PROCEEDINGS OF THE OCEAN DRILLING PROGRAM

INITIAL REPORTS

VOLUME 130
18 January 1990–26 March 1990

NATIONAL SCIENCE FOUNDATION

JOINT OCEANOGRAPHIC INSTITUTIONS, INC.

best copy available

130

DRILLING LOCATIONS

LEG	LOCATION	REP	SITES
100	Gulf of Mexico	E	625A–625C
101	Bahamas	E	626–636
102	Bermuda Rise	E	418
103	Galicia Margin	E	637–641
104	Norwegian Sea	E	642–644
105	Baffin Bay–Labrador Sea	E	645–647
106	Mid-Atlantic Ridge	E	648–649
107	Tyrrhenian Sea	E	650–656
108	Eastern Tropical Atlantic	E	657–668
109	Mid-Atlantic Ridge	E	669–670, 395, 648
110	Northern Barbados Ridge	E	671–676
111	Costa Rica Rift	G	677–678, 504B
112	Peru Continental Margin	G	679–688
113	Weddell Sea, Antarctica	E	689–697
114	Subantarctic South Atlantic	E	698–704
115	Mascarene Plateau	G	705–716
116	Distal Bengal Fan	G	717–719
117	Oman Margin	G	720–731
118	Southwest Indian Ridge	G	732–735
119	Kerguelen Plateau–Prydz Bay	E	736–746
120	Central Kerguelen Plateau	E	747–751
121	Broken Ridge & Ninetyeast Ridge	G	752–758
122	Exmouth Plateau	G	759–764
123	Argo Abyssal Plain–Exmouth Plateau	G	765–766
124	Celebes & Sulu Seas	G	767–771
124E	Philippine Sea	G	772–777
125	Bonin/Mariana Region	G	778–786
126	Bonin Arc-Trench System	G	787–793
127	Japan Sea	G	794–797
128	Japan Sea	G	794, 798–799
129	Old Pacific Crust	G	800–802
130	Ontong Java Plateau	G	803–807

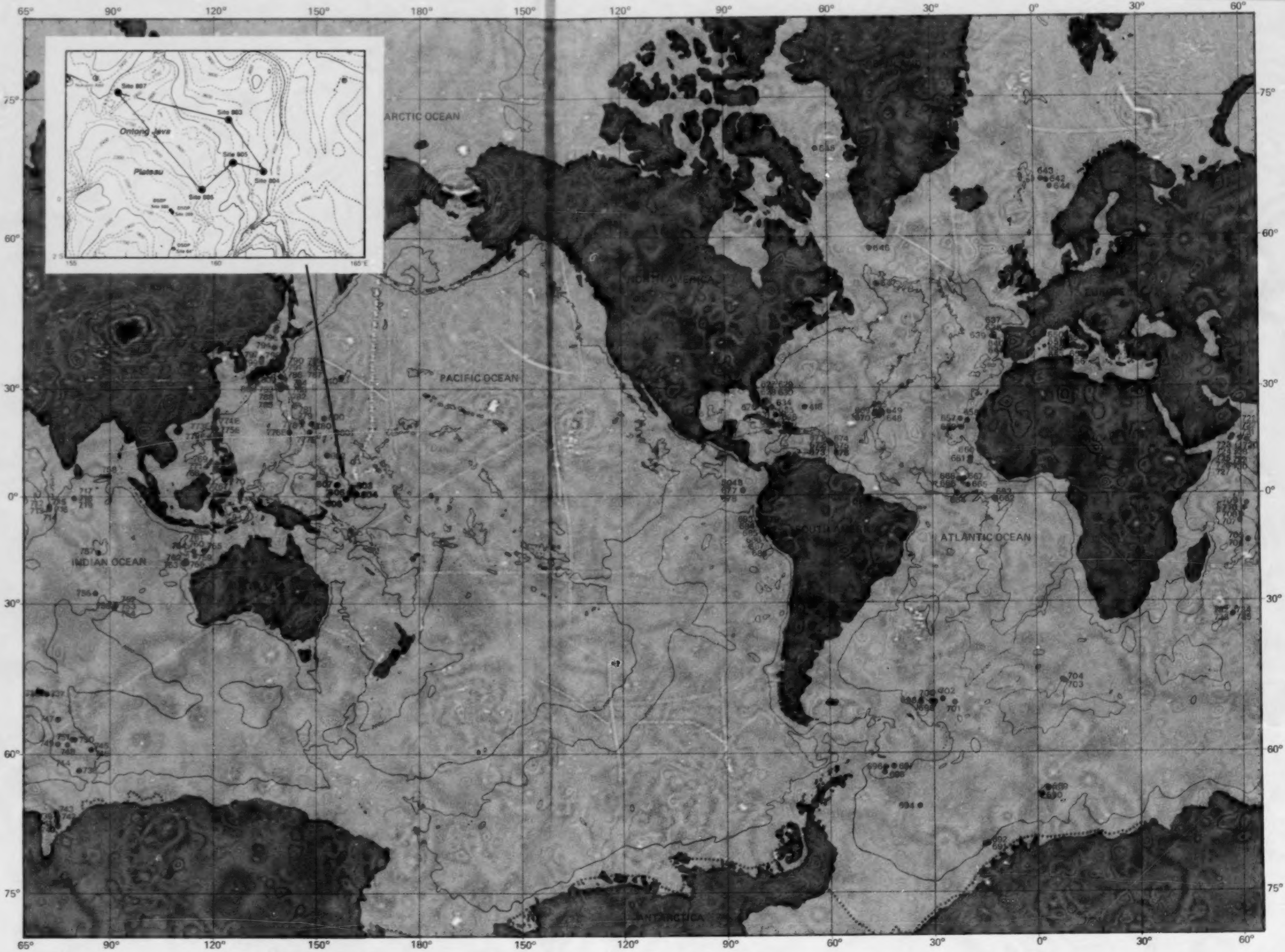
Site 807
Site 803
Site 805
Site 804
Site 806
Ontong Java
Plateau
155
160
165°E
ARCTIC OCEAN
PACIFIC OCEAN
NORTH AMERICA
SOUTH AMERICA
ATLANTIC OCEAN
INDIAN OCEAN
ANTARCTICA
65°
90°
120°
150°
180°
150°
120°
90°
60°
30°
0°
30°
60°
75°
60°
30°
0°
30°
60°
75°

STORAGE

E - East Coast Repository
G - Gulf Coast Repository

OCEAN DRILLING PROGRAM

NS 1.38/2:

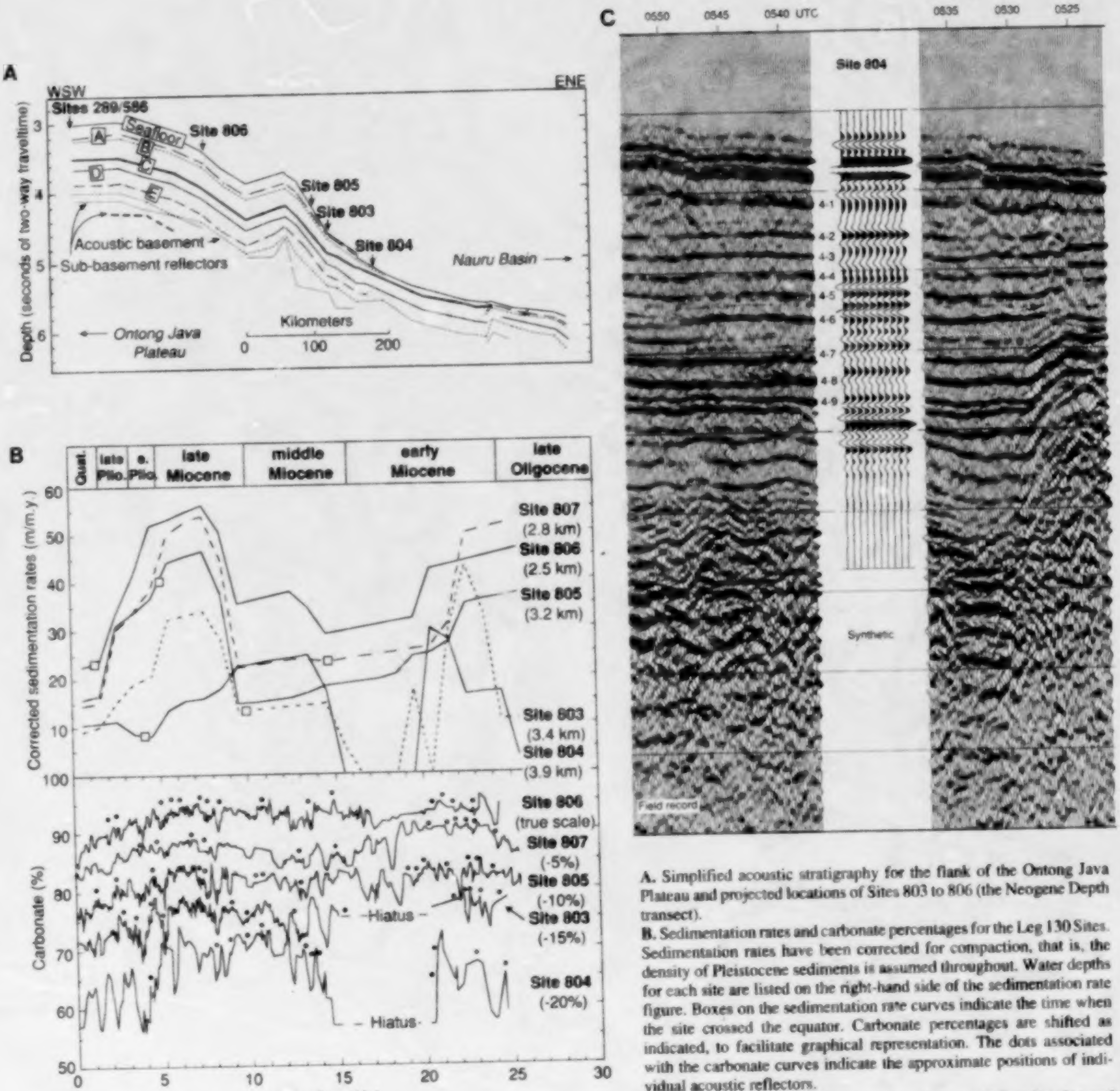

A. Simplified acoustic stratigraphy for the flank of the Ontong Java Plateau and projected locations of Sites 803 to 806 (the Neogene Depth transect).

B. Sedimentation rates and carbonate percentages for the Leg 130 Sites. Sedimentation rates have been corrected for compaction, that is, the density of Pleistocene sediments is assumed throughout. Water depths for each site are listed on the right-hand side of the sedimentation rate figure. Boxes on the sedimentation rate curves indicate the time when the site crossed the equator. Carbonate percentages are shifted as indicated, to facilitate graphical representation. The dots associated with the carbonate curves indicate the approximate positions of individual acoustic reflectors.

C. Comparison of synthetic seismogram (generated from logging and physical property data) with the field record at Site 804. Matching of the synthetic with the field record provides a powerful test of the correctness of age assignments given to the reflectors.

A. Core photo of typical nannofossil ooze recovered during Leg 130 (Sections 130-805B-29X-1 through -5). Note the alternating light/dark intervals throughout the core.
B. Example of spectral analysis of the GRAPE data from Hole 806C (25–34 mbsf) and the global stack of tropical planktonic $\delta^{18}O$ (SPECMAP stack, Imbrie et al., 1984). Note the strong power associated with periods of ≈ 100, 41, and 21 k.y. in both records.
C. Cretaceous/Tertiary boundary transition at Site 807 (Interval 130-807C-54R-3, 125–145 cm). The boundary was placed in the interval represented by the black bar based on the first occurrence, rapid rise, and subsequent decline of the calcareous dinoflagellate *Thoracosphaera*.
D. Cretaceous/Tertiary boundary transition at Site 803 (Interval 130-803D-68R-1, 40–60 cm). The boundary was placed in the interval represented by the black bar.
E. Basalt pillow penetrated by rotary drilling at Site 803. Note glassy rim (at top), fractures, vein-fill, and signs of alteration of phenocrysts within the fine-grained matrix (Interval 130-803D-69R-2, 0–40 cm).

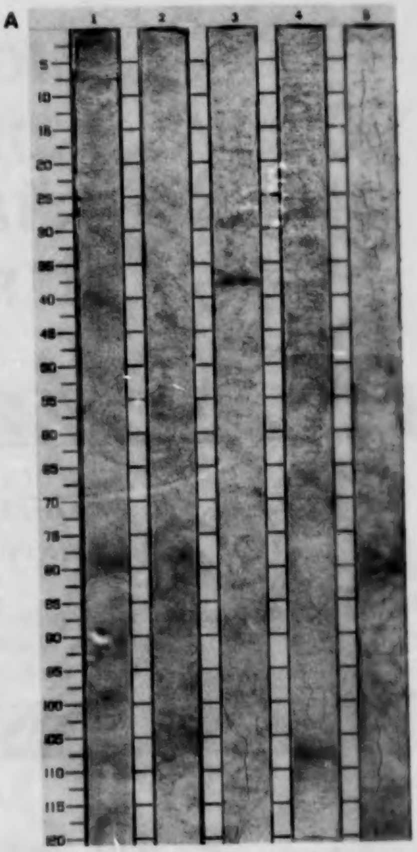
A
1
2
3
4
5
5
10
15
20
25
30
35
40
45
50
55
60
65
70
75
80
85
90
95
100
105
110
115
120

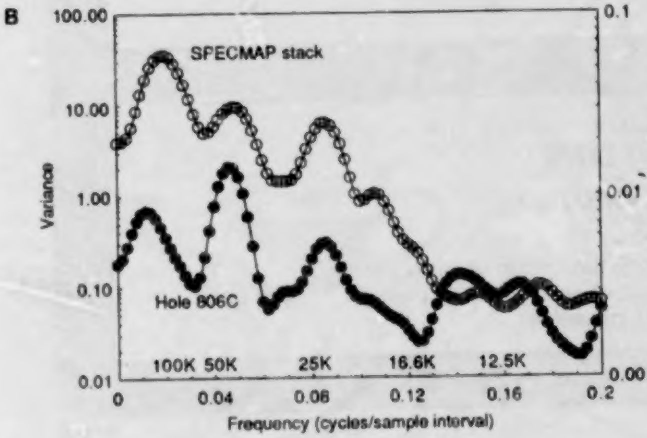

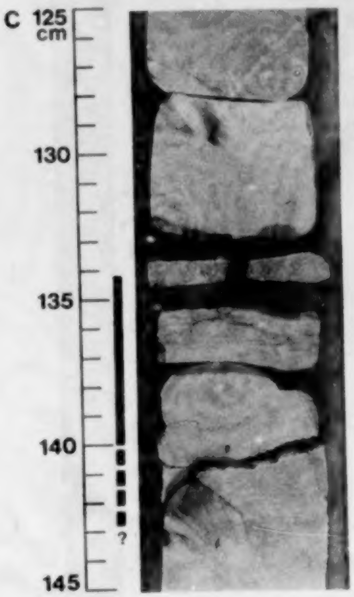
C
125 cm
130
135
140
145
?

D
40 cm
45
50
55
60

E
cm
10
20
30
40

PROCEEDINGS
OF THE
OCEAN DRILLING
PROGRAM

VOLUME 130
INITIAL REPORTS
ONTONG JAVA PLATEAU

Covering Leg 130 of the cruises of the Drilling Vessel *JOIDES Resolution*,
Apra Harbor, Guam, to Apra Harbor, Guam, Sites 803–807,
18 January 1990–26 March 1990

Loren W. Kroenke, Wolfgang H. Berger, Thomas R. Janecek,
Jan Backman, Franck Bassinot, Richard M. Corfield, Margaret Lois Delaney,
Rick Hagen, Eystein Jansen, Lawrence A. Krissek, Carina Lange, Robert Mark Leckie,
Ida Lykke Lind, Mitchell W. Lyle, John J. Mahoney, Janice C. Marsters,
Larry Mayer, David C. Mosher, Robert Musgrave, Michael L. Prentice,
Johanna M. Resig, Heike Schmidt, Rainer Stax, Michael Storey,
Kozo Takahashi, Toshiaki Takayama, John A. Tarduno,
Roy H. Wilkens, Guoping Wu
Shipboard Scientific Party

Thomas R. Janecek
Shipboard Staff Scientist

Prepared by the
OCEAN DRILLING PROGRAM
TEXAS A&M UNIVERSITY

Eva M. Barbu
Volume Editor

in Cooperation with the
NATIONAL SCIENCE FOUNDATION
and
JOINT OCEANOGRAPHIC INSTITUTIONS, INC.

PROCEEDINGS OF THE OCEAN DRILLING PROGRAM

VOLUME 130

INITIAL REPORTS

ONTONG JAVA PLATEAU

Covering Leg 130 of the cruises of the Drilling Vessel *JOIDES Resolution*,
Apra Harbor, Guam, to Apra Harbor, Guam, Sites 803–807,
18 January 1990–26 March 1990

Loren W. Kroenke, Wolfgang H. Berger, Thomas R. Janecek,
Jan Backman, Franck Bassinot, Richard M. Corfield, Margaret Lois Delaney,
Rick Hagen, Eystein Jansen, Lawrence A. Krissek, Carina Lange, Robert Mark Leckie,
Ida Lykke Lind, Mitchell W. Lyle, John J. Mahoney, Janice C. Marsters,
Larry Mayer, David C. Mosher, Robert Musgrave, Michael L. Prentice,
Johanna M. Resig, Heike Schmidt, Rainer Stax, Michael Storey,
Kozo Takahashi, Toshiaki Takayama, John A. Tarduno,
Roy H. Wilkens, Guoping Wu
Shipboard Scientific Party

Thomas R. Janecek
Shipboard Staff Scientist

Prepared by the
OCEAN DRILLING PROGRAM
TEXAS A&M UNIVERSITY

Eva M. Barbu
Volume Editor

in Cooperation with the
NATIONAL SCIENCE FOUNDATION
and
JOINT OCEANOGRAPHIC INSTITUTIONS, INC.

This publication was prepared by the Ocean Drilling Program, Texas A&M University, as an account of work performed under the international Ocean Drilling Program, which is managed by Joint Oceanographic Institutions, Inc., under contract with the National Science Foundation. Funding for the program was provided by the following agencies at the time of this cruise:

Canada/Australia Consortium for the Ocean Drilling Program, Department of Energy, Mines and Resources (Canada) and Department of Primary Industries and Energy (Australia)

Deutsche Forschungsgemeinschaft (Federal Republic of Germany)

European Science Foundation Consortium for the Ocean Drilling Program (Belgium, Denmark, Finland, Iceland, Italy, Greece, the Netherlands, Norway, Spain, Sweden, Switzerland, and Turkey)

Institut Français de Recherche pour l'Exploitation de la Mer (France)

National Science Foundation (United States)

Natural Environment Research Council (United Kingdom)

University of Tokyo, Ocean Research Institute (Japan)

Any opinions, findings, and conclusions or recommendations expressed in this publication are those of the author(s) and do not necessarily reflect the views of the National Science Foundation, the participating agencies, Joint Oceanographic Institutions, Inc., Texas A&M University, or Texas A&M Research Foundation.

It is recommended that reference to the whole or to part of this volume be made in one of the following forms, as appropriate:

Kroenke, L. W., Berger, W. H., Janecek, T. R., et al. 1991. *Proc. ODP, Init. Repts.*, 130: College Station, TX (Ocean Drilling Program).

Shipboard Scientific Party, 1991. Site 803. *In* Kroenke, L. W., Berger, W. H., Janecek, T. R., et al., *Proc. ODP, Init. Repts.*, 130: College Station, TX (Ocean Drilling Program), 101–176.

Effective Publication Dates of ODP *Proceedings*

According to the International Code of Zoological Nomenclature, the date of publication of a work and of a contained name or statement affecting nomenclature is the date on which the publication was mailed to subscribers, placed on sale, or when the whole edition is distributed free of charge, mailed to institutions and individuals to whom free copies are distributed. The mailing date, *not the printed date*, is the correct one.

The mailing dates of recent *Proceedings of the Ocean Drilling Program* are as follows:

Volume 127 (*Initial Reports*): September 1990
Volume 128 (*Initial Reports*): September 1990
Volume 129 (*Initial Reports*): December 1990
Volume 114 (*Scientific Results*): February 1991
Volume 115 (*Scientific Results*): September 1990
Volume 116 (*Scientific Results*): September 1990
Volume 117 (*Scientific Results*): February 1991

Distribution

Copies of this publication may be obtained from Publications Distribution Center, Ocean Drilling Program, 1000 Discovery Drive, College Station, Texas 77845-9547. Orders for copies will require advance payment. See current ODP publication list for price and availability of this publication.

Printed March 1991

ISSN 0884-5883
Library of Congress 87-655-674

The paper used in this publication meets the minimum requirements of American National Standard for Information Sciences—Permanence of Paper for Printed Library Materials, ANSI Z39.48–1984∞™

Foreword

By the National Science Foundation

The scientists of the Ocean Drilling Program (ODP) have embarked on what could prove to be one of the most important earth science initiatives of the decade—an initiative rivaling in scope and impact the exploration of the frontiers of outer space. The program explores our planet's last frontier—the Earth's structure and history as it is revealed beneath the oceans. The scope of the program's scientific goals excites the imagination, challenges the intellect, and enhances the spirit of cooperation among peoples in countries around the world.

Between 1872 and 1876, HMS *Challenger* undertook the world's first major oceanographic expedition. That expedition greatly expanded man's knowledge of the world's oceans and revolutionized our ideas about planet Earth. From 1968 to 1983, another ship named *Challenger* logged more than 375,000 miles on 96 voyages across every ocean for the Deep Sea Drilling Project (DSDP), operated by Scripps Institution of Oceanography. Among the project's many remarkable discoveries were the confirmation of seafloor spreading and the establishment of the relative youth of the seafloor, thus verifying the dynamic and changing nature of the Earth's crust.

Today, the Ocean Drilling Program, which began in 1983, brings new resources to bear on scientific ocean drilling. A new drillship is in operation—the *JOIDES Resolution*—one of the world's most modern and best equipped drillships with enhanced capability for drilling and coring in polar areas and rough weather, expanded laboratory space, facilities for more scientists, and a major drill-hole logging program. The name of the ship was derived from the international scientific partnership that directs the program—the Joint Oceanographic Institutions for Deep Earth Sampling (JOIDES)—and from the flagship of Captain Cook's second voyage to the Pacific Ocean in the late 18th century. Texas A&M University is responsible for science operations in the program, and Lamont-Doherty Geological Observatory is responsible for the logging program.

The Ocean Drilling Program truly has international participation. In 1975, the International Phase of Ocean Drilling began with member nations—the U.S.A., U.S.S.R., Federal Republic of Germany, Japan, United Kingdom, and France—all providing funds and scientific guidance for the project. Today, ODP partners include the U.S.A., the Canada/Australia Consortium for the Ocean Drilling Program, France, the Federal Republic of Germany, Japan, the United Kingdom, and the European Science Foundation, which represents Sweden, Finland, Norway, Iceland, Denmark, Belgium, the Netherlands, Spain, Switzerland, Italy, Greece, and Turkey. The National Science Foundation, with funds contributed by the United States and international partners, supports the scientific operations and planning for the ODP through a contract with Joint Oceanographic Institutions, Inc. (JOI).

The information gained by the program leads to a better understanding of the Earth and its dynamic processes. Drilled sediment cores and logs reveal clues to past climatic history and tie into parallel studies of paleoclimates from glacial ice cores drilled on the continents. Understanding these sediment cores will enable scientists to complete the map of major geologically active regions of the Earth, and to identify processes that lead to dynamic change such as earthquakes, volcanic eruptions, and mountain and continental growth. We are far from being able to predict such changes accurately now; but with the new tools and understanding, the accuracy of such predictions can be improved. This better understanding of the Earth's system(s) will allow us to identify regions of potential mineral and energy resource development, an issue of worldwide human interest. The Ocean Drilling Program is not in itself aimed at finding resources, but the knowledge of the Earth's processes that is gained through such a basic research program will inevitably provide pieces of information required for such resource discovery and exploitation.

The program is fully under way in its aim to further the understanding of the Earth's dynamic systems. People of our planet will benefit directly and indirectly from this research in both their daily living and work activities. This multinational endeavor will perhaps foster other cooperative efforts in science or among societies. The Ocean Drilling Program has distinguished ancestors in the original *Resolution* and *Challenger* expeditions and the Deep Sea Drilling Project. The National Science Foundation is proud to be playing a leading role in this program, and we are looking forward to significant and innovative science for many years to come.

Erich Bloch
Director
National Science Foundation

Washington, D.C.

Foreword

By Joint Oceanographic Institutions, Inc.

This volume presents results from the Ocean Drilling Program (ODP), where scientists use a specially equipped ocean drilling ship to sample and measure the properties of the submerged part of the Earth's crust. These data are then synthesized with other information to yield new insights into earth processes.

These results address the scientific goals of the program, which include providing a global description of geological and geophysical structures and materials, studying in detail areas of major geophysical activity such as mid-ocean ridges and the associated hydrothermal circulations, and studying passive and active continental margins. In addition, the ODP data support the study of sea-level and ocean-circulation changes, the effects of the Earth's orbital variations on climate, and the study of processes and mechanisms of evolution from the biological records in the cores which are recovered from drilling.

The Ocean Drilling Program is a partnership of scientists and governments. Overall scientific policy and management guidance is provided by Joint Oceanographic Institutions for Deep Earth Sampling (JOIDES), which consists of committees and panels made up of representatives of the participating institutions and other scientific and engineering experts. The JOIDES Executive Committee (EXCOM) provides general oversight; the JOIDES Planning Committee (PCOM) is the focal point for all scientific planning for the ODP and is key to the scientific success of the program.

The PCOM has a network of panels and working groups which screen drilling proposals, evaluate instrumentation and measurement techniques, and assess geophysical survey data and other safety and siting information. PCOM uses the recommendations of these panels and committees to select drilling targets, to specify the major scientific objectives of each two-month drilling segment or leg, and to provide the science operator with nominations for co-chief scientists. The science operator, Texas A&M University, in turn is responsible for planning the detailed ship's operations, actual drilling schedules, and final scientific rosters, which are developed in close cooperation with PCOM and the cognizant panels.

Many of the scientific goals can be met only with new technology. Thus the program has identified engineering goals, which include the ability to start a hole and to core on bare rock at mid-ocean ridge sites, to drill in high-temperature and corrosive regions typical of hydrothermal areas, and to core in high latitudes with minimum interference from high seas and sea ice. To meet these needs, the program operates a specially equipped drillship, the *JOIDES Resolution*, which contains laboratories and equipment that are state-of-the-art, and carries a major new logging program.

The ship, registered as SEDCO/BP 471 after her owners and her length in feet (144 meters), is 70 feet (21 meters) wide, and has a displacement of 16,595 long tons. Her derrick towers 200 feet (61 meters) above the waterline, and a computer-controlled dynamic-positioning system stabilizes the ship over a specific location while drilling in water depths up to 27,000 feet (8230 meters). The drilling system collects cores from beneath the seafloor with a derrick and drawworks that can handle 30,000 feet (9144 meters) of drill pipe. More than 12,000 square feet (1115 square meters) of space distributed throughout the ship is devoted to scientific laboratories and equipment. The ship sails with a scientific and technical crew of 50 and a ship's crew of 65.

Logging is a major part of the overall operation. The program provides a full suite of geochemical and geophysical measurements for every hole deeper than 1300 feet (400 meters). For each such hole, there are lowerings of basic oil-industry tools: nuclear, sonic, and electrical. In addition, a borehole televiewer is available for imaging the well-bore wall, a 12-channel logging tool provides accurate velocity and elastic property measurements as well as sonic waveforms for spectral analysis of energy propagation near the well bore, and a vertical seismic profiler records reflectors from below the total depth of the hole.

Texas A&M University serves as science operator for the Ocean Drilling Program. In this capacity, they operate and staff the drillship to collect cores from JOIDES-designated sites from around the world. The science operator also ensures that adequate scientific analyses are performed on the cores by maintaining the shipboard scientific laboratories and by providing logistical and technical support for shipboard scientific teams. Onshore, Texas A&M manages scientific activities after each leg, is curator for the cores, distributes samples, and coordinates the editing and publication of the scientific results. Lamont-Doherty Geological Observatory (LDGO) of Columbia University manages the program's logging operations, which include processing the data and provision of assistance to scientists in data analysis. The ODP Data Bank, a repository for geophysical data, is also managed by LDGO. Core samples from ODP and the previous Deep Sea Drilling Project are stored for future investigation at three sites: ODP Pacific and Indian Ocean cores at Texas A&M University, ODP and DSDP Atlantic and Antarctic cores at Lamont-Doherty Geological Observatory, and DSDP Pacific and Indian Ocean cores at Scripps Institution of Oceanography.

International oversight and coordination are provided by the ODP Council, a governmental consultative body of partner country representatives, chaired by the United States, which periodically reviews the general progress of the program and discusses financial plans and other management issues. Joint Oceanographic Institutions, Inc., a nonprofit consortium of U.S. oceanographic institutions, serves as the National Science Foundation's prime contractor and manages the ODP. JOI is responsible for seeing that the scientific objectives and plans are translated into scientific operations consistent with JOIDES recommendations and budgetary constraints.

Scientific achievements of the ODP already include new data on early seafloor spreading and how continents separate and their margins evolve. We have new insight into glacial cycles and the fluctuations of currents throughout geological time. Technical achievements include the first bare-rock coring, and logging data more accurate and complete than ever before. JOI is pleased to have played a facilitating role in the Ocean Drilling Program.

DJames Baker

D. James Baker
President
Joint Oceanographic Institutions, Inc.

Washington, D.C.

OCEAN DRILLING PROGRAM

MEMBER ORGANIZATIONS OF THE JOINT OCEANOGRAPHIC INSTITUTIONS FOR DEEP EARTH SAMPLING (JOIDES):

University of California at San Diego, Scripps Institution of Oceanography

Columbia University, Lamont-Doherty Geological Observatory

University of Hawaii, Hawaii Institute of Geophysics

University of Miami, Rosenstiel School of Marine and Atmospheric Science

Oregon State University, College of Oceanography

University of Rhode Island, Graduate School of Oceanography

Texas A&M University, College of Geosciences

University of Texas at Austin, Institute for Geophysics

University of Washington, College of Ocean and Fishery Sciences

Woods Hole Oceanographic Institution

Canada/Australia Consortium for the Ocean Drilling Program, Department of Energy, Mines and Resources (Canada) and Department of Primary Industries and Energy (Australia)

European Science Foundation Consortium for Ocean Drilling, Belgium, Denmark, Finland, Iceland, Italy, Greece, the Netherlands, Norway, Spain, Sweden, Switzerland, and Turkey

Federal Republic of Germany, Bundesanstalt für Geowissenschaften und Rohstoffe

France, Institut Français de Recherche pour l'Exploitation de la Mer

Japan, University of Tokyo, Ocean Research Institute

United Kingdom, Natural Environment Research Council

PRIME CONTRACTOR

Joint Oceanographic Institutions, Inc.
Washington, D.C.

Thomas E. Pyle
Director, Ocean Drilling Programs

OPERATING INSTITUTION

College of Geosciences
Texas A&M University
College Station, Texas

Melvin Friedman
Principal Investigator

OCEAN DRILLING PROGRAM

Philip D. Rabinowitz
Director

Timothy J. G. Francis
Deputy Director

Richard G. McPherson
Administrator

Audrey W. Meyer, Manager
Science Operations

Barry W. Harding, Manager
Engineering and Drilling Operations

Russell B. Merrill, Curator and Manager
Science Services

Robert E. Olivas, Manager
Technical and Logistics Support

LOGGING OPERATOR

Borehole Research Group
Lamont-Doherty Geological Observatory
Columbia University
Palisades, New York

Roger N. Anderson, Head

PARTICIPANTS ABOARD *JOIDES RESOLUTION* FOR LEG 130*

Loren W. Kroenke
Co-Chief Scientist
Hawaii Institute of Geophysics
University of Hawaii
2525 Correa Road
Honolulu, Hawaii 96822

Wolfgang H. Berger
Co-Chief Scientist
Fachbereich Geowissenschaften
Universität Bremen
Postfach 330440
D-2800 Bremen 33
Federal Republic of Germany

Thomas R. Janecek
ODP Staff Scientist/Sedimentologist
Ocean Drilling Program
Texas A&M University
1000 Discovery Drive
College Station, Texas 77845-9547

Jan Backman
Paleontologist (nannofossils)
Department of Geology
University of Stockholm
S-10691 Stockholm
Sweden

Franck Bassinot
Physical Properties Specialist
Département de Géologie Dynamique
Université Pierre et Marie Curie
4 Place Jussieu
75252 Paris Cedex 05
France

Richard M. Corfield
Paleontologist (foraminifers)
Department of Earth Sciences
University of Oxford
Parks Road
Oxford OX1 3PR
United Kingdom

Margaret Lois Delaney
Inorganic Geochemist
Institute of Marine Sciences
University of California, Santa Cruz
Santa Cruz, California 95064

Rick Hagen
Geophysicist
Hawaii Institute of Geophysics
University of Hawaii
2525 Correa Road
Honolulu, Hawaii 96822

Eystein Jansen
Sedimentologist
Department of Geology
University of Bergen
Allegaten 41
N-5007 Bergen
Norway

Lawrence A. Krissek
Sedimentologist
Department of Geology and Mineralogy
Ohio State University
125 South Oval Mall
Columbus, Ohio 43210-1298

Carina Lange
Paleontologist (diatoms)
Scripps Institution of Oceanography
University of California, San Diego
La Jolla, California 92093-0215

Robert Mark Leckie
Paleontologist (foraminifers)
Department of Geology and Geography
University of Massachusetts
Amherst, Massachusetts 01003

Ida Lykke Lind
Sedimentologist
Instituttet for Teknisk Geologi
DTH, Bygning 204
DK2800 Lyngby
Denmark

Mitchell W. Lyle
LDGO Logging Scientist
Borehole Research Group
Lamont-Doherty Geological Observatory
Columbia University
Palisades, New York 10964

John J. Mahoney
Igneous Petrologist
Hawaii Institute of Geophysics
University of Hawaii
2525 Correa Road
Honolulu, Hawaii 96822

Janice C. Marsters
Physical Properties Specialist
Hawaii Institute of Geophysics
University of Hawaii
2525 Correa Road
Honolulu, Hawaii 96822

---

*Addresses at time of cruise.

Larry Mayer
Logging Scientist
Department of Oceanography
Dalhousie University
Halifax, Nova Scotia B3H 4J1
Canada

David C. Mosher
Sedimentologist
Department of Oceanography
Dalhousie University
Halifax, Nova Scotia B3H 4J1
Canada

Robert Musgrave
Paleomagnetist
Geology Department
University of Tasmania
G.P.O. Box 252C
Hobart, Tasmania 7001
Australia

Michael L. Prentice
Sedimentologist
Department of Geological Sciences
University of Maine
Orono, Maine 04469

Johanna M. Resig
Paleontologist (foraminifers)
Department of Geology and Geophysics
University of Hawaii
2525 Correa Road
Honolulu, Hawaii 96822

Heike Schmidt
Sedimentologist
Fachbereich Geowissenschaften
Universität Bremen
Postfach 330440
D-2800 Bremen 33
Federal Republic of Germany

Rainer Stax
Organic Geochemist
Institut für Geowissenschaften und Lithosphärenforschung
Universität Giessen
Senckenbergstrasse 3
D-6300 Giessen
Federal Republic of Germany

Michael Storey
Igneous Petrologist
Department of Geology
University of Keele
Keele, Staffordshire ST5 5BG
United Kingdom

Kozo Takahashi
Paleontologist (radiolarians)
Department of Geology and Geophysics
Woods Hole Oceanographic Institution
Woods Hole, Massachusetts 02543

Toshiaki Takayama
Paleontologist (nannofossils)
Department of Geology
College of Liberal Arts
Kanazawa University
1-1 Marunouchi
Kanazawa 920
Japan

John A. Tarduno
Paleomagnetist
Scripps Institution of Oceanography
University of California, San Diego
La Jolla, California 92093-0215

Roy H. Wilkens
Physical Properties Specialist/Logging Scientist
Hawaii Institute of Geophysics
University of Hawaii
2525 Correa Road
Honolulu, Hawaii 96822

Guoping Wu
Sedimentologist
Scripps Institution of Oceanography
University of California, San Diego
La Jolla, California 92093-0215

SEDCO OFFICIALS

Captain Edwin G. Oonk
Master of the Drilling Vessel
Underseas Drilling, Inc.
707 Texas Avenue South
Suite 103D
College Station, Texas 77840-1917

Kenneth D. Horne
Drilling Superintendent
Underseas Drilling, Inc.
707 Texas Avenue South
Suite 103D
College Station, Texas 77840-1917

ODP ENGINEERING AND OPERATIONS PERSONNEL

Eugene Pollard	Drilling Superintendent
Mark Robinson	Engineer

ODP TECHNICAL AND LOGISTICS PERSONNEL

Wendy J. Autio	Marine Technician/Paleomagnetics Laboratory
Stacey Cervantes	Photographer
David Cunningham	Marine Technician/Core Laboratory
MaryAnn Cusimano	Chemistry Technician
Kenneth du Vall	Marine Technician/Marine Geophysics Laboratory
John R. Eastlund	Computer Systems Manager
Ted ("Gus") Gustafson	Marine Technician/Marine Geophysics Laboratory
Burney Hamlin	Laboratory Officer
Michiko Hitchcox	Yeoperson
Matt Mefferd	Assistant Laboratory Officer
Peggy Myre	Curatorial Representative
Carie Rivers	Marine Technician/Core Laboratory
Mark C. Simpson	Chemistry Technician
Donald Sims	X-ray Technician
William Stevens	Electronics Technician
Mark Watson	Electronics Technician
Barry Weber	Electronics Technician
Charles Williamson	Marine Technician/Shipping/Storekeeper

Ocean Drilling Program Publications Staff

Publications Supervisor
William D. Rose

Chief Editor
Norman J. Stewart

Editors
Eva M. Barbu
Lona Haskins Dearmont
Sondra K. Stewart
William R. Winkler

Chief Production Editor
Jennifer Pattison Hall

Production Editors
Janna C. Abel
Jaime A. Gracia (this volume)

Publications Coordinator
Janalisa Braziel Soltis

Assistant Publications Coordinator
Jill Mutschler-Fontenot

Hole Summary Coordinator
Laura Hammond Young

Publications Distribution Specialist
Fabiola Muñoz Byrne

Senior Photographer
John W. Beck

Photographer
Roy T. Davis

Chief Illustrator
Deborah Partain

Illustrators
Michelle Curtis
Linda C. De Leon
Garnet D. Gaither
Cynthia M. Mullican

Compositor
Mary Elizabeth Betz

Production Assistants
Gudelia ("Gigi") Delgado
Lisa L. Tirey

TABLE OF CONTENTS

VOLUME 130—INITIAL REPORTS

Acknowledgments 1

SECTION 1: INTRODUCTION

1. Introduction 5
Shipboard Scientific Party

2. Explanatory Notes 15
Shipboard Scientific Party

3. SeaBeam and Seismic Reflection Surveys on the Ontong Java Plateau 45
L. A. Mayer, T. H. Shipley, E. L. Winterer, D. Mosher, and R. A. Hagen

4. Underway Geophysics 77
R. A. Hagen and Shipboard Scientific Party

SECTION 2: SITE REPORTS

5. Site 803 101
Shipboard Scientific Party

    Principal results 102
    Background and objectives 102
    Operations 103
    Lithostratigraphy 107
    Biostratigraphy 118
    Paleomagnetism 127
    Sedimentation rates 132
    Inorganic geochemistry 132
    Carbon geochemistry 139
    Physical properties 139
    Igneous petrology 146
    Logging 149
    Seismic stratigraphy 155
    Summary and conclusions 164
    References 166

6. Site 804 177
Shipboard Scientific Party

    Principal results 177
    Background and objectives 178
    Operations 181
    Lithostratigraphy 181
    Biostratigraphy 187
    Paleomagnetism 193
    Sedimentation rates 196
    Inorganic geochemistry 200
    Carbon geochemistry 202
    Physical properties 202

Seismic stratigraphy 207
Summary and conclusions 215
References 221

7. Site 805 223
Shipboard Scientific Party

Principal results 223
Background and objectives 224
Operations 226
Lithostratigraphy 230
Biostratigraphy 232
Paleomagnetism 245
Sedimentation rates 248
Inorganic geochemistry 248
Organic geochemistry 254
Physical properties 256
Logging 260
Seismic stratigraphy 266
Summary and conclusions 270
References 278

8. Site 806 291
Shipboard Scientific Party

Principal results 291
Background and objectives 292
Operations 295
Lithostratigraphy 297
Biostratigraphy 307
Paleomagnetism 316
Sedimentation rates 320
Inorganic geochemistry 320
Carbon geochemistry 326
Physical properties 326
Logging 329
Seismic stratigraphy 335
Summary and conclusions 339
References 354

9. Site 807 369
Shipboard Scientific Party

Principal results 369
Background and objectives 371
Operations 374
Lithostratigraphy 375
Biostratigraphy 393
Paleomagnetism 408
Sedimentation rates 414
Inorganic geochemistry 417
Carbon geochemistry 419
Physical properties 420
Igneous petrology 428
Logging 439
Seismic stratigraphy 444
Summary and conclusions 448
References 462

SECTION 3: SYNTHESIS

10. Ontong Java Plateau, Leg 130: Synopsis of Major Drilling Results 497
W. H. Berger, L. W. Kroenke, L. A. Mayer, and Shipboard Scientific Party

SECTION 4: SUMMARY

11. High-resolution, Whole-core Magnetic Susceptibility Data from Leg 130, Ontong Java Plateau .541
J. A. Tarduno, L. A. Mayer, R. Musgrave, and Shipboard Scientific Party

12. Inorganic Geochemistry Summary 549
M. L. Delaney and Shipboard Scientific Party

13. GRAPE Density Records and Density Cyclicity 553
E. Jansen, L. A. Mayer, and Shipboard Scientific Party

SECTION 5: CORES

Core description forms and core photographs for:

Site 803 559

Site 804 671

Site 805 725

Site 806 839

Site 807 981

SECTION 6: POLICY

JOIDES Advisory Groups 1235

Sample-distribution Policy 1239

BACK-POCKET FOLDOUTS

Chapter 11: Figure 1. Whole-core magnetic susceptibility data from Holes 805A, 806A, and 807A to 35 mbsf using an 80-mm Bartington MS2C sensor
Chapter 11: Figure 2. Correlation between Holes 805A and 805C using whole-core magnetic susceptibility data
Chapter 11: Figure 3. Correlation between Holes 806A, 806B, and 806C to 15.0 mbsf using whole-core magnetic susceptibility data
Chapter 11: Figure 4. Comparison of whole-core magnetic susceptibility data for Site 806A using an 80-mm Bartington MS2C sensor and a 100-mm MS1C Bartington sensor
Chapter 11: Figure 11. Correlation between Holes 807A and 807B using whole-core magnetic susceptibility data
Chapter 11: Figure 13. Correlation between Holes 807A, 805C, and 806A/C down to 7.0 mbsf using whole-core magnetic susceptibility data

BACK-POCKET MICROFICHE

Formation microscanner images for Leg 130 (fiche 1–11):

Hole 803D: Main log (pass 2), depth range, 92–307 mbsf
Hole 803D: Main log (pass 1), depth range, 299–611 mbsf
Hole 807C: Main log (pass 2), depth range 1097–1504 mbsf

Chapter 4: Table 1. Navigation data
Chapter 5: Table 9. Carbonate and inorganic carbon data, Site 803
Chapter 5: Table 11. Laboratory vane shear strength, Site 803
Chapter 5: Table 12. Laboratory compressional wave velocity, Site 803
Chapter 5: Table 13. Discrete index properties, Site 803
Chapter 6: Table 5. Carbonate and inorganic carbon data, Site 804
Chapter 6: Table 7. Shear strength data, Site 804
Chapter 6: Table 9. Index properties data, Site 804
Chapter 6: Table 10. *P*-wave velocity data, Site 804
Chapter 7: Table 8. Carbonate and inorganic carbon data, Holes 805B and 805C
Chapter 7: Table 9. Laboratory vane shear strength, Holes 805B and 805C
Chapter 7: Table 10. Discrete index properties, Holes 805B and 805C
Chapter 7: Table 11. *P*-wave velocity data, Holes 805B and 805C
Chapter 8: Table 6. Concentrations of total carbon and inorganic carbon, Hole 806B
Chapter 8: Table 7. Shear strength data, Holes 806B and 806C
Chapter 8: Table 8. Index properties data, Holes 806B and 806C
Chapter 8: Table 9. *P*-wave velocity data, Holes 806B and 806C
Chapter 9: Table 14. *P*-wave velocity data, Site 807

ACKNOWLEDGMENTS

The Leg 130 Scientific Party of the Ocean Drilling Program expresses its thanks to the great number of people and organizations who helped us plan and complete a very successful drilling program. This summary of shipboard results represents one tangible product of their efforts.

In particular, we thank Carl Brenner and the staff of the JOIDES/ODP Site Survey Data Bank, Lamont-Doherty Geological Observatory, for providing us with the extensive site survey data that aided in our site selection. We extend our gratitude to Captain Ed Oonk and his officers, engineers, and crew for getting us safely there and back. We are grateful to Gene Pollard, ODP Operations Superintendent, and Ken Horne, SEDCO drilling superintendent, for their dedicated and enthusiastic efforts. The skill and good spirits of the drill floor crew are very much appreciated. Their drilling efforts resulted in a record amount of recovery of both pelagic ooze and plateau basalt.

Our special thanks goes to the ODP technical staff, who had more work on their hands than could reasonably be expected. Their skill, devotion, and good humor were of crucial importance to our success (and sanity).

Finally, we wish to express our appreciation to the shore-based ODP staff for all of their pre- and post-cruise efforts.

SECTION 1: INTRODUCTION

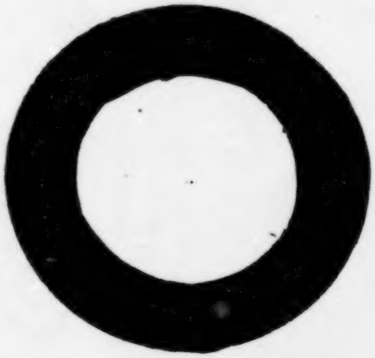

Kroenke, L. W., Berger, W. H., Janecek, T. R., et al., 1991
Proceedings of the Ocean Drilling Program, Initial Reports, Vol. 130

1. INTRODUCTION[1]

Shipboard Scientific Party[2]

MAIN GOALS

The area drilled on the northeastern margin of the Ontong Java Plateau during Ocean Drilling Program (ODP) Leg 130 (Fig. 1) was chosen to provide a depth transect of carbonate deposition in the western equatorial Pacific. Our intent was to recover a complete record of Neogene, Paleogene, and Late Cretaceous ocean history along this transect, with the goal of achieving a detailed reconstruction of paleoceanography and paleoclimate in a well-constrained time frame. The unique geological setting of the plateau led to the accumulation and preservation of a thick cover of pelagic sediments, apparently undisturbed in many areas. Thus, this region appeared to be eminently suited for high-resolution studies of globally significant paleoceanographic signals. In addition, there was the expectation that paleoceanographic events could be traced in the physical properties of the sediment, and that a link to the seismic record would allow three-dimensional regional mapping as well as long-distance correlation. Last, but not least, the origin and tectonic history of the Ontong Java Plateau itself constituted an important objective of our studies.

ONTONG JAVA PLATEAU

The Ontong Java Plateau in the western equatorial Pacific is a broad mid-oceanic submarine plateau striking northwest and paralleling the Solomon Islands to the south (Fig. 1). Its name is taken from an exceptionally large atoll north of these islands. The plateau occupies an extensive area (1000 × 1500 km) and rises to unusually shallow depths in its central region (around 1700 m). The physiography along the margin is complex, with atolls or seamounts located near the western and southwestern edges (Kroenke, 1972).

Pelagic carbonate deposits of Mesozoic and Cenozoic age, well stratified and more than 1000 m thick, cover a large portion of the plateau. Although considerable evidence exists for disturbance, including mass wasting (Berger and Johnson, 1976), one can find many virtually undisturbed sections that display a layer-cake seismic stratigraphy (Fig. 2). The age and origin of these layers has long been a matter of investigation; the suggestion is that they reflect distinct paleoceanographic events (Mayer et al., 1986).

Previous drilling expeditions established the general stratigraphy of the sediment cover (Deep Sea Drilling Project [DSDP] Site 64: Winterer, Riedel, et al., 1971; DSDP Sites 288 and 289: Andrews, Packham, et al., 1975; DSDP Site 586: Moberly, Schlanger, et al., 1986; see Fig. 1), as well as the age of the oldest sediment overlying basalt (Aptian at Site 289). Wide-angle reflection and refraction measurements indicate a remarkably uniform sedimentary velocity structure within the sediment stack, with values ranging from 1.7 to 3.78 km/s over the entire plateau (Maynard et al., 1973). The sediments are carried by anomalously thick oceanic crust (Hussong et al., 1979) that appears to be more than 40 km thick near the center of the plateau. The thickness of the crust bears importantly on the apparent depth stability of the plateau, as seen in the carbonate record.

In addition to the broad, flat-lying, undeformed central part of the plateau, a variety of complex deformational styles that include faulting, folding, and diapiric intrusions are displayed mainly on its southwestern and southern margins (Fig. 3). Presumably, these reflect the collisional relationship of the plateau with the Solomon Island Arc, which also may be responsible for much of the sediment disturbance observed elsewhere.

Three of the DSDP sites mentioned (Sites 64, 288, and 289) were rotary drilled; Site 64 was spot cored and Sites 288 and 289 were continuously cored. Site 586, drilled adjacent to Site 289, was cored with the advanced hydraulic piston corer (APC) to 300 m below seafloor (mbsf), reaching the lowest upper Miocene. This site also was drilled ahead and logged to 623 mbsf (lower Miocene). The most continuous deep sampling of the section was at Site 289 (Leg 30) near the crest of the plateau in a water depth of 2206 m (Fig. 4). Drilling at Site 289 ended at 1271 mbsf in Aptian tholeiitic basalt (113 Ma; R. Duncan, pers. comm., 1990) with vitric tuff directly overlying the basalt. Above the tuff are 1260 m of Campanian to Pleistocene biogenous sediments; from 1262 to 969 mbsf are Lower Cretaceous to upper Eocene radiolarian-bearing limestones, nannofossil-foraminifer chalks, and nodular cherts; and from 969 mbsf to the seafloor are upper Eocene to Pleistocene nannofossil-foraminifer chalks and oozes. A number of unconformities were found in the older part of the section, but from the lower Oligocene to Holocene the section is continuous, with diverse and well-preserved microfossils (Andrews, Packham, et al., 1975).

Well-preserved nannofossil ooze was recovered from the upper 300 m of the section at Site 586, with the first chalky layers appearing at 260 m. This site provides a high-resolution Neogene record beginning about 11 Ma that can be compared in detail with our own records. Sedimentation rates at Site 586 vary between 13 and 39 m/m.y., suggesting considerable fluctuations in carbonate productivity or preservation, or both. The amount of reworking and redeposition that occurred at Site 586, however, is in doubt. As reported by the Leg 89 shipboard scientific party, evidence for substantial admixture of sediments from elsewhere was found throughout the section at Hole 586A (Moberly, Schlanger, et al., 1986). In contrast, as described by the Leg 90 shipboard scientific party, evidence for extensive reworking or turbidite layers was not found at Hole 586B, although numerous thin, foraminifer-rich zones ascribed to winnowing were observed in the upper 45 m of the section (Kennett, von der Borch, et al., 1986).

Based on previous drilling results and on tectonic reconstructions of the region (e.g., Kroenke, 1984; Kroenke et al., 1986), a provisional history of the plateau can be compiled. The Ontong Java Plateau apparently began to form before 113 Ma, probably along a west-northwest-aligned spreading ridge. Pelagic sediments were deposited on the plateau as it formed; a shift from Austral to Tethyan assemblages at about 100 Ma (Site 289) reflects the northward movement of the plateau. During its jour-

---

[1] Kroenke, L. W., Berger, W. H., Janecek, T. R., et al., 1991. *Proc. ODP, Init. Repts.,* 130: College Station, TX (Ocean Drilling Program).

[2] Shipboard Scientific Party is as given in the list of participants preceding the contents.

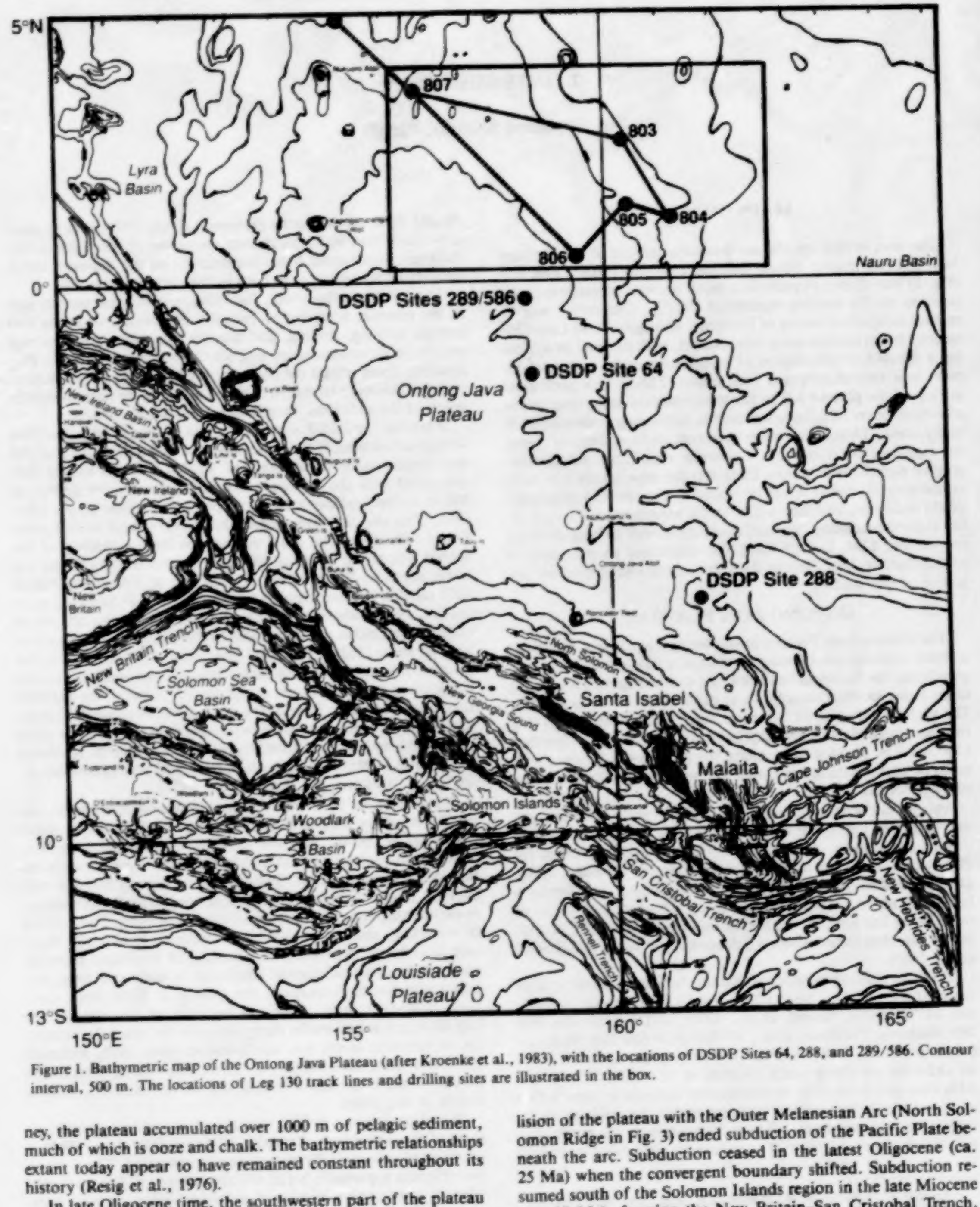
5°N
0°
10°
13°S
150°E
155°
160°
165°
807
803
805
804
806
Lyra Basin
Nauru Basin
DSDP Sites 289/586
DSDP Site 64
Ontong Java Plateau
DSDP Site 288
New Ireland Basin
New Ireland
New Britain
New Britain Trench
Solomon Sea Basin
North Solomon
Santa Isabel
New Georgia Sound
Malaita
Cape Johnson Trench
Solomon Islands
Woodlark Basin
San Cristobal Trench
Rennell Trench
New Hebrides Trench
Louisiade Plateau

Figure 1. Bathymetric map of the Ontong Java Plateau (after Kroenke et al., 1983), with the locations of DSDP Sites 64, 288, and 289/586. Contour interval, 500 m. The locations of Leg 130 track lines and drilling sites are illustrated in the box.

ney, the plateau accumulated over 1000 m of pelagic sediment, much of which is ooze and chalk. The bathymetric relationships extant today appear to have remained constant throughout its history (Resig et al., 1976).

In late Oligocene time, the southwestern part of the plateau encountered the Outer Melanesian (North Solomon) subduction zone, resulting in an intrusion of dikes and sills along the outer trench rise (Roncador Homocline–Stewart Arch in Fig. 3). Collision of the plateau with the Outer Melanesian Arc (North Solomon Ridge in Fig. 3) ended subduction of the Pacific Plate beneath the arc. Subduction ceased in the latest Oligocene (ca. 25 Ma) when the convergent boundary shifted. Subduction resumed south of the Solomon Islands region in the late Miocene (ca. 10 Ma), forming the New Britain–San Cristobal Trench. Eastward subduction of the Indo-Australia Plate beneath the Pacific Plate brought about the subsequent collision of the Wood-

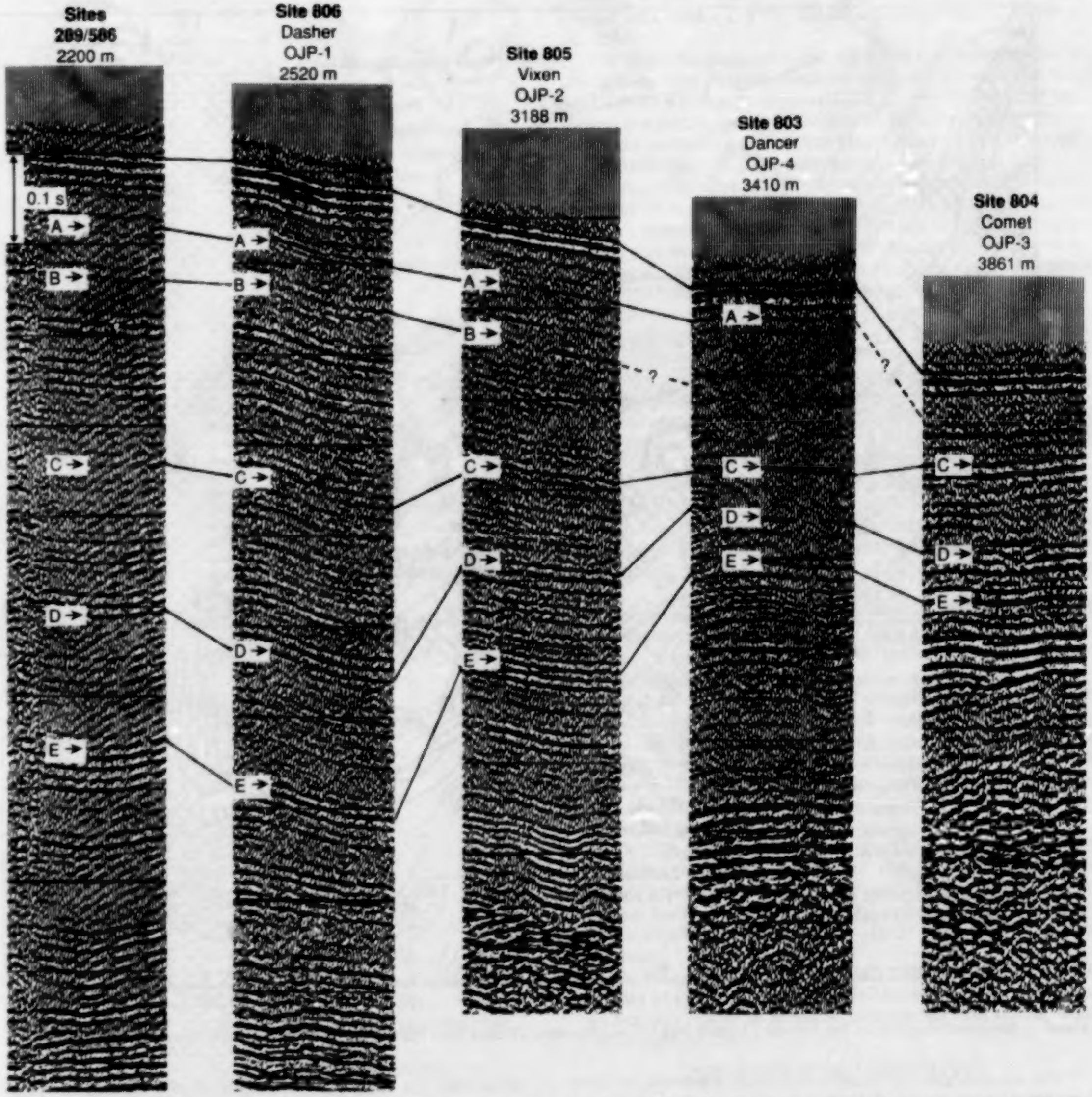

Figure 2. Relationships of seismic sections and marker reflectors on the northeastern flank of the Ontong Java Plateau (after Mayer et al., this volume). Horizontal lines within each section represent 0.1 s of two-way traveltime (twt). See text for discussion of acoustic reflectors (A, B, C, D, and E).

lark Spreading Ridge with the Solomon Islands Arc (ca. 4 Ma). That collision led to the elevation and folding of the southwestern margin of the Ontong Java Plateau, culminating in the formation of the Malaita Anticlinorium (Fig. 3), the overthrusting of the Solomon Arc by plateau oceanic crust, and the emplacement of ophiolites on the islands of Malaita and Santa Isabel (Fig. 1). This overthrusting probably is still occurring.

PALEOCEANOGRAPHIC BACKGROUND

The Ontong Java Plateau has long been a focal point for paleoceanographic studies for several reasons. First and foremost is its remarkable combination of geographic location and bathymetry. For a good part of its Neogene history, the plateau has been located close to the equator, a region characterized by unusually vigorous production of biogenic sediments. Rates of sediment supply to the seafloor are high, potentially providing an expanded sedimentary record. More important, the fact that the plateau rises well above the carbonate compensation depth (CCD), and did so for most of its history, has resulted in the accumulation of a thick pile of calcareous sediment little affected by dissolution. On the flanks of the plateau, however, similar sediments have been affected by dissolution. The contrast between these sections contains clues to the saturation history of the deep Pacific and, hence, to the global ocean carbon cycle.

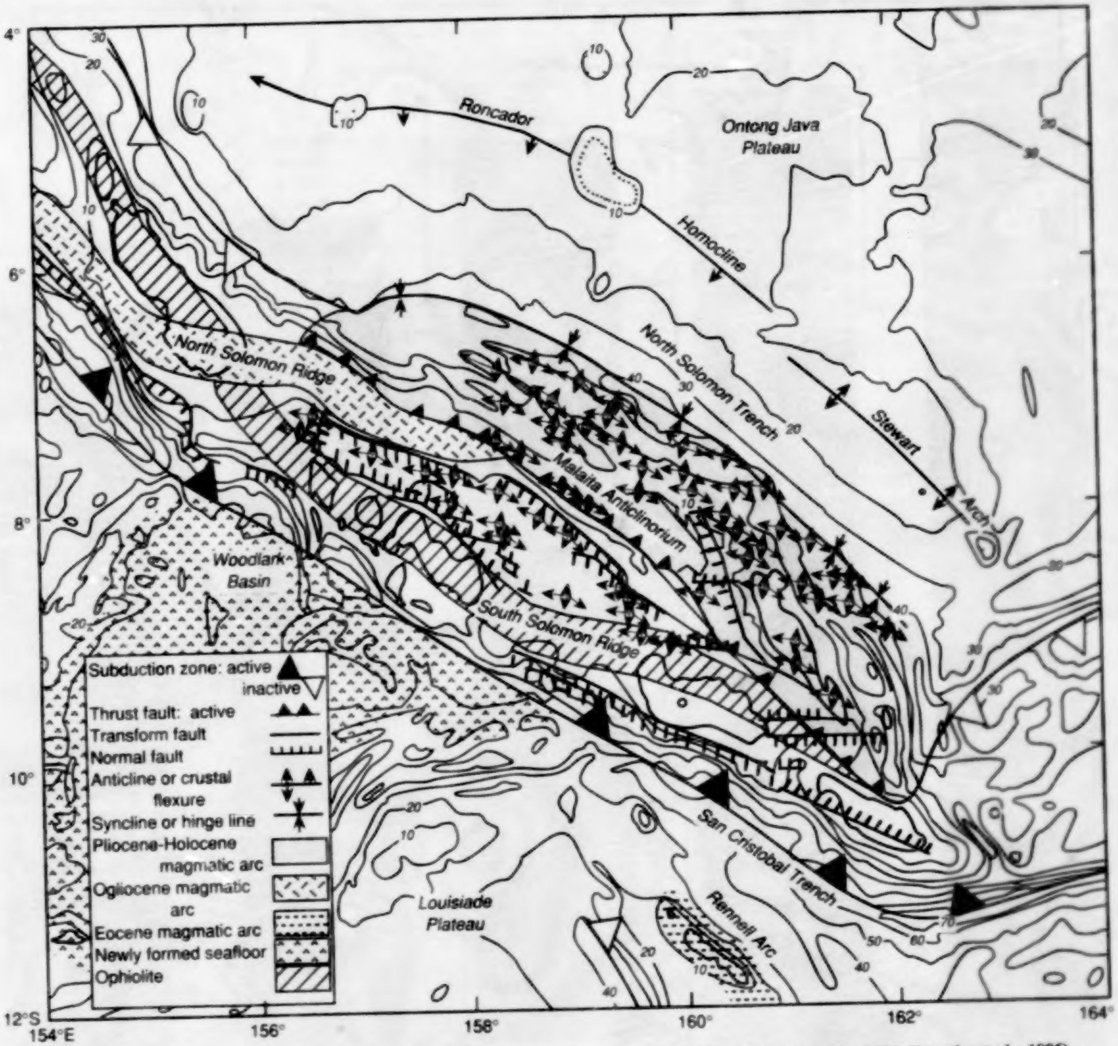
4°
6°
8°
10°
12°S
154°E
156°
158°
160°
162°
164°
Roncador
Ontong Java Plateau
Homocline
North Solomon Trench
Stewart Arch
North Solomon Ridge
Malaita Anticlinorium
South Solomon Ridge
Woodlark Basin
San Cristobal Trench
Rennell Arc
Louisiade Plateau
Subduction zone: active
inactive
Thrust fault: active
Transform fault
Normal fault
Anticline or crustal flexure
Syncline or hinge line
Pliocene-Holocene magmatic arc
Ogliocene magmatic arc
Eocene magmatic arc
Newly formed seafloor
Ophiolite

Figure 3. Structural elements of the Solomon Islands and the southwestern Ontong Java Plateau (after Kroenke, 1984; Kroenke et al., 1986).

The accumulation of pelagic carbonate sediments in open-ocean environments is primarily dependent on the rate of production and dissolution of foraminifers and calcareous nannofossils. Productivity is determined by the availability of nutrients, which, in turn, depends on the concentration of phosphate and nitrate in deep waters, and the rates of upward mixing to the photic zone. On a global scale, carbonate productivity controls carbonate dissolution through the requirement that carbonate supplied to the seafloor in excess of input to the ocean must be redissolved for recycling. Thus, a general increase in production also increases the overall dissolution rate. On a regional scale, high production results in increased carbonate deposition and a deepening of the CCD, as observed along the equator (Arrhenius, 1952; Berger and Winterer, 1974; van Andel et al., 1975). Therefore, increased production along the equator results in the increased accumulation of carbonate. Deposition rates for calcareous sediments on the Ontong Java Plateau, consequently, contain global and regional signals of ocean productivity.

NEOGENE OBJECTIVES

A major goal of Leg 130 was to drill four sites down the northeastern flank of the plateau (Fig. 5) to collect a series of continuous sedimentary sequences that would provide a depth transect of Neogene sediments. A series of equatorial drill sites from the top of the Ontong Java Plateau to near its base (Fig. 6) spans a depth range of 2000 m within a short distance. Most of the sediments sampled would have been produced under the same surface-water conditions and deposited from the same pelagic rain material. The depth interval bracketed by our sites (2500–3900 m) contains the depth range in which changes in dissolution gradients through time are most pronounced, with con-

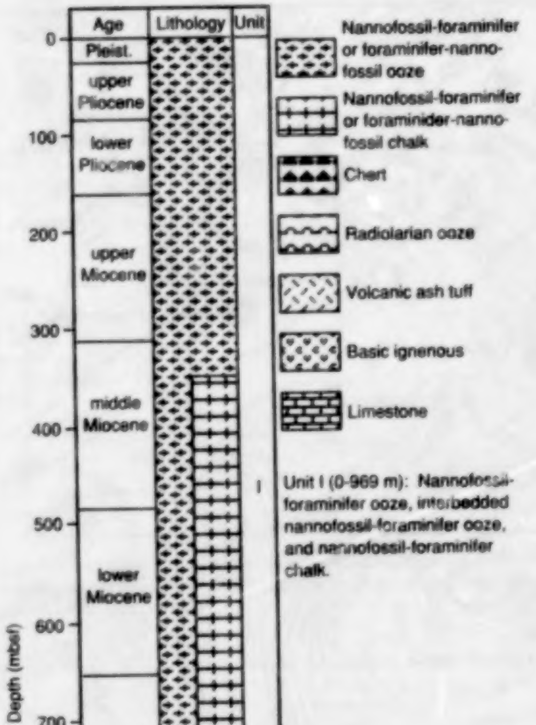
Age
Lithology
Unit
Depth (mbsf)
0
100
200
300
400
500
600
700
800
900
1000
1100
1200
1275
Pleist.
upper Pliocene
lower Pliocene
upper Miocene
middle Miocene
lower Miocene
upper Oligocene
lower Oligocene
upper Eocene
middle Eocene
l. Eocene
upper Paleo.
l. Paleo.
middle Maastr.
l. Maastr.
Campanian
Aptian
u. Cret.
l. Cret.
I
IIA
IIB
III
Nannofossil-foraminifer or foraminifer-nannofossil ooze
Nannofossil-foraminifer or foraminider-nannofossil chalk
Chert
Radiolarian ooze
Volcanic ash tuff
Basic igneous
Limestone
Unit I (0-969 m): Nannofossil-foraminifer ooze, interbedded nannofossil-foraminifer ooze, and nannofossil-foraminifer chalk.
Unit II (969-1262 m): Radiolarian-bearing limestone, siliceous limestone, nannofossil- foraminifer chalk, nannofossil-foraminifer limestone, and nodular chert, and tuff.
Subunit IIA (969-1321 m): Radiolarian-bearing limestone, siliceous limestone, nannofossil-foraminifer chalk, nannofossil-foraminifer limestone, and nodular chert.
Subunit IIB (1231-1262 m) Limestone and tuff.
Unit III (1262-1271 m): Basalt.

Figure 4. Site 289 stratigraphic column (from Andrews, Packham, et al., 1975).

siderable effects on physical properties and seismic reflectors (Berger and Johnson, 1976; Berger and Mayer, 1978; Mayer et al., 1986).

The favorable geographic and bathymetric characteristics of the Ontong Java Plateau eliminate many of the variables that may influence pelagic sedimentation (i.e., productivity and latitudinal gradients), thereby providing a nearly ideal natural laboratory for evaluating the vertical (depth) distribution of a variety of parameters of paleoceanographic significance.

Beside the patterns of sediment accumulation contained within these deposits, a large amount of information concerning the physical, chemical, paleontological, and sedimentological properties is also stored within them. The paleomagnetic record contains signals pertaining to the sedimentation of magnetic minerals and the history of the Earth's magnetic field. Other physical properties measurements reveal details about the diagenetic history. Stable isotope studies of foraminifer species permit the reconstruction of paleotemperature, strength of the thermocline and oxygen minimum, origin of deep waters, global ice volume, and other parameters important for ocean and climate history. Micropaleontological analyses provide additional paleoenvironmental data and allow high-resolution correlation between cores. The site reports and individual contributions present an introduction to these interpretations, but much remains to be extracted.

With regard to the Neogene objectives, the study of sediments drilled and cored along the depth transect was expected to yield the following:

1. high-resolution stratigraphic records across intervals of major paleoceanographic changes (Table 1) by evaluating variations of primary paleoceanographic indicators (isotopes, carbonate, biota);
2. a detailed record of vertical oceanic gradients and their links to climatic parameters and bottom-water properties;
3. a detailed sedimentary record that will provide a better understanding of the nature and role of carbonate dissolution in the deep sea and that will attempt to quantify amounts of dissolution (which is necessary to address the CO_2 problem and related questions);
4. a high-resolution sedimentary record necessary for the completion of a global network of equatorial depth transects that will yield a better understanding of basin-basin fractionation and biotic evolution as well as a pelagic standard for comparison with marginal transects to clarify basin-shelf fractionation; and
5. a sedimentary record that will contribute to our understanding of the origin of seismic reflectors on oceanic plateaus and that will enable us to make comparisons with seismic horizons in oceanic basins.

PRE-NEOGENE OBJECTIVES

The Cretaceous-Paleogene section also was important to us because of the intrinsic interest of unfamiliar ocean conditions outside of the range of the Neogene, and also because this record provides a reference for Southern Hemisphere paleoceanography and bears on the early history of the plateau itself. Major hiatuses were encountered in Upper Cretaceous-Paleogene sediments at DSDP Sites 288 and 289, which makes it unlikely that complete sequences are readily available. However, many of the unconformities at Site 288 do not correlate with those at Site 289 (or the shallower, spot-cored Site 64), implying that they represent local events of limited areal extent (Andrews, Packham, et al., 1975). Drilling at other locations on top of the plateau, therefore, may recover key sections missed at earlier sites. Such additional data may allow us to be able to differentiate

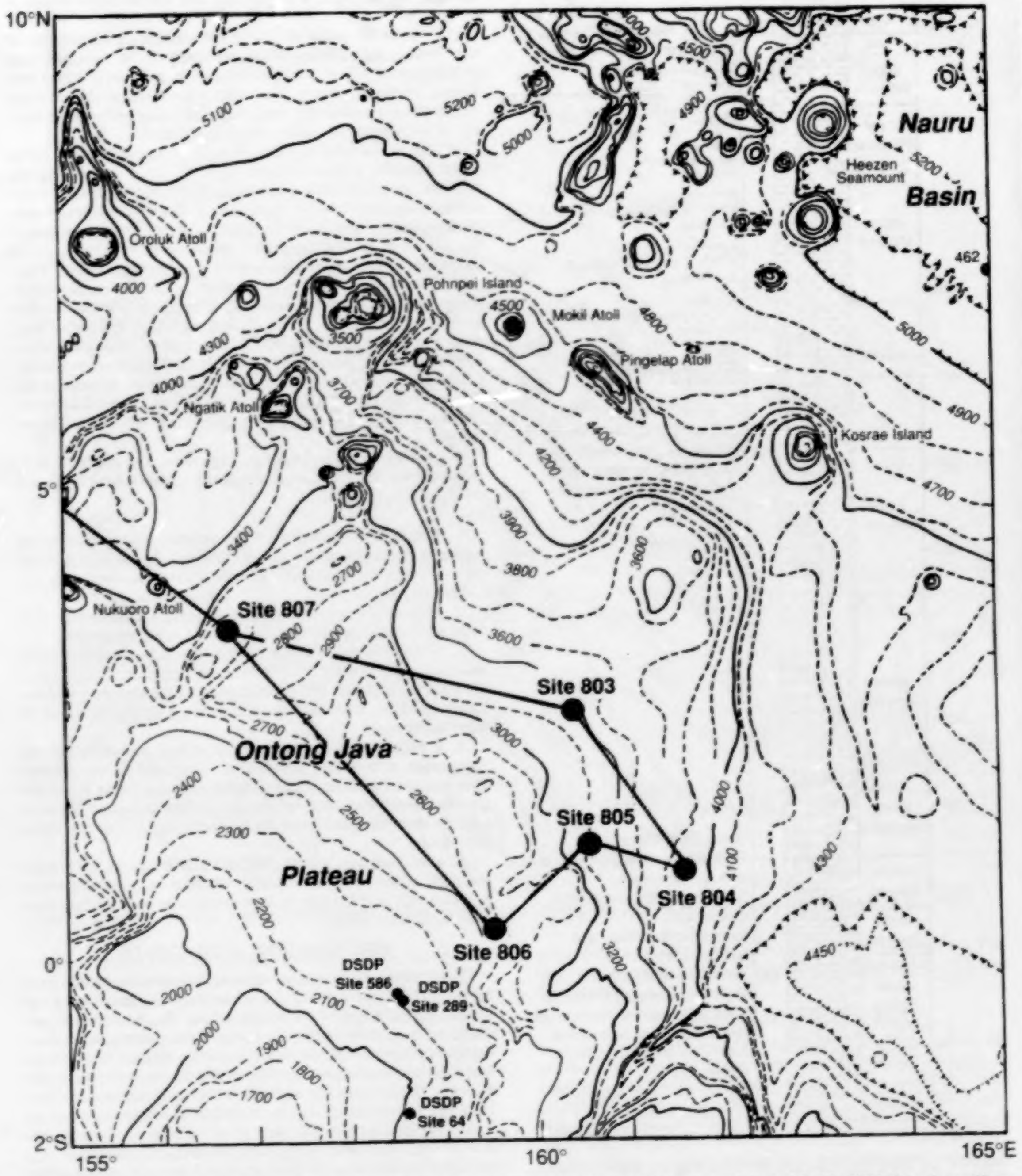
10°N
5°
0°
2°S
155°
160°
165°E
5100
5200
5000
4500
4900
Nauru
Heezen Seamount
5200
Basin
462
Oroluk Atoll
4000
Pohnpei Island
4500
Mokil Atoll
4800
5000
4300
3500
Pingelap Atoll
4000
Ngatik Atoll
3700
4400
4900
Kosrae Island
4200
4700
3400
3800
3600
2700
3800
Nukuoro Atoll
Site 807
2800
2900
3600
Site 803
2700
3000
Ontong Java
2400
2600
4000
2500
Site 805
2300
4100
4300
Plateau
Site 804
2200
Site 806
3200
4450
DSDP Site 586
DSDP Site 289
2000
2100
2000
1900
1800
1700
DSDP Site 64

Figure 5. Bathymetric map (in meters) of the northwestern part of the Ontong Java Plateau (after Mammerickx and Smith, 1985). Locations of Leg 130 drill sites as well as sites drilled on DSDP Legs 7 (Site 64), 30 (Site 289), and 89 (Site 586) are provided for reference.

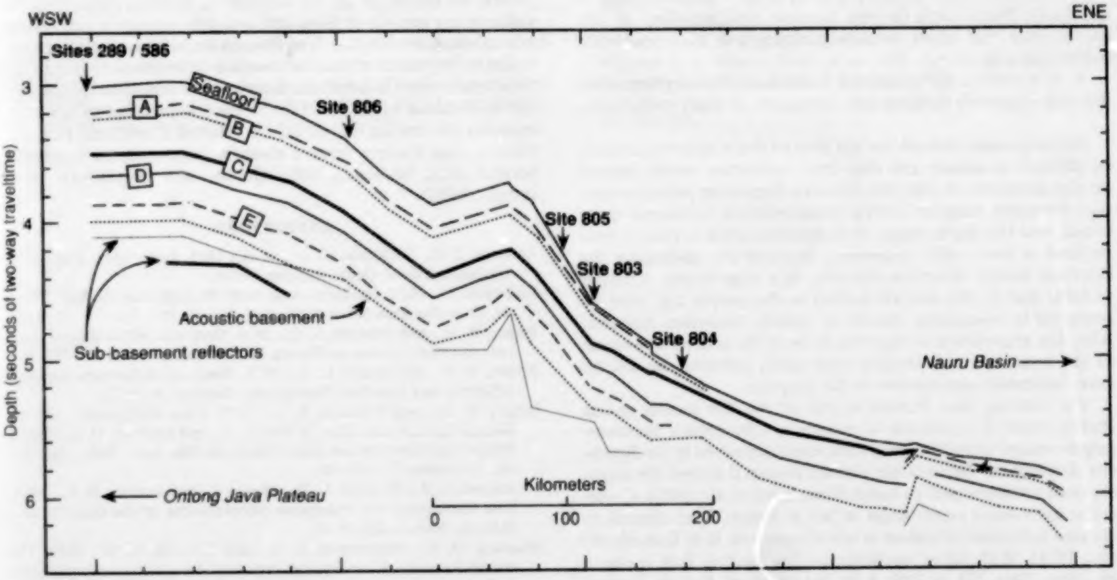

Figure 6. Generalized single-channel seismic (SCS) profile down the northeastern flank of the Ontong Java Plateau with the projected locations of Neogene transect Sites 803–806. See Mayer et al. (this volume) and seismic stratigraphy sections in each site report for discussions of acoustic reflectors labeled A–E in this figure.

Table 1. Events in the central equatorial Pacific, their age, sedimentary causes, and associated events.

Approximate age (Ma)	Geochemical events	Hiatus	Paleoceanographic events	Primary cause of relector
3.0–3.5	Benthic ^{18}O enrichment. $CaCO_3$ dissolution.		Closing of Panama Isthmus. North Hemisphere glaciation? North Atlantic erosion.	Carbonate miminum.
6.5–7.5	Chron 6 ^{13}C depletion	NH6	Increased isolation of Mediterranean Sea. Climatic deterioration.	Carbonate minimum.
8.5–9.5	Benthic ^{18}O enrichment. Mid-Chron 10 $CaCO_3$ dissolution event.	NH5 NH4?	Major North Atlantic erosion. Increase of siliceous deposition in Pacific. Major cooling. Major drop in sea level.	Extreme carbonate minimum.
13.5–14.5	15c $CaCO_3$ dissolution event. Benthic ^{18}O enrichment.	NH3?	Ice buildup in Antarctica. Intensification of Antarctic Bottom Water production.	Carbonate minimum.
16.5–17.5	16g $CaCO_3$ dissolution Chron 16 ^{13}C enrichment.	NH1b	Closing of Tethys. Norwegian Sea spillover. Intensified Pacific upwelling.	Carbonate minimum.
20.5–22.5		NH1a?	Opening of Drake Passage. Establishment of Circum-Atlantic Current and of a steep Southern Hemisphere thermal gradient.	Diagenesis.

Note: Source of data is from Theyer et al., 1989.

widespread (water-mass-controlled) unconformities from those produced locally by tectonic events or bottom currents.

With regard to Leg 130 objectives for Cretaceous and Paleogene sediments on the Ontong Java Plateau, our goals were as follows:

1. to fill critical gaps in Cretaceous biostratigraphy and paleobiogeography;
2. to estimate the original basement depth of the plateau and its subsequent bathymetric change from benthic foraminifers and, possibly, from the history of carbonate dissolution;

3. to investigate the record of Cretaceous anoxic events in the South Pacific and thereby increase understanding of the mechanisms that cause oceanwide deposition of organic-rich sediments; and

4. to recover a well-preserved Cretaceous/Tertiary boundary that might provide insights into the causes of mass extinctions.

We were aware that all but the first of these objectives would be difficult to achieve and that their realization would depend on circumstances of sediment recovery. Regarding paleobathymetry, the depth range of bathyal foraminifers is commonly quite broad, and the depth range of dissolution levels is poorly constrained in these older sequences. Successfully addressing the third and fourth objectives above is, to a large extent, a matter of luck; that is, the desired section of the proper age must be preserved in a sequence known to contain abundant hiatuses. Also, the appropriate section has to be in the recovered portion of the cored interval. Despite such odds, however, we did recover sediments appropriate to the purpose.

The Ontong Java Plateau is one of the few locales in the Pacific where it is possible to recover a fully pelagic biostratigraphic record from Mesozoic carbonates deposited in the Southern Hemisphere. Because the plateau migrated toward the equator from southern mid-latitudes (Hammond et al., 1975), Cretaceous microfossil assemblages reflect a change from Austral to Tethyan provincial affinities in mid-Cretaceous time (Scheibnerova, 1974). With better resolution of this interval than is possible from Sites 288 or 289, a boundary point for the Austral realm in the Pacific can be established.

BASEMENT OBJECTIVES

Drilling into basement and recovering a substantial amount of basalt was the final item on our list of objectives. The origin of the old, oceanic Pacific plateaus (Ontong Java, Manihiki, Shatsky, Hess, Magellan) is poorly understood, and progress in this field on Ontong Java would be crucial. The Ontong Java Plateau has an unusually thick crust of truly continental proportions (~40 km thick on the main high plateau; e.g., Hussong et al., 1979). Even on the edges of the plateau, the crust is still well within the continental range (~30 km, for instance, near the island of Malaita; e.g., Nixon and Boyd, 1979; Kroenke, 1972, and unpubl. data, 1989). If there is continental crust on any of the large Pacific intraoceanic plateaus (as has been surmised by some), the Ontong Java Plateau, with by far the thickest crust, would seem to be one of the most favorable places to find it. A deep basement hole on the main high plateau (Fig. 5, Site 807) would go far toward settling this issue.

We drilled into basement on Ontong Java Plateau for the following reasons:

1. to determine the nature of the crust on the Ontong Java Plateau, that is, to establish the lithology, petrogenesis, and sources of Ontong Java Plateau crustal material;

2. to determine the age of the basement and paleolatitudes of the Ontong Java Plateau so that we can understand the origin and subsequent movement of the plateau better; and

3. to compare the basement composition of the Ontong Java Plateau with that of the extensive "mid-Cretaceous" volcanic events of the Pacific for insights into the origin of both features.

Age information on a deep basement hole can be obtained from radiometric dating (Ar-Ar), possibly from microfossils in sediments overlying the igneous rocks, and the M-series magnetic-polarity record. In conjunction with age dating, paleomagnetic measurement of basement rocks will provide important insights on the paleolatitudes of the Ontong Java Plateau during the period of crustal formation. Existing data from the sedimentary records at Sites 288 and 289 indicate a substantial migration of the Ontong Java Plateau from higher southern latitudes to its present equatorial location (Hammond et al., 1975). New results from a deep basement section would reveal the earlier migrational history of the plateau, knowledge of which is essential for testing the currently debated hypothesis that the Ontong Java Plateau formed above a ridge-centered Louisville hotspot (e.g., Mahoney, 1987; Gordon and Henderson, pers. comm., 1987).

REFERENCES

Andrews, J. E., Packham, G. H., et al., 1975. *Init. Repts. DSDP,* 30: Washington (U.S. Govt. Printing Office).

Arrhenius, G., 1952. Sediment cores from the East Pacific. *Rep. Swedish Deep-Sea Expedition 1947–1948,* Vol. 5, Pts. 1–3.

Berger, W. H., and Johnson, T. C., 1976. Deep-sea carbonates: dissolution and mass wasting on Ontong Java Plateau. *Science,* 192:785–787.

Berger, W. H., and Mayer, L. A., 1978. Deep-sea carbonates: acoustic reflectors and lysocline fluctuations. *Geology,* 6:11–15.

Berger, W. H., and Winterer, E. L., 1974. Plate stratigraphy and the fluctuating carbonate line. *In* Hsü, K. J., and Jenkyns, H. C. (Eds.), *Pelagic Sediments on Land and Under the Sea.* Spec. Publ., Int. Assoc. Sedimentol., 1:11–48.

Hammond, S. R., Kroenke, L. W., Theyer, F., and Keeling, D. L., 1975. Late Cretaceous and Paleogene paleolatitudes of the Ontong Java Plateau. *Nature,* 255:46–47.

Hussong, D. M., Wipperman, L. K., and Kroenke, L. W., 1979. The crustal structure of the Ontong Java and Manahiki oceanic plateaus. *J. Geophys. Res.,* 84:6003–6010.

Kennett, J. P., von der Borch, C. C., et al., 1986. *Init. Repts. DSDP,* 90, Pts. 1 and 2: Washington (U.S. Govt. Printing Office).

Kroenke, L. W., 1972. Geology of the Ontong Java Plateau [Ph.D. dissert.]. Univ. of Hawaii, HIG-72-5.

———, 1984. *Cenozoic Tectonic Development of the Southwest Pacific.* U.N. ESCAP/CCOP/SOPAC, Tech. Bull. No. 6.

Kroenke, L. W., Jouannic, C., and Woodward, P., 1983. Bathymetry of the Southwest Pacific, Chart I: The Geophysical Atlas of the Southwest Pacific, Mercator Projection, Scale 1:6,442,192 at 0 degrees: Suva, Fiji (U.N. ESCAP/CCOP/SOPAC).

Kroenke, L. W., Resig, J. M., and Cooper, P. A., 1986. Tectonics of the southeastern Solomon Islands: formation of the Malaita Anticlinorium. *In* Vedder, J. G., Pound, K. S., and Boundy, S. Q. (Eds.), *Geology and Offshore Resources of Pacific Island Arcs, Central and Western Solomon Islands.* Circum-Pacific Counc. Energy Mineral Resour., Earth Sci. Ser., 4:109–116.

Mahoney, J. J., 1987. An isotopic survey of Pacific oceanic plateaus: implications for their nature and origin. *In* Batiza, R., Keating, B., and Fryer, P. (Eds.), *Seamounts, Islands, and Atolls: The Menard Volume.* Am. Geophys. Union, Monogr. Ser., 43:207–220.

Mammerickx, J., and Smith, S. M., 1985. *Bathymetry of the North Central Pacific:* Boulder, CO (Geological Society of America), Map and Chart Ser., No. MC-52.

Mayer, L. A., Shipley, T. H. and Winterer, E. L., 1986. Equatorial Pacific seismic reflectors as indicators of global oceanographic events. *Science,* 233:761–764.

Maynard, G. L., Sutton, G. H., Hussong, D. M., and Kroenke, L. W., 1973. Seismic wide-angle reflection and refraction investigation of the sediments on the Ontong Java Plateau. *Eos,* 54(4):378.

Moberly, R., Schlanger, S. O., et al., 1986. *Init. Repts. DSDP,* 89: Washington (U.S. Govt. Printing Office).

Nixon, P. H., and Boyd, F. R., 1979. Garnet bearing lherzolites and discrete nodule suites from the Malaita alnoite, Solomon Islands, S.W. Pacific, and their bearing on oceanic mantle composition and geotherm. *In* Boyd, F. R. and Meyer, H.O.A. (Ed.), *The Mantle Sample: Inclusions in Kimberlite and Other Volcanics.* Proc. 2nd Int. Kimberlite Conf., Am. Geophys. Union, 2:400–423.

Resig, J., Buyannanonth, V., and Roy, K., 1976. Foraminiferal stratigraphy and depositional history of the Ontong Java Plateau. *Deep-Sea Res.,* 23:441–456.

Scheibnerova, V., 1974. Aptian-Albian benthonic foraminifera from DSDP Leg 27, Sites 259, 260, and 263, eastern Indian Ocean. *In*

Veevers, J. J., Heirtzler, J. R., et al., *Init. Repts. DSDP,* 27: Washington (U.S. Govt. Printing Office), 697–741.

Theyer, F., Vincent, E., and Mayer, L. A., 1989. Sedimentation and paleoceanography of the central equatorial Pacific. *In* Winterer, E. L., Hussong, D. M., and Decker, R. W. (Eds.), *The Geology of North America* (Vol. N): *The Eastern Pacific Ocean and Hawaii*: Boulder, CO (Geological Society of America), 347–372.

van Andel, T. H., Heath, G. R. and Moore, T. C., Jr., 1975. Cenozoic history and paleoceanography of the central equatorial Pacific Ocean. *Mem. Geol. Soc. Am.*, No. 143.

Winterer, E. L., Riedel, W. R., et al., 1971. *Init. Repts. DSDP,* 7: Washington (U.S. Govt. Printing Office).

Ms 130A-101

Kroenke, L. W., Berger, W. H., Janecek, T. R., et al., 1991
Proceedings of the Ocean Drilling Program, Initial Reports, Vol. 130

2. EXPLANATORY NOTES[1]

Shipboard Scientific Party[2]

INTRODUCTION

In this chapter, we have assembled information regarding the recovery of materials, the presentation of results, and the conventions used to identify samples. This information concerns only shipboard operations and analyses described in the site reports in the *Initial Reports* volume of the Leg 130 *Proceedings of the Ocean Drilling Program*. The methods used by various investigators for shore-based analysis of Leg 130 data will be detailed in the individual scientific contributions published in the *Scientific Results* volume.

AUTHORSHIP OF SITE CHAPTERS

The separate sections of the site chapters were written by the following shipboard scientists (authors are listed in alphabetical order in parentheses; no seniority is implied). Authors who participated in the editing of this volume at the first Leg 130 postcruise meeting are denoted with an asterisk.

Site Summary (Berger*, Kroenke*)
Background and Objectives (Berger, Kroenke)
Operations (Janecek*, Pollard)
Sedimentology and Lithostratigraphy (Janecek, Jansen, Krissek*, Lind, Mosher, Prentice, Schmidt, Wu)
Biostratigraphy (Backman, Corfield, Lange, Leckie*, Resig, Takahashi, Takayama)
Paleomagnetics (Musgrave, Tarduno)
Sediment Accumulation Rates (Backman)
Inorganic Geochemistry (Delaney)
Carbon Geochemistry (Stax)
Igneous Petrology (Mahoney, Storey)
Physical Properties (Bassinot, Marsters, Mayer, Wilkens)
Downhole Measurements (Lyle*, Mayer, Wilkens)
Seismic Stratigraphy (Mayer*)
Summary and Conclusions (Berger, Kroenke)
Appendix (Shipboard Scientific Party)

Following the text of each site chapter are summary core descriptions ("barrel sheets" and igneous rock visual core descriptions) and photographs of each core.

SURVEY AND DRILLING DATA

Use of "Ma" vs "m.y."

The abbreviation "Ma" is equivalent to and replaces m.y. B.P. (million years before present); for example, 35–40 Ma. The abbreviation "m.y." is used in such sentences as "...for 4 m.y. in the early Miocene" to denote a number of years rather than a specific point in time.

Drilling Characteristics

Information concerning sedimentary stratification in uncored or unrecovered intervals may be inferred from seismic data and wireline-logging results as well as from an examination of the behavior of the drill string as observed and recorded on the drilling platform. Typically, the harder a layer, the slower and more difficult it is to penetrate. A number of other factors may determine the rate of penetration, so it is not always possible to relate the drilling time directly to the hardness of the layers. Bit weight and revolutions per minute, recorded on the drilling recorder, also influence the penetration rate.

Drilling Deformation

When cores are split, many show signs of significant sediment disturbance, including the concave-downward appearance of originally horizontal bands, haphazard mixing of lumps of different sediment types (mainly at the tops of cores), and the near-fluid state of some sediments recovered from tens to hundreds of meters below the seafloor. Core deformation probably occurs during cutting, retrieval (with accompanying changes in pressure and temperature), and core handling on deck. A detailed discussion of slumplike drilling disturbance is given in the "Core Description" section of this chapter.

SHIPBOARD SCIENTIFIC PROCEDURES

Numbering of Sites, Holes, Cores, and Samples

Ocean Drilling Program (ODP) drill sites are numbered consecutively. A site consists of one or more holes drilled while the ship was positioned over one acoustic beacon. Multiple holes may be drilled at a single site by pulling the drill pipe above the seafloor (out of the hole), moving the ship some distance from the previous hole, and then drilling another hole.

For all ODP drill sites, a letter suffix distinguishes each hole drilled at the same site. The first hole drilled is assigned the site number modified by the suffix A, the second hole has suffix B, and so forth. Note that this procedure differs slightly from that used by Deep Sea Drilling Project (DSDP) Sites 1 through 624 in which the first hole has no suffix. Adding a suffix for each hole prevents ambiguity between site- and hole-number designations. It is important to distinguish among holes drilled at a site, because recovered sediments or rocks from different holes usually do not have equivalent depths for equivalent stratigraphic positions.

The cored interval is measured in meters below seafloor (mbsf). The depth interval assigned to an individual core begins with the depth below the seafloor that the coring operation began and extends to the depth that the coring operation ended (see Fig. 1). For example, each coring interval is generally up to 9.5 m long, which is the length of a core barrel. Coring intervals may be shorter than that. Also, cores are not adjacent if separated by drilled intervals. In soft sediments, the drill string can be "washed ahead" with the core barrel in place, without recovering sediments. This is achieved by pumping water down the pipe at high pressure to wash the sediment out of the way of the bit and up the space between the drill pipe and the wall of the hole. If thin, hard, rock layers are present, then it is possible to get "spotty" sampling of these resistant layers within the washed interval and thus have a cored interval greater than 9.5 m. In drilling hard rock, a center bit may replace the core barrel if it is necessary to drill without core recovery.

---

[1] Kroenke, L. W., Berger, W. H., Janecek, T. R., et al., 1991. *Proc. ODP, Init. Repts.*, 130: College Station, TX (Ocean Drilling Program).

[2] Shipboard Scientific Party is as given in the list of participants preceding the contents.

Cores taken from a hole are numbered serially from the top of the hole downward. Core numbers and their associated cored intervals in mbsf usually are unique in a given hole; however, this may not be true if an interval must be cored twice because of the caving of cuttings or other hole problems. The maximum full recovery for a single core is 9.5 m of rock or sediment contained in a plastic liner (6.6-cm internal diameter) plus about 0.2 m (without a plastic liner) in the core catcher (Fig. 2). The core catcher is a device at the bottom of the core barrel that prevents the core from sliding out when the barrel is being retrieved from the hole. In certain situations (e.g., when coring gas-charged sediments that expand while being brought on deck), recovery may exceed the 9.5-m maximum.

A recovered core is divided into 1.5-m sections that are numbered serially from the top (Fig. 2). When full recovery is obtained, the sections are numbered from 1 through 7, with the last section possibly being shorter than 1.5 m (rarely, an unusually long core may require more than 7 sections). When less than full recovery is obtained, there will be as many sections as needed to accommodate the length of the core recovered (e.g., 4 m of core would be divided into two 1.5-m sections and one 1-m section). If cores are fragmented (recovery < 100%), sections are numbered serially and intervening sections are noted as void, whether shipboard scientists believe that the fragments were contiguous *in situ* or not. In rare cases, a section < 1.5 m may be cut to preserve features of interest (e.g., lithologic contacts).

By convention, material recovered from the core catcher is placed below the last section when the core is described and labeled core catcher (CC); in sedimentary cores, it is treated as a

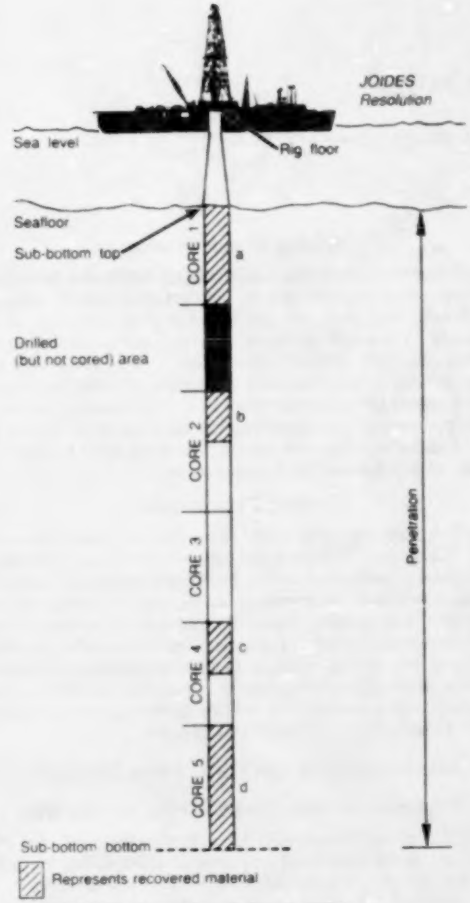
JOIDES
Resolution
Sea level
Rig floor
Seafloor
Sub-bottom top
CORE 1
a
Drilled
(but not cored) area
CORE 2
b
CORE 3
CORE 4
c
CORE 5
d
Penetration
Sub-bottom bottom
Represents recovered material

BOTTOM FELT	distance from rig floor to seafloor
TOTAL DEPTH	distance from rig floor to bottom of hole (sub-bottom bottom)
PENETRATION	distance from seafloor to bottom of hole (sub-bottom bottom)
NUMBER OF CORES	total of all cores recorded, including cores with no recovery
TOTAL LENGTH OF CORED SECTION	distance from sub-bottom top to sub-bottom bottom minus drilled (but not cored) areas in between
TOTAL CORE RECOVERED	total from adding a, b, c, and d in diagram
CORE RECOVERY (%)	equals TOTAL CORE RECOVERED divided by TOTAL LENGTH OF CORED SECTION times 100

Figure 1. Coring and depth intervals.

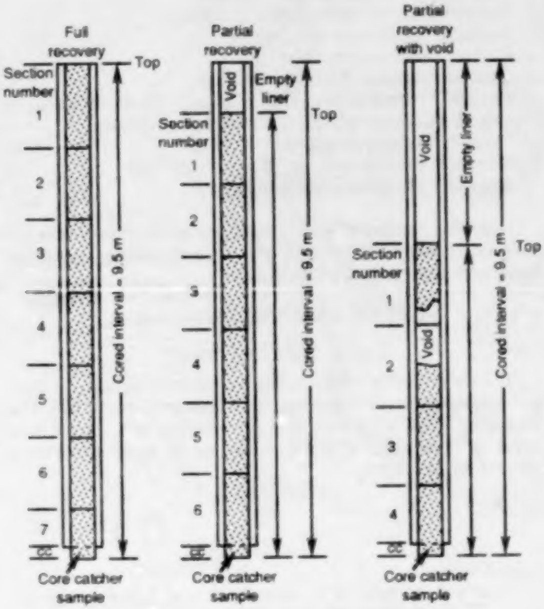
Full recovery
Section number
Top
1
2
3
4
5
6
7
CC
Cored interval = 9.5 m
Core catcher sample
Partial recovery
Void
Empty liner
Section number
Top
1
2
3
4
5
6
CC
Cored interval = 9.5 m
Core catcher sample
Partial recovery with void
Void
Empty liner
Section number
Top
1
Void
2
3
4
CC
Cored interval = 9.5 m
Core catcher sample

Figure 2. Examples of numbered core sections.

separate section. The core catcher is placed at the top of the cored interval in cases where material is only recovered in the core catcher. However, information supplied by the drillers or by other sources may allow for more precise interpretation as to the correct position of core-catcher material within an incompletely recovered cored interval.

Igneous rock cores are also cut into 1.5-m sections that are numbered serially; each piece of rock is then assigned a number. Fragments of a single piece are assigned a single number, and individual fragments are identified alphabetically. The core-catcher sample is placed at the bottom of the last section and is treated as part of the last section, rather than separately. Scientists completing visual core descriptions describe each lithologic unit, noting core and section boundaries only as physical reference points.

When the recovered core is shorter than the cored interval, the top of the core is equated with the top of the cored interval by convention to achieve consistency in handling analytical data derived from the cores. Samples removed from the cores are designated by distance measured in centimeters from the top of the section to the top and bottom of each sample removed from that section. In curated hard rock sections, sturdy plastic spacers are placed between pieces that did not fit together to protect them from damage in transit and in storage; therefore, the centimeter interval noted for a hard rock sample has no direct relationship to that sample's depth within the cored interval, but is only a physical reference to the location of the sample within the curated core.

A full identification number for a sample consists of the following information: leg, site, hole, core number, core type, section number, piece number (for hard rock), and interval in centimeters measured from the top of section. For example, a sample identification of "130-803A-25R-1, 10–12 cm" would be interpreted as representing a sample removed from the interval between 10 and 12 cm below the top of Section 1 in Core 25 (R designates that this core was taken during rotary drilling) of Hole 803A during Leg 130.

All ODP core and sample identifiers indicate core type, using the following abbreviations: H = advanced hydraulic piston corer (APC); R = rotary core barrel (RCB); P = pressure core barrel; X = extended core barrel (XCB); B = drill-bit recovery; C = center-bit recovery; I = *in-situ* water sample; S = sidewall sample; W = wash-core recovery; and M = miscellaneous material. APC, XCB, RCB, and W cores were cut on Leg 130.

Core Handling

Sediments

As soon as a core was retrieved on deck, a sample was taken from the core catcher and given to the paleontological laboratory for an initial age assessment. The core was then placed on a long horizontal rack, and gas samples were taken by piercing the core liner and withdrawing gas into a vacuum tube. Voids within the core were sought as sites for gas sampling. Some of the gas samples were stored for shore-based study, but others were analyzed immediately as part of the shipboard safety and pollution-prevention program. Next, the core was marked into section lengths, each section was labeled, and the core was cut into sections. Interstitial water (IW), organic geochemistry (OG), and whole-round physical properties (PP) samples were also taken at this time. In addition, some headspace gas samples were scraped from the ends of cut sections on the catwalk and sealed in glass vials for light hydrocarbon analysis. Afterward, each section was sealed at the top and bottom by gluing on color-coded plastic caps: blue to identify the top of a section and clear for the bottom. A yellow cap was placed on the section ends from which a whole-round sample was removed. The caps were usually attached to the liner by coating the end liner and the inside rim of the cap with acetone and then attaching the caps to the liners.

The cores then were carried into the laboratory, where the sections were labeled with an engraver to mark the full designation of the section permanently. The length of the core in each section and the core-catcher sample were measured to the nearest centimeter; this information was logged into the shipboard CORELOG data-base program.

Whole-round sections from APC and XCB cores were normally run through the multisensor track (MST). The MST includes the gamma-ray attenuation porosity evaluator (GRAPE), the *P*-wave logger, and a volume magnetic susceptibility meter. After the core had equilibrated to room temperature (approximately 3 hr), thermal conductivity measurements were performed on fairly soft sediments, and the cores were split.

Cores of soft material were split lengthwise into working and archive halves. The softer cores were split with a wire or saw, depending on the degree of induration. Harder cores were split with a band saw or diamond saw. The wire-cut cores were split from the bottom to top, so investigators should be aware that older material could have been transported up the core on the split face of each section.

The working half of the core was sampled for shipboard and shore-based laboratory studies. Each sample extracted was logged into the sampling data-base program by the location and the name of the investigator receiving the sample. Records of all of the samples removed are kept by the curator at ODP headquarters. The extracted samples were sealed in plastic vials or bags and labeled. Samples were routinely taken for shipboard physical property analysis. These samples were subsequently used for calcium carbonate (coulometric) and organic carbon (CNS elemental) analyses; these data are reported in the site chapters.

The archive half was then described visually. Smear slides were made from samples taken from the archive half and were supplemented by thin sections taken from the working half. Most archive sections were run through the cryogenic magnetometer. The archive half was photographed with both black-and-white and color film, a whole core at a time. Close-up photographs (black-and-white) were taken of particular features, as requested by individual scientists, for illustrations in the summary of each site.

Both halves of the core were put into labeled plastic tubes, which were then sealed and transferred to cold-storage space aboard the drilling vessel. At the end of the leg, the cores were transferred from the ship in refrigerated air-freight containers to cold storage at the Gulf Coast Repository of the Ocean Drilling Program, Texas A&M University, College Station, Texas.

Igneous and Metamorphic Rocks

Igneous and metamorphic rock cores were handled differently from sedimentary cores. Once on deck, the core-catcher was placed at the bottom of the core liner and total core recovery was calculated by shunting the rock pieces together and measuring to the nearest centimeter; this information was logged into the shipboard CORELOG data-base program. The core then was cut into 1.5-m-long sections and transferred into the laboratory.

The contents of each section were transferred into 1.5-m-long sections of split core liner, where the bottom of oriented pieces (i.e., pieces that clearly could not have rotated top to bottom about a horizontal axis in the liner) were marked with a red wax pencil to ensure that orientation was not lost during the splitting and labeling process. The core was then split into archive and working halves. A plastic spacer was used to separate individual pieces and/or reconstructed groups of pieces in the core liner. These spacers may represent a substantial interval of no recovery. Each piece was numbered sequentially from the top of each section, beginning with number 1; reconstructed groups of pieces were assigned the same number but were lettered consecutively. Pieces were labeled only on external surfaces. If the piece was oriented, an arrow was added to the label pointing to the top of the section.

The working half of the hard-rock core was sampled for shipboard laboratory studies. Records of all samples are kept by the curator at ODP headquarters. Minicore samples were taken routinely for physical properties and magnetic studies. Some of these samples were subdivided at a later time for X-ray fluorescence (XRF) analysis and thin-sectioning, so that as many measurements as possible were made on the same pieces of rock. At least one minicore was taken per lithologic unit when recovery permits, generally from the freshest areas of core. Additional thin sections, X-ray diffraction (XRD) samples, and XRF samples were selected from areas of particular interest. Samples for shore-based studies were selected in a sampling party held after drilling had ended.

The archive half was described visually, then photographed with both black-and-white and color film, one core at a time. Both halves of the core were then shrink-wrapped in plastic to prevent rock pieces from vibrating out of sequence during transit, put into labeled plastic tubes, sealed, and transferred to cold-storage space aboard the drilling vessel.

VISUAL CORE DESCRIPTION

Sediment "Barrel Sheets"

The core description forms (Fig. 3), or "barrel sheets," summarize the data obtained during shipboard analysis of each sediment core. The following discussion explains the ODP conventions used in compiling each part of the core description forms and the exceptions to these procedures adopted by the Leg 130 scientific party.

Shipboard sedimentologists were responsible for visual core logging, smear slide analyses, and thin-section descriptions of sedimentary and volcaniclastic material. Mineral composition data, determined by X-ray diffraction, were used to augment the visual core descriptions. Data on biostratigraphy (age), geochemistry ($CaCO_3$, C_{org}), paleomagnetics, and physical properties (wet-bulk density and porosity) were integrated with the sedimentological information.

Core Designation

Cores are designated using leg, site, hole, core number, and core type as discussed in the section on "Numbering of Sites, Holes, Cores, and Samples" (this chapter). The cored interval is specified in terms of meters below seafloor (mbsf). Based on drill-pipe measurements (dpm) reported by the SEDCO coring technician and the ODP operations superintendent, depths are corrected for the height of the rig floor dual elevator stool above sea level to give true water depth and correct depth in meters below sea level (mbsl).

Paleontological Data

Microfossil abundance, preservation, and zone assignment appear on the core description form under the heading "Biostrat. Zone/Fossil Character." The chronostratigraphic unit, as recognized on the basis of paleontological results, is shown in the "Time-Rock Unit" column. Detailed information on the zonations and terms used to report abundance and preservation is presented in the "Biostratigraphy" section (this chapter).

Paleomagnetic, Physical Properties, and Chemical Data

Columns are provided on the core description form for recording paleomagnetic results (normal, reversed, or unknown polarity, shown as "N," "R," or "?", respectively), physical properties values (wet-bulk density and porosity), and chemical data (percentages of $CaCO_3$ determined with the Coulometrics analyzer). Additional information on shipboard procedures for collecting these types of data appears in the "Paleomagnetism," "Physical Properties," and "Organic Geochemistry" sections (this chapter).

Graphic Lithology Column

The lithology of the material recovered is represented on the core description forms by a single symbol or by two or more symbols (see Fig. 4) in the column titled "Graphic Lithology." Where an interval of sediment or sedimentary rock is a homogeneous mixture, the constituent categories are separated by a solid vertical line, with each category represented by its own symbol. Constituents comprising <25% of the sediment are not put in the graphic lithology column but are listed in the "Lithologic Description" section of the barrel sheet. In an interval composed of two or more sediment types that have quite different composition, such as thin-bedded and highly variegated sediments, the average relative abundances of the constituents are represented graphically by dashed lines that vertically divide the interval into appropriate fractions, as described above.

The graphic lithology column only shows the composition of layers or intervals exceeding 10 cm in thickness. Information on finer scale lithologic variations is included in the visual core description (VCD) forms available from ODP upon request.

Where sedimentary material was intercalated with igneous rocks, the igneous petrologists described the igneous section and recorded the results in "Hard Rock Core Description Forms." These are referred to on the sedimentary barrel sheets as "igneous rock" or "basalt."

Sedimentary Structures

In sediment cores, natural structures and structures created by the coring process can be difficult to distinguish. Natural structures observed are indicated in the "Sedimentary Structure" column of the core description form. The symbols used to describe the primary biogenic and physical sedimentary structures, and secondary structures such as microfaults, dewatering veinlets, and mineral-filled fractures, are given in Figure 5. In describing sediments recovered during Leg 130, the use of two of these symbols was modified:

1. Throughout most of the recovered intervals, the symbol for "planar laminae" is used to indicate the presence of color bands. True planar laminae were observed only in the basal clastic sediments at Sites 803 and 807; in all cases, the meaning of this symbol is described in the barrel sheet text.
2. In deeper portions of the recovered intervals, the symbol for "Convoluted/Contorted Beds" is used to indicate the presence of stylolites. Each feature (true convoluted/contorted beds and stylolites) is also noted in the appropriate barrel sheet text, so that the meaning of the symbol on each barrel sheet can be clarified by consulting its text.

Sediment Disturbance

Sediment disturbance resulting from the coring process is illustrated in the "Drilling Disturbance" column on the core description form (using the symbols in Fig. 5). Blank regions indicate a lack of drilling disturbance. The degree of drilling disturbance is described for soft and firm sediments using the following categories:

1. Slightly deformed: bedding contacts are slightly bent.
2. Moderately deformed: bedding contacts have undergone extreme bowing.

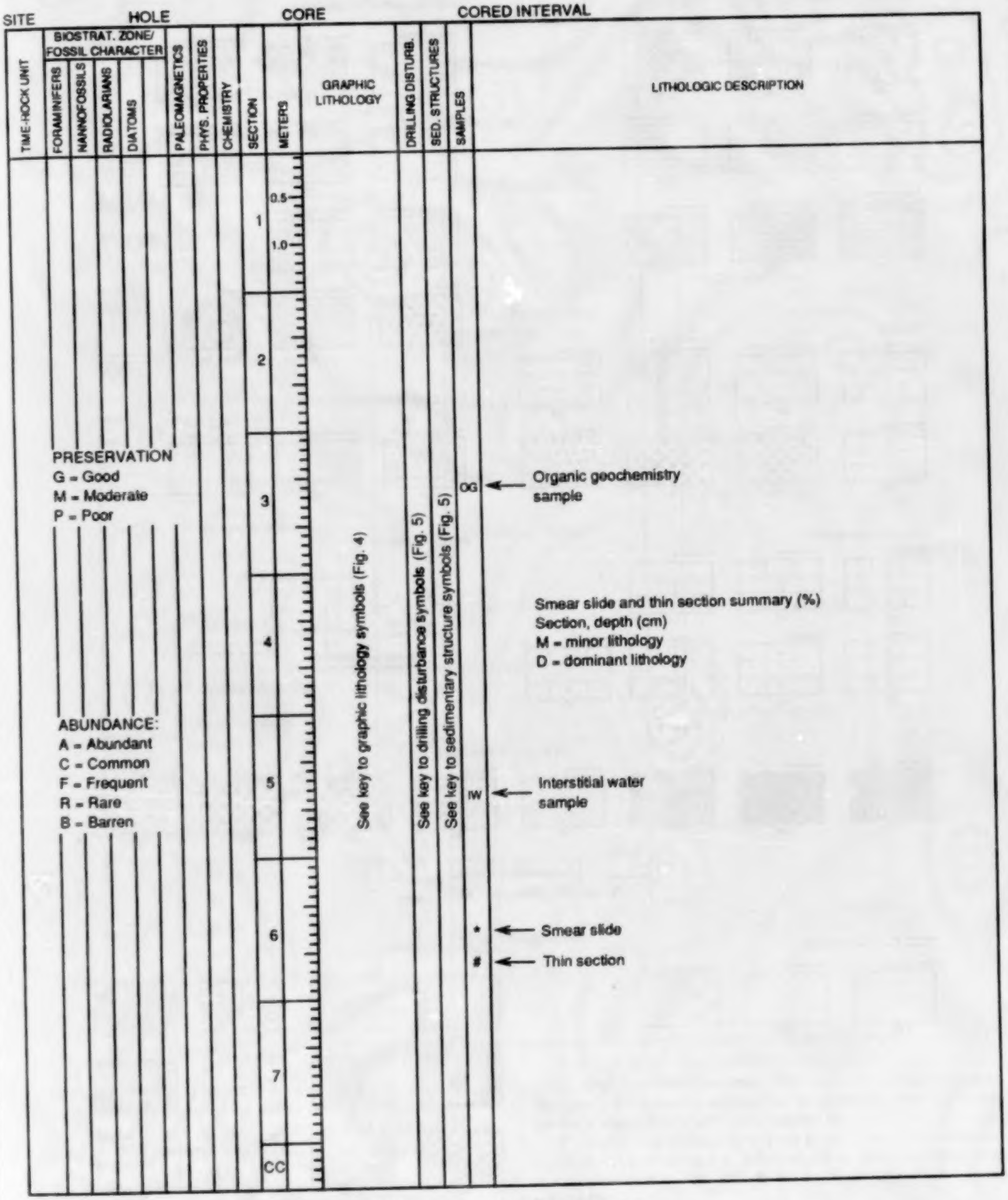
SITE
HOLE
CORE
CORED INTERVAL
TIME-ROCK UNIT
BIOSTRAT. ZONE/ FOSSIL CHARACTER
FORAMINIFERS
NANNOFOSSILS
RADIOLARIANS
DIATOMS
PALEOMAGNETICS
PHYS. PROPERTIES
CHEMISTRY
SECTION
METERS
GRAPHIC LITHOLOGY
DRILLING DISTURB.
SED. STRUCTURES
SAMPLES
LITHOLOGIC DESCRIPTION
0.5
1.0
1
2
3
4
5
6
7
CC
PRESERVATION
G = Good
M = Moderate
P = Poor
ABUNDANCE:
A = Abundant
C = Common
F = Frequent
R = Rare
B = Barren
See key to graphic lithology symbols (Fig. 4)
See key to drilling disturbance symbols (Fig. 5)
See key to sedimentary structure symbols (Fig. 5)
OG
Organic geochemistry sample
Smear slide and thin section summary (%)
Section, depth (cm)
M = minor lithology
D = dominant lithology
IW
Interstitial water sample
*
Smear slide
#
Thin section

Figure 3. Core description form ("barrel sheet") used for sediments and sedimentary rocks.

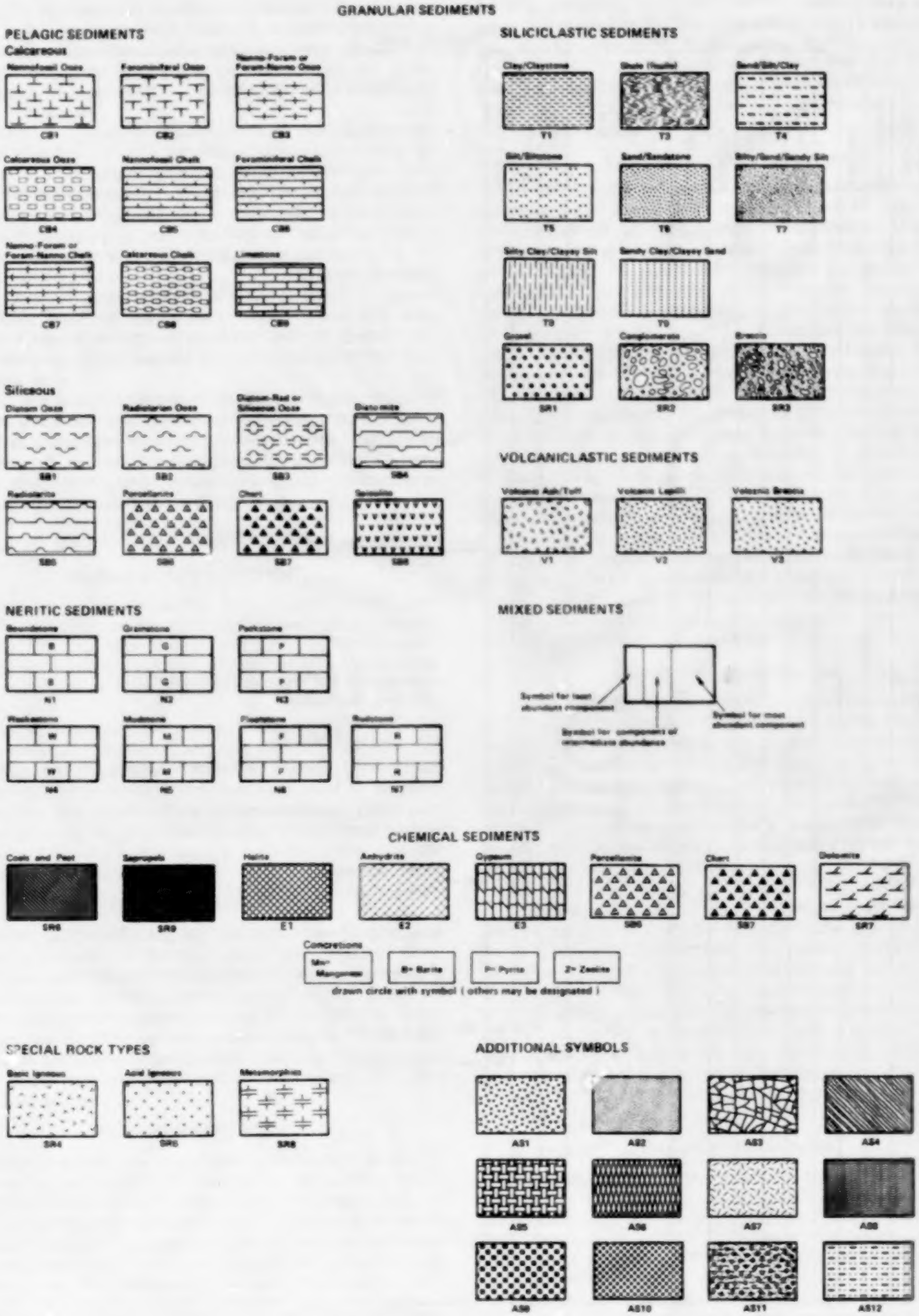
GRANULAR SEDIMENTS
PELAGIC SEDIMENTS
Calcareous
Nannofossil Ooze
CB1
Foraminiferal Ooze
CB2
Nanno-Foram or Foram-Nanno Ooze
CB3
Calcareous Ooze
CB4
Nannofossil Chalk
CB5
Foraminiferal Chalk
CB6
Nanno-Foram or Foram-Nanno Chalk
CB7
Calcareous Chalk
CB8
Limestone
CB9
Siliceous
Diatom Ooze
SB1
Radiolarian Ooze
SB2
Diatom-Rad or Siliceous Ooze
SB3
Diatomite
SB4
Radiolarite
SB5
Porcellanite
SB6
Chert
SB7
Spiculite
SB8
NERITIC SEDIMENTS
Boundstone
B
N1
Grainstone
G
N2
Packstone
P
N3
Wackestone
W
N4
Mudstone
M
N5
Floatstone
F
N6
Rudstone
R
N7
SILICICLASTIC SEDIMENTS
Clay/Claystone
T1
Shale (fissile)
T3
Sand/Silt/Clay
T4
Silt/Siltstone
T5
Sand/Sandstone
T6
Silty/Sand/Sandy Silt
T7
Silty Clay/Clayey Silt
T8
Sandy Clay/Clayey Sand
T9
Gravel
SR1
Conglomerate
SR2
Breccia
SR3
VOLCANICLASTIC SEDIMENTS
Volcanic Ash/Tuff
V1
Volcanic Lapilli
V2
Volcanic Breccia
V3
MIXED SEDIMENTS
Symbol for least abundant component
Symbol for component of intermediate abundance
Symbol for most abundant component
CHEMICAL SEDIMENTS
Coals and Peat
SR6
Sapropels
SR9
Halite
E1
Anhydrite
E2
Gypsum
E3
Porcellanite
SB6
Chert
SB7
Dolomite
SR7
Concretions
Mn= Manganese
B= Barite
P= Pyrite
Z= Zeolite
drawn circle with symbol (others may be designated)
SPECIAL ROCK TYPES
Basic Igneous
SR4
Acid Igneous
SR5
Metamorphics
SR8
ADDITIONAL SYMBOLS
AS1
AS2
AS3
AS4
AS5
AS6
AS7
AS8
AS9
AS10
AS11
AS12

Figure 4. Key to symbols used in the "graphic lithology" column on the core description form shown in Figure 3.

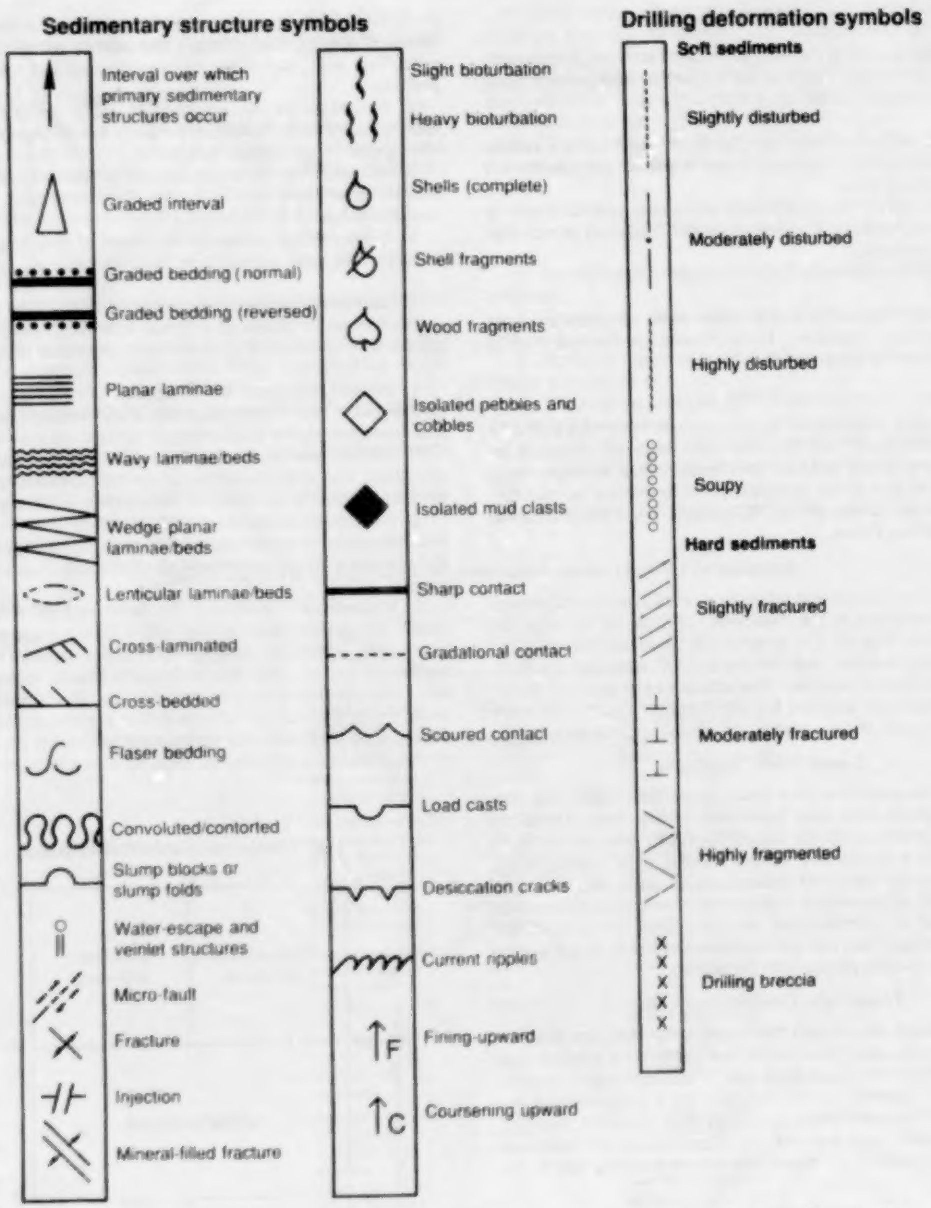
Sedimentary structure symbols
Interval over which primary sedimentary structures occur
Graded interval
Graded bedding (normal)
Graded bedding (reversed)
Planar laminae
Wavy laminae/beds
Wedge planar laminae/beds
Lenticular laminae/beds
Cross-laminated
Cross-bedded
Flaser bedding
Convoluted/contorted
Slump blocks or slump folds
Water-escape and veinlet structures
Micro-fault
Fracture
Injection
Mineral-filled fracture
Slight bioturbation
Heavy bioturbation
Shells (complete)
Shell fragments
Wood fragments
Isolated pebbles and cobbles
Isolated mud clasts
Sharp contact
Gradational contact
Scoured contact
Load casts
Desiccation cracks
Current ripples
F
Fining-upward
C
Coarsening upward
Drilling deformation symbols
Soft sediments
Slightly disturbed
Moderately disturbed
Highly disturbed
Soupy
Hard sediments
Slightly fractured
Moderately fractured
Highly fragmented
Drilling breccia

Figure 5. Key to symbols used for drilling disturbance and sedimentary structure on core description form shown in Figure 3.

3. Highly deformed: bedding is completely disturbed, sometimes showing symmetrical diapirlike or flow structures.

4. Soupy: intervals are water saturated and have lost all aspects of original bedding.

The degree of fracturing in indurated sediments and igneous rocks is described using the following categories:

1. Slightly fractured: core pieces are in place and contain little drilling slurry or breccia;

2. Moderately fragmented: core pieces are in place or partly displaced, but original orientation is preserved or recognizable (drilling slurry may surround fragments);

3. Highly fragmented: pieces are from the interval cored and probably in correct stratigraphic sequence (although they may not represent the entire section), but original orientation is completely lost;

4. Drilling breccia: core pieces have lost their original orientation and stratigraphic position and may be mixed with drilling slurry.

Induration

The criteria used to determine the induration of pelagic sediments found during Leg 130 are subjective and provide three classes for pelagic oozes:

1. Soft: sediments that have little strength and are readily deformed under the finger or broad blade of the spatula are termed oozes or clay;
2. Firm: partly lithified pelagic sediments such as oozes or clays that are readily deformed under the fingernail or the edge of a spatula blade;
3. Hard: nonfriable, cemented rocks.

The suffix "-stone" is added to the name of cemented rocks (e.g., limestone, claystone). Hard siliceous sedimentary rocks are called chert or porcellanite.

Color

Colors were determined by comparison with Munsell soil-color charts immediately after the cores were split because redox-associated color changes may occur when deep-sea sediments are exposed to the atmosphere. Information on core colors is given in the text of the "Lithologic Description" on the core description forms.

Samples

The position of samples taken from each core for shipboard analysis is indicated in the "Samples" column on the core description form (Fig. 3). The symbol "★" indicates the location of smear slide samples, and the symbol "#" indicates the location of thin-section samples. The notations IW and OG designate the location of samples for whole-round, interstitial-water geochemistry and frozen organic geochemistry, respectively.

Smear Slide Summary

A table summarizing data from smear slides and thin sections appears on each core barrel description form. The table includes information on the sample location, whether the sample represents a dominant ("D") or a minor ("M") lithology in the core, and the estimated percentages of sand, silt, and clay, together with all identified components. Note that smear slide analyses tend to underestimate the abundance of foraminifers and volcaniclastic-detrital material because these larger grains are difficult to incorporate into the smear.

Lithologic Description—Text

The lithologic description that appears on each core description form (barrel sheet) consists of two parts: (1) a heading that lists all the major sediment types (see "Sedimentology" section, this chapter) observed in the core; and (2) a more detailed description of these sediments, including data on color, location in the core, significant features, etc. Descriptions and locations of thin, interbedded, or minor lithologies are included in the text.

SEDIMENTOLOGY

The new sediment classification scheme for ODP by Mazzullo et al. (1988), partly reproduced below, was used during Leg 130. The sediment classification scheme described here defines two basic sediment types: (1) granular and (2) chemical.

Granular Sediments

Classes of Granular Sediments

Four types of grains are recognized in granular sediments: *pelagic, neritic, siliciclastic,* and *volcaniclastic* grains.

1. Pelagic grains are composed of the fine-grained skeletal debris of open-marine siliceous and calcareous microfauna and microflora (e.g., radiolarians, nannofossils) and associated organisms.
2. Neritic grains are composed of coarse-grained calcareous skeletal debris (e.g., bioclasts, peloids), and fine-grained calcareous grains of nonpelagic origin.
3. Siliciclastic grains are composed of mineral and rock fragments that were derived from plutonic, sedimentary, and metamorphic rocks.
4. Volcaniclastic grains are composed of rock fragments and minerals that were derived from volcanic sources.

Variations in the relative proportions of the four grain types define five major classes of granular sediments: *pelagic, neritic, siliciclastic, volcaniclastic,* and *mixed sediments* (Fig. 6).

1. Pelagic sediments are composed of >60% pelagic and neritic grains and <40% siliciclastic and volcaniclastic grains, and contain a higher proportion of pelagic than neritic grains.
2. Neritic sediments are composed of >60% pelagic and neritic grains and <40% siliciclastic and volcaniclastic grains, and contain a higher proportion of neritic than pelagic grains.
3. Siliciclastic sediments are composed of >60% siliciclastic and volcaniclastic grains and <40% pelagic and neritic grains, and contain a higher proportion of siliciclastic than volcaniclastic grains.
4. Volcaniclastic sediments are composed of >60% siliciclastic and volcaniclastic grains and <40% pelagic and neritic grains, and contain a higher proportion of volcaniclastic than siliciclastic grains. This class includes epiclastic sediments (volcanic detritus that is produced by erosion of volcanic rocks by wind, water, and ice), pyroclastic sediments (the products of the degassing of magmas), and hydroclastic sediments (the products of the granulation of volcanic glass by steam explosions).

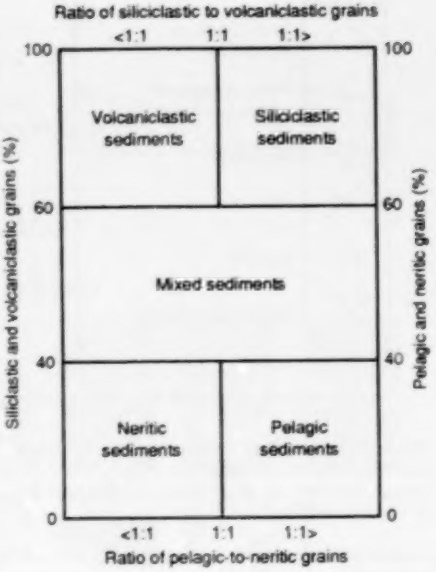
Ratio of siliciclastic to volcaniclastic grains
<1:1
1:1
1:1>
100
100
Volcaniclastic sediments
Siliciclastic sediments
Siliciclastic and volcaniclastic grains (%)
60
60
Mixed sediments
Pelagic and neritic grains (%)
40
40
Neritic sediments
Pelagic sediments
0
0
<1:1
1:1
1:1>
Ratio of pelagic-to-neritic grains

Figure 6. Diagram showing classes of granular sediment (modified from Mazzullo et al., 1988).

5. Mixed sediments are composed of 40%–60% siliciclastic and volcaniclastic grains, and 40%–60% pelagic and neritic grains.

Classification of Granular Sediment

A granular sediment can be classified by designating a *principal name* and *major* and *minor modifiers*. The principal name of a granular sediment defines its granular sediment class; the major and minor modifiers describe the texture, composition, fabric, and/or roundness of the grains themselves (Table 1).

Principal Names

Each granular sediment class has a unique set of principal names, which are outlined below.

For pelagic sediment, the principal name describes the composition and degree of consolidation using the following terms:

1. *Ooze:* unconsolidated calcareous and/or siliceous pelagic sediments.
2. *Chalk:* firm pelagic sediment composed predominantly of calcareous pelagic grains.
3. *Limestone:* hard pelagic sediment composed predominantly of calcareous pelagic grains.
4. *Radiolarite, diatomite,* and *spiculite:* firm pelagic sediment composed predominantly of siliceous radiolarians, diatoms, and sponge spicules, respectively.
5. *Porcellanite:* a well-indurated rock with abundant authigenic silica but less hard, lustrous, or brittle than chert (in part, such rocks may represent mixed sedimentary rock).
6. *Chert:* vitreous or lustrous, conchoidally fractured, highly indurated rock composed predominantly of authigenic silica.

For neritic sediment, the principal name describes the texture and fabric, using the following terms (from Dunham, 1962):

1. *Boundstone:* components organically bound during deposition.
2. *Grainstone:* grain-supported fabric, no mud, grains <2 mm in size.
3. *Packstone:* grain-supported fabric, with intergranular mud, grains <2 mm in size.
4. *Wackestone:* mud-supported fabric, with >10% grains, grains <2 mm in size.
5. *Mudstone:* mud-supported fabric, with <10% grains.
6. *Floatstone:* matrix-supported fabric, grains >2 mm in size.
7. *Rudstone:* grain-supported fabric, grains >2 mm in size.

Table 1. Outline of granular-sediment classification scheme (modified from Mazzullo et al., 1988).

Sediment class	Major modifiers	Principal names	Minor modifiers
Pelagic	1. Composition of pelagic and neritic grains present in major amounts 2. Texture of clastic grains present in major amounts	1. Ooze 2. Chalk 3. Limestone 4. Radiolarite 5. Diatomitie 6. Spiculite 7. Chert	1. Composition of pelagic and neritic grains present in minor amounts 2. Texture of clastic grains present in minor amounts
Neritic	1. Composition of neritic and pelagic grains present in major amounts 2. Texture of clastic grains present in major amounts	1. Boundstone 2. Grainstone 3. Packstone 4. Wackestone 5. Mudstone 6. Floatstone 7. Rudstone	1. Composition of neritic and pelagic grains present in minor amounts 2. Texture of clastic grains present in minor amounts
Siliciclastic	1. Composition of all grains present in major amounts 2. Grain fabric (gravels only) 3. Grain shape (optional) 4. Sediment color (optional)	1. Gravel 2. Sand 3. Silt 4. Clay (etc.)	1. Composition of all grains present in minor amounts 2. Texture and composition of siliciclastic grains present as matrix (for coarse-grained clastic sediments)
Volcaniclastic	1. Composition of all volcaniclasts present in major amounts 2. Composition of all pelagic and neritic grains present in major amounts 3. Texture of siliciclastic grains present in major amounts	1. Breccia 2. Lapilli 3. Ash/tuff	1. Composition of all volcaniclasts present in minor amounts 2. Composition of all neritic and pelagic grains present in minor amounts 3. Texture of siliciclastic grains present in minor amounts
Mixed	1. Composition of neritic and pelagic grains present in major amounts 2. Texture of clastic grains present in major amounts	1. Mixed sediments	1. Composition of neritic and pelagic grains present in minor amounts 2. Texture of clastic grains present in minor amounts

For siliciclastic sediment, the principal name describes the texture and is assigned according to the following guidelines:

1. The Udden-Wentworth grain-size scale (Wentworth, 1922; Table 2) defines the grain-size ranges and the names of the textural groups (*gravel, sand, silt,* and *clay*) and subgroups (*fine sand, coarse silt,* etc.) that are used as the principal names of siliciclastic sediment.
2. When two or more textural groups or subgroups are present in a siliciclastic sediment, they are listed as principal names in order of increasing abundance.
3. The suffix "*-stone*" is affixed to the principal names *sand, silt,* and *clay* when the sediment is lithified. *Conglomerate* and *breccia* are used as principal names of gravels with well-rounded and angular clasts, respectively.

For volcaniclastic sediment, the principal name describes the texture. The names and ranges of three textural groups (from Fisher and Schmincke, 1984) are as follows:

1. *Volcanic breccia:* pyroclasts >64 mm in diameter.
2. *Volcanic lapilli:* pyroclasts from 2 to 64 mm in diameter; when lithified, the term "*lapillistone*" is used.
3. *Volcanic ash:* pyroclasts <2 mm in diameter; when lithified, the term "*tuff*" is used.

Table 2. Udden-Wentworth grain-size scale for siliciclastic sediments (Wentworth, 1922).

Millimeters		Micrometers	Phi (ϕ)	Wentworth size class	
			−20		Gravel
	4096		−12	Boulder (−8 to −12ϕ)	
	1024		−10		
	256		−8		
				Cobble (−6 to −8ϕ)	
	84		−6		
	16		−4	Pebble (−2 to −6ϕ)	
	4		−2		
	3.36		−1.75		
	2.83		−1.5	Granule	
	2.36		−1.25		
	2.00		−1.0		
	1.58		−0.75		Sand
	1.41		−0.5	Very coarse sand	
	1.19		−0.25		
	1.00		0.0		
	0.84		0.25		
	0.71		0.5	Coarse sand	
	0.59		0.75		
1/2	0.50	500	1.0		
	0.42	420	1.25		
	0.35	350	1.5	Medium sand	
	0.30	300	1.75		
1/4	0.25	250	2.0		
	0.210	210	2.25		
	0.177	177	2.5	Fine sand	
	0.149	149	2.75		
1/8	0.125	125	3.0		
	0.106	106	3.25		
	0.088	88	3.5	Very fine sand	
	0.074	74	3.75		
1/16	0.0625	63	4.0		
	0.063	83	4.25		Mud
	0.044	44	4.5	Coarse silt	
	0.037	37	4.75		
1/32	0.031	31	5.0		
1.64	0.0156	15.6	6.0	Medium silt	
1/128	0.0078	7.8	7.0	Fine silt	
1/256	0.0039	3.9	8.0	Very fine silt	
	0.0020	2.0	9.0		
	0.00096	0.96	10.0	Clay	
	0.00049	0.49	11.0		
	0.00024	0.24	12.0		
	0.00012	0.12	13.0		
	0.00006	0.06	14.0		

For mixed sediment, the principal name describes the degree of consolidation, with the term "*mixed sediment*" used for unlithified sediment, and the term "*mixed sedimentary rock*" used for lithified sediment.

Major and Minor Modifiers

The principal name of a granular sediment class is preceded by major modifiers and followed by minor modifiers (preceded by the term "with") that describe the lithology of the granular sediment in greater detail (Table 1). The most common uses of major and minor modifiers are to describe the composition and textures of grain types that are present in major (>25%) and minor (10%-25%) proportions. In addition, major modifiers can be used to describe grain fabric, grain shape, and sediment color. The nomenclature for the major and minor modifiers is outlined below.

The composition of pelagic grains can be described with the major and minor modifiers *diatom(-aceous), radiolarian, spicules(-ar), siliceous, nannofossil, foraminifer, and calcareous.* The terms *siliceous* and *calcareous* are used to describe sediments that are composed of siliceous or calcareous pelagic grains of uncertain origin.

The composition of neritic grains can be described with the following major and minor modifiers:

1. *Ooid* (or *oolite*): spherical or elliptical nonskeletal particles <2 mm in diameter that have a central nucleus surrounded by a rim with concentric or radial fabric.
2. *Bioclast* (or *bioclastite*): fragment of skeletal remains (specific names such as *molluscan* or *algal* can also be used).
3. *Pellet(-al)*: fecal particles from deposit-feeding organisms.
4. *Intraclast:* reworked carbonate-rock fragment or rip-up clast.
5. *Pisolite:* spherical or ellipsoidal, nonskeletal particle, commonly >2 mm in diameter, with or without a central nucleus but displaying multiple concentric layers of carbonate.
6. *Peloid* (or *pel*): micritized carbonate particle of unknown origin.
7. *Calcareous, dolomitic, aragonitic,* and *sideritic:* used to describe the composition of carbonate muds or mudstones (micrite) of nonpelagic origins.

The texture of siliciclastic grains is described by the major and minor modifiers *gravel(-ly), sand(-y), silt(-y),* and *clay(-ey).* The composition of siliciclastic grains can be described by:

1. Mineralogy: with such modifiers as "quartz," "feldspar," "glauconite," "mica," "kaolinite," "zeolitic," "lithic" (for rock fragments), "calcareous," "gypsiferous," or "sapropelic" (for detrital clasts of calcium carbonate, gypsum, and organic matter, respectively).
2. Provenance: the source of rock fragments (particularly in gravels, conglomerates, and breccias) can be described by such modifiers as volcanic, sed-lithic, meta-lithic, gneissic, basaltic, etc.

The composition of volcaniclastic grains is described by the major and minor modifiers *lithic* (rock fragments), *vitric* (glass and pumice), and *crystal* (mineral crystals), or by modifiers that describe the compositions of the lithic grains and crystals (e.g., *feldspar* or *basaltic*). The fabric of the sediment can be described by the major modifiers *grain-supported, matrix-supported,* and *imbricated.* Generally, fabric descriptors are applied only to gravels, conglomerates, and breccias for they provide useful information on their transport history.

Chemical Sediments

Classes of Chemical Sediments

Chemical sediments are composed of minerals that formed by inorganic processes, such as precipitation from solution or colloidal suspension, deposition of insoluble precipitates, or recrystallization of detrital evaporites and siliceous, calcareous, or carbonaceous (plant) biogenic debris. They generally have a crystalline (i.e., nongranular) texture.

There are five classes of chemical sediments: carbonaceous sediments, evaporites, silicates, carbonates, and metalliferous sediments. Each class of chemical sediment has its own distinctive classification scheme. The following chemical sediments were encountered on Leg 130.

Silicates and Carbonates

Silicates and carbonates are defined as sedimentary rocks that are nongranular and nonbiogenic in appearance and composed of silicate and carbonate minerals. Silicates and carbonates may have formed from the recrystallization of siliceous and calcareous grains, but they are distinguished by the absence of clearly identifiable granular and biogenic components. They may also form as primary precipitates, as in the case of dolomite or proto-dolomite or as hydrothermal alteration products, such as in the case of zeolites. They are classified according to their mineralogy, using principal names such as chert (microcrystalline quartz), calcite, and dolomite. They should also be modified with terms that describe their crystalline (as opposed to granular) nature, such as crystalline, microcrystalline, massive, and amorphous.

Grain Size Analyses

Bulk grain-size analyses were conducted on approximately one sample per section on unconsolidated APC cores. These results are presented in tabular and graphic form in each site report. The analyses were conducted using an eight-channel Lasentec Lab-Tec 100 particle-size analyzer. Data were collected at the following size intervals: <4, 4–8, 8–16, 16–32, 32–63, 63–125, 125–250, and >250 μm. Standard dispersal techniques were used to disaggregate the samples for analysis.

BIOSTRATIGRAPHY

Preliminary age assignments were established primarily on core-catcher samples. Samples from within the cores were examined when a critical shipboard age determination was necessary. Four microfossil groups were examined for biostratigraphic purposes: calcareous nannofossils, planktonic foraminifers, radiolarians, and diatoms. Benthic foraminifers provided preliminary paleoenvironmental information. Sample position and the abundance, preservation, and age or zone for each fossil group were recorded on the barrel sheets for each core.

Time scales by Berggren et al. (1985a, 1985b) for the Cenozoic and Kent and Gradstein (1985) for the Cretaceous provide the correlation between magnetostratigraphy and absolute time used in this report. Tables 3, 4, and 5 summarize the nannofossil, planktonic foraminifers, and diatom datums, respectively, used for Leg 130. Figures 7 and 8 show the correlation of Cenozoic chronostratigraphy, biostratigraphy, and magnetostratigraphy used for Leg 130.

Calcareous Nannofossils

The chief purpose of Leg 130 was to recover sedimentary sequences that represent a continuous stratigraphic column encompassing the interval from the present to the Lower Creta-

Table 3. Calcarous nannofossil species events and their assigned age estimates.

Event	Species	Zone (top)	Age (Ma)	References
OA	*Emiliania huxleyi*		0.09	1
FO	*Emiliania huxleyi*	NN20	0.28	1
LO	*Pseudoemiliania lacunosa*	NN19	0.46	1
LO	*Reticulofenestra asanoi*		0.83	2
FO	*Gephyrocapsa parallela*		0.90	2
FO	*Reticulofenestra asanoi*		1.06	2
LO	large *Gephyrocapsa*		1.10	2
LO	*Helicosphaera sellii*		1.19	2
FO	large *Gephyrocapsa*		1.36	2
LO	*Calcidiscus macintyrei*		1.45(1.57)	3(2)
FO	*Gephyrocapsa oceanica*		1.57	2
FO	*Gephyrocapsa caribbeanica*		1.66	2
Pleistocene/Pliocene boundary			1.66	4
LO	*Discoaster brouweri*	NN18	1.89	3
LO	*Discoaster triradiatus*		1.89	3
OA	*Discoaster triradiatus*		2.07	5
LO	*Discoaster pentaradiatus*	NN17	2.35	3
LO	*Discoaster surculus*	NN16	2.41	3
LO	*Reticulofenestra ampla*		2.62	2
LO	*Discoaster tamalis*		2.65	3
LO	*Sphenolithus* spp.		3.45	3
LO	*Reticulofenestra pseudoumbilica*	NN15	3.56	3
LO	*Amaurolithus tricorniculatus*	NN14	3.7	6a
FO	*Discoaster asymmetricus*	NN13	4.1	6a
LO	*Amaurolithus primus*		4.4	6a
FO	*Ceratolithus rugosus*	NN12	4.6	3
LO	*Ceratolithus acutus*		4.6	3
FO	*Ceratolithus acutus*		4.9(4.85)	7
LO	*Triquetrorhabdulus rugosus*		4.9	7
Pliocene/Miocene boundary			4.9	8
LO	*Discoaster quinqueramus*	NN11	5.0	7
LO	*Amaurolithus amplificus*		5.4	9
FO	*Amaurolithus amplificus*		6.0	9
FO	*Amaurolithus primus*		6.7	9
FO	*Discoaster quinqueramus*	NN10	7.5	7
FO	*Discoaster berggrenii*		8.2	6a
LO	*Discoaster hamatus*	NN9	8.7	7
LO	*Catinaster* spp.		8.8	7
FO	*Discoaster neohamatus*		9.0	7
FO	*Catinaster calyculus*		10.0	6a
FO	*Discoaster hamatus*	NN8	10.5	7
FO	*Catinaster coalitus*	NN7	11.1	7
FO	*Discoaster kugleri*	NN6	12.2	7
LO	*Coronocyclus nitescens*		12.8	9
LO	*Cyclicargolithus floridanus*		13.1	7
LO	*Sphenolithus heteromorphus*	NN5	13.6	7
LO	*Helicosphaera ampliaperta*	NN4	16.0	6a
TA	*Discoaster deflandrei* group		16.1	9
FO	*Sphenolithus heteromorphus*		18.6	7
LO	*Sphenolithus belemnos*	NN3	18.8	7
LO	*Triquetrorhabdulus carinatus*	NN2	19.5	7
FO	*Sphenolithus belemnos*		20.0	7
FO	*Discoaster druggii*	NN1	23.6	7
TA	*Sphenolithus delphix*		23.6	10
Miocene/Oligocene boundary			23.7	6a
OA	*Sphenolithus delphix*		24.7	10
LO	*Sphenolithus ciperoensis*		25.2	6b
OA	*Triquetrorhabdulus carinatus*		27.0	10
LO	*Sphenolithus distentus*	NP24	27.5(28.2)	10(6b)
AS	*S. ciperoensis/S. distentus*		28.8	10
FO	*Sphenolithus ciperoensis*	NP23	30.2	6b
FO	*Sphenolithus distentus*		34.2	6b
LO	*Reticulofenestra umbilica*	NP22	33.8(34.2)	11(6b)
LO	*Ericsonia formosa*	NP21	34.9	11
Oligocene/Eocene boundary			36.6	6b
LO	*Discoaster saipanensis*	NP20	37.7	11
LO	*Discoaster barbadiensis*		37.0	11
FO	*Chiasmolithus oamaruensis*	NP17	39.8	6b
LO	*Chiasmolithus grandis*		40.0	6b
LO	*Chiasmolithus solitus*	NP16	42.3	6b
FO	*Dictyococcites hesslandii*		42.9	11
LO	*Nannotetrina* spp.		44.2	11
FO	*Reticulofenestra umbilica* (>14 μm)		44.4	11
LO	*Chiasmolithus gigas*		47.0	6b
FO	*Chiasmolithus gigas*		48.8	12
FO	*Nannotetrina fulgens*	NP14	49.5	12

Table 3 (continued).

Event	Species	Zone (top)	Age (Ma)	References
Oligocene/Eocene boundary (Cont.)				
LO	*Discoaster sublodoensis*		49.7	12
FO	*Nannotetrina* spp.		50.3	12
LO	*Discoaster lodoensis*		50.4	12
FO	*Discoaster sublodoensis*	NP13	52.3	12
LO	*Tribrachiatus orthostylus*	NP12	54.0	12
FO	*Discoaster lodoensis*	NP11	55.0	12
FO	*Sphenolithus radians*		56.0	12
AS	*T. orthostylus–T. contortus*	[a]NP10	56.2	12
Eocene/Paleocene boundary			[b]56.4	
FO	*Triquetrorhabdulus contortus*		56.5	12
FO	*Triquetrorhabdulus bramlettei*	NP9	56.7	12
FO	*Discoaster diastypus*		56.7	12
FO	*Rhomboaster* spp.		56.8	12
LO	*Fasciculithus* spp.		56.9	12
LO	*Ericsonia robusta*		57.8	12
FO	*Campylosphaera eodela*		59.2	6b
FO	*Discoaster multiradiatus*	NP8	59.0	12
FO	*Discoaster okadai*		59.3	12
FO	*Discoaster nobilis*		59.4	12
LO	*Heliolithus kleinpellii*		60.1	12
FO	*Discoaster mohleri*	NP6	60.2	12
LO	*Chiasmolithus danicus*		61.0	6b
FO	*Heliolithus kleinpellii*	NP5	61.0	12
FO	*Heliolithus cantabriae*		61.5	12
LO	*Fasciculithus pileatus*		61.8	12
LO	*Cruciplacolithus tenuis*		61.8	6b
FO	*Fasciculithus* spp.		62.4	12
FO	*Ellipsolithus macellus*	NP3	62.8	12
FO	*Sphenolithus* spp.		62.9	12
FO	*Chiasmolithus danicus*	NP2	64.8	6b
FO	*Cruciplacolithus tenuis*	NP1	65.9	6b
FO	*Cruciplacolithus primus*		66.1	6b
Tertiary/Cretaceous boundary			66.4	6b

Notes: FO = first occurrence, LO = last occurrence, OA = onset acme, TA = termination acme, and AS = abundance shift. Zonal codes are those of Martini (1971). Age column references represent (1) Thierstein et al., 1977; (2) Sato et al., 1991; (3) Backman and Shackleton, 1983; (4) Rio et al., in press; (5) Backman and Pestiaux, 1986; (6a) Berggren et al., 1985a; (6b) Berggren et al., 1985b; (7) Backman et al., 1990; Zijderveld et al., 1986; (9) Rio et al., 1990; (10) Fornaciari et al., 1990; (11) Backman, 1987; (12) Backman, 1986.

[a] Martini (1971) defined the top of NP10 by the LO of *T. contortus*. A proclivity to diagenetic overgrowth in combination with a subtle evolutionary transition into the descendant species *T. orthostylus* prevents precise determination of the NP10/NP11 boundary. The abundance cross-over between these closely related forms, however, provides a biostratigraphic indication that is easier to recognize than the LO of *T. contortus*.

[b] Berggren et al. (1985b) originally suggested that the Eocene/Paleocene boundary is coincident with the biostratigraphic NP9/NP10 boundary, and provided an age estimate of 57.8 Ma for these two boundaries. Subsequent developments in late Paleocene/early Eocene biochronology indicate that the NP9/NP10 boundary is about 56.7 Ma (Backman, 1986), an estimate that was derived using the geomagnetic polarity history of Berggren et al. (1985b). Aubry et al. (1988) recently argued that the Eocene/Paleocene boundary does not fall at the NP9/NP10 boundary but well within NP10. Aubry and others consequently conclude that Berggren's et al. (1985b) estimate of 57.8 Ma is too old (by 0.7 m.y. in their opinion). Our biochronology in the pertinent interval differs from that of Aubry and others; however, we have adopted their argument that the Eocene/Paleocene boundary is associated with the middle to upper part of Zone NP10 (see their text on p. 735 and fig. 6). For these reasons, we will use an age of 56.4 Ma for the Eocene/Paleocene boundary.

ceous. In terms of calcareous nannofossil biostratigraphy, the classification of Leg 130 sediments was expressed through a single Cenozoic zonal scheme. Cretaceous sediments were classified biostratigraphically using a composite zonal scheme.

Chronological Framework

The age estimates of calcareous nannofossil zonal boundaries, or marker events, have been derived largely from the geomagnetic polarity time scale (GPTS) of Berggren et al. (1985a, 1985b). Their polarity history covers the time interval from the present to 84 Ma (termination of Chron 34). The GPTS of Kent and Gradstein (1985) was used in the Cretaceous time interval

Table 4. Cenozoic planktonic foraminifer species events.

Event	Species	Zone (top)	Age (Ma)
LO	*Globorotalia tosaensis*		0.6
FO	*Pulleniatina finalis*		1.3
LO	*Globigerinoides fistulosus*		1.6
Pleistocene/Pliocene boundary			1.6
FO	*Globorotalia truncatulinoides*	N21/*G. tosaensis*	1.9
LO	*Globorotalia exilis*		2.1
LO	*Globorotalia miocenica*		2.2
LO	*Globorotalia pertenuis*		2.5
LO	*Globorotalia multicamerata*		2.9
LO	*Globoquadrina altispira*		2.9
FO	*Globigerinoides fistulosus*		2.9
LO	*Sphaeroidinellopsis* spp.		3.0
FO	*Sphaeroidinella dehiscens* s.s.		3.0
FO	*Globorotalia inflata*		3.0
LO	*Globorotalia conomiozea*		3.0
FO	*Globorotalia tosaensis*	N19/*G. miocenica*	3.1
FO	*Globorotalia crassula*		3.1
FO	*Globorotalia pertenuis*		3.3
FO	*Globorotalia miocenica*		3.4
LO	*Globorotalia margaritae*		3.4
LO	*Pulleniatina primalis*		3.5
Coiling change in *Pulleniatina* (S to D)			3.8
LO	*Globigerina nepenthes*		3.9
FO	*Globorotalia crassiformis* s.s.		4.1
FO	*Globorotalia crassiformis* s.l.		4.3
FO	*Globorotalia puncticulata*		4.4
LO	*Globorotalia cibaoensis*		4.4
FO	*Sphaeroidinella dehiscens* s.l.	N18	5.1
FO	*Globorotalia tumida*		5.2
FO	*Pulleniatina spectabilis*		5.2
Pliocene/Miocene boundary			5.3
FO	*Globigerinoides conglobatus*	N17b	5.3
FO	*Globorotalia cibaoensis*	N17b	5.3
LO	*Globoquadrina dehiscens*	N17b	5.3
LO	*Globorotalia lenguaensis*	N17b	5.3
FO	*Globorotalia margaritae*		5.6
FO	*Pulleniatina primalis*	N17a	5.8
FO	*Globorotalia conomiozea*		6.1
FO	*Globorotalia plesiotumida*	N16	7.1
FO	*Neogloboquadrina dutertrei* s.l.	*N. acostaensis*	8.0
FO	*Neogloboquadrina acostaensis*	N15/*G. menardii*	10.2
LO	*Globorotalia siakensis* (= *mayeri*)	N14/*G. mayeri*	10.4
FO	*Globigerina nepenthes*	N13	11.3
LO	*G. fohsi lobata* and *G. fohsi robusta*	N12	11.5
FO	*Globorotalia fohsi robusta*		12.6
FO	*G. fohsi lobata* (= *G. fohsi fohsi*)	N11	13.1
FO	*Globorotalia praefohsi*	N10	13.9
LO	*Globorotalia peripheroronda*		14.6
FO	*Globorotalia peripheroacuta*	N9/*G. peripheroronda*	14.9
LO	*Praeorbulina sicana*	N9/*G. peripheroronda*	14.9
LO	*Praeorbulina glomerosa*	N9/*G. peripheroronda*	14.9
FO	*Orbulina suteralis*	N8/*P. glomerosa*	15.2
FO	*Praeorbulina glomerosa*	*G. insueta*	16.3
FO	*Praeorbulina sicana*	N7	16.6
FO	*Globorotalia miozea*		16.8
LO	*Globorotalia zealandica*		16.8
FO	*Globorotalia birnageae*		17.0
LO	*Catapsydrax stainforthi*		17.4
FO	*Globorotalia zealandica*	N6/*C. stainforthi*	17.6
LO	*Globorotalia incognita*	N6/*C. stainforthi*	17.6
LO	*Catapsydrax dissimilis*	N6/*C. stainforthi*	17.6
FO	*Globorotalia praescitula*		17.7
FO	*Globigerinatella insueta*	N5	19.0
FO	*Globigerinoides altiaperturus*		20.9
LO	*Globorotalia kugleri* s.s.	N4/*G. kugleri*	21.8
FO	*Globoquadrina dehiscens*		23.2
FO	*Globorotalia incognita*		23.2
LO	*Globigerina angulisuturalis*		23.2
LO	*Globorotalia pseudokugleri*		23.2
Miocene/Oligocene boundary			23.7
FO	*Globorotalia kugleri* s.s.	P22/*G.ciperoensis*	23.7
FO	*Globigerinoides primordius* (common)		24.5
FO	*Globigerinoides primordius* (rare)		25.8
FO	*Globorotalia pseudokugleri*		[b]26.3
LO	*Globorotalia opima*	P21b/*G. opima*	28.2
LO	*Chiloguembelina* spp.	P21a	30.0
FO	*Globigerina angulisuturalis*	P20	[b]31.6
LO	*Globigerina angiporoides*		32.0

Table 4 (continued).

Event	Species	Zone (top)	Age (Ma)
Miocene/Oligocene boundary (Cont.)			
FO	*Globigerina opima*	*G. ampliapertura*	32.7
LO	*Globigerina ampliapertura*	P19	[b]32.8
LO	*Pseudohastigerina* spp.	P18/*C. chip.–P. micra*	34.0
Oligocene/Eocene boundary			36.6
LO	*Globorotalia cocoaensis*	P17/*G. cerroazulensis*	[b]36.6
LO	*Globorotalia cerroazulensis*	*G. cerroazulensis*	36.6
LO	*Hantkenina* spp.	*G. cerroazulensis*	36.6
LO	*Globigerapsis* spp.		37.0
LO	*Cribrohantkenina inflata*	P16	[b]37.2
LO	*Porticulasphaera semiinvoluta*	*P. semiinvoluta*	37.6
FO	*Cribrohantkenina inflata*	P15	[b]38.1
LO	*Acarinina* and *Truncorotaloides rohri*		40.6
LO	*Morozovella spinulosa*		41.1
FO	*Porticulasphaera semiinvoluta*	P14/*T. rohri*	41.3
LO	*Subbotina frontosa*		42.0
LO	*Globigerapsis beckmanni*	P13/*G. beckmanni*	42.6
FO	*Globigerapsis beckmanni*	P12/*M. lehneri*	43.0
LO	*Acarinina bullbrooki*	P12/*M. lehneri*	43.0
FO	*Globorotalia pomeroli*		44.7
FO	*Globigerapsis index*		45.0
FO	*Morozovella lehneri*	P11/*G. subconglobata*	46.0
LO	*Morozovella aragonensis*	P11/*G. subconglobata*	46.0
FO	*Globigerapsis kugleri*	P10/*H. aragonensis*	[a]49.0
FO	*Hantkenina* spp.	P9/*A. pentacamerata*	52.0
FO	*Planorotalites palmerae*	P8/*M. aragonensis*	53.4
FO	*Morozovella aragonensis*	P7/*M. formosa formosa*	[a]54.0
FO	*Morozovella formosa*	P6b/*M. subbotinae*	[a]55.2
Eocene/Paleocene boundary			56.4
LO	*Morozovella velascoensis*	P6a/*M. velascoensis*	57.8
FO	*Morozovella subbotinae*	P5	[b]58.2
LO	*Planorotalites pseudomenardii*	P4/*P. pseudomenardii*	58.8
FO	*Planorotalites pseudomenardii*	P3b/*P. pusilla pusilla*	61.0
FO	*Morozovella velascoensis*		61.7
FO	*Morozovella albeari*		61.7
LO	*Subbotina pseudobulloides*		61.7
FO	*Morozovella pusilla*	P3a/*M. angulata*	62.0
FO	*Morozovella conicotruncata*	P3a/*M. angulata*	62.0
FO	*Morozovella angulata*	P2/*M. uncinata*	62.3
FO	*Morozovella uncinata*	P1c/*S. trinidadensis*	63.0
LO	*Globastica daubjergensis*		64.0
LO	*Planorotalites compressus*	P1b/*S. pseudobulloides*	64.5
FO	*S. praecursoria (trinidadensis)*	P1b/*S. pseudobulloides*	64.5
FO	*Subbotina triloculinoides*	P1a	[b]65.5
FO	*Subbotina pseudobulloides*	Pα/*P. eugubina*	[b]66.1
FO	*Parvularugoglobigerina eugubina*		66.35
LO	*Globotruncana*		66.4

Notes: FO = first occurrence and LO = last occurrence. Most datums are from Berggren et al. (1985a, 1985b). Refer to Table 3 for comments on the placement of the Eocene/Paleocene boundary.

[a] From Aubry et al. (1988).

[b] From Berggren and Miller (1988).

Table 5. Diatom species events and their assigned age estimates.

Event	Species	Zone (top)	Age (Ma)	References
LO	*Nitzschia reinholdii*	NTD 16	0.65	1
LO	*Rhizosolenia praebergonii* var. *robusta*		1.55	1
FO	*Pseudoeunotia doliolus*	NTD 15	1.8	1
LO	*Thalassiosira convexa* var. *aspinosa*		2.1	1
LO	*Nitzschia jouseae*		2.6	1
FO	*Rhizosolenia praebergonii*	NTD 14	3.0	1
FO	*Asteromphalus elegans*		3.9	1
LO	*Nitzschia cylindrica*		4.35	1
FO	*N. jouseae*	NTD 13	4.5	2
FO	*Thalassiosira oestrupii*		5.2 (5.1)	4
LO	*Asterolampra acutiloba*		5.35	2
LO	*Nitzschia miocenica*		5.6	2
LO	*Thalassiosira praeconvexa*		5.8	2
FO	*T. convexa* var. *aspinosa*	NTD 12	6.1	2
LO	*Nitzschia porteri*		7.2 (6.7)	2
FO	*N. miocenica*	NTD 11	7.3 (6.8)	2
LO	*Rossiella paleacea*		7.4 (6.9)	2
LO	*Coscinodiscus nodulifer* var. *cylcopus*		7.9	3
LO	*Thalassiosira burckliana*		8.0 (7.0)	2
LO	*Actinocylcus ellipticus* var. *javanica*		8.0	3
LO	*Coscinodiscus yabei*	NTD 10	8.6 (7.5)	2
FO	*T. burckliana*		9.0 (8.0)	2
LO	*Coscinodiscus temperei* var. *delicata*		9.8 (8.2)	2
LO	*C. vetustissimus* var. *javanica*		10.7 (8.5)	2
LO	*Actinocyclus moronensis*	NTD 9	11.3 (8.9)	2
LO	*Denticulopsis punctata* f. *hustedtii*		12.2 (10.7)	2
LO	*Synedra jouseana*		12.3 (12.1)	3
LO	*Craspedodidscus coscinodiscus*	NTD 8	12.2 (10.7)	2
LO	*Actinocyclus ellipticus* var. *spiralis*		12.4 (12.3)	3
FO	*Hemidiscus cuneiformis*		12.6 (11.2)	2
FO	*Coscinodiscus temperei* var. *delicata*	NTD 7	12.8	
LO	*Coscinodiscus lewisianus*	NTD 6	13.5 (12.9)	2
LO	*Denticulopsis hustedtii*		13.7	2
LO	*Cestodiscus pulchellus* var. *maculatus*		13.9	3
LO	*Cestodiscus peplum*	NTD 5	14.1	2
FO	*A. ellipticus* var. *spiralis*		14.2 (14.1)	3
LO	*Annellus californicus*		15.0	2
FO	*Actinocyclus ingens*		15.5	2
LO	*C. lewisianus* var. *similis*		15.7	3
FO	*C. peplum*	NTD 4	16.4	2
LO	*Raphidodiscus marylandicus*		16.7	3
FO	*Denticulopsis nicobarica*	NTD 3	17.8	
LO	*Craspedodiscus elegans*	NTD 2	18.7	2
LO	*Borgorovia veniamini*	NTD 1	19.9	2
LO	*C. lewisianus* var. *rhomboides*		22.5	2
FO	*Rossiella paleacea*	*Rocella gelida* Zone	22.7	2
LO	*Rocella vigilans*		22.7?	3
FO	*B. veniamini*		24.0?	3
LO	*Coscinodiscus excavatus*	*C. excavatus*	33.0?	3

Notes: FO = first occurrence and LO = last occurrence. Zonal codes are those of Barron (1985). Age column references represent (1) Barron, 1985a; (2) summary in Barron et al., 1985a; (3) Barron et al., 1985b; (4) Baldauf, 1985.

older than Chron 34 (T). This particular event in time connects the two time scales. A few age estimates shown in Table 3 are taken directly from Berggren et al. (1985a, 1985b). The increasing availability of Cenozoic bio- and magnetostratigraphies in deep-sea sediments has resulted in improved correlations between nannofossil biostratigraphy and the geomagnetic polarity history, improvements that are accounted for in Table 3.

The biochronology of Cretaceous calcareous nannofossil marker events still lacks much of the detail that exists for Cenozoic markers, simply because the direct correlations between bio- and magnetostratigraphy are fewer in number in the Cretaceous. For this reason, we have only listed age assignments for Cenozoic marker events. It should be pointed out, however, that Cenozoic age estimates in many cases also are associated with serious uncertainties. One of the major reasons is the lack, or limited availability, of adequate magnetostratigraphic records from tropical/equatorial environments. As a consequence, we have few data on the bio- and magnetostratigraphic correlations from those regions in which the highest rates of taxonomic evolution have occurred; the data in Berggren et al. (1985a, 1985b), for example, predominantly represent mid-latitude estimates.

Cenozoic Zonation

From the zonal schemes available for the subdivision of nannofossils in Cenozoic sediments, we chose the scheme of Martini (1971). This scheme does not represent the ultimate resolution (e.g., the number of evolutionary appearances/disappearances per unit time) that can be achieved in Cenozoic deep-sea sediments, because deep-sea biostratigraphy has developed rapidly over the past two decades and continues to do so. Yet this zonal scheme does provide a simple picture of biostratigraphic relationships in the cored sequences. The fact that most marine

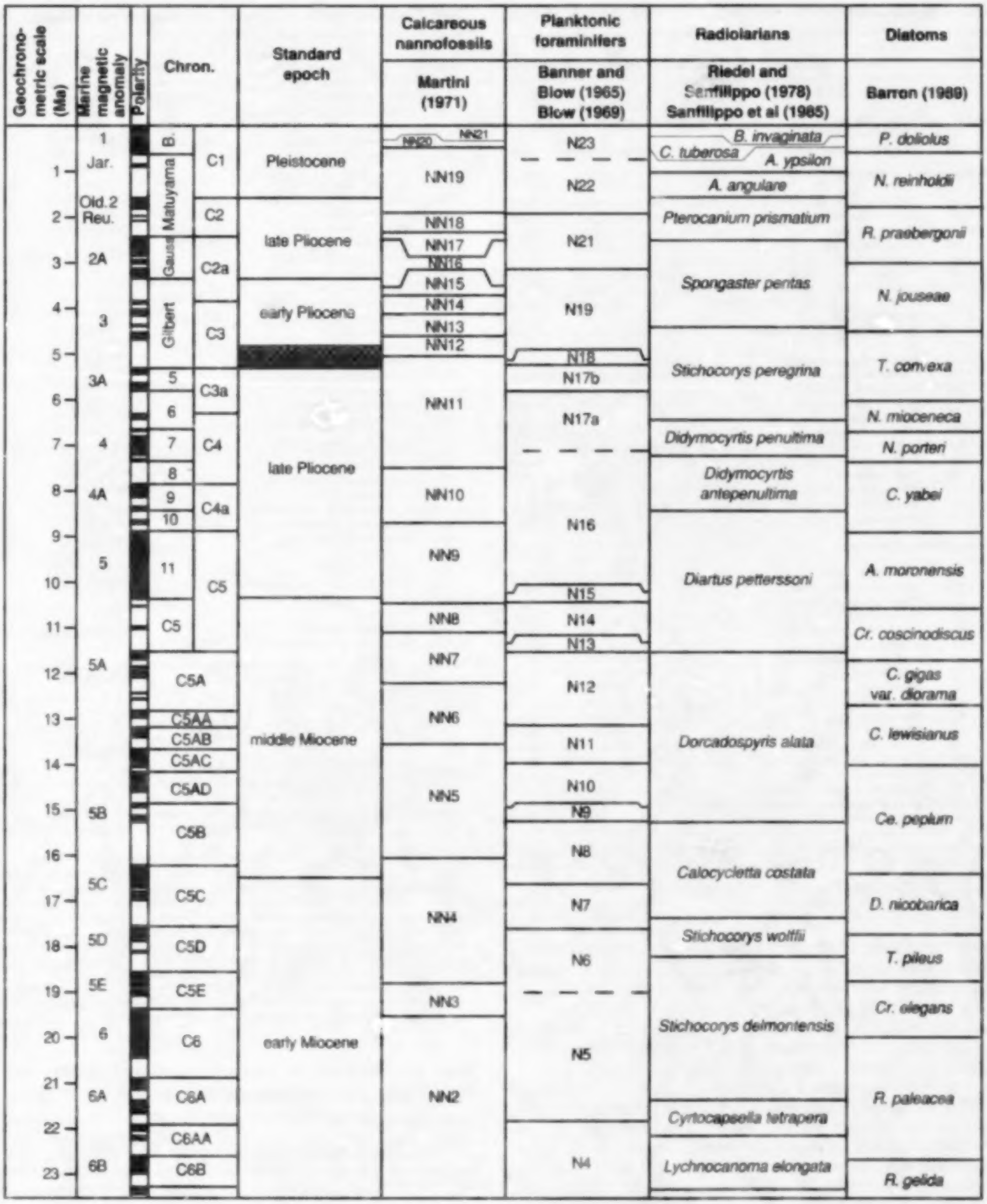
Geochronometric scale (Ma)
Marine magnetic anomaly
Polarity
Chron.
Standard epoch
Calcareous nannofossils
Martini (1971)
Planktonic foraminifers
Banner and Blow (1965) Blow (1969)
Radiolarians
Riedel and Sanfilippo (1978) Sanfilippo et al (1985)
Diatoms
Barron (1989)
1
2
3
4
5
6
7
8
9
10
11
12
13
14
15
16
17
18
19
20
21
22
23
1
Jar.
Old.2
Reu.
2A
3
3A
4
4A
5
5A
5B
5C
5D
5E
6
6A
6B
B.
Matuyama
Gauss
Gilbert
5
6
7
8
9
10
11
C5
C1
C2
C2a
C3
C3a
C4
C4a
C5
C5A
C5AA
C5AB
C5AC
C5AD
C5B
C5C
C5D
C5E
C6
C6A
C6AA
C6B
Pleistocene
late Pliocene
early Pliocene
late Pliocene
middle Miocene
early Miocene
NN20
NN21
NN19
NN18
NN17
NN16
NN15
NN14
NN13
NN12
NN11
NN10
NN9
NN8
NN7
NN6
NN5
NN4
NN3
NN2
N23
N22
N21
N19
N18
N17b
N17a
N16
N15
N14
N13
N12
N11
N10
N9
N8
N7
N6
N5
N4
B. invaginata
C. tuberosa
A. ypsilon
A. angulare
Pterocanium prismatium
Spongaster pentas
Stichocorys peregrina
Didymocyrtis penultima
Didymocyrtis antepenultima
Diartus petterssoni
Dorcadospyris alata
Calocycletta costata
Stichocorys wolffii
Stichocorys delmontensis
Cyrtocapsella tetrapera
Lychnocanoma elongata
P. doliolus
N. reinholdii
R. praebergonii
N. jouseae
T. convexa
N. miocenica
N. porteri
C. yabei
A. moronensis
Cr. coscinodiscus
C. gigas var. diorama
C. lewisianus
Ce. peplum
D. nicobarica
T. pileus
Cr. elegans
R. paleacea
R. gelida

Figure 7. Correlation of Neogene chronostratigraphy, biostratigraphy, and magnetostratigraphy used during Leg 130. Magnetic chron terminology follows that adopted by Leg 108 (Shipboard Scientific Party, 1988a). Correlation of the magnetic polarity record, epoch boundaries, and planktonic foraminifer zones follows Berggren et al. (1985b). Nannofossil zonal boundaries are based on datums presented in Table 3. Correlation of the late Miocene–Pleistocene radiolarian zones with the magnetic polarity record follows Shipboard Scientific Party (1989a). Correlation of the early Miocene–middle Miocene radiolarian zones with the magnetic polarity record follows Barron (1989). Diatom events are presented in Table 3. Correlation of diatom zones with magnetic polarity follows Barron (1989). The hatchured area at the Miocene/Pliocene boundary shows that the range in age of the boundary is between 5.3 (Berggren et al., 1985b) and 4.9 Ma (Zijderveld et al., 1986).

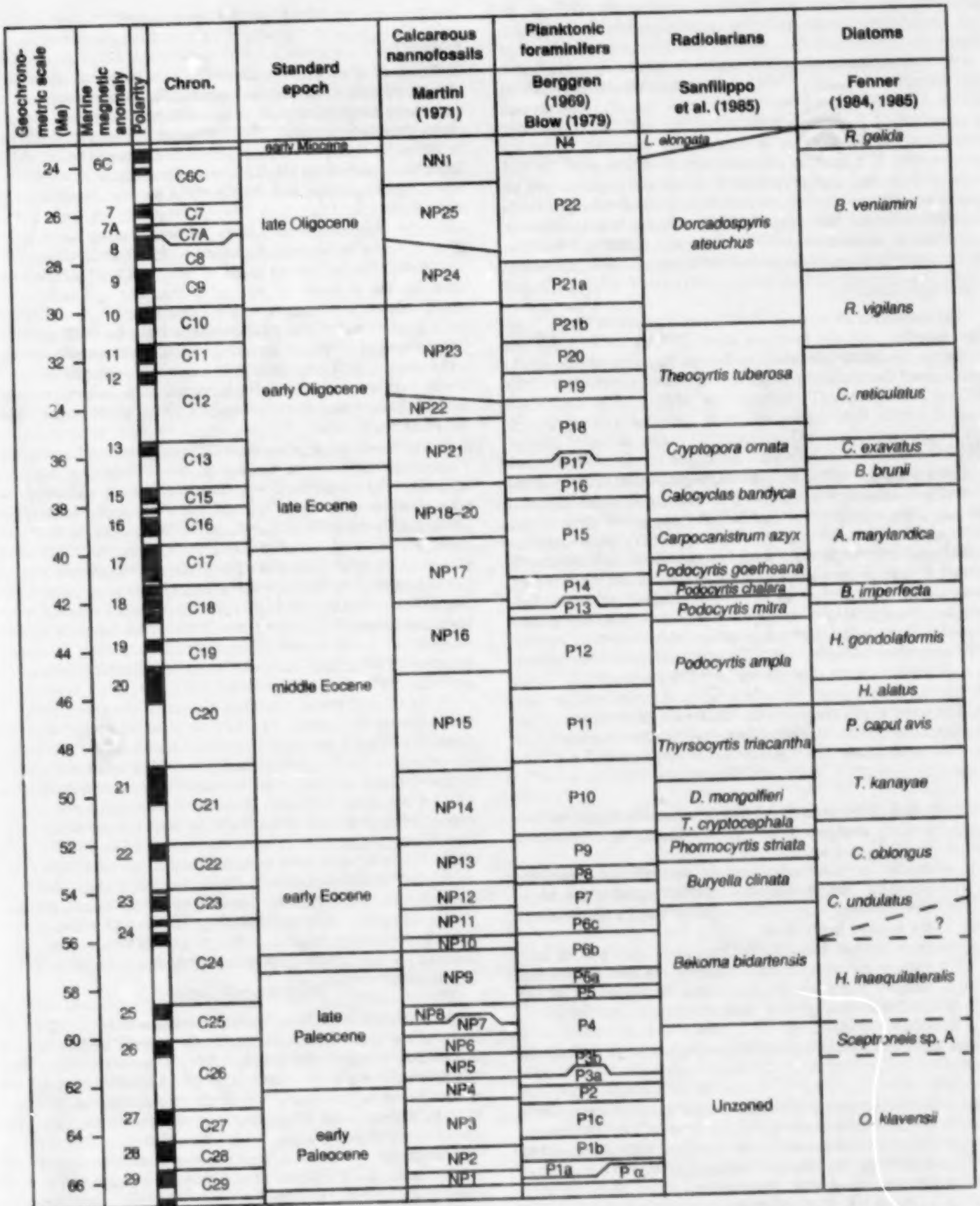
Geochronometric scale (Ma)
Marine magnetic anomaly
Polarity
Chron.
Standard epoch
Calcareous nannofossils
Martini (1971)
Planktonic foraminifers
Berggren (1969) Blow (1979)
Radiolarians
Sanfilippo et al. (1985)
Diatoms
Fenner (1984, 1985)
24
26
28
30
32
34
36
38
40
42
44
46
48
50
52
54
56
58
60
62
64
66
6C
7
7A
8
9
10
11
12
13
15
16
17
18
19
20
21
22
23
24
25
26
27
28
29
C6C
C7
C7A
C8
C9
C10
C11
C12
C13
C15
C16
C17
C18
C19
C20
C21
C22
C23
C24
C25
C26
C27
C28
C29
early Miocene
late Oligocene
early Oligocene
late Eocene
middle Eocene
early Eocene
late Paleocene
early Paleocene
NN1
NP25
NP24
NP23
NP22
NP21
NP18–20
NP17
NP16
NP15
NP14
NP13
NP12
NP11
NP10
NP9
NP8
NP7
NP6
NP5
NP4
NP3
NP2
NP1
N4
P22
P21a
P21b
P20
P19
P18
P17
P16
P15
P14
P13
P12
P11
P10
P9
P8
P7
P6c
P6b
P6a
P5
P4
P3b
P3a
P2
P1c
P1b
P1a
P α
L. elongata
Dorcadospyris ateuchus
Theocyrtis tuberosa
Cryptopora ornata
Calocyclas bandyca
Carpocanistrum azyx
Podocyrtis goetheana
Podocyrtis chalara
Podocyrtis mitra
Podocyrtis ampla
Thyrsocyrtis triacantha
D. mongolfieri
T. cryptocephala
Phormocyrtis striata
Buryella clinata
Bekoma bidartensis
Unzoned
R. gelida
B. veniamini
R. vigilans
C. reticulatus
C. exavatus
B. brunii
A. marylandica
B. imperfecta
H. gondolaformis
H. alatus
P. caput avis
T. kanayae
C. oblongus
C. undulatus
?
H. inaequilateralis
Sceptroneis sp. A
O. klavensii

Figure 8. Correlation of Paleogene chronostratigraphy, biostratigraphy, and magnetostratigraphy used during Leg 130. Hatchured area at the Paleocene/Eocene boundary shows that range in age of the boundary is between 57.7 (Berggren et al., 1985a) and 56.4 Ma (Table 3). Correlation of the magnetic polarity record, epoch boundaries, and planktonic foraminifer zones follows Berggren et al. (1985a), as modified by Aubry et al. (1988) and Berggren and Miller (1988). Nannofossil zonal boundaries are based on the datums presented in Table 3. Correlation of radiolarian zones follows Berggren et al. (1985a) and Barron (1989) for the Oligocene, and Aubry et al. (1988) for the Eocene and Paleocene. Diatom zonation is correlated with nannofossil and radiolarian zones following Fenner (1984) and Bolli et al. (1985, chapter 2).

geologists are familiar with Martini's scheme also adds to its value as an initial framework for Leg 130 nannofossil biostratigraphy.

We have, however, also used numerous biostratigraphic events that are not in Martini's (1971) zonal boundary definitions (Table 3). These additional events represent a resource that creates a substantially improved biostratigraphic and biochronologic resolution, which becomes important, for example, in the reconstruction of Cenozoic sediment accumulation rates. In this context, it should be emphasized that many arguments can be raised for continuous revision and further subdivision of existing zonal schemes, including Martini's scheme, but it is likewise important to emphasize that this approach invariably leads to an infinitely growing set of code systems and/or code numbers.

Cretaceous Zonation

The zonations of Sissingh (1977) and Thierstein (1976) were used together with the Berggren et al. (1985c) GPTS from the Cretaceous/Tertiary boundary to the termination of Chron 34, and beyond there together with the Kent and Gradstein (1985) GPTS.

Methods

Calcareous nannofossils were examined by means of standard light microscope techniques (under crossed nicols or transmitted light at about 790×, or 1250×, magnification).

A peculiar characteristic among calcareous nannofossil assemblages is that individual samples may show signs of strong etching as well as strong overgrowth; more dissolution-resistant forms simply add secondary calcite provided by more dissolution-prone morphotypes. Qualitative descriptions of calcareous nannofossil preservational states commonly involve a sophisticated code system that accounts for dissolution and overgrowth on a progressive scale (e.g., Roth and Thierstein, 1972). When considering the purposes of the shipboard descriptions, and the Leg 130 water depth range, we have adopted the simplest possible, but nevertheless effective, code system for characterizing preservational states. Thus, preservation was recorded with one of the following three letter designations:

G = good (little or no evidence of dissolution and/or secondary overgrowth of calcite; diagnostic characteristics fully preserved);
M = moderate (dissolution and/or secondary overgrowth; partially altered primary morphological characteristics; however, nearly all specimens can be identified at the species level); and
P = poor (severe dissolution, fragmentation, and/or secondary overgrowth with primary features largely destroyed; many specimens cannot be identified at the species and/or generic level).

Five different levels of relative abundance were defined as follows:

A = abundant (the taxonomic category comprises >10% of the total assemblage);
C = common (the taxonomic category comprises from 1% to 10% of the total assemblage);
F = few (the taxonomic category comprises from 0.1% to 1.0% of the total assemblage); and
R = rare (the taxonomic category comprises <0.1% of the total assemblage); and
B = barren.

Planktonic Foraminifers

Zonation

Berggren et al. (1985a, 1985b) present the most comprehensive compilation of Cenozoic planktonic foraminifer zonal schemes and their correlation with magnetostratigraphy and the geochronometric time scale. The Paleogene has subsequently been modified by Aubry et al. (1988) and Berggren and Miller (1988). Table 4 presents a list of planktonic foraminifer first (FO) and last (LO) occurrence datums for the Cenozoic based on these studies.

In the Neogene, we primarily followed the zonal scheme of Blow (1969) ("N" zones), as modified by Kennett and Srinivasan (1983). Species datum levels of Berggren et al. (1985c) were used for the purpose of assigning absolute age estimates to zonal boundaries (Table 4). However, we note two modifications to the placement of the "N" zonal boundaries on Figure 2 of Berggren et al. (1985c) depicting the compilation of Neogene geochronology: (1) the N19/N21 boundary was placed at 3.1 Ma, based on the FO of *Globorotalia tosaensis;* and (2) the N11/N12 boundary was placed at 13.1 Ma, based on the FO of *Globorotalia fohsi.*

We followed Berggren et al. (1985c) in placing the Pliocene/Pleistocene boundary at the top of the Olduvai Subchron (1.6 Ma). The FO of *Globorotalia truncatulinoides* commonly has been used to define the base of the Pleistocene (e.g., Blow, 1969; Bolli and Premoli Silva, 1973; Stainforth et al., 1975; Kennett and Srinivasan, 1983; Bolli and Saunders, 1985). Berggren et al. (1985c) placed the FO of *G. truncatulinoides* at 1.9 Ma. The Pliocene/Pleistocene boundary was recognized in the Leg 130 material by the LO of *Globigerinoides fistulosus* (1.6 Ma according to Berggren et al., 1985c). This taxon is well developed in the northern Ontong Java Plateau area. The co-occurrence of *G. fistulosus* and *G. truncatulinoides* defined the uppermost Pliocene part of Zone N22.

Within the Pliocene, a coiling change in the genus *Pulleniatina* (sinistral to dextral) was used to separate undifferentiated Zones N19–N20 from undifferentiated Zones N18–N19. We did not recognize *Globorotalia pseudopima,* used by Blow (1969) to define the base of Zone N20, in material recovered during Leg 130. In the lower Pliocene, *Sphaeroidinella dehiscens* s.l. occurred only rarely and sporadically in Leg 130 material; therefore, it was not possible to separate Zones N18 and N19 consistently. Some workers have used the total range of *Globorotalia margaritae* to define the lower Pliocene interval (e.g., Bolli and Premoli Silva, 1973; Stainforth et al., 1975; Bolli and Saunders, 1985). Berggren et al. (1985c) placed the FO of *G. margaritae* at 5.6 Ma (uppermost Miocene). We placed the Miocene/Pliocene boundary at the LO of *Globoquadrina dehiscens* and the FO of *Globorotalia tumida.*

The placement of the Oligocene/Miocene boundary based on planktonic foraminifers has experienced a long history of interpretation and varied application (see reviews by Berggren et al., 1985c; Berggren and Miller, 1988). Kennett and Srinivasan (1983) used the FO of *Globoquadrina dehiscens* to mark the boundary for both tropical and temperate zonations. Berggren et al. (1985c) used the FO of *Globorotalia kugleri* s.s., citing the FO of *G. dehiscens* slightly subsequent to that of *G. kugleri* in the stratotype of the Aquitanian Stage. Berggren and Miller (1988) noted that the FO of *G. dehiscens* is about 0.5 m.y. after the FO of *G. kugleri* s.s. Therefore, the FO of *G. dehiscens* also is useful for approximating the Oligocene/Miocene boundary, as suggested by Kennett and Srinivasan (1983, p. 184) and Berggren et al. (1985c, p. 219); however, this taxon occurs only sporadically in the basal Miocene material recovered during Leg

130. The problem in using the *G. kugleri* datum has stemmed from differentiating between *G. kugleri* s.l. (including *G. pseudokugleri* and *G. mendacis*) and *G. kugleri* s.s. In this report, we followed Berggren et al. (1985c) in using the FO of *G. kugleri* s.s. to define the Oligocene/Miocene boundary (P22/N4).

In the Paleogene, we primarily followed the zonal scheme of Berggren (1969) and Blow (1979) ("P" Zones), as recently modified by Berggren and Miller (1988).

For the Cretaceous, the zonal schemes of Caron (1985) and Sliter (1989) were used. Sliter (1989) has correlated the zones with the magneto-geochronology of Kent and Gradstein (1985). It should be noted that substage boundaries, and especially biostratigraphic zonal boundaries, are fixed poorly with the geochronometric time scale.

Methods

Unlithified ooze was soaked briefly in a weak Calgon solution and afterward was washed directly over a 63-μm mesh sieve and dried. Semilithified ooze and chalk was first broken up by hand and soaked in a weak Calgon solution; afterward, these samples were washed over a 63-μm mesh sieve and dried. Large chunks of dried chalk were crushed with a pestle first and then processed a second time. The samples were again soaked in a weak Calgon solution, placed in an ultrasonic bath for about 1 min, and then washed over a 63-μm mesh sieve and dried. The extraction of foraminifers from limestone was difficult, but some success has resulted from crushing the rock first using a Carver hydraulic press. The crushed limestone was ground up even finer with the mortar and pestle. The fine sediment was then soaked in a hot Calgon solution, placed in an ultrasonic bath for about 1 min, and washed over a 63-μm mesh sieve and dried. The crushing method was particularly successful using limestones with obvious clay or ash content.

Planktonic species abundances were estimated (no actual counts were made) using the following categories:

R = rare (<3%);
F = few (3%-15%);
C = common (15%-30%); and
A = abundant (>30%).

Preservational characteristics were divided into three categories:

G = good (>90% of the specimens unbroken);
M = moderate (30%-90% of the specimens showing dissolved or broken chambers); and
P = poor (with samples dominated by fragments and specimens with broken or dissolved chambers).

Benthic Foraminifers

Core-catcher samples for benthic foraminifers were processed by wet sieving through a 63-μm mesh screen and drying the sand fraction on a hot plate. Sediment treatment methods before sieving varied with the amount of consolidation of the calcareous ooze, as described under the section on planktonic foraminifers. Because the low frequency of benthic specimens relative to planktonic microfossils makes any estimate of species content difficult, census data were prepared on representative samples of various ages; their principal taxa are listed in the site reports. These data are mostly based on counts of 100-300 specimens portioned from the sample by microsplitter. The intent of this census is to present an overview of the changes in the benthic assemblages through time along the plateau transect and to provide a background for detailed studies of the paleobathymetric history of the plateau and its paleoceanographic record.

The generic classification of Loeblich and Tappan (1987) was used where possible. Pacific modern and fossil deep-water benthic species are identified in the works of Douglas (1973), Burke (1981), Resig (1981), Thomas (1985), van Morkhoven et al. (1986), and Hermelin (1989).

Radiolarians

Zonation

During Leg 130, the low-latitude zonations of Sanfilippo et al. (1985) and Saunders et al. (1984) were used for the Cenozoic. Zonations proposed by Sanfilippo and Riedel (1985) were used for the Cretaceous. Radiolarian species events published by Riedel and Sanfilippo (1978), Sanfilippo et al. (1985), and Shipboard Scientific Party (1989a) were used to establish a biochronology for Leg 130.

Methods

For most upper Neogene samples, the standard treatment with hydrochloric acid and hydrogen peroxide, as described by Sanfilippo et al. (1985), was applied. This procedure did not disaggregate radiolarians from the pelagic clay matrix in most middle Miocene and older samples. For these samples, several cubic centimeters of sediment were placed in a 400-ml beaker and 2 teaspoons of Calgon were added, followed by the addition of hot water and 5 ml of 30% hydrogen peroxide. The sample was treated in an ultrasonic bath for about 3 min. This method was especially essential for cleaning Cretaceous radiolarians. Paleogene and Cretaceous limestones were crushed using a Carver hydraulic press. Some of these samples were ground further with a mortar and pestle (see also foraminifer methods above). All samples were sieved with 63-μm mesh stainless sieve. Strewn slides were prepared to examine the radiolarians.

The abundance recorded is based on qualitative examinations. The following criteria were used:

A = abundant (>100 specimens);
C = common (50-100 specimens);
F = few (5-50 specimens); and
R = rare (<5 specimens).

The preservation states of radiolarians were defined as follows:

G = good (no sign of dissolution);
M = moderate (minor dissolution); and
P = poor (strong dissolution).

Diatoms

Zonation

Significant contributions to the understanding of the Neogene diatom biostratigraphy from the equatorial Pacific include studies by Burckle (1972) and Barron (1985b), among others. The low-latitude diatom zonation used for Leg 130 is that proposed by Barron (1985b) and Barron et al. (1985a, 1985b) for the upper Oligocene through Holocene sequence in the central equatorial Pacific, and the low-latitude zonation summarized by Fenner (1985) for the Upper Cretaceous through Oligocene sequence. Diatom species events published by Baldauf (1985), Barron (1985a), and Barron et al. (1985a, 1985b) were used on Leg 130 and are summarized in Table 5.

Methods

Each core-catcher sample (approximately 10 cm^3 of sediment) was processed in a 400-ml beaker with hydrogen peroxide and hydrochloric acid, using heat to speed the chemical reaction. The sample was then diluted by adding 300 ml of distilled water and decanted after settling for 2 hr. The dilution/decanting process was repeated until a pH of 6 was reached. The preparation of Cretaceous samples was the same as for radiolarians (see above), although the sample was not sieved. Strewn slides of acid-cleaned material were prepared on 22- × 50-mm cover glasses and mounted on glass slides using Hyrax or Piccolyte mounting media. They were examined with a Zeiss compound microscope under Phase Contrast illumination at 500× to check for the presence of biostratigraphic marker species. The identification of species was routinely checked at 1250×.

Species were considered abundant (A) when two or more specimens were present in one field of view at 500×; common (C) if one specimen was encountered in two fields of view; few (F) if one specimen was observed in one horizontal traverse across the slide; and rare (R) if less than one was observed per traverse. If no diatoms were encountered, the sample was recorded as barren.

The preservation of diatoms was classified according to three major categories based on the presence of complete or broken, thinly to heavily silicified valves, as follows:

G = good, well-preserved specimens, thinly silicified valves present, only minor signs of dissolution or even none at all;
M = moderate, some thinly silicified valves present, slight to moderate dissolution; and
P = poor, only heavily silicified valves present, abundant broken specimens, severe dissolution.

The criteria for distinguishing whole from partial diatoms follow Schrader and Gersonde (1978).

PALEOMAGNETICS

Paleomagnetic studies on Leg 130 measured the natural remanent magnetization (NRM) and the remanence after stepwise demagnetization of continuous sections of the archive half-core in both sediments and basement. Alternating field (AF) demagnetization was applied to half-core sections with NRM measurements that indicated probable stable remanence and intensity levels above the lower operational limit of the shipboard cryogenic magnetometer (about 0.01 $\mathrm{mAm^{-1}}$). Demagnetization allowed directions of the characteristic remanent (primary) magnetization (ChRM) to be isolated from the NRM of both sediments and igneous rocks by removing secondary components, predominantly viscous remanent magnetizations (VRMs), and magnetizations acquired during drilling.

Measurement of the ChRM fulfilled two complementary purposes. First, magnetic polarity throughout the sediment column was determined to allow the construction of a magnetostratigraphy. Reference was made to the magnetostratigraphies of Berggren et al. (1985b) and Kent and Gradstein (1985) (Tables 6 and 7). Second, the direction of the ChRM provided a history of the motion of the Ontong Java Plateau in the geomagnetic reference frame. Declinations from unoriented cores are indeterminate, so these cores could only contribute paleoinclinations, from which paleolatitudes were directly calculated. Paleoinclinations from Pliocene to Eocene sites were too low and scattered to allow a clear distinction of individual measurements into normal and reversed sets, so direct calculation of paleoinclinations was not possible; instead, the frequency distribution of inclination was plotted, and peaks in this distribution sought.

Table 6. Geomagnetic polarity time scale for the Cenozoic and Late Cretaceous (after Berggren et al., 1985a, 1985b, 1985c).

Normal polarity interval (Ma)	Anomaly	Normal polarity interval (Ma)	Anomaly
0–0.73	1	23.55–23.79	6C
0.91–0.98		24.04–24.21	6C
1.66–1.88	2	25.50–25.60	7
2.02–2.04		25.67–25.97	7
2.12–2.14		26.38–26.56	7A
2.47–2.92	2A	26.86–26.93	8
2.99–3.08	2A	27.01–27.74	8
3.18–3.40	2A	28.15–28.74	9
3.88–3.97	3	28.80–29.21	9
4.10–4.24	3	29.73–30.03	10
4.40–4.47	3	30.09–30.33	10
4.57–4.77	3	31.23–31.58	11
5.35–5.53	3A	31.64–32.06	11
5.68–5.89	3A	32.46–32.90	12
6.37–6.50		35.29–35.47	13
6.70–6.78	4	35.54–35.87	13
6.85–7.28	4	37.24–37.46	15
7.35–7.41	4	37.48–37.68	15
7.90–8.21	4A	38.10–38.34	16
8.41–8.50	4A	38.50–38.79	16
8.71–8.80		38.83–39.24	16
8.92–10.42	5	39.53–40.43	17
10.54–10.59		40.50–40.70	17
11.03–11.09		40.77–41.11	17
11.55–11.73	5A	41.29–41.73	18
11.86–12.12	5A	41.80–42.23	18
12.46–12.49		42.30–42.73	18
12.58–12.62		43.60–44.06	19
12.83–13.01		44.66–46.17	20
13.20–13.46		48.75–50.34	21
13.69–14.08		51.95–52.62	22
14.20–14.66		53.88–54.03	23
14.87–14.96	5B	54.09–54.70	23
15.13–15.27	5B	55.14–55.37	24
16.22–16.52	5C	55.66–56.14	24
16.56–16.73	5C	58.64–59.24	25
16.80–16.98	5C	60.21–60.75	26
17.57–17.90	5D	63.03–63.54	27
18.12–18.14	5D	64.29–65.12	28
18.56–19.09	5E	65.50–66.17	29
19.35–20.45	6	66.74–68.42	30
20.88–21.16	6A	68.52–69.40	31
21.38–21.71	6A	71.37–71.65	32
21.90–22.06		71.91–73.55	32
22.25–22.35		73.96–74.01	
22.57–22.97	6B	74.30–80.17	33
23.27–23.44	6C	84.00–118.00	34

Absolute declinations were determined for cores oriented by the multishot orientation tool. Complete declination-inclination data allow the determination of an apparent polar wander path (APWP), but directly oriented data were limited to cores younger than the middle Miocene. It may prove possible to orient deeper cores by reference to VRMs acquired by these cores in the direction of the axial dipole field; this will require detailed, land-based demagnetization studies.

Discrete samples were taken as cubes in the oozes and as minidrill cores in the chalks, radiolarian silts, and basalts. Magnetization in most of the sediments was very weak, frequently $<0.1\ \mathrm{mAm^{-1}}$. Measurement of discrete samples, therefore, was reserved for land-based studies, for which more sensitive magnetometers would be available. Measurement of most of the archive-half cores in the basalt basement indicated a stable magnetization with little overprinting; demagnetization was restricted to a few cores with exceptional NRMs. Discrete samples of the basement rocks also were reserved for land-based studies to allow demagnetization in closely spaced stages.

Magnetic susceptibility of the half-core sections was measured as part of the physical properties package (see Tarduno et al., this volume). Measurements were collected at 3 to 10 cm intervals with a Bartington Instruments Magnetic Susceptibility

Table 7. Geomagnetic polarity time scale for the Early Cretaceous and Late Jurassic (after Kent and Gradstein, 1985).

Anomaly (reversed polarity)	Normal polarity interval (Ma)	Anomaly (normal polarity)
	84.00-118.00	Cretaceous Quiet Zone
M0	118.70-121.81	
M1	122.25-123.03	M2
M3	125.36-126.46	M4
M5	127.05-127.21	
M6	127.34-127.52	
M7	127.97-128.33	
M8	128.60-128.91	
M9	129.43-129.82	
M10	130.19-130.57	
	130.63-131.00	
	131.02-131.36	
M10N	131.65-132.53	
M11	133.03-133.08	
M11	133.50-134.01	
	134.42-134.75	
M12	135.56-135.66	
	135.88-136.24	
	136.37-136.64	
M13	137.10-137.39	
M14	138.30-139.01	
M15	139.58-141.20	
M16	141.85-142.27	
M17	143.76-144.33	
M18	144.75-144.88	
	144.96-145.98	
M19	146.44-146.75	
	146.81-147.47	
M20	148.33-149.42	
M21	149.89-151.46	
	151.51-151.56	
	151.61-151.69	
M22	152.53-152.66	
	152.84-153.21	
	153.49-153.52	
M23	154.15-154.48	
	154.85-154.88	
M24	155.08-155.21	
	155.48-155.84	
	156.00-156.29	
M25	156.55-156.70	
	156.78-156.88	
	156.96-157.10	
	157.20-157.30	
	157.38-157.46	
	157.53-157.61	
	157.66-157.85	
PM26	158.01-158.21	
PM27	158.37-158.66	
PM28	158.87-159.80	
PM29	160.33-(169.00)	Jurassic Quiet Zone

Meter (Model MS1, using a MS1/CX, 80-mm, whole-core sensor loop set to 0.47 kHz). Severe drift problems with the existing susceptibility loop required its replacement during Leg 130. Signal clipping was found to be a problem with many of the weakly magnetized sediments on the "1" sensitivity range; when there was an indication that this was obscuring a real signal, sensitivity was switched to "0.1".

Instruments

Magnetic remanence on Leg 130 was measured with the shipboard 2-G Enterprises (Model 760R), three-axis, pass-through cryogenic superconducting rock magnetometer, which is integrated with an on-line AF demagnetizer (Model 2G600) capable of alternating fields as high as 25 mT. ODP policy limits demagnetization of the archive half-core to 15 mT or the mean destructive field, whichever is the smaller. Communications between superconducting quantum interference devices (SQUIDs), the AF degaussing system, and the drive motor were linked through a FASTCOM4 multiserial communications board in an IBM PC-AT compatible computer. All devices and actual measurements of archive half-cores were controlled by a modified version of the Rhode Island University BASIC program. Program commands enable the magnetometer to operate at the 1× scale with flux counting for weakly magnetized sediments and 100× for basement. Some calibration error may occur at the 100× scale, resulting in incorrect declinations and inclinations; comparative calibration between the 1× and 100× scales on Leg 123 (Shipboard Scientific Party, 1990a, p. 46) showed this error to be <5%.

The SQUID sensors in the cryogenic magnetometer measured magnetization over an interval approximately 15 cm long. Each axis has a slightly different response curve. The widths of the sensor regions imply that as much as 150 cm^3 of core contributes to the sensor signals. The large volume of core material within the sensor region permits an accurate determination of remanence for weakly magnetized cores despite the high background noise levels related to the ship's motion. Declinations and inclinations are best determined by deconvolution of the x,y,z data. No deconvolution program was available on Leg 130, however, so declination and inclination were calculated directly from the x,y,z data; on the other hand, intensity was calculated by dividing the magnetic moment by the volume of the sample within the sensors (i.e., the length within the sensor region by the cross-sectional area of the core).

Sediments

Remanence measurements of sediments were performed by passing continuous archive-half core sections through the cryogenic magnetometer. Depending on the resolution desired and on the backlog of cores to be processed, measurements were taken at 1-, 3-, 5-, or 10-cm spacings. Demagnetization was normally carried out at 15 mT.

Basalt

Basaltic rocks were measured in much the same fashion as sediments. In cases where basalt recovery was fragmentary, individual continuous pieces were run through the magnetometer. Otherwise, whole sections of the basalt cores were run. Basalt cores were AF demagnetized at 15 mT only when anomalous inclinations indicated overprinting.

CARBON GEOCHEMISTRY

Shipboard carbon geochemistry analyses were conducted to monitor volatile hydrocarbons for safety considerations on a real-time basis and to characterize the initial content and type of organic matter in the sediments.

Hydrocarbon Gases

As required by safety considerations, concentrations of methane (C_1), ethane (C_2), and propane (C_3) hydrocarbons were monitored in the sediment cores at intervals of approximately 10 m. Headspace samples were obtained by removing a 5-cm^3 plug of sediment from the core as it arrived on deck with a No. 8 cork borer. The sample was placed immediately in a 21-ml glass vial that was sealed with a septum and metal crimp and then heated to 60°C for at least 45 min. The gas driven off was drawn into a syringe and analyzed.

The gas samples obtained were injected into a Hach-Carle AGC Series 100 Model 211 gas chromatograph equipped with a flame ionization detector and a 6-ft × $^1/_8$-in. steel column packed with Porapak N:Q (80%/20%). Details of this method and the complete configuration of the gas chromatograph are given in the "Explanatory Notes" chapter for Leg 112 (Shipboard Scientific Party, 1988c).

Elemental Analysis

Sediments were analyzed on board ship for inorganic carbon and for total nitrogen, carbon, and sulfur.

Inorganic carbon was determined with a Coulometrics 5011 carbon dioxide coulometer equipped with a System 140 carbonate carbon analyzer. A known mass, ranging from 15 to 70 mg of dried and ground sediment, was reacted in a 2N HCl solution. The liberated CO_2 was titrated in a monoethanolamine solution with a colorimetric indicator, and the change in light transmittance was monitored with a photodetection cell. The percentage of carbonate was calculated from the inorganic carbon content assuming that all carbonate occurs as calcium carbonate:

$$CaCO_3 = IC \cdot 8.334.$$

Total nitrogen, carbon, and sulfur were determined using a N/C/S analyzer (Model NA 1500) from Carlo Erba Instruments. Mixtures of vanadium pentoxide and crushed samples were combusted in an oxygen atmosphere at 1000°C, converting organic and inorganic carbon to CO_2, sulfur to SO_2, and nitrogen to NO_2. The NO_2 was reduced to N_2 using copper. The gases were then separated by gas chromatography and measured with a thermal conductivity detector. Total organic carbon (TOC) was calculated from the difference between total carbon (TC) in the N/C/S analyzer and inorganic carbon (IC) in the coulometer:

$$TOC = TC - IC.$$

Rock-Eval Analysis

Organic matter type, thermal maturity, and hydrocarbon-producing potential were assessed with a Delsi, Inc., Rock-Eval II Plus T.O.C. instrument (Espitalie et al., 1977). Approximately 100 mg of dried and ground whole sediments were analyzed according to the standard procedures described in Emeis and Kvenvolden (1986).

INORGANIC GEOCHEMISTRY

Interstitial Water Sampling and Chemistry

For interstitial water sampling, 5- to 10-cm-long, whole-round sections were cut immediately after the cores arrived on deck, generally from the shallowest six cores and then from every third core thereafter. We sampled different holes at each site as needed to cover the entire depth range drilled at each site. Before squeezing, whole-round surfaces were carefully scraped with spatulas to remove potentially contaminated exteriors. Whole rounds were then placed into stainless steel squeezing devices (Manheim and Sayles, 1974) and squeezed with a hydraulic press. Interstitial water samples were filtered through 0.45-μm disposable filters and collected in plastic syringes.

Interstitial water samples were routinely analyzed for salinity as total dissolved solids with a Goldberg optical hand-held refractometer (Reichart); for pH and alkalinity by Gran titration with a Brinkmann pH electrode and a Metrohm autotitrator; for Cl, Ca, and Mg concentrations by titration; for SO_4 concentrations by ion chromatography with a Dionex 2120i chromatograph; and for Si, PO_4, and NH_4 concentrations by spectrophotometric methods with a Milton Roy Spectronic 1001 spectrophotometer using the analytical techniques described by Gieskes and Peretsman (1985). International Association of Physical Sciences Organizations (IAPSO) standard seawater was used for calibrating most techniques. The reproducibility of these techniques, expressed as 1 standard deviation of the means of multiple determinations of IAPSO standard seawater or of another standard, is as follows: alkalinity, 3%; Cl, 0.4%; Ca, <1%; Mg, 0.5%; SO_4, <2%; and Si, PO_4, and NH_4, 2%–3%.

We used flame spectrophotometric techniques with a Varian SpectrAA-20 atomic absorption unit to quantify concentrations of Na, K, Li, Sr, Rb, and Mn. Na and K were determined on 1/500 diluted aliquots by flame emission using an air-acetylene flame with Cs as an ionization suppressant. Li and Sr were determined on 1/6 diluted aliquots. Li was determined by emission using an air-acetylene flame, and Sr by atomic absorption using an air-acetylene flame with La as a realizing agent. Rb was determined directly on undiluted interstitial water samples by emission using an air-acetylene flame. Mn was determined by atomic absorption on 1/5 diluted aliquots with La added. Standards for all flame spectrophotometric techniques were matched in matrix composition to the samples. The reproducibility of these techniques, expressed as 1 standard deviation of the means of multiple determinations of IAPSO standard seawater or of another standard treated as samples, is as follows: Na, <1%–2%; K, <2%–3%; Li, <1%–2%; Rb, <1%–2%; Sr, <2%; and Mn, 2%–3%.

Chemical data for interstitial waters are reported in molar units in each site report.

IGNEOUS ROCKS

Core Curation and Shipboard Sampling

Igneous rocks were split into archive and working halves using a rock saw with a diamond blade. The petrologists decided on the orientation of each cut so as to preserve unique features and/or expose important structures. The archive half was described, and samples for shipboard and shore-based analyses were removed from the working half. Each piece was numbered sequentially from the top of each section, beginning with the number 1. Pieces that could be fitted together (like a jigsaw puzzle) were assigned the same number but were lettered consecutively (e.g., 1A, 1B, 1C, etc.).

Spacers were placed between pieces with different numbers but not between those with different letters and the same number. The presence of a spacer may represent a substantial interval of no recovery. Whenever the original unsplit piece was sufficiently large that the top and bottom could be distinguished before being removed from the core liner (i.e., the piece could not have rotated about a horizontal axis in the liner during drilling), a red wax cross was marked on the base of each piece.

Before the rock dried, sampling was conducted for shipboard physical properties, magnetics, X-ray diffraction (XRD), X-ray fluorescence (XRF), and thin-section studies. Minicores were taken from the working half and stored in seawater before measuring the physical properties. Nondestructive measurements of magnetic susceptibility and sometimes thermal conductivity were made on the archive half of the core. The archive half was then described in detail on the visual core description (VCD) form and photographed before storage.

Visual Core Descriptions

Hard rocks sampled from the basement were graphically represented on VCD forms specific to igneous and metamorphic rocks (see the VCD forms following the core barrel sheets). Copies of the VCD forms, as well as other prime data collected during Leg 130, are available on microfilm at all three ODP repositories. The left-hand column of the VCD (Fig. 9) is a graphical representation of the archive half. A horizontal line across the entire width of this column denotes a plastic spacer glued between rock pieces inside the liner. The number of each piece was also recorded, with oriented pieces indicated by the presence of an upward-pointing arrow to the right of the rele-

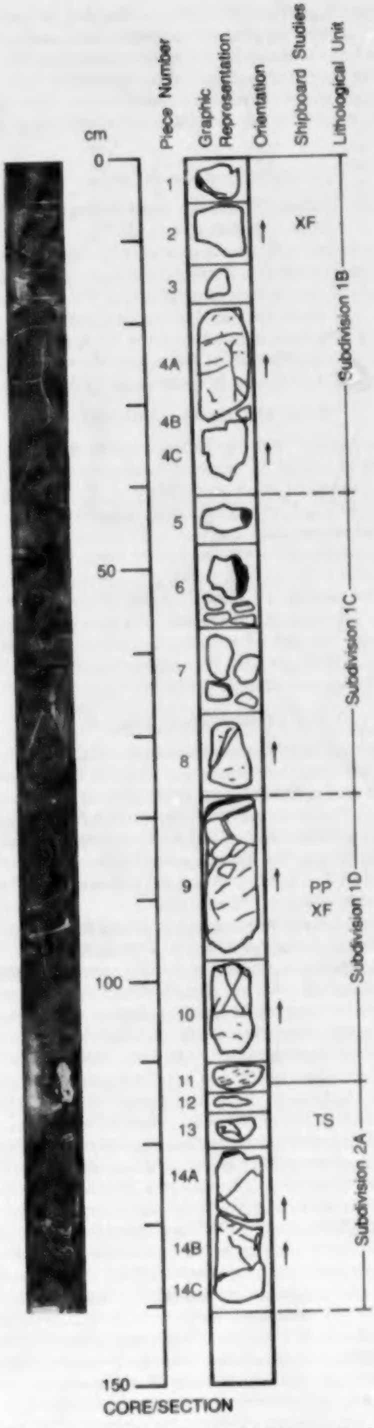
cm
Piece Number
Graphic Representation
Orientation
Shipboard Studies
Lithological Unit
0
50
100
150
1
2
3
4A
4B
4C
5
6
7
8
9
10
11
12
13
14A
14B
14C
XF
PP
XF
TS
Subdivision 1B
Subdivision 1C
Subdivision 1D
Subdivision 2A
CORE/SECTION

130-803D-69R-1

SUBDIVISION 1B: APHYRIC BASALT

Pieces 1-4

CONTACTS: None.
PHENOCRYSTS: Aphyric.
GROUNDMASS: Fine grained.
VESICLES: Nonvesicular.
COLOR: Gray to light-medium orange-brown.
STRUCTURE: Pillow.
ALTERATION: Highly altered, mottled appearance with light orange-brown patches.
VEINS/F RACTURES: <5%; 0.2-2 mm; subvertical and subhorizontal; calcite veins in Piece 4.

SUBDIVISION 1C: APHYRIC BASALT

Pieces 5-8

CONTACTS: Top of basalt pillow.
PHENOCRYSTS:
Pyroxene - <1%; ~1 mm; euhedral laths.
GROUNDMASS: Fine grained with glass rims.
VESICLES: Nonvesicular.
COLOR: Gray to dark gray, light-medium orange-brown, black glass rims.
STRUCTURE: Pillow.
ALTERATION: Moderately to highly altered with mottled and banded appearance.
VEINS/FRACTURES: <1-5%; <0.5-5 mm; irregular-subhorizontal; green mineral (celadonite?).

SUBDIVISION 1D: APHYRIC BASALT

Pieces 9, 10

CONTACTS: Margin of pillow.
PHENOCRYSTS: Aphyric.
GROUNDMASS: Fine grained with glassy rims.
VESICLES: Nonvesicular.
COLOR: Gray to dark gray, light-medium orange-brown, black glass rims.
STRUCTURE: Pillow.
ALTERATION: Moderately to highly altered.
VEINS/FRACTURES: <5%; <5 mm; subhorizontal; calcite-filled.

SUBDIVISION 2A: APHYRIC BASALT

Pieces 11-14

CONTACTS: Pieces 11-13 are a mixture of calcite and completely altered green basaltic glass (celadonite, serpentine, chlorite?). Probably the contact between pillow and limestone.
PHENOCRYSTS: Aphyric.
GROUNDMASS: Fine grained, glassy rim to top of Piece 14.
VESICLES: Nonvesicular.
COLOR: Medium gray-brown to light gray-brown/orange-brown.
STRUCTURE: Pillow.
ALTERATION: Very highly altered, mottled and banded appearance.
VEINS/FRACTURES: <5%; 0.5-5 mm; irregular; calcite.

Figure 9. Example of a completed VCD form for igneous rocks.

vant piece. Shipboard samples and studies were indicated in the "shipboard studies" column, using the following system of notation:

XD = X-ray diffraction analysis,
XF = X-ray fluorescence analysis,
PM = paleomagnetic measurements,
TS = thin-section billet, and
PP = physical properties measurement.

When the cores were described, checklists of macroscopic features were used to ensure consistent and complete descriptions, one for fine- and medium-grained extrusives and dikes, and another for plutonic rocks. The VCD form for fine- and medium-grained igneous rocks required the following information:

1. The leg, site, hole, core number and type, and section number.
2. A graphic representation of the core, including the rock piece numbers and positions of shipboard samples.
3. Lithologic unit boundaries, based on criteria such as the occurrence of glassy and quenched margins, trends of marked grain-size variation, and changes in petrographic type and phenocryst assemblages.

The following checklist was used for fine- and medium-grained igneous rocks. For each lithologic unit defined, the following were noted:

1. Unit number (consecutive downhole), including the numbers of the top and bottom pieces in the unit.
2. Rock name.
3. Contact type: glassy, intrusive, depositional, etc.
4. Phenocrysts: whether homogeneous or heterogeneous throughout the unit. For each phenocryst phase the following were given: abundance (%), average size (in millimeters), shape, degree of alteration (%), type and secondary phases, and any other comments.
5. Groundmass texture: glassy, microcrystalline, fine-grained (<1 mm), and medium-grained (1-5 mm). Any relative grain size changes within the unit from piece to piece were noted.
6. Color (dry).
7. Vesicles: size, shape, percentage, distribution, and nature of any fillings. Similar data for miaroles (vugs).
8. Structure: massive, pillowed, thin, or sheetlike, brecciated.
9. Alteration: type, form, distribution, and degree, ranging from fresh (<2% alteration present) to slightly altered (2%-10%), moderately altered (10%-40%), highly altered (40%-80%), very highly altered (80%-95%), and completely altered (95%-100%).
10. Veins/fractures: type, width, orientation, percentage present, and nature of infillings.

Finally, other comments were added, including continuity of the unit within the core and interrelationship between units. When the VCD form was complete and agreed upon by the igneous petrologists, the same information was then recorded in the VAX computer data-base HARVI. Each record was checked by the data-base program for consistency and printed in a format that could be pasted directly onto the final VCD record for subsequent curatorial handling.

Igneous rocks were classified mainly on the basis of mineralogy and texture. Basalts (fine-grained) and dolerites (medium-grained) were termed aphyric if phenocrysts were lacking or if they amounted to <1% of the rock. If porphyritic, the rock was designated as sparsely phyric (phenocryst content of 1%-2%), moderately phyric (2%-10%), or highly phyric (>10%). Estimates of phenocryst proportions were based on those visible with a hand lens or binocular microscope of about 10× power. Basaltic rocks were further classified by phenocryst type: a moderately plagioclase-olivine phyric basalt contains 2%-10% total phenocrysts, most of which are plagioclase with lesser amounts of olivine.

Thin-section Description

Thin-section billets of basaltic rocks recovered during Leg 130 were examined to help define subunit boundaries indicated on the VCDs and to confirm the identity of petrographic groups and/or alteration products. Petrographic descriptions, together with estimates of the various mineral phases (both primary and secondary), were made on the igneous thin-section description forms, which also were entered into the VAX computer database HRTHIN. Identification of secondary phases, such as clays and zeolites, was augmented in some cases by XRD.

X-ray Diffraction Analysis

A Philips ADP 3520 X-ray diffractometer was used for the XRD analysis of unknown, generally secondary, mineral phases. Instrument conditions were as follows: CuK-alpha radiation with Ni filter, 40 kV, 35 mA, goniometer scan from 2° to 50° 2θ, step size 0.02°, count time 2 s.

Samples were ground with water in an agate pestle and mortar until reduced to a very fine slurry. A suspension was then pipetted onto the surface of a glass slide and allowed to air dry before analysis. The resulting diffractograms were interpreted, in a few cases, with the aid of a computerized search-and-match routine using JCPDS powder files and tabulated data for clay minerals (Brindley and Brown, 1980).

X-ray Fluorescence Analysis

Samples from Site 803, considered to be either representative of individual lithologic subdivisions or possibly of unusual composition, were analyzed for major oxides and selected trace elements by XRF. The on-board XRF system is a fully automated, wave-length-dispersive, ARL 8420 spectrometer using a 3-kW rhodium X-ray tube as the excitation source for major and trace elements. Table 8 lists the elements analyzed as well as the operating conditions used.

Sample preparation involved (a) crushing the sample to a powder and (b) producing glass disks (for major element analysis) and pressed powder pellets (for trace element analysis). Initially, about 10 cm^3 of rock was removed from the core, and unwanted saw marks were erased by wet-grinding on a silicon carbide disk mill. Each sample was then ultrasonically washed in distilled water and methanol for 10 min and dried at 110°C for 2 hr. Larger pieces were reduced to <1-cm diameter by crushing them between two plastic disks in a hydraulic press. Powders were produced by grinding pieces in a motorized alumina mortar and pestle (to minimize contamination) for 10-30 min.

Major elements were determined on fused glass disks (Norrish and Hutton, 1969) to reduce matrix effects and variations in background. The disks are made by mixing 6 g of dry, lanthanum-doped (20% La_2O_3), lithium tetraborate flux (Spex #FF28-10) with 0.5 g of rock powder that has been ignited at about 1000°C in platinum-gold crucibles for 6-10 min and then poured into Pt-Au molds using a modified Claisse Fluxer apparatus. This 12:1 flux-to-sample ratio reduces matrix effects to the point where matrix corrections are unnecessary for normal basaltic to granitic compositions. Hence, the relationship between X-ray intensity and concentration becomes linear and can be described by:

$$C_i = (I_i \times m_i) - b_i,$$

Table 8. X-ray fluorescence analytical conditions, Leg 130.

Element	Detector	Collimator	Crystal	2θ	CT (s)
Fe	FC	F	LiF	57.52	40
Mn	KrC	F	LiF	62.98	40
Ti	FC	F	LiF	86.14	40
Ca	FC	C	LiF	113.16	40
K	FC	F	LiF	136.65	40
Si	FC	C	PET	109.25	40
Al	FC	C	PET	145.27	100
P	FC	C	Ge	140.94	200
Mg	FC	C	TlAP	44.87	200
Na	FC	C	TlAP	54.71	200
Nb	SC	F	LiF	21.37	200
Zr	SC	F	LiF	21.53	100
Y	SC	F	LiF	23.78	100
Sr	SC	F	LiF	25.13	100
Rb	SC	F	LiF	26.60	100
Zn	SC	F	LiF	41.79	60
Cu	SC	F	LiF	45.02	60
Ni	SC	C	LiF	48.67	60
Cr	FC	F	LiF	69.35	60
V	FC	F	LiF*	122.84	60

Notes: All elements measured on K-alpha line, using a rhodium X-ray tube operated at 60 kV and 50 mA. SC = NaI scintillation counter; FC = flow proportional counter (P10 gas); KrC = sealed krypton gas counter; F = fine and C = coarse; LiF = LiF (200) and LiF* = LiF (220); CT = counting time. Source: Shipboard Scientific Party, 1989b.

where

C_i = concentration of oxide i (wt%),
I_i = net peak X-ray intensity of oxide i,
m_i = slope of calibration curve for oxide i (wt%/cps), and
b_i = apparent background concentration for oxide i (wt%).

The slope m_i was calculated from a calibration curve derived from the measurement of well-analyzed reference rocks (BHVO-1, G-2, AGV-1, JGB-1, JP-1, Br, and DRN). The background b_i was determined on blanks or was derived by regression analysis from the calibration curves.

Trace elements were determined on pressed-powder pellets made by mixing 6 g of fresh rock powder with 1 g of wax. This mixture was then pressed into an aluminium cap with 7 tons of pressure. A minimum of 5 g of sample ensures the pellet will be "infinitely thick" for rhodium K-series radiation. For the computation of trace element concentrations from measured X-ray intensities, an off-line calculation program, based on routines from Bougault et al. (1977) and written by T. L. Grove and M. Loubet, was used.

SEDIMENTATION RATES

Sedimentation rate computations represent an important piece in the modern paleoceanographic puzzle because they add the element of time dimension to the lithostratigraphic column. We have chosen the time scales of Berggren et al. (1985a, 1985b), and Kent and Gradstein (1985) for the sedimentation rate method of transforming rock units into time units, as these scales are among the most complete syntheses available.

The correlation of biostratigraphic events to the geomagnetic polarity history is a key element in marine time scales; moreover, it is critically valuable in tropical regions where the rate of taxonomic evolution of sediment-forming marine microplankton has been greatest. A modest number of tropical deep-sea sediment sections are presently available that possess adequate magnetostratigraphies encompassing the past few million years. Thus, many Pliocene and Pleistocene biostratigraphic events are tied directly to the magnetic polarity zones in a low-latitude setting and, therefore, are considered to provide reasonably accurate biochronologies.

In contrast to this latest Neogene situation, it is perhaps surprising to note that we still do not possess a single continuous Miocene section with adequate magnetostratigraphy from a tropical/equatorial environment to refine biochronology in this interval. The compilation of Berggren et al. (1985b) of Miocene age estimates of the calcareous microfossil datums predominantly represents correlations in mid-latitude North and South Atlantic sections (e.g., DSDP Sites 516, 519, 521, 558, and 563). Recent ODP coring in the Indian Ocean, however, provided some insight into correlations of Miocene calcareous nannofossil biostratigraphy to magnetostratigraphy from an equatorial region, results that have been adopted here. Thus, it appears tenable to conclude that the established age estimates of many Miocene biostratigraphic events are associated with comparatively large uncertainties and, therefore, are poorly suited for establishing highly resolved sedimentation rate histories.

Shipboard biostratigraphy included information from two siliceous and two calcareous microfossil groups, implying that over 100 potential age-depth indicators were available for the Neogene. For a number of reasons, this wealth of information does not imply that we possess one control point every 0.25 m.y. over the past 25 Ma, but rather the existence of a fairly wide scatter of points in the age-depth graphs. This is so despite the fact that we have limited the uncertainties of the age-depth indications to depth (i.e., sample spacing) alone. It will be seen that the different microfossil groups commonly provide age discrepancies of about 1 m.y. for identical sample depths, discrepancies that are on the order of 10%–20% of the age of the sediment even in the late Miocene and Pliocene time interval. Such differences are considered to reflect problems largely associated with the assigned ages of the biostratigraphic events, implying that it is necessary to use selected age-depth indicators when estimating the sedimentation rate history.

The highly resolved, and fairly precise, Pliocene and Pleistocene biochronology allows a corresponding degree of detail to be included in the sedimentation rate estimates of these time intervals. In the Miocene, we have chiefly tried to recognize consistent linear scatters of age-depth indicators and, toward the extremes of these scatters, to select the marker events that describe a generalized, constant rate within the areas of scatter. For purposes of intersite comparison, it would be advantageous to rely on an identical set of biostratigraphic events when establishing sedimentation rates. This approach, therefore, will be adopted when permitted by the distribution of the critical age-depth points. An obvious consequence is that this procedure allows a fair amount of scatter of points around the proposed rate lines; this scatter reflects the biochronological uncertainty range at any given period of time for any given, or all, microfossil groups. Nevertheless, consistent offsets of points from the rate line then imply that the assigned age estimate of either the selected marker or the offset point needs revision.

Until the day when we possess a more accurate Miocene biochronology, which can be created only through the retrieval and direct correlation of adequate magnetostratigraphies, it will remain difficult to improve the resolution of Miocene sedimentation rate histories. It follows (1) that the low-resolution sedimentation rate records presented here make it possible to decipher the general pattern of change, but hardly to view the entire chain of details making up the pattern; and (2), that we still cannot properly assess the rates of many of the important processes that characterized the development of the Miocene deep-sea environment.

All of the available biostratigraphic information from each hole cored during Leg 130 has been listed in table format and portrayed graphically as age-depth plots. Clusters of points in some sections are shown at enlarged scales to help identify individual points. Those graphs with enlarged scales of holes have grids in contrast to the graphs with the complete hole information. To emphasize the sedimentation rate variability through time, sedimentation rates were plotted vs. age for one or several holes at each site. That variability depended entirely on the selected control points indicating rate changes, and hence involved subjective bias.

All sedimentation rates were calculated using mid-points in the observed depth uncertainty range, and rates between control points were obtained through linear interpolation.

PHYSICAL PROPERTIES

Shipboard measurements of physical properties provided information that aids characterization of lithologic units, correlation of lithology with downhole geophysical logging results, and interpretation of seismic reflection and other geophysical data. The goal of the physical properties program of Leg 130, in addition to providing a link between lithologic and geophysical data, was to identify the physical signals in the sediments that result from carbonate dissolution and diagenesis.

Several types of measurements were performed on the whole-round core sections. Measurements of bulk density, compressional wave velocity, and magnetic susceptibility were provided by the multisensor track (MST). The MST incorporated a gamma-ray attenuation porosity evaluator (GRAPE), a compressional wave (*P*-wave) core logger (PWL), and a magnetic susceptibility monitor. Thermal conductivity measurements with the needle probe method were performed at discrete intervals in whole-round sections of soft sediments.

Physical properties measurements made on samples obtained from the split cores included vane shear strength, electrical resistivity, compressional wave velocity and attenuation, and index properties. Samples were chosen to be representative of the core or section in undisturbed sediment. Measurements and samples were obtained generally at a frequency of two per section in the oozes, one per section deeper in the hole.

Multisensor Track

The MST incorporated the GRAPE, *P*-wave logger, and magnetic susceptibility devices in scans of the whole-round core sections. Individual unsplit core sections were placed horizontally on the MST, which moved the section through the three sets of sensors.

The GRAPE measured average bulk density over 1-cm intervals by comparing the attenuation of gamma rays through the cores with attenuation through an aluminum standard (Boyce, 1976). The GRAPE data were most reliable in the APC cores. The drilling slurry between the core and liner and between the XCB "biscuits" yielded lower bulk densities, and thus GRAPE data from the XCB cores could be used only as an indication of trends and highs in bulk densities. GRAPE data were useful in correlating between holes and sites by observing peak-to-peak spacings and general trends in the data.

Wet-bulk density was also determined by means of the GRAPE special 2-min count technique, as described by Boyce (1976). The GRAPE measurements were made perpendicular to bedding on half-round samples cut from the cores using the double-bladed saw. All counts for the samples and accompanying air (background) counts were made in duplicate and averaged. Grain density values from gravimetric measurements were used to correct the wet-bulk density determined by the GRAPE for deviation of the grain density of the sample from that of quartz. The precision estimated for this technique is ±1.5% (Boyce, 1976).

The PWL transmitted a 500-kHz compressional wave pulse through the core at a repetition rate of 1 kHz. The transmitting and receiving transducers were aligned perpendicular to the core axis. A pair of displacement transducers monitored the separation between the compressional wave transducers; therefore, variations in the outside diameter of the liner did not degrade the accuracy of the velocities. Measurements were taken at 2-cm intervals. Generally, only the APC cores were measured, as the XCB and RCB cores had voids between the core and the liner that caused transmission losses. Weak returns with signal strengths below a threshold value of 100 were removed.

The MST magnetic susceptibility procedures are included in the "Paleomagnetics" section of this chapter (this volume).

Thermal Conductivity

Thermal conductivity measurement techniques used during Leg 130 have been described by Von Herzen and Maxwell (1959) and Vacquier (1985). Measurements were made with a Woods Hole Thermcon-85 unit, and all data are reported in units of W/m · K. The estimated error in the measurements is about 5%–10%. Data were not corrected for *in-situ* pressure and temperature.

To reduce background thermal transients, cores were allowed to equilibrate in their liners until the sediments reached a stable temperature. Needle probes were inserted in sections 2, 3, 4, and 5 of every soft sediment section through holes drilled through the liners. Sample temperatures were monitored with the thermistors in the probes, without applying a current to the heater wires. The actual test sequence was started once the background temperature drift was reduced to 0.04°C/min. Thermal conductivity was calculated from the rate of temperature rise in the probe while a heater current was flowing. The temperature rise in the probe varies logarithmically with time as:

$$T(t) = (q/4\pi k)\ \ln(t) + \text{const.},$$

where k is the thermal conductivity, T and t are temperature and time, respectively, and q is the heat generated per unit length of the probe. From this equation, we can derive thermal conductivity from the slope of temperature vs. the logarithm of time.

Measurements of thermal conductivity were performed until the sediment became too lithified to insert the needle probes. Unfortunately, many problems were encountered when using the probes, and no spares were available. One of the probes malfunctioned while measuring cores from Site 803, allowing only three sections to be measured per core. Another probe yielded data with high drift, so the number of sections measured per core was decreased when we measured the cores from Site 806. Thermal conductivity was not measured in Site 807 cores. Analyses of data from the first site showed considerable scatter in the data, even within individual cores. This is probably related to the problem with the probe calibrations, but no time was available to correct for this. The data given are the mean values calculated for each core; thus, only one value per core is given.

Electrical Resistivity

The Wayne-Kerr precision component analyzer was used to measure resistivity, following the procedures outlined in the "Explanatory Notes" chapter of Leg 127 (Shipboard Scientific Party, 1990b). We measured the electrical resistivity of the sediments once per section using a four-electrode configuration, which consists of four 2-mm stainless steel rods with an electrode spacing of 13 mm. A 20-kHz square wave current was applied to the outer electrodes, and the difference in potential between the two inner electrodes was measured. The size of the current (typically 50 mA) was measured over a resistor in the outer circuit.

The electrodes were buried approximately 1 cm into the split-core surface after measuring the resistance of seawater in another split liner, thus avoiding geometric differences between sediment and water samples. Measurements were made in two directions (horizontal and vertical). Unfortunately, erroneous readings of resistance began during the measurement of cores from Site 803. This problem was probably caused by epoxy leaking into the assembly in which the probes were embedded. Unfortunately, there was no time to repair the probe assembly. Analyses of the data before this malfunction showed a great deal of scatter, apparently the result of different measurement techniques used by different workers. In light of these problems, and because good resistivity logs were obtained at Site 803, the laboratory electrical resistivity program was suspended for the duration of Leg 130.

Vane Shear Strength

The undrained shear strength of the sediment was determined with the ODP motorized miniature vane shear device following the procedures of Boyce (1976). The vane rotation rate was set to 60°/min. The vane used for all measurements had a 1:1 blade ratio with a dimension of 1.27 cm.

The vane shear device measured the torque and strain at the vane shaft with a torque transducer and potentiometer, respectively. Output for torque and strain was recorded on a Hewlett-Packard XY recorder in volts. The shear strength reported was the peak strength determined from the torque vs. the strain plot, as detailed in the "Explanatory Notes" chapter of Leg 110 (Shipboard Scientific Party, 1988b). In addition to the peak shear strength, residual strength was determined from the same plot when the failure was not dominated by cracking of the sample (Pyle, 1984).

When we analyzed the vane tests, we assumed that a cylinder of sediment was uniformly sheared about the axis of the vane in an undrained condition, with cohesion as the principal contributor to shear strength. Departures from this assumption included progressive cracking within and outside of the failing specimen, uplift of the failing core cylinder, drainage of local pore pressures (i.e., the test can no longer be considered as undrained), and stick-slip behavior. Also, silts and sands provided increased friction effects. Because the sediments cored during Leg 130 were predominantly silt-, sandy silt-, or clayey silt-sized, friction effects and sample draining during testing were likely. The rate of rotation was increased to that recommended by Boyce (1976) to allow a faster test, which we hoped would minimize the problem of draining. In light of these problems, and because of the expected disturbance during drilling, the minivane test cannot be considered a measure of the true shear strength of the sediment. In a laboratory situation, only properly controlled or simple shear tests can be used to provide adequate *in-situ* strength. The minivane test does, however, provide an estimate of strength and a means of comparing downcore and between-hole parameters.

Compressional Wave Velocity

We obtained compressional *P*-wave velocity measurements by means of two different systems during Leg 130, depending on the degree of lithification of the sediment. *P*-wave velocities were measured in unconsolidated sediment using a Dalhousie University/Bedford Institute of Oceanography Digital Sound Velocimeter (DSV; Mayer et al., 1987). The system used on Leg 130 was provided by the Departmente de Geologie Dynamique, Université de Paris VI, and funded by CNRS, France. Velocity calculations were based on the accurate measurement of the time of flight of an impulsive acoustic signal traveling between a pair of piezoelectric transducers inserted in the split sediment cores. The signal used was a 2-μs square wave; the transducers have resonances at about 250 and 750 kHz. A dedicated microcomputer controlled all functions of the velocimeter. The transmitted and received signals were digitized by a Nicolet 320 digital oscilloscope and transferred to the microcomputer for processing. The DSV software selected the first arrival and calculated sediment velocity; the full waveform was stored for later calculation of attenuation.

Four transducers were used; two of them, separated by approximately 7 cm, measured the vertical (along the core axis) *P*-wave velocity, and the other two, separated by approximately 3.5 cm, measured the horizontal (parallel to bedding) velocity. The transducers were firmly fixed at one end on a steel plate so that their separation would not change during velocity determinations. Thermistors in the transducer probes monitored temperatures while measurements were being taken.

Periodically, the separation was precisely evaluated by running a calibration procedure in distilled water. A value of sound velocity in distilled water was determined (based on standard equations) for the measured temperature, with the computer calculating the transducer separation using the signal traveltime. At each sampling interval (usually two per section), the transducers were carefully inserted into the split section and velocity was measured in both directions.

The Hamilton Frame velocimeter was used to measure compressional wave velocities at 500 kHz in discrete sediment samples when induration made it difficult to insert the DSV transducers without making any perturbations around them and in lithified sediments and basement rocks when insertion became impossible. Samples were carefully cut using a double-bladed diamond saw to obtain parallel faces. Sample thickness was measured directly from the velocimeter-frame lead screw. Zero traveltimes for the velocity transducers were estimated by linear regression of traveltime vs. distance for a series of aluminum and lucite standards. Filtered seawater was used to improve the acoustic contact between the sample and the transducers. The DSV oscilloscope and processing software was used to digitize waveforms, calculate velocities, and store the waveforms for later attenuation calculations.

Measurements were performed after the cores had equilibrated to room temperature (approximately 3 hr). Thus, *P*-wave velocity data are given at laboratory conditions (1 atm., 26°C approximately).

Index Properties

Index properties (bulk density, grain density, water content, porosity, and dry density) were calculated from measurements of wet and dry weights and dry volume. Samples of approximately 10 cm^3 were taken to determine the index properties. Soft sediment samples were placed in precalibrated aluminum containers before being measured for weight and volume. Index properties measurements for lithified sediment and basement rock samples were made on crushed portions of the sample cubes cut for velocity determinations.

Sample weights were determined aboard ship to a precision of ±0.01 g using a Scitech electronic balance. Volumes were determined using a Quantachrome Penta-Pycnometer, a helium-displacement pycnometer. The Quantachrome pycnometer measured volumes to an approximate precision of 10^{-4} cm^3.

It has been observed that the frequent air pressure drops in the lab stack affect the performance of the pycnometer. Another problem in the consistency of the pycnometer arises as a result of slightly different pressures measured during different calibration runs. The variability associated with pressure drops was minimized by repeating the measurements until two volumes for the same cell agreed to within 0.05 cm^3. To correct for the differences associated with changes in calibration pressure, a standard was included in every other pycnometer run. The standard was rotated through each of the cells so that changes in the cells could be monitored. The sample volumes were then corrected by the difference between the measured standard volume and the known standard volume.

The entire set of beakers was painstakenly calibrated during transit to the first site. This recalibration was conducted by calculating the densities of the beakers, using weights and volumes already present in the data base. Because the beakers are made of aluminum, their densities should be near 2.7 g/cm^3. However, many of the calculated densities were off by 0.1 g/cm^3 or more. Thus, the beakers were all weighed and run through the pycnometer, and the densities recalculated. These values were entered into the "physprops" data base.

At Site 803, wet and dry volumes were measured for each sample. It quickly became apparent that the samples from subsequent sites could only be run once through the pycnometer if we were to keep up with the desired sampling frequency. Examination of the data indicated that the dry volumes measured by the pycnometer are more accurate than the wet volumes, because of the presence of volatiles in the wet samples that apparently result in erroneous pressure readings. Therefore, for subsequent sites, only dry samples were run through the pycnometer. Dry weight and volume measurements were obtained after the samples were oven dried at 110°C for 24 hr and allowed to cool in a desiccator. A salt correction, assuming 35-ppt interstitial fluid salinity, was applied to density and porosity computations as per Hamilton (1971).

Wet-bulk density was calculated from the wet and dry weights (W_w and W_d, respectively) and dry volumes (V_d). The wet volume (V_w), used to calculate bulk density, was calculate by adding the weight of the water lost through drying of the sample to the dry volume, using the following equation:

$$V_w = V_d + (W_w - W_d)/\delta_f,$$

where δ_f is the density of evaporated water and is assumed to be equal to 1. The dry volume, V_d, includes both the volume of the sediment or rock constituents and the volume of salt remaining in the sample upon drying. Then, wet-bulk density was calculated in the normal manner as follows:

$$\delta_{bw} = W_w/V_w.$$

Porosity, water content (calculated as a percentage of dry weight), grain density, and dry-bulk density were also calculated using the calculated wet volume, according to the equations of Boyce (1976).

DOWNHOLE MEASUREMENTS

General

Downhole logs can be used to characterize the geophysical, geochemical, and structural properties of a drilled sequence. Log measurements have a distinct advantage over core-based measurements in that they represent continuous and *in-situ* measurements of the borehole. After coring is completed in a particular hole, a combination of sensors is lowered downhole on a seven-conductor cable, and each of several measuring devices continuously monitors properties of the adjacent formation. Under rough sea conditions, a wireline heave compensator can be used to minimize the effects of ship heave on the tool position in the borehole. The depths of investigation are sensor-dependent, and data are typically recorded at 15-cm intervals.

Three different tool strings of Schlumberger sensors were used on Leg 130: (1) a "geophysical" tool string, (2) a "geochemical" tool string, and (3) the formation microscanner (FMS). The Lamont-Doherty temperature tool was also attached at the base of each tool string to obtain heat-flow information.

The Geophysical Tool String

The geophysical tool string typically consists of the natural gamma-ray spectrometry tool (NGT), the phasor dual-induction tool (DITE), the long-spacing digital sonic velocity tool (LSS), and the lithodensity tool (HLDT). At Hole 803D, because of tool failures, a borehole-compensated sonic velocity tool (BHC) was also used. The geophysical tool string is designed to measure the sonic-wave propagation properties of the borehole through measurements in the formation of the compressional wave velocity; the deep, intermediate, and shallow resistivity; and the formation density. The sonic velocity data, when combined with the information on density, are used to calculate an impedance log and generate a synthetic seismogram for the logged sequence. The natural gamma radiation tool is run on each combination tool string to provide a common basis for log correlations.

The dual induction tool (DITE) provides three different measurements of electrical resistivity, each with a different radial depth of investigation. Two induction devices ("deep" and "medium" resistivity) send high-frequency alternating currents through transmitter coils, creating magnetic fields that induce secondary (Foucalt) currents in the formation. These ground-loop currents produce new inductive signals, proportional to the conductivity of the formation, that are recorded by a series of receiving coils. The measured conductivities are converted to resistivity. A third device (the "spherically focused" resistivity [SFR] tool) measures the current necessary to maintain a constant voltage drop across a fixed interval. The vertical resolution is on the order of 2 m for the two induction devices and about 1 m for the SFR. The data can be corrected for irregularities in borehole diameter.

In general, resistivity responds to the inverse square root of porosity (Archie, 1942). Water salinity, clay content, hydrocarbon content, and temperature are also important factors in controlling the electrical resistivity of rocks. Other factors that may influence the resistivity of a rock include the concentration of hydrous and metallic minerals, formation vesicularity, and the geometry of the interconnected pore space.

The long-spacing digital sonic tool (LSS) uses two acoustic transmitters and two receivers to measure the time required for sound waves to travel along the borehole wall over source-receiver distances of 8, 10, and 12 ft (2.4, 3.0, and 3.6 m). First arrivals for the individual source-receiver paths are used to calculate the velocities of the waves traveling in the formation; the tool measures four traveltimes at each measurement depth as there are four possible paths. The borehole-compensated sonic tool (BHC; also known as the short spacing sonic tool) has two sources and two receivers configured to provide four symmetric and redundant measurements of acoustic traveltime. The source-receiving spacing on this tool provides two 3-ft- and two 5-ft-interval transit time measurements. In poor hole conditions, such as are often experienced by ODP, the LSS provides more reliable data than the BHC. Only compressional wave velocities are determined aboard the ship, but full sonic waveforms are recorded for post-cruise processing to determine shear wave and Stonely wave velocities. The vertical resolution of the LSS and the BHC is about 2 ft (0.61 m). Logs can be corrected for cycle skipping (misidentified arrivals) because of the four-way measurement redundancy. Compressional wave velocity is dominantly controlled by porosity and lithification; decreases in porosity and increases in lithification typically cause velocity to increase with depth in a sedimentary sequence.

The lithodensity tool (HLDT) uses a 0.66 MeV ^{137}Ce gamma-ray source for its density measurements. The source is mounted in the tool body and a caliper arm presses it and a pair of detectors against the borehole wall. The density measurement is based upon Compton scattering of the gamma rays within the formation and, thus, actually is a measurement of electron density. Because most rock-forming elements have atomic weights that are twice their atomic numbers, the electron density can be converted directly to bulk density. In addition, the tool also records a photoelectric effect index. Photoelectric absorption occurs in the energy window below 150 KeV and depends upon the energy of the incident gamma ray, the atomic cross section, and the nature of the atom. The measurement is almost independent of porosity and can therefore be used directly as a matrix lithology indicator. The density and photoelectric effect measurements require excellent contact with the borehole wall; the tool provides a measure of this and corrections can be made for excessive borehole roughness. The vertical resolution of the measurement is about 0.3 m.

The Geochemical Tool String

The geochemical tool string used on Leg 130 consists of a natural gamma-ray tool (NGT), an induced gamma-ray spectroscopy tool (GST), and the aluminum clay tool (ACT). Relative concentrations of Si, Ca, Fe, S, H, and Cl can be derived on shipboard, as well as weight percent abundance of K, U, Th, and Al. Further shore-based processing can produce abundance logs of the first six elements mentioned plus Gd and Ti.

The NGT measures the natural radioactivity of the formation. Most gamma rays are emitted by the naturally occurring radioactive isotope ^{40}K and by a series of U and Th isotopes and their daughters. The gamma radiation originating in the formation close to the borehole wall is measured by a sodium iodide scintillation detector mounted inside the sonde. The energy spectrum measured by the sodium iodide detector is divided into five discrete energy windows. The total counts recorded in each window, for a specified depth in the well, are processed at the surface to give elemental abundances of K, U, and Th. The tool has a depth of investigation of about 0.3–0.5 m. The NGT data are also corrected for borehole diameter variations. The tool is run on every combination tool string to serve as a basis for depth correlations between separate runs.

The elements K, U, and Th tend to be most abundant in clay minerals, and consequently the gamma-ray curve is commonly used to estimate the sediment clay content. Uranium tends to be concentrated in organic-rich sediments because of its redox chemistry (Fertl, 1983) and can be an indirect indicator of sapropelic layers. However, silicic volcaniclastics and potassium-feldspar-rich sandstones also can have high abundances of these three elements.

The GST consists of a pulsed 14-MeV neutron generator and a gamma-ray scintillation detector. The incident neutrons lose energy through inelastic scattering in the formation and eventually are captured by elemental nuclei when they reach thermal energy levels (about 0.02 eV). After capture, gamma rays are emitted; these gamma rays are detected by the tool. The 256-channel energy spectrum is deconvoluted to determine the relative abundance of Ca, Si, Fe, Cl, H, and S on board the ship. The raw logs were extensively reprocessed post-cruise by the Borehole Research Group at Lamont-Doherty Geological Observatory to produce percentage data for these elements as well as Gd and Ti. Because the depth being investigated is shallow, the logs also had to be corrected for variability in borehole diameter.

Aluminum abundance is measured by the ACT, which uses a different form of neutron activation analysis than the GST. When aluminum absorbs a neutron from the 2.5-MeV ^{252}Cf source, it forms an unstable nucleus with a half-life of about 2 min. When it decays, a characteristic gamma ray is emitted within the energy windows of the natural gamma tool. The contribution to the gamma-ray spectrum caused by natural radiation is removed by running NGT tools both above and below the neutron source; the detector above measures the natural radiation before activation, and the detector below measures the induced radiation.

The Formation Microscanner

The formation microscanner (FMS) produces high-resolution images of the microresistivity character of the borehole wall that can be used for detailed sedimentological or structural interpretations (Ekstrom et al., 1986; Pezard and Luthi, 1988). Schlumberger originally introduced the tool in 1986, but it was not suitable for use in the narrow-gauge drill pipe used by the ODP. A modified sensor was consequently developed by Schlumberger and first deployed during Leg 126.

The FMS tool consists of 16 electrode "buttons" on each of four orthogonal pads that are pressed against the borehole wall. The electrodes are spaced about 2.5 mm apart and are arranged in two diagonally offset rows of eight electrodes each. Shore-based processing corrects the offset rows to one level, which doubles the horizontal resolution to about 1.25 mm. The FMS tool string contains a general purpose inclinometry tool (GPIT) that spatially orients the resistivity measurements through the use of an accelerometer and from the declination and inclination of the Earth's magnetic field vector. The raw data undergo extensive processing to transform the individual microresistivity traces into complete, spatially oriented images. Because of limited shipboard capabilities for processing on Leg 130, only limited reprocessing was carried out at sea.

Possible applications of the FMS-derived images include (1) making detailed correlations between coring and logging depths; (2) finding the orientation of cores; (3) mapping fractures, faults, foliations, and formation structures; and (4) determining strikes and dips of bedding. The FMS can also be used to measure stress in the borehole. The FMS provides precise measurements of borehole diameter in two orthogonal directions. In an isotropic, linearly elastic rock subjected to an anisotropic stress field, breakouts form along the borehole wall as a result of compressive stress concentrations exceeding the strength of the rock. Under these conditions, the breakout orientation develops in the direction of the least principal horizontal stress. It has been demonstrated previously that stress orientations deduced from rock breakouts are consistent with other independent stress indicators (Bell and Gough, 1979; Zoback et al., 1988).

REFERENCES

Archie, G. E., 1942. The electrical resistivity log as an aid in determining some reservoir characteristics. *J. Petrol. Tech.*, 5:1–8.

Aubry, M.-P., Berggren, W. A., Kent, D. V., Flynn, J. J., Klitgord, K. D., Obradovich, J. D., and Prothero, D. R., 1988. Paleogene geochronology: an integrated approach. *Paleoceanography*, 3:707–742.

Backman, J., 1986. Late Paleocene to middle Eocene calcareous nannofossil biostratigraphy from the Shatsky Rise, Walvis Ridge and Italy. *Palaeogeogr., Palaeoclimatol., Palaeoecol.*, 57:43–59.

________, 1987. Quantitative calcareous nannofossil biochronology of middle Eocene through early Oligocene sediment from DSDP Sites 522 and 523. *Abh. Geol. Bundesanst. Austria*, 39:21–31.

Backman, J., and Pestiaux, P., 1986. Pliocene *Discoaster* abundance variations, Deep Sea Drilling Project Site 606: biochronology and paleoenvironmental implications. *In* Ruddiman, W. F., Kidd, R. B., Thomas, E., et al., *Init. Repts. DSDP*, 94, Pt. 2: Washington (U.S. Govt. Printing Office), 903–910.

Backman, J., and Shackleton, N. J., 1983. Quantitative biochronology of Pliocene and early Pleistocene calcareous nannofossils from the Atlantic, Indian and Pacific oceans. *Mar. Micropaleontol.*, 8:141–170.

Backman, J., Schneider, D. A., Rio, D., and Okada, H., 1990. Neogene low-latitude magnetostratigraphy from Site 710 and revised age estimates of Miocene nannofossil datum events. *In* Duncan, R. A., Backman, J., Peterson, L. C., et al., *Proc. ODP, Sci. Results*, 115: College Station, TX (Ocean Drilling Program), 217–276.

Baldauf, J. G., 1985. A high resolution late Miocene–Pliocene diatom biostratigraphy for the eastern equatorial Pacific. *In* Mayer, L., Theyer, F., Thomas, E., et al., *Init. Repts. DSDP,* 85: Washington (U.S. Govt. Printing Office), 457–475.

Barron, J. A., 1985a. Late Eocene to Holocene diatom biostratigraphy of the equatorial Pacific Ocean, Deep Sea Drilling Project Leg 85. *In* Mayer, L., Theyer, F., Thomas, E., et al., *Init. Repts. DSDP,* 85: Washington (U.S. Govt. Printing Office), 413–447.

________, 1985b. Miocene to Holocene planktic diatoms. *In* Bolli, H. M., Saunders, J. B., and Perch-Nielsen, K. (Eds.), *Plankton Stratigraphy:* Cambridge (Cambridge Univ. Press), 763–809.

________, 1989. The late Cenozoic stratigraphic record and hiatuses of the northeast Pacific: results from the Deep Sea Drilling Project. *In* Winterer, E. L., Hussong, D. M., and Decker, R. W. (Eds.), *The Eastern Pacific Ocean and Hawaii* (Vol. N): Boulder, CO (Geol. Soc. Am.), 311–322.

Barron, J. A., Keller, G., and Dunn, D. A., 1985a. A multiple microfossil biochronology for the Miocene. *In* Kennett, J. P. (Ed.), *The Miocene Ocean: Paleoceanography and Biogeography.* Mem. Geol. Soc. Am., 163:21–36.

Barron, J. A., Nigrini, C. A., Pujos, A., Saito, T., Theyer, F., Thomas, E., and Weinreich, N., 1985b. Synthesis of biostratigraphy, central equatorial Pacific, Deep Sea Drilling Project Leg 85: refinement of Oligocene to Quaternary biochronology. *In* Mayer, L., Theyer, F., Thomas, E., et al., *Init. Repts. DSDP,* 85: Washington (U.S. Govt. Printing Office), 905–934.

Bell, J. S., and Gough, D. I., 1979. Northeast-southwest compressive stress in Alberta: evidence from oil wells. *Earth Planet. Sci. Lett.,* 45:475–482.

Berggren, W. A., 1969. Rates of evolution in some Cenozoic planktonic foraminifera. *Micropaleontology,* 15(3):351–365.

Berggren, W. A., Kent, D. V., and Flynn, J. J., 1985a. Jurassic to Paleogene: Part 2. Paleogene geochronology and chronostratigraphy. *In* Snelling, N. J. (Ed.), *The Chronology of the Geological Record.* Mem. Geol. Soc. (London), 10:141–195.

Berggren, W. A., Kent, D. V., Flynn, J. J., and Van Couvering, J. A., 1985b. Cenozoic geochronology. *Geol. Soc. Am. Bull.,* 96:1407–1418.

Berggren, W. A., Kent, D. V., and Van Couvering, J. A., 1985c. The Neogene: Part 2. Neogene geochronology and chronostratigraphy. *In* Snelling, N. J. (Ed.), *The Chronology of the Geological Record.* Mem. Geol. Soc. (London), 10:211–260.

Berggren, W. A., and Miller, K. G., 1988. Paleogene tropical planktonic foraminiferal biostratigraphy and magnetobiochronology. *Micropaleontology,* 34(4):362–380.

Blow, W. H., 1969. Late middle Eocene to Recent planktonic foraminiferal biostratigraphy. *In* Brönniman, P., and Renz, H. H., (Eds.), *Proceedings of the First International Conference on Planktonic Microfossils, Geneva:* Leiden (E. J. Brill), 1:199–422.

________, 1979. *The Cainozoic Globigerinida:* Leiden (E. J. Brill).

Bolli, H. M., and Premoli-Silva, I., 1973. Oligocene to Recent planktonic foraminifera and stratigraphy of the Leg 15 sites in the Caribbean Sea. *In* Edgar, N. T., Saunders, J. B., et al., *Init. Repts. DSDP,* 15: Washington (U.S. Govt. Printing Office), 475–497.

Bolli, H. M., and Saunders, J. B., 1985. Oligocene to Holocene low latitude planktonic foraminifera. *In* Bolli, H. M., Saunders, J. B., and Perch-Nielsen, K. (Eds.), *Plankton Stratigraphy:* Cambridge (Cambridge Univ. Press), 155–262.

Bougault, M., Cambon, P., and Toulhoat, H., 1977. X-ray spectrometric analysis of trace elements in rocks: correction for instrumental interferences. *X-Ray Spectrom.,* 6:66–72.

Boyce, R. E., 1976. Definitions and laboratory techniques of compressional sound velocity parameters and wet-water content, wet-bulk density, and porosity parameters by gravimetric and gamma ray attenuation techniques. *In* Schlanger, S. O., Jackson, E. D., et al., *Init. Repts. DSDP,* 33: Washington (U.S. Govt. Printing Office), 931–958.

Brindley, G. W., and Brown, G. (Eds.), 1980. *Crystal Structures of Clay Minerals and Their X-ray Identification.* Mineral. Soc. Monogr., No. 5.

Burckle, L. H., 1972. Late Cenozoic planktonic diatom zones from the eastern equatorial Pacific. *Nova Hedwigia Beih.,* 39:217–246.

Burke, S. C., 1981. Recent benthic foraminifera of the Ontong Java Plateau. *J. Foraminiferal Res.,* 11:1–19.

Caron, M., 1985. Cretaceous planktonic foraminifera. *In* Bolli, H. M., Saunders, J. B., and Perch-Nielsen, K. (Eds.), *Plankton Stratigraphy:* Cambridge (Cambridge Univ. Press), 17–86.

Douglas, R., 1973. Benthic foraminiferal biostratigraphy in the central North Pacific, Leg 17, Deep Sea Drilling Project. *In* Winterer, E., Ewing, J., et al., *Init. Repts. DSDP,* 17: Washington (U.S. Govt. Printing Office), 607–672.

Dunham, R., 1962. Classification of carbonate rocks according to depositional texture. *In* Ham, W. E. (Ed.), *Classification of Carbonate Rocks:* Tulsa, OK (AAPG), 108–121.

Ekstrom, M. P., Dahan, C. A., Chen, M.-Y., Lloyd, P. M., and Rossi, D. J., 1986. Formation imaging with microelectrical scanning arrays. *Trans. SPWLA Annu. Logging Symp.,* 27th, Paper BB.

Emeis, K.-C., and Kvenvolden, K. A., 1986. Shipboard organic geochemistry on *JOIDES Resolution. ODP Tech. Note,* No. 7.

Espitalié, J., Laporte, J. L., Madec, M., Marquis, F., Leplat, P., Paulet, J., and Boutfeu, A., 1977. Method rapide de caracterisation des roches mère de leur potentiel petrolier et de leur degree d'evolution. *Rev. Inst. Fr. Pet.,* 32:23–42.

Fenner, J., 1984. Eocene-Oligocene planktic diatom stratigraphy in the low latitudes and high southern latitudes. *Micropaleontology,* 30: 319–342.

________, 1985. Late Cretaceous to Oligocene planktic diatoms. *In* Bolli, H. M., Saunders, J. B., and Perch-Nielsen, K. (Eds.), *Plankton Stratigraphy:* Cambridge (Cambridge Univ. Press), 713–762.

Fertl, W. H., 1983. Gamma ray spectral logging: a new evaluation frontier. *World Oil,* 197:99–112.

Fisher, R. V., and Schmincke, H.-U., 1984. *Pyroclastic Rocks:* Berlin-Heidelberg-New York (Springer-Verlag).

Fornaciari, E., Raffi, I., Rio, D., Villa, G., Backman, J., and Olafsson, G., 1990. Quantitative distribution patterns of Oligocene and Miocene calcareous nannofossils from western equatorial Indian Ocean. *In* Duncan, R. A., Backman, J., Peterson, L. C., et al., *Proc. ODP, Sci. Results,* 115: College Station, TX (Ocean Drilling Program), 237–254.

Gieskes, J. M., and Peretsman, G., 1985. Water chemistry procedures aboard *JOIDES Resolution*—some comments. *ODP Tech. Note,* No. 5.

Hamilton, E. L., 1971. Prediction of *in-situ* acoustic and elastic properties of marine sediments. *Geophysics,* 36:266–284.

Hermelin, J.O.R., 1989. Pliocene benthic foraminifera from the Ontong-Java Plateau (western equatorial Pacific Ocean): faunal response to changing paleoenvironment. *Spec. Publ., Cushman Found. Foraminiferal Res.,* 26:1–143.

Kennett, J. P., and Srinivasan, M. S., 1983. *Neogene Planktonic Foraminifera: A Phylogenetic Atlas:* Stroudsburg, PA (Hutchinson Ross).

Kent, D. V., and Gradstein, F. M., 1985. A Cretaceous and Jurassic geochronology. *Geol. Soc. Am. Bull.,* 96:1419–1427.

Loeblich, A., and Tappan, H., 1987. *Foraminiferal Genera and Their Classification:* New York (Van Nostrand).

Manheim, F. T., and Sayles, F. L., 1974. Composition and origin of interstitial waters of marine sediments based on deep sea drill cores. *In* Goldberg, E. D. (Ed.), *The Sea* (Vol. 5): *Marine Chemistry:* New York (Wiley-Interscience), 527–568.

Martini, E., 1971. Standard Tertiary and Quaternary calcareous nannoplankton zonation. *In* Farinacci, A. (Ed.), *Proceedings of the Second International Conference on Planktonic Microfossils, Roma:* Rome (Ed. Technoscienza), 2:739–785.

Mayer, L. A., Courtney, R. C., and Moran, K., 1987. Ultrasonic measurements of marine sediment properties. *Proc. Oceanogr.,* 87 1:139.

Mazzullo, J. M., Meyer, A., and Kidd, R., 1988. New sediment classification scheme for the Ocean Drilling Program. *In* Mazzullo, J., and Graham, A. G., *Handbook for Shipboard Sedimentologists.* ODP Tech. Note, 8:45–67.

Norrish, K., and Hutton, J. T., 1969. An accurate X-ray spectrographic method for the analysis of a wide range of geological samples. *Geochim. Cosmochim. Acta,* 33:431–453.

Pezard, P. A., and Luthi, S. M., 1988. Borehole electrical images in the basement of the Cajon Pass Scientific Drillhole, California; fracture identification and tectonic implications. *Geophys. Res. Lett.*, 15: 1017–1020.

Pyle, M. R., 1984. Vane shear data on undrained residual strength. *J. Tech. Div., Am. Soc. Civ. Eng.*, 110:543–547.

Resig, J., 1981. Biogeography of benthic foraminifera on the northern Nazca Plate and adjacent continental margin. *Mem. Geol. Soc. Am.*, 154:619–666.

Riedel, W. R., and Sanfilippo, A., 1978. Stratigraphy and evolution of tropical Cenozoic radiolarians. *Micropaleontology,* 24:61–96.

Rio, D., Backman, J., and Raffi, I., in press. *Calcareous Nannofossil Biochronology and the Pliocene/Pleistocene Boundary:* Cambridge (Cambridge Univ. Press).

Rio, D., Fornaciari, E., and Raffi, I., 1990. Late Oligocene through early Pleistocene calcareous nannofossils from western equatorial Indian Ocean (Leg 115). *In* Duncan, R. A., Backman, J., Peterson, L. C., et al., *Proc. ODP, Sci. Results*, 115: College Station, TX (Ocean Drilling Program), 175–236.

Roth, P. H., and Thierstein, H. R., 1972. Calcareous nannoplankton: Leg 14 of the Deep Sea Drilling Project. *In* Hayes, D. E., Pimm, A. C., et al., *Init. Repts. DSDP,* 14: Washington (U.S. Govt. Printing Office), 421–485.

Sanfilippo, A., and Riedel, W. R., 1985. Cretaceous radiolaria. *In* Bolli, H. M., Saunders, J. B., and Perch-Nielsen, K. (Eds.), *Plankton Stratigraphy:* Cambridge (Cambridge Univ. Press), 573–630.

Sanfilippo, A., Westberg-Smith, M. J., and Riedel, W. R., 1985. Cenozoic radiolaria. *In* Bolli, H. M., Saunders, J. B., and Perch-Nielsen, K. (Eds.), *Plankton Stratigraphy:* Cambridge (Cambridge Univ. Press), 631–712.

Sato, T., Kameo, K., and Takayama, T., 1991. Coccolith biostratigraphy of the Arabian Sea and a new nannofossil zonal scheme for the Quaternary. *In* Prell, W. L., Niitsuma, N., et al., *Proc. ODP, Sci. Results*, 117: College Station, TX (Ocean Drilling Program).

Saunders, J. B., Bernoulli, D., Müller-Merz, E., Oberhänsli, H., Perch-Nielsen, K., Riedel, W. R., Sanfilippo, A., and Torrini, R., Jr., 1984. Stratigraphy of late middle Eocene to early Oligocene in the Bath Cliff section, Barbados, West Indies. *Micropaleontology,* 30: 390–425.

Schrader, H.-J., and Gersonde, R., 1978. Diatoms and silicoflagellates. *Utrecht Micropaleontol. Bull.*, 17:129–176.

Shipboard Scientific Party, 1988a. Introduction and explanatory notes. *In* Ruddiman, W., Sarnthein, M., et al., *Proc. ODP, Init. Repts.*, 108: College Station, TX (Ocean Drilling Program), 5–28.

________, 1988b. Introduction and explanatory notes. *In* Mascle, A., Moore, J. C., et al., *Proc. ODP, Init. Repts.*, 110: College Station, TX (Ocean Drilling Program), 5–25.

________, 1988c. Explanatory notes: Leg 112. *In* Suess, E., von Huene, R., et al., *Proc. ODP, Init. Repts.*, 112: College Station, TX (Ocean Drilling Program), 25–44.

________, 1989a. Explanatory notes. *In* Prell, W. L., Niitsuma, N., et al., *Proc. ODP, Init. Repts.*, 117: College Station, TX (Ocean Drilling Program), 11–33.

________, 1989b. Introduction and explanatory notes. *In* Robinson, P. T., Von Herzen, R., et al., *Proc. ODP, Init. Repts.*, 118: College Station, TX (Ocean Drilling Program), 3–24.

________, 1990a. Explanatory notes. *In* Gradstein, F. M., Ludden, J. N., et al., *Proc. ODP, Init. Repts.*, 123: College Station, TX (Ocean Drilling Program), 27–59.

________, 1990b. Explanatory notes. *In* Tamaki, K., Pisciotto, K., Allan, J., et al., *Proc. ODP, Init. Repts.*, 128: College Station, TX (Ocean Drilling Program), 35–60.

Sissingh, W., 1977. Biostratigraphy of Cretaceous calcareous nannoplankton. *Geol. Mijnbouw,* 56:37–65.

Sliter, W. V., 1989. Biostratigraphic zonation for Cretaceous planktonic foraminifers examined in thin section. *J. Foraminiferal Res.*, 19:1–19.

Stainforth, R. M., Lamb, J. L., Luterbacher, H. P., Beard, J. H., and Jeffords, R. M., 1975. Cenozoic planktonic foraminiferal zonation and characteristics of index forms. *Univ. Kans. Paleontol. Contrib. Art.*, 62:1–425.

Thierstein, H. R., 1976. Mesozoic calcareous nannoplankton biostratigraphy of marine sediments. *Mar. Micropaleontol.*, 1:325–362.

Thierstein, H. R., Geitzenauer, K. R., Molfino, B., and Shackleton, N. J., 1977. Global synchroneity of late Quaternary coccolith datum levels: validation by oxygen isotopes. *Geology,* 5:400–405.

Thomas, E., 1985. Late Eocene to Recent deep-sea benthic foraminifers from the central equatorial Pacific Ocean. *In* Mayer, L., Theyer, F., Thomas, E., et al., *Init. Repts. DSDP,* 85: Washington (U.S. Govt. Printing Office), 655–694.

van Morkhoven, F.P.C.M., Berggren, W. A., and Edwards, A. S., 1986. Cenozoic cosmopolitan deep-water benthic foraminifera. *Bull. Cent. Rech. Explor.-Prod. Elf-Aquitaine,* Mem. No. 11.

Vacquier, V., 1985. The measurement of thermal conductivity of solids with a transient linear heat source on the plane surface of a poorly conducting body. *Earth Planet. Sci. Lett.*, 74:275–279.

Von Herzen, R. P., and Maxwell, A. E., 1959. The measurement of thermal conductivity of deep-sea sediments by a needle probe method. *J. Geophys. Res.*, 65:1557–1563.

Wentworth, C. K., 1922. A scale of grade and class terms of clastic sediments. *J. Geol.*, 30:377–390.

Zijderveld, J.D.A., Zachariasses, J. W., Verhallen, P.J.J.M., and Hilgen, F. J., 1986. The age of the Miocene-Pliocene boundary. *Newsl. Stratigr.*, 16:169–181.

Zoback, M. D., Zoback, M. L., Mount, V. S., Suppe, J., Eaton, J. P., Healy, J. H., Oppenheimer, D., Reasenberg, P., Jones, L., Raleigh, C. B., Wong, I. G., Scotti, O., and Wentworth, C., 1988. New evidence on the state of stress of the San Andreas Fault. *Science*, 238: 1105–1111.

Ms 130A-102

Kroenke, L. W., Berger, W. H., Janecek, T. R., et al., 1991
Proceedings of the Ocean Drilling Program, Initial Reports, Vol. 130

3. SEABEAM AND SEISMIC REFLECTION SURVEYS ON THE ONTONG JAVA PLATEAU[1]

L. A. Mayer,[2] T. H. Shipley,[3] E. L. Winterer,[4] D. Mosher,[2] and R. A. Hagen[5]

INTRODUCTION

In support of Leg 130 drilling, a site survey program was conducted between 17 and 31 December 1988 aboard the *Thomas Washington* (ROUNDABOUT Cruise 11; E. L. Winterer, T. Shipley, and L. Mayer, Principal Investigators). During this cruise over 3000 km of digitally recorded, single-channel water-gun seismic, magnetic, and SeaBeam bathymetric data were collected in the western equatorial Pacific. Because of the large steaming distances to and from port (Majuro to Majuro), only approximately half of this data set was actually collected on the Ontong Java Plateau (OJP) (Fig. 1).

The goal of the site survey cruise was to find a route from the top of the plateau to the bottom along which the seismic (and thus sedimentary) section would be minimally disturbed by mass wasting and redeposition. Our plan was to identify those areas with the most expanded sedimentary sections and conduct detailed site surveys suitable for drill site selection. Ideally, sites would be at depth intervals of 400–600 m, spanning the depth range of the plateau. In addition to the seismic and SeaBeam surveys, an extra day of ship time was provided by Scripps Institution of Oceanography for the collection of piston cores. We collected four piston cores; their lengths and locations are listed in Table 1.

The site survey cruise was funded specifically to select sites for the Neogene objectives of the Leg 130 drilling program. Thus, ship time constraints precluded surveying a region 300 km west of Sites 289/586 where it is thought that an expanded Mesozoic section might be found. We were, however, well aware of the important pre-Neogene and lithosphere objectives associated with OJP drilling and attempted to accommodate these objectives with the little flexibility that we had. Our approach was to review all existing OJP seismic data, select a route that would provide the best chance of finding undisturbed sections, and then parallel that route as we left Majuro and began to climb up the plateau.

A review of existing seismic data revealed that, although disturbance on the plateau is nearly ubiquitous, at certain depth intervals it is especially pronounced. Complications are common near 3000–3500 mbsl where there is commonly a sharp break in slope, and near 4000 mbsl where there seems to be significant disturbance in the deeper part of the section (Fig. 2). Based on existing seismic data, the best hope for finding a desirable path up the plateau was near the track taken by *Vema* Cruise 24-05 in 1967. This air-gun record (single-channel 40 in.^{3}) showed little disturbance (bearing around 250°) over a large portion of the plateau. We departed Majuro on 17 December and began our survey up the plateau, paralleling the *Vema* track on the 20th of December (Fig. 1).

The traverse up the plateau with the high-resolution water-gun seismic reflection system revealed that the section was more complex than originally thought. Scattered throughout the plateau are examples of mass wasting, scour and channel fill, and complex tectonic and possibly igneous activity. Particularly difficult was the 3000–3500 mbsl depth interval (which is, interestingly, the approximate depth of the lysocline in this region; Berger and Mayer, 1978). The difficulty in finding appropriate sites at this depth range forced us to deviate from the *Vema* track after tying our line to Sites 289/586. We chose to head northeast so that we could follow a bathymetric promontory that might be free of mass wasting and have an expanded older section. Also, surveys to the north would cover sites that are off the isochron of Site 289 and thus be beneficial to lithosphere objectives.

Despite the complexities of the plateau (which make for an interesting story in their own right), the preliminary analysis of the seismic data led us to think that we could find potential sites through which the seismic stratigraphy could be traced (and thus provide a general idea of our location in the section) as well as sites that experienced a minimum amount of disruption. The sedimentary cover on the plateau thins from ~1200 m in thickness at 2200 m water depth to <450 m at 4300 m water depth (averaging about 100 m loss in thickness for every 200 m of water depth; Figs. 2 and 3). The determination of the manner in which this thinning takes place is one of the important goals of the drilling.

During our traverse from the top of the plateau (Sites 289/586) to Majuro, five detailed site surveys were conducted, and, in the spirit of the season, these were named after Santa's reindeer. Surveys were conducted at the following depth intervals: 2600–2800 mbsl (A = Dasher, OJP-1, Site 806); 3040–3180 mbsl (C = Prancer); 3100–3300 mbsl (D = Vixen, OJP-2, Site 805); 3400–3600 mbsl (B = Dancer, OJP-4, Site 803); and 4120–4200 mbsl (E = Comet, OJP-3) (Fig. 1). A preliminary bathymetric chart was produced for each survey area as well as an "avoidance" chart, that is, a chart that details areas avoided in the site selection process. Criteria used to select potential sites included the avoidance of those sites with evidence of modern or past erosion (i.e., hyperbolae or channel structures), displacement or disruption in the sediment column, major faulting and seismic anomalies (Figs. 4 and 5).

Also included as targets to be avoided were the strongly reverberant layers that commonly occur mid-section at water depths greater than 3000 m. These mid-section reflections have a seismic character similar to the chert and basement found near the bottom of Site 289 (Reflectors "F" and "G"; see below and Fig. 6), and may be related to basement complexities, tectonic disruption, igneous intrusion, erosion and early chertification, or some combination of these. Their origin is not yet understood, but certainly they will be the subject of future investigation. Preference was given to those sites with expanded sections and with high-quality seismic images.

---

[1] Kroenke, L. W., Berger, W. H., Janecek, T. R., et al., 1991. *Proc. ODP, Init. Repts.*, 130: College Station, TX (Ocean Drilling Program).

[2] Department of Oceanography, Dalhousie University, Halifax, Nova Scotia, Canada B3H 4J1.

[3] Institute for Geophysics, University of Texas at Austin, 8701 Mopac Boulevard, Austin, TX 78759-8345, U.S.A.

[4] Scripps Institution of Oceanography, Geological Research Division, University of California, San Diego, La Jolla, CA 92093-0215, U.S.A.

[5] Hawaii Institute of Geophysics, University of Hawaii, 2525 Correa Road, Honolulu, HI 96822, U.S.A.

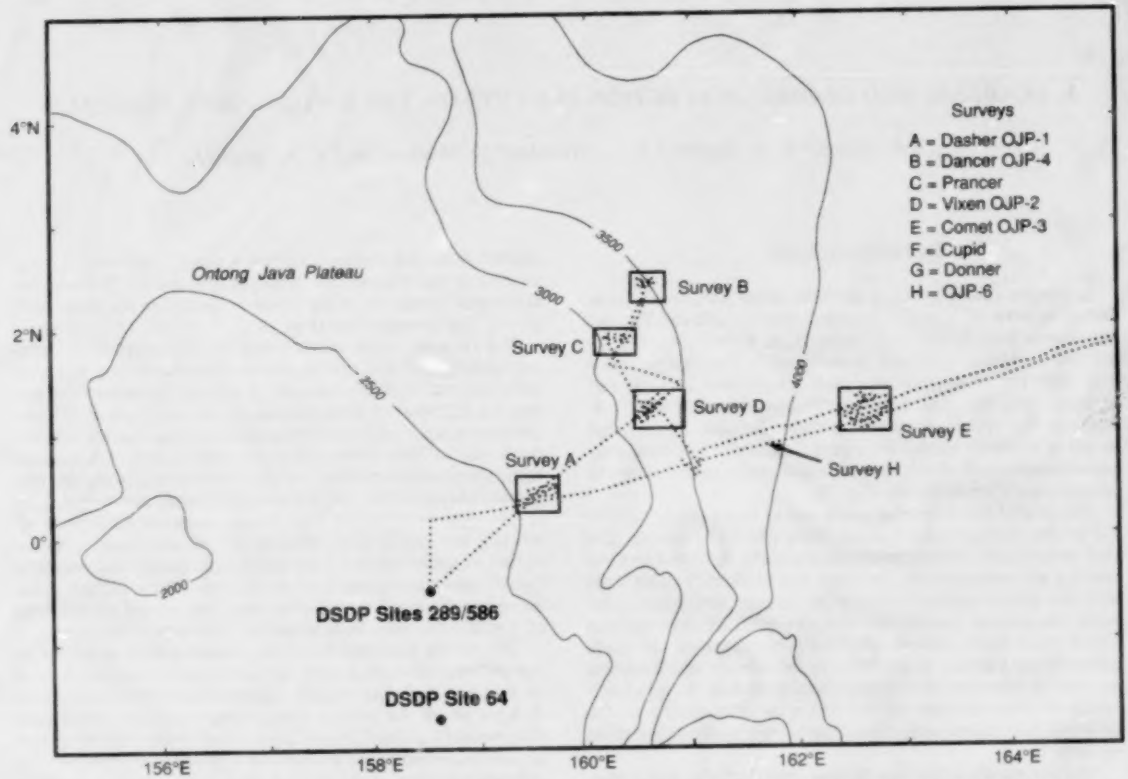

Figure 1. Bathymetry of northeast Ontong Java Plateau and ship track of ROUNDABOUT Cruise 11 with the locations of the detailed site survey areas for the Leg 130 drill sites.

Table 1. Locations of piston cores collected during ROUNDABOUT Cruise 11.

Core	Latitude	Longitude	Water depth (m)	Length (m)
PC 74	00°20.48′N	159°22.49′E	2547	8.5
PC 75	01°53.15′N	160°11.49′E	3078	8.5
PC 76	01°10.10′N	160°40.20′E	3290	7.6
PC 77	00°35.64′N	161°00.66′E	3490	8.5

METHODS

Seismic data were collected with an SSI, 80-in.^{3} water gun fired at 2000 psi. The seismic records were digitized aboard the research vessel at a 1-ms digitization rate by the data acquisition systems of the Scripps Institution of Oceanography as well as the University of Texas. All records presented in this chapter were band-pass filtered at 70–250 kHz and displayed at the same (constant) gain. Navigation was provided by transit satellite and, when available, the global positioning system (GPS).

An NGDC77 data tape, microfilm of analog seismic data, and the cruise report are on file with the Ocean Drilling Program (ODP) Site Survey Data Bank. Data tapes shipped back from Majuro were received at the University of Texas in February 1989, and Tom Shipley and Dave Mosher completed preliminary processing (filtering and display optimization) by early March.

Bathymetric data were collected with SeaBeam, a 16-narrow-beam echo sounder that collects detailed depth information in a swath parallel to the ship and with a width of about 80% of the water depth (Renard and Allenou, 1979). A 20-m contour interval was used for all surveys presented here. The SeaBeam data were adjusted on board the ship to reconcile it with the "best" available navigation for a given survey. The maps presented here are hand-contoured, based on the SeaBeam maps.

SURVEY AREAS

DSDP Sites 289/586

The starting point for our analyses of the site survey data for the Ontong Java Plateau was the line collected over Deep Sea Drilling Project (DSDP) Sites 289/586 (Fig. 7). With the results from DSDP Legs 30 and 89 (Fig. 8) (Shipboard Scientific Party, 1975, 1986) and ODP Leg 130, it is possible to make a preliminary interpretation of the seismic record and assign approximate ages to some of the major reflectors. Seven reflectors were chosen for mapping (A through G; Fig. 3), the deepest two representing the recovery, at Site 289, of chert (F) and basaltic basement (G), respectively. By attempting to trace these seismic horizons throughout the Ontong Java Plateau survey data, we hoped to gain some idea of the stratigraphy within the detailed survey areas.

It must be noted that this sort of seismic interpretation is subjective and, considering the complex nature of the Ontong Java Plateau seismic stratigraphy, a time-consuming task. Given

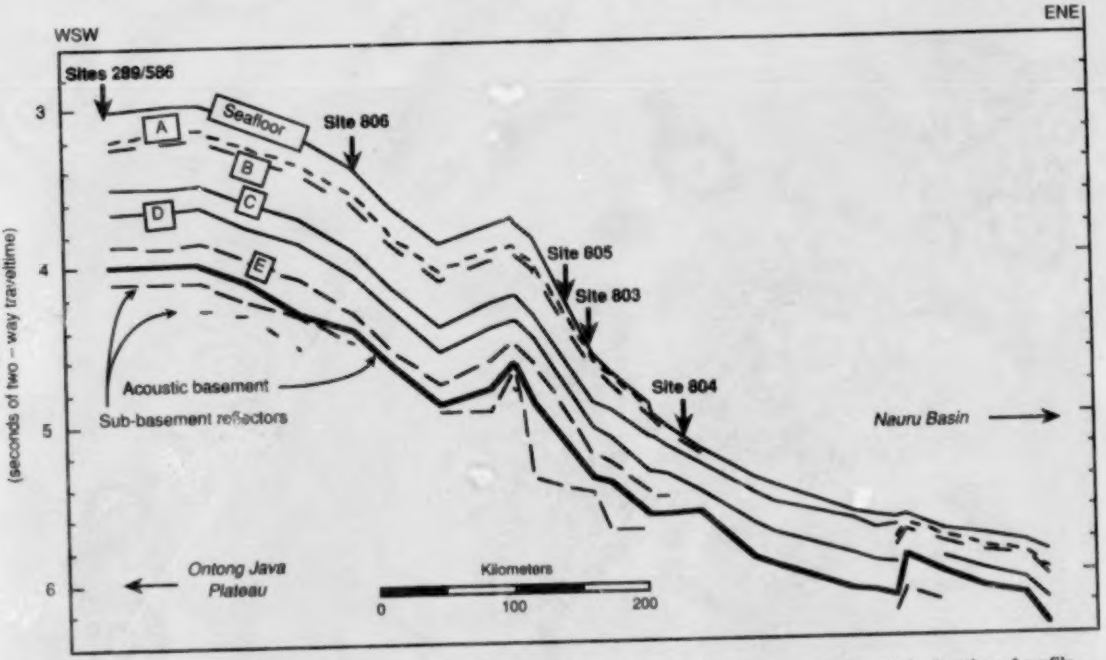

Figure 2. Line interpretation of seismic stratigraphy of the northeastern flank of the Ontong Java Plateau. See Figure 1 for location of profile.

the limited time that we have had to analyze these data, we emphasize the preliminary nature of our interpretations.

Dasher, 2600–2800 mbsl (OJP-1)—Site 806

Using Sites 289/586 (at 2200 m) as an upper plateau reference point, the traverse from Sites 289/586 to the Dasher region is quite straightforward. The "layer-cake" like, seismic stratigraphy of the upper plateau remains virtually constant; individual reflectors can be traced directly along the approximately 139 km between the sites (Figs. 2 and 3). There is virtually no reduction in the thickness of the section between Site 289 and proposed Site OJP-1 except for the deepest part of the section. Bathymetry in the Dasher survey region shows a fairly gentle but steady increase in depth from about 2500 mbsl in the southwest quadrant to 2860 mbsl in the northeast (Fig. 9); a channel-like feature is found in the northern part of the survey area. Areas avoided for site selection in this area consisted mostly of regions of surface erosion (hyperbolic echoes; Figs. 10, 11, and 12). Site OJP-1 (Site 806), in the southwest corner of the survey area, was selected as a primary target because it showed a slightly expanded section and was removed from apparent modern erosion (Fig. 13).

Prancer, 3040–3180 mbsl

The fairly continuous stratigraphy of the upper plateau continues on from Dasher until approximately the 2850-m contour. At this point there is a 150-m drop in the bathymetry (bringing the plateau to depths >3000 m; Fig. 2). Associated with this bathymetric step is a loss of about 0.2 s in the seismic section (Fig. 3). Reflectors are difficult to trace at this point, but it appears that most of the loss is in the upper part of the section (although all of the marker reflectors are still present). Soon after crossing this bathymetric step, the mid-section reverberations (MSRs) discussed earlier were observed. The MSRs continue between the 3000- and 3500-m contours along with extremely rugged surficial topography and much surface erosion. The Prancer region appears to be a small window with no MSR and only minor (though ubiquitous) surface erosion.

The Prancer area is gently sloping to the southeast with a large, deep depression in the northeast section (Fig. 14). Areas avoided in site selection included those that displayed faulting and surface erosion (Figs. 15, 16, and 17). Sites were difficult to select, but OJP-16 (Figs. 16 and 17) was proposed as a first priority site in this region and OJP-17 was suggested as an alternative. The regional seismic correlation (Fig. 3) indicates that the section has thinned by almost 30% between 2600 and 3050 mbsl and that most of the thinning has taken place between about 8 and 20 Ma and in the very deepest part of the section. Because of time constraints, OJP-16 and OJP-17 were not selected as drilling targets.

Vixen, 3100–3300 mbsl (OJP-2)—Site 805

The surface topography in the Vixen area is a bit more complex than that in the other areas (Fig. 18). A zone of rough surficial topography associated with an MSR and possible basement roughness is found in the southeast section of the survey area (Figs. 19, 20, and 21). Targets that were avoided in site selection included the numerous MSRs in the western portion of the survey area, surface erosion in the south (Figs. 21 and 22), and faulting in the northeast (Fig. 21). The seismic section is similar to that found in the Prancer survey area (though of better quality here) with the section appearing to be slightly thinner from 0 to about 8 Ma, and somewhat expanded between 8 and 20 Ma (Fig. 3). The deeper part of the section may also be thicker here than at Prancer. Site OJP-2 (Site 805) is located in the eastern part of the survey area in a region that shows an expanded and complication-free section.

Dancer, 3400–3600 mbsl (OJP-4)—Site 803

The bathymetry in the Dancer area is flat (Fig. 23), with several regions of very rugged topography (northeast and southwest) that appear to be related to basement features (Figs. 24

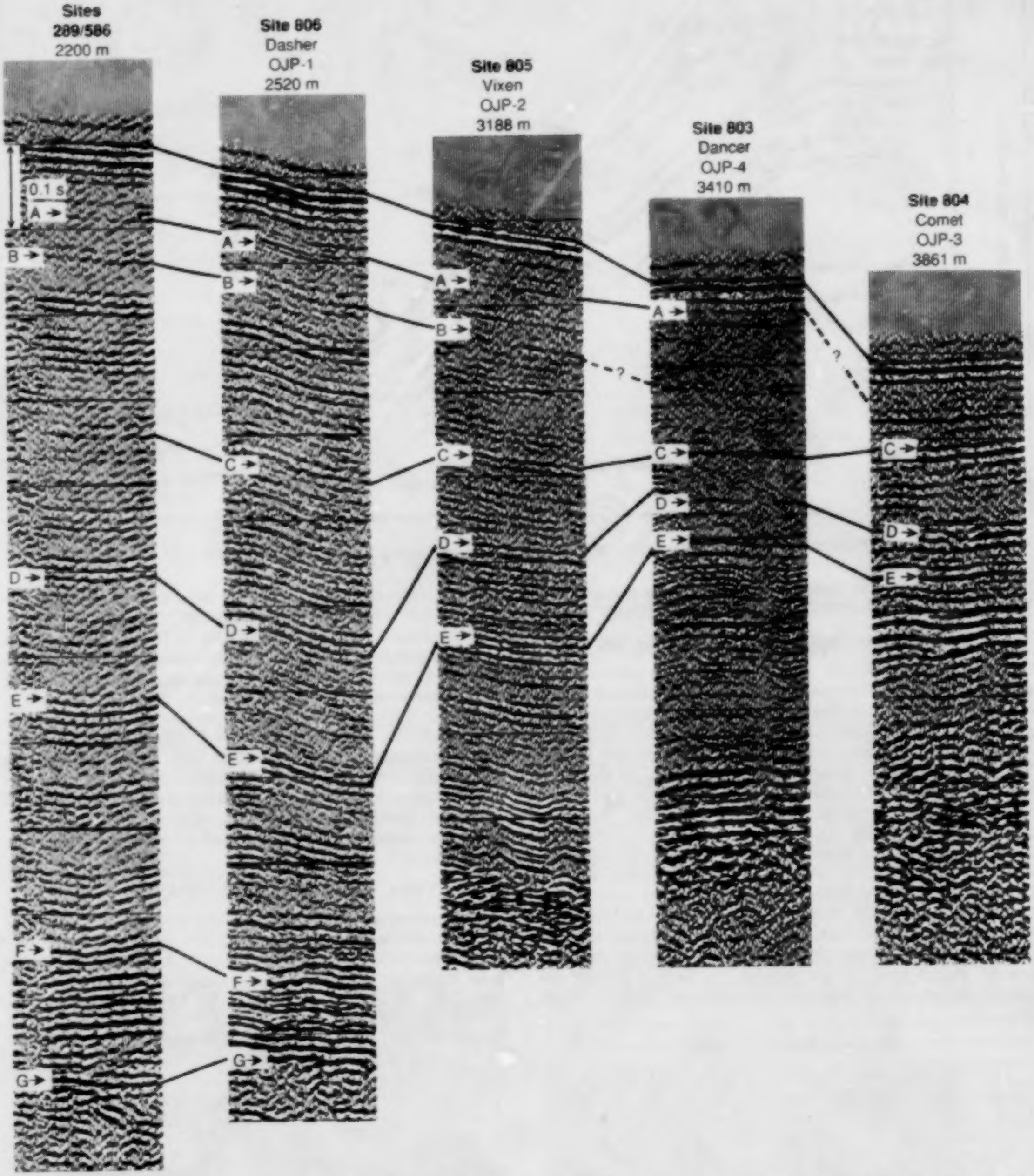

Figure 3. Relationships of seismic sections and marker reflectors down the northeastern edge of the Ontong Java Plateau. Horizontal lines within each section represent 0.1 s (two-way traveltime). Seven major reflectors (A through G) were chosen at this site for correlation throughout the survey area.

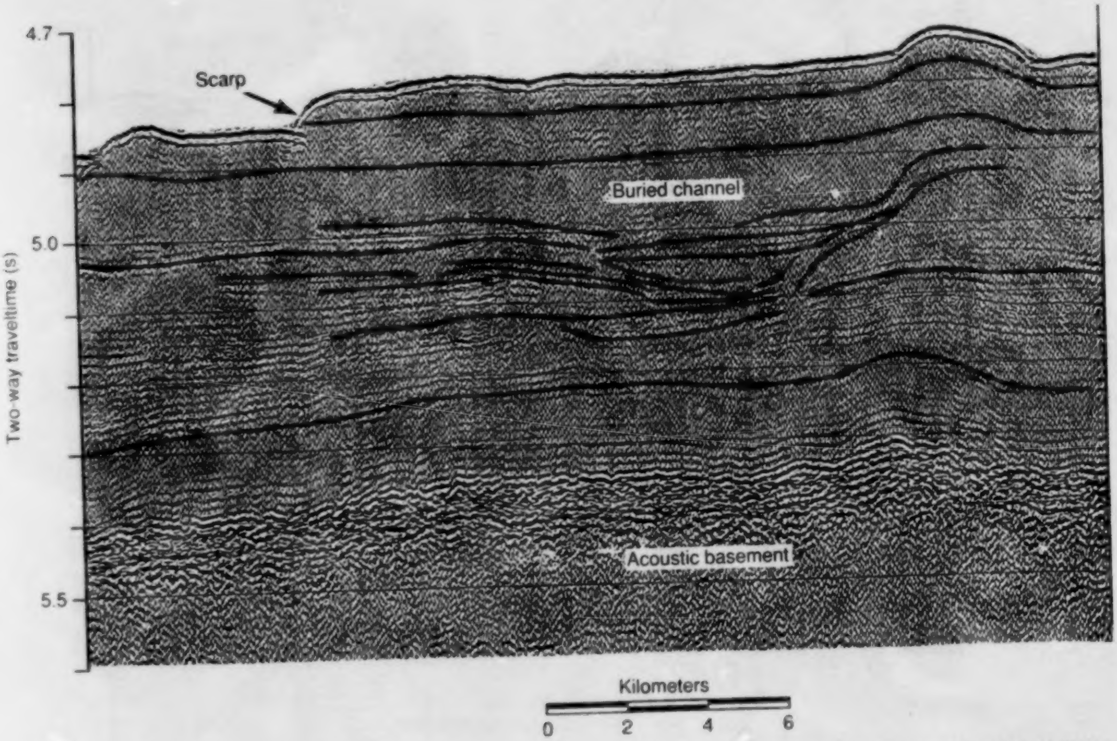

Figure 4. Sample seismic profile with examples of internal structures and surface erosional features that are considered to be undesirable for drill sites.

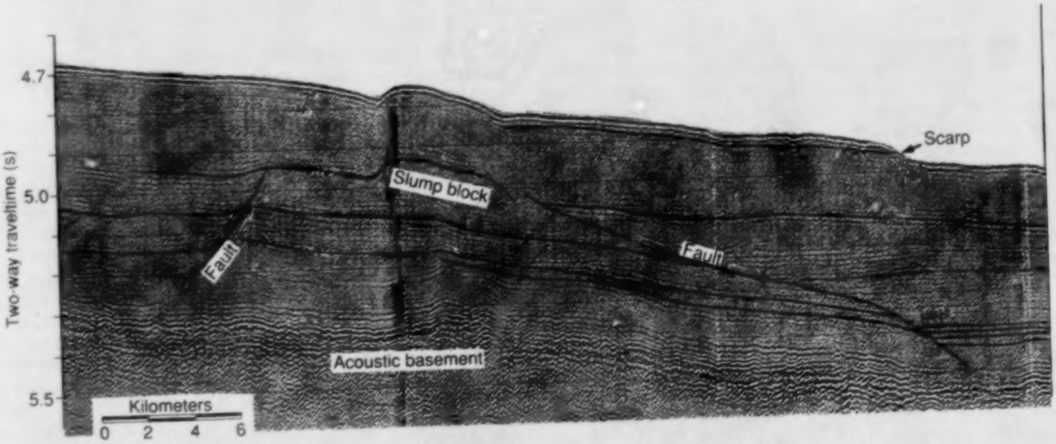

Figure 5. Sample seismic profile with evidence of faulting and slump structures.

and 25). Targets that were avoided in site selection included numerous MSRs (the site is located between two MSRs; Fig. 25), rough basement, and numerous small faults (Fig. 26). These small faults do not appear to disrupt the seismic stratigraphy. At this depth the section is 60% thinner than it was at Sites 289/586 (Figs. 2 and 3). We also can no longer trace, with confidence, the upper two marker reflectors (A and B). That we can no longer pick up these reflectors does not necessarily mean that this part of the section is missing. It may be that the section is compressed to the point that the seismic character is now substantially different. Site CJP-4 (Site 803) is located in the middle of the survey area in a fairly expanded section, close to an MSR.

Comet, 4120–4200 mbsl (OJP-3)

At depths greater than 4000 mbsl, the sediment column on the Ontong Java Plateau thins substantially and evidence for

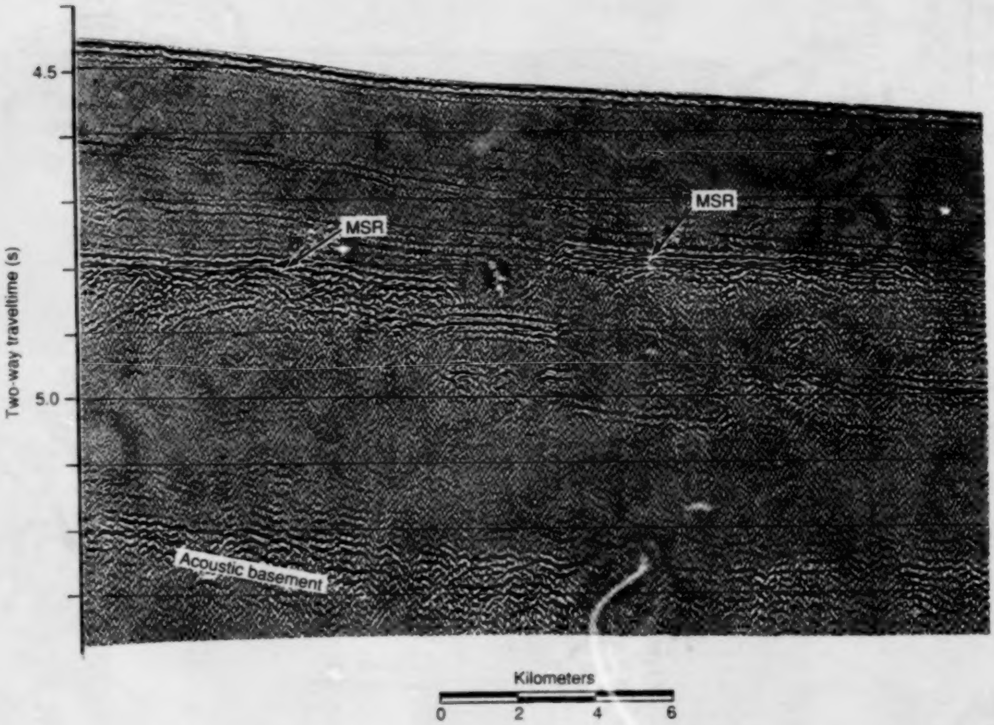

Figure 6. Sample seismic profile with examples of strongly reverberant, mid-section layers (MSRs), which are common between 3000 and 3500 m water depth.

strong erosion is common. In the vicinity of survey area Comet, however, we found, amid a region of extremely complex (and interesting) structures, an almost enclosed basin (graben?) containing a thick sedimentary fill. At first we thought that this fill might represent redeposited material from surrounding highs, but the seismic character of the fill appears to correlate with the section outside of the basin, indicating that the section should be predominantly pelagic. The basin itself is very flat (Fig. 27); rough topography can be found outside of it (to the northeast), associated with the outcrop or near outcrop of basement(?) (Fig. 28). Figure 29 shows the boundaries of the fill. Proposed Site OJP-3 (Figs. 30 and 31) was selected at the point of thickest fill.

The section here is significantly less than half of what it was at 2200 mbsl (Figs. 2 and 3). Most of this thinning appears to take place above Reflector "C," estimated to be about 10 Ma. This is quite consistent with the record of equatorial Pacific carbonate stratigraphy, which shows a major change in the nature of carbonate chemistry in the Pacific at about the middle/late Miocene boundary (Mayer et al., 1985, 1986). In sediments older than the middle/late boundary, carbonate values remain generally high, even in the deep Pacific, but younger sediments typically show major fluctuations in carbonate content.

DISCUSSION

The site survey data from the Ontong Java Plateau reveal a picture of the complex interactions among the processes of pelagic sedimentation, carbonate dissolution, tectonism, and redeposition. Although a detailed understanding of this picture will have to wait on a careful analysis of these data, several preliminary observations can be made.

The top of the northeast quadrant of the Ontong Java Plateau is characterized by a thick (~ 1200 m) sediment cover with numerous, closely spaced, parallel seismic reflectors. Individual reflectors can be correlated easily over large distances with only rare, small vertical displacements observed. Seafloor topography is generally flat, with rugged topography only in those regions where basement shows substantial relief. In general, the acoustic basement (probably chert overlying basalt) shows moderate relief. The parallel reflectors draping over basement topography indicate that this portion of the plateau is dominated by pelagic sedimentation processes. Although a full understanding of the origin of the closely spaced seismic events must await the analysis of drilling results, we can speculate that the reflectors in this portion of the plateau are the result of physical property contrasts caused by subtle changes in grain size (winnowing and dissolution), carbonate content (winnowing and ocean chemistry), and original microfossil assemblages (productivity). As such, they represent a record of paleoceanographic change that, on the top of the plateau, should be fairly continuous for the Neogene (Figs. 2 and 3).

The parallel, "layer-cake" like seismic stratigraphy of the upper plateau continues beyond the slope break between the plateau and the flank (at about 2250 m) to a depth of about 2800 m. At this depth there is a sharp break in the continuity of the reflectors, with reflectors on the downslope side having a hum-

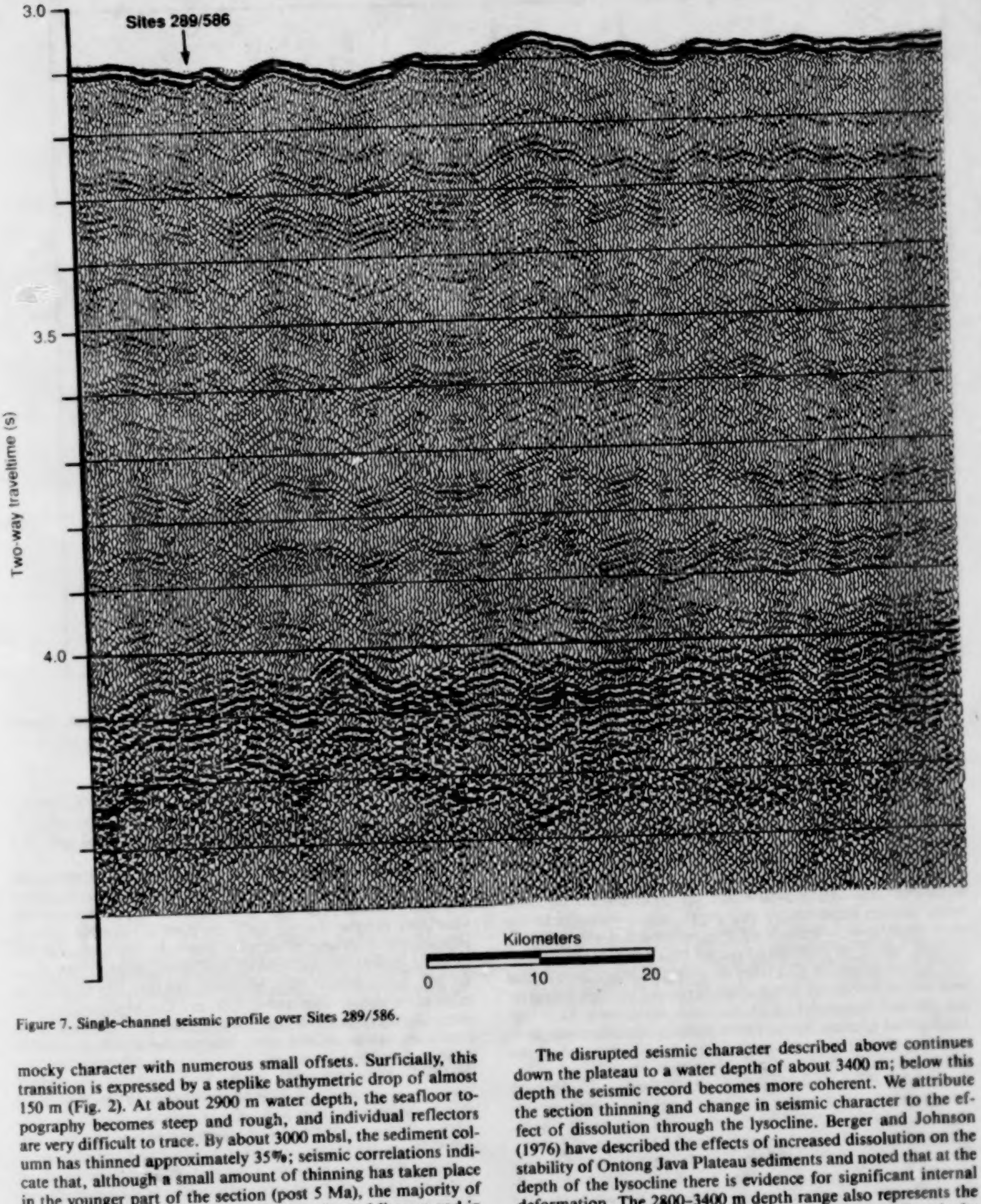

Figure 7. Single-channel seismic profile over Sites 289/586.

mocky character with numerous small offsets. Surficially, this transition is expressed by a steplike bathymetric drop of almost 150 m (Fig. 2). At about 2900 m water depth, the seafloor topography becomes steep and rough, and individual reflectors are very difficult to trace. By about 3000 mbsl, the sediment column has thinned approximately 35%; seismic correlations indicate that, although a small amount of thinning has taken place in the younger part of the section (post 5 Ma), the majority of thinning has taken place in the middle to lower Miocene and in the pre-early Oligocene section (Fig. 3).

The disrupted seismic character described above continues down the plateau to a water depth of about 3400 m; below this depth the seismic record becomes more coherent. We attribute the section thinning and change in seismic character to the effect of dissolution through the lysocline. Berger and Johnson (1976) have described the effects of increased dissolution on the stability of Ontong Java Plateau sediments and noted that at the depth of the lysocline there is evidence for significant internal deformation. The 2800–3400 m depth range also represents the depth interval over which the vertical dissolution gradient is the

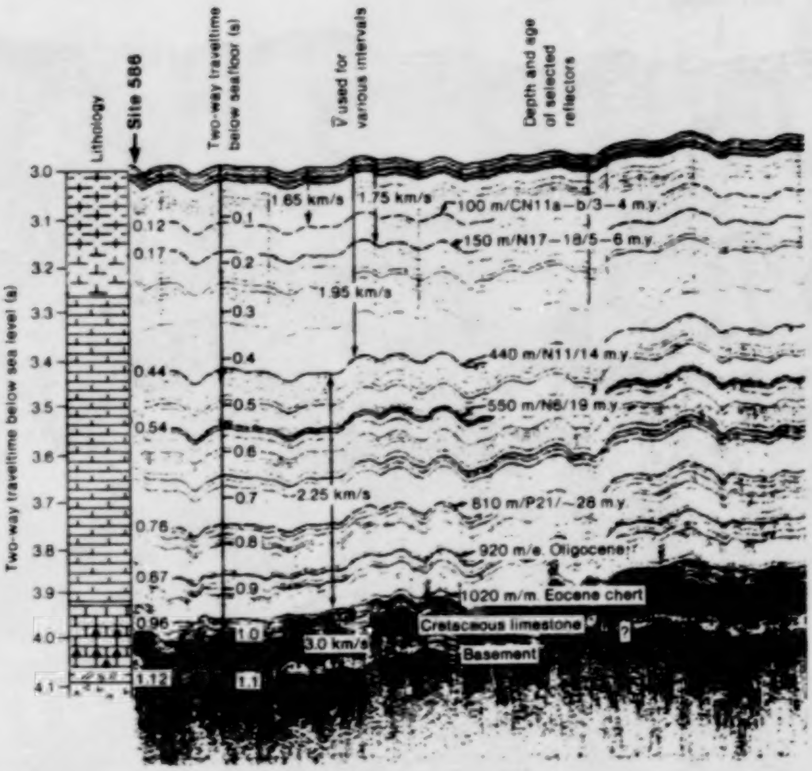
Lithology
Site 586
Two-way traveltime below seafloor (s)
V̄ used for various intervals
Depth and age of selected reflectors
Two-way traveltime below sea level (s)
3.0
3.1
3.2
3.3
3.4
3.5
3.6
3.7
3.8
3.9
4.0
4.1
0.12
0.17
0.44
0.54
0.76
0.87
0.96
1.12
0.1
0.2
0.3
0.4
0.5
0.6
0.7
0.8
0.9
1.0
1.1
1.65 km/s
1.75 km/s
1.95 km/s
2.25 km/s
3.0 km/s
100 m/CN11a–b/3–4 m.y.
150 m/N17–18/5–6 m.y.
440 m/N11/14 m.y.
550 m/N6/19 m.y.
610 m/P21/~26 m.y.
920 m/e. Oligocene
1020 m/m. Eocene chert
Cretaceous limestone
Basement
?

Figure 8. Interpretation of seismic profile over Sites 289/586 based on the drilling results of Leg 89 (Moberly, Schlanger, et al., 1986). Based on Leg 130 seismic stratigraphy, the ages of the 0.42- and 0.54-sbsf events have been reinterpreted to be ca. 11 and 16 Ma, respectively.

steepest. Thus, changes in the depth of the lysocline over time would tend to result in significant vertical changes in the state of preservation of the accumulating sediment. The superposition of sediments with significantly different states of preservation may contribute to the instability of the sediments in this depth range.

Deeper than about 3400 mbsl, the sediment section once again changes character. At this depth range, we begin to see more evidence of tectonic disruption of the sedimentary section (faults), as well as evidence of buried channels (Figs. 4 and 5). The reflection profile also takes on a characteristic appearance with several horizontal low-amplitude zones (relatively transparent sections) bounded by high-amplitude reflections. The most pronounced of these zones occurs in the lower Oligocene sediments. Also at this depth range is the first occurrence of the MSRs, the high-amplitude reflections that typically occur between 0.2 and 0.5 s below seafloor (sbsf). Features of this type have been observed before and have been interpreted as sills (Kroenke, 1972), lithified carbonates, and diagenetic "hardgrounds" associated with erosive events (Shipley et al., 1985). The restriction of the MSRs to certain stratigraphic intervals and depth ranges implies that they may be associated with periods of increased tectonic activity related to the subduction of the southwest portion of the plateau. The grabenlike features that are found at the base of the plateau (see discussion of OJP-3) and are restricted to between 3800 and 4200 mbsl may be a flexural response to this subduction.

The preliminary interpretation of the seismic stratigraphy on the Ontong Java Plateau indicates that the sedimentary section has thinned from ~1200 m on the crest to about 450 m at the base (4300 m water depth). Although there is a general decrease in sediment thickness at all time intervals, the nature of the thinning varies with time interval and depth range. In the younger part of the section (post Miocene), the majority of thinning takes place deeper than about 3500 m. The Miocene and pre-early Oligocene sections, on the other hand, begin to thin at depths as shallow as 2800 mbsl, whereas the middle to late Oligocene section remains remarkably constant in thickness throughout the entire depth range of the plateau. Even these rough correlations present a picture of the history of the equatorial dissolution surfaces that is consistent with the carbonate-compensation depth (CCD) history presented by van Andel et al. (1975). From the results of drilling, logging, and seismic modeling, we hope to put together a detailed picture of the temporal and spatial history of carbonate dissolution in the western equatorial Pacific.

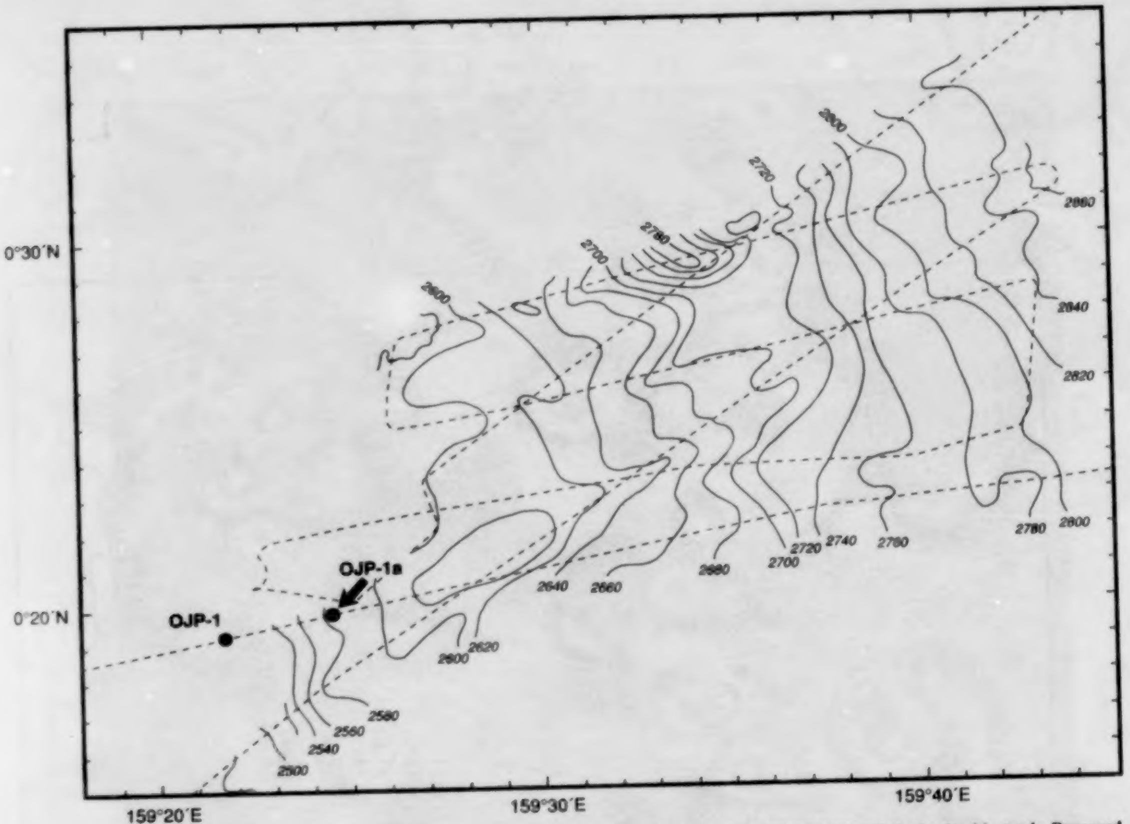

Figure 9. SeaBeam bathymetry in the Dasher survey area. Contour interval is 20 m. Dashed line is ROUNDABOUT Cruise 11 ship track. Proposed Sites OJP-1 and 1a are shown.

REFERENCES

Berger, W. H., and Johnson, T. C., 1976. Deep-sea carbonates: dissolution and mass wasting on Ontong Java Plateau. *Science*, 192:785–787.

Berger, W. H., and Mayer, L. A., 1978. Deep-sea carbonates: acoustic reflectors and lysocline fluctuations. *Geology*, 6:11–15.

Kroenke, L., 1972. Geology of the Ontong Java Plateau [Ph.D. dissert.]. Univ. of Hawaii, HIG-72-5.

Mayer, L. A., Shipley, T. H., Theyer, F., Wilkens, R. H., and Winterer, E. L., 1985. Seismic modeling and paleoceanography at Deep Sea Drilling Project Site 574. *In* Mayer, L. A., Theyer, F., Thomas, E., et al., *Init. Repts. DSDP*, 85: Washington, (U.S. Govt. Printing Office), 947–970.

Mayer, L. A., Shipley, T. H., and Winterer, E. L., 1986. Equatorial Pacific seismic reflectors as indicators of global oceanographic events. *Science*, 233:761–764.

Moberly, R., Schlanger, S. O., et al., 1986. *Init. Repts. DSDP*, 89: Washington (U.S. Govt. Printing Office).

Renard, V., and Allenou, J. P., 1979. SeaBeam multi-beam echo sounding in "Jean Charcot" description, evaluation and first results. *Int. Hydrogr. Rev.*, 56:35–67.

Shipboard Scientific Party, 1975. Site 289. *In* Andrews, J. E., Packham, G., et al., *Init. Repts. DSDP*, 30: Washington (U.S. Govt. Printing Office), 231–398.

Shipboard Scientific Party, 1986. Site 586. *In* Moberly, R., Schlanger, S. O., et al., *Init. Repts. DSDP*, 89: Washington (U.S. Govt. Printing Office), 213–281.

Shipley, T. H., Winterer, E. L., Goud, M., Hills, S. J., Metzler, C. V., Paull, C. K., and Shay, J. T., 1985. SeaBeam bathymetric and water-gun seismic reflection surveys in the equatorial pacific. *In* Mayer, L. A., Theyer, F., Thomas, E., *Init. Repts. DSDP*, 85: Washington (U.S. Govt. Printing Office), 825–835.

van Andel, T. H., Heath, G. R., and Moore, T. C., Jr., 1975. Cenozoic history and paleoceanography of the central equatorial Pacific. *Mem. Geol. Soc. Am.*, 143:1–134.

Ms 130A-103

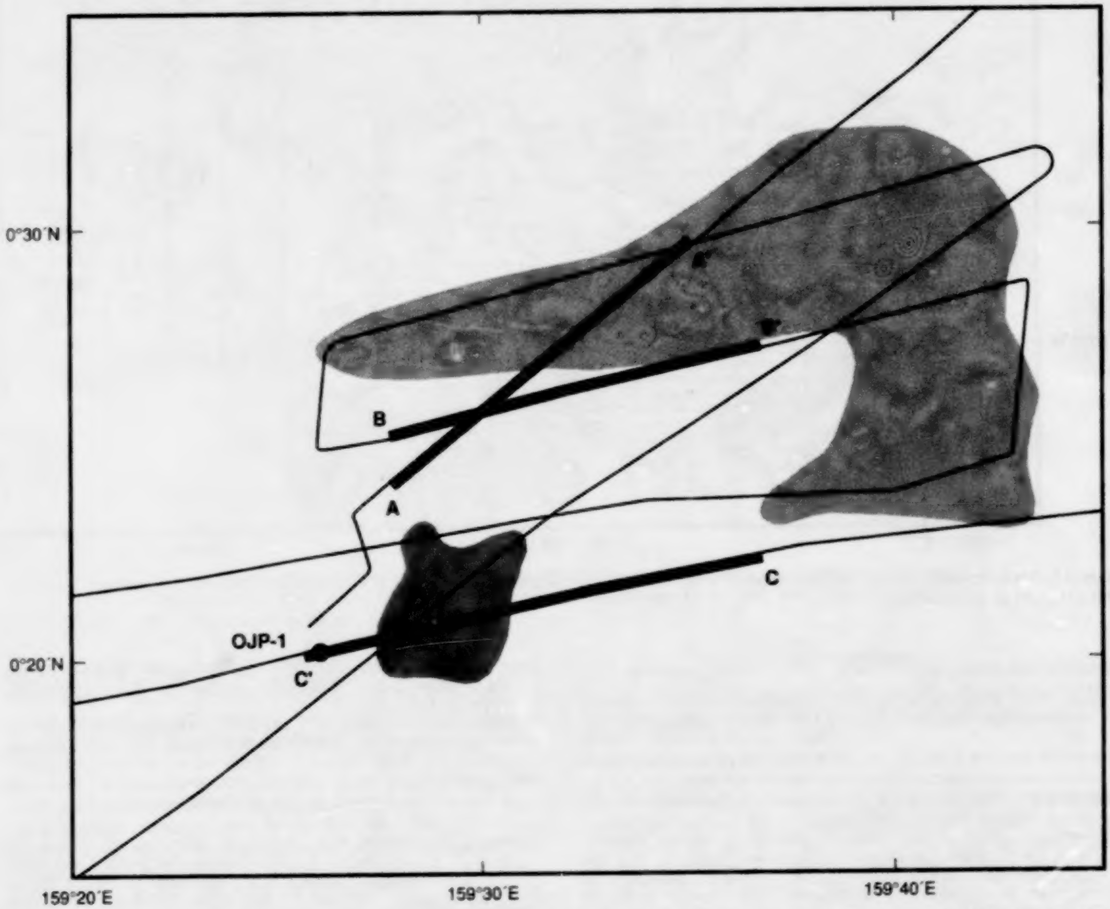
0°30´N
0°20´N
159°20´E
159°30´E
159°40´E
A
B
C
C'
OJP-1

Figure 10. Drilling "avoidance" map of the Dasher survey area based on seismic reflection profiles. Stippled areas were avoided for site selection.

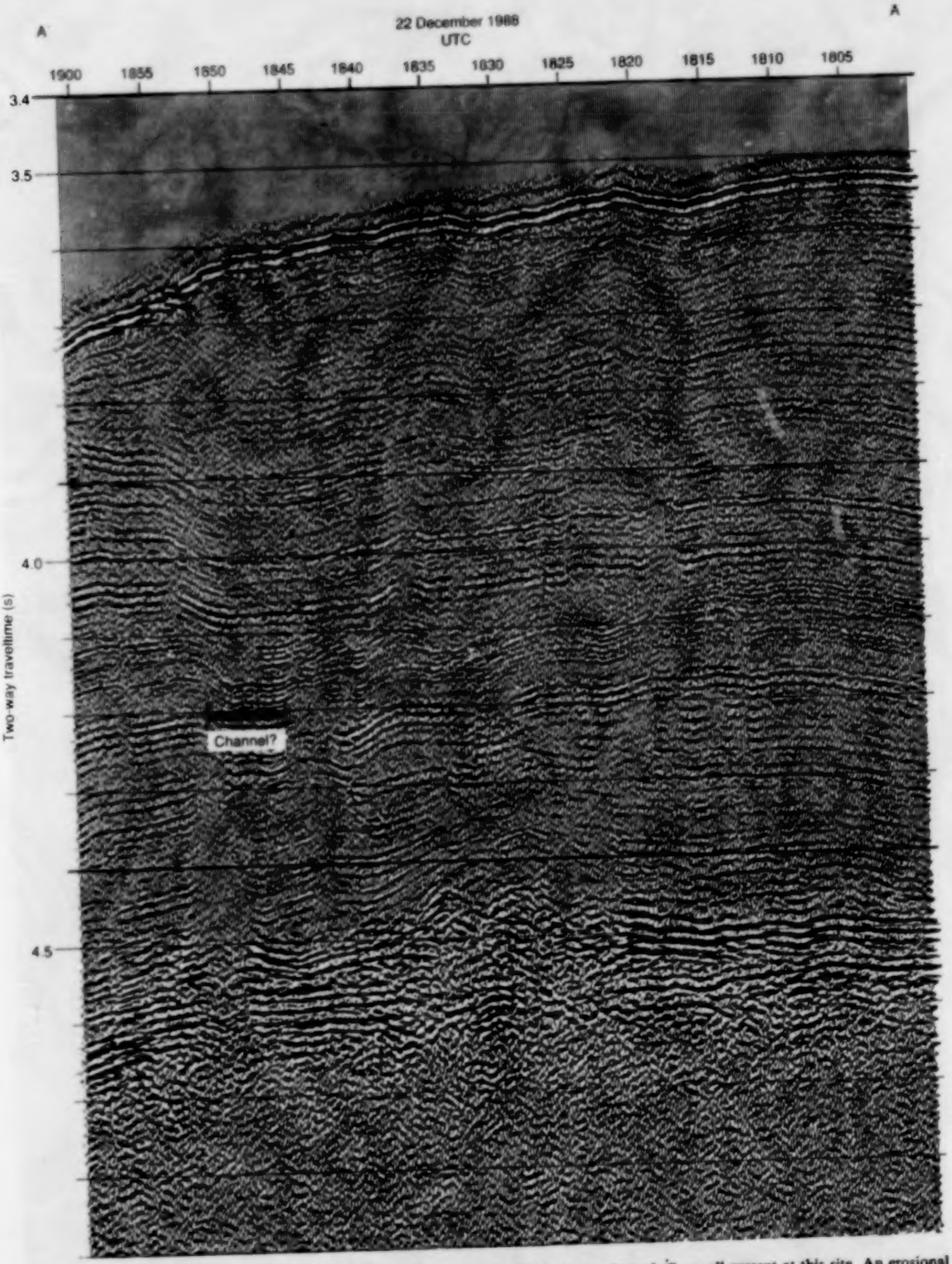

Figure 11. Single-channel seismic profile A-A′ in the Dasher survey area. Reflectors A through G are all present at this site. An erosional channel is visible at the left of the figure. See Figure 10 for location of line.

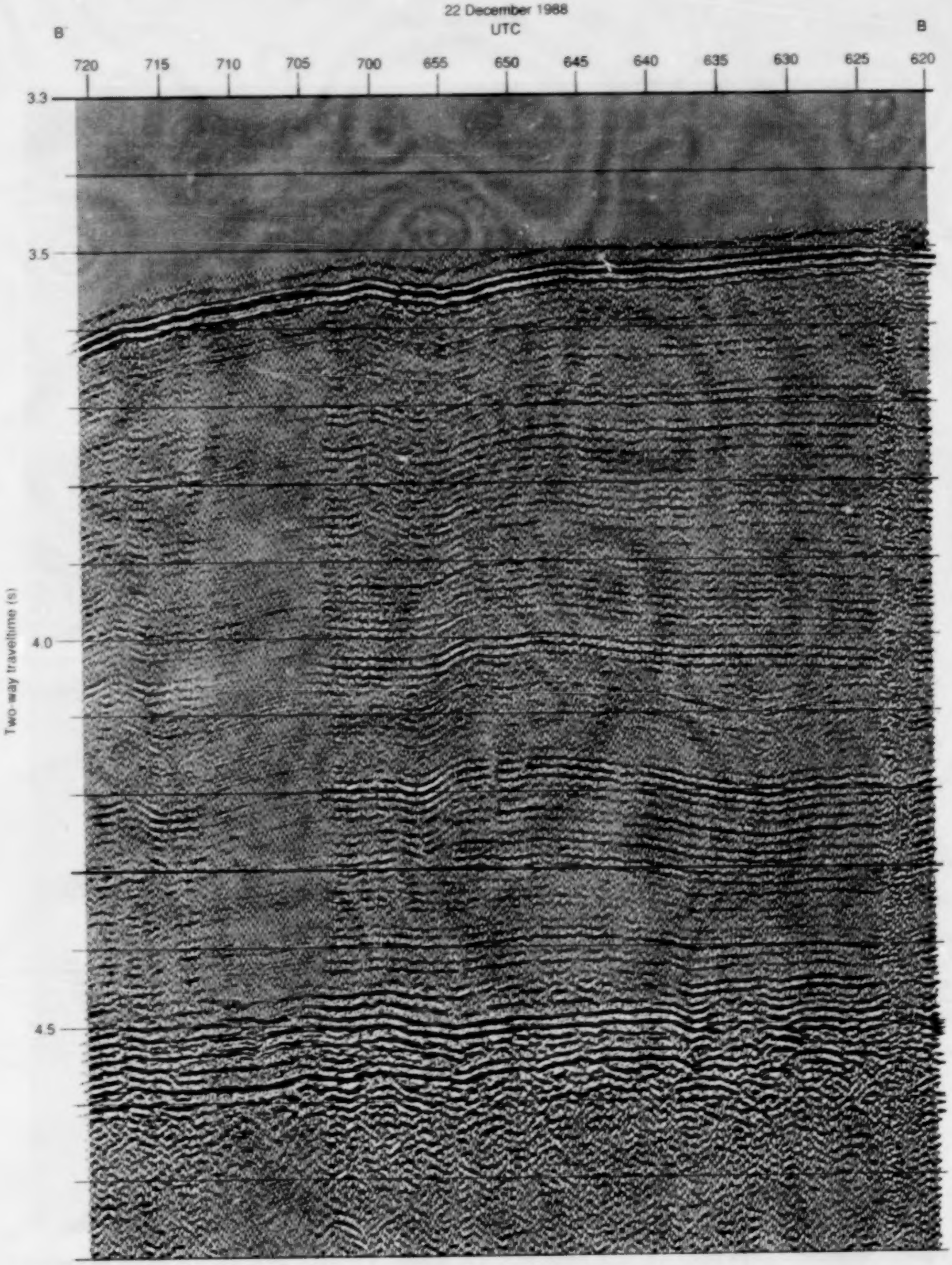

Figure 12. Single-channel seismic profile B-B′ in the Dasher survey area. See Figure 10 for location of line.

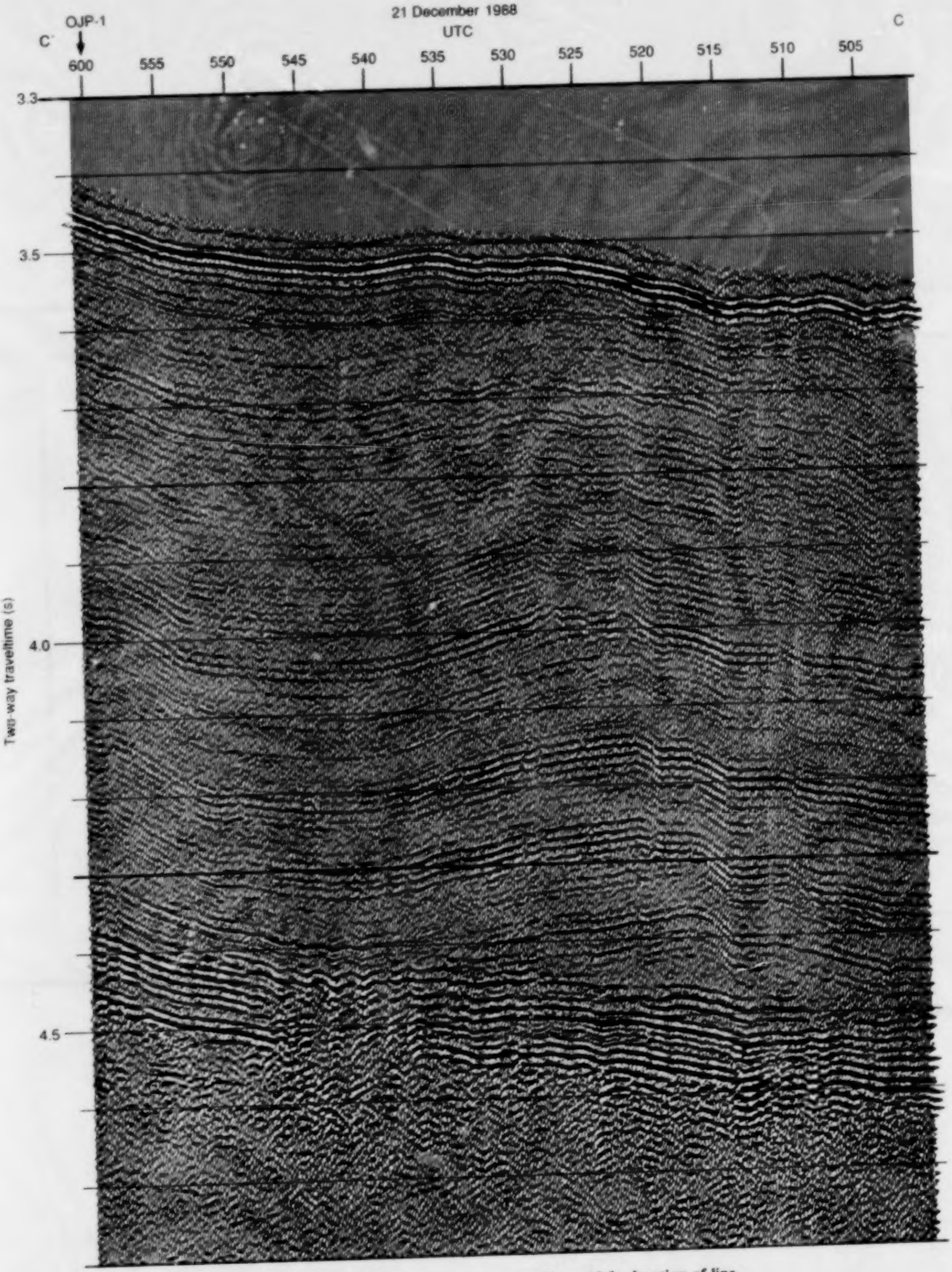

Figure 13. Single-channel seismic profile C-C′ in the Dasher survey area. See Figure 10 for location of line.

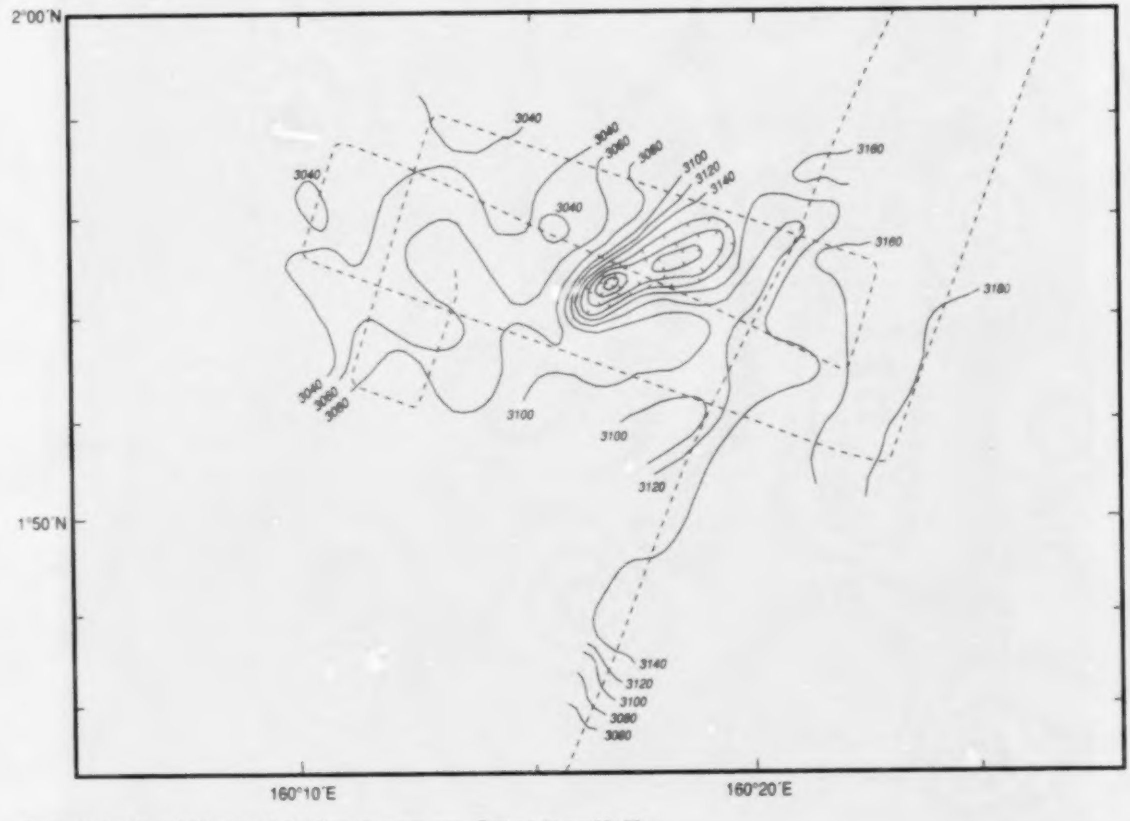
2°00'N
1°50'N
160°10'E
160°20'E
3040
3040
3060
3080
3040
3040
3100
3120
3140
3160
3160
3180
3040
3060
3080
3100
3100
3120
3140
3120
3100
3080
3060

Figure 14. SeaBeam bathymetry in the Prancer survey area. Contour interval is 20 m.

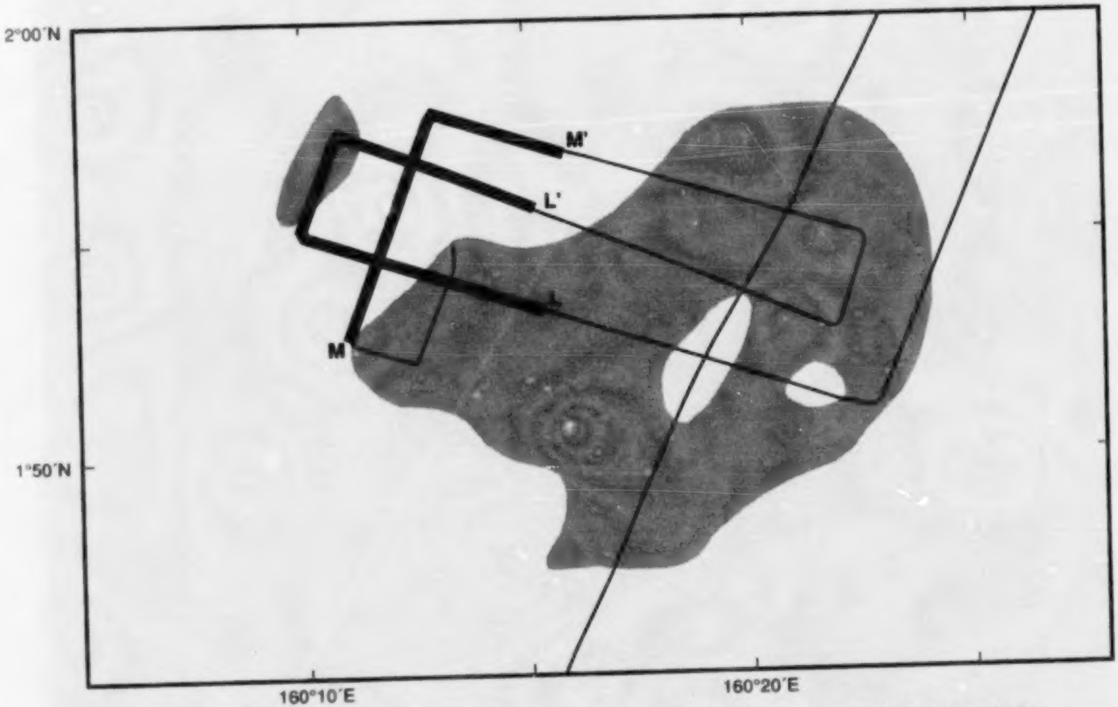
2°00´N
1°50´N
160°10´E
160°20´E
M'
L'
L
M

Figure 15. Drilling "avoidance" map of the Prancer survey area based on seismic profiles. Stippled areas were avoided for site selection.

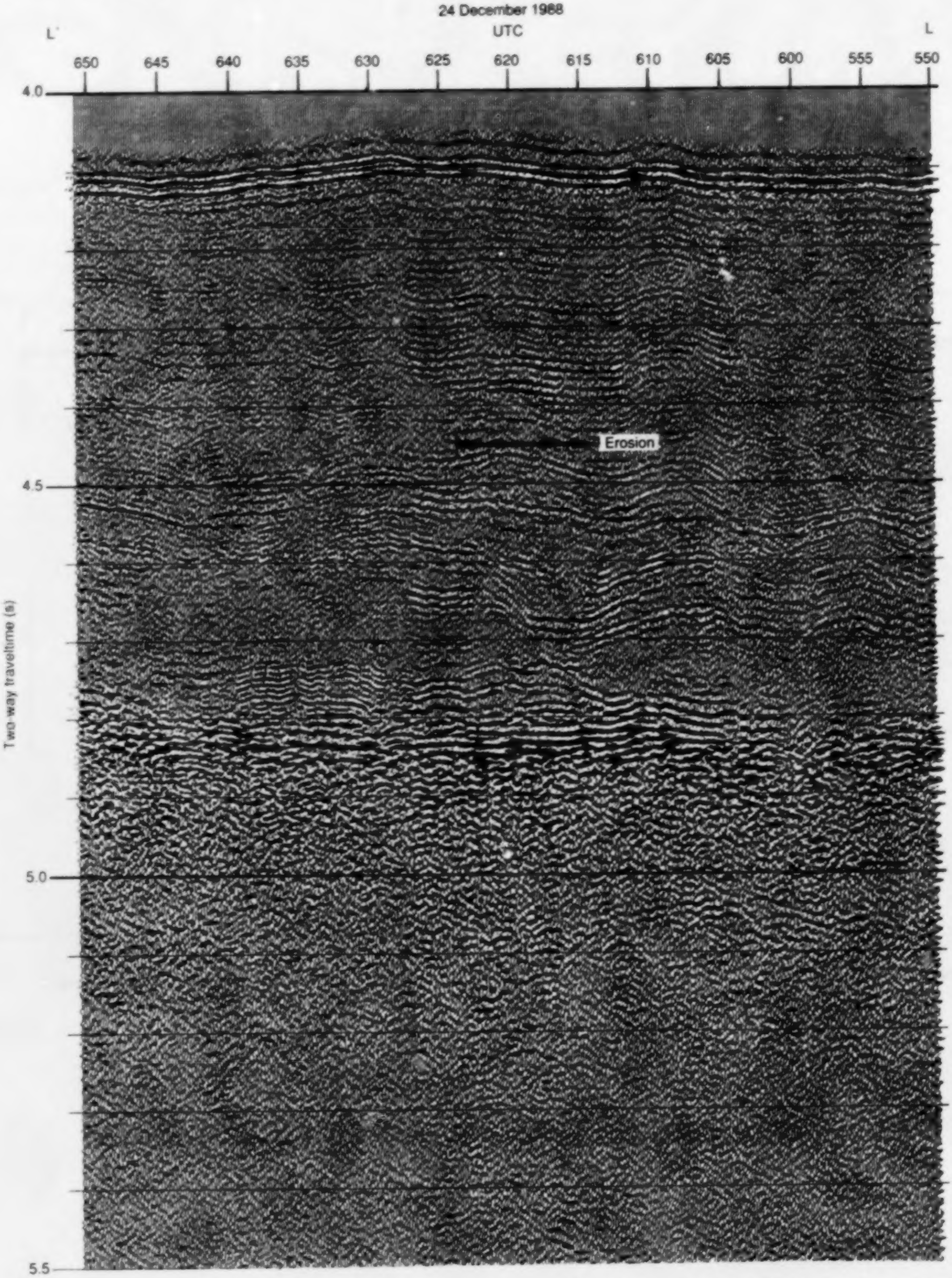

Figure 16. Single-channel seismic profile L-L' in the Prancer survey area. A possible buried channel structure is visible near the center of the figure. See Figure 15 for location of line.

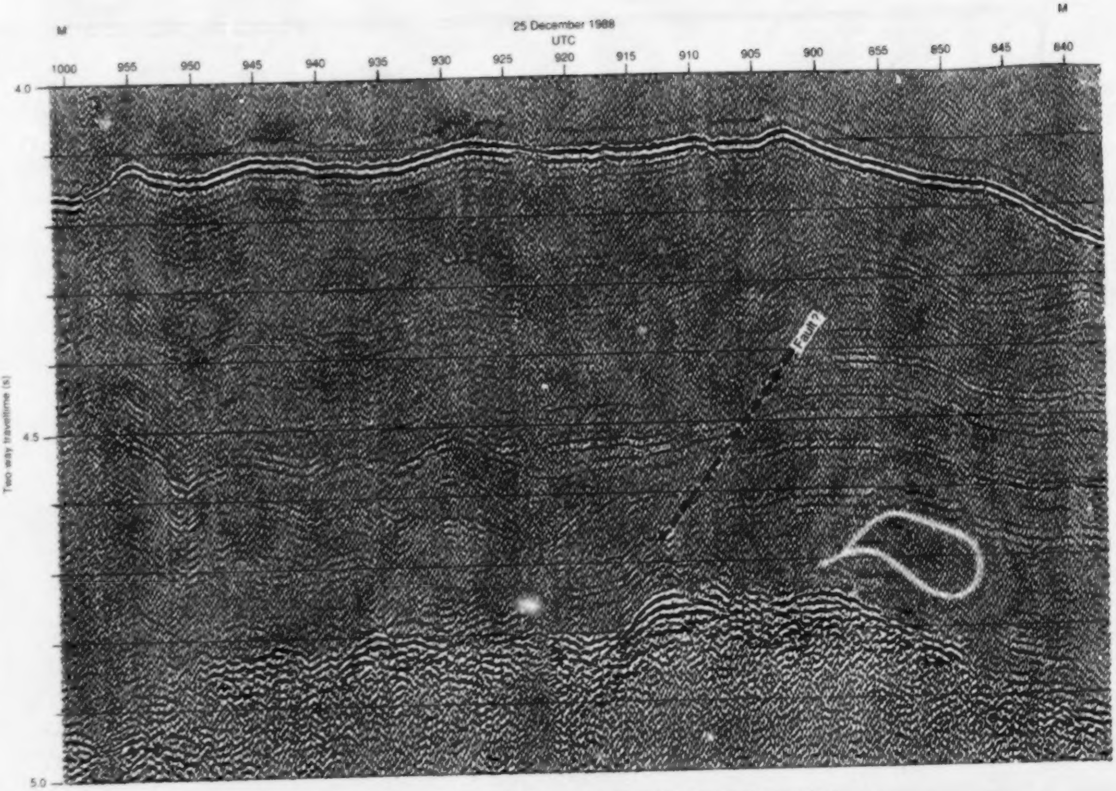

Figure 17. Single-channel seismic profile M-M′ in the Prancer survey area. See Figure 15 for location of line.

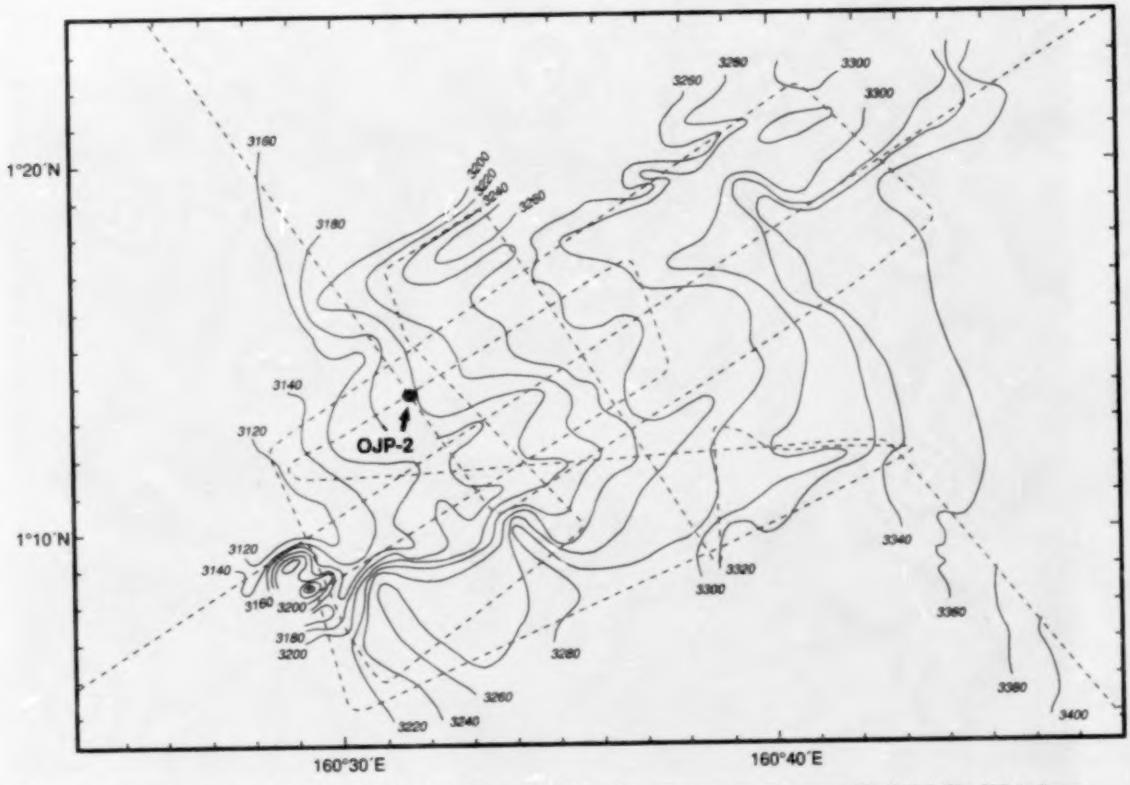
3260
3280
3300
3300
3160
1°20'N
3200
3220
3240
3260
3180
3140
3120
OJP-2
1°10'N
3120
3140
3160
3200
3180
3200
3340
3320
3300
3360
3280
3260
3380
3400
3220
3240
160°30'E
160°40'E

Figure 18. SeaBeam bathymetry of the Vixen survey area. Contour interval is 20 m. The location of proposed Site OJP-2 (Site 805) is shown.

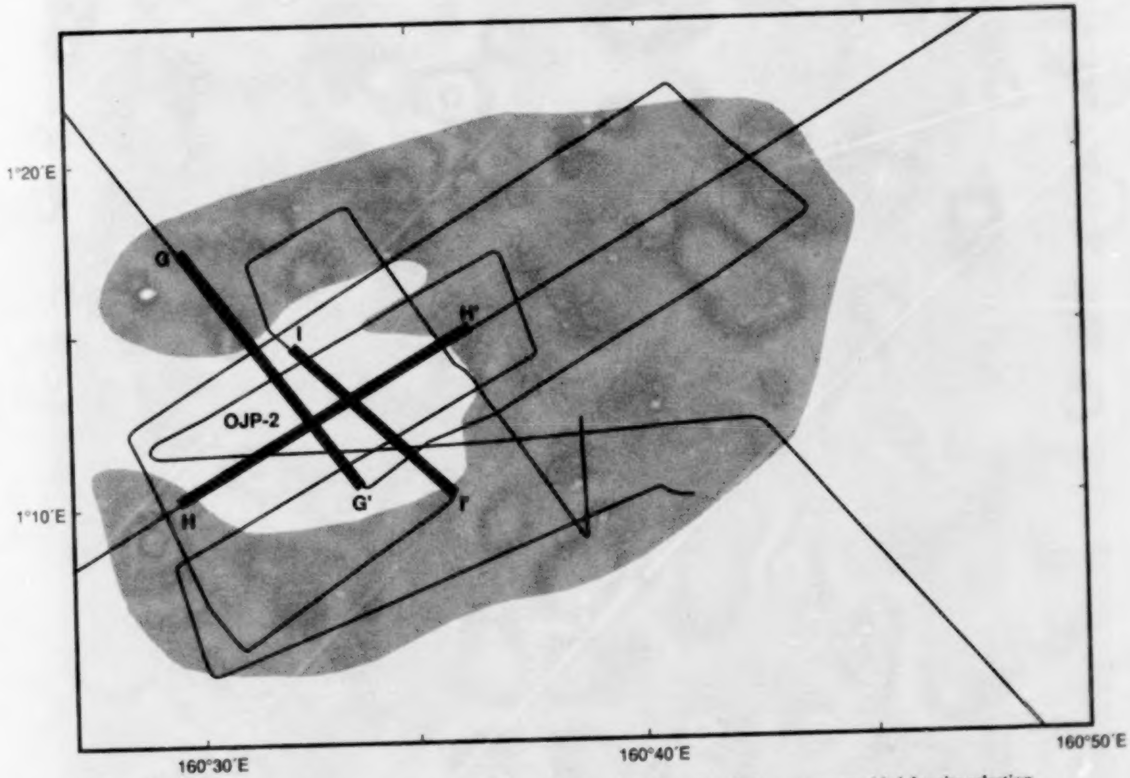
G
H'
I
OJP-2
H
G'
I'
1°20'E
1°10'E
160°30'E
160°40'E
160°50'E

Figure 19. Drilling "avoidance" map of the Vixen survey area based on seismic profiles. Stippled areas were avoided for site selection.

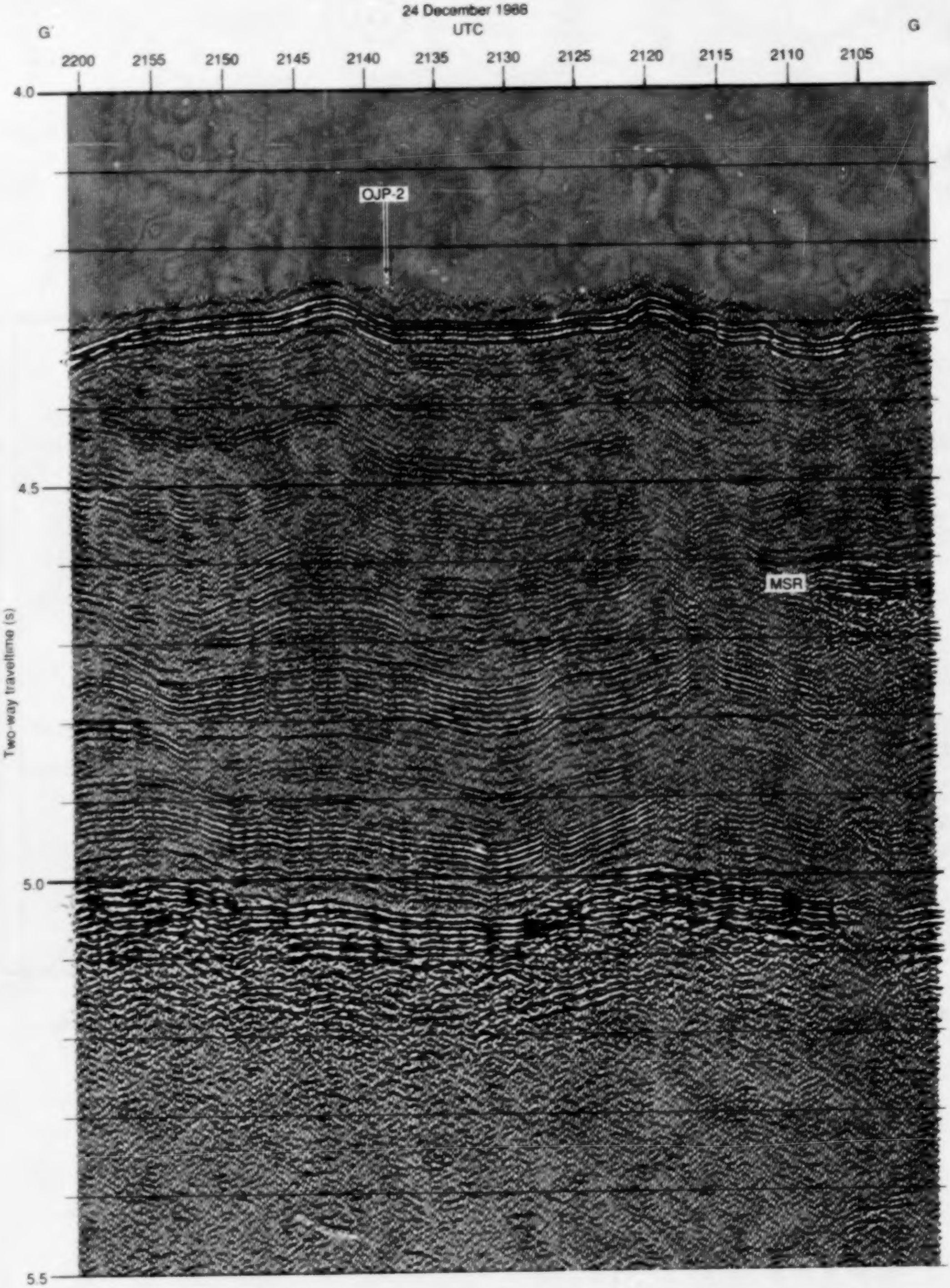

Figure 20. Single-channel seismic profile G-G′ in the Vixen survey area. An MSR is visible on the right side of the figure. See Figure 19 for location of line.

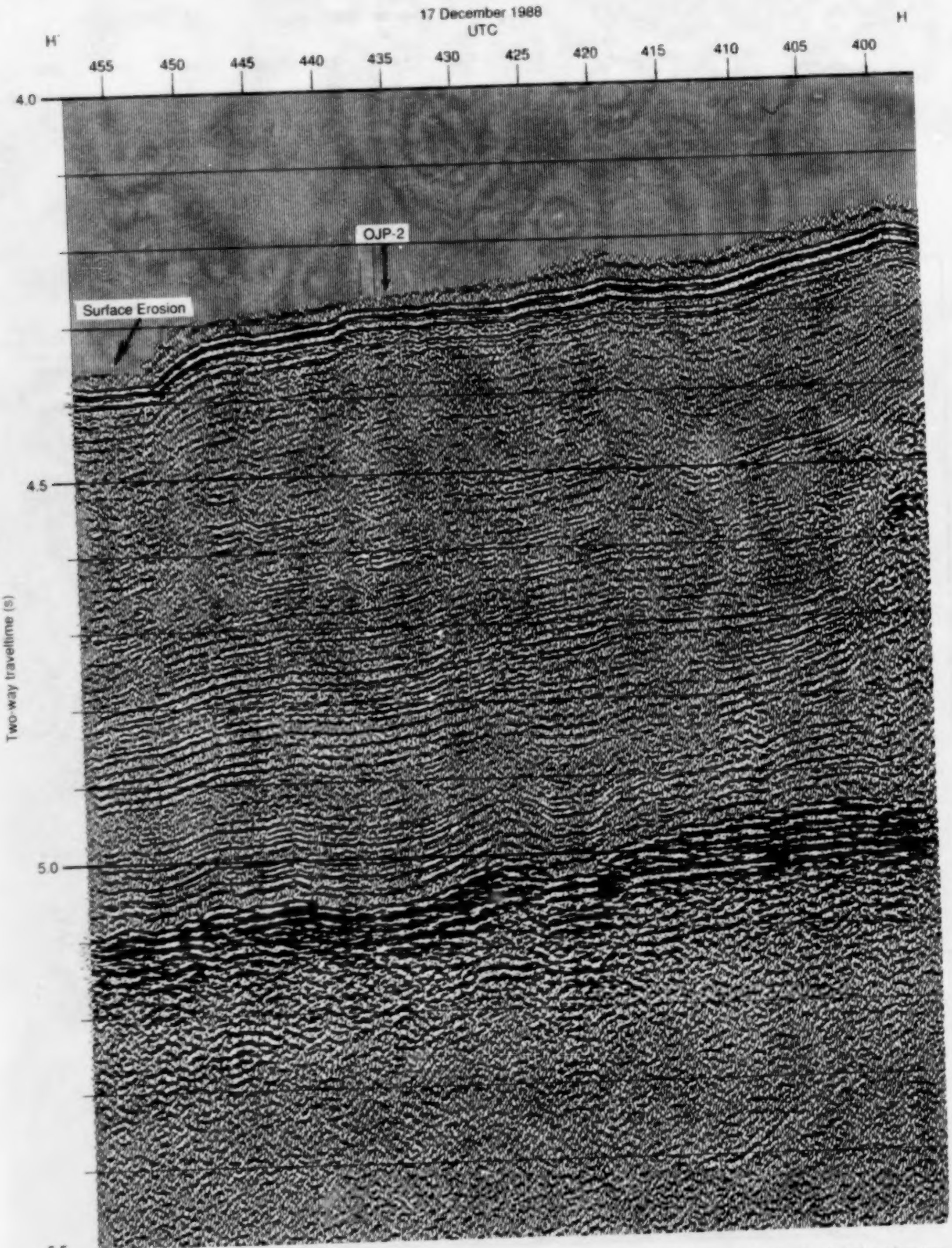

Figure 21. Single-channel seismic profile H-H′ in the Vixen survey area. The MSR on the right side of the figure is associated with surface erosional features. See Figure 19 for location of line.

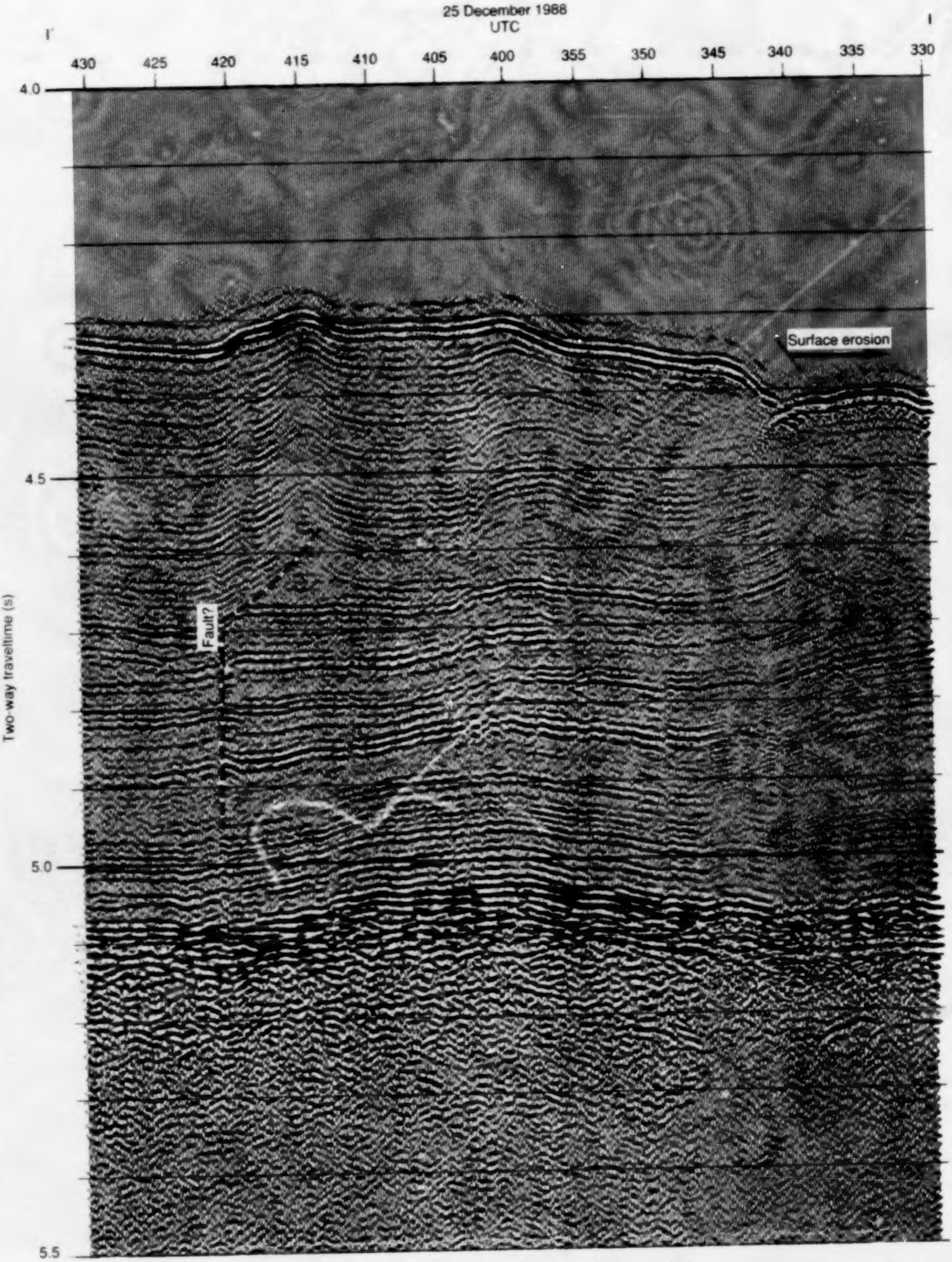

Figure 22. Single-channel seismic profile I-I' in the Vixen survey area. See Figure 19 for location of line.

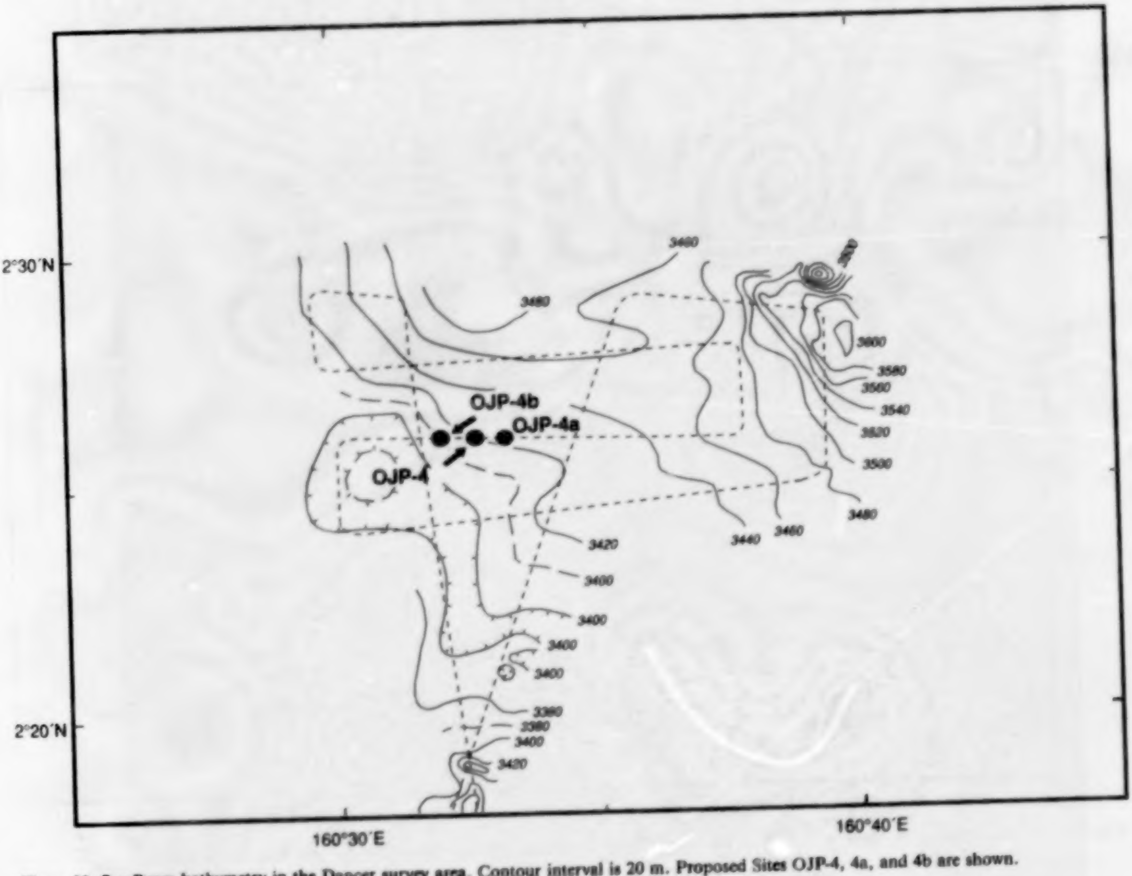
2°30'N
2°20'N
160°30'E
160°40'E
OJP-4b
OJP-4a
OJP-4
3460
3480
3600
3580
3560
3540
3520
3500
3480
3440
3460
3420
3400
3400
3400
3400
3380
3380
3400
3420

Figure 23. Sea Beam bathymetry in the Dancer survey area, Contour interval is 20 m. Proposed Sites OJP-4, 4a, and 4b are shown.

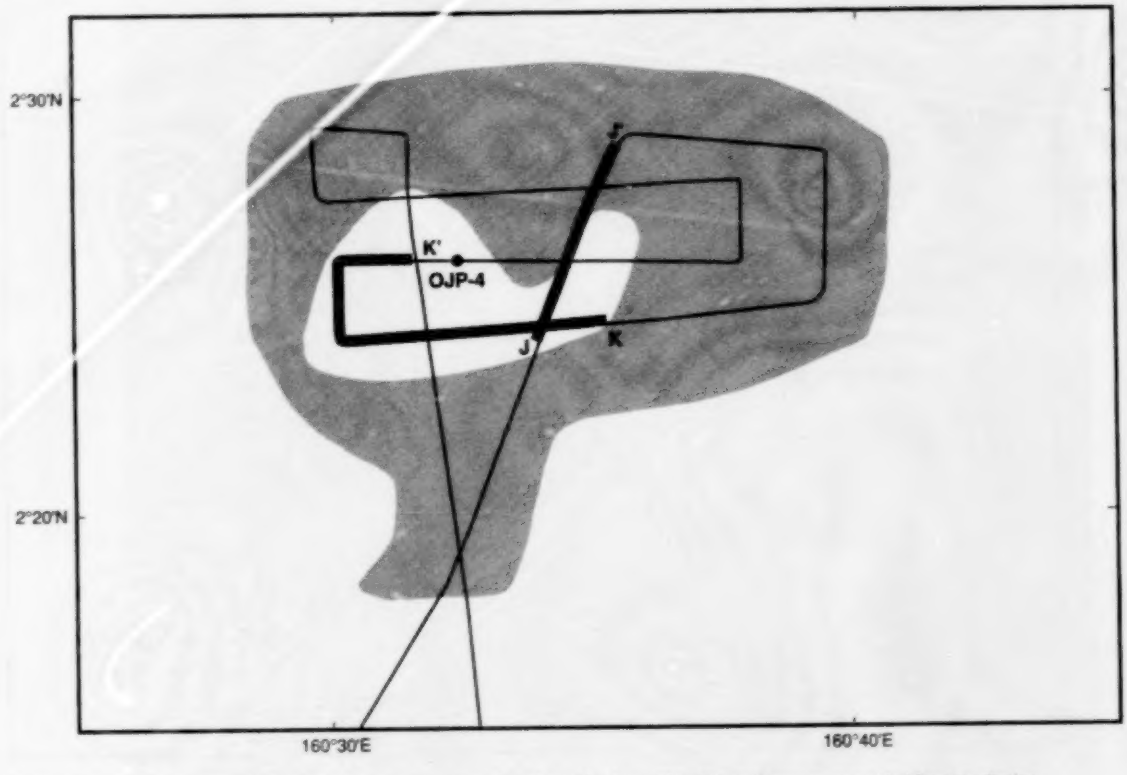
2°30'N
2°20'N
160°30'E
160°40'E
J'
K'
OJP-4
J
K

Figure 24. Drilling "avoidance" map of the Dancer survey area based on seismic profiles. Stippled areas were avoided for site selection.

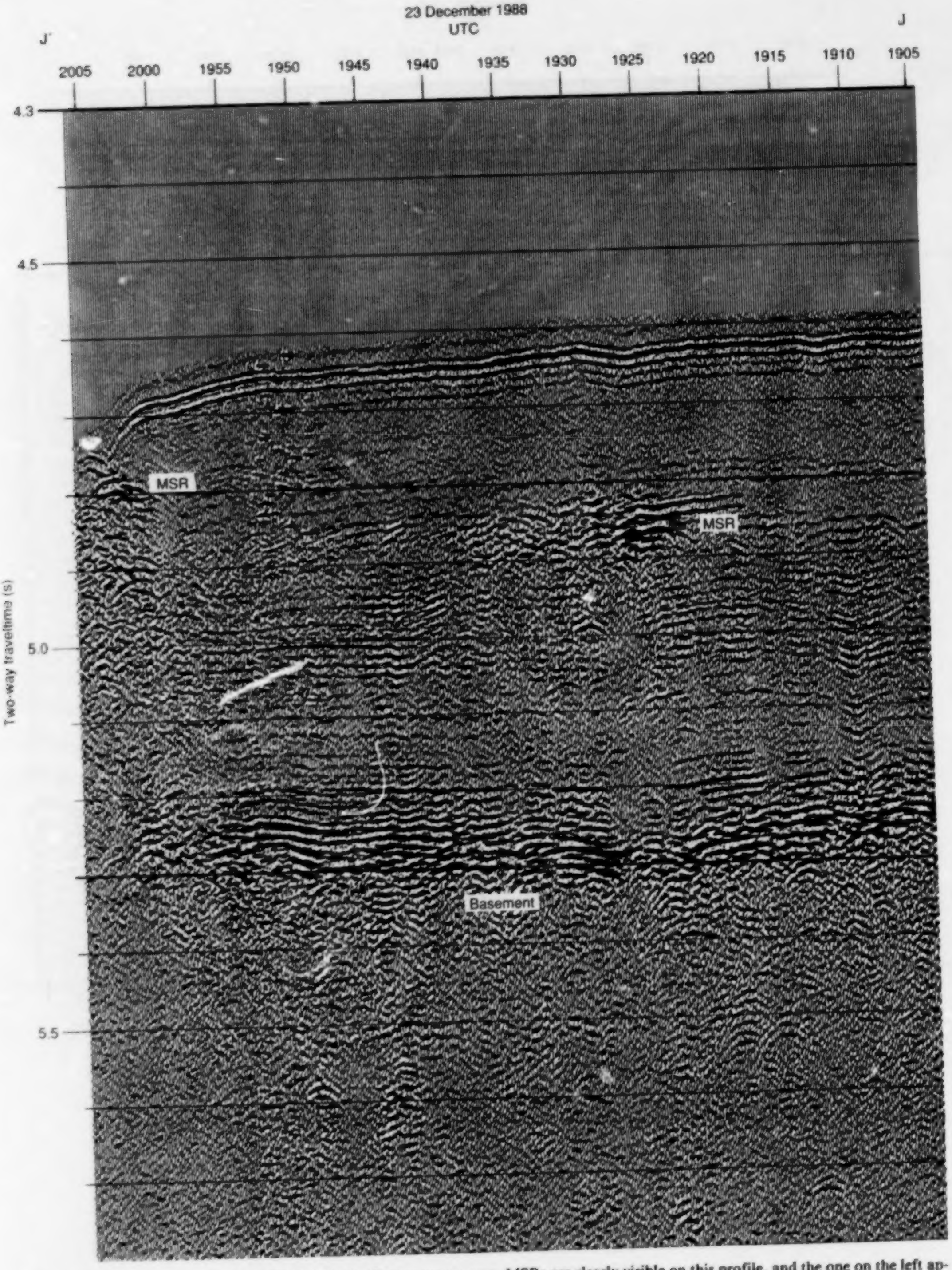

Figure 25. Single-channel seismic profile J-J′ in the Dancer survey area. MSRs are clearly visible on this profile, and the one on the left appears to outcrop at the surface. See Figure 24 for location of line.

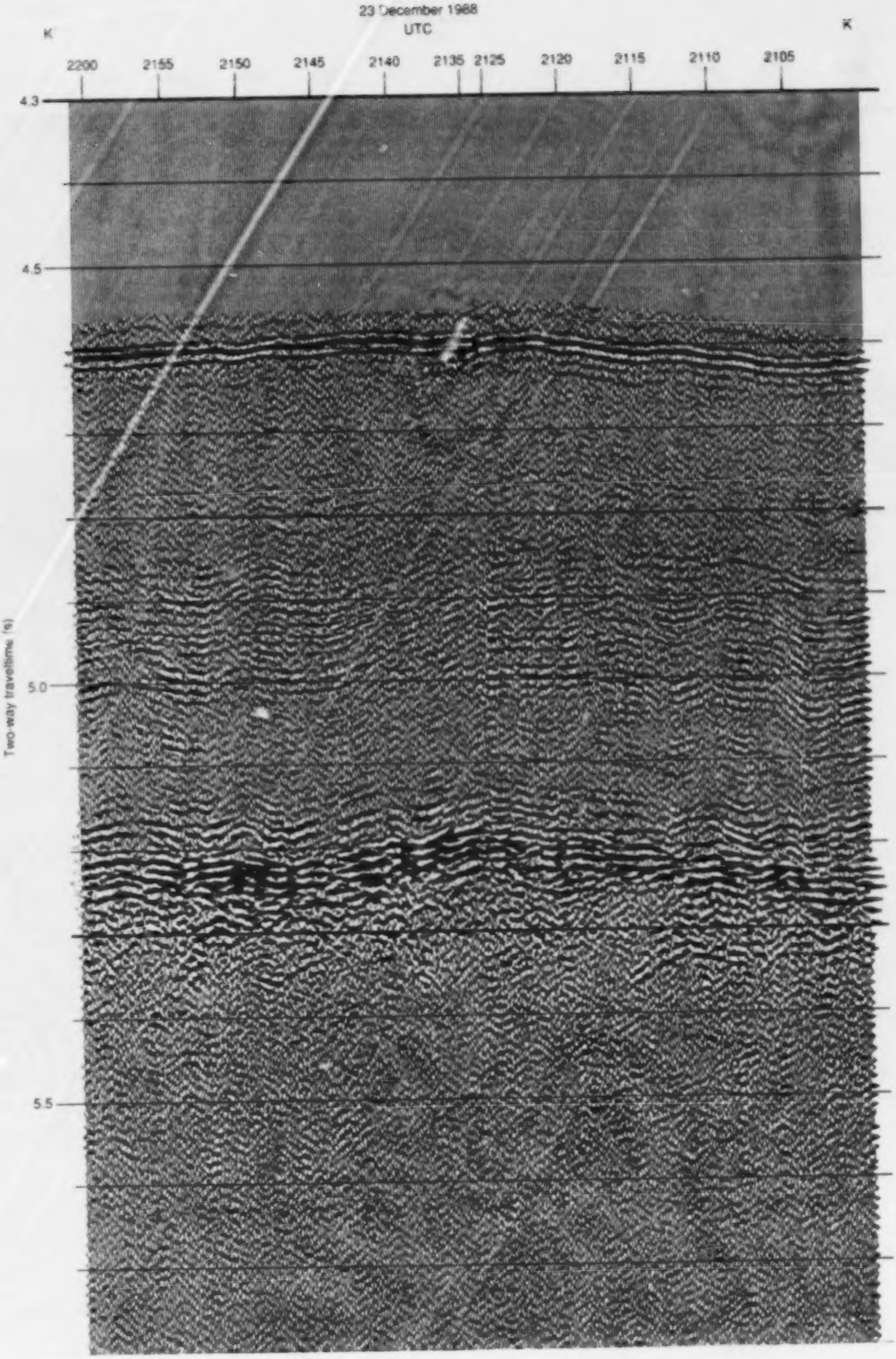

Figure 26. Single-channel seismic profile K-K' in the Dancer survey area. See Figure 24 for location of line.

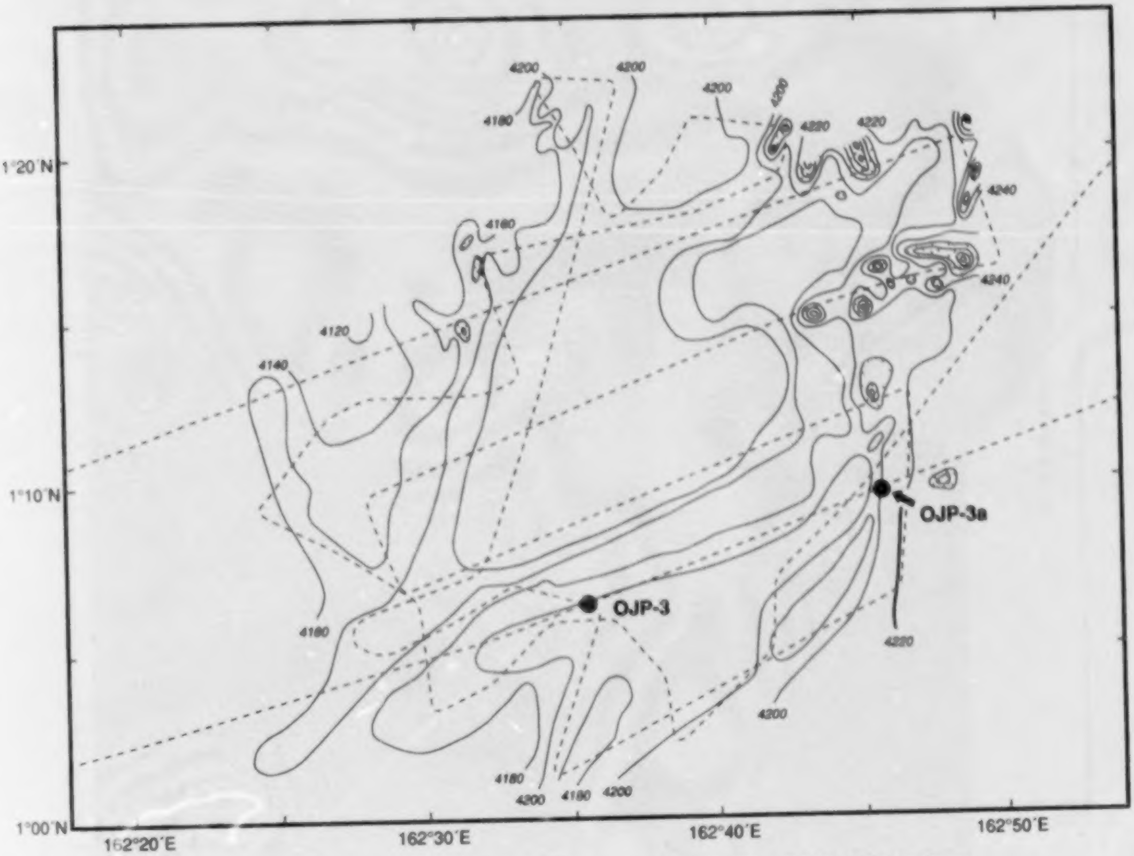
1°20'N
1°10'N
1°00'N
162°20'E
162°30'E
162°40'E
162°50'E
OJP-3
OJP-3a
4120
4140
4160
4180
4200
4220
4240

Figure 27. SeaBeam bathymetry in the Comet survey area. Contour interval is 20 m. Proposed Sites OJP-3 and 3a are shown.

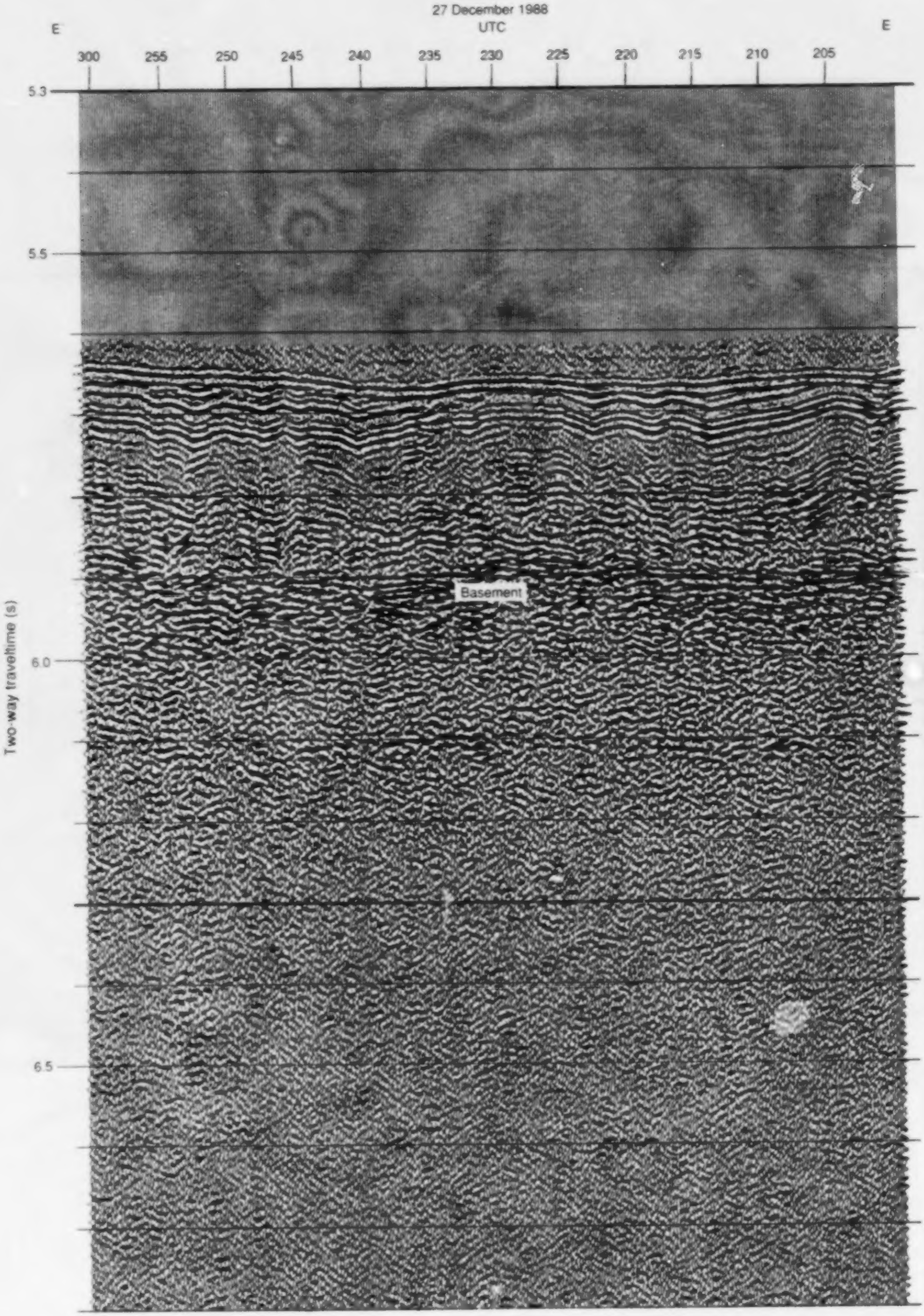

Figure 28. Single-channel seismic profile E-E′ in the Comet survey area. The uplift(?) of basement in this area has caused erosional truncation of surface layers and rough bathymetry. See Figure 29 for location of line.

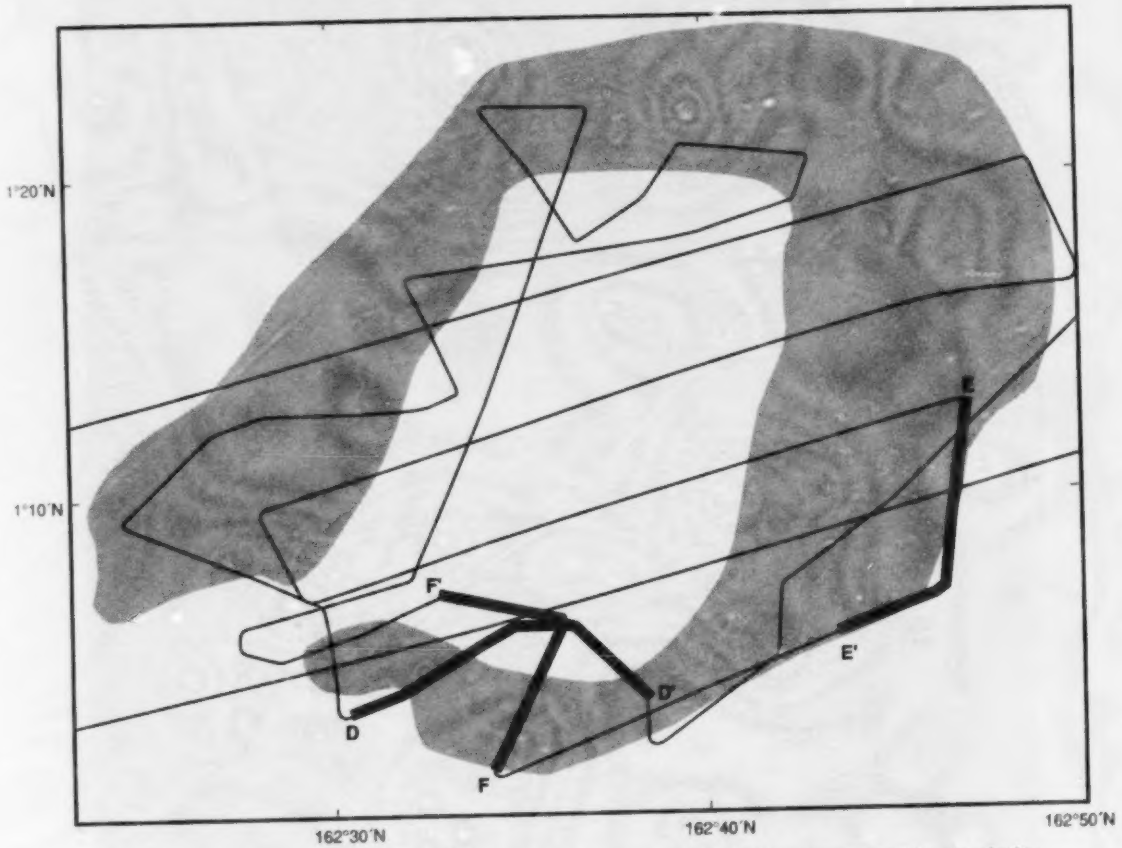
1°20′N
1°10′N
162°30′N
162°40′N
162°50′N
D
D′
E
E′
F
F′

Figure 29. Drilling "avoidance" map of the Comet survey area based on seismic profiles. Stippled areas were avoided for site selection.

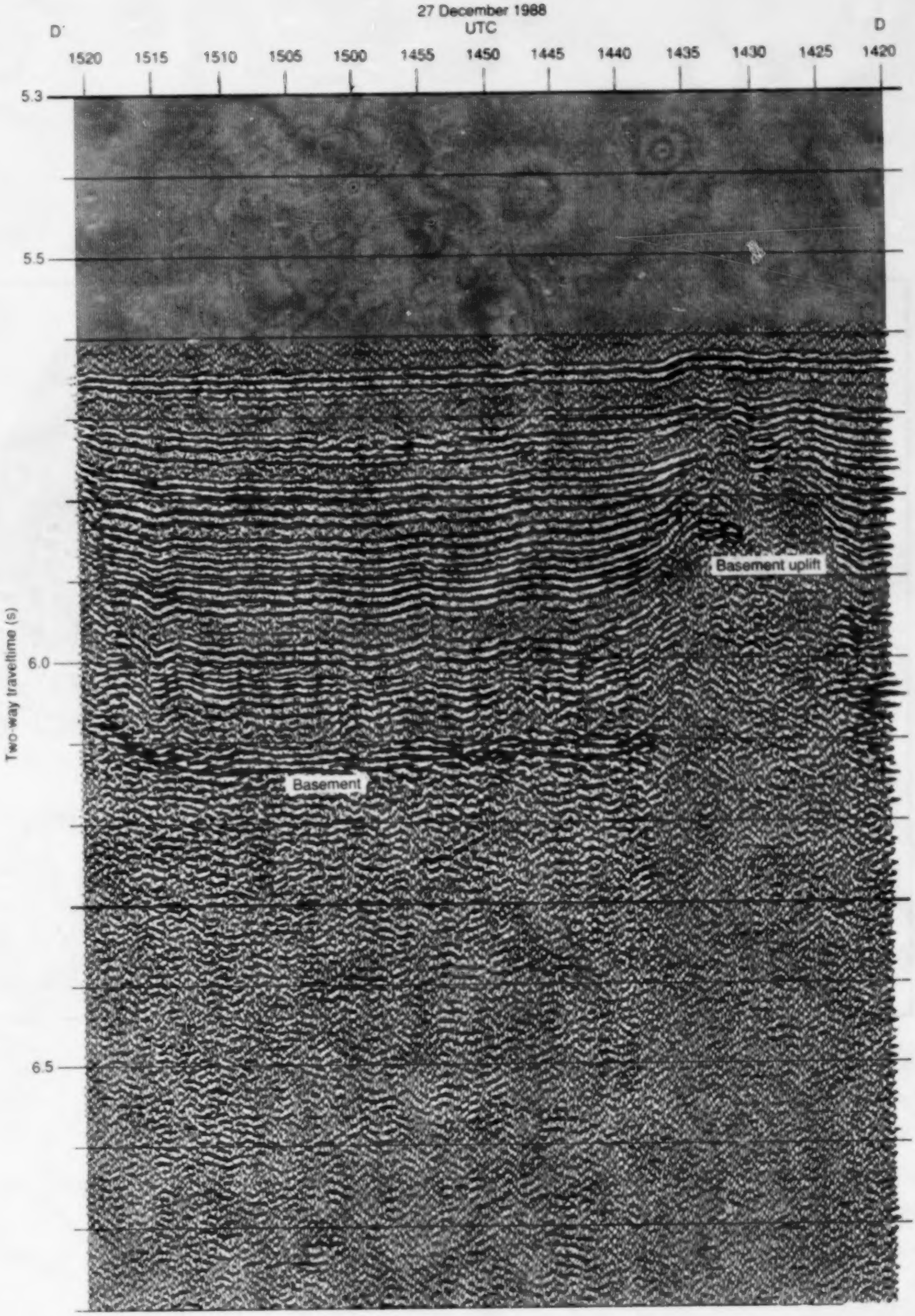

Figure 30. Single-channel seismic profile D-D' in the Comet survey area. A thick sedimentary section occurs in a small graben structure. See Figure 29 for location of line.

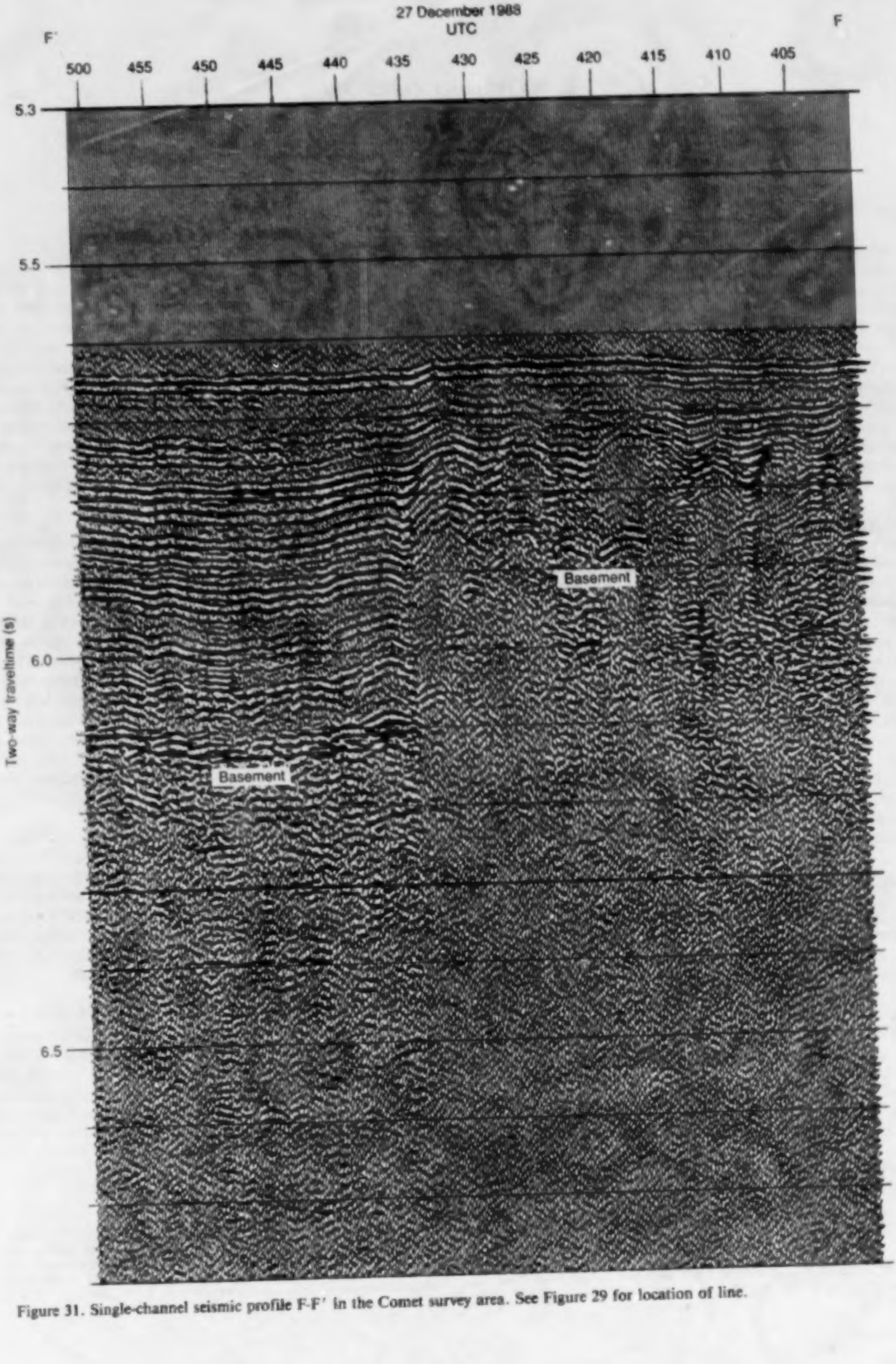

Figure 31. Single-channel seismic profile F-F′ in the Comet survey area. See Figure 29 for location of line.

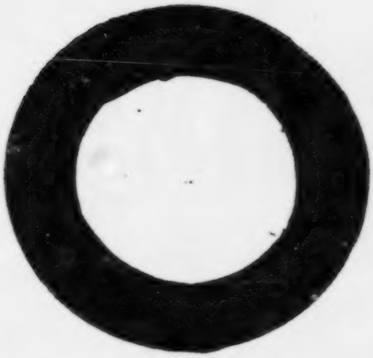

Kroenke, L. W., Berger, W. H., Janecek, T. R., et al., 1991
Proceedings of the Ocean Drilling Program, Initial Reports, Vol. 130

4. UNDERWAY GEOPHYSICS[1]

Rick A. Hagen[2] and Shipboard Scientific Party[3]

INTRODUCTION

Geophysical data were collected during Ocean Drilling Program (ODP) Leg 130. Of the 2767 nmi traveled during the round trip from and to Guam, we collected bathymetric data for 2753 nmi, magnetic data for 2741 nmi; and seismic reflection data for 863 nmi. Of the 62.7 total days spent at sea, 11.5 days were spent in transit.

Shipboard geophysical instruments included two precision echo-sounders (3.5 and 12 kHz), a proton precession magnetometer, single-channel seismic profilers, and a satellite navigation system. These instruments were maintained and operated by ODP marine technicians, in cooperation with the scientific party and the officers and crew of the *JOIDES Resolution*.

NAVIGATION DATA

Navigation data were collected in the underway geophysics lab by a Magnavox 1107 satellite navigation system (SATNAV). We obtained the ship's positions with this system during the entire 62.7 days at sea and received 1702 satellite fixes during the cruise (Table 1, back pocket microfiche).

A plot of the general navigation for Leg 130 is shown in Figure 1. This plot was generated from satellite navigation and course- and speed-change information. These data were compiled from the shipboard bridge log, the underway geophysical log, and the satellite navigation sheets. Course and speed information came from the digital-seismic tape headers. The Geological Data Center at Scripps Institution of Oceanography produced this navigation compilation.

BATHYMETRIC DATA

Bathymetric data were obtained with 3.5-kHz (EDO-248C recorder system) and 12-kHz (Raytheon recorder system) echo-sounders. We operated both systems with a CESP-III correlator system to improve signal strength. The quality of the recorded data was poor when the ship traveled at speeds greater than about 8 kt. A summary of the bathymetric data collected during Leg 130 is displayed in Figure 2.

MAGNETIC DATA

A Geometrics 801 proton-precession magnetometer was towed approximately 300 m astern during transits between sites and during the transits from and to Guam. The data were recorded in analog format on a graphics recorder, digitally in the header of the seismic tapes and manually every 5 min in the underway geophysics log. The magnetic field values were reduced to anomaly values by subtracting the 1985 IGRF value. A summary of the results is shown in Figure 2.

SEISMIC REFLECTION DATA

At least one single-channel seismic line was run across each site before it was occupied. Single-channel seismic lines also were run during several of the transits between sites to provide seismic stratigraphic continuity across the Ontong Java Plateau.

The seismic sources used aboard the *JOIDES Resolution* during Leg 130 usually consisted of two synchronized 80-in.[3] Seismic Systems Inc. water guns firing at a 10-5 rep rate. The seismic receiver, deployed from the fantail and towed approximately 300 m behind the vessel, consisted of a 100-m-long Teledyne model 178 streamer, containing 60 active sections. Towing depth was usually 10 m and was set by weighting the streamer and by adjusting the ship's speed. Hydrophone elements were combined to produce a single signal, which was recorded on both analog and digital records.

Seismic data were displayed in real time in analog format on two EDO-550, dry-paper recorders, using only the streamer, amplifiers, and two band-pass filters (Table 2). These data also were recorded digitally using a supermicro 561 Masscomp computer, which functioned as the central unit for recording, processing, and displaying the data. Raw data were recorded on nine-track tapes with a Cipher drive, using SEG-Y format and a density of 1600 bpi. The header for each shot contains the following information: shot number, date, time, wind speed, wind direction, ship's speed, ship's gyro heading, cumulative distance traveled, streamer and gun depth, and information on the timing of the guns.

Digital data were processed and displayed in real time on a 15-in.-wide Printronix, high-resolution graphic printer (160 dots/in.). The digital profiles were reprocessed on site using the Masscomp computer and the SIOSEIS processing system. The reprocessed lines were displayed on a 22-in. Versatec electrostatic plotter (200 dots/in.).

SINGLE-CHANNEL SEISMIC REFLECTION PROFILES

A map view of the bathymetry of the Ontong Java Plateau traversed on Leg 130 is shown together with the ship's track in Figure 3. The single-channel seismic reflection profiles with their corresponding track segments are shown in Figures 4 through 31. The digital data were analog, band-pass filtered (25–250 Hz) and collected at a 1-ms digitization rate. The quality of the data is somewhat variable as it depended on the ship's speed and sea conditions. Further filtering did not improve the quality of the digital data, so additional filtering was not applied to the reprocessed data. A three-trace, center-weighted running mix and automatic gain control were applied to all traces. Bad traces were deleted. The signal was muted to the seafloor on all of the profiles. The parameters used in collecting and reprocessing the seismic data are listed in Table 2. We collected 10 seismic lines during the cruise, as follows.

Seismic Line 1

Seismic Line 1 was collected across Site 807 en route to Site 803 (Julian Day [JD] 026/1117 Universal Time Coordinated

---

[1] Kroenke, L. W., Berger, W. H., Janecek, T. R., et al., 1991. *Proc. ODP, Init. Repts.*, 130: College Station, TX (Ocean Drilling Program).

[2] Hawaii Institute of Geophysics, University of Hawaii, 2525 Correa Road, Honolulu, HI 96822, U.S.A.

[3] Shipboard Scientific Party is as given in the list of participants preceding the contents.

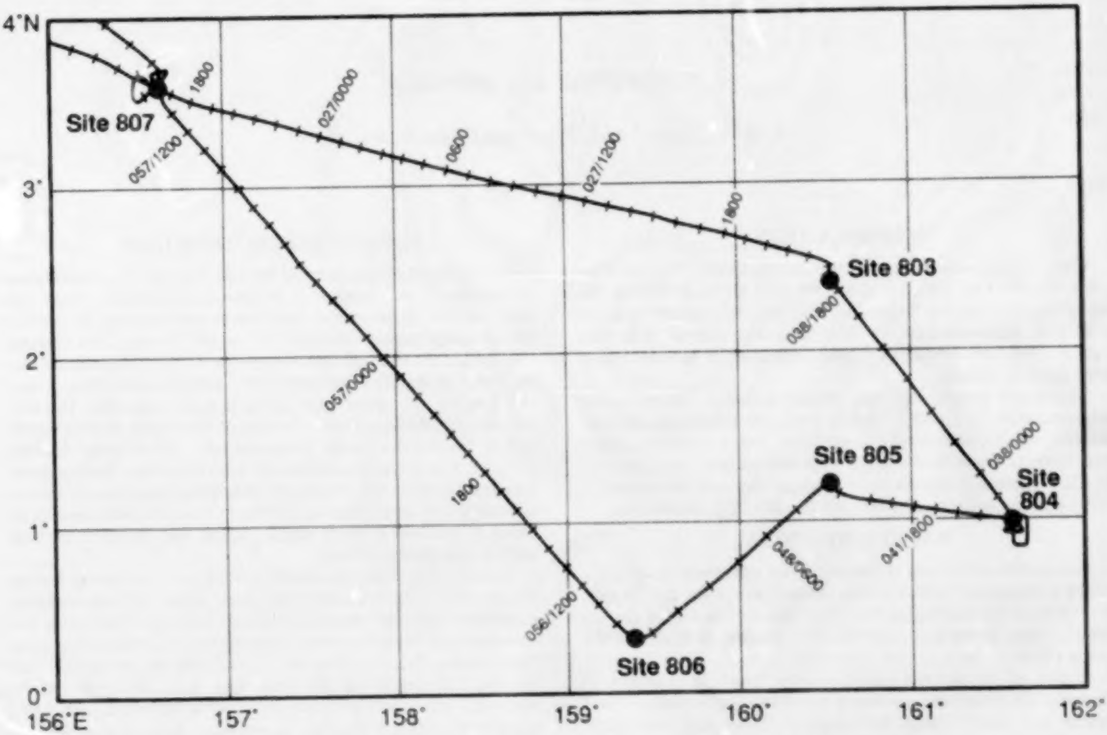

Figure 1. Leg 130 track line on the Ontong Java Plateau. The locations of Sites 803 through 807 are also shown.

[UTC] to JD 026/1737 UTC). A short survey (Fig. 4) was conducted at this site, which had not been covered by the ROUNDABOUT site survey (see Mayer et al., this volume). Water depth ranges from 2700 to 2775 m and the thickness of the sedimentary section ranges from 0.9 to 1.3 s (two-way traveltime [twt]) on this profile. The processed digital seismic profiles (Figs. 5 and 6) clearly show the drilling target, a small basement depression that had been identified on a 1975 analog seismic profile (*Thomas Washington*, EURYDICE 9 Cruise). Thickening of the sedimentary section occurs mid-section (about 4.2 s) at the site and at the base of the section in the basement depression. The data do not resolve the sedimentary section very well, however, because the eel was towed too deep (15–18 m) and at a slow speed (about 7 kt), resulting in a low-frequency-dominated record.

Seismic Line 2

Seismic Line 2 was collected during the transit from Site 807 to Site 803 (JD 026/1737 UTC to JD 027/1900 UTC). The ship's speed was greater during this transit (about 8.5 kt) than during the survey of Site 807; thus, the eel rode at a shallower depth, increasing the frequency content and the resolution of the data. The ship's track for Seismic Line 2 is shown in Figure 7, and the processed digital-seismic profiles are presented in Figures 8, 9, 10, 11, and 12. This long seismic profile was collected to tie the seismic stratigraphy of Site 807 to that of the other sites, which had been more thoroughly surveyed. Water depth on this profile ranges from 1875 to 3340 m, and the thickness of the sedimentary section from 0 to 1.05 s.

Most of the sedimentary section revealed by Seismic Line 2 was undisturbed, with uniform, flat-lying reflectors. However, several areas were highly disturbed, characterized by pinch and swell of layers, surface erosion, and internal deformation. Some portions of the line have numerous mid-section reverberant layers (MSRs), which are especially common near the east flank of a small rugged seamount (approximately 30 km across and 1100 m high) located near JD 027/1630 UTC (Fig. 12). The MSRs occur at a common depth in the section (0.25–0.3 s below sea floor [sbsf]) and appear to extend out from the flank of the seamount. Their acoustic character is also quite similar to that of the basement, leading us to infer that they might be sills or extrusive lava flows.

Alternatively, the MSRs may be diagenetically altered layers ("hardgrounds") created by fluid circulation. The MSRs also occur near three small acoustically transparent, diapirlike structures that are located between JD 027/0130 UTC and JD 027/0400 UTC (Figs. 8 and 9). The largest of these features, which we tentatively interpret as mud volcanoes, is about 3.5 km across and 375 m high. If the MSRs are recently intruded sills, the mud volcanoes may have been created by hydrothermal remobilization of sediment.

Seismic Line 3

Seismic Line 3 was collected on the approach and survey of Site 803 (JD 027/1900 UTC to JD 028/0133 UTC). The ship's track for Seismic Line 3 is shown in Figure 13, and the processed digital-seismic profiles are presented in Figures 14 and 15. The survey crossed the site from north to south and then

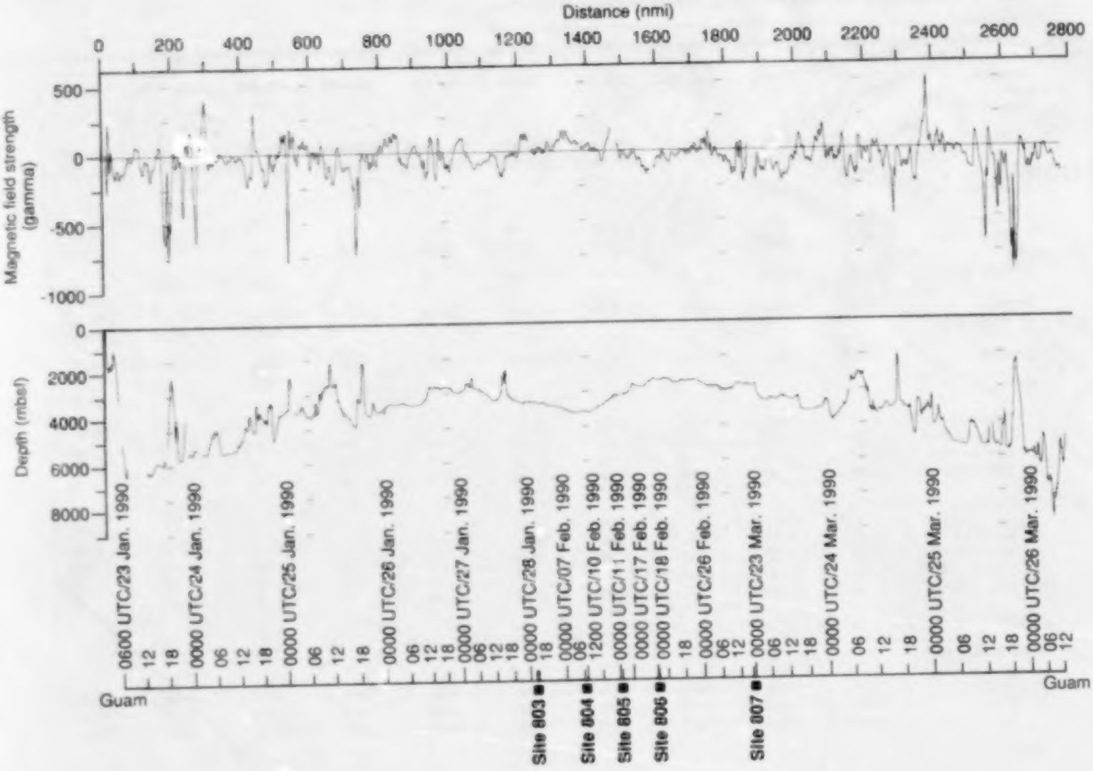

Figure 2. Summary of magnetic anomaly and bathymetry data for Leg 130.

approached the site from the east along one of the ROUNDABOUT site survey profiles. Water depth on this profile ranges from 3340 to 3490 m and sediment thickness from 0.65 to 0.75 s. The section is undisturbed near the site but very disturbed elsewhere with pinching and thinning of layers, MSRs, and deformation. The beacon was dropped at JD 028/0128 UTC, as the ship came off a prominent MSR layer and passed over an undisturbed section.

The depth of the eel was greater than normal because the ship reduced speed during the survey. This resulted in a low-resolution, low-frequency-dominated record.

Seismic Line 4

Seismic Line 4 was collected on the approach and survey of Site 804 (JD 038/0103 UTC to JD 038/0606 UTC). The ship's track for Seismic Line 4 is shown in Figure 16, and the processed digital-seismic profiles are presented in Figures 17 and 18. The survey was designed to cross two pre-existing profiles from the ROUNDABOUT site survey. The ship crossed the site from north to south and then approached the site from the east. Water depth on this profile varies from 3825 to 3925 m, and the thickness of the sedimentary section ranges from 0.25 to 0.65 s. The main structural feature of the site is a narrow northwest-striking basement depression that has a basement relief of about 0.3 s. The section is very disturbed, consisting of rough basement topography, faults and folds of the graben flanks, and evidence of sliding and slumping in the graben. These slump deposits can be identified in the record by their semitransparent, "chaotic" acoustic character. The site was located in the center of this small graben structure where the section appeared to be the least disturbed.

After our experience with the earlier surveys, the eel towing depth was reduced and the survey speed increased slightly, resulting in a higher frequency record and improved resolution.

Seismic Line 5

Seismic Line 5 was a post-site survey of Site 804 (JD 041/1205 UTC to JD 041/1833 UTC) (Fig. 16). The line was run to provide more information on the area around Site 804, an alternate site that had not been surveyed extensively by the ROUNDABOUT site survey. The ship left the site heading southwest, turned to the east, passed along the axis of the narrow graben drilled at Site 804, and headed northwest on the way to Site 805.

Water depth along this profile ranges from 3600 to 3915 m, and sediment thickness ranges from 0.35 to 0.65 s. This profile looks very similar to Seismic Line 4 in the area near the site. The section becomes significantly more compressed out of the graben and away from the site to the northwest (Fig. 19). The section gradually thickens again with decreasing water depth on the transit to Site 805 (Fig. 20). This thickening occurs throughout the section, but it appears to be greatest at the top of the section (Fig. 21).

Table 2. Seismic data, real-time recording, and reprocessing parameters.

Line Number	Line 1	Line 2	Line 3	Line 4	Line 5	Line 6	Line 7	Line 8	Line 9	Line 10
Location	Site 807	Transit	Site 803	Site 804	Transit	Site 805	Site 806	Transit	Site 807	Transit
Time (UTC)										
Start	026/1117	026/1737	027/1900	038/0103	041/1205	041/1833	048/0950	056/0915	057/1045	082/0030
End	026/1737	027/1900	028/0133	038/0606	041/1833	042/0134	048/1100	057/1045	057/1630	082/2202
Shotpoints										
Start	5050	6951	14559	541	59	1972	414	1	7657	9381
End	6950	14558	16509	2055	1971	3609	770	7656	9380	17013
Distance (nmi)	45	205	48	87	45	42	9	191	40	151
Source (water guns)	2 80 in.^{3}	2 80 in.^{3}	2 80 in.^{3}	2 80 in.^{3}	2 80 in.^{3}	2 80 in.^{3}	2 80 in.^{3}	1 80 in.^{3} 1 200 in.^{3}	1 80 in.^{3} 1 200 in.^{3}	1 80 in.^{3} 1 200 in.^{3}
Streamer	Port	Port	Port	Port	Port	Port	Port	Port	Port	Port
Analog 1:										
Range (s)	0–10	0–10	0–10	0–10	4–7	4–7	3–6	3–6	3–6	3–6
High cut (Hz)	150	150	150	150	150	150	150	150	150	150
Low cut (Hz)	30	30	30	30	30	30	30	30	30	30
Gain (dB)	40	40	40	40	40	40	40	40	40	40
Analog 2:										
Range (s)	2–8	2–8	2–8	2–8	0–10	0–10	0–10	0–10	0–10	0–10
High cut (Hz)	150	150	150	150	150	150	150	150	150	150
Low cut (Hz)	30	30	30	30	30	30	30	30	30	30
Gain (dB)	40	40	40	40	40	40	40	40	40	40
Digital:										
Data window (ms)										
Length	5000	5000	5000	5000	5000	5000	5000	5000	5000	5000
From	3000	Varied	4000	4000	4000	4000	3000	3000	3000	3000
To	8000	Varied	9000	9000	9000	9000	8000	8000	8000	8000
Filter										
High cut (Hz)	250	250	250	250	250	250	250	250	250	250
Low cut (Hz)	25	25	25	25	25	25	25	25	25	25
Mix										
Traces	3	3	3	3	3	3	3	3	3	3
Weights	131	131	131	131	131	131	131	131	131	131
AGC										
Window (ms)	2000	2000	2000	2000	2000	2000	2000	2000	2000	2000

Seismic Line 6

Seismic Line 6 (JD 041/1833 UTC to JD 042/0134 UTC) was collected on the transit to, as well as on, the survey of Site 805 (Fig. 22). Only a single crossing of the site was planned, as it had been well surveyed previously. A beacon failure on the first pass, however, led to a second crossing of the site.

Water depth along this profile ranges from 3170 to 3600 m, and the thickness of the sedimentary section ranges from 0.65 to 0.8 s. The section is moderately disturbed, with pinching of layers throughout the section, deformation, and surface erosion channels (Fig. 23). Site 805 was located west of a zone of surface erosion in an area of slightly thicker sediments.

The change in character of the seismic record at about 2217 UTC (Fig. 23) is the result of a decrease in ship speed.

Seismic Line 7

Seismic Line 7 (JD 48/0950 UTC to JD 48/1100 UTC) was collected during the site survey of Site 806 (Fig. 24). Water depth on this profile ranges from 2475 to 2620 m, and the thickness of the sedimentary section is 1.00–1.03 s. The section is uniform with no indication of significant thickening or thinning of layers (Fig. 25). A small surface erosion channel occurs about 7 km east-northeast of the site (about 1006 UTC; Fig. 25). Although there is a distinct slope to the bottom (and the seismic section) and the seismic layering is undulating, there is no obvious seismic evidence of slumping or internal deformation of the section at the site.

Seismic Line 8

Seismic Line 8 (JD 056/0915 UTC to JD 057/1045 UTC) was collected on the transit from Site 806 to Site 807 (Fig. 26). This long profile was collected to help tie together the seismic stratigraphy of the individual sites. This line also was used to test one of the new 200-in.^{3} HAMCO water guns, which was towed in conjunction with one of the 80-in.^{3} guns. The increased power of the larger gun, particularly in the low frequencies, made a definite improvement in our ability to separate the basement reflector from the heavy reverberations that occur just above it. At the same time, the 80-in.^{3} gun provided the higher frequency energy that resolves the sedimentary layering.

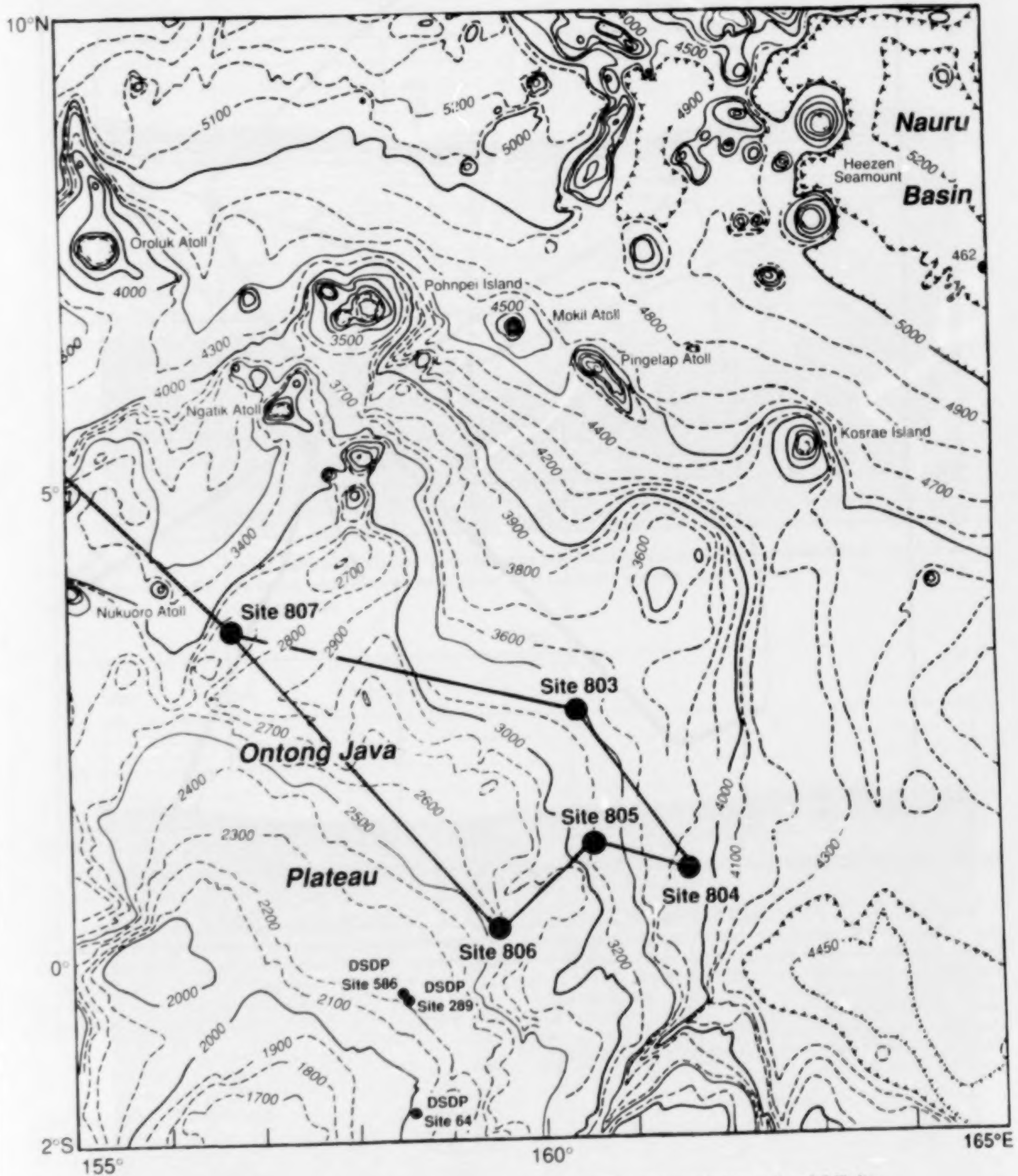
10°N
5°
0°
2°S
155°
160°
165°E
Nauru
Basin
Heezen Seamount
462
Oroluk Atoll
Pohnpei Island
Mokil Atoll
Pingelap Atoll
Ngatik Atoll
Kosrae Island
Nukuoro Atoll
Site 807
Site 803
Site 805
Site 804
Site 806
Ontong Java
Plateau
DSDP Site 586
DSDP Site 289
DSDP Site 64
5100
5200
5000
4500
4900
5200
4000
4300
4500
3500
4800
5000
4000
3700
4900
4400
4200
4700
3900
3400
3600
2700
3800
2800
2900
3600
3000
2700
2400
2600
2500
4000
2300
4100
4300
2200
3200
4450
2000
2100
2000
1900
1800
1700

Figure 3. Bathymetric map of the Ontong Java Plateau (Mammerickx and Smith, 1985) with Leg 130 ship track and drill sites.

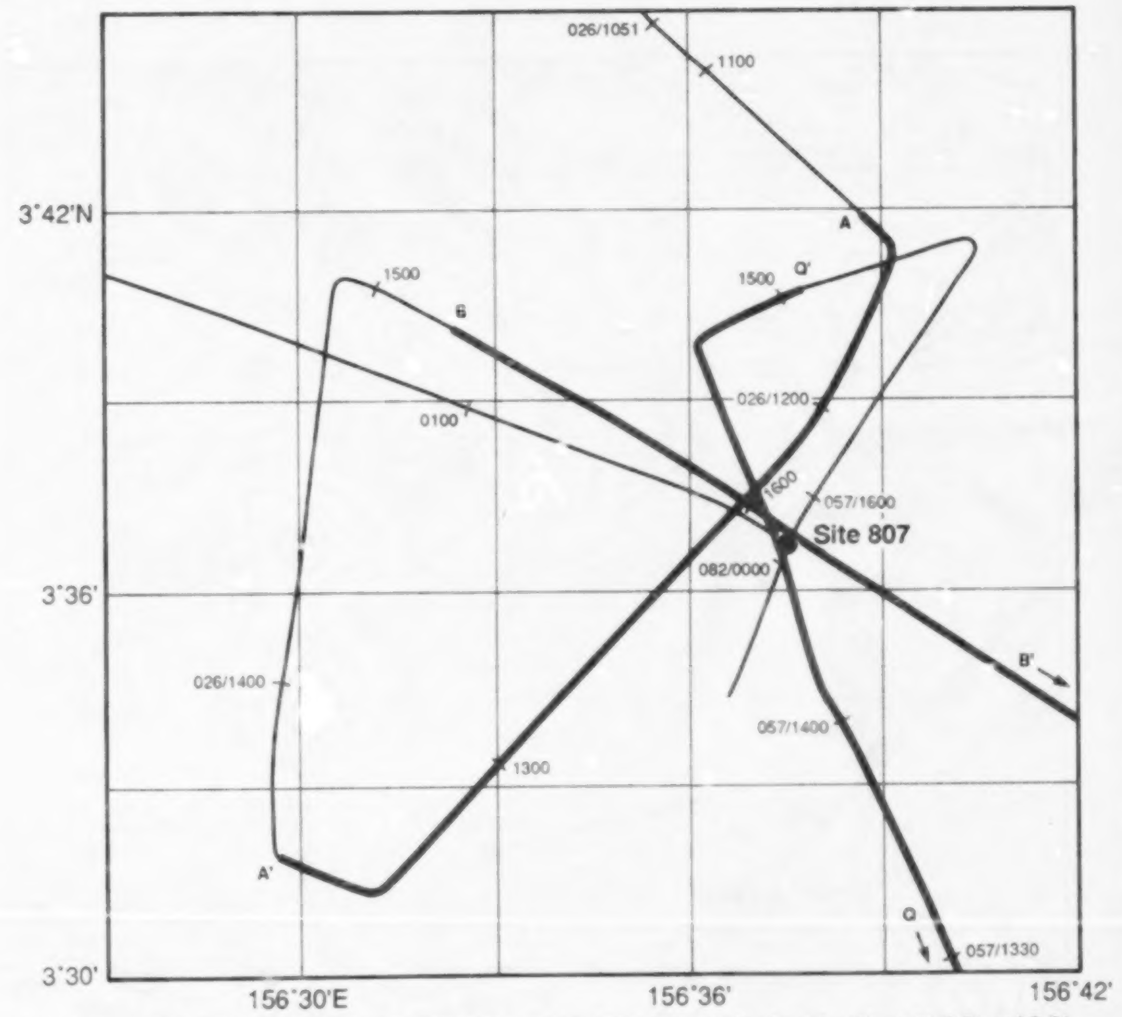

Figure 4. Ship track for single-channel Seismic Lines 1 (JD 026) and 9 (JD 057), including the locations of profiles A-A', B-B', and Q-Q'.

Water depth on this profile ranges from 2475 to 3008 m, and the thickness of the sedimentary section ranges from 0.9 to 1.16 s. Figure 27 shows a portion of this seismic line (P-P'; Fig. 26). The undisturbed stratigraphy shown in Figure 27 is typical of the line as a whole. The increased power of the larger water gun is evident at depth where the heavy reverberations that typically occur just above basement (see earlier seismic profiles) have been resolved into a crisp upper horizon and a heavy, sharp basement reflection.

Seismic Line 9

Seismic Line 9 (JD 057/1045 UTC to JD 057/1630 UTC) was collected on the site survey of Site 807 (Fig. 4). The 200-in.^{3} water gun also was used with one of the 80-in.^{3} guns on this line. Water depth on this profile ranges from 2700 to 2830 m, and the thickness of the sedimentary section ranges from 0.92 to 1.2 s. The small basement depression drilled at Site 807 is shown near the center of Figure 28. Although the deep reflectors in the depression are less reverberant and are more clearly defined, the overall quality of the section and the resolution of the upper stratigraphy is much poorer with this water gun combination (Figs. 5, 6, and 28).

Seismic Line 10

Seismic Line 10 (JD 082/0030 UTC to JD 082/2202 UTC) was collected during the early part of the transit to Guam following drilling at Site 807 (Fig. 29). Water depth on this profile ranges from 2775 to 3750 m, and the thickness of the sedimentary section is 0.0–1.2 s. The water depth increases sharply by

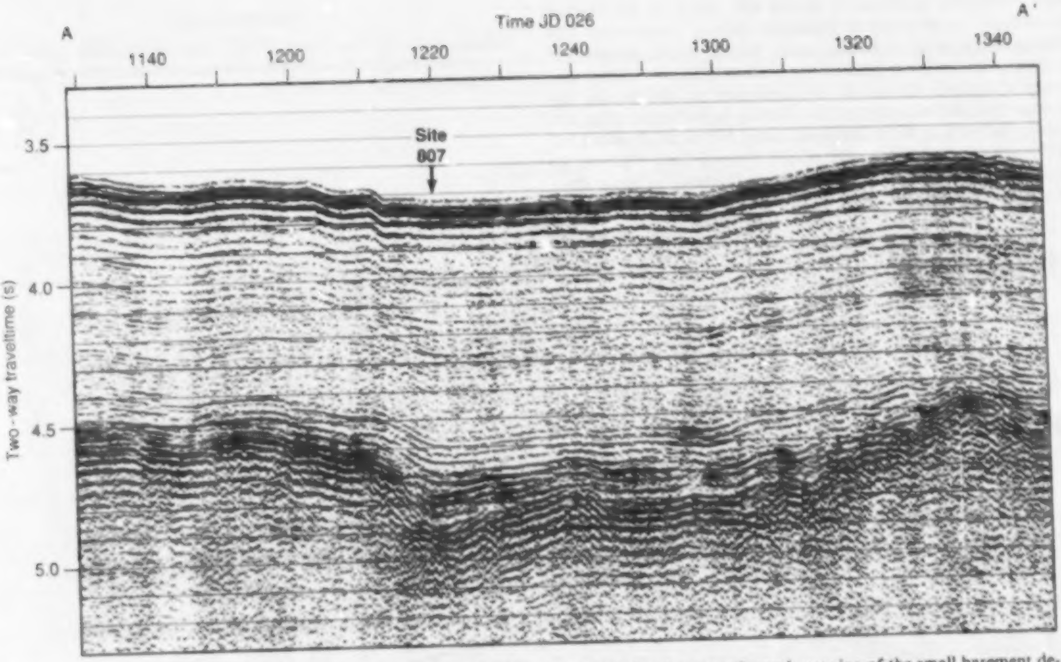

Figure 5. Profile A-A' of processed digital single-channel seismic reflection Line 1 showing a north-south crossing of the small basement depression drilled by Site 807. The section thickens in the middle (about 4.2 s) and in the basement depression (about 4.8 s). JD = Julian Day throughout.

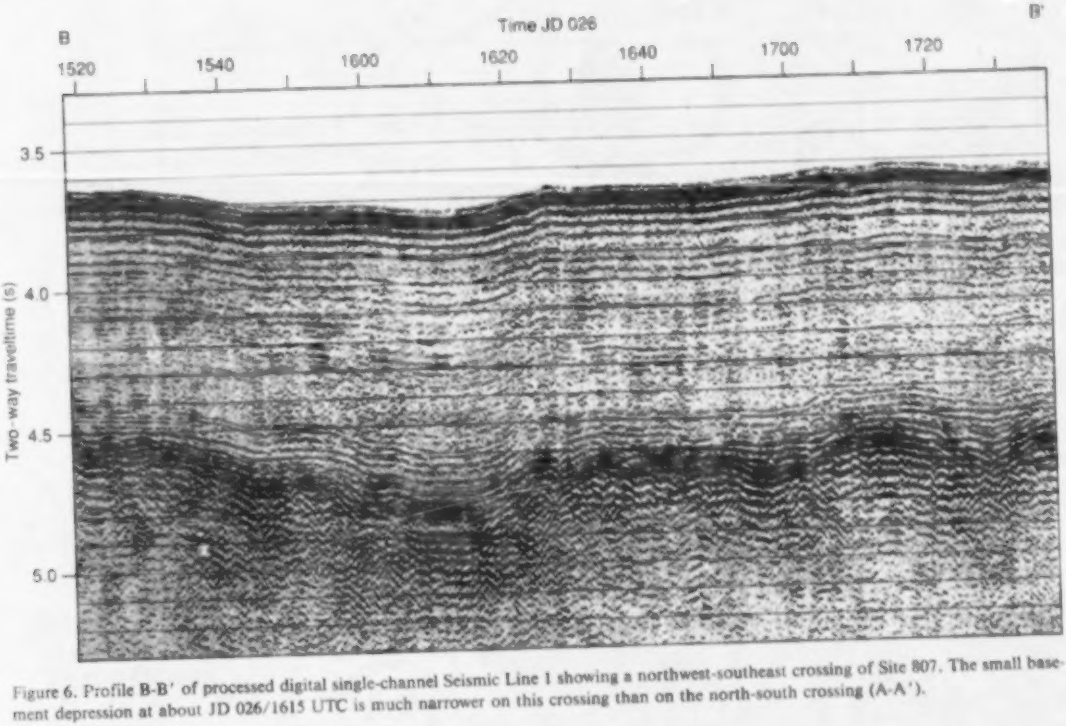

Figure 6. Profile B-B' of processed digital single-channel Seismic Line 1 showing a northwest-southeast crossing of Site 807. The small basement depression at about JD 026/1615 UTC is much narrower on this crossing than on the north-south crossing (A-A').

about 700 m just to the north of Site 807. Much of this change results from the thinning of the upper part of the section. The sedimentary section increases again farther north because of thickening in the lower part of the section (Fig. 30). Horst and graben structures appear in the basement as the profile approaches the northern edge of the Ontong Java Plateau (Fig. 31). A sharp increase in water depth of about 550 m at JD 082/1515 UTC marks the northern edge of the Ontong Java Plateau. To the north of this drop-off, the section thickens to more than 1.2 s and internal reflectors become highly distorted.

REFERENCES

Mammerickx, J., and Smith, S. M., 1985. *Bathymetry of the North Central Pacific*: Boulder, CO (Geological Society of America), Map and Chart Ser., No. MC-52.

Ms 130A-104

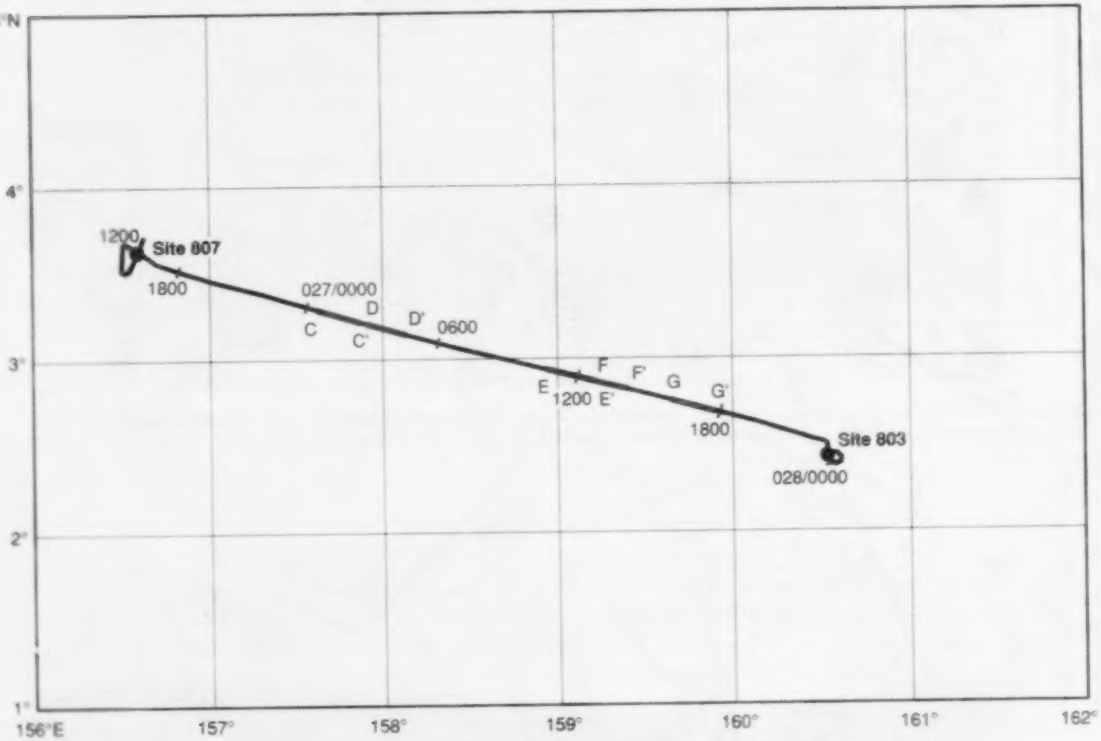
5°N
4°
3°
2°
1°
156°E
157°
158°
159°
160°
161°
162°
1200
Site 807
1800
027/0000
C
D
C'
D'
0600
E
F
1200 E'
F'
G
G'
1800
Site 803
028/0000

Figure 7. Ship track for single-channel Seismic Line 2, showing the locations of profiles C-C', D-D', E-E', F-F', and G-G'.

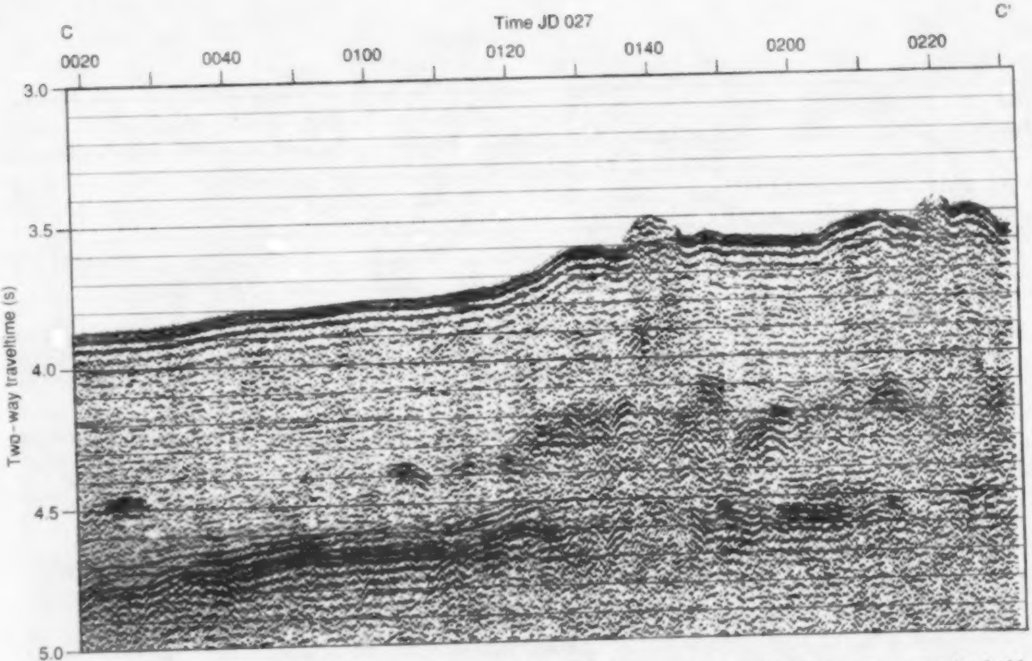

Figure 8. Profile C-C′ of processed digital single-channel Seismic Line 2 showing two of the small diapirlike structures associated with mid-section reverberant layers (MSRs). The transparent seismic character of these features leads us to interpret them as mud volcanoes.

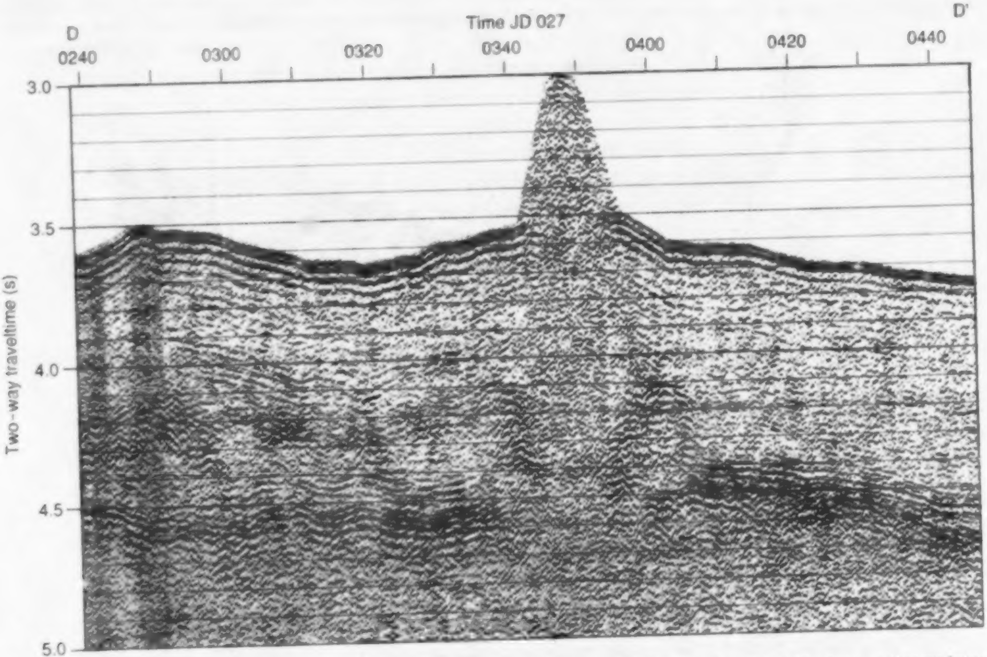

Figure 9. Profile D-D′ of processed digital single-channel Seismic Line 2 showing the largest of the diapirlike features that we interpret as mud volcanoes.

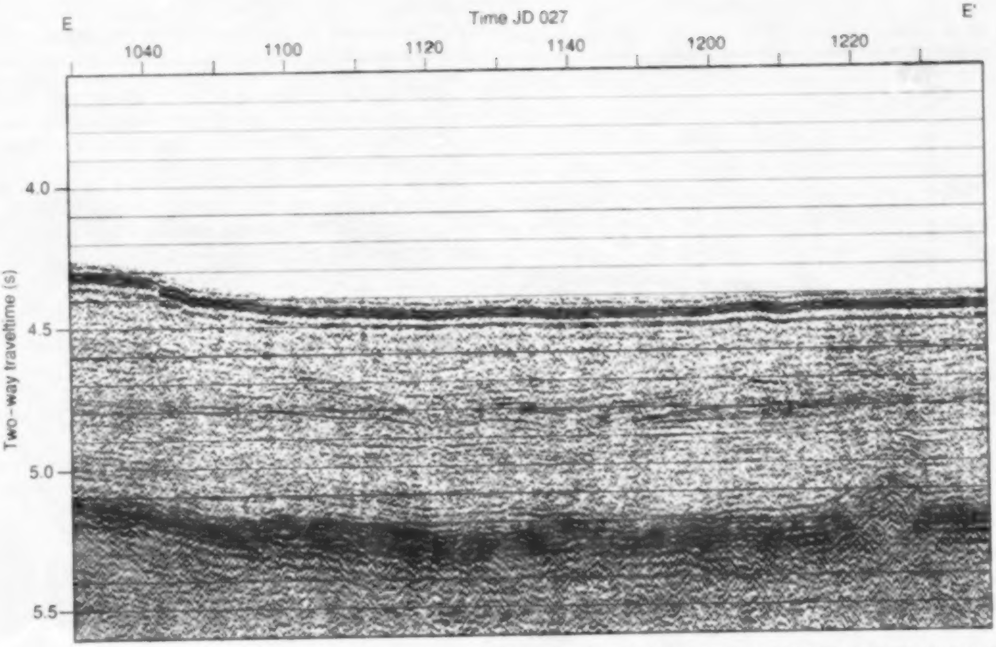

Figure 10. Profile E-E' of processed digital single-channel Seismic Line 2 showing pinching and swelling of seismic layers mid-section (4.7–5.0 s).

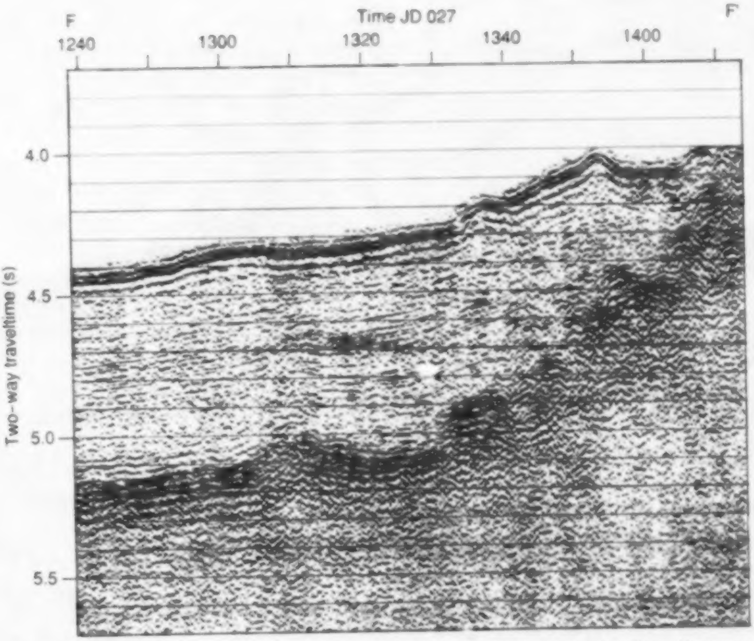

Figure 11. Profile F-F' of processed digital single-channel Seismic Line 2 showing the sedimentary section on the western flank of a small uncharted seamount. The sediment appears to drape over the seamount with only minor surface disruption.

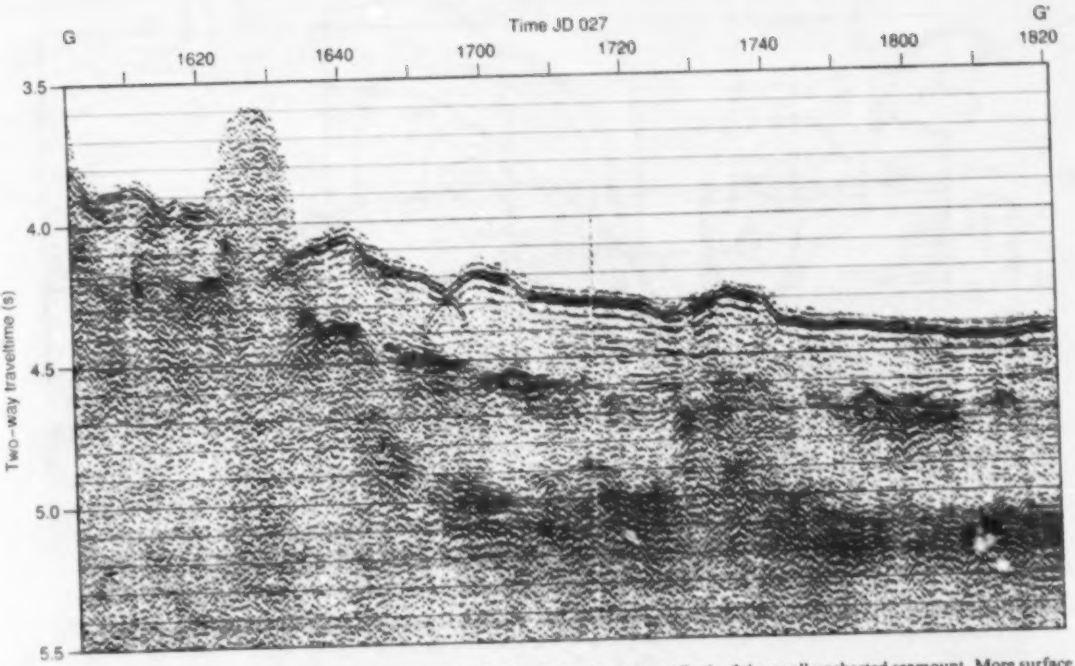

Figure 12. Profile G-G′ of processed digital single-channel Seismic Line 2 showing the east flank of the small uncharted seamount. More surface disturbance occurs on this flank of the seamount than the western flank, which may be associated with the occurrence of MSRs. The MSRs occur at a common level in the section (about 0.3 sbsf).

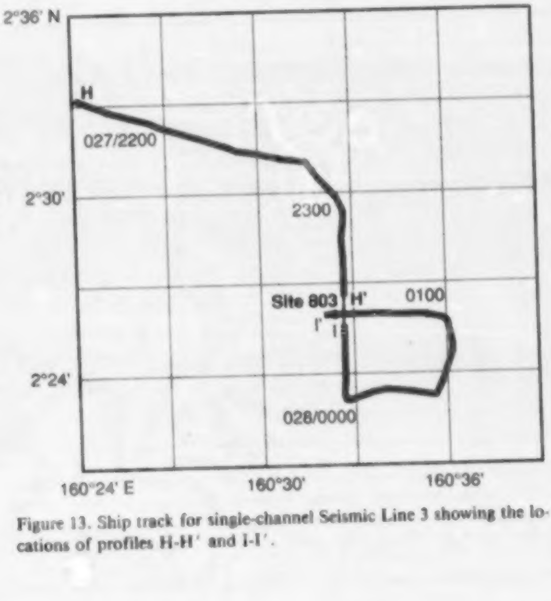
2°36' N
2°30'
2°24'
160°24' E
160°30'
160°36'
H
027/2200
2300
Site 803
H'
0100
I'
I
028/0000

Figure 13. Ship track for single-channel Seismic Line 3 showing the locations of profiles H-H′ and I-I′.

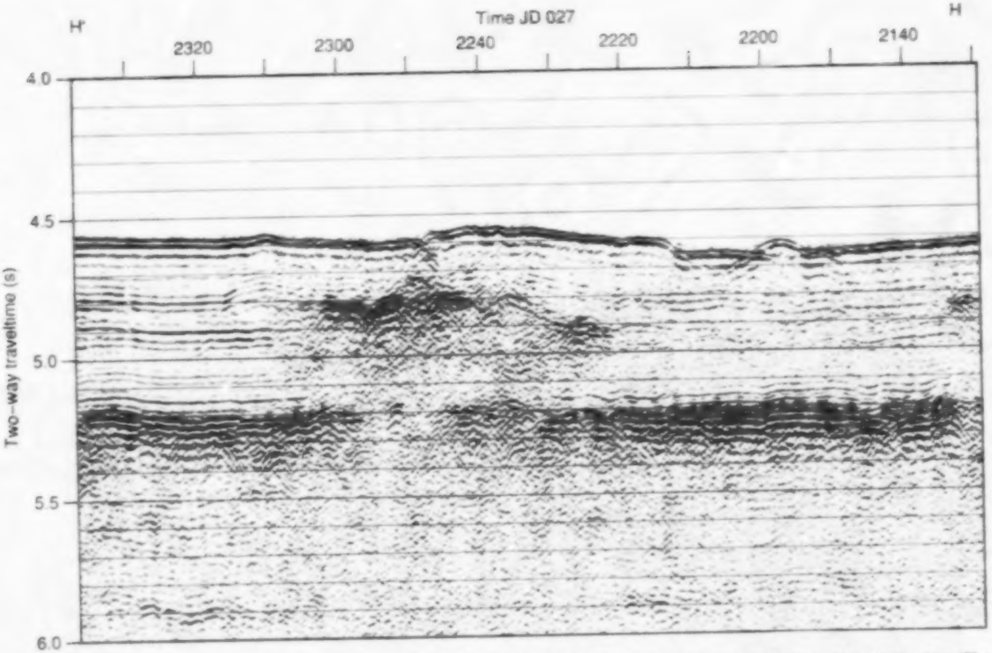

Figure 14. Profile H-H' of processed digital single-channel Seismic Line 3 showing an MSR associated with surface disruption. The MSR has a rough seismic character, similar to basement, and clearly deforms the overlying sediment. This implies that it may be a volcanic sill.

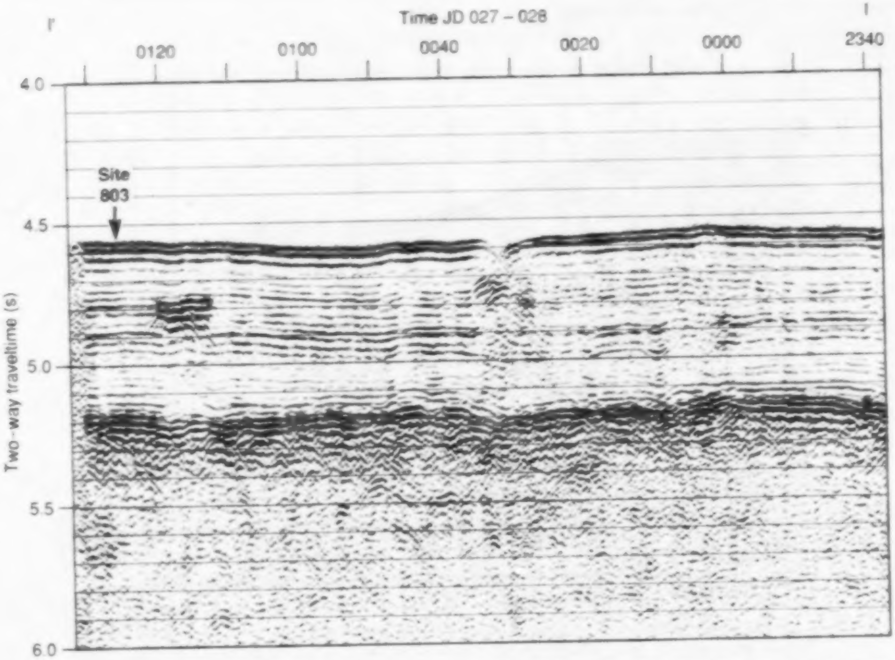

Figure 15. Profile I-I' of processed digital single-channel Seismic Line 3. A small surface erosional channel is located at about 0033 UTC. Site 803 is located just to the left (west) of a small MSR.

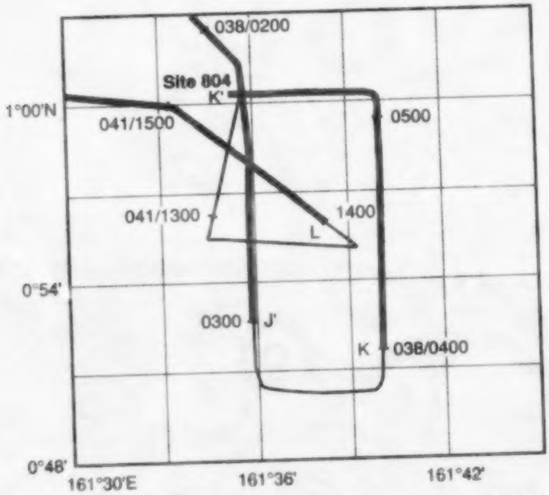
038/0200
Site 804
K'
1°00'N
041/1500
0500
041/1300
1400
L'
L
0°54'
0300
J'
K
038/0400
0°48'
161°30'E
161°36'
161°42'

Figure 16. Ship track for single-channel Seismic Lines 4 (JD 038) and 5 (JD 041) showing the locations of profiles J-J′, K-K′, and L-L′.

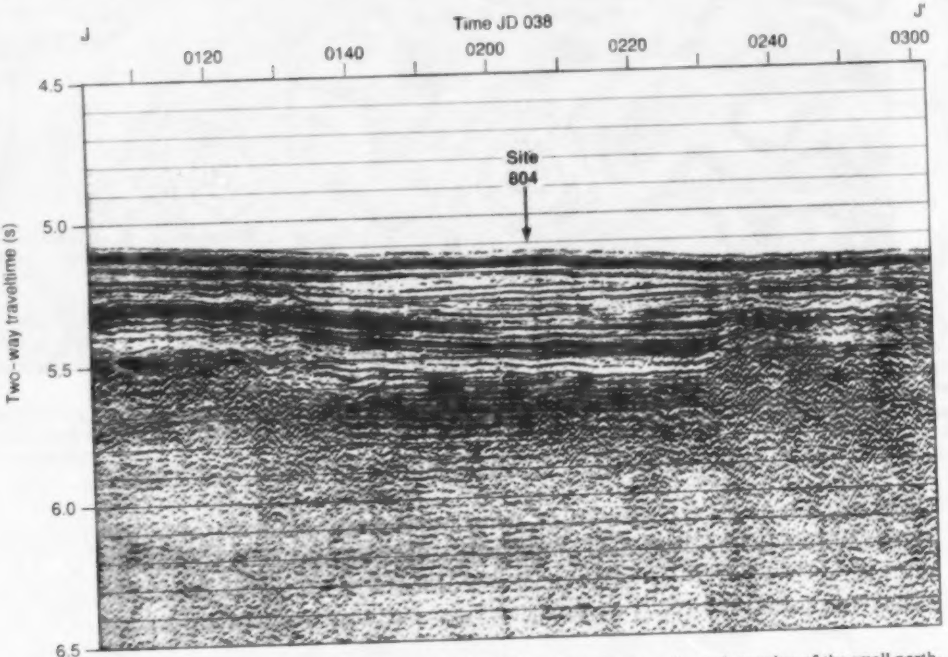

Figure 17. Profile J-J′ of processed digital single-channel Seismic Line 4 showing a north-south crossing of the small north-west-trending graben drilled by Site 804. Minimal disruption of the sediment on the flanks of the graben implies that it is an original basement feature that has been infilled by sediment. The sediment fill includes several disturbed zones and lens-shaped layers indicative of slumping. Small faults and disruption on the edges of the feature probably result from differential sediment compaction.

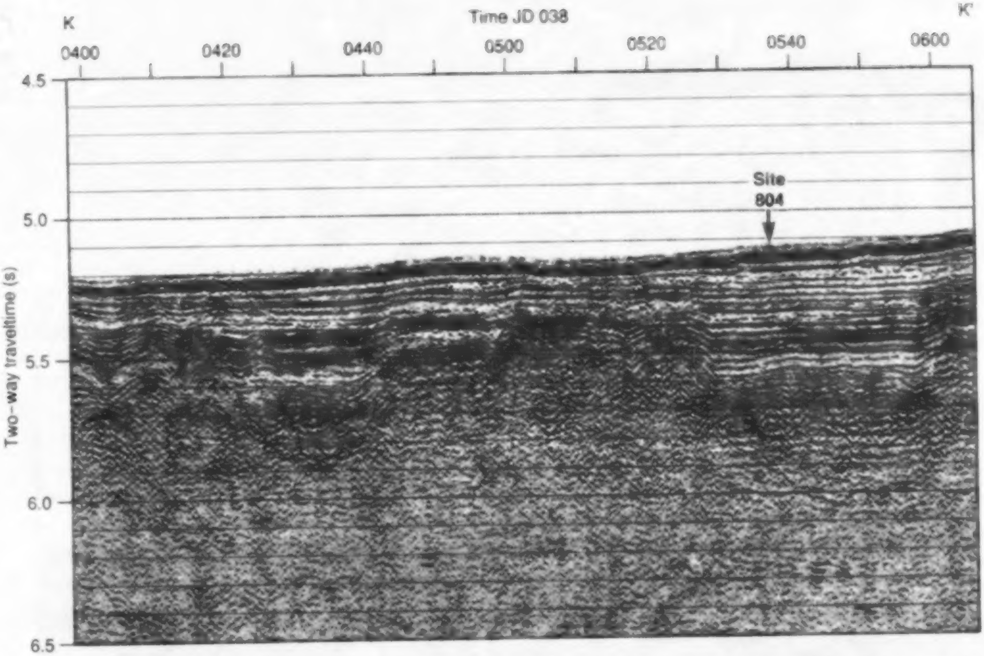

Figure 18. Profile K-K′ of processed digital single-channel Seismic Line 4 showing an east-west crossing of the small graben (right edge of figure). The sediment filling the graben appears to be much less disturbed in this crossing. Faulting is clearly evident on the left (east) edge of the graben. A south-north crossing of the same graben to the south (left portion of figure) shows much more deformation of the sediment filling the graben.

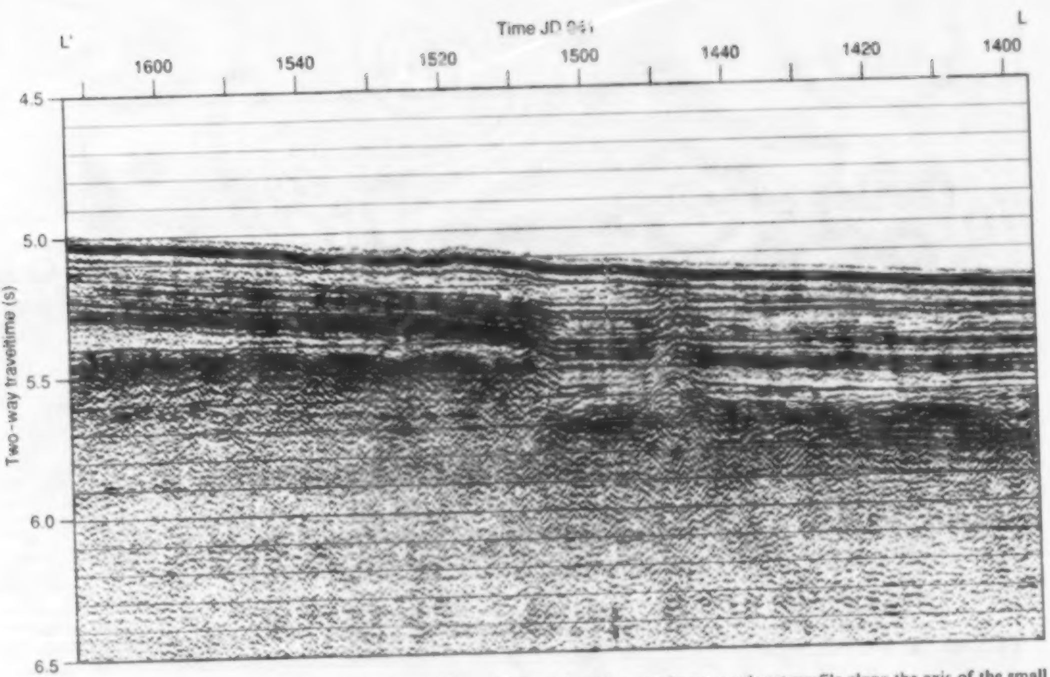

Figure 19. Profile L-L' of processed digital single-channel Seismic Line 5. This is a northwest-southeast profile along the axis of the small graben showing the transition to the more compressed section on the northwest flank of the feature.

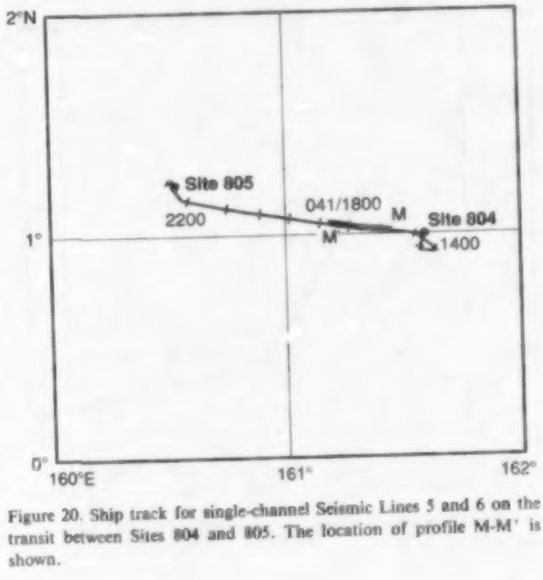
2°N
1°
0°
160°E
161°
162°
Site 805
2200
041/1800
M
M'
Site 804
1400

Figure 20. Ship track for single-channel Seismic Lines 5 and 6 on the transit between Sites 804 and 805. The location of profile M-M' is shown.

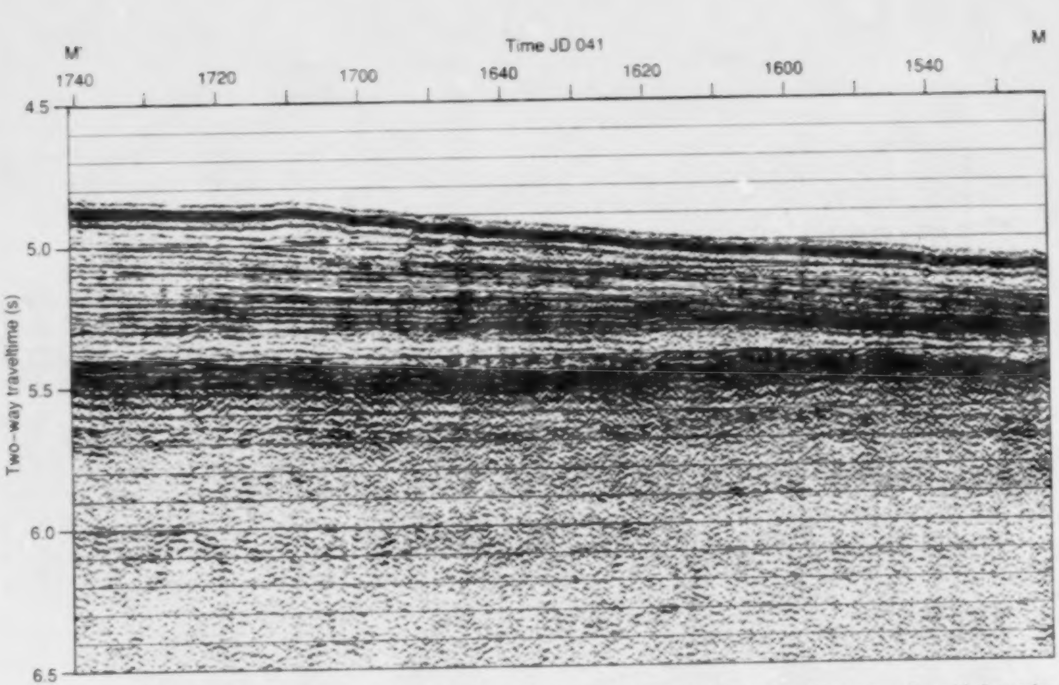

Figure 21. Profile M-M' of processed digital single-channel Seismic Line 5 showing the thickening of the sedimentary section with decreasing water depth. Thickening occurs at all levels in the section but is most pronounced at the top.

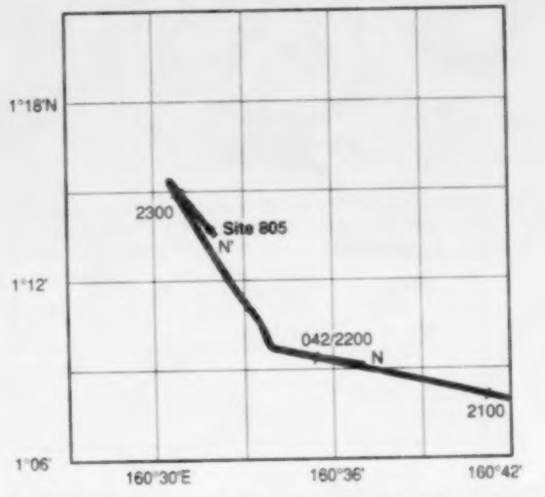
1°18'N
1°12'
1°06'
160°30'E
160°36'
160°42'
2300
Site 805
N'
042/2200
N
2100

Figure 22. Ship track for single-channel Seismic Line 6 showing the location of profile N-N'.

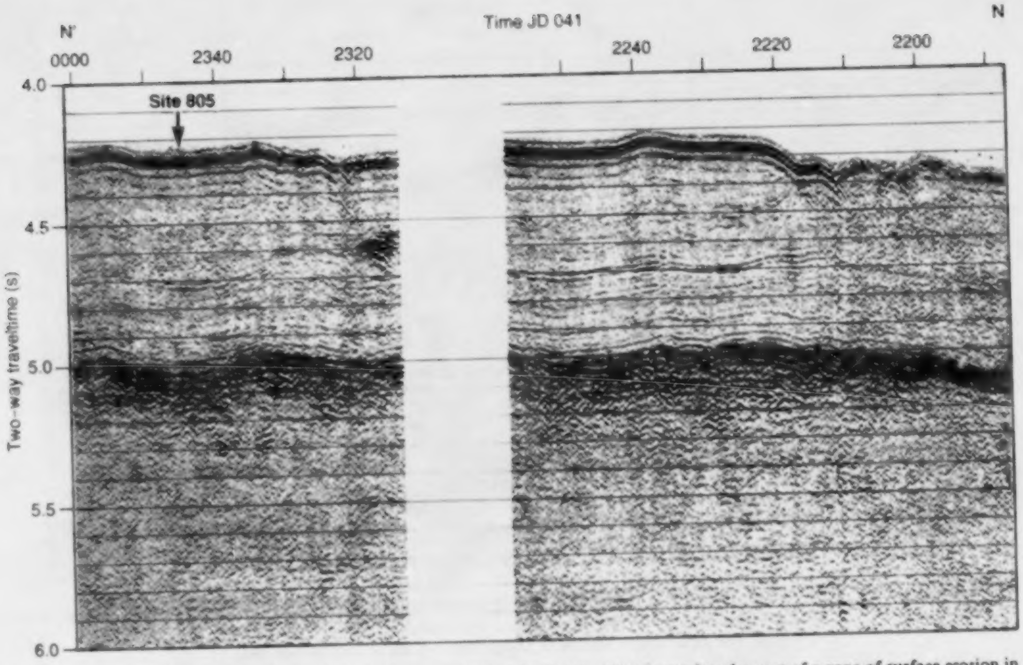

Figure 23. Profile N-N' of processed digital single-channel Seismic Line 6. Site 805 is located to the west of a zone of surface erosion in an area of slightly thicker sediments.

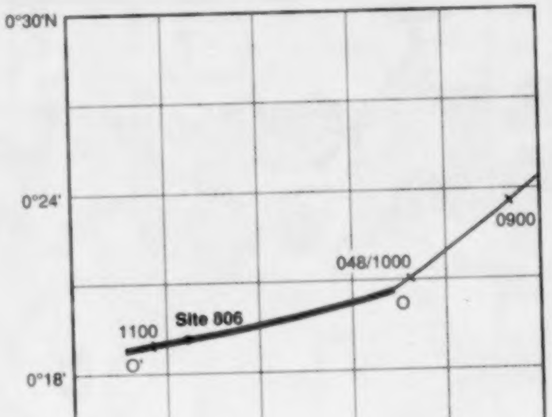
0°30'N
0°24'
0°18'
159°18'E
159°24'
159°30'
0900
048/1000
O
Site 806
1100
O'

Figure 24. Ship track for single-channel Seismic Line 7 showing the location of profile O-O'.

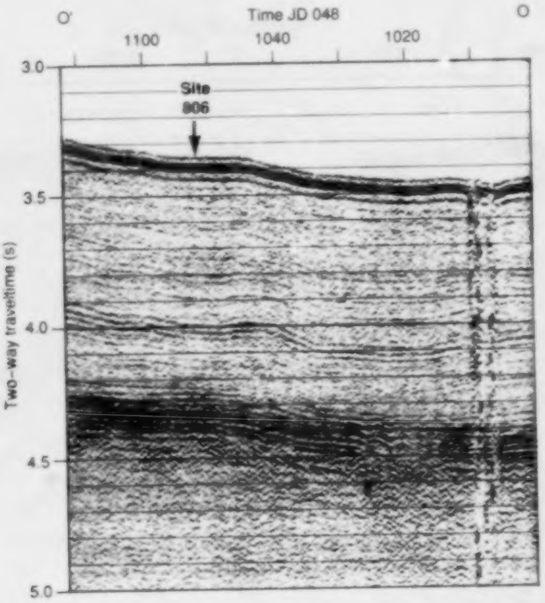

Figure 25. Profile O-O′ of processed digital single-channel Seismic Line 7. The sedimentary section is undulating but fairly undisturbed near Site 806.

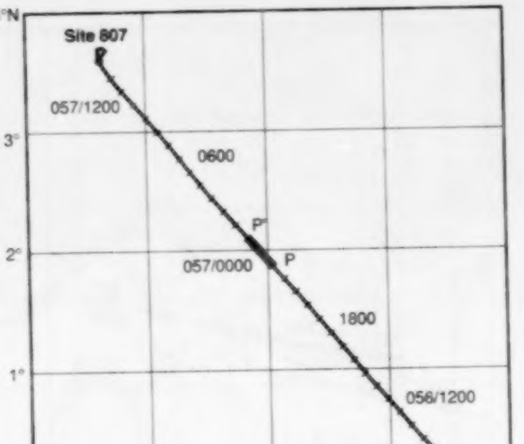
4°N
3°
2°
1°
0°
156°E
157°
158°
159°
160°
Site 807
057/1200
0600
P'
057/0000
P
1800
056/1200
Site 806

Figure 26. Ship track for single-channel Seismic Line 8 showing the location of profile P-P′.

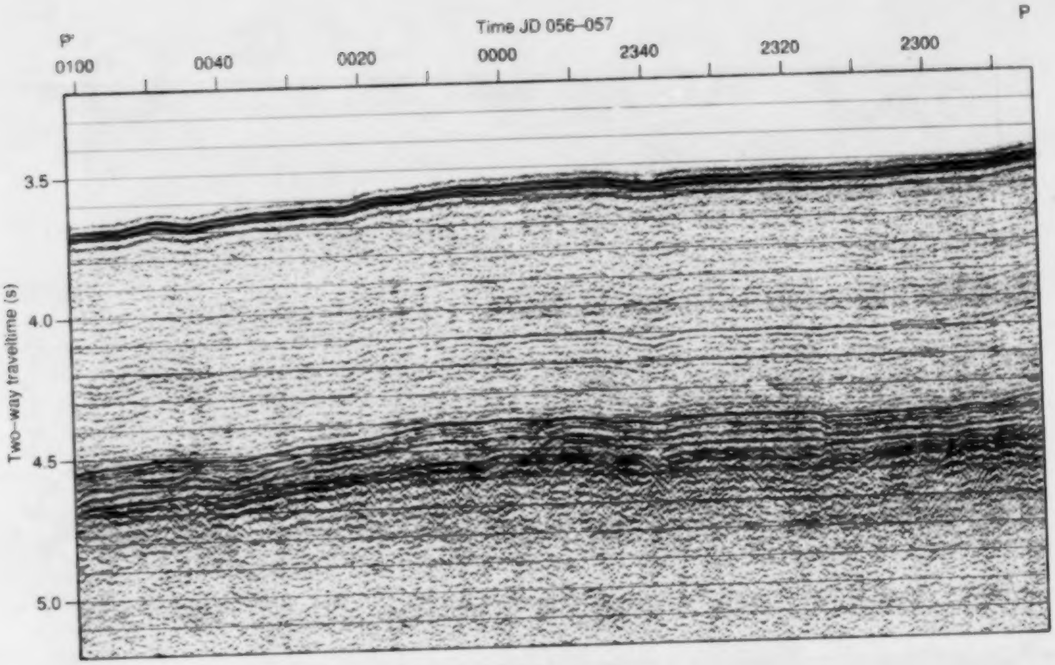

Figure 27. Profile P-P′ of processed digital single-channel Seismic Line 8.

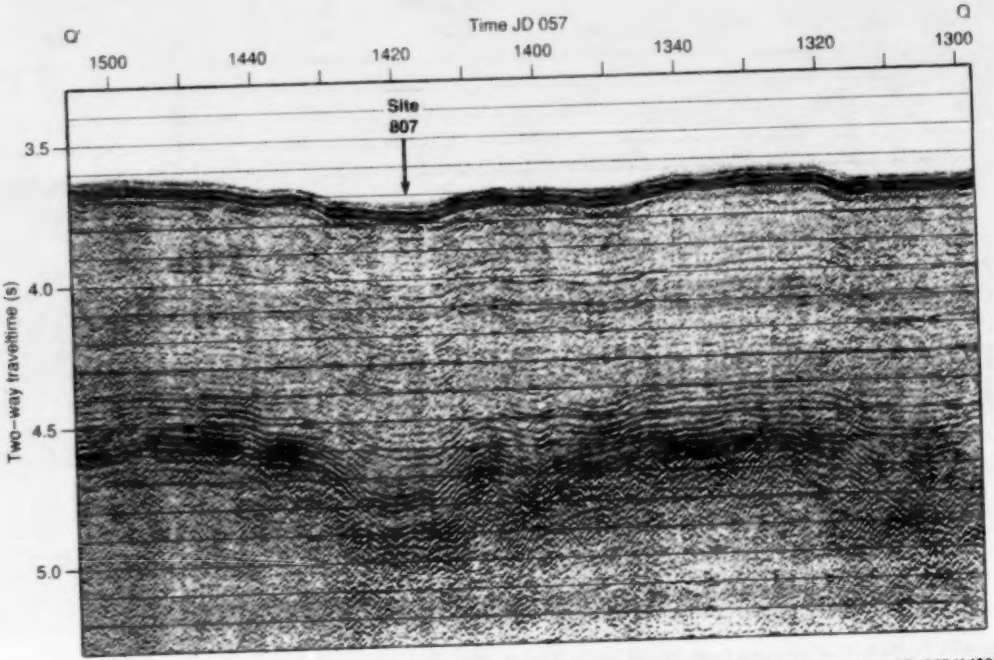

Figure 28. Profile Q-Q′ of processed digital single-channel Seismic Line 9 across the basement depression, at about JD 057/1420 UTC, drilled at Site 807.

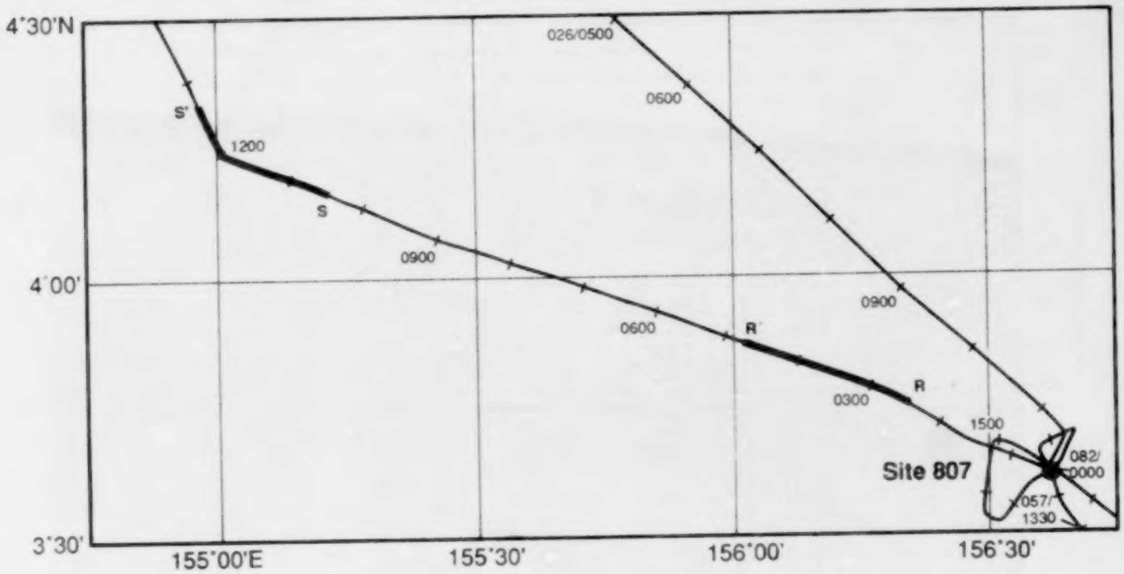
4°30'N
4°00'
3°30'
155°00'E
155°30'
156°00'
156°30'
026/0500
0600
S'
1200
S
0900
0600
R'
0900
R
0300
1500
082/
0000
Site 807
057/
1330

Figure 29. Ship track for single-channel Seismic Line 10 showing the locations of profiles R-R' and S-S'.

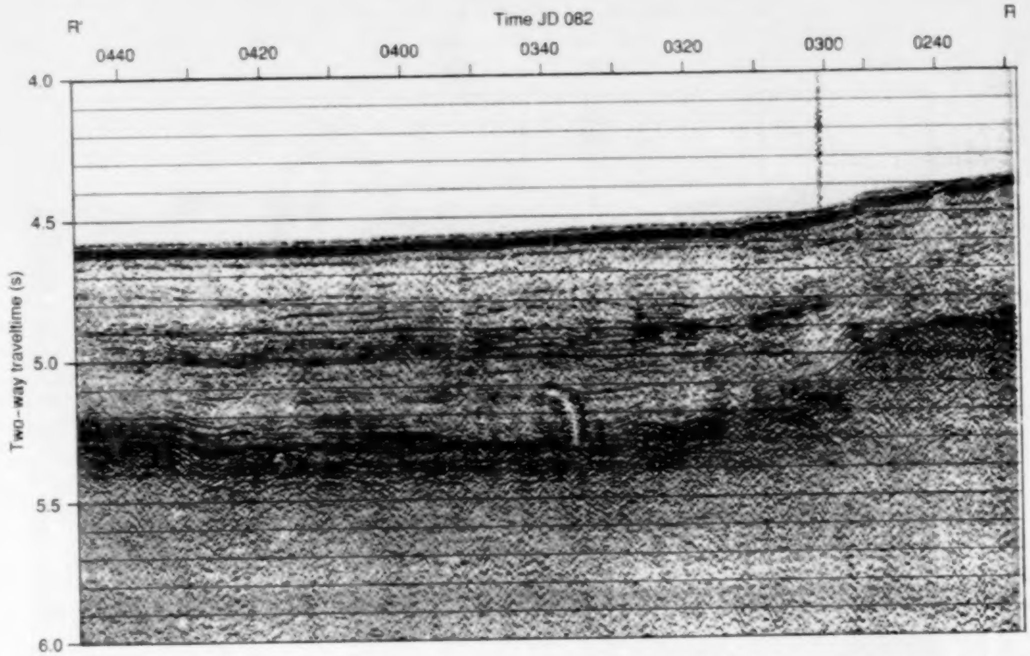

Figure 30. Profile R-R' of processed single-channel Seismic Line 10. The lower portion of the section thickens as the plateau slowly increases in depth to the north.

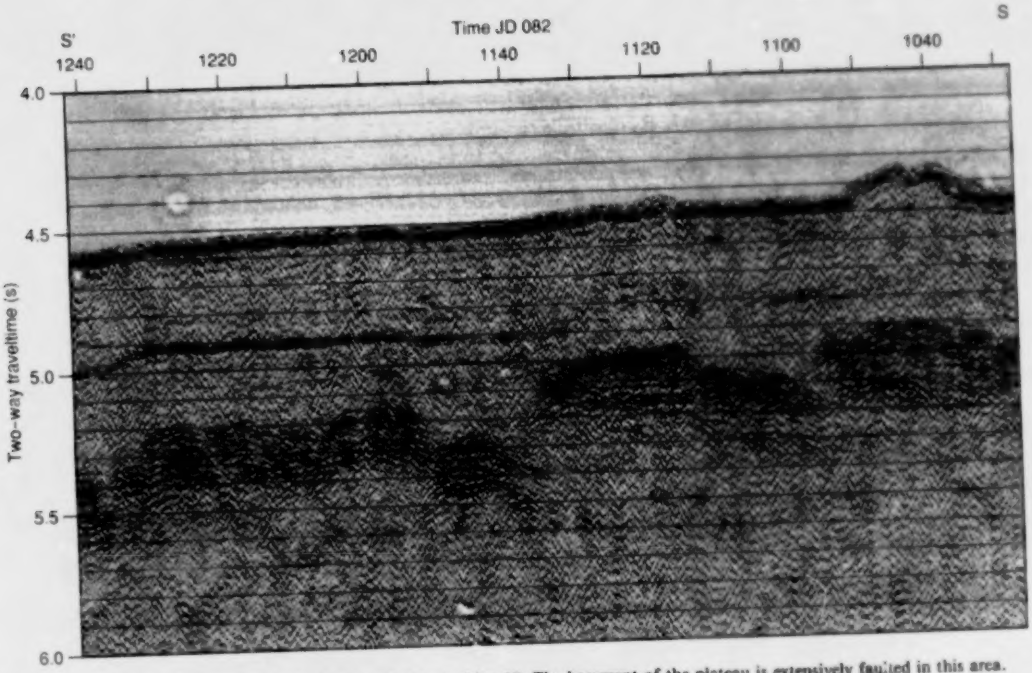

Figure 31. Profile S-S' of processed single-channel Seismic Line 10. The basement of the plateau is extensively faulted in this area.

SECTION 2: SITE REPORTS

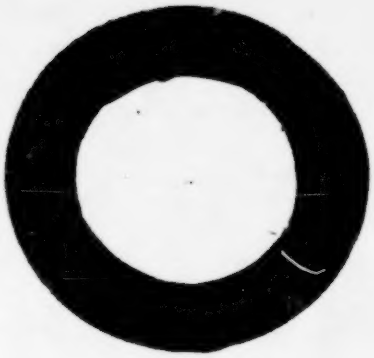

Kroenke, L. W., Berger, W. H., Janecek, T. R., et al., 1991
Proceedings of the Ocean Drilling Program, Initial Reports, Vol. 130

5. SITE 803[1]

Shipboard Scientific Party[2]

HOLE 803A

Date occupied: 28 January 1990

Date departed: 28 January 1990

Time on hole: 18 hr, 10 min

Position: 2°25.98′N, 160°32.40′E

Bottom felt (rig floor; m, drill-pipe measurement): 3421.5

Distance between rig floor and sea level (m): 11.80

Water depth (drill-pipe measurement from sea level, m): 3409.7

Total depth (rig floor; m): 3477.00

Penetration (m): 55.50

Number of cores (including cores with no recovery): 6

Total length of cored section (m): 55.50

Total core recovered (m): 57.99

Core recovery (%): 104.5

Oldest sediment cored:
  Depth (mbsf): 55.50
  Nature: nannofossil ooze
  Youngest age: Quaternary
  Oldest age: early Pliocene
  Measured velocity (km/s): 1.55

HOLE 803B

Date occupied: 28 January 1990

Date departed: 29 January 1990

Time on hole: 10 hr

Position: 2°25.98′N, 160°32.40′E

Bottom felt (rig floor; m, drill-pipe measurement): 3422.2

Distance between rig floor and sea level (m): 11.80

Water depth (drill-pipe measurement from sea level, m): 3410.4

Total depth (rig floor; m): 3483.50

Penetration (m): 61.30

Number of cores (including cores with no recovery): 7

Total length of cored section (m): 61.30

Total core recovered (m): 58.18

Core recovery (%): 94.9

Oldest sediment cored:
  Depth (mbsf): 61.30
  Nature: nannofossil ooze
  Youngest age: Quaternary
  Oldest age: Pliocene
  Measured velocity (km/s): 1.54

HOLE 803C

Date occupied: 29 January 1990

Date departed: 30 January 1990

Time on hole: 1 day, 9 hr, 15 min

Position: 2°25.98′N, 160°32.40′E

Bottom felt (rig floor; m, drill-pipe measurement): 3422.2

Distance between rig floor and sea level (m): 11.80

Water depth (drill-pipe measurement from sea level, m): 3410.4

Total depth (rig floor; m): 3659.70

Penetration (m): 237.50

Number of cores (including cores with no recovery): 23

Total length of cored section (m): 218.50

Total core recovered (m): 226.31

Core recovery (%): 103.6

Oldest sediment cored:
  Depth (mbsf): 218.50
  Nature: nannofossil ooze
  Youngest age: upper Pliocene
  Oldest age: middle/late Miocene
  Measured velocity (km/s): 1.62

HOLE 803D

Date occupied: 30 January 1990

Date departed: 6 February 1990

Time on hole: 7 days, 2 hr, 45 min

Position: 2°25.98′N, 160°32.46′E

Bottom felt (rig floor; m, drill-pipe measurement): 3424.0

Distance between rig floor and sea level (m): 11.80

Water depth (drill-pipe measurement from sea level, m): 3412.2

Total depth (rig floor; m): 4080.00

Penetration (m): 656.00

Number of cores (including cores with no recovery): 71

Total length of cored section (m): 656.00 (APC, 217.1; XCB, 394.9; RCB, 44)

Total core recovered (m): 494.96 (APC, 228.88; XCB, 248.47; RCB, 17.61)

Core recovery (%): 75.5 (APC, 105.4%; XCB, 62.9%; and RCB, 40.0%)

Oldest sediment cored:
  Depth (mbsf): 630.98
  Nature: claystone
  Youngest age: Quaternary
  Oldest age: Late Cretaceous
  Measured velocity (km/s): 1.87

Basement:
  Depth (mbsf): 630.98
  Nature: highly altered, fine grained, and pyroxene phyric pillow basalt
  Measured velocity (km/s): 4.18

---

[1] Kroenke, L. W., Berger, W. H., Janecek, T. R., et al., 1991. *Proc. ODP, Init. Repts.*, 130: College Station, TX (Ocean Drilling Program).

[2] Shipboard Scientific Party is as given in the list of participants preceding the contents.

Principal results: Site 803 (proposed Site OJP-4) is located near the equator on the northeastern margin of the Ontong Java Plateau (latitude 2°26.0′N, longitude 160°32.4′E) in 3410 m of water, roughly 400 km northeast of DSDP Site 289/586. Site 803 was occupied with three major objectives: (1) to serve as a deep-water anchor site on a Neogene depth transect designed to detect depth-related paleoceanographic signals; (2) to provide Paleogene and Cretaceous sediments for studies of pre-Neogene paleoceanography; and (3) to obtain basement rock for studies of the origin of the Ontong Java Plateau.

The site is located on a single-channel seismic (SCS) line acquired by the *Thomas Washington* during the ROUNDABOUT Cruise 11 "DANCER" survey. The site was positioned on the SCS line at 2205 hr UTC (Universal Time Coordinated) on 23 December 1989, between proposed Sites OJP-4 and OJP-4B.

Four holes were drilled at Site 803. Hole 803A, a dedicated hole, was cored with the advanced hydraulic piston corer to 55.5 m below seafloor (mbsf). Average recovery was 104%. Hole 803B was cored with the APC to 61.3 mbsf, at which point a core barrel became stuck and was left in the hole, which forced us in turn to abandon the hole. Average recovery was 95%. Hole 803C, after washing down 19 m, was cored with the APC to 237.5 mbsf; below this depth an APC rod parted during an 100,000-lb. overpull on Core 130-803C-24H, again forcing us to abandon a hole. Average recovery was 104%. We cored Hole 803D with the APC and the extended core barrel (XCB) to 612.0 mbsf; at this depth an 170,000-lb. overpull occurred that ended further XCB coring in the hole. After we dropped a free-fall funnel (FFF) in Hole 803D, it was successfully reentered using the slimline sonar reentry tool. We then cored Hole 803D with the rotary core barrel (RCB) to a total depth of 656.0 mbsf; this included 25.6 m of basement, of which 9.6 m was recovered. Average recovery at Hole 803D was 76%. The hole was successfully logged and a good suite of geophysical measurements was obtained.

The following lithostratigraphic units were recognized:

Unit I (0-563.7 mbsf): Pleistocene–upper Eocene nannofossil ooze and chalk to foraminifer nannofossil ooze and chalk, divisible into two subunits.

Subunit IA (0–217.1 mbsf): Pleistocene–middle Miocene nannofossil ooze to foraminifer nannofossil ooze. The ooze ranges in color from pale yellowish brown (at the top) through light gray to white. Bioturbation is ubiquitous. Faint color bands in various shades of green, purple, and red are common.

Subunit IB (217.1–563.7 mbsf): middle Miocene–upper Eocene nannofossil and foraminifer nannofossil chalk. Colors range from light gray to white. Bioturbation is common. Absent above 409 mbsf, color banding becomes more abundant, more intense, and more distinct downhole.

Unit II (563.7–621.8 mbsf): upper Eocene to middle Eocene nannofossil chalk with radiolarians, radiolarian nannofossil chalk, and nannofossil radiolarite. Sparse chert is present. Colors range from white to light brownish gray. Bioturbation is slight to heavy.

Unit III (621.8–626.3 mbsf): middle Eocene–lower Upper Cretaceous claystone and clayey siltstone, with minor nannofossil-bearing to radiolarian-rich intervals. Colors vary in intervals from brown to dark brown to very dark brown, with minor intervals of dark yellowish brown. Sharp contacts between colored intervals may represent significant unconformities. The discrepancy in the lower depth of Unit III and the upper depth of Unit IV is the result of using an "ODP-curated" depth for the base of Unit III and a "best guess" depth for basement based on drilling information.

Unit IV (630.4–656.0 mbsf): Cenomanian? or older tholeiitic basalts that are predominantly aphyric, fine grained, and nonvesicular. The basalts consist of multiple pillow lavas, which together make up a sequence roughly equivalent to one "subunit" at Site 807. Here at Site 803, the sequence was divided into nine subdivisions on the basis of interpillow limestones, suggesting flows distinctly separated in time. Average basalt recovery was 38%. Alteration varies from severe to mild, and small amounts of fresh glass are present.

Shipboard X-ray fluorescence (XRF) measurements indicate that the basalt units are chemically uniform and distinct from normal mid-ocean ridge basalt (MORB) (e.g., Zr/Nb = 14–17 vs. >30 for normal MORB). They are, however, quite similar to the basalt drilled at Site 289 on the Ontong Java Plateau, to the few analyzed basement lavas of Malaita (eastern Solomon Islands), and to the basalts drilled at Site 462 in the Nauru Basin (i.e., within the range of variation displayed by the flow and sill complex).

The severe alteration of the uppermost lava flow of Unit IV suggests the presence of a considerable hiatus between basaltic basement and Unit III. Moreover, the basal sediments of Unit III, which directly overlie basaltic basement, are not metalliferous. This situation also suggests that a significant hiatus may exist between the underlying basalt and the overlying basal sediments of Unit III. Additional hiatuses also may occur at overlying sharp color contacts in Unit III.

Despite the occurrence of dark-colored intervals in the siliciclastic sediments of Unit III, no evidence for the presence of black shales was detected. Because of the likelihood of significant hiatuses within the condensed section, however, their formation and deposition on the Ontong Java Plateau cannot be excluded.

The Cretaceous/Tertiary (K/T) boundary occurs near the top of Unit III. Remarkably, the entire K/T transition zone appears to have been preserved in Section 130-803D-68R-1. Initially restricted to the interval between 53 and 38 cm in Section 130-803D-68R-1 by nannofossil dating, the K/T boundary was finally placed at 45 cm in Section 130-803D-68R-1, based on the first appearance of *Thoracosphaera* at 46.5 cm in the section coupled with a peak in magnetic susceptibility at 45 cm in the section.

Above the K/T transition zone at the top of Unit III, a major hiatus occurs that encompasses most of the Paleocene and all of the lower Eocene. Sedimentation rates during the middle Eocene, about 7 m/m.y., almost doubled to 13 m/m.y. at 40 Ma, and increased to 25 m/m.y. at 35 Ma. In the late Oligocene, they dropped to below 10 m/m.y. but rose again dramatically during the Oligocene-Miocene transition, attaining 30 m/m.y. for a brief period just preceding the hiatus. Paleomagnetic analyses of the Oligocene sediments have resulted in a tentative magnetostratigraphy spanning Chrons 7 through 11. Preliminary analyses suggest a paleolatitude of 4.5°S for Site 803 during the Oligocene, which, in turn, suggests that the Ontong Java Plateau has been part of the Pacific Plate for the last 30 m.y.

A significant hiatus (or rather hiatus pair) occurred in the early Miocene within the interval from 22 to 15 Ma. Sedimentation rates in the middle Miocene are typically near 10 m/m.y. In the late Miocene, the rates abruptly increased, reaching a maximum near 30 m/m.y. between 6 and 8 Ma. After 5 Ma, sedimentation rates decreased rapidly, falling to near 10 m/m.y. in the late Pleistocene.

Pass-through cryogenic magnetometer measurements have yielded a virtually complete magnetostratigraphic sequence from 3.4 Ma to the present, including the Mammoth, Kaena, Olduvai, and Jaramillo subchrons. Sedimentation rates based on this magnetostratigraphy decreased from 15 to 10 m/m.y. at the base of the Olduvai Subchron (1.88 Ma), averaging 10 m/m.y. to the present. The cause of this drop in sedimentation rate is not obvious.

Hole 803D logging data, in conjunction with a detailed suite of physical property measurements obtained from the split cores, confirm the depth of the ooze-chalk transition and reveal the presence of local maxima and minima in velocity that correlate with chert horizons and radiolarian-rich zones deep in the section. The logs also provide important data for the generation of synthetic seismograms.

Results from interstitial water geochemistry at Site 803 suggest that, in contrast to Site 289, there is no evidence of nonconservative behavior of Mg, despite the presence of a noticeable ash layer. Calcium and magnesium depth gradients are larger, and the maximum dissolved strontium concentrations are higher at Site 803 than at Site 289.

BACKGROUND AND OBJECTIVES

Overview

The general background for all sites is contained in the "Introduction" chapter of this volume. Site 803 (proposed Site OJP-4), the first of the Leg 130 sites to be drilled on the Ontong Java Plateau, was scheduled as one of the deep-water sites for a depth transect of Neogene sediments along the equator. The transect was designed for the study of paleoceanographic events of global significance. The pelagic sediment cover of the plateau is uniquely suited for such studies. The maximum thickness of the cover is more than 1200 m; moreover, it occurs below the crest of the plateau in water depths greater than 2200 m. The water depth at the site (near the lysocline) promised a large carbonate dissolution signal, as reflected in the various sediment properties.

We anticipated that the section would be reasonably complete, despite the loss from carbonate dissolution, at least above the Eocene. This site also was planned for drilling to basement, and our hope was to recover Paleogene and Cretaceous sediments, as well as basement rock, for pre-Neogene paleoceanography and for studies on the origin of the Ontong Java Plateau. Within the upper portion of the section, we drilled multiple holes to provide material for concurrent detailed studies and to provide for overlap between cores.

We reached basement after penetrating 630 m of sediment. The proportional decrease in thickness of sediment that occurs with increasing depth of the seafloor varies between the different sediment layers, as can be seen on the seismic profiles (see "Introduction" chapter, this volume). The linkage of paleoceanographic events to acoustic stratigraphy will allow three-dimensional mapping as well as correlation into distant sediment sections throughout the Pacific basin.

Background

The Ontong Java Plateau (see Fig. 1, "Introduction" chapter, this volume) is a broad, shallow, mid-ocean submarine plateau in the western equatorial Pacific. Its shallowest regions lie above 2000 m, and its flanks reach depths in excess of 4500 m. With an area of 1.5 million km^2, it is the largest of the "classic" Pacific plateaus. The plateau has a crustal thickness on the order of 40 km, yet it is in isostatic equilibrium, apparently maintaining its depth over much of its history. Crustal seismic velocities are in the range of oceanic crust (Hussong et al., 1979).

The Ontong Java Plateau has long been the focus of paleoceanographic studies based on conventional coring and on seismic profiling. Leg 130 is the fourth drilling expedition to sample the sediment cover here: four Deep Sea Drilling Project (DSDP) sites were drilled earlier on the plateau. Three sites were rotary drilled, with Site 64 spot cored during Leg 7 (Winterer, Riedel, et al., 1971) and Sites 288 and 289 continuously cored during Leg 30 (Andrews, Packham, et al., 1975). Site 289, which was drilled in a water depth of 2206 m, ended at 1271 mbsf in tholeiitic basalt overlain by Aptian sediments. Sediment thickness at Site 289 was 1262 m, of which the lowermost 293 m were mid-Cretaceous to upper Eocene radiolarian-bearing limestones, nannofossil foraminifer chalks, and nodular cherts. The upper 969 m consisted of upper Eocene to Pleistocene nannofossil foraminifer chalks and oozes, with a continuous section down to the lower Oligocene. Semilithified chalk was first encountered near 250 mbsf, in the upper Miocene part of the section. Site 586, drilled on Leg 89 next to Site 289, was piston-cored to 305 mbsf, the lowermost upper Miocene (Moberly, Schlanger, et al., 1986), and recovered a complete section of well-preserved nannofossil ooze.

Objectives

Site 803, roughly 400 km northeast of DSDP Sites 289/586 on the northeastern margin of the Ontong Java Plateau, was planned as the first of the four Leg 130 sites that constitute a Neogene depth transect (Sites 803–806; Fig. 1). This transect, complementary to similar ODP transects elsewhere along the equator, was designed to allow detection of depth-related paleoceanographic signals. The sediments sampled along the transect would have been produced in the same surface-water conditions and thus in the same pelagic rain; any differences in accumulation and preservation could be attributed to depth effects. The depth sampled at Site 803 (Fig. 1), near the lysocline (around the 3400 m), is that at which dissolution gradients are most pronounced, so that saturation fluctuations should leave a maximum imprint in physical properties (Johnson et al., 1977). In turn, this imprint should be detectable in the acoustic stratigraphy (Berger and Mayer, 1978; Mayer et al., 1986).

With regard to Paleogene and Cretaceous sediments, ocean-wide coverage leaves much to be desired. Recovery has been much less comprehensive than in the Neogene. Substantial hiatuses exacerbate this situation. Major hiatuses were encountered in Upper Cretaceous to Paleogene sediments previously drilled at DSDP Sites 288 and 289, lowering expectations for finding complete sequences. However, many of the unconformities at Site 288 do not correlate with those at Site 289 (or the shallower, spot-cored Site 64), implying that they represent local events of limited areal extent (Andrews, Packham, et al., 1975). There was some hope, therefore, that drilling at Site 803 would recover key sections missed earlier. There was also the expectation that we would find clues to the extent of Cretaceous anoxic events in the South Pacific and to the original basement depth of the Ontong Java Plateau and subsequent bathymetric change. Although we assigned a low probability of success to the goal of recovering a well-preserved Cretaceous/Tertiary boundary and despite the presence of a foreshortened section, the K/T boundary was indeed recovered at this site.

We planned to sample basement at Site 803 for dating purposes and petrologic analyses. Basement previously had been drilled at Site 289, recovering basalt samples of varying texture from several meters of penetration. Recently, a ^{40}Ar/^{39}Ar date of 113 Ma was obtained on one sample of this basalt (R. Duncan, pers. comm., 1990). With a second basement sample from Site 803, and a third from Site 807, the nature and origin of the Ontong Java Plateau could be determined on a much sounder basis.

The criteria used to select Site 803 included the avoidance of erosion (i.e., reflection hyperbolae or channel structures), displacement or disruption in the sediment column, faulting, and such seismic anomalies as the strongly reverberant mid-section reflectors (MSRs) that commonly occur throughout the area (see Mayer et al., this volume). Site 803 is located in 3410 m of water, about one mile west of a small MSR (Fig. 2). The thickness of the sedimentary section at the site is 0.65 s (two-way traveltime [twt]), approximately 60% of that at Sites 289/586. The section is well stratified and appears to include most of the Neogene seismic reflection horizons that had been previously mapped on the Ontong Java Plateau.

OPERATIONS

Guam to Site 803

The *JOIDES Resolution* left Guam at 0215 hr (UTC) on 23 January 1990 and steamed toward Site 803 (proposed Site OJP-4), 1180 nmi southeast of Guam. The magnetometer was streamed at 0255 hr. The first leg of the transit covered 932 nmi to proposed Site OJP-5 (future Site 807) at an average speed of 11.4 kt. Seas were moderate at 5–9 ft, with winds gusting 28–40 kt and side currents running at 3 kt. A 42-nmi seismic survey was run at 8 kt over the OJP-5 site, and a 239-nmi seismic survey was run at 8 kt to Site 803 (OJP-4) (see "Underway Geophysics" chapter, this volume). The entire transit to the first site covered 1213 nmi in 120 hr at an average speed of 10.1 kt.

Site 803

A 19-nmi, pre-site seismic survey was run over the site area under optimal global positioning system (GPS) windows. The first beacon was dropped at 0120 hr on 28 January 1990 over proposed Site OJP-4A. A second beacon was dropped at 0126 hr to mark proposed Site OJP-4.

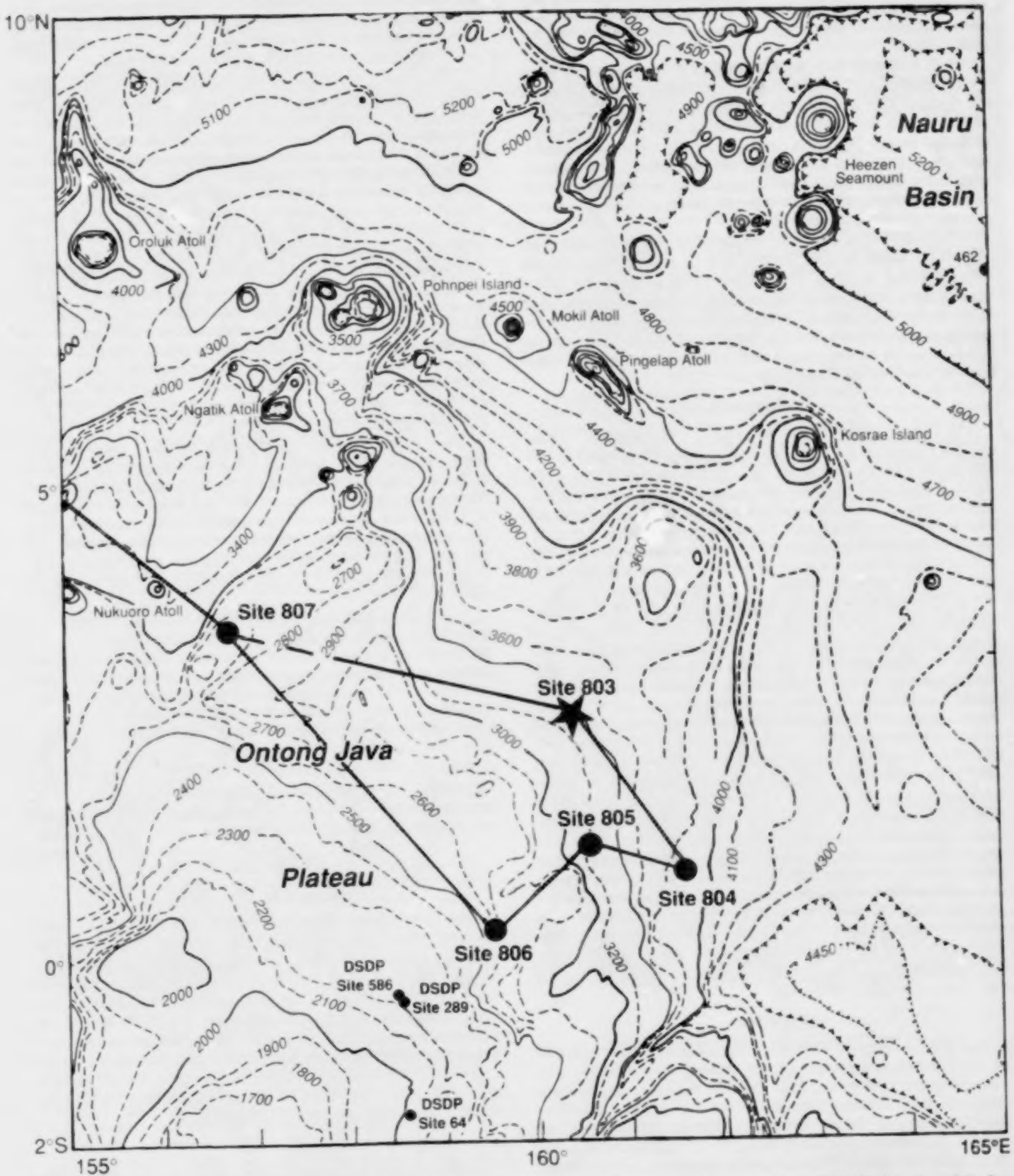
10°N
5°
0°
2°S
155°
160°
165°E
Nauru
Basin
Heezen Seamount
462
Oroluk Atoll
Pohnpei Island
Mokil Atoll
Pingelap Atoll
Ngatik Atoll
Kosrae Island
Nukuoro Atoll
Site 807
Site 803
Site 805
Site 804
Site 806
Ontong Java
Plateau
DSDP Site 586
DSDP Site 289
DSDP Site 64
5100
5200
5000
4500
4900
5200
4000
4300
3500
4500
4800
5000
4900
4000
3700
4400
4200
4700
3400
3900
3800
3600
2700
2800
2900
3600
3000
2700
2400
2500
2600
2300
4000
4100
4300
2200
3200
4450
2000
2100
2000
1900
1800
1700

Figure 1. Bathymetry in meters of the northwestern part of the Ontong Java Plateau (after Mammerickx and Smith, 1985). The location of the Leg 130 sites together with those from DSDP Legs 7, 30, and 89 are shown for reference. Contour interval is 100 m.

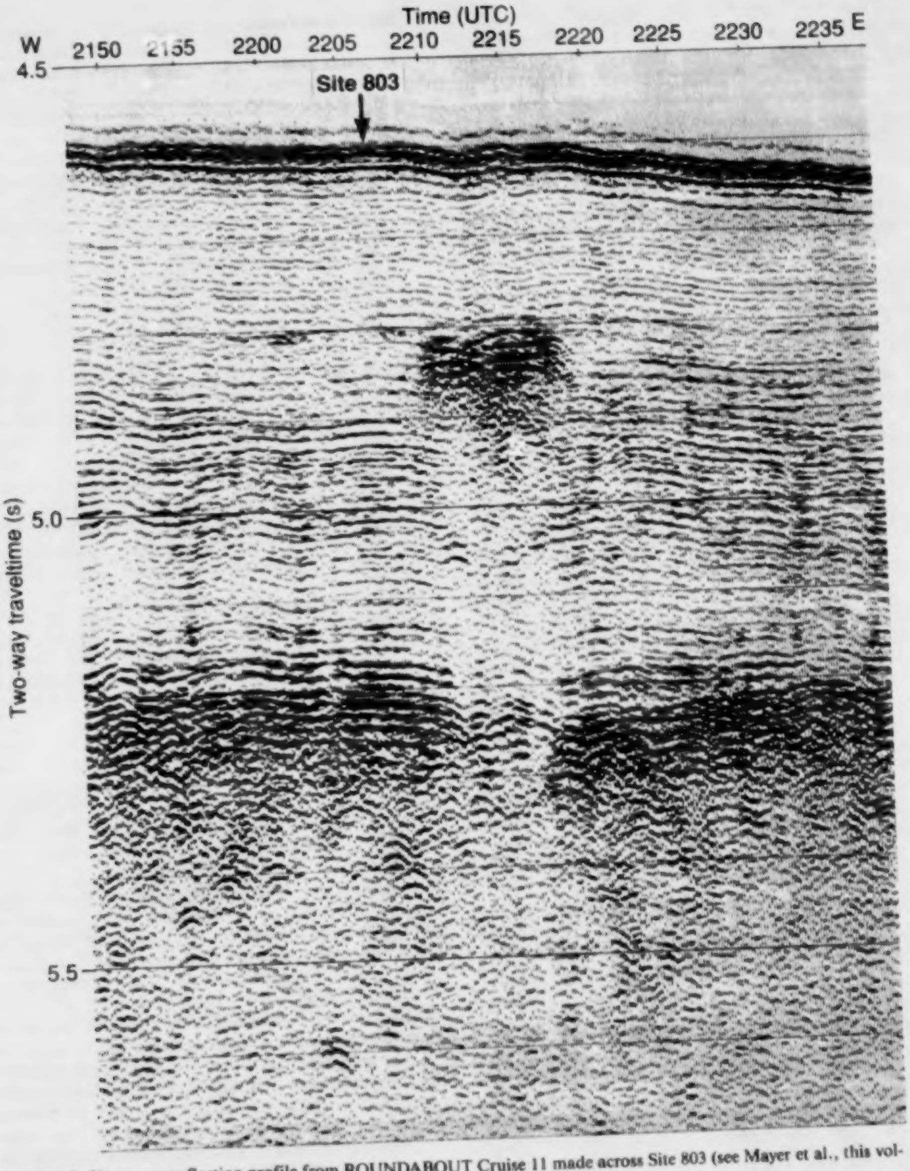

Figure 2. Site survey reflection profile from ROUNDABOUT Cruise 11 made across Site 803 (see Mayer et al., this volume).

Hole 803A

The ship was positioned 100 m east of the second beacon, and Hole 803A was spudded at 1300 hr on 28 January 1990 at 2°25.98′N and 160°32.40′E in 3409.7 m of water.

Cores 130-803A-1H through -6H were taken from 0 to 55.5 mbsf with 55.5 m of sediment cored and 57.99 m recovered (104.49% recovery; see Table 1). Orientation surveys were taken during Cores 130-803A-3H through -6H, but the orientation sleeve broke during the surveys, and the orientation data are questionable. The new, stronger APC piston-rod assembly was tested in this hole and was used throughout Leg 130. The hole was terminated per program after Core 130-803A-6H. The pipe was pulled out of the hole and the bit cleared the seafloor at 1930 hr on 28 January 1990, ending Hole 803A.

Hole 803B

The ship was offset 20 m east of Hole 803A, and Hole 803B was spudded at 2050 hr on 28 January 1990 in 3410.4 m of water. Cores 130-803B-1H through -7H were taken from 0 to 61.3 mbsf with 61.3 m of sediment cored and 58.18 m recovered (94.91% recovery; see Table 1). Orientation surveys were taken

Table 1. Coring summary, Site 803.

Core no.	Date (1990)	Time (UTC)	Depth (mbsf)	Cored (m)	Recovered (m)	Recovery (%)
130-803A-						
1H	Jan. 28	1325	0–8.0	8.0	6.04	100.0
2H	28	1430	8.0–17.5	9.5	9.90	104.0
3H	28	1545	17.5–27.0	9.5	10.05	105.8
4H	28	1645	27.0–36.5	9.5	10.02	105.5
5H	28	1745	36.5–46.0	9.5	9.89	104.0
6H	28	1845	46.0–55.5	9.5	10.09	106.2
Coring totals				55.5	57.99	104.5
130-803B-						
1H	28	2115	0–4.3	4.3	4.36	101.0
2H	28	2200	4.3–13.8	9.5	9.89	104.0
3H	28	2300	13.8–23.3	9.5	9.82	103.0
4H	29	0015	23.3–32.8	9.5	9.85	103.0
5H	29	0115	32.8–42.3	9.5	10.06	105.9
6H	29	0215	42.3–51.8	9.5	6.85	72.1
7H	29	0315	51.8–61.3	9.5	7.35	77.3
Coring totals				61.3	58.18	94.9
130-803C-						
1H	29	1300	19.0–28.5	9.5	9.80	103.0
2H	29	1350	28.5–38.0	9.5	9.56	100.0
3H	29	1450	38.0–47.5	9.5	9.88	104.0
4H	29	1610	47.5–57.0	9.5	9.92	104.0
5H	29	1705	57.0–66.5	9.5	9.92	104.0
6H	29	1800	66.5–76.0	9.5	9.30	97.9
7H	29	1920	76.0–85.5	9.5	10.13	106.6
8H	29	2030	85.5–95.0	9.5	10.10	106.3
9H	29	2130	95.0–104.5	9.5	9.79	103.0
10H	29	2230	104.5–114.0	9.5	10.03	105.6
11H	29	2315	114.0–123.5	9.5	10.04	105.7
12H	30	0110	123.5–133.0	9.5	9.74	102.0
13H	30	0210	133.0–142.5	9.5	10.07	106.0
14H	30	0310	142.5–152.0	9.5	9.38	98.7
15H	30	0400	152.0–161.5	9.5	9.77	103.0
16H	30	0445	161.5–171.0	9.5	10.15	106.8
17H	30	0530	171.0–180.5	9.5	10.03	105.6
18H	30	0630	180.5–190.0	9.5	10.13	106.6
19H	30	0730	190.0–199.5	9.5	9.83	103.0
20H	30	0930	199.5–209.0	9.5	10.14	106.7
21H	30	1030	209.0–218.5	9.5	9.83	103.0
22H	30	1120	218.5–228.0	9.5	8.81	92.7
23H	30	1205	228.0–237.5	9.5	9.96	105.0
Coring totals				218.5	226.31	103.6
130-803D-						
1H	30	1700	0–2.5	2.5	2.53	101.0
2H	30	1830	2.5–12.0	9.5	9.94	104.0
3H	30	1940	12.0–21.5	9.5	9.84	103.0
4H	30	2100	21.5–31.0	9.5	10.01	105.3
5H	30	2155	31.0–40.5	9.5	9.92	104.0
6H	30	2300	40.5–46.1	5.6	9.87	176.0
7H	31	0000	46.1–55.6	9.5	9.98	105.0
8H	31	0100	55.6–65.1	9.5	9.93	104.0
9H	31	0215	65.1–74.6	9.5	9.82	103.0
10H	31	0315	74.6–84.1	9.5	9.86	104.0
11H	31	0400	84.1–93.6	9.5	9.68	102.0
12H	31	0445	93.6–103.1	9.5	9.61	101.0
13H	31	0545	103.1–112.6	9.5	9.81	103.0
14H	31	0630	112.6–122.1	9.5	9.51	100.0
15H	31	0715	122.1–131.6	9.5	9.54	100.0
16H	31	0745	131.6–141.1	9.5	9.57	101.0
17H	31	0915	141.1–150.6	9.5	9.97	105.0
18H	31	1015	150.6–160.1	9.5	9.72	102.0
19H	31	1110	160.1–169.6	9.5	9.55	100.0
20H	31	1155	169.6–179.1	9.5	10.00	105.2
21H	31	1250	179.1–188.6	9.5	10.06	105.9
22H	31	1335	188.6–198.1	9.5	10.07	106.0
23H	31	1440	198.1–207.6	9.5	10.10	106.3
24H	31	1730	207.6–217.1	9.5	9.99	105.0
25X	31	1910	217.1–226.8	9.7	6.34	65.3
26X	31	2045	226.8–236.5	9.7	9.21	94.9
130-803D- (Cont.)						
27X	31	2230	236.5–245.9	9.4	4.32	45.9
28X	31	2345	245.9–255.5	9.6	6.90	71.9
29X	Feb. 1	0045	255.5–265.1	9.6	7.46	77.7
30X	1	0145	265.1–274.7	9.6	6.00	62.5
31X	1	0245	274.7–284.3	9.6	5.81	60.5
32X	1	0345	284.3–294.1	9.8	7.98	81.4
33X	1	0430	294.1–303.3	9.2	7.85	85.3
34X	1	0515	303.3–313.0	9.7	9.54	98.3
35X	1	0555	313.0–322.7	9.7	9.01	92.9
36X	1	0645	322.7–332.3	9.6	9.16	95.4
37X	1	0740	332.3–342.0	9.7	9.63	99.3
38X	1	0810	342.0–351.6	9.6	8.44	87.9
39X	1	0855	351.6–361.3	9.7	9.06	93.4
40X	1	0955	361.3–371.0	9.7	7.51	77.4
41X	1	1045	371.0–380.7	9.7	5.50	56.7
42X	1	1135	380.7–390.4	9.7	7.05	72.7
43X	1	1225	390.4–400.0	9.6	7.28	75.8
44X	1	1320	400.0–409.7	9.7	8.28	85.3
45X	1	1430	409.7–419.3	9.6	9.18	95.6
46X	1	1530	419.3–429.0	9.7	8.39	86.5
47X	1	1630	429.0–438.6	9.6	7.20	75.0
48X	1	1730	438.6–447.8	9.2	6.01	65.3
49X	1	1830	447.8–457.5	9.7	6.03	62.1
50X	1	1930	457.5–467.2	9.7	6.17	63.6
51X	1	2030	467.2–476.9	9.7	4.60	47.4
52X	1	2145	476.9–486.6	9.7	4.52	46.6
53X	1	2245	486.6–496.3	9.7	5.66	58.3
54X	1	2345	496.3–506.0	9.7	6.63	68.3
55X	2	0045	506.0–515.6	9.6	6.37	66.3
56X	2	0145	515.6–525.3	9.7	9.10	93.8
57X	2	0230	525.3–534.6	9.3	5.66	60.8
58X	2	0345	534.6–544.3	9.7	1.26	13.0
59X	2	0430	544.3–554.0	9.7	3.90	40.2
60X	2	0535	554.0–563.7	9.7	2.50	25.8
61X	2	0645	563.7–573.4	9.7	0.80	8.3
62X	2	0800	573.4–583.0	9.6	0.40	4.2
63X	2	1215	583.0–588.7	5.7	0.37	6.5
64X	2	1505	588.7–598.4	9.7	0.55	5.7
65X	2	1715	598.4–601.9	3.5	0.48	13.7
66X	2	1940	601.9–612.0	10.1	0.36	3.6
67R	4	0645	612.0–621.8	9.8	2.52	24.7
68R	4	0810	621.8–631.4	9.6	4.95	51.5
69R	4	1140	631.4–641.1	9.7	3.91	40.3
70R	4	1555	641.1–650.8	9.7	3.10	31.9
71R	4	1910	650.8–656.0	5.2	3.13	60.2
Coring totals				656.0	494.96	75.5

during Cores 130-803B-3H through -7H, but the camera malfunctioned and no data were recovered.

Cores 130-803B-6H and -7H were taken using the new APC breakaway piston head (BPH), with 19.0 m of sediment cored and 14.20 m recovered (74.74% recovery; see Table 1). The BPH separated successfully on both runs.

While putting the APC core-barrel assembly into position for Core 130-803B-8H, the core barrel became stuck and could not be pulled out with an air tugger. Several attempts to free the core barrel were unsuccessful, and the drill pipe was finally tripped out of the hole to recover the core barrel. The bit cleared the seafloor at 0530 hr on 29 January 1990, ending Hole 803B.

Hole 803C

The ship was offset 20 m east of Hole 803B for further APC coring. We intended to run the drill pipe 19 mbsf to spud the hole, but the first two APC attempts were water cores. A recheck of the drill pipe revealed that one stand had been left out of the string. The additional stand was run in the hole, and

Hole 803C was spudded at 1130 hr, 29 January 1990; the hole was washed to 19.0 mbsf.

Cores 130-803C-1H through -23H were taken from 19.0 to 237.5 mbsf, with 218.5 m of sediment cored and 226.31 m recovered (103.6% recovery; see Table 1). Orientation surveys were taken on Cores 130-803C-1H through -23H. Directional surveys at 28.5 and 57.0 mbsf indicated 1° of vertical drift. After Core 130-803C-24H (247.0 mbsf) was fired, the core would not pull free, even with 100,000 lb of overpull. The new, "stronger" APC piston rod parted in the top thread, leaving the core barrel, with Core 130-803C-24H, in the hole. The drill pipe was pulled out of the hole to retrieve the core barrel, and it cleared the seafloor at 1445 hr on 30 January 1990, thus ending Hole 803C.

Hole 803D

The ship was offset 20 m east of Hole 803C, and Hole 803D was spudded at 1630 hr on 30 January 1990 in 3412.2 m of water. Cores 130-803D-1H through -24H were taken from 0 to 217.1 mbsf, with 217.1 m of sediment cored and 228.88 m recovered (105.43% recovery). Orientation surveys were taken on Cores 130-803D-3H through -24H.

Core 130-803D-24H did not fully stroke out, and the core barrel temporarily became stuck in moderately stiff nannofossil ooze. Attempts to drill over the core barrel proved unsuccessful. Repeated overpulls, up to 170,000 lb, finally freed the core barrel.

We ended APC coring at this point and began coring with the XCB. Cores 130-803D-25X through -66X were taken from 217.1 to 612.0 mbsf with 394.9 m of sediment cored and 248.47 m recovered (62.92% recovery). Various flapper and finger core catchers and XCB bits were tried in an effort to improve the XCB recovery of the stiff white nannofossil/chalk sediments. Good core recovery (62.79%) was obtained with six-tooth, hard-formation (sharp) carbide bits using two, hard-formation core catchers with soft springs. Recovery dropped to 15.69% below Core 130-803D-57X (534 mbsf) as a result of the core jamming in the bit. Poor circulation through the bit was suspected, and the bit seal was found to be severely cut (after sustaining 90 core barrel runs).

An FFF was dropped in Hole 803D so that we could core into basement with an RCB reentry in the same hole, rather than wash down a new RCB hole. The purpose in using the FFF was not only to save time but also to test the televiewer (TV) camera and coaxial cable, which would be required later at proposed Site OJP-5. The TV picture was fuzzy but usable on deck. However, the picture was lost at 140 meters below sea level (mbsl), despite repair attempts. Although the loss of the TV picture was critical, the FFF was equipped with four floats and a sonar target as a precaution, and through-the-drill-pipe slimline sonar was available as a reentry backup tool. The bottom hole assembly (BHA) was run in to 8 m above the sea floor, the Schlumberger logging line was rigged up, and the sonar was run through the drill pipe. The sonar acquired the FFF target, and reentry was successfully completed. This was the first known reentry of an FFF using the through-the-drill-pipe slimline sonar tool.

Cores 130-803D-67R through -71R were taken from 612.0 to 656.0 mbsf. Basalt was encountered at 630.4 mbsf, and a total of 9.59 m of hard rock was recovered. At this point, we had achieved our scientific objectives; therefore, we terminated coring and released the bit at the bottom of the hole. After a short trip to condition the hole, a viscous mud sweep was circulated to clean the hole. The seafloor was unconsolidated down to 55 mbsf, so the open-ended BHA was pulled up to only 109 mbsf for logging.

Downhole logs were run as follows:

Run No. 1 (NGT/DIT/HLDT/LSS/TLT). The log was run from a depth of 649.2 to 534.9 mbsf at a speed of 900 ft/hr. Because the HLDT/LSS tools were not functioning properly, the tool was run at a speed of 1800 ft/hr to 98.7 mbsf.

Run No. 2 (NGT/FMS/TLT). The connector head on the FMS tool flooded as the tool was run in the hole. The tool was pulled out of the hole and dried out, and a successful run was made from 609.8 to 98.7 mbsf. A repeat log was run from 191.7 to 98.7 mbsf.

Run No. 3 (NGT/ACT/GST/HLDT). The log was run from 610.5 to 464.8 mbsf at 600 ft/hr. Because the GST was not functioning properly, the log was run at 900 ft/hr from 464.8 to 98.7 mbsf.

Run No. 4 (NGT/BHC/TLT). Two logs, one from 605.6 to 98.7 mbsf and another from 606.8 to 101.1 mbsf, were run successfully.

When the logging program was completed, the pipe was pulled out of the hole and the BHA cleared the rotary table at 1730 hr, 6 February 1990, ending Hole 803D.

LITHOSTRATIGRAPHY

Introduction

Four holes were drilled at Site 803. Holes 803A and 803B were cored with the APC, and approximately 60 m of sediment was recovered from the top of the section in each. The recovery rate averaged 99.5% at these two holes. Hole 803C was cored with a combination of APC and XCB methods; sediments were recovered to 226 mbsf, with a recovery rate of 103.6%. The complete section was cored at Hole 803D with a combination of APC, XCB, and RCB methods, and sediments were recovered throughout the entire thickness of 626 m. The average recovery rate was 75.7%, but it gradually decreased downhole. The cored sequence is composed predominantly of nannofossil ooze and chalk, with variable abundances of foraminifers. Radiolarian abundances increase below 564 mbsf, and siliciclastic rocks dominate the basal 4.5 m of sediment. The recovered sediments range in age from Pleistocene to early Late Cretaceous and overlie basaltic rocks, which were recovered in Section 130-803D-68R-4 through Core 130-803D-71R. The basalts are described elsewhere in this chapter (see "Igneous Petrology" section, this chapter).

The sedimentary section at Site 803 has been divided into three lithologic units (Table 2 and Fig. 3). Unit I (0–563.7 mbsf) is composed of Pleistocene to upper Eocene nannofossil ooze and chalk to foraminifer nannofossil ooze and chalk and is divided into two subunits on the basis of degree of consolidation. Subunit IA is composed of ooze, whereas Subunit IB contains chalk; the ooze-chalk transition is located between 210 and 220 mbsf (near the base of Core 130-803D-24H), the level at which cores could no longer be split with a wire. Unit II is composed of approximately 58 m of nannofossil chalk with radiolarians, radiolarian nannofossil chalk, nannofossil radiolarite, and minor amounts of chert, and is late Eocene to middle Eocene in age. Unit III is composed of approximately 4.5 m of claystone, clayey siltstone, and minor radiolarite of latest Paleocene to early Late Cretaceous age; this unit is severely condensed and contains several major unconformities.

Description of Units

Unit I

Intervals: Hole 803A, Cores 130-803A-1H to -6H; Hole 803B, Cores 130-803B-1H to -7H; Hole 803C, Cores 130-803C-1H to -23H; Hole 803D, Cores 130-803D-1H to -60X
Age: Pleistocene-late Eocene
Depth: 0–563.7 mbsf

Table 2. Lithologic summary, Site 803.

Lithologic unit	Cores	Depth (mbsf)	Age	Lithology
IA	803A-1H to -6H 803B-1H to -7H 803C-1H to -23H 803D-1H to -24H	0–217.1	Pleistocene to middle Miocene	Nannofossil ooze to foraminifer nannofossil ooze
IB	803D-25 to -60X	217.1–563.7	middle Miocene to late Eocene	Nannofossil chalk to nannofossil chalk with foraminifers
II	803D-61X to -67R	563.7–621.8	late Eocene to middle Eocene	Nannofossil chalk with radiolarians to nannofossil radiolarite and chert
III	803D-68R-1 to -68R-3	621.8–626.3	middle Eocene to early Late Cretaceous	Claystone and clayey siltstone

Unit I is composed of nannofossil ooze and chalk to foraminifer nannofossil ooze and chalk and has been divided into two subunits. Subunit IA (0–217.1 mbsf) comprises the nannofossil ooze to foraminifer nannofossil ooze, whereas Subunit IB (217.1–563.7 mbsf) contains the nannofossil chalk to foraminifer nannofossil chalk.

Subunit IA

Intervals: Hole 803A, Cores 130-803A-1H to -6H; Hole 803B, Cores 130-803B-1H to -7H; Hole 803C, Cores 130-803C-1H to -23H; Hole 803D, Cores 130-803D-1H to -24H
Age: Pleistocene–middle Miocene
Depth: 0–217.1 mbsf

Subunit IA contains 217.1 m of nannofossil ooze, nannofossil ooze with foraminifers, and foraminifer nannofossil ooze. Foraminifer abundances decrease downhole through the first 30–60 m of Subunit IA, producing a lithologic transition from foraminifer nannofossil ooze to nannofossil ooze with foraminifers to nannofossil ooze. Foraminifer abundances remain low (<10%) through the remainder of Subunit IA, with a slight increase in Cores 130-803D-17H and -18H (upper Miocene sediments).

Dominant colors are various types of white (2.5Y N8/, 2.5Y 8/2, 5Y 8/1, 10YR 8/1, and 10YR 8/2) and light gray (2.5Y N7/, 5Y 7/1, and N7/). The uppermost 20 m, the Pleistocene section, also exhibits pale yellowish brown (10YR 6/3) to pale yellow (10YR 7/3) colors. Primary depositional sedimentary structures were not observed in Subunit IA. Bioturbation is ubiquitous, ranging in intensity from slight to heavy (Fig. 4). Faint color bands, one centimeter to several tens of centimeters thick in various shades of green, purple, and red, are common in most of Subunit IA (Fig. 5). Only Cores 130-803C-20H, -21H, and -23H, and Cores 130-803D-23H and -24H, in the lowermost portion of Subunit IA, do not contain these color bands.

Small faults with centimeter-scale offsets were observed in Sections 130-803B-6H-3 through -7H-2 (45–55 mbsf), 130-803C-9H-1 through -4 (95–101 mbsf), and 130-803D-16H-4 (136–138 mbsf) (Fig. 6). Angular discordances in color banding not attributed to coring disturbance were observed in Sections 130-803C-7H-4 through -6 (81–86 mbsf), 130-803C-14H-1 through -3 (142–147 mbsf), 130-803C-18H-6 through -19H-2 (188–193 mbsf), 130-803C-22H-3 through -6 (221–228 mbsf), and 130-803D-22H-2 through -7 (190–198 mbsf). These angular discordances are commonly overlain by an interval, one to several meters thick, that contains 5%–10% more foraminifers than the underlying sediments.

The only significant occurrence of a different lithology within Subunit IA is a thin (<1 cm thick) volcanic ash layer recovered in Sections 130-803C-18H-2, 77 cm, and 130-803D-21H-2, 61 cm (Figs. 7 and 8). In both holes, the ash layer is underlain by approximately 6 cm of very dark gray (5Y 3/1) nannofossil ooze with minor amounts of apatite and zeolites. This ash is a clear marker horizon in natural gamma-ray logging data obtained at Hole 803D (see "Logging" section, this chapter).

Subunit IA is predominantly composed of nannofossils and variable amounts of foraminifers (Fig. 9). On average, the calcareous biogenic constituents form more than 95% of these sediments. The dominance of carbonates in these sediments is also indicated by the results of shipboard carbonate analyses (Fig. 10) and X-ray diffraction (XRD) scans. Accessory biogenic components include radiolarians, silicoflagellates, sponge spicules, and diatoms, whereas quartz, feldspar, volcanic ash, and clay minerals are the common terrigenous components. Texturally, the sediments are predominantly silts and clayey silts. Shipboard grain-size determinations (Fig. 11 and Table 3) indicate that mean grain size generally decreases downhole through the first 100 m, reflecting the decrease in foraminifer abundance described previously. The mean grain size then increases by a factor of 2 over the interval from 100 to 150 mbsf, as foraminifers become more abundant in Cores 130-803D-17H and -18H (upper Miocene sediments). Grain size again decreases below 150 mbsf as foraminifer abundances decrease.

During visual description of Subunit IA, a qualitative transition from "soft" ooze to "stiff" ooze was noted at approximately 150 mbsf. This transition exists as a zone of change in grain size, physical properties (see "Physical Properties" section, this chapter), and log signatures (resistivity and velocity; see "Logging" section, this chapter) from 135 to 145 mbsf, and produces a major horizon on seismic reflection profiles in this area (see "Seismic Stratigraphy" section, this chapter).

Subunit IB

Intervals: Hole 803D, Cores 130-803D-25X to -60X
Age: middle Miocene–late Eocene
Depth: 217.1–563.7 mbsf

Subunit IB consists of 346.6 m of nannofossil chalk and nannofossil chalk with foraminifers and is distinguished from Subunit IA on the basis of the ooze-chalk transition. Sediment recovery was good (77% average) over most of the interval, but decreased drastically in the last three cores of Subunit IB (26% average; Fig. 3), in which minor amounts of chert were recovered. In these last three cores of Subunit IB, a marked decrease

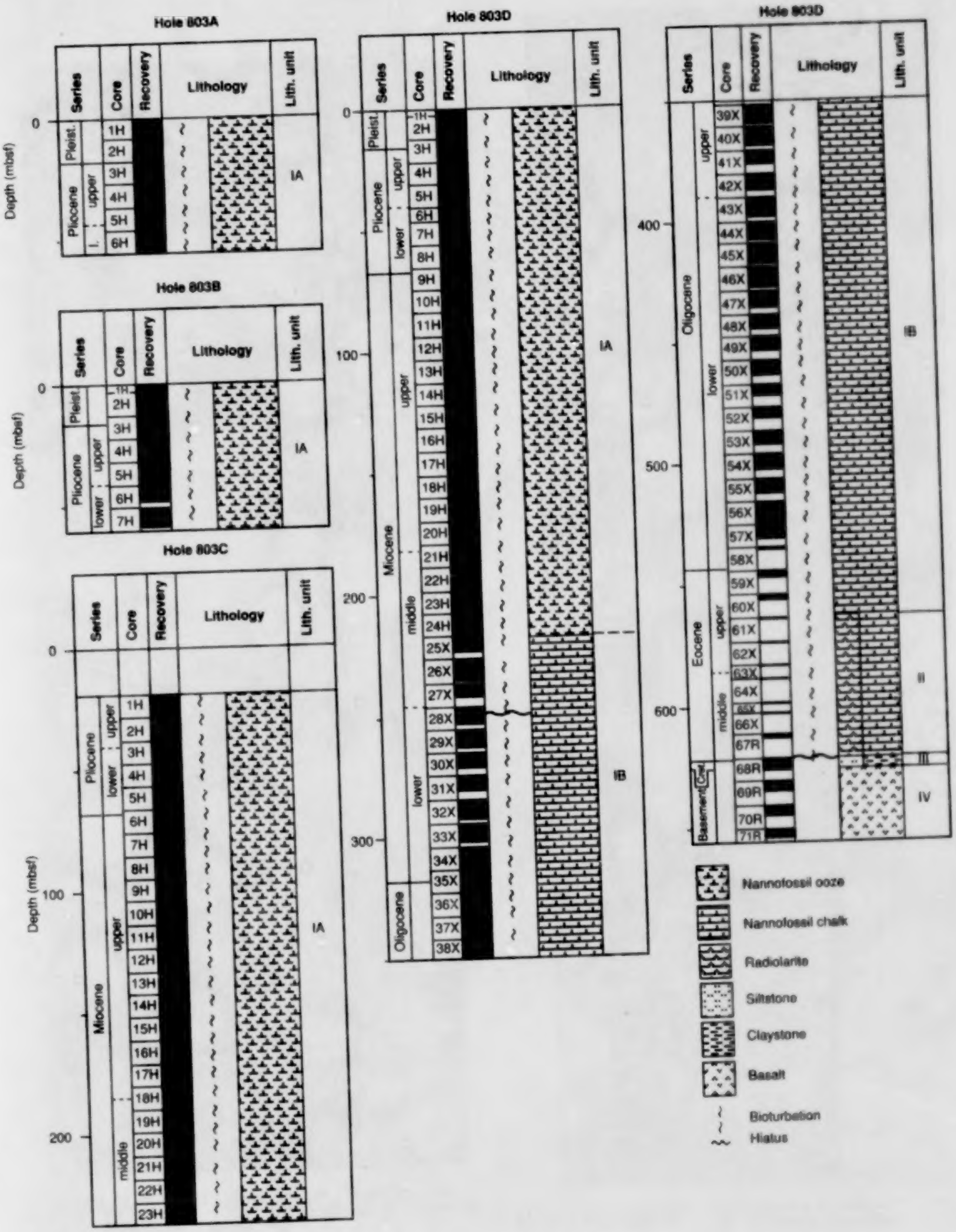
Hole 803A
Depth (mbsf)
0
Series
Core
Recovery
Lithology
Lith. unit
Pleist.
Pliocene
upper
l.
1H
2H
3H
4H
5H
6H
IA
Hole 803B
Depth (mbsf)
0
Series
Core
Recovery
Lithology
Lith. unit
Pleist.
Pliocene
upper
lower
1H
2H
3H
4H
5H
6H
7H
IA
Hole 803C
Depth (mbsf)
0
100
200
Series
Core
Recovery
Lithology
Lith. unit
Pliocene
upper
lower
Miocene
upper
middle
1H
2H
3H
4H
5H
6H
7H
8H
9H
10H
11H
12H
13H
14H
15H
16H
17H
18H
19H
20H
21H
22H
23H
IA
Hole 803D
0
100
200
300
Series
Core
Recovery
Lithology
Lith. unit
Pleist.
Pliocene
upper
lower
Miocene
upper
middle
lower
Oligocene
1H
2H
3H
4H
5H
6H
7H
8H
9H
10H
11H
12H
13H
14H
15H
16H
17H
18H
19H
20H
21H
22H
23H
24H
25X
26X
27X
28X
29X
30X
31X
32X
33X
34X
35X
36X
37X
38X
IA
IB
Hole 803D
400
500
600
Series
Core
Recovery
Lithology
Lith. unit
Oligocene
upper
lower
Eocene
upper
middle
Basement
Cret.
39X
40X
41X
42X
43X
44X
45X
46X
47X
48X
49X
50X
51X
52X
53X
54X
55X
56X
57X
58X
59X
60X
61X
62X
63X
64X
65X
66X
67R
68R
69R
70R
71R
IB
II
III
IV
Nannofossil ooze
Nannofossil chalk
Radiolarite
Siltstone
Claystone
Basalt
Bioturbation
Hiatus

Figure 3. Lithologic summary, Site 803.

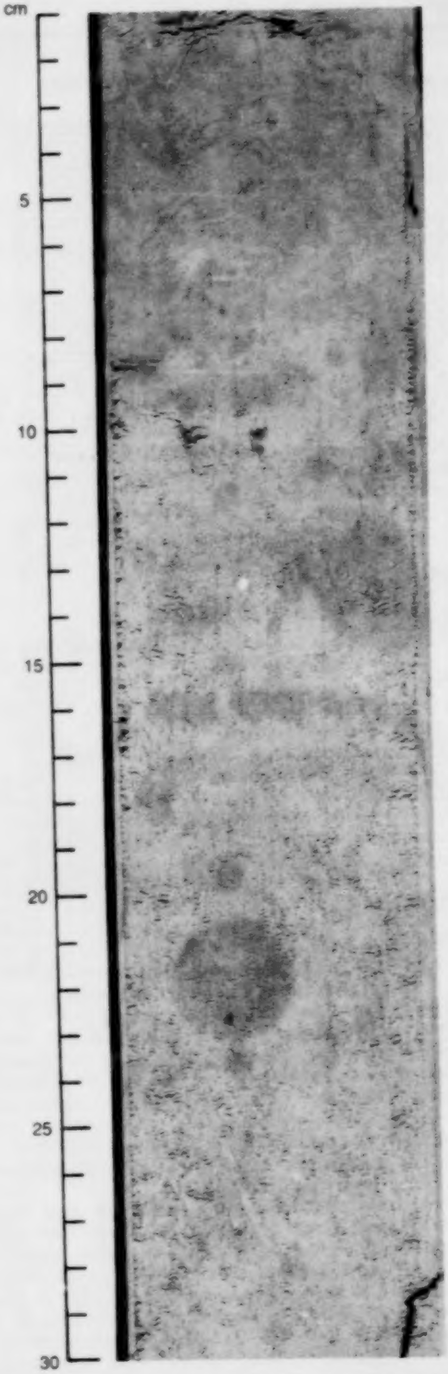
cm
5
10
15
20
25
30

Figure 4. Photograph of general nature of bioturbation in Subunit IA (Section 130-803C-3H-6, 1–30 cm).

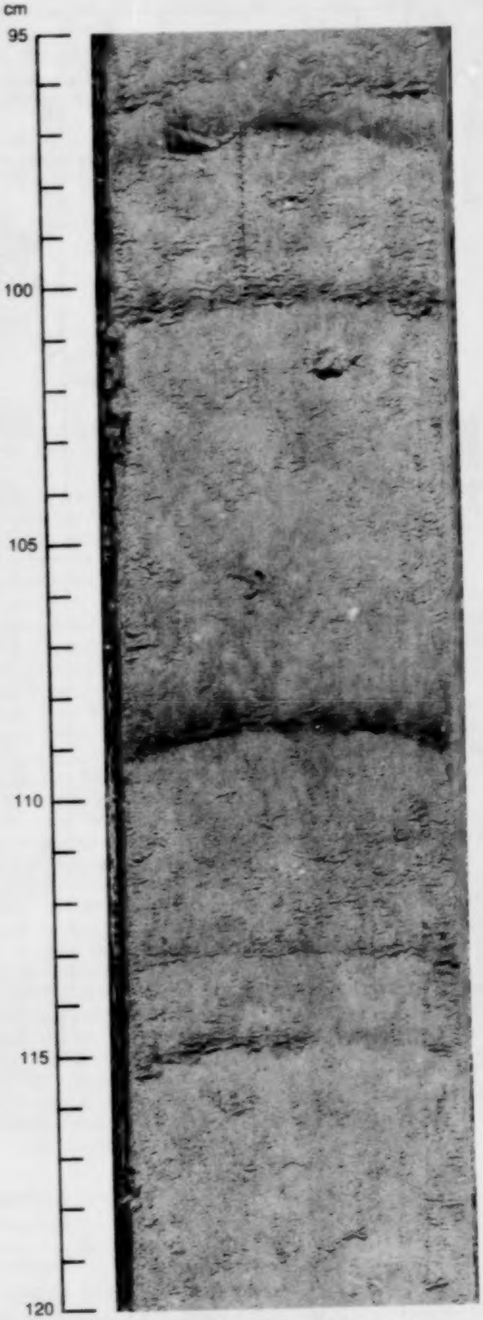
cm
95
100
105
110
115
120

Figure 5. Photograph of color banding in Subunit IA (Section 130-803D-4H-1, 95–120 cm).

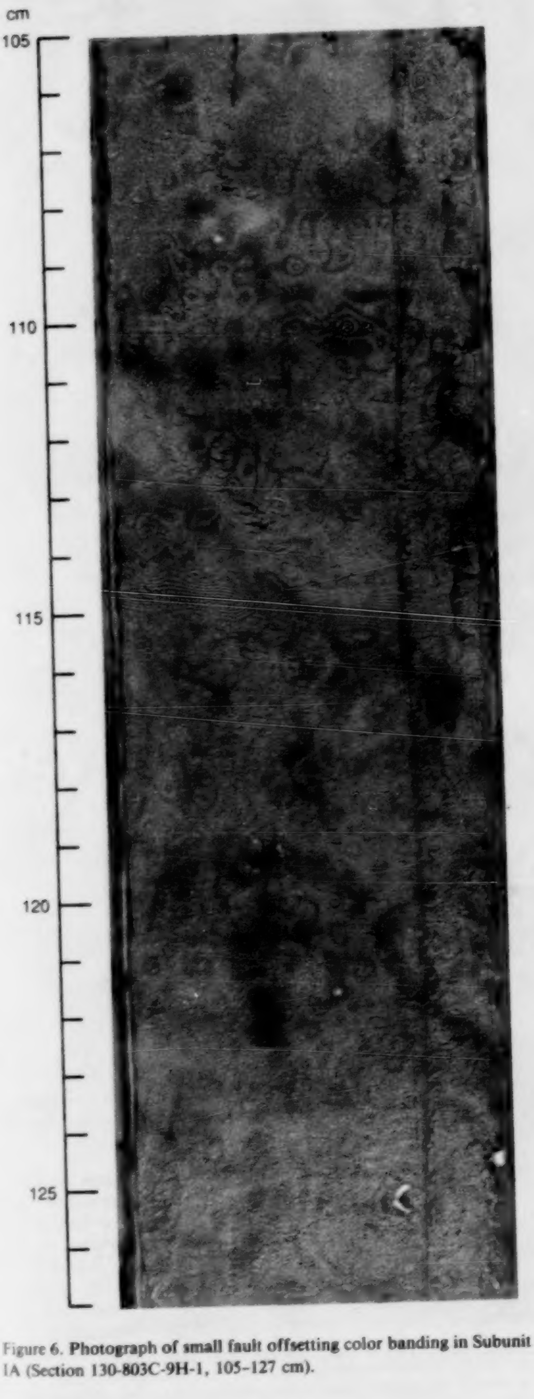
cm
105
110
115
120
125

Figure 6. Photograph of small fault offsetting color banding in Subunit IA (Section 130-803C-9H-1, 105–127 cm).

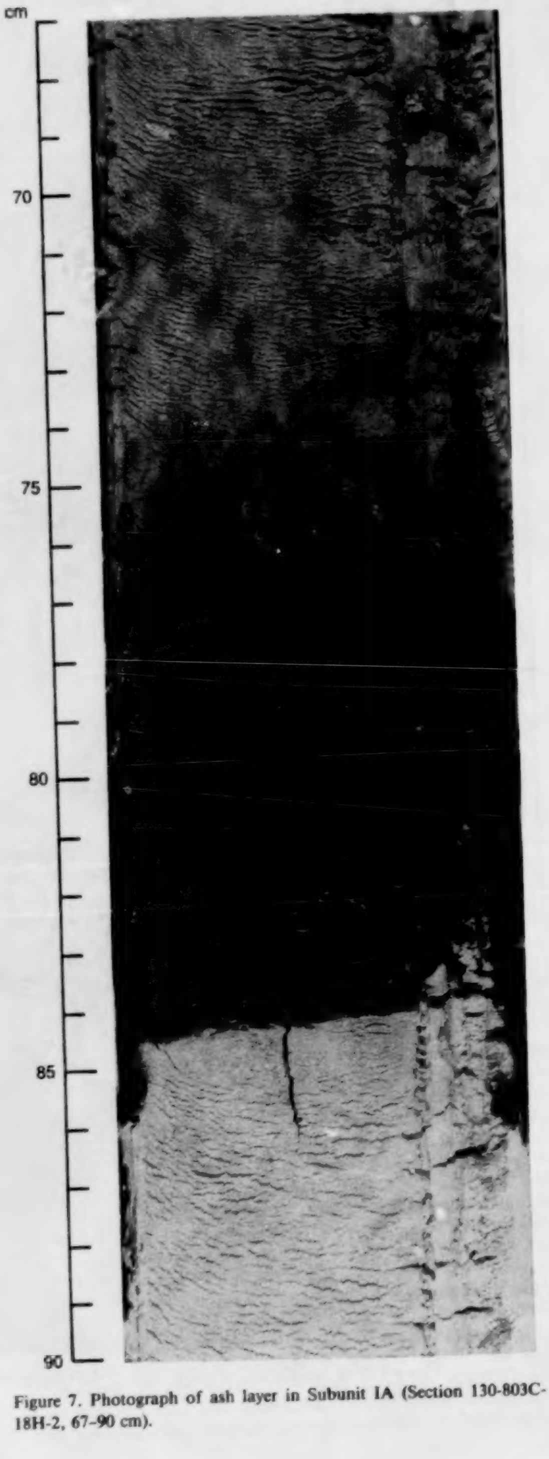
cm
70
75
80
85
90

Figure 7. Photograph of ash layer in Subunit IA (Section 130-803C-18H-2, 67–90 cm).

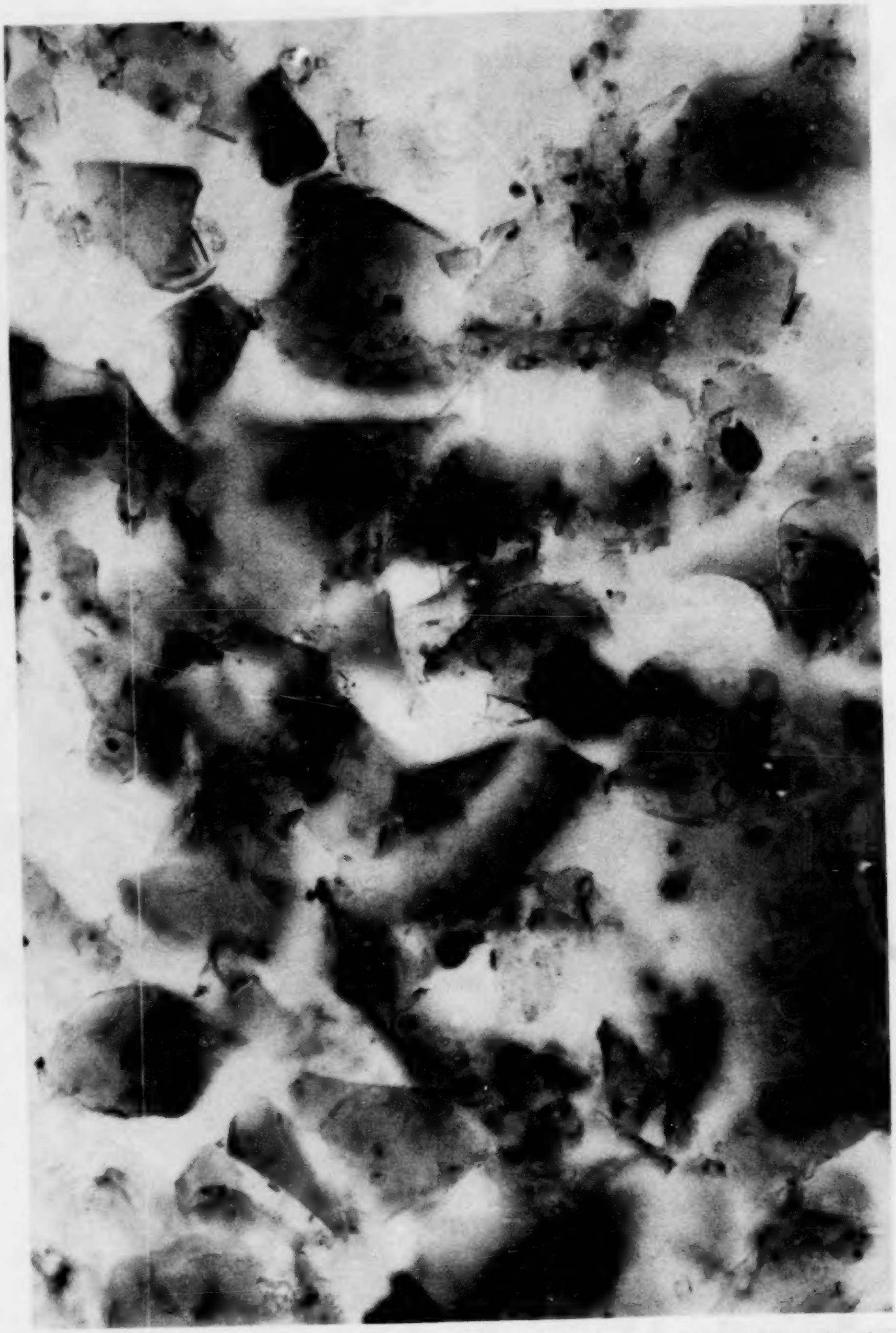

Figure 8. Photomicrograph of smear slide of ash layer in Subunit IA. Field of view is approximately 1 mm wide; plane polarized light.

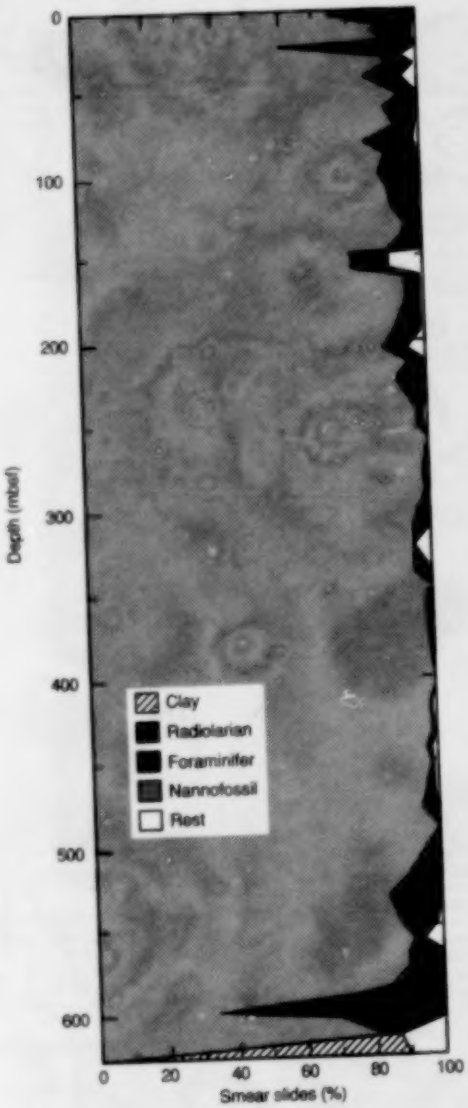

Figure 9. Composition of sediments at Hole 803D as compiled from smear slide data.

in pore-water silica concentration indicates the onset of silica reprecipitation (see "Inorganic Geochemistry" section, this chapter), and the irregular nature of velocity and density logs suggests interbedding of hard and soft sediment types below 520 mbsf (see "Logging" section, this chapter). All of these data suggest that well-cemented biosiliceous sediments first appear as thin beds near the base of Subunit IB, and that the presence of interbedded hard and soft sediment types reduced the coring effectiveness of the XCB.

The primary colors of Subunit IB are essentially the same as those of Subunit IA. Indicators of bioturbation are common to abundant throughout Subunit IB (Fig. 12) and include diffuse mottling, disseminated pyritic burrow linings, millimeter-scale simple burrows, and large, more complex and identifiable discrete trace fossils. Among the latter are several excellent examples of *Zoophycos* and *Chondrites* (Fig. 13). The faint color banding characteristic of Subunit IA is absent in Cores 130-803D-25X through -44X (217–409 mbsf), but is present in the next 100 m below (lower Oligocene sediments of Cores 130-803D-45X to -55X). The color bands become more abundant, intense, and distinct downhole. In intervals that contain both color bands and bioturbation features, the color bands are continuous across and through burrows.

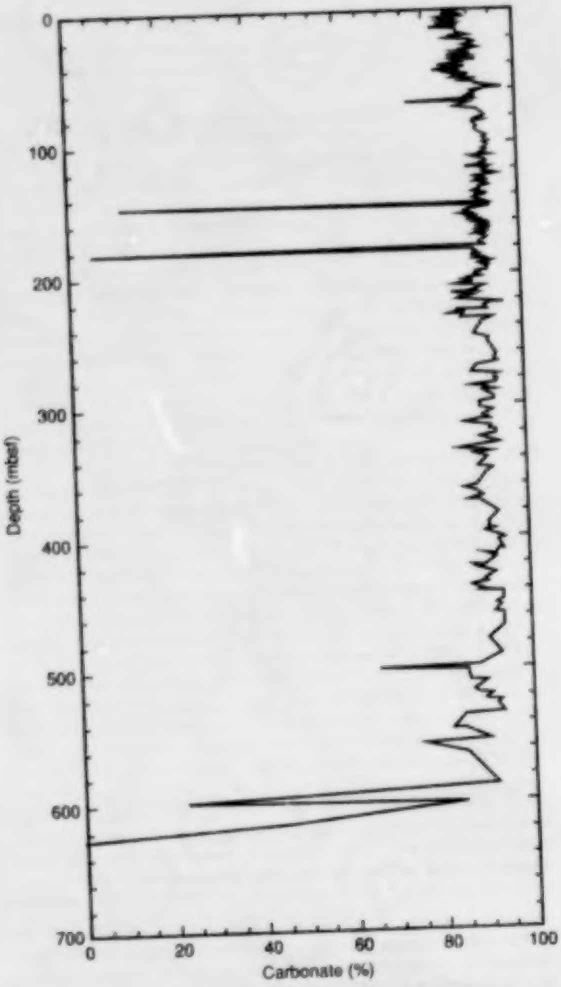

Figure 10. Calcium carbonate content of sediments at Hole 803D, as determined by shipboard analyses.

As in Subunit IA, the composition of Subunit IB is dominated by biogenic carbonate, as demonstrated by smear-slide examination, shipboard carbonate analyses, and XRD scans (Figs. 9 and 10). Foraminifer abundances are low throughout most of Subunit IB and exceed 10% only in Cores 130-803D-57X through -59X (525–554 mbsf), which span the Eocene/Oligocene boundary. Radiolarians are the most common biogenic sili-

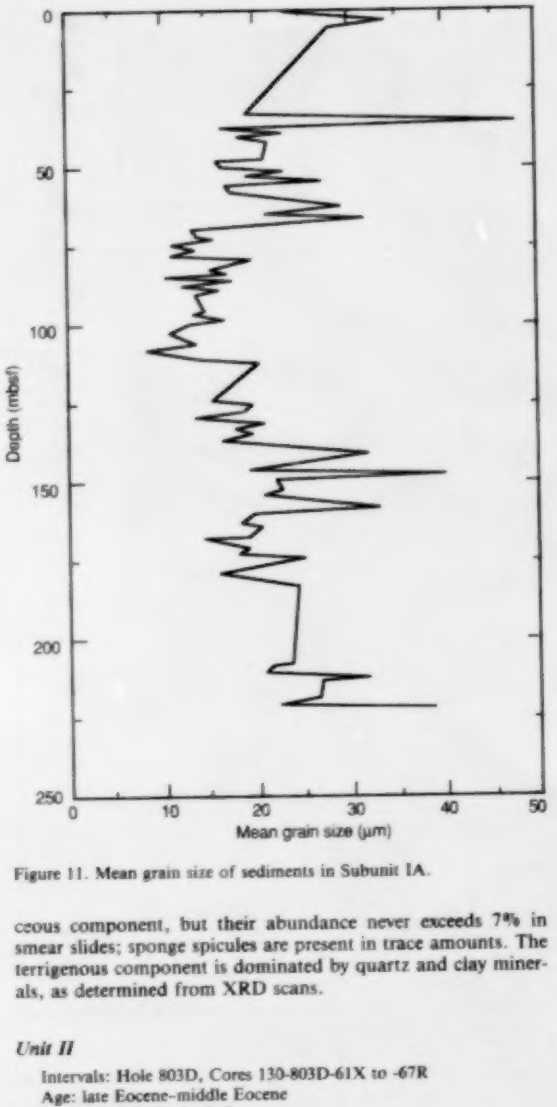

Figure 11. Mean grain size of sediments in Subunit IA.

ceous component, but their abundance never exceeds 7% in smear slides; sponge spicules are present in trace amounts. The terrigenous component is dominated by quartz and clay minerals, as determined from XRD scans.

Unit II

Intervals: Hole 803D, Cores 130-803D-61X to -67R
Age: late Eocene-middle Eocene
Depth: 563.7–621.8 mbsf

Unit II consists of approximately 58 m of nannofossil chalk with radiolarians, radiolarian nannofossil chalk, nannofossil radiolarite, and minor amounts of chert. Radiolarian abundances generally increase downhole from Cores 130-803D-61X to -65X and decrease below that level (Fig. 9), although chert was recovered in Section 130-803D-67R-CC. The nannofossil radiolarite and the chert provide useful markers for correlating the lithostratigraphy to other shipboard measurements. The nannofossil radiolarite appears as a high-porosity, low-velocity zone in physical properties data (see "Physical Properties" and "Logging" sections, this chapter) and a low-density interval from 595 to 597 mbsf in logging data (see "Logging" section, this chapter). The chert appears as a thin resistive bed on the electrical resistivity log (see "Logging" section, this chapter), has high measured velocities (see "Physical Properties" section, this chapter), and is identifiable as a major reflector on seismic profiles (see "Seismic Stratigraphy" section, this chapter).

Table 3. Grain size results. Hole 803D.

Core, section, interval (cm)	Depth (mbsf)	Mean grain size (µm)
130-803D-		
1H-1, 123	1.2	23.2
1H-2, 38	1.9	34.0
2H-2, 37	4.4	27.5
5H-1, 106	32.1	19.0
5H-2, 131	33.8	47.3
5H-3, 106	35.1	30.0
5H-4, 110	36.6	16.6
5H-5, 111	38.1	22.6
5H-6, 112	39.6	18.3
5H-7, 36	40.4	21.2
7H-1, 36	46.5	20.7
7H-1, 111	47.2	15.8
7H-2, 110	48.7	16.2
7H-3, 113	50.2	22.9
7H-4, 111	51.7	18.9
7H-5, 111	53.2	26.9
7H-6, 110	54.7	16.8
8H-1, 112	56.7	17.4
8H-2, 110	58.2	22.3
8H-3, 110	59.7	25.1
8H-4, 111	61.2	28.8
8H-5, 111	62.7	26.5
8H-6, 110	64.2	20.9
8H-7, 35	64.9	31.5
9H-1, 111	66.2	21.2
9H-2, 110	67.7	15.0
9H-3, 109	69.2	12.9
9H-4, 106	70.7	13.6
9H-5, 114	72.2	15.0
9H-6, 111	73.7	11.2
10H-1, 99	75.6	13.4
10H-2, 108	77.2	11.0
10H-3, 108	78.7	19.3
10H-5, 109	81.7	14.9
10H-6, 109	83.2	16.7
10H-7, 36	84.0	10.4
11H-1, 110	85.2	17.0
11H-2, 109	86.7	12.1
11H-3, 108	88.2	15.6
11H-4, 109	89.7	13.5
12H-1, 110	94.7	14.5
12H-2, 110	96.2	13.2
12H-3, 110	97.7	16.6
12H-4, 110	99.2	12.7
12H-5, 112	100.7	11.6
12H-6, 110	102.2	10.8
13H-2, 111	105.7	13.6
13H-3, 111	107.2	8.4
130-803D-(Cont.)		
13H-4, 102	108.6	12.1
13H-5, 108	110.2	13.9
13H-6, 110	111.7	20.0
15H-1, 113	123.2	15.3
15H-2, 112	124.7	19.2
15H-3, 112	126.2	18.6
15H-4, 113	127.7	16.1
15H-5, 107	129.2	13.4
15H-6, 107	130.7	20.5
16H-1, 106	132.7	17.7
16H-2, 111	134.2	19.4
16H-3, 112	135.7	17.8
16H-4, 31	136.4	16.2
16H-5, 111	138.7	23.3
16H-6, 112	140.2	31.7
17H-1, 111	142.2	26.3
17H-3, 109	145.2	19.2
17H-4, 105	146.7	39.9
17H-5, 112	148.2	22.2
17H-6, 102	149.6	22.1
18H-1, 110	151.7	22.6
18H-2, 115	153.2	20.8
18H-3, 110	154.7	22.3
18H-4, 110	156.2	28.8
18H-5, 110	157.7	32.9
18H-6, 110	159.2	28.0
18H-7, 30	159.9	19.4
19H-1, 110	161.2	19.2
19H-2, 111	162.7	18.2
19H-3, 115	164.2	20.5
19H-5, 110	167.2	18.7
19H-5, 110	167.2	14.1
19H-6, 110	168.7	14.8
20H-1, 111	170.7	19.2
20H-2, 110	172.2	18.0
20H-3, 110	173.7	25.1
20H-5, 111	176.7	18.1
20H-7, 31	178.9	15.6
21H-3, 109	183.2	24.1
23H-7, 39	207.5	23.3
24H-1, 116	208.8	21.1
24H-2, 104	210.1	20.7
24H-3, 104	211.6	31.6
24H-4, 104	213.1	26.4
24H-6, 104	216.1	26.0
25H-1, 107	218.2	26.4
25H-3, 72	220.8	22.0
25H-4, 41	222.0	38.8

These sediments are white (2.5Y 8/0, 10YR 8/1, and 10YR 8/2) to light brownish gray (10YR 7/3) in color and are slightly to heavily bioturbated. No physical sedimentary structures were observed in Unit II, although any structures present may have been obscured by the poor recovery and significant drilling disturbance of sediments from this interval.

Sediment compositions in Unit II are more variable than those in Unit I (Fig. 9) because of the wide range of nannofossil and radiolarian contents. Nannofossil abundances range from 35% to 90%, whereas radiolarian abundances range from 15% to 65%. Foraminifers and sponge spicules are present in trace amounts. The lower average carbonate content of Unit II and its increased variability are also expressed in shipboard carbonate analyses (Fig. 10). Terrigenous components in Unit II include clays and quartz; the diffractograms also indicate the increased abundance of opal in Cores 130-803D-63R through -66R. On the basis of smear-slide estimates, the sediments of Unit II are classified texturally as silts and sandy silts.

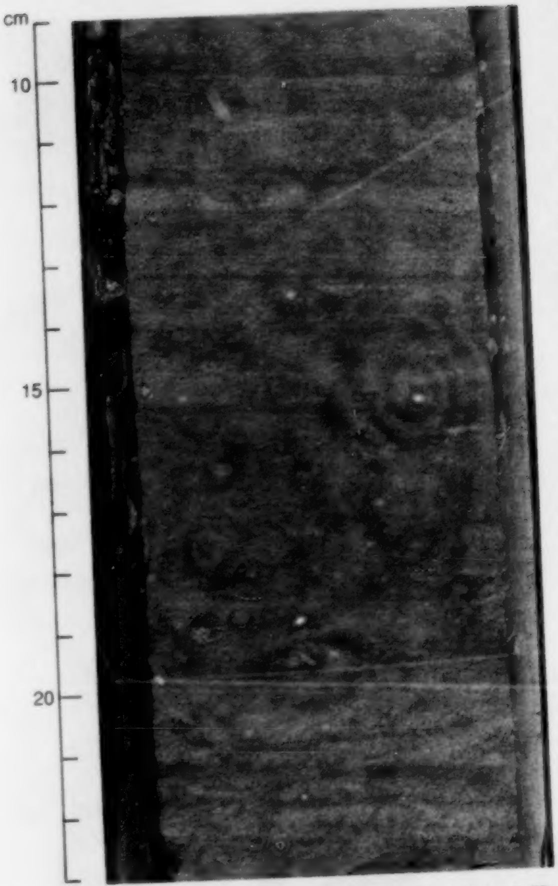

Figure 12. Photograph of general nature of bioturbation in Subunit IB (Section 130-803D-58X-CC, 9–23 cm).

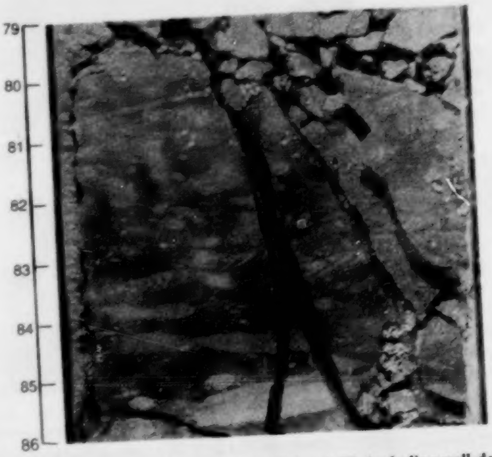

Figure 13. Photograph of bioturbation in Subunit IB, including well-developed *Zoophycos* trace fossils (Section 130-803D-55X-4, 79–86 cm).

Unit III

Intervals: Hole 803D, Sections 130-803D-68R-1 to -3
Age: middle Eocene–early Late Cretaceous
Depth: 621.8–626.3 mbsf

Unit III is composed of claystone and clayey siltstone, with minor radiolarian-rich intervals. We recovered 4.5 m of sediment from Unit III, but resistivity logs suggest that this lithology continues from 621.8 mbsf to basement at 632 mbsf (see "Logging" section, this chapter). Dominant colors are very dark brown (10YR 2/2), dark brown (10YR 3/3, 7.5YR 4/2, and 7.5YR 4/4), and brown (7.5YR 5/4), with minor intervals of dark yellowish brown (10YR 4/4). The radiolarian-rich sediments (radiolarian clayey siltstone to radiolarite) are dark yellowish brown, whereas the radiolarian-poor sediments exhibit more reddish colors. Sharp contacts separate intervals of different color in Sections 130-803D-68R-1 and -3 and may represent significant unconformities (Fig. 14). Bioturbation is common to abundant throughout most of Unit III, but distinct millimeter-scale lamination is present in parts of the Cretaceous interval (Sections 130-803D-68R-2 and -3; Fig. 15).

The siliciclastic sediments of Unit III are composed of 80% or more silica-rich grains and clays, with iron-oxide coatings common to abundant. Many of the silica-rich grains exhibit unusual internal heterogeneity in extinction under cross-polarized light, similar to the characteristics of chert. XRD scans identify quartz, plagioclase and potassium feldspar, illite, and mixed-layer clays as the dominant siliciclastic components. Nannofossil abundances in Unit III are low (20% or less), as indicated by smear-slide examination (Fig. 9), shipboard carbonate analyses (Fig. 10), and XRD scans. Radiolarians are abundant to dominant in the dark yellowish-brown intervals, but rare to absent in the remainder of Unit III (Fig. 16). Although Unit III directly overlies basaltic basement, these sediments are not metalliferous. This evidence suggests that a significant hiatus exists between the basal sediments and the underlying basalts. The limited thickness of Unit III and the available biostratigraphic data (see "Biostratigraphy" section, this chapter) indicate that significant hiatuses also exist within Unit III. Despite the presence of such hiatuses, shipboard biostratigraphic data indicate that a continuous Cretaceous/Tertiary boundary was recovered within Interval 130-803D-68R-1, 38–53 cm. The boundary lies near Section 130-803D-68R-1, 46.5 cm (Fig. 17).

Discussion

The depositional history of Site 803 began with a period of slow and discontinuous siliciclastic sedimentation, which extended from the Cretaceous into the Eocene. Since that time, Site 803 has been dominated by pelagic sedimentation, with evidence for significant variations in water-column productivity, dissolution, and/or sediment reworking. These environmental variations are recorded by changes in sediment composition, sediment grain size, and accumulation rates, and by the presence and extent of hiatuses.

Formation of the Ontong Java Plateau is interpreted to have begun during the middle Jurassic (approximately 160 Ma; Kroenke et al., 1986). Crust in the vicinity of Site 803 was probably erupted in Late Cretaceous time or earlier based on paleontological information and on an $^{40}Ar/^{39}Ar$ date (113 Ma) on a basalt sample from nearby DSDP Site 289 (see "Background and Objectives" section, this chapter). Initial sedimentation at Site 803 was dominated by siliciclastic rocks, as observed in lithologic Unit III. The presence of radiolarians, the extent and nature of bioturbation, and the preservation of laminated intervals in Unit III all indicate that it was deposited under marine conditions.

Stratigraphic control within Unit III is limited at present, but the available data indicate that Unit III ranges from early Late

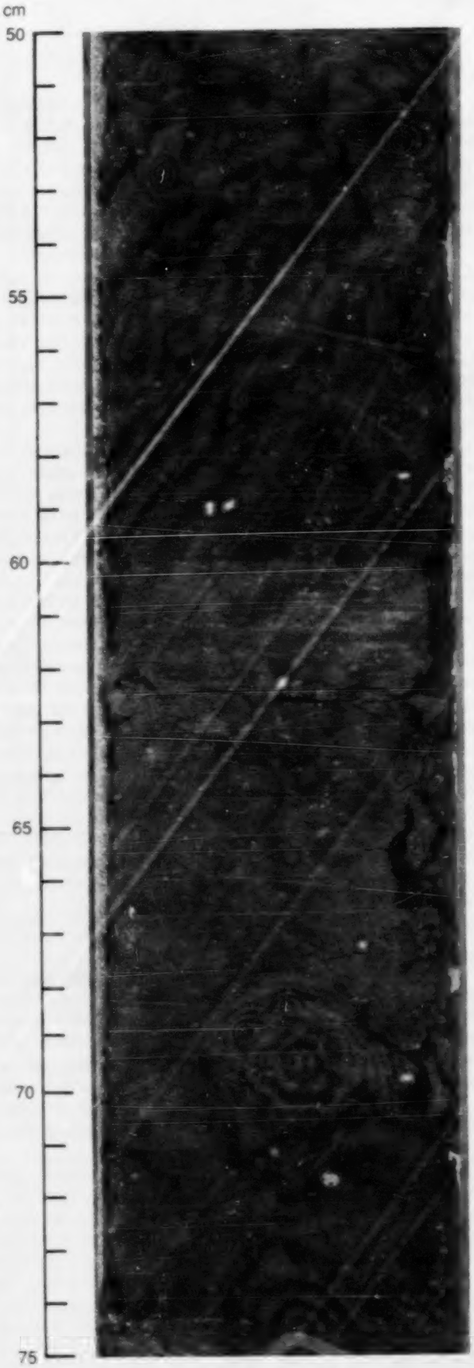
cm
50
55
60
65
70
75

Figure 14. Photograph of sharp color contacts in Unit III (Section 130-803D-68R-1, 50–75 cm).

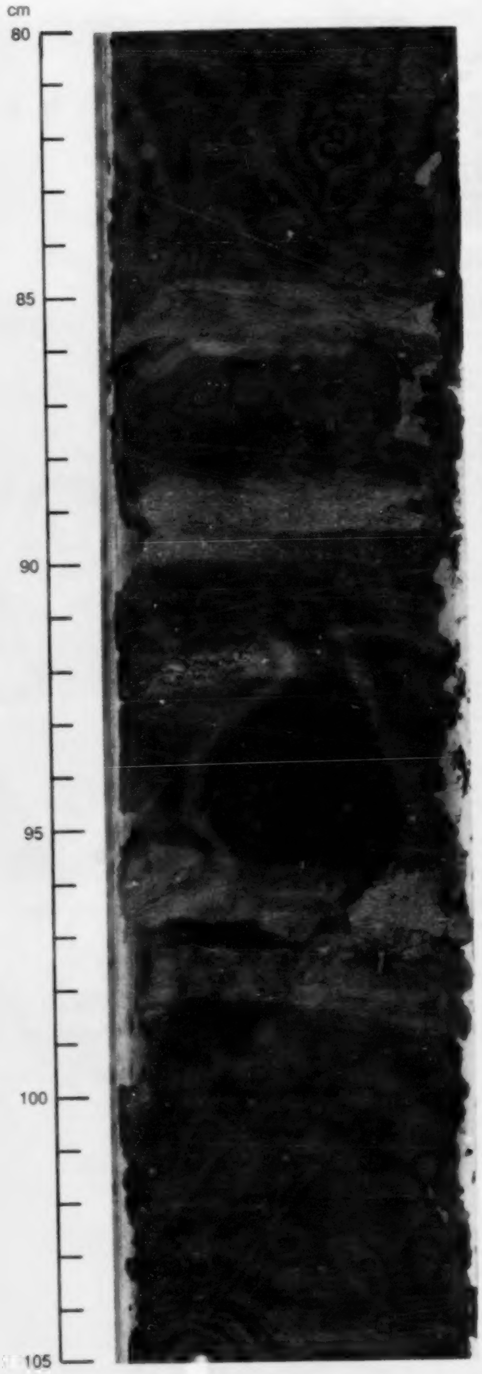
cm
80
85
90
95
100
105

Figure 15. Photograph of bioturbated and laminated intervals in Unit III (Section 130-803D-68R-3, 80–105 cm). The contacts between the bioturbated and laminated intervals are sharp.

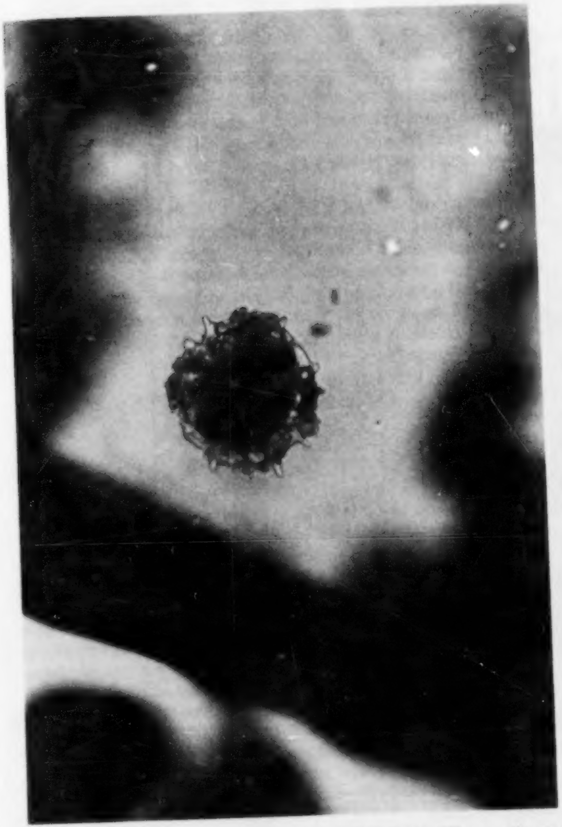

Figure 16. Photomicrograph of radiolarian from Unit III; note the extent of recrystallization exhibited. Field of view is approximately 0.5 mm wide.

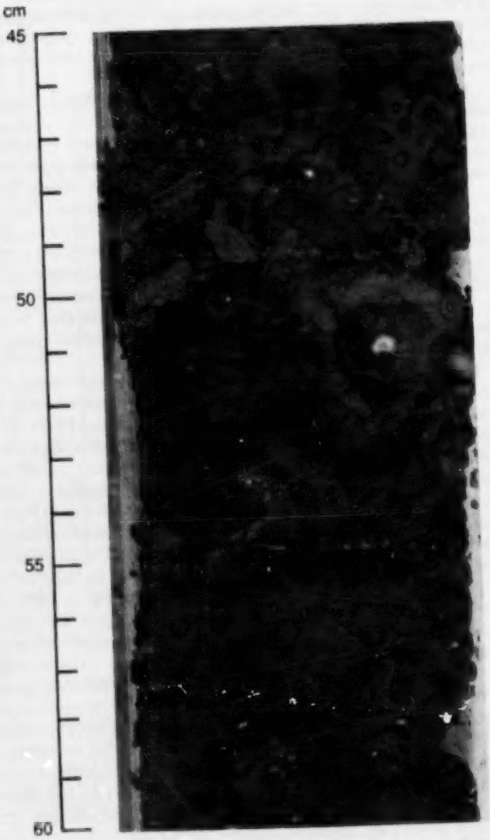

Figure 17. Photograph of interval in Unit III that contains the Cretaceous/Tertiary boundary (Section 130-803D-68R-1, 45–60 cm). Shipboard biostratigraphic analysis places the boundary at Section 130-803D-68R-1, 46.5 cm.

Cretaceous to middle Eocene in age. As Unit III is only 4.5 m thick, extremely slow sedimentation rates and/or major hiatuses clearly are indicated. The absence of metalliferous sediments directly overlying basalt suggests a hiatus of unknown origin and duration. Shipboard biostratigraphic studies have identified a hiatus that encompasses most of the Paleocene and part of the Eocene, which is located near the top of Unit III (see "Biostratigraphy" section, this chapter). Additional unconformities may be located at the sharp color contacts described previously.

The siliciclastic component in Unit III includes a significant number of silica-rich grains, with characteristics similar to chert. The largest of these grains are sand-sized and spherical and appear to be altered radiolarians (Fig. 16). The presence of the silica-rich grains indicates that at least a portion of the siliciclastic component was derived from a chert source, although the location of such a source (autochthonous vs. allochthonous) is unknown. Biogenic carbonate is rare to absent in Unit III, indicating deposition near or below the carbonate compensation depth (CCD). The removal of carbonate by dissolution probably was one important mechanism in maintaining the low sedimentation rates in Unit III. Additional periods of erosion and/or nondeposition within Unit III also are evident, although the reasons for such hiatuses are unknown at this time.

Conditions favorable for the deposition of biogenic pelagic sediments were initiated by Eocene time, as recorded in the mixed biosiliceous-calcareous sediments of lithologic Unit II. The increased carbonate content of Unit II indicates deposition above the CCD, at least episodically throughout the Eocene. Radiolarians are common to abundant throughout Unit II and are present at the base of Unit I, indicating conditions favorable for the supply and preservation of silica. Similar conditions were found for Eocene sediments at Site 289 and were interpreted as a signal of enhanced productivity (Andrews, Packham, et al., 1975). The Eocene record at Site 289 also was interrupted by several intervals of erosion and/or nondeposition.

Pelagic carbonate deposition has dominated Site 803 from the late Eocene to the Quaternary. Deposition in the Oligocene appears to have been rather continuous and little affected by major changes in carbonate preservation or removal. A major episode of dissolution/erosion produced a hiatus in the early to middle Miocene (15–21 Ma; see "Biostratigraphy" section, this chapter). This hiatus can be correlated with extensive unconformities in other areas (Keller and Barron, 1983). Such extensive gaps in the marine record presumably reflect climatic and/or tectonic events that caused major changes in oceanic circulation and chemistry. Conditions favoring pelagic sedimentation were reestablished by middle Miocene time and have generally been maintained since then.

Microfaulted, dipping, and contorted color bands were observed in Subunit IA, and these disturbed intervals were often overlain by beds of homogeneous nannofossil ooze enriched in foraminifers. These features may record sediment mass movements of various types, including slumps and debris flows. Mass wasting processes have previously been reported from the flanks of the Ontong Java Plateau (Berger and Johnson, 1976; Berger et al., 1977), and seismic reflection profiles provide abundant evidence for sediment faulting and slumping near Site 803 (see "Seismic Stratigraphy" section, this chapter). Berger and Johnson (1976) suggest that sediment failure may be produced by undercutting of downslope support by dissolution, by seismic activity, or by both.

Deposition at Site 289 was interpreted to be continuous from the Oligocene to the Quaternary, based on both nannofossil and foraminifer zonations (Andrews, Packham, et al., 1975). Foraminifers were reported as abundant throughout this interval. In contrast, the equivalent record at Site 803 is interrupted by a major unconformity, and foraminifers are rare, except in lowermost Oligocene, upper Miocene, and upper Pliocene/Pleistocene sediments. In detail, foraminifers become more abundant moving upcore through the upper Pliocene-to-Pleistocene section at Site 803. These data suggest differences in the histories of productivity, preservation, and/or winnowing at Sites 289 and 803, resulting, at least in part, from the deeper location of Site 803. Subtle variations of productivity/preservation conditions at Site 803 also may be recorded by the color banding common in Unit I. The origin of this color banding is not known, but a working hypothesis focuses on diagenetic enhancement of subtle primary compositional differences (especially organic carbon content) by preferential redox reactions of iron and manganese. Shore-based studies will examine the nature and origin of these variations, to help interpret the chemical and physical history of sedimentation on the Ontong Java Plateau from the Oligocene to the Pleistocene.

BIOSTRATIGRAPHY

Introduction

The sediments recovered at Site 803 yielded a continuous stratigraphic record from the present back to the middle Eocene (0–46 Ma), with the exception of one distinct hiatus across the middle/lower Miocene boundary (approximately 15.5–21.3 Ma). These Holocene to Eocene sediments are chiefly of biogenic origin. The five major microfossil groups that make up the bulk of the material (calcareous nannofossils, planktonic and benthic foraminifers, diatoms, and radiolarians) occur in varying proportions and show variable states of preservation.

In contrast to the upper section of the drilled sequence, hiatuses of substantial duration characterize the lowermost part of the sediment section, as follows:

1. The Paleocene/Eocene boundary, the entire lower Eocene, and the lower half of the middle Eocene are missing. The middle Eocene is underlain by a mere 1-cm-thick sediment layer of late Paleocene age (about 58 Ma). This hiatus is estimated to span over some 12 m.y.
2. Almost all of the Paleocene is missing. The uppermost Paleocene is underlain by basal Paleocene sediments that presumably were deposited shortly (probably <0.5 m.y) after the Cretaceous/Tertiary boundary, implying a Paleocene hiatus representing about 8 m.y.
3. The Cretaceous is poorly represented. Less than 5 m of condensed(?) and virtually carbonate-free sediments rest on the volcanic basement. Occurrences of radiolarians in a few discrete layers in these deep-sea clays suggest an early Cenomanian age within a meter of the basement. These few meters of nearly nonfossiliferous sediments thus represent a time interval spanning at least 30 m.y. (approximately 67–97 Ma); presumably several substantial hiatuses are present.

Considering the fact that the time interval from 45 Ma to roughly 100 Ma is represented by <5 m of sediment, it appears all the more remarkable that the Cretaceous/Tertiary (K/T) boundary is preserved intact in this section.

Detailed information on biostratigraphic assignments, abundance, and preservation of the different microfossil groups is presented below. A generalized picture of the biostratigraphy is shown in Figure 18.

Calcareous Nannofossils

Hole 803A

Pleistocene

Pelagic oozes in Hole 803A contain well to moderately preserved, diverse assemblages of nannofossils. The youngest assemblage observed from this hole belongs to Zone NN20 and is present in Sample 130-803A-1H-3, 0–1 cm, in which *Gephyrocapsa caribbeanica* and *Gephyrocapsa oceanica* occur together with abundant small *Gephyrocapsa*. Rare *Helicosphaera inversa* is also found in this sample. A single reworked specimen of the Cretaceous species *Watznaueria barnesae* was recognized. Samples 130-803A-1H-CC and -2H-CC are assigned to Zone NN19 based on the presence of abundant *Pseudoemiliania lacunosa*, common to abundant Pleistocene gephyrocapsids, and the absence of the Pliocene discoasters. Both *Helicosphaera sellii* and *Calcidiscus macintyrei* are present in Sample 130-803A-2H-CC, placing this sample in the very basal Pleistocene or the very topmost Pliocene.

Pliocene

Sample 130-803A-3H-CC contains *Discoaster brouweri* and is assigned to Zone NN18. The Pliocene/Pleistocene boundary falls approximately midway between the successive last occurrences (LOs) of *D. brouweri* and *C. macintyrei* and lies, therefore, between Samples 130-803A-2H-CC and -3H-CC. The former sample also contains the uppermost observed presence of *Coccolithus pelagicus,* which is a typical cool-water species in the present oceans. Specimens of the genus *Gephyrocapsa* were not observed in or below Sample 130-803A-3H-CC. *Discoaster pentaradiatus,* the LO of which defines the NN17/NN18 zonal boundary, occurs in and below Sample 130-803A-4H-CC, placing this sample in Zone NN17. A single specimen of *Discoaster surculus* was recognized, which was considered reworked. Sample 130-803A-5H-CC contains comparatively diversified discoasters such as *D. asymmetricus, D. brouweri, D. challengeri, D. pentaradiatus, D. surculus, D. tamalis, D. triradiatus,* and *D. variabilis.* This sample was assigned to Zone NN16. We recognized a few sphenoliths; therefore, this sample was placed in the lowermost part of Zone NN16 (between the LOs of *Sphenolithus* spp. and *Reticulofenestra pseudoumbilica*).

The first downhole observation of common *Reticulofenestra pseudoumbilica* was made in Sample 130-803A-6H-1, 75 cm, marking the top of lower Pliocene Zone NN15. The bottom of Hole 803A contains a typical lower Pliocene assemblage, with abundant placoliths (*Calcidiscus leptoporus, R. pseudoumbilica,* small morphotypes of *Reticulofenestra*) and sphenoliths, and a varied asterolith association. *Discoaster asymmetricus*

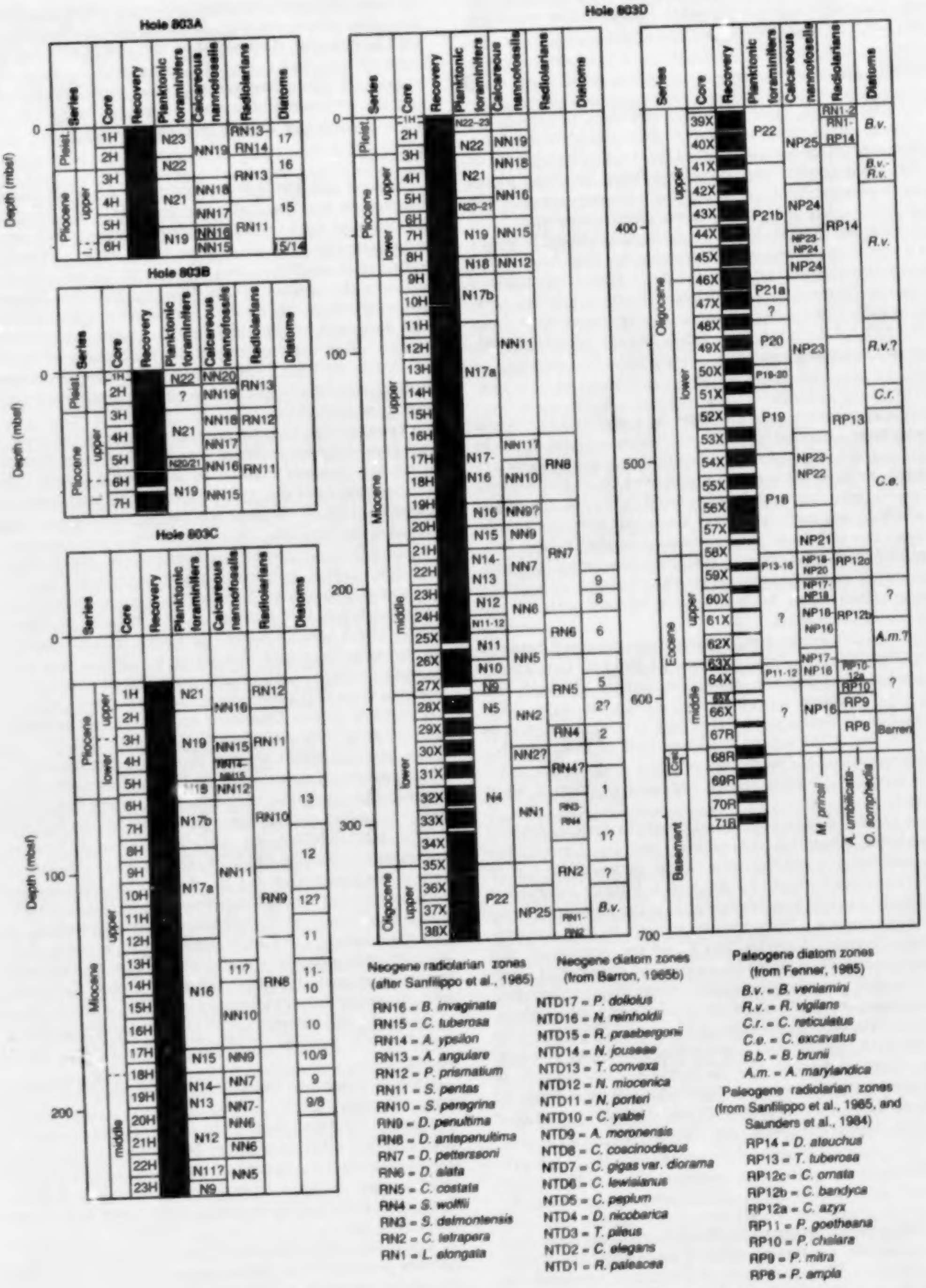

Neogene radiolarian zones
(after Sanfilippo et al., 1985)

RN16 = *B. invaginata*
RN15 = *C. tuberosa*
RN14 = *A. ypsilon*
RN13 = *A. angulare*
RN12 = *P. prismatium*
RN11 = *S. pentas*
RN10 = *S. peregrina*
RN9 = *D. penultima*
RN8 = *D. antepenultima*
RN7 = *D. petterssoni*
RN6 = *D. alata*
RN5 = *C. costata*
RN4 = *S. wolffii*
RN3 = *S. delmontensis*
RN2 = *C. tetrapera*
RN1 = *L. elongata*

Neogene diatom zones
(from Barron, 1985b)

NTD17 = *P. doliolus*
NTD16 = *N. reinholdii*
NTD15 = *R. praebergonii*
NTD14 = *N. jouseae*
NTD13 = *T. convexa*
NTD12 = *N. miocenica*
NTD11 = *N. porteri*
NTD10 = *C. yabei*
NTD9 = *A. moronensis*
NTD8 = *C. coscinodiscus*
NTD7 = *C. gigas var. diorama*
NTD6 = *C. lewisianus*
NTD5 = *C. peplum*
NTD4 = *D. nicobarica*
NTD3 = *T. pileus*
NTD2 = *C. elegans*
NTD1 = *R. paleacea*

Paleogene diatom zones
(from Fenner, 1985)

B.v. = *B. veniamini*
R.v. = *R. vigilans*
C.r. = *C. reticulatus*
C.e. = *C. excavatus*
B.b. = *B. brunii*
A.m. = *A. marylandica*

Paleogene radiolarian zones
(from Sanfilippo et al., 1985, and Saunders et al., 1984)

RP14 = *D. ateuchus*
RP13 = *T. tuberosa*
RP12c = *C. ornata*
RP12b = *C. bandyca*
RP12a = *C. azyx*
RP11 = *P. goetheana*
RP10 = *P. chalara*
RP9 = *P. mitra*
RP8 = *P. ampla*

Figure 18. Biostratigraphic hole summaries, Site 803. RN = radiolarian Neogene zone, NTD = Neogene tropical diatom zone, RP = radiolarian Paleogene zone, and NN = nannofossil Neogene zone.

and *Ceratolithus rugosus* are present, but *Amaurolithus* spp. were not observed. Core 130-803A-6H, hence, can be referred to the NN15–NN13 zonal interval.

Hole 803B

Pleistocene

An upper Pleistocene assemblage with abundant gephyrocapsids characterizes Sample 130-803B-1H-CC. The absence of both *Emiliania huxleyi* and *Pseudoemiliania lacunosa* places this sample in Zone NN20. *Helicosphaera inversa* also occurs in this sample. The LO of *P. lacunosa* was observed between Samples 130-803B-1H-CC and -2H-1, 70 cm. Sample 130-803B-2H-CC contains some specimens of *Gephyrocapsa* that have distal shield sizes in excess of 6 μm; this sample is accordingly referred to the interval between the LOs of large *Gephyrocapsa* and *Helicosphaera sellii*. *Calcidiscus macintyrei* disappears between Samples 130-830B-3H-2, 10 cm, and -3H-2, 145 cm, placing the latter layer in the basal Pleistocene.

Pliocene

The last appearances of *Discoaster brouweri* and *Discoaster triradiatus* were observed between the 10- and 82-cm levels in Section 130-803B-3H-4. As the Pliocene/Pleistocene boundary roughly falls midway between the successive LOs of *D. brouweri* and *C. macintyrei*, this boundary is placed in Section 130-803B-3H-3, which agrees with magnetostratigraphic information obtained from this hole (with the termination of the Olduvai Subchron at 130-803B-3H-3, 10 cm; see "Paleomagnetics" section, this chapter). *Coccolithus pelagicus* was observed only below the Pliocene/Pleistocene boundary, in agreement with the observation from Hole 803A.

The LO of *Discoaster pentaradiatus* was observed between Samples 130-803B-4H-2, 103 cm, and -4H-3, 5 cm. Rare *Discoaster surculus* and *Discoaster tamalis* in Sample 130-803B-4H-CC, therefore, indicate a position well within the upper Pliocene Zone NN16. Sample 130-803B-5H-CC is also assigned to Zone NN16, but it belongs to the lower half of that zone because of the presence of *Discoaster variabilis*. Indeed, rare sphenoliths in Sample 130-803B-5H-CC suggest a position at basal Zone NN16.

Sample 130-803B-6H-CC contains common *Reticulofenestra pseudoumbilica*, abundant sphenoliths, and few *Ceratolithus rugosus*, indicating a position somewhere between the top of Zone NN15 and the bottom of Zone NN13. Further subdivision in that interval was not possible because of the absence of critical marker species (i.e., *Discoaster asymmetricus* and *Amaurolithus* spp.). Sample 130-803B-7H-CC, at the bottom of this hole, is assigned to Zone NN12 because of the presence of *Ceratolithus acutus* in an otherwise typical lower Pliocene low-latitude assemblage, with abundant sphenoliths and small placoliths (particularly *Reticulofenestra* <5 μm and *Dictyococcites productus*). Both *Ceratolithus rugosus* and *Discoaster quinqueramus* are absent in Sample 130-803B-7H-CC. The absence of *Reticulofenestra pseudoumbilica*, however, must be a result of ecological exclusion, and these unfavorable conditions must have ended during Zone NN13 time (see Hole 803A).

Hole 803C

Pliocene

Hole 803C was washed down to 19 mbsf, but from there on it shows an apparently continuous upper Pliocene through middle Miocene sequence. The occurrences of *Discoaster pentaradiatus* together with *D. surculus* indicate Zone NN16 for Samples 130-803C-1H-CC and -2H-CC. The latter sample contains rare *Discoaster tamalis*. The occurrences of *Reticulofenestra pseudoumbilica* and *Sphenolithus abies* in Sample 130-803C-3H-CC shows that this sample belongs to Zone NN15. Sample 130-803C-4H-CC contains *Amaurolithus tricorniculatus* and *Discoaster asymmetricus* and is accordingly assigned to Zone NN14. The absence of *Discoaster asymmetricus* and *Ceratolithus rugosus* and the presence of *Ceratolithus acutus* in Sample 130-803C-5H-CC places this sample in Zone NN12.

Miocene

Section 130-803C-6H-2 contains the LO of *Triquetrorhabdulus rugosus* and the first occurrence (FO) of *Ceratolithus acutus*, whereas the LO of *Discoaster quinqueramus* was observed in Section 130-803C-6H-4. This latter section, therefore, is assigned to Zone NN11, and the top of this zone approximately indicates the position of the Miocene/Pliocene boundary. The characteristic central knob in *Discoaster quinqueramus* is not so well developed in the oldest and youngest associations of this species, often making precise determinations of its entry and exit levels difficult. Sample 130-803C-6H-CC contains abundant specimens of *Coccolithus pelagicus* relative to other samples from Hole 803C.

Amaurolithus spp. are consistently rare in the lower Pliocene and upper Miocene sediments, and primary morphological characters are typically masked by substantial calcite overgrowth. Representatives of this group could be followed down to Sample 130-803C-11H, 5 cm, but not deeper; the deepest species observed is *Amaurolithus tricorniculatus*.

The LO of *Discoaster neohamatus* was observed in Section 130-803C-11H-6, and shorter rayed variants of *Discoaster quinqueramus* (*Discoaster berggrenii*) become progressively more common below that section. It was difficult to determine the NN10/NN11 zonal boundary precisely; well-developed *Discoaster quinqueramus* and *Discoaster berggrenii* were observed in Sample 130-803C-12H-CC, whereas intermediate morphotypes between these two knob-possessing species and their knob-lacking ancestor species *Discoaster bellus* occur abundantly in Sample 130-803C-13H-CC. Sample 130-803C-14H-CC clearly belongs to Zone NN10 because the above-mentioned five-rayed, knob-possessing morphotypes as well as *Discoaster hamatus* are absent. Therefore, the uncertainty in placing the NN10/NN11 zonal boundary encompasses the length of two full cores.

The NN9/NN10 zonal boundary (LO of *Discoaster hamatus*) occurs in Section 130-803C-17H-2. The nominate species is rare in the uppermost 3–4 m of its range, and some samples contain triradiate morphovariants of the five-rayed *Discoaster hamatus*. A shift in dominance between *Discoaster hamatus* and the six-rayed *Discoaster neohamatus*, an event that probably is biochronologically useful once properly evaluated, occurs in the upper part of Section 130-803C-17H-4. *Catinaster calyculus* disappears between Samples 130-803C-17H-4, 100 cm, and -17H-4, 150 cm, whereas the FO of *Discoaster neohamatus* occurs between Samples 130-803C-17H-5, 125 cm, and -17H-6, 75 cm.

Discoaster hamatus has its FO (defining the NN8/NN9 boundary) in Section 130-803C-18H-5. Overgrown specimens of *Catinaster coalitus* were observed in rare numbers throughout Section 130-803C-18H-6, and the NN7/NN8 zonal boundary is placed between that sample and Sample 130-803C-18H-CC. The middle/upper Miocene boundary is defined as falling within Zone NN8 and thus can be placed in the lower part of Core 130-803C-18H.

The middle Miocene assemblages contain abundant *Dictyococcites perplexus* and small reticulofenestrids. The *Triquetrorhabdulus* assemblage increases in diversity and the distinct, large *Coccolithus miopelagicus* has its LO in Sample 130-803C-18H-CC. Calcite overgrowth on discoasters prevents accurate identification of *Discoaster kugleri*, the FO of which defines the

NN6/NN7 boundary. The successive LOs of *Coronocyclus nitescens* and *Cyclicargolithus floridanus* can be used to subdivide the NN6–NN7 zonal interval. Neither of these events falls chronologically near the NN6/NN7 boundary, although the former species event is closer (0.6 m.y. older than the NN6/NN7 boundary estimate).

The LOs of *Cyclicargolithus floridanus* and *Sphenolithus heteromorphus* were both observed between Samples 130-803C-22H-3, 15 cm, and -22H-3, 50 cm. The latter species event defines the NN5/NN6 zonal boundary. Large-sized (>7 μm) *Reticulofenestra pseudoumbilica* appear within upper Zone NN5. This event was observed in Core 130-803C-22H. Sample 130-803C-23H-CC, which ends Hole 803C, still is within Zone NN5 because the ratio of the *Discoaster deflandrei* group/total number of discoasters is <30% (see Rio et al., 1990).

Hole 803D

Middle and Lower Miocene

Only core-catcher samples were investigated in the upper 24 cores of Hole 803D (i.e., in the Pleistocene to middle Miocene interval). The results from these core catchers are similar to the results obtained from Holes 803A through 803C, results that are summarized in Figure 18.

The NN5/NN6 boundary falls in Section 130-803D-25X-2, and a stable Zone NN5 assemblage is maintained throughout Sample 130-803D-27X-CC. This assemblage is composed mainly of abundant *Cyclicargolithus floridanus* and reticulofenestrids, common *Sphenolithus heteromorphus, Sphenolithus moriformis*, and *Coccolithus pelagicus*, few to rare discoasters, *Coccolithus miopelagicus, Coronocyclus nitescens, Helicosphaera granulata*, and *Triquetrorhabdulus rugosus*. The ratio of the *Discoaster deflandrei* group/total number of discoasters is <30% in Sample 130-803D-27X-CC, suggesting placement within Zone NN5 (i.e., younger than about 16 Ma) for this sample (see Rio et al., 1990).

A major change in taxonomic composition that is of biostratigraphic importance occurs between Samples 130-803D-27X-CC and -28X-1, 140 cm. The middle Miocene NN5 assemblage of the former sample is replaced by a typical early Miocene assemblage belonging to the NN2 *Discoaster druggii* Zone in the latter sample. The biostratigraphically most critical components in the older Zone NN2 assemblage include *Sphenolithus belemnos, Discoaster druggii*, and *Triquetrorhabdulus carinatus*. The co-occurrences of these taxa indicate an age ranging between 19.5 and 20.0 Ma for upper Core 130-803D-28X, and the presence of a hiatus between the bottom of Core 130-803D-27X and the top of Core 130-803D-28X. This hiatus, therefore, has a minimum duration of approximately 3.4 m.y.

Sphenolithus belemnos has its FO in the core break separating Core 130-803D-28X from the next underlying core. A prominent feature of the lower Miocene is that this part of the stratigraphic column still provides, at least in terms of nannofossil biostratigraphy, few reliable species events. The NN1/NN2 zonal boundary is difficult to recognize because of inconsistent occurrences and poor preservation (severe overgrowth disguising primary characters) of *Discoaster druggii*. Nonetheless, some potentially useful biostratigraphic events were observed: in Core 130-803D-29X, the LO of *Ericsonia obruta;* in Section 130-803D-31X-1, the LO of large-sized (>11 μm) *Cyclicargolithus* spp.; and in Core 130-803D-34X, the LO of abundant to dominant *Triquetrorhabdulus carinatus*. None of these events are directly correlated to magnetostratigraphy.

Oligocene

The distinct acme interval of *Sphenolithus delphix*, lasting from shortly above the LO of *Sphenolithus ciperoensis* to the Oligocene/Miocene boundary in the equatorial Indian Ocean (Rio et al., 1990) was not observed. Neither *Helicosphaera recta* (which defines the NP25/NN1 boundary) nor *Dictyococcites bisectus* was observed in the Miocene to Oligocene transitional interval, implying that the next deeper tie point was provided by the LO of *Sphenolithus ciperoensis* at the core break separating the bottom of Core 130-803D-39X from the top of Core 130-803D-40X.

Sphenolith species events that are critical for several Oligocene zonal boundary definitions were generally rare in Hole 803D. *Sphenolithus distentus* was observed (looking downhole) from Core 130-803D-42X, thus indicating Zone NP24. Sample 130-803D-45X-CC was also assigned to Zone NP24 because of the presence of rare *Sphenolithus ciperoensis*.

The sequence ranging from Samples 130-803D-46X-CC to -52X-CC is characterized by the absence of *Sphenolithus ciperoensis* and *Reticulofenestra umbilica*, and this section belongs to Zone NP23. *Sphenolithus pseudoradians* was observed in Sample 130-803D-48X-CC. Samples 130-803D-53X-CC through -55X-CC contain forms similar to *Reticulofenestra hillae;* therefore, these samples tentatively were placed in the NP23/NP22 zonal interval. Sample 130-803D-56X-CC contains *Ericsonia formosa* together with the first downhole occurrence of typical, large *Reticulofenestra hillae*. Thus, this sample is assigned to Zone NP21; typical *Reticulofenestra umbilica*, however, was not observed in Sample 130-803D-56X-CC. Sample 130-803D-58X-CC still belongs to Oligocene Zone NP21, with common *Bramlettius serraculoides, Dictyococcites bisectus/Dictyococcites hesslandii, Ericsonia formosa, Reticulofenestra umbilica, Reticulofenestra hillae*, and abundant *Cyclicargolithus floridanus*.

Eocene

The bottom of Core 130-803D-59X contains an upper Eocene assemblage, with *Discoaster saipanensis, Discoaster barbadiensis*, and *Cribrocentrum reticulatum*. Of these, only *Discoaster saipanensis* remains present at the top of this core, suggesting that the sample is located shortly below the Eocene/Oligocene boundary.

Preservation becomes progressively poorer (both dissolution and overgrowth) downhole throughout the Eocene sequence, and placolith fragments are common. Martini's (1971) zonal scheme does not work well in open-ocean, low-latitude sediments in the upper half of the Eocene. The composition of the Eocene assemblages, however, is generally stable in Hole 803D. *Calcidiscus protoannulus* has its LO in Core 130-803D-62X and *Chiasmolithus grandis* has its LO in the next deeper core. The latter event marks the middle/upper Eocene boundary. The *Dictyococcites bisectus/Dictyococcites hesslandii* complex has been a common to abundant member of the lower Oligocene and Eocene assemblages; the FO of this taxonomic category was observed in Core 130-803D-65X. The FO of *Reticulofenestra umbilica* (>14 μm) falls in the core break below Core 130-803D-66X. Core 130-803D-67X, however, contains well-developed, large *Coccolithus eopelagicus* and/or *Chiasmolithus gigas*. Rare occurrences, in combination with preservation problems, prevented identification of the central area structure of these similarly constructed morphotypes, and hence they could not be distinguished. If specimens of *Nannotetrina* spp. were present, they could not be recognized, even at the generic level, because of severe calcite overgrowth. Nevertheless, it is important to note that Sample 130-803D-67X-CC belongs to the middle Eocene interval between the FOs of *Chiasmolithus gigas* and *Reticulofenestra umbilica*.

Paleocene

Sample 130-803D-68R-1, at 0.1 and 0.9 cm, contains an assemblage characteristic of the uppermost Paleocene that includes common *Discoaster multiradiatus*, few *Discoaster nobilis*, abundant *Fasciculithus tympaniformis* (and other late Paleocene fasciculith morphotypes), and rare *Ellipsolithus macellus*. These samples are assigned to Zone NN9. The next sample from only 1 cm further downcore is barren except for a single, poorly preserved specimen that probably belongs to the Cretaceous genus *Micula*. See the "Lithostratigraphy" section of this chapter for a description of the major change in sediment lithology occurring between Cores 130-803D-67R and -68R.

Cretaceous/Tertiary Boundary

The sediments in Hole 803D are barren of calcareous nannofossils below Sample 130-803D-68R-1, 73 cm. From this sample and upward to Sample 130-803D-68R-1, 3 cm, the poorly preserved and low-diversity assemblages (presumably preservational artifact) are predominantly of uppermost Cretaceous origin. About 40 smear slides were examined from this interval to obtain adequate representation of the different sediment types. The stratigraphic distribution of selected species in this upper part of Section 130-803D-68R-1 is illustrated in Table 4.

The dissolution-resistant genus *Micula* is a major component throughout the pertinent interval, with the consistent presence of *Micula prinsii*. This conspicuous species has its FO shortly before the K/T boundary and disappears together with other Cretaceous taxa at the boundary. At Shatsky Rise Site 577, the FO of *Micula prinsii* can be calculated to 65.5–66.6 Ma, combining data from Monechi (1985) and Bleil (1985). This evolutionary event consequently occurred only shortly before the K/T boundary (66.4 Ma; Berggren et al., 1985a) in the western Pacific Ocean.

Monechi (1985) used the FO and subsequent rapid increase in abundance of the calcareous dinoflagellate *Thoracosphaera* spp. for recognition of the K/T boundary, an event that coincides precisely with the iridium spike at DSDP Site 577 (Wright et al., 1985). Monechi's criterion for recognition of the K/T boundary is adopted here, partly because *Thoracosphaera* (fragments, mostly) is one of the few taxonomic categories that is preserved in the strongly dissolved sediments encountered in Section 130-803D-68R-1.

Pure upper Maestrichtian assemblages (with *Micula prinsii*) were observed between in Sample 130-803D-68R-1, between 53 and 73 cm. Fragments of *Thoracosphaera* spp. appear in Sample 130-803D-68R-1, 46.5 cm, become abundant in the next higher Sample 130-803D-68R-1, 38 cm, and remain abundant above that sample (Table 4). *Markalius astroporus* is present in Sample 130-803D-68R-1, 29.5 cm. This sample also contains another basal Danian marker, namely *Biantholithus sparsus*. The FO of the former species was observed about 20 cm above the K/T boundary at Site 577 (Monechi, 1985).

If using the data and definitions described above, the conclusion is reached that the K/T boundary is preserved intact in Sample 130-803D-68R-1, between 38 and 53 cm, and that this boundary lies near Sample 130-803D-68R-1, 46.5 cm. It follows that the Cretaceous calcareous nannofossils occurring above the boundary must be considered to be reworked.

Planktonic Foraminifers

The discussion of planktonic foraminifers that follows is a composite summary of the zones recognized at Site 803 and their diagnostic taxa. Problems regarding dissolution and missing marker species also are discussed. Figure 18 summarizes the planktonic foraminifer zonation of the four holes drilled at Site 803 and their correlation with those of the calcareous nannofossils, diatoms, and radiolarians. Hole 803D represents the complete sequence drilled at this site; therefore, it is used as the reference hole.

We found that planktonic foraminifers were abundant from the surface to well within middle Miocene Zone N10 (Sections

Table 4. Range chart of calcareous nannofossil species across the Cretaceous/Tertiary boundary interval (Section 130-803D-68R-1).

Species	Interval (cm)																
	0.1	0.9	5	10	15	25	26	30	38	47	53	59	60	61	63	68	73
upper Paleocene:																	
C. pelagicus	X	X								K/T							
D. mohleri	X	X															
D. multiradiatus	X	X								L							
D. nobilis	X	X								A							
E. macellus	X	X								Y							
F. tympaniformis	X	X								E							
S. primus	X	X								R							
lower Paleocene:																	
B. sparsus								X									
Thoracosphaera			X	X	X	X	X	X	X	X							
M. astroporus								X									
Cretaceous:																	
A. cymbiformis											X	X		X			
C. aculeus					X					X		X			X		X
C. ehrenbergii					X							X					
C. margerelii										X					X	X	X
L. quadratus					X	X											
Micrantholithus				X		X											
M. decussata				X	X	X			X			X	X	X	X	X	X
M. murus			X		X	X		X		X	X	X	X	X	X	X	X
M. prinsii					X					X	X	X	X	X	X	X	X
P. cretacea										X		X	X				
Q. trifidium			X														
W. barnesae			X	X	X	X	X	X	X	X	X	X	X	X	X	X	X

Note: The importance of the thoracosphaerids for recognition of the boundary is discussed in the text.

130-803D-1H-CC to -25X-CC). The sediments become distinctly more chalky from Sections 130-803D-25X-CC to -26X-CC (about 230 mbsf). Preservation in this upper part of the section at Site 803 ranges from moderate to good. Selective dissolution of planktonic foraminifer tests is responsible for the absence of some taxa, including several marker species, and for the breakage of tests. Estimates of foraminifer fragmentation range between 20% and 50% for this interval. Although *Globigerinoides sacculifer* is one of the most abundant species, its test often appears thin and fragile, as do the tests of *Orbulina universa*.

Foraminifer abundance, in general, decreases from "abundant" to "few" and "common" in the lower middle Miocene through Oligocene interval (Samples 130-803D-26X-CC to -58X-CC). Preservation is generally moderate, although slightly poorer preservation is noted in the lowermost Miocene (*Globorotalia kugleri* Zone N4) through upper Oligocene (*Globigerina ciperoensis* Zone P22) interval (130-803D-32X-CC to -40X-CC). Foraminifers are very rare in the upper to middle Eocene interval (130-803D-59X-CC to -66X-CC), and the assemblages contain only solution-resistant taxa.

The Pliocene/Pleistocene boundary is difficult to locate based on the planktonic foraminifers recovered at Site 803. According to Berggren et al. (1985b), the FO of *Globorotalia truncatulinoides* is in the uppermost Pliocene and marks the boundary between Zones N21 and N22 (base of the *Globorotalia truncatulinoides* Zone). Other workers use the FO of *G. truncatulinoides* to mark the Pliocene/Pleistocene boundary (e.g., Bolli and Saunders, 1985; Kennett and Srinivasan, 1983). The LO of *Globigerinoides fistulosus* would serve as a good marker of the Pliocene/Pleistocene boundary according to Berggren et al. (1985b), but we did not record the co-occurrence of *G. truncatulinoides* and *G. fistulosus* in core-catcher samples examined from Site 803.

Globigerinoides fistulosus is a good upper Pliocene (uppermost N19 and N21) marker species at Site 803. Its presence most likely represents the lower *Globorotalia tosaensis* Zone and the upper part of the *Globorotalia miocenica* Zone (1.9–2.9 Ma according to Berggren et al., 1985b). *Globorotalia miocenica* does not occur in the Pacific (Berggren et al., 1985b), but *G. tosaensis* does occur consistently throughout much of the upper Pliocene section. The presence of *Sphaeroidinellopsis* spp. in the absence of *Globorotalia margaritae* also marks the upper Pliocene *G. miocenica* Zone (uppermost N19).

The LO of *Globorotalia margaritae* marks the top of lower Pliocene Zone N19. However, the nominate taxon was not observed in the lower part of the zone, perhaps because of dissolution effects. Other diagnostic taxa of this zone include *Sphaeroidinella dehiscens* s.l., *Sphaeroidinellopsis paenedehiscens, S. seminulina, Globoquadrina altispira, Globorotalia tumida, G. plesiotumida, G. menardii, G. multicamerata, Globigerinoides extremus, Pulleniatina primalis*, and *Globigerina venezuelana*. *Pulleniatina spectabilis* is present in the lower part of the zone. *Globigerina nepenthes* is noticeably absent or found only in very small numbers, which again is attributed to dissolution. The FO of *S. dehiscens* s.l. marks the top of Zone N18.

The Miocene/Pliocene boundary (N17/N18) is marked by the FO of *Globorotalia tumida* and the LO of *Globoquadrina dehiscens*. The upper Miocene *Neogloboquadrina dutertrei* s.l. Zone (N17) is characterized by *Globigerinoides* spp., *Neogloboquadrina acostaensis, Globoquadrina dehiscens, G. altispira, Sphaeroidinellopsis seminulina, Globorotalia plesiotumida, G. merotumida*, the *G. menardii* group, and *G. lenguaensis*. *Pulleniatina primalis* is present in the uppermost part of this zone and can be used to subdivide N17 (e.g., Kennett and Srinivasan, 1983).

The FO of *Globorotalia plesiotumida* marks the top of the upper Miocene *Neogloboquadrina acostaensis* Zone (N16). The differentiation of *G. plesiotumida* and *G. merotumida* is obscured by numerous transitional forms. As a result, the position of the N16/N17 boundary is rather tenuous at Site 803. The *N. acostaensis* Zone has a similar fauna to that of the overlying *N. dutertrei* s.l. Zone. The lower upper Miocene *Globorotalia menardii* Zone (N15) is characterized by the absence of *Neogloboquadrina acostaensis* (FO at the base of Zone N16) and the absence of *Globorotalia siakensis* (LO at the top of Zone N14).

The upper middle Miocene *Globorotalia mayeri* Zone (N14) is characterized by *Globorotalia siakensis* (= *G. mayeri*), *Sphaeroidinellopsis* spp., *Globoquadrina dehiscens, G. altispira*, and *Neogloboquadrina continuosa*. Numerous *G. siakensis* and species of *Globigerina* replace species of *Globigerinoides* as the dominant taxa of the sediment assemblages. This may be a preservational or paleoecological signal, or a combination of both. The FO of *Globigerina nepenthes* defines the top of Zone N13, but this taxon is very rare in material from Site 803. Therefore, the recognition of the N13/N14 boundary is not certain based on shipboard results.

The *Globorotalia fohsi* lineage defines several zones within the middle Miocene (N10–N12): *G. fohsi robusta, G. fohsi lobata*, and *G. fohsi fohsi* are characteristic of Zone N12; *G. fohsi praefohsi* and *G. peripheroacuta* are diagnostic of Zone N11; and the presence of *G. peripheroacuta* in the absence of *G. fohsi praefohsi* distinguishes Zone N10. Other diagnostic taxa of Zones N10–N12 include *Globorotalia siakensis*, the *G. archeomenardii-praemenardii* plexus, *Globoquadrina altispira, G. dehiscens, Catapsydrax parvulus*, and *Neogloboquadrina continuosa*.

The FO of *Globorotalia peripheroacuta* and the LO of *Globigerinoides sicanus* define the top of middle Miocene *Globorotalia peripheroronda* Zone N9. However, the *Praeorbulina-Orbulina* lineage is poorly represented in the Site 803 material, probably the consequence of dissolution. As a result, it is difficult to differentiate the lowermost zones of the middle Miocene (N8 and N9).

A significant stratigraphic break between Sections 130-803D-27X-CC and -28X-CC separates sediments of lower middle Miocene Zone N9 from sediments of the lower Miocene *Catapsydrax dissimilis* Zone (N5). The lower part of Zone N5 is indicated by the presence of *Globoquadrina binaiensis*. Therefore, sediment, representing approximately 4–6 m.y. of time, is missing in the disconformity. The diagnostic taxa of Zone N5 include *Catapsydrax dissimilis, C. stainforthi, Globoquadrina binaiensis, G. dehiscens, Globorotalia siakensis*, and *Globigerinoides primordius*. *Globorotalia kugleri* Zone N4 is characterized by *G. kugleri* s.s., *G. siakensis, Catapsydrax dissimilis, Globoquadrina dehiscens, G. binaiensis*, and *Globigerina sellii*. *Globorotalia peripheroronda* is present in the upper part of the zone.

The Oligocene/Miocene boundary (P22/N4) is based on the FO of *Globorotalia kugleri* s.s. (see "Explanatory Notes" chapter, this volume). Upper Oligocene *Globigerina ciperoensis* Zone P22 is distinguished by the absence of both *G. kugleri* s.s. and *Globorotalia opima opima* in the Site 803 material. The nominate taxon, as well as *Globigerina angulisuturalis* and *Globigerinoides primordius*, are absent, probably a result of selective dissolution. Species present include *Globorotalia opima nana, Catapsydrax dissimilis, C. unicavus*, and *Globigerina venezuelana*. *Globorotalia kugleri* s.l. and *G. siakensis* are present in the upper part of the zone.

The LO of *Globorotalia opima opima* defines the top of the mid-Oligocene *G. opima opima* Zone (P21). The assemblage is very similar to that of the overlying *Globigerina ciperoensis* Zone. Furthermore, *G. opima opima* is present consistently throughout the zone. Subzones P21a and P21b could not be differentiated during shipboard work because of the absence of

Chiloguembelina cubensis, the LO of which would normally be used to recognize the top of Subzone P21a (lower Oligocene/upper Oligocene boundary). Its absence is probably related to selective dissolution. The FO of *Globigerina angulisuturalis* defines the top of Zone P20; however, because this taxon was not observed in material from Site 803, the differentiation of Zone P20 and the lower part of Zone P21 is not precise. The LO of *Globigerina angiporoides* in the absence of *Globigerina ampliapertura* does, however, serve as a proxy for Zone P20 at this site.

The FO of *Globigerina opima opima* is used to identify the top of the lower Oligocene *Globigerina ampliapertura* Zone. The LO of *G. ampliapertura* defines the top of Zone P19. These two datums occur within 0.1 m.y. of each other, according to Berggren et al. (1985a). In addition to the nominate taxon, *Globorotalia opima nana, Catapsydrax dissimilis,* and *C. unicavus* also are present within Zone P19. *Globigerina angiporoides* is present sporadically. Specimens transitional between *G. ampliapertura* and *Globorotalia increbescens* are present in the lower part of the zone.

The top of the lower Oligocene *Cassigerinella chipolensi-Pseudohastigerina micra* Zone P18 is defined by the LO of *Pseudohastigerina*. Preservation is good throughout this zone at Site 803, and this is perhaps why *P. micra* and *Chiloguembelina cubensis* are present throughout the zone. *Globigerina ampliapertura, Catapsydrax dissimilis,* and *Globigerina eocaena* also are present.

The Eocene/Oligocene boundary could not be identified at Site 803 based on planktonic foraminifers. Foraminifer preservation is generally poor and abundance is low throughout the middle and upper Eocene interval (Sections 130-803D-58X-CC to -67R-CC). Diversity is very low and only solution-resistant forms are found. A general late middle Eocene–late Eocene age (P13–P16) is suggested by the presence of *Catapsydrax dissimilis, Globigerina eocaena,* and *G. tripartita* in Section 130-803D-59X-CC. A general middle Eocene age (P11–P12) is assigned to Section 130-803D-64X-CC based on the presence of *Acarinina broedermanni, Globorotalia* cf. *bolivariana* (Toumarkine and Luterbacher, 1985), and *Globigerina senni.*

Basal Tertiary and Cretaceous sediments of Core 130-803D-68R represent a highly condensed interval, including an apparently complete K/T boundary sequence in the upper part of Section 130-803D-68R-1, according to the calcareous nannofossil data. No foraminifer samples were taken in the boundary interval for shipboard analysis. Below the K/T boundary interval, planktonic foraminifers are absent. Deep-water, agglutinated benthic foraminifers are present in very low abundances. The agglutinated taxa *Trochamminoides proteus* and *T. irregularis* from Sample 130-803D-68R-1, 110–112 cm, indicate a Maestrichtian-Paleocene age according to the range data of Kaminski et al. (1986). Agglutinated taxa are present in Sample 130-803D-68R-3, 143–145 cm, but they are not age diagnostic based on shipboard analysis.

Benthic Foraminifers

Core-catcher samples from Hole 803D were examined for benthic foraminifers. Benthic specimens are present in all of the Quaternary through middle Eocene core-catcher samples from Sections 130-803D-1H-CC through -67R-CC. Near the base of the hole, Samples 130-803D-68R-1, 110–112 cm, and -68R-3, 143–145 cm, contain agglutinated foraminifers of mid-Cretaceous to Late Cretaceous age, based on nannofossil and radiolarian data.

Benthic foraminifers generally are well preserved in all of these samples and vary in abundance relative to planktonic specimens according to the amount of dissolution affecting the planktonic components. Intervals of strong dissolution with a high concentration of radiolarians contain greater than the 1%–2% benthic foraminifers, relative to the total foraminifer fauna, that would be expected for a deep-water site lying above the foraminifer lysocline. These intervals are represented mainly in Samples 130-803D-13H-CC and -14H-CC (upper Miocene), 130-803D-28X-CC through -42X-CC (lower Miocene through upper Oligocene), 130-803D-44X-CC through -55X-CC (lower Oligocene), and 130-803D-59X-CC through -67X-CC (lower upper Eocene through middle Eocene). Because the benthic assemblages from this site are consistently of lower bathyal to abyssal biofacies, as detailed below, water-mass changes rather than tectonic movements are indicated by the preservational state and relative proportions of the microfossil components of the pelagic ooze and chalk comprising the stratigraphic section.

The lowest Eocene sample, Sample 130-803D-67R-CC, of middle Eocene age, is a radiolarian ooze that contains a few rare specimens of calcareous benthic foraminifers, including the species *Alabamina dissonata,* which ranges from the upper Paleocene through the upper Eocene. In contrast to the good preservation of benthic specimens throughout the younger section, most of the specimens in this sample are broken and etched; no planktonic foraminifers are present. This sample was deposited below the middle Eocene CCD.

Listed in Table 5 are the most frequent species present in sand fraction (>63 µm) samples representative of the various time-stratigraphic units. Their percent frequencies among the benthic fauna are given, as well as the names of some less frequent members of the assemblages. The basic trend of these data indicates an upper Eocene through lower Oligocene species assemblage, an upper Oligocene through lower Miocene transitional assemblage, followed by a middle Miocene through Quaternary modern assemblage, all of deep-water origin (Woodruff, 1985; Thomas, 1990).

Diatoms

Neogene

Diatoms were examined in three (Holes 803A, 803C, and 803D) out of the four holes drilled at Site 803. As with planktonic foraminifers, the discussion of diatoms is also a composite summary of the diatom zones recognized in the Quaternary-Pliocene (Hole 803A), early Pliocene–late Miocene (Hole 803C), and middle Miocene–Oligocene (Hole 803D). Assignment of Site 803 samples to the low-latitude diatom zonation is summarized in Figure 18.

Diatoms are abundant to common (few) above 236.5 mbsf (Samples 130-803A-1H-CC to 130-803D-25X-CC), whereas large fluctuations in their abundance are seen below that level. In general, preservation is moderate to good, although poorer preservation is noted in the lower middle Miocene (Sample 130-803D-26X-CC) and upper Oligocene (Samples 130-803D-36X-CC through -39X-CC).

The sequence is complete from the Quaternary NTD 17 (for Neogene Tropical Diatom zone; Barron, 1985) *Pseudoeunotia doliolus* Zone (Sample 130-803A-1H-CC) through the lower middle Miocene NTD 5 *Cestodiscus peplum* Zone (Sample 130-803D-27X-CC), and from approximately early Miocene Sample 130-803D-29X-CC to -53X-CC. The diatom data suggest a hiatus in the early Miocene of approximately 4–6 m.y.

Two diatom zones, NTD 4 *Denticulopsis nicobarica* and NTD 3 *Triceratium pileus,* are completely missing at Site 803. This hiatus would correspond, in part, to Hiatus NH2 and Hiatus NH1b of Keller and Barron (1983), lumped together. This conclusion also is supported by nannofossil and planktonic foraminifer evidence.

The uppermost core-catcher sample (130-803A-1H-CC) is assigned to the NTD 17 *P. doliolus* zone. The Pliocene/Pleistocene boundary is difficult to locate, as diatom abundance is low and the valves are not well preserved.

Table 5. **Benthic foraminifers as a percentage of total foraminifers.**

Age and sample data	Species name	Sample (%)
Quaternary (N22) Sample 130-803D-1H-CC B = 3% *N* = 312 T = 9,984	*Pseudoparrella exigua*	15%
	Nuttallides umbonifera	11%
	Pullenia bulloides	9%
	Globocassidulina subglobosa	7%
	Cassidulina sp.	6%
	Oridorsalis umbonatus	6%
	Alabaminella weddellensis	5%
	(Others: *Cassidulina complanata*, *Uvigerina bradyana*, *Fontbotia wuellerstorfi*)	
early Pliocene (N18) Sample 130-803D-6H-CC B = 1% *N* = 208 T = 1,664	*Nuttallides umbonifera*	7%
	Globocassidulina subglobosa	6%
	Cibicidoides mundulus	6%
	Melonis affinis	6%
	Pleurostomella acuminata	6%
	(Others: *Sigmoilina edwardsi*, *Uvigerina proboscidea*, *Favocassidulina favus*)	
late Miocene (N17) Sample 130-803D-12H-CC B = <1% *N* = 161 T = 644	*Globocassidulina subglobosa*	11%
	Oridorsalis umbonatus	6%
	Nuttallides umbonifera	6%
	Pullenia bulloides	6%
	Sigmoilina edwardsi	6%
	Eggerella bradyi	6%
	Pleurostomella subnodosa	6%
	Siphouvigerina sp.	6%
	(Others: *Fontbotia wuellerstorfi*)	
middle Miocene (N11) Sample 130-803D-24H-CC B = <1% *N* = 154 T = 1,232	*Oridorsalis umbonatus*	16%
	Melonis affinis	10%
	Globocassidulina subglobosa	8%
	Nuttallides umbonifera	8%
	Cibicidoides sp.	7%
	(Others: *Parrelloides bradyi*, *Gyroidinoides neosoldanii*)	
early Miocene (N4) Sample 130-803D-31X-CC B = 4% *N* = 229 T = 458	*Nuttallides umbonifera*	19%
	Oridorsalis umbonatus	14%
	Linaresia pseudogrosserugosa	9%
	Globocassidulina subglobosa	7%
	Globocassidulina sp.	6%
	(Others: *Parrelloides bradyi*, *Gyroidinoides zealandicus*, *Bolivinopsis cubensis*)	
late Oligocene (P21–P22) Sample 130-803D-38X-CC B = 16% *N* = 280 T = 1,120	*Oridors alis umbonatus*	16%
	Cassidulina subglobosa	11%
	Pseudoparrella aff. *exigua*	8%
	Nuttallides umbonifera	7%
	Pullenia bulloides	6%
	Gyroidinoides zealandicus	6%
	(Others: *Anomalinoides spissiformis*, *Parrelloides bradyi*, *Bolivinopsis cubensis*	
early Oligocene (P18) Sample 130-803D-58X-CC B = <1% *N* = 143 T = 143	*Oridorsalis umbonatus*	13%
	Nonion havanense	10%
	Dorothia chapapotensis	10%
	Pullenia bulloides	8%
	Cibicidoides praemundulus	7%
	(Others: *Cibicidoides grimsdalei*, *Anomalinoides spissiformis*)	
late Eocene (P13–P16) Sample 130-803D-59X-1, 3–5 cm B = 82% *N* = 73 T = 73	*Cibicidoides praemundulus*	22%
	Oridors alis umbonatus	19%
	Cibicidoides grimsdalei	10%
	Nonion havanense	7%
	Anomalinoides spissiformis	7%
	Gyroidinoides lamarckianus	7%
	(Others: *Dorothia chapapotensis*, *Alabamina dissonata*, no *Nuttallides truempyi*)	
late Eocene (P13–P16) Sample 130-803D-60X-CC B = 85% *N* = 449 T = 449	*Oridorsalis umbonatus*	20%
	Cibicidoides grimsdalei	18%
	Nuttallides truempyi	8%
	Globocassidulina subglobosa	6%
	Cibicidoides sp.	6%
	Gyroidinoides sp.	6%
	(Others: *Alabamina dissonata*, *Anomalinoides spissiformis*, *Nonion havanense*, *Buliminella grata*)	

Notes: B = the percentage of representation of benthic specimens relative to total foraminifer content; *N* = the number of specimens counted for the percent frequency data; and T = the total number of benthic specimens in each approximately 20-cm^3 core-catcher sample, calculated from the sample split used for the census data.

The late Pliocene NTD 15 ***Rhizosolenia praebergonii*** **Zone** is found in Samples 130-803A-3H-CC, -4H-CC, and -5H-CC. The FO of *R. praebergonii*, the presence of *Thalassiosira convexa* var. *aspinosa*, and the LO of *Actinocyclus ellipticus* f. *lanceolatus* are in the lower late Pliocene samples (NTD 15/NTD 14 *Nitzschia jouseae* boundary: Sample 130-803A-6H-CC).

We could not resolve the subzones of NTD 13 *Thalassiosira convexa* defined by Burckle (1972). However, the LO of *Nitzschia miocenica*, the presence of *N. cylindrica* and members of the *T. convexa* group, and the FO of *Thalassiosira oestrupii* are contained in Samples 130-803C-5H-CC and -6H-CC assigned to this zone. The Miocene marker *Thalassiosira miocenica* was not observed. The NTD 12 *Nitzschia miocenica* Zone is rather large and expands possibly over at least three cores (Samples 130-803C-7H-CC through -9H-CC). Sample 130-803-10H-CC may represent the base of the NTD 12 Zone, slightly above the LO of *Nitzschia porteri*. The short overlap in the ranges of *N. miocenica* and *N. porteri* is seen in Sample 130-803C-11H-CC. This sample and Samples 130-803C-12H-CC and -13H-CC tentatively are assigned to the NTD 11 *N. porteri* Zone. The presence of *N. porteri* and *N. cylindrica* and the absence of *N. marina* leads us to do so. However, *Thalassiosira burckliana* was not observed.

The presence of *Coscinodiscus yabei* and the restricted range of *C. vetustissimus* var. *javanicus* fall within the NTD 10 *C. yabei* Zone (Samples 130-803C-15H-CC through -17H-CC). *Coscinodiscus nodulifer* var. *cyclopus* is present in this zone.

Sample 130-803C-17H-CC may represent the NTD 10/NTD 9 (*Actinocyclus moronensis*) boundary. The ranges of this species and *C. vetustissimus* var. *javanicus* overlap here. The species *Denticulopsis hustedtii* is missing. The late/middle Miocene boundary occurs within the NTD 9 Zone. The NTD 8 *Craspedodiscus cosinodiscus* Zone is contained in Sample 130-803D-23H-CC. At Site 803, the zone is characterized by the presence of *C. coscinodiscus* and *Synedra jouseana*, the LOs of *Denticulopsis punctata* f. *hustedtii* and *Actinocylcus ingens*, and the absence of *Hemidiscus cuneiformis*. The NTD 7 *Coscinodiscus gigas* var. *diorama* Zone may be compressed into the NTD 6 Zone, as only fragments of this species are recorded in the same sample (130-803D-24H-CC) in which the LOs of *Coscinodiscus lewisianus* and *Cestodiscus pulchellus* were observed. The NTD 6 *C. lewisianus* Zone extends from Samples 130-803D-24H-CC through -25X-CC. The occurrence of *Cestodiscus peplum* (NTD 5) is limited to Sample 130-803D-27X-CC.

As mentioned above, Zones NTD 4 and NTD 3 are missing. The LO of *Craspedodiscus elegans* in Sample 130-803D-29X-CC assigns this sample to the NTD 2 Zone. However, low diatom abundances and poor preservation prevents precise dating of this sample. The characteristic diatom *Thalassiosira fraga* is missing. The presence of *Rosiella paleacea* and the few to common abundances of *Synedra jouseana*, *Coscinodiscus lewisianus* var. *rhomboides*, *C. marginatus*, and *C. oligocenicus* would assign Samples 130-803D-31X-CC through -34X-CC to the NTD 1 *R. paleacea* Zone.

The poor preservation of Sample 130-803D-35X-CC does not allow dating of this sample. The *Rocella gelida* Zone may be removed or compressed (?) at Site 803. The Oligocene/Miocene boundary cannot be identified. Samples 130-803D-36X-CC through -40X-CC are assigned to the *Borgorovia veniamini* Zone. The interval of the *Rocella vigilans* Zone (Samples 130-803D-42X-CC to -47X-CC) is moderately to well preserved at Site 803. *R. vigilans* is the most consistently present species throughout the zone. *Cestodiscus reticulatus* is present in Sample 130-803D-51X-CC. The LO of *Coscinodiscus excavatus* is in Sample 130-803D-52X-CC, and its FO is in Sample 130-803D-59X-CC. We could not recognize the late Eocene *Baxteriopsis brunii* Zone proposed by Fenner (1984) in Hole 803D, and the

Eocene/Oligocene boundary could not be identified. Samples 130-803D-62X-CC and -63X-CC are tentatively assigned to the *Asterolampra marylandica* Zone. This assignment, however, is uncertain and is based mainly on the FO of *A. marylandica* in Sample 130-803D-63X-CC and the presence of *Triceratium inconspicuum* var. *inconspicuum* in Sample 130-803D-62X-CC. Diatoms are rare in Samples 130-803D-64X-CC to -66X-CC. *A. marylandica* is absent, and no other biostratigraphic marker species could be found in these samples. Sample 130-803D-67X-CC is barren.

Cretaceous

The 19 samples of Core 130-803D-68R used for radiolarian studies (see "Radiolarians" section, this chapter) were also used for diatom analysis. They contain no diatoms.

Radiolarians

Radiolarians were observed in all of the recovered core-catcher samples of Cenozoic age. Their preservational states generally deteriorate with increasing depth throughout the Neogene. They generally are well preserved in the Pleistocene to middle Miocene nannoplankton/foraminifer oozes. Moderate to poorly preserved radiolarians are present in the underlying middle Miocene–lower Miocene oozes and chalks. Chalky sediments, sometimes silicified, recovered from the Oligocene and the Eocene contain poorly preserved radiolarians. Zonal assignments were possible for all the Cenozoic samples, although in some cases more than one zone could not be differentiated. In the radiolarian record, sequential zones from the Pleistocene to the middle Eocene were found, and no significant hiatus was recognized above the middle Eocene at this site. A major hiatus occurs in the lowermost Tertiary. Cretaceous radiolarians were found in the sediment layers overlying the basement. Several samples yielded useful stratigraphic information. Figure 18 summarizes the radiolarian zonation of Holes 803A, 803B, 803C, and 803D as well as their correlation with the zones of other taxa.

Neogene

The following core-catcher samples, ranging from the seafloor to 361.3 mbsf in depth, were determined to be of Neogene age: 130-803A-1H-CC through -6H-CC; 130-803B-1H-CC through -7H-CC; 130-803C-1H-CC through -15H-CC; and 130-803D-16H-CC through -39X-CC. The upper Miocene sediments (i.e., the *Didymocyrtis antepenultima* Zone) were the thickest unit observed at this site.

Pleistocene

The two uppermost core-catcher samples from Hole 803B (130-803B-1H-CC and -2H-CC) can be assigned to the *Anthocyrtidium angulare* Zone of the lowermost Quaternary. The presence of *Lamprocyrtis neoheteroporos* and *Theocorythium trachelium* and the absence of *Collosphaera tuberosa* suggests that these samples are in the *A. angulare* Zone. Thus, it is apparent that the Holocene and upper Pleistocene sections are condensed (or missing) in the top several meters.

Pliocene

Samples 130-803B-3H-CC and 130-803C-1H-CC are placed in the uppermost Pliocene radiolarian zone (the *Pterocanium prismatium* Zone). The *Spongaster pentas* Zone is found in Samples 130-803B-4H-CC through -7H-CC and 130-803C-2H-CC through -4H-CC. Age-diagnostic taxa (and their FOs and LOs) found in these samples are *Spongaster tetras* (FO), *Spongaster berminghami* (LO), *S. pentas* (FO), *Stichocorys peregrina* (LO), and *Didymocyrtis penultima* (LO). The *S. peregrina* Zone begins from Sample 130-803C-5H-CC and extends into Sample 130-803C-8H-CC. Diagnostic taxa found in these samples are *S. peregrina*, *D. penultima*, *S. berminghami*, and *Solenosphaera omnitubus* (LO). As the *S. peregrina* Zone ranges from the lower Pliocene to the upper Miocene, the Miocene/Pliocene boundary lies between Cores 130-803C-5H and -8H.

Upper Miocene

Samples 130-803C-9H-CC through -11H-CC are assigned to the *Didymocyrtis penultima* Zone. The FO of *S. omnitubus* and the LOs of *Didymocyrtis antepenultima* and *Stichocorys delmontensis* are found in these samples. Samples 130-803C-12H-CC through -15H-CC and Samples 130-803D-16H-CC through -18H-CC are placed in the *D. antepenultima* Zone. In this zone, we recognized the following six datum levels: the LOs of *Dictyocoryne ontogenesis, Diartus hughesi, Didymocyrtis laticonus*, and *Diartus petterssoni;* and the FOs of *D. antepenultima* and *S. berminghami.*

Reworked middle Eocene specimens were recognized in three core-catcher samples: 130-803C-10H-CC (*Podocyrtis phyxis* [F = few]), 130-803C-11H-CC (*P. phyxis* [C = common]), and 130-803C-12H-CC (*Theocotyle cryptocephala* [F]). Species belonging to younger ages (e.g., Pliocene) were encountered in Sample 130-803C-14H-CC: *S. tetras* (F), *S. pentas* (R), and *D. penultima* (R). Pliocene specimens of *Anthocyrtidium prolatum* (F) and *S. pentas* (F) were also found in Sample 130-803D-17H-CC. Both of these are considered to be downcore contaminations during coring procedures.

Middle Miocene

Samples 130-803D-19H-CC through -23H-CC were assigned to the *D. petterssoni* Zone of the uppermost middle Miocene. In these samples, the FOs of following species were found: *Dictyocoryne ontogenesis, Diartus hughesi*, and *Diartus petterssoni.* Sample 130-803D-24H-CC lies in the upper part of the *Dorcadospyris alata* Zone; this zone continues to the next sample (130-803D-25X-CC). In these samples, the FOs of *D. laticonus* and *S. delmontensis* and the LOs of *Lithopera renzae* and *Lithopera neotera* are located.

Lower Miocene

The uppermost part of the *Calocycletta costata* Zone begins at Sample 130-803D-26X-CC; the same zone continues to Sample 130-803D-27X-CC, and the lower part of the zone is in Sample 130-803D-28X-CC. The LOs of *Didymocyrtis mammifera, Dorcadospyris dentata, Dorcadospyris forcipata, Liriospyris parkerae, Cyrtocapsella japonica*, and *Calocycletta caepa* were found in these samples. Datum levels of the FOs in the zone are *D. dentata* and *L. parkerae*. Samples 130-803D-29X-CC through -31X-CC are located in the *Stichocorys wolffii* Zone.

Samples 130-803D-32X-CC and -33X-CC cannot be differentiated between the *S. wolffii* and *Stichocorys delmontensis* Zones because of the lack of key species. Nevertheless, either of the zones would give no problem in terms of continuity in sedimentation. Sample 130-803D-34X-CC contains a radiolarian assemblage corresponding to the top of the *Cyrtocapsella tetrapera* Zone. Samples 130-803D-35X-CC and -36X-CC are also placed in the C. tetrapera Zone. Samples 130-803D-37X-CC and -38X-CC can be assigned to either the *C. tetrapera* or the *Lychnocanoma elongata* Zones, as they cannot be differentiated. Sample 130-803D-39X-CC belongs in the lower part of the *L. elongata* to the upper part of *Dorcadospyris ateuchus* Zones.

Paleogene

Paleogene sediments recovered from Hole 803D, composed of nannofossil chalks to foraminifer nannofossil chalks, generally contain poorly preserved radiolarians. Zonal assignments were usually possible. With increasing age and depth, the chalks increased in degree of consolidation, and they were best treated with calgon, hydrogen peroxide, and ultrasonic disaggregation after boiling in a hydrochloric acid solution (see "Explanatory Notes" chapter, this volume).

Oligocene

Samples 130-803D-40X-CC through -48X-CC can be placed in the *D. ateuchus* Zone of the Oligocene. Diagnostic taxa in these samples include *Lithocyclia angusta, D. ateuchus,* and *Theocyrtis annosa.* Samples 130-803D-49X-CC through -58X-CC are placed in the *Theocyrtis tuberosa* Zone of the lower Oligocene. These samples usually include *Tristylospyris triceros, L. angusta,* and *Artophormis gracilis.* In the lower part of this zone, *Lithocyclia crux* and *Centrobotrys gravida* were present.

Upper Eocene

Sample 130-803D-59X-CC can be assigned to the *Cryptoprora ornata* Zone (Saunders et al., 1984, equivalent to the uppermost part of the *Thyrsocyrtis bromia* Zone of Sanfilippo et al., 1985) of the upper Eocene. This sample contains *T. triceros, Artophormis balbadensis, Calocyclas turris, C. ornata,* the *Sethochytris babylonis* group, *Dictyoprora mongolfieri, Dictyoprora pirum, Dictyoprora armadillo, Lophocyrtis jacchia,* and *Lychnocanoma amphitrite.* The *Calocyclas bandyca* Zone (Saunders et al., 1984; equivalent to the middle part of the *Thyrsocyrtis bromia* Zone of Sanfilippo et al., 1985) of the upper Eocene is placed in Samples 130-803D-60X-CC through -63X-CC, based on the presence of *T. bromia, C. turris, C. bandyca, C. ornata,* and *Cryptoprora azyx.*

Middle Eocene

Sample 130-803D-64X-CC tentatively is assigned from the *Podocyrtis chalara* to the *Cryptoprora azyx* Zones (Saunders et al., 1984, equivalent to the basal part of the *Thyrsocyrtis bromia* Zone of Sanfilippo et al., 1985), which cannot be differentiated. The diagnostic taxa present in this sample include *Eusyringium fistuligerum, Lithocyclia ocellus, Thyrsocyrtis triacantha, Thyrsocyrtis rhizodon, Dictyoprora mongolfieri,* and *Podocyrtis papalis.* Sample 130-803D-65X-CC is placed in the lower part of the *P. chalara* Zone as it contains *E. fistuligerum, Podocyrtis trachodes,* and *P. chalara.* Sample 130-803D-66X-CC, which contains *P. mitra* together with several other middle Eocene species, is placed in the *Podocyrtis mitra* Zone. Sample 130-803D-67X-CC is assigned to the *Podocyrtis ampla* Zone based on the presence of *P. mitra, Podocyrtis sinuosa, D. mongolfieri, Theocotylissa ficus,* and *Pterocodon lex.*

Cretaceous

We examined 19 samples from Core 130-803D-68R for radiolarians. Among them only three samples yielded useful, but poorly preserved, radiolarians for stratigraphic information. They can be found in Sample 130-803D-68R-3 at intervals of 86–87, 89–90, and 96–98 cm, all of which are light brown (10YR 4/4) soft sediments. Among these three samples, Sample 130-803D-68R-3, 89–90 cm, presents the best preservation as well as a large number (>100 specimens/slide) of specimens. The sample can be assigned with reasonable confidence to the interval from the upper *Acaeniotyle umbilicata* Zone to the lower *Abesacapsula sophedia* Zone, which corresponds with the upper Albian to the lower Cenomanian (~103–95 m.y.) (Sanfilippo and Riedel, 1985). Three key species found in the sample include *Thanarla veneta* (A = abundant), *Thanarla elegantissima* (C = common), and *Pseudodictyomitra pseudomacrocephala* (A). Although most of the specimens are casts of silica filled all the way to the center of the specimens, and therefore their preservational states are defined as "poor," their original shapes (and thus outlines) as well as surface ornamentations are preserved, which made the species identification possible. One sample lower in the section (130-803D-86R-3, 96–89 cm) yielded fewer radiolarians of poorer preservation. *Thanarla elegantissima* (R = rare) and *P. pseudomacrocephala* (F = few) in this sample present the same age bracket as the above sample. Furthermore, Sample 130-803D-68R-3, 86–87 cm, contained *P. pseudomacrocephala*? (R), but the species identification is tentative because of the very poor preservation. It may be possible that this sample also belongs to the same age as the above-mentioned two samples. There are several other nassellarian species preserved in all of the above three samples. However, it is not possible to provide further information because of the poor preservation.

PALEOMAGNETISM

Introduction

Pass-through magnetometer measurements were taken on all APC split-core archive sections recovered from Holes 803A, 803B, 803C, and 803D and on all XCB cores recovered from Hole 803D. Pass-through magnetometer measurements were also taken on RCB sediment split-core archive sections recovered from Hole 803D. Rotary coring of basalt at Hole 803D resulted in the recovery of continuous pieces 25–75 cm in length that could be unambiguously oriented with respect to the top, separated by smaller pieces with questionable orientations. To address this problem, a different measuring technique was adopted. A single, continuous segment of basalt was chosen from each section of the split-core archives and measured with the pass-through magnetometer.

Pass-through magnetometer measurements were taken at 1-, 3-, 5- and 10-cm intervals, depending on the interval of interest. The natural remanent magnetization was measured for all cores and the magnetization after treatment at 15 mT for most cores. On critical intervals, demagnetizations were carried out at 5, 10, and 15 mT. Pass-through magnetic susceptibility measurements were also taken on all unsplit core sections recovered at Site 803. These measurements were done at 3-, 5-, and 10-cm increments.

The multishot core orientation device failed at Hole 803A when difficulties in drilling resulted in the loss of a camera. This left only one operational camera for orientation. Orientations were attempted on Hole 803B but judged unreliable by the drilling crew. Orientations were recorded on Cores 130-803C-3H, -4H, and -5H of Hole 803C and below Core 130-803D-6H in Hole 803D.

Results

One of the most conspicuous characteristics of the pass-through magnetometer measurements of APC cores was an anomalously high magnetic intensity recorded for the top of the first section of each core. This high intensity gradually decreased downcore to a value similar to that of the remainder of the core at 50–100 cm within the first section. This effect was not entirely surprising as it corresponded roughly with the zone of physical disruption ("draw-in") caused by the hydraulic coring process. What was surprising, however, was that this effect sometimes extended beyond any visible signs of disruption, suggesting that the drilling disturbance in APC cores can be quite subtle. Therefore, the directional results from the first meter of recovery in each core were interpreted with caution. Alternating field (AF) demagnetization generally produced little change in direction in the Pliocene-Pleistocene cores. Occasionally, however, large changes were noted and were most probably the result of the removal of a present-day viscous magnetization.

Despite minor problems with core disturbance, the pass-through magnetometer measurements of APC cores yielded correlatable reversal boundaries at each hole for Pliocene-Pleistocene sediments. The magnetic intensity decreased before some reversal boundaries and slowly increased afterward with transitional directional behavior recorded during the reversal (Fig. 19). This high-resolution record deteriorated rapidly below approximately 46 mbsf in each core, marked with a rapid decrease in intensity to very low levels (1×10^{-7} to 5×10^{-8} emu/cm^3) (Fig. 20).

Intensities for much of the Miocene sediments were at these low levels; therefore, AF demagnetization was halted. In the Oligocene sediments, intensities increased to interpretable values and AF demagnetization was resumed. Although the Oligocene sediments were cored with the XCB, the pass-through magnetometer measurements yielded intervals of constant inclination that can be tentatively interpreted as a magnetostratigraphy. The single Cretaceous RCB core yielded fairly strong intensities, and we think that at least one reversal boundary present in the section contains the Cretaceous/Tertiary boundary (Section 130-803D-68R-1). The RCB basalt pieces also yielded results that are interpretable in terms of polarity.

Pass-through magnetic susceptibility measurements yielded high-resolution data for Pliocene-Pleistocene cores that allowed

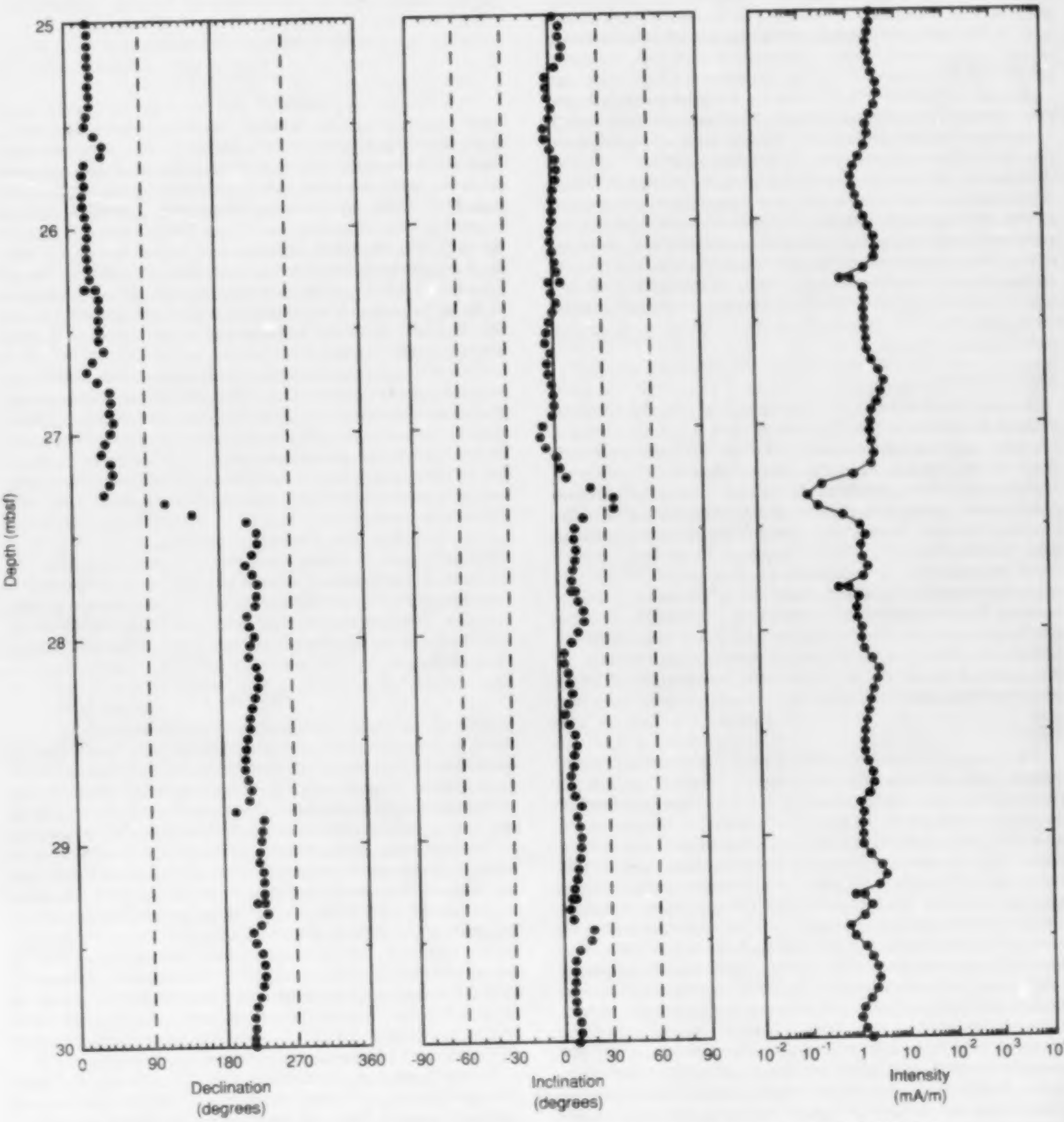

Figure 19. Reversal boundary between the Matuyama and Gauss chrons (2.47 Ma) observed at 27.4 mbsf in Core 130-803B-4H.

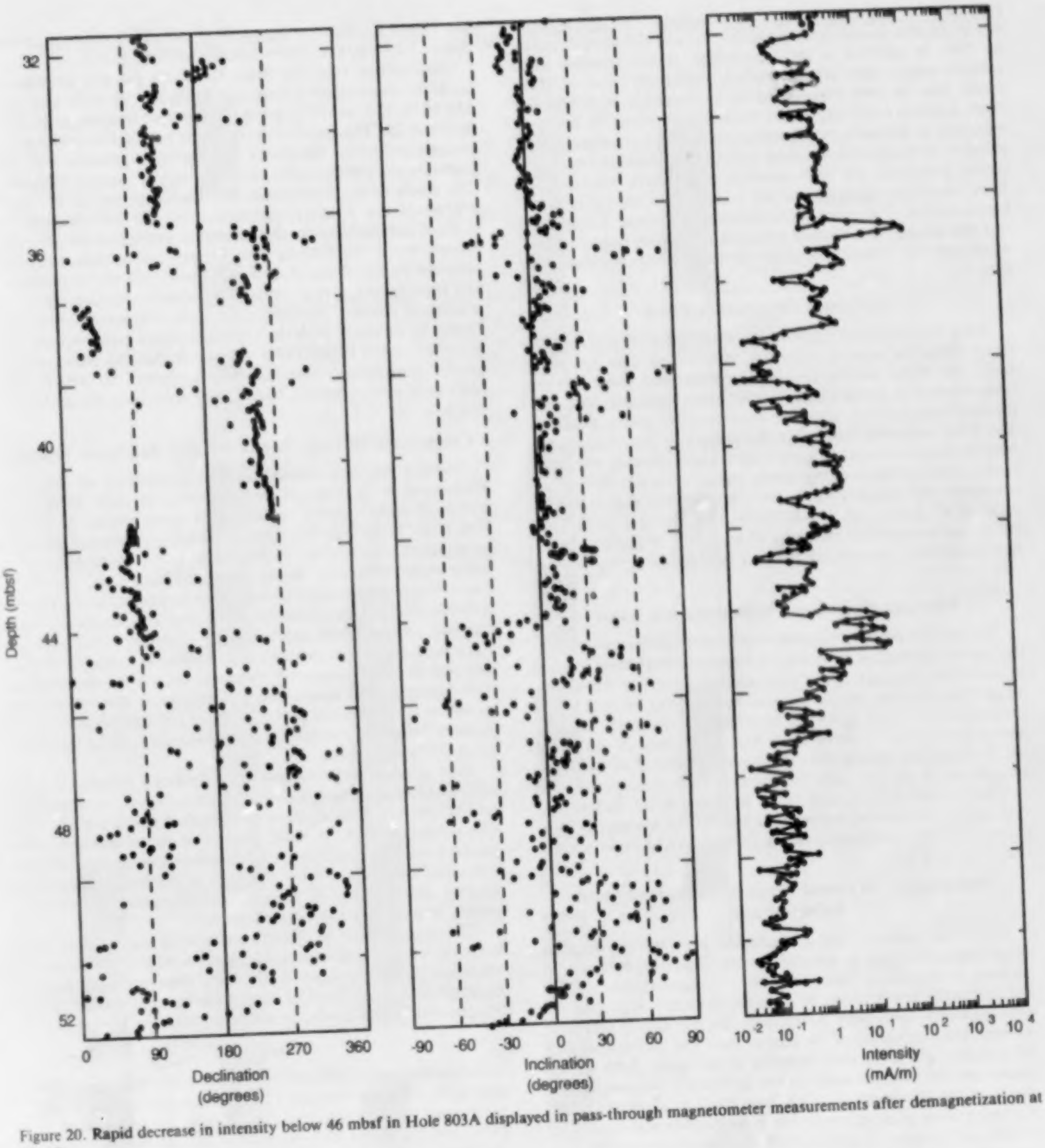

Figure 20. **Rapid decrease in intensity below 46 mbsf in Hole 803A displayed in pass-through magnetometer measurements after demagnetization at 15 mT.**

detailed correlations. Susceptibility measurements mirrored the magnetic intensity values, however, and became extremely low to negative in the Miocene sediments, clearly influenced by the diamagnetic calcite content. Severe drift problems with the M.S.1 susceptibility meter were suspected during measurements on Hole 803D. These suspicions were confirmed by measurements on a MnO_2 standard. Such behavior was monitored carefully, but some intervals in the data base are clearly dominated by this unusually high drift.

Correlation Between Holes 803A, 803B, 803C, and 803D: A Pliocene-Pleistocene Magnetostratigraphy

Site 803 is situated at 2°N; therefore, we could not use paleomagnetic inclinations for polarity determinations. As orientations were unavailable for many of the Pliocene-Pleistocene cores, a relative polarity scheme based on magnetic declination was developed to produce a composite magnetostratigraphy, independent of paleontological determinations. The first polarity in a given core was assigned polarity "A" and the second, polarity "B". In addition to these polarities, several possible short polarity events were also identified. Although some of these events may be true polarity zones or magnetic excursions of short duration (< 50 ka), many are artifacts caused by the local reduction in intensity, remagnetization in zones of increased dissolution of magnetite, or local sediment disruption caused by coring processes. All such possible events have been omitted from the current analysis and will be examined further in shore-based studies. The magnetostratigraphic approach adopted for this site resulted in a stacked sequence of relative polarity determinations that is easily correlated to the geomagnetic time scale (Fig. 21).

Multishot Orientation Error

After we completed the Pliocene-Pleistocene magnetostratigraphy based on relative polarities, orientation data for Holes 803C and 803D were available. Unfortunately, these orientations resulted in declinations 75°–90° from expected. The drilling crew was notified, and they examined the coring assembly. The T-bar assembly that holds the camera to the pressure-case bottom plug was found to have rotated approximately 90° counterclockwise (when looking down the core barrel). When this correction was applied to Cores 130-803C-2H and -3H from Hole 803C and Cores 130-803D-3H through -5H from Hole 803D, the declinations were near 0° and 180°, suggesting polarities identical to the relative polarity interpretation.

Pliocene-Pleistocene Sedimentation Rates

The relative polarity magnetostratigraphy allows us to calculate the sedimentation rates for the Pliocene-Pleistocene interval in each hole (Fig. 22). These rates average 1 cm/k.y. for the interval from the base of the Olduvai Subchron (1.88 Ma) to the present and 1.5 cm/k.y. for the interval from the top of the Gilbert reversed polarity chron (3.40 Ma) to the base of the Olduvai. Fluctuations during the Pleistocene, suggested by using the boundaries of the Jaramillo Subchron as calibration points, are seen in the records from both Holes 803B and 803D. Sedimentation rates in the interval between the base of the Mammoth Subchron (3.18 Ma) and the top of the Gilbert may be slightly lower than 1.5 cm/k.y.

Preliminary Oligocene Magnetostratigraphy and Paleolatitude

Below the point at which multishot orientations were no longer available, polarity determinations could only be made on the basis of the sign of the inclination. Paleoinclinations for Site 803 during the Miocene can be expected to be low, reflecting the near-equatorial latitudinal position of the site during this time interval. Discrimination of the sign of such low inclinations was not possible, given the weak intensity of the cores. Both the intensity and the absolute value of the inclination increased sufficiently in the Oligocene cores of Hole 803D to allow the tentative recognition of intervals in which inclination was consistent in sign and magnitude after 15-mT demagnetization (Fig. 23). Assuming that the Ontong Java Plateau moved with the Pacific Plate over the interval from the Oligocene to the present (an assumption at variance with the results from DSDP Site 289; Hammond et al., 1975), normal polarity can be assigned to negative inclinations, from which the Oligocene magnetostratigraphy follows (Fig. 24). Paleontological dates are consistent with this magnetostratigraphy.

Age was determined as a function of stratigraphic depth from this magnetostratigraphy (Fig. 25). Sedimentation rates averaged 3.1 cm/k.y. during the early Oligocene, between Anomalies 13 and 12, but they slowed later in the Oligocene to an average of 1.57 cm/k.y. between Anomalies 11 and 7.

Inclinations from the cores for which polarity information could be determined (Cores 130-803D-36X to -41X and Cores 130-803D-45X to -50X) are distributed by frequency, as shown in Figure 26. The distribution is biased toward low positive inclinations, reflecting the dominantly reversed polarity over these intervals and possibly also some unremoved viscous remanence. The mode of the inclination distribution occurs at 9°. If this represents the primary magnetization, the paleolatitude was 4.5°. Which hemisphere this represents cannot be directly determined, but if the Ontong Java Plateau has remained coherent with the Pacific Plate, then this paleolatitude was in the Southern Hemisphere, giving a total displacement for this site on the plateau of about 7° northward since the Oligocene. This is consistent to within 2° with the Pacific apparent polar wander path (Gordon, 1983; Sager, 1987). It appears that the paleomagnetic results from DSDP Site 289, which showed no paleolatitude shift until approximately 30 Ma, may have been biased in some fashion.

Cretaceous/Tertiary Boundary and Basement Polarity

Volume magnetic susceptibility measurements on the single Cretaceous RCB sediment core recovered at Hole 803D (Core 130-803D-68R) revealed values 10–40 times greater (k = 100–400 × 10^{-6} cgs) than the values recorded on the previous 622 m of sediment. In Section 130-803D-68R-1, two peaks in susceptibility occur (Fig. 27). Based on nannofossil ages, the Cretaceous/Tertiary boundary is thought to be present in the Interval 130-803D-68R-1, 38–53 cm. The first peak in susceptibility at 45 cm may correlate with the boundary since the Cretaceous-Tertiary boundary often exhibits high magnetic susceptibility values due to the presence of magnetic spherules. However, the high background magnetic susceptibility must also be explained as well as the additional peak in Section 130-803D-68R-1, 95 cm. A more definitive interpretation of these data awaits the results from discrete sampling.

Pass-through magnetometer measurements revealed a polarity transition at Section 130-803D-68R-1, 70 cm, as denoted by an 180° shift in declination in an unbroken portion of the core. The polarity record, however, cannot be unambiguously determined from the pass-through measurements because of the relative rotations between other portions of the cores and possible viscous overprinting. A polarity determination will be conducted as part of a shore-based study.

The measurement of discrete continuous segments of basalt from each section was successful in determining the dominant basement polarity. All pieces measured displayed clear negative inclinations indicative of normal polarity, as the Ontong Java Plateau was in the Southern Hemisphere in the Cretaceous.

Discussion

Given the low to intermediate sedimentation rates, the detail seen in the Pliocene through Pleistocene magnetostratigraphy is surprising. The magnetostratigraphic record is remarkably complete. The calculated 50% decrease in sedimentation rate before the base of the Olduvai Subchron (1.88 Ma) may record increased carbonate dissolution in the Pleistocene. Comparison of these records with those expected from shallower sites should provide further clues to the nature of this substantial change in carbonate sedimentation at the onset of the Pleistocene. The drilling of sites at different depths will also provide constraints on the origin of the transition from high-resolution magnetostratigraphic data to low-intensity signals observed at 46 mbsf at this site. This phenomenon may be either a result of the dissolution of magnetite with depth or the lack of an initial magnetite input relative to the carbonate accumulation.

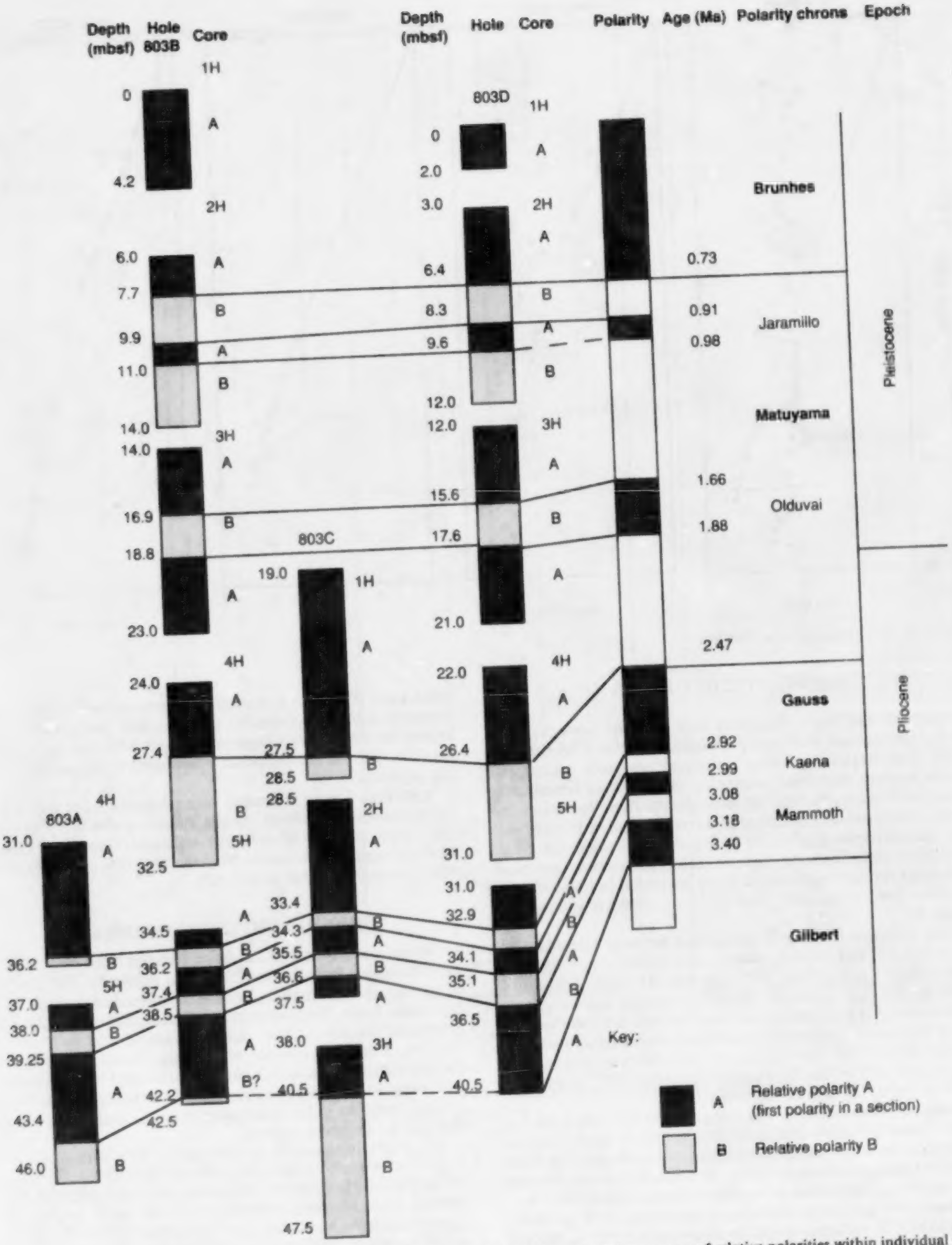
Depth (mbsf)
Hole 803B
Core
Depth (mbsf)
Hole
Core
Polarity
Age (Ma)
Polarity chrons
Epoch
803A
803C
803D
1H
2H
3H
4H
5H
0.73
0.91
0.98
1.66
1.88
2.47
2.92
2.99
3.08
3.18
3.40
Brunhes
Jaramillo
Matuyama
Olduvai
Gauss
Kaena
Mammoth
Gilbert
Pleistocene
Pliocene
Key:
A Relative polarity A (first polarity in a section)
B Relative polarity B

Figure 21. Preliminary Pliocene-Pleistocene magnetostratigraphy for Site 803 based on stacked sequences of relative polarities within individual sites. The first polarity in a core is labeled "A" and the second, "B". Possible short polarity intervals have been excluded in this analysis. No cores are oriented and inclination cannot be used for polarity determinations. The magnetostratigraphic column is based upon stacked cores containing relative polarity information.

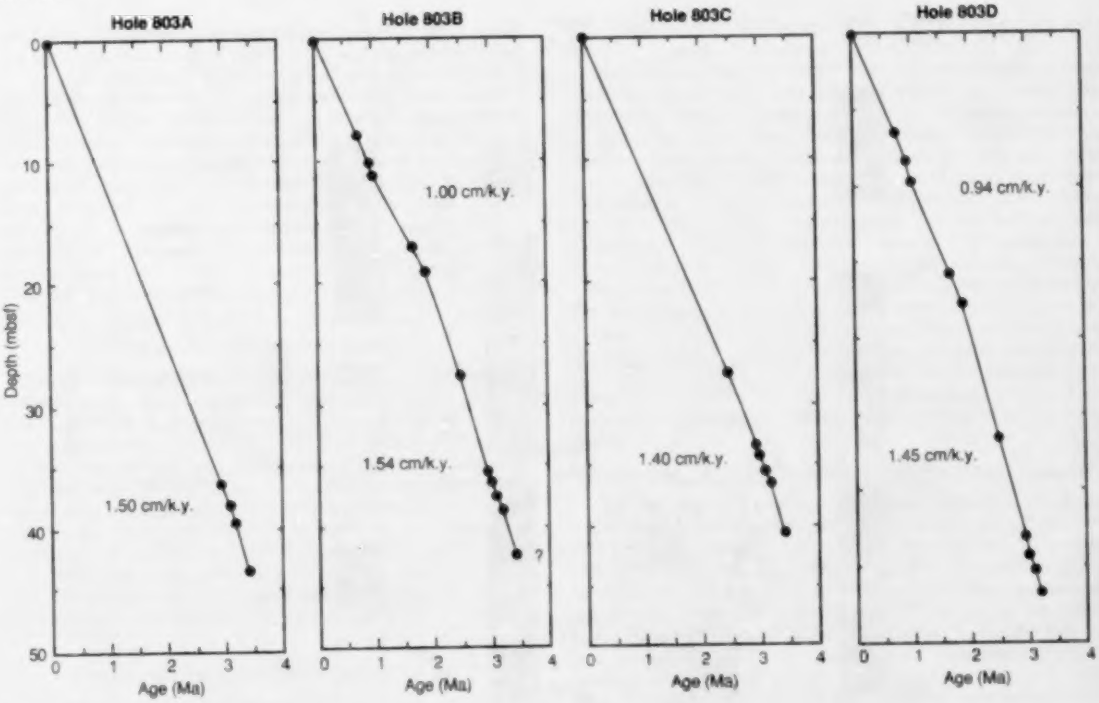

Figure 22. Sedimentation rates, Site 803.

SEDIMENTATION RATES

Over 200 age/depth indicators were gathered from the middle Eocene through Holocene sediments of Holes 803A through 803D. The majority of these indicators represent microfossil events because magnetostratigraphic data were obtained only from the Pliocene/Pleistocene intervals. All these age/depth indicators are listed as a function of increasing age in Table 6, and they are portrayed graphically in Figures 28 through 32. Sedimentations rates from the Eocene-Holocene interval have been calculated for all four holes and are presented in Table 7, and the rates from Holes 803C and 803D are shown graphically in Figure 33.

One Neogene hiatus was recognized between Samples 130-803D-27X-CC and -28X-1, 140 cm. The recovery rate for Core 130-803D-27X was 45.9%, implying that the hiatus falls somewhere between 241.5 and 247.3 mbsf. by making a downhole extrapolation of the sedimentation rate that was derived from the LO of *Discoaster hamatus* and the FO of *Globorotalia peripheroacuta* (Table 7), an age estimate of 15.4 Ma was obtained for the younger side of the Miocene hiatus. Hole 803C ended precisely at the young side of the hiatus.

Another Miocene hiatus was recognized at the core break between Cores 130-803D-28X and -29X at 255.5 mbsf. A minimum sedimentation rate of 17.8 m/m.y. was obtained in Core 130-803D-28X, which separates the two hiatuses. Thus, the old side of the upper hiatus is estimated to be about 19.5 Ma, whereas the young side of the lower hiatus is placed at 20.0 Ma. The old side of the lower hiatus is placed at 21.8 Ma, at the LO level of *Globorotalia kugleri*.

The age-depth relationships of two late Oligocene and one Oligocene/Miocene boundary marker (Fig. 30) suggest that a large portion of the late Oligocene (23.7–28.2 Ma) is somewhat condensed. The rates in the adjacent intervals are similar, which probably points to a similar surface-water productivity input across the entire late Oligocene–earliest Miocene interval and signifies that the condensation was caused by processes operating at depth.

Less than 5 m of sediments were preserved from the time interval between 45 (oldest middle Eocene sediments recovered) and about 100 Ma (Cretaceous sediment/basement contact). The age/depth relationships from the pertinent core (130-803D-68R) are not presented graphically.

INORGANIC GEOCHEMISTRY

We collected 24 interstitial water samples from Hole 803D at depths ranging from 8.5 to 623.2 mbsf (Table 8). The majority of the samples are from the nannofossil ooze and chalk of lithologic Unit I (see "Lithostratigraphy" section, this chapter); the lowermost sample is from the basal siliciclastic sediments of Unit III, 3 m above contact with basalt. Chemical gradients in the interstitial waters at this site are influenced by the biogenic-rich, organic-carbon-poor character of the sediments and by alteration reactions in the underlying basalt by means of diffusion through the sediment column.

Chlorinity increases by approximately 10% with depth (Fig. 34), as does salinity, measured refractively as total dissolved solids (Table 8). Sodium concentrations measured by flame emission spectrophotometry (Table 8) and those estimated by charge balance calculations agree to within <1.5% and are approximately constant with increasing depth. Alkalinity increases slightly to 3.9 mM by 166 mbsf in Core 130-803D-19H, then decreases to 2.4 mM at 509 mbsf in Core 130-803D-55X, with a sharp decrease to 0.36 mM at 623 mbsf in Core 130-803D-68R (Fig. 34).

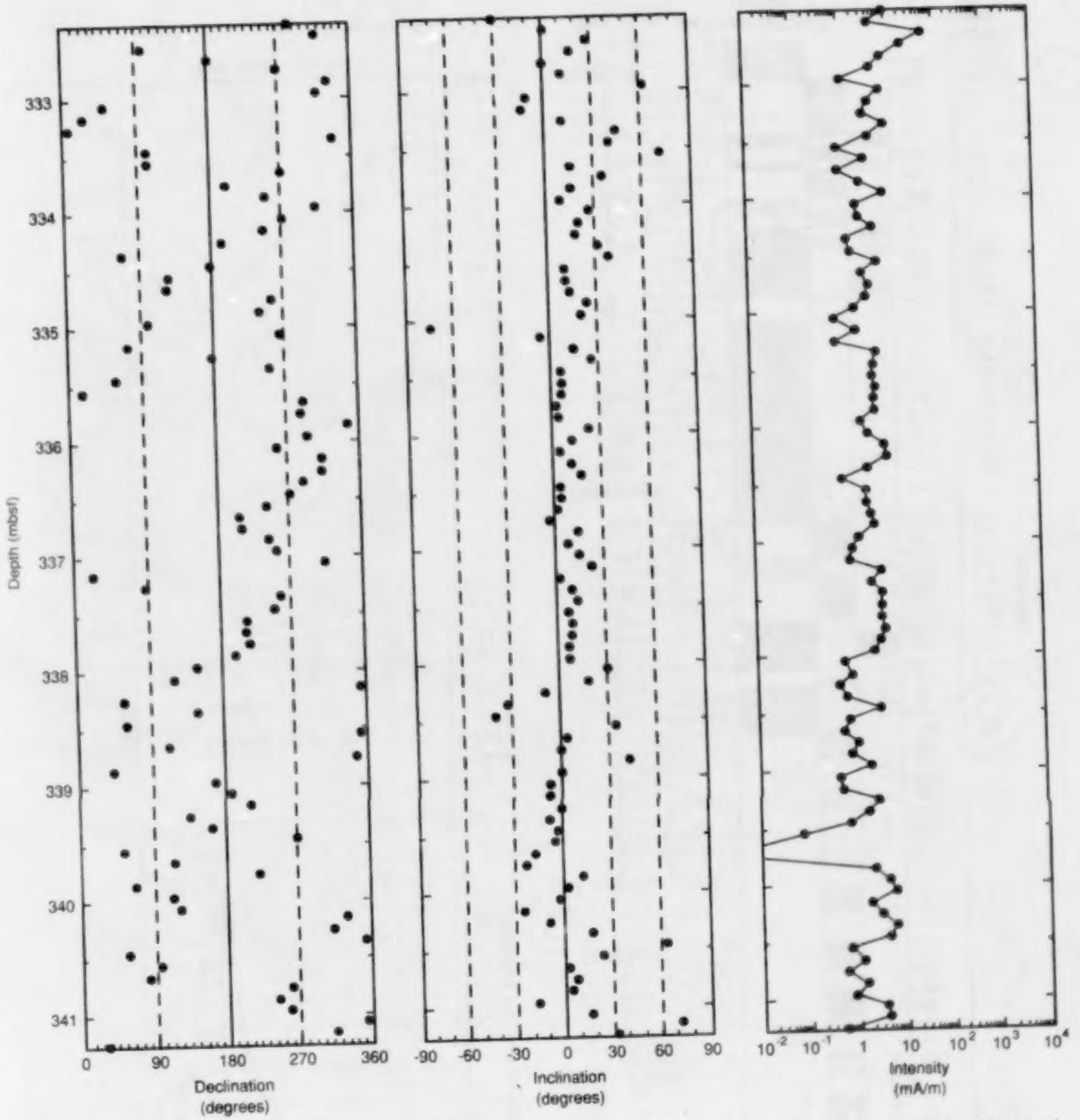

Figure 23. Declination, inclination, and intensity in Core 130-803D-37X, showing intervals of consistent low positive (335–338 mbsf) and low negative (338.7–339.5 mbsf) inclinations, together with intervals of scattered inclinations.

Sulfate concentrations decrease by approximately 20% to 195 mbsf and are essentially constant below that depth (Fig. 34). The extent of SO_4^{2-} depletion is limited, presumably because of the relatively low organic carbon content of these sediments. This interpretation is supported by the profiles of the labile nutrients, as well as by the limited alkalinity increase. Phosphate concentrations are below the detection limit of 1-2 μM in all samples analyzed (Table 8). Ammonia concentrations are generally low (from 10 to 110 μM), increasing from the surface to 195 mbsf and then decreasing slightly or remaining constant with increasing depth (Fig. 34).

Dissolved silica concentrations increase downcore from 470 μM at 8.5 mbsf to over 1200 μM at 546 mbsf, and then decrease sharply to 600 μM in the lowermost sample at 623 mbsf (Fig. 34). The increase in dissolved Si concentration with depth is consistent with continuous dissolution of biogenic silica; the dissolved Si decrease in the deepest interstitial water sample suggests precipitation and agrees with the discovery of chert in the

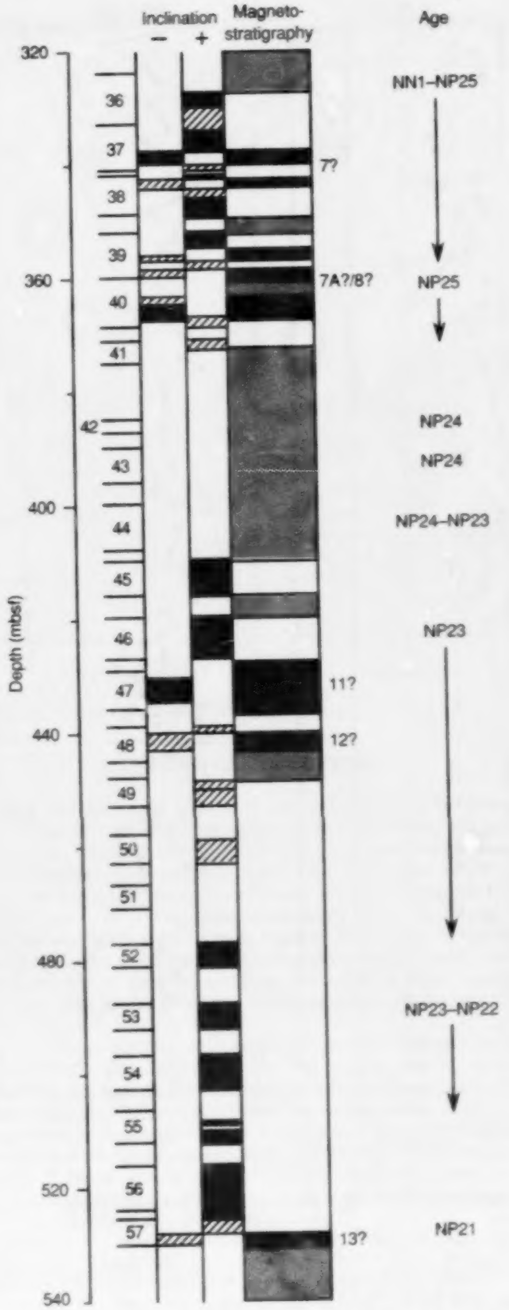

Figure 24. Record of intervals of consistent low positive and low negative inclinations, and corresponding magnetostratigraphy. Black sections of inclination column indicate confident polarity; hatched regions are probable, but uncertain; white sections are unknown. Black sections of magnetostratigraphy are normally polarized, white reversed, and hatched unknown.

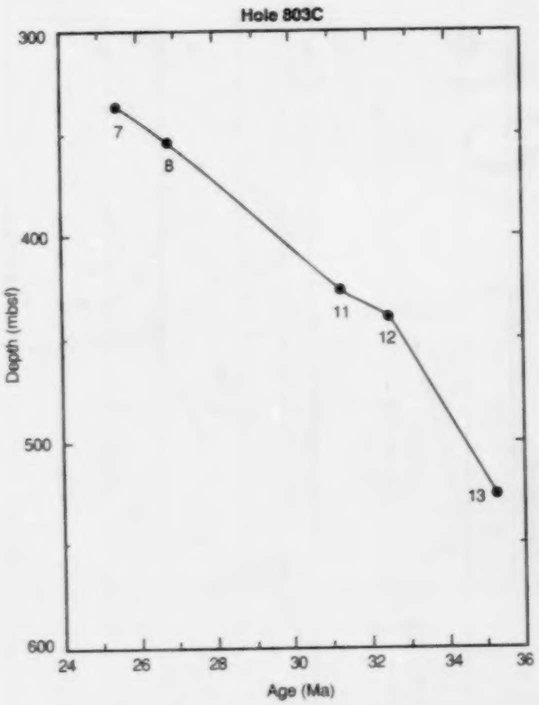

Figure 25. Age vs. depth for the Oligocene. Chron numbers are indicated.

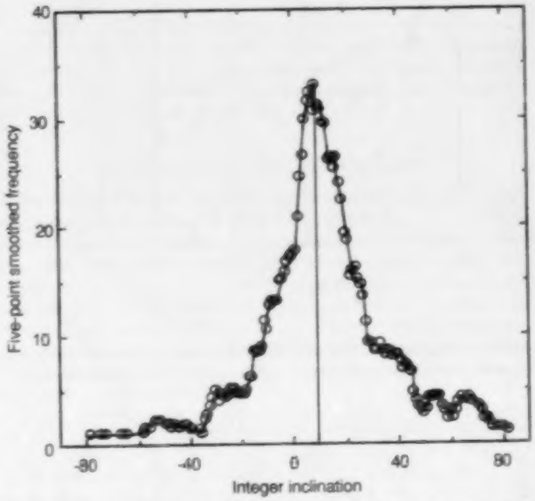

Figure 26. Frequency plot of inclination, smoothed over five integral divisions. The mode of the inclination at +9° is indicated.

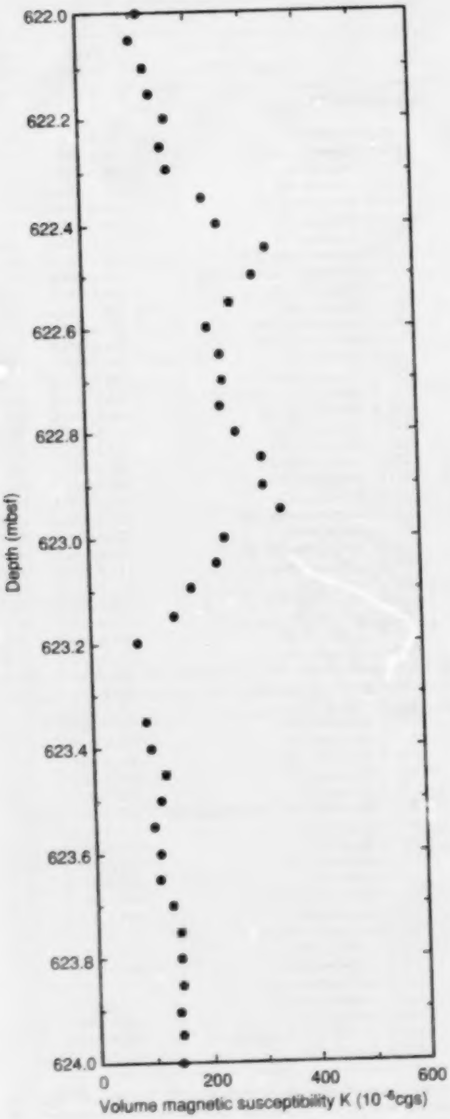

Figure 27. Volume magnetic susceptibility measurements from Section 130-803D-68X-1, which is thought to contain the Cretaceous/Tertiary boundary on the basis of nannofossil analyses.

lowermost sediments (see "Lithostratigraphy" section, this chapter). Manganese concentrations are below the detection limit (<2-3 μM) in samples from 8.5 to 546 mbsf, showing no enrichment with the increase in dissolved Si (Table 8). The elevated Mn concentration of 37 μM at 623 mbsf suggests the presence of a source in the sediments of Unit III or in the underlying basalt.

Calcium concentrations increase with depth, with an average gradient of 8 mM/100 m, and magnesium concentrations decrease with depth, with an average gradient of 4 mM/100 m (Fig. 34). Ca and Mg concentrations are correlated linearly (R^2

Table 6. Bio- and magnetostratigraphic events determined at Site 803.

Event	Depth (mbsf)	Age (Ma)
Hole 803A:		
FO *E. huxleyi* (N)	0.0–3.0	0.27
LO *P. lacunosa* (N)	3.0–8.0	0.46
LO *G. tosaensis* (F)	8.0–17.5	0.60
LO *N. reinholdii* (D)	8.0–17.5	0.65
LO *C. macintyrei* (N)	8.0–17.5	1.45
LO *R. praebergonii* var. *robusta* (D)	17.5–27.0	1.55
FO *P. doliolus* (D)	17.5–27.0	1.80
LO *D. brouweri* (N)	17.5–27.0	1.89
FO *G. truncatulinoides* (F)	17.5–27.0	1.90
LO *D. surculus* (N)	27.0–36.5	2.45
LO *G. multicamerata* (F)	17.5–27.0	2.90
LO *G. altispira* (F)	27.0–36.5	2.90
Kaena (T)	36.2–36.2	2.92
LO *Sphaeroidinellopsis* spp. (F)	36.5–46.0	3.00
FO *R. praebergonii* (D)	46.0–55.5	3.00
FO *Sphaeroidinella dehiscens* (F)	46.0–55.5	3.00
Mammoth (O)	39.25–39.25	3.18
LO *R. pseudoumbilica* (N)	46.0–46.8	3.56
Gauss (O)	43.4–43.4	3.40
Hole 803B:		
LO *P. lacunosa* (N)	4.3–5.0	0.46
LO *G. tosaensis* (F)	0.0–4.3	0.60
Brunhes (O)	7.7–7.7	0.73
Jaramillo (T)	9.9–9.9	0.91
Jaramillo (O)	12.2–12.2	0.98
LO *C. macintyrei* (N)	15.4–16.8	1.45
Olduvai (T)	16.9–16.9	1.66
Olduvai (O)	18.8–18.8	1.88
LO *D. brouweri* (N)	18.4–19.1	1.89
LO *D. pentaradiatus* (N)	25.8–26.4	2.35
Gauss (T)	27.4–27.4	2.47
LO *G. multicamerata* (F)	23.3–32.8	2.90
LO *G. altispira* (F)	32.8–42.3	2.90
Kaena (T)	35.4–35.4	2.92
Kaena (O)	36.2–36.2	2.99
LO *Sphaeroidinellopsis* spp. (F)	42.3–51.8	3.00
Mammoth (T)	37.4–37.4	3.08
Mammoth (O)	38.5–38.5	3.18
Gauss (O)	42.2–42.2	3.40
LO *R. pseudoumbilica* (N)	42.3–51.8	3.56
LO *C. acutus* (N)	51.8–61.3	4.60
Hole 803C:		
LO *P. prismatium* (R)	28.5–38.0	2.43
Gauss (T)	27.5–27.5	2.47
LO *S. peregrina* (R)	28.5–38.0	2.63
LO *D. tamalis* (N)	28.5–38.0	2.65
LO *G. altispira* (F)	28.5–38.0	2.90
Kaena (T)	33.4–33.4	2.92
Kaena (O)	34.3–34.3	2.99
LO *Sphaeroidinellopsis* spp. (F)	38.0–47.5	3.00
Mammoth (T)	35.5–35.5	3.08
Mammoth (O)	36.6–36.6	3.18
LO *P. fistula* (R)	38.0–47.5	3.27
LO *L. audax* (R)	38.0–47.5	3.34
Gauss (O)	40.5–40.5	3.40
LO *P. primalis* (F)	38.0–47.5	3.50
LO *P. doliolum* (R)	38.0–47.5	3.54
LO *R. pseudoumbilica* (N)	38.0–47.5	3.56
LO *S. pentas* (R)	38.0–47.5	3.78
FO *A. ypsilon* (R)	38.0–47.5	3.78
LO *S. berminghami* (R)	47.5–57.0	3.86
FO *S. pentas* (R)	57.0–66.5	4.25
LO *C. acutus* (N)	57.0–66.5	4.60
LO *S. omnitobus* (R)	57.0–66.5	4.75
LO *T. rugosus* (N)	67.4–68.6	4.90
LO *D. quinqueramus* (N)	68.6–71.6	5.00
LO *S. corona* (R)	66.5–76.0	5.05
FO *Sphaeroidinella dehiscens* s.l. (F)	57.0–66.5	5.10
FO *G. tumida* (F)	66.5–76.0	5.20
FO *P. spectabilis* (F)	66.5–76.0	5.20
LO *G. dehiscens* (F)	66.5–76.0	5.30
LO *A. tritubus* (R)	76.0–85.5	5.35

Table 6 (continued).

Event	Depth (mbsf)	Age (Ma)
Hole 803C: (Cont.)		
LO *N. miocenica* (D)	66.5–76.0	5.60
FO *P. primalis* (F)	85.5–95.0	5.80
FO *T. convexa* var. *aspinosa* (D)	85.5–95.0	6.10
LO *C. caepa* (R)	95.0–104.5	6.40
FO *S. omnitubus* (R)	114.0–123.5	6.40
LO *N. porteri* (D)	114.0–123.5	6.70
FO *Amaurolithus* spp. (N)	115.6–118.6	6.70
FO *N. miocenica* (D)	123.5–133.0	6.80
LO *D. hughesi* (R)	123.5–133.0	7.15
LO *N. porteri* (D)	114.0–123.5	7.20
FO *N. miocenica* (D)	123.5–133.0	7.30
LO *T. ontogenesis* (R)	123.5–133.0	7.45
LO *C. yabei* (D)	161.5–171.0	7.50
FO *D. quinqueramus/berggrenii* (N)	133.0–142.5	7.50
FO *A. tritubus* (R)	133.0–142.5	7.74
LO *D. laticonus* (R)	133.0–142.5	8.15
LO *B. miralestensis* (R)	142.5–152.0	8.15
LO *D. petterssoni* (R)	152.0–161.5	8.15
LO *C. vetustissimus* var. *javanicus* (D)	152.0–161.5	8.50
LO *C. yabei* (D)	161.5–171.0	8.60
LO *D. hamatus* (N)	172.7–174.0	8.70
LO *Catinaster* spp. (N)	176.0–177.0	8.80
LO *A. moronensis* (D)	171.0–180.5	8.90
FO *D. neohamatus* (N)	178.3–179.3	9.00
FO *N. acostaensis* (F)	171.0–180.5	10.20
LO *G. siakensis* (F)	180.5–190.0	10.40
FO *D. hamatus* (N)	187.0–188.5	10.50
LO *C. vetustissimus* var. *javanicus* (D)	152.0–161.5	10.70
LO *C. coscinodiscus* (D)	180.5–190.0	10.70
FO *C. coalitus* (N)	189.5–190.0	11.10
LO *A. moronensis* (D)	171.0–180.5	11.30
LO *G. fohsi lobata* (F)	199.5–209.0	11.50
LO *C. coscinodiscus* (D)	180.5–190.0	12.20
FO *G. fohsi lobata* (F)	218.5–228.0	13.10
LO *S. heteromorphus* (N)	218.0–221.5	13.60
FO *G. praefohsi* (F)	228.0–237.5	13.90
LO *G. peripheroronda* (F)	228.0–237.5	14.60
FO *G. peripheroacuta* (F)	228.0–237.5	14.90
LO *Praeorbulina sicana* (F)	228.0–237.5	14.90
Hole 803D:		
LO *P. lacunosa* (N)	2.5–12.0	0.46
Brunhes (O)	6.4–6.4	0.73
Jaramillo (T)	8.3–8.3	0.91
Jaramillo (O)	9.6–9.6	0.98
LO *C. macintyrei*	12.0–21.5	1.45
Olduvai (T)	15.6–15.6	1.66
Olduvai (O)	17.6–17.6	1.88
LO *D. brouweri* (N)	12.0–21.5	1.89
FO *G. truncatulinoides* (F)	12.0–21.5	1.90
LO *D. pentaradiatus* (N)	21.5–31.0	2.35
Gauss (T)	26.4–26.4	2.47
LO *D. tamalis* (N)	21.5–31.0	2.65
LO *G. multicamerata* (F)	21.5–31.0	2.90
LO *G. altispira* (F)	31.0–40.5	2.90
Kaena (T)	32.9–32.9	2.92
Kaena (O)	34.1–34.1	2.99
LO *Sphaeroidinellopsis* (F)	31.0–40.5	3.00
FO *Sphaeroidinella dehiscens* (F)	40.5–46.1	3.00
Mammoth (T)	35.1–35.1	3.08
FO *G. tosaensis* (F)	31.0–40.5	3.10
Mammoth (O)	36.5–36.5	3.18
LO *Sphenolithus* spp. (N)	31.0–40.5	3.45
LO *R. pseudoumbilica* (N)	40.5–46.1	3.56
LO *C. acutus* (N)	55.6–65.1	4.60
LO *D. quinqueramus* (N)	65.1–74.6	5.00
FO *G. tumida* (F)	65.1–74.6	5.20
FO *P. spectabilis* (F)	65.1–74.6	5.20
LO *G. dehiscens* (F)	74.6–84.1	5.30
FO *P. primalis* (F)	84.1–93.6	5.80
FO *Amaurolithus* spp. (N)	112.2–122.1	6.70
FO *G. plesiotumida* (F)	160.1–169.6	7.10
FO *D. quinqueramus* (N)	131.6–141.1	7.50
FO *S. berminghami* (R)	160.1–169.6	7.95

Table 6 (continued).

Event	Depth (mbsf)	Age (Ma)
Hole 803D: (Cont.)		
LO *S. wolffii* (R)	225.5–265.1	8.15
LO *D. hamatus* (N)	169.6–179.1	8.70
FO *D. hughesi* (R)	169.6–179.1	8.75
LO *C. japonica* (R)	179.1–188.6	10.15
FO *N. acostaensis* (F)	169.6–179.1	10.20
LO *G. siakensis* (F)	179.1–188.6	10.40
FO *D. hamatus* (N)	179.1–188.6	10.50
LO *C. coscinodiscus* (D)	198.1–207.6	10.70
LO *D. punctata* f. *hustedtii* (D)	198.1–207.6	10.70
LO *L. thornburgi* (R)	188.6–198.1	11.00
FO *C. coalitus* (N)	179.1–188.6	11.10
FO *H. cuneiformis* (D)	198.1–207.6	11.20
LO *G. fohsi lobata* (F)	198.1–207.6	11.50
LO *C. cornuta* (R)	198.1–207.6	11.75
LO *C. coscinodiscus* (D)	198.1–207.6	12.20
LO *D. punctata* f. *hustedtii* (D)	198.1–207.6	12.20
FO *H. cuneiformis* (D)	198.1–207.6	12.50
LO *C. nitescens* (N)	198.1–207.6	12.80
LO *C. lewisianus* (D)	217.1–226.8	12.90
FO *G. fohsi lobata* (F)	207.6–217.1	13.10
LO *C. floridanus* (N)	207.6–217.1	13.10
LO *C. lewisianus* (D)	217.1–226.8	13.50
LO *S. heteromorphus* (N)	217.1–226.8	13.60
FO *G. praefohsi* (F)	226.8–236.5	13.90
LO *G. peripheroronda* (F)	226.8–236.5	14.60
FO *G. peripheroacuta* (F)	237.3–241.0	14.90
LO *P. sicana* (F)	236.5–245.9	14.90
LO *A. californicus* (D)	245.9–255.5	15.00
FO *C. peplum* (D)	245.9–255.5	16.40
LO *C. stainforthi* (F)	245.9–255.5	17.40
LO *C. dissimilis* (F)	245.9–255.5	17.60
LO *S. wolffii* (R)	225.5–265.1	8.15
FO *S. heteromorphus* (N)	245.9–247.3	18.60
LO *C. elegans* (D)	245.9–255.5	18.70
LO *S. belemnos* (N)	245.9–247.3	18.80
LO *T. carinatus* (N)	245.9–247.3	19.50
LO *B. veniamini* (D)	255.5–265.1	19.90
FO *S. belemnos* (N)	255.5–255.7	20.00
LO *G. kugleri* (F)	255.5–265.1	21.80
LO *C. lewisianus* var. *rhomboides* (D)	255.5–265.1	22.50
FO *R. paleacea* (D)	313.0–322.7	22.70
FO *G. kugleri* (F)	313.0–322.7	23.70
LO *S. ciperoensis* (N)	322.7–332.3	25.20
LO *G. opima* (F)	342.0–351.6	28.20
LO *G. ampliapertura* (F)	457.5–467.2	32.80
LO *R. umbilica* (N)	486.6–496.3	33.80
LO *Pseudohastigerina* (F)	515.6–525.3	34.00
LO *E. formosa* (N)	515.6–525.3	34.90
LO *D. saipanensis* (N)	544.3–544.3	36.70
LO *D. barbadiensis* (N)	544.3–554.0	37.00
LO *C. reticulatum* (N)	544.3–554.0	37.70
LO *C. grandis* (N)	583.0–588.7	40.00
LO *D. bisectus/D. hesslandii* (N)	601.9–612.0	42.90
FO *R. umbilica* (N)	612.0–612.2	44.40

Notes: The depth uncertainty predominantly represents sampling intervals used. References for the age estimates are presented in the Explanatory Notes. N = nannofossil, F = foraminifer, D = diatom, R = radiolarian, FO = first occurrence, and LO = last occurrence. Magnetostratigraphic reversal boundaries followed by designation (T) or (O) refer to "termination" or "onset," respectively.

= 0.97) with a $\Delta Ca/\Delta Mg$ ratio of approximately -2. The linear correlation is indicative of the conservative nature of these profiles, with Ca and Mg gradients controlled by reactions in the underlying basalt and diffusion between this boundary and overlying seawater (McDuff and Gieskes, 1976; McDuff, 1981). These gradients are larger than those observed at shallower Sites 288 and 289 (Leg 30) from the Ontong Java Plateau (Elderfield et al., 1982), presumably a result of the difference in sediment thickness between these sites (McDuff, 1981; for sedimentation

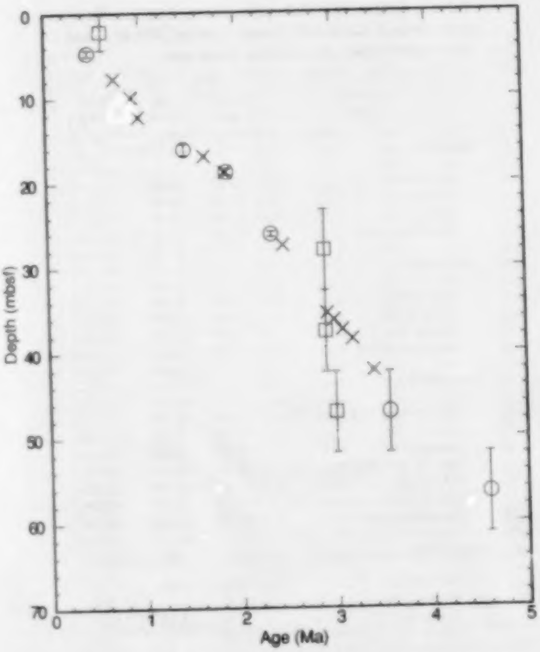

Figure 28. Age/depth relationships of bio- and magnetostratigraphic markers in Hole 803B. Error bars show sample interval uncertainties. Circle = nannofossils, square = foraminifers, and x = magnetostratigraphic reversal boundary.

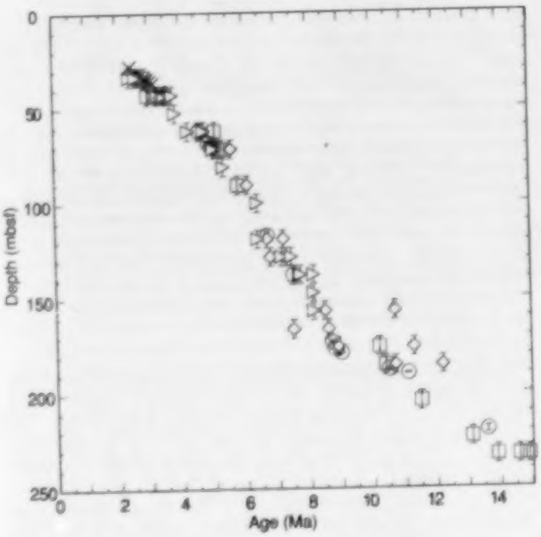

Figure 29. Age/depth relationships of bio- and magnetostratigraphic markers in Hole 803C. Error bars show sample interval uncertainties. Circle = nannofossil, square = foraminifers, diamond = diatom, triangle = radiolarian, and × = magnetostratigraphic reversal boundary.

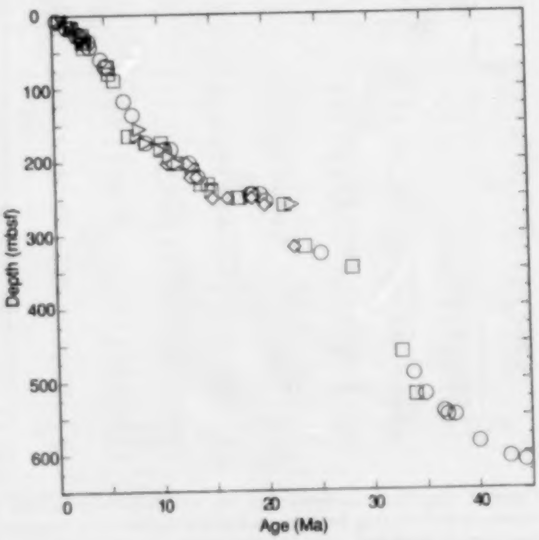

Figure 30. Age/depth relationships of bio- and magnetostratigraphic markers in Hole 803D. Symbol size approximates maximum sample interval uncertainties. Symbols are as in Figure 29.

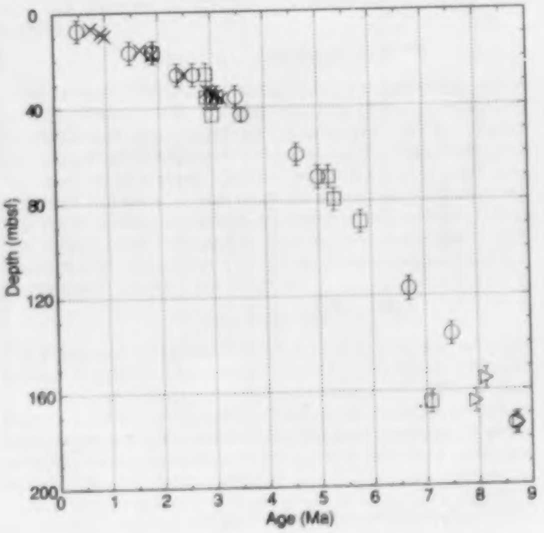

Figure 31. Age/depth relationships of bio- and magnetostratigraphic markers in Hole 803D in the late Miocene through Holocene time interval. Error bars show sample interval uncertainties. Symbols are as in Figure 29.

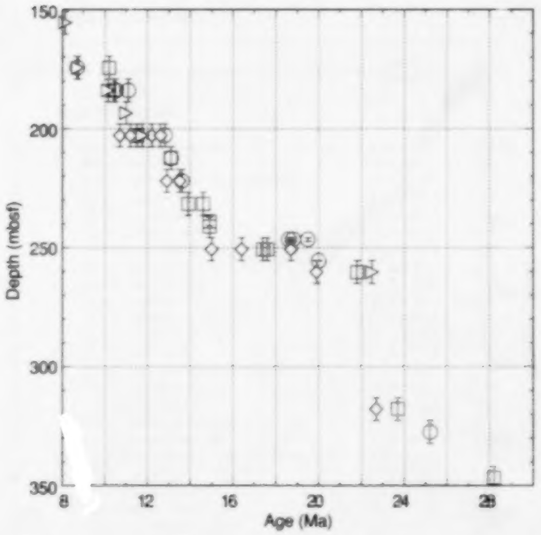

Figure 32. Age/depth relationships of bio- and magnetostratigraphic markers in Hole 803D in the early late Miocene through early Miocene time interval. Error bars show sample interval uncertainties. Symbols are as in Figure 29.

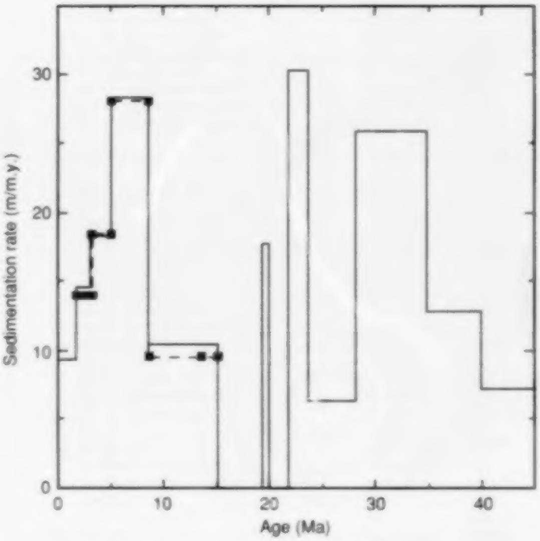

Figure 33. Sedimentation rate history, Site 803.

rates at these sites, see Andrews, Packham, et al., 1975, in particular the chapter on Site 288; and the "Sedimentation Rates" section of this chapter). There is no nonconservative behavior apparent in the Mg gradient from reaction with the thin (< 1 cm) volcanic ash layer found at Section 130-803D-21H-2, 61 cm.

Table 7. Estimated sedimentation rates from the Holocene through the middle Eocene interval, Site 803, and the control points determining those rates.

Control point	Depth (mbsf)	Age (Ma)	Rate (m/m.y.)
Hole 803A:			
Top section	0.00	0.00	
Mammoth (O)	39.25	3.18	12.3
Gauss (O)	43.40	3.40	18.9
Terminal depth	55.50	4.04	
Hole 803B:			
Top section	0.00	0.00	
Olduvai (O)	18.80	1.88	10.0
Gauss (O)	42.20	3.40	15.4
Terminal depth	61.30	4.64	
Hole 803C:			
Top section (top Core 1H)	19.00	1.86	
Gauss (T)	27.50	2.47	
Gauss (O)	40.50	3.40	14.0
LO *D. quinqueramus* (N)	69.90	5.00	18.4
LO *D. hamatus* (N)	173.40	8.70	28.0
LO *S. heteromorphus* (N)	220.25	13.60	9.6
Terminal depth	237.50	15.40	
Hole 803D:			
Top section	0.00	0.00	
Olduvai (O)	17.60	1.88	9.4
Mammoth (O)	36.50	3.18	14.5
LO *D. quinqueramus* (N)	69.85	5.00	18.3
LO *D. hamatus* (N)	174.35	8.70	28.2
FO *G. peripheroacuta* (F)	239.15	14.90	10.5
Young side hiatus	244.40	15.40	
Old side hiatus	244.40	19.50	
LO *T. carinatus* (N)	246.60	19.50	
FO *S. belemnos* (N)	255.50	20.00	17.8
Young side hiatus	255.50	20.00	
Old side hiatus	255.50	21.80	
LO *G. kugleri* (F)	260.30	21.80	30.3
FO *G. kugleri* (F)	317.85	23.70	30.3
LO *G. opima* (F)	346.80	28.20	6.4
LO *E. formosus* (N)	519.95	34.90	25.8
LO *C. grandis* (N)	585.90	40.00	12.9
FO *D. hesslandii* (N)	606.70	42.90	7.2
130-803D-67R-CC	621.80	45.01	

Notes: Age estimates for terminal depths of the different holes were obtained through linear extrapolation from the nearest shallower control point, using the sedimentation rates at that point. The Paleocene and Cretaceous sediments overlying the volcanic basement in Core 130-803D-68R are discussed in the "Biostratigraphy" section of this chapter. N = nannofossil, F = foraminifer, FO = first occurrence, and LO = last occurrence. Magnetostratigraphic reversal boundaries followed by the designation "T" or "O" refer to "termination" and "onset," respectively. See "Explanatory Notes" chapter (this volume) for a discussion of Leg 130 sedimentation rate philosophy.

Strontium concentrations increase with depth to a broad plateau (850–960 μM) below 150 m; they decrease slightly below 509 mbsf to 830 μM in the sample at 623 mbsf (Fig. 34). The gradient and broad maximum are typical of Sr profiles controlled by the release of Sr to interstitial water during recrystallization of biogenic calcite to inorganic calcite (e.g., Gieskes, 1981). Maximum Sr concentrations at this site are higher than those at Sites 288 and 289 (Leg 30) from the Ontong Java Plateau (Elderfield et al., 1982).

Lithium concentrations decrease from 21 μM near the surface to a minimum of 15 μM from 138 to 166 mbsf and then increase downcore with depth to ~35 μM in the deepest samples,

Table 8. Interstitial water geochemical data, Hole 803D.

Core, section, interval (cm)	Depth (mbsf)	pH	Alk. (mM)	Sal. (g/kg)	Cl^- (mM)	Na (mM)	SO_4^{2-} (mM)	PO_4^{3-} (μM)	NH_4^+ (μM)	SiO_2 (μM)	Mn (μM)	Ca^{2+} (mM)	Mg^{2+} (mM)	Sr (μM)	Li (μM)	K (mM)	Rb (μM)
130-803D-																	
2H-4, 145-150	8.45	7.6	3.59	35.0	554	471	29.4	LD	12	472	LD	10.9	52.1	175	20.8	11.6	1.80
3H-4, 145-150	17.95	7.9	3.23	35.0	561	475	27.5	LD	24	543	LD	11.5	51.6	263	19.6	11.9	1.86
4H-4, 145-150	27.45	7.3	3.44	35.0	562	480	26.9	LD	29	543	LD	12.3	51.5	338	18.8	11.3	1.80
5H-4, 145-150	36.95	7.4	3.42	35.5	562	480	26.6	LD	39	575	LD	12.9	50.8	399	18.8	10.9	1.68
6H-4, 145-150	46.45	7.4	3.60	35.5	561	479	26.8	LD	43	615	LD	13.1	50.7	448	18.6	11.3	1.76
7H-4, 145-150	52.05	7.5	3.56	35.5	562	487	26.0	LD	51	652	LD	13.6	50.0	503	18.3	11.3	1.83
10H-4, 145-150	80.55	7.6	3.60	35.0	562	482	24.2	LD	68	723	LD	14.7	48.9	643	17.0	10.8	1.81
13H-4, 145-150	109.05	7.6	3.76	35.5	565	479	24.0	LD	87	763	LD	16.4	47.1	747	15.7	10.4	1.69
16H-4, 145-150	137.55	7.6	3.78	36.0	565	479	23.1	LD	96	853	LD	18.0	45.9	806	15.4	10.5	1.79
19H-4, 145-150	166.05	7.2	3.88	35.2	566	479	23.6	LD	99	838	LD	20.0	45.5	864	15.4	10.1	1.65
22H-4, 145-150	194.55	7.6	3.65	35.5	569	479	22.9	LD	114	903	LD	21.5	43.8	868	16.9	10.0	1.58
25X-3, 145-150	221.55	7.5	3.45	35.5	568	482	22.9	LD	105	861	LD	22.8	43.3	868	17.4	9.53	1.49
28X-3, 145-150	250.35	7.1	3.69	36.0	576	479	22.8	LD	105	907	LD	24.5	42.1	887	18.5	9.39	1.48
31X-2, 145-150	277.65	ND	ND	36.0	576	481	23.5	LD	ND	936	LD	26.7	41.3	921	18.6	9.03	ND
34X-4, 145-150	309.25	7.6	3.15	36.0	581	484	23.1	LD	ND	943	LD	28.6	40.5	953	17.7	8.91	1.40
37X-5, 140-150	339.70	7.6	2.89	39.0	586	483	23.7	LD	ND	959	LD	30.0	40.0	959	20.1	8.72	ND
40X-2, 140-150	364.20	7.6	2.68	36.5	584	490	22.9	LD	111	1016	LD	30.5	38.0	933	22.2	8.92	1.32
43X-3, 140-150	394.80	7.6	2.74	38.5	588	482	22.8	LD	ND	1018	LD	31.5	41.0	922	22.3	8.27	1.30
46X-4, 140-150	425.20	7.6	2.46	36.5	593	482	23.2	LD	111	1068	LD	35.3	37.4	931	22.3	8.13	1.28
49X-3, 140-150	452.20	ND	ND	35.5	593	492	24.1	ND	ND	1001	LD	35.3	38.5	884	26.3	8.28	ND
52X-1, 140-150	478.30	ND	ND	ND	594	487	23.2	ND	ND	1148	LD	38.5	36.3	920	28.2	7.93	ND
55X-2, 140-150	508.90	7.6	2.44	37.0	589	479	23.3	ND	97	1193	LD	40.4	35.0	932	29.0	7.40	1.08
59X-1, 140-150	545.70	ND	ND	38.0	596	484	22.5	ND	96	1264	LD	44.1	33.5	902	36.4	7.11	1.01
68R-1, 138-150	623.18	7.1	0.36	41.0	608	476	23.5	ND	98	594	37	61.7	26.4	830	34.5	4.31	0.47

Note: Alk. = alkalinity, Sal. = salinity, LD = concentrations lower than detection limit, and ND = not determined.

values greater than seawater concentrations (Fig. 34). There is no Li enrichment with the increase in dissolved silica, despite previous reports that biogenic silica dissolution is an important source of Li for interstitial waters (e.g., Gieskes, 1981). Potassium and rubidium concentrations both decrease with depth (Fig. 34) and are linearly correlated with the Ca increase with depth, suggesting that the decreases are related to uptake in low-temperature basalt alteration reactions.

CARBON GEOCHEMISTRY

Shipboard carbon geochemical analyses of samples from Site 803 included routine determinations of volatile hydrocarbons in sediments, inorganic carbon measurements on 481 samples, and 21 Rock-Eval analyses. The NCS elemental analyzer was inoperable during the time that we drilled Site 803; consequently, no shipboard nitrogen and sulphur data are available for this site. The methods used for these analyses are outlined in the "Explanatory Notes" chapter (this volume). Background and detailed descriptions are given by Emeis and Kvenvolden (1986). For safety considerations, hydrocarbon gases were routinely monitored by using the headspace technique. No volatile hydrocarbons were detected in the sediments of Site 803.

Inorganic carbon concentrations (see "Explanatory Notes" chapter, this volume) were determined on physical property samples. All data are summarized in Table 9 (microfiche, back pocket), and the carbonate values for Hole 803D are plotted vs. depth in Figure 10 (see "Lithostratigraphy" section, this volume). Unit I is characterized by very high carbonate concentrations ranging from 80% to 95%. Two ash layers, one at 146 and one at 181 mbsf (Sections 130-803D-17H-4 and -21H-2, respectively; Miocene), have low carbonate contents ($\leq 10\%$; Fig. 10). In the opal-rich sediments of lithologic Unit II (middle and upper Eocene; Fig. 10), carbonate values range from 20% to 90% (Table 9). The Mesozoic sediments of Unit III have very low amounts of carbonate ($<1\%$; Fig. 10 and Table 9).

Because the NCS analyzer was inoperable during Site 803, the contents of total organic carbon (TOC) in the sediments were estimated by means of the Rock-Eval pyrolysis technique (Espitalié et al., 1977). However, the measured amount of TOC in the sediments collected at Site 803 was always less than 0.05% (i.e., below the detection limit of the shipboard Rock-Eval pyrolysis). Because the TOC measurements made with the Rock-Eval pyrolysis are generally lower than those measured with the NCS analyzer (see "Site Summary" section, "Site 798" chapter, in Ingle, Suehiro, et al., 1990), the organic carbon contents will have to be verified independently by shore-based analyses.

PHYSICAL PROPERTIES

An intensive physical properties program was conducted at Site 803. Whole-round analyses consisted of measurements on the multisensor track (MST; see "Explanatory Notes" chapter, this volume) and needle-probe thermal conductivity. Split cores were used for vane shear, electrical resistivity, and velocity measurements and samples were taken for index properties analyses. This effort resulted in data that correlated well with the downhole logging data ("Logging" section, this chapter) and contributed to the construction of synthetic seismograms ("Seismic Stratigraphy" section, this chapter).

Multisensor Track

All sections of the four holes drilled at Site 803 were run through the MST. The GRAPE data for the upper 240 m in Holes 803C and 803D are presented in Figure 35. GRAPE data provide a good estimate of sediment bulk density and can be used as a means of making correlations between holes. The bars on Figure 35 denote the interval of the first section of each core, and the GRAPE profiles indicate that this section is often disturbed. Deeper sections also are affected in many of the cores, as demonstrated by the gradual increase of bulk density over several meters beneath many core breaks. This apparent disturbance problem is discussed further in the section on vane shear strength.

Despite the overprint of low-density spikes and the gradual rebound to undisturbed values on the profiles, other significant trends in the GRAPE data were observed. For example, the profiles show a trend of increasing GRAPE density from the seafloor to 100 mbsf. At this depth the profile changes character,

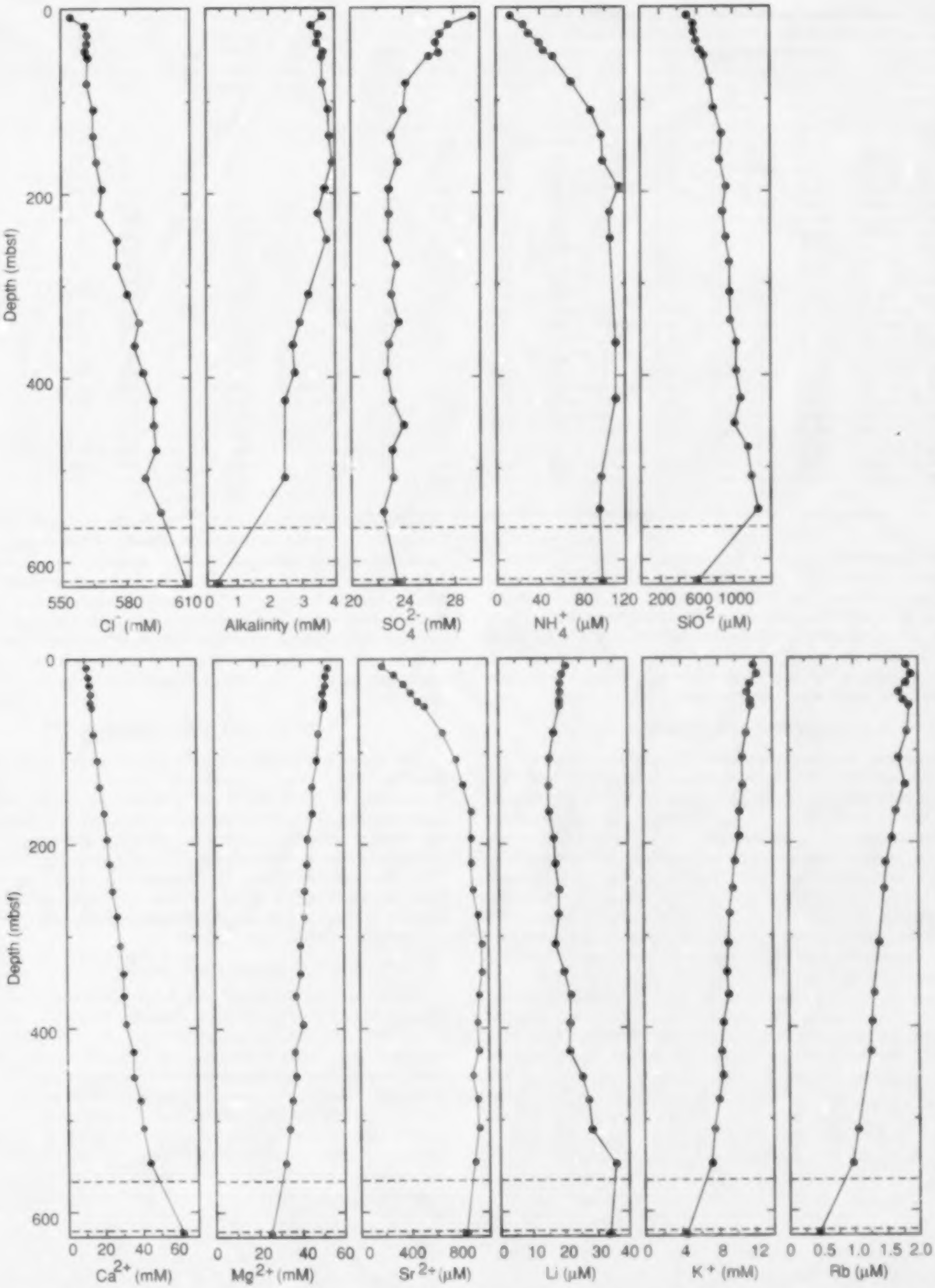

Figure 34. Interstitial water geochemical data vs. depth, Hole 803D. The two horizontal dashed lines represent depth boundaries between lithologic Units I, II, and III; the depth at the base of the plots is that of the contact of Unit III with basalt.

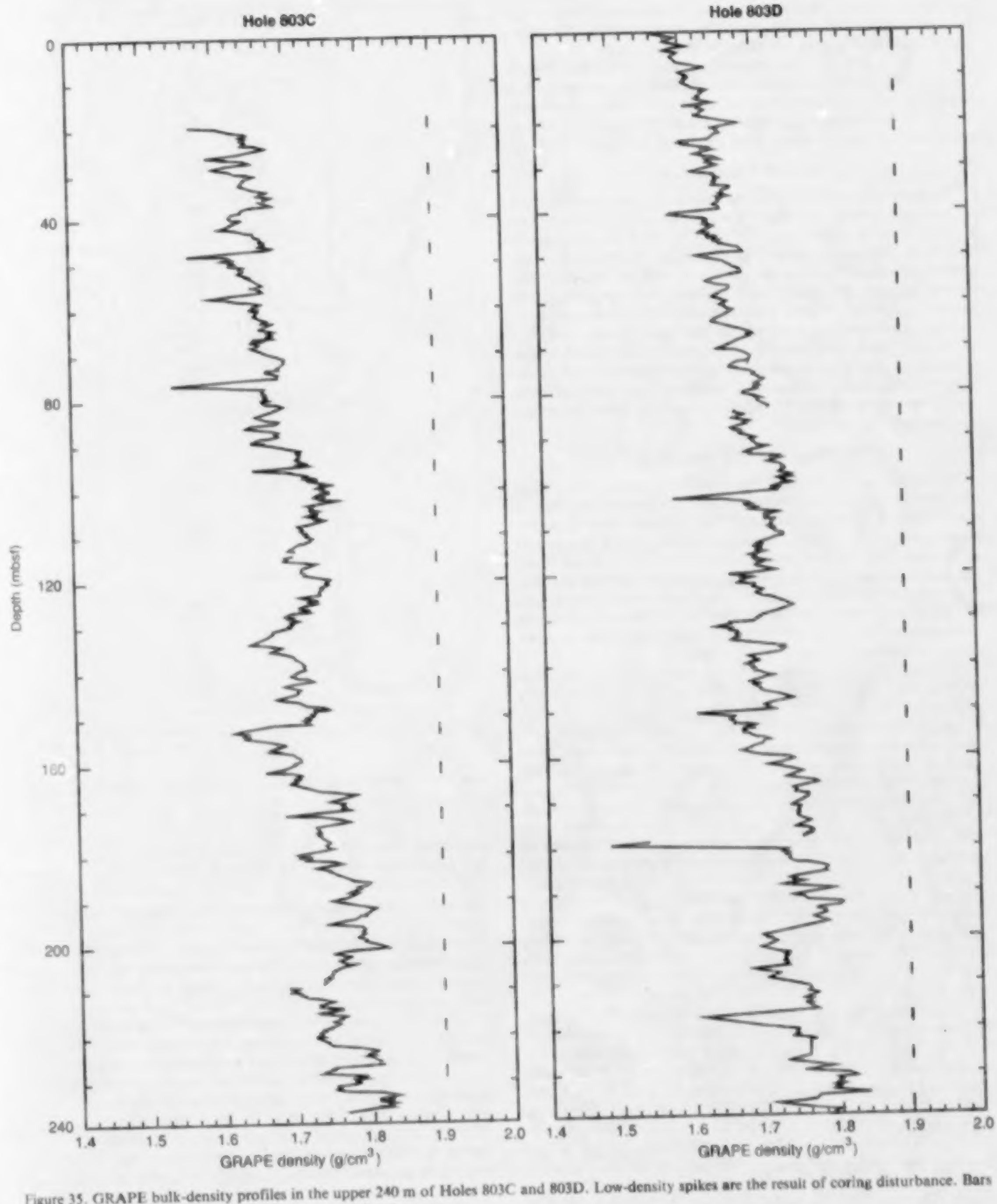

Figure 35. GRAPE bulk-density profiles in the upper 240 m of Holes 803C and 803D. Low-density spikes are the result of coring disturbance. Bars denote the depth interval of the first section of each core.

with average density decreasing to a depth near 160 mbsf. These trends appear to alternate downhole and may be related to alternations in calcium carbonate content, as discussed below with respect to the discrete index properties measurements. The quality of the GRAPE data deteriorates in XCB cores.

The MST also includes magnetic susceptibility and *P*-wave velocity sensors. The magnetic susceptibility data also provide a means of making correlations between holes and is discussed further in the "Paleomagnetism" section (this chapter). The *P*-wave velocity data have not been processed yet.

Thermal Conductivity

Thermal conductivity was measured in three sections per core in each hole at Site 803; values are given in Table 10. Profiles of thermal conductivity (W/m · K) with depth in Holes 803C and 803D are presented in Figure 36. Problems were encountered with calibrating the probes as well as with malfunctioning probes; thus, the data show considerable scatter. The thermal conductivity value is a mean calculated by averaging the thermal conductivities measured on the third, fourth, and fifth sections of each core (see "Explanatory Notes" chapter, this volume). In general, thermal conductivity values increase downhole, corresponding to decreasing porosity. This crude relationship is shown in Figure 37, which presents a plot of thermal conductivity vs. porosity.

Vane Shear Strength

Undrained shear strength was measured using a motorized minivane in split core sections (see the procedures outlined in the "Explanatory Notes" chapter, this volume). Vane measurements were made in APC cores and in competent biscuits of XCB cores until the sediment became too stiff. In many cases, progressive cracking of the sediment occurred during the test, thus negating the assumption that a cylinder of sediment is uniformly sheared about the axis of the vane. Where failure was dominated by cracking, the post-peak values could not be interpreted as residual strengths (Pyle, 1984).

Drilling-induced disturbance in the cores has a considerable effect on the peak shear strength values. As discussed previously with respect to the GRAPE data, the upper section(s) of many of the piston cores are disturbed. This is evident in the GRAPE profiles from core-length cycles consisting of a low-density spike followed by a gradual increase in the upper few sections to "undisturbed" values (recognizing that disturbance occurs during the coring process). It might be expected that the peak strength values obtained in the upper sections of those disturbed cores would be lower than those obtained in the deeper sections of each core. Examination of the peak strength data on a core-by-core basis, however, indicates that, in some cases, the first section has a peak strength higher than that measured for deeper sections in the core. Figure 38 shows peak shear strength vs. section number for Hole 803D. In most cases, the first section has a higher shear strength than the second and third sections, with the strength values increasing again in the last three to four sections of each core.

It is possible the soil skeleton in the upper section is compressed, resulting in an increase of the friction component of the shear strength. Thus, shear strength is actually increased despite disturbance. This conclusion, however, seems at odds with the GRAPE data, which show a low-density spike in the upper section(s) of most cores. Examination of the upper section on each core shows water and soupy mud between the sediment and liner. It appears that water trapped between the piston and the sediment surface has been forced between the core and the liner, while also resulting in some compression of the sediment in the upper sections. The water between the liner and sediment explains the low GRAPE density values; compression of the sediment explains the higher vane shear strength values measured.

Table 10. Thermal conductivity data, Site 803.

Depth (mbsf)	Thermal conductivity (W/m · K)
Hole 803A:	
7.8	1.09
17.2	1.16
26.6	1.14
45.7	1.09
55.2	1.07
Hole 803B:	
22.4	1.10
31.8	1.16
41.4	1.06
52.4	1.32
61.8	1.12
71.4	1.12
79.4	1.25
90.4	1.22
99.9	1.33
109.4	1.40
120.4	1.43
128.4	1.37
137.9	1.39
147.4	1.41
156.9	1.27
166.4	1.22
175.9	1.48
185.4	1.46
194.9	1.42
213.9	1.46
223.4	1.36
232.9	1.41
Hole 803C:	
6.6	1.09
15.4	1.14
26.4	1.21
34.4	1.28
45.4	1.21
51.0	1.38
60.4	1.42
70.0	1.30
79.5	1.34
89.0	1.30
98.5	1.35
108.0	1.30
117.5	1.33
127.0	1.28
136.5	1.43
174.5	1.33
193.5	1.30
212.5	1.45

Profiles of undrained shear strength for Holes 803B, 803C, and 803D are presented in Figure 39. Residual strengths were obtained where cracking did not dominate failure. Both peak and residual values are given in Table 11 (microfiche, back pocket). Measurements in Holes 803C and 803D were performed until the sediment was judged to be too stiff, near 240 mbsf. The low shear strengths observed for these sediments, relative to other marine sediments, reflect their lack of cohesion and the associated susceptibility to coring disturbance (Lee, 1982). Shear strengths are slightly higher in the ooze from approximately 15 to 60 mbsf, corresponding to a larger mean grain size caused by an increase in foraminifer content (see "Lithostratigraphy" section, this chapter). This relationship of higher shear strength with increased preservation of foraminifers has also been shown in vane shear strength data from box cores obtained on the Ontong Java Plateau (Berger and Johnson, 1976).

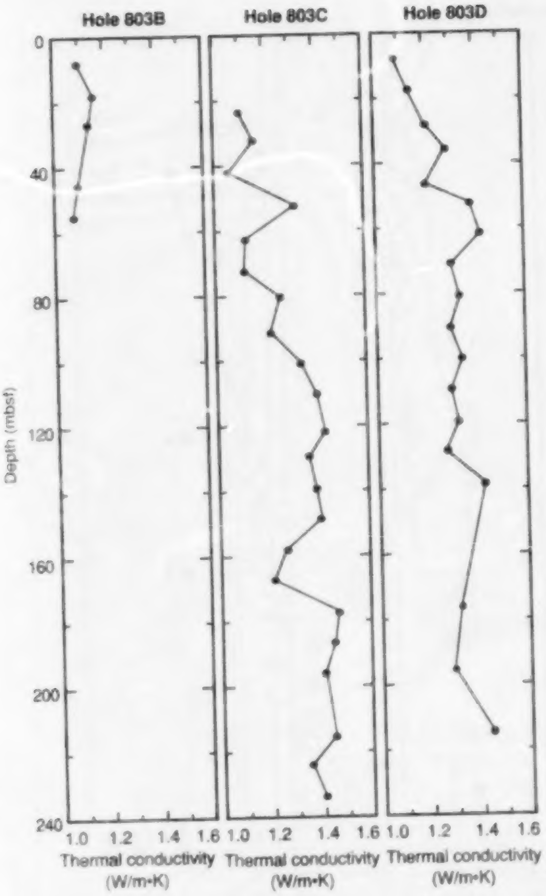

Figure 36. Thermal conductivity vs. depth, Holes 803B, 803C, and 803D.

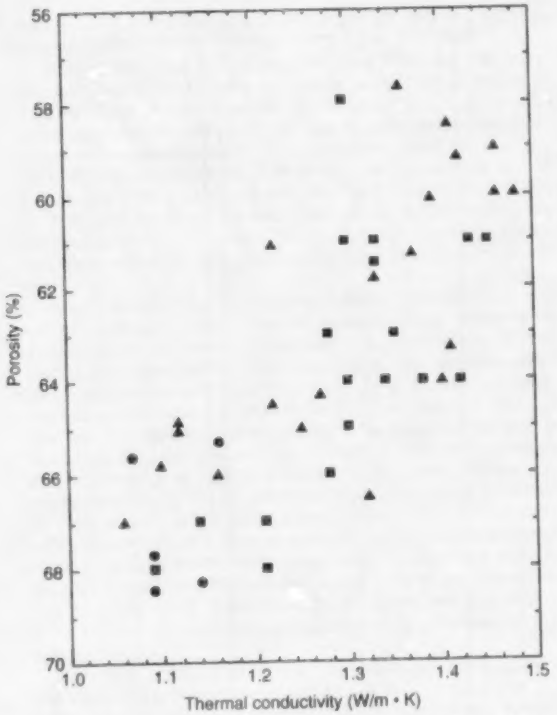

Figure 37. Thermal conductivity vs. porosity, Site 803. Dot = Hole 803B, triangle = Hole 803C, and square = Hole 803D.

Peak shear strengths increase just below 150 mbsf, indicating the onset of lithification. The transition zone between ooze and chalk has been defined as 210–220 mbsf (see "Lithostratigraphy" section, this chapter). The observed change in shear strength could be caused by either chemical (the onset of cementation) or mechanical (the interaction of granular particles and higher friction effects after reaching a critical porosity) effects.

Formation Factor

Electrical resistivity measurements were made in Holes 803A, 803B, and 803C using a four-electrode arrangement in split cores (see the procedures outlined in the "Explanatory Notes" chapter, this volume). The probe system malfunctioned during measurements in Hole 803D, giving unstable readings of resistivity. This problem was caused by a leak in the epoxy holding the probes. Because of the high-resolution velocity measurements and the extensive index properties sampling program, time was not available to fix the probes and measurements were stopped at this point. Furthermore, analyses of the data showed variation that could not be correlated between holes but seemed, instead, to be operator dependent. In light of these problems, and the fact that good downhole resistivity logs were obtained (see "Logging" section, this chapter), the electrical resistivity data obtained from the probe measurements are not presented.

Velocity

Compressional wave (*P*-wave) velocities were measured on split cores in two directions to give vertical (parallel to core axis) and horizontal (perpendicular to core axis) velocity and attenuation. Measurements were performed with the Dalhousie sediment velocimeter (DSV; see "Explanatory Notes" chapter, this volume) at a sample frequency of two per section in APC cores. The system used with this apparatus provides storage of waveforms to allow for subsequent attenuation analysis. This will be performed as a shore-based project. The Hamilton Frame apparatus was used to measure velocity in lithified sediment. In general, the lithified sediment at Site 803 withstood the processes of XCB and RCB coring quite well; thus, Hamilton Frame measurements could generally be conducted at a rate of one per section, with velocities measured in both the vertical and horizontal directions. Waveform data from the Hamilton Frame were also captured by the DSV oscilloscope, allowing the possibility of future analysis for attenuation.

Profiles of vertical and horizontal *P*-wave velocity with depth for Holes 803C and 803D are shown in Figure 40. Table 12 (microfiche, back pocket) presents the velocity data for all Site 803 holes. Velocities remain close to 1550 m/s in the upper 150 m of sediment at Site 803, with some slight variations caused by changes in the carbonate content and grain size. Detailed examination of these trends must await shore-based investigation of

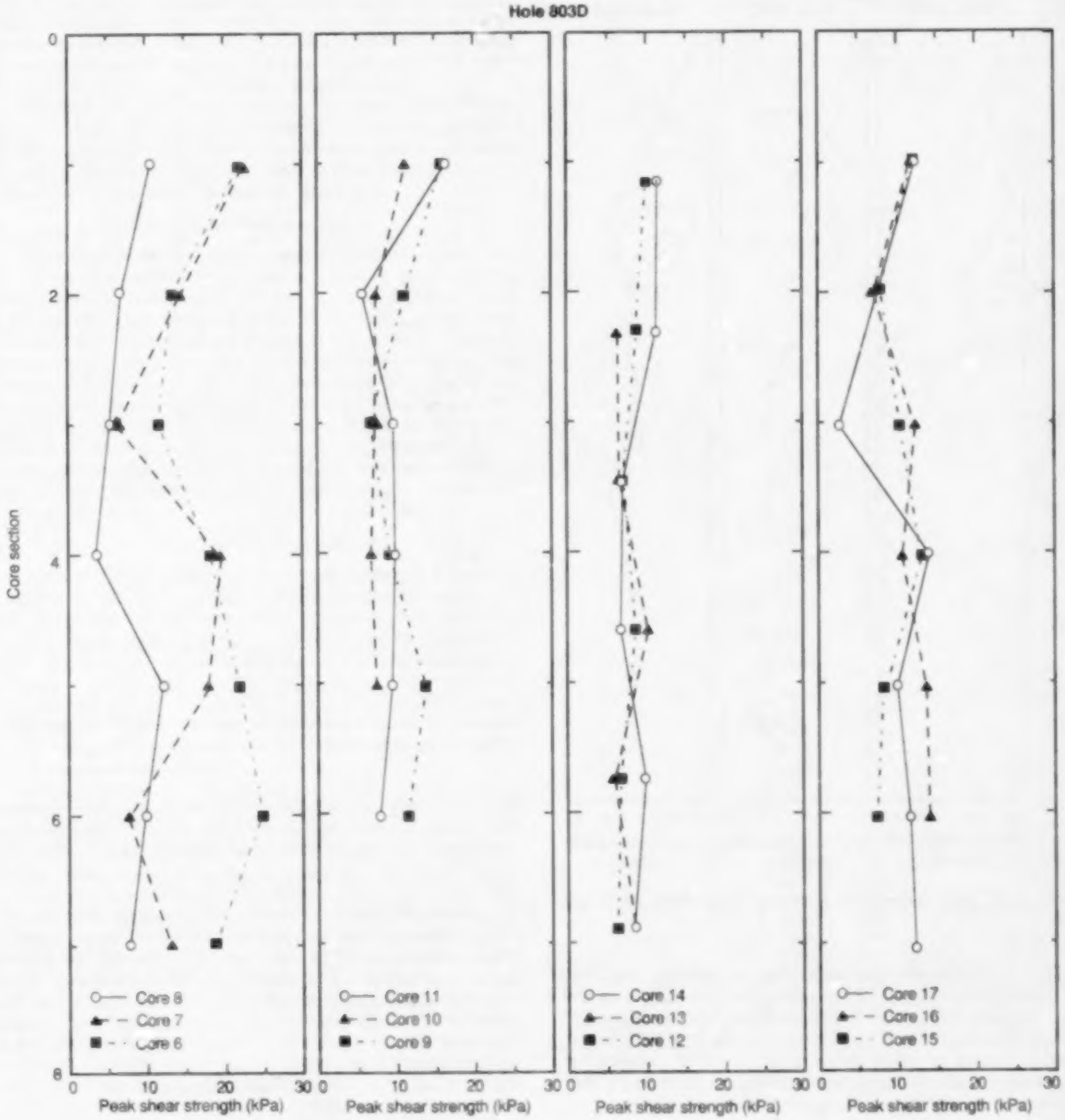

Figure 38. Vane shear strength vs. section number for Cores 130-803D-6H through -17X.

grain size, carbonate content, crystallinity, and isotopes. In many cases, the relationship between carbonate content, grain size, and velocity is not clear.

Velocities increased near 175 mbsf, indicating the onset of lithification. Although the transition between ooze and chalk has been defined at 210–220 mbsf, velocity is a sensitive indicator of increases in rigidity of the sediment framework. The depth of increase of *P*-wave velocity corresponds to the increase in vane shear strength. Variations in velocity over the next 100 m probably reflect changes in the degree of cementation. Near the bottom of Hole 803D, several intervals of radiolarites occur. These highly siliceous layers result in velocities much lower (ca. 1500 m/s) than the surrounding carbonate sequences, which have velocities greater than 2000 m/s. The last measurement in Hole 803D was obtained on basalt, thus the sudden increase in velocity to 4300 m/s.

Laboratory velocity data are compared with log sonic velocity data in the "Logging" section of this chapter. Laboratory velocities were expected to be lower than log velocities because of the removal of overburden and coring disturbance, and this re-

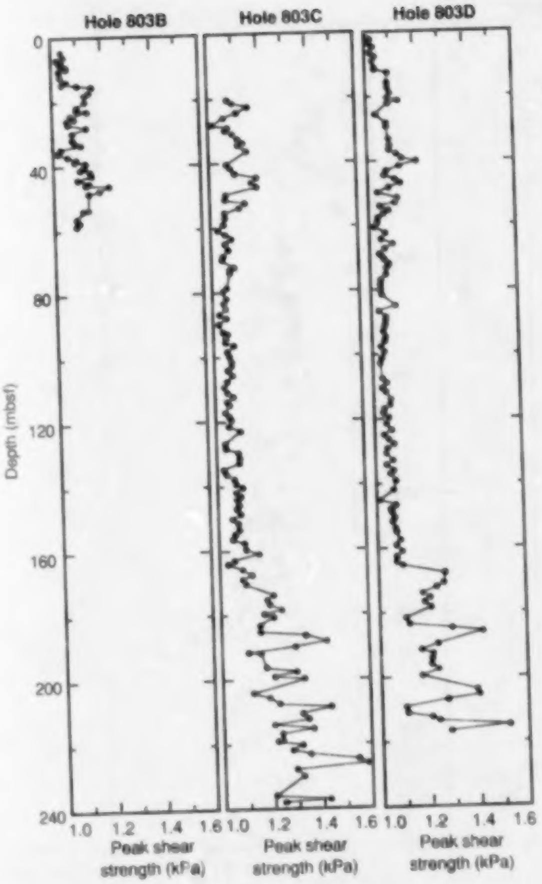

Figure 39. Laboratory vane peak shear strength vs. depth, Site 803.

lationship was seen. Most of the trends in the laboratory data are echoed in the log data, however, lending credibility to both data sets.

Index Properties

The index properties calculated from the weight and volume data for Site 803 samples are wet-bulk density, grain density, water content (based on dry weight), porosity, and dry-bulk density (see "Explanatory Notes" chapter, this volume). These data are presented in Table 13 (microfiche, back pocket).

Because of the high calcite content of these sediments (generally >85%; see Fig. 10), the grain density is generally constant with depth, with values near 2.7 g/cm^3. The bulk density of calcareous sediment is affected by the grain shape, level of dissolution, grain size, stress history, and overburden pressure (Lee, 1982). A preliminary comparison of bulk-density profiles with calcium carbonate content data indicates a strong relationship. In fact, the bulk-density profiles closely mimic the carbonate profiles for most of the Site 803 sediments.

Laboratory bulk-density profiles were compared with log bulk-density results (see "Logging" section, this chapter). These data show a closer relationship than the laboratory and logging velocity data, and correlation between the two data sets is exceptionally good.

Bulk-density data for Holes 803C and 803D are shown vs. depth in Figure 41. Porosity and water content are presented in Figures 42 and 43, respectively. In the upper 20 m of the sediment column, there are rapid changes in index properties, associated with consolidation of young sediment. Over this interval, bulk density increases from 1.45 g/cm^3 near the seafloor to 1.55 g/cm^3 at 20 mbsf, whereas water content decreases from 110% to 75% over the same interval. Between 20 and 110 mbsf, the gradients are not as strong, with bulk density increasing gradually from values of 1.55 g/cm^3 at 20 mbsf to 1.65 gcm^3 at 110 mbsf.

Near 110 mbsf, there is a change in the profile from the trend usually associated with a normally consolidating sediment sequence. Over the interval of approximately 110–155 mbsf, bulk density decreases slightly. This phenomenon is associated with a major dissolution event (see "Biostratigraphy" section, this chapter) and corresponds to a decrease in carbonate content over this interval. The relationship between density and dissolution has previously been documented for carbonates from the equatorial Pacific (Mayer et al., 1986). From 155 to 210 mbsf, a steady increase in bulk density corresponds to an increase in carbonate content, the two curves again showing similar trends. One interesting anomaly in this interval is an ash layer, measured in both Holes 803C and 803D. Bulk densities in the ash layer drop to near 1.5 g/cm^3, whereas porosity jumps to 75% and water content to 110%. Bulk densities decrease again over the interval from 195 to 210 mbsf, again corresponding to a decrease in carbonate content.

Bulk density begins to increase rapidly with increasing depth near 210 mbsf, from approximately 1.6 to 1.85 g/cm^3 at 255 mbsf. Porosity decreases from 62% to 50% and water content decreases from 53% to 40% over this interval. This corresponds to the zone of increasing cementation. Bulk density increases gradually (from 1.85 to 1.95 g/cm^3) down to 560 mbsf, with some variation caused by the slight changes in carbonate content. Porosity and water content show corresponding decreases over this interval.

Changes in sediment type between 595 to 640 mbsf result in extremes in index properties over this interval. A radiolarite, measured at 598 mbsf, has a bulk-density value of 1.46 g/cm^3. Water content and porosity increase sharply at this depth, and grain density is 2.24 g/cm^3. These results agree with those of equatorial Pacific sediments that have high radiolarian contents (Mayer et al., 1986). The remaining measurements, except for the last one in Hole 803D, were on lithified red clay. The final measurement in Hole 803D, at 632 mbsf, is on a basalt, yielding a bulk density of 2.71 g/cm^3, a grain density of 2.82 g/cm^3, and a porosity of 2.4%.

If compaction of the sediment in the upper section of core is occurring, as suggested by the vane shear data, a decrease in discrete sample porosities would also be expected in this section. Examination of the index properties data on a core-by-core basis shows this to be true for many cores. The first section of each of those cores has a lower porosity, with the next few sections having higher porosities, below which the porosity returns to the general trend of the sediment interval containing that particular core.

Summary

The intensive physical properties program conducted at Site 803 has resulted in a suite of data that correlates well with the log data and that can be used with confidence in the construction of synthetic seismograms. This chapter describes the major trends in the physical properties data. Detailed investigation of

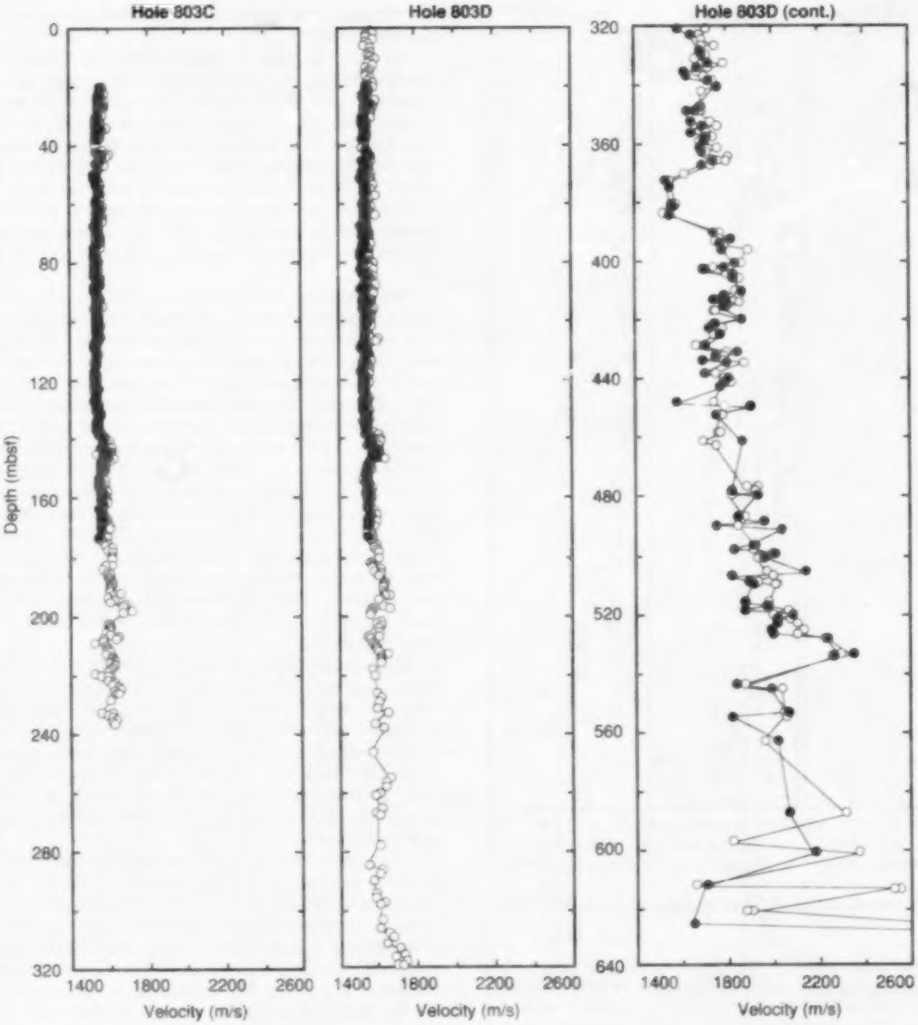

Figure 40. Laboratory compressional wave velocity (m/s) vs. depth in Holes 803C (0–320 mbsf) and 803D (0–640 mbsf). Filled circles = vertical measurements (parallel to core axis); open circles = horizontal measurements (perpendicular to core axis).

the physical causes of these trends, and their relationship to paleoceanographic events, will be conducted on shore.

Coring disturbance in the upper sections of many cores is clearly evidenced by the GRAPE and vane shear strength data. Despite the influence of this disturbance on the profiles of the various physical properties measured, correlation of physical properties trends between holes and with trends in calcium carbonate and grain size is possible.

IGNEOUS PETROLOGY

Introduction

Tholeiitic basalts were encountered in Hole 803D at a depth of 631.0 mbsf below brown Albian clay in Section 130-803D-68R-4. Note that this depth does not correspond to the curated depth of 626.3 mbsf but refers to the depth at which the drillers "felt" basement. Coring of basalt continued until drilling was stopped at 656.0 mbsf in Core 130-803D-71R; recovery averaged 38% (Fig. 44). The rocks mainly consist of successive pillow lavas. They are predominantly nonvesicular, hypocrystalline, fine-grained, aphyric to very sparsely plagioclase-, clinopyroxene-, or olivine-phyric; rare, large phenocrysts of plagioclase and clinopyroxene as large as 0.5–1.0 cm across were observed in three instances (Sections 130-803D-69R-1, Piece 9; -70R-3, Piece 6; and -71R-1, Piece 2). Alteration ranges from severe to moderate within pillow interiors, where the development of smectite and other secondary minerals typically gives a mottled brown and gray, or blotchy reddish brown and gray appearance. Pillow rims

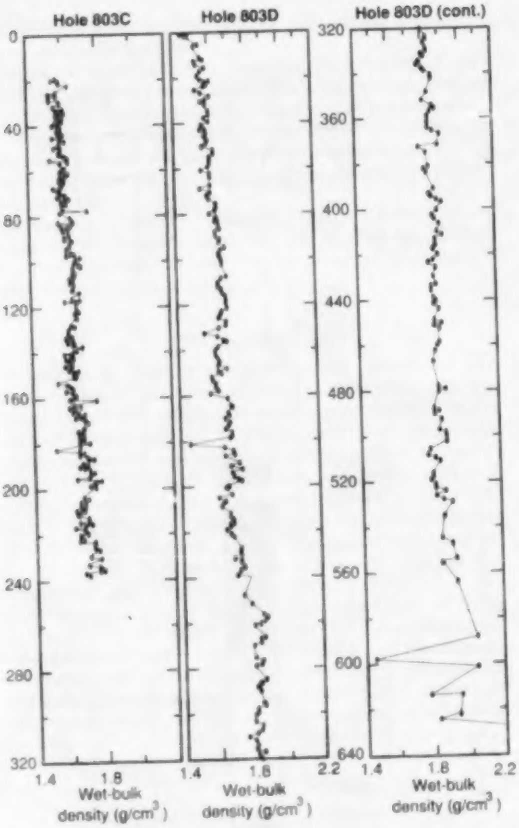

Figure 41. Laboratory bulk density (g/cm^3) vs. depth in Holes 803C (0–320 mbsf) and 803D (0–640 mbsf).

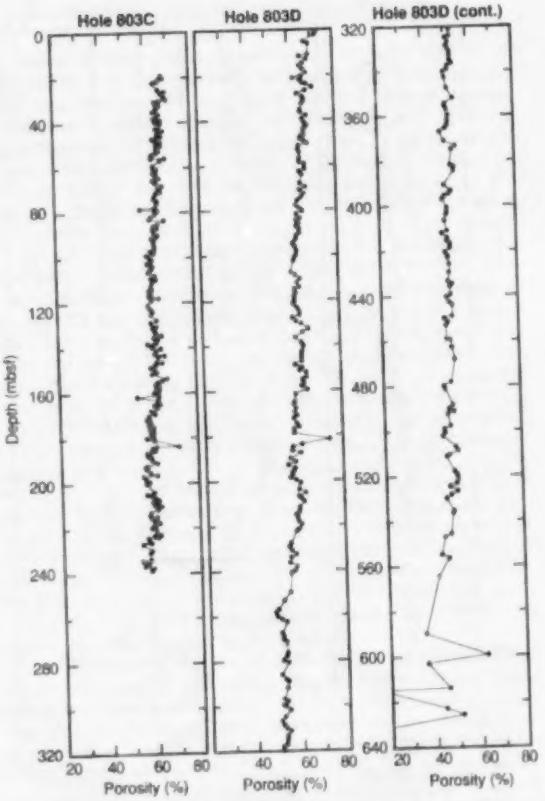

Figure 42. Laboratory porosity (%) vs. depth in Holes 803C (0–320 mbsf) and 803D (0–640 mbsf).

tend to be much less altered, and although most glass is at least partially devitrified, small amounts of fresh glass are present on many rims.

In general, alteration decreases slightly going downward in the hole. The most altered interval is Section 130-803D-68R-4, directly below the sediment contact. At the contact, the basalt is capped by a flat, ~2-cm-thick hydrothermal(?) layer consisting of several alternating bands of calcite and a bright green clay mineral, probably celadonite. Fractures and calcite-filled veins (0.5–5 mm thick) are fairly numerous throughout the basalt section and mainly appear to represent remnants of cooling cracks in individual pillows; basalt alteration tends to be more intense near such veins.

Several thin (< 20 cm thick) interpillow limestones are present. Of these, several are best described as breccias, as they contain variable proportions of bright to dark green lapilli-size clasts (celadonite?), which appear to be completely altered fragments of spalled-off basaltic glass. Microfossils in these limestones, although present, have been recrystallized beyond specific recognition, probably by baking during emplacement of the overlying lava.

The entire basalt section at Site 803 roughly corresponds to a single stratigraphic "subunit" at Site 807, given that three of the subunits at Site 807 are thicker than the entire basement interval cored at Site 803. Although the basalts are similar macroscopically throughout the recovered section, the cores were divided into nine subdivisions (as opposed to "subunits" at Site 807) on the basis of intercalated limestones or breccias, which suggest a passage of time greater than that for a single eruption. These subdivisions are numbered 1 through 9 below. The distribution of these subdivisions relative to core recovered is shown in Figure 44.

Following ODP guidelines, it was possible to divide the cores on an even finer scale (e.g., 9a, 9b, etc.) according to the presence of glassy or chilled pillow tops or changes in phenocryst type or abundance. Several of these secondary subdivisions probably represent individual pillows. This classification does not necessarily imply that all of the secondary subdivisions within a given primary subdivision reflect the same eruption; only that definitive macroscopic evidence to the contrary was lacking in the recovered portion of the core. Indeed, chemical data indicate that some of the secondary subdivisions comprising individual primary subdivisions are derived from different magmas. Detailed visual core descriptions with subdivision and secondary subdivision boundaries are appended at the end of this chapter.

Subdivision Thickness, Designation, and Alteration Summary

Subdivision 1: 150 cm thick (Sections 130-803D-68R-4, 7 cm, to -69R-1, 110 cm); aphyric, very fine-grained, nonvesicular basalt; highly to intensely altered.

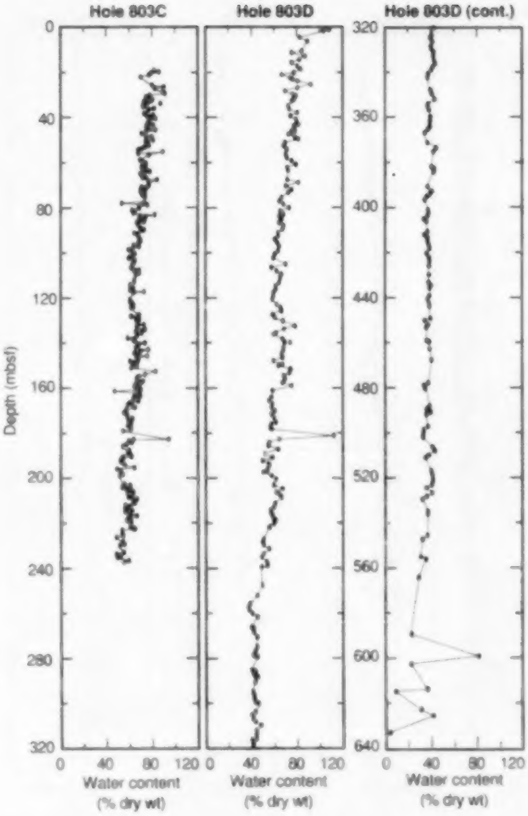

Figure 43. Laboratory water content (% dry wt) vs. depth in Holes 803C (0–320 mbsf) and 803D (0–640 mbsf).

Subdivision 2: 53 cm thick (Sections 130-803D-69R-1, 120 cm, to -69R-2, 40 cm); aphyric, very fine-grained, nonvesicular basalt with glassy pillow rims; alteration high overall but less than Subdivision 1.

Subdivision 3: 40 cm thick (Sections 130-803D-69R-2, 50 cm, to -69R-2, 90 cm); aphyric, fine-grained, nonvesicular basalt with glassy pillow rim; highly altered.

Subdivision 4: 90 cm thick (Cores 130-803D-69R-2, 110 cm, to -69R-3, 50 cm); aphyric, fine-grained, nonvesicular basalt with glassy pillow rims to sparsely plagioclase-olivine(?) phyric basalt; highly to moderately altered interiors, fairly fresh rims.

Subdivision 5: 193 cm thick (Sections 130-803D-69R-3, 70 cm, to -70R-1, 90 cm); aphyric to sparsely plagioclase phyric to sparsely clinopyroxene (?) phyric, nonvesicular basalt; alteration varies from moderate to high in interiors with fresher pillow rims.

Subdivision 6: 18 cm thick (Sections 130-803D-70R-1, 100–120 cm); aphyric, very fine-grained, nonvesicular basalt; very highly to moderately altered, decreasing toward pillow rim.

Subdivision 7: 23 cm thick (Sections 130-803D-70R-1, 130 cm, to -70R-2, 10 cm); aphyric, very fine-grained, nonvesicular basalt; very highly to moderately altered, decreasing toward pillow rims.

Subdivision 8: 88 cm thick (Sections 130-803D-70R-2, 20–110 cm); aphyric, very fine-grained basalt; moderately to very

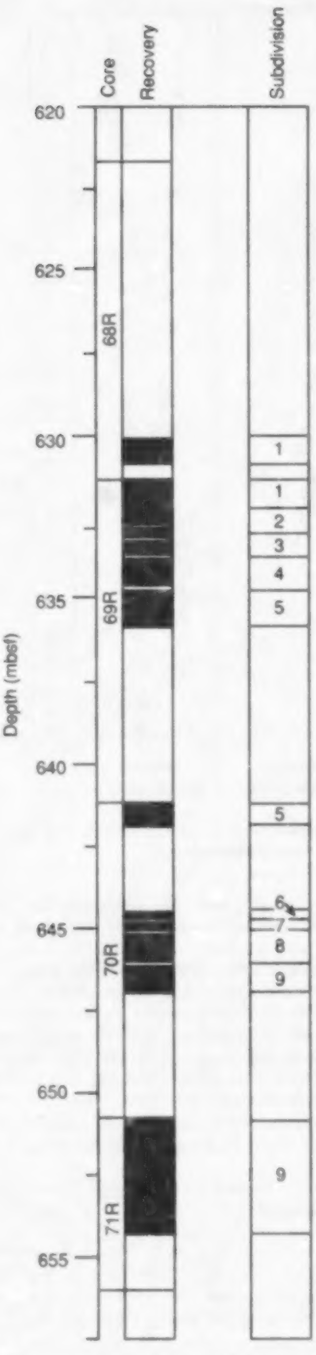

Figure 44. Basalt recovery at Site 803, showing proportion of material recovered (in black) and division into nine main subdivisions.

highly altered near veins and fractures; one calcite-filled amygdule (~1 mm) near bottom.

Subdivision 9: 454 cm thick (Sections 130-803D-70R-2, 140 cm, to -71R-3, 80 cm); aphyric to sparsely clinopyroxene-plagioclase phyric basalt; rare subhedral phenocrysts of plagioclase up to 8 mm across in 9b (Section 130-803D-71R-1, Piece 2); 9b also contains rare, 1–4-mm-thick, calcite-filled amygdules at top and bottom; highly to moderately altered with patches of less altered massive material.

Note that the "curated" recovery is 11.09 m whereas the actual amount of basement recovery was 9.59 m. This discrepancy results from "curated" recovery figure including the spacers that separate the pieces of basalt.

Petrography

Thin-section examination of pillow interiors from several subdivisions confirmed their fine-grained, typically aphyric, hypocrystalline nature (see attached thin-section descriptions at the end of this book in Section 5). Phenocrysts observed include rare subhedral (<0.5 mm across) pseudomorphs of olivine in Section 130-803D-68R-4, 45–47 cm, and rare, fairly fresh, 3–5 mm thick, subhedral to anhedral, compositionally zoned clinopyroxene in Sample 130-803D-70R-3, 60–62 cm; the clinopyroxene is notable for numerous, fresh inclusions of basaltic glass up to 0.05 mm across. A large, fairly fresh (1 cm thick) subhedral plagioclase crystal occurs in Sample 130-803D-69R-1, 87–90 cm. Once-glassy groundmasses are generally altered to dark, cryptocrystalline material, probably smectite; plagioclase laths, sometimes skeletal, also are somewhat altered, and groundmass clinopyroxene grains often are partially replaced by brownish to reddish clays. Despite alteration, textures are well preserved; they are mainly intersertal (hyalophitic) and are subordinately intergranular or subophitic. The most noteworthy petrographic aspect of these rocks, however, is the scarcity of phenocryst phases.

Shipboard Chemical Analyses

Major and trace elements were determined by X-ray fluorescence spectrometry (see "Explanatory Notes" chapter, this volume) on 13 specimens from pillow interiors representing most of the subdivisions; water loss on ignition (LOI) was determined gravimetrically on the same samples. Data are presented in Table 14. The basalts are all fairly evolved (Mg-number = 35–53), mildly quartz- to olivine-normative tholeiites. They possess MORB-like Ti/Zr (111–116 vs. ~100 for normal MORB) and Zr/Y (2.9–3.5 vs. ~3.0 for normal MORB) ratios, but rather high Sr (145–197 vs. 100–120 ppm for normal MORB), CaO (11.07–13.66 wt%), and K_2O (0.30–1.44 wt%) concentrations. Zr/Nb ratios are distinctly low compared with normal MORB (15–17 vs. ~30 or more), as are TiO_2, Zr, and Y abundances for the level of differentiation indicated by Mg-number (Figs. 45 and 46).

In general, the major elements and compatible trace elements do not display simple interelement relationships, suggesting that the rocks may represent more than one liquid line of descent or parental magma. For example, Fe_2O_3 and MgO do not define a single trend; nor do Ni and Cr vary coherently with Mg-number (Fig. 46). The incompatible elements Nb, Zr, Y, and Ti display very limited overall variations in abundance, and ratios between them remain almost constant within analytical uncertainties. Rubidium and potassium, and to a lesser extent phosphorus, exhibit significantly greater ranges and define rough positive correlations with water LOI (Fig. 47), indicating that some of the measured variation is a result of alteration by seawater. Loss on ignition is between 1.19 and 3.17 wt% for all but one sample; such values are typical of moderately altered lavas.

Preliminary Conclusions

Several different eruptions are represented in Hole 803D. All the basalts are moderately differentiated tholeiites, and they may have been derived from more than one parental magma. There is no evidence at this site for the thick, massive flood lavas postulated to compose the upper levels of basement over much of the plateau (e.g., Kroenke, 1972); instead, the thin, pillowed nature of the flows implies that their feeder vents were not very distant and eruption rates were low. This feature may be related to the location of this site on the flank of the plateau.

The rocks are distinct from normal MORB (see above), but also distinct from typical oceanic-island tholeiites. The latter are much more enriched in immobile incompatible elements (such as Zr, Nb, and Ti), have higher Zr/Y (generally >4), and much lower Zr/Nb ratios (commonly <12). The closest resemblance of the Site 803 lavas is to the few available basalts from other Pacific plateaus (see Fig. 45, for example); in particular, those from the Manihiki Plateau (Jackson et al., 1976) and the single flow of Ontong Java basalt recovered at Site 289 (Stoeser, 1975). They also are quite similar to lavas from the islands of Malaita and Santa Isabel (J. Mahoney, unpubl. data, 1989), which may represent an uplifted portion of the western edge of the Ontong Java Plateau (e.g., Kroenke, 1972), and to the Cretaceous sill and flow complex in the Nauru Basin to the east of the plateau (e.g., Floyd, 1986; Saunders, 1986). In conjunction with Nd and Sr isotopic studies, the above chemical characteristics have been interpreted to reflect mantle sources that are a combination of MORB and oceanic-island-type components (Mahoney, 1987; P. Castillo, pers. comm., 1990).

Significantly, as with the other Pacific plateau samples (Mahoney, 1987), the Site 803 basalts show no evidence of having interacted with continental crust, although several workers (e.g., Nur and Ben-Avraham, 1982) have proposed on the basis of seismic refraction data that the Ontong Java Plateau is a subsided continental fragment. Finally, we note that the poorly defined Cretaceous age of the lowermost sediments at Site 803 does not allow any firm conclusions regarding the duration of late-stage volcanism at this site vs. Site 289 or 807.

LOGGING

Logging Operations

An almost complete set of high-quality logging data was collected at Hole 803D despite abundant technical problems. The logging operations are summarized in Table 15; acronyms used are listed in Table 16. Four logging runs were made during the course of 32 hr, one each with a geophysical and a geochemical tool string, one with an electrical resistivity imaging tool (the formation microscanner or FMS), and one with a sonic velocity tool. Each of the tool strings also carried the natural gamma-ray tool so as to correlate depths between individual runs.

The first run employed a geophysical tool string that consisted of a sonic tool (LSS), a resistivity tool (DIT), a density tool (HLDT), and a natural gamma-ray tool (NGT). In addition, the string carried the Lamont temperature tool (TLT) at its base. The LSS malfunctioned when we had a minor problem passing the bit release at the end of the drill string; the malfunction not only made it impossible to record sound velocities, but also made it impossible to command the caliper on the density tool to open. The caliper is needed to push the HLDT sensors against the borehole wall and receive proper density readings of the formation. Because of the tool failures, good data were acquired only from the natural gamma-ray, resistivity, and temperature tools. The tool string was able to reach within 10 m of the base of the hole (653 mbsf) and thus was able to log the upper 20 m of basalt and the lowermost sedimentary section.

Table 14. Major element, trace element, and CIPW-normative compositions of basalts from Hole 803D analyzed on board ship.

Core, section Interval (cm) Subdivision	68R-4 38–41 1A	69R-1 6–8 1B	69R-1 88–90 1D	69R-2 135–137 4A	69R-3 48–50 4B	69R-3 83–85 5A	69R-4 28–30 5C	70R-1 62–64 5D	70R-2 32–34 8A	70R-3 61–62 9B	71R-1 129–131 9D	71R-2 86–88 9F	71R-3 37–39 9H
Major elements (wt%):													
SiO_2	48.94	49.46	48.67	50.25	49.11	49.43	50.86	50.02	49.32	50.02	49.57	49.89	49.71
TiO_2	1.44	1.31	1.31	1.32	1.31	1.31	1.47	1.34	1.38	1.31	1.27	1.33	1.26
Al_2O_3	16.62	14.96	15.19	15.00	14.87	15.29	16.70	15.07	15.72	15.24	14.77	15.19	14.26
$^{a}Fe_2O_3$	12.88	12.05	12.89	10.70	12.58	12.04	9.68	11.51	11.56	10.16	11.74	10.70	11.84
MnO	0.15	0.17	0.19	0.17	0.18	0.16	0.11	0.17	0.16	0.18	0.20	0.17	0.24
MgO	3.94	5.87	5.39	6.95	5.59	5.58	5.29	6.54	6.41	6.57	6.93	6.06	7.12
CaO	11.63	12.76	13.62	12.69	12.47	12.84	11.17	12.24	11.11	12.92	12.82	12.93	12.49
Na_2O	2.19	1.92	1.89	1.92	1.78	1.97	2.18	2.01	2.27	1.97	1.84	2.05	1.89
K_2O	1.04	0.36	0.45	0.31	0.61	0.64	1.44	0.66	0.84	0.31	0.35	0.42	0.42
P_2O_5	0.21	0.11	0.12	0.11	0.13	0.13	0.37	0.13	0.15	0.12	0.11	0.12	0.10
Total	99.02	98.97	99.70	99.42	98.61	99.37	99.26	99.67	98.90	98.99	99.59	98.85	99.30
LOI	3.17	1.62	2.83	1.19	1.72	2.31	8.49	1.66	2.41	1.63	1.34	1.59	1.76
N	2	1	4	1	2	2	4	2	2	2	4	2	2
ᵇCIPW norms:													
Quartz	0.48	1.57		1.76	1.63	0.61	1.72	0.60		1.84	0.67	1.42	0.64
Orthoclase	6.25	2.17	2.70	1.86	3.67	3.85	8.65	3.96	5.07	1.84	2.11	2.54	2.50
Albite	18.86	16.57	16.22	16.47	15.38	16.89	18.72	17.17	19.59	16.96	15.77	17.69	16.21
Anorthite	33.13	31.75	32.02	31.83	31.56	31.49	31.98	30.52	30.81	32.49	31.41	31.61	29.68
Diopside	20.58	26.62	29.73	25.70	25.75	26.91	18.19	24.85	20.19	26.39	26.61	27.23	26.89
Hypersthene	14.83	16.08	13.29	17.42	16.61	15.00	15.15	17.72	16.46	15.60	18.36	14.50	19.04
Olivine			0.66						2.50				
Apatite	0.47	0.25	0.27	0.24	0.29	0.28	0.81	0.29	0.33	0.26	0.25	0.27	0.22
Ilmenite	2.79	2.54	2.52	2.55	2.54	2.53	2.83	2.57	2.68	2.54	2.44	2.58	2.43
Magnetite	2.62	2.45	2.60	2.16	2.57	2.44	1.96	2.32	2.35	2.06	2.37	2.17	2.40
Mg#	35.01	46.09	42.29	53.21	43.80	44.87	49.02	49.89	49.32	53.06	50.81	49.79	51.17
Trace elements (ppm):													
Nb	4.8	5.0	4.4	4.4	4.7	4.7	5.2	4.4	4.6	4.8	4.5	4.2	4.7
Zr	83.0	73.9	72.8	73.4	75.3	75.6	85.5	75.4	79.1	75.4	71.3	73.1	77.5
Y	26.9	21.5	22.0	20.8	23.1	23.5	29.3	23.8	24.2	23.5	23.0	22.5	24.0
Sr	196.6	157.8	159.0	154.0	160.6	163.0	187.5	162.2	168.1	158.0	144.6	148.1	154.5
Rb	22.7	8.7	8.1	4.8	13.3	13.3	18.1	12.7	13.8	2.5	6.1	6.8	6.7
Zn	219.9	111.2	116.5	99.3	129.8	102.5	72.7	110.8	88.0	77.1	89.1	89.4	100.3
Cu	70.1	87.1	92.1	59.1	124.6	59.1	71.2	55.4	83.5	135.1	37.9	37.9	53.9
Ni	182.8	134.2	108.9	119.8	90.0	93.4	91.1	105.3	95.5	135.2	103.8	107.2	115.6
Cr	284.0	239.4	232.8	231.9	237.7	238.4	255.1	230.9	247.5	233.0	224.0	227.5	260.4
V	294.5	298.6	298.7	278.3	268.3	288.1	251.2	252.1	272.9	258.0	265.4	270.5	278.1

Notes: CIPW-normative after Johanssen, 1931, for example. LOI = loss on ignition, *N* = number of analyses.

[a] All Fe expressed as Fe_2O_3.

[b] Fe_2O_3/FeO set at 0.15 and Mg# = (atomic) 100 Mg/Mg + Fe^{2+}.

The formation microscanner (FMS) was used in the second logging run. The FMS can be used to image bedding and fractures downhole. About halfway to the seafloor, a connector flooded and shorted the tool out. The FMS was brought back on deck, the pressure casings were opened, the tool was dried, and the run was repeated. By the time the tool string passed to a lower part of the hole, it encountered a bridge at 610 mbsf. Thus, no further logging data were acquired from the basement or lower sedimentary section. The main logging run collected FMS, natural gamma-ray, and temperature data (TLT) to the drill pipe. The uppermost section of the hole was washed out to such an extent that the caliper arms of the FMS lost contact with the borehole wall and no usable data were collected over this interval. The tools were lowered to 192 mbsf, repeating measurements in the upper, soft sedimentary section to ascertain the reliability of the FMS data in these unconsolidated sediments.

The third run consisted of the geochemical tool string, modified to include the HLDT. The tool configuration was, from the top down, NGT (natural gamma-ray), HLDT (density), ACT (aluminum), GST (eight-element, fast-capture, neutron activation spectroscopy). Although the entire tool string checked out correctly on deck, when the GST was calibrated at the mud line the spectra were out of tolerance and could not be deconvolved into elemental data. The run was continued to collect density data and aluminum percentages in the section. The interval from 610.5 mbsf to the pipe at 98.7 mbsf was logged on the main logging pass and the section from 311.1 to 98.7 mbsf was logged again.

The fourth logging run consisted of the NGT (natural gamma-ray), a mechanical caliper to help center the tool, the BHC (borehole-compensated sonic tool), and the TLT (temperature). The BHC sonic tool was used because the backup LSS malfunctioned on deck. The main logging pass recorded data from 605.6 to 98.7 mbsf. A section from 606.8 to 101.1 mbsf was logged a second time to check the reproducibility of the BHC in this soft formation. After this run, the sonic string was pulled out of the hole and logging was concluded.

The logs show that the hole was in good condition below 250 mbsf, but the hole had widened considerably above this depth. Above 200 mbsf, the hole was significantly wider than the maximum opening of the density tool caliper. Hence, above this depth the log density measurements average about 1.4 g/cm^3, compared with core measurements of about 1.6 g/cm^3 (see Fig.

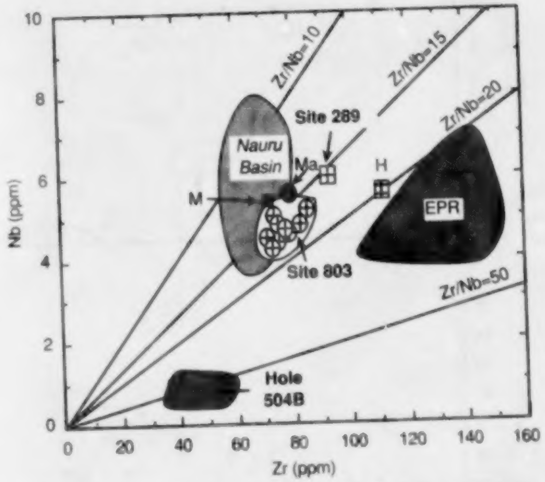

Figure 45. Plot of Zr vs. Nb for Site 803 tholeiites. For comparison, fields are shown for the East Pacific Rise (EPR; Humphries et al., 1980), Hole 504B on the Costa Rica Rift (Kempton et al., 1985), and the Nauru Basin (Floyd, 1986; Saunders, 1986). Averages for Manihiki Plateau lavas ("M"; Jackson et al., 1976) and Malaita basement basalts ("Ma"; J. Mahoney, unpubl. data, 1989) are also plotted, as are data for the single basalt flows recovered at Site 289 (Stoeser, 1975) and on Hess Rise ("H"; Seifert et al., 1981).

48). Below this depth, core and log measurements are in better agreement. Density measurements from the logs above 200 mbsf are suspect.

The original logs were recorded in depth increments of feet below rig floor. Each logging tool combination contained a natural gamma-ray detector (NGT) that recorded a prominent spike produced by the thick ash layer seen at 181.3 mbsf in the core (see "Lithostratigraphy" section, this chapter). All logging depths were converted to meters and adjusted to align the gamma-ray peaks at 181.3 mbsf.

Log Stratigraphic Units

Well-log data defined the extent of sediment types that were poorly recovered at Site 803. Perhaps of greater importance, the logs illustrated the nature of transitions in the sedimentary column, such as ooze to chalk, which could not be recorded in great detail from core observations or measurements. These transitions strongly influence the seismic character of the site.

Rather than describe the behavior of the well logging data in terms of the rock stratigraphic units recognized in the recovered core, the data have been subdivided into log stratigraphic units based solely on internal consistencies of the logging profiles. Log stratigraphic units do not necessarily coincide with lithologic units. The units (described as A, B, C, etc., to distinguish them from lithologic Units I, II, III) are described in Table 17. All of the logs, with the log stratigraphic units defined, are displayed in Figures 49 through 52. Correlations between density, electrical resistivity, and compressional wave velocity are fairly consistent (i.e., they all exhibit changes and inflections near the same depths).

Gamma-ray activity is somewhat independent of the other properties and has different trends. This difference may be a result of the extremely low signal seen in the gamma-ray logs and the portion of the sediments that produce the signal. Normal gamma-ray counts from continental margin carbonates are in the tens of API units; shale counts are about 100. Whatever component is producing the gamma radiation in the Site 803 sediments (probably windblown clay or volcanic ash) is very dilute.

Although the concentration variations may be enough to produce the regular changes that are found in the gamma-ray log, they are not enough to effect such other properties as density seriously, as these are a sum of all components of the sediments. Aluminum, another log associated with clay content in these sediments, is plotted along with the "noncarbonate content" (100 − %$CaCO_3$) from core samples (Fig. 50). Visually, there appears to be correlation between the two signals. Temperature logs (Fig. 51) show an increase from 1.6°C at the mud line to near 7.0°C at the bottom of the hole.

Logging Unit A extends from the top of the logged interval (106 mbsf) to approximately 199 mbsf. It includes the ash layer depth tie point at 181.3 mbsf (labeled "Ash" in Fig. 49). Logging Unit A is defined by generally increasing compressional wave velocity (1.65–1.85 km/s) and gamma-ray activity (3.5–5.0 API). Unexpected (from core descriptions) features of logging Unit A are the two zones of increased electrical resistivity (132.2–144.9 and 182.9–199.2 mbsf). These intervals of increased resistivity correlate with small but significant increases in compressional wave velocity at the same depths. No marked reduction in porosity was observed in core samples from these intervals (see "Physical Properties" section, this chapter).

Gradients in bulk density, electrical resistivity, and gamma-ray activity characterize logging Unit B. Wet-bulk density increases from 1.60 to 1.85 g/cm^3 in the depth range from 199 to 259 mbsf. Resistivity also increases, with a local maximum at approximately 259 mbsf. Gamma-ray activity continues to increase from about 150 mbsf, in logging Unit A, to a local maximum within logging Unit B at 248 mbsf, and drops sharply in the bottom 11 m of the unit. Logging Unit B also increases in overall compressional wave velocity (1.85 km/s at 200.3 mbsf and 2.11 km/s at 259.4 mbsf), but the increase is more discontinuous over the interval, with several local maxima and minima. The velocity fluctuations, coupled with density variations, are the source of strong reflectors seen in the seismic section (see "Seismic Stratigraphy" section, this chapter).

Between 259 and 521 mbsf in Hole 803D (logging Unit C), there is a gradual increase in velocity (2.11–2.28 km/s), almost constant density (1.85 g/cm^3), and two broad minima in gamma-ray activity and electrical resistivity. The resistivity and gamma-ray minima are approximately coincident at around 320 and 470 mbsf. A slight velocity minimum appears to correlate with the shallower of the two resistivity and gamma-ray minima. In general, this section of the sediment column behaves as might be expected of normally compacting carbonate sediments.

Logging Unit D (521–596 mbsf) is again a depth interval of increased gradients and irregular log response. Bulk density increases from 1.85 to 2.07 g/cm^3 by 583 mbsf. Compressional wave velocity increases over the same depth range (2.28–2.62 km/s) with a peak at 583 mbsf. Resistivity also increases with depth over the interval. All three of these properties do not increase smoothly, but rather show local maxima and minima that are seen in the seismic record as the strong reflectors near the bottom of the sedimentary column (see "Seismic Stratigraphy" section, this chapter).

The short interval between 596 and 601 mbsf is singled out as an individual unit (logging Unit E) because of the extreme drop in velocity and electrical resistivity occurring over these 5 m. Logging Unit E corresponds to the recovery of a nannofossil radiolarite with an equally anomalous low laboratory velocity (see "Lithostratigraphy" and "Physical Properties" sections, this chapter).

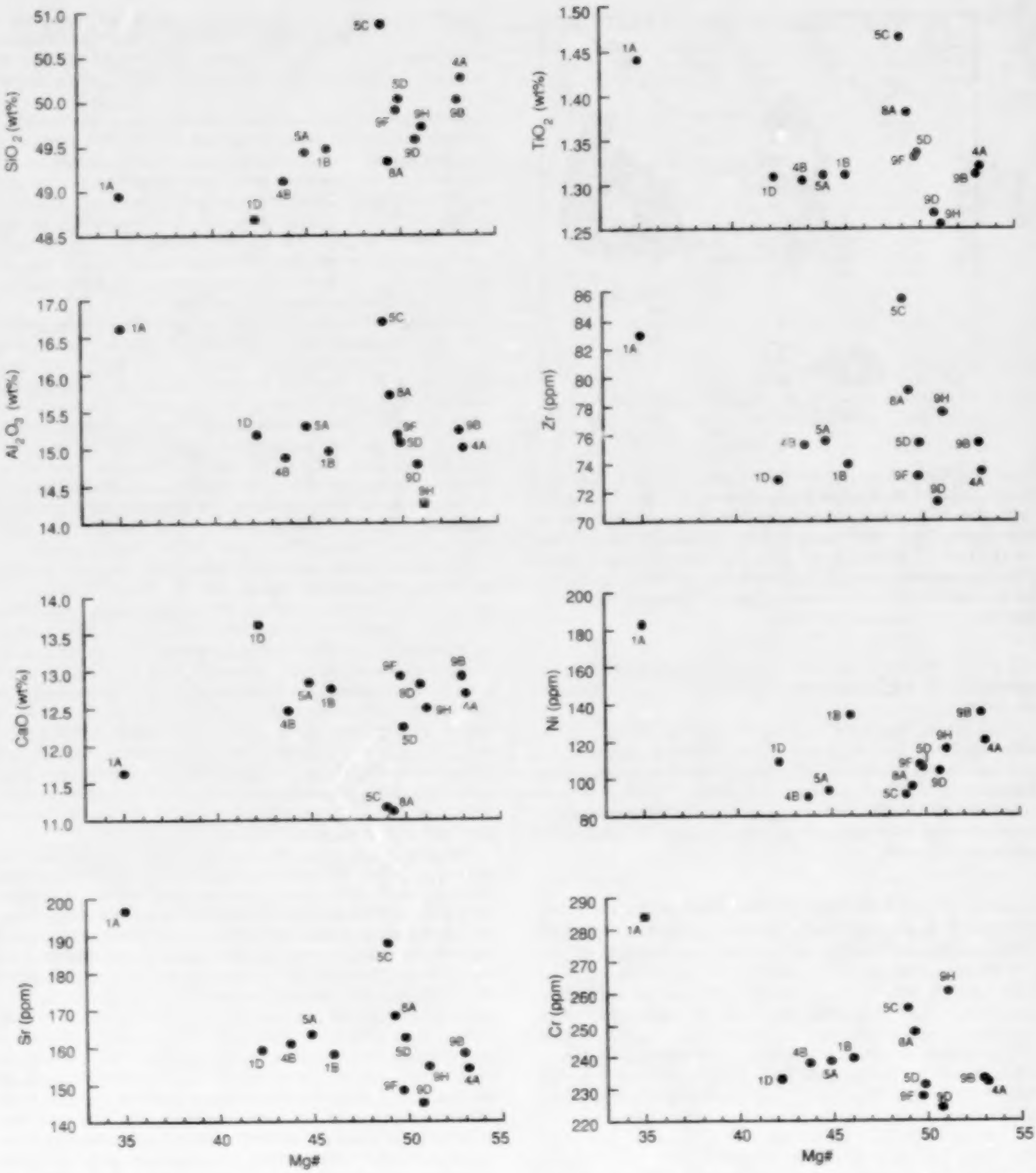

Figure 46. Variation of selected major and trace elements vs. Mg-number for Site 803 basalts. Numbers and letters next to points indicate subdivisions and secondary subdivisions, respectively.

The remaining sedimentary unit, logging Unit F, extends from 601 mbsf to basement at approximately 630.4 mbsf. It is defined solely by electrical logs (Fig. 52) as no other logs could be taken over this interval. Resisting the urge to break the bottom 30 m of the hole into three logging units, we note that there is a minimum in resistivity at 615 mbsf and a rather strong maximum at 618–620 mbsf. The minimum may be associated with another silica-rich interval; the maximum appears to coincide with a continuous chert layer partially recovered in the core (see "Lithostratigraphy" section, this chapter).

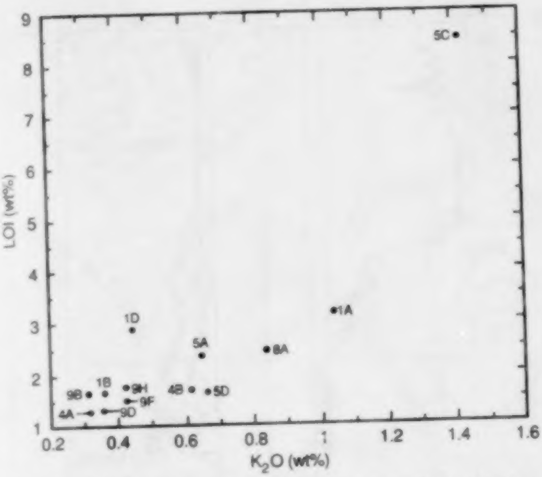

Figure 47. K$_2$O vs. weight loss on ignition (LOI) for Site 803 tholeiites. Numbers and letters next to points indicate subdivisions and secondary subdivisions, respectively.

Basement appears in the resistivity logs at a depth of 631.4 mbsf. It is characterized by resistivities in the range from 10 to 1000 ohmm, typical of weathered oceanic pillow basalts.

Correlation with Lithostratigraphy

Although the log stratigraphic unit boundaries do not coincide with the lithostratigraphic unit boundaries, there are some correlations. The two lithostratigraphic unit boundaries (IA/IB and IB/II) that fall within the intervals of comprehensive logging coverage (Fig. 49) are located in log stratigraphic units defined by strong property gradients. Thus, the ooze-to-chalk transition at 217.1 mbsf described from the recovered core is seen as a true transition zone in the logs (logging Unit B), extending over 60 m. The transition also has an irregular character, suggestive of hard and soft intervals, as the oozes above grade into the chalks below. Logging Unit D, containing the Subunit IB/Unit II boundary, appears to be another zone of enhanced gradients caused by diagenetic change; in this case, the onset of precipitation of authigenic silica as opal-CT cement and/or chert.

In at least three instances, the logs add detail of structure and sediment distribution where core recovery was low near the base of the hole. Poor core recovery began with Core 130-803D-57X, coinciding with the top of logging Unit D (521 mbsf). Nodular chert first appeared in the cores at this level. Chert formation and enhanced grain cementation in general are probably responsible for the local high-velocity layers within logging Unit D at 521–541, 546–558, and the generally higher velocity values below 564 mbsf (where the break is made between lithostratigraphic Subunit IB and Unit II). Similarly, the chert horizon in Unit F (partially recovered in Core 130-803D-67X) is defined by a zone of high resistivity about 2 m thick. Core 130-803D-65X recovered only a few centimeters of radiolarite, but the logs indicate that there may be an interval of radiolarite that is nearly 5 m thick (logging Unit E).

Finally, the fairly constant electrical resistivity log data between 621.8 mbsf and basement at 631.4 mbsf implies that lithologic Unit III is uniform. The recovered 5 m of the section are representative of a 10-m-thick unit.

Comparison with Laboratory Data

Compressional wave velocity and bulk density data recorded *in situ* during well logging at Hole 803D are directly comparable with laboratory measurements of the same properties made on

Table 15. Diary of logging operations, Hole 803D.

Local day	Local time	Cumulative hours	[a]Depth (mbsf)	
2/5/90	5:10			Last core on deck
2/5/90	13:45	0.0		RIH with Quad Combo (NGT/DIT/HLDT/LSS/TLT)
2/5/90	15:09	1.4		At mud line
2/5/90	16:49	3.1	649.2	On bottom of hole, 9 m above total drilled section
2/5/90	17:15	3.5		Main log pass; only NGT/DIT/TLT functioning; up at 900 ft/hr
2/5/90	17:41	3.9	534.9	Change speed to 1800 ft/hr as HLDT not functioning
2/5/90	18:30	4.7	98.7	Tool in pipe at 3516 mbrf (11,539 ft); POOH
2/5/90	20:00	6.2		Tool string on deck
2/5/90	21:15	7.5		RIH with NGT/FMS/TLT; connector head flooded at 6000 ft
2/6/90	0:53	11.1		RIH with NGT/FMS/TLT
2/6/90	2:47	13.0	609.8	At bottom of hole; hole bridged
2/6/90	2:59	13.2		Up log of FMS
2/6/90	4:59	15.2	98.7	Enter pipe; end main FMS log
2/6/90	5:20	15.6	191.7	Repeat uplog from 11,850 ft to pipe at 11,539 ft
2/6/90	5:48	16.0	98.7	POOH with FMS
2/6/90	7:50	18.1		RIH with geochemical string (NGT/ACT/GST/HLDT)
2/6/90	9:30	19.7		Pause at mud line; GST has spectra out of tolerance
2/6/90	10:30	20.7		Decide to go down with nonfunctioning GST
2/6/90	11:02	21.3	610.5	Start log up; 600 ft/hr (NGT/ACT/HLDT)
2/6/90	11:49	22.1	464.8	GST not coming up; change logging speed to 900 ft/hr
2/6/90	13:10	23.4	98.7	Into pipe
2/6/90	13:25	23.7	311.1	Start repeat section logging up
2/6/90	14:15	24.5	98.7	Back into pipe; POOH
2/6/90	16:23	26.6		RIH for second attempt at sonic run (NGT/BHC/TLT)
2/6/90	17:54	28.1	605.6	Hit bottom of hole at 13,214 ft
2/6/90	18:03	28.3		Start up log
2/6/90	18:45	29.0	98.7	End up log
2/6/90	19:09	29.4	606.8	Start repeat of sonic run from 13,216 ft
2/6/90	19:50	30.1	101.1	End repeat sonic run 11,557 ft; POOH
2/6/90	22:00	32.3		Rigged down from logging runs.

[a] Based on correlation of ash layer observed at 181.3 m in core to NGT spike at 11,810 ft in quad combo; 11,816 ft in FMS main; 11,824 ft in geochemical string; 11,822 ft in sonic main; 11,820 ft in sonic repeat.

Table 16. Acronyms used in well logging.

Acronym	Definition or meaning
ACT	Aluminum clay tool
API	American Petroleum Institute standard units of gamma activity calibrated to test pit in Houston, TX
BHC	Borehole compensated sonic tool
DIT	Phasor dual induction tool
fbrf	Feet below rig floor
FMS	Formation microscanner
GST	Geochemical spectral tool
HLDT	High-temperature lithodensity tool
LSS	Long-spaced sonic logging tool
mbrf	Meters below rig floor
mbsf	Meters below sea floor
NGT	Natural gamma tool
POOH	Pull out of hole
RIH	Run into hole
SDT	Long-spaced sonic digital tool
TLT	LDGO temperature logging tool

Table 17. Log-stratigraphic units defined at Hole 803D.

Logging unit	Depth range	Description
A	<199	Velocity gradient (1.65–1.85 km/s) Resistivity relatively constant (0.7 ohmm)
B	199–259	Gradients in density (1.60–1.85 g/cm^3) Resistivity (0.7–0.8 ohmm) Velocity (1.85–2.11 km/s)
C	259–521	Velocity gradient (2.11–2.28 km/s) Resistivity varies (0.8–1.0 ohmm) Density varies between (1.8–1.9 g/cm^3)
D	521–596	Density gradient (1.9–2.1 g/cm^3) Velocity increase (2.28–2.62 km/s) Resistivity increase (1.0–1.6 ohmm)
E	596–601	Velocity and resistivity minima (1.79 km/s, 0.7 ohmm)
F	601–630.4	Variable resistivity No sonic, density
Basement	630.4	

discrete sections of recovered core. Plots of superimposed logging and laboratory data vs. depth are presented in Figure 48. The laboratory data are uncorrected for ocean-bottom temperature and pressure. The corrected laboratory data (to *in-situ* conditions) will have slightly higher velocities and densities. Comparison of the laboratory and logging data allow both logging specialists and the physical properties specialists to evaluate the effects of hole conditions and core disturbance on their data.

Laboratory wet-bulk density values agree well with density logs below 200 mbsf. Above this level the density log is shifted toward unrealistically low values (<1.40 g/cm^3). Based on the comparison of the two sets of data, the density logs are unreliable above 200 mbsf. The compressional wave velocity logs can be used to edit both logging and shipboard sample results. Within the upper 250 mbsf at Hole 803D, there are several relative maxima and minima in both data sets. Excursions that are seen in the results of both experiments have been retained. Low-velocity intervals in the well logs from 121.1 to 126.1, 187.8 to 188.7, 223.7 to 227.6, and 243.1 to 247.7 mbsf have been discounted. For similar reasons, the low velocities measured in five laboratory samples between 370 and 390 mbsf are attributed to core disturbance rather than to an *in-situ* occurrence. On a positive note, many local maxima and minima that might have been suspect in either individual laboratory or logging data are confirmed as real events by the data comparison (e.g., a local velocity maximum between 138 and 147 mbsf and an extreme velocity minimum between 596.9 and 600.8 mbsf).

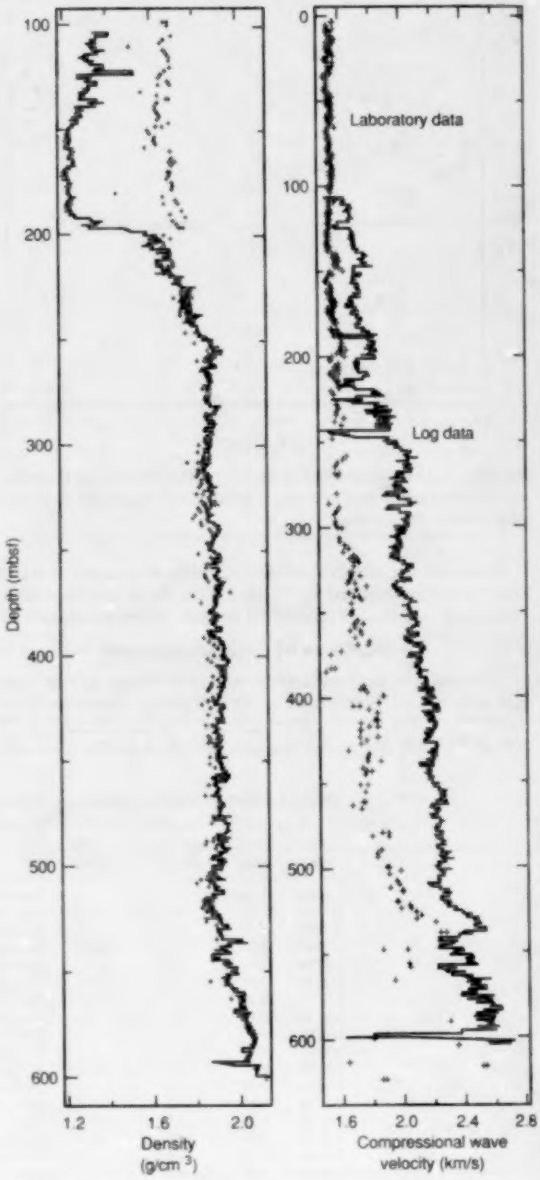

Figure 48. Logging and laboratory velocity and density data, Hole 803D. Laboratory data at STP.

Velocity-Resistivity Relationship

Compressional wave velocity is plotted vs. electrical resistivity in Figure 53. The figure illustrates this relationship as well as that of velocity to porosity in the sediment column as diagenesis takes place. We have used a 1-m running average value of the logs in Figure 53 to reduce the number of points and to clarify the diagram. The different log-stratigraphic units have been identified in the plot. Electrical resistivity is used because it is

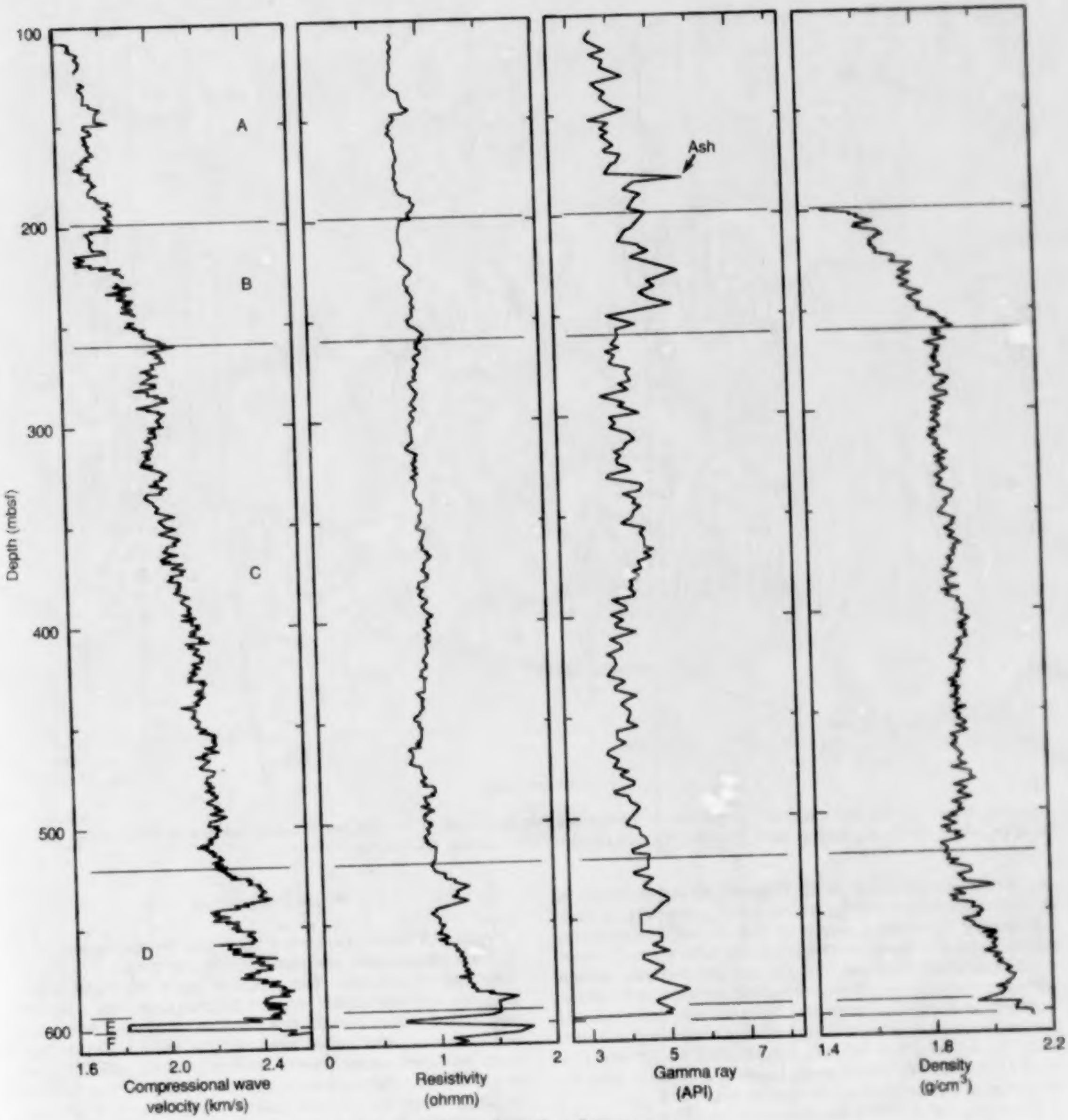

Figure 49. Well logging data, Hole 803D. Logging units A–D are shown for reference.

an analog of porosity in these sediments. The different units occupy overlapping fields that tend toward lower porosities (higher resistivities) and increasing velocities with depth. The velocity-resistivity relationship illustrates the change from a regime where there is a substantial change in velocity (1.55–2.40 km/s) with very little change in resistivity (0.7–1.0 ohmm, logging Units A, B, and C) to one in which there is a much smaller change in velocity 2.40–2.60 km/s) over a wider range of resistivity (1.0–1.8 ohmm, logging Units D and F). The rapid rise in velocity with little change in resistivity represents the effects of increasing cementation on sediment grains in the upper part of the column. The harder sediments follow a normal porosity-velocity relationship.

The formation microscanner images are presented on microfiche at the back of this volume (see back pocket).

SEISMIC STRATIGRAPHY

Introduction

The seismic character of the Ontong Java Plateau in the vicinity of Site 803 is transitional between the "layer cake" stratigraphy of the thick section at the top of the plateau and the more

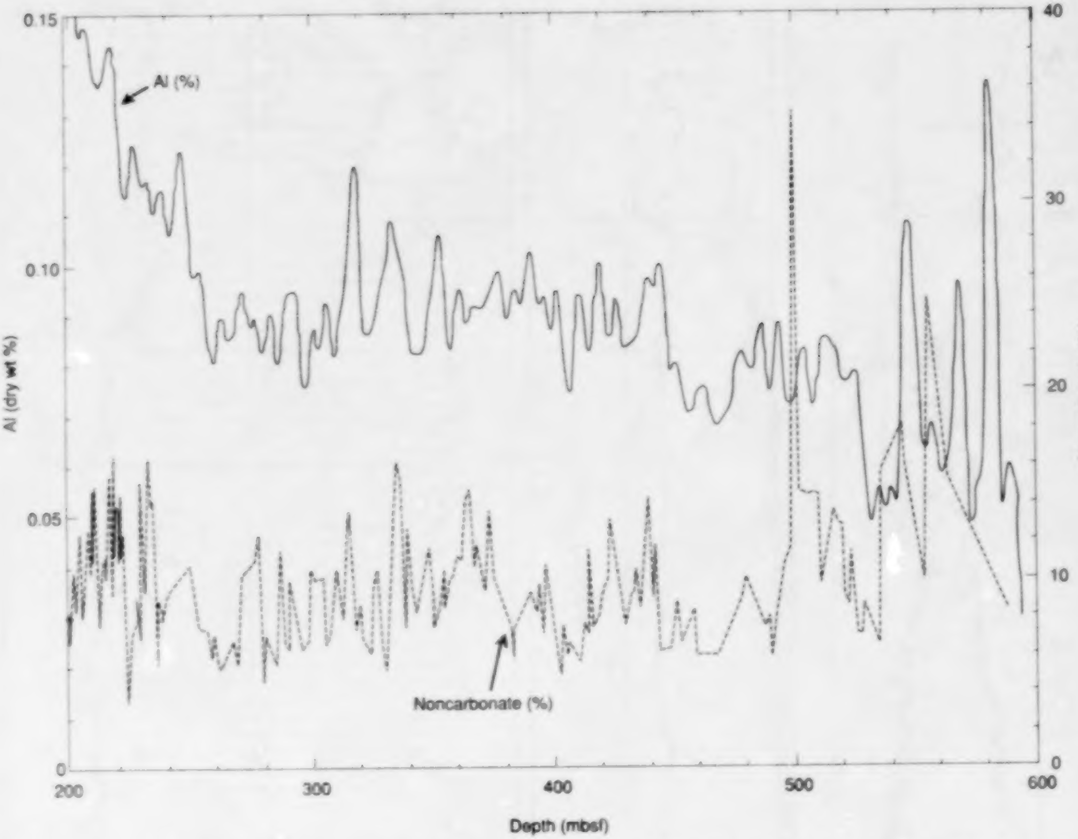

Figure 50. Aluminum log (solid line) and noncarbonate fraction (dashed line), Hole 803D. The noncarbonate fraction is calculated as 100 − %$CaCO_3$, where the $CaCO_3$ value is taken from the "Carbon Geochemistry" section, this chapter.

variable seismic signature of the thinned flanks (see Mayer et al., this volume). Site 803 lies within a depth range that is characterized by numerous examples of mid-section reverberations (MSRs); some of these reverberant layers have a rough, basementlike acoustic character that disrupts the overlying section whereas others are more flat-lying and do not seem to affect the sediments above. The former may be basalt sills and the latter may represent local, diagenetically enhanced features (see Mayer et al., this volume). Site 803 lies approximately 1.6 km west of a small MSR (Fig. 54). This feature, however, appears to have little influence on the seismic stratigraphy at the drill site.

Slumping and sediment remobilization are ubiquitous on the plateau, and several small zones of apparently displaced sediments were found in the cores recovered at Site 803. The seismic record at Site 803, however, shows little evidence of major mass movement events. Seismically, the section is well stratified and, at 0.65 s thick, is approximately 40% thinner than the section at Sites 289/586 (on the top of the plateau; Andrews, Packham, et al., 1975). In this section, we will look at the origin of some of the major reflectors at Site 803 and thus gain insight into the nature of this thinning. In combining these results with those from the other Ontong Java Plateau sites, we hope to lay the groundwork for future studies that will use the seismic record to extract a detailed record of the tectonic and paleoceanographic history of the Ontong Java Plateau.

Seismic Modeling

Although the seismic record often has the appearance of a geologic cross-section and can easily be interpreted in terms of structural relationships, two problems make the direct stratigraphic use of the seismic record a difficult task. First, the seismic section presents events as a function of traveltime and not depth. Second, the limited bandwidth of seismic systems prevents resolution on the scale of the true geologic variability; instead, seismic reflections are commonly interference composites resulting from the complex interaction of the true geologic structure and the outgoing pulse of the seismic system (Mayer, 1979). Both of these problems are particularly serious in the pelagic carbonate sequences of the Ontong Java Plateau where low sedimentation rates and the subtle physical response of the sediment to paleoceanographic change result in a seismic section that is composed of numerous closely spaced reflectors. Interference must clearly play a role in producing the seismic record here and, given the closely-spaced nature of the reflectors, an inaccurate traveltime-to-depth conversion would easily result in the miscorrelation of a reflector with a geologic event.

To convert a seismic section into a depth section (and thus to know where in the borehole record to look for the cause of a particular seismic event), we must accurately determine the true sonic velocity structure of the sediment column. At Site 803, we

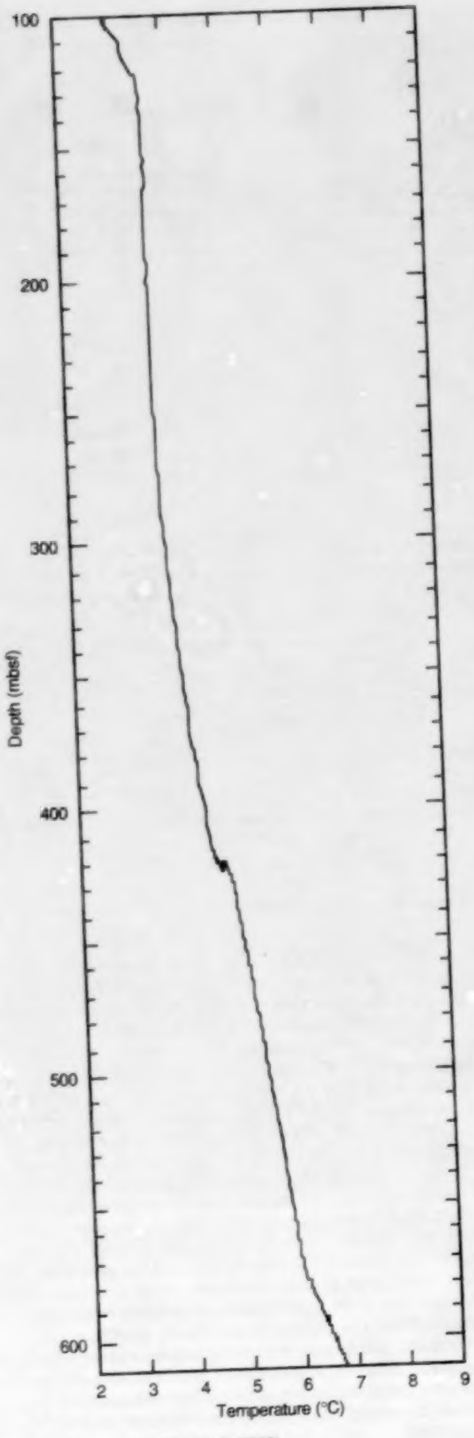

Figure 51. Temperature log, Hole 803D.

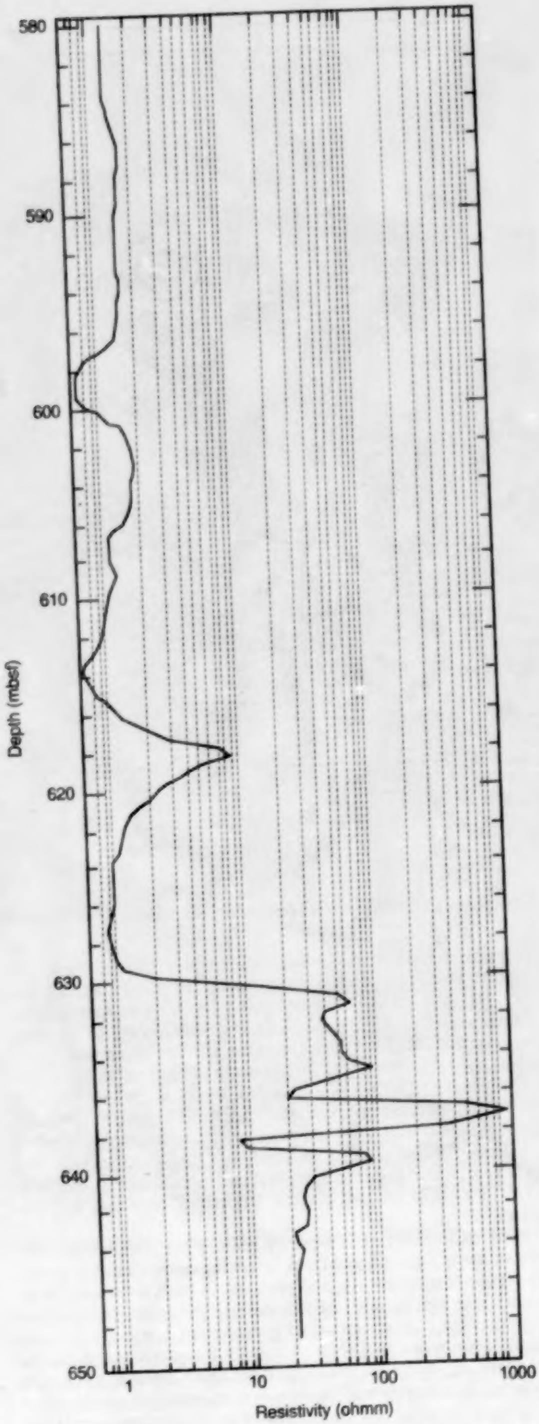

Figure 52. Resistivity log from the lower part of Hole 803D.

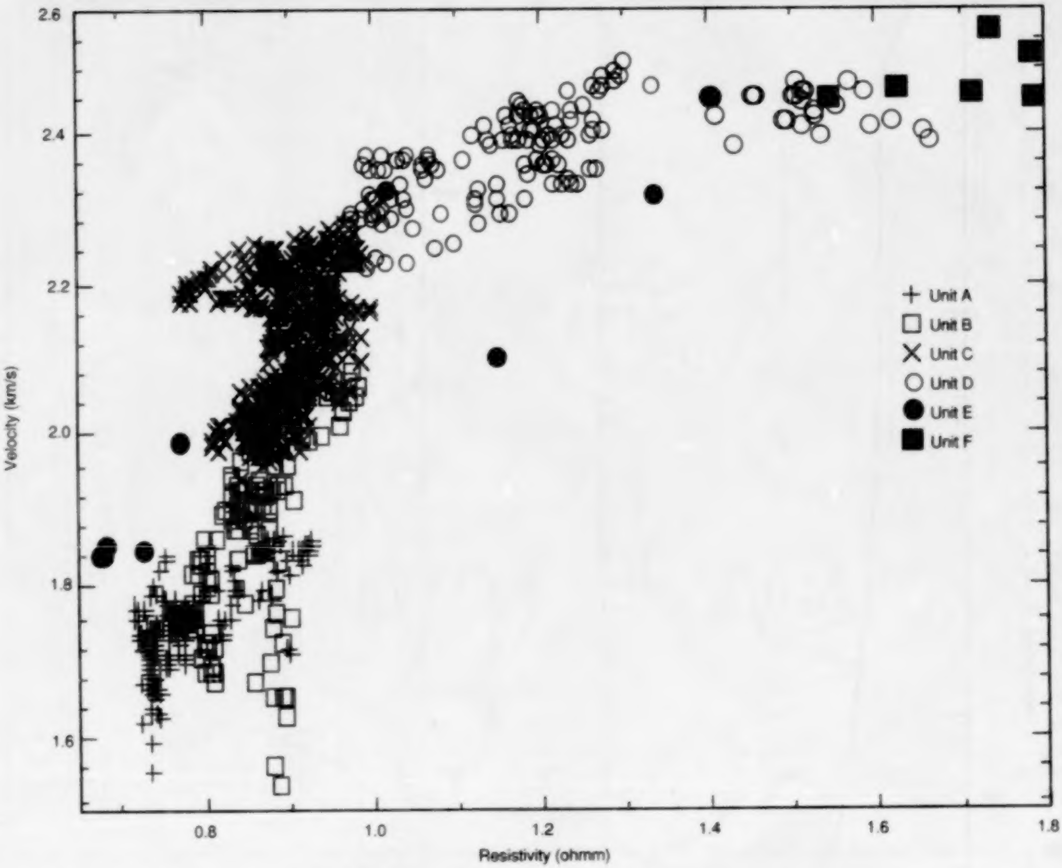

Figure 53. Cross-plot of velocity and resistivity logging data, Hole 803D. Key on figure denotes logging units.

have several sources of data available to us for this purpose. The most accurate source of velocity data is downhole logging that provides an *in-situ* measure of sonic velocity. A successful sonic log was collected in Hole 803D that provided us with high-quality, *in-situ* velocity data for the interval from about 100 to 605 mbsf; the sample interval for this data is approximately 15 cm (60-cm sensor spacing; see "Logging" section, this chapter). To fill the gap in the upper part of the section, laboratory velocity data collected with the Dalhousie digital sediment velocimeter (DSV; see "Physical Properties" section, this chapter) were corrected to *in-situ* values and merged with the logging data (Fig. 55); the sample interval for the laboratory data was approximately 60 cm.

The adjustment of laboratory velocity measurements to *in-situ* values is a complicated task involving corrections for porosity rebound, temperature, and pressure. A carbonate-specific rebound relationship was used to correct the measured porosity for the effect of the removal of overburden, a velocity-porosity relationship was established to correct the velocity, and finally, standard equations for the change of sound speed as a function of pressure and temperature were used to calculate *in-situ* velocity (the same procedure was applied for the adjustment of laboratory density values). Failure to make these adjustments can lead to errors in the traveltime-to-depth conversion of as much as 15%. Details of these corrections can be found in Mayer et al. (1985). Once *in-situ* velocities are calculated, seismic traveltimes can be converted to depth.

The veracity of the traveltime-to-depth conversion can be evaluated through the generation of synthetic seismograms and the comparison of the synthetic seismogram to the actual seismic record collected over the site. Synthetic seismograms were generated using the corrected laboratory velocity and density data merged with the log velocity and density data. These data were resampled at a 1-ms sample interval (approximately 75 cm) and then used to calculate acoustic impedance (the product of velocity and density) and reflection coefficients (the rate of change of the acoustic impedance; Fig. 56). In principle, the reflection coefficient profile represents what a seismic profile would look like if we had a source of infinite bandwidth (perfect resolution). The reflection coefficient profile is convolved with the water-gun seismic source signature measured on the site survey cruise (Fig. 57) to generate a synthetic seismogram. The model assumes plane waves, no multiples, and no attenuation; details of the model are described in Mayer et al. (1985).

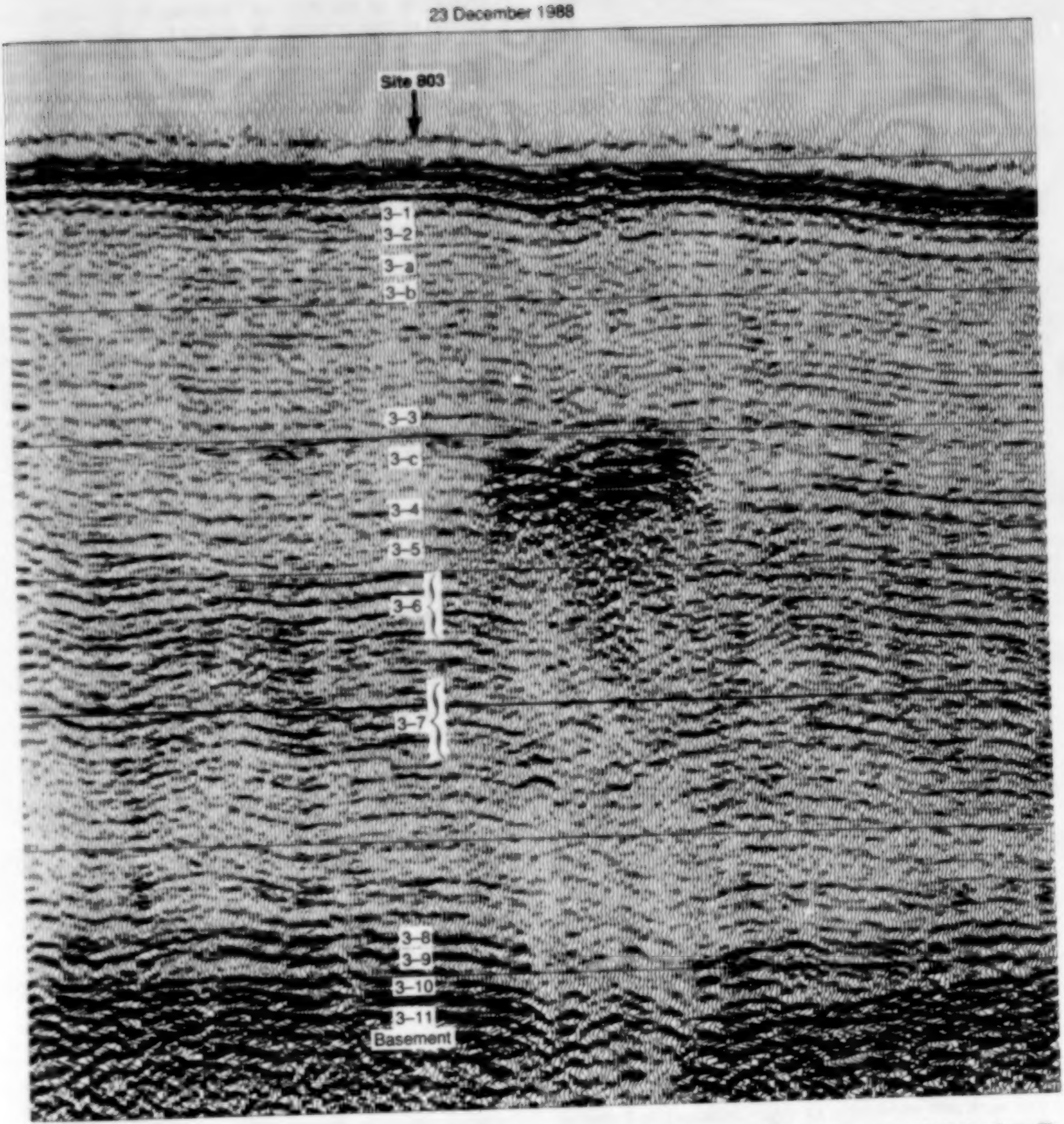

Figure 54. Seismic record collected on the ROUNDABOUT Cruise 11 site survey over Site 803 using the 80-in.^{3} water gun, 70–250 Hz bandpass filter. For details of reflectors (e.g., 3-1, 3-2, 3-a), see Table 18.

Results

A comparison of the synthetic seismogram (filtered with the same filter parameters as the field record) with the seismic profile collected at Site 803 reveals an excellent match between the two (Fig. 58). The seismic data presented here was that collected on the site survey cruise aboard the *Thomas Washington* (see Mayer et al., this volume). There is almost a one-to-one correspondence between reflectors, with the larger reflectors clearly identifiable on both the synthetic seismogram and the field record. Deeper in the section, the synthetic seismogram shows a few smaller events that do not appear on the field record. This is probably caused by the lack of attenuation in the model and thus the preservation of low-amplitude, high-frequency events

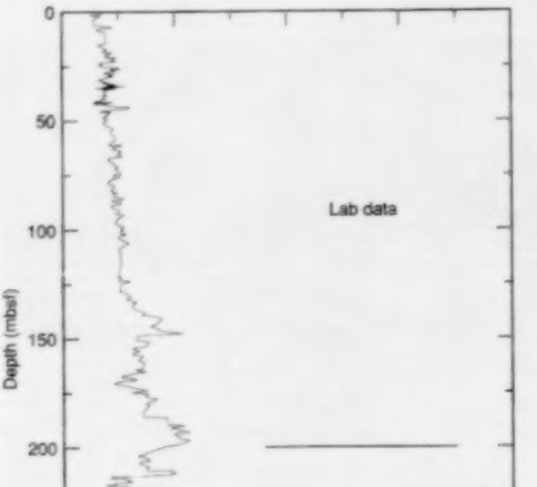

Figure 55. Merged laboratory and log velocity profile. Laboratory values are from 0 to 200 mbsf, log values from 200 to 605 mbsf.

at depth. Nonetheless, the correlation between the field record and the synthetic seismogram indicates that the traveltime-to-depth conversion is fairly accurate (close examination reveals that the model-determined velocities are about 1.2% too high).

Two sets of synthetics were generated, one including the physical properties measured on the few centimeter-thick ash layers found at 181 mbsf and one without these ash values. Although the approximately 1-cm-thick ash layer is probably too thin to be resolved on the field seismic record, the strongly contrasting physical properties associated with it and the interpolation process involved in generating the synthetic make it a clearly distinguishable event on the synthetic seismogram and thus provides a good tie point between the synthetic seismogram and the drilling results.

Given an acceptable traveltime-to-depth conversion, we can now look at the origin of some of the reflectors at Site 803. We emphasize that these are preliminary results that will undoubtedly be modified after more careful analysis.

We were able to identify 11 major reflectors or reflector packages (3-1 through 3-11) on the field record at Site 803 (Fig. 54). These reflectors were selected based on their amplitude and lateral coherency within the immediate area of Site 803. No effort has been made to select reflectors that appear to be regionally correlatable (see Mayer et al., this volume). In addition, three reflectors (a–c) that are large-amplitude events on the synthetic record but are less well defined on the field record (at least at the exact location of Site 803) have been identified. Reflectors were not picked in the upper 30 ms of the seismic record because of the disrupting effect of the outgoing pulse. The depths (in both traveltime and mbsf) as well as the ages (based on the biostratigraphy of Site 803; see "Biostratigraphy" section, this chapter) of these reflectors are presented in Table 18.

Although a detailed understanding of the origin and paleoceanographic significance of these events must await careful shore-based studies, we can use the preliminary physical properties, lithologic, and biostratigraphic data to speculate on the cause of the reflectors. Associated with each major reflector is a change in acoustic impedance. Occasionally, a large reflector can result from the constructive interference of several small impedance contrasts, or a large impedance contrast does not show up as a reflector because of destructive interference (e.g., the impedance contrast at 77 mbsf [95 ms] that does not appear on either the field record or the synthetic). For the most part, however, the major reflectors are associated with a significant change in acoustic impedance (Fig. 56).

The youngest reflectors identified (3-1 and 3-2) are associated with small but rapid increases in bulk density that correspond to carbonate content maxima (Fig. 59) and, in the case of 3-1, a large increase in mean grain size (Fig. 59). No grain size measurements were made over the interval of 3-2. In contrast, the 3-a and 3-b events are the result of density shifts related to carbonate and grain size minima. The association of high carbonate content and large grain size (Reflectors 3-1 and 3-2) probably indicates increased preservation that results from the greater abundance of whole foraminifer tests. The decrease in grain size and carbonate minima associated with Reflectors 3-a and 3-b, on the other hand, probably represent periods of enhanced dissolution.

At 153 mbsf, Reflector 3-3 has yet a different signal with a low carbonate content and a grain size maximum. There is also a sharp increase in velocity at this depth, in opposition to the normal association of increasing velocity with increasing carbonate content and indicative of the dominant role that grain size variations can have in controlling the physical properties of sediments. This association of physical properties may indicate the removal of nannofossils by current winnowing. Reflector 3-c, like its letter-named counterparts, shows a dissolution signal characterized by low carbonate content, small mean grain size, and low velocity. On the synthetic seismogram that includes the ash layer, the ash occurs a few meters above Reflector 3-c. The level of the ash layer precisely corresponds to the top of the MSR (Fig. 54) and may indicate that volcanism was associated with the emplacement of the MSR. This association may also place an age constraint on the MSR.

Reflector 3-4 is at a velocity, density, and carbonate minimum; grain size data is ambiguous with the reflector lying in a transitional position between a small change from fairly coarse to fine-grained sediments. The signal appears to be one of dissolution. The sedimentologists place the ooze-chalk transition several meters below Reflector 3-4 (see "Lithostratigraphy" section, this chapter). This transition is clearly seen in the sharp change in slope of both the velocity and density curves (Fig. 56). Reflector 3-5, at about 240 mbsf, presents more of a mystery. Although it lies several meters below a large change in carbonate content, the reflector appears to be more related to the rapid changes in velocity in this part of the section. Carbonate data is spotty and no grain size information is available for this interval, so it is difficult to speculate on the origin of these velocity changes. It is possible, however, that these are the result of high-frequency changes in the degree of cementation.

Reflector 3-5 lies at the top of a major hiatus (see "Biostratigraphy" section, this chapter); the large contrast in age across this stratigraphic break may result in a rather sharp jump in the state of induration of the sediment and thus the velocity and density structure (Fig. 56). Early cementation has a large effect on the rigidity of the sediment; rigidity is the dominant parameter in determining the sonic velocity of a material. Thus, small

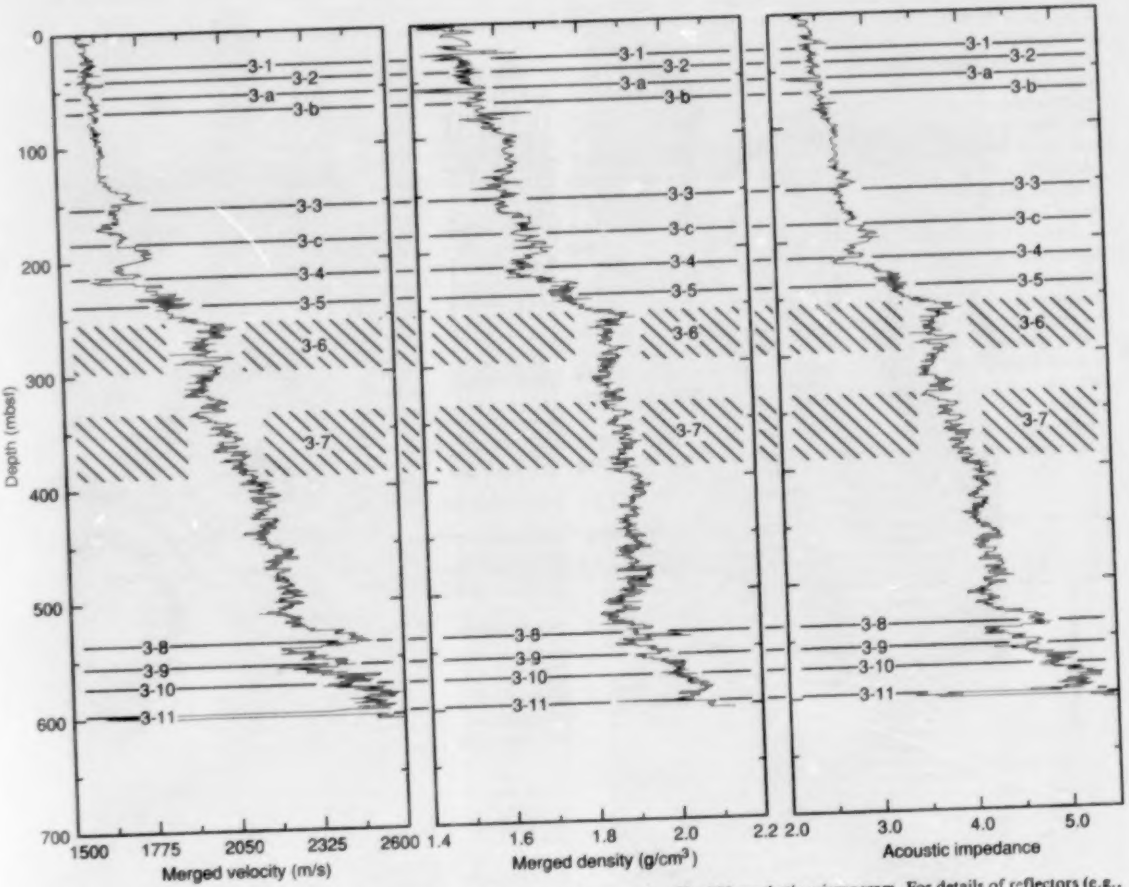

Figure 56. Velocity, density, acoustic impedance, and reflectivity data used for generating Site 803 synthetic seismogram. For details of reflectors (e.g., 3-1, 3-2, 3-a), see text.

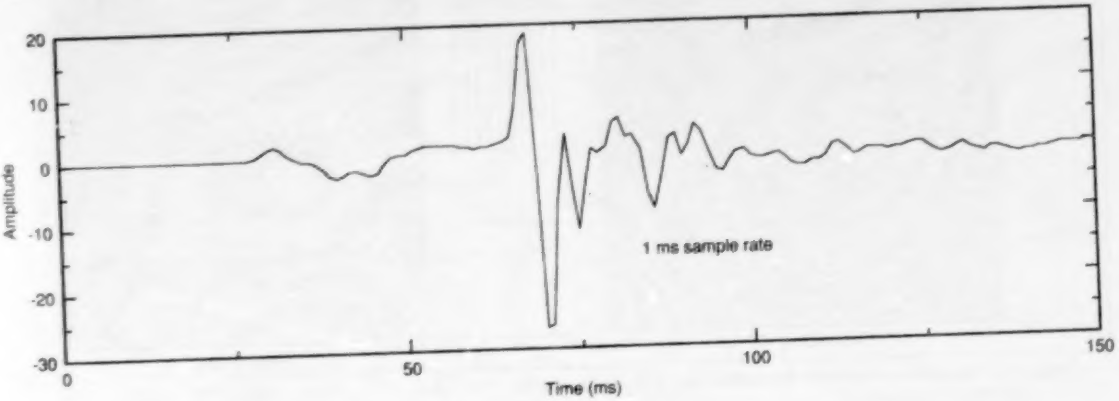

Figure 57. *Thomas Washington* 80-in.^{3} water-gun, farfield source signature.

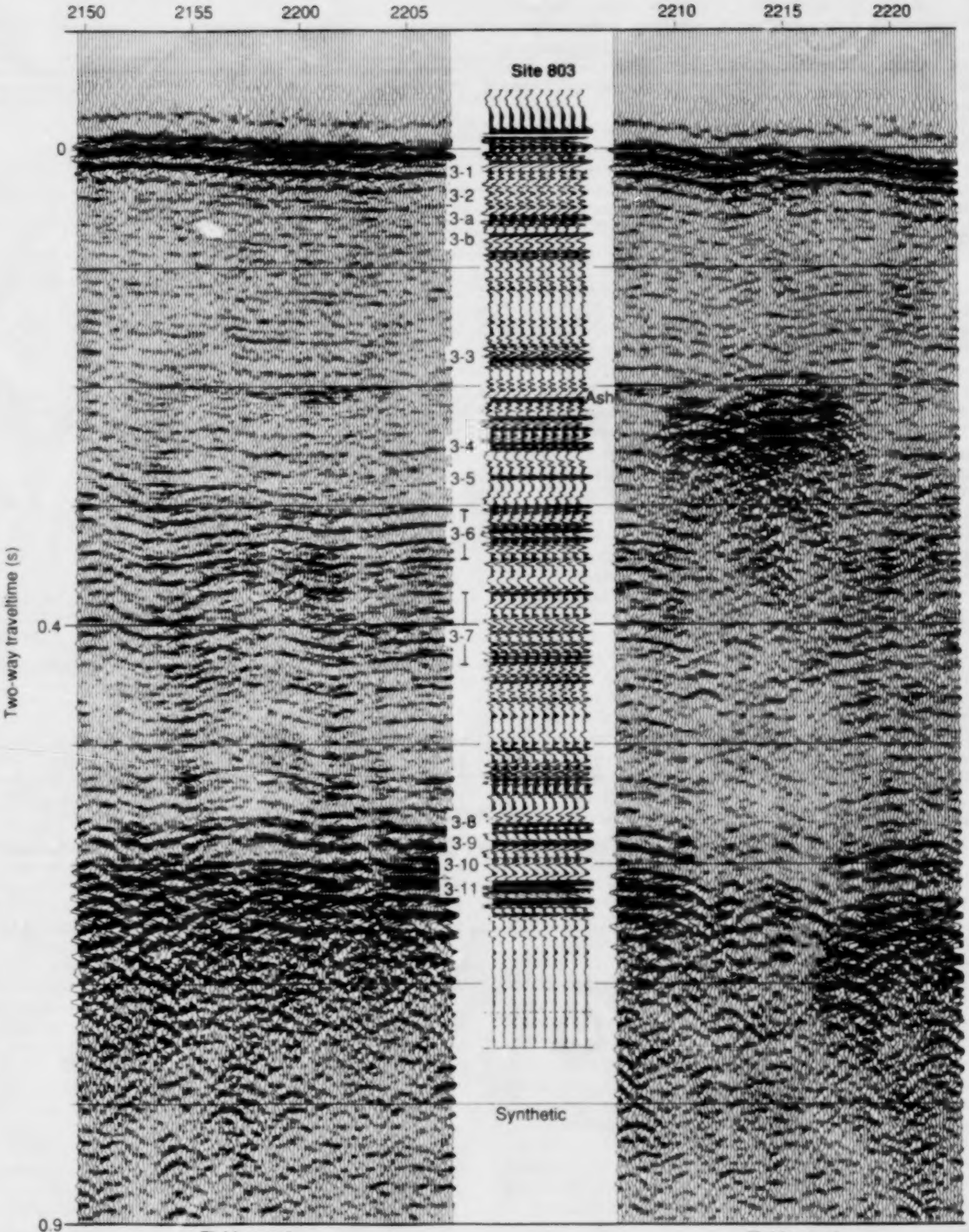

Figure 58. Comparison of synthetic seismogram and field record, Site 803.

Table 18. Summary of traveltimes, depths, and ages for Site 803 reflectors.

Reflector	Two-way seismic (s)	Traveltime synthetic (s)	Depth		Age (Ma)
			Seismic (mbsf)	Synthetic (mbsf)	
3-1	0.036	0.037	29	30	2.58
3-2	0.051	0.052	41	42	3.3–3.4
3-3	0.188	0.190	153	156	8.0–8.1
3-4	0.256	0.250	212	215	12.3–12.5
3-5	0.282	0.288	234	240	14.5–14.83
3-6	0.300–0.345	0.305–0.350	254–296	255–297	21.5–23.02
3-7	0.385–0.440	0.385–0.440	335–392	335–392	24.3–27.25
3-8	0.569	0.572	534	538	36.5–37.00
3-9	0.585	0.589	552	558	38.00
3-10	0.605	0.605	576	576	39.00
3-11	0.620	0.622	595	598	40.83
3-a		0.072		57	4.3
3-b		0.087		70.6	5.03
3-c		0.222		183	9.72

Notes: Depths and traveltimes to seismic events are picked on both the synthetic seismograph (synthetic) and the field record (seismic). Ages are from sedimentation rate curves (see "Sedimentation Rates" section, this chapter).

cyclic variations in the degree of cementation can result in a velocity structure much like that observed near Reflector 3-5.

Reflectors 3-6 and 3-7 are the two reverberant reflector packages in the lower part of the section at Site 803. Although the synthetic seismogram allows for the identification of individual reflectors within these packages, such detail is beyond the scope of this report and will be deferred to shore-based study. These reverberant packages occur within a zone of fairly high, but strongly fluctuating carbonate values (Fig. 59) that result in a highly variable density and, in particular, velocity structure. Carbonate content, velocity, and density all increase together, but a full understanding of the oceanographic processes responsible for this signal will have to await more detailed study.

The deepest reflectors (3-8 to 3-11) are the result of large decreases in velocity and density that accompany decreases in carbonate content and the appearance of significant amounts of biogenous silica. Biogenic silica typically results in decreased densities and velocities because of the low grain density of the siliceous tests (2.1 g/cm^3) and the ability of siliceous tests to maintain an open structure despite substantial overburden. This is borne out by the changes in the log resistivity (a porosity proxy) that correlate with these low-velocity zones (see "Logging" section, this chapter). The relative roles of productivity

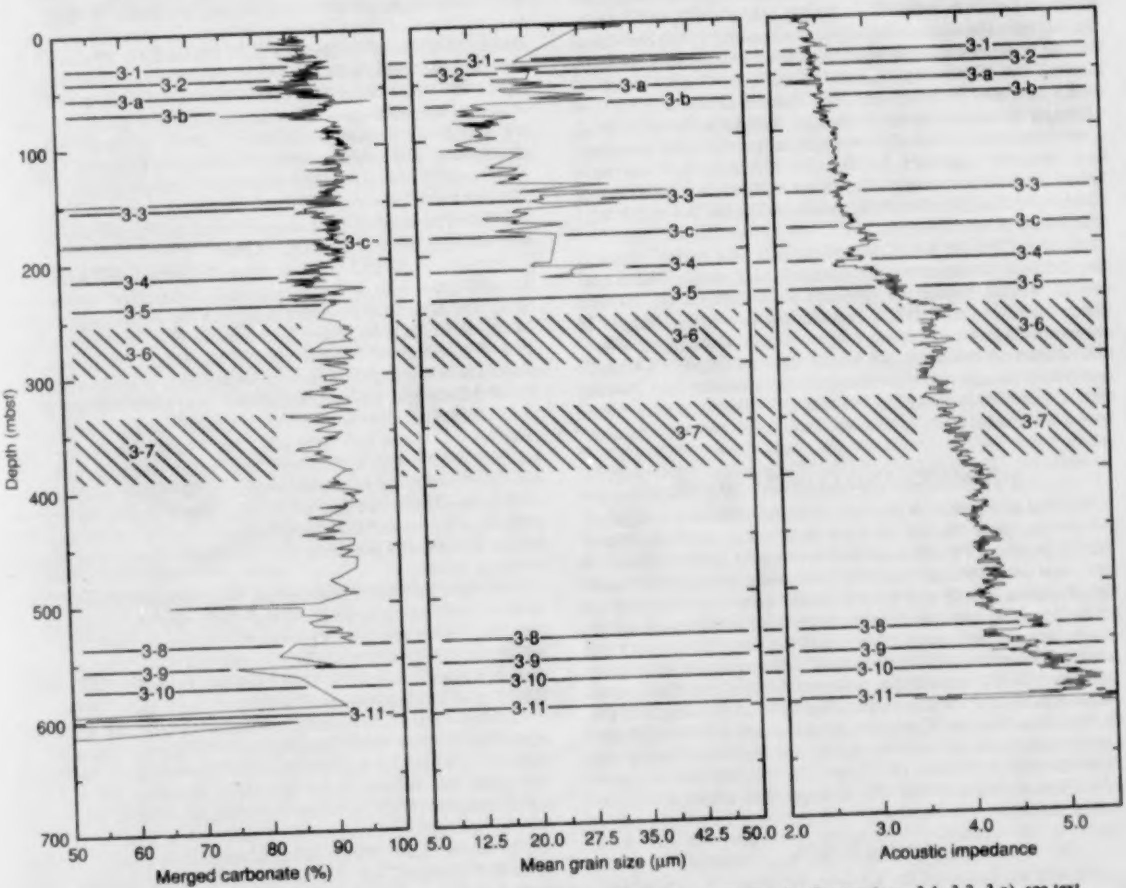

Figure 59. Carbonate content, grain size, and acoustic impedance vs. depth at Site 803. For details of reflectors (e.g., 3-1, 3-2, 3-a), see text.

and dissolution in determining the sedimentary composition of this interval must await further study. The density and velocity logs, and thus the seismic modeling, stopped short of a thin chert layer partially recovered and clearly identified on the logs, a 4.5-m-thick claystone, and finally basalt recovered at 626 mbsf. Extrapolating from existing data places basement at approximately 640 m/s below seafloor (Fig. 54).

Although the regional and global significance of the seismic events examined at Site 803 cannot be evaluated until more sites are drilled, it is interesting to speculate on the possible paleoceanographic significance of some of these events. Reflectors 3-1 and 3-2 are events that appear to be related to increases in carbonate preservation in the western equatorial Pacific. Reflector 3-1 at 2.58 Ma is within 10,000 yr of the time cited by Jansen and Sjoholm (1990) for the initiation of true Northern Hemisphere glaciation and the 3.3–3.4 Ma age for Reflector 3-2 corresponds to a time noted for increased North Atlantic Deep Water (NADW) and a shift in the benthic $\delta^{18}O$ record possibly related to increased Antarctic Bottom Water (AABW) activity (Backman, 1979; Prell, 1985).

In contrast, Reflectors 3-a and 3-b at 4.3 and 5.03 Ma, respectively, which indicate dissolution events in the Pacific, are associated with peaks in carbonate preservation in the Atlantic (Jansen and Sjoholm, 1990). The 5.03-Ma event may be related to the isolation of the Mediterranean (the Messinian interval). As noted before (Berger, 1970; Mayer et al., 1986), the chemistry, and thus the seismic response of sediments of the equatorial Pacific, appears closely linked with the history of Atlantic water masses. The winnowing indicated as the cause for Reflector 3-3 (8–8.1 Ma) may be a regional phenomenon as this is not a time of major paleoceanographic change. Reflector 3-c (9.72 Ma), apparently another dissolution event, is, on the other hand, coincident with a central Pacific-wide reflector that has been linked to global oceanographic events and, in particular, major changes in NADW circulation as is Reflector 3-4 (12.3–12.5 Ma; Mayer et al., 1986).

Reflector 3-5 (15.8 Ma) lies at the end of a major hiatus at Site 803 (see "Biostratigraphy" section, this chapter); this hiatus (in varying degrees of severity) is widespread (Keller and Barron, 1983) and also has been linked to major changes in ocean circulation and seismic events. Finally, the deepest reflectors, including Reflector 3-8 at the Eocene/Oligocene boundary, clearly represent major changes in productivity and dissolution at Site 803. Although it is likely that these too may correspond to regional if not global events, it is too early to speculate at this point.

SUMMARY AND CONCLUSIONS

Site 803 is situated on the equatorial northeastern margin of the Ontong Java Plateau in 3410 m of water at 2°26′N and 160°32′E. It was drilled as part of a Neogene depth transect to serve as a deep-water anchor site. The primary objective was to sample a section affected by substantial carbonate dissolution, yet sufficiently complete to provide a record of dissolution gradients, events, and cycles, that could be tied into a biostratigraphic framework. Other objectives were to provide Paleogene and Cretaceous sediments for paleoceanographic studies and to obtain basement rock that might shed light on the origin of the Ontong Java Plateau. The site was located on a *Thomas Washington* single-channel seismic (SCS) line acquired during the ROUNDABOUT Cruise 11 "DANCER" survey between proposed Sites OJP-4 and OJP-4B, upslope from a mid-section reflector (MSR).

Coring Results

Site 803 was occupied for 8.7 days. We cored 991.3 m of sediments: 552.4 m with the APC (103% recovery), 394.9 m with the XCB (63% recovery), and 7.0 m with the RCB (38% recovery). Also, we cored 25.6 m of basalt, recovering a total of 9.6 m in all (38% recovery). Total core recovery was 837.4 m. We drilled four holes as follows: Hole 803A with the APC from 0 to 55.5 mbsf; Hole 803B with the APC from 0 to 61.3 mbsf; Hole 803C with the APC from 19 to 237.5 mbsf; and Hole 803D with the APC from 0 to 217.1 mbsf, with the XCB from 217.1 to 612.0 mbsf, and with the RCB from 612.0 to 656.0 mbsf.

The recovered sediments range in age from Pleistocene to early Late Cretaceous; they were divided into three units. The uppermost unit, Unit I, takes up most of the section (0–563.7 mbsf); it ranges from late Eocene to Pleistocene in age and consists of nannofossil ooze and chalk to foraminifer nannofossil ooze and chalk. Unit II (563.7–621.8 mbsf) ranges from the middle to the late Eocene in age and consists of approximately 58 m of nannofossil chalk with radiolarians, radiolarian nannofossil chalk, nannofossil radiolarite, and minor amounts of chert. Unit III (621.8–626.3 mbsf) ranges from the early Late Cretaceous to the middle Eocene in age and is composed of claystone and clayey siltstone, with minor radiolarian-rich intervals. Resistivity logs suggest that this lithology continues from 621.8 mbsf to basement at 630.4 mbsf.

The record is continuous from the Pleistocene to the lower Miocene, where there is a significant stratigraphic break at 245.9 mbsf with a double hiatus within the period from 22 to 15 Ma, the first of three major stratigraphic breaks encountered above the Cretaceous/Tertiary (K/T) boundary. The other two stratigraphic breaks occur across the Paleocene/Eocene boundary (~45–~58 Ma) at 621.8 mbsf and in the Paleocene (~58–~66 Ma) immediately below. The section below the K/T boundary, which was penetrated at 622.25 mbsf, is condensed and, presumably, also contains several substantial hiatuses.

In Unit I, the ooze-chalk transition occurs between 210 and 220 mbsf and provides the basis for division into Subunits IA and IB. The logging data suggest that this transition extends over 60 m in the sedimentary column.

Subunit IA (0–217 mbsf) consists of nannofossil ooze, nannofossil ooze with foraminifers, and foraminifer nannofossil ooze. The foraminifer content is high in the Pleistocene and adjacent upper Pliocene ooze and decreases downhole through the first 30 to 60 mbsf, so that most of the subunit is nannofossil ooze. There is a slight increase in foraminifer content within the upper Miocene sediments, somewhat below the middle of the section. Bioturbation is ubiquitous. Colors are dominantly various types of white and light gray; the Pleistocene section also exhibits colors with a yellowish hue. Faint green, purple, and red color bands are common, except in the upper middle Miocene nannofossil ooze (ca. 14–10 Ma). These appear to have an origin analogous to "Liesegang" rings, which arise through diffusion along redox gradients that surround objects that contain reducing matter.

Sediment instability is indicated by microfaulted and discordant color banding at several levels in the section, especially in the lower Pliocene and uppermost Miocene ooze, but also within the upper and middle Miocene portions. One thin discrete ash layer is present in Unit I (at 181.2 mbsf in Hole 803D) that clearly ties the recovered section to the logging data.

Subunit IB (217–564 mbsf) consists of nannofossil chalk and nannofossil chalk with foraminifers. Its upper boundary is marked by a shift to higher velocity in the log data, with only one more low-velocity layer downhole between 240 and 250 mbsf. Subunit IB is much like the younger Subunit IA, except for the presence of lithification. Colors are similar, as is intensity of bioturbation. Color banding appears in lower Oligocene sediments (around 420–520 mbsf). The bands become more abundant, intense, and distinct downhole in this interval. They are continuous across and through burrows.

Radiolarians are present in low proportions throughout the section and their abundance never exceeds 7% in smear slide analyses. Minor amounts of chert were recovered at 546.15 mbsf in lowermost Oligocene sediments. A marked decrease in pore-water silica near this level indicates the onset of silica precipitation. Chert formation and enhanced grain cementation in the upper Eocene chalk is probably responsible for the local high-velocity layers detected in the logs at 521–541 and 546–558 mbsf and below 564 mbsf.

Unit II (564–622 mbsf) consists of interbedded upper to middle Eocene nannofossil chalk with radiolarians, radiolarian nannofossil chalk, and nannofossil radiolarite. Drilling disturbance was significant in this unit. Minor amounts of chert were recovered. These sediment types produce distinctive records in the physical properties measurements, logging data, and seismic reflection profiles. Chert presumably is more abundant than coring reveals: it may appear as a thin bed with high values in the resistivity log and with high sound velocities; furthermore, it may be responsible for a major reflector on the seismic profiles at that depth.

Unit III (622–626 mbsf) is surprisingly thin for the age range (middle Eocene–early Late Cretaceous). It is composed of dark-colored claystone and siltstone, predominated by deep-sea siliciclastic sediments. Unit III also contains a complete Cretaceous/Tertiary boundary sequence as well as several major unconformities.

In Unit IV, nine basalt subdivisions were recognized based on the presence of intercalated limestones or breccias. The age, based on paleontology, is probably Cenomanian or older. The basalts are predominantly aphyric, fine-grained, and nonvesicular tholeiites. Shipboard XRF measurements indicate that the basalts are fairly evolved and, in terms of their Zr/Nb ratio (15–17), distinct from both normal mid-ocean-ridge basalt (Zr/Nb greater than 30) and typical oceanic-island tholeiites (Zr/Nb commonly less than 12). Slight compositional variations within the basalts indicate that they may have been derived from more than one parental magma.

Seismic Stratigraphy

Site 803 is characterized by a layer-cake seismic stratigraphy. The 14 reflectors that have been identified in the synthetic seismograms, generated from Site 803 physical property and logging data, almost exactly match those in the SCS survey profiles (see "Seismic Stratigraphy" section, this chapter). Reflectors 3-1 and 3-2 (at 2.6 and 3.3–3.4 Ma, respectively) appear to be related to fluctuations in carbonate preservation in the western equatorial Pacific and possibly linked to the initiation of Northern Hemisphere glaciation and the increased activity of North Atlantic Deep Water (NADW) (cf. Mayer et al., 1986). Reflectors 3-a and 3-b (at 4.3 and 5.0 Ma, respectively) are believed to be indicative of dissolution events.

The winnowing suggested to be the possible cause for Reflector 3-3 (at 8–8.1 Ma), as indicated by the high sand content at about 146 mbsf at Site 803, may be a regional phenomenon unrelated to a major paleoceanographic change. However, a similar winnowing event is indicated in DSDP Site 586 at about that time. Reflector 3-c (9.7 Ma) apparently coincides with a central Pacific-wide reflector that has been linked to global oceanographic events, in particular, to major changes in NADW production. The same is true for Reflector 3-4 (at 12.3–12.5 Ma; Mayer et al., 1986). Reflector 3-5 (at 15.1–15.5 Ma) coincides with a major hiatus, typical for this period of Antarctic cooling. Reflector packages 3-6 and 3-7 mark the late Oligocene to early Miocene transition period. They presumably arose in response to carbonate fluctuations produced as a consequence of climatic change when the Drake passage opened. The deepest reflectors, including 3-8 near the Eocene/Oligocene boundary, clearly represent major changes in depositional style and diagenesis at Site 803, especially in the accumulation of silica.

Sequence of Events

Widespread volcanism occurred in the region of the Ontong Java Plateau in Aptian-Albian time. At Site 803 on the flank of the plateau, the thin, pillowed nature of the flows implies that their feeder vents were not very distant and that eruption rates were low. The severe alteration of the uppermost lava flow of Unit IV coupled with the absence of metalliferous sediments directly overlying the basalt indicates the presence of a hiatus of unknown origin and duration.

The depositional history at Site 803 began in the early Late Cretaceous with slow and/or discontinuous siliciclastic sedimentation below the CCD. Sedimentation apparently was continuous across the K/T boundary. The fact that these sediments are preserved is remarkable and calls for an explanation. We propose early lithification as an answer. The presence of a major hiatus, occupying most of the Paleocene to early Eocene time, suggests erosional activity within or at the end of this period. The hiatus ended with the onset of pelagic sedimentation in the middle Eocene, suggesting a deepening of the CCD, as well as the return of conditions favorable for the production and preservation of biogenic silica (cf. Berger and Winterer, 1974; van Andel et al., 1975). Since the late Eocene, carbonate deposition has dominated in this location. Sedimentation rates, about 7 m/m.y. during the middle Eocene, doubled in the late Eocene, to 13 m/m.y. at 40 Ma.

Sedimentation at Site 803, continuous across the Eocene/Oligocene boundary, remained near 13 m/m.y. into the early Miocene. Paleomagnetic analyses of the Oligocene sediments have resulted in a tentative magnetostratigraphy spanning Chrons 11 through 7. Preliminary analyses indicate a paleolatitude of 4.5°S for Site 803 during the Oligocene, which, in turn, implies that the Ontong Java Plateau has been part of the Pacific Plate for the past 30 m.y. In the early Miocene, the one significant Neogene hiatus developed, involving the record between 22 and 15 Ma (NH2 of Keller and Barron, 1983). The sediments above the hiatus, of middle Miocene age, were deposited at rates near 10 m/m.y. The hiatus may be related to earthquake activity associated with a resurgence of transcurrent motion along nearby fracture zones caused by a change in Indo-Australia plate motion. This event, which took place about 16 Ma, resulted in renewed convergence along the Melanesian Subduction Zone (Manus–North Solomon–Vitiaz trenches) and a rejuvenation of volcanism along the Melanesian Arc (Kroenke, 1984).

In the late middle Miocene, ash was erupted from a not-too-distant source, a source that may also have been responsible for the emplacement of a nearby mid-section reflector. Although possibly related to incipient Solomon Island Arc volcanism, the ash more likely is the product of nearby tectonic volcanism, resulting from transtensive stress release, linked again to a resurgence of transcurrent motion along nearby fracture zones that was caused by still another change in Indo-Australian Plate motion. The latter event, occurring roughly ca. 10–12 Ma, also probably coincided with the formation of the new Solomon Island Subduction Zone (along the New Britain–San Cristobal trenches). In the late Miocene, sedimentation rates abruptly increased to between 25 and 30 m/m.y., with peak rates centered on ~7 Ma. In the Pliocene, sedimentation rates decreased to 15 m/m.y.; in the Pleistocene, they decreased still further to about 10 m/m.y. The magnetic stratigraphy shows that the decrease takes place at the base of the Olduvai Subchron (1.88 Ma).

Comparison of Site 803 with Sites 288, 289/586, and 462

Of the sites previously drilled on the Ontong Java Plateau, Sites 289/586 are the nearest to Site 803 and contain the most complete and well-studied sections. In comparing the sites, a few notable similarities were observed. The basement basalts at Site 803 are compositionally quite similar (at least in terms of Zr and Nb) to the basalt drilled at Site 289 as well as to the few analyzed basement lavas of Malaita (eastern Solomon Islands) and to the basalt flows and sills drilled at Site 462 in the Nauru Basin northeast of the Ontong Java Plateau.

Numerous hiatuses were encountered in the lower Paleogene and Upper Cretaceous sections drilled at DSDP Sites 288 and 289 on the Ontong Java Plateau that may well correlate with missing intervals at Site 803. These hiatuses may be associated with tectonic events that occurred around the region during Late Cretaceous and early Paleogene time. For example, hiatuses that occur deep in the section at Sites 288 and 289, and perhaps even at Site 807, may be related to the Campanian volcanic events recorded at Site 462 in the Nauru Basin (Moberly, Schlanger, et al., 1986). Early Paleogene hiatuses at all three sites may be related, in part, to the initiation of subduction along the Papuan–New Caledonia trenches and the end of seafloor spreading in the Tasman and Coral Sea basins (Kroenke, 1984).

With regard to Paleogene sediments, it appears that similar conditions, favorable for the supply and preservation of silica, existed in the Eocene at Sites 803 and 289. Such conditions are typical of the entire central Pacific (Berger, 1973; van Andel et al., 1975). Likewise, the Eocene record at both sites was interrupted by several intervals of erosion and/or nondeposition. The descriptions of the Neogene nannofossil oozes and chalks with their various subordinate components also are quite similar for these two sites. However, there are substantial differences in detail, especially with regard to sedimentation rates. These differences may be summarized as follows:

1. The basalts at Site 803 are pillow basalts that comprise many thin flows in contrast to the single massive flow drilled at Site 289.
2. In the sediments, no chert was observed in the Miocene at Site 803, and the amount of chert encountered deep in the hole was minor in contrast to the massive cherts encountered at Site 289 in the middle Eocene–Upper Cretaceous section.
3. A complete K/T transition sequence was found at Site 803 (albeit within a claystone-siltstone sequence) as opposed to the hiatus encountered at Site 289.
4. Significantly, and in contrast to Site 289, no stratigraphic break was observed at the Eocene/Oligocene boundary at Site 803.
5. On the other hand, sedimentation rates were higher at Sites 289/586 than at Site 803 because of the shallower depth of the former (2200 vs. 3400 m) and no Miocene hiatus was observed at Sites 289/586.

When comparing overall sedimentation rate patterns of Site 803 with those of Sites 289/586, one notes striking changes in the ratios for the Neogene sediments. This ratio ranges from 0.32 (for the lower Pliocene) to 0.77 (for the upper Miocene). Expressed inversely, the rates at Site 289 are higher by a factor of between 3 and 1.3. Some of this variation is quite probably a result of the changing intensity of winnowing on top of the plateau, but most of it must be ascribed to the changing intensity of dissolution below 3000 m depth.

REFERENCES

Andrews, J. E., Packham, G., et al., 1975. *Init. Repts. DSDP,* 30: Washington (U.S. Govt. Printing Office).

Backman, J., 1979. Pliocene biostratigraphy of DSDP Sites 111 and 116 from the North Atlantic Ocean and the age of the Northern Hemisphere Glaciation. *Stockholm Contrib. Geol.*, 32:115–137.

Barron, J. A., 1985. Miocene to Holocene planktonic diatoms. *In* Bolli, H. M., Saunders, J. B., and Perch-Nielsen, K. (Eds.), *Plankton Stratigraphy:* Cambridge (Cambridge Univ. Press), 763–809.

Berger, W. H., 1970. Biogenous deep-sea sediments: fractionation by deep-sea circulation. *Geol. Soc. Am. Bull.*, 81:1385–1401.

________, 1973. Cenozoic sedimentation in the eastern tropical Pacific. *Geol. Soc. Am. Bull.*, 84:1941–1954.

Berger, W. H., and Johnson, T. C., 1976. Deep-sea carbonates: dissolution and mass wasting on Ontong Java Plateau. *Science,* 192:785–787.

Berger, W. H., Johnson, T. C., and Hamilton, E. L., 1977. Sedimentation on Ontong-Java Plateau: observations on a classic "carbonate monitor." *In* Anderson, N. R., and Malahoff, A. (Eds.), *The Fate of Fossil Fuel* CO_2 *in the Oceans:* New York (Plenum Press), 543–567.

Berger, W. H., and Mayer, L. A., 1978. Deep-sea carbonates: acoustic reflectors and lysocline fluctuations. *Geology,* 6:11–15.

Berger, W. H., and Winterer, E. L., 1974. Plate stratigraphy and the fluctuating carbonate line. *In* Hsü, K. J., and Jenkyns, H. C. (Eds.), *Pelagic Sediments on Land and Under the Sea.* Spec. Publ., Int. Assoc. Sedimentol., 1:11–48.

Berggren, W. A., Kent, D. V., and Flynn, J. J., 1985a. Jurassic to Paleogene: Part 2. Paleogene geochronology and chronostratigraphy. *In* Snelling, N. J. (Ed.), *The Chronology of the Geological Record.* Mem. Geol. Soc. (London), 10:141–195.

Berggren, W. A., Kent, D. V., and Van Couvering, J. A., 1985b. The Neogene: Part 2. Neogene geochronology and chronostratigraphy. *In* Snelling, N. J. (Ed.), *The Chronology of the Geological Record.* Mem. Geol. Soc. (London), 10:211–260.

Bleil, U., 1985. The magnetostratigraphy of northwest Pacific sediments, Deep Sea Drilling Project Leg 86. *In* Heath, G. R., Burckle, L. H., et al., *Init. Repts. DSDP,* 86: Washington (U.S. Govt. Printing Office), 441–458.

Bolli, H. M., and Saunders, J. B., 1985. Oligocene to Holocene low latitude planktic foraminifera. *In* Bolli, H. M., Saunders, J. B., and Perch-Nielsen, K. (Eds.), *Plankton Stratigraphy:* Cambridge (Cambridge Univ. Press), 155–262.

Burckle, L. H., 1972. Late Cenozoic planktonic diatom zones from the eastern equatorial Pacific. *Nova Hedwigia Beih.*, 39:217–246.

Elderfield, H., Gieskes, J. M., Baker, P. A., Oldfield, R. K., Hawkesworth, C. J., and Miller, R., 1982. $^{87}Sr/^{86}Sr$ and $^{18}O/^{16}O$ ratios, interstitial water chemistry and diagenesis in deep-sea carbonate sediments of the Ontong-Java Plateau. *Geochim. Cosmochim. Acta,* 46:2259–2268.

Emeis, K.-C., and Kvenvolden, K. A., 1986. Shipboard organic geochemistry on *JOIDES Resolution.* ODP Tech. Note, No. 7.

Espitalié, J., Laporte, J. L., Madec, M., Marquis, F., Leplat, P., Paulet, J., and Boutfeu, A., 1977. Method rapide de caracterisation des roches mère de leur potentiel petrolier et de leur degree d'evolution. *Rev. Inst. Fr. Pet.*, 32:23–42.

Fenner, J., 1984. Eocene-Oligocene planktic diatom stratigraphy in the low latitudes and the high southern latitudes. *Micropaleontology,* 30:319–342.

Floyd, P. A., 1986. Petrology and geochemistry of oceanic intraplate sheet-flow basalts, Nauru Basin, Deep Sea Drilling Project Leg 89. *In* Moberly, R., Schlanger, S. O., et al., *Init. Repts. DSDP,* 89: Washington (U.S. Govt. Printing Office), 471–497.

Gieskes, J. M., 1981. Deep-sea drilling interstitial water studies: implications for chemical alteration of the oceanic crust, Layers I and II. *In* Warme, J. E., Douglas, R. G., and Winterer, E. L. (Eds.), *The Deep Sea Drilling Project: A Decade of Progress.* Spec. Publ., Soc. Econ. Paleontol. Mineral., 32:149–167.

Gordon, R. G., 1983. Late Cretaceous apparent polar wander of the Pacific plate: evidence for a rapid shift of the Pacific hotspots with respect to the spin axis. *Geophys. Res. Lett.*, 10:709–712.

Hammond, S. R., Kroenke, L. W., and Theyer, F., 1975. Northward motion of the Ontong-Java Plateau between -110 and -30 m.y.: a paleomagnetic investigation of DSDP Site 289. *In* Andrews, J. E., Packham, G., et al., *Init. Repts. DSDP,* 30: Washington (U.S. Govt. Printing Office), 415–418.

Humphris, S. E., Thompson, R. N., Gibson, I. L., and Marriner, G. F., 1980. Comparison of geochemistry of basalts from the East Pacific Rise, OCP Ridge and Siqueiros Fracture Zone, Deep Sea Drilling Project, Leg 54. *In* Rosendahl, B. R., Hekinian, R., et al., *Init. Repts. DSDP,* 54: Washington (U.S. Govt. Printing Office), 635–649.

Hussong, D. M., Wipperman, L. K., and Kroenke, L. W., 1979. The crustal structure of the Ontong Java and Manihiki oceanic plateaus. *J. Geophys. Res.*, 84:6003–6010.

Ingle, J. C., Jr., Suehiro, K., von Breymann, M. T., et al., 1990. *Proc. ODP, Init. Repts.*, 128: College Station, TX (Ocean Drilling Program).

Jackson, E. D., Bargar, K. E., Fabbi, B. P., and Heropoulos, C., 1976. Petrology of the basaltic rocks drilled on Leg 33 of the Deep Sea Drilling Project. *In* Schlanger, S. O., Jackson, E. D., et al., *Init. Repts. DSDP,* 33: Washington (U.S. Govt. Printing Office), 571–630.

Jansen, E., and Sjoholm, J., 1990. Late Miocene–Pleistocene evolution of Northern Hemisphere and global glaciations. *Nature*.

Johanssen, A., 1931. *A Descriptive Petrography of the Igneous Rocks* (Vol. 1): Chicago (Univ. of Chicago Press).

Johnson, T. C., Hamilton, E. L., and Berger, W. H., 1977. Physical properties of calcareous ooze: control by dissolution at depth. *Mar. Geol.*, 24:259–277.

Kaminski, M. A., Gradstein, F. M., Berggren, W. A., Geroch, S., and Beckmann, J. P., 1986. Flysch-type agglutinated foraminiferal assemblages from Trinidad: taxonomy, stratigraphy and paleobathymetry. *Proc. Second Int. Workshop on Agglutinated Foraminifera,* Vienna.

Keller, G., and Barron, J. A., 1983. Paleoceanographic implications of Miocene deep sea hiatuses. *Geol. Soc. Am. Bull.*, 94:590–613.

Kempton, P. D., Autio, L. K., Rhodes, J. M., Holdaway, M. J., Dungan, M. A., and Johnson, P., 1985. Petrology of basalts from Hole 504B, Deep Sea Drilling Project, Leg 83. *In* Anderson, R. N., Honnorez, J., et al., *Init. Repts. DSDP,* 83: Washington (U.S. Govt. Printing Office), 129–164.

Kennett, J. P., and Srinivasan, M. S., 1983. *Neogene Planktonic Foraminifera: A Phylogenetic Atlas:* Stroudsburg, PA (Hutchinson Ross).

Kroenke, L. W., 1972. Geology of the Ontong Java Plateau. *Hawaii Inst. Geophys. Rep.*, HIG 72-5.

———, 1984. Cenozoic Tectonic Development of the Southwest Pacific. *U.N. ESCAP, COOP/SOPAC, Tech. Bull.*, No. 6.

Kroenke, L. W., Jouannic, C., and Woodward, P. (Comps.), 1983. Bathymetry of the Southwest Pacific: Chart 1 of the Geophysical Atlas of the Southwest Pacific, CCOP/SOPAC.

Kroenke, L. W., Resig, J., and Cooper, P. A., 1986. Tectonics of the southeastern Solomon Islands: formation of the Malaita Anticlinorium. *In* Vedder, J. G., Pound, K. S., and Boundy, S. Q. (Eds.), *Geology and Offshore Resources of Pacific Island Arcs, Central and Western Solomon Islands.* Circum-Pacific Counc. Energy Mineral Resourc., Earth Sci. Ser., 4:109–116.

Lee, H. J., 1982. Bulk density and shear strength of several deep-sea calcareous sediments. *In* Demars, K. R., and Chaney, R. C. (Eds.), *Geotechnical Properties, Behavior, and Performance of Calcareous Soils.* ASTM Spec. Tech. Publ., 777:54–78.

McDuff, R. E., 1981. Major cation gradients in DSDP interstitial waters: the role of diffusive exchange between seawater and upper ocean crust. *Geochim. Cosmochim. Acta,* 45:1705–1713.

McDuff, R. E., and Gieskes, J. M., 1976. Calcium and magnesium in DSDP interstitial waters: diffusion or reaction? *Earth Planet. Sci. Lett.*, 33:1–10.

Mahoney, J. J., 1987. An isotopic survey of Pacific oceanic plateaus: implications for their nature and origin. *In* Keating, B. H., Fryer, P., Batiza, R., and Boehlert, G. W. (Eds.), *Seamounts, Islands, and Atolls.* Am. Geophys. Union Monogr., 43:207–220.

Mammerickx, J., and Smith, S. M., 1985. *Bathymetry of the North Central Pacific*: Boulder, CO (Geological Society of America), Map and Chart Ser., No. MC-52.

Martini, E., 1971. Standard Tertiary and Quaternary calcareous nannoplankton zonation. *In* Farinacci, A. (Ed.), *Proceedings of the Second International Conference on Planktonic Microfossils, Roma:* Rome (Ed. Technoscienza), 2:739–785.

Mayer, L. A., 1979. The origin of fine scale acoustic stratigraphy in deep-sea carbonates. *J. Geophys. Res.*, 804:6177–6184.

Mayer, L. A., Shipley, T. S, Theyer, F., Wilkens, R. W., and Winterer, E. L., 1985. Seismic modeling and paleoceanography at Deep Sea Drilling Project Site 574. *In* Mayer, L. A., Theyer, F., Thomas, E., et al., *Init. Repts. DSDP,* 85: Washington, (U.S. Govt. Printing Office), 947–970.

Mayer, L. A., Shipley, T. H., and Winterer, E. L., 1986. Equatorial Pacific seismic reflectors as indicators of global oceanographic events. *Science,* 233:761–764.

Moberly, R., Schlanger, S. O., et al., 1986. *Init. Repts. DSDP,* 89: Washington (U.S. Govt. Printing Office), 213–235.

Monechi, S., 1985. Campanian to Pleistocene calcareous nannofossil stratigraphy from the northwest Pascific Ocean, Deep Sea Drilling Project Leg 86. *In* Heath, G. R., Burckle, L. H., et al. *Init. Repts. DSDP,* 86: Washington (U.S. Govt. Printing Office), 301–336.

Nur, A., and Ben-Avraham, Z., 1982. Oceanic plateaus, the fragmentation of continents, and mountain building. *J. Geophys. Res.*, 87: 3644–3661.

Prell, W. L., 1985. Pliocene stable isotope and carbonate stratigraphy (Holes 572C and 573A): paleoceanographic data bearing on the question of Pliocene glaciation. *In* Mayer, L., Theyer, F., Thomas, E., et al., *Init. Repts. DSDP,* 85: Washington (U.S. Govt. Printing Office), 723–734.

Pyle, M. R., 1984. Vane shear data on undrained residual strength. *J. Tech. Div. Am. Soc. Civ. Eng.*, 110:543–547.

Rio, D., Fornaciari, E., and Raffi, I., in press. Late Oligocene through early Pleistocene calcareous nannofossils from western equatorial Indian Ocean (ODP Leg 115). *In* Duncan, R. A., Backman, J., Peterson, L. C., et al., *Proc. ODP, Sci. Results,* 115: College Station, TX (Ocean Drilling Program).

Sager, W. W., 1987. Late Eocene and Maastrichtian paleomagnetic poles for the Pacific plate: implications for the validity of seamount paleomagnetic data. *Tectonophysics,* 144:301–314.

Sanfilippo, A., and Riedel, W. R., 1985. Cretaceous radiolaria. *In* Bolli, H. M., Saunders, J. B., and Perch-Nielsen, K. (Eds.), *Plankton Stratigraphy:* Cambridge (Cambridge Univ. Press), 573–630.

Sanfilippo, A., Westberg-Smith, M. J., and Riedel, W. R., 1985. Cenozoic radiolaria. *In* Bolli, H. M., Saunders, J. B., and Perch-Nielsen, K. (Eds.), *Plankton Stratigraphy:* Cambridge (Cambridge Univ. Press), 631–712.

Saunders, A. D., 1986. Geochemistry of basalts from the Nauru Basin, Deep Sea Drilling Project Legs 61 and 89: implications for the origin of oceanic flood basalts. *In* Moberly, R., Schlanger, S. O., et al., *Init. Repts. DSDP,* 89: Washington (U.S. Govt. Printing Office), 499–517.

Saunders, J. B., Bernoulli, D., Müller-Merz, E., Oberhänsli, H., Perch-Nielsen, K., Riedel, W. R., Sanfilippo, A., and Torrini, R., Jr., 1984. Stratigraphy of late middle Eocene to early Oligocene in the Bath Cliff section Barbados, West Indies. *Micropaleontology,* 30: 390–425.

Seifert, K. E., Vallier, T. L., Windom, K. E., and Morgan, S. R., 1981. Geochemistry and petrology of igneous rocks, Deep Sea Drilling Project Leg 62. *In* Thiede, J., Vallier, T. L., et al., *Init. Repts. DSDP,* 62: Washington (U.S. Govt. Printing Office), 945–954.

Stoeser, D. B., 1975. Igneous rocks from Leg 30 of the Deep Sea Drilling Project. *In* Andrews, J. E., Packham, G., et al., *Init. Repts. DSDP,* 30: Washington (U.S. Govt. Printing Office), 401–414.

Thomas, E., 1990. Late Cretaceous through Neogene deep-sea benthic foraminifers (Maud Rise, Weddell Sea, Antarctica). *In* Barker, P. F., Kennett, J. P., et al., *Proc. ODP, Sci. Results,* 113: College Station, TX (Ocean Drilling Program), 571–591.

Toumarkine, M., and Luterbacher, H., 1985. Paleocene and Eocene planktic foraminifera. *In* Bolli, H. M., Saunders, J. B., and Perch-Nielsen, K. (Eds.), *Plankton Stratigraphy:* Cambridge (Cambridge Univ. Press), 87–154.

van Andel, T. H., Heath, G. R., and Moore, T. C., Jr., 1975. Cenozoic history and paleoceanography of the central equatorial Pacific. *Mem. Geol. Soc. Am.*, 143:1–134.

Winterer, E. L., Riedel, W. R., et al., 1971. *Init. Repts. DSDP,* 7: Washington (U.S. Government Printing Office).

Woodruff, F., 1985. Changes in Miocene deep-sea benthic foraminiferal distribution in the Pacific Ocean: relationship to paleoceanography. *In* Kennett, J. P. (Ed.), *The Miocene Ocean: Paleoceanography and Biogeography.* Mem. Geol. Soc. Am., 163:131–175.

Wright, A. A., Bleil, U., Monechi, S., Michel, H. V., Shackleton, N. J., Simoneit, B.R.T., and Zachos, J. C., 1985. Summary of Cretaceous/Tertiary boundary studies, Deep Sea Drilling Project Site 577, Shatsky Rise. *In* Heath, G. R., Burckle, L. H., et al., *Init. Repts. DSDP,* 86: Washington (U.S. Govt. Printing Office), 799–804.

Ms 130A-105

NOTE: All core description forms ("barrel sheets") and core photographs have been printed on coated paper and bound as Section 5, near the back of the book, beginning on page 559.

Hole 803D: Resistivity-Sonic-Gamma Ray Log Summary

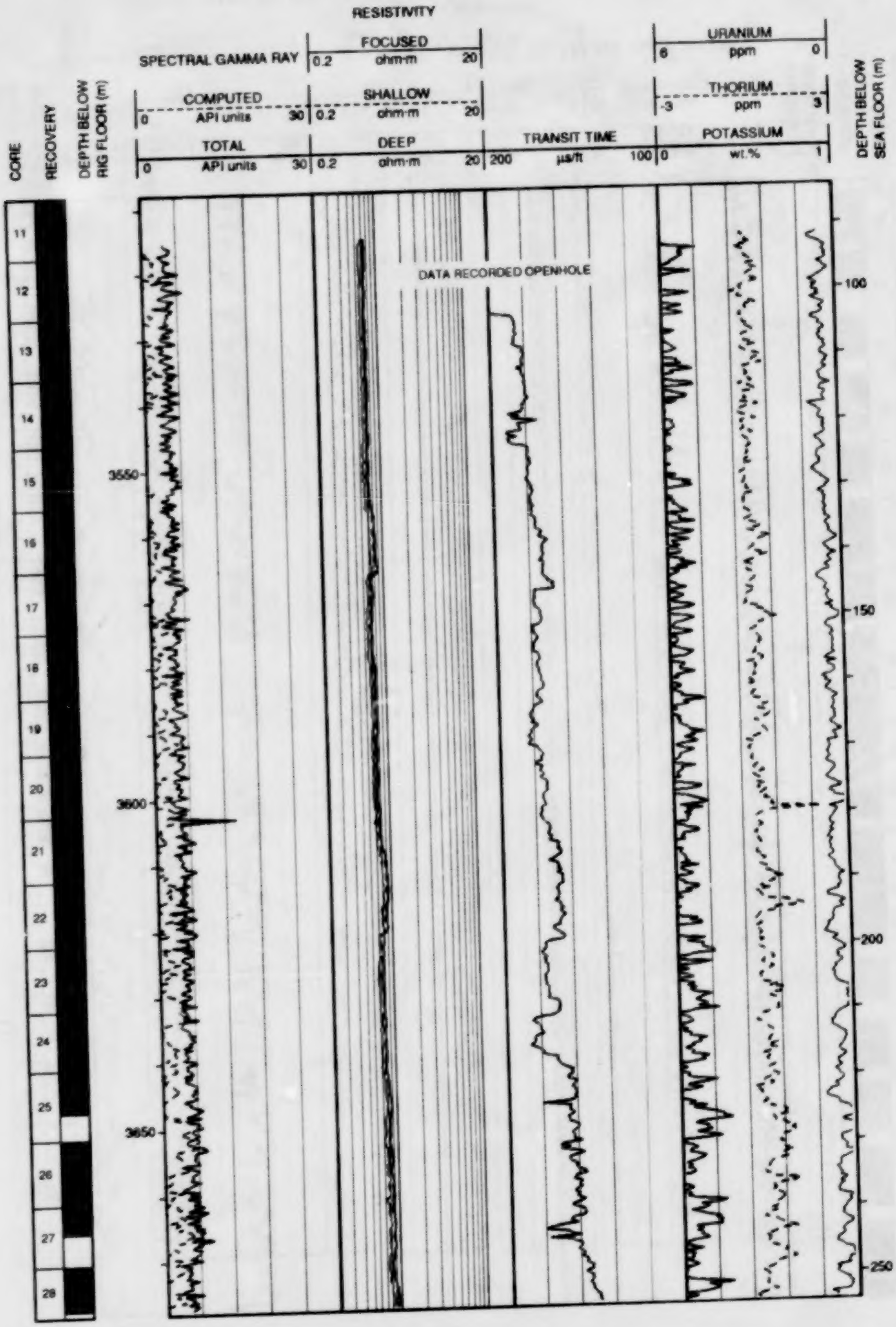

Hole 803D: Resistivity-Sonic-Gamma Ray Log Summary (continued)

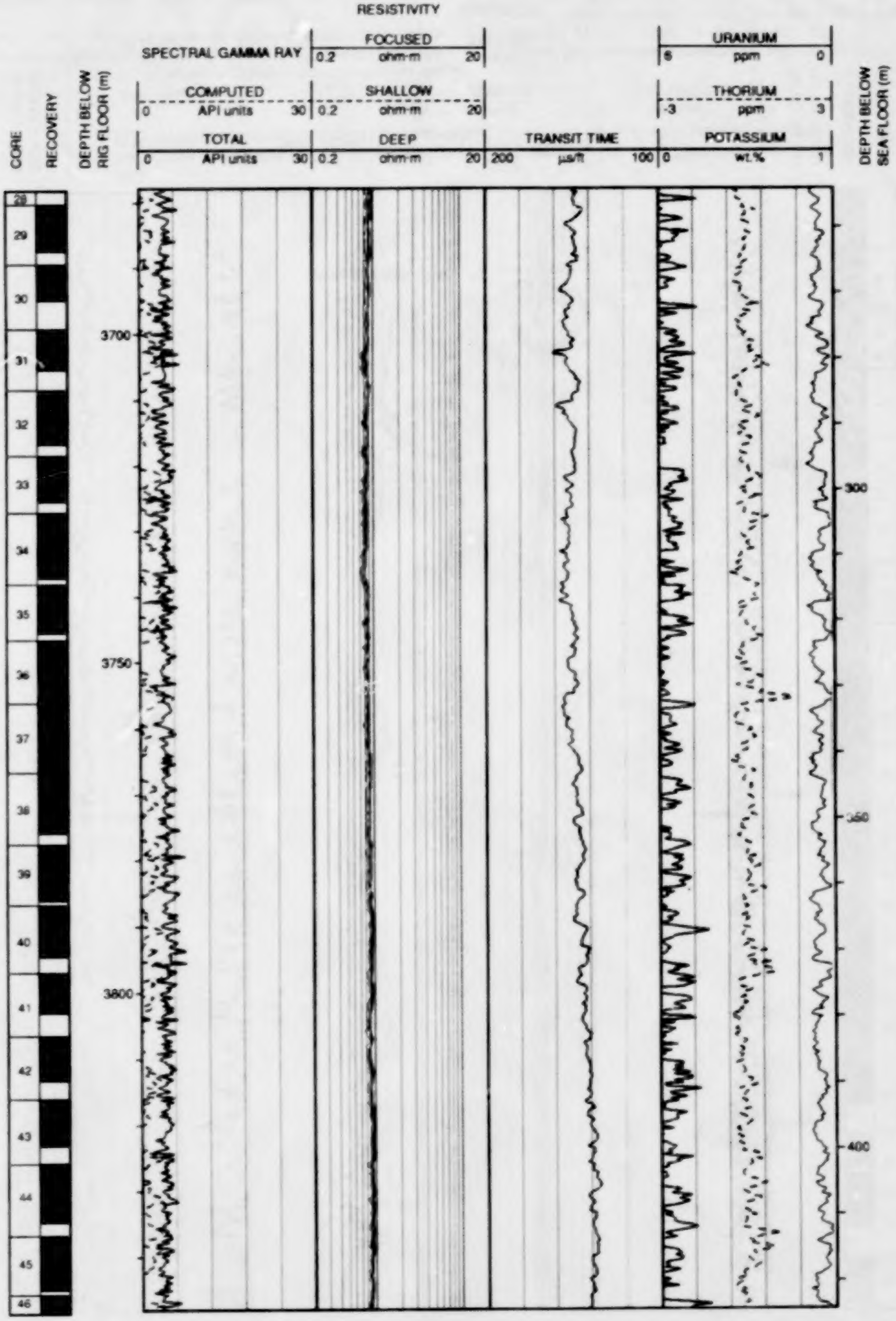

Hole 803D: Resistivity-Sonic-Gamma Ray Log Summary (continued)

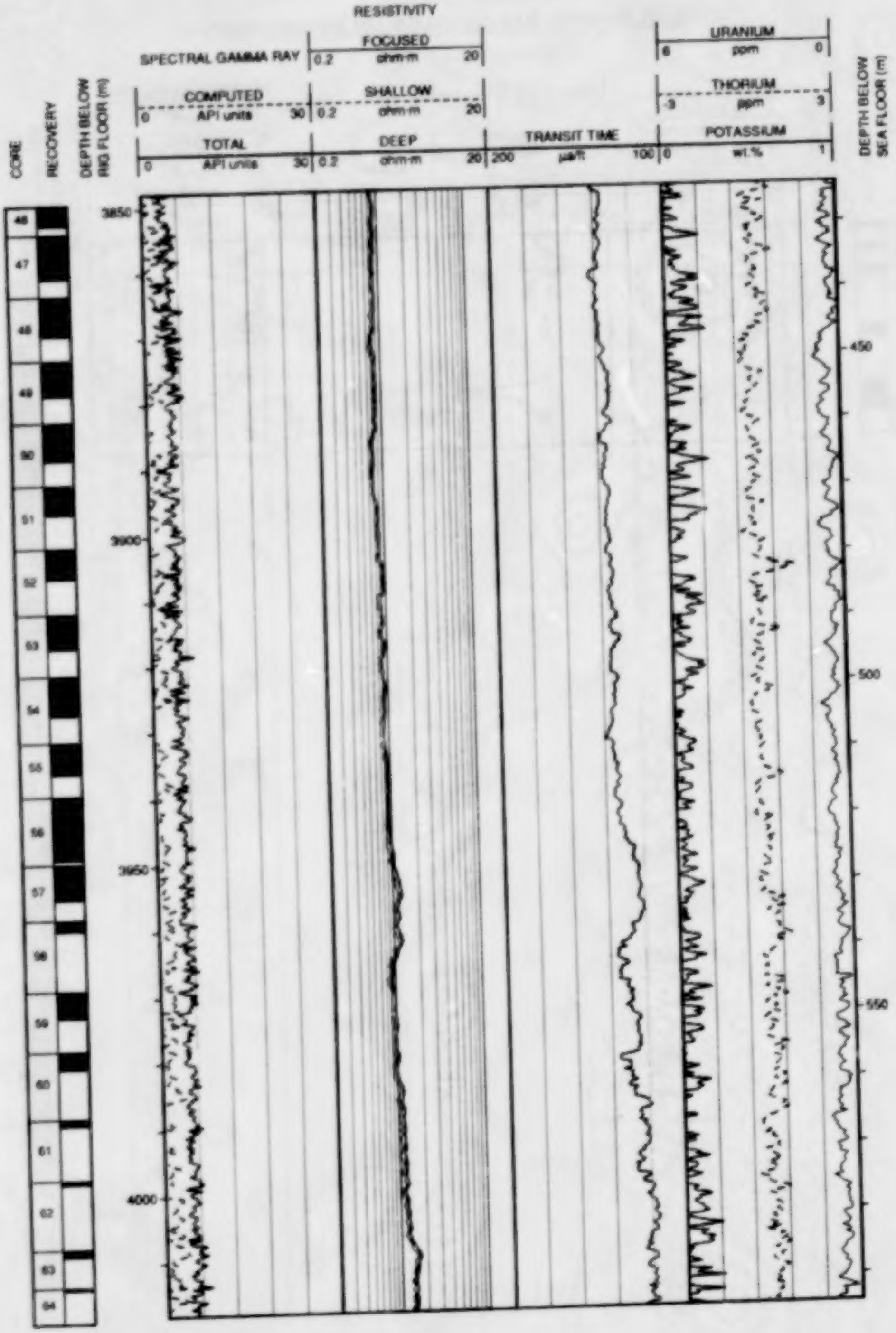

Hole 803D: Resistivity-Sonic-Gamma Ray Log Summary (continued)

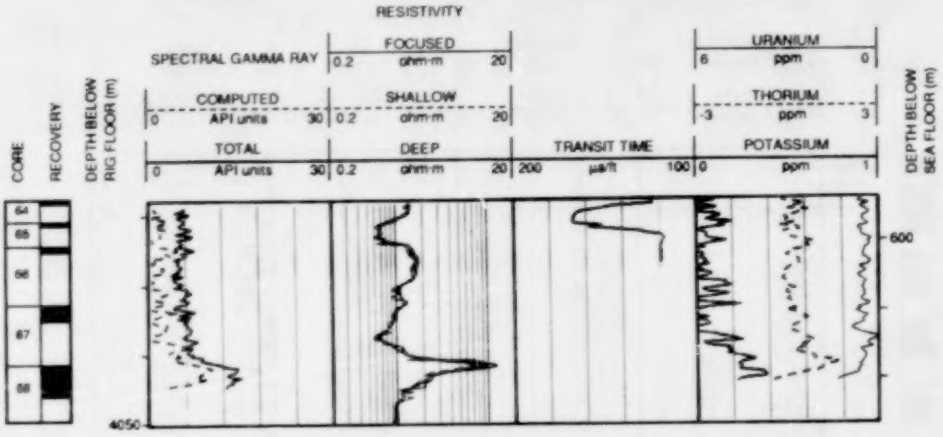

Hole 803D: Density-Gamma Ray-Aluminum Log Summary

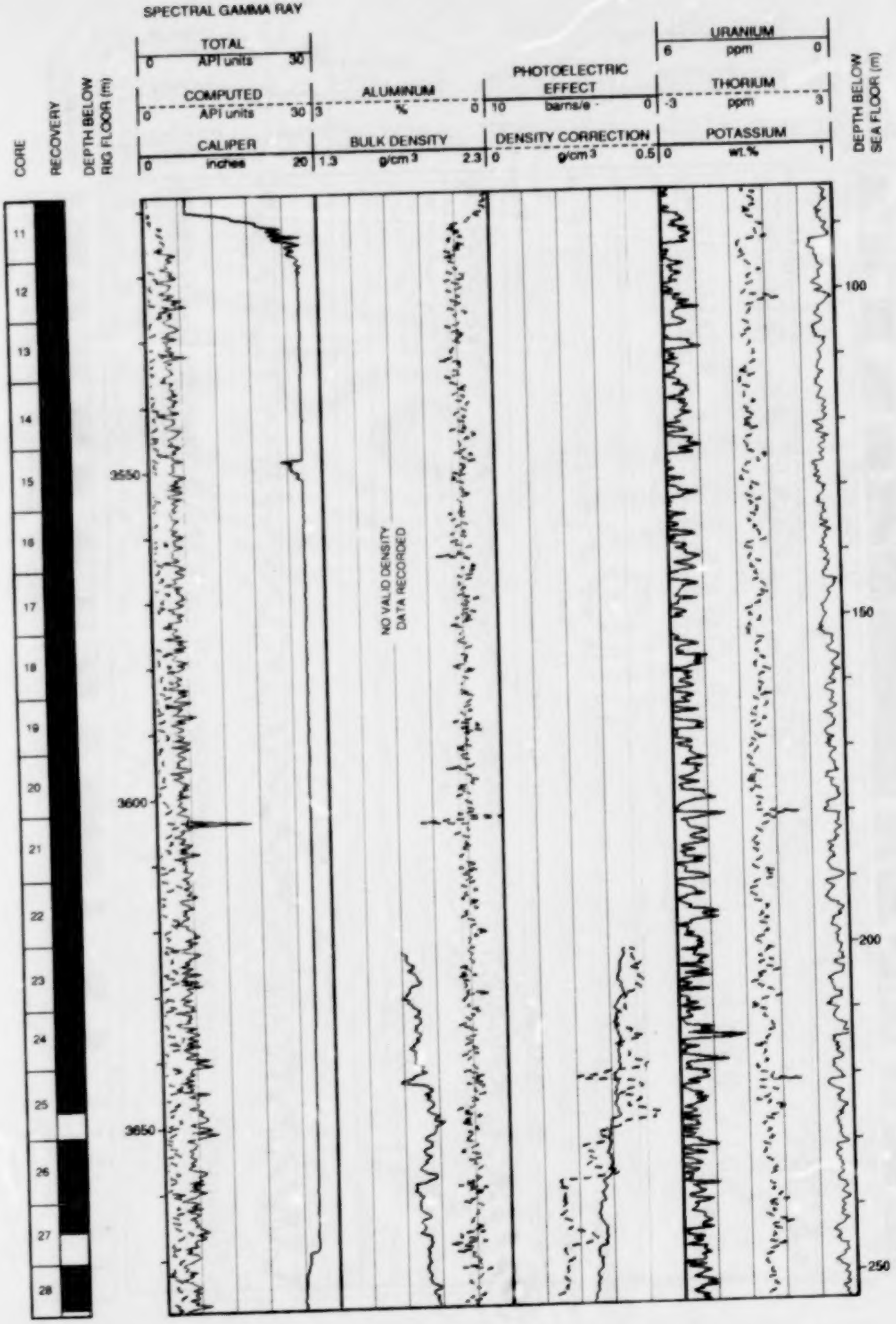

Hole 803D: Density-Gamma Ray-Aluminum Log Summary (continued)

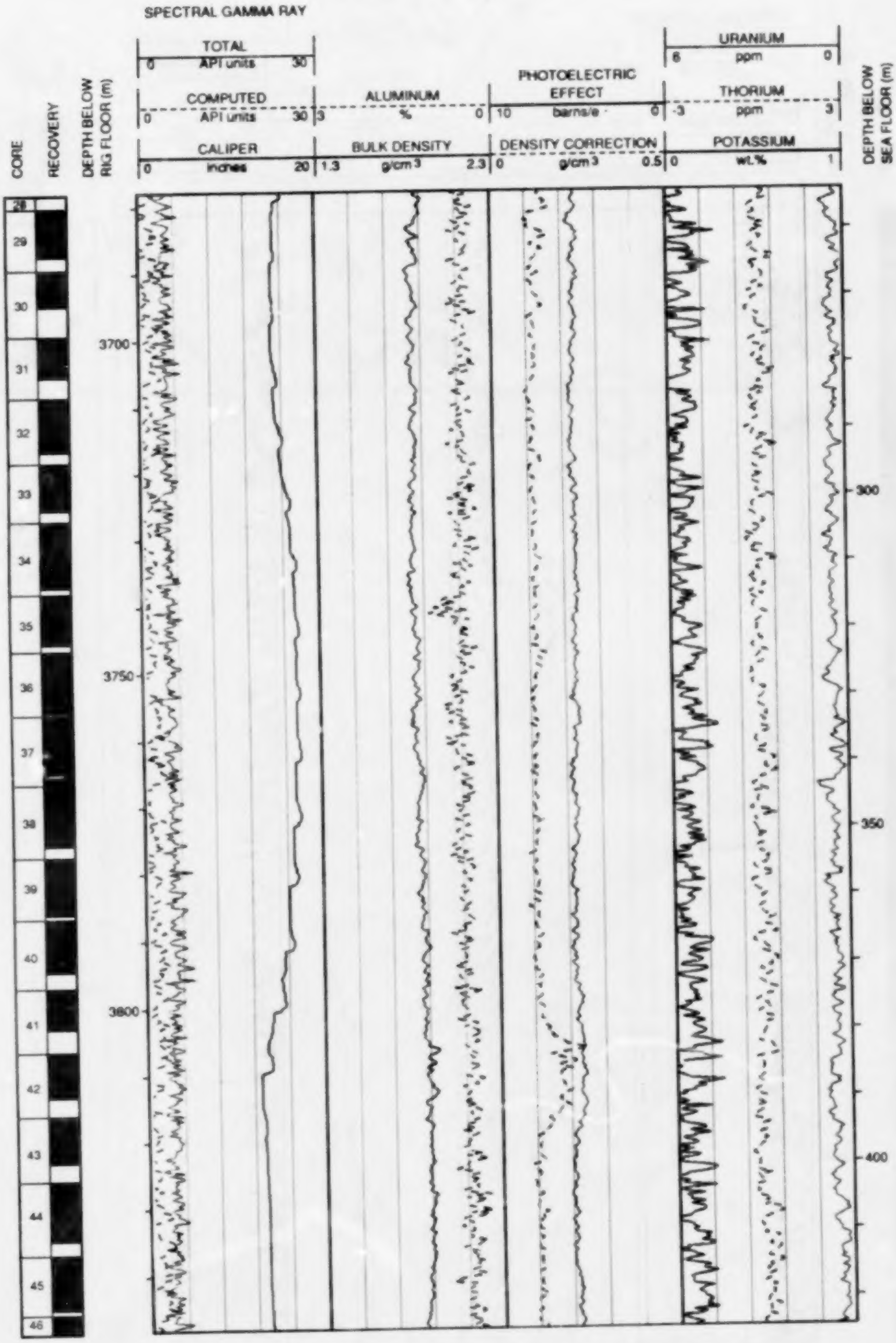

Hole 803D: Density-Gamma Ray-Aluminum Log Summary (continued)

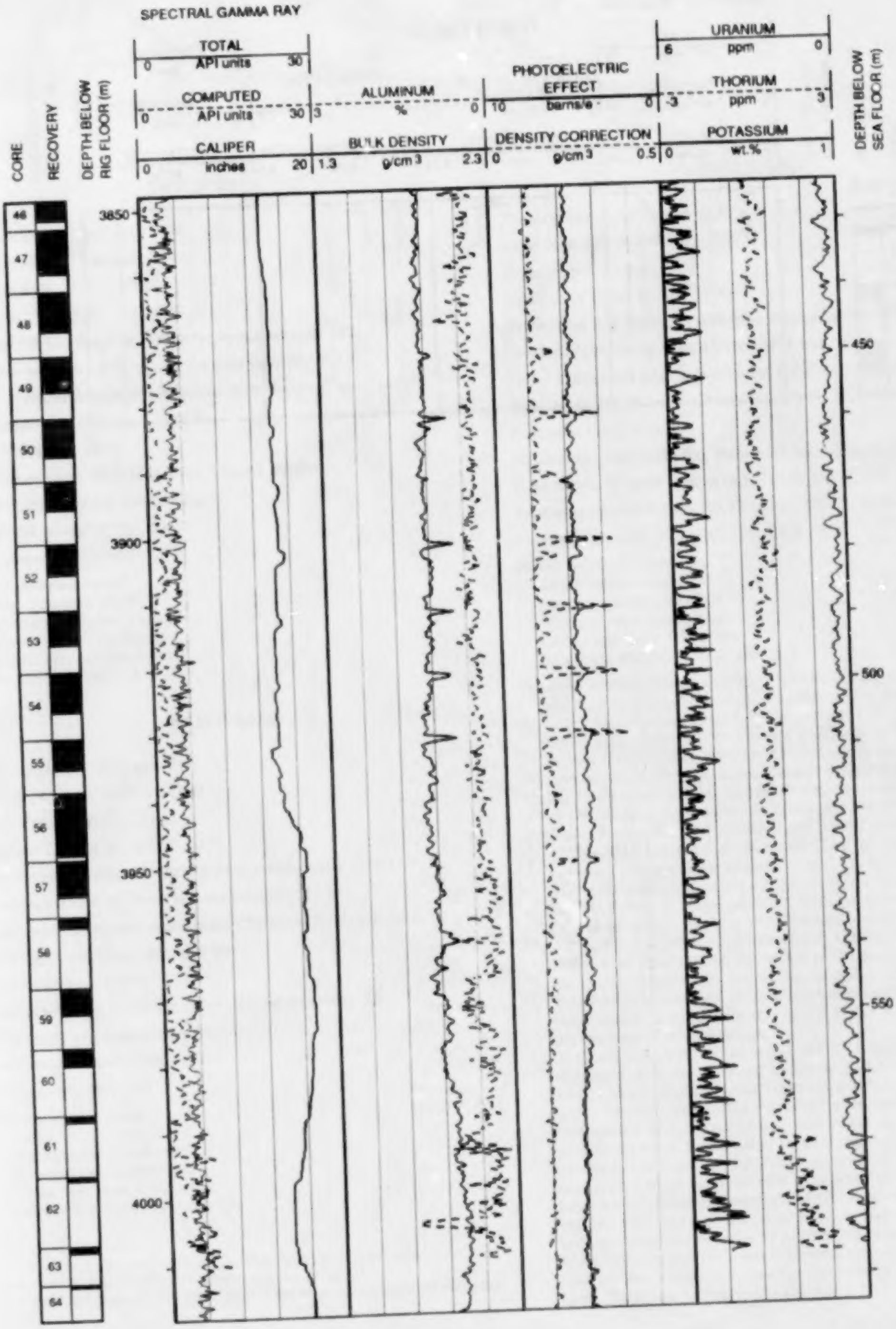

Hole 803D: Density-Gamma Ray-**Aluminum** Log Summary (continued)

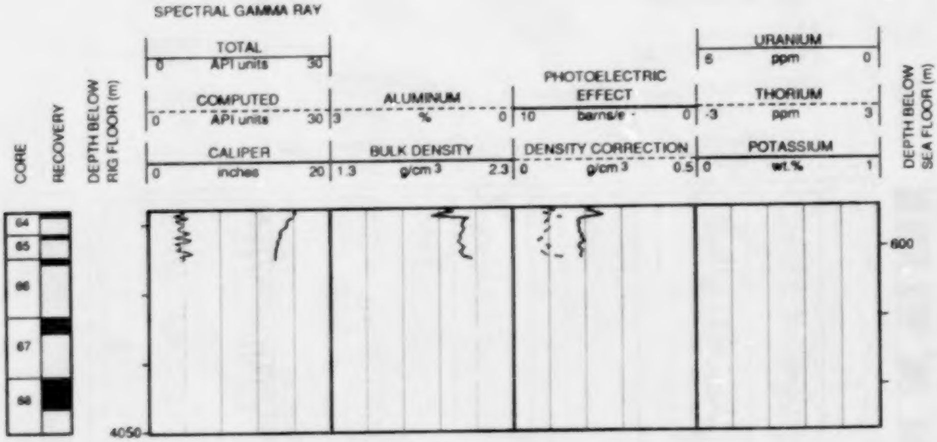

Kroenke, L. W., Berger, W. H., Janecek, T. R., et al., 1991
Proceedings of the Ocean Drilling Program, Initial Reports, Vol. 130

6. SITE 804[1]

Shipboard Scientific Party[2]

HOLE 804A

Date occupied: 7 February 1990

Date departed: 7 February 1990

Time on hole: 15 hr, 15 min

Position: 1°00.28′N, 161°35.62′E

Bottom felt (rig floor; m, drill-pipe measurement): 3872.8

Distance between rig floor and sea level (m): 11.08

Water depth (drill-pipe measurement from sea level, m): 3861.7

Total depth (rig floor; m): 3921.50

Penetration (m): 48.70

Number of cores (including cores with no recovery): 6

Total length of cored section (m): 48.70

Total core recovered (m): 50.52

Core recovery (%): 104

Oldest sediment cored:
Depth (mbsf): 48.70
Nature: nannofossil ooze
Youngest age: Quaternary
Oldest age: late Miocene
Measured velocity (km/s): 1.53

HOLE 804B

Date occupied: 7 February 1990

Date departed: 8 February 1990

Time on hole: 16 hr, 30 min

Position: 1°00.28′N, 161°35.62′E

Bottom felt (rig floor; m, drill-pipe measurement): 3871.8

Distance between rig floor and sea level (m): 11.08

Water depth (drill-pipe measurement from sea level, m): 3860.7

Total depth (rig floor; m): 4009.50

Penetration (m): 137.70

Number of cores (including cores with no recovery): 15

Total length of cored section (m): 137.70

Total core recovered (m): 141.61

Core recovery (%): 103

Oldest sediment cored:
Depth (mbsf): 128.20
Nature: nannofossil ooze
Youngest age: Quaternary
Oldest age: middle Miocene
Measured velocity (km/s): 1.58

HOLE 804C

Date occupied: 8 February 1990

Date departed: 10 February 1990

Time on hole: 1 day, 19 hr

Position: 1°00.28′N, 161°35.62′E

Bottom felt (rig floor; m, drill-pipe measurement): 3872.2

Distance between rig floor and sea level (m): 11.08

Water depth (drill-pipe measurement from sea level, m): 3861.1

Total depth (rig floor; m): 4184.70

Penetration (m): 312.50

Number of cores (including cores with no recovery): 33

Total length of cored section (m): 312.50 (APC, 120.3; XCB, 192.2)

Total core recovered (m): 273.78 (APC, 120.27; XCB, 153.51)

Core recovery (%): 87 (APC, 100; XCB, 79.9)

Oldest sediment cored:
Depth (mbsf): 312.50
Nature: nannofossil chalk
Youngest age: Quaternary
Oldest age: early Oligocene
Measured velocity (km/s): 1.65/1.7

Principal results: Ocean Drilling Program (ODP) Site 804 (proposed Site OJP-6) is located near the equator on the northeastern margin of the Ontong Java Plateau (1°00.3′N, 161°35.6′E) in 3861 m of water, approximately 375 km east-northeast of Deep Sea Drilling Project (DSDP) Sites 289/586. The site serves as the deep-water end member on a Neogene depth transect designed to detect depth-related paleoceanographic signals. It was occupied with the objective of obtaining a high-resolution carbonate record in a sublysoclinal setting for studies of dissolution and biostratigraphy.

Site 804 is located near the center of a slight depression about 4.5 km wide, along a single-channel seismic (SCS) line acquired by the *Thomas Washington* during ROUNDABOUT Cruise 11. It was positioned upslope of proposed Site OJP-6, on the *JOIDES Resolution* SCS crossing line, about 1′N of the intersection with the ROUNDABOUT line (1145 UTC, 23 December 1989) (see Hagen et al., and Mayer et al., this volume, for details of the surveys). Our SCS crossing profile showed that the section would not be ideal, that is, it would include disturbed zones and possibly hiatuses. Unfortunately, this situation is normal for this region at this water depth, even under the best of circumstances.

Three holes were drilled at Site 804. Hole 804A, a dedicated hole, was cored with the advanced hydraulic piston corer (APC) to 48.7 meters below seafloor (mbsf) into upper Miocene sediments, with 104% recovery. Hole 804B was cored with the APC to 137.7 mbsf into middle Miocene sediments, with 103% recovery. The hole was abandoned when a core barrel became stuck and required 80,000 lb of overpull to free it after drilling 5 m over it. A major unconformity occurs near this level. Hole 804C was cored with the APC to 120.3 mbsf for an average recovery rate of 100%, as over- and under-recovery just balanced over the cored interval. Below this depth, coring with the extended core barrel (XCB) proceeded to 312.5 mbsf, at which point it ended in lower Oligocene sediments; the upper Oligocene was not represented. Average recovery for the XCB section was 80%. There was no logging at this site.

---

[1] Kroenke, L. W., Berger, W. H., Janecek, T. R., et al., 1991. *Proc. ODP, Init. Repts.*, 130: College Station, TX (Ocean Drilling Program).

[2] Shipboard Scientific Party is as given in the list of participants preceding the contents.

The entire sequence encountered is considered as one lithologic unit, consisting of nannofossil ooze and chalk with varying abundances of foraminifers. Below 158 mbsf (ca. 11 Ma), the sediments contain significant abundances of radiolarians. The ooze/chalk transition was placed at 181 mbsf in the middle Miocene (ca. 13 Ma).

Two lithostratigraphic subunits were recognized, as follows:

Subunit IA (0–181 mbsf): Pleistocene to middle Miocene nannofossil ooze with foraminifers, nannofossil ooze, and nannofossil ooze with radiolarians. Colors are light brown in the top 20–40 m, grading into white with color banding below. The color banding (green and reddish hues) is best expressed between 44 and 59 mbsf (uppermost Miocene and lowermost Pliocene). It is well developed between 71 and 90 mbsf, and persists to about 100 mbsf. Disturbed layers, which include disrupted and distorted color banding, occur over a wide interval (42–110 mbsf) in the upper Miocene. These features are prominent between 70 and 80 mbsf in the uppermost Miocene (ca. 8 Ma). Two turbidites near 93 mbsf attest to redeposition within the middle upper Miocene (ca. 11 Ma).

Subunit IB (181–313 mbsf): middle Miocene to upper lower Oligocene nannofossil chalk and nannofossil chalk with radiolarians. Colors are yellowish white, pale brown, and white. The main difference from the overlying unit is the greater lithification. Also, radiolarian-bearing sediments are more common in this subunit. At depths near 200 mbsf, there are indications of ooze/chalk clasts (glide breccia?) and distorted bioturbation features.

The sediments in the deepest core (130-804C-33X, 303.30–312.50 mbsf) were well indurated but posed no problem for XCB coring, which recovered a nearly full core of chunks and chips, with evidence of chalk grinding on chalk. This type of recovery was typical for the lowermost 100 m of the section. Sedimentation rates for this chalk are between 10 and 15 m/m.y. The Oligocene/Miocene boundary was located near 270 mbsf, with foraminifer-poor, low-carbonate, lower Miocene chalk overlying lower Oligocene chalks. There is evidence for the presence of microbreccia and fault gouge at this boundary.

In the lowermost Miocene, there are zones with greatly reduced foraminifer content. Thick layers of nannofossil chalk alternate with equally thick layers of nannofossil chalk containing radiolarians for much of the lower Miocene. A high radiolarian content was noted in the middle portion of this section (near 265 mbsf). The boundary between the lower and middle Miocene (near 200 mbsf) lies within a hiatus spanning the time from 20.0 to 14.7 Ma. The hiatus is bracketed by low-carbonate sediment highly enriched in radiolarians. The associated sediment (190–210 mbsf) also shows evidence of strong deformation, presumably by a gliding of the overlying section on the lower Miocene deposits. Pieces of nannofossil-radiolarite occur here. Foraminifers show signs of severe dissolution.

The ooze/chalk transition was located just a few meters above the glide zone, near the base of foraminifer Zone N12 (ca. 13.5 Ma). At Site 803, this transition was picked at a greater depth but at about the same age (ca. 13 Ma). Sedimentation rates between the hiatus at 197 mbsf (20–15 Ma) and the base of Zone NN9 at 154 mbsf (ca. 10.5 Ma) are near 18 m/m.y. Above this level, carbonate content increases (toward its maximum values of over 90%), as does foraminifer abundance. Radiolarians become less abundant. Sedimentation rates decline in upper Miocene time, dropping back to near 10 m/m.y. in the Pliocene and Pleistocene.

There is a condensed section (or a hiatus) in the lowermost Pliocene, marked by low carbonate values. After this event, carbonate values fluctuate greatly, and foraminifer abundance increases substantially. Detailed paleomagnetic stratigraphies for Pliocene-Pleistocene sediments in the three holes identified small changes in sedimentation rates and their between-hole variations.

Chemical gradients in interstitial waters at this site are generally similar to those at Site 803, reflecting the calcareous/siliceous nature of the sediments and the paucity of organic material. Calcium and magnesium gradients were influenced by basalt alteration reactions at depth and show the usual negative correlation ($R^2 = 0.97$). Strontium concentrations are lower than at Site 803, presumably reflecting diminished recrystallization intensity at Site 804. Dissolved silica increases with depth, indicating continuing dissolution of siliceous fossils. Near-maximum levels are reached at 100 mbsf, suggesting that below that level dissolution is reduced or balanced by precipitation.

Physical properties, including wet-bulk density and sound velocity, show greater variability at this site than at Site 803. Distinct minima in density occur near or within the intervals identified to include hiatuses. Clearly, this has implications for the positioning of associated reflectors within the seismic profiles.

BACKGROUND AND OBJECTIVES

Overview

Site 804, the deepest site of the Neogene depth transect on the Ontong Java Plateau, was drilled near target Site OJP-6 (3920 m), which was scheduled as an alternate to Site OJP-3 (4200 m) (Fig. 1). Both of these sites were expected to contain a record of the severe effects of varying dissolution on Neogene carbonates but at a level well short of complete removal. Thus, the saturation history of deep waters, and its ramifications for physical properties, would be contained in these sediments, as well as sufficiently preserved benthic foraminifers for bathyal paleoceanography. Triplicate APC-cored holes were planned at the site for the upper portion of the section (Quaternary and Neogene): two holes to 250 mbsf, and a third hole to 50 mbsf. Triple APC coring provides overlap between cores and sufficient material for concurrent high-resolution studies.

Background

The general background to this site is contained in the "Introduction" chapter (this volume; also see Kroenke, 1972). The Ontong Java Plateau is a broad, shallow, mid-ocean highland in the western equatorial Pacific. Its shallowest regions lie above 2000 m, and its flanks reach depths in excess of 4500 m. With an area greater than 1.5 million km^2, it is the largest of the "classic" Pacific plateaus. The plateau has a crustal thickness on the order of 40 km. Apparently, it maintained its present depth over much of its history, indicating isostatic equilibrium. Crustal seismic velocities are in the range of that of oceanic crust (Hussong et al., 1979).

The pelagic sediment cover of the Ontong Java Plateau is uniquely suited for paleoceanographic studies. The maximum thickness of the sediment cover is over 1200 m and occurs below the top of the plateau, in water depths between 2000 and 2500 m. The cover thins by roughly 100 m for every 200 m of water depth increase below 2200 m (Berger and Johnson, 1976). At Site 804 (3861 m) the sediment is approximately 500 m thick.

Site 804 is the deep-water end member of a depth transect along the equatorial portion of the Ontong Java Plateau, designed for the study of paleoceanographic events of global significance (Fig. 2). Two sites were proposed for drilling (OJP-3 and OJP-6). After drilling Site 803, we realized that considerable disturbance and/or the presence of unconformities were to be expected at both of the proposed deep-water sites, but that the shallower of the two might hold the better record. Thus, the alternate site, OJP-6, was chosen for drilling. Drilling continued to just below 300 mbsf, revealing several substantial hiatuses, and ended within early Oligocene sediments.

Unfortunately, problems arising from the creep of large sediment bodies are ubiquitous at these depths, because of a combination of tectonic and stratigraphic factors. The site location is close to a significant offset in basement levels between the plateau and the deep ocean floor (Fig. 2). Occasional earthquakes are to be expected in such a setting. Episodic shaking, basement relief, and perhaps increased mobility of deep-water sediments, from the presence of carbonate-poor layers, apparently create large-scale slumping and debris flow on the flanks of the plateau. Removal of support at greater water depths also may play

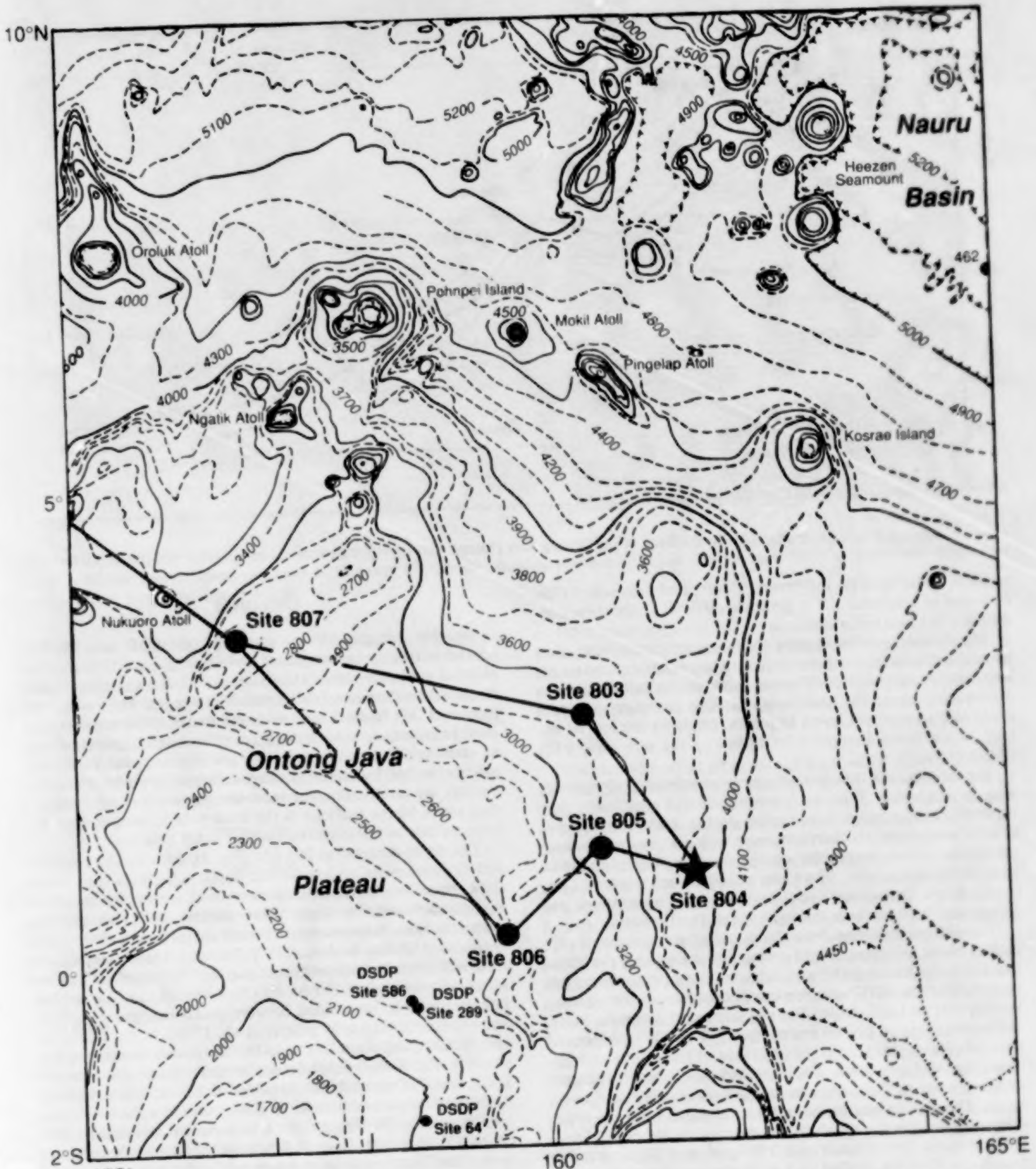
10°N
5°
0°
2°S
155°
160°
165°E
Nauru
Basin
Heezen Seamount
462
Oroluk Atoll
Pohnpei Island
Mokil Atoll
Pingelap Atoll
Ngatik Atoll
Kosrae Island
Nukuoro Atoll
Ontong Java
Plateau
Site 807
Site 803
Site 805
Site 804
Site 806
DSDP Site 586
DSDP Site 289
DSDP Site 64
5100
5200
5000
4500
4900
4000
4300
3500
4600
3700
4400
4200
4700
3900
3800
3600
3400
2700
2800
2900
3000
2400
2600
2500
2300
2200
2100
2000
1900
1800
1700
3200
4100
4450

Figure 1. Bathymetry in meters of the northwestern part of the Ontong Java Plateau (after Mammerickx and Smith, 1985). The location of the Leg 130 sites and DSDP Sites 64 and 289/586 is shown. Contour interval is 100 m.

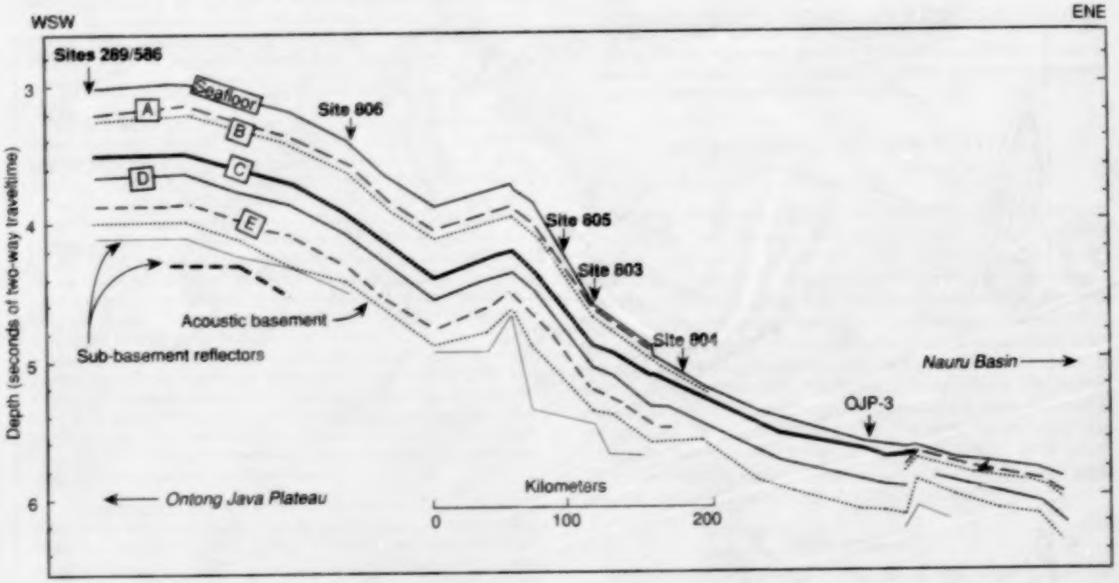

Figure 2. Simplified acoustic stratigraphy for the flank of the Ontong Java Plateau, and approximate location of Sites 803–806 (the depth transect).

a role in fostering mass movement (Berger and Johnson, 1976). Selection of a suitable site to drill was difficult under these conditions.

The seismic profiles across the proposed deep-water sites show the effects of mass movement. They exhibit crenulate reflectors ("crinkly horizons") at several levels, as well as evidence for wedging along the basin margins. The crenulate reflectors grade into transparent layers in places, implying the loss of energy return from disruption or tilting of the reflecting units (Fig. 3).

Indications exist that disturbance is associated preferentially with certain layers. Thus, we hypothesized that such layers may be predisposed, through conditioning during deposition, to serve as glide strata later. Furthermore, even with disturbance by mass movement, paleoceanographic (dissolution) events may be linked by acoustic stratigraphy. If we can establish such a connection, it will allow three-dimensional mapping and correlation into distant sediment sections throughout the Pacific basin.

The plateau has long been the focus of paleoceanographic studies based on conventional coring and on seismic profiling. Leg 130 is the fourth drilling expedition to sample the sediment cover here: four DSDP sites were drilled earlier on the plateau. Participants on Leg 7 drilled Site 64 (Shipboard Scientific Party, 1971), and those on Leg 30 drilled Sites 288 and 289 (Shipboard Scientific Party, 1975a, 1975b). All three of these sites were rotary-drilled and spot-cored. The upper 969 m in Site 289 consisted of late Eocene to Pleistocene nannofossil foraminifer chalks and oozes. The section was found to be continuous from the lower Oligocene on, the top of which was reached at 890 mbsf. Semilithified chalk first appears near 250 mbsf (late Miocene). The fourth site (Site 586, drilled on Leg 89 next to Site 289) was hydraulically piston cored to 305 mbsf and reached upper Miocene sediments (Shipboard Scientific Party, 1986a, 1986b). Well-preserved nannofossil ooze was recovered at this site.

Objectives

Site 804, roughly 375 km northeast of DSDP Sites 289/586 on the northeastern margin of the Ontong Java Plateau, was planned as the deepest of the four Leg 130 sites that constitute a Neogene depth transect (Sites 803–806; Fig. 1). The general objective of this transect was to detect and reconstruct depth-related paleoceanographic signals, such as the changing gradients of carbonate dissolution intensity and the deep-water $\delta^{13}C$ signals in benthic foraminifers. The sediments sampled along the transect are produced in the same surface-water conditions and thus arrive on the seafloor in the same pelagic rain, so that differences can be attributed to depth-related effects.

The depth sampled at Site 804 (Fig. 1), between the lysocline and the carbonate compensation depth (CCD), is that which shows the effects of dissolution most dramatically, yet preserves enough carbonate to study these effects. Thus, all physical properties should be severely affected by carbonate dissolution at this level (Johnson et al., 1977). In turn, this imprint should be detectable in the acoustic stratigraphy. Our hope was that the effects of dissolution would be strata-bound, so that a clear linkage could be established between paleoceanographic events and acoustic stratigraphy (Mayer et al., 1986). In the case of severe dissolution pulses, one would expect hiatus formation, presumably also linked to paleoceanographic events (Barron and Keller, 1982). The combination of dissolution effects (which apparently decreases resistance to shear) and the local tectonics (which provide for tilting and earthquakes) is inimical to these objectives regarding acoustic stratigraphy. Thus, it is necessary to find and sample minimally disturbed sediments. As it turned out, sediment disturbances identified as minor when studying seismic profiles proved to be quite substantial upon drilling. Nevertheless, the objectives regarding acoustic linkage and hiatus formation remain valid.

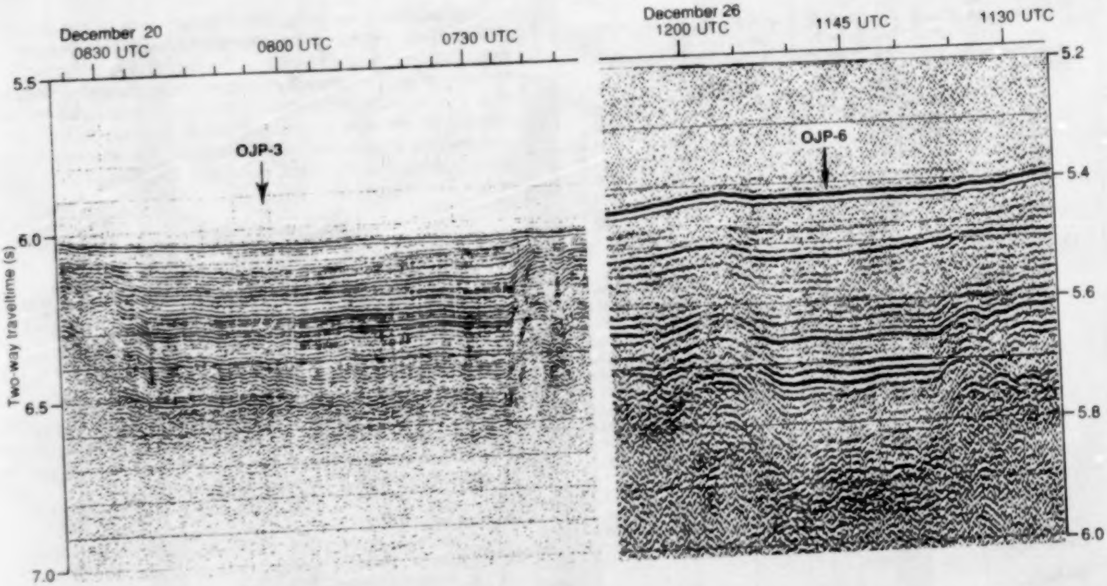

Figure 3. Seismic profiles across proposed drilling sites for Site 804, showing evidence of planar disturbance (crinkly horizons) and debris flow (wedges next to basin rim). Site OJP-3 was not drilled.

Regarding biofacies objectives, we expected that changes in the preservation of calcareous fossils would provide clues to changes in the intensity of dissolution, with wide implications for the study of deep-water history and the oceanic carbon cycle (e.g., Berger, 1981). In addition, we hypothesized that preserved benthic foraminifers would record deep-water properties directly in their abundances and chemical composition. The effects of partial dissolution on biostratigraphic zonation (by selective removal of marker species) also is important.

OPERATIONS

Site 804

The transit to Site 804 (proposed Site OJP-6) started at 1730 hr, 6 February 1990, and covered 98 nm over 7.5 hr at an average speed of 13.0 kt. Upon arrival, a 47-nmi pre-site seismic survey was run over the proposed site (for more details of the survey, see the "Underway Geophysics" chapter, this volume). The beacon was dropped at 0537 hr, 7 February 1990, initiating Site 804.

Hole 804A

The ship was positioned 20 m east of the beacon. Core 130-804A-1H was spudded at 1520 hr, 7 February 1990, in a water depth of 3861.7 m. Cores 130-804A-1H through -6H were taken from 0 to 48.7 mbsf, with 48.7 m of sediment cored and 50.52 m recovered (103.74% recovery; see Table 1). We conducted orientation surveys during Cores 130-804A-3H through -6H. Hole 804A was ended when the depth objective of 50 mbsf was reached.

Hole 804B

The ship was offset 40 m east of the beacon. Core 130-804B-1H was taken at 2215 hr, 7 February 1990, in a water depth of 3860.7 m. Cores 130-804C-1H through -15H were taken from 0 to 137.7 mbsf, with 137.7 m of sediment cored and 141.61 m recovered (102.84% recovery). Orientation surveys were taken on Cores 130-804-3H through -15H. Hole 804B was terminated when Core 130-803B-15H required 80,000 lb of overpull to free it after drilling 5 m over the core barrel.

Hole 804C

The ship was offset 60 m east of the beacon. Core 130-804C-1H was taken at 1500 hr, 8 February 1990, in a water depth of 3861.1 m. Cores 130-804C-1H through -13H were taken from 0 to 120.3 mbsf, with 120.3 m of sediment cored and 120.27 m recovered (99.98% average recovery).

The breakaway piston head was tested in Cores 130-804C-9H through -11H, but the piston came off in all three cores, in spite of passing deck tests with the outside and inner holes plugged. Recovery for the three cores was reduced from an average of 9.95 to 8.34 m. Orientation surveys were taken on Cores 130-804C-3H through -13H. Cores 130-804C-14X through -33X were taken from 120.3 to 312.5 mbsf with 192.2 m of sediment cored and 153.51 m recovered (79.92% recovery). Hole 804C was terminated after reaching the depth/age objectives.

The drill string was pulled out of the hole, and the bit cleared the rotary table at 0830 hr, 10 February 1990, ending Hole 804C. Before departing Site 804, the vibration-isolated television (VIT) frame was run to the seafloor to test the televiewer (TV) camera and coaxial cable. After successful completion of this test, the TV was pulled, and the ship got underway at 1200 hr, 10 February 1990.

LITHOSTRATIGRAPHY

Introduction

Three holes were drilled at Site 804. Holes 804A and 804B were cored with the APC to 49 mbsf and 138 mbsf, respectively.

Table 1. Coring summary, Site 804.

Core no.	Date (Feb. 1990)	Time (UTC)	Depth (mbsf)	Cored (m)	Recovered (m)	Recovery (%)
130-804A-						
1H	7	1520	0–1.2	1.2	1.26	105.0
2H	7	1620	1.2–10.7	9.5	9.83	103.0
3H	7	1725	10.7–20.2	9.5	10.03	105.6
4H	7	1825	20.2–29.7	9.5	9.92	104.0
5H	7	1925	29.7–39.2	9.5	9.98	105.0
6H	7	2100	39.2–48.7	9.5	9.50	100.0
Coring totals				48.7	50.52	103.7
130-804B-						
1H	7	2215	0–4.7	4.7	4.64	98.7
2H	7	2315	4.7–14.2	9.5	9.95	105.0
3H	8	0015	14.2–23.7	9.5	10.03	105.6
4H	8	0220	23.7–33.2	9.5	9.91	104.0
5H	8	0310	33.2–42.7	9.5	10.12	106.5
6H	8	0400	42.7–52.2	9.5	9.85	103.0
7H	8	0500	52.2–61.7	9.5	9.82	103.0
8H	8	0545	61.7–71.2	9.5	9.89	104.0
9H	8	0630	71.2–80.7	9.5	9.70	102.0
10H	8	0730	80.7–90.2	9.5	9.87	104.0
11H	8	0810	90.2–99.7	9.5	10.01	105.3
12H	8	0900	99.7–109.2	9.5	9.78	103.0
13H	8	0950	109.2–118.7	9.5	7.95	83.7
14H	8	1050	118.7–128.2	9.5	10.01	105.3
15H	8	1215	128.2–137.7	9.5	10.08	106.1
Coring totals				137.7	141.61	102.8
130-804C-						
1H	8	1500	0–6.3	6.3	6.31	100.0
2H	8	1600	6.3–15.8	9.5	10.00	105.2
3H	8	1710	15.8–25.3	9.5	9.78	103.0
4H	8	1815	25.3–34.8	9.5	9.98	105.0
5H	8	2030	34.8–44.3	9.5	10.05	105.8
6H	8	2130	44.3–53.8	9.5	10.07	106.0
7H	8	2230	53.8–63.3	9.5	9.99	105.0
8H	9	0000	63.3–72.8	9.5	9.79	103.0
9H	9	0100	72.8–82.3	9.5	8.14	85.7
10H	9	0200	82.3–91.8	9.5	7.98	84.0
11H	9	0300	91.8–101.3	9.5	8.91	93.8
12H	9	0400	101.3–110.8	9.5	9.77	103.0
13H	9	0500	110.8–120.3	9.5	9.50	100.0
14X	9	0545	120.3–129.8	9.5	6.92	72.8
15X	9	0630	129.8–139.3	9.5	4.75	50.0
16X	9	0715	139.3–148.8	9.5	2.51	26.4
17X	9	0800	148.8–158.3	9.5	9.26	97.5
18X	9	0920	158.3–168.0	9.7	8.60	88.6
19X	9	1045	168.0–177.7	9.7	8.30	85.5
20X	9	1130	177.7–187.4	9.7	8.10	83.5
21X	9	1230	187.4–197.1	9.7	6.58	67.8
22X	9	1310	197.1–206.8	9.7	9.06	93.4
23X	9	1355	206.8–216.5	9.7	8.38	86.4
24X	9	1505	216.5–226.2	9.7	4.84	49.9
25X	9	1610	226.2–235.8	9.6	9.31	97.0
26X	9	1715	235.8–245.4	9.6	9.15	95.3
27X	9	1820	245.4–255.1	9.7	8.58	88.4
28X	9	1920	255.1–264.7	9.6	8.95	93.2
29X	9	2020	264.7–274.4	9.7	7.81	80.5
30X	9	2130	274.4–284.0	9.6	8.49	88.4
31X	9	2230	284.0–293.7	9.7	7.98	82.2
32X	9	2340	293.7–303.3	9.6	7.47	77.8
33X	10	0045	303.3–312.5	9.2	8.47	92.0
Coring totals				312.5	273.78	87.6

At Hole 804C, the interval from 0 to 120 mbsf was cored with the APC and the interval from 120 to 313 mbsf was cored with the XCB. Recovery was near 100% in the intervals cored with the APC and near 80% in the intervals cored with the XCB.

The entire sedimentary sequence consists of nannofossil ooze and chalk with varying abundances of foraminifers. Significant abundances of radiolarians (10%–25%) are noted below 158 mbsf. The oldest sediment recovered is of late early Oligocene age.

The sediments are relatively homogeneous in composition; thus, they were grouped into one lithostratigraphic unit and divided into two subunits based on the degree of lithification (Fig. 4). Subunit IA is composed of nannofossil ooze and nannofossil ooze with varying abundances of foraminifers and radiolarians. Subunit IB contains nannofossil chalk and nannofossil chalk with varying abundances of radiolarians. The ooze/chalk transition is located at 181 mbsf, in Section 130-804C-20X-3, and is of middle Miocene age.

Description of Units

Unit I

Intervals: Hole 804A, Cores 130-804A-1H to -6H; Hole 804B, Cores 130-804B-1H to -15H; Hole 804C, Cores 130-804C-1H to -33X
Age: Pleistocene–late early Oligocene
Depth: 0–313 mbsf

The sediments recovered at Site 804 consist of nannofossil ooze and chalk. Foraminifers and radiolarians generally are present in abundances of less than 25%. The sequence was divided into two subunits to distinguish between oozes and chalks.

Subunit IA

Intervals: Hole 804A, Cores 130-804A-1H to -6H; Hole 804B, Cores 130-804B-1H to -15H; Hole 804C, Core 130-804C-1H to Section 130-804C-20X-3
Age: Pleistocene–middle Miocene
Depth: 0–181 mbsf

Subunit IA is 181 m thick and is composed of (in decreasing order of abundance) nannofossil ooze, nannofossil ooze with foraminifers, nannofossil ooze with radiolarians, foraminifer nannofossil ooze, and nannofossil foraminifer ooze.

Drilling disturbance was generally minor, although several sections in Cores 130-804C-4H through -6H contained flow-in.

Nannofossil ooze with foraminifers and foraminifer nannofossil ooze were found at the top of Subunit IA; they graded into nannofossil ooze at approximately 20–40 mbsf. Foraminifer abundances remain near 5% in the interval from 40 to 120 mbsf and increase below 120 mbsf, whereas radiolarian abundances increase to 10% or more below 158 mbsf. As a result, nannofossil ooze with foraminifers alternates with nannofossil ooze with radiolarians on a scale of 5–10 m between 120 and 182 mbsf.

The dominant sediment color is white (2.5Y 8/0), except for the uppermost Pleistocene section (the first two cores in each hole), which is pale brown (10YR 6/3). Most cores of Subunit IA also contain pale yellowish green (10GY 7/2), light gray (5Y 7/1), and reddish gray (5R 7/1), millimeter- to centimeter-scale, diffuse color bands of varying intensity. Between 42 and 110 mbsf (Cores 6H through 12H in each hole), numerous color bands are dipping and show evidence of microfaulting and contortion. These characteristics do not appear to be caused by the drilling process or bioturbation and may be evidence of mass displacement.

Other evidence for mass movement is the presence of three graded beds 10, 12, and 50 cm thick that are interpreted to be turbidites. The first graded bed is located in the interval dominated by nannofossil ooze approximately 93 mbsf (upper Miocene) in both Holes 804B and 804C (Sections 130-804B-11H-2 and 130-804C-11H-2, respectively); it consists of sand-rich nannofossil foraminifer ooze (Fig. 5). The other two graded beds are located in Sections 130-804C-19X-1 and -3, respectively (middle Miocene), within an interval of nannofossil ooze with foraminifers between 168 and 174 mbsf. They consist of nannofossil foraminifer ooze.

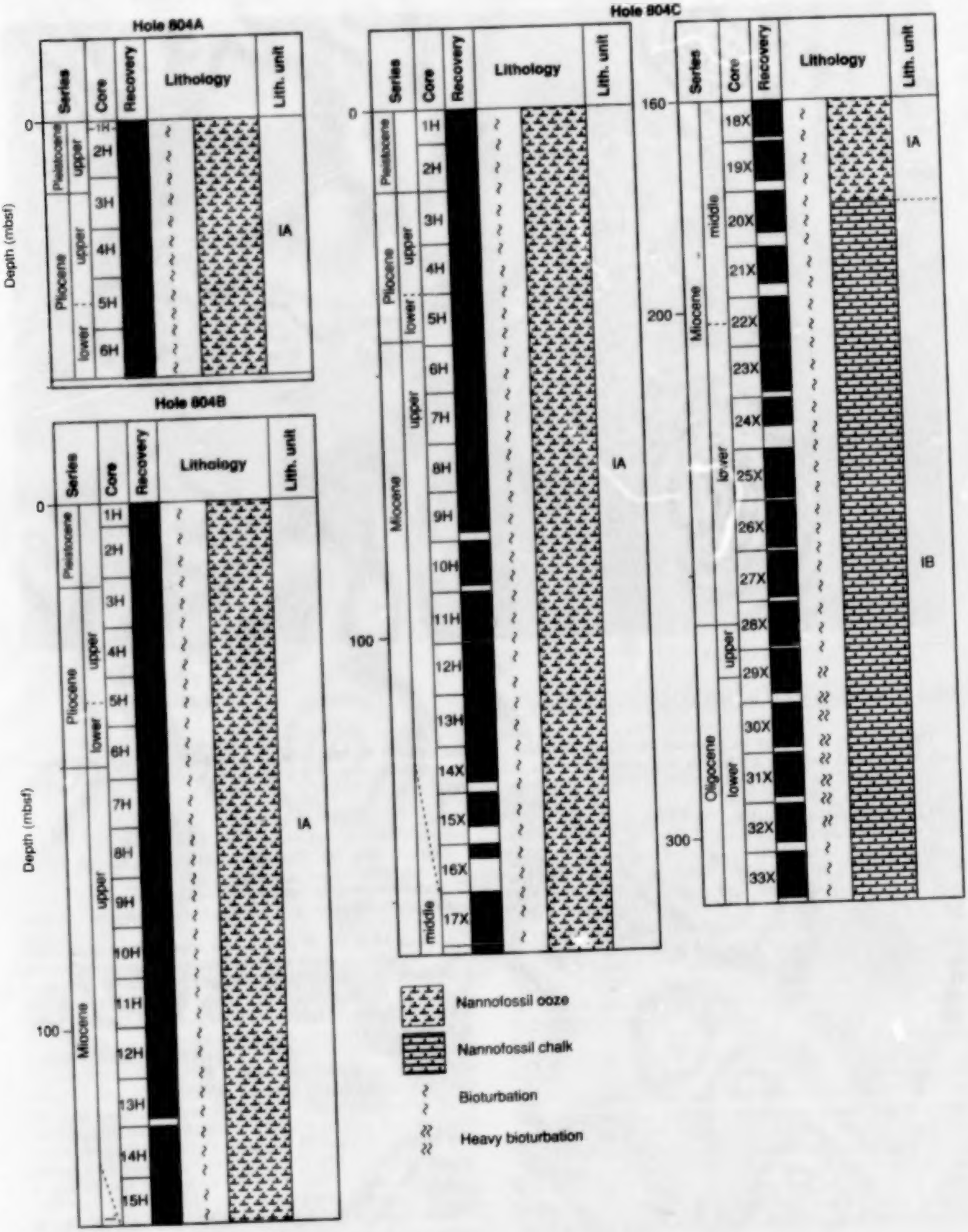
Hole 804A
Depth (mbsf)
0
Series
Core
Recovery
Lithology
Lith. unit
Pleistocene
upper
Pliocene
lower
1H
2H
3H
4H
5H
6H
IA
Hole 804B
Depth (mbsf)
0
100
Pleistocene
Pliocene
upper
lower
Miocene
upper
1H
2H
3H
4H
5H
6H
7H
8H
9H
10H
11H
12H
13H
14H
15H
IA
Hole 804C
0
100
160
200
300
Pleistocene
Pliocene
upper
lower
Miocene
upper
middle
lower
Oligocene
1H
2H
3H
4H
5H
6H
7H
8H
9H
10H
11H
12H
13H
14X
15X
16X
17X
18X
19X
20X
21X
22X
23X
24X
25X
26X
27X
28X
29X
30X
31X
32X
33X
IA
IB
Nannofossil ooze
Nannofossil chalk
Bioturbation
Heavy bioturbation

Figure 4. Lithologic summary, Site 804.

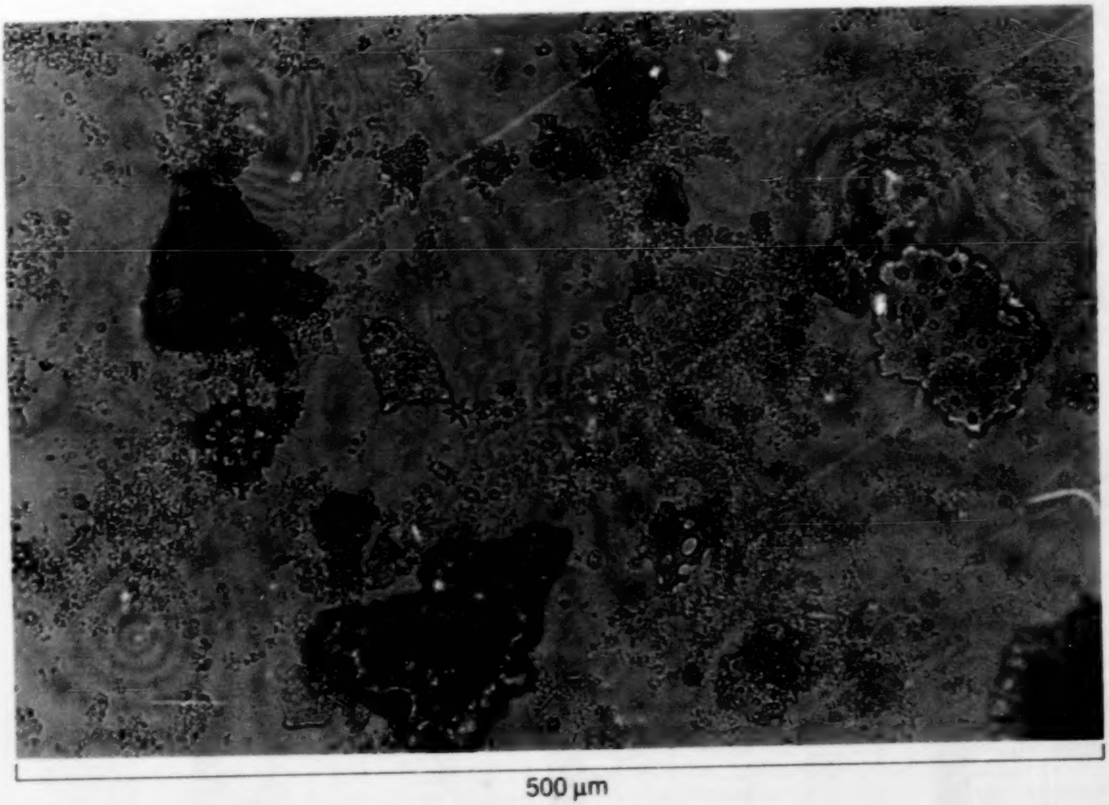

Figure 5. Photomicrograph of turbidite sediment (Section 130-804C-11H-2).

The sediments of Subunit IA generally are slightly to moderately bioturbated, but they are heavily bioturbated in a few intervals. Bioturbation is indicated by burrow mottles of a material that exhibits a different color and is often coarser grained than the surrounding sediments; the burrows and trace structures sometimes are filled by pyrite.

As estimated from visual observation and smear slide descriptions (Fig. 6), texturally these sediments are silts with a few intervals of clayey silts; the sand content rarely exceeds 5%. Carbonate contents generally range between 78% and 93% (Fig. 7). The transition from nannofossil ooze with foraminifers to nannofossil ooze at 40 mbsf is marked by an average increase of approximately 7% in carbonate content. The interval composed of nannofossil ooze shows fairly constant and high carbonate values (around 91%). Fluctuations in the carbonate content increase below 158 mbsf as radiolarians become a significant component of the sediment.

The siliceous biogenic components, mainly radiolarians and diatoms, make up less than 5% of the sediment in Subunit IA, except in the intervals of nannofossil ooze with radiolarians. Abundances of nonbiogenic components identified in smear slides (zeolite, quartz, volcanic ash) are always below 3%. X-ray diffraction (XRD) scans indicate the dominance of calcite throughout Subunit IA, but also record the more detailed variations described previously. Above 40 mbsf, the terrigenous fraction is abundant and includes illite, 7Å and 14Å clays, quartz, and feldspar. Below approximately 40 mbsf, the terrigenous fraction is less abundant and consists predominantly of mixed-layer clays and quartz. The presence of opal is indicated in an XRD sample taken below 158 mbsf.

Subunit IB

Intervals: Hole 804C, Section 130-804C-20X-4 to Core 130-804C-33X
Age: middle Miocene–late early Oligocene
Depth: 181–313 mbsf

Subunit IB is 132 m thick and is composed of nannofossil chalk, nannofossil chalk with radiolarians, radiolarian nannofossil chalk, and nannofossil radiolarite, in order of decreasing abundance. Drilling disturbance is seen as moderately fractured to highly fragmented cores with a few brecciated sections (especially Sections 130-804C-26X-2 through -6).

Nannofossil chalk in the upper part of this subunit graded into radiolarian nannofossil chalk at 197 mbsf (top of Core 130-804C-22X) in the middle Miocene. Within the interval of radiolarian nannofossil chalk, two minor sediment types were encountered that appeared only once and in very small quantities: (1) a drilling fragment of nannofossil radiolarite was found in Section 130-804C-22X-5, and (2) very stiff and structureless nannofossil ooze, heavily disturbed by drilling, was located in Sections 130-804C-23X-5 and -6.

Three intervals of nannofossil chalk, each several meters to several tens of meters thick, alternate with 10- to 25-m-thick in-

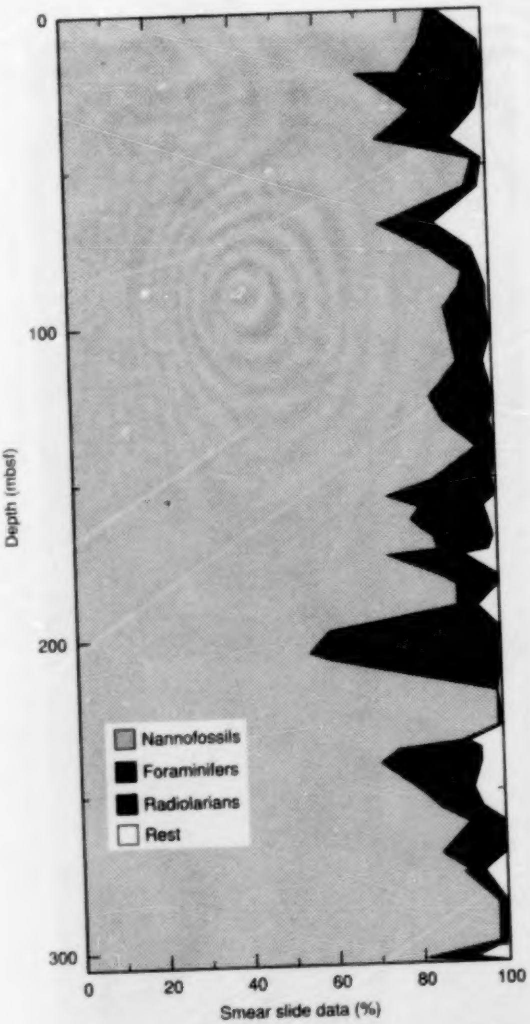

Figure 6. Composition of sediments at Hole 804C, as compiled from smear slide data.

tervals of nannofossil chalk with radiolarians below 226 mbsf in lower Miocene sediments. The base of Subunit IB consists of nannofossil chalk with radiolarians and is of late early Oligocene age.

Bioturbation is generally moderate throughout the subunit, but it is heavy in a few sections. Bioturbation is indicated by color mottles, simple discrete burrows, and well-developed *Zoophycos* trace fossils (e.g., Section 130-804C-33X-1). In Section 130-804C-24X-2, a few centimeter-long pieces of a pyritized burrow fill (around 1 cm in diameter) were noted. Color differences helped us to distinguish between nannofossil chalk and nannofossil chalk with radiolarians in Subunit IB. Pure nannofossil chalk is white (2.5Y 8/0) to light gray (5Y 7/1), whereas nannofossil chalk with radiolarians is white (5Y 8/2, appears yellowish) to very pale brown (10YR 7/3).

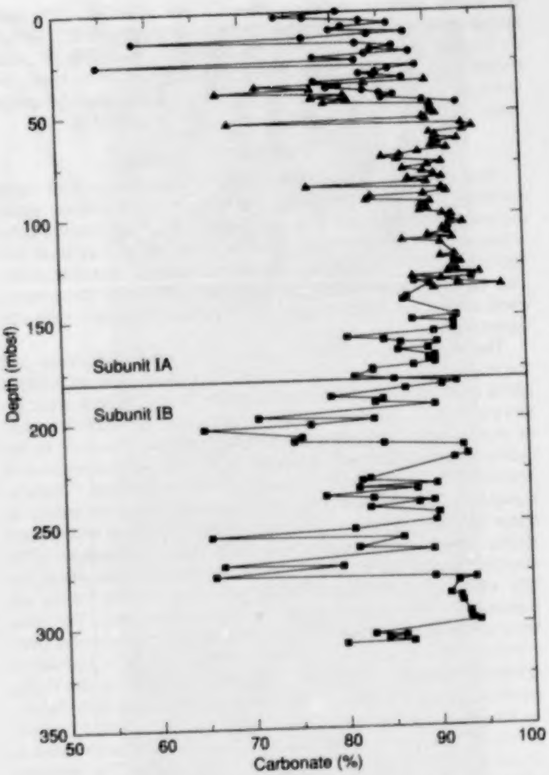

Figure 7. Calcium carbonate content of sediments at Site 804, as determined by shipboard analyses. The profile is a composite of data from Holes 804A (dots), 804B (triangles), and 804C (squares).

Grain-size distributions, estimated from smear slides, indicate that texturally nannofossil chalks are silts whereas nannofossil chalks with radiolarians are clayey silts. Most samples contained more than 5% sand, which was as high as 15% in some cores.

Shipboard carbonate analyses reflect the changes in sediment composition described above (Fig. 7). The radiolarian-rich interval at the top of Subunit IB (197–226 mbsf) appears as a minimum in the carbonate profile, with concentrations between 65% and 75%. The underlying interval of alternating nannofossil chalk and nannofossil chalk with radiolarians is apparent in both the smear slide and the carbonate profiles (Figs. 6 and 7).

Siliceous biogenic components other than radiolarians include diatoms, siliceous sponge spicules, silicoflagellates, and unidentified fragments, each of which contributed less than 5% to the sediments. The XRD scans of samples from Subunit IB indicate the continued importance of calcite, together with the presence and variable abundances of clays, quartz, feldspar, and opal.

Cores 130-804C-21X and -22X are unique in Subunit IB for the evidence of sediment disturbance that they contain. In Core 130-804C-21X, this included elongate (2–5 cm long) features and irregularly shaped mottles with faint outlines that are slightly different in color than the surrounding sediment. Some of these features appear to be compressed burrow fills, but others may be poorly defined sediment clasts. Core 130-804C-22X contained several disturbed zones, with highly contorted, swirled, or fragmented trace fossils and sediment clasts (Fig. 8); distorted (stretched, microfaulted, rotated) thin color bands or laminae (Fig. 9); and angular, centimeter-scale, slightly darker clasts distributed irregularly throughout the core (Fig. 10).

Discussion

The sedimentary sequence at Site 804 is composed of fairly homogeneous nannofossil oozes and chalks with varying abundances of foraminifers and radiolarians. The lithostratigraphic sequence at this site consists of one lithologic unit divided into two subunits (IA and IB) to distinguish between ooze and chalk. The primary sedimentary process that produced the interval cored at Site 804 is interpreted to be pelagic, biogenic sedimentation.

The sedimentary column between the upper Oligocene and the middle Miocene (Subunit IB and the lower part of Subunit IA) is characterized by alternating radiolarian-rich and -poor intervals, implying variations in surface-water productivity and/or dissolution. Carbonate preservation generally is poor in the radiolarian-rich intervals, as indicated by the low abundances of foraminifers and their poor state of preservation (see "Biostratigraphy" section, this chapter). Calcium carbonate values in these intervals are 10%–20% lower than in the pure nannofossil chalks. Intervals with significant radiolarian abundances (>10%) also are recognized by their color; nannofossil chalks are generally white, as compared with the yellowish or pale brown appearance of the nannofossil chalks with radiolarians. The combination of low foraminifer abundances, poor foraminifer preservation, and darker color can be interpreted as an indication of extensive dissolution because of deposition close to the CCD, resulting in the relative enrichment of radiolarians and clays.

Evidence for sediment disturbance (slump blocks, microfaults, dipping, and contorted color bands) is concentrated in Cores 130-804C-21X and -22X (187–207 mbsf). The elongate features in Core 130-804C-21X can be interpreted as clasts that were transported, perhaps only a short distance, and redeposited when both the clasts and the matrix were still soft (ooze). The distortion of trace fossils and color bands or laminae observed in Core 130-804C-22X may represent a shear zone between semilithified sediment packages. Seismic reflection profiles from this area (see "Seismic Stratigraphy" section, this chapter) indicate the effects of major slumping at approximately 80 and 200 mbsf, which coincide with the disturbed intervals in the cores described above. Biostratigraphic data indicate the presence of a hiatus at the top of Core 130-804C-22X (197 mbsf; see "Biostratigraphy" section, this chapter); this hiatus encompasses the time interval from 15 to 20 Ma and occurs at an interval of low measured sonic velocities (see "Physical Properties" section, this chapter). Based on the evidence for mass failures and dissolution and the presence of stratigraphic hiatuses, sedimentation in Subunit IB is considered to be noncontinuous.

The upper portion of Subunit IA appears to be a complete section of upper middle Miocene to Pleistocene sediments (see "Biostratigraphy" section, this chapter), which are dominated by nannofossils with varying abundances of foraminifers. Evidence for some carbonate dissolution is seen in foraminifer test preservation, but the carbonate content remains high (Fig. 7) and radiolarian abundances are insignificant.

Microfaulting and distortion of color bands in the upper Miocene interval (42–110 mbsf) and the presence of turbidites at 93, 178, and 180 mbsf indicate the effects of sediment mass-movement processes. Further evidence for mass-wasting and reworking comes from the mixing observed in the biostratigraphic record (see "Biostratigraphy" section, this chapter) and from the incoherent and transparent zones on the seismic reflection

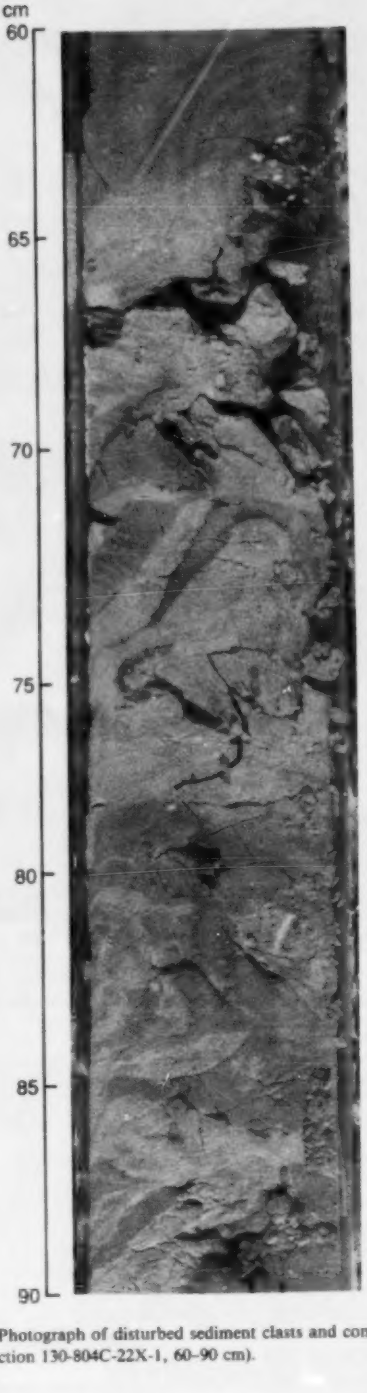

Figure 8. Photograph of disturbed sediment clasts and contorted trace fossils (Section 130-804C-22X-1, 60–90 cm).

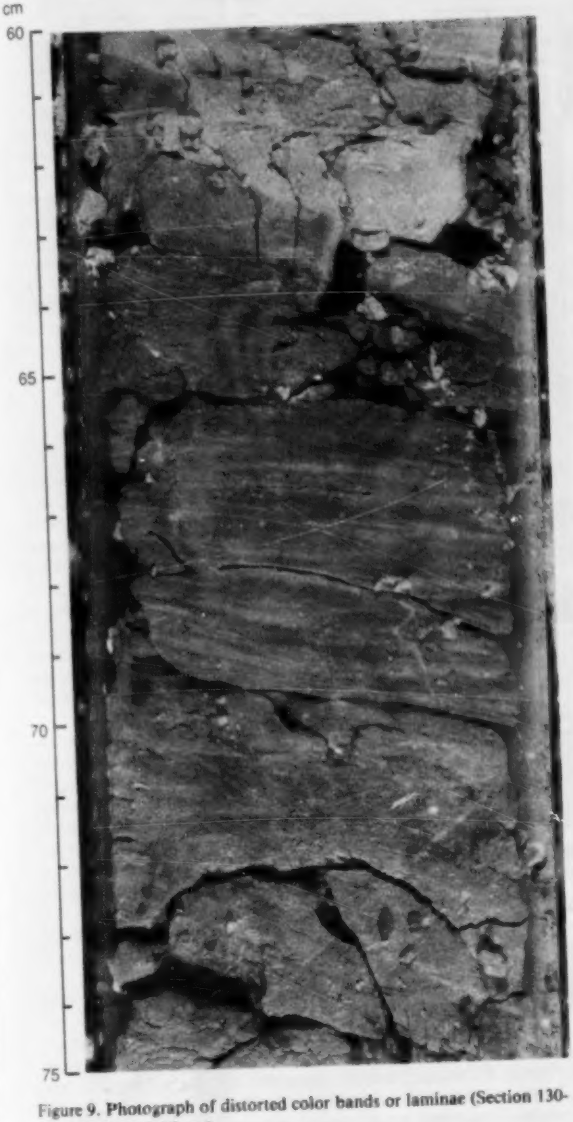

Figure 9. Photograph of distorted color bands or laminae (Section 130-804C-22X-4, 60–75 cm).

profiles taken through the site (see "Seismic Stratigraphy" section, this chapter).

The lithologic and microfossil evidence indicates that carbonate dissolution may have been less severe since the late middle Miocene than before that time. The style of sedimentation, however, which was largely pelagic, biogenic deposition with infrequent slope failures and resedimentation events, remained constant from the late early Oligocene to the Pleistocene.

BIOSTRATIGRAPHY

Introduction

Of the three holes drilled at Site 804, Hole 804A penetrated sediments of Pliocene and Pleistocene age. An apparently com-

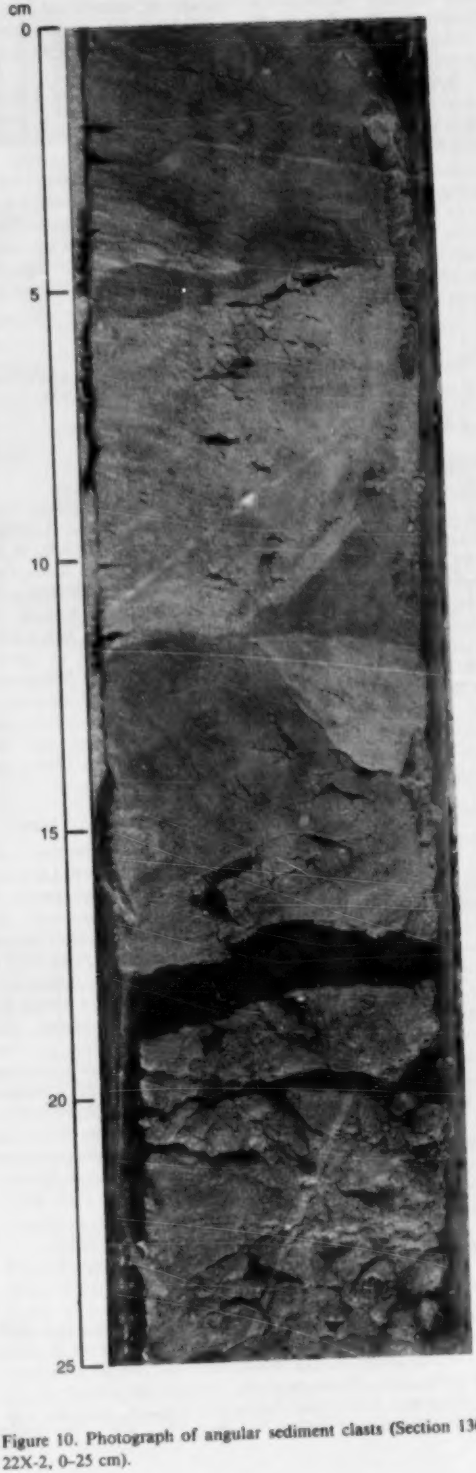

Figure 10. Photograph of angular sediment clasts (Section 130-804C-22X-2, 0–25 cm).

plete sequence was retrieved (Fig. 11). We placed the Pliocene/Pleistocene boundary in Core 130-804A-3H on the basis of planktonic foraminifer, calcareous nannofossil, radiolarian, and diatom evidence.

Hole 804B was drilled to a depth of 137.7 mbsf and penetrated into sediment of late middle Miocene age (Fig. 11). Evidence of downhole contamination and reworking was found in Hole 804B based on evidence from all four fossil groups.

The deepest hole at this site, Hole 804C, penetrated strata of early Oligocene age (Fig. 11). However, we recognized a hiatus at the lower/middle Miocene boundary in this section. The selective dissolution of planktonic foraminifers across this critical interval has removed several important time-diagnostic taxa. The Oligocene/Miocene boundary lies within the interval from Cores 130-804C-27X to -29X (255.1–274.4 mbsf).

Calcareous Nannofossils

Neogene and Oligocene calcareous nannofossil assemblages were recovered from the three holes drilled at Site 804.

Hole 804A

Pleistocene

Sample 130-804A-1H-CC, 0–1 cm, contains abundant *Emiliania huxleyi* together with *Calcidiscus leptoporus, Gephyrocapsa oceanica, Syracosphaera,* and *Umbilicosphaera;* it was placed in Zone NN21. Because of the absence of *E. huxleyi* and *Pseudoemiliania lacunosa,* we assigned Sample 130-804A-1H-CC to Zone NN20. The presence of *P. lacunosa* in Sample 130-804A-2H-CC indicates the Pleistocene Zone NN19. This sample also contains *Reticulofenestra asanoi* (see Sato et al., 1991), which is concentrated in the middle part of Zone NN19, and thus has its range in the upper half of the Matuyama reversed epoch. *Coccolithus pelagicus* and *Discoaster brouweri* were found as high as Samples 130-804A-3H-4, 36–37 cm, and -3H-5, 110–111 cm, respectively. Therefore, the Pliocene/Pleistocene boundary was placed in Core 130-804A-3H.

Pliocene

Sample 130-804A-3H-CC contains *Discoaster brouweri* together with *D. triradiatus;* therefore, this sample was assigned to the uppermost Pliocene Zone NN18. *Discoaster* species in Sample 130-804A-4H-CC consist of *Discoaster brouweri, D. pentaradiatus,* and *D. asymmetricus* and a single specimen of *D. tamalis.* Consequently, we placed this sample in Zone NN17. In contrast to this sample, a diverse discoaster assemblage consisting of such species as *D. asymmetricus, D. brouweri, D. challengeri, D. pentaradiatus, D. surculus, D. triradiatus,* and *D. variabilis* was recognized in Sample 130-804A-5H-CC. This discoaster assemblage, together with the presence of abundant *Reticulofenestra pseudoumbilica* and the absence of *Amaurolithus* species, places Sample 130-804A-5H-CC in Zone NN15. A few beautiful specimens of *D. tristellifer* are also present in this sample. The co-occurrences of *Discoaster quinqueramus, D. berggrenii,* and *Triquetrorhabdulus rugosus* place Sample 130-804A-6H-CC, which is the deepest sample from Hole 804A, in Zone NN11.

Hole 804B

Pleistocene

The nannofossil assemblages of the upper Pliocene and Pleistocene in Hole 804B are similar to those observed in Hole 804A. The extinction of *P. lacunosa* was observed between Sample 130-804B-1H-3, 75 cm, and the core-catcher sample of this core. *Calcidiscus macintyrei* disappears between Samples 130-804B-2H-1, 75 cm, and -3H-1, 74 cm.

Pliocene

Discoaster brouweri and *D. triradiatus* disappear between the 74- and 94-cm levels in Section 130-804B-3H-4, thus placing the Pliocene/Pleistocene boundary in the upper part of Core 130-804B-3H. The NN18/NN17 and NN17/NN18 zonal boundaries fall within Core 130-804B-4H; *D. asymmetricus, D. tamalis,* and *D. variabilis* were observed in Sample 130-804B-4H-CC, placing this sample in the lower half of Zone NN16 (2.9-3.5 Ma). Sample 130-804B-5H-CC contains *Ceratolithus rugosus* and *Discoaster asymmetricus,* together with abundant *Reticulofenestra pseudoumbilica* and sphenoliths, placing this sample in the lower Pliocene. The rare and/or inconsistent occurrences of *D. asymmetricus* and *Amaurolithus* spp. prevent a reliable subdivision of the Zone NN13–NN15 interval in the lower Pliocene. *Cyclicargolithus floridanus* was observed in Sample 130-804B-5H-CC, indicating reworking from Miocene or Oligocene strata.

Miocene

Discoaster quinqueramus was observed from Sample 130-804B-6H-CC through -9H-CC, placing these samples in Zone NN11. The presence of *Discoaster asymmetricus* and several species of ceratoliths, such as *Ceratolithus rugosus* and *C. acutus,* was considered to be the result of downhole contamination. The absence of both *Discoaster quinqueramus* and *Discoaster hamatus* in the two next underlying samples (130-804B-9H-CC and -10H-CC) places these samples in Zone NN10. Sample 130-804B-9H-CC also shows signs of downhole contamination because Pliocene species like *Discoaster tamalis* and *Ceratolithus acutus* are observed within the Miocene Zone NN10 assemblage. One noteworthy character of the Zone NN10 assemblages is the bloomlike, high abundances of small sphenoliths (*Sphenolithus neoabies*?).

Sample 130-804B-11H-CC contains both *Discoaster hamatus* and *Discoaster neohamatus,* whereas Sample 130-804B-12H-CC lacks the latter species. These samples were placed, therefore, in the upper and lower parts of Zone NN9, respectively. Sample 130-804B-13H-CC contains neither *Catinaster coalitus* nor *Sphenolithus heteromorphus,* placing this sample in the NN7–NN6 zonal interval. *Discoaster kugleri* was not observed. The rare and inconsistent occurrences of this species, however, prevent a reliable separation of the NN6 and NN7 Zones. Reworked forms (*Reticulofenestra umbilica* and *Dictyococcites bisectus*) from Eocene or Oligocene strata also occur in Sample 130-804B-13H-CC.

Samples from the two deepest cores of Hole 804B (130-804B-14H-CC and -15H-CC) show mixed assemblages of varying ages. *Discoaster hamatus, Discoaster neohamatus, Catinaster coalitus,* and *Discoaster bellus* represent the late Miocene, whereas *Discoaster druggii* represents the early Miocene, and *Dictyococcites bisectus* must have had an Oligocene or Eocene origin. These taxa are all mixed into sediment of middle Miocene age (Zones NN6/NN7).

Hole 804C

Miocene

The nannofossil assemblages from the Pleistocene to the upper Miocene are similar to those observed in Hole 804B.

We assigned Samples 130-804C-8H-CC through -10H-CC to Zone NN10 because *Discoaster quinqueramus* and *Discoaster hamatus* are both absent in an otherwise early late Miocene assemblage that contains exceptionally abundant sphenoliths, for example. The underlying Zone NN9 interval is remarkably thick, lasting from Samples 130-804C-11H-CC through -16H-CC. The last occurrence (LO) of *Catinaster* spp. was observed between

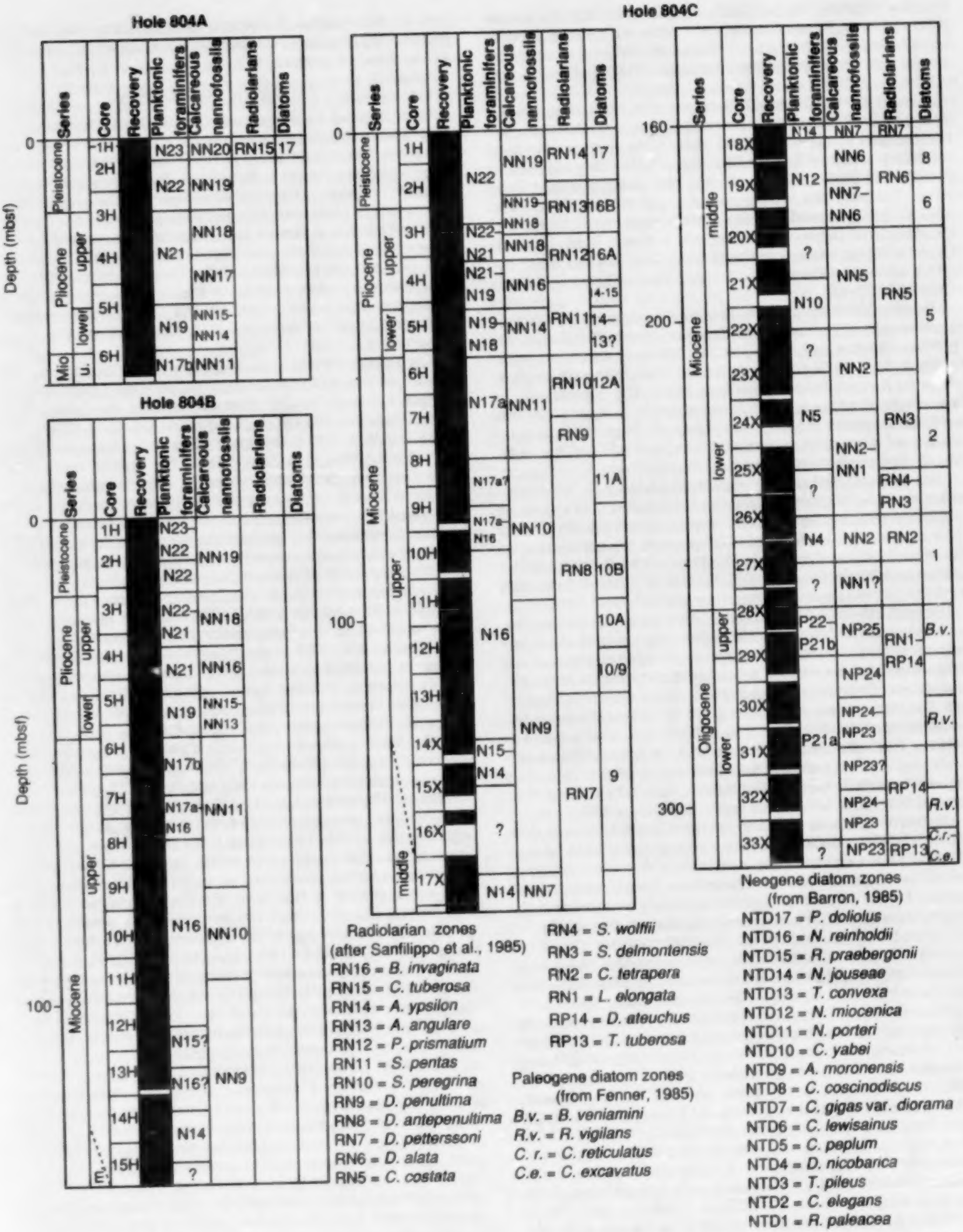

Figure 11. Biostratigraphic hole summaries, Site 804. RN = radiolarian Neogene zone, NTD = Neogene tropical diatom zone, RP = radiolarian Paleogene zone, and NN = nannofossil Neogene zone.

Samples 130-804C-10H-CC and -11H-CC, the first occurrence (FO) of *Discoaster neohamatus* was observed between Samples 130-804C-14X-CC and -15X-CC, and the FO of *Catinaster calyculus* was observed between Samples 130-804C-16X-CC and -17X-CC.

Sample 130-804C-16X-CC is characterized by strong dissolution. The fairly dissolution-resistant discoasters, therefore, are concentrated in abundance and show little or no evidence of secondary overgrowth. Rare *Discoaster kugleri* were observed in Sample 130-804C-17X-CC, placing this sample within Zone NN7. The two next deeper samples (130-804C-18X-CC and -19X-CC) were placed in Zone NN6, not so much because of the absence of *Discoaster kugleri*, which clearly is an unreliable biostratigraphic marker in the Ontong Java Plateau area, but rather because of the LO of *Coronocyclus nitescens* in Sample 130-804C-18X-CC.

Sample 130-804C-20X-CC contains abundant *Sphenolithus heteromorphus* and common *Cyclicargolithus floridanus*, together with other typical early middle Miocene assemblage components, such as *Discoaster deflandrei*, *Coccolithus miopelagicus*, and *Reticulofenestra pseudoumbilica*. The presence of the last species together with *S. heteromorphus* indicates that this sample belongs to the uppermost part of Zone NN5, because the top of this zone contains the evolutionary FO of "normal-sized" *Reticulofenestra pseudoumbilica* (>7 μm).

We also observed that sphenoliths, including *S. heteromorphus*, were abundant in Sample 130-803C-21X-CC. The lack of *Helicosphaera ampliaperta* in Miocene sediments in the Ontong Java region (see also Shafik, 1973) prevents the subdivision of the NN4/NN5 zonal interval. The presence of *Reticulofenestra pseudoumbilica* in Sample 130-803C-21X-CC, however, suggests that this sample represents the upper part of Zone NN5.

Sample 130-803C-22X-CC lacks *Sphenolithus heteromorphus* and *Sphenolithus belemnos*, but it does contain such characteristic lower Miocene species as *Triquetrorhabdulus carinatus* and *Triquetrorhabdulus milowii*, as well as the ubiquitous lower Neogene taxa, *Discoaster deflandrei* and *Cyclicargolithus floridanus*. This implies that perhaps as much as 10% of the lower Neogene is represented in Core 130-803C-22X or that a hiatus is present. The latter seems to be true because *Sphenolithus heteromorphus* is missing already 8 cm into the top of that core. This hiatus across the lower/middle Miocene boundary in Hole 804C has a similar extension to that observed in Hole 803D.

Triquetrorhabdulus carinatus increases in abundance in Core 130-803C-24X, and *Discoaster druggii* was observed in Sample 130-803C-26X-CC, indicating a position within Zone NN2 and above the Oligocene/Miocene boundary. Reliable nannofossil markers for the Oligocene/Miocene boundary are missing in the Ontong Java region. When considering the position of the FO of *Discoaster druggii* and the fact that *Sphenolithus ciperoensis* has its LO in Core 130-803C-29X, which gives this core a position well into the Oligocene, it follows that the Oligocene/Miocene boundary must lie within the two intervening cores.

The presence of intergrading morphotypes within the sphenolith lineage used in Oligocene zonal schemes usually results in poor biostratigraphic precision when determining zonal boundaries (see recent reviews by Okada, 1990; Fornaciari et al., 1990). Unfortunately, this problem also affects the Oligocene biostratigraphy of Leg 130 sediments. Thus, the NP24/NP25 zonal boundary was tentatively placed in Core 130-804C-31X because of the presence of *Sphenolithus distentus* in the core-catcher sample. *Sphenolithus* cf. *S. ciperoensis* was observed in Sample 130-804C-32X-CC, together with *Sphenolithus distentus*, suggesting a position within Zone NP24.

Hole 804C reached its terminal depth at Sample 130-804C-33X-CC, a sample that also contains *Sphenolithus predistentus* and *Sphenolithus pseudoradians*, abundant *Coccolithus pelagicus*, *Cyclicargolithus floridanus*, few *Discoaster tanii*, and *Coccolithus eopelagicus*. This sample was assigned to Zone NP23 of the lower Oligocene.

Planktonic Foraminifers

The preservation of the abundant planktonic foraminifers in Hole 804A ranges between moderate and poor. The time span represented in the six cores retrieved covers the interval from Zone N22 (Pleistocene) to Zone N17b (just below the Miocene/Pliocene boundary). Figure 11 illustrates the stratigraphic distribution of the planktonic foraminifers recovered from Site 804.

The Pleistocene section in this site is characterized by a diverse assemblage of planktonic foraminifers with clear tropical affinities. Sample 130-804A-1H-CC does not contain *Globorotalia tosaensis* and so is of latest Pleistocene age (upper N22). The co-occurrence of *G. tosaensis* and *Globorotalia truncatulinoides* in Sample 130-804A-2H-CC indicates a lower Pleistocene age within Zone N22.

The Pliocene/Pleistocene boundary, as defined by the presence of planktonic foraminifers, is within Core 130-804A-3H as Sample 130-804A-3H-CC does not contain specimens of *G. truncatulinoides*. We referred Samples 130-804A-3H-CC and -4H-CC to Zone P21 in the upper Pliocene, and we placed Sample 130-804A-5H-CC in Zone N18 on the basis of the presence of *G. tumida* in the absence of *Sphaeroidinella dehiscens*. Sample 130-804A-6H-CC was assigned to Zone N17b based on the presence of *Pulleniatina primalis*. Given the distribution of this species, it appears that part of the Pliocene (Zones 19/20) is missing in the recovered section or has failed to be resolved with a sampling density of one sample per core.

The abundance and preservation of planktonic foraminifers in Hole 804B is highly variable. The total age range of the 15 cores retrieved at this hole covers the time interval from the early Pleistocene (N22) to the late middle Miocene (N14). The fauna in Sample 130-804B-1H-CC lacks *G. truncatulinoides* and *G. tosaensis*; however, Sample 130-804B-2H-CC is placed in Zone N22 (Pleistocene). The co-occurrence of *G. truncatulinoides* and *Globigerinoides fistulosus* indicates a latest Pliocene age for Sample 130-804B-3H-CC, although it is still within Zone N22. Sample 130-804B-4H-CC was assigned to Zone N21. It is not possible to assign a zone to Sample 130-804B-5H-CC.

Sample 130-804B-6H-2, 135–137 cm, was placed within Zone N19, whereas the core catcher from the same section was assigned to Zone N17. This implies either the presence of a hiatus covering much of the Pliocene within Core 130-804B-6H or insufficient sampling resolution, as noted in Hole 804A. Zone N16 was expanded in this hole, and time-diagnostic fossils of this interval (the absence of *Globorotalia plesiotumida* and the presence of *Neogloboquadrina acostaensis*) were found from Samples 130-804B-7H-CC through -13H-CC. Sample 130-804B-12H-CC was difficult to date because of the poor preservation. We assigned Sample 130-804B-14H-CC to Zone N14 based on the presence of *Globorotalia siakensis*. Hence, the implication is that Zone N15 is either missing in this hole or was missed in our preliminary core-catcher examination.

Hole 804C is the deepest hole drilled at this site and covers the interval from the Pleistocene (N22) to the early Oligocene (P21b). The abundance of planktonic foraminifers declines downhole, reaching a minimum between Samples 130-804C-21X-CC and -28X-CC. Further downhole, the abundance of the planktonic foraminifers increases. The preservation of planktonic foraminifers is variable in Hole 804C, but it is best between Samples 130-804C-12H-CC and -15H-CC. The poorest preservation occurs between Samples 130-804C-16H-CC and -24X-CC.

Samples 130-804C-1H-CC through -3H-CC are of Pleistocene age within Zone N22. Sample 130-804C-4H-CC was placed in lower Zone N21 or upper Zones N19–N20. As was the case with the previous two holes at this site, much of the Pliocene of Zone N19/N20 appears to be missing or condensed. Sample 130-804C-5H-CC was assigned to Zone N18 because of the presence of *Globorotalia tumida* and the lack of *Sphaeroidinella dehiscens*. Zone N17a occupies Samples 130-804C-6H-CC through -9H-CC because the index species for Zone N17b (*Pulleniatina primalis*) was not observed. Samples 130-804C-10H-CC to -13H-CC were assigned to Zone N16 based on the absence of *G. plesiotumida* and the presence of *N. acostaensis*.

It was not possible to assign an age to Sample 130-804C-14X-CC because of the downhole contamination that is evident (the presence of *Neogloboquadrina humerosa* and *N. acostaensis* in a sample containing *G. siakensis* is particularly revealing in this regard). Sample 130-804C-15X-CC is partially dissolved and devoid of age-diagnostic planktonic foraminifer taxa, and Sample 130-804C-16X-CC is barren of foraminifers, implying that dissolution intensified. Sample 130-804C-17X-CC also shows evidence of downhole contamination with the co-occurrence of *G. siakensis* and *N. acostaensis*. Sample 130-804C-18X-CC is of Zone N12 age, based on the presence of *Globorotalia fohsi lobata*, and Sample 130-804C-19X-CC was assigned to Zone N12 based on the presence of *Globorotalia fohsi*. The poor preservation in Sample 130-804C-20X-CC precluded a zonal assignment.

The poor preservation inherent in this portion of Hole 804C probably has selectively removed more delicate morphotypes, as suggested by the low diversity of foraminifers in Sample 130-804C-21X-CC. Hence, the presence of *Globorotalia* cf. *peripheroacuta* suggests an age range of Zones N10 through N12, but the more delicate *Globorotalia praefohsi*, which would indicate Zone N11, may have been dissolved out of the sample. Poor preservation in Sample 130-804C-22X-CC has reduced species diversity to only the most robust members of the fauna. This sample contained only single specimens each of the species *Globorotalia venezuelana* and *Sphaeroidinella disjuncta*. It was not possible, therefore, to assign an age to it.

Samples 130-804C-23X-CC and -24X-CC were assigned to Zone N5. The lack of age-diagnostic fossils in 130-804C-25X-CC precluded an age assignment for this sample. Sample 130-804C-26X-CC was assigned to Zone N4 based on the presence of *Globorotalia kugleri*. Samples 130-804C-27X-CC and -28X-CC are barren of planktonic foraminifers. Samples 130-804C-29X-CC to -32X-CC are of early Oligocene age (Zone P21a), based on the presence of *Globorotalia opima*. Sample 130-804C-33X-CC is barren. Much of the upper Oligocene is missing at this site.

Diatoms

We also examined diatoms in Hole 804C and found that Quaternary through Oligocene specimens were present. The assignment of samples to low-latitude diatom zonation is summarized in Figure 11.

Above 101.3 mbsf (Cores 130-804C-1H to -11H), diatoms are common to abundant, and preservation is generally good. Below Sample 130-804C-11H-CC, diatoms are less abundant and preservation is generally poor to moderate. Diatoms decreased sharply in abundance and preservation from Samples 130-804C-27X-CC (lowest early Miocene) through -30X-CC (early Oligocene). This interval contains only sparse, poorly preserved diatoms that are difficult to assign to any particular zone. Thereafter, diatoms increase in abundance again, and preservation is good from Sample 130-804C-32X-CC to the base of the hole.

As at Site 803, the sequence is complete from the Quaternary NTD 17 *Pseudoeunotia doliolus* Zone (Sample 130-804C-1H-CC) through the lower middle Miocene NTD 5 *Cestodiscus peplum* Zone (Sample 130-804C-22X-CC). At this point, we observed a break in the sequence, and Sample 130-804C-24X-CC was assigned to the NTD 2 *Craspedodiscus elegans* Zone. The sequence is complete from the lower middle Miocene through the early Oligocene (Sample 130-804C-33X-CC). Two diatom zones, NTD 4 *Denticulopsis nicobarica* and NTD 3 *Triceratium pileus*, are completely missing at Site 804; therefore, a hiatus in the early Miocene has been suggested to account for this gap (see "Biostratigraphy" section, "Site 803" chapter, this volume).

Sample 130-804C-1H-CC was assigned to the NTD 17 Zone. The Pliocene/Pleistocene boundary is located in the NTD 16 *Nitzschia reinholdii* Zone (Samples 130-804C-2H-CC and -3H-CC) and is coincident with a peak in the abundance of *Thalassiosira oestrupii*.

Sample 130-804C-4H-CC was placed in the late Pliocene TD 15 *Rhizosolenia praebergonii* Zone (Subzone A). The LO of *Nitzschia jouseae* falls within Subzone A. Sample 130-804C-4H-CC is contaminated with Pleistocene specimens. The Miocene species *Coscinodiscus nodulifer* var. *cyclopus* is present in Samples 130-804C-5H-CC and -6H-CC and is probably reworked. The Pliocene/Miocene boundary could not be identified with the present sampling resolution.

The presence of *Nitzschia miocenica* and the absence of members of the *Thalassiosira convexa* group allowed us to assign Sample 130-804C-6H-CC to the NTD 12 *N. miocenica* Zone, Subzone A. The overlap between the FO of *N. miocenica* and the LOs of *Nitzschia porteri* and *Rossiella paleacea* and the presence of *Thalassiosira burckliana* is noted in Sample 130-804C-8H-CC. This sample was assigned to the NTD 11 *N. porteri* Zone, base of Subzone A, with some uncertainty.

The NTD 10 *Coscinodiscus yabei* Zone extends over Cores 130-804C-10H (Subzone B: *T. burckliana* present) and 130-804C-11H (Subzone A: *Coscinodiscus temperei* var. *delicata* present). The LOs of *Actinocyclus moronensis* and *Denticulopsis hustedtii* and the FO(?) of *Coscinodiscus vetustissimus* var. *javanicus* were observed in Sample 130-804C-12H-CC. Samples 130-804C-13H-CC through -16X-CC were assigned to the NTD 9 *Actinocyclus moronensis* Zone (middle Miocene/late Miocene boundary). Sample 130-804C-18X-CC is contained in the NTD 8 *Craspedodiscus coscinodiscus* Zone. In Hole 804C the LOs of *Synedra jouseana*, *Actinocyclus ingens*, and *Actinocyclus ellipticus* var. *spiralis* also fall within this zone.

The LOs of *Coscinodiscus lewisianus* and *Cestodiscus pulchellus* were recorded in Sample 130-804C-19X-CC. Sample 130-804C-20X-CC falls within Subzone B of the NTD 5 *Cestodiscus peplum* Zone, and Sample 130-804C-22X-CC is within Subzone A, which contains *Annellus californicus*. The middle Miocene/early Miocene boundary is also contained within Subzone A.

The LO of *Craspedodiscus elegans* (NTD 2 Zone) was found in Sample 130-804C-24X-CC. In Sample 130-804C-26X-CC, the next downcore sample analyzed, *Rosiella paleacea* and *Borgorovia veniamini* are common, and *Coscinodiscus oligocenicus* and *C. lewisianus* var. *rhomboides* are present. *Thalassiosira primalabiata* is present in Sample 130-804C-27X-CC. The presence of this flora allowed us to assign this interval to the NTD 1 *Rosiella paleacea* Zone.

The *Rocella gelida* Zone seems to be missing or compressed at Hole 804C. Therefore, we could not identify the Miocene/Oligocene boundary. However, *Rocella vigilans* becomes abundant in Sample 130-804C-28X-CC and remains common throughout Sample 130-804-32X-CC. *Borgorovia veniamini* is also present in Sample 130-804C-28X-CC. Preservation in Cores 130-804C-28X through -30X is too poor to allow recognition of the subzones of the *R. vigilans* Zone.

Sample 130-804C-33X-CC contains lower Oligocene flora and was placed in the *Cestodiscus reticulatus–Coscinodiscus excavatus* Zones sensu Fenner (1985) and the *C. excavatus* Zone sensu Barron (1985).

Radiolarians

Radiolarians examined from core-catcher samples at Holes 804A and 804C range in age from the Pleistocene in the uppermost cores to the Oligocene at the base of Hole 804C (312.5 mbsf). The following discussion is based on the zonal assignment of stratigraphically important taxa examined in core-catcher samples. Also discussed is the state of radiolarian preservation. The radiolarian zonation of Hole 804C and the correlation of these zonations with other taxa is summarized in Figure 11. The radiolarian biostratigraphic data from this site show a sequential zonal succession throughout the Neogene and the Oligocene, except for one zone that was not recorded (between Samples 130-804C-22X-CC and -23X-CC).

Pleistocene

Sample 130-804A-1H-CC was assigned to the *Collosphaera tuberosa* Zone of the late Pleistocene as it contains *C. tuberosa, Lamprocyrtis nigriniae,* and *Theocorythium trachelium trachelium,* key taxa to this zone. Core 130-804C-1H-CC, however, does not contain either *C. tuberosa* or *T. t. trachelium,* but one specimen of *L. nigriniae* was found. Therefore, this sample belongs to the *Amphirhopalum ypsilon* Zone. The next lower sample (130-804C-2H-CC) was assigned to the *Anthocyrtidium angulare* Zone of the lower Pleistocene because *A. angulare, Lamprocyrtis neoheteroporos,* and *T. t. trachelium* are present.

Pliocene

The LO of *Pterocanium prismatium* was recorded in Sample 130-804C-3H-CC together with the presence of *Lamprocyrtis heteroporos* (FO) as well as *Spongaster tetras* and *Didymocyrtis tetrathalamus,* which lead us to assign this sample to the *P. prismatium* Zone. The specimen of *Calocycletta virginis* found in this sample is either the result of reworking or contamination. The LO of *Stichocorys peregrina* was located in Sample 130-804C-4H-CC. The presence of *D. tetrathalamus, P. prismatium,* and *Anthocyrtidium jenghisi* leads to an assignment of this sample to the *Spongaster pentas* Zone.

The next lower sample (130-804C-5H-CC) contains the LOs of *Phormostichoartus doliolum* and *Didymocyrtis avita* as well as the presence of *S. pentas* and *P. prismatium.* One specimen of *Diartus hughesi* and a few specimens of *Didymocyrtis avita* found in this sample are probably the result of reworking. This sample was placed in the *S. tetras* Zone. Sample 130-804C-6H-CC was placed in the *Stichocorys peregrina* Zone as it contains the LO of *Spongaster berminghami* and the presence of *S. peregrina, S. delmontensis, D. avita,* and *Solenosphaera omnitubus.* This zone extends from 4.3–4.4 to 6.1–6.7 Ma and contains the Miocene/Pliocene boundary.

Late Miocene

We assigned Sample 130-804C-7H-CC to the *Didymocyrtis penultima* Zone mainly because of the presence of *S. omnitubus,* although *Didymocyrtis antepenultima* and *D. laticonus* are also present, most likely the result of reworking. Sample 130-804C-8H-CC was unambiguously placed in the *Didymocyrtis antepenultima* Zone because abundant *S. peregrina, D. laticonus,* and *D. hughesi* as well as common *S. delmontensis* and rare *Dictyocoryne ontogenesis* are present. This zone continues through Sample 130-804C-12H-CC.

Middle Miocene

Sample 130-804C-13H-CC was placed in the *Diartus petterssoni* Zone based on the occurrences of *Lithopera thornburgi, Liriospyris elevata, Stichocorys wolffii,* and *D. petterssoni.* The specimen of *Lithopera renzae* found in this sample is considered to be reworked. Samples 130-804C-14H-CC and -16H-CC were also assigned to this zone. Sample 130-804C-18X-CC is considered to be in the *Calocycletta alata* Zone because of the presence of *D. laticonus, Lithopera neotera, L. renzae,* and *S. wolffii.*

Abundant specimens of *Stichocorys* cf. *peregrina* are present in this sample, but *S. peregrina* is thought to be extinct slightly before 7.2 Ma (Shipboard Scientific Party, 1989). Thus, it should not be placed in this sample but, rather, assigned to the *D. antepenultima* Zone or to a younger zone. An alternative explanation is that *Stichocorys* cf. *peregrina* is a form quickly evolved from *S. delmontensis,* which went extinct soon after. Therefore, this form is considered to be a variant of *S. delmontensis* or a taxon other than *S. peregrina.*

Early Miocene

Sample 130-804C-20X-CC belongs to the upper part of the *Calocycletta costata* Zone as *Dorcadospyris dentata* (LO), *D. forcipata* (LO), *Lithospyris parkerae,* and *Didymocyrtis violina* are present. This zone continues into Sample 130-804C-22X-CC. The *Stichocorys wolffii* Zone, the next sequential radiolarian zone, was not recorded in either Sample 130-804C-22X-CC or -23X-CC. Therefore, it is possible that a hiatus exists within Core 130-804C-23X. Sample 130-804C-23X-CC was placed in the *Stichocorys delmontensis* Zone, the next lower zone, as this sample contains the LO of *D. ateuchus* and the FO of *Cyclampterium leptetrum.* Sample 130-804C-24X-CC is also in the same zone.

The next lower sample examined (130-804C-26X-CC) is bracketed by the FO of *Cyrtocapsella cornuta* and the LO of *Theocyrtis annosa,* which leads to the *Cyrtocapsella tetrapera* Zone. It should be noted that the FOs of *S. delmontensis, D. violina,* and *Lychocanoma elongata* were all recorded in this sample, which indicates that the ranges of the former two taxa extend into this zone rather than end at the bottom of the *S. delmontensis* Zone (Sanfilippo et al., 1985).

Sample 130-804C-27X-CC contains *D. ateuchus, T. annosa,* and *Dendrospyris bursa* and the LO of *Artophormis gracilis,* which places this sample in the *Lychocanoma elongata* and/or *D. ateuchus* Zone. According to Nigrini and Lombari (1984), *D. bursa* ranges from the *L. elongata* Zone in the late Oligocene to the *D. alata* Zone in the middle Miocene, based on a study in the western tropical Pacific. However, several stratigraphically deeper samples, assignable to the Oligocene, contain this species. Therefore, we conclude that the range of this species is older than previously thought (see below for documentation of this taxon).

Sample 130-804C-28X-CC belongs to the lower part of the *L. elongata* Zone and to the upper part of the *D. ateuchus* Zone as four specimens of *Dorcadospyris papilio* were found, in addition to the presence of *Dorcadospyris forcipata, D. ateuchus,* and *D. praeforcipata* in the >250-μm size fraction. (Several samples of this age were specifically processed with either the 125- or 250-μm sieve in addition to a 63-μm sieve because of the large size of the species belonging to the genus *Dorcadospyris.*) Sample 130-804C-29X-CC cannot be differentiated from either the *L. elongata* or the *D. ateuchus* zones because this sample only contains such taxa as *A. gracilis, D. ateuchus, D. forcipata,* and *T. annosa.* Sample 130-804C-30X-CC was placed in the *L. elongata* or *D. ateuchus* zones based on the presence of *D. ateuchus, C. pegetrum,* and *D. bursa.*

Oligocene

Sample 130-804C-31X-CC was unambiguously placed in the *D. ateuchus* Zone because of the presence of *D. ateuchus, D. forcipata, Theocyrtis annosa,* and *Lithocyclia angusta.* One specimen of *Dorcadospyris triceros* recorded in this sample is present in the next older zone. This specimen is considered to be an evolutionary form because the change from *D. triceros* to *D. ateuchus* is an evolutionary transition. Sample 130-804C-32X-CC was assigned to the *D. ateuchus* Zone as it contains *D. ateuchus, D. forcipata, C. pegetrum,* and *T. annosa*. One specimen of *Dorcadospyris triceros* found in this sample is probably the result of evolutionary transition.

Abundant *Centrobotrys petrushevskayae* in this sample (observed continuously from Sample 130-804C-23X-CC downward) warrants further study in revising the ranges of this taxon, as it is should be present only in the lower part of the *Theocyrtis tuberosa* Zone of the Oligocene. Based on data from this site alone, the younger limit of *C. petrushevskayae* extends to the *S. delmontensis* Zone. Sample 130-804C-33X-CC, from the last core in the hole, was assigned to the *T. tuberosa* Zone because of the presence of *Dorcadospyris pseudopapilio* and *Lithocyclia crux*. *D. bursa*, also found in this sample, ranges from the *T. tuberosa* Zone (FO) to the *S. delmontensis* Zone (LO) and revises the published range of Nigrini and Lombari (1984).

Preservation

The preservation of radiolarians at this site is generally better than that of specimens studied at Site 803. Site 804 (3920 m) is 520 m deeper than Site 803 (3400 m), resulting in significantly greater dissolution of both calcareous nannoplankton and planktonic foraminifers at this site. This, in turn, may have provided higher concentrations of cations (e.g., Fe, Mn, and Al) remineralized from biogenic minerals in interstitial waters. Although the sedimentation rate at this site is less than that at Site 803, the predicted higher concentrations of these elements may have resulted in increased cation coating and, hence, a lower rate of silica dissolution; this hypothesis is supported by the better preservation of diatoms at Site 804 than at 803.

As at Site 803, the preservational state of radiolarians deteriorates in the older samples. Generally, Pleistocene and Pliocene radiolarians are well preserved and early Miocene and Oligocene radiolarians are poorly preserved. It appears that once the biogenic opal contents of the sediment decrease beyond a critical level, siliceous fossils start dissolving at a higher rate, thereby resulting in poorer preservation. This may be related to changes in paleoproductivity that controlled supply rates of biogenic opal to the seafloor.

PALEOMAGNETISM

Introduction

Pass-through cryogenic magnetometer measurements were conducted on all cores from the three holes drilled at Site 804. As at Site 803, the Pliocene-Pleistocene sequence yielded stable magnetizations after alternating field (AF) demagnetization, from which a detailed magnetostratigraphy was recognized (Fig. 12). Intensities diminished in all three holes from average values of 1–10 $\mathrm{mAm^{-1}}$ above Cores 130-804A-6H, 130-804B-6H, and 130-804C-6H to values generally $<0.1\ \mathrm{mAm^{-1}}$ below Cores 130-804A-7H, 130-804B-7H, and 130-804C-7H; this drop in intensity corresponds to an age of about 5 Ma. Reduced natural remanent magnetization (NRM) intensities, and the presence of a steeply inclined viscous overprint probably originating during drilling, precluded any interpretation of the Miocene sequence.

Measurements were taken at 3- and 5-cm intervals throughout the Quaternary and Pliocene sequence, but the interval was increased to 10 cm in the weakly magnetized Miocene sequence. The NRM was measured on all cores as well as the magnetization after 15-mT AF demagnetization on all but the most weakly magnetized cores.

Multishot orientations were carried out on Cores 130-804A-3H to -6H, 130-804B-3H to -6H, and 130-804C-3H to -13H. Careful examination of the multishot tool by the drilling team after each use largely avoided the orientation problems encountered at Site 803, but orientation errors nevertheless appeared to affect Cores 130-804B-4H and 130-804C-13H. The declinations of intervals of the same polarity frequently increase by about 20°–30° from the top to the base of a core (e.g., Core 130-804A-3H; Fig. 13); this is evidently a result of rotation within the core barrel, either during or after drilling. An additional error arose through the formation of air bubbles within the multishot magnetic compass. Core orientations are based on a photographic image of this compass, and bubbles obscured this record to the extent that some core orientations were uncertain by as much as ±20°.

Section 130-804A-4H-2 was cut along the wrong orientation lines, resulting in an incorrect reference declination; this was corrected in constructing the magnetostratigraphy.

Pliocene-Pleistocene Magnetostratigraphy

Magnetostratigraphic columns were constructed for each of the three holes (Fig. 12) and were generally in good agreement with each other. Cores 130-804A-1H and -2H, 130-804B-1H and -2H, and 130-804C-1H and -2H were unoriented; their polarities were inferred by extension from the polarity sequence of the underlying oriented cores. No coherent polarity record could be recognized below Core 6H in all three holes. Holes 804A and 804B preserve nearly complete polarity records over the Brunhes, Matuyama, and Gauss chrons. Continuous magnetostratigraphy in Hole 804B may extend as far as the Nunivak Subchron in the Gilbert Chron. Interruptions to the magnetostratigraphic record in Hole 804C (the result of disturbed sections in Cores 130-804C-4H and -5H) limit the resolution of the Gauss and Gilbert chrons in this hole.

Preservation of major polarity events is good in all three holes. We identified the Jaramillo and Olduvai subchrons within the Matuyama Chron and the Kaena and Mammoth subchrons within the Gauss Chron in all three holes. Near the base of Core 130-804B-5H, we could also identify the Cochiti Subchron of the Gilbert Chron. A short but prominent normal polarity event occurs within the Matuyama Chron at a similar stratigraphic level in all three holes at this site; this probably represents one of the two normal events within the Réunion Subchron, but which one is not clear.

A short interval of intermediate polarity overlies the prominent Réunion Event in both Holes 804A and 804B (Fig. 13). This may correspond to the upper Réunion Event, but no corresponding event is present in Hole 804C. An interval of intermediate polarity, which may correspond to the lower Réunion Event, occurs between 23.8 and 24.5 mbsf in Hole 804C. Correct identification of the Réunion events is important, as they occur near the time a change in sedimentation rate is indicated by the magnetostratigraphy of Site 803. The correlation indicated in Figure 12 results in the simplest pattern of change in the sedimentation rate, and so is preferred here, at least for Holes 804A and 804B.

The oldest polarity event that can be definitely correlated among the holes is the Cochiti Subchron, between 42.5 and 41.7 mbsf in Hole 804B. Greater than 100% recovery leads to an overlap of about 30 cm between the sub-bottom depths indicated for the base of Core 130-804B-5H and the top of Core 130-804B-6H. Within this overlap, the polarity indicated in Core 130-804B-5H is reversed, whereas in Core 130-804B-6H it is normal. It is possible that a very short normal polarity event has been recovered here. Alternatively, either some recovery may have been lost, or the section is locally compressed, so that the Nunivak Subchron is represented by only a 50-cm interval, and the lowest interval recorded in this hole is the Sidufjall Subchron.

Intensities decrease rapidly below 43–45 mbsf in all three holes, dropping by an order of magnitude over a few meters. Core 130-804A-6H appears to record a pattern of continuous

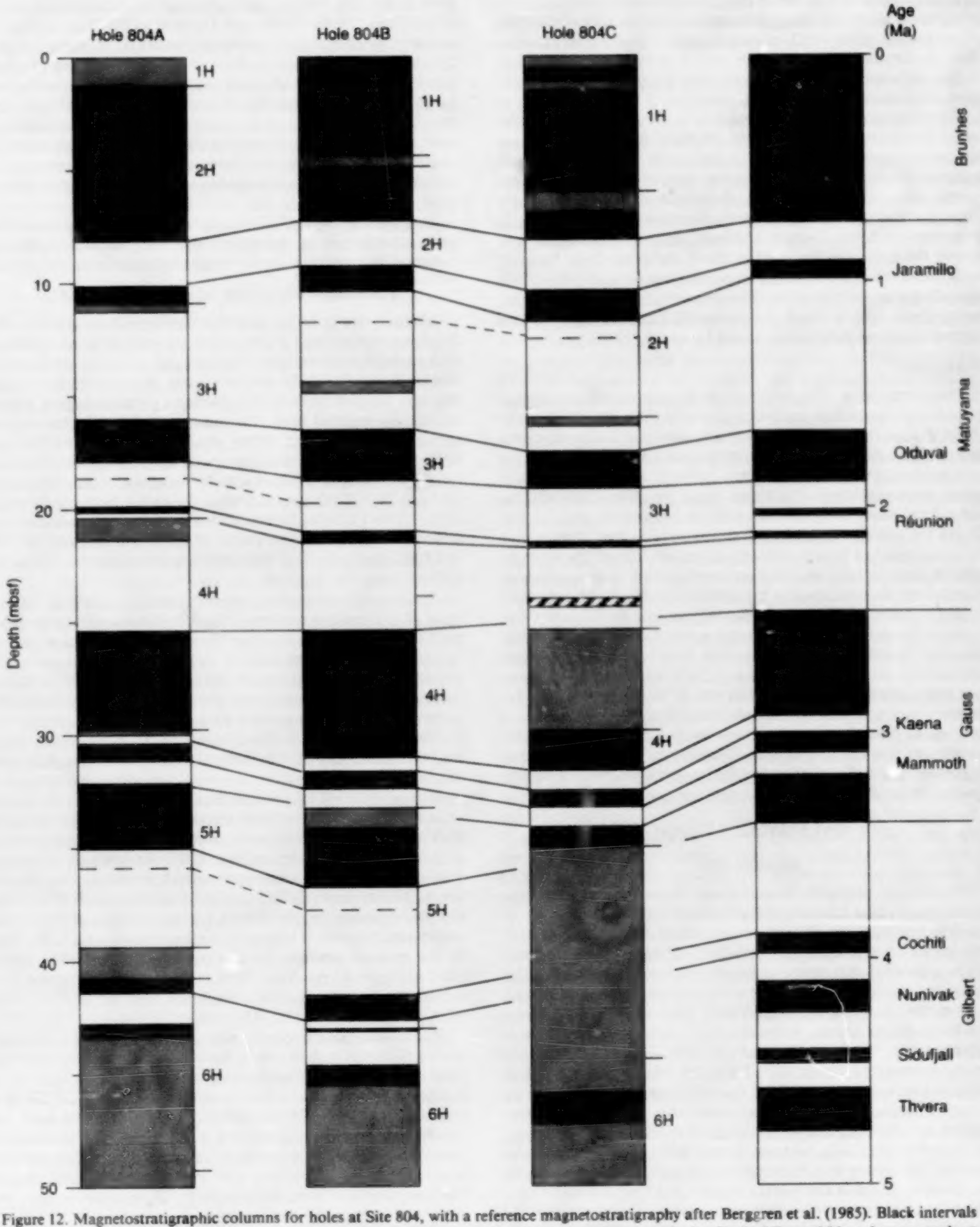

Figure 12. Magnetostratigraphic columns for holes at Site 804, with a reference magnetostratigraphy after Berggren et al. (1985). Black intervals indicate normal polarization; white, reverse polarization. Half-tone shading indicates unknown polarity. Dashed lines within columns are short events; diagonally hatched interval is of intermediate polarity. Confident ties between columns are shown by an unbroken line; dashed lines indicate ties between minor events.

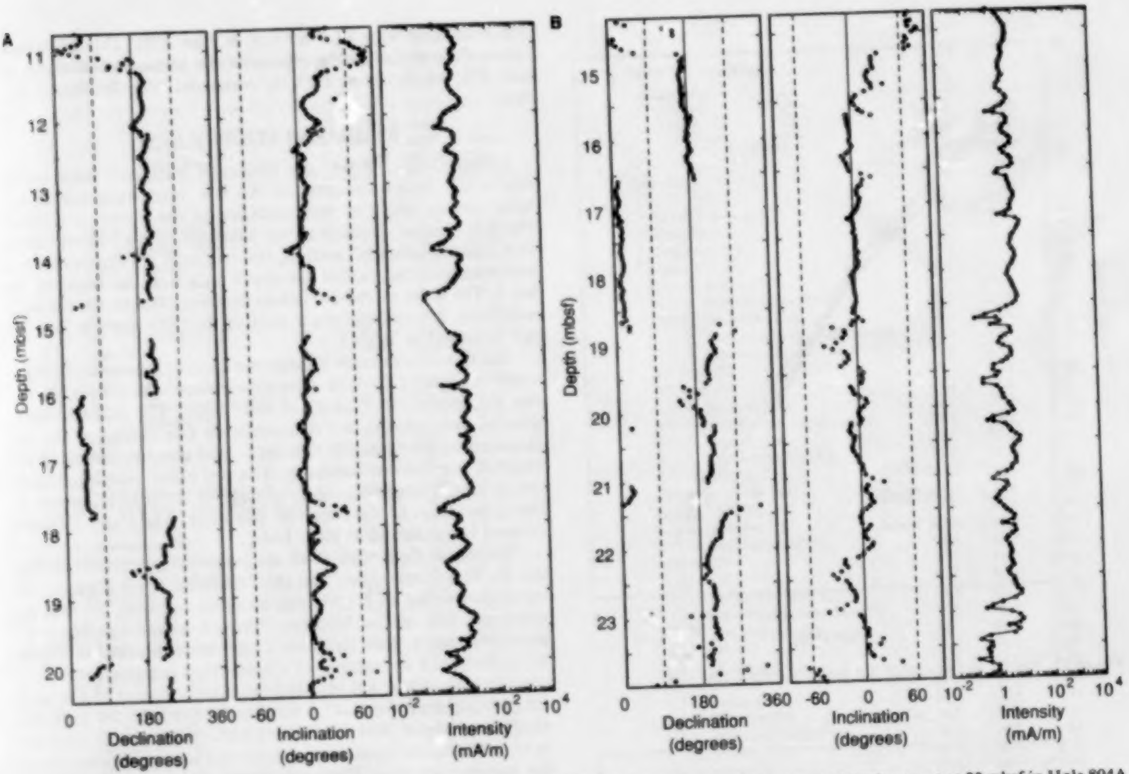

Figure 13. Oriented data from (A) Core 130-804A-3H and (B) Core 130-804B-3H. Note the prominent normal Réunion event at 20 mbsf in Hole 804A and at 21.2 mbsf in Hole 804B, and the weaker, intermediately polarized event at 18.6 mbsf in Hole 804A and 19.8 mbsf in Hole 804B.

normal polarity below 43.5 mbsf (Fig. 14). This normal interval is far too long to fit in with the rest of the Pliocene magnetostratigraphy and so is suspect. In addition, both the declination and inclination patterns through this interval are noisy, and the intensity record has a cyclic series of alternations with a spatial frequency of about 20 cm superimposed on the general decline in intensity. It is possible that this interval within Core 130-804A-6H represents remobilized material, perhaps a slump or mudflow, that was remagnetized when it was partially fluidized at the time of its redeposition. Alternatively, the cyclicity also may be related to depth variations in the concentration of pyrrhotite (see "Site 806" chapter for a further discussion of pyrrhotite generation).

Pliocene-Pleistocene Sedimentation Rates

Comparative age vs. depth plots of the three holes at this site are shown in Figure 15. Some variation between the three holes is evident, but this does not exceed about 2 m and probably reflects only imprecision in sub-bottom depth measurement. Age-depth picks from Holes 804A and 804C cluster around the trend of Hole 804B, which represents the most complete and internally consistent record.

Age-depth data from Hole 804B fall into two intervals, which are characterized by linear sedimentation rates that intersect at about 2 Ma (Fig. 16). As was the case at Site 803, sedimentation rates at Site 804 declined at this time, but the change is less marked at Site 804. Sedimentation rates over the interval from 0 to 2 Ma average 10 m/m.y. at Sites 803 and 804, but the rates for the earlier Pliocene are lower at Site 804 (11.6 m/m.y. at Site

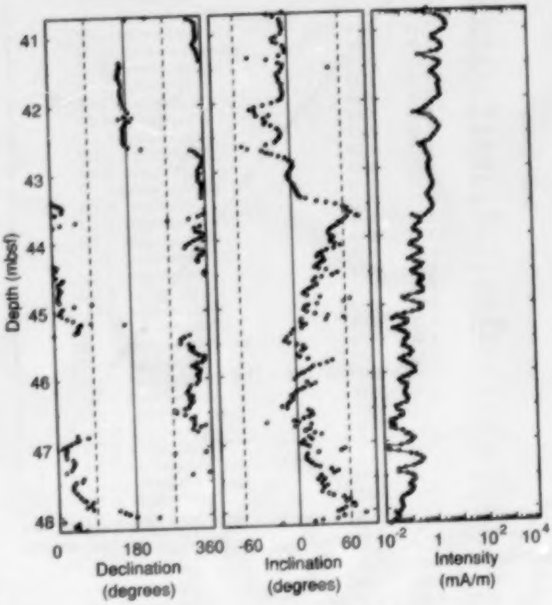

Figure 14. Oriented data from Core 130-804A-6H.

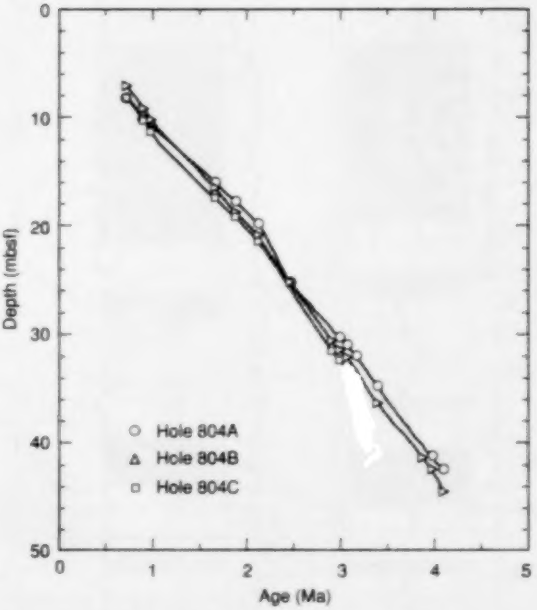

Figure 15. Plot of age vs. depth for polarity events, Site 804.

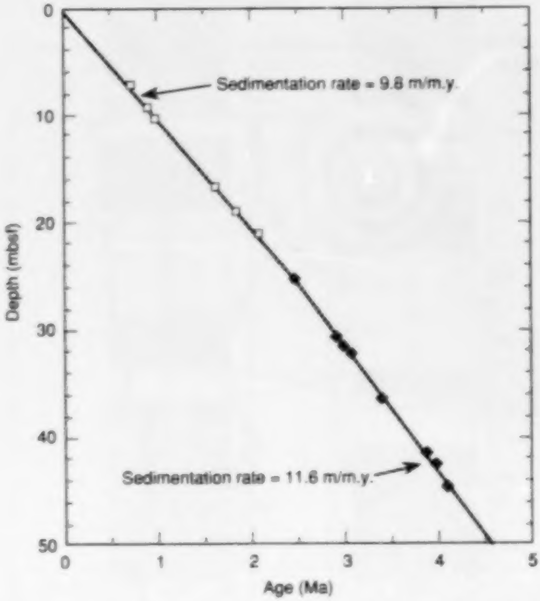

Figure 16. Age vs. depth for events from Hole 804B, showing alignment of events on two linear trends. Corresponding sedimentation rates are indicated.

804 compared with 15.4 m/m.y. at Site 803). This difference may reflect dissolution processes at the greater water depth of Site 804, which lies at 3861 m, compared with 3410 m at Site 803.

SEDIMENTATION RATES

Lower Oligocene through Holocene sediments were recovered at the three holes cored at Site 804. Interpretable geomagnetic reversal histories were obtained in the Pleistocene–lower Pliocene interval, to the Nunivak Subchron of the Gilbert Chron (see "Paleomagnetics" section, this chapter). All shipboard bio- and magnetostratigraphic age-depth indicators are listed in Table 2. The series of control points that were chosen for the sedimentation rate calculations in each of the three holes at Site 804 are presented in Table 3.

The Pliocene through Pleistocene interval is presented graphically in Figure 17, which presents age-depth data from the entire sequence (0–48.7 mbsf) of Hole 804A. The magnetostratigraphic data indicate one sedimentation rate change at the termination of the Jaramillo Subchron, and another change at the onset of the Olduvai Subchron. The two oldest biostratigraphic points clearly suggest a major change in sedimentation rate at the termination of the Nunivak Subchron. The lower Pliocene interval is condensed at Hole 804A.

The results from Hole 804B are presented graphically in Figure 18. This graph shows that the condensed lower Pliocene interval that ended at 4.1 Ma has its onset at about 5.0 Ma, almost precisely at the Miocene/Pliocene boundary. Two age-depth indicators from Hole 804A have been included in Figure 18, namely, the appearance of *Ceratolithus rugosus* (44.6–45.8 mbsf in Hole 804A; 4.6 Ma) and the disappearance of *Discoaster quinqueramus* (45.8–47.3 mbsf in Hole 804A; 5.0 Ma), because these events were determined with closer sample intervals in Hole 804A, and because they constrain sedimentation rates in the pertinent interval. These two events occur with the Gilbert/Nunivak boundary within a single core in Holes 804A (130-804A-6H) and 804B (130-804B-6H). This reversal boundary lies exactly 2 m deeper in Hole 804B than in Hole 804A; therefore, 2 m are added to the depths of the two biostratigraphic events as observed in Hole 804A to derive their depths in Hole 804B. Both of these inferred depths are within the uncertainty ranges of the events as determined in Hole 804B. The extra points taken from Hole 804A argue for a somewhat condensed, but continuous Miocene/Pliocene transition interval rather than for the presence of a hiatus.

Plots of age-depth indicators from Hole 804C are shown in Figure 19, and the plots are shown at enlarged scales in Figures 20 (0–9 Ma) and 21 (8–22 Ma). The scatter of points, particularly those represented by radiolarian events, is wide in the upper Miocene through Holocene interval (Fig. 20), but throughout that scatter the trend from Holes 804A and 804B is clearly recognizable. Several species events representing widely distributed middle to early Miocene ages were observed at a single depth level around 200 mbsf (Fig. 21), thus indicating the presence of a hiatus. This hiatus was placed in the center of Core 130-804C-22X (197.1–206.8 mbsf). An age estimate of 14.7 Ma was obtained for the young side of the hiatus through extrapolation of the sedimentation rate from the nearest overlying control point (LO of *Sphenolithus heteromorphus;* 182.55 mbsf, 13.6 Ma; see Table 3).

The older side of the Miocene hiatus is less well constrained biostratigraphically. Nevertheless, it is obvious that the entire range of *Sphenolithus belemnos* is masked by the hiatus, implying that the youngest possible age estimate for the old side of the hiatus is identical to the age estimate of the first evolutionary appearance of *S. belemnos* (20.0 Ma). The LO event of *Glo-*

Table 2. Bio- and magnetostratigraphic events determined at Site 804.

Event	Upper depth (mbsf)	Lower depth (mbsf)	Age (Ma)
Hole 804A:			
FO *E. huxleyi* (N)	0	1.2	0.28
LO *P. lacunosa* (N)	1.2	10.7	0.46
LO *G. tosaensis* (F)	1.2	10.7	0.60
Brunhes (O)	8.2	8.2	0.73
Jaramillo (T)	10.15	10.2	0.91
Acme *R. asanoi*	10.7	10.7	1.00
LO *C. macintyrei* (N)	10.7	15.2	1.45
Olduvai (T)	16.0	16.0	1.66
Olduvai (O)	17.8	17.8	1.88
LO *D. brouweri* (N)	15.2	20.2	1.89
FO *G. truncatulinoides* (F)	10.7	20.2	1.90
LO *D. surculus* (N)	20.2	29.7	2.45
Gauss (T)	25.3	25.3	2.47
LO *G. altispira*	29.7	39.2	2.90
Kaena (O)	30.4	30.4	2.99
LO *Sphaeroidinellopsis* spp. (F)	29.7	39.2	3.00
FO *Sphaeroidinella dehiscens* (F)	29.7	39.2	3.00
Mammoth (T)	31.2	31.2	3.08
Mammoth (O)	32.2	32.2	3.18
Gauss (O)	35.0	35.0	3.40
LO *R. pseudoumbilica* (N)	29.7	39.2	3.56
Cochiti (O)	41.4	41.4	3.97
Nunivak (T)	42.7	42.7	4.10
FO *C. rugosus*	44.6	45.8	4.60
LO *D. quinqueramus*	45.8	47.3	5.00
Hole 804B:			
LO *P. lacunosa* (N)	3.8	4.7	0.46
LO *G. tosaensis* (F)	4.7	14.2	0.60
Brunhes (O)	7.2	7.2	0.73
Jaramillo (T)	9.3	9.3	0.91
Jaramillo (O)	10.3	10.3	0.98
LO *C. macintyrei* (N)	14.2	15.0	1.45
LO *G. fistulosus* (F)	14.2	23.7	1.60
Olduvai (T)	16.6	16.6	1.66
LO *G. extremus* (F)	4.7	14.2	1.80
Olduvai (O)	18.8	18.8	1.88
LO *D. brouweri* (N)	19.4	19.6	1.89
FO *G. truncatulinoides* (F)	23.7	33.2	1.90
LO *D. surculus* (N)	23.7	33.2	2.45
Gauss (T)	25.4	25.4	2.47
LO *D. variabilis* (N)	23.7	33.2	2.90
LO *G. multicamerata* (F)	33.2	42.7	2.90
LO *G. altispira* (F)	23.7	33.2	2.90
FO *G. fistulosus* (F)	23.7	33.2	2.90
Kaena (T)	30.8	30.8	2.92
Kaena (O)	31.6	31.6	2.99
LO *Sphaeroidinellopsis* spp. (F)	33.2	42.7	3.00
FO *S. dehiscens* (F)	42.7	45.6	3.00
Mammoth (T)	32.4	32.4	3.08
FO *G. tosaensis* (F)	23.7	33.2	3.10
Gauss (O)	36.6	36.6	3.40
LO *P. primalis* (F)	33.2	42.7	3.50
LO *R. pseudoumbilica* (N)	33.2	42.7	3.56
Cochiti (T)	41.6	41.6	3.88
LO *G. nepenthes* (F)	42.7	52.2	3.90
LO *P. spectabilis* (F)	33.2	42.7	3.90
Cochiti (O)	42.7	42.7	3.97
Nunivak (T)	44.7	44.7	4.10
LO *C. acutus* (N)	42.7	52.2	4.6
LO *D. quinqueramus* (N)	42.7	52.2	5.0
FO *S. dehiscens* (F)	42.7	52.2	5.1
FO *G. tumida* (F)	45.6	52.2	5.2
FO *P. spectabilis* (F)	45.6	52.2	5.2
LO *G. dehiscens* (F)	33.2	42.7	5.3
FO *P. primalis* (F)	52.2	61.7	5.8
FO *D. quinqueramus* (N)	71.2	80.7	7.5
LO *D. hamatus* (N)	90.2	99.7	8.7
LO *G. siakensis* (F)	118.7	128.2	10.4

Table 2 (continued).

Event	Upper depth (mbsf)	Lower depth (mbsf)	Age (Ma)
Hole 804C:			
LO *P. lacunosa* (N)	0	6.3	0.46
Brunhes (O)	8.2	8.2	0.73
Jaramillo (T)	10.3	10.3	0.91
Jaramillo (O)	11.3	11.3	0.98
LO *A. angulare* (R)	6.3	15.8	0.99
LO *L. neoheteroporos* (R)	6.3	15.8	1.11
LO *C. macintyrei* (N)	11.5	15.8	1.45
LO *R. praebergonii* var. *robusta* (D)	15.8	25.3	1.55
FO *A. angulare* (R)	15.8	25.3	1.58
Olduvai (T)	17.5	17.5	1.66
Olduvai (O)	19.2	19.2	1.88
LO *D. brouweri* (N)	24.1	25.3	1.89
LO *T. convexa* var. *aspinosa* (D)	25.3	34.8	2.10
LO *D. surculus* (N)	30.3	31.9	2.45
FO *L. neoheteroporos* (R)	15.8	25.3	2.52
LO *N. jouseae* (D)	25.3	34.8	2.60
LO *S. peregrina* (R)	25.3	34.8	2.63
LO *D. variabilis* (N)	31.9	33.4	2.90
LO *G. altispira* (F)	25.3	34.8	2.90
LO *G. multicamerata* (F)	44.3	53.8	2.90
Kaena (T)	31.7	31.7	2.92
Kaena (O)	32.5	32.5	2.99
LO *Sphaeroidinellopsis* (F)	34.8	44.3	3.00
FO *Sphaeroidinella dehiscens* (F)	34.8	44.3	3.00
FO *R. praebergonii* (D)	34.8	44.3	3.00
Mammoth (T)	33.2	33.2	3.08
FO *G. tosaensis* (F)	25.3	34.8	3.10
Mammoth (O)	34.2	34.2	3.18
LO *L. audax* (R)	44.3	53.8	3.34
LO *P. doliolum* (R)	34.8	44.3	3.54
LO *R. pseudoumbilica* (N)	34.8	46.1	3.56
FO *A. ypsilon* (R)	34.8	44.3	3.78
LO *S. pentas* (R)	34.8	44.3	3.78
LO *S. berminghami* (R)	44.3	53.8	3.86
FO *A. elegans* (D)	44.3	53.8	3.90
FO *S. pentas* (R)	44.3	53.8	4.25
LO *C. acutus* (N)	34.8	46.1	4.60
LO *S. omnitubus* (R)	44.3	53.8	4.75
LO *S. delmontensis* (R)	44.3	53.8	5.00
LO *D. quinqueramus* (N)	34.8	46.1	5.00
LO *S. corona* (R)	53.8	63.3	5.05
FO *G. tumida* (F)	44.3	53.8	5.20
FO *P. spectabilis* (F)	44.3	53.8	5.20
LO *G. dehiscens* (F)	44.3	53.8	5.30
LO *A. tritubus* (R)	53.8	63.3	5.35
FO *S. omnitubus* (R)	63.3	72.8	6.40
LO *C. caepa* (R)	72.8	82.3	6.40
FO *Amaurolithus* spp. (N)	63.3	72.8	6.70
LO *N. porteri* (D)	63.3	72.8	6.70
LO *R. paleacea* (D)	63.3	72.8	6.90
LO *T. burckliana* (D)	63.3	72.8	7.00
FO *G. plesiotumida* (F)	72.8	82.3	7.10
LO *D. hughesi* (R)	53.8	63.3	7.15
LO *N. porteri* (D)	63.3	72.8	7.20
LO *R. paleacea* (D)	63.3	72.8	7.40
LO *D. ontogenesis* (R)	63.3	72.8	7.45
FO *D. quinqueramus* (N)	63.3	72.8	7.50
FO *A. tritubus* (R)	53.8	63.3	7.74
FO *S. berminghami* (R)	91.8	101.3	7.95
LO *T. burckliana* (D)	63.3	72.8	8.00
LO *D. petterssoni* (R)	110.8	120.3	8.15
LO *D. laticonus* (R)	53.8	63.3	8.15
LO *S. wolffii* (R)	91.8	101.3	8.15
LO *C. temperei* var. *delicata* (D)	91.8	101.3	8.20
LO *D. hamatus* (N)	91.8	101.3	8.70
FO *D. hughesi* (R)	129.8	139.3	8.75
LO *A. moronensis* (D)	101.3	110.8	8.90
FO *T. burckliana* (D)	91.8	101.3	9.00
LO *C. temperei* var. *delicata* (D)	91.8	101.3	9.80
FO *N. acostaensis* (F)	120.3	129.8	10.20
LO *G. siakensis* (F)	120.3	129.8	10.40
FO *D. hamatus* (N)	148.8	158.3	10.50

Table 2 (continued).

Event	Upper depth (mbsf)	Lower depth (mbsf)	Age (Ma)
Hole 804C: (Cont.)			
LO *C. coscinodiscus* (D)	158.3	168.0	10.70
LO *D. punctata* f. *hustedtii* (D)	158.3	168.0	10.70
FO *L. thornburgi* (R)	110.8	120.3	10.95
FO *H. cuneiformis* (D)	158.3	168.0	10.20
LO *A. moronensis* (D)	101.3	110.8	11.30
LO *G. fohsi lobata* (F)	158.3	163.0	11.50
LO *C. cornuta* (R)	158.3	168.0	11.75
LO *C. coscinodiscus* (D)	158.3	168.0	12.20
LO *D. punctata* f. *hustedtii* (D)	158.3	168.0	12.20
FO *H. cuneiformis* (D)	158.3	168.0	12.60
FO *C. lewisianus* (D)	177.7	187.4	12.90
FO *G. fohsi lobata* (F)	168.0	177.7	13.10
FO *C. lewisianus* (D)	177.7	187.4	13.50
LO *S. heteromorphus* (N)	177.7	187.4	13.60
FO *G. praefohsi* (F)	177.7	187.4	13.90
LO *C. peplum* (F)	177.7	187.4	14.10
LO *G. peripheroronda* (F)	197.1	216.5	14.60
FO *C. peplum* (D)	206.8	216.5	16.30
LO *C. dissimilis* (F)	197.1	216.5	17.60
FO *S. heteromorphus* (N)	197.1	206.8	18.60
LO *C. elegans* (D)	216.5	226.2	18.70
LO *B. veniamini* (D)	226.2	235.8	19.90
FO *S. belemnos* (N)	197.1	206.8	20.00
LO *G. kugleri* (F)	226.2	245.4	21.80
FO *D. druggii* (N)	245.4	255.1	23.60
FO *G. kugleri* (F)	245.4	255.1	23.70
LO *S. ciperoensis* (N)	264.7	274.4	25.20
LO *G. opima* (F)	264.7	274.4	28.20

Notes: The depth uncertainty predominantly represents sampling intervals used. References for the age estimates are presented in the "Explanatory Notes" chapter (this volume). N = nannofossil, F = foraminifer, D = diatom, R = radiolarian, FO = first occurrence, and LO = last occurrence. Magnetostratigraphic reversal boundaries followed by the designation (T) or (O) refer to "termination" or "onset," respectively.

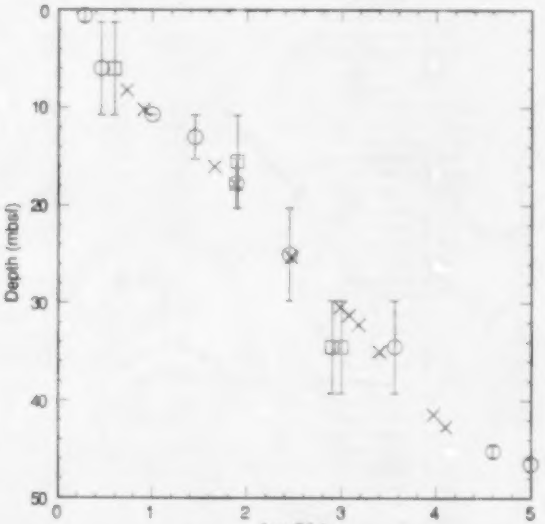

Figure 17. Age/depth relationships of bio- and magnetostratigraphic markers in Hole 804A. Error bars show sample interval uncertainties. Open circles = nannofossils, open squares = foraminifers, and × = magnetostratigraphic reversal boundary.

Table 3. Estimated sedimentation rates, Site 804, and the control points determining those rates.

Control point	Depth (mbsf)	Age (Ma)	Sedimentation rate (m/m.y.)
130-804A-			
Top section	0	0	
Jaramillo (T)	10.15	0.91	11.2
Olduvai (O)	17.80	1.88	7.9
Nunivak (T)	42.70	4.10	11.2
LO D. quinqueramus (N)	46.55	5.00	4.3
Terminal depth	48.70	5.50	
130-804B-			
Top section	0	0	
Brunhes (O)	7.20	0.73	9.9
Jaramillo (O)	10.30	0.98	12.4
Olduvai (O)	18.80	1.88	9.4
Nunivak (T)	44.70	4.10	11.7
LO D. quinqueramus (N)	47.45	5.00	3.1
LO D. hamatus (N)	94.95	8.70	12.8
Terminal depth	137.7	<10.5	>23.8
130-804C-			
Top section	0	0	
Brunhes (O)	8.20	0.73	11.2
Olduvai (O)	19.20	1.88	9.6
Mammoth (O)	34.20	3.18	11.5
Insufficient resolution	34.2–49.05	3.18–5.2	
LO P. spectabilis (F)	49.05	5.20	
LO D. hamatus (N)	94.95	8.70	13.1
LO S. heteromorphus (N)	182.55	13.60	17.9
Hiatus young side	201.95	14.69	
Hiatus old side	201.95	20.00	
FO S. belemnos (N)	201.95	20.00	
LO G. kugleri (F)	235.80	21.80	18.8
LO S. ciperoensis (N)	269.55	25.20	9.9
Hiatus young side	269.55	25.20	
LO G. opima (F)	269.55	28.20	
Hiatus old side	269.55	28.20	
Terminal depth	312.50	<33.8	?

Notes: N = nannofossil, F = foraminifer, D = diatom, R = radiolarian, FO = first occurrence, and LO = last occurrence. Magnetostratigraphic reversal boundaries followed by the designation (T) or (O) refer to "termination" or "onset," respectively. See "Explanatory Notes" chapter (this volume) for Leg 130 philosophy on sedimentation rates.

borotalia kugleri at 21.8 Ma lies well below the hiatus, implying that the old side of the hiatus begins between 20.0 and 21.8 Ma.

Another hiatus is implied in the upper Oligocene that encompasses the time interval from at least 25.2 (LO of *Sphenolithus ciperoensis*) to at least 28.2 Ma (LO of *Globorotalia opima*). The young side of the hiatus lies somewhere between the *S. ciperoensis* event and the FO of *G. kugleri* at 23.7 Ma. The youngest possible age for the old side of this Oligocene hiatus coincides with the *G. opima* event, although it appears likely that the old side of the hiatus is older than 28.2 Ma. About 43 m of sediment of early Oligocene age (<33.8 Ma) were cored below the hiatus. If they represent continuous deposition, these 43 m of sediments were deposited at a minimum rate of 7.7 m/m.y.

The sedimentation rates indicated for the lower Miocene/uppermost Oligocene interval that separates the two hiatuses are poorly constrained. Several alternatives to the sedimentation rates suggested in Table 3 can be deduced from the distribution of the available age-depth indicators.

The sedimentation rates for all three holes from Site 804 are plotted vs. age in Figure 22. The condensed lower Pliocene interval stands out clearly. Data from Hole 804C has been omitted above 5 Ma, simply because the data available do not permit us to identify the condensed lower Pliocene interval and because

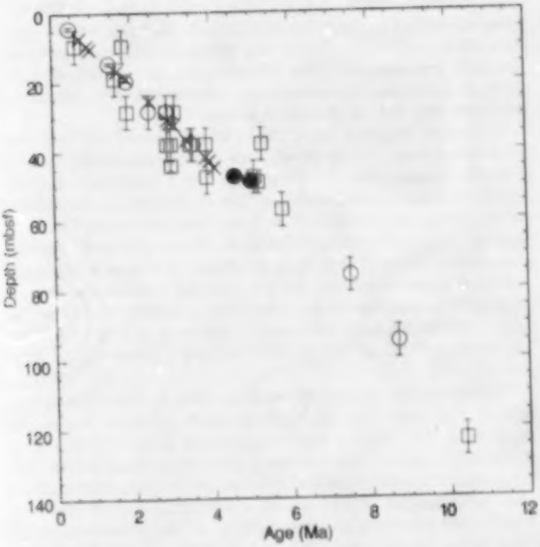

Figure 18. Age/depth relationships of bio- and magnetostratigraphic markers in Hole 804B. Error bars show sample interval uncertainties. Open circles = nannofossils, open squares = foraminifers, and × = magnetostratigraphic reversal boundary. Two nannofossil events (filled circles) are derived from Hole 804A (see explanation in text).

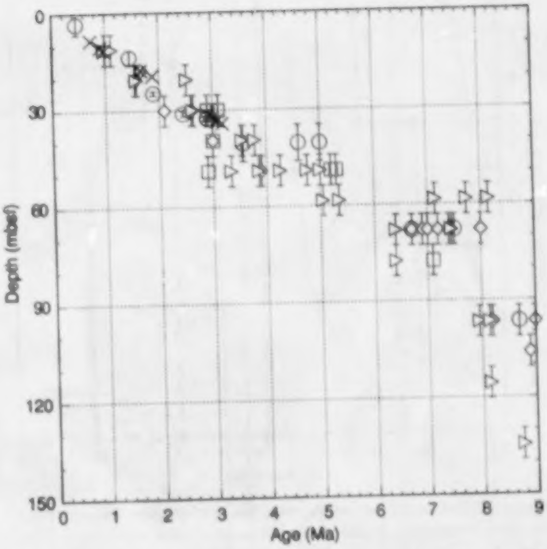

Figure 20. Late Miocene through Holocene age/depth relationships of bio- and magnetostratigraphic markers in Hole 804C. Error bars show sample interval uncertainties. Open circles = nannofossils, open squares = foraminifers, open diamonds = diatoms, open triangles = radiolarians, and × = magnetostratigraphic reversal boundary.

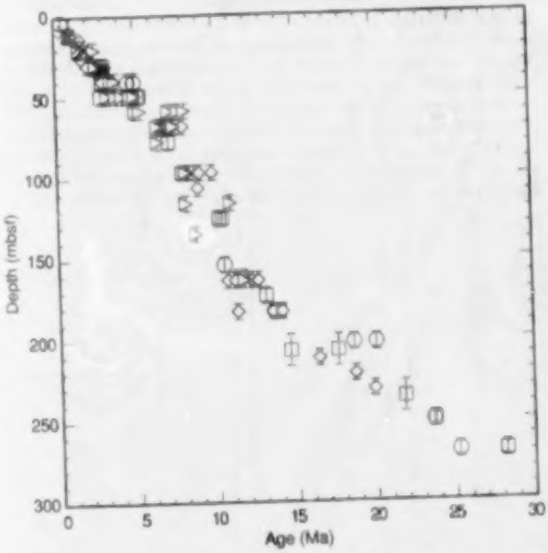

Figure 19. Age/depth relationships of bio- and magnetostratigraphic markers in Hole 804C. Error bars show sample interval uncertainties. Open circles = nannofossils, open squares = foraminifers, open diamonds = diatoms, open triangles = radiolarians, and × = magnetostratigraphic reversal boundary.

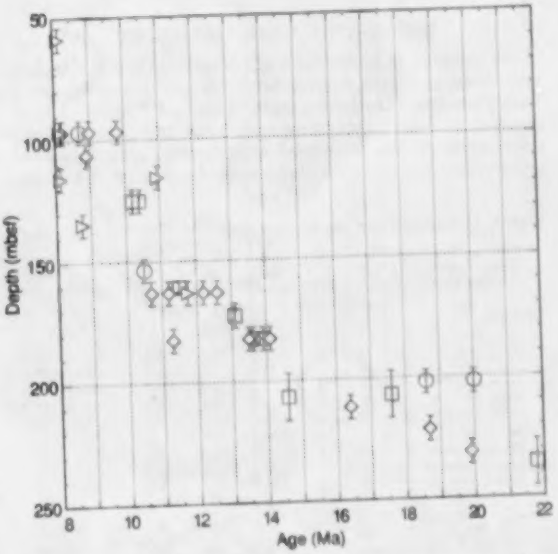

Figure 21. Early through late Miocene age/depth relationships of biostratigraphic markers in Hole 804C. Error bars show sample interval uncertainties. Open circles = nannofossils, open squares = foraminifers, open diamonds = diatoms, and open triangles = radiolarians.

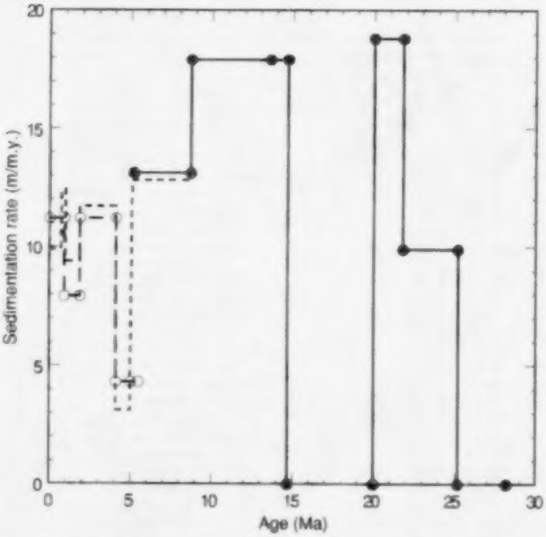

Figure 22. Sedimentation rate history, Site 804. Dashed line with open circles = Hole 804A, dashed line = Hole 804B, and solid line = Hole 804C.

the Pliocene and Pleistocene intervals are well represented by the sections from Holes 804A and 804B.

The sedimentation rate and its change in the 20- to 25-Ma interval (Fig. 22) should be regarded as but one possible way to connect four points.

INORGANIC GEOCHEMISTRY

We collected 15 interstitial water samples at Site 804: 9 from Hole 804B at depths ranging from 3.0 to 134.2 mbsf, and 6 from Hole 804C at depths ranging from 161.3 to 307.5 mbsf (Table 4). For this report, these are considered as constituting a single depth profile. Interstitial water samples span almost the entire drilled interval of the Unit I nannofossil oozes and chalks, the single lithologic unit recognized at Site 804 (see "Lithostratigraphy" section, this chapter). Chemical gradients in the interstitial waters at this site are generally similar to those at Site 803, being influenced by the biogenic-rich, organic-carbon-poor character of the sediments and by the diffusive influence of basalt alteration reactions at depth. However, the magnitudes of some chemical gradients and maxima are lower at Site 804 than at the shallower Site 803, as described below.

Chlorinity increases by $<1\%$ to values around 560 mM over the interval from 0 to 20 mbsf, with a small additional increase at depths greater than 250 mbsf (Fig. 23). Chlorinity values are similar to those at comparable depths at Site 803, as are salinity values, measured refractively as total dissolved solids (Table 4). Sodium concentrations measured by flame emission spectrophotometry (Table 4) and those estimated by charge balance calculations agree to within $<1.5\%$ and are approximately constant with increasing depth. Alkalinity is relatively constant at values around 3.6 mM, with small maxima at 10.7 mbsf in Core 130-804B-2H and at 246.9 mbsf in Core 130-804C-27X (Fig. 23).

Sulfate concentrations decrease by 10% to values around 25 mM at 100 mbsf and are approximately constant below that depth (Fig. 23). Sulfate concentrations at given depths and at comparable ages in Site 804 are higher than those at Site 803, suggesting that the rates and total extent of SO_4 depletion are even more limited at Site 804 by low organic carbon contents. The limited alkalinity increase as well as phosphate concentrations below the detection limit of 1–2 μM in all the samples (Table 4) support this interpretation. Ammonia concentrations are low, with the peak value observed in a single sample at 217.9 mbsf in Core 130-804C-24X similar to the maximum at Site 803. There are generally lower concentrations than at Site 803 throughout this profile (Fig. 23).

Dissolved silica concentrations increase with depth to around 900 μM (Fig. 23). The increase in dissolved Si concentrations, presumably a result of the continuous dissolution of biogenic silica, is similar to that observed at Site 803. Manganese concentrations are generally below the detection limit (<2–3 μM) in most samples, except for higher values in the upper 20 m and slightly elevated values around 217.9–246.9 mbsf in Cores 130-804C-24X and -27X (Table 4). Manganese profiles in interstitial waters often show complex structures with depth, probably caused by the occurrence of different zones in which Mn can be mobilized by reduction into its dissolved state (Gieskes, 1981).

Table 4. Interstitial water geochemical data, Site 804.

Core, section, interval (cm)	Depth (mbsf)	pH	Alk. (mM)	Sal. (g/kg)	Cl^- (mM)	Na (mM)	SO_4^{2-} (mM)	PO_4^{3-} (μM)	NH_4^+ (μM)	SiO_2 (μM)	Mn (μM)	Ca^{2+} (mM)	Mg^{2+} (mM)	Sr (μM)	Li (μM)	K (mM)	Rb (μM)
130-804B-																	
1H-2, 145-150	2.95	7.5	3.53	35.0	554	474	27.7	LD	8	450	21	10.7	51.4	108	25.9	10.5	1.77
2H-4, 145-150	10.65	7.4	4.55	35.5	557	475	27.4	LD	13	462	12	11.2	51.7	158	21.8	10.6	1.81
3H-4, 145-150	20.15	7.4	3.77	35.0	561	484	28.0	LD	19	531	4	11.6	51.6	201	20.9	11.2	1.74
4H-4, 145-150	29.65	7.8	3.53	35.5	559	485	27.7	LD	26	636	LD	11.9	50.8	242	20.9	11.2	1.89
5H-4, 145-150	39.15	7.6	3.54	35.5	561	481	27.2	LD	31	679	LD	12.2	50.2	272	20.4	11.1	1.83
6H-4, 145-150	48.65	7.6	3.64	35.5	560	477	26.4	LD	45	690	LD	12.5	49.8	300	19.5	10.9	1.82
9H-4, 145-150	77.15	7.8	3.77	35.0	558	480	26.5	LD	49	774	LD	13.5	48.8	392	17.2	10.6	1.76
12H-4, 145-150	105.65	7.6	3.75	35.0	560	483	25.7	LD	48	809	LD	14.7	47.5	460	15.9	11.9	1.78
15H-4, 145-150	134.15	7.6	3.56	35.5	561	481	25.1	LD	55	851	LD	15.8	46.1	514	15.0	10.8	1.81
130-804C-																	
18X-2, 145-150	161.25	7.6	3.39	35.5	561	479	25.7	LD	57	801	LD	16.2	45.8	521	15.9	9.91	1.69
21X-1, 145-150	188.85	ND	ND	ND	561	480	25.3	ND	79	836	ND	17.7	43.8	577	15.9	9.89	1.58
24X-1, 140-150	217.90	7.9	3.76	35.0	561	478	24.9	LD	113	843	7	18.5	43.6	573	18.7	9.40	1.54
27X-2, 0-10	246.90	7.8	4.28	35.5	561	495	26.6	LD	62	901	3	19.9	42.1	608	18.3	9.63	1.54
30X-3, 140-150	278.80	7.6	3.74	35.5	567	491	24.8	LD	62	930	LD	21.3	42.1	608	18.3	9.72	1.48
33X-3, 140-150	307.49	7.6	3.64	35.5	568	486	25.4	ND	67	909	ND	22.4	41.8	621	18.3	8.70	1.46

Notes: Alk. = alkalinity, Sal. = salinity, LD = concentration lower than detection limit, and ND = not determined.

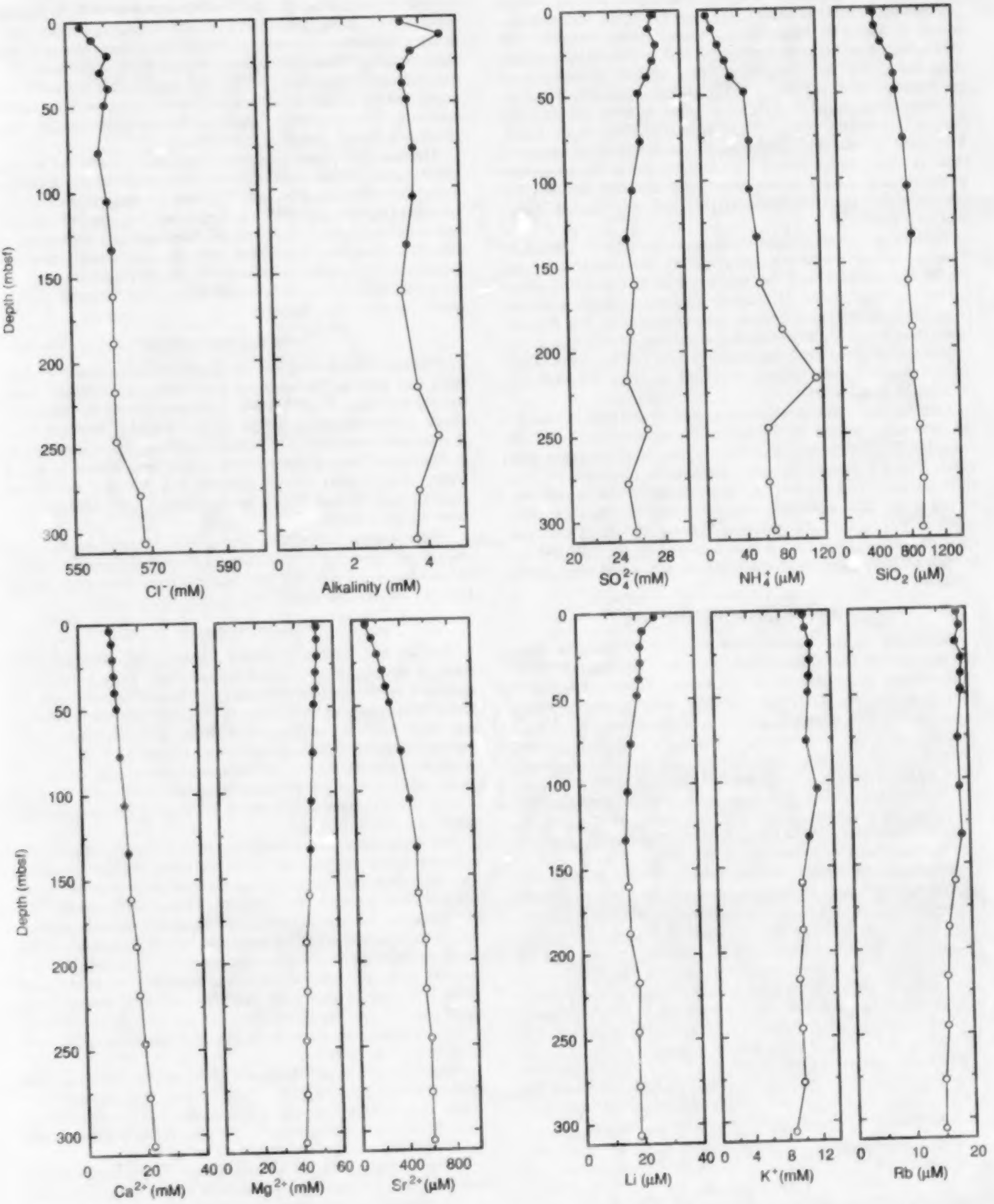

Figure 23. Interstitial water geochemical data vs. depth, Holes 804B and 804C. Closed circles indicate samples from Hole 804B; open circles, samples from Hole 804C. The depth at the base of the plots is that of the deepest sediment drilled.

Calcium concentrations increase with depth, with an average gradient of 4 mM/100 m (Fig. 23), approximately half that observed at Site 803. Magnesium concentrations decrease with depth, with a gradient of 4 mM/100 m (Fig. 23), similar to that observed at Site 803. Magnesium and calcium concentrations are linearly correlated ($R^2 = 0.97$), with a $\Delta Ca/\Delta Mg$ ratio approximately equal to -1, similar to those at Sites 288 and 289 (Leg 30) from the Ontong Java Plateau (Elderfield et al., 1982). The linear correlation is indicative of the conservative nature of these profiles, with Ca and Mg gradients primarily controlled by reactions in the underlying basalt and diffusion between this boundary and overlying seawater (McDuff and Gieskes, 1976; McDuff, 1981).

Strontium concentrations increase with depth to maximum observed values around 600 μM (Fig. 23). The character of the profile is consistent with the release of Sr to interstitial water during recrystallization of biogenic calcite to inorganic calcite (e.g., Gieskes, 1981). Strontium concentrations at Site 804 are lower than those at corresponding depths at Site 803, and the maximum observed concentrations at Site 804 are lower than the maximum concentrations observed at Sites 288 and 289 (Elderfield et al., 1982).

Lithium concentrations decrease from 26 μM near the top of the sediment column to minimum values around 15–16 μM from 105.7 to 188.9 mbsf and then slightly increase again with depth (Fig. 23). Potassium concentrations first increase slightly, then decrease with depth (Fig. 23), similar to the profile observed at Site 803. Rubidium concentrations also decrease with depth (Fig. 23), with this decrease linearly correlated with the Ca increase, implying that it is also caused by the diffusive influence of basalt alteration reactions on interstitial water composition.

CARBON GEOCHEMISTRY

Shipboard carbon geochemical analyses of samples from Site 804 include determinations of inorganic carbon (189 samples), volatile hydrocarbons in sediments (10 samples), and 8 Rock-Eval analyses. The NCS elemental analyzer was not operational at Site 804; therefore, there are no shipboard data for total carbon, sulfur, and nitrogen. The analytical methods are outlined in the "Explanatory Notes" chapter (this volume). More detailed descriptions of the methods are given by Emeis and Kvenvolden (1986). The sediments were routinely monitored for the presence of hydrocarbon gases as required by safety considerations. As in the sediments from Site 803, no volatile hydrocarbons were detected at Site 804.

Inorganic carbon (IC; see "Explanatory Notes" chapter, this volume) was measured on samples collected for physical properties analyses. The carbon data are presented in Table 5 (microfiche, back pocket) and plotted vs. depth in Figure 7. The sediments at Site 804 are characterized by carbonate values ranging from 55% to 95%. Lower carbonate contents (55%–70%) between 200 and 300 mbsf (upper Oligocene to lower Miocene) and between 0 and 100 mbsf (upper Miocene to Holocene) correlate with radiolarian-rich intervals and may reflect greater dissolution of carbonate in these sections.

Rock-Eval pyrolysis (Espitalié et al., 1977) was used for total organic carbon (TOC) determinations. The TOC values are below the detection limit of the shipboard Rock-Eval pyrolysis (0.05%; see "Site 803" chapter, this volume).

PHYSICAL PROPERTIES

Introduction

Physical properties were measured on whole rounds and split cores at Site 804. Whole-round analyses included gamma-ray attenuation porosity evaluator (GRAPE) and *P*-wave logger (PWL) measurements (using the multisensor track) as well as thermal conductivity. Index properties (wet-bulk density, porosity, grain density, and water content), undrained vane shear strength, and compressional wave velocity were measured on split cores. The digital sound velocimeter (DSV) was used in soft sediment sections, and the Hamilton Frame on discrete samples in indurated intervals. The methods of analyses are described in the "Explanatory Notes" chapter (this volume).

The intensive physical properties program conducted on Leg 130 concentrated on making closely spaced laboratory measurements and therefore provided little time for data processing. We recorded GRAPE and PWL data on board the ship but will process them on shore. No downhole measurements were made at Site 804; therefore, laboratory velocity and density measurements corrected to *in-situ* values were the only data available for the calculation of synthetic seismograms (see "Seismic Stratigraphy" section, this chapter).

Thermal Conductivity

Thermal conductivity was measured on whole-round sections using the needle-probe technique (see "Explanatory Notes" chapter, this volume). As at Site 803, problems caused by inaccurate needle calibration led to a high degree of scatter. For each core, the thermal conductivity reported is a mean value calculated by averaging the thermal conductivity values for Sections 3, 4, and 5 (see "Explanatory Notes" chapter, this volume). Results are given in Table 6, and Figure 24 shows changes in thermal conductivity with depth.

There is some indication that thermal conductivity increases with depth, presumably as a consequence of decreases in porosity and water content, but the measurements show little change between 40 and 240 mbsf.

Shear Strength

At Site 804, undrained shear strength was normally measured at an interval of one per split section, using a motorized minivane apparatus (see "Explanatory Notes" chapter, this volume). Measurements were made by inserting the vane in the soft sediment in the intervals cored with the APC and into undisturbed coherent blocks of sediment ("biscuits") in intervals cored with the XCB until the sediment became too stiff (at approximately 140 mbsf in Hole 804B and 160 mbsf in Hole 804C). The sediment at Site 804 is principally silt or clayey silt, similar to that at Site 803.

The vane shear test is designed for clay measurements, with cohesion being the main factor in the shear strength equation. The vane shear test, however, may be used as an estimate of undrained shear strength (see "Physical Properties" section, "Site 803" chapter, for a detailed discussion). Residual shear strength data were obtained wherever cracking did not dominate failure. Shear strength results are presented in Table 7 (microfiche, back pocket); mean grain size in the top of Hole 804B is presented in Table 8. Figure 25 shows the variations of shear strength with depth, and Figure 26 shows the changes with depth of mean grain size and shear strength in the upper portion of the sediment section at Hole 804B.

Shear strength values measured in the three holes range from approximately 5 to 50 kPa. There is a general increase with depth as a result of sediment consolidation (Fig. 25). Differences in the shear strength curves between Holes 804B and 804C below 80 mbsf may reflect coring disturbance.

From 0 to 80 mbsf, the shear strength curves from all three holes at Site 804 have the same basic shape (Fig. 25). Exact "peak-to-peak" correlations are very difficult, however, as coring-induced disturbance has considerable effect on the peak shear strength values (see discussion in "Physical Properties" section, "Site 803" chapter, this volume). The three curves show

Table 6. Thermal conductivity data, Site 804.

Core, section, interval (cm)	Depth (mbsf)	Thermal conductivity (W/m · K)	Corrected (mean per core)
130-804A-			
2H-3, 35	4.55	1.1567	
2H-4, 35	6.05	1.2426	1.2091
2H-5, 35	7.55	1.2280	
3H-3, 35	14.05	1.0420	
3H-4, 35	15.55	1.2043	1.1519
3H-5, 35	17.05	1.2095	
4H-3, 35	23.55	1.1338	
4H-4, 35	25.05	1.3144	1.2286
4H-5, 35	26.55	1.2375	
5H-3, 35	33.05	1.2387	
5H-4, 35	34.55	1.1817	1.2296
130-804B-			
2H-3, 35	8.05	1.2786	
2H-4, 35	9.55	1.2955	1.2531
2H-5, 35	11.05	1.1851	
4H-3, 35	27.05	1.3100	
4H-3, 35	28.55	1.2463	
4H-5, 35	30.05	1.1827	
6H-3, 35	46.05	1.2441	
6H-3, 35	47.55	1.3073	
6H-5, 35	49.05	1.3705	
8H-3, 35	65.05	1.3801	
8H-4, 35	66.55	1.2422	1.3010
8H-5, 35	68.05	1.2805	
9H-3, 35	74.55	1.2724	
9H-4, 35	76.05	1.1637	1.1600
9H-5, 35	77.55	1.0438	
10H-4, 35	85.55	1.2940	
	86.03	1.3730	
10H-5, 35	87.05	1.4520	
11H-3, 35	93.55	1.2525	
11H-4, 35	95.05	1.4145	1.3379
11H-5, 35	96.55	1.3466	
12H-3, 35	103.05	1.3372	
12H-4, 35	104.55	1.4353	1.4089
12H-5, 35	106.05	1.4543	
13H-3, 35	112.55	1.3003	
13H-4, 35	114.05	1.3947	1.2990
13H-5, 35	115.55	1.2021	
14H-3, 35	122.05	1.3805	
	122.80	1.3412	
14H-4, 35	123.55	1.3020	
15H-3, 35	131.55	1.3750	
15H-4, 35	133.05	1.4321	1.3538
15H-5, 35	134.55	1.2544	
130-804C-			
2H-3, 35	9.65	1.1854	
2H-4, 35	11.15	1.1280	1.1556
2H-5, 35	12.65	1.1535	
3H-3, 35	19.15	1.2286	
3H-4, 35	20.65	1.1654	1.2379
3H-5, 35	22.15	1.3198	
4H-3, 35	28.65	1.1949	
4H-3, 35	29.40	1.1750	
4H-4, 35	30.15	1.1552	
5H-3, 35	38.15	1.1882	
5H-4, 35	39.65	1.1215	1.1762
5H-5, 35	41.15	1.2190	
6H-3, 35	47.65	1.3962	
6H-4, 35	49.15	1.2984	1.3621
6H-5, 35	50.65	1.3918	
7H-3, 35	57.15	1.3010	
7H-4, 35	58.65	1.4224	1.3344
7H-5, 35	60.15	1.2798	
8H-3, 40	66.70	1.3698	
8H-4, 40	68.20	1.2739	1.2768
8H-5, 40	69.70	1.1867	
10H-3, 35	85.65	1.5051	
10H-4, 35	87.15	1.4132	1.4097
10H-5, 35	88.65	1.3108	
11H-3, 35	95.15	1.3116	
130-804C- (Cont.)			
11H-4, 35	96.65	1.3322	1.3105
11H-5, 35	98.15	1.2878	
12H-4, 35	106.15	1.1912	
12H-4, 35	106.90	1.3249	
12H-5, 35	107.65	1.4586	
13H-3, 35	114.15	1.2298	
13H-4, 35	115.65	1.3117	1.3066
13H-5, 35	117.15	1.3784	
18X-3, 35	161.65	1.0240	
18X-4, 35	163.15	1.1899	1.2292
18X-5, 35	164.65	1.4736	
19X-3, 35	171.35	1.2268	
19X-4, 35	172.85	1.4120	1.2972
19X-5, 35	174.35	1.2528	
20X-3, 35	181.05	1.2091	
20X-3, 35	181.80	1.1826	
20X-4, 35	182.55	1.1561	
22X-3, 35	200.45	1.2620	
22X-3, 35	201.20	1.3086	
22X-4, 35	201.95	1.3553	
25X-3, 35	229.55	1.3429	
25X-4, 35	231.05	1.2136	1.2639
25X-5, 35	232.55	1.2352	
26X-3, 35	239.15	1.3305	
26X-3, 35	239.90	1.3595	
26X-4, 35	240.65	1.3885	
28X-3, 35	258.45	1.5486	
28X-4, 35	259.95	1.4803	1.4646
28X-5, 35	261.45	1.3651	
29X-3, 35	268.05	1.6781	
29X-3, 35	268.80	1.5562	
29X-4, 35	269.55	1.4343	
30X-3, 35	277.75	1.5816	
30X-4, 35	279.25	1.6533	1.5268
30X-5, 35	280.75	1.3456	

the same interval of anomalously high shear strength values (30 kPa) between approximately 20 and 45 mbsf. This interval is characterized by a marked increase in the mean grain size (Fig. 26). Smear slide examination reveals a greater abundance of foraminifers in this interval (see "Lithostratigraphy" section, this chapter). Enhanced grain-to-grain contact in this coarser sediment section may explain the higher shear strength values (through an increase in friction).

Index Properties

The sampling frequency for index properties at Site 804 was two samples per section in Holes 804A and 804B and one sample per section in Hole 804C (at the same locations as the velocity measurements). Intervals showing evidence of "flow-in" or any other coring disturbance were not sampled (usually, the top of Section 1 in many cores). Results of the index property measurements are presented in Table 9 (microfiche, back pocket). Figures 27 through 30 show the downhole profiles for bulk density, porosity, water content, and grain density in each hole; superimposed on Figure 31 are the merged porosity curve for Site 804 and a generalized porosity curve for calcareous sediments (Hamilton, 1976). On the whole, shipboard data appear to be of good quality. The very high bulk density (2.01 g/cm³), low porosity, and low water content value at 125 mbsf is questionable. Comparison with GRAPE data will be necessary to check its validity.

The lithology at Site 804 is fairly uniform (see "Lithostratigraphy" section, this chapter). The mineralogical composition of the sediments is dominated by biogenic calcite, with variable,

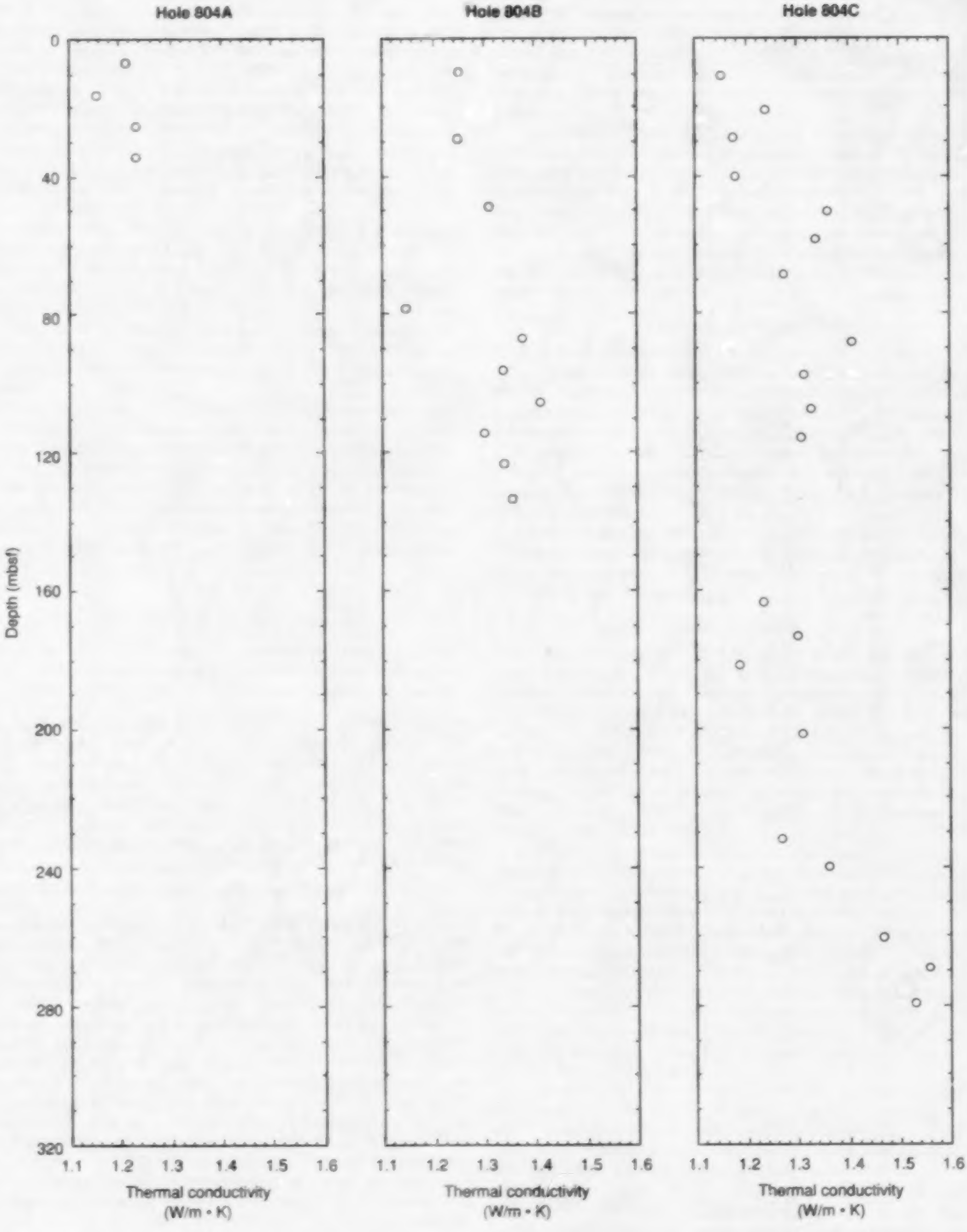

Figure 24. Thermal conductivity vs. depth, Site 804.

Table 8. Mean grain size data, Hole 804B.

Core, section, interval (cm)	Depth (mbsf)	Mean grain size (μm)
130-804B-		
1H-1, 28	0.28	15.2
1H-1, 99	0.99	13.6
1H-2, 22	1.72	20.0
1H-2, 101	2.51	26.8
1H-3, 37	3.37	13.3
1H-3, 121	4.21	13.5
2H-1, 43	5.13	24.6
2H-1, 104	5.74	6.9
2H-2, 30	6.50	21.5
2H-2, 110	7.30	10.6
2H-3, 22	7.92	17.8
2H-3, 123	8.93	11.2
2H-4, 28	9.48	10.5
2H-4, 101	10.21	9.8
2H-5, 33	11.03	11.2
2H-5, 126	11.96	12.1
2H-6, 27	12.47	13.1
2H-6, 112	13.32	13.1
2H-7, 53	14.23	9.0
3H-1, 110	15.30	9.0
3H-2, 31	16.01	11.7
3H-2, 111	16.81	8.9
3H-3, 42	17.62	9.8
3H-3, 114	18.34	12.2
3H-4, 37	19.07	37.1
3H-4, 103	19.73	20.3
3H-5, 38	20.58	25.8
3H-5, 111	21.31	17.2
3H-6, 43	22.13	18.6
3H-6, 107	22.77	15.5
3H-7, 49	23.69	21.8
4H-1, 46	24.16	25.5
4H-1, 105	24.75	25.8
4H-2, 36	25.56	48.4
4H-3, 38	27.08	18.6
4H-3, 109	27.79	17.5
4H-4, 36	28.56	14.2
4H-4, 111	29.31	24.0
4H-5, 27	29.97	19.7
4H-7, 33	33.03	25.3
5H-1, 122	34.42	10.0
5H-2, 38	35.08	9.3
5H-2, 111	35.81	14.7
5H-4, 38	38.08	63.8
5H-4, 107	38.77	25.8
5H-5, 32	39.52	61.6
5H-5, 112	40.32	58.3
5H-6, 31	41.01	56.4
5H-6, 106	41.76	72.7
5H-7, 41	42.61	61.0
6H-1, 39	43.09	39.4
6H-1, 117	43.87	41.8
6H-2, 44	44.64	21.5
6H-2, 108	45.28	22.6
6H-2, 109	45.29	12.6
6H-3, 110	46.80	27.0
6H-4, 112	48.32	23.4
6H-5, 33	49.03	22.8
6H-5, 108	49.78	16.9
6H-6, 33	50.53	13.7
6H-6, 38	50.58	27.5
6H-6, 107	51.27	17.3
6H-7, 37	52.07	15.6

but minor, amounts of biogenic silica; nonbiogenic components are always below 3% in abundance. Grain density reflects the contribution of these two end-members (calcite with a grain density of 2.7 g/cm^3 and silica with a grain density of 2.2 g/cm^3 [Fig. 30]); thus, there is a good correspondence of grain density to the carbonate profile (Fig. 30). Grain density values average 2.68 g/cm^3 when carbonate content is high (around 90%). They decrease to 2.55 g/cm^3 in intervals of lower carbonate content (65%–70%), presumably related to carbonate dissolution or to changes in productivity that result in an enrichment of siliceous microfossils (see "Lithostratigraphy" section, this chapter). Below 200 mbsf, fluctuations in the grain density curve reflect the alternation of nannofossil chalk sections with intervals of nannofossil chalk with radiolarians (see "Lithostratigraphy" section, this chapter).

Wet-bulk density at Site 804 appears to be controlled mainly by porosity changes ($R^2 = 0.98$; see Fig. 32). The reason for the high correlation can be seen from the equation relating wet-bulk density (D) to porosity (Θ) and grain density (D_g):

$$D = \Theta \cdot D_w + (1 - \Theta) \cdot D_g,$$

where D_w = density of interstitial water. The dominant effect of porosity on wet-bulk density at Site 804 can be readily appreciated when considering that the only variable showing large amplitude changes in the above equation is porosity (50%–70%).

Wet-bulk density values measured at Site 804 range from 1.42 g/cm^3 at about 39 mbsf to 1.97 g/cm^3 at 286.70 mbsf (Fig. 27), generally increasing with depth. This increase is not linear but overlain by steps and cycles. Porosity and water content have the same trends (but inverse from that of the wet-bulk density). Regions of anomalously low (or high) values are superimposed on these downhole trends. These anomalous regions are also characterized by marked anomalies in *P*-wave velocity, shear strength, and carbonate content.

In the uppermost 110 mbsf, consolidation effects lead to a constant decrease in porosity and water content (with a correlative increase in wet-bulk density). In a gross sense, the trend of the porosity-depth curve is similar to Hamilton's generalized consolidation curve for calcareous sediments (Fig. 31). The interval between 110 and 210 mbsf shows a marked difference from Hamilton's curve, with essentially no reduction of porosity or water content (increase of wet-bulk density) within that depth.

Several factors may explain this departure from the generalized trend. Beginning at 110 mbsf, sediment becomes stiff enough to create problems inserting the DSV transducers for *P*-wave velocity measurements, possibly a result of the onset of sediment induration. The ooze/chalk transition occurs at about 180 mbsf (see "Lithostratigraphy" section, this chapter), but chalk nodules in ooze were observed significantly shallower. Thus, the deviation of the Site 804 data from the Hamilton curve between 110 and 210 mbsf may be related to the progressive increase of cementation over this interval. Cementation increases the rigidity of the sediment framework, thereby improving its resistance to compaction.

Variations in radiolarian abundance may play a role in the absence of a porosity reduction with depth between 110 and 210 mbsf. Below approximately 150 mbsf, radiolarian abundance increases more or less continuously until about 200 mbsf (see "Lithostratigraphy" section, this chapter). In central equatorial Pacific sediments, porosity generally increases with increasing radiolarian content (Mayer, 1979). High porosities associated with radiolarian content may tend to cancel the reduction trend in the porosity profile by offsetting compaction effects.

Below 210 mbsf, high-amplitude fluctuations related to changes in sediment composition make it difficult to estimate a general trend in index property profiles. It seems, however, that porosity and water content decrease slightly with depth. This reduction is probably no longer an effect of consolidation but, rather, the results of pore-space infilling with calcite cementation.

Second-order, higher frequency fluctuations are superimposed on the general trend described above. These fluctuations take

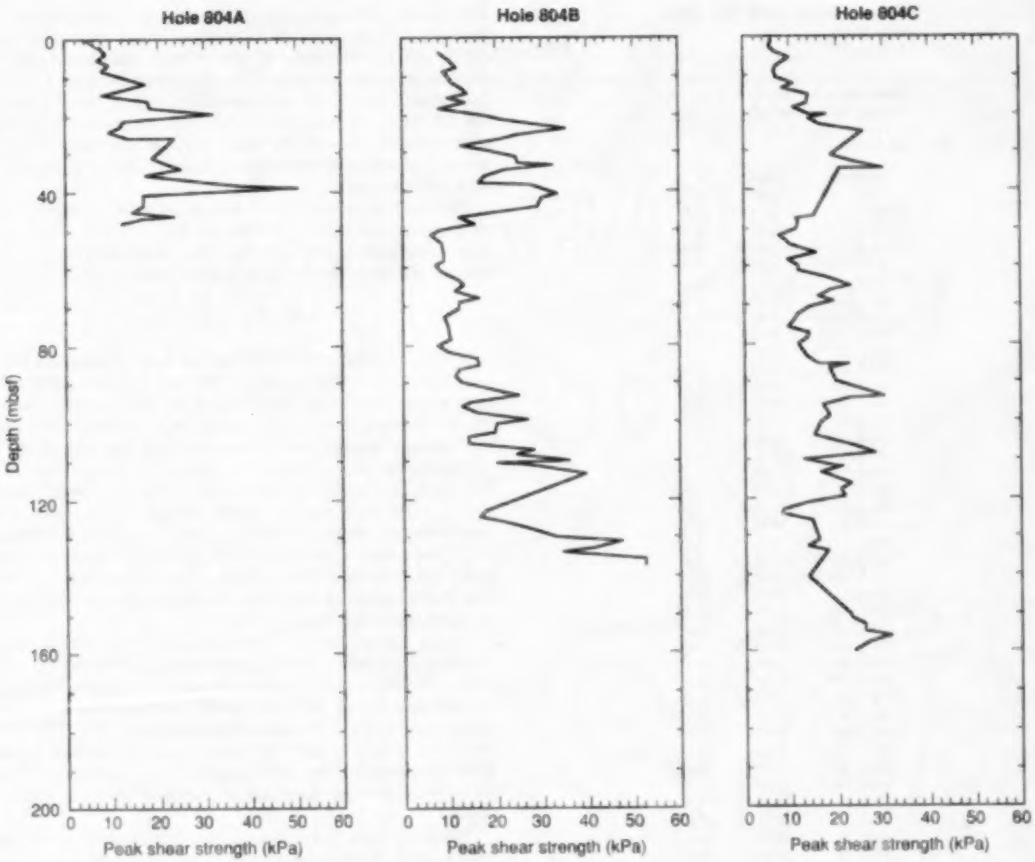

Figure 25. Laboratory vane peak shear strength vs. depth, Site 804.

place over intervals of a few meters to approximately 10 m. They appear to be related to changes in the carbonate content profile, with low porosities (high densities) measured in intervals of high carbonate content. The amplitude of these fluctuations increases with depth below 210 mbsf. Here, fluctuations in the index property profiles reflect the alternation between nannofossil chalk and nannofossil chalk with radiolarians (see "Lithostratigraphy" section, this chapter).

Two shallower intervals, 25–45 and 45–70 mbsf, depart from the Hamilton consolidation curve. The interval between 25 and 45 mbsf has high values of porosity and water content (low wet-bulk density). An increase in mean grain size was measured between 20 and 45 mbsf that corresponds to an increase in foraminifer content (Fig. 26). This increase in foraminifer content may lead to a more open sediment framework, with higher porosity and water content. Grain-to-grain contact between foraminifers also was proposed to explain the anomalously high shear strength values measured in this interval (see section on "Shear Strength" above). More detailed grain size analyses will be conducted post cruise to test these hypotheses.

The second anomalous interval, from 45 to 70 mbsf, shows a marked decrease in porosity and water content (increase in wet-bulk density), compared with the Hamilton consolidation curve (Fig. 31). This anomaly may reflect the effect of rapid consolidation caused by enhanced dewatering during slumping (see "Seismic Stratigraphy" section, this chapter).

Compressional Wave Velocity

Horizontal (parallel to bedding) and vertical (perpendicular to bedding) *P*-wave velocities were measured twice per section in all of Hole 804A and through 110 mbsf in Holes 804B and 804C (Cores 130-804B-13H and 130-804C-13H). Beginning at 110 mbsf, the sediment became stiff and insertion of the DSV probes created fractures along the bedding planes that made it difficult to transmit and receive the acoustic signal for vertical *P*-wave measurements. In Hole 804C, the DSV apparatus was replaced by the Hamilton Frame at the ooze/chalk transition near 180 mbsf (Section 130-804C-20X-2). Measurements were made on coherent and undisturbed blocks of chalk that were cut using the parallel-blade diamond saw. Good samples for Hamilton Frame measurements were sometimes difficult to obtain because of coring disturbance. Weakly cemented chunks also fractured easily when inserted between the Hamilton transducers, making measurements inaccurate or impossible. Results of velocity analyses are presented in Table 10 (microfiche, back pocket). Figure 33 shows the changes of velocity with depth.

The absence of downhole logging data at Site 804 makes it difficult to determine the validity of the anomalously high (or

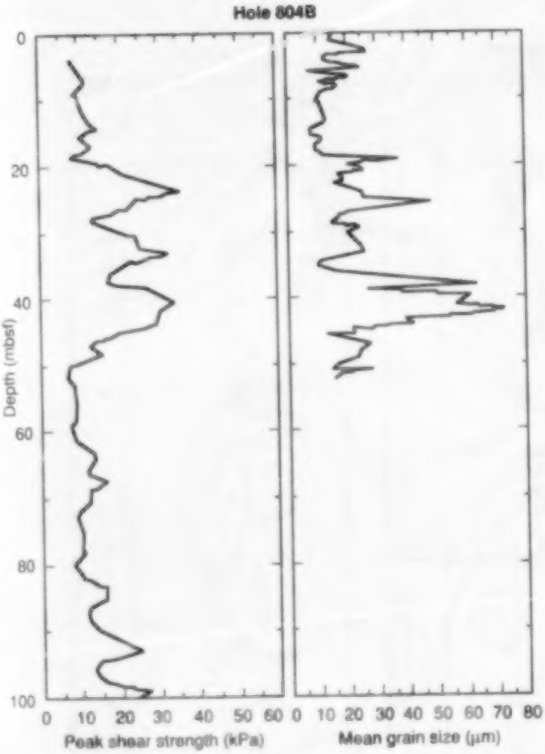

Figure 26. Vane shear strength and mean grain size vs. depth, Hole 804B.

low) laboratory velocity values. A cross correlation with PWL data within undisturbed intervals will be attempted on shore. Most of the velocity data recorded at Site 804 seem reliable; they compare well with those of Site 803. Two sharp decreases in the velocity values measured at Hole 804C (between 130 and 140 mbsf and at 160 mbsf) are, however, questionable. Signals transmitted between DSV transducers were weak, and we suspect that these low values are related to coring disturbance and/or internal fracturing caused by probe insertion.

Velocity values measured at Site 804 generally increase with depth, from 1530 m/s at the mud line to values greater than 1800 m/s at about 300 mbsf. In detail, between 0 and 50 mbsf, velocities do not appear to increase, with values averaging 1530 m/s. From 50 mbsf to the bottom of Hole 804C, velocities increase linearly with depth. Second-order fluctuations (changes occurring over intervals of a few meters to around 10 m) appear to be related to changes in the carbonate content, with high velocities measured in high carbonate content intervals. The amplitude of these fluctuations increases with depth.

Intervals of anomalous velocity values are superimposed on the depth trend. Beginning at approximately 170 mbsf, a decrease in *P*-wave velocity values correlates with a gradual decrease in the carbonate content (Fig. 33). Velocity values change from 1650 m/s at 170 mbsf to 1525 m/s at 200 mbsf. The base of this low velocity zone is difficult to determine because of the paucity of data. The vertical *P*-wave velocity data in Hole 804C (Fig. 33) implies that it may extend to 220 mbsf. It is interesting to note that the ooze/chalk transition boundary was placed at 180 mbsf (see "Lithostratigraphy" section, this chapter) and is located in the decreasing velocity interval, which begins at 170 mbsf. This result is opposite to what is expected, and the reason for it remains unexplained, at present.

SEISMIC STRATIGRAPHY

Site 804 is approximately 2 km northwest of proposed Site OJP-6, a site selected as a slightly shallower alternative to proposed Site OJP-3 (see "Underway Geophysics" chapter and Mayer et al., this volume). The location of proposed Site OJP-6 was chosen based on a single high-resolution seismic profile collected during the *Thomas Washington* site survey cruise (see Mayer et al., this volume), but the final position of Site 804 is off the site survey cruise line and based solely on the data collected by the *JOIDES Resolution* during its pre-beacon-deployment survey. Because the profile of the *JOIDES Resolution* is the only one that crosses the drilling site, discussion of seismic stratigraphy at Site 804 will be based on this line rather than the *Thomas Washington* line. A comparison of the *JOIDES Resolution* seismic line over Site 804 and a *Thomas Washington* line approximately 2 km from the site is presented in Figure 34.

At 3861 m, Site 804 represents the deepest site of the Ontong Java Plateau depth transect. As discussed in Mayer et al. (this volume), it is extremely difficult to find thick, undisturbed accumulations of sediment in this depth range; the only thick sequences present are found in a series of grabenlike features that are common on the plateau between about 3800 and 4200 m (see Mayer et al., this volume; Fig. 35). Both Site 804 and proposed Site OJP-3 (at 4200 m) are located in these grabenlike features and, although only limited surveying was done at Site 804, a detailed survey of OJP-3 revealed many of their characteristics. These small basins are typically oriented roughly north-south and are about 10–16 km wide and about 20–25 km long. They are full grabens in that the basement high completely encloses them (Fig. 36). The offset in acoustic basement between the "horst" and the graben is approximately 300 m at Site OJP-3 and 200 m at Site 804. Although it is not yet clear whether these features are original basement topography that has differentially filled or whether they are related to more recent tectonic activity, the ability to trace seismic units from graben to horst as well as clear evidence of erosion on top of the horst (e.g., OJP-3; Fig. 37) implies that fairly recent movement may, at least in part, be responsible for these structures.

In a gross sense, the seismic stratigraphy at Site 804, as at proposed Sites OJP-3 and OJP-6, can be tied together with the seismic stratigraphy of the rest of the plateau. These deep sites all show a thinned post-Miocene section (relative to the upper part of the plateau; see Mayer et al., this volume). Upon closer examination, however, it is clear that superimposed on this more general seismic stratigraphy is a clear signal of local sediment disturbance. This is particularly obvious in the north-south crossing of Site 804 where a lens of disrupted sediment can be seen between 0.051 and 0.250 sbsf (between Reflectors 4-1 and 4-7; 44–215 mbsf; Fig. 38). Both the upper and lower surfaces of this zone show a particularly incoherent (crenulate) reflector pattern; the upper surface is represented biostratigraphically as a condensed section (ca. 4.3 Ma), whereas the lower surface is a hiatus (ca. 20–15 Ma; see "Biostratigraphy" section, this chapter).

There are also several regions within the lens that have a more disturbed, incoherent reflector pattern (e.g., 0.051–0.103 sbsf at 44–85 mbsf and 0.120–0.190 sbsf at 100–160 mbsf). A number of small faults may be identified, implying that the mass has moved from the northwest to the southeast (from upslope) along a slip plane at about 207 mbsf. The movement does not appear to be large, but enough to cause internal deformation in the sedimentary section. This movement may represent

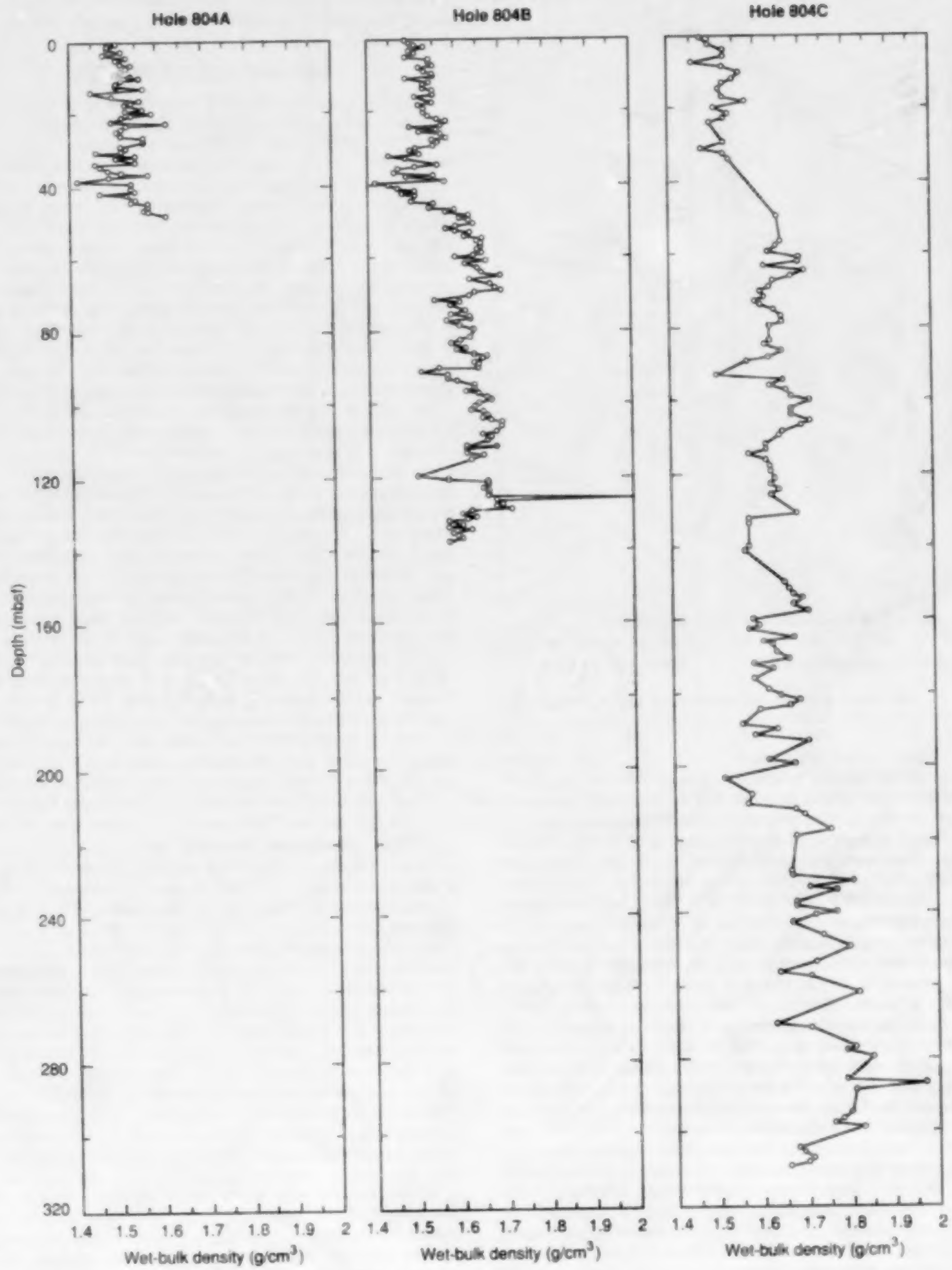

Figure 27. Laboratory wet-bulk density vs. depth, Site 804.

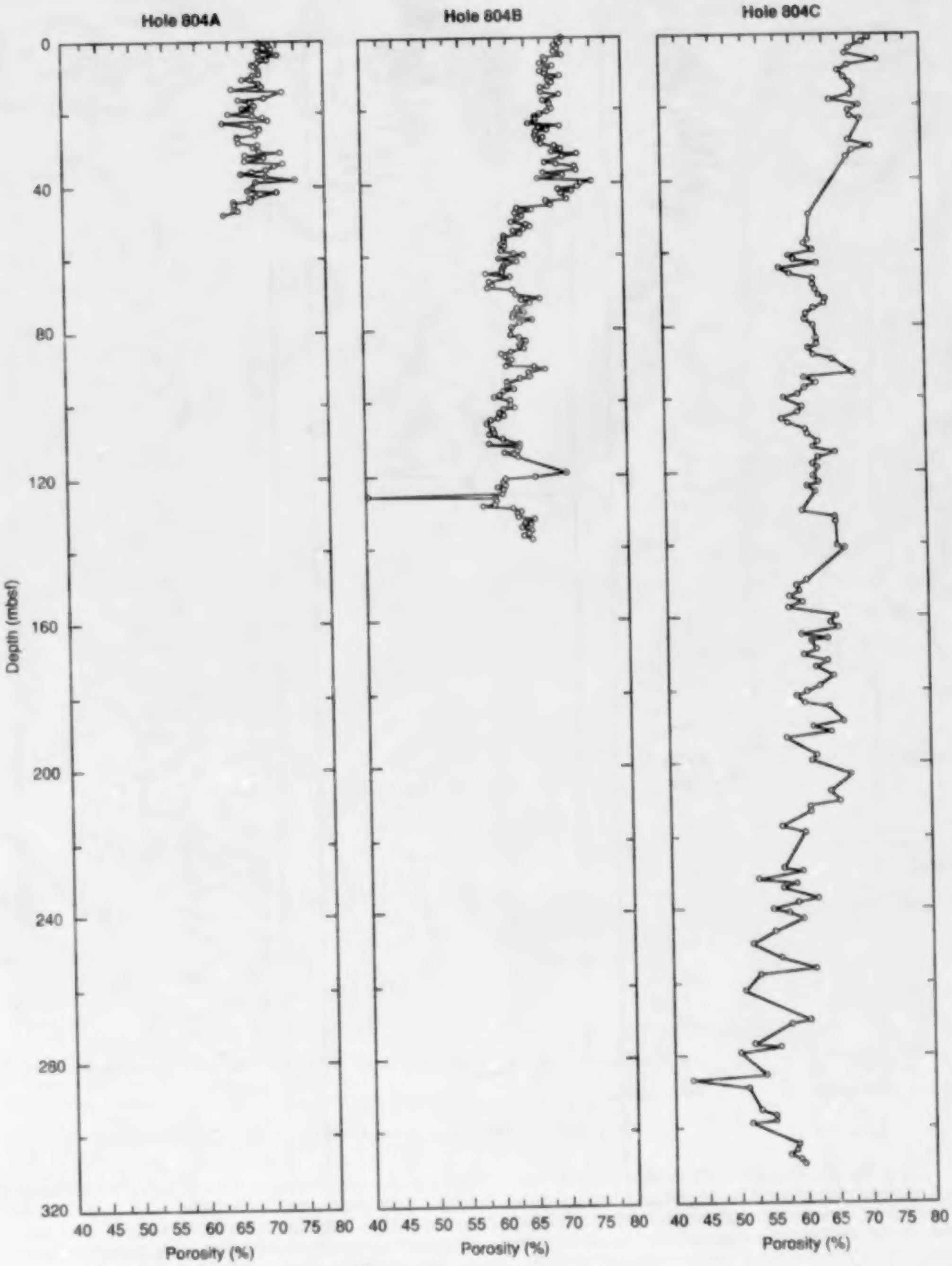

Figure 28. Laboratory porosity vs. depth, Site 804.

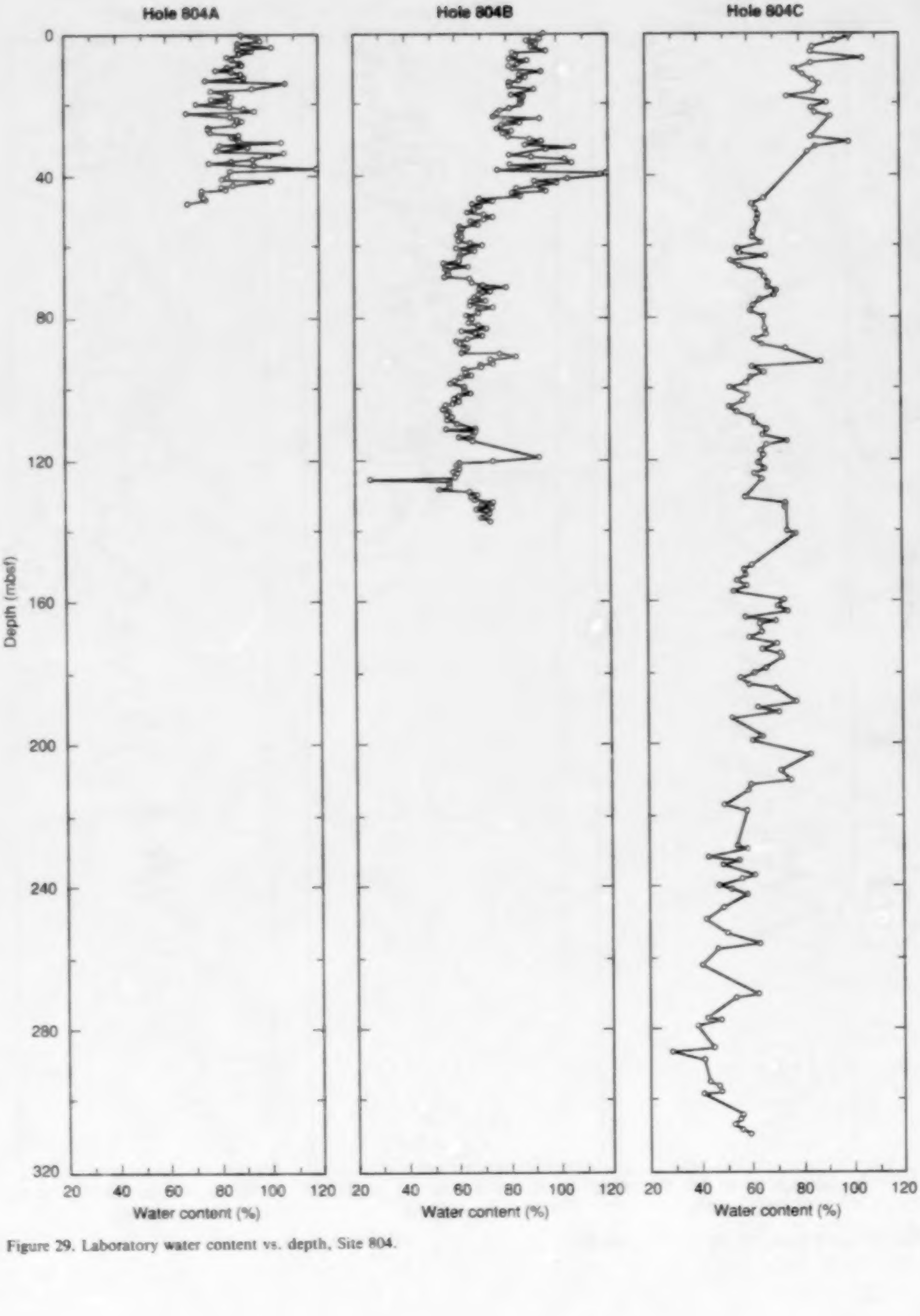

Figure 29. Laboratory water content vs. depth, Site 804.

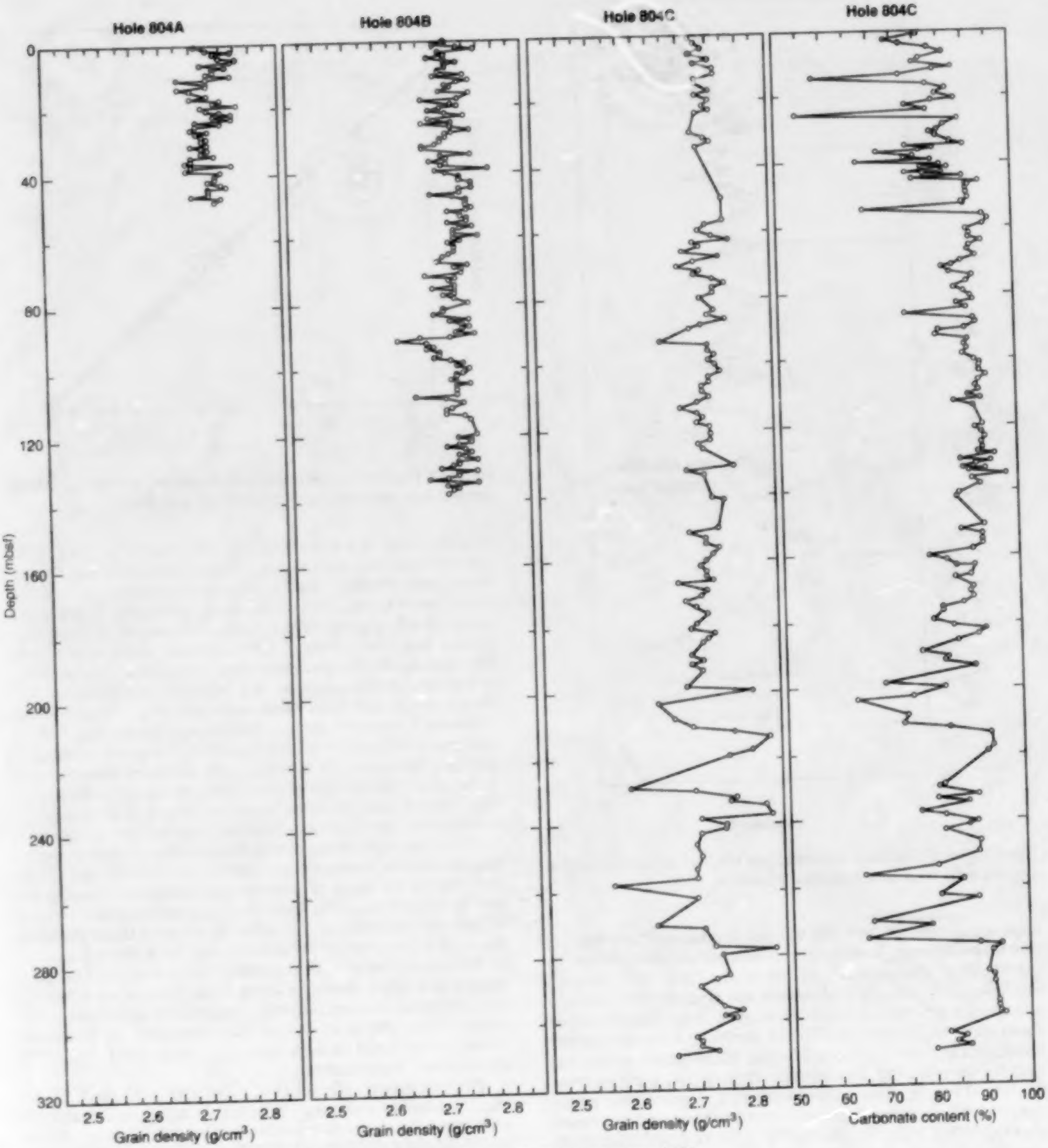

Figure 30. Grain density (Holes 804A, 804B, and 804C) and merged carbonate content vs. depth.

the response of the sediment column to earthquakes (e.g., Berger and Johnson, 1976), to differential compaction over pre-existing basement topography (e.g., Mayer, 1980), or to faulting. If faulting is the cause, the stratigraphic relationships within the disturbed lens imply that the faulting is fairly recent (see below).

Drilling results support the interpretation of mass movement within the sedimentary section. Microfaulted, dipping, and contorted beds are described in cores recovered between 42 and 110 mbsf (see "Lithostratigraphy" section, this chapter). Although there is clear evidence for movement and disruption within the sediment column, the section appears to be stratigraphically intact (see "Biostratigraphy" section, this chapter); thus, the conclusions drawn from the seismic stratigraphy should prove to be relevant to the more general questions of regional paleoceanography.

To relate drill hole results to the seismic record accurately, seismic modeling, as described in Mayer et al. (1985, 1986; see "Seismic Stratigraphy" section, "Site 803" chapter, this vol-

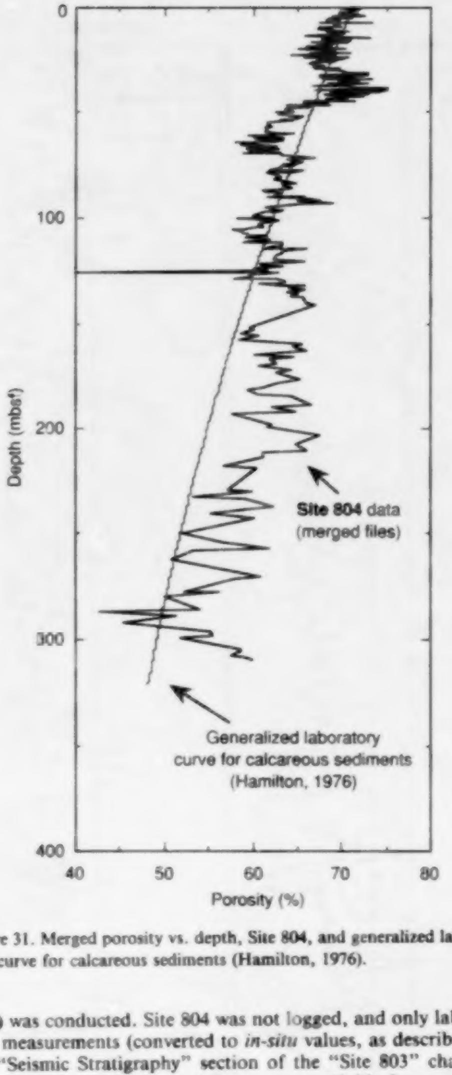

Figure 31. Merged porosity vs. depth, Site 804, and generalized laboratory curve for calcareous sediments (Hamilton, 1976).

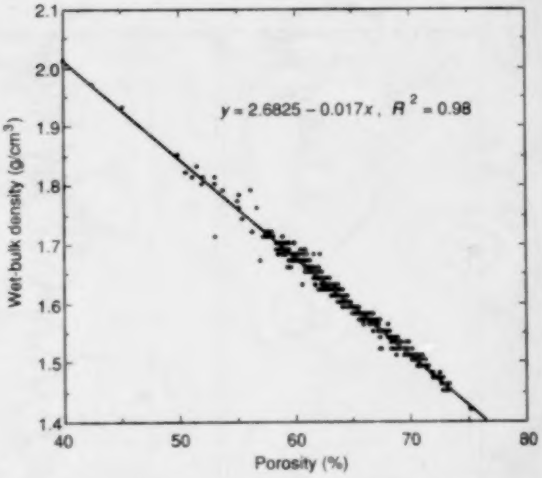

Figure 32. Regression of saturated bulk density vs. porosity for Site 804 (merged data sets from Holes 804A, 804B, and 804C).

ume) was conducted. Site 804 was not logged, and only laboratory measurements (converted to *in-situ* values, as described in the "Seismic Stratigraphy" section of the "Site 803" chapter, this volume) of velocity and density are available for synthetic seismogram generation. In addition, there is no seismic source signature available for the *JOIDES Resolution* seismic system; therefore, the signature of the *Thomas Washington*'s system was used for the modeling. The decrease in resolution resulting from the lack of logging data and the somewhat inappropriate source signature will inevitably degrade the synthetic seismogram. Nonetheless, there is still a reasonable match between the field record and the synthetic seismogram (Fig. 38), giving us some confidence in the traveltime-to-depth conversion.

Based on the *JOIDES Resolution* profile, nine reflectors (4-1 through 4-9; Table 11 and Fig. 39) were identified within the interval drilled (309 m). Most of these can be identified on the synthetic seismogram, with the exception of Reflector 4-8 (see discussion below).

As with Site 803 (and with all such analyses), the uppermost part of the section (upper 30 m/s) is dominated by the outgoing seismic pulse; the shallowest identifiable reflector beyond the outgoing pulse is 4-1 at 0.052 sbsf (42 mbsf; Figs. 34 and 39). This reflector, seen on both the *JOIDES Resolution* and *Thomas Washington* profiles, marks the upper boundary of the displaced lens of sediment. In the synthetic record, it appears as several closely spaced events; on the field record, it is a discontinuous (crenulate) surface. This reflector, dated at about 4.3 Ma, also marks the boundary of a 10-m-thick zone with low carbonate content, density, and velocity and generally high shear strength and large mean grain size (Figs. 39 and 40; see "Physical Properties" section, this chapter, for details). The unusual association of low carbonate with increased mean grain size and shear strength may imply an increased abundance of radiolarians, though this was not noted by the sedimentologists. This interval does, however, show an increased abundance of foraminifers (see "Lithostratigraphy" section, this chapter).

The reflector itself appears to be the result of closely spaced, large-amplitude changes from high to low velocity and density that may be the result of decreased sedimentation rates at this time (see "Sedimentation Rates" section, this chapter). Immediately below the depth of this reflector, we see a sharp change in the slope of the density vs. depth curve. Such slope breaks are to be expected with normal consolidation, but this change in slope is at a much shallower depth (and younger age) than the first change in slope at Site 803. Perhaps the movement of the sediment lens served to dewater the upper part of the section (where water could escape) and thus cause these apparently anomalously high densities.

The next deeper reflector (4-2, 0.100 sbsf at 83 mbsf, ca. 8.1 Ma) is marked by a density, velocity, and carbonate decrease; no grain size information is available for this interval (Figs. 40 and 41). Until grain size data are collected, it will be difficult to determine whether this event represents dissolution, winnowing, or a combination of both. Reflector 4-2 also marks the lower boundary of the upper disrupted zone of the large mass of displaced sediment (Fig. 38). A sharp increase in shear strength occurs at this depth (see "Physical Properties" section, this chapter).

Reflector 4-3 (0.121 sbsf, at 98 mbsf, ca. 9.1 Ma) marks the upper boundary of the lower disrupted zone (Fig. 38). There is a small increase in carbonate content and velocity at this level but a major increase in density, which probably accounts for the re-

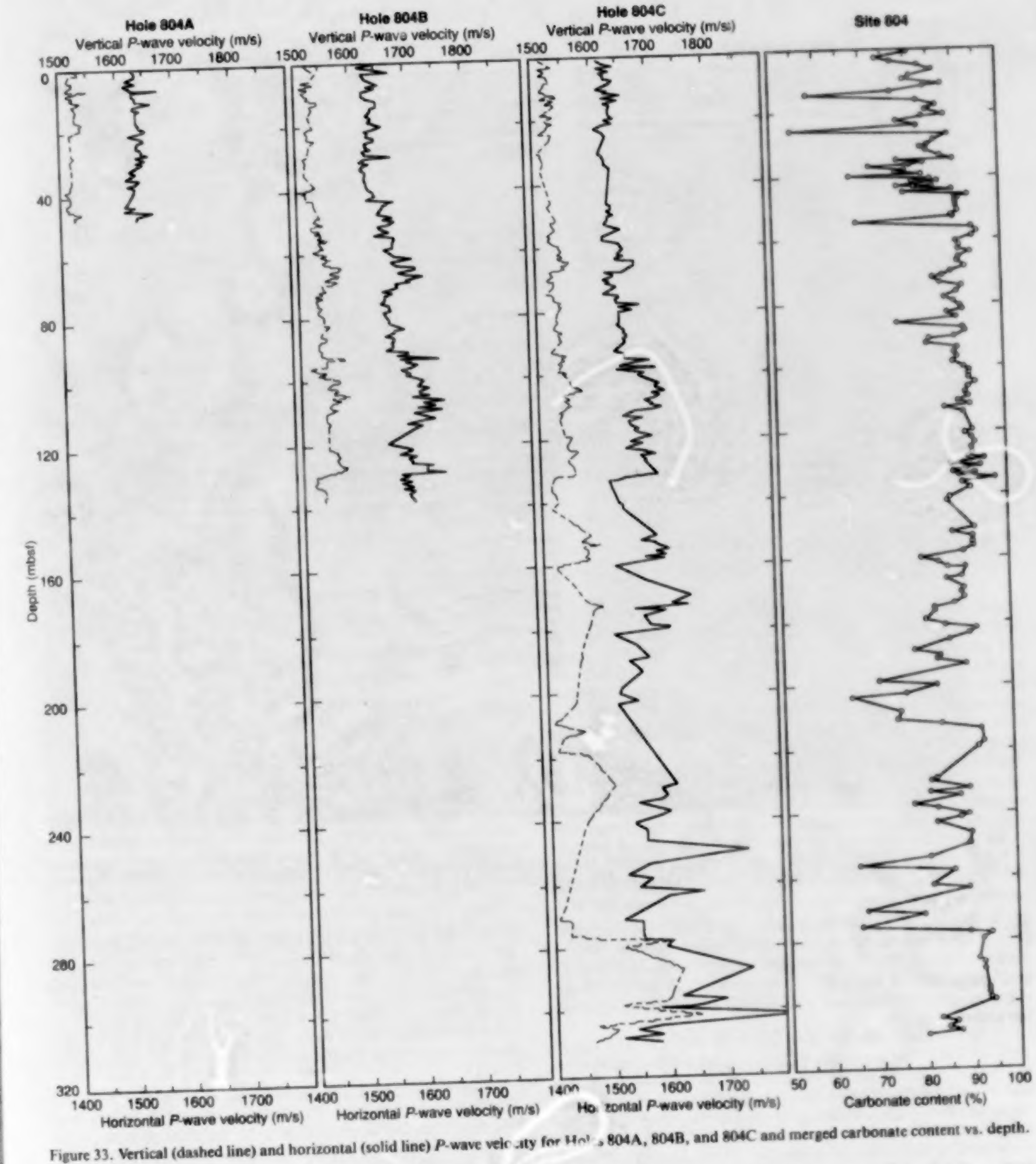

Figure 33. Vertical (dashed line) and horizontal (solid line) *P*-wave velocity for Holes 804A, 804B, and 804C and merged carbonate content vs. depth.

flector (Figs. 40 and 41). As with Reflector 4-1, there appears to be an increase in density moving into the more deformed zone.

Reflector 4-4 (0.148–0.150 sbsf at 125–129 mbsf, 9.68–9.78 Ma) is characterized by rapidly changing density, velocity, and carbonate content (low to high). Again, grain size will be a key in deciphering the paleoceanographic significance of this signal. Although Reflector 4-4 is difficult to trace within the graben (it is broken up by sediment movement), it is of the same age as a major reflector found at Site 803 and in the central equatorial Pacific (Mayer et al., 1986) and may be representative of a global oceanographic event.

Reflector 4-5 (0.170 sbsf at 145–150 mbsf, 10.3–10.6 Ma) is associated with a change from high to low carbonate and velocity. A large (1 point) density spike (decrease) is observed at

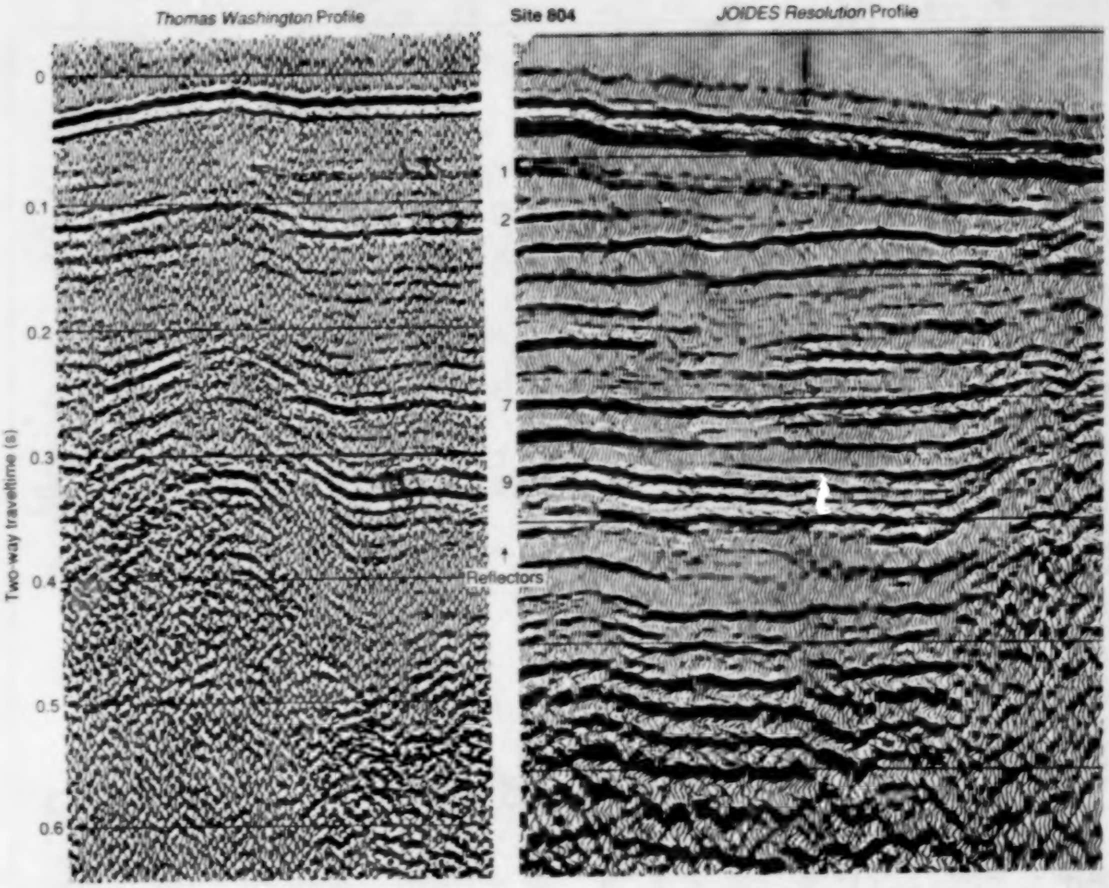

Figure 34. Seismic record collected on ROUNDABOUT Cruise 11 site survey approximately 2 km south of Site 804 (80-in.^{3} water gun, 70–250 Hz band-pass filter) and *JOIDES Resolution* profile at Site 804. For details of reflector picks, see Table 11.

about this level (Fig. 40). This excursion is not, however, supported by a change in velocity or carbonate content, which makes it suspect; further investigation will be necessary to evaluate the validity of this point. Reflector 4-5 is in the middle of the lower disrupted zone and is broken up toward the margins of the graben (Fig. 38).

A very strong reflector (4-6, 0.200 sbsf at 170–175 mbsf, 13.2–13.7 Ma) that also quickly fades out toward the margins of the graben is found within the lower disrupted zone (Figs. 34 and 39). There is a slight increase in carbonate content at this depth but no significant change in density. There is, however, a large change in velocity (Figs. 40 and 41). An increase in velocity without a large change in density is indicative of the early stages of cementation when the rigidity of the sediment is increased (and thus the velocity) without a substantial increase in the bulk density (Mayer et al., 1985). In support of this, the sedimentologists place the ooze-chalk transition several meters below the depth of this reflector (181 mbsf; see "Lithostratigraphy" section, this chapter).

Beneath Reflector 4-6 is a highly disturbed zone that is represented stratigraphically as a hiatus (15.7–20.9 Ma; see "Biostratigraphy" section, this chapter). Significantly, the carbonate content is extremely low in this zone, suggesting pervasive dissolution. This is the same hiatus found at Site 803; its global distribution is discussed by Keller and Barron (1983) and its relationship to a central Pacific-wide seismic event by Mayer et al. (1986).

Directly beneath this disturbed zone is Reflector 4-7 (0.250 sbsf, 215 mbsf, 20.2–20.5 Ma), a strong reflector traceable outside the graben and also identifiable on the *Thomas Washington* profile. This reflector appears to be the primary focus of the large, lens-shaped sediment mass. Reflector 4-7 is associated with a rapid rise in carbonate content (there is limited velocity and density data in this interval, but we would expect the carbonate increase to give rise to an increase in both velocity and density). We propose that the large lens of sediment discussed above slid on the carbonate-poor, radiolarian-rich zone above Reflector 4-7; the more porous, dissolution-weakened sediment

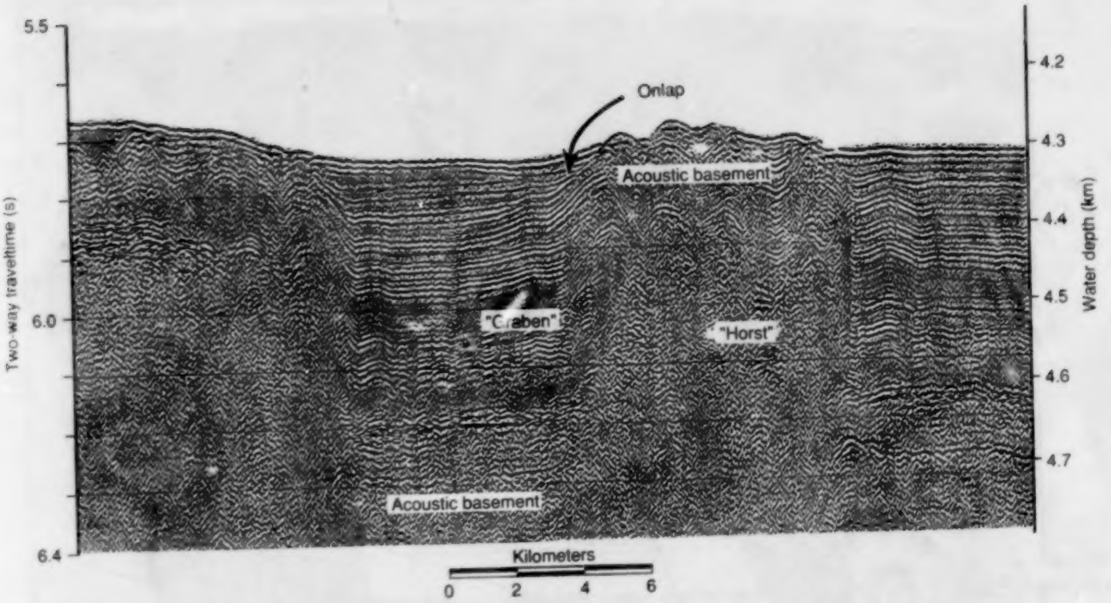

Figure 35. Seismic profile collected aboard the *Thomas Washington* showing grabenlike feature at proposed Site OJP-3.

was severely disrupted whereas the high-carbonate-content material below remained intact.

The deepest reflector within the drilled section (4-9; 0.305 sbsf at 270 mbsf, 24.6–28.36 Ma) is a strong doublet that is also identifiable on the *Thomas Washington* profile. This reflector is the result of a sharp decrease in velocity, density, and carbonate content and is coincident with a major hiatus just below the Miocene/Oligocene boundary. This same horizon is marked by a series of reverberant reflectors at the shallower Site 803.

Although drilling ended at 309 mbsf, we can use the results of Site 803 to estimate the depths and ages of the deeper reflectors. Beneath Reflector 4-9 is another transparent zone with an incoherent and crenulate appearance, possibly representing another period of sediment movement. These sediments are probably early Oligocene in age, ranging from 28 to 36 Ma. Below the transparent zone are several reverberant reflectors (0.420–0.480 sbsf) that are probably equivalent to Reflectors 3-8 through 3-10 at Site 803 and represent the large changes in carbonate/silica content between 36 and 39 Ma. The first really strong deep reflector (0.480 sbsf) is probably the first occurrence of limestone or massive chert and, if the section is similar to the one at Site 803, basement should be close below at about 0.515 sbsf or approximately 505 mbsf.

Site 804 is far from ideal for seismic stratigraphic studies in the context of Leg 130: (1) it was not surveyed with the high-resolution profiling system used for the other sites; (2) we do not have a source signature for the seismic system used; and (3) most unfortunately, its seismic record is overprinted by a series of local mass movement events. Nonetheless, there are some similarities between the seismic stratigraphy at Sites 803 and 804 that imply that, with careful study, it may be possible to extract a regional paleoceanographic picture from the seismic record even at these depths. The long outgoing pulse and the poor results from the *JOIDES Resolution* seismic system prevent us from examining the younger events that were found at Site 803 (3-1 at 2.58 Ma and 3-2 at 3.3–3.4 Ma). However, given the preliminary nature of both the seismic picks and the biostratigraphy, it is possible that Site 803 Reflector 3-a (4.3 Ma) and Site 804 Reflector 4-1 (4.1 Ma) represent the same event. The 5-Ma reflector at Site 803 (3-b) is not found in the *JOIDES Resolution* seismic record at Site 804, but it is clearly present on the synthetic seismogram and can be seen in the higher resolution *Thomas Washington* profile (Figs. 34 and 39). Reflectors 3-4 (8.0–8.1 Ma) and 4-2 (8.0–8.1 Ma) are precisely the same age, which is intriguing because at both sites they appeared to be local events. If a reflector continues to be found at this time, we will have to look carefully for a regional mechanism. The central-Pacific-wide middle/late Miocene boundary reflector (Mayer et al., 1986) is present at both sites (3-c at Site 803 and 4-4 at Site 804) as is the Miocene/Oligocene boundary reflector (3-7 at Site 803 and 4-9 at Site 804). Given the preliminary nature of our seismic analyses, the physical properties studies, and the biostratigraphy, it is still too early to do anything more than speculate on the possible regional significance of these events. If, however, they continue to appear at future sites, the arguments become more compelling.

SUMMARY AND CONCLUSIONS

Location and Objectives

Site 804 is located in the western equatorial Pacific, on the northeastern margin of the Ontong Java Plateau (latitude 1°00.3′N, longitude 161°35.6′E) in 3861 m of water, 375 km east-northeast of DSDP Sites 289/586. Our objective in drilling this site was to obtain a continuous sedimentary record to serve as the deep-water end member on a Neogene depth transect, designed to recover depth-related paleoceanographic signals. It was anticipated that we would encounter a high-resolution carbonate record in a sublysoclinal setting for studies of dissolution and biostratigraphy.

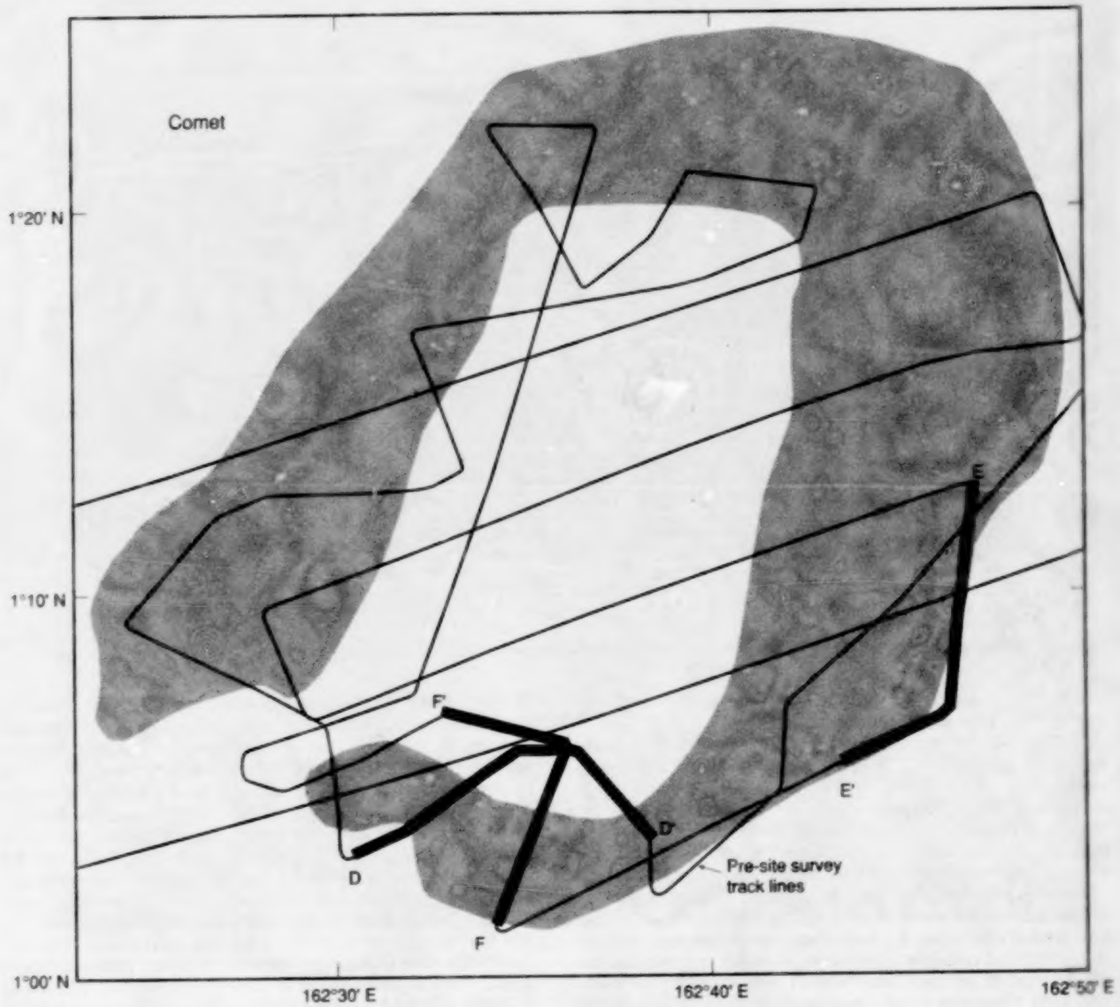

Figure 36. Map of distribution of grabenlike feature at proposed Site OJP-3. White area denotes downdropped block; gray area, upthrown block. See Mayer et al. (this volume) for details.

We positioned the site using a single-channel seismic (SCS) line acquired by the *Thomas Washington* during ROUNDABOUT Cruise 11, on the SCS crossing line of *JOIDES Resolution*. The site is located near the center of a slight depression about 4.5 km wide. The location is close to a significant offset in basement levels between the plateau and the deep ocean floor (Fig. 2). Episodic shaking from earthquakes, basement relief, and perhaps the presence of clay-rich layers at this water depth apparently create conditions favorable for large-scale slumping and debris flow on the flanks of the plateau. Removal of support at greater water depths by carbonate dissolution also may play a role in fostering mass movement (Berger and Johnson, 1976). Selection of a suitable site to drill was difficult under these conditions, and the site chosen was less than ideal for the purposes of the transect.

Coring Results

We spent 3.25 days at this site, coring 499 m of sediment and recovering 466 m. Three holes were drilled. Hole 804A, a dedicated hole, was cored with the APC to 48.7 mbsf into upper Miocene sediments, with 103.7% recovery. Hole 804B was cored with the APC to 137.7 mbsf into middle Miocene sediments, with 102.8% recovery. It was abandoned when the core barrel became stuck in the hole. Hole 804C was cored with the APC to 120.3 mbsf with a recovery of 100% on average. Below this depth, coring continued with the XCB to 312.5 mbsf, at which point it ended in lower Oligocene sediments. Average recovery for the XCB section was 80%. There was no logging.

Neogene sediments were retrieved, except for the four deepest cores in Hole 804C, which recovered early Oligocene chalk

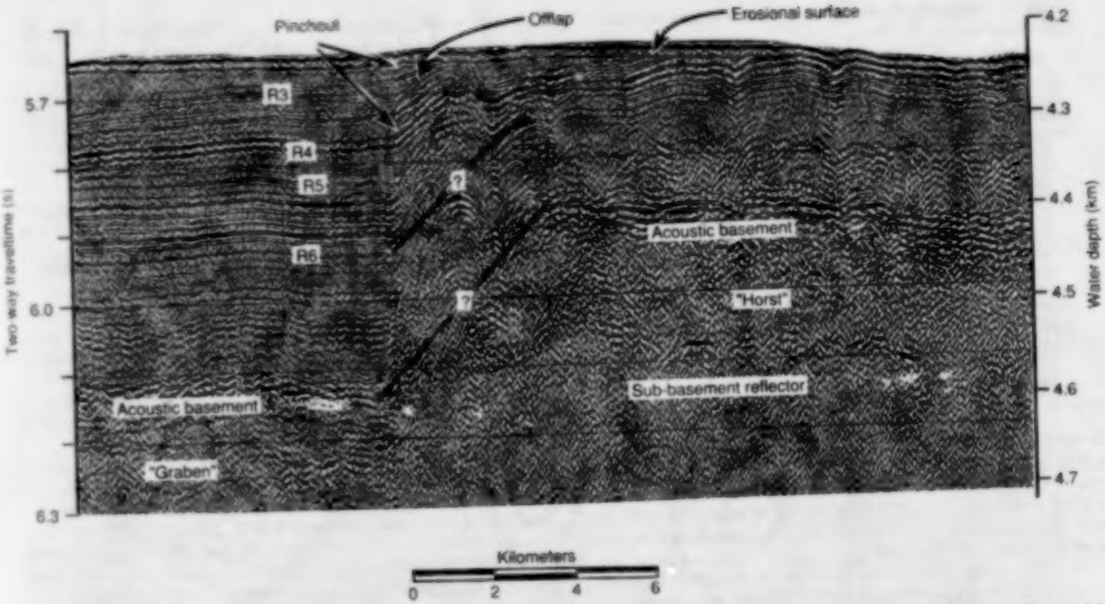
Pinchout
Offlap
Erosional surface
R3
R4
R5
R6
?
?
Acoustic basement
"Horst"
Sub-basement reflector
Acoustic basement
"Graben"
Two-way traveltime (s)
5.7
6.0
6.3
Water depth (km)
4.2
4.3
4.4
4.5
4.6
4.7
Kilometers
0
2
4
6

Figure 37. Detail of seismic stratigraphic relationships at margin of grabenlike feature at proposed Site OJP-3. See text for details of reflector picks.

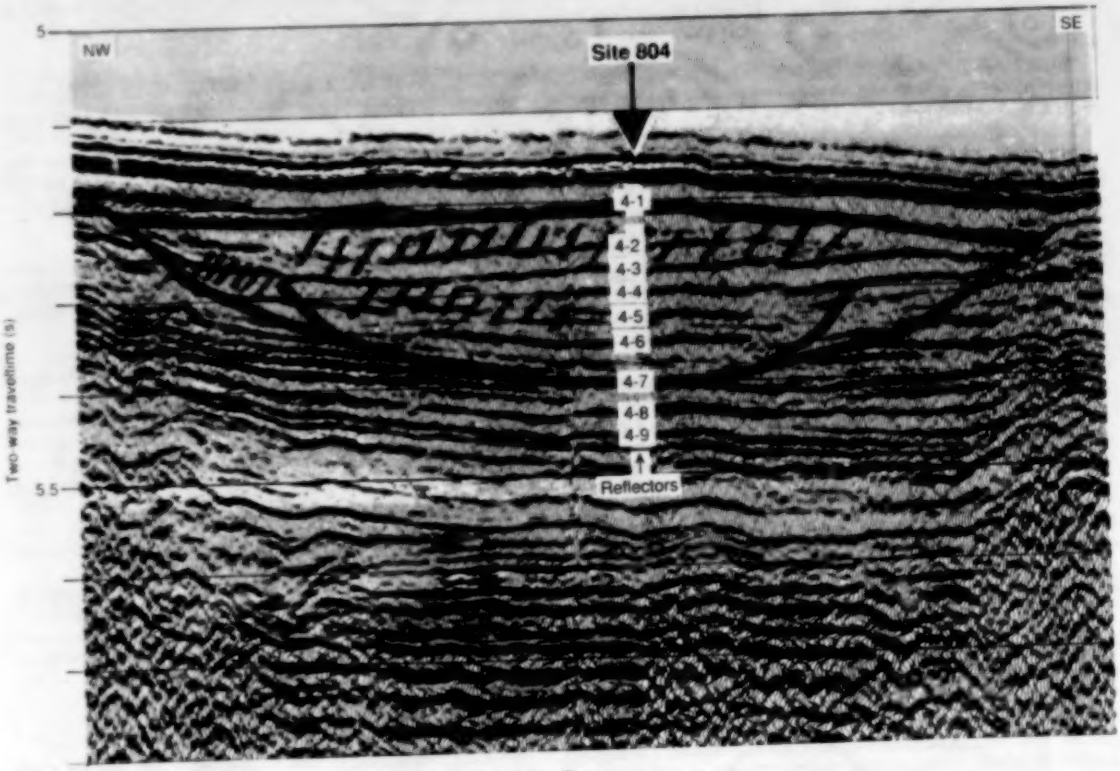
5
NW
SE
Site 804
4-1
4-2
4-3
4-4
4-5
4-6
4-7
4-8
4-9
Reflectors
Two-way traveltime (s)
5.5

Figure 38. Intervals of disrupted sediments at Site 804 outlined in heavy lines.

Table 11. Summary of traveltimes, depths, and ages for Site 804 reflectors.

	Traveltime		Depth		
Reflector	Seismic (sbsf)	Synthetic (sbsf)	Seismic (mbsf)	Synthetic (mbsf)	Age (Ma)
4-1	0.052	0.052	42	42	4.1
4-2	0.100	0.100	83	83	8.0–8.1
4-3	0.121	0.122	98	100	8.9–9.0
4-4	0.148	0.150	124	128	9.68–9.78
4-5	0.170	0.178	145	150	10.3–10.6
4-6	0.200	0.210	173	182	13.1–13.7
4-7	0.250	0.255	215	217	20.2–20.5
4-8	0.280	?	239	?	22.8–23.0
4-9	0.305	0.310	267	270	24.6–28.4

Notes: Depths and traveltimes to seismic events are picked on both the synthetic seismogram (synthetic) and the field record (seismic). Ages are from sedimentation rate curves (see "Sedimentation Rates" section, this chapter).

(Cores 130-804C-29X to -33X). The entire column, from the earliest deposits to the seafloor, was classified as nannofossil ooze and chalk and is considered to be one lithologic unit. Major breaks occur in the upper Oligocene (hiatus at 270 mbsf, ca. 28–25 Ma) and at the lower-to-middle Miocene transition (hiatus at 197 mbsf, ca. 20–15 Ma).

There is a condensed section or hiatus in the lower Pliocene, between 5 and 4 Ma (46–43 mbsf), and possibly within the middle Miocene, between 13 and 11 Ma (near 160 mbsf). Disturbance of layers (other than from coring) was evident in the section containing the major hiatus from the early to middle Miocene (210–187 mbsf), and also between 42 and 110 mbsf (most of the upper Miocene). It was especially prominent between 70 and 80 mbsf (7–8 Ma).

Two subunits were recognized in this rather uniform section of bioturbated ooze and chalk. They are separated by the ooze/chalk transition at 181 mbsf (middle Miocene, ca. 13 Ma).

The younger section of the unit (Subunit IA, 0–181 mbsf) comprises Pleistocene to middle Miocene nannofossil ooze with foraminifers, nannofossil ooze, and nannofossil ooze with radiolarians. The oozes are light brown in the top 20–40 mbsf, grading into white ooze, with color banding (green and reddish hues) down to 100 mbsf. The banding (related to Liesegang diffusion rings) is best expressed between 44 and 59 mbsf (uppermost Miocene and lowermost Pliocene) and is well developed between 71 and 90 mbsf. Banding is disrupted and distorted in the disturbed layers mentioned, within sediments of uppermost Miocene age (ca. 7–8 Ma). Two turbidites near 93 mbsf attest to redeposition within the middle upper Miocene sequence (ca. 11 Ma).

The older portion of the unit (Subunit IB, 181–313 mbsf) consists of middle Miocene to upper lower Oligocene nannofossil chalk and nannofossil chalk with radiolarians. Colors are yellowish white, pale brown, and white. Radiolarian-bearing sediments are common in this subunit, with a strong radiolarian maximum in the lower Miocene (near 200 mbsf) just below the early/middle Miocene hiatus. Also at this depth, there are indications of ooze/chalk clasts and distorted bioturbation features, as mentioned.

Seismic Stratigraphy

Seismic profiles across the site show the effects of mass movement. These profiles exhibit incoherent crenulate reflections at several levels, as well as evidence for wedging along the basin margins (see Fig. 38). Disturbance is first clearly noticeable at 0.05 sbsf (0.05 two-way traveltime from the seafloor, around 40 mbsf), where part of the section seems to be condensed or missing. At that level, or slightly below it, there is an unconformity that is expressed as a termination of tilted deeper reflectors against the overlying section (upper unconformity; see Fig. 38). Disturbance continues down to 0.1 sbsf (around 80 mbsf) but may include the next deeper interval (to 0.12 sbsf) as well. This would correspond to the disruptions seen in the cores, especially at 70–80 mbsf (7–8 Ma), in the upper portion of the tilted block composing the upper and middle Miocene section.

Disturbance is again seen in the lower part of the block, near 0.21 sbsf (ca. 170 mbsf). At 0.22 s, there is a strong reflector that is weakly developed outside the depression; however, within the graben it is bowl shaped and concentrates energy. This reflector coincides with, or is situated immediately above, the ooze/chalk transition as located in the cores. The lower boundary of the tilted block is probably a slip plane at 0.23 sbsf (lower unconformity; see Fig. 38). In the cored sediments, there is a major hiatus at this level (197 mbsf, ca. 20–15 Ma). On either side, groups of reflectors are disrupted, presumably because of mass movement. This series of strong reflectors probably represents ooze/chalk alternations in the lower Miocene.

The Miocene/Oligocene hiatus is well expressed as a strong double reflector, with the first return at 0.30–0.31 sbsf (around 270 mbsf). Judging from the lack of strong reflectors below, a section of more than 100 m of lower Oligocene sediments might be expected here, with the (unconformable) Eocene/Oligocene boundary appearing near 0.42 sbsf. If so, another 200 or perhaps 250 m of sediment (depending on the basement pick) would be expected in this graben before reaching basement. The first strong deep reflector (at 0.48 sbsf) presumably would mark the location of Eocene limestone and chert. Outside of the basin, the apparent paucity of pre-Oligocene deposits would suggest widespread erosion early in the Cenozoic and in the Late Cretaceous, as was the case at Site 803.

There is some indication that disturbance is associated preferentially with certain layers. This gives rise to the hypothesis that such layers may be predisposed, through conditioning during deposition, to serve as slip planes later. Inasmuch as hiatus formation is contingent on paleoceanographic events, the tracing of these features by seismic profiling should yield valuable information on the nature of such events (Mayer et al., 1986).

Special Studies

Physical properties, including wet-bulk density and sound velocity, show greater variability at this site than at Site 803. Distinct minima in density occur near or within the intervals identified to have hiatuses.

Chemical gradients in interstitial waters at this site are generally similar to those at Site 803, reflecting the calcareous/siliceous nature of the sediments and the paucity of organic material. Calcium and magnesium gradients are influenced by basalt alteration reactions at depth and show the usual negative correlation ($R^2 = 0.97$). Strontium concentrations are lower than at Site 803, presumably reflecting diminished recrystallization intensity at Site 804. Dissolved silica increases with depth, indicating the continued dissolution of siliceous fossils. Near-maximum levels are reached at 100 mbsf, suggesting that below that level dissolution is reduced or balanced by precipitation.

A comparison of detailed magnetostratigraphic profiles for the Pliocene-Pleistocene sediments in the three holes allowed us to detect small changes in sedimentation rates and between-hole variations. There appears to be a small decrease in the sedimentation rate at the Pliocene/Pleistocene boundary from 11.6 to 9.8 m/m.y.

Sequence of Events

Faulting presumably started during initial cooling and sinking of the newly formed crust, early in the history of the pla-

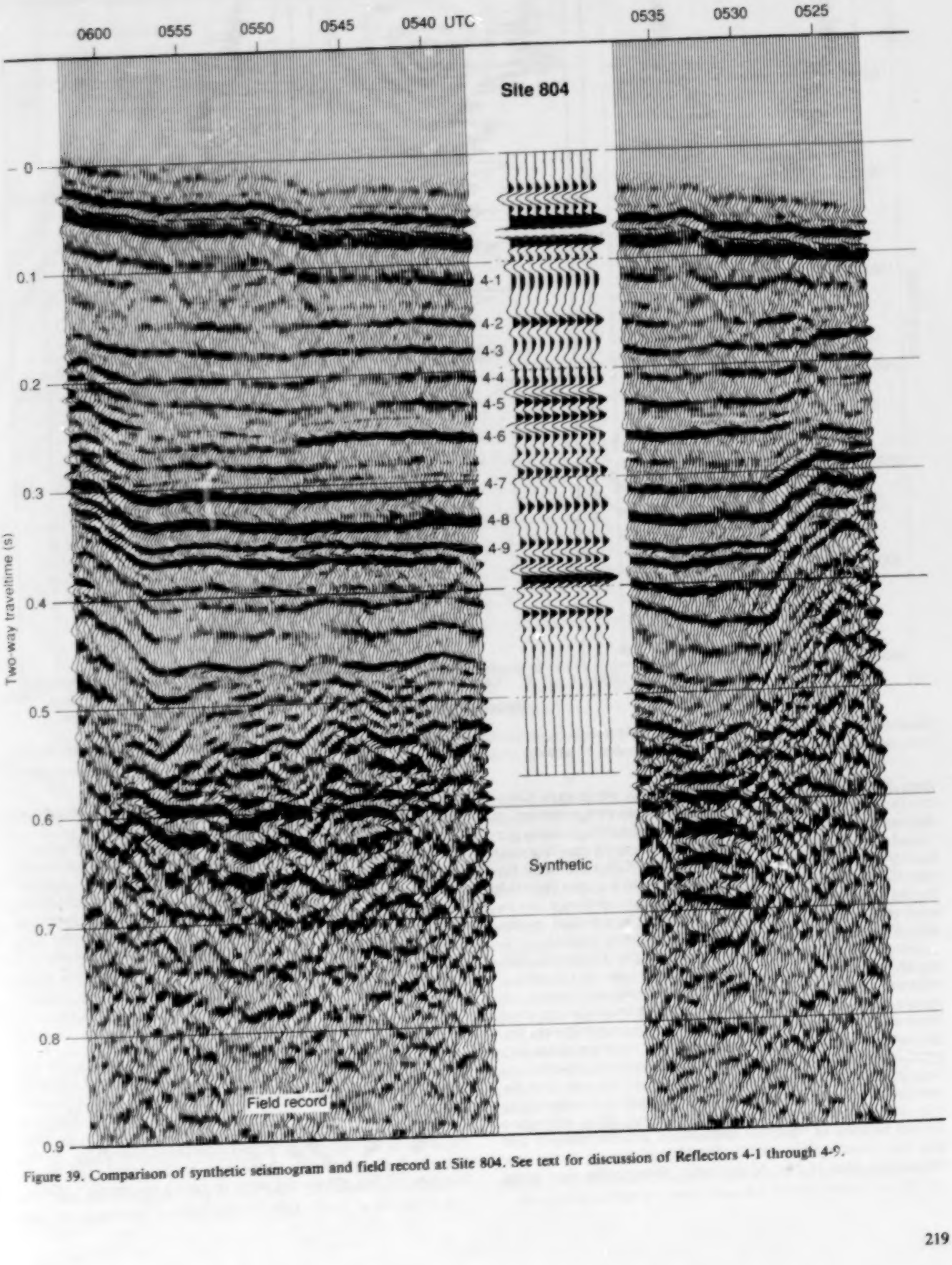

Figure 39. Comparison of synthetic seismogram and field record at Site 804. See text for discussion of Reflectors 4-1 through 4-9.

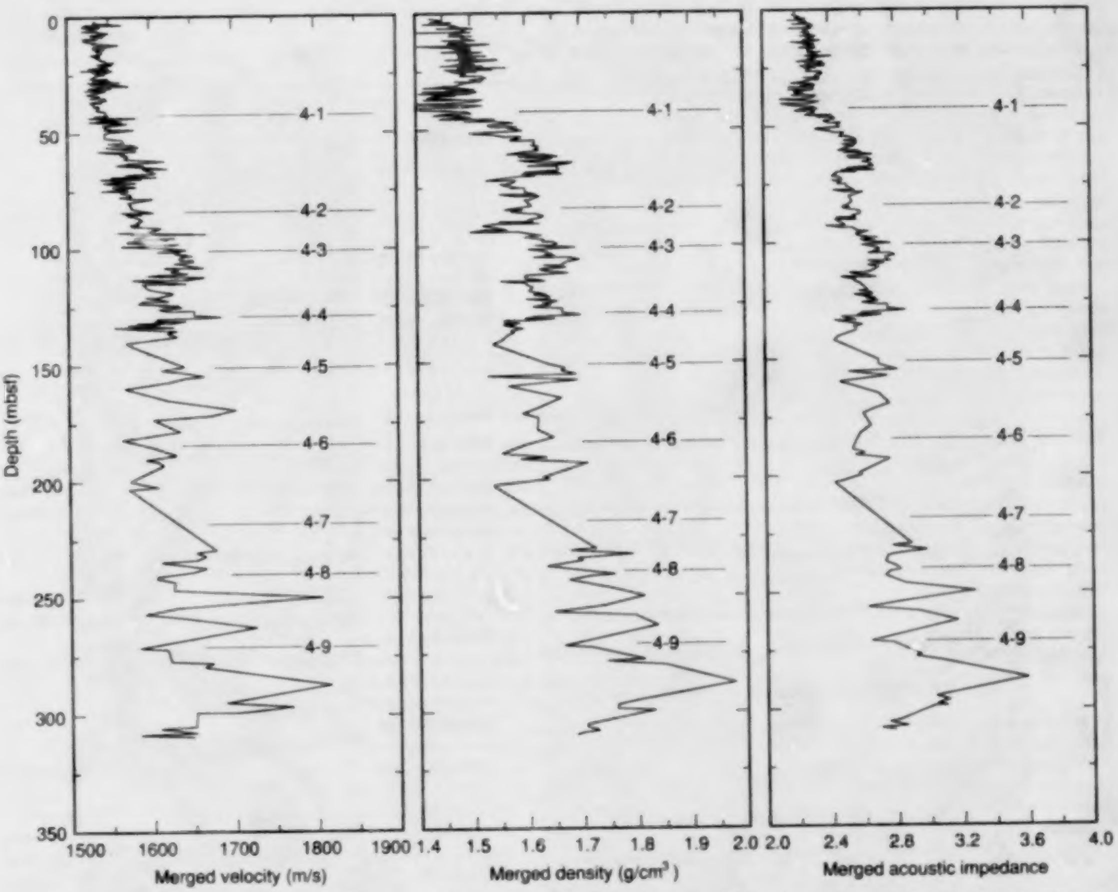

Figure 40. Merged velocity, density, and impedance records vs. depth, Site 804. Measurements are laboratory values corrected to *in situ*. Numbers refer to correlatable reflectors. See text for a discussion of reflector origins.

teau. This faulting initiated the basin within which early Cenozoic (and perhaps Late Cretaceous) sediments were preserved, as seen on the seismic profiles. Elsewhere in the area, erosion prevented deposition or removed much sediment in pre-Oligocene time. With the downward excursion of the CCD in the latest Eocene (Berger and Winterer, 1974), conditions became favorable for the accumulation of calcareous sediments, so that a continuous record could be generated, in principle, albeit at moderately low sedimentation rates (about 10 m/m.y. overall).

Sometime in the earliest Miocene, upper Oligocene sediments were removed. Low carbonate values near the Oligocene/Miocene boundary suggest that chemical erosion played a role in this process. Despite the high carbonate values in the lower Miocene (commonly >85%), dissolution apparently was important in keeping sedimentation rates low: there are zones with greatly reduced foraminifer content. Radiolarian abundances became quite high at times. In the latest early Miocene (just below the hiatus at 197 mbsf), foraminifer-poor and radiolarian-rich ooze was deposited. From that time on, silica deposition seemed to wane as silica was sequestered into the margins and into high-latitude sinks that became active because of the general cooling after 16 Ma. At this point, foraminifers also began to become more abundant, with a peak near 10 Ma and a sustained increase since the end of the Miocene.

The increase in foraminifers, and hence the possibility of fluctuations in the sand content, has important implications for the development of physical properties in the latest Cenozoic, which in turn controls acoustic stratigraphy. There is little doubt that an increase in sand supply parallels an increase in upwelling and, hence, foraminifer productivity. The question is why nannofossil supply did not keep pace. Increased winnowing and improved carbonate preservation must also be considered when trying to explain these patterns (Johnson et al., 1977).

Comparison with Sites 803 and 289

The lithology of Site 804 is the same as that at Site 803 for the total depth drilled (into the lower Oligocene) and presumably is the same back in the upper Eocene also. The carbonate content at Site 803 is somewhat higher on average. Upward from the base of the upper Miocene, both sites show roughly the same trends in foraminifer and radiolarian abundance. However, the high radiolarian abundances in the middle and lower Miocene of Site 804 do not seem to have a counterpart in Site

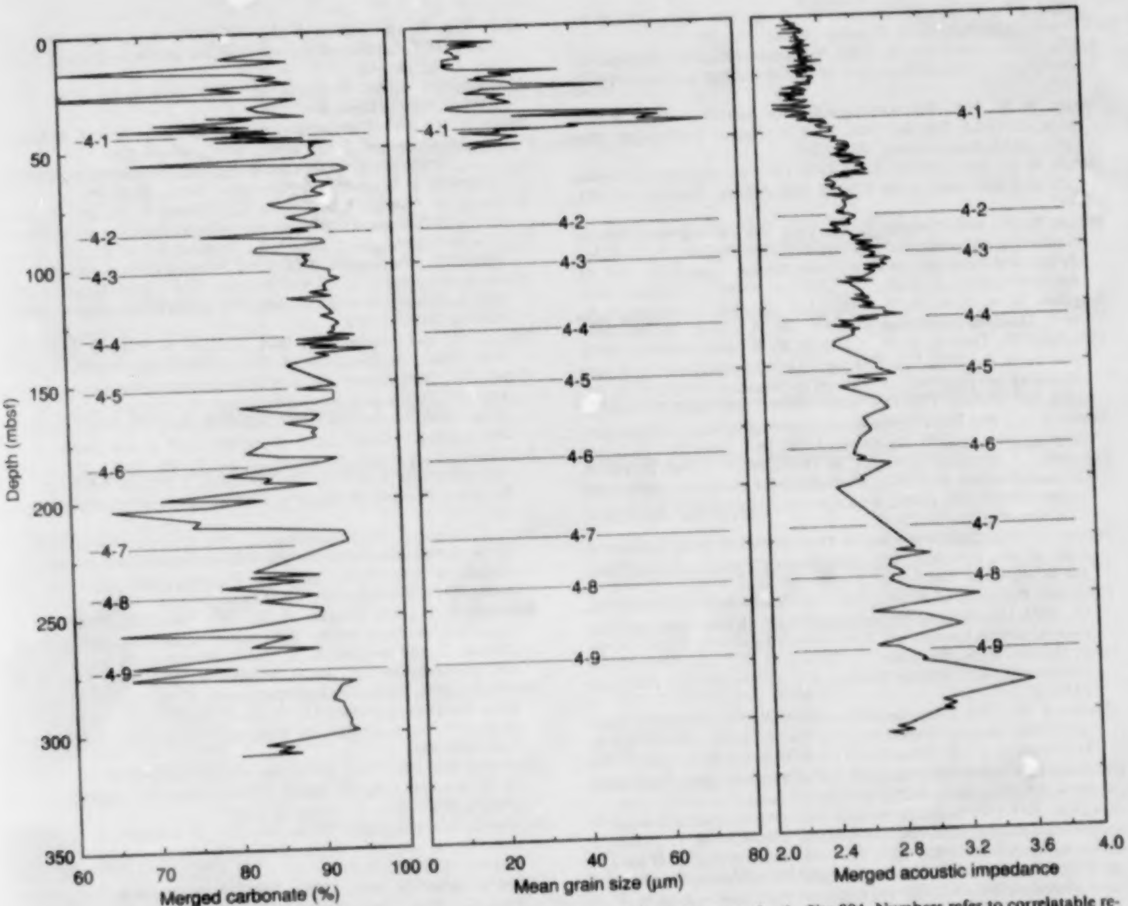

Figure 41. Carbonate content, mean grain size (from Hole 804B only), and acoustic impedance vs. depth, Site 804. Numbers refer to correlatable reflectors. See text for a discussion of reflector origins.

803. Thus, considering the distinctly lower carbonate values in Site 804 in the radiolarian-rich horizons, it appears that the difference is a result mainly of the enhanced carbonate dissolution at Site 804 in those intervals.

At DSDP Site 289, the section equivalent to the one cored at Site 804 is nannofossil foraminifer ooze and interbedded nannofossil foraminifer ooze and nannofossil foraminifer chalk. The facies (Unit I) extends down into the lower Oligocene, where it ends at a hiatus with upper Eocene limestone and chalk (Shipboard Scientific Party, 1975b). Foraminifers are much more abundant at Site 289 than at Site 804. Two processes must be considered: (1) increased winnowing at the depth of Site 289 (2200 m), and (2) the destruction of tests at the depth of Site 804 (3400 m). Radiolarian content is low throughout Unit I of Site 289. However, in the lower Miocene radiolarian concentrations are somewhat increased, just as they are at Site 804.

The ooze/chalk transition is located at 181 mbsf at Site 804. It is shallower here than at Site 803 (217 mbsf), but it has about the same age (13–14 Ma), supporting the hypothesis of Schlanger and Douglas (1974) that conditioning during the time of deposition is an important parameter in the rate of lithification. At Site 289, the transition was found near 350 mbsf in sediments that are somewhat younger (12–11 Ma). Thus, a distinctly increased overburden may accelerate the process of lithification, but not all that much.

Site 804 has a number of breaks in the stratigraphic record (near 4.5 Ma, between ca. 19–15 Ma, and between ca. 28–25 Ma), one of which is close to a hiatus in Site 803 (ca. 22–15 Ma). This hiatus is correlative with NH1 through NH2 of Keller and Barron (1987). There may be a condensed section in the uppermost lower Miocene of Site 289 that overlaps somewhat with the hiatus seen in Site 804. Rates of accumulation are about 10% lower at Site 804 than at Site 803, on the whole, in keeping with the greater depth of Site 804. In addition, about 10% of the sediment column is missing at Site 804, compared with Site 803, above the early-to-middle Miocene hiatus. Compared with those of Site 289, sedimentation rates at Site 804 are lower by a factor of 2 to 3, not counting the effect of hiatuses. This would suggest that more than one half of the carbonate at Site 804 has been removed by dissolution, on average. Thus, the high carbonate values here are not caused by the lack of dissolution, but by the lack of dilution by noncalcareous particles.

REFERENCES

Barron, J. A., 1985. Late Eocene to Holocene diatom biostratigraphy of the equatorial Pacific Ocean, Deep Sea Drilling Project Leg 85. *In*

Mayer, L., Theyer, F., Thomas, E., et al., *Init. Repts. DSDP*, 85: Washington (U.S. Govt. Printing Office), 413–456.

Barron, J. A., and Keller, G., 1982. Widespread Miocene deep-sea hiatuses: coincidence with periods of global cooling. *Geology*, 10:577–581.

Berger, W. H., 1981. Paleoceanography: the deep-sea record. *In* Emiliani, C. (Ed.), *The Sea* (Vol. 7): *The Oceanic Lithosphere:* New York (Wiley-Interscience), 1437–1519.

Berger, W. H., and Johnson, T. C., 1976. Deep-sea carbonates: dissolution and mass wasting on Ontong Java Plateau. *Science*, 192:785–787.

Berger, W. H., and Winterer, E. L., 1974. Plate stratigraphy and the fluctuating carbonate line. *In* Hsü, K. J., and Jenkyns, H. C. (Eds.), *Pelagic Sediments on Land and Under the Sea*. Spec. Publ., Int. Assoc. Sedimentol., 1:11–48.

Berggren, W. A., Kent, D. V., Flynn, J. J., and Van Couvering, J. A., 1985. Cenozoic geochronology. *Geol. Soc. Am. Bull.*, 96:1407–1418.

Elderfield, H., Gieskes, J. M., Oldfield, R. K., Hawkesworth, C. J., and Miller, R., 1982. $^{87}Sr/^{86}Sr$ and $^{18}O/^{16}O$ ratios, interstitial water chemistry and diagenesis in deep-sea carbonate sediments of the Ontong Java Plateau. *Geochim. Cosmochim. Acta*, 46:2259–2268.

Emeis, K.-C., and Kvenvolden, K. A., 1986. Shipboard organic geochemistry on *JOIDES Resolution*. *ODP Tech. Note*, No. 7.

Espitalié, J., Laporte, J. L., Madec, M., Marquis, F., Leplat, P., Paulet, J., and Boutfeu, A., 1977. Method rapide de caracterisation des roches mère de leur potentiel petrolier et de leur degree d'evolution. *Rev. Inst. Fr. Pet.*, 32:23–42.

Fenner, J., 1985. Late Cretaceous to Oligocene planktonic diatoms. *In* Bolli, H. M., Saunders, J. B., and Perch-Nielsen, K. (Eds.), *Plankton Stratigraphy:* Cambridge (Cambridge Univ. Press), 713–762.

Fornaciari, E., Raffi, I., Rio, D., Villa, G., Backman, J., and Olafsson, G., 1990. Quantitative distribution patterns of Oligocene and Miocene calcareous nannofossils from western equatorial Indian Ocean. *In* Duncan, R. A., Backman, J., Peterson, L. C., et al., *Proc. ODP, Sci. Results*, 115: College Station, TX (Ocean Drilling Program), 237–254.

Gieskes, J. M., 1981. Deep-sea drilling interstitial water studies: implications for chemical alteration of the oceanic crust, Layers I and II. *In* Warme, J. E., Douglas, R. G., and Winterer, E. L. (Eds.), *The Deep Sea Drilling Project: A Decade of Progress*. Soc. Econ. Paleontol. Mineral. Spec. Publ., 32:149–167.

Hamilton, E. L., 1976. Variations of density and porosity with depth in deep-sea sediments. *J. Sediment. Petrol.*, 46:280–300.

Hussong, D. M., Wipperman, L. K., and Kroenke, L. W., 1979. The crustal structure of the Ontong Java and Manahiki oceanic plateaus. *J. Geophys. Res.*, 84:6003–6010.

Johnson, T. C., Hamilton, E. L., and Berger, W. H., 1977. Physical properties of calcareous ooze: control by dissolution at depth. *Mar. Geol.*, 24:259–277.

Keller, G., and Barron, J. A., 1983. Paleoceanographic implications of Miocene deep-sea hiatuses. *Geol. Soc. Am. Bull.*, 94:590–613.

________, 1987. Paleodepth distribution of Neogene deep-sea hiatuses. *Paleoceanography*, 2:697–713.

Kroenke, L., 1972. Geology of the Ontong Java Plateau [Ph.D. dissert.]. Univ. of Hawaii, HIG .

McDuff, R. E., 1981. Major cation gradients in DSDP interstitial waters: the role of diffusiv exchange between seawater and upper ocean crust. *Geochim. Cosmochim. Acta*, 45:1705–1713.

McDuff, R. E., and Gieskes, J. M., 1976. Calcium and magnesium profiles in DSDP interstitial waters: diffusion or reaction? *Earth Planet. Sci. Lett.*, 33:1–10.

Mammerickx, J., and Smith, S. M., 1985. *Bathymetry of the North Central Pacific*. Geol. Soc. Am.

Mayer, L. A., 1979. Deep sea carbonates: acoustic, physical, and stratigraphic properties. *J. Sediment. Petrol.*, 49:819–836.

________, 1980. Erosional troughs in deep-sea carbonates and their relationship to basement structure. *Mar. Geol.*, 39:59–80.

Mayer, L. A., Shipley, T. S., Theyer, F., Wilkens, R. W., and Winterer, E. L., 1985. Seismic modelling and paleoceanography at DSDP Site 574. *In* Mayer, L. A., Theyer, F., Thomas, E., et al., *Init. Repts. DSDP*, 85: Washington, (U.S. Govt. Printing Office), 947–970.

Mayer, L. A., Shipley, T. H., and Winterer, E. L., 1986. Equatorial Pacific seismic reflectors as indicators of global oceanographic events. *Science*, 233:761–764.

Nigrini, C., and Lombari, G., 1984. *A Guide to Miocene Radiolaria*. Spec. Publ., Cushman Found. Foraminiferal Res., No. 22.

Okada, H., 1990. Quaternary and Paleogene calcareous nannofossils, Leg 115. *In* Duncan, R. A., Backman, J., Peterson, L. C., et al., *Proc. ODP, Sci. Results*, 115: College Station, TX (Ocean Drilling Program), 129–174.

Sanfilippo, A., Westberg-Smith, M. J., and Riedel, W. R., 1985. Cenozoic radiolaria. *In* Bolli, H. M., Saunders, J. B., and Perch-Nielsen, K. (Eds.), *Plankton Stratigraphy:* Cambridge (Cambridge Univ. Press), 631–712.

Sato, T., Kameo, K., and Takayama, T., 1991. Coccolith biostratigraphy of the Arabian Sea and a new nannofossil zonal scheme for the Quaternary. *In* Prell, W. L., Niitsuma, N., et al., *Proc. ODP, Sci. Results*, 117: College Station, TX (Ocean Drilling Program), 37–54.

Schlanger, S. O., and Douglas, R. G., 1974. The pelagic ooze-chalk-limestone transition and its implication for marine stratigraphy. *In* Hsü, K. J., and Jenkyns, H. C. (Eds.), *Pelagic Sediments: On Land and Under the Sea*. Int. Assoc. Sedimentol. Spec. Publ., 1:117–148.

Shafik, S., 1973. Nannofossil biostratigraphy of the southwest Pacific, Deep Sea Drilling Project Leg 30. *In* Andrews, J. E., Packham, G., et al., *Init. Repts. DSDP*, 30: Washington (U.S. Govt. Printing Office), 549–598.

Shipboard Scientific Party, 1971. Site 64. *In* Winterer, E. L., Riedel, W. R., et al., *Init. Repts. DSDP*, 7: Washington (U.S. Govt. Printing Office), 473–606.

Shipboard Scientific Party, 1975a. Site 288. *In* Andrews, J. E., Packham, G., et al., *Init. Repts. DSDP*, 30: Washington (U.S. Govt. Printing Office), 175–229.

Shipboard Scientific Party, 1975b. Site 289. *In* Andrews, J. E., Packham, G., et al., *Init. Repts. DSDP*, 30: Washington (U.S. Govt. Printing Office), 231–398.

Shipboard Scientific Party, 1986a. Site 586. *In* Moberly, R., Schlanger, S. O., et al., *Init. Repts. DSDP*, 89: Washington (U.S. Govt. Printing Office), 213–281.

Shipboard Scientific Party, 1986b. Site 586: western equatorial Pacific. *In* Kennett, J. P., von der Borch, C. C., et al., *Init. Repts DSDP*, 90: Washington (U.S. Govt. Printing Office), 19–114.

Shipboard Scientific Party, 1989. Explanatory notes. *In* Prell, W. L., Niitsuma, N., et al., *Proc. ODP, Init. Repts.*, 117: College Station, TX (Ocean Drilling Program), 11–33.

Ms 130A-106

NOTE: All core description forms ("barrel sheets") and core photographs have been printed on coated paper and bound as Section 5, near the back of the book, beginning on page 559.

Kroenke, L. W., Berger, W. H., Janecek, T. R., et al., 1991
Proceedings of the Ocean Drilling Program, Initial Reports, Vol. 130

7. SITE 805[1]

Shipboard Scientific Party[2]

HOLE 805A

Date occupied: 11 February 1990

Date departed: 11 February 1990

Time on hole: 11 hr, 30 min

Position: 1°13.68′N, 160°31.76′E

Bottom felt (rig floor; m, drill-pipe measurement): 3199.5

Distance between rig floor and sea level (m): 11.02

Water depth (drill-pipe measurement from sea level, m): 3188.5

Total depth (rig floor; m): 3250.00

Penetration (m): 50.50

Number of cores (including cores with no recovery): 6

Total length of cored section (m): 50.50

Total core recovered (m): 52.22

Core recovery (%): 103.4

Oldest sediment cored:
Depth (mbsf): 50.50
Nature: nannofossil ooze
Youngest age: Quaternary
Oldest age: late Pliocene
Measured velocity (km/s):

HOLE 805B

Date occupied: 11 February 1990

Date departed: 13 February 1990

Time on hole: 1 day, 21 hr, 45 min

Position: 1°13.68′N, 160°31.76′E

Bottom felt (rig floor; m, drill-pipe measurement): 3197.8

Distance between rig floor and sea level (m): 11.02

Water depth (drill-pipe measurement from sea level, m): 3186.8

Total depth (rig floor; m): 3671.10

Penetration (m): 473.30

Number of cores (including cores with no recovery): 50

Total length of cored section (m): 473.30 (APC, 263.2; XCB, 210.1)

Total core recovered (m): 444.89 (APC, 271.30; XCB, 173.59)

Core recovery (%): 93 (APC, 103.1; XCB, 82.6)

Oldest sediment cored:
Depth (mbsf): 473.30
Nature: nannofossil chalk
Youngest age: Quaternary
Oldest age: early Miocene
Measured velocity (km/s): 1.8

HOLE 805C

Date occupied: 13 February 1990

Date departed: 17 February 1990

Time on hole: 3 days, 18 hr, 45 min

Position: 1°13.69′N, 160°31.77′E

Bottom felt (rig floor; m, drill-pipe measurement): 3198.7

Distance between rig floor and sea level (m): 11.02

Water depth (drill-pipe measurement from sea level, m): 3187.7

Total depth (rig floor; m): 3809.70

Penetration (m): 611.00

Number of cores (including cores with no recovery): 64

Total length of cored section (m): 611.00 (APC, 235.8; XCB, 375.2)

Total core recovered (m): 495.46 (APC, 236.34; XCB, 259.12)

Core recovery (%): 81 (APC, 100.2; XCB, 69.1)

Oldest sediment cored:
Depth (mbsf): 611.00
Nature: nannofossil chalk
Youngest age: Quaternary
Oldest age: late Oligocene
Measured velocity (km/s): 1.9

Principal results: Ocean Drilling Program (ODP) Site 805 (proposed Site OJP-2) is located on the northeastern margin of the Ontong Java Plateau, close to the equator (latitude 1°13.7′N, longitude 160°31.8′E) in 3188 m of water, roughly 270 km northeast of Deep Sea Drilling Project (DSDP) Sites 289/586. The site represents the intermediate-to-deep member on a transect that was designed to detect depth-related paleoceanographic signals in Neogene sediments. It was occupied with the objective to obtain a high-resolution carbonate record in a lysoclinal setting for studies of ocean history, including biostratigraphy, chemostratigraphy, and acoustic stratigraphy.

Site 805 was positioned at the proposed location (OJP-2), within a gently sloping valley about 3.5 km wide and flanked by low ridges along either side. We used crossing *Thomas Washington* single-channel seismic (SCS) lines acquired during ROUNDABOUT Cruise 11 (2130 UTC, 24 December 1989, and 1700 UTC, 25 December). The seismic profiles showed continuous reflectors, with little or no disturbance.

Three holes were drilled using either the advanced hydraulic piston corer (APC) or the extended core barrel (XCB), with full recovery on the APC cores. Hole 805A, a dedicated hole, was cored with the APC to 50.5 mbsf into upper Pliocene sediments. Hole 805B was cored with the APC to 263.2 mbsf, where refusal occurred at the boundary between the middle and upper Miocene. The hole was continued with XCB coring to 473.3 mbsf, with 210.1 m of sediment cored and 173.6 m recovered. Coring ended about half-way through a thick section of lower Miocene sediments. Hole 805C was cored with the APC to 235.8 mbsf, at which point we began to core with the XCB. Drilling ended in upper Oligocene sediments at 611.0 mbsf, with 259.1 m cored with the XCB (69% recovery). The hole was then logged.

The entire sedimentary sequence encountered is considered as one lithologic unit (Unit I), consisting of nannofossil ooze and chalk with varying abundances of foraminifers. Radiolarians are a minor constituent throughout the section. The ooze-chalk transition is placed be-

---

[1] Kroenke, L. W., Berger, W. H., Janecek, T. R., et al., 1991. *Proc. ODP, Init. Repts.*, 130: College Station, TX (Ocean Drilling Program).

[2] Shipboard Scientific Party is as given in the list of participants preceding the contents.

tween 283 and 294 mbsf; it is gradational and shows alternation of layers of varying induration. The age of this interval is ca. 11 Ma. Sedimentation throughout the time interval represented seems to have been continuous at this site.

The ooze-chalk transition divides Unit I into two subunits, as follows:

Subunit IA (0–293.7 mbsf) consists of Pleistocene to middle Miocene nannofossil ooze with foraminifers, and foraminifer nannofossil ooze, with 90%–95% carbonate. The dominant color is white; the upper 30 m of the section is light gray. Bioturbation is common throughout, ranging from slight to heavy. Some well-developed burrows have concentric color rings, indicating redox gradients as the cause for color banding. Banding is common throughout the unit and is especially well expressed in the uppermost Miocene. For the most part, color bands are coarse and irregular in Subunit IA. Microfaulting was observed in Core 130-805B-18H at 166 mbsf (middle upper Miocene), and tilting is seen at the middle to upper Miocene boundary. Sediments are generally soft, but in the lowermost portion of Subunit IA (283–293 mbsf) more lithified intervals appear. A shift toward higher velocities occurs near the top of that zone, and another at the ooze-chalk transition at about 294 mbsf.

Subunit IB (293.7–611 mbsf) consists of middle Miocene to upper Oligocene nannofossil chalk, nannofossil chalk with foraminifers, and foraminifer nannofossil chalk. Foraminifer content is high down to about 380 mbsf (boundary of middle to lower Miocene) and decreases below that level, reaching a minimum in the lower Miocene. Radiolarian content is low; a moderate peak occurs near 400 mbsf, in the uppermost lower Miocene. The color is dominantly white. Color banding occurs throughout but becomes rare below 504 mbsf in the lowermost Miocene. It includes bundles of pseudo-laminae, that is, fine-scale banding showing sharp individual boundaries. Microfaulting is generally absent, except near 310 mbsf (ca. 12 Ma).

The sediments in the chalk section posed no problem for coring with the XCB down to the upper Oligocene, at which point recovery became low. Even where recovery is very good, core contents are largely disjointed chunks and chips, with evidence for grinding of chalk on chalk. This type of recovery is typical for the material below 370 mbsf. The Oligocene/Miocene boundary is located near 525 mbsf, apparently without any evidence of a hiatus (although recovery is poor at this level). Sedimentation rates for the deep chalk section are between 10 and 20 m/m.y., with the higher rates occurring in the Oligocene and the lower ones in the middle Miocene.

The middle Miocene is characterized by rather high foraminifer abundances, with a broad maximum near 12 Ma. Sedimentation rates are between 10 and 15 m/m.y. Carbonate values are quite variable, fluctuating between 85% and 95%. At the transition to the upper Miocene, there is a carbonate minimum, which also is a minimum in foraminifer content. This feature correlates with a zone of increased dissolution in the eastern equatorial Pacific (Barron et al., 1985). Carbonate values reach a maximum (near 95%) in the middle portion of the upper Miocene and tend to decrease to the present, with increasing variability reflecting increasing fluctuations in the carbon chemistry of the ocean. Sedimentation rates in the upper Miocene are very high (35–40 m/m.y.) and drop in the Pliocene (25–30 m/m.y.). They decrease again within the Pleistocene (to below 20 m/m.y.).

Paleomagnetic stratigraphies were produced for the uppermost section of the two holes. Only the Brunhes and part of the Matuyama chrons could be identified. The sedimentation rate since 1.7 Ma was determined to be 17.1 m/m.y.

Chemical gradients in interstitial waters at this site are generally similar to those at Sites 803 and 804, reflecting the calcareous/siliceous nature of the sediments and the paucity of organic material. A somewhat higher supply of organic matter at this shallower site, close to the equator, tends to produce slightly stronger gradients. Calcium and magnesium gradients are influenced by basalt alteration reactions at depth and show the usual negative correlation. Strontium concentrations reflect recrystallization processes, which take place in younger sediments at this site than at the other two as a result of the higher sedimentation rates. Dissolved silica shows a steady increase with depth, except for a minor reversal of this trend just above the ooze-chalk transition.

Excellent logs were obtained for sound velocity and density at Site 805. The fact that this site has continuous sedimentation makes these logs especially valuable for the interpretation of seismic profiles. The geochemical log for the bottom 200 m (lower to middle Miocene) shows cycles, apparently with frequencies in the Milankovitch spectrum.

BACKGROUND AND OBJECTIVES

Overview

Site 805, the second lysocline site of the Neogene depth transect on Ontong Java Plateau, was drilled near the target Site OJP-2 (3200 m) (Fig. 1). The site is similar in water depth to Site 803 (3410 m), but it differs in being closer to the equator and just above (rather than below) the modern lysocline. At this level, contrasts in preservational state are expected to be close to maximum. Thus, the saturation history of deep waters, and its ramifications for physical properties, would be optimally recorded in sediments accumulating at a rate of some 15 m/m.y. Rich tropical assemblages of pelagic and benthic microfossils would be recovered from these sediments for use in paleoceanographic and biostratigraphic studies, covering the entire Neogene as well as the transition into the Paleogene.

The site was planned for multiple coring in the upper portion of the section (Neogene and Quaternary): two hydraulic piston-core holes to 250 mbsf, a third hole to 50 mbsf, and coring with the XCB to 500 mbsf. The multiple coring provides for overlap between cores and for sufficient material for concurrent high-resolution studies.

Background

The general background to this site is contained in the "Introduction" chapter of this volume (also see Kroenke, 1972). The Ontong Java Plateau is a broad, shallow, mid-ocean highland in the western equatorial Pacific. Its shallowest regions lie above 2000 m, and its flanks reach depths in excess of 4500 m. With an area of 1.5 million km^2, it is the largest of the "classic" Pacific plateaus. The plateau has a crustal thickness on the order of 40 km. Apparently, it roughly maintained its present depth over much of its history, indicating isostatic equilibrium. Crustal seismic velocities are in the range of that of oceanic crust (Hussong et al., 1979).

The pelagic sediment cover of the plateau is uniquely suited for paleoceanographic studies. The maximum thickness of the sediment is typically near 1200 m and occurs below the top of the plateau, in water depths between 2000 and 2500 m. The sediment thins by roughly 100 m for every 200 m of water depth increase, below 2200 m (Berger and Johnson, 1976). At Site 805 (3188 m), the sediment is approximately 700 m thick.

Site 805 was planned as a companion site to Site 803 as part of a Neogene depth transect in the equatorial portion of Ontong Java Plateau and was designed to study paleoceanographic events of global significance. Somewhat higher sedimentation rates were expected here, nearer to the equator, and at the slightly shallower depth, compared with Site 803. Gradients for physical, chemical, and paleontological properties are especially strong at this depth level (Shackleton and Opdyke, 1976; Johnson et al., 1977; Wu and Berger, 1989). Unfortunately, problems arising from the creep of large sediment bodies are ubiquitous in this depth range because of a combination of tectonic and stratigraphic factors. The site location is close to a significant offset in basement levels between the plateau and the deep ocean floor (Fig. 2). Earthquakes are to be expected in such a setting, at least occasionally. Episodic shaking, basement relief, and increased mobility of sediments at depth (because of preconditioning by partial dissolution of carbonate in certain horizons) apparently create large-scale slumping and debris flow on the flanks of the plateau. Removal of support at greater water

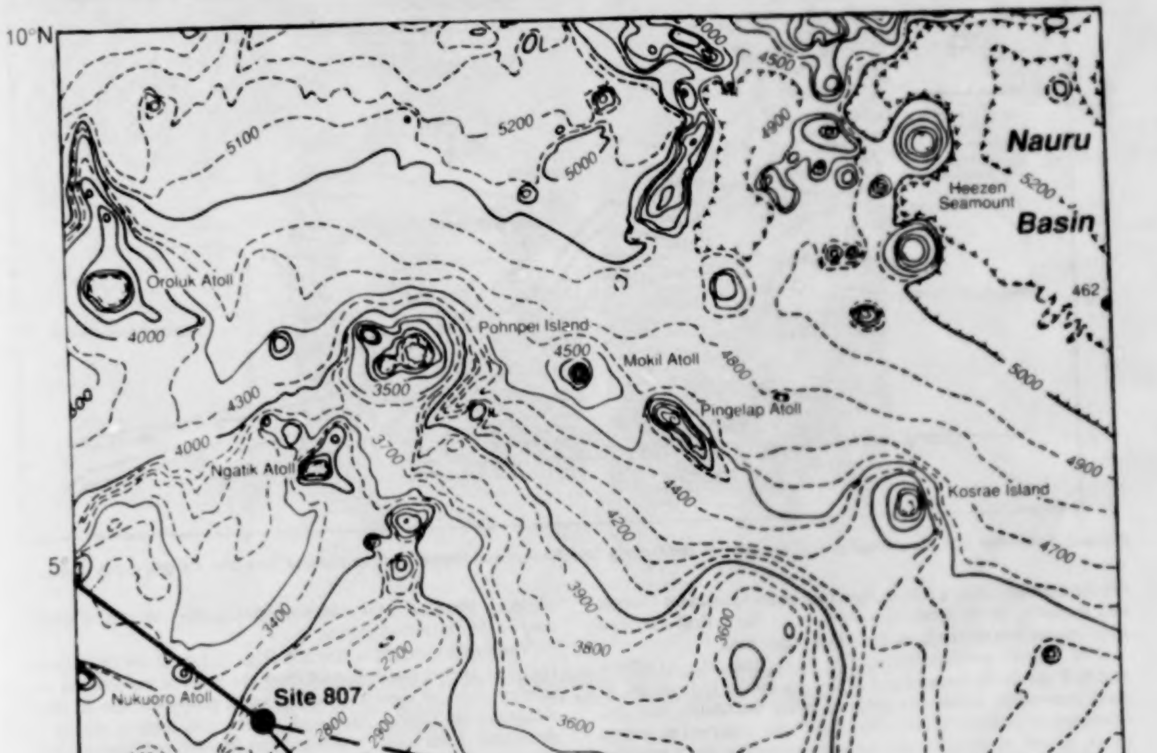
10°N
5°
0°
2°S
155°
160°
165°E
Nauru
Basin
Heezen Seamount
462
Oroluk Atoll
Pohnpei Island
Mokil Atoll
Pingelap Atoll
Ngatik Atoll
Kosrae Island
Nukuoro Atoll
Site 807
Site 803
Site 805
Site 804
Site 806
DSDP Site 586
DSDP Site 289
DSDP Site 64
Ontong Java
Plateau
5100
5200
5000
4500
4900
4000
4300
3500
3700
4800
4400
4200
4900
4700
3900
3800
3600
3400
2700
2800
2900
3000
2600
2500
2400
2300
2200
2000
2100
1900
1800
1700
4100
3200
4450

Figure 1. Bathymetry in meters of the northwestern part of the Ontong Java Plateau (after Mammerickx and Smith, 1985). The location of the Leg 130 sites together with those from DSDP Legs 7, 30, and 89 are shown for reference. Contour interval is 100 m.

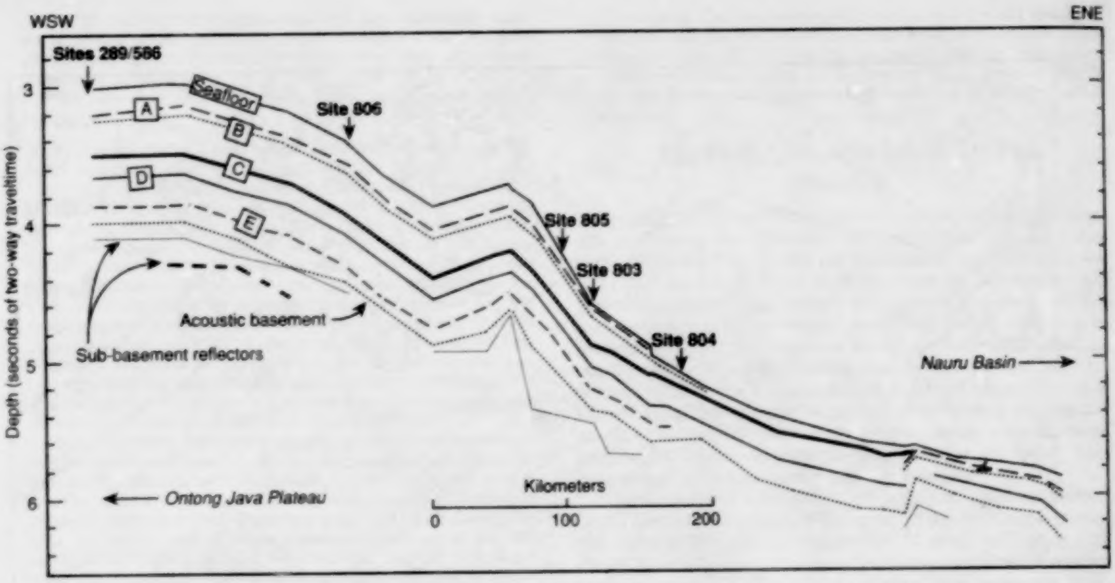

Figure 2. Simplified acoustic stratigraphy of the flank of the Ontong Java Plateau and approximate location of Sites 803–806 (the depth transect).

depths may also play a role in fostering mass movement (Berger and Johnson, 1976). Selection of a suitable site to drill a continuous record was difficult under these conditions.

The seismic profiles across Site 805 (from the ROUNDABOUT survey in December 1989) show subtle indications of mass movement within the sloping valley harboring the site. Crenulate reflectors ("crinkly horizons") are observed at several levels, as well as evidence for wedging along the basin margins (Fig. 3). Despite these indications for disturbance, a rather complete section was expected to be encountered based on these profiles, as the overall coherency of the seismic reflectors is quite good.

The plateau has long been the focus of paleoceanographic studies based on conventional coring and on seismic profiling. Leg 130 is the fourth drilling expedition to sample the sediment cover here: four DSDP sites were drilled earlier on the plateau. Leg 7 drilled Site 64 (Shipboard Scientific Party, 1971), and Leg 30 drilled Sites 288 and 289 (Shipboard Scientific Party, 1975a, 1975b). All three sites were rotary-drilled and spot-cored. The upper 969 m in Site 289 consisted of upper Eocene to Pleistocene nannofossil-foraminifer chalks and oozes. The section was found to be continuous from the lower Oligocene on, the top of which was reached at 890 mbsf. Semilithified chalk first appears near 250 mbsf (late Miocene). Site 586, drilled on Leg 89 next to Site 289, was cored with the APC to 305 mbsf, reaching upper Miocene sediments (Shipboard Scientific Party, 1986a, 1986b). It recovered well-preserved nannofossil ooze.

Objectives

Site 805, roughly 140 km northeast of DSDP Sites 289/586 on the northeastern margin of the Ontong Java Plateau, was planned as the shallower of the two lysocline sites (803 and 805) within the series of four equatorial sites that constitute a Neogene depth transect (Sites 803–806; Fig. 1). The general objective of this transect was to detect depth-related paleoceanographic signals. The sediments sampled along the transect were produced in the same surface-water conditions and thus arrived on the seafloor in the same pelagic rain, so that differences in physical, chemical, and paleontological properties can be attributed to depth-related effects.

The depth sampled at Site 805 (Fig. 1), just above the modern lysocline, is that which should show the greatest variation in dissolution-induced signals. Thus, physical properties should show maximum amplitudes here, and in turn, this imprint should be detectable in the acoustic stratigraphy (Berger and Mayer, 1978). The objective is to explore whether through such effects of dissolution a clear linkage can be established between paleoceanographic events and acoustic stratigraphy (Mayer et al., 1986). In the case of severe dissolution pulses, one would expect hiatus formation, presumably also linked to paleoceanographic events (Barron and Keller, 1982). Establishing such linkages will allow three-dimensional mapping and correlation into distant sediment sections throughout the Pacific basin.

Regarding biostratigraphic objectives at this site, we expected that changes in the preservation of calcareous fossils would provide clues to changes in the intensity of dissolution, with wide implications for the study of deep-water history and the oceanic carbon cycle. Recovery of preserved benthic foraminifers should allow reconstruction of deep-water properties directly, in their abundances and chemical composition. The effects of partial dissolution on biostratigraphic zonation (by selective removal of marker species) should be a minor problem at this depth level, but could be important during upward excursions of the carbonate compensation depth (CCD).

OPERATIONS

Site 805

Upon leaving Site 804, a 20-nmi, 2.75-hr seismic survey was run over the site at 7.3 kt. The transit from Sites 804 to 805 covered 63 nmi in 7.5 hr at an average speed of 8.4 kt. A 22-nmi, 2.75-hr, pre-site seismic survey was run over the proposed site at 8.4 kt (see "Underway Geophysics" chapter, this volume, for further details of surveys). Minimal satellite positioning was available. A beacon was dropped at 2250 hr, 10 February 1990, but the weight came off the beacon, and it floated back to the

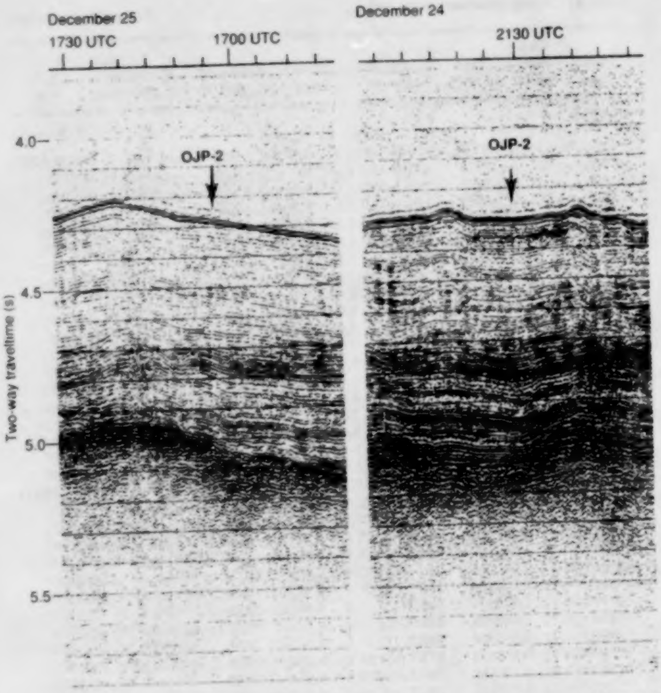

Figure 3. Seismic profiles across proposed drilling sites for Site 805, showing evidence of planar disturbance (crinkly horizons) and debris flow (wedges next to basin rim). See Mayer et al. (this volume) for details.

surface. An additional 6-nmi survey track was run, and a second beacon was dropped at 2345 hr, 10 February 1990, on the proposed site, initiating Site 805.

Hole 805A

The ship was positioned 100 m south of the beacon. Core 130-805A-1H was taken at 0700 hr, 11 February 1990, in 3188.5 m of water. Cores 130-805A-1H through -6H were taken from 0 to 50.5 mbsf, with 50.5 m of sediment cored and 52.22 m recovered (103.41% recovery; Table 1). Orientation surveys were taken during Cores 130-805A-3H through -6H. Hole 805A was terminated when we reached our depth objective of 50 mbsf. At this point, the drill pipe was pulled out of the hole and the bit cleared the seafloor at 1115 hr, 11 February 1990.

Hole 805B

The ship was positioned 100 m south and 30 m east of the beacon. Core 130-805B-1H was taken at 1155 hr, 11 February 1990, in a water depth of 3186.8. Cores 130-805C-1H through -28H were taken from 0 to 263.2 mbsf, with 263.2 m of sediment cored and 271.3 m recovered (103.08% recovery; Table 1). Orientation surveys were taken during Cores 130-805B-3H through -28H.

APC refusal was reached at Core 130-805B-28H (263.2 mbsf) when the core barrel would not pull free with 100,000 lbs of overpull. The APC core barrel was washed over for 7 m but still required 80,000 lbs of overpull to pull it free. This was another successful test of the new APC equipment, which included a stronger piston rod and washover capability. Core 130-805B-28H was recovered with 9.96 m of sediment and no damage to the core barrel.

We initiated XCB coring at this point, and Cores 130-805B-29X through -50X were taken from 263.2-473.3 mbsf, with 210.1 m of sediment cored and 173.59 m recovered (82.62% recovery). The sonic core monitor (SCM) was tested on Core 130-805B-47X. A 9.5-m section was cored but only 0.70 m of sediment was recovered. The SCM electronics performed properly but the core jammed in the cutting shoe. Hole 805B was terminated after reaching Miocene sediments.

Hole 805C

The ship was positioned 100 m south and 60 m east of the beacon. Core 130-805C-1H was taken at 1015 hr, 13 February 1990, in 3187.7 m of water. Cores 130-805C-1H through -25H were taken from 0 to 235.8 mbsf with 235.8 m of sediment cored and 236.34 m recovered (100.23% recovery; Table 1). Orientation surveys were taken during Cores 130-805C-3H through -10H.

APC coring was interrupted for 45 min after Core 130-805C-7H, when the beacon signal became intermittent at 1540 hr, 13 February 1990. A backup beacon was launched at 1552 hr, 13 February 1990.

The breakaway piston head was tested in Cores 130-805C-21H and -23H. Recovery was reduced from an average of 9.78 to 5.82 m during these test runs.

Coring with the APC ended at 235.8 m, a shallower depth than in the previous hole, to avoid getting the core barrel stuck and having to drill over the core again. Coring with the XCB began at this point, and Cores 130-805C-26X through -55X were drilled from 235.8 to 523.9 mbsf, with an average recovery of 80%. Below 523.9 mbsf, the sediment repeatedly jammed in the cutting shoe and reduced recovery in Cores 130-805C-56X

Table 1. Coring summary, Site 805.

Core no.	Date (Feb. 1990)	Time (UTC)	Depth (mbsf)	Cored (m)	Recovered (m)	Recovery (%)	Age
130-805A-							
1H	11	0700	0–3.0	3.0	2.99	99.6	NN20–NN21
2H	11	0735	3.0–12.5	9.5	9.94	104.0	NN19
3H	11	0925	12.5–22.0	9.5	9.86	104.0	NN19
4H	11	0905	22.0–31.5	9.5	9.74	102.0	NN18?
5H	11	0950	31.5–41.0	9.5	9.73	102.0	NN18
6H	11	1035	41.0–50.5	9.5	9.96	105.0	NN16
Coring totals				50.5	52.22	103.4	
130-805B-							
1H	11	1155	0–6.7	6.7	6.70	100.0	NN20
2H	11	1230	6.7–16.2	9.5	9.77	103.0	NN19
3H	11	1320	16.2–25.7	9.5	9.70	102.0	
4H	11	1400	25.7–35.2	9.5	10.05	105.8	NN18
5H	11	1455	35.2–44.7	9.5	10.00	105.2	NN16
6H	11	1600	44.7–54.2	9.5	9.96	105.0	NN16
7H	11	1655	54.2–63.7	9.5	9.65	101.0	NN16
8H	11	1745	63.7–73.2	9.5	9.83	103.0	NN16
9H	11	1850	73.2–82.7	9.5	10.10	106.3	NN15
10H	11	1940	82.7–92.2	9.5	10.12	106.5	NN15–NN14
11H	11	2040	92.2–101.7	9.5	9.90	104.0	
12H	11	2135	101.7–111.2	9.5	9.56	100.0	NN12
13H	11	2220	111.2–120.7	9.5	9.89	104.0	NN12
14H	11	2300	120.7–130.2	9.5	9.91	104.0	NN11
15H	12	0015	130.2–139.7	9.5	9.77	103.0	NN11
16H	12	0200	139.7–149.2	9.5	10.06	105.9	NN11
17H	12	0245	149.2–158.7	9.5	9.68	102.0	NN11
18H	12	0330	158.7–168.2	9.5	9.50	100.0	NN11
19H	12	0415	168.2–177.7	9.5	8.41	88.5	NN11
20H	12	0500	177.7–187.2	9.5	9.80	103.0	NN11
21H	12	0535	187.2–196.7	9.5	9.59	101.0	NN11
22H	12	0615	196.7–206.2	9.5	9.79	103.0	
23H	12	0700	206.2–215.7	9.5	9.79	103.0	NN11
24H	12	0745	215.7–225.2	9.5	9.83	103.0	NN10
25H	12	0815	225.2–234.7	9.5	9.81	103.0	NN10
26H	12	0845	234.7–244.2	9.5	9.99	105.0	NN10
27H	12	0940	244.2–253.7	9.5	10.18	107.1	
28H	12	1135	253.7–263.2	9.5	9.96	105.0	
29X	12	1230	263.2–272.9	9.7	8.41	86.7	NN9
30X	12	1315	272.9–282.5	9.6	9.13	95.1	NN9
31X	12	1400	282.5–292.2	9.7	9.02	93.0	NN9?
32X	12	1445	292.2–301.4	9.2	7.24	78.7	NN7–NN6
33X	12	1530	301.4–311.0	9.6	8.97	93.4	NN6
34X	12	1620	311.0–320.5	9.5	7.78	81.9	NN6
35X	12	1705	320.5–330.0	9.5	7.81	82.2	
36X	12	1750	330.0–339.7	9.7	7.90	81.4	NN5
37X	12	1835	339.7–349.4	9.7	8.41	86.7	NN5
38X	12	1930	349.4–359.0	9.6	7.51	78.2	NN5
39X	12	2030	359.0–368.7	9.7	8.99	92.7	NN5
40X	12	2140	368.7–378.3	9.6	8.33	86.8	NN5
41X	12	2245	378.3–388.0	9.7	7.47	77.0	NN5–NN4
42X	13	0045	388.0–397.7	9.7	8.06	83.1	NN2
43X	13	0130	397.7–407.3	9.6	9.13	95.1	NN2
44X	13	0215	407.3–417.0	9.7	9.22	95.0	NN2
45X	13	0320	417.0–426.5	9.5	8.44	88.8	NN2
46X	13	0430	426.5–436.0	9.5	8.36	88.0	NN1
47X	13	0520	436.0–445.5	9.5	0.70	7.4	NN1?
48X	13	0600	445.5–455.1	9.6	6.92	72.1	NN1?
49X	13	0645	455.1–464.8	9.7	8.42	86.8	NN1?
50X	13	0740	464.8–473.3	8.5	7.37	86.7	NN1?
Coring totals				473.3	444.89	94.0	
130-805C-							
1H	13	1015	0–7.8	7.8	7.80	100.0	NN19
2H	13	1050	7.8–17.3	9.5	9.88	104.0	
3H	13	1145	17.3–26.8	9.5	9.40	98.9	NN19
4H	13	1230	26.8–36.3	9.5	9.96	105.0	
5H	13	1320	36.3–45.8	9.5	9.67	102.0	NN17
6H	13	1410	45.8–55.3	9.5	10.09	106.2	
7H	13	1510	55.3–64.8	9.5	9.92	104.0	NN16
8H	13	1625	64.8–74.3	9.5	9.78	103.0	NN16
9H	13	1720	74.3–83.8	9.5	9.95	105.0	NN15
10H	13	1845	83.8–93.3	9.5	9.94	104.0	NN15
11H	13	1940	93.3–102.8	9.5	9.88	104.0	NN13–NN12

Table 1 (continued).

Core no.	Date (Feb. 1990)	Time (UTC)	Depth (mbsf)	Cored (m)	Recovered (m)	Recovery (%)	Age
130-805C- (Cont)							
12H	13	2040	102.8–112.3	9.5	9.71	102.0	NN12
13H	13	2115	112.3–121.8	9.5	9.98	105.0	NN12
14H	13	2245	121.8–131.3	9.5	9.93	104.0	NN11
15H	14	0000	131.3–140.8	9.5	9.77	103.0	NN11
16H	14	0055	140.8–150.3	9.5	10.01	105.3	NN11
17H	14	0110	150.3–159.8	9.5	9.78	103.0	NN11
18H	14	0250	159.8–169.3	9.5	9.83	103.0	NN11
19H	14	0335	169.3–178.8	9.5	9.83	103.0	NN11
20H	14	0415	178.8–188.3	9.5	9.73	102.0	NN11
21H	14	0450	188.3–197.8	9.5	9.56	100.0	NN11
22H	14	0530	197.8–207.3	9.5	9.93	104.0	NN11
23H	14	0620	207.3–216.8	9.5	2.07	21.8	NN11
24H	14	0650	216.8–226.3	9.5	9.87	104.0	NN10?
25H	14	0740	226.3–235.8	9.5	10.07	106.0	NN10
26X	14	0825	235.8–245.4	9.6	9.34	97.3	NN10
27X	14	0910	245.4–255.1	9.7	1.54	15.9	NN10
28X	14	0955	255.1–264.7	9.6	8.70	90.6	NN10?
29X	14	1045	264.7–274.4	9.7	8.97	92.5	NN9
30X	14	1145	274.4–284.0	9.6	8.07	84.0	NN8
31X	14	1220	284.0–293.7	9.7	9.10	93.8	NN6–NN7
32X	14	1300	293.7–302.9	9.2	9.18	99.8	NN6–NN7
33X	14	1345	302.9–312.6	9.7	9.08	93.6	NN6–NN7
34X	14	1435	312.6–322.3	9.7	8.64	89.1	NN6
35X	14	1525	322.3–331.8	9.5	8.02	84.4	NN5
36X	14	1620	331.8–341.5	9.7	8.80	90.7	NN5
37X	14	1710	341.5–351.2	9.7	7.27	74.9	NN5
38X	14	1805	351.2–360.9	9.7	9.38	96.7	NN5–NN4
39X	14	1900	360.9–370.6	9.7	9.19	94.7	NN5–NN4
40X	14	1950	370.6–380.3	9.7	8.67	89.4	NN5–NN4
41X	14	2050	380.3–389.9	9.6	6.33	65.9	NN5–NN4
42X	14	2145	389.9–399.5	9.6	6.86	71.4	NN3–NN2
43X	14	2230	399.5–409.1	9.6	8.62	89.8	NN2
44X	14	2310	409.1–418.7	9.6	9.51	99.0	NN2
45X	15	0000	418.7–428.4	9.7	8.90	91.7	NN2
46X	15	0050	428.4–438.1	9.7	8.70	89.7	NN2–NN1
47X	15	0140	438.1–447.7	9.6	9.44	98.3	NN2–NN1
48X	15	0220	447.7–457.4	9.7	7.25	74.7	NN2
49X	15	0310	457.4–467.0	9.6	5.02	52.3	NN1–NN2
50X	15	0400	467.0–475.5	8.5	6.92	81.4	NN1–NN2
51X	15	0445	475.5–485.2	9.7	7.23	74.5	NN1–NN2
52X	15	0545	485.2–494.9	9.7	5.83	60.1	NN2
53X	15	0640	494.9–504.6	9.7	7.19	74.1	NN1–NN2
54X	15	0740	504.6–514.2	9.6	6.51	67.8	NN1–NN2
55X	15	0840	514.2–523.9	9.7	4.14	42.7	NN1–NN2
56X	15	0940	523.9–533.5	9.6	0.80	8.3	NN1–NN2
57X	15	1035	533.5–543.2	9.7	2.93	30.2	NN1–NN2
58X	15	1210	543.2–552.9	9.7	0.92	9.5	NN2–NN1
59X	15	1340	552.9–562.6	9.7	2.22	22.9	NP25
60X	15	1520	562.6–572.3	9.7	0.99	10.2	NP25
61X	15	1700	572.3–582.0	9.7	9.61	99.1	NP24–NP23
62X	15	1900	582.0–591.7	9.7	5.11	52.7	NP23
63X	15	2050	591.7–601.3	9.6	2.68	27.9	NP23
64X	15	2300	601.3–611.0	9.7	1.46	15.0	
Coring totals				611.0	495.46	81.1	

through -64X to 16%. The Polypak seal in the bit seal (ring) was later found to be completely eroded away, explaining why the XCB bit nozzles were plugging and the core was jamming in the bit throat. Hole 805C was terminated after penetrating into Oligocene sediments.

A short pipe trip to 100 mbsf was made to condition the hole (no fill or drag was encountered), and a mud sweep was made to clean the hole. The bit was pulled up to 116.3 mbsf and logging began. Logs were run as follows:

Run No. 1: NGT/DIT/LSS. The first pass was run successfully at 900 ft/hr from 609.9 mbsf (1.2 m off the bottom) to 100.3 mbsf. A second, successful run was made at 900 ft/hr from 199.9 to 100.3 mbsf.

Run No. 2: NGT/ACT/HLDT/GST. The tool was run into the hole but was pulled out when it was discovered that a bullnose, used to open the lockable flapper valve, had not been run. The tool then was lowered to a depth of 609.3 mbsf, and the logging run was started. This run was aborted at 331.6 mbsf as the GST was not operating properly. The tool was lowered to 443.8 mbsf (the depth where the GST began to malfunction) and a repeat log was run. The GST did not produce neutrons properly during this repeat run. The tool was lowered to 199.9 mbsf to determine if the formation had been activated. There was no sign of neutron activation, so the string was pulled out of the hole.

Upon completion of the logging program, the pipe was pulled to the surface, and the bottom hole assembly (BHA) cleared the rotary table at 0345 hr, 17 February 1990, ending Hole 805C.

LITHOSTRATIGRAPHY

Introduction

Site 805 is located at a water depth of 3188 m, a shallower water depth than Sites 803 and 804. It was intended to occupy an intermediate position on the Neogene depth transect on the flank of the Ontong Java Plateau. Three holes were drilled at Site 805. Hole 805A was drilled with the APC to 50.5 mbsf with greater than 100% recovery. Cores from Hole 805A were stored unopened. Hole 805B was drilled to 473.3 mbsf. The upper 263.2 m were drilled with the APC and the remaining portion was drilled with the XCB. Recovery in the APC section was generally 100% or more, except for Core 130-805B-19H, and recovery in the XCB section averaged 83%. Hole 805C covered the same section as Hole 805B and was further extended to 611 mbsf. It was cored with the APC to 235.8 mbsf and with the XCB throughout the rest of the section. Recovery was 100% in the section cored with the APC, except for Core 130-805C-23H, which only recovered 2 m of sediment. Flow-in was observed in the upper five sections of Core 130-805C-7H and in all of Core 130-805C-8H. Shorter intervals of Cores 130-805C-10H, -11H, -14H, -16H, and -17H also exhibit flow-in structures and sediment distortion. This reduces the quality of the recovered material in this hole. Recovery in the part of Hole 805C drilled with the XCB was generally above 70% through Core 130-805C-54X (514.2 mbsf). Below this level, recovery was drastically reduced but variable, ranging from 8% (Core 130-805C-56X) to 99% (Core 130-805C-61X).

Nannofossil ooze and chalk are the predominant sediment types recovered at Site 805. Intervals of foraminifer nannofossil ooze and chalk are also present. Radiolarians are the most significant minor constituent of the sediments. Site 805 differs from Sites 803 and 804 in having a higher foraminifer content and in lacking intervals with high radiolarian abundances. The sedimentary section at Site 805 is stratigraphically complete, covering the Pleistocene to the upper Oligocene (see "Biostratigraphy" section, this chapter).

The sediments at Site 805 were grouped into one lithologic unit (Unit I) (Table 2 and Fig. 4). This unit is composed of upper Oligocene to Pleistocene nannofossil chalk and ooze and foraminifer nannofossil chalk and ooze. The unit was divided into two subunits (IA and IB) based on the degree of consolidation. Subunit IA is composed of ooze, whereas Subunit IB is composed of chalk. The Subunit IA/IB boundary is located at 282.5 mbsf in Hole 805B (base of Core 130-805B-30X), and at 293.7 mbsf (base of Core 130-805C-31X) in Hole 805C, and is gradational within each hole. Semi-indurated layers and stiffer portions are embedded in the softer ooze in the lower cores of Subunit IA, and the uppermost cores of Subunit IB include intervals of ooze.

Description of Units

Unit I

Intervals: Hole 805B, Cores 130-805B-1H to -50X, and Hole 805C, Cores 130-805C-1H to -64X
Age: Pleistocene–late Oligocene
Depth: 0–611 mbsf

Unit I is composed of nannofossil ooze and chalk to foraminifer nannofossil ooze and chalk and has been divided into two subunits. Subunit IA (0–293.7 mbsf) consists of nannofossil ooze and foraminifer nannofossil ooze, whereas Subunit IB (293.7–611 mbsf) contains nannofossil chalk and foraminifer nannofossil chalk.

Subunit IA

Intervals: Hole 805B, Cores 130-805B-1H to -30X, and Hole 805C, Cores 130-805C-1H to -31X
Age: Pleistocene–middle Miocene
Depth: 0–293.7 mbsf

Subunit IA is composed of 293.7 m of nannofossil ooze, nannofossil ooze with foraminifers, and foraminifer nannofossil ooze. The average foraminifer content is noticeably higher than at Sites 803 and 804. Foraminifer abundance is variable, with foraminifer-rich intervals in the Pleistocene and the Pliocene sections. Foraminifer abundances are low in parts of the upper Miocene section (Cores 130-805B-19H to -22H and 130-805C-19H to -22H) between 169 and 207 mbsf (Fig. 5), and increase again below this interval (Cores 130-805B-25H to -27H and Cores 130-805C-24H to -27H; 225–254 mbsf), and in parts of Core 130-805B-29X (263.2–272.9 mbsf), close to the ooze-chalk transition. Foraminifer abundances are variable at the middle/upper Miocene boundary, as seen in the alternations between nannofossil ooze and foraminifer nannofossil ooze in Figure 4. There is no clear relationship between the shipboard estimates of carbonate content and foraminifer content; carbonate content is low (82%–94%) and foraminifer content is high in the upper 150 m of the section (Fig. 6) (last 5–6 m.y.), whereas high foraminifer and high carbonate contents coincide in other portions of the section. Radiolarians are commonly present as a minor constituent in Subunit IA, but at concentrations too low to estimate abundance changes from smear slide analyses (Fig. 5).

The dominant color of the sediments of Subunit IA is white (2.5Y 8/0, 5Y 8/1), although the upper 30 m are light gray (5Y 7/1, 2.5Y 7/1). Bioturbation, ranging from slight to heavy, is common throughout the subunit, as evidenced by burrow mottling, pyritized burrow fills and specks, and numerous trace fossils that range in size from several millimeters to almost 10 cm in length (Fig. 7). As at Sites 803 and 804, the sediments through-

Table 2. Lithologic summary, Site 805.

Lithologic unit	Cores	Depth (mbsf)	Age	Lithology
IA	805B-1H to -30X 805C-1H to -31X	0–293.7	Pleistocene to middle Miocene	Nannofossil ooze to foraminifer nannofossil ooze
IB	805B-31X to -50X 805C-32X to -64X	293.7–611.0	middle Miocene to late Oligocene	Nannofossil chalk to foraminifer nannofossil chalk

out Subunit IA display numerous faint to sharp color bands that are light gray (5Y 7/2), pale blue (5PB 7/2), pale purple (5P 6/2), grayish blue (5PB 5/2), and light greenish gray (5G 7/1). The color bands are normally horizontal, but a few steeply inclined bands were also observed. In some instances, these bands clearly spread as concentric rings from well-developed burrows. The vertical bands were observed to cut through horizontal bands in some cases, apparently changing or diminishing the color of the horizontal band in the process. An example of this relationship is shown in Figure 8. This style of banding indicates that either the vertical or both the vertical and horizontal bands were formed diagenetically along diffusion gradients. The sediments at Site 805 appear to be much less influenced by microfaulting and distorted bedding than those at Sites 803 and 804. Only a few microfaults were observed, particularly in Section 130-805B-18H-5 (Fig. 9).

A thin, bioturbated ash-layer was observed at 260.29 mbsf in Hole 805C (Core 130-805C-28X-4, 69 cm) (see also Fig. 5). This ash was not found in Hole 805B either because of the disseminated nature of the ash or the loss at a core break.

The dominance of carbonate in the sediments of Subunit IA is clearly reflected by X-ray diffraction (XRD) scans and calcium carbonate contents (Fig. 6). Relative peak intensities from the XRD analyses agree with the general trends of the shipboard carbonate measurements and indicate somewhat lower calcite content in Cores 130-805B-15H to -21H, which generally coincides with the interval of low foraminifer content. Clays, quartz, and feldspars are the important nonbiogenic constituents of Subunit IA.

The predominance of nannofossils in the sediments of Subunit IA produces a silty texture. This observation is supported by shipboard grain-size analyses (Table 3). Figure 10 shows that mean grain size varies within the fine to medium silt-size range (10–30 μm) as a series of high-frequency, grain-size fluctuations throughout the upper 300 m of sediment, superimposed on longer intervals of variation. The most noticeable of these longer term changes is a trend toward coarser mean values below 200 mbsf. This trend is probably the result of increased foraminifer abundances (see Fig. 5 for comparison).

In the lower portion of Subunit IA (283–293.7 mbsf), the sediment gradually becomes stiffer, as seen by the development of interbedded semi-indurated layers and more lithified, nodule-like intervals. The downhole velocity log (see "Logging" section, this chapter) documents a marked shift toward higher velocities at 250 mbsf, which probably reflects the onset of such interbedding. Spikes in the velocity log between 250 and 300 mbsf may reflect the variable degree of lithification in lower Subunit IA. The ooze-chalk transition at about 294 mbsf is also reflected by a steplike increase in sonic velocity in the downhole log.

Subunit IB

Intervals: Hole 805B, Cores 130-805B-31X to -50X, and Hole 805C, Cores 130-805C-32X to -64X
Age: middle Miocene–late Oligocene
Depth: 293.7–611 mbsf

Subunit IB is composed of 317.3 m of nannofossil chalk, nannofossil chalk with foraminifers, and foraminifer nannofossil chalk. The average foraminifer content is high throughout the upper 90 m of Subunit IB (to Core 130-805C-41X), an interval composed of alternations of foraminifer nannofossil chalk and nannofossil chalk with foraminifers. The foraminifer content decreases below this level, and nannofossil chalk forms the remainder of the section (Figs. 4 and 5). Radiolarians are present in minor quantities in Subunit IB except for Core 130-805B-43X, in which radiolarian abundances as high as 10% were observed in smear slides.

The dominant color of Subunit IB sediment is white (2.5Y 8/0). As in Subunit IA, the sediments of Subunit IB display numerous faint to sharp color bands, which are light gray (5Y 7/2), pale blue (5PB 7/2), pale purple (5P 6/2), grayish blue (5PB 7/2), and light greenish gray (5G 7/1) in color. The color bands of this subunit are commonly sharply defined and concentrated in groups of millimeter-scale thin bands (Fig. 11). Color bands are not common below 504 mbsf (below Core 130-805C-54X), where the sediments are fairly homogeneous. The lack of color banding in this interval could also be the result of reduced recovery in the lower part of the hole. Concentric color rings that form "haloes" around burrows are common (Fig. 12). Bioturbation ranges from slight to heavy throughout the section. This is documented by the presence of numerous burrows, which range in size from several millimeters to almost 10 cm, and by burrow mottles, pyritized burrow fills, and disseminated pyrite that locally color the sediment pale blue (5PB 7/2) to pale purple (5P 6/2). The effects of heavy bioturbation are generally most visible in the darker layers, as shown in Figure 13.

Microfaulting and contortion of color bands generally were not observed in Subunit IB. The only noticeable exception is in Core 130-805C-33X (309.2–312.6 mbsf), which contains wispy laminations and smeared banding (Fig. 14). It is unclear whether these structures were the result of drilling disturbance or if they record sediment destabilization that occurred before drilling began.

Small nodules of chert, each a few centimeters thick, were recorded at 344.35 (Interval 130-805C-37X-2, 135–137 cm) and 370.6 mbsf (Interval 130-805C-40X-1, 0–10 cm). The absence of cherts at these levels in Hole 805B suggests that the cherts are nodular and do not form continuous layers. Shipboard pore-water measurements indicate that the dissolved silica content is high and close to saturation throughout Subunit IB, making the precipitation of chert likely. The levels that contain chert, however, are not accompanied by any noticeable change in pore-water silica concentrations (see "Inorganic Geochemistry" section, this chapter), suggesting that only a minor amount of chert precipitation has occurred. High pore-water silica is probably caused by dissolution of sedimentary silica, but no silica-enriched sediments were recovered at this site; for that reason, the silica source is interpreted to lie below the bottom of Hole 805C.

A thin ash layer was observed at 295.96 mbsf (Section 130-805C-32X-2, 76 cm). With the exception of the chert nodules and the ash layer, Subunit IB is composed almost entirely of calcareous sediments, although the poor recovery in the lower portion of the hole may indicate the presence of cherts in that interval.

The compositional predominance of carbonate is evident in the XRD scans and the shipboard carbonate measurements (Fig. 6). Calcite peak intensities are especially large in diffractograms of samples from the uppermost cores of Subunit IB, in accordance with their high foraminifer content. Nonbiogenic components, which include clays, quartz, and feldspar, are minor constituents in Subunit IB.

The uppermost 2–3 cores of Subunit IB exhibit variable degrees of lithification and contain interbeds of chalk and ooze. Below this interval, the section is composed of more uniformly firm chalk, which becomes increasingly stiff downhole. This transitional interval from ooze to chalk is expressed as a zone of fluctuations in the sonic velocity and density logs (see "Logging" section, this chapter). Much of the remaining variation in the apparent hardness of the sediments can be attributed to the extent of drilling disturbance.

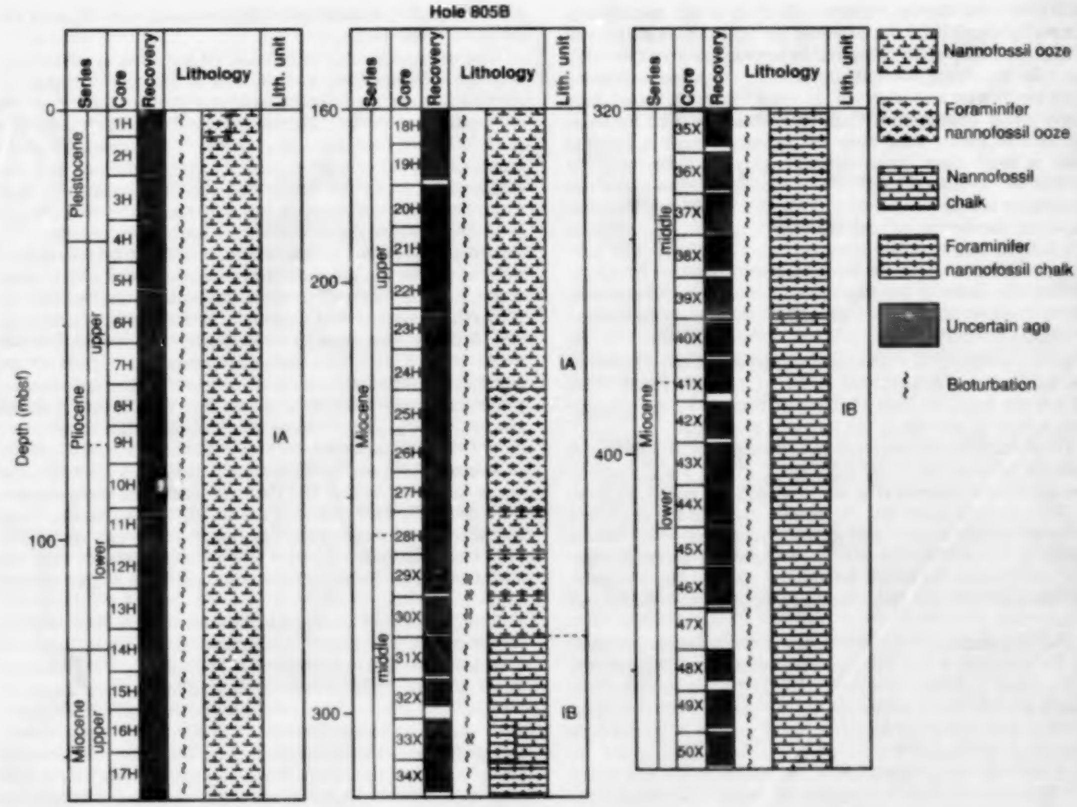
Hole 805B
Series
Core
Recovery
Lithology
Lith. unit
Depth (mbsf)
0
100
160
200
300
320
400
Pleistocene
Pliocene
upper
lower
Miocene
upper
middle
lower
IA
IB
1H
2H
3H
4H
5H
6H
7H
8H
9H
10H
11H
12H
13H
14H
15H
16H
17H
18H
19H
20H
21H
22H
23H
24H
25H
26H
27H
28H
29X
30X
31X
32X
33X
34X
35X
36X
37X
38X
39X
40X
41X
42X
43X
44X
45X
46X
47X
48X
49X
50X
Nannofossil ooze
Foraminifer nannofossil ooze
Nannofossil chalk
Foraminifer nannofossil chalk
Uncertain age
Bioturbation

Figure 4. Lithologic summary, Holes 805B and 805C.

Discussion

Site 805 has been characterized by continuous biogenic, pelagic deposition above the CCD since the late Oligocene. This history is documented by the stratigraphic continuity of the recovered pelagic sediments, their generally high sedimentation rates, and the predominance of biogenic carbonate in the sediments. Intervals of reduced sedimentation rate, probably caused by increased dissolution and closer proximity to the CCD, occurred at approximately 10 and 20 Ma (see "Biostratigraphy" section, this chapter).

The most noticeable variation in the sediments of Site 805 is the change in foraminifer content. Foraminifer abundance is generally low in the Oligocene and lower Miocene sections of the record, and it increases in the upper parts of the middle Miocene, in parts of the upper Miocene, and in intervals of the Pleistocene. The changes in foraminifer content may have been caused by variations in the relative production of the different fossil groups, by preservational effects, or by variations in winnowing. Enhanced dissolution can reduce the relative importance of foraminifers in the sediments (Berger, 1976; Berger et al., 1977), because foraminifer preservation is more sensitive than calcareous nannofossil preservation to the position of the calcite lysocline. Changes in the depth of the lysocline and the thickness of the interval from the lysocline to the CCD, therefore, will affect the dissolution of nannofossils and foraminifers differently (Berger et al., 1977). As a result, the foraminifer-rich intervals may indicate times of better foraminifer preservation caused by reduced dissolution. Long-term trends in the relative abundances of the various microfossil groups may be linked to movement of the Ontong Java Plateau into the equatorial zone.

The ooze-chalk transition is located deeper in the sediment column at Site 805 than at Sites 803 and 804, suggesting that this boundary depends on sediment age as well as depth of burial. The depth of the ooze-chalk transition may also be related to the original sediment composition, such as the extent of dissolution experienced before burial (Schlanger and Douglas, 1974). The transition from ooze to chalk is gradational and occurs through a change in the relative abundances of interbedded soft and indurated layers. It is noted that intensively burrowed intervals are often the first to become indurated.

BIOSTRATIGRAPHY

Introduction

Site 805, in 3200 m water depth, is intermediate in position on the Ontong Java Plateau depth transect. A 611 m sedimentary section was drilled and an apparently continuous stratigraphic section of calcareous ooze and chalk of Holocene to late Oligocene age was recovered (Fig. 15). The strata contain a mixture of calcareous and siliceous microfossils suitable for correlation between zonal schemes of the various groups. These microfossil assemblages have various states of preservation pertinent to the interpretation of paleoceanography and/or diagen-

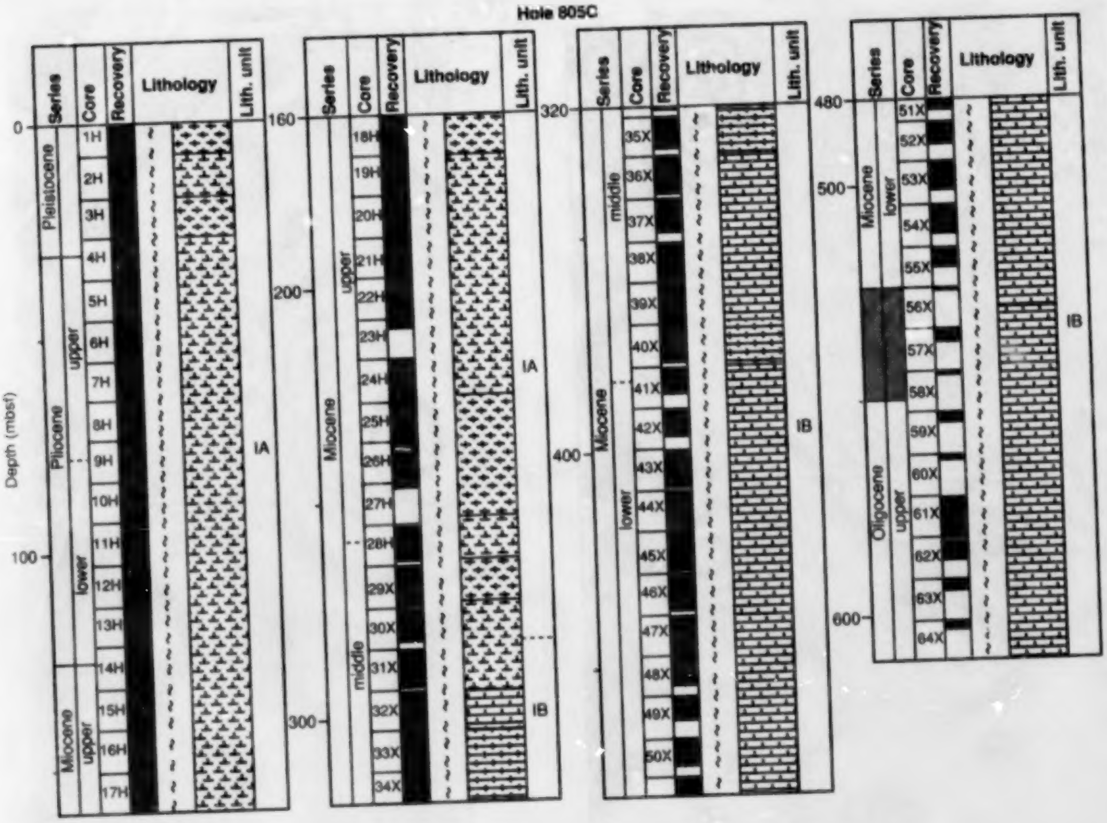
Hole 805C
Depth (mbsf)
Series
Core
Recovery
Lithology
Lith. unit
0
100
160
200
300
320
400
480
500
600
Pleistocene
Pliocene
upper
lower
Miocene
middle
Oligocene
IA
IB
1H
2H
3H
4H
5H
6H
7H
8H
9H
10H
11H
12H
13H
14H
15H
16H
17H
18H
19H
20H
21H
22H
23H
24H
25H
26H
27H
28H
29X
30X
31X
32X
33X
34X
35X
36X
37X
38X
39X
40X
41X
42X
43X
44X
45X
46X
47X
48X
49X
50X
51X
52X
53X
54X
55X
56X
57X
58X
59X
60X
61X
62X
63X
64X

Figure 4 (continued).

esis at intermediate depths on the flanks of the Ontong Java Plateau. The 135-m lower Miocene section is unusually thick, only about 15 m less than that recovered on the upper surface of the Ontong Java Plateau at DSDP Site 289.

Evidence for a significant amount of reworked microfossils was found only among the Quaternary radiolarian assemblages. Problems encountered among all the microfossil groups are the occasional absence of index fossils to differentiate zones and some intervals of poor preservation. These problems are limited and probably can be resolved through examination of sectional samples. Detailed discussion of the stratigraphy as well as the condition of the samples examined follows.

Calcareous Nannofossils

Hole 805A

Pleistocene

The uppermost sample of this hole (Sample 130-805A-1H-CC) contains a Pleistocene to Holocene coccolith assemblage without *Pseudoemiliania lacunosa*. This sample is placed in the NN21/NN20 zonal interval. The assemblages in the next lower two samples (Samples 130-805A-2H-CC and -3H-CC) are characterized by the presence of abundant *Pseudoemiliania lacunosa* and the absence of discoasters. These two samples are placed in Zone NN19. The last occurrence (LO) of *Helicosphaera sellii* was observed in Core 130-805A-3H.

Pliocene

Sample 130-805A-4H-CC contains *Calcidiscus macintyrei*, *Discoaster brouweri*, and *D. triradiatus*, implying that the Pliocene/Pleistocene boundary falls in Core 130-805A-4H. Sample 130-805A-5H-CC lies below the acme interval of *D. triradiatus* but still belongs to Zone NN18. The bottom of this hole (Sample 130-805A-6H-CC) is late Pliocene in age (the upper part of Zone NN16), based on the occurrences of *Discoaster brouweri*, *D. pentaradiatus*, *D. surculus*, and *D. asymmetricus* and the absence of *D. tamalis* and *Reticulofenestra pseudoumbilica*.

Hole 805B

The nannofossil assemblages in the uppermost six cores in this hole are similar to those observed in Hole 803A, and this description of the nannofossil biostratigraphy begins in the upper Pliocene where the NN17/NN18 zonal boundary was observed between Samples 130-805B-5H-6, 70 cm, and -5H-7, 70 cm. The NN16/NN17 boundary falls between the latter sample and Sample 130-805B-5H-CC.

Although the relative abundances of *Discoaster tamalis* and *Discoaster asymmetricus* have not been investigated systematically at closely spaced sample intervals in the upper Pliocene sediments of Leg 130, it is nevertheless obvious that these morphotypes did not thrive in this region because they are notoriously rare. *Discoaster tamalis* is found only in Sample 130-805B-6H-CC.

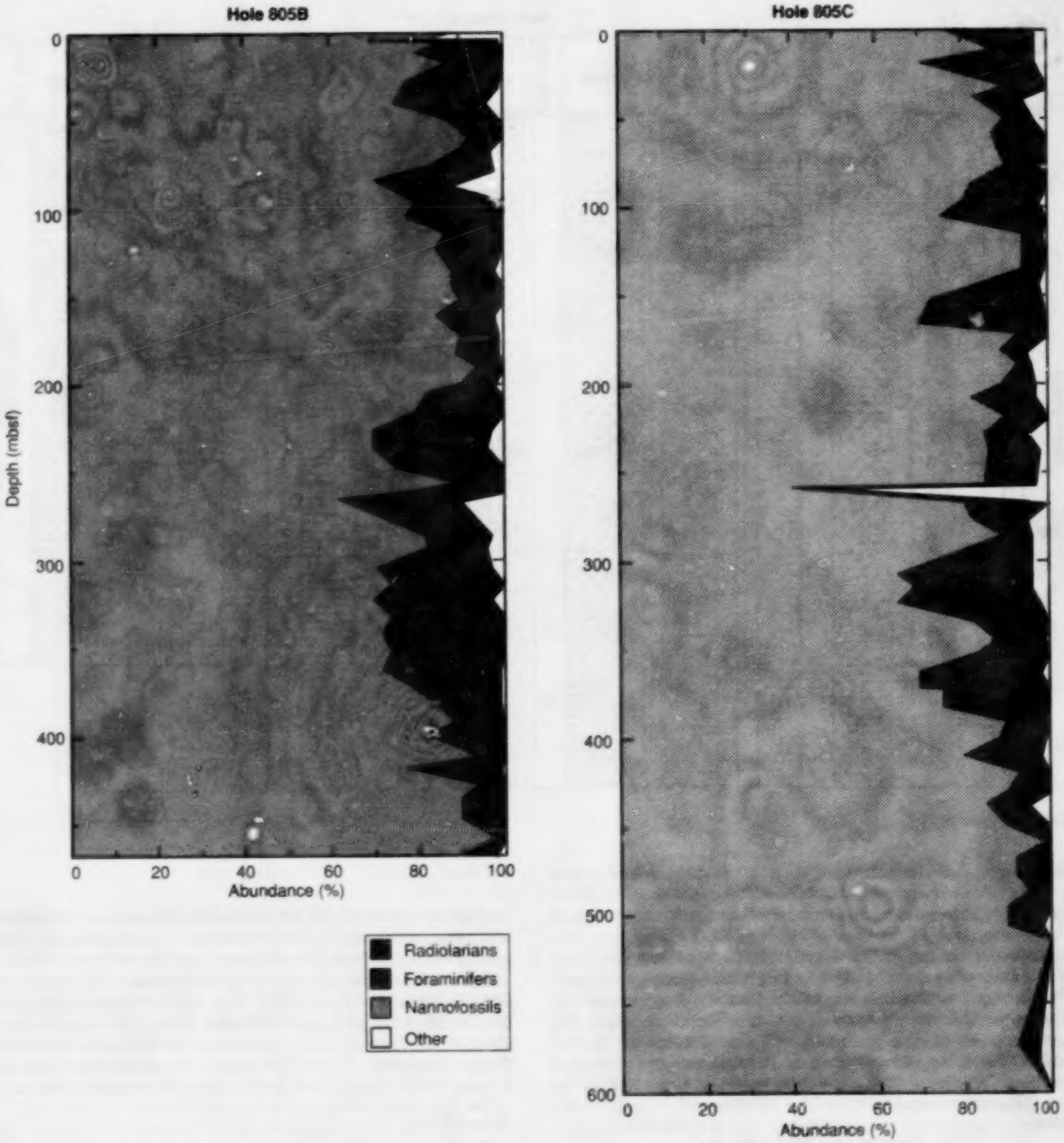

Figure 5. Abundances of major sediment components at Site 805, as determined by smear slide analysis.

Reticulofenestra pseudoumbilica occurs within and below Sample 130-805B-9H-CC. This sample and the next lower sample (130-805B-10H-CC) contain *Discoaster asymmetricus*. The NN15/NN14 boundary cannot be distinguished because *Amaurolithus* is very rare or absent. Therefore, these two samples are tentatively placed in the NN15/NN14 zonal interval. The assemblage in the next deeper sample (Sample 130-805B-11H-CC) is characterized by the presence of *Reticulofenestra pseudoumbilica, Ceratolithus acutus*, and a specimen similar to *Discoaster asymmetricus*. Moreover, this sample lacks *Ceratolithus rugosus* and *Discoaster quinqueramus*. Taken together, this assemblage clearly indicates Zone NN12 of the lowermost Pliocene. The two next deeper samples (Samples 130-805B-12H-CC and -13H-CC) are also considered to belong to Zone NN12 because of the absence of *Ceratolithus rugosus* and *Discoaster quinqueramus*. In Samples 130-805B-11H-CC, -12H-CC, and -13H-CC, peculiar subcircular *Reticulofenestra* specimens are fairly abundant; for example, they occupy nearly 50% of the total assemblage in the former two samples.

Miocene

The section ranging from Samples 130-805B-14H-CC through -23H-CC is referred to Zone NN11 based on the continuous occurrence of *D. quinqueramus*. As mentioned previously, the top

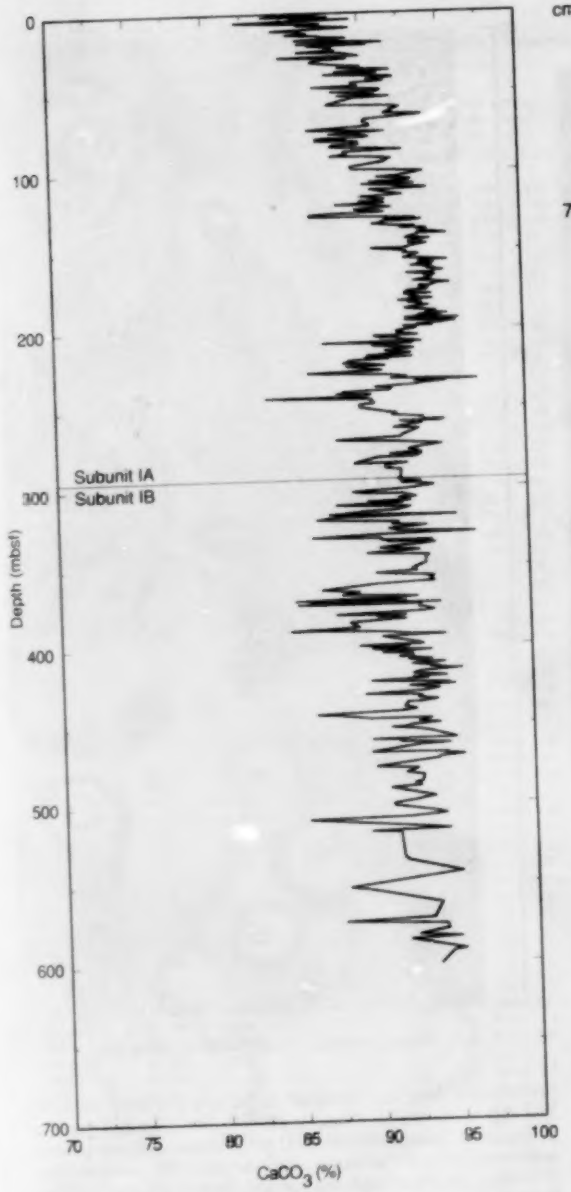

Figure 6. Calcium carbonate content, Hole 805B, based on shipboard measurements.

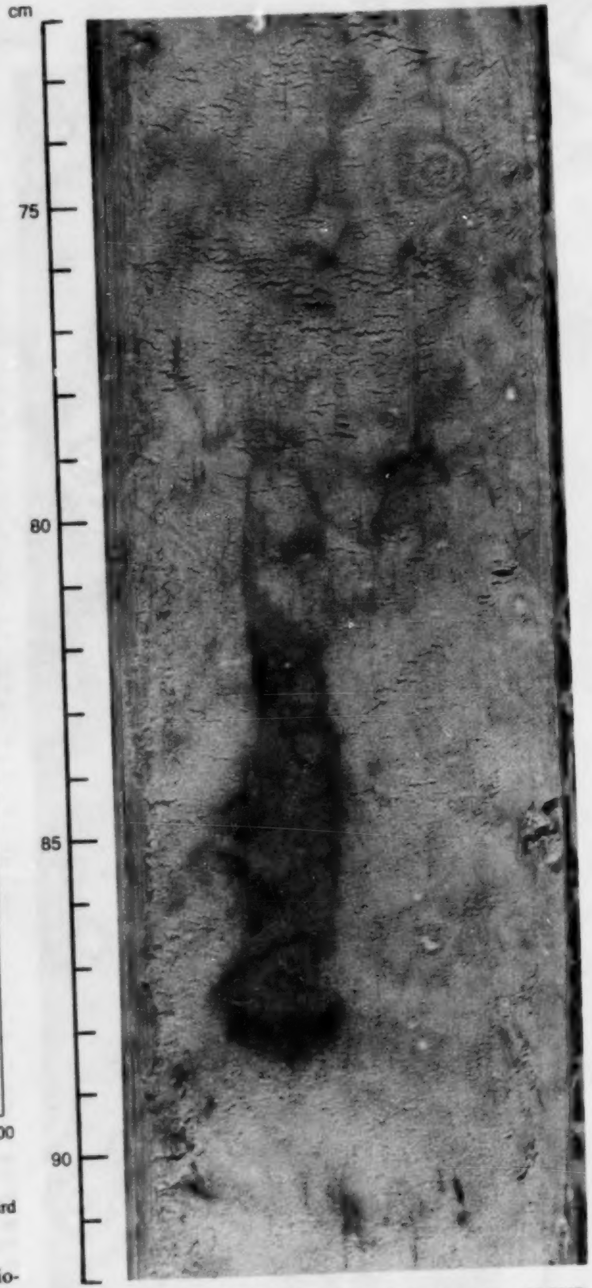

Figure 7. Photograph of large burrow in Subunit IA (Section 130-805B-21H-3, 72–92 cm).

of this zone approximately indicates the position of the Miocene/Pliocene boundary. Specimens belonging to *Amaurolithus* are rare and poorly preserved; their first occurrence (FO) was observed in the interval between Cores 130-806B-22H to -23H. The latter core contains the LO of *Discoaster neohamatus*. The underlying Zone NN10 is represented by the stratigraphic interval ranging from Samples 130-805B-24H-CC through -28H-CC because of the absence of *Discoaster quinqueramus* and *D. hamatus*. The lower part of Zone NN11 and the upper part of Zone NN10 (Samples 130-805B-22H-CC down to -25H-CC) is characterized by a bloomlike abundance of small sphenolith species, such as *Sphenolithus abies* and *S. neoabies*.

The first downhole observation of *Discoaster hamatus* was made in Sample 130-805B-29X-CC, marking the top of Zone NN9. *Catinaster coalitus*, *Catinaster calyculus*, and *Discoaster*

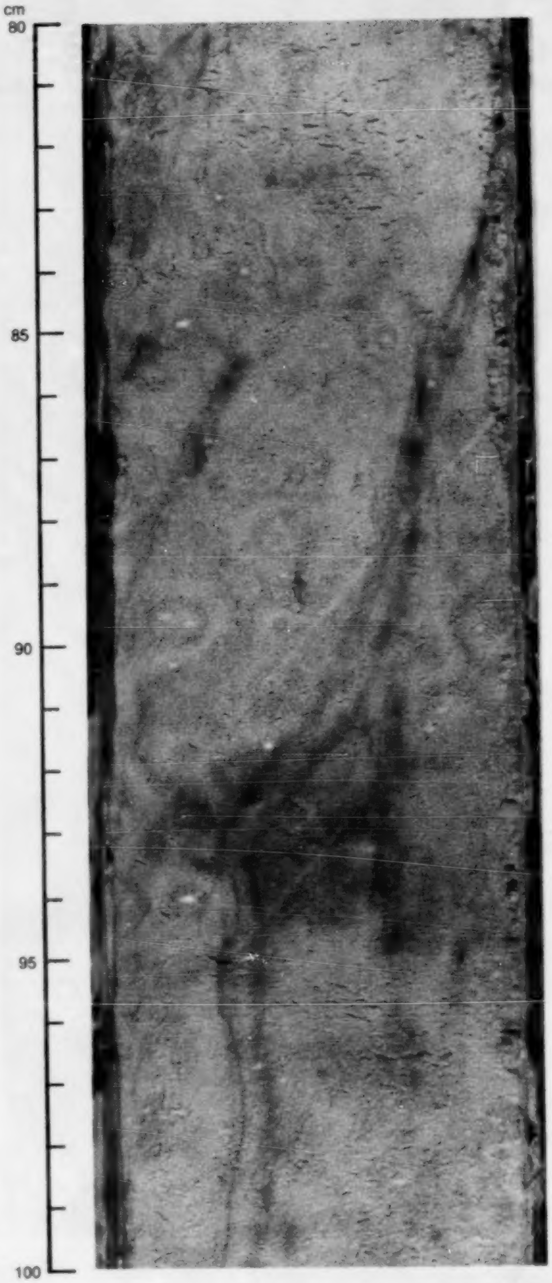

Figure 8. Photograph of a vertical color band in Subunit IA (Section 130-805B-20H-1, 80–100 cm). Formation of the vertical band appears to have changed the color of the horizontal band across the width of the core.

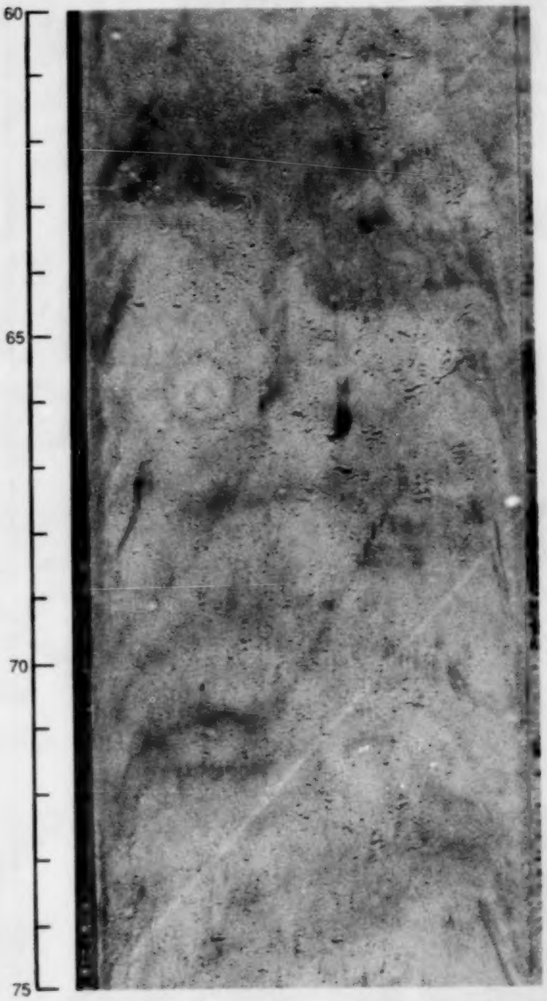

Figure 9. Microfaulting (Section 130-805B-18H-5, 60–75 cm).

neohamatus were also observed in Sample 130-805B-29H-CC. The next lower sample (Sample 130-805-30X-CC) also contains *D. hamatus*. Sample 130-805B-31X-CC contains neither *Discoaster hamatus* nor *Catinaster coalitus*. As at the previous sites, secondary calcite overgrowth on discoasters prevents accurate identification of *Discoaster kugleri*. In addition, this species is a warm-water form (Wise, 1973) but it is generally rare in oceanic sediments (Hay, 1970). Therefore, we were unable to recognize the NN6/NN7 boundary in this hole.

Sample 130-805B-32X-CC is rich in typical *Reticulofenestra pseudoumbilica* and *Dictyococcites perplexus*, as well as typical middle Miocene discoasters that predominantly belong to the *Discoaster variabilis* complex. Having passed through Zone NN8 and not yet reached Zone NN5, and not relying on *Discoaster kugleri* as a marker species, Core 130-806B-32X was placed in the NN6/NN7 zonal interval. Samples 130-805B-33X-CC and -34X-CC lie between the LOs of *Coronocyclus nitescens* and *Cyclicargolithus floridanus*, and between the LOs of *Cyclicargo-*

Table 3. Mean grain size of sediments, Subunit IA.

Core, section, interval (cm)	Depth (mbsf)	Mean grain size (µm)
130-805B-		
1H-1, 10	0.10	31.30
1H-3, 10	3.10	12.50
1H-4, 10	4.60	15.90
1H-5, 11	6.11	16.20
2H-1, 10	6.80	14.60
2H-2, 10	8.30	15.30
2H-3, 118	10.88	12.90
2H-4, 111	12.31	18.60
2H-5, 111	13.81	12.00
2H-6, 111	15.31	8.70
3H-1, 70	16.90	12.50
3H-2, 70	18.40	15.60
3H-3, 70	19.90	31.60
3H-4, 70	21.40	18.30
3H-5, 70	22.90	17.30
3H-6, 70	24.40	17.70
3H-7, 70	25.40	15.80
4H-1, 145	27.15	25.60
4H-2, 145	28.65	23.30
4H-3, 145	30.15	17.30
4H-4, 145	31.65	22.40
4H-5, 145	33.15	16.30
4H-6, 145	34.65	20.50
4H-7, 70	35.40	19.00
5H-1, 70	35.90	14.10
5H-2, 70	37.40	16.20
5H-3, 70	38.90	18.20
5H-4, 70	40.40	18.40
5H-5, 70	41.90	21.80
5H-6, 70	43.40	17.10
6H-1, 122	45.92	20.30
6H-2, 70	46.90	24.70
6H-2, 70	46.90	29.20
6H-3, 70	48.40	15.60
6H-4, 70	49.90	20.40
6H-4, 70	49.90	22.90
6H-5, 70	51.40	11.30
6H-5, 70	51.40	14.00
6H-6, 70	52.90	17.10
6H-6, 70	52.90	16.70
8H-2, 106	66.26	13.70
8H-3, 106	67.76	14.00
8H-4, 106	69.26	17.20
8H-5, 100	70.70	21.40
8H-6, 91	72.11	19.90
9H-1, 114	74.34	10.90
9H-2, 114	75.84	15.30
9H-3, 114	77.34	14.30
9H-4, 114	78.84	22.00
9H-5, 114	80.34	16.80
9H-6, 80	81.50	14.80
10H-1, 104	83.74	12.10
10H-2, 104	85.24	13.30
10H-3, 104	86.74	18.40
10H-4, 104	88.24	19.40
10H-5, 104	89.74	15.70
10H-6, 104	91.24	16.60
10H-7, 60	92.40	21.80
11H-1, 108	93.28	16.40
11H-2, 108	94.78	10.60
11H-3, 106	96.26	12.00
11H-4, 106	97.76	12.20
11H-5, 106	99.26	12.80
11H-6, 106	100.76	15.40
12H-1, 10	101.80	11.50
12H-2, 10	103.30	20.60
12H-3, 10	104.80	15.10
12H-4, 10	106.30	17.20
12H-5, 10	107.80	12.80
12H-6, 10	109.30	16.30
12H-7, 10	110.80	14.10
13H-1, 110	112.30	16.90
13H-2, 110	113.80	23.30
13H-3, 110	115.30	20.70
13H-4, 110	116.80	14.80
13H-5, 110	118.30	13.90
13H-6, 110	119.80	14.60
13H-7, 35	120.55	18.90
14H-1, 111	121.81	12.50
14H-2, 111	123.31	15.60
14H-3, 111	124.81	17.20
14H-4, 116	126.36	22.00
14H-5, 109	127.79	13.40
14H-6, 110	129.30	16.30
14H-7, 45	130.15	17.70
15H-1, 111	131.31	17.80
15H-2, 109	132.79	19.00
15H-3, 110	134.30	18.70
15H-4, 110	135.80	19.10
15H-5, 110	137.31	17.80
15H-6, 106	138.76	26.10
15H-7, 46	139.66	27.00
16H-1, 35	140.05	29.30
16H-2, 35	141.55	21.40
16H-3, 35	143.05	28.50
16H-4, 35	144.55	10.80
16H-5, 35	146.05	10.00
16H-6, 35	147.55	15.00
16H-7, 35	149.05	16.30
17H-1, 110	150.30	12.40
17H-2, 110	151.80	16.90
17H-4, 110	154.80	16.70
17H-5, 110	156.30	14.10
17H-6, 110	157.80	15.50
18H-1, 10	158.80	15.10
18H-2, 10	160.30	19.60
18H-2, 108	161.28	16.70
18H-3, 10	161.80	16.30
18H-3, 110	162.80	17.00
18H-4, 10	163.30	17.50
18H-4, 110	164.28	14.10
18H-5, 10	164.80	17.70
18H-5, 110	165.80	15.40
18H-6, 10	166.30	12.50
18H-6, 110	167.30	11.40
18H-7, 10	167.80	21.80
18H-7, 35	168.05	14.40
19H-2, 10	169.80	24.80
19H-3, 10	171.30	25.30
19H-4, 10	172.80	21.00
19H-5, 10	174.30	23.60
19H-6, 10	175.80	20.40
20H-1, 50	178.20	16.70
20H-2, 50	179.70	12.70
20H-3, 50	181.20	13.10
20H-4, 50	182.70	14.60
20H-5, 50	184.20	14.60
20H-6, 50	185.70	10.20
20H-7, 50	186.80	14.80
21H-1, 60	187.80	17.60
21H-2, 60	189.30	22.10
21H-3, 60	190.80	17.40
21H-4, 60	192.30	19.20
21H-5, 60	193.80	26.90
21H-6, 60	195.30	21.30
22H-2, 50	198.70	14.60
22H-3, 50	200.20	27.90
22H-4, 50	201.70	25.80
22H-5, 50	203.20	23.20
22H-6, 50	204.70	23.80
23H-1, 83	207.03	19.80
23H-2, 83	208.53	24.00
23H-3, 83	210.03	22.20
23H-4, 83	211.53	25.50
23H-5, 83	213.03	27.40
23H-6, 83	214.53	24.60
24H-1, 88	216.58	18.00
24H-2, 88	218.08	24.40
24H-3, 88	219.58	22.30
24H-4, 88	221.08	17.30
24H-5, 88	222.58	17.90
24H-6, 88	224.08	17.70
25H-1, 130	226.50	18.30
25H-2, 105	227.75	27.60
25H-3, 107	229.27	27.70
25H-4, 104	230.74	30.10
25H-5, 108	232.28	23.50
25H-6, 103	233.73	24.00
26H-2, 107	237.27	18.70
26H-3, 113	238.83	23.80
26H-4, 86	240.06	30.80
26H-5, 101	241.71	23.40
26H-6, 106	243.26	27.10
27H-3, 118	248.38	20.70
27H-4, 98	249.68	30.40
27H-5, 109	251.29	21.90
27H-6, 109	252.79	26.50
27H-7, 106	254.26	15.50
28H-1, 100	254.70	25.70
28H-2, 100	256.20	15.90
28H-3, 100	257.70	15.70
28H-4, 60	258.80	17.50
28H-6, 100	262.20	23.00
28H-7, 40	263.10	22.80
29H-1, 33	263.53	21.80
29H-2, 46	265.16	22.20
29H-3, 46	266.66	29.20
29H-4, 45	268.15	15.40
29H-5, 45	269.65	17.20
29H-6, 19	270.89	25.30
30H-4, 60	278.00	19.90
30H-5, 60	279.50	18.50
30H-6, 65	281.05	27.80

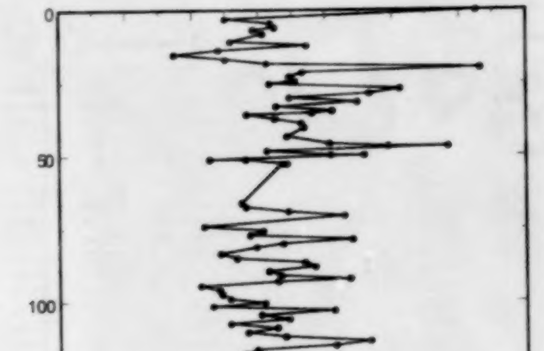

Figure 10. Mean grain size of sediments in Subunit IA (Hole 805B), based on shipboard measurements.

lithus floridanus and *Sphenolithus heteromorphus*, respectively. Therefore, these two samples are considered to belong to Zone NN6. The NN6/NN5 boundary was observed in Core 130-805B-35X. The absence of *Helicosphaera ampliaperta* prevents recognition of the NN4/NN5 boundary in this hole. The change in ratio of the *Discoaster deflandrei* group to total discoasters, however, was observed in Core 130-805B-39X.

The FO of *Sphenolithus heteromorphus* was found between Samples 130-805B-41X-CC and -42X-1, 92 cm. Therefore, the section ranging from Samples 130-805B-35X-CC through -41X-CC was referred to Zones NN5 and NN4. *Triquetrorhabdulus carinatus* was found as high as Sample 130-805B-42X-CC, although a common abundance was observed first in Core 130-805B-45X. *Sphenolithus belemnos* was observed in Core 130-805B-42X. The interval from this core down to Sample 130-805B-45X-CC was placed in the lower Miocene Zone NN2 based on the co-occurrence of *T. carinatus* and *D. druggii*. The section below this zone probably belongs to the NN1 *Triquetrorhabdulus carinatus* Zone. A single specimen of *Sphenolithus ciperoensis* in Sample 130-805B-48X-CC is considered to be reworked.

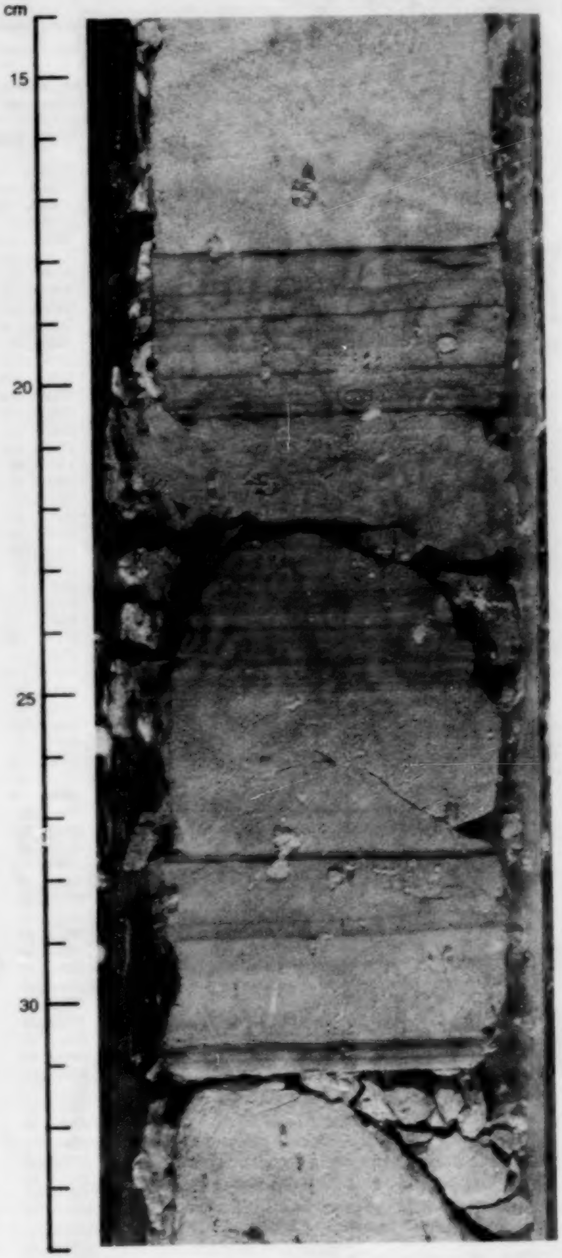

Figure 11. Concentration of well-defined, millimeter-sized color bands in Subunit IB (Section 130-805B-45X-6, 14–34 cm).

Hole 805C

Only core-catcher samples were investigated in the upper 50 cores of Hole 805C (i.e., in the Pleistocene to lower Miocene interval). The results from these core-catcher samples are quite

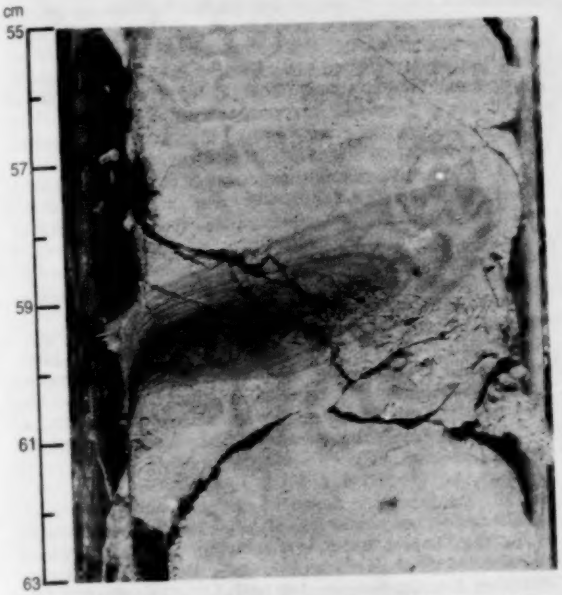

Figure 12. Concentric color bands surrounding a pyritized burrow (Section 130-805B-46X-1, 55–63 cm).

similar to the results obtained from the previous hole and are summarized in Figure 15.

The blooms of the peculiar *Reticulofenestra* morphotype and small sphenoliths again are found in this hole in Samples 130-805C-10H-CC through -12H-CC and in Samples 130-805C-24H-CC and -25H-CC, respectively.

Lower Miocene and Oligocene

Sporadic occurrences of *Discoaster druggii* were recognized in the interval ranging from Samples 130-805C-42X-CC through 130-805C-52X-CC. This interval is also characterized by the continuous occurrences of *Triquetrorhabdulus carinatus*, indicating Zone NN2. The underlying six samples (Samples 130-805C-53X-CC through -58X-CC) contain no age-diagnostic species. These samples may be assigned to the NN2/NN1 zonal interval. A few specimens of *Sphenolithus ciperoensis* were observed in Sample 130-805C-59X-CC, suggesting a late Oligocene age for this sample. Sample 130-805C-60X-CC contains *Sphenolithus ciperoensis* together with *Cyclicargolithus abisectus*, *C. floridanus*, *Discoaster deflandrei*, and *Sphenolithus moroformis*.

Neither *Helicosphaera recta*, which defines the NN1/NP25 boundary, nor *Dictyococcites bisectus* were found in the Miocene to Oligocene transitional interval. Therefore, this sample was placed in Zone NP25. The state of preservation becomes poor with abundant fragments below Sample 130-805C-61X-CC. *Sphenolithus ciperoensis* and *S. distentus* were observed in Sample 130-805C-61X-CC, which was placed in Zone NP24. The deepest three samples obtained from this hole, Samples 130-805C-62X-CC through -64X-CC contain both *S. distentus* and *S. predistentus* and are placed in early Oligocene Zone NP23.

Planktonic Foraminifers

Planktonic foraminifers were recovered from all of the core-catcher samples from Holes 805A, 805B, and 805C, but they are few in number in some of the lowermost Miocene and all of the upper Oligocene strata at the base of Hole 805C.

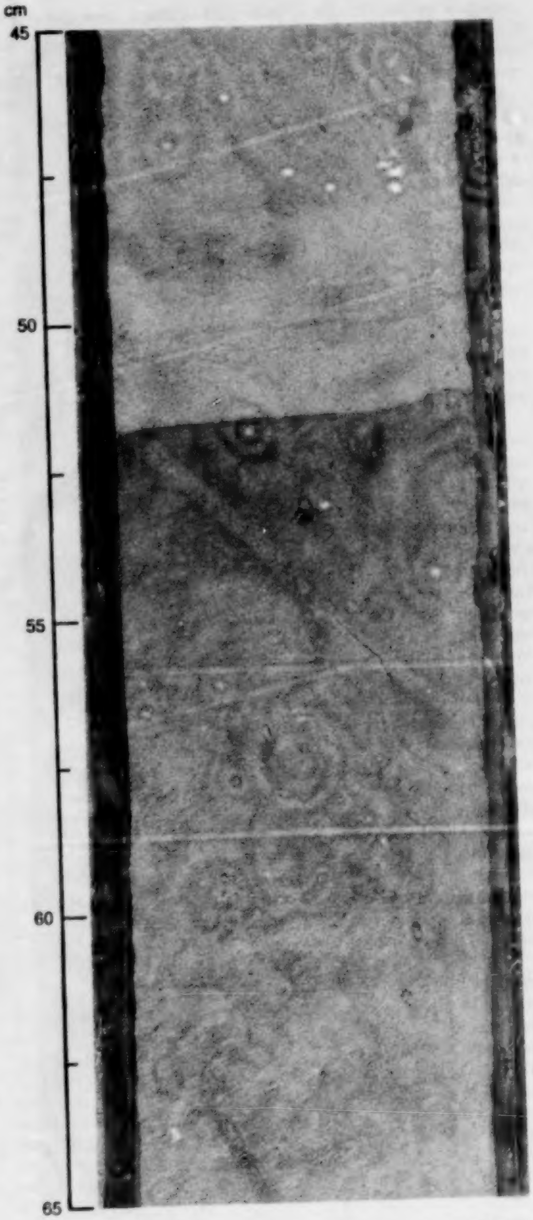

Figure 13. Example of bioturbation (*Zoophycos* trace fossils) easily observed in a darker interval (Section 130-805C-31X-1, 45–65 cm). Note the possible truncation of a burrow at the boundary between the light- and dark-colored intervals.

The section appears to be complete, but that spanning the lower/middle Miocene boundary may be condensed, or contain a hiatus, as at Sites 803 and 804. Zone N15, an interval zone,

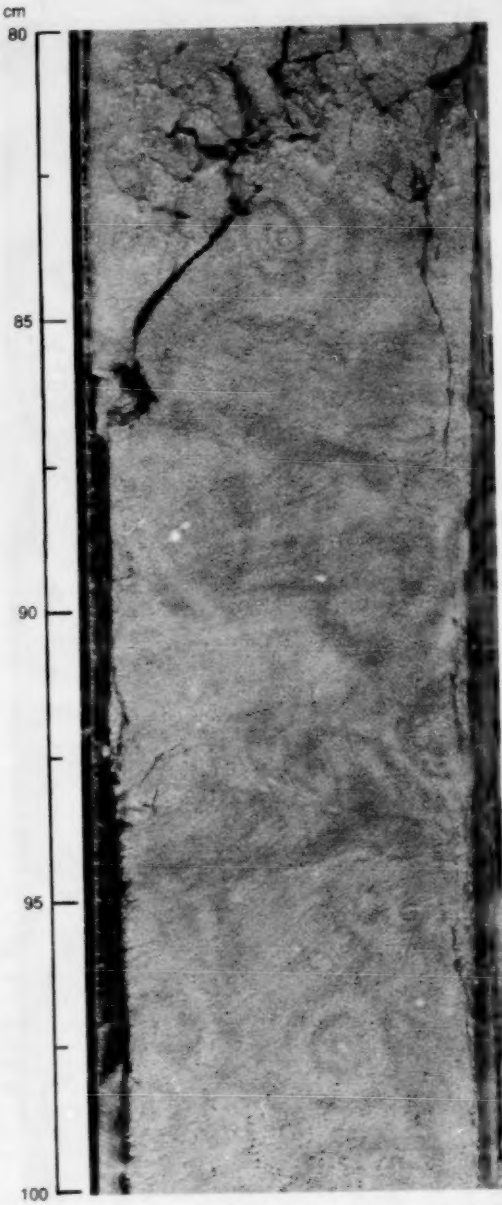

Figure 14. Wispy and contorted(?) laminations (Section 130-805C-33X-4, 80–100 cm). The origin and significance of these features are unclear.

also was not recognized at this site, but it may be represented in a part of Core 130-805B-28X. The lack of diagnostic species in the core-catcher samples examined prevents the resolution of these problems at this time.

The stratigraphy of the three holes is shown in Figure 15 and is discussed below. Remarks concerning the condition of the assemblages and the basis for zonation are also included.

Hole 805A

Planktonic foraminifers are abundant and assemblages are moderately well preserved in the Pleistocene and uppermost Pliocene strata; they are abundant but poorly preserved because of dissolution in the middle Pliocene strata at the base of the hole. The assemblages contain a diversity of tropical species, including many representatives of the genus *Globigerinoides*.

The Pliocene/Pleistocene boundary was placed between Samples 130-805A-2H-CC and -3H-CC, based on the FO of *Globorotalia truncatulinoides*. Sample 130-805A-1H-CC is without *G. tosaensis* and falls within the late part of Zone N22 or within N23. Sample 130-805A-2H-CC contains *G. tosaensis* and *G. truncatulinoides*, which are definitive for Zone N22. Samples 130-805A-3H-CC and -5H-CC contain *G. tosaensis* without *G. truncatulinoides* and are in Zone N21. Between these samples, Sample 130-805A-4H-CC does not contain *G. tosaensis*, possibly because of dissolution, as the assemblage appears more fragmented than assemblages in the adjoining core-catcher samples. The final sample of the hole, Sample 130-805A-6H-CC, is without *G. tosaensis*, but it contains *Sphaeroidinella dehiscens* and was assigned to Zones N19–N20, therefore.

Hole 805B

The first six cores in Hole 805B duplicate the section in Hole 805A. The Pliocene/Pleistocene boundary was placed between Samples 130-805B-2H-CC and -3H-CC; the Miocene/Pliocene boundary between Samples 130-805B-13H-CC and -14H-CC; the middle Miocene/upper Miocene boundary between Samples 130-805B-28H-4, 74–76 cm, and -28H-7, 40–42 cm; and the lower/middle Miocene boundary between Samples 130-805B-40X-CC and -41X-CC. The hole terminated in lower Miocene strata.

Zones N19–N20 were recognized from abundant, moderately well- to well-preserved foraminifers in Samples 130-805B-7H-CC through -9H-CC by the presence of *Sphaeroidinella dehiscens* combined with coiling trends in *Pulleniatina*. The left-to-right coiling change of *Pulleniatina* at 3.8 Ma within this zone was located between Samples 130-805B-9H-CC (left) and -8H-CC (right). *Sphaeroidinella* was not observed below Sample 130-805B-7H-CC. All Pliocene-Pleistocene samples examined contain *Globorotalia tumida*, which has its FO at the base of Zone N18. Sample 130-805B-13H-CC contains *Globorotalia* cf. *tumida* and was assigned to the base of Zone N18.

Upper Miocene Zone N17 was represented in Samples 130-805B-14H-CC through -20H-CC by assemblages containing *Globorotalia plesiotumida* and *G. merotumida*. The presence of *Pulleniatina*, which has been used to divide the zone into A and B units, was noted as low as Sample 130-805B-16H-CC; therefore, its FO at 5.8 Ma falls within Core 130-805B-17H. Except for the assemblages at the base of this zone that show considerable fragmentation, the planktonic foraminifers are moderately well to well preserved. This high degree of fragmentation was also noted in the uppermost core of Zone N16, below which the planktonic foraminifer assemblages are well preserved. Zone N16, recognized through the presence of *Globorotalia merotumida* in the absence of *G. plesiotumida* includes Samples 130-805B-21H-CC through -28H-4, 74–76 cm. *Globorotalia acostaensis* is well represented in these samples; morphologies transitional from *G. continuosa* are present in the lowest sample. Specimens of *Streptochilus* are well represented in this zone. The change from *S. subglobigerum* to *S. latum*, which occurs in about the middle of Zone N16 (Resig, 1989), takes place in Sample 130-805B-24H-CC.

Middle Miocene Zone N14, with abundant *Globorotalia siakensis* (LO at top of N14), was recognized in Samples 130-805B-28H-7, 40–42 cm, through -31X-CC. Only the last sample shows the concurrence of *Globigerina nepenthes* and *G. siakensis*, which defines the zone. This last sample also marks a change in consolidation of the sediment from nannofossil ooze above to nannofossil chalk below. Zones N9 through N12 were assigned to Samples 130-805B-32X-CC through -39X-CC based on the phylogenetic series *Globorotalia peripheroronda*, *G. peripheroacuta*, *G. praefohsi*, and *G. fohsi* and its variants, which occur in stratigraphic succession. Planktonic foraminifers are abundant in this interval and their preservation is moderate. Sample 130-805B-40X-CC is assigned to Zone N8 or N9 on the presence of *Globorotalia archeomenardii* and *Praeorbulina sicana*. *Catapsydrax unicavus* appears to be reworked into this assemblage.

Lower Miocene Zones N6 and N7 cannot be differentiated in Sample 130-805B-41X-CC, which, like the sample above, contains many small specimens of undetermined stratigraphic significance. The age assignment of the sample was based on the absence of *P. sicana* (FO in Zone N8) and of *Globoquadrina binaiensis* (LO in Zone N5). *Catapsydrax unicava* (LO in Zone N6) is rare in the assemblage but may have been reworked as it appears to have been in the stratigraphically next higher sample. *Globigerinatella insueta*, used to define these zones, is not present in the samples from this site. Samples 130-805B-42X-CC through -46X-CC were assigned to Zone N5 based on the presence of *Globoquadrina binaiensis* and the absence of *Globorotalia kugleri*. Within this zone, radiolarians are particularly abundant in Sample 130-805B-43X-CC and horizons of strong fragmentation of specimens are present in Samples 130-805B-42X-CC and -46X-CC. Zone N4 is represented in Samples 130-805B-47X-CC through -50X-CC, the bottom of the hole, based on the presence of common *Globorotalia kugleri* s.s. Many small planktonic specimens are present in these samples. The preservation of the tests is moderate to good.

Hole 805C

The repeated section of this hole into Zone N4 closely parallels that of Hole 805B in planktonic foraminifer abundance, preservation, and stratigraphy, but a few of the zonal boundaries are slightly offset. In this section, an unusual Zone N16 assemblage, in which there are no keeled species, is present in Sample 130-805C-22H-CC. This may reflect a climatic change, as the foraminifers in the sample are well preserved. In a departure from the stratigraphy of Hole 805B, Samples 130-805C-30X-CC through -32X-CC were tentatively assigned to Zone N13 based on the presence of *Globorotalia siakensis* in the absence of *Globigerina nepenthes*. Because *G. nepenthes* is not consistently present, this assignment is preliminary.

The boundary between lower Miocene Zones N4 and N5 is between Samples 130-805C-47X-CC and -48X-CC based on the LO of *Globorotalia kugleri* s.s. The Oligocene/Miocene boundary was placed between Samples 130-805C-55X-CC and -56X-CC, based on the FO of *G. kugleri* s.s. Below this boundary to Sample 130-805C-58X-CC, specimens of similar morphology to *G. kugleri* are present. These specimens are differentiated from *G. kugleri* s.s. by the greater convexity of their spiral sides and their less inclined sutures. The upper part of Zone P22 is characterized by these *G. kugleri* ancestors, which occur with *Globorotalia opima nana*. *G. opima opima*, which marks the top of Zone P21b, is present in Sample 130-805C-61X-CC and the remainder of the core-catcher samples to the bottom of the hole. No *Chiloguembelina* are present in these samples from Zone P21b. Only a few specimens of planktonic foraminifers are present in the lowermost Miocene and in the Oligocene section from Sample 130-805C-55X-CC to the bottom of the hole. These samples contain abundant radiolarians.

Benthic Foraminifers

The core-catcher samples from the Quaternary to lower Miocene section of Hole 805B were examined for benthic foraminifers, which were found to be present in all samples. In addition, a single sample from Hole 805C (Sample 130-805C-60X-CC) was examined to evaluate the upper Oligocene benthic assemblage. Preservation of the benthic tests generally is good, even when the planktonic foraminifers show fragmentation. However, Samples 130-805B-14H-CC (top of the Miocene), -42X-CC, -43X-CC, -46X-CC, and -48X-CC (lower Miocene), and Sample 130-805C-60X-CC (upper Oligocene) contain 50% or more broken benthic tests. Large concentrations of radiolarians in these samples, as well as a low planktonic foraminifer content, indicate carbonate dissolution has occurred. The intervals of increased dissolution appear to be fewer than at Site 803, which lies 200 m deeper, but parts of the lower Miocene and upper Oligocene section at both sites experienced extensive dissolution, resulting in a concentration of benthic tests.

At Site 805, as at Site 803, the benthic assemblages represent lower bathyal to abyssal biofacies. No evidence of transported tests was noted. Articulated whole ostracode valves in Samples 130-805B-13H-CC (lower Pliocene) and -17H-CC (upper Miocene) indicate *in-situ* assemblages.

The stratigraphic succession of assemblages is similar to that at Site 803; the upper Oligocene and lower Miocene assemblages are transitional in that they contain species common in the Paleogene such as *Cibicidoides grimsdalei* and *Buliminella grata* along with a high percentage of *Nuttallides*, a genus that is generally prominent in the Neogene assemblages. The Quaternary assemblages examined from Sites 805 and 803 differ significantly in that *Uvigerina* is better represented at Site 805 and *Nuttallides umbonifera* and *Pseudoparrella exigua* are better represented at Site 803. This may be a result of differences between the two sites in deep-water masses or in surface productivity, hence organic input, or to a combination of these environmental factors. At 3200-m water depth, Site 805 is close to the modern boundary between Pacific Deep Water and Pacific Bottom Water that lies at approximately 3000 m. The Site 805 Quaternary assemblage may be at least partly controlled by the deep-water mass, whereas the Site 803 assemblage has bottom-water affiliation. However, Site 805 (1°13′N) lies nearer the band of equatorial upwelling and may receive more organic flux than Site 803 (2°26′N), which would also favor uvigerinid populations. Although the organic content of the carbonate sediment in the Ontong Java Plateau is low, a small increase in organic carbon from <0.01% to 0.35% was linked to an onset of uvigerinids in the Pliocene section at DSDP Site 586 (Hermelin, 1989).

Listed in Table 4 are the most frequent benthic species present in sand fraction (>0.063 mm) samples representative of the various time-stratigraphic units. Their percent frequencies among the benthic fauna are given, as well as the names of some less frequent members of the assemblages. The following data also are given: B = the percent representation of benthic specimens relative to total foraminiferal content; N = the number of specimens counted for the percent frequency data; and T = the total number of benthic specimens in each approximately 20-cm^3 core-catcher sample, calculated from the sample split used for the census data.

Diatoms

Diatoms were examined in Hole 805B (Samples 130-805B-20H-CC through -50X-CC) and in Hole 805C (Samples 130-805C-1H-CC through -20H-CC and Samples 130-805C-50X-CC through -64X-CC). Quaternary through Oligocene diatoms are present. The assignment of samples to a low-latitude diatom zonation is summarized in Figure 15.

Diatoms are few (rare) and poorly preserved in the Pleistocene sediments (Samples 130-805C-1H-CC through -3H-CC). Between 45 (Sample 130-805C-5H-CC, upper Pliocene) and 426.5 mbsf (Sample 130-805B-45X-CC, middle early Miocene), diatoms are

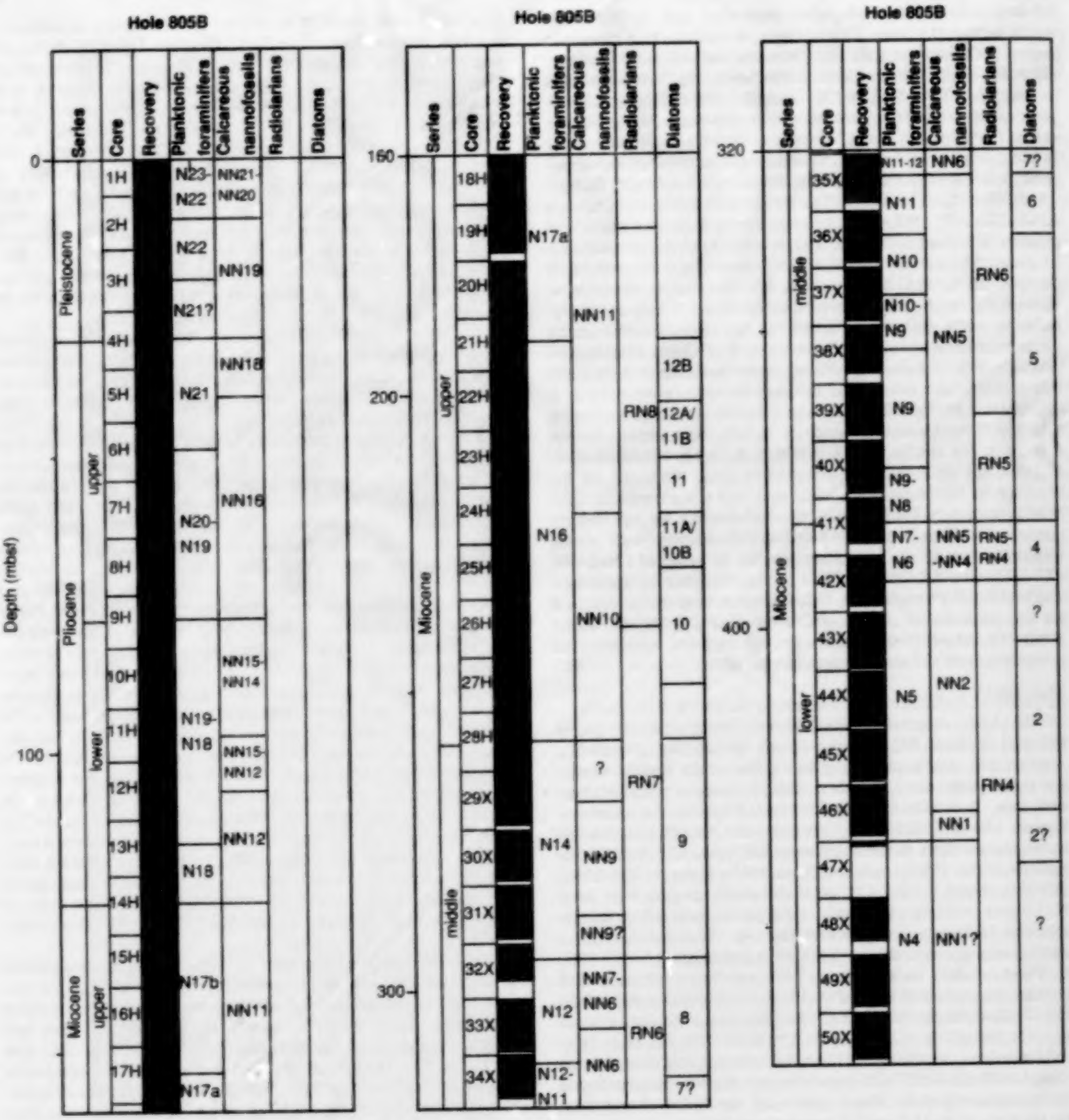

Figure 15. Biostratigraphic hole summaries, Holes 805B and 805C. RN = radiolarian Neogene zone, NTD = Neogene tropical diatom zone, RP = radiolarian Paleogene zone, and NN = nannofossil Neogene zone.

common to abundant, and preservation is generally good. A sharp decrease in abundance and preservation was observed in the early Miocene (Samples 130-805B-46X-CC through -50X-CC) and upper Oligocene (Samples 130-805C-56X-CC through -64X-CC).

Site 805 is the first site on this depth transect with an apparently complete sediment sequence, from the Quaternary NTD *Pseudoeunotia doliolus* Zone (Sample 130-805C-1H-CC) through the Oligocene *Rocella vigilans* Zone (Sample 130-805C-62X-CC). However, poor preservation and low diatom abundances prevented the precise dating of the sediment in the lower Miocene (Samples 130-805B-47X-CC through -50X-CC) and across the Miocene/Oligocene boundary (Sample 130-805C-55X-CC; the *Rocella gelida* Zone may be missing).

Unlike Sites 803 and 804, Site 805 has a complete Miocene sediment sequence (Fig. 15), which includes diatom Zones NTD 13 *Thalassiosira convexa* (Sample 130-805C-14H-CC) through NTD 1 *Rosiella paleacea* (Sample 130-805C-54X-CC). The late Miocene/middle Miocene boundary is located in Sample 130-805B-28H-CC at the top of the NTD 9 *Actinocyclus moronensis*

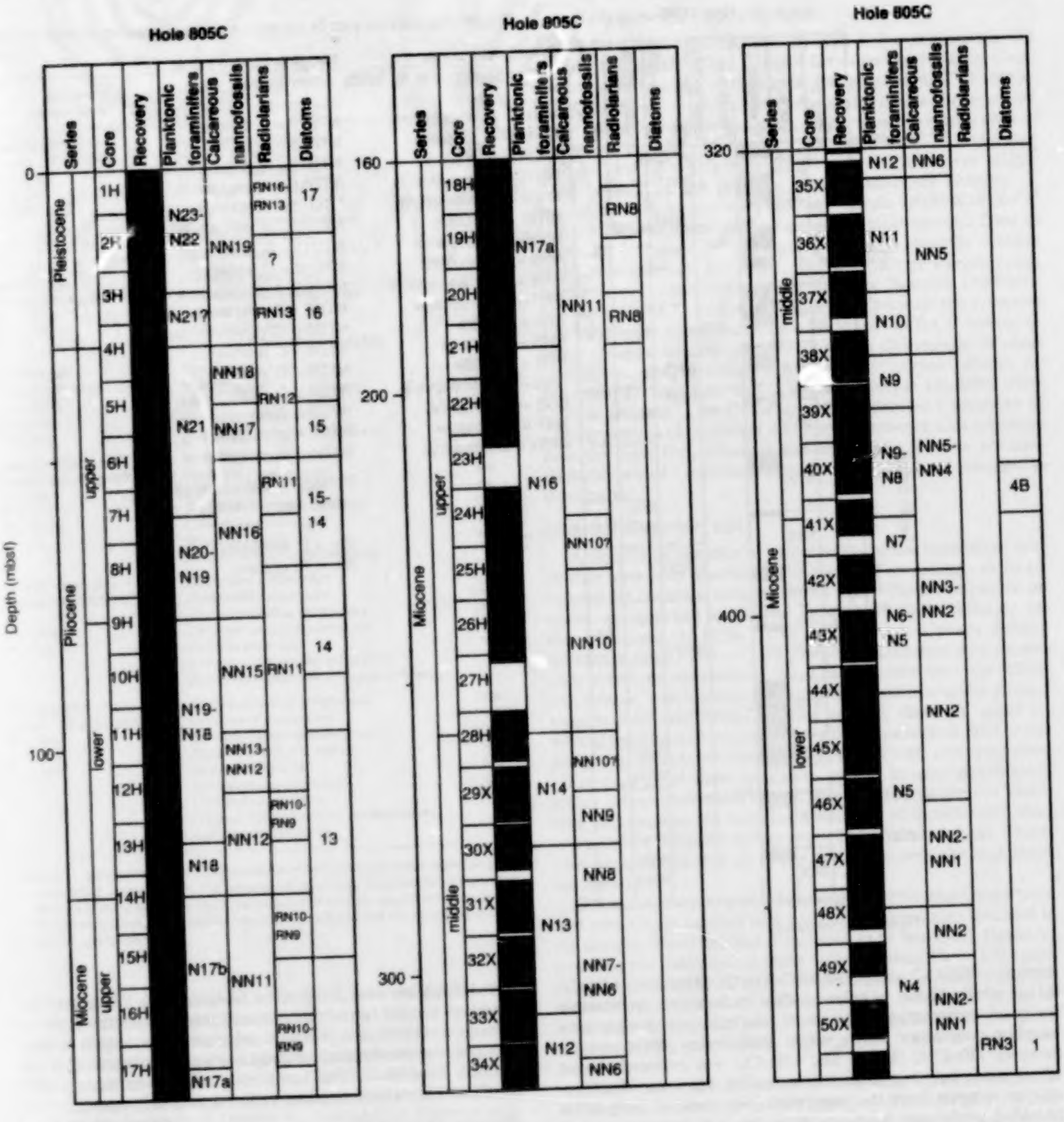

Figure 15 (continued).

Zone. The middle/early Miocene boundary is difficult to locate at Site 805. It may be contained in the basal NTD 5 *Cestodiscus peplum* Zone in Sample 130-805B-40X-CC. The next sample downhole (Sample 130-805B-41X-CC) was assigned to the NTD 4 *Denticulopsis nicobarica* Zone (upper early Miocene). This zone was missing at Sites 803 and 804. The NTD 3 *Triceratium pileus* Zone may be compressed, and the next dated sample (Sample 130-805B-44X-CC) falls within the NTD 2 *Craspedodiscus elegans* Zone.

Diatoms are poorly preserved in the Oligocene samples. Samples 130-805C-56X-CC and -57X-CC are assigned to the *Borgorovia veniamini* Zone, and Samples 130-805C-58X-CC through -62X-CC fall within the *Rocella vigilans* Zone. The age of the last core-catcher sample (Sample 130-805C-64X-CC) could not be determined because of the poor preservation of the diatom assemblage.

Radiolarians

Samples from the three holes at Site 805 were combined to examine a continuous stratigraphic sequence. The following core-catcher samples were examined: 130-805A-1H-CC and -2H-CC; 130-805B-20H-CC through -50H-CC; 130-805C-1H-CC

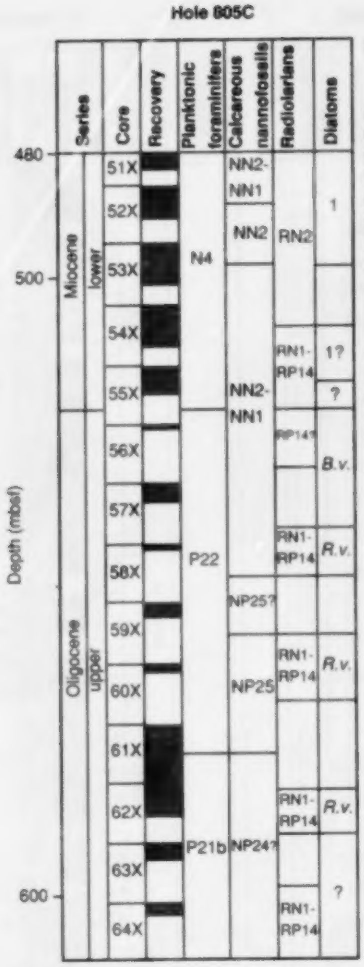

Radiolarian zones
(after Sanfilippo et al., 1985)

RN16 = *B. invaginata*
RN15 = *C. tuberosa*
RN14 = *A. ypsilon*
RN13 = *A. angulare*
RN12 = *P. prismatium*
RN11 = *S. pentas*
RN10 = *S. peregrina*
RN9 = *D. penultima*
RN8 = *D. antepenultima*
RN7 = *D. pettersoni*
RN6 = *D. alata*
RN5 = *C. costata*
RN4 = *S. wolffii*
RN3 = *S. delmontensis*
RN2 = *C. tetrapera*
RN1 = *L. elongata*
RP14 = *D. ateuchus*

Neogene diatom zones
(from Barron, 1985)

NTD17 = *P. doliolus*
NTD16 = *N. reinholdii*
NTD15 = *R. praebergonii*
NTD14 = *N. jouseae*
NTD13 = *T. convexa*
NTD12 = *N. miocenica*
NTD11 = *N. porteri*
NTD10 = *C. yabei*
NTD9 = *A. moronensis*
NTD8 = *C. coscinodiscus*
NTD7 = *C. gigas* var. *diorama*
NTD6 = *C. lewisianus*
NTD5 = *C. peplum*
NTD4 = *D. nicobarica*
NTD3 = *T. pileus*
NTD2 = *C. elegans*
NTD1 = *R. paleacea*

Paleogene diatom zones
(from Fenner, 1985)

B.v. = *B. veniamini*
R.v. = *R. vigilans*

Figure 15 (continued).

through -20H-CC; and 130-805C-50X-CC through -64X-CC (611.0 mbsf). These samples contain radiolarians in variable states of preservation. For most intervals, age assignments based on radiolarians were possible. Radiolarian preservation in Samples 130-805C-1H-CC and -2H-CC was extremely poor, which made age determination uncertain. However, the core-catcher samples from the uppermost two cores of Hole 805A provided useful age information as the radiolarians are preserved in moderate and good condition, respectively.

The following discussion pertains to the zonal assignment of the core-catcher samples examined and their stratigraphically important taxa. Figure 15 summarizes the radiolarian zonation of Holes 805A, 805B, and 805C and correlates these zonations with the zones of other taxa. Evidence for sediment reworking is also discussed.

Quaternary

Sample 130-805A-1H-CC was assigned to the *Buccinosphaera invaginata* Zone, which extends from 0.21 Ma to the present as it contains *B. invaginata*. Significant amounts (18%–19%) of radiolarians are considered to be reworked (see "Sediment Reworking" section below, this chapter). Sample 130-805A-2H-CC belongs to the *Anthocyrtidium angulare* Zone, which is indicated by the presence of *A. angulare* and *Theocorythium trachelium trachelium*. The same zone extends to Sample 130-805C-3H-CC, which contains *Lamprocyrtis heteroporos*.

Pliocene Through Upper Miocene

Sample 130-805C-4H-CC was placed in the *Pterocanium prismatium* Zone because of the presence of *Lamprocyrtis neoheteroporos*, *L. heteroporos*, and *Pterocanium prismatium*. The presence of both species of *Lamprocyrtis* indicates that this sample belongs to the uppermost part of the assigned zone because the change from *Lamprocyrtis heteroporos* to *L. neoheteroporos* is evolutionary. Sample 130-805C-5H-CC was also placed in that zone, but it contains reworked *Stichocorys peregrina* and *Didymocyrtis antepenultima* from upper Miocene and lower Pliocene intervals. Samples 130-805C-6H-CC through -11H-CC were assigned to the *Spongaster pentas* Zone because of the presence of *S. pentas* and *Didymocyrtis avita*.

Table 4. Benthic foraminifers as a percentage of total foraminifers, Site 805.

Age and sample data	Species name	Sample (%)
Quaternary (N22)	*Oridorsalis umbonatus*	10%
Sample 130-805B-2H-CC	*Pullenia bulloides*	8%
B = 1%	*Uvigerina bradyana*	8%
N = 211	*Pseudoparrella exigua*	7%
T = 3,376	*Cassidulina* sp.	6%
	Pacinonion novozealandicum	6%
	Melonis pompilioides	5%
	(Others: *Cibicidoides mundulus*)	
early Pliocene (N18)	*Nuttallides umbonifera*	10%
Sample 130-805B-13H-CC	*Globocassidulina subglobosa*	7%
B = <1%	*Pullenia bulloides*	5%
N = 296	*Eggerella bradyi*	5%
T = 2,368	(Others: *Cibicidoides mundulus*)	
late Miocene (N17)	*Siphouvigerina* sp.	10%
Sample 130-805B-18H-CC	*Melonis affinis*	6%
B = <1%	*Pleurostomella acuminata*	6%
N = 195	*Nuttallides umbonifera*	5%
T = 780	(Others: *Cibicidoides mundulus*)	
middle Miocene (N11)	*Nuttallides umbonifera*	10%
Sample 130-805B-35X-CC	*Oridorsalis umbonatus*	9%
B = 1%	*Eggerella bradyi*	7%
N = 172	*Globocassidulina subglobosa*	6%
T = 1,376	*Cibicidoides mundulus*	6%
	Brizalina pusilla	5%
	(Others: *Bolivinopsis cubensis*)	
early Miocene (N4)	*Nuttallides umbonifera*	17%
Sample 130-805B-50X-CC	*Oridorsalis umbonatus*	14%
B = <1%	*Globocassidulina subglobosa*	13%
N = 174	*Linaresia pseudogrosserugosa*	6%
T = 348	*Pullenia bulloides*	6%
	(Others: *Cibicidoides grimsdalei*, *Buliminella grata*, *Bolivinopsis cubensis*)	
late Oligocene (P22)	*Globocassidulina subglobosa*	24%
Sample 130-805C-60X-CC	*Oridorsalis umbonatus*	10%
B = 5%	*Linaresia pseudogrosserugosa*	7%
N = 375	*Pseudoparrella* aff. *exigua*	6%
T = 375	*Siphonodosaria* sp.	6%
	Gyroidinoides girardanus	6%
	Cassidulina spinifera	6%
	(Others: *Cibicidoides* cf. *subhaidingeri*, *Bolivinopsis cubensis*)	

Notes: B = the percentage of representation of benthic specimens relative to total foraminifer content; N = the number of specimens counted for the percent frequency data; and T = the total number of benthic specimens in each approximately 20-cm^3 core-catcher sample, calculated from the sample split used for the census data.

Samples 130-805C-12H-CC, -14H-CC, and -16H-CC are in either the *Didymocyrtis penultima* Zone or the *S. peregrina* Zone as these zones cannot be differentiated. The samples contain *D. penultima*, *S. peregrina*, *Spongaster berminghami*, and *Solenosphaera omnitubus*. Samples 130-805C-18H-CC through -25H-CC were placed in the *Didymocyrtis antepenultima* Zone, based on the presence of *Diartus hughesi* and/or *Didymocyrtis antepenultima*.

Middle Miocene

Sample 130-805B-26X-CC was placed in the upper part of the *Diartus petterssoni* Zone because of the presence of *Didymocyrtis laticonus* and *D. petterssoni*. Samples 130-805B-28X-CC, -30X-CC, and -31X-CC also belong to the *D. petterssoni* Zone, an assignment further substantiated by the presence of *Lithopera neotera*, in addition to the two taxa already mentioned. Samples 130-805B-32X-CC through -38X-CC were placed in the *Dorcadospyris alata* Zone as they all contain *D. alata* and/or *Lithopera renzae*.

Lower Miocene Through Oligocene

Samples 130-805B-39X-CC and -40X-CC were placed in the *Calocycletta costata* Zone because it can be bracketed by *Calocycletta costata* and *Dorcadospyris forcipata*. Sample 130-805B-41X-CC belongs to either the *Calocycletta costata* Zone or the upper part of the *Stichocorys wolffii* Zone as it contains *Dorcadospyris dentata*. Samples 130-805B-42X-CC through -50X-CC (473.3 mbsf) were placed in the *Stichocorys wolffii* Zone because of the presence of *Dorcadospyris simplex*, *S. wolffii*, and *Cyclampterium pegetrum*. Sample 130-805C-50X-CC (475.5 mbsf) was placed in the *Stichocorys delmontensis* Zone as it can be bracketed by the presence of *Cyrtocapsella cornuta* and *Cyclampterium leptetrum*. The presence of *Cyrtocapsella tetrapera* and *Theocyrtis annosa* brackets Samples 130-805C-51X-CC, -52X-CC, and -53X-CC in the *Cyrtocapsella tetrapera* Zone. Samples 130-805C-54X-CC through -64X-CC belong to either the *Lychnocanoma elongata* or the *Dorcadospyris ateuchus* zones. They typically contain *Dorcadospyris papilio*, *D. forcipata*, *D. ateuchus*, *and T. annosa*. Sample 130-805C-56X-CC was assigned to the *D. ateuchus* Zone because a specimen of *Lychnocanoma* cf. *trifolium* was found. However, this specimen does not have feet, although the rest of the features are conformable with *L. trifolium*, and therefore the zonal assignment is tentative.

Sediment Reworking

A significant number of radiolarians in the uppermost core catcher have been reworked. The extent of reworking can be estimated by counting radiolarians of two different refractive indexes, as reworked specimens have significantly different indexes. Sample 130-805A-1H-CC, mounted in Canada Balsam (refractive index, ND = 1.53), contains abundant and moderately preserved radiolarians. Most radiolarians have low refractive indexes, which makes them nearly transparent under a transmission light microscope. In this sample, there are many reworked specimens of late Miocene radiolarians such as *Stichocorys peregrina*, *S. delmontensis*, and *Didymocyrtis antepenultima*. More than 20 of these specimens appear to have significantly higher refractive indexes than upper Pleistocene and/or Holocene radiolarians. No reworked specimens of significantly older age with low refractive indexes have been found thus far. Therefore, we assumed that all of the specimens with the high index are reworked.

There are many species of Quaternary, Pliocene-Quaternary, and even longer ranging taxa with high indexes also admixed in the sample. These are also considered to be reworked. Based on counting the specimens in three different areas (N = 139 specimens in each area) at 100× magnification of each slide, the following percentages of radiolarians are considered to be reworked: from 63 to 125 μm, N = 18.3% and standard deviation (SD) = 1.5%; greater than 125 μm, N = 19.1% and SD = 3.3%.

The reworked radiolarians must have been buried once (probably upslope somewhere) as they remain well preserved. At a later time (<0.21 Ma, during the *Buccinosphaera invaginata* Zone), these specimens were transported to the present site. Because these radiolarians were buried once and probably have a cation coating on their skeletal surfaces, they were not subjected to further dissolution to a significant extent.

PALEOMAGNETISM

Introduction

Paleomagnetic analysis in Hole 805B began in Cores 130-805B-1H and -2H at 1-cm intervals, with measurement of both the natural remanent magnetization (NRM) and the remanence

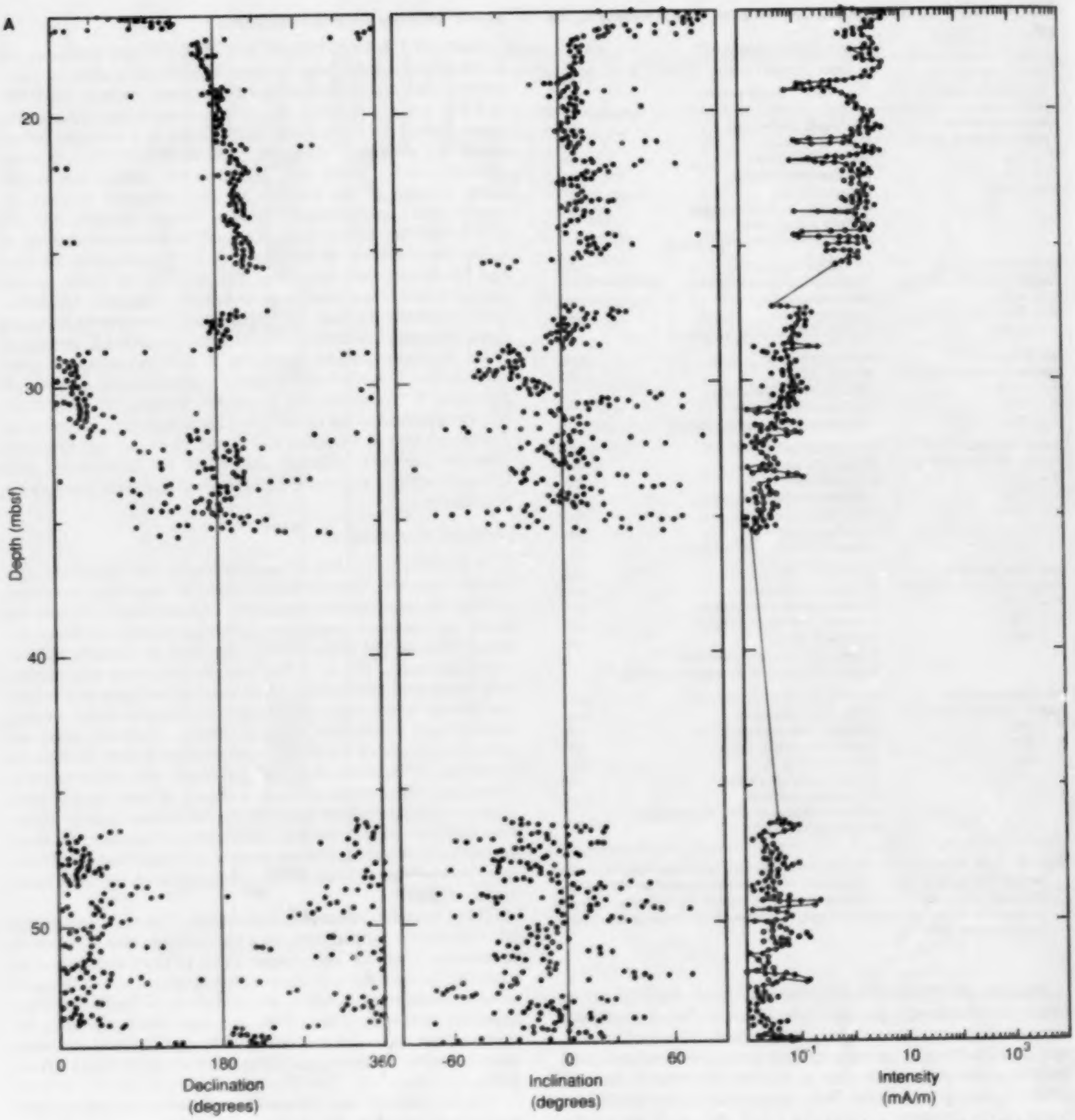

Figure 16. Oriented declination, inclination, and intensity plots for (A) Cores 130-805B-3H to -6H and (B) Cores 130-805C-3H to -5H. Note the difference in the depth scales.

after 15-mT alternating field (AF) demagnetization. Measurement intervals were increased to 3 cm at Core 130-805B-3H, to 5 cm at Core 130-805B-5H, and to 10 cm at Core 130-805B-10H. Magnetization intensity after AF demagnetization in Hole 805B drops to less than 0.1 mA/m at depths below 32 mbsf (Fig. 16). This corresponds to a magnetic moment less than 1 order of magnitude greater than that of the sample holder, and thus below the practical limit of measurement on the shipboard cryogenic magnetometer. Therefore, AF demagnetization in this hole was limited to one section per core after Core 130-805B-10H. The behavior of each demagnetized section, and of the NRM of the whole core, was monitored throughout the remainder of Hole 805B for evidence of an increase in intensity and/or an improvement in the magnetization direction record. Most cores below Core 130-805B-4H show evidence of a magnetic overprint, with a steep negative inclination (between −60° and −80°), that was largely removed by 15-mT AF demagnetization. Intensities after demagnetization are frequently <10% of the NRM

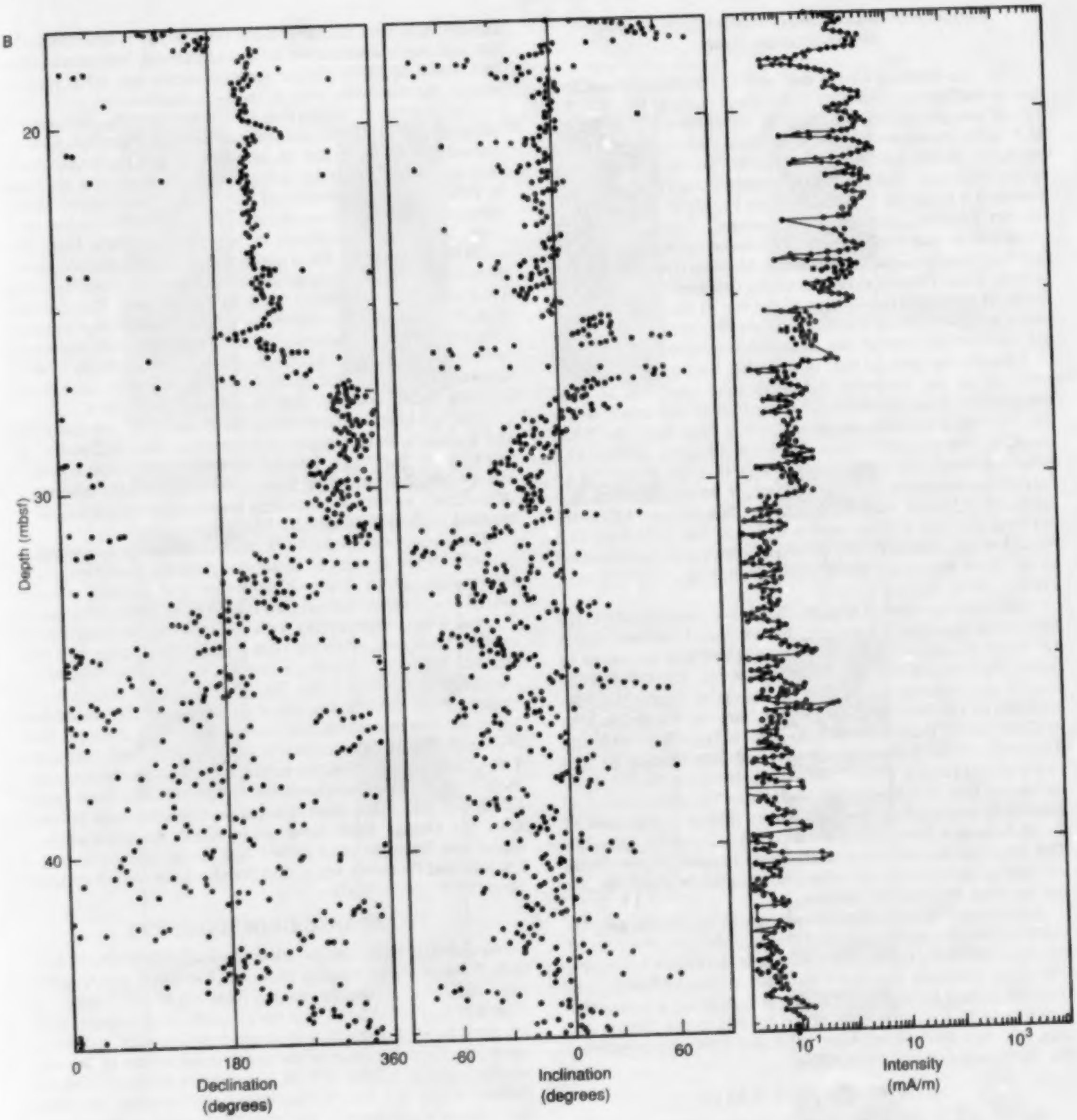

Figure 16 (continued).

intensity. It is suspected that this component was acquired during or after drilling, possibly within the regions near the base and the top of the drill string where the ambient field is concentrated. No consistent primary magnetizations are present below Core 130-805B-5H. Demagnetization of the first few cores of Hole 805C follows a similar pattern to that of Hole 805B (Fig. 16). It was clear that nothing would be gained by the measurement of cores from Hole 805C over most of the Miocene sequence, so measurement was discontinued after Core 130-805C-10H. Measurement in Hole 805C began again at Core 130-805C-58X and continued to 130-805C-64X, but no consistent primary magnetization could be determined from this interval.

Cores from the dedicated Hole 805A were not to be demagnetized and thus were not included in the routine paleomagnetic analysis. The NRM of whole-round Cores 130-805A-3H and -4H was measured, however. Both cores show evidence of overprinting, resulting in anomalously high negative inclinations. Polarities can be tentatively identified in Core 130-805A-3H and in part of Core 130-805A-4H, but these are subject to confirmation by demagnetization.

Pliocene-Holocene Magnetostratigraphy and Sedimentation Rate

Only the Brunhes Chron and part of the Matuyama Chron can be confidently identified in the three holes at Site 805 (Fig. 17). A normal interval within Core 130-805B-4H from 28.6 to 31.6 mbsf correlates with the Olduvai Subchron; the lower boundary of this subchron is the oldest datable magnetic event in the sequence. Although recognizable polarity extends for a further 3.9 m to the bottom of Core 130-805B-4H, neither of the two Réunion events can be recognized. The Jaramillo Subchron can be tentatively identified in Holes 805B and 805C, but it unfortunately spans the core break between Cores 2H and 3H in both holes. Flow-in at the top of the first section of Core 130-805B-3H prevented recognition of the top of the Jaramillo Subchron in Hole 805B, and a similar disruption in Core 130-805C-3H obscured the base of the Jaramillo Subchron in Hole 805C.

Both the top and the base of what has been provisionally interpreted as the Jaramillo Subchron were identified in Hole 805A within Core 130-805A-3H from 15.4 to 16.9 mbsf. Below this interval, a second interval of normal polarity in the NRM record is present within Core 130-805A-3H from 18.8 to 19.6 mbsf. Although this event does not appear in the record for either of the two other holes at this site, it does correlate with a normally polarized interval seen at Site 804 in Core 130-804B-2H from 11.5 to 11.7 mbsf and in Core 130-804C-2H from 12.3 to 12.5 mbsf. This normally polarized interval may correspond to the Cobb Mountain Event (Mankinen et al., 1978; Jacobs, 1984, p. 165).

Three minor events of apparently normal polarity within the Matuyama Reversed Chron can be correlated between Cores 130-805B-3H and 130-805C-3H; two of these also appear to be present in Core 130-805A-3H. A minor event, <1 m below the base of the Brunhes Chron, can be correlated from Core 130-805B-2H to 130-805C-2H. Two other minor events near the base of Core 130-805B-2H have no equivalent in the other two holes. The nature of all these minor events, and their relation (if any) to the global polarity record, is unclear. However, the three minor events seen in Cores 130-805B-3H and 130-805C-3H are all marked by sudden decreases in intensity from a background of 2-3 mA/m to a value at the event of 0.1-0.2 mA/m (Fig. 18). This behavior may suggest a relationship between events of this sort and zones of increased reduction potential in which magnetite has been removed by solution.

Age controls on the sedimentation rate in Hole 805B are provided by the base and top of the Olduvai Subchron, the base of the Jaramillo Subchron, and the Brunhes/Matuyama boundary. The three youngest age-depth data are nearly collinear, and their line of best fit intersects the origin, indicating a sedimentation rate of 17.1 m/m.y. from about 1.7 Ma to the present day (Fig. 19). Age controls in Holes 805A and 805C are consistent, but very limited, with this rate.

SEDIMENTATION RATES

The biostratigraphic age-depth indicators observed in the cored sediments at Site 805 suggest a continuous depositional history from the present to approximately the lower Oligocene/upper Oligocene boundary at about 30 Ma. The rates by which these sediments were deposited varied by a factor of 3; the average rate over the entire 30-m.y. interval was estimated to be 23 m/m.y.

All age-depth indicators observed in the three holes cored are listed in Table 5, and the results from Holes 805B and 805C are shown graphically in Figures 20 and 21, respectively. In the 5-15-Ma interval, the data from Hole 805C appear somewhat more coherent than the corresponding plots from Hole 805B, which simply reflects the fact that more (and more widely spread) data were available from Hole 805B. When comparing the age-depth distribution of the calcareous indicators alone, this results in highly similar patterns of the age-depth progression in the two holes, also in the 5-15-Ma interval.

The maximum penetration of the stratigraphic column was obtained in Hole 805C, and shorter intervals from this hole are plotted in Figures 22 and 23, respectively. The particular events used as control points for sedimentation rate changes are listed in Table 6. The distribution of the age-depth indicators clearly indicates a rate change at about 2 Ma (Fig. 22) in the late Pliocene. The stepwise increase in sedimentation rate from that point and back to 8.7 Ma is perhaps less well constrained, as the distribution of points in principle would allow a uniform rate (36.5 m/m.y.) to be drawn from 2.07 to 8.7 Ma. The distribution of the age-depth indicators in the lower Neogene-upper Oligocene interval, however, offers many possible alternative sedimentation rates to the ones suggested in Table 6; the inferred constant rate from 18.8 to 29.9 Ma, for example, presumably contains more variability than is indicated in Table 6.

The rate histories from Holes 805B and 805C are compared in Figure 24. The two largest changes occur close to 2 and 9 Ma, respectively. The 7-m.y. interval between these points of major change is characterized by high sedimentation rates (about 25-40 m/m.y.), and the surrounding intervals are characterized by medium high rates (about 10-20 m/m.y.).

The transition period into the high sedimentation rate regime just after 9 Ma appears to be shorter than the transition out of this regime, which clearly is smoother and perhaps even occurred in a stepwise fashion throughout most of the Pliocene (5, 3.5, and 2 Ma, respectively). This Pliocene change from high to medium high sedimentation rates is considered to be well constrained biochronologically, a fact that cannot be claimed for the sharp change at 8.7 Ma. Yet, both the shape and timing of change of this curve closely mimic paleomagnetically constrained sedimentation rate curves that recently have been obtained from the western equatorial Indian Ocean (Peterson and Backman, 1990). This suggests that the productivity and preservation patterns changed on an interbasinal scale, presumably from related causes and hence that these changes were synchronous. If this is true, the change from lower early-middle Miocene rates to higher late Miocene rates indeed was sharp, occurring over a few hundred thousand years, and the change probably occurred closer to 8 than to 9 Ma.

INORGANIC GEOCHEMISTRY

We collected 24 interstitial water samples at Site 805: 11 from Hole 805B at depths ranging from 183.7 to 469.2 mbsf, and 13 from Hole 805C at depths ranging from 6.0 to 165.7 mbsf and from 449.3 to 578.2 mbsf. For the purpose of this report, these are considered to constitute a single depth profile. Interstitial water samples cover most of the depth range drilled of the nannofossil ooze and chalk of Unit I, the single lithologic unit recognized at Site 805 (see "Lithostratigraphy" section, this chapter). Chemical gradients in the interstitial waters at this site (Table 7) are generally similar to those at Sites 803 and 804, being governed by the biogenic, organic-carbon-poor character of the sediments and by diffusive influence of basalt alteration reactions at depth. The magnitude of the chemical gradients at Site 805, the shallowest of the first three sites drilled on Leg 130, are generally equal to or larger than those at Site 803. The chemical gradients in Site 803 are, in turn, larger than those at the deepest site, Site 804. These differences are consistent with more organic carbon burial at shallower water depths; or, because Site 805 is closer to the equator, the sedimentation rate at Site 805 is the highest of the first three sites.

Chlorinity increases almost 3% to 570 mM at 32.8 mbsf (Core 130-805C-4H) and increases further to values greater than

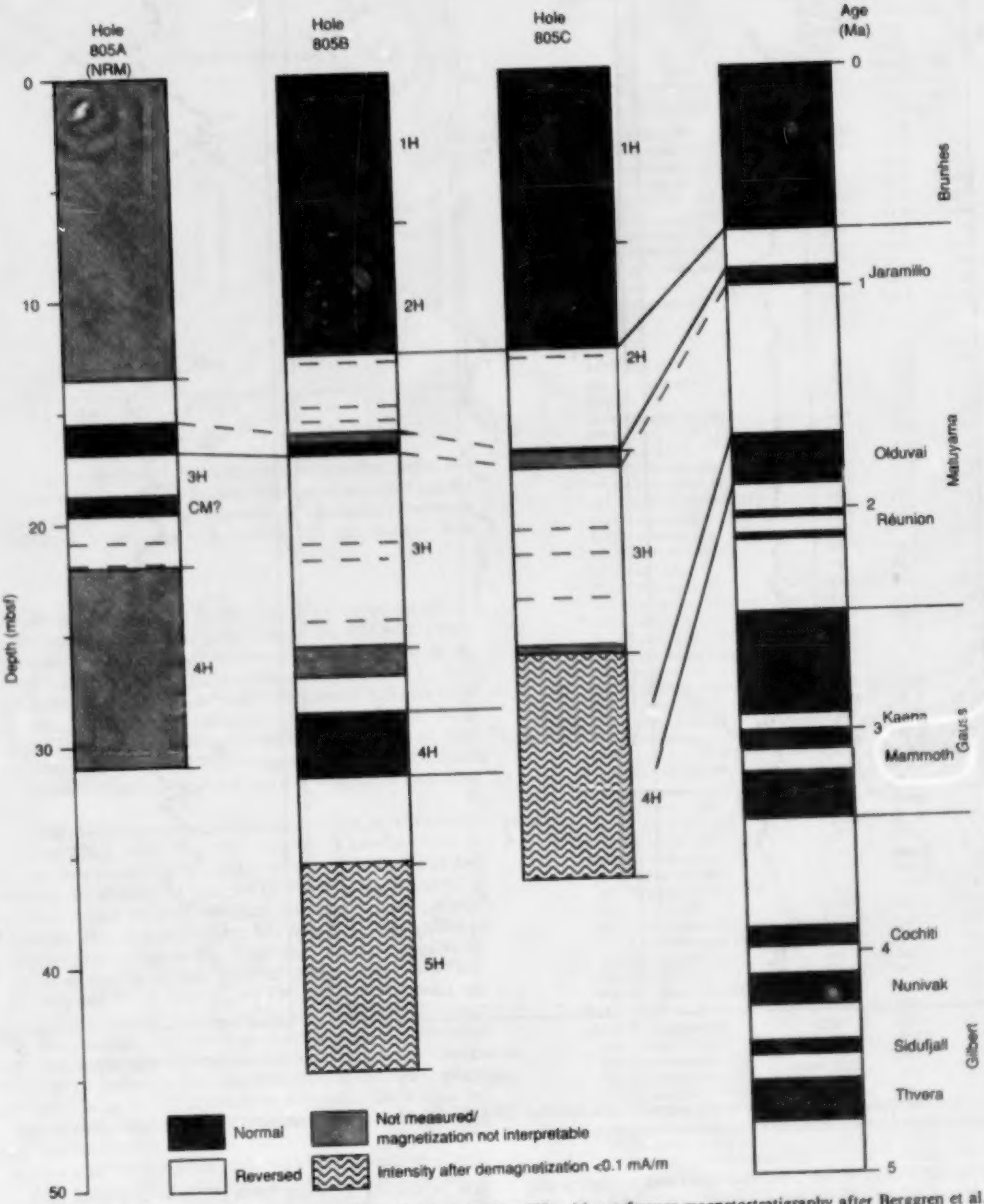

Figure 17. Pliocene-Holocene magnetostratigraphy for holes at Site 805, with a reference magnetostratigraphy after Berggren et al. (1985). Black intervals indicate normal polarization; white, reversed polarization. Half-tone shading indicates unknown polarity. Dashed lines within columns are short events; areas with wavy lines indicate that intensity after demagnetization is <0.1 mA/m. Confident ties between columns are shown by an unbroken line; dashed lines indicate ties between minor events.

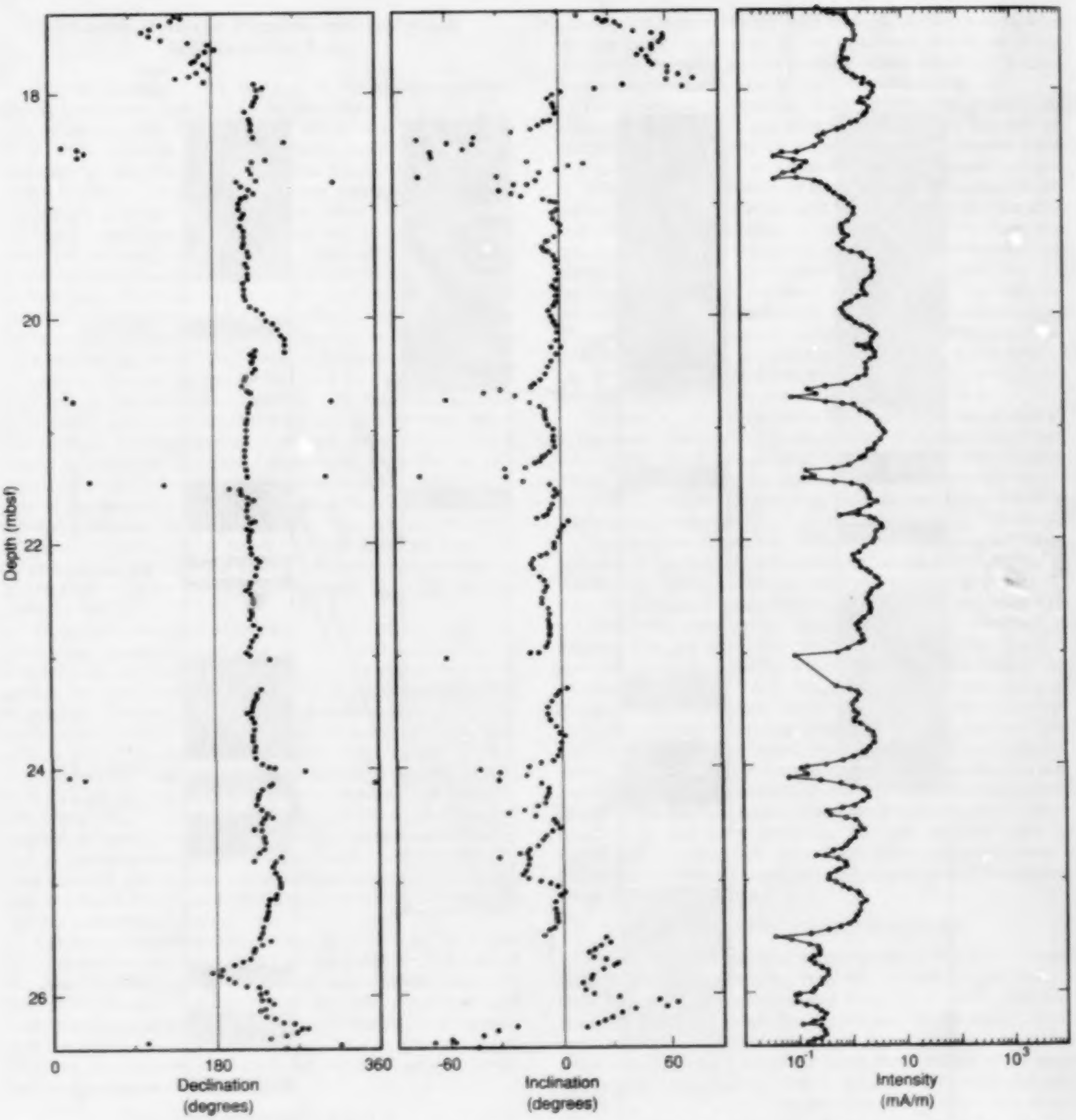

Figure 18. Oriented declination, inclination, and intensity plots for Core 130-805C-3H. Note the three apparent polarity events at 20.7, 21.4, and 24.1 mbsf, and the large decrease in intensity associated with each.

580 mM by 165.7 mbsf (Core 130-805C-18H) and as high as 590 mM at depths below 450 m, for a total increase of 6.5% (Fig. 25). Chlorinity at Site 805 is greater than that at Site 804, with a depth profile roughly similar to that at Site 803. Salinity, measured refractively as total dissolved solids, increases with depth from 35.0 to 36.5 g/kg (Table 7). Sodium concentrations measured by flame emission spectrophotometry (Table 7) and those estimated by charge balance calculations generally agree to within <1.5%. Sodium concentrations increase 4% to 500 mM from 6.0 to 578.2 mbsf and are higher than those at Sites 803 and 804. Alkalinity increases from ~3 mM to a peak of 5 mM at 80.3 mbsf, then decreases to values around 4 mM. There is a small secondary alkalinity maximum of 4.8 mM at 324.9 mbsf, and a further decrease to 2.6 mM at 578.2 mbsf (Fig. 25). Alkalinity values at Site 805 are consistently larger, and the peak value occurs at a greater depth than at Site 804, the deepest site drilled. Alkalinity values at Site 805 are generally similar to those at Site 803, but the maximum is larger here at Site 805.

Sulfate concentrations decrease by nearly 25% from 28.5 mM at 6.0 mbsf to values around 22 mM by 165.7 mbsf and

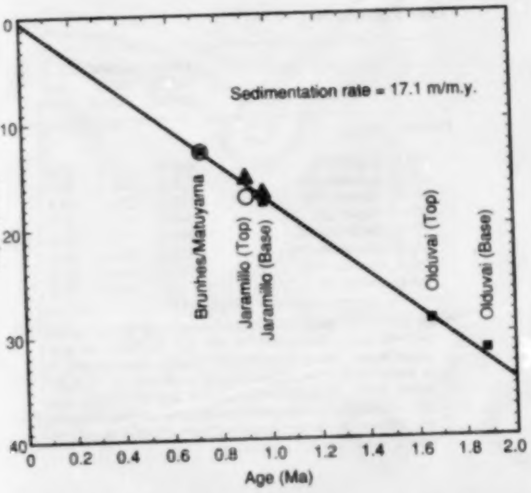

Figure 19. Age vs. depth plot, Site 805, with linear sedimentation rate fitted to Hole 805B data for the Brunhes/Matuyama boundary and the base of the Jaramillo and the top of the Olduvai subchrons. Filled triangle = Hole 805A, filled square = Hole 805B, and open circle = Hole 805C.

then are fairly constant with depth (Fig. 25). The extent of sulfate depletion at Site 805 is greater than at Site 804 and is similar to that at Site 803. Phosphate concentrations are below the detection limit of 1-2 μM in all samples analyzed (Table 7). Ammonia concentrations reach a maximum around 250 μM from 183.7 to 295.1 mbsf and decrease to 150-160 μM with depth (Fig. 25). These concentrations are higher than those at Sites 803 and 804, suggesting that more organic matter was oxidized or that the sedimentary sinks for ammonia were more limited at Site 805.

Dissolved silica concentrations increase with depth to around 1200 μM at 578.2 mbsf (Fig. 25). The depth profile, both in shape and concentration, is similar to those at Sites 803 and 804, despite the absence at Site 805 of the intervals enriched in radiolarians found at Sites 803 and 804 (see "Lithostratigraphy" section, this chapter). There are no obvious dissolved Si decreases corresponding to the occurrence of small chert nodules found at depths of 344.35 mbsf (Core 130-805C-37X-2, 135-137 cm) and 370.6 mbsf (Core 130-805C-40X-1, 0-10 cm) in Hole 805C (but not in Hole 805B; see "Lithostratigraphy" section, this chapter). The extent of chert formation is probably limited. Manganese concentrations are generally below the detection limit (<2-3 μM), with the exception of the two shallowest samples (Table 7). No increase in dissolved Mn is apparent with the increase in dissolved Si, despite previous reports suggesting this correlation (Gieskes, 1981).

Calcium concentrations increase with depth, with an average gradient of 4 mM/100 m (Fig. 26), similar to that observed at Site 804. The Ca depth profile is generally similar to that at Site 803 as well, except below 500 mbsf. The profile at Site 803 is steeper than that from Site 805, presumably because of decreased diffusion coefficients as sediment porosity decreases. Magnesium concentrations decrease with depth, with a gradient of −3.4 mM/100 m (Fig. 25), similar to those at Sites 803 and 804. Magnesium and Ca concentrations are linearly correlated (R^2 = 0.98), with a ΔCa/ΔMg ratio approximately equal to −1.2. The linear correlation is indicative of the conservative

Table 5. Bio- and magnetostratigraphic events determined at Site 805.

Event	Upper depth (mbsf)	Lower depth (mbsf)	Age (Ma)
130-805A-			
FO *E. huxleyi* (N)	0	3.0	0.28
LO *P. lacunosa* (N)	3.0	12.5	0.46
LO *C. tuberosa* (R)	3.0	12.5	0.50
LO *G. tosaensis* (F)	3.0	12.5	0.60
LO *N. reinholdii* (D)	3.0	12.5	0.65
LO *C. macintyrei* (N)	22.0	31.5	1.45
LO *D. brouweri* (N)	22.0	31.5	1.89
OA *D. triradiatus* (N)	22.0	31.5	2.07
FO *G. truncatulinoides* (F)	12.5	22.0	1.90
LO *D. surculus* (N)	41.0	50.5	2.45
FO *G. tosaensis* (F)	41.0	50.5	3.10
130-805B-			
LO *P. lacunosa* (N)	6.7	16.2	0.46
LO *G. tosaensis* (F)	6.7	16.2	0.60
Brunhes (O)	12.6	12.6	0.73
LO *C. macintyrei* (N)	33.9	35.2	1.45
Olduvai (T)	28.6	28.6	1.66
Olduvai (O)	31.6	31.6	1.88
LO *D. brouweri* (N)	33.9	35.7	1.89
OA *D. triradiatus* (N)	33.9	35.7	2.07
FO *G. truncatulinoides* (F)	16.2	25.7	1.90
LO *D. pentaradiatus* (N)	43.4	44.7	2.35
LO *D. surculus* (N)	43.4	44.7	2.45
LO *D. tamalis* (N)	44.7	54.2	2.65
LO *G. altispira* (F)	54.2	63.7	2.90
FO *G. fistulosus* (F)	63.7	73.2	2.90
LO *Sphaeroidinellopsis* spp. (F)	54.2	63.7	3.00
FO *S. dehiscens* (F)	63.7	73.2	3.00
LO *R. pseudoumbilica* (N)	73.2	82.7	3.56
LO *G. nepenthes* (F)	92.2	101.7	3.90
LO *C. acutus* (N)	101.7	111.2	4.6
LO *D. quinqueramus* (N)	120.7	130.2	5.0
FO *G. tumida* (F)	120.7	130.2	5.2
FO *P. spectabilis* (F)	120.7	130.2	5.2
LO *G. conglobatus* (F)	120.7	130.2	5.3
FO *P. primalis* (F)	149.2	158.7	5.8
FO *S. omnitubus* (R)	196.7	206.2	6.4
FO *Amaurolithus* (N)	196.7	206.2	6.7
LO *N. porteri* (D)	196.7	206.2	6.7
LO *T. burckliana* (D)	215.7	225.2	7.0
FO *G. plesiotumida* (F)	177.7	187.2	7.1
LO *N. porteri* (D)	196.7	206.2	7.2
LO *D. hughesi* (R)	196.7	206.2	7.2
FO *D. quinqueramus* (N)	215.7	225.2	7.5
LO *C. yabei* (D)	234.7	244.2	7.5
LO *T. burckliana* (D)	215.7	225.2	8.0
FO *S. berminghami* (R)	234.7	244.2	8.0
LO *D. pettersoni* (R)	253.7	263.2	8.2
LO *S. wolfii* (R)	282.5	292.2	8.2
FO *N. dutertrei* s.l. (F)	187.2	196.7	8.0
LO *C. yabei* (D)	234.7	244.2	8.6
LO *D. hamatus* (N)	263.2	272.9	8.7
LO *Catinaster* (N)	263.2	272.9	8.8
LO *A. moronensis* (D)	253.7	263.2	8.9
FO *D. neohamatus* (N)	272.9	282.5	9.0
FO *N. acostaensis* (F)	260.4	263.1	10.2
LO *G. siakensis* (F)	260.4	263.1	10.4
LO *L. thornburgi*	292.2	301.4	10.5
FO *D. hamatus* (N)	282.5	292.2	10.5
LO *D. punctata* f. *hustedtii* (D)	320.5	330.0	10.7
LO *C. coscinodiscus* (D)	292.2	301.4	10.7
FO *H. cuneiformis* (D)	292.2	301.4	11.2
LO *A. moronensis* (D)	253.7	263.2	11.3
FO *G. nepenthes* (F)	292.2	301.4	11.3
LO *G. fohsi lobata/robusta* (F)	292.2	301.4	11.5
LO *C. cornuta* (R)	301.4	311.0	11.8
LO *D. punctata* f. *hustedtii* (D)	320.5	330.0	12.2
LO *C. coscinodiscus* (D)	292.2	301.4	12.2
FO *H. cuneiformis* (D)	292.2	301.4	12.6
LO *C. nitescens* (N)	301.4	311.0	12.8
LO *C. lewisianus* (D)	320.5	330.0	12.9
LO *C. floridanus* (N)	311.0	320.5	13.1

Table 5 (continued).

Event	Upper depth (mbsf)	Lower depth (mbsf)	Age (Ma)
130-805B- (Cont)			
LO *C. lewisianus* (D)	320.5	330.0	13.5
LO *S. heteromorphus* (N)	320.5	330.0	13.6
FO *G. praefohsi* (F)	330.0	339.7	13.9
LO *C. peplum* (D)	330.0	339.7	14.1
LO *G. peripheroronda* (F)	330.0	339.7	14.6
FO *G. peripheroacuta* (F)	349.4	359.0	14.9
FO *C. peplum* (D)	368.7	378.3	16.4
LO *C. dissimilis* (F)	397.7	407.3	17.6
FO *S. heteromorphus* (N)	388.0	397.7	18.6
LO *C. elegans* (D)	407.3	417.0	18.7
LO *S. belemnos* (N)	388.0	397.7	18.8
FO *S. belemnos* (N)	407.3	417.0	20.0
LO *G. kugleri* (F)	436.0	445.5	21.8
130-805C-			
LO *P. lacunosa* (N)	0	7.8	0.46
Brunhes (O)	12.7	12.7	0.73
LO *L. neoheteroporus* (R)	17.3	26.8	1.11
LO *C. macintyrei* (N)	26.8	36.3	1.45
LO *D. brouweri* (N)	26.8	36.3	1.89
OA *D. triradiatus* (N)	26.8	36.3	2.07
FO *G. truncatulinoides* (F)	17.3	26.8	1.90
LO *D. pentaradiatus* (N)	36.3	45.8	2.35
LO *D. surculus* (N)	45.8	55.3	2.45
FO *L. neoheteroporus* (R)	36.3	45.8	2.52
LO *D. tamalis* (N)	45.8	55.3	2.65
LO *G. altispira* (F)	45.8	55.3	2.90
FO *G. fistulosus* (F)	55.3	64.8	2.90
LO *Sphaeroidinellopsis* spp. (F)	64.8	74.3	3.00
LO *G. margaritae* (F)	64.8	74.3	3.40
LO *Sphenolithus* (N)	64.8	74.3	3.45
LO *P. doliolum* (R)	74.3	83.8	3.54
LO *R. pseudoumbilica* (N)	74.3	83.8	3.56
LO *S. pentas* (R)	64.8	74.3	3.78
FO *A. ypsilon* (R)	74.3	83.8	3.78
LO *S. berminghami* (R)	93.3	102.8	3.86
FO *S. pentas* (R)	112.3	121.8	4.25
LO *C. acutus* (N)	102.8	112.3	4.6
LO *S. omnitubus* (R)	102.8	112.3	4.8
LO *D. quinqueramus* (N)	121.8	131.3	5.0
LO *S. corona* (R)	55.3	64.8	5.1
FO *G. tumida* (F)	112.3	121.8	5.2
FO *P. spectabilis* (F)	121.8	131.3	5.2
LO *G. conglobatus* (F)	140.8	150.3	5.3
FO *G. cibaoensis*	140.8	150.3	5.3
LO *A. tritubus* (R)	169.3	178.8	5.4
FO *P. primalis* (F)	150.3	159.8	5.8
LO *C. caepa* (R)	169.3	178.8	6.4
FO *Amaurolithus* (N)	197.8	207.3	6.7
FO *G. plesiotumida* (F)	188.3	197.8	7.1
FO *D. quinqueramus* (N)	216.8	235.8	7.5
FO *A. tritubus* (R)	188.3	197.8	7.7
LO *D. laticonus* (R)	169.3	178.8	8.2
LO *D. hamatus* (N)	264.7	274.4	8.7
LO *Catinaster* (N)	264.7	274.4	8.8
FO *D. neohamatus* (N)	264.7	274.4	9.0
FO *N. acostaensis* (F)	255.1	264.7	10.2
LO *G. siakensis* (F)	255.1	264.7	10.4
FO *D. hamatus* (N)	274.4	284.0	10.5
FO *Catinaster* (N)	284.0	293.7	11.1
FO *G. nepenthes* (F)	274.4	284.0	11.3
LO *G. fohsi lobata/robusta* (F)	302.9	312.6	11.5
LO *C. nitescens* (N)	312.6	322.3	12.8
LO *C. floridanus* (N)	312.6	322.3	13.1
LO *S. heteromorphus* (N)	322.3	331.8	13.6
FO *G. praefohsi* (F)	341.5	351.2	13.9
LO *G. peripheroronda* (F)	351.2	360.9	14.6
FO *G. peripheroacuta* (F)	351.2	360.9	14.9
LO *P. sicana* (F)	351.2	360.9	14.9
FO *P. sicana* (F)	380.3	389.9	16.6
LO *C. dissimilis* (F)	389.9	399.5	17.6
FO *S. heteromorphus* (N)	389.9	399.5	18.6
LO *S. belemnos* (N)	389.9	399.5	18.8
FO *S. belemnos* (N)	399.5	409.1	20.0
130-805C- (Cont)			
LO *G. kugleri* (F)	447.7	457.4	21.8
FO *R. paleacea* (D)	523.9	533.5	22.7
LO *R. vigilans* (D)	523.9	533.5	22.7
FO *G. kugleri* (F)	523.9	533.5	23.7
FO *B. veniamini* (D)	543.2	552.9	24.0
LO *S. ciperoensis* (N)	552.9	562.6	25.2
LO *S. distentus* (N)	572.3	582.0	27.5
LO *G. opima* (F)	572.3	582.0	28.2

Notes: The depth uncertainty predominantly represents sample intervals used. References for the age estimates are presented in the "Explanatory Notes" chapter (this volume). N = nannofossil, F = foraminifer, D = diatom, R = radiolarian, FO = first occurrence, LO = last occurrence, and OA = onset acme. Magnetostratigraphic reversal boundaries followed by the designation (T) or (O) refer to "termination" and "onset," respectively.

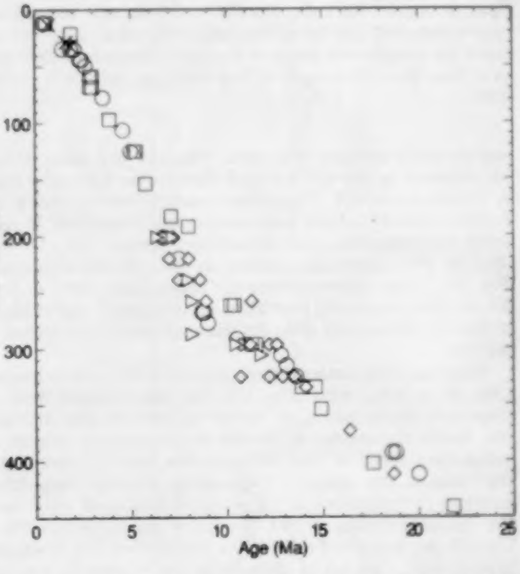

Figure 20. Age-depth relationships of bio- and magnetostratigraphic markers, Hole 805B. Sample interval uncertainties correspond closely to the symbol size used. Circle = nannofossil, square = foraminifer, diamond = diatom, triangle = radiolarian, and × = magnetostratigraphic reversal boundary.

nature of these profiles, with Ca and Mg gradients primarily controlled by reactions in the underlying basalt and diffusion between this boundary and overlying seawater (McDuff and Gieskes, 1976; McDuff, 1981).

Strontium concentrations increase with depth to maximum values >900 μM by 108.8 mbsf and persist to 578.2 mbsf, the deepest sample (Fig. 25). Strontium concentrations at this site are always larger than those at the deeper Site 804, where sediments accumulate more slowly. The Sr increase with depth at this site is steeper than that at Site 803, with the maximum con-

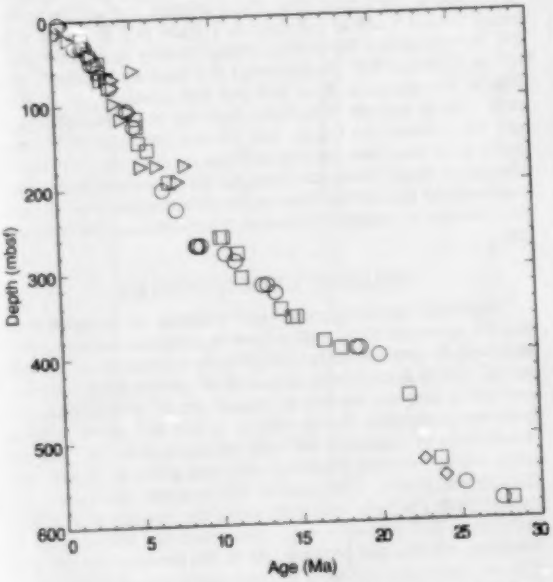

Figure 21. Age-depth relationships of biostratigraphic markers, Hole 805C. Sample interval uncertainties correspond closely to the symbol size used. Symbols used are as in Figure 20.

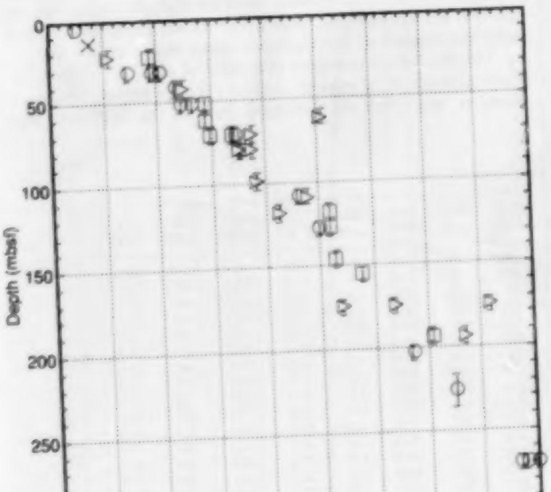

Figure 22. Age-depth relationships of biostratigraphic markers from the upper Miocene through Holocene interval in Hole 805C. Error bars show sample interval uncertainties. Symbols used are as in Figure 20.

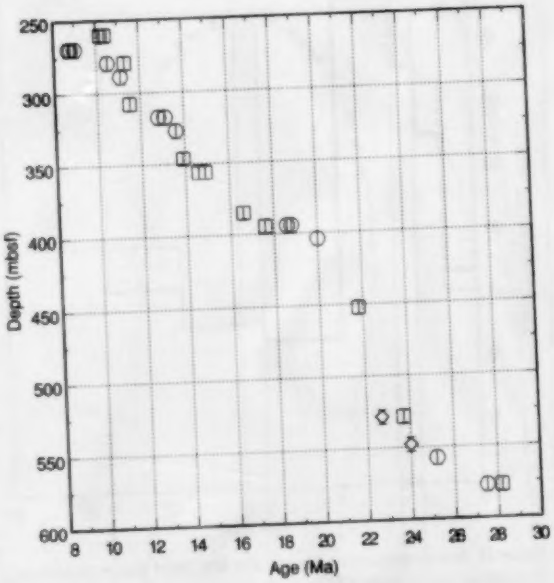

Figure 23. Age-depth relationships of biostratigraphic markers from the upper Oligocene through the lower upper Miocene interval, Hole 805C. Error bars show sample interval uncertainties. Symbols used are as in Figure 20.

Table 6. Estimated sedimentation rates, Site 805, and the control points determining those rates.

Control point	Depth (mbsf)	Age (Ma)	Sedimentation rate (m/m.y.)
130-805B-			
Top section	0	0	
Olduvai (O)	31.60	1.88	16.8
LO *R. pseudoumbilica* (N)	77.95	3.56	27.6
LO *D. quinqueramus* (N)	125.45	5.00	33.0
LO *D. hamatus* (N)	268.05	8.70	38.5
LO *S. heteromorphus* (N)	325.25	13.60	11.7
LO *S. belemnos* (N)	392.85	18.80	13.0
LO *G. kugleri* (F)	440.75	21.80	16.0
Terminal depth	473.30	23.84	
130-805C-			
Top section	0	0	
OA *D. triradiatus* (N)	31.55	2.07	15.2
LO *R. pseudoumbilica* (N)	79.05	3.56	31.9
LO *D. quinqueramus* (N)	126.55	5.00	33.0
LO *D. hamatus* (N)	269.55	8.70	38.6
LO *S. heteromorphus* (N)	327.05	13.60	11.7
LO *S. belemnos* (N)	394.70	18.80	13.0
LO *G. opima* (F)	577.15	28.20	19.4
Terminal depth	611.00	29.94	

Notes: References for the age estimates are presented in the "Explanatory Notes" chapter (this volume), as well as the Leg 130 philosophy for determining the sedimentation rates. N = nannofossil, F = foraminifer, FO = first occurrence, LO = last occurrence, and OA = onset acme. Magnetostratigraphic reversal boundaries followed by the designation (T) or (O) refer to "termination" or "onset," respectively.

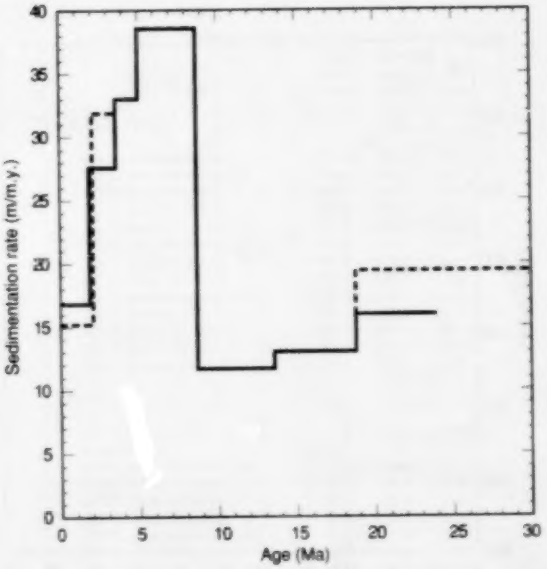

Figure 24. Sedimentation rate history, Site 805. Solid line = Hole 805B and dashed line = Hole 805C.

centrations at Site 803 similar to these, but not reached until >300 mbsf. This is consistent with previous observations for carbonate-rich sites, suggesting that the depth of the Sr maximum, although not necessarily its concentration, is inversely related to sedimentation rate, with deeper maxima for slower sedimentation rates (Gieskes, 1981).

Lithium concentrations decrease from 22.5 μM near the top of the sediment column to a minimum of 14.6 μM at 165.7-12.2 mbsf. The Li profile then increases to 22.2 μM at 578.2 mbsf (Fig. 25). The profile is similar to those at Sites 803 and 804, suggesting that the controls on these profiles must also be similar. Potassium concentrations decrease from 12 mM at 6.0 mbsf to 6.8 mM at 578.2 mbsf (Fig. 25). Rubidium concentrations decrease from 1.9 μM at 6.0 mbsf to 1.1 μM at 578.2 mbsf (Fig. 25). Potassium and Rb concentrations linearly correlate with Ca (R^2 = 0.95 and 0.85, respectively) and have similar depth profiles at this site as at Sites 803 and 804. Lithium, at all three sites, clearly behaves differently than the other two alkalis, K and Rb. Increases in Ca, K, and Rb and decreases in Mg with depth at all three sites are apparently a result of the diffusive influence of basalt alteration reactions on interstitial water composition; the similarities between the sites suggests that the general histories of basalt alteration at these sites must be comparable.

ORGANIC GEOCHEMISTRY

Shipboard carbon geochemical analyses of samples from Site 805 consisted of determinations of inorganic carbon on 510 samples, 40 determinations of volatile hydrocarbons in sediments, and 10 Rock-Eval analyses. Total carbon (TC), nitrogen, and sulfur were not measured because the NCS-elemental analyzer was inoperable during drilling at Site 805. More detailed descriptions of analytical methods are outlined in the "Explanatory Notes" chapter (this volume) and given by Emeis and Kvenvolden (1986). The volatile hydrocarbon gases were extracted from the bulk sediment, using the headspace-sampling technique, and routinely were monitored for abundances of methane, ethane, and propane. As in the previous sites of Leg 130, no significant amounts of these gases were detected.

Analyses of total inorganic carbon (IC) were performed on physical properties samples. Percent $CaCO_3$ is calculated as IC · 8.334. The data are presented in Table 8 (microfiche, back pocket) and are plotted vs. depth in Figure 6. The sediments at Site 805 generally show very high carbonate contents ranging from 85% to 95%. Compared with Site 804, carbonate values at Site 805 are less variable, which may reflect lower carbonate dissolution because of the shallower water depth at Site 805.

The Rock-Eval pyrolysis (Espitalié et al., 1977) was used to determine the total organic carbon (TOC) content. The values, however, are below the detection limit of the shipboard Rock-

Table 7. Interstitial water geochemical data, Holes 805B and 805C.

Core, section, interval (cm)	Depth (mbsf)	pH	Alk. (mM)	Sal. (g/kg)	Cl^- (mM)	Na (mM)	SO_4^{2-} (mM)	PO_4^{3+} (μM)	NH_4^+ (μM)	SiO_2 (μM)	Mn (μM)	Ca2+ (mM)	Mg^{2+} (mM)	Sr (μM)	Li (μM)	K (mM)	Rb (μM)
130-805C-1H-4, 145-150	5.95	7.5	2.90	35.0	554	480	28.5	LD	28	528	10	10.6	50.4	175	22.5	12.1	1.92
130-805C-2H-4, 145-150	13.75	7.5	3.59	35.0	561	482	28.5	LD	54	530	4	11.7	50.2	281	21.0	11.4	1.79
130-805C-3H-4, 145-150	23.25	7.4	3.60	35.0	567	483	26.9	LD	83	558	LD	12.7	49.2	407	21.0	11.5	1.71
130-805C-4H-4, 145-150	32.75	7.2	3.91	35.0	569	484	25.8	LD	105	585	LD	13.6	48.1	495	20.1	11.2	1.75
130-805C-5H-4, 145-150	42.25	7.2	4.09	35.5	570	491	26.0	LD	127	625	LD	14.6	47.1	603	19.1	11.0	1.70
130-805C-6H-4, 145-150	51.75	7.5	4.14	35.0	570	490	24.8	LD	146	678	LD	15.3	45.2	672	18.6	11.2	1.75
130-805C-9H-4, 145-150	80.25	7.1	5.36	35.5	575	483	23.6	LD	178	736	LD	17.7	42.8	837	16.6	10.6	1.67
130-805C-12H-4, 145-150	108.75	7.6	4.48	35.5	569	492	22.8	LD	209	835	LD	21.3	40.1	939	15.1	10.4	1.72
130-805C-15H-4, 140-150	137.20	7.6	4.57	35.5	575	493	22.6	LD	222	865	LD	22.0	38.7	989	15.1	10.1	1.63
130-805C-18H-4, 140-150	165.70	7.1	4.43	36.0	581	494	21.5	LD	231	893	LD	23.6	37.3	963	14.6	9.68	1.60
130-805B-20H-4, 145-150	183.65	7.7	4.33	35.5	575	506	22.0	LD	247	931	LD	24.3	36.4	959	14.7	10.1	1.61
130-805B-23H-4, 145-150	212.15	6.9	4.34	36.0	582	497	22.9	LD	252	965	LD	26.2	35.1	959	14.7	9.25	1.52
130-805B-26H-4, 145-150	240.65	7.5	3.76	36.0	582	495	21.8	LD	251	1032	LD	26.8	34.6	932	15.3	9.41	1.62
130-805B-29X-4, 145-150	269.15	7.6	ND	36.5	582	493	22.4	LD	260	960	LD	28.7	34.1	923	15.8	8.79	1.47
130-805B-32X-2, 140-150	295.10	7.1	4.19	36.5	582	491	22.7	LD	247	975	LD	29.0	33.4	904	16.8	8.88	1.47
130-805B-35X-3, 140-150	324.90	7.1	4.80	36.5	583	487	21.9	LD	238	1008	LD	29.5	33.2	904	17.3	8.56	1.43
130-805B-38X-3, 140-150	353.80	7.1	3.82	36.5	584	493	21.8	LD	234	1043	LD	30.3	32.9	921	18.4	8.45	1.43
130-805B-41X-3, 140-150	382.70	7.6	3.24	36.5	585	493	21.8	LD	206	1084	LD	29.6	33.0	888	21.0	8.46	1.34
130-805B-44X-5, 140-150	414.70	ND	ND	36.5	577	494	21.7	ND	202	1077	LD	30.8	32.2	924	18.4	7.94	1.35
130-805B-48X-3, 140-150	449.90	ND	ND	ND	585	497	23.3	ND	195	1092	LD	32.2	31.6	952	20.0	7.65	1.26
130-805B-50X-3, 140-150	469.20	ND	ND	ND	596	497	22.5	ND	ND	1075	LD	32.3	32.6	937	20.0	7.55	1.24
130-805C-53X-3, 140-150	499.30	7.6	2.90	36.5	588	505	22.4	ND	166	1138	LD	32.8	31.8	979	21.1	7.28	1.17
130-805C-57X-2, 0-10	535.00	ND	ND	ND	593	500	22.7	ND	158	1158	LD	32.7	31.3	940	21.1	7.14	1.18
130-805C-61X-4, 140-150	578.20	7.6	2.59	36.5	590	500	22.3	ND	153	1205	LD	33.9	30.8	952	22.2	6.82	1.08

Notes: LD = concentration lower than detection limit, and ND = not determined.

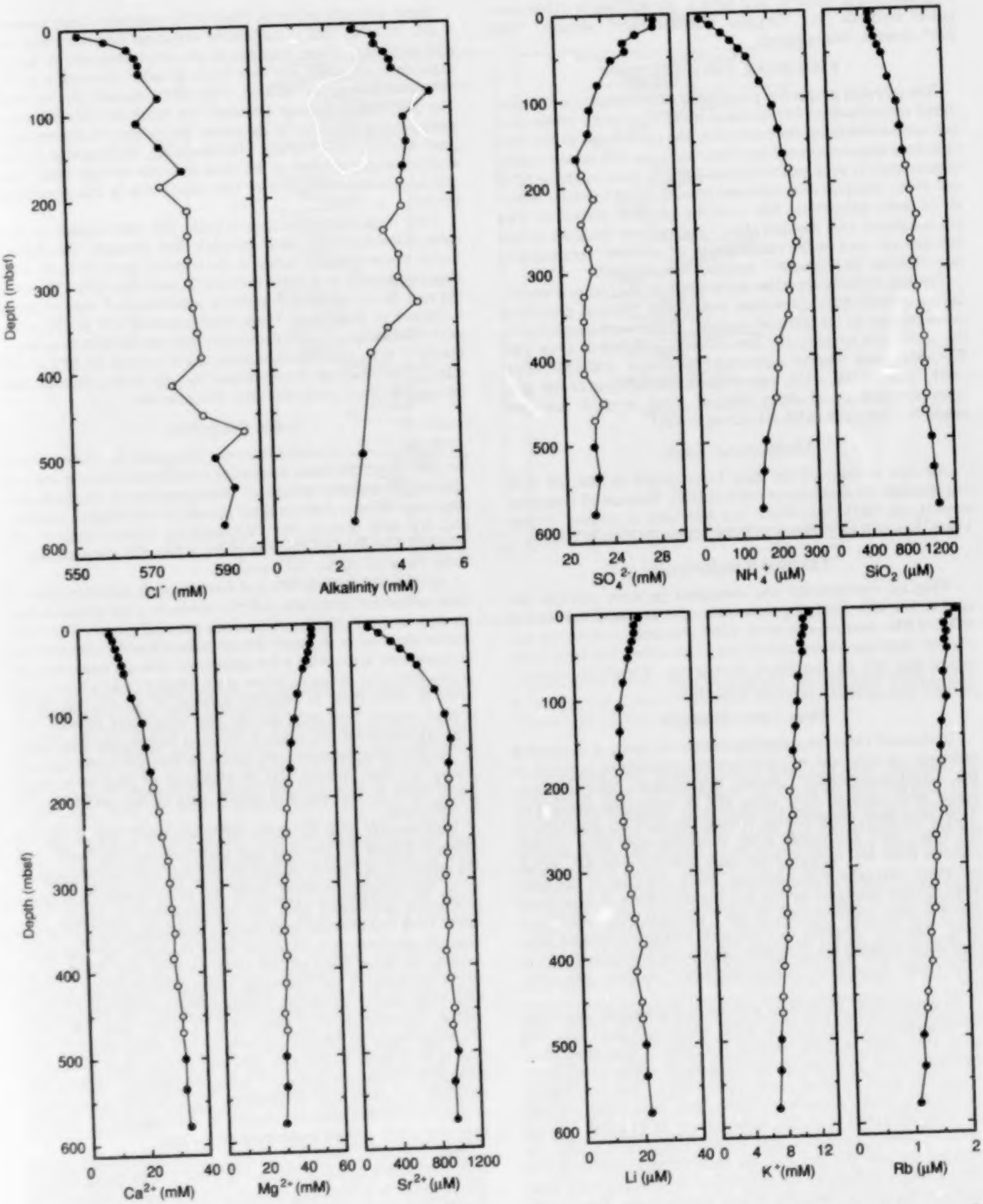

Figure 25. Interstitial water geochemical data vs. depth, Holes 805B and 805C. Open circles = samples from Hole 805B; closed circles = samples from Hole 805C. The depth at the base of the plots is that of the deepest sediment drilled.

Eval instrument (0.05%) and have to be verified by other analytical methods (see "Organic Geochemistry" section, "Site 803" chapter, this volume).

PHYSICAL PROPERTIES

The physical properties program at Site 805 included whole-round measurements (multisensor track and needle-probe thermal conductivity) on the cores from the three holes at Site 805. Split-core measurements (vane shear strength and velocity probe measurements) were performed on the split cores of Holes 805B and 805C. Samples were obtained from the split cores for analysis of index properties. The resulting physical properties data are compared with the downhole logging data obtained at Site 805 and are used in the construction of synthetic seismograms (see "Seismic Stratigraphy" section, this chapter).

Drilling disturbance (flow-in) in many of the piston cores obtained in Hole 805C prevented meaningful physical properties measurements in the affected sections. This disturbance involved the upper five sections of Core 130-805C-7H, all of Core 130-805C-8H, and shorter intervals in Cores 130-805C-10H, -11H, -13H, -14H, -16H, and -17H. A malfunction of the vane shear strength electronics prevented shear strength measurements in Cores 130-805B-1H through -21H.

Multisensor Track

All core sections of the three holes drilled at Site 805 were run through the multisensor track (MST). Because of time constraints, no MST data from Site 805 were processed at sea. These data will be presented in the *Scientific Results* volume.

Thermal Conductivity

Thermal conductivity was measured in three sections per core at Site 805. However, as was the case for results from Site 803 and 804, considerable work is still required to adjust the values for improper probe calibration. This effort has been postponed and will be completed post-cruise. Therefore, thermal conductivity data are not presented here.

Vane Shear Strength

Undrained shear strength was measured using a motorized minivane on split-core sections (see the procedures outlined in the "Explanatory Notes" chapter, this volume). Vane measurements were made in APC cores and in competent biscuits of XCB cores until the sediment became too stiff for insertion of the vane, near 240 mbsf. Table 9 (microfiche, back pocket) presents peak and residual vane shear data for Site 805. Residual shear strengths were obtained where cracking of the sediment did not dominate failure (see the discussion of vane shear strength data interpretation in the "Physical Properties" section, "Site 803" chapter, this volume). Figure 26 presents peak vane shear strength for Hole 805C and mean grain size for Hole 805B (taken from the "Lithostratigraphy" section, this chapter).

As noted above, equipment malfunction prevented vane shear measurements in most of Hole 805B. Many data gaps also exist in the Hole 805C profiles because of coring disturbance. Measurements were obtained in the apparently undisturbed lower sections in some of those cores where flow-in was observed in the upper sections; however, in some cases these lower sections also were disturbed (e.g., the measurement at 91 mbsf, Section 130-805C-10H-5, yielded a peak shear strength of 2.3 kPa). As observed for Sites 803 and 804, the shear strength profile at Site 805 is strongly influenced by disturbance of the calcareous sediments during coring, resulting in core-length cycles. These problems with the vane shear strength data set at Site 805 make it difficult to interpret the data with respect to changes in grain size or carbonate content.

Shear strength values at Hole 805C generally range between 5 and 20 kPa, with considerable variation between these two end members. Shear strength in silt-sized sediment is largely dependent on grain size (see more detailed discussion in the "Physical Properties" section, "Site 803" chapter, this volume). The observed variations are likely the result of high-frequency grain-size fluctuations in the upper 300 m (see "Lithostratigraphy" section, this chapter). Unfortunately, shipboard grain-size samples were not taken at the same intervals as vane shear measurements, so verification of this correlation is not possible at present.

Low-frequency variations in grain size also appear to have some effect on vane shear strength. For example, the slightly higher shear strength values in the interval from 20 to 45 mbsf may correspond to a slight increase in grain size (Fig. 26). Over the next 80 m, correlation between grain size and shear strength is limited by data gaps. From approximately 125 to 185 mbsf, peak vane shear strength decreases from near 20 kPa to approximately 8 kPa, and then increases again to near 25 kPa at 220 mbsf. This trend can be correlated loosely with a decrease and increase in mean grain size over this interval.

Index Properties

Samples were obtained from the split cores for index properties analyses. The index properties calculated from the wet and dry weights and dry volume of these samples are wet-bulk density, grain density, water content (based on dry weight), porosity, and dry bulk density (see "Explanatory Notes" chapter, this volume). The data for the four holes at Site 805 are presented in Table 10 (microfiche, back pocket).

As observed at Sites 803 and 804, the high calcite content of these sediments (generally >85%) results in grain densities that are constant with depth, with values near 2.7 g/cm^3. The slight scatter observed in the grain density values is within the scope of measurement error, with a few exceptions that are unexplainable at this time. For example, a low grain density (2.47 g/cm^3) at 45 mbsf in Hole 805C is possibly a result of an improperly recorded weight. Low bulk density and high water content were also calculated for this sample. We have resisted the temptation to discard unexplainable data spikes at this time; the GRAPE profile for this interval will be examined as part of a shore-based study so that this and similar data spikes can be verified or discarded.

Bulk-density data for Holes 805B and 805C are plotted vs. depth in Figure 27. Porosity and water content for these holes are presented in Figures 28 and 29, respectively. In the upper 10 m of the sediment column, there are steep gradients in index properties, associated with the consolidation of young sediment. Over this interval, bulk density increases from 1.45 g/cm^3 near the seafloor to 1.55 g/cm^3 near 10 mbsf, whereas water content decreases from almost 110% to 80% over the same interval. Between 15 and 180 mbsf, the gradients are not as high, with bulk density increasing gradually from values near 1.55 g/cm^3 at approximately 10 mbsf to 1.72 g/cm^3 near 190 mbsf. High-frequency variations are seen in the index property profiles in both holes of this site, and may be the result of fluctuations in the carbonate content ("Lithostratigraphy" section, this chapter). To verify this relationship, bulk density must be corrected for porosity rebound caused by the removal of overburden; this study will be completed post-cruise.

Near 190 mbsf there is a change in the bulk density profile (Fig. 27) from a trend of increasing density with depth (the expected trend for a normally consolidating sediment sequence) to one of decreasing density with depth. A similar change was observed at Site 803 at approximately 110 mbsf and at Site 804 near 50 mbsf. This trend continues to 260 mbsf. As discussed for Site 803, this phenomenon appears to be associated with a

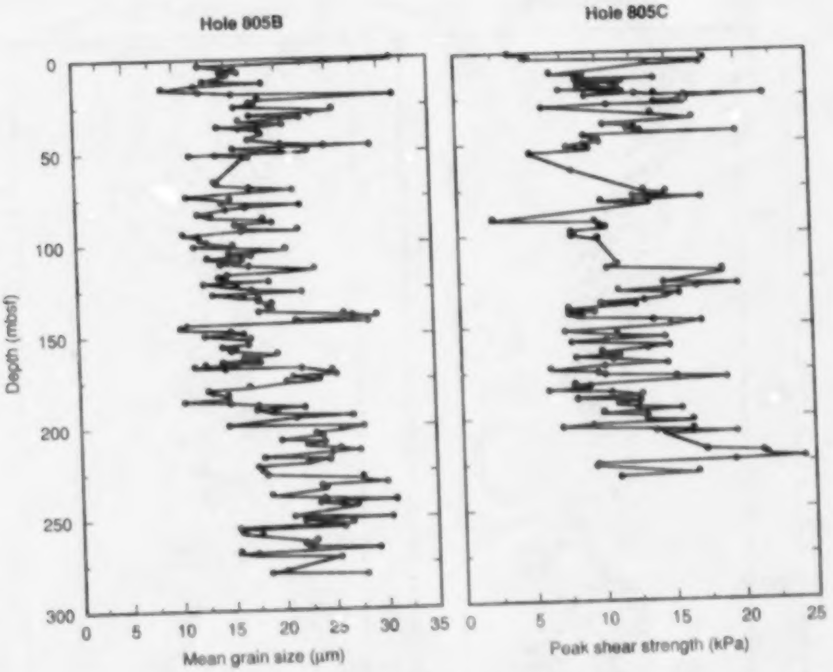

Figure 26. Laboratory vane peak shear strength vs. depth, Hole 805B, and mean grain size vs. depth, Hole 805C.

major dissolution event and corresponds to a notable decrease in carbonate content over this interval.

Bulk density begins to increase with depth again below 260 mbsf, from values of approximately 1.72 g/cm^3 near 260 mbsf to 1.77 g/cm^3 near 390 mbsf. Porosity decreases from 60% to 55% and water content decreases from 55% to 45% over this interval. This zone of fairly constant index property gradients crosses the ooze-chalk boundary, near 290 mbsf (see "Lithostratigraphy" section, this chapter). The decreases in porosity may be a result, in part, of consolidation as a consequence of overburden and, in part, of chemical cementation. Alternations between softer ooze and more cemented sediments in the ooze-chalk transition zone probably result in much of the variation seen in the profiles of index properties.

At 390 mbsf, bulk density values increase sharply to 1.9 g/cm^3, whereas porosity and water contents measurements show a steplike decrease; porosity values decrease to 50% and water contents to 35%. The index properties values then remain constant at these levels, with a few variations caused by local variations in grain size, to a depth of approximately 500 mbsf. The slight scatter observed may be the result of local grain-size variations. This interval of constant index properties is possibly a result of increased cementation, which prevents continued mechanical consolidation.

Between 500 and 600 mbsf bulk density values increase again but with less of a gradient than in the zones of increasing bulk density discussed above. Near 600 mbsf, bulk density values reach levels near 2 g/cm^3, whereas porosity values decrease to 45% and water contents decrease to 30%. These changes in the properties of already-cemented sediments probably represent the result of infilling of voids by calcite overgrowths. The explanations given for the various zones of physical properties will be tested by post-cruise crystallinity analyses and scanning electron microscope (SEM) studies.

Velocity

Compressional wave (*P*-wave) velocities were measured on split cores both perpendicular to (vertical) and parallel with (horizontal) bedding. Measurements were performed using the Digital Sediment Velocimeter (DSV) or the Hamilton Frame, depending on the degree of lithification of the sediment (see "Explanatory Notes" chapter, this volume).

Profiles of vertical and horizontal *P*-wave velocity with depth for Holes 805B and 805C are shown in Figure 30 and listed in Table 11 (microfiche, back pocket). Data gaps in the upper 100 m of Holes 805C are the result of coring disturbance, as previously discussed. As at Sites 803 and 804, velocities remain close to 1550 m/s in the upper 200 m of sediment at Site 805, similar to the previous two sites. Detailed examination of variations within this interval must await shore-based investigation of grain size, carbonate content, crystallinity, and isotopes.

Velocities begin to increase near 240 mbsf, indicating the upper limit of lithification, reaching 1700 m/s near 310 mbsf. After this initial increase in velocity, there is a sharp decrease to values below 1550 m/s near 330 mbsf. Shipboard grain size data are not available deeper than 280 mbsf, and thus the reason for this decrease in velocity is unknown at this time.

Velocity increases sharply from 1550 m/s at 325 mbsf to near 2000 m/s at 380 mbsf. This increase corresponds to a marked increase in bulk density over this interval and can be attributed to increased cementation. Fluctuations in velocity are possibly the results of variations in the degree of cementation of the

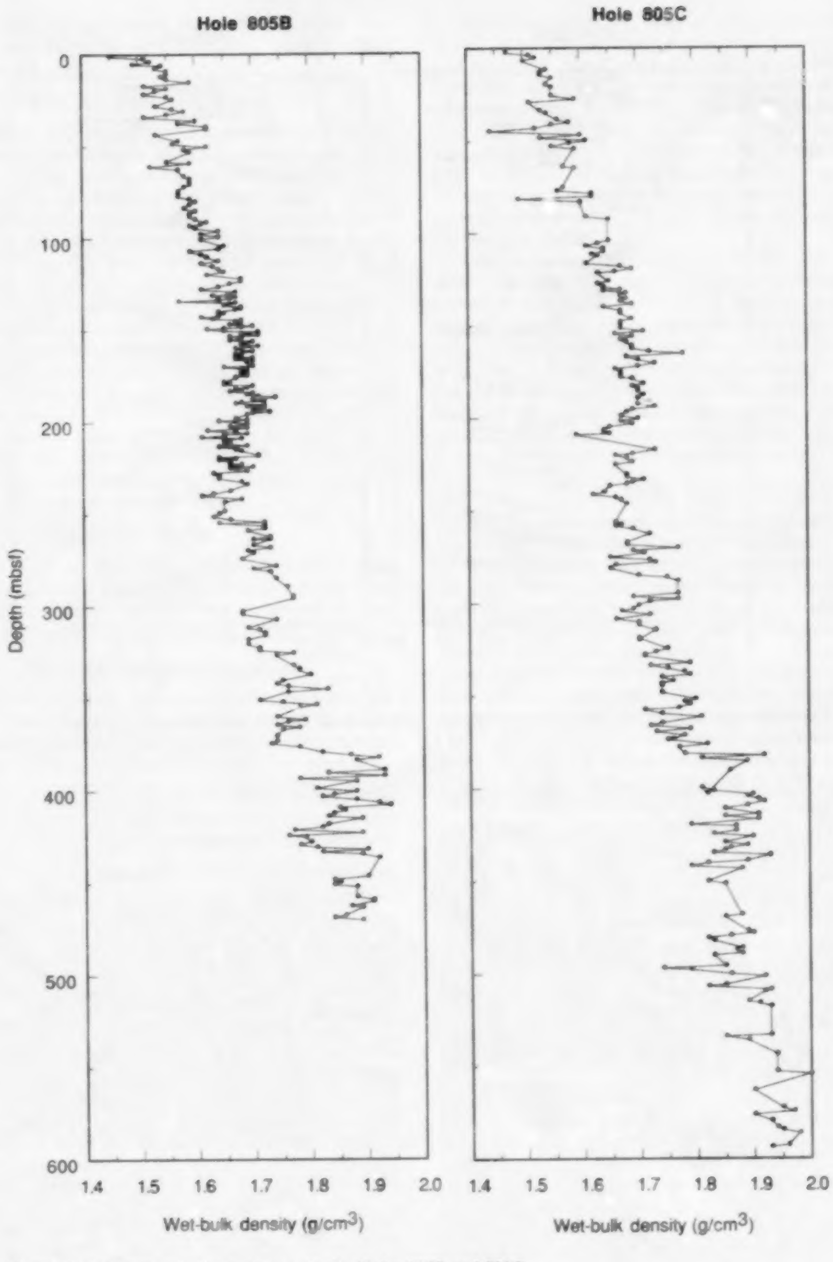

Figure 27. Laboratory bulk density vs. depth, Holes 805B and 805C.

measured samples. The interval between approximately 400 and 500 mbsf may represent a zone in which cementation is sufficient to prevent further consolidation, as discussed above with regard to the index properties data.

A zone of velocity anisotropy (with vertical velocities significantly greater than horizontal velocities) was observed between 440 and 490 mbsf. This, however, may be an artifact of testing. If small horizontal cracks exist in the sample, the force of the Hamilton Frame transducers applied in the vertical direction may close the fractures, thus increasing the measured velocity. Conversely, the force of the transducers applied in the horizontal direction may open the fractures and decrease the measured velocity.

Velocity increases over the interval from 500 to 600 mbsf. This increase in velocity would be expected if calcite is filling the voids in this interval, thus increasing the rigidity of the sedi-

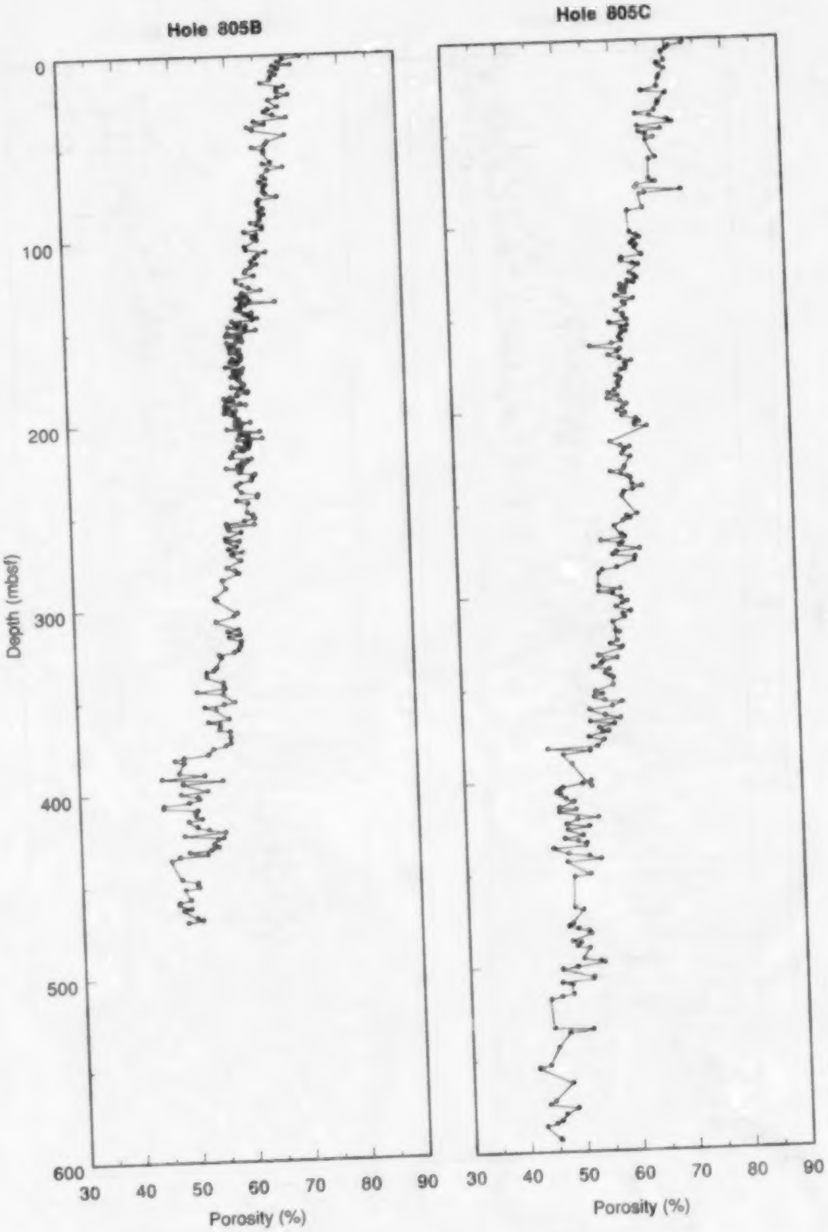

Figure 28. Laboratory porosity vs. depth, Holes 805B and 805C.

ment. Laboratory *P*-wave velocities reach values near 2000 m/s at the bottom of the hole, near 600 mbsf.

Laboratory velocity data for Site 805 are compared with log sonic velocity data for this site in the "Logging" section (this chapter). In general, there is good agreement in the shape of the curves, although laboratory velocities are lower than log velocities because of coring disturbances and the removal of overburden that resulted in porosity rebound of the cored sediments.

Summary

This brief examination of the shipboard physical properties data for Site 805 identifies the major trends in peak vane shear strength, index properties, and *P*-wave velocity. Detailed study of the high-frequency variations observed will be performed post-cruise with the aid of additional analyses such as grain size, crystallinity, SEM, triaxial shear strength, and consolida-

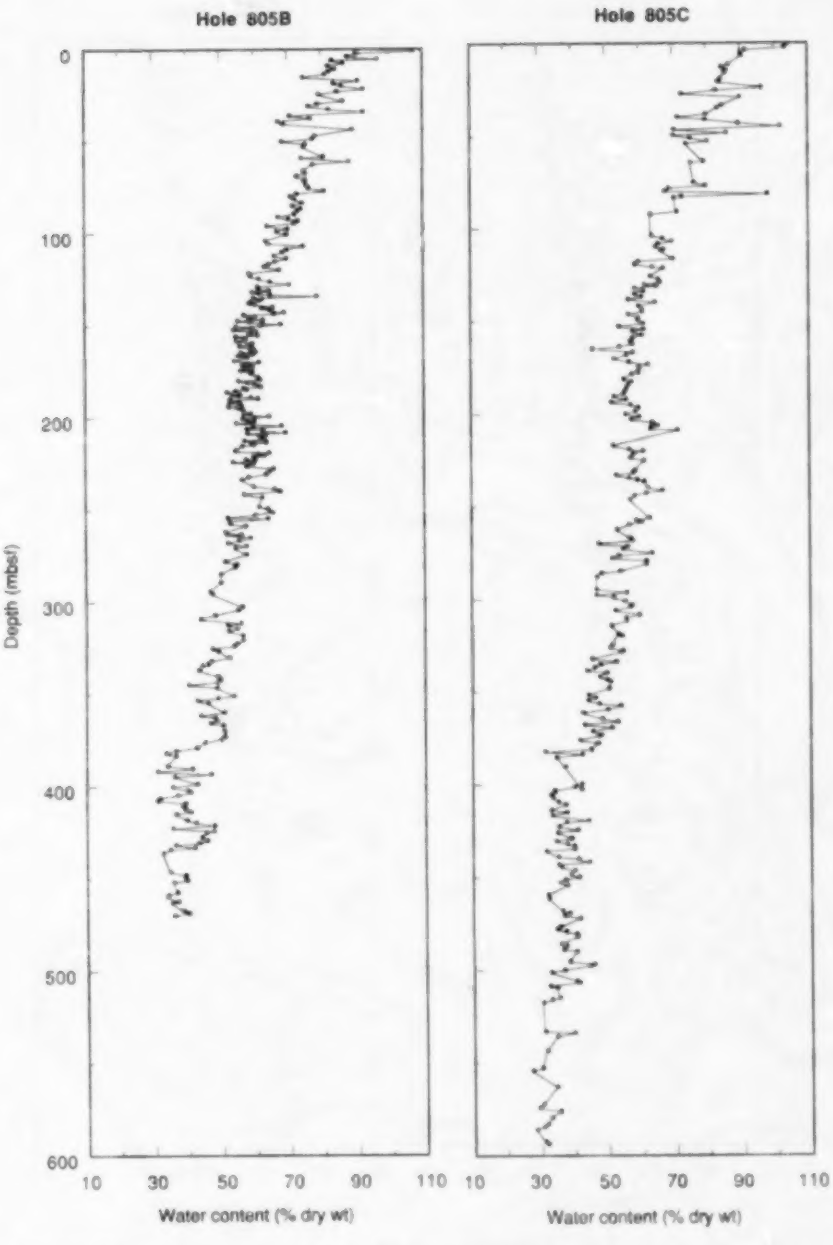

Figure 29. Laboratory water content vs. depth, Holes 805B and 805C.

tion. The major physical properties trends in the carbonate ooze appear related to dissolution events that are also evident in grain size and carbonate content data. Observed trends in the chalk sequences appear closely related to the degree of lithification and diagenesis.

LOGGING

Logging Operations

Logging at Site 805 went much more smoothly than at Site 803. Nevertheless, logging of Hole 805C was not without its

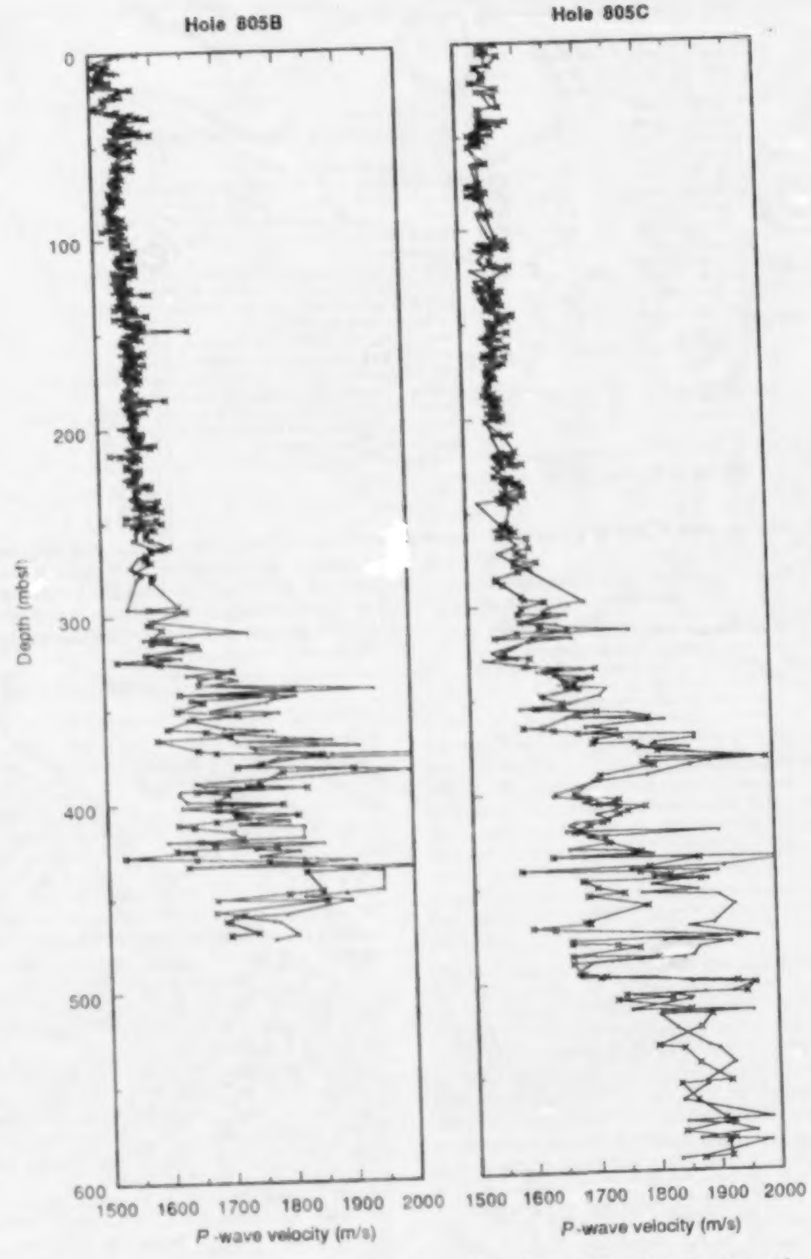

Figure 30. Laboratory compressional wave velocity vs. depth, Holes 805B and 805C. Lines with squares represent vertical (longitudinal) measurements (perpendicular to bedding), and lines with crosses represent horizontal (transverse) measurements (parallel to bedding).

problems. Table 12 lists the sequence of events during the logging of Hole 805C, and Table 13 lists the acronyms used in that table and this chapter. The first logging run consisted of a sonic velocity tool (LSS), resistivity tool (DITE), and the natural gamma-ray tool (NGT). The geophysical tool string was lowered to within 2 m of the bottom of the hole (609 mbsf), and it collected data up to the drill pipe at 100 mbsf. The section between 200 and 100 mbsf was logged a second time to establish the repeatability of the measurements. All tools functioned well on this run.

Table 12. Sequence of events during logging, Site 805.

Local day	Local time	Cumulative hour	Depth (mbsf)	Comments
2/16/90	9:00			Last core on deck
2/16/90	16:00	0.0		RIH with geophysical string tool (NGT/DIT/LSS)
2/16/90	17:02	1.0		At mud line
2/16/90	17:47	1.8	609.0	On bottom of hole, <2 m fill
2/16/90	17:50	1.8	609.9	Main log pass; NGT/DIT/LSS all working; up at 900 ft/hr
2/16/90	19:25	3.4	100.3	Tool in pipe at 3,300 m (10823 ft); run down for repeat
2/16/90	19:45	3.8	199.9	Start up on repeat section; NGT/DIT/LSS all working; 900 ft/hr
2/16/90	20:10	4.2	100.3	Tool in pipe at 3,300 m (10,823 ft); POOH
2/16/90	21:00	5.0		Tool string on deck
2/16/90	21:44	5.7		RIH with geochemical string tool (NGT/ACT/HLDT/GST)
2/16/90	22:34	6.6		POOH; put bullnose on to lock back flapper
2/16/90	23:12	7.2		RIH with geochemical string tool (NGT/ACT/HLDT/GST)
2/17/90	0:49	8.8	609.3	At bottom of hole; start log up
2/17/90	2:29	10.5	331.6	Trouble with GST after 11,900 ft (428 m); stop log
2/17/90	2:41	10.7	443.8	Dropped back to this depth; start repeat log up
2/17/90				GST misbehaving; not putting out many neutrons for this run
2/17/90	4:55	12.9	100.3	Enter pipe; end repeat geochemical string tool
2/17/90	5:32	13.5	199.9	Second repeat; go down to 11,150 ft to see if formation activated
2/17/90	5:59	14.0	100.3	No sign of neutrons; POOH with geochemical string tool
2/17/90	8:25	16.4		Rigged down from logging runs

Note: Depth is based on a seafloor depth of 3199 mbrf.

Table 13. Acronyms used in describing logging at Hole 805C.

Acronym	Description
ACT	Aluminum clay tool
API Units	American Petroleum Institute standard unit for gamma-ray activity
BHC	Borehole compensated sonic tool
DIT	Phasor dual induction resistivity tool
FMS	Formation microscanner
GST	Geochemical spectral tool
HLDT	High temperature lithodensity tool
LSS	Long-spaced sonic digital tool
NGT	Natural gamma-ray tool
TLT	LDGO temperature logging tool
fbrf	Feet below rig floor
mbrf	Meters below rig floor
mbsf	Meters below sea floor
POOH	Pull out of hole
RIH	Run (tool) into hole

The second logging run was the combined geochemical tool string (geochemical spectral tool [GST], aluminum clay tool [ACT], and the natural gamma tool [NGT]), the lithodensity tool (HLDT), and the Lamont temperature tool (TLT). The tool string was lowered almost halfway to the mud line before we realized that the bullnose (which insures that the flapper valve on the XCB bit locks out of the way) was not attached to the base of the tool. The string was pulled back to the surface, the bullnose was attached, and the tool string was sent down again, to within 2 m of the base of Hole 805C. During the upward logging run, the GST went out of tolerance near 428 mbsf, and the up log was stopped at 331 mbsf. The tool was lowered again to 443 mbsf, and an attempt was made to calibrate the GST. The GST continued to malfunction and failed to obtain any new data for the rest of the logging run. The ACT, NGT, HLDT, and TLT continued to function for the remainder of the upward logging run to pipe. After the tool string entered pipe (100 mbsf), we pulled it from the hole and concluded logging 23.5 hr after the last core was on deck.

Even though the GST malfunctioned, the other logs are of excellent quality and most cover the entire hole from 609 to 100 mbsf. The density log is good only between 609 and 120 mbsf because the upper hole was broadened by washing. A step in the velocity profile at 240 mbsf also may be traced to bad hole conditions, as is discussed in more detail below. An ash layer was recorded at 544 mbsf in both NGT runs that provides a stratigraphic tie point between the two logs. Unfortunately, because this interval was poorly recovered by coring, we were unable to tie the logs definitively to core.

Log Stratigraphic Units

The lithology of the recovered section at Site 805 was described as a monotonous single unit (subdivided at the ooze chalk boundary; see "Lithostratigraphy" section, this chapter) but the detailed resolution of the logs showed a wide range of sedimentological changes at a number of scales. Following the procedure established at Site 803, the logging results were divided into log stratigraphic units based on internal consistencies within the logging records. These log stratigraphic units were then compared with the lithostratigraphic units and the basis for their similarities or differences were evaluated. Figure 31 presents the primary geophysical log data (velocity, density, resistivity, and natural gamma ray), and Figures 32 through 37 present the geochemical log results (calcium, silica, and aluminum). Because the GST only worked properly between 600 and about 400 mbsf, the log stratigraphic units were based solely on the geophysical log suite.

The logging data were divided into four log stratigraphic units (A, B, C, and D) based on the geophysical logs, with the exception of the natural gamma-ray log. Although changes in velocity, density, and resistivity generally correlate with each other, their relationship to the gamma-ray data is unclear. As discussed in the logging section of Site 803 (this volume), the natural gamma-ray levels in these sediments are extremely low (probably representing the low content of clay or ash) and, therefore, do not significantly influence the other parameters.

Logging Unit A

Unit A begins at the depth of the shallowest log data (100 mbsf) and continues to between 240 and 260 mbsf, depending on which log is being examined. This unit has fairly constant resistivity and density profiles, and a gently increasing velocity profile (the low-velocity zone between 140 and 160 mbsf is probably an artifact of poor hole conditions; see the comparison with laboratory data below). The numerous low-amplitude, high-frequency changes in all properties may be related to changes in

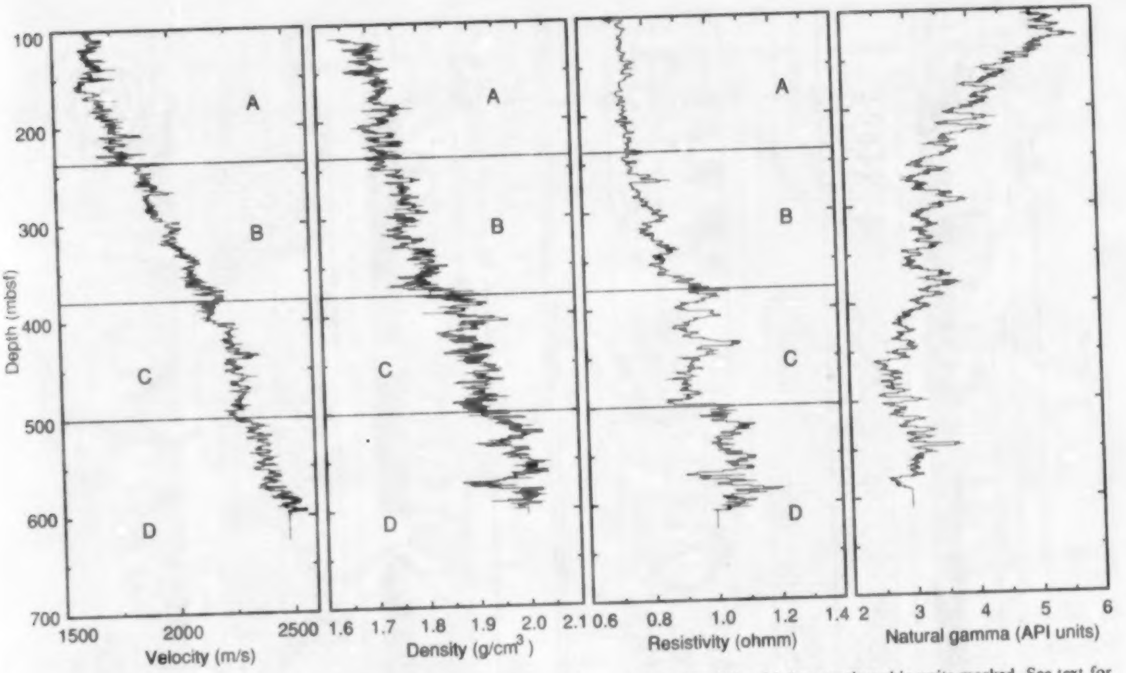

Figure 31. Logs of velocity, density, resistivity, and natural gamma-ray activity vs. depth, Site 805, with log-stratigraphic units marked. See text for description of units.

foraminifer content, although detailed correlations are not possible at this point. Below about 200 mbsf, high-amplitude changes in density and velocity are seen. These appear to be related to changes in induration noted by the sedimentologists (see "Lithostratigraphy" section, this chapter). As at Site 803, there are small zones of high resistivity (low porosity) that correspond to increases in velocity and density (e.g., between 210 and 240 mbsf).

Logging Unit B

Unit B is marked by an offset (increase) in velocity, density, and resistivity. This offset occurs at slightly different depths depending on the log: 240 mbsf in the velocity log, 250 mbsf in the density log, and 260 mbsf in the resistivity log. Analyses of the borehole sonic data indicate that this offset may be an artifact of a rapid change in borehole diameter. The velocity data shallower than 240 mbsf should be considered suspect. The change in borehole conditions is, in itself, probably indicative of changes in the properties of the sediment; thus, we have chosen to maintain this boundary as a log-stratigraphic-unit boundary. This offset roughly corresponds to a time of transition from high to low sedimentation rates (see "Sedimentation Rates" section, this chapter).

Beneath the offset, density, velocity, and resistivity values all increase slowly with depth, probably because of compaction. Superimposed on this steady increase with depth are high-frequency, low-amplitude fluctuations in all parameters, probably related to changes in sediment properties in response to variations in oceanographic conditions.

Logging Unit C

Unit C begins with another offset, an increase in velocity, density, and resistivity. The log profiles are characterized by high-amplitude excursions, particularly resistivity. Within the unit, the gradients decrease with depth. The top of Unit C (380 mbsf) is the depth at which there is a sharp decline in foraminifer content from about 30% to about 10% (see "Lithostratigraphy" section, this chapter). The decrease in grain size associated with the disappearance of foraminifers is consistent with the increase in velocity, density, and resistivity (resulting from decreased pore space) that is seen in the logs. The high-amplitude fluctuations are probably related to changes in the induration of the sediment.

Logging Unit D

Unit D is marked by another offset (increase) in velocity, density, and resistivity. Within this unit are several high-amplitude, low-frequency excursions in all properties, resulting in decreases in density and resistivity. Although recovery was poor in these intervals, the logs imply that these zones are probably less indurated than the surrounding material.

Correlation with Lithostratigraphy

Examination of the logs has revealed much variability, more than can be noted in the visual description of the cores. Given the internal consistency between the logs, the variations observed are probably significant in terms of changes in paleoceanographic conditions. The section at Site 805 was divided into a single lithologic unit with a subdivision at the ooze-chalk transition that was placed between 283 and 293 mbsf (see "Lithostratigraphy" section, this chapter). The logs indicate that this transition began somewhat higher in the section. The velocity log shows a shift to higher values at about 240 mbsf, the density log at 250 mbsf, and the resistivity log at 260 mbsf. Although we have discussed that this may, in part, be an artifact of borehole conditions, the different logs apparently reflect different stages

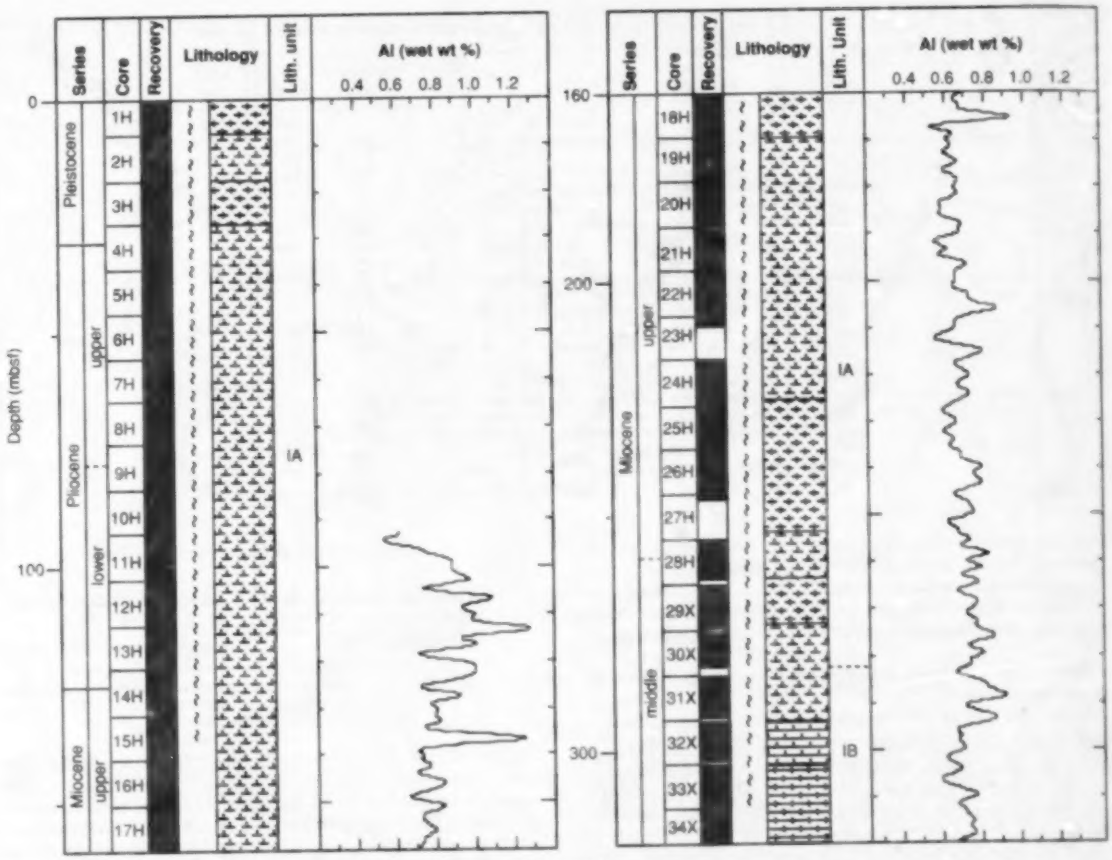

Figure 32. Log-derived aluminum record and lithologic column, Hole 805C.

of lithification. At the onset of cementation (240 mbsf), the rigidity of the sediment is rapidly changed (and thus the velocity) without substantial change to the density or resistivity. At a more advanced stage (250 mbsf), cementation begins to affect the density and then finally (at 260 mbsf) the resistivity. The alterations of induration noted by the sedimentologists above the zone of the ooze-chalk transition are clearly seen on the logs.

A major break in the logs takes place at 380 mbsf (Units B/C boundary), correlating with a change in foraminifer content downhole. This level also corresponds to a change in the style of recovery; below this depth the recovered material consists of disjointed chunks and chips whereas above it recovery is more continuous. The offset in the logs at 500 mbsf has no counterpart in the lithologic description, but this is a zone of poor recovery. The logs imply that there are significant changes in the sediment in the deepest log stratigraphic unit (D).

Small nodules of chert were recovered in Hole 805C at 344 mbsf, but there is no evidence of massive chert layers in the logs at this depth. Chert was not recovered from Hole 805B at this depth, supporting the notion that the chert is patchy.

Comparison with Laboratory Data

Figure 38 shows the comparison of log velocity and density data to uncorrected and corrected laboratory values (for details of the correction procedure, see "Seismic Stratigraphy" section, "Site 803" chapter, this volume). As was noted at Site 803, these comparisons serve to test the quality of both laboratory and log values. Wherever the high-frequency components of the curves have the same shape, we can be reasonably confident that both sets of measurement are good. When there is a discrepancy between the two, we must examine each to see where the problem could lie. The lack of a low-velocity zone between 140 and 160 mbsf in the laboratory data led us to question the log values over this interval. Examination of caliper data here suggests that borehole conditions may have been poor.

Chemical Logs

Three separate logs provided *in-situ* chemical information in Hole 805C: the natural gamma-ray tool, the aluminum clay tool, and the geochemical spectral tool. Presented below are preliminary observations on aluminum distribution (ACT) from 100 to 580 mbsf (Fig. 32) and the calcium data (GST) for the lower 200 m of the hole (Fig. 33).

Aluminum and Natural Gamma Logs

The aluminum data in Figure 32 are presented as wet-weight percent. The profile has been smoothed by a 15-point Gaussian filter to remove noise associated with the low absolute aluminum content. The aluminum concentration in Hole 805C is low and has high-frequency variability, but only subtle low-frequency

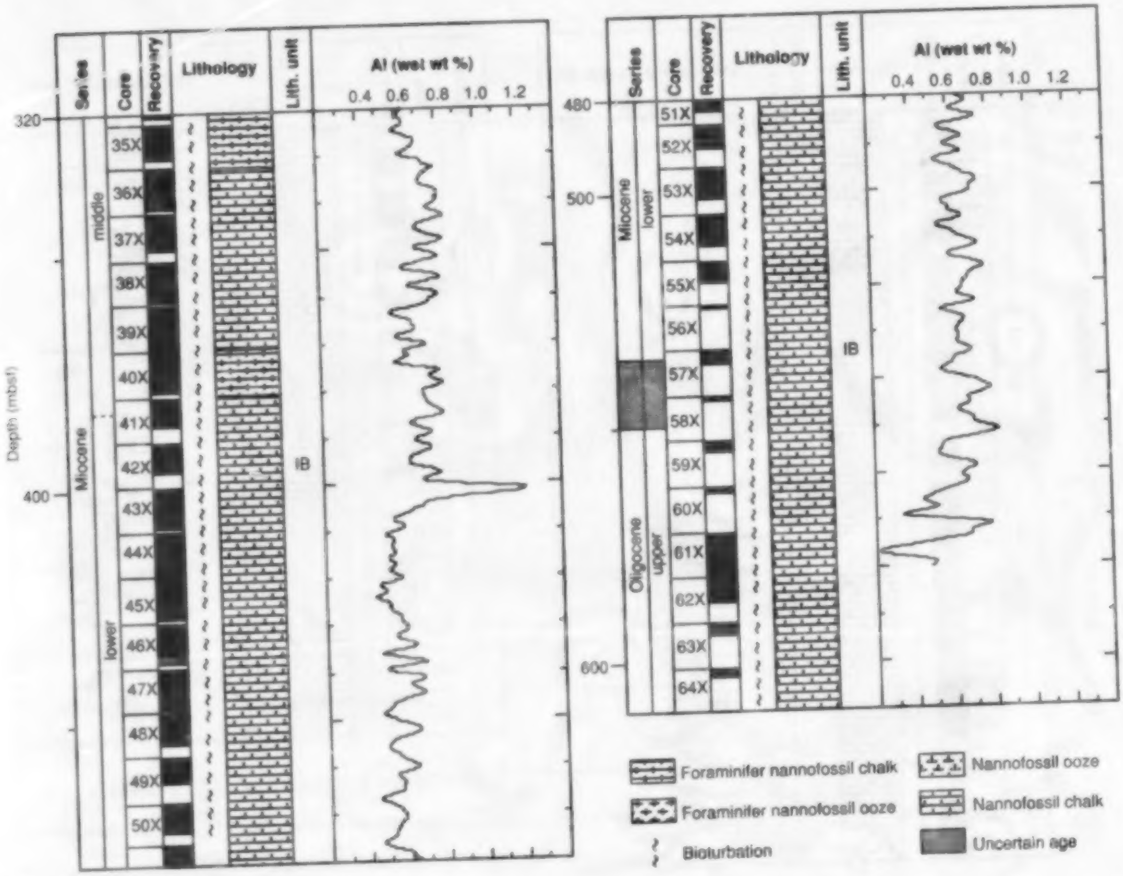

Figure 32 (continued).

trends. In Figure 34, the aluminum data are compared with the natural-gamma information. Because Al and natural gamma-ray activity both indicate the amount of terrigenous debris, one would expect that the two should be correlated. Below 260 mbsf we do see such a correlation between the two records. Between 160 and 260 mbsf the logs diverge strongly for reasons not yet well understood.

As calcite dilutes the other sediment fractions in these sediments, there should be a perfect correlation between the noncalcite fraction in the sediment and the aluminum content, provided that the aluminum content of the noncalcite fraction is constant. Figure 35 is a plot of these two parameters vs. depth in Hole 805C. The noncalcite fraction was determined by subtracting core measurements of calcite from 100%. As illustrated in the figure, there is general agreement between the two variables. The comparison suffers, however, from differences in sampling density. The log information was collected at 15-cm intervals, whereas the core data were collected on a meter spacing at best. Downhole, where recovery became poorer, the core data are more widely spaced. Better comparisons and more rigorous validation of the aluminum log must await shore-based studies.

The GST Calcium Log

Only preliminary processing of the GST data was available on board the ship. The GST collects data for Ca, Si, Fe, K, Ti, S, Gd, Cl, and H. However, the sediments of Hole 805C are so highly calcareous that only Ca and Si in the solid phases and Cl and H in the pore waters will most likely be above detection limits. We present the data for the shipboard comparison as counts of Ca/(Ca + Si) to normalize any variations in neutron capture by the solid phases.

Figure 33 shows the calcium log plotted vs. the lithologic column from 405 mbsf to the base of the hole. The uppermost port of the section (~425–405 mbsf) was logged as the tool began to exceed its tolerances and may be invalid. It is obvious that most of the variation seen on the profile is in the higher frequency range, even though fluctuations at periodicities of several million years are also apparent. The Ca/(Ca + Si) data and the aluminum data (Fig. 36) are inversely correlated, at least for lower frequencies. At shorter periods, on the order of 1–5 m, the correlation is not good, probably because of the low aluminum content.

A comparison of the log of Ca/(Ca + Si) to the core carbonate data is presented in Figure 37. The two data sets compare in a general way through the interval from 405 to 510 mbsf, where core recovery was quite good. Below 510 mbsf the core and log records diverge, but as core recovery was poor in this interval, one must be concerned about the positioning of core data in terms of depth below seafloor as well as whether the recovered core represents a biased sample of the sedimentary record (e.g., lithified sections only).

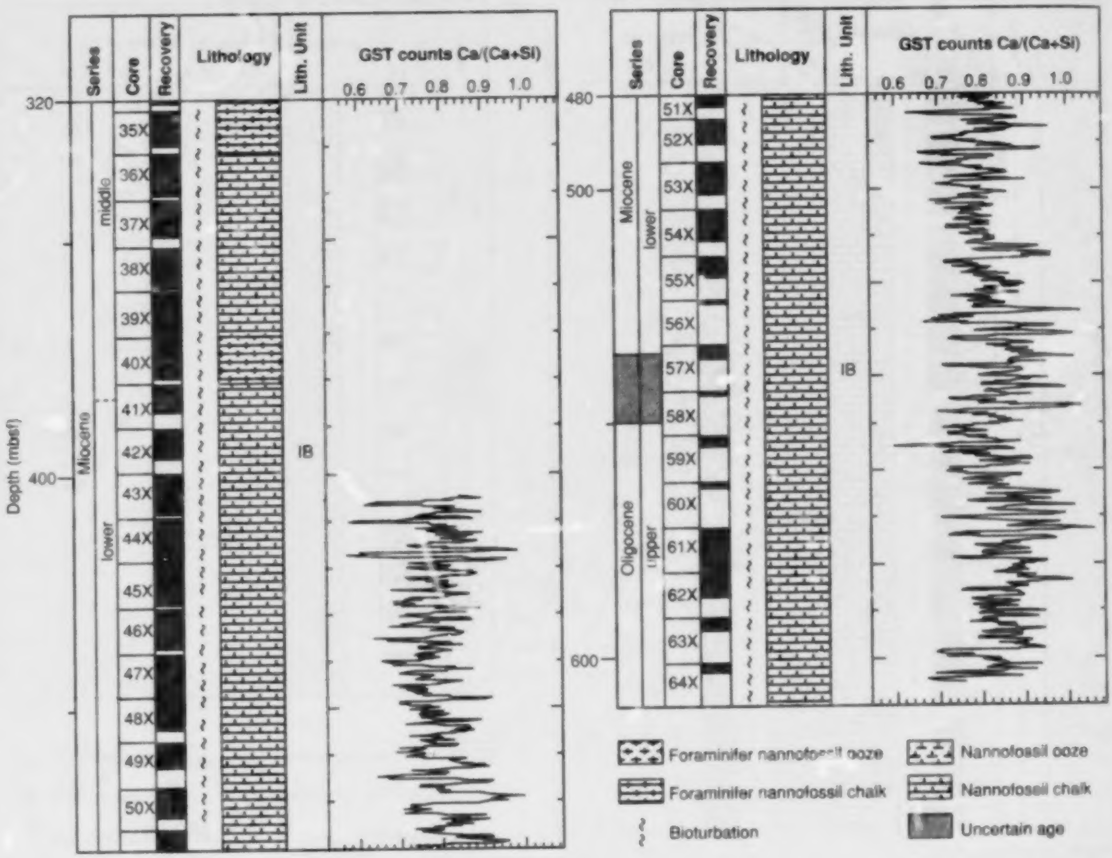

Figure 33. Log-derived calcium/(calcium + silica) ratio and lithologic column, Hole 805C.

The data records presented in Figure 37 cover an interval that has major sedimentation rate changes; in addition, they provide a way to check if the high-frequency information in the calcite log is consistent across the interval of sedimentation rate changes. Between 404 and 453 mbsf, the sedimentation rate is estimated to be 26.8 m/m.y., based upon the LO of the foraminifer *Globorotalia kugleri* and the FO of the nannofossil *Sphenolithus belemnos* (Table 5, "Sedimentation Rates" section, this chapter), as is shown in Figure 37 by the bar representing 1 m.y. of time. During a typical 1-m.y. interval in this section, 9–10 high-amplitude calcium cycles occur, perhaps equivalent to the 100-k.y. period observed in Pacific Pleistocene carbonate sediments.

Between 453 and 529 mbsf, the estimated sedimentation rate based upon the FO and LO of *G. kugleri* is 40.1 m/m.y. (Fig. 37). The high-amplitude calcium cycles continue to occur at frequencies of about 9–10/m.y., even though the cycles are much broader when viewed along a depth axis. Below 529 and above 558 mbsf, the sedimentation rate (based upon the LO of the nannofossil *S. ciproensis* and the FO of *G. kugleri*) is estimated to be 19.4 m/m.y. Here too, calcium variations occur at frequencies of 9–10 cycles/m.y. These observations are very encouraging with regard to carbonate cycle information contained in these records, which will be investigated after shore-based reprocessing of the data sets.

SEISMIC STRATIGRAPHY

The seismic section at Site 805 has the "layer-cake" appearance of the thick, shallow regions of the Ontong Java Plateau. Despite the similarity in appearance to the top of the plateau, the section here is approximately 25% thinner than that at Sites 289/586 (see Mayer et al., this volume). As discussed in Mayer et al., it is not possible to trace individual reflectors from the top of the plateau beyond depths of about 3000 m. Nonetheless, a preliminary analysis of the site survey seismic records indicates that the majority of the thinning takes place in the Miocene and Pliocene intervals and in the pre-Oligocene. Although the section in the vicinity of Site 805 is fairly flat-lying and undisturbed, displacements and faulting can be seen on either side of the site. In addition, a small MSR (see Mayer et al., this volume) is located slightly downslope from the site (Fig. 39).

As at the previous sites, we used the results of laboratory and log measurements to convert seismic traveltime to depth-in-section as well as seismic modeling to check on the accuracy of this traveltime-to-depth conversion. For Site 805, laboratory measurements of velocity and density were made approximately every 75 cm (see "Physical Properties" section, this chapter), and velocity and density logs (15-cm sample interval; around 60-cm sensor spacing) were run for the section between 100 and 609

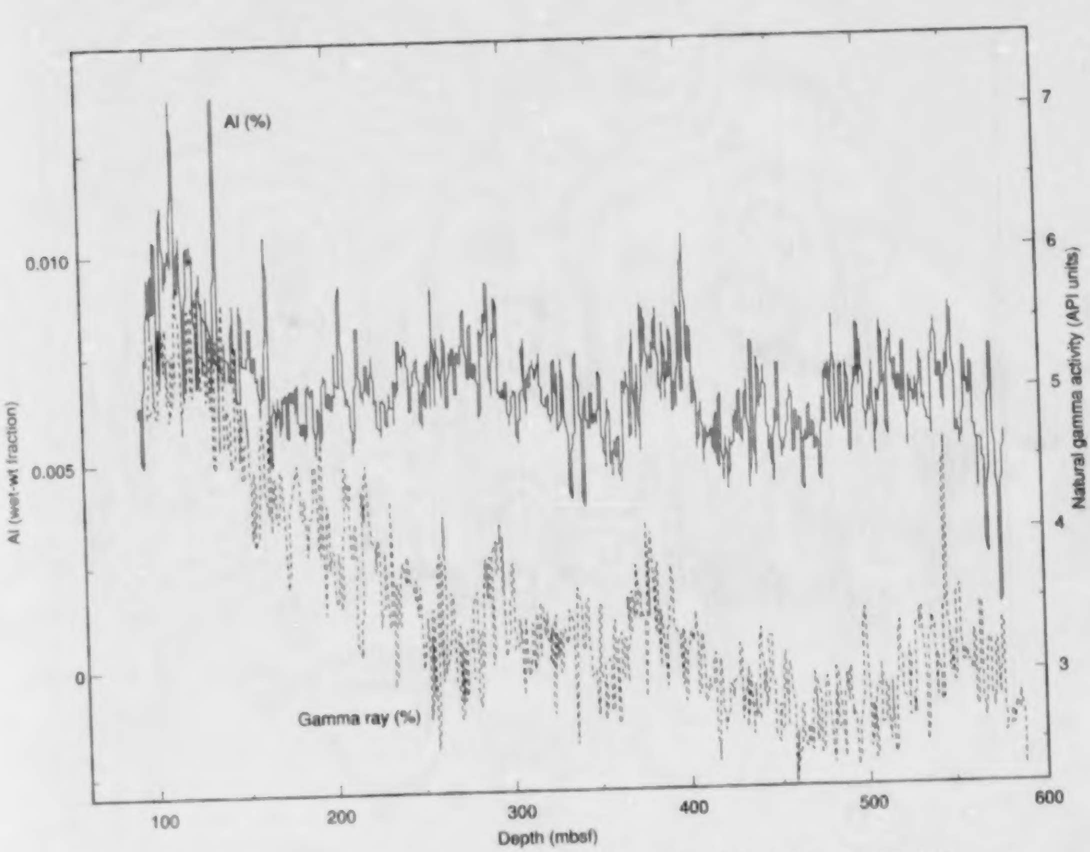

Figure 34. Wet-weight fraction of aluminum (solid line) compared with natural gamma-ray activity (dashed line), Hole 805C.

mbsf (see "Logging" section, this chapter). Laboratory measurements of velocity and density were converted to *in-situ* values using the methods described in Mayer et al. (1985) and merged with the log data. If we assume that the log measurements represent *in-situ* values, then the good match seen between the corrected laboratory measurements and log data implies that the *in-situ* correction is reasonable (Fig. 38). A comparison of log and corrected laboratory data also reveals that between 140 and 160 mbsf there is a zone where log velocity values decrease but laboratory values do not. A close examination of the log data over this interval suggests that the borehole in this section was extremely wide and thus the log data may be questionable; log data, therefore, were replaced by corrected laboratory data over this interval.

The merged, corrected laboratory and log data (velocity and density) were used to calculate acoustic impedance (Fig. 40), which was then convolved with a seismic source signature to generate a synthetic seismogram (see "Site 803" chapter, this volume, or Mayer et al., 1985, for details). The synthetic seismogram is compared to the field seismic profile to evaluate the accuracy of the traveltime-to-depth conversion. The field records used for this study are those collected by the *Thomas Washington* (ROUNDABOUT Cruise 11) during the site surveys for Leg 130 (see Mayer et al., this volume).

As is typical for equatorial Pacific deep-sea carbonates, the seismic record at Site 805 is composed of numerous closely spaced reflectors (there are more than 90 at Sites 289/586). It would be far beyond the scope of this report to discuss the possible origin of each of these reflectors. Instead, we select a few representative reflectors and look at their origin and stratigraphic significance. The criteria for selection of these reflectors is simply that they have high amplitudes and are laterally coherent within the immediate area of Site 805. No effort has been made to select reflectors that are regionally correlatable (e.g., see Mayer et al., this volume) and thus the regional paleoceanographic significance of the selected reflectors remains uncertain.

A comparison of the synthetic seismogram to the field record at Site 805 (Fig. 41) produces a reasonable match, although not one that is without ambiguities. In the absence of a clear tie point like basement or chert (as at Site 803), there are several possible fits of the synthetic record to the field data. We have chosen a fit that maximizes the number of matches, particularly in the deeper part of the section (Fig. 41). We have selected 11 reflectors in the 611-m thick section; their traveltimes, depths, and ages are listed in Table 14. To facilitate discussion, the seismic section has been divided into six groups (Panama, Tethys, Antarctic, Drake, Texas, and Ontong Java). These groups have been given labels based on major oceanographic events that influence oceanographic processes during the time of their formation. The rationale for this naming scheme is discussed in the "Summary and Conclusions" section of this chapter.

The high Pleistocene sedimentation rates at Site 805 allow us to pick the first Pleistocene reflector of Leg 130 (at Sites 803 and 804 all of the Pleistocene was obscured by the signal of the

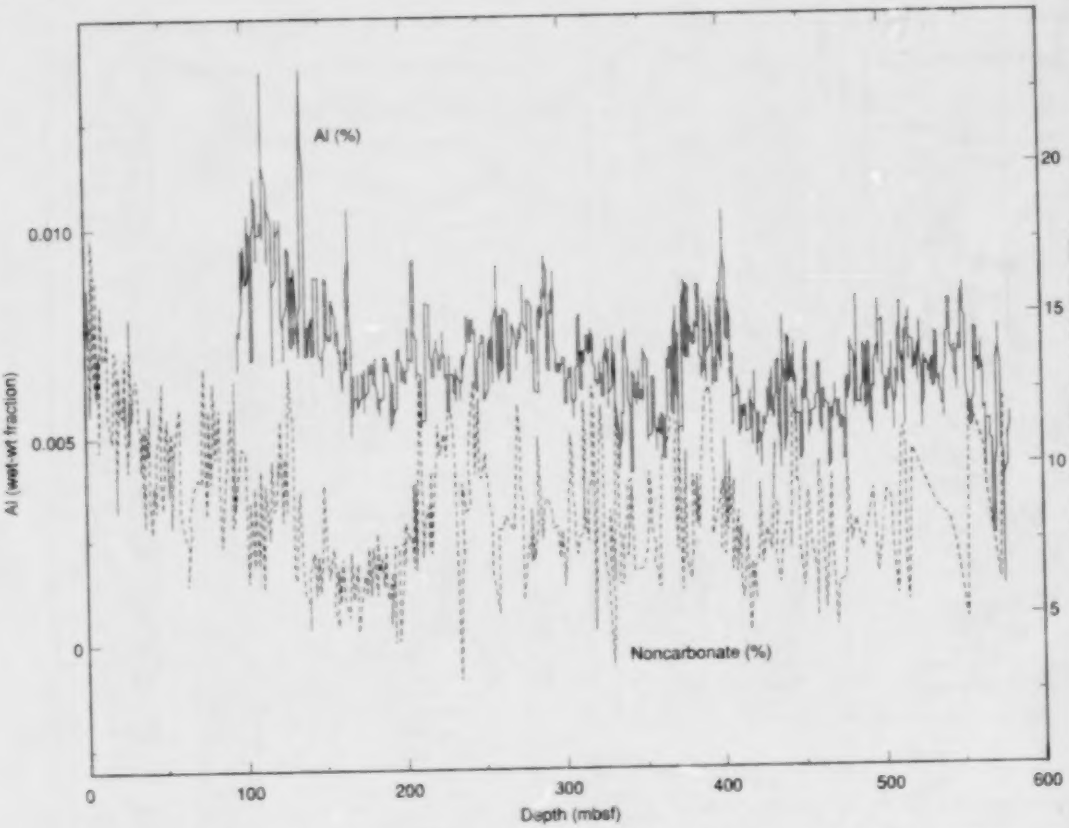

Figure 35. Log-derived aluminum wet-weight fraction (solid line) compared with shipboard measurements of the noncarbonate fraction (100 − %CaCO$_3$) (dashed line), Hole 805C.

outgoing pulse). Reflector 5-1 (0.026 s below seafloor [sbsf], 20 mbsf, 1.2 Ma) is characterized by an increase in density and velocity (and thus acoustic impedance; Fig. 41). These changes correlate with an increase in grain size and a decrease in carbonate content (Fig. 42). The association of increased grain size with decreased carbonate content is unusual and may indicate the removal of nannofossils by currents. The same set of physical property relationships characterize the next two deeper reflectors (5-2, 45 mbsf, 2.4–2.5 Ma, and 5-3, 80 mbsf, 3.7 Ma) assigned to the "Panama" series of reflectors (see "Summary and Conclusions" section, this chapter).

In the next three deeper reflectors (5-4, 101 mbsf, 4.4–4.5 Ma; 5-5, 218 mbsf, 7.1–7.3 Ma; and 5-6, 280 mbsf, 10.3–10.6 Ma), members of the "Tethyan Series" (see "Summary and Conclusions" section, this chapter), grain size no longer appears to play a dominant role. Here, velocity and density seem to be responding to changes in carbonate content that may be a function of variations in productivity and dissolution. All records begin to show cyclic, moderate-amplitude fluctuations (particularly evident in the density record) that give rise to the numerous closely spaced reflectors that characterize this interval. Within this reflector series is the ooze-chalk transition, at about 282 mbsf, roughly at Reflector 5-6 (see "Lithostratigraphy" section, this chapter). The alternations in induration state noted by the sedimentologists are evident in the physical property records and are expressed as high-amplitude peaks in density and particularly in velocity.

In the middle of this interval, there is a large offset in the log-derived velocity (237 mbsf) that results in a high impedance contrast and a large reflector on the synthetic seismogram (Figs. 40 and 41). A depth below seafloor of 237 m should correspond to a seismic traveltime of approximately 0.280 s, a time at which we do not see a high-amplitude, well-developed reflector on the field profile. Laboratory velocity data over this interval do not show a similar effect, and several quality control parameters in the log imply that this velocity offset may be an artifact of poor borehole conditions (see "Logging" section, this chapter). It should be noted, however, that variations in hole conditions often correspond to variations in lithology. Closer examination of this interval will be a subject of shore-based study.

The next four reflectors (5-7, 5-8, 5-9, and 5-10), associated with the "Drake" and "Antarctic" series (see "Summary and Conclusions" section, this chapter), are all the result of rapid, high-amplitude increases in velocity that are superimposed on lower frequency velocity and density excursions (Fig. 40). Carbonate data are sketchy in this interval, but carbonate content apparently plays no role here. Velocity and density fluctuations are perfectly in phase, indicating that cementation and induration are becoming more advanced. The deepest selected reflector (5-11, 530 mbsf, 23.7–23.9 Ma) is also the result of a high-

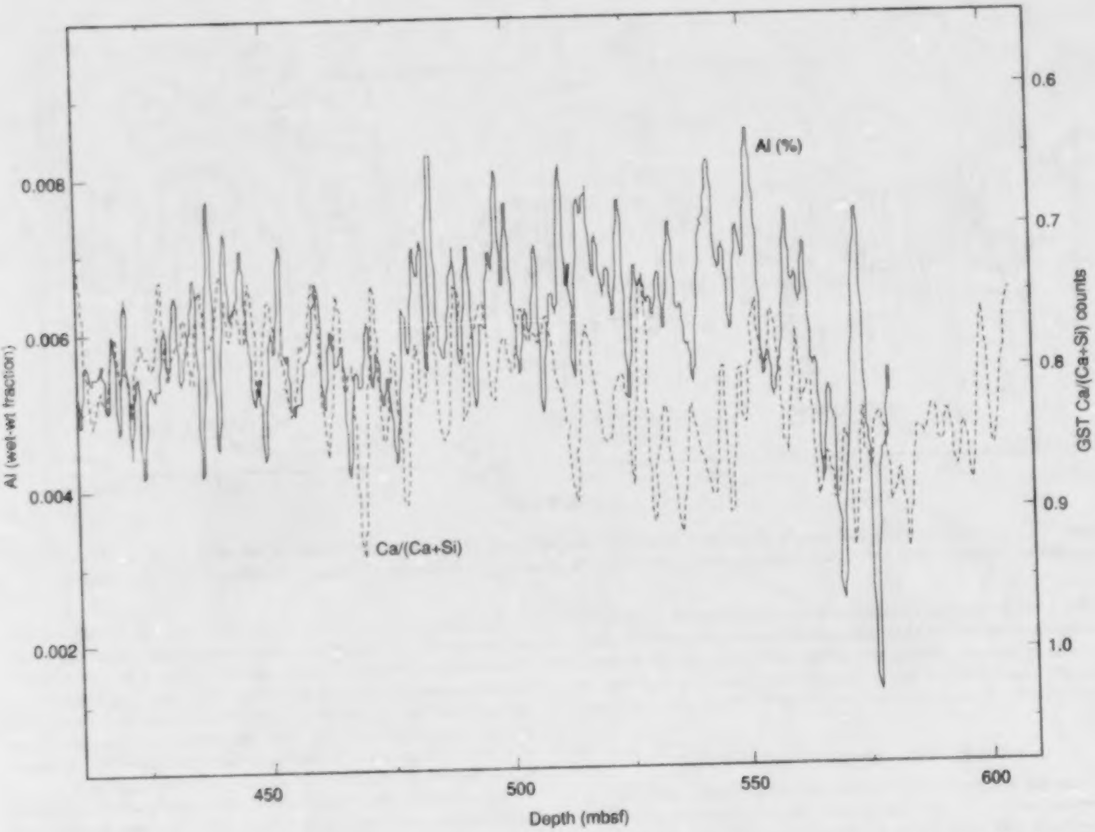

Figure 36. Log-derived calcium/(calcium + silica) ratio (dashed line) compared with log-derived aluminum wet-weight fraction (solid line).

amplitude change in velocity, but, in this case, a decrease rather than an increase.

Drilling stopped at Site 805 at 611 mbsf. Using the results of Site 803, we can estimate that the Eocene/Oligocene boundary should be found at approximately 0.650 sbsf (660 m) and that the strongly reverberant reflectors of the "Ontong Java Series" (see "Summary and Conclusions" section, this chapter) represent the large fluctuations in carbonate content and induration (alternations between limestone and chert) typical of many Eocene sections. Acoustic basement at this site is complex; there are two very strong reverberant zones, one at 0.758 sbsf and the second at 0.845 sbsf. The upper zone may represent massive chert and the lower one basalt, or we may be seeing two basaltic flow units separated by sediments.

The ultimate goal of our seismic stratigraphic effort was to use the seismic record as a paleoceanographic tool by producing detailed maps of the distribution, in time and space, of various parameters that reflect paleoceanographic processes. The achievement of this goal involved, among other things, the careful mapping of selected seismic horizons over large distances, a project well beyond the scope of a shipboard report. We have, however, already noticed identifiable patterns in the seismic character of the Ontong Java Plateau sites and, to facilitate future discussions, have given these reflector patterns names. Reflectors have been grouped and the groups given labels based on the major geographic events that influenced oceanographic processes at that time. Thus, we adopt (tentatively) the hypothesis of Mayer et al. (1985, 1986), which proposes that certain central Pacific-wide seismic reflectors were the result of global oceanographic events. We do not imply, however, by this naming, that our analyses of Ontong Java seismic stratigraphy suffices for ascribing particular reflectors to particular events.

The youngest named group of reflectors (4–2 Ma) are called the Panama Series because of the influence of the closing of the Isthmus of Panama on global oceanography at this time. Also dominating global oceanographic processes during this period was the onset of Northern Hemisphere Glaciation and associated reorganizations of North Atlantic Deep Water. The next group, the Tethyan Series, spans a time interval (10.5–4 Ma) affected by the closing of the Tethyan Seaway and including the isolation of the Mediterranean and a fundamental change in the partitioning of silica and carbonate between the Atlantic and the Pacific.

The Antarctic Series (19–10.5 Ma) represents that period of time dominated by the buildup of ice in Antarctica and perhaps the initiation of Norwegian Sea overflow into the Atlantic. This is followed, downsection, by the Drake Series (22.5–19 Ma), during which the Drake Passage opened up and steep north-south thermal gradients and circumpolar circulation began. Beneath the Drake Series are the Texas Interval (35–23 Ma), a long period of comparatively little oceanographic change that resulted in a reflector-free seismic interval, and the Ontong Java

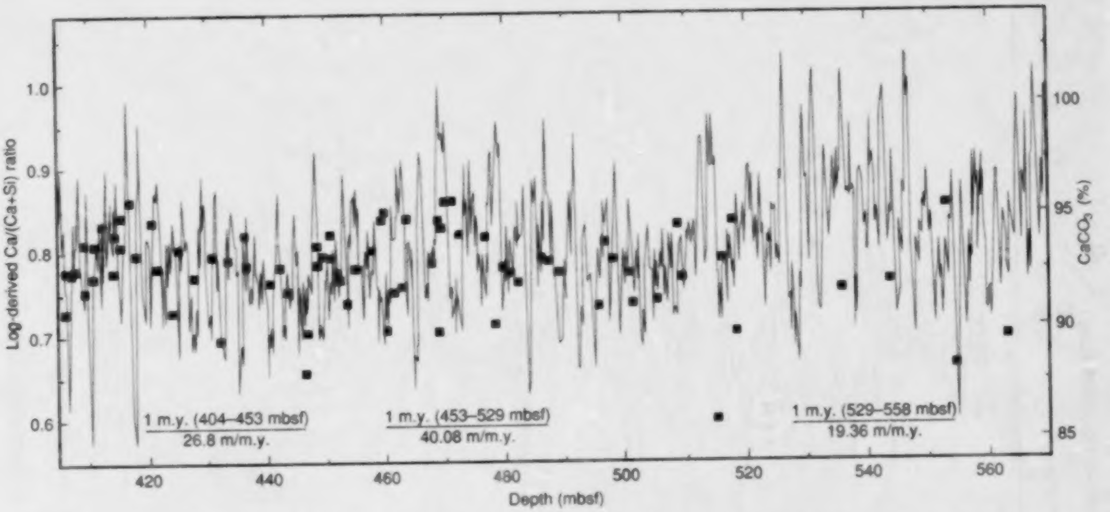

Figure 37. Log-derived calcium/(calcium + silica) ratio (solid line) compared with shipboard measurements of %CaCO$_3$ (squares) for the interval from 400 to 590 mbsf, Hole 805C. Bars represent 1-m.y. time intervals. Note change in spacing of cyclicity as sedimentation rate changes.

Series (middle and late Eocene), which is characterized by strongly reverberant reflectors that are indicative of the large fluctuations in carbonate content and induration typical of the Eocene. Further discussion of the rationale for these divisions can be found in the "Summary and Conclusions" section of this chapter.

SUMMARY AND CONCLUSIONS

Site 805 is located in the western equatorial Pacific on the northeastern margin of the Ontong Java Plateau (latitude 1°13.7′N, longitude 160°31.8′E) in 3188 m of water. Our objective in drilling this site was to obtain a continuous record that would serve as the intermediate member of a depth transect of Neogene sediments, designed to recover depth-related paleoceanographic signals. We anticipated that we would encounter a high-resolution carbonate record in a near-lysoclinal setting for our studies of dissolution history and biostratigraphy.

The site was positioned based on two intersecting single-channel seismic (SCS) lines acquired by the *Thomas Washington* during ROUNDABOUT Cruise 11 (2130 UTC, 24 December 1989, and 1700 UTC, 25 December 1989). The site was located within a gently sloping valley about 3.5 km wide, flanked by low ridges along either side where the SCS profiles showed continuous reflectors with little or no disturbance.

Coring Results

We spent 6.17 days on this site, drilling three holes and coring 1135 m of sediment, of which 993 m were recovered. Hole 805A, a dedicated hole, was cored with the APC to 50.5 mbsf into upper Pliocene sediments, with 103% recovery. Hole 805B was cored with the APC to 263.2 mbsf, where refusal occurred, at the boundary between upper and middle Miocene sediments; recovery was 103%. The hole was continued with XCB coring to 473.3 mbsf, with 210.1 m of sediment cored and 173.6 m recovered (83% recovery). Coring ended about half-way through a thick section of lower Miocene sediments. Hole 805C was cored with the APC to 235.8 mbsf (100% recovery), at which point XCB coring was initiated. Drilling ended in upper Oligocene sediments at 611.0 mbsf, with 259.1 m cored with the XCB (69% recovery). The hole was then logged.

The sediment retrieved is Neogene in age, except for the nine deepest cores in Hole 805C, which recovered Oligocene chalk. The entire column, from the earliest deposits to the seafloor, was considered to be one lithologic unit and was classified as nannofossil and foraminifer nannofossil ooze and chalk. The average sedimentation rate over the entire interval is ~20 m/m.y. No stratigraphic breaks were detected. However, sedimentation rates fell to rather low values (almost 10 m/m.y.).

Two subunits were recognized in this quite uniform section of bioturbated ooze and chalk. They are separated by the ooze-chalk transition at 282.5 mbsf in Hole 805B (base of Core 130-805B-30X) and at 293.7 mbsf in Hole 805C (base of Core 130-805C-31X) (upper middle Miocene, ca. 11.4 Ma). The transition is gradational and shows alternating layers with varying degrees of lithification.

The younger section of the unit (Subunit IA, 0–293.7 mbsf) comprises Pleistocene to middle Miocene nannofossil ooze, nannofossil ooze with foraminifers, and foraminifer nannofossil ooze. Radiolarian content was low on the whole. The oozes are light gray in the top 30 mbsf, grading into white ooze. Color banding is common throughout the unit and is especially well expressed in the uppermost Miocene. For the most part, color bands are coarse and irregular in Subunit IA. Some large burrows have well-developed concentric color rings ("Liesegang rings"), indicating redox gradients as the cause for color banding. Microfaulting was observed in Core 130-805B-18H at 166 mbsf (middle upper Miocene), and color band tilting was seen at the middle/upper Miocene boundary.

Sediments are generally soft, but in the lowermost portion of Subunit IA (283–293 mbsf) more lithified intervals appear. A shift toward higher velocities occurred near the top of that zone, and another at the ooze-chalk transition at about 294 mbsf.

The older section of the unit, Subunit IB (293.7–611 mbsf), consists of approximately 317 m of nannofossil chalk, nannofossil chalk with foraminifers, and foraminifer nannofossil chalk of middle Miocene to late Oligocene age. The color is dominantly white. Color banding occurs throughout but becomes rare below 504 mbsf in the lowermost Miocene. It includes bundles of pseudolaminae, that is, fine-scale Liesegang banding, that show sharp individual boundaries. Microfaulting is gener-

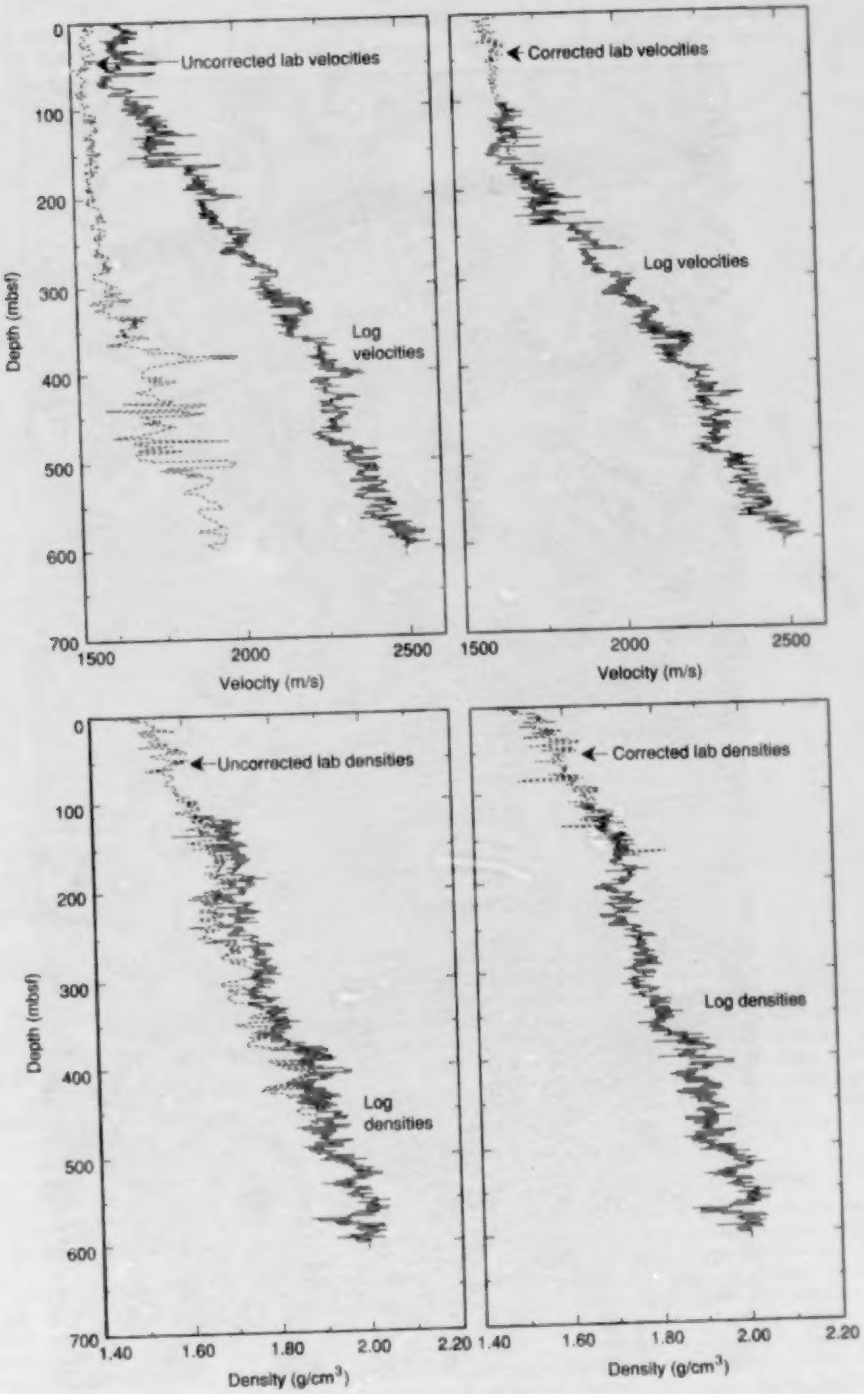

Figure 38. Comparison of velocity and density logs with uncorrected and corrected laboratory measurements, Hole 805C. Dashed line represents laboratory measurements. Comparison of velocity log with corrected laboratory velocity measurements.

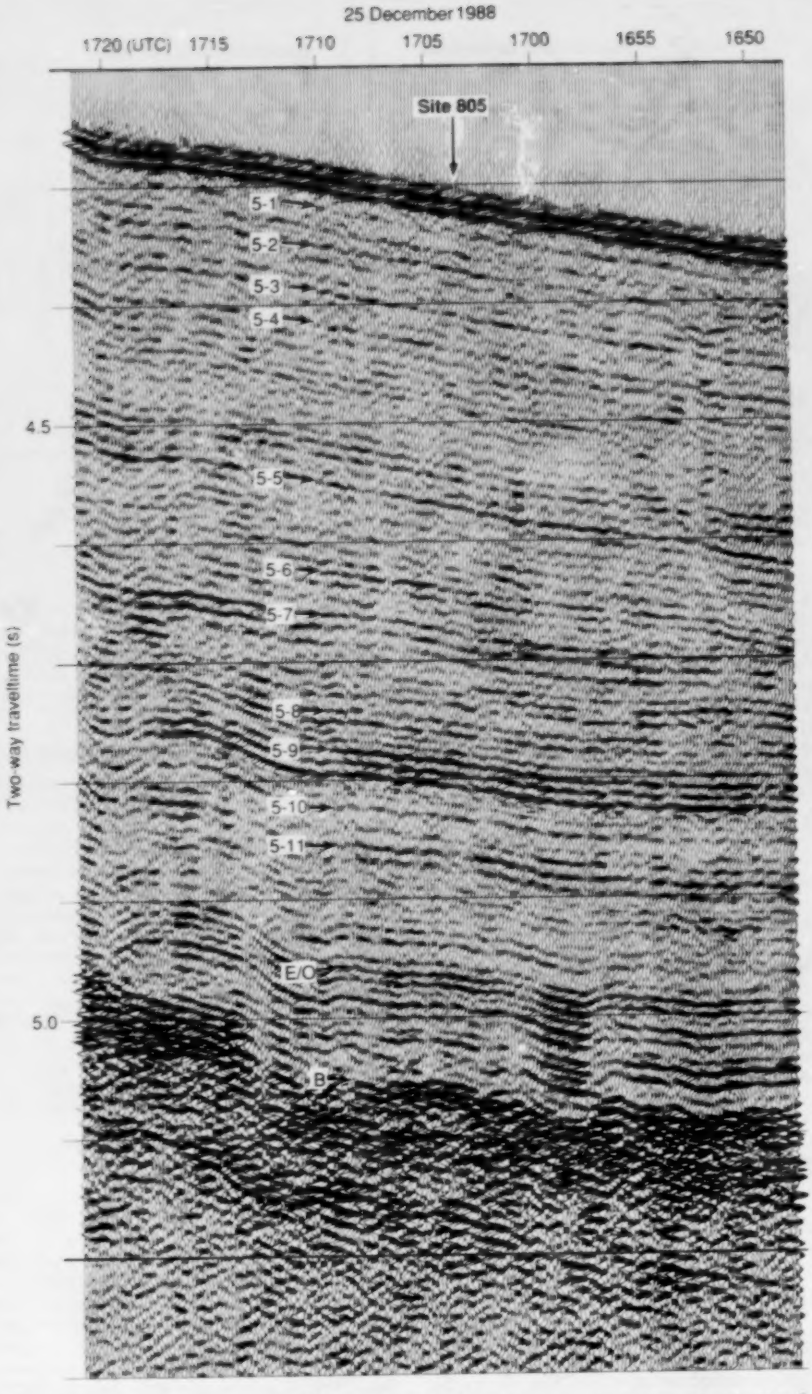

Figure 39. Seismic record collected on ROUNDABOUT Cruise 11 site survey over Site 805 using the 80-in.^{3} water gun, 70–250 Hz band-pass filter. For details of reflectors, see Table 14.

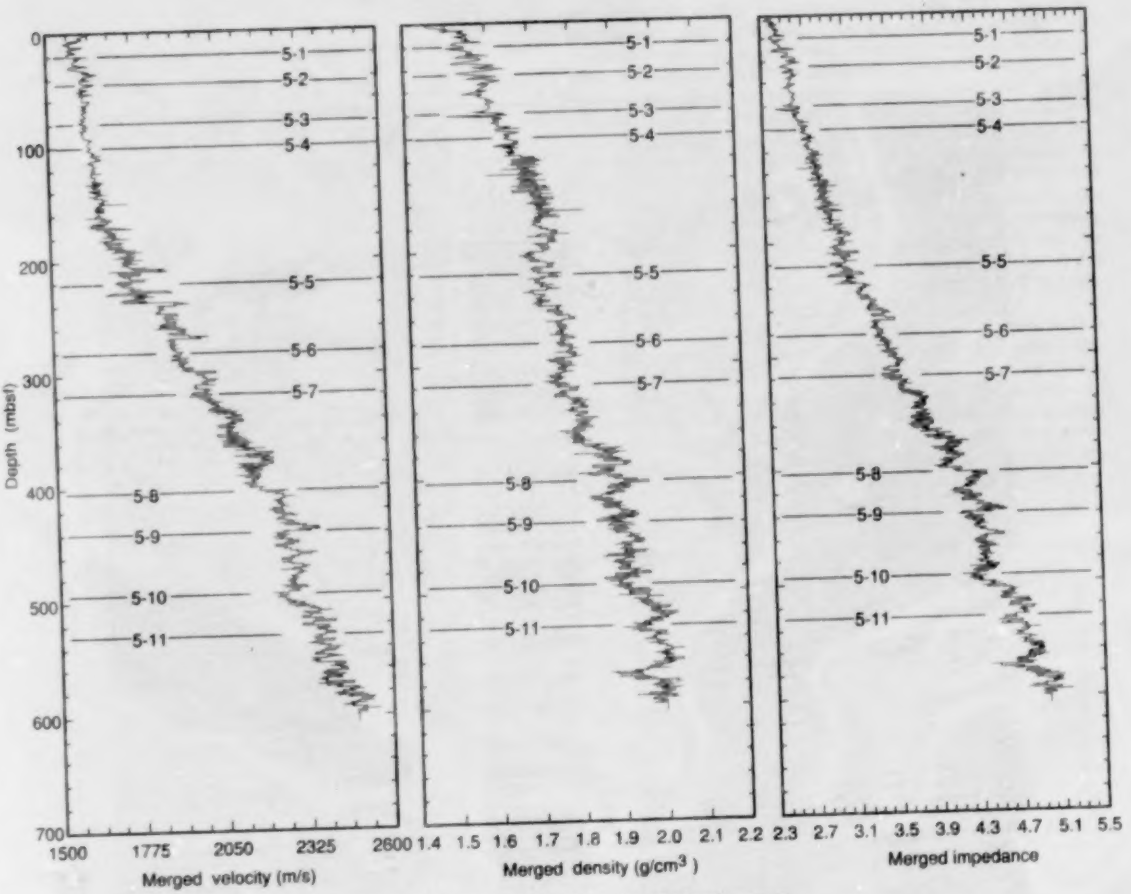

Figure 40. Velocity, density, and acoustic impedance used for generating Site 805 synthetic seismogram.

ally absent, except at ~310 mbsf (ca. 12 Ma), near the top of the subunit.

Recovery in the chalk subunit was good down into lower Miocene sediments. Here it dropped noticeably below 450 mbsf (Core 130-805C-47X) and became quite poor below 520 mbsf (Core 130-805C-55X) near the Oligocene/Miocene boundary. Even where recovery is very good, core contents are largely disjointed chunks and chips, with evidence for grinding of chalk on chalk. This type of recovery is typical for the material below 370 mbsf. The Oligocene/Miocene boundary was located near 525 mbsf and apparently is without hiatus. Sedimentation rates for the deep chalk section are typically between 7 and 30 m/m.y., with the lower rates occurring in the Oligocene and the higher ones in the lower middle Miocene.

Special Studies

Magnetostratigraphy was produced for the uppermost section of Holes 805B and 805C. Only the Brunhes Chron and part of the Matuyama could be identified. The sedimentation rate since 1.7 Ma was determined to be 17.1 m/m.y.

Chemical gradients in the interstitial waters at this site are generally similar to those at Sites 803 and 804, reflecting the calcareous/siliceous nature of the sediments and the paucity of organic material. A somewhat higher supply of organic matter at this shallower site, perhaps a result of the shallower depth, tends to produce slightly stronger gradients. Calcium and magnesium gradients are influenced by basalt alteration reactions at depth and show the usual negative correlation. Strontium concentrations reflect recrystallization processes, which take place in younger sediments at this site than at the other two because of the higher sedimentation rates. Dissolved silica shows a steady increase with depth, except for a minor reversal of this trend just above the ooze-chalk transition.

Seismic Stratigraphy

Site 805 was the first of the Leg 130 sites to deliver a complete stratigraphic record without hiatuses. It is, therefore, of great interest with respect to a central objective of the leg: to determine the nature of the acoustic reflectors seen on seismic profiles. Guidance in attempting this was provided by the velocity and density profiles recovered during logging and by the age controls determined during biostratigraphic analyses.

A great number of reflectors were observed in the profile taken by the *Thomas Washington* during the ROUNDABOUT pre-site survey (Fig. 43). Depth assignment and dating shows that at least some of the reflectors are associated with pale-

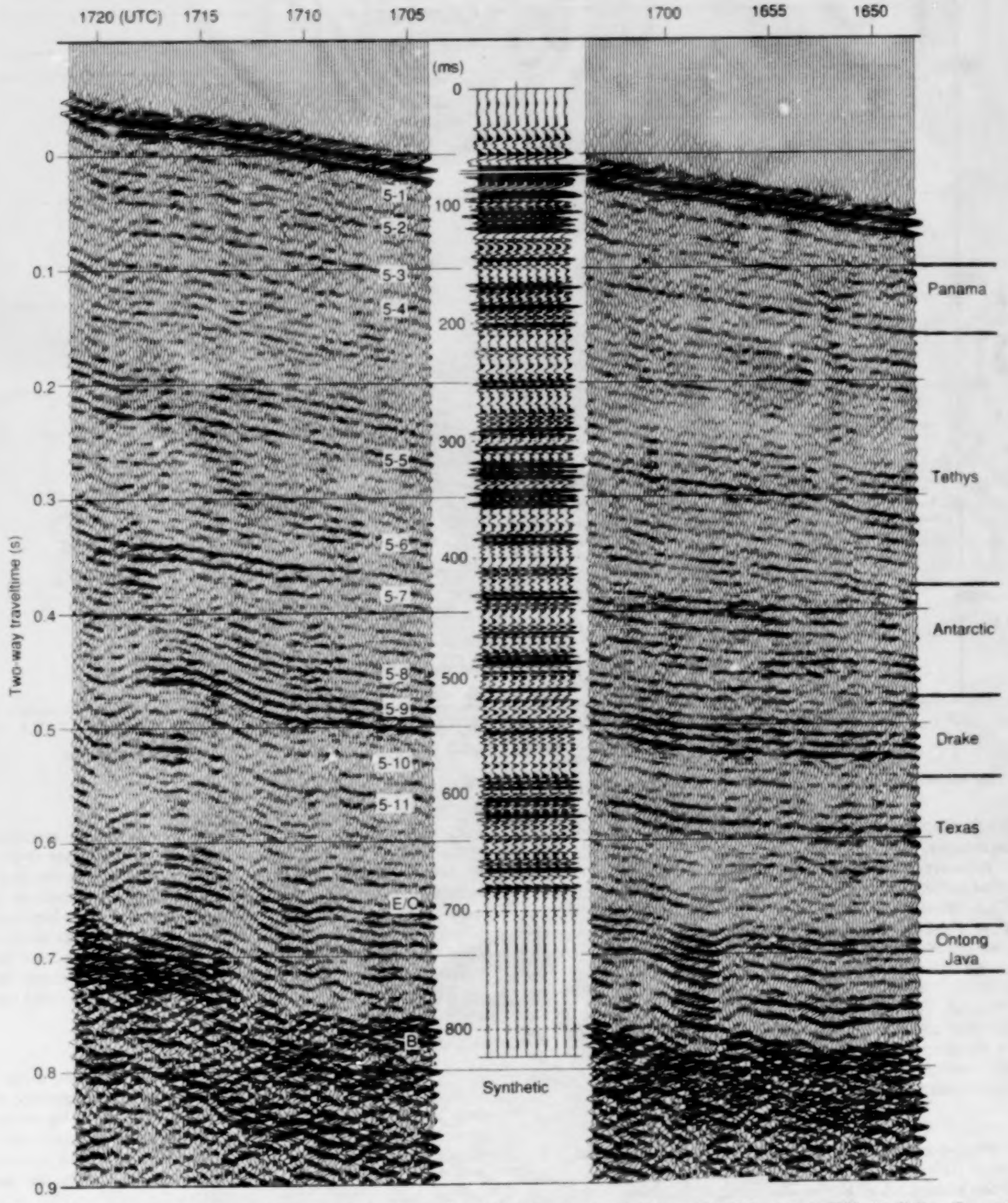

Figure 41. Comparison of synthetic seismogram and field records, Site 805. For details of reflectors (5-1, 5-2, etc.), see Table 14. E/O = Eocene/Oligocene boundary and B = basement. Names to the right refer to distinct groups of reflectors. See text for details.

Table 14. Summary of traveltimes, depths, and ages for Site 805 reflectors.

	Traveltime		Depth		
Reflector	Seismic (s)	Synthetic (s)	Seismic (m)	Synthetic (m)	Age (Ma)
5-1	0.027	0.025	21	20	1.2
5-2	0.060	0.057	48	45	2.4–2.5
5-3	0.100	0.100	80	80	3.7
5-4	0.124	0.124	101	101	4.4–4.5
5-5	0.260	0.267	215	221	7.1–7.36
5-6	0.328	0.332	278	281	10.3–10.6
5-7	0.367	0.368	317	319	12.8–12.9
5-8	0.442	0.449	396	403	19.0–19.9
5-9	0.479	0.482	436	440	21.2–21.3
5-10	0.522	0.530	486	495	22.6–22.9
5-11	0.559	0.561	528	531	23.7–23.9

Notes: Depths and traveltimes to seismic events are picked on both the synthetic seismogram (synthetic) and the field record (seismic). Ages are from sedimentation rate curves (see "Sedimentation Rates" section, this chapter).

oceanographic events, as suggested by Mayer et al. (1986) for the central equatorial Pacific. They proposed the closing of the Panama Isthmus, reorganization of deep circulation in the Atlantic, climatic events surrounding the Antarctic, and the opening of Drake Passage as important paleoceanographic themes reflected in the acoustic properties of Pacific pelagic sediments. Accordingly (but without prejudging the question about origins), we refer to reflectors aged 2–4 Ma as "Panama Series," to those aged 10–19 Ma as "Antarctic Series," and to those aged 19–23 Ma as "Drake Series." These ages are approximate; the criterion is grouping, not dating. The advantage of considering groups of reflectors in addition to single members is that the variability of properties within a given section is being addressed, rather than only an individual excursion of velocity and/or density within the sediment profile.

The interval between the Panama and the Drake reflectors is the "Tethys Interval," which contains sediments deposited during mountain building in the closing Tethys Belt. Below the Drake Series is an acoustically quiet zone, the "Texas Interval," named in appreciation of Texan know-how in deep-sea drilling, which saved enough time in a crowded schedule to allow entering this zone on several occasions during Leg 130. Below the Texas Interval is the "Ontong Java Series," a group of strong re-

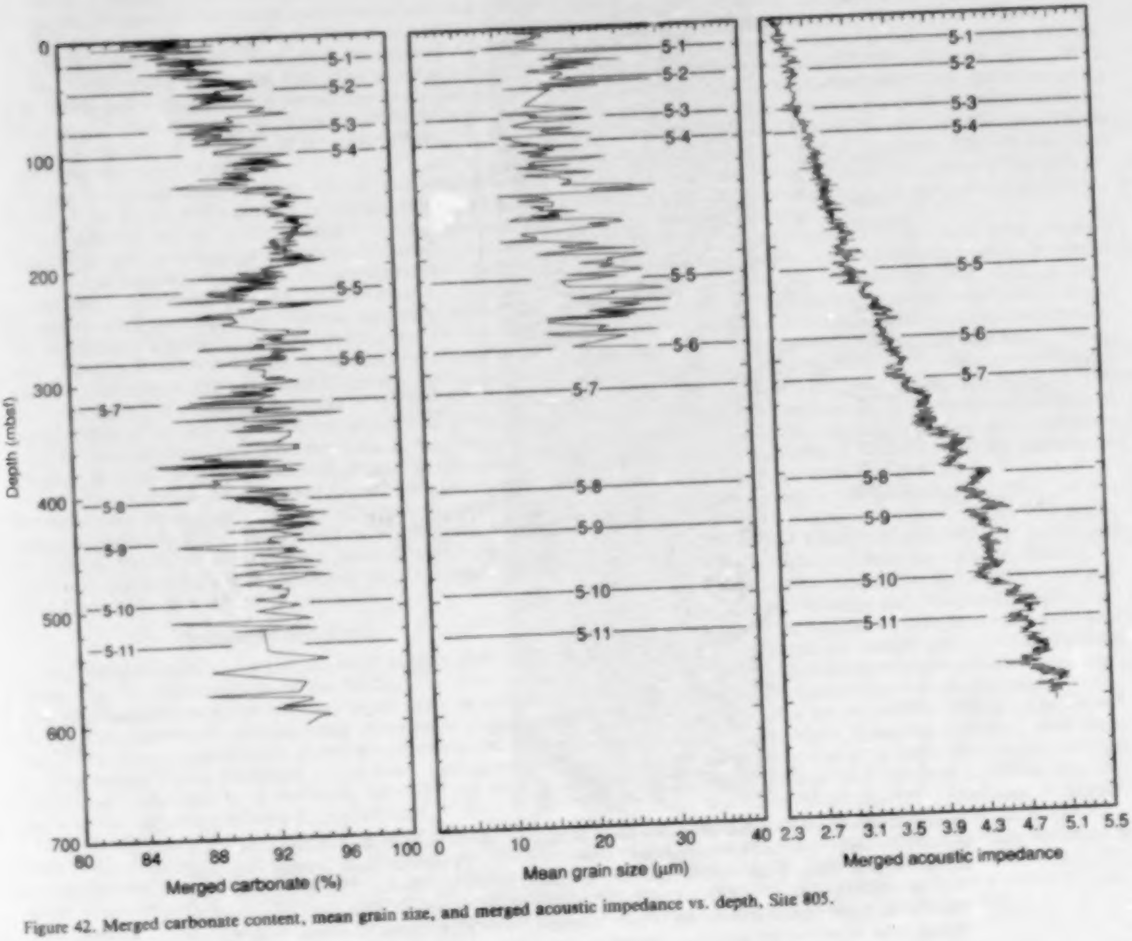

Figure 42. Merged carbonate content, mean grain size, and merged acoustic impedance vs. depth, Site 805.

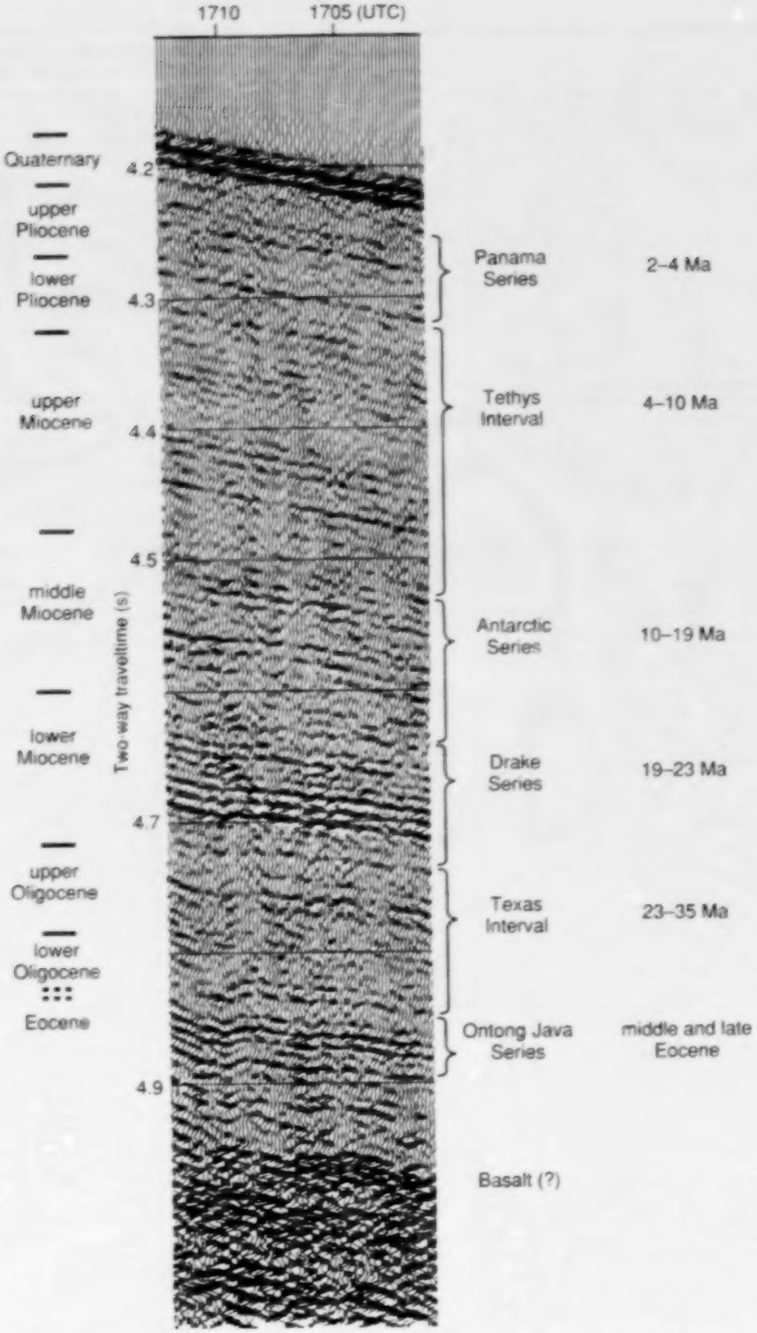

Figure 43. Seismic profile at Site 805, taken on 25 December 1989 on the *Thomas Washington* ROUNDABOUT Cruise 11 (see "Seismic Stratigraphy" section, this chapter), with time scale assigned from drilling and logging results. Names to the right refer to distinct groups of reflectors ("series") and to zones with no distinct groups of reflectors ("intervals"). Three of the names are taken from suggestions by Mayer et al. (1986) regarding the origin of such reflectors (Panama, Antarctic, and Drake Passage). Although these hypotheses are appealing, our use of these names does not imply that we consider them proved. For "Tethys" and "Texas" intervals, see text. Numbers to the left refer to two-way traveltime. Numbers at top refer to time of day.

flectors, ubiquitous on the plateau, that are derived from impedance changes caused by limestone and chert formation.

The Panama Series contains reflectors dated near 2, 2.4, and 3.7 Ma. The age of 2.4 Ma corresponds to a deep-water cooling event and the onset of North Atlantic ice buildup (Backman, 1979; Shackleton et al., 1984). Reflectors dated at 2.4 and 3.7 Ma can be identified in the seismic record across DSDP Site 586 (near Site 289) using the velocity profile obtained from logging that site (Shipboard Scientific Party, 1986a). The Tethys Interval (Fig. 43) contains a number of lesser reflectors, one of which apparently corresponds to lithification (near 210 m, age 7 Ma). The presumed condensed section just below 10 Ma (see "Sedimentation Rate" section, this chapter) has a less than prominent group of reflectors at the base of the Tethys Interval (270–290 mbsf). Also, the ooze-chalk transition does not seem to be strongly expressed, although it is possible to find reflecting horizons in the vicinity of 290 mbsf.

The next group of strong reflectors, going downsection in Figure 43, is the upper part of the Antarctic Series, in the middle of the middle Miocene (13 Ma). It starts with a distinct reflector between 310 and 320 mbsf (dated 12.5–13 Ma). The lower part of this series is somewhat weaker and belongs to the lowermost middle Miocene and uppermost lower Miocene (360–385 mbsf, 15–18 Ma). This entire zone is characterized by a major climatic change and associated excursions in carbonate content and other sediment properties (Barron et al., 1985). These changes, presumably, are associated with the onset of Antarctic Bottom Water production at that time. The group of reflectors immediately below the Antarctic Series, the Drake Series, has the strongest reflector members. Ages range from about 18.5 Ma for the uppermost members of the group (390 mbsf) to 22 Ma for the deepest (460 mbsf).

Below this group there is a thick section, the Texas Interval (up to 180 m thick), which is more or less transparent acoustically. The reason for this is the absence of abrupt changes in sediment properties within the Oligocene. This period was also noted by the biostratigraphers for the paucity of evolutionary events. One lone reflector (Fig. 43; 520–530 mbsf, ca. 23.6 Ma) appears to mark the Oligocene/Miocene boundary. Below this interval, there is a group of strong reflectors, the Ontong Java Series, the top of which is thought to represent the change from chalk to limestone in the lowermost Oligocene and upper Eocene, especially the occurrence of chert in the middle Eocene. The thickness of this acoustic unit is on the order of 100 m. Another 50 m or so down, acoustic basement is reached, which probably consists of basalt or perhaps of chert and limestone.

In summary, the results of Site 805 support, in a general way, the hypothesis that many reflectors represent the effects of global paleoceanographic events and can be correlated across the tropical Pacific. Other reflectors, however, may be regionally strong expressions of minor events or may be related to diagenetic processes that are not synchronous.

Sedimentation Rates

The oldest sediments cored, at 611 mbsf in Hole 805C, were of latest early Oligocene age (Zone NP23). The distance to acoustic basement below this level may be estimated as approximately 0.15-s two-way traveltime, which corresponds to roughly 190 m of sediment at that depth. If this is all the sediment there is, considerable hiatus formation in the lower Paleogene and Cretaceous would seem to be indicated, assuming that the uncored section represents at least 80 m.y. of time.

Since early Oligocene time, Site 805 has received nannofossil ooze, with rather minor admixtures of siliceous fossils. Sedimentation rates typically varied between 12 m/m.y. (middle and upper Miocene) and almost 40 m/m.y. (upper Pliocene), the overall average being near 20 m/m.y. Two condensed sections may be present, based on nannofossils and foraminifers (see "Biostratigraphy" section, this chapter): one between 10 and 9 Ma (lowermost upper Miocene), and the other centered on 17.5 Ma (uppermost lower Miocene). Both these periods are characterized by strong carbonate dissolution events in the central Pacific (Barron et al., 1985); the younger one is commonly a time of hiatus formation (NH4 of Keller and Barron, 1983).

Comparisons with Sites 289, 803, and 804

The lithology of Site 805 was the same as that of the comparison sites. The carbonate content at Site 805 typically reached values above 90% throughout the section except in the Pleistocene portion and at the upper and lower boundaries of the middle Miocene. In the Pliocene values hover around 90%. The carbonate stratigraphy of Site 803 is quite similar in long-term trends as well as in some of the details. Site 804 also has similar trends, although they are disturbed there by hiatus formation. On the whole, percentages in Site 804 are between 5% and 10% lower, and fluctuate more strongly, than in Site 805.

Mean grain size is typically between 12 and 25 μm at Site 805, with maxima near the Pleistocene/Pliocene boundary and in the uppermost and lowermost upper Miocene. Minima occur in the middle of the lower Pliocene and in the upper half of the upper Miocene. No measurements are available for pre-mid-Miocene sediments. Patterns are quite different for Sites 803 and 804. Site 803 has distinctly higher values in post-Miocene time, despite its greater depth and lower sedimentation rate. Dissolution should decrease sand content there (Johnson et al., 1977), so differences in local winnowing, or in the rate of receiving fines from upslope, may be indicated. In the upper Miocene the situation is reversed: Site 805 has the coarser sediments. This is as expected if dissolution effects dominate. Site 804 has mean grain sizes that are quite comparable with those of Site 805, except for a pronounced coarsening in the section surrounding the hiatus in the lower Pliocene.

Smear slide abundance patterns of the major fossil groups—nannofossils, foraminifers, and radiolarians—are quite similar between Sites 803 and 805. To establish differences, a more quantitative analysis than has been done on board will be necessary. For Site 804, the abundance patterns are quite different, presumably because of carbonate dissolution and hiatus formation at that site. At DSDP Site 289, foraminifers are much more abundant than at Site 805 (Shipboard Scientific Party, 1975b). Several processes must be considered: increased winnowing at Site 289 (2200 m), and the destruction of tests and the delivery of upslope fines at the depth of Site 805 (3200 m). Radiolarian content is low throughout Unit 1 of Site 289.

The ooze-chalk transition was located at 290 mbsf (ca. 11–11.5 Ma) in Site 805. It is deeper and younger here than at Site 803 (217 mbsf, ca. 14–14.5 Ma), but shallower than its location in Site 289 although roughly synchronous with it (350 mbsf, ca. 11.5 Ma). Thus, the comparison of Site 805 with Site 289 supports the hypothesis of Schlanger and Douglas (1974) that age (i.e., conditioning during deposition) is an important parameter in the rate of lithification; the comparison with Site 803 does not. It appears that a distinctly increased overburden may accelerate the process of lithification but not all that much.

Rates of accumulation are about 10%–30% lower in Site 805 than in Site 289, on the whole, in keeping with the greater depth of Site 805. The rates are distinctly higher than in Site 803 by a factor of between 1.2 (upper Miocene) and 1.9 (lower Pliocene and middle and lower Miocene). For Pleistocene sediments, rates are unusually low at all three sites (289, 803, and 805). Also, for this period, the sedimentation rate of Site 805 actually exceeds that of Site 289. This suggests strong winnowing during this period, with downslope transport of fine material presumably mitigating the winnowing effect at Site 805.

REFERENCES

Backman, J., 1979. Pliocene biostratigraphy of DSDP Sites 111 and 116 from the North Atlantic Ocean and the age of the Northern Hemisphere Glaciation. *Stockholm Contrib. Geol.*, 32:115–137.

Barron, J. A., and Keller, G., 1982. Widespread Miocene deep-sea hiatuses: coincidence with periods of global cooling. *Geology*, 10:577–581.

Barron, J. A., Keller, G., and Dunn, D. A., 1985. A multiple microfossil biochronology for the Miocene. *In* Kennett, J. P. (Ed.), *The Miocene Ocean: Paleoceanography and Biogeography.* Mem. Geol. Soc. Am., 163:21–36.

Berger, W. H., 1976. Biogenous deep sea sediments: production, preservation, and interpretation. *In* Riley, J. P., and Chester, R. (Eds.), *Chemical Oceanography* (Vol. 5): New York (Academic Press), 265–328.

Berger, W. H., and Johnson, T. C., 1976. Deep-sea carbonates: dissolution and mass wasting on Ontong Java Plateau. *Science*, 192:785–787.

Berger, W. H., Johnson, T. C., and Hamilton, E. L., 1977. Sedimentation on Ontong-Java Plateau: observations on a classic "carbonate monitor." *In* Anderson, N. R., and Malahoff, A. (Eds.), *The Fate of Fossil Fuel* CO_2 *in the Oceans:* New York (Plenum Press), 543–567.

Berger, W. H., and Mayer, L. A., 1978. Deep-sea carbonates: acoustic reflectors and lysocline fluctuations. *Geology*, 6:11–15.

Berggren, W. A., Kent, D. V., Flynn, J. J., and Van Couvering, J. A., 1985. Cenozoic geochronology. *Geol. Soc. Am. Bull.*, 96:1407–1418.

Emeis, K.-C., and Kvenvolden, K. A., 1986. Shipboard organic geochemistry on *JOIDES Resolution*. *ODP Tech. Note*, No. 7.

Espitalié, J., Laporte, J. L., Madec, M., Marquis, F., Leplat, P., Paulet, J., and Boutfeu, A., 1977. Method rapide de caracterisation des roches mère de leur potentiel petrolier et de leur degree d'evolution. *Rev. Inst. Fr. Pet.*, 32:23–42.

Gieskes, J. M., 1981. Deep-sea drilling interstitial water studies: implications for chemical alteration of the oceanic crust, layers I and II. *In* Warme, J. E., Douglas, R. G., and Winterer, E. L. (Eds.), *The Deep Sea Drilling Project: A Decade of Progress*. Spec. Publ., Soc. Econ. Paleontol. Mineral., 32:149–167.

Hay, W. W., 1970. Calcareous nannofossils from cores recovered on DSDP Leg 4. *In* Bader, R. G., Gerard, R. D., et al., *Init. Repts. DSDP*, 4: Washington (U.S. Govt. Printing Office), 455–501.

Hermelin, J.O.R., 1989. Pliocene benthic foraminifera from the Ontong Java Plateau (western equatorial Pacific Ocean): faunal response to changing paleoenvironment. *Spec. Publ., Cushman Found. Foraminiferal Res.*, 26:1–143.

Hussong, D. M., Wipperman, L. K., and Kroenke, L. W., 1979. The crustal structure of the Ontong Java and Manihiki oceanic plateaus. *J. Geophys. Res.*, 84:6003–6010.

Jacobs, J. A., 1984. *Reversals of the Earth's Magnetic Field:* Bristol (Adam Hilger).

Johnson, T. C., Hamilton, E. L., and Berger, W. H., 1977. Physical properties of calcareous ooze: control by dissolution at depth. *Mar. Geol.*, 24:259–277.

Keller, G., and Barron, J. A., 1983. Paleoceanographic implications of Miocene deep-sea hiatuses. *Geol. Soc. Am. Bull.*, 94:590–613.

Kroenke, L., 1972. Geology of the Ontong Java Plateau [Ph.D. dissert.]. Univ. of Hawaii.

Mammerickx, J., and Smith, S. M., 1985. *Bathymetry of the North Central Pacific:* Boulder, CO (Geological Society of America), Map and Chart Ser., No. MC-52.

Mankinen, E. A., Donnelly, J. M., and Grommé, C. S., 1978. Geomagnetic polarity event recorded at 1.1. m.y.r. B.P. on Cobb mountain, Clear Lake volcanic field, California. *Geology*, 6:653–656.

Mayer, L. A., Shipley, T. S, Theyer, F., Wilkens, R. W., and Winterer, E. L., 1985. Seismic modelling and paleoceanography at DSDP Site 574. *In* Mayer, L. A., Theyer, F., Thomas, E., et al., *Init. Repts. DSDP*, 85: Washington (U.S. Govt. Printing Office), 947–970.

Mayer, L. A., Shipley, T. H., and Winterer, E. L., 1986. Equatorial Pacific seismic reflectors as indicators of global oceanographic events. *Science*, 233:761–764.

McDuff, R. E., 1981. Major cation gradients in DSDP interstitial waters: the role of diffusive exchange between seawater and upper ocean crust. *Geochim. Cosmochim. Acta*, 45:1705–1713.

McDuff, R. E., and Gieskes, J. M., 1976. Calcium and magnesium profiles in DSDP interstitial waters: diffusion or reaction? *Earth Planet. Sci. Lett.*, 33:1–10.

Peterson, L. C., and Backman, J., 1990. Late Cenozoic carbonate accumulation and the history of the carbonate compensation depth in the western equatorial Indian Ocean. *In* Backman, J., Duncan, R. A., Peterson, L. C., et al., *Proc. ODP, Sci. Results*, 115: College Station, TX (Ocean Drilling Program), 467–507.

Resig, J. M., 1989. Stratigraphic distribution of late Neogene species of the planktonic foraminifer *Streptochilus* in the Indo-Pacific. *Micropaleontology*, 35:49–62.

Sanfilippo, A., Westberg-Smith, M. J., and Riedel, W. R., 1985. Cenozoic radiolaria. *In* Bolli, H. M., Saunders, J. B., and Perch-Nielsen, K. (Eds.), *Plankton Stratigraphy:* Cambridge (Cambridge Univ. Press), 631–712.

Schlanger, S. O., and Douglas, R. G., 1974. The pelagic ooze-chalk-limestone transition and its implication for marine stratigraphy. *In* Hsü, K. J., and Jenkyns, H. C. (Eds.), *Pelagic Sediments: On Land and Under the Sea*. Spec. Publ., Int. Assoc. Sedimentol., 1:117–148.

Shackleton, N. J., Backman, J., Zimmerman, H., Kent, D. V., Hall, M. A., Roberts, D. G., Schnitker, D., Baldauf, J., Desprairies, A., Homrighausen, R., Huddlestun, P., Keene, J. B., Kaltenback, A. J., Krumsiek, K.A.O., Morton, A. C., Murray, J. W., and Westberg-Smith, J., 1984. Oxygen isotope calibration of the onset of ice-rafting in DSDP Site 552A: history of glaciation in the North Atlantic region. *Nature*, 307:620–623.

Shackleton, N. J., and Opdyke, N. D., 1976. Oxygen-isotope and paleomagnetic stratigraphy of Pacific Core V28-239: late Pliocene to latest Pleistocene. *In* Cline, R. M., and Hays, J. D. (Eds.), *Investigations of Late Quaternary Paleoceanography and Paleoclimatology.* Mem. Geol. Soc. Am., 145:449–464.

Shipboard Scientific Party, 1971. Site 64. *In* Winterer, E. L., Riedel, W. R., et al., *Init. Repts. DSDP*, 7: Washington (U.S. Govt. Printing Office), 473–606.

Shipboard Scientific Party, 1975a. Site 288. *In* Andrews, J. E., Packham, G., et al., *Init. Repts. DSDP*, 30: Washington (U.S. Govt. Printing Office), 175–229.

Shipboard Scientific Party, 1975b. Site 289. *In* Andrews, J. E., Packham, G., et al., *Init. Repts. DSDP*, 30: Washington (U.S. Govt. Printing Office), 231–398.

Shipboard Scientific Party, 1986a. Site 586. *In* Moberly, R., Schlanger, S. O., et al., *Init. Repts. DSDP*, 89: Washington (U.S. Govt. Printing Office): 213–235.

Shipboard Scientific Party, 1986b. Site 586: western equatorial Pacific. *In* Kennett, J. P., von der Borch, C. C., et al., *Init. Repts DSDP*, 90: Washington (U.S. Govt. Printing Office), 19–114.

Wise, S. W., Jr., 1973. Calcareous nannofossils from cores recovered during Leg 18, Deep Sea Drilling Project: biostratigraphy and observations of diagenesis. *In* Kulm, L. D., von Huene, R., et al., *Init. Repts. DSDP*, 18: Washington (U.S. Govt. Printing Office), 569–615.

Wu, G., and Berger, W. H., 1989. Planktonic foraminifera: differential dissolution and the Quaternary stable isotope record in the west-equatorial Pacific. *Paleoceanography*, 4:181–198.

Ms 130A-107

NOTE: All core description forms ("barrel sheets") and core photographs have been printed on coated paper and bound as Section 5, near the back of the book, beginning on page 559.

Hole 805C: Resistivity-Sonic-Gamma Ray Log Summary

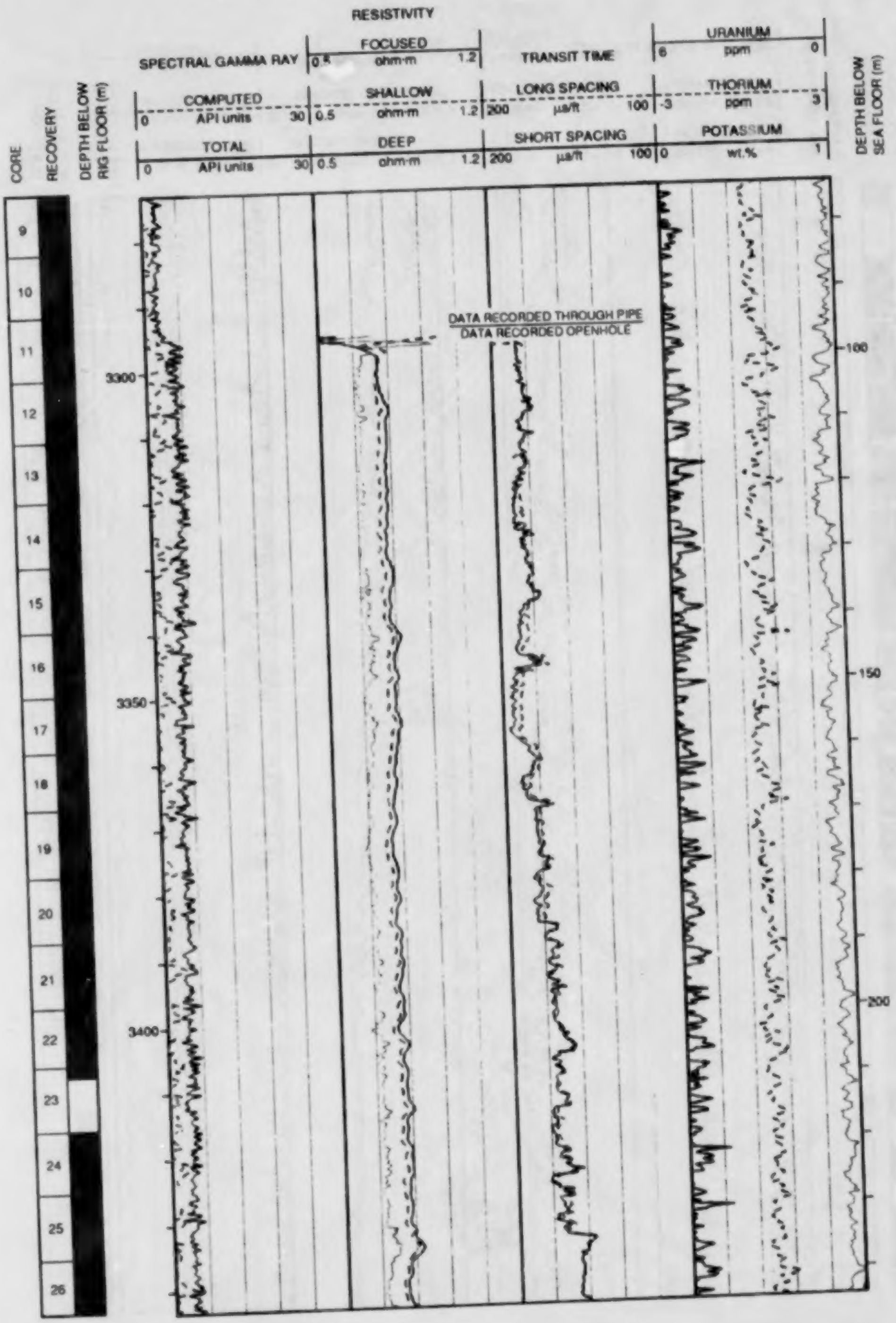

Hole 805C: Resistivity-Sonic-Gamma Ray Log Summary (continued)

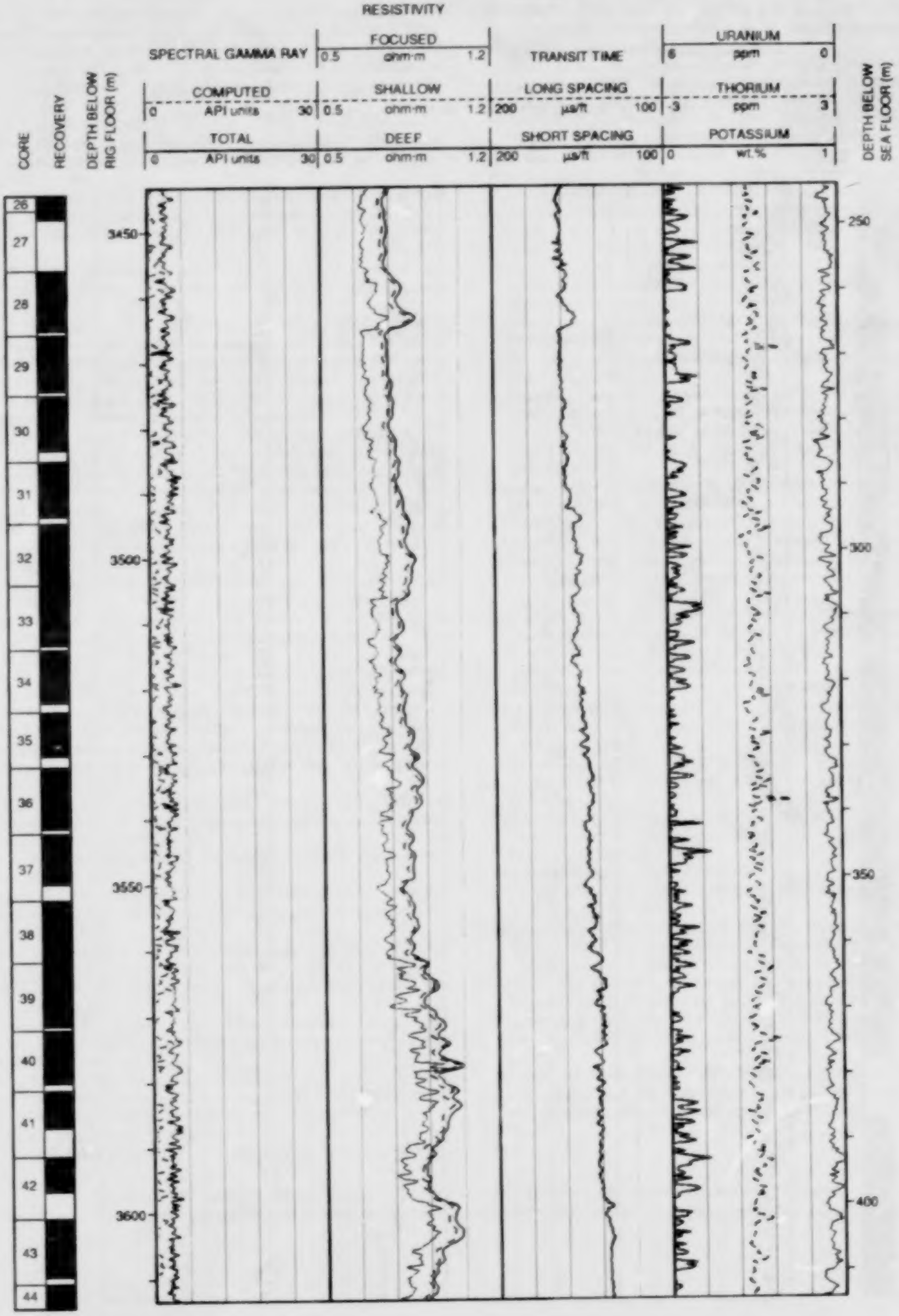

Hole 805C: Resistivity-Sonic-Gamma Ray Log Summary (continued)

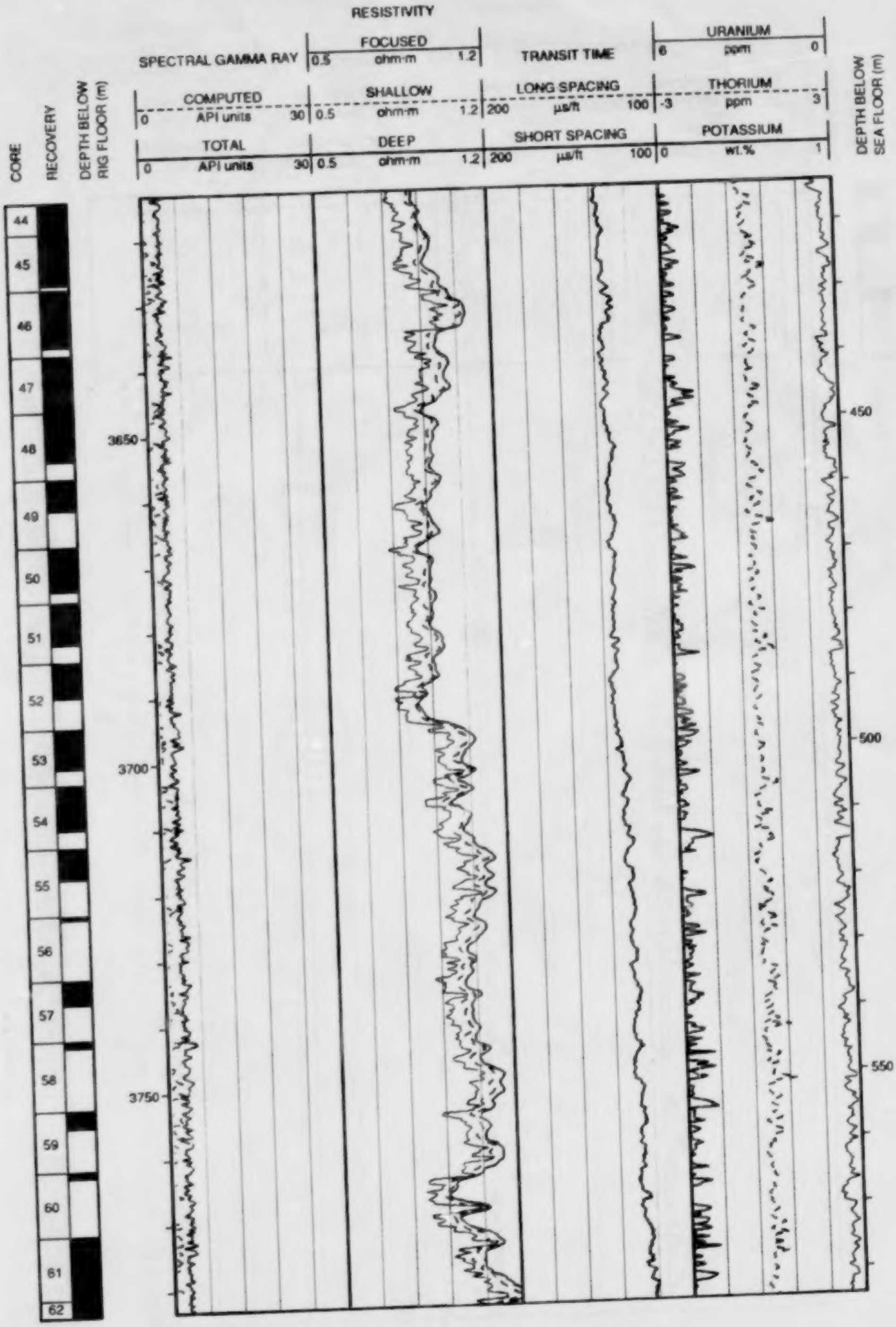

Hole 805C: Resistivity-Sonic-Gamma Ray Log Summary (continued)

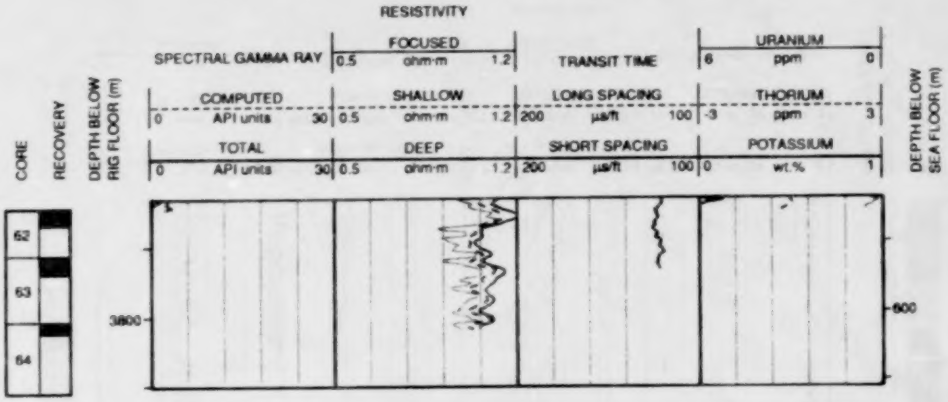

Hole 805C: Density-Gamma Ray Log Summary

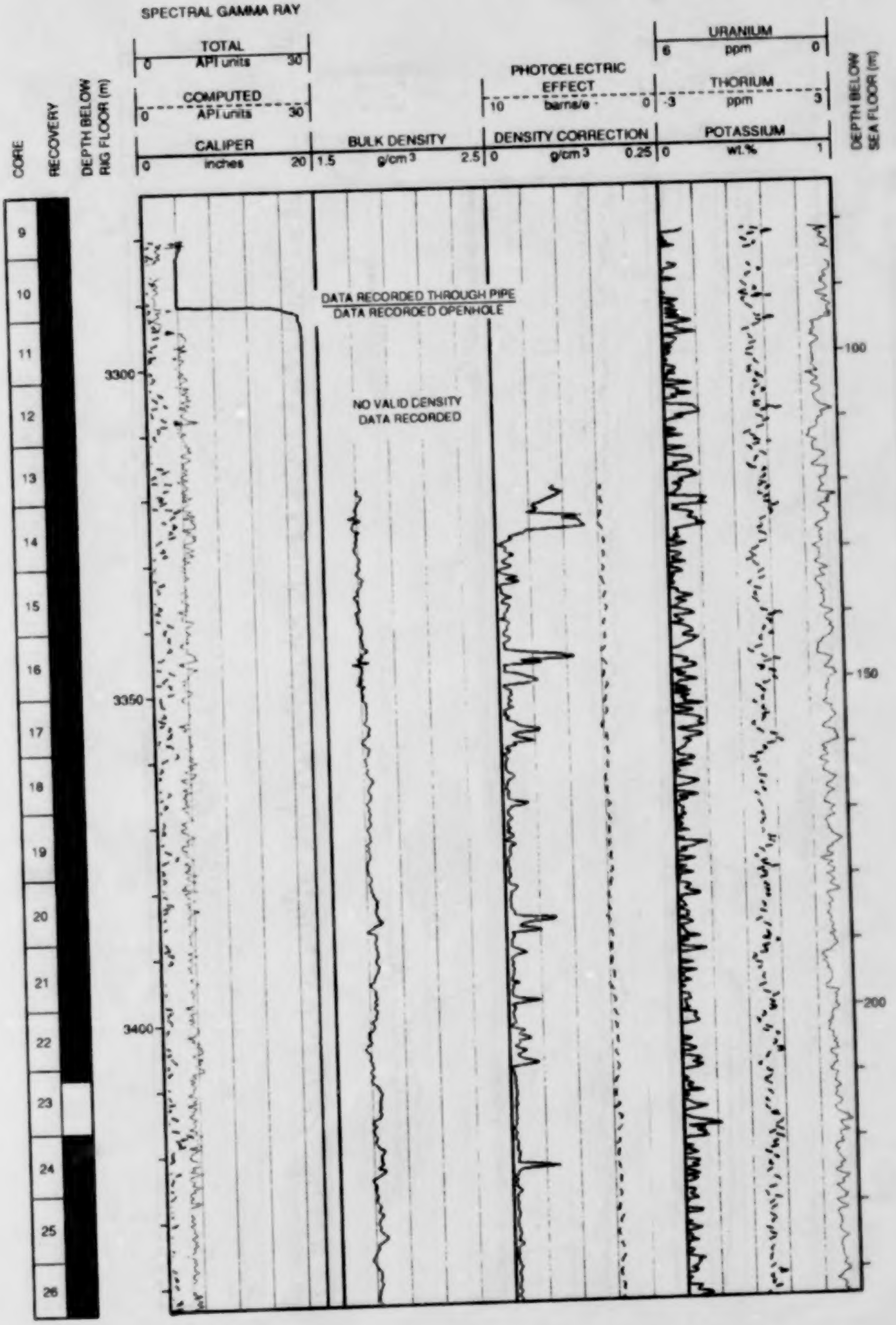

Hole 805C: Density-Gamma Ray Log Summary (continued)

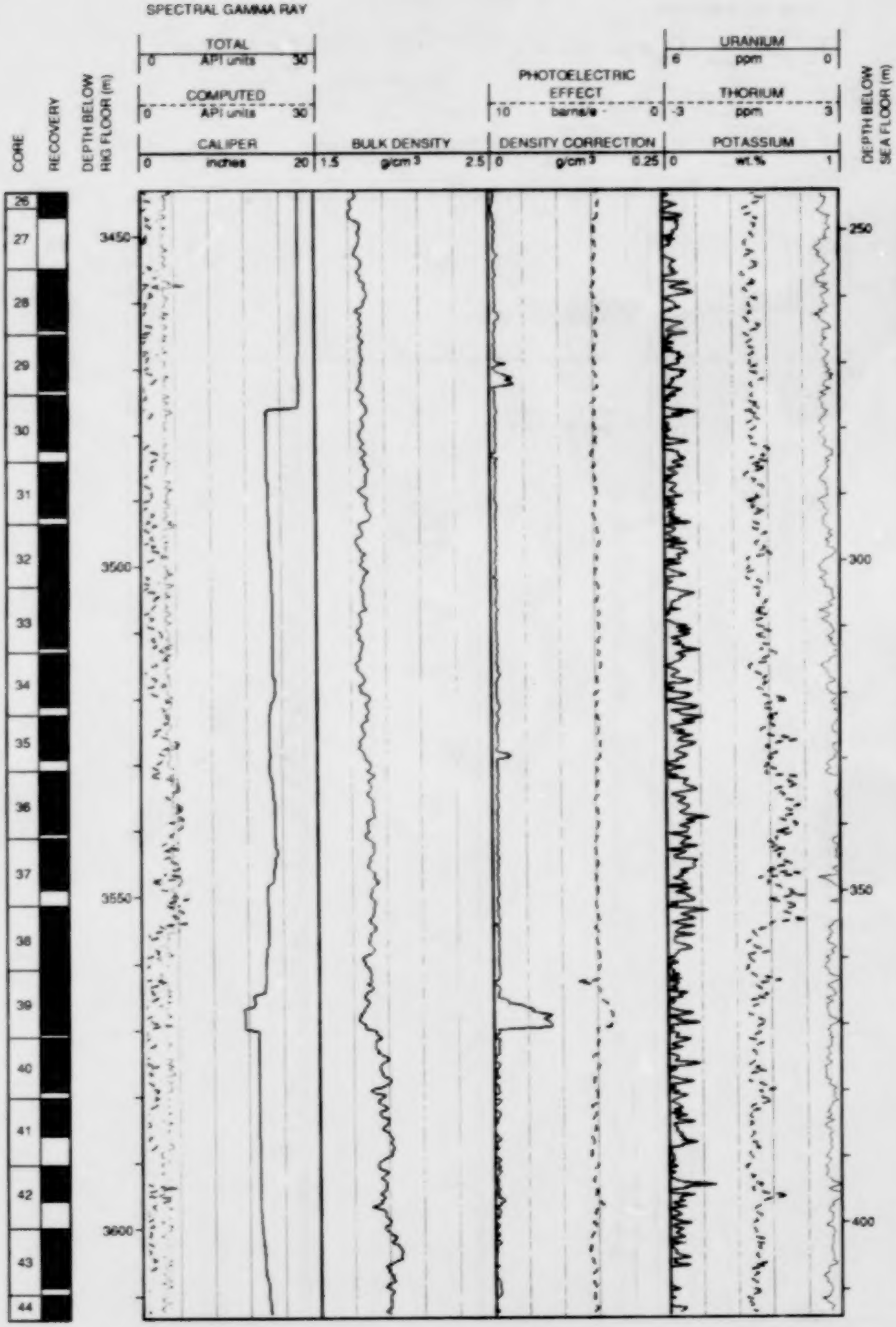

Hole 805C: Density-Gamma Ray Log Summary (continued)

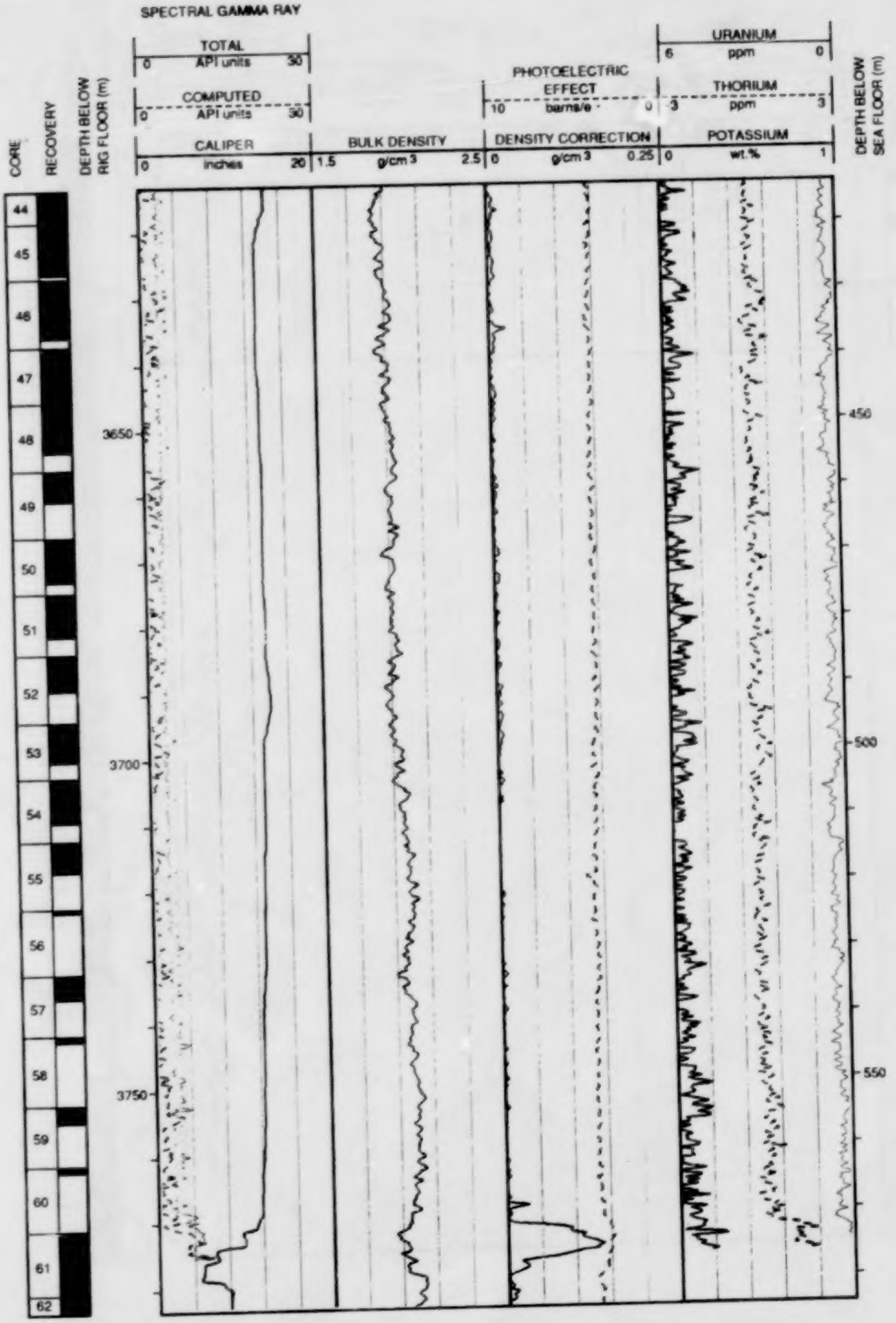

Hole 805C: Density-Gamma Ray Log Summary (continued)

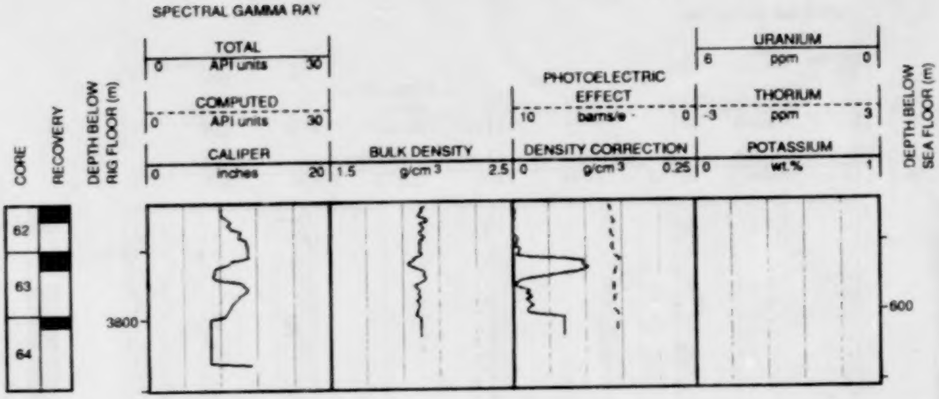

Hole 805C: Geochemical Log Summary

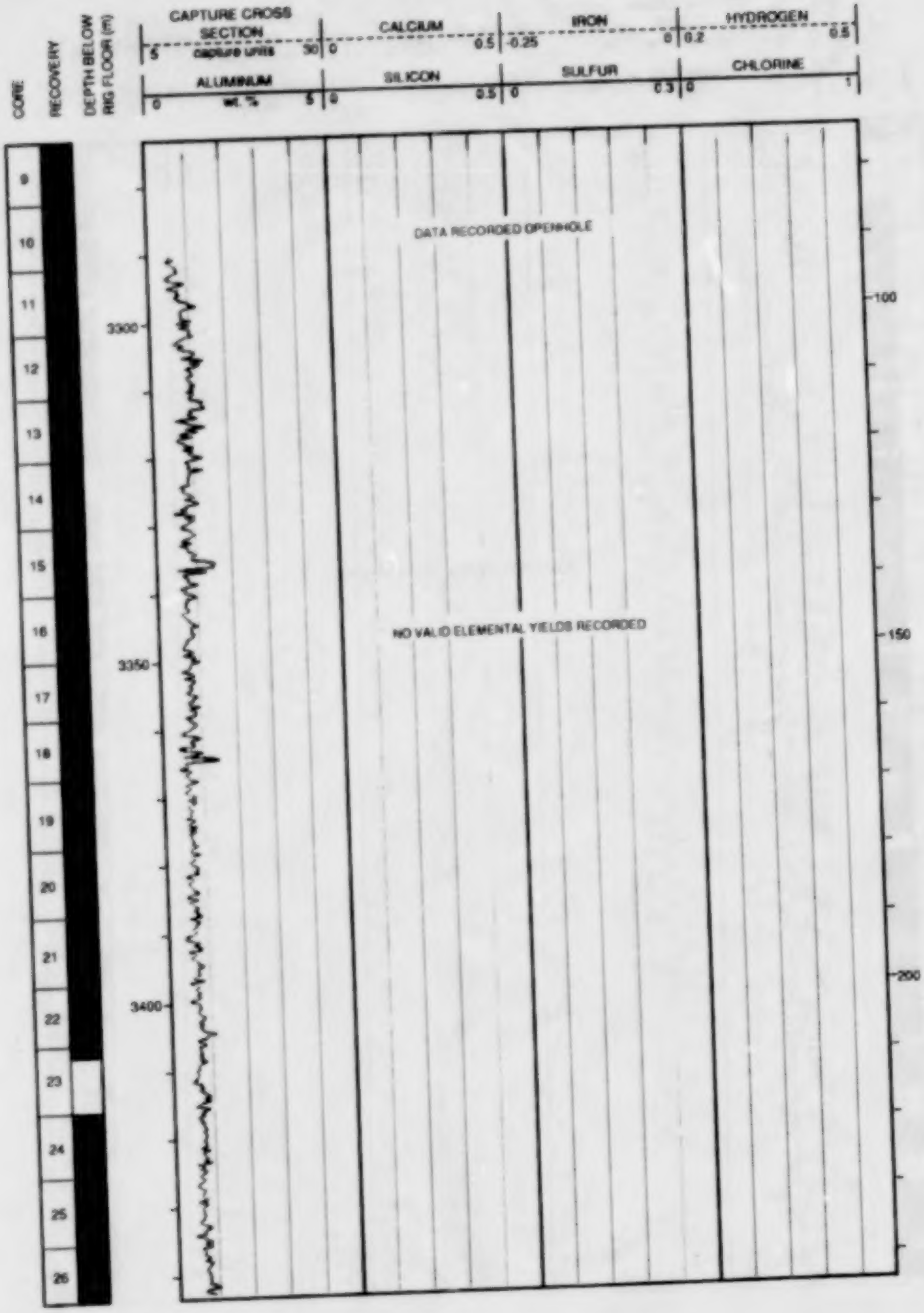

Hole 805C: Geochemical Log Summary (continued)

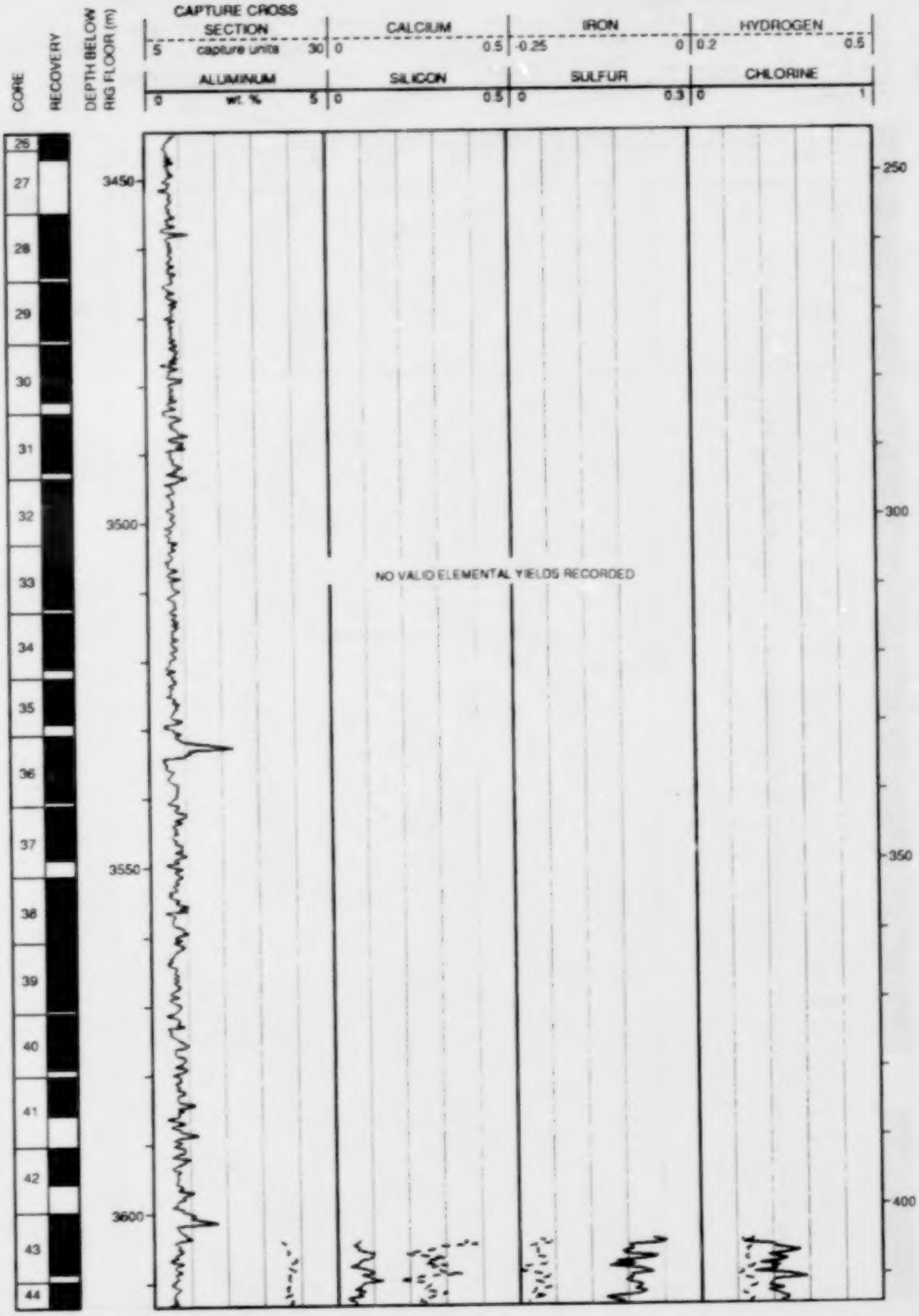

Hole 805C: Geochemical Log Summary (continued)

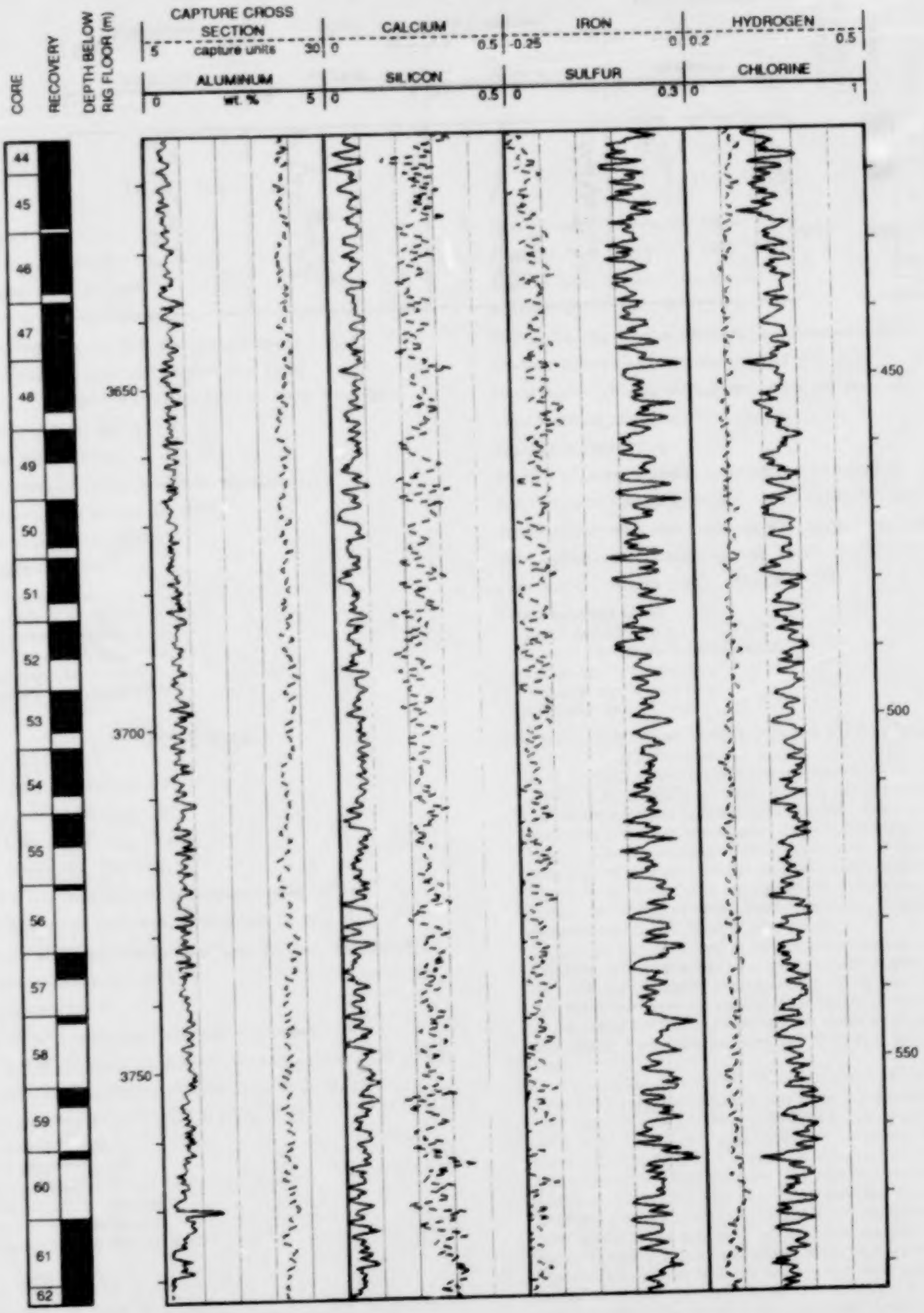

Hole 805C: Geochemical Log Summary (continued)

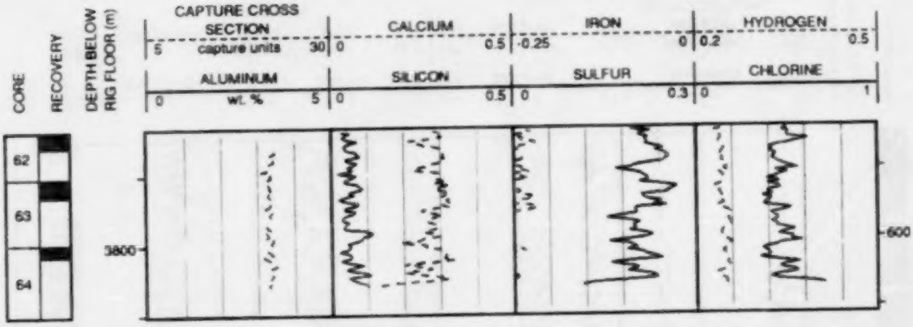

Kroenke, L. W., Berger, W. H., Janecek, T. R., et al., 1991
Proceedings of the Ocean Drilling Program, Initial Reports, Vol. 130

8. SITE 806[1]

Shipboard Scientific Party[2]

HOLE 806A

Date occupied: 17 February 1990

Date departed: 18 February 1990

Time on hole: 1 day, 15 min

Position: 0°19.11′N, 159°21.68′E

Bottom felt (rig floor; m, drill-pipe measurement): 2531.8

Distance between rig floor and sea level (m): 11.14

Water depth (drill-pipe measurement from sea level, m): 2520.7

Total depth (rig floor; m): 2615.50

Penetration (m): 83.70

Number of cores (including cores with no recovery): 9

Total length of cored section (m): 83.70

Total core recovered (m): 85.95

Core recovery (%): 102.7

Oldest sediment cored:
Depth (mbsf): 83.70
Nature: nannofossil ooze
Oldest age: late Pliocene
Youngest age: Quaternary
Measured velocity (km/s): ND

HOLE 806B

Date occupied: 18 February 1990

Date departed: 22 February 1990

Time on hole: 4 days, 4 hr, 30 min

Position: 0°19.11′N, 159°21.69′E

Bottom felt (rig floor; m, drill-pipe measurement): 2531.0

Distance between rig floor and sea level (m): 11.14

Water depth (drill-pipe measurement from sea level, m): 2519.9

Total depth (rig floor; m): 3274.10

Penetration (m): 743.10

Number of cores (including cores with no recovery): 78

Total length of cored section (m): 743.10 (APC, 320.0; XCB, 423.1)

Total core recovered (m): 666.36 (APC, 335.20; XCB, 331.15.)

Core recovery (%): 89 (APC, 104.8; XCB, 78.3)

Oldest sediment cored:
Depth (mbsf): 743.10
Nature: nannofossil chalk with foraminifers
Oldest age: early Miocene
Youngest age: Quaternary
Measured velocity (km/s): 2.2

HOLE 806C

Date occupied: 22 February 1990

Date departed: 25 February 1990

Time on hole: 2 days, 17 hr, 30 min

Position: 0°19.11′N, 159°21.70′E

Bottom felt (rig floor; m, drill-pipe measurement): 2531.9

Distance between rig floor and sea level (m): 11.14

Water depth (drill-pipe measurement from sea level, m): 2520.8

Total depth (rig floor; m): 3308.30

Penetration (m): 776.40

Number of cores (including cores with no recovery): 62

Total length of cored section (m): 587.60 (APC, 309.6; XCB, 278)

Total core recovered (m): 523.62 (APC, 320.61; XCB, 203.01)

Total section drilled without coring: 188.8

Core recovery (%): 89 (APC, 103.6; XCB, 73)

Oldest sediment cored:
Depth (mbsf): 776.4
Nature: foraminifer nannofossil chalk
Oldest age: late Oligocene
Youngest age: Quaternary
Measured velocity (km/s): 2.1

Principal results: Ocean Drilling Program (ODP) Site 806 (proposed Site OJP-1) is located on the northeastern margin of the Ontong Java Plateau, close to the equator (latitude 0°19.1′N, longitude 159°21.7′E) in 2520 m of water, roughly 125 km northeast of Deep Sea Drilling Project (DSDP) Sites 289/586. The site represents the shallow end member on a transect that was designed to detect depth-related paleoceanographic signals in Neogene sediments. We occupied this site with the objective to obtain a high-resolution carbonate record in an undisturbed setting, which could serve as a standard section for studies of ocean history, including biostratigraphy, chemostratigraphy, and acoustic stratigraphy.

Site 806 was positioned at the proposed location (OJP-1), on a 2-km-wide terrace interrupting a gentle incline sloping to the northeast. We used a single-channel-seismic (SCS) line acquired by the *Thomas Washington* during ROUNDABOUT Cruise 11 (0600 UTC, 21 December 1989). The seismic profile shows a full set of reflectors, comparable with those at Sites 289/586, with little or no disturbance.

Three holes were drilled, using the advanced hydraulic piston corer (APC) and the extended core barrel (XCB), with full recovery with the APC. Hole 806A, a dedicated hole, was cored with the APC to 83.7 mbsf into upper Pliocene sediments. Hole 806B was cored with the APC to 320 mbsf, at which point refusal occurred within the lower upper Miocene. The hole was continued with XCB coring to 743.1 mbsf, with 423.1 m of sediment cored and 331.2 m recovered (78%). Coring ended in the lowermost Miocene because of poor recovery. The hole was then logged. Hole 806C was cored with the APC to 309.6 mbsf and coring with the XCB was then begun. The aim was to core with the XCB to the lower middle Miocene a second time, and then drill ahead to search for the Oligocene/Miocene boundary. The attempt was successful. Drilling terminated in uppermost Oligocene sediments at 776.4 mbsf, with 278 m cored for a recovery rate of 73% and 188.8 m drilled without coring.

---

[1] Kroenke, L. W., Berger, W. H., Janecek, T. R., et al., 1991. *Proc. ODP, Init. Repts.*, 130: College Station, TX (Ocean Drilling Program).

[2] Shipboard Scientific Party is as given in the list of participants preceding the contents.

The entire sedimentary sequence encountered is considered as one lithologic unit (Unit I), consisting of upper Oligocene to Pleistocene foraminifer nannofossil ooze and chalk to nannofossil ooze and chalk with foraminifers. Foraminifer abundances mostly range between 15% and 30%, with occasional excursions to 10% and 50%. Radiolarians are a minor constituent throughout the section. The ooze-chalk transition was placed between 338 and 340 mbsf; it is gradational and shows alternation of layers of varying induration, beginning at about 200 mbsf. The age of the sediments at the transition is ca. 10 Ma. Sedimentation throughout the time interval represented seems to have been continuous at this site.

Unit I is divided into two subunits at the ooze-chalk transition, as follows:

> Subunit IA (0–339 mbsf) consists of Pleistocene to upper middle Miocene foraminifer nannofossil ooze to nannofossil ooze with foraminifers. Carbonate content generally ranges from 90% to 95%, except in the Pleistocene where it drops to 85%–90%. The dominant color is white, but the topmost several meters are very pale brown grading to light gray below, and then to white. Bioturbation is common throughout, ranging from slight to heavy. Liesegang banding is common throughout the subunit, although it appears to be fainter and more diffuse in appearance than at Sites 803–805. The best examples are near the bottom of the subunit. Authigenic pyrite was found, associated with burrows, and a slight odor of H_2S was occasionally noted on opening the cores. Microfaulting is rare. Sediments are generally soft, but in the lowermost portion of Subunit IA intervals of greater lithification appear (below 200 mbsf). Coring was impeded in one instance because of porcellanite nodules (Core 130-806C-34X) near the level of APC refusal. The shallowest porcellanite nodules were found at 240 mbsf (ca. 8 Ma). A change in the velocity-depth gradient occurs at this level. Deeper in the section, at the ooze-chalk transition, the character of the velocity profile noticeably changes: above this level, high-frequency variations are distinct; below it, they are subdued.
>
> Subunit IB (339–776 mbsf) consists of lower upper Miocene to upper Oligocene foraminifer nannofossil chalk to nannofossil chalk with foraminifers, with a few intervals of nannofossil chalk. Foraminifer content is high (around 30%) down to about 600 mbsf (ca. 20 Ma) and decreases somewhat below that level. Radiolarian content is low. Carbonate content typically fluctuates between 90% and 95%. The color is dominantly white. Color banding occurs throughout; bands become thinner and more distinct with depth in the subunit. Small-scale flaser structures are present. Bioturbation is ubiquitous. Rare, centimeter-size porcellanite nodules were observed at several levels (350 and 510 mbsf). The depth gradient of dissolved silica is reduced at 350 mbsf and between 450 and 550 mbsf, possibly in response to precipitation.

The sediments in the chalk section posed no problem for coring with the XCB, down to the Oligocene/Miocene boundary zone, where recovery decreased. However, even where recovery is very good, core contents are largely broken up and brecciated, with evidence for grinding of chalk on chalk. This type of recovery is typical for the material below 320 mbsf, that is, the section cored with the XCB. The Oligocene/Miocene boundary is located between 740 and 750 mbsf, and apparently is without hiatus (although recovery is poor at this level). Sedimentation rates for the deep chalk section vary between 20 and 30 m/m.y., the same as for the upper portion of the chalk subunit.

The entire Miocene section exhibits little change in foraminifer content, carbonate percentage, and grain size; it also shows a steady increase in density and velocity with depth. The middle Miocene is characterized by rather high foraminifer abundances, with a minimum at the transition to the upper Miocene. Sedimentation rates increase from around 20 m/m.y. in the lower Miocene to more than 40 m/m.y. in the upper Miocene. Above the middle Miocene/upper Miocene boundary, there is a carbonate minimum. This feature correlates with a zone of increased dissolution in the eastern equatorial Pacific. Carbonate values reach a maximum (near 95%) in the middle portion of the upper Miocene and tend to decrease to the present, with increasing variability reflecting increasing fluctuations in the carbon chemistry of the ocean. Sedimentation rates decrease in the late Pliocene (to around 20 m/m.y. for the Pleistocene), despite the fact that the site was further off the equator in the late Miocene.

Magnetostratigraphies were produced for the uppermost section of the two holes. The high productivity experienced at this site, however, is not conducive to the retention of a magnetic signal.

Chemical gradients in interstitial waters at this site are generally similar to those at Site 803 and 805, reflecting the calcareous/siliceous nature of the sediments and the paucity of organic material. A somewhat higher supply of organic matter at this shallower site, close to the equator, tends to produce slightly stronger gradients. Calcium and magnesium gradients, influenced by basalt alteration reactions at depth, show the usual negative correlation. Strontium concentrations reflect recrystallization processes, which appear to be more vigorous at this site than at the other two, because of the higher sedimentation rates and the higher supply of organic matter. Dissolved silica shows a steady increase with depth, except for the minor reversals mentioned.

Excellent logs were obtained for sound velocity and density at Site 806. The fact that this site has continuous sedimentation at high rates will make these logs especially valuable for the interpretation of seismic profiles and for the study of Milankovitch cycles.

BACKGROUND AND OBJECTIVES

Overview

Site 806, the shallow-water anchor site of the Neogene depth transect on the Ontong Java Plateau, was drilled near target Site OJP-1 (2600 m) (Fig. 1). The site lies half-way between Site 805 and DSDP Site 586, and is intermediate in depth between the two. It is well above the present lysocline and just slightly north of the equator, in the region of maximum Pleistocene sediment supply rate. Effects of varying dissolution are expected to be subdued at this depth, and the high rate of accumulation should provide for maximum resolution within the Neogene record. Thus, the productivity history, and its ramifications for physical properties, should be optimally recorded in sediments accumulating at rates of 20–40 m/m.y. We expected to recover rich tropical assemblages of pelagic and benthic microfossils from these sediments, for use in paleoceanographic and biostratigraphic studies of the Neogene.

The site was planned for multiple coring in the upper portion of the section (Neogene and Quaternary), including two APC-cored holes to 250 mbsf, a third hole to 50 mbsf, and XCB-coring to 600 mbsf. The multiple coring was expected to provide for overlap between cores and for sufficient material for concurrent high-resolution studies. Logging was to provide the information necessary to interpret seismic reflection profiles, for correlation between holes, and for three-dimensional reconstruction of sedimentation rates.

Background

The general background to this site is contained in the "Introduction" chapter (this volume; also see Kroenke, 1972). The Ontong Java Plateau is a broad, shallow, mid-ocean highland in the western equatorial Pacific. Its shallowest regions lie above 2000 m, and its flanks reach depths in excess of 4500 m. With an area of 1.5 million km^2, it is the largest of the "classic" Pacific plateaus. The plateau has a crustal thickness on the order of 40 km. Apparently, it roughly maintained its present depth over much of its history, indicating isostatic equilibrium. Crustal seismic velocities are in the range of that of oceanic crust (Hussong et al., 1979).

The pelagic sediment cover of the plateau is uniquely suited for paleoceanographic studies. The maximum thickness of the sediment is over 1200 m and occurs below the top of the plateau, in water depths between 2000 and 2500 m. The sediment thins by roughly 100 m for every 200 m of water depth increase below 2200 m (Berger and Johnson, 1976). At Site 806, the sediment is approximately 1200 m thick.

Site 806 was planned as the shallow-water, end-member site of a Neogene depth transect in the equatorial portion of the On-

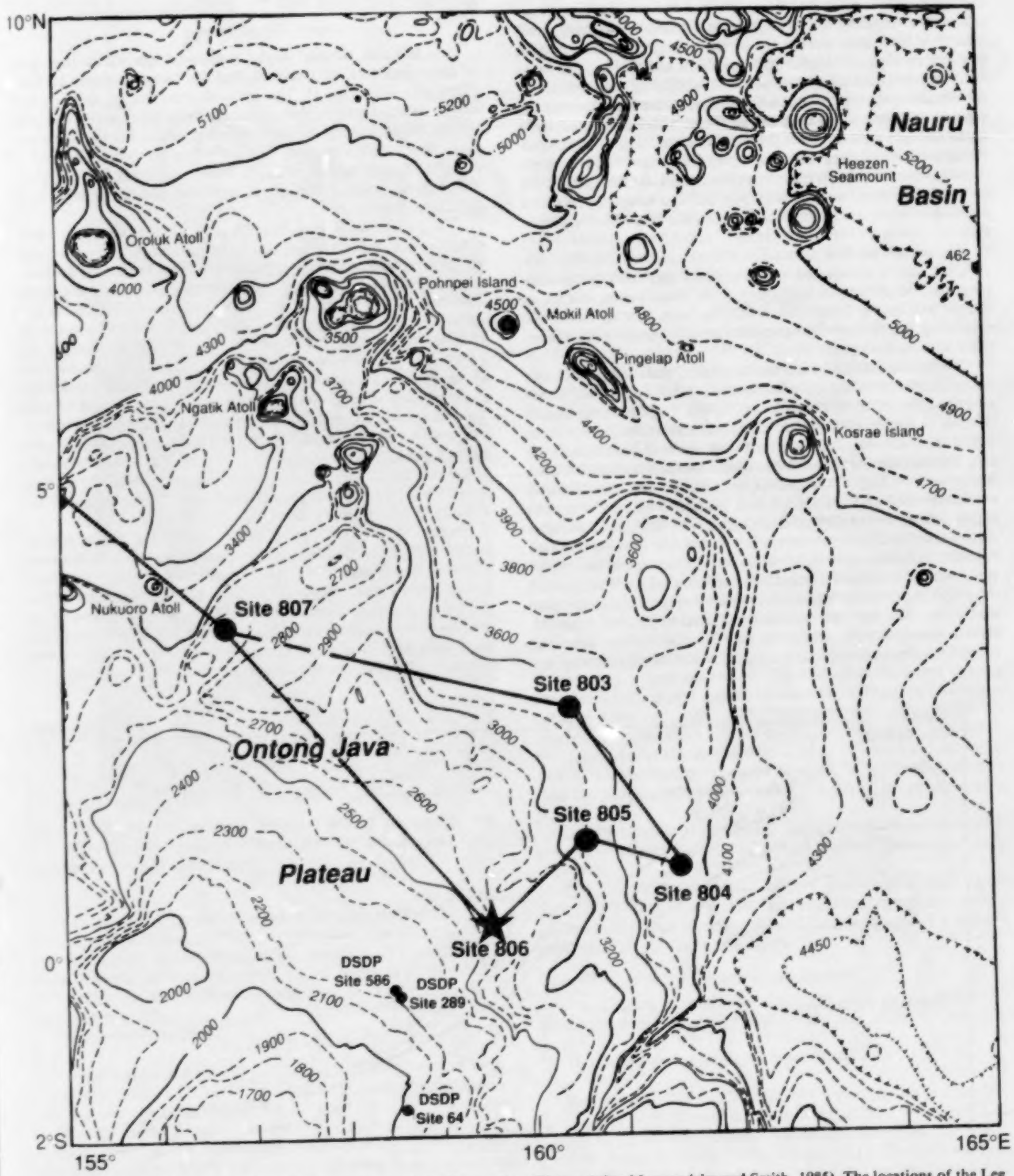
10°N
5°
0°
2°S
155°
160°
165°E
Nauru
Basin
Heezen Seamount
462
Oroluk Atoll
Pohnpei Island
Mokil Atoll
Pingelap Atoll
Ngatik Atoll
Kosrae Island
Nukuoro Atoll
Site 807
Site 803
Site 805
Site 804
Site 806
Ontong Java
Plateau
DSDP Site 586
DSDP Site 289
DSDP Site 64
5100
5200
5000
4500
4900
4000
4300
3500
4800
3700
4400
4200
3900
3800
3600
3400
2700
2800
2900
3000
2400
2500
2600
2300
2200
2000
2100
1900
1800
1700
3200
4100
4700
4450

Figure 1. Bathymetry in meters of the northwestern part of the Ontong Java Plateau (after Mammerickx and Smith, 1985). The locations of the Leg 130 sites as well as DSDP Sites 64 and 289/586 are shown. Contour interval is 100 m.

tong Java Plateau, designed for the study of paleoceanographic events of global significance. In this transect, this site should have the highest sedimentation rates and the best preserved carbonates, containing the most complete paleoceanographic record. Problems arising from the creep of large sediment bodies, ubiquitous at water-depths between 3000 and 4000 m, seem to be of much reduced importance at this shallower depth. The site is well above the significant offset between the basement of the plateau and that of the deep ocean floor, which influences sediment stability further down the plateau flank (Fig. 2). Thus, although earthquakes presumably affect the area occasionally, the damage they can do is more restricted in extent (Berger et al., 1977). Selection of a suitable site to drill a continuous record is much less difficult under these conditions than in the deeper sites.

The seismic profiles across Site 806 (taken from the ROUNDABOUT survey conducted in December 1989) show gently dipping parallel reflectors with very little disturbance, except at depths well below the section of interest here, that is, below 800 mbsf (Fig. 3). We therefore expected to encounter a rather complete section at this site.

The plateau has long been the focus of Quaternary paleoceanographic studies based on conventional coring (e.g., Shackleton and Opdyke, 1976; Wu and Berger, 1989). Leg 130 is the fourth drilling expedition to sample the sediment cover here. Three DSDP sites on the plateau were rotary-drilled: participants on Leg 7 drilled and spot-cored Site 64 (Shipboard Scientific Party, 1971); and on Leg 30 the participants drilled and continuously cored Sites 288 and 289 (Shipboard Scientific Party, 1975). The upper 969 m in Site 289 consisted of upper Eocene to Pleistocene nannofossil foraminifer chalks and oozes. The section was found to be continuous from the lower Oligocene on, the top of which was reached at 890 mbsf. Semilithified chalk first appears near 250 mbsf (late Miocene). Results of paleoceanographic studies on Site 289 are reported in Kennett (1985). A fourth DSDP site, Site 586, drilled on Leg 89 next to Site 289, was cored with the hydraulic piston corer to 305 mbsf, reaching upper Miocene sediments (Shipboard Scientific Party, 1986). Well-preserved nannofossil ooze was recovered.

Objectives

Site 806 was planned as the shallowest site within the series of four equatorial sites constituting the Neogene depth transect (Sites 803–806; Fig. 1). The general objective of this transect was to detect depth-related paleoceanographic signals. The sediments sampled along the transect are produced in the same surface-water conditions and thus arrive on the seafloor more or less in the same pelagic rain. Differences in physical, chemical, and paleontological properties, therefore, can be largely attributed to a depth effect.

The depth sampled at Site 806 (Fig. 1), well above the modern lysocline in this region, is that which should show the greatest preservation and the least influence from variations in dissolution intensity. Thus, physical properties should show a signal that can serve as a standard, for comparison with the deeper sites. In turn, this would allow the identification of the factors that are responsible for producing the lithologic changes and which are detectable in the acoustic stratigraphy (productivity changes, dissolution events). The objective was to explore whether through such effects a clear linkage can be established between paleoceanographic events and acoustic stratigraphy (Mayer et al., 1986). Hiatus formation (presumably also linked to paleoceanographic events; Barron and Keller, 1982) should be at a minimum here. Establishing such linkages should allow three-dimensional mapping and correlation into distant sediment sections throughout the Pacific basin.

Regarding biostratigraphic objectives at this site, it was expected that changes in the relative abundance of calcareous and siliceous fossils and in the isotopic composition of planktonic foraminifers should provide clues to changes in intensity of productivity. An important objective is the determination of the original sedimentation rates, as a function of productivity history, with attendant implications for the study of the oceanic carbon cycle. The recovery of benthic foraminifers should allow

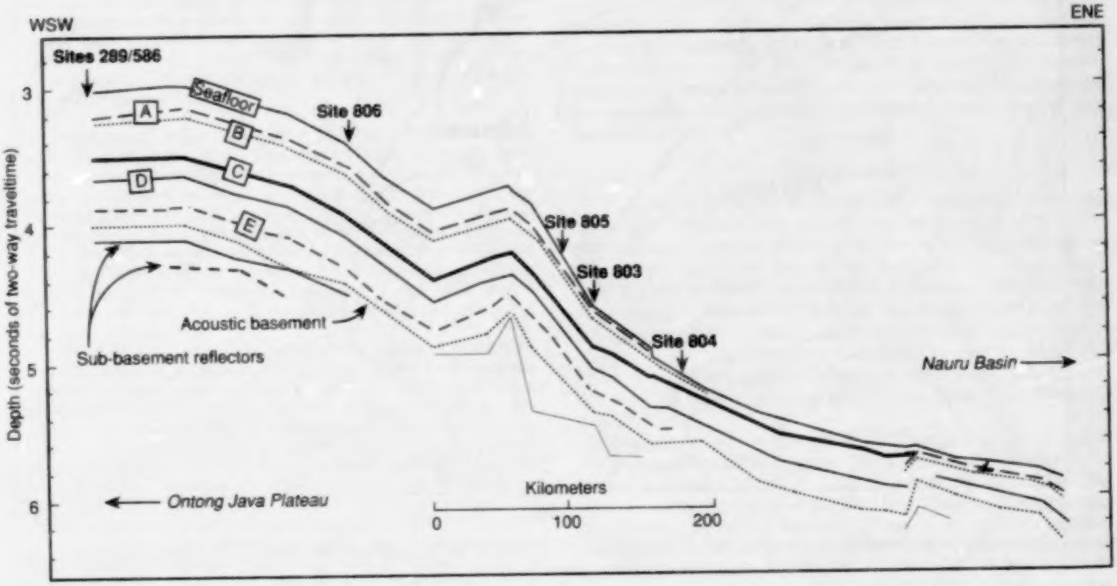

Figure 2. Simplified acoustic stratigraphy for the flank of the Ontong Java Plateau, and approximate location of Sites 803–806 (the depth transect).

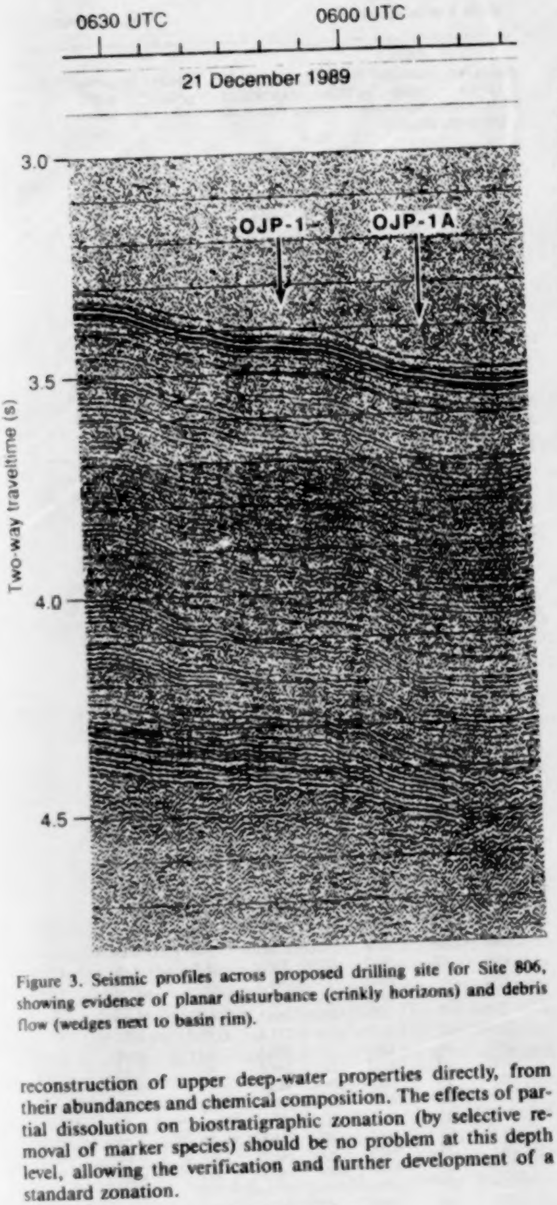

Figure 3. Seismic profiles across proposed drilling site for Site 806, showing evidence of planar disturbance (crinkly horizons) and debris flow (wedges next to basin rim).

reconstruction of upper deep-water properties directly, from their abundances and chemical composition. The effects of partial dissolution on biostratigraphic zonation (by selective removal of marker species) should be no problem at this depth level, allowing the verification and further development of a standard zonation.

OPERATIONS

The transit from Sites 805 to 806 covered 81 nmi in 6.25 hr at an average speed of 13.0 kt. A 17-nmi, pre-site seismic survey was run over the proposed site for 2.0 hr at 8.5 kt (details of site surveys are found in the "Underway Geophysics" chapter, this volume). Good global positioning system (GPS) satellite navigation was available for the site survey. The beacon was dropped at 1052 hr, 17 February 1990, on the proposed site, initiating Site 806.

Hole 806A

The ship was positioned 30 m east of the beacon. After the first core was taken, the core barrel became stuck in the pipe while being retrieved and could not be jarred loose or knocked loose by pumping. The drill string had to be pulled, and the outer-shear-pin sub dogs were found to have broken off and jammed the core barrel in the drill pipe. The core barrel was empty and thus was considered a water core. Core 130-806A-1H was taken at 0530 hr, 18 February 1990, in 2520.7 m of water. Cores 130-806A-1H through -9H (Table 1) were taken from 0 to 83.7 mbsf with 83.7 m of sediment cored and 85.95 m recovered (102.69% recovery). Orientation surveys were conducted during Cores 130-806A-3H through -9H. Hole 806A ended when the depth objective of 83 mbsf was reached. At this point, the pipe was pulled out of the hole, and the bit cleared the seafloor at 1100 hr, 18 February 1990.

Hole 806B

The ship was positioned 60 m east of the beacon. Core 130-806B-1H was taken at 1140 hr, 18 February 1990, in a water depth of 2519.9 m. Cores 130-806B-1H through -34H were taken from 0 to 320.0 mbsf with 320.0 m of sediment cored and 335.20 m recovered (104.75% recovery). Orientation surveys were conducted during Cores 130-806B-3H through -17H. Refusal of the APC was reached at Core 130-806B-34H when the core barrel became stuck and would not pull free, even with 100,000 lb of overpull. At this point, the core barrel was washed over 8 m and finally pulled free with 20,000 lb of overpull.

Cores 130-806B-35X through -78X were taken from 320.0 to 743.1 mbsf with 423.1 m of sediment cored and 331.16 m recovered (78.27% recovery). The XCB bit nozzles started plugging at Core 130-806B-40X (378.2 mbsf), and the sinker-bar assembly was removed to permit pump pressures up to 900 psi. This adjustment succeeded in improving core recovery until Core 130-806B-63X (598.6 mbsf) when the chalk became much harder and started jamming in the shoe. Attempts to improve recovery by reducing weight on bit (WOB) and using different cutting shoes met with mixed results because the formation alternated between hard and soft chalk. The sonic core monitor (SCM) was tested during Core 130-806B-77X, but the target jammed in the liner support sleeve and only 0.35 m of core was recovered. The SCM electronics appeared to work properly and showed that the blockage occurred during the first part of the coring process.

Coring ended in Hole 806B at 743.1 m in lower Miocene sediments, with recovery totaling 666.36 m (89.67% average recovery).

The first air drop in ODP history was made at 0420 hr, 20 February 1990, resulting in the successful delivery of a magnetic susceptibility coil, directional survey camera, and TV camera parts (but no ice cream machine).

Hole 806B Logging

After coring operations ceased, the pipe was pulled to 92 mbsf and a high-viscosity mud sweep was made to clean the hole.

The following logging runs were made:

Run No. 1: NGT/DIT/LSS. Two logs were run successfully from 741.0 to 90.2 mbsf at a rate of 900 ft/hr (306 m/hr). Less than 2 m of fill were found at the base of the hole.

Run No. 2: NGT/ACT/HLDT/GST/TLT. The tool was lowered down the hole to a depth of 740.1 mbsf and pulled back up at a rate of 600 ft/hr (204 m/hr). The GST malfunctioned at

Table 1. Coring summary, Site 806.

Core no.	Date (Feb. 1990)	Time (UTC)	Depth (mbsf)	Cored (m)	Recovered (m)	Recovery (%)
130-806A-						
1H	18	0530	0–7.7	7.7	7.75	100.0
2H	18	0610	7.7–17.2	9.5	9.69	102.0
3H	18	0655	17.2–26.7	9.5	9.89	104.0
4H	18	0730	26.7–36.2	9.5	9.79	103.0
5H	18	0755	36.2–45.7	9.5	9.85	103.0
6H	18	0835	45.7–55.2	9.5	9.76	103.0
7H	18	0915	55.2–64.7	9.5	9.73	102.0
8H	18	0945	64.7–74.2	9.5	9.74	102.0
9H	18	1020	74.2–83.7	9.5	9.75	102.0
Coring totals				83.7	85.95	102.7
130-806B-						
1H	18	1140	0–6.5	6.5	6.54	100.0
2H	18	1210	6.5–16.0	9.5	9.84	103.0
3H	18	1255	16.0–25.5	9.5	9.99	105.0
4H	18	1330	25.5–35.0	9.5	9.92	104.0
5H	18	1415	35.0–44.5	9.5	9.98	105.0
6H	18	1500	44.5–54.0	9.5	10.02	105.5
7H	18	1555	54.0–63.5	9.5	9.96	105.0
8H	18	1640	63.5–73.0	9.5	9.79	103.0
9H	18	1720	73.0–82.5	9.5	10.05	105.8
10H	18	1835	82.5–92.0	9.5	9.81	103.0
11H	18	1930	92.0–101.5	9.5	10.06	105.9
12H	18	2020	101.5–111.0	9.5	9.99	105.0
13H	18	2100	111.0–120.5	9.5	10.03	105.6
14H	18	2150	120.5–130.0	9.5	9.85	103.0
15H	18	2240	130.0–139.5	9.5	9.92	104.0
16H	18	2315	139.5–149.0	9.5	9.94	104.0
17H	19	0005	149.0–158.5	9.5	9.91	104.0
18H	19	0040	158.5–168.0	9.5	10.00	105.2
19H	19	0115	168.0–177.5	9.5	10.02	105.5
20H	19	0200	177.5–187.0	9.5	9.97	105.0
21H	19	0235	187.0–196.5	9.5	9.90	104.0
22H	19	0310	196.5–206.0	9.5	9.91	104.0
23H	19	0345	206.0–215.5	9.5	9.98	105.0
24H	19	0430	215.5–225.0	9.5	10.00	105.2
25H	19	0500	225.0–234.5	9.5	9.96	105.0
26H	19	0535	234.5–244.0	9.5	9.91	104.0
27H	19	0615	244.0–253.5	9.5	9.95	105.0
28H	19	0640	253.5–263.0	9.5	10.00	105.2
29H	19	0715	263.0–272.5	9.5	9.88	104.0
30H	19	0745	272.5–282.0	9.5	10.12	106.5
31H	19	0820	282.0–291.5	9.5	10.01	105.3
32H	19	0850	291.5–301.0	9.5	9.91	104.0
33H	19	0925	301.0–310.5	9.5	9.96	105.0
34H	19	1030	310.5–320.0	9.5	10.12	106.5
35X	19	1120	320.0–329.7	9.7	9.27	95.5
36X	19	1155	329.7–339.4	9.7	9.64	99.4
37X	19	1230	339.4–349.1	9.7	8.45	87.1
38X	19	1310	349.1–358.8	9.7	6.33	65.2
39X	19	1345	358.8–368.5	9.7	8.73	90.0
40X	19	1430	368.5–378.2	9.7	7.46	76.9
41X	19	1510	378.2–387.9	9.7	7.27	74.9
42X	19	1635	387.9–397.5	9.6	9.74	101.0
43X	19	1805	397.5–407.2	9.7	9.62	99.2
44X	19	1915	407.2–416.9	9.7	9.55	98.4
45X	19	2045	416.9–426.5	9.6	9.37	97.6
46X	19	2300	426.5–436.1	9.6	9.50	98.9
47X	20	0005	436.1–445.8	9.7	6.93	71.4
48X	20	0115	445.8–455.5	9.7	9.76	100.0
49X	20	0210	455.5–463.6	8.1	9.74	120.0
50X	20	0315	463.6–473.3	9.7	8.43	86.9
51X	20	0400	473.3–482.6	9.3	9.75	105.0
52X	20	0500	482.6–492.3	9.7	7.73	79.7
53X	20	0620	492.3–501.9	9.6	6.20	64.6
54X	20	0725	501.9–511.6	9.7	9.65	99.5
55X	20	0810	511.6–521.3	9.7	9.77	101.0
56X	20	0910	521.3–530.9	9.6	5.87	61.1
57X	20	1005	530.9–540.5	9.6	9.74	101.0
58X	20	1105	540.5–550.2	9.7	9.72	100.0
59X	20	1205	550.2–559.9	9.7	9.74	100.0
60X	20	1305	559.9–569.6	9.7	6.99	72.0
61X	20	1410	569.6–579.3	9.7	9.73	100.0

Table 1 (continued).

Core no.	Date (Feb. 1990)	Time (UTC)	Depth (mbsf)	Cored (m)	Recovered (m)	Recovery (%)
130-806B- (Cont.)						
62X	20	1530	579.3–589.0	9.7	9.80	101.0
63X	20	1650	589.0–598.6	9.6	9.78	102.0
64X	20	1815	598.6–608.3	9.7	3.03	31.2
65X	20	1945	608.3–617.9	9.6	8.25	85.9
66X	20	2100	617.9–627.5	9.6	9.64	100.0
67X	20	2215	627.5–637.2	9.7	3.35	34.5
68X	20	2340	637.2–646.5	9.3	1.31	14.1
69X	21	0100	646.5–656.2	9.7	6.23	64.2
70X	21	0215	656.2–665.8	9.6	5.17	53.8
71X	21	0335	665.8–675.5	9.7	4.48	46.2
72X	21	0455	675.5–685.2	9.7	6.09	62.8
73X	21	0605	685.2–694.8	9.6	9.75	101.0
74X	21	0710	694.8–704.5	9.7	4.52	46.6
75X	21	0810	704.5–714.1	9.6	8.50	88.5
76X	21	0925	714.1–723.7	9.6	4.93	51.3
77X	21	1045	723.7–733.4	9.7	0.35	3.6
78X	22	1205	733.4–743.1	9.7	1.30	13.4
Coring totals				743.1	666.36	89.7
130-806C-						
1H	22	1840	0–5.6	5.6	5.58	99.6
2H	22	1925	5.6–15.1	9.5	9.93	104.0
3H	22	2020	15.1–24.6	9.5	9.98	105.0
4H	22	2050	24.6–34.1	9.5	9.98	105.0
5H	22	2120	34.1–43.6	9.5	9.11	95.9
6H	22	2210	43.6–53.1	9.5	9.48	99.8
7H	22	2245	53.1–62.6	9.5	9.81	103.0
8H	22	2325	62.6–72.1	9.5	9.91	104.0
9H	23	0000	72.1–81.6	9.5	10.00	105.2
10H	23	0045	81.6–91.1	9.5	9.98	105.0
11H	23	0145	91.1–100.6	9.5	10.07	106.0
12H	23	0215	100.6–110.1	9.5	9.98	105.0
13H	23	0240	110.1–119.6	9.5	9.81	103.0
14H	23	0310	119.6–129.1	9.5	9.72	102.0
15H	23	0340	129.1–138.6	9.5	9.67	102.0
16H	23	0405	138.6–148.1	9.5	9.87	104.0
17H	23	0435	148.1–157.6	9.5	9.92	104.0
18H	23	0500	157.6–167.1	9.5	9.89	104.0
19H	23	0530	167.1–176.6	9.5	9.57	101.0
20H	23	0600	176.6–186.1	9.5	9.79	103.0
21H	23	0630	186.1–195.6	9.5	9.29	97.8
22H	23	0700	195.6–205.1	9.5	9.75	102.0
23H	23	0730	205.1–214.6	9.5	9.94	104.0
24H	23	0800	214.6–224.1	9.5	9.86	104.0
25H	23	0835	224.1–233.6	9.5	9.85	103.0
26H	23	0905	233.6–243.1	9.5	9.97	105.0
27H	23	0935	243.1–252.6	9.5	9.86	104.0
28H	23	1005	252.6–262.1	9.5	10.18	107.1
29H	23	1035	262.1–271.6	9.5	9.91	104.0
30H	23	1105	271.6–281.1	9.5	9.96	105.0
31H	23	1135	281.1–290.6	9.5	9.93	104.0
32H	23	1205	290.6–300.1	9.5	9.94	104.0
33H	23	1235	300.1–309.6	9.5	10.12	106.5
34X	23	1315	309.6–319.3	9.7	0.02	0.2
35X	23	1345	319.3–328.9	9.6	9.09	94.7
36X	23	1425	328.9–338.5	9.6	9.33	97.2
37X	23	1500	338.5–348.2	9.7	6.98	71.9
38X	23	1545	348.2–357.9	9.7	7.64	78.7
39X	23	1625	357.9–367.6	9.7	8.20	84.5
40X	23	1730	367.6–377.3	9.7	6.71	69.2
41X	23	1840	377.3–387.0	9.7	6.69	68.9
42X	23	2000	387.0–396.7	9.7	9.43	97.2
43X	23	2055	396.7–406.3	9.6	9.50	98.9
44X	23	2200	406.3–415.9	9.6	9.47	98.6
45X	23	2300	415.9–425.6	9.7	9.57	98.6
46X	23	2350	425.6–435.2	9.6	9.31	97.0
47X	24	0045	435.2–444.9	9.7	9.43	97.2
48X	24	0140	444.9–454.6	9.7	4.20	43.3
49X	24	0245	454.6–464.5	9.9	6.79	68.6
50X	24	0340	464.5–474.3	9.8	9.54	97.3
51X	24	0445	474.3–483.7	9.4	6.33	67.3
52X	24	0515	483.7–493.3	9.6	5.10	53.1

Table 1 (continued).

Core no.	Date (Feb. 1990)	Time (UTC)	Depth (mbsf)	Cored (m)	Recovered (m)	Recovery (%)
130-806C- (Cont.)						
53X	24	0630	493.3–503.0	9.7	8.19	84.4
54X	24	0740	503.0–512.7	9.7	5.47	56.4
55X	24	0820	512.7–522.4	9.7	6.23	64.2
56X	24	0920	522.4–532.0	9.6	9.32	97.1
57X	24	1140	532.0–541.7	9.7	9.54	98.3
58X	24	1530	599.0–608.5	9.5	9.04	95.1
59X	24	2205	740.0–749.5	9.5	0.81	8.5
60X	24	2340	749.5–759.2	9.7	0.79	8.1
61X	25	0110	759.2–766.7	7.5	9.12	121.0
62X	25	0250	766.7–776.4	9.7	1.17	12.0
Coring totals				587.6	523.62	89.1

702.9 mbsf and was again lowered to 740.7 mbsf to restart the run. The second run up the hole proceeded smoothly until 486.5 mbsf, at which point the GST lost resolution. The tool string was lowered to 504.4 mbsf and the run restarted a third time. This third run was completed to a depth of 88.4 mbsf but the GST did not recalibrate properly. The tool was lowered one final time, to a depth of 334.1 mbsf, in order to restart the GST, but this attempt also was unsuccessful. The tool string was finally pulled on deck, the pipe was pulled out of the hole, and the bottom hole assembly (BHA) cleared the seafloor at 1830 hr, 22 February 1990, ending Hole 806B.

Hole 806C

The ship was positioned 90 m east of the beacon. Core 130-806C-1H was taken at 1840 hr, 22 February 1990, in 2520.8 m of water. Cores 130-806C-1H through -33H were taken from 0 to 309.6 mbsf with 309.6 m of sediment cored and 320.61 m recovered (103.56% recovery). Orientation surveys were taken during Cores 130-806C-3H through -12H. Coring with the APC ended at Core 130-806A-33H (309.6 m) to avoid getting the core barrel stuck in the hole.

Cores 130-806C-34X through -57X were taken from 309.6 to 541.7 mbsf. From that point, the hole was drilled ahead with a center bit to 599.0 mbsf. A spot core (Core 130-806C-58X) was taken from 599.0 to 608.5 mbsf to obtain a sedimentary interval not recovered in the previous hole. The spot core was successful in obtaining the interval. The hole was drilled further with a center bit to a depth of 740.0 mbsf. Cores 130-806C-59X through -62X were taken from 740.0 to 776.4 mbsf. The XCB coring operation drilled 278.0 m and recovered 203.01 m of sediment (73.02% average recovery).

Coring was terminated in Hole 806C after reaching the Miocene/Oligocene boundary. At Hole 806C, a total of 587.6 m of sediment was cored and 523.62 m recovered (89.11% recovery). After coring operations ceased, the pipe was pulled out of the hole and the BHA cleared the rotary table at 0900 hr, 25 February 1990, ending Site 806.

LITHOSTRATIGRAPHY

Introduction

Three holes were drilled at Site 806. Hole 806A was cored with the APC to a sub-bottom depth of 83.7 m. Cores from this hole were not split on board the ship. Hole 806B was cored with the APC to a sub-bottom depth of 320 m and was then cored with the XCB to a total depth of 743.1 mbsf. Hole 806C was cored with the APC to a sub-bottom depth of 309.6 m, cored with the XCB to 541.7 mbsf, drilled to 599 mbsf, cored with the XCB to 608.5 mbsf, drilled to 740 mbsf, and cored again with the XCB to a total sub-bottom depth of 776.4 m. Recovery was 100% in the APC-cored intervals and averaged 78% and 73% in the XCB-cored intervals of Holes 806B and 806C, respectively.

The sediments described from Site 806 are grouped into one lithostratigraphic unit (Unit I), as were the sediments from Sites 804 and 805, and the sediments from equivalent intervals at Sites 289 and 586 (Shipboard Scientific Party, 1975, 1986). This unit is composed of upper Oligocene to Pleistocene foraminifer nannofossil ooze and chalk to nannofossil ooze and chalk with foraminifers (Fig. 4). Foraminifer abundances range between 10% and 50% of the constituent grains in most of the smear slides analyzed (Fig. 5). The cored interval at Site 806 apparently comprises a complete stratigraphic section from the upper Oligocene to the Pleistocene (see "Biostratigraphy" section, this chapter).

Description of Units

Unit I

Intervals: Hole 806B, Cores 130-806B-1H through -62X;
Hole 806C, Cores 130-806C-1H through -78X
Age: Pleistocene–late Oligocene
Depth: 0–776.4 mbsf

Unit I is composed of foraminifer nannofossil ooze and chalk to nannofossil ooze and chalk with foraminifers. The unit is divided into two subunits: (1) Subunit IA (0–339 mbsf) is foraminifer nannofossil ooze to nannofossil ooze with foraminifers, and (2) Subunit IB (339–776.4 mbsf) is foraminifer nannofossil chalk to nannofossil chalk with foraminifers.

Subunit IA

Intervals: Hole 806B, Cores 130-806B-1H through -36X;
Hole 806C, Cores 130-806C-1H through -37X
Age: Pleistocene–early late Miocene
Depth: 0–339 mbsf

Subunit IA is composed of 339 m of foraminifer nannofossil ooze to nannofossil ooze with foraminifers. Foraminifer content, on the basis of smear slide estimates, generally fluctuates between 15% and 30% and only rarely dips below 10% (Fig. 5). These values are significantly higher than the foraminifer abundances at previous Leg 130 sites (Sites 803, 804, and 805). The sediments are, therefore, classified as foraminifer nannofossil ooze to nannofossil ooze with foraminifers.

The sediments of Subunit IA are described texturally as clayey silts to sandy clayey silts. The main constituent of the sediment is nannofossils, as reflected by the predominance of medium silt mean grain sizes determined by shipboard particle size analyses (Fig. 6 and Table 2). The coarser grains (fine sand and coarse silt) at this site are foraminifers, so that fluctuations in the mean grain size are a good indicator of the relative abundances of foraminifers and nannofossils. The foraminifers appear to be well preserved from smear slide observations. The smear slide abundances (Fig. 5) and the grain-size curve (Fig. 6) show large, repeated, and closely spaced fluctuations in the foraminifer content. Other constituents are typically observed in only trace amounts. These grains include radiolarians, siliceous sponge spicules, diatoms, silicoflagellates, volcanic glass, quartz, accessory minerals, and clay, in general order of decreasing abundance.

The carbonate abundance curve for Site 806 is similar to that from Site 805 (Fig. 7; cf. with Fig. 6, "Site 805" chapter, this volume). Carbonate contents range between 83% and 95% and are above 90% through most of the hole. The lowest carbonate values are found at the top of the hole, and X-ray diffraction (XRD) analyses suggest an abundance of terrigenous components (clays, quartz, and feldspars) in this interval. The carbonate

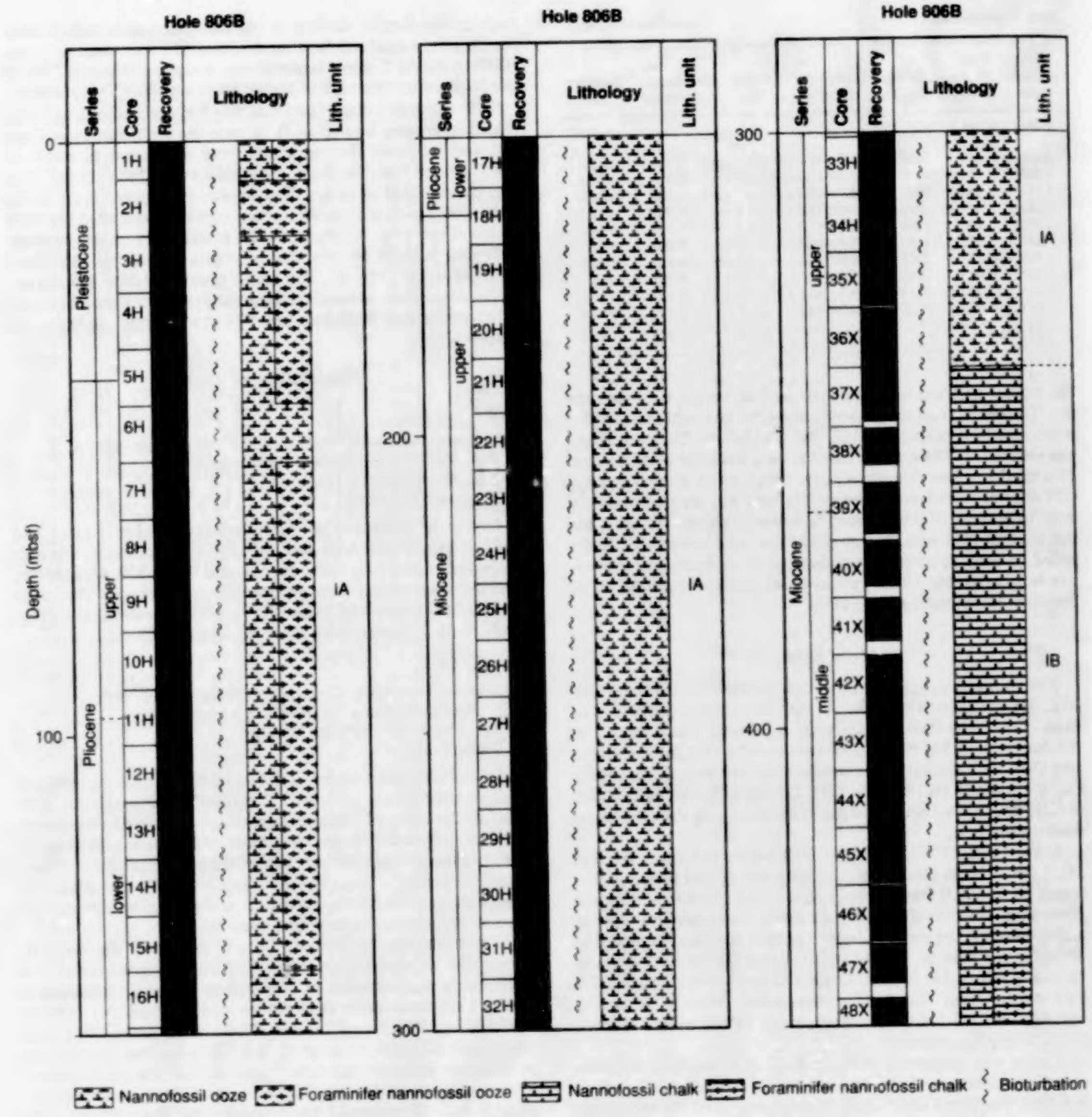
Hole 806B
Series
Core
Recovery
Lithology
Lith. unit
Depth (mbsf)
0
100
200
300
400
Pleistocene
Pliocene
upper
lower
Miocene
middle
1H
2H
3H
4H
5H
6H
7H
8H
9H
10H
11H
12H
13H
14H
15H
16H
17H
18H
19H
20H
21H
22H
23H
24H
25H
26H
27H
28H
29H
30H
31H
32H
33H
34H
35X
36X
37X
38X
39X
40X
41X
42X
43X
44X
45X
46X
47X
48X
IA
IB
Nannofossil ooze
Foraminifer nannofossil ooze
Nannofossil chalk
Foraminifer nannofossil chalk
Bioturbation

Figure 4. Lithologic summary, Holes 806B and 806C.

content gradually increases with depth to a value of approximately 94% near 250 mbsf, but decreases significantly at 100–120 mbsf (3.5–4.0 Ma), 150–170 mbsf (5.0–5.5 Ma), and 260–320 mbsf (7.0–8.5 Ma). These decreases are not yet explained in terms of dilution versus carbonate dissolution as no obvious relation exists between the carbonate content and the mean grain size, nor between the carbonate and the foraminifer contents (Figs. 5, 6, and 7).

The dominant color of the sediments in Subunit IA is white (2.5Y 8/0, 5Y 8/1, 7.5YR 8/1, and 10YR 8/1). The uppermost several meters at both Holes 806B and 806C are, however, very pale brown (10YR 7/3) and grade rapidly to light gray (10YR 7/2) and then to white. Color banding is common throughout Subunit IA, although the banding appears to be less frequent, fainter, and more diffuse than at Sites 803 to 805. These color bands are typically light greenish gray (5G 7/1) to pale yellowish green (10GY 7/2), light gray (N7/) to reddish gray (5R 6/1), and grayish blue (5PB 5/2) to pale purple (5P 6/2). They are generally 0.5–2 cm thick and horizontal and form groups distributed throughout a core. The groups of color bands are positioned at regular intervals in some parts of Subunit IA, but are apparently randomly distributed in others.

Bioturbation, ranging in intensity from moderate to heavy, is evident throughout the subunit. It is recognized by the presence

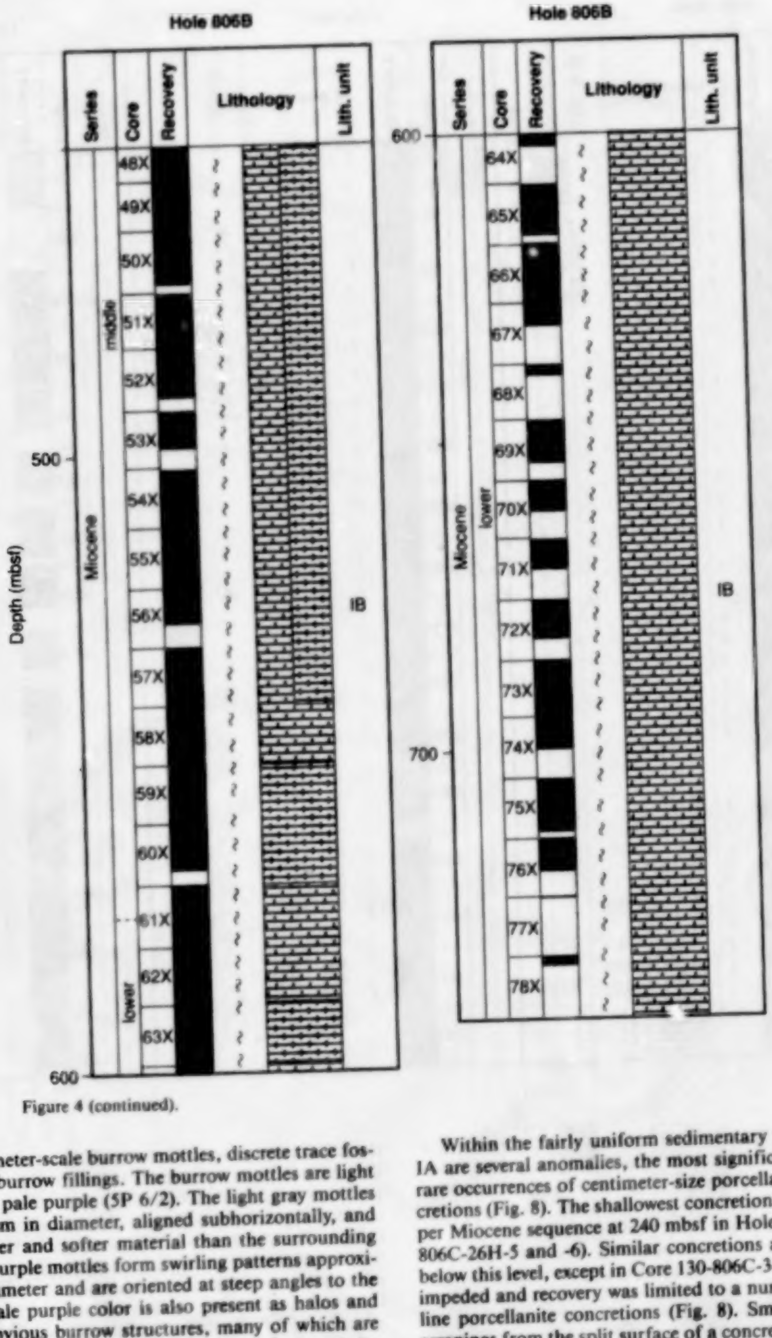
Hole 806B
Series
Core
Recovery
Lithology
Lith. unit
Depth (mbsf)
500
600
Miocene
middle
lower
48X
49X
50X
51X
52X
53X
54X
55X
56X
57X
58X
59X
60X
61X
62X
63X
IB
Hole 806B
600
700
Miocene
lower
64X
65X
66X
67X
68X
69X
70X
71X
72X
73X
74X
75X
76X
77X
78X
IB

Figure 4 (continued).

of abundant centimeter-scale burrow mottles, discrete trace fossils, and pyritized burrow fillings. The burrow mottles are light gray (2.5Y 7/2) or pale purple (5P 6/2). The light gray mottles are typically 1–3 cm in diameter, aligned subhorizontally, and infilled with coarser and softer material than the surrounding matrix. The pale purple mottles form swirling patterns approximately 1 cm in diameter and are oriented at steep angles to the horizontal. The pale purple color is also present as halos and borders around obvious burrow structures, many of which are filled with authigenic pyrite. Pale purple color rings, greater than 10 cm in diameter, are also apparent in the cores. Bioturbation structures appear to be larger and more abundant than at Sites 803 and 804, though comparable with those observed at Site 805. A slight odor of H_2S was noted upon opening most cores from Subunit IA.

Within the fairly uniform sedimentary sequence of Subunit IA are several anomalies, the most significant of which are the rare occurrences of centimeter-size porcellanite nodules or concretions (Fig. 8). The shallowest concretion was found in the upper Miocene sequence at 240 mbsf in Hole 806C (Sections 130-806C-26H-5 and -6). Similar concretions are found only rarely below this level, except in Core 130-806C-34X, where coring was impeded and recovery was limited to a number of microcrystalline porcellanite concretions (Fig. 8). Smear slide analyses of scrapings from the split surface of a concretion showed the presence of nannofossils, and the concretion contains 14% $CaCO_3$.

Other features worthy of note within Subunit IA are microfaults, pumice, and thin (centimeter-scale) beds of well-sorted foraminifer ooze. Microfaults were observed as offsets in color bands at 290 mbsf in Hole 806B (Section 130-806B-31H-6) and

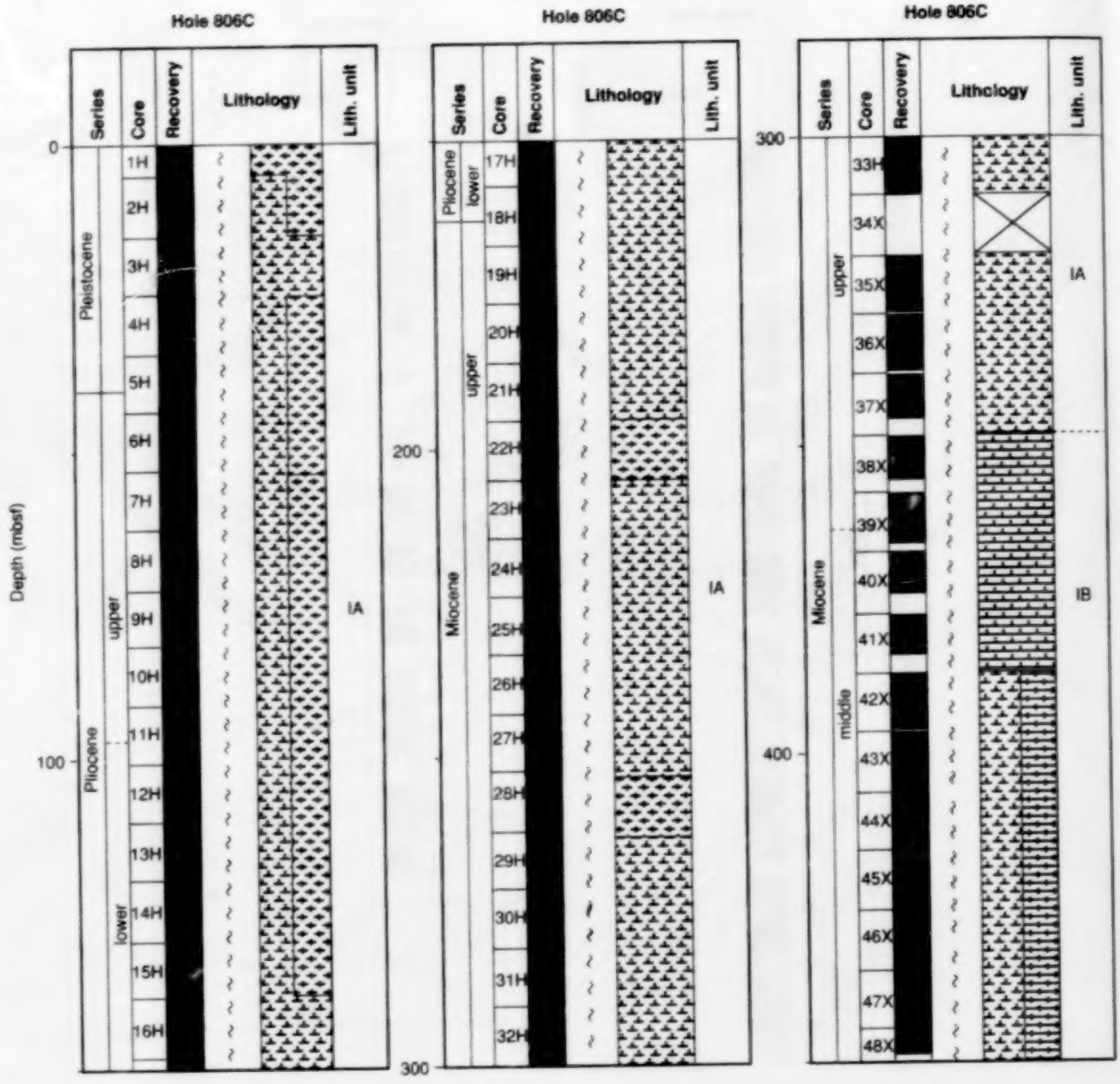
Hole 806C
Series
Core
Recovery
Lithology
Lith. unit
Depth (mbsf)
0
100
200
300
400
Pleistocene
Pliocene
upper
lower
Miocene
middle
IA
IB
1H
2H
3H
4H
5H
6H
7H
8H
9H
10H
11H
12H
13H
14H
15H
16H
17H
18H
19H
20H
21H
22H
23H
24H
25H
26H
27H
28H
29H
30H
31H
32H
33H
34X
35X
36X
37X
38X
39X
40X
41X
42X
43X
44X
45X
46X
47X
48X

Figure 4 (continued).

at 190 and 299 mbsf in Hole 806C (Sections 130-806C-21H-4 and -32H-6). A pumice pebble, 2–3 cm in diameter, was found at 56.6 mbsf in Hole 806C (Section 130-806C-7H-3, 52 cm; Fig. 9). At 39.4 and 45.1 mbsf within Hole 806C (Sections 130-806C-5H-4 and -6H-2, respectively), thin (1 and 3 cm) beds of well-sorted foraminifer tests were observed. The lower contacts of these beds are sharp and even, and the upper contacts are obscured by bioturbation. The material within the beds is primarily whole foraminifer tests and grading is not obvious. Grain size analyses were conducted on samples from the bed at 39.4 mbsf (Fig. 10) and demonstrate the coarser, well-sorted nature of the bed relative to the surrounding sediment.

At approximately 200 mbsf (upper Miocene) in Holes 806B and 806C, the first signs of sediment induration were observed as thin (centimeter-scale), stiff to hard layers interspersed within the softer ooze matrix. These harder intervals appear to be nodular rather than continuous, although it is not known if this pattern is primary or a function of the coring process. With increasing depth these stiff intervals gradually become harder and thicker. The placement of the ooze-chalk transition is subjective, but it normally coincides with the level at which the saw, rather than the pull-wire, is necessary to split the core. Given this criterion, the ooze-chalk transition at Site 806 was placed at approximately 340 mbsf in both holes, even though sediments at this level are still interbedded chalks and oozes. Several additional lines of evidence, however, support placing this transition at 320 mbsf:

1. The downhole caliper log shows that the hole is narrower and more stable at 320 mbsf than above, perhaps because of the

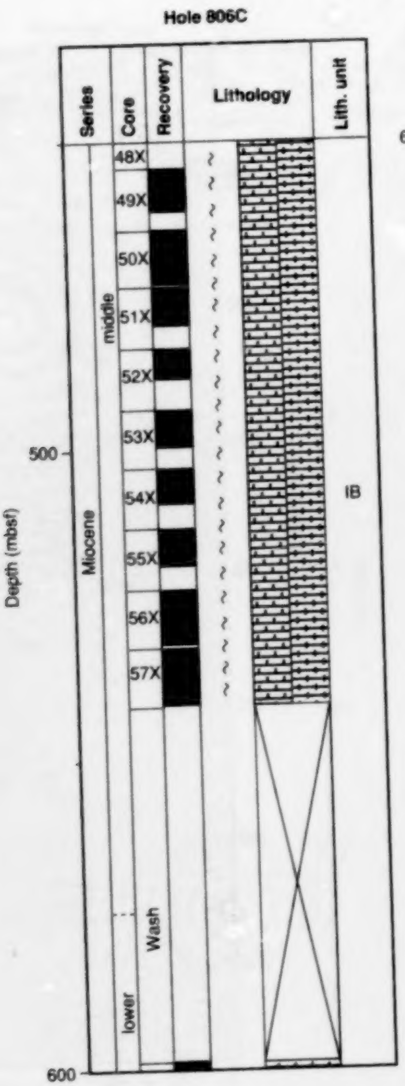
Hole 806C
Series
Core
Recovery
Lithology
Lith. unit
Depth (mbsf)
500
600
Miocene
middle
lower
48X
49X
50X
51X
52X
53X
54X
55X
56X
57X
Wash
IB

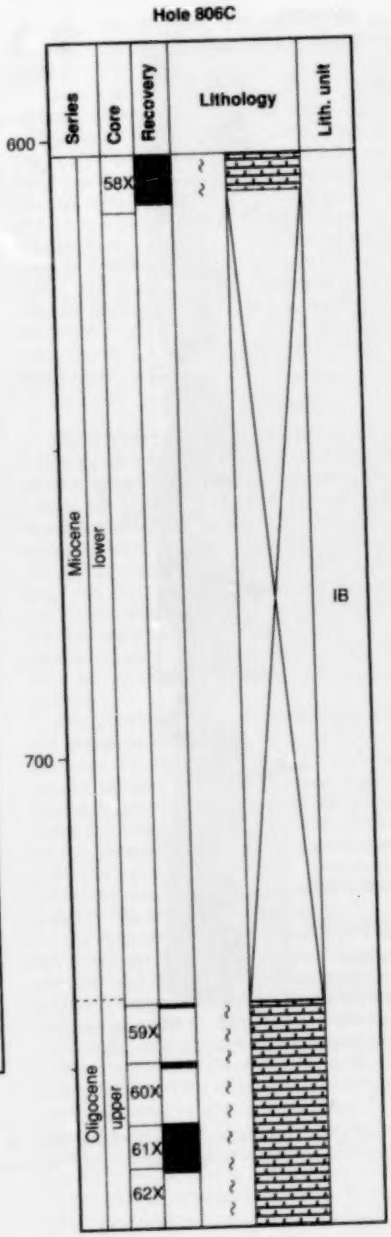
Hole 806C
Series
Core
Recovery
Lithology
Lith. unit
600
700
Miocene
lower
Oligocene
upper
58X
59X
60X
61X
62X
IB

Figure 4 (continued).

transition from ooze to chalk (see "Logging" section, this chapter).

2. Sonic velocities measured on board ship increase markedly for samples recovered below 320 m (see "Physical Properties" section, this chapter), but these measurements have not been corrected for *in-situ* conditions. Because porosity rebound caused by the removal of overburden is greater in unlithified material than in cemented chalks, this velocity increase is a function of cementation and correlates well with the ooze-chalk transition chosen from evidence in the recovered sediments. Sonic velocities from the downhole velocity log increase gradually and show no obvious correlation with the onset of lithification, since these measurements were made under conditions of existing overburden.

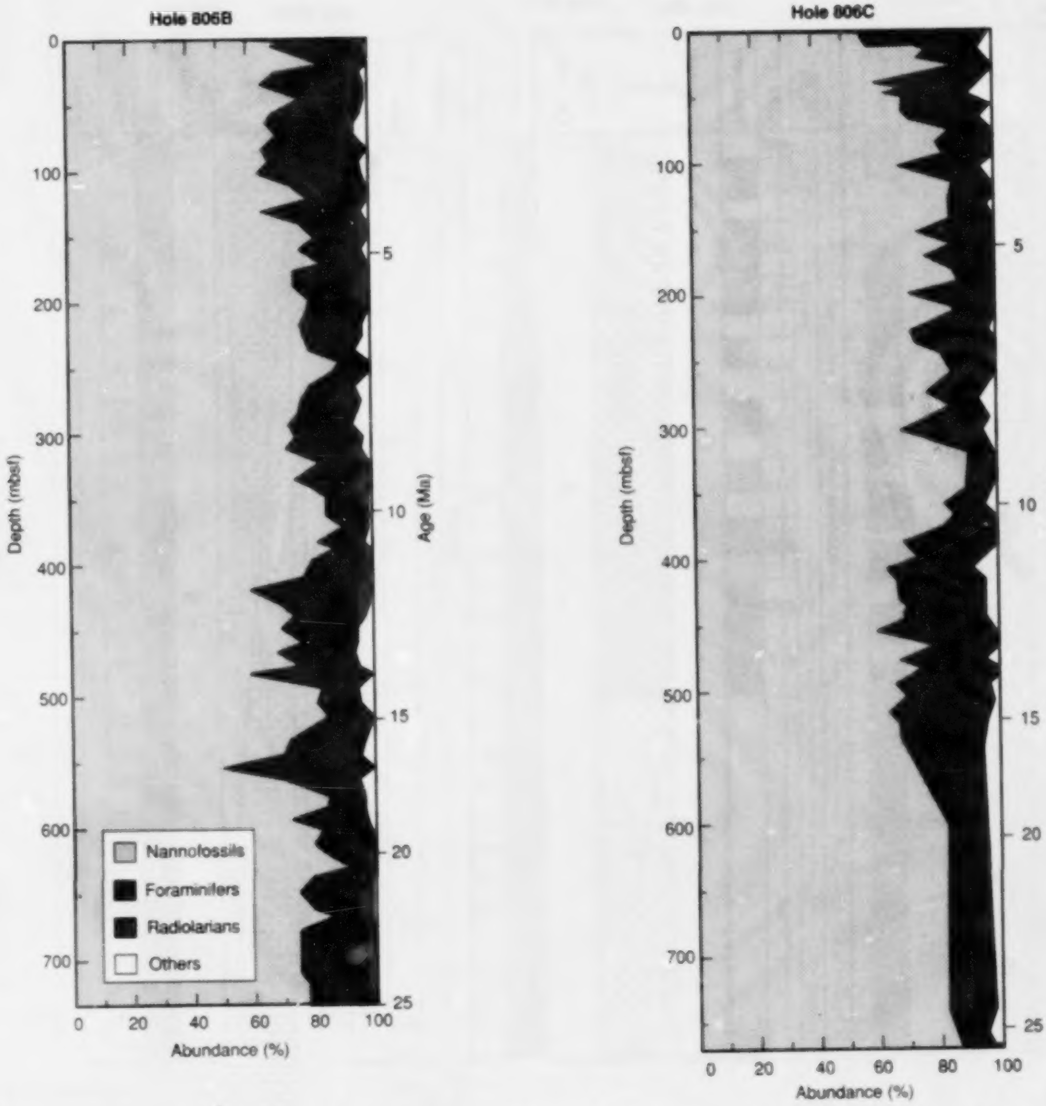

Figure 5. Abundances of major components, Holes 806B and 806C, as determined from smear slide analyses. Age designations are from the sedimentation rate data provided in the "Sedimentation Rates" section (this chapter).

Subunit IB

Intervals: Hole 806B, Cores 130-806B-37X through -78X;
Hole 806C, Cores 130-806C-38X through -62X
Age: early late Miocene-late Oligocene
Depth: 339-776.4 mbsf

Subunit IB, from 339 to 560 mbsf (lower upper Miocene to lower Miocene), is composed of foraminifer nannofossil chalk to nannofossil chalk with foraminifers, with a few intervals of nannofossil chalk. From 560 mbsf to the base of Hole 806C at 776.4 mbsf (lower Miocene to upper Oligocene), Subunit IB contains nannofossil chalk with foraminifers. The foraminifer content of Subunit IB, which varies between 10% and 50%, is high relative to that of equivalent intervals at Sites 803, 804, and 805 (Fig. 5). The amounts of other components, such as radiolarians, remain low (<5% to trace), as in Subunit IA. The mean carbonate content in this interval (Fig. 7) remains high at approximately 94%, but the short-term fluctuations are more extreme than in Subunit IA, ranging between values of 88% and 95%.

The dominant sediment color of Subunit IB is white (2.5Y 8/0 and 10YR 8/1). A few intervals (20-30 cm thick) are pale pink (5RP 8/2) to light pale purple (5P 6/2) in color. Thin (<0.1-1 cm thick), faint, and distinct color bands are common. These bands are light gray (5Y 7/2), pale blue (5PB 7/2), pale purple (5P 6/2), and greenish gray (5G 7/1) in color. The color

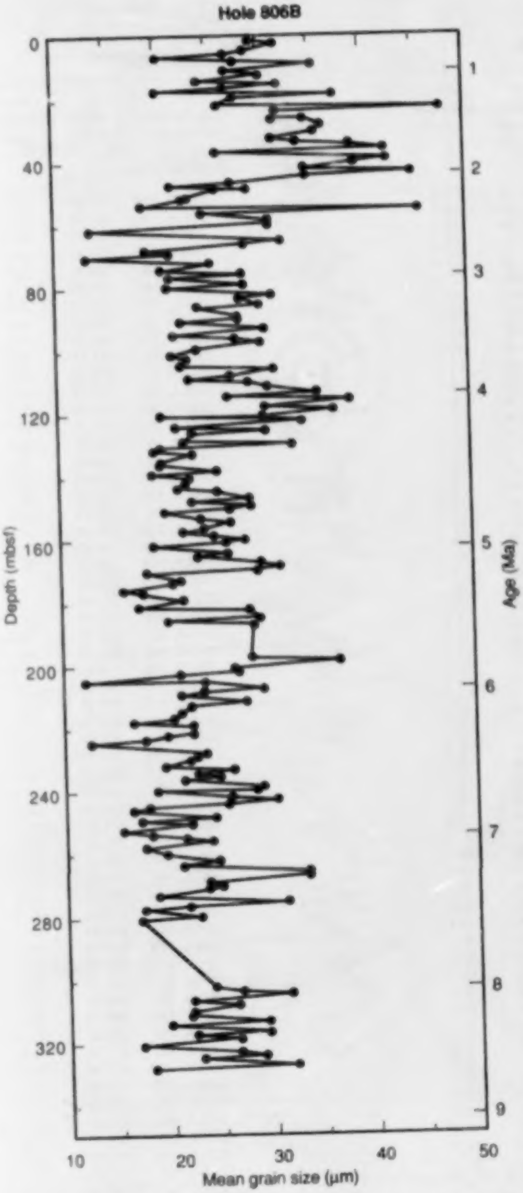

Figure 6. Mean grain-size curve, Hole 806B. Age designations are from the sedimentation rate data provided in the "Sedimentation Rates" section (this chapter).

bands become thinner, more distinct, and wavy in shape (approaching flaser structures) with depth in the subunit.

The sediments of Subunit IB are moderately to heavily bioturbated, as evident from burrow mottles, pyrite-filled trace structures and burrows, and discrete trace fossils (e.g., *Zoophycos*) (Fig. 11). Rare, centimeter-size porcellanite nodules were observed within this subunit, located at approximately 350 mbsf in Hole 806C (Sections 130-806C-38X-1 and -2), and at 509 mbsf and 514 mbsf in Hole 806B (Sections 130-806B-54X-5 and -55X-2).

The top of Subunit IB consists of soft chalk with interbeds of ooze. Color bands at this depth are faint, diffuse, and typically about 1 cm thick. The chalk intervals gradually become thicker and more lithified with depth. The color banding is millimeter-scale in thickness and very distinct by about 370 mbsf. By approximately 530 mbsf the sediment is composed of 100% chalk (no ooze) and is well lithified. Burrow traces at this depth are flattened, and color bands are very thin ($\ll 0.1$ cm) and wavy in appearance, forming flaser structures. The bands typically occur in groups from about 1 to 3 cm thick (Fig. 12), and become thinner and more braided with increasing depth. Furthermore, single, very thin ($\ll 0.1$ cm) light gray (N7/), slightly wavy bands are apparent (Fig. 13). Fracturing occurs readily along these surfaces.

Discussion

The sedimentary column at Site 806 is composed of homogeneous nannofossil oozes and chalks with foraminifers to foraminifer nannofossil oozes and chalks. The foraminifer abundances are high relative to those observed at the sites drilled in deeper water during Leg 130 (Sites 803–805), and typically range between 15% and 30%. The foraminifer tests are generally well preserved in comparison with those from Sites 803–805 (Fig. 14). This evidence, combined with biostratigraphic data (see "Biostratigraphy" section, this chapter) and the absence of primary sedimentary structures, suggests that the sedimentary section at this site was deposited by biogenic pelagic processes since the late Oligocene, without interruption or significant dissolution.

The most significant variation in the sediments at Site 806 is the change in foraminifer content, and consequently in mean grain size. On a large scale, foraminifer abundance is low in the upper Oligocene and lower Miocene, highest in the middle Miocene, low again in the upper Miocene, and high through the Pliocene and Pleistocene (Fig. 5). On a smaller scale, the high-frequency variations in foraminifer content appear on a scale of meters to tens of meters. Higher resolution grain-size and smear slide information, however, will be necessary to describe or quantify this variability adequately.

The fluctuations in the foraminifer content and mean grain size reflect the interplay of several factors, including overall productivity and the relative production rates of the different fossil groups, climatic conditions, changes in surface-water circulation, and changes in the effects preservation/dissolution and/or winnowing. It is difficult to determine the importance of each of these processes at this time. The good state of preservation of foraminifers and the water depth of this site suggest that dissolution has been of minor importance, but detailed work is required to document degrees of dissolution. The sediments exhibit little evidence of winnowing, although heavy bioturbation may have obscured such sedimentary structures. Two thin beds of well-sorted foraminifer ooze in Hole 806C (39.4 and 45.1 mbsf) may provide limited evidence for bottom current activity. These beds are well sorted, contain whole foraminifer tests, and are apparently ungraded. Because of their ungraded nature and uniform composition of foraminifers, these beds are interpreted as lag deposits formed by strong winnowing events, rather than as turbidites. In contrast, the turbidites at Site 804 contain numerous fragments of foraminifers mixed with other constituents and are graded (see "Lithostratigraphy" section, "Site 804" chapter, this volume).

Foraminifer abundance fluctuations may also be explained by changes in relative productivity, but it is difficult to imagine a bloom in foraminifers without an accompanying bloom in the

Table 2. Mean grain size of sediments from Subunit IA, as determined by shipboard analyses.

Core, section, interval (cm)	Depth (mbsf)	Mean grain size (µm)
130-806B-		
1H-1, 112	1.12	29.3
1H-2, 110	2.60	31.8
1H-3, 96	3.96	29.0
1H-4, 110	5.60	26.8
1H-5, 23	6.23	20.4
2H-1, 108	7.58	27.7
2H-2, 109	9.09	35.2
2H-3, 110	10.60	27.1
2H-4, 111	12.11	30.1
2H-5, 111	13.61	24.5
2H-6, 111	15.11	32.0
2H-7, 49	15.99	27.0
3H-1, 75	16.75	20.4
3H-2, 75	18.25	37.3
3H-3, 75	19.75	27.6
3H-4, 75	21.25	26.1
3H-5, 75	22.75	47.5
3H-6, 75	24.25	31.9
3H-7, 74	25.74	31.5
4H-1, 70	26.20	34.4
4H-2, 70	27.70	36.1
4H-4, 70	30.70	35.7
4H-5, 70	32.20	31.3
4H-6, 70	33.70	33.6
4H-7, 60	35.10	39.0
5H-1, 75	35.75	42.2
5H-2, 75	37.25	26.0
5H-3, 75	38.75	42.3
5H-4, 75	40.25	39.3
5H-5, 75	41.75	34.6
5H-6, 75	43.25	44.7
6H-1, 10	44.60	34.6
6H-2, 10	46.10	27.3
6H-3, 10	47.60	21.4
6H-4, 10	49.10	28.8
6H-4, 10	49.10	25.8
6H-5, 10	50.60	23.4
6H-6, 10	52.10	22.6
6H-7, 10	53.60	18.7
7H-1, 109	55.09	45.5
7H-2, 110	56.60	24.8
7H-3, 110	58.10	30.7
7H-4, 109	59.59	30.6
7H-5, 111	61.11	13.5
8H-1, 110	64.60	31.9
8H-2, 110	66.10	28.6
8H-3, 110	67.60	18.9
8H-4, 110	69.10	21.1
8H-5, 110	70.60	12.9
8H-6, 110	72.10	24.9
9H-1, 109	74.09	20.4
9H-2, 109	75.59	28.2
9H-3, 109	77.09	21.1
9H-4, 109	78.59	28.2
9H-5, 109	80.09	20.8
9H-6, 109	81.59	31.0
10H-1, 69	83.19	28.0
10H-2, 110	85.10	29.6
10H-3, 109	86.59	23.9
10H-4, 109	88.09	27.3
10H-5, 110	89.60	27.6
10H-6, 109	91.09	22.3
11H-1, 110	93.10	30.0
11H-2, 110	94.60	21.4
11H-3, 109	96.09	27.3
11H-4, 125	97.75	29.6
11H-5, 111	99.11	23.7
12H-1, 10	101.60	21.2
12H-2, 10	103.10	22.4
12H-3, 10	104.60	22.1
12H-4, 10	106.10	31.0
12H-5, 10	107.60	26.8
12H-6, 10	109.10	22.8
12H-7, 10	110.60	28.8
13H-1, 59	111.59	30.3
13H-2, 59	113.09	35.1
13H-3, 59	114.59	26.6
13H-4, 59	116.09	38.2
13H-5, 59	117.59	30.0
13H-6, 59	119.09	36.7
13H-7, 59	120.59	29.7
14H-1, 40	120.90	20.0
14H-2, 40	122.40	33.6
14H-3, 36	123.86	21.3
14H-4, 34	125.34	30.1
14H-5, 34	126.84	23.1
14H-6, 36	128.36	22.2
14H-7, 24	129.74	32.7
15H-1, 35	130.35	19.9
15H-2, 35	131.85	19.2
15H-3, 35	133.35	22.9
15H-4, 40	134.90	20.1
15H-5, 41	136.41	19.7
15H-6, 40	137.90	25.3
15H-7, 40	139.40	19.1
16H-1, 110	140.60	22.4
16H-2, 110	142.10	22.1
16H-3, 110	143.60	21.8
16H-4, 110	145.10	25.3
16H-5, 110	146.60	28.2
16H-6, 110	148.10	22.9
16H-7, 75	149.25	28.6
17H-1, 110	150.10	26.6
17H-2, 109	151.59	20.2
17H-3, 110	153.10	23.5
17H-4, 110	154.60	26.3
17H-5, 110	156.10	23.9
17H-6, 110	157.60	22.0
17H-7, 40	158.40	24.8
18H-1, 96	159.46	27.8
18H-2, 96	160.96	26.0
18H-3, 96	162.46	18.9
18H-4, 96	163.96	26.1
18H-5, 96	165.46	23.2
18H-6, 96	166.96	29.4
19H-1, 10	168.10	31.1
19H-2, 10	169.60	29.1
19H-3, 10	171.10	18.5
19H-4, 10	172.60	21.4
19H-5, 10	174.10	20.8
19H-6, 10	175.60	16.0
20H-1, 15	177.65	18.0
20H-2, 15	179.15	21.7
20H-3, 110	181.60	17.5
20H-4, 110	183.10	28.3
20H-5, 110	184.60	29.1
20H-6, 110	186.10	20.4
20H-7, 15	186.65	28.5
22H-1, 110	197.60	28.3
22H-2, 110	199.10	36.7
22H-3, 110	200.60	26.6
22H-4, 110	202.10	26.9
22H-5, 110	203.60	21.3
22H-6, 110	205.10	12.3
22H-7, 10	205.60	23.6
23H-1, 105	207.05	29.3
23H-2, 109	208.59	23.6
23H-3, 38	209.38	21.4
23H-4, 109	211.59	27.7
23H-5, 105	213.05	22.4
23H-6, 105	214.55	21.5
24H-1, 110	216.60	20.7
24H-2, 110	218.10	16.9
24H-3, 109	219.59	22.5
24H-4, 106	221.06	22.5
24H-5, 110	222.60	20.2
24H-6, 110	224.10	18.0
24H-7, 40	224.90	12.5
25H-2, 108	227.58	23.6
25H-3, 108	229.08	22.8
25H-4, 109	230.59	22.2
25H-5, 119	232.19	19.8
25H-6, 111	233.61	26.2
25H-7, 48	234.48	22.7
26H-1, 108	235.58	24.9
26H-2, 104	237.04	21.7
26H-3, 109	238.59	29.0
26H-4, 109	240.09	28.5
26H-4, 109	240.09	19.1
26H-5, 110	241.60	26.1
26H-6, 109	243.09	30.3
26H-7, 39	243.89	25.7
27H-1, 110	245.10	18.2
27H-2, 110	246.60	16.6
27H-3, 110	248.10	24.4
27H-4, 105	249.55	17.4
27H-5, 105	251.05	21.9
27H-6, 108	252.58	15.4
27H-7, 40	253.40	18.2
28H-1, 109	254.59	21.7
28H-2, 109	256.09	24.0
28H-3, 115	257.65	17.6
28H-5, 115	260.65	19.7
28H-6, 109	262.09	24.6
29H-1, 109	264.09	21.2
29H-2, 109	265.59	33.5
29H-3, 113	267.13	33.4
29H-4, 99	268.49	23.8
29H-5, 104	270.04	25.1
29H-6, 116	271.66	23.8
30H-1, 111	273.61	18.6
30H-2, 111	275.11	31.2
30H-3, 111	276.61	21.9
30H-4, 111	278.11	17.6
30H-5, 110	279.60	22.7
30H-6, 111	281.11	17.1
33H-1, 110	302.10	24.1
33H-2, 110	303.60	26.7
33H-3, 110	305.10	31.6
33H-4, 110	306.60	21.9
33H-5, 110	308.10	26.5
33H-6, 110	309.60	21.9
34H-1, 102	311.52	21.8
34H-2, 109	313.09	29.4
34H-3, 110	314.60	19.9
34H-4, 110	316.10	29.4
34H-5, 110	317.60	22.2
34H-6, 110	319.10	26.2
35X-1, 104	321.04	17.1
35X-2, 104	322.54	26.6
35X-3, 106	324.06	28.9
35X-4, 107	325.57	23.1
35X-5, 108	327.08	31.7
35X-6, 91	328.41	18.2

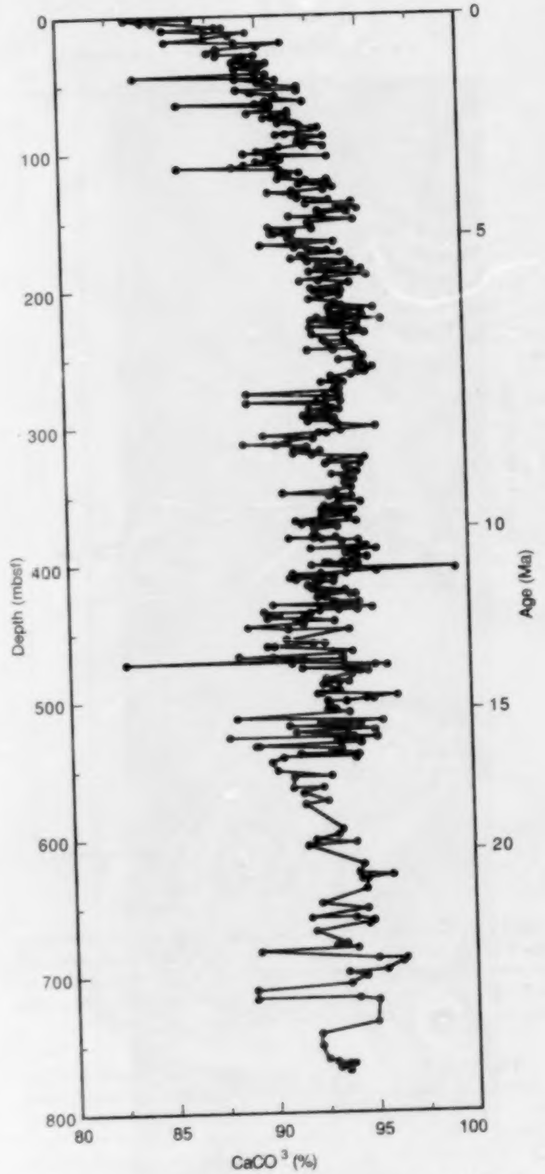

Figure 7. Carbonate contents, Hole 806B. Age designations are from the sedimentation rate data provided in the "Sedimentation Rates" section (this chapter).

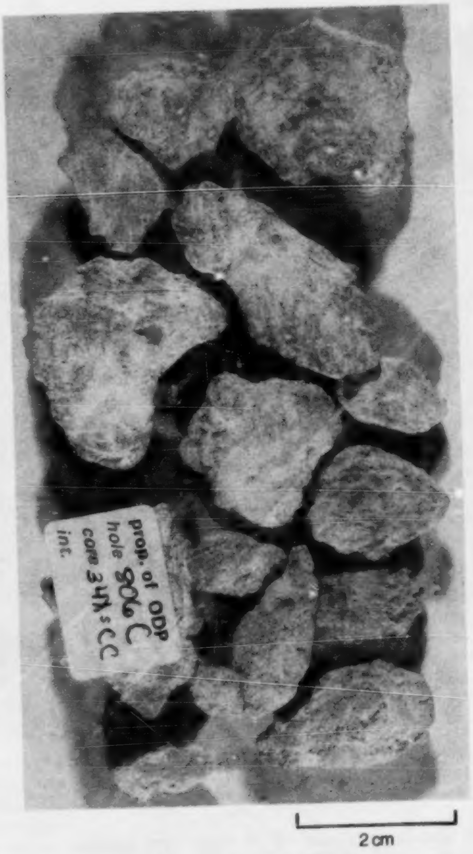

Figure 8. Porcellanite nodules (Core 130-806C-34X; 309.6 mbsf; upper middle Miocene). These nodules were the only material recovered in Core 130-806C-34X.

nannofossils. In addition, the intervals with high sedimentation rates do not correlate well with the periods of higher foraminifer abundance (see "Sedimentation Rates" section, this chapter). Instead, the intervals with low sedimentation rates correlate with high foraminifer abundances, supporting the winnowing hypothesis for the concentration of foraminifers. Further detailed work is necessary before the relative effects of productivity and winnowing on sedimentation rates and foraminifer abundances can be quantified. Changes in climate or surface-water masses may alter the composition of an assemblage, resulting in the production of more resistant forms that are preserved in the sedimentologic record. As a result, the grain-size change would reflect this change in foraminifer assemblage composition.

The abundance of foraminifers, which affects the grain size and is, in part, controlled by productivity and dissolution, may also affect the lithification process by influencing the diagenetic potential of the sediment. The processes involved in the ooze to chalk transition are, however, not well understood (Schlanger and Douglas, 1974). At Site 806, the transition was placed at 340 mbsf (lower upper Miocene), which is deeper and younger than the ooze-chalk transitions at Sites 803, 804, and 805. In fact, the transition occurs gradually over an interval of approximately 250 m. The first significant evidence of lithification is the presence of thin intervals of stiffer material within softer ooze. These intervals become thicker and harder downsection until they become chalk, which is intercalated with stiff ooze. The transition proceeds by a reduction in the abundance of ooze, until the sediment is eventually all converted to chalk. Smear slide observations of lithified samples provide little evidence of grain-to-grain cementation, although the difficulty of disaggregating those grains when making smear slides suggests that some cementation has occurred. The potential for cementa-

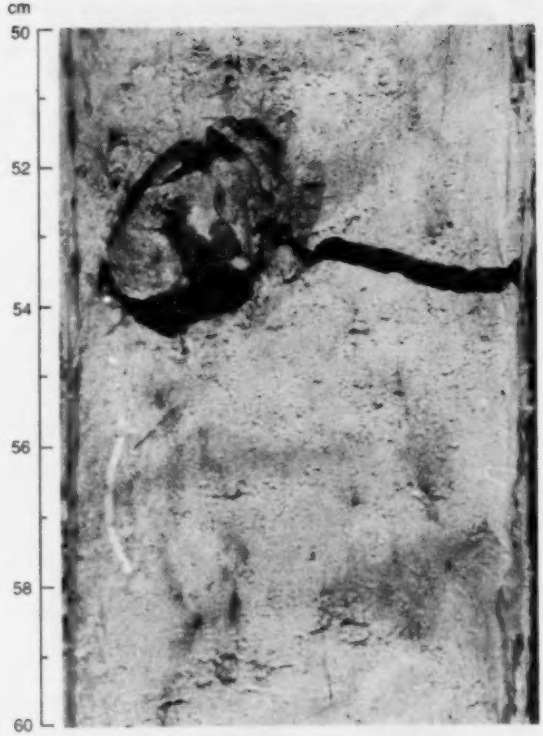

Figure 9. A dropstone of pumice (Section 130-806C-7H-3, 52 cm; 56.6 mbsf).

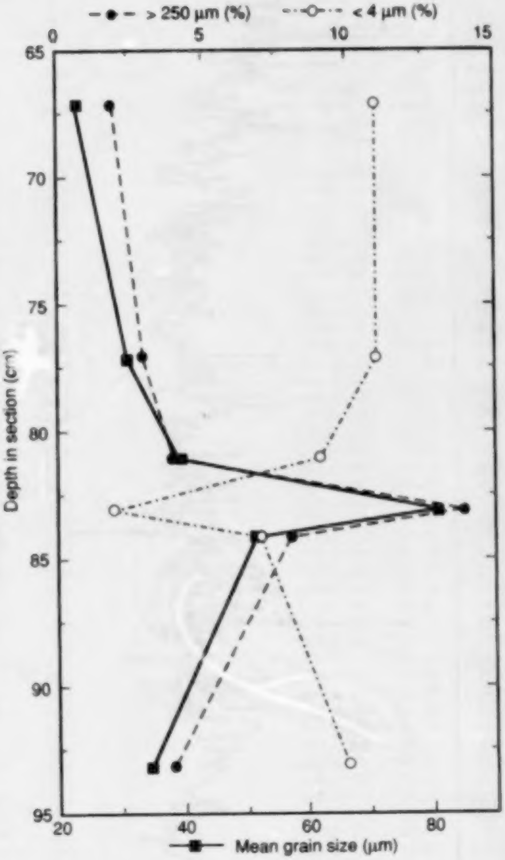

Figure 10. Profiles of mean grain size and coarse sand (>250 µm) and clay (<4 µm) abundances found in a well-sorted bed of foraminifer tests at Section 130-806C-5H-4, 83 cm (39.4 mbsf). Depth is measured as the position within Section 130-806C-5H-4. This bed is interpreted as having been formed by a strong winnowing event.

tion is also demonstrated by the significant amounts of calcite precipitated onto nannofossil tests during lithification, which gradually make the nannofossils appear thicker downhole (Fig. 15).

Other signs of lithification include porcellanite concretions that are distributed in low abundances below 240 mbsf. The silica comprising these nodules appears to have been precipitated. Although pore-water silica concentrations are not significantly higher at the levels where concretions were recovered, the pore-water silica levels are consistently high enough to allow precipitation (see "Inorganic Geochemistry" section, this chapter). It is not known at this time why the concretion abundances are so low nor what the catalyst is for their formation.

The chalk becomes more lithified below approximately 500 mbsf. Sediment compaction, both mechanical and chemical, results in the flattened appearance of bioturbation structures and color-band thinning. Below 600 mbsf the color bands become wavy and braided in appearance (Fig. 14), probably because of chemical compaction by dissolution and reprecipitation, which produces flaser structures. These features are not interpreted as primary sedimentary structures, caused by oceanic bottom currents, as was suggested for Site 289 on the Ontong Java Plateau (Shipboard Scientific Party, 1975). We interpret these structures as postdepositional for three reasons: (1) the color bands thin and intensify with depth; (2) the color bands frequently cross bioturbation structures, suggesting that they formed after the bioturbation; and (3) the color bands are braided at depth in Site 806, whereas primary sedimentary structures cannot cross and intertwine with one another.

Thin (<0.1 mm), single, gray, wavy color bands were also observed occasionally (Fig. 15). Fracturing occurred readily along the irregular contacts formed by these bands. These bands cross bioturbation features in some cases, such as is shown in Figure 13. In these cases, the trace fossil is slightly offset across the band, implying that some material has been lost through chemical compaction. This observation supports the interpretation of these structures as incipient stylolites.

Summary

The sedimentary section at Site 806, which extends from the upper Oligocene to the Pleistocene, is a complete stratigraphic section of biogenic pelagic sediments, with no evidence of interruption, hiatus, or significant reworking other than bioturbation. As a result, this site offers an excellent type section for correlation to sites lower on the slope of the Ontong Java Plateau. The sedimentary column was classified as one lithostratigraphic unit (Unit I), but was divided into two subunits on the basis of the states of lithification. Subunit IA is composed of foramini-

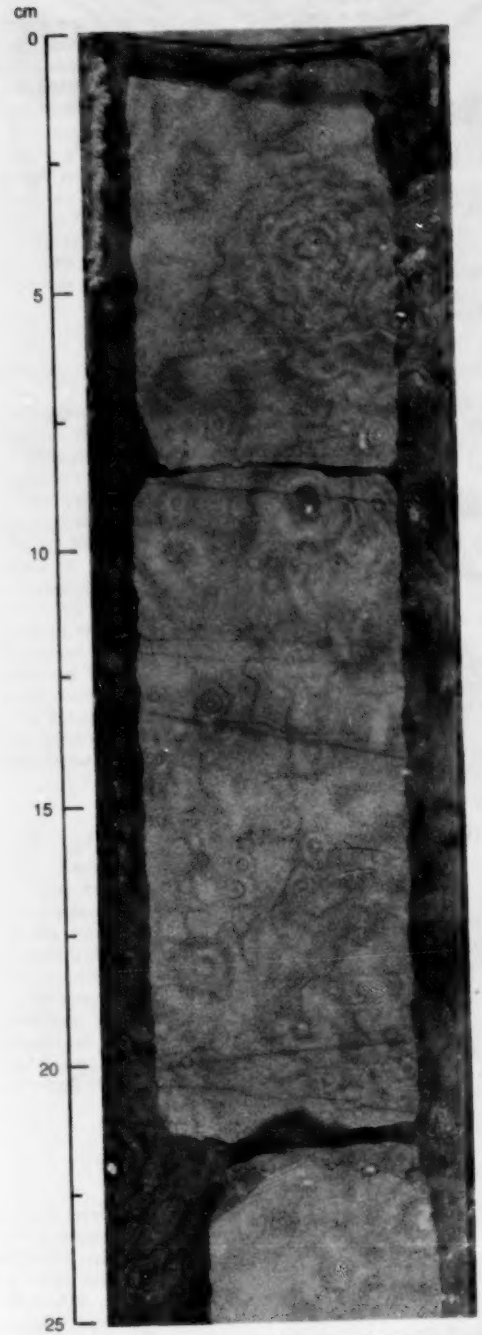

Figure 11. Distinct *Zoophycos* trace fossils common in the chalks deep in Site 806 (Section 130-806B-70X-4, 0–25 cm; 662 mbsf).

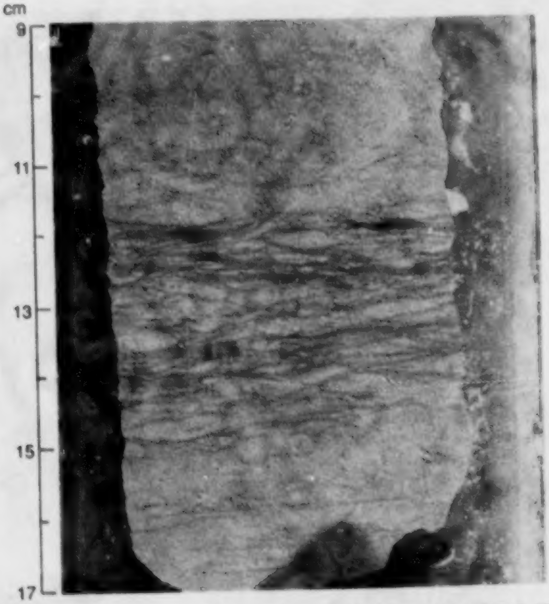

Figure 12. Photograph of color bands (Section 130-806B-70X-CC, 9–17 cm; 656 mbsf). These bands are described as flaser structures because of their wavy, braided appearance and are interpreted as resulting from chemical compaction.

fer nannofossil ooze to nannofossil ooze with foraminifers, with some intervals of nannofossil ooze. Subunit IB is composed of foraminifer nannofossil chalk to nannofossil chalk with foraminifers.

BIOSTRATIGRAPHY

Introduction

Site 806, in a water depth of 2520 m, is nearest to the equator and is the shallowest site on the Ontong Java Plateau depth transect. Three holes were drilled at Site 806. Hole 806A penetrated sediments of Quaternary to Pliocene age, and an apparently complete sequence was retrieved. The Pliocene/Pleistocene boundary was placed within Core 130-806A-5H on the basis of the calcareous nannofossil evidence. Hole 806B was drilled to a depth of 743.1 mbsf and retrieved an apparently continuous sequence of sediments of Pleistocene to early Miocene age (Fig. 16). The deepest hole at this site, Hole 806C, penetrated sediments of Pleistocene to late Oligocene age (Fig. 16). Much of the lower Miocene was not cored at this hole, which was washed ahead below 542 mbsf to retrieve the Oligocene/Miocene boundary. This boundary was placed within Core 130-806C-59X (interval 740.0–749.5 mbsf) on the basis of the planktonic foraminifer and diatom evidence. As at Site 805, this site has an unusually thick middle and lower Miocene section (approximate thickness = 380 m).

The microfossils show various states of preservation. Calcareous nannofossils, planktonic foraminifers, diatoms, and radiolarians are generally well to moderately well preserved throughout much of the sediment sequence. However, the preservation of diatoms and radiolarians is generally moderate to poor in the lower Miocene. Poor preservation of foraminifers, diatoms, and radiolarians was seen in Oligocene samples.

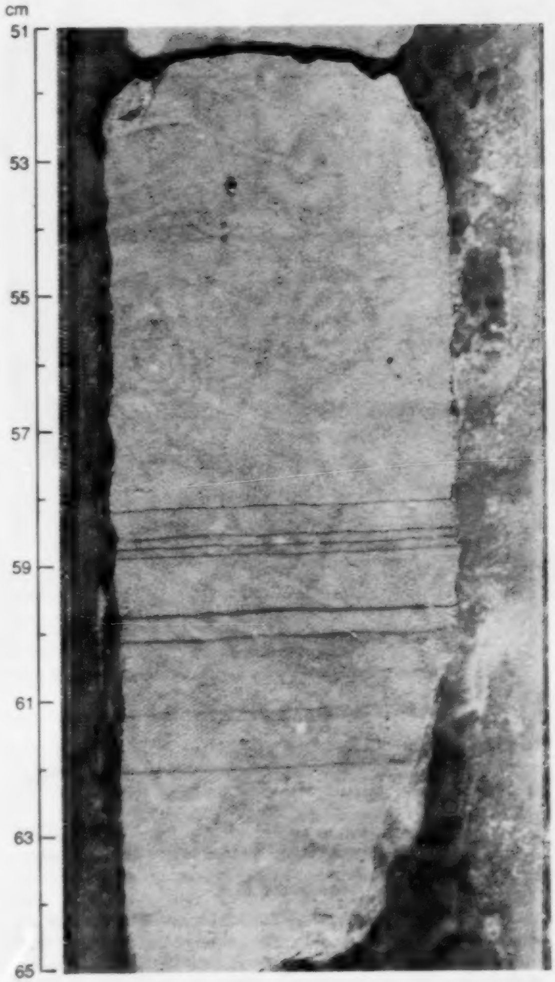

Figure 13. A photograph of very thin (<<0.1 cm), wavy, gray bands observed in the highly consolidated chalks deep in Site 806 (Section 130-806B-70X-3, 51–65 cm; 659 mbsf). Fractures occur readily along these bands, which are interpreted as incipient stylolites. Note that the color band crosses through the *Zoophycos* trace fossil without interruption; the trace fossil, however, is offset slightly across the band, suggesting the loss of material through chemical compaction.

Details on biostratigraphy as well as on abundance and preservation of the different microfossil groups are presented below.

Calcareous Nannofossils

The sediments at Site 806 yielded abundant calcareous nannofossils from an apparently continuous Neogene and uppermost Oligocene sequence. The section can be characterized as presenting a "text-book" type of stratigraphy with virtually all zonal markers present and no signs of sedimentological or drilling disturbance. Only three markers in the zonal schemes of Martini (1971) and Okada and Bukry (1980) were observed to be missing, namely *Helicosphaera ampliaperta* (NN4/NN5 boundary), *Helicosphaera recta* (NP25/NN1 boundary), and *Dictyococcites bisectus* (CP19/CN1 boundary).

Preservation is good in the Pleistocene and the upper Pliocene, and moderate in the remainder of the section. The chief problem was that primary morphological characters of the discoasters commonly were blurred by calcite overgrowth. The calcareous dinoflagellate genus *Thoracosphaera* was observed in low but varying abundances throughout the section.

The following discussion represents a composite summary of the nannofossil biostratigraphy as recognized in the Quaternary to upper Pliocene (Hole 806A), the lower Pliocene to lower Miocene (Hole 806B), and the middle Miocene to upper Oligocene sections (Hole 806C). Figure 16 summarizes the calcareous nannofossil zones of the three holes drilled at Site 806 and their correlation to those of the planktonic foraminifers, diatoms, and radiolarians.

Hole 806A

Pleistocene

Sample 130-806A-1H-CC contains a late Pleistocene to Holocene assemblage, including such forms as *Calcidiscus leptoporus, Ceratolithus telesmus, Helicosphaera carteri, Syracosphaera,* and abundant small *Gephyrocapsa.* This sample lies above the stratigraphic range of *Pseudoemiliania lacunosa* and was placed in the NN20/NN21 zonal interval, therefore. This interval was not subdivided because *Emiliania huxleyi* cannot be reliably identified using light microscopy. The presence of abundant *Pseudoemiliania lacunosa* and the absence of discoasters place Samples 130-806A-2H-CC through -4H-CC in Zone NN19. Among these samples, Sample 130-806A-3H-CC contains many specimens of *Pontosphaera,* even though it is still referred to as "few" in abundance (0.1%–1.0 % of the total assemblage). Sample 130-806A-4H-CC contained the first downhole observations of *Coccolithus pelagicus, Calcidiscus macintyrei,* and *Helicosphaera sellii,* and therefore corresponds to the lower part of Zone NN19. One reworked specimen (*Discoaster variabilis*) was also observed in this core-catcher sample.

Pliocene

The Pliocene/Pleistocene boundary was placed in Core 130-806A-5H. Sample 130-806A-5H-CC contained a few specimens of *Discoaster brouweri* and was assigned to the upper Pliocene Zone NN18. *Discoaster brouweri* and *D. pentaradiatus* co-occur in Sample 130-806A-6H-CC (Zone NN17). Below this level, the assemblage is characterized by a more diversified discoaster association, including *Discoaster surculus.* Samples 130-806A-7H-CC through -9H-CC were assigned to the upper Pliocene Zone NN16. Rare *Discoaster asymmetricus* and *D. tamalis* were observed in Sample 130-806A-8H-CC. *Discoaster variabilis* was absent in this discoaster-rich sample, placing this sample in the upper half of Zone NN16. Hole 806A ended within Zone NN16 of the upper Pliocene (Core 130-806A-9H).

Hole 806B

Pliocene

The last occurrence (LO) of *Discoaster brouweri* is in the lower part of Core 130-806B-5H. The onset of the acme interval of *Discoaster triradiatus* appears to begin in Section 130-806B-6H-1, and the NN18/NN17 zonal boundary falls between Samples 130-806B-7H-1, 70 cm, and 130-806B-7H-2, 70 cm. The single specimen of *Discoaster pentaradiatus* observed in Sample 130-806B-6H-CC was considered to be reworked. Sample 130-806B-7H-CC contains *Discoaster surculus.* Samples 130-806B-7H-CC through -10H-CC are all placed in Zone NN16. Within that interval, Sample 130-806B-9H-CC yielded such diversified

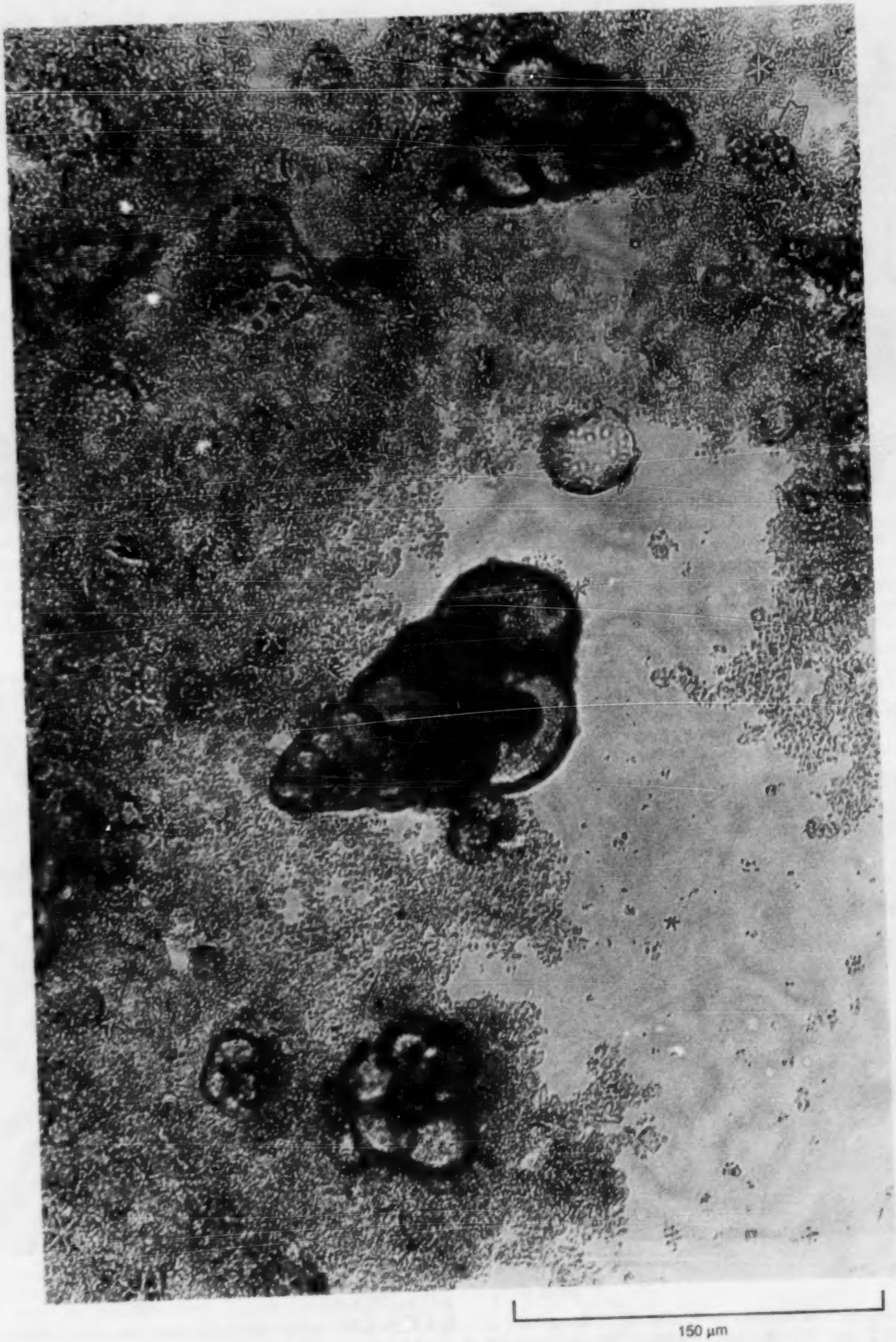

Figure 14. Photomicrograph of well-preserved foraminifer tests abundant in all of the sediments recovered from Site 806 (Section 130-806B-24H-3, 74 cm; 218 mbsf). Pyrite infilling of test chambers is also abundant. The prominent biserial foraminifers are *Streptochilus latum*.

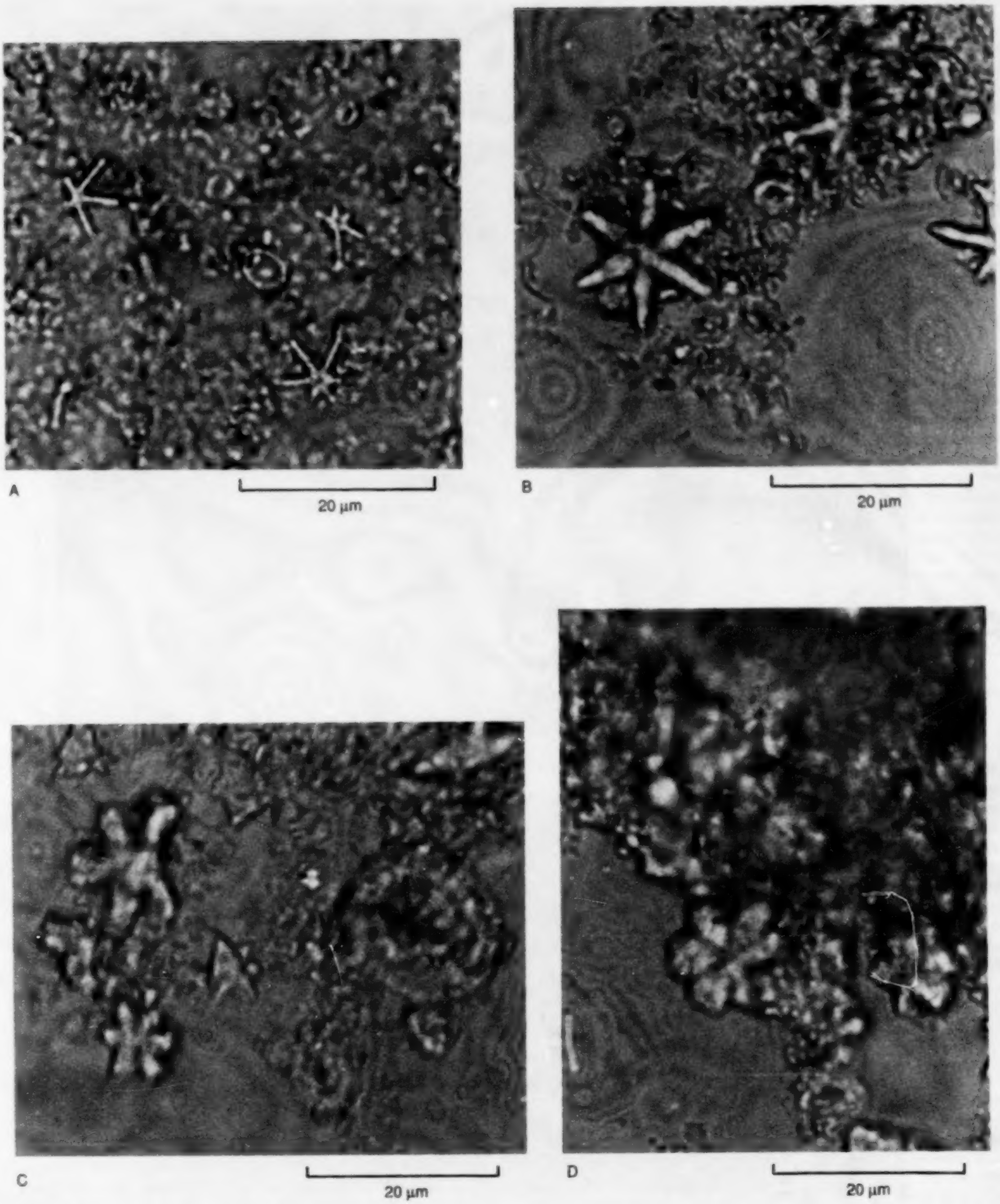

Figure 15. Photomicrographs showing the calcification of nannofossil tests (*Discoaster*) as the sediment in transformed from ooze to chalk. **A**. Section 130-806A-6H-CC; 54 mbsf. **B**. Section 130-806B-24H-3; 219 mbsf. **C**. Section 130-806C-51X-3; 478 mbsf. **D**. Section 130-806B-65X-3; 611 mbsf. Note the gradual thickening of the arms of the *Discoaster* tests with depth in the hole, which results from calcite precipitation onto the tests.

discoaster species as *Discoaster asymmetricus, D. brouweri, D. challengeri, D. decorus, D. surculus, D. tamalis, D. triradiatus,* and *D. variabilis*. Some specimens of *D. challengeri* and *D. variabilis* are unusually large in size.

The LO of *Sphenolithus abies* is between Samples 130-806B-10H-5, 75 cm, and -6, 75 cm, indicating an approximate position of the upper/lower Pliocene boundary. The highest occurrence of *Reticulofenestra pseudoumbilica* was observed between Samples 130-806B-11H-2, 75 cm, and -3, 75 cm, indicating the NN15/NN16 zonal boundary. Samples 130-806B-12H-CC through -14H-CC contain *R. pseudoumbilica* and *Discoaster asymmetricus*, placing these samples in the NN15/NN14 zonal interval. This interval is not subdivided because members of the genus *Amaurolithus* are rare or absent in this section. *Sphenolithus abies* and *S. neoabies* are abundant in these samples belonging to the upper part of the lower Pliocene. A bloomlike abundance of small reticulofenestrid placoliths (<3 μm) was observed in Sample 130-806B-14H-4, 40 cm.

Ceratoliths are comparatively rare in the lower Pliocene. Nevertheless, the change from the descendant *Ceratolithus rugosus* to the ancestral form *Ceratolithus acutus* was observed between Samples 130-806B-16H-6, 40 cm, and -7, 40 cm. Thus, these samples mark the NN12/NN13 zonal boundary. *Triquetrorhabdulus rugosus* has its LO in Section 130-806B-17H-5, indicating a position within the bottom part of Zone NN12 and near the Miocene/Pliocene boundary.

Sediments between Samples 130-806B-14H-CC and -16H-CC are characterized by fairly abundant occurrences of peculiar subcircular *Reticulofenestra* specimens in addition to abundant *Scyphosphaera* spp., *Sphenolithus abies*, and *S. neoabies*.

Miocene

Samples 130-806B-18H-CC down to -29H-CC contain *Discoaster quinqueramus*, the total range of which defines the late Miocene Zone NN11. The uppermost part of the range of *D. quinqueramus* was difficult to recognize, partly because of calcite overgrowth that blurred the distinct and characteristic central knob of this species, but partly also because the critical central knob was less clearly developed among the uppermost representatives of what we take to be *D. quinqueramus*. The lowermost occurrence of *Amaurolithus* was observed in Sample 130-806B-24H-CC, which lies in the middle part of Zone NN11. Representatives of this genus are consistently rare in the upper Miocene sediments of the Ontong Java Plateau. Yet, by judging from the results of the previous Leg 130 sites, one would expect a somewhat lower position for the evolutionary appearance of *Amaurolithus*.

Discoaster neohamatus disappears in Core 130-806B-29H. Sample 130-806B-30H-CC contains rare *Discoaster quinqueramus* together with *D. berggrenii*. Samples 130-806B-31H-CC through -35X-CC contain neither *Discoaster quinqueramus* nor *D. hamatus*, indicating a position of the NN10/NN11 zonal boundary in the former core. The lower part of Zone NN11 and the upper part of Zone NN10 (i.e., Samples 130-806B-29H-CC through -31H-CC) are characterized by bloomlike abundances of small *Sphenolithus abies* and *S. neoabies*. *Minylitha convallis* and sphenoliths are abundant in Sample 130-806B-33H-CC, whereas *Thoracosphaera* is rather common in Sample 130-806B-34H-CC.

Samples 130-806B-36X-CC through -38X-CC are characterized by continuous occurrences of *Discoaster hamatus*, the total range of which defines Zone NN9. Sample 130-806B-39X-CC is characterized by the presence of *Catinaster coalitus* and the absence of *Discoaster hamatus*, and hence belongs to Zone NN8; the middle/late Miocene boundary was placed within Zone NN8.

The sediments from Sample 130-806B-40X-CC through Sample -44X-CC lack primary marker species except for a single specimen of *Discoaster* cf. *D. kugleri* in Sample 130-806B-43X-CC. This interval, however, is characterized by a typical upper middle Miocene assemblage, including *Calcidiscus leptoporus* and abundant *Calcidiscus macintyrei*, few *Coccolithus miopelagicus*, common to abundant members of the *Discoaster variabilis* group, common to abundant *Reticulofenestra pseudoumbilica* and *Reticulofenestra gelida*, and few to common *Triquetrorhabdulus rugosus*. The LO of *C. miopelagicus* appears to fall immediately below Zone NN8. The NN6/NN7 zonal interval is difficult to subdivide because of the absence or rare occurrence of the nominate species *Discoaster kugleri*. If present, calcite overgrowth on discoasters tends to prevent accurate identification of *D. kugleri*.

Coronocyclus nitescens was observed in and below Sample 130-806B-45X-CC. The LO of this species is supposed to lie near the first occurrence (FO) of *Discoaster kugleri*. Samples 130-806B-45X-CC down to 130-806B-50X-CC contains *Coronocyclus nitescens* but not *Sphenolithus heteromorphus*, and therefore these samples may belong to Zone NN6. The LOs of *Cyclicargolithus floridanus* and *Sphenolithus heteromorphus* are both observed between Samples 130-806B-50X-CC and 130-806B-51X-CC. Samples 130-806B-51X-CC through 130-806B-61X-CC contain *S. heteromorphus*.

Helicosphaera ampliaperta, the last occurrence of which is used to define the top of Zone NN4, has not been observed in any of the Leg 130 samples taken from the pertinent stratigraphic interval and must have been ecologically excluded from this region. It follows that the combination of Zones NN4 and NN5 results in a long biostratigraphic interval that straddles the lower/middle Miocene boundary. Bukry's (1973) end-of-acme concept of *Discoaster deflandrei*, that recently was quantified and defined by Rio et al. (in press) as the decrease to <30% of *D. deflandrei* of the total discoaster assemblage, allows splitting of the NN4/NN5 zonal interval into two parts of approximately equal duration. This abundance transition was observed in Core 130-806B-57X.

The FO of *Sphenolithus heteromorphus* occurs in Core 130-806B-62X, a core that also contains the LO of *Sphenolithus belemnos*, and thus marks the NN3/NN4 zonal boundary. Sample 130-806B-63X-CC also contains *Sphenolithus belemnos*, indicating that the FO of this species lies above Sample 130-806B-64X-CC. Rare specimens of *Triquetrorhabdulus carinatus* were observed in this former sample (reworked?). The first observation of common *T. carinatus* was made in Sample 130-806B-66X-CC, which probably marks the top of the lower Miocene Zone NN2.

The nannofossil assemblages in the deepest part of Hole 806B are abundant but moderate to poorly preserved (Samples 130-806B-64X-CC to 130-806B-78X-CC). This rather monotonous flora is composed of abundant *Discoaster deflandrei, Cyclicargolithus floridanus* and forms belonging to the *Sphenolithus moriformis* group. A few specimens of *Discoaster druggii* were observed in Samples 130-806B-66X-CC and 130-806B-77X-CC, placing this interval in Zone NN2. Sample 130-806B-78X-CC, which was taken from the bottom of the Hole 806B, contains neither *D. druggii* nor *Sphenolithus ciperoensis*. The lack of *D. druggii* in this sequence, however, does not necessarily imply a position within Zone NN1 because of calcite overgrowth problems.

Hole 806C

Sphenolithus heteromorphus disappears together with *Cyclicargolithus floridanus* in Core 130-806C-50X; the NN5/NN6 zonal boundary thus lies in this core. *Discoaster deflandrei* is abundant in and below Sample 130-806C-56X-CC, accounting

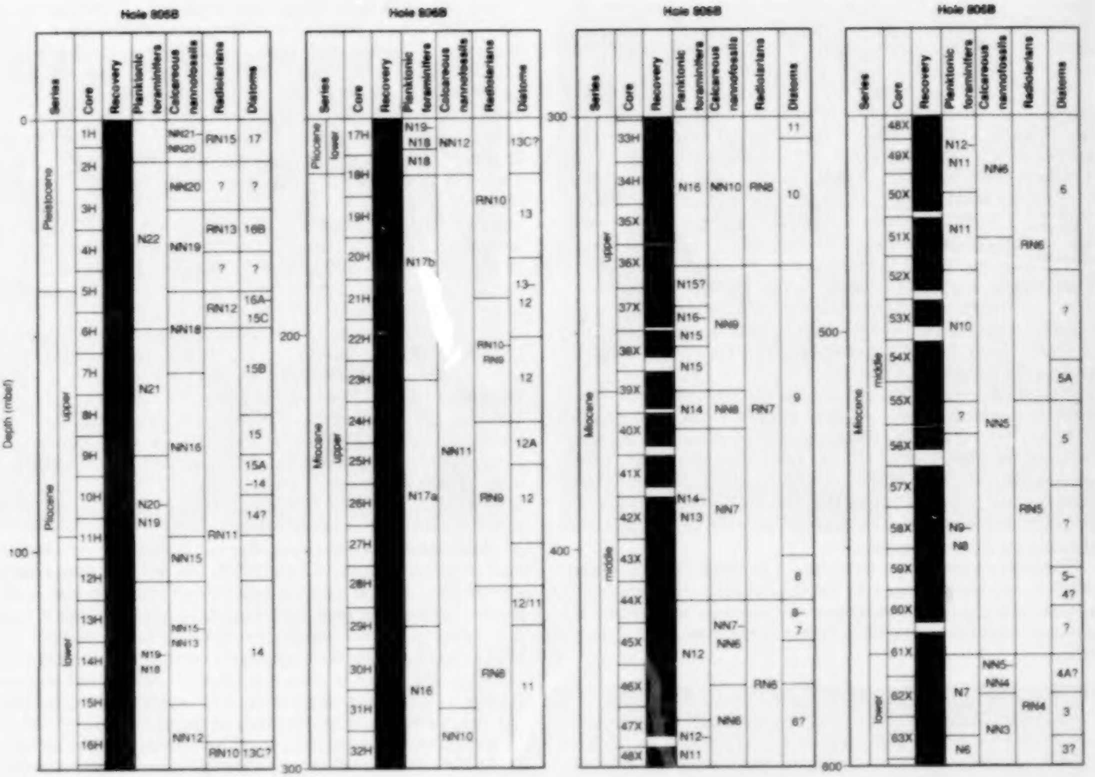

Figure 16. Biostratigraphic hole summaries, Site 806. RN = radiolarian Neogene zone, NTD = Neogene tropical diatom zone, RP = radiolarian Paleogene zone, and NN = nannofossil Neogene zone.

for >30% of the total discoaster assemblage. The decrease in abundance to values that are substantially less than 30% in Core 130-806C-56X approximately indicates the lower/middle Miocene boundary and the NN4/NN5 zonal boundary. *Sphenolithus heteromorphus* is abundant in Sample 130-806C-57X-CC, which lies at 541.7 mbsf.

Core 130-806C-58X was recovered after washing down to 599.0 mbsf. This core contains the FO of *Sphenolithus belemnos* between Samples 130-806C-58X-1, 75 cm, and -58X-CC, implying that the FO of *Sphenolithus heteromorphus* and the LO of *Sphenolithus belemnos* (NN3/NN4 boundary) fall in the washed interval. Both *Triquetrorhabdulus carinatus* and *Discoaster druggii* were observed in Sample 130-806C-58X-CC; *T. carinatus* was observed also from the top of this core, in Sample 30-806C-58X-1, 5 cm, together with *S. belemnos*, placing the core in the lower Miocene Zone NN2.

The interval from 608.5 to 740.0 mbsf was drilled without coring. Sample 130-806C-59X-CC contains a typical upper Oligocene/lower Miocene assemblage, with common to abundant *Coccolithus pelagicus*, *Cyclicargolithus floridanus*, *Discoaster deflandrei*, and sphenoliths, including abundant *Sphenolithus moriformis*, common *S. dissimilis*, and rare *S. delphix* and *S. conicus*. Sample 130-806C-61X-CC was dominated by *Cyclicargolithus floridanus* and *Sphenolithus moriformis*. A few specimens of *Sphenolithus ciperoensis* were also observed in this sample. *Helicosphaera recta* and *Dictyococcites bisectus* are absent in the upper Oligocene sediments from the Ontong Java Plateau. The rare occurrences of *Sphenolithus ciperoensis*, however, suggest that Core 130-806C-61X belongs to upper Oligocene Zone NP25. Sample 130-806C-62X-CC represents the bottom of Hole 806C; the assemblage is similar to that observed in the next higher core and is considered to represent Zone NP25 despite the fact that *Sphenolithus ciperoensis* was not observed.

Planktonic Foraminifers

Planktonic foraminifers are abundant in the Pleistocene to lower Pliocene sequence of Hole 806A, and the preservation is good. Exceptions to this are the Samples 130-806A-7H-CC and -8H-CC where the preservation is poor.

Hole 806B penetrated an apparently continuous sequence of sediments of Pleistocene to early Miocene age (Fig. 16). With the exception of Sample 130-806B-1H-CC where the preservation of planktonic foraminifers is poor, abundance and preservation are generally good from the top of the section through Sample 130-806B-38X-CC in the middle Miocene. In the remainder of the middle Miocene sequence, from Sample 130-806B-38X-CC to -56X-CC, planktonic foraminifers are abundant and the preservation is moderate to good. Below Core 130-806B-58X-CC, abundance and preservation of planktonic foraminifers are more variable but in general are also good.

The sediment recovered in Hole 806C ranges in age from Pleistocene to late Oligocene (Fig. 16). Like Hole 806B, this hole possesses an expanded middle and lower Miocene section. Much of the lower Miocene (N4 and N5) was not cored at this

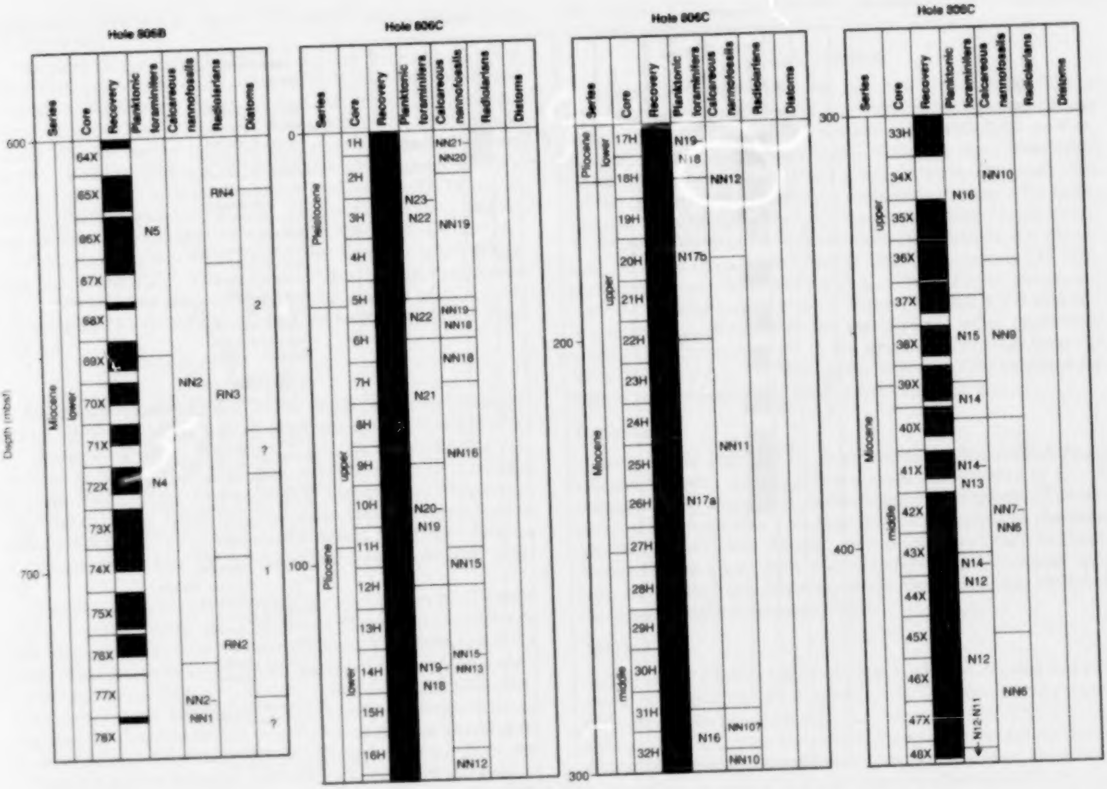

Figure 16 (continued).

hole. Planktonic foraminifers are generally abundant and well preserved. Preservation is poor only in the bottom two samples in the hole (upper Oligocene).

Hole 806A

Sample 130-806A-1H-CC is void of the Pleistocene–latest Pliocene marker species *Globorotalia truncatulinoides*. This absence may be environmentally controlled, as there was no sign of dissolution in this sample. However, *G. truncatulinoides* is present in stratigraphically lower samples. The Pliocene/Pleistocene boundary was placed within Core 130-806A-4H on the basis of the LO of *Globigerinoides fistulosus*.

Hole 806B

The Pliocene/Pleistocene boundary was placed in Core 130-806B-5H on the basis of the FO of *G. truncatulinoides*. The base of the upper Pliocene was placed within Core 130-806B-9H on the basis of the FO of *G. tosaensis*. The base of Zone N19–N20 occurs within Core 130-806B-12H. The FO of *Globorotalia tumida* occurs in Sample 130-806B-17H-CC; therefore, the base of Zone N18 and the lower Pliocene is within Core 130-806B-18H. The base of Subzone 17b occurs within Core 130-806B-23H on the basis of the FO of *Pulleniatina primalis*. Subzone 17a extends to within Core 130-806B-29H (i.e., the core below the last core-catcher sample to contain *Globorotalia plesiotumida*). The FO of *Neogloboquadrina acostaensis* occurs within Core 130-806B-38X, which therefore defines the base of Zone N16. The zonal marker *Globorotalia siakensis* defines the base of Zone N15 and is found within Core 130-806B-39X. Therefore, Zone N15, typically of short duration, occupies an attenuated interval of sediment between these two marker species. The base of Zone N14 is defined on the basis of the FO of *Globigerina nepenthes*. This species was not observed in the core-catcher samples of Hole 806B and so it is not possible to subdivide the N14/N13 interval.

The LO of the *Globorotalia fohsi* plexus was observed in Sample 130-806B-44X-CC; therefore, the base of Zone N13 occurs within Core 130-806B-44X. Members of the *G. fohsi* lineage are well developed at Site 806, although they do not form a dominant part of the fauna. Gradational forms are common, making the distinction between *G. fohsi* and *G. praefohsi*, and therefore the Zone N12/N11 transition, difficult to recognize. For practical purposes, however, we placed this boundary in Core 130-806B-47X. Zone N11 (based on the FO of *G. praefohsi*) covers the interval from Cores 130-806B-48X to -52X. Zone N10 was defined on the FO of *G. peripheroacuta*, which occurs in Core 130-806B-55X. However, Core 130-806B-55X itself is chalky and difficult to disaggregate, so that no age-diagnostic taxa were observed within it.

No members of the *Orbulina* lineage were observed in the lower middle Miocene part of this hole; therefore, it is not possible to distinguish the boundary between Zones N8 and N9. Assemblages diagnostic of Zone N7 were identified in Cores 130-806B-61X and -62X. Although *Praeorbulina sicanus* was not observed in this hole, these two samples are devoid of *Catapsydrax dissimilis*, indicating an approximate Zone N7 age. The

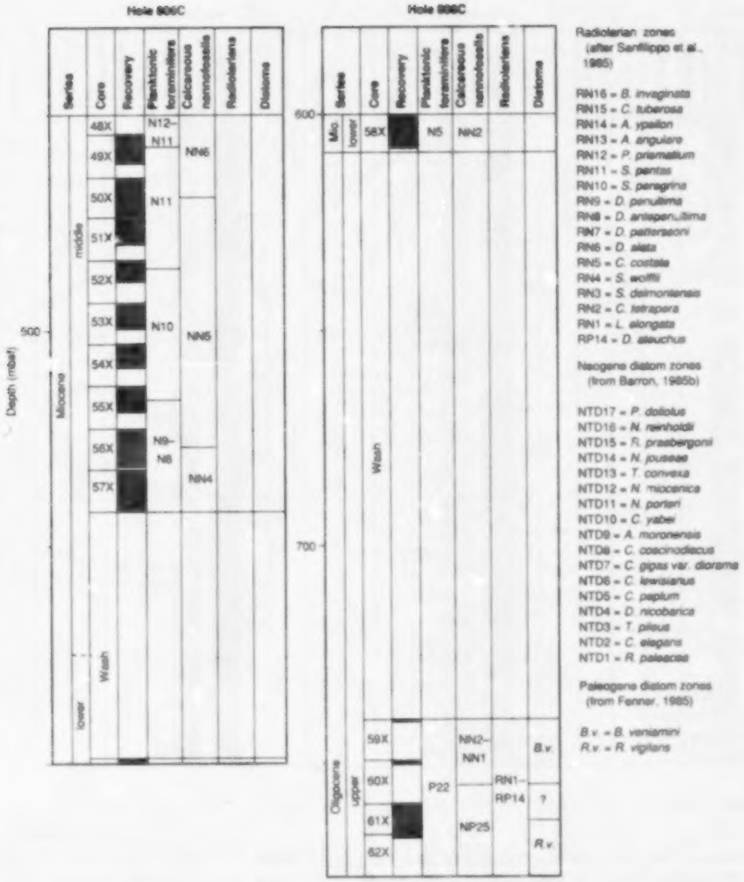
Hole 806C
Series
Core
Recovery
Planktonic foraminifers
Calcareous nannofossils
Radiolarians
Diatoms
Depth (mbsf)
500
600
700
Miocene
middle
lower
Wash
48X
49X
50X
51X
52X
53X
54X
55X
56X
57X
N12–N11
N11
N10
N9–N8
NN6
NN5
NN4
Hole 806C
Mio.
lower
58X
N5
NN2
Oligocene
upper
59X
60X
61X
62X
P22
NN2–NN1
NP25
RN1–RP14
B.v.
?
R.v.
Radiolarian zones
(after Sanfilippo et al., 1985)
RN16 = B. invaginata
RN15 = C. tuberosa
RN14 = A. ypsilon
RN13 = A. angulare
RN12 = P. prismatium
RN11 = S. pentas
RN10 = S. peregrina
RN9 = D. penultima
RN8 = D. antepenultima
RN7 = D. petterssoni
RN6 = D. alata
RN5 = C. costata
RN4 = S. wolffii
RN3 = S. delmontensis
RN2 = C. tetrapera
RN1 = L. elongata
RP14 = D. ateuchus
Neogene diatom zones
(from Barron, 1985b)
NTD17 = P. doliolus
NTD16 = N. reinholdii
NTD15 = R. praebergonii
NTD14 = N. jouseae
NTD13 = T. convexa
NTD12 = N. miocenica
NTD11 = N. porteri
NTD10 = C. yabei
NTD9 = A. moronensis
NTD8 = C. coscinodiscus
NTD7 = C. gigas var. diorama
NTD6 = C. lewisianus
NTD5 = C. peplum
NTD4 = D. nicobarica
NTD3 = T. pileus
NTD2 = C. elegans
NTD1 = R. paleacea
Paleogene diatom zones
(from Fenner, 1985)
B.v. = B. veniamini
R.v. = R. vigilans

Figure 16 (continued).

LO of *C. dissimilis* was placed in Sample 130-806B-63X-CC, and this event marks the base of Zone N7. Core 130-806B-63X, therefore, contains part of Zone N6. An indicator species that has been used as a proxy for Zone P5 is the presence of *Globoquadrina binaiensis* in the absence of *Globorotalia kugleri*. The LO of *G. binaiensis* was observed in Sample 130-806B-64X-CC, and Zone N5 extends down to Core 130-806B-69X or Sample 130 806B-69X-CC, where the LO of *G. kugleri* was observed. Zone N4 was recognized in sediment from Core 130-806B-69X to the base of the hole in Sample 130-806B-78X-CC.

Hole 806C

Cores 130-806C-1H through -5H were placed in Pleistocene-uppermost Pliocene Zone N22. The FO of *G. truncatulinoides* occurs within Core 130-806C-6H. Core 130-806C-6H to within Core 130-806C-9H-CC were placed within Zone N21. Because of the absence of *G. tosaensis* in Sample 130-806C-6H-CC and -7H-CC, this zone was also recognized on the presence of *G. fistulosus*. The distinction between Zones N19/20 and N18 was difficult to recognize in this hole because of the sporadic occurrence of *S. dehiscens*. However, on the basis of the change from sinistral to dextral coiling within the *Pulleniatina* lineage, we placed the Zone N19–N20 to Zone N18–N19 boundary within Core 130-806C-12H. The base of Zone N18 (the FO of *G. tumida*) occurs within Core 130-806C-18H. The boundary between Subzones N17a and N17b (the FO of *P. primalis*) occurs within Core 130-806C-22H. The boundary between Subzone N17a and N16 was based on the FO of *G. plesiotumida*, which occurs within Core 130-806C-31H.

The base of Zone N16 was defined according to the FO of *N. acostaensis*, which occurs within Core 130-806C-37X, as it was first observed in Sample 130-806C-36X-CC. The LO of *G. siakensis* (and therefore the base of N15) occurs within Core 130-806C-39X. The base of Zone N14 is normally defined on the FO of *G. nepenthes*, but because of the paucity of this taxon in Leg 130 material, it was not possible to discriminate Zone N13 from Zone N14 reliably on the basis of the core-catcher samples. The LO of the subspecies *Globorotalia fohsi lobata* and *Globorotalia fohsi robusta* occurs within Core 130-806C-43X and thus defines the base of Zone N13. Zone N12 extends to Core 130-806C-48X, although precise recognition of this zonal boundary was obscured by the occurrence of transitional morphotypes between *Globorotalia praefohsi* and *G. fohsi*. The FO of *G. praefohsi* occurs within Core 130-806C-52X. This event defines the base of Zone N11. Zone N10 in this hole was found from Cores 130-806C-52X to -56X. The FO of *G. peripheroa-*

cuta, which defines the base of Zone N10, occurs within Core 130-806C-56X.

Members of the *Orbulina* lineage are not well represented in Hole 806C (as was the case in Hole 806B); therefore, it was not possible to distinguish Zones N8 and N9. Together, these two zones occupy Cores 130-806C-56X and -57X. The hole was drilled without coring much of the lower Miocene. The next sample examined (Sample 130-806C-58X-CC at 608.5 mbsf) is within Zone N5, the base of which is defined by the LO of *G. kugleri*. Further washing took place below this sample, and the next sample to be examined (Sample 130-806C-59X-CC at 749.5 mbsf) contains a planktonic foraminifer fauna of upper Oligocene age (Zone P22). The critical marker species designating P22 is *Globorotalia pseudokugleri* in the absence of *G. kugleri* s.s. Samples 130-806C-60X-CC and -61X-CC are also of Zone P22 age.

Diatoms

Diatoms were examined in Holes 806B (Samples 130-806B-1H-CC through -78X-CC) and 806C (Samples 130-806C-59X-CC through -62X-CC). Quaternary through lower Miocene diatoms are present in Hole 806B (Fig. 16). The sediment recovered in Hole 806C ranges in age from Pleistocene to Oligocene. Much of the lower Miocene section was drilled without coring to retrieve the Oligocene/Miocene boundary. Oligocene diatoms are present in the four samples analyzed from Hole 806C (Fig. 16).

Diatoms are common to abundant and preservation generally is moderate from the Pleistocene (Sample 130-806B-1H-CC) through the middle Miocene (Sample 130-806B-51X-CC). Large fluctuations in abundance (abundant to few) and preservation (moderate to poor) were seen below Core 130-806B-52X. Furthermore, only one fragment of *Synedra jouseana* and one fragment of *Craspedodiscus coscinodiscus* (coarse form) were found in Sample 130-806C-78X-CC. Preservation is poor in uppermost Oligocene Samples 130-806C-59X-CC and -60X-CC.

As at Site 805, Site 806 has a complete and expanded sediment sequence, from the Quaternary NTD 17 *Pseudoeunotia doliolus* Zone (Sample 130-806B-1H-CC) throughout the Oligocene *Rocella vigilans* Zone (Sample 130-806C-62X-CC). However, the *Rocella gelida* Zone across the Miocene/Oligocene boundary may be missing. This also has been the case in all the previous sites (803, 804, and 805).

The Pliocene/Pleistocene boundary, as defined on the basis of diatoms, is within Core 130-806B-5H, as Sample 130-806B-5H-CC does not contain specimens of *P. doliolus*. Samples 130-806B-5H-CC through 130-806B-9H-CC are all referable to the NTD 15 *R. praebergonii* Zone in the upper Pliocene.

The Pliocene/Miocene boundary was located in the NTD 13 *Thalassiosira convexa* Zone, and it coincides with the FO of *T. oestrupii* in Sample 130-806B-18H-CC.

The late Miocene/middle Miocene boundary falls within the NTD 9 *Actinocyclus moronensis* Zone and may be contained in Core 130-806B-39X. Poor preservation and low diatom abundance hinders exact recognition of the middle Miocene/lower Miocene boundary. It may be placed in Core 130-806B-59X as the next downcore sample analyzed (Sample 130-806B-59X-CC) contains the LO of *Raphidodiscus marylandicus* (16.7 Ma) within the lower Miocene. The thick Miocene section at Site 806 allowed us to recognize two diatom zones previously missing at Sites 803 and 804: the NTD 4 *Denticulopsis nicobarica* Zone and the NTD 3 *Triceratium pileus* Zone (Samples 130-806B-57X-CC (?) to -63X-CC).

The Oligocene flora of Hole 806C is preserved poorly. Sample 130-806C-59X-CC tentatively was assigned to the *Borgorovia veniamini* Zone, and Samples 130-806C-61X-CC and -62X-CC were assigned to the *Rocella vigilans* Zone.

Radiolarians

Radiolarians recovered from Site 806 ranged from well to poorly preserved, and most of the samples provided useful age information. All core-catcher samples from Hole 806B were examined. Four core-catcher samples recovered from Hole 806C (the bottom of which is at 776.4 mbsf) were also examined. The following discussion concerns the zonal assignments of the stratigraphically important taxa and the age of their datum levels. The radiolarian datums with absolute ages cited in the discussion are taken from those listed by Nigrini in the Leg 117 "Explanatory Notes" chapter (Prell et al., 1989). Figure 16 summarizes the radiolarian zonation of Holes 806B and 806C and correlates these zonations with the zones of the other microfossil groups. The radiolarian zones are continuous at least from the lower Pleistocene to the early lower Miocene. No evidence for significant sediment reworking is found at this site.

Quaternary

Sample 130-806B-1H-CC was placed in the *Collosphaera tuberosa* Zone of the Quaternary, given the presence of *C. tuberosa* and the absence of *Buccinosphaera invaginata*. The uppermost Pleistocene section appears to be condensed. Samples 130-806B-2H-CC and -4H-CC did not contain enough key radiolarian taxa to assign ages. Core 130-806B-3H-CC, which contains *A. angulare* and *Theocorythium trachelium*, was placed in the *Anthocyrtidium angulare* Zone.

Pliocene

The LO of *Pterocanium prismatium* (1.52–1.56 Ma) was observed in Sample 130-806B-5H-CC, which places it in the upper part of the *P. prismatium* Zone. Samples 130-806B-6H-CC through -15H-CC were assigned to the *Spongaster pentas* Zone. This zone contains the following radiolarian events: the LO of *S. pentas* (3.74–3.82 Ma) in Sample 130-806B-6H-CC; the LO of *Stichocorys peregrina* (2.62–2.64 Ma) in Sample 130-806B-7H-CC; the FO of *Amphirhopalum ypsilon* (3.77–3.79 Ma) in Sample 130-806B-8H-CC; the FO of *Spongaster tetras* (3.83–3.85 MA) in Sample 130-806B-11H-CC; and the LO of *Spongaster berminghami* (3.85–3.87 Ma) in Sample 130-806B-16H-CC. Samples 130-806B-16H-CC through -20H-CC were placed in the *Stichocorys peregrina* Zone. Radiolarian events found in this zone include the LO of *Solenosphaera omnitubus* (4.7–4.8 Ma) in Sample 130-806B-16H-CC; the FO of *S. pentas* (4.2–4.3 Ma) in Sample 130-806B-18H-CC; and the LO of *Acrobotrys tritubus* (5.3–5.4 Ma) in Sample 130-806B-20H-CC.

Upper Miocene

Samples 130-806B-21H-CC through -23H-CC were assigned to the *Didymocyrtis penultima* or the *S. peregrina* Zones, which cannot be differentiated. These samples contain the following key taxa: *S. peregrina*, *S. berminghami*, *S. omnitubus*, *A. tritubus*, and *D. penultima*. Samples 130-806B-24H-CC through -27H-CC belong to the *D. penultima* Zone. Radiolarian events found in these samples include the LO of *Calocycletta caepa* (6.2–6.6 Ma) in Sample 130-806B-24H-CC and the FO of *S. omnitubus* (6.3–6.5 Ma) in Sample 130-806B-26H-CC. Samples 130-806B-28H-CC through -35X-CC were placed in the *Didymocyrtis antepenultima* Zone. The LOs of the following five taxa were found: *Diartus hughesi* (7.1–7.2 Ma) in Sample 130-806B-29H-CC; *Dictyocoryne ontogenesis* (7.2–7.7 Ma) in Sample 130-806B-31H-CC; *Didymocyrtis laticonus* (8.1–8.2 Ma) in Sample 130-806B-31H-CC; *Diartus petterssoni* (8.1–8.2 Ma) in

Sample 130-806B-34H-CC; and *Stichocorys wolffii* (8.1–8.2 Ma) in Sample 130-806B-35H-CC. Also, the FO of *S. berminghami* (7.9–8.0 Ma) was observed in Sample 130-806B-35X-CC.

Middle Miocene

Samples 130-806B-36X-CC through -43X-CC were assigned to the *D. petterssoni* Zone. In this zone, the FO of *D. hughesi* (8.7–8.8 Ma) in Sample 130-806B-35X-CC and the LO of the following three taxa were observed: *Cyrtocapsella japonica* (10.0–10.3 Ma) in Sample 130-806B-38X-CC, *Lithopera thornburgi* (10.3–11.6 Ma) in Sample 130-806B-42X-CC, and *Cyrtocapsella cornuta* (11.6–11.9 Ma) in Sample 130-806B-43X-CC. The *Dorcadospyris alata* Zone begins in Sample 130-806B-44X-CC and extends through Sample 130-806B-54X-CC. Several LOs and FOs of *Dorcadospyris* species are in this zone, but exact datum levels are yet to be determined.

Lower Miocene and Oligocene

Samples 130-806B-56X-CC through -60X-CC were placed in the *Calocycletta costata* Zone. Around this depth and below, radiolarian preservation is generally moderate to poor; however, age assignments are still possible because of the preservation of sufficient key taxa. The *Stichocorys wolffii* Zone occurs between the base of *C. costata* and the base of *S. wolffii* (Riedel and Sanfilippo, 1978), and Samples 130-806B-61X-CC through -66X-CC were placed in it. *S. wolffii* was generally found in high abundance in this zone. A critical evaluation of *S. wolffii* morphology (i.e., the number of pores in the cephalis that are <12) was needed to bracket this zone because other morphological features of this taxon are identical to those of *Stichocorys delmontensis* (Riedel and Sanfilippo, 1978).

Samples 130-806B-67X-CC through -73X-CC were placed in the *S. delmontensis* Zone, which is followed by the *Cyrtocapsella tetrapera* Zone in Samples 130-806B-74X-CC through -77X-CC. Sample 130-806B-78X-CC (743.1 mbsf) and Samples 130-806C-59X-CC (749.5 mbsf) through -62X-CC (776.4 mbsf) were assigned to either the *Dorcadospyris ateuchus* or the *C. tetrapera* Zone, which cannot be differentiated. It is notable that *Dorcadospyris riedeli* appears just above the occurrence of *Dorcadospyris papilio*, which has been noted at other sites. The radiolarian evidence suggests that the bottom of Hole 806C may or may not be in the Oligocene because of the zonal assignment, which ranges from the middle Oligocene to the early lower Miocene.

PALEOMAGNETISM

Introduction

Stable magnetic polarity at Site 806 can be traced downward with confidence only to about 10 mbsf in Holes 806B and 806C and does not extend to the Brunhes/Matuyama Chron boundary in either hole, representing the trend toward a shorter magnetostratigraphic record with decreasing water depth in the three near-equatorial sites (804, 805, and 806). Two factors combine to reduce the age limit of the preserved magnetostratigraphy: (1) an increase in sedimentation rates extending the record, so that a given magnetic datum occurs at a greater subbottom depth; and (2) a decrease in the sub-bottom depth at which the primary magnetic remanence fades to the point that polarity information is lost (Fig. 17). In response to this behavior, detailed paleomagnetic analysis at Site 806 was curtailed at any early stage.

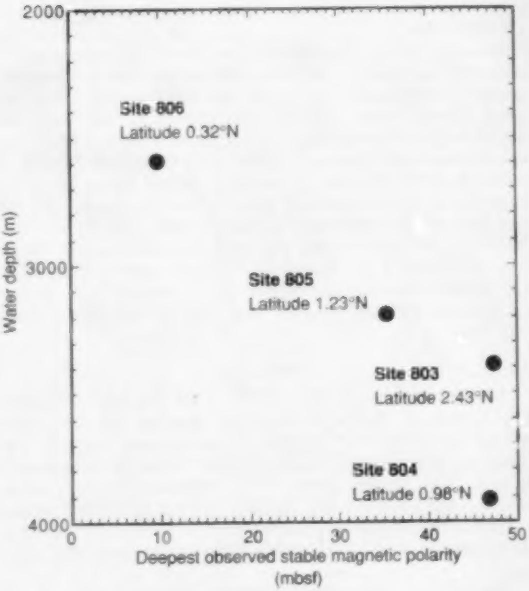

Figure 17. Relationship between water and sub-bottom depths to the deepest point at which stable magnetic polarity was observed for Sites 803–806. The depth to which magnetic polarity is preserved lessens with decreasing water depth and increased proximity to the equatorial zone of high biogenic productivity.

Natural remanent magnetization (NRM) and 15-mT alternating field (AF) demagnetized runs were measured in the cryogenic magnetometer at 1-cm intervals in the first two cores in both Holes 806B and 806C (Cores 130-806B-1H and -2H and Cores 130-806C-1H and -2H). The measurement interval was expanded to 3 cm for the third and fourth cores (Cores 130-806B-3H and -4H and Cores 130-806C-3H and -4H), and to 5 cm for the fifth core (Cores 130-806B-5H and 130-806C-5H). Measurement was expanded to 10-cm intervals from Core 130-806B-11H in Hole 806B, and from Core 130-806C-7H in Hole 806C, whereas demagnetization was restricted to one section per core. Paleomagnetic measurements in Hole 806C were discontinued after Core 130-806C-10H.

Magnetization Record

Plots of AF-demagnetized declination, inclination and intensity for Holes 806B and 806C are shown in Figure 18. Cores 130-806B-1H and -2H and Cores 130-806C-1H and -2H were not oriented; these cores represent the upper 16 m in Hole 806B and the upper 15.3 m in Hole 806C. The intensity record in cores from Hole 806B, subjected to 15-mT magnetic cleaning, remains fairly constant at values of 2–4 mA/m from the surface to 10.3 mbsf, at which point the intensity values decrease to 0.1–0.2 mA/m over an interval of about 0.5 m. Demagnetized intensity in Hole 806B then increases with sub-bottom depth, peaking at values of 0.5 mA/m at 20 mbsf, before declining again to 0.01–0.02 mA/m by 30 mbsf, and recovering to about 0.5 mA/m at about 37 mbsf. Demagnetized intensities of cores from Hole 806C also decrease sharply at 10 mbsf, declining from 3 mA/m at 9.8 mbsf to 0.3 mA/m at 10.5 mbsf. Below 10.5 mbsf, intensity declines more steadily in Hole 806C than in Hole 806B.

Although both the declination and inclination records are noisy, AF-cleaned magnetizations in Holes 806B and 806C appear to be stable down to about 10 mbsf, the depth at which intensity values suddenly decline. Continuity of the declination record from within a meter of the seafloor implies that the polarity to 10 mbsf is normal, despite the lack of orientation over

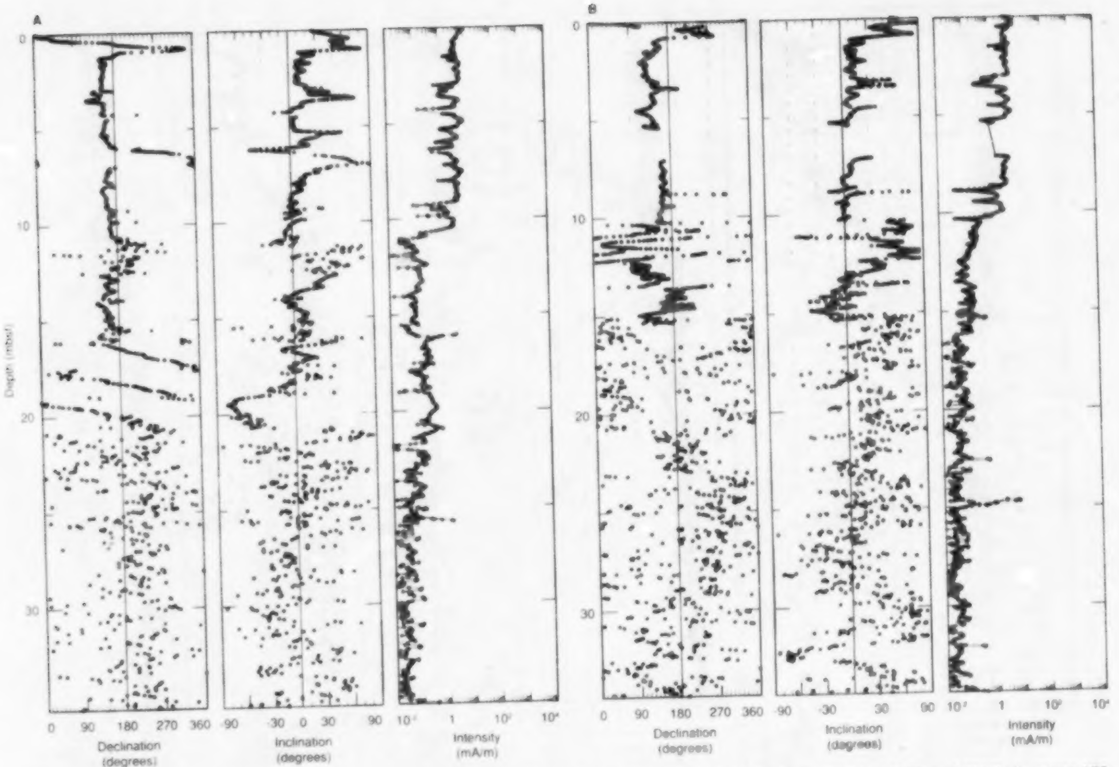

Figure 18. Unoriented, AF-demagnetized declination, inclination, and intensity charts for the first four cores in Holes 806B and 806C. **A.** Cores 130-806B-1H to -4H. **B.** Cores 130-806B-1H to -4H.

this interval, and that the Brunhes/Matuyama boundary is deeper than 10 mbsf in both holes. Below 10 mbsf, the AF-cleaned magnetization records in both holes are difficult to interpret. Within Core 130-806B-2H, immediately below the sharp drop in intensity at 10.5 mbsf, the AF-cleaned declination and inclination records are complex and remain so until about 12.5 mbsf. Inclination values reach about +80° at 11.2 mbsf before decreasing to 0° at 13.6 mbsf. Declination and inclination records remain constant from 13.6 mbsf to the base of Core 130-806B-2H at 16.0 mbsf.

Declination values follow an extraordinary spiraling path through three complete revolutions from the top of Core 130-806B-3H at 16.0 mbsf down to 21 mbsf. Over this interval, inclination varies from about +60° to about −70° in a continuous but complex fashion, and intensity increases as noted above. Below 21 mbsf the AF-cleaned record in Hole 806B becomes chaotic, and intensities decrease again. Complex magnetization features also appear in the record from Hole 806C, beginning immediately below the sharp drop in intensity values at 10.3 mbsf. Between 10.3 and ~12.3 mbsf in Core 130-806C-2H, the AF-cleaned declination record swings through a series of short-wavelength, large variations, whereas the inclination data form a noisy grouping around +60°. From 12.3 mbsf to the base of Core 130-806C-2H at 15.1 mbsf, declination data continue to oscillate, with a wavelength of about 30 cm and a range of about 60°–140°, whereas the inclination values trend downward from about +80° to about −30°.

Visual examination of these intervals of complex magnetization in Holes 806B and 806C shows no evidence for physical disruption or internal rotation of the cores. It is difficult to envisage how these features could have arisen as part of the primary magnetization of the sediments. It is also clear from an examination of the records from Sites 803, 804, and 805 that the loss of recognizable polarity normally accompanies a sudden drop in intensity of the type seen at about 10 mbsf in Holes 806B and 806C. NRM measurements have steep negative inclinations over each of these intervals of complex magnetization (Fig. 19), similar to those identified as drilling-induced remanence in other, deeper cores (see below). The spiraling declination values seen in Core 130-806B-3H may be artifacts caused by the passage of the core past a locally intense field source while the source was rotating relative to the core. Intervals of less disturbed, apparently normal polarity below 10 mbsf in Holes 806B and 806C may have been magnetized by viscous remanence acquired during the Brunhes Chron.

It appears unlikely that any of the magnetization measured either as NRM or after 15-mT cleaning in the magnetically complex region between about 10 and 20 mbsf in Holes 806B and 806C is of primary origin. The unusual magnetization pattern of these intervals, their apparent susceptibility to VRM and drilling-related remanences, and the resistance of these secondary magnetizations to AF cleaning (i.e., their high coercivity) may indicate an unusual magnetic mineralogy in this interval.

The NRMs of many of the cores below 30 mbsf in Holes 806B and 806C have inclinations of about −60° to −80° (Fig. 20), a pattern similar to that seen at Site 805. Drilling-induced remanence reported by Sallomy and Briden (1975) in a borehole core was aligned with the borehole axis, although drilling in this

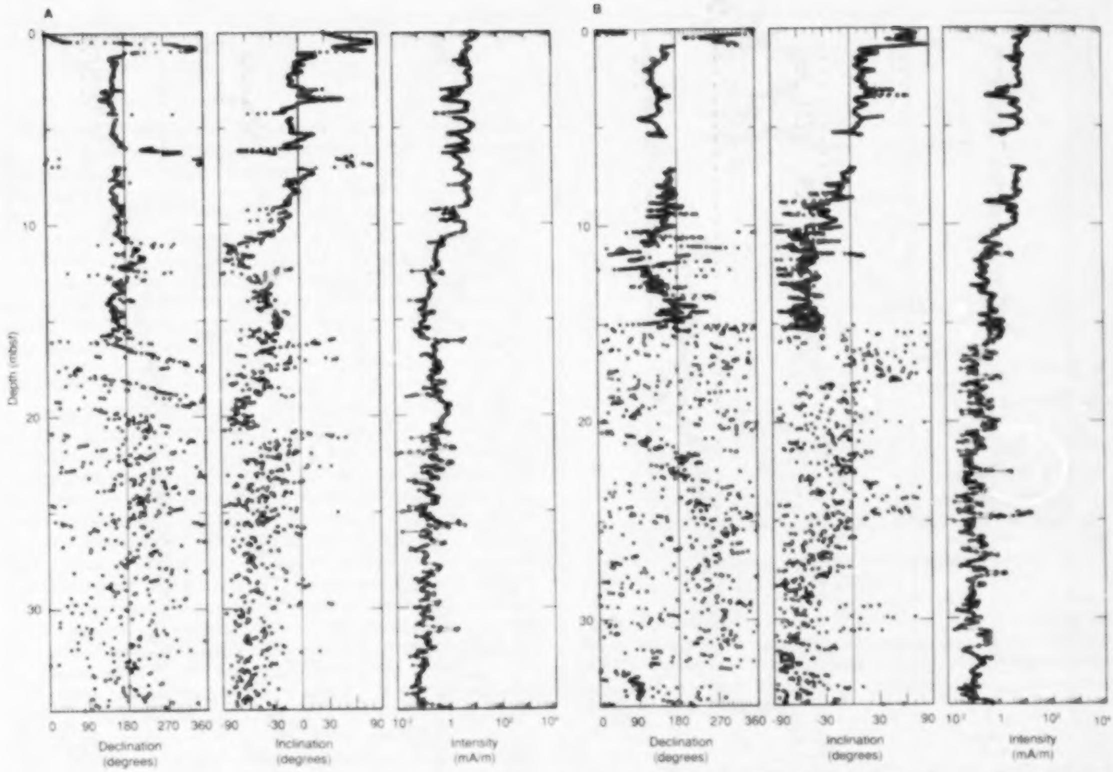

Figure 19. Unoriented NRM declination, inclination, and intensity charts for the first four cores in Holes 806B and 806C. **A**. Cores 130-806B-1H to -4H. **B**. Cores 130-806C-1H to -4H.

case was in harder rocks in which drilling-induced heating was a likely factor in the magnetization. Steeply negative NRM inclinations in weakly magnetized cores from Leg 130 sites probably reflect the presence of a similar borehole-parallel component dominating a presumably shallowly inclined pre-drilling remanence.

SO_4^{2-} Reduction and Magnetization Intensity

Interstitial water SO_4^{2-} levels and remanence intensity in Hole 806B appear to be positively correlated (Fig. 21). The abundance of the SO_4^{2-} ion has a trend similar to that of the log intensity, particularly after demagnetization. An SO_4^{2-} concentration of about 26.6 mM appears to be critical; as this value is first crossed at about 10.3 mbsf, the demagnetized remanence intensity drops sharply from about 3 to about 0.15 mA/m. An upward inflection in the SO_4^{2-} abundance at a sub-bottom depth of 20 mbsf is accompanied by a local increase in intensity, as noted above. Remanence intensities of 0.02 mA/m are reached when the SO_4^{2-} concentration drops to about 25 mM, at which point remanence measurements reach the limit of resolution of the shipboard cryogenic magnetometer.

Reduction of magnetite, producing dissolved and reduced Fe, and the reduction of sulfate to sulfide (both of which were caused by microbial activity) result in the precipitation of iron sulfide minerals, principally pyrite. These reactions appear to be the possible mechanism that links the decline in remanence intensity to the decrease in SO_4^{2-} concentration (e.g., Karlin and Levi, 1983, 1985). Two successive phases of downhole alteration of the magnetic mineralogy in Hole 806B are implied by the presence of the interval of complex magnetization between the sharp decrease in intensity at about 10.3 mbsf and the beginning of random weak magnetizations at 20 mbsf.

Little dissolution of magnetite occurs from the surface to about 10 mbsf, at which point rapid dissolution over the next 0.5 m appears to remove almost all magnetite much larger than the critical "blocking diameter" of 0.025 μm (Dunlop, 1981). At this point, primary magnetization becomes too weak to measure. The interval between 10 and 20 mbsf, in which high coercivity secondary components appear to have been acquired, may correspond to an interval observed by Sager (1988) in carbonate oozes in Holes 632A and 633A from ODP Leg 101. Mean destructive fields increased in these holes as intensities decreased downhole. Sager attributed this behavior to the possible development of a metastable, magnetic iron sulfide such as greigite or pyrrhotite along with pyrite as the sulfate reduction reactions progress.

A similar mechanism may operate between 10 and 20 mbsf in Holes 806B and 806C. The local inflection in SO_4^{2-} concentration at 20 mbsf is presumably related to changes in the rate of SO_4^{2-} reduction over the interval in which these metastable iron sulfides are produced. The accompanying peak in magnetic intensity in both the NRM and AF-cleaned records is a function of the acquisition of high-coercivity secondary remanences by these metastable phases. Below 20 mbsf, magnetite may be

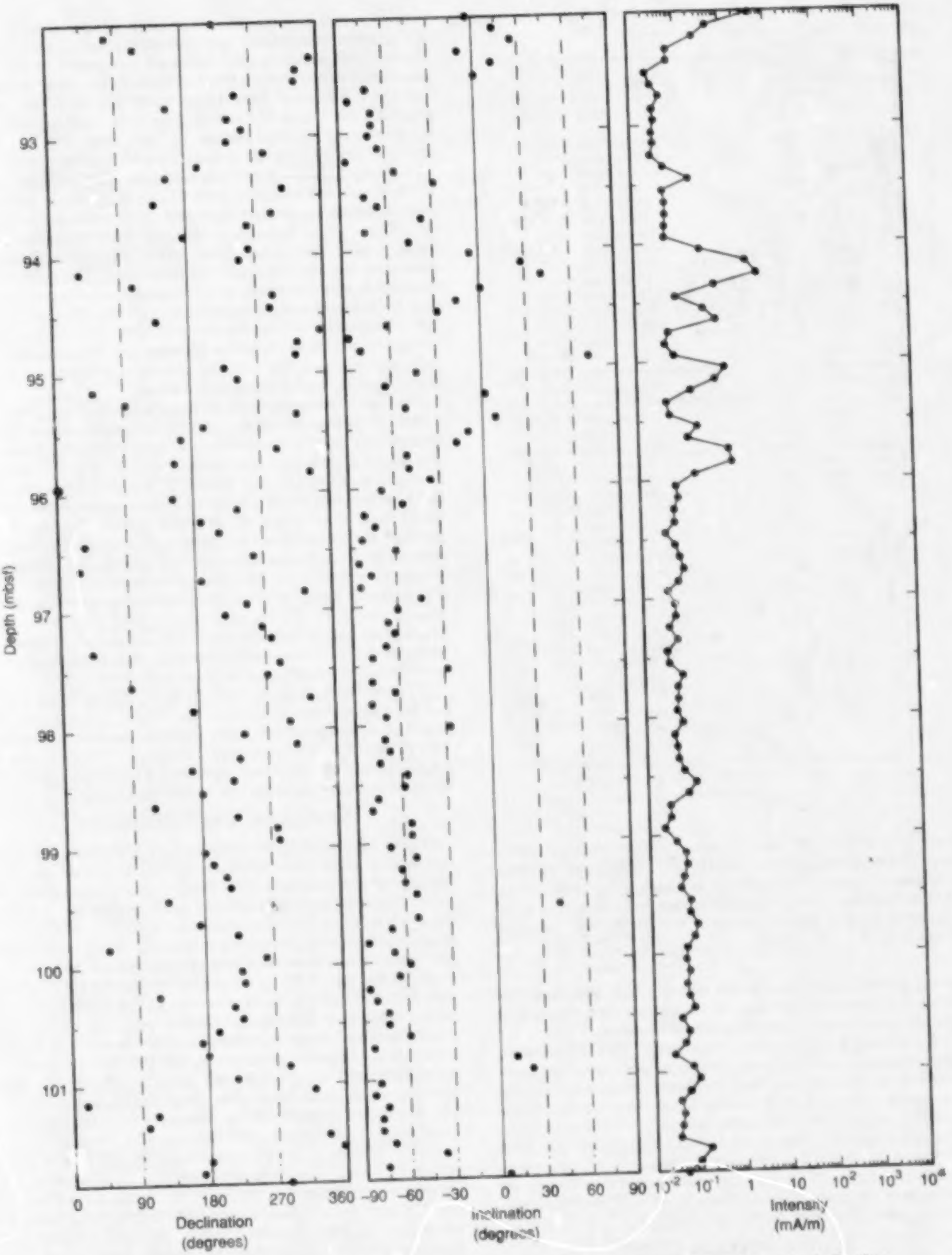

Figure 20. Declination, inclination, and intensity chart of the NRM of Core 130-806B-11H. Note the steeply negative inclinations.

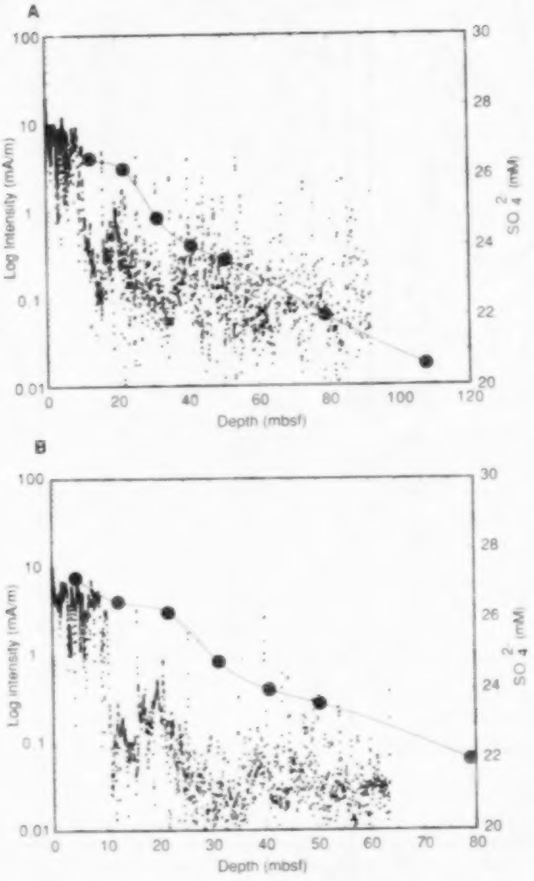

Figure 21. Correlation between remanence intensity (dots) and sulfate ion concentration (closed circles, fitted by cubic splines) (see "Inorganic Geochemistry" section, this chapter) vs. depth, Hole 806B, for (A) NRM and (B) after 15-mT demagnetization. Note the increase in demagnetized intensity and the change in the rate of SO_4^{2-} reduction around 20 mbsf.

present as very fine-grained relicts within pyrite, and large proportions of the remanence may be carried by magnetite grains with low coercivities and short relaxation times.

Fine-grained pyrrhotite may also persist and contribute a higher coercivity component to the remanence. Although Lowrie and Heller (1982) noted that pyrrhotite was rarely a significant source of remanence in marine limestones, pyrrhotite, occurring as minute inclusions within pyrite, has been reported as the major magnetic carrier in the Helvetic Limestones (Kligfield and Channell, 1981). The pervasive drilling-induced remanence observed in the weakly magnetized cores may be carried by either or both of these minerals. Shore-based studies of the magnetic mineralogy should clarify these matters.

SEDIMENTATION RATES

An apparently continuous uppermost Oligocene through Holocene sediment sequence was cored at Site 806. The average sedimentation rate is about 30 m/m.y., as estimated from the biostratigraphic information (see "Biostratigraphy" section, this chapter). All datum events that were recognized in the three holes cored at Site 806 are listed in Table 3. The biostratigraphic age-depth indicators from Holes 806B and 806C are shown graphically in Figures 22 and 23. The large depth uncertainties for some early Miocene datums of Hole 806C (Fig. 23) represent two washed intervals separated by a single spot core.

Age-depth data representing calcareous and siliceous microfossil groups are available from Hole 806B. These data have been replotted for shorter time and depth intervals in Figures 24, 25, and 26, so that every individual biostratigraphic datum listed in Table 3 can be identified, and so that points where sedimentation rate changes occur can be selected. The different microfossil groups commonly provide age discrepancies of about 1 m.y. for identical sample depths (i.e., Fig. 24). These discrepancies consequently are on the order of 10%–20% of the age of the sediment even in the upper Miocene and Pliocene intervals. Presumably, they largely reflect problems associated with the assigned ages to the biostratigraphic events.

Sedimentation rates from all three holes that have been calculated from selected calcareous biostratigraphic events and are presented in Table 4. These rates are plotted vs. age in Figure 27. The shape of this age/rate curve is similar to those obtained from previous Leg 130 sites (Sites 803, 804, and 805). This similarity implies that the rate histories indeed were alike at the different sites, but to some extent it also reflects the fact that, if possible, the same series of control points were chosen for the sedimentation rate calculations at the different sites. Minor differences in the rate histories between Holes 806B and 806C (Fig. 27) primarily stem from the large sample intervals used. The greatest rate difference between the two holes falls in the 20–25 Ma interval and is probably caused by the use of different datums: the LO of *Globorotalia kugleri* in Hole 806B, and the LO of *Sphenolithus ciperoensis* in Hole 806C.

The marked increase in sedimentation rates at about 8.7 Ma has been also observed at all of the deeper transect sites. Assuming the change at the fairly shallow Site 806 is associated with moderate to little carbonate dissolution, it follows that the major portion of that signal represents a significant productivity increase in the early part of late Miocene time.

INORGANIC GEOCHEMISTRY

Thirty interstitial water samples were collected at Site 806, twenty-nine from Hole 806B at depths ranging from 4.5 to 706.0 mbsf and one from Hole 806C at 765.1 mbsf, which was patched into the profile. Interstitial water samples cover most of the depth range of the nannofossil ooze and chalk of Unit I, the single lithologic unit recognized at Site 806 (see "Lithostratigraphy" section, this chapter). Chemical gradients in the interstitial waters at this site (Table 5) are similar to those at the first three sites drilled on this leg, being governed by the biogenic-rich, organic-carbon-poor character of the sediments and by the diffusive influence of basalt alteration reactions at depth. The magnitude of the chemical gradients at Site 806, the site nearest to the equator and at the shallowest depth drilled on this leg, is generally equal to or larger than those at the first three sites. The differences in gradients are consistent with the differences in geography, water depth, and sedimentation rates.

Going downhole, chlorinity increases by almost 2% to 565 mM at 41.0 mbsf (Core 180-806B-5H) and increases further to values close to 600 mM at depths >500 m, for a total increase of 8.5% over the sampled interval (Fig. 28). Salinity, measured refractively as total dissolved solids, is fairly constant with depth at 35.0–35.5 g/kg over the interval from 4.5 to 564.4 mbsf, with the exception of a high, possibly errant, value of 40 g/kg at 450.2 mbsf (Core 130-806B-48X); there are a few higher values in the interval from 594.9 to 679.9 mbsf (Table 5).

Table 3. Biostratigraphic events observed at Site 806.

Event	Upper depth (mbsf)	Lower depth (mbsf)	Age (Ma)
130-806A-			
LO *P. lacunosa* (N)	7.7	17.2	0.46
LO *G. tosaensis* (F)	7.7	17.2	0.60
LO *C. macintyrei* (N)	26.7	36.2	1.45
LO *G. fistulosus* (F)	26.7	36.2	1.60
LO *D. brouweri* (N)	36.2	45.7	1.89
OA *D. triradiatus* (N)	36.2	45.7	2.07
LO *D. pentaradiatus* (N)	45.7	55.2	2.35
LO *D. surculus* (N)	55.2	64.7	2.45
LO *D. tamalis* (N)	64.7	74.2	2.65
LO *G. multicamerata* (F)	64.7	74.2	2.90
LO *G. altispira* (F)	64.7	74.2	2.90
FO *G. fistulosus* (F)	74.2	83.7	2.90
130-806B-			
LO *P. lacunosa* (N)	6.5	16.0	0.46
FO *C. tuberosa* (R)	6.5	16.0	0.50
LO *G. tosaensis* (F)	6.5	16.0	0.60
LO *N. reinholdii* (D)	16.0	25.5	0.65
LO *A. angulare* (R)	25.5	35.0	0.99
LO *C. macintyrei* (N)	32.3	35.0	1.45
LO *P. prismatium* (R)	35.0	44.5	1.54
FO *A. angulare* (R)	16.0	25.5	1.58
LO *G. fistulosus* (F)	35.0	44.5	1.60
LO *R. praebergonii* var. *robusta* (D)	35.0	44.5	1.55
LO *D. brouweri* (N)	38.8	41.8	1.89
FO *G. truncatulinoides* (F)	44.5	54.0	1.90
OA *D. triradiatus* (N)	44.5	46.8	2.07
LO *T. convexa* var. *aspinosa* (D)	44.5	54.0	2.10
LO *D. pentaradiatus* (N)	54.7	56.2	2.35
LO *N. jouseae* (D)	73.0	82.5	2.60
LO *S. peregrina* (R)	54.0	63.5	2.63
LO *G. multicamerata* (F)	44.5	54.0	2.90
LO *G. altispira* (F)	63.5	73.0	2.90
FO *G. fistulosus* (F)	73.0	82.5	2.90
LO *Sphaeroidinellopsis* spp. (F)	73.0	82.5	3.00
FO *R. praebergonii* (D)	73.0	82.5	3.00
FO *S. dehiscens* (F)	73.0	82.5	3.00
FO *G. tosaensis* (F)	73.0	82.5	3.10
LO *P. fistula* (R)	92.0	101.5	3.27
LO *G. margaritae* (F)	73.0	82.5	3.40
LO *Sphenolithus* (N)	89.3	90.8	3.45
LO *P. doliolum* (R)	92.0	101.5	3.54
LO *R. pseudoumbilica* (N)	94.3	95.8	3.56
FO *A. ypsilon* (R)	73.0	82.5	3.78
FO *S. tetrus* (R)	101.5	111.0	3.84
LO *S. berminghami* (R)	139.5	149.0	3.86
FO *A. elegans* (D)	73.0	82.5	3.90
FO *S. pentas* (R)	168.0	177.5	4.25
LO *N. cylindrica* (D)	139.5	149.0	4.35
FO *N. jouseae* (D)	139.5	149.0	4.50
LO *C. acutus* (N)	147.4	148.9	4.60
LO *S. omnitubus* (R)	139.5	149.0	4.75
LO *D. quinqueramus* (N)	158.5	168.0	5.00
LO *S. delmontensis* (R)	196.5	206.5	5.00
LO *S. corona* (R)	215.5	225.0	5.05
FO *S. dehiscens* (F)	92.0	101.5	5.10
FO *G. tumida* (F)	158.5	168.0	5.20
FO *P. spectabilis* (F)	158.5	168.0	5.20
LO *A. acutiloba* (D)	158.5	168.0	5.40
LO *A. tritubus* (R)	177.5	187.0	5.35
LO *N. miocenica* (D)	168.0	177.5	5.60
LO *T. praeconvexa* (D)	168.0	177.5	5.80
FO *P. primalis* (F)	206.0	215.5	5.80
LO *C. caepa* (R)	215.5	225.0	6.40
FO *S. omnitubus* (R)	244.0	253.5	6.40
FO *Amaurolithus* (N)	215.5	225.0	6.70
FO *G. plesiotumida* (F)	263.0	272.5	7.10
LO *D. hughesi* (R)	263.0	272.5	7.15
FO *D. quinqueramus* (N)	263.0	282.0	7.50
LO *C. yabei* (D)	301.0	310.5	7.50
LO *D. ontogenesis* (R)	282.0	291.5	7.50
FO *S. berminghami* (R)	329.7	339.4	7.95
LO *A. ellipticus* var. *javanica* (D)	263.0	272.5	8.00
LO *B. miralestensis* (R)	320.0	329.7	8.15
130-806B- (Cont.)			
LO *D. laticonus* (R)	282.0	291.5	8.15
LO *D. petterssoni* (R)	310.5	320.0	8.15
LO *S. wolffii* (R)	320.0	329.7	8.15
LO *C. yabei* (D)	301.0	310.5	8.60
LO *D. hamatus* (N)	329.7	339.4	8.70
FO *D. hughesi* (R)	329.7	339.4	8.75
LO *A. moronensis* (D)	329.7	339.4	8.90
LO *C. japonica* (R)	349.1	358.8	10.15
FO *N. acostaensis* (F)	349.1	358.8	10.20
LO *G. siakensis* (F)	358.8	368.5	10.40
FO *D. hamatus* (N)	358.8	368.5	10.50
LO *C. coscinodiscus* (D)	397.5	407.2	10.70
LO *L. thornburgi* (R)	387.9	397.5	11.00
FO *C. coalitus* (N)	368.5	378.2	11.10
LO *A. moronensis* (D)	329.7	339.4	11.30
LO *G. fohsi lobata/robusta* (F)	407.2	416.9	11.50
LO *C. cornuta* (R)	397.5	407.2	11.75
LO *C. coscinodiscus* (D)	397.5	407.2	12.20
LO *C. nitescens* (N)	426.5	436.1	12.80
LO *C. lewisianus* (D)	426.5	436.1	12.90
FO *G. fohsi fohsi* (F)	445.8	455.5	13.10
LO *C. floridanus* (N)	473.3	482.6	13.10
LO *C. lewisianus* (D)	426.5	436.1	13.50
LO *S. heteromorphus* (N)	473.3	482.6	13.60
FO *D. hustedtii* (D)	455.5	463.6	13.70
FO *G. praefohsi* (F)	501.9	511.6	13.90
LO *C. peplum* (D)	501.9	511.6	14.10
LO *A. californicus* (D)	501.9	511.6	14.80
FO *G. peripheroacuta* (F)	511.6	521.3	14.90
LO *C. lewisianus* var. *similis* (D)	511.6	521.3	15.70
TA *D. deflandrei* (N)	530.9	540.5	16.10
LO *R. marylandicus* (D)	550.2	559.9	16.70
LO *C. dissimilis* (F)	589.0	598.6	17.60
FO *S. heteromorphus* (N)	579.3	589.0	18.60
LO *C. elegans* (D)	608.3	617.9	18.70
LO *S. belemnos* (N)	579.3	589.0	18.80
FO *S. belemnos* (N)	598.6	608.3	20.00
LO *G. kugleri* (F)	646.5	656.2	21.80
FO *R. paleacea* (D)	733.4	743.1	22.70
130-806C-			
LO *P. lacunosa* (N)	5.6	11.6	0.46
LO *G. tosaensis* (F)	0	5.6	0.60
LO *C. macintyrei* (N)	34.1	43.6	1.45
LO *G. fistulosus* (F)	34.1	43.6	1.60
LO *D. brouweri* (N)	34.1	43.6	1.89
FO *G. truncatulinoides* (F)	43.6	53.1	1.90
OA *D. triradiatus* (N)	43.6	53.1	2.07
LO *D. pentaradiatus* (N)	53.1	62.6	2.35
LO *D. surculus* (N)	53.1	62.6	2.45
LO *G. altispira* (F)	62.6	72.1	2.90
FO *G. fistulosus* (F)	72.1	81.6	2.90
LO *Sphaeroidinellopsis* spp. (F)	72.1	81.6	3.00
FO *S. dehiscens* (F)	72.1	81.6	3.00
FO *G. tosaensis* (F)	72.1	81.6	3.10
LO *G. margaritae* (F)	72.1	81.6	3.40
LO *Sphenolithus* (N)	81.6	91.1	3.45
LO *R. pseudoumbilica* (N)	91.1	100.6	3.56
LO *C. acutus* (N)	138.6	148.1	4.60
FO *C. acutus* (N)	176.6	186.1	4.90
LO *D. quinqueramus* (N)	176.6	186.1	5.00
FO *S. dehiscens* (F)	81.6	91.1	5.10
FO *G. tumida* (F)	157.6	167.1	5.20
FO *P. primalis* (F)	195.6	205.1	5.80
FO *Amaurolithus* (N)	233.6	243.1	6.70
FO *G. plesiotumida* (F)	281.1	290.6	7.10
FO *D. quinqueramus* (N)	281.1	290.6	7.50
LO *D. hamatus* (N)	328.9	338.5	8.70
LO *Catinaster* (N)	328.9	338.5	8.80
FO *D. neohamatus* (N)	338.5	348.2	9.00
FO *N. acostaensis* (F)	338.5	348.2	10.20
LO *G. siakensis* (F)	357.9	367.6	10.40
FO *D. hamatus* (N)	367.6	377.3	10.50
FO *Catinaster* (N)	367.6	377.3	11.10

Table 3 (continued).

Event	Upper depth (mbsf)	Lower depth (mbsf)	Age (Ma)
130-806C- (Cont.)			
LO *G. fohsi lobata/robusta* (F)	406.3	415.9	11.50
LO *C. nitescens* (N)	415.9	425.6	12.80
FO *G. fohsi fohsi*	444.9	454.6	13.10
LO *C. floridanus* (N)	464.5	474.3	13.10
LO *S. heteromorphus* (N)	464.5	474.3	13.60
FO *G. praefohsi* (F)	483.7	493.3	13.90
FO *G. peripheroacuta* (F)	512.7	522.4	14.90
TA *D. deflandrei*	522.4	532.0	16.10
LO *C. dissimilis* (F)	541.7	608.5	17.60
FO *S. heteromorphus* (N)	541.7	608.5	18.60
LO *S. belemnos* (N)	541.7	608.5	18.80
FO *S. belemnos* (N)	599.8	608.5	20.00
LO *G. kugleri* (F)	608.5	749.5	21.80
FO *G. kugleri* (F)	608.5	749.5	23.70
LO *S. ciperoensis* (N)	759.2	766.7	25.20

Notes: The depth uncertainty predominantly represents sample intervals used. References for the age estimates are presented in the "Explanatory Notes" chapter (this volume). N = nannofossil, F = foraminifer, D = diatom, R = radiolarian, FO = first occurrence, LO = last occurrence, OA = onset acme, and TA = termination acme. Magnetostratigraphic reversal boundaries followed by the designation (T) or (O) refer to "termination" and "onset," respectively.

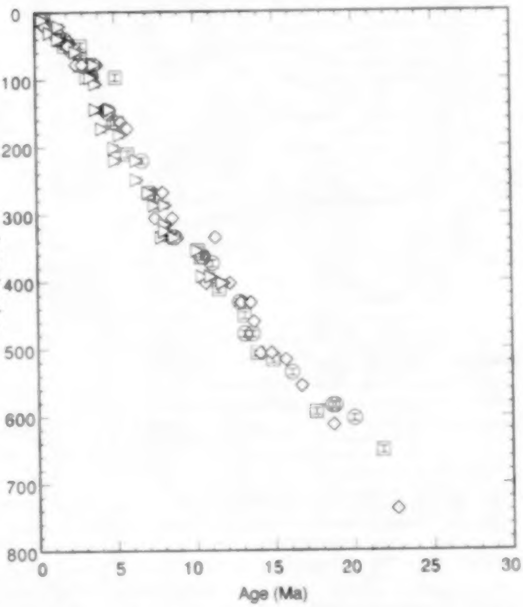

Figure 22. Age-depth relationships of biostratigraphic markers, Hole 806B. Circles = nannofossil, squares = foraminifer, diamonds = diatom, and triangles = radiolarian.

Sodium concentrations measured by flame emission spectrophotometry (Table 5) and those estimated by charge balance calculations generally agree to within <1.5%. Sodium concentrations increase from 471 mM at 4.5 mbsf to ~520 mM at 650.9-706.0 mbsf, a total increase of 10%. Sodium concentrations at

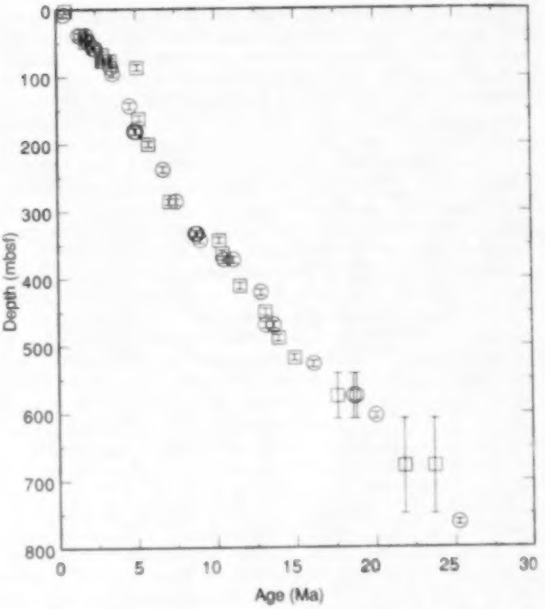

Figure 23. Age-depth relationships of biostratigraphic markers, Hole 806C. Large error bars show uncored interval. Symbols used are as in Figure 22.

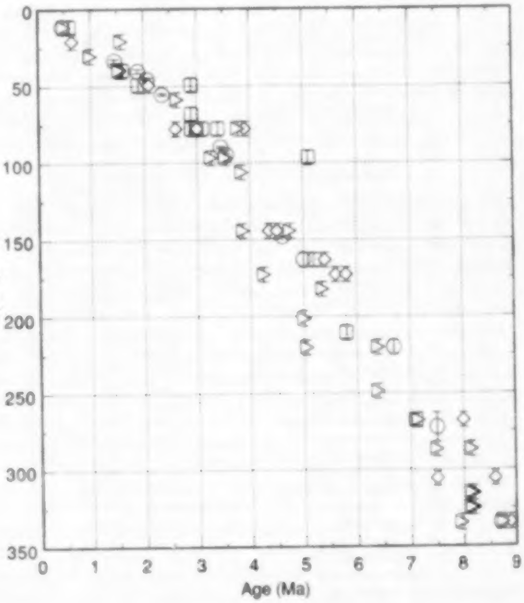

Figure 24. Age-depth relationships of biostratigraphic markers from the upper Miocene through Holocene interval, Hole 806B. Error bars show sample interval uncertainties. Symbols used are as in Figure 22.

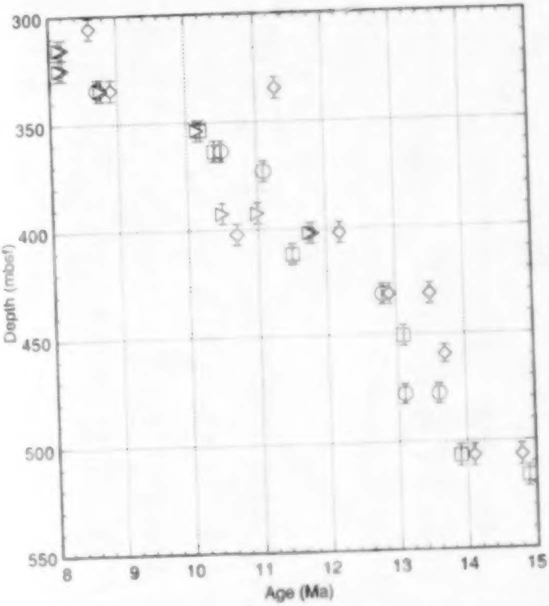

Figure 26. Age-depth relationships of biostratigraphic markers from the lower through middle Miocene interval, Hole 806B. Error bars show sample interval uncertainties. Symbols used are as in Figure 22.

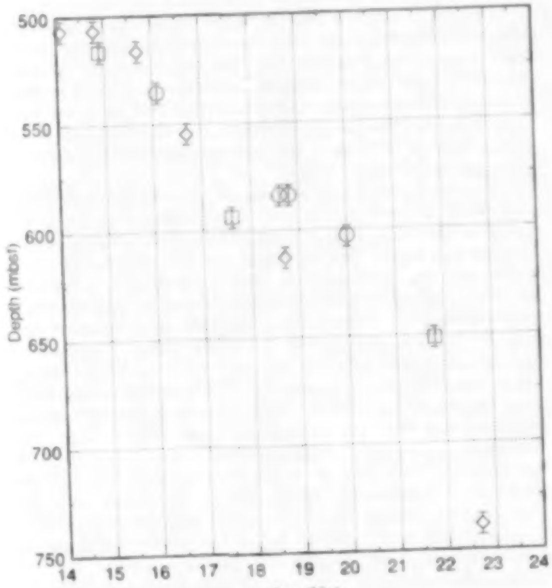

Figure 25. Age-depth relationships of biostratigraphic markers from the middle through lower upper Miocene interval, Hole 806B. Error bars show sample interval uncertainties. Symbols used are as in Figure 22.

Table 4. Estimated sedimentation rates, Site 806, and the control points determining those rates.

Control points	Depth (mbsf)	Age (Ma)	Sedimentation rate (m/m.y.)
130-806A-			
Top section	0	0	
OA D. triradiatus	41.05	2.07	19.8
LO G. altispira	69.55	2.90	34.3
Terminal depth	83.70	3.31	
130-806B-			
Top section	0	0	
LO D. brouweri (N)	40.25	1.89	21.3
LO R. pseudoumbilica (N)	95.00	3.56	32.8
LO D. hamatus (N)	334.55	8.70	46.6
LO S. heteromorphus (N)	477.95	13.60	29.3
FO S. belemnos (N)	603.45	20.00	19.6
LO G. kugleri (F)	651.35	21.80	26.6
Terminal depth	743.10	25.25	
130-806C-			
Top section	0	0	
OA D. triradiatus (N)	48.35	2.07	23.4
LO R. pseudoumbilica (N)	95.85	3.56	31.9
LO D. hamatus (N)	333.70	8.70	46.3
LO S. heteromorphus (N)	469.40	13.60	27.7
FO S. belemnos (N)	603.38	20.00	20.9
LO S. ciperoensis (N)	762.95	25.20	30.7
Terminal depth	776.40	25.64	

Notes: References for the age estimates are presented in the "Explanatory Notes" chapter (this volume). N = nannofossil, F = foraminifer, D = diatom, R = radiolarian, FO = first occurrence, LO = last occurrence, and OA = onset acme. Magnetostratigraphic reversal boundaries followed by the designation (T) or (O) refer to "termination" and "onset," respectively.

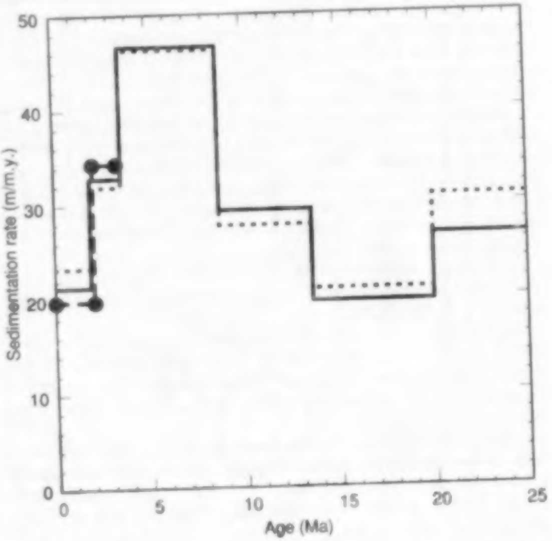

Figure 27. Sedimentation rate history, Site 806. Dashed line with filled circle = Holes 806A; solid line = Hole 806B; and dashed line = Hole 806C.

Table 5. Interstitial water geochemical data, Holes 806B and 806C.

Core, section, interval (cm)	Depth (mbsf)	pH	Alk. (mM)	Sal. (g/kg)	Cl^- (mM)	Na (mM)	SO_4^{2-} (mM)	PO_4^{3-} (μM)	NH_4^+ (μM)	SiO_2 (μM)	Mn (μM)	Ca^{2+} (mM)	Mg^{2+} (mM)	Sr (μM)	Li (μM)	K (mM)	Rb (μM)
130-806B-																	
1H-3, 145–150	4.45	7.6	3.73	35.5	553	471	27.2	2.9	37	469	9	10.7	52.3	140	24.5	10.8	1.62
2H-4, 145–150	12.45	7.6	4.07	35.5	559	472	26.5	2.7	92	506	4	10.7	51.9	223	22.8	10.9	1.68
3H-4, 145–150	21.95	7.6	4.53	35.5	562	483	26.2	2.5	140	539	3	10.9	51.0	317	22.3	11.1	1.58
4H-4, 145–150	31.45	7.6	4.72	35.5	563	475	24.8	2.3	182	552	3	11.1	50.2	396	21.9	11.1	1.72
5H-4, 145–150	40.95	7.6	5.08	35.5	565	479	24.0	LD	218	595	LD	11.3	49.3	475	21.0	11.3	1.74
6H-4, 145–150	50.45	7.6	5.25	35.5	564	487	23.6	LD	247	637	LD	11.4	48.5	540	20.6	11.4	1.76
9H-4, 145–150	78.95	7.6	5.80	35.5	564	484	22.0	LD	325	676	LD	12.3	45.9	723	18.9	11.1	1.70
12H-4, 145–150	107.45	7.6	6.23	35.0	568	490	20.6	LD	379	728	LD	13.2	43.5	861	17.2	10.8	1.70
15H-4, 145–150	135.95	7.6	6.31	35.0	567	484	20.1	LD	430	796	LD	14.3	41.6	983	15.9	10.6	1.70
18H-4, 145–150	164.45	7.6	6.43	35.0	567	492	19.2	LD	462	842	LD	15.2	39.7	1055	15.4	10.6	1.66
21H-4, 145–150	192.95	7.6	6.33	35.0	569	488	18.4	LD	502	871	LD	16.2	37.7	1069	14.1	10.5	1.69
24H-4, 145–150	221.45	7.1	6.34	35.0	578	493	17.4	LD	528	896	LD	16.9	36.6	1070	13.7	10.3	1.71
27H-4, 145–150	249.95	7.6	6.33	35.0	576	491	17.3	LD	543	956	LD	17.8	35.8	1048	13.3	10.3	1.70
30H-5, 145–150	279.95	7.6	6.24	35.0	575	500	17.1	LD	579	995	LD	18.6	34.3	1057	13.3	10.3	1.74
33H-4, 145–150	306.95	7.6	5.93	ND	576	503	17.3	LD	589	1010	LD	19.6	34.1	1082	12.8	10.3	1.72
36X-4, 145–150	335.65	7.8	5.74	35.0	577	498	16.9	LD	601	1033	LD	20.2	33.1	1094	13.7	10.7	1.72
39X-4, 140–150	364.70	7.1	5.67	35.0	580	503	16.9	LD	610	1022	LD	21.2	32.3	1102	14.1	10.1	1.70
42X-3, 140–150	392.30	7.6	5.63	35.0	581	503	16.7	LD	618	1058	LD	21.7	31.0	1089	15.4	10.0	1.72
45X-3, 140–150	421.30	7.0	5.14	35.5	584	506	16.4	LD	644	1109	LD	22.7	30.5	1106	16.7	10.0	1.69
48X-3, 140–150	450.20	7.6	5.60	40.0	591	519	16.7	LD	646	1147	LD	23.7	29.7	1132	18.4	10.0	1.69
52X-4, 140–150	488.50	ND	ND	ND	592	506	16.3	ND	644	1132	ND	24.9	28.5	1148	20.9	9.63	1.62
54X-5, 140–150	509.30	7.6	4.46	ND	596	511	16.1	LD	649	1132	LD	25.1	28.2	1138	21.8	9.78	1.60
57X-2, 140–150	533.80	ND	ND	ND	599	511	16.3	ND	642	1139	ND	26.1	27.5	1143	23.9	9.77	1.65
60X-4, 0–7	564.40	6.6	ND	35.5	582	501	16.1	LD	611	1136	LD	26.1	26.6	1111	26.5	9.56	1.65
63X-4, 140–150	594.90	7.7	3.88	37.5	597	517	15.9	LD	648	1192	LD	27.7	25.0	1172	27.3	9.53	1.55
66X-4, 140–150	623.80	7.1	3.75	36.0	594	514	15.6	ND	657	1263	LD	28.6	24.4	1180	29.0	9.30	1.53
69X-3, 140–150	650.90	ND	ND	ND	595	519	15.6	ND	646	1248	LD	29.9	23.5	1197	28.6	9.09	1.40
72X-3, 140–150	679.90	7.6	3.13	35.5	597	525	16.0	ND	631	1242	LD	30.0	23.3	1172	26.9	9.16	1.40
75X-2, 0–10	706.00	ND	ND	ND	604	522	15.4	ND	633	1221	ND	30.0	23.4	1165	26.5	9.03	1.42
130-806C-																	
61X-4, 140–150	765.10	ND	ND	ND	590	519	14.3	ND	708	1347	ND	31.5	20.5	1191	24.2	9.08	1.33

Notes: LD = concentration lower than detection limit, and ND = not determined.

Site 806 below 300 mbsf are higher than those at Site 805, which in turn were higher than those at Sites 803 and 804.

Alkalinity increases from 3.7 mM at 4.5 mbsf to a broad maximum (>6 mM) from 107.5 to 280.0 mbsf; it then decreases with depth to 3.1 mM at 679.9 mbsf (Fig. 28). Site 806 has a deeper and broader alkalinity maximum with higher concentrations than Sites 803, 804, and 805, suggesting a larger supply of organic matter for oxidation at this fairly shallow site, the closest to the equator of those drilled on the Ontong Java Plateau.

Sulfate concentrations decrease by almost 50% from 27.2 mM at 4.5 mbsf to 14.3 mM at 765.1 mbsf; most of the decrease occurs by 221.5 mbsf, where the concentration is 17.4 mM (Fig. 28). The sulfate depletion at this site is nearly a factor of 2 larger than at Sites 803 and 805 and larger still than that at the deepest site (804), consistent with the patterns of the alkalinity profiles for these sites.

Phosphate concentrations are 2–3 μM in the upper 31.5 mbsf, with concentrations at greater depths below the detection limit of 1–2 μM (Table 5).

Ammonia concentrations increase to a broad maximum >610 μM by 392.3 mbsf, persisting at these levels throughout the depth range sampled (Fig. 28). These concentrations are twice those at Site 805, which are in turn higher than those at Sites 803 and 804.

Measurable phosphate concentrations in the shallowest samples, higher ammonia concentrations, higher alkalinities, and greater sulfate depletion all suggest a greater supply of organic matter to the sediments at Site 806, which is then oxidized downcore.

Dissolved silica concentrations increase with depth to 1200 μM or greater by 623.8 mbsf (Fig. 28). The depth profile, both in shape and concentration, is similar to those at Sites 803, 804, and 805. No decreases in dissolved Si are seen, but there are only sparse occurrences of porcellanite below 240 mbsf (see "Lithostratigraphy" section, this chapter).

Dissolved manganese concentrations are generally below the detection limit of 2–3 μM, with the exception of samples in the depth range from 4.5 to 31.5 mbsf. The higher dissolved manganese concentrations are consistent with the reduction of manganese oxides during organic matter oxidation shallow in the core. There is no increase in dissolved Mn with the dissolved Si increase, perhaps because of the organic-carbon-poor nature of the sediments (Gieskes, 1981).

Calcium concentrations increase with depth, with an average gradient of 2.7 mM/100 m (Fig. 28), smaller than those observed at Sites 803, 804, and 805. Magnesium concentrations decrease with depth, with an overall gradient of −4.2 mM/100 m (Fig. 28), similar to gradients observed at Sites 803, 804, and 805. Although the Ca and Mg concentrations are linearly correlated overall ($R^2 = 0.96$), with a ΔCa/ΔMg ratio approximately equal to −0.7, there is clear evidence in a plot of this relationship for nonconservative behavior of Mg in the upper 136 m. The extent of Mg depletion relative to Ca increase in that depth range is greater than expected from a strictly linear correlation, indicating that there must be an additional sink for Mg in the shallowest sediments, such as dispersed volcanic ash (McDuff and Gieskes, 1976). Nonconservative Mg behavior was also observed in the upper section of Site 289 on the Ontong Java Plateau (Leg 30), though not at Site 288 (Elderfield et al., 1982). The correlation of Mg and Ca below 136 mbsf is linear ($R^2 = 0.99$) with a ΔCa/ΔMg ratio approximately equal to −0.9.

Strontium concentrations increase with depth to >1000 μM by 164.5 mbsf and to maximum values of >1100 μM by 364.7 mbsf, persisting to the deepest sample (Fig. 28). The maximum concentrations here are higher than at Sites 803, 804, and 805, where sediments accumulate more slowly.

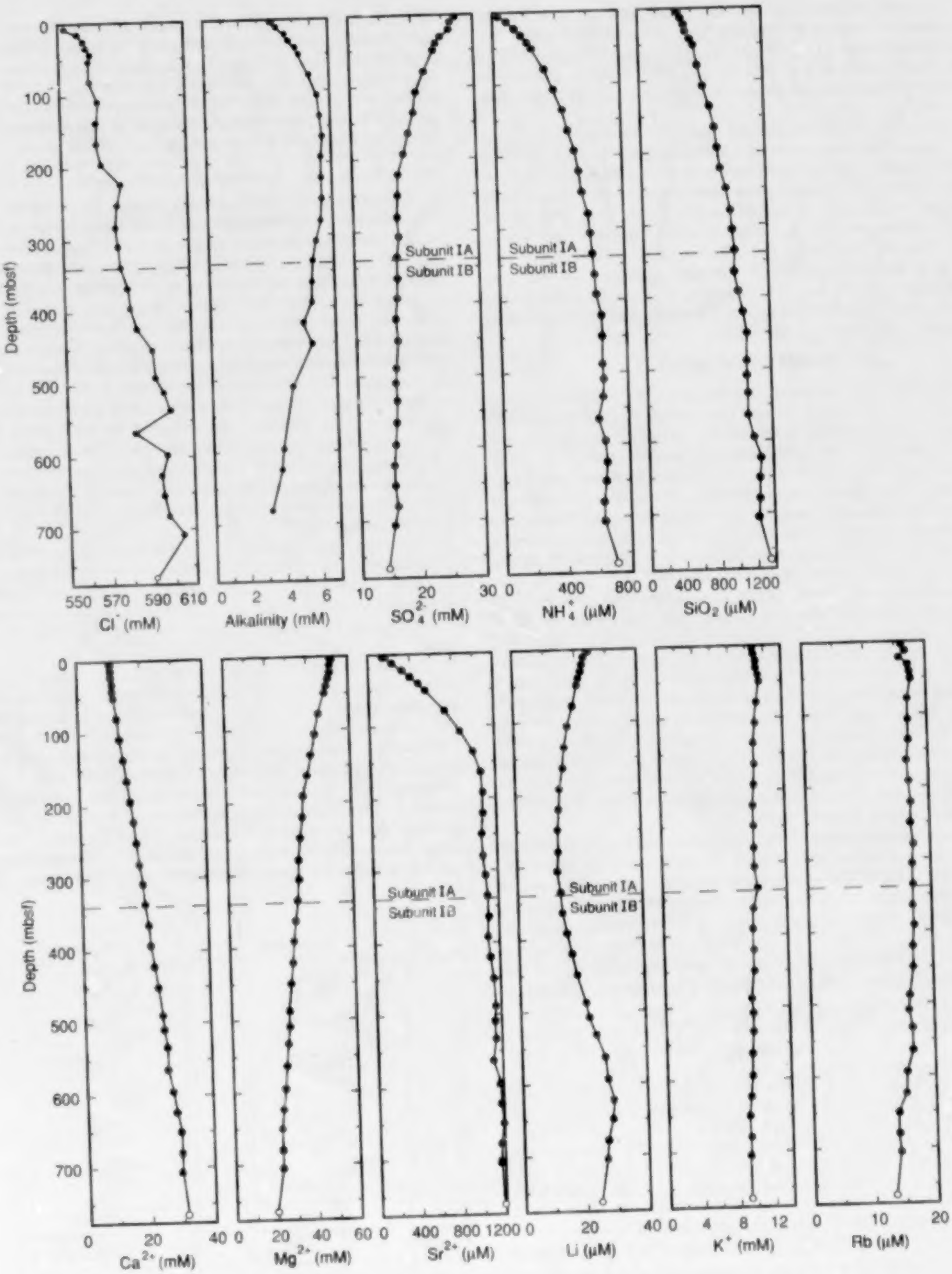

Figure 28. Interstitial water geochemical data, Site 806. Filled circles = Hole 806B and open circle = Hole 806C. The depth at the base of the plots is that of the deepest sediment drilled.

Lithium concentrations decrease from 24.5 μM at 4.5 mbsf to a broad minimum of < 15 μM from 193.0 to 364.7 mbsf; values then increase to 24–29 μM from 564.4 to 765.1 mbsf (Fig. 28). The Li minimum at this site has lower concentrations persisting to somewhat greater depths than those at Sites 803, 804, and 805.

Potassium concentrations decrease with depth from 10.8 mM at 4.5 mbsf to values around 9.0–9.1 mM from 650.9 to 765.1 mbsf (Fig. 28) and correlate well with the increase in Ca (R^2 = 0.93). Rubidium concentrations also decrease with depth from 1.6 μM at 4.5 mbsf to 1.3 μM at 765.1 mbsf (Fig. 28). The K and Rb decreases with depth are smaller than those observed at Sites 803, 804, and 805. The differences between Site 806 and the first three sites drilled in the magnitudes of Ca increases with depth and K and Rb decreases with depth suggest that there must be differences in the history of basalt alteration at Site 806 compared with the others.

CARBON GEOCHEMISTRY

The shipboard carbon geochemical analyses included determinations of inorganic carbon (342 samples), total carbon (50 samples), and volatile hydrocarbons (43 samples). A detailed description of the analytical methods used is given in the "Explanatory Notes" chapter (this volume) and by Emeis and Kvenvolden (1986). Volatile hydrocarbons were routinely monitored every third core. The samples were taken using the headspace-technique and were measured for the occurrence of methane, ethane, and propane. As at the previous Leg 130 sites, no significant amounts of these gases were detected.

Inorganic carbon (IC) analyses were conducted on physical properties samples. Percent $CaCO_3$ was calculated as IC · 8.334, assuming that all carbonate is calcite. The results are summarized in Table 6 and presented in Figure 7. The sediments at Site 806 contain very high amounts of $CaCO_3$, with values ranging from 85% to 97%. The range and variation of the values is much lower when compared with previous sites on Leg 130. Carbonate contents increase downhole from 85% to 95% over the interval from 0 to 250 mbsf, similar to the trend seen at all of the previous Leg 130 sites. In the lower part of the section (250–740 mbsf), $CaCO_3$ values average 92%. Table 6 is on microfiche in back pocket.

Total organic carbon (TOC) was calculated as the difference between total carbon (TC) values (as determined by means of the Carlo Erba NCS Analyzer) and inorganic carbon. The downhole distribution of total organic carbon in the sediments of Site 806 is characterized by very low values ranging between 0.02% and 0.6%. Most of the shipboard organic carbon data are near the detection limit of the analytical methods used. They will have to be verified by independent shore-based analyses.

PHYSICAL PROPERTIES

Introduction

At a depth of 2520 mbsl, Site 806 is the shallowest of the four sites devoted to the Neogene transect of the Ontong Java Plateau. GRAPE and *P*-wave velocity (using the multisensor track), and thermal conductivity measurements were made on whole rounds from all cores at Site 806. Physical property measurements were made on split cores from Holes 806B and 806C (cores from Hole 806A were not split on board the ship). These measurements included undrained shear strength, index properties (wet-bulk density, porosity, grain density, water content), and *P*-wave velocity.

The intensive physical properties program conducted on Leg 130 concentrated on making closely spaced laboratory measurements and afforded little time for processing data. Problems caused by improper needle calibration led to a significant scatter in the thermal conductivity data at Site 806. Correction of these thermal conductivity values will be attempted on shore. GRAPE and *P*-wave logger (PWL) data were recorded in the three holes at Site 806, but only a few intervals of the GRAPE data set were processed on board. No comparison of the GRAPE data with index properties is attempted in this chapter. The entire GRAPE and PWL data set also will be processed on shore.

Shear Strength

Undrained shear strength was typically measured at a sampling interval of one per split section in Holes 806B and 806C, using a motorized minivane apparatus (see "Explanatory Notes" chapter, this volume). Between 0 and approximately 200 mbsf, measurements were performed by inserting the vane in the soft sediment. Below 200 mbsf, shear strength was measured in undisturbed coherent blocks of sediment (or "biscuits") interspersed within the softer ooze matrix. Measurements were made until the sediment became too stiff (at approximately 315 mbsf in Hole 806B and 310 mbsf in Hole 806C).

Residual shear strength data were obtained at points where cracking did not dominate the sediment failure (see discussion of vane shear strength data interpretation in the "Physical Properties" section, "Site 803" chapter, this volume). Shear strength results are presented in Table 7, and Figure 29 shows a plot of the variations of shear strength with depth. Table 7 is on microfiche in backpocket.

Shear strength measured at Site 806 ranges from 5 to 25 kPa. Profiles from the two holes are similar; some minor differences, however, are possibly a result of coring-induced disturbance (see detailed discussion of disturbance effects on shear strength in the "Physical Properties" section, "Site 803" chapter, this volume).

Between 0 and 200 mbsf, shear strength values generally range between 5 and 15 kPa. Below 200 mbsf, the constant increase in shear strength reflects the progressive induration of the sediment. High-amplitude, low-frequency shear strength fluctuations (wavelength of around 40–60 m) and high-amplitude, high-frequency fluctuations (wavelength of around a few meters to 10 m) are superimposed on the general trend described above. Below 200 mbsf, the low-frequency fluctuations in shear strength data decrease in amplitude. High-frequency fluctuations, however, begin to dominate the record and may be the result of interspersed layers of different induration states. Some

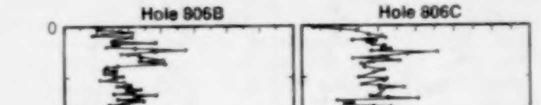

Figure 29. Peak shear strength vs. depth, Holes 806B and 806C.

of the lower values are probably caused by internal cracking in the stiffer intervals.

Index Properties

In Hole 806B, the sampling frequency for index property measurements in soft sediments was two samples per section until Core 130-806B-15H (139 mbsf), and one sample per section in the deeper cores. The sampling frequency in Hole 806C was generally one sample per section in APC cores and less frequently in the chalk interval. Index property samples were always taken at the same locations as the velocity measurements. Intervals showing evidence of "flow-in" or any other coring disturbance were not sampled (usually, the top of Section 1 in many cores). Results of index property measurements are presented in Table 8. Figures 30 through 33 show the downhole profiles of wet-bulk density, porosity, water content and grain density in each hole; superimposed on Figure 34 are the merged porosity curve for Site 806 (Holes 806B and 806C) and a generalized porosity curve for calcareous sediments (Hamilton, 1976). Table 8 is on microfiche in back pocket.

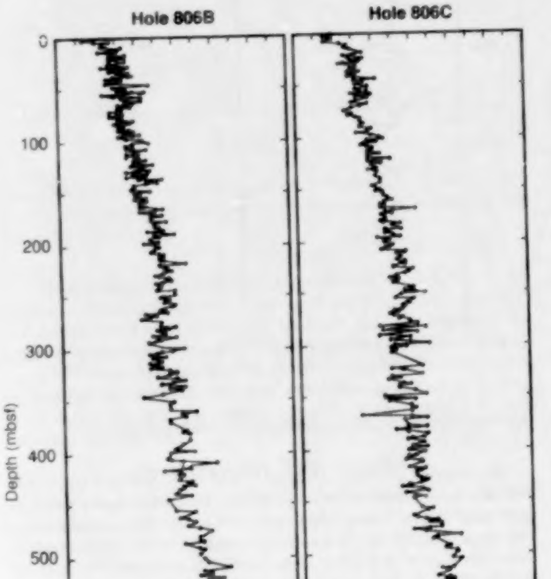

Figure 30. Wet-bulk density vs. depth, Holes 806B and 806C.

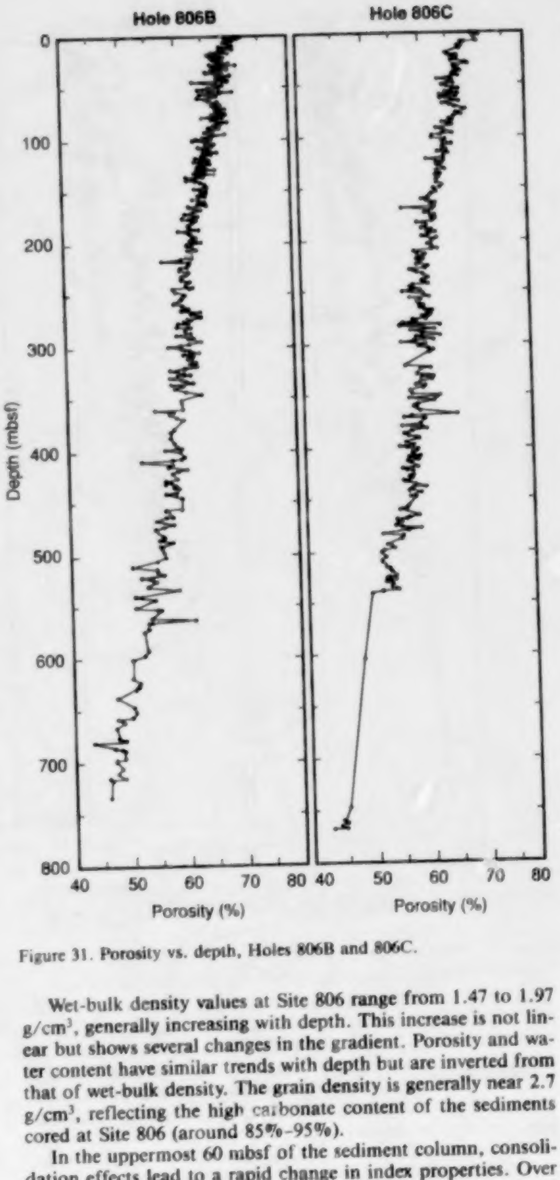

Figure 31. Porosity vs. depth, Holes 806B and 806C.

Wet-bulk density values at Site 806 range from 1.47 to 1.97 g/cm^3, generally increasing with depth. This increase is not linear but shows several changes in the gradient. Porosity and water content have similar trends with depth but are inverted from that of wet-bulk density. The grain density is generally near 2.7 g/cm^3, reflecting the high carbonate content of the sediments cored at Site 806 (around 85%–95%).

In the uppermost 60 mbsf of the sediment column, consolidation effects lead to a rapid change in index properties. Over this interval, porosity decreases from 72% at the mud line to ~66% at 60 mbsf (water content decreases from 100% to 75% and wet-bulk density increases from 1.47 to 1.58 g/cm^3). The trend of the porosity-depth curve in this interval is similar to the generalized curve of Hamilton (1976) for calcareous sediments (Fig. 34).

At about 60 mbsf, a small step in the index property curves (a decrease in bulk density and an increase in porosity) marks the beginning of an important divergence from the general trend of the Hamilton curve. Between 60 and ~240 mbsf, consolidation effects on the index properties were still observed but with diminished amplitude. Compared to the Hamilton curve, the re-

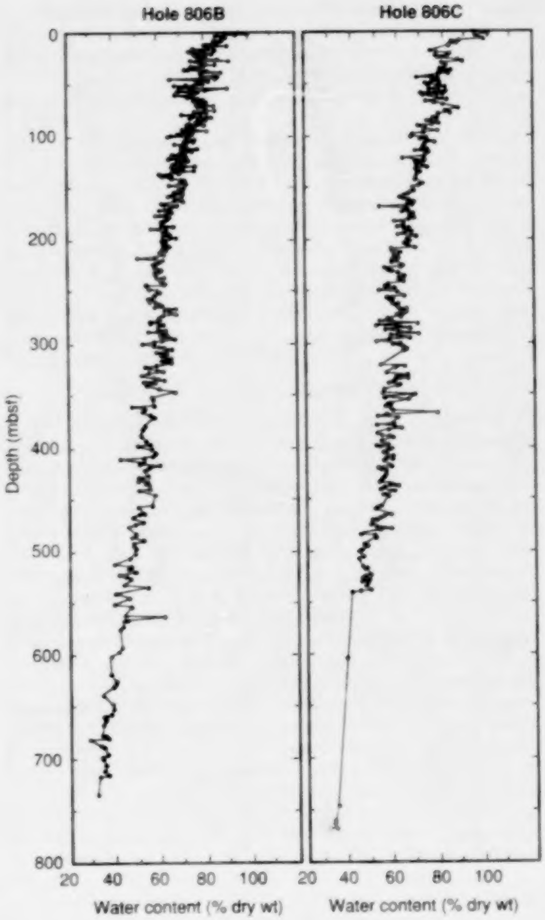

Figure 32. Water content vs. depth, Holes 806B and 806C.

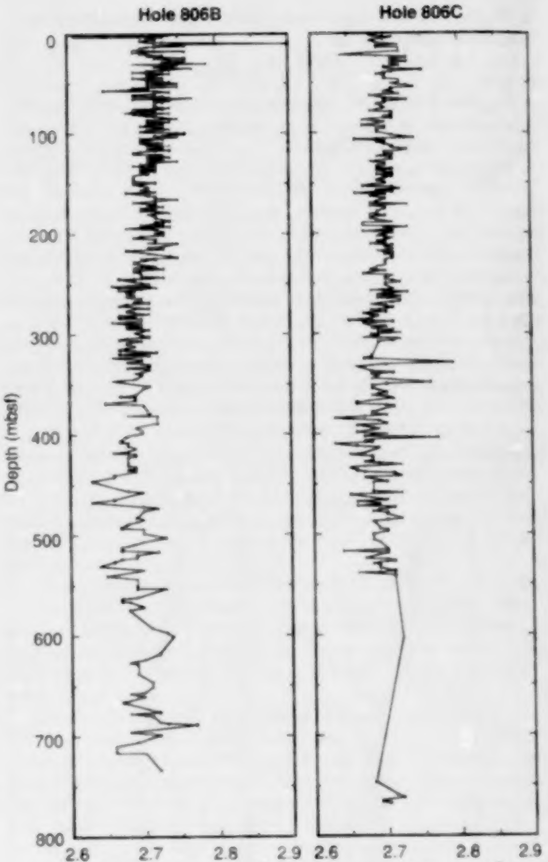

Figure 33. Grain density vs. depth, Holes 806B and 806C.

duction of porosity with depth at Site 806 is low (Fig. 34). At 240 mbsf, the porosity at Site 806 reaches 61% and is, therefore, 10% higher than the porosity value in the Hamilton curve. An increase of sediment rigidity because of early cementation may explain the small reduction of porosity in this depth interval. The low shear strength values measured in this interval do not, however, support this argument. Another possible explanation for this low gradient in the porosity-depth curve is the fact that the sediment is richer in foraminifers at Site 806 than at the previous Leg 130 sites (see "Lithostratigraphy" section, this chapter).

An important contribution to the porosity measured at Site 806 may come from intraparticle porosity (foraminifer chambers). Between 0 and 60 mbsf, consolidation effects led to a rapid reduction of the interparticle porosity. At about 60 mbsf, the sediment may become grain supported and thus further interparticle porosity reduction below 60 mbsf would be less important. Intraparticle porosity in foraminifer tests is not reduced by mechanical compaction; total porosity is, therefore, unaffected by compaction until breakdown of foraminifer tests occurs or test are filled by remobilized calcite.

The interval between 240 and ~440 mbsf shows little reduction of porosity and water content and little increase in wet-bulk density with depth (Figs. 30 through 32). The first occurrence of "biscuits" interspersed in soft ooze was observed slightly above the beginning of this interval (around 200 mbsf) and reflects the visible onset of lithification (see "Lithostratigraphy" section, this chapter). The ooze-chalk transition occurs at about 340 mbsf. The small amount of compaction between 240 and 440 mbsf is, therefore, probably a result of the progressive increase of cementation over this interval. Cementation increases the rigidity of the sediment, thereby improving its resistance to compaction.

A slight increase in porosity (decrease in density) was observed between approximately 250 and 320 mbsf (Figs. 30 and 31), which correlates with a major decrease in carbonate content. This trend also was observed in the index property curves at previous Leg 130 sites.

Below 440 mbsf, bulk density increases rapidly with depth. Reduction of porosity because of mechanical compaction is presumably very low, as it was in the previous interval (240–440 mbsf). Thus, the reduction of porosity with depth (and the increase in bulk density) was possibly a result of pore spaces infilling with calcite as the chalk became more indurated.

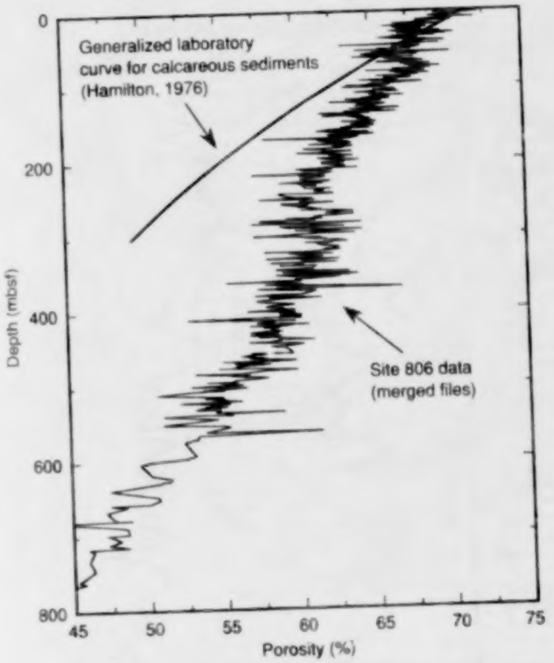

Figure 34. Merged porosity (Holes 806B and 806C) vs. depth for Site 806 and generalized laboratory curve for calcareous sediments (Hamilton, 1976).

High-frequency fluctuations (wavelength of around a few meters to 30 m) are superimposed on the general index property trends described above (Figs. 30 through 32). The study of the origin of major seismic reflectors at Site 806 (see "Seismic Stratigraphy" section, this chapter) shows that these fluctuations in index property values result from a complex interplay of at least three major factors: carbonate content, mean grain size, and sediment induration.

Compressional Wave Velocity

Horizontal (parallel to bedding) and vertical (perpendicular to bedding) *P*-wave velocities were measured on split cores at Site 806. The DSV apparatus was replaced by the Hamilton Frame at 324 mbsf in Hole 806B and at 387 mbsf in Hole 806C. Results of velocity analyses are shown in Table 9 and listed in Figure 35. Figure 36 shows changes with depth of horizontal *P*-wave velocity and mean grain size in the top 350 mbsf at Hole 806B, and Figure 37 shows a smoothed version of these two curves (5-point running average). Table 9 is on microfiche in back pocket.

Velocities measured at Site 806 range from 1530 to about 2400 m/s, generally increasing with depth. In the upper part of the section, however, between 0 and 120 mbsf, velocity actually decreases slightly. In this depth interval, the general trend and the high-amplitude, low-frequency fluctuations of *P*-wave velocities correlate well with changes in mean grain size (Fig. 37). The trend of slightly decreasing velocity corresponds to the progressive decrease in mean grain size over this interval.

Below 120 mbsf, velocity and mean grain size are poorly correlated, with the mean grain size trend showing only minor changes with depth whereas velocity values increase. This increase in the velocity values is presumably caused by consolidation and cementation.

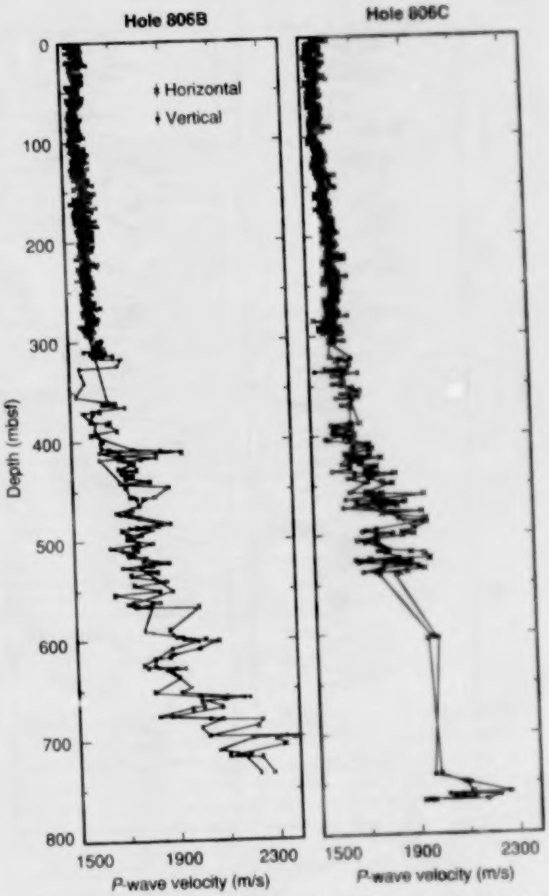

Figure 35. *P*-wave velocity (vertical and horizontal) vs. depth, Holes 806B and 806C.

The gradient of laboratory *P*-wave velocities is weak between 120 and 310 mbsf. It begins to increase rapidly below about 310 mbsf, slightly above the ooze/chalk transition (340 mbsf). Very low velocity values recorded between 320 and 340 mbsf in Hole 806B and at about 390 mbsf in Hole 806C correspond to the first measurements made with the Hamilton Frame and are probably the result of chalk fracturing.

LOGGING

Logging at Site 806 followed the same protocol as at Site 805 and achieved similar results (Tables 10 and 11). The first tool string was the Leg 130 geophysical string consisting of an NGT (natural gamma-ray), LSS (long spaced sonic), and DITE (electrical resistivity) combination. Logging data were collected from the base of the hole (741 mbsf) to pipe (90.2 mbsf; Table 10). All data on this run are of good quality.

The next tool string consisted of the NGT (natural gamma-ray), ACT (aluminum clay tool), HLDT (lithodensity tool), GST (geochemical spectral tool), and TLT (temperature) combination. After reaching the bottom of the hole at 741 mbsf and beginning this logging run, the GST would not calibrate properly. The tool string was lowered back to the bottom of the hole, recalibrated, and the logging run started from 740 mbsf with all

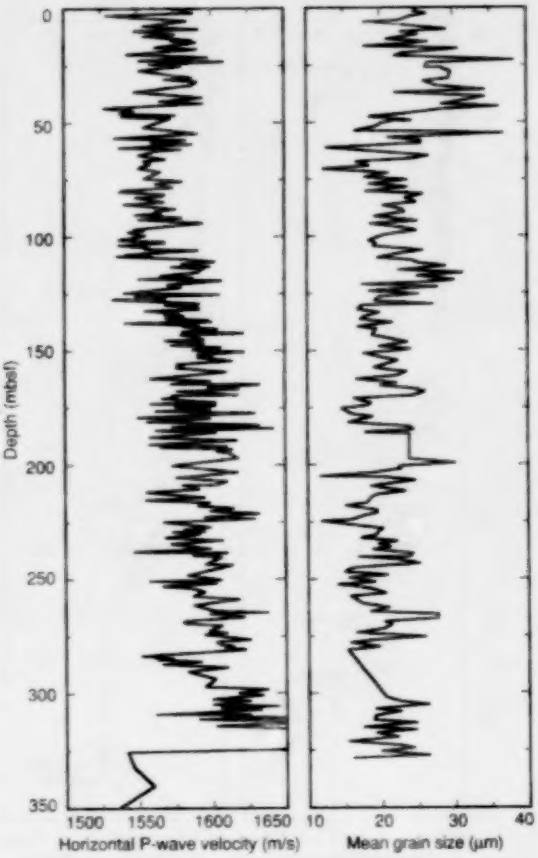

Figure 36. Horizontal *P*-wave velocity and mean grain size vs. depth, Hole 806B.

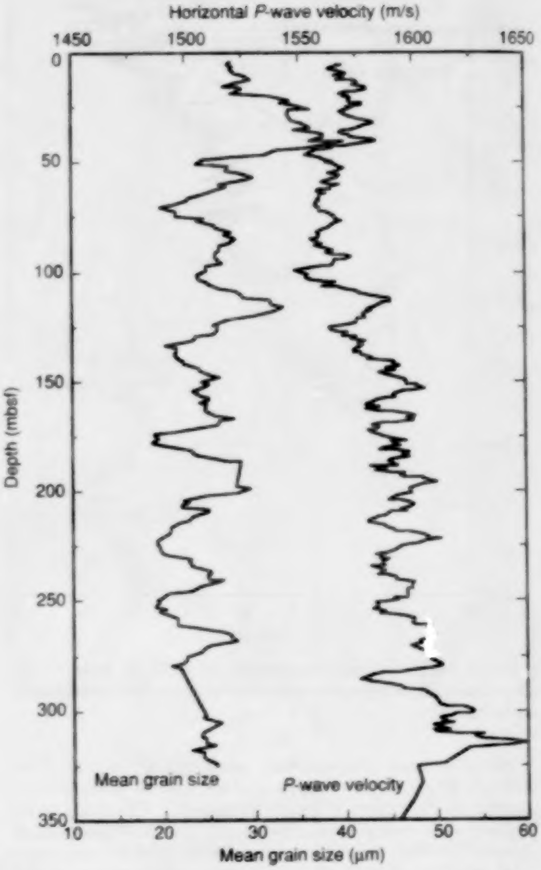

Figure 37. Smoothed curves (5-point running average) of horizontal *P*-wave velocity and mean grain size vs. depth, Hole 806B.

tools functioning. Because the formation was activated by the GST on the first (aborted) pass, the NGT and ACT logs of the bottom 38 m (741-703 mbsf) are suspect. The decay of unstable nuclei created by the high neutron flux from the GST produced gamma radiation that was measured by these two tools.

Logging proceeded smoothly until about 485 mbsf, where the GST again began to show poor resolution. By 442 mbsf, resolution was sufficiently bad to require the loggers to stop logging operations. The tool string was lowered back down to 496 mbsf and an attempt was made to recalibrate the GST. The GST would not function properly after 30 min of recalibration effort, so the GST was shut down and logging continued upward with the other tools. The tool string entered pipe at 88.4 mbsf.

The GST, when checked in pipe, appeared to function. For this reason, the tool string was lowered to repeat the section not logged with the GST. The tool string was lowered to 334 mbsf, but after an additional 15 min of recalibration the GST still malfunctioned. The tool string was raised to 244 mbsf for a repeat logging section (without the GST) of the NGT/ACT/HLDT/TLT from 244 to 121 m without the heave compensator as swells were low. Apparently, the caliper on the HLDT jammed into the wall of the hole on a down swell and broke off at about 160 mbsf during this final run.

Because of GST failures, the geochemical logs of Hole 806B are not continuous and are pieced together in sections. Spikes in the natural gamma activity logs and the aluminum logs may be present because of GST-induced hot spots in the hole. Nevertheless, the NGT and ACT logs are of good quality for the most part. The density log suffers from one major dropout between 290 and 320 mbsf and from suspect intervals between 290 and 180 mbsf. On the repeat section, the density log data is useless above 160 mbsf, the point at which the caliper broke off.

Log Stratigraphic Units

The stratigraphic column recovered at Site 806 is nannofossil ooze with foraminifers, grading into chalk at about 320 mbsf. We recognized three logging units, similar to the top three units at Site 805 (Fig. 38 and Site 805, Figs. 30-32).

Logging Unit A

Unit A (90-340 mbsf) is marked by low resistivity values that remain at about 0.8 ohmm throughout the interval. Wet-bulk density values increase downcore only slightly, from 1.6 to 1.7 g/cm^3. A comparison of log and laboratory density reveals unreliable logging data from 190 to 320 mbsf (Fig. 49, "Seismic

Table 10. Logging operations, Hole 806B.

Local day	Local time	Cumulative hours	ᵃDepth (mbsf)	
2/21/90	22:30			Last core on deck
2/22/90	7:50	0.0		RIH with geophysical tool string (NGT/DIT/LSS)
2/22/90	8:53	1.0	96.3	Out of pipe; start downlog to base of hole
2/22/90	9:37	1.8	741.0	On bottom of hole, <2 m fill
2/22/90	9:38	1.8	741.0	Main log pass; NGT/DIT/LSS all working; up at 900 ft/hr; heave compensator not on
2/22/90	12:11	4.3	71.9	Tool in pipe at 90.2 mbsf (600 ft), end up log at 71.9 mbsf
2/22/90	12:11	4.3		Run down for repeat section
2/22/90	12:20	4.5	212.1	Start up on repeat section; NGT/DIT/LSS all working; 900 ft/hr
2/22/90	12:46	4.9	71.9	Tool in pipe at 90.2 mbsf (8,600 ft); POOH
2/22/90	13:50	6.0		Tool string on deck
2/22/90	14:52	7.0		RIH with geochemical tool string (NGT/ACT/HLDT/GST/TLT)
2/22/90	16:15	8.4	740.1	At bottom of hole; heave compensator on; start log up, 600 ft/hr
2/22/90	16:31	8.7	702.9	Trouble with GST; stop up log at 10,610 fbrf; this section neutroned
2/22/90	16:46	8.9	740.7	Dropped back to this depth; got GST started, HLDT caliper closed
2/22/90	16:57	9.1	716.9	HLDT caliper fully open, all logs good
2/22/90	18:28	10.6	486.5	GST starts to lose resolution
2/22/90	18:37	10.8	442.9	Stop up log, go back down to 9,960 fbrf (504.4 mbsf)
2/22/90	19:09	11.3	495.6	Start up log; GST would not recalibrate, not functioning
2/22/90	21:24	13.6	88.4	Enter pipe; end repeat geochemical string
2/22/90	21:27	13.6	82.3	Stop in pipe for recalibration; some response
2/22/90	22:03	14.2	334.1	Run back in hole to try to GST started; no luck, run back up for repeat
2/22/90	22:03	14.2	244.1	Repeat up log (NGT/ACT/HLDT/TLT) GST not functioning; heave compensator sticky, not turned on
2/22/90	23:05	15.2	120.7	End repeat section; POOH
2/23/90	0:00	16.2		Geochemical string at wellhead
2/23/90	1:15	17.4		Riggnd down from logging runs

ᵃ Based on a seafloor depth of 2531 mbrf.

Table 11. Acronyms used in text describing logging at Hole 806B.

Acronym	Definition or meaning
ACT	Aluminum clay tool
API units	American Petroleum Institute standard units for gamma-ray activity calibrated to test pit in Houston, TX
BHC	Borehole compensated sonic tool
DIT	Phasor dual induction tool
fbrf	Feet below rig floor
FMS	Formation microscanner
GST	Geochemical spectral tool
HLDT	High-temperature lithodensity tool
LSS	Long-spaced sonic digital tool
mbrf	Meters below rig floor
mbsf	Meters below seafloor
NGT	Natural gamma tool
POOH	Pull out of hole
RIH	Run into hole
SDT	Long-spaced sonic digital tool
TLT	LDGO temperature logging tool

Stratigraphy" section, this chapter). Most of the large-amplitude variations observed in the HLDT density data between 190 and 320 mbsf are suspect.

Natural gamma-ray activity decreases throughout the entire interval of Unit A, indicative of increasing calcite contents with depth. To a certain extent, a similar pattern was observed for aluminum. As in Hole 805C, however, the Al trend stops before that of the natural gamma-ray activity, at about 280 mbsf. The lowermost part of the unit between 300 and 320 mbsf has some of the highest Al values.

Velocities in Unit A increase from just above 1.6 km/s at 90 mbsf to about 1.95 km/s at the base of this unit. Superimposed upon this linear velocity change are high-frequency (10–20 m period) velocity variations of about 0.1 km/s. These high-frequency variations may, in part, be artifacts resulting from hole-width variations or coring (see below). The transition between Units A and B also has a section of very high-frequency velocity variations between 320 and 340 mbsf. A few porcellanite nodules were the only recovered material in this interval in Hole 806C. In Hole 806B, which was logged, a single porcellanite nodule was found in a full core of chalk. We speculate that the high-frequency velocity variations are indicative of one or more chert-rich horizons at this depth.

Logging Unit B

Unit B (340–600 mbsf) is characterized by gradients in all physical properties and flat chemical logs. Resistivity values increase from 0.8 to 1.1 ohmm and have larger amplitude fluctuations than in Unit A. The velocity gradient also is greater in this unit. In the lower portion of the unit, between 460 and 600 mbsf, small-amplitude, low-frequency (30–40 m period) variations were observed. The density gradient increases somewhat from Units A to B, and the density log is marked by low-frequency variations. In the lower part of Unit B, between 500 and 600 m, the low-frequency density and velocity variations are inversely correlated. However, there is no correlation between the two data sets over the entire unit, except for the compaction-imposed linear increase of both density and velocity with depth.

Logging Unit C

Unit C (600–720 mbsf) is marked by a decrease in resistivity, velocity, and density gradients with depth and by high-amplitude, low-frequency (30–40 m period) variations in density and resistivity. The chemical logs show little distinction between logging Units B and C. Unit C, in Hole 806B, resembles logging Unit C in Hole 805C and may represent a common depositional lithology. The Unit B-C transition, located at 380 mbsf in Hole 805C, marks the level of a condensed section between 17 and 20 Ma (see "Sedimentation Rates" section, "Site 805" chapter, this

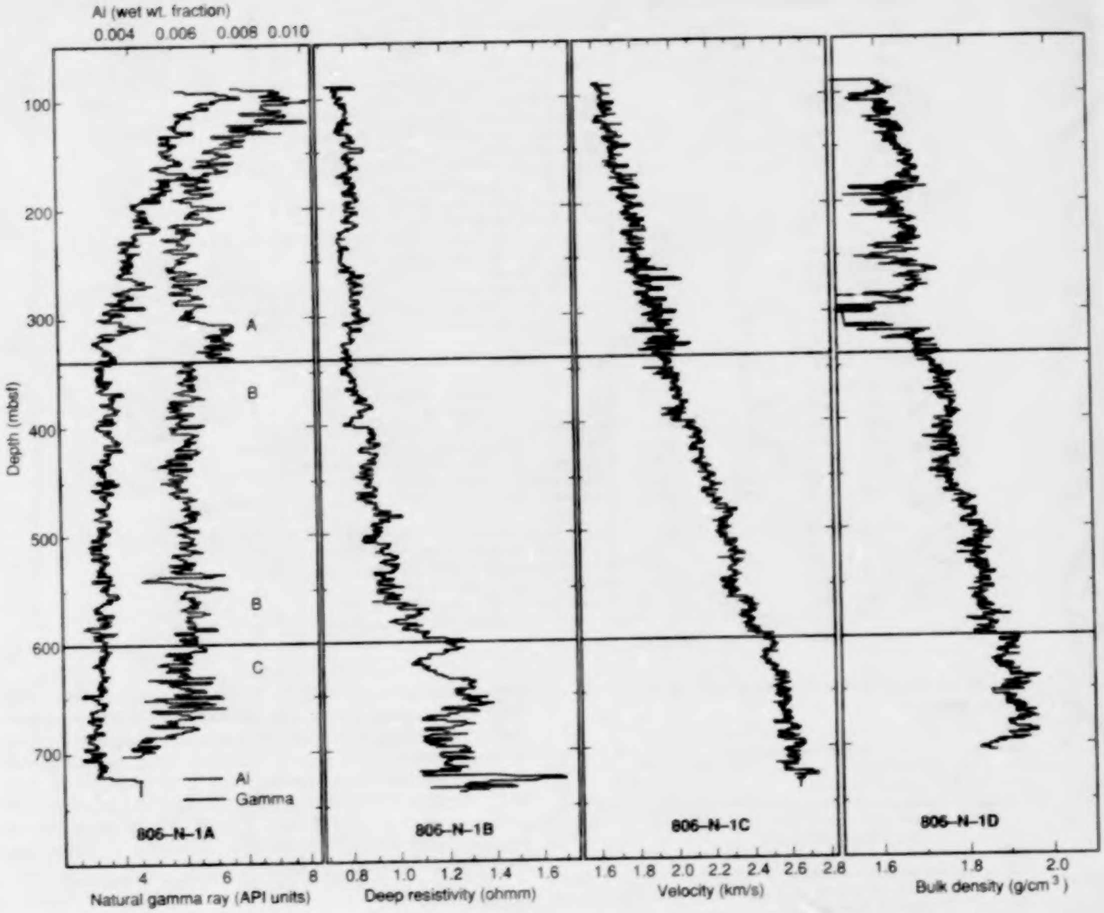

Figure 38. Logging profiles of aluminum content, natural gamma ray, resistivity, velocity, and bulk density, Hole 806B. Logging units are marked by heavy black lines.

volume); in Hole 806B, the Unit B-C transition is located at 600 mbsf, the level of a condensed section of about the same age.

Logging Artifacts in Unit A

Unit A contains artifacts in the logs, induced or enhanced by hole conditions. The caliper on the density tool (HLDT), which holds the instrument against the wall of the hole, reached its maximum extension of 18 in. at depths above 350 mbsf, and gave little information about the size of the upper part of the hole. The separate travel paths from the long-spaced sonic tool, however, gave information about hole width in the upper part of Hole 806B (Fig. 39). The LSS has three different source-receiver spacings: 8, 10, and 12 ft. Thus, at any point in the hole we can perform a small refraction experiment. If the sound velocity for fluid in the borehole is known, the distance to the wall of the borehole can be solved. Assuming that Hole 806B was filled with seawater, the hole width varied as shown in Figure 39.

The mechanical and sonic calipers give similar information qualitatively, although there is some offset between the two. Above 320 mbsf the hole has washed out more than the $11^{3}/_{4}$-in. drill bit size. The washouts are not randomly spaced, at least below 170 mbsf, nor are they necessarily associated with the recovery of individual cores either. From 190 to 265 mbsf, washouts are spaced about 18–20 m apart. Below 265 mbsf to the APC/XCB core change at 320 mbsf, the washout spacing decreases to about 10 m.

There is a definite correlation between sonic velocities and hole width (Fig. 40), based upon a comparison between the sonic caliper and the upper part of the sonic log. A narrow hole is correlated with higher velocities. This in itself is not necessarily an artifact, since better indurated horizons should have higher sound velocities than neighboring units and, because of their competence, should be less prone to washout. There is a definite 9.5-m periodicity in the velocity record over the interval from 100 to 340 mbsf that does not correlate with the washouts except below 250 mbsf. The largest amplitudes occur when the washouts also have about a 10-m spacing. This is best illustrated in Figure 41, in which the core breaks are marked by the verticals of a square wave. At each core break, we can recognize a couplet of high- and low-velocity spikes. In most cases, the

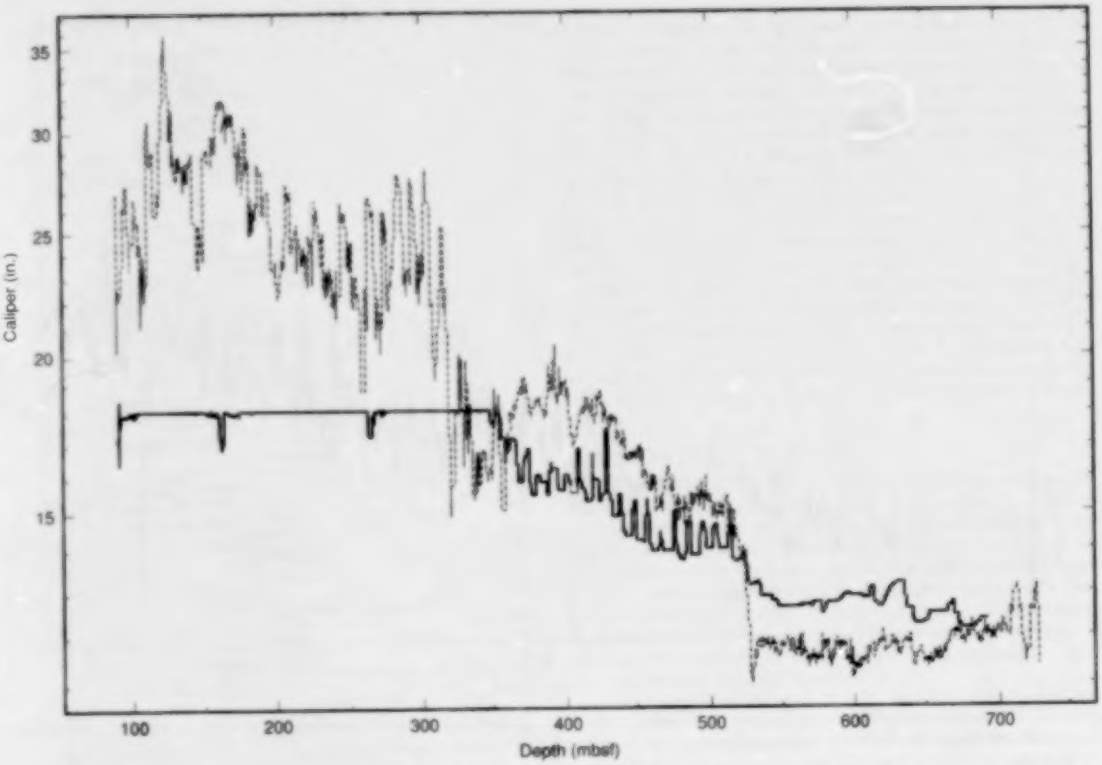

Figure 39. HLDT hole width measured by caliper (solid line) compared with hole width inferred from the sonic velocity log (dashed line) (see text), Hole 806B. The HLDT caliper has a maximum extension of 18 in. All information about hole width in the upper portion of the hole must be based upon the sonic velocity measurements.

high-velocity spike is most prominent. The 9.5-m couplets most probably are coring artifacts, as they are precisely the length of the APC.

The strong density artifacts in Unit A are probably the hole width. The HLDT can only get accurate density readings when positioned near the core wall. Figure 38 shows a large dropout that occurred between 290 and 320 mbsf. Above this interval, between 180 and 290 mbsf, comparison with lab data shows that the logging data are invalid (see "Seismic Stratigraphy" section, this chapter).

Chemical Logging at Site 806

In addition to the ACT aluminum data and the natural gamma-ray activity data already described, a geochemical spectral tool (GST) log was obtained over the interval from 445 to 735 mbsf. This represents a time interval from about 12.4 to 25.5 Ma. As at Site 805, only Ca and Si are present in sufficient abundance in the solid phases for the data to be considered reliable. Figure 42 shows the GST counts of Ca normalized to the total Ca + Si counts, an indicator of calcite abundance in the sediments. Two main features are apparent from the logging data: (1) a trend to higher calcite toward the base of the hole and (2) abundant high-frequency variations of calcite throughout the interval.

By simple inspection (Fig. 43), it appears that much of this high-frequency variation may occur at the 100-k.y. Milankovitch period. Figure 43 incorporates a 100-k.y. signal based upon sedimentation rates from Table 11 (see "Sedimentation Rates" section, this chapter). The large-amplitude signal in this part of the record appears to occur at this periodicity. Spectral analysis techniques provide an objective approach to examine the periodicity, as shown in Figure 44. In this case, we have used only eight nannofossil datum levels to establish a time scale for Hole 806B. Despite the crude time scale, 100-k.y. periodicity is apparent in the 13-m.y. long record. Weak, but significant, power occurs near the 41-k.y. Milankovitch period. Strong power also occurs at 313, 209, 84, 68, and 49.5 k.y. Some of these periodicities may be resonant periods of the climate system amplifying harmonics of the orbital periods. All or part of them could be artifacts introduced by the crude time scale, however.

Correlation Between Sites 586, 805, and 806

Comparison of Sites 586 and 806

Site 586 (0°29.84′S, 158°29.89′E, 2208 m water depth; Shipboard Scientific Party, 1986a, 1986b) and Site 806 (0°19.11′N, 159°21.69′E, 2521 m water depth) are both located on the top of the Ontong Java Plateau, on opposite sides of the equator but within 75 nmi of each other. The two sites should have highly similar records. Figure 45 is a comparison of the two velocity profiles. A simple linear stretch of the Site 586 depth axis with respect to depth in Site 806 has been used for the comparison. Note also that the velocity axes have been offset so that the two records could lie side by side. From the excellent correlation of the two records, one can infer that the two sites had the same depositional history over the entire common interval, essentially

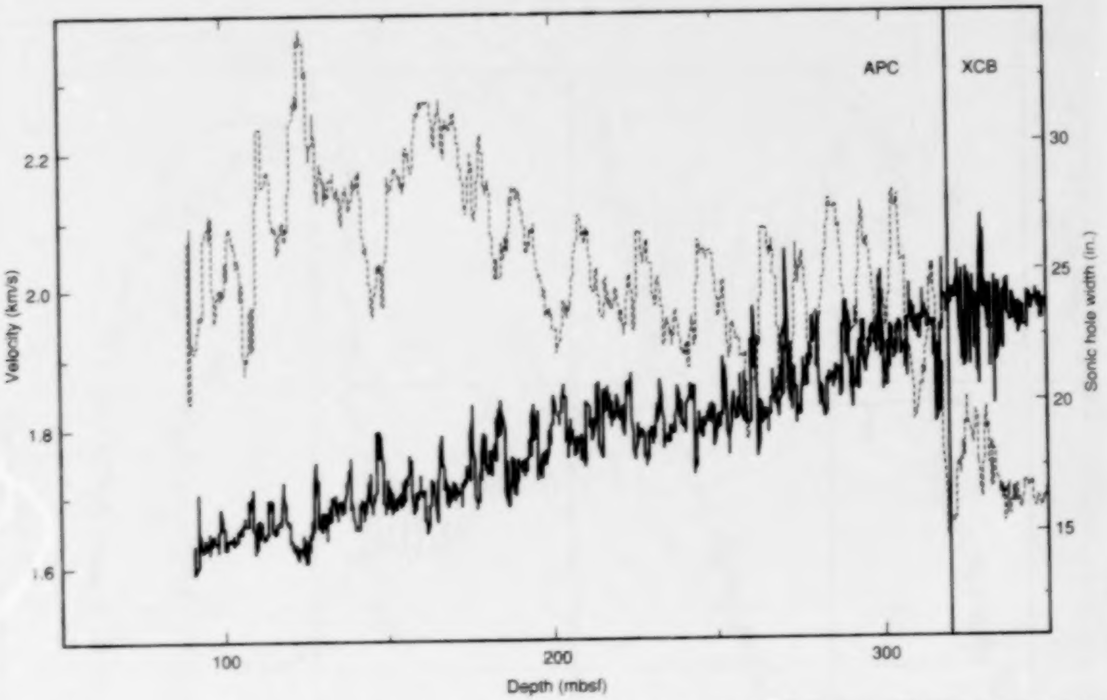

Figure 40. Comparison of velocity profile (solid line) to sonic hole width (dashed line) from the same logging data, Hole 806B. A narrow hole is generally correlated with fast sonic velocities. Coring artifacts, with a 9.5-m spacing, can also be seen.

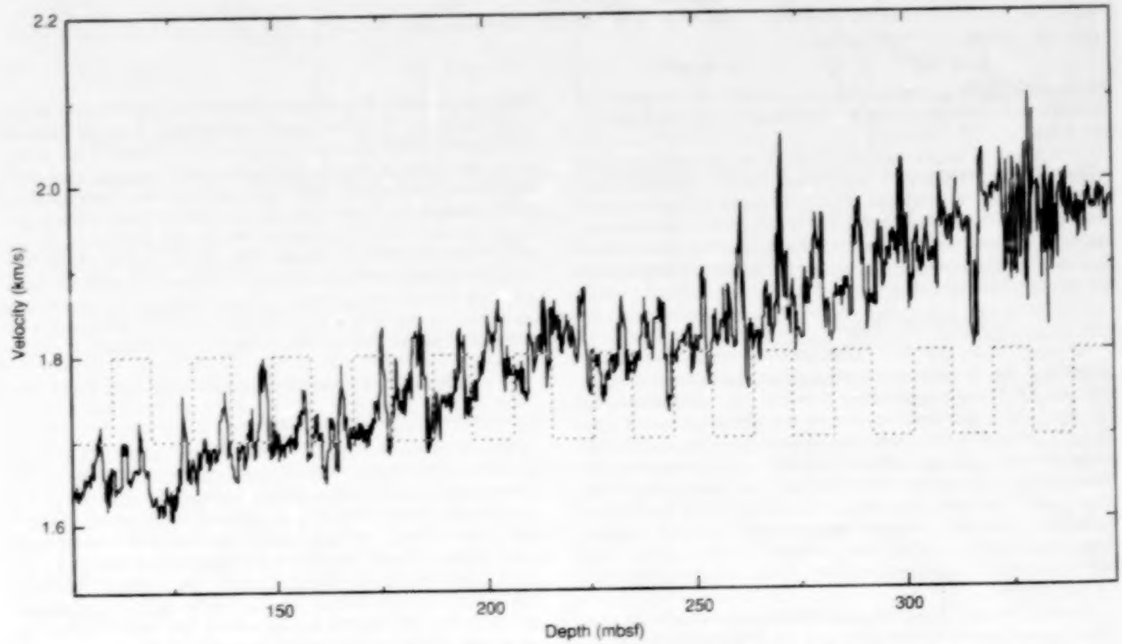

Figure 41. Velocity profile from Hole 806B compared with core breaks in the hole. Core breaks are marked by vertical lines of the square wave. Note that a couplet of high- and low-velocity spikes are consistently associated with the core breaks.

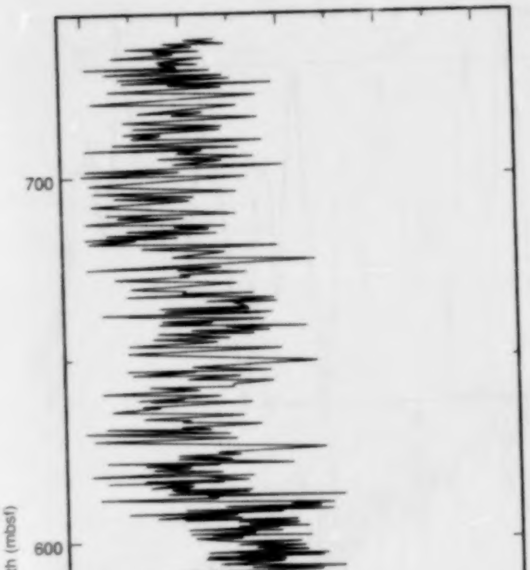

Figure 42. GST record of calcium variations, Hole 806B. The data are presented as Ca/(Ca + Si) counts to normalize borehole effects in the shipboard-processed data. There is a trend throughout the interval toward higher calcium in older sediments. In addition, there are abundant large-amplitude, high-frequency variations.

all of the Miocene. This observation argues against local winnowing events at either site. Instead, any resuspension or other sediment loss must be regional in scale.

Site 586 does have lower sedimentation rates than Site 806 for the entire logged interval, consistent with their positions relative to the equator. Assuming an absolute latitudinal motion for the Ontong Java Plateau of about 0.25°/m.y. northward during the Neogene (R. Musgrave, pers. comm.) Site 806 was located about 1°S, and Site 586 was located about 2°S when the sediments at the top of the logged interval were being deposited. The difference in sediment deposition at the two sites may in part reflect the sedimentation rate gradient away from the equator. Expansion and contraction of the equatorial high-productivity zone during the Miocene may eventually be discerned from detailed correlations of these two sites.

Even though velocity data from Holes 586C and 806C were offset for clarity in Figure 45, they converge at depth. The two records apparently have different velocity gradients. This is an artifact of the presentation in the figure, however. Common depths have similar velocities at either site. Thus, the two sites have similar compaction trends, which are mostly a result of burial depth. Superimposed upon the compaction trend are the variations in the physical properties caused by changes in sedimentation. These variations, which have paleoceanographic significance, will be easy to separate from the diagenetic information.

Comparison of Sites 805 and 806

Correlation of Sites 805 and 806 should yield important insights about dissolution gradients in the Miocene. Dissolution- and sedimentation-induced differences between Sites 805 and 806 make the correlation more difficult than for the sites on top of the Ontong Java Plateau, however. The correlation will be dependent upon stratigraphic ties and age control provided by micropaleontological studies. This should pose little problem, as the two sites have two of the best Neogene micropaleontological records ever recovered in ODP (see "Biostratigraphy" section, this chapter and Site 805 chapter).

The comparisons between Site 805 and 806 velocity and density, respectively, are illustrated in Figures 46 and 47. Both figures are drawn assuming that Site 806 averages a factor of 1.44 higher sedimentation rate than Site 805. An examination of either figure indicates that there have been many relative changes in sedimentation rate between the sites. Mesoscale features, such as the small 30–40-m wavelength velocity variations in the interval from 420 to 640 mbsf in Hole 806B and from 300 to 440 mbsf in Hole 805C will provide a means to refine the correlation and look for higher frequency ties between the records.

SEISMIC STRATIGRAPHY

The seismic section at Site 806, the shallowest of the Ontong Java Plateau depth transect sites, is characterized by a thick sequence of parallel, closely spaced reflectors that mirror the gently sloping seafloor and basement topography (Fig. 48). The section shows little evidence of disturbance or mass wasting, and individual reflectors can be traced continuously to Sites 289/586 (Shipboard Scientific Party, 1975b, 1986a), 139 km west and 400 m shallower than Site 806. The section at Site 806 is only slightly thinner than those at Sites 289/586, and its thickness exceeds that at Site 805 by a factor of 1.35. Between Sites 289/586 and 806, the minor thinning that was observed occurs in the deep (pre-Oligocene) part of the section; between Sites 806 and 805 the thinning takes place throughout the section, with the possible exception of the Oligocene (see Mayer et al., this volume).

As at the previous sites, we have used the results of laboratory and logging measurements to convert seismic traveltime to depth-in-section, and we have employed seismic modeling to check on the accuracy of this traveltime-to-depth conversion. Site 806 laboratory measurements of velocity and density were made approximately every 75 cm (see "Physical Properties" section, this chapter), and velocity and density logs (15-cm sample interval, 60-cm sensor spacing) were run for the section between 100 and 710 mbsf (see "Logging" section, this chapter). Labo-

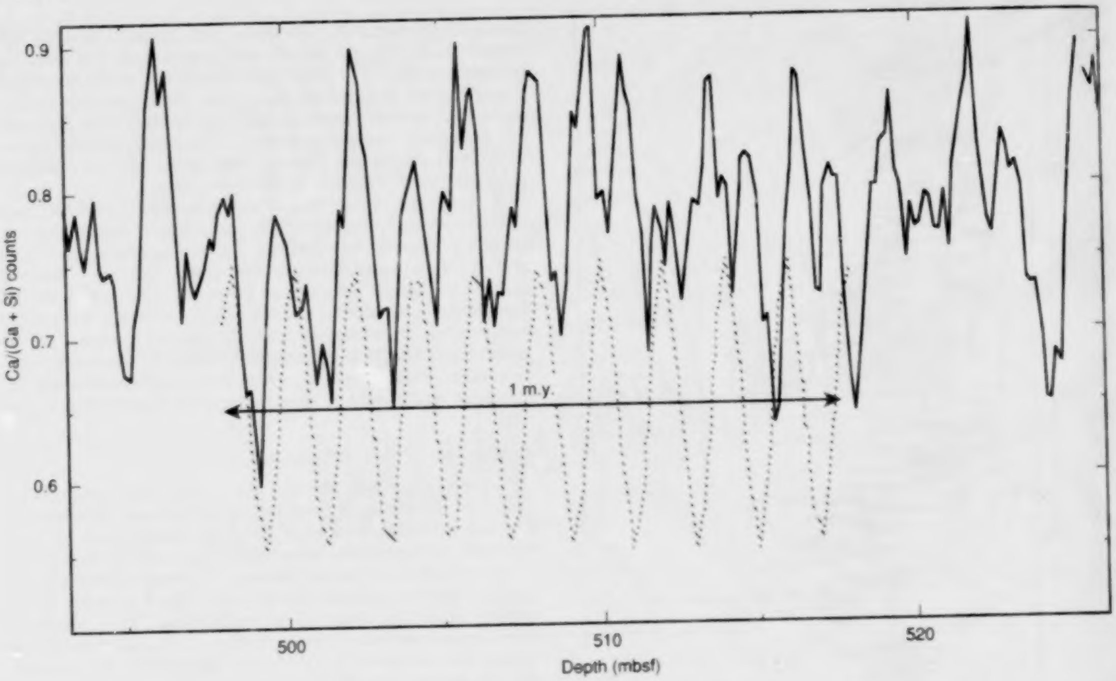

Figure 43. A plot of a small interval of the GST Ca/Ca + Si (solid line) data (Hole 806B), which shows that much of the variation in calcium occurs at a period of approximately 100 k.y. The dashed line represents a 100-k.y. cycle based on sedimentation rates listed in Table 4.

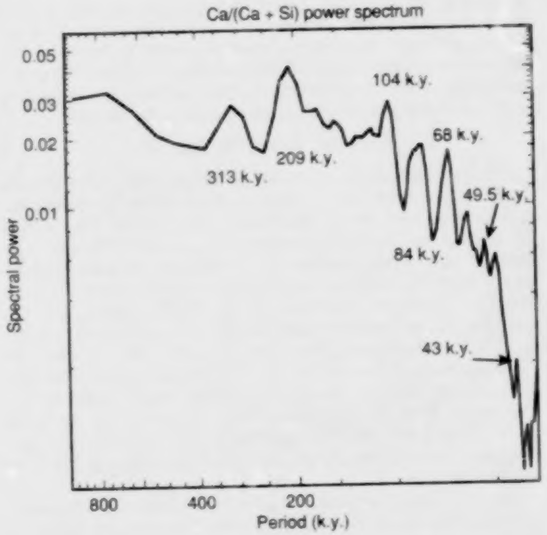

Figure 44. Power spectrum of the GST calcium record interpolated to a 7500-yr sample spacing. The time scale used for the spectral analysis is based upon only eight nannofossil age control points (Table 4). Milankovitch-type periodicity near 41 and 100 k.y. can be found, as well as a large amount of power in lower frequencies.

ratory measurements of velocity and density were converted to *in-situ* values using the methods described in Mayer et al. (1985) and merged with the logging data. A comparison of *in-situ* corrected laboratory data with log data reveals several inconsistencies that must be addressed before the data can be properly merged (Fig. 49).

If we assume that the log-derived velocities and densities represent *in-situ* values, then laboratory measurements, properly corrected to *in situ*, should be the same as the logging values. At the previous sites, the corrected laboratory values have, for the most part, been in good agreement with the logging data, implying that the procedure used to correct laboratory data to *in-situ* values is reasonable. Discrepancies between the laboratory and logging values (e.g., at Site 805 between 140 and 160 mbsf; see "Logging" section, "Site 805" chapter, this volume) have been attributed to poor hole conditions that have degraded the logs in certain intervals.

A comparison of log and laboratory velocity measurements (Fig. 49) reveals that between 100 and 180 mbsf the logging data are also in agreement with the corrected laboratory measurements and below 180 mbsf the two data sets diverge. Deeper than about 180 mbsf, the laboratory velocities are consistently lower than the logged velocities, but we have little confidence in the *in-situ* correction process at these depths (once cementation begins). A detailed look at several indicators of borehole conditions reveals that there are changes in the borehole behavior at 180 and 340 mbsf (see "Logging" section, this chapter). A full understanding of the effect of these borehole changes will have to await further study.

Comparing the logs from Site 806 with the laboratory data reveals that between 100 and 180 mbsf the corrected density values are in good agreement with the logging data; however, below

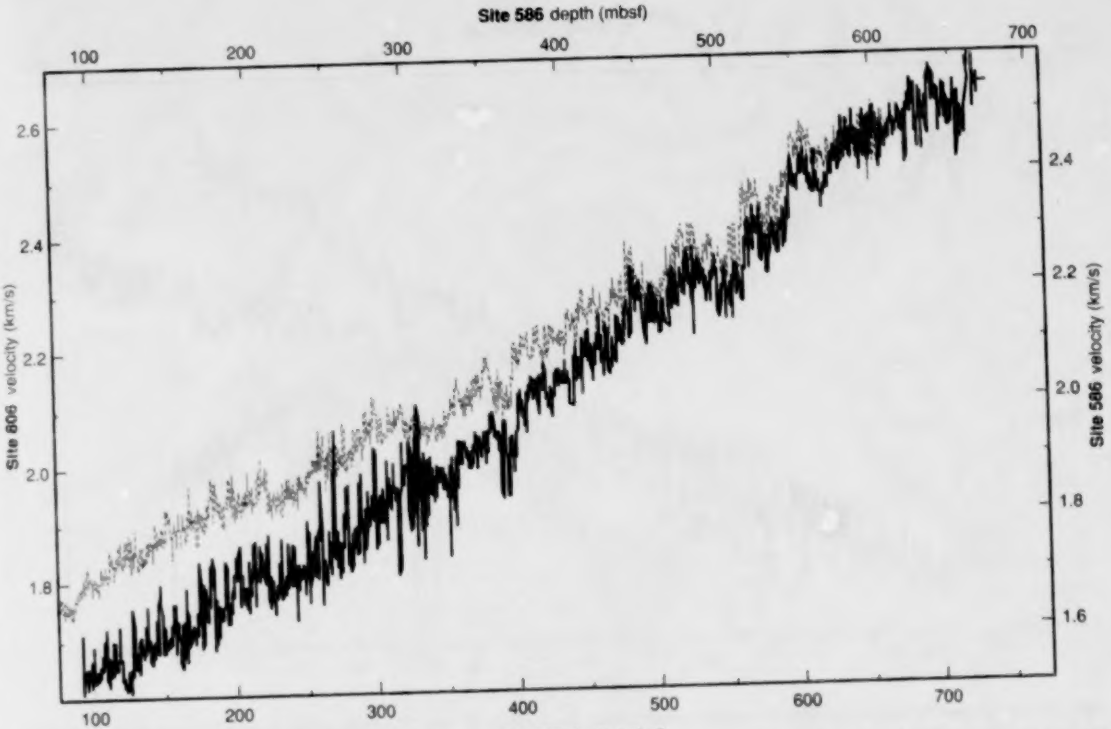

Figure 45. Comparison of velocity profiles, Holes 586C (dashed line) and 806B (solid line). Site 586 is approximately 135 km to the southwest of Site 806. Note that the two sites have separate depth axes so as to eliminate first-order sedimentation rate differences between the two sites. In the figure, the Site 586 velocity data have been offset by 0.1 km/s for clarity.

that depth the logging values are significantly lower than the lab measurements (Fig. 49). Between 280 and 340 mbsf, the logged densities are so low that they are unquestionably in error.

To obtain the best possible data base for the seismic model, we have used laboratory density data from the seafloor to 360 mbsf (and downhole density data deeper than that) and laboratory velocity data from the seafloor to 180 mbsf (and downhole velocity data deeper down). The compromise that we make in doing this is the loss of detailed density sampling provided by logging, particularly in the interval from 200 to 360 mbsf where the laboratory sampling interval was reduced (Fig. 49).

The merged, corrected laboratory and logging data (velocity and density) were used to calculate acoustic impedance (Fig. 50), which was then convolved with a seismic source signature to generate a synthetic seismogram (see "Seismic Stratigraphy" section, "Site 803" chapter, this volume, or Mayer et al., 1985, for details). The synthetic seismogram was compared with the field seismic profile to evaluate the accuracy of the traveltime-to-depth conversion. The field records used for this study are those collected by the *Thomas Washington* (ROUNDABOUT Cruise 11) during the site surveys for Leg 130 (see Mayer et al., this volume).

As at previous sites, we have looked in detail at several representative reflectors within the section. By examining the age and possible origin of these reflectors, we hope to place the seismic record in a stratigraphic framework. The criteria for the selection of these reflectors is simply that they have large amplitudes and are laterally coherent within the immediate area of Site 806. No effort has been made to select reflectors that are regionally correlatable (e.g., see Mayer et al., this volume), although the regional distribution of the named reflector patterns is evident (see "Summary and Conclusions" section, this chapter). As at Site 805, we will refer to the six named reflector series (Panama, Tethys, Antarctic, Drake, Texas, and Ontong Java; see "Seismic Stratigraphy" and "Summary and Conclusions" sections, "Site 805" chapter, this volume) to place the selected reflectors within a regional stratigraphic framework.

The comparison of the synthetic seismogram to the field profile at Site 806 (Fig. 50) produces a reasonable match, though not one that is without ambiguities. In the absence of a clear tie point such as basement or chert (as at Site 803), there are several possible fits of the synthetic record to the field data. We have chosen a fit that maximizes the number of matches, particularly in the deeper part of the section (Fig. 50). We have selected 13 reflectors in the 740 m of logged section; they are labeled on the plot of reflection coefficient vs. traveltime (Fig. 51), and their traveltimes, depths, and ages are listed in Table 12.

The three shallowest reflectors picked (6-1, 6-2, and 6-3) are associated with the "Panama Series" of reflectors. The youngest two (6-1, ca. 1.9–2.0 Ma., and 6-2, ca. 2.4 Ma.) are correlated with large grain size, low carbonate, high velocity, and low density (Figs. 52 and 53), a physical property association that appears to indicate winnowing. Increased currents remove the fine components (which may preferentially remove nannofossils and could reduce the measured carbonate content, depending

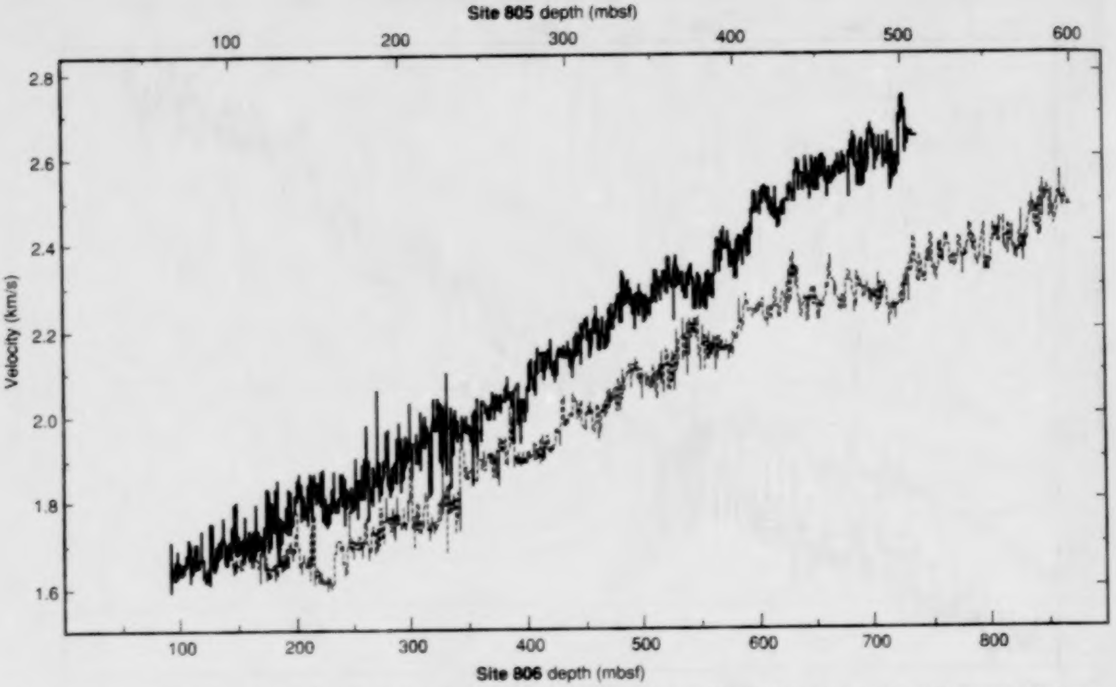

Figure 46. Comparison of velocity profiles, Holes 805C (dashed line) and 806B (solid line). The offset in the data at 220 mbsf in the Hole 805C profile is an artifact of the logging data (see "Seismic Stratigraphy" section, "Site 805" chapter, this volume).

on the composition of the noncarbonate components), resulting in a coarse-grained system that does not pack well (thus, the low density) and yet has a high velocity (because of the large grain size). The third reflector of this group (6-3, ca. 3.8–3.9 Ma) has the same set of physical property relationships except that it is associated with a high carbonate content, which may indicate that it is the result of increased productivity rather than winnowing.

Within the "Tethys Series," six reflectors (6-4 through 6-9) have been picked. The youngest of these (6-4, ca. 5.1 Ma) shows the physical property association that we suggest represents winnowing (high in grain size and velocity with a low in carbonate content and density; Figs. 52 and 53). The next deepest reflector (6-5, ca. 5.8–6 Ma) is the only one associated with a marked low in grain size (and thus velocity); density and carbonate content vary only slightly (Figs. 52 and 53). This interval may represent a period of particularly quiescent current activity. At about the same depth (200 mbsf), there is a marked change in the shape of the velocity vs. depth curve with a sharp increase in velocity (Fig. 52). The rapid increase in velocity with depth is probably indicative of the onset of cementation (induration is first reported by the sedimentologists at about 200 mbsf, see "Lithostratigraphy" section, this chapter).

At about the same level, we also see a change in the slope of the density curve with density increasing at a slower rate below 200 mbsf (Fig. 52). This change in the shape of the density curve may also be indicative of a change from a compaction-dominated system (above 200 mbsf) to one where grain-to-grain contacts and induration begin to support the sediment column, or it may simply be a reflection of the increase in carbonate content with depth (Fig. 53).

Deeper than 200 mbsf, the state of induration begins to play an important role in reflector formation. Reflector 6-6 (265 mbsf, ca. 7.2 Ma) still shows some indication of a grain-size influence (large grain size and high velocity), but at this depth there is also a peak in density, perhaps the result of enhanced cementation. Deeper than 250 mbsf, induration variations become the dominant mechanism for reflector formation. Reflector 6-7 (280 mbsf, ca. 7.5–7.6 Ma) is associated with rapid, in-phase, alternations between high and low velocity, density, and carbonate content. These variations in induration (as shown by the rapid, large-amplitude changes in velocity and density) apparently are a response to fluctuations in carbonate content (and thus more fundamental oceanographic factors such as dissolution and productivity). Reflector 6-8 (320 mbsf, ca. 8.2–8.4 Ma), with its low velocity and density, probably represents the unindurated end member of this system.

All of the deeper reflectors (6-9 through 6-13), which include representatives of the "Antarctic," "Drake," and "Texas" series, are characterized by synchronous, large-amplitude fluctuations in velocity, density, and carbonate content that appear to represent the diagenetic enhancement of an original carbonate signal. Interestingly, the "Texas Interval," which has been characterized by few large-amplitude reflectors at previous sites, shows a number of large-amplitude events here. It is possible that this is a result of the increased thickness of the section here and thus the increased potential for diagenetic enhancement of the original sediment variability.

The logging record at Site 806 ends at approximately 740 mbsf. We can, however, use the results of Site 803 to estimate that the Eocene/Oligocene boundary is at about 120 m below Reflector 6-13, at approximately 0.88 s below seafloor (sbsf).

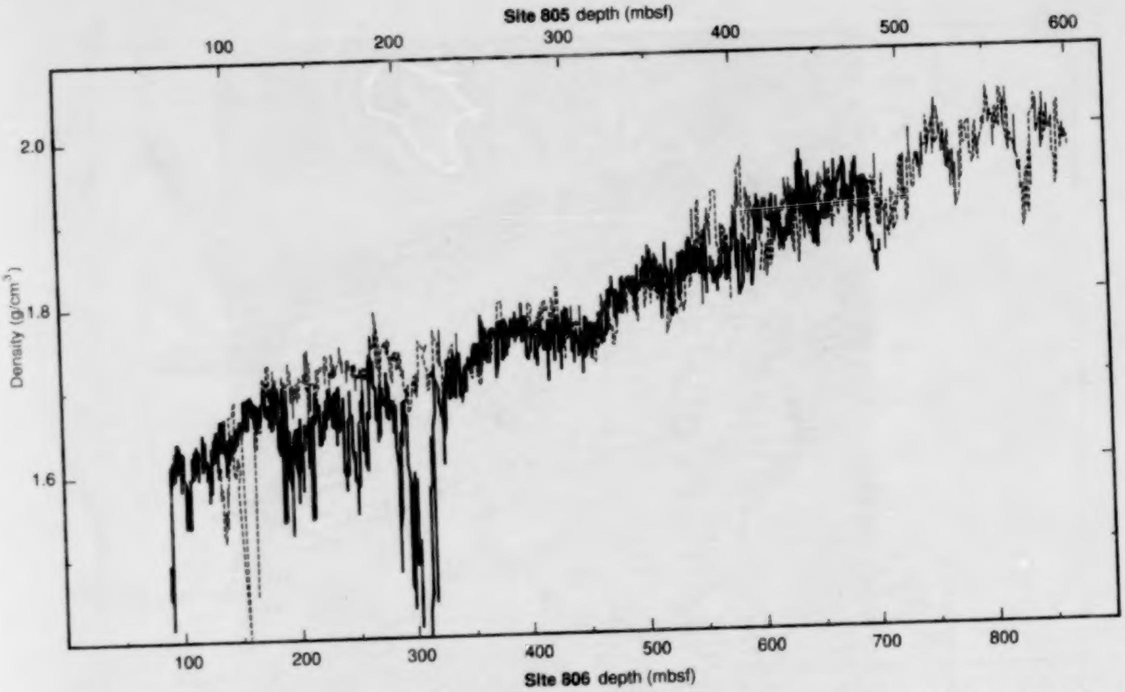

Figure 47. Comparison of wet-bulk density profiles, Holes 805C (dashed line) and 806B (solid line). The overall shape of the two records is similar.

Basement should then be at 1.03 sbsf or approximately 1000 mbsf.

SUMMARY AND CONCLUSIONS

Site 806 is located on the northeastern margin of the Ontong Java Plateau, close to the equator (latitude 0°19.1′N, longitude 159°21.7′E) in 2520 m of water. The site represents the shallow end member on a transect that was designed to detect depth-related paleoceanographic signals in Neogene sediments. The objective in drilling at this location was to obtain a continuous record in an undisturbed setting, with maximum sedimentation rates, that could serve as a standard section against which all others could be measured. The setting was considered ideal for high-resolution studies of ocean history, including biostratigraphy, chemostratigraphy, and acoustic stratigraphy. This expectation proved well founded.

Positioning was based on a SCS line acquired by the *Thomas Washington* during ROUNDABOUT Cruise 11 (0600 UTC, December 21 1989). The site is located at the proposed location (OJP-1) on a 2-km-wide terrace interrupting a gentle incline sloping to the northeast. The sedimentary sequence apparently is complete and undisturbed, with the seismic profile showing a full set of reflectors that are readily correlatable with those at Sites 289/586.

Coring Results

We spent 7.5 days at this site, drilling three holes and coring 1414 m of sediment, of which 1276 m were recovered. Hole 806A, a dedicated hole, was cored with the APC to 83.7 mbsf into upper Pliocene sediments, with 103% recovery. Hole 806B was cored with the APC to 320.0 mbsf, where refusal occurred, within the lower upper Miocene; recovery was 105%. The hole was continued with XCB coring to 743.1 mbsf, with 423.1 m of sediment cored and 331.2 m recovered (78% recovery). Coring was terminated within lowermost Miocene sediments when the objective (recovery of the Neogene section) was judged to have been reached. The hole was then logged, with the pipe pulled to 92 mbsf.

Hole 806C was cored with the APC to 309.6 mbsf (104% recovery), at which point coring with the XCB was initiated. Cores were taken from 309.6 to 541.7 mbsf; from that point, we drilled ahead with a center bit to 599.0 mbsf, where a spot core was taken to obtain sediments from an interval with poor recovery in Hole 806B. A full core was obtained. Drilling was then continued with a center bit to 740 mbsf, at which point four cores were taken (740.0–776.4 mbsf), spanning the Oligocene/Miocene boundary. The XCB-coring operation drilled 278 m and recovered 203 m of sediment (73% recovery) at this hole.

The sediment retrieved is Neogene in age, except for the three deepest cores in Hole 806C, which recovered Oligocene chalk (Cores 130-806C-60X to -62X). The entire column, from the oldest deposits to the seafloor, is considered as one lithologic unit and was classified as foraminifer nannofossil ooze and chalk to nannofossil ooze and chalk with foraminifers. No stratigraphic breaks were detected; apparently depositional history was continuous between the upper Oligocene (ca. 27 Ma) and the present. The average sedimentation rate over the entire Neogene may be estimated as 32 m/m.y, the highest of any site drilled on Leg 130. Depending on assumptions made about the age of biostratigraphic tie points, the range of fluctuation lies between 15 and 55 m/m.y., or between 20 and 45 m/m.y.

Two subunits were recognized in this rather uniform section of bioturbated ooze and chalk, on the basis of degree of consolidation. They are separated by the ooze-chalk transition, placed

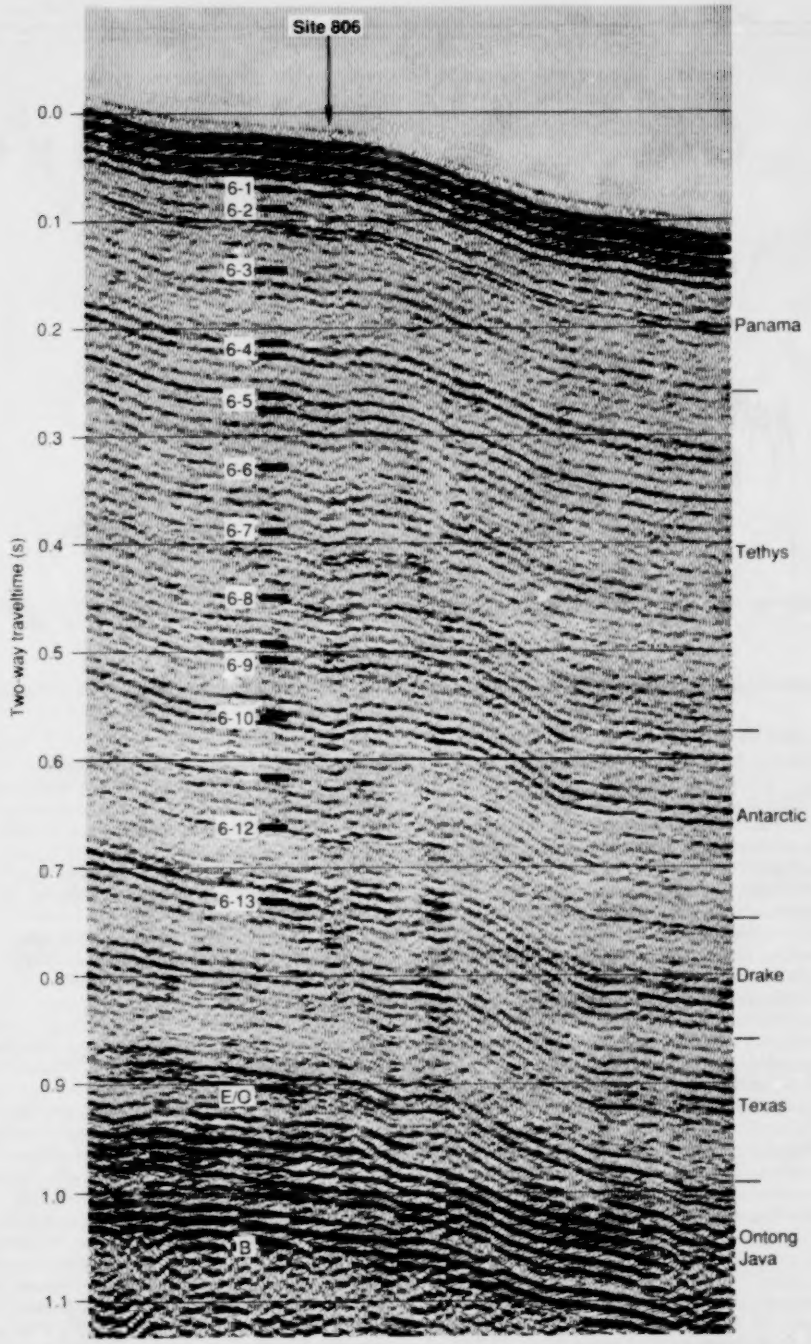

Figure 48. Seismic record collected on the ROUNDABOUT Cruise 11 site survey over Site 806, using the 80-in.^{3} water gun, 70–250 Hz band-pass filter. For details of reflector picks, see Table 12. E/O = Eocene/Oligocene boundary and B = basement.

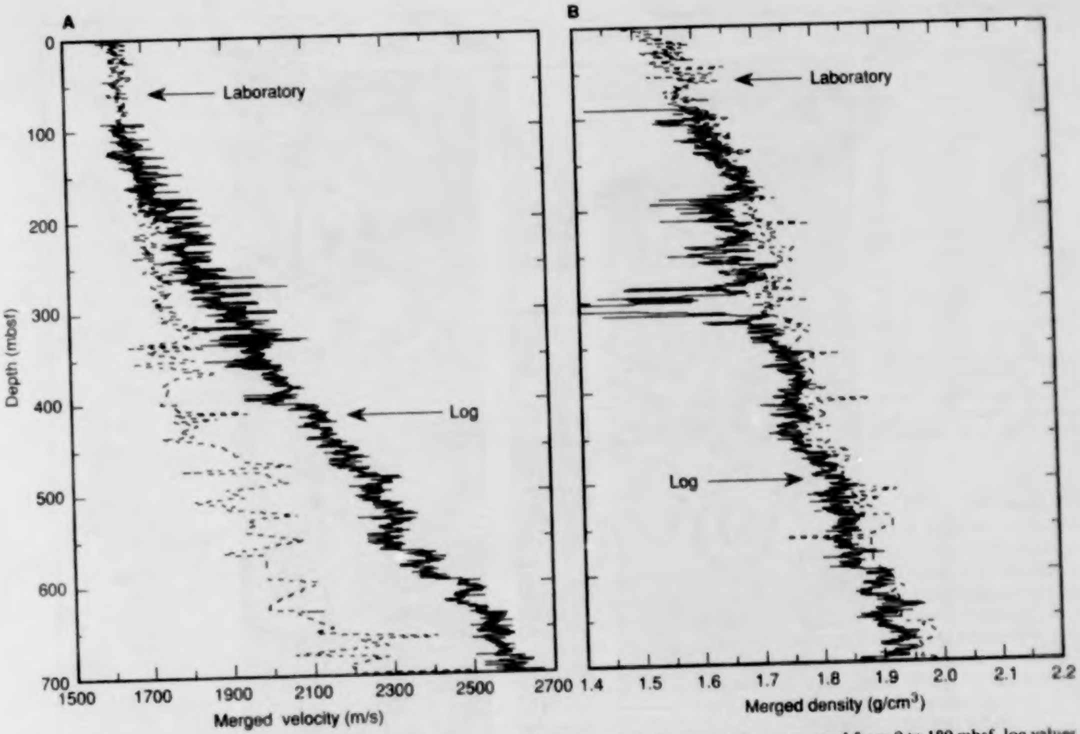

Figure 49. **A.** Merged laboratory (dashed line) and log velocity (solid line) profiles. Laboratory values were used from 0 to 180 mbsf, log values from 180 to 740 mbsf. **B.** Merged laboratory (dashed line) and log density (solid line) profile. Laboratory values were used from 0 to 360 mbsf, log values from 360 to 750 mbsf.

at 339.4 mbsf in Hole 806B (Core 130-806B-37X) and at 338.5 mbsf in Hole 806C (Core 130-806C-37X) (lowermost upper Miocene, ca. 10 Ma). The transition is gradational and shows alternating layers of varying degree of lithification, beginning at about 200 mbsf in both holes, looking downhole.

The younger section of the unit (Subunit IA, 0-339 mbsf) comprises Pleistocene to upper middle Miocene foraminifer nannofossil ooze to nannofossil ooze with foraminifers. Foraminifer content is significantly higher than at previous Leg 130 sites (Sites 803-805) and is estimated to be between 15 and 30%, on average. Radiolarian content is low throughout. Bioturbation is common throughout; it appears to be more strongly expressed than at the previous sites (803-805). Liesegang banding is common throughout the subunit, although it appears to be fainter and more diffuse in appearance than at Sites 803-805. The best examples are near the bottom of the subunit. Authigenic pyrite was found, associated with burrows, and a slight odor of H_2S was noted on occasion, upon opening the cores. Microfaulting is rare. Sediments are generally soft, but in the lowermost portion of Subunit IA more lithified intervals appear (below 200 mbsf). Coring was impeded in one instance because of porcellanite nodules (310 mbsf, ca. 8.2 Ma, Core 130-806C-34X) near the level of APC refusal. The shallowest porcellanite nodules were found at 240 mbsf (ca. 6.7 Ma). A marked change in the velocity-depth gradient (associated with a brief reversal) occurs just above this depth level (at 220 mbsf). At the ooze-chalk transition (339 mbsf), the character of the velocity profile changes: above this level, high-frequency variations are pronounced; below it, they are indistinct.

The older section of the unit, Subunit IB (339-776 mbsf), consists of 437 m of foraminifer nannofossil chalk to nannofossil chalk with foraminifers, with a few intervals of nannofossil chalk, ranging from the lower upper Miocene to the upper Oligocene. Foraminifer content is high down to about 600 mbsf (ca. 20 Ma) and decreases below that level. Radiolarian content is low throughout. The color is predominantly white. Color banding occurs throughout; bands become thinner and more distinct with depth in the subunit. Small-scale flaser bedding is present. Bioturbation is ubiquitous. Rare, centimeter-size porcellanite nodules were observed at several levels (350 and 510 mbsf). The depth gradient of dissolved silica is reduced at 350 mbsf and between 450 and 550 mbsf, possibly in response to precipitation.

The sediments in the chalk section posed no problem for XCB-coring down to the Oligocene/Miocene boundary zone, at which point recovery decreased. However, even where recovery is very good, the chalk is broken up and brecciated by drilling, with evidence for grinding of chalk on chalk. This type of recovery is typical for the material below 320 mbsf, that is, the section cored with the XCB. The Oligocene/Miocene boundary is located between 740 and 750 mbsf and apparently is without hiatus (although recovery is poor at this level). Sedimentation rates for the deep chalk section vary between 20 and 30 m/m.y., the same as for the upper portion of the chalk subunit.

Special Studies

An attempt was made to construct magnetostratigraphies for the uppermost section of Holes 806B and 806C. Although the

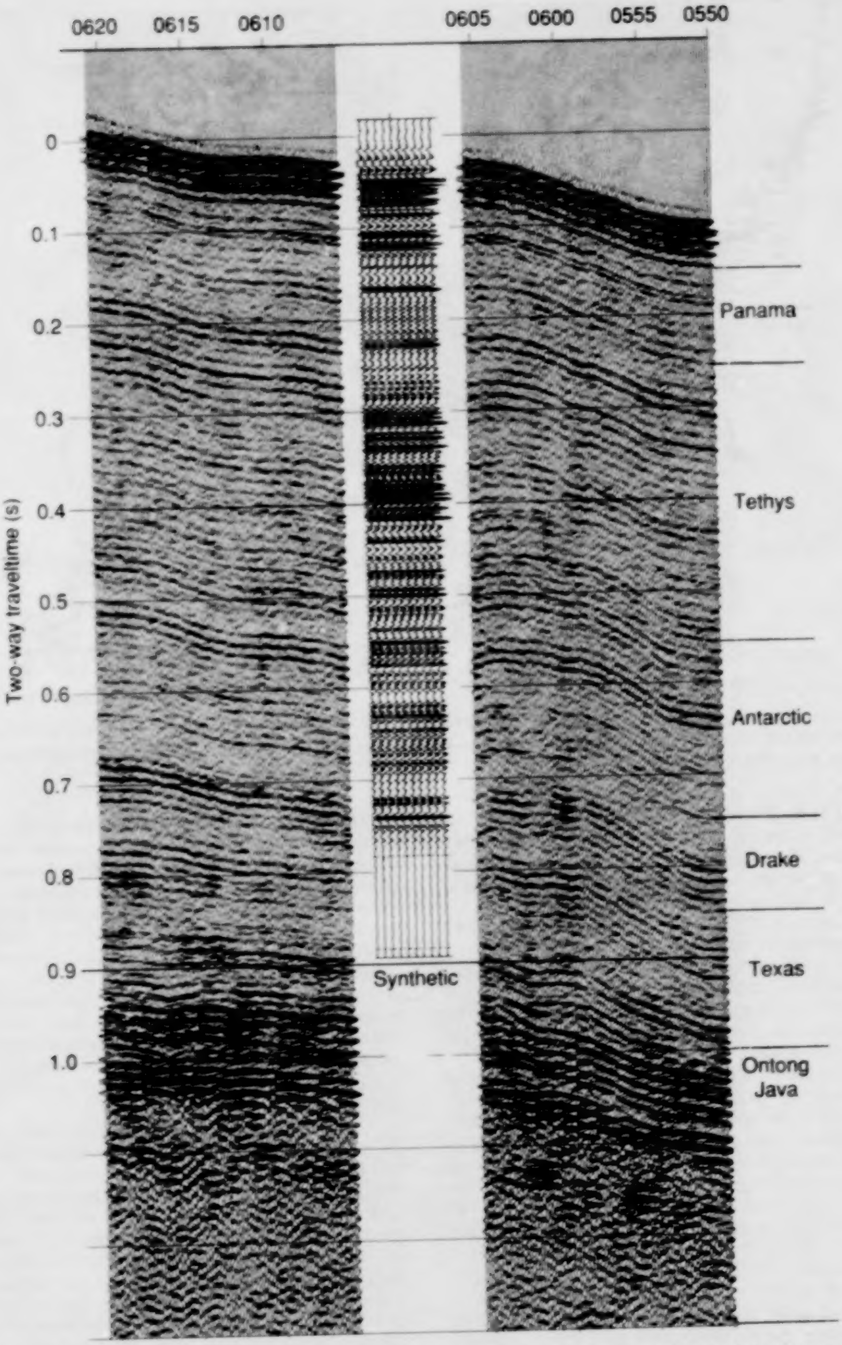

Figure 50. Comparison of synthetic seismogram and field record at Site 806. Names to the right of the diagram refer to groups of reflectors or zones with reflector groups. See Site 805 "Summary and Conclusions" section for significance of names.

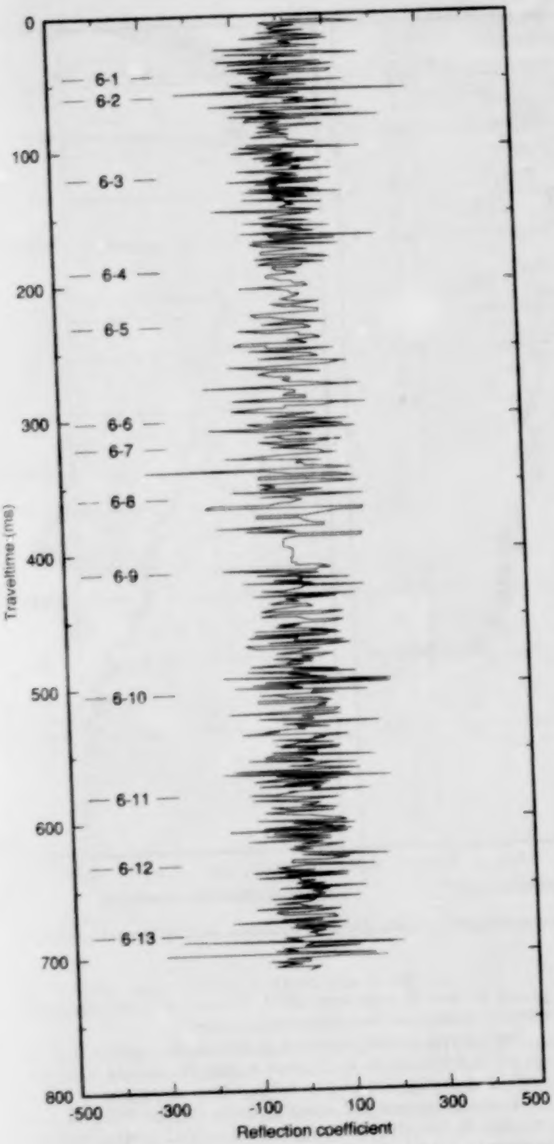

Figure 51. Reflection coefficient vs. traveltime, Site 806. For details of reflector picks, see Table 12.

Brunhes/Matuyama boundary could not be identified, magnetic susceptibility seems to be measurable well into the Pliocene, opening the possibility for the study of Milankovitch-type cycles using magnetic properties.

Chemical gradients in interstitial waters at this site are generally similar to those at Sites 803–805, reflecting the calcareous/siliceous nature of the sediments and the paucity of organic material. A somewhat higher supply of organic matter at this site, presumably because of the shallower depth, tends to produce slightly stronger gradients. Sulfate concentrations, especially, show this influence of organic supply. Concentrations decrease by almost 50% over the length of Hole 806C, with most of the decrease occurring by 222 mbsf. Alkalinity increases correspondingly in the upper section but decreases below 250 mbsf, presumably in response to precipitation of carbonate. Calcium and magnesium gradients are influenced by basalt alteration reactions at depth and show the usual negative correlation. Strontium concentrations reflect recrystallization processes, which apparently are more vigorous here than at the previous sites because of the higher sedimentation rates. Dissolved silica shows a steady increase with depth, except for a minor reversal of this trend near the ooze/chalk transition (350–360 mbsf).

Table 12. Summary of traveltimes, depth, and ages for Site 806 reflectors.

	Traveltime		Depth		
Reflector	Seismic (s)	Synthetic (s)	Seismic (m)	Synthetic (m)	Age (Ma)
6-1	0.050	0.055	41	45	1.9–2.0
6-2	0.068	0.070	56	57	2.4
6-3	0.129	0.131	106	108	3.8
6-4	0.200	0.200	167	167	5.1
6-5	0.235–0.24	0.24–0.024	196	213	5.7–[illegible]
6-6	0.310	0.312	264	265	7.2
6-7	0.326	0.332	278	284	7.5–7.6
6-8	0.360	0.370	311	321	8.2–8.4
6-9	0.425	0.425	375	375	10.8
6-10	0.514	0.515	469	470	13.3
6-11	0.591	0.590	556	555	17.6
6-12	0.635	0.641	610	617	20.3–20.5
6-13	0.690	0.694	678	685	22.8–22.9

Notes: Depths and traveltimes to seismic events are picked on both the synthetic seismograph (synthetic) and the field record (seismic). Ages are from sedimentation rate curves (see "Sedimentation Rates" section, this chapter).

Excellent logs were obtained for sound velocity and density at Site 806. The fact that this site has continuous sedimentation makes these logs especially valuable. Laboratory velocities and bulk densities provide control for the upper portion of the record, which could not be logged. Bulk density and sound velocity increase with depth more or less as expected. Bulk density values are near 1.6 g/cm^3 at 100 mbsf and increase to 1.9 g/cm^3 by 700 mbsf. If expressed as average density increase per age interval (0.15 g/cm^3 per 10 Ma) the overall gradient is exactly identical to that in Site 586. It is noticeably higher than that in Site 805, which has a distinctly lower sedimentation rate. Thus, both depth of burial and age govern this parameter. Sound velocity is 1.65 km/s at 100 mbsf and increases by 0.13 km/s per 100 m down to 250 mbsf, where the gradient changes to 0.18 km/s. The stronger gradient, presumably, shows the effects of carbonate precipitation below 250 mbsf, as seen in the interstitial water measurements.

Seismic Stratigraphy

Site 806 is characterized by the highest sedimentation rate of any of the Leg 130 sites. A complete section, without hiatuses, is also present, as is true for Site 805. This site, therefore, is of great interest with respect to a central objective of the leg: to determine the nature of the acoustic reflectors seen on seismic profiles.

The reflector groups identified at Site 805 can also be recognized at Site 806, in the SCS profiles taken by the *Thomas Washington* during the ROUNDABOUT pre-site survey (Fig. 54). In addition, there are others, not seen in the Site 805 profiles. Dating shows that at least some reflectors are associated with paleoceanographic events, as suggested by Mayer et al. (1986) for the central equatorial Pacific. They proposed the

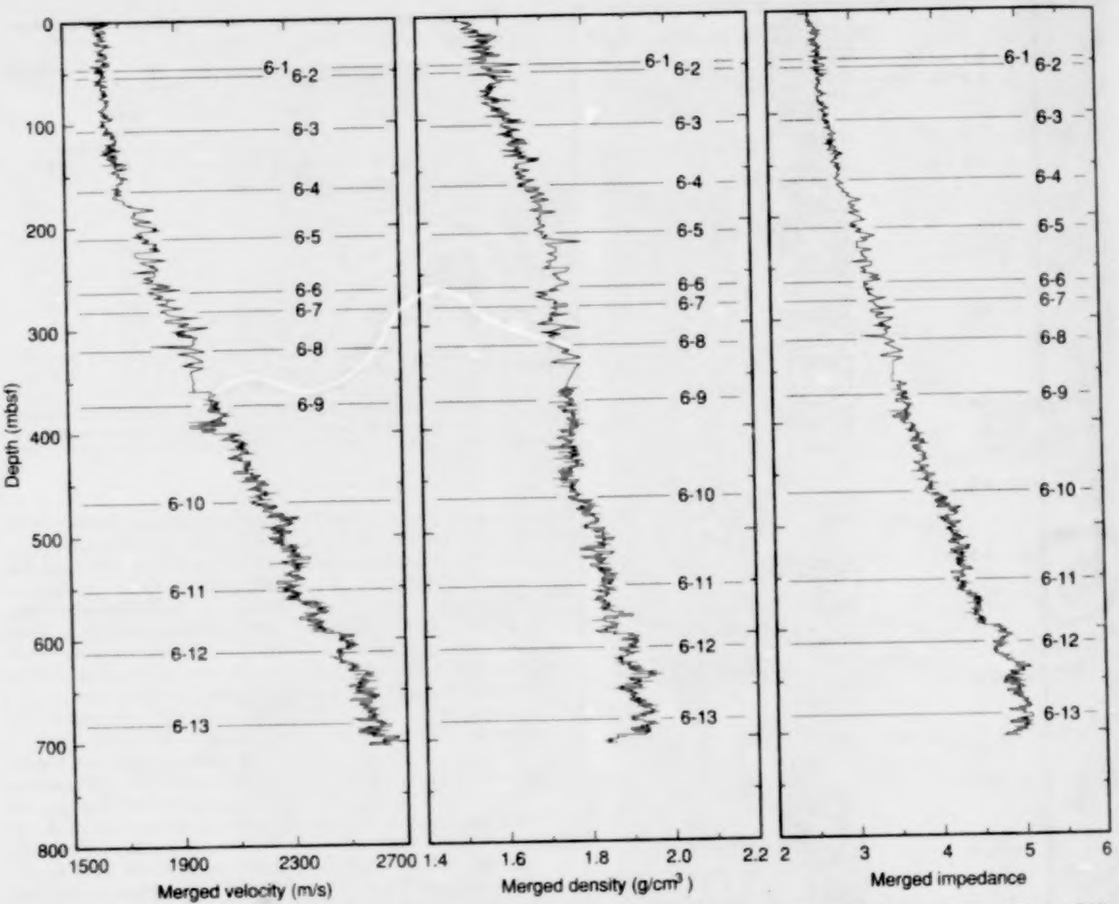

Figure 52. Merged velocity, density, and acoustic impedance used to generate synthetic seismogram, Site 806. For details of reflector picks, see Table 12.

closing of the Panama Isthmus, reorganization of deep circulation in the Atlantic, climatic events surrounding the Antarctic, and the opening of the Drake Passage as important paleoceanographic themes reflected in the acoustic properties of Pacific pelagic sediments. The names for three reflector groups were chosen for these propositions (without necessarily implying endorsement). The advantage of considering groups of reflectors in addition to single members is obvious: it is then the variability of sediment properties within a given section that is being addressed, rather than an individual excursion of velocity and/or density. For explanation of the names "Tethys Interval" and "Texas Interval," see the "Summary and Conclusions" section of the Site 805 chapter (this volume).

The match of reflectors shown in Figure 54 is readily obtained by assuming that the traveltime to equivalent reflectors in Site 806 is 1.37 times that in Site 805. The success of the match allows dating by correlation and also allows the statement that sedimentation rates between these two sites are likely to differ by a certain factor for the entire Neogene and Oligocene. This result is quite surprising, considering that the effects of dissolution are thought to be responsible for the difference in overall sedimentation rate, and that dissolution intensity might be expected to have a long-term trend, producing a corresponding trend in differences in sedimentation rates.

The general match proposed in Figure 54 predicts that the age of 22.0 Ma found at .50 sbsf at Site 805 should appear at 0.685 sbsf at Site 806 (0.5 · 1.37), which corresponds to 676 mbsf, using a generalized velocity profile for Site 806 (based on logging). In fact, the biostratigraphic age of 22.0 Ma in Site 806 appears at 665 mbsf (with an uncertainty of 5 m). At 676 mbsf (the guess), the age is 22.3 Ma according to shipboard biostratigraphy. The result of this exercise suggests that the matching of reflectors on the Ontong Java Plateau produces correlations that are comparable in quality with those from biostratigraphic control. To check this proposition, additional matches were picked as follows (each comparison shows Site 805 first, then Site 806):

1. 0.044 sbsf, 35 mbsf, 1.95 Ma; 0.061 sbsf, 48 mbsf, 2.05 Ma;
2. 0.128 sbsf, 103 mbsf, 4.44 Ma; 0.170 sbsf, 139 mbsf, 4.49 Ma;
3. 0.258 sbsf, 216 mbsf, 7.17 Ma; 0.332 sbsf, 285 mbsf, 7.64 Ma; and

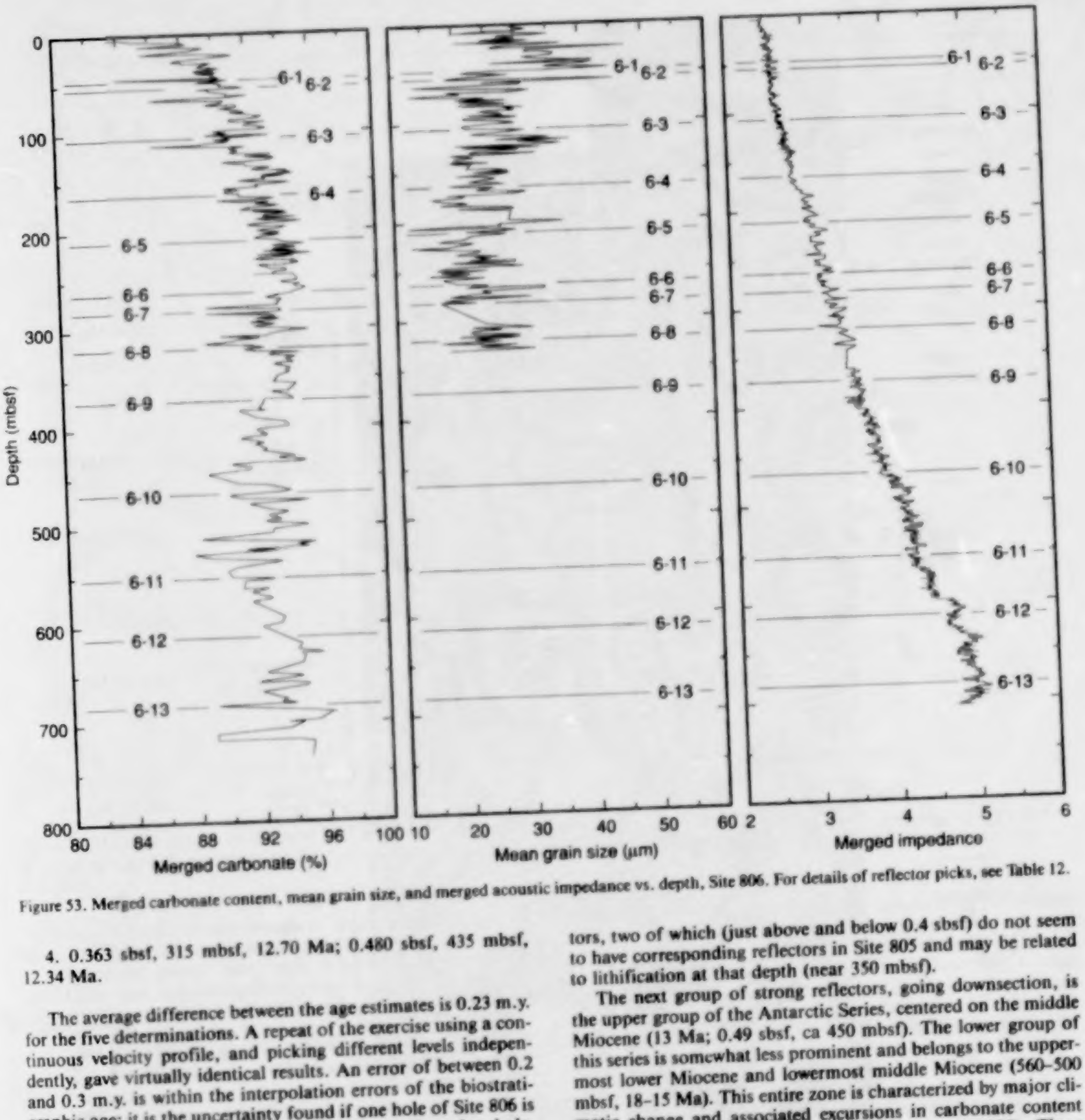

Figure 53. Merged carbonate content, mean grain size, and merged acoustic impedance vs. depth, Site 806. For details of reflector picks, see Table 12.

4. 0.363 sbsf, 315 mbsf, 12.70 Ma; 0.480 sbsf, 435 mbsf, 12.34 Ma.

The average difference between the age estimates is 0.23 m.y. for the five determinations. A repeat of the exercise using a continuous velocity profile, and picking different levels independently, gave virtually identical results. An error of between 0.2 and 0.3 m.y. is within the interpolation errors of the biostratigraphic age; it is the uncertainty found if one hole of Site 806 is used to predict the age at the same depth in the other hole. Thus, as far as we can tell, the correlative reflectors of Sites 805 and 806 are identical in age. The demonstration of this synchroneity is an important result; it is greatly simplified by the fact that near-equivalent levels in the two sites are readily found because of the similarity of sedimentation rate patterns (Fig. 55).

The Panama Series (Fig. 54) contains reflectors that we dated near 2, 2.4, and 3.7 Ma. The age of 2.4 Ma corresponds to a deep-water cooling event and the onset of North Atlantic ice buildup (Backman, 1979; Shackleton et al., 1984). The reflectors dated at 2.4 and 3.7 Ma can be identified in the seismic record from DSDP Site 586 using the velocity profile provided by the logging of DSDP Site 586 (Shipboard Scientific Party, 1986a). The Tethys Interval contains a number of lesser reflectors, two of which (just above and below 0.4 sbsf) do not seem to have corresponding reflectors in Site 805 and may be related to lithification at that depth (near 350 mbsf).

The next group of strong reflectors, going downsection, is the upper group of the Antarctic Series, centered on the middle Miocene (13 Ma; 0.49 sbsf, ca 450 mbsf). The lower group of this series is somewhat less prominent and belongs to the uppermost lower Miocene and lowermost middle Miocene (560–500 mbsf, 18–15 Ma). This entire zone is characterized by major climatic change and associated excursions in carbonate content and other sediment properties (Barron et al., 1985). These changes, presumably, are associated with the onset of Antarctic Bottom Water production at that time. The group of reflectors immediately below the Antarctic Series, the Drake Series, has the strongest reflector members. Dates range from about 22.5 Ma for the deepest of the group (680 mbsf) to 18.5 for the uppermost (570 mbsf).

Below this group there is a thick section, the Texas Interval (250–270 m thick), which shows another series of reflectors, almost as strong as the Drake Series. At Site 805 these reflectors are much less pronounced. The reason for the difference is not known; it may be related to the higher diagenetic potential in Site 806, which could be stemming from better preservation of

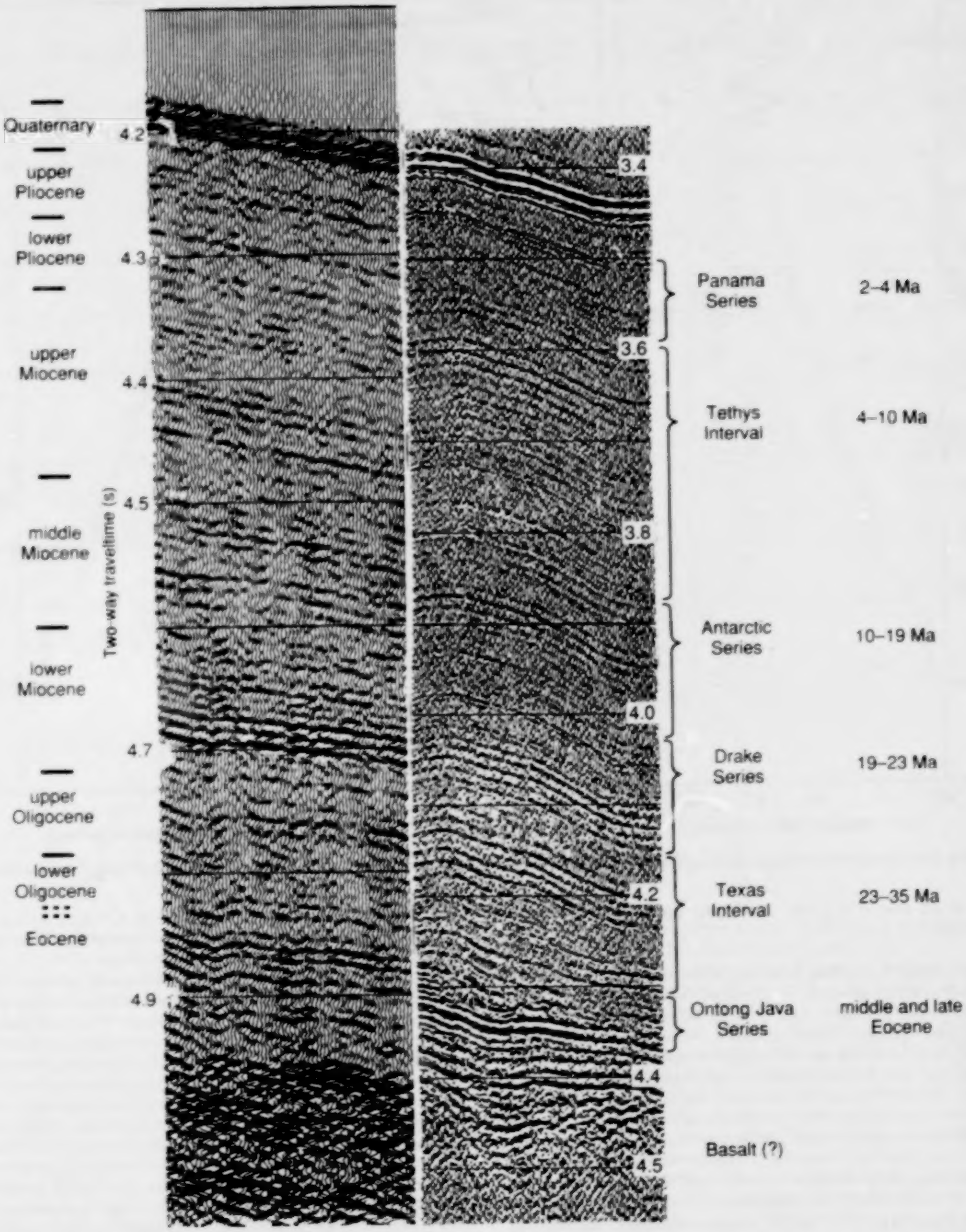

Figure 54. Comparison of seismic profiles at Sites 805 and 806. Profiles taken by the *Thomas Washington* on ROUNDABOUT Cruise 11 (see "Seismic Stratigraphy" section, this chapter), with time scale assigned from drilling and logging results as well as biostratigraphic studies (see "Biostratigraphy" section, this chapter). Names to the right refer to groups of reflectors ("series") and zones with less distinct groups ("intervals"). See the "Summary and Conclusions" section of the Site 805 chapter (this volume) for the significance of names. The record of Site 806 is to the right; its traveltime scale was reduced by a factor of 0.73 to match reflectors as best as possible without individual adjustments.

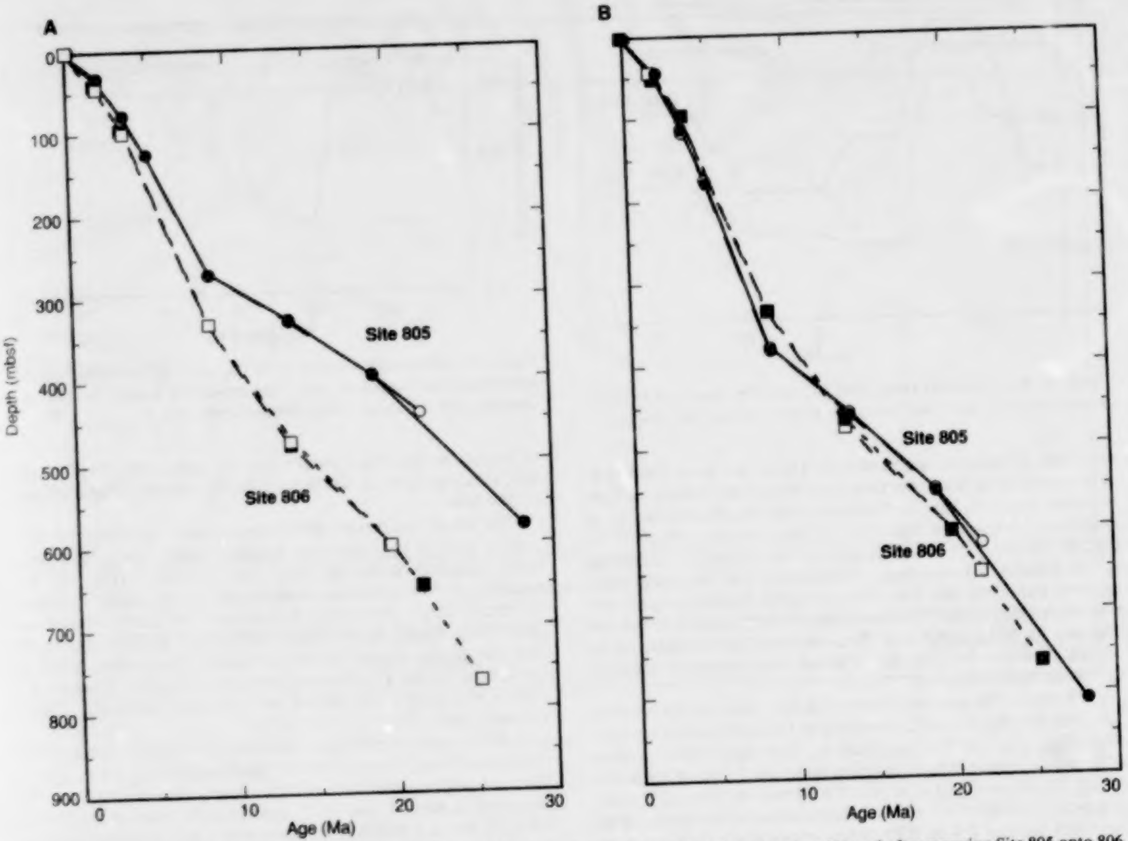

Figure 55. Age-depth plots, Sites 805 (solid line) and 806 (dashed line), as given by biostratigraphic tie points (**A**) and after mapping Site 805 onto 806 by multiplying depth by a factor of 1.4 (**B**). Solid squares = Hole 806B, open squares = Hole 806C, solid circles = Hole 805C, and open circles = Hole 805B.

carbonate or from a greater supply of organic matter, or both. Below this interval is the Ontong Java Series, which is thought to represent the change from chalk to limestone in the lowermost Oligocene, and—somewhat deeper in the section—the occurrence of chert. As at Site 805, acoustic basement lies a short distance below this sequence.

In summary, there is good correlation between Sites 805 and 806, and good agreement in biostratigraphic dates for equivalent reflectors or reflector groups, regardless of the overall difference in sedimentation rates. This observation provides strong support for the hypothesis that many reflectors represent the effects of paleoceanographic events felt over a wide depth range and, hence, are of global significance. Other reflectors may be regionally strong expressions of minor events or may be related to diagenetic processes that are not synchronous.

Sedimentation Rates

The oldest sediments cored, at 776 mbsf in Hole 806C, were of latest Oligocene age (Zones NP25 and P22). The distance to acoustic basement below this level (0.75 sbsf) may be estimated as approximately 0.23 s two-way traveltime, which corresponds to roughly 340 m of sediment at that depth. Assuming that the uncored section represents at least 80 Ma of time, the presence of condensed intervals or hiatuses, or both, would seem to be indicated for the early Paleocene and Upper Cretaceous.

Since late Oligocene time, Site 806 has received nannofossil ooze with, on the whole, rather minor admixtures of siliceous fossils. Sedimentation rates typically varied between 20 (lower Miocene) and 46 m/m.y. (upper Miocene), the overall average being near 30 m/m.y. (Fig. 56). These numbers are somewhat misleading, inasmuch they are not corrected for mass flux, and contain the trend of decreasing porosity with depth. If one corrects for this trend, one will find that the mass flux in the late Oligocene is of the same magnitude as in the late Neogene. Spikes in sedimentation rate may be present between 8 and 6 Ma (uppermost Miocene), and between 14 and 13 Ma (middle Miocene) (see "Sedimentation Rates" section, Figs. 22 through 26) but cannot be fully substantiated at this time because of uncertainties in absolute ages for biostratigraphic tie-points. The two intervals in question are characterized by maximum carbonate values. There seem to be no condensed sections at Site 806 (whereas thinning was observed at Site 805 for the upper lower Miocene).

Comparisons Between Sites 805 and 806

Carbonate Stratigraphy

Of the sites drilled during Leg 130, Sites 805 and 806 are the most similar with respect to reflector patterns (Fig. 54) and sedimentation rate patterns (Figs. 55 and 56). The lithologies of the

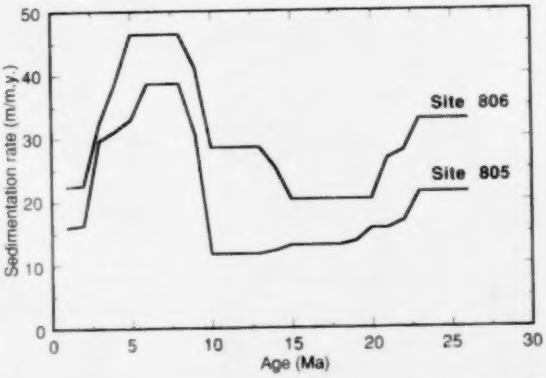

Figure 56. Sedimentation rates, Sites 805 and 806, based on biostratigraphic tie-points (see "Sedimentation Rates" section, this chapter).

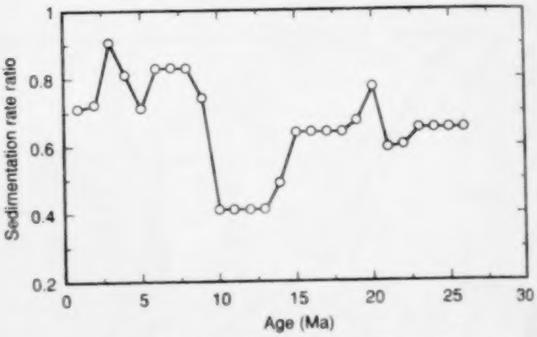

Figure 57. Sedimentation rate ratio between Sites 805 and 806, based on biostratigraphic tie-points (see "Sedimentation Rates" section, this chapter). The circles are 1-m.y. interpolation steps.

two sites, in essence, are identical. These two sites, therefore, offer a unique opportunity to study one central objective of the Neogene program, that is, the depth effect on the deposition of carbonate. A question that arises in this context is to what extent are fluctuations in sedimentation rate caused by variations in the intensity of carbonate dissolution. The following brief analysis addresses this question, using the biostratigraphic tie-points provided in the "Sedimentation Rate" sections of the site chapters for 805 and 806 and the carbonate data available on 15 March 1990 and listed in the "Carbon Geochemistry" sections of the same site chapters.

The overall Neogene sedimentation rate ratio (SRR) between Sites 806 and 805 is ~ 1.4, according to biostratigraphic correlation (Fig. 55). The inverse—that is, SRR (805/806)—is then 0.71, which means that on average there are 7.1 m of sediment at Site 805 for every 10 m at Site 806. Based on biostratigraphy, it appears that there are marked fluctuations in this ratio, ranging from around 0.4 to 0.85, when considering time spans of several million years (Fig. 57). There is a general resemblance of the (bio-)SRR curve to the sedimentation rate curves of both sites (cf. Figs. 56 and 57). This indicates that the depth factor reducing sedimentation at Site 805 (presumably carbonate dissolution) tends to be less important during intervals when sedimentation rates are high. If this proves to be true, one would conclude that dissolution gradient and supply rate are negatively correlated. This is opposite actual expectations (van Andel et al., 1975; Berger, 1979).

Carbonate dissolution, presumably, is largely responsible for the average SRR of 0.71, that is, the reduction of sedimentation at Site 805 with respect to that at Site 806. To explore further the importance of this factor as a source of variability in sedimentation pattern, we next turn to the carbonate record. By multiplying depths between 0 and 200 mbsf in Site 805 by 1.35, a tolerably good match between the two carbonate records is obtained for this interval (Fig. 58). Likewise, multiplying depths between 200 and 400 mbsf in Site 805 by 1.28 matches the carbonate records closely enough for the purpose of the discussion that follows (Fig. 58).

The carbonate content at Site 806 typically fluctuates between 90% and 95% throughout the section except in the Pleistocene portion, where it drops to values as low as 86% (Fig. 58). Values below 90% also are seen in the lower upper Miocene (280–320 mbsf, 7.5–8.5 Ma) (Fig. 58), and again in the lower middle Miocene (490–550 mbsf, 14–16.5 Ma). The pattern in Site 805 is quite similar, percentage values being commonly 1%%-2% lower and amplitudes slightly greater. Strong lows in carbonate at Site 806 typically line up with strong lows at Site 805, although lows at Site 805 do not necessarily have a partner in Site 806.

The major carbonate minimum periods are initiated by a sudden drop in the carbonate content, which can be extremely steep, especially at Site 805 (e.g., near 170 mbsf) (Fig. 58). Termination of low carbonate acme events can be equally sudden. In detail, large carbonate fluctuations are superimposed on these steep ramps, accentuating differences in physical properties (the figure shows 7-point averages). Ten sudden drops in carbonate values ("carbonate reduction events" [CREs]) are readily recognized (numbered with Roman numerals, CRE-I through CRE-X).

CRE-I, near 10 mbsf (ca. 0.5 Ma), presumably initiates the "Brunhes Dissolution Cycle" of Adelseck (1977). CRE-II (1–2 Ma; not well matched on the figure) apparently leads into the Dissolution Acme Event M17, described by Saito et al. (1975). CRE-III (ca. 2.4 Ma) is correlative with a major glacial buildup event in the North Atlantic (Backman 1979; Shackleton et al., 1984), and is seen as a strong reflector in the Panama Interval. CRE-IV (ca. 3.2 Ma) is correlative to a period of cooling and increase in North Atlantic Deep Water production. The event presumably leads into the GU3 minimum in the carbonate stratigraphy of Saito et al. (1975). It marks the time of the closure of the Panama Straits (Keigwin, 1978).

The next three major CREs each mark a descent into a different substantial minimum carbonate period. CRE-V (ca. 4.0 Ma) apparently coincides with a major warming and transgression (Ingle, 1973; Whitman, 1989). The deepest of the Panama Series reflectors, near 3.7 Ma, may mark recovery from this event. CRE-VI (ca. 4.4 Ma) apparently is associated with that same warming, representing an earlier step. CRE-VII (ca. 5.2 Ma) leads into a major dissolution acme, labeled "X" in Saito et al. (1975). This event is associated with a strong reflector, identified at 0.17 mbsf in Site 586 (labeled 150 m/N17–N18/5–6 m.y.), by Shipboard Scientific Party (1986a). Our own data show a strong triple reflector at 0.20–0.22 sbsf (5.1–5.4 Ma) in the upper part of the Tethys Series. A moderate cooling is indicated in the oxygen isotope data for Site 586 at this level (Whitman, 1989) as well as a rapid increase in sand content, which peaks shortly thereafter (Whitman, 1989). Hiatus formation in the central Pacific is indicated for this period (NH7 of Keller and Barron, 1987).

The next deeper CRE (VIII) is not strongly expressed, possibly because of the very high initial carbonate values. It occurs near 245 mbsf (ca. 6.8 Ma). Site 806 does not show a strong reflector here, but Site 805 does (0.25 sbsf; 6.9 Ma). The event ap-

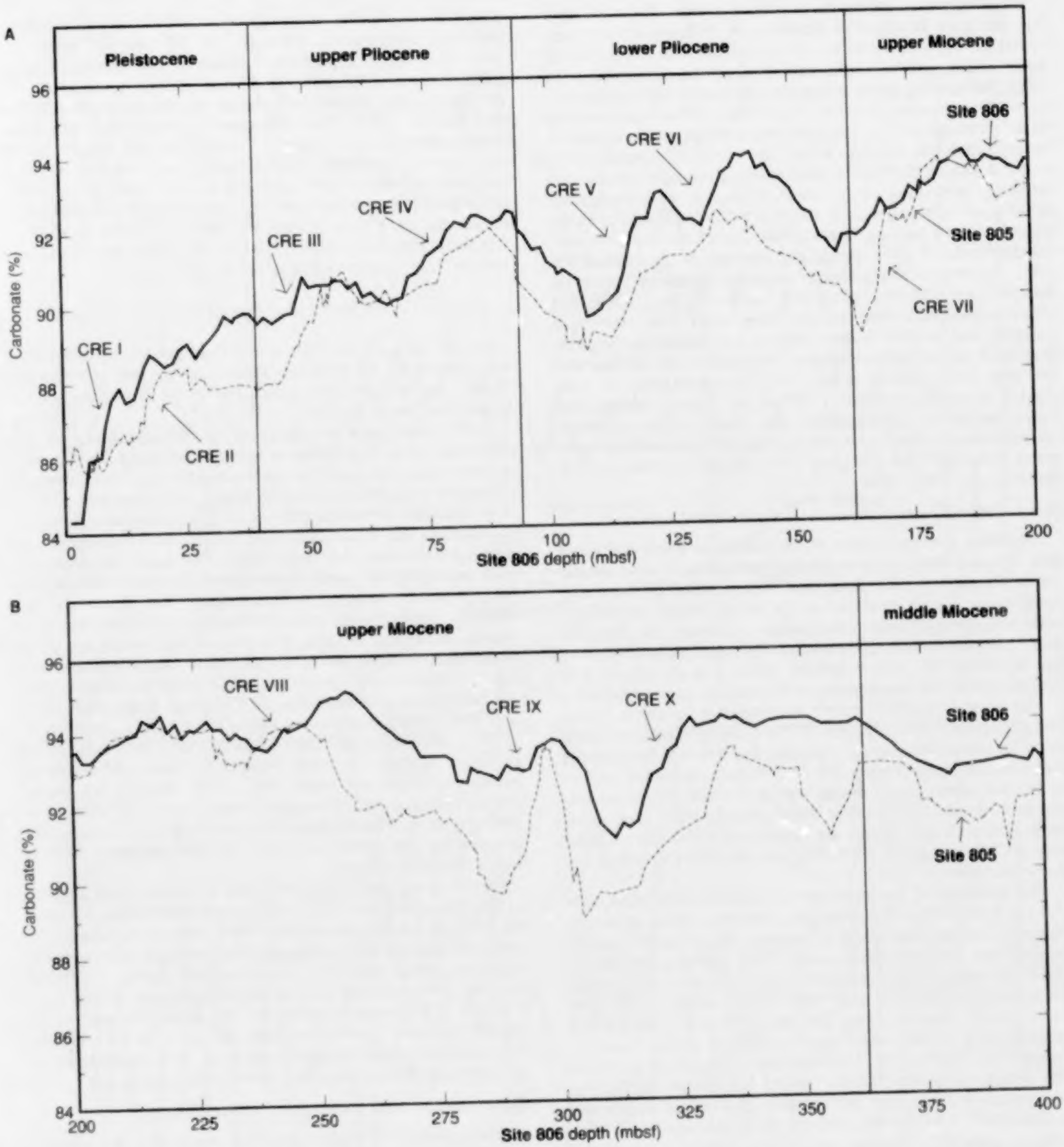

Figure 58. Comparison of the carbonate stratigraphies, Sites 805 and 806 (upper 400 mbsf). The carbonate reduction events are numbered from CRE-I in the upper Pleistocene to CRE-X at the beginning of the upper Miocene. The events are characterized by a sudden decrease in carbonate in one or both of the sites (see text). From 0 to 200 mbsf, the depth-in-hole values of Site 805 were multiplied by 1.35 for an approximate match; from 200 to 400 mbsf, the depth-in-hole values of Site 805 were multiplied by 1.28.

pears correlative with Hiatus NH6 of Keller and Barron (1987). CRE-IX and CRE-X are major events, occurring within the N16 Zone, notorious for poor preservation elsewhere in the Pacific. At Site 806 they are dated near 7.5 Ma and 8.5 Ma, respectively, suggesting a close association with Hiatus NH5 (Keller and Barron (1987). The extreme carbonate minimum in the eastern central Pacific labeled 10e (Barron et al., 1985) and Hiatus NH5 appear to be correlative. Thus, CRE-IX or CRE-X, or both, appear to be equivalent to 10e and NH5. A cooling step is reported for this interval at Site 289 (Savin et al., 1985). A moderately strong reflector is seen at Site 806 at the level of CRE-X (0.37 sbsf; Fig. 54), but only a weak one shows up in Site 805.

With regard to carbonate reduction events, then, we note that they have Pacific-wide significance, in lining up with carbonate lows in the central Pacific, as well as with Pacific hiatus events. Also, acoustic reflectors tend to be associated with CREs, presumably because they are responsible for creating surfaces of contrasting physical properties, within the sediment stack. As to causes, we note that several of the events appear to be associated with cooling, and at least one (CRE-V) with a pronounced warming. Cooling and warming changes the sites of carbonate deposition of the ocean, leading to a reorganization of sedimentation patterns. In principle, this could lead to either an increase or a decrease in carbonate deposition at a given site. On the flanks of the Ontong Java Plateau, in the tropical Pacific, a cooling event apparently produces sudden carbonate reduction (although the cooling trend, after 10 Ma, is associated with increased carbonate sedimentation rates). The response to warming seen at CRE-V may stem from a change in the partitioning of carbonate between shelf and deep-ocean (Berger and Winterer, 1974; Davies et al., 1977) environments, or from sharply reduced carbonate production. These findings lend strong support to the hypothesis that many acoustic reflectors on the Ontong Java Plateau are the result of paleoceanographic events (Schlanger and Douglas, 1974; Berger and Mayer, 1978; Mayer et al., 1985, 1986).

Curve Matching and Difference in Carbonate Content

The close correspondence of the carbonate stratigraphies of Sites 805 and 806 permits a detailed feature-for-feature matching on a scale somewhat finer than that provided by biostratigraphy alone. Figure 59 shows such a match, based on peak-to-peak and ramp-to-ramp correlations. Although all available data were used to make the match, only paired data are shown, that is, values that have a partner within 4 m of the matched level (i.e., Site 806 depth-in-hole). Resolution varies depending on the variability of the record; it is taken to be about 1 Ma. The stratigraphy of differences in the carbonate content in the two sites (based on paired, averaged data) shows fluctuations with a typical range between 0% and 3% (the carbonate content of Site 806 minus the carbonate content of Site 805, at equivalent depth levels). The greatest differences, and the most variable portions of the record, are associated with major CREs, such as CRE-II, CRE-V, CRE-VII, and the CRE-IX/X interval, discussed above.

The maximum difference is seen at 510 mbsf (Site 806), near 15.5 Ma (CRE-XVI). This event coincides with the rapid change in oxygen isotopes that marks the acme of the Antarctic cooling event (Zones N9/N10; Savin et al., 1985; Vincent and Berger, 1985). The maximum is preceded (in time) by two smaller peaks (belonging to CRE-XVII and CRE-XVIII), one near 550 mbsf (ca. 17.5 Ma), the other near 585 mbsf (19 Ma). CRE-XVII is centered on Zone N8, which marks the onset of the Antarctic cooling event (Savin et al., 1985) and the maximum of the Monterey carbon isotope excursion (Vincent and Berger, 1985). Hiatus formation is common in this interval (NH2 of Keller and Barron, 1987). CRE-XVIII occurs in the uppermost lower Miocene, in Zone N7. Cooling and ^{13}C enrichment is correlated with this event, as well as a carbonate minimum in the central Pacific (16g; Barron et al., 1985). CRE-XVI through CRE-XVIII define a period of reduced sedimentation rate in Site 806, whereas at Site 805 there is a condensed section, and at Sites 803 and 804 the interval is not represented in the record at all.

Surprisingly, the events surrounding CRE-XVI to CRE-XVIII are not strongly expressed in the acoustic reflection records of Sites 805 and 806. There is, however, a strong double reflector in the profile at Site 586, farther up on the plateau. It is labeled 550/N6/19 m.y. (Shipboard Scientific Party, 1986a) and probably corresponds to CRE XVII/CRE XVIII. At Site 806, there is a group of strong reflectors in the middle of the Antarctic Series (at ca. 3.9 sbsf; Fig. 54) near 435 mbsf (Site 806). This series apparently belongs to the interval between CRE-XIII and CRE-XIV (12–13 Ma), which corresponds to a period of hiatus formation in the central Pacific (NH3 of Keller and Barron, 1987). The differences in carbonate content between matching depth levels of Sites 806 and 805 imply a loss of carbonate at the deeper site. Assuming that this loss occurred by carbonate dissolution, and that noncarbonate material was not affected, we can calculate the proportion of sediment lost at the deeper site ("Loss") from the carbonate fluxes in the shallow site ("initial carbonate") and in the deeper one ("final carbonate"), at corresponding depth levels:

$$\text{Loss} = (\text{Initial carb.}) - (\text{Final carb.}) = 1 - NC_i/NC_f,$$

where NC_i and NC_f are initial and final percent of noncarbonate, respectively. To determine the percentage loss of carbonate, "Loss" would have to be multiplied by the percentage of carbonate content at Site 806.

The "Loss" curve should repeat the pattern of the carbonate difference curve (Fig. 59A), as it is a function of the difference in carbonate. The result of calculating the loss of sediment by the above equation is shown in Figure 59B, together with the two smoothed carbonate curves, on the same scale. First, one should note that small differences in carbonate between the two sites are translated into large losses. The reason for this is the great sensitivity of "Loss" in the above equation to the quotient NC_i/NC_f when these numbers are small. This also means that errors in measurement, or in matching the carbonate curves, are greatly amplified. Second, it is evident that losses are pulsed rather than being smoothly distributed through time. We know this is true for the Milankovitch scale, where dissolution cycles are common (e.g., Thompson, 1976; Moore et al., 1977; Farrell and Prell, 1989). Apparently, unless the results shown here are artifacts stemming from spotty data and poor matching, similar pulsing is indicated on scales between 0.5 and 1 Ma in our carbonate curves (cf. van Andel et al., 1975). Finally, this analysis reveals that loss by carbonate dissolution in the manner assumed (that is, without involving loss of noncarbonate) cannot account for the overall difference in sedimentation rates between Sites 805 and 806.

If the stratigraphy of Site 805 were to be generated from that of Site 806 solely according to carbonate dissolution, the differences in carbonate percentages would have to be greater than observed. For a general sedimentation rate ratio of 0.71, the average loss would have to come out as 29% (100% − 71%). In fact, we get about one-half of that (Pleistocene, 8.5%; upper Pliocene, 6.3%; lower Pliocene, 13.9%; upper Miocene, 13.9%, middle Miocene, 13.0%, and lower Miocene, 16.8%). We shall next adduce further evidence regarding this discrepancy and subsequently discuss possible causes for its origin.

Sedimentation Rate Ratios from Curve Matching

The match of carbonate curves shown in Figure 59 implies that we know which depth levels at Sites 805 and 806 correspond to each other. If this knowledge is accurate, we can next turn to the ratios in sedimentation rates that are implied for each 10-m section in Site 806 (10 m is an arbitrary interpolation interval). Note that the resulting curve (Fig. 60) is independent of age assignments. The overall SRR is given as 0.71, from biostratigraphy. Down to about 400 mbsf (Site 806), the SRR found by carbonate matching agrees well with that based on biostratigraphy. Below this depth, the carbonate data have too many gaps for confident matching.

Down into the uppermost upper Miocene, the deviations of the SRR from the average are minor. For the Quaternary, there

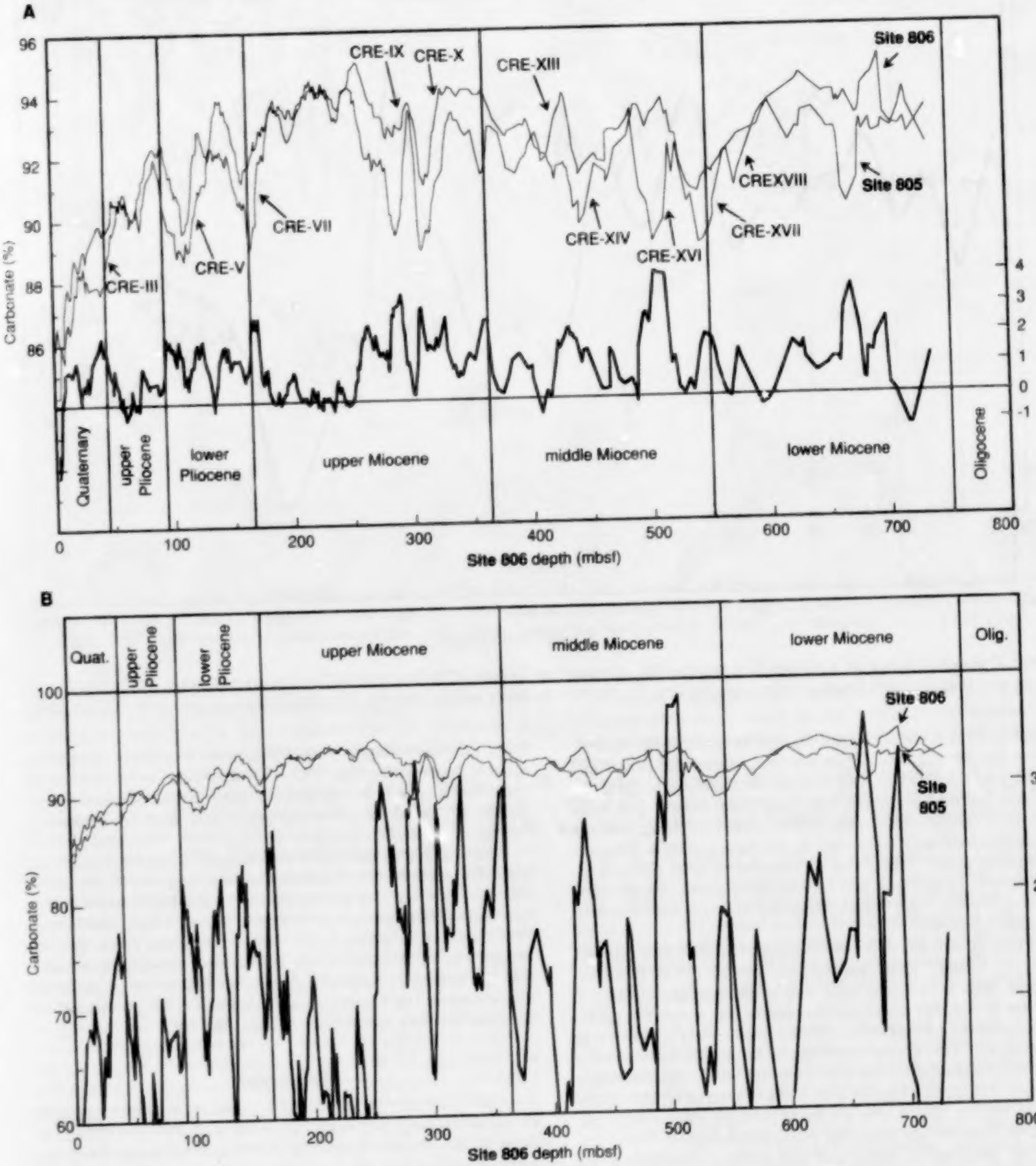

Figure 59. Carbonate difference stratigraphy of Sites 805 and 806. **A**. Match of carbonate curves for the two sites, by adjusting the Site 805 curve at roughly 20-m intervals, fit by eye. Only paired data are shown, as well as the difference in carbonate (scale on right). Carbonate reduction events for the times preceding the upper Miocene are tentative as the data are spotty in that interval. CRE-I to CRE-X, as in Figure 58. CRE-XIII to CRE-XVIII, see text. **B**. Loss of sediment calculated on the assumption that the difference between the sedimentation rates of Sites 805 and 806 is entirely a result of the dissolution of carbonate and that the initial supply of sediment is the same at both sites. The uppermost two curves are the paired carbonate data, for orientation.

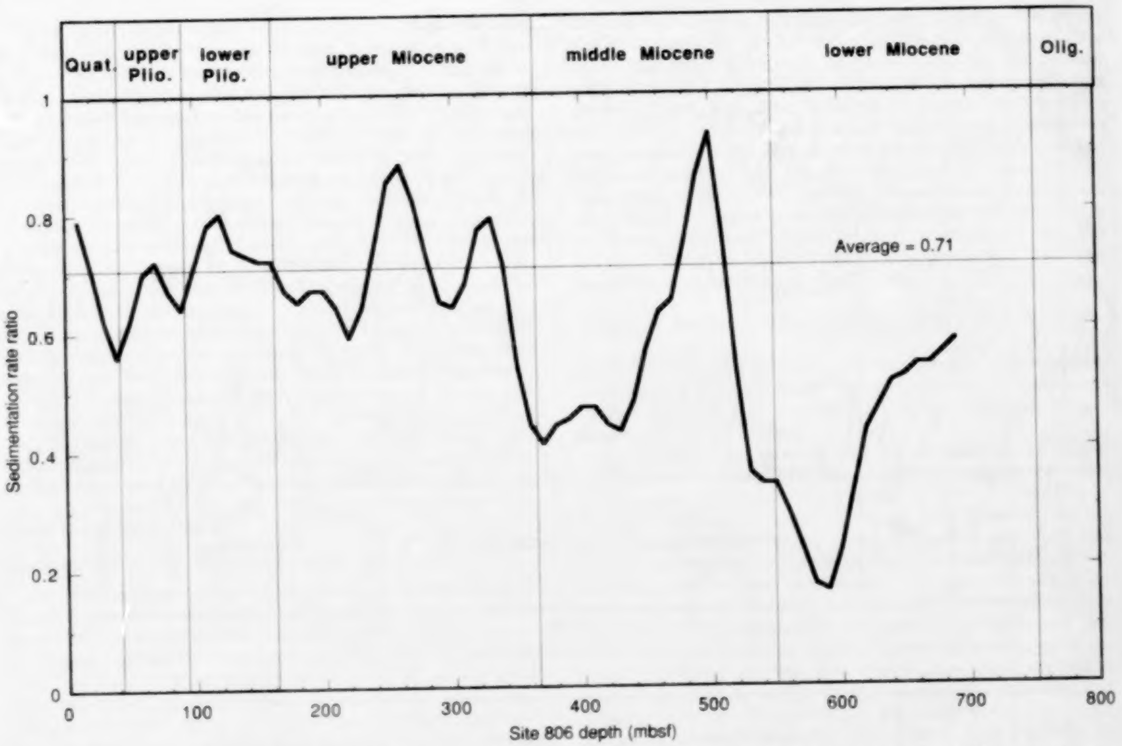

Figure 60. Sedimentation rate ratio between Sites 805 and 806, calculated on the basis of the match of carbonate curves shown in Figure 59. Note the similarity with the SRR curve based on biostratigraphy (Fig. 57) down to the upper middle Miocene. For older sediments, carbonate data are spotty.

is a tendency for a low SRR, presumably because of the equatorial position of Site 806. There are two substantial peaks and one valley in SRR within the interval with sufficient data for discussion (above 500 mbsf). The first peak is near 240 mbsf (6.5–7 Ma), the second is near 490 mbsf (14–15 Ma), and the valley is centered near 400 mbsf, in the upper middle Miocene (11 Ma). The peaks signify that sedimentation rates differed little between Sites 805 and 806 during those particular periods; the valley, on the other hand, indicates a major difference in sedimentation rates.

The first peak (near 240 mbsf) marks the time when Site 805 crossed the equator while Site 806 had moved off it. If we assume that Site 805 should have had a sedimentation rate 0.7 times that of 806, the discrepancy suggests that the difference in sedimentation rate between the equator and 1° to the south was a factor of 1.2. This appears reasonable for an equator-to-south comparison (a similar distance to the north would have virtually no effect). The period centered on 6–7 Ma falls in Hiatus Interval NH6 (Keller and Barron, 1987); perhaps this is why the equatorial effect is not expressed more strongly.

The second peak of SRR, near 490 mbsf, is centered on the Antarctic cooling event, as seen in oxygen isotopes (Savin et al., 1985; Vincent and Berger, 1985) and marks a time of substantial dissolution in Site 805. It is quite possible that this peak is spurious, at least in its extent above the average SRR. A slight adjustment of the match between Sites 805 and 806 could readily reduce the peak and at the same time fill the trough to its right, without eliminating it, of course. Not much credence can be given to the exact shape of the SRR minimum in the uppermost lower Miocene because the carbonate data base deteriorates quickly below 450 mbsf. The SRR minimum is most probably present (based on biostratigraphy, there is a condensed section in Site 805 centered at this period), but it does not necessarily extend to values below 0.3.

The broad SRR minimum in the upper middle Miocene, and extending into the lowermost upper Miocene, marks the end of the Antarctic cooling period (Savin et al., 1985) and contains two hiatus-prone periods (NH3 and NH4 of Keller and Barron, 1987), as well as evidence for major carbonate removal in the central Pacific (Barron et al., 1985). This coincidence suggests that the late-stage Antarctic cooling steps resulted in carbonate dissolution in the western equatorial Pacific, and that such dissolution affected Site 805 more than Site 806.

Discussion

A comparison of the carbonate-based stratigraphies is shown in Figure 61. The carbonate curves for Sites 805 and 806 are the same as in Figure 59 (showing only matching pairs). Note that correlation between the two curves is good to about 10 Ma ($R^2 = 0.81$), and becomes quite poor in sediments older than this ($R^2 = 0.16$). It is not clear to what extent this reflects a change in climate dynamics, and to what extent it is a function of poor data coverage. The matching technique also needs to be improved. Note for example that a slight shift of the Site 805 curve at 16 Ma to the left would improve the fit with the Site 806 curve between 15 and 17 Ma. This would have the beneficial effect of decreasing the apparent 15-Ma peak in the SRR (Fig. 60, 490

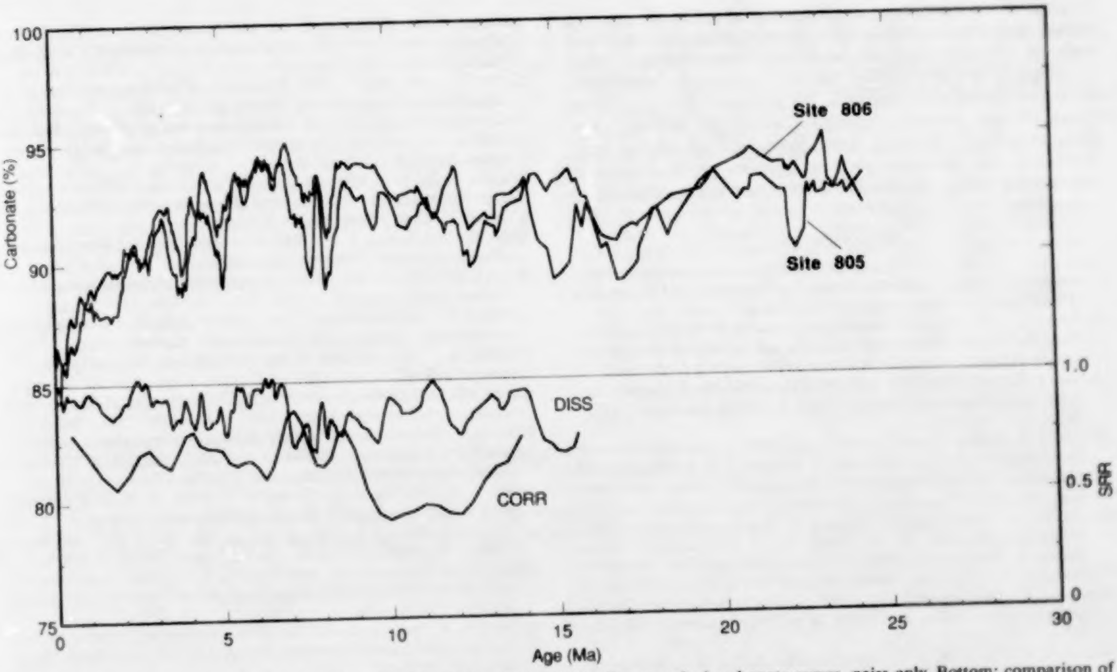

Figure 61. Summary graph of the carbonate stratigraphy of Sites 805 and 806. Top: matched carbonate curves, pairs only. Bottom: comparison of sedimentation rate ratios (SRR) between the two sites, one based on carbonate differences ("DISS"), the other on the match of the carbonate profiles ("CORR"). SRR values were left off for the deeper part of the section, where they are believed to be unreliable. Note that the two SRRs do not agree.

mbsf) while reducing the minimum in the SRR to the right (Fig. 60, 580 mbsf). Nevertheless, a strong dynamic component is believed to be present in the factors responsible for the change in carbonate correlation near 10 Ma, but this effect must be substantiated by work on shore.

The data density and the match based on it are thought to be quite good back to 13.5 Ma, so the two derivative curves are shown back to this time in the summary figure (Fig. 61). DISS is the SRR based on LOSS, where LOSS is calculated from the ratio of noncarbonate values (see equation above) (Fig. 59B), and CORR is the SRR based on matching the carbonate curves (Fig. 60). It is quite evident that the two independent SRR estimates only agree in three intervals: near 3.5–5, near 7–8.5, and near 14 Ma. These intervals contain well-defined periods of strong carbonate dissolution (CRE-V and CRE-VII, CRE-IX and CRE-X, and CRE-XVI; see Fig. 59A), all of which affect Site 805 much more than Site 806. During such times, then, the dissolution gradient dominates the differences in sedimentation rate. During the rest of the time (most of it, actually), changes in the carbonate dissolution gradient do not seem to be the controlling factor governing changes in sedimentation rates, or, if they are, carbonate dissolution does not result in sufficient reduction of carbonate percentages at the deeper site to allow calculation of the loss sustained.

The latter point was raised earlier, when discussing Figure 59B. The carbonate percentages in Site 805 are too similar to those of Site 806, considering the difference in sedimentation rates between the two sites. It is as though much noncarbonate loss occurred at Site 805 also, in addition to carbonate loss (which, of course, must bear the bulk of the difference between the two sites). An alternative hypothesis for explaining the discrepancy, namely, the addition of "trickle-down" carbonate from higher up the slope, cannot stand up to scrutiny. If sufficient nannofossil carbonate were to be added to Site 805 to bring the percentages back up, the rate of sedimentation would then go up proportionally, changing both SRR indexes in the same direction.

We need to find a mechanism that removes noncarbonate dilutants at the same time, and at the same measure, as carbonate is removed. Several mechanisms can be envisaged, as follows:

1. The reduction of carbonate accumulation from dissolution may lead to greater exposure of siliceous fossils, coupling their dissolution rate to that of carbonate. In this case, the diatoms at Site 805 should be less well preserved that those at Site 806, at least in the upper portion of the section, before diagenesis destroys the signal. The diatom preservation differences between Sites 805 and 806 are being checked for this predicted effect.

2. Dissolution of carbonate changes the physical properties of the sediment in such a fashion that mechanical removal of noncarbonate is more easily accomplished by a combination of biosuspension and current transport. In this case, the diatom-to-radiolarian ratio should be less in Site 805 than in Site 806, and there should also be less clay per radiolarian weight.

3. Much of the loss at Site 805 could be caused by solifluction, engendered by carbonate dissolution, which increases porosity and decreases shear strength. In this scenario, the bioturbated layer moves downslope during repeated short dissolution pulses and microhiatuses are produced, especially during earthquakes. Such a mechanism would result in loss of sediment without fractionating between carbonate and noncarbonate, reducing the "true" SRR, but not the one based on carbonate difference.

Evidence for the operation of these (or related) processes has to be collected onshore. It is unlikely that the raw grain size data available will throw light on the subject. The mean size values are higher in Site 806 than at Site 805, presumably because of the higher foraminifer content at the shallower site. This is the reverse of what would be expected if winnowing were the most important factor. However, breakdown of foraminifers from dissolution will produce a decrease in mean size in calcareous sediments (Johnson et al., 1977), overriding any effect from winnowing.

REFERENCES

Adelseck, C. G., Jr., 1977. Recent and late Pleistocene sediments from the eastern equatorial Pacific Ocean: sedimentation and dissolution [Ph.D. dissert.]. Univ. California, San Diego.

Backman, J., 1979. Pliocene biostratigraphy of DSDP Sites 111 and 116 from the North Atlantic Ocean and the age of the Northern Hemisphere Glaciation. *Stockholm Contrib. Geol.*, 32:115–137.

Barron, J. A., and Keller, G., 1982. Widespread Miocene deep-sea hiatuses: coincidence with periods of global cooling. *Geology,* 10:577–581.

Barron, J. A., Keller, G., and Dunn, D. A., 1985. A multiple microfossil biochronology for the Miocene. *In* Kennett, J. P. (Ed.), *The Miocene Ocean: Paleoceanography and Biogeography.* Mem. Geol. Soc. Am., 163:21–36.

Berger, W. H., 1979. Impact of deep-sea drilling on paleoceanography. *In* Talwani, M., Hay, W., and Ryan, W.B.F. (Eds.), *Deep Drilling Results in the Atlantic Ocean: Continental Margins and Paleoenvironment.* Am. Geophys. Union, Maurice Ewing Ser., 3:297–314.

Berger, W. H., and Johnson, T. C., 1976. Deep-sea carbonates: dissolution and mass wasting on Ontong Java Plateau. *Science,* 192:785–787.

Berger, W. H., Johnson, T. C., and Hamilton, E. L., 1977. Sedimentation on Ontong Java Plateau: observations on a classic "carbonate monitor." *In* Anderson, N. R., and Malahoff, A. (Eds.), *The Fate of Fossil Fuel CO_2 in the Oceans:* New York (Plenum Press), 543–567.

Berger, W. H., and Mayer, L. A., 1978. Deep-sea carbonates: acoustic reflectors and lysocline fluctuations. *Geology,* 6:11–15.

Berger, W. H., and Winterer, E. L., 1974. Plate stratigraphy and the fluctuating carbonate line. *In* Hsü, K. J., and Jenkyns, H. C. (Eds.), *Pelagic Sediments on Land and Under the Sea:* Spec. Publ., Int. Assoc. Sedimentol., 1:11–48.

Bukry, D., 1973. Low-latitude coccolith biostratigraphic zonation. *In* Edgar, N. T., Saunders, J. B., et al., *Init. Repts. DSDP,* 15: Washington (U.S. Govt. Printing Office), 685–703.

Davies, T. A., Hay, W. W., Southam, J. R., Worsley, T. R., 1977. Estimates of Cenozoic oceanic sedimentation rates. *Science,* 197:53–55.

Dunlop, D. J., 1981. The rock magnetism of fine particles. *Phys. Earth Planet. Inter.,* 26:1–26.

Elderfield, H., Gieskes, J. M., Baker, P. A., Oldfield, R. K., Hawkesworth, C. J., and Miller, R., 1982. $^{87}Sr/^{86}Sr$ and $^{18}O/^{16}O$ ratios, interstitial water chemistry and diagenesis in deep-sea carbonate sediments of the Ontong-Java Plateau. *Geochim. Cosmochim. Acta,* 46:2259–2268.

Emeis, K.-C., and Kvenvolden, K. A., 1986. Shipboard organic geochemistry on *JOIDES Resolution. ODP Tech. Note,* No. 7.

Farrell, J. W., and Prell, W. L., 1989. Climatic change and $CaCO_3$ preservation: an 800,000 year bathymetric reconstruction from the central equatorial Pacific Ocean. *Paleoceanography,* 4:447–466.

Gieskes, J. M., 1981. Deep-sea drilling interstitial water studies: implications for chemical alteration of the oceanic crust, Layers I and II. *In* Warme, J. E., Douglas, R. G., and Winterer, E. L. (Eds.), *The Deep Sea Drilling Project: A Decade of Progress.* Spec. Publ., Soc. Econ. Paleontol. Mineral., 32:149–167.

Hamilton, E. L., 1976. Variations in density and porosity with depth in deep-sea sediments. *J. Sediment. Petrol.,* 46:280–300.

Hussong, D. M., Wipperman, L. K., and Kroenke, L. W., 1979. The crustal structure of the Ontong Java and Manahiki oceanic plateaus. *J. Geophys. Res.,* 84:6003–6010.

Ingle, J. C., 1973. Summary comments on Neogene biostratigraphy, physical stratigraphy and paleo-oceanography in the marginal northeastern Pacific Ocean. *In* Kulm, L. D., von Huene, R., et al., *Init. Repts. DSDP,* 18: Washington (U.S. Govt. Printing Office), 949–960.

Johnson, T. C., Hamilton, E. L., and Berger, W. H., 1977. Physical properties of calcareous ooze: control by dissolution at depth. *Mar. Geol.,* 24:259–277.

Karlin, R., and Levi, S., 1983. Diagenesis of magnetic minerals in recent hemipelagic sediments. *Nature,* 303:327–330.

Karlin, R., and Levi, S., 1985. Geochemical and sedimentological control of the magnetic properties of hemipelagic sediments. *J. Geophys. Res.,* 90:10,373–10,392.

Keigwin, L. D., 1978. Pliocene closing of the Isthmus of Panama, based on biostratigraphic evidence from nearby Pacific and Caribbean sea cores. *Geology,* 6:630–634.

Keller, G., and Barron, J. A., 1987. Paleodepth distribution of Neogene deep-sea hiatuses. *Paleoceanography,* 2:697–713.

Kennett, J. P. (Ed.), 1985. *The Miocene Ocean: Paleoceanography and Biogeography.* Mem. Geol. Soc. Am., No. 163.

Kligfield, R., and Channell, J.E.T., 1981. Widespread remagnetization of Helvetic Limestones. *J. Geophys. Res.,* 86:1888–1900.

Kroenke, L., 1972. Geology of the Ontong Java Plateau [Ph.D. dissert.]. Univ. of Hawaii.

Lowrie, W., and Heller, F., 1982. Magnetic properties of marine limestones. *Rev. Geophys. Space Phys.,* 20:171–192.

Martini, E., 1971. Standard Tertiary and Quaternary calcareous nannoplankton zonation. *In* Farinacci, A. (Ed.), *Proc. 2nd Planktonic Conf. Roma:* Rome (Ed. Technosci.), 2:739–785.

Mayer, L. A., Shipley, T. H., Theyer, F., Wilkens, R. W., and Winterer, E. L., 1985. Seismic modelling and paleoceanography at DSDP Site 574. *In* Mayer, L. A., Theyer, F., Thomas, E., et al., *Init. Repts. DSDP,* 85: Washington (U.S. Govt. Printing Office), 947–970.

Mayer, L. A., Shipley, T. H., and Winterer, E. L., 1986. Equatorial Pacific seismic reflectors as indicators of global oceanographic events. *Science,* 233:761–764.

McDuff, R. E., and Gieskes, J. M., 1976. Calcium and magnesium profiles in DSDP interstitial waters: diffusion or reaction? *Earth Planet. Sci. Lett.,* 33:1–10.

Moore, T. C., Pisias, N. G., and Heath, G. R., 1977. Climate changes and lags in Pacific carbonate preservation, sea surface temperature and global ice volume. *In* Malahoff, A., and Anderson, N. (Eds.), *The Fate of Fossil Fuel CO_2 in the Oceans:* New York (Plenum Press), 145–165.

Okada, H., and Bukry, D., 1980. Supplementary modification and introduction of code numbers to the low latitude coccolith biostratigraphic zonation (Bukry, 1973; 1975). *Mar. Micropaleontol.,* 5:321–325.

Riedel, W. R., and Sanfilippo, A., 1978. Stratigraphy and evolution of tropical Cenozoic radiolarians. *Micropaleontology,* 24:61–96.

Rio, D., Fornaciari, E., and Raffi, I., 1990. Late Oligocene through early Pleistocene calcareous nannofossils from western equatorial Indian Ocean (ODP Leg 115). *In* Backman, J., Duncan, R. A., et al., *Proc. ODP, Sci. Results,* 115: College Station, TX (Ocean Drilling Program), .

Sager, W. W., 1988. Paleomagnetism of Ocean Drilling Program Leg 101 Sediments: magnetostratigraphy, magnetic diagenesis, and paleolatitudes. *In* Austin, J. A., Jr., Schlager, W., et al., *Proc. ODP, Sci. Results,* 101: College Station, TX (Ocean Drilling Program), 327–360.

Saito, T., Burckle, L. H., and Hays, J. D., 1975. Late Miocene to Pleistocene biostratigraphy of equatorial Pacific sediments. *In* Saito, T., and Burckle, L. H. (Eds.), *Late Neogene Epoch Boundaries.* Spec. Publ., Micropaleontol., 1:226–244.

Sallomy, J. T., and Briden, J. C., 1975. Palaeomagnetic studies of Lower Jurassic rocks in England and Wales. *Earth Planet. Sci. Lett.,* 24:369–376.

Savin, S. M., Abel, L., Barrera, E., Hodell, D., Kennett, J. P., Murphy, M., Keller, G., Killingley, J., and Vincent, E., 1985. The evolution of Miocene surface and near-surface marine temperatures: oxygen isotopic evidence. *In* Kennett, J. P. (Ed.), *The Miocene Ocean: Paleoceanography and Biogeography.* Mem. Geol. Soc. Am., 163:49–82.

Schlanger, S. O., and Douglas, R. G., 1974. The pelagic ooze-chalk-limestone transition and its implication for marine stratigraphy. *In* Hsü, K. J., and Jenkyns, H. C. (Eds.), *Pelagic Sediments: On Land and Under the Sea.* Spec. Publ., Int. Assoc. Sedimentol., 1:117–148.

Shackleton, N. J., Backman, J., Zimmerman, H., Kent, D. V., Hall, M. A., Roberts, D. G., Schnitker, D., Baldauf, J., Desprairies, A., Homrighausen, R., Huddlestun, P., Keene, J. B., Kaltenback, A. J., Krumsiek, K.A.O., Morton, A. C., Murray, J. W., and Westberg-Smith, J., 1984. Oxygen isotope calibration of the onset of ice-rafting in DSDP Site 552A: history of glaciation in the North Atlantic region. *Nature*, 307:620–623.

Shackleton, N. J., and Opdyke, N. D., 1976. Oxygen-isotope and paleomagnetic stratigraphy of Pacific Core V28-239: late Pliocene to latest Pleistocene. *In* Cline, R. M., and Hays, J. D. (Eds.), *Investigations of Late Quaternary Paleoceanography and Paleoclimatology.* Mem. Geol. Soc. Am., 145:449–464.

Shipboard Scientific Party, 1971. Site 64. *In* Winterer, E. L., Riedel, W. R., et al., *Init. Repts. DSDP,* 7: Washington (U.S. Govt. Printing Office), 473–606.

Shipboard Scientific Party, 1975a. Site 288. *In* Andrews, J. E., Packham, G., et al., *Init. Repts. DSDP,* 30: Washington (U.S. Govt. Printing Office), 175–229.

Shipboard Scientific Party, 1975b. Site 289. *In* Andrews, J. E., Packham, G., et al., *Init. Repts. DSDP,* 30: Washington (U.S. Govt. Printing Office), 231–398.

Shipboard Scientific Party, 1986a. Site 586. *In* Moberly, R., Schlanger, S. O., et al., *Init. Repts. DSDP,* 89: Washington (U.S. Govt. Printing Office), 213–281.

Shipboard Scientific Party, Leg 90, 1986b. Site 586: western equatorial Pacific. *In* Kennett, J. P., von der Borch, C. C., et al., *Init. Repts DSDP,* 90: Washington (U.S. Govt. Printing Office), 19–114.

Shipboard Scientific Party, 1989. Explanatory Notes. *In* Prell, W. L., Niitsuma, N., et al., *Proc. ODP, Init. Repts.*, 117: College Station, TX (Ocean Drilling Program), 11–33.

Thompson, P. R., 1976. Planktonic foraminiferal dissolution and the progress towards a Pleistocene equatorial Pacific transfer function. *J. Foraminiferal Res.*, 6:208–227.

van Andel, T. H., Heath, G. R., and Moore, T. C., Jr., 1975. Cenozoic history and paleoceanography of the central equatorial Pacific. *Mem. Geol. Soc. Am.*, No. 143.

Vincent, E., and Berger, W. H., 1985. Carbon dioxide and polar cooling in the Miocene: the Monterey Hypothesis. *In* Sundquist, E., and Broecker, W. S. (Eds.), *The Carbon Cycle and Atmospheric* CO_2*: Natural Variations Archean to Present:* Am. Geophys. Union, Geophys. Monogr. Ser., 32:455–468.

Whitman, J. M, 1989. Stable isotope record of foraminifera from Ontong Java Plateau for the last 6 million years, DSDP Site 586 [Ph.D. dissert.]. Univ. California, San Diego.

Wu, G., and Berger, W. H., 1989. Planktonic foraminifera: differential dissolution and the Quaternary stable isotope record in the west-equatorial Pacific. *Paleoceanography,* 4:181–198.

Ms 130A-108

NOTE: All core description forms ("barrel sheets") and core photographs have been printed on coated paper and bound as Section 5, near the back of the book, beginning on page 559.

Hole 806B: Resistivity-Sonic-Gamma Ray Log Summary

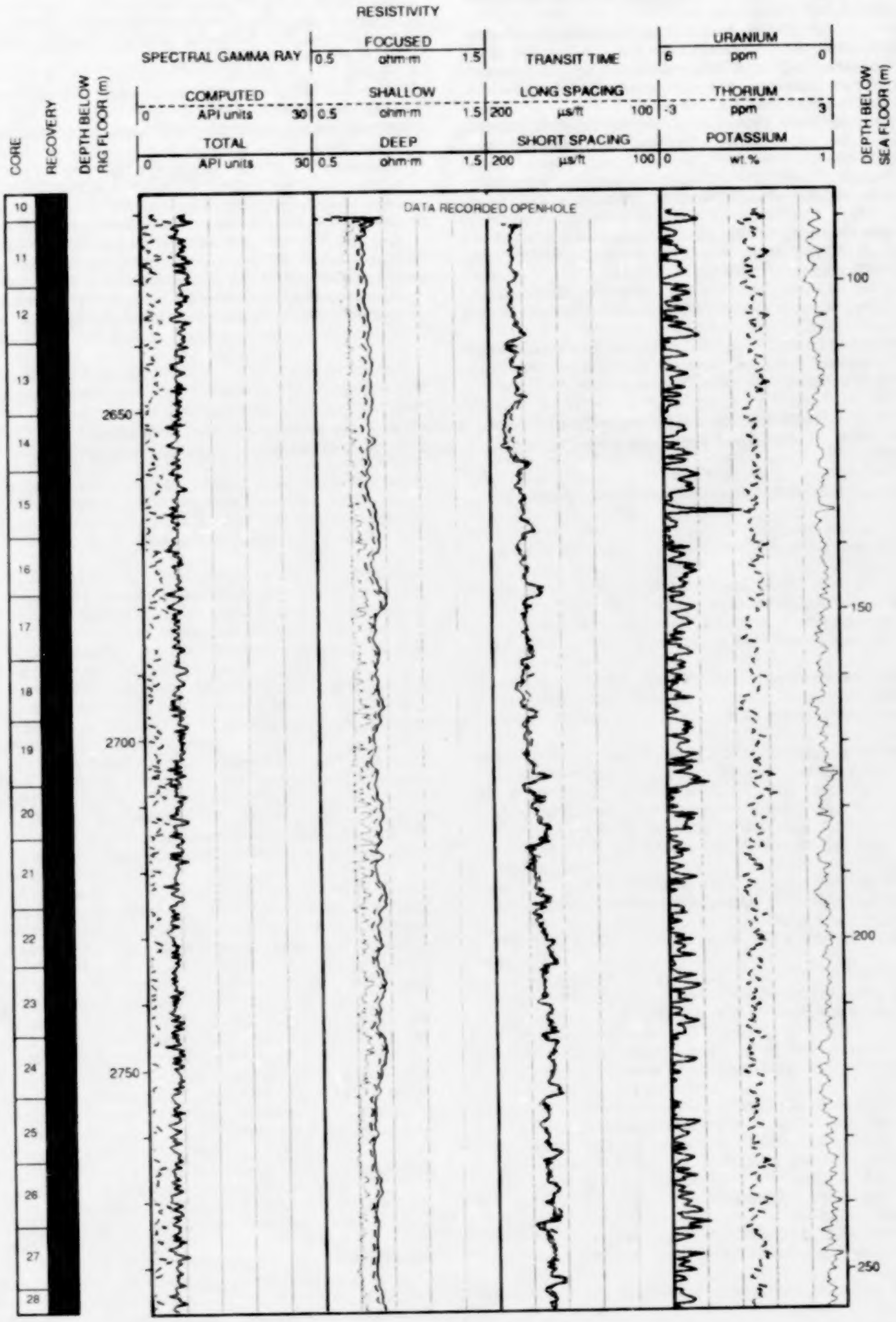

Hole 806B: Resistivity-Sonic-Gamma Ray Log Summary (continued)

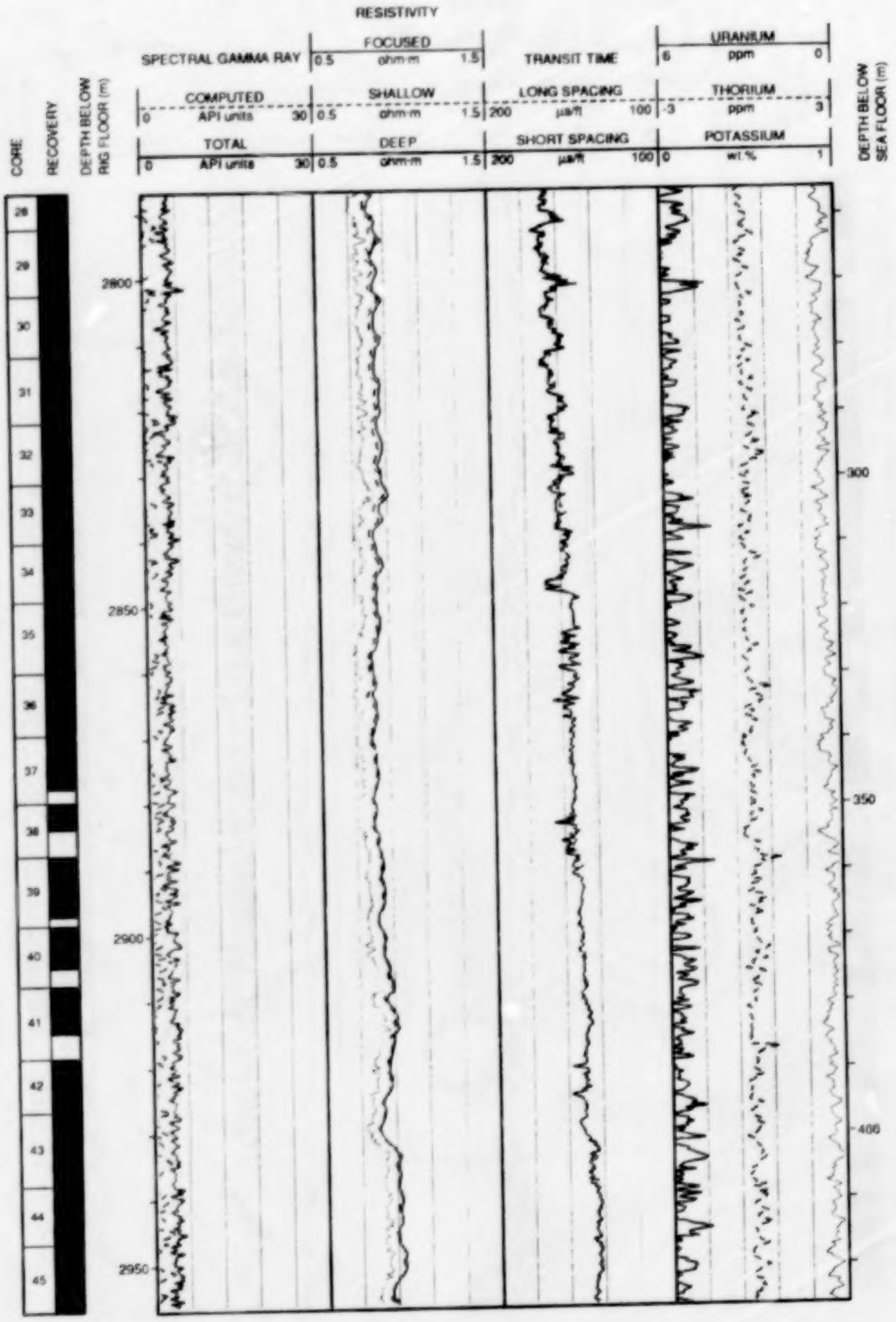

Hole 806B: Resistivity-Sonic-Gamma Ray Log Summary (continued)

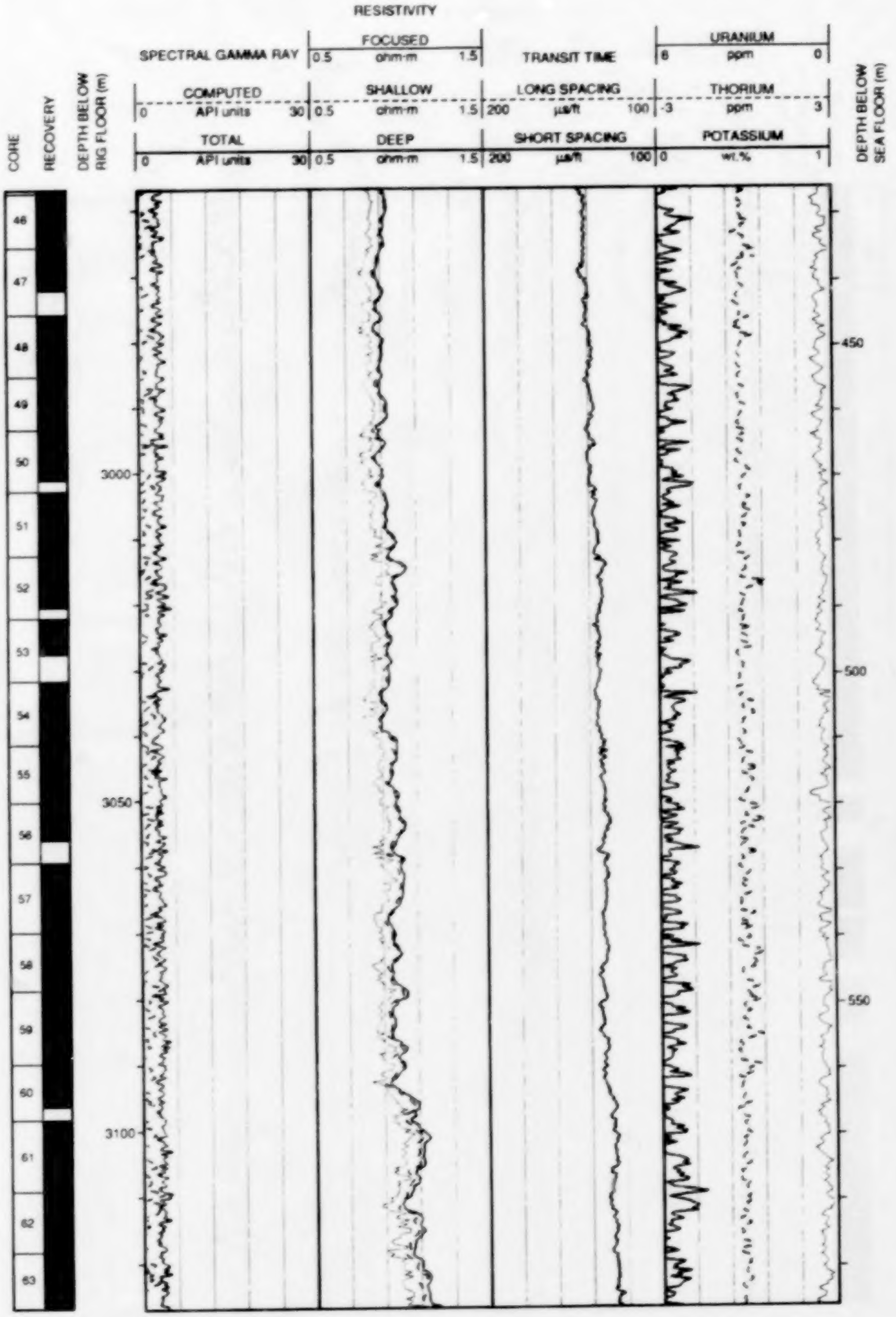

Hole 806B: Resistivity-Sonic-Gamma Ray Log Summary (continued)

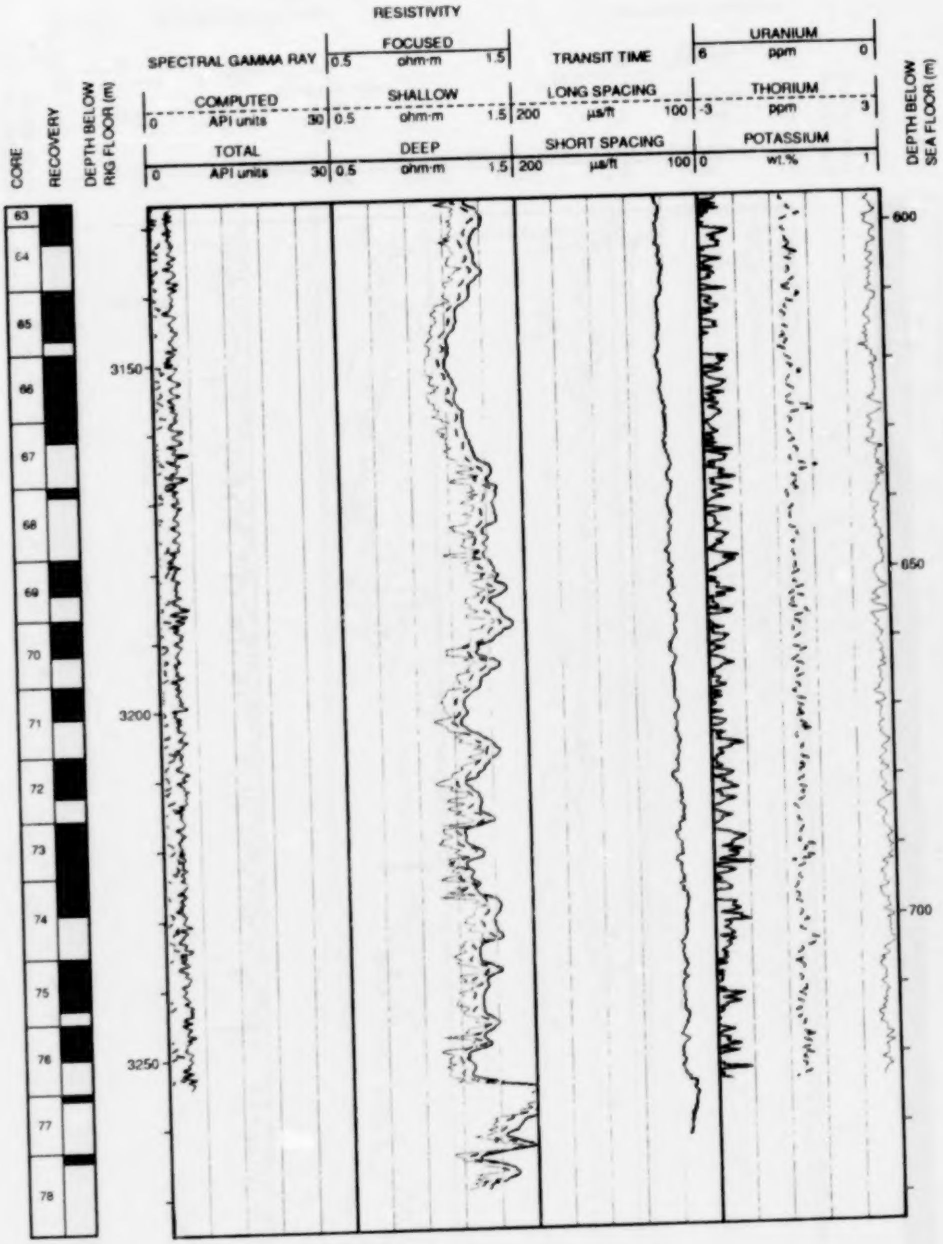

Hole 806B: Density-Gamma Ray Log Summary

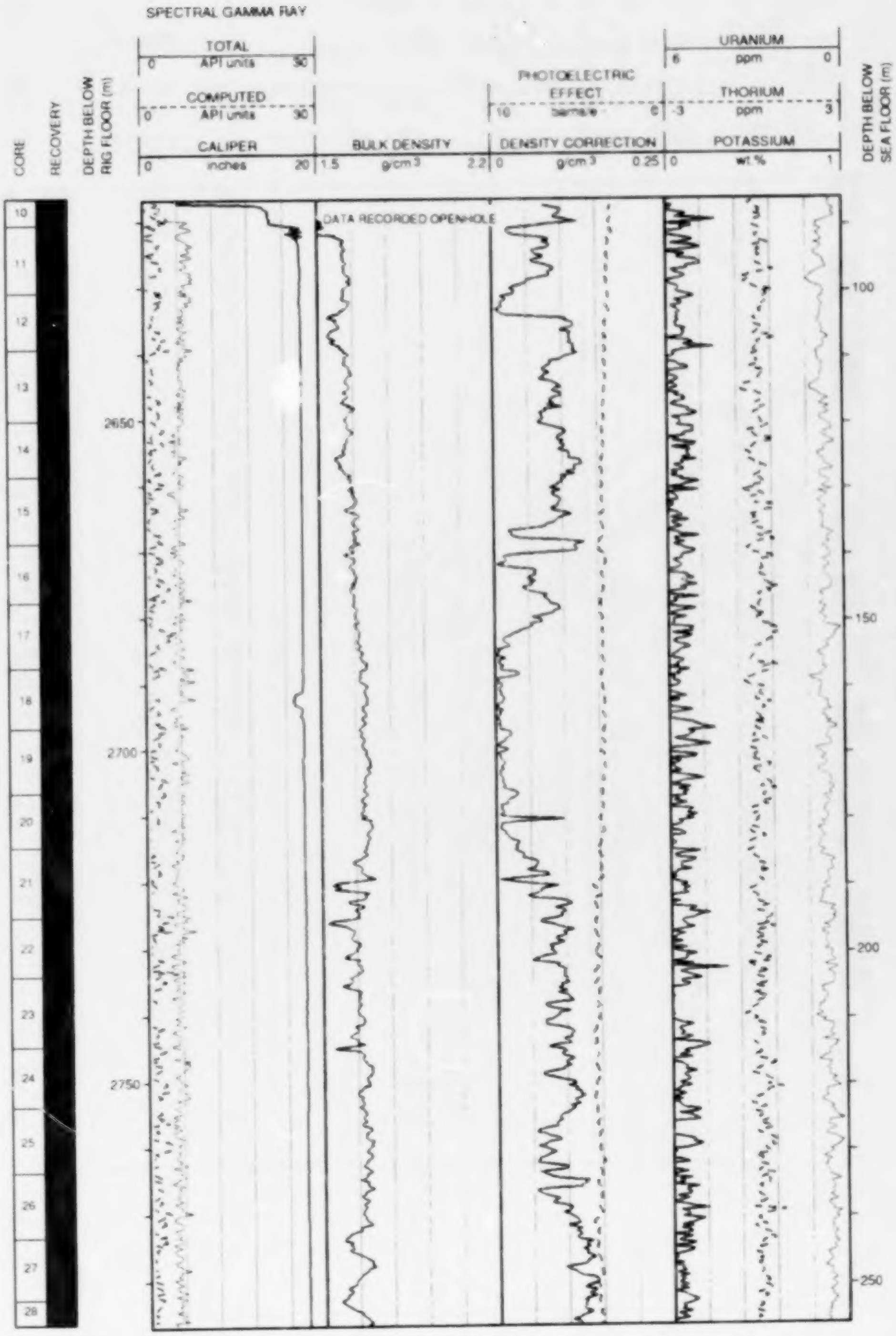

Hole 806B: Density-Gamma Ray Log Summary (continued)

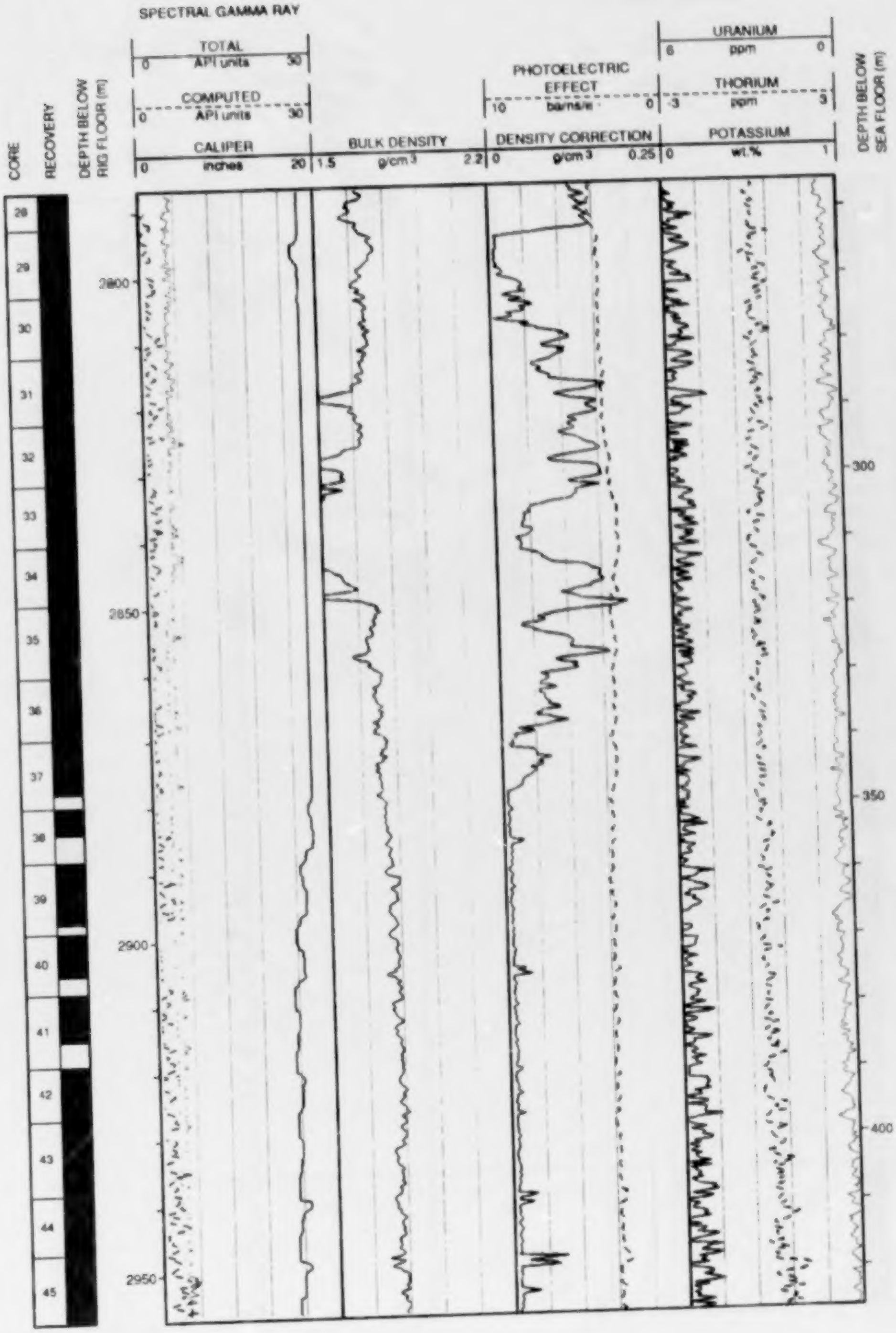

Hole 806B: Density-Gamma Ray Log Summary (continued)

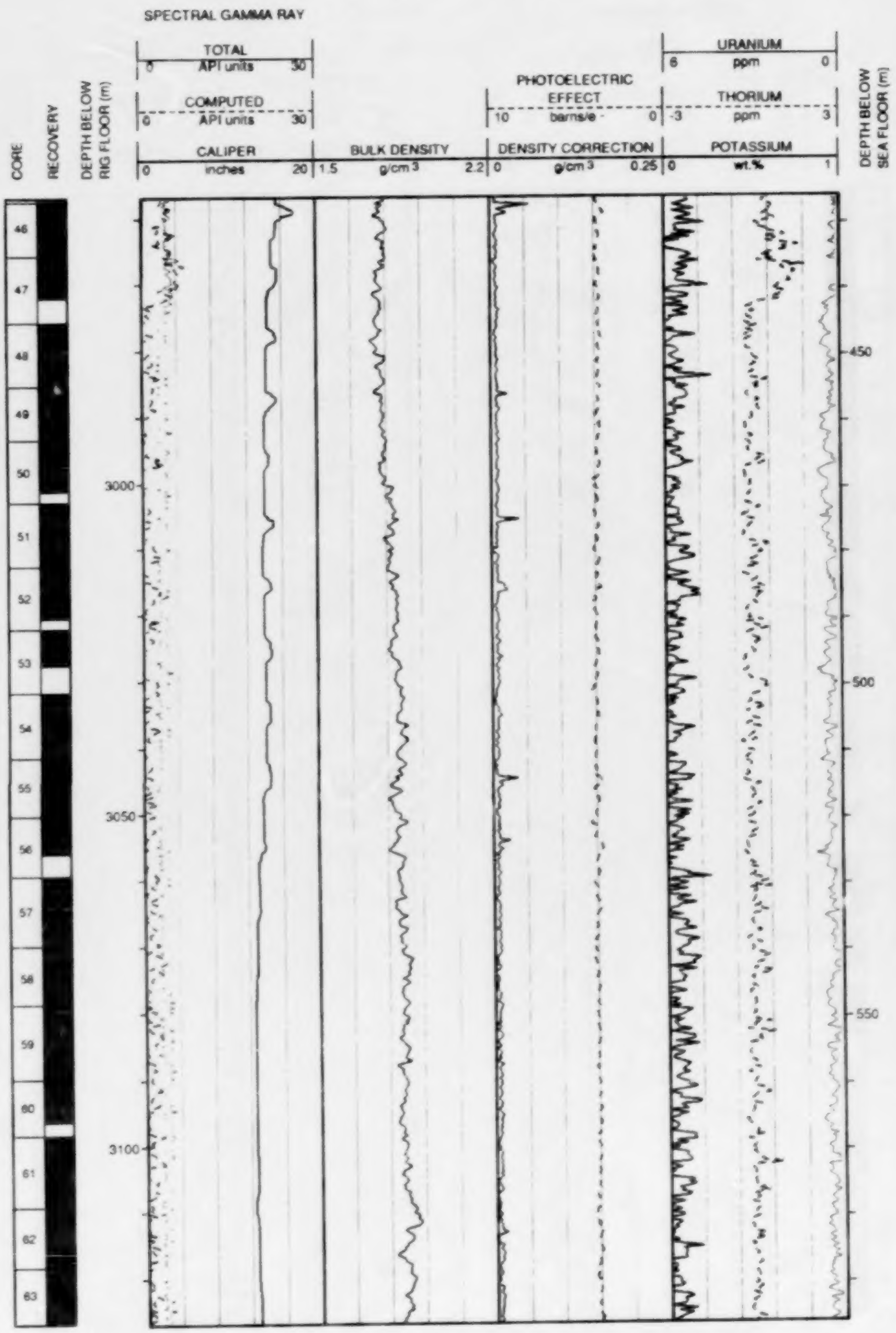

Hole 806B: Density-Gamma Ray Log Summary (continued)

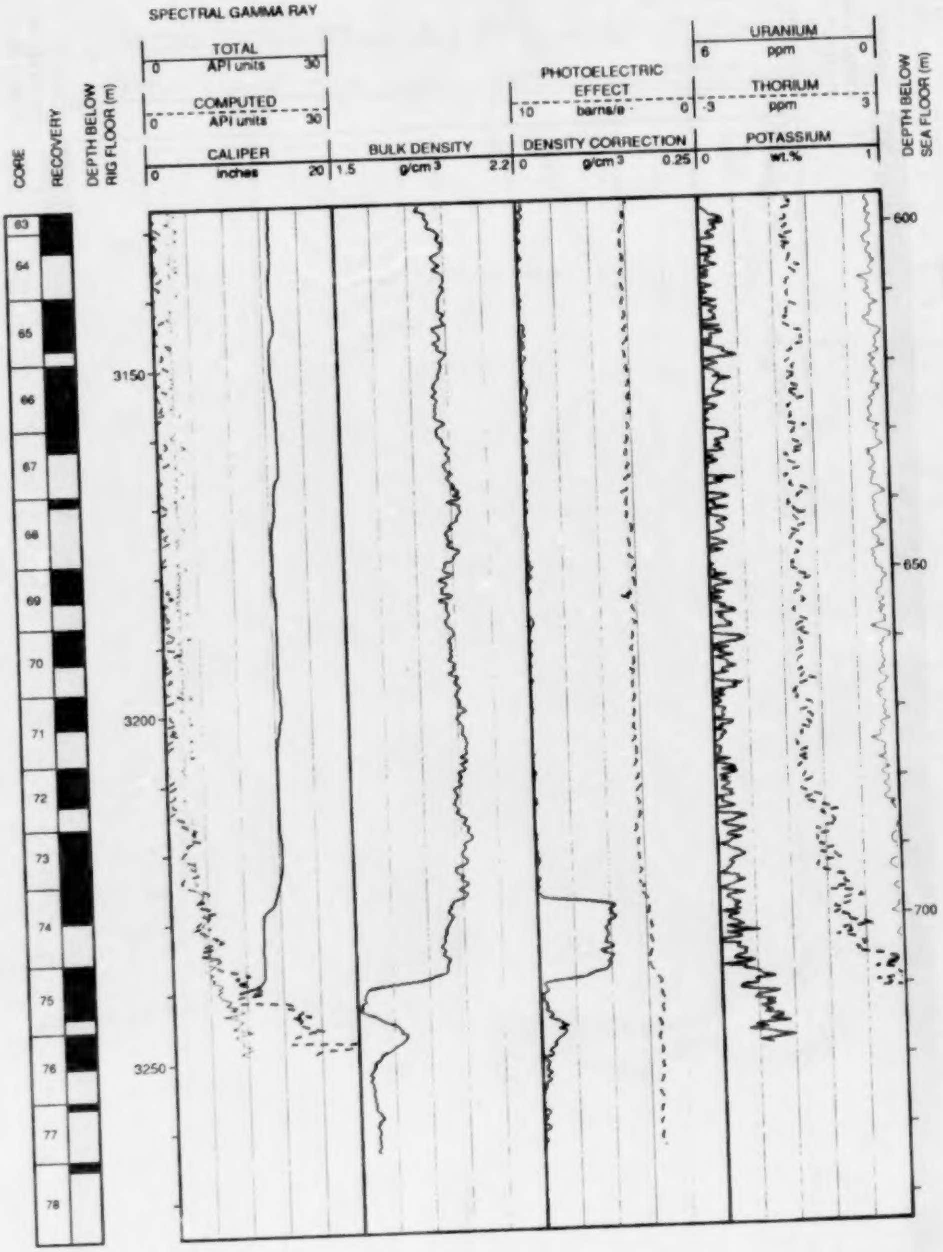

Hole 806B: Geochemical Log Summary

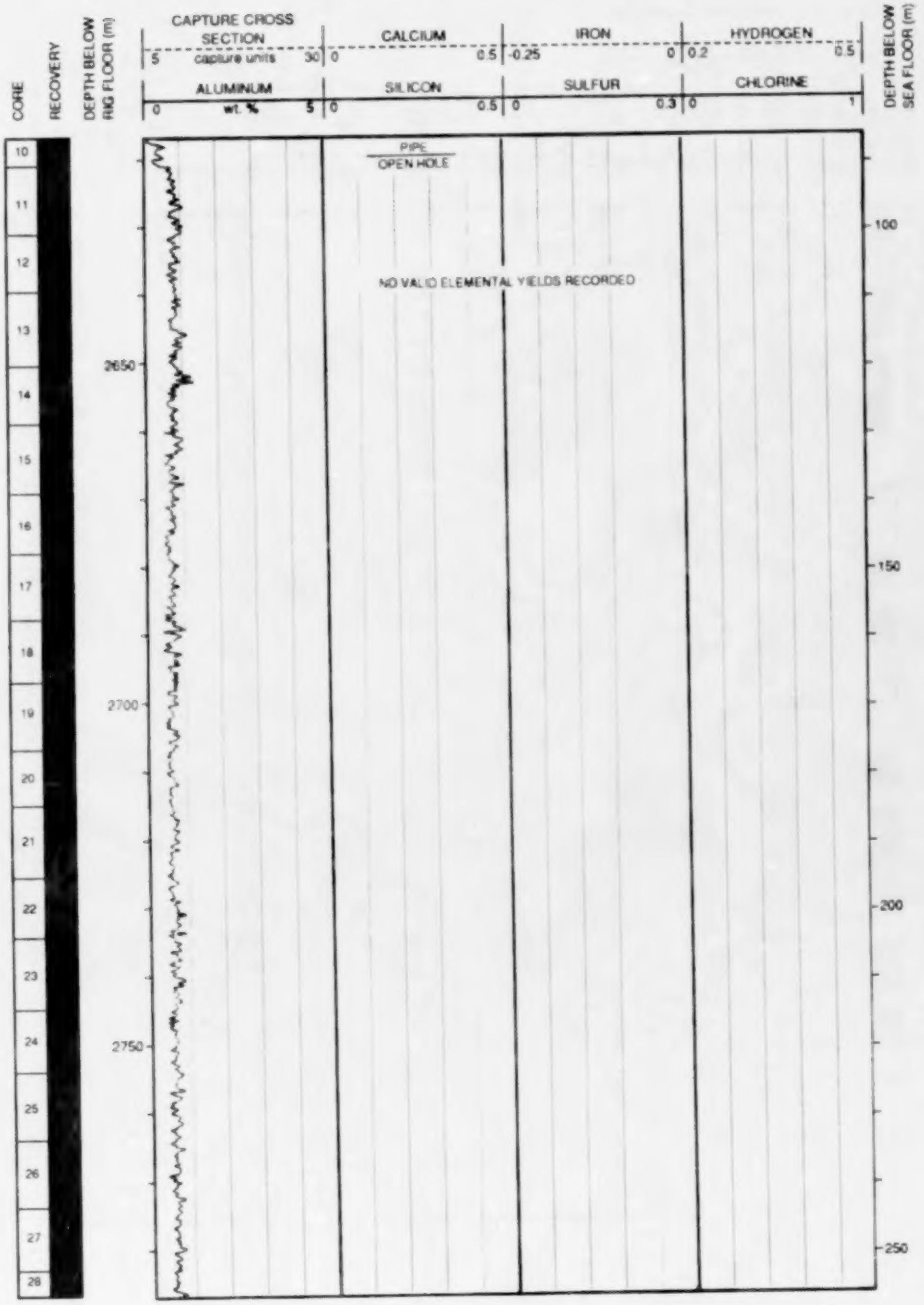

Hole 806B: Geochemical Log Summary (continued)

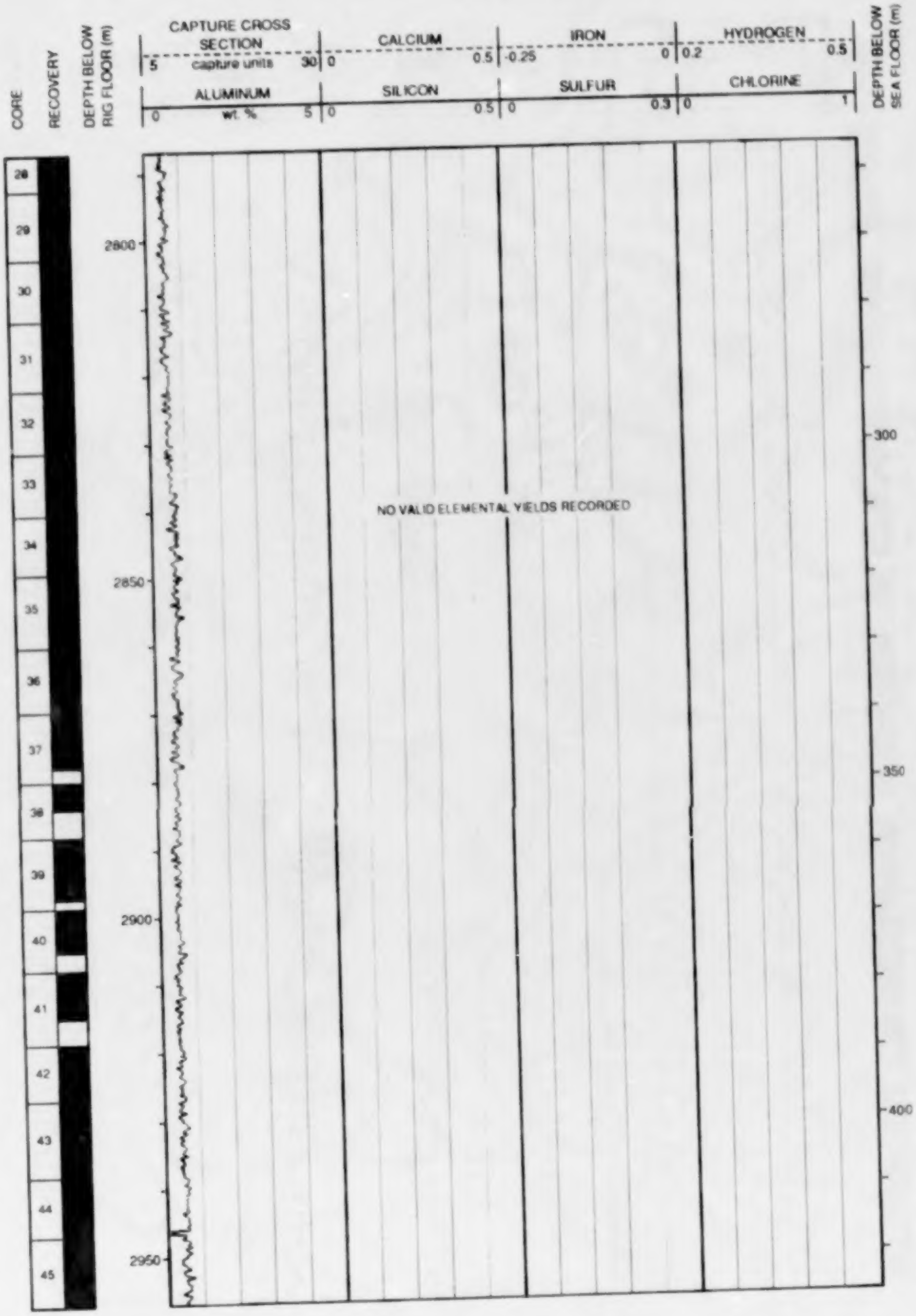

Hole 806B: Geochemical Log Summary (continued)

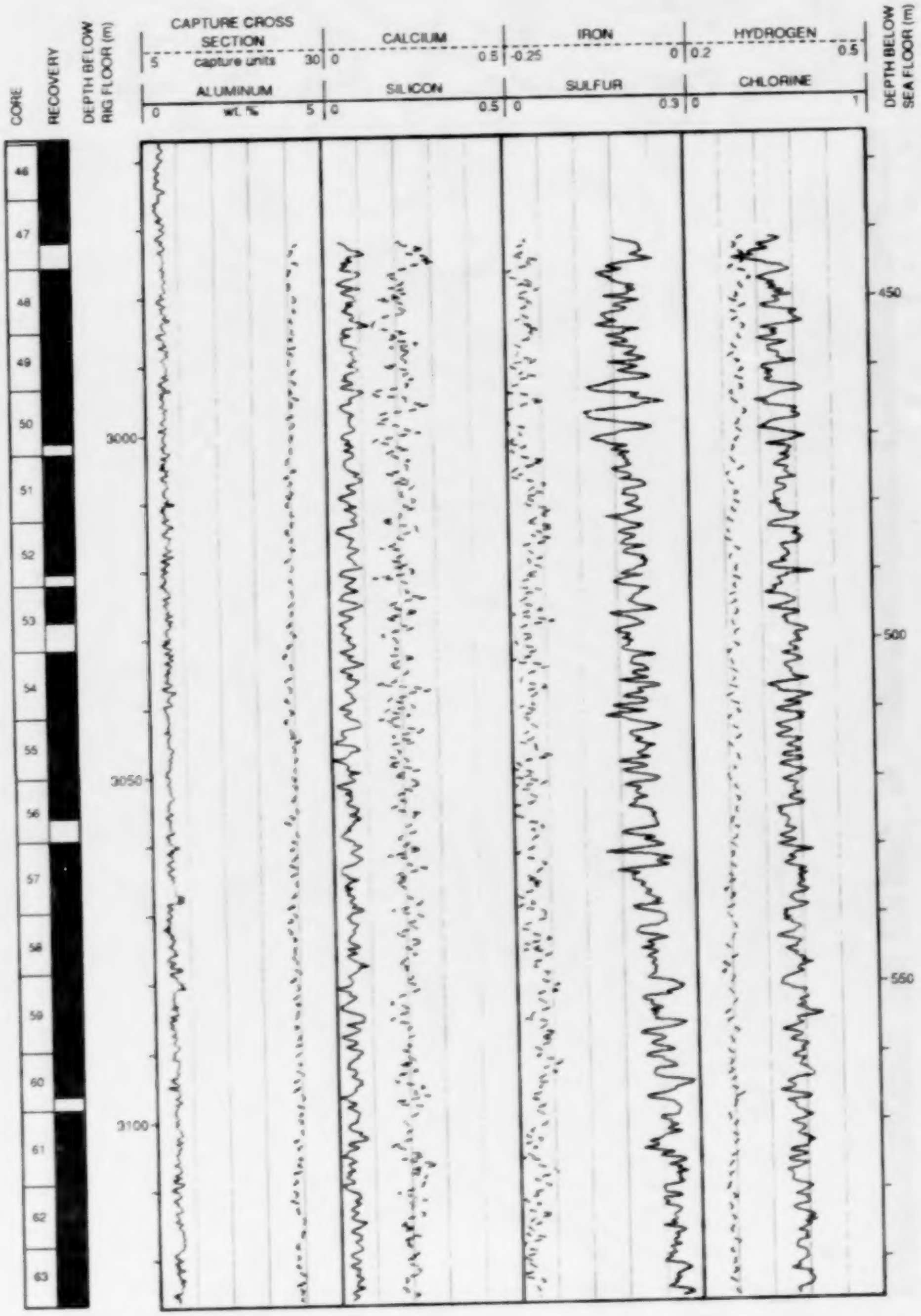

Hole 806B: Geochemical Log Summary (continued)

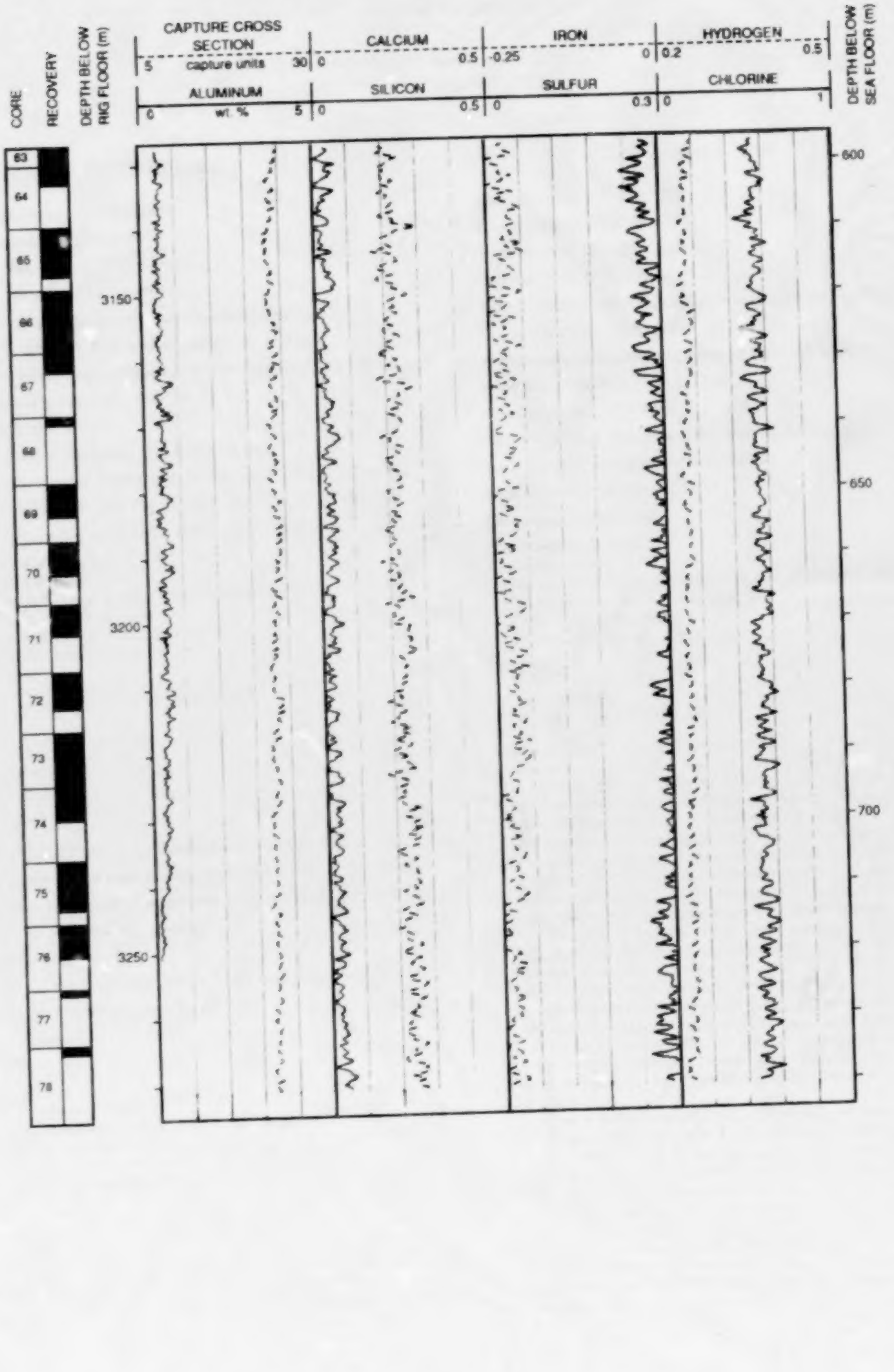

Kroenke, L. W., Berger, W. H., Janecek, T. R., et al., 1991
Proceedings of the Ocean Drilling Program, Initial Reports, Vol. 130

9. SITE 807[1]

Shipboard Scientific Party[2]

HOLE 807A

Date occupied: 26 February 1990

Date departed: 2 March 1990

Time on hole: 4 days, 4 hr, 52 min

Position: 3°36.42′N, 156°37.49′E

Bottom felt (rig floor; m, drill-pipe measurement): 2815.1

Distance between rig floor and sea level (m): 11.32

Water depth (drill-pipe measurement from sea level, m): 2803.8

Total depth (rig floor; m): 3638.00

Penetration (m): 822.90

Number of cores (including cores with no recovery): 86

Total length of cored section (m): 822.90 (APC, 254.4; XCB, 568.5)

Total core recovered (m): 716.74 (APC, 263.11; XCB, 453.63)

Core recovery (%): 87.1 (APC, 103.4; XCB, 79.8)

Oldest sediment cored:
Depth (mbsf): 822.90
Nature: nannofossil ooze with foraminifers
Youngest age: Quaternary
Oldest age: early Oligocene
Measured velocity (km/s): 1.9

HOLE 807B

Date occupied: 2 March 1990

Date departed: 4 March 1990

Time on hole: 1 day, 4 hr, 30 min

Position: 3°36.39′N, 156°37.49′E

Bottom felt (rig floor; m, drill-pipe measurement): 2817.4

Distance between rig floor and sea level (m): 11.32

Water depth (drill-pipe measurement from sea level, m): 2806.1

Total depth (rig floor; m): 3096.00

Penetration (m): 278.60

Number of cores (including cores with no recovery): 30

Total length of cored section (m): 278.60

Total core recovered (m): 280.18

Core recovery (%): 100.6

Oldest sediment cored:
Depth (mbsf): 278.60
Nature: nannofossil ooze with foraminifers
Youngest age: Quaternary
Oldest age: late Miocene
Measured velocity (km/s): 1.6

HOLE 807C

Date occupied: 4 March 1990

Date departed: 23 March 1990

Time on hole: 18 days, 22 hr

Position: 3°36.39′N, 156°37.48′E

Bottom felt (rig floor; m, drill-pipe measurement): 2817.0

Distance between rig floor and sea level (m): 11.32

Water depth (drill-pipe measurement from sea level, m): 2805.7

Total depth (rig floor; m): 4345.40

Penetration (m): 1528.40

Number of cores (including cores with no recovery): 93

Total length of cored section (m): 748.40

Total core recovered (m): 252.84

Core recovery (%): 33.8

Oldest sediment cored:
Depth (mbsf): 1379.70
Nature: limestone, claystone, radiolarian siltstone, and minor chert
Youngest age: lower Oligocene
Oldest age: Aptian-Albian
Measured velocity (km/s): 2.0

Basement:
Depth (mbsf): 1379.7
Nature: basalt
Measured velocity (km/s): 5.0

Principal results: Site 807 (proposed Site *OJP-5A*) is located on the northern rim of the Ontong Java Plateau (latitude 3°36.4′N, longitude 156←37.5′E) in 2805 m of water, roughly 475 km northwest of Deep Sea Drilling Project (DSDP) Sites 289/586. Site 807 was occupied with three major objectives: (1) to provide Paleogene and Cretaceous sediments for studies of pre-Neogene paleoceanography; (2) to obtain basement rock for studies of the origin of the Ontong Java Plateau; and (3) to provide a second shallow-water site, off the equator, for comparison with Sites 803 and 806 on the Neogene equatorial depth transect.

The site is located on a single-channel seismic (SCS) line acquired by the *Thomas Washington* during the EURYDICE Cruise 9 survey at 0255 UTC, 11 April 1975. The site was resurveyed on 26 January 1990 from 1117 to 1737 UTC and crossed again on 26 February during the approach to the site and before dropping the beacon. The beacon was dropped at 1608 UTC, 26 February 1990, in a location believed to be protected from bottom-current activity (i.e., within a shallow basement graben about 0.5 km from the footwall of the northern side of the graben).

Three holes were drilled at Site 807 between 1608 UTC, 26 February 1990, and 1800 UTC, 23 March 1990. Hole 807A was cored with the advanced hydraulic piston corer (APC) and the extended core barrel (XCB) to 822.9 mbsf with 87.1% recovery (103.4% in the section cored with the APC [0–254.4 mbsf], and 79.8% in the section cored with the XCB [254.4–822.9 mbsf]). The hole was successfully logged and a good suite of geophysical measurements was obtained. Hole 807B was cored with the APC to 278.6 mbsf, at which point 120,000-lb. of overpull was encountered on Core 130-807B-30H, forcing abandonment of the hole. Average recovery was 100.6%.

---

[1] Kroenke, L. W., Berger, W. H., Janecek, T. R., et al., 1991. *Proc. ODP, Init. Repts.*, 130: College Station, TX (Ocean Drilling Program).

[2] Shipboard Scientific Party is as given in the list of participants preceding the contents.

A reentry cone with about 58 m of 16.5-in. casing was set at Hole 807C and, after running in and cementing about 350 m of 11.75-in. casing, the hole was washed to 780.0 mbsf. Coring with the rotary core barrel (RCB) then began. Hole 807C was cored with the RCB to 1528.4 mbsf with 33.8% recovery. Hole 807C was also successfully logged to the total depth drilled, and a complete set of geophysical measurements, including formation microscanner (FMS) data, was obtained. Preliminary analyses of the shipboard data indicate that a complete, undisturbed record of the last 10 m.y. was recovered in the uppermost 280 m of sediment obtained from the two holes cored with the APC.

The Neogene section is around 591 m thick, and recovery in the Neogene and upper Oligocene sediments cored with the APC and the XCB (APC, 100.6% and 103.4%; XCB, 79.8%) was excellent. The Paleogene section is around 602 m thick, but recovery was significantly decreased in the lower Oligocene–Paleocene sediments cored with the RCB (averaging 26.8%). Recovery averaged 46.6% over the 186.5-m-thick Cretaceous section. Basalt was encountered at 1379.7 mbsf in Core 130-807C-74R. Total penetration into basement was 149.7 m, and 87.6 m of basalt (60% recovery) and 0.6 m of interbedded sediment were recovered.

The sedimentary sequence at Site 807 consists of three lithologic units, as follows:

Unit I (0–968.0 mbsf) is composed mainly of Pleistocene to upper/middle Eocene nannofossil ooze and chalk with foraminifers, with lesser amounts of foraminifer nannofossil ooze and chalk as well as nannofossil ooze and chalk. Unit I is divided into Subunits IA and IB, based on the depth of the ooze-chalk transition. The boundary between the two subunits is placed at 293 mbsf, which corresponds to an age of middle/late Miocene (ca. 10.4 Ma).

Unit II (968.0–1351.4 mbsf) is composed of upper/middle Eocene to upper Campanian limestone, chert, nannofossil chalk, and nannofossil chalk with foraminifers. Unit II is divided into Subunits IIA and IIB, based on the transition from chalk to limestone. The boundary between the two subunits is placed at 1098.0 mbsf, where a limestone lithology is indicated by the presence of over 50% nonbiogenic carbonate in smear slides. The transition is also reflected in the substantial increase in average core recovery, from about 7% in Subunit IIA to about 44% in Subunit IIB.

Unit III (1351.4–1379.7 mbsf) is composed of lower Cenomanian to upper Albian–Aptian claystone, siltstone with varying amounts of radiolarians, and limestone. Unit III is divided into Subunits IIIA and IIIB at the claystone/limestone boundary.

Unit IV (1379.7–1528.4 mbsf), comprising igneous basement at Site 807, is composed of Albian-Aptian basalt and interbedded limestone. Unit IV is further divided into seven subunits (IVA through IVG), five of which are igneous (IVA, IVC, IVE, IVF, and IVG), and two of which are sedimentary (IVB and IVD). All of the igneous subunits are composed of sightly altered tholeiitic basalts.

Subunit IVA (1379.7–1424.6 mbsf) consists of aphyric pillow lavas and thin (<2 m thick), massive flows with rare plagioclase phenocrysts up to 3 mm long, superficially similar to lavas at Site 803. Subunits IVC (1425.1–1441.9 mbsf), IVE (1442.0–1447.0 mbsf), IVF (1447.0–1475.0 mbsf), and IVG (1475.0–1528.4 mbsf) are also aphyric, but they contain sparse, euhedral to subhedral, olivine microphenocrysts (<1 mm long) as well, largely replaced by green and black clays. Like Subunit IVA, Subunits IVC, IVE, and IVG are successions of pillow lavas and thin (<3 m thick) massive flows. Subunit IVF, however, consists of a single massive flow, approximately 28 m thick. This flow documents the presence of thick flood basalt lavas on the Ontong Java Plateau.

The sedimentary interbeds, Subunits IVB (1424.6–1425.1 mbsf) and IVD (1441.9–1442.0 mbsf), are Albian-Aptian limestone interbedded with vitric tuff, and limestone containing quartz and illite/glauconite, respectively. Another sedimentary interbed, detected during logging at 1434 mbsf but unsampled in the coring, is located within Subunit IVC. Flecks of native copper were observed in several of the basalt cores below the sedimentary interbeds of Subunit IVB, particularly in vein material in Section 130-807C-82R-2 at 40 and 58 cm. Disseminated pyrite also was observed in glassy pillow rims and fractures.

The Albian-Aptian age of the sediments overlying the basalt suggests that the volcanic sequence will be useful in refining the Pacific Plate apparent polar-wander path. Three factors make the study of Unit IV basalts especially promising: (1) the presence of three sedimentary interbeds (which suggests that the sequence represents sufficient time to average a significant amount of secular variation in the paleofield direction); (2) the remarkably fresh state of many of the rocks; and (3) the occurrence of thick flows interbedded with pillows (which should permit recognition of tilting within the pillow basalts). The inclinations of natural remanent magnetizations (NRMs) of the basalts are dominantly steeper than 20°. If the NRM is dominated by a primary remanence, as suggested in accordance with the freshness of the rocks, the entire basalt sequence is of normal polarity.

Above the basalt and basal limestones, the overall interbedded pattern of the upper Albian to lower Cenomanian claystone/siltstone sequence may indicate the importance of periodic mass transport or cyclical deposition at Site 807. Much of the lower part of the Upper Cretaceous could be missing. The upper Campanian-Maestrichtian limestone apparently contains a signal of changing dissolution levels in the Cretaceous ocean, with good preservation of foraminifers observed in the Maestrichtian in places. The section is barren of radiolarians. Sedimentation rates decreased from 10 to 20 m/m.y. in the late Maestrichtian to less than 5 m/m.y. in the early Paleocene. The Cretaceous/Tertiary (K/T) boundary is located in Core 130-807C-54R. The sequence recovered is thought to be complete, with volcanic ash marking the transition.

Much of the Paleocene–middle Eocene is condensed, with the exception of part of the upper Paleocene (NP9) where sedimentation rates reach 30 m/m.y. Preservation of fossils below the upper Eocene generally is poor. The section is barren of diatoms, but radiolarians occur sporadically in the middle Eocene. After an initial low of 1 m/m.y. in the early middle Eocene (ca. 54–51 Ma), sedimentation rates increased again, peaking near 30 m/m.y. in the late middle Eocene (ca. 45–43 Ma). Hiatuses are present in the Paleogene section: two in the middle Eocene and one in the middle of the Oligocene. The latter hiatus immediately follows a jump in sedimentation rate to over 35 m/m.y. (ca. 30–32 Ma).

The Neogene section appears complete, albeit somewhat thinned in the upper part of the lower Miocene. Sedimentation rates range from near 30 m/m.y. across the Oligocene/Miocene boundary (ca. 28–22 Ma), to 15–20 m/m.y. in the early to early late Miocene (ca. 22–8 Ma), to more than 40 m/m.y. in the late Miocene (ca. 8–5 Ma), before dropping to about 15 m/m.y. in the Pleistocene. The overall sedimentation rate pattern for the Neogene is quite similar to those of Sites 805 and 806, with Site 807 having intermediate values. Surprisingly, the equatorial crossing of Site 807 (ca. 10–12 Ma) does not seem to affect the sedimentation rate greatly.

Hole 807C logging data, in conjunction with a detailed suite of physical properties measurements obtained from the split cores, confirm the depths of the ooze-chalk and chalk-limestone transitions based upon sediment descriptions and reveal the presence of local maxima and minima in velocity that correlate with chert or silicified chalk horizons and with the claystone/siltstone beds deep in the section. The logs allow an estimate of the amount of chert present in the section, which is thought to vary between 20% and 70% at any one interval, the higher values signifying the presence of massive cherts or beds of highly silicified limestone. The logs from different holes at Site 807 correlate well over intervals of 15 cm or less, instilling confidence in the interpretation of high-frequency events at Milankovitch time scales.

Gamma-ray logs and the FMS data confirm the presence of a single, massive flow in Subunit IVF and help identify the presence of sedimentary interbeds in the overlying pillowed-flow subunits, including one unsampled by the coring operation. Resistivity logs, moreover, indicate that another massive flow might be present at the bottom of the hole. The logs provide important constraints on the generation of synthetic seismograms. Duplication of logging runs in the paired Holes 807A and 807C allows assessment of the precision of the logging data.

A reasonably complete seismic stratigraphy is present at Site 807. Evidence for small-scale mass movement was observed at 0.14–0.24 s below seafloor (sbsf) and at 0.28–0.41 sbsf (4.7–6.7

and 7.5–12.5 Ma, respectively). Thickened wedges of sediment occur between 0.44 and 0.53 sbsf (14.5–20.5 Ma) and around 1.00–1.02 sbsf (about 50.4 Ma). Basement occurs at approximately 1.13 sbsf (1379.7 mbsf).

Magnetic susceptibility was measurable well into Pliocene sediments. These data will be useful for fine-scale correlation and for studies of Milankovitch-type cycles.

Results from interstitial water geochemistry at Site 807 are similar to the data obtained from Sites 803 and 804. The conservative gradients (Ca and Mg) compare favorably with those of Sites 288 and 289, suggesting similar basalt-alteration diffusion rates. These and other gradients reflect the dominance of biogenic sediments and the paucity of organic carbon. Calcium and magnesium depth gradients are the least pronounced at Site 807, however, and the magnesium profile at Site 807 is anomalous with the other Ontong Java sites in the lower part of the section where magnesium concentrations remain constant with increasing depth. Dissolved silica concentrations generally increase with depth down to 900 mbsf (ca. 36 Ma) and then decrease and level off at 1000 mbsf (ca. 42 Ma) in the silicified sediments of Unit II.

BACKGROUND AND OBJECTIVES

Overview

Site 807 (proposed Site OJP-5A) was the last of the Leg 130 sites to be drilled on the Ontong Java Plateau. It was scheduled as the primary site for deep penetration into basement. The site is located on the northern rim of the high plateau, in water shallow enough to ensure a high sedimentation rate, yet far enough away from Sites 288 and 289 to avoid the local hiatuses in the sedimentary sections at those sites. It was selected in a region of fairly smooth basement and sedimentary topography, away from such complicating features as seamounts, structural complexities, and canyons so as to maximize the chances of recovering little-disturbed sediment and basement sections. Also, the site was placed as far off the postulated isochron passing through Site 289 as possible to allow evaluation of the proposed north-south age progression across the Ontong Java Plateau. The goal was to drill a thick, well-preserved Cenozoic and Mesozoic sedimentary section before penetrating as deeply into basement as time allowed.

The maximum sedimentary thickness on the Ontong Java Plateau, which is more than 1200 m, occurs below the crest of the plateau in water depths greater than 2200 m. Site 807 was located on the northern rim of the high plateau to retain a thick sedimentary section yet avoid the problems of current-winnowing and bottom transport encountered at other drilling sites on the plateau, as well as the type of slope instability observed on the flanks of the plateau. Despite its shallow depth, the apparent thinning in the upper part of the section observed in the SCS reflection profile leading up to the site, as well as the apparent thickening observed in the lower part of the section, led us to expect the presence of a slightly thinner Neogene section and a slightly thicker Paleogene-Cretaceous section. The site was positioned in a shallow basement graben in the hope that the sediment laid down immediately following eruption of the final basement-capping flows was protected from erosion and thus preserved.

Site 807 was planned for drilling into basement, and our hope was to recover a complete section of Paleogene and Cretaceous sediments and as much basement rock as feasible, for pre-Neogene paleoceanography and for studies on the origin of the Ontong Java Plateau. We reached basement after penetrating 1379.7 m of sediment and continued to drill into basalt for 149 m. The Neogene is about 591 m thick, and recovery was excellent in the Neogene and upper Oligocene sediments (averaging 101%–103% in the 254- and 279-m sections cored with the APC, and 80% for the section cored with the XCB). The Paleogene is about 602 m thick, but recovery was significantly decreased in the lower Oligocene–Paleocene sediments (averaging 27.4% in the section cored with the RCB).

Background

The general background for all sites is contained in the "Introduction" chapter (this volume; also see Kroenke, 1972). The Ontong Java Plateau is a broad, shallow, mid-ocean highland in the western equatorial Pacific. Its shallowest regions lie above 2000 m, and its flanks reach depths in excess of 4500 m. With an area in excess of 1.5 million km^2, it is the largest of the "classic" Pacific plateaus. The plateau has a crustal thickness on the order of 40 km, yet it is in isostatic equilibrium, apparently maintaining its depth over much of its history. Crustal seismic velocities are in the range of oceanic crust (Hussong et al., 1979). Age estimates for basement have varied from Aptian (113–117 Ma) for the entire plateau to a succession of ages ranging from earliest Early Cretaceous (145 Ma) along the northernmost rim of the plateau to latest Late Cretaceous on Santa Isabel (see Fig. 1, "Introduction" chapter, this volume) along the southern margin of the plateau.

The oldest sediments overlying basalt are known to be Aptian at Site 289 and Aptian or older at Site 288. Paleontological dates of Albian or older were obtained for the oldest sediments overlying upraised plateau basement on Malaita, and dates of Eocene or older for the oldest sediments overlying plateau basement exposed on Santa Isabel. One radiometric date of 66 Ma has been obtained for a basement sample of uncertain affinity from Santa Isabel.

Leg 130 is the fourth drilling expedition to sample the sediment cover here; four DSDP sites were drilled earlier on the plateau. Three sites were rotary-drilled, with Site 64 spot cored during Leg 7 (Shipboard Scientific Party, 1971) and Sites 288 and 289 continuously cored during Leg 30 (Shipboard Scientific Party, 1975a, 1975b). Site 289, drilled in a water depth of 2206 m, terminated at 1271 mbsf in tholeiitic basalt overlain by Aptian sediments. Sediment thickness is 1262 m, of which the lowermost 293 m are mid-Cretaceous to upper Eocene radiolarian-bearing limestones, nannofossil foraminifer chalks, and nodular cherts. The upper 969 m consists of upper Eocene to Pleistocene nannofossil foraminifer chalks and oozes, with a continuous section down to the lower Oligocene. Semilithified chalk was first encountered near 250 m in the section (late Miocene age).

Site 586, drilled on Leg 89 next to Site 289, was piston cored to 305 mbsf and reached the lowermost upper Miocene (Shipboard Scientific Party, 1986a, 1986b). Well-preserved nannofossil ooze was recovered from the upper 300 m of the section, the first chalky layers appearing at 260 m (age, earliest late Miocene, ca. 10 Ma). Sedimentation rates in Site 586 vary between 13 and 39 m/m.y.

Objectives

Site 807 is located in 2805 m of water, roughly 475 km northwest of DSDP Sites 289/586 on the northern margin of the Ontong Java Plateau (Fig. 1). The site was originally positioned on a single-channel seismic (SCS) profile collected by the *Thomas Washington* during EURYDICE Cruise 9 at 0255 UTC, 11 April 1975 (Berger et al., 1977). It is located within a shallow basement graben about 0.5 km from the foot wall on the northern side of the graben (Fig. 2). The thickness of the sedimentary section at this site is roughly 1.20 s (two-way traveltime), approximately 7%–10% thicker than observed at Sites 289/586. The section is well stratified and appears to include most of the Neogene seismic reflection horizons that have been previously mapped on the Ontong Java Plateau and in other areas of the equatorial Pacific. The

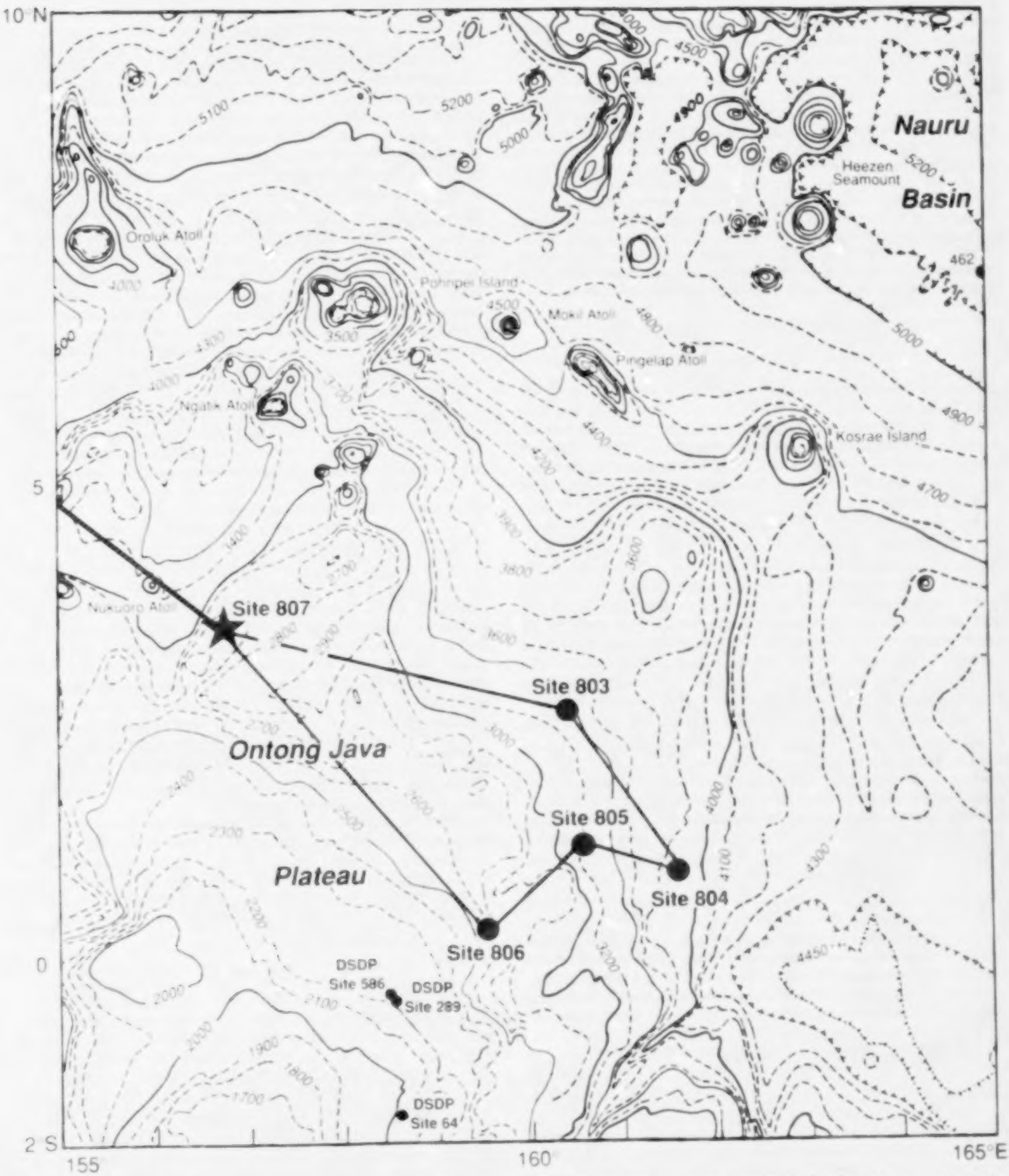
10°N
5
0
2°S
155°
160°
165°E
Nauru
Basin
Heezen Seamount
462
Oroluk Atoll
Pohnpei Island
Mokil Atoll
Pingelap Atoll
Ngatik Atoll
Kosrae Island
Nukuoro Atoll
Site 807
Site 803
Site 805
Site 804
Site 806
Ontong Java
Plateau
DSDP Site 586
DSDP Site 289
DSDP Site 64
5100
5200
5000
4500
4900
5200
4000
4300
3500
4500
4800
5000
4900
4700
4400
4200
3700
3400
2700
3800
3600
3600
2800
2900
3000
2700
2400
2500
2600
2300
2200
2000
2100
2000
1900
1800
1700
3200
4000
4100
4300
4450

Figure 1. Bathymetry in meters of the northwestern part of the Ontong Java Plateau (after Mammerickx and Smith, 1985). The location of the Leg 130 sites together with those from DSDP Legs 7, 30, and 89 are shown for reference. Contour interval is 100 m.

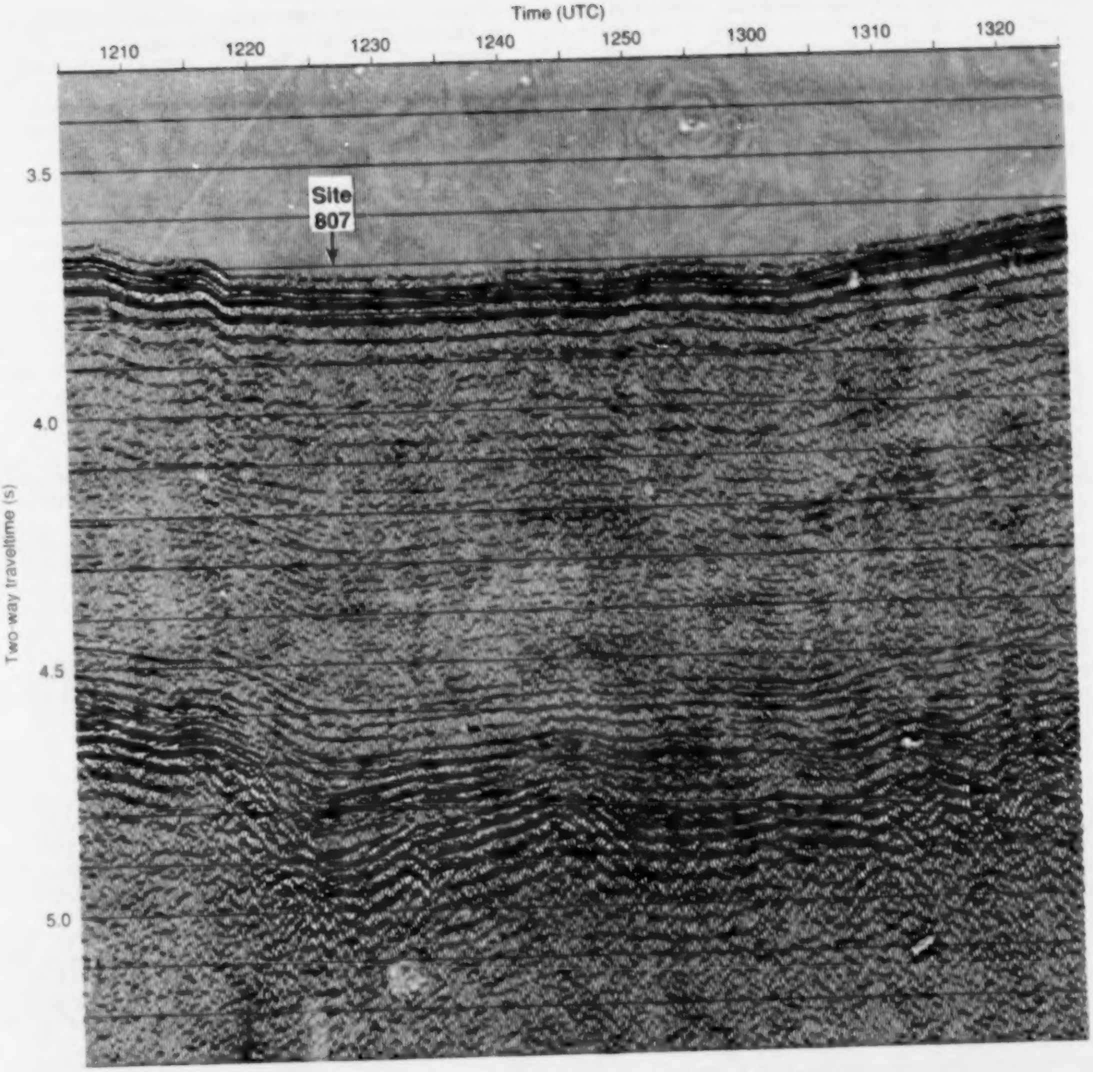

Figure 2. Site survey reflection profile across Site 807 (see "Underway Geophysics" chapter, this volume).

lower part of the section, preserved within a basement graben, has only minor sedimentary deformation, restricted for the most part to small compaction folds and subtle growth faults.

The site was planned to penetrate the entire sedimentary section and as far into basement as feasible. Drilling here was expected to provide a study in latitudinal contrasts between this site north of the equator and the other, more equatorial sites drilled across the northeastern flank of the Ontong Java Plateau on the Neogene depth transect. Water depth at Site 807 is intermediate between Sites 805 and 806, facilitating the comparison of changes in sedimentation caused by differences in latitude between the sites. The latitude of Site 807 is only slightly north of Site 803, however, facilitating comparison of depth-related paleoceanographic signals. Neogene objectives were to be achieved at Site 807 by double coring with the APC as deep as possible and then coring with the XCB to refusal.

Concerning Paleogene and Cretaceous sediments, the poor coverage in the Pacific leaves much to be desired. Substantial hiatuses exacerbate this situation. Major hiatuses were encountered in Upper Cretaceous to Paleogene sediments drilled at DSDP Sites 288 and 289, lowering our expectations with regard to finding complete sequences. However, many of the unconformities at Site 288 do not correlate with those at Site 289 (or the shallower, spot-cored Site 64), implying that they represent local events of limited areal extent (Shipboard Scientific Party, 1975a, 1975b). There was hope, therefore, that drilling at Site 807 could recover key sections missed earlier. There was also the expectation that we would find clues to the extent of Cretaceous anoxic events in the South Pacific and to the original basement depth of the plateau and subsequent bathymetric change.

If recovery were adequate, paleomagnetic investigations of Cretaceous sediments from the Ontong Java Plateau might also provide the opportunity to examine short polarity events within the Cretaceous normal polarity superchron (Tarduno, in press). Furthermore, if age estimates of early Aptian through Hauterivian for the basal sediments at Site 807 were correct, the basal sediments and basalt could be independently dated by magnetostratigraphy, complementing radiometric and isotopic studies.

Basement samples also were to be recovered at Site 807 for dating and geochemical/petrologic analyses. Previously, basement had been drilled at Site 289, recovering a scant 4.5 m of basalt of varying textures from a single flow. Recently, an $^{40}Ar/^{39}Ar$ date of 113 Ma was obtained on a sample of this basalt (R. Duncan, pers. comm., 1989). With a second suite of basaltic basement samples from Site 803, and a third and more comprehensive suite from Site 807, new light will be thrown on the question of the nature and origin of the Ontong Java Plateau. Problems to be addressed include whether the plateau formed at a hotspot during a short interval of time and over a single thermal plume (Mahoney, 1987); whether the plateau formed by ridge crest processes over a prolonged span of time and along a slowly spreading ridge system (Kroenke, 1984); or whether we have some combination of both processes, as in the example of the comparatively small Icelandic Plateau.

It was also hoped that a good paleolatitude might be obtained for the Ontong Java Plateau by sampling multiple flow units at Site 807. At present, the only absolute paleolatitudes for the Pacific Plate for the Early Cretaceous are based on marine magnetic anomaly skewness data (Gordon, in press). The reliability of these paleolatitudes is in doubt, however, because of possible systematic errors, as observed in other data sets (Petronotis and Gordon, 1989). Because only a single flow was sampled at Site 289, a biased estimate of the paleolatitude for the Ontong Java Plateau was obtained. By sampling multiple flows at Site 807, therefore, we hoped to obtain a benchmark Early Cretaceous paleolatitude for the Pacific Plate as well as the Ontong Java Plateau. Furthermore, if a viscous present-day overprint were to be present on the basalt, as has been observed in the western central Pacific (Tarduno et al., 1989), it might also be possible to construct a paleomagnetic pole for this period.

OPERATIONS

The transit from Sites 806 to 807 covered 251 nmi in 28.5 hr at an average speed of 8.81 kt. A 30-nmi seismic survey was run over the proposed site in 4.0 hr at 7.5 kt. The 200-in.^{3} water gun was used on the transit and site survey (see the "Underway Geophysics" chapter, this volume, for details of the surveys). The global positioning satellite (GPS) system was not available for the site survey but was available for the final positioning. The beacon was dropped at 1608 hr UTC, 26 February 1990, on the proposed site, initiating Site 807.

Hole 807A

The ship was positioned 30 m south-southwest of the beacon. Core 130-807A-1H was taken at 0005 hr, 27 February 1990 in a water depth of 2803.8 m. Cores 130-807A-1H through -27H were taken from 0 to 254.4 mbsf, with 254.4 m of sediment cored and 263.11 m recovered (103.4% recovery; see Table 1). Orientation surveys were taken during Cores 130-807A-3H through -27H. Coring with the APC ended at Core 130-807A-27H when overpull increased to 100,000 lb.

Cores 130-807A-28X through -86X were taken from 254.4 to 822.9 mbsf, with 568.5 m of sediment cored and 453.63 m recovered (79.8% recovery; see Table 1). Coring with the XCB ended when core recovery dropped below probable recovery with the RCB system. The sonic core monitor was run successfully on Cores 130-807A-74X, -76X, and -79X (recovery 5.46, 8.44, and 2.40 m, respectively). Problems with chalk jamming in the shoe were noted in Core 130-807A-69X (659.2 mbsf; 1.46-m recovery). The sinker bars were removed at that point, and a modified standard XCB shoe with a smaller inner diameter was used with good results.

Hole 807A Logging

Upon completion of coring at Hole 807A, the pipe was pulled to 100 mbsf and a high-viscosity mud sweep was made to clean the hole. The bit was pulled to 85.6 mbsf and logging operations began.

The following logs were completed:

Run No. 1: NGT/LSS/DIT/TLT; a successful logging run was made over the interval from 820.5 to 89.6 mbsf at 900 ft/hr. Approximately 2.4 m of fill was encountered at the base of the hole.

Run No. 2: NGT/ACT/HLDT; the log was run at 600 ft/hr from 821.1 to 323.4 mbsf, at which point problems with the heave compensator were encountered. The tool was lowered to 354.8 mbsf, the heave compensator turned back on, and logging data were collected to a depth of 75.6 mbsf.

At the end of logging operations, the pipe was pulled out of the hole, and the bottom hole assembly (BHA) cleared the seafloor at 2100 hr, 2 March 1990, ending Hole 807A.

Hole 807B

The ship was positioned 60 m south-southwest of the beacon. A jet-in test was conducted to a depth of 69 mbsf. The ship was then positioned 90 m south-southwest of the beacon. Core 130-807B-1H was taken at 2345 hr, 2 March 1990, in a water depth of 2806.1 m. Cores 130-807B-1H through -30H were taken from 0 to 278.6 mbsf, with 278.6 m of sediment cored and 280.18 m recovered (100.57% recovery).

Orientation surveys were taken during Cores 130-807B-3H- through -10H. Refusal of the APC was reached at Core 130-807B-30H (278.6 mbsf) when overpull reached 120,000 lb. At this point, the pipe was pulled out of the hole and the BHA cleared the rotary table at 0115 hr, 4 March 1990, ending Hole 807B.

Hole 807C

The ship was positioned 120 m south-southwest of the beacon. A new-style reentry cone was positioned under the rotary table; and a casing shoe, four joints of 16-in. casing, and the hanger were assembled and landed in the cone. The assembly was picked up and run slowly into the moonpool at 1000 hr, 4 March 1990. Seas were mild with 2–7 ft swells and 8-s periods. The cone was lowered about 3 m below the water surface when the driller observed the weight fluctuate between 36,000 and 15,000 lb, followed by a gradual loss of weight. A large surge was observed and a heavy dull thump was heard in the moonpool area. The cone had become unjayed and had sunk to the seafloor.

A second, new-style reentry cone was built, with the addition of two 10 × 10 in. holes in each of four mud-skirt plates and four 1 × 24 in. vertical slots in the reentry funnel to reduce surge effects while lowering the cone below the moonpool. An identical four-joint, 16-in. casing string and BHA were jayed into the cone. Entry into the water was smoother (the holes seemed to reduce the heave surge effect), and the cone was run to just above the seafloor 150 m from the beacon.

Hole 807C was spudded at 0700 hr, 5 March 1990, when the 16-in. casing was jetted-in to a sub-bottom depth of 58.1 mbsf. The bit was unjayed and a hole was drilled to 360.0 mbsf. A mud sweep was then made and the pipe pulled out of the hole.

Twenty-five joints of 11.75-in. casing were made up and run to the seafloor. The reentry cone was located with the televiewer (TV) camera after a 1.75-hr search, and the cone was reentered. The casing was run into the hole to 349.8 mbsf and cemented in place. The cementing string was pulled out, and an RCB bit with a 12 drill-collar BHA was run to the seafloor. The cone was reentered after a 1.5-hr TV camera search.

The casing shoe was drilled out in 2.25 hr, and a hole was drilled without coring to 780.0 mbsf in hard chalk in 5.0 hr. Coring with the RCB began at this point, and Cores 130-807C-1R through -56R (780.0–1216.3 mbsf) recovered 93.30 m of hard chalk (Cores 130-807C-1R through -24R), hard limestone (Cores 130-807C-25R through -41R), and chert (Cores 130-807C-42R through -56R). Poor recovery often resulted from the hard chalk fracturing and jamming in the bit throat. The bit deplugger was run three times. The bit was pulled after 44.65 hr of rotation time.

A four-cone insert bit was run to the seafloor and the reentry cone was entered after a short search. Cores 130-807C-57R through -79R (1216.3–1423.9 mbsf) were taken with 91.25 m of core recovered in hard limestone. Basalt was encountered at 1380 mbsf. The bit was pulled after rotating 42.0 hr, and two shanks were found to have broken welds.

A second four-cone insert bit was run to the seafloor, and the reentry cone was entered after a short search. Cores 130-807C-80R through -88R (1423.9–1503.0 mbsf) were cut, with 50.59 m of basalt recovered. The bit was pulled after 35.08 hr of rotation time, and one shank weld was found to have failed.

A third four-cone insert bit was run to the seafloor, and the reentry cone was entered after a short search. Cores 130-807C-89R through -93R (1503.0–1528.4 mbsf) were cut, with 13.10-m basalt recovered, and the bit was pulled after rotating 18.16 hr when it torqued up once again. The bit was examined with the TV camera at the seafloor and was found to have two shanks and cones missing; presumably they were left in Hole 807C. The bit was dropped on the seafloor by activating the mechanical bit release and the cone was reentered for logging. The pipe was set to 169 mbsf in preparation for logging.

Logs were run as follows:

Log No. 1: NGT/LSS/DIT/TLT; the log data were collected from 330.4 to 1492.9 mbsf and from 1528.3 to 348.7 mbsf at a rate of 900 ft/hr. Approximately 0.6 m of bottom fill were encountered.

Log No. 2: NGT/ACT/HLDT; the log was started at a depth of 1525.8 mbsf and run at a speed of 600 ft/hr. At 1467.9 mbsf, the caliper became jammed with debris and the logging run was stopped. The tool was lowered again to 1527.0 mbsf, and the logging run restarted. No further complications were encountered, and data were collected up to a depth of 348.7 mbsf.

Log No. 3: NGT/FMS/GPIT/TLT; the first log with this tool was made at 900 ft/hr over the interval from 1509.1 to 947.3 mbsf, at which point the hole was too wide for the FMS caliper. The tool was lowered again to the base of the hole, and a second log was collected from 1507.8 to 1095.5 mbsf.

After logging, the pipe was pulled out of the hole and the BHA cleared the rotary table at 0000 hr, 23 March 1990, ending Site 807.

Site 807 to Guam

The thrusters and hydrophones were pulled, and the ship began a post-site survey toward Guam at 0000 hr, 23 March 1990. A 203-nmi underway geophysics survey was conducted enroute to Guam.

The *JOIDES Resolution* arrived outside Apra Harbor, Guam, on 26 March 1990. The harbor pilot arrived on board at 1930 hr, 26 March. The first line ashore was at 2030 hr, 26 March 1990, ending Leg 130.

LITHOSTRATIGRAPHY

Introduction

The sedimentary sequence at Site 807 was divided into three lithologic units (Fig. 3 and Table 2). Unit I (0–968 mbsf) is composed predominantly of Pleistocene to upper Eocene nannofossil ooze and chalk with foraminifers, with lesser amounts of foraminifer nannofossil ooze and chalk and nannofossil ooze and chalk. This unit was divided into Subunits IA and IB, based on the degree of induration. The boundary between the two subunits was placed at 293 mbsf, the top of Core 130-807A-32X, which corresponds to a middle-late Miocene age of 10–11 Ma (see "Biostratigraphy" section, this chapter). The basal 30 m of Subunit IA contains a significant amount of chalk as isolated nodules and layers.

Unit II (968–1351.4 mbsf) is composed of Eocene to upper Campanian limestone, chert, nannofossil chalk, and nannofossil chalk with foraminifers. The boundary between Units I and II was placed at the level where chert becomes a significant component in the recovered sediment. Unit II was divided into Subunits IIA and IIB, based on the transition from chalk to limestone. The boundary between the two subunits was placed at 1098 mbsf, the top of Core 130-807C-41R, which corresponds to an early middle Eocene age of approximately 40 Ma (see "Biostratigraphy" section, this chapter). The transition in sediment induration is also reflected in a substantial increase in recovery, from 7% in Subunit IIA to 44% in Subunit IIB.

Unit III (1351.4–1379.7 mbsf) is composed of lower Cenomanian to upper Albian claystone and siltstone with varying amounts of radiolarians, and Albian to Aptian limestone. The unit was divided into Subunits IIIA and IIIB at the transition from claystone to limestone. The boundary between the two subunits was placed at 1369.7 mbsf (Section 130-807C-73R-2, 82 cm). Limestone beds were also recovered as interlayers in the basalt at 1424.6–1425.1 mbsf (Section 130-807C-80R-1, 70–120 cm) and at 1439 mbsf (Section 130-807C-82R-3, 72–79 cm).

Description of Units

Unit I

Intervals: Hole 807A, Cores 130-807A-1H through -86X; Hole 807B, Cores 130-807B-1H through -30H; Hole 807C, Cores 130-807C-1R through -26R
Age: Pleistocene–late Eocene
Depth: 0–968 mbsf

Unit I consists predominantly of nannofossil ooze and chalk with foraminifers and lesser amounts of foraminifer nannofossil ooze and chalk and nannofossil ooze and chalk. Unit I was divided into two subunits. Subunit IA (0–293 mbsf) is primarily nannofossil ooze with foraminifers and foraminifer nannofossil ooze, but it grades to nannofossil ooze in some intervals. The basal 30 m of Subunit IA contains a significant percentage of chalk. Subunit IB (293–968 mbsf) grades downward from foraminifer nannofossil

Table 1. Coring summary, Site 807.

Core no.	Date (1990)	Time (UTC)	Depth (mbsf)	Cored (m)	Recovered (m)	Recovery (%)
130-807A-						
1H	Feb. 27	0005	0–7.4	7.4	7.37	99.6
2H	27	0050	7.4–16.9	9.5	9.90	104.0
3H	27	0125	16.9–26.4	9.5	9.91	104.0
4H	27	0215	26.4–35.9	9.5	9.94	104.0
5H	27	0250	35.9–45.4	9.5	9.85	103.0
6H	27	0345	45.4–54.9	9.5	9.93	104.0
7H	27	0420	54.9–64.4	9.5	9.96	105.0
8H	27	0500	64.4–73.9	9.5	9.95	105.0
9H	27	0535	73.9–83.4	9.5	9.70	102.0
10H	27	0615	83.4–92.9	9.5	9.87	104.0
11H	27	0655	92.9–102.4	9.5	9.85	103.0
12H	27	0730	102.4–111.9	9.5	9.74	102.0
13H	27	0820	111.9–121.4	9.5	9.66	101.0
14H	27	0845	121.4–130.9	9.5	9.84	103.0
15H	27	0930	130.9–140.4	9.5	9.93	104.0
16H	27	1005	140.4–149.9	9.5	9.97	105.0
17H	27	1045	149.9–159.4	9.5	9.92	104.0
18H	27	1125	159.4–168.9	9.5	9.73	102.0
19H	27	1210	168.9–178.4	9.5	9.92	104.0
20H	27	1250	178.4–187.9	9.5	9.71	102.0
21H	27	1325	187.9–197.4	9.5	9.40	98.9
22H	27	1405	197.4–206.9	9.5	9.89	104.0
23H	27	1455	206.9–216.4	9.5	9.98	105.0
24H	27	1540	216.4–225.9	9.5	9.80	103.0
25H	27	1625	225.9–235.4	9.5	9.90	104.0
26H	27	1715	235.4–244.9	9.5	9.89	104.0
27H	27	1810	244.9–254.4	9.5	9.60	101.0
28X	27	1900	254.4–264.1	9.7	9.04	93.2
29X	27	2000	264.1–273.8	9.7	9.58	98.7
30X	27	1945	273.8–283.5	9.7	9.30	95.9
31X	27	2130	283.5–292.7	9.2	8.12	88.2
32X	27	2215	292.7–302.3	9.6	8.02	83.5
33X	27	2245	302.3–312.0	9.7	9.41	97.0
34X	27	2335	312.0–321.2	9.2	9.71	105.0
35X	28	0010	321.2–330.9	9.7	8.56	88.2
36X	28	0055	330.9–340.6	9.7	9.48	97.7
37X	28	0125	340.6–350.2	9.6	9.77	102.0
38X	28	0210	350.2–359.9	9.7	9.13	94.1
39X	28	0250	359.9–369.7	9.8	8.51	86.8
40X	28	0325	369.7–379.5	9.8	9.62	98.1
41X	28	0400	379.5–389.2	9.7	9.02	93.0
42X	28	0452	389.2–398.9	9.7	8.33	85.9
43X	28	0530	398.9–408.6	9.7	8.76	90.3
44X	28	0600	408.6–418.3	9.7	8.14	83.9
45X	28	0635	418.3–427.8	9.5	9.87	104.0
46X	28	0715	427.8–437.5	9.7	8.97	92.5
47X	28	0750	437.5–447.1	9.6	9.05	94.3
48X	28	0830	447.1–456.8	9.7	9.66	99.6
49X	28	0905	456.8–466.4	9.6	7.93	82.6
50X	28	0950	466.4–476.1	9.7	9.45	97.4
51X	28	1030	476.1–485.8	9.7	8.94	92.1
52X	28	1110	485.8–495.4	9.6	8.59	89.5
53X	28	1150	495.4–505.1	9.7	8.50	87.6
54X	28	1225	505.1–514.8	9.7	8.74	90.1
55X	28	1305	514.8–524.0	9.2	9.23	100.0
56X	28	1340	524.0–533.7	9.7	8.58	88.4
57X	28	1420	533.7–543.4	9.7	8.42	86.8
58X	28	1500	543.4–553.0	9.6	7.85	81.8
59X	28	1540	553.0–562.6	9.6	7.01	73.0
60X	28	1620	562.6–572.3	9.7	7.48	77.1
61X	28	1700	572.3–581.9	9.6	8.84	92.1
62X	28	1740	581.9–591.6	9.7	7.93	81.7
63X	28	1820	591.6–601.3	9.7	6.92	71.3
64X	28	1905	601.3–611.0	9.7	7.55	77.8
65X	28	2000	611.0–620.6	9.6	7.36	76.6
66X	28	2045	620.6–630.3	9.7	6.65	68.5
67X	28	2120	630.3–639.9	9.6	5.15	53.6
68X	28	2215	639.9–649.6	9.7	6.88	70.9
69X	28	2335	649.6–659.2	9.6	1.46	15.2
70X	Mar 1	0040	659.2–668.9	9.7	8.44	87.0
71X	1	0150	668.9–678.2	9.3	8.01	86.1
72X	1	0300	678.2–687.8	9.6	5.99	62.4
73X	1	0415	687.8–697.5	9.7	9.04	93.2
74X	1	0520	697.5–707.2	9.7	5.46	56.3
75X	1	0615	707.2–716.9	9.7	7.04	72.6
76X	1	0730	716.9–726.5	9.6	8.44	87.9

Table 1 (continued).

Core no.	Date (1990)	Time (UTC)	Depth (mbsf)	Cored (m)	Recovered (m)	Recovery (%)
77X	1	0820	726.5–736.2	9.7	8.21	84.6
78X	1	0930	736.2–745.5	9.3	8.08	86.9
79X	1	1035	745.5–755.2	9.7	2.40	24.7
80X	1	1155	755.2–764.9	9.7	4.11	42.4
81X	1	1305	764.9–774.5	9.6	1.09	11.3
82X	1	1430	774.5–784.2	9.7	5.91	60.9
83X	1	1540	784.2–793.9	9.7	6.29	64.8
84X	1	1700	793.9–803.6	9.7	9.65	99.5
85X	1	1820	803.6–813.2	9.6	3.48	36.2
86X	1	1940	813.2–822.9	9.7	2.48	25.5
Coring totals				822.9	716.74	87.1
130-807B-						
1H	Mar. 2	2345	0–3.1	3.1	3.04	98.0
2H	3	0020	3.1–12.6	9.5	9.75	102.0
3H	3	0100	12.6–22.1	9.5	9.64	101.0
4H	3	0145	22.1–31.6	9.5	9.59	101.0
5H	3	0220	31.6–41.1	9.5	9.73	102.0
6H	3	0300	41.1–50.6	9.5	9.83	103.0
7H	3	0350	50.6–60.1	9.5	9.79	103.0
8H	3	0430	60.1–69.6	9.5	9.88	104.0
9H	3	0505	69.6–79.1	9.5	9.72	102.0
10H	3	0550	79.1–88.6	9.5	9.78	103.0
11H	3	0630	88.6–98.1	9.5	10.06	105.9
12H	3	0705	98.1–107.6	9.5	9.76	103.0
13H	3	0745	107.6–117.1	9.5	9.87	104.0
14H	3	0805	117.1–126.6	9.5	9.33	98.2
15H	3	0845	126.6–136.1	9.5	9.23	97.1
16H	3	0920	136.1–145.6	9.5	9.91	104.0
17H	3	1000	145.6–155.1	9.5	9.97	105.0
18H	3	1030	155.1–164.6	9.5	9.67	102.0
19H	3	1135	164.6–174.1	9.5	7.33	77.1
20H	3	1215	174.1–183.6	9.5	5.67	59.7
21H	3	1255	183.6–193.1	9.5	9.79	103.0
22H	3	1325	193.1–202.6	9.5	9.82	103.0
23H	3	1400	202.6–212.1	9.5	9.95	105.0
24H	3	1440	212.1–221.6	9.5	9.93	104.0
25H	3	1520	221.6–231.1	9.5	9.91	104.0
26H	3	1555	231.1–240.6	9.5	9.93	104.0
27H	3	1635	240.6–250.1	9.5	9.84	103.0
28H	3	1720	250.1–259.6	9.5	9.94	104.0
29H	3	1820	259.6–269.1	9.5	9.72	102.0
30H	3	1900	269.1–278.6	9.5	9.80	103.0
Coring totals				278.6	280.18	100.6
130-807C-						
1R	Mar. 8	0930	780.0–789.7	9.7	0.20	2.1
2R	8	1030	789.7–799.3	9.6	2.52	26.2
3R	8	1140	799.3–809.0	9.7	0.04	0.4
4R	8	1300	809.0–818.6	9.6	2.68	27.9
5R	8	1400	818.6–828.3	9.7	0.02	0.2
6R	8	1525	828.3–838.0	9.7	7.59	78.2
7R	8	1650	838.0–847.7	9.7	0.19	2.0
8R	8	1805	847.7–857.4	9.7	0.01	0.1
9R	8	2000	857.4–867.1	9.7	0.62	6.4
10R	8	2200	867.1–872.3	5.2	0.00	0.0
11R	8	2300	872.3–876.6	4.3	0.00	0.0
12R	9	0145	876.6–881.9	5.3	0.59	11.1
13R	9	0300	881.9–888.9	7.0	0.22	3.1
14R	9	0400	888.9–893.9	5.0	0.15	3.0
15R	9	0500	893.9–898.9	5.0	0.72	14.4
16R	9	0600	898.9–903.9	5.0	1.36	27.2
17R	9	0700	903.9–908.9	5.0	3.47	69.4
18R	9	0800	908.9–913.9	5.0	0.23	4.6
19R	9	0900	913.9–918.9	5.0	0.67	13.4
20R	9	1000	918.9–923.9	5.0	0.23	4.6
21R	9	1220	923.9–933.7	9.8	0.39	4.0
22R	9	1415	933.7–938.7	5.0	0.36	7.2
23R	9	1520	938.7–943.7	5.0	5.21	104.0
24R	9	1630	943.7–948.4	4.7	2.94	62.5
25R	9	1745	948.4–958.1	9.7	1.29	13.3
26R	9	1900	958.1–967.8	9.7	1.53	15.8
27R	9	2015	967.8–977.5	9.7	0.09	0.9
28R	9	2130	977.5–987.1	9.6	0.15	1.6
29R	9	2300	987.1–996.8	9.7	0.32	3.3

Table 1 (continued).

Core no.	Date (1990)	Time (UTC)	Depth (mbsf)	Cored (m)	Recovered (m)	Recovery (%)
30R	10	0200	996.8–1006.5	9.7	1.52	15.7
31R	10	0345	1006.5–1016.1	9.6	0.78	8.1
32R	10	0500	1016.1–1025.4	9.3	0.22	2.4
33R	10	0620	1025.4–1034.6	9.2	0.40	4.4
34R	10	0740	1034.6–1044.3	9.7	0.47	4.8
35R	10	0850	1044.3–1054.0	9.7	0.82	8.5
36R	10	1010	1054.0–1063.7	9.7	0.41	4.2
37R	10	1135	1063.7–1073.2	9.5	0.31	3.3
38R	10	1250	1073.2–1082.4	9.2	0.68	7.4
39R	10	1415	1082.4–1092.0	9.6	0.42	4.4
40R	10	1520	1092.0–1097.7	5.7	1.72	30.2
41R	10	1700	1097.7–1102.4	4.7	0.94	20.0
42R	10	1845	1102.4–1106.4	4.0	1.65	41.2
43R	10	2100	1106.4–1116.0	9.6	1.20	12.5
44R	10	2340	1116.0–1125.6	9.6	1.08	11.2
45R	11	0220	1125.6–1135.2	9.6	2.84	29.6
46R	11	0500	1135.2–1140.2	5.0	3.86	77.2
47R	11	0725	1140.2–1145.2	5.0	2.51	50.2
48R	11	0940	1145.2–1150.2	5.0	3.19	63.8
49R	11	1220	1150.2–1155.2	5.0	1.23	24.6
50R	11	1420	1155.2–1160.2	5.0	1.97	39.4
51R	11	1800	1160.2–1169.8	9.6	5.11	53.2
52R	11	2300	1169.8–1179.4	9.6	4.58	47.7
53R	12	0400	1179.4–1188.8	9.4	5.75	61.2
54R	12	0845	1188.8–1196.9	8.1	6.00	74.1
55R	12	1450	1196.9–1206.6	9.7	6.05	62.4
56R	12	1915	1206.6–1216.3	9.7	3.80	39.2
57R	13	1600	1216.3–1222.5	6.2	2.87	46.3
58R	13	1900	1222.5–1232.2	9.7	0.57	5.9
59R	13	2215	1232.2–1241.8	9.6	3.34	34.8
60R	13	0115	1241.8–1251.5	9.7	0.22	2.3
61R	14	0400	1251.5–1261.2	9.7	2.84	29.3
62R	14	0645	1261.2–1270.8	9.6	4.72	49.1
63R	14	0920	1270.8–1280.5	9.7	5.49	56.6
64R	14	1210	1280.5–1290.1	9.6	3.75	39.0
65R	14	1515	1290.1–1299.8	9.7	3.34	34.4
66R	14	1800	1299.8–1309.5	9.7	4.60	47.4
67R	14	2100	1309.5–1319.1	9.6	6.93	72.2
68R	14	2335	1319.1–1328.8	9.7	3.64	37.5
69R	15	0230	1328.8–1338.4	9.6	7.08	73.7
70R	15	0520	1338.4–1348.0	9.6	6.37	66.3
71R	15	0800	1348.0–1357.7	9.7	9.31	96.0
72R	15	0945	1357.7–1367.4	9.7	3.31	34.1
73R	15	1145	1367.4–1375.4	8.0	2.71	33.9
74R	15	1545	1375.4–1385.2	9.8	5.67	57.8
75R	15	2045	1385.2–1394.8	9.6	6.02	62.7
76R	16	0050	1394.8–1404.5	9.7	1.45	14.9
77R	16	0300	1404.5–1409.5	5.0	2.70	54.0
78R	16	0600	1409.5–1414.5	5.0	3.56	71.2
79R	16	1030	1414.5–1423.9	9.4	5.36	57.0
80R	17	1050	1423.9–1433.6	9.7	4.43	45.7
81R	17	1405	1433.6–1438.2	4.6	3.72	80.8
82R	17	1850	1438.2–1447.2	9.0	6.95	77.2
83R	18	0145	1447.2–1455.9	8.7	8.51	97.8
84R	18	0825	1455.9–1465.6	9.7	7.03	72.5
85R	18	1355	1465.6–1475.3	9.7	8.84	91.1
86R	18	1905	1475.3–1485.0	9.7	3.91	40.3
87R	18	2345	1485.0–1494.7	9.7	2.28	23.5
88R	19	0515	1494.7–1503.0	8.3	4.92	59.3
89R	20	0400	1503.0–1509.1	6.1	3.25	53.3
90R	20	0845	1509.1–1515.3	6.2	3.90	62.9
91R	20	1115	1515.3–1516.8	1.5	0.44	29.3
92R	20	1415	1516.8–1518.8	2.0	2.40	120.0
93R	20	2130	1518.8–1528.4	9.6	3.11	32.4
Coring totals				748.4	252.84	33.8

chalk to nannofossil chalk with foraminifers and, at greater depth, to nannofossil chalk.

Subunit IA

Intervals: Hole 807A, Cores 130-807A-1H through -31X; Hole 807B, Cores 130-807B-1H through -30H
Age: Pleistocene–middle/late Miocene boundary
Depth: 0–293 mbsf

Subunit IA consists of 293 m of foraminifer nannofossil ooze, nannofossil ooze with foraminifers, and minor amounts of nannofossil ooze. Smear slide data indicate that nannofossil content in the ooze averages about 75% (Fig. 4A). Foraminifer abundance averages approximately 23% (Table 3) and ranges between 8% and 40%. Maxima in foraminifer abundance were noted in both Holes 807A and 807B from 20 to 40 mbsf (1.0–2.0 Ma), from 60 to 90 mbsf (ca. 2.5 Ma), from 155 to 170 mbsf (ca. 6 Ma), and from 220 to 250 mbsf (ca. 8 Ma). Foraminifer abundances are low in both holes at approximately 50 (2.0–2.5 Ma), 135 (ca. 5.2 Ma), and 190–210 mbsf (ca. 7.5 Ma). Constituents present in trace amounts include radiolarians, diatoms, siliceous sponge spicules, silicoflagellates, volcanic glass, quartz, accessory minerals, and clay.

Texturally, Subunit IA is composed of silts that range from sandy silt to rare clayey silt (Table 3).The high proportion of silt reflects the abundance of nannofossils. Mean grain size averages 28 µm (medium silt) throughout Subunit IA and exhibits crude positive covariation with the estimates of foraminifer abundance based on smear slides (Figs. 4 and 5; Tables 3 and 4). For instance, both mean grain size and foraminifer abundance are high between 60 and 90 mbsf and between 220 and 250 mbsf. Fluctuations in the relative abundance of foraminifers can be further illustrated by analysis of the coarse (>125 µm) and intermediate (63–125 µm) size fractions, which are dominated by foraminifers (Fig. 5B). The size fraction data and smear slide data correlate well with foraminifer abundance.

Calcium carbonate contents in Subunit IA range between 88% and 94% and average 92% (Fig. 6A). The top 30 m of the subunit, representing the Pleistocene (see "Paleomagnetics" section, this chapter), have the lowest carbonate contents of the subunit; below that level, carbonate contents gradually increase to a maximum at 165–210 mbsf. The carbonate contents then decrease over the interval from 210 mbsf to the base of the subunit. X-ray diffraction (XRD) analyses indicate that the relative abundances of terrigenous components, including clays, quartz, and feldspar, are higher in the upper portion of the subunit and decrease below approximately 70 mbsf. Long-term changes in carbonate content and in the abundances of the coarse- and intermediate-size fractions generally correspond throughout Subunit IA. Mean carbonate contents and coarse/intermediate fraction abundances are low above 60 mbsf and high between 60 and 130 mbsf. Between 210 and 260 mbsf, carbonate content is low and coarse/intermediate fraction abundances are high.

Colors in Subunit IA grade from pale brown (10YR 6/3) in the top 50 cm to light gray (10YR 7/2) from 0.5 to 3 mbsf, to predominantly white (2.5Y 8/0, 5Y 8/1, 7.5YR 8/1, and 10YR 8/1) below 3 mbsf. As at Sites 803, 804, 805 and 806, color bands are pervasive. The colors of the bands are either various shades of green, such as light greenish gray (5G 7/1) and pale yellowish green (10GY 7/2), or purple, including reddish gray (5R 6/1), grayish blue (5PB 5/2), and pale purple (5P 6/2). The bands are horizontal, up to 2 cm thick, and commonly occur as green and purple pairs separated by white ooze. The bands first appear at about 9 mbsf and increase in frequency downhole to a maximum at approximately 200 mbsf, corresponding to the upper Miocene. The abundance of bands decreases over the interval from 200 mbsf to the base of Subunit IA (Fig. 7).

Subunit IA is extensively bioturbated. The evidence includes burrows, cylindrical pyrite concretions, and abundant trace fossils. Burrows are commonly surrounded by pale purple (5P 6/2) elliptical halos. In some instances, halo diameters are as large as 20 cm. As a result, it is possible that many of the dipping and horizontal color streaks and bands observed in Subunit IA are fragments of large halos. Color bands were observed to pass through burrows but to be overprinted by the burrow-ringing halo (Fig. 8). These relationships indicate that the color bands and halos reflect different generations of diagenesis.

Other noteworthy features in Subunit IA are the presence of microfaults and a nodule of porcellanite. The porcellanite nodule that was found at 252 mbsf (Core 130-807B-27X-5, 110 cm) is 2–3 cm in diameter and microcrystalline in texture. Similar concretions were found at Site 806 as shallow as 240 mbsf (see "Lithostratigraphy" section, "Site 806" chapter, this volume). Microfaults are present below 49 mbsf as offsets of up to 5 cm in color bands. Several microfaults were also observed between 101 and 107 mbsf (Sections 130-807B-12H-2 and -6); between 132 and 133 mbsf (Core 130-807B-15H); between 191 and 198 mbsf (Sections 130-807A-21H-3 and -4 and Sections 130-807B-22H-1 and -3); and between 242 and 246 mbsf (Sections 130-807A-26H-5 and -6 and Section 130-807B-27H-4).

At a depth of approximately 253 mbsf, 40 m above the base of Subunit IA, the increased induration of ooze is indicated by the first recovery of chalk biscuits. Between 253 and 264 mbsf, the proportion of indurated layers and chalk nodules increases to approximately 10% of the sediment. The abundance of chalk nodules increases throughout the basal 30 m of Subunit IA, and the sediment is predominantly chalk at 294 mbsf.

Support for the division of Unit I into subunits based on induration also comes from the logging results (see "Logging" section, this chapter). Log stratigraphic Unit A2 was chosen with upper and lower boundaries at 254 and 306 mbsf, depths that correspond closely to those chosen from visual examination. Log stratigraphic Unit A2 is characterized by velocities intermediate between those in overlying and underlying sediments. Sonic velocities measured onboard ship increase markedly for samples recovered below 290 m, probably reflecting the change from ooze to chalk (see "Physical Properties" section, this chapter).

Subunit IB

Intervals: Hole 807A, Cores 130-807A-32X through -86X; Hole 807C, Cores 130-807C-1R through -26R
Age: late middle Miocene–late Eocene
Depth: 293–968 mbsf

Subunit IB is composed primarily of nannofossil chalk with foraminifers, foraminifer nannofossil chalk, and nannofossil chalk (Fig. 3). Smear slide analyses indicate that nannofossils compose approximately 80% of Subunit IB (Fig. 4B). Foraminifer abundances are high, approximately 20%, from 350 to 500 mbsf (13–21 Ma) and from 690 to 840 mbsf (middle Oligocene). Foraminifer content is low from 300 to 350 mbsf (11–13 Ma), from 525 to 675 mbsf (22–27 Ma), and from 915 to 968 mbsf (upper Eocene).

Nine ash layers, composed of altered glass and opaque minerals, are present in Subunit IB between 639 and 759 mbsf (ca. 26–32 Ma) (Table 5). The ash layers are dark gray (2.5Y 4/0) and strongly bioturbated (Fig. 9). Other components in Subunit IB, such as radiolarians and diatoms, are present in trace quantities. One chert nodule, 2–3 cm in diameter, was found at 494 mbsf (Section 130-807A-52X-6) and another at 543 mbsf (Section 130-807A-58X-1). Four layers or nodules of chert, each 3–7 cm thick, were found between 959 and 961 mbsf; each contained a partially silicified exterior of chalk (Fig. 10).

Carbonate contents are less than approximately 91% above 415 mbsf (Fig. 7), increase to approximately 95% from 415 to 460 mbsf (14–17 Ma), and decrease below 575 mbsf. In Subunit IB carbonate contents vary inversely with the large shifts in foraminifer abundance estimated from smear slide analyses.

Subunit IB is predominantly white (2.5Y 8/0, 5Y 8/0, 7.5YR 8/0, and 10YR 8/1), but it grades in color to intervals (20–30 cm thick) of pale pink (5RP 8/2) and pale blue (5PB 7/2). Alternate faint and distinct color bands in various shades of green (5G 7/1 and 5GY 7/2) are apparent at the top of Subunit IB (Fig. 8), but they disappear almost completely below 300 mbsf. Purple (5P 6/2) and gray bands fluctuate in abundance throughout the subunit but are concentrated at approximately 350 and 760 mbsf. The color bands become thinner with depth

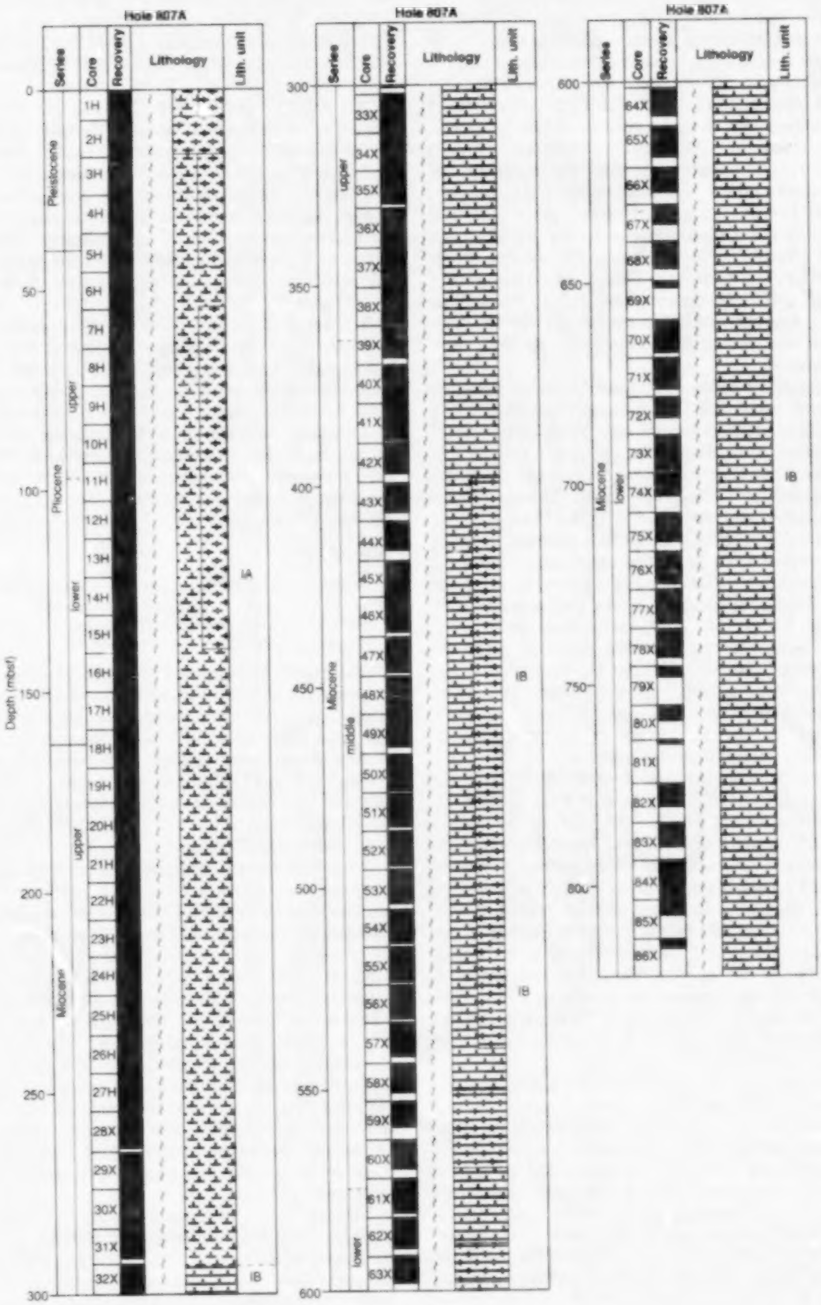

Figure 3. Lithologic summary. Site 807.

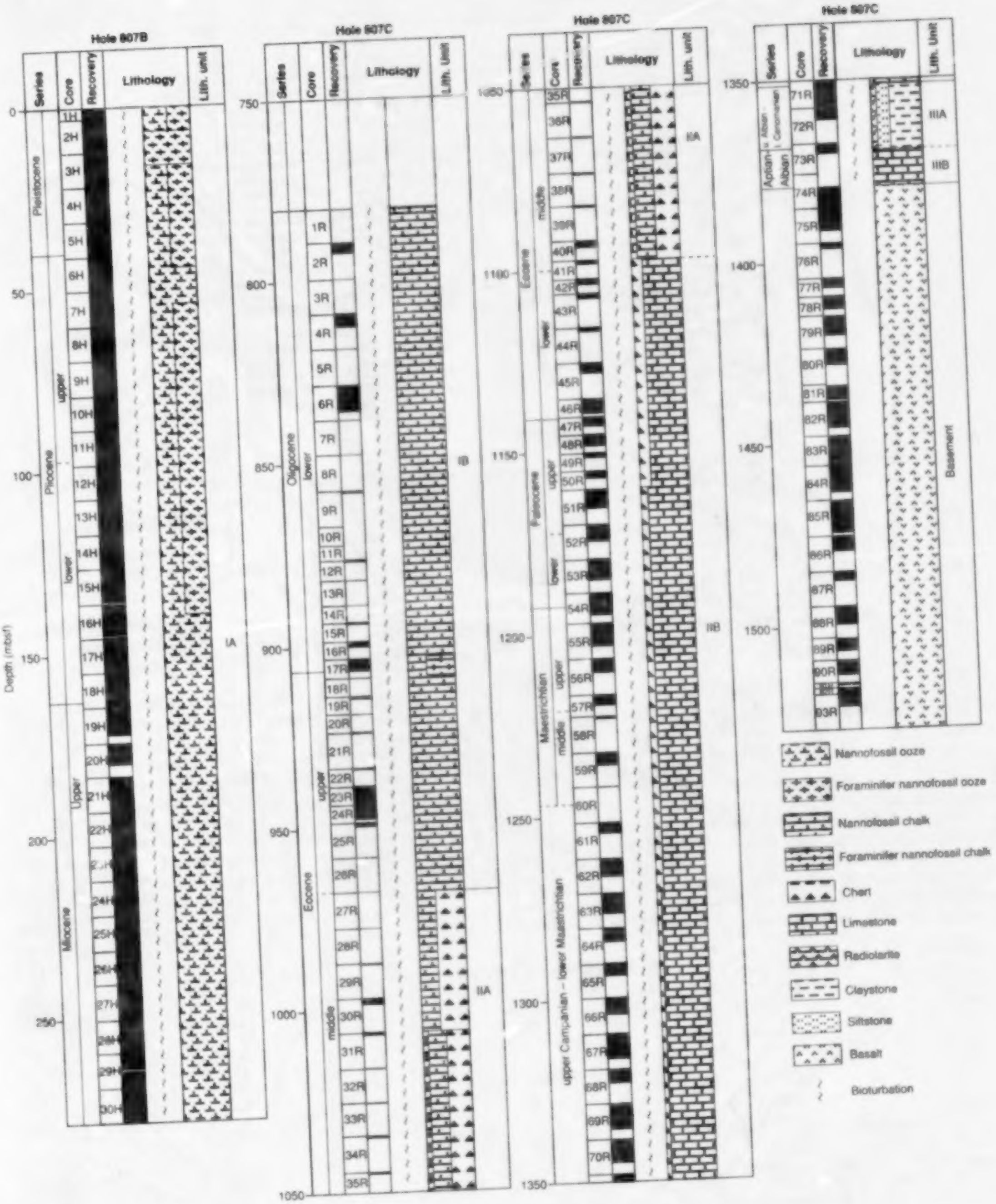
Hole 807B
Hole 807C
Hole 807C
Hole 807C
Series
Core
Recovery
Lithology
Lith. unit
Depth (mbsf)
Pleistocene
Pliocene
upper
lower
Miocene
Upper
Oligocene
Eocene
middle
Paleocene
Maastrichtian
upper Campanian – lower Maastrichtian
Albian – Cenomanian
Aptian – Albian
IA
IB
IIA
IIB
IIIA
IIIB
Basement
Nannofossil ooze
Foraminifer nannofossil ooze
Nannofossil chalk
Foraminifer nannofossil chalk
Chert
Limestone
Radiolarite
Claystone
Siltstone
Basalt
Bioturbation

Figure 3 (continued).

Table 2. Lithologic summary, Site 807.

Lithologic unit	Cores	Depth (mbsf)	Age	Lithology
IA	807A-1H to -31X 807B-1H to -30H	0–293	Pleistocene to middle/late Miocene	Foraminifer nannofossil ooze to nannofossil ooze with foraminifers
IB	807A-32X to -86X 807C-1R to -26R	293–968	middle/late Miocene to late Eocene	Nannofossil chalk to foraminifer nannofossil chalk
IIA	807C-27R to -40R	968–1098	middle Eocene	Chert, nannofossil chalk to nannofossil chalk with foraminifers, limestone
IIB	807C-41R to -71R, 45 cm	1098–1351.4	Eocene to late Campanian	Limestone
IIIA	807C-71R-3, 45 cm, to -73R-2, 82 cm	1351.4–1369.7	early Cenomanian to late Albian	Claystone, radiolarian siltstone
IIIB	807C-73R-2, 82 cm, to -74R-1, 25 cm	1369.7–1379.7	Early Cretaceous (Albian/Aptian)	Limestone

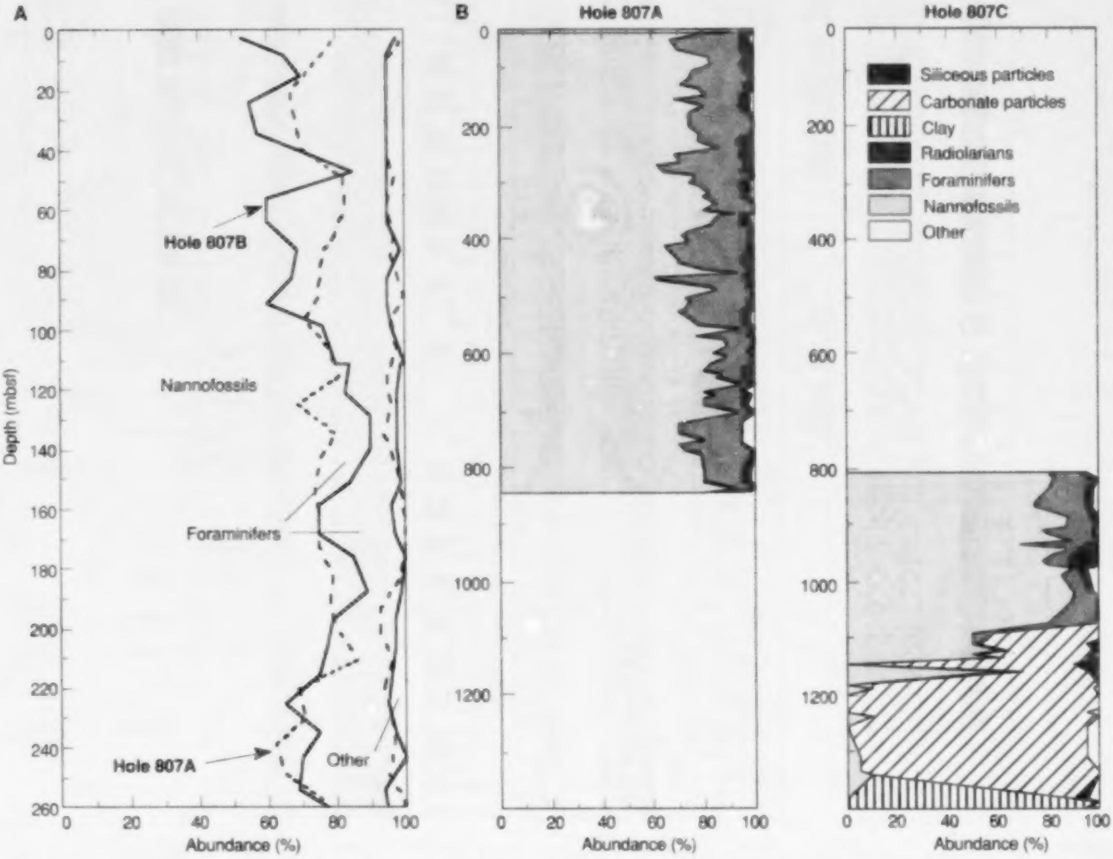

Figure 4. Abundances of major sediment components estimated from smear slides. A. Subunit IA, Hole 807A (dashed lines) and Hole 807B (solid lines) (0–260 mbsf). B. All units, Holes 807A and 807C.

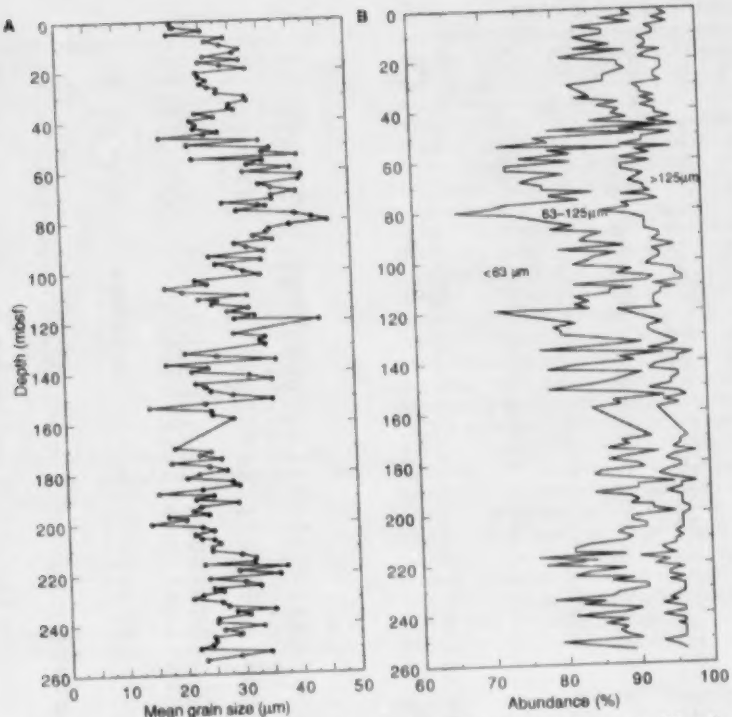

Figure 5. A. Mean grain size of Subunit IA sediments, Hole 807A. B. Coarse (>125 µm), intermediate (63–125 µm), and fine (<63 µm) fraction abundances, Subunit IA, Hole 807A.

and average 1–2 mm in thickness. In the upper part of Subunit IB, the bands have planar outlines and are closely spaced (Fig. 11). Below 700 mbsf, however, the color bands are developed either as gray microstylolitic swarms or as wavy, braided patterns of thin bands that grade to diagenetic flaser structures (Fig. 12) or dissolution seams (Fig. 13).

Bioturbation is pervasive in Subunit IB. The evidence includes mottling in shades of white, trace fossils (e.g., *Zoophycos*) (Fig. 14), disseminated pyrite, and rare pyritized burrow linings. Burrows commonly become more flattened with increasing depth. Where thin color bands and bioturbation structures intersect, color bands are continuous throughout (and so postdate) the bioturbation structures (Fig. 15).

Unit II

Intervals: Hole 807C, Core 130-807C-27R through Section 130-807C-71R-3, 45 cm
Age: middle Eocene–late Campanian
Depth: 968–1351.4 mbsf

Unit II is dominated by limestone and chert but also contains nannofossil chalk and nannofossil chalk with foraminifers. Unit II was divided into two subunits. Subunit IIA (968–1098 mbsf) was primarily recovered as chert and nannofossil chalk to nannofossil chalk with foraminifers, but limestone and silicified limestone are present as minor constituents below 1006 mbsf. Subunit IIB (1098–1351.4 mbsf) is predominantly limestone,

Table 3. Summary statistics for sedimentary parameters, Site 807.

Subunit	Mean size	Sand (%)	Silt (%)	Clay (%)	>125 µm (%)	63–125 µm (%)	Foraminifers (%)	$CaCO_3$ (%)
IA:							22	92
Mean	28.3	14.9	79.9	5.1	6.0	9.0	8	1.7
Sigma	6.2	5.4	5.8	2.9	2.2	3.5	59	170
N	170	170	170	170	170	170		
IB:							17	93
Mean							8	23
Sigma							54	223
N								

Notes: Mean grain size is reported in microns. Mean size and sand, silt, and clay (>125 and 63–125 µm fraction) abundances are from shipboard grain-size analyses. Foraminifer contents are from smear slide estimates. Carbonated contents are from shipboard carbonate analyses. *N* = number of analyses.

Table 4. Grain-size data for sediments in Subunit IA, Hole 807A.

Core, section, interval (cm)	Depth (mbsf)	Mean	Sand (%)	Silt (%)	Clay (%)	>125 μm (%)
130-807A-						
1H-1, 95	0.95	20.0	10	78	13	95
1H-2, 95	2.45	20.5	9	81	9	96
1H-3, 95	3.95	25.3	13	79	8	94
1H-4, 95	5.45	19.5	9	87	5	96
1H-5, 95	6.95	29.2	17	78	6	93
2H-1, 95	8.35	26.0	13	80	7	94
2H-2, 95	9.85	28.5	13	85	1	94
2H-3, 95	11.35	31.7	17	77	6	92
2H-4, 95	12.85	30.7	15	78	7	93
2H-5, 95	14.35	25.6	12	86	2	93
2H-6, 95	15.85	31.7	17	78	6	92
2H-7, 18	16.58	24.8	10	83	6	95
3H-1, 95	17.85	28.5	15	81	6	93
3H-2, 95	19.35	32.8	19	77	5	92
3H-3, 95	20.85	24.3	11	80	8	95
3H-4, 95	22.35	24.7	11	81	7	95
3H-5, 95	23.85	25.9	10	87	2	95
3H-6, 95	25.35	24.9	12	81	8	94
3H-7, 64	26.54	26.2	13	80	7	94
4H-1, 95	27.35	27.8	13	81	6	94
4H-2, 95	28.85	27.7	13	87	1	95
4H-3, 95	30.35	32.5	18	76	6	91
4H-4, 95	31.85	32.9	17	76	7	92
4H-5, 95	33.35	29.9	16	78	7	92
4H-6, 95	34.85	29.8	15	83	1	94
4H-7, 10	35.50	30.6	17	76	6	92
5H-1, 109	36.99	23.9	11	86	3	94
5H-2, 110	38.50	27.1	14	85	1	92
5H-3, 109	39.99	23.0	11	86	4	94
5H-4, 109	41.49	23.9	11	87	1	94
5H-5, 109	42.99	23.5	10	82	8	96
5H-6, 109	44.49	27.7	15	78	7	93
5H-7, 30	45.20	25.3	11	86	3	94
6H-1, 109	46.49	17.6	6	92	2	97
6H-2, 112	48.02	34.7	21	70	10	89
6H-3, 111	49.51	22.4	9	90	1	96
6H-4, 110	51.00	36.5	23	71	6	92
6H-5, 111	52.51	35.3	21	78	1	92
6H-6, 111	54.01	41.2	28	68	3	89
6H-7, 70	55.10	23.1	11	87	2	96
7H-1, 110	56.00	35.2	21	76	2	91
7H-2, 110	57.50	32.6	18	78	3	93
7H-3, 110	59.00	40.0	25	69	5	89
7H-4, 110	60.50	31.8	18	75	7	93
7H-5, 110	62.00	41.9	27	68	5	89
7H-6, 110	63.50	41.4	27	67	6	89
8H-1, 110	65.50	34.5	19	78	2	92
8H-2, 110	67.00	36.6	23	72	6	91
8H-3, 110	68.50	40.8	25	68	6	90
8H-4, 110	70.00	36.6	22	76	1	92
8H-5, 110	71.50	36.7	22	76	1	92
8H-6, 85	72.75	28.0	15	74	10	93
8H-7, 45	73.85	34.3	21	70	10	89
9H-1, 35	74.25	35.6	21	72	6	92
9H-2, 35	75.75	30.5	17	81	2	94
9H-3, 35	77.25	40.6	27	67	6	89
9H-4, 35	78.75	43.4	29	66	5	90
9H-5, 35	80.25	46.2	34	63	4	86
9H-6, 35	81.75	39.6	26	69	6	90
9H-7, 35	83.25	36.1	23	71	6	92
10H-1, 109	84.49	35.6	21	74	4	92
10H-2, 109	85.99	33.3	18	77	5	92
10H-3, 109	87.49	36.6	21	79	0	92
10H-4, 109	88.99	30.0	14	79	6	94
10H-5, 109	90.49	32.1	16	82	0	94
10H-6, 109	91.99	35.0	17	76	6	93
11H-1, 109	93.99	25.5	11	85	3	96
11H-2, 108	95.48	34.5	20	74	6	93
11H-3, 108	96.98	26.6	12	81	7	94
11H-4, 107	98.47	29.6	15	85	1	94
11H-5, 107	99.97	31.5	16	78	6	93
11H-6, 107	101.47	34.2	18	78	5	92
12H-1, 106	103.46	23.0	10	89	1	96
12H-2, 107	104.97	25.0	12	86	2	96
12H-3, 107	106.47	17.8	7	92	2	97
12H-4, 116	108.06	20.8	8	91	1	97

Table 4 (continued).

Core, section, interval (cm)	Depth (mbsf)	Mean	Sand (%)	Silt (%)	Clay (%)	>125 μm (%)
12H-5, 110	109.50	31.9	18	82	1	93
12H-6, 106	110.96	23.5	10	89	0	96
12H-7, 22	111.62	26.7	13	82	4	94
13H-1, 107	112.97	25.8	13	78	9	94
13H-2, 107	114.47	32.1	18	74	6	93
13H-3, 107	115.97	28.4	16	77	7	93
13H-4, 107	117.47	33.1	18	81	1	93
13H-5, 107	118.97	29.6	16	79	5	94
13H-6, 10	119.50	44.2	29	68	3	88
14H-3, 31	124.71	29.4	18	75	4	94
14H-4, 31	126.21	34.8	21	73	6	92
14H-5, 31	127.71	33.9	20	75	5	92
14H-6, 31	129.21	34.8	20	76	3	93
15H-2, 121	132.36	20.9	9	86	5	96
15H-3, 109	133.74	26.4	14	80	7	95
15H-4, 109	135.24	36.5	23	72	4	92
15H-5, 109	136.74	17.6	6	87	6	98
15H-6, 109	138.24	24.8	12	82	7	96
15H-7, 109	139.74	22.0	10	82	8	96
16H-1, 108	141.48	31.8	18	81	1	93
16H-2, 108	142.98	35.8	22	71	7	92
16H-3, 108	144.48	22.6	9	83	8	95
16H-4, 108	145.98	24.3	11	81	8	96
16H-5, 108	147.48	25.2	13	80	7	95
16H-6, 123	149.13	29.0	16	76	7	95
17H-1, 100	150.90	35.8	22	71	7	92
17H-2, 100	152.40	24.2	11	80	8	96
17H-3, 100	153.90	14.5	6	94	0	97
17H-4, 100	155.40	25.2	13	79	8	94
17H-5, 100	156.90	25.4	12	81	7	96
17H-6, 100	158.40	29.0	16	78	7	93
19H-1, 103	169.93	18.7	8	84	8	97
19H-2, 103	171.43	24.9	12	80	7	96
19H-3, 103	172.93	22.9	11	82	8	96
19H-4, 103	174.43	26.7	14	79	7	95
19H-5, 103	175.93	18.0	7	83	9	98
19H-6, 103	177.43	24.5	11	82	7	95
20H-1, 55	178.95	27.6	14	79	6	94
20H-2, 55	180.45	22.8	10	89	0	96
20H-3, 55	181.95	20.7	9	85	7	96
20H-4, 55	183.45	28.5	15	80	5	94
20H-5, 55	184.95	29.6	16	82	2	93
20H-6, 55	186.45	23.3	11	83	6	95
20H-7, 55	187.95	15.7	5	85	11	98
21H-1, 100	188.90	25.1	10	88	1	96
21H-2, 100	190.40	22.1	10	87	3	96
21H-3, 100	191.90	29.4	16	78	6	94
21H-4, 100	193.40	22.9	11	79	10	96
21H-5, 100	194.90	21.6	10	81	10	96
21H-6, 100	196.40	24.2	11	89	0	96
21H-7, 10	197.00	17.3	8	79	13	96
22H-1, 100	198.40	20.3	8	91	1	97
22H-2, 100	199.90	14.2	5	83	13	97
22H-3, 100	201.40	23.1	11	81	9	96
22H-4, 100	202.90	25.0	11	82	6	96
22H-5, 100	204.40	21.7	9	81	10	96
22H-6, 100	205.90	22.8	9	86	5	96
22H-7, 10	206.50	25.0	12	86	2	96
23H-1, 106	207.96	26.0	13	88	1	95
23H-2, 110	209.50	24.6	11	88	1	96
23H-4, 111	212.51	29.7	17	76	6	95
23H-3, 108	210.98	24.6	12	81	8	95
23H-5, 109	213.99	32.1	19	81	1	93
23H-6, 110	215.50	31.8	19	74	6	94
23H-7, 50	216.40	23.3	12	76	11	95
24H-1, 109	217.49	37.5	24	71	6	90
24H-2, 109	218.99	29.1	16	77	7	94
24H-3, 109	220.49	36.2	23	76	1	92
24H-4, 109	221.99	24.0	12	81	7	96
24H-5, 109	223.49	30.2	17	82	1	94
24H-6, 109	224.99	32.8	19	76	5	94
24H-7, 50	225.90	24.7	11	86	3	96
25H-1, 105	226.95	26.3	14	81	6	94
25H-2, 105	228.45	22.8	9	84	7	96
25H-3, 105	229.95	21.1	9	89	3	96
25H-4, 105	231.45	26.1	13	81	6	96
25H-5, 105	232.95	27.1	14	79	7	95

Table 4 (continued).

Core, section, interval (cm)	Depth (mbsf)	Mean	Sand (%)	Silt (%)	Clay (%)	>125 μm (%)
25H-6, 105	234.45	35.2	22	73	4	94
25H-7, 15	235.05	28.6	15	84	1	95
26H-1, 105	236.45	30.8	18	76	7	93
26H-2, 105	237.95	25.3	10	84	6	96
26H-3, 105	239.45	25.2	12	87	2	96
26H-4, 105	240.95	33.2	19	81	1	93
26H-5, 105	242.45	26.3	12	81	7	96
26H-6, 105	243.95	29.3	15	79	5	96
26H-7, 10	244.50	28.9	14	81	5	95
27H-1, 43	245.33	24.6	12	82	6	96
27H-2, 43	246.83	24.9	13	83	5	96
27H-3, 43	248.33	24.3	12	84	5	96
27H-4, 43	249.83	22.1	10	82	7	96
27H-5, 43	251.33	34.3	21	76	4	93
27H-6, 43	252.83	29.1	16	80	6	95
27H-7, 43	254.33	23.2	11	84	6	96

although chert is presented as a minor constituent throughout. The boundary between the two subunits is placed at 1098 mbsf, below which limestone dominates.

Subunit IIA

Intervals: Hole 807C, Core 130-807C-27R through -40R
Age: middle Eocene
Depth: 968–1098 mbsf

Recovery from Subunit IIA was low, ranging from 1% to 30%. Approximately 50% of the recovered sediment was chert, but the low recovery hinders an evaluation of the actual abundance of each lithology in the cored interval (Fig. 3). Estimates from the wireline log velocity data indicate a chert content of approximately 20% through Subunit IIA. The chert is gray (N5/ and 5Y 6/1) and apparently nodular, as demonstrated by chalk coatings on outer surfaces and by chalk inclusions, 1 mm to 1 cm in size (Fig. 16). The remainder of the recovered material was approximately 40% nannofossil chalk to nannofossil chalk with foraminifers and 10% limestone.

The chalk is commonly brecciated by drilling, but larger pieces were recovered from 997.0 to 998.1 mbsf (Core 130-807C-30R), from 1006.5 to 1007.1 mbsf (Core 130-807C-31R), from 1044.0 to 1045.0 mbsf (Core 130-807C-35R), from 1063.7 to 1064.0 mbsf (Core 130-807C-37R), and from 1073.2 to 1073.7 mbsf (Core 130-807C-38R). The chalk is white (2.5Y 8/0) and moderately bioturbated. Burrows are commonly flattened and subhorizontal in orientation. Isolated greenish gray (5GY 6/1) and gray (N7/) microstylolitic braided patterns are present, occasionally grading to diagenetic flaser structures.

A few single stylolites, with amplitudes of less than 1 mm, were observed. The white (2.5Y 8/0) limestone and silicified limestone were recovered only as drilling rubble. The chalks, limestones, and silicified limestones are interlayered. XRD analyses indicate that zones of pure calcite, <20 m thick, alternate with zones that are dominated by calcite but also contain cristobalite, quartz, and clay. Carbonate contents indicate a similar pattern of fluctuation through this subunit (Fig. 6C). Evidence for the silicification of chalk by cementation or replacement of microfossils and for calcite cementation and recrystallization is seen in thin section (Figs. 17 and 18).

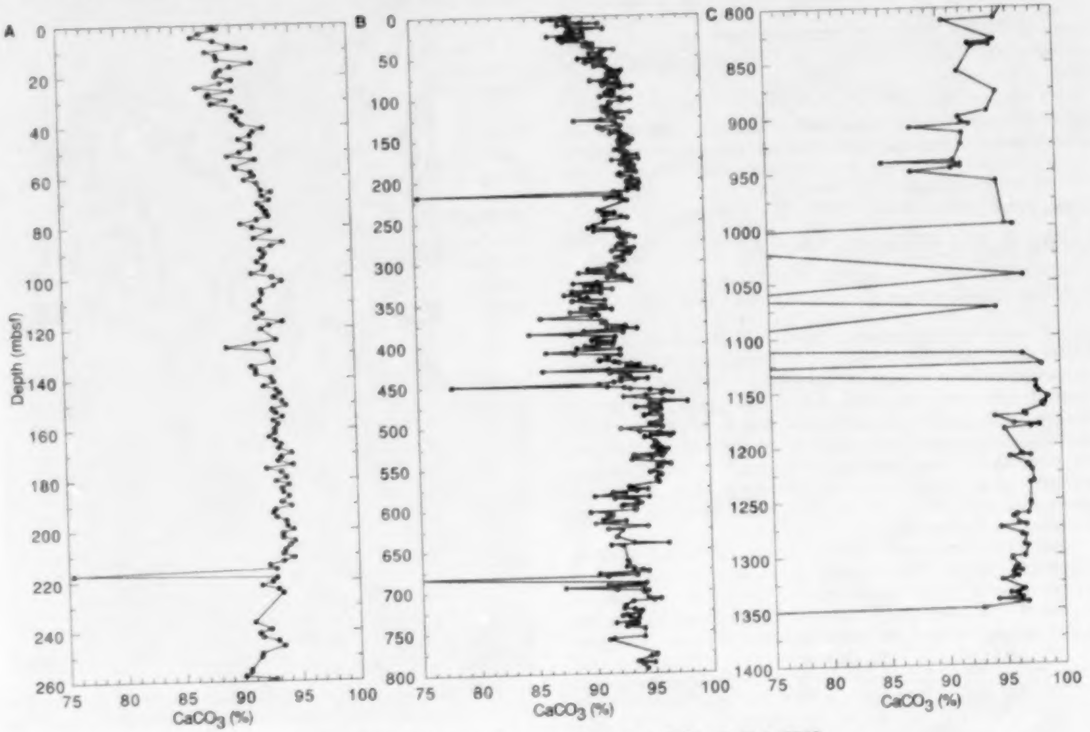

Figure 6. Carbonate contents, Site 807. **A.** Subunit IA, Hole 807A. **B.** Unit I, Hole 807A. **C.** Hole 807C.

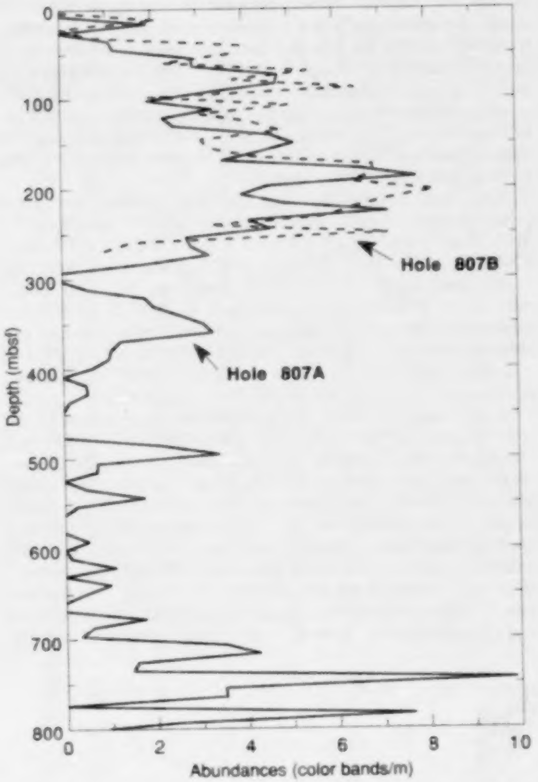

Figure 7. Abundances of color bands, Holes 807A and 807B. The number of color bands has been estimated from core photographs.

Subunit IIB

Intervals: Hole 807C, Core 130-807C-41R through Section 130-807C-71R-3, 45 cm
Age: Eocene to late Campanian
Depth: 1098–1351.4 mbsf

Subunit IIB is composed primarily of limestone (Fig. 3). Smear slide data indicate a transition from material dominated by nannofossils to material dominated by carbonate particles between 1060 and 1140 mbsf (Fig. 4). Silicified limestone is present to a depth of 1140 mbsf and contains abundant cristobalite (and quartz), as indicated by XRD traces. Carbonate contents are low episodically through Subunit IIB, superimposed on a general decrease downhole (Fig. 6C). Only minor clay and quartz are seen in XRD traces of samples taken below 1140 mbsf.

Chert is present as nodules or in layers, up to 7 cm thick, in all cores of Subunit IIB. Chert abundance rarely exceeds 10% of the recovered material, however, and constitutes <5% of the recovered sediment below 1270 mbsf. The chert exhibits various shades of gray and red, including light gray (N6/ and N7/), gray (5Y 5/1, 2.5Y 5/0, and N5/), dark gray (5YR 4/1), reddish gray (5YR 4/2 and 5YR 5/2), weak red (2.5YR 4/2), dusky red (10R 3/3), reddish brown (4YR 4/2 and 5YR 4/3), dark brown (10YR 4/3 and 7.5YR 4/2), brownish gray (10YR 6/2 and 5YR 6/1), grayish blue (5PB 5/2), and dusky blue (5PB 3/2).

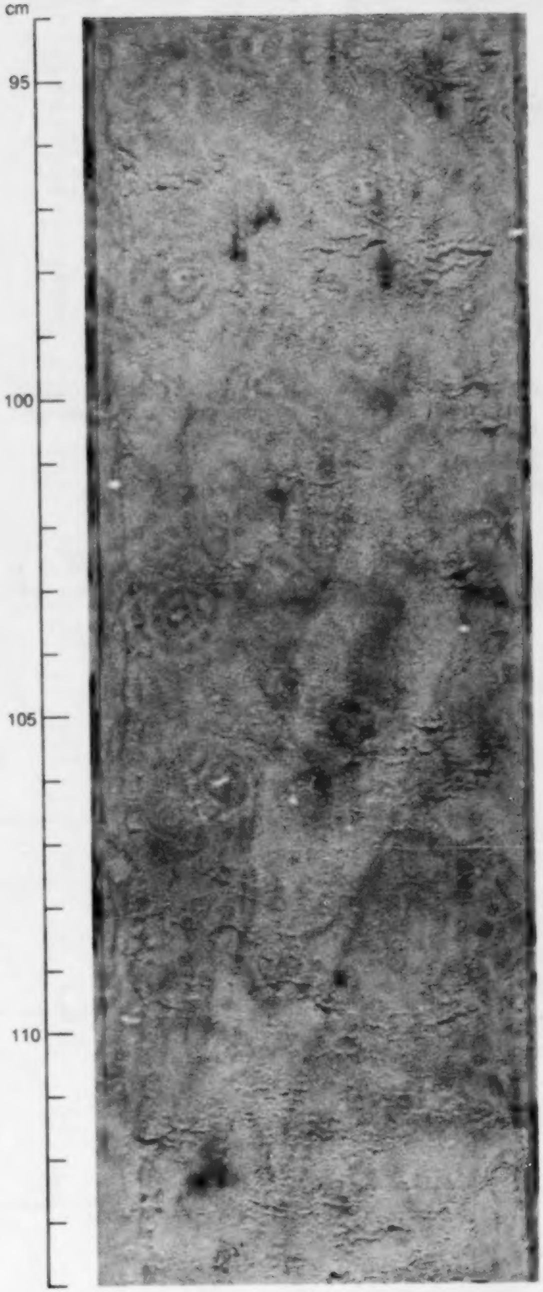

Figure 8. Photograph of color band passing through burrow, Hole 807A (Section 130-807A-25H-2, 94–114 cm; 228 mbsf). Note that redox haloes around the burrow overprint the color bands.

Table 5. Inventory of ash layers, Site 807.

Core, section, interval (cm)	Depth (mbsf)
130-807A-	
67X-CC, 20–23	639.70
70X-5, 110–116	666.33
71X-5, 63–70	675.57
72X-4, 66–69	683.32
72X-4, 94–98	683.66
73X-CC, 56–61	697.50
77X-4, 56–61	731.60
78X-5, 45–47	742.67
80X-3, 48–50	758.71
130-807C-	
47R-1, 40–41	1140.60
50R-1, 14–17	1155.34
52R-3, 67–100	1173.64
54R-1, 40–41	1189.20
54R-1, 63–64	1189.43
54R-1, 138–139	1190.18
54R-2, 13–14	1190.43
54R-2, 16–17	1190.46
54R-2, 60–61	1190.90
54R-2, 70–71	1191.00
54R-2, 83–84	1191.13
54R-2, 115–116	1191.45
54R-3, 27–28	1192.07
54R-3, 134–135	1193.14
55R-1, 27–28	1197.17
55R-1, 87–88	1197.77
66R-1, 102–103	1300.82

At least 15 layers of gray (N4/, N5/, and N5/1) ash are present between 1140 and 1200 mbsf (Table 5). One layer, located at 1156.6 mbsf, is 3 cm thick whereas the other layers are <1 cm thick. Several bioturbated ash layers are present at 1174 mbsf (Core 130-807C-52R; Fig. 19). Diagenesis may have produced flaserlike structures in the ash. At least 10 dark gray (N3/1, 10YR4/1, and 5Y 4/1), brown (7.5YR 3/3), and grayish brown (10YR 4/2) layers of ash and clay, which may be altered volcanic ash, are located between 1300 and 1351 mbsf. Only the layers composed obviously of volcanic glass layers are included in Table 5.

Subunit IIB is predominantly white (2.5Y 8/0, 5Y 8/1, 5YR 8/0, 5YR 8/1, 7.5YR 8/0, 10YR 8/0, and 10YR 8/1) in color with isolated light gray (5Y 7/1) intervals. In the interval between 1116 and 1135 mbsf (Cores 130-807C-44R and -45R), white limestone clasts up to 5 mm in diameter were found. Nannofossils from one such clast at 1127 mbsf are of Late Cretaceous age, whereas nannofossils in the surrounding matrix are a mixture of Paleocene and Cretaceous species. The clasts, therefore, are reworked, older sediments. At approximately the same level, a 5-cm-thick finely laminated bed was composed of only lower Eocene nannofossils. Between 1197 and 1232 mbsf (Cores 130-807C-55R to -58R), 1-mm- to 1-cm-scale bands or pseudolaminae of well-sorted carbonate particles exhibit low-angle truncation surfaces (Fig. 20). Clasts 1–5 cm in diameter are common below 1232 mbsf (Cores 130-807C-59R to -70R). Most of the clasts are white limestone (Fig. 21), but gray limestone clasts become more abundant below 1271 mbsf, and angular green, noncalcareous, clay-rich clasts are present below 1290 mbsf (Fig. 22). Dark brown claystone clasts are common below 1321 mbsf. The clast-bearing intervals alternate with clast-free intervals at a scale of 1 to 5 m. A fold overlying a microfault at 1264 mbsf (Core 130-807C-62R; Fig. 23) underlies a 1-m-thick, graded, clast-bearing interval.

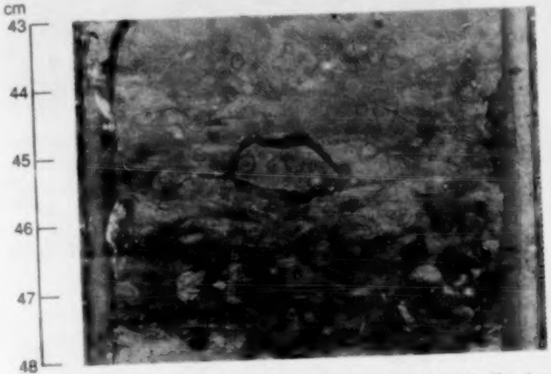

Figure 9. Photograph of bioturbated ash layer, Hole 807A (Section 130-807A-78X-5, 43–48 cm; 743 mbsf).

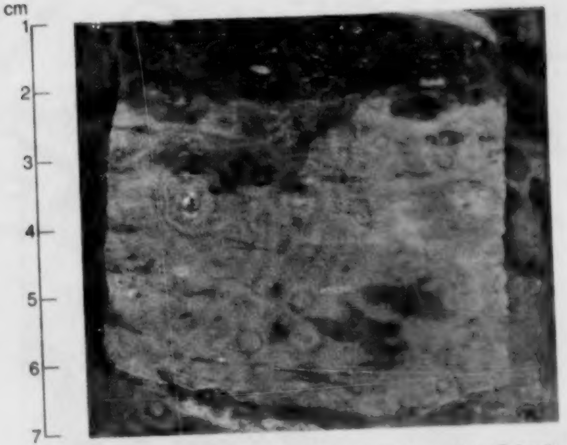

Figure 10. Photograph of chert, probably of nodular origin, Subunit IB, Hole 807C (Section 130-807C-26R-1, 1–7 cm; 960 mbsf).

Stylolites, with up to 5-mm amplitude and dark greenish gray (5G 4/1) or gray (N5/) drapes, are present throughout Subunit IIB (Fig. 24). Differential compaction, possibly of chemical origin, is evident at 1184 mbsf (Section 130-807C-53R-3), where burrows exist as uncompacted lenses in the more heavily compacted, clay-rich matrix (Fig. 25).

An apparently complete K/T boundary section was recovered at approximately 1193.14 mbsf (Section 130-807C-54R-3, 135 cm). This section is composed of limestone and silicified limestone with minor chert, similar to the rest of Subunit IIB; however, the section is notable for the presence of a 0.5-cm-thick ash at the actual position of the K/T boundary (Fig. 26 and Table 5).

Unit III

Intervals: Hole 807C, Section 130-807C-71R-3, 45 cm, through -74R-1, 25 cm
Age: early Cenomanian to Albian-Aptian
Depth: 1351.4–1379.7 mbsf

Unit III consists of upper Albian to lower Cenomanian claystone and siltstone with varying amounts of radiolarians, and Aptian to Albian limestone. The unit is divided into two subunits on the basis of claystone and limestone abundances. Subunit IIIA (1351.4–1369.7 mbsf) contains claystone inter-

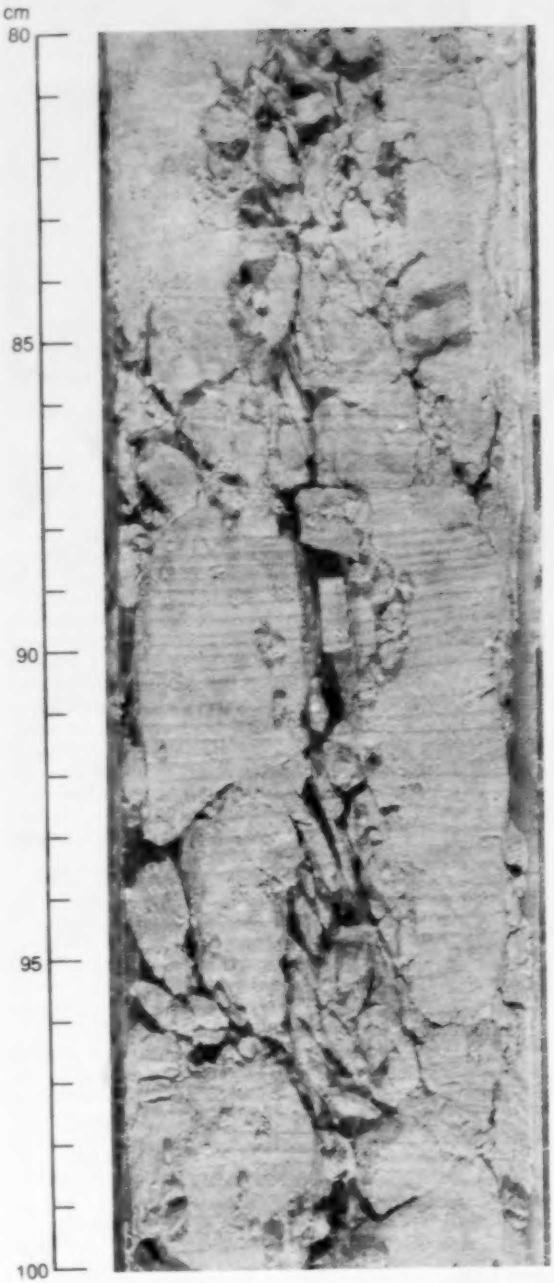

Figure 11. Photograph of thin color bands, Hole 807A (Section 130-807A-34X-6, 80–100 cm; 318 mbsf).

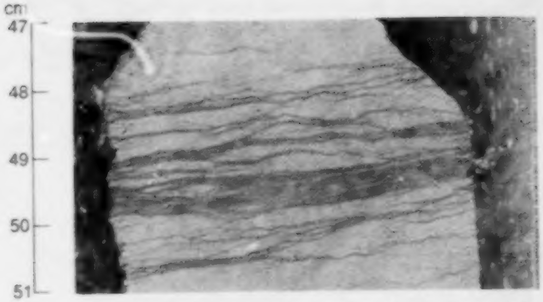

Figure 12. Photograph of a braided swarm of microstylolites in chalk, Subunit IB, Hole 807C (Section 130-807C-12R-1, 47–51 cm, 877 mbsf). These bands exhibit flaser-type structures caused by their wavy, braided appearance and are interpreted as a product of chemical compaction.

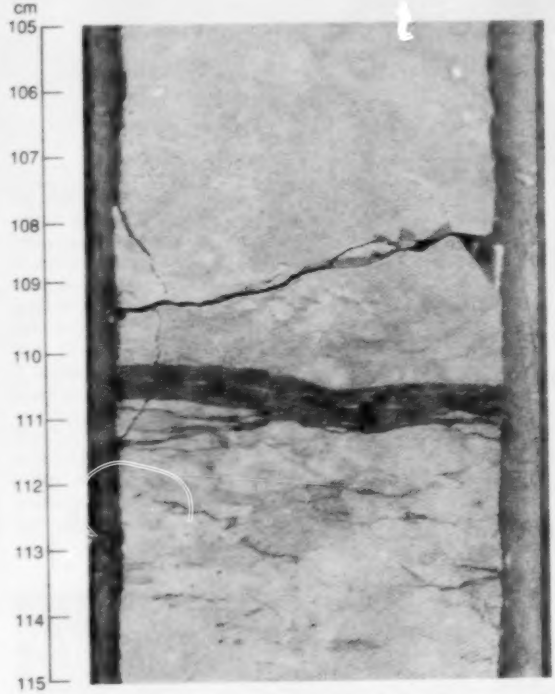

Figure 13. Photograph of microstylolitic dissolution seam, Hole 807C (Section 130-807C-6R-4, 105–115 cm; 834 mbsf). Burrows in the chalk matrix are truncated by dissolution at the seam boundaries.

bedded with siltstone; Subunit IIIB (1369.7–1379.7 mbsf) consists of limestone.

Subunit IIIA

Intervals: Hole 807C, Section 130-807C-71R-3, 45 cm, through -73R-2, 82 cm
Age: early Cenomanian to late Albian
Depth: 1351.4-1369.7 mbsf

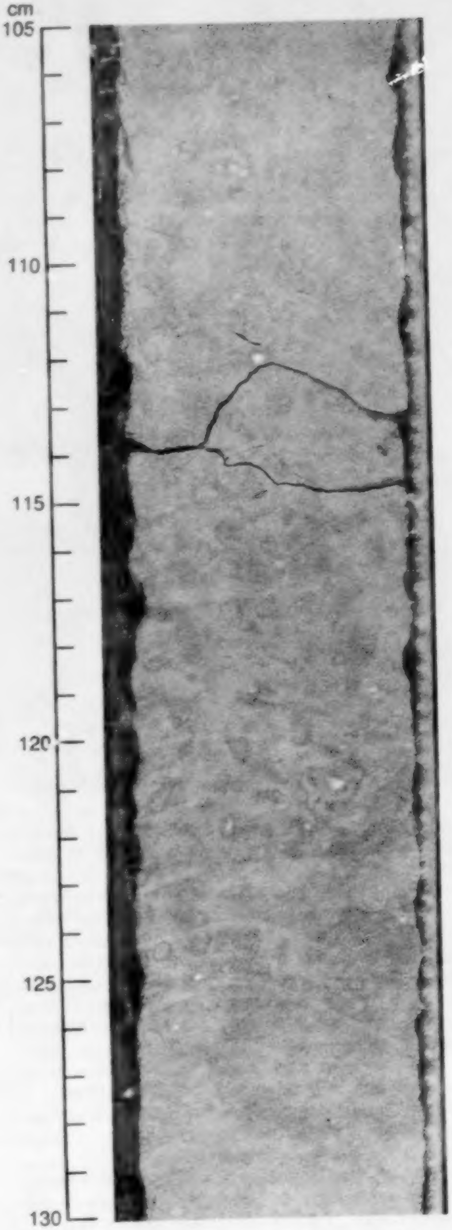

Figure 14. *Zoophycos* burrow. Hole 807C (Section 130-807C-2R-1, 105–130 cm; 791 mbsf). The helical burrow structure is demonstrated by the presence of small traces near the top and wider/thicker traces near the base.

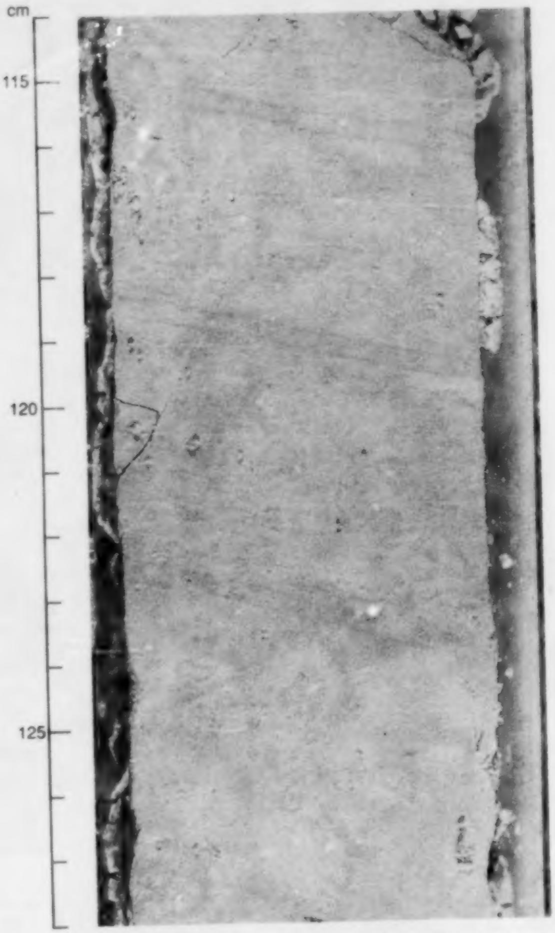

Figure 15. Photograph of very thin (1 mm) horizontal color bands passing through inclined trace fossils, Hole 807A (Section 130-807A-71X-3, 114–128 cm, 659 mbsf).

Subunit IIIA contains claystone, siltstone with radiolarians, radiolarian siltstone, and radiolarian sandy siltstone. The claystone is predominantly very dark grayish brown (10YR 3/2), but reddish brown (5YR 4/4) and black (10YR 2/1, 10YR 3/1) intervals are also present. Isolated heavily bioturbated intervals are indicated by mottling and burrows as large as 2 cm in diameter. XRD analyses indicate the presence of quartz, illite, and feldspar in the claystones.

The siltstone interbeds are pale blue green (5BG 7/2), reddish brown (5YR 4/4), pink (7.5YR 7/4), pinkish gray (7.5YR 7/2), light gray (N7/), grayish brown (10YR 5/2), gray (10YR 6/1), and light brownish gray (10YR 6/2). The radiolarian content of the siltstones increases downcore. XRD analyses indicate that quartz is the major component of the siltstones and that cristobalite is present. Siltstone beds are rare at the top of Subunit IIIA and become more abundant with depth. The downcore increase in siltstone frequency produces an overall upward-fining sequence in Subunit IIIA. The contacts between the claystone and siltstone intervals are pre-

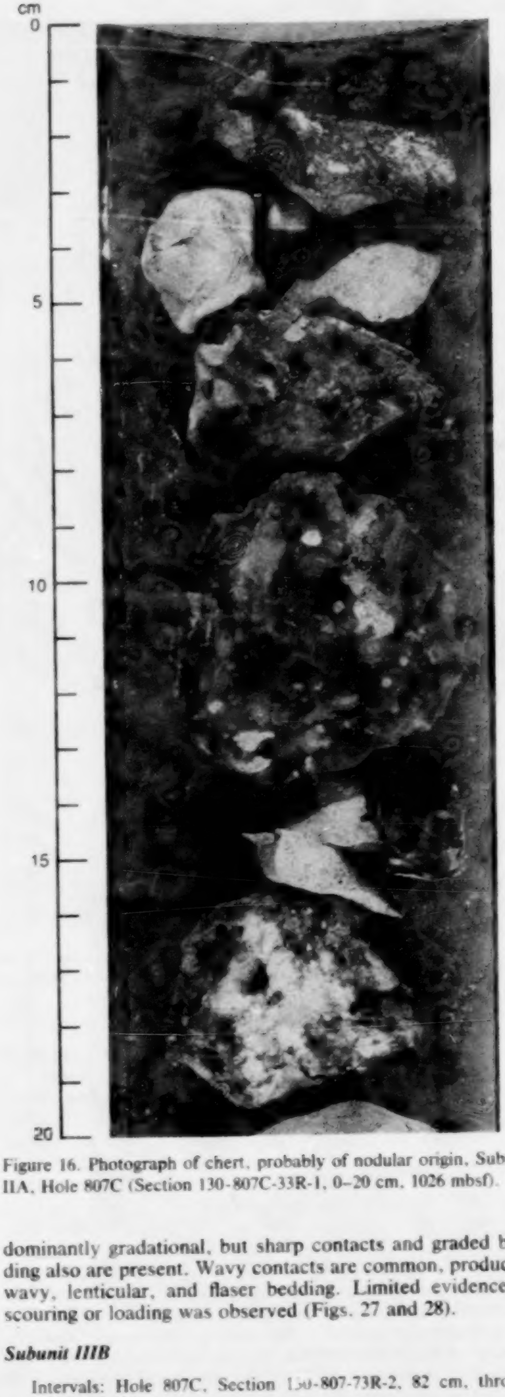

Figure 16. Photograph of chert, probably of nodular origin, Subunit IIA, Hole 807C (Section 130-807C-33R-1, 0–20 cm, 1026 mbsf).

dominantly gradational, but sharp contacts and graded bedding also are present. Wavy contacts are common, producing wavy, lenticular, and flaser bedding. Limited evidence of scouring or loading was observed (Figs. 27 and 28).

Subunit IIIB

Intervals: Hole 807C, Section 130-807-73R-2, 82 cm, through -74R-1, 25 cm
Age: Early Cretaceous, Albian-Aptian
Depth: 1369.7–1379.7 mbsf

Subunit IIIB is composed of bioturbated limestone. Limestone was recovered in the interval from 1369.7 to 1375.7 mbsf, but a distinct decrease in drilling rate at 1379.7 mbsf suggests that the latter depth is the contact between limestone and basalt. The limestone is gray (10YR 6/1) to light gray (10YR 7/2) in color. The upper part of the recovered section contains vertical, very fine, anastomosing fractures, whereas the lower part of the section contains pervasive wavy and lenticular bedding on a scale of 0.5 to 3 cm, as well as microfaults and abundant healed tensional cracks (Fig. 28). Both intervals contain black (2.5Y 2.5/0) to dark gray (N/5) chert, apparently of nodular origin.

Two limestone beds were recovered as interlayers in the basalt. The upper bed (Section 130-807C-80R-1, 70–120 cm) is white (10YR 8/1 to 10YR 8/2) interbedded with dark reddish brown (5YR 3/3) to reddish brown (5YR 4/3) vitric tuff, and contains numerous healed fractures. XRD analyses indicate that the lower, olive brown (2.5Y 4/4) clayey limestone (Section 130-807C-82R-3, 72–79 cm) also contains quartz and illite/glauconite.

Discussion

The sediments overlying basalt at Site 807 consist of 10 m of limestone (Subunit IIIB), overlain by 18 m of siliciclastic sediments (Subunit IIIA) and 1351 m of carbonate sediments (Units II and I). The basal limestone of Early Cretaceous age overlies basalt directly without a metalliferous interbed, indicating a hiatus of unknown duration. The wavy and lenticular bedding of the limestone (Fig. 28) may be primary depositional structures, but diagenetic alteration of burrowed pelagic sediment can produce similar structures.

The radiolarian-bearing nature of the upper Albian to lower Cenomanian claystone and interbedded siltstones that directly overlie the limestone indicates the marine origin of these siliciclastics. The upward fining of these sediments, their interbedded pattern, and the sedimentary structures seen (Figs. 27 and 28) indicate the importance of repeated mass transport events during the deposition of these sediments.

The overlying carbonates span the period from the late Campanian to the present. At Site 803, the early Late Cretaceous to middle Eocene is represented by a 4.5-m-thick siliciclastic interval at a depth of 621.8–626.3 mbsf, corresponding to a depth of approximately 4020 m below the present sea level. At Site 807, the same time interval is represented by more than 200 m of carbonate sediments, the base of which is approximately 4150 m below the present sea level. At Site 807, the K/T boundary is located in carbonate sediments that are 4000 m below the present sea level, whereas at Site 803 the K/T boundary is present in siliclastic sediments that are 4020 m below the present sea level. The apparent difference in the late Campanian to Maestrichtian carbonate-compensation depth (CCD) deduced from these depth values may be explained by post-Cretaceous tectonic movement of Site 807 relative to Site 803. On seismic sections, Site 807 is seen to be located on down-dropped basement, so that Site 807 may have been shallower than Site 803 for part of the time since the late Campanian.

The carbonate sediments of Site 807 were divided into two units based on the degree of diagenesis. Limestone and chert dominate Unit II, whereas only minor chert and porcellanite were found in the chalks and oozes of Unit I. The transition from chert-rich Unit II to chert-poor Unit I at 968 mbsf is also reflected in a marked upsection increase in dissolved silica in the pore water (see "Inorganic Geochemistry" section, this chapter; Fig. 47). An equivalent lithologic boundary was defined at approximately the same depth at nearby Site 289 (Shipboard Scientific Party, 1975b). Unit II is further subdi-

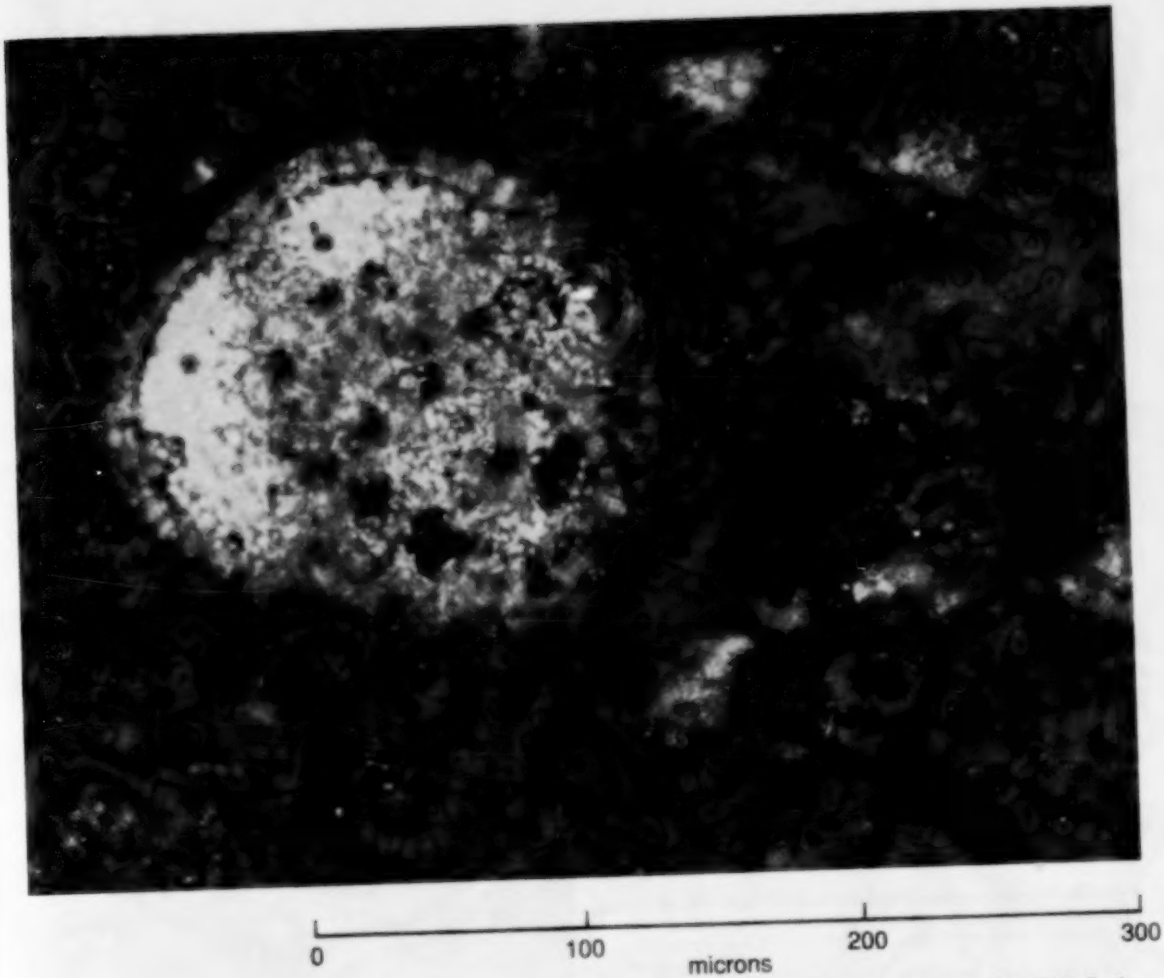

Figure 17. Photomicrograph of silicified chalk, illustrating cementation and/or replacement of microfossils by silica, Hole 807C (Section 130-807C-41R-1, 47 cm; 1098 mbsf).

vided into the 253-m-thick Subunit IIB, which consists of limestone with a low chert content, and the 130-m-thick Subunit IIA, which is composed predominantly of chert and chalk. The extent of carbonate recrystallization decreases upsection.

The interbedded and graded clast-bearing intervals in the lower 120 m of Subunit IIB and the presence of a fold at 1264 mbsf beneath a 1-m-thick, graded, clast-bearing interval indicate mass movement events and deposition. The claystone clasts, which are common in the lower 30 m, may have been derived from deposits equivalent to the siliciclastic rocks of Subunit IIIA. The angular green clasts in the lower 60 m are probably altered fragments of basalt. The presence of these mass-flow deposits may indicate that Site 807 was already partially downfaulted in the late Campanian. The overlying, 35-m-thick limestone interval contains laminae of well-sorted carbonate particles; those laminae may be primary sedimentary structures. Some of the bands include low-angle truncation surfaces and may have been produced by winnowing during deposition. The upper 100 m of Subunit IIB is composed of bioturbated limestone, which probably originated as pelagic carbonate sediment with isolated interbeds of mass-flow deposited material.

The low recovery in the overlying 130 m of middle Eocene Subunit IIA complicates the interpretation of its depositional history. The interval may be a sequence of pelagic carbonates with a generally high initial content of siliceous material that subsequently acted as the source material for chert formation.

Unit I is an apparently continuous, 968-m-thick sequence of well-preserved biogenic carbonate deposited from the late Eocene to the Pleistocene. The principal lithologic characteristics of Unit I, such as mean grain size, foraminifer abundance, and carbonate content, reflect changes in carbonate productivity, dissolution, winnowing, dilution, and climate change. Detailed shore-based study is required to resolve the relative influences of these processes. A further influence on the long-term changes in Unit I composition is the plate-tectonic drift of Site 807 northwestward through the equatorial

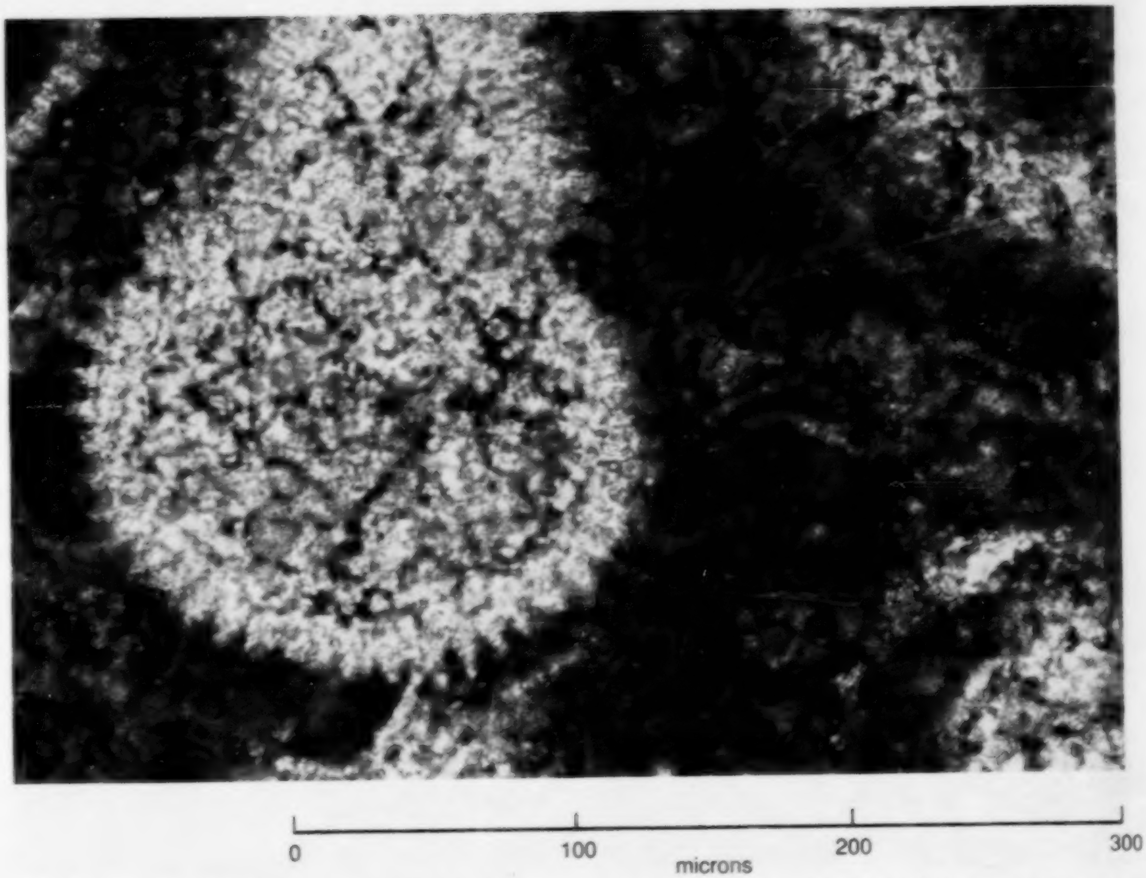

Figure 18. Photomicrograph of material from the chalk-limestone transition zone, Hole 807C, illustrating the effects of calcite cementation and/or recrystallization (Section 130-807C-45R-1, 45 cm; 1126 mbsf).

high-productivity zone, which is presently confined within 1° of the equator.

The lithologic characteristics of Subunit IA at the Leg 130 sites provide preliminary evidence for long-term changes in the depth-related carbonate dissolution gradient, as well as the latitude-related productivity gradient, in the western tropical Pacific Ocean. The decrease in mean grain size from Sites 806 and 807, which are well above the lysocline, to Site 805, at a lysoclinal water depth of 3188 m, probably reflects an increase in carbonate dissolution with depth (Fig. 29). The effects of dissolution also explain some of the decrease in sedimentation rates with increasing water depth (see "Sedimentation Rates" section, this chapter, as well as in the chapters for Sites 803 through 806, this volume). As a result, temporal changes in the gradient of mean grain size with water depth may record temporal changes in the carbonate dissolution gradient.

At the same time, contrasts between sedimentation rates at Sites 806 and 807 hold promise for resolving changes in productivity in the western equatorial Pacific upwelling zone. For example, foraminifer abundances, mean grain sizes, and carbonate contents in Subunit IA at Sites 806 and 807 are very similar (Fig. 29), suggesting that carbonate dissolution at Site 807 is not significantly greater than at Site 806. The sedimentation rates for Subunit IA at Site 807 are only 70% of those at Site 806, however. Because the decrease in sedimentation rate cannot be explained by a significant dissolution gradient between Sites 806 and 807, the difference in sedimentation rate may be driven predominantly by greater productivity at Site 806. This hypothesis is consistent with present productivity patterns in the western equatorial Pacific Ocean, which show that Site 806 is located within a narrow belt of high productivity whereas Site 807 is located just north of this belt (Berger, 1989). A further complication is that the two sites, which are widely separated on the Ontong Java Plateau, may have different winnowing histories.

A comparison of the ooze-chalk transformation at Site 807 with the ooze-chalk transformations at the other Leg 130 sites provides insight into the carbonate lithification process (Fig. 30). The ooze-chalk transition at Site 807 is evident over a 60-m interval, from 252 to 312 mbsf, with the critical change placed at 293 mbsf (near the middle/late Miocene boundary). This pattern is consistent with a trend established from Sites 803 to 806, which shows that the depth of the ooze-chalk transition decreases and the age of the transition increases as

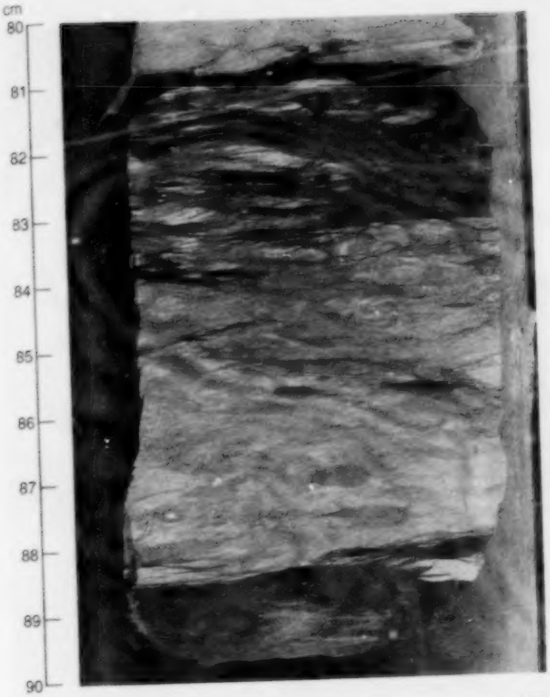

Figure 19. Bioturbated ash(?) layers, Hole 807C (Section 130-807C-52R-3, 80–90 cm, 1174 mbsf). The wispy ("flaser") structures suggest recrystallization and possible chemical compaction.

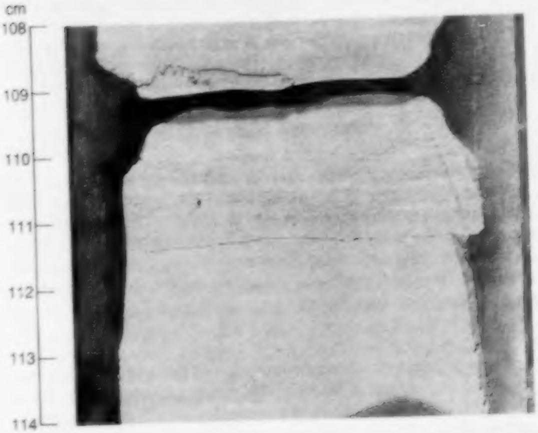

Figure 20. Zone with wispy laminae of well-sorted carbonate particles, Hole 807C (Section 130-807C-56R-2, 108–114 cm; 1209 mbsf).

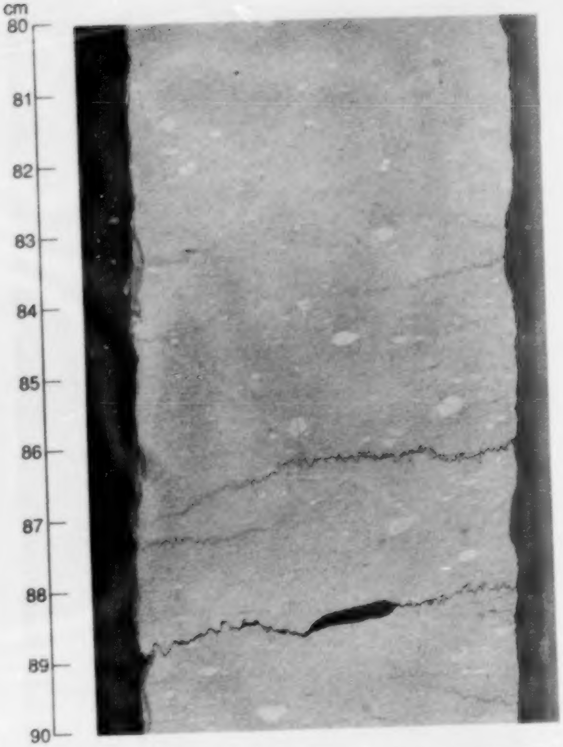

Figure 21. Clast-bearing limestone, Hole 807C (Section 130-807C-59R-2, 80–90 cm; 1235 mbsf). White limestone clasts are dominant, but a single flattened claystone clast is present in the middle of the stylolite at 89 cm.

water depth increases. In general, this suggests that the depth of the transition is strongly influenced by burial depth and age, and that a decrease in the depth of burial can be overcome by the increased time allowed for the diagenetic process. More detailed comparisons between these sites should identify other factors that affect the rate of conversion from ooze to chalk. These factors may include the increasing effects of carbonate dissolution at increasing water depth, as well as variations in the mass wasting and winnowing histories with water depth.

BIOSTRATIGRAPHY

Introduction

The Neogene section at Site 807 (lithologic Subunit IA and part of Subunit IB) is virtually complete, based on the shipboard analyses of calcareous nannofossils, planktonic foraminifers, diatoms, and radiolarians from core-catcher samples (Fig. 31). However, the sequence is somewhat condensed in the upper part of the lower Miocene. This same interval is absent at Sites 803 and 804 and likewise is thin at Site 805. Microfossil preservation is good to moderate throughout the Neogene for all groups studied, except in the interval from the middle part of the middle Miocene through the lower Miocene where diatom preservation is poor.

All fossil groups are well represented in the Oligocene and upper Eocene chalk (part of lithologic Subunit IB). In contrast to the Neogene, the Paleogene section contains several hiatuses and condensed intervals (see "Sedimentation Rates" section, this chapter). A hiatus or condensed interval is present in the lower part of the upper Oligocene. Two hiatuses are recognized in the middle Eocene. Much of the middle Eocene through Paleocene section is condensed with the

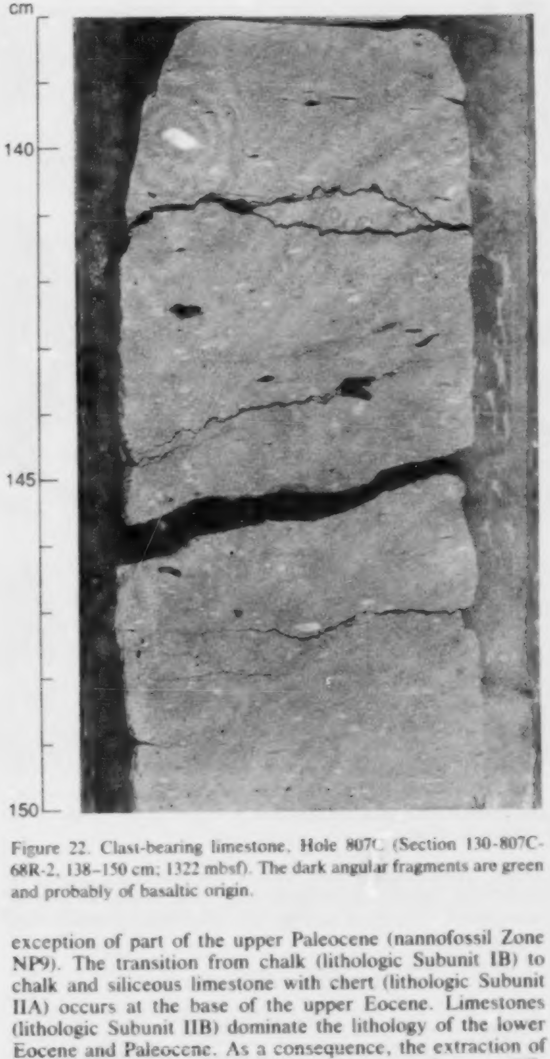

Figure 22. Clast-bearing limestone, Hole 807C (Section 130-807C-68R-2, 138–150 cm; 1322 mbsf). The dark angular fragments are green and probably of basaltic origin.

exception of part of the upper Paleocene (nannofossil Zone NP9). The transition from chalk (lithologic Subunit IB) to chalk and siliceous limestone with chert (lithologic Subunit IIA) occurs at the base of the upper Eocene. Limestones (lithologic Subunit IIB) dominate the lithology of the lower Eocene and Paleocene. As a consequence, the extraction of planktonic foraminifers for shipboard analyses became difficult in sediments older than the late Eocene. Sediments older than latest Eocene are barren of diatoms. Radiolarians occur sporadically through the middle Eocene but are absent in lower Eocene and Paleocene strata at Site 807. Calcareous nannofossils provided the most consistent and reliable shipboard age determinations for the middle Eocene–Paleocene interval.

An apparently complete K/T boundary sequence is preserved in Core 130-807C-54R. The boundary interval is recognized principally on an acme of the calcareous dinoflagellate *Thoracosphaera* in the lower part of Section 130-807C-54R-3 (Table 6). Upper Campanian and Maestrichtian limestones of Site 807 (lithologic Subunit IIB) are barren of siliceous microfossils but generally contain common to abundant populations of poorly preserved calcareous nannofossils. Planktonic foraminifers were successfully extracted from part of the Maestrichtian limestones. Radiolarians provide age controls throughout the sequence of lower Cenomanian–upper Albian brown mudstones (lithologic Subunit IIIA). A hiatus of unknown duration separates the limestones and mudstones. A thin sequence of limestones (lithologic Subunit IIIB) overlies basalt and yields a loosely defined Albian-Aptian age on the basis of calcareous nannofossils and radiolarians.

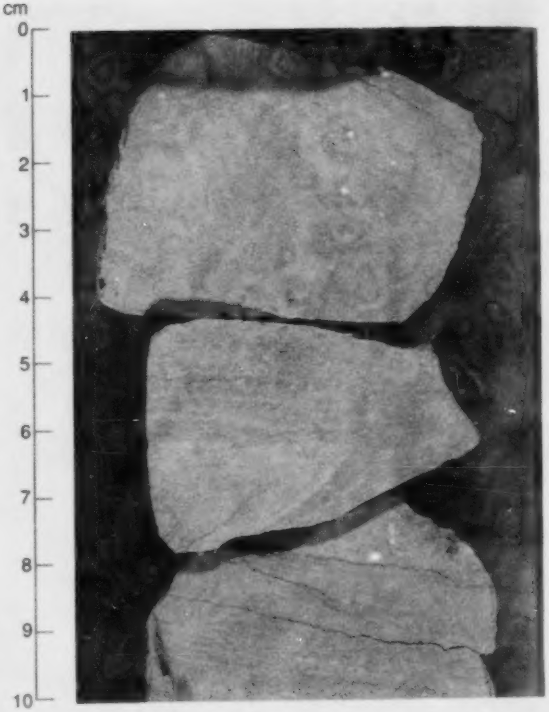

Figure 23. Folded limestone, Hole 807C (Section 130-807C-62R-3, 0–10 cm; 1264 mbsf).

Calcareous Nannofossils

Hole 807A

The section recovered from this hole ranges in age from late Pleistocene to early Oligocene. Calcareous nannofossils are abundant throughout the core. Preservation is good in the Pleistocene and generally moderate in the remainder of the section, the chief problem being overgrowth of calcite on many discoaster specimens.

Pleistocene

The youngest calcareous nannofossil flora in this hole was observed in Sample 130-807A-1H-CC and belongs to Zones NN21–NN20, where abundant gephyrocapsid specimens occur together with *Calcidiscus leptoporus*, *Helicosphaera carteri*, *Syracosphaera pulchra*, and *Umbilicosphaera mirabilis*. Trace amounts of reworked *Calcidiscus macintyrei*, *Cyclicargolithus floridanus*, and *Discoaster* spp. were also observed in Sample 130-807A-1H-CC. The presence of abundant *Pseudoemiliania lacunosa* and the absence of discoasters place Samples 130-807A-2H-CC and -3H-CC in Zone NN19. The former sample contains comparatively abundant *Reticulofenestra asanoi*, but no *Gephyrocapsa parallela*, suggesting an age of this sample that is between 0.83 and 1.06 Ma. The

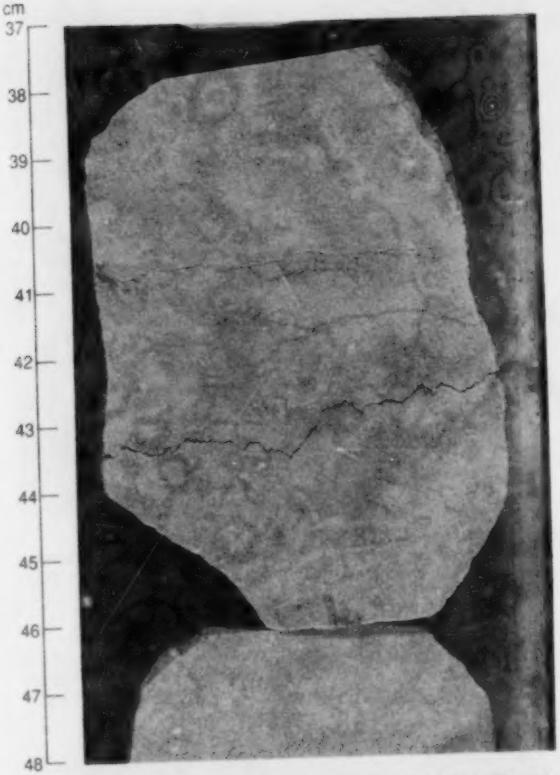

Figure 24. Well-developed stylolite in limestone, Hole 807C (Section 130-807C-48R-1, 37–48 cm; 1146 mbsf).

latter sample contains both *Helicosphaera sellii* and *Calcidiscus macintyrei* and therefore corresponds to the lower part of Zone NN19.

Pliocene

Sample 130-807A-4H-CC contains *Discoaster brouweri* and rare *Discoaster triradiatus* and is assigned to latest Pliocene Zone NN18. The Pliocene/Pleistocene boundary lies within Core 130-807A-4H. The assemblages in the next lower four samples, Samples 130-807A-5H-CC through -8H-CC, are characterized by the occurrences of *Discoaster brouweri*, *Discoaster pentaradiatus*, and *Discoaster surculus*, which place these samples in the upper Pliocene Zone NN16. The long sample intervals used did not permit recognition of the short Zone NN17 in Hole 807A. Sample 130-807A-6H-CC is older than 2.65 Ma because of the presence of *Discoaster tamalis*. Similarly, because of the presence of *Sphenolithus abies* and the absence of *Reticulofenestra pseudoumbilica*, Sample 130-807A-8H-CC was referred to the basal part of Zone NN16, which approximates the lower/upper Pliocene boundary. Sample 130-807A-9H-CC contains *Reticulofenestra pseudoumbilica*, *Sphenolithus abies*, *Amaurolithus delicatus*, and rare *Discoaster asymmetricus*, together with abundant small placoliths. This sample was placed in Zones NN13–NN14.

Samples 130-807A-10H-CC through -13H-CC do not contain *Discoaster quinqueramus*. *Ceratolithus acutus* was observed in Samples 130-807A-10H-CC and -12H-CC, placing

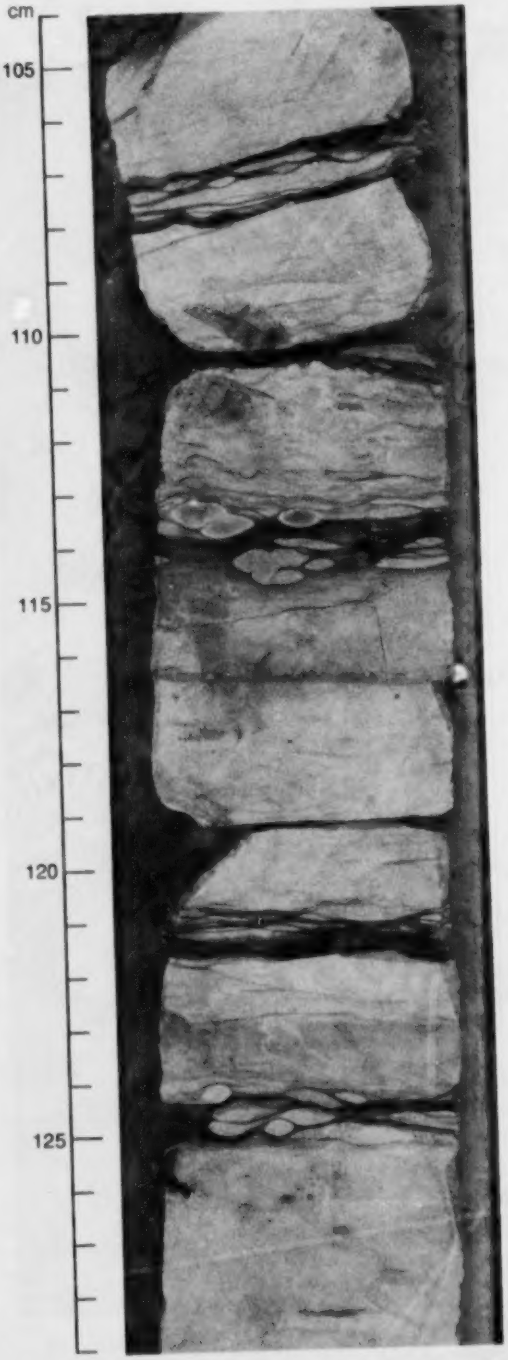

Figure 25. Illustration of the effects of differential compaction between more compacted clay-rich matrix, possibly caused by chemical compaction, and less compacted limestone lenses, which probably represent burrows, Hole 807C (Section 130-807C-53R-3, 104–129 cm; 1184 mbsf).

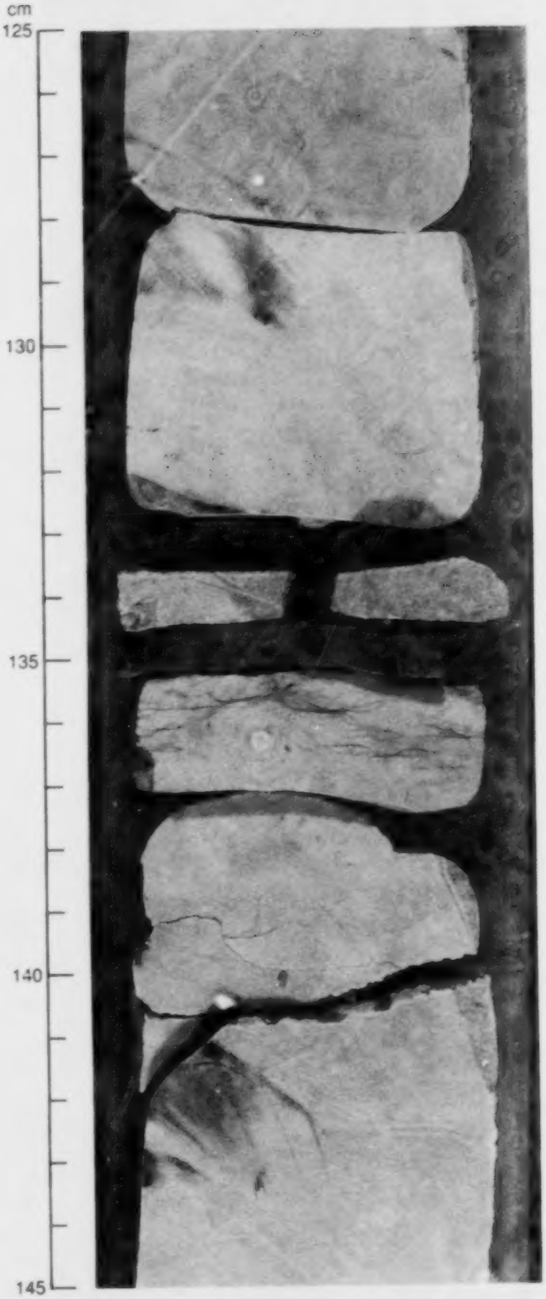

Figure 26. Photograph of Cretaceous/Tertiary boundary interval, Hole 807C. Biostratigraphic data place the actual boundary at the volcanic ash layer in Section 130-807C-54R-3 at 135 cm (1193.14 mbsf).

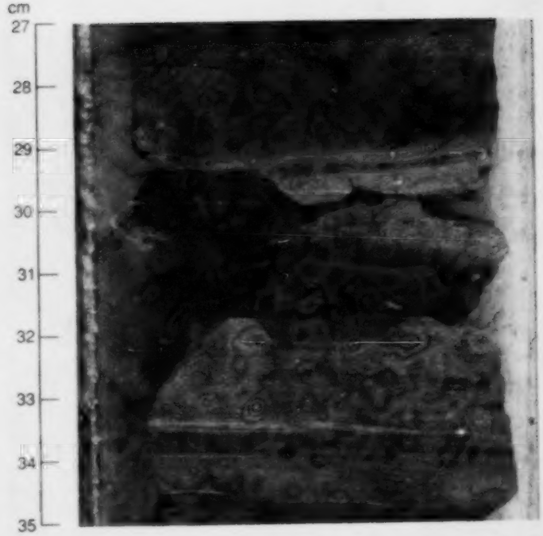

Figure 27. Graded and lenticular bedding in claystone and radiolarian siltstone, Subunit IIIA, Hole 807C (Section 130-807C-72R-2, 27–35 cm; 1360 mbsf).

them in Zone NN12. The absence of *Triquetrorhabdulus rugosus* and *Discoaster quinqueramus* in Sample 130-807A-13H-CC suggests that this sample also belongs to Zone NN12.

Miocene

Discoaster quinqueramus is considered to be present in Sample 130-807A-14H-CC, although the central knob is not as prominent as in Sample 130-807A-15H-CC and below. *Discoaster quinqueramus* was observed down through Sample 130-807A-25H-CC, indicating Zone NN11. Samples 130-807A-17H-CC through -19H-CC contain *Amaurolithus amplificus*. Samples 130-807A-17H-CC and -18H-CC contain fairly abundant sphenoliths and small placoliths. A couple of large specimens of *Discoaster neorectus* that were nearly 25 mm in diameter were observed in Sample 130-807A-21H-CC. Samples 130-807A-26H-CC through -30X-CC contain neither *Discoaster quinqueramus* nor *D. hamatus* and were placed in upper Miocene Zone NN10. The sediments around the Zone NN9/NN10 boundary (Samples 130-807A-24H-CC through -26H-CC) are characterized by bloomlike abundances of small *Sphenolithus abies* and *S. neoabies*. This distinct acme event has been observed at the identical stratigraphic level in all Leg 130 sites.

The occurrence of *Discoaster hamatus* places Samples 130-807A-31X-CC and -32X-CC in Zone NN9. The former sample contains *Discoaster neohamatus*, whereas the latter sample contains fairly common *Catinaster coalitus*. Thus, Core 130-807A-32X contains the middle/upper Miocene boundary. The next lower four samples, Samples 130-807A-33X-CC through -36X-CC, contain neither *Discoaster hamatus* nor *Sphenolithus heteromorphus*. *Coronocyclus nitescens* occurs in and below Sample 130-807A-37X-CC. The last occurrence (LO) of *Coronocyclus nitescens* is supposed to fall near the first occurrence (FO) event of *Discoaster kugleri*, which defines the Zone NN6/NN7 boundary. In the absence of *Discoaster kugleri* in the Leg 130 sediments, the former event has been used as a substitute marker that approximates

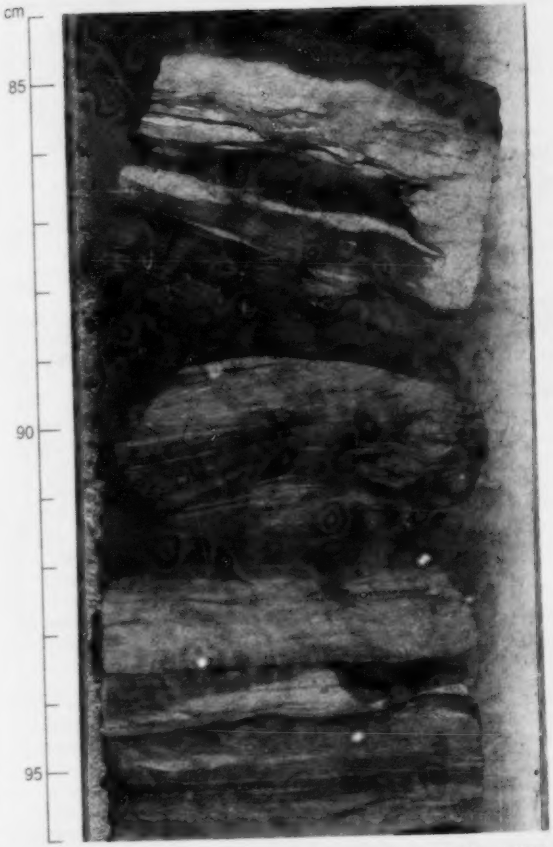

Figure 28. Wavy and lenticular bedding in limestone, Subunit IIIB, Hole 807C (Section 130-807C-73R-2, 84–96 cm, 1370 mbsf).

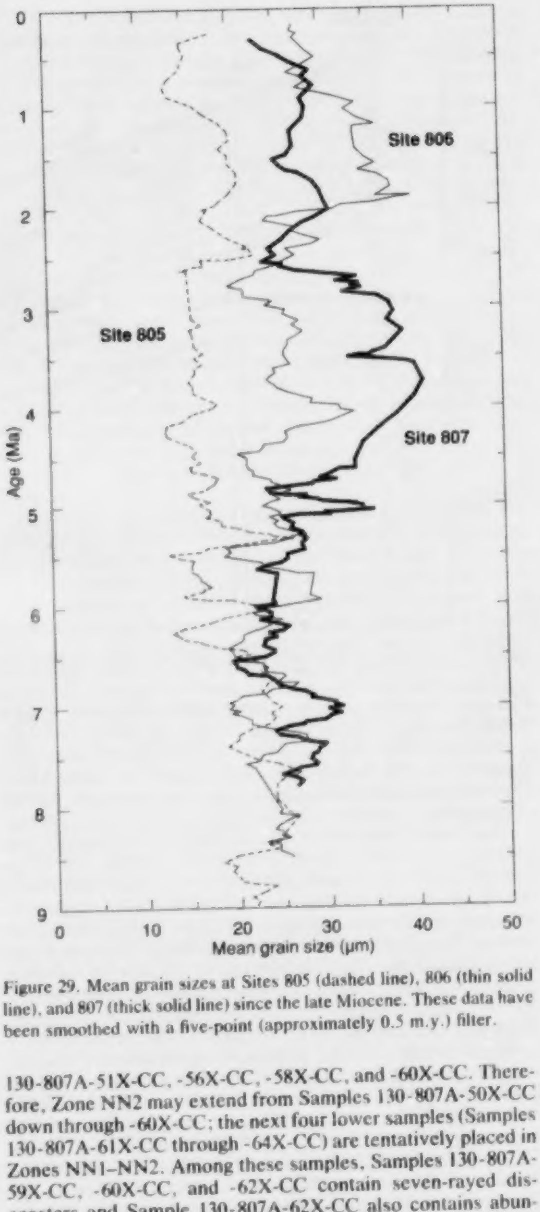

Figure 29. Mean grain sizes at Sites 805 (dashed line), 806 (thin solid line), and 807 (thick solid line) since the late Miocene. These data have been smoothed with a five-point (approximately 0.5 m.y.) filter.

the NN6–NN7 boundary. Samples 130-807A-37X-CC through -39X-CC were referred to Zone NN6 because of the presence of *Coronocyclus nitescens* and the absence of *Sphenolithus heteromorphus*. *Reticulofenestra pseudoumbilica* and *Reticulofenestra gelida* are fairly large in size in Sample 130-807A-34X-CC. Samples 130-807A-40X-CC through -48X-CC contain *Sphenolithus heteromorphus* together with *Cyclicargolithus floridanus*, indicating Zone NN5.

The LO of *Helicosphaera ampliaperta*, which marks the Zone NN4/NN5 boundary, is also lacking at Site 807. The top of the acme of *Discoaster deflandrei*, however, was observed between Samples 130-807A-45X-CC and -46X-CC. The interval from Samples 130-807A-40X-CC through -45X-CC was placed in Zone NN5, whereas the interval from Samples 130-807A-46X-CC through -48X-CC was placed in Zone NN4. The calcareous nannofossil assemblages are poorly preserved in Samples 130-807A-45X-CC and -46X-CC.

A short-range sphenolith species, *Sphenolithus milanetti*, was observed in Sample 130-807A-47X-CC. The presence of *Sphenolithus belemnos* and the absence of *Sphenolithus heteromorphus* and *Triquetrorhabdulus carinatus* place Sample 130-807A-49X-CC in Zone NN3. The latter species was observed up through Sample 130-807A-50X-CC. *Discoaster druggii* occurs only occasionally in small numbers in Samples 130-807A-51X-CC, -56X-CC, -58X-CC, and -60X-CC. Therefore, Zone NN2 may extend from Samples 130-807A-50X-CC down through -60X-CC; the next four lower samples (Samples 130-807A-61X-CC through -64X-CC) are tentatively placed in Zones NN1–NN2. Among these samples, Samples 130-807A-59X-CC, -60X-CC, and -62X-CC contain seven-rayed discoasters and Sample 130-807A-62X-CC also contains abundant *Sphenolithus delphix*. The highest occurrence of *Cyclicargolithus abisectus* was recognized in Sample 130-807A-64X-CC.

Oligocene

The LO of the upper Oligocene species *Sphenolithus ciperoensis* between Samples 130-807A-64X-CC and -65X-CC, and the fact that *Sphenolithus delphix* is common in Core 130-807A-62X, indicates that the Oligocene/Miocene boundary probably lies within Core 130-807A-63X. *Sphenolithus ciperoensis* was observed in Samples 130-807A-

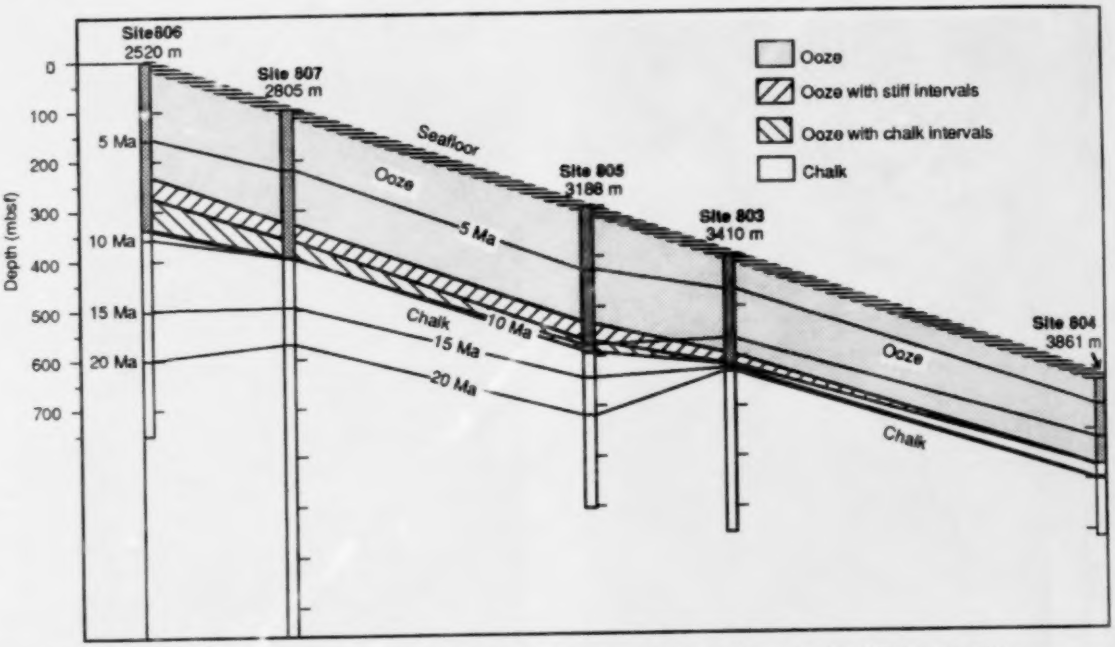

Figure 30. Summary of the bathymetry, ages, and sub-bottom depths of the ooze-chalk transition at the sites drilled on Leg 130.

65X-CC through -72X-CC. *Sphenolithus distentus* occurs together with *S. ciperoensis* in Sample 130-807A-72X-CC. Samples 130-807A-65X-CC through -71X-CC were placed in Zone NP25, and Sample 130-807A-72X-CC in Zone NP24. Throughout Zone NP25, *Cyclicargolithus abisectus* occurs occasionally.

The highest occurrence of *Coccolithus eopelagicus* was observed in Sample 130-807A-68X-CC. Sample 130-807A-73X-CC contains several specimens of transitional forms between *Sphenolithus distentus* and *Sphenolithus ciperoensis* and must lie close to the Zone NP23–NP24 boundary. This implies that Zone NP24 is exceptionally thin relative to surrounding Zones NP25 (above) and NP23 (below). Nevertheless, the lower/upper Oligocene boundary probably lies within Core 130-807A-73X. The interval from Sample 130-807A-74X-CC down to the bottom of the hole was assigned to lower Oligocene Zone NP23 because of the absence of *Sphenolithus ciperoensis* and *Reticulofenestra umbilica*. *Sphenolithus distentus* was observed in Samples 130-807A-74X-CC through -81X-CC. The highest occurrence of *Sphenolithus pseudoradians* was observed in Sample 130-807A-80X-CC. The interval from Sample 130-807A-82X-CC down to the bottom of the hole contains *Dictyococcites bisectus* and *Zygrhablithus bijugatus*. *Coccolithus eopelagicus* occurs sporadically in the upper part of Zone NP23, but continuously in and below Sample 130-807A-83X-CC. *Helicosphaera bramlettei* was observed in Sample 130-807A-79X-CC, and *Helicosphaera compacta* was observed in Samples 130-807A-84X-CC and -86X-CC.

Hole 807B

Hole 807B was cored continuously with the APC to refusal at 278.6 mbsf (Core 130-807B-30H). The nannofossil assemblages in Hole 807B are similar to those observed in the corresponding interval in Hole 807A, and the biostratigraphic relationships of these two holes are shown in Figure 31. The sediments obtained from the bottom of this hole contain *Calcidiscus leptoporus*, *Calcidiscus macintyrei*, *Cotinaster calyculus*, *Coccolithus pelagicus*, various discoasters (such as *D. bellus*, *D. brouweri*, *D. challengeri*, and *D. variabilis*), *Helicosphaera carteri*, *Reticulofenestra* spp., *Sphenolithus abies*, and *Triquetrorhabdulus rugosus*. This assemblage is characterized by the absence of *Discoaster quinqueramus* and *Discoaster hamatus*, which places these sediments in upper Miocene Zone NN10. This zone extended over five cores in Hole 807A. The deepest core of Hole 807B (Core 130-807B-30H) is the fifth core representing Zone NN10, implying that Hole 807B probably ended shortly above the Zone NN9/NN10 boundary.

Hole 807C

Oligocene

The nannofossil assemblages in depth correlative Samples 130-807A-86X-CC and 130-807C-1R-CC are similar in composition and abundance: *Cyclicargolithus floridanus* and *Sphenolithus moriformis* are abundant, whereas *Coccolithus pelagicus*, *Coccolithus eopelagicus*, *Dictyococcites bisectus*, *Dictyococcites hesslandii*, *Helicosphaera compacta*, *Sphenolithus predistentus*, and *Zygrhablithus bijugatus* range in abundance between common and rare. This basic composition of the nannofossil assemblages, representing Zone NP23, continues down through Core 130-807C-8R, although the proportions between species change between samples. Lower Oligocene species such as *Discoaster tanii*, *Ericsonia fenestratus*, *Ericsonia obruta*, *Helicosphaera reticulata*, and *Rhabdosphaera tenuis* were observed in several samples from Zone NP23. Moreover, a sphenolith species that resembles *Sphenolithus distentus* but has its entire range below the continuous range of *Sphenolithus distentus* s.s. was observed in

Cores 130-807C-7R through -15R. These two morphotypes, therefore, do not overlap stratigraphically. Okada (1990) recently observed this morphotype from the identical stratigraphic interval in the equatorial Indian Ocean. For the time being, we follow Okada's designation of this species as *Sphenolithus* aff. *distentus*.

The LO of the *Reticulofenestra umbilica–Reticulofenestra hillae* complex, and hence the Zones NP22/NP23 boundary, was observed in Core 130-807C-9R. There was no recovery in Cores 130-807C-10R and -11R, although they also must lie in the Zone NP22 interval as the underlying Core 130-807C-12R belongs to that zone. The LO of *Ericsonia formosa* was observed in Core 130-807C-13R. The *Dictyococcites bisectus–Dictyococcites hesslandii* complex has its first continuous occurrence in the lower Oligocene. This group increases in abundance, together with *Bramlettius serraculoides*, through the lower Oligocene.

Eocene

Discoaster preservation is consistently poor throughout the lower Oligocene and Eocene, making a precise determination of the LO of *Discoaster saipanensis* difficult. Thus, the NP20/NP21 boundary, which approximates the Eocene/Oligocene boundary, is difficult to determine precisely. We consider, however, that rare *Discoaster saipanensis* is present as high as Sample 130-807C-18R-CC. Typical *Discoaster barbadiensis* was observed up to Sample 130-807C-19R-CC. This upper Eocene sample also yields abundant *Bramlettius serraculoides*, *Coccolithus pelagicus*, *Cyclicargolithus floridanus*, and common *Reticulofenestra umbilica–Reticulofenestra hillae*. Common discoasters belonging to the six-rayed *Discoaster deflandrei* group and the five-rayed *Discoaster tanii* group were also observed. A few helicosphaerid species and *Ericsonia formosa* formed the less abundant members of this upper Eocene assemblage.

The LO of *Cribrocentrum reticulatum* was observed in Core 130-807C-22R, whereas the last "*Calcidiscus*" *protoannulus* was observed in Core 130-807C-24R. Rare *Chiasmolithus solitus* was observed in Sample 130-807C-29R-CC, suggesting a position within Zone NP16. This sample also contains the LO of *Chiasmolithus grandis*, the extinction of which closely approximates the middle Eocene/upper Eocene boundary. The LO of *Campylosphaera dela* was observed in Core 130-807C-30R. The taxonomic diversity increased through the upper Eocene down through the middle Eocene, and the upper middle Eocene assemblages cored at Site 807 typically contain about 20 easily recognizable species, a number that would increase had preservation been better.

The biostratigraphically important *Dictyococcites bisectus–Dictyococcites hesslandii* complex has its first evolutionary appearance in Core 130-807C-31R. Large reticulofenestrids (i.e., *Reticulofenestra umbilica*), appeared in Core 130-807C-36R. *Sphenolithus furcatolithoides* was observed in Core 130-807C-37R, whereas the LO of *Nannotetrina alata* falls in Core 130-807C-38R. This core is also characterized by the presence of abundant *Coccolithus pelagicus* and *Pseudotriquetrorhabdulus inversus*, common (relatively small) chiasmoliths and *Reticulofenestra dictyoda*, and few to rare *Chiasmolithus grandis*, *Coccolithus eopelagicus*, *Ericsonia formosa*, and *Sphenolithus radians*. The smaller nannotetrinas were not recognized because of severe calcite overgrowth. Rare and poorly preserved *Chiasmolithus gigas* were added to this general assemblage in Sample 130-807C-39R-CC, thus providing an important biostratigraphic control point within the middle Eocene Zone NP15. This sample also contains *Nannotetrina alata*.

Poor preservation and severe calcite overgrowth prevents confident identification of the nannotetrinas, including *Nannotetrina alata*, in Sample 130-807C-40R-CC. The presence of *Discoaster sublodoensis*, however, places this sample in Zone NP14 or lowermost Zone NP15. *Discoaster lodoensis* co-occurred with *Discoaster sublodoensis* in Sample 130-807C-41R-CC, indicating Zone NP14. Hence, the lower Eocene/middle Eocene boundary must be located in Core 130-807C-41R. This is also the deepest core containing representatives of the genus *Reticulofenestra*, a genus that is considered to appear within Zone NP13 (Romein, 1979).

Sample 130-807C-42R-CC, therefore, lacks reticulofenestrids, but severely overgrown specimens of *Tribrachiatus orthostylus* were observed together with *Discoaster lodoensis*, implying that the sample belongs to Zone NP12 and that Zone NP13 is condensed and lies within Core 130-807C-42R. The diversity in this sample is low, which partly is caused by poor preservation. Sample 130-807C-43R-CC was taken from a silicified limestone and is virtually barren of nannofossils. The co-occurrence of typical *Discoaster diastypus*, *Discoaster keupperi*, *Discoaster lodoensis*, and overgrown *Tribrachiatus orthostylus*, places Sample 130-807C- 44R-CC in Zone NP12.

Core 130-807C-45R has biostratigraphic relationships that indicate the influence of turbiditic or debris-flow deposition. Sample 130-807C-45R-1, 10 cm, yielded an upper Paleocene assemblage (Zone NP9; including the only *Ellipsolithus macellus* specimens observed from Site 807), intermixed with Cretaceous forms (e.g., *Micula* spp. and *Watznaueria barnesae*). Investigation of a small white clast (Sample 130-807C-45R-1, 34 cm) yielded an assemblage composed almost exclusively of Cretaceous forms, whereas the surrounding grayish matrix at the same level contains a predominantly Zone NP9 flora with little Cretaceous representation. Sample 130-807C-45R-1, 114–116 cm, however, represents the lower Eocene Zone NP12 (*Discoaster lodoensis* and *Tribrachiatus orthostylus* are both present). The presence of *Discoaster diastypus* and *Tribrachiatus orthostylus* in Core 130-807C-46R indicates Zone NP11.

Paleocene

Discoaster multiradiatus was observed in Samples 130-807C-47R-CC and -48R-CC, together with representatives of the genera *Toweius* and, possibly, *Rhomboaster*. Poor preservation prevents a reliable identification of rhomboasters, which share a tendency with the descendant *Tribrachiatus* lineage to being prone to secondary calcite overgrowth. The biostratigraphic assignment of these two samples into upper Zone NP9, therefore, must rely also on the absence of *Discoaster diastypus*, which indicates a position below Zone NP10, and the absence of fasciculiths, which indicates a position in uppermost Zone NP9 when, as here, *Discoaster multiradiatus* is present. It follows that Zone NP10 probably is condensed, and that both this zone and the Paleocene/Eocene boundary lie within Core 130-807C-47R.

Cores 130-807C-49R and -50R were also assigned to Zone NP9 because of the co-occurrences of abundant and diverse fasciculiths, including *Fasciculithus tympaniformis* and *Discoaster multiradiatus*. One of the best preserved samples in that depth interval consisted of an easily disintegrated chalk clast taken from within a chert layer. This sample (130-807C-50R-1, 116 cm) contained abundant fasciculiths; common *Coccolithus pelagicus*, *Discoaster multiradiatus*, *Toweius* spp., and *Sphenolithus moriformis*; and few to rare *Discoaster nobilis*, chiasmoliths, thoracosphaerids, and one of the few observations of *Neochiastozygus*.

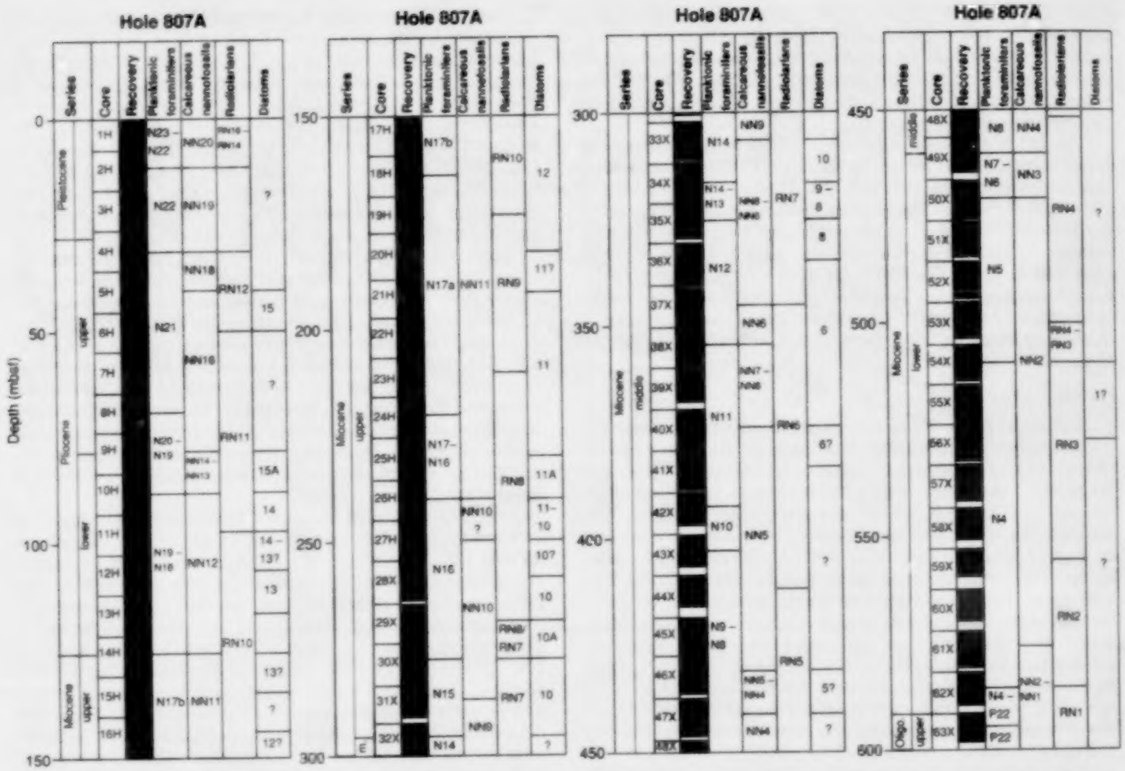

Figure 31. Biostratigraphic hole summaries, Site 807. RN = radiolarian Neogene zone, NTD = Neogene tropical diatom zone, RP = radiolarian Paleogene zone, and NN = nannofossil Neogene zone.

The LO of *Ericsonia robusta* was observed between Samples 130-807C-51R-1, 90 cm, and -2, 88 cm. *Discoaster multiradiatus* is common and fasciculiths are abundant in these samples, indicating a position in lower Zone NP9. Rare *Heliolithus riedelii* were observed in Sample 130-807C-51R-CC; a long search for *Discoaster multiradiatus* in this sample yielded one possible specimen. This sample, therefore, is considered to lie close to the NP8/NP9 boundary.

Core 130-807C-52R contained the NP5–NP7 zonal interval. The lowermost occurrence of *Discoaster mohleri*, the FO of which defines the NP6/NP7 boundary, was observed through Sample 130-807C-52R-3, 20–22 cm. This sample contained rare, fairly small, *Heliolithus kleinpellii*, a species that was observed also at a level 10 cm further downcore; its ancestor, *Heliolithus cantabriae*, was present in Sample 130-807C-52R-3, 75 cm. Thus, the NP6/NP7 and NP5/NP6 boundaries both lie in the upper half of Section 130-807C-52R-3. Abundant fasciculiths, including rare *Fasciculithus pileatus*, were observed in Sample 130-807C-52R-CC, indicating Zone NP5.

Sample 130-807C-53R-2, 130 cm, contained an evolutionary young fasciculith association, including *Fasciculithus bitectus*, *Fasciculithus magnicordis*, and *Fasciculithus ulii*. This association lacks *Fasciculithus tympaniformis*, thus indicating Zone NP4. The next lower sample (Sample 130-807C-53R-3, 23 cm) lies below the ranges of both fasciculiths and sphenoliths, but contains rare specimens of Danian (lower Paleocene) species, such as *Cruciplacolithus primus*, *Cruciplacolithus tenuis*, and *Prinsius bisulcus*.

The abundance of nannofossils decreases markedly through Core 130-807C-53R from "abundant" to "few" or "rare"; preservation is consistently poor and diversity is low. Nevertheless, characteristic lower Paleocene species (i.e., *Cruciplacolithus primus*) were observed in several samples from the lower part of this core, and one would expect, therefore, to find abundant small placoliths (e.g., *Biscutum* spp.) in these lower Paleocene limestones. Their absence is interpreted to represent diagenetic destruction and reduction of the original assemblage. Despite the fact that the lower Paleocene forms are rare, their presence indicates that the observed Cretaceous species must be reworked.

General conditions of low abundance, low diversity, and poor preservation also characterized Core 130-807C-54R, in which an apparently continuous K/T boundary transition was recovered.

The Cretaceous/Tertiary Boundary

The wealth of small Tertiary placolith taxa (i.e., *Biscutum*, *Cruciplacolithus*, and *Toweius*) emerging immediately after the mass extinction of Cretaceous forms (e.g., Romein, 1979; Thierstein and Okada, 1979; Manivit and Feinberg, 1984; Monechi, 1985) essentially have been dissolved in the nearest 8 m above the assigned K/T boundary horizon at Site 807. Trace amounts of such Danian placoliths, however, are con-

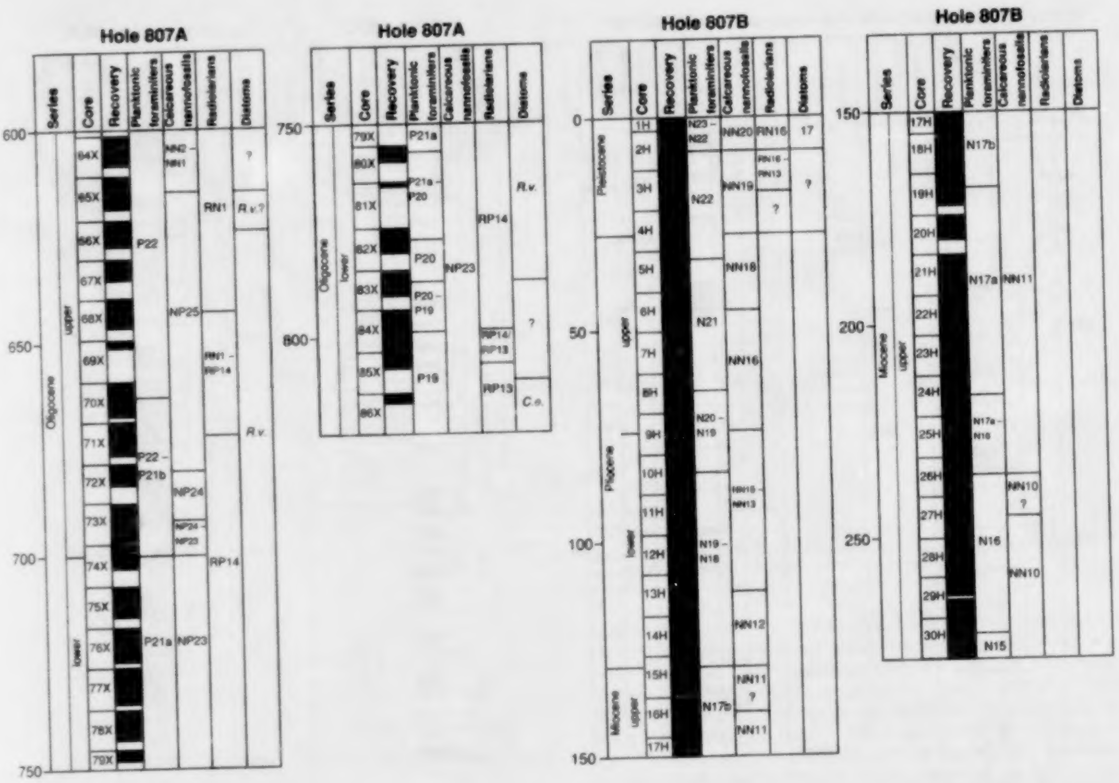

Figure 31 (continued).

sistently present from 1.1 m above the boundary horizon. The boundary was placed within a 16-cm interval at the base of Section 130-807C-54R-3 because of the FO, rapid rise, and subsequent rapid decline in abundance (acme) of the calcareous dinoflagellate *Thoracosphaera* (Table 6). Only fragments of these dissolution-resistant morphotypes were preserved in the deeply buried (1193 mbsf) K/T sequence at Site 807. Moreover, the lowermost Danian sediments contain abundant Cretaceous specimens, in comparison with the low abundance of indigenous species, reflecting the fact that the Cretaceous-source sediments are rich in such dissolution-resistant morphotypes as *Watznaueria* and *Micula* (Thierstein, 1981).

Cretaceous

The abundance of Upper Cretaceous assemblages varies from few to common, whereas the preservation varies between poor and moderate. Cores 130-807C-55R through -57R contain *Micula murus* and hence belong to the upper Maestrichtian; Sample 130-807C-55R-1, 86 cm, yielded a few specimens of *Micula prinsii*, indicating a position immediately below the K/T boundary. Other typical forms in these poorly preserved upper Maestrichtian assemblages include *Arkhangelskiella cymbiformis*, *Cretarhabdus crenulatus*, *Cribrosphaerella ehrenbergii*, *Lithraphidites quadratus*, and the ubiquitous *Watznaueria barnesae*. *Microrhabdulus decoratus*, *Prediscosphaera cretacea*, and *Ceratolithoides aculeus* were observed occasionally in the Maestrichtian cores. The latter species, however, is a fairly regular member of assemblages from Samples 130-807C-60R-CC to -70R-CC, whereas *Parhabdolithus embergeri* was observed in Core 130-807C-61R and downhole.

Quadrum trifidium has its LO in Core 130-807C-61R. This important marker species is consistently present throughout its observed range; its FO level was observed between Samples 130-807C-70R-CC and -71R-1, 37–38 cm. *Quadrum gothicum* occurs consistently from Sample 130-807C-59R-CC through the continuous carbonate-bearing sediments, to the sharp red clay contact in Section 130-807C-71R-3. Thus, the age range of this interval is limited to the early Maestrichtian–late Campanian.

A short interval of nannofossil-bearing limestones in basal Core 130-807C-73R and topmost Core 130-807C-74R separates the barren red and brown zeolitic clays above from the igneous basement below. The nannofossils in this limestone are abundant but poorly preserved, and *Watznaueria barnesae* appears to occupy over 90% of the total assemblage. The presence of a few specimens of *Rucinolithus irregularis*, which had a stratigraphic range restricted to the Aptian and Albian, places Sample 130-807C-73R-CC in the Lower Cretaceous. Therefore, it appears reasonable to assume that the red clay interval, which separates these Aptian- Albian limestones from the overlying upper Campanian limestones in Core 130-807C-71R, is associated with hiatus(es) of considerable duration (on the order of 10^7 yr). *Parhabdolithus embergeri* and, possibly, *Watznaueria britannica* are rare members of the assemblage in Sample 130-807C-73R-CC. If the latter species, indeed, is a member of this assemblage, its presence supports the Lower Cretaceous assignment.

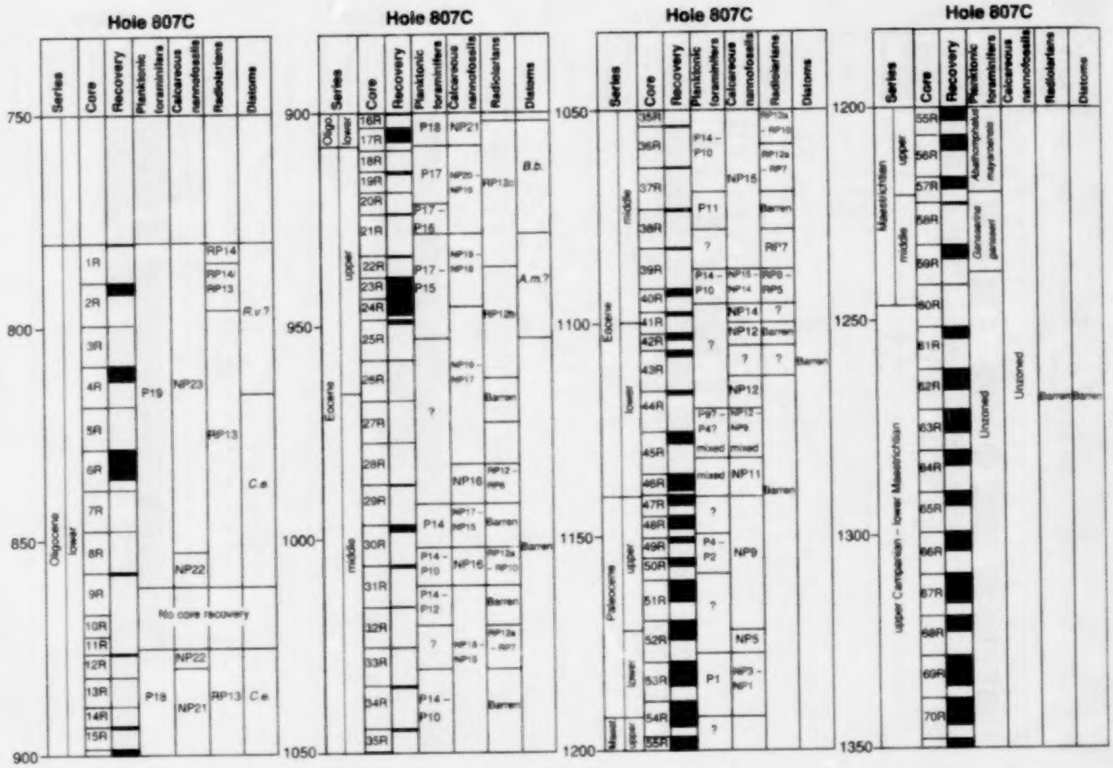

Figure 31 (continued).

Basement was reached about 20 cm below Sample 130-807C-73R-CC, and the Aptian-Albian age assignment for the overlying limestone presumably also applies for the basalt. The basal sedimentary sequence cored in Hole 807C has some interesting characteristics in common with the sequence cored at neighboring Site 289 (see Shipboard Scientific Party, 1975b). A fairly extended Maestrichtian through upper Campanian carbonate-rich sequence ends in a short interval of red clays (described as a vitric tuff bed). The tuff bed is underlain by a short interval of limestones, which, in turn, rests on basaltic basement. The age of these lower limestones is uncertain. They are referred to as being "... probably Aptian ..." (Shafik, 1975, p. 598), or upper Albian (Shafik, 1975, p. 583), because "... only the *Eiffellithus turriseiffeli* Zone from the Lower Cretaceous has been identified among Leg 30 material" (implying that the sediments cannot be older than late Albian). Nevertheless, both estimates are coherent with the less precise Aptian-Albian assignment suggested for the basal limestones in Hole 807C.

A few pieces of limestone were retrieved from within the basalt sequence. The limestones from Section 130-807C-80R-1 yielded poorly preserved nannofossils, although the presence of both *Watznaueria barnesae* and some distinct specimens of *Watznaueria britannica* indicate an Early Cretaceous age for these limestone pieces, as well as the adjacent basalts. It appears likely that this estimate can be considerably refined.

Planktonic Foraminifers

Neogene

Neogene sediments are present to a depth of approximately 592 mbsf in Hole 807A. The Oligocene/Miocene boundary (P22/N4) can probably be placed in the upper part of Core 130-807A-63X. Hole 807B ended in basal upper Miocene sediments (Zone N15). Planktonic foraminifers are generally abundant and well to moderately well preserved through the Neogene section at Site 807. The sequence appears to be complete except in the upper part of the lower Miocene (Zones N6 and N7) where the section is thin either because of reduced sediment accumulation or gaps in the sediment record (Fig. 31).

Pleistocene–uppermost Pliocene Zones N22–N23 are characterized by the presence of *Globorotalia truncatulinoides*, although the occurrence of this taxon is often sporadic in the holes drilled during Leg 130. The LO of *Globigerinoides fistulosus* marks the Pliocene/Pleistocene boundary. The co-occurrence of *G. truncatulinoides* and *G. fistulosus* defines the uppermost Pliocene part of Zone N22 (e.g., Sample 130-807B-4H- CC). Upper Pliocene Zone N21 is characterized by the presence of *G. fistulosus* and *Sphaeroidinella dehiscens*. The FO of *Globorotalia tosaensis* defines the base of Zone N21, but this taxon occurs only sporadically at this site; therefore, the FO of *S. dehiscens* s.s. is used as a proxy for the base of the zone. The LO of *Globoquadrina altispira* and the LO of

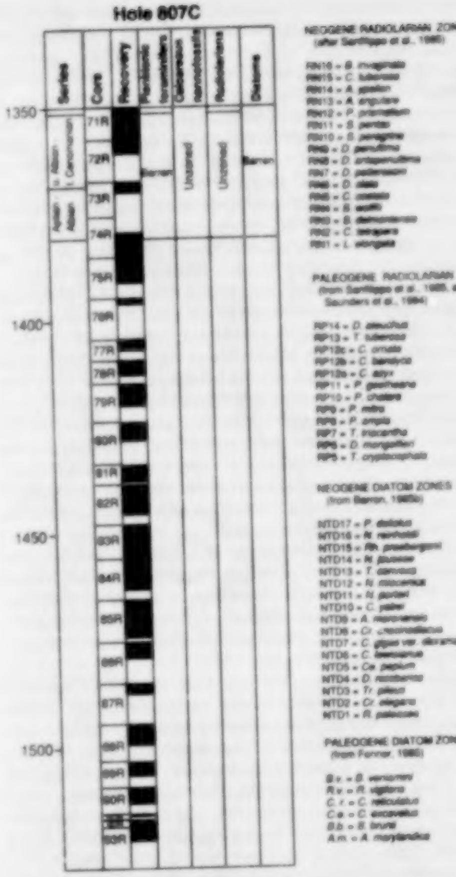

Figure 31 (continued).

Sphaeroidinellopsis spp. are present in the lower part of Zone N21.

The mid-Pliocene interval (Zones N19–N20) is characterized by the presence of right-coiled *Pulleniatina*. The LO of *Globorotalia margaritae* is in this zone. *Sphaeroidinella dehiscens* s.l. (*S. dehiscens immaturus*) would normally be used to differentiate Zones N18 and N19. However, this taxon is very rare in the lower Pliocene of Site 807. The coiling change in *Pulleniatina* is used to mark the boundary between Zones N19–N20 and Zones N18–N19 (undifferentiated) at this site. Characteristic taxa of Zones N18–N19 include *Globorotalia margaritae*, *G. tumida*, *G. plesiotumida*, *G. menardii*, *Globoquadrina altispira*, *Sphaeroidinellopsis seminulina*, *S. paenedehiscens*, *Globigerinoides extremus*, *G. conglobatus*, and left-coiled *Pulleniatina primalis*, *P. praecursor*, and *P. spectabilis*. The FO of *Globorotalia tumida* marks the Miocene/Pliocene boundary at this site.

Upper Miocene Zone N17 is divided into Subzones N17a and N17b based on the FO of *Pulleniatina primalis*, which is restricted to Subzone N17b. The faunal composition of Subzones N17a and N17b is otherwise similar and includes *Globorotalia menardii*, *G. plesiotumida*, *G. merotumida*, *Globoquadrina dehiscens*, *G. altispira*, *Globigerinoides* spp., *Sphaeroidinellopsis* spp., *Neogloboquadrina humerosa*, and *N. acostaensis*. The FO of *Globorotalia plesiotumida* was used to define the base of Subzone N17a. However, the presence of forms transitional to *G. merotumida* make the exact placement of this boundary tenuous. Coiling changes in the *Globorotalia menardii* group in Subzone N17a and the FO of *Neogloboquadrina humerosa* in Zone N16 (Berggren et al., 1985) help to bracket the boundary. The composition of the Zone N16 assemblage is similar to that of Subzone N17a with the exception of the FOs noted above. The FO of *Neogloboquadrina acostaensis* marks the N15/N16 zonal boundary. The interval with neither *N. acostaensis* nor *Globorotalia siakensis* corresponds to basal upper Miocene Zone N15. The LO of *Globorotalia continuosa* is in Zone N15. *Streptochilus* occurs commonly throughout the upper Miocene of this site.

The uppermost zone of the middle Miocene (N14) is recognized by the LO of *Globorotalia siakensis*. Other characteristic taxa of this zone include *Globorotalia continuosa*, *G. menardii*, *G. praemenardii*, *G. lenguaensis*, *Globoquadrina dehiscens*, *G. altispira*, *Globigerinoides sacculifer*, *G. trilobus*, *G. subquadratus*, *Globigerina woodi*, and rare *G. nepenthes*. The FO of *Globigerina nepenthes* differentiates Zones N13 and N14. *Globorotalia fohsi*, *G. fohsi lobata*, and *G. fohsi robusta* are diagnostic of middle Miocene Zone N12. The FO of the *G. fohsi* group marks the base of the zone. Zone N11 is characterized by the presence of *Globorotalia praefohsi*, whereas *Globorotalia peripheroacuta* in the absence of *G. praefohsi* characterizes Zone N10. The FO of *G. peripheroacuta* marks the base of Zone N10. Other taxa present in Zones N10–N12 include *Globorotalia siakensis*, *G. praemenardii*, *G. lenguaensis*, *Globoquadrina dehiscens*, *G. altispira*, *Sphaeroidinellopsis seminulina*, *S. kochii*, *Globigerinoides trilobus*, *G. subquadratus*, and *Globigerina woodi*. The LO of *Globorotalia peripheroronda* is present within Zone N10. The lowest zones of the middle Miocene (N8 and N9) could not be differentiated at Site 807 because of the general absence of species of the *Praeorbulina-Orbulina* lineage. However, *Praeorbulina sicanus* is present and its FO marks the base of Zone N8.

Table 6. Relative abundances of Tertiary and Cretaceous calcareous nannofossils and the calcareous dinoflagellate *Thoracosphaera* in Core 130-807C-54R.

Core, section, interval (cm)	Depth (mbsf)	Cretaceous	Tharacosphaera	Tertiary
130-807C-				
54R-2, 12	1190.42	Common	—	Trace
54R-2, 29	1190.59	Common	—	Trace
54R-2, 115	1191.45	Common	Rare	Trace
54R-2, 120	1191.50	Common	Rare	Trace
54R-3, 27	1192.07	Common	Rare	Trace
54R-3, 51	1192.31	Rare	Rare	—
54R-3, 56	1192.36	Rare	Rare	—
54R-3, 84	1192.39	—	Common	Trace
54R-3, 116	1192.64	Few	Rare	—
54R-3, 127	1193.07	Common	Abundant	—
54R-3, 134	1193.14	Rare	Rare	—
54R-3, 135.5	1193.16	Rare	Rare	—
54R-3, 137	1193.17	Common	Rare	—
54R-3, 150	1193.30	Abundant	Rare	—
54R-4, 3	1193.33	Few	—	—
54R-4, 29	1193.59	Few	—	—
54R-4, 60	1193.90	Common	—	—
54R-4, 101	1194.31	—	—	—
54R-CC	1196.90	Common	—	—
55R-1, 86	1197.76	Rare	—	—

Note: The Cretaceous/Tertiary boundary interval is recognized by the first occurrence and the rapid rise of *Thoracosphaera*.

The upper part of the lower Miocene is thin at Site 807. Only one core-catcher sample contains a fauna indicative of either Zone N7 or N6 (Sample 130-807A-49X-CC). This sample contains *Globorotalia birnageae*, *G. peripheroronda*, *G. siakensis*, *Catapsydrax stainforthi*, and *C. dissimilis*. This part of the section could represent a condensed interval with a mixed fauna, as evidenced by the co-occurrence of *G. birnageae* (FO in Zone N7) and *C. dissimilis* (LO at the top of Zone N6). The remainder of the lower Miocene, including most of Zone N5 and all of Zone N4, is thick and apparently complete. Zone N5 is recognized by the presence of *Globoquadrina binaiensis* in the absence of *Globorotalia kugleri*. Zone N4 is defined by the total range of *G. kugleri* s.s. Other taxa found within Zones N4 and N5 include *Catapsydrax dissimilis*, *C. unicavus*, and *Globorotalia siakensis*. *Globigerinoides altiaperturus* occurs in Zone N5, and the LO of *Globorotalia nana* is in Zone N4. The base of the Miocene probably occurs within Core 130-807A-63X.

Paleogene

Upper Oligocene Zone P22 is recognized by the absence of *Globorotalia kugleri* and *G. opima*. Taxa present throughout the zone include *Globorotalia nana*, *G. siakensis*, *Catapsydrax* spp., *Globigerina angustiumbilicata*, and *Cassigerinella chipolensis*. *Globorotalia pseudokugleri* is present in the upper part of the zone. The top of Zone P21 is defined by the LO of *Globorotalia opima*. Zone P21 is subdivided into upper Oligocene Subzone P21b and lower Oligocene Subzone P21a based on the LO of *Chiloguembelina*, which is restricted to Subzone P21a. Core-catcher samples from Cores 130-807A-70X to -73X contain specimens transitional between *G. nana* and *G. opima*. Because these samples apparently do not contain *G. opima* s.s., it is not clear whether they belong to Zone P22 or Subzone P21b. Other taxa present in this interval, including *Globigerina angulisuturalis* and *G. ciperoensis*, do not help to resolve the uncertainty. Sample 130-807A-74X-CC contains both *G. opima* s.s. and *Chiloguembelina*, indicative of Subzone P21a. A hiatus within the lower part of the upper Oligocene sequence is one interpretation of the data (see "Sedimentation Rates" section, this chapter).

The base of lower Oligocene Subzone P21a is defined by the FO of *Globigerina angulisuturalis*, which is a rare component of these Oligocene sediments. Zone P20 is recognized by the presence of *Globorotalia opima* in the absence of *G. angulisuturalis* and *Globigerina ampliapertura*. The LO of *G. ampliapertura* defines the top of Zone P19. Other taxa present in Zone P19 include *Chiloguembelina*, *Cassigerinella chipolensis*, *Catapsydrax* spp., *Globigerina yeguaensis*, *G. tripartita*, and *Globorotalia nana*. The lowest zone of the Oligocene (Zone P18) is characterized by the presence of *Pseudohastigerina micra* in the absence of late Eocene taxa. Additional taxa noted in Zone P18 include *Globorotalia increbescens*, *Cassigerinella chipolensis*, *Catapsydrax* spp., *Globigerina ampliapertura*, *G. gortanii*, and *G. yeguaensis*. The upper Eocene (Zones P15–P17) is recognized by the co-occurrence of *Globorotalia cerroazulensis*, *Hantkenina* spp. (primarily observed as spines), and *Globigerina angiporoides*.

Chert with little surrounding matrix dominates the recovered sediment through the middle Eocene (Zones P10–P14) (Fig. 31). The matrix consists mostly of chalky limestone that becomes more siliceous adjacent to cherts. It is very difficult to extract planktonic foraminifers from this material, but rare specimens in most samples provide a crude age determination. Some samples appear to be barren. This, however, may largely be an artifact of the harsh mechanical treatment needed to extract foraminifer tests, including grinding with a mortar and pestel and ultrasonic vibration. Thin-section analyses would probably permit resolution of the planktonic foraminifer zones through this interval and the underlying limestones.

Taxa indicative of middle Eocene Zone P14 in Sample 130-807C-30R-CC include *Truncorotaloides rohri*, *Morozovella spinulosa*, *Acarinina bullbrooki*, *Globigerinatheka* spp., spines of *Hantkenina*, and *Subbotina eocaena*. An assemblage indicative of middle Eocene Zone P11 was found in Sample 130-807C-38R-CC that includes *Morozovella aragonensis*, *Acarinina bullbrooki*, *Globigerinatheka index*, and *G. subconglobatus*. Other core-catcher samples in the middle Eocene are mostly characterized by the presence of robust, indeterminate species of *Subbotina* and *Globigerinatheka*.

The zones of the lower Eocene were not clearly recognized on the basis of planktonic foraminifers. This interval contains evidence of slumping and/or reworking based on nannofossil and foraminifer evidence. Mixed floras and faunas were noted in several samples. For example, Sample 130-807C-45R-1, 30–32 cm, contains a mixed foraminifer assemblage that indicates a late Paleocene (P4–P6a) to early Eocene (P6b–P9) age based on the presence of *Planorotalites pseudomenardii*, *P. chapmani*, *Morozovella velascoensis*, *M. angulata*, *M. aequa*, and *M. quetra*. This sample also contains about 5%–10% reworked, middle Maestrichtian species, including *Globotruncana esnehensis*, *G. mariei*, *G. arca*, *G. rosetta*, *Rugoglobigerina* sp., *Pseudoguembelina costulata*, and *Pseudotextularia elegans*. A thin-section sample from Sample 130-807C-46R-CC similarly contains a mixed Paleocene–lower Eocene assemblage, including such lower Paleocene species as *Morozovella trinidadensis*. No Cretaceous taxa were noted in this sample.

Foraminifers provided spotty age controls in the Paleocene strata of Site 807. To facilitate the extraction of planktonic foraminifers from the limestone matrix, the core-catcher samples were first crushed with a Carver hydraulic press and then crushed again with a mortar and pestel. This method was particularly successful where the limestone contains wispy gray horizons of volcanic ash or clay. The more homogeneous white limestones yielded the fewest specimens with the crushing method. Thin-section analyses would undoubtedly yield the best results for zoning these rocks with planktonic foraminifers. Sample 130-807C-49R-CC contains *Morozovella* cf. *M. conicotruncata*, indicating Zone P3 or P4. The presence of *Planorotalites pseudomenardii* and *Morozovella* cf. *M. angulata* in Sample 130-807C-50R-CC indicates Zone P4. Subzone P1b was suggested by the presence of *Subbotina pseudobulloides* and *S. triloculinoides* in Sample 130-807C-53R-4, 97–98 cm, whereas the presence of *Eoglobigerina fringa* in Sample 130-807C-54R-2, 120–122 cm, suggests Subzone P1a.

According to calcareous nannofossil data, the K/T boundary is present in the lower 16 cm of Core 130-807C-54R-3. A foraminifer assemblage from Sample 130-807C-54R-3, 56–58 cm, is composed of small indeterminate planktonic foraminifers along with a couple of small specimens of indeterminate Upper Cretaceous globotruncanids. This may represent a basal Tertiary Pα assemblage with recycled(?) Upper Cretaceous elements. Thin-section analyses through Core 130-807C-54R are needed to define the boundary more clearly, relative to the interval of elevated Thoracosphaera abundance recognized in the microflora (Table 6).

Cretaceous

Shipboard analyses of Cretaceous planktonic foraminifers were problematic because of the indurated nature of the limestones. However, specimens were extracted from part of the Maestrichtian section by the crushing technique outlined above. Sample 130-807C-57R-CC contains *Abathomphalus* *mayaroensis*, *Rosita contusa* s.l., and *Pseudoguembelina costulata* of the upper Maestrichtian *Abathomphalus mayaroensis* Zone (lower part). The mid-Maestrichtian *Gansserina gansseri* Zone was indicated by the presence of *Gansserina wiedenmayeri*, the *Globotruncana orientalis-falsostuarti* plexus, *Globotruncanita stuartiformis*, *Rugoglobigerina hexacamerata*, *Rosita fornicata*, *Globigerinelloides* sp., *Pseudotextularia elegans*, and *Pseudoguembelina costulata* in Sample 130-807C-59R-CC. Sample 130-807C-60R-CC contains a similar assemblage with the addition of *Globotruncanita subspinosa*. Samples 130-807C-59R-CC and -60R-CC are indicative of the lower to mid-Maestrichtian.

Very few foraminifers were extracted from the lower Maestrichtian–upper Campanian limestones in Cores 130-807C-61R to -71R, as dated by calcareous nannofossils. Cut slabs of limestone in this interval contain fewer tests of planktonic foraminifers than are present in higher stratigraphic levels, as observed by means of a stereo-zoom microscope. The greater relative abundance of planktonic foraminifers in part of the Maestrichtian may record a primary signal of changing dissolution levels in the Cretaceous ocean. The CCD was elevated from Aptian through Campanian time (Thierstein, 1979; Tucholke and Vogt, 1979). The increase in planktonic foraminifer preservation in the Maestrichtian of Site 807 may record the rapid depression of the Maestrichtian CCD observed in the Atlantic (Tucholke and Vogt, 1979). Diagenetic factors, including the clay content of limestones, may also be responsible for the apparent changes in relative abundances of planktonic foraminifers.

The lower Cenomanian–upper Albian red mudstones of Cores 130-807C-71R, -72R, and -73R, as dated by radiolarians, are barren of foraminifers. Aptian-Albian carbonates overlying basalt in Core 130-807C-74R, dated by calcareous nannofossils and radiolarians, are likewise barren of planktonic foraminifers. Sample 130-807C-73R-CC contains a few calcareous benthic foraminifers that are overgrown with calcite. A thin limestone between basalt flows in Core 130-807C-80R also contains only a few poorly preserved, overgrown calcareous benthic foraminifers.

Benthic Foraminifers

All core-catcher samples from Hole 807A (Samples 130-807A-1H-CC through -86X-CC) and those from Hole 807C in which the chalks could be readily disaggregated (Samples 130-807C-1R-CC through -38R-CC) contain benthic foraminifers. Some of the lower Eocene, Paleocene, and Cretaceous limestones below Core 130-807C-38R probably contain small numbers of benthic specimens, but they were not seen in cursory examinations of the surfaces of the siliceous limestones. Two sectional samples from the claystone above the basalt basement (130-807C-71R-3, 74–76 cm, and -71R-5, 127–129 cm) were barren of foraminifers.

Benthic specimens comprise <1% of the foraminifers in the sand fraction of almost all of the samples examined, except for small percentage increases in intervals of moderate dissolution (Samples 130-807A-4H-CC, -5H-CC, -30X-CC, -49X-CC, and -63X-CC) and high percentages of benthic specimens in intervals of strong dissolution of planktonic foraminifers (Samples 130-807C-32R-CC and -34R-CC) in the middle Eocene section. Few foraminifers are present in a part of the upper Eocene section that contains abundant radiolarians (Samples 130-807C-24R-CC and -25R-CC). A comparison with Sites 803 and 805 shows a general increase with depth of site in the percentage of benthic specimens, reflecting selective dissolution of planktonic components through time. Exceptions are the lower Oligocene and upper Miocene samples, in which benthic foraminifers are well preserved at all three sites.

The benthic specimens are well preserved down to the lower Oligocene, at which time they begin to appear in a recrystallized form. This deterioration in preservation corresponds with an increase in radiolarians. The frequency of breakage also increases in the lower Oligocene through middle Eocene part of the section. Some of this breakage is probably a result of sample processing.

The stratigraphic distribution of taxa is comparable with that of Sites 803 and 805, in which lower bathyal to abyssal assemblages characteristic of the upper Eocene–lower Oligocene, upper Oligocene–lower Miocene transition, and middle Miocene–Quaternary transitions were recognized. Just as at Site 803, *Alabamina dissonata*, but not *Nuttallides truempyi*, is present in the latest Eocene sample. However, *N. truempyi* was noted lower in the section at both sites. Prominent Eocene species that continue into the Oligocene include *Cibicidoides grimsdalei*, *Anomalinoides spissiformis*, *Nonion havanense*, *Gyroidinoides girardanus*, and *Cibicidoides praemundulus*. All three sites analyzed (803, 805, and 807) are characterized by *Linaresia* (= *Anomalinoides*) *pseudogrosserugosa* in the lower Miocene and *Brizalina pusilla* in the middle Miocene, high percentages of *Nuttallides umbonifera* from the lower Miocene through the lower Pliocene, and rare uvigerinids from the Oligocene through the middle Miocene. Uvigerinids decrease in frequency away from the equator in Quaternary and upper Miocene samples, presumably related to upwelling and organic flux of the sediments. The lower Pliocene sample at Site 807, however, contains more uvigerinids than comparable samples at the two deeper sites, perhaps a reflection of shifts in water mass boundaries or in the equatorial divergence zone.

Listed in Table 7 are the most frequent species present in sand-fraction (63 μm) samples representative of the various time-stratigraphic units. Their percent frequencies among the benthic fauna are given, as well as the names of some less frequent members of the assemblages. The following data are also given: *B* = the percent representation of benthic specimens relative to total foraminifer content; *N* = the number of specimens counted for the percent frequency data; and *T* = the total number of benthic specimens in each approximately 20-cc core-catcher sample, calculated from the sample split used for the census data.

Diatoms

Diatoms were examined in Holes 807A and 807C. The assignment of Site 807 samples to low-latitude diatom zonations is summarized in Figure 31.

Hole 807A

Above 83.4 mbsf (Pleistocene to upper Pliocene, Cores 130-807A-1H to -9H), diatoms are rare and poorly preserved. An exception was found in Sample 130-807A-5H-CC, in which diatoms are abundant and moderately preserved. This sample was assigned to the NTD 15 *Rhizosolenia praebergonii* Zone; it is characterized by a diverse flora dominated by *Coscinodiscus nodulifer* and *Nitzschia marina*. *Rhizosolenia praebergonii*, *Asteromphalus elegans*, *Hemidiscus cuneiformis*, *Thalassiosira convexa* var. *aspinosa*, *T. oestrupii*, *T. leptopus*, *T. eccentrica*, *Nitzschia fossilis*, *N. reinholdii*, and *Thalassionema nitzschioides* are also characteristic of NTD 15. Diatoms increase sharply in abundance and preservation from Samples 130-807A-9H-CC (middle Pliocene NTD 15A *R. praebergonii* Zone) through -40X-CC (middle Miocene NTD 6 *Coscinodiscus lewisianus* Zone). The poor preservation of diatoms between 389.2 mbsf (middle Miocene, Sample 130-807A-41X-CC) and 620.6 mbsf (upper Oligocene, Sample 130-807A-65X-CC) and the lack of age-diagnostic fossils

Table 7. Benthic foraminifers as a percentage of total foraminifers, Site 807.

Age and sample data	Species name	Sample (%)
Quaternary (N22)	*Pullenia bulloides*	18%
Sample 130-807A-2H-CC	*Globocassidulina subglobosa*	12%
B = <1%	*Pseudoparrella exigua*	10%
N = 197	*Oridorsalis umbonatus*	7%
T = 3,152	*Melonis affinis*	6%
	Pacinonion novozealandicum	5%
	(Others: *Fontbotia wuellerstorfi*, *Nuttallides umbonifera*)	
lower Pliocene (N18)	*Globocassidulina subglobosa*	13%
Sample 130-807A-13H-CC	*Nuttallides umbonifera*	13%
B = <1%	*Siphouvigerina* sp.	9%
N = 152	*Pullenia bulloides*	7%
T = 2,432	*Cibicidoides mundulus*	6%
	(Others: *Fontbotia wuellerstorfi*, *Parrelloides bradyi*)	
upper Miocene (N17a)	*Globocassidulina* sp.	9%
Sample 130-807A-23H-CC	*Globocassidulina subglobosa*	7%
B = <1%	*Favocassidulina favus*	7%
N = 236	*Cibicidoides mundulus*	6%
T = 1,888	*Oridorsalis umbonatus*	6%
	Siphonodosaria sp.	6%
	(Others: *Siphouvigerina* sp., *Uvigerina bradyana*, *Nuttallides umbonifera*)	
middle Miocene (N11)	*Nuttallides umbonifera*	10%
Sample 130-807A-40X-CC	*Globocassidulina subglobosa*	9%
B = <1%	*Fontbotia wuellerstorfi*	6%
N = 133	*Globocassidulina* sp.	5%
T = 2,128	*Brizalina pusilla*	5%
	Oridorsalis umbonatus	5%
	(Others: *Uvigerina gracilliformis*, *Parrelloides bradyi*)	
lower Miocene (N4)	*Globocassidulina subglobosa*	14%
Sample 130-807A-56X-CC	*Nuttallides umbonifera*	8%
B = <1%	*Linaresia pseudogrosserugosa*	7%
N = 134	*Stilostomella* sp.	7%
T = 536	*Gyroidinoides zealandicus*	6%
	Pyrulinoides sp.	6%
	Pullenia bulloides	5%
	(Others: *Parrelloides bradyi*, *Cibicidoides* sp., *Nonion havanense*, *Uvigerina gracilliformis*)	
upper Oligocene (P22)	*Cibicidoides praemundulus*	14%
Sample 130-807A-65X-CC	*Globocassidulina subglobosa*	13%
B = <1%	*Eggerella bradyi*	9%
N = 109	*Gyroidinoides lamarckianus*	7%
T = 436	*Pleurostomella subnodosa*	6%
	Oridorsalis umbonatus	5%
	(Others: *Parrelloides bradyi*, *Anomalinoides spissiformis*, *Uvigerina gracilliformis*, *Cassidulina spinifera*, *Bulimina glomarchallengeri*)	
lower Oligocene (P19)	*Globocassidulina subglobosa*	22%
Sample 130-807A-85X-CC	*Cibicidoides praemundulus*	8%
B = <1%	*Pacinonion* sp.	8%
N = 129	*Gyroidinoides girardanus*	7%
T = 516	*Oridorsalis umbonatus*	6%
	Pleurostomella sp.	6%
	Parrelloides bradyi	5%
	Bulimina cf. *microcostata*	5%
	(Others: *Cibicidoides grimsdalei*, *Anomalinoides spissiformis*)	
upper Eocene (P17)	*Anomalinoides spissiformis*	11%
Sample 130-807C-18R-CC	*Gyroidinoides girardanus*	10%
B = <1%	*Globocassidulina subglobosa*	10%
N = 209	*Cibicidoides praemundulus*	9%
T = 209	*Oridorsalis umbonatus*	8%
	Alabamina dissonata	5%
	Cibicidoides grimsdalei	5%
	Pleurostomella sp.	5%
	(Others: *Nonion havanense*, *Uvigerina havanensis*, *Cibicidoides eocaenus*)	

Notes: *B* = the percentage of representation of benthic specimens relative to total foraminifer content; *N* = the number of specimens counted for the percent frequency data; and *T* = the total number of benthic specimens in each approximately 20-cm^3 core-catcher sample, calculated from the sample split used for the census data.

precludes an age assignment for this rather large interval. Samples 130-807A-66X-CC through -81X-CC were assigned to the *Rocella vigilans* Zone. The LO of *Coscinodiscus excavatus* was found in Sample 130-807A-86X-CC (early Oligocene *C. excavatus* Zone).

Hole 807C

The diatom assemblages of Samples 130-807A-82X-CC through -86X-CC and Samples 130-807C-1R-CC through -5R-CC are very similar in composition and abundance. The LO of *C. excavatus* was found in Sample 130-807C-5R-CC at 828.3 mbsf.

Diatoms are common to abundant and moderately to well preserved from the Oligocene (Sample 130-807C-1R-CC) to the upper middle Eocene (Sample 130-807C-24R-CC). The following diatom zones were recognized (Fig. 31): *C. excavatus* Zone (Samples 130-807C-5R-CC through -16R-CC), *Baxteriopsis brunii* Zone (Samples 130-807C-17R-CC to -21R-CC), and *Asterolampra marylandica*(?) Zone (Samples 130-807C-22R-CC through -25R-CC). For the purposes of this report, the *C. excavatus* Range Zone of Barron (1985) was used here without recognition of Fenner's (1984) *Cestodiscus reticulatus* Zone. *Cestodiscus reticulatus* seems to be absent in Hole 807C, or this species may have been confused with *Cestodiscus robustus* (see comments in Barron, 1985).

A sharp decrease in abundance and preservation was seen in Sample 130-807C-25R-CC, below which the stratigraphic section is barren of diatoms.

Radiolarians

At Site 807, radiolarians were recovered from essentially all (except for several Pleistocene samples) of the section down to the middle Eocene, but generally none (or only trace amounts) were recovered from limestones below the upper middle Eocene. The radiolarians in the oozes (Pleistocene to middle Miocene) and chalks (middle Miocene to middle Eocene) are well to poorly preserved, and they provide useful age information in most cases. Radiolarian preservation in Neogene sediments at Site 807 is generally the worst of all the sites drilled during Leg 130. Nevertheless, zonal assignments for the Oligocene to lower Miocene were best accomplished at Site 807, among all sites of Leg 130, because of the presence of key taxa and high sedimentation rates, despite the poor preservation of radiolarians during this time interval.

Radiolarian-barren intervals become common downcore in the middle Eocene. Essentially all of the limestone samples are barren of radiolarians, including those from the Cretaceous/Tertiary boundary (see "Calcareous Nannofossil" section, this chapter). Below the Maestrichtian and Campanian limestones, the lithology changed into radiolarian siltstones and radiolarian sandy siltstones, just above the basement basalts. In these siltstones, abundant radiolarians were recovered that provided important zonal information.

Core-catcher samples from Hole 807A were examined throughout the interval drilled, down to the base of the hole (822.9 mbsf). Three core-catcher samples recovered from Hole 807B were also examined and used to make a stratigraphic composite, as the uppermost three core-catcher samples from Hole 807A did not provide well-defined age information because of the dissolution. In Hole 807C, sediments were washed to 780.0 mbsf and cores were recovered thereafter; core-catcher samples throughout the hole (from 789.7 to 1375.4 mbsf) were examined. In addition, samples from within Cretaceous cores were examined to determine ages otherwise not obtainable because of the absence of all other microfossil groups. Zonal assignments (Saunders et al., 1984; Sanfilippo and Riedel, 1985; Sanfilippo et al., 1985) of the samples with stratigraphically important taxa are discussed below. The radiolarian datums with absolute ages cited in this discussion are taken from those listed by Nigrini in the "Explanatory Notes" chapter of Leg 117 (Shipboard Scientific Party, 1989). Figure 31 summarizes the radiolarian zonation of the Holes 807A, 807B, and 807C as well as provides correlation with zones of other taxa. The radiolarian zones are continuous from at least the lower Pleistocene to the base of the upper Eocene. No evidence for significant sediment reworking was found at this site.

Quaternary

Sample 130-807B-1H-CC was placed in the *Buccinosphaera invaginata* Zone of the Quaternary based on the presence of *B. invaginata*. Sample 130-807B-2H-CC contains *Theocorythium trachelium*, suggesting that it is in the *Anthocyrtidium angulare* Zone or younger. Neither Sample 130-807A-3H-CC nor 130-807B-3H-CC contains enough radiolarians (thus lacking key taxa) to assign ages.

Pliocene

Sample 130-807A-4H-CC belongs to the *Pterocanium prismatium* Zone, which contains *Lamprocyrtis heteroporos* and the LO of *Theocalyptra davisiana*. Sample 130-807A-5H-CC was also placed in the same zone and contains the LO of *P. prismatium* (1.52–1.56 Ma). This datum level, however, may be in one or two shallower cores as dissolution has affected the assemblages. Thus, this datum level, which may not be reliable, was not used in the sedimentation rate estimates (see "Sedimentation Rates" section, this chapter). Samples 130-807A-6H-CC through -10H-CC contain assemblages that place them in the *Spongaster pentas* Zone. This zone contains the following radiolarian events: the LO of *Stichocorys peregrina* (2.62–2.64 Ma) in Sample 130-807A-6H-CC; the FO of *Amphirhopalum ypsilon* (3.77–3.79 Ma) in Sample 130-807A-8H-CC; the LO of *Phormostichoartus fistula* in Sample 130-807A-8H-CC; the LO of *S. pentas* (3.74–3.82 Ma) in Sample 130-807A-9H-CC; the FO of *Spongaster tetras* (3.83–3.85 Ma) in Sample 130-807A-9H-CC; and the LO of *Phormostichoartus doliolum* (3.53–3.55 Ma) in Sample 130-807A-10H-CC. Samples 130-807A-11H-CC through -18H-CC were placed in the *S. peregrina* Zone. Radiolarian events found in this zone include the following: the LO of *Spongaster berminghami* (3.85–3.87 Ma) in Sample 130-807A-11H-CC; the LO of *Solenosphaera omnitubus* (4.7–4.8 Ma) in Sample 130-807A-11H-CC; the FO of *S. pentas* (4.2–4.3 Ma) in Sample 130-807A-13H-CC; and the LO of *Acrobotrys tritubus* (5.3–5.4 Ma) in Sample 130-807A-16H-CC.

Upper Miocene

Samples 130-807A-19H-CC through -22H-CC were assigned to the *Didymocyrtis penultima* Zone. Radiolarian events found in these samples include the LO of *Stichocorys delmontensis* (5 Ma) in Sample 130-807A-19H-CC; the LO of *Siphostichartus corona* (5.0–5.1 Ma) in Sample 130-807A-20H-CC; the LO of *Calocycletta caepa* (6.2–6.6 Ma) in Sample 130-807A-21H-CC; and the FO of *Solenosphaera omnitubus* (6.3–6.5 Ma) in Sample 130-807A-21H-CC. Samples 130-807A-23H-CC through -28H-CC were placed in the *Didymocyrtis antepenultima* Zone. The LOs of the following six taxa were found in this zone: *Diartus hughesi* (7.1–7.2 Ma) in Sample 130-807A-23H-CC; *Dictyocoryne ontogenesis* (7.2–7.7 Ma) in Sample 130-807A-23H-CC; *Didymocyrtis laticonus* (8.1–8.2 Ma) in Sample 130-807A-25H-CC; *Botryostrobus miralestensis* (8.1–8.2 Ma) in Sample 130-807A-27H-CC; *Diartus petterssoni* (8.1–8.2 Ma) in Sample 130-807A-29H-CC; and *Stichocorys wolffii* (8.1–8.2 Ma) in Sample 130-807A-28H-CC. The FOs of two taxa were also found in this zone: *A. tritubus* (7.7–7.78 Ma) in Sample 130-807A-24H-CC and *S. berminghami* (7.9–8.0 Ma) in Sample 130-807A-28H-CC. Sample 130-807A-29X-CC was placed at the boundary (8.3–8.5 Ma) between the *D. petterssoni* and *D. antepenultima* zones, as this sample is located one core below the FO of *S. berminghami* (7.9–8.0 Ma) and the LO of *D. petterssoni* (8.1–8.2 Ma) and contains both *D. hughesi* and *D. petterssoni*. This boundary, therefore, was defined as the evolutionary transition from *D. petterssoni* to *D. hughesi* (Sanfilippo et al., 1985).

Middle Miocene

Samples 130-807A-29H-CC through -36X-CC were placed in the *D. petterssoni* Zone. The FO of *D. hughesi* (8.7–8.8 Ma) in Sample 130-807A-30H-CC and the LOs of *Lithopera thornburgi* (10.3–11.6 Ma) in Sample 130-807A-32H-CC, *Cyrtocapsella japonica* (10.0–10.3 Ma) in Sample 130-807A-33H-CC, and *Cyrtocapsella cornuta* (11.6–11.9 Ma) in Sample 130-807A-36X-CC were found in this zone. Samples 130-807A-37X-CC through -43X-CC were placed in the *Dorcadospyris alata* Zone. Several FOs and LOs of *Dorcadospyris* species are in this zone, but exact datum levels are yet to be determined.

Lower Miocene

Samples 130-807A-44X-CC through -47X-CC were placed in the *Calocycletta costata* Zone. Samples 130-807A-48X-CC through -52X-CC were placed in the *Stichocorys wolffii* Zone. Sample 130-807A-53X-CC was assigned to either the *Stichocorys delmontensis* Zone or the *S. wolffii* Zone, which could not be differentiated because of the lack of key taxa. Diagnostic taxa found in this sample include *Cyrtocapsella tetrapera*, *Cyrtocapsella japonica*, *Dorcadospyris ateuchus*, and *Dorcadospyris simplex*. Samples 130-807A-54X-CC through -58X-CC were placed in the *S. delmontensis* Zone, followed by the *Cyrtocapsella tetrapera* Zone in which Samples 130-807A-59X-CC through -61X-CC were placed. Samples 130-807A-62X-CC through -67X-CC were placed in the *Lychnocanoma elongata* Zone. Zonal assignment for the earliest lower Miocene was best accomplished at Site 807, among all sites of Leg 130, because of the presence of key taxa and high sedimentation rates, despite the generally poor radiolarian preservation. At this site, *Dorcadospyris riedeli* appears just above the occurrence of *Dorcadospyris papilio*. This has been a consistent occurence at all sites drilled during Leg 130. The range of *D. riedeli* on the Ontong Java Plateau appears within the duration of *L. elongata* Zone. This will serve as a useful time marker near the Oligocene/Miocene boundary in future studies.

Oligocene

Samples 130-807A-68X-CC through -70X-CC belong to either the *Dorcadospyris ateuchus* Zone or the *L. elongata* Zone, which also could not be differentiated because of the lack of key taxa. Samples 130-807A-71X-CC through -82X-CC and 130-807C-1R-CC (789.7 mbsf) were assigned to the *D. ateuchus* Zone of the upper Oligocene. These samples usually contain the following key taxa: *Dorcadospyris forcipata*, *D. ateuchus*, *Theocyrtis annosa*, *Lithocyclia angusta*, and *Artophormis gracilis*. Samples 130-807A-84X-CC (803.6 mbsf) and 130-807C-2R-CC (799.3 mbsf) were placed at the boundary between the *Theocyrtis tuberosa* Zone and the *D. ateuchus* Zone as both contained *Dorcadospyris circulus* and *Dorcadospyris quadripes* (Moore, 1971), together with *A. gracilis* and *L. angusta*. The match between Holes 807A and 807C is very good as documented by the boundary depths indicated above. Samples 130-807A-85X-CC and -86X-CC and 130-807C-3R-CC through -16R-CC belong to the *T. tuberosa* Zone of the lower Oligocene; diagnostic taxa include *Artophormis gracilis*, *Centrobotrys gravida*, *Cyclampterium milowi*, *Tristylospyris triceros*, *Lithocyclia crux*, and *L. angusta*.

Upper Eocene

Samples 130-807C-17R-CC through -22R-CC, all of which contain *Cryptoprora ornata*, were placed in the *C. ornata* Zone (= upper *Thyrsocyrtis bromia* Zone of Sanfilippo et al., 1985) of the uppermost Eocene (Saunders et al., 1984). Samples from the upper part of this zone contain *L. aristotelis* group (varieties with three and four wide arms). Samples 130-807C-23R-CC through -26R-CC, bearing *Calocyclas bandyca*, are placed in the *C. bandyca* Zone. Other age-diagnostic taxa co-occurring with *C. bandyca* include *Calocyclas turris*, *Artophormis balbadensis*, *Lophocyrtis jacchia*, *Thyrsocyrtis tetracantha*, *T. bromia*, and *Thyrsocyrtis rhizodon*. In Core 130-807C-26R the first chert nodules were found (for more details, see the "Lithostratigraphy" section, this chapter). Below this core, the occurrence of cherts generally increased.

Middle Eocene

Coincidental with the occurrence of cherts and silicified chalk, radiolarian abundance decreased with depth; apparently the result of the dissolution of biogenic opal and the remobilization of silica during chert formation. Cores 130-807C-27R through -39R, containing chalk or a mixture of chalk and limestone, have poorly preserved radiolarians or are barren. Thus, zonal assignments were possible only for the following samples. Sample 130-807C-28R-CC was placed in the *Dictyoprora mongolfieri* Zone to the *Cryptoprora ornata* Zone of the middle Eocene to the upper Eocene, which could not be resolved because only *D. mongolfieri*, *Dictyoprora armadillo*, and *Lithochytris vespertilio* were present. Samples 130-807C-31R-CC and -36R-CC belong to the *Podocyrtis chalara* Zone of the middle Eocene up to the *Carpocanistrum azyx* Zone of the basal late Eocene, which also could not be resolved further, as only *P. chalara*, *T. rhizodon*, *L. vespertilio*, *Eusyringium fistuligerum*, and members of the *Sethochytris babylonis* group were present. Samples 130-807C-33R-CC and -37R-CC were placed in the *T. triacantha* Zone up to the *C. azyx* Zone as they contain *E. fistuligerum*. Sample 130-807C-39R-CC belongs to the *T. triacantha* Zone as *T. triacantha*, *Theocotyle venezuelensis*, and *Podocyrtis sinuosa* were present. Sample 130-807C-40R-CC was assigned to a range from the *Theocotyle cryptecephala* Zone to the *Pterocodon ampla* Zone, based on the presence of *P. sinuosa*. Samples 130-807C-27R-CC, -30R-CC, -32R-CC, -34R-CC, -35R-CC, and -38R-CC were barren of radiolarians.

Cores 130-807C-40R through -70R are limestones with intermittent occurrences of cherts, especially in the Tertiary. Core-catcher samples in this long interval were usually devoid of radiolarians and only occasionally contained trace amounts of radiolarian fragments or radiolarian casts. Thus, no age information was obtained from these cores or from Core 130-807C-54R, which was examined in several sectional samples.

Cretaceous

Radiolarian abundance increased with a drastic change in lithology from limestone to brown siltstone. Samples 130-807C-71R-CC; -72R-1, 89–91 and 144–146 cm; -72R-2, 121–123 cm; and -73R-1, 100–102 cm, were placed in the upper *Acaeniotyle umbilicata* Zone of the upper Albian to the lower *Abesacapsula sophedia* Zone of the lower Cenomanian (103–95 Ma) (Sanfilippo and Riedel, 1985). They contain opal CT or quartz-filled (e.g., inside of shells) radiolarians of the following taxa: *Pseudodictyomitra pseudomacrocephala*, *Thanarla veneta*, *T. elegantissima*, *T. pulchra* (of Sanfilippo and Riedel, 1985), *Thanarla* sp., *Archaeodictyomitra* cf. *vulgaris*, *Archaeodictyomitra* sp. A (of Thurow, 1988), and *Novixitus*[00a0]sp. Although the range of *T. pulchra* (of Sanfilippo and Riedel, 1985) was illustrated as Berriasian to Barremian by Sanfilippo and Riedel (1985), Thurow (1988, p. 407) points out that ". . . their text figure 8 (2d) shows Pessagno's (1977) type specimen, which is from the lower Cenomanian . . . ." Thus, the above co-occurrence of the two taxa presents no problem, and zonal assignment from the upper Albian to the lower Cenomanian is justified. Specimens of the two species of *Thanarla* showed distensions both greater than and less than 25% (see Sanfilippo and Riedel, 1985), so they were placed into *T. pulchra* and *T. elegantissima*, according to the definitions of Sanfilippo and Riedel (1985). Thurow's (1988) definition of this species is slightly different: both forms of the genus observed here fall into Thurow's *T. elegantissima*. In either case, specimens with distensions greater than 25% (i.e., *T. pulchra* or *T. elegantissima*) are Albian-Cenomanian in age.

Basalt was recovered in Core 130-807C-74R, and a thin layer of limestone occurred at the top of the core. Sample 130-807C-74R-1, 0–2 cm, contains a small number of poorly preserved radiolarians and was tentatively given an Aptian to Cenomanian age based on the presence of the following taxa and the evolutionary changes mentioned below: *Thanarla* sp. A aff. *T. conica* (Thurow, 1988, pl. 7, figs. 7 and 8), *Thanarla* sp. B aff. *T. conica* (Thurow, 1988, pl. 7, fig. 12), ?*Archaeodictyomitra vulgaris*, and *Cyrtocapsa* sp. cf. *C. grutterinki*. All the taxa mentioned in this sample are illustrated in plates 7 and 8 of Thurow (1988), which are characteristic of the Hauterivian to the lower Aptian. With increasing depth, changes in the morphology of the genus *Thanarla* from a *T. elegantissima* type to a *Thanarla conica* type were noticed. Sample 130-807C-73R-1, 100–102 cm, contains *Thanarla conica*. It appears that we are seeing a gradual evolutionary change in *Thanarla* morphology: among the five samples assigned from the upper Albian to the lower Cenomanian, Sample 130-807C-73R-1, 100–102 cm (the deepest one) is slightly older than the rest of the four. By the same token, Sample 130-807C-74R-1, 0–2 cm, is slightly older (but not substantially) than the five samples from Cores 130-807C-71R through -73R.

Two sedimentary layers composed of limestones were found in Sections 130-807C-80R-1 and -82R-3 between pillow basalts. Sample 130-807C-80R-1, 70–72 cm, contains rare, poorly preserved, non-age-diagnostic spumellarians. Sample 130-807C-80R-1, 74–75 cm, is barren of radiolarians, and spherical cavities in rock matrices were found during standard acidified slide procedures. Nonacidified foraminifer preparation of this sample yielded spherical spumellarian-like specimens. Thus, we consider that the specimens were replaced by calcium carbonate. Sample 130-807C-82R-1, 75–76 cm, is also barren of radiolarians. No age information, therefore, can be given to any of the three samples interbedded in the basalt layers.

PALEOMAGNETISM

Introduction

Pass-through magnetometer measurements were taken on the split-archive sections cored with the APC in Hole 807A, all of which were oriented except Cores 130-807A-1H and -2H. A sharp drop in magnetic intensity, similar to that seen at the other Leg 130 sites, was observed at approximately 32 mbsf.

Below that depth, magnetic intensities were close to the noise level of the pass-through cryogenic magnetometer, and the paleomagnetic directional information useful for polarity determination was lost. In response to this behavior, only Cores 130-807B-1H through -10H were measured from Hole 807B.

All XCB and RCB cores from Hole 807C were measured, except those lacking a substantial number of sufficiently long pieces that were likely to have remained aligned in the core. Certain intervals cored with the RCB had exceptional recovery, and both inclination and relative declination information were available. Unlike Site 803, basalts recovered from Site 807 commonly contained numerous continuous pieces in a given section. Therefore, split archive sections were measured rather than representative pieces from a section. These sections were measured after the individual section pieces had been numbered for curatorial purposes. Measurement intervals for Site 807 paleomagnetic analyses varied between 1, 3, 5 and 10 cm. Basalt sections generally were measured at 1-cm sampling intervals. This detailed sampling interval should allow the examination of individual numbered pieces in the data.

Sediments

Pleistocene

The loss of an interpretable paleomagnetic polarity signal appears to be related in a simple fashion to the drop in magnetic remanence at Site 807. Loss of signal and decrease of remanence coincide at approximately 32 mbsf. Above the decrease in intensity, the Brunhes/Matuyama boundary as well as the Jaramillo and Olduvai subchrons were recognized (Fig. 32). Sedimentation rates, based on an age control provided by these polarity boundaries, average 15.6 m/m.y. (Hole 807B) over the interval from 1.88 Ma to the present (Fig. 33).

Sulfate Reduction and Magnetization

By analogy with other studies with detailed supporting rock magnetic data (e.g., Karlin and Levi, 1985), we think that the drop in magnetic intensity displayed in the Site 807 data is a result of the dissolution of magnetite by postdepositional reduction diagenesis. As at Site 806, there also appears to be a relationship between sulfate concentration measured by means of interstitial water geochemistry and the point at which magnetic intensity is lost (Fig. 34). Sulfate reduction increases more slowly with depth at Site 807 than at Site 806 (see "Inorganic Geochemistry" section, this chapter), but the sudden decrease in magnetization intensity and the accompanying loss of an interpretable polarity signal occurs at a similar sulfate concentration at both sites (about 26.6 mM at Hole 806B and about 26.8 mM at Hole 807A) (Fig. 34). Over the interval from approximately 18 to 27 mbsf, the natural remanent magnetization (NRM) inclination record is steeply negative (Fig. 32A), perhaps caused by the acquisition of a drill-string remanence. After 15-mT demagnetization, the inclination of this interval remains anomalously high (Fig. 32B). This may indicate the presence of a diagenetic mineral phase related to reduction.

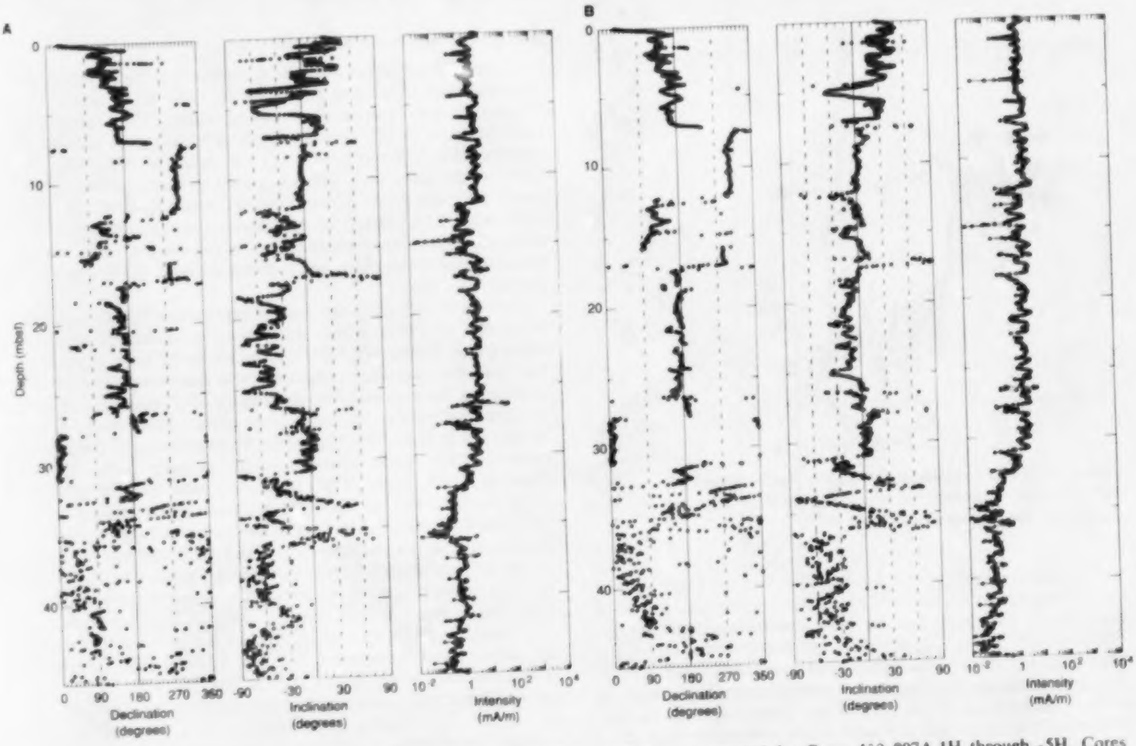

Figure 32. NRM (A) and AF-demagnetized (B) declination, inclination, and intensity record for Cores 130-807A-1H through -5H. Cores 130-807A-1H and -2H (0–16.9 mbsf) have not been oriented.

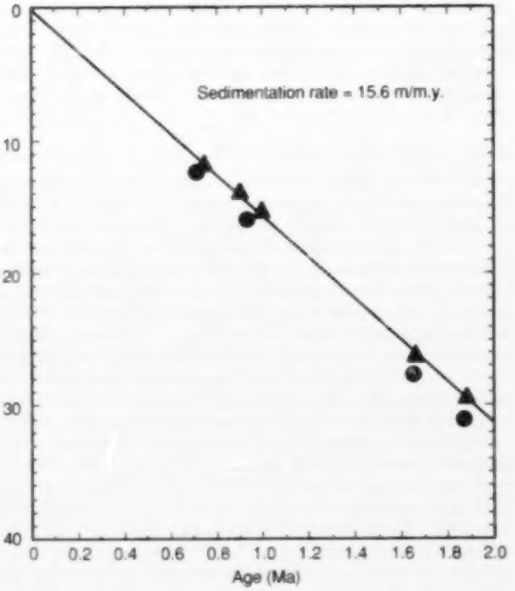

Figure 33. Depth vs. age plot derived from magnetostratigraphic data, Holes 807A (dots) and 807B (triangles). See discussion in text for details of magnetostratigraphic boundaries.

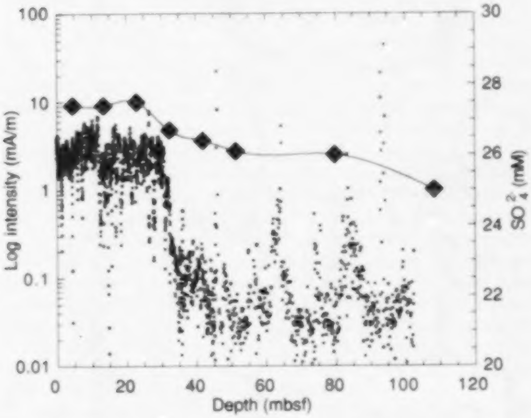

Figure 34. AF-demagnetized (15-mT) remanence intensity (circles) and sulfate ion concentration (diamonds, fitted by cubic splines) as a function of sub-bottom depth, Hole 807A.

The paleomagnetic record at Site 807, like the other sites of the Ontong Java Plateau, indicates a loss of magnetic intensity and polarity information at the same sub-bottom depth for the different APC holes, but at a different depth when comparing sites (Fig. 35). In general, decreasing water depth and latitude (i.e., proximity to the equatorial zone of upwelling) coincide with a decrease in the length of the paleomagnetic record. Differences in reduction are most likely ultimately caused by the supply of organic carbon: the greater the supply, the lesser the chance of retaining a magnetic signature.

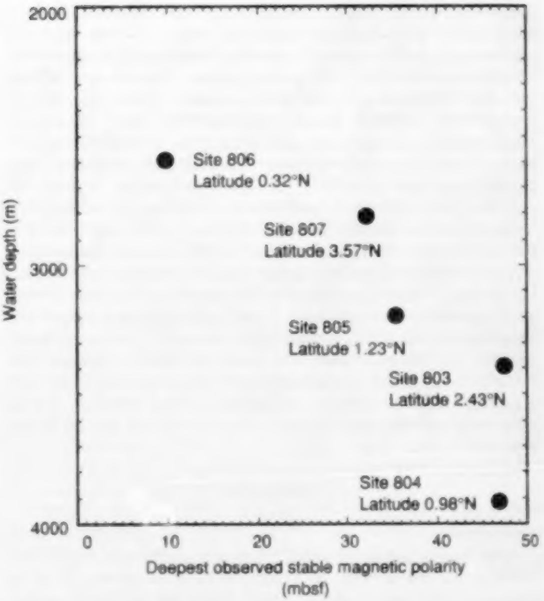

Figure 35. Depth at which paleomagnetic polarity information is lost vs. site water depth and latitude.

Miocene, Oligocene, and Eocene

Several intervals of consistent inclination were seen in the Miocene and Oligocene sequence in Hole 807A and in the Oligocene and Eocene sequence in Hole 807C. Inclination records after 15-mT demagnetization from Cores 130-807A-46X to -49X, 130-807A-64X to -71X, and 130-807C-4R, -6R, -17R, -23R, -24R, and- 26R all appear to record a consistent, stable magnetization. Rotary-drilled Cores 130-807C-4R, -6R, -17R, and -23R consist of continuous pieces as long as 3 m (two sections). Declination records following 15-mT demagnetization in these cores are continuous over these unbroken pieces (Fig. 36).

Paleolatitudes over the period represented by Cores 130-807A-46X to -49X, which date to early to middle Miocene nannofossil Zones NN5–NN3, are likely to have been very low, and the magnetostratigraphy was not determined on the inclination data alone. The frequency of 1° intervals of AF-cleaned inclination summed over these four cores peaks between +2° and −10° (Fig. 37A). Extrapolation of the 39-Ma point on the Pacific apparent polar wander path (APWP) (Gordon, 1983; Sager, 1987) predicts a paleolatitude of about 1.7°S for Site 807 at Zone NN4 time, corresponding to an inclination of ±3.4°. The frequency analyses suggest that the distribution of inclinations is shifted with respect to these values toward slightly steeper negative values. This could be a result of either an unremoved drill-string remanence or a sampling of more normal polarity samples than reversed.

Cores 130-807A-64X to -72X span the interval in the late Oligocene from foraminifer Subzone P21b to P22. Interpolation from the Pacific APWP places Site 807 from 4°S to 5.7° over this interval, corresponding to paleo-inclinations of ±8° to ±11.3°. The frequency distribution of 1° intervals of AF-cleaned inclination for this set of cores (Fig. 37B) has a broader maximum than that for the Miocene cores, perhaps reflecting the increased separation between normal and re-

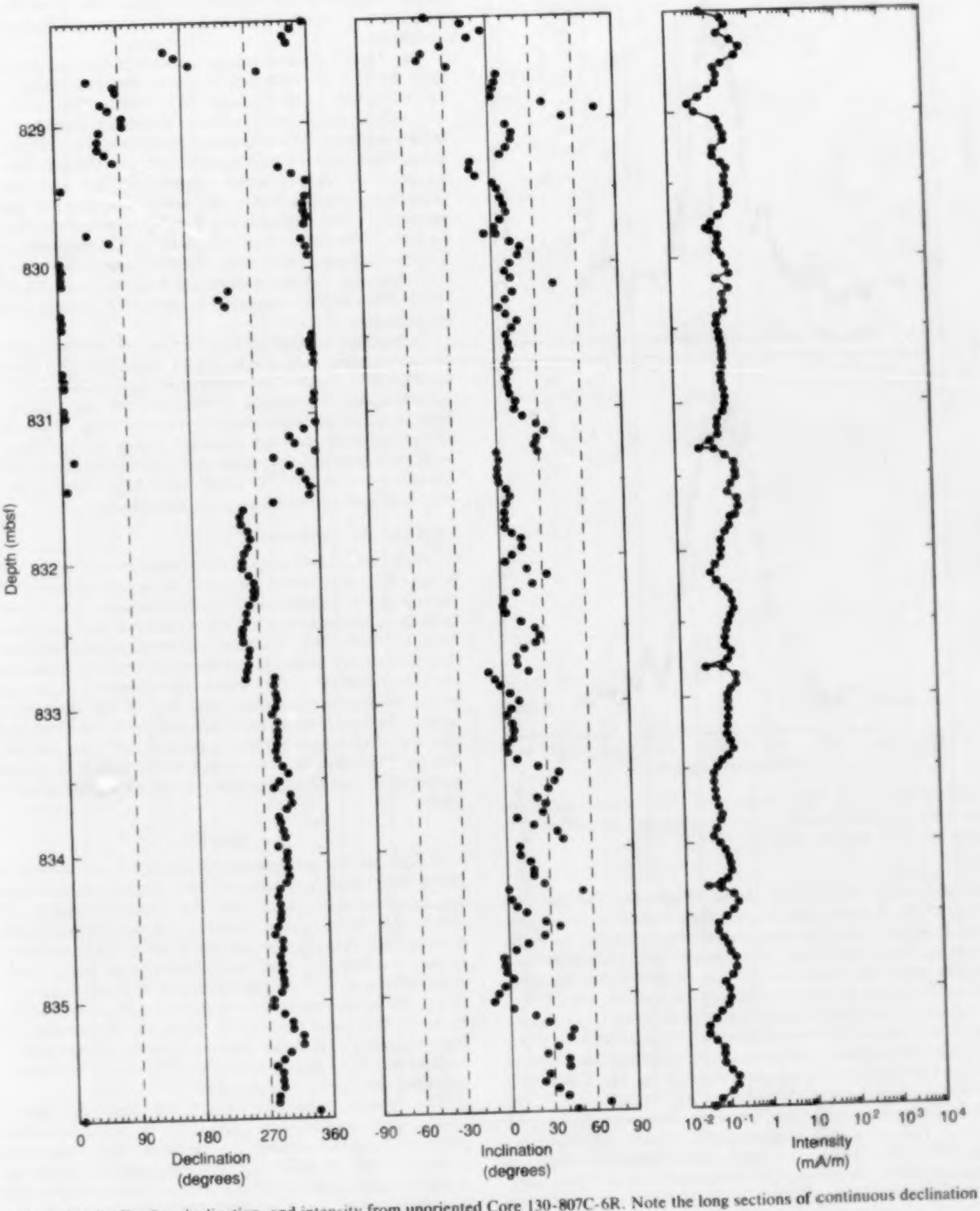

Figure 36. Declination, inclination, and intensity from unoriented Core 130-807C-6R. Note the long sections of continuous declination marking unbroken intervals within the core.

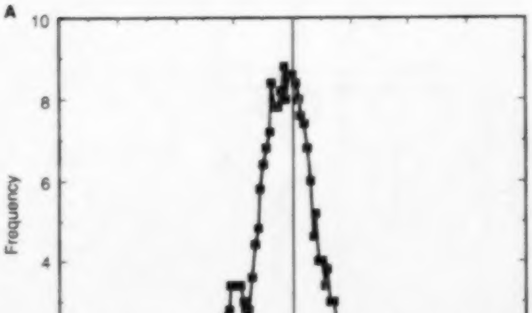

Figure 37. Frequency of 1° intervals of 15-mT-cleaned inclination after five-point smoothing. **A.** Cores 130-807A-46X through -49X. **B.** Cores 130-807A-64X through -72X.

versed polarity inclinations in the Oligocene. The simplest explanation of these data is that they represent the Pacific paleofield direction of normal and reversed polarity. As in the Miocene data, however, distribution has shifted toward steeper negative values, which may reflect either an unremoved overprint or a predominantly normal-field sampling.

Although the rotary-drilled cores of Hole 807C preserve a continuous record of both inclination and declination in many instances, inclinations are commonly variable within cores as well as between closely adjacent cores (Fig. 38). Combining data from all of the early Oligocene cores from Hole 807C for which there was sufficient recovery to enable processing through the cryogenic magnetometer (Cores 130-807C-2R, -4R, -6R, -9R, -12R, -15R, and -17R) yields the graph of frequency vs. 1° intervals of inclination shown in Figure 39A. Extrapolation of the Pacific APWP indicates a latitude of 6° to 7° for Site 807 during the early Oligocene, equating to an inclination of about ±12° to ±14°. The major peak of the inclination frequency graph occurs at +6°, essentially the inclination expected for a viscous remanent magnetization (VRM) acquired over the Brunhes Chron. Although a minor peak does occur at +14° AF-cleaned magnetizations in this set of cores appear to have recorded a present-day field overprint that can probably be removed with higher peak-field demagnetization.

The 15-mT-cleaned magnetizations of Eocene cores from Hole 807C with sufficient recovery for processing (Cores 130-807C-19R, -23R through -26R, -30R, -35R, -37R, -38R, and -40R through -44R) yield the inclination frequency graph shown in Figure 39B. In contrast to a bimodal distribution that would be expected if both normal and reversed direction were recorded in roughly equal proportion, the data define a skewed distribution with a maximum inclination at approximately 22°. Paleolatitudes for Site 807 extrapolated from the Pacific APWP range from about 13° at the beginning of the Eocene to about 8° at its end. The maximum is therefore in the expected range of inclinations for a normal polarity record, but overprinting as suggested in the other frequency graphs could also be present.

In summary, it appears that two factors limit interpretation of the available data. First, 15-mT demagnetization appears insufficient to remove overprinting in many intervals. Second, the expected inclinations of Site 807 on the Ontong Java Plateau are commonly too shallow to allow a clear distinction of normal and reversed polarity groups in the frequency analyses presented. It is suspected that samples from Site 289 (Hammond et al., 1975), which were AF-cleaned to only 10 mT, may suffer from these same limitations.

Paleocene and Cretaceous

Most Paleocene-Campanian sections recovered were composed of section pieces too small to be interpreted with our pass-through magnetometer measurements. The transition from these limestones to the brown and red clays recovered in Core 130-807C-71R, however, deserves special mention. In this core nearly complete recovery allowed an evaluation of the clay NRM (Fig. 40), which was observed to be several orders of magnitude greater than that of the adjacent limestone. The NRM has an extremely consistent shallow inclination that may record a viscous present-day overprint. If this can be confirmed in shore-based studies, it may provide a means of orienting any primary declination present in these rocks.

Basalts

Basalt NRMs are dominantly negative and steeper than 20°. If the NRM is dominated by a primary remanence, as suggested in accordance with the unaltered nature of the flows, the entire basalt sequence is of normal polarity. Several intervals that do not show these NRM inclinations display inclinations that are positive and fairly shallow. After stepwise AF demagnetization at 5, 10, and 15 mT steps, these intervals have negative inclinations similar to those of the rest of the basalts. As in the claystones, if this low-coercivity overprint can be shown to represent the present-day field direction at Site 807, it may be useful for orienting the primary declination.

The Aptian-Albian age of the sediments overlying the basalts recovered at Hole 807C give the volcanic sequence great potential for refining the Pacific APWP. Three factors make the study of Hole 807C basalts especially promising in shore-based studies: (1) the presence of two to three sediment interbeds, which suggests that the sequence may represent enough time to average a significant amount of secular variation; (2) the unaltered state of the rocks; and (3) the occurrence of massive flows interbedded with pillow flows that can provide control on possible tilting of individual pillows.

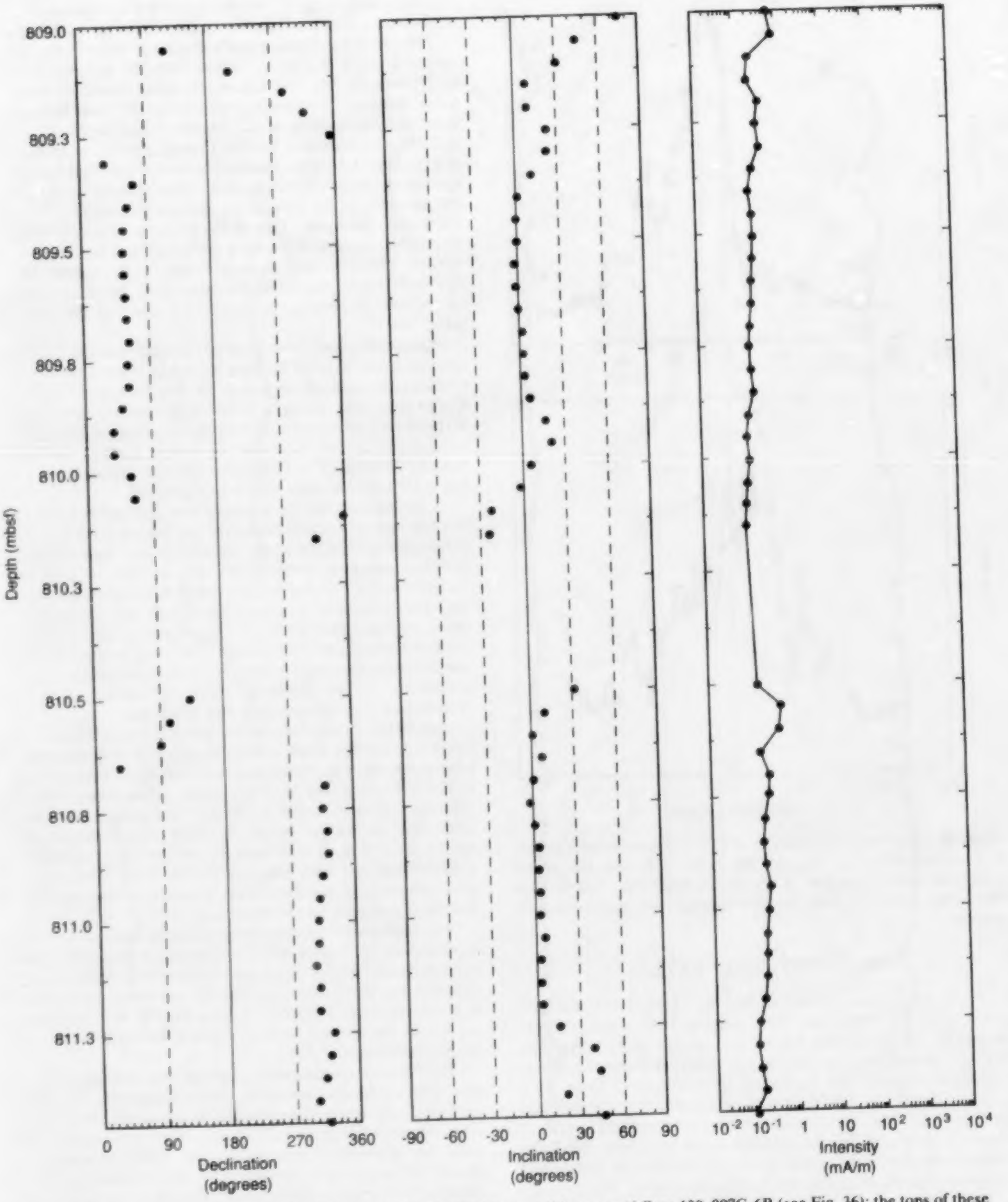

Figure 38. Core 130-807C-4R. Note the difference in inclination between this core and Core 130-807C-6R (see Fig. 36); the tops of these two cores are less than 20 m apart.

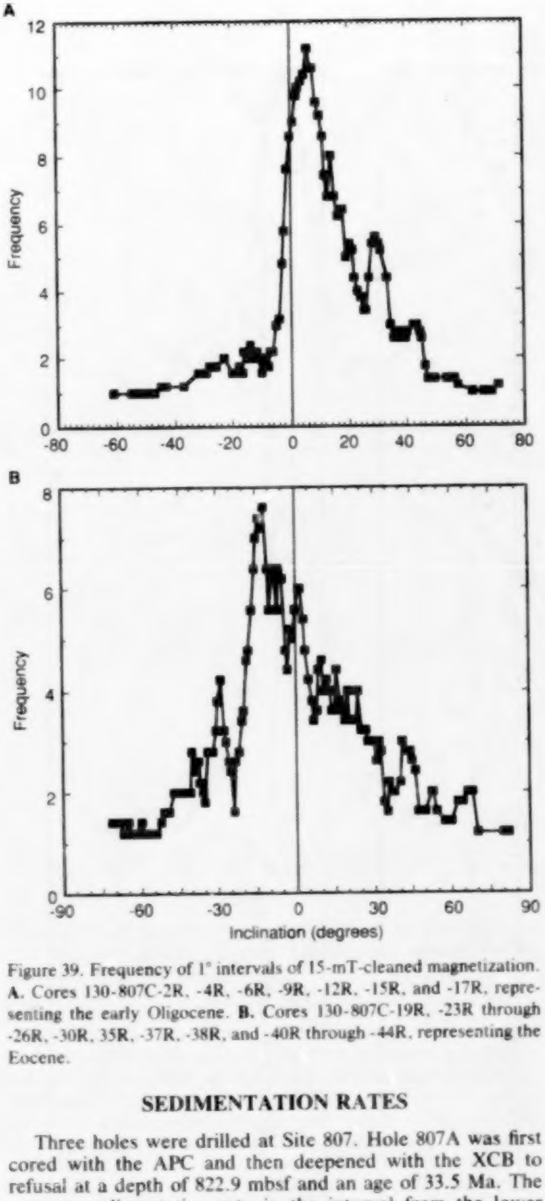

Figure 39. Frequency of 1° intervals of 15-mT-cleaned magnetization. **A.** Cores 130-807C-2R, -4R, -6R, -9R, -12R, -15R, and -17R, representing the early Oligocene. **B.** Cores 130-807C-19R, -23R through -26R, -30R, 35R, -37R, -38R, and -40R through -44R, representing the Eocene.

SEDIMENTATION RATES

Three holes were drilled at Site 807. Hole 807A was first cored with the APC and then deepened with the XCB to refusal at a depth of 822.9 mbsf and an age of 33.5 Ma. The average sedimentation rate in the interval from the lower Oligocene through the Holocene is 24.6 m/m.y. Hole 807B was cored with the APC to refusal at a depth of 278.6 mbsf and an age of 8.3 Ma, yielding an average sedimentation rate of about 33.6 m/m.y. in the interval from the lower Miocene through the Holocene. Hole 807C was washed to 780.0 mbsf and then cored with the RCB into basement. An average sedimentation rate of 17.7 m/m.y. was calculated for the biogenous sediments between the seafloor and the red clay contact at 1351.5 mbsf. This average rate is substantially lower than the Neogene rates. Increasing compaction with depth, condensed Paleogene sections, and the presence of several shorter Paleogene hiatuses all help to explain the apparent decrease in sedimentation rate with increasing age. Variable input rates of biogenic sediment components through time also have contributed to create the observed differences.

The biostratigraphic results from the three holes are presented in Table 8, and age-depth plots for Site 807 are shown in Figures 41–44. The age-depth plots from this hole have many features in common with Sites 805 and 806. First, a major change in slope of the age-depth indicators occurs close to 2 Ma, subsequently leading to peak rates of over 40 m/m.y. in the upper Miocene. Another general slope change occurs in the lower upper Miocene, indicating reduced sedimentation (on the order of 15–20 m/m.y.) through the middle and most of the lower Miocene. The basal Miocene through Oligocene interval is characterized by a doubling in sedimentation rates (30–40 m/m.y.), approaching those of the upper Miocene (Table 9). One 2-m.y.-long hiatus is indicated in the basal part of the late Oligocene, between 28.2 and 30.0 Ma (at 702.35 mbsf).

Age-depth plots from Hole 807C, representing the 50-m.y. interval from 30 to 80 Ma, are shown in Figure 42. This graph displays the general structure of the Paleogene and Upper Cretaceous rate history: rather high rates in the Oligocene through middle Eocene and Upper Cretaceous intervals, and comparatively low rates in the lower Eocene through Paleocene interval. The Oligocene through lower Eocene interval is shown in greater detail in Figure 43.

A hiatus that has its younger end precisely at the middle Eocene–upper Eocene boundary (40 Ma) is clearly indicated, although the position of its old end is less well constrained. Another hiatus, in combination with an extremely condensed section, occurs at about 1100 mbsf, between about 47 to 54 Ma. These hiatuses are associated with the termination and onset of the chert interval, respectively. The entire chert interval from about 970 through 1100 mbsf is characterized by anomalously low core recovery, which introduces large uncertainties in the depth positions of marker events and, consequently, sedimentation rate estimates.

Age-depth constraints in the lower Eocene through Upper Cretaceous interval are shown graphically in Figure 44. Sedimentation rates decrease progressively from about 17 m/m.y. in the lower Eocene to 2–3 m/m.y. in the basal Paleocene. This interval is preceded by Maestrichtian–upper Campanian rates that are on the order of 13–20 m/m.y. Sedimentation rates have not been established from the upper Albian–lower Cenomanian red clay interval (below 1351.5 mbsf), or the short interval of Albian-Aptian limestones that underlie the red clays and rest on the basement.

The sedimentation rates from all three holes at Site 807 are summarized in Figure 45. The difference in upper Miocene rates between Holes 807A and 807B stems from the use of different marker events (Hole 807B was terminated above the nannofossil Zone NN9/NN10 boundary at 8.7 Ma). The age control in the cross-over interval from Holes 807A to 807C is poorly constrained.

The Neogene sedimentation rate histories from all Leg 130 sites (Sites 803–807) are compared in Figure 46. The sites are listed as a function of increasing water depth, from Site 806 (shallowest) to Site 804 (deepest). This comparison clearly indicates a trend of decreasing rate with increasing water depth, at least back to almost 9 Ma. Assuming that the productivity input remained fairly similar at these sites at any given time; and, considering the fact that the sediments in these sections mainly consist of biogenous carbonate, it appears reasonable to conclude that the substantial decrease in sedimentation rate with depth reflects loss of carbonate by means of dissolution.

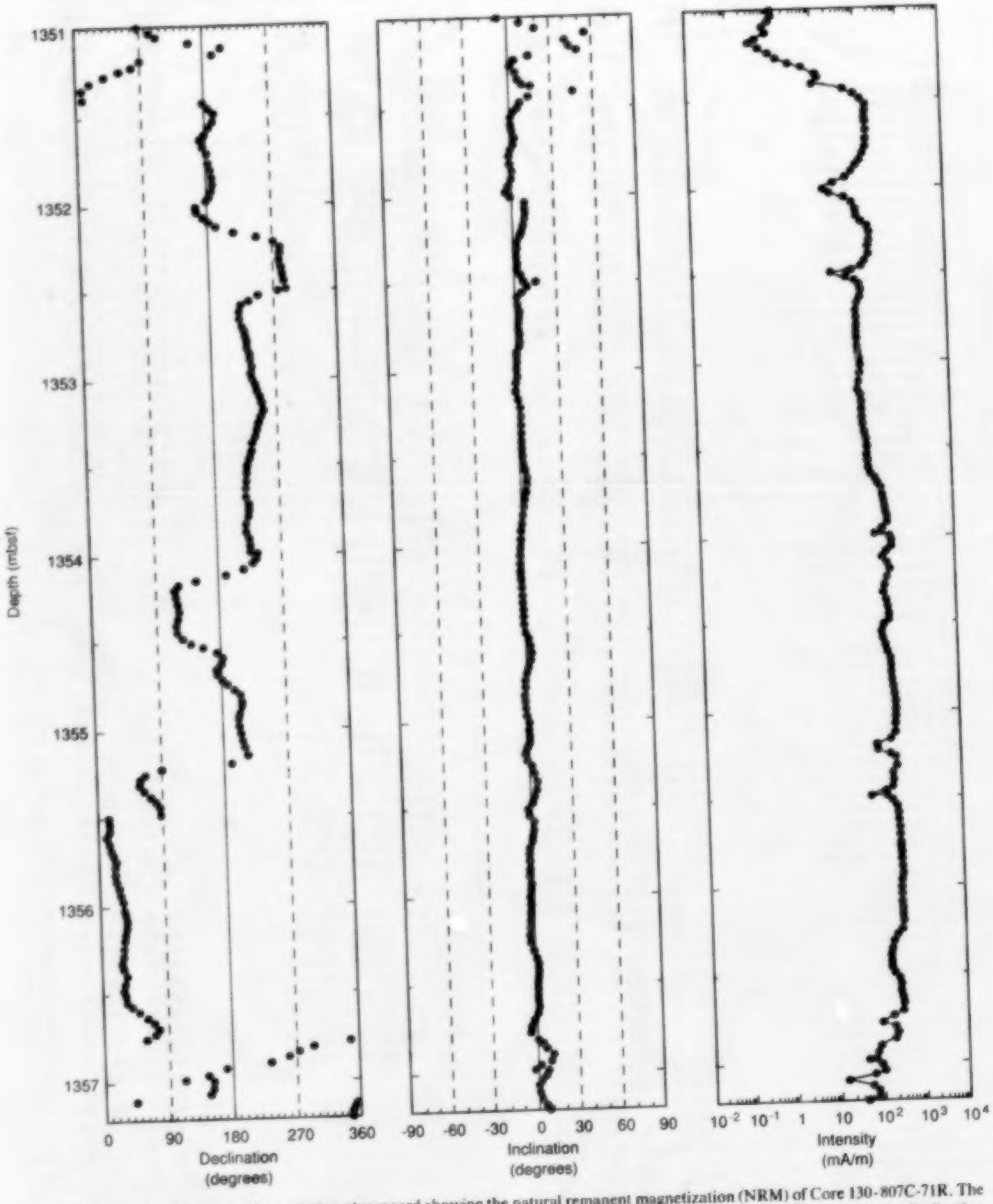

Figure 40. Pass-through cryogenic magnetometer record showing the natural remanent magnetization (NRM) of Core 130-807C-71R. The increase in intensity between 1351.0 and 1351.5 mbsf corresponds to the transition from limestone to claystone. Shifts in the declination record are caused by breaks between continuous pieces.

Table 8. Biostratigraphic events determined at Site 807.

Events	Upper depth (mbsf)	Lower depth (mbsf)	Age (Ma)
130-807A-			
LO *P. lacunosa* (N)	7.40	16.90	0.46
LO *G. tosaensis* (F)	7.40	16.90	0.60
LO *C. macintyrei* (N)	16.90	26.40	1.45
LO *G. fistulosus* (F)	26.40	35.90	1.60
LO *D. brouweri* (N)	26.40	35.90	1.89
FO *G. truncatulinoides* (F)	26.40	35.90	1.90
OA *D. triradiatus* (N)	26.40	35.90	2.07
LO *T. convexa* var. *aspinosa* (D)	16.90	26.40	2.10
LO *T. davisiana* (R)	35.90	45.40	2.43
LO *D. surculus* (N)	35.90	45.40	2.45
LO *S. peregrina* (R)	45.40	54.90	2.63
LO *D. tamalis* (N)	35.90	45.40	2.65
LO *G. altispira* (F)	54.90	64.40	2.90
FO *G. fistulosus* (F)	64.40	73.90	2.90
LO *Sphaeroidinellopsis* spp. (F)	35.90	45.40	3.00
FO *S. dehiscens* s.s. (F)	64.40	73.90	3.00
LO *P. fistula* (R)	64.40	73.90	3.27
LO *G. margaritae* (F)	64.40	73.90	3.40
LO *Sphenolithus* (N)	64.40	73.90	3.45
LO *P. doliolum* (R)	83.40	92.90	3.54
LO *R. pseudoumbilica* (N)	73.90	83.40	3.56
FO *A. ypsilon* (R)	73.90	83.40	3.78
LO *S. pentas* (R)	73.90	83.40	3.78
FO *S. tetras* (R)	83.40	92.90	3.84
LO *S. berminghami* (R)	92.90	102.40	3.86
FO *S. pentas* (R)	121.40	130.90	4.25
FO *N. jouseae* (D)	102.40	111.90	4.50
LO *C. acutus* (N)	83.40	92.90	4.60
LO *S. omnitubus* (R)	92.90	102.40	4.75
LO *D. quinqueramus* (N)	121.40	130.90	5.00
LO *S. delmontensis* (R)	168.90	178.40	5.00
LO *S. corona* (R)	178.40	187.90	5.05
FO *S. dehiscens* s.l. (F)	130.90	140.40	5.10
FO *G. tumida* (F)	121.40	130.90	5.20
LO *G. dehiscens* (F)	140.40	149.90	5.30
LO *A. tritubus* (R)	140.40	149.90	5.35
LO *N. miocenica* (D)	102.40	111.90	5.60
FO *P. primalis* (F)	159.40	168.90	5.80
FO *S. omnitubus* (R)	197.40	206.90	6.40
LO *C. caepa* (R)	187.90	197.40	6.40
LO *N. porteri* (D)	178.40	187.90	6.70
LO *D. hughesi* (R)	206.90	216.40	7.15
LO *N. porteri* (D)	178.40	187.90	7.20
FO *D. quinqueramus* (N)	235.40	244.90	7.50
LO *D. ontogenesis* (R)	206.90	216.40	7.45
LO *C. yabei* (D)	244.90	254.40	7.50
FO *A. tritubus* (R)	225.90	235.40	7.74
LO *C. nodulifer* var. *cyclopus* (D)	197.40	206.90	7.90
FO *S. berminghami* (R)	264.10	273.80	7.95
LO *A. ellipticus* var. *javanica* (D)	197.40	206.90	8.00
LO *D. peterssoni* (R)	264.10	273.80	8.15
LO *S. wolffii* (R)	254.40	264.10	8.15
LO *B. miralestensis* (R)	244.90	254.40	8.15
LO *D. laticonus* (R)	225.90	235.40	8.15
LO *C. yabei* (D)	244.90	254.40	8.60
LO *D. hamatus* (N)	283.50	292.70	8.70
FO *D. hughesi* (R)	283.50	292.70	8.75
LO *Catinaster* spp. (N)	283.50	292.70	8.80
LO *A. moronensis* (D)	312.00	321.20	8.90
FO *D. neohamatus* (N)	292.70	302.30	9.00
LO *C. japonica* (R)	302.30	312.00	10.15
FO *N. acostaensis* (F)	273.80	283.50	10.20
LO *G. siakensis* (F)	292.70	302.30	10.40
LO *L. thornburgi* (R)	292.70	302.30	10.45
FO *D. hamatus* (N)	302.30	312.00	10.50
LO *L. thornburgi* (R)	292.70	302.30	11.00
FO *C. coalitus* (N)	302.30	312.00	11.10
LO *A. moronensis* (D)	312.00	321.20	11.30
FO *G. nepenthes* (F)	312.00	321.20	11.30
LO *G. fohsi lobata* (F)	321.20	330.90	11.50
LO *C. cornuta* (R)	330.90	340.60	11.75
LO *S. jouseana* (D)	321.20	330.90	12.30
LO *A. ellipticus* var. *spiralis* (D)	321.20	330.90	12.30
LO *C. nitescens* (N)	340.60	350.20	12.80
LO *C. lewisianus* (D)	330.90	340.60	12.90
FO *G. fohsi lobata* (F)	350.20	359.90	13.10
LO *C. floridanus* (N)	369.70	379.50	13.10
LO *C. lewisianus* (D)	330.90	340.60	13.50
LO *S. heteromorphus* (N)	369.70	379.50	13.60
LO *C. pulchellus* var. *maculatus* (D)	330.90	340.60	13.90
FO *G. praefohsi* (F)	389.20	396.90	13.90
FO *A. ellipticus* var. *spiralis* (D)	379.50	389.20	14.10
LO *G. peripheroronda* (F)	389.20	398.90	14.60
FO *G. peripheroacuta* (F)	398.90	408.60	14.90
FO *A. ingens* (D)	408.60	418.30	15.50
TA *D. deflandrei* (N)	427.80	437.50	16.10
FO *S. heteromorphus* (N)	456.80	466.40	18.60
LO *S. belemnos* (N)	456.80	466.40	18.80
FO *S. belemnos* (N)	476.10	485.80	20.00
LO *G. kugleri* (F)	505.10	514.80	21.80
FO *D. druggii* (N)	553.00	562.60	23.60
FO *G. kugleri* (F)	581.90	601.30	23.70
LO *S. ciperoensis* (N)	611.00	620.60	25.20
FO *G. pseudokugleri* (F)	639.90	649.60	26.30
LO *S. distentus* (N)	678.20	687.80	27.50
LO *G. opima* (F)	659.20	668.90	28.20
LO *G. opima* (F)	697.50	707.20	28.20
LO *Chiloguembelina* spp. (F)	697.50	707.20	30.00
FO *G. angulisuturalis* (F)	755.20	764.90	31.60
FO *G. opima* (F)	784.20	793.90	32.70
LO *G. ampliapertura* s.s. (F)	793.90	803.60	32.80
LO *C. excavatus* (D)	813.20	822.90	33.00
130-807B-			
LO *P. iacunosa* (N)	3.10	12.60	0.46
LO *G. tosaensis* (F)	3.10	12.60	0.60
LO *C. macintyrei* (N)	12.60	22.10	1.45
LO *G. fistulosus* (F)	22.10	31.60	1.60
LO *D. brouweri* (N)	22.10	31.60	1.89
FO *G. truncatulinoides* (F)	31.60	41.10	1.90
OA *D. triradiatus* (N)	31.60	41.10	2.07
LO *D. surculus* (N)	50.60	60.10	2.45
LO *G. altispira* (F)	50.60	60.10	2.90
FO *S. dehiscens* s.s. (F)	79.10	88.60	3.00
FO *G. tosaensis*	41.10	50.60	3.10
LO *Sphenolithus* (N)	60.10	69.60	3.45
LO *R. pseudoumbilica* (N)	69.60	79.10	3.56
LO *C. acutus* (N)	107.60	117.10	4.60
LO *D. quinqueramus* (N)	126.60	145.60	5.00
FO *G. tumida* (F)	126.60	131.60	5.20
LO *G. dehiscens* (F)	98.10	107.60	5.30
FO *P. primalis* (F)	155.10	164.60	5.80
FO *G. plesiotumida* (F)	221.60	231.10	7.10
FO *D. quinqueramus* (N)	231.10	250.10	7.50
FO *G. acostaensis* (F)	269.10	278.60	10.20
130-807C-			
LO *R. umbilica* (N)	857.40	867.10	33.80
LO *Pseudohastegerina* (F)	876.60	881.90	34.00
LO *E. formosa* (N)	881.90	888.90	34.90
LO *G. cerroazulensis* (F)	908.90	913.90	36.60
LO *Hantkenina* (F)	908.90	913.90	36.60
LO *D. saipanensis* (N)	908.90	913.90	36.70
LO *D. barbadiensis* (N)	908.90	913.90	37.00
LO *C. reticulatum* (N)	933.70	938.70	37.70
LO *C. protoannula* (N)	943.70	948.40	38.20
LO *C. grandis* (N)	987.10	996.80	40.00
LO *Acarinina* (F)	987.10	1006.50	40.60
LO *T. rohri* (F)	987.10	1006.50	40.60
LO *M. spinulosa* (F)	987.10	1006.50	41.10
LO *C. solitus* (N)	987.10	996.80	42.30
FO *D. hesslandii* (N)	1006.50	1016.10	42.90
LO *A. bullbrooki* (F)	987.10	1006.50	43.00
FO *R. umbilica* (N)	1054.00	1063.70	44.40
FO *G. pomeroli* (F)	1063.70	1082.40	44.70
LO *N. alata* (N)	1073.20	1082.40	45.40
LO *M. aragonensis* (F)	1063.70	1082.40	46.00
LO *C. gigas* (N)	1082.40	1092.00	47.00
FO *C. gigas* (N)	1092.00	1097.70	47.40
FO *N. alata* (N)	1092.00	1097.70	49.80
LO *D. sublodoensis* (N)	1092.00	1097.70	49.70

Table 8 (continued).

Events	Upper depth (mbsf)	Lower depth (mbsf)	Age (Ma)
LO *D. lodoensis* (N)	1097.70	1102.40	50.40
LO *T. orthostylus* (N)	1102.40	1106.40	54.00
LO *D. sublodoensis* (N)	1092.00	1097.70	49.70
LO *D. lodoensis* (N)	1097.70	1102.40	50.40
LO *T. orthostylus* (N)	1102.40	1106.40	54.00
FO *D. lodoensis* (N)	1126.75	1137.10	55.00
FO *T. orthostylus* (N)	1140.20	1145.20	56.10
FO *D. diastypus* (N)	1140.20	1145.20	56.60
LO *Fasciculithus* (N)	1150.20	1155.20	56.80
LO *E. robusta* (N)	1161.10	1162.60	57.70
FO *D. multiradiatus* (N)	1162.60	1169.80	58.90
LO *H. kleinpellii* (N)	1172.36	1173.01	60.10
FO *D. mohleri* (N)	1173.01	1173.12	60.20
FO *H. kleinpellii* (N)	1173.12	1173.60	60.90
FO *H. cantabriae* (N)	1173.55	1179.40	61.40
FO *Fasciculithus* spp. (N)	1182.20	1182.63	62.30
FO *Sphenolithus* spp. (N)	1182.20	1182.63	62.80
K/T (FO abund. *Thoracosphaera*)	1193.14	1193.33	66.40
LO *T. trifidium* (N)	1261.20	1270.80	71.90
FO *T. trifidium* (N)	1348.00	1348.37	76.00

Notes: The depth uncertainty predominantly represents sampling intervals used. References for the age estimates are presented in the "Explanatory Notes" chapter (this volume). N = nannofossil, F = foraminifer, D = diatom, R = radiolarian, FO = first occurrence, LO = last occurrence, OA = onset acme, and K/T = Cretaceous/Tertiary. Magnetostratigraphic reversal boundaries followed by designation (T) or (O) refer to "termination" or "onset," respectively.

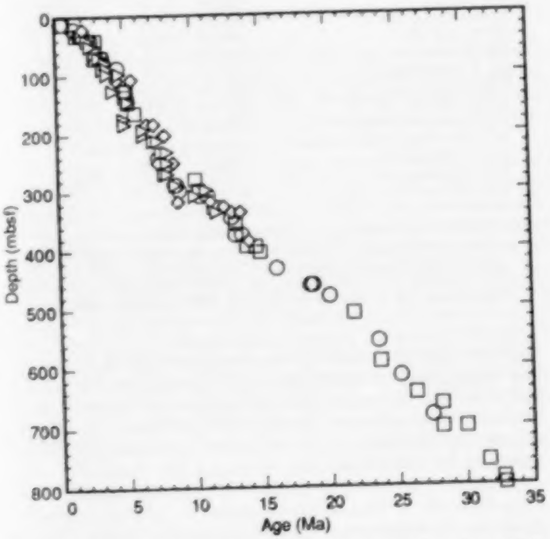

Figure 41. Age-depth relationships of biostratigraphic markers, Hole 807A. Circles = nannofossils, squares = foraminifers, diamonds = diatoms, and triangles = radiolarian.

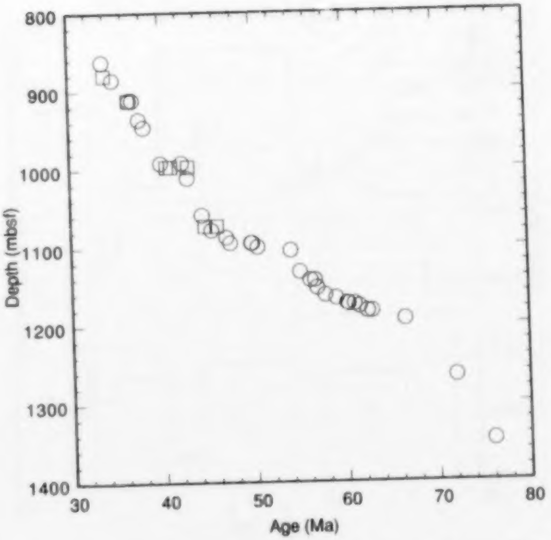

Figure 42. Age-depth relationships of biostratigraphic markers, Hole 807C. Symbols used are as in Figure 41.

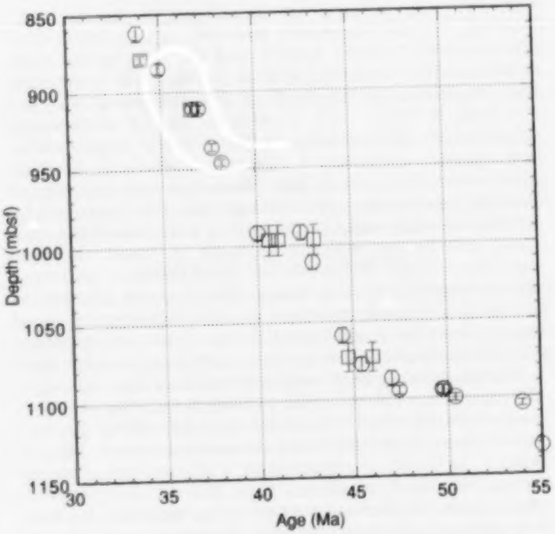

Figure 43. Age-depth relationships of biostratigraphic markers from the Oligocene through lower Eocene interval, Hole 807C. Error bars show sample interval uncertainties. Symbols used are as in Figure 41.

The deepest site (804) exhibits one anomalous time interval, between approximately 4 and 5 Ma (lower Pliocene). This interval is characterized by enhanced dissolution and perhaps by minor hiatus formation.

The difference in rate histories between Site 806 and Sites 803, 805, and 807 between about 9 and 13 Ma presumably reflects the combined effect of increasing dissolution gradients with depth as well as the paleolocation of the individual sites relative to the equatorial zone of divergence, upwelling, and high productivity. Site 804 has a higher sedimentation rate in the 9–13-Ma interval than the next three shallower sites. This fact presumably reflects the effect of mass wasting.

INORGANIC GEOCHEMISTRY

Thirty-six interstitial water samples were collected at Site 807, thirty-one from Hole 807A at depths ranging from 4.5 to 778.9 mbsf, and five from Hole 807C at depths ranging from

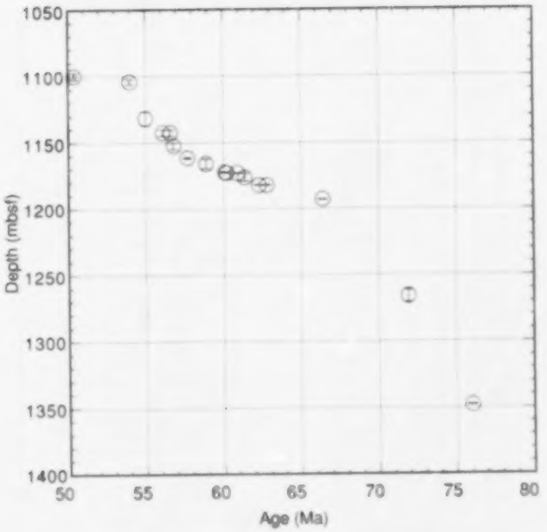

Figure 44. Age-depth relationships of biostratigraphic markers from the lower Eocene through upper Campanian interval, Hole 807C. Error bars show sample interval uncertainties. Symbols used are as in Figure 41.

Table 9. Estimated sedimentation rates, Site 807, and the control points determining those rates.

Control point	Depth (mbsf)	Age (Ma)	Sedimentation rate (m/m.y.)
130-807A-			
Top section	0	0	
OA *D. triradiatus* (N)	31.15	2.07	15.05
LO *D. quinqueramus* (N)	126.15	5.00	32.42
LO *D. hamatus* (N)	288.10	8.70	43.77
LO *S. heteromorphus* (N)	374.60	13.60	17.65
LO *G. kugleri* (F)	509.95	21.80	16.51
LO *G. opima* (F)	702.35	28.20	30.06
Hiatus younger side	702.35	28.20	—
Hiatus older side	702.35	30.20	—
LO *Chiloguembelina* spp. (F)	702.35	30.20	37.08
LO *G. ampliapertura* s.s. (F)	798.75	32.80	37.08
Terminal depth	822.90	33.45	
130-807B-			
Top section	0	0	
LO *D. brouweri* (N)	26.85	1.89	14.21
LO *R. pseudoumbilica* (N)	74.35	3.56	28.44
FO *G. tumida* (F)	129.10	5.20	33.38
FO *D. quinqueramus* (N)	240.60	7.50	48.48
Terminal depth	278.60	8.28	
130-807C-			
LO *R. umbilica* (N)	862.25	33.80	
LO *C. cerroazulensis* (F)	911.40	36.60	17.55
LO *C. grandis* (N)	991.95	40.00	23.69
Hiatus young side	991.95	40.00	—
Hiatus old side	991.95	42.30	—
LO *C. solitus* (N)	991.95	42.30	31.86
FO *R. umbilica* (N)	1058.85	44.40	31.86
FO *C. gigas* (N)	1094.85	47.40	12.00
Hiatus young side	1094.85	47.40	—
Hiatus old side	1094.85	49.80	—
FO *N. alata* (N)	1094.85	49.80	2.27
LO *T. orthostylus* (N)	1104.40	54.00	2.27
LO *Fasciculithus* (N)	1152.70	56.80	17.25
LO *E. robusta* (N)	1161.85	57.70	10.17
FO *Fasciculithus* spp. (N)	1182.42	62.30	4.47
K/T (FO abund. *Thoracosphaera*)	1193.24	66.40	2.64
LO *T. trifidium* (N)	1266.00	71.90	13.23
FO *T. trifidium* (N)	1348.19	76.00	20.05
Red clay contact	1351.50	76.17	

Notes: References for the age estimates are presented in the "Explanatory Notes" chapter (this volume), as well as the Leg 130 philosophy for determining the sedimentation rates. N = nannofossil, F = foraminifer, D = diatom, R = radiolarian, FO = first occurrence, LO = last occurrence, OA = onset acme, and K/T = Cretaceous/Tertiary.

810.4 to 1092.2 mbsf. For this report, these samples are considered as constituting a single depth profile. Interstitial water samples cover the depth range of the nannofossil ooze and chalk of Unit I, with the two deepest interstitial water samples from the limestones of Unit II (see "Lithostratigraphy" section, this chapter). Chemical gradients in the interstitial waters at this site (Table 10) are similar in character to those at the other sites drilled on this leg, being governed by the biogenic-rich, organic-carbon-poor character of the sediments and by the diffusive influence of basalt alteration reactions at depth. The interstitial water chemistry (dissolved silica concentrations) also reflects the extensive silicification in Unit II. The gradients at this site, the northernmost drilled and at the second shallowest water depth, are generally intermediate in magnitude relative to those at the other sites.

Chlorinity increases downhole by almost 2% to 563 mM at 22.9 mbsf (Core 130-807A-3H) and increases further to values greater than 580 mM by 681.1 mbsf (Core 130-807A-72X), for a total increase of almost 6% over the sampled interval (Fig. 47). Salinity, measured by refraction as total dissolved solids, increases with depth to values around 36.5–37.0 g/kg by 681.1 mbsf (Table 10). Sodium concentrations measured by flame emission spectrophotometry (Table 10) and those estimated by charge balance calculations generally agree to within 2%. Sodium concentrations increase from 476 mM at 4.5 mbsf to values around 510 mM at depths greater than 713.1 mbsf, a total increase of 7%. Sodium concentrations at depth in this site are lower than those at Site 806 and similar to those at Site 805. Alkalinity increases from 3.5 mM at 4.5 mbsf to >6 mM from 306.7 to 335.3 mbsf; it then decreases with depth to <4 mM by 681.1 mbsf (Fig. 47). The alkalinity maximum at this site occurs at a greater depth below the seafloor and is broader than the maxima at the sites drilled in deeper water. At depths <300 mbsf, alkalinity is lower at this site than at Site 806; at depths >300 mbsf, alkalinity is equal to or greater than at Site 806.

Sulfate concentrations decrease more than 20% to values <22 mM by 306.7 mbsf (Fig. 47). Sulfate depletion at this site continues to greater depths and is equal to or slightly larger than that at the sites in deeper water. Sulfate depletion here is less than at Site 806 by a factor of about 2, presumably because of the shallower water depth at Site 806 being favorable for a higher organic carbon supply to the sediments or because Site 806 is nearly on the equator and Site 807 is at 3.5°N.

Phosphate concentrations are below the detection limit of 1–2 μM in all but the shallowest sample (4.5 mbsf; Table 10). Ammonia concentrations increase to a quasi-constant level of >300 μM by 280 mbsf, persisting at these values throughout the depth range sampled (Fig. 47). In the upper 200 m, the ammonia profile is similar to that at Site 805 at a greater water depth; however, at greater sub-bottom depths, concentrations are higher at Site 807. Ammonia concentrations at Site 807 are a factor of 2 lower than those at Site 806, similar to sulfate depletion.

Dissolved silica concentrations increase with depth to over 1500 μM by 905.3 mbsf, with a depth profile similar to those at the other sites drilled (Fig. 47). From the sample at 940.1 mbsf near the base of lithologic Unit I continuing to the deepest sample at 1092.2 mbsf in Unit II, dissolved silica concentra-

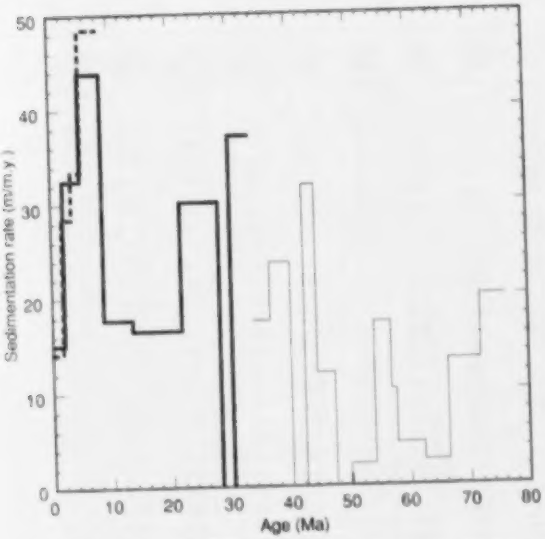

Figure 45. Sedimentation rate history, Site 807. Heavy solid line = Hole 807A, dashed line = Hole 807B, and thin solid line = Hole 807C.

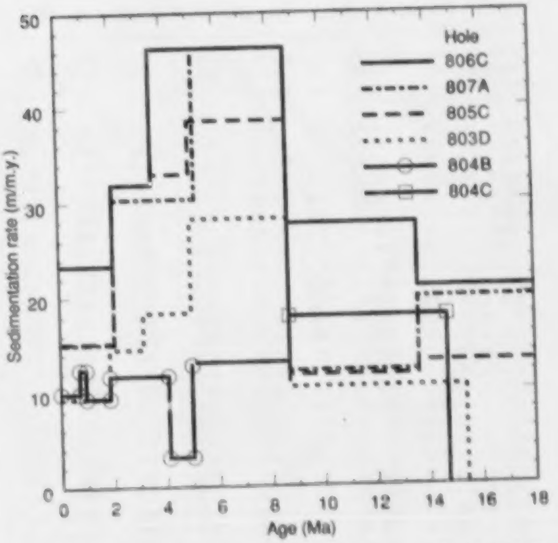

Figure 46. Comparison of Leg 130 sedimentation rate histories (0–18 Ma).

tions decrease rapidly by over a factor of 2, presumably as the result of the extensive limestone silicification and chert formation observed in Unit II (see "Lithostratigraphy" section, this chapter).

Dissolved manganese concentrations are below the detection limit of 2–3 μM in all but the shallowest two samples (Table 10). There is no increase in dissolved Mn with the dissolved Si increase, possibly reflecting the organic-carbon-poor nature of the sediments (Gieskes, 1981).

Calcium concentrations increase with depth by a factor of just over 2 to 22.1 mM at 1092.2 mbsf, with an average gradient of 1.1 mM/100 m (Fig. 47). This is the smallest depth gradient observed in the Leg 130 sites. There seems to be no simple pattern in the Ca gradients related to latitude or to sedimentation rate variation. Magnesium concentrations decrease with depth, with an overall gradient of -1.4 mM/100 m (Fig. 47), the smallest overall depth gradient observed. Calcium and Mg concentrations are linearly correlated overall ($R^2 = 0.95$) with a ΔCa/ΔMg ratio of −0.78, but there is some evidence of nonconservative Mg behavior throughout, indicating a sink for Mg in the sediments as well as in the underlying basalt (McDuff and Gieskes, 1976).

Strontium concentrations increase with depth to >900 μM by 165.4 mbsf, are generally consistent to 451.5 mbsf, and then slightly decrease with depth (Fig. 47). The Sr profile is similar throughout its depth range to that at Site 803, but it increases less with depth below the seafloor in the upper sediment column than do Sites 805 and 806.

Lithium concentrations decrease from 24.2 μM at 4.5 mbsf to minimum values of <13 μM from 137.1 to 279.7 mbsf; they then increase to close to 20 μM around 425.7–451.5 mbsf (Fig. 47). Minimum concentrations of lithium were the lowest observed in the Leg 130 sites. Lithium concentrations display a complex structure with depth below 451.5 mbsf.

Potassium concentrations decrease from ~11 mM at 4.5 mbsf to 8.4 mM at 1092.2 mbsf (Fig. 47); they linearly correlate with Ca ($R^2 = 0.85$). The potassium depth gradient is comparable with that at Site 806 over equivalent depth ranges; these are the smallest observed in these sites. Rubidium concentrations also decrease with depth from 1.7 μM at 4.5 mbsf to 1.0 μM by 1092.2 mbsf (Fig. 47); they linearly correlate with Ca ($R^2 = 0.87$). The rubidium depth gradient is steeper than that at Site 806 and smaller than at Sites 803, 804, and 805.

Although basalt alteration as indicated in the interstitial water signature apparently differs from site to site, there is no simple pattern relating the magnitudes of all the various gradients (Ca, Mg, K, and Rb) that reflects the degree of influence from basalt alteration from site to site.

CARBON GEOCHEMISTRY

Shipboard carbon geochemical analyses of sediments from Site 807 included determinations of inorganic carbon (503 samples), total carbon (61 samples), and volatile hydrocarbons (44 samples). The inorganic carbon and total carbon measurements were performed on dried ground samples collected for physical properties analyses. The methods used are outlined in the "Explanatory Notes" chapter (this volume), whereas background and detailed descriptions are given in Emeis and Kvenvolden (1986).

Volatile hydrocarbons in the sediments were routinely monitored as required by safety and pollution considerations. Samples were collected using the headspace-sampling technique and measured for methane, ethane, and propane. As in the previous Leg 130 sites, no significant amounts of these gases were detected. Inorganic carbon (IC) was determined using a Coulometrics carbon dioxide coulometer. Percent $CaCO_3$ is calculated according to the equation: $CaCO_3 = IC \cdot 8.334$. The data are presented in Table 11 and plotted vs. depth in Figure 6.

The carbonate curve closely reflects the lithostratigraphic units described in the "Lithostratigraphy" section (this chapter). Unit I (0–968 mbsf, Holocene to upper Eocene) consists of nannofossil-rich oozes and chalks and is characterized by very high carbonate contents, ranging from 85% to 95%. Long-term variations with noticeably higher values (up to 95%

Table 10. Interstitial water geochemical data, Holes 807A and 807C.

Core, section, interval (cm)	Depth (mbsf)	pH	Alk. (mM)	Sal. (g/kg)	Cl^- (mM)	Na^+ (mM)	SO_4^{2-} (mM)	PO_4^{3-} (μM)	NH_4^+ (μM)	SiO_2 (μM)	Mn^{2+} (μM)	Ca^{2+} (mM)	Mg^{2+} (mM)	Sr^{2+} (μM)	Li (μM)	K^+ (mM)	Rb (μM)
130-807A-																	
1H-3, 145–150	4.45	7.5	3.51	35.0	553	476	27.4	3.0	6	401	13	10.6	52.3	130	24.2	10.8	1.67
2H-4, 145–150	13.35	7.5	3.64	36.0	558	484	27.4	LD	47	480	4	10.9	52.3	208	21.0	11.4	1.65
3H-4, 145–150	22.85	7.5	4.17	37.5	563	487	27.5	LD	55	503	LD	11.3	51.8	284	20.1	11.2	1.55
4H-4, 145–150	32.35	7.6	4.04	35.5	564	487	26.7	LD	88	543	LD	11.3	51.4	356	19.6	11.4	1.73
5H-4, 145–150	41.85	7.6	4.16	35.5	561	487	26.4	LD	96	570	LD	11.4	50.9	425	18.2	11.4	1.72
6H-4, 145–150	51.35	7.6	4.29	35.5	565	487	26.1	LD	111	592	LD	11.7	50.6	476	17.3	11.3	1.68
9H-4, 145–150	79.85	7.6	4.69	35.0	561	486	26.0	LD	161	673	LD	12.2	48.6	619	15.5	11.4	1.66
12H-4, 145–150	108.35	7.2	5.08	35.0	561	483	25.0	LD	193	723	LD	12.7	47.6	753	13.2	11.0	1.64
15H-5, 145–150	137.10	7.2	5.36	35.0	565	488	23.6	LD	224	773	LD	13.3	46.9	840	12.3	10.7	1.63
18H-4, 145–150	165.35	7.6	5.63	35.0	567	488	22.9	LD	236	800	LD	13.9	45.7	904	11.4	10.9	1.62
21H-4, 145–150	193.85	7.6	5.78	34.5	561	487	22.6	LD	268	852	LD	14.6	44.4	927	11.4	10.9	1.60
24H-4, 145–150	222.35	7.6	5.97	35.0	565	492	22.2	LD	290	915	LD	15.0	43.6	905	11.3	10.7	1.56
27H-4, 145–150	250.85	7.8	5.92	37.5	563	486	22.5	LD	286	948	LD	15.5	43.2	896	11.3	10.9	1.59
30X-4, 140–150	279.70	7.1	5.80	35.0	561	491	22.0	LD	302	919	LD	15.8	42.2	896	12.2	10.8	1.53
33X-3, 140–150	306.70	7.1	6.23	35.5	569	493	21.8	LD	300	950	LD	16.4	41.8	907	13.6	10.7	1.47
36X-3, 140–150	335.30	7.1	6.32	35.5	571	490	21.6	LD	305	969	LD	16.8	41.6	899	14.9	10.5	1.46
39X-2, 140–150	362.80	7.6	5.73	36.0	574	493	21.4	LD	320	994	LD	17.2	41.1	907	15.8	10.5	1.47
42X-4, 140–150	395.10	7.6	5.26	35.3	573	497	21.4	LD	319	1014	LD	17.6	40.3	896	18.3	10.4	1.47
45X-5, 140–150	425.70	7.1	5.24	35.5	570	502	21.9	LD	315	1025	LD	18.0	40.3	876	19.4	10.4	1.45
48X-3, 140–150	451.50	7.6	ND	35.5	578	503	21.5	LD	314	1091	LD	18.4	40.0	900	19.9	10.3	1.40
51X-3, 140–150	480.50	7.6	5.01	35.5	580	503	21.8	LD	331	1081	LD	19.0	39.4	896	17.6	10.3	1.43
54X-4, 0–10	509.60	7.5	5.05	35.5	579	497	21.4	LD	331	1104	LD	19.0	39.6	878	16.2	10.2	1.38
57X-4, 140–150	539.60	7.7	4.25	36.0	576	502	21.6	LD	329	1104	LD	19.3	40.0	860	15.3	10.1	1.39
60X-4, 140–150	568.50	7.1	5.30	36.0	577	502	21.8	LD	333	1143	LD	19.5	39.2	874	14.0	9.96	1.39
63X-4, 0–10	596.10	7.2	5.01	36.0	583	499	21.1	LD	322	1158	LD	19.7	39.0	836	15.3	9.95	1.33
66X-2, 140–150	623.50	7.6	4.85	36.0	575	498	21.4	LD	307	1158	LD	19.6	39.5	800	15.3	9.82	1.32
70X-4, 140–150	665.10	7.6	4.36	36.0	579	501	21.0	LD	326	1228	LD	19.9	39.3	817	13.5	9.70	1.30
72X-2, 140–150	681.10	7.6	3.94	36.5	582	507	21.0	LD	340	1266	LD	20.2	38.8	862	12.1	9.85	1.36
75X-4, 140–150	713.10	ND	ND	ND	585	515	21.2	LD	330	1262	LD	20.5	38.5	853	11.7	9.81	1.31
78X-2, 0–10	737.70	ND	ND	ND	585	516	21.2	ND	333	1289	ND	20.8	38.2	866	12.1	9.62	1.31
82X-3, 140–150	778.90	7.6	4.00	36.5	583	505	21.5	LD	342	1364	LD	21.2	38.9	865	11.7	9.35	1.26
130-807C-																	
4R-1, 140–150	810.40	7.6	3.94	36.5	581	503	21.5	ND	328	1442	LD	21.2	38.0	883	11.7	9.39	1.22
17R-1, 140–150	905.30	7.6	3.68	36.3	583	511	21.4	ND	343	1517	LD	21.8	37.5	901	11.3	9.25	1.16
23R-1, 140–150	940.10	ND	ND	35.5	586	505	21.4	ND	320	1317	ND	21.2	38.0	840	14.0	8.87	1.12
30R-1, 71–76	997.51	ND	ND	ND	585	510	22.1	ND	327	725	ND	21.7	37.9	844	14.4	8.87	1.09
40R-1, 23–31	1092.23	ND	ND	37.0	584	504	21.8	ND	309	688	LD	22.1	37.4	789	15.8	8.42	1.01

Note: LD = concentration lower than detection limit and ND = not determined.

$CaCO_3$) from 90 to 300 mbsf (late Pliocene to upper Miocene) and from 450 to 550 mbsf (middle to lower Miocene; Fig. 6 and Table 11) were observed. In Samples 130-807A-25H-1, 108–110 cm, -48X-2, 99–101 cm, and -72X-4, 67–69 cm (217.5, 449.5, and 683.4 mbsf, respectively), the carbonate content is significantly lower than in the surrounding samples (73%–78%). None of these samples represent the dominant lithology of their respective sections. The upper two samples were taken from interbedded silica-rich layers and the lower one from an ash-rich layer.

The chert-rich limestones in Subunit IIA and the upper part of Subunit IIB (968–1351.4 mbsf; middle and lower Eocene) have $CaCO_3$ values between 51% and 97% $CaCO_3$, whereas the chert-poor limestones of the lower part of Subunit IIB (1140–1350 mbsf; lower Eocene to upper Cenomanian) are characterized by high carbonate values from 95% to almost 99%.

The dark claystones in Subunit IIIA (1351.4–1369.7 mbsf; lower Cenomanian to upper Albian) have carbonate contents less than 0.3% (Fig. 6 and Table 11), which is similar to equivalent intervals recovered in Hole 803D.

Total organic carbon (TOC) was determined only for samples from Hole 807A and is defined as the difference between total carbon (NCS-analyzer) and inorganic carbon (Coulometer). TOC values range from 0.02% to 0.6% and are similar to TOC values observed in sediments of Site 806. It should be noted that the measurements are near the detection limit of the shipboard analytical methods used. They will be verified by shore-based analyses.

PHYSICAL PROPERTIES

The physical properties program at Site 807 included multisensor track (MST) measurements of whole-round cores, and index property, vane shear strength and *P*-wave velocity measurements of split cores. Methods for these measurements are described in the "Explanatory Notes" chapter (this volume). One vane shear strength measurement per section was taken in Holes 807A and 807B to the depth at which induration prevented vane insertion (around 280 mbsf). *P*-wave velocity measurements were made and index properties samples taken at a sampling interval of two per section in the upper 150 m of Hole 807A, and one per section in the rest of Hole 807A and in Holes 807B and 807C. In general, the recovery of APC cores at Holes 807A and 807B allowed us to obtain a complete suite of physical properties measurements. Recovery decreased in the XCB cores and deteriorated significantly in the RCB cores; this lack of recovery is reflected in gaps in the physical properties data sets.

Vane Shear Strength

The ODP motorized minivane was used to measure undrained shear strength in split core sections (see "Explanatory Notes" chapter, this volume). Measurements were performed in successive APC and XCB cores until the sediment became too lithified (near 280 mbsf). Residual shear strengths were obtained where cracking of the sediment around the vane did not dominate failure (see discussion of vane shear strength data in the

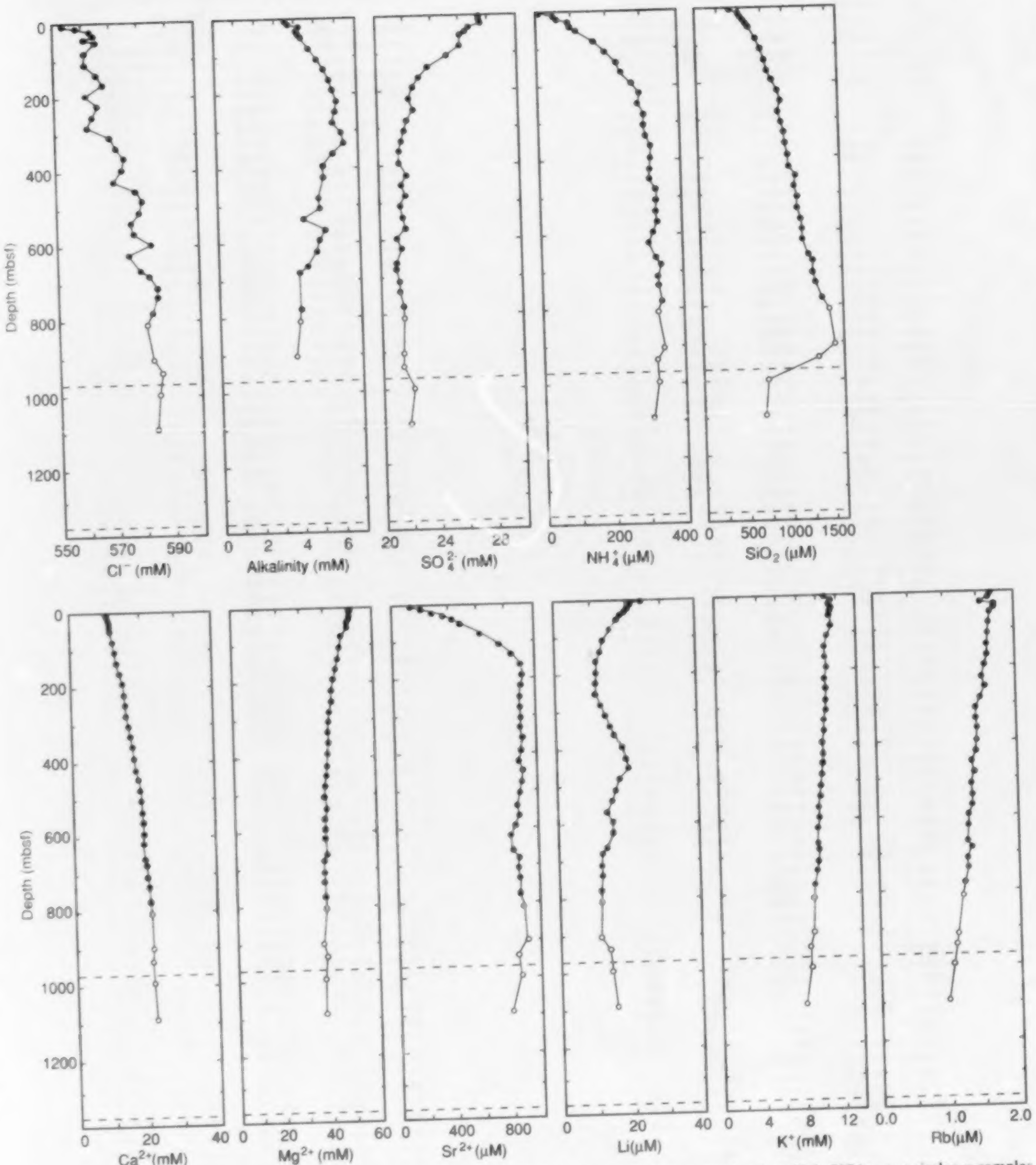

Figure 47. Interstitial water geochemical data vs. depth, Holes 807A and 807C. Closed circles = samples from Hole 807A; open circles = samples from Hole 807C. The two horizontal dashed lines represent depth boundaries between lithologic Units I, II, and III; the depth at the base of the plots is that of the contact of Unit III with basalt.

Table 11. Concentrations of total carbon and inorganic carbon, Holes 807A and 807B.

Core, section, interval (cm)	Depth (mbsf)	Inorganic carbon (%)	$CaCO_3$ (%)
130-807A-			
1H-1, 95–97	0.95	10.61	88.4
1H-2, 8–10	1.58	10.65	88.7
1H-3, 13–15	3.13	10.48	87.3
1H-4, 14–16	4.64	10.40	86.6
1H-5, 13–15	6.13	10.63	88.5
2H-1, 94–96	8.34	10.78	89.8
2H-2, 14–16	9.04	10.96	91.3
2H-3, 14–16	10.54	10.54	87.8
2H-4, 14–16	12.04	10.65	88.7
2H-5, 14–16	13.54	10.66	88.8
2H-6, 14–16	15.04	11.01	91.7
2H-7, 14–16	16.54	10.79	89.9
3H-1, 94–96	17.84	10.70	89.1
3H-2, 15–17	18.55	10.66	88.8
3H-3, 14–16	20.04	10.64	88.6
3H-4, 21–23	21.61	10.81	90.0
3H-5, 14–16	23.04	10.68	89.0
3H-6, 15–17	24.55	10.43	86.9
3H-7, 24–26	26.14	10.80	90.0
4H-1, 94–96	27.34	10.56	88.0
4H-2, 15–17	28.05	10.55	87.9
4H-3, 15–17	29.55	10.75	89.5
4H-4, 15–17	31.05	10.59	88.2
4H-5, 14–16	32.54	10.84	90.3
4H-6, 15–17	34.05	10.90	90.8
4H-7, 30–32	35.70	10.80	90.0
5H-1, 108–110	36.98	10.85	90.4
5H-2, 35–37	37.75	10.85	90.4
5H-3, 40–42	39.30	10.90	90.8
5H-4, 39–41	40.79	11.12	92.6
5H-5, 39–41	42.29	11.01	91.7
5H-6, 40–42	43.80	10.99	91.5
5H-7, 29–31	45.19	10.87	90.5
6H-2, 33–35	47.23	10.99	91.5
6H-3, 35–37	48.75	10.99	91.5
6H-4, 35–37	50.25	10.88	90.6
6H-5, 35–37	51.75	10.74	89.5
6H-6, 35–37	53.25	11.03	91.9
7H-1, 108–110	55.98	10.82	90.1
7H-2, 33–35	56.73	10.83	90.2
7H-3, 33–35	58.23	10.98	91.5
7H-4, 33–34	59.73	11.01	91.7
7H-5, 33–35	61.23	10.91	90.9
7H-6, 33–35	62.73	11.05	92.0
8H-1, 107–109	65.47	11.08	92.3
8H-2, 34–36	66.24	11.19	93.2
8H-3, 33–35	67.73	11.09	92.4
8H-4, 42–44	69.32	11.17	93.0
8H-5, 39–41	70.79	11.05	92.0
8H-6, 39–41	72.29	11.09	92.4
8H-7, 34–36	73.74	11.13	92.7
9H-1, 33–35	74.23	11.12	92.6
9H-2, 33–35	75.73	11.15	92.9
9H-3, 33–35	77.23	11.03	91.9
9H-4, 33–35	78.73	10.87	90.5
9H-5, 33–35	80.23	10.98	91.5
9H-6, 33–35	81.73	11.17	93.0
10H-1, 108–110	84.48	11.00	91.6
10H-2, 108–110	85.98	11.30	94.1
10H-3, 108–110	87.48	11.18	93.1
10H-4, 108–110	88.98	11.06	92.1
10H-5, 108–110	90.48	11.10	92.5
10H-6, 108–110	91.98	11.08	92.3
11H-1, 106–108	93.96	11.02	91.8
11H-2, 107–109	95.47	11.11	92.5
11H-3, 107–109	96.97	11.09	92.4
11H-4, 107–109	98.47	10.96	91.3
11H-5, 107–109	99.97	11.18	93.1
11H-6, 107–109	101.47	11.27	93.9
12H-1, 106–108	103.46	11.19	93.2
12H-2, 107–109	104.97	11.06	92.1
12H-3, 106–108	106.46	11.07	92.2
12H-5, 106–108	109.46	11.04	92.0
12H-6, 106–108	110.96	10.98	91.5
13H-2, 106–108	114.46	11.07	92.2
13H-3, 106–108	115.96	11.00	91.6
13H-4, 106–108	117.46	11.27	93.9
13H-5, 108–110	118.98	11.13	92.7
13H-6, 108–110	120.48	11.05	92.0
14H-3, 31–33	124.71	11.20	93.3
14H-4, 30–32	126.20	10.97	91.4
14H-5, 31–33	127.71	10.68	89.0
14H-6, 30–32	129.20	11.11	92.5
15H-3, 108–110	133.73	11.17	93.0
15H-4, 109–111	135.24	10.94	91.1
15H-5, 107–109	136.72	10.99	91.5
15H-6, 107–109	138.22	10.98	91.5
15H-7, 107–109	139.72	11.14	92.8
16H-1, 107–109	141.47	11.16	93.0
16H-2, 107–109	142.97	11.06	92.1
16H-3, 107–109	144.47	11.19	93.2
16H-4, 107–109	145.97	11.23	93.5
16H-5, 107–109	147.47	11.17	93.0
16H-6, 118–120	149.08	11.25	93.7
17H-1, 73–75	150.63	11.28	94.0
17H-2, 89–91	152.29	11.14	92.8
17H-3, 75–77	153.65	11.18	93.1
17H-4, 89–91	155.29	11.25	93.7
17H-5, 74–76	156.64	11.15	92.9
17H-6, 75–77	158.15	11.20	93.3
18H-1, 74–76	160.14	11.16	93.0
18H-2, 75–77	161.65	11.16	93.0
18H-3, 72–74	163.12	11.11	92.5
18H-4, 74–76	164.64	11.17	93.0
18H-5, 74–76	166.14	11.22	93.5
18H-6, 75–77	167.65	11.20	93.3
19H-1, 73–75	169.63	11.33	94.4
19H-2, 72–74	171.12	11.22	93.5
19H-3, 71–73	172.61	11.19	93.2
19H-4, 85–87	174.25	11.34	94.5
19H-5, 72–74	175.62	11.07	92.2
19H-6, 74–76	177.14	11.22	93.5
20H-1, 75–77	179.15	11.27	93.9
20H-2, 74–76	180.64	11.16	93.0
20H-3, 72–74	182.12	11.30	94.1
20H-4, 74–76	183.64	11.23	93.5
20H-5, 72–74	185.12	11.24	93.6
20H-6, 74–76	186.64	11.30	94.1
21H-1, 115–117	189.05	11.22	93.5
21H-2, 107–109	190.47	11.32	94.3
21H-3, 110–112	192.00	11.15	92.9
21H-4, 90–92	193.30	11.13	92.7
21H-5, 107–109	194.97	11.17	93.0
21H-6, 109–111	196.49	11.26	93.8
22H-1, 109–111	198.49	11.27	93.9
22H-2, 99–101	199.89	11.33	94.4
22H-3, 110–112	201.50	11.23	93.5
22H-4, 109–111	202.99	11.22	93.5
22H-5, 110–112	204.50	11.35	94.5
22H-6, 112–114	206.02	11.30	94.1
23H-1, 105–107	207.95	11.25	93.7
23H-2, 109–111	209.49	11.23	93.5
23H-3, 107–109	210.97	11.33	94.4
23H-4, 110–112	212.50	11.22	93.5
23H-5, 108–110	213.98	11.08	92.3
23H-6, 109–111	215.49	11.15	92.9
26H-1, 109–111	236.49	10.91	90.9
26H-3, 108–110	239.48	11.08	92.3
26H-4, 109–111	240.99	10.96	91.3
26H-5, 109–111	242.49	11.00	91.6
26H-6, 109–111	243.99	11.15	92.9
27H-1, 109–111	245.99	11.21	93.4
27H-3, 109–111	248.99	10.99	91.5
27H-4, 109–111	250.49	10.97	91.4
28X-1, 94–96	255.34	10.86	90.5
28X-2, 30–32	256.20	10.86	90.5
28X-3, 52–54	257.92	10.80	90.0
28X-4, 30–32	259.20	11.12	92.6
28X-5, 100–102	261.40	10.87	90.5

Table 11 (continued).

Table 11 (continued).

Core, section, interval (cm)	Depth (mbsf)	Inorganic carbon (%)	$CaCO_3$ (%)
28X-6, 29–30	262.19	11.11	92.5
29X-1, 61–64	264.71	11.16	93.0
29X-2, 109–112	266.69	11.23	93.5
29X-3, 70–73	267.80	11.12	92.6
29X-4, 66–68	269.26	11.29	94.0
29X-5, 84–86	270.94	11.15	92.9
29X-6, 60–63	272.20	11.18	93.1
30X-2, 56–58	275.86	11.19	93.2
30X-3, 87–89	277.67	11.12	92.6
30X-4, 65–67	278.95	11.16	93.0
30X-5, 100–102	280.80	11.09	92.4
30X-6, 70–72	282.00	11.27	93.9
31X-1, 95–97	284.45	11.21	93.4
31X-2, 123–125	286.23	11.04	92.0
31X-3, 66–68	287.16	11.24	93.6
31X-4, 68–71	288.68	11.22	93.5
31X-5, 70–72	290.20	11.16	93.0
32X-1, 144–146	294.14	11.08	92.3
32X-2, 110–112	295.30	11.15	92.9
32X-3, 126–128	296.96	11.16	93.0
32X-4, 93–95	298.13	11.15	92.9
33X-1, 35–37	302.65	11.02	91.8
33X-2, 135–137	305.15	11.09	92.4
33X-3, 53–55	305.83	11.02	91.8
33X-4, 127–129	308.07	10.79	89.9
33X-5, 145–147	309.75	10.88	90.6
33X-6, 77–79	310.57	11.06	92.1
34X-1, 68–70	312.68	10.70	89.1
34X-2, 73–75	314.23	11.06	92.1
34X-3, 100–102	316.00	11.16	93.0
34X-4, 107–109	317.57	11.08	92.3
34X-5, 42–44	318.42	11.00	91.6
34X-6, 131–133	320.81	11.19	93.2
36X-1, 133–134	332.23	11.04	92.0
36X-2, 141–143	333.81	10.83	90.2
36X-3, 107–109	334.97	10.62	88.5
36X-4, 135–137	336.75	10.93	91.0
36X-5, 113–115	338.03	10.70	89.1
36X-6, 81–83	339.21	10.54	87.8
37X-2, 87–89	342.97	10.78	89.8
37X-3, 95–97	344.55	10.71	89.2
37X-4, 50–52	345.60	10.96	91.3
37X-5, 8–9	346.68	10.62	88.5
38X-1, 140–142	351.60	10.91	90.9
38X-2, 112–113	352.82	10.96	91.3
38X-3, 142–144	354.62	10.95	91.2
38X-4, 96–98	355.66	10.72	89.3
38X-5, 78–80	356.98	11.03	91.9
39X-1, 37–39	360.27	10.60	88.3
39X-2, 91–93	362.31	10.86	90.5
39X-3, 114–116	364.04	10.89	90.7
39X-4, 47–49	364.87	10.82	90.1
39X-5, 142–144	367.32	10.29	85.7
40X-1, 80–82	370.50	10.93	91.0
40X-2, 57–59	371.77	10.96	91.3
40X-3, 59–61	373.29	10.93	91.0
40X-4, 145–147	375.65	10.97	91.4
40X-5, 121–123	376.91	11.17	93.0
40X-6, 109–111	378.29	11.03	91.9
41X-1, 90–92	380.40	11.28	94.0
41X-2, 75–77	381.75	10.97	91.4
41X-3, 72–74	383.22	10.73	89.4
41X-4, 76–78	384.76	11.14	92.8
41X-5, 83–85	386.33	10.17	84.7
41X-6, 84–86	387.84	10.60	88.3
42X-1, 106–108	390.26	11.06	92.1
42X-2, 102–104	391.72	10.86	90.5
42X-3, 106–108	393.26	10.88	90.6
42X-4, 79–81	394.49	10.82	90.1
42X-5, 60–62	395.80	11.05	92.0
42X-6, 40–42	397.10	10.88	90.6
43X-1, 81–83	399.71	11.03	91.9
43X-2, 56–58	400.96	10.75	89.5
43X-3, 67–69	402.57	10.88	90.6
43X-4, 67–69	404.07	10.66	88.8
43X-5, 76–78	405.66	11.11	92.5

Table 11 (continued).

Core, section, interval (cm)	Depth (mbsf)	Inorganic carbon (%)	$CaCO_3$ (%)
44X-1, 75–77	409.35	10.34	86.1
44X-2, 141–143	411.51	10.64	88.6
44X-3, 110–112	412.70	11.11	92.5
44X-4, 102–104	414.12	10.96	91.3
44X-5, 124–126	415.84	10.99	91.5
45X-1, 98–100	419.28	10.89	90.7
45X-2, 97–99	420.77	11.04	92.0
45X-3, 90–92	422.20	11.09	92.4
45X-4, 95–97	423.75	11.21	93.4
45X-5, 57–59	424.87	11.30	94.1
45X-6, 65–67	426.45	11.18	93.1
46X-1, 116–118	428.96	11.45	95.4
46X-2, 112–114	430.42	10.98	91.5
46X-3, 107–109	431.87	10.30	85.8
46X-4, 108–110	433.38	11.51	95.9
46X-5, 81–83	434.61	11.00	91.6
46X-6, 78–80	436.08	11.18	93.1
47X-1, 111–113	438.61	11.20	93.3
47X-2, 122–124	440.22	11.10	92.5
47X-3, 111–112	441.61	11.38	94.8
47X-4, 113–115	443.13	11.25	93.7
47X-5, 103–105	444.53	11.10	92.5
47X-6, 51–53	445.51	11.03	91.9
48X-1, 100–102	448.10	10.88	90.6
48X-2, 99–101	449.59	9.35	77.9
48X-3, 101–103	451.11	10.96	91.3
48X-4, 93–95	452.53	11.14	92.8
48X-5, 84–86	453.94	11.20	93.3
48X-6, 100–102	455.60	11.40	95.0
49X-1, 53–55	457.33	11.55	96.2
49X-2, 92–94	459.22	11.63	96.9
49X-3, 65–67	460.45	11.52	96.0
49X-4, 74–76	462.04	11.36	94.6
49X-5, 72–74	463.52	11.13	92.7
50X-1, 89–91	467.29	11.39	94.9
50X-2, 93–95	468.83	11.54	96.1
50X-3, 89–91	470.29	11.79	98.2
50X-4, 100–102	471.90	11.42	95.1
50X-5, 97–99	473.37	11.39	94.9
50X-6, 98–100	474.88	11.50	95.8
51X-1, 34–36	476.44	11.25	93.7
51X-2, 40–42	478.00	11.40	95.0
51X-3, 43–44	479.53	11.51	95.9
51X-4, 38–40	480.98	11.43	95.2
51X-5, 33–35	482.43	11.48	95.6
51X-6, 16–18	483.76	11.40	95.0
52X-1, 108–110	486.88	11.33	94.4
52X-2, 14–16	487.44	11.51	95.9
52X-5, 61–63	492.41	11.51	95.9
53X-1, 105–107	496.45	11.39	94.9
53X-2, 93–95	497.83	11.49	95.7
53X-3, 97–99	499.37	11.45	95.4
53X-4, 90–92	500.80	11.53	96.0
53X-5, 91–93	502.31	11.09	92.4
54X-1, 84–86	505.94	11.29	94.0
54X-2, 97–99	507.57	11.49	95.7
54X-3, 114–116	509.24	11.63	96.9
54X-4, 113–115	510.73	11.41	95.0
54X-5, 80–82	511.90	11.60	96.6
54X-6, 27–29	512.87	11.33	94.4
55X-3, 61–63	518.41	11.44	95.3
55X-4, 65–67	519.95	11.45	95.4
55X-5, 103–105	521.83	11.44	95.3
55X-6, 43–45	522.73	11.48	95.6
56X-1, 146–148	525.46	11.42	95.1
56X-2, 110–112	526.60	11.51	95.9
56X-3, 53–55	527.53	11.57	96.4
56X-4, 131–133	529.81	11.47	95.5
56X-6, 49–50	531.99	11.54	96.1
57X-1, 85–87	534.55	11.23	93.5
57X-2, 86–88	536.06	11.51	95.9
57X-3, 95–97	537.65	11.41	95.0
57X-4, 65–67	538.85	11.25	93.7
57X-5, 56–58	540.26	11.20	93.3
58X-1, 105–107	544.45	11.53	96.0
58X-2, 104–106	545.94	11.60	96.6

Table 11 (continued).

Core, section, interval (cm)	Depth (mbsf)	Inorganic carbon (%)	$CaCO_3$ (%)
58X-3, 143–145	547.83	11.47	95.5
58X-4, 138–140	549.28	11.50	95.8
59X-2, 124–126	555.74	11.38	94.8
59X-3, 107–109	557.07	11.48	95.6
59X-4, 135–137	558.85	11.50	95.8
60X-1, 11–13	562.71	11.45	95.4
60X-3, 38–40	565.98	11.46	95.5
60X-4, 72–74	567.82	11.48	95.6
61X-1, 97–99	573.27	11.16	93.0
61X-2, 111–113	574.91	11.21	93.4
61X-3, 121–123	576.51	11.36	94.6
61X-4, 145–147	578.25	11.24	93.6
61X-5, 143–145	579.73	11.00	91.6
61X-6, 92–94	580.72	11.12	92.6
62X-2, 113–115	584.53	10.80	90.0
62X-3, 100–102	585.90	11.37	94.7
62X-4, 96–98	587.36	11.01	91.7
62X-5, 88–90	588.78	11.24	93.6
63X-1, 110–112	592.70	11.28	94.0
63X-2, 32–34	593.42	11.25	93.7
63X-3, 32–34	594.92	11.11	92.5
63X-4, 59–61	596.69	11.08	92.3
63X-5, 46–48	598.06	11.22	93.5
64X-1, 9–11	601.39	11.22	93.5
64X-2, 109–111	603.89	10.76	89.6
64X-3, 124–126	605.54	10.99	91.5
64X-4, 81–83	606.61	10.94	91.1
64X-5, 59–61	607.89	10.99	91.5
65X-1, 67–69	611.67	10.94	91.1
65X-2, 62–64	613.12	10.89	90.7
65X-3, 73–75	614.73	11.12	92.6
65X-4, 65–67	616.15	11.02	91.8
65X-5, 52–54	617.52	10.80	90.0
66X-1, 85–87	621.45	11.34	94.5
66X-3, 79–81	624.39	10.94	91.1
66X-4, 85–87	625.95	11.08	92.3
67X-3, 92–94	634.22	11.02	91.8
68X-1, 105–107	640.95	11.20	93.3
68X-2, 111–113	642.51	11.56	96.3
68X-3, 105–107	643.95	10.96	91.3
68X-4, 89–91	645.29	11.09	92.4
70X-3, 60–62	662.80	11.13	92.7
70X-5, 70–72	665.90	11.14	92.8
71X-1, 126–128	670.16	11.12	92.6
71X-2, 123–125	671.63	11.19	93.2
71X-3, 109–111	672.99	11.19	93.2
71X-4, 112–114	674.52	11.28	94.0
71X-5, 108–110	675.98	11.34	94.5
72X-1, 74–76	678.94	10.84	90.3
72X-2, 66–68	680.36	11.22	93.5
72X-3, 78–80	681.98	10.93	91.0
72X-4, 67–69	683.37	8.87	73.9
73X-2, 90–92	690.20	11.32	94.3
73X-3, 86–88	691.66	11.22	93.5
73X-4, 80–82	693.10	10.93	91.0
73X-5, 75–77	694.55	11.28	94.0
73X-6, 35–37	695.65	10.48	87.3
74X-1, 62–64	698.12	11.01	91.7
74X-2, 59–61	699.59	11.33	94.4
74X-3, 63–65	701.13	11.29	94.0
75X-1, 73–75	707.93	11.33	94.4
75X-2, 86–88	709.56	11.46	95.5
75X-3, 72–74	710.92	11.39	94.9
75X-4, 83–85	712.53	11.18	93.1
76X-1, 94–96	717.84	11.09	92.4
76X-2, 120–122	719.60	11.09	92.4
76X-3, 114–116	721.04	11.08	92.3
76X-4, 95–97	722.35	11.19	93.[illegible]
76X-5, 82–84	723.72	11.26	93.8
77X-1, 83–85	727.33	11.24	93.6
77X-2, 105–107	729.05	11.10	92.5
77X-3, 78–80	730.28	11.06	92.1
77X-4, 75–77	731.75	11.14	92.8
77X-5, 73–75	733.23	11.22	93.5
78X-1, 110–112	737.30	11.18	93.1
78X-2, 88–90	738.58	11.00	91.6

Table 11 (continued).

Core, section, interval (cm)	Depth (mbsf)	Inorganic carbon (%)	$CaCO_3$ (%)
78X-3, 27–29	739.47	11.21	93.4
78X-4, 110–112	741.80	11.18	93.1
78X-5, 65–67	742.85	11.11	92.5
79X-1, 35–37	745.85	11.29	94.0
80X-1, 43–45	755.63	11.28	94.0
80X-2, 93–95	757.63	10.97	91.4
80X-3, 79–81	758.99	10.93	91.0
82X-2, 69–71	776.69	11.41	95.0
82X-3, 109–111	778.59	11.41	95.0
82X-4, 73–75	779.73	11.34	94.5
83X-2, 4–6	785.74	11.21	93.4
83X-3, 3–5	787.23	11.38	94.8
83X-4, 23–25	788.93	11.26	93.8
84X-1, 48–52	794.38	11.31	94.2
130-807C-			
2R-1, 35	790.05	11.40	95.0
2R-2, 26	791.46	11.53	96.1
4R-1, 51	809.51	11.40	95.0
4R-2, 66	811.16	10.86	90.5
6R-1, 91	829.21	11.39	94.9
6R-2, 92	830.72	11.34	94.5
6R-3, 91	832.21	11.12	92.7
6R-4, 91	833.71	11.34	94.5
6R-5, 80	835.10	11.16	93.0
9R-1, 21	857.61	11.00	91.7
12R-1, 26	876.86	11.40	95.0
15R-1, 17	894.07	11.30	94.2
16R-1, 58	899.48	11.00	91.7
17R-1, 31	904.21	11.04	92.0
17R-2, 48	905.88	11.11	92.6
18R-CC, 8	908.98	10.50	87.5
19R-1, 34	914.24	11.04	92.0
21R-1, 4	923.94	11.03	91.9
23R-1, 49	939.19	10.94	91.2
23R-2, 42	940.62	10.20	85.0
23R-3, 43	942.13	11.02	91.8
23R-4, 37	943.57	10.98	91.5
24R-1, 70	944.40	11.02	91.8
24R-2, 70	945.90	10.92	91.0
25R-1, 35	948.75	10.50	87.5
26R-1, 56	958.66	11.38	94.8
49R-1, 75	1150.95	11.77	98.1
50R-1, 71	1155.91	11.87	98.9
51R-1, 70	1160.90	11.83	98.6
51R-2, 67	1162.37	11.81	98.4
51R-3, 70	1163.90	11.82	98.5
52R-1, 82	1170.62	11.62	96.8
52R-2, 119	1172.49	11.64	97.0
52R-3, 31	1173.11	11.32	94.3
53R-1, 68	1180.08	11.51	95.9
53R-2, 74	1181.64	11.77	98.1
53R-3, 62	1183.02	11.69	97.4
53R-4, 122	1185.09	11.41	95.1
56R-1, 134	1207.94	11.58	96.5
56R-2, 140	1209.50	11.68	97.3
56R-3, 50	1210.10	11.46	95.5
57R-1, 115	1217.45	11.64	97.0
57R-2, 98	1218.78	11.65	97.1
58R-1, 10	1222.60	11.69	97.4
59R-1, 54	1232.74	11.70	97.5
59R-2, 68	1234.38	11.66	97.2
61R-1, 57	1252.07	11.66	97.2
61R-2, 89	1253.89	11.66	97.2
62R-1, 83	1262.03	11.64	97.0
62R-2, 63	1263.33	11.52	96.0
62R-3, 94	1265.14	11.48	95.7
63R-1, 28	1271.08	11.54	96.2
63R-2, 57	1272.87	11.62	96.8
63R-3, 90	1274.70	11.35	94.6
64R-1, 95	1281.45	11.57	96.4
64R-2, 70	1282.70	11.60	96.7
65R-1, 51	1290.61	11.59	96.6
65R-2, 41	1292.01	11.63	96.9
66R-1, 125	1301.05	11.59	96.6
66R-2, 73	1302.03	11.46	95.5

Table 11 (continued).

Core, section, interval (cm)	Depth (mbsf)	Inorganic carbon (%)	$CaCO_3$ (%)
66R-3, 85	1303.65	11.46	95.5
67R-1, 74	1310.24	11.52	96.0
67R-2, 111	1312.05	11.50	95.8
67R-3, 73	1313.17	11.50	95.8
67R-4, 66	1314.60	11.56	96.3
67R-5, 36	1315.80	11.47	95.6
68R-1, 67	1319.77	11.52	96.0
68R-2, 28	1320.88	11.46	95.5
68R-3, 58	1322.68	11.35	94.6
69R-2, 106	1331.36	11.58	96.5
69R-3, 3	1331.83	11.56	96.3
69R-4, 86	1334.16	11.52	96.0
69R-5, 15	1334.95	11.44	95.3
70R-1, 69	1339.09	11.56	96.3
70R-2, 108	1340.98	11.32	94.3
70R-3, 97	1342.37	11.56	96.3
70R-4, 52	1343.42	11.62	96.8
71R-1, 45	1348.45	11.16	93.0
71R-2, 130	1350.80	7.54	62.8
71R-3, 106	1352.06	0.036	0.3
71R-4, 59	1353.09	0.024	0.2
71R-5, 47	1354.47	0.036	0.3
71R-6, 27	1355.77	0.024	0.2
72R-2, 47	1359.67	0.024	0.2
73R-1, 67	1368.07	0.024	0.2
73R-2, 55	1369.45	0.024	0.2

Note: A description of the method for determining $CaCO_3$ can be found in the "Explanatory Notes" chapter (this volume).

"Physical Properties" section, "Site 803" chapter, this volume). Peak vane shear strength data are plotted vs. depth in Figure 48 for Holes 807A and 807B and are listed in Table 12.

As has been noted in the previous reports of vane shear strength data for Leg 130, the strength profiles are strongly influenced by the overprint of core-length cycles of disturbance. This problem is discussed in greater detail in the "Physical Properties" section of the "Site 803" chapter (this volume).

The peak vane shear strengths at Site 807 generally range from 5 to 20 kPa. The sediments at this site are predominantly silt-sized (see "Lithostratigraphy" section, this chapter), and shear strength is expected to be highly dependent on changes in grain size. However, shipboard grain size data were not routinely obtained near the vane test intervals, so the relationship between the two parameters is difficult to examine at present. Peak vane strengths increase below 240 mbsf in response to the onset of cementation.

Index Properties

Index properties samples were taken from split cores at those locations where the velocity measurements were made. Wet and dry weights and dry volumes of these samples were measured and used to calculate wet-bulk density, grain density, water content (based on dry weight), porosity, and dry-bulk density. The procedures and calculations used are outlined in the "Explanatory Notes" chapter (this volume). Table 13 presents the index properties data for the three holes at Site 807.

Figure 49 presents calcium carbonate content and grain density for Holes 807A and 807C. Carbonate content, measured on the dried index properties samples, is generally greater than 85%, as it was for other Leg 130 sites. Grain densities reflect this high carbonate content, with values near 2.7 g/cm³ for most of the recovered sediments. Grain density minima are generally correlated with minima in carbonate content. The association of low-carbonate content with low-grain density reflects the higher silica content of these samples (grain density of biogenic silica is 2.2 g/cm³). For example, the zone between 1000 and 1130 mbsf (chert-rich interval) shows a peak-to-peak correlation between carbonate content and grain density measurements performed over this interval. Between 1350 and 1370 mbsf, carbonate content decreases suddenly, corresponding to the presence of claystones in this interval. Grain density also decreases in this interval, reflecting an increase in radiolarian concentration.

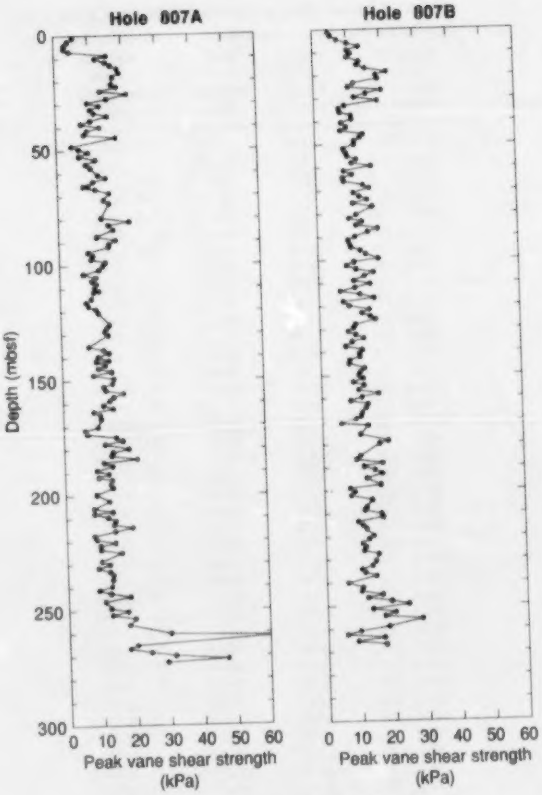

Figure 48. Shear strength vs. depth, Holes 807A and 807B.

Figure 50 presents wet-bulk density, porosity, and water content (calculated as a percentage of dry weight) vs. depth for Holes 807A and 807C. The ooze-chalk transition is located at approximately 290 mbsf, with interbedded ooze and chalk from about 250 to 290 mbsf (see "Lithostratigraphy" section, this chapter). In general, bulk density increases with depth (corresponding to decreases in porosity and water content) through the ooze and chalk sequences. From approximately 950 to 1150 mbsf, the interval of transition from ooze to limestone, the index properties change sharply. Large fluctuations in the index properties were observed and are probably a result of variations in the relative amounts of silica. From approximately 1180 to 1350 mbsf, in the interval containing limestones, bulk density decreases downhole (with corresponding increases of porosity and water content). The reason for this is not understood, at present. The downhole trend in the resistivity logging profile also reverses in this interval (see "Logging" section, this chapter). Finally, the abrupt change in the index properties below 1350 mbsf is caused by the

Table 12. Shear strength data, Holes 807A and 807B.

Core, section, interval (cm)	Depth (mbsf)	Peak shear strength (kPa)	Residual shear strength (kPa)
130-807A-			
1H-1, 120	1.20	5.6	1.12
1H-2, 135	2.85	4.0	1.12
1H-3, 135	4.35	3.1	0.67
1H-4, 135	5.85	2.9	0.45
1H-5, 110	7.10	4.5	0.90
2H-1, 136	8.76	15.5	6.96
2H-2, 135	10.25	12.1	4.72
2H-3, 135	11.75	15.1	5.17
2H-4, 135	13.25	16.7	7.41
2H-5, 110	14.50	18.6	
2H-6, 136	16.26	19.1	7.64
3H-1, 135	18.25	17.2	7.64
3H-3, 136	21.26	16.8	
3H-4, 114	22.54	18.3	8.31
3H-5, 135	24.25	13.3	
3H-6, 132	25.72	21.3	12.80
4H-1, 135	27.75	15.3	6.07
4H-2, 135	29.25	9.4	3.82
4H-3, 135	30.75	13.0	
4H-4, 135	32.25	10.3	
4H-5, 135	33.75	11.3	4.72
4H-6, 136	35.26	15.3	
5H-1, 120	37.10	10.3	
5H-2, 116	38.56	7.4	2.81
5H-3, 117	40.07	13.0	4.27
5H-4, 119	41.59	9.1	2.02
5H-5, 119	43.09	8.2	1.17
5H-6, 119	44.59	17.7	
6H-2, 118	48.08	4.5	0.34
6H-3, 120	49.60	6.7	
6H-4, 100	50.90	9.3	2.92
6H-5, 120	52.60	6.7	1.35
6H-6, 120	54.10	11.5	3.82
7H-1, 120	56.10	8.5	2.92
7H-2, 120	57.60	9.9	2.47
7H-4, 120	60.60	12.1	4.04
7H-5, 120	62.10	14.4	6.29
7H-6, 120	63.60	10.6	4.27
8H-1, 119	65.59	9.0	2.02
8H-1, 122	65.62	7.6	3.15
8H-2, 120	67.10	11.2	
8H-3, 122	68.62	15.3	6.51
8H-5, 122	71.62	13.5	3.59
8H-6, 117	73.07	15.1	3.59
9H-4, 100	79.40	12.8	4.27
9H-5, 120	81.10	21.1	6.74
9H-6, 120	82.60	14.8	4.72
10H-1, 120	84.60	16.2	
10H-3, 120	87.60	11.2	3.15
10H-4, 120	89.10	16.8	6.07
10H-5, 120	90.60	14.8	5.62
10H-6, 120	92.10	14.6	
11H-1, 135	94.25	8.5	1.80
11H-2, 135	95.75	9.9	2.25
11H-3, 135	97.25	9.4	1.80
11H-4, 135	98.75	13.7	3.15
11H-5, 130	100.20	12.8	
11H-6, 137	101.77	11.7	3.48
12H-1, 135	103.75	7.0	
12H-2, 135	105.25	10.8	2.92
12H-3, 135	106.75	9.4	2.47
12H-4, 115	108.05	10.8	2.92
12H-5, 131	109.71	10.3	3.59
12H-6, 121	111.11	11.5	
12H-7, 21	111.61	9.9	3.37
13H-2, 113	114.53	9.2	2.70
13H-3, 120	116.10	7.6	2.47
13H-4, 135	117.75	8.3	2.02
13H-5, 113	119.03	10.4	3.59
13H-6, 121	120.61	11.2	3.37
14H-3, 135	125.75	14.4	5.17
14H-4, 135	127.25	13.5	4.27
14H-5, 141	128.81	12.9	3.15
14H-6, 140	130.30	13.9	4.27
15H-3, 136	135.26	8.0	1.80
15H-4, 136	136.76	12.4	2.92
15H-5, 115	138.05	14.0	6.51
15H-6, 136	139.76	10.8	2.47
15H-7, 140	141.30	13.9	3.82
16H-1, 135	141.75	10.1	1.12
16H-2, 139	143.29	12.8	2.70
16H-3, 140	144.80	10.8	2.47
16H-4, 136	146.26	14.6	3.15
16H-5, 136	147.76	9.2	2.70
16H-6, 136	149.26	15.3	4.72
17H-1, 136	151.26	14.8	6.74
17H-2, 135	152.75	12.1	
17H-3, 136	154.26	12.8	6.29
17H-4, 136	155.76	18.0	8.09
17H-5, 134	157.24	15.1	4.72
17H-6, 135	158.75	13.9	
18H-1, 135	160.75	11.9	
18H-2, 135	162.25	14.8	3.82
18H-3, 135	163.75	9.0	
18H-4, 116	165.06	11.0	4.04
18H-5, 135	166.75	11.2	2.47
19H-1, 135	170.25	10.2	2.70
19H-2, 135	171.75	6.3	
19H-3, 135	173.25	7.0	1.57
19H-4, 136	174.76	15.5	3.59
19H-5, 135	176.25	17.5	
19H-6, 135	177.75	12.1	5.17
20H-1, 136	179.76	19.1	
20H-2, 135	181.25	14.5	
20H-3, 135	182.75	13.9	
20H-4, 135	184.25	21.6	10.11
20H-5, 135	185.75	11.7	3.37
20H-6, 135	187.25	14.2	6.29
21H-1, 122	189.12	9.5	2.47
21H-2, 123	190.63	13.0	3.82
21H-3, 122	192.12	9.9	3.15
21H-4, 110	193.50	14.0	
21H-5, 115	195.05	13.5	
21H-6, 121	196.61	14.2	
22H-1, 124	199.64	9.2	
22H-3, 121	202.61	13.0	
22H-5, 120	205.60	8.3	
22H-6, 125	207.15	13.8	
23H-1, 112	208.02	8.4	
23H-2, 123	209.63	12.4	
23H-3, 125	211.15	14.6	
23H-4, 130	212.70	14.2	
23H-5, 125	214.15	19.7	
23H-6, 122	215.62	14.4	
24H-1, 120	217.60	8.2	
24H-2, 120	219.10	8.8	
24H-3, 120	220.60	14.4	
24H-4, 100	221.90	9.9	
24H-5, 120	223.60	10.1	
24H-6, 120	225.10	16.2	
25H-2, 120	228.60	10.2	
25H-3, 120	230.10	12.6	
25H-4, 120	231.60	9.2	
25H-5, 120	233.10	12.6	
25H-6, 120	234.60	13.5	
26H-1, 120	236.60	13.4	
26H-3, 120	239.60	13.0	
26H-4, 120	241.10	9.2	
26H-5, 120	242.60	12.6	
26H-6, 120	244.10	18.4	
27H-1, 120	246.10	11.0	
27H-3, 120	249.10	12.6	
27H-4, 100	250.40	17.7	
27H-5, 120	252.10	13.0	
27H-6, 120	253.60	19.8	
28X-2, 39	256.29	18.0	
28X-4, 135	260.25	30.3	
28X-5, 119	261.59	64.0	

Table 12 (continued).

Core, section, interval (cm)	Depth (mbsf)	Peak shear strength (kPa)	Residual shear strength (kPa)
29X-1, 120	265.30	20.2	
29X-2, 126	266.86	18.0	
29X-3, 125	268.35	24.3	
29X-4, 133	269.93	31.5	
29X-5, 116	271.26	47.2	
29X-6, 123	272.83	29.2	
130-807B-			
1H-1, 120	1.20	4.7	
1H-2, 120	2.70	5.4	
2H-1, 120	4.30	7.2	
2H-2, 120	5.80	10.3	
2H-3, 120	7.30	13.7	
2H-4, 120	8.80	10.2	
2H-5, 120	10.30	11.2	
2H-6, 120	11.80	10.1	
3H-1, 120	13.80	13.7	
3H-2, 120	15.30	13.1	
3H-3, 120	16.80	15.5	
3H-4, 120	18.30	21.8	
3H-5, 120	19.80	18.6	
3H-6, 120	21.30	19.1	
4H-1, 120	23.30	11.9	
4H-2, 130	24.90	10.3	
4H-3, 130	26.40	20.2	
4H-4, 120	27.80	15.5	
4H-5, 120	29.30	12.0	
4H-6, 120	30.80	18.9	
5H-1, 120	32.80	9.0	
5H-2, 120	34.30	7.2	
5H-3, 120	35.80	7.6	
5H-4, 120	37.30	11.0	
5H-5, 120	38.80	11.1	
5H-6, 120	40.30	7.9	
6H-1, 120	42.30	9.4	
6H-2, 120	43.80	7.6	
6H-3, 120	45.30	14.4	
6H-4, 120	46.80	13.4	
6H-5, 120	48.30	11.7	
6H-6, 120	49.80	11.6	
7H-1, 120	51.80	8.3	
7H-2, 120	53.30	9.0	
7H-3, 120	54.80	9.5	
7H-4, 120	56.30	12.1	
7H-5, 120	57.80	10.8	
7H-6, 120	59.30	16.5	
8H-1, 120	61.30	8.3	
8H-2, 120	62.80	10.7	
8H-3, 120	64.30	7.9	
8H-4, 120	65.80	8.2	
8H-5, 120	67.30	13.9	
8H-6, 120	68.80	15.7	
9H-1, 120	70.80	11.0	
9H-2, 120	72.30	12.8	
9H-3, 120	73.80	15.1	
9H-4, 120	75.30	10.8	
9H-5, 120	76.80	16.5	
10H-1, 120	80.30	11.7	
10H-2, 120	81.80	9.4	
10H-3, 120	83.30	13.2	
10H-4, 120	84.80	11.5	
10H-5, 120	86.30	18.0	
10H-6, 120	87.80	14.9	
11H-1, 120	89.80	11.1	
11H-2, 120	91.30	9.0	
11H-3, 120	92.80	9.4	
11H-4, 120	94.30	9.8	
11H-5, 120	95.80	12.6	
11H-6, 120	97.30	14.2	
12H-1, 120	99.30	17.9	
12H-2, 120	100.80	10.6	
12H-3, 120	102.30	8.3	
12H-4, 120	103.80	11.2	
12H-5, 120	105.30	16.4	
12H-6, 120	106.80	13.6	

Table 12 (continued).

Core, section, interval (cm)	Depth (mbsf)	Peak shear strength (kPa)	Residual shear strength (kPa)
13H-1, 122	108.82	10.4	
13H-2, 116	110.26	15.3	
13H-3, 120	111.80	10.7	
13H-4, 125	113.35	6.3	
13H-5, 128	114.88	12.2	
13H-6, 120	116.30	16.4	
13H-7, 125	117.85	7.1	
14H-2, 118	119.78	8.8	
14H-3, 118	121.28	14.8	
14H-4, 128	122.88	12.6	
14H-5, 113	124.23	15.1	
14H-6, 116	125.76	16.7	
15H-1, 120	127.80	10.6	
15H-2, 120	129.30	9.9	
15H-3, 120	130.80	8.3	
15H-4, 120	132.30	10.6	
15H-5, 120	133.80	13.0	
15H-6, 120	135.30	9.5	
16H-1, 120	137.30	7.4	
16H-2, 120	138.80	12.4	
16H-3, 120	140.30	11.5	
16H-4, 120	141.80	11.7	
16H-5, 120	143.30	8.5	
16H-6, 120	144.80	8.3	
17H-1, 120	146.80	13.0	
17H-2, 120	148.30	11.7	
17H-3, 120	149.80	11.2	
17H-4, 120	151.30	12.4	
17H-5, 120	152.80	9.4	
17H-6, 120	154.30	12.6	
18H-1, 121	156.31	11.0	
18H-2, 124	157.84	17.0	
18H-3, 123	159.33	11.9	
18H-4, 135	160.95	8.5	
18H-5, 135	162.45	13.7	
18H-6, 134	163.94	13.1	
19H-1, 135	165.95	11.9	
19H-2, 135	167.45	11.6	
19H-3, 135	168.95	10.0	
19H-4, 135	170.45	5.6	
19H-5, 108	171.68	13.5	
20H-1, 135	175.45	11.2	
20H-3, 123	178.33	19.5	
20H-4, 89	179.49	16.8	
21H-1, 135	184.95	11.0	
21H-2, 135	186.45	9.7	
21H-3, 135	187.95	17.6	
21H-4, 135	189.45	11.9	
21H-5, 135	190.95	15.2	
21H-6, 135	192.45	17.5	
22H-1, 135	194.45	12.8	
22H-3, 135	197.45	16.8	
22H-4, 135	198.95	7.6	
22H-5, 135	200.45	9.0	
22H-6, 135	201.95	7.9	
23H-1, 137	203.97	14.2	
23H-3, 135	206.95	12.4	
23H-4, 135	208.45	11.8	
23H-5, 135	209.95	16.8	
23H-6, 135	211.45	17.3	
24H-1, 135	213.45	9.8	
24H-2, 135	214.95	11.2	
24H-3, 135	216.45	12.2	
24H-5, 135	219.45	14.3	
24H-6, 135	220.95	12.9	
25H-1, 135	222.95	11.0	
25H-2, 135	224.45	12.0	
25H-3, 142	226.02	11.3	
25H-4, 140	227.50	15.7	
25H-6, 140	230.50	14.8	
26H-1, 140	232.50	13.7	
26H-2, 140	234.00	10.6	
26H-3, 130	235.40	11.5	
26H-4, 140	237.00	14.8	
26H-6, 138	239.98	6.3	

Table 12 (continued).

Core, section, interval (cm)	Depth (mbsf)	Peak shear strength (kPa)	Residual shear strength (kPa)
27H-1, 140	242.00	10.8	
27H-2, 140	243.50	10.3	
27H-3, 140	245.00	16.6	
27H-4, 140	246.50	12.1	
27H-5, 137	247.97	19.1	
27H-6, 128	249.38	24.3	
28H-1, 128	251.38	13.5	
28H-2, 124	252.84	20.2	
28H-3, 124	254.34	17.1	
28H-4, 115	255.75	28.3	
28H-6, 136	258.96	18.2	
29H-1, 120	260.80	9.7	
29H-2, 120	262.30	5.8	
29H-3, 120	263.80	16.8	
29H-4, 120	265.30	8.8	
29H-5, 120	266.80	17.3	

occurrence of claystones with radiolarites. No index property measurements were obtained on the basalt.

Figure 51 presents wet-bulk density data vs. depth for the upper 350 m in Holes 807A and 807B. In general, these profiles are similar to those observed at the other sites of Leg 130 within carbonate ooze. They are characterized by a general increase with depth. Bulk density increases sharply in the upper 20 m of the sediment column. A slight decrease in bulk density over the next 30 m corresponds to a sharp decrease in mean grain size over this interval (see "Lithostratigraphy" section, this chapter). Below this anomalous section, bulk density increases with depth, to values near 1.65 g/cm^3 at approximately 200 mbsf. From 200 to approximately 260 mbsf, bulk density decreases. This decrease corresponds to a notable decrease in carbonate content over this interval. Similar decreases were observed at other Leg 130 sites, although at slightly different depths in the sediment column.

P-wave Velocity

Horizontal (parallel to bedding) and vertical (perpendicular to bedding) *P*-wave velocities were measured at Site 807. Velocity measurements were performed with the digital sound velocimeter (DSV) and the Hamilton Frame, depending on the degree of lithification. In Hole 807A, the DSV apparatus was replaced by the Hamilton Frame at approximately 275 mbsf, slightly above the ooze-chalk transition at 290 mbsf (see "Lithostratigraphy" section, this chapter). The DSV apparatus was used in all cores from Hole 807B that contained ooze, and the Hamilton Frame was used on all cores from Hole 807C. Results of the velocity analyses are given in Table 14. Figure 52 shows the changes of velocity with depth at Site 807 (merged data sets from Hole 807A and 807C). Figure 53 shows changes of velocity in Holes 807A and 807B in the uppermost 350 mbsf. Table 14 is on microfiche (back pocket).

Velocity measured at Site 807 ranges from 1530 m/s (calcareous ooze) to 5500 m/s (basalt). Velocity values generally increase with depth, although there are major changes in the velocity-depth gradient. There are also intervals of anomalously low (or high) values that reflect major lithologic changes.

In the ooze, horizontal velocity values are usually higher than vertical velocity values (Fig. 53). This may result from anisotropy in the sediment fabric, or from the opening of fine cracks parallel to bedding that result from the release of overburden pressure during core recovery. These fine cracks would tend to reduce *P*-wave propagation in a vertical direction. In the indurated sediment section at Site 807, beginning at the ooze-chalk transition (around 290 mbsf), anisotropy is reversed, with vertical velocities usually higher than horizontal velocities (Figs. 52 and 53). The reason for this anisotropy in lithified sediment is, as yet, unknown.

In the uppermost 100 mbsf, velocities do not change much, with values averaging 1560 m/s. The low velocities measured between 103 and 117 mbsf in Hole 807A (Fig. 53) are probably a result of improper DSV calibration and will be corrected on shore.

Between 100 and approximately 300 mbsf, velocity increases slowly but continuously with depth (Fig. 53), with values ranging from about 1580 m/s at 100 mbsf to 1650 m/s at 300 mbsf. This increase in velocity presumably reflects the increase of sediment consolidation and the onset of cementation in this interval. The first visible effect of cementation on lithology is the occurrence, below 250 mbsf, of chalk "biscuits" interspersed in the soft ooze. The ooze-chalk transition occurs at about 290 mbsf (see "Lithostratigraphy" section, this chapter). Anomalously low velocity values recorded between 275 and 286 mbsf correspond to the first measurements made with the Hamilton Frame. The sediment in this interval is weakly cemented and fractures easily when inserted between the Hamilton Frame transducers, thus affecting *P*-wave propagation.

Between 300 and approximately 1000 mbsf, velocity increases at a greater rate than in the previous interval. The general trend is linear, with extreme velocity values ranging from 1650 m/s at 300 mbsf to about 2000 m/s at 1000 mbsf. Two zones of generally higher velocity values are superimposed on this depth trend; one between 400 and 500 mbsf, and the other between approximately 620 and 780 mbsf. The interval between 300 and 1000 mbsf roughly corresponds to Subunit IB (chalk interval) (see "Lithostratigraphy" section, this chapter). The velocity increase over this interval is probably caused by the progressive induration of chalk. The two zones of higher velocity values presumably reflect local increases of this induration.

Because of poor recovery in the interval between 970 and 1100 mbsf (see "Lithostratigraphy" section, this chapter), velocity data are sparse. *P*-wave velocities generally increase between 1000 and 1100 mbsf (Fig. 52). Below 1100 mbsf, velocities are highly variable (Fig. 52). The interval between 1100 and 1350 mbsf is divided into two zones of different velocities, even though there is no major lithologic difference in this interval (limestone Subunit IIB; see "Lithostratigraphy" section, this chapter). Velocities average 4100 m/s, but are highly variable, between 1100 and 1240 mbsf. Velocities decrease rapidly at 1240 mbsf, and between 1250 and 1350 mbsf they average 3500 m/s, also with large fluctuations.

The claystone interval between 1350 and 1370 mbsf is marked by an interval of low velocity (around 2000 m/s). Basalt drilled at the bottom of Hole 807C leads to a drastic increase in the velocity profile, with values reaching 5200 m/s at 1400 mbsf.

IGNEOUS PETROLOGY

Introduction

Igneous basement was reached at 1379.7 mbsf in Hole 807C (Section 130-807C-74R-1). Basement coring continued for 149.7 m until drilling ceased at 1528.4 mbsf (Section 130-807C-93R-3); average recovery was 60.2%. The basement rocks are predominantly tholeiitic basalts (Albian-Aptian? in age), consisting of both pillow and massive lavas, the latter mostly <3 m thick but including one 28-m-thick flow. In addition, two thin sedimentary horizons were cored and partially recovered: (1) an Aptian(?) limestone and tuff and (2) a soft, yellow-brown, smectite-rich limestone (Intervals 130-807C-80R-1, 70–120 cm, and -82R-3, 72–79 cm, respectively). Well-logging information indicates that there is a third sedimentary bed between these two that was not recovered (see "Logging" section, this chapter).

We have divided the basalts into five main stratigraphic subunits based on (1) the two recovered inter-lava sedimentary layers, themselves designated as basement Subunits B and D, and (2) the pronounced change in flow character between the thick, massive lava (Subunit F) and the flow packets above and below it, which are dominated by thin massive flows and pillows (Fig. 54). All the basalts are very fine grained to fine grained, nonvesicular, hypocrystalline, and aphyric to sparsely phyric. Subunit A rocks are characterized by rare phenocrysts of plagioclase as much as 3 mm in length, superficially similar to the lavas at Site 803; whereas basalts of the lower subunits (C, E, F, and G) have small (<1 mm wide), euhedral to subhedral, olivine microphenocrysts that are generally replaced with green or black clays.

Remarkably, in view of their age, most of the rocks are altered only slightly, and alteration rarely exceeds a moderate level. For the most part, alteration is restricted to the vicinity of veins, most of which are small (<5 mm thick) and filled with clays or calcite. Several thicker veins (up to 7 cm thick) of dark blue, blue-green, or brown clays and iron oxides or hydroxides are present, particularly in Sections 130-807C-88R-3 and -88R-4; similar, but much thinner, veins occur elsewhere. These veins appear to record the passage of hydrothermal fluids derived from greater depths. Two fragments of what appear to be chertified basalt were found in association with these veins. Small (1 mm long) blebs of metallic copper were identified in Section 130-807C-82R-2 at 40 and 58 cm. Several 2- to 5-cm-thick green or yellow-brown veins (containing celadonite, smectite, chert, and/or calcite) also were encountered; these may represent thin, baked, inter-lava sediment layers when they occur between glassy pillow rims or breccias (Intervals 130-807C-88R-3, 7–12 cm; -89R-1, 143–150 cm, and -88R-4, 95–103 cm) or sediment injected into fractures in the basalts (Interval 130-807C-83R-6, 78–86 cm).

A summary of the main features of the igneous stratigraphic subunits is given below. Sedimentary Subunits B and D are described in the "Lithostratigraphy" section (this chapter). Based on the presence of chilled glassy rinds, each of the basaltic subunits - except for Subunit F - is composed of multiple cooling "units" comparable with the fine-scale basement subdivisions at Site 803. Some of these cooling "units" probably represent individual eruptions, particularly the thicker massive flows; others undoubtedly are merely local sheets and pillows comprising parts of larger eruptions. Detailed visual core descriptions are appended at the end of this volume.

Summary of Igneous Subunits

Subunit A: 46 m thick (Sections 130-807C-74R-1, 25 cm, to -80R-1, 70 cm); contains at least 35 glass-bounded pillows and thin massive cooling "units" or subdivisions (<2 m thick); all aphyric, very fine-grained basalt with rare euhedral plagioclase phenocrysts up to 3 mm long; superficially similar to Site 803 basalts.

Subunit C: 16 m thick (Sections 130-807C-80R-1, 120 cm, to -82R-3, 70 cm); pillow lavas and thin massive flows (<3 m thick) forming at least 9 cooling "units"; aphyric, very fine-grained to fine-grained basalt with sparse euhedral to subhedral olivine microphenocrysts (0.2–1 mm across) that are largely replaced by green and black clays.

Subunit E: 5 m thick (Sections 130-807C-82R-3, 79 cm, to -82R-6, 120 cm); mineralogically and morphologically like Subunit C; contains at least 6 glass-rimmed cooling "units" or subdivisions.

Subunit F: 28 m thick (Sections 130-807C-82R-6, 120 cm, to -85R-7, 125 cm); a single massive flow, very fine-grained at its glassy top and bottom, and fine-grained in the interior; similar to Subunits C and E mineralogically.

Subunit G: 53 m thick (Sections 130-807C-85R-7, 125 cm, to -93R-3, 55 cm); like Subunits C and E morphologically and mineralogically; contains at least 34 cooling "units" or subdivisions, which tend to be slightly thicker (up to 3 m thick) with increasing depth; well-log gamma-ray results suggest that a second thick flow may lie beneath this subunit only slightly below the bottom of the hole (see "Logging" section, this chapter).

Petrography

Shipboard thin-section studies of representative samples from each subunit emphasized the comparatively mild degree of alteration in these basalts, and the general paucity of phenocrysts (detailed visual core descriptions are attached at the end of this volume). Textures are intersertal to intergranular, with minor subophitic patches. Groundmasses are fairly fresh, though glass largely has been replaced with dark cryptocrystalline material, probably mainly smectite. In addition to the altered olivine microphenocrysts already mentioned, Subunits C, E, F, and G contain rare, fresh plagioclase and clinopyroxene microphenocrysts. Unlike Subunit A, however, larger phenocrysts are essentially absent in the 103 m of the lower basement sequence.

Shore-based Chemical Analyses of Shipboard Samples

Because the shipboard X-ray fluorescence (XRF) spectrometer was inoperable by the time the ship reached Site 807, chemical analyses were done onshore at the University of Keele, following standard methods (e.g., Floyd, 1986). What follows is a very preliminary report of the data. Nineteen samples representing all subunits but "E" were analyzed for major and trace elements by XRF; water loss on ignition (LOI) was determined gravimetrically. The results are listed in Table 15.

The fresher condition of the Site 807 lavas as compared with those at Site 803 is reflected in their lower LOI values (<0.67 vs. 1.19–3.17 wt%). Like the Site 803 basalts, the Site 807 basalts are somewhat evolved tholeiites, but they have slightly higher average Mg contents (7.3 vs. 6.0 wt%). Four are mildly quartz-normative; three of these are from Subunit A and the lower subunits. The former is characterized by somewhat lower MgO and SiO_2 concentrations; higher Na_2O, TiO_2, and Y values; and markedly higher Sr and Zr concentrations than the lower subunits (see Table 15 and Fig. 55). Likewise, ratios of Ti/Zr (96–99) and Zr/Y (3.2–3.4) for Subunit A are, respectively, slightly greater than for the lower subunits (102–107 and 2.6–3.0), although all values are within the range exhibited by normal MORB.

K_2O and Rb concentrations are higher in Subunit A, but the largest K_2O value (0.63 wt%) was observed in Subunit C. Several of the samples from Subunits F and G have very low K_2O contents (0.03–0.06 wt%), values that are at the very low end of the spectrum for normal MORB. Similar basalts were found on the Manihiki Plateau (Jackson et al., 1976), in the Nauru Basin to the east of Site 807 (e.g., Floyd, 1986), and on the island of Malaita and Santa Isabel at the western edge of the Ontong Java Plateau (J. Mahoney, unpubl. data, 1989).

Chemical variations within individual subunits generally appear to be smaller than in the single stratigraphic subunit

Table 13. Index properties data, Site 807.

Core, section, interval (cm)	Depth (mbsf)	Wet-bulk density (g/cm^3)	Grain density (g/cm^3)	Water content (% dry wt)	Porosity (%)	Dry-bulk density (g/cm^3)
130-807A-						
1H-1, 95	0.95	1.52	2.65	87.3	69.1	0.81
1H-2, 8	1.58	1.51	2.67	89.4	69.7	0.80
1H-2, 94	2.44	1.47	2.67	100.3	72.1	0.74
1H-3, 13	3.13	1.51	2.67	90.9	70.1	0.79
1H-3, 93	3.93	1.48	2.66	97.8	71.5	0.75
1H-4, 14	4.64	1.54	2.70	83.9	68.6	0.84
1H-4, 94	5.44	1.56	2.71	79.8	67.6	0.87
1H-5, 13	6.13	1.52	2.69	90.0	70.1	0.80
1H-5, 95	6.95	1.48	2.68	100.0	72.1	0.74
2H-1, 94	8.34	1.54	2.67	81.8	67.8	0.85
2H-2, 14	9.04	1.53	2.65	84.2	68.3	0.83
2H-2, 94	9.84	1.52	2.70	88.0	69.6	0.81
2H-3, 14	10.54	1.53	2.69	85.9	69.1	0.82
2H-4, 14	12.04	1.54	2.72	84.2	68.9	0.84
2H-4, 94	12.84	1.55	2.65	80.4	67.3	0.86
2H-5, 14	13.54	1.53	2.69	86.3	69.2	0.82
2H-5, 94	14.34	1.53	2.65	83.8	68.3	0.83
2H-6, 14	15.04	1.55	2.68	82.0	68.0	0.85
2H-6, 94	15.84	1.53	2.62	83.9	68.0	0.83
2H-7, 14	16.54	1.52	2.70	88.6	69.8	0.81
3H-1, 94	17.84	1.55	2.71	81.6	68.1	0.85
3H-2, 15	18.55	1.56	2.73	81.9	68.4	0.86
3H-2, 95	19.35	1.50	2.67	92.7	70.5	0.78
3H-3, 14	20.04	1.52	2.67	87.3	69.3	0.81
3H-3, 95	20.85	1.56	2.68	78.3	67.0	0.88
3H-4, 21	21.61	1.58	2.68	74.8	66.0	0.90
3H-4, 84	22.24	1.55	2.73	83.1	68.7	0.85
3H-5, 14	23.04	1.55	2.68	80.8	67.7	0.86
3H-5, 96	23.86	1.58	2.70	75.1	66.3	0.90
3H-6, 15	24.55	1.55	2.67	80.9	67.6	0.86
3H-6, 95	25.35	1.54	2.68	83.8	68.4	0.84
3H-7, 24	26.14	1.54	2.71	85.8	69.2	0.83
4H-1, 94	27.34	1.53	2.69	86.7	69.2	0.82
4H-2, 15	28.05	1.57	2.68	77.0	66.6	0.89
4H-2, 94	28.84	1.56	2.70	78.9	67.3	0.87
4H-3, 95	30.35	1.52	2.67	89.0	69.7	0.80
4H-3, 95	30.35	1.50	2.70	94.1	71.0	0.77
4H-4, 15	31.05	1.51	2.68	91.9	70.4	0.78
4H-4, 95	31.85	1.51	2.68	91.7	70.4	0.79
4H-5, 14	32.54	1.54	2.71	85.7	69.2	0.83
4H-5, 95	33.35	1.54	2.68	84.0	68.5	0.84
4H-6, 15	34.05	1.55	2.72	82.1	68.3	0.85
4H-6, 95	34.85	1.53	2.68	84.6	68.7	0.83
4H-7, 30	35.70	1.56	2.71	80.9	68.0	0.86
5H-1, 108	36.98	1.52	2.68	87.4	69.3	0.81
5H-2, 35	37.75	1.52	2.67	89.1	69.7	0.80
5H-2, 109	38.49	1.55	2.66	81.2	67.6	0.85
5H-3, 40	39.30	1.55	2.68	82.3	68.1	0.85
5H-3, 108	39.98	1.57	2.68	78.0	66.9	0.88
5H-4, 39	40.79	1.56	2.69	78.4	67.1	0.88
5H-4, 108	41.48	1.55	2.68	80.6	67.6	0.86
5H-5, 39	42.29	1.53	2.70	87.5	69.6	0.81
5H-5, 108	42.98	1.53	2.65	84.3	68.3	0.83
5H-6, 40	43.80	1.53	2.67	85.6	68.9	0.82
5H-6, 108	44.48	1.51	2.66	90.5	69.9	0.79
5H-7, 29	45.19	1.52	2.66	87.9	69.3	0.81
6H-2, 33	47.23	1.53	2.69	86.3	69.2	0.82
6H-3, 35	48.75	1.54	2.71	84.2	68.8	0.84
6H-3, 110	49.50	1.56	2.66	77.7	66.6	0.88
6H-4, 35	50.25	1.54	2.73	86.7	69.5	0.82
6H-4, 109	50.99	1.53	2.65	85.0	68.5	0.83
6H-5, 35	51.75	1.55	2.69	81.4	67.9	0.85
6H-5, 110	52.50	1.53	2.66	84.0	68.4	0.83
6H-6, 35	53.25	1.55	2.68	80.9	67.7	0.86
6H-6, 109	53.99	1.54	2.72	85.7	69.2	0.83
7H-1, 108	55.98	1.55	2.68	80.1	67.5	0.86
7H-2, 33	56.73	1.52	2.68	88.5	69.6	0.81
7H-2, 108	57.48	1.53	2.68	84.9	68.7	0.83
7H-3, 33	58.23	1.52	2.66	86.5	69.0	0.82
7H-3, 108	58.98	1.52	2.65	86.4	68.9	0.82
7H-4, 33	59.73	1.53	2.67	86.1	69.0	0.82
7H-4, 110	60.50	1.55	2.68	81.3	67.8	0.85
7H-5, 33	61.23	1.55	2.66	81.0	67.6	0.86
7H-5, 110	62.00	1.54	2.67	83.8	68.4	0.84

Table 13 (continued).

Core, section, interval (cm)	Depth (mbsf)	Wet-bulk density (g/cm^3)	Grain density (g/ cm^3)	Water content (% dry wt)	Porosity (%)	Dry-bulk density (g/cm^3)
7H-6, 33	62.73	1.53	2.67	86.1	69.0	0.82
7H-6, 108	63.48	1.54	2.71	84.5	68.9	0.83
8H-1, 107	65.47	1.54	2.65	82.1	67.8	0.85
8H-2, 34	66.24	1.55	2.64	79.2	66.9	0.87
8H-2, 110	67.00	1.53	2.66	85.2	68.6	0.83
8H-3, 33	67.73	1.54	2.70	83.2	68.4	0.84
8H-3, 110	68.50	1.54	2.66	82.7	68.0	0.84
8H-4, 42	69.32	1.53	2.67	84.7	68.6	0.83
8H-4, 110	70.00	1.54	2.68	84.3	68.6	0.83
8H-5, 39	70.79	1.54	2.67	82.5	68.1	0.85
8H-5, 110	71.50	1.56	2.71	80.7	67.9	0.86
8H-6, 39	72.29	1.56	2.68	79.2	67.3	0.87
8H-6, 100	72.90	1.52	2.66	88.4	69.4	0.80
8H-7, 34	73.74	1.54	2.68	84.0	68.5	0.84
9H-1, 33	74.23	1.56	2.69	79.2	67.3	0.87
9H-1, 108	74.98	1.58	2.70	75.0	66.2	0.90
9H-2, 33	75.73	1.58	2.68	75.0	66.0	0.90
9H-2, 108	76.48	1.58	2.69	74.7	66.0	0.91
9H-3, 33	77.23	1.54	2.68	82.6	68.1	0.85
9H-3, 108	77.98	1.60	2.68	71.3	64.9	0.93
9H-4, 33	78.73	1.52	2.62	86.4	68.6	0.81
9H-4, 108	79.48	1.54	2.66	82.3	67.9	0.85
9H-5, 33	80.23	1.55	2.67	81.0	67.6	0.86
9H-5, 108	80.98	1.59	2.69	73.3	65.6	0.92
9H-6, 33	81.73	1.56	2.68	78.9	67.1	0.87
9H-6, 108	82.48	1.55	2.67	81.7	67.8	0.85
10H-1, 108	84.48	1.58	2.70	76.5	66.6	0.89
10H-2, 108	85.98	1.54	2.70	84.3	68.8	0.84
10H-3, 108	87.48	1.56	2.67	78.5	67.0	0.87
10H-5, 108	90.48	1.60	2.69	70.9	64.9	0.94
10H-6, 108	91.98	1.57	2.69	78.1	67.0	0.88
11H-1, 106	93.96	1.56	2.66	77.7	66.7	0.88
11H-2, 107	95.47	1.57	2.64	74.4	65.5	0.90
11H-3, 107	96.97	1.54	2.69	82.8	68.3	0.84
11H-4, 107	98.47	1.58	2.66	74.6	65.7	0.90
11H-5, 107	99.97	1.55	2.66	79.3	67.1	0.87
11H-6, 107	101.47	1.58	2.67	73.5	65.5	0.91
12H-1, 106	103.46	1.60	2.70	70.8	64.9	0.94
12H-2, 107	104.97	1.59	2.68	71.9	65.1	0.93
12H-3, 106	106.46	1.61	2.69	69.5	64.4	0.95
12H-5, 106	109.46	1.58	2.69	74.8	66.1	0.90
12H-6, 106	110.96	1.58	2.67	73.7	65.5	0.91
13H-2, 106	114.46	1.59	2.69	72.7	65.4	0.92
13H-3, 106	115.96	1.59	2.70	72.9	65.5	0.92
13H-4, 106	117.46	1.61	2.69	69.6	64.5	0.95
13H-5, 106	118.96	1.60	2.70	72.1	65.3	0.93
13H-6, 106	120.46	1.59	2.71	73.7	65.9	0.92
14H-3, 31	124.71	1.62	2.71	68.5	64.3	0.96
14H-3, 108	125.48	1.59	2.71	73.1	65.7	0.92
14H-4, 30	126.20	1.61	2.72	69.5	64.6	0.95
14H-4, 108	126.98	1.62	2.73	70.0	64.9	0.95
14H-5, 31	127.71	1.59	2.72	74.4	66.2	0.91
14H-5, 108	128.48	1.60	2.69	71.2	64.9	0.93
14H-6, 30	129.20	1.62	2.71	68.7	64.3	0.96
14H-6, 108	129.98	1.61	2.69	69.9	64.6	0.95
15H-3, 108	134.98	1.59	2.73	75.5	66.6	0.90
15H-4, 109	136.49	1.57	2.69	78.2	67.0	0.88
15H-5, 107	137.97	1.63	2.69	65.8	63.2	0.98
15H-6, 107	139.47	1.62	2.70	67.2	63.7	0.97
15H-7, 107	140.97	1.63	2.71	67.4	63.9	0.97
16H-1, 107	141.47	1.60	2.68	71.1	64.9	0.93
16H-2, 107	142.97	1.63	2.69	66.6	63.4	0.98
16H-3, 107	144.47	1.63	2.67	64.6	62.5	0.99
16H-4, 107	145.97	1.64	2.70	65.1	63.0	0.99
16H-5, 107	147.47	1.63	2.69	65.0	62.8	0.99
16H-6, 118	149.08	1.67	2.70	59.4	60.8	1.05
17H-1, 73	150.63	1.64	2.72	65.9	63.4	0.99
17H-2, 89	152.29	1.61	2.68	69.2	64.2	0.95
17H-3, 75	153.65	1.61	2.68	68.4	63.9	0.96
17H-4, 89	155.29	1.65	2.70	63.4	62.4	1.01
17H-5, 74	156.64	1.66	2.71	62.4	62.1	1.02
17H-6, 75	158.15	1.66	2.73	62.3	62.2	1.02
18H-1, 74	160.14	1.62	2.69	67.6	63.8	0.97
18H-2, 75	161.65	1.63	2.71	66.0	63.4	0.98
18H-3, 72	163.12	1.61	2.73	70.9	65.2	0.94
18H-4, 74	164.64	1.63	2.67	65.3	62.8	0.98

Table 13 (continued).

Core, section, interval (cm)	Depth (mbsf)	Wet-bulk density (g/cm^3)	Grain density (g/cm^3)	Water content (% dry wt.)	Porosity (%)	Dry-bulk density (g/cm^3)
18H-5, 74	166.14	1.63	2.71	67.2	63.9	0.97
18H-6, 75	167.65	1.63	2.71	66.6	63.6	0.98
19H-1, 73	169.63	1.63	2.69	64.9	62.8	0.99
19H-2, 72	171.12	1.65	2.72	63.8	62.7	1.01
19H-3, 71	172.61	1.65	2.72	63.9	62.8	1.01
19H-4, 85	174.25	1.64	2.71	65.1	63.1	0.99
19H-5, 72	175.62	1.64	2.73	66.2	63.6	0.98
19H-6, 74	177.14	1.67	2.70	60.4	61.3	1.04
20H-1, 75	179.15	1.64	2.73	66.0	63.5	0.99
20H-2, 74	180.64	1.64	2.69	64.5	62.7	1.00
20H-3, 72	182.12	1.67	2.71	60.7	61.4	1.04
20H-4, 74	183.64	1.64	2.72	65.2	63.2	0.99
20H-5, 72	185.12	1.68	2.70	58.6	60.5	1.06
20H-6, 74	186.64	1.67	2.73	61.1	61.8	1.04
21H-1, 115	189.05	1.65	2.72	63.4	62.6	1.01
21H-2, 107	190.47	1.64	2.69	63.6	62.3	1.00
21H-3, 110	192.00	1.65	2.71	64.1	62.7	1.00
21H-4, 90	193.30	1.64	2.71	64.6	62.9	1.00
21H-5, 107	194.97	1.64	2.70	64.9	63.0	0.99
21H-6, 109	196.49	1.69	2.72	58.1	60.5	1.07
22H-1, 109	199.49	1.68	2.71	59.3	60.9	1.05
22H-2, 99	200.89	1.66	2.72	62.3	62.1	1.02
22H-3, 110	202.50	1.68	2.71	58.7	60.7	1.06
22H-4, 109	203.99	1.67	2.72	60.7	61.6	1.04
22H-5, 110	205.50	1.68	2.71	59.3	60.9	1.05
22H-6, 112	207.02	1.68	2.70	58.0	60.3	1.07
23H-1, 105	207.95	1.67	2.72	61.2	61.7	1.03
23H-2, 109	209.49	1.64	2.70	64.0	62.6	1.00
23H-3, 107	210.97	1.68	2.68	58.4	60.3	1.06
23H-4, 110	212.50	1.66	2.73	62.1	62.2	1.03
23H-5, 108	213.98	1.72	2.71	53.6	58.5	1.12
23H-6, 109	215.49	1.65	2.69	63.2	62.2	1.01
26H-1, 109	236.49	1.65	2.72	63.3	62.5	1.01
26H-3, 108	239.48	1.64	2.69	64.7	62.8	1.00
26H-4, 109	240.99	1.64	2.66	63.5	62.1	1.00
26H-5, 109	242.49	1.62	2.68	68.0	63.8	0.96
26H-6, 109	243.99	1.65	2.69	62.6	62.0	1.02
27H-1, 109	245.99	1.66	2.69	60.5	61.3	1.04
27H-3, 109	248.99	1.65	2.69	62.2	61.9	1.02
27H-4, 109	250.49	1.61	2.68	68.5	64.0	0.96
27H-5, 109	251.99	1.64	2.70	64.4	62.8	1.00
27H-6, 109	253.49	1.62	2.69	66.7	63.4	0.97
28X-1, 94	255.34	1.64	2.69	63.8	62.4	1.00
28X-2, 30	256.20	1.61	2.67	68.2	63.8	0.96
28X-3, 52	257.92	1.61	2.65	68.0	63.6	0.96
28X-4, 30	259.20	1.62	2.66	65.9	63.0	0.98
28X-5, 100	261.40	1.60	2.62	68.5	63.5	0.95
28X-6, 27	262.17	1.61	2.65	67.2	63.3	0.97
29X-1, 61	264.71	1.65	2.67	61.2	61.3	1.03
29X-2, 109	266.69	1.68	2.68	57.4	59.8	1.07
29X-3, 70	267.80	1.64	2.68	63.3	62.2	1.01
29X-4, 66	269.26	1.67	2.72	60.5	61.5	1.04
29X-5, 84	270.94	1.66	2.66	59.6	60.6	1.04
29X-6, 60	262.50	1.69	2.68	56.8	59.6	1.08
30X-2, 56	275.86	1.64	2.69	63.8	62.5	1.00
30X-3, 87	277.67	1.68	2.68	57.8	60.1	1.07
30X-4, 65	278.95	1.67	2.69	59.6	60.9	1.05
30X-5, 100	280.80	1.61	2.67	67.9	63.7	0.96
30X-6, 70	282.00	1.64	2.65	63.4	62.0	1.00
31X-1, 95	284.45	1.65	2.66	61.0	61.2	1.03
31X-3, 66	287.16	1.67	2.69	60.0	61.0	1.04
31X-4, 68	288.68	1.63	2.67	65.1	62.7	0.99
31X-5, 70	290.20	1.62	2.66	65.6	62.8	0.98
32X-1, 144	294.14	1.63	2.64	63.2	61.7	1.00
32X-2, 110	295.30	1.68	2.68	57.8	60.0	1.06
32X-3, 126	296.96	1.68	2.71	58.0	60.3	1.07
32X-4, 93	298.13	1.70	2.72	56.2	55.7	1.09
33X-1, 35	302.65	1.65	2.67	62.2	61.7	1.02
33X-2, 53	304.33	1.69	2.67	56.2	59.3	1.08
33X-3, 135	306.65	1.67	2.68	59.5	60.7	1.05
33X-4, 127	308.07	1.72	2.71	52.9	58.2	1.13
33X-5, 145	309.75	1.70	2.70	55.2	59.1	1.10
33X-6, 77	310.57	1.60	2.66	69.5	64.1	0.95
34X-1, 68	312.68	1.72	2.68	51.9	57.5	1.13
34X-2, 73	314.23	1.69	2.67	56.7	59.5	1.08
34X-3, 100	316.00	1.68	2.66	57.5	59.7	1.06

Table 13 (continued).

Core, section, interval (cm)	Depth (mbsf)	Wet-bulk density (g/cm^3)	Grain density (g/ cm^3)	Water content (% dry wt)	Porosity (%)	Dry-bulk density (g/cm^3)
34X-4, 107	317.57	1.72	2.68	52.7	57.8	1.12
34X-5, 42	318.42	1.75	2.67	47.8	55.3	1.18
34X-6, 131	320.81	1.67	2.71	59.6	61.0	1.05
35X-1, 133	322.53	1.72	2.70	53.5	58.4	1.12
35X-2, 140	324.10	—	—	58.3	—	—
35X-3, 111	325.31	1.69	2.69	56.5	59.5	1.08
35X-4, 144	327.14	1.68	2.70	57.9	60.3	1.07
35X-5, 104	328.24	1.68	2.69	58.5	60.4	1.06
36X-1, 133	332.23	1.69	2.69	56.3	59.5	1.08
36X-2, 141	333.81	1.67	2.69	59.4	60.8	1.05
36X-3, 107	334.97	1.70	2.71	55.4	59.2	1.10
36X-4, 135	336.75	1.68	2.75	60.2	61.6	1.05
36X-5, 113	338.03	1.72	2.68	52.9	57.9	1.12
36X-6, 82	339.22	1.67	2.69	59.6	60.9	1.05
37X-2, 87	342.97	1.70	2.72	55.7	59.5	1.09
37X-3, 95	344.55	1.69	2.69	56.6	59.6	1.08
37X-4, 50	345.60	1.70	2.74	56.8	60.1	1.09
37X-5, 8	346.68	1.71	2.71	53.9	58.6	1.11
38X-1, 140	351.60	1.68	2.73	60.1	61.4	1.05
38X-2, 112	352.82	1.68	2.73	59.9	61.3	1.05
38X-3, 142	354.62	1.67	2.72	60.2	61.3	1.04
38X-4, 96	355.66	1.60	2.74	72.1	65.6	0.93
38X-5, 78	356.98	1.66	2.70	61.0	61.5	1.03
39X-1, 37	360.27	1.63	2.63	64.0	62.0	0.99
39X-2, 91	362.31	1.67	2.72	60.3	61.4	1.04
39X-3, 114	364.04	1.60	2.64	69.2	63.9	0.95
39X-4, 47	364.87	1.69	2.77	59.0	61.3	1.06
39X-5, 142	367.32	1.67	2.68	59.4	60.7	1.05
39X-6, 141	368.81	1.67	2.69	59.7	60.9	1.05
40X-1, 80	370.50	1.69	2.70	56.9	59.8	1.08
40X-2, 57	371.77	1.71	2.69	54.0	58.5	1.11
40X-3, 59	373.29	1.69	2.68	55.7	59.2	1.09
40X-4, 145	375.65	1.68	2.67	57.7	59.9	1.06
40X-5, 121	376.91	1.71	2.68	53.2	58.0	1.12
40X-6, 109	378.29	1.73	2.68	50.7	56.9	1.15
41X-1, 90	380.40	1.75	2.70	49.7	56.6	1.17
41X-2, 75	381.75	1.76	2.72	48.2	56.0	1.19
41X-3, 72	383.22	1.68	2.67	57.0	59.6	1.07
41X-4, 76	384.76	1.76	2.70	48.3	55.8	1.18
41X-5, 83	386.33	1.73	2.70	51.4	57.4	1.14
41X-6, 84	387.84	1.79	2.76	46.7	55.5	1.22
42X-1, 106	390.26	1.77	2.71	47.0	55.3	1.21
42X-2, 102	391.72	1.78	2.72	46.5	55.1	1.21
42X-3, 106	393.26	1.83	2.88	46.0	56.3	1.25
42X-4, 79	394.49	1.79	2.71	44.8	54.1	1.24
42X-5, 60	395.80	1.78	2.74	46.6	55.3	1.22
42X-6, 40	397.10	1.77	2.74	48.8	56.5	1.19
43X-1, 81	399.71	1.75	2.68	48.6	55.9	1.18
43X-2, 57	400.97	1.74	2.70	50.0	56.7	1.16
43X-3, 67	402.57	1.78	2.71	45.9	54.7	1.22
43X-4, 67	404.07	1.81	2.70	42.6	52.8	1.27
43X-5, 76	405.66	1.78	2.74	47.3	55.7	1.21
44X-1, 75	409.35	1.76	2.68	46.8	54.9	1.20
44X-2, 141	411.51	1.85	2.71	39.3	50.9	1.33
44X-3, 110	412.70	1.75	2.69	48.3	55.8	1.18
44X-4, 102	414.12	1.74	2.73	50.8	57.4	1.16
44X-5, 124	415.84	1.84	2.70	39.9	51.1	1.31
45X-1, 98	419.28	1.82	2.69	41.5	52.1	1.28
45X-2, 97	420.77	1.78	2.70	45.7	54.5	1.22
45X-3, 90	422.20	1.81	2.68	41.7	52.1	1.28
45X-4, 95	423.75	1.84	2.73	40.4	51.7	1.31
45X-5, 57	424.87	1.76	2.70	47.7	55.6	1.19
45X-6, 65	426.45	1.77	2.70	47.1	55.2	1.20
46X-1, 116	428.96	1.78	2.74	46.7	55.4	1.22
46X-2, 112	430.42	1.78	2.70	45.3	54.3	1.23
46X-3, 107	431.87	1.82	2.66	40.0	50.9	1.30
46X-4, 108	433.38	1.75	2.71	48.9	56.3	1.18
46X-5, 81	434.61	1.85	2.70	39.2	50.7	1.33
46X-6, 78	436.08	1.79	2.68	43.6	53.2	1.25
47X-1, 111	438.61	1.75	2.70	49.5	56.5	1.17
47X-2, 122	440.22	1.78	2.69	45.6	54.4	1.22
47X-3, 110	441.60	1.80	2.69	43.5	53.2	1.25
47X-4, 113	443.13	1.81	2.67	41.5	51.9	1.28
47X-5, 103	444.53	1.79	2.69	44.5	53.8	1.24
47X-6, 51	445.51	1.79	2.71	45.1	54.3	1.23
48X-1, 100	448.10	1.80	2.68	43.5	53.1	1.25

Table 13 (continued).

Core, section, interval (cm)	Depth (mbsf)	Wet-bulk density (g/cm^3)	Grain density (g/ cm^3)	Water content (% dry wt)	Porosity (%)	Dry-bulk density (g/cm^3)
48X-2, 99	449.59	1.79	2.65	43.0	52.6	1.25
48X-3, 101	451.11	1.82	2.71	41.5	52.2	1.29
48X-4, 93	452.53	1.81	2.69	42.1	52.4	1.28
48X-5, 84	453.94	1.83	2.72	41.7	52.4	1.29
48X-6, 100	455.60	1.80	2.70	43.5	53.3	1.26
49X-1, 53	457.33	1.74	2.70	49.9	56.6	1.16
49X-2, 92	459.22	1.78	2.70	45.2	54.2	1.23
49X-3, 65	460.45	1.81	2.70	42.4	52.7	1.27
49X-4, 74	462.04	1.82	2.69	40.7	51.5	1.30
49X-5, 72	463.52	1.88	2.70	36.2	48.8	1.38
50X-1, 89	467.29	1.84	2.71	39.6	51.1	1.32
50X-2, 93	468.83	1.82	2.72	41.9	52.5	1.28
50X-3, 90	470.30	1.78	2.71	45.9	54.6	1.22
50X-4, 100	471.90	1.84	2.71	40.3	51.5	1.31
50X-5, 99	473.39	1.81	2.71	42.6	52.8	1.27
50X-6, 98	474.88	1.87	2.73	37.6	49.9	1.36
51X-1, 33	476.43	1.84	2.70	39.9	51.2	1.31
51X-2, 41	478.01	1.83	2.72	40.9	51.9	1.30
51X-3, 42	479.52	1.83	2.68	40.4	51.3	1.30
51X-4, 38	480.98	1.86	2.68	36.9	49.0	1.36
51X-5, 33	482.43	1.81	2.71	42.7	52.9	1.27
51X-6, 18	483.78	1.84	2.71	40.4	51.6	1.31
52X-1, 108	486.88	1.79	2.69	44.3	53.7	1.24
52X-3, 14	488.94	1.84	2.71	39.7	51.1	1.32
52X-5, 61	492.41	1.77	2.69	46.7	55.0	1.21
53X-1, 105	496.45	1.84	2.70	39.3	50.8	1.32
53X-2, 93	497.83	1.79	2.69	44.0	53.4	1.24
53X-3, 97	499.37	1.80	2.72	44.3	54.0	1.25
53X-4, 90	500.80	1.79	2.71	44.9	54.2	1.24
53X-5, 91	502.31	1.90	2.70	34.3	47.4	1.42
54X-1, 96	506.06	1.79	2.73	45.1	54.4	1.24
54X-2, 97	507.57	1.78	2.71	46.3	54.9	1.22
54X-3, 114	509.24	1.80	2.73	44.2	53.9	1.25
54X-4, 113	510.73	1.77	2.73	47.8	55.8	1.20
54X-5, 80	511.90	1.74	2.72	50.8	57.3	1.15
54X-6, 27	512.87	1.72	2.67	51.5	57.2	1.14
55X-2, 116	517.46	1.77	2.70	46.9	55.1	1.20
55X-3, 61	518.41	1.77	2.71	47.2	55.4	1.20
55X-4, 65	519.95	1.83	2.72	41.3	52.2	1.29
55X-5, 103	521.83	1.75	2.70	49.5	56.5	1.17
55X-6, 43	522.73	1.76	2.69	47.7	55.5	1.19
56X-1, 146	525.46	1.79	2.70	44.3	53.8	1.24
56X-2, 110	526.60	1.78	2.70	45.8	54.6	1.22
56X-3, 53	527.53	1.81	2.71	42.9	53.0	1.27
56X-4, 131	529.81	1.85	2.74	39.9	51.5	1.32
56X-6, 49	531.99	1.83	2.69	40.1	51.2	1.31
57X-1, 85	534.55	1.79	2.71	44.6	54.0	1.24
57X-2, 86	536.06	1.79	2.71	44.7	54.1	1.24
57X-4, 65	538.85	1.79	2.72	45.2	54.4	1.23
57X-5, 56	540.26	1.76	2.68	47.3	55.1	1.20
58X-1, 105	544.45	1.79	2.70	44.3	53.8	1.24
58X-2, 104	545.94	1.79	2.75	46.1	55.2	1.23
58X-3, 143	547.83	1.79	2.74	46.2	55.1	1.22
58X-4, 136	549.26	1.80	2.74	45.0	54.5	1.24
59X-2, 124	555.74	1.83	2.72	41.5	52.3	1.29
59X-3, 107	557.07	1.66	2.79	63.7	63.2	1.02
59X-4, 135	558.85	1.83	2.73	41.8	52.6	1.29
60X-1, 11	562.71	1.81	2.70	42.2	52.5	1.28
60X-3, 38	565.98	1.81	2.72	43.8	53.6	1.26
60X-4, 72	567.82	1.84	2.74	40.3	51.7	1.31
61X-1, 97	573.27	1.79	2.72	45.6	54.6	1.23
61X-2, 111	574.91	1.77	2.70	46.9	55.2	1.21
61X-3, 121	576.51	—	—	48.7	—	—
61X-4, 145	578.25	1.81	2.70	42.9	52.9	1.26
61X-5, 143	579.73	1.80	2.72	44.3	53.9	1.25
61X-6, 92	580.72	1.77	2.67	45.5	54.1	1.22
62X-3, 100	585.90	1.79	2.69	44.0	53.5	1.25
62X-4, 96	587.36	1.80	2.71	43.8	53.5	1.25
62X-5, 88	588.78	1.83	2.71	41.5	52.2	1.29
63X-1, 110	592.70	1.83	2.71	41.0	51.9	1.30
63X-2, 50	593.60	1.85	2.72	39.4	51.0	1.33
63X-3, 32	594.92	1.84	2.72	40.2	51.5	1.31
63X-4, 59	596.69	1.89	2.72	36.1	48.8	1.39
63X-5, 46	598.06	1.86	2.71	37.6	49.7	1.36
64X-1, 9	601.39	1.84	2.70	39.7	51.0	1.32
64X-2, 109	603.89	1.91	2.70	33.3	46.6	1.43

Table 13 (continued).

Core, section, interval (cm)	Depth (mbsf)	Wet-bulk density (g/cm^3)	Grain density (g/ cm^3)	Water content (% dry wt)	Porosity (%)	Dry-bulk density (g/cm^3)
64X-3, 124	605.54	1.87	2.70	37.0	49.2	1.36
64X-4, 81	606.61	1.82	2.69	41.2	51.8	1.29
64X-5, 59	607.89	1.84	2.72	40.7	51.9	1.30
65X-1, 67	611.67	1.82	2.68	41.2	51.8	1.29
65X-2, 62	613.12	1.86	2.70	38.1	50.0	1.35
65X-3, 73	614.73	1.78	2.67	44.6	53.6	1.23
65X-4, 65	616.15	1.84	2.68	38.6	50.1	1.33
65X-5, 52	617.52	1.81	2.69	42.6	52.7	1.27
66X-1, 85	621.45	1.83	2.72	40.9	52.0	1.30
66X-3, 79	624.39	1.86	2.71	38.2	50.2	1.34
66X-4, 85	625.95	1.82	2.69	40.8	51.6	1.30
67X-3, 92	634.22	1.78	2.67	45.1	53.9	1.23
68X-1, 105	640.95	1.84	2.72	40.0	51.4	1.31
68X-2, 111	642.51	1.88	2.71	36.6	49.1	1.37
68X-3, 105	643.95	1.84	2.71	39.7	51.1	1.32
68X-4, 89	645.29	1.84	2.69	39.6	50.8	1.32
70X-3, 60	662.80	1.86	2.68	37.4	49.3	1.35
70X-4, 17	663.87	1.86	2.68	36.9	49.0	1.36
70X-5, 70	665.90	1.91	2.70	33.4	46.7	1.43
71X-1, 126	670.16	1.86	2.69	37.4	49.4	1.35
71X-2, 123	671.63	1.87	2.70	36.6	49.0	1.37
71X-3, 109	672.99	1.87	2.71	37.5	49.6	1.36
71X-4, 112	674.52	1.85	2.73	39.5	51.1	1.33
71X-5, 108	675.98	1.85	2.71	38.9	50.6	1.33
72X-1, 74	678.94	1.86	2.70	37.6	49.6	1.35
72X-2, 66	680.36	1.84	2.70	39.1	50.7	1.33
72X-3, 78	681.98	1.88	2.72	36.4	49.1	1.38
72X-4, 67	683.37	1.83	2.62	37.8	49.1	1.33
73X-2, 90	690.20	1.81	2.72	42.6	52.9	1.27
73X-3, 85	691.65	1.84	2.69	39.1	50.6	1.32
73X-4, 78	693.08	1.86	2.69	37.8	49.7	1.35
73X-5, 75	694.55	1.85	2.70	38.5	50.2	1.34
73X-6, 35	695.65	1.87	2.67	36.2	48.4	1.37
74X-1, 62	698.12	1.88	2.68	35.2	47.8	1.39
74X-2, 59	699.59	1.85	2.72	38.8	50.6	1.34
74X-3, 63	701.13	1.84	2.66	38.3	49.8	1.33
75X-1, 73	707.93	1.85	2.71	39.4	51.0	1.32
75X-2, 86	709.56	1.85	2.72	39.2	50.9	1.33
75X-3, 73	710.93	1.89	2.70	35.3	48.1	1.40
75X-4, 83	712.53	1.87	2.69	36.4	48.7	1.37
76X-1, 94	717.84	1.86	2.70	37.5	49.6	1.36
76X-2, 120	719.60	1.91	2.70	33.5	46.8	1.43
76X-3, 114	721.04	1.86	2.71	38.0	50.0	1.35
76X-4, 95	722.35	1.90	2.71	34.7	47.7	1.41
76X-5, 82	723.72	1.87	2.71	36.9	49.3	1.37
77X-1, 83	727.33	1.88	2.69	35.8	48.4	1.38
77X-2, 105	729.05	1.85	2.70	38.6	50.3	1.33
77X-3, 78	730.28	1.85	2.67	37.9	49.6	1.34
77X-4, 75	731.75	1.84	2.6[illegible]	39.5	50.7	1.32
77X-5, 73	733.23	1.87	2.72	37.7	49.9	1.36
78X-1, 110	737.30	1.86	2.71	37.9	49.9	1.35
78X-2, 88	738.58	1.86	2.69	37.6	49.6	1.35
78X-3, 27	739.47	1.82	2.68	41.9	51.7	1.29
78X-4, 110	741.80	1.83	2.70	40.2	51.3	1.31
78X-5, 65	742.85	1.82	2.69	41.0	51.7	1.29
79X-1, 35	745.85	1.83	2.70	40.5	51.5	1.30
79X-3, 31	748.81	1.90	2.71	35.1	48.1	1.40
80X-1, 43	755.63	1.81	2.70	42.8	52.9	1.27
80X-2, 93	757.63	1.82	2.69	41.4	52.0	1.29
80X-3, 79	758.99	1.81	2.67	41.1	51.6	1.29
82X-2, 69	776.69	1.85	2.71	39.0	50.6	1.33
82X-3, 109	778.59	1.78	2.70	45.6	54.5	1.22
82X-4, 73	779.73	1.79	2.72	45.7	54.7	1.23
83X-2, 4	785.54	1.82	2.69	41.4	52.0	1.29
83X-3, 3	787.03	1.85	2.70	38.5	50.3	1.34
83X-4, 23	788.73	1.81	2.70	42.3	52.6	1.27
130-807B-						
1H-1, 109	1.09	1.52	2.69	87.8	69.5	0.81
1H-2, 104	2.54	1.51	2.69	91.2	70.3	0.79
2H-1, 109	4.19	1.52	2.70	90.4	70.2	0.80
2H-2, 96	5.56	1.45	2.70	109.9	74.0	0.69
2H-3, 111	7.21	1.54	2.76	87.7	70.0	0.82
2H-4, 107	8.67	1.57	2.72	79.3	67.6	0.87
2H-5, 110	10.20	1.54	2.70	84.5	68.8	0.83
2H-6, 110	11.70	1.53	2.73	86.8	69.6	0.82

Table 13 (continued).

Core, section, interval (cm)	Depth (mbsf)	Wet-bulk density (g/cm^3)	Grain density (g/ cm^3)	Water content (% dry wt)	Porosity (%)	Dry-bulk density (g/cm^3)
3H-1, 109	13.69	1.50	2.70	94.1	71.0	0.77
3H-2, 109	15.19	1.56	2.72	81.3	68.1	0.86
3H-3, 109	16.69	1.54	2.71	85.5	69.1	0.83
3H-4, 109	18.19	1.52	2.70	89.7	70.0	0.80
3H-5, 112	19.72	1.56	2.71	79.6	67.6	0.87
3H-6, 110	21.20	1.55	2.69	82.0	68.1	0.85
4H-1, 126	23.36	1.58	2.72	76.6	66.8	0.89
4H-2, 109	24.69	1.52	2.69	87.8	69.5	0.81
4H-3, 137	26.47	1.60	2.70	71.9	65.3	0.93
4H-4, 105	27.65	1.54	2.72	84.6	69.0	0.84
4H-5, 110	29.20	1.51	2.68	90.2	70.0	0.79
4H-6, 110	30.70	1.53	2.74	88.7	70.1	0.81
5H-1, 111	32.71	1.56	2.70	78.8	67.3	0.87
5H-2, 107	34.17	1.58	2.70	75.9	66.5	0.90
5H-3, 110	35.70	1.57	2.70	77.5	66.9	0.88
5H-4, 109	37.19	1.56	2.73	80.0	67.9	0.87
5H-5, 126	38.86	1.58	2.75	76.7	67.1	0.90
5H-6, 128	40.38	1.57	2.71	77.9	67.1	0.88
6H-1, 115	42.25	1.55	2.70	81.9	68.1	0.85
6H-2, 110	43.70	1.51	2.67	90.0	69.9	0.79
6H-3, 114	45.24	1.60	2.72	73.4	65.9	0.92
6H-4, 112	46.72	1.56	2.69	78.7	67.2	0.87
6H-5, 110	48.20	1.55	2.72	81.7	68.2	0.86
6H-6, 110	49.70	1.57	2.69	77.1	66.8	0.89
7H-1, 106	51.66	1.55	2.70	81.4	68.0	0.86
7H-2, 107	53.17	1.56	2.70	79.6	67.5	0.87
7H-3, 107	54.67	1.54	2.71	83.6	68.7	0.84
7H-4, 109	56.19	1.54	2.69	85.1	68.9	0.83
7H-5, 109	57.69	1.56	2.69	80.3	67.6	0.86
7H-6, 109	59.19	1.56	2.72	79.7	67.7	0.87
8H-1, 109	61.19	1.57	2.71	79.1	67.5	0.87
8H-2, 109	62.69	1.57	2.71	79.0	67.4	0.87
8H-3, 107	64.17	1.54	2.71	83.8	68.7	0.84
8H-4, 110	65.70	1.58	2.72	77.0	67.0	0.89
8H-5, 110	67.20	1.56	2.70	78.8	67.3	0.87
8H-6, 108	68.68	1.58	2.70	76.2	66.5	0.89
9H-1, 108	70.68	1.55	2.69	80.4	67.6	0.86
9H-2, 109	72.19	1.59	2.69	73.1	65.5	0.92
9H-3, 109	73.69	1.63	2.73	67.3	64.0	0.97
9H-4, 110	75.20	1.59	2.70	74.4	66.0	0.91
9H-5, 109	76.69	1.56	2.72	79.7	67.7	0.87
9H-6, 109	78.19	1.58	2.67	73.3	65.4	0.91
10H-1, 108	80.18	1.59	2.72	74.8	66.3	0.91
10H-2, 108	81.68	1.59	2.71	74.9	66.3	0.91
10H-3, 108	83.18	1.58	2.66	74.8	65.9	0.90
10H-4, 108	84.68	1.58	2.73	77.4	67.1	0.89
10H-5, 108	86.18	1.60	2.70	72.4	65.4	0.93
10H-6, 108	87.68	1.59	2.70	73.5	65.7	0.92
11H-1, 108	89.68	1.59	2.69	72.6	65.4	0.92
11H-2, 108	91.18	1.59	2.69	73.8	65.8	0.91
11H-3, 108	92.68	1.56	2.73	80.9	68.2	0.86
11H-4, 108	94.18	1.59	2.67	73.2	65.4	0.92
11H-5, 108	95.68	1.60	2.68	70.6	64.7	0.94
11H-6, 108	97.18	1.63	2.72	66.8	63.8	0.98
12H-1, 108	99.18	1.60	2.69	70.8	64.8	0.94
12H-2, 108	100.68	1.60	2.68	71.1	64.8	0.93
12H-3, 108	102.18	1.61	2.70	70.2	64.7	0.95
12H-4, 108	103.68	1.60	2.70	72.6	65.5	0.92
12H-5, 108	105.18	1.61	2.72	69.6	64.7	0.95
12H-6, 108	106.68	1.61	2.70	70.1	64.7	0.95
13H-1, 109	108.69	1.62	2.73	68.7	64.5	0.96
13H-2, 109	110.19	1.59	2.69	72.8	65.5	0.92
13H-3, 113	111.73	1.59	2.71	73.4	65.8	0.92
13H-4, 110	113.20	1.59	2.70	73.2	65.6	0.92
13H-5, 139	114.99	1.58	2.73	76.8	67.0	0.89
13H-6, 111	116.21	1.60	2.68	71.1	64.9	0.93
14H-1, 108	118.18	1.58	2.67	74.3	65.8	0.91
14H-2, 110	119.70	1.61	2.75	71.1	65.5	0.94
14H-3, 104	121.14	1.58	2.65	73.0	65.2	0.92
14H-4, 109	122.69	1.59	2.68	72.8	65.4	0.92
14H-5, 106	124.16	1.60	2.71	71.4	65.2	0.94
14H-6, 106	125.66	1.58	2.69	74.7	66.0	0.91
15H-1, 109	127.69	1.62	2.71	69.2	64.5	0.96
15H-2, 108	129.18	1.61	2.69	69.6	64.4	0.95
15H-3, 109	130.69	1.59	2.70	73.2	65.7	0.92
15H-4, 109	132.19	1.61	2.70	70.3	64.7	0.94

Table 13 (continued).

Core, section, interval (cm)	Depth (mbsf)	Wet-bulk density (g/cm^3)	Grain density (g/ cm^3)	Water content (% dry wt)	Porosity (%)	Dry-bulk density (g/cm^3)
15H-5, 109	133.69	1.60	2.68	71.1	64.8	0.93
15H-6, 109	135.19	1.58	2.69	74.9	66.1	0.90
16H-1, 108	137.18	1.61	2.69	68.7	64.2	0.96
16H-2, 109	138.69	1.63	2.70	66.1	63.3	0.98
16H-3, 109	140.19	1.66	2.71	62.4	62.1	1.02
16H-4, 109	141.69	1.64	2.72	65.5	63.3	0.99
16H-5, 109	143.19	1.64	2.72	65.4	63.2	0.99
16H-6, 109	144.69	1.64	2.70	65.0	63.0	0.99
17H-1, 109	146.69	1.64	2.77	67.4	64.3	0.98
17H-2, 109	148.19	1.64	2.69	64.4	62.7	1.00
17H-3, 109	149.69	1.63	2.71	66.3	63.5	0.98
17H-4, 109	151.19	1.61	2.70	69.4	64.5	0.95
17H-5, 109	152.69	1.64	2.72	64.5	62.9	1.00
17H-6, 109	154.19	1.63	2.71	66.5	63.5	0.98
18H-1, 111	156.21	1.63	2.72	66.8	63.8	0.98
18H-2, 108	157.68	1.61	2.69	69.8	64.5	0.95
18H-3, 109	159.19	1.59	2.68	71.8	65.1	0.93
18H-4, 108	160.68	1.62	2.71	67.8	64.0	0.97
18H-5, 108	162.18	1.61	2.69	70.0	64.6	0.95
18H-6, 108	163.68	1.61	2.72	70.4	65.0	0.94
19H-1, 107	165.67	1.63	2.73	67.5	64.1	0.97
19H-2, 107	167.17	1.68	2.77	60.5	61.9	1.05
19H-3, 108	168.68	1.66	2.74	63.2	62.6	1.02
19H-4, 108	170.18	1.60	2.69	70.9	64.8	0.94
19H-5, 83	171.43	1.65	2.72	64.2	62.9	1.00
20H-1, 107	175.17	1.65	2.72	62.8	62.3	1.02
20H-2, 107	176.67	1.68	2.71	58.9	60.7	1.06
20H-3, 107	178.17	1.65	2.70	62.7	62.1	1.02
20H-4, 50	179.10	1.68	2.72	58.9	60.8	1.06
21H-1, 106	184.66	1.68	2.74	60.4	61.6	1.04
21H-2, 106	186.16	1.65	2.68	62.2	61.7	1.02
21H-3, 106	187.66	1.64	2.71	64.4	62.8	1.00
21H-4, 106	189.16	1.65	2.71	62.6	62.1	1.02
21H-5, 106	190.66	1.64	2.69	64.1	62.5	1.00
21H-6, 106	192.16	1.62	2.68	66.9	63.5	0.97
22H-1, 106	194.16	1.68	2.73	59.1	61.0	1.06
22H-2, 106	195.66	1.70	2.69	55.3	59.1	1.09
22H-3, 106	197.16	1.67	2.72	60.0	61.3	1.05
22H-4, 106	198.66	1.65	2.72	64.3	62.8	1.00
22H-5, 106	200.16	1.67	2.70	60.4	61.3	1.04
22H-6, 106	201.66	1.68	2.74	59.5	61.2	1.05
23H-1, 106	203.66	1.69	2.70	57.4	60.0	1.07
23H-2, 106	205.16	1.67	2.73	60.9	61.7	1.04
23H-3, 106	206.66	1.68	2.71	58.1	60.4	1.06
23H-4, 106	208.16	1.66	2.70	61.0	61.5	1.03
23H-5, 122	209.82	1.65	2.72	64.6	63.0	1.00
23H-6, 122	211.32	1.68	2.70	57.7	60.2	1.07
24H-1, 122	213.32	1.63	2.70	66.9	63.7	0.97
24H-2, 106	214.66	1.65	2.71	62.4	62.1	1.02
24H-3, 118	216.28	1.62	2.71	68.4	64.2	0.96
24H-4, 118	217.78	1.62	2.68	66.5	63.3	0.98
24H-5, 106	219.16	1.68	2.68	57.4	59.9	1.07
24H-6, 106	220.66	1.63	2.70	66.6	63.5	0.98
25H-1, 105	222.65	1.66	2.70	60.6	61.3	1.04
25H-3, 105	225.65	1.64	2.71	64.7	63.0	1.00
25H-4, 106	227.16	1.60	2.68	70.0	64.5	0.94
25H-5, 107	228.67	1.61	2.69	68.4	64.0	0.96
25H-6, 123	230.33	1.61	2.68	70.0	64.5	0.94
26H-1, 106	232.16	1.63	2.70	65.4	63.1	0.99
26H-2, 124	233.84	1.63	2.67	65.5	62.9	0.98
26H-3, 108	235.18	1.64	2.71	65.4	63.2	0.99
26H-4, 107	236.67	1.63	2.68	65.6	63.0	0.98
26H-6, 115	239.75	1.66	2.68	60.7	61.2	1.03
27H-1, 106	241.66	1.66	2.69	61.6	61.7	1.03
27H-2, 106	243.16	1.64	2.70	63.9	62.6	1.00
27H-3, 85	244.45	1.66	2.71	62.4	62.1	1.02
27H-4, 106	246.16	1.65	2.69	62.1	61.8	1.02
27H-5, 86	247.46	1.62	2.66	66.1	63.0	0.98
27H-6, 101	249.11	1.60	2.68	70.7	64.7	0.94
28H-1, 119	251.29	1.61	2.66	67.7	63.5	0.96
28H-2, 103	252.63	1.63	2.68	66.1	63.2	0.98
28H-3, 103	254.13	1.67	2.67	59.3	60.6	1.05
28H-4, 103	255.63	1.63	2.73	66.8	63.9	0.98
28H-5, 104	257.14	1.65	2.68	61.8	61.6	1.02
28H-6, 61	258.21	1.60	2.69	70.7	64.8	0.94
29H-1, 109	260.69	1.68	2.71	58.4	60.5	1.06

Table 13 (continued).

Core, section, interval (cm)	Depth (mbsf)	Wet-bulk density (g/cm^3)	Grain density (g/ cm^3)	Water content (% dry wt)	Porosity (%)	Dry-bulk density (g/cm^3)
29H-2, 109	262.19	1.65	2.68	62.2	61.7	1.02
29H-3, 106	263.66	1.67	2.69	58.9	60.5	1.05
29H-4, 109	265.19	—	—	62.5	—	—
29H-5, 109	266.69	1.64	2.69	64.0	62.5	1.00
29H-6, 109	268.19	—	—	58.5	—	—
30H-1, 109	270.19	1.71	2.69	53.5	58.2	1.12
30H-2, 109	271.69	1.65	2.72	63.6	62.6	1.01
30H-3, 109	273.19	1.66	2.69	61.4	61.5	1.03
30H-4, 109	274.69	1.69	2.72	57.6	60.3	1.07
30H-5, 109	276.19	—	—	60.0	—	—
30H-6, 104	277.64	—	—	60.4	—	—
130-807C-						
2R-1, 35	790.05	1.82	2.68	40.8	51.6	1.29
2R-2, 26	791.46	1.85	2.72	39.3	51.0	1.33
4R-1, 55	809.55	1.82	2.70	41.3	52.0	1.29
4R-2, 66	811.16	1.87	2.68	36.1	48.5	1.38
6R-1, 91	829.21	1.77	2.70	46.5	55.0	1.21
6R-2, 92	830.72	1.79	2.71	45.0	54.2	1.23
6R-3, 91	832.21	1.80	2.69	43.5	53.2	1.25
6R-4, 91	833.71	1.78	2.71	46.5	55.0	1.21
6R-5, 80	835.10	1.80	2.71	43.7	53.5	1.25
9R-1, 21	857.61	1.80	2.70	43.5	53.2	1.25
12R-1, 26	876.86	1.83	2.73	41.8	52.5	1.29
15R-1, 17	894.07	1.86	2.70	37.3	49.5	1.36
16R-1, 58	899.48	1.92	2.71	33.2	46.6	1.44
17R-1, 31	904.21	1.83	2.68	40.5	51.4	1.30
17R-2, 48	905.88	1.83	2.67	39.2	50.5	1.32
18R-CC, 8	—	1.84	2.65	38.1	49.5	1.33
19R-1, 33	914.23	1.83	2.71	40.7	51.7	1.30
21R-1, 4	923.94	1.91	2.71	33.7	47.0	1.43
23R-1, 49	939.19	1.84	2.68	38.8	50.2	1.33
23R-2, 42	940.62	1.92	2.65	31.2	44.6	1.46
23R-3, 43	942.13	1.89	2.70	35.4	48.1	1.39
23R-4, 37	943.57	1.88	2.69	35.9	48.4	1.38
24R-1, 70	944.40	1.88	2.68	35.4	48.0	1.39
24R-2, 70	945.90	1.82	2.67	40.2	51.0	1.30
25R-1, 35	948.75	1.90	2.69	34.0	47.1	1.42
26R-1, 56	958.66	2.10	2.70	21.0	35.6	1.74
30R-1, 34	997.14	1.98	2.72	29.0	43.4	1.54
30R-2, 49	998.79	1.96	2.70	29.5	43.7	1.52
31R-1, 26	1006.76	2.22	2.55	11.1	21.7	1.99
35R-1, 20	1044.50	1.94	2.71	31.7	45.5	1.47
37R-1, 3	1063.73	2.11	2.55	16.5	29.1	1.81
38R-1, 38	1073.58	2.02	2.74	26.5	41.4	1.60
40R-1, 89	1092.89	2.18	2.62	15.1	27.8	1.89
41R-1, 32	1098.02	2.25	2.62	11.8	23.2	2.01
42R-1, 41	1102.81	2.21	2.63	13.7	26.0	1.95
43R-1, 18	1106.58	2.28	2.53	8.1	16.7	2.11
44R-1, 44	1116.44	2.20	2.72	16.4	30.2	1.89
45R-1, 62	1126.22	2.29	2.69	11.7	23.4	2.05
45R-2, 49	1127.59	2.38	2.66	7.9	16.9	2.21
47R-2, 65	1142.35	2.44	2.73	7.5	16.5	2.27
48R-2, 98	1147.68	2.46	2.72	6.6	14.8	2.31
49R-1, 77	1150.97	2.51	2.73	5.6	13.0	2.37
50R-1, 71	1155.91	2.56	2.79	5.4	12.7	2.43
51R-1, 70	1160.90	2.45	2.72	6.9	15.5	2.30
51R-2, 67	1162.37	2.47	2.71	6.1	14.0	2.33
51R-3, 71	1163.91	2.56	2.71	3.8	9.2	2.46
52R-1, 82	1170.62	2.46	2.71	6.6	14.8	2.31
52R-2, 119	1172.43	2.56	2.75	4.5	10.8	2.45
52R-3, 31	1173.11	2.54	2.71	4.4	10.3	2.43
53R-1, 68	1180.08	2.61	2.75	3.3	8.2	2.52
53R-2, 74	1181.64	2.65	2.73	1.9	4.8	2.60
53R-3, 62	1183.02	2.30	2.69	11.3	22.8	2.07
53R-4, 122	1185.12	2.52	2.71	4.8	11.2	2.41
56R-1, 134	1207.94	2.50	2.72	5.7	13.1	2.36
56R-2, 140	1209.50	2.54	2.78	5.9	13.9	2.39
56R-3, 50	1210.10	2.48	2.74	6.5	14.8	2.33
57R-1, 115	1217.45	2.45	2.73	7.4	16.5	2.28
57R-2, 98	1218.78	2.47	2.74	6.9	15.5	2.31
58R-1, 10	1222.60	2.48	2.71	6.0	13.7	2.34
59R-1, 55	1232.75	2.40	2.71	8.6	18.5	2.21
59R-2, 68	1234.38	2.40	2.74	9.2	19.6	2.20
61R-1, 56	1252.06	2.43	2.78	9.1	19.8	2.23
61R-2, 88	1253.88	2.43	2.76	8.7	18.9	2.23

Table 13 (continued).

Core, section, interval (cm)	Depth (mbsf)	Wet-bulk density (g/cm^3)	Grain density (g/cm^3)	Water content (% dry wt)	Porosity (%)	Dry-bulk density (g/cm^3)
62R-1, 83	1262.03	2.34	2.74	11.0	22.7	2.11
62R-2, 63	1263.33	2.38	2.74	9.7	20.5	2.17
62R-3, 93	1265.13	2.38	2.75	10.0	21.2	2.17
63R-1, 28	1271.08	2.40	2.74	9.2	19.8	2.19
63R-2, 57	1272.87	2.40	2.73	8.9	19.2	2.21
63R-3, 88	1274.68	2.38	2.77	10.4	21.9	2.16
64R-1, 95	1281.45	2.39	2.72	9.1	19.5	2.19
64R-2, 72	1282.72	2.40	2.75	9.5	20.4	2.19
65R-1, 53	1290.63	2.36	2.75	10.8	22.5	2.13
65R-2, 41	1292.01	2.34	2.74	11.3	23.2	2.11
66R-1, 127	1301.07	2.32	2.74	11.9	24.2	2.07
66R-2, 74	1302.04	2.30	2.72	12.1	24.3	2.05
66R-3, 84	1303.64	2.31	2.73	12.0	24.2	2.06
67R-1, 75	1310.25	2.35	2.72	10.4	21.7	2.13
67R-2, 109	1312.09	2.38	2.72	9.5	20.1	2.17
67R-3, 73	1313.23	2.35	2.71	10.1	21.1	2.14
67R-4, 82	1314.82	2.34	2.71	10.5	21.8	2.12
67R-5, 37	1315.87	2.33	2.73	11.4	23.3	2.09
68R-1, 67	1319.77	2.32	2.72	11.5	23.4	2.08
68R-2, 28	1320.88	2.31	2.70	11.4	23.1	2.08
68R-3, 58	1322.68	2.37	2.71	9.6	20.2	2.16
69R-2, 106	1331.36	2.38	2.73	9.7	20.5	2.17
69R-3, 3	1331.83	2.38	2.72	9.3	19.8	2.18
69R-4, 86	1334.16	2.38	2.74	10.0	21.1	2.16
69R-5, 15	1334.95	2.38	2.74	9.8	20.8	2.17
70R-1, 69	1339.09	2.36	2.71	10.1	21.0	2.14
70R-2, 108	1340.98	2.42	2.74	8.6	18.7	2.22
70R-3, 97	1342.37	2.35	2.73	10.8	22.4	2.12
70R-4, 52	1343.42	2.26	2.58	10.4	20.8	2.04
71R-1, 45	1348.45	2.33	2.71	11.0	22.5	2.10
71R-2, 130	1350.80	2.32	2.73	11.6	23.6	2.08
71R-3, 106	1352.06	2.10	2.81	23.9	39.5	1.69
71R-4, 59	1353.09	2.02	2.70	25.7	40.3	1.61
71R-5, 47	1354.47	2.03	2.71	25.4	40.1	1.62
71R-6, 27	1355.77	2.04	2.63	22.3	36.4	1.67
72R-2, 42	1359.62	1.75	2.44	39.9	48.6	1.25
73R-1, 67	1368.07	1.84	2.45	31.3	42.7	1.40
73R-2, 55	1369.45	2.07	2.67	21.7	36.1	1.70

sampled at Site 803 (i.e., the entire basement section cored at Site 803). Variations between Subunits C, E, F, and G are limited as well and are illustrated in the Zr vs. TiO_2 plot in Figure 56. Site 803 results lie in an intermediate position between the data for the upper and lower Site 807 subunits; the same is true for the Sr data. More detailed comparisons are premature at present, in view of the different levels of alteration at the two sites, the lack of Nb data for Site 807, and the absence of intercalibration between the shipboard and Keele XRF machines.

Preliminary Conclusions

In contrast to Site 803, basement Subunit F in Hole 807C provides clear evidence for the existence of thick basalt flows on the Ontong Java Plateau comparable with those typical of major continental flood basalt provinces. The general lack of large phenocrysts also is reminiscent of some continental flood basalts, such as those of the Grande Ronde Formation in the Columbia River province of the western United States (e.g., Hooper, 1988). Moreover, even the thinner massive, olivine-bearing flows at Site 807 tend to be markedly thicker than those at Site 803 (up to 3 m vs. <1 m), which lies on the edge of the Ontong Java Plateau. Because of the absence of large phenocrysts in the lower subunits, the samples recovered can generally be treated as representative of erupted liquid compositions. Their little-altered nature and the lack of substantial sedimentary interbeds in the lower portion of the basement section suggest that they were erupted over a short time interval and were effectively sealed off from significant interaction with seawater by overlying flows and sediments. The plagioclase-bearing lavas of Subunit A are fairly enriched in Sr, Ti, and Zr and are chemically distinct from those of the lower subunits, which are depleted in these elements. The passage of a somewhat greater interval of time between Subunits C and A than between the eruption of the lower subunits may be indicated by the mineralogical and chemical differences and the presence of a >0.6-m-thick limestone layer between them. Both the upper and lower subunits appear distinct from the basalts at Site 803.

LOGGING

Logging Operations

Hole 807A

Logging operations at Hole 807A are summarized in Table 16. As at all sites on Leg 130, a wiper trip was made to clear the hole before logging. In addition, the hole was first flushed with bentonite, after which seawater was circulated to clean the hole. The first logging run was made with the geophysical logging string, consisting of the natural gamma-ray tool (NGT), the long-spaced sonic digital tool (LSS), the resistivity tool (DIT), and the temperature tool (TLT).

The tool string was run to the end of pipe, and a down log was recorded from 85.6 (just before leaving pipe) to 802.6 mbsf. The down log was stopped short of the bottom of the hole to prepare for the main logging run up the hole. The tool

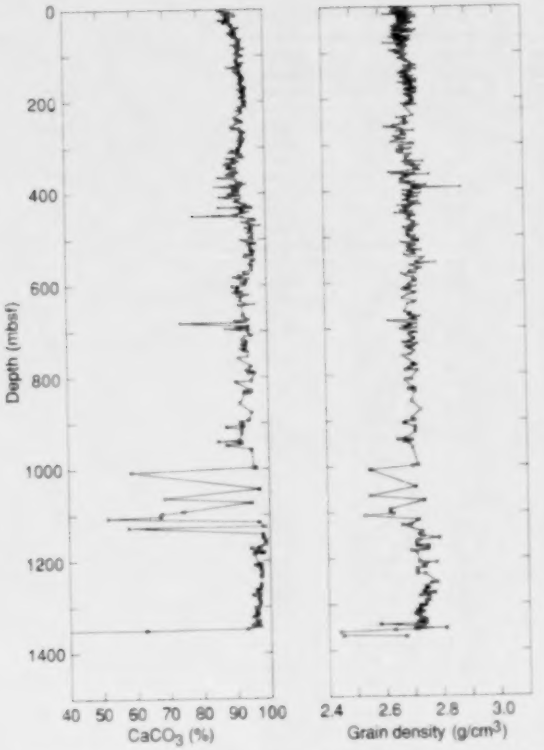

Figure 49. Carbonate content and grain density vs. depth, Site 807 (merged data sets from Holes 807A [dots] and 807C [crosses]).

string set down at the base of the hole at 820.5 mbsf, or <2.5 m short of the total drilled section. The heave compensator was turned on and the uplog begun, with all tools operating normally. The entire section from 820 mbsf to the base of pipe at 89.6 mbsf was logged successfully. No repeat log was run as Hole 807C also was to be logged.

The second logging run was conducted with an abbreviated geochemical tool string consisting of the NGT, the aluminum clay tool (ACT), and the density tool (HLDT). The geochemical spectral tool (GST) was left out of the string because it failed deck tests. During the rig-up, the bullnose, an assembly at the end of the tool string that allows the string to pass in and out of the XCB bit, sheared a bolt and was lost overboard. A substitute assembly was built, and the hole was reentered after a 1.5-hr delay.

The geochemical logging run was relatively trouble-free. However, there was some debris at the bottom of the hole that kept the HLDT caliper from fully opening until 785 mbsf. As a result, the density data are unreasonably low below this depth. The only other problem during this run occurred when power was accidentally cut to the heave compensator while the tool string was at 323.4 mbsf. The tool string was lowered slightly, the heave compensator was restarted, and the logging run continued. Some spikes in the NGT logs appear at this level.

Hole 807C

Upon completion of coring at Hole 807C, the drill string was pulled out of the hole, the rotary core bit was mechanically released, and the drill pipe was run back into the hole to a depth of 170 mbsf. The tool strings used in Hole 807C and a summary of the operations are presented in Table 16; acronyms used are listed in Table 17.

The first two logging runs (the geophysical string [NGT/LSS/DIT/TLT] and the geochemical string [NGT/ACT/HLDT]) were completed successfully from the base of the hole at 1528 mbsf to the casing at 350 mbsf. In the first run, the quality of the sonic log suffered because the hard and perhaps irregular nature of the borehole wall in the lower part of the hole induced many dropouts and cycle skips in the recorded data. Density data only are recorded from 1508 mbsf upward because debris at the bottom of the hole prevented the HLDT caliper from opening.

On the third run, the FMS (an imaging resistivity tool) was used to obtain detailed information about the structure of the basalts, *in-situ* stress (by means of breakouts), and the thickness of the chert layers in the sediments. The GPIT, an orientation recording tool, was attached to the string and was used to ascertain the hole inclination and deviation and to record the absolute orientation of the FMS resistivity pads. The base of the hole was logged twice with the tool string, once from 1509 to 947 mbsf, and again from 1508 to 1096 mbsf. The FMS images are presented on microfiche in the back pocket of this volume.

Both logging passes were stopped by a bridge that blocked the lower part of the hole. The upper boundary of the logged intervals was determined by the diameter of the borehole. The HLDT caliper data from the previous logging run indicated that the hole above 950 mbsf was washed out to at least 18 in. The FMS can only extend its pads to 15 in.; thus, it could not be used in the upper section of the borehole. The second run was stopped at 1096 mbsf because roughly half of the section above was wider than the FMS calipers. Sections in the logs affected by washouts can be recognized by intervals in which the FMS tool string twisted rapidly in the hole.

Log Stratigraphic Units at Hole 807A

Results of gamma-ray, electrical resistivity, sonic velocity, and bulk density logging in Hole 807A are shown in Figure 57. Each of the logs show some degree of downhole variability, but there are no common events in the profiles that clearly define individual log stratigraphic units. The lack of distinctive character in the logs reflects the uniform composition of these carbonate-rich sediments. The upper 950+ m of sediments were placed in a single lithostratigraphic unit (see "Lithostratigraphy" section, this chapter), with a subdivision at 293 mbsf identified as the ooze-chalk transition.

The log stratigraphic units shown in Figure 57 are based on natural subdivisions of logging data, which can be seen in a cross-plot of velocity and electrical resistivity (Fig. 58). Electrical resistivity is an analog of porosity in sediments and sedimentary rocks (Archie, 1942), although the correlation between the two properties is not constant or well understood in sediments that are undergoing compaction and lithification. The velocity vs. resistivity data show different, subparallel trends that relate to compaction and diagenesis. These data have been used as the basis for division of the Hole 807A data into the two major units with six subdivisions that are shown by different symbols in Figure 58 and are characterized in Table 18.

Logging Unit A represents the part of the sediment column that is undergoing the most significant change in physical properties. The rate of change is reflected in the values of the depth gradients for each of the properties listed in Table 18. Velocity, resistivity, and density all increase within Logging Unit A (top of logged interval to 474 mbsf). In Logging Unit B,

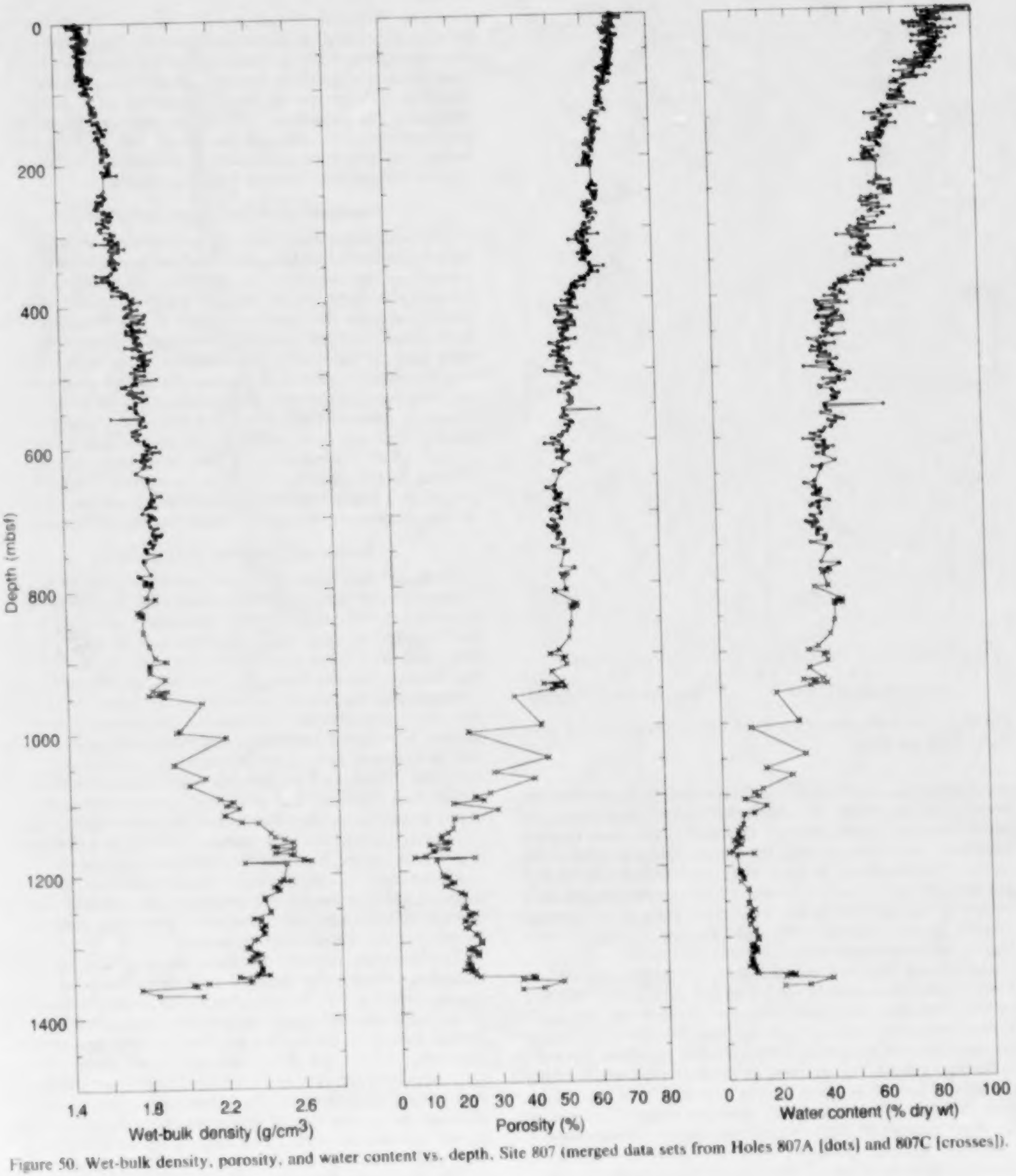

Figure 50. Wet-bulk density, porosity, and water content vs. depth, Site 807 (merged data sets from Holes 807A [dots] and 807C [crosses]).

the changes from 474 mbsf to the bottom of the logged interval (approximately 810 mbsf, depending on the position of the tool in the string and the logging run) are very small or negative. Only within Logging Subunit B2 are depth gradients of the logged properties near those of the subunits of Logging Unit A.

Comparison with Laboratory Data

Logging and laboratory data for compressional wave velocity and bulk density are plotted vs. depth in Figure 59. There is good agreement between the two determinations of density and an increase in the difference between laboratory

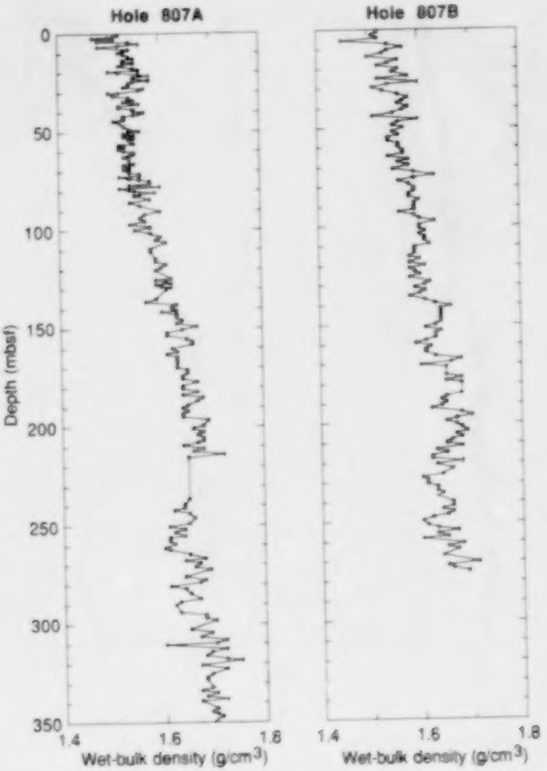

Figure 51. Wet-bulk density vs. depth for the uppermost 350 mbsf, Holes 807A and 807B.

and logging velocity with depth. Laboratory bulk densities are lower than log values by about 0.05 g/cm^3 throughout the entire column. Most changes in density are seen in both laboratory and well-log data, lending credence to both of the results. The minimum in log density centered on 240 mbsf is not entirely supported by laboratory measurements and may be lower than *in-situ* values. However, there is definitely a density decrease between 220 and 240 mbsf, as seen in both logging and laboratory data.

Agreement between velocity data are less systematic. A velocity minimum seen in the log at 140 mbsf is not reflected in the laboratory measurements and is probably not real. Lower in the section (e.g., 410–450 and 480–520 mbsf), there are variations in laboratory velocities that are either not seen in the log or are not as extreme in the log as in the laboratory samples. These differences in the two data sets may result from the state of preservation of the cored material or because the most competent, and therefore probably the acoustically "fastest," samples generally are removed from the core for velocity determination. Fracturing of rock samples has a significant effect on measurements of velocity out of proportion to the change in porosity the fractures might induce (Toksöz et al., 1976). Thus, the differences in fractured and unfractured samples on the surface will tend to amplify more subtle differences in logging data caused by microstructural changes in the sediments *in situ*.

Gamma-ray activity, aluminum counts (from the ACT), and determinations of carbonate content of laboratory samples (see "Inorganic Geochemistry" section, this chapter) are roughly correlated, as shown in Figure 60. Broad maxima and minima in gamma-ray activity are matched by peaks in aluminum counts, suggesting clay or volcanic glass (aluminosilicates) as the source of the radioactivity. The maxima in aluminum and gamma-ray activity are mirrored by minima in carbonate content, although the abrupt nature of the shift in gamma-ray and aluminum values in the logs at 450 mbsf is not seen in the calcium carbonate content record.

Comparison with Lithostratigraphy

The approximate location of the boundary between lithologic Subunits IA and IB is indicated in Figures 57 and 58. The position of the boundary in the cross plot is approximate because the depth of the Subunit IA/IB boundary does not cleanly separate the data in the case of the cross-plots. The level assigned to the ooze/chalk boundary is somewhat arbitrary (see "Lithostratigraphy" section, this chapter) and is actually within a zone of transition. The transitional nature of the zone can be seen particularly well in Figure 58, where the lithologic Subunit IA/IB boundary lies in the middle of the logging Unit A2 field. Most of the points within lithologic Subunit IA have lower velocities and resistivities than those in Subunit IB, but all of the data from the interval of logging Unit A2 fall on a single velocity/resistivity trend and are indicative of a single process or state of microstructure of the sediment.

Results of Logging at Hole 807C

Sediment logs from the lower section of Hole 807C (750–1400 mbsf) and logs from the basement (1350–1530 mbsf) are presented in Figures 61 and 62. The upper part of the log has been omitted because of the excellent agreement of the Hole 807C logs with those recorded in Hole 807A (see below for discussion). The well logs from Hole 807C provide substantial evidence that the cores recovered in the lower parts of the hole are representative of the lithology in general. Lithostratigraphic boundaries have been superimposed on the logging data in Figure 61 (see "Lithostratigraphy" section, this chapter). The boundary between lithologic Units I and II was picked at a depth of 968 mbsf in the recovered core. This depth is approximately 13 m below the depth where velocity and resistivity logs abruptly increase and define a unit boundary. The lithologic Unit I/II boundary is based on the transition from chalk to cherty chalk. Velocity, density, and resistivity all increase across this boundary because of the lower porosity of the chert and the effect of increased cementation by silica of the calcareous sediments.

The boundary between lithologic Subunits IIA and IIB is located at 1098 mbsf in both the core descriptions and in the logging data (Fig. 61). The transformation across the boundary of chalk and silicified chalks to limestone is clearly seen in the logging data as an increase in velocity, density, and electrical resistivity. There are local maxima in all three of these properties between 1150 and 1200 mbsf that do not correspond to anything mentioned in the lithostratigraphic discussion, although the appearance of limestone clasts in the core does appear to correlate with stable logging values between 1230 mbsf and the base of lithologic Unit II at 1351 mbsf.

The claystone, siltstone, and limestone of lithologic Unit III appear in the logs as an interval of reduced velocity, resistivity, and density. Local maxima in the profiles are interpreted as limestone stringers within a predominantly silt- and claystone unit. The boundary of the sediments with basaltic basement is well defined at 1380 mbsf.

Basement logs are presented in Figure 62. Velocity data are not presented because of excessive noise in the unprocessed logs. Smoothed gamma-ray data are shown because of the

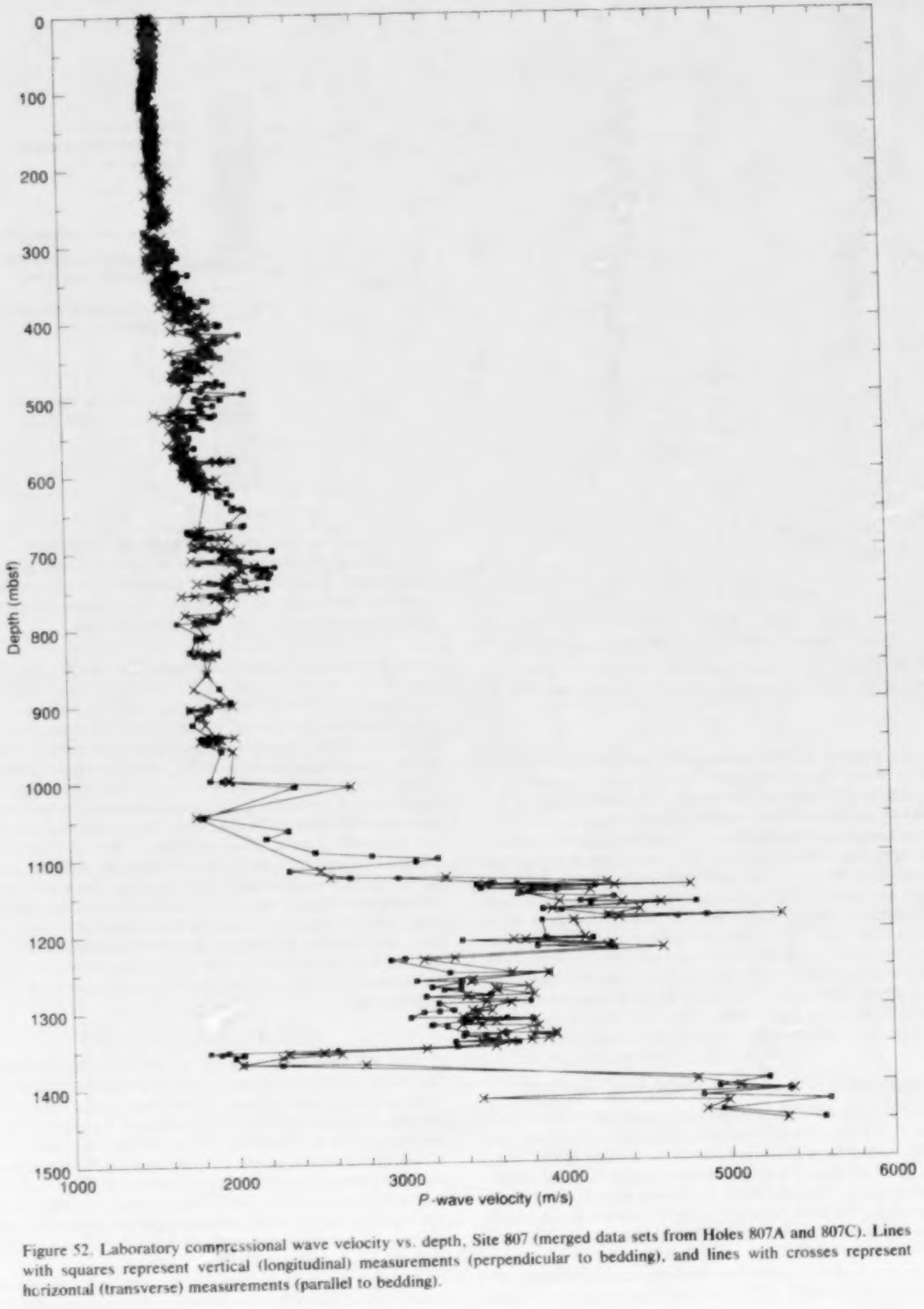

Figure 52. Laboratory compressional wave velocity vs. depth, Site 807 (merged data sets from Holes 807A and 807C). Lines with squares represent vertical (longitudinal) measurements (perpendicular to bedding), and lines with crosses represent horizontal (transverse) measurements (parallel to bedding).

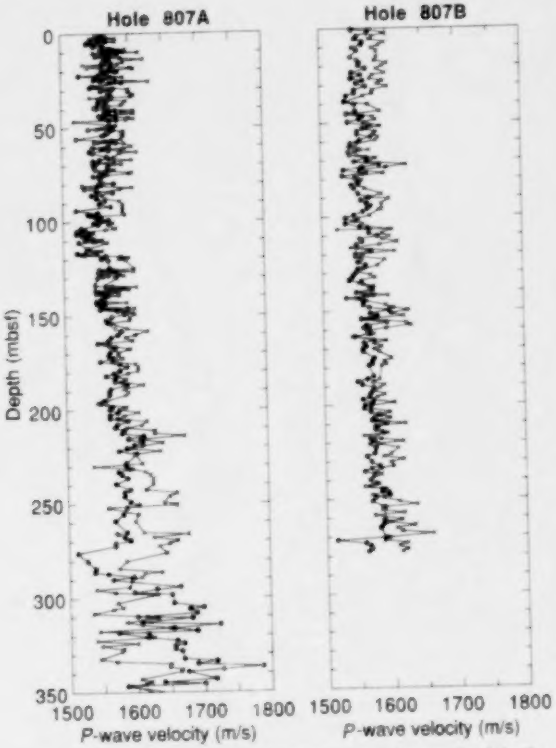

Figure 53. Laboratory compressional wave velocity vs. depth in the uppermost 350 mbsf, Holes 807A and 807B. Symbols used are as in Figure 52.

generally greater level of gamma-ray activity in the altered sections of the basaltic basement and the spikes produced by thin pockets or layers of sediment. The basement is clearly defined by an increase in density and resistivity at 1380 mbsf. A distinctive feature in the logs is the definition of the massive basalt flow that is characterized by a minimum in gamma-ray activity between 1447 and 1471 mbsf. Sediment layers or pockets are seen in the logs as maxima in gamma-ray activity and minima in density and electrical resistivity. Two of the intervals (1425 and 1439 mbsf) correspond to sediments recovered in the core. A third interval at 1435 mbsf is seen in the logs but was not recovered. Finally, the increase in resistivity at the bottom of Hole 807C (1562 mbsf) may represent the top of another massive basalt unit, although this interpretation cannot be supported as other measurements did not reach this depth.

Comparison of Logs from Holes 807A and 807C

Logs in Hole 807C overlapped the logs from Hole 807A in the interval from 350 to 803 mbsf. Coincident sections from 550 to 650 mbsf have been presented side-by-side in Figure 63. Correlation of data between the two holes is remarkable. Electrical resistivity data show an almost perfect match, with a difference of approximately 1 m between matching peaks at the top of the section and almost 2 m at the bottom, for a 1% difference in section thickness. Density and velocity logs show almost as much correspondence although the data vary at a shorter wavelength. There are two factors that may cause some degradation in the fit between the velocity and density logs from the two holes: (1) data from Hole 807C were decimated by 50% for the plot (i.e., there are twice as many data points in the Hole 807A data set as there are in the Hole 807C data) to save computer space; and (2) the state of the sea at the time of logging. Hole 807C was logged in seas that were almost flat, whereas there was a larger swell during logging operations at Hole 807A. In parts of the density and velocity sections, the Hole 807A data look like a smoothed version of the Hole 807C data. This could be a natural "smoothing" caused by small (around 0.5 m) oscillations of the logging tool downhole during the Hole 807A logging. The resistivity tool investigates a larger volume of the formation surrounding the hole, and thus may be somewhat less sensitive to ship's heave than the velocity or density tools. Regardless of the minor details, the overall agreement of the logs from two adjacent holes lends validity to even the minor peaks seen in the well logging data.

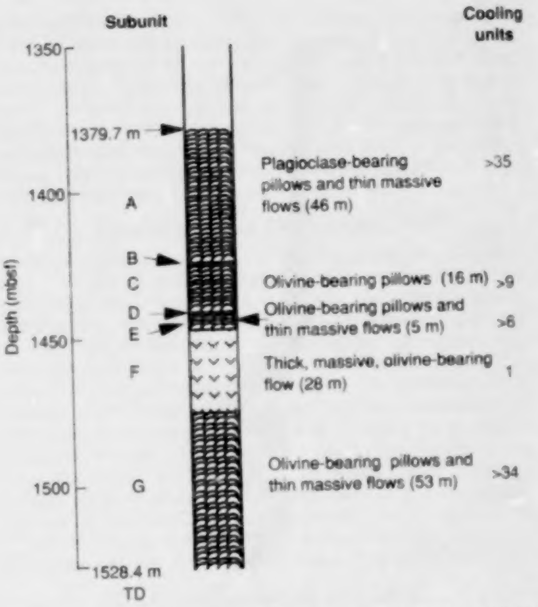
Subunit
Cooling units
1350
1379.7 m
1400
1450
1500
Depth (mbsf)
A
B
C
D
E
F
G
Plagioclase-bearing pillows and thin massive flows (46 m)
>35
Olivine-bearing pillows (16 m)
>9
Olivine-bearing pillows and thin massive flows (5 m)
>6
Thick, massive, olivine-bearing flow (28 m)
1
Olivine-bearing pillows and thin massive flows (53 m)
>34
1528.4 m TD

Figure 54. Lithologic column of basement, Hole 807C, showing distribution of pillows and thin, massive flows (Subunits A, C, E, and G) and thick, massive flow (Subunit F) as well as two thin sedimentary interbeds (Subunits B and D). Cooling "units" estimated from glassy chilled rinds are given on the right for each subunit.

SEISMIC STRATIGRAPHY

Site 807, the northernmost of the Leg 130 drill sites, is characterized by a thick sequence of parallel, closely spaced reflectors that are typical of the top of the Ontong Java Plateau. Located over a small basement basin, the selected site has one of the thickest (1.13 s) sections in the area. Most of the thickening is in the deepest part of the section where material from surrounding highs appears to have moved into the basement low (Fig. 64). The asymmetry of the basement structure is partly preserved through the sediment column, resulting in a pronounced surficial topographic feature directly over the basement high.

At several levels within the section, the loss of lateral coherency of the reflectors provides evidence of minor sedi-

Table 15. Major element, trace element, and CIPW-normative compositions of basalts from Hole 807C.

Core, section	74R-1	75R-2	76R-1	77R-1	78R-2	79R-5	80R-1	81R-2	82R-2	83R-2	84R-2	85R-5	86R-1	87R-2	88R-1	89R-1	90R-3	92R-2	93R-1
Interval (cm)	124–127	61–64	69–71	48–51	69–72	28–30	49–51	74–77	42–45	30–33	111–115	112–115	100–103	37–40	70–75	38–42	72–76	100–103	25–28
Subunit	A	A	A	A	A	A	A	C	C	F	F	F	G	G	G	G	G	G	G
Major elements (wt%):																			
SiO_2	48.65	48.17	49.06	48.88	48.76	49.46	48.44	50.21	50.57	50.07	50.48	50.01	49.19	50.45	50.22	49.44	49.37	50.35	50.17
TiO_2	1.66	1.59	1.61	1.61	1.59	1.65	1.66	1.20	1.21	1.14	1.14	1.10	1.14	1.20	1.15	1.17	1.15	1.16	1.15
Al_2O_3	14.73	14.07	14.35	14.33	14.05	14.62	14.79	15.08	14.91	13.91	13.95	13.85	14.25	15.20	14.08	14.10	14.09	14.46	14.24
$^aFe_2O_3$	12.54	13.51	13.33	13.27	13.49	12.75	12.77	10.53	10.96	12.88	12.64	12.99	12.92	10.25	13.24	13.05	12.64	12.28	12.72
MnO	0.18	0.20	0.18	0.19	0.27	0.18	0.40	0.22	0.23	0.19	0.19	0.18	0.22	0.19	0.21	0.22	0.21	0.20	0.21
MgO	6.05	7.26	6.42	6.70	7.18	6.45	7.02	8.01	7.61	7.41	7.55	7.89	7.20	7.93	7.22	7.73	7.71	7.40	7.45
CaO	12.43	11.77	11.94	11.99	11.75	12.30	12.27	11.42	11.84	11.85	11.77	11.89	11.94	12.51	12.14	12.28	12.30	12.02	12.15
Na_2O	2.45	2.32	2.43	2.49	2.34	2.49	2.41	2.28	2.29	2.08	2.05	2.01	2.15	2.40	2.17	2.08	2.16	2.17	2.13
K_2O	0.41	0.35	0.12	0.13	0.31	0.11	0.07	0.63	0.41	0.06	0.06	0.06	0.35	0.06	0.19	0.03	0.06	0.05	0.15
P_2O_5	0.14	0.14	0.13	0.14	0.14	0.14	0.14	0.11	0.10	0.09	0.10	0.09	0.11	0.10	0.10	0.10	0.09	0.09	0.10
Total	99.91	99.99	99.78	99.99	100.30	100.57	100.07	100.34	100.51	99.63	100.07	100.12	99.49	100.36	100.53	100.18	99.65	100.13	100.18
LOI	0.66	0.62	0.20	0.27	0.40	0.41	0.10	0.67	0.38	0.05	0.15	0.03	0.02	0.07	−0.19	−0.02	−0.13	−0.07	−0.29
^{b}CIPW norms:																			
Quartz										0.71	1.09	0.17						0.47	
Orthoclase	2.42	2.07	0.71	0.77	1.83	0.65	0.41	3.72	2.42	0.35	0.35	0.35	2.07	0.35	1.12	0.18	0.35	0.30	0.89
Albite	20.73	19.63	20.56	21.07	19.80	21.07	20.39	19.29	19.38	17.60	17.35	17.01	18.19	20.31	18.36	17.60	18.28	18.36	18.02
Anorthite	27.99	26.95	27.90	27.55	26.92	28.40	29.34	29.06	29.20	28.45	28.69	28.60	28.21	30.53	28.12	29.06	28.58	29.57	28.86
Diopside	27.08	25.16	25.21	25.62	25.11	26.17	25.22	21.92	23.63	24.50	23.91	24.50	24.99	25.16	25.95	25.68	26.18	24.22	25.32
Hypersthene	8.65	10.27	15.76	12.76	12.91	14.38	10.66	16.24	18.55	22.35	23.08	23.77	16.25	16.03	20.37	19.17	17.21	21.65	21.13
Olivine	5.63	8.45	2.60	5.14	6.45	2.71	7.16	4.19	1.58				3.99	2.73	0.94	2.67	3.50		0.53
Magnetite	2.16	2.33	2.30	2.29	2.33	2.20	2.20	1.89	1.89	2.22	2.23	2.24	2.23	1.77	2.29	2.25	2.18	2.12	2.20
Ilmenite	3.15	3.02	3.06	3.06	3.02	3.13	3.15	2.28	2.30	2.17	2.17	2.09	2.17	2.28	2.18	2.22	2.18	2.20	2.18
Apatite	0.32	0.32	0.30	0.32	0.32	0.32	0.32	0.25	0.23	0.21	0.23	0.21	0.25	0.23	0.23	0.23	0.21	0.21	0.23
Trace elements (ppm):																			
Zr	102	99	99	99	97	102	101	67	68	68	67	62	65	69	65	67	64	68	67
V	331	327	325	316	305	332	327	347	346	331	321	323	343	347	339	346	331	337	348
Sr	218	198	173	172	16	175	176	121	123	113	110	107	109	115	107	110	107	110	108
Rb	10	8	3	2	6	2	1	9	7	2	2		1	7	1	5	1	1	03
Zn	100	99	93	96	91	98	98	93	105	88	90	82	97	103	92	98	93	93	93
Cu	146	139	137	139	137	138	144	42	98	150	141	143	131	147	141	144	143	143	139
Ni	96	115	100	99	95	97	97	103	99	86	86	90	92	118	87	94	103	90	96
Cr	170	154	156	153	143	150	146	167	140	120	126	152	157	169	154	144	155	156	157
Y	30	29	30	29	30	31	30	24	23	26	25	22	25	27	24	23	24	26	24
Ga	19	21	17	20	20	21	18	19	19	17	15	18	18	19	15	18	17	17	17

Notes: Analyses were conducted at the University of Keele. CIPW-normative after Johanssen, 1931, for example. LOI = loss on ignition.

[a] All Fe expressed as Fe_2O_3.

[b] Fe_2O_3/FeO set at 0.15 and Mg number = (atomic) 100 Mg/Mg + Fe^{2+}.

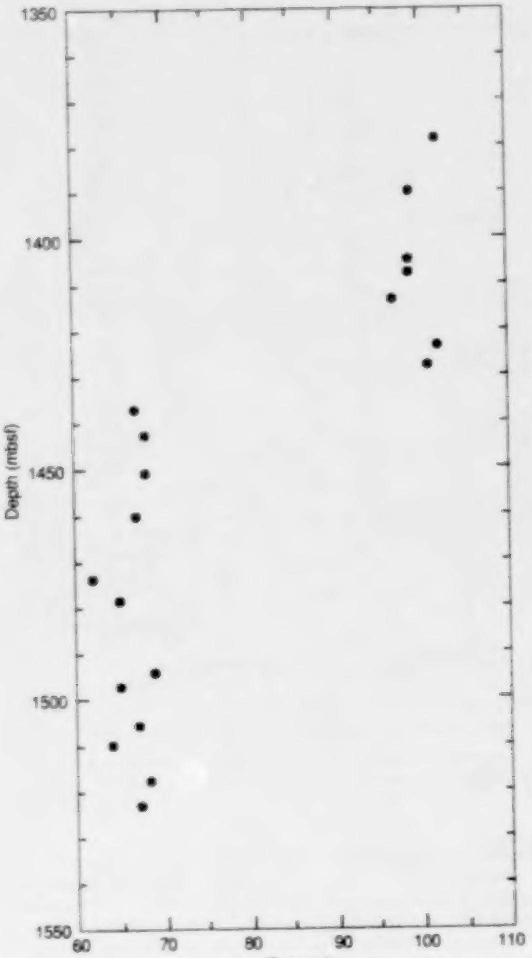

Figure 55. *Zr* vs. depth for Site 807 basalts. Note the abrupt break between high and low Zr lavas, which corresponds to Subunit A and Subunits C, E, F, and G, respectively.

ment disruption. These occur between 0.14 and 0.24 sbsf and between 0.28 and 0.41 sbsf. In each of these intervals, the sedimentologists noted an abundance of microfaults (see "Lithostratigraphy" section, this chapter). A third interval (0.44–0.53 sbsf) also shows seismic evidence of minor disruption and thickening, but a sedimentological expression of this disturbance was not observed.

Site 807 was not surveyed by the *Thomas Washington* during its Leg 130 site survey cruise (see Mayer et al., this volume); thus, a brief survey of the site was conducted by the *JOIDES Resolution* before beacon deployment. Details of this survey and of the seismic system used are presented in the "Underway Geophysics" chapter (this volume).

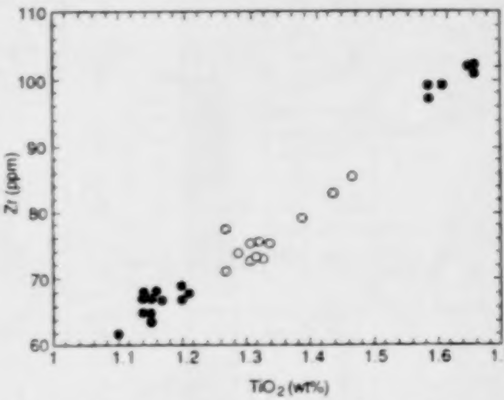

Figure 56. Zr vs. TiO_2 for Site 803 (open circles) and 807 (closed circles) basalts.

As at the previous sites, we have used the results of both laboratory and logging measurements to convert seismic traveltime to depth-in-section, and we employ seismic modeling to check on the accuracy of this traveltime-to-depth conversion. For Site 807, laboratory measurements of velocity and density were made approximately every 75 or 150 cm (see "Physical Properties" section, this chapter), and velocity and density logs (15-cm sample interval, 60-cm sensor spacing) were run for the section between 90 and 1530 mbsf (see "Logging" section, this chapter). Two separate logging runs were made at Site 807, the first on the section from 90 to 800 mbsf and the second from approximately 350 to 1530 mbsf. In this section, we will only use the results of the first logging run and physical properties data from Hole 807A. The results from Hole 807C will be incorporated into shore-based studies.

Laboratory measurements of density and velocity were converted to *in-situ* values using the methods described in Mayer et al. (1985) and merged with the logging data. A comparison of the *in-situ* corrected laboratory data with the log data reveals several inconsistencies that must be addressed before the data can be properly merged (Figs. 65 and 66).

If we assume that the log-derived densities and velocities represent *in-situ* values, then laboratory measurements, properly corrected to *in situ*, should be the same as the logging values. At the previous sites, the corrected laboratory values have, for the most part, been in good agreement with the logging data, implying that the procedure used to correct laboratory data to *in-situ* values is reasonable. Discrepancies between the laboratory and logging values (e.g., at Site 805 between 140 and 160 mbsf; see "Logging" section, "Site 805" chapter, this volume) have, at previous sites, been attributed to poor hole conditions that have degraded the logs in certain intervals. Comparing the Site 807 logs with the laboratory data reveals that between 90 and 200 mbsf the corrected density values are in reasonable agreement with the logging data; however, between 200 and 260 mbsf the logging values are significantly lower than the lab measurements (Fig. 65). Between 220 and 250 mbsf, the logged densities are so low that they are unquestionably in error.

A comparison of the log and laboratory velocity measurements (Fig. 66) reveals that between 90 and 140 mbsf the logging data are in agreement with the corrected laboratory

Table 16. Logging operations, Holes 807A and 807C.

Local day	Local time	Cumulative hours	[a]Depth (mbsf)	
130-807A-				
3/2/90	5:40			Last core on deck
3/2/90	12:21			Start rig up
3/2/90	13:44	0		RIH with geophysical tool string (NGT/LSS/DIT/TLT)
3/2/90	14:45	1.0		At mud line
3/2/90	14:55	1.2	85.6	Start downlog
3/2/90	16:08	2.4	802.8	Stop downlog
3/2/90	16:10	2.4	820.5	At bottom of hole; 2.4 m of fill
3/2/90	16:10	2.4	820.5	Start uplog; NGT/LSS/DIT/TLT; up at 900 ft/hr; heave compensator on
3/2/90	18:51	5.1	89.6	Tool in pipe at 9530 fbrf; POOH
3/2/90	20:02	6.3		Tool string on deck
3/2/90	20:38	6.9		Dropped bullnose down mousehole when bolt sheared
3/2/90	21:55	8.2		Substitute bullnose built; tool string being built up
3/2/90	22:05	8.4		RIH with NGT/ACT/HLDT
3/2/90	23:13	9.5	0	Passing mud line going down
3/2/90	23:45	10.0	821.1	On bottom with NGT/ACT/HLDT; start uplog, heave compensator on; 600 ft/hr
3/3/90	2:30	12.8	323.4	Power pulled to winch shack from engine room; heave compensator down
3/3/90	2:40	12.9	354.8	Drop to 354.8 mbsf to turn heave compensator back on continue log
3/3/90	3:57	14.2	109.4	Heave compensator turned off
3/3/90	4:09	14.4	75.6	Tool string in pipe; POOH
3/3/90	5:23	15.7		NGT/ACT/HLDT at wellhead; sources removed
3/3/90	6:30	16.8		Rigged down from logging runs on Hole 807A
130-807C-				
3/21/90	19:30	0		Start rig up
3/21/90	20:54	1.4		RIH with geophysical tool string (NGT/LSS/DIT/TLT)
3/21/90	21:59	2.5		At mud line
3/21/90	22:13	2.7	330.4	Start downlog; heave compensator on
3/21/90	23:36	4.1	1492.9	Stop downlog
3/21/90	23:39	4.1	1528.3	At bottom of hole; 0.6 m of fill
3/21/90	23:39	4.1	1528.3	Start uplog; NGT/LSS/DIT/TLT; up at 900 ft/hr
3/22/90	3:58	8.5	348.7	Tool in casing; POOH
3/22/90	5:25	9.9		Tool string on deck
3/22/90	6:19	10.8		RIH with NGT/ACT/HLDT
3/22/90	7:53	12.4	1525.8	On bottom with NGT/ACT/HLDT; start uplog, heave compensator on; 600 ft/hr
3/22/90	8:11	12.7	1467.9	Caliper jammed by debris in lower section, stop log
3/22/90	8:16	12.8	1527.0	On bottom again; start main uplog; 600 ft/hr
3/22/90	14:25	18.9	348.7	Tool string in casing; POOH
3/22/90	16:44	21.2		RIH with NGT/FMS/GPIT/TLT
3/22/90	18:06	22.6	0	Passing mud line, pause for TLT tie point
3/22/90	19:14	23.7	1509.1	Set down on bridge; start main uplog, heave compensator on, 900 ft/hr
3/22/90	21:23	25.9	947.3	Stop main uplog; hole above too wide for FMS caliper go down for repeat
3/22/90	21:50	26.3	1507.8	Start repeat uplog from same bridge; 900 ft/hr
3/22/90	23:11	27.7	1095.5	Stop repeat uplog; POOH
3/23/90	1:20	29.8		NGT/FMS/GPIT/TLT at wellhead
3/23/90	2:09	30.7		Rigged down from logging runs on Hole 807C

[a] Depth in Hole 807A based on mud-line depth below rigfloor of 2815.1 m, and depth in Hole 807C based on mud-line depth below rigfloor of 2817.0 m.

measurements and below 140 mbsf the two data sets diverge. Deeper than about 140 mbsf, the corrected laboratory velocities are consistently lower than the logged velocities. A detailed look at several indicators of borehole conditions reveals that there are changes in borehole behavior between 220 and 250 mbsf (see "Logging" section, this chapter). A full understanding of the effect of these borehole changes will have to await further study. It is clear, however, that the *in-situ* correction used throughout Leg 130 does not work at Sites 806 and 807 as well as it worked at previous sites (and in the central equatorial Pacific where it was derived). We speculate that this is a result of the fundamental difference in the consolidation behavior between the sediments that accumulate on the top of the plateau and those that accumulate in deeper water. These differences may be a result of variations in grain size (foraminifer abundance), early cementation, or clay content in these two environments.

To obtain the best possible data base for the seismic model, we eliminated the logging density values that were clearly inaccurate and used laboratory density data from the seafloor to 260 mbsf (and downhole density data deeper than that). The logging velocity data do not appear to be corrupted by borehole problems; thus, we used corrected laboratory velocity data only from the seafloor to 90 mbsf where no logging data was available. The compromise that we make in doing this is the loss of the detailed density sampling provided by

Table 17. Acronyms used in well logging.

Acronym	Definition or meaning
ACT	Aluminum clay tool
API	American Petroleum Institute standard units of gamma activity calibrated to test pit in Houston, TX
BHC	Borehole compensated sonic tool
DIT	Phasor dual induction tool
fbrf	Feet below rig floor
FMS	Formation microscanner
GPIT	Three-axis magnetometer-inclinometer logging tool
GST	Geochemical spectral tool
HLDT	High-temperature lithodensity tool
LSS	Long-spaced sonic logging tool
mbrf	Meters below rig floor
mbsf	Meters below seafloor
NGT	Natural gamma tool
POOH	Pull out of hole
RIH	Run into hole
SDT	Long-spaced sonic digital tool
TLT	LDGO temperature logging tool

logging, particularly in the interval from 200 to 260 mbsf where the laboratory sampling interval was reduced (Figs. 65 and 66).

The merged, corrected laboratory and logging data (velocity and density) were used to calculate acoustic impedance (Fig. 67), which was then convolved with a seismic source signature to generate a synthetic seismogram (see "Seismic Stratigraphy" section, "Site 803" chapter, this volume or Mayer et al., 1985, for details). The synthetic seismogram was compared to the field seismic profile to evaluate the accuracy of the traveltime-to-depth conversion. The field records used for this study are those collected by the *JOIDES Resolution* during the pre-drilling survey (see "Underway Geophysics" chapter, this volume). Because no source signature was available for the *JOIDES Resolution*'s seismic system, we used the source signature of the *Thomas Washington* seismic system. The *Thomas Washington* system appears to have a somewhat greater bandwidth than does the *JOIDES Resolution*, and thus the synthetic seismogram generated has a higher resolution than the field profile (Fig. 68).

As has been done at the previous sites, we looked in detail at several representative reflectors within the section. By examining the age and possible origin of these reflectors, we hoped to place the seismic record in a stratigraphic framework. The criteria for the selection of these reflectors were simply that they have large amplitudes and be laterally coherent *within the immediate area of Site 807*. No effort was made to select reflectors that were regionally correlatable (e.g., see Mayer et al., this volume), although the regional distribution of the named reflector patterns is evident (see "Summary and Conclusions" section, this chapter). As at Sites 805 and 806, we referred to the six named reflector series and intervals (Panama, Tethys, Antarctic, Drake, Texas, and Ontong Java; see "Seismic Stratigraphy" and "Summary and Conclusions" sections, "Site 805" chapter, this volume) to place the selected reflectors within a regional stratigraphic framework.

The comparison of the synthetic seismogram to the field profile at Site 807 (Fig. 68) produced a reasonable match, implying that the traveltime-to-depth conversion was acceptable. We have selected 11 reflectors in the 800 m of logged section; they are labeled on the plot of reflection coefficient vs. traveltime (Fig. 69); their traveltimes, depths, and ages are listed in Table 19.

Because of the longer outgoing pulse of the *JOIDES Resolution* seismic system, the youngest reflector that we could pick at Site 807 is associated with the "Panama" Series (7-1) at 3.6–3.8 Ma. This reflector has most of the characteristics of the "winnowing" physical property association (high velocity because of the large grain size and low density and carbonate content because of the removal of nannofossils, leaving an enrichment of silica), except that it has a high density rather than a low one (Figs. 67 and 70). This may mean that the grain size increase at this time is not a response to increased currents but, rather, is a function of a primary increase in foraminifer abundance or is associated with the increase in terrigenous components noted by the sedimentologists (see "Lithostratigraphy" section, this chapter).

In contrast, the next deeper reflector (7-2; 4.6–4.8 Ma) shows the complete "winnowing" physical property association but with extremely small changes in carbonate and density, which lead us to question whether winnowing is indeed the reflector-forming mechanism here. In an analysis of grain-size distribution parameters, the sedimentologists found no evidence for winnowing at Site 807 (see "Lithostratigraphy" section, this chapter). The mechanisms responsible for these physical property changes will be the subject of future study.

Reflector 7-3 (6.7 Ma) has all the indications of a diagenetically enhanced reflector (high velocity, high density, fine grain size, and a small increase in carbonate content), but it occurs at a depth at which the sedimentologists have not yet indicated the occurrence of chalk (Figs. 67 and 70). This may be the result of the greater sensitivity of the physical properties measurements to the onset of cementation, or a misinterpretation of the physical properties interrelationships. Again, shore-based studies of the physical properties interrelationships should resolve this issue. The final reflector of the "Tethys" series (7-4; 7.4–7.5 Ma) is once again associated with a grain size and velocity peak but no change in carbonate (there is little density data in this interval). A peak in foraminifer abundance was noted at this depth that may indicate a change in productivity or winnowing.

All of the deeper reflectors (7-5 through 7-11), with the exception of 7-9 (24.1–24.3 Ma), have the same physical properties associations, with density and velocity increasing or decreasing synchronously. As at Site 806, we interpret this to represent the diagenetic enhancement of an original oceanographic signal. Unlike Site 806, however, the carbonate content does not seem to vary in unison with the density and velocity, suggesting that the original oceanographic signal here may be somewhat different from that at Site 806. Reflector 7-9 is in the middle of an interval (570–630 mbsf) in which the velocity and density signals go out of phase. The reason for this is not yet understood but will be the subject of future study.

SUMMARY AND CONCLUSIONS

Site 807, located on the northern margin of the Ontong Java Plateau (latitude 3°36.4′N, longitude 156°37.5′E, 2805 m water depth) was drilled to answer questions regarding the origin and tectonic development of oceanic plateaus in general and the geologic history and paleoceanography of the Ontong Java Plateau in particular. Drilling objectives were (1) to provide Paleogene and Cretaceous sediments for studies of pre-Neogene paleoceanography; (2) to obtain basement rock for studies of the origin of the Ontong Java Plateau; and (3) to provide a second shallow-water site, off the equator, for comparison with Sites 803 and 806 on the Neogene equatorial depth transect. Criteria used to select Site 807 included (1) a position on the northern rim of the high plateau as far from Site 289 as feasible; (2) a location in fairly shallow water to obtain a well-preserved carbonate section; (3) the presence of

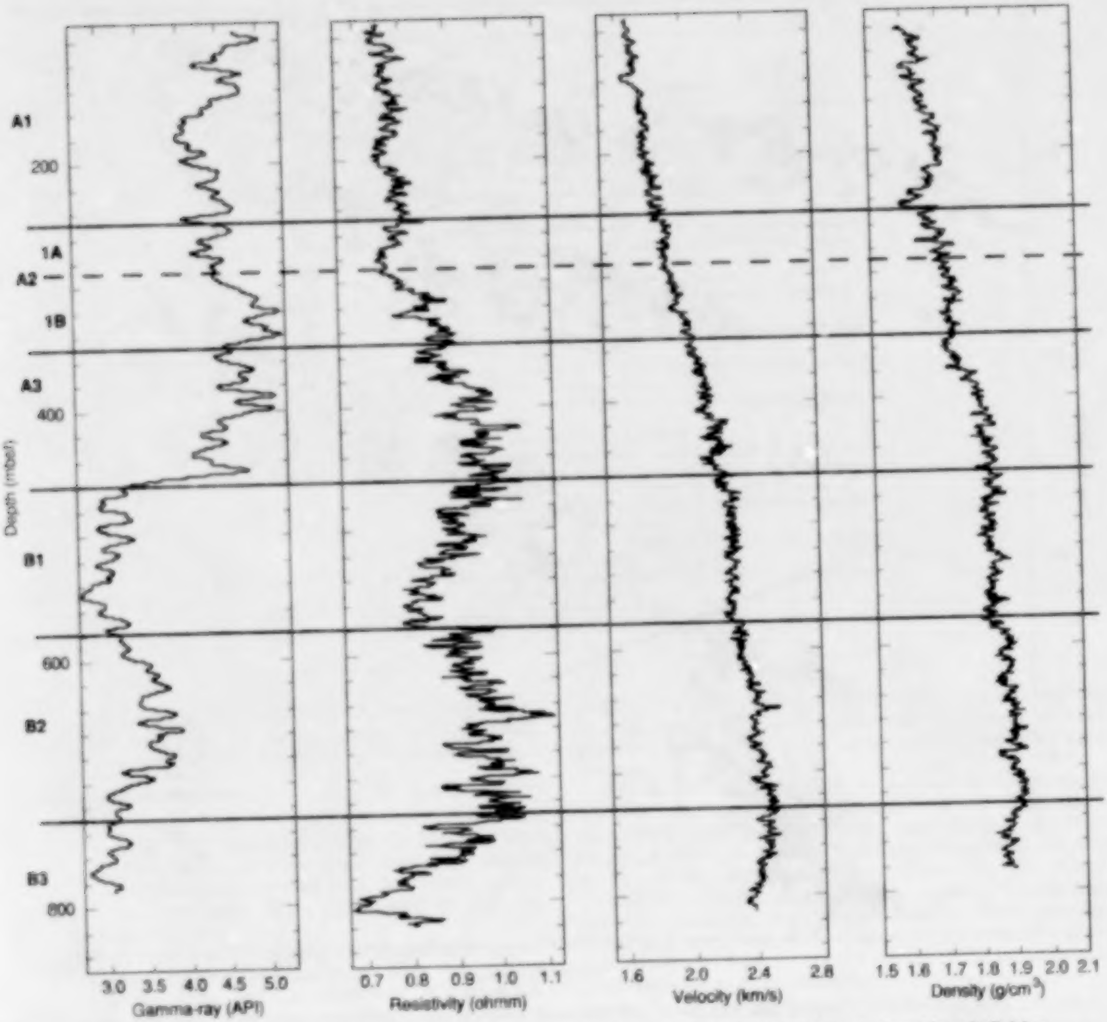

Figure 57. Well logging data, Hole 807A. Solid lines identify log stratigraphic units, dashed line defines lithostratigraphic unit division.

a thick section showing thinning in the upper layers and thickening in the lower layers in the seismic reflection profiles; and (4) the presence of an undeformed sedimentary and basement section in a location protected from potential bottom-current activity.

The site was positioned by means of a single-channel seismic (SCS) line acquired by the *Thomas Washington* during the EURYDICE Cruise 9 survey at 0255 UTC on 11 April 1975; it was resurveyed during Leg 130 (see "Underway Geophysics" chapter, this volume). Site 807 is located on the northern rim of a high plateau, roughly 475 km northwest of Sites 289/586, within a shallow basement graben about 0.5 km from the footwall of the northern side of the graben. The sedimentary section is thick, about 1.18 s of two-way traveltime in the SCS profile (see "Underway Geophysics" chapter, this volume) and shows well-behaved layering, disturbed by only minor thickening along the graben walls in the lower portion of the section, and a sheltered location from the ubiquitous bottom currents of the plateau. Thus, this site appeared to offer the best opportunity for recovering one of the most complete depositional sequences present on the plateau as well as representative basement samples.

Coring Results

Overview

Site 807 was occupied for 24.3 days. We cored 1701.6 m of Neogene, Paleogene, and Upper Cretaceous sediments, 533.0 m by APC (averaging 102% recovery), 568.5 m by XCB (80% recovery), and 599.7 m by RCB (27.4% recovery). We also cored 148.7 m of basement (dated as Lower Cretaceous), representing the deepest basement penetration yet achieved on a Pacific oceanic plateau (Fig. 71), and recovered 87.6 m of basalt and 0.6 m of interbedded sediment. Three holes were

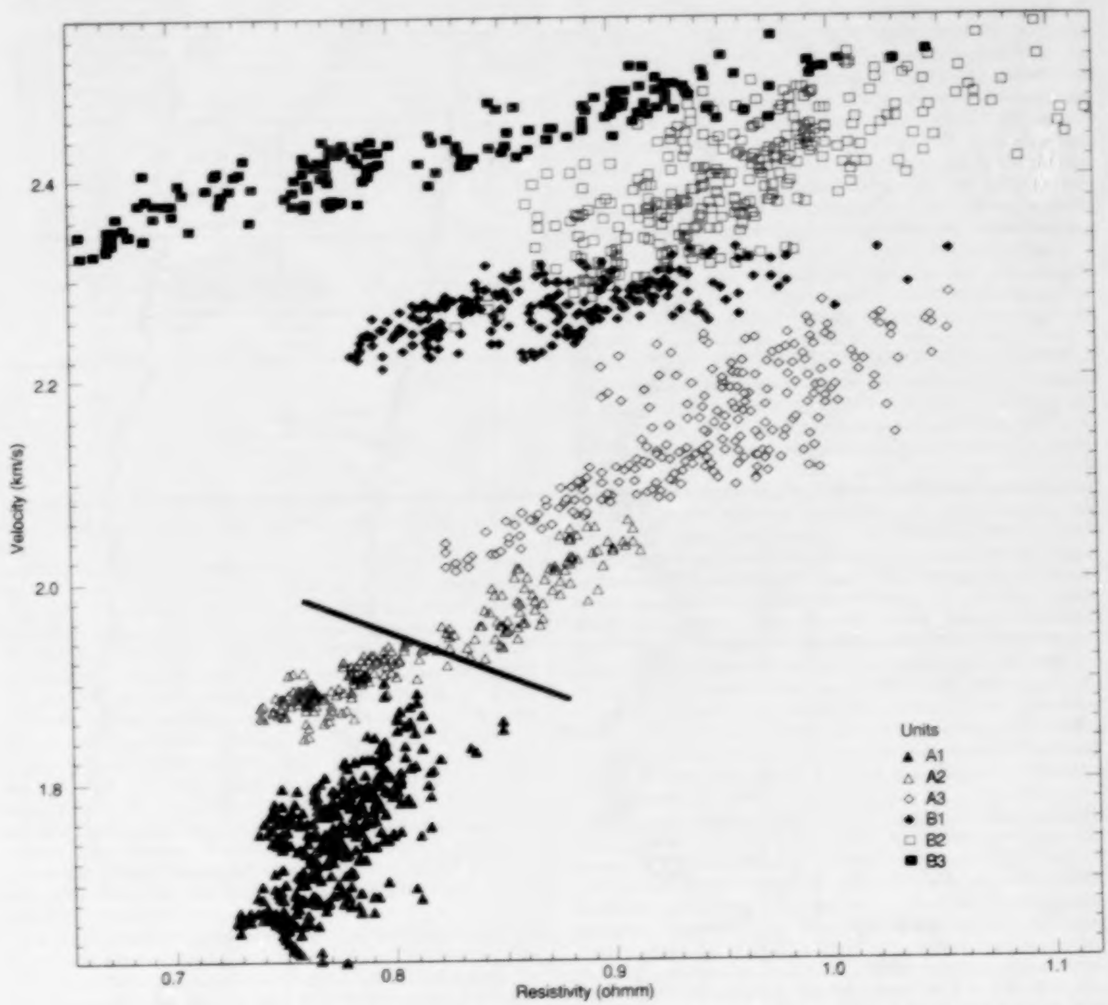

Figure 58. Electrical resistivity logging data plotted vs. compressional wave velocity logging data, Hole 807A. Solid bar represents the approximate location of the ooze-chalk transition identified in the recovered core.

drilled as follows: Hole 807A was cored with the APC to 254.4 mbsf and with the XCB to 822.9 mbsf; Hole 807B was cored with the APC to 278.6 mbsf; and Hole 807C was cored with the RCB from 780.0 to 1528.4 mbsf. Holes 807A and 807C were also successfully logged to total depth drilled, and a complete set of geophysical measurements were obtained (including FMS data in Hole 807C).

The sediments recovered range in age from Pleistocene to Early Cretaceous; they were divided into three lithologic units. Unit I (0–968.0 mbsf) is composed mainly of Pleistocene to upper/middle Eocene nannofossil ooze and chalk with foraminifers, with lesser amounts of foraminifer nannofossil ooze and chalk as well as nannofossil ooze and chalk. Unit II (968.0–1351.4 mbsf) is composed of upper/middle Eocene to upper Campanian limestone, chert, nannofossil chalk, and nannofossil chalk with foraminifers. Unit III (1351.4–1379.7 mbsf) is composed of lower Cenomanian to upper Albian–Aptian claystone, siltstone with varying amounts of radiolarians, and limestone. Igneous basement at Site 807 is represented by one lithologic unit, Unit IV (1379.7–1528.4 mbsf), which is predominantly composed of Albian-Aptian basalt.

The record is continuous from the Pleistocene to the upper Oligocene, at which time a stratigraphic break occurs at 702.4 mbsf (ca. 28–30 Ma), the first of three major stratigraphic breaks encountered above the Cretaceous/Tertiary boundary. Other breaks occur in the middle Eocene at 996.8, 1073.0, and 1094.8 mbsf (ca. 40–42 and 47–50 Ma). Much of the Paleocene-to-middle Eocene section is condensed, with the exception of part of the upper Paleocene. The K/T boundary was crossed at 1193.1 mbsf, and an apparently complete boundary sequence was recovered. The section below the K/T boundary also probably includes one or more stratigraphic breaks, in particular between the upper Campanian limestone

Table 18. Log stratigraphic units, Hole 807A.

Unit	Depth range (mbsf)	Gradient (km^{-1})	Characteristics
A1	?–253.5	0.5	Resistivity: gradual increase from 0.72 to 0.80 ohmm
		1.3	Velocity: gradient of 1.65–1.85 km/s
		0.7	Density: increasing from 1.60 to 1.70 g/cm^3, suspect minimum at lower boundary
A2	253.5–352	1.2	Resistivity: relative minimum of about 0.75 ohmm at 280 mbsf, increase to 0.87 ohmm
		2.0	Velocity: increase from 1.85 to 1.90 km/s at upper boundary, then generally constant, varying about 1.90 km/s, with an increase to 2.05 km/s at the lower boundary
		0.7	Density: increasing from 1.65 to 1.72 g/cm^3
A3	352–474	0.7	Resistivity: increasing from 0.87 to 0.95 ohmm at 400 mbsf, then constant with a scatter of 0.1 ohmm
		1.2	Velocity: increasing from 2.05 to 2.25 km/s at 415 mbsf, then varying about 2.20 km/s
		0.9	Density: constant to 380 mbsf, where there is a step from 1.72 to 1.80 g/cm^3, then increasing to 1.83 g/cm^3
B1	474–580	−1.2	Resistivity: decreasing from 0.95 to 0.80 ohmm about scatter of 0.1 ohmm
		0.0	Velocity: constant about 2.25 km/s
		0.2	Density: step increase from 1.83 to 1.85 g/cm^3 at 530 mbsf
B2	580–730.5	1.0	Resistivity: sharp increase from 0.85 to 0.95 ohmm at upper boundary, then gradual increase to 1.00 ohmm
		1.3	Velocity: increase at upper boundary to 2.25 to 2.30 km/s, then gradual increase to 2.50 km/s
		0.7	Density: increasing to 1.85 g/cm^3 within 10 m of upper boundary, then gradually increasing to 1.95 g/cm^3
B3	730.5–?	−1.7	Resistivity: decreasing from 0.95 to 0.70 ohmm, with less scatter at lower resistivities
		−1.7	Velocity: decreasing from 2.50 to 2.35 km/s
		−1.4	Density: decreasing from 1.92 to 1.85 g/cm^3 at 780 mbsf, bad data below this depth

and the lower Cenomanian claystone-siltstone sequences at 1351.4 mbsf and near the Aptian-Albian limestone-basalt contact encountered at 1379.7 mbsf in Core 130-807C-74R.

Stratigraphy of the Sediments

Unit I was divided into Subunits IA and IB, based on the depth of the ooze-chalk transition at 293 mbsf (ca. 10.4 Ma). The boundary is transitional, as the lower 30 m of Subunit IA contains a significant percentage of chalk in isolated nodules and layers and the upper 20 m of Subunit IB contains numerous thin intervals of ooze.

Subunit IA (0–293 mbsf) consists of Pleistocene to upper/middle Miocene foraminifer nannofossil ooze, nannofossil ooze with foraminifers, and minor amounts of nannofossil ooze, mostly ranging from sandy silt to silt and, only rarely, to silty clay. Foraminifer abundances vary from 4% to 40% and average about 23%. Significant maxima in mean grain size and foraminifer abundance were noted in Holes 807A and 807B at 25 mbsf (ca. 2 Ma), from 60 to 90 mbsf (ca. 4 Ma), at 160 mbsf (ca. 6 Ma), and between 220 and 250 mbsf (ca. 7–8 Ma). Significant minima were observed at 50 mbsf (2.5–3 Ma), at 135 mbsf (ca. 5 Ma), and between 190 and 210 mbsf (ca. 6.5 Ma). Carbonate content increases downhole from 88% in the Pleistocene section to an average of 92% in the Miocene section. Radiolarians and diatoms are present in trace amounts. Colors range from white (in the top 3 m) through pale brown to light gray. Horizontal color bands are pervasive, occurring in various shades of green or purple. Up to 2 cm thick and commonly in green and purple pairs, the bands first appear at 9 mbsf and increase in frequency downhole to a maximum in the upper Miocene, between 90 and 200 mbsf, below which they decrease in frequency. Bioturbation is extensive, as indicated by burrow structures, authigenic pyrite pellets, and trace fossils. The odor of H_2S also was detected upon splitting some of the cores. Burrows are commonly surrounded by discrete purple halos that crosscut and overprint color bands, suggesting the presence of redox gradients emanating from the burrows. Minor microfaulting is present.

Subunit IB (293–968.0 mbsf) consists of upper/middle Miocene to upper Eocene nannofossil chalk with foraminifers, foraminifer nannofossil chalk, and nannofossil chalk. Foraminifer abundances are high, about 20%, from 350 to 500 mbsf (ca. 13–21 Ma) and from 680 to 740 mbsf (ca. 27–31 Ma). Foraminifer abundances are low at the top of the subunit from 300 to 350 mbsf (ca. 11–13 Ma) and from 525 to 675 mbsf (ca. 22–27 Ma). Mean carbonate content for the subunit is about 93%. Carbonate maxima occur from 450 to 575 mbsf; minima occur from 325 to 425 mbsf and below 575 mbsf. Nine separate ash layers are present between 639 and 759 mbsf (ca. 26–32 Ma). The ash layers are dark gray and show the effects of bioturbation well. Radiolarians and diatoms are present in trace quantities. The chalk is predominantly white. Faint to distinct green color bands are common at the top of the subunit but are rare below 300 mbsf. The purple bands fluctuate in abundance throughout the subunit but are more frequent between 700 and 760 mbsf. The bands thin with depth to a thickness of <1 mm. Swarms of thin bands exhibiting wavy, braided, flaserlike patterns are common. Bioturbation is common as indicated by burrow mottles, trace fossils, and pyritized burrow linings that become flattened with depth.

Unit II was divided into Subunits IIA and IIB, based on the transition from chalk to limestone. The boundary between the two subunits is placed at 1098.0 mbsf, where a limestone lithology is indicated by the presence of over 50% nonbiogenic carbonate in the smear slides. The transition is also reflected in a substantial increase in average core recovery, from about 7% in Subunit IIA to about 44% in Subunit IIB.

Subunit IIA (968.0–1098.0 mbsf) consists of middle Eocene nannofossil chalk, nannofossil chalk with foraminifers, lime-

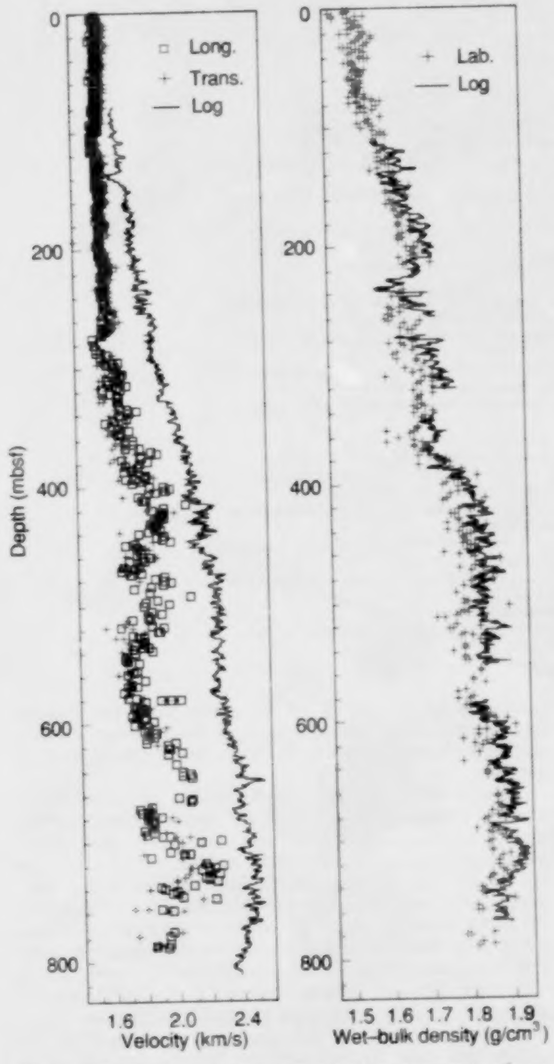

Figure 59. Comparison of laboratory sample measurements of compressional wave velocity and bulk density with logging data, Hole 807A. Laboratory data are plotted vs. depth but are not corrected for *in-situ* conditions. Long = longitudinal, trans = transverse, and lab = laboratory.

stone, silicified limestone, and chert. The chalk is white and moderately bioturbated. Burrows are commonly flattened and predominantly horizontal. Isolated occurrences of gray, anastomosing color bands or flaser structures were observed. Both the limestone and the silicified limestone are white. The chert is gray, apparently nodular, and commonly occurs with chalk coatings and millimeter- to centimeter-size chalk inclusions.

Subunit IIB (1098.0–1351.4 mbsf) consists of middle Eocene to upper Campanian limestone and chert. The limestone is predominantly white and moderately to highly bioturbated, as evidenced by weak mottling, finely disseminated pyrite, and flattened horizontal burrows. Stylolites occur throughout the subunit. Gray and red chert nodules and minor chert layers are present in all cores. At least 15 ash layers were found between 1140 and 1200 mbsf (ca. 56–67 Ma). The thickest is a 3-cm layer encountered at 1156.6 mbsf (ca. 57 Ma), whereas the remaining layers are about 1 cm thick. At least 10 dark gray to brown clay layers were found between 1300 and 1351 mbsf (ca. 74–76 Ma); these may represent altered volcanic ash (the upper 2 layers contain volcanic glass). Evidence for redeposition is ubiquitous below 1116 mbsf. Clasts of white limestone, about 5 mm in diameter, are dispersed throughout a slightly darker matrix from 1116 to 1197 mbsf, indicating a steady input of debris from the flanks of the graben. Nannofossils from a clast at 1127 mbsf are of Late Cretaceous age, whereas nannofossils in the matrix are of mixed Paleocene and Cretaceous age. Evidence for mass transport is pervasive below 1197 mbsf. Laminae or beds of well-sorted carbonate grains, 5 mm to 5 cm thick, were observed between 1197 and 1232 mbsf. Low-angle truncation surfaces and the well-sorted nature of the grains suggest that some of the parallel laminae are primarily formed by redeposition of winnowing. Clast-bearing intervals alternating with clast-free intervals over thicknesses of 1–5 m are common below 1232 mbsf. Most of the clasts, ranging from 1 to 5 cm in diameter, are white limestone, but gray clasts become more abundant below 1271 mbsf, and green clasts are present below 1290 mbsf. The green clasts may be altered basaltic glass. Dark brown claystone clasts are common below 1321 mbsf. The clast-bearing intervals probably represent debris-flow deposits. A fold at 1264 mbsf, underlying a 1-m-thick, graded, clast-bearing interval, supports the debris flow interpretation.

Unit III was divided into Subunits IIIA and IIIB, based on the relative abundances of claystone and limestone.

Subunit IIIA (1351.4–1369.7 mbsf) consists of lower Cenomanian to upper Albian claystone interbedded with siltstone with radiolarians, radiolarian siltstone, and radiolarian sandy siltstone. The claystone is very dark grayish brown. Bioturbated intervals are indicated by the presence of mottling and burrows, about 1 cm long. The siltstone interbeds, which are generally gray, are rare at the top of the subunit, but they become more abundant and increase in radiolarian content downhole. The contacts between the claystone and the siltstone interbeds are predominantly gradational, but sharp contacts and graded bedding are also present. Although few scour marks or load structures were observed, the overall interbedded pattern emphasizes the importance of episodic deposition at Site 807.

Subunit IIIB (1369.7–1379.7 mbsf) consists of upper Albian–Aptian limestone and chert. Although the limestone was recovered from 1369.7 to 1375.6 mbsf, as measured from the cores, a distinct decrease in the drilling rate at 1379.7 mbsf suggests that this depth is the contact between the limestone and the underlying basalt. The recovered limestone is generally gray and bioturbated. The upper part contains very fine, vertical, anastomosing fractures. The lower part contains wavy, lenticular beds, about 0.5–3 cm thick, as well as microfaults and abundant healed tensional cracks. The chert, found in both intervals, is black to dark gray and nodular in origin.

Basement Stratigraphy

Unit IV (1379.7–1528.4 mbsf), comprising basement at Site 807, is composed of Albian-Aptian tholeiitic basalt and interbedded limestone, and is divided into seven subunits, IVA through IVG, five of which are igneous (IVA, IVC, IVE, IVF, and IVG), and two of which are sedimentary (IVB and IVD).

Subunit IVA (1379.7–1424.6 mbsf): aphyric pillow lavas and thin (<2 m thick) massive flows with rare plagioclase phenocrysts up to 3 mm long, superficially similar to lavas at Site 803.

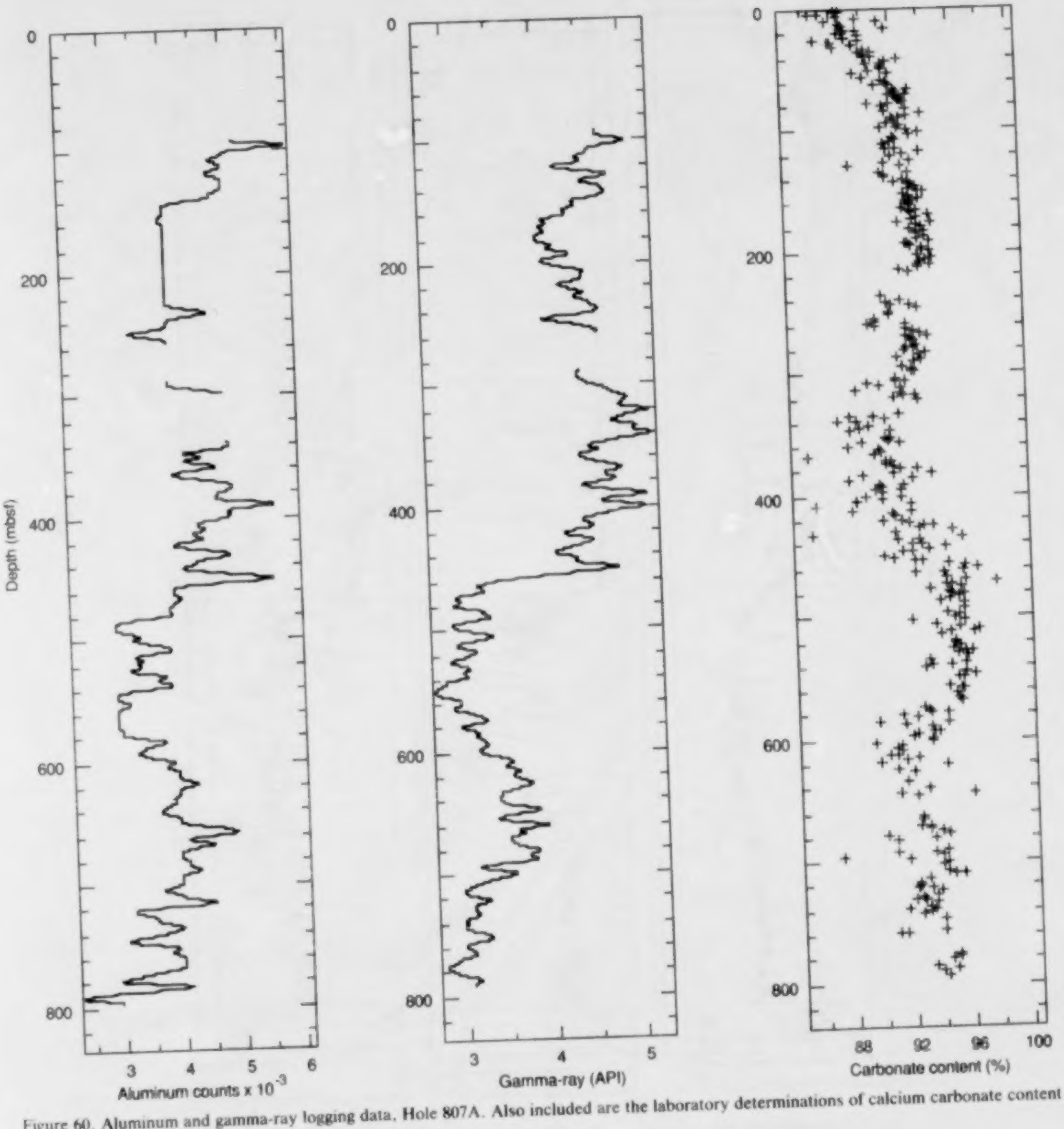

Figure 60. Aluminum and gamma-ray logging data, Hole 807A. Also included are the laboratory determinations of calcium carbonate content from the physical properties samples.

Subunit IVB (1424.6–1425.1 mbsf): Albian-Aptian limestone interbedded with vitric tuff. The limestone is white and contains numerous healed fractures. The tuff is dark reddish brown to reddish brown.

Subunit IVC (1425.1–1441.9 mbsf): aphyric pillow lavas and thin (<3 m thick) massive flows with sparse, euhedral to subhedral, olivine microphenocrysts (<1 mm long), largely replaced by green and black clays.

Subunit IVD (1441.9–1442.0 mbsf): Albian-Aptian limestone, which is olive brown and contains quartz and illite/glauconite.

Subunit IVE (1442.0–1447.0 mbsf): aphyric pillow lavas and thin (<3 m thick) massive flows with sparse, euhedral to subhedral, olivine microphenocrysts (<1 mm long), largely replaced by green and black clays.

Subunit IVF (1447.0–1475.0 mbsf): aphyric massive flow with sparse, euhedral to subhedral, olivine microphenocrysts (<1 mm long), largely replaced by green and black clays.

Subunit IVG (1475.0–1528.4 mbsf): aphyric pillow lavas and thin (<3 m thick) massive flows with sparse, euhedral to subhedral, olivine microphenocrysts (<1 mm long), largely replaced by green and black clays.

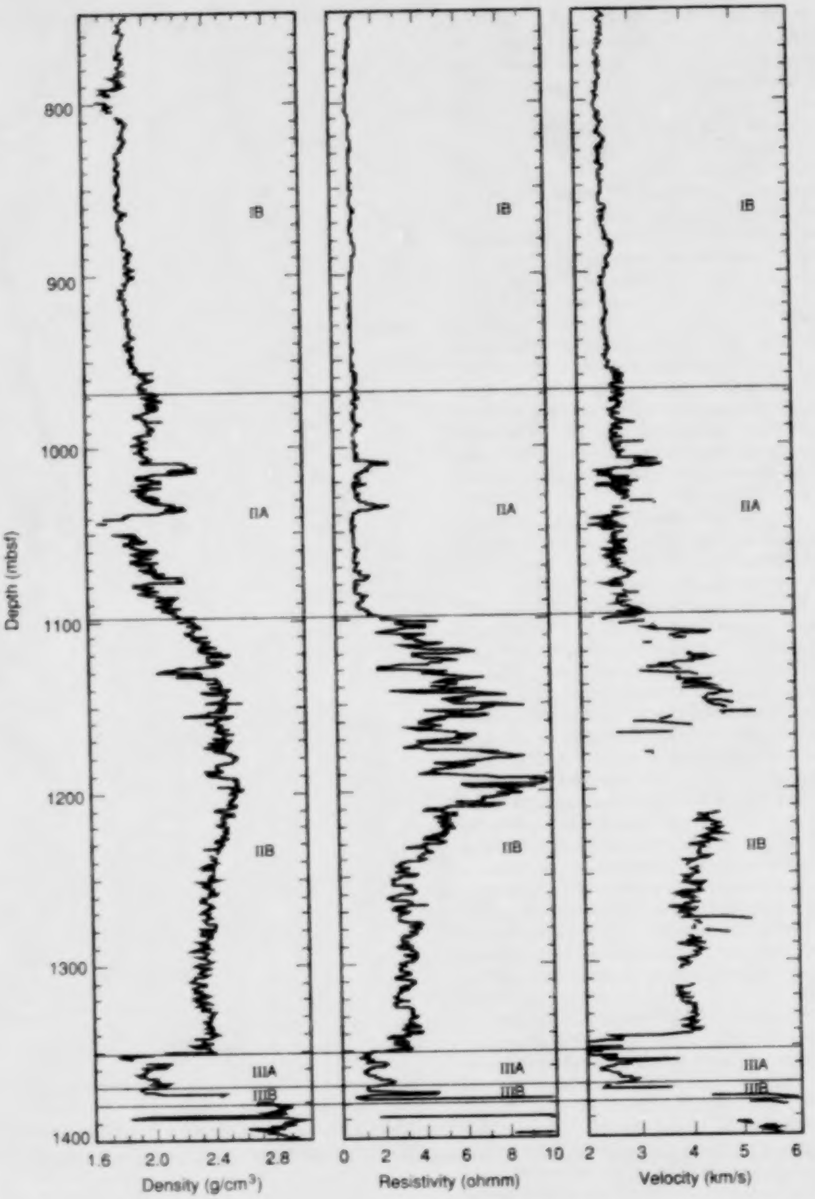

Figure 61. Compressional wave velocity, electrical resistivity, and bulk density logging data from the lower sedimentary section, Hole 807C. Basement depth is 1380 mbsf. Lithostratigraphic unit boundaries are superimposed on the plot.

Flecks of native copper were observed in several of the basalt cores below the sedimentary interbeds of Subunit IVB, particularly in vein material in Section 130-807C-82R-2 at 40 and 58 cm. Disseminated pyrite also was observed in glassy pillow rims and fractures. Another sedimentary interbed, unsampled in the coring but detected during logging, occurs within Subunit IVC at 1434 mbsf. All of the igneous subunits of Unit IV are composed of tholeiitic basalt, generally only slightly altered. Subunits IVA, IVC, IVE, and IVG are successions of pillow and thin (<3 m thick) massive flows. Subunit IVF, however, consists of a single massive flow, approximately 28 m thick. This flow documents the presence of thick flood basalt lavas on the Ontong Java Plateau. The general paucity of phenocrysts is reminiscent of some continental flood basalts, notably the Grande Ronde formation of the Columbia River Basalt Group.

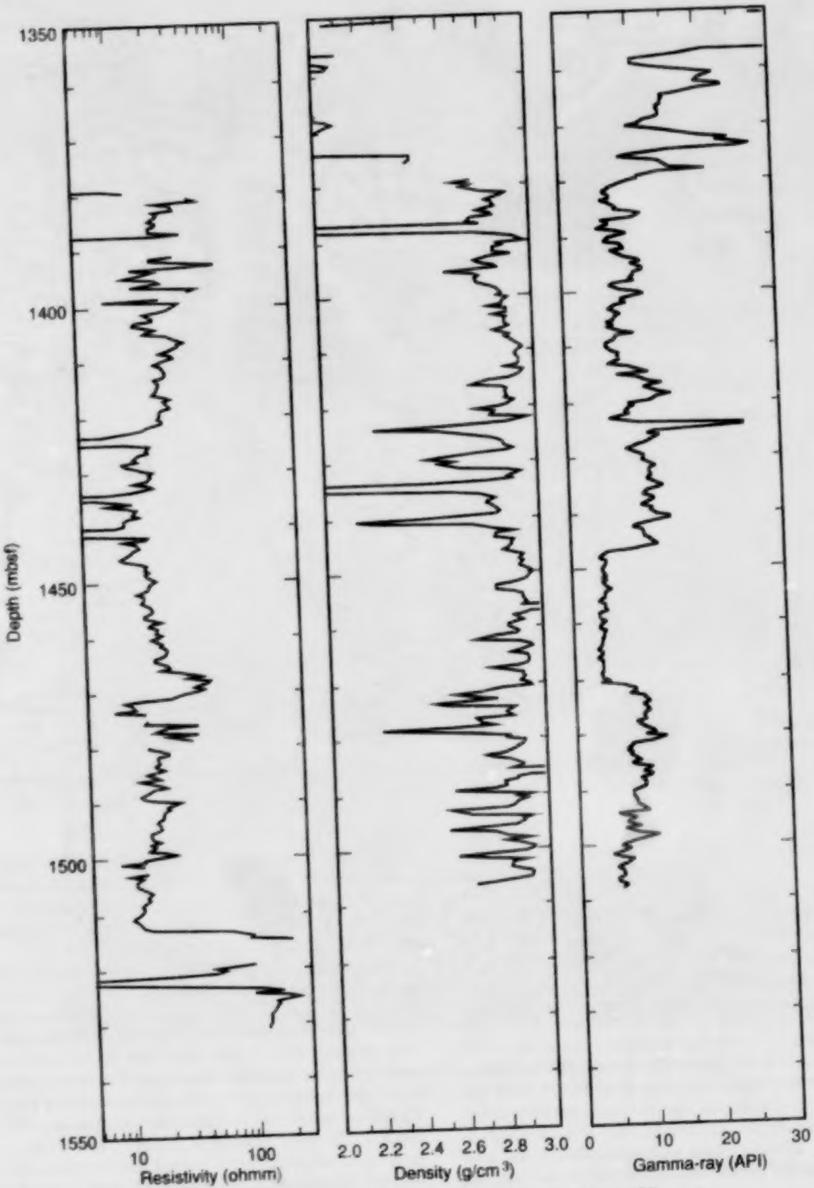

Figure 62. Basement logs of gamma-ray, resistivity, and bulk density, Hole 807C.

Special Studies

Paleomagnetic measurements were made on all APC and XCB cores from Hole 807A, on Cores 130-807B-1H through -10H from Hole 807B, and on all RCB cores from Hole 807C. The Pleistocene sediments of Holes 807A and 807B contain a well-defined record of the Brunhes/Matuyama boundary as well as the Jaramillo and Olduvai subchrons. These polarity boundaries enable a precise determination of Pleistocene sedimentation rates. Parts of the Miocene section, as well as parts of the Oligocene, Eocene, and Paleocene, also look promising for paleolatitude determinations. At the base of the sedimentary section in Hole 807C, the brown claystone/siltstone sequence has NRMs dominated by a viscous present-day overprint that may permit determination of a Cenomanian-Campanian paleodeclination. The Aptian-Albian age of the sediments overlying the basalt suggests that we have recovered a volcanic sequence that is especially promising for refining the Pacific Plate APWP. The NRMs of the basalts are dominantly steeper than 20° in inclination. If the NRMs are

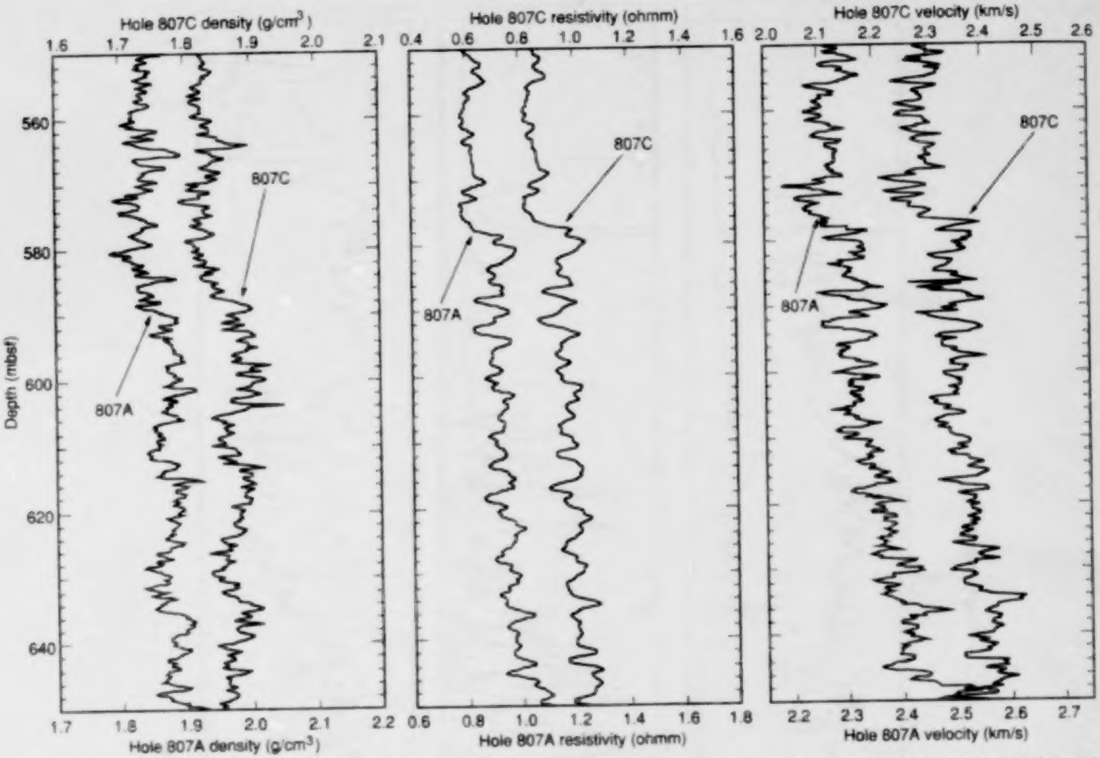

Figure 63. Comparison of logging data from Holes 807A and 807C over the interval from 550 to 650 mbsf from each log. Note that the Hole 807A data have been offset as follows in each instance to facilitate comparison: density by 0.1 g/cm^3, resistivity by 0.2 ohmm, and velocity by 0.15 km/s.

dominated by a primary remanence, as suggested in accordance with the freshness of the rocks, then the entire basalt sequence is of normal polarity.

Magnetic susceptibility measurements yielded good results well into Pliocene sediments. These data will be useful for fine-scale correlation and for studies of Milankovitch-type cycles.

Results from interstitial water geochemistry at Site 807 are similar to those obtained at Sites 803 and 804. The conservative gradients (Ca and Mg) compare favorably with those of Sites 288 and 289, suggesting similar rates for basalt alteration and diffusion. These and other gradients reflect the dominance of biogenic sediments and the paucity of organic carbon. Ca- and Mg-depth gradients are the least pronounced at Site 807, as compared with the other sites, and the Mg profile at Site 807 is anomalous in the lower part of the section where Mg concentrations remain constant with increasing depth. Dissolved silica concentrations generally increase with depth down to 900 mbsf (ca. 36 Ma), then decrease and level off at 1000 mbsf (ca. 42 Ma) in the silicified sediments of Unit II.

The combined carbonate content curve for Holes 807A and 807C (Fig. 72) closely reflects the lithostratigraphic units described at Site 807. The nannofossil oozes and chalks of Unit I are characterized by very high carbonate contents ranging from 85% to 95%. The chert-rich limestones in Subunit IIA and the upper part of Subunit IIB vary widely in carbonate content, ranging from 51% to 97%, whereas the chert-poor limestones of Subunit IIB are characterized by consistently high values ranging from 95% to almost 99%. In contrast, the claystones/siltstones of Subunit IIIA have carbonate contents <0.3% and are similar to equivalent intervals recovered above basement at Site 803.

Excellent well-log data were obtained from Holes 807A and 807C. The logs from both holes correlate well over scales of decimeters, instilling confidence in the measurements and also in the interpretation of cyclicity for Milankovitch time scales. The logging data from Hole 807A, in conjunction with a detailed suite of physical properties measurements obtained from the split cores, confirm the depth of the ooze-chalk transition based upon sediment descriptions. The logging data from Hole 807C likewise confirm the depth of the chalk-limestone transition and reveal the presence of local maxima and minima in velocity that correlate with chert/silicified chalk horizons and the claystone/siltstone beds deep in the section. Velocity, density, and resistivity all increase across the Unit I/II boundary because of the lower porosity of the chert and the effect of increased cementation of the calcareous sediment by silica. The Subunit IIA/IIB boundary is clearly seen in the logging data as an increase in velocity, density, and electrical resistivity and reflects the transformation of chalk and silicified chalk to limestone.

The logs allow an estimate of the amount of chert present in the section, which is seen to vary between 20% and 70% (Fig. 73), the higher values signifying the presence of massive cherts or beds of highly silicified limestone. The claystone,

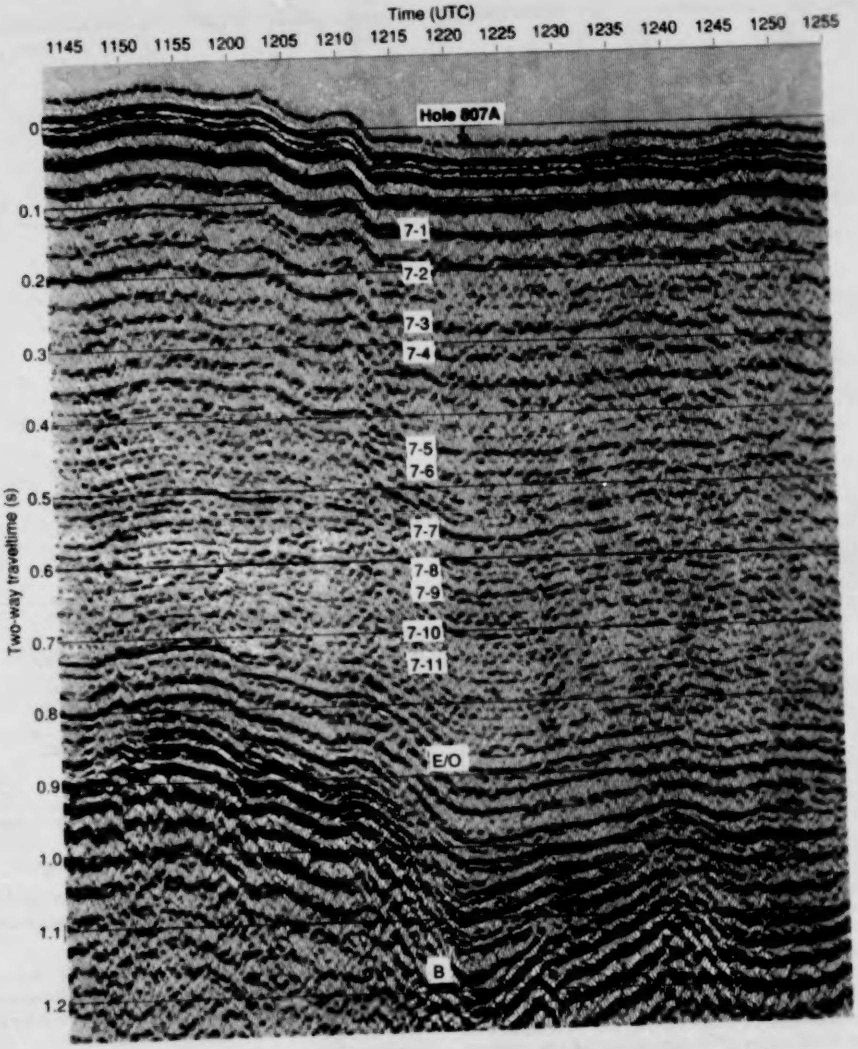

Figure 64. Seismic record collected by *JOIDES Resolution* over Site 807, using the 80- and 200-in.^{3} water guns, 70–250 Hz band-pass filter. For details of reflector picks, see Table 19. E/O = Eocene/Oligocene boundary and B = basement.

siltstone, and limestone of lithologic Unit III appear in the logs as an interval of reduced velocity, resistivity, and density. Basement is clearly defined as an increase in density, resistivity, and velocity. Gamma-ray, density, and resistivity logs together with the FMS data confirm the presence of a single massive flow in Subunit IVF and help identify the presence of sedimentary interbeds in the overlying pillowed flow subunits, including the one unsampled by the coring operation. Resistivity logs, moreover, suggest that another massive flow might be present at the bottom of the hole. For the sedimentary section, the logs provide important constraints on the generation of synthetic seismograms. Duplication of logging runs in the paired Holes 807B and 807C allows assessment of the precision of the logging data.

A reasonably complete seismic stratigraphy is present at Site 807. Comparison of the synthetic seismogram to the field profile (Fig. 68) produces a good match, implying that the traveltime-to-depth conversion is acceptable. Evidence for small-scale mass movement was observed at 0.14–0.24 and 0.28–0.41 sbsf (4.7–6.7 and 7.5–12.5 Ma, respectively). Thickened wedges of sediment occur between 0.44 and 0.53 sbsf (14.5–20.5 Ma) and around 1.00–1.02 sbsf (about 50.4 Ma). Basement occurs at approximately 1.18 sbsf (1379.7 mbsf, based on the drilling).

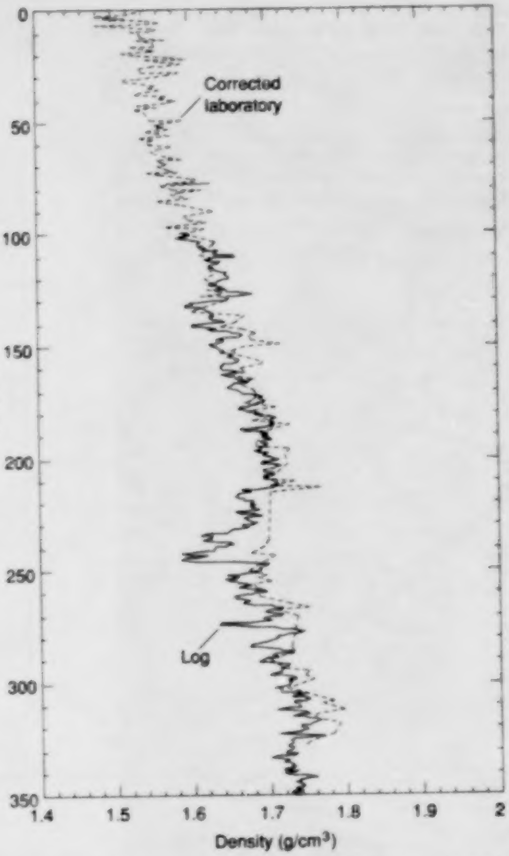

Figure 65. Merged laboratory and log density profile, Hole 807A. Laboratory values, corrected to *in situ*, are used from 0 to 260 mbsf, and log values are used from 260 to 783 mbsf.

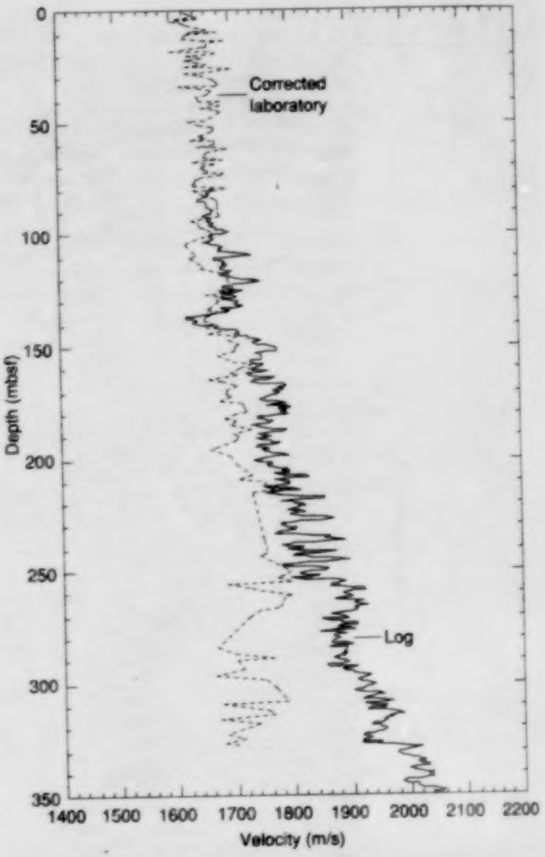

Figure 66. Merged laboratory and log velocity profile, Hole 807A. Laboratory values, corrected to *in situ*, are used from 0 to 90 mbsf, and log values are used from 180 to 783 mbsf.

Sequence of Events

The sequence of events as deduced from the drilling at Site 807 portrays the final stage of development of the world's largest submarine flood basalt plateau. The Ontong Java Plateau evidently formed, for the most part, by widespread effusion of massive flood basalts into deep water during Aptian time. The sequence of eruptive events that occurred toward the end of the formation of the plateau, as recorded at Sites 803 and 807, are as follows.

The final phase of flood basalt effusion was characterized by the eruption of a massive flow, which was closely followed by the eruption of a series of thin pillowed flows. This sequence was followed, in turn, by the eruption of another massive flow, again closely followed by the eruption of another series of thin pillowed flows. After an interval of time (of uncertain duration), represented by the deposition of a limestone-claystone facies at Site 807, the eruption of a late-stage sequence of pillowed flows occurred. Based on phenocryst assemblages, these probably are of a more evolved composition and represent the waning phase of volcanism at the site.

The first sediments to accumulate at the thermally elevated site were limestones and vitric tuffs, deposited above (but probably close to) the Early Cretaceous CCD (i.e., above 3000 mbsl). As the plateau cooled and contracted, the seafloor subsided, and a radiolarian ooze-clay facies began to accumulate as the site rapidly sank below the CCD. The graben that probably developed around the site during plateau subsidence apparently provided a sediment trap and sheltered accumulating sediment at the site from bottom-current activity, thus preserving the early depositional history of the Ontong Java Plateau.

Following deposition of the upper Albian–lower Cenomanian claystone-siltstone facies, there appears to be a major hiatus, possibly caused by deposition below the CCD. Subsequently, the upper Campanian–Maestrichtian limestones were laid down, presumably in response to a rapidly falling CCD. Sedimentation rates decreased from 10–20 m/m.y. in the late Maestrichtian to <5 m/m.y. in the early Paleocene. Mid-ocean volcanism apparently began on or near the Ontong Java Plateau in latest Maestrichtian time, as evidenced by the ash layer deposited just below the K/T boundary at Site 807. The volcanism, increasing in intensity (or proximity to the site),

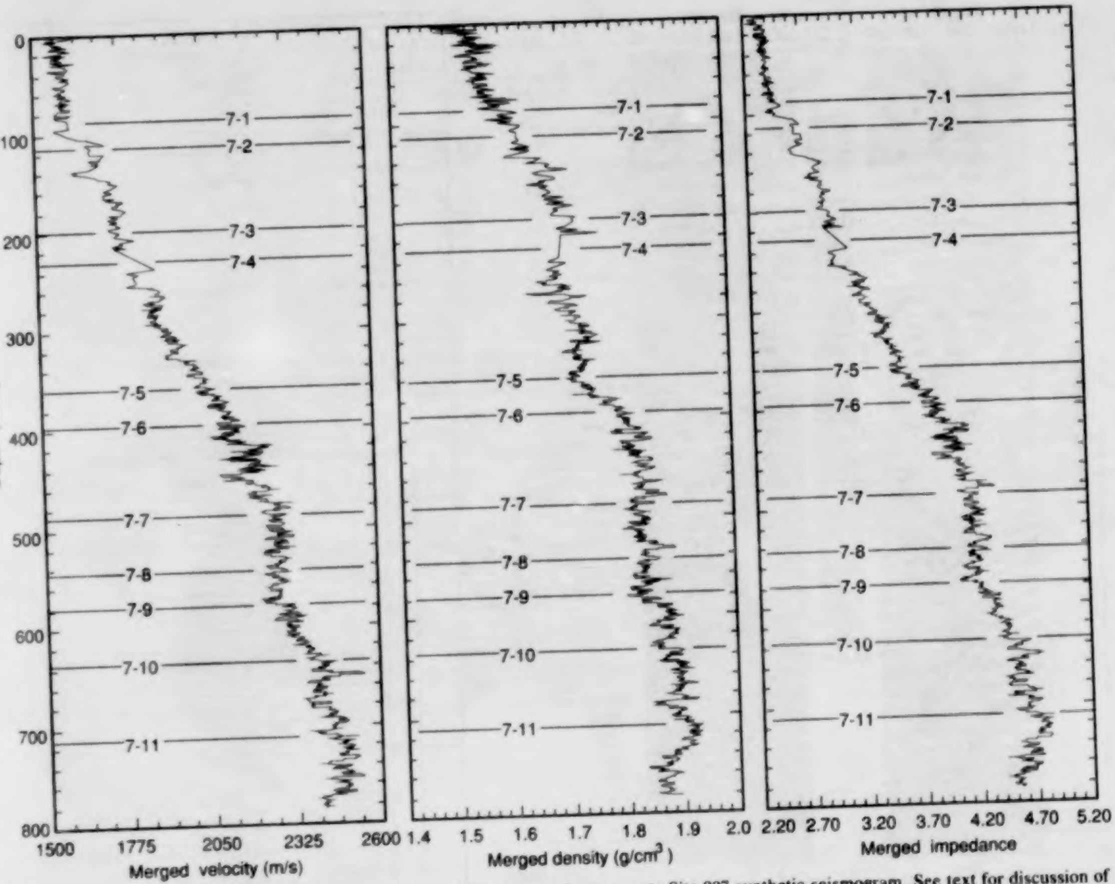

Figure 67. Velocity, wet-bulk density, and acoustic impedance data used to generate Site 807 synthetic seismogram. See text for discussion of reflector picks.

peaked in the late Paleocene (ca. 57 Ma) and then receded, disappearing entirely by middle Eocene time (ca. 54 Ma). After an initial low of near 1 m/m.y. in the early/middle Eocene (ca. 54–51 Ma), sedimentation rates increased in the Paleogene, peaking near 30 m/m.y. in the late middle Eocene (ca. 45–43 Ma). Hiatuses, however, also apparently occurred in the middle Eocene (ca. 50–47 and 43–40 Ma).

Volcanism began again in early-late Oligocene time (ca. 32–26 Ma), as the Ontong Java Plateau docked against the Melanesian Arc (Kroenke, 1984). A jump in sedimentation rate between 20 and 35 m/m.y. occurred in the early Oligocene (ca. 32–30 Ma), followed by another hiatus (ca. 28–30 Ma). Deposition thereafter was uninterrupted. Sedimentation rates ranged from 30 m/m.y. across the Oligocene/Miocene boundary (ca. 28–22 Ma), through 16–18 m/m.y. in the early to early late Miocene (ca. 22–4 Ma), to 44 m/m.y. in the late Miocene (ca. 8–5 Ma), before dropping to the Quaternary rate of about 15 m/m.y.

Comparison with Other Sites

Site 807 was the last site to be drilled on Leg 130, providing an opportunity for comparison with the results obtained previously. Only Neogene sedimentation patterns will be considered here; for additional topics, see Berger et al. (this volume).

The Neogene carbonate stratigraphy of Site 807 (Fig. 72; above 600 mbsf) shows the same general pattern as the profiles of Sites 805 and 806 (see "Summary and Conclusions" section, "Site 806" chapter, this volume). The major features are the broad carbonate maxima centered on the upper Miocene and the lowermost Miocene, and a minima in the middle Miocene and the Quaternary. The upper lower Miocene minimum seen in Site 805, and represented by hiatus formation in Sites 803 and 804, is not well expressed in Site 807. Additional measurements are necessary to check whether this discrepancy was caused by spotty sampling or by differences in carbonate patterns at different water depths, during the time when cold deep-water formation began.

The rather small depth difference between Sites 807 and 806 (300 m), at depths well above the present lysocline (3.3 km; Berger et al., 1982), results in very small absolute differences in carbonate percentages. The same is true for the comparison of carbonate values between Sites 807 and 805 (depth difference near 400 m). Averages for the last 15 m.y. are as follows (sequence is in the order of water depth):

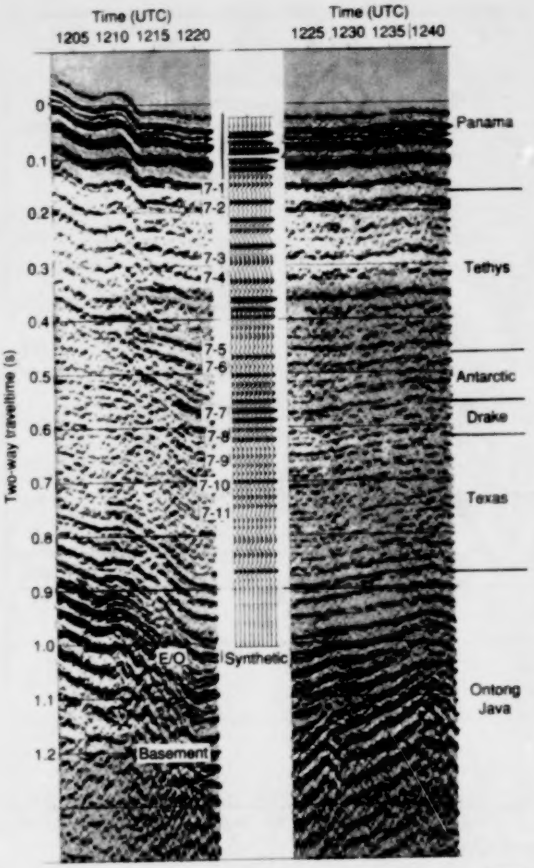

Figure 68. Comparison of synthetic seismogram and field record, Site 807.

Age	Site 806	Site 807	Site 805
0–5 Ma	90.65 ± 2.22	91.02 ± 1.768	9.52 ± 2.34
5–10 Ma	93.40 ± 1.26	92.80 ± 1.10	92.38 ± 2.04
10–15 Ma	92.95 ± 1.68	90.56 ± 1.85	91.40 ± 2.10

It can be seen that the carbonate percentages change very little over the interval, and that they overlap with each other's standard deviations. For the last 5 m.y., Site 807 has the highest carbonate values, presumably because of having less dilutant material than the shallower, equatorial Site 806 (volcanic input, silica). Between 5 and 10 Ma, the sequence is as expected from the depth differences. However, between 10 and 15 Ma, Site 807 has the lowest carbonate values of the three sites, presumably because at that period it is the closest to the equator, receiving an increased proportion of diatoms and radiolarians.

A comparison of sediment thicknesses of Site 807 with the other sites, for the major biostratigraphic subdivisions, is shown in Figure 74. The sedimentation rate trends are much clearer than the ones in the carbonate percentages. For the Neogene, Site 807 has 80% of the sediment accumulation of Site 806 and exceeds that of Site 805 by 11%. The proportional difference to Site 806 is greatest in the Pleistocene (70%) and is least in the late Pliocene and late Miocene (88% and 85%, respectively). The late Miocene "agreement" is presumably caused by the positions of Sites 807 and 806 relative to the equator. The close agreement in the late Pliocene is surprising, especially as it is followed by the strong difference in sedimentation rates in the Pleistocene. Apparently, the belt of high productivity was much wider in the late Pliocene than in the Pleistocene.

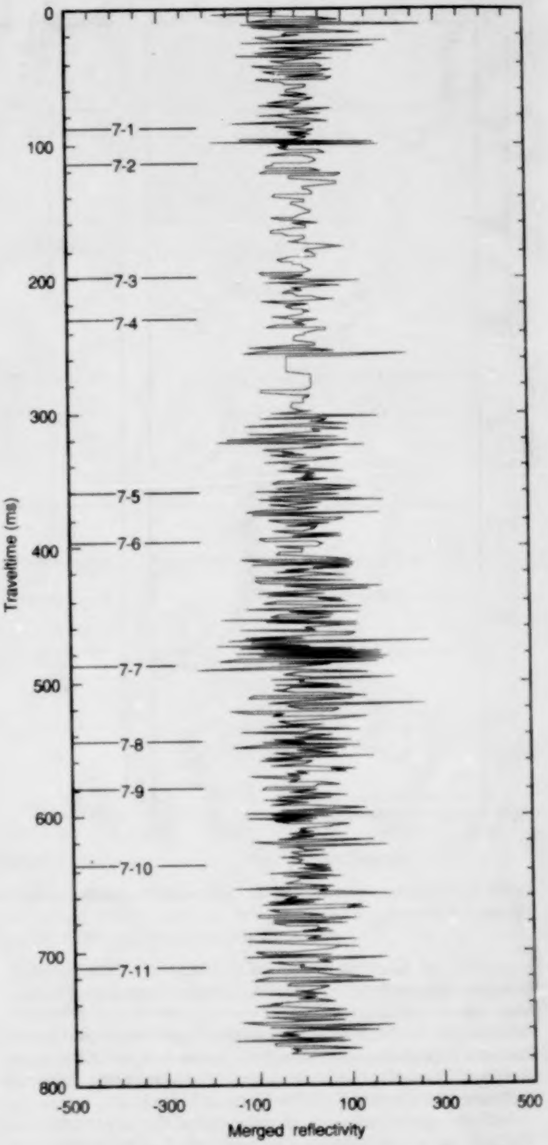

Figure 69. Reflection coefficient vs. traveltime, Hole 807A. See text for discussion of reflector picks.

A crude index of the Neogene dissolution gradient may be found by considering the ratios of the sediment thicknesses at

Table 19. Summary of traveltimes, depths, and ages for Site 807 reflectors.

	Traveltime		Depth			
Reflector	Seismic (s)	Synthetic (s)	Seismic (m)	Synthetic (m)	Age (Ma)	Series interval
7-1	0.100	0.110	80	87	3.6–3.8	Panama
7-2	0.150	0.140	120	114	4.6–4.8	Tethys
7-3	0.240	0.240	199	199	6.7	Tethys
7-4	0.278	0.275	235	230	7.4–7.5	Tethys
7-5	0.405	0.410	355	360	12.5–12.8	Antarctic
7-6	0.440	0.445	391	396	14.6–14.9	Antarctic
7-7	0.523	0.528	482	487	20.1–20.4	Drake
7-8	0.580	0.578	547	544	22.9–23.0	Drake
7-9	0.613	0.608	585	579	24.1–24.3	Texas
7-10	0.665	0.658	646	637	26.0–26.3	Texas
7-11	0.725	0.720	719	713	30.5–30.6	Texas

Notes: Depth and traveltimes to seismic events are picked on both the synthetic seismogram (synthetic) and the field record (seismic). Ages are from sedimentaiton rate curves (see "Sedimentation Rates" section, this chapter).

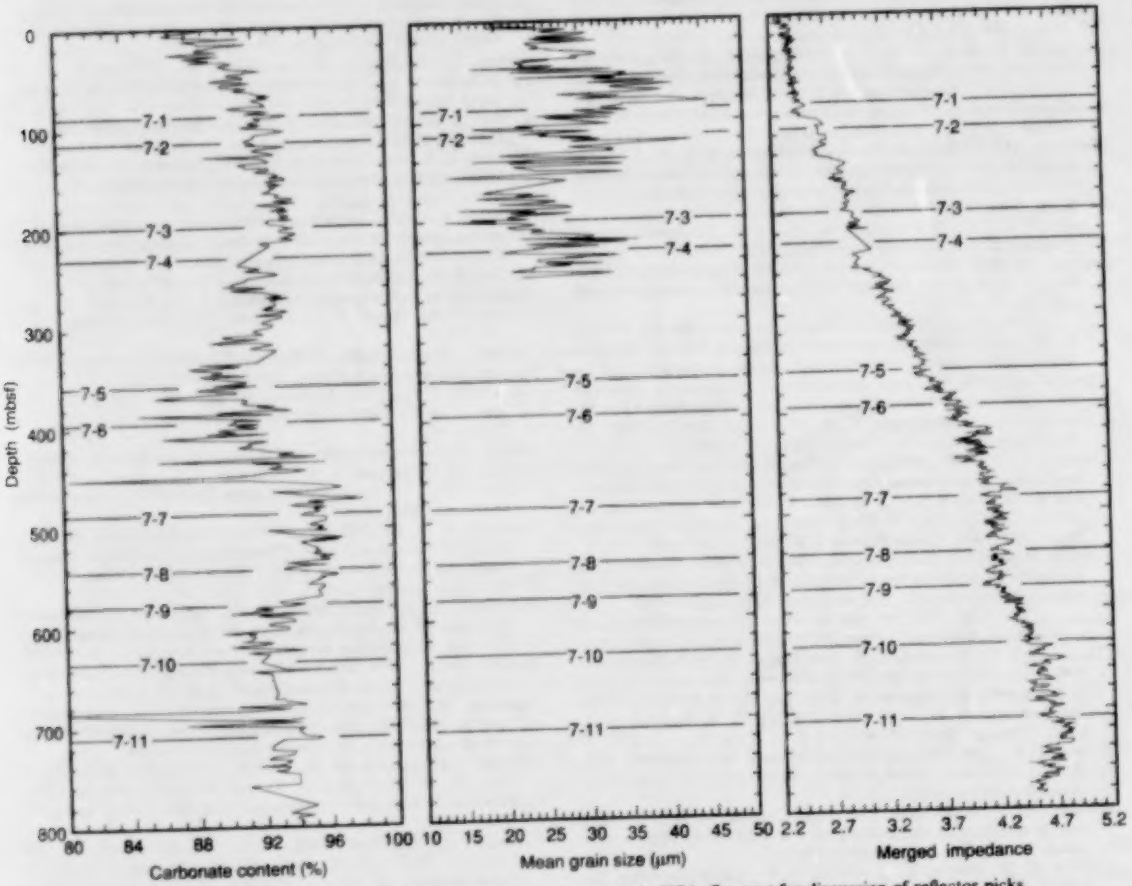

Figure 70. Carbonate content, grain size, and acoustic impedance vs. depth, Hole 807A. See text for discussion of reflector picks.

Site 806, 807, and 805. The gradient is supposed to increase over the last 25 m.y. (van Andel et al., 1975). No clear trend emerges from our data, however. The gradient appears to be greatest in the late early Miocene and early middle Miocene at the time of hiatus formation in the deeper sites. This time corresponds to NH2 in the hiatus scheme of Keller and Barron (1983) and to the onset of major Antarctic cooling (Savin et al., 1985).

The question why the pre-Neogene section is so much more riddled with hiatuses than the Neogene one must remain open. Of course, age itself is correlated with probability of removal (Moore and Heath, 1977). However, the history of the plateau, and especially its tectonic history as reflected in earthquakes, will have to be considered when discussing the distribution of major hiatuses. Regional mapping of seismic reflectors should help in this endeavor.

REFERENCES

Archie, G. E., 1942. The electrical resistivity log as an aid in determining some reservoir characteristics. *J. Petrol. Tech.*, 5:1–8.

Barron, J. A., 1985a. Late Eocene to Holocene diatom biostratigraphy of the equatorial Pacific Ocean, Deep Sea Drilling Project Leg 85. In Mayer, L., Theyer, F., Thomas, E., et al., *Init. Repts. DSDP*, 85: Washington (U.S. Govt. Printing Office), 413–456.

———, 1985b. Late Eocene to Holocene diatom biostratigraphy of the equatorial Pacific Ocean, Deep Sea Drilling Project Leg 85. *In* Mayer, L., Theyer, F., Thomas, E., et al., *Init. Repts. DSDP*, 85: Washington (U.S. Govt. Printing Office), 413–456.

Berger, W. H., 1989. Global maps of ocean productivity. *In* Berger, W. H., Smetacek, V. S., and Wefer, G. (Eds.), *Productivity of the Oceans: Present and Past:* New York (Wiley and Sons), 429–455.

Berger, W. H., Bonneau, M.-C., and Parker, F. L., 1982. Foraminifera on the deep-sea floor: lysocline and dissolution rate. *Oceanol. Acta*, 5:249–258.

Berger, W. H., Johnson, T. C., and Hamilton, E. L., 1977. Sedimentation on Ontong-Java Plateau: observations on a classic "carbonate monitor." *In* Anderson, N. R., and Malahoff, A. (Eds.), *The Fate of Fossil Fuel CO2* in the Oceans: New York (Plenum Press), 543–567.

Berggren, W. A., Kent, D. V., and Van Couvering, J. A., 1985. The Neogene: Part 2. Neogene geochronology and chronostratigraphy. *In* Snelling, N. J. (Ed.), *The Chronology of the Geological Record.* Mem. Geol. Soc. (London), 10:211–260.

Emeis, K.-C., and Kvenvolden, K. A., 1986. Shipboard organic geochemistry on *JOIDES Resolution*. *ODP Tech. Note*, No. 7.

Fenner, J., 1984. Eocene-Oligocene planktic diatom stratigraphy in the low latitudes and the high southern latitudes. *Micropaleontology*, 30:319–342.

———, 1985. Late Cretaceous to Oligocene planktic diatoms. *In* Bolli, H. M., Saunders, J. B., and Perch-Nielsen, K. (Eds.), *Plankton Stratigraphy:* Cambridge (Cambridge Univ. Press), 713–762.

Floyd, P. A., 1986. Petrology and geochemistry of oceanic intraplate sheet-flow basalts, Nauru Basin, Deep Sea Drilling Project Leg 89. *In* Moberly, R., Schlanger, S. O., et al., *Init. Repts. DSDP*, 89: Washington (U.S. Govt. Printing Office), 471–497.

Gieskes, J. M., 1981. Deep-sea drilling interstitial water studies: implications for chemical alteration of the oceanic crust, Layers I and II. *In* Warme, J. E., Douglas, R. G., and Winterer, E. L. (Eds.), *The Deep Sea Drilling Project: A Decade of Progress.* Spec. Publ., Soc. Econ. Paleontol. Mineral., 32:149–167.

Gordon, R. G., 1983. Late Cretaceous apparent polar wander of the Pacific Plate: evidence for a rapid shift of the Pacific hotspots with respect to the spin axis. *Geophys. Res. Lett.*, 10:709–712.

———, in press. Test for bias in paleomagnetically determined paleolatitudes from Pacific Plate DSDP sediments. *J. Geophys. Res.*

Hammond, S. R., Kroenke, L. W., and Theyer, F., 1975. Northward motion of the Ontong-Java Plateau between 110 and 30 m.y.: a paleomagnetic investigation of DSDP Site 289. *In* Andrews, J. E., Packham, G., et al., *Init. Repts. DSDP*, 30: Washington (U.S. Govt. Printing Office) 415–418.

Hooper, P. R., 1988. The Columbia River basalt. *In* Macdougall, J. D. (Ed.), *Continental Flood Basalts:* Dordrecht, The Netherlands (Kluwer Academic Publ.), 1–34.

Hussong, D. M., Wipperman, L. K., and Kroenke, L. W., 1979. The crustal structure of the Ontong Java and Manihiki oceanic plateaus. *J. Geophys. Res.*, 84:6003–6010.

Jackson, E. D., Bargar, K. E., Fabbi, B. P., and Heropoulos, C., 1976. Petrology of the basaltic rocks drilled on Leg 33 of the Deep Sea Drilling Project. *In* Schlanger, S. O., Jackson, E. D., et al., *Init. Repts. DSDP*, 33: Washington (U.S. Govt. Printing Office), 571–630.

Johanssen, A., 1931. *A Descriptive Petrography of the Igneous Rocks* (Vol. 1): Chicago (Univ. of Chicago Press).

Karlin, R., and Levi, S., 1985. Geochemical and sedimentological control of the magnetic properties of hemipelagic sediments. *J. Geophys. Res.*, 90:10,373–10,392.

Keller, G., and Barron, J. A., 1983. Paleoceanographic implications of Miocene deep-sea hiatuses. *Geol. Soc. Am. Bull.*, 94:590–613.

Kroenke, L. W., 1972. Geology of the Ontong-Java Plateau. *Hawaii Inst. Geophys. Rep.*, HIG 72-5.

———, 1984. Cenozoic tectonic development of the Southwest Pacific. *U. N. ESCAP, CCOP/SOPAC, Tech. Bull.*, No. 6.

Kroenke, L. W., Jouannic, C., and Woodward, P. (Comps.), 1983. Bathymetry of the Southwest Pacific: Chart 1 of the Geophysical Atlas of the Southwest Pacific, CCOP/SOPAC.

Mahoney, J. J., 1987. An isotopic survey of Pacific oceanic plateaus: implications for their nature and origin. *In* Keating, B. H., Fryer, P., Batiza, R., and Boehlert, G. W. (Eds.), *Seamounts, Islands, and Atolls.* Am. Geophys. Union Monogr., 43:207–220.

Mammerickx, J., and Smith, S. M., 1985. *Bathymetry of the North Central Pacific:* Boulder, CO (Geological Society of America), Map and Chart Ser., No. MC-52.

Manivit, H., and Feinberg, H., 1984. Correlation of magnetostratigraphy and nannofossil biostratigraphy in Upper Cretaceous and lower Paleocene sediments of the Walvis Ridge area. *In* Moore, T. C., Jr., Rabinowitz, P. D., et al., *Init. Repts. DSDP*, 74: Washington (U.S. Govt. Printing Office), 469–474.

Mayer, L. A., Shipley, T. H., Theyer, F., Wilkens, R. W., and Winterer, E. L., 1985. Seismic modeling and paleoceanography at Deep Sea Drilling Project Site 574. *In* Mayer, L. A., Theyer, F., Thomas, E., et al., *Init. Repts. DSDP*, 85: Washington, (U.S. Govt. Printing Office), 947–970.

McDuff, R. E., and Gieskes, J. M., 1976. Calcium and magnesium in DSDP interstitial waters: diffusion or reaction? *Earth Planet. Sci. Lett.*, 33:1–10.

Monechi, S., 1985. Campanian to Pleistocene calcareous nannofossil stratigraphy from the northwest Pacific Ocean, Deep Sea Drilling Project Leg 86. *In* Heath, G. R., Burckle, L. H., et al., *Init. Repts. DSDP*, 86: Washington (U.S. Govt. Printing Office), 301–336.

Moore, T., 1971. Radiolaria. *In* Tracey, J. I., Jr., Sutton, G. H., et al., *Init. Repts. DSDP*, 8: Washington (U.S. Govt. Printing Office), 727–775.

Moore, T. C., and Heath, G. R., 1977. Survival of deep-sea sedimentary sections. *Earth Planet. Sci. Lett.*, 37:71–80.

Ogushwitz, P. R., 1985. Applicability of the Biot theory. III. Wave speeds versus depth in marine sediments. *J. Acoust. Soc. Am.*, 77:453–463.

Okada, H., 1990. Quaternary and Paleogene calcareous nannofossils, Leg 115. *In* Duncan, R. A., Backman, J., Peterson, L. C., et al., *Proc. ODP, Sci. Results*, 115: College Station, TX (Ocean Drilling Program), 129–174.

Pessagno, E. A., Jr., 1977. *Lower Cretaceous Radiolarian Biostratigraphy of the Great Valley Sequence and Franciscan Complex, California Coast Ranges.* Spec. Publ., Cushman Found. Foraminiferal Res., No. 15.

Petronotis, K. E., and Gordon, R. G., 1989. Age dependence of skewness of magnetic anomalies above seafloor formed at the Pacific-Kula spreading center. *Geophys. Res. Lett.*, 16:315–318.

Romein, A.J.T., 1979. Lineages in early Paleogene calcareous nannoplankton. *Utrecht Micropaleontol. Bull.*, 22:1–231.

Sager, W. W., 1987. Late Eocene and Maestrichtian paleomagnetic poles for the Pacific plate: implications for the validity of seamount paleomagnetic data. *Tectonophysics*, 144:301–314.

Sanfilippo, A., and Riedel, W. R., 1985. Cretaceous Radiolaria. *In* Bolli, H. M., Saunders, J. B., and Perch-Nielsen, K. (Eds.), *Plankton Stratigraphy:* Cambridge (Cambridge Univ. Press), 573–630.

Sanfilippo, A., Westberg-Smith, M. J., and Riedel, W. R., 1985. Cenozoic Radiolaria. *In* Bolli, H. M., Saunders, J. B., and Perch-Nielsen, K. (Eds.), *Plankton Stratigraphy:* Cambridge (Cambridge Univ. Press), 631–712.

Saunders, J. B., Bernoulli, D., Müller-Merz, E., Oberhänsli, H., Perch-Nielsen, K., Riedel, W. R., Sanfilippo, A., and Torrini, R., Jr., 1984. Stratigraphy of late middle Eocene to early Oligocene in the Bath Cliff section Barbados, West Indies. *Micropaleontology*, 30:390–425.

Savin, S. M., Abel, L., Barrera, E., Hodell, D., Kennett, J. P., Murphy, M., Keller, G., Killingley, J., and Vincent, E., 1985. The evolution of Miocene surface and near-surface marine temperatures: oxygen isotopic evidence. *In* Kennett, J. P. (Ed.), *The Miocene Ocean: Paleoceanography and Biogeography*. Mem. Geol. Soc. Am., 163:49–82.

Schlanger, S. O., and Douglas, R. G., 1974. The pelagic ooze-chalk-limestone transition and its implication for marine stratigraphy. *In* Hsü, K. J., and Jenkyns, H. C. (Eds.), *Pelagic Sediments: On Land and Under the Sea*. Spec. Publ., Int. Assoc. Sedimentol., 1:117–148.

Shafik, S., 1975. Nannofossil biostratigraphy of the southwest Pacific, Deep Sea Drilling Project Leg 30. *In* Andrews, J. E., Packham, G., et al., *Init. Repts. DSDP*, 30: Washington (U.S. Govt. Printing Office), 549–598.

Shipboard Scientific Party, 1971. Site 64. *In* Winterer, E. L., Riedel, W. R., et al., 1971. *Init. Repts. DSDP*, 7: Washington (U.S. Govt. Printing Office), 473–606.

_______, 1975a. Site 288. *In* Andrews, J. E., Packham, G., et al., *Init. Repts. DSDP*, 30: Washington (U.S. Govt. Printing Office), 175–229.

_______, 1975b. Site 289. *In* Andrews, J. E., Packham, G., et al., *Init. Repts. DSDP*, 30: Washington (U.S. Govt. Printing Office), 231–281.

_______, 1986a. Site 586. *In* Moberly, R., Schlanger, S. O., et al., *Init. Repts. DSDP*, 89: Washington (U.S. Govt. Printing Office), 213–281.

_______, 1986b. Site 586: western equatorial Pacific. *In* Kennett, J. P., von der Borch, C. C., et al., *Init. Repts. DSDP*, 90: Washington (U.S. Govt. Printing Office), 19–114.

_______, 1989. Explanatory notes. *In* Prell, W. L., Niitsuma, N., et al., *Proc. ODP, Init. Repts.*, 117: College Station, TX (Ocean Drilling Program), 11–33.

Tarduno, J. A., in press. Brief reversed polarity interval during the Cretaceous Normal Polarity Superchron. *Geology*.

Tarduno, J., Sliter, W. V., Bralower, T. J., McWilliams, M., Premoli Silva, I., and Ogg, J. G., 1989. M-sequence reversals recorded in DSDP sediment cores from the western Mid-Pacific Mountains and Magellan Rise. *Geol. Soc. Am. Bull.*, 101:1306–1316.

Thierstein, H. R., 1979. Paleoceanographic implications of organic carbon and carbonate distribution in Mesozoic deep sea sediments. *In* Talwani, M., Hay, W., and Ryan, W.B.F. (Eds.), *Deep Drilling Results in the Atlantic Ocean:* Am. Geophys. Union, Maurice Ewing Ser., 3:249–274.

_______, 1981. Late Cretaceous nannoplankton and the change at the Cretaceous/Tertiary boundary. *In* Warme, J. E., et al. (Eds.), *The Deep Sea Drilling Project: A Decade of Progress*. Spec. Publ., Soc. Econ. Paleontol. Mineral., 32:355–394.

Thierstein, H. R., and Okada, H., 1979. The Cretaceous/Tertiary boundary event in the North Atlantic. *In* Tucholke, B. E., Vogt, P. R., et al., *Init. Repts. DSDP*, 43: Washington (U.S. Govt. Printing Office), 601–616.

Thurow, J., 1988. Cretaceous radiolarians of the North Atlantic Ocean: ODP Leg 103 (Sites 638, 640, and 641) and DSDP Legs 93 (Site 603) and 47B (Site 398). *In* Boillot, G., Winterer, E. L., et al., *Proc. ODP, Sci. Results*, 103: College Station, TX (Ocean Drilling Program), 379–418.

Toksöz, M. N., Cheng, C. H., and Timur, A., 1976. Velocities of seismic waves in porous rocks. *Geophysics*, 41:621–645.

Tucholke, B. E., and Vogt, P. R., 1979. Western North Atlantic: sedimentation evolution and aspects of tectonic history. *In* Tucholke, B. E., Vogt, P. R., et al., *Init. Repts. DSDP*, 43: Washington (U.S. Govt. Printing Office), 791–825.

van Andel, T. H., Heath, G. R., and Moore, T. C., Jr., 1975. Cenozoic history and paleoceanography of the central equatorial Pacific. *Mem. Geol. Soc. Am.*, 143:1–134.

Wood, A. B., 1930. *A Textbook of Sound:* London (G. Bell and Sons).

Wylie, M.R.J., Gregory, A. R., and Gardner, G.H.F., 1958. An experimental investigation of factors affecting elastic wave velocities in porous media. *Geophysics*, 23:459–493.

Ms 130A-109

NOTE: All core description forms ("barrel sheets") and core photographs have been printed on coated paper and bound as Section 5, near the back of the book, beginning on page 559.

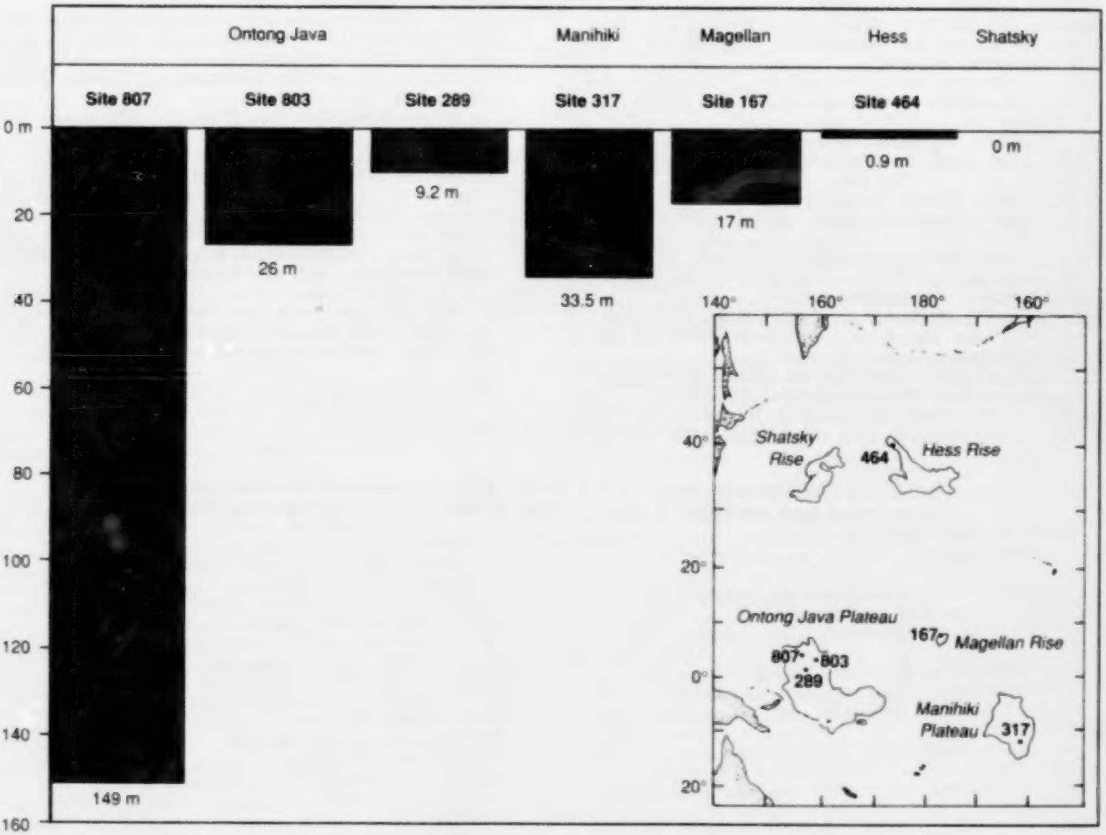

Figure 71. Basement penetration of oceanic flood basalt plateaus in the Pacific. The locations of the Leg 130 drilling sites are shown in the figure inset. The Icelandic Plateau in the Atlantic is slightly smaller than the Magellan Plateau, the smallest of the Pacific plateaus.

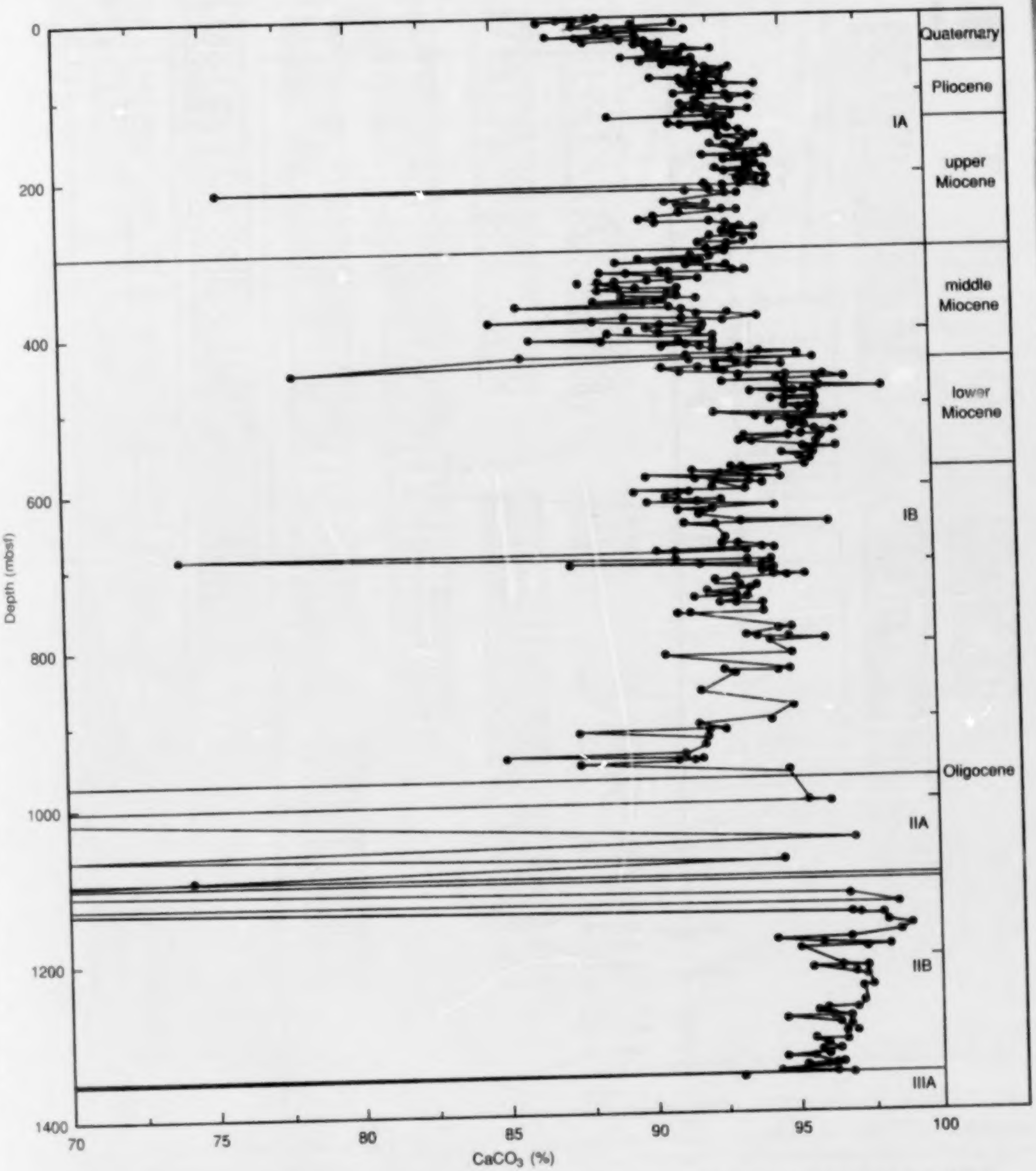

Figure 72. Carbonate content, Site 807 (from Holes 807A and 807C). Lithologic units and ages are shown on the right side of the figure.

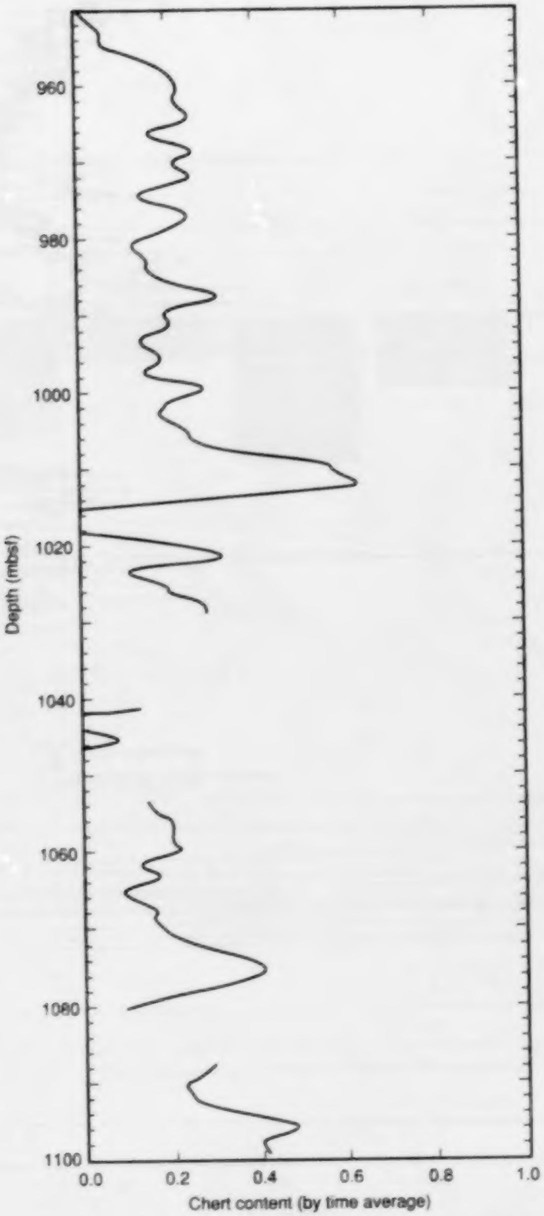

Figure 73. Chert content, Hole 807C, based on a time average of the velocity logging data (chert = 4.0 km/s, limestone = 2.5 km/s).

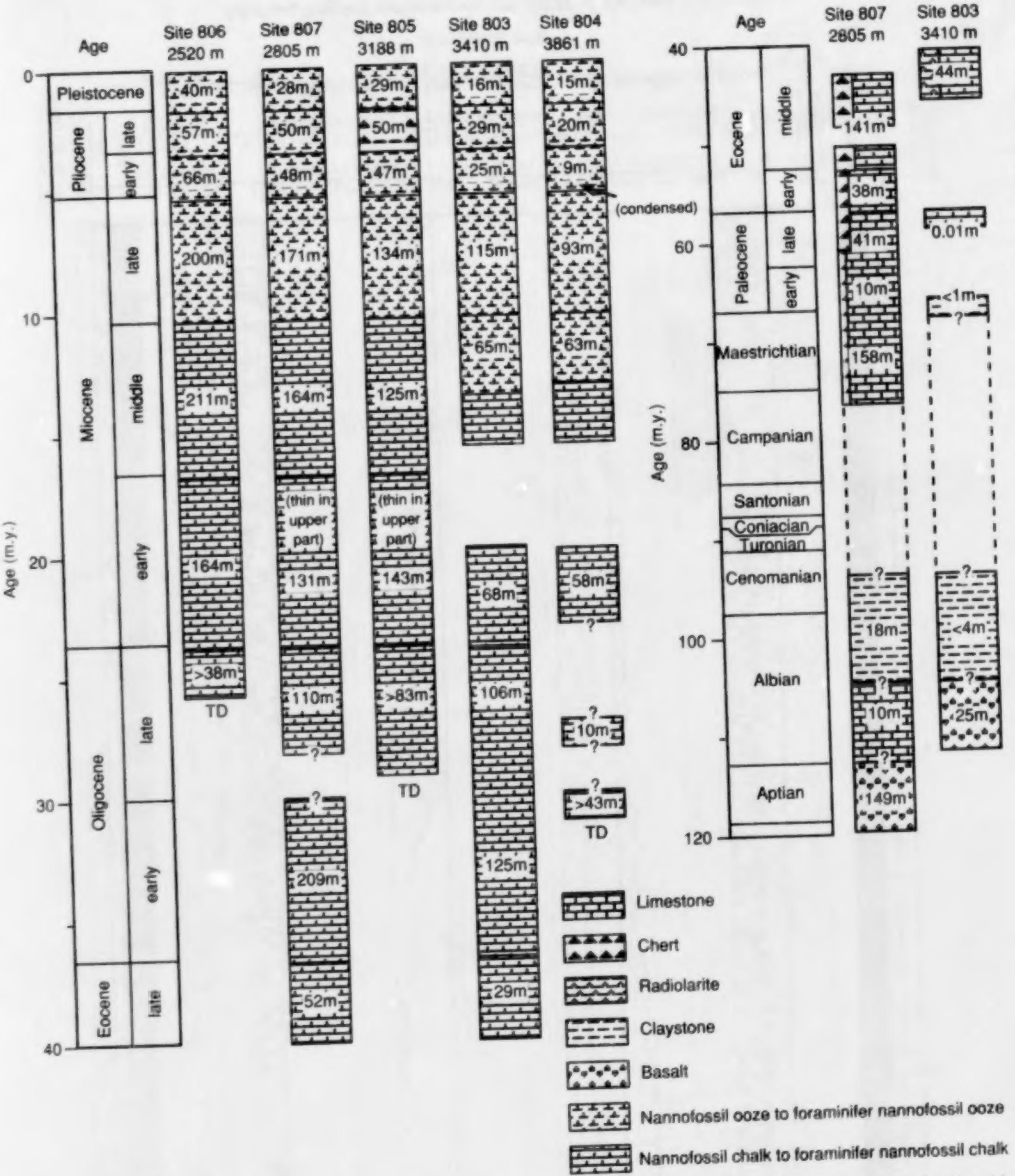

Figure 74. Leg 130 sites drilled on the Ontong Java Plateau, western equatorial Pacific, arranged according to depth. Recovered sediment is shown as a function of age rather than as depth below seafloor to highlight hiatuses within the drilled section. Sediment thicknesses given in the columns are approximate values based on shipboard biostratigraphy. Note, for example, that the upper Miocene at Site 806 is approximately 200 m thick and thins downslope to approximately 93 m at Site 804. Age control through much of the Cretaceous is poor as a result of the dissolution of calcareous microfossils.

Hole 807A: Resistivity-Sonic-Gamma Ray Log Summary

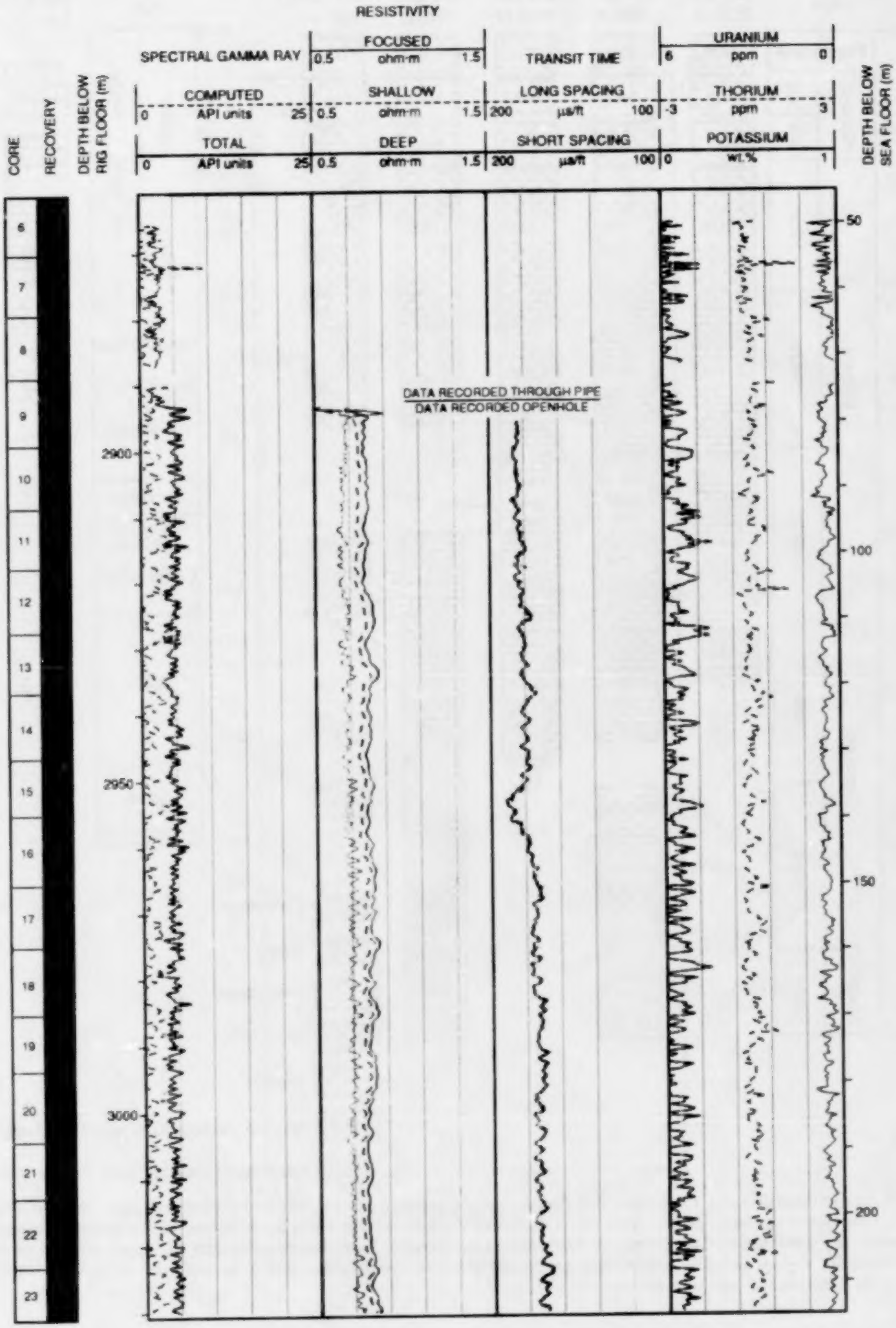

Hole 807A: Resistivity-Sonic-Gamma Ray Log Summary (continued)

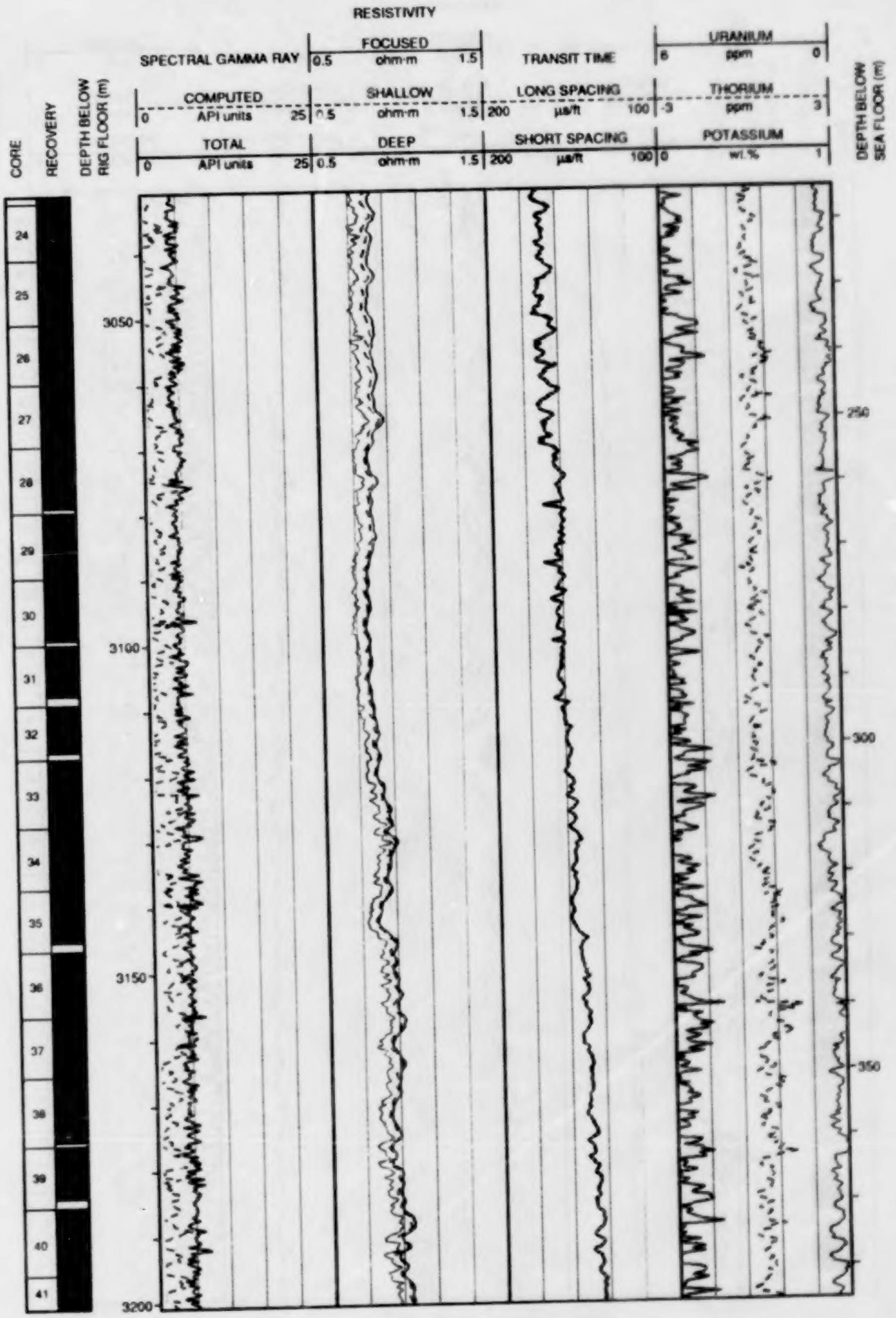

Hole 807A: Resistivity-Sonic-Gamma Ray Log Summary (continued)

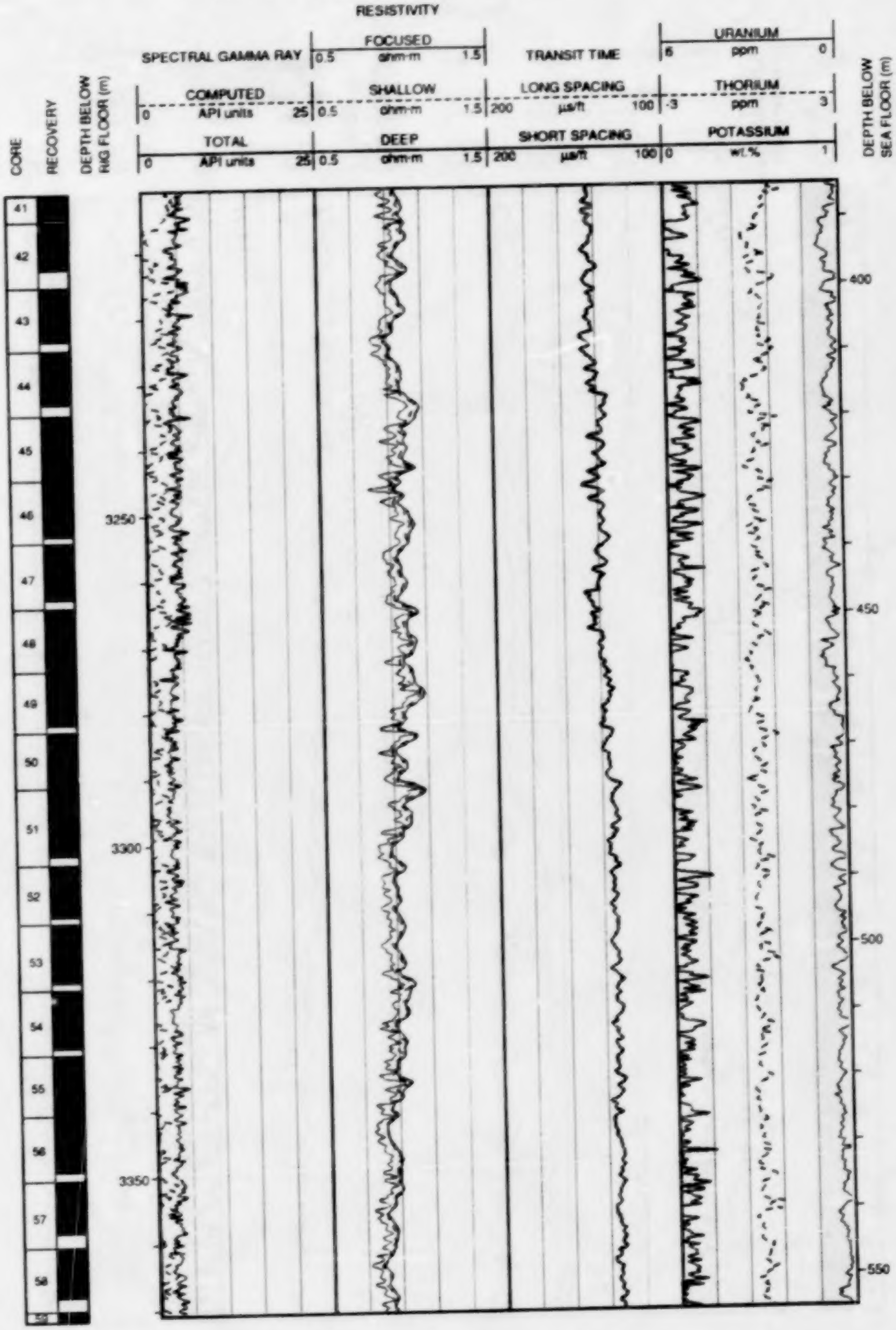

Hole 807A: Resistivity-Sonic-Gamma Ray Log Summary (continued)

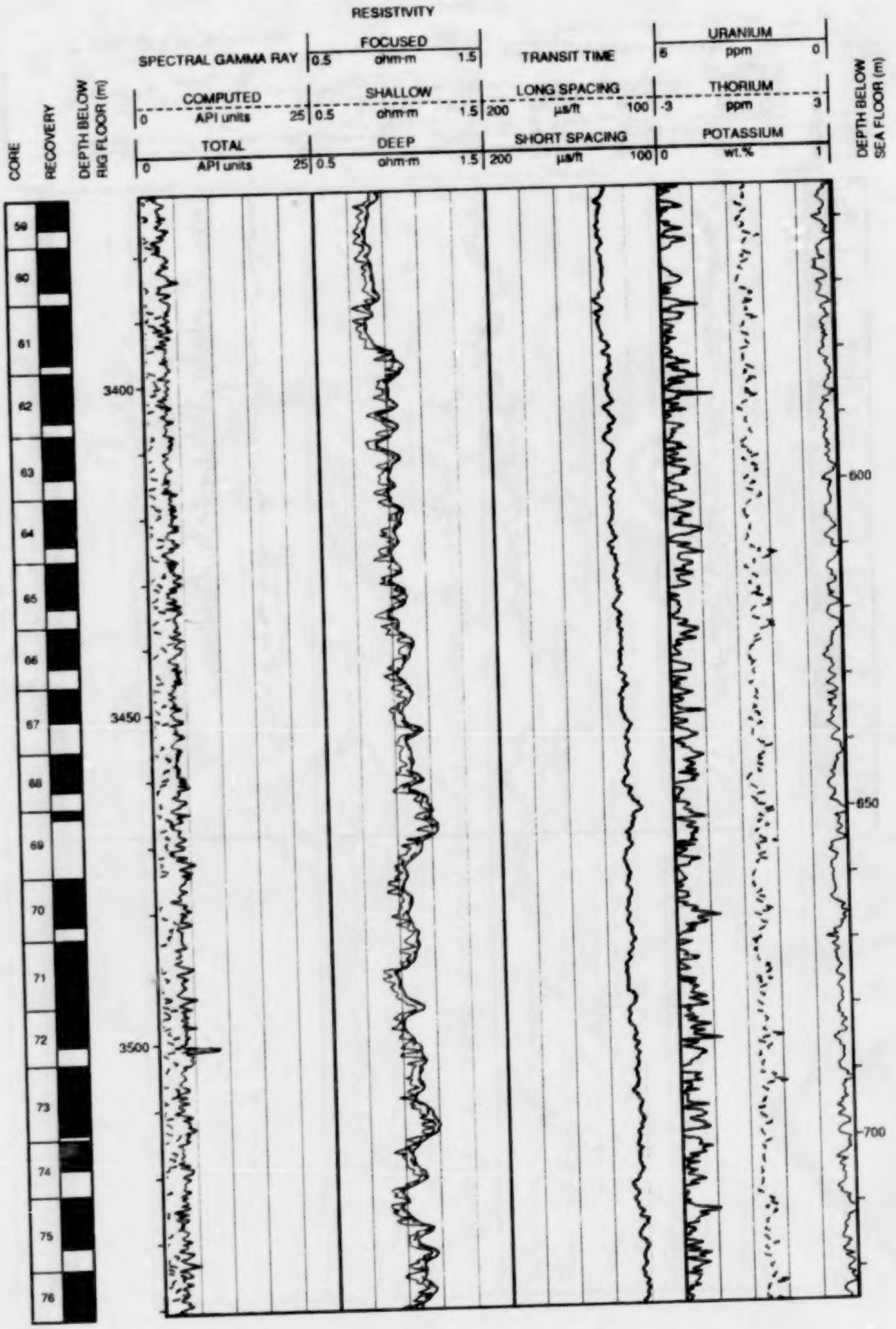

Hole 807A: Resistivity-Sonic-Gamma Ray Log Summary (continued)

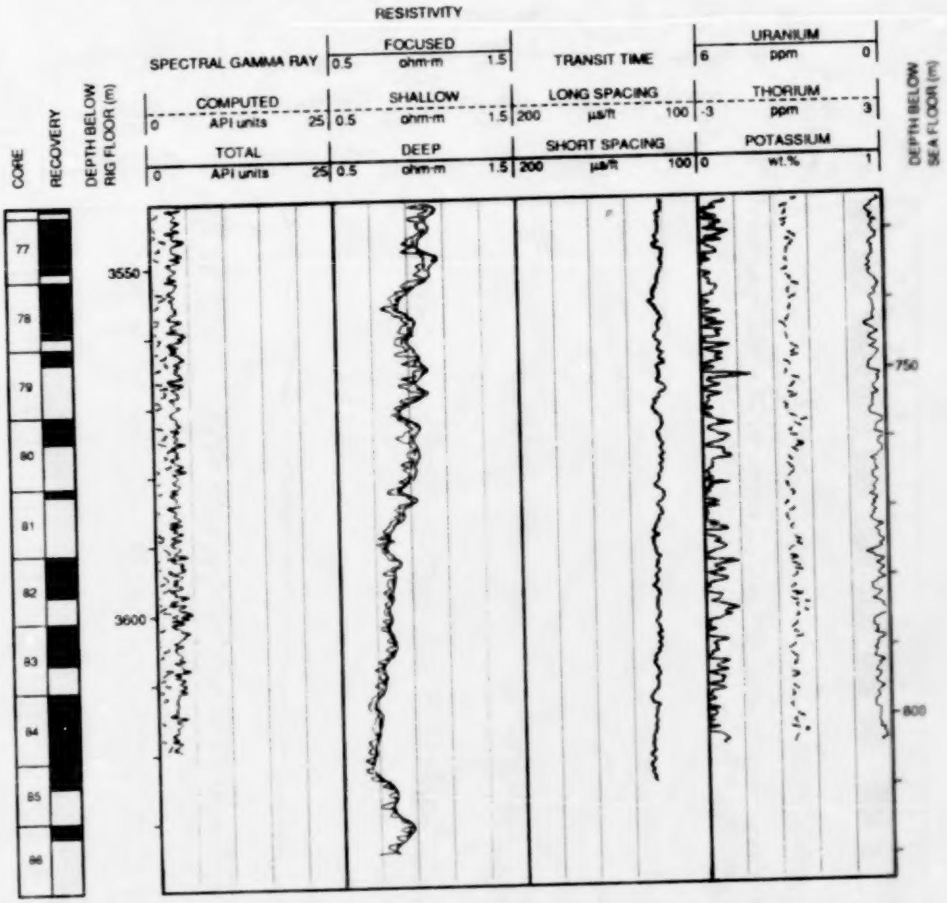

Hole 807A: Density-Gamma Ray-Aluminum Log Summary

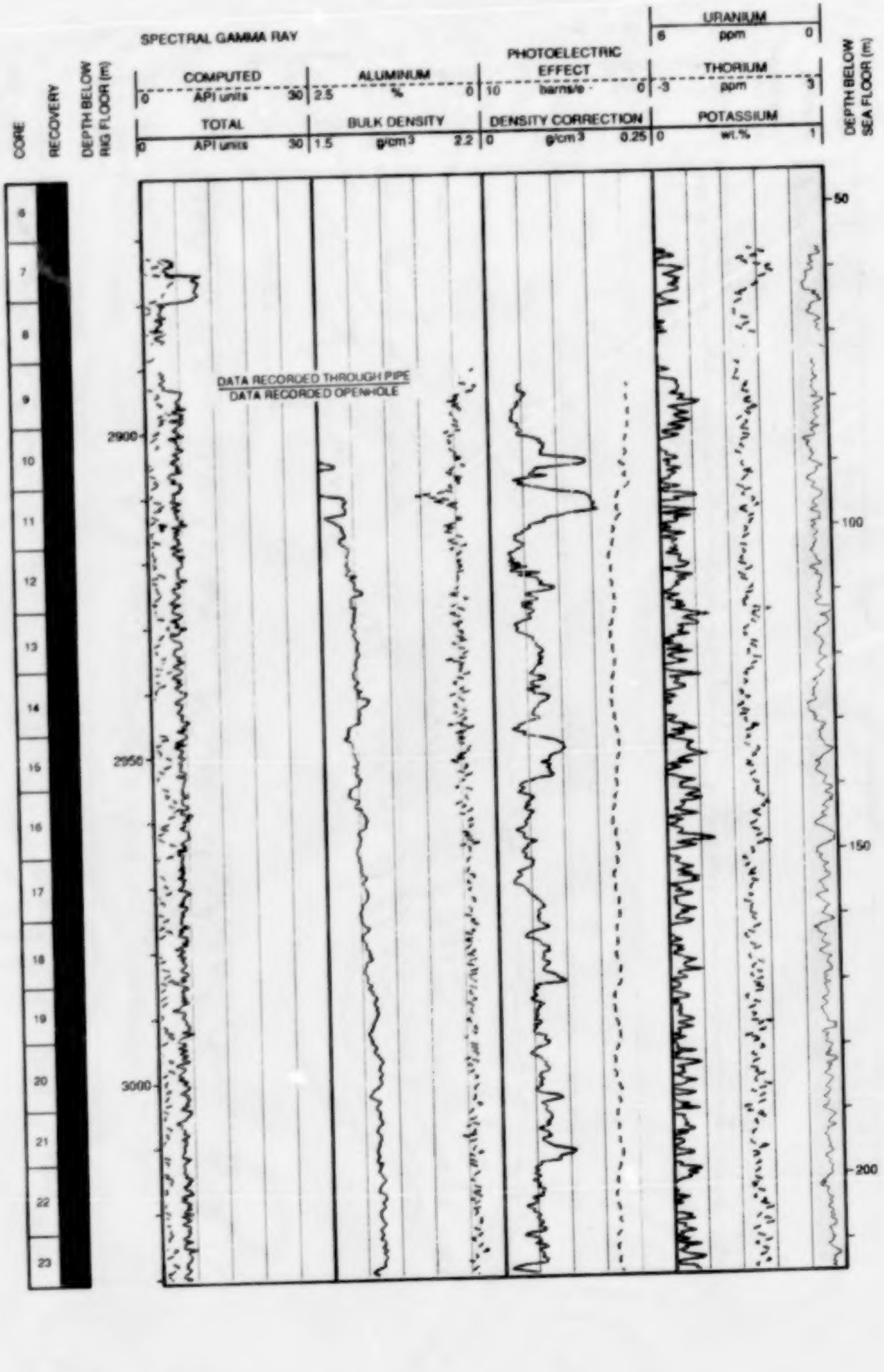

Hole 807A: Density-Gamma Ray-Aluminum Log Summary (continued)

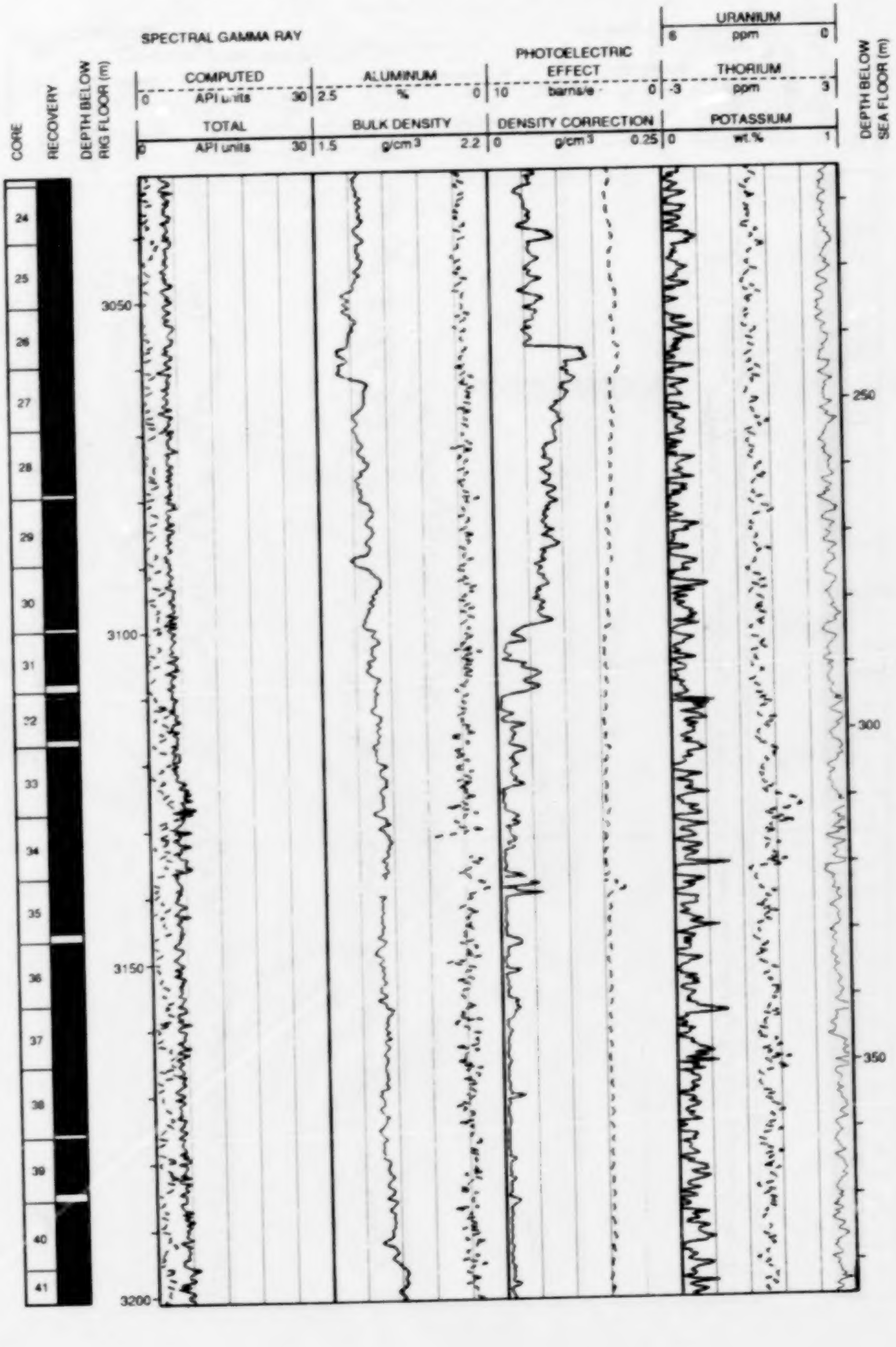

Hole 807A: Density-Gamma Ray-Aluminum Log Summary (continued)

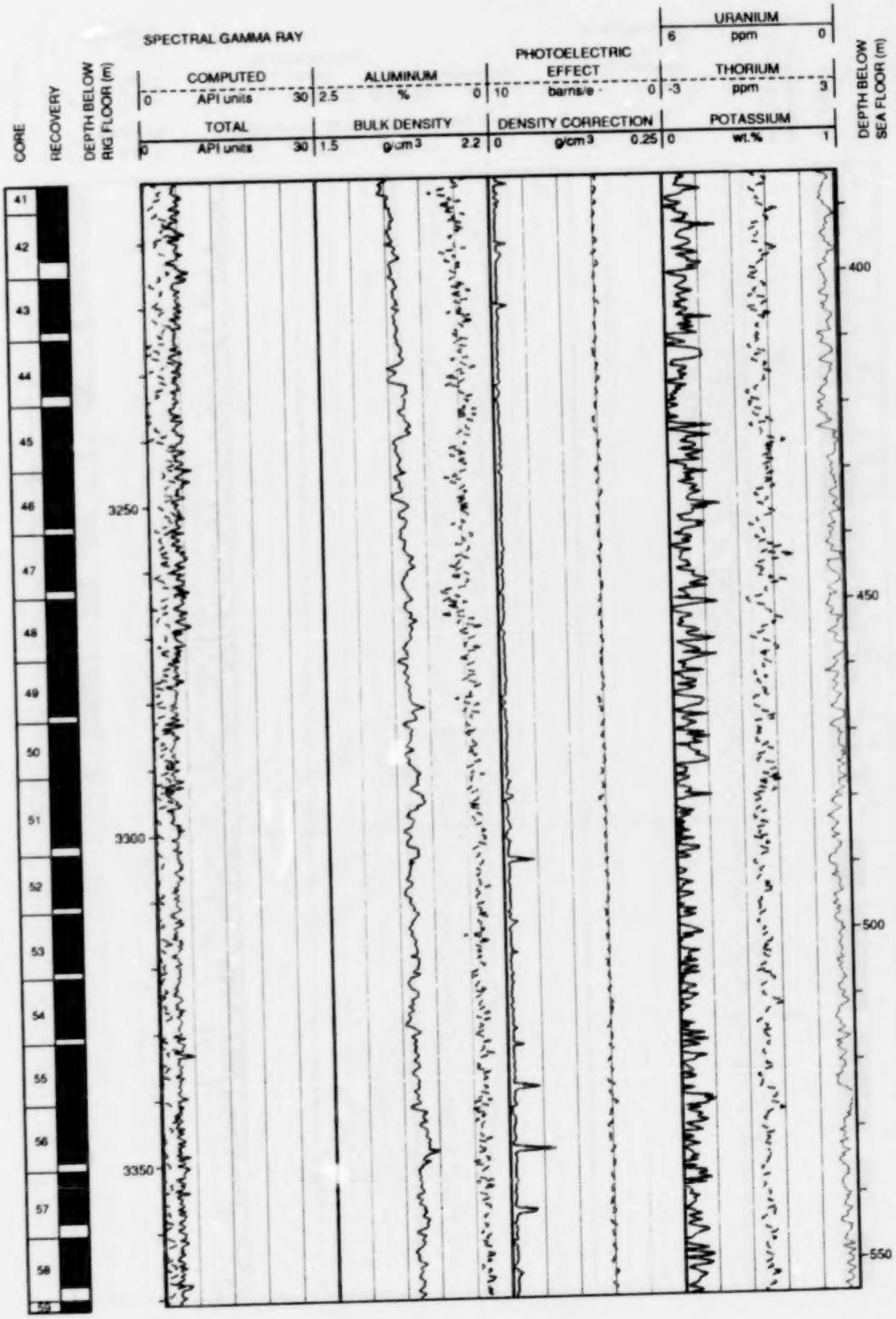

Hole 807A: Density-Gamma Ray-Aluminum Log Summary (continued)

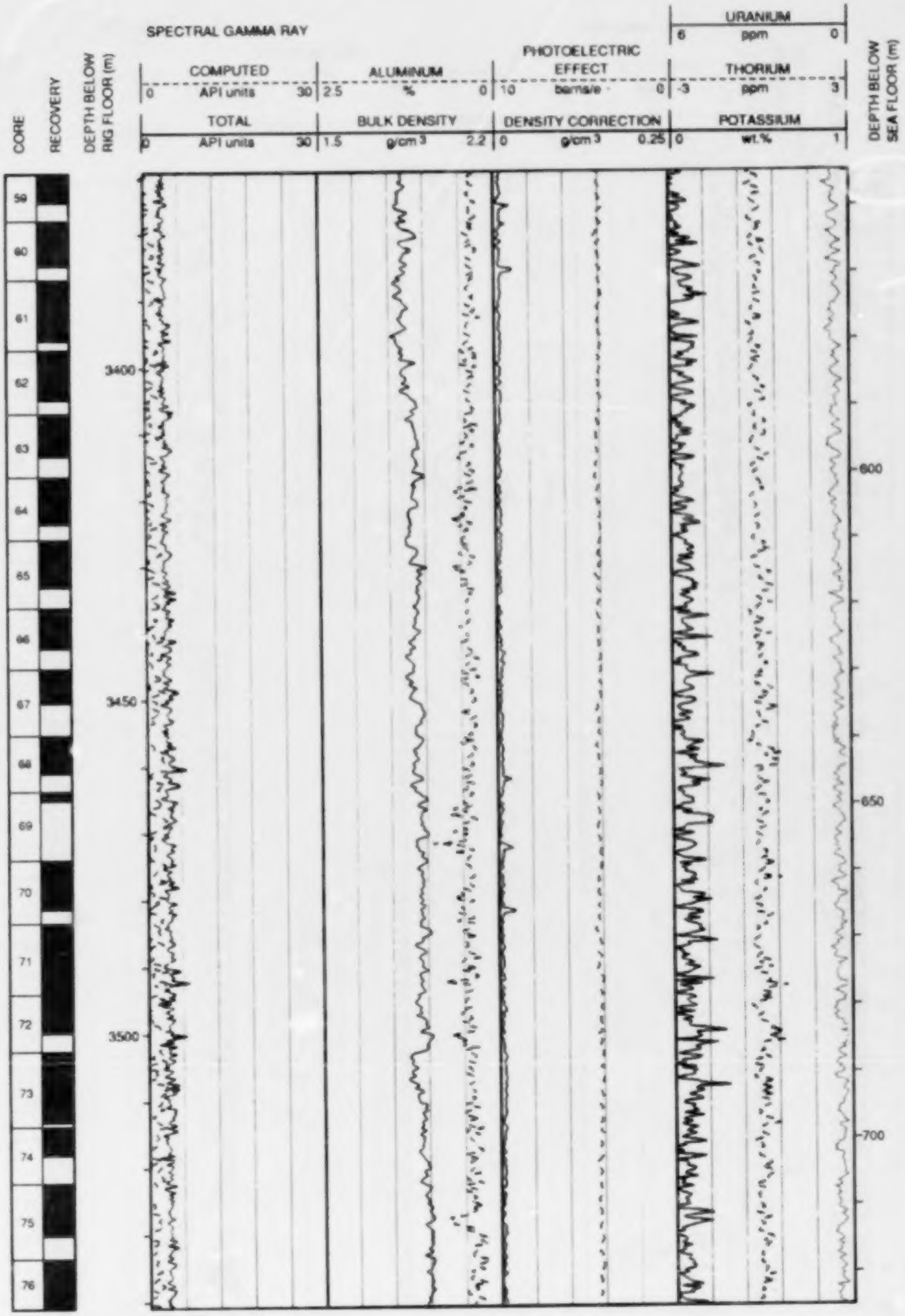

Hole 807A: Density-Gamma Ray-Aluminum Log Summary (continued)

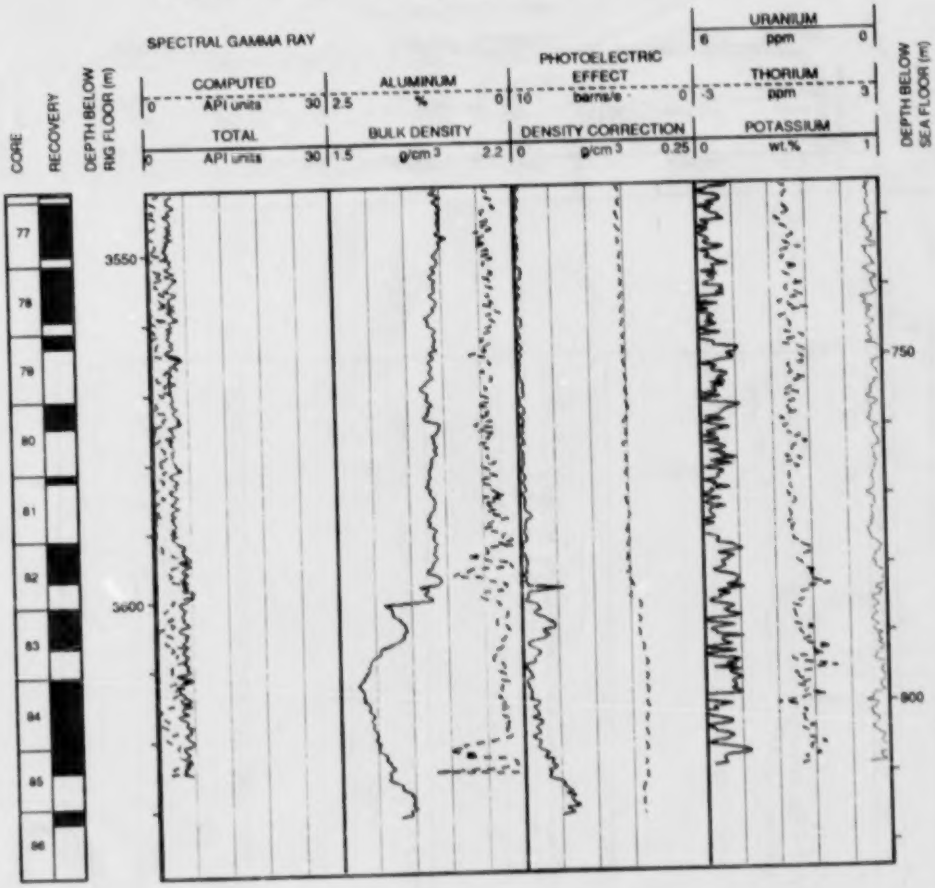

Hole 807C: Resistivity-Sonic-Gamma Ray Log Summary

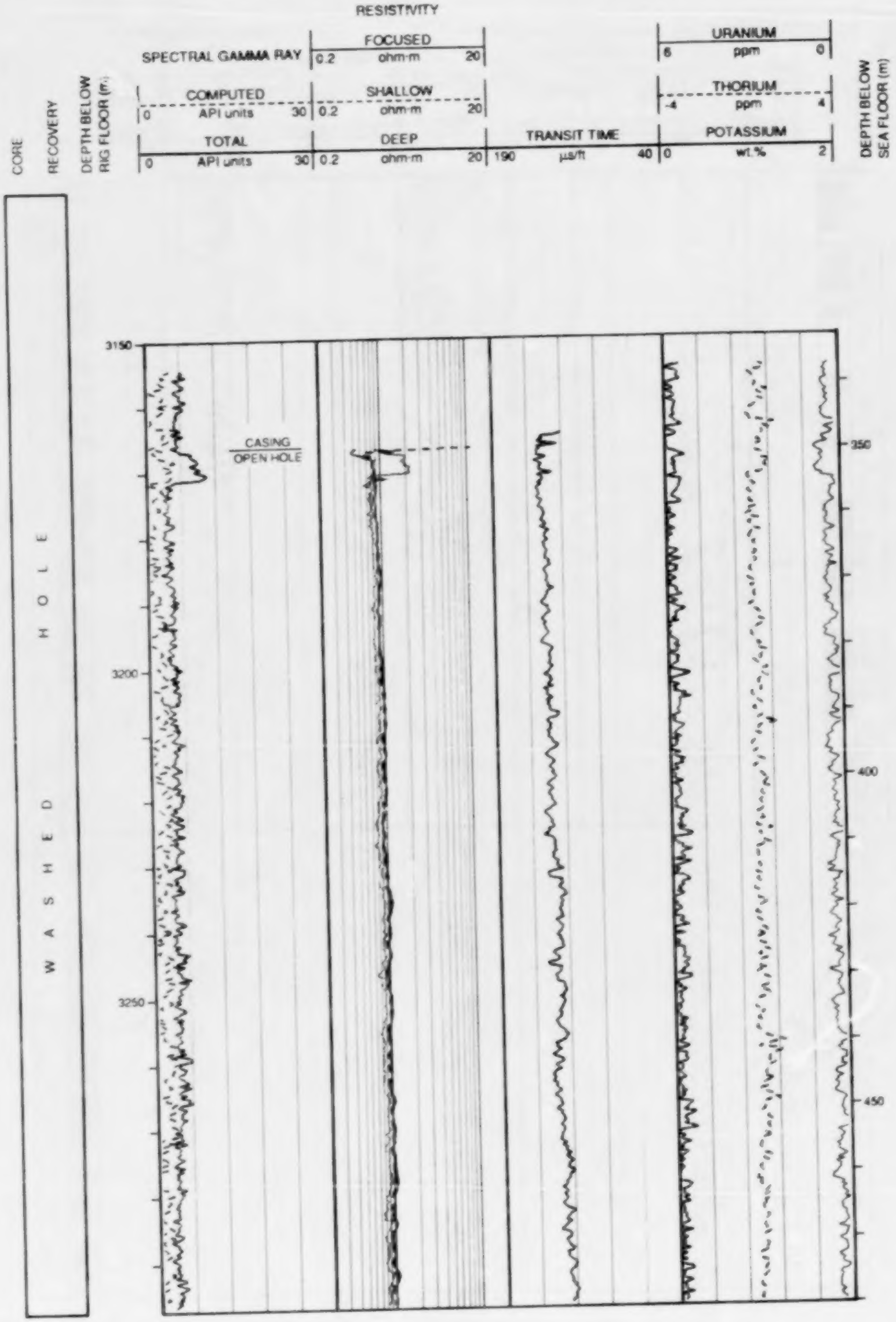

Hole 807C: Resistivity-Sonic-Gamma Ray Log Summary (continued)

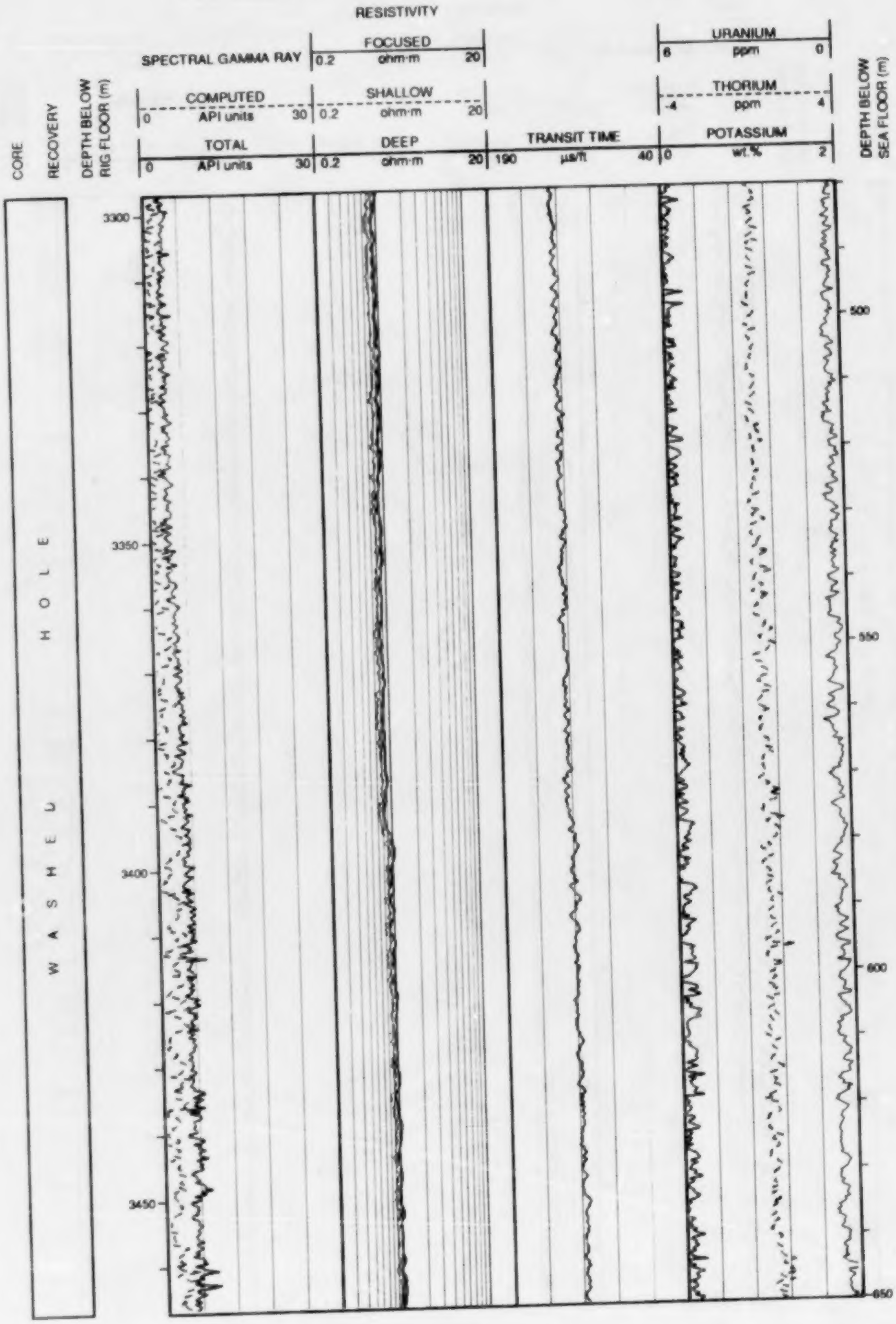

Hole 807C: Resistivity-Sonic-Gamma Ray Log Summary (continued)

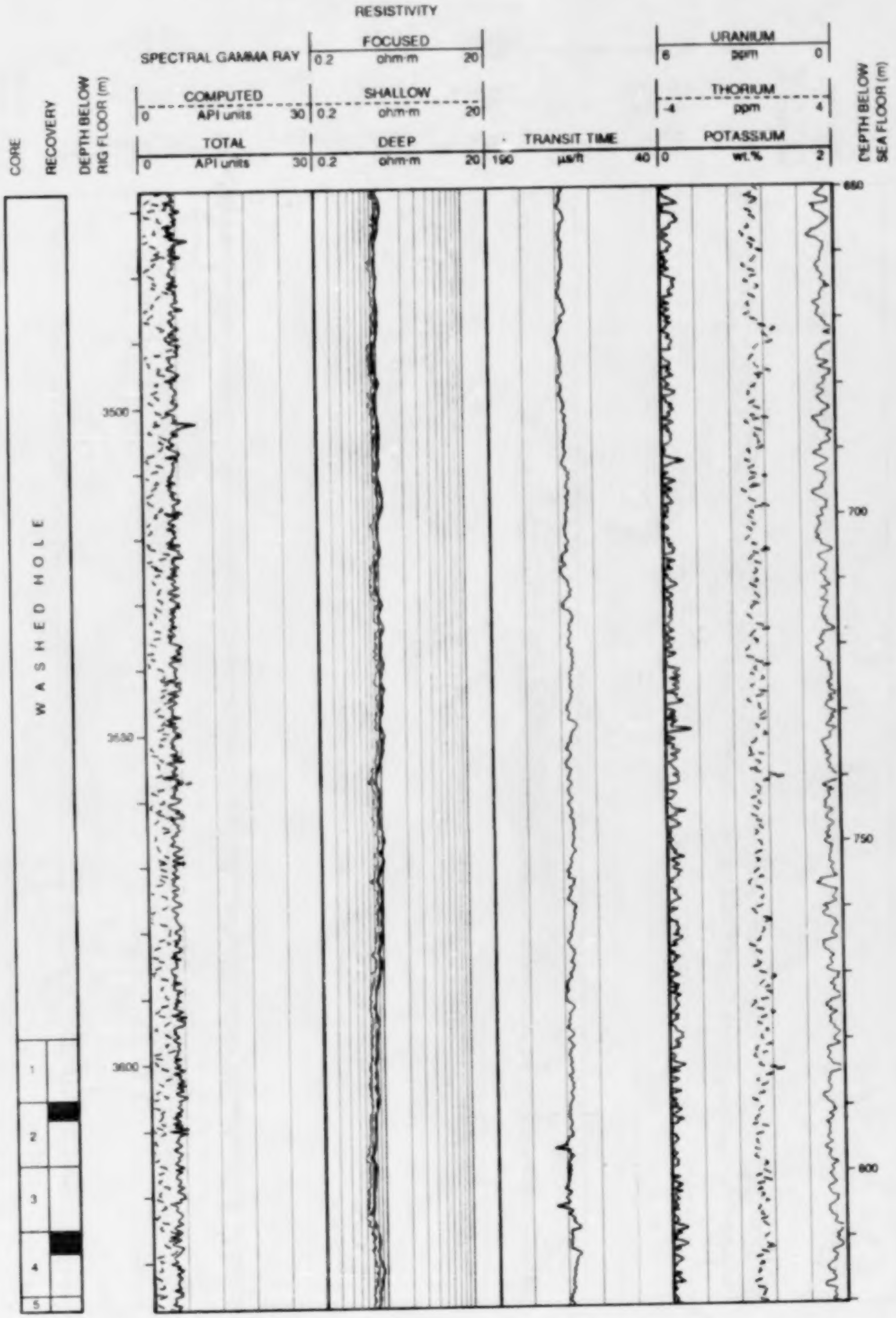

Hole 807C: Resistivity-Sonic-Gamma Ray Log Summary (continued)

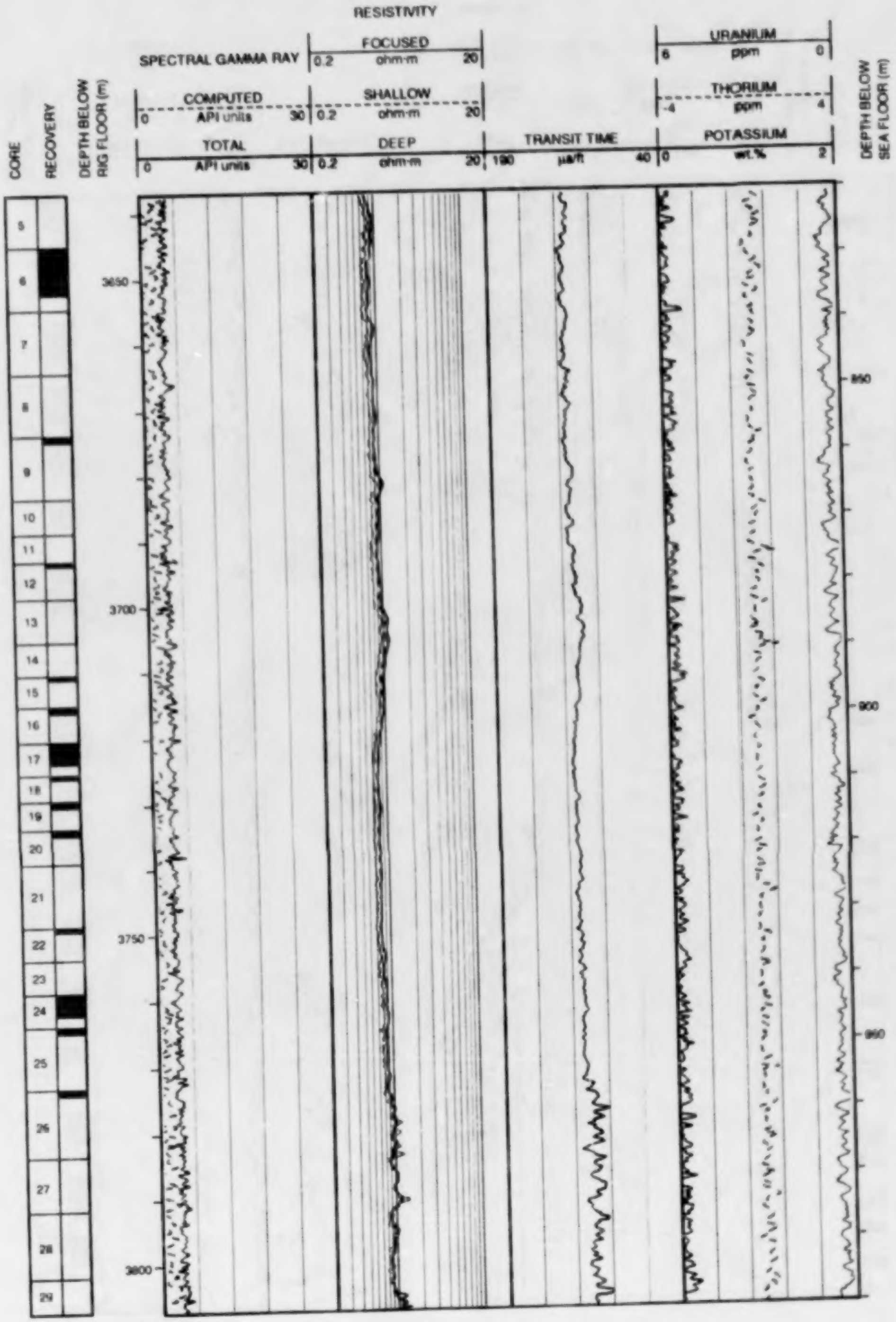

Hole 807C: Resistivity-Sonic-Gamma Ray Log Summary (continued)

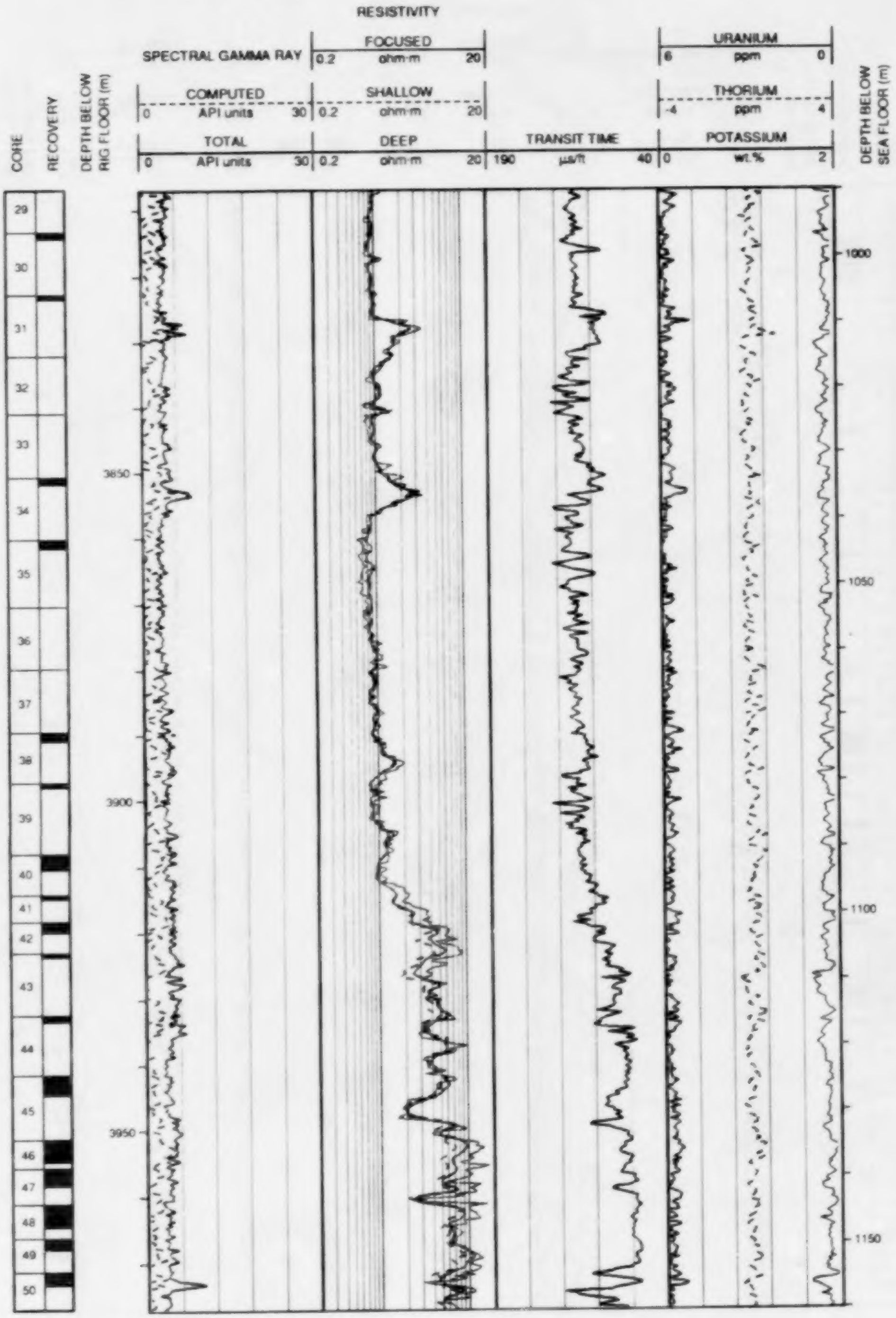

Hole 807C: Resistivity-Sonic-Gamma Ray Log Summary (continued)

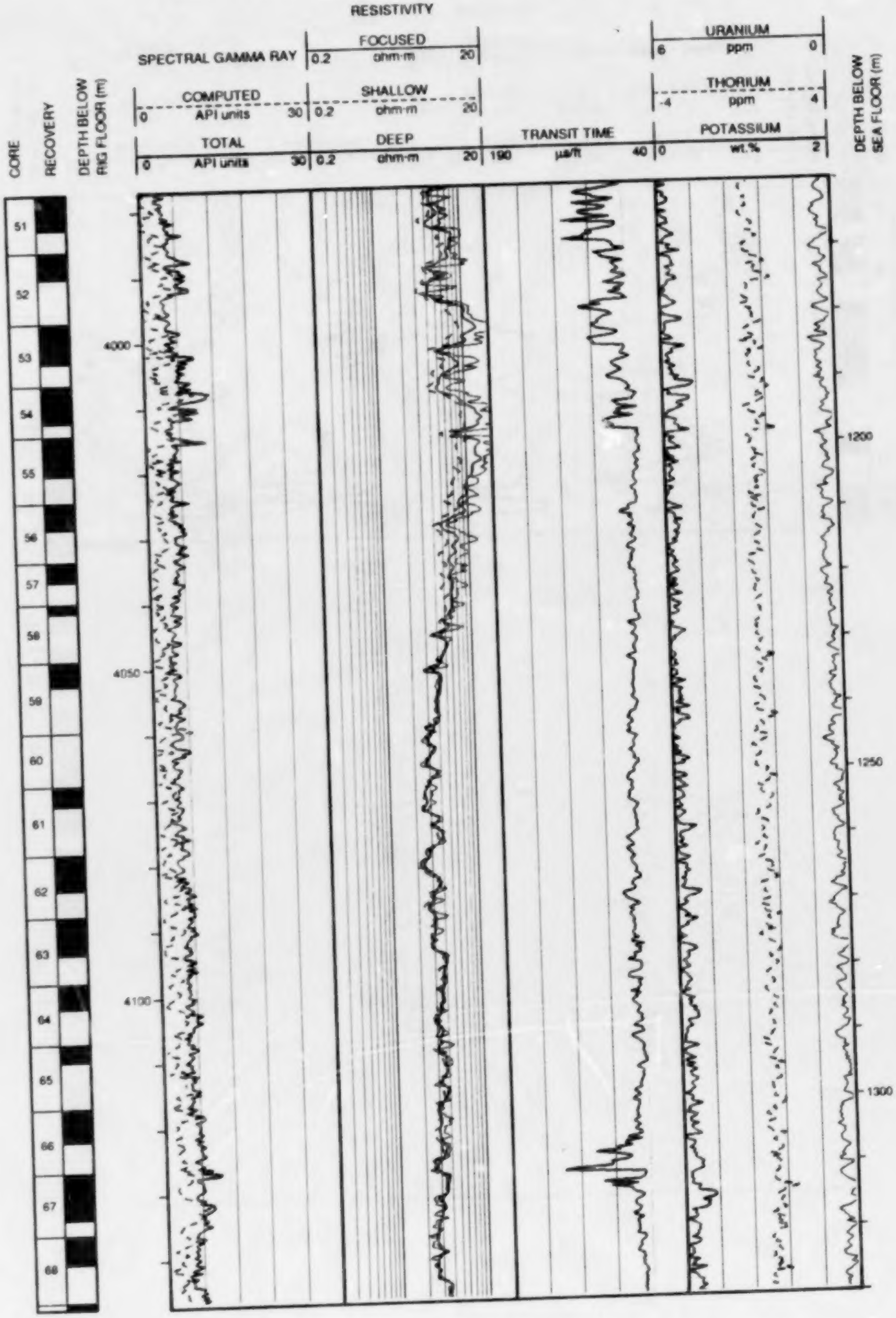

Hole 807C: Resistivity-Sonic-Gamma Ray Log Summary (continued)

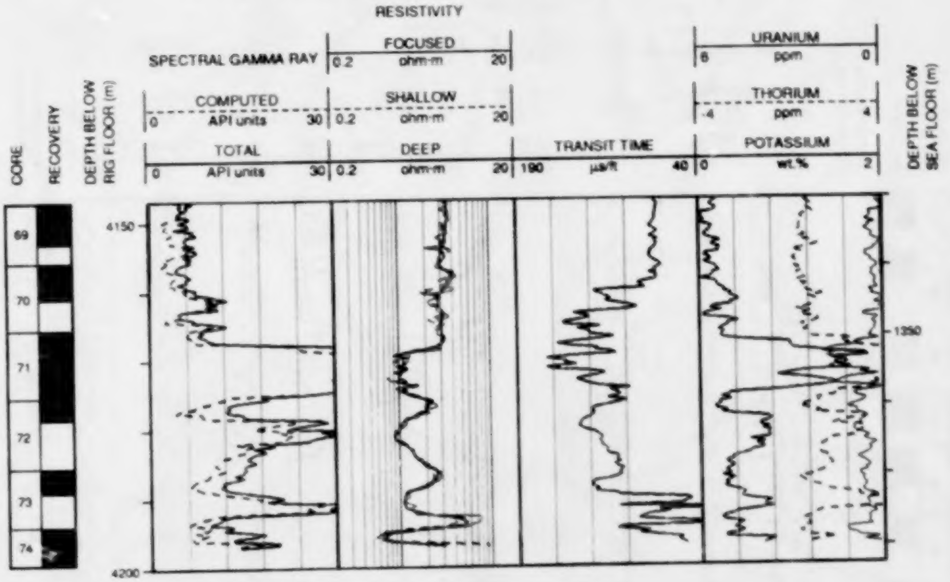

Hole 807C: Resistivity-Sonic-Gamma Ray Log Summary (continued)

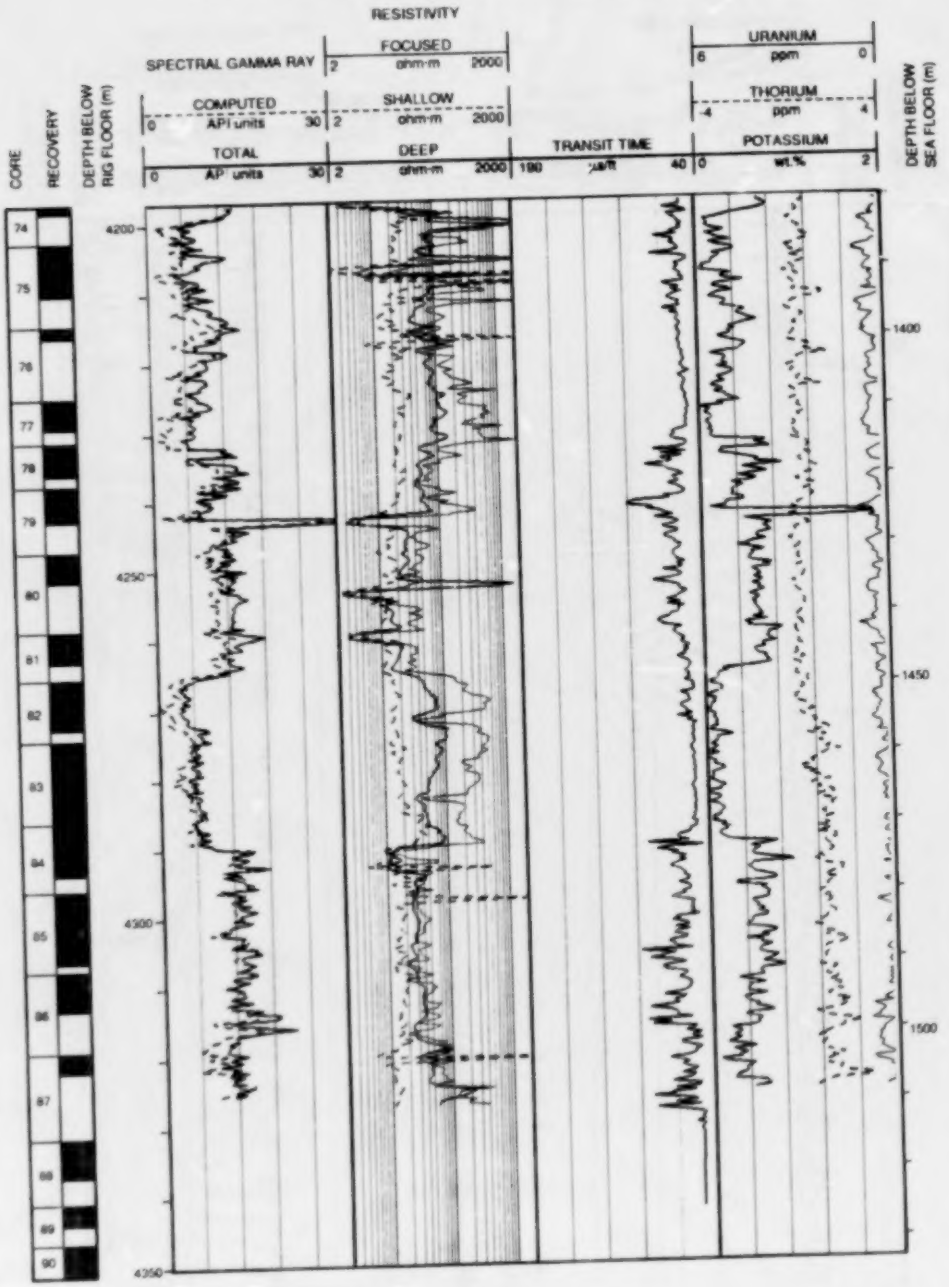

Hole 807C: Density-Gamma Ray-Aluminum Log Summary

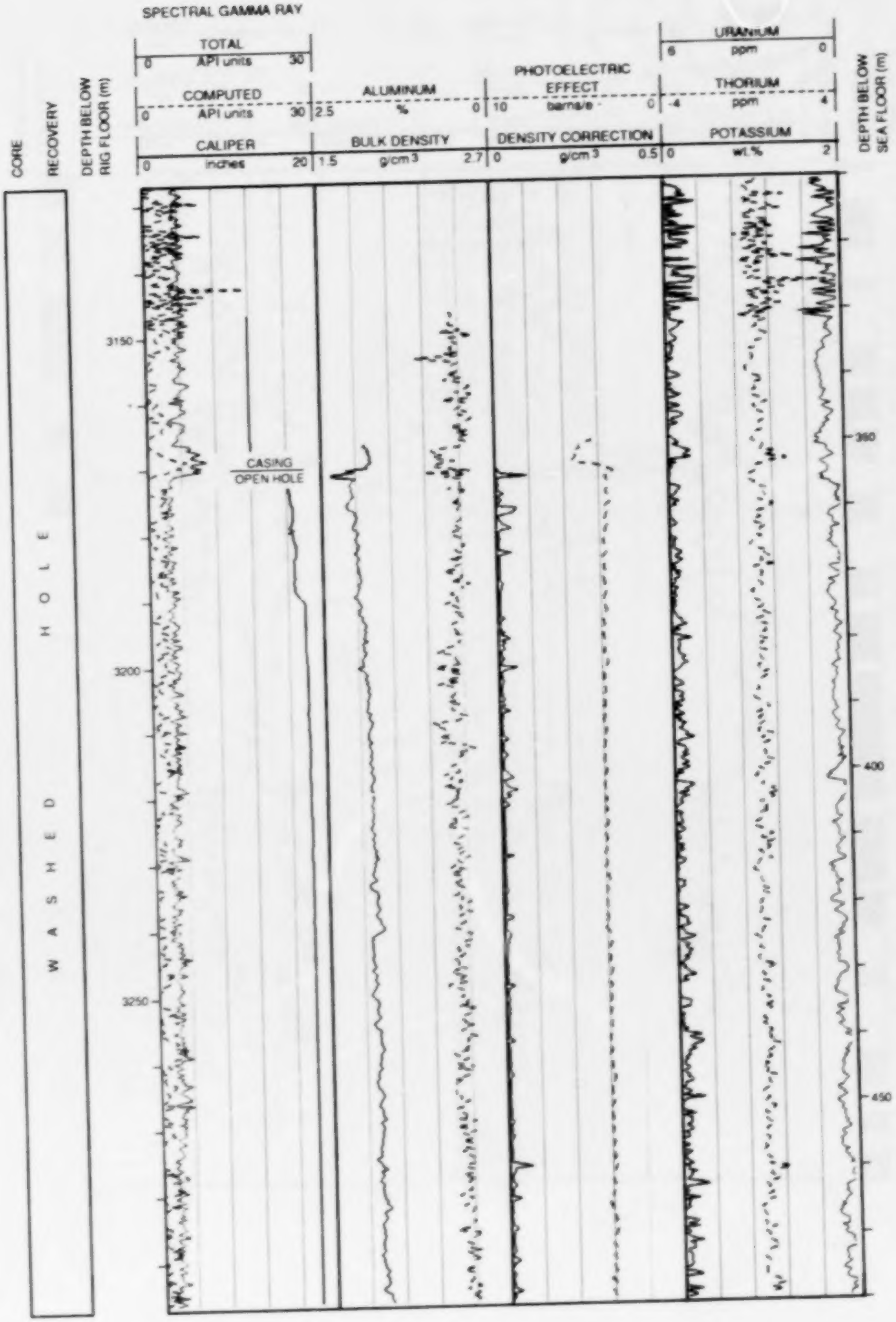

Hole 807C: Density-Gamma Ray-Aluminum Log Summary (continued)

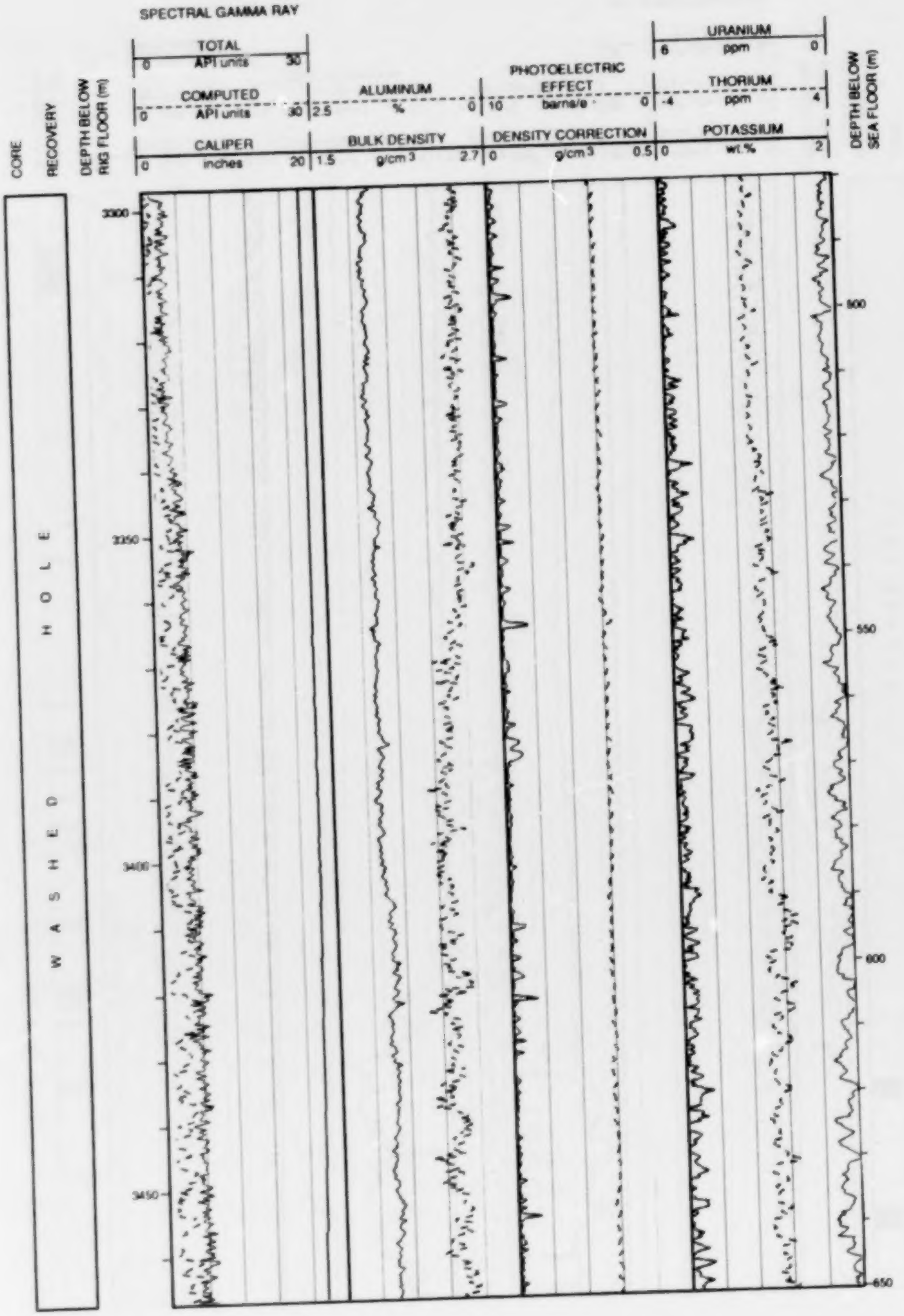

Hole 807C: Density-Gamma Ray-Aluminum Log Summary (continued)

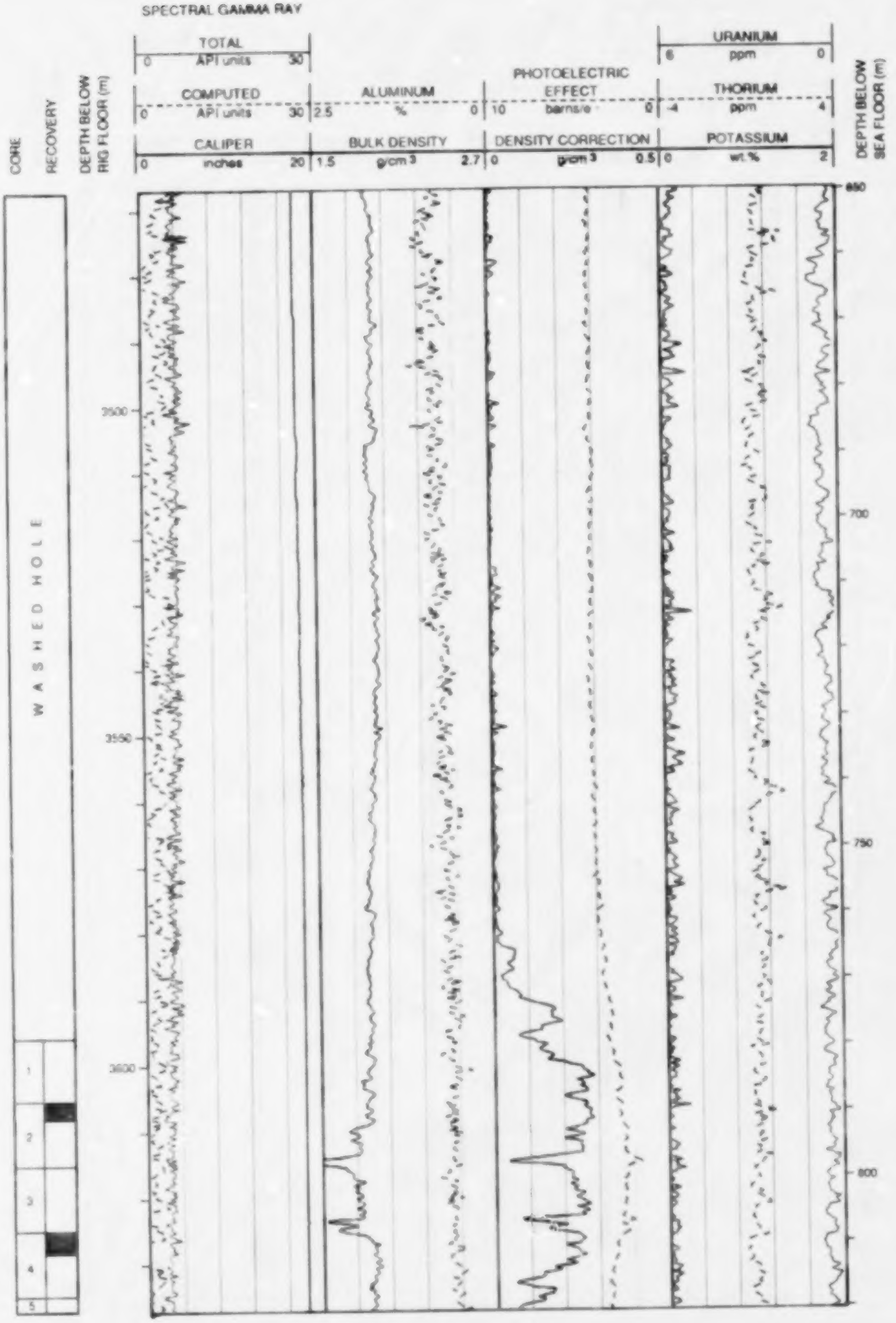

Hole 807C: Density-Gamma Ray-Aluminum Log Summary (continued)

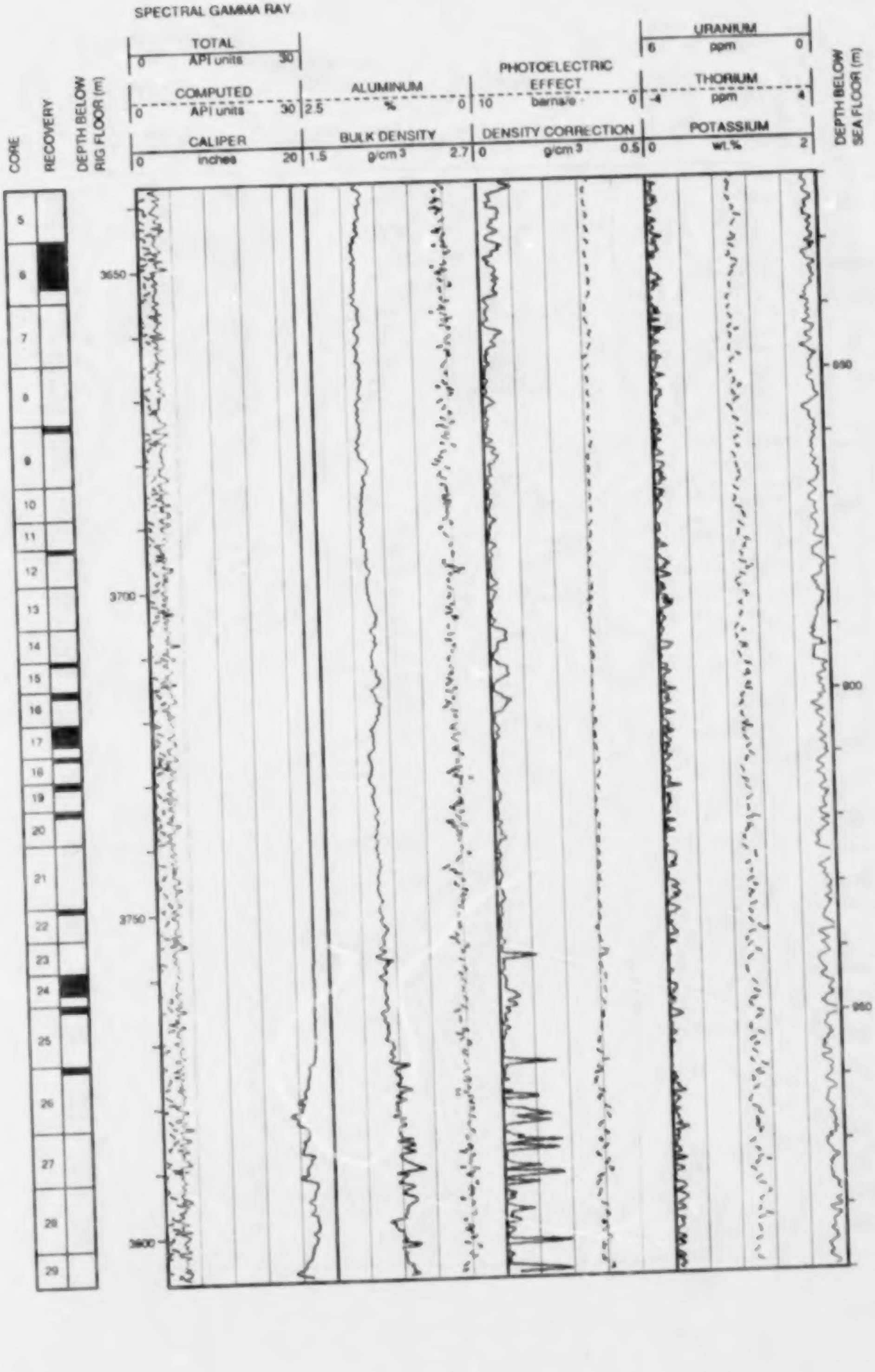

Hole 807C: Density-Gamma Ray-Aluminum Log Summary (continued)

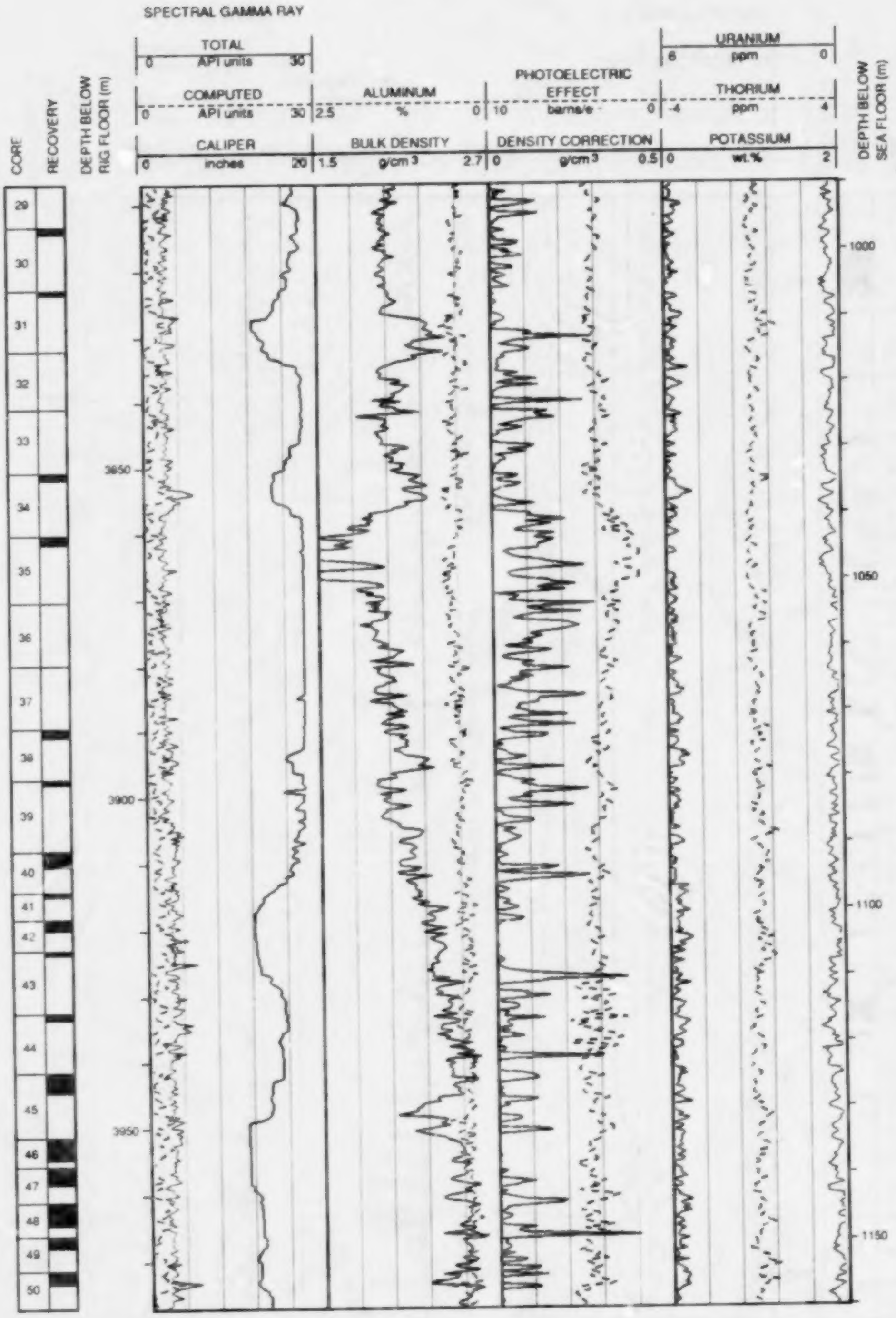

Hole 807C: Density-Gamma Ray-Aluminum Log Summary (continued)

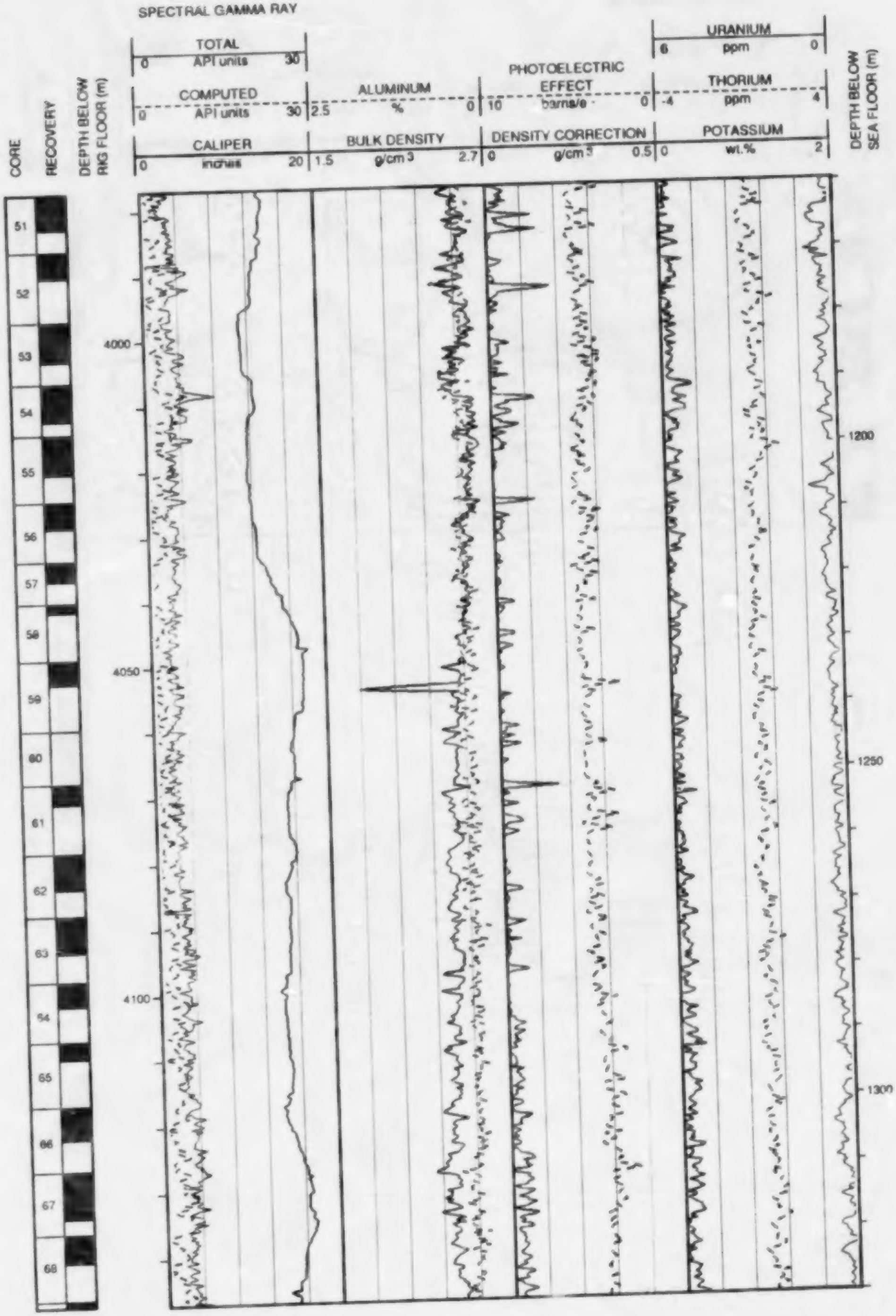

Hole 807C: Density-Gamma Ray-Aluminum Log Summary (continued)

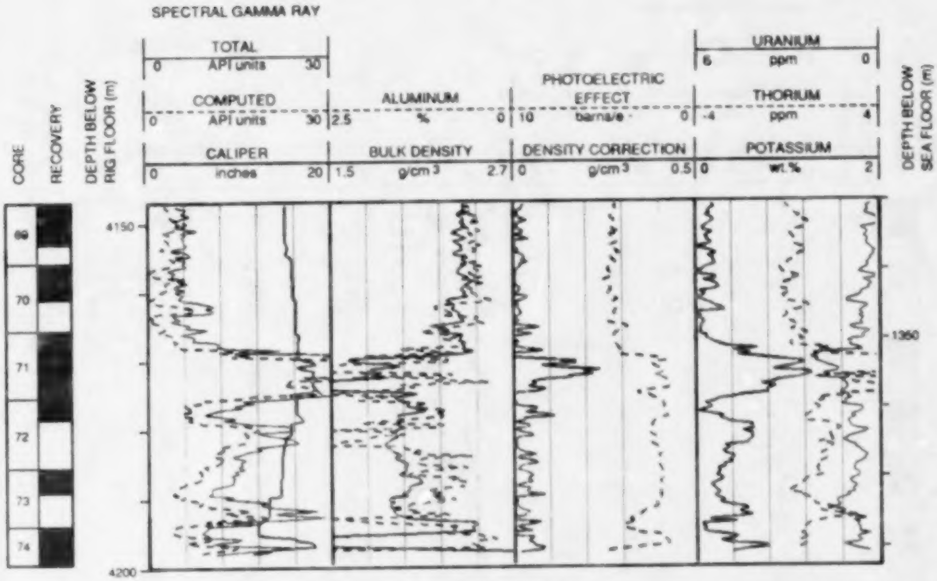

Hole 807C: Density-Gamma Ray-Aluminum Log Summary (continued)

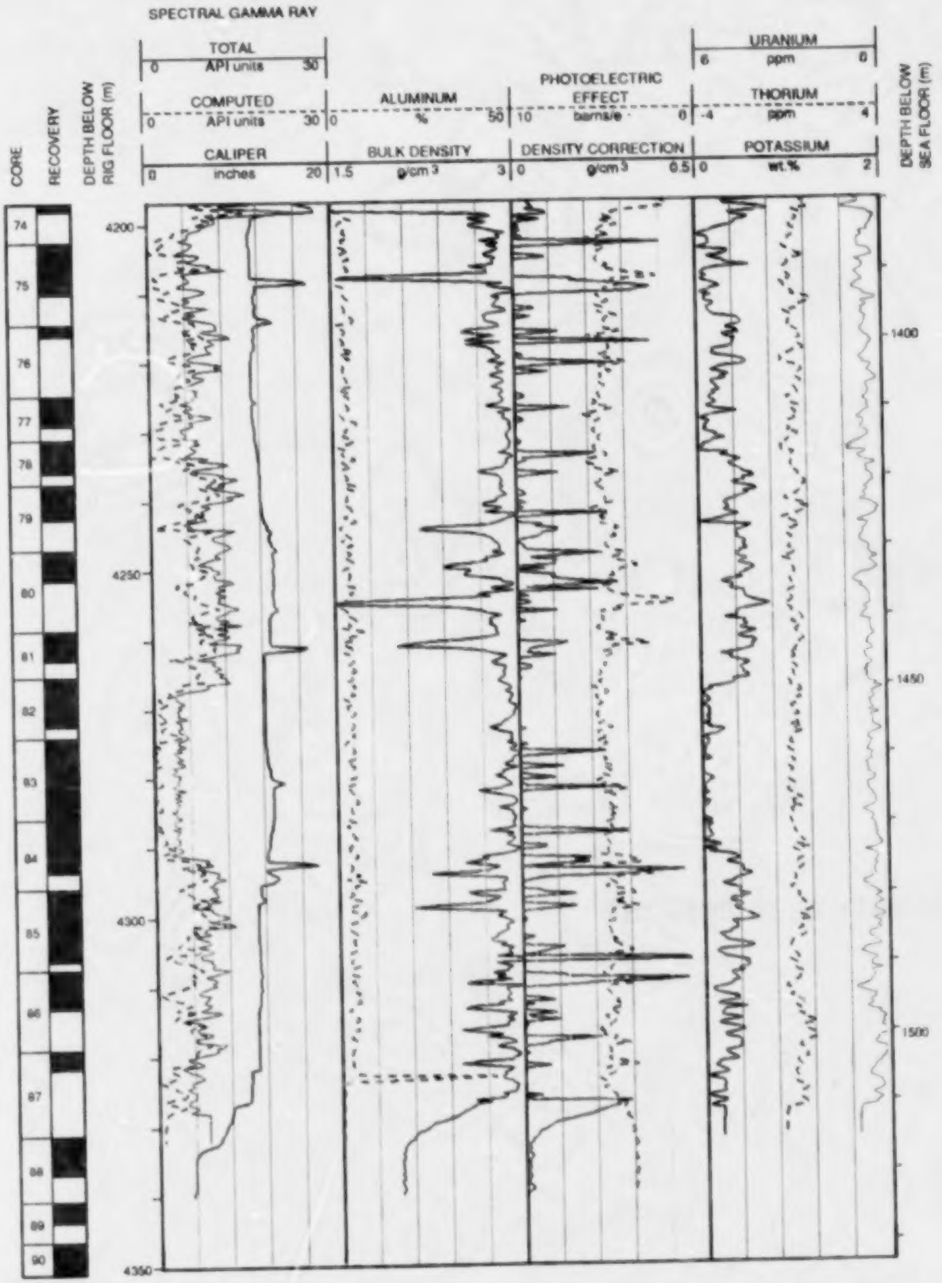

SECTION 3: SYNTHESIS

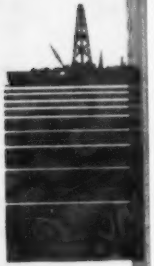

Kroenke, L. W., Berger, W. H., Janecek, T. R., et al., 1991
Proceedings of the Ocean Drilling Program, Initial Reports, Vol. 130

10. ONTONG JAVA PLATEAU, LEG 130: SYNOPSIS OF MAJOR DRILLING RESULTS[1]

W. H. Berger,[2] L. W. Kroenke,[3] L. A. Mayer,[4] and Shipboard Scientific Party[5]

ABSTRACT

Sixteen holes were drilled at five sites on the northeastern flank of Ontong Java Plateau during Leg 130 (Sites 803 through 807). All of these sites are near the equator, but are at different depths (803: 02°26.0′N, 3410 m; 804: 01°00.3′N, 3861 m; 805: 01°13.7′N, 3188 m; 806: 00°19.1′N, 2520 m; and 807: 03°36.4′N, 2805 m). One of our goals was to obtain a depth transect of Neogene carbonate deposition for reconstructing the history of ocean climate, chemistry, and productivity, and for understanding the origin of acoustic reflectors. Another goal was to achieve considerable penetration into basement for elucidating the origin of the plateau.

All sites yielded multiple Neogene sequences, which were cored using the advanced hydraulic piston corer (APC) to the ooze-chalk transition (10–14 Ma) and with the extended core barrel (XCB) below that. Sites 803 and 807 were drilled to basement and yielded incomplete Paleogene and Cretaceous sections. Penetration into basement was 25 m at Site 803 and 149 m at Site 807; 98 m of basalt was recovered. In all, we cored 5889 m, taking 639 cores. Of the record 4822 m recovered, 55% was taken with the APC, 39% with the XCB, and 6% with the rotary core barrel (RCB). All sites except Site 804 were logged.

Neogene sedimentation rates were found to vary by more than a factor of 2, with a striking maximum in the latest Miocene to early Pliocene and a strong minimum in the Pleistocene. Fluctuations in carbonate content on the million-year scale are highly coherent among depths over the last 12 m.y., perhaps less so before that. Many acoustic reflectors appear synchronous with carbonate reduction events (CREs) and other paleoceanographic events. Other reflectors are tied to diagenesis (e.g., the ooze-chalk transformation, which is diachronous).

Recovery of the Cretaceous/Tertiary (K/T) boundary at Sites 803 and 807 demonstrates the presence of a deep carbonate-compensation depth (CCD) across the transition: one sequence is calcareous, the other is not. Because the K/T sections occur below and above major hiatuses, we postulate that special conditions for preservation existed during the transition. In addition, there is evidence of volcanic activity at that time.

The basalts cored at Sites 803 and 807 are predominantly olivine-bearing and were erupted during the mid-Cretaceous. At Site 807, pillow lavas buried sediments. One thick flow (at about 28 m) was penetrated here, apparently a flood basalt. Magnetic paleolatitudes suggest that the Ontong Java Plateau has moved coherently with the Pacific Plate since the Early Cretaceous.

INTRODUCTION

The five sites drilled during Ocean Drilling Program (ODP) Leg 130 are situated on the northeastern flank of the Ontong Java Plateau in the western equatorial Pacific, a region well known for its excellent pelagic record (Fig. 1). This record was explored during three previous Deep Sea Drilling Project (DSDP) expeditions that provided information on Sites 64, 288, 289, and 586 to the south of the Leg 130 area (Shipboard Scientific Party, 1971, 1975a, 1975b, 1986).

The unique geological setting of the plateau, a region long elevated above the surrounding seafloor because of its anomalously thick crust (Hussong et al., 1979), led to the accumulation and preservation of a thick cover of calcareous sediments. Situated well away from special boundary conditions, a pelagic record has collected on the plateau that is eminently suited for high-resolution studies of global ocean signals. In addition, there are indications that paleoceanographic events can be traced in the physical properties of sediments, providing a link to the seismic record that allows both three-dimensional regional mapping and long-distance correlation. Last, but not least, the tectonic history of the Ontong Java Plateau, the largest plateau in the Pacific, has been studied frequently (see Kroenke, 1972, 1984). The plateau is of subcontinental size (e.g., it is much larger than the Iberian peninsula), and its origin is of considerable interest in the context of large-scale tectonics.

Leg 130 scientists had two major goals that differed from those of previous cruises: (1) the cruise was designed to furnish a depth transect for the Neogene portion of the sediment cover, and (2) it was planned to penetrate deeply into basement. Both these goals were fully met. In addition, our intent was to recover as much of the Paleogene and Cretaceous record as time would permit, given the priorities mentioned, with the aim of obtaining the means for detailed reconstruction of paleoceanography and paleoclimate for these earlier periods as well. Leg 130 also succeeded in this aim when all sites penetrated into pre-Neogene sediments and samples from throughout the Paleogene and Cretaceous were recovered from two sites. In addition, complete (or nearly complete) records (one calcareous, the other noncalcareous) of the Cretaceous/Tertiary (K/T) boundary were recovered from Sites 803 and 807.

DRILLING STRATEGY AND MAIN RESULTS

Objectives

As mentioned, a major goal of Leg 130 was to sample sedimentary sequences at different depths along the equator for a Neogene depth transect (Figs. 2 and 3). This transect was planned so as to procure the material for high-resolution stratigraphic studies of paleoceanographic changes (water temperature, productivity, carbonate chemistry) (1) for assessing the equatorial dynamics of the western Pacific, (2) for comparing results with

---

[1] Kroenke, L. W., Berger, W. H., Janecek, T. R., et al., 1991. *Proc. ODP, Init. Repts.*, 130: College Station, TX (Ocean Drilling Program).

[2] Research Associate, University of Bremen, D2800 Bremen, Federal Republic of Germany (permanent address: Scripps Institution of Oceanography, La Jolla, CA 92093, U.S.A.).

[3] Hawaii Institute of Geophysics, Honolulu, HI 96822, U.S.A.

[4] Dalhousie University, Halifax, Nova Scotia, B3H-4J1, Canada.

[5] Shipboard Scientific Party is as given in the list of participants preceding the contents.

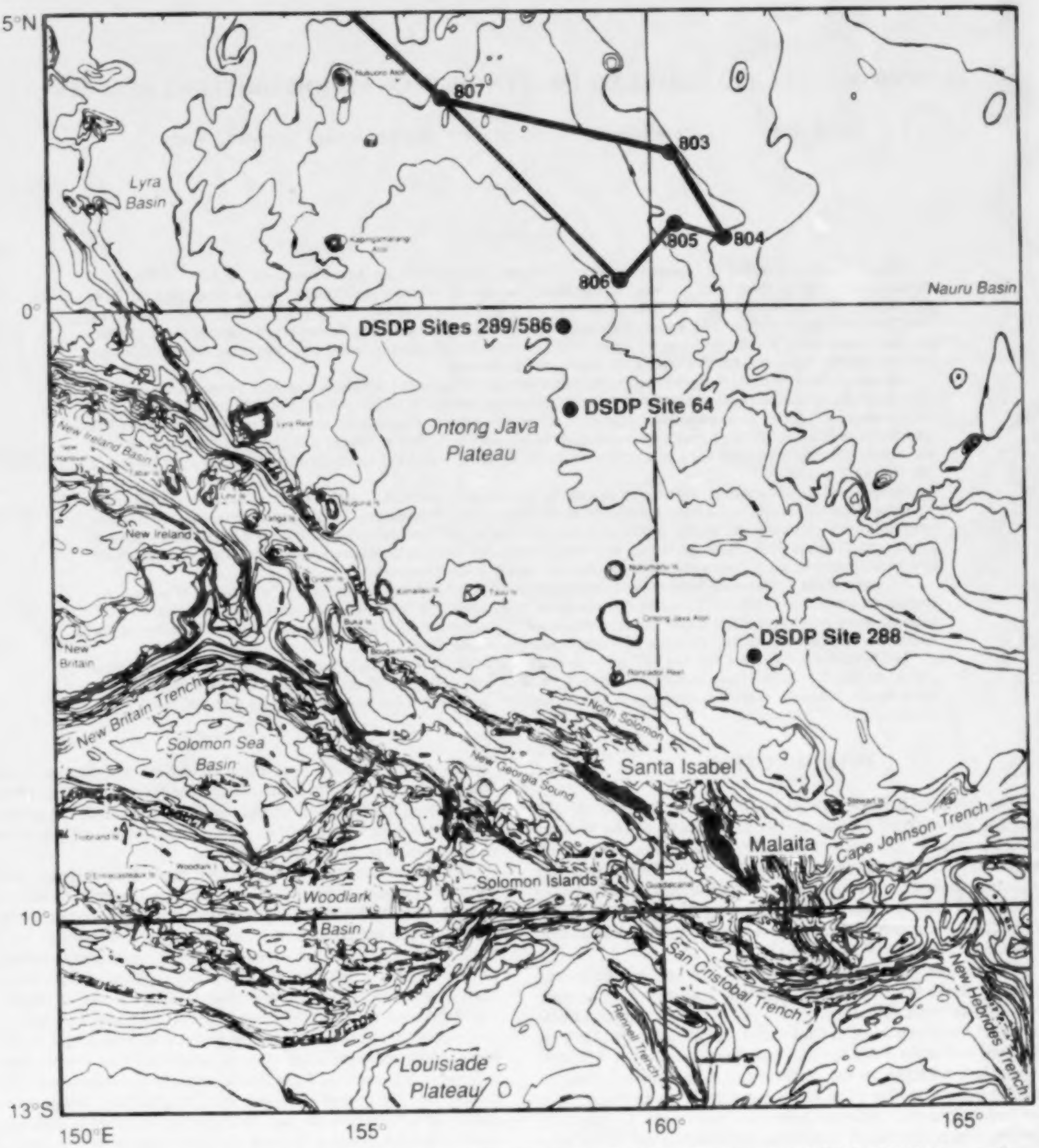
5°N
0°
10°
13°S
150°E
155°
160°
165°
807
803
805
804
806
Lyra Basin
Nauru Basin
DSDP Sites 289/586
DSDP Site 64
Ontong Java Plateau
New Ireland Basin
New Ireland
New Britain
DSDP Site 288
New Britain Trench
Solomon Sea Basin
North Solomon
New Georgia Sound
Santa Isabel
Malaita
Cape Johnson Trench
Solomon Islands
Woodlark Basin
San Cristobal Trench
Rennell Trench
New Hebrides Trench
Louisiade Plateau

Figure 1. Geographic setting of Leg 130 sites, and relationship to DSDP Sites 64 (Leg 7), 288 and 289 (Leg 30), and 586 (Leg 89). Bathymetry from Kroenke et al. (1983). Contour interval is 500 m.

other equatorial depth transects, and (3) for clarifying the origin and significance of the ubiquitous subparallel reflectors in pelagic carbonates here and elsewhere, with the hope that an understanding of the origin of these reflectors would provide a valuable paleoceanographic tool.

Four ODP sites (803, 804, 805, and 806) address this. Including DSDP Sites 289/586, then, there are five equatorial sites that span a depth interval of almost 2000 m. The sediments thus sampled essentially were produced in the same surface-water conditions and have been derived from the same pelagic rain. The depth interval bracketed by our sites (2500–3900 m) contains the depth range in which changes in dissolution gradients are most pronounced, with considerable effects on physical properties and, hence, seismic properties (Berger and Johnson, 1976; Johnson et al., 1977; Berger and Mayer, 1978; Mayer et al., 1985, 1986).

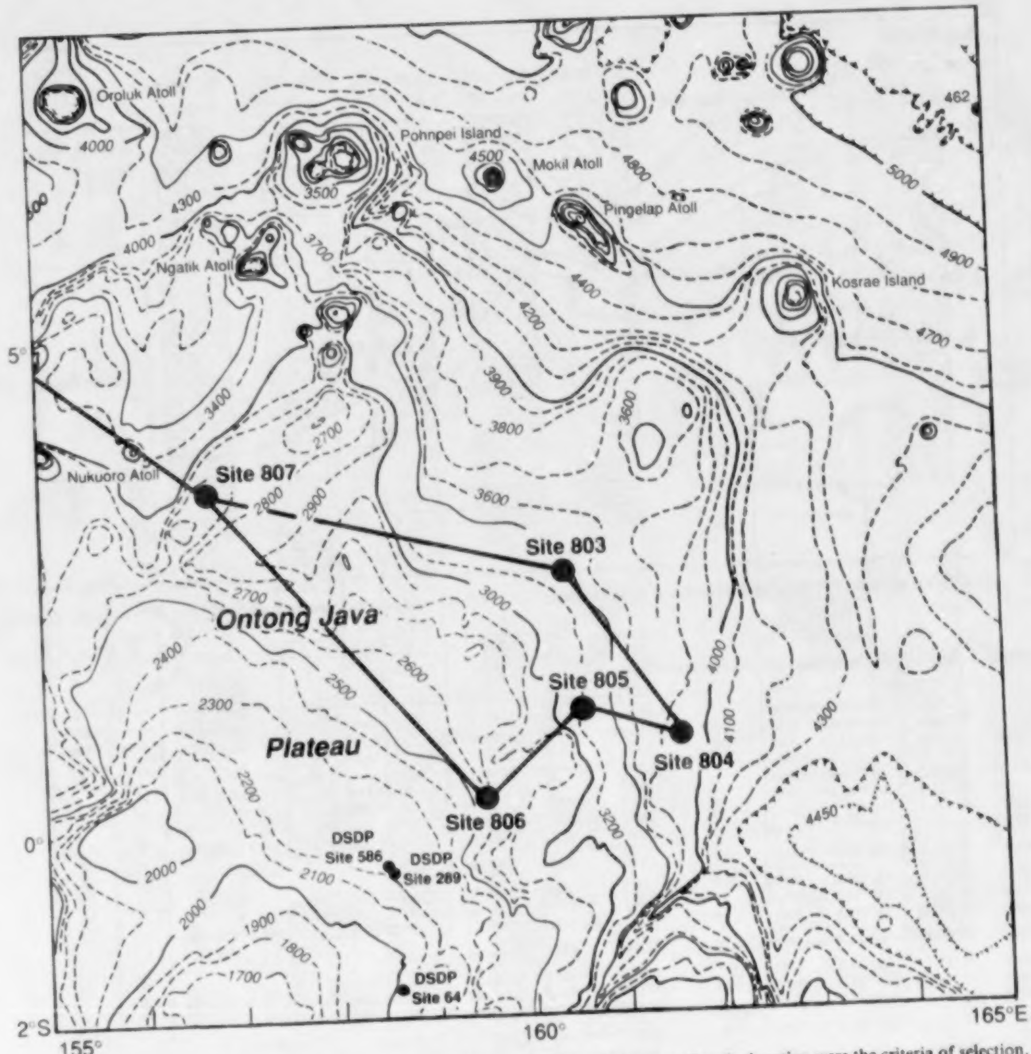
Oroluk Atoll
Pohnpei Island
Mokil Atoll
Pingelap Atoll
Ngatik Atoll
Kosrae Island
Nukuoro Atoll
462
4000
4300
3500
4500
4800
5000
4900
4700
3700
4400
4200
3900
3800
3600
3400
2700
Site 807
2800
2900
Site 803
3000
Ontong Java
2600
2500
2400
2300
Site 805
4000
4100
4300
Site 804
Plateau
2200
Site 806
4450
3200
DSDP
Site 586
DSDP
Site 289
2100
2000
1900
1800
1700
DSDP
Site 64
5°
0°
2°S
155°
160°
165°E

Figure 2. Location of Sites 803–807. Proximity to equator and a spread of depths in an undisturbed section were the criteria of selection. Bathymetry after Mammerickx and Smith (1985). Contour interval is 100 m.

The Cretaceous-Paleogene section was another of our objectives because of the intrinsic interest of ocean conditions outside of the range of those of the more familiar Neogene and also because this record provides a reference for Southern Hemisphere paleoceanography and bears on the early history of the plateau itself. Major hiatuses previously were encountered in that section, which made it unlikely that we would find complete sequences. Yet, scientists thought that many of these hiatuses are of local extent, so that additional drilling might be expected to fill at least some of the gaps.

Drilling into basement was a high priority. The origin of the old oceanic Pacific plateaus (Ontong Java, Manihiki, Shatsky, Hess, Magellan) is a problem with many implications for mantle processes and the evolution of the seafloor. The relationship of the plateau basalts to the extensive "mid-Cretaceous" volcanic events of the Pacific is of special interest. There also are implications for climatic change (CO_2 influx, hydrothermal activity) and possibly for the origin of continental crust in general (Kroenke, 1974).

Drilling Statistics

The *JOIDES Resolution* sailed from Guam on 23 January 1990 and returned to Guam on 27 March 1990, after 62.7 days at sea. Of these, 51.2 days were spent on site; the rest was spent while the ship was under way, including seismic profiling and site positioning. A total of 16 holes were drilled at five sites (Table 1).

All sites yielded multiple Neogene sequences using the advanced hydraulic piston corer (APC) to refusal (near the ooze-chalk transition), and the extended core barrel (XCB) below

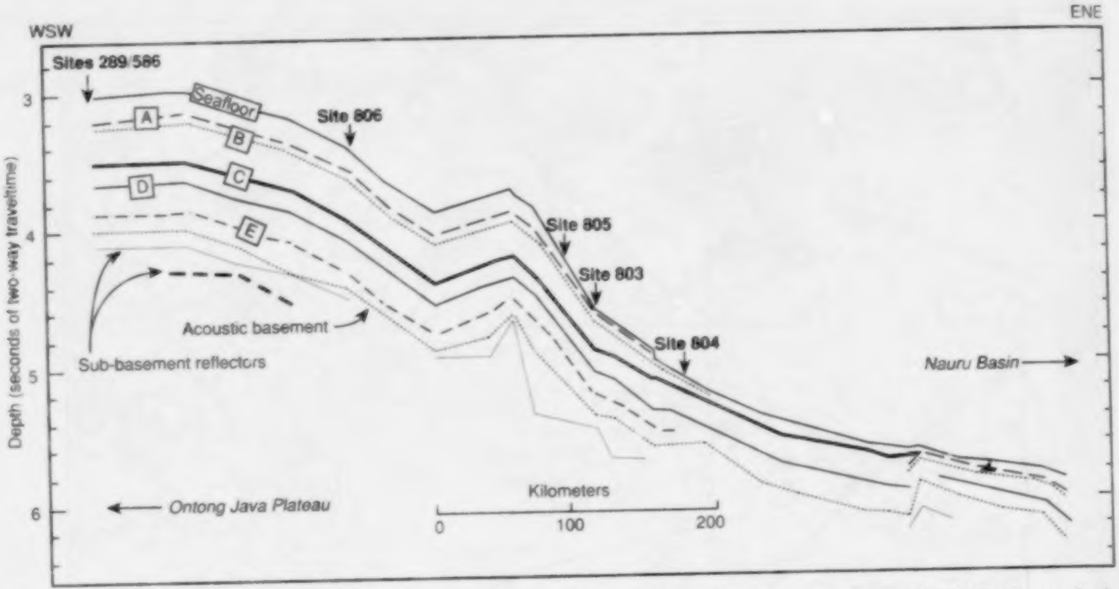

Figure 3. Simplified acoustic stratigraphy for the flank of the Ontong Java Plateau, and approximate locations of Sites 803–806 (the Neogene depth transect).

Table 1. Leg 130 site locations and drilling statistics.

Hole	Latitude (north)	Longitude (east)	Water depth (m)	Cores (*N*)	Maximum penetration (m)	Interval cored (m)	Core recovered (m)	Recovered with APC (m)	Recovered with XCB (m)	Recovered with RCB (m)	Time (days)
803A	02°26.0	160°32.5	3410	6	55.5	55.50	57.99	57.99 (104.5%)	0	0	
803B	02°26.0	160°32.5	3410	7	61.3	61.30	58.18	58.18 (94.9%)	0	0	
803C	02°26.0	160°32.5	3410	23	237.5	218.50	226.31	226.31 (105.4%)	0	0	
803D	02°26.0	160°32.5	3412	71	656.0	656.0	494.96	228.88 (103.6%)	248.47 (62.9%)	17.61 (40.0%)	
803	02°26.0	160°32.5	3410	107	656.0	991.3	837.44	571.36	248.47	17.61	9.7
804A	01°00.3	161°35.6	3862	6	48.7	48.7	50.52	50.52 (103.7%)	0	0	
804B	01°00.3	161°35.6	3861	15	137.7	137.7	141.61	141.61 (102.8%)	0	0	
804C	01°00.3	161°35.6	3861	33	312.5	312.5	273.78	120.27 (100%)	153.51 (79.9%)	0	
804	01°00.3	161°35.6	3861	54	312.5	498.9	465.91	312.40	153.51		3.1
805A	01°13.7	160°31.8	3189	6	50.5	50.5	52.22	52.22 (103.4%)	0	0	
805B	01°13.7	160°31.8	3187	50	473.3	473.3	444.89	271.30 (103.1%)	173.59 (82.6%)	0	
805C	01°13.7	160°31.8	3188	64	611.0	611.0	495.46	236.34 (100.2%)	259.12 (69.1%)	0	
805	01°13.7	160°31.8	3188	120	611.0	1134.8	992.57	559.86	432.71		6.2
806A	00°19.1	159°21.7	2521	9	83.7	83.7	85.95	85.95 (102.7%)	0	0	
806B	00°19.1	159°21.7	2520	78	743.1	743.1	666.36	335.20 (104.8%)	331.16 (78.3%)	0	
806C	00°19.1	159°21.7	2520	62	776.4	587.6	523.62	320.61 (103.6%)	203.01 (73.0%)	0	
806	00°19.1	159°21.7	2520	149	776.4	1414.4	1275.93	741.76	534.17		7.9
807A	03°36.4	156°37.5	2804	86	822.9	822.9	716.74	263.11 (103.4%)	453.63 (79.8%)	0	
807B	03°36.4	156°37.5	2806	30	278.6	278.6	280.18	280.18 (100.6%)	0	0	
807C	03°36.4	156°37.5	2806	93	1528.4	748.4	252.84	0	0	252.84 (33.8%)	
807	03°36.4	156°37.5	2805	209	1528.4	1849.9	1249.76	543.29	453.63	252.84	24.3
Grand totals				639	3884.3	5889.3	4821.58	2728.67	1822.49	270.45	51.2

that. Sites 803 and 807 were deepened by rotary core barrel (RCB) drilling, reaching basement and yielding Paleogene and Cretaceous sections (Fig. 4). Penetration into basement was 25 m at Site 803 and 149 m at Site 807; 98 m of basalt was recovered. In all, we cored 5889 m, taking 639 cores. Of the record 4822 m recovered, 56.5% was by taken with the APC, 38% with the XCB, and 5.5% with the RCB. Four sites were logged extensively.

Main Results

Site 803

Four holes were drilled at Site 803 (2°26.0′N, 160°32.5′E; water depth, 3410 m), the last of which (803D) was drilled into basement and terminated at 656.0 m below seafloor (mbsf) (see Table 1 for drilling and recovery statistics). The acoustic thickness of the sediment is about 0.64 s (two-way traveltime [TWT];

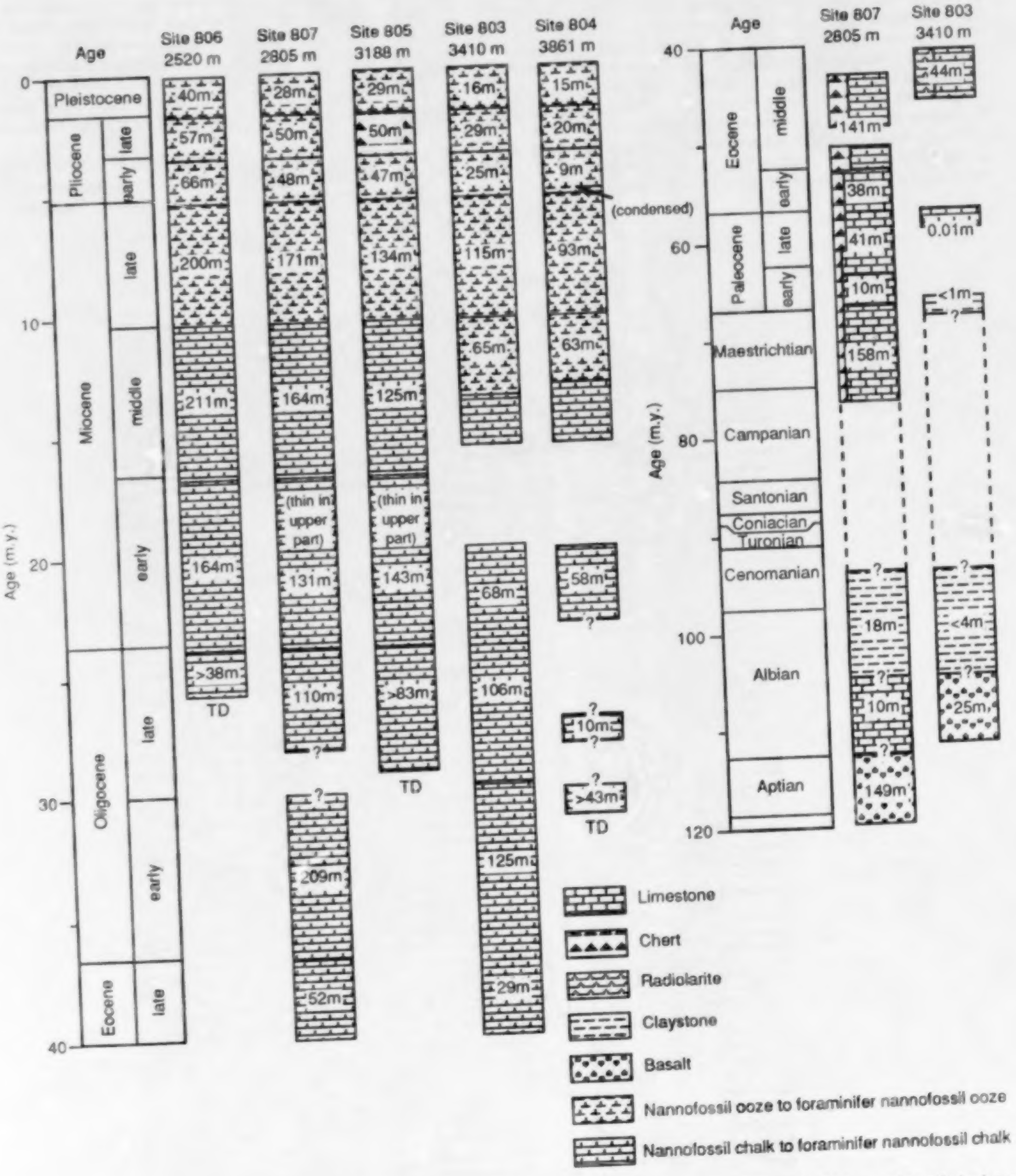
Age
Site 806
2520 m
Site 807
2805 m
Site 805
3188 m
Site 803
3410 m
Site 804
3861 m
Age (m.y.)
0
10
20
30
40
Pleistocene
Pliocene
late
early
Miocene
late
middle
early
Oligocene
late
early
Eocene
late
40m
57m
66m
200m
211m
164m
>38m
TD
28m
50m
48m
171m
164m
(thin in upper part)
131m
110m
?
?
209m
52m
29m
50m
47m
134m
125m
(thin in upper part)
143m
>83m
TD
16m
29m
25m
115m
65m
68m
106m
125m
29m
15m
20m
9m
(condensed)
93m
63m
58m
?
?
10m
?
?
>43m
TD
Age
Site 807
2805 m
Site 803
3410 m
40
60
80
100
120
Eocene
middle
early
Paleocene
late
early
Maestrichtian
Campanian
Santonian
Coniacian
Turonian
Cenomanian
Albian
Aptian
141m
38m
41m
10m
158m
?
18m
?
10m
?
149m
44m
0.01m
<1m
?
?
<4m
?
25m
Limestone
Chert
Radiolarite
Claystone
Basalt
Nannofossil ooze to foraminifer nannofossil ooze
Nannofossil chalk to foraminifer nannofossil chalk

Figure 4. Sites drilled on Ontong Java Plateau during Leg 130. Sites are arranged according to depth: note decrease in thickness of correlative intervals, from left to right, and hiatus formation at the two deep sites. Sediment thicknesses listed are approximate values based on shipboard biostratigraphy. Age control through much of the Cretaceous is poor because of the poor preservation of calcareous microfossils.

Fig. 5). The site was drilled near a strong "mid-section reverberation" (MSR), the origin of which is unknown. Reflectors were numbered from the top down at this site to identify them uniquely for subsequent correlation with other sites.

The recovered sediments range in age from Pleistocene to early Late Cretaceous; they were divided into three units. The uppermost Unit I takes up most of the section (0–563.7 mbsf); it ranges from upper Eocene to Pleistocene and consists of nannofossil ooze and chalk to foraminifer nannofossil ooze and chalk. The ooze-chalk transition occurs between 210 and 220 mbsf and provides the basis for dividing the unit into Subunits IA and IB. The logging data suggest that this transition ranges through 60 m or more in the sedimentary column. The foraminifer content is high in the Pleistocene and adjacent upper Pliocene ooze and decreases downhole through the first 30–60 mbsf, where it remains low throughout the rest of the section. The oozes and chalks of Unit I are uniform, although depositional cycles are evident in places where redox fluctuations are expressed as Liesegang color banding, which is thought to result from changing concentrations and states of oxidation of iron and manganese (Fig. 6).

Unit II (563.7–621.8 mbsf) ranges from middle to upper Eocene and consists of approximately 58 m of nannofossil chalk with radiolarians, radiolarian nannofossil chalk, nannofossil ra-

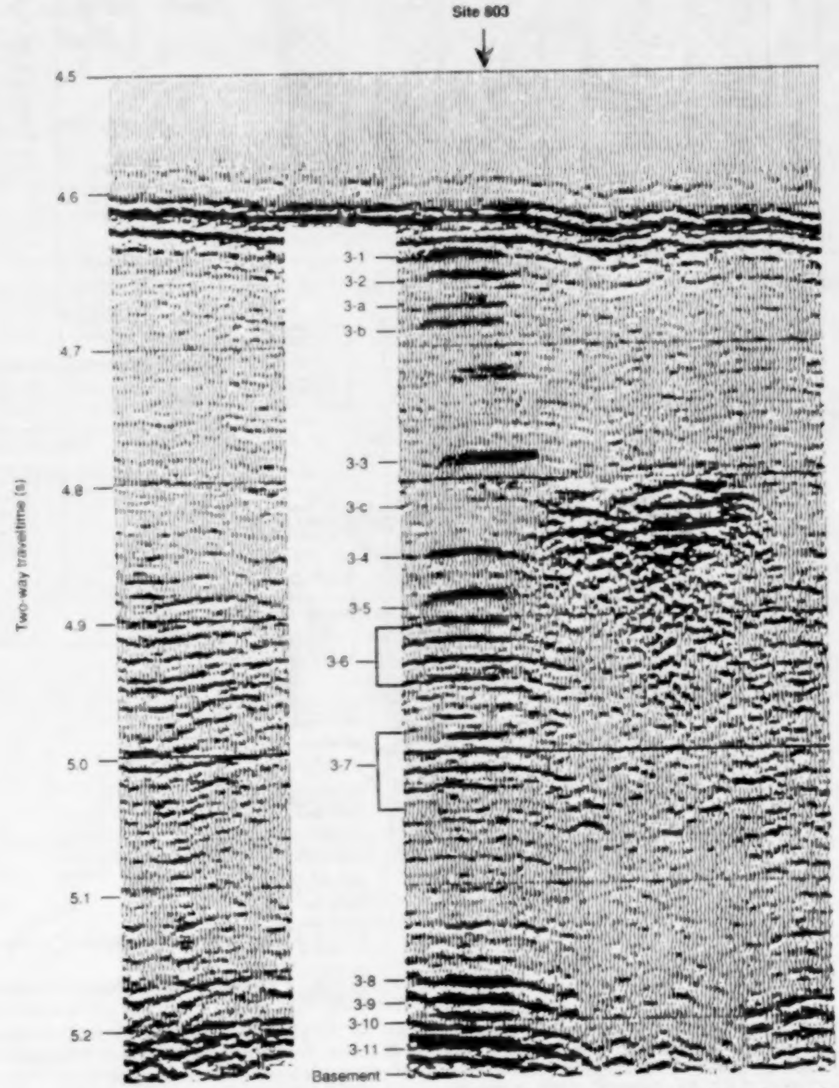

Figure 5. Seismic record at Site 803, collected by scientists on board the *Thomas Washington* during the ROUNDABOUT Cruise 11 site survey, using the 80-in.^{3} water gun, 70–250 Hz band-pass filter. Numbers refer to reflectors and reflector groups.

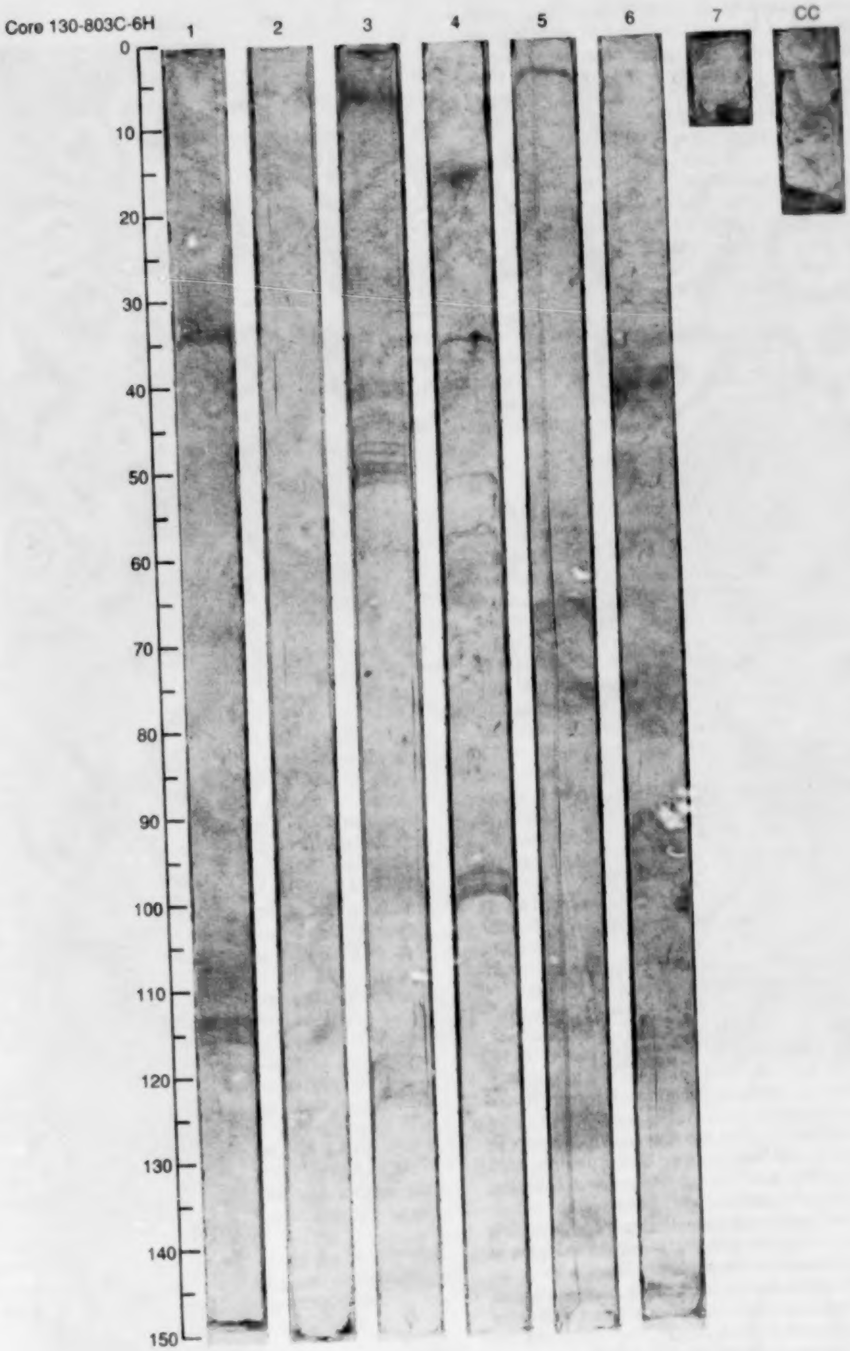
Core 130-803C-6H
1
2
3
4
5
6
7
CC
0
10
20
30
40
50
60
70
80
90
100
110
120
130
140
150

Figure 6. Liesegang color banding from Core 130-803C-6H (66.0–76.0 mbsf) in Subunit IA, nannofossil ooze. Bands are reddish gray, greenish gray, and pale green, and are believed to be caused by changes in concentrations and oxidation states in iron and manganese.

diolarite, and minor amounts of chert. Unit III (621.8–626.3 mbsf) ranges from lower Upper Cretaceous to middle Eocene and is composed of claystone and clayey siltstone, with minor radiolarian-rich intervals. Resistivity logs suggest that this lithology continues from 621.8 mbsf to basement at 630.4 mbsf. The K/T boundary was crossed at 622.25 mbsf, where an apparently complete boundary sequence was recovered.

The record is continuous from the Pleistocene to the lower Miocene section, where a significant stratigraphic break appears at 245.9 mbsf (about 15–20 Ma), the first of three major stratigraphic breaks encountered above the K/T boundary. The other two breaks occur across the Paleocene/Eocene boundary (~ 45–~ 58 Ma) at 621.8 mbsf and in the Paleocene (~ 58– ~ 66 Ma) immediately below. The section below the K/T boundary, which was penetrated at 622.25 mbsf, is condensed and presumably also contains several substantial hiatuses.

Nine basalt subunits were recognized within basement rocks (Unit IV) on the basis of intercalated limestones or breccias. Their age is Cenomanian–upper Albian or older. These basalts are pillowed (Fig. 7) and are predominantly aphyric, fine-grained, and nonvesicular tholeiites.

Site 804

Three holes were drilled at Site 804 (1°00.3′N, 161°35.6′E; water depth, 3861 m), with the deepest terminating at 312.5 mbsf in lower Oligocene nannofossil chalk (see Table 1 for drilling and recovery statistics). The seismic record (Fig. 8) shows an acoustic thickness of sediments of about 0.65 s TWT, similar to Site 803. There is evidence for disturbance from mass movement.

The sediment retrieved is Neogene in age, except for the five deepest cores in Hole 804C, in which Oligocene chalk was recovered (Cores 130-804C-29X to -33X). The entire column, from the oldest to the youngest deposits cored, was classified as nannofossil ooze and chalk and is considered as one lithologic unit. Major breaks are found in the upper Oligocene (hiatus at 270 mbsf, about 28–25 Ma) and at the lower-to-middle Miocene transition (hiatus at 197 mbsf, about 15–20 Ma). There is a condensed section or hiatus from the lower Pliocene section that occurred between 5 and 4 Ma (46–43 mbsf) and one possibly within the middle Miocene, between 13 and 11 Ma (near 160 mbsf).

The ooze-chalk transition appears near 181 mbsf and serves as a boundary between the two subunits recognized within the nannofossil ooze and chalk. Here, the age is middle Miocene (about 13 Ma). Radiolarians are more common in the lower subunit, with a maximum in the lower Miocene section (near 200 mbsf), just below the lower/middle Miocene hiatus. Disturbance of layers (other than from coring) is evident in the section spanning the major hiatus from lower to middle Miocene (210–187 mbsf) and between 42 and 110 mbsf (most of the upper Miocene). This disturbance is especially prominent between 70 and 80 mbsf (7–8 Ma).

The site is characterized by mass movement, which limits its utility as a sublysoclinal standard section. Unfortunately, such movement is typical of this depth range (Berger and Johnson, 1976), so that undisturbed sediments will not be readily found. Seismic profiles exhibit incoherent crenulate reflections at several levels, as well as evidence for wedging along the margins of the basin or valley that contains the deposits. There is some indication that disturbance is associated preferentially with certain layers. This leads us to suspect that such layers may have been predisposed through conditioning during deposition to serve as slip planes when the opportunity arose (e.g., during earthquake activity).

Site 805

At Site 805 (1°13.7′N, 160°31.8′E; water depth, 3188 m), three holes were drilled, with the deepest reaching upper Oligo-

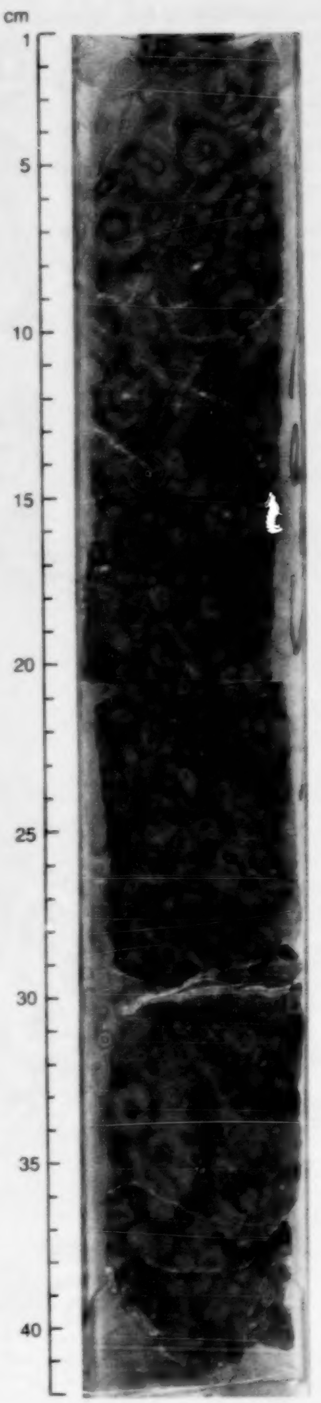

Figure 7. Basalt pillow penetrated by rotary drilling, at Site 803 (Interval 130-803D-69R-2, 1–42 cm). Note glassy rim (at top), fractures, vein fill, and signs of alteration of phenocrysts within fine-grained matrix.

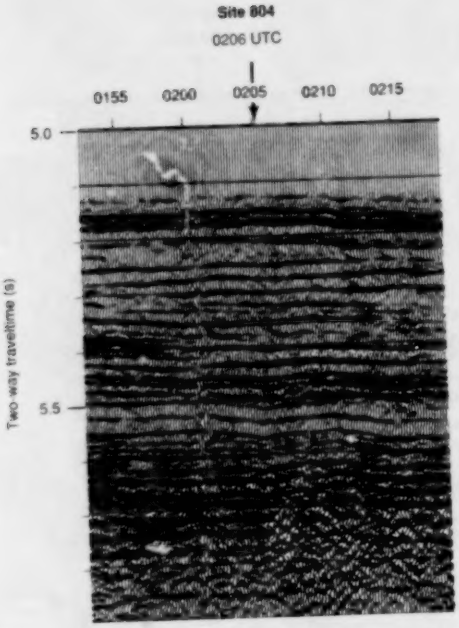

Figure 8. Seismic record at Site 804 collected by the *JOIDES Resolution* before drilling, using the 80-in.^{3} water gun, 25–250 Hz band-pass filter.

cene nannofossil chalk before total depth at 611 mbsf (see Table 1 for drilling and recovery statistics). The seismic record shows an acoustic sediment thickness of 0.85 to 0.90 s TWT (Fig. 9).

The retrieved sediment is Neogene in age, except for the eight deepest cores in Hole 805C, where Oligocene chalk was recovered. The entire column, from the oldest deposits recovered to the seafloor, was considered as one lithologic unit and was classified as nannofossil and foraminifer nannofossil ooze and chalk. The average sedimentation rate for the unit was estimated as 21.5 m/m.y. No stratigraphic breaks were detected. However, sedimentation rates decrease to low values (below 10 m/m.y.) near 10 and 18 Ma.

Two subunits were recognized on the basis of induration in this remarkably uniform section. These are separated by the ooze-chalk transition near 288 m (± 6 m). The age of the transition is late middle Miocene (about 11.4 Ma). The transition is gradational and has alternating layers, with varying degrees of lithification. Recovery is incomplete in the chalk sections because of the grinding of chalk on chalk during coring (Fig. 10A). Fine-scale color banding is common in places and is thought to be related to Liesegang banding (Fig. 10B), that is, diffusion across redox gradients. One should not confuse such color banding with laminations (which would indicate an absence of bioturbation).

The apparent completeness of its section makes Site 805 most valuable as a lysoclinal monitor of carbonate preservation through the entire Neogene and back into the upper Oligocene.

Site 806

Three holes were drilled at Site 806 (0°19.1′N, 159°21.7′E; water depth, 2520 m), with the deepest reaching upper Oligocene nannofossil chalk before being terminated at 776.4 m (see Table 1 for drilling and recovery statistics). The seismic record

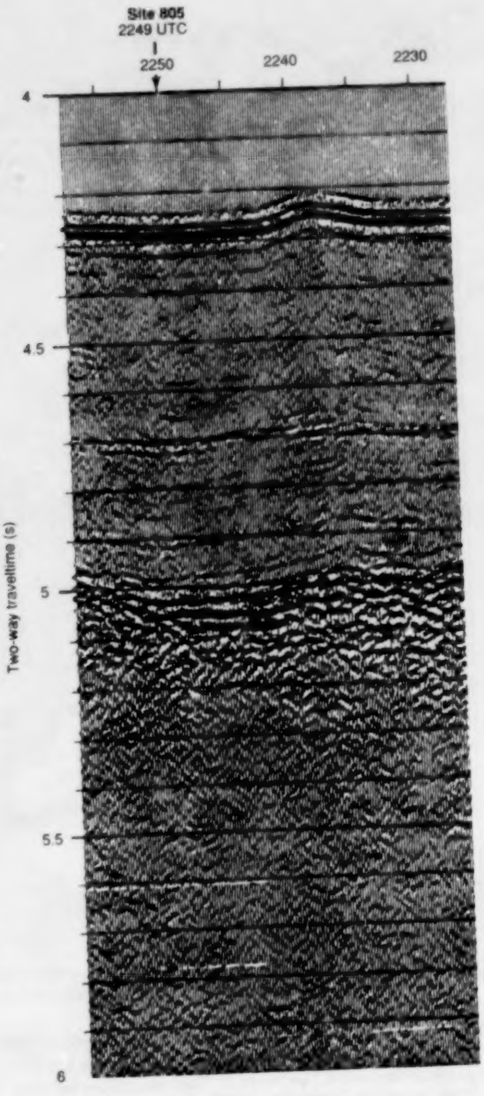

Figure 9. Seismic record at Site 805, collected by the *JOIDES Resolution* before drilling, using the 80-in.^{3} water gun, 25–250 Hz band-pass filter.

shows an undisturbed sediment section having an acoustic thickness of 1.00–1.05 s TWT (Fig. 11).

The sediment retrieved is Neogene in age, except for the four deepest cores in Hole 806C, where Oligocene chalk was recovered. The entire column, from the oldest deposits recovered to the seafloor, was considered as one lithologic unit and was classified as foraminifer nannofossil ooze and chalk to nannofossil ooze and chalk with foraminifers. No stratigraphic breaks were detected; apparently, the depositional history was continuous from the upper Oligocene (about 27 Ma) to the present. The average sedimentation rate over the entire Neogene has been esti-

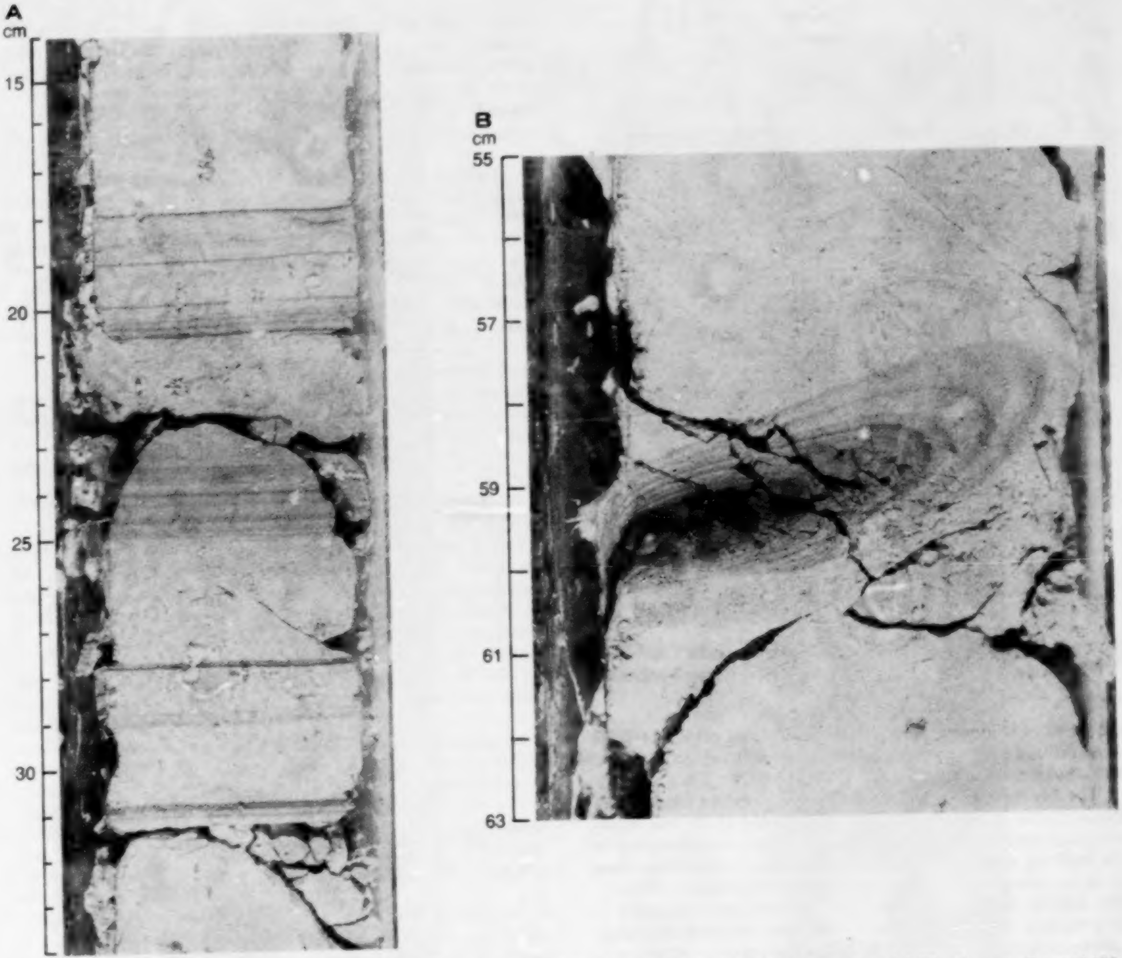

Figure 10. Fine-scale color banding in lower Miocene nannofossil chalk, Site 805, demonstrating (**A**) the formation of drilling lacunae (Interval 130-805B-45X-6, 14–34 cm). **B.** The banding is analogous to the more familiar Liesegang rings (Interval 130-805B-46X-1, 55–63 cm).

mated as 31.6 m/m.y, the highest rate of any site drilled during Leg 130. Depending on assumptions made about the age of biostratigraphic tie-points, the range of fluctuation lies between 15 and 55 m/m.y. or between 20 and 45 m/m.y.

We placed the ooze-chalk transition at 339 mbsf (lowermost upper Miocene, about 10 Ma). This transition is gradational and shows alternating layers of varying degree of lithification below about 200 mbsf. Again, the boundary was used to distinguish two subunits within the ooze-chalk sequence. Foraminifer content is significantly higher here than at Sites 803, 804, or 805, which we estimated as between 15% and 30%, on average. The completeness of the section at Site 806 and the excellent preservation of calcareous fossils, especially the abundantly occurring foraminifers, make this site extremely valuable as a standard against which to compare the other stratigraphies.

We obtained excellent logs for sound velocity and density for all except the uppermost part of Site 806. Laboratory velocities and bulk densities provide control for the upper portion of the record, which could not be logged.

Site 807

Three holes were drilled at Site 807 (3°36.4′N, 156°37.5′E; water depth, 2805 m), with the deepest one penetrating the entire sedimentary section and well into basement (dated as Early Cretaceous) and terminating at 1528.4 mbsf (see Table 1 for drilling and recovery statistics). The seismic record shows an undisturbed upper section and a somewhat disturbed lower section in a basement graben. The acoustic thickness is near 1.15 s TWT (Fig. 12).

The sediments recovered range in age from Pleistocene to Early Cretaceous; these were divided into three lithologic units. Unit I (0–968.0 mbsf) is composed mainly of Pleistocene to upper/middle Eocene nannofossil ooze and chalk with foraminifers, with lesser amounts of foraminifer nannofossil ooze and chalk as well as nannofossil ooze and chalk. Unit II (968.0–1351.4 mbsf) is composed of upper/middle Eocene to upper Campanian limestone, chert, nannofossil chalk, and nannofossil chalk with foraminifers. Unit III (1351.4–1379.7 mbsf) is

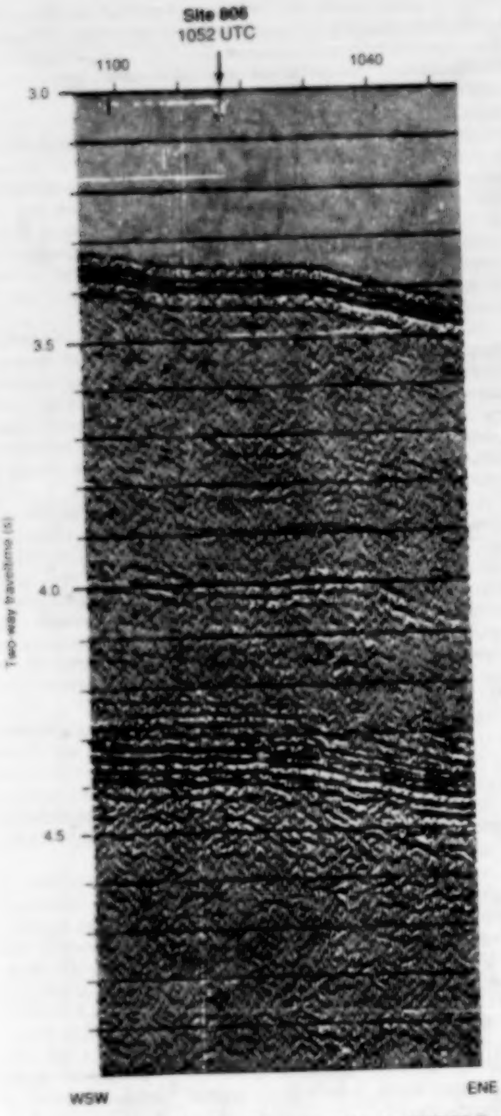

Figure 11. Seismic record at Site 806, collected by the *JOIDES Resolution* before drilling, using the 80-in.^{3} water gun, 25–250 Hz band-pass filter.

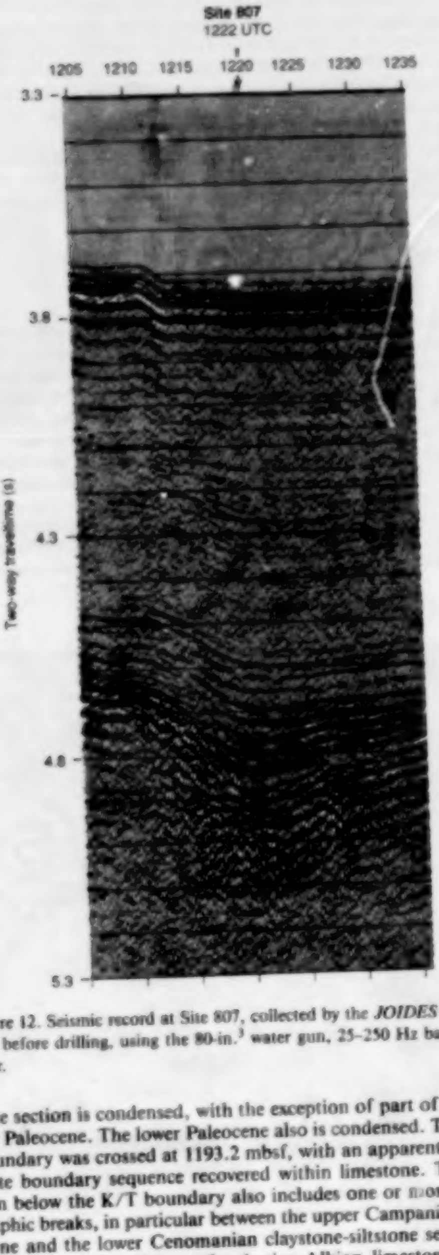

Figure 12. Seismic record at Site 807, collected by the *JOIDES Resolution* before drilling, using the 80-in.^{3} water gun, 25–250 Hz band-pass filter.

composed of lower Cenomanian to upper Albian-Aptian(?) claystone, siltstone containing varying amounts of radiolarians, and limestone. Igneous basement at Site 807 is represented by one lithologic unit, Unit IV (1379.7–1528.4 mbsf), which is predominantly composed of Albian-Aptian(?) basalt.

The record is continuous from the Pleistocene to the upper Oligocene, at which time a stratigraphic break occurs at 702.4 mbsf (about 28–30 Ma), the first of three stratigraphic breaks that were encountered above the K/T boundary. Other breaks occur in the middle Eocene at 991.9 and 1094.8 mbsf (about 40–43 Ma and 47–50 Ma). Much of the Paleocene to middle Eocene section is condensed, with the exception of part of the upper Paleocene. The lower Paleocene also is condensed. The K/T boundary was crossed at 1193.2 mbsf, with an apparently complete boundary sequence recovered within limestone. The section below the K/T boundary also includes one or more stratigraphic breaks, in particular between the upper Campanian limestone and the lower Cenomanian claystone-siltstone sequences at 1351.4 mbsf and near the Aptian-Albian limestone-basalt contact encountered at 1379.7 mbsf.

The depth of the ooze-chalk transition within Unit I was placed at 293 mbsf (about 10.4 Ma), where it separates Subunits IA and IB. This transition is not well defined and includes the lower 30 m of Subunit IA and the upper 20 m of Subunit IB. Silicified limestones and chert appear in Unit II below 968 mbsf, first interbedded with chalk and deeper down without chalk (below 1098 mbsf). The limestone has stylolites in places that form on clay-rich surfaces (Fig. 13). The sediments of Unit II, which range from the upper Eocene to the upper Campanian, are underlain by Subunit IIIA (1351.4–1369.7 mbsf), which is characterized by interbedded claystones and radiolarian-bearing siltstones (lower Cenomanian to upper Albian). Below these deposits, limestone and chert are predominant (upper Albian to Aptian, 1369.7–1379.7 mbsf).

Unit IV (1379.7–1528.4) is composed of Albian-Aptian tholeiitic basalt and interbedded limestone and has been divided into seven subunits, five of which are igneous and two of which are sedimentary.

NEOGENE DEPTH TRANSECT

Goals and Setting

For a good part of its Neogene history, the Ontong Java Plateau was located near the equator, where production of biogenous sediments has been unusually vigorous. Thus, rates of supply to the seafloor are high and provide an expanded carbonate record. On the upper portions of the plateau, sediments have been affected little by the dissolution of carbonate; however, on the lower portions of the flanks, these have been affected. The contrast between these sections provides clues to the saturation history of the deep Pacific, hence, to that ocean's carbon cycle. Carbonate sedimentation is strongly cyclic and is closely tied to climatic fluctuations (Moore et al., 1977). Thus, each individual record also provides clues to climate history.

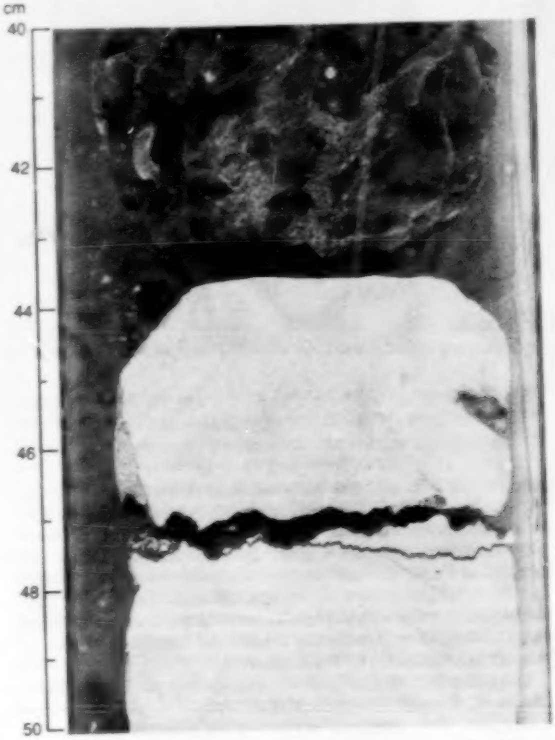

Figure 13. White limestone of Paleocene age showing parting along a stylolite surface. Chert is present in this section but not in abundance (Interval 130-807C-53R-3, 40–50 cm).

On a global scale, the carbonate deposited by the global ocean must equal the carbonate influx in the ocean. Thus, carbonate productivity and carbonate dissolution are linked through the requirement that carbonate supplied to the seafloor in excess of influx must be redissolved. Therefore, a general increase in production increases the overall dissolution rate. In contrast, on a regional scale, an increased supply of pelagic carbonate results in increased carbonate deposition and a deepening of the carbonate-compensation depth (CCD), as is observed along the equator (Arrhenius, 1952; Berger and Winterer, 1974; van Andel et al., 1975). Regionally, then, increased production results in the increased accumulation of carbonate. Consequently, the deposition rates of calcareous sediments of the Ontong Java Plateau include both a global and a regional signal with respect to ocean productivity.

In addition, signals reflect the regional dynamics of physical oceanography, especially bottom-water flow. Evidence exists for regular fluctuations in conditions that affect sediment composition and for abrupt change and/or reorganizations in the structure of supply, dissolution, and mechanical disturbance. These fluctuations and steps are of great significance in any attempt to understand the workings of the ocean system, that is, its role in climatic change.

A major goal of Leg 130 was to collect a series of continuous sedimentary sequences down the northeastern flank of the plateau. The sites were chosen to minimize the effects of latitudinal productivity gradients and to provide a means for evaluating the vertical distribution of a range of parameters of paleoceanographic significance, including physical properties, isotopic compositions, and micropaleontologic abundances. Shipboard studies permit the preliminary comparison of depth series of two important parameters: sedimentation rate and carbonate content (Fig. 14).

The most striking features of the sedimentation rate patterns are (1) the late Miocene to early Pliocene maximum and (2) the fact that equatorial position seems to have little influence on the patterns. A striking feature of the carbonate record is that so little difference exists among sites, although amplitudes of fluctuations increase with water depth, as expected. In the following, we elaborate on these observations.

Two sites are especially well suited for comparisons along a depth gradient: Sites 805 and 806. Each offers an apparently unbroken record for the last 25 m.y. These two sites are close enough to the equator to compare directly the quantity and quality of the supply of sediment, so that differences can be ascribed to depth of deposition without reservations. A third site (807) also appears to have a complete record, but its latitudinal position is distinctly different, implying a difference in supply of sediment to the seafloor. In turn, about 12–16 m.y. ago, this latter site recorded equatorial conditions, whereas the others were farther south, reflecting the general northward motion of the Pacific Plate.

The two remaining sites (803 and 804) also contain important information about depth effects: they are located below the lysocline, so that exposure to carbonate dissolution is severe. However, this also makes these sequences more susceptible to removal of entire sections. Substantial hiatuses were detected; however, more may be present.

Sedimentation Rates

Sedimentation rates are derived from ages assigned mainly on the basis of inspection of core-catcher samples, largely following the zonal scheme of Berggren et al. (1985). Calcareous nannofossils and planktonic foraminifers provide the main chronological framework (Fig. 15). In many cases, estimated Cenozoic ages are associated with serious uncertainties because of a lack, or limited availability, of adequate magnetostratigraphic

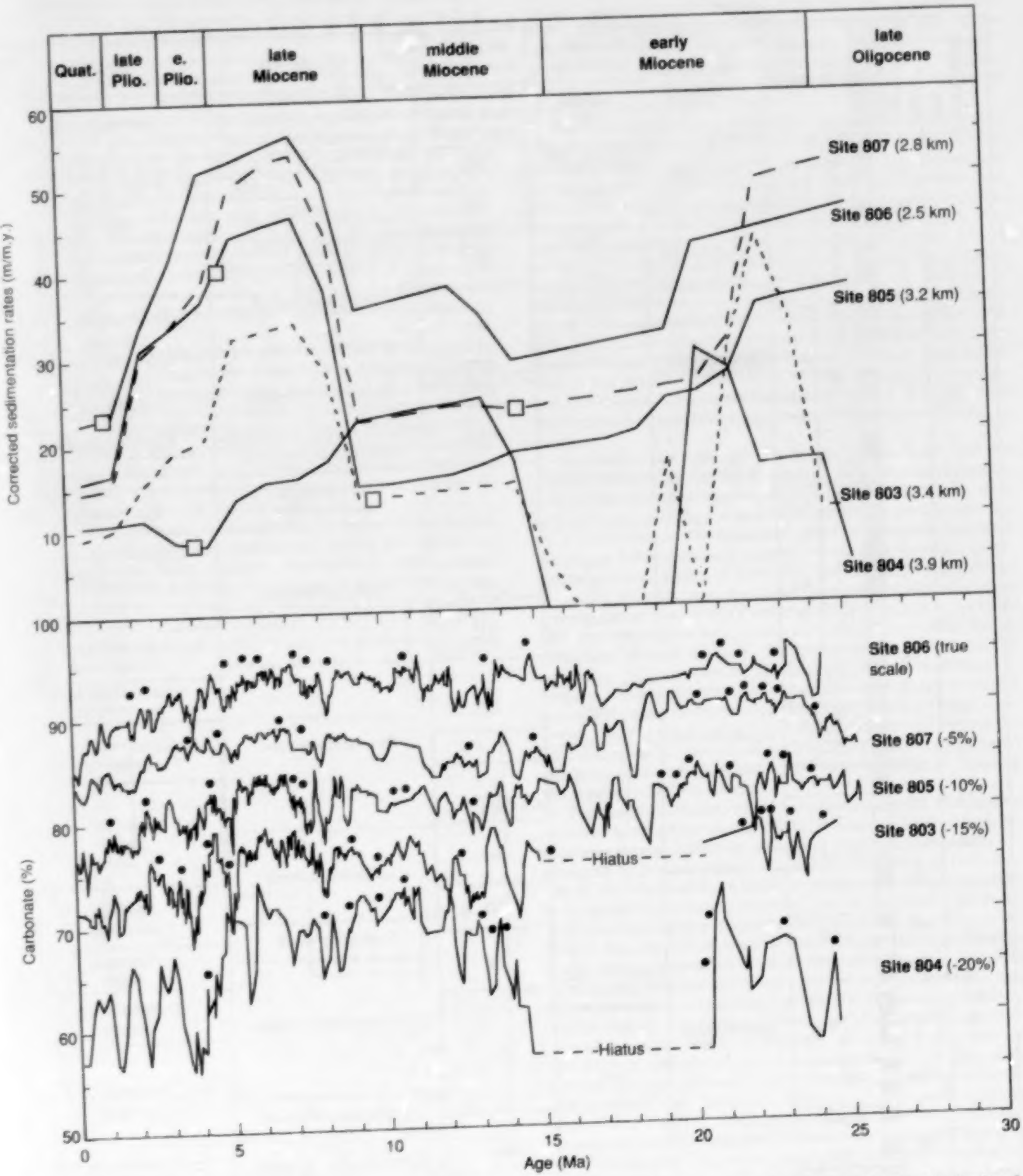

Figure 14. Sedimentation rates and carbonate percentages, Leg 130 sites. Sedimentation rates have been corrected for compaction (i.e., the density of Pleistocene sediments is assumed throughout for the calculation). Water depths for each site are listed on the right-hand side of the sedimentation rate figure. Boxes on the sedimentation rate curves indicate the time when the site crossed the equator. Carbonate percentages were shifted as indicated to aid graphical presentation. The dots associated with the carbonate curves indicate the approximate positions of individual acoustic reflectors.

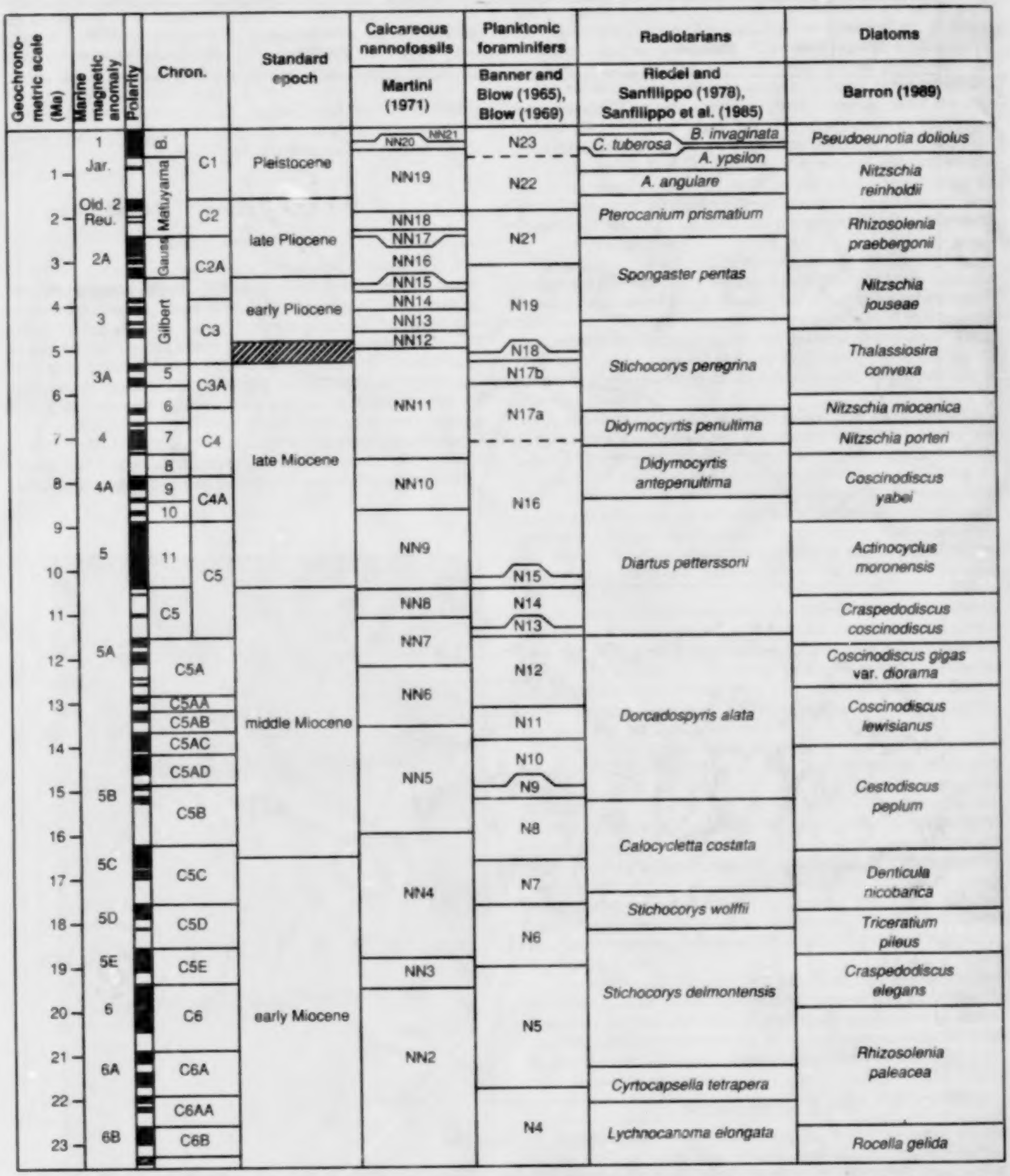
Geochronometric scale (Ma)
Marine magnetic anomaly
Polarity
Chron.
Standard epoch
Calcareous nannofossils
Martini (1971)
Planktonic foraminifers
Banner and Blow (1965), Blow (1969)
Radiolarians
Riedel and Sanfilippo (1978), Sanfilippo et al. (1985)
Diatoms
Barron (1989)
1
2
3
4
5
6
7
8
9
10
11
12
13
14
15
16
17
18
19
20
21
22
23
1
Jar.
Old. 2
Reu.
2A
3
3A
4
4A
5
5A
5B
5C
5D
5E
6
6A
6B
B.
Matuyama
Gauss
Gilbert
5
6
7
8
9
10
11
C5
C1
C2
C2A
C3
C3A
C4
C4A
C5
C5A
C5AA
C5AB
C5AC
C5AD
C5B
C5C
C5D
C5E
C6
C6A
C6AA
C6B
Pleistocene
late Pliocene
early Pliocene
late Miocene
middle Miocene
early Miocene
NN20
NN21
NN19
NN18
NN17
NN16
NN15
NN14
NN13
NN12
NN11
NN10
NN9
NN8
NN7
NN6
NN5
NN4
NN3
NN2
N23
N22
N21
N19
N18
N17b
N17a
N16
N15
N14
N13
N12
N11
N10
N9
N8
N7
N6
N5
N4
B. invaginata
C. tuberosa
A. ypsilon
A. angulare
Pterocanium prismatium
Spongaster pentas
Stichocorys peregrina
Didymocyrtis penultima
Didymocyrtis antepenultima
Diartus petterssoni
Dorcadospyris alata
Calocycletta costata
Stichocorys wolffii
Stichocorys delmontensis
Cyrtocapsella tetrapera
Lychnocanoma elongata
Pseudoeunotia doliolus
Nitzschia reinholdii
Rhizosolenia praebergonii
Nitzschia jouseae
Thalassiosira convexa
Nitzschia miocenica
Nitzschia porteri
Coscinodiscus yabei
Actinocyclus moronensis
Craspedodiscus coscinodiscus
Coscinodiscus gigas var. diorama
Coscinodiscus lewisianus
Cestodiscus peplum
Denticula nicobarica
Triceratium pileus
Craspedodiscus elegans
Rhizosolenia paleacea
Rocella gelida

Figure 15. Biostratigraphic scheme for the Neogene, used during Leg 130. Drawn by Mark Leckie. See "Explanatory Notes" chapter (this volume) for sources of references given in the figure.

records from tropical environments. Unfortunately, the cores recovered during Leg 130 proved to be unsuitable for constructing detailed magnetostratigraphies for sections older than the upper Pliocene. The high productivity near the equator, and the resulting diagenetic processes, apparently are inimical to the preservation of signals pertaining to geomagnetic polarity history. Thus, problems of resolution in dating must be kept in mind when contemplating the history of sedimentation rates: small changes in the age control points can substantially change the picture.

The overall sedimentation rate pattern for the last 25 m.y. is best reflected in that of Site 806 (Fig. 16). This site is dominated by a distinct low in the late early to early middle Miocene (ca. 20–15 Ma) and a prominent peak in the late Miocene to earliest Pliocene. As mentioned, equatorial position apparently does not influence major trends strongly. The period of low rates is characterized by hiatus formation at Sites 803 and 804, suggesting a causal association between rate reduction and sediment removal.

The onset of the low rate period after 20 Ma corresponds to the beginning of a long period dominated by a highstand in sea level, according to the sea-level curve of Haq et al. (1987). This period also roughly coincided with a major excursion in the carbon isotope composition of the ocean (Vincent and Berger, 1985), which marked a strong increase in coastal ocean production. Thus, it appears that the early Neogene carbonate drought had global causes: the lack of supply from continents and the sequestration of carbon on shelves and in margins.

The upper Miocene sediments display some of the highest rates yet recorded in open-ocean pelagic sediments. The timing of this carbonate flood suggests a strong relationship to major phases in mountain building. An increase in supply from emerging continents must be assumed: lowstands of sea level characterize the period (Vail and Hardenbol, 1979; Haq et al., 1987). Cooling and an increase in trade winds, and hence in equatorial upwelling, is likely as well, an interpretation supported by the optimal preservation of diatoms in the interval. A strong east-west gradient in productivity developed during this time in the equatorial Pacific (Leinen, 1979; Kennett, 1985), an asymmetry that has implications for the dynamics of the equatorial undercurrent (Barron and Baldauf, 1989) and, indeed, for the entire equatorial system (Flohn, 1985).

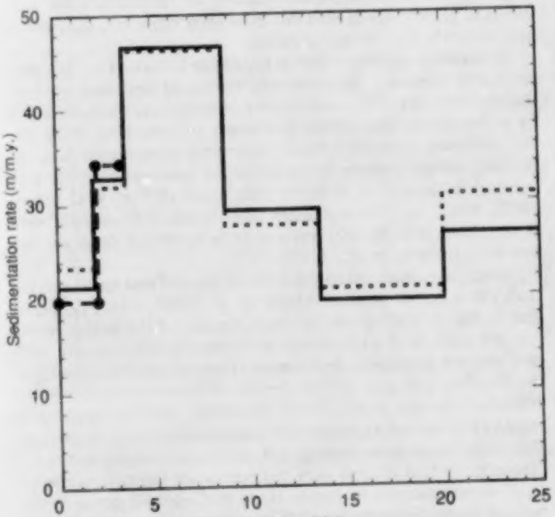

Figure 16. Sedimentation rates for Holes 806A, 806B, and 806C, based on the ratio of sediment thickness to the biostratigraphic time interval (uncorrected for compaction). Note the differences from hole to hole. Dashed line with filled circles = Hole 806A, solid line = Hole 806B, and dashed line = Hole 806C. Drawn by Jan Backman.

The remarkable decrease in carbonate accumulation in the Pliocene, and especially in the Quaternary, was accompanied by decreasing diatom and radiolarian preservation. This decline may reflect decreased production from the removal of nutrients and silica, presumably by coastal-ocean pumping in response to increased seasonal upwelling generated by monsoonal winds. The equatorial upwelling mill, driven by strong trade winds, turned as fast as ever, but its grist was diminished, being trapped in the ocean margins. Alternatively, or in addition, the increase in northern trade winds (the southern ones being strong already) now led to a pile-up of shallow warm water in the western Pacific, making the upwelling process less efficient by deepening the thermocline. There are indications from the increased difference in the oxygen isotope values of *Globigerinoides sacculifer* and *Pulleniatina obliquiloculata*, 2 m.y. ago at Site 586, that this mechanism was indeed important (Whitman and Berger, in press).

An increase in foraminifer content during the latest Neogene suggests yet another factor for reducing sedimentation rates: increased winnowing. Resuspension of fine material (that is, nannofossils) by bioturbation and local turbulence presumably is a ubiquitous process. The resuspended material imparts increased density to bottom-contact waters, which flow downhill in response, creating a type of katabatic flow familiar from cold air in contact with glaciers. Katabatic deep-sea currents should be favored during lowstands of sea level. Tidal energy is most readily destroyed in shelf seas, which are greatly diminished during periods of lowered sea level. Thus, this energy is available for enhancing tidal currents in the deep sea, which would help in keeping fine-grained material suspended (even if not powerful enough to create resuspension). Transport would be from shallow depths to greater ones, where dissolution would remove the advected material. One corollary of such a process is increased alkalinity of the ocean, which would have the effect of reducing the atmospheric CO_2 content.

The orderly arrangement of sedimentation rates among sites since the middle Miocene, according to depth of deposition, indicates a strong carbonate saturation gradient, presumably established by the increasing influence of formation of cold deep water. That the position relative to the equator seems unimportant is surprising. Again, we recall the earlier caveat about assigning biostratigraphic ages before attempting to interpret details of these curves. A sense of the changing ratios in sedimentation rates, independent of exact time scale, may be obtained by assuming that Site 806 is standard and by expressing the rates of the other sites as fractions (i.e., thickness ratios; see Table 2).

The overall change in thicknesses for the Neogene is a function of the water depth, as expected. However, trends between the different periods are by no means identical. An interesting reversal occurred between Sites 805 and 807 during the early Miocene, which may disappear, however, when one corrects for compaction (Fig. 14). There is a maximum difference in the sedimentation rates between Sites 805 and 806 during the late middle Miocene (Fig. 14), which affects the thickness ratio for the middle Miocene, making it unusually low (0.59). The two sublysoclinal sites also have low ratios for this interval, but not Site 807. Again, correction for density differences and refinements of biostratigraphy may change this picture. Assuming that the trend is real, one should consider that the late middle Miocene was a time of globally shallowed CCD (Berger and Winterer,

Table 2. Sediment thickness ratios of Leg 130 sites.

Site	806	807	805	803	804
Depth (km)	2.5	2.8	3.2	3.4	3.9
Pleistocene	1.0	0.70	0.73	0.40	0.38
late Pliocene	1.0	0.88	0.88	0.51	0.35
early Pliocene	1.0	0.73	0.71	0.38	0.14
late Miocene	1.0	0.86	0.67	0.58	0.47
middle Miocene	1.0	0.78	0.59	0.31	0.30
early Miocene	1.0	0.80	0.87	0.41	0.35
Neogene	1.0	0.80	0.72	0.43	0.35

Note: Denominator = Site 806.

1974). Thus, one may infer that increased production (Site 806) was compensated by increased dissolution in the deeper sites (Sites 803, 804, and 805). This compensation may reflect negative feedback to achieve global carbonate balance (van Andel et al., 1975), or it may represent a fortuitous combination of regional and global effects.

Carbonate Stratigraphy

The carbonate curves (Fig. 14) show broad coherency, as well as good correlation in detail, at least back to about 12 m.y. ago. The deeper sites show the lower values and the larger fluctuations, as one would predict. The increased range of fluctuations in the sublysoclinal sites, as compared with the shallow ones, suggests a strong imprint from changes in dissolution rates.

We note that correlations in carbonate content are good for the last 12 m.y. and are poor earlier. In part, spotty sampling in the earlier sections may be responsible, and greater sampling density will be necessary to find the exact change in the quality of correlations as a function of time. It appears that fluctuations in carbonate increase in amplitude within the upper Miocene sediments, especially during post-Miocene time, and that such fluctuations are strongly felt, even within the shallowest site (806). Two especially large oscillations can be seen between 9 and 8 m.y. ago, at the exact time when sedimentation rates increased sharply (Fig. 14).

One outstanding problem is why the carbonate values of the deeper sites differ so little from the high values of the shallower sites. A detailed comparison of Site 806 with Site 805 (Fig. 17) shows that these differences vary only between 0% and 3% on the whole, although the differences in depth and in sedimentation rates (Fig. 14) are not subtle at all. Despite the small amplitude of the carbonate fluctuations and the small difference between the two sites, the patterns track closely, suggesting a cause active over a large depth interval. Assuming that fluctuating dissolution intensity is the underlying cause, we have labeled the levels of sudden carbonate decrease "carbonate reduction events" (CREs) and numbered the main events with Roman numerals, going downhole in the usual fashion. Should CREs prove to be dilution events (which we think unlikely), the "reduction" would be strictly relative to the noncarbonate fraction.

If we assume that the difference in carbonate content between the two sites represents excess removal of carbonate at Site 805 and allow no other factors, we can calculate the expected ratio in sedimentation rates between the two sites. The sedimentation rate ratio (SRR) rarely falls below a value of 0.8 (Fig. 18, curve marked DISS; scale to right) for the last 15 m.y. The ratio seen in the biostratigraphy is distinctly smaller, with an average of nearly 0.67 for this same interval (385/574; see Fig. 4). Correlation of carbonate peaks with valleys also yields values for the SRR. On the whole, these are close to the ones obtained from biostratigraphy and, consequently, are distinctly below the ratios calculated on the basis of carbonate differences alone (Fig. 18, curve marked CORR). (It is true that accumulation rates should be compared, rather than sedimentation rates; here, we are neglecting the difference in gradient of porosity reduction, which introduces a small error: CORR and SRR are affected, whereas DISS is not.)

We conclude from this exercise that carbonate removal by dissolution alone cannot explain the differences in sedimentation rates among the sites as well as the differences in carbonate content. To explain the differences in sedimentation rates, sediment removal at Site 805 must be invoked. To explain the absence of a corresponding difference in carbonate, one must assume both the removal of carbonate and of dilutant. Thus, the pattern can be explained if one postulates that carbonate dissolution cannot proceed alone but implies the removal of noncarbonate dissolution as well.

Much more will be learned about this point by reconstructing sedimentation rates at high resolution using Milankovitch tuning. Shipboard measurements of physical properties, logging results, and stable isotope analyses to be performed onshore will be available for this purpose.

SEISMIC STRATIGRAPHY

Goals and Setting

One important objective of Leg 130 was to obtain data about the origin of the acoustic reflectors, which characterize the layer-cake stratigraphy on the plateau. Many of the reflectors seen at each individual site can be traced over considerable distances, and certain reflectors, or reflector groups, appear to be exactly equivalent from one site to the next. A selection of seismic profiles from different depths is shown in Figure 19 (see Mayer et al., this volume).

Reflectors in the area of DSDP Sites 289 and 586 had been tentatively dated, based on Site 289 drilling results (Shipboard Scientific Party, 1975b) and Site 586 logging results (Shipboard Scientific Party, 1986; see Fig. 20). An important objective of Leg 130 was to establish correlations of reflectors from sediments at greater depth into this published sequence, if possible, and to verify the age assignments.

It has been suggested that many of the reflectors are synchronous and represent diagenetically enhanced sediment contrast derived from previous conditioning of sediments on the seafloor by paleoceanographic events (Schlanger and Douglas, 1974). For the shallower reflectors, where diagenesis presumably is unimportant, abrupt changes in conditions of preservation alone were invoked as agents of reflector formation (Berger and Mayer, 1978), based on the knowledge that dissolution changes sand content and thus directly governs velocity within deep-sea carbonates (Johnson et al., 1977).

Taking a view simultaneously more general and more specific than these earlier studies, Mayer et al. (1985, 1986) proposed that in the central equatorial Pacific many of the major reflectors are associated with certain paleoceanographic events, with or without diagenetic enhancement. They selected the closing of the Panama Isthmus, reorganization of deep circulation in the Atlantic, climatic events in the Antarctic, and the opening of the Drake Passage as important paleoceanographic themes reflected in the acoustic stratigraphy of Pacific pelagic sediments (Table 3). In this general view, reflectors are the tangible large-scale manifestations of major steps in Cenozoic ocean evolution, as driven by tectonics (Berggren and Hollister, 1977; Keigwin, 1978; Kennett, 1982, 1985) and by internal climatic feedback mechanisms translating tectonic change into climate steps (Berger et al., 1981). If it is true that globally important events can be seen in the seismic reflectors of the central equatorial Pacific, then these events should be similarly represented in the sediments of the western equatorial Pacific, even though the

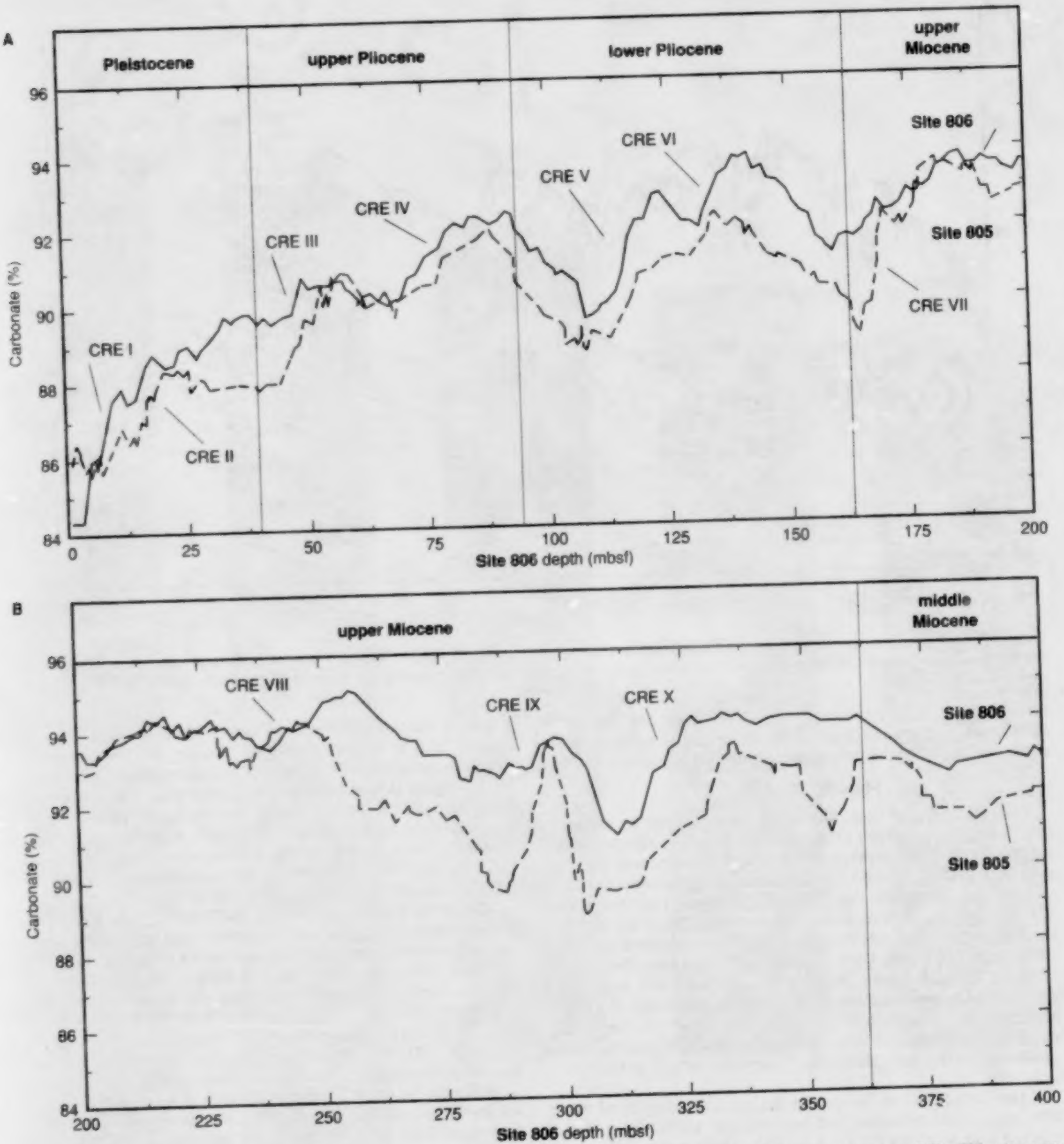

Figure 17. Detailed comparison of the carbonate contents of Sites 806 and 805. CRE = carbonate reduction event. Mapping of Site 805 pattern on the Site 806 pattern was done by eye. Based on measurements by R. Stax; drawn by E. Jansen.

physical causes for generating the echo potential might be different in these shallower and more carbonate-rich sediments.

The task is to map the reflectors for each site by seismic profiling and to assign them to the correct depth in the sediment column, using the appropriate downhole velocity profile. Based on both density and velocity profiles, a synthetic seismogram can be generated (Mayer et al., 1985) that will simultaneously express the expected position and strength of the reflectors (Fig. 21). Matching the synthetic profile with the real profile provides a powerful test of the correctness of the depth assignments. Bio-

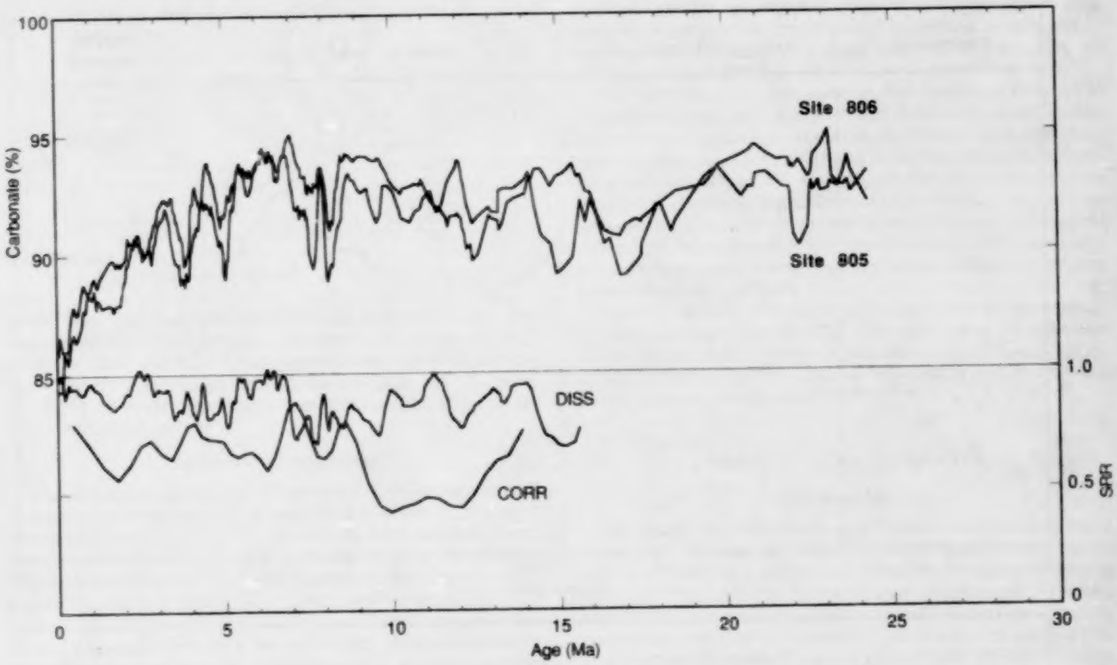

Figure 18. Sedimentation rate ratios from carbonate stratigraphy. Top: carbonate curves for Sites 805 and 806. Bottom: sedimentation rate ratios (SRRs) calculated from the differences between carbonate contents (DISS) and from mapping the curve of Site 805 over that of Site 806 (CORR).

stratigraphic dating provides ages for the reflectors. Detailed sedimentologic, paleontologic, and chemostratigraphic studies allow one to assess the paleoceanographic significance.

Sites 803 and 804

Like all the other sites, Site 803 is characterized by a layer-cake seismic stratigraphy (Fig. 5). In this region, disturbances commonly interrupt the regular layering. The prominent feature seen between 4.8 and 4.9 s TWT is discussed as "mid-section reverberation" (MSR) in the "Site 803" chapter (this volume). The level of an ash layer apparently corresponds to the top of the MSR, which suggests that volcanism was associated with its formation. Elsewhere, there is some indication that these features are associated with faults in the basement and that they represent enhanced diagenesis (i.e., increased velocity). We suggest that the circulation of fluids through cracks in the basement during times of volcanism accelerated lithification, thus producing MSRs (i.e., these are "diagenetic dikes" or "diagenetic sills").

Many reflectors can be seen in the regular sequence of Site 803. Nine single reflectors and two reflector groups have been marked with numbers from 3-1 to 3-11. Three minor reflectors are marked 3-a, 3-b, and 3-c. These marked reflectors have well-matched counterparts in the synthetic seismogram that was generated from physical property and logging data for Site 803.

From the ages of the reflectors, possible clues emerge regarding their paleoceanographic significance. Reflectors 3-1 and 3-2 occur at depths dated at 2.6 and 3.3–3.4 Ma, respectively. These periods are well established as steps of cooling and buildup of ice in the Northern Hemisphere (Backman, 1979; Shackleton et al., 1984). In nearby DSDP Site 586, oxygen isotopes have heavier values in both planktonic and benthic forms for both events (Whitman and Berger, in press). Marked changes in sand content and in carbonate content also are indicated. Presumably, the initiation of Northern Hemisphere glaciation was felt in this region through changes in productivity (caused by wind field changes; Arrhenius, 1952) and changes in bottom-water properties (increased activity of North Atlantic Deep Water [NADW], with corresponding downstream effects in the Pacific; Berger, 1970). These results are in good agreement with the propositions of Mayer et al. (1986; Table 3).

Reflectors 3-a and 3-b (at 4.3 and 5.0 Ma, respectively) are tied to strong changes in carbonate and sand content. Ice melting and warming trends are indicated in the oxygen isotope data for the 4.3-Ma event (Whitman and Berger, in press), and a major rise in sea level has been postulated for about this time (Vail and Hardenbol, 1979). The transition from the Miocene to the Pliocene is marked by a pronounced dissolution spike (Saito et al., 1975; CRE VII, Fig. 17A). Thus, for these reflectors, too, the paleoceanographic connection holds up well.

Reflector 3-c (at 9.7 Ma) corresponds to a major decrease in sea level (Vail and Hardenbol, 1979; Haq et al., 1987) and with a reorganization of much deep-sea sedimentation (an increase in the dust supply, an increase in NADW production, closure of the Indo-Pacific passage, a shift in silica to high-latitude sinks; see Janecek and Rea, 1983; Miller and Fairbanks, 1985; Romine and Lombari, 1985; and references therein). Hiatus formation is common near this level (NH4 of Keller and Barrón, 1987). Reflector 3-4 (12.3-12.5 Ma) lines up with the NH3 level. Reflector 3-5 (15.8 Ma) coincides with a major hiatus at Site 803 and lines up with level NH2 of Keller and Barron (1987). The period between 16 and 15 Ma can be characterized by major fluctuations in sea level (Haq et al., 1987) and by the initiation of major cooling of abyssal waters; that is, a major increase in Antarctic

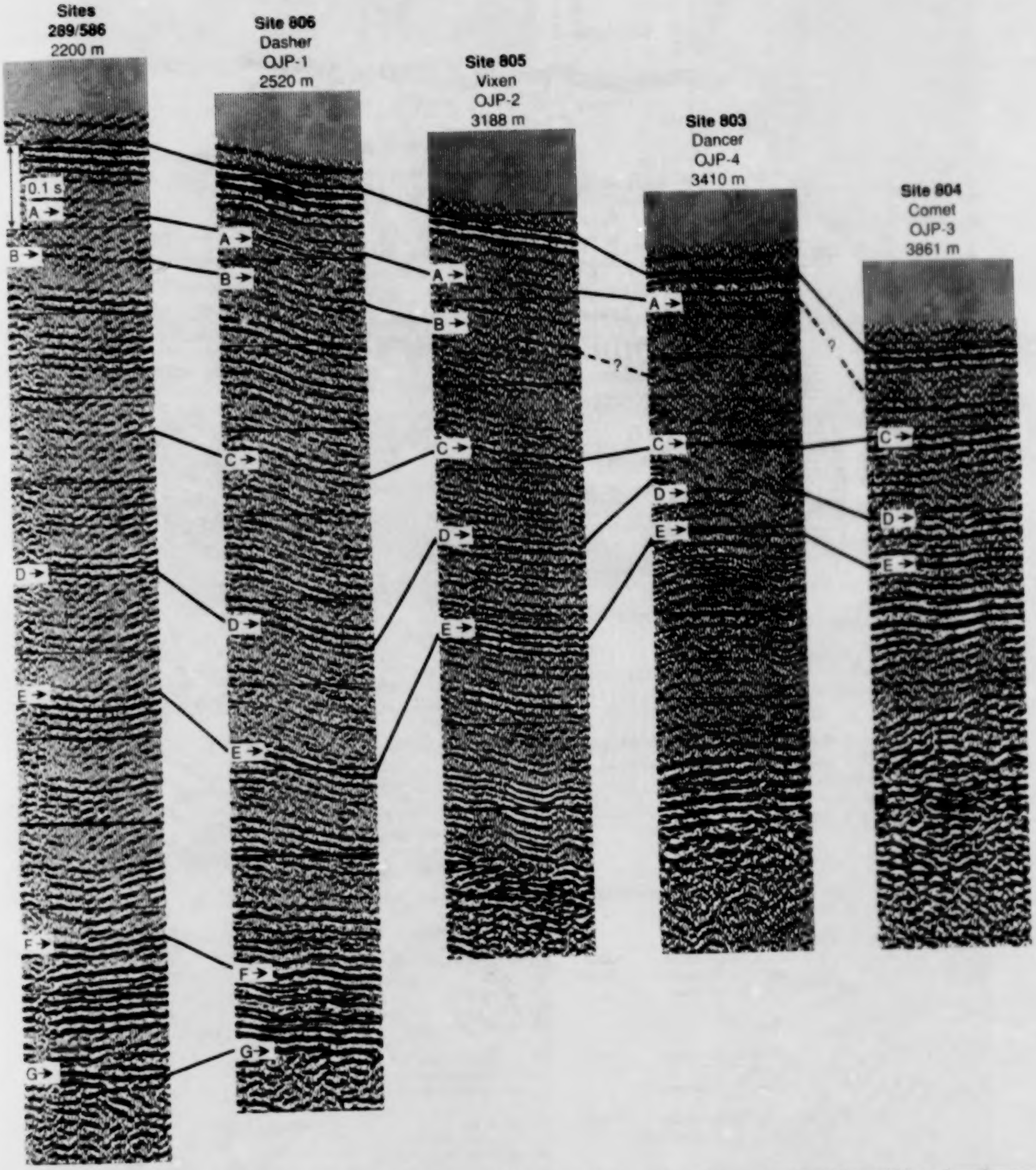

Figure 19. Relationships of seismic sections and marker reflectors down the flank of Ontong Java Plateau. Horizontal lines within each section represent 0.1 s of two-way traveltime. See Mayer et al. (this volume) for discussion of Reflectors A–G.

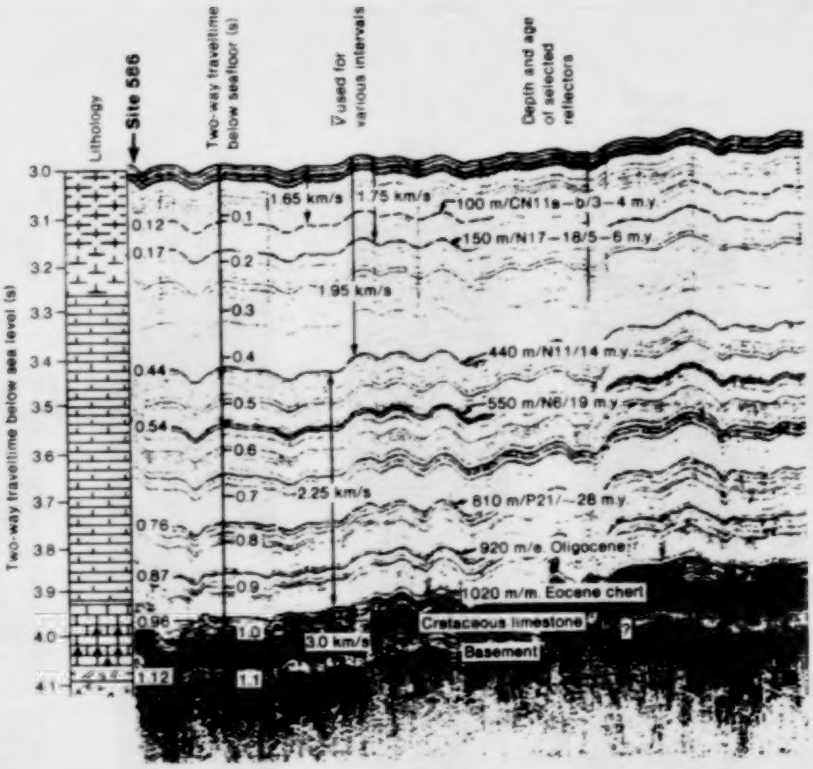

Figure 20. Interpretation of Leg 89 seismic profile over Site 586 (from Shipboard Scientific Party, 1986). Survey speed was 7 kt.

Table 3. Reflectors in the central Pacific and their paleoceanographic significance.

Approximate age (Ma)	Geochemical events	Hiatus	Paleoceanographic events	Primary cause of relector
3.0-3.5	Benthic ^{18}O enrichment. $CaCO_3$ dissolution.		Closing of Panama Isthmus. North Hemisphere glaciation? North Atlantic erosion.	Carbonate miminum.
6.5-7.5	Chron 6 ^{13}C depletion	NH6	Increased isolation of Mediterranean Sea. Climatic deterioration.	Carbonate minimum.
8.5-9.5	Benthic ^{18}O enrichment. Mid-Chron 10 $CaCO_3$ dissolution event.	NH5 NH4?	Major North Atlantic erosion. Increase of siliceous deposition in Pacific. Major cooling. Major drop in sea level.	Extreme carbonate minimum.
13.5-14.5	15c $CaCO_3$ dissolution event. Benthic ^{18}O enrichment.	NH3?	Ice buildup in Antarctica. Intensification of Antarctic Bottom Water production.	Carbonate minimum.
16.5-17.5	16g $CaCO_3$ dissolution Chron 16 ^{13}C enrichment.	NH1b	Closing of Tethys. Norwegian Sea spillover. Intensified Pacific upwelling.	Carbonate minimum.
20.5-22.5		NH1a?	Opening of Drake Passage. Establishment of Circum-Atlantic Current and of a steep Southern Hemisphere thermal gradient.	Diagenesis.

Note: Source of data is from Theyer et al. (1989).

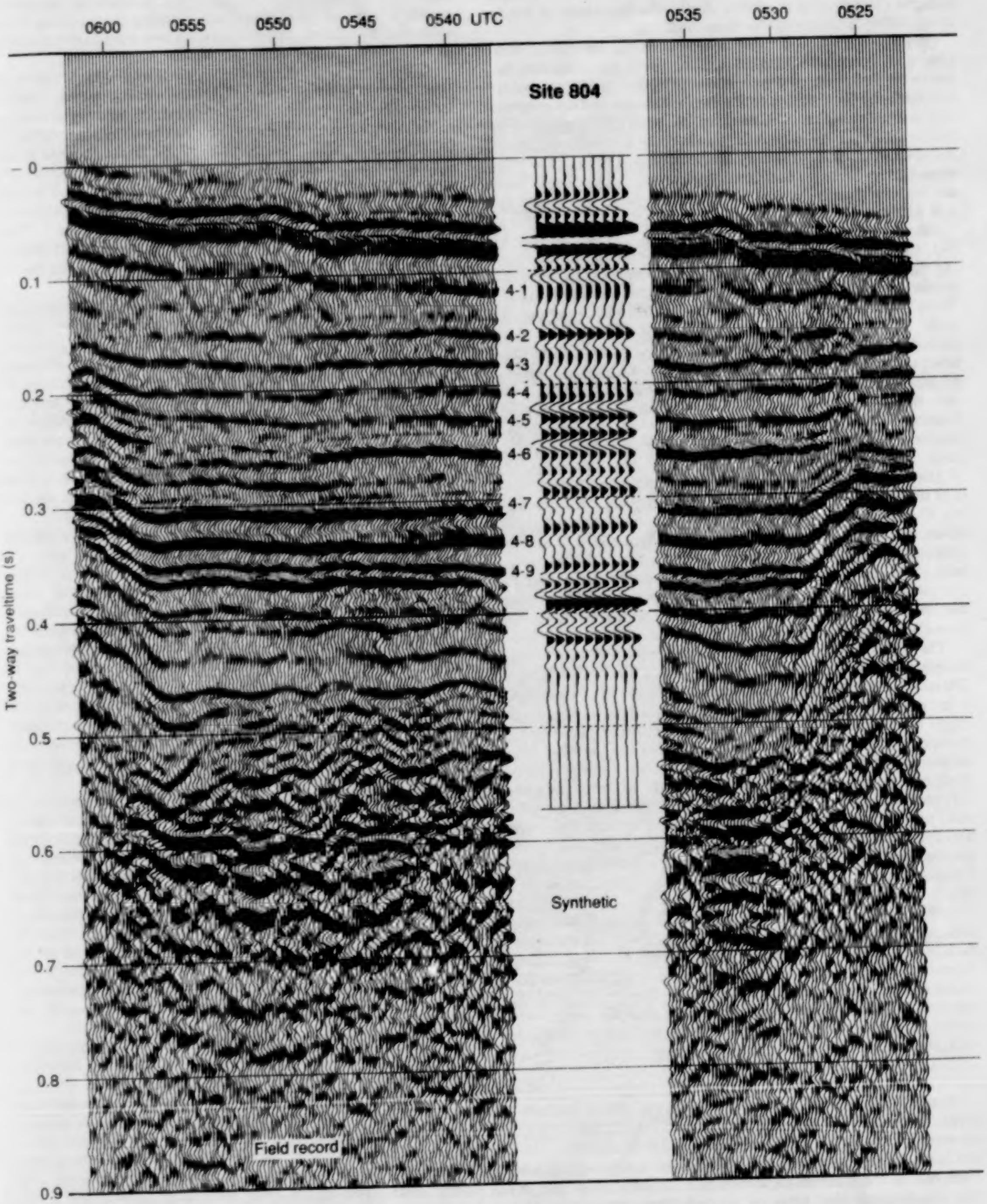

Figure 21. Comparison of synthetic seismogram and field record at Site 804. See text for discussion of reflector numbers.

Bottom Water (AABW) production, as seen in benthic oxygen isotopes (Woodruff et al., 1981). Again, the hypothesis of Mayer et al. (1986) is supported by these findings.

Reflectors 3-6 and 3-7 are developed in the lowermost Miocene and uppermost Oligocene. They mark the transition between the Paleogene and Neogene, a period of great changes associated with the opening of the Drake Passage and the progressive thermal isolation of Antarctica. No particular events can be assigned to the individual reflectors in these groups at this time. We shall see similar groups in Sites 805 and 806, which will be discussed in greater detail later. Reflector 3-8 and deeper ones are associated with the velocity jumps produced by the formation of chert and limestone.

Site 804 was not ideally suited for studying seismic stratigraphy; nevertheless, it contained some important lessons concerning the ease of correlation among the sites. Seismic profiles across the site (Fig. 21) show the effects of mass movement. These profiles exhibit disturbed crenulate reflections at several levels, as well as evidence for wedging along the basin margins. Disturbance is first clearly noticeable at 0.05 s below seafloor (sbsf; about 40 mbsf), where the lower Pliocene section seems to be condensed or missing (near 4.5 Ma). An unconformity occurs at that level or slightly below it. Disturbance continues down to 0.1 sbsf (about 80 mbsf) and also may include deeper intervals. This would correspond to the disruptions seen in the cores, especially at 70–80 mbsf (7–8 Ma).

Disturbance is seen again in the lower part of the block, near 0.21 sbsf (about 170 mbsf). At 0.22 sbsf, there is a strong reflector. This reflector essentially coincides with the ooze-chalk transition, as located in the cores. Another reflector at 0.23 sbsf is probably a slip plane. In the cored sediments, a major hiatus is seen at this level (197 mbsf, 18.6–14.6 Ma). On either side of this plane, reflectors have been disrupted, presumably from mass movement. This series of strong reflectors probably represents ooze-chalk alternations in the lower Miocene.

The Miocene/Oligocene hiatus is well expressed as a strong double reflector, with the first return at 0.30–0.31 sbsf (about 270 mbsf). Judging from the absence of strong reflectors below, a section of more than 100 m of lower Oligocene sediments might be expected here, with the (unconformable) Eocene/Oligocene boundary appearing near 0.42 sbsf. If so, another 200, or perhaps 250, m of sediment (depending on where the basement reflector is assigned) would be expected in this graben before reaching basement. The first strong deep reflector (at 0.48 sbsf) presumably would mark the location of Eocene limestone and chert. Outside of the basin, the apparent paucity of pre-Oligocene deposits would suggest widespread erosion early in the Cenozoic and in the Late Cretaceous, as was the case at Site 803.

There is some indication that disturbance is associated preferentially with certain layers. This supports the hypothesis that such layers may be predisposed, through preconditioning during deposition, to serve as slip planes later. If so, the connection between reflectors and paleoceanographic events is strengthened, but also confused, because unconformities and slip planes will give the appearance of a complete sequence within a seismic section, even though the sequence is incomplete.

Sites 805 and 806

Sites 805 and 806 are similar with respect to their seismic records, except that the record is compressed by a factor of 0.73 on average in Site 805. Both sites have complete records, without hiatuses. In fact, this is one of the reasons why correlation from one to the other is so readily accomplished (Fig. 22). A case can be made that many of the paleoceanographically significant reflectors identified at Site 803 also can be identified here. Taking advantage of this finding and following the general suggestions of Mayer et al. (1986) regarding the meaning of the reflectors in terms of global events, we now turn to the grouping of reflectors and their overall pattern.

Going back in time, the themes put forward by Mayer et al. (1985, 1986; Table 3) included (1) the closing of the Panama Isthmus and the concomitant reorganization of deep circulation in the Atlantic, (2) climatic events surrounding the cooling of the Antarctic, and (3) the opening of the Drake Passage as important paleoceanographic sets of events. Accordingly (but without prejudging their origins), we refer to reflectors aged 2–4 Ma as "Panama Series," to those aged 10–19 Ma as "Antarctic Series," and to those aged 19–23 Ma as "Drake Series." These ages are approximate: the criterion is grouping, not dating. Roughly, these groups correspond to the Pliocene, the middle Miocene, and the lower Miocene.

The interval between the Panama and Antarctic series is the "Tethys Interval," which contains sediments deposited during mountain building in the closing Tethys belt. This interval includes the entire upper Miocene and the lowermost Pliocene. Below the Drake Series is the "Texas Interval," which is acoustically subdued in Site 805, but which has two distinct reflector groups in Site 806. In essence, the Texas Interval brackets the Oligocene. (It is so named to honor Texan drilling know-how.) Below this interval is the "Ontong Java Series," a group of strong reflectors, ubiquitous on the plateau, that derives from impedance changes caused by the formation of limestone and chert in the upper Eocene.

The Panama Series contains the reflectors already discussed for Site 803; these can also be identified at Site 586, using the velocity profile provided by Shipboard Scientific Party (1986). The Tethys Interval contains a number of reflectors of lesser strength. Lithification occurs in the upper Miocene at both sites, presumably producing weak reflectors through the alternation of ooze and chalk layers. Throughout this interval, Site 806 has the stronger reflectors. The presumed condensed section near 10 Ma (see "Sedimentation Rate" section, "Site 805" chapter, this volume) has a less than prominent group of reflectors at the base of the Tethys Interval. In Site 806, again, the equivalent section is more strongly reflecting. In either site, the ooze-chalk transition (as determined visually) does not seem to be strongly expressed.

The next group of strong reflectors (traveling downsection) is the upper part of the Antarctic Series, which is centered on the middle Miocene (13 Ma). The lower part of this series is somewhat weaker and belongs to the lowermost middle Miocene and uppermost lower Miocene (15–18 Ma). This entire zone is characterized by a major climatic change, with associated excursions in carbonate content and other sediment properties (Barron et al., 1985). Presumably, these changes are associated with the onset of AABW production at that time. The group of reflectors immediately below the Antarctic Series, the Drake Series, has the strongest reflectors in both sites. Ages range from about 18.5 Ma for the uppermost part of the group to 22.5 Ma for the deepest.

The Texas Interval is more or less transparent acoustically in Site 805, suggesting the absence of significant events. However, in Site 806, the interval has two strong reflector groups. Presumably, the reason for the difference is diagenetic enhancement in Site 806, providing an augmentation of contrast that is missing in Site 805. The diagenetic enhancement in Site 806 may result from the presence of more reactive carbonate or from the greater thickness of the sediment, or both. The zone of lithologic uniformity that makes up the Texas Interval also was noted by the Leg 130 biostratigraphers for its paucity of evolutionary events. Below this interval, a group of strong reflectors, the Ontong

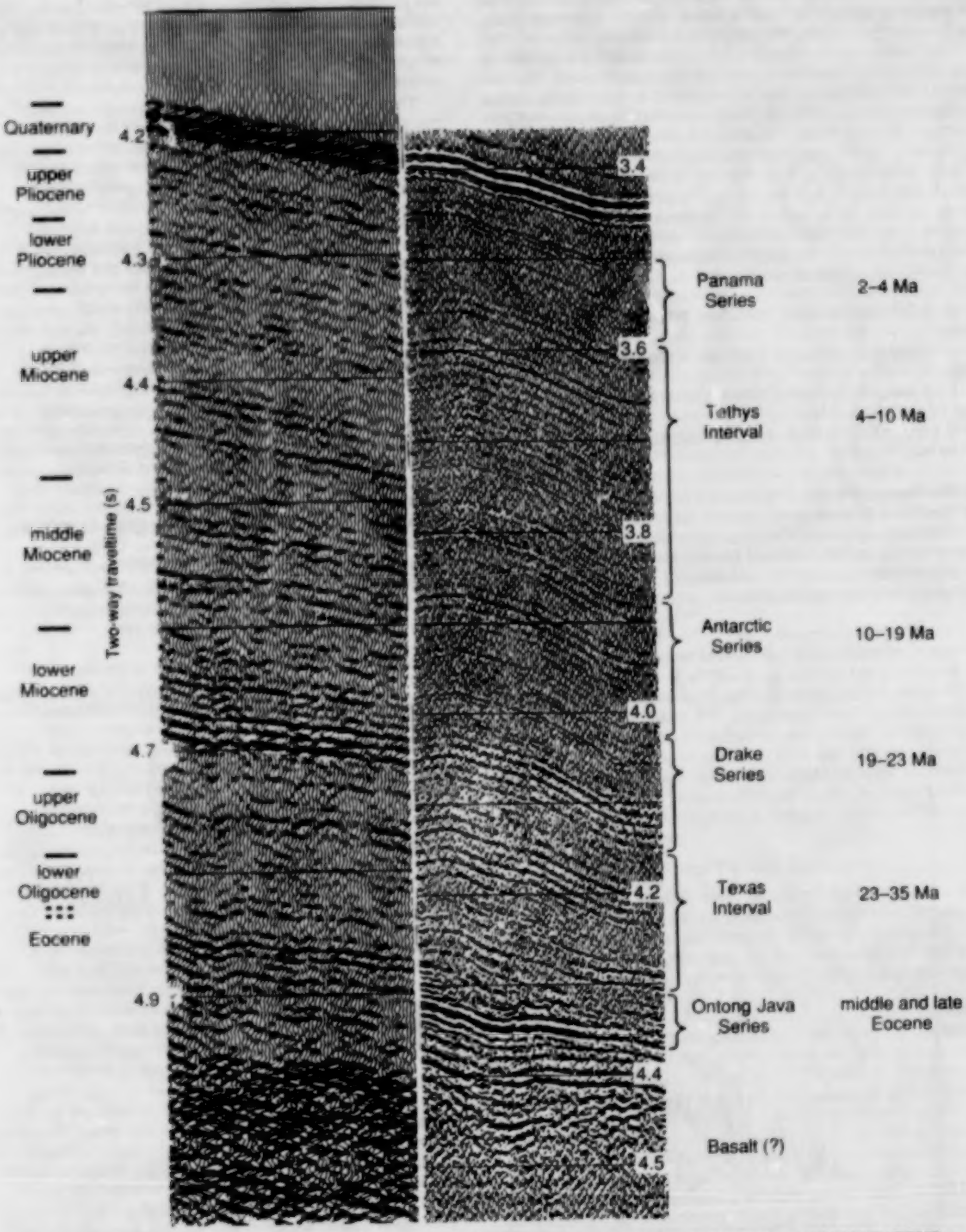

Figure 22. Correlation of seismic reflectors at Sites 805 and 806. Profiles taken by the *Thomas Washington* on ROUNDABOUT Cruise 11 site survey, with the time scale assigned from drilling and logging results and biostratigraphy. Names to the right refer to groups of reflectors ("series") and to zones with less distinct groups ("intervals"). The record of Site 806 is to the right; its scale was reduced by a factor of 0.73 with respect to that of Site 805, in order to obtain an approximate match for the reflectors.

Java Series, is thought to represent the change from chalk to limestone in the lowermost Oligocene, as well as the occurrence of Eocene chert somewhat deeper in the section.

The quality of the match achieved by simple correlation of the reflectors in Sites 805 and 806 is surprisingly good. The positions of the reflectors can be calculated in detail on the basis of velocity profiles (Fig. 23). Tests show that mismatches of correlated reflectors are on the order of 10 m—about the same as the quality of biostratigraphic correlation. For example, a reflector (0.50 sbsf) dated at 22.0 Ma in Site 805 was correlated with a reflector in Site 806; its age turned out to be 22.3 Ma, 10 m too deep for a perfect fit. To check this proposition further, specific matches were selected and dated independently. For a perfect match, the dates on the same line should be identical (each comparison shows Site 805 first, then Site 806):

1. 0.044 sbsf, 35 mbsf, 1.95 Ma; 0.061 sbsf, 48 mbsf, 2.05 Ma;
2. 0.128 sbsf, 103 mbsf, 4.44 Ma; 0.170 sbsf, 139 mbsf, 4.49 Ma;
3. 0.258 sbsf, 216 mbsf, 7.17 Ma; 0.332 sbsf, 285 mbsf, 7.64 Ma; and
4. 0.363 sbsf, 315 mbsf, 12.70 Ma; 0.480 sbsf, 435 mbsf, 12.34 Ma.

The average difference among the age estimates is 0.23 m.y. for the five determinations, close to the interpolation errors of the biostratigraphic age. Thus, as far as we can tell, the correlative reflectors of Sites 805 and 806 are identical in age.

This demonstration of synchroneity of the reflectors of Sites 805 and 806 is an important result. It provides strong support for the hypothesis that many reflectors represent the effects of paleoceanographic events that are felt over a wide depth range and, hence, are of global significance. Other reflectors may be regionally strong expressions of minor events or may be related to diagenetic processes that are not synchronous.

The fact that reflectors occur in groups suggests that the ocean system, when in transition from one state to another, does so in steps marked by reversals toward the original state or by assuming a sequence of strange states before finding the target state. This is as expected if we are dealing with a chaotic system characterized by quasi-stable substates ("attractors"). Any one set of boundary conditions, governed by geography, will have a set of attractors whose presence is revealed mainly by Milankovitch forcing. Because plate tectonics and volcanism change the boundary conditions, another set of attractors gradually emerges. If the distance between the two sets is great (as when opening or closing a major ocean passage), the system has the opportunity for large-amplitude fluctuations, even though forcing has not changed. At such times, facies changes in any one place also will be large, so that physical properties likewise will fluctuate greatly. This "transitional hypersensitivity" is subsequently recognized as reflector groups, especially after diagenesis has enhanced the signal. If these suggestions have merit, it is immediately obvious why the correlation of reflector groups is a useful approach to acoustic stratigraphy.

PALEOGENE AND CRETACEOUS SEDIMENTS

Goals and Recovery

Objectives for the pre-Neogene record centered on improvement of the biostratigraphic record, on diagenesis, on the origin

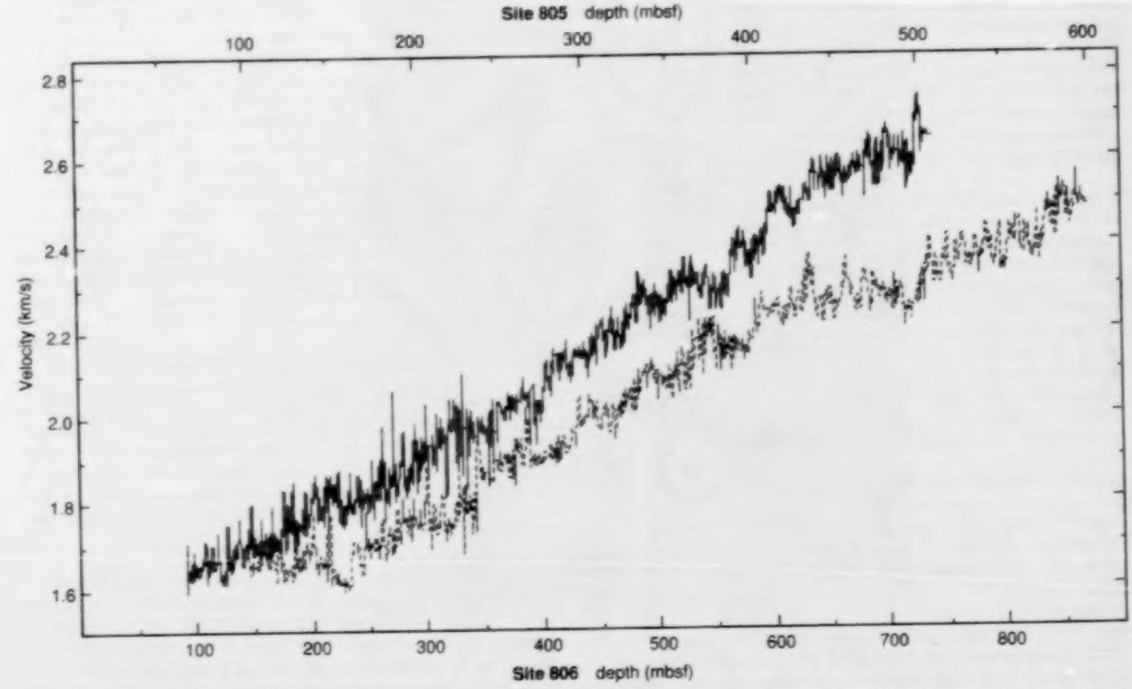

Figure 23. Velocity profiles in Sites 805 (dashed line) and 806 (solid line), plotted to emphasize correlation of fluctuations. Note linear offset of depth axis to aid the graphical comparison. Drawn by M. Lyle.

of hiatuses, and on the nature and extent of anoxic events in the Pacific. We also hoped to learn more about the Cretaceous/Tertiary boundary. Prospects for complete sections were not good, based on the abundance of substantial hiatuses found in the pre-Oligocene record in DSDP Site 289 (Shipboard Scientific Party, 1975b).

Oligocene material was recovered at all five sites, but pre-Oligocene deposits at the only two (803 and 807) that were drilled into basement. In the deeper site (803, 3410 m), hiatus formation was extensive below the middle Eocene. Only short sections of the record were recovered between the Eocene and the Aptian?. Fortuitously, one of these sections contains a complete K/T transition in a sub-CCD setting (but with traces of carbonate). In the shallower site (807, 2805 m), the Paleogene is well represented, and there is an apparently complete section for the Maestrichtian. Again, the K/T boundary section is complete (within the biostratigraphic resolution). The record between the Maestrichtian and the Cenomanian is missing, whereas those of the Cenomanian and Albian are poorly represented (<30 m), considering the length of time involved (20 m.y.).

Paleogene Sediments

Oligocene sediments were penetrated in all sites and were invariably assigned to lithologic Subunit IB, nannofossil chalk. Overall sedimentation rates can be determined in Sites 803 and 807, where they are 18 and 25 m/m.y., respectively. The latter value is low because of a mid-Oligocene hiatus (Fig. 4). If these rates are corrected for compaction, they are fully equivalent to average Neogene sedimentation rates. Peak rates also are of comparable magnitude. The transition from the late Oligocene to the early Miocene is uneventful; in fact, it is so gradual that considerable difficulties were encountered when identifying the boundary.

Oligocene sediments are homogeneous and have uniformly high carbonate values. In regions near the lysocline, the differences in diagenetic potential (Schlanger and Douglas, 1974) may be low, judging from the weakness of reflectors (Texas Interval at Site 805 and at deeper sites). Farther upslope, differential diagenetic processes (incipient limestone and chert formation) apparently enhance subtle lithologic contrasts, greatly increasing the echo potential. In essence, the formation of limestone and chert is a recrystallization process that feeds on fossils. Preservation of both nannofossils and diatoms deteriorates, therefore, as diagenesis proceeds (and the echo potential rises).

Eocene sediments, in contrast to those of the Oligocene, exhibit great diversity of lithology. The late Eocene record is not much different from that of the early Oligocene, except for somewhat increased lithification. This was included in the nannofossil chalk unit that spans the last 40 m.y. However, siliceous material became much more important before that time, and the rest of the Eocene record is characterized by interbedded radiolarian-bearing chalks, calcareous radiolarites, and various types of limestones and chert. These deposits are readily seen as strong reflectors over broad reaches of the plateau.

The top of these reflectors (the Ontong Java Series) marks a major reorganization of the silica budget of the ocean. This reorganization traces out a transition from global silica glut to global silica starvation at about 40 Ma. On the whole, this starvation has prevailed since. Silica starvation may be caused by a general lack of supply to the ocean or to localized excess consumption. To call on increased silica supply in the Eocene, one can point to the evidence for increased volcanism (Kennett et al., 1977) and to increased chemical leaching of continental bedrock during a warm climate with low-lying continents (van Houten, 1982). To find excess consumption during post-Eocene time, one would have to look to the Antarctic Ocean and to the ocean margins. The fact that the ocean acquired cold, deep waters at about 40 Ma (Shackleton and Kennett, 1974) shows that a strong increase in the planetary temperature gradient occurred, which inevitably resulted in upwelling (and in silica removal) in high latitudes and along the ocean margins.

High, scattered concentrations of silica in the pelagic sediments of the Eocene ocean may have been produced, in part, by episodic carbonate buildup on widespread Eocene shelf seas, which would have removed the major dilutant. Occasional global nitrate deficiency, the result of denitrification in a warm, low-oxygen ocean, would have increased concentrations of silica in the water by decreasing the removal of silica by diatoms, which would have needed this nitrate for growth (Berger and Roth, 1975).

The striking difference in sectional preservation between post-Eocene and pre-Oligocene deposits may be related to the overall change in silica content. In the sections we drilled (803 and 807), hiatuses and condensed sections were common throughout Paleocene to middle Eocene time, and similar observations have been made elsewhere on the plateau. We postulate that the presence of silica-rich layers in the older Paleogene sediments led to early lithification within selected beds, impeding dewatering of the formations. When earthquakes shook the plateau (e.g., as a consequence of its collision with the Melanesian subduction system), high interstitial water pressures below semilithified beds facilitated wholesale removal of extensive sediment blocks by mass wasting. In contrast, when silica starvation set in, bedding became much less pronounced, and lithification increased cohesion in a three-dimensional framework without impeding dewatering. Thus, the sediment stack became much more stable. Earthquakes then mainly affected sediments on the steeper slopes, at the lower flanks of the plateau. Farther up toward the top of the plateau, shaking resulted in dewatering, rather than in sliding.

The silica hypothesis of sectional preservation may be generalized to a bedding-plane hypothesis: when bedding is strong, removal is more likely. If so, horizons having strong acoustic reflectors are more likely to harbor hiatuses (which in turn enhance the echo potential). The hypothesis (involving either silica or carbonate removal) also offers an explanation for the observation that *reorganization* of the system can produce hiatuses: during such transitions, bedding develops because the system jumps back and forth between climatic states. In turn, bedding increases the sensitivity to mass movement during earthquakes by hindering dewatering.

Cretaceous/Tertiary Transition

Given that the pre-Oligocene record on the Ontong Java Plateau is riddled with hiatuses, as seen at Sites 64 and 289 and on seismic profiles, we hardly expected to recover a complete section across the K/T boundary. In fact, we recovered not one, but two such sections, one each from the two holes that penetrated into the Cretaceous.

At Site 803, the K/T boundary occurs near 622.3 mbsf within dark brown claystone (in part silty) with signs of reworking (Fig. 24). The section has a low carbonate content and some poorly preserved radiolarian remains. The depth of deposition, assuming isostatic adjustment of the basement under the increasing sediment load, would have been somewhere near 3.5 km. At Site 807, the boundary is near 1193.1 mbsf, within white to gray limestone with variable amounts of silica cement. Lithified volcanic ash is associated with the boundary (Fig. 24). The depth of deposition, assuming isostatic adjustment, would have been near 3 km, considering that a graben was still forming at the time of deposition of lower Tertiary sediments. Thus, the most probable depth for the CCD during the time of the K/T transition would have been somewhere between 3 and 3.5 km.

The lithologic change across the K/T boundary at Site 803 is unremarkable, with traces of carbonate, chert fragments, and glass present in smear slides above and below. There is a trend

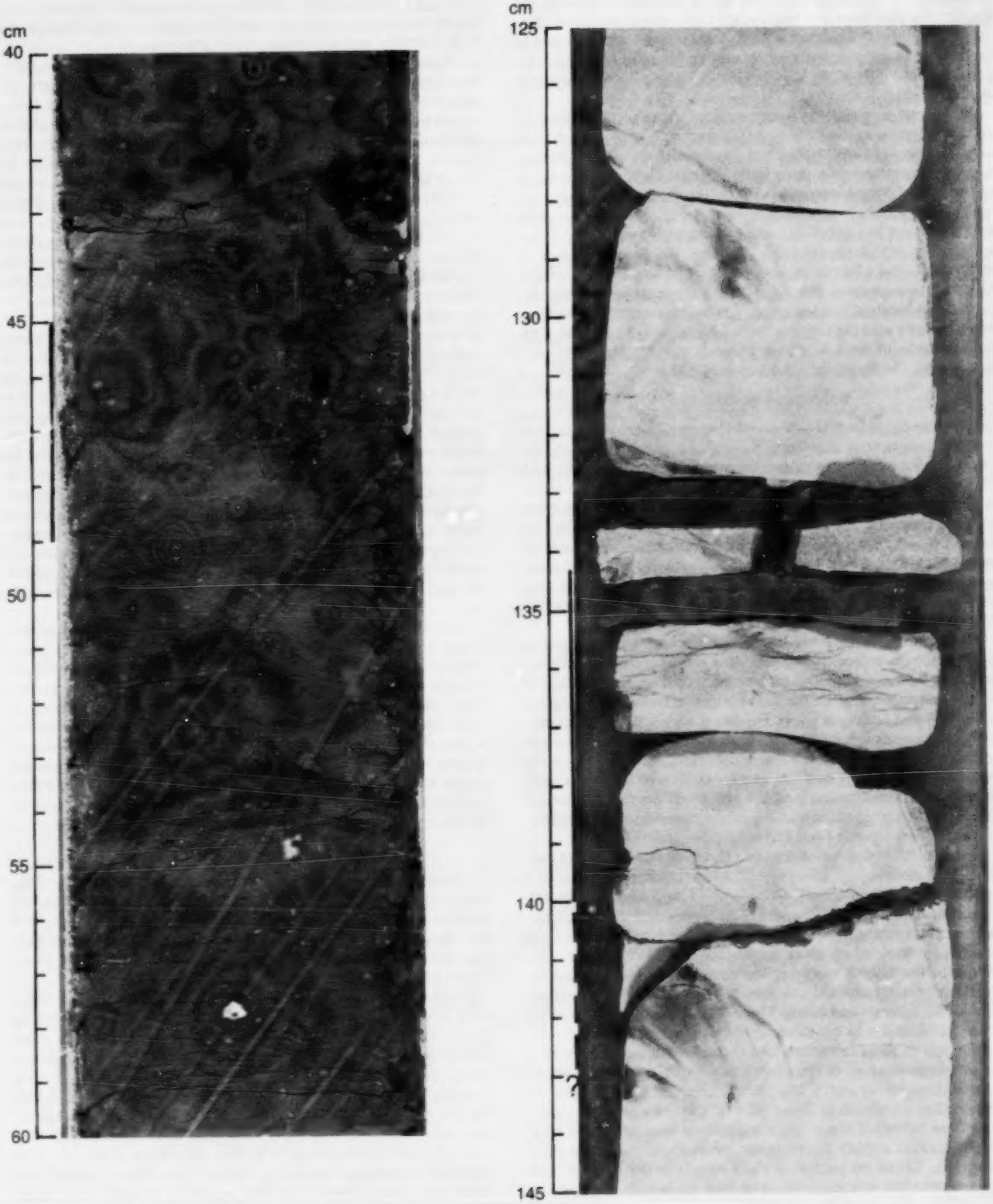

Figure 24. Cretaceous-Tertiary transitions at Sites 803 (Interval 130-803-68R-1, 40–60 cm; left) and 807 (Interval 130-807C-54R-3, 125–145 cm; right). The first is noncalcareous; the second occurs within limestone. Note the presence of lithified volcanic ash at Site 807. Cretaceous/Tertiary boundary intervals are indicated by a bar on each figure.

toward increasing carbonate on approaching the boundary (i.e., the CCD moves to greater depth), and a distinct jump in carbonate content coincides with the appearance of *Thoracosphaera*. Above this jump, carbonate content fluctuates, and radiolarian remains (and glass) appear better preserved than below the jump.

The position of the K/T boundary was identified by means of calcareous nannofossils from a poorly preserved and low-diversity assemblage (see "Biostratigraphy" section, "Site 803" chapter, this volume). The criterion used to place the boundary was the appearance of *Thoracosphaera*, a dinoflagellate cyst presumably indicating conditions of stress. Also at that level, Cretaceous nannofossil species, including *Micula prinsii*, decrease in abundance drastically. The presence of *Micula prinsii* signals that the latest Maestrichtian was indeed recovered (Monechi, 1985). The presence of *Markalius astroporus* and that of *Biantholithus sparsus* indicate that basal Danian material was recovered. Reworked Cretaceous species also are common in the basal Danian section.

The lithologic change across the boundary at Site 807 also is unremarkable, except for the ash layer associated with the boundary (Fig. 24). The limestone above and below is moderately to highly bioturbated with millimeter- to centimeter-scale, subhorizontal, compacted burrow traces. Submillimeter-scale flaser structures are common. Below the boundary, faint, light grayish bands and stylolites can be seen. Dark reddish gray chert is present throughout as fragments of continuous layers up to 6 cm thick and as irregularly shaped masses in limestone pieces.

On the basis of nannofossils, the K/T boundary was placed (see "Biostratigraphy" section, "Site 807" chapter, this volume) within a 16-cm interval at the base of Section 130-807C-54R-3. The first appearance, rapid rise in abundance, and subsequent decline of *Thoracosphaera* are the chief criteria. Within this boundary interval, *Thoracosphaera* is rare, but it is abundant immediately afterward. Cretaceous forms are common throughout the section, from uppermost Maestrichtian to lowermost Danian. In fact, they increase again in abundance after a decline within the vicinity of the boundary itself. Thus, reworking across the boundary is indicated, as well as an increase in preservation, which allowed the reworked material (from upslope) to remain abundant. In contrast, the Tertiary forms are present in subdued numbers, having been delivered from surface production, rather than from downslope reworking, and being more susceptible to dissolution as well.

At Site 807 as at Site 803, a decline of the CCD across the transition is indicated, perhaps by roughly 200 m. The presence of uppermost Maestrichtian is documented by *Micula prinsii*, which is present in a sample taken just about 1 m below the boundary. From about 1 m above the boundary upward, trace amounts of Danian placoliths (*Biscutum*, *Cruciplacolithus*, and *Toweis*) are present.

In sum, the great change in the nannofossil flora, described by Bramlette (1965) and many since, is represented in both sections, although in a condition of poor fossil preservation. The sudden disappearance of a rich nannofossil flora, and the appearance of abundant *Thoracosphaera*, has been extensively commented on. In our samples, it appears that *Thoracosphaera* is abundant because it was resistant to dissolution. Its dominance may owe more to the fact that nannofossils were no longer available for delivery to the seafloor. Thus, the commonly used term "bloom" for these mass occurrences may be misleading: even if production of *Thoracosphaera* was low, it would show the dominance pattern seen in the absence of a viable nannoflora. An interpretation that *Thoracosphaera* represents stressful conditions after the K/T event, while appealing, cannot be based on these observations. For all we know, conditions may have been excellent for the growth of Cretaceous nannofossils. However, they were no longer around to take advantage of any such opportunity.

The K/T boundary at Site 807 is embedded in a limestone sequence that does not seem to have major hiatuses in the immediate vicinity of the transition, although the poor preservation of nannofossils and low sedimentation rates indicate a position near the CCD of the time. In contrast, the K/T boundary at Site 803 is uniquely situated between major hiatuses and greatly condensed sections. The a priori probability of finding any particular section of 100,000–200,000 yr in this great record void cannot be estimated. Given that one such preserved layer is present, the probability that it contains the K/T boundary would be on the order of 1 in 1000. Thus, our finding the K/T boundary must be ascribed either to incredible luck or to a process that made the sedimentary record of this particular time interval unusually preservable.

We suggest that a case can be made for preservation-enhancing circumstances at the K/T boundary at this sub-CCD level. Two conditions had to be fulfilled. First, the site had to be close enough to the CCD to preserve enough nannofossils for identification. This was a matter of luck—at a greater depth, we might have recovered the K/T boundary without realizing it. Second, the deposited material had to be cemented early, so that it was not removed during erosion episodes. We assume that such quasi-contemporaneous episodes are responsible for the removal of extensive sequences in the Late Cretaceous and early Tertiary in this setting.

We think that the early cementation was accomplished by silica supersaturation and possibly by increased metal precipitation (iron and manganese). The mechanism we postulate is simple: when biological activity was greatly reduced at the end of the Cretaceous by making the ocean unsuitable for pelagic plankton, the ocean tended to revert to its thermodynamic state. In this state, saturation with silicate was achieved in the deep sea, and supersaturation thus could be achieved in interstitial waters. Early cementation by silicification was then possible. Volcanism, indicated by the ash layer in Site 807, may have been a contributing factor by releasing silica and metals to deep waters. In favor of the silica-enrichment hypothesis, note that some evidence exists for enhanced preservation of radiolarians. Early cementation also would have trapped metals that could have added to the erosional resistance.

There is evidence from magnetic studies for iron enrichment exactly at the boundary: a strong peak in magnetic susceptibility in Section 130-803D-68R-1, at 45 cm. The presence of magnetic spherules may be responsible (see "Site 803" chapter, "Paleomagnetics" section, this volume). The high background and an additional spike deeper in the section suggest generally increased iron flux to the seafloor, supporting the suggestion regarding increased volcanic activity.

The evidence for volcanism in Site 807, in the form of lithified ash associated with the boundary, is of some interest, considering the possible role of volcanism in changing the Earth's habitability during K/T time (e.g., McLean, 1985). The deeper site exhibits evidence of volcanic activity throughout, not just right at the boundary. Presumably, if Earth was hit by a bolide during the event (Alvarez et al., 1980), volcanism would surely have been stimulated. Thus, there is no point in entering a debate that poses the question in terms of bolide vs. volcanism. In any case, without chemical and petrological studies, a plain mid-ocean origin for the volcanism observed cannot be excluded and, indeed, remains an attractive possibility. After all, the plateau is of volcanic origin, and the record shows evidence for volcanic activity well into the Paleogene.

Cretaceous Sediments

The contrast between the two sites that have Cretaceous sediments is surprising, considering the moderate difference in depth of deposition that apparently prevailed at the time: on the order of 500 m (see above). If dissolution below the CCD was the cause for the difference in sediment accumulation, the dissolution gradient across this depth must have been strong, which has implications for global ocean productivity. There is no need to dissolve and recycle carbonate in a stagnant ocean, and dissolution gradients should be weak, were productivity low. Contrasting carbonate contents across moderate depth differences indicate conditions that, if widespread, should disagree with the ocean-desert hypothesis of Bralower and Thierstein (1984).

The deeper site contains less than 4 m of the Cretaceous section, all of which is noncalcareous, dark brown claystone. This material represents the entire time span between the K/T boundary and the top of the last basalt, about 40 m.y. Within the last core section above the basalt, there are several centimeter-thick layers of soft, dark, yellowish brown radiolarite (Fig. 25). These layers contain radiolarians of late Albian to early Cenomanian age. The shallower site has 186 m of limestones and claystones, representing mainly the Maestrichtian (limestones) and the Cenomanian and Albian (claystone and limestones). A hiatus spanning up to 20 m.y. between these periods apparently is indicated. Sedimentation rates in the Maestrichtian are high (about 20 m/m.y.), which corresponds to accumulation rates comparable with those in the late Neogene.

Why was sectional preservation 40 times better at Site 807 than at Site 803? Was it because carbonate sedimentation at the shallower site allowed for earlier lithification? Was it the result of local tectonic effects? With the small number of sites available, and in the absence of mapping of Cretaceous sections by seismic methods, we were unable to address these questions. Reworked clasts containing older fossils are present in lower Tertiary rocks at Site 807, as well as in Cretaceous rocks (Fig. 25). This indicates the effects of erosion from the rims of the graben, the formation of which preserved the sequence we found.

The upper Albian and lower Cenomanian claystone with radiolarians, found at Sites 803 and 807, suggests that the CCD stood high at that time, possibly as high as or higher than 3 km (cf. Thierstein, 1979) (Fig. 26). Limestone remains are associated with the basaltic basement at both sites, indicating a lower CCD (or a higher plateau) during the time of the last lava flows, in late Aptian(?), or in Albian time. There is no indication of anoxic events, although their presence cannot be excluded because of the spotty record.

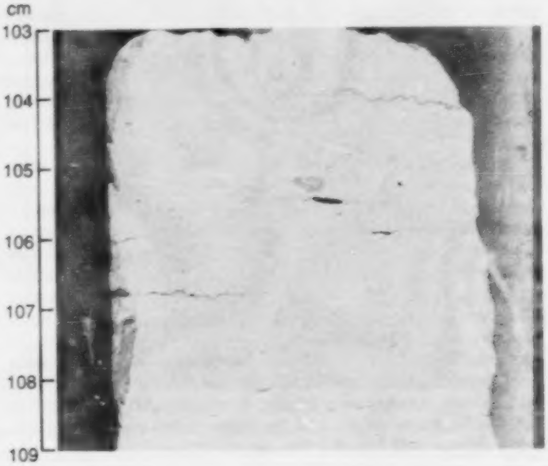

Figure 25. Upper Campanian to lower Maestrichtian limestone, with limestone clasts presumably derived from the erosion of the graben rim and redeposition within the graben at Site 807 (Interval 130-807C-65R-2, 103-109 cm).

BASEMENT DRILLING RESULTS

Objectives and Setting

The main goals for drilling into basement concerned the question of the origin of Ontong Java Plateau (the world's largest oceanic plateau) and the origin of oceanic plateaus in general. When was the basalt emplaced? At what rate? What was its source? These are questions that can only be solved when sufficient material has been recovered. The significance of oceanic plateaus in general, inter alia, pertains to their possible role in the growth of continents (Kroenke, 1974; Storey et al., in press).

The Ontong Java Plateau, with an areal extent of roughly 1 million km^2 (the same as Spain and France combined), is more than twice the size of the next largest flood basalt province, the Deccan Traps. The enormous outpourings of basalt during the middle Cretaceous, which appear to be indicated by our results, should have raised the sea level and, if sufficiently concentrated in time, may have affected the circulation and chemistry of the ocean and, therefore, also the chemistry of the atmosphere, producing large-scale climatic warming (see Arthur et al., 1985). A volume of more than 25 million km^3 of basaltic crust may be estimated for Ontong Java Plateau, based on seismic refraction data (roughly the same as the volume of ice on Antarctica). Rapid emplacement of this basalt, without isostatic adjustment, might have raised the sea level by more than 50 m.

Recovery and Rock Types

So far, penetration into basement of Pacific plateaus has been moderate (Fig. 27). Thus, the two sites of Leg 130 at which basalt was recovered provide a substantial increase in material for attacking questions regarding the origin of plateau basalts. The Leg 130 scientists recovered 11 m of basalt at Site 803 and 92 m at Site 807.

Basalts at both sites are tholeiites. At Site 803, the rocks mainly consist of successive pillow lavas, whereas at Site 807, both pillow and massive lavas occur, the latter mostly less than 3 m thick, but including one 28-m-thick flow (Fig. 28). In places, sedimentary layers occur between flows. Calcareous fossils are present, but they have been recrystallized beyond specific recognition. Basalts are nonvesicular, hypocrystalline, fine grained, and aphyric to sparsely phyric. At Site 803, alteration ranges from severe to moderate within pillow interiors, whereas at Site 807, alteration rarely exceeds a moderate level and is restricted to the vicinity of veins, presumably marking ducts for hydrothermal fluids from greater depths.

Petrography and Chemical Properties

Thin-section examination of pillow interiors confirmed the fine-grained, typically aphyric, hypocrystalline nature of the basalt. Phenocrysts observed include rare subhedral (<0.5 mm) pseudomorphs of olivine, zoned clinopyroxene, and plagioclase laths. The deeper units at Site 807 also contain altered olivine microphenocrysts. The most noteworthy petrographic aspect of these rocks, however, is the scarcity of phenocrysts. In the lower 103 m of the basement sequence at Site 807, these are essentially absent.

Major and trace elements on pillow interiors were determined by X-ray fluorescence spectrometry on board the ship for Site 803. For Site 807, analyses were performed at the University of Keele. At Site 803, the basalts are fairly evolved (Mg# = 35–53), mildly quartz- to olivine-normative tholeiites. These basalts have MORB-type Ti/Zr and Zr/Y ratios and high Sr, Ca, and K concentrations. Zr/Nb ratios are distinctly low compared with nor-

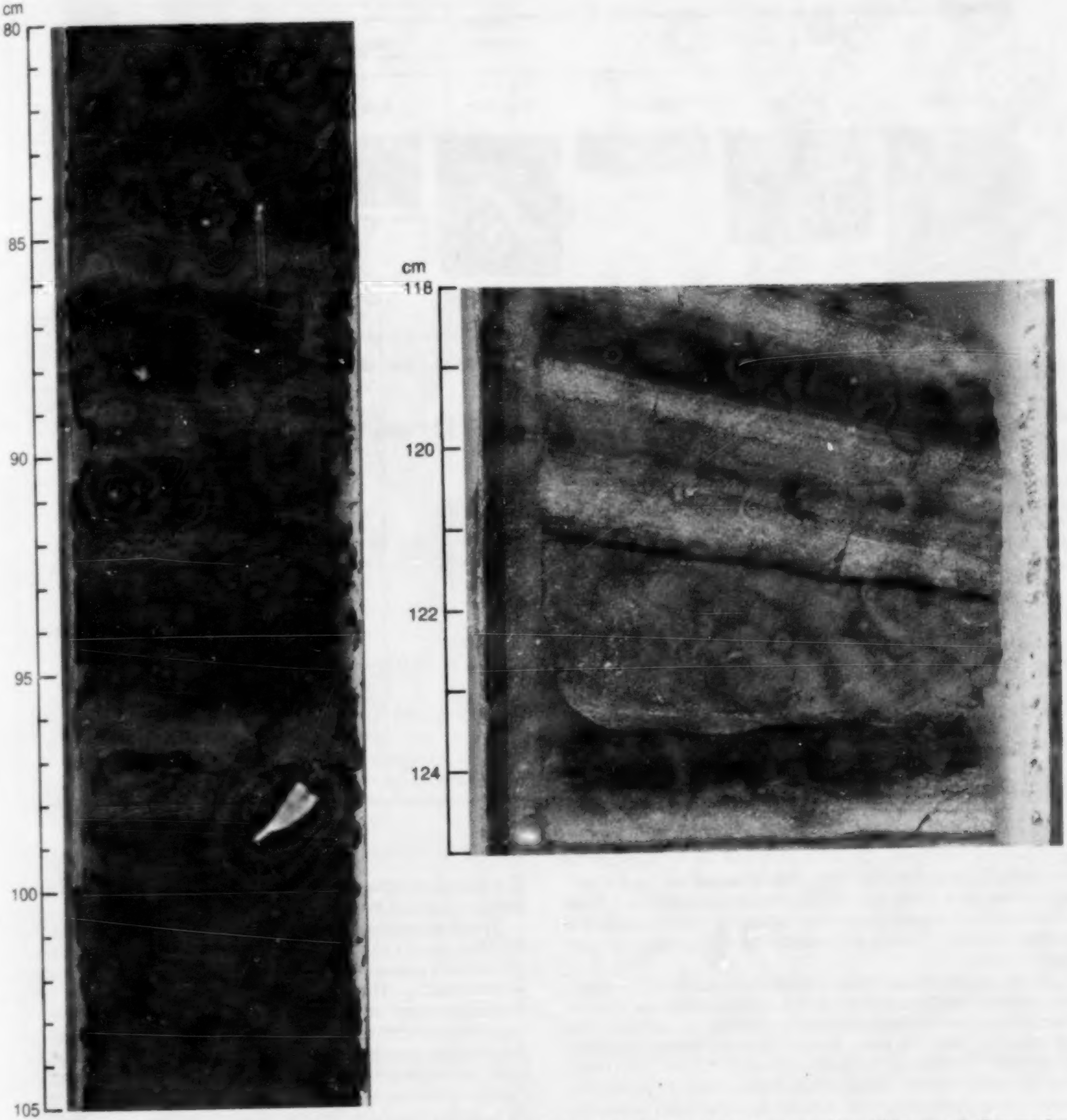

Figure 26. Barren dark brown claystones with lighter colored radiolarian-rich layers. Radiolarians indicate an age of late Albian to early Cenomanian. Left: Site 803 (Interval 130-803D-68X-3, 80–105 cm); right: Site 807 (Interval 130-807C-72R-1, 118–125 cm).

mal MORBs, as are Ti, Zr, and Y abundances, for the level of differentiation indicated by the Mg#. Thus, these rocks are distinct from normal MORBs. They also are distinct from typical oceanic-island tholeiites by being much less enriched in immobile incompatible elements, such as Zr, Nb, and Ti, and by having higher Zr/Y and much lower Zr/Nb ratios (Fig. 29). The closest resemblance is to the few available basalts from other Pacific plateaus, in particular those of the Manihiki Plateau (Jackson et al., 1976) and the rocks recovered at Site 289, not far away (Stoeser, 1975).

In general, the major and compatible trace elements do not display simple inter-element relationships, suggesting that the rocks may represent more than one liquid line of descent or parental magma. In conjunction with Nd and Sr isotopic studies, the type of chemical signature found in these rocks has been interpreted to reflect mantle sources that are a combination of MORB- and oceanic-island-type components (Mahoney, 1987).

At Site 807, the plagioclase basalts of the uppermost subunit are enriched in Sr, Ti, and Zr, making them distinct from those of the lower subunits, which are depleted in these elements. The

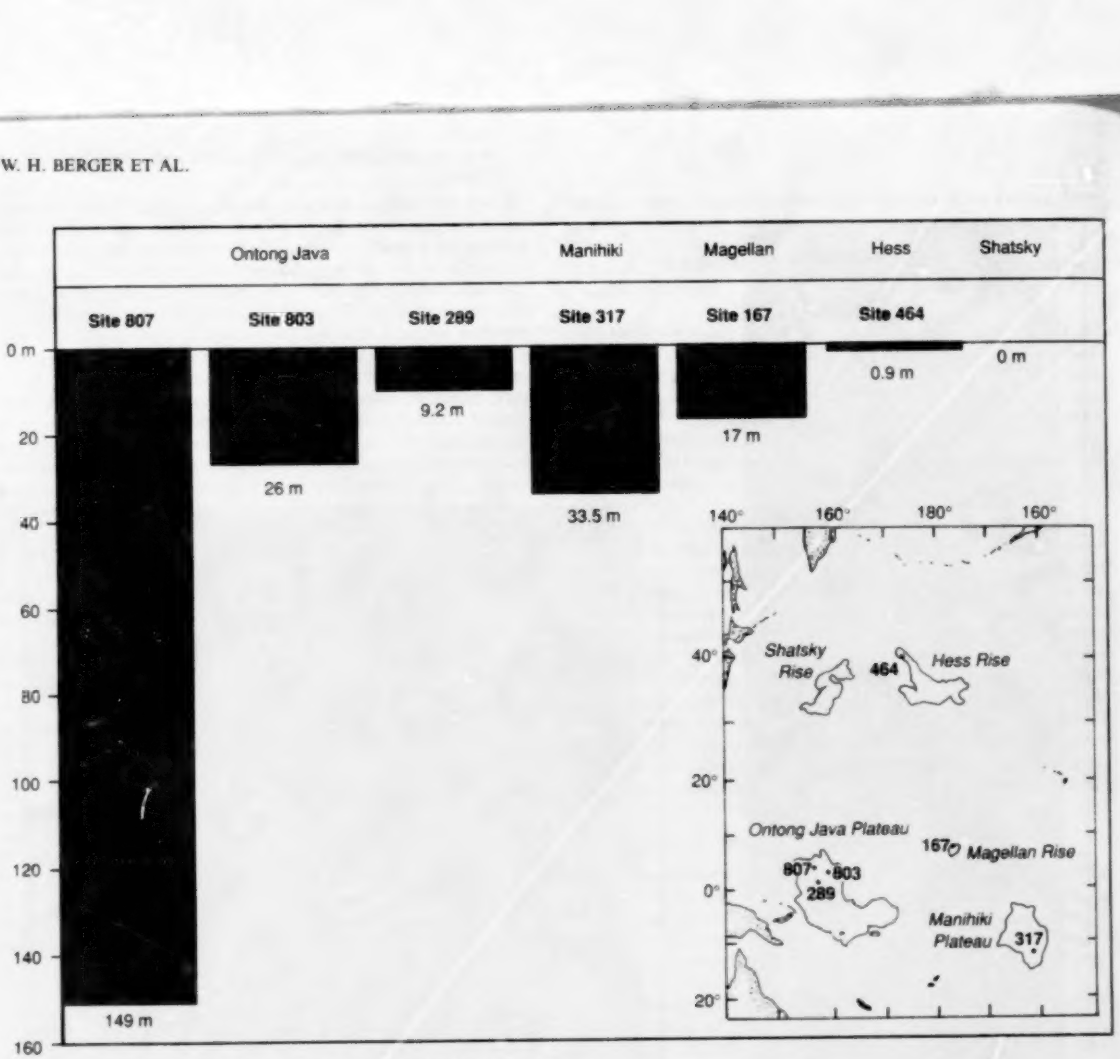

Figure 27. Basement penetration of oceanic plateau basalts in the Pacific.

mineralogical and chemical differences observed for the last and next-to-last lava flows and the limestone layer between them (>0.6 m thick) suggest the passage of considerable time before the last eruption. There is no evidence for similar separation of earlier flows.

Basalts at Site 807 are distinct from those at Site 803. Chemical variations within subunits at Site 807 generally are smaller than those within the unit sampled at Site 803. In addition, the variations between the older flows at Site 807 (below the limestone layer) are limited, as illustrated in the Zr vs. TiO_2 field (Fig. 30). Note that the basalt at Site 803 occupies a position between the uppermost flow in Site 807 and the flows below the limestone layer at Site 807. The same is true for the Sr data (see "Site 807" chapter, "Igneous Petrology" section, this volume).

Preliminary Conclusions

Several eruptions are represented in Site 803. All basalts are moderately differentiated tholeiites that may have been derived from more than one parental magma. The thin, pillowed nature of the flows suggests that their feeder vents were not distant and that eruption rates were low. This feature may be related to the location of this site on the flank of the plateau. In contrast, the thick basalt unit at Site 807 provides clear evidence for the presence of massive flows on the Ontong Java Plateau that are comparable with those of major continental flood basalt provinces. The general absence of large phenocrysts also is reminiscent of some continental flood basalts.

The flows at Site 807 generally are thicker than those at Site 803 (3 m vs. <1 m); their sparse but ubiquitous olivine microphenocrysts indicate that the lavas at Site 807 may be primitive in composition. The absence of much alteration and of sedimentary interbeds in the deeper portion of the recovered section suggests emplacement over a short period of time, so that any one flow was exposed to seawater only a short time. The uppermost unit at Site 807 apparently was emplaced after passage of considerable time, as indicated by both mineralogical and chemical differences and the presence of a 0.6-m-thick limestone layer at its base.

The late Aptian to Albian age of the upper basement at the sites where basalt was recovered (DSDP Site 289 and ODP Sites 803 and 807) suggests that volcanism was widespread across the Ontong Java Plateau during that time. This final phase of flood basalt effusion was characterized by the eruption of massive flows, interspersed with and followed by the eruption of a series of thin, pillowed flows. The last flows that occurred are scattered after quiescence (as shown by the sediment layers between the pillow lavas), and these late-stage eruptions have a more evolved composition, as seen in the phenocryst assemblage. The first sediments to accumulate on the thermally elevated plateau were deep-water limestones and vitric tuffs that were deposited

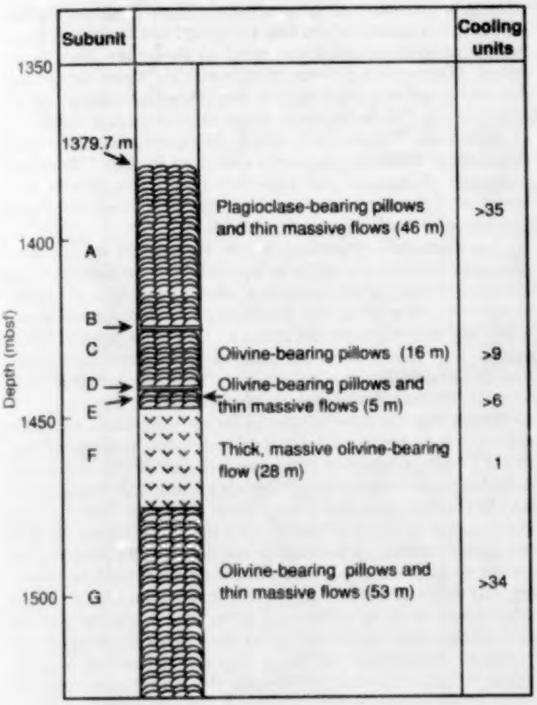
Subunit
Cooling units
Depth (mbsf)
1350
1379.7 m
1400
1450
1500
A
B
C
D
E
F
G
Plagioclase-bearing pillows and thin massive flows (46 m)
>35
Olivine-bearing pillows (16 m)
>9
Olivine-bearing pillows and thin massive flows (5 m)
>6
Thick, massive olivine-bearing flow (28 m)
1
Olivine-bearing pillows and thin massive flows (53 m)
>34

Figure 28. Lithologic column of basement drilled in Hole 807C, showing distribution of pillows and thin, massive flows (A, C, E, G); a thick, massive flow (F), as well as two thin sedimentary interbeds (B, D). Cooling "units" are estimated from glassy chilled rinds and are given on the right for each subunit. Figure by J. Mahoney and M. Storey.

above, but probably near, the Early Cretaceous CCD (2500–3000 mbsl).

Paleolatitudes from magnetic inclinations in the basalt suggest that Ontong Java Plateau moved coherently with the Pacific Plate because its construction was completed in the Early Cretaceous.

SPECIAL STUDIES

Paleomagnetism

Pass-through cryogenic magnetometer measurements were performed for selected APC split-core archive sections, XCB cores, and RCB cores where available, the choice being dictated by the quality of the material. *In-situ* orientations were attempted in cores where this was deemed profitable. Although the attempt was not always successful, the majority of APC cores that yielded directional data are oriented.

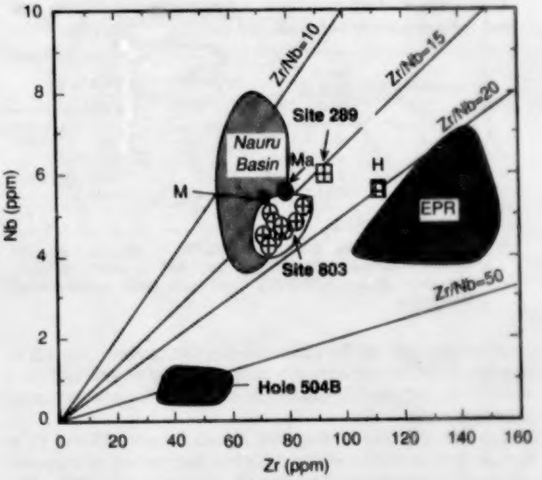

Figure 29. Plot of Zr vs. Nb for Site 803 tholeiites. For comparison, fields are shown for the East Pacific Rise ("EPR"), Hole 504B on the Costa Rica Rift, and the Nauru Basin. Averages for Manihiki Plateau lavas ("M") and Malaita basement basalts ("Ma") are also plotted, as are data for the single basalt flows recovered at Site 289 and on Hess Rise ("H"). Plotted by J. Mahoney and M. Storey.

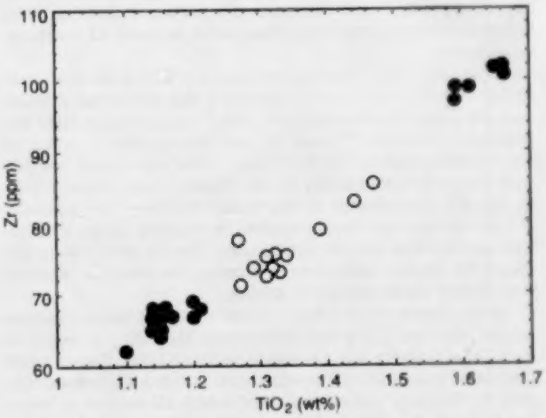

Figure 30. Composition of lava flows, Sites 803 (open circles) and 807 (closed circles), Zr vs. TiO_2. Plotted by J. Mahoney and M. Storey.

A conspicuous characteristic of the pass-through magnetometer measurements on APC cores was an anomalously high magnetic intensity in the top 50–100 cm of the first section of each core, signifying physical disturbance through "draw-in" caused by the hydraulic coring process. Despite this problem, APC cores yielded correlatable reversal boundaries at Sites 803, 804, 805, and 807. No reversal could be identified in Site 806. The high-resolution records in the various sites deteriorate rapidly below a sub-bottom depth of between 15 and 50 m, with the exact level depending on the site and with Site 806 presenting the worst case.

The level at which the intensity decreases below 0.3 mA/m and approaches 0.1 mA/m commonly marks the depth interval below which the directional data are uninterpretable. Because of the proximity to the equator, inclinations could not be used to place reversals in the Pliocene-Pleistocene sediments. Changes in the polarity of declination were used instead.

Results for Neogene sediments are summarized in Table 4. A distinct trend can be seen in these data, such that shallower sites and those nearer the equator show deterioration of the magnetic signals at a lesser age of sediment. Two factors combine to re-

Table 4. Depth of deterioration of magnetic signal, age at that level, and sedimentation rates for selected intervals.

Site	Level of deterioration (m)	Age at level (Ma)	Sedimentation rates (m/m.y.)			
			Brun	M/B-Old.	Old.-M/G	Gauss
803	49	4.0	10	10	15	15
804	47	4.3	10	10	12	12
805	33	1.9	17	17	—	—
806	16	(0.7)	(20–23) (no reversal determined)			
807	32	2.0	16	16	—	—

Notes: Intervals are: Brun, 0–0.73 Ma; M/B-Old. = Brunhes/Matuyama boundary to Olduvai, 0.73–1.66 Ma; Old.-M/G = Olduvai to Matuyama/Gauss boundary, 1.88–2.47 Ma; and Gauss: Gauss normal interval, 2.47–3.40 Ma.

duce the age limit of the preserved magnetostratigraphy: (1) an increase in sedimentation rates to expand the record and (2) a decrease in the sub-bottom depth at which the primary magnetic remanence fades.

The deterioration of magnetic signals between 15 and 50 m downhole presumably results from the destruction of magnetic minerals by the reduction of iron (Karlin and Levi, 1985). This is indicated both because the sites with higher sedimentation rates (= higher productivity and higher organic carbon supply) show the greater effect and because sulfate reduction is highly correlated with magnetic signal deterioration.

Although magnetic intensities in Miocene sediments were generally at low levels, making interpretations difficult or impossible, Paleogene and Cretaceous sediments and basalt yielded interesting magnetic data. In places, intensities increased to interpretable values, and intervals of constant inclination were found that can be tentatively interpreted in terms of magnetostratigraphy.

In Site 803, mid-Oligocene sediments exhibit a mode of inclination distribution at +9°. Assuming this represents primary magnetization, the paleolatitude is 4.5°, suggesting a total displacement of about 7° since the last 30 Ma; that is, a rate of northward movement of 0.23°/m.y. This rate agrees roughly with earlier determinations for the Pacific Plate (Sager, 1987). In Site 807, the attempt to determine Oligocene paleolatitudes did not yield unique results within the expected range. Present-field overprinting may be responsible. Similar results were obtained for Eocene sediments, indicating the need for detailed shore-based demagnetization studies.

In the basalts of Site 807, natural remanent magnetizations are predominantly negative and steeper than 20°, as expected for normal polarity and a position south of 10°S. Pass-through magnetic susceptibility measurements yielded high-resolution data for Pliocene-Pleistocene cores, which allowed us to correlate in detail. However, in Miocene sediments, susceptibility values became extremely low to negative and were clearly influenced by the diamagnetic calcite content.

For several sites (805, 806, and 807), high-resolution, whole-core, magnetic susceptibility data were obtained for APC cores and were recorded at 3-cm intervals (Tarduno et al., this volume). These data allowed us to correlate in detail among the different holes at the same site and among sites (Fig. 31). The variations in susceptibility show Milankovitch spectral properties, indicating that abundances of magnetic minerals follow the fluctuations of climate (e.g., Bloemendal et al., 1988). Variations in source regions, wind regime, and diagenesis may be responsible.

Diagenesis and Physical Properties

Several diagenetic phenomena are of special interest when interpreting the sedimentary record: (1) the conversion of ooze to chalk, (2) the conversion of chalk to limestone, and (3) the mobility, precipitation, and aging of silica. These processes strongly influence the quality of the historic record and the echo properties of the sediment stack that result in the seismic profiles obtained. Diagenesis is a destructive process riding on the thermodynamic gradient toward equilibrium. However, timing and circumstances of lithification may retain clues to original conditions of deposition. The degree to which different sediments are predisposed to undergo diagenetic alteration is their "diagenetic potential" (Schlanger and Douglas, 1974). This should be a function of the amount of reactive materials preserved during the time of deposition and first burial.

The ooze-chalk transition is not represented by a sudden change in firmness (as might be implied from the specific depth assignment) but, rather, involves a substantial length of section, about 100–200 m (Fig. 32). Invariably, the transition is gradational and shows alternating layers of varying degrees of lithification. With this in mind, the patterns of the ooze-chalk transition and of silicification (as seen in the first appearance of chert nodules, looking downhole) are summarized in Table 5.

Notice that the range of depths for the ooze-chalk transition (182–339 m, a factor of 1.86) is greater than the range of ages (9.5–13.8 Ma, a factor of 1.45) and that the two run in opposite directions (the deepest transition also being the youngest). It may be that the transition from ooze to chalk was favored by aging as well as by depth of burial, with the product between these two factors tending to be roughly constant in this data set. The greater range in the depth factor might be interpreted as indicating that depth of burial was less important than age in causing lithification in these sediments. Alternatively, noting that the ages of the chalk transition are in the same rank order as the depths of deposition, one might argue that the sites least affected by carbonate dissolution were the most active diagenetically, as postulated by Schlanger and Douglas (1974).

Finding the rare chert nodules that occurred in the Neogene portion of the record is a matter of luck. Still, the shallowest occurrence of such nodules is indeed in the site having the most preserved silica and the highest sedimentation rates (Site 806). The inference that silica abundance was crucial to chert formation is strengthened by the observation that chert beds invariably appear in the Eocene record, when silica was abundant (ODP Sites 803 and 807 and DSDP 289). In addition, the "radiolarite" noted in Site 804 at 200 mbsf occurs in connection with a hiatus, where carbonate was removed and silica was concentrated.

Limestones first appear just below 1000 m in Site 807 and dominate below 1100 m. Site 803 has no limestone sequence, either because it was below the CCD for much of pre-Oligocene time or because carbonate was removed during periods of erosion within that interval.

The significance of diagenesis to distribution of physical properties was mentioned above in the context of seismic stratigraphy. Lithification affects both rigidity and density, which govern the *P*-wave velocity. In Site 807, for example, a distinct increase occurs in the trend of increasing velocity below 300 mbsf (marked "R" in Fig. 33), whereas density jumps to higher values at 380 mbsf (marked "B" in Fig. 33). Rigidity increased rapidly and pore space was eliminated in this interval. The "official" transition at 293 mbsf (as determined visually) most closely corresponds to a sudden increase in velocity, as measured on board the ship, suggesting that interparticle binding at this point was strong enough to withstand the stress of recovery and pressure release.

In Site 806, a marked change in the velocity-depth gradient also occurs near the level where lithification first became important, as seen by the occurrence of porcellanite nodules (240 mbsf, 6–7 Ma; Fig. 23). At the ooze-chalk transition (339 mbsf), the character of the velocity profile changes: above this level,

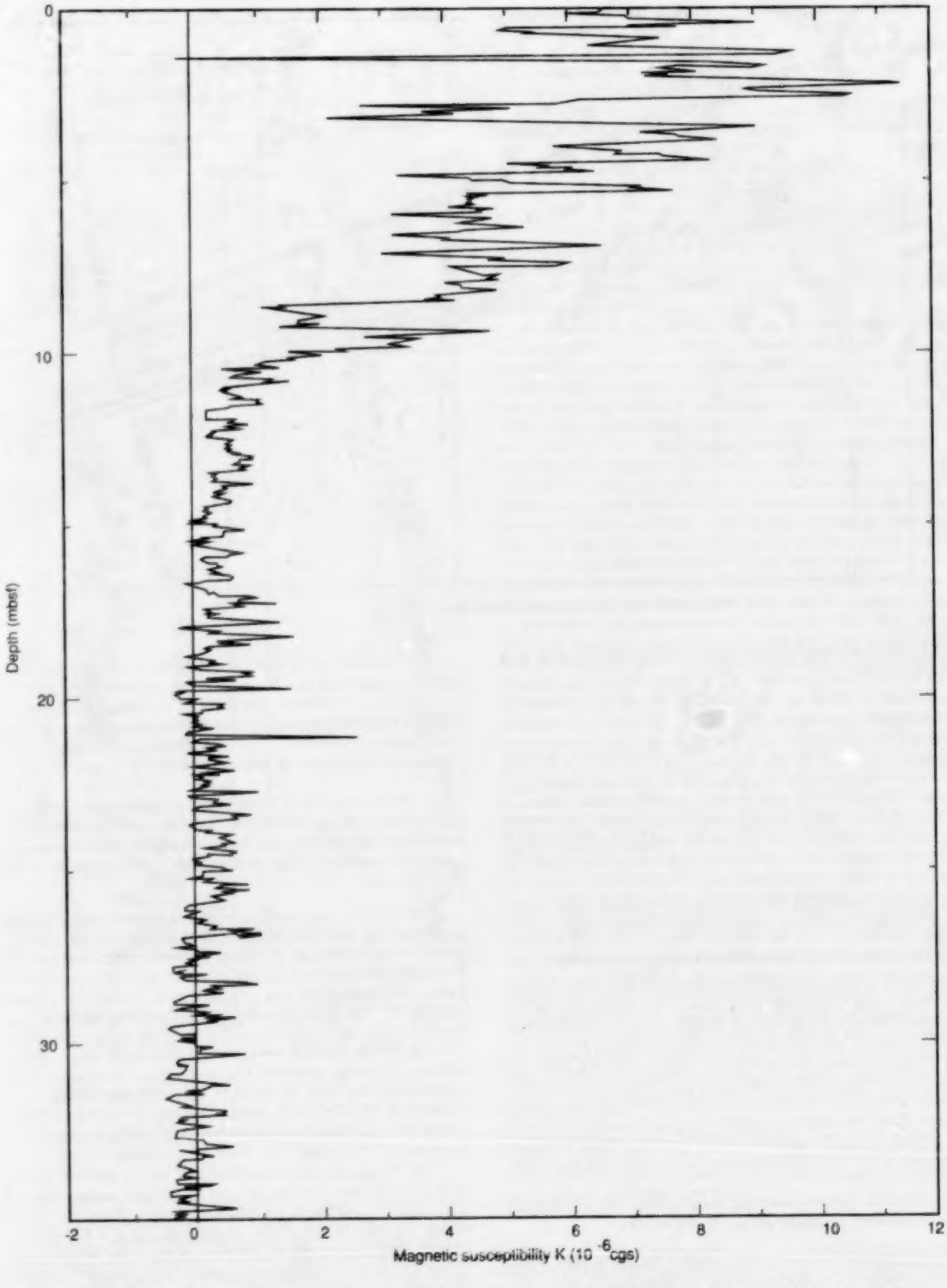

Figure 31. Whole-core magnetic susceptibility for Hole 806A using an 80-mm MS2C Bartington sensor. Note the rapid reduction below 10 mbsf and indications of cyclicity at low levels of susceptibility. From Tarduno et al. (this volume).

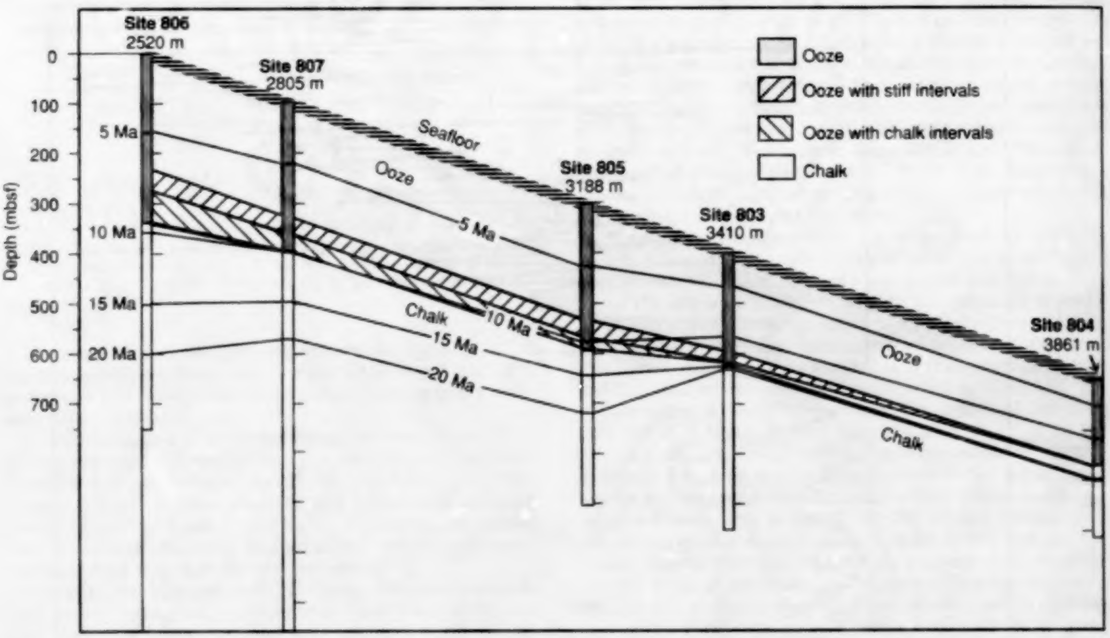

Figure 32. Location of ooze-chalk transition at each Leg 130 site. Drawn by D. Masher.

Table 5. Depth of ooze-chalk transition and occurrences of chert at each Leg 130 site.

			Chert nodules		
Site	Ooze-chalk level (m)	Age (Ma)	Level (m)	Age (Ma)	Other shallow occurrences
803	217	13	540	37	Chert beds, mid-Eocene
804	182	13.5–14			"Radiolarite," 200 m
805	288	10.5–11.5	344	14	"Chert?", late Oligocene
806	339	9–10	240	6–7	Also 310, 509, and 514 m
807	293	10–10.5	252	8	Chert bed, 960 m, 39 Ma

high-frequency variations are pronounced; below it, they are indistinct. Similar phenomena were observed at the other sites.

Diagenesis and Interstitial Water Chemistry

Diagenetic processes involve mobilization and precipitation of carbonate and silica and thus should be observable in the composition of interstitial waters; that is, in the concentrations of calcium, strontium, and silica. Much of the reactivity of sediments owes to the presence of organic matter, which is reflected in profiles of oxygen and sulfate (Fig. 34). Reduction of sulfate is evident down into uppermost Miocene sediments. Reduction increases alkalinity, whereas carbonate precipitation decreases it. Of special interest is the dissolved strontium, which increases in response to the recrystallization of biogenic carbonate (Gieskes, 1981; Fig. 35).

The chemical species analyzed show one of three patterns, mostly as follows:

1. "Hingepoint" patterns, with a rapid change in concentration from a value set by bottom-water composition to some typical value inside the sediment, commonly in an interval between 6 and 8 Ma old. Below, the hingepoint concentrations stay more or less constant or have a low gradient. Sulfate, ammonia, silica, and strontium profiles exhibit this pattern (Figs. 34 and 35).
2. Patterns similar to the those of the hingepoint, but which display a marked decrease below the hingepoint; that is, a maximum occurs. Alkalinity shows this type of distribution, with the maximum appearing in sediments between 4 and 14 Ma (Fig. 34).
3. Patterns that can be represented approximately by stating the surface concentration and another concentration near the bottom of the section; that is, a general trend with depth. Both potassium and rubidium profiles exhibit this type of distribution (Fig. 36).

The first two patterns (hingepoint and maximum) are related to diagenesis, and the third (general trend), for the most part, presumably reflects an exchange between ocean and basement. Calcium and alkalinity exhibit a mixed pattern, somewhere between the hingepoint and general trend, indicating a complex origin. In these cases, the effects of sulfate reduction, carbonate precipitation, and basement influence must be considered. Sites 806 and 807 show the greatest initial increases in alkalinity within the section younger than 10 Ma, as expected from sulfate reduction values (Fig. 34). In contrast, Sites 803 and 804 show little increase in alkalinity. All values decrease deeper in the section below the mid-Neogene maximum, suggesting precipitation of carbonate or exchange with basement or both.

The hingepoint may be interpreted as the bottom part of a reaction zone that moved upward as sedimentation proceeded. The reactive sediments are younger than 8 Ma on the whole. Along the gradient above the hingepoint, there is diffusional exchange with bottom water. Below it, a tendency exists for reprecipitation, as interstitial water concentrations slowly increase toward equilibrium values. There may be a decrease in permeability below the hingepoint, allowing for concentrations below to build up to higher levels, despite a decrease in reaction rates.

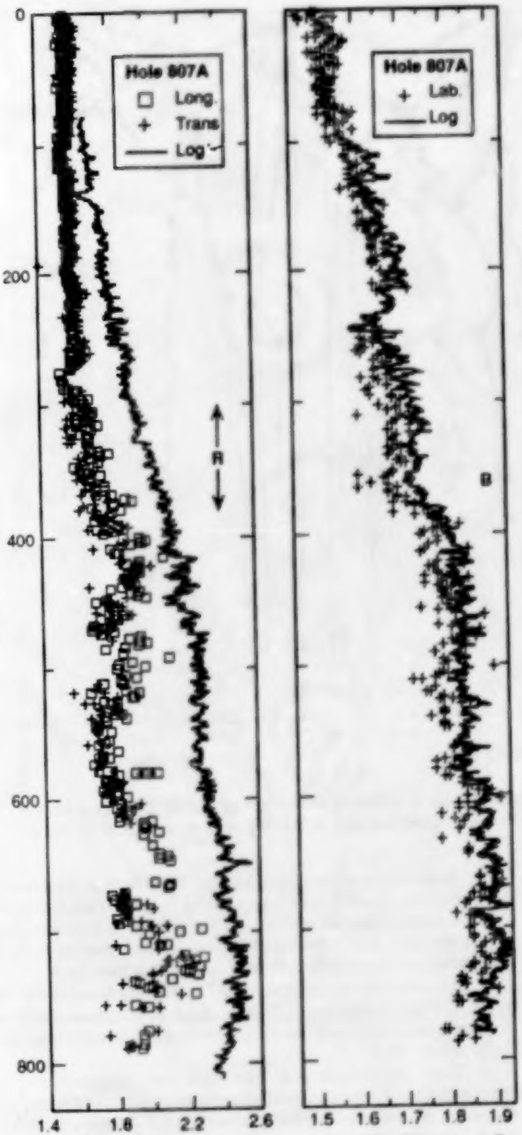

Figure 33. Velocity and bulk density profiles, Site 807, as measured by logging and on deck. The breaks in trends (R = ramp and B = break) appear between 300 and 380 mbsf, suggesting a change in the nature of lithification at that depth.

Major trends in the composition of interstitial water bearing on diagenesis are summarized below (Table 6). Note that, in essence, the patterns are identical for all rows shown, except for calcium. The last two rows refer to sedimentation rate and water depth of the sites, respectively. Thus, sedimentation rates for the last 5 Ma, as well as depth of deposition, are correlated with the factors controlling sulfate reduction and with silica and strontium content in the late Neogene portion of the section, but less so for calcium content. The equatorial position of Site 805 makes up for its greater depth, in comparison with Site 807, so that sedimentation rates are identical over the last 5 Ma, and reactivity tends to be slightly greater in Site 805.

In Site 806, the high values of missing sulfate, of silica concentration, and of strontium indicate that (at the 5-Ma age level) the sediments were bathed in interstitial waters that differed more from the composition of seawater than those in the other sites. Thus, at the same age level within this interval, (1) the reduction of iron mineral should be more advanced, (2) the likelihood of silica precipitation should increase, and (3) the recrystallization of carbonate should be faster at Site 806 than at the other sites. The problem with postulating statements about the relative speed of reaction rates is that at some age level, concentrations alone cannot give this information.

If we assume that the coefficients of diffusion are roughly the same in the various sites in sediments less than 5 Ma old, we can make some observations about the relative rates of diffusion of dissolved substances out of the sediment. One can see from the normalized values in parentheses in Table 6 that the gradients of missing sulfate are about the same for the different sites, except for Site 807, which has a distinctly weaker gradient. Presumably, this relates to its position well off the equator (3.5°). This would seem to indicate that oxidation of organic matter proceeds at about the same pace in the different sites, because the same amount of sulfate deficit was generated. This implies that Site 806, with considerably more organic matter delivered (because of its shallow depth), should retain more of this matter than the other sites, so that in principle sulfate reduction continued much longer here.

For silica, the gradients are similar for Sites 805, 806, and 807, but they are considerably greater for deeper Sites 803 and 804. Perhaps the greater abundance of opal in these sites (from dissolution of carbonate) is the reason. If the coating of opal surfaces or the alteration by surface reactions is important for determining dissolution rates, then a sediment having a higher opal content (and lower contaminant content) should provide silica at a higher rate and, hence, show the greater depth gradient. In any case, the sites having the higher sedimentation rates appear to release silica at a lesser rate. This suggests that rapid burial is an advantage for retaining siliceous fossils in sediment.

Strontium gradients are similar for the different sites (except for being somewhat high in Site 803). Thus, recrystallization of carbonate should proceed at about the same pace in the various sites. However, this does involve the younger sediments in the sites having the higher sedimentation rates, so that one might contend that recrystallization was favored by the initial preservation of reactive carbonate in those sites. Presumably, calcium content was affected by this process. However, calcium values tend to be erratic, indicating that a number of different processes were involved when determining the patterns.

The pattern for ammonia mirrors that of sulfate, except with the opposite sign. Thus, the same factor may be responsible; that is, the availability of organic matter. The stoichiometry suggests that ammonia was being lost, presumably to uptake by clay minerals.

Magnesium gradients were influenced by basalt alteration reactions at depth and exhibit the usual negative correlation (R = 0.97) with calcium (Fig. 36). Thus, calcium concentrations likewise reflect reactions with basalt.

GRAPE Density Variations

The gamma-ray attenuation porosity evaluator (GRAPE) portion of the multisensor track (MST) unit measures the saturated bulk density of sediments in unopened cores by tracking the amount of attenuation of gamma rays aimed at the core, with a

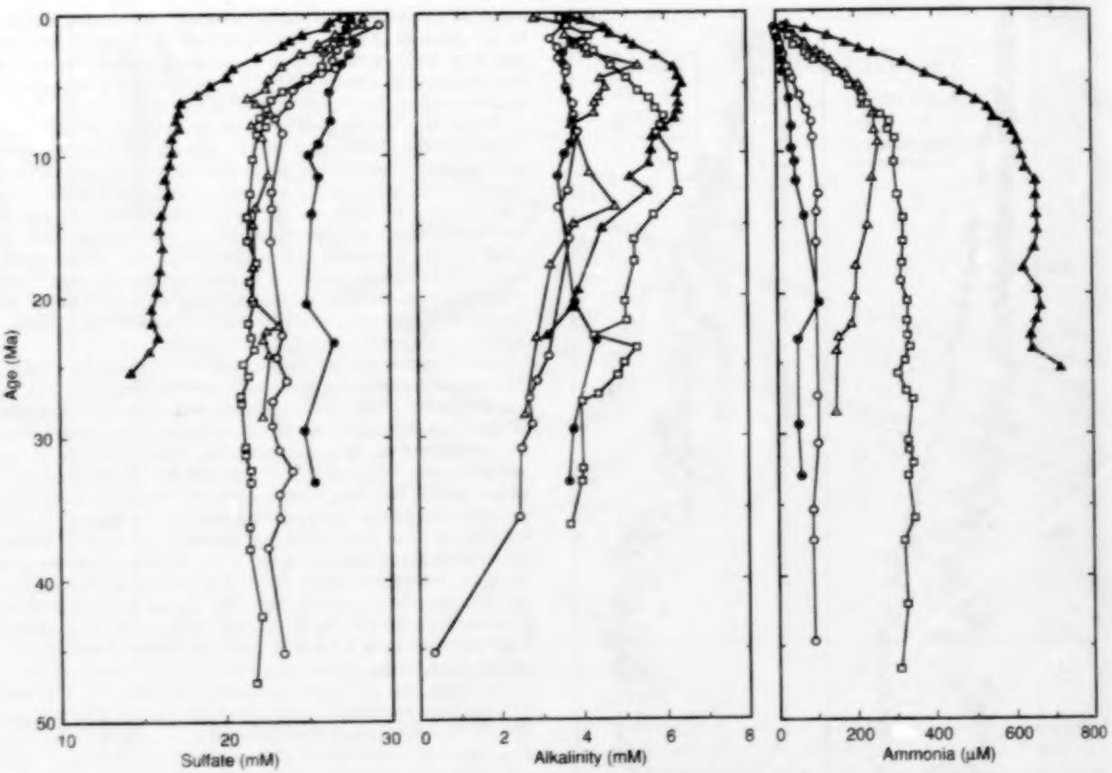

Figure 34. Dissolved sulfate, alkalinity, and ammonia in the Leg 130 sites, plotted vs. age of sediment. Data and figures from Delaney et al., this volume. Open circles = Site 803, closed circles = Site 804, open triangles = Site 805, closed triangles = Site 806, and open squares = Site 807.

sampling interval from 2 to 3 cm. Although the exact relationship of attenuation to true density is a matter of calibration, results yield a reliable index of density variations that can be used for hole-to-hole and site-to-site correlations within the APC range (Fig. 37). In addition, these data provide information about the nature of Milankovitch cycles as a function of age within the Neogene record (Jansen et al., this volume).

The extraction of Milankovitch frequencies from these records allows one to check on the time scale adopted. If the tie-points for the time scale are correct, the fluctuations should show peak power at the standard periods (eccentricity, obliquity, precession); if not, the peaks should be shifted in a systematic manner. Such a test was performed for the data from the upper 25 mbsf in Hole 806B; it gave excellent results (Fig. 38). The Pleistocene record shows the expected peaks, although the power distributions exhibit some idiosyncracies that warrant study.

SUMMARY AND OUTLOOK

Highlights

Important first results of Leg 130 include the following:

1. Recovery of complete Neogene sections at several depths that provided materials for detailed biostratigraphic and paleoceanographic studies and already has yielded new insights about the global ocean carbon cycle.
2. Acquisition of extensive logging records and high-resolution, physical properties data (including magnetic susceptibility) that permitted detailed correlation from hole to hole and from site to site and that provided the basis for interpreting acoustic reflectors, which now appear significant in a new light.
3. Recovery of two complete K/T boundary transitions, one above and one below the CCD, which raises questions about the unusual preservation of the K/T transition in this setting, especially below the CCD.
4. Deep penetration into basement and unprecedented recovery of basalt on an oceanic plateau, which opens the way for thorough investigations of the origin and early history of Ontong Java Plateau (and by analogy other oceanic plateaus).

Drilling results suggest that changes in the global ocean climate and in the carbon cycle govern productivity and preservation patterns and that these changes exceed in amplitude the effects of equatorial position and depth of deposition. In the Neogene deposits, what is reflected in the sedimentation rate patterns are changes in the entire ocean-climate system rather than regional changes. We infer this from the pronounced coherency among patterns, independent of depth or position relative to the equator. Although an erroneous age scale can produce coherency in rates artificially, we think that the errors inherent in the scale used are not large enough to create all or most of this effect. In any case, carbonate stratigraphy, which

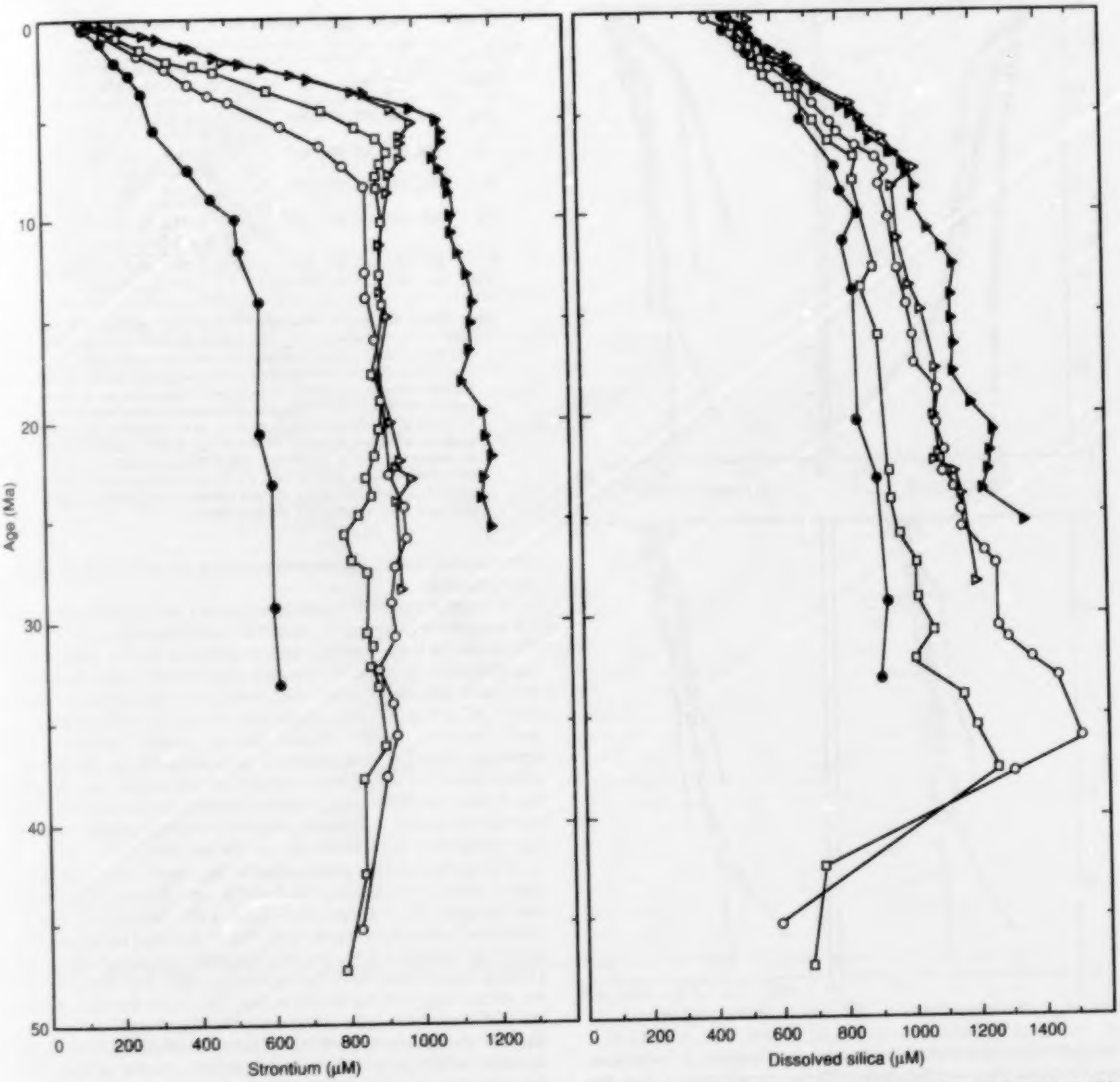

Figure 35. Concentrations of dissolved strontium and silica in the Leg 130 sites, plotted vs. age of sediment. Data and figures from Delaney et al. (this volume). See Figure 34 for an explanation of symbols used.

depends much less on the age scale, exhibits the same sort of across-depth and across-latitude coherency in greater detail.

Sedimentation rates in the Neogene were found to vary by more than a factor of 2, with a striking maximum (50–60 m/m.y.) in the latest Miocene to early Pliocene sections throughout the depth transect sampled. Fluctuations in carbonate on the million-year scale are highly coherent among depths over the last 12 Ma, but they are less so before that. A striking decline in sedimentation rate occurred at the end of the Pliocene. This decline (previously noted in Site 586 sediments higher up on the plateau by Shipboard Scientific Party, 1986) is surprising for two reasons: (1) the great increase in planetary temperature gradient in the Northern Hemisphere, which set in with the closure of the Panama Straits and the buildup of northern ice after 3.5 Ma, should have increased the trade winds and the strength of equatorial upwelling, and (2) the increased erosion of northern continents, resulting from the onset of the northern ice ages, should have delivered an increased amount of material, including calcium carbonate, thus predisposing the entire ocean system for increased sedimentation rates.

We propose that both these factors were active, but that they led (1) to a pile-up of warm water in the western equatorial Pacific, making upwelling less effective; (2) to an increase in the deposition of continental slope sediments, where increased coastal productivity and increased terrigenous influx conspired to sequester organic matter and the nutrients contained within it; and (3) to a shifting of remaining nutrients from upper waters to deep waters by increased coupling between intermediate and

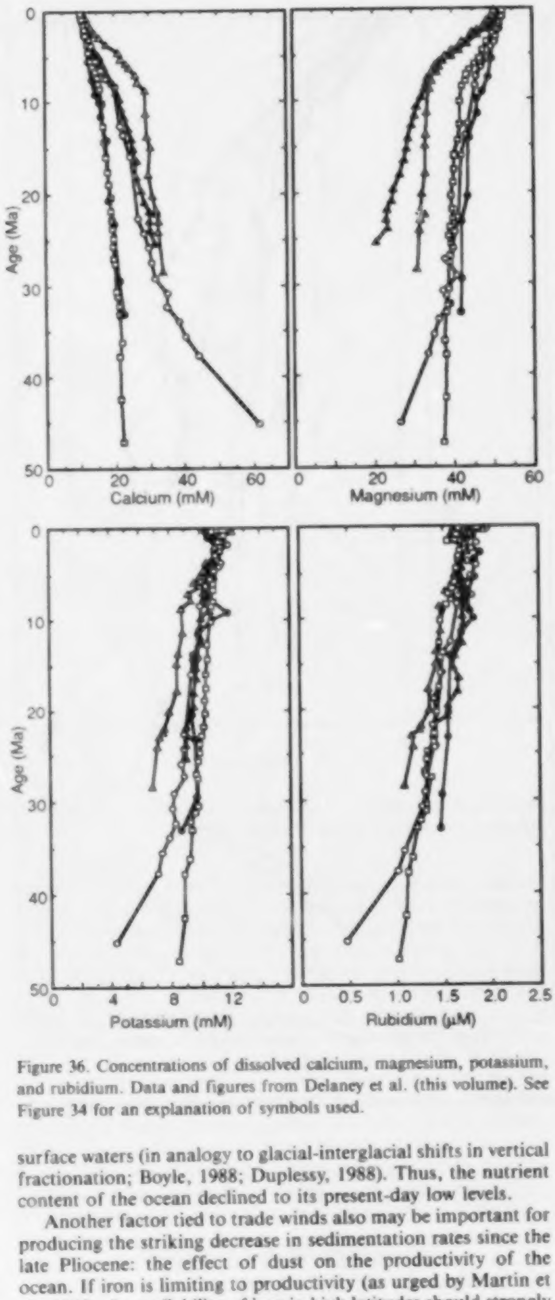

Figure 36. Concentrations of dissolved calcium, magnesium, potassium, and rubidium. Data and figures from Delaney et al. (this volume). See Figure 34 for an explanation of symbols used.

Table 6. Summary of interstitial water composition.

Type	Rank	Values in mM at 5 Ma (normalized gradient)
SO_4	806, 805, 807, 803, 804	11.0, 7.5, 6, 5.7, 3.3 (1.0, 0.88, 0.71, 1.2, 1.1)
SiO_2	806, 805, 807, 803, 804	0.85, 0.85, 0.76, 0.70, 0.70 (1.0, 1.3, 1.2, 1.9, 3.0)
Sr	806, 805, 807, 803, 804	1.06, 0.99, 0.82, 0.62, 0.3 (1.0, 1.2, 1.0, 1.4, 1.0)
Ca	805, 806, 803, 807, 804	22.5, 15.4, 15.0, 13.0, 13.0 (1.0, 0.5, 1.2, 0.6, 1.7)
SR	806, 805, 807, 803, 804	32.6, 25.2, 25.2, 14.0, 8.8 m/m.y.
WD	806, 807, 805, 803, 804	2.5, 2.8, 3.2, 3.4, 3.9 km

Notes: Shown are species measured, the rank order of sites with respect to concentrations, and the values at the 5-Ma level for each site in that same order. In parentheses are normalized concentration values, that is, indexes of the actual downhole gradients, in the late Neogene sediments. Normalization was done by dividing the concentrations at 5 Ma by the sedimentation rate, then setting the value of the first site equal to unity. If all sites have the same gradient, all values are unity. Sulfate is shown as the difference of the measured amount to 30 mM; this difference is assumed to be the sulfate consumed. The data are from the summary of inorganic chemistry (Delaney et al., this volume). Sedimentation rates (SR) and water depth (WD) are also shown.

surface waters (in analogy to glacial-interglacial shifts in vertical fractionation; Boyle, 1988; Duplessy, 1988). Thus, the nutrient content of the ocean declined to its present-day low levels.

Another factor tied to trade winds also may be important for producing the striking decrease in sedimentation rates since the late Pliocene: the effect of dust on the productivity of the ocean. If iron is limiting to productivity (as urged by Martin et al., 1990), the availability of iron in high latitudes should strongly modify the amount of preformed nutrients in intermediate waters, which would bear on tropical productivity. As the planet entered the modern ice age, some 3 m.y. ago, iron-containing dust should have become more abundant in the atmosphere, in analogy to what happens during glacial conditions (Janecek, 1985; Petit et al., 1990). Surface waters in high latitudes then might have been stripped of nutrients more efficiently, leaving intermediate waters barren and reducing the efficiency of tropical upwelling.

A large number of acoustic reflectors are synchronous and are associated in time with important paleoceanographic events. These can be traced among sites at different depths, despite being produced by different mechanisms in some cases. Extensive downhole logging provides the control for calculating the exact depth of reflectors; thus, they can be tied to biostratigraphic and lithostratigraphic datum points. Some reflectors are strongly related to diagenesis or are enhanced by diagenesis, others mark the position of hiatuses, which in turn line up with condensed sections, emphasizing the importance of carbonate dissolution pulses. Such pulses tend to occur in groups, suggesting transitional hypersensitivity of the system.

The hypothesis that paleoceanographic events ultimately dominated seismic stratigraphy on Ontong Java Plateau (Schlanger and Douglas, 1974; Berger and Mayer, 1978; Mayer et al., 1985, 1986) has been amply confirmed. The uppermost reflectors of a group of reflectors (second only to basement in strength, the Ontong Java Series) mark the time of a major reorganization of the silica budget of the ocean within the upper Eocene. As for the record of Ontong Java Plateau, this was when the world began to look "modern." Since that time, sedimentation has been uniform with regard to rates and types of material delivered: it consists of pure calcareous ooze that was delivered at a rate of almost 30 m/m.y.. Thus, some time during the late Eocene, the great geochemical fractionation machine was turned on, silica was sequestered into the margins and high latitudes, and little else except carbonate was left for the tropical pelagic ocean. From that time on, changes were mainly recorded as changes in carbonate supply, dissolution, and winnowing, and these effects (by default) became the basis for making reflectors.

The ooze-chalk transformation occurs earlier in the thicker sediment stacks at shallower water depths. Overburden, the initial condition of sediments at burial, and age are all important for controlling the rates of diagenesis. This transformation is invariably transitional and is marked by the alternation of chalk and ooze. In this zone, contrasts of density and sound velocity are enhanced and thus are favorable for the development of seemingly diachronous reflectors.

Recovery of the K/T boundary, apparently in complete sections, at Sites 803 and 807, demonstrates the presence of a deep

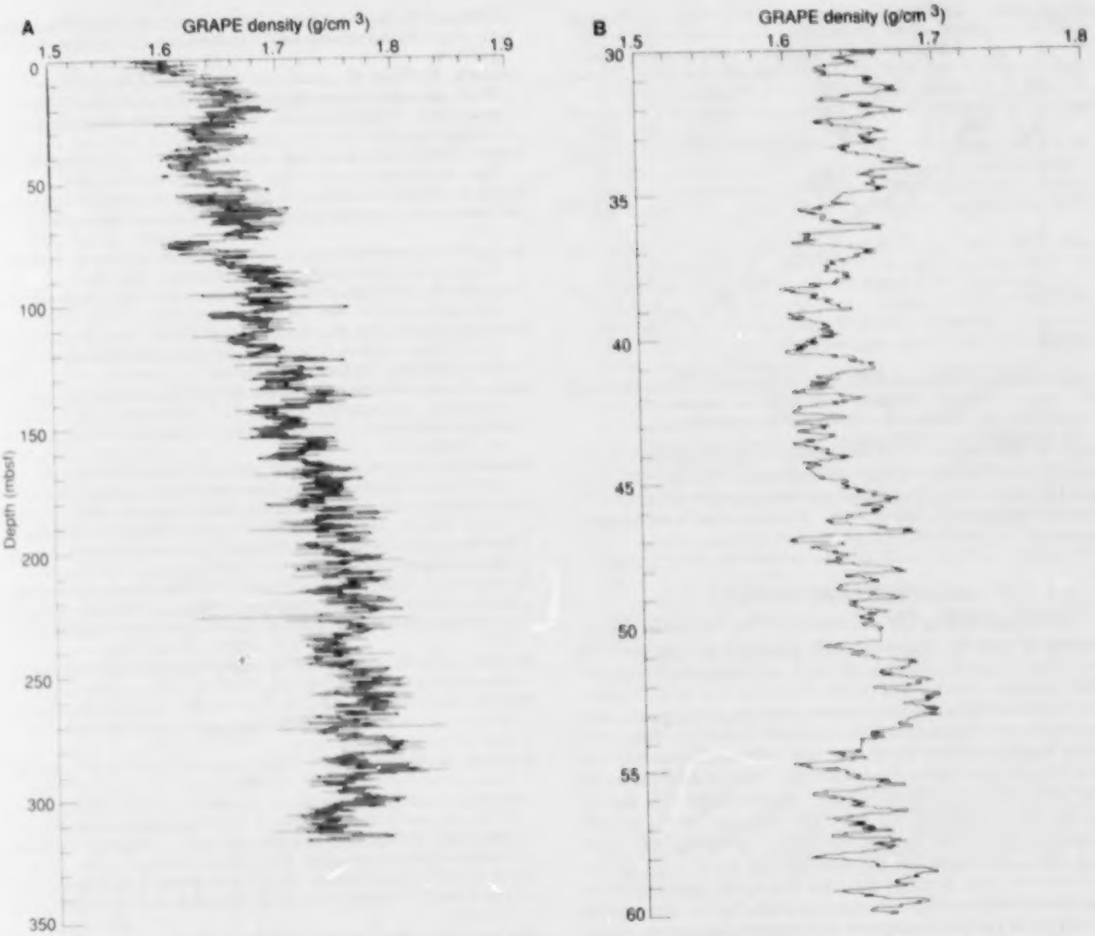

Figure 37. GRAPE density data from Hole 806B. Data are smoothed by a 10-pt Gaussian filter. Figure by Jansen et al. (this volume).

CCD across the transition: one sequence is calcareous, the other is noncalcareous. Estimating the depth of deposition at the shallower site as nearly 3 km and that of the deeper site as approximately 3.5 km brackets the position of the CCD at that time. The shallower site shows a volcanic ash layer immediately preceding the K/T boundary (as placed by microfossil content and verified by stable isotopes; R. Corfield, pers. comm., 1990). The deeper site shows evidence of volcanic activity throughout the K/T transition. This volcanism may be partly responsible for the striking fact that the K/T boundary was preserved as the only short sequence within an extensive hiatus. Alternatively or in addition, excess silica built up in deep waters because of the demise of diatoms and thus facilitated early cementation.

The basalts cored at Sites 803 and 807 (26 and 149 m penetration, respectively) are predominantly fine grained, aphyric, and olivine bearing. They represent flows that may have been erupted from submarine vents in rapid succession during the mid-Cretaceous. Late stages of eruption also are indicated as occurring after a lapse of considerable time. At Site 807, pillowed lava flows buried sediments at least twice. One thick flow (28 m) was penetrated at Site 807, indicating that flood basalts were an important element in the construction of the plateau. In fact, these flows may have been dominant in the makeup of the plateau. However, our sampling mainly recovered the products of late-stage volcanism (with numerous pillow lavas) and evidence for hydrothermal activity. The latest flows show signs of having been derived from more evolved magma. Paleolatitudes from magnetic inclinations in the basalt suggest that the Ontong Java Plateau moved coherently with the Pacific Plate since the Early Cretaceous.

Outlook

A vast array of measurements were performed on board the *JOIDES Resolution*, including extensive logging. The analysis of these data has just begun, and much additional information is expected from sedimentological, petrological, geophysical, chemical, paleontological, and isotopic studies of the material collected. The major results presented here help to define the questions that need answers and indicate the directions in which future studies might follow.

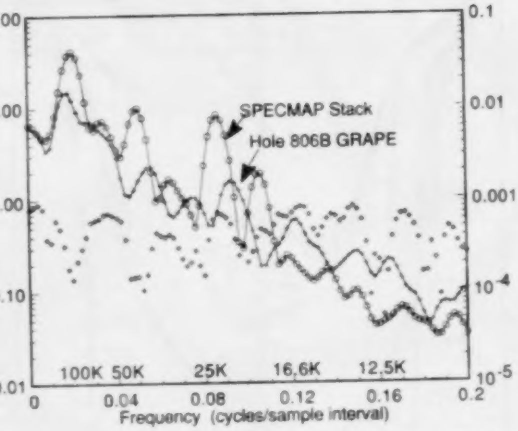

Figure 38. Spectral analysis of the smoothed GRAPE record from the upper 25 m in Hole 806B (Pleistocene), compared with the SPECMAP record of Imbrie et al. (1984). Time scale based on shipboard age model. Figure by Jansen et al. (this volume). Unconnected open diamonds = coherency.

ACKNOWLEDGMENTS

The success of Leg 130 was a result of the efforts of a great number of people, beginning with planning and preparation and culminating in drilling, recovery, sampling, and analysis. This summary of shipboard results represents one tangible product of these efforts. We thank those who worked in committee and those who surveyed the sites and helped to plan them. We thank Captain Edwin Oonk and his officers, engineers, and crew for getting us safely there and back. We are grateful to the Operations Manager, Gene Pollard, and his engineers, and to Ken Horne and his drilling crew. The alertness of the drillers during repetitive and routine operations saved the day more than once. We appreciate the alacrity and good spirit of the rigfloor crew, who saved us the time that made record recovery possible for both pelagic ooze and plateau basalt. Our special thanks go to the ODP technical and logistics personnel, whose skills and devotion were of crucial importance and who had more on their hands than what might be reasonably expected. We thank ODP staff for special efforts in onshore support. Last but not least, we are grateful to the stewards and the baker for making things comfortable on board SEDCO/BP 471, the *JOIDES Resolution*.

REFERENCES

Alvarez, L. W., Alvarez, W., Asaro, F., and Michel, H. V., 1980. Extraterrestrial cause for the Cretaceous-Tertiary extinction. *Science*, 208:1095–1108.

Arrhenius, G., 1952. Sediment cores from the east Pacific. *Rep. Swed. Deep-Sea Exped. 1947–1948*, 5:1–227.

Arthur, M. A., Dean, W. E., and Schlanger, S. O., 1985. Variations in the global carbon cycle during the Cretaceous related to climate, volcanism, and changes in atmospheric CO_2. *In* Sundquist, E. T., and Broecker, W. S. (Eds.), *The Carbon Cycle and Atmospheric CO_2: Natural Variations Archean to Present*. Am. Geophys. Union Monogr., 32:504–529.

Backman, J., 1979. Pliocene biostratigraphy of DSDP Sites 111 and 116 from the North Atlantic Ocean and the age of the Northern Hemisphere Glaciation. *Stockholm Contrib. Geol.*, 32:115–137.

Barron, J. A., and Baldauf, J. G., 1989. Tertiary cooling steps and paleoproductivity as reflected by diatoms and biosiliceous sediments. *In* Berger, W. H., Smetacek, V. S., and Werfer, G. (Eds.), *Productivity of the Oceans: Present and Past*: New York (Wiley-Interscience), 341–354.

Barron, J. A., Keller, G., and Dunn, D. A., 1985. A multiple microfossil biochronology for the Miocene. *In* Kennett, J. P. (Ed.), *The Miocene Ocean: Paleoceanography and Biogeography.* Mem. Geol. Soc. Am., 163:21–36.

Berger, W. H., 1970. Biogenous deep-sea sediments: fractionation by deep-sea circulation. *Geol. Soc. Am. Bull.*, 81:1385–1401.

Berger, W. H., and Johnson, T. C., 1976. Deep-sea carbonates: dissolution and mass wasting on Ontong Java Plateau. *Science*, 192:785–787.

Berger, W. H., and Mayer, L. A., 1978. Deep-sea carbonates: acoustic reflectors and lysocline fluctuations. *Geology*, 6:11–15.

Berger, W. H., and Roth, P. H., 1975. Oceanic micropaleontology: progress and prospects. *Rev. Geophys. Space Phys.*, 13:561–635.

Berger, W. H., Vincent, E., and Thierstein, H. R., 1981. The deep-sea record: major steps in Cenozoic ocean evolution. *Spec. Publ., Soc. Econ. Paleontol. Mineral.*, 32:489–504.

Berger, W. H., and Winterer, E. L., 1974. Plate stratigraphy and the fluctuating carbonate line. *In* Hsü, K. J., and Jenkyns, H. C. (Eds.), *Pelagic Sediments on Land and Under the Sea*. Spec. Publ., Int. Assoc. Sedimentol., 1:11–48.

Berggren, W. A., and Hollister, C. D., 1977. Plate tectonics and paleocirculation—commotion in the ocean. *Tectonophysics*, 38:11–48.

Berggren, W. A., Kent, D. V., and Van Couvering, J. A., 1985. The Neogene: Part 2, Neogene geochronology and chronostratigraphy. *In* Snelling, N. J. (Ed.), *The Chronology of the Geological Record*. Mem. Geol. Soc. (London), 10:211–260.

Bloemendal, J., Lamb, B., and King, J., 1988. Paleoenvironmental implications of rock-magnetic properties of late Quaternary sediment cores from the eastern equatorial Atlantic. *Paleoceanography*, 3:61–87.

Boyle, E. A., 1988. Vertical oceanic nutrient fractionation and glacial/interglacial CO_2 cycles. *Nature*, 331:55–56.

Bralower, T. J., and Thierstein, H. R., 1984. Low productivity and slow deep-water circulation in mid-Cretaceous oceans. *Geology*, 12:614–618.

Bramlette, M. N., 1965. Massive extinctions in biota at the end of Mesozoic time. *Science*, 148:1696–1699.

Duplessy, J. C., Shackleton, N. J., Fairbanks, R. G., Labeyrie, L., Oppo, D., and Kallel, N., 1988. Deep-water source variations during the last climatic cycle and their impact on global deep-water circulation. *Paleoceanography*, 3:343–360.

Flohn, H., 1985. *Das Problem der Klimaänderungen in Vergangenheit und Zukunft*: Wissenschaftliche Buchgesellschaft Darmstadt, BRD Germany.

Gieskes, J. M., 1981. Deep-sea drilling interstitial water studies: implications for chemical alteration of the oceanic crust, Layers I and II. *In* Warme, J. E., Douglas, R. G., and Winterer, E. L. (Eds.), *The Deep Sea Drilling Project: A Decade of Progress*. Spec. Publ., Soc. Econ. Paleontol. Mineral., 32:149–167.

Haq, B. U., Hardenbol, J., and Vail, P. R., 1987. Chronology of fluctuating sea levels since the Triassic. *Science*, 235:1156–1167.

Hussong, D. M., Wipperman, L. K., and Kroenke, L. W., 1979. The crustal structure of the Ontong Java and Manihiki oceanic plateaus. *J. Geophys. Res.*, 84:6003–6010.

Imbrie, J., Hays, J. D., Martinson, D. G., McIntyre, A., Mix, A. C., Morley, J. J., Pisias, N. G., Prell, W. L., and Shackleton, N. J., 1984. The orbital theory of Pleistocene climate: support from a revised chronology of the marine delta $\delta^{18}O$ record. *In* Berger, A., Imbrie, J., Hays, J., Kukla, G., and Saltzman, B. (Eds.), *Milankovitch and Climate* (Pt. 1): Dordrecht, The Netherlands (D. Reidel), 269–305.

Jackson, E. D., Bargar, K. E., Fabbi, B. P., and Heropoulos, C., 1976. Petrology of the basaltic rocks drilled on Leg 33 of the Deep Sea Drilling Project. *In* Schlanger, S. O., Jackson, E. D., et al., *Init. Repts. DSDP*, 33: Washington (U.S. Govt. Printing Office), 571–630.

Janecek, T. R., 1985. Eolian sedimentation in the Northwest Pacific Ocean: a preliminary examination of the data from Deep Sea Drilling Project Sites 576 and 578. *In* Heath, G. R., Burckle, L. H., et al., *Init. Repts. DSDP*, 86: Washington (U.S. Govt. Printing Office), 589–603.

Janecek, T. R., and Rea, D. K., 1983. Eolian deposition in the northeast Pacific Ocean: Cenozoic history of atmospheric circulation. *Geol. Soc. Am. Bull.*, 94:730–738.

Johnson, T. C., Hamilton, E. L., and Berger, W. H., 1977. Physical properties of calcareous ooze: control by dissolution at depth. *Mar. Geol.*, 24:259–277.

Karlin, R., and Levi, S., 1985. Geochemical and sedimentological control of the magnetic properties of hemipelagic sediments. *J. Geophys. Res.*, 90:10,373–10,392.

Keigwin, L. D., 1978. Pliocene closing of the Isthmus of Panama, based on biostratigraphic evidence from nearby Pacific and Caribbean Sea cores. *Geology*, 6:630–634.

Keller, G., and Barron, J. A., 1987. Paleodepth distribution of Neogene deep-sea hiatuses. *Paleoceanography*, 2:697–713.

Kennett, J. P., 1982. *Marine Geology*: Englewood Cliffs, NJ (Prentice Hall).

Kennett, J. P. (Ed.), 1985. *The Miocene Ocean: Paleoceanography and Biogeography.* Mem. Geol. Soc. Am., No. 163.

Kennett, J. P., McBirney, A. R., and Thunell, R. C., 1977. Episodes of Cenozoic volcanism in the circum-Pacific region. *J. Volcanol. Geotherm. Res.*, 2:145–163.

Kroenke, L., 1972. Geology of the Ontong Java Plateau. *Hawaii Inst. Geophys Rep.*, HIG 72-5.

_______, 1974. Origin of continents through development and coalescence of oceanic flood basalt plateaus. *Eos*, 55:443.

_______, 1984. Cenozoic tectonic development of the southwest Pacific. *U. N. ESCAP, CCOP/SOPAC, Tech. Bull.*, No. 6.

Kroenke, L. W., Jouannic, C., and Woodward, P. (Comps.), 1983. Bathymetry of the Southwest Pacific: Chart 1 of the Geophysical Atlas of the Southwest Pacific, CCOP/SOPAC.

Leinen, M., 1979. Biogenic silica accumulation in the central equatorial Pacific and its implications for Cenozoic paleoceanography. *Geol. Soc. Am. Bull.*, 90(Pt. 2):1310–1376.

Mahoney, J. J., 1987. An isotopic survey of Pacific oceanic plateaus: implications for their nature and origin. *In* Keating, B. H., Fryer, P., Batiza, R., and Boehlert, G. W. (Eds.), *Seamounts, Islands, and Atolls.* Am. Geophys. Union Monogr., 43:207–220.

Mammerickx, J., and Smith, S. M., 1985. *Bathymetry of the North Central Pacific*: Boulder, CO (Geological Society of America), Map and Chart Ser., No. MC-52.

Martin, J. H., Gordon, R. M., and Fitzwater, S. E., 1990. Iron in Antarctic waters. *Nature*, 345:156–158.

Mayer, L. A., Shipley, T. H., Theyer, F., Wilkens, R. W., and Winterer, E. L., 1985. Seismic modeling and paleoceanography at Deep Sea Drilling Project Site 574. *In* Mayer, L. A., Theyer, F., Thomas, E., et al., *Init. Repts. DSDP*, 85: Washington (U.S. Govt. Printing Office), 947–970.

Mayer, L. A., Shipley, T. H., and Winterer, E. L., 1986. Equatorial Pacific seismic reflectors as indicators of global oceanographic events. *Science*, 233:761–764.

McLean, D. M., 1985. Mantle degassing induced dead ocean in the Cretaceous-Tertiary transition. *In* Sundquist, E. T., and Broecker, W. S. (Eds.), *The Carbon Cycle and Atmospheric CO_2: Natural Variations Archean to Present.* Am. Geophys. Union Monogr., 32:493–503.

Miller, K. G., and Fairbanks, R. G., 1985. Oligocene to Miocene carbon isotope cycles and abyssal circulation changes. *In* Sundquist, E. J., and Broecker, W. S. (Eds.), *The Carbon Cycle and Atmospheric CO_2: Natural Variations Archean to Present.* Am. Geophys. Union Monogr., 32:469–486.

Monechi, S., 1985. Campanian to Pleistocene calcareous nannofossil stratigraphy from the northwest Pascific Ocean, Deep Sea Drilling Project Leg 86. *In* Heath, G. R., Burckle, L. H., et al., *Init. Repts. DSDP*, 86: Washington (U.S. Govt. Printing Office), 301–336.

Moore, T. C., Pisias, N. G., and Heath, G. R., 1977. Climate changes and lags in Pacific carbonate preservation, sea surface temperature and global ice volume. *In* Malahoff, A., and Anderson, N. (Eds.), *The Fate of Fossil Fuel CO_2 in the Oceans*: New York (Plenum Press), 145–165.

Petit, J. R., Mounier, L., Jouzel, J., Korotkevich, Y. S., Kotlyakov, V. I., and Lorius, C., 1990. Paleoclimatological and chronological implications of the Vostok core dust record. *Nature*, 343:56–58.

Romine, K., and Lombari, G., 1985. Evolution of Pacific circulation in the Miocene: radiolarian evidence from DSDP Site 289. *In* Kennett, J. P. (Ed.), *The Miocene Ocean: Paleoceanography and Biogeography.* Mem. Geol. Soc. Am., 163:273–290.

Sager, W. W., 1987. Late Eocene and Maastrichtian paleomagnetic poles for the Pacific plate: implications for the validity of seamount paleomagnetic data. *Tectonophysics*, 144:301–314.

Saito, T., Burckle, L. H., and Hays, J. D., 1975. Late Miocene to Pleistocene biostratigraphy of equatorial Pacific sediments. *In* Saito, T., and Burckle, L. H. (Eds.), *Late Neogene Epoch Boundaries.* Spec. Publ., Micropaleontol., 1:226–244.

Schlanger, S. O., and Douglas, R. G., 1974. The pelagic ooze-chalk-limestone transition and its implication for marine stratigraphy. *In* Hsü, K. J., and Jenkyns, H. C. (Eds.), *Pelagic Sediments: On Land and Under the Sea.* Spec. Publ., Int. Assoc. Sedimentol., 1:117–148.

Shackleton, N. J., Backman, J., Zimmerman, H., Kent, D. V., Hall, M. A., Roberts, D. G., Schnitker, D., Baldauf, J., Desprairies, A., Homrighausen, R., Huddlestun, P., Keene, J. B., Kaltenback, A. J., Krumsiek, K.A.O., Morton, A. C., Murray, J. W., and Westberg-Smith, J., 1984. Oxygen isotope calibration of the onset of ice-rafting in DSDP Site 552A: history of glaciation in the North Atlantic region. *Nature*, 307:620–623.

Shackleton, N. J., and Kennett, J. P., 1974. Paleotemperature history of the Cenozoic and the initiation of Antarctic glaciation: oxygen and carbon isotope analyses in DSDP Sites 277, 279 and 281. *In* Kennett, J. P., Houtz, R. E., et al., *Init. Repts. DSDP*, 29: Washington (U.S. Govt. Printing Office), 743–755.

Shipboard Scientific Party, 1971. Site 64. *In* Winterer, E. L., Riedel, W. R., et al., *Init. Repts. DSDP*, 7: Washington (U.S. Govt. Printing Office), 473–606.

_______, 1975a. Site 288. *In* Andrews, J. E., Packham, G., et al., *Init. Repts. DSDP*, 30: Washington (U.S. Govt. Printing Office), 175–229.

_______, 1975b. Site 289. *In* Andrews, J. E., Packham, G., et al., *Init. Repts. DSDP*, 30: Washington (U.S. Govt. Printing Office), 231–398.

_______, 1986. Site 586. *In* Moberly, R., Schlanger, S. O., et al., *Init. Repts. DSDP*, 89: Washington (U.S. Govt. Printing Office), 213–281.

Stoeser, D. B., 1975. Igneous rocks from Leg 30 of the Deep Sea Drilling Project. *In* Andrews, J. E., Packham, G., et al., *Init. Repts. DSDP*, 30: Washington (U.S. Govt. Printing Office), 401–414.

Storey, M., Mahoney, J. J., Kroenke, L. W., and Saunders, A. D., in press. Are oceanic plateaus sites of komatiite formation? *Geology.*

Theyer, F., Vincent, E., and Mayer, L. A., 1989. Sedimentation and paleoceanography of the central equatorial Pacific. *In* Winterer, E. L., Hussong, D. M., and Decker, R. W. (Eds.), *The Geology of North America* (Vol. N): *The Eastern Pacific Ocean and Hawaii*: Boulder, CO (Geological Society of America), 347–372.

Thierstein, H. R., 1979. Paleoceanographic implications of organic carbon and carbonate distribution in Mesozoic deep sea sediments. *In* Talwani, M., Hay, W., and Ryan, W.B.F. (Eds.), *Deep Drilling Results in the Atlantic Ocean*: Am. Geophys. Union, Maurice Ewing Ser., 3:249–274.

Vail, P. R., and Hardenbol, J., 1979. Sea-level changes during the Tertiary. *Oceanus*, 22:71–79.

van Andel, T. H., Heath, G. R., and Moore, T. C., Jr., 1975. Cenozoic history and paleoceanography of the central equatorial Pacific. *Mem. Geol. Soc. Am.*, 143:1–134.

van Houten, F. B., 1982. Ancient soils and ancient climates. *In* Berger, W. H., and Crowell, J. C. (Eds.), *Climate in Earth History*: Washington (National Academy Press), 112–117.

Vincent, E., and Berger, W. H., 1985. Carbon dioxide and polar cooling in the Miocene: the Monterey Hypothesis. *In* Sundquist, E., and Broecker, W. S. (Eds.), *The Carbon Cycle and Atmospheric CO_2: Natural Variations Archean to Present*: Am. Geophys. Union Monogr., 32:455–468.

Whitman, J., and Berger, W. H., in press. Pliocene-Pleistocene oxygen isotope record, Site 586, Ontong Java Plateau. *Mar. Micropaleontol.*

Woodruff, F., Savin, S. M., and Douglas, R. G., 1981. Miocene stable isotope record: a detailed deep Pacific Ocean study and its paleoclimatic implications. *Science*, 212:665–668.

Wu, G., and Berger, W. H., in press. Pleistocene $\delta^{18}O$ records from Ontong Java Plateau: effects of winnowing and dissolution. *Mar. Geol.*

Ms 130A-110

SECTION 4: SUMMARY

Kroenke, L. W., Berger, W. H., Janecek, T. R , et al., 1991
Proceedings of the Ocean Drilling Program, Initial Reports, Vol. 130

11. HIGH-RESOLUTION, WHOLE-CORE MAGNETIC SUSCEPTIBILITY DATA FROM LEG 130, ONTONG JAVA PLATEAU[1]

John A. Tarduno,[2] Larry A. Mayer,[3] Robert Musgrave,[4] and Shipboard Scientific Party[5]

ABSTRACT

High-resolution, whole-core magnetic susceptibility data, recorded at 3-cm intervals, were obtained for advanced hydraulic piston (APC) cores at Sites 805, 806, and 807 of Leg 130 on the Ontong Java Plateau. In this initial report, we present a preliminary evaluation of these data for their use in core correlations and paleoclimatic studies. The data allow detailed intrasite correlations between the offset APC cores and provide a means for intersite correlations of Pleistocene sediments. Variations in magnetic susceptibility values probably mirror variations in terrestrial influx and may act as proxy indicators of climate. Highly coherent cyclicity, representing Milankovitch orbital frequencies, is exhibited in some intervals and provides the potential to tune sedimentation rates. Postdepositional dissolution of magnetite by reduction diagenesis, which is also reflected in the magnetic susceptibility data, may be a limiting factor in these studies.

INTRODUCTION

Variations in rock magnetic parameters commonly reflect changes in terrestrial influx that can be related to environmental change (Thompson et al., 1980; Thompson and Oldfield, 1986). One of the principal goals of high-resolution magnetic susceptibility measurements during Ocean Drilling Program (ODP) Leg 130 was to determine whether the recovered sediments contained a climatically driven rock-magnetic signature. As such records commonly provide fine detail, they also provide a means of correlating the various sites as well as the offset advanced hydraulic piston (APC) cores at a single site (e.g., Bloemendal et al., 1988b).

The Ontong Java Plateau is an ideal setting to obtain a magnetic susceptibility record that reflects climatic change. The bathymetry of the plateau has produced a stable sedimentary environment that probably preserves global signals rather than the local events that have been a limiting factor in previous efforts to obtain a rock-magnetic characterization of glacial-interglacial cycles (e.g., King, 1986). The near-equatorial position of the Leg 130 sites has resulted in the accumulation of a thick Neogene sequence of calcium-carbonate-rich sediments thought to record major paleoceanographic changes by means of calcite dissolution gradients. Therefore, the influence of diamagnetic calcite is expected to be especially pronounced in these sediments.

Two other factors that are not the products of variations in terrestrial influx can also influence magnetic susceptibility (e.g., Hall et al., 1989). First, the production of magnetite in the single-domain size range by magnetotactic bacteria can be an important process in deep-sea sediments (Kirschvink and Chang, 1984; Petersen et al., 1986; Stoltz et al., 1986; Worm and Weinreich, 1988). These particles sometimes display distinctive shapes. Recent rock-magnetic experiments conducted on piston cores from the Ontong Java Plateau (Tauxe and Wu, 1990) have addressed this point. Although no magnetite with shapes characteristic of those produced by magnetotactic bacteria were observed, Tauxe and Wu (1990) did find compelling evidence for magnetite of pseudosingle domain size. The source of this magnetite could be volcanic grains as such particles were observed by transmission electron microscopy (Tauxe and Wu, 1990); however, other sources such as bacteria that produce magnetite extracellularly (Lovley et al., 1987) could not be excluded.

The second factor not directly related to terrestrial influx that can influence magnetic susceptibility measurements is post-depositional dissolution of magnetite by reduction diagenesis (Karlin, 1983; Karlin and Levi, 1983, 1985; Canfield and Berner, 1987). This process appears to be an important control on the magnetic polarity records (e.g., see "Paleomagnetics" section, "Site 805" chapter, this volume) and, as discussed below, the magnetic susceptibility records for Leg 130 sites.

INSTRUMENTATION AND METHODS

Low-field volume magnetic susceptibility measurements of whole-core sections were taken with a Bartington Instruments Magnetic Susceptibility Meter (model MS1). Anomalously high drift exhibited by an initial loop sensor resulted in the use of two substitute sensor loops with different diameters and frequencies (Table 1). We used the automated shipboard multisensor track (MST) set at 3-cm intervals and the 0.1 × range of the Bartington meter to record all the measurements discussed in this report. At the 0.1 × range, the magnetic susceptibility precision is 2×10^{-7} cgs, using an 80-mm sensor. The MST also includes measurements of *P*-wave velocity and saturated bulk density by means of the gamma-ray attenuation porosity evalua-

Table 1. Magnetic susceptibility sensor diameters and operating frequencies used during Leg 130.

Site	Cores	Sensor	Diameter (mm)	Frequency (kHz)
805A	1H-4H	MS1C	100	0.86
805C	1H-2H	MS1C	100	0.86
806A	1H-4H	MS1C	100	0.86
806A	1H-9H	MS2C	80	0.565
806B	1H-8H	MS1C	100	0.86
806C	1H-21H	MS2C	80	0.565
807A	1H-27H	MS2C	80	0.565
807B	1H-30H	MS2C	80	0.565

---

[1] Kroenke, L. W., Berger, W. H., Janecek, T. R., et al., 1991. *Proc. ODP, Init. Repts.*, 130: College Station, TX (Ocean Drilling Program).

[2] Scripps Institution of Oceanography, University of California, San Diego, La Jolla, CA 92093-0215, U.S.A.

[3] Department of Oceanography, Dalhousie University, Halifax, Nova Scotia, Canada B3H 4J1.

[4] Geology Department, The University of Tasmania, G.P.O. Box 252C, Hobart, Tasmania, 7001, Australia.

[5] Shipboard Scientific Party is as given in the list of participants preceding the contents.

tor (GRAPE). Background measurements were taken before and after the measurement of each core section. The measurement time for one 1.5-m core section, with the *P*-wave and GRAPE data also collected, was 13 min.

The data were collected on a DEC PRO 350 microcomputer and stored on floppy diskettes. After transferal to a VAX 11/750 computer, the background readings for each section were used to calculate a linear drift correction. Raw data were calibrated for a sensor diameter of 80 mm using a MnO_2 standard. The values derived from the use of the 100-mm sensor were adjusted by measuring the same standard and calculating a correction factor (2.7) relative to the 80-mm sensor. The difference in frequency between the two sensors used is negligible for the expected range of contributions to the susceptibility of Leg 130 sediments. Sensor diameter, however, could influence the resolving power of the measured data. Therefore, raw data were collected on the same interval from Hole 806A (Cores 130-806A-1H to -4H) with the two different sensors for a sensitivity comparison.

RESULTS

Volume magnetic susceptibility values from Sites 805, 806, and 807 are generally low (less than 10×10^{-6} cgs), probably reflecting a low ferrimagnetic content as well as a high diamagnetic calcium carbonate content. Nevertheless, a distinct series of variations are present in the data from Pleistocene sediments at all sites, allowing detailed correlations between offset APC cores.

Anomalously high values of magnetic susceptibility are commonly associated with sediment located 10–20 cm below or above core breaks. The origin of these magnetic susceptibility "spikes" is visible rust contamination, a common feature in some APC cores (Sager, 1986, 1988). Such contamination was not observed far from the core breaks *within* the APC cores. Artifacts in the magnetic susceptibility data caused by such contamination can easily be addressed by filtering these values in future studies.

The high-amplitude variations in magnetic susceptibility exhibit rapid decay at a sub-bottom depth that is the same in the offset APC holes of a single site but different between sites (Fig. 1, back pocket). This depth also corresponds to the level at which the intensity of magnetic remanence decays by several orders of magnitude and directional information useful for paleomagnetic polarity determinations is lost. The cause of this transition in the character of the magnetic susceptibility signal appears to be postdepositional dissolution of magnetite by reduction diagenesis (Karlin, 1983; Karlin and Levi, 1983, 1985; Canfield and Berner, 1987). Rather than being a gradual transition, the proposed dissolution manifests itself as an abrupt drop in magnetic susceptibility values, perhaps related to the point at which buffers to reduction diagenesis are exceeded. This scenario is further supported by the interstitial water geochemistry from these sites, which shows a decrease in SO_4^{-2} concentration at a depth (see the "Inorganic Geochemistry" sections of Sites 805, 806, and 807) that coincides with the drop in magnetic remanence (see the "Paleomagnetics" sections of Sites 806 and 807). The variable water depths and latitudes (and, therefore, the distance from the equatorial zone of upwelling) appear directly related to the depth at which the magnetic susceptibility data exhibit the prominent decrease.

Correlation of the paleomagnetic record cannot be continued below the abrupt drop in magnetic remanence, but correlatable variations in susceptibility are sometimes present below this depth. The magnetic susceptibility decrease, however, does lower the measured susceptibility values much closer to the precision of the sensors used in this study and therefore represents an inherent limitation of the data. The features of the magnetic susceptibility data that can be correlated at each site are summarized below.

Site 805

The limited high-resolution magnetic susceptibility data from Site 805 allow detailed correlation of Holes 805A and 805C down to 10 m below seafloor (mbsf) (Table 2 and Fig. 2, back pocket). Above 3 mbsf, the offset between the two holes is approximately 20 cm. This offset increases to 39–40 cm at 3 mbsf, presumably because of material lost in the core break in Hole 805A.

Site 806

Distinct variations in magnetic susceptibility values above 10.5 mbsf allow detailed correlations between the offset holes at Site 806 (Fig. 3, back pocket). For correlation purposes, data collected with the 80-mm Bartington MS2C sensor (Table 1) from Holes 806A and 806C were compared with each other as well as with data from Hole 806B collected using the 100-mm Bartington MS1C sensor. This comparison allows the Site 806 section to be divided into four intervals separated by core breaks (Table 3). Differences in sub-bottom depth between the cores are always less than 0.7 m. Variations within a correlated interval may reflect differential compaction (or expansion) during recovery.

An additional interval can be correlated between Holes 806A and 806C, below the prominent drop in magnetic susceptibility values in these holes at 10.48 and 10.60 mbsf, respectively. Hole 806B has higher magnetic susceptibility values within this interval, different from those observed at either Hole 806A or Hole 806C. The data for Hole 806B, however, were collected with the 100-mm sensor, which, as discussed further below, appears to have less resolution than those collected with the 80-mm sensor.

Comparison of Data from Hole 806A Using 80- and 100-mm Sensors

A comparison of the 80- and 100-mm Bartington sensors (Fig. 4, back pocket) was made using cores from Hole 806A. The records from the two sensors are nearly identical above 10.48 mbsf but differ at greater sub-bottom depths. In particular, the 100-mm sensor appears to have low- and high-frequency characteristics not observed in the data using the 80-mm sensor. When these data sets are next compared with the data collected with the 80-mm Bartington sensor on Hole 806C (Fig. 4, back pocket), it is clear that these characteristics are unique to the

Table 2. Correlation between Holes 805A and 805C based on whole-round magnetic susceptibility measurements.

Correlation	Type	Hole, Core	Depth (mbsf)	Hole, Core	Depth (mbsf)	A-C
A1	Peak	805A-1H	0.47	805C-1H	0.41	0.06
A2	Peak	805A-1H	1.28	805C-1H	1.10	0.18
A3	Peak	805A-1H	1.91	805C-1H	1.73	0.18
A4	Peak	805A-1H	2.18	805C-1H	1.97	0.21
A5	Peak	805A-1H	2.60	805C-1H	2.39	0.21
		Core break	3.00			
B1	Peak	805A-2H	3.35	805C-1H	2.96	0.39
B2	Trough	805A-2H	4.25	805C-1H	3.86	0.39
B3	Peak	805A-2H	4.43	805C-1H	4.04	0.39
B4	Peak	805A-2H	5.15	805C-1H	4.79	0.36
B5	Peak	805A-2H	5.54	805C-1H	5.21	0.33
B6	Trough	805A-2H	5.75	805C-1H	5.45	0.30
B7	Peak	805A-2H	7.04	805C-1H	6.68	0.36
B8	Trough	805A-2H	7.28	805C-1H	6.92	0.36
B9	Peak	805A-2H	7.76	805C-1H	7.40	0.36
				Core break	7.80	

Note: See Figure 2 for locations of correlative peaks and troughs.

Table 3. Correlation between Holes 806A, 806C, and 806B based upon whole-round magnetic susceptibility measurements.

Correlation	Type	Hole, Core	Depth (mbsf)	Hole, Core	Depth (mbsf)	Hole, Core	Depth (mbsf)	A-C	A-B	B-C
A1	Peak	806A-1H	0.38	806C-1H	0.47	806B-1H	0.53	−0.0	−0.15	0.06
A2	Peak	806A-1H	0.89	806C-1H	1.40	806B-1H	—	−0.15	—	
A3	Trough	806A-1H	1.07	806C-1H	1.19	806B-1H	1.25	−0.12	−0.18	0.06
A4	Peak	806A-1H	1.22	806C-1H	1.37	806B-1H	—	−0.15	—	
A5	Trough	806A-1H	1.49	806C-1H	1.49	806B-1H	1.73	0.00	−0.24	0.24
A6	Peak	806A-1H	2.18	806C-1H	2.39	806B-1H	2.36	−0.21	−0.18	−0.03
A7	Trough	806A-1H	2.33	806C-1H	2.51	806B-1H	2.66	−0.18	−0.33	0.15
A8	Peak	806A-1H	2.51	806C-1H	2.75	806B-1H	2.81	−0.24	−0.30	0.06
A9	Trough	806A-1H	2.81	806C-1H	3.11	806B-1H	3.17	−0.30	−0.36	0.06
A10	Peak	806A-1H	2.93	806C-1H	3.29	806B-1H	3.26	−0.36	−0.33	−0.03
A11	Trough	806A-1H	3.17	806C-1H	3.50	806B-1H	3.56	−0.33	−0.39	0.06
A12	Peak	806A-1H	3.44	806C-1H	3.77	806B-1H	3.92	−0.33	−0.48	0.15
A13	Peak	806A-1H	3.80	806C-1H	4.13	806B-1H	—	−0.33	—	
A14	Trough	806A-1H	4.01	806C-1H	4.49	806B-1H	—	−0.48	—	
A15	Peak	806A-1H	4.40	806C-1H	4.79	806B-1H	4.85	−0.39	−0.45	0.06
A16	Trough	806A-1H	4.49	806C-1H	5.00	806B-1H	5.06	−0.51	−0.57	0.06
A17	Trough	806A-1H	4.82	806C-1H	5.30	806B-1H	5.33	−0.48	−0.51	0.03
				Core break	5.60					
B1	Trough	806A-1H	5.42	806C-2H	5.95	806B-1H	5.93	−0.53	−0.51	−0.02
B2	Peak	806A-1H	5.48	806C-2H	6.04	806B-1H	5.96	−0.56	−0.48	−0.08
B3	Peak	806A-1H	5.84	806C-2H	6.28	806B-1H	—	−0.44	—	
						Core break	6.50			
C1	Peak	806A-1H	6.35	806C-2H	6.70	806B-2H	7.00	−0.35	−0.65	0.30
C2	Trough	806A-1H	6.56	806C-2H	7.00	806B-2H	7.21	−0.44	−0.65	0.21
C3	Peak	806A-1H	7.31	806C-2H	7.57	806B-2H	7.93	−0.26	−0.62	0.36
C4	Peak	806A-1H	7.43	806C-2H	7.72	806B-2H	8.11	−0.29	−0.68	0.39
		Core break	7.70							
D1	Peak	806A-2H	8.17	806C-2H	8.32	806B-2H	8.77	−0.15	−0.60	0.45
D2	Peak	806A-2H	8.47	806C-2H	8.68	806B-2H	9.10	−0.21	−0.63	0.42
D3	Trough	806A-2H	8.71	806C-2H	8.86	806B-2H	9.28	−0.15	−0.57	0.42
D4	Peak	806A-2H	9.40	806C-2H	9.55	806B-2H	9.97	−0.15	−0.57	0.42
D5	Peak	806A-2H	9.79	806C-2H	9.91	806B-2H	10.36	−0.12	−0.57	0.45
D6	Trough	806A-2H	10.48	806C-2H	10.60	806B-2H	10.90	−0.12	−0.42	0.30
E1	Peak	806A-2H	10.81	806C-2H	11.02			−0.21		
E2	Peak	806A-2H	11.47	806C-2H	11.59			−0.12		
E3	Peak	806A-2H	13.36	806C-2H	13.51			−0.15		
E4	Peak	806A-2H	13.78	806C-2H	13.90			−0.12		
E5	Peak	806A-2H	14.32	806C-2H	14.44			−0.12		

Note: See Figure 3 for locations of correlative peaks and troughs.

100-mm sensor. These features, which may be some combination of long-term drift and noise, suggest that magnetic susceptibility values below 2 × 10^{-6} cgs using the 100-mm sensor should be interpreted with considerable caution.

Cyclicity in the Site 806 Magnetic Susceptibility Data

Intervals in the high-resolution data from Holes 806A and 806C, below the large decrease in magnetic susceptibility, exhibit cyclic variations. These variations are especially apparent in Core 130-806A-4H (Fig. 5). To examine this cyclicity, spectral analyses were performed using the standard techniques adopted by the SPECMAP program. The result of this analysis for Core 130-806A-4H (using the 80-mm sensor) shows that the magnetic susceptibility data display a dominant period of approximately 41 k.y. (see "Sedimentation Rate" section, "Site 806" chapter, this volume, for age controls) (Fig. 6A). When this is compared to a composite profile of Pleistocene isotopic data sets representing an ice volume signal (Imbrie et al., 1984), it is clear how well these data match the 41-k.y. obliquity cycle. The lower resolution magnetic susceptibility data from the same core, collected with the 100-mm sensor, were also analyzed (Fig. 6B). As expected from our initial observations, lower frequency energy not observed in the data collected with the 80-mm sensor is present and is believed to be an artifact. Moreover, the 41-k.y. cycle is still clearly seen.

To test the apparent cyclicity in Core 130-806A-4H further, two other data sets were examined. First, magnetic susceptibility data from the equivalent core of Hole 806C (Core 130-806C-4H) were also analyzed (Fig. 7). Again, a dominant 41-k.y. cycle was observed (Fig. 8) and a cross-correlation of the data from Cores 130-806A-4H and 130-806C-4H shows the cycles to be highly coherent (Fig. 9). Second, GRAPE density data from Hole 806C were examined to see if a similar cyclicity was present in an independent data set. Again, a 41-k.y. cycle was observed together with other Milankovitch cycles (Fig. 10). The presence of the obliquity cycle in the magnetic susceptibility data suggests that the approach has potential for the tuning of sedimentation rates in the upper section at Site 806.

Site 807

Distinct variations in whole-core magnetic susceptibility data above 30 mbsf allow a detailed correlation of Holes 807A and 807B (Fig. 11, back pocket). Unlike Hole 806C, shifts in the correlated sub-bottom depths, which coincide with the core breaks, are often greater than 1 m (Fig. 12 and Table 4). Hole 807B displays higher susceptibility values between 16.0 and 24.0 mbsf than those observed at Hole 807A. Variations superimposed on these higher background values, however, correlate well with variations present in the data from Hole 807A.

Correlation of Holes 805C, 806A, and 807A

To compare the magnetic susceptibility data between sites, the data from the offset holes at a given site first must be spliced together to avoid the problem of missing a section because of gaps at the core breaks. To examine whether sites could be correlated with the whole-round magnetic susceptibility data de-

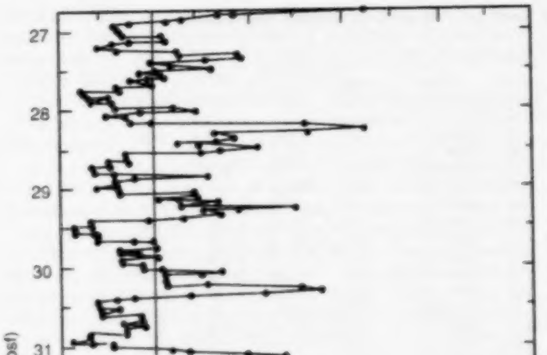

Figure 5. Whole-core volume magnetic susceptibility record from Core 130-806A-4H exhibiting cyclic variations. High values below 36.0 mbsf are probably caused by rust contamination at the core break.

scribed above, the first cores from one hole at each site were compared (Fig. 13, back pocket), avoiding the need to splice together records in this study. Each record shows a prominent drop in magnetic susceptibility values near 1.5 mbsf. Several other features appear to be common between the records, as shown in a preliminary correlation (Table 5).

SUMMARY

In this initial report, we evaluated the usefulness of the high-resolution, whole-round magnetic susceptibility data collected during Leg 130 for core correlations and paleoclimatic studies. The data appear useful for both of these applications with certain limitations. These limitations and our preliminary observations and conclusions follow.

High-resolution volume magnetic susceptibility data were collected at Sites 805, 806, and 807. Measured values decay rapidly at a sub-bottom depth that is common to the offset APC cores at a given site but different between sites. This rapid decay is probably a result of postdepositional dissolution of magnetite by reduction diagenesis (e.g., Karlin and Levi, 1983).

At sub-bottom depths shallower than the rapid drop in magnetic susceptibility, distinct fluctuations allow detailed correlation between the offset cores at a single site. The correlations record differences in compaction and expansion within single cores created during coring and recovery and provide a means of measuring gaps in recovery caused by core breaks. Correlations are sometimes possible below the prominent drop in magnetic susceptibility, but the sensitivity of the sensor used to collect the data must also be considered.

A preliminary analysis of data from Core 130-806A-4H shows that these data record at least the 41-k.y. obliquity cycle. This conclusion is supported by identifying this same cyclicity in another hole at an equivalent depth (Core 130-806C-4H) and by identifying similar cyclicity in an independent data set (i.e., the GRAPE data from Core 130-806C-4H). The interval from which these analyses were performed corresponds to the Matuyama Epoch, in which the 41-k.y. obliquity period in paleoclimatic data sets commonly dominates (Ruddiman et al., 1986a, 1986b; Henrich, 1989). The presence of orbitally driven frequencies in the magnetic susceptibility data suggest that such data have potential in tuning sedimentation rates. Furthermore, these magnetic susceptibility data may represent a near-continuous record of a paleoclimatic proxy.

It is tempting to speculate that the variations in magnetic susceptibility that can be correlated between sites are related to glacial-interglacial cycles, as observed in studies in the Atlantic (Robinson, 1986; Bloemendal et al., 1988a). A more definitive analyses of these data awaits the generation of high-resolution time scales using oxygen isotope variations. In addition, complementary rock magnetic analyses are needed to determine the probable contributors to the magnetic susceptibility signal, which may be different above and below the prominent magnetic susceptibility decrease.

ACKNOWLEDGMENTS

We thank ODP technicians Wendy Autio, Dave Cunningham, Ken du Vall, Matt Mefferd, Carie Rivers, Mark Simpson, Don Sims, Chuck Williamson, and the Leg 130 Shipboard Scientific Party for making many of the measurements described in this report.

REFERENCES

Bloemendal, J., Lamb, B., and King, J., 1988a. Paleoenvironmental implications of rock-magnetic properties of late Quaternary sediment cores from the eastern equatorial Atlantic. *Paleoceanography,* 3:61–87.

Bloemendal, J., Tauxe, L., Valet, J.-P., and Shipboard Scientific Party, 1988b. High-resolution, whole-core magnetic susceptibility logs from Leg 108. *In* Ruddiman, W., Sarnthein, M., Baldauf, J., et al., *Proc. ODP, Init. Repts.*, 108: College Station, TX (Ocean Drilling Program), 1005–1013.

Canfield, D. E., and Berner, R. A., 1987. Dissolution and pyritization of magnetite in anoxic marine sediments. *Geochim. Cosmochim. Acta,* 51:645–659.

Hall, F. R., Busch, W. H., and King, J. W., 1989. The relationship between variations in rock-magnetic properties and grain size of sediments from ODP Hole 645C. *In* Srivastava, S. P., Arthur, M., Clement, B., et al., *Proc. ODP, Sci. Results,* 105: College Station, TX (Ocean Drilling Program), 837–838.

Henrich, R., 1989. Glacial/interglacial cycles in the Norwegian Sea: sedimentology, paleoceanography, and evolution of late Pliocene to Quaternary Northern Hemisphere climate. *In* Eldholm, O., Thiede, J., Taylor, E., et al., *Proc. ODP, Sci. Results,* 104: College Station, TX (Ocean Drilling Program), 189–253.

Imbrie, J., Hays, J. D., Martinson, D. G., McIntyre, A., Mix, A. C., Morley, J. J., Pisias, N. G., Prell, W. L., and Shackleton, N. J., 1984. The orbital theory of Pleistocene climate: support from a revised chronology of the marine $\delta^{18}O$ record. *In* Berger, A. L., Imbrie, J., Hays, J., Kukla, G., and Saltzman, B. (Eds.), *Milankovitch and Climate: Understanding the Response to Astronomical Forcing* (Vol. 1): Dordrecht-Boston-Lancaster (D. Riedel Publ. Co.), 269–305.

Karlin, R., 1983. Paleomagnetism and diagenesis of hemipelagic sediments in the northeast Pacific Ocean and the Gulf of California [Ph.D. dissert.]. Oregon State Univ., Corvallis.

Karlin, R., and Levi, S., 1983. Diagenesis of magnetic minerals in recent hemipelagic sediments. *Nature,* 303:327–330.

________, 1985. Geochemical and sedimentological control of the magnetic properties of hemipelagic sediments. *J. Geophys. Res.,* 90: 10,373–10,392.

King, J. W., 1986. Paleomagnetic and rock-magnetic stratigraphy of Pigmy Basin, Deep Sea Drilling Project Site 619, Leg 96. *In* Bouma, A. H., Coleman, J. M., Meyer, A. W., et al., *Init. Repts. DSDP,* 96: Washington (U.S. Govt. Printing Office), 677–684.

Kirschvink, J. L., and Chang, S.-B. R., 1984. Ultrafine-grained magnetite in deep-sea sediments: possible bacterial magnetofossils. *Geology,* 12:559–562.

Lovley, D. R., Stolz, J. F., Nord, G. L., Jr., and Phillips, E.J.P., 1987. Anaerobic production of magnetite by a dissimilatory iron-reducing microorganism. *Nature,* 330:252–254.

Petersen, N., von Dobeneck, T., and Vali, H., 1986. Fossil bacterial magnetite in deep-sea sediments from the South Atlantic Ocean. *Nature,* 320:611–615.

Robinson, S. G., 1986. The late Pleistocene paleoclimatic record of North Atlantic deep-sea sediments revealed by mineral-magnetic measurements. *Phys. Earth Planet. Int.,* 42:22–47.

Ruddiman, W. F., McIntyre, A., and Raymo, M., 1986a. Paleoenvironmental results from North Atlantic Sites 607 and 609. *In* Ruddiman, W. F., Kidd, R. B., Thomas, E., et al., *Init. Repts. DSDP,* 94, Pt. 2: Washington (U.S. Govt. Printing Office), 855–878.

Ruddiman, W. F., Raymo, M., and McIntyre, A., 1986b. Matuyama 41,000-year cycles: North Atlantic Ocean and Northern Hemisphere ice sheets. *Earth Planet. Sci. Lett.,* 80:117–129.

Sager, W. W., 1986. Magnetic-susceptibility measurements of metal contaminants in ODP Leg 101 cores. *In* Austin, J. A., Jr., Schlager, W., Palmer, A. A., et al., *Proc. ODP, Init. Repts.,* 101: College Station, TX (Ocean Drilling Program), 39–45.

________, 1988. Paleomagnetism of Ocean Drilling Program Leg 101 sediments: magnetostratigraphy, magnetic diagenesis, and paleotides. *In* Austin, J. A., Jr., Schlager, W., Palmer, A. A., et al., *Proc. ODP, Sci. Results,* 101: College Station, TX (Ocean Drilling Program), 327–343.

Stoltz, J. F., Chang, S.-B. R., and Kirschvink, J. L., 1986. Magnetotactic bacteria and single-domain magnetite in hemipelagic sediments. *Nature,* 321:849–851.

Tauxe, L., and Wu, G., 1990. Normalized remanence in sediments of the western equatorial Pacific: relative paleointensity of the geomagnetic field? *J. Geophys. Res.,* 95:12,337–12,350.

Thompson, R., Bloemendal, J., Dearing, J. A., Oldfield, F., Rummery, T. A., Stober, J. C., and Turner, G. M., 1980. Environmental applications of magnetic measurements. *Science,* 207:481–486.

Thompson, R., and Oldfield, F., 1986. *Environmental Magnetism:* New York (Allen and Unwin).

Worm, H.-U., and Weinreich, N., 1988. Rock magnetism of pelagic sediments from the equatorial Pacific. *Earth Planet. Sci. Lett.,* 89:184–192.

Ms 130A-111

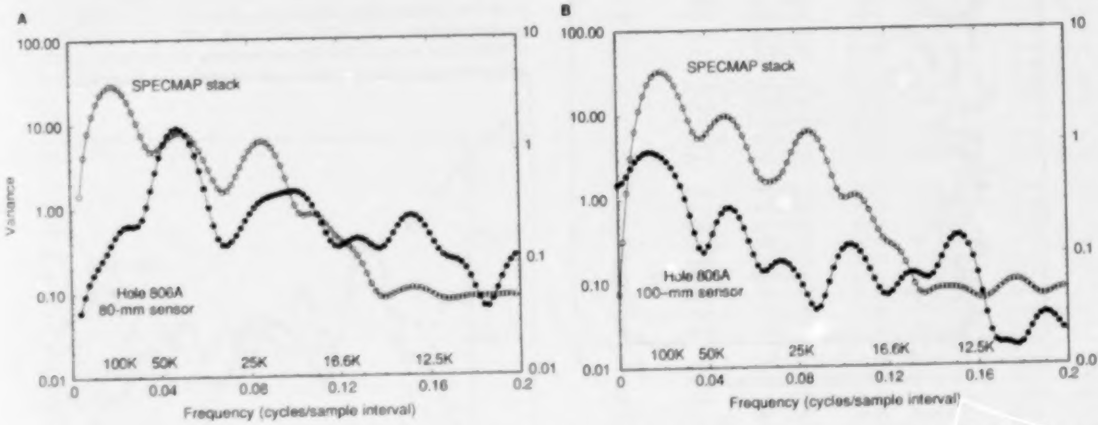

Figure 6. Spectral analysis of whole-core magnetic susceptibility data from Core 130-806A-4H between 27.0 and 36.0 mbsf using **(A)** the "high-resolution" 80-mm Bartington MS2C sensor and **(B)** the "low-resolution" 100-mm Bartington MS1C sensor. Also shown for comparison is the spectral analysis of the SPECMAP stack, which is a composite profile of Pleistocene isotopic data sets representing an ice-volume signal. Periodicity (in thousands of years) is shown above the frequency values.

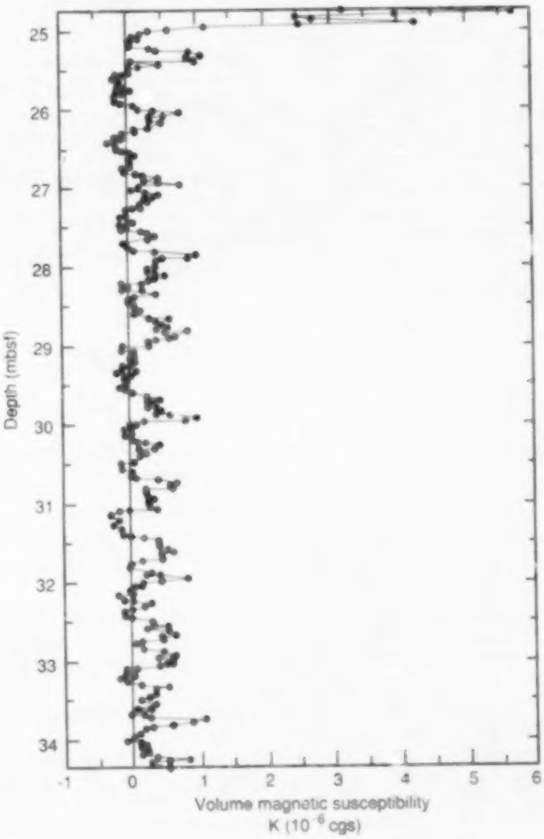

Figure 7. Whole-core magnetic susceptibility record from Core 130-806C-4H exhibiting cyclic variations similar to those observed in Core 130-806A-4H over the same range of sub-bottom depths. High values above 25.0 mbsf are probably caused by rust contamination at the core break.

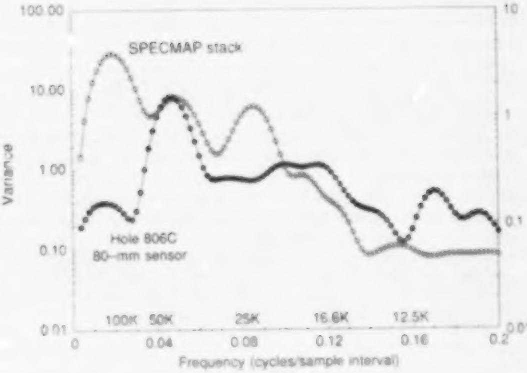

Figure 8. Spectral analyses of whole-core magnetic susceptibility data from Core 130-806C-4H between 25.0 and 34.0 mbsf using the "high-resolution" 80-mm Bartington sensor. Also shown for comparison is the spectral analysis of the SPECMAP stack, which is a composite profile of Pleistocene isotopic data sets representing an ice-volume signal. Periodicity (in thousands of years) is shown above the frequency values.

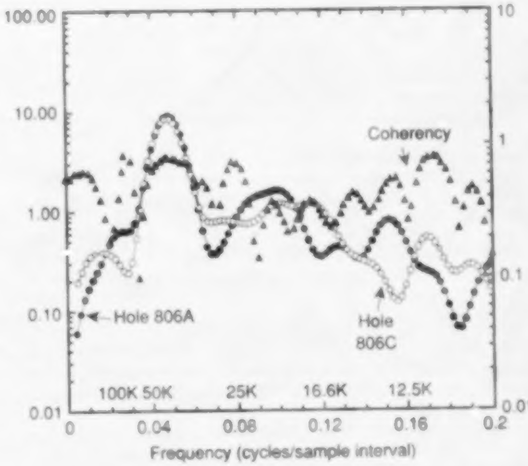

Figure 9. Cross correlation of "high-resolution" whole-core magnetic susceptibility records from Cores 130-806A-4H and 130-806C-4H. Periodicity (in thousands of years) is shown above the frequency values.

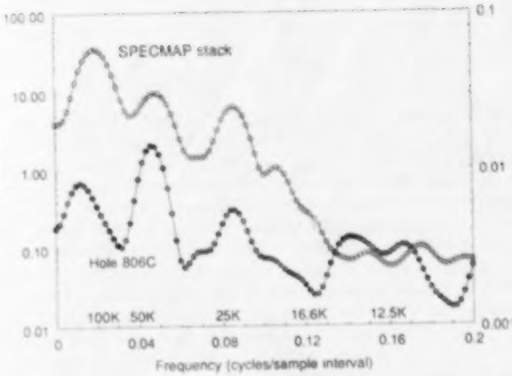

Figure 10. Spectral analyses of GRAPE data from Core 130-806C-4H between 25.0 and 34.0 mbsf. Also shown for comparison is the spectral analysis of the SPECMAP stack, which is a composite profile of Pleistocene isotopic data sets representing an ice-volume signal. Periodicity (in thousands of years) is shown above the frequency values.

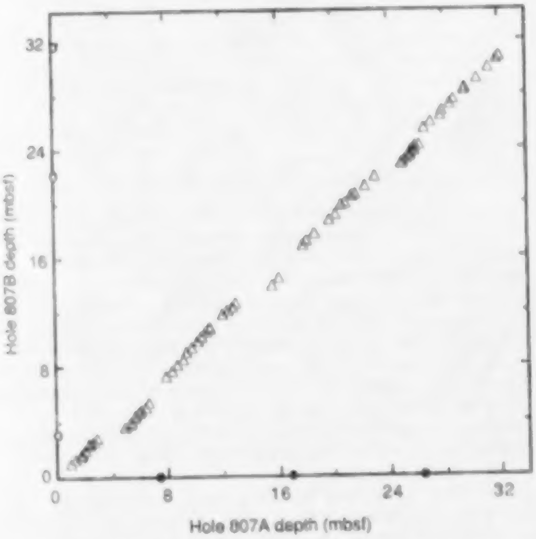

Figure 12. Correlation of Hole 807A and 807B using whole-core magnetic susceptibility data. Offsets in the correlation are caused by the loss of material at the core breaks (filled circles = Hole 807A and open circles = Hole 807B).

Table 4. Correlation between Holes 807A and 807B based upon whole-round magnetic susceptibility measurements.

Correlation	Type	Hole, Core	Depth (mbsf)	Hole, Core	Depth (mbsf)	A-B
A1	Peak	807A-1H	1.10	807B-1H	0.95	0.15
A2	Trough	807A-1H	1.43	807B-1H	1.19	0.24
A3	Trough	807A-1H	1.73	807B-1H	1.49	0.24
A4	Peak	807A-1H	1.85	807B-1H	1.67	0.18
A5	Peak	807A-1H	2.12	807B-1H	1.91	0.21
A6	Trough	807A-1H	2.39	807B-1H	2.12	0.27
A7	Peak	807A-1H	2.54	807B-1H	2.27	0.27
A8	Trough	807A-1H	2.81	807B-1H	2.54	0.27
A9	Peak	807A-1H	2.96	807B-1H	2.75	0.21
				Core break	3.10	
B1	Trough	807A-1H	4.94	807B-2H	3.54	1.40
B2	Trough	807A-1H	5.33	807B-2H	3.87	1.46
B3	Peak	807A-1H	5.48	807B-2H	3.99	1.49
B4	Trough	807A-1H	5.72	807B-2H	4.26	1.46
B5	Peak	807A-1H	5.87	807B-2H	4.44	1.43
B6	Trough	807A-1H	6.11	807B-2H	4.59	1.52
B7	Peak	807A-1H	6.20	807B-2H	4.77	1.43
B8	Peak	807A-1H	6.50	807B-2H	5.04	1.46
B9	Peak	807A-1H	6.77	807B-2H	5.28	1.49
		Core break	7.40			
C1	Peak	807A-2H	8.02	807B-2H	7.26	0.76
C2	Peak	807A-2H	8.44	807B-2H	7.71	0.73
C3	Peak	807A-2H	8.80	807B-2H	8.07	0.73
C4	Peak	807A-2H	9.22	807B-2H	8.49	0.73
C5	Peak	807A-2H	9.55	807B-2H	9.00	0.55
C6	Peak	807A-2H	9.82	807B-2H	9.24	0.58
C7	Peak	807A-2H	10.30	807B-2H	9.78	0.52
C8	Peak	807A-2H	10.63	807B-2H	10.14	0.49
C9	Peak	807A-2H	10.93	807B-2H	10.50	0.43
C10	Trough	807A-2H	11.14	807B-2H	10.65	0.49
C11	Peak	807A-2H	11.23	807B-2H	10.77	0.46
C12	Peak	807A-2H	12.13	807B-2H	11.70	0.43
C13	Peak	807A-2H	12.52	807B-2H	12.06	0.46
C14	Peak	807A-2H	12.82	807B-2H	12.30	0.52
C15	Peak	807A-2H	13.09	807B-2H	12.57	0.52
				Core break	12.60	
D1	Peak	807A-2H	15.70	807B-3H	13.82	1.88
D2	Peak	807A-2H	16.12	807B-3H	14.30	1.82
		Core break	16.90			
E1	Trough	807A-3H	18.00	807B-3H	16.79	1.21
E2	Peak	807A-3H	18.24	807B-3H	17.06	1.18
E3	Peak	807A-3H	18.84	807B-3H	17.66	1.18
E4	Trough	807A-3H	19.89	807B-3H	18.59	1.30
E5	Peak	807A-3H	20.31	807B-3H	19.04	1.27
E6	Trough	807A-3H	20.85	807B-3H	19.61	1.24
E7	Peak	807A-3H	21.09	807B-3H	19.85	1.24
E8	Trough	807A-3H	21.57	807B-3H	20.30	1.27
E9	Peak	807A-3H	21.81	807B-3H	20.54	1.27
E10	Peak	807A-3H	22.41	807B-3H	21.08	1.33
E11	Peak	807A-3H	23.13	807B-3H	21.74	1.39
				Core break	22.10	
F1	Peak	807A-3H	25.08	807B-4H	22.60	2.48
F2	Peak	807A-3H	25.26	807B-4H	22.81	2.45
F3	Peak	807A-3H	25.56	807B-4H	23.14	2.42
F4	Trough	807A-3H	25.68	807B-4H	23.23	2.45
F5	Peak	807A-3H	25.83	807B-4H	23.38	2.45
F6	Trough	807A-3H	25.89	807B-4H	23.59	2.30
F7	Peak	807A-3H	25.98	807B-4H	23.68	2.30
F8	Trough	807A-3H	26.19	807B-4H	23.83	2.36
F9	Peak	807A-3H	26.37	807B-4H	24.01	2.36
		Core break	26.40			
G1	Peak	807A-4H	26.78	807B-4H	25.21	1.57
G2	Peak	807A-4H	27.26	807B-4H	25.69	1.57
G3	Trough	807A-4H	27.89	807B-4H	26.26	1.63
G4	Peak	807A-4H	28.07	807B-4H	26.50	1.57
G5	Trough	807A-4H	28.64	807B-4H	26.98	1.66
G6	Peak	807A-4H	28.85	807B-4H	27.25	1.60
G7	Peak	807A-4H	29.60	807B-4H	28.00	1.60
G8	Trough	807A-4H	29.72	807B-4H	28.09	1.63
G9	Peak	807A-4H	30.53	807B-4H	28.84	1.69
G10	Peak	807A-4H	31.40	807B-4H	29.68	1.72
G11	Peak	807A-4H	32.12	807B-4H	30.31	1.81
G12	Trough	807A-4H	32.18	807B-4H	30.40	1.78
G13	Peak	807A-4H	32.27	807B-4H	30.46	1.81
				Core break	31.60	

Note: See Figure 11 for locations of correlative peaks and troughs.

Table 5. Correlation between Holes 807A, 805C, and 806A based upon whole-round magnetic susceptibility measurements.

Correlation	Type	Hole, Core	Depth (mbsf)	Hole, Core	Depth (mbsf)	Hole, Core	Depth (mbsf)	807-805 (m)	807-806 (m)	805-806 (m)
A1	Peak	807A-1H	0.41	805C-1H	0.41	806A-1H	0.38	0.00	0.03	0.03
A2	Peak	807A-1H	1.10	805C-1H	1.10	806A-1H	0.89	0.00	0.21	0.21
A3	Trough	807A-1H	1.43	805C-1H	1.49	806A-1H	1.49	−0.06	−0.06	0.00
A4	Peak	807A-1H	1.67	805C-1H	1.73	806A-1H	—	−0.06	—	—
A5	Trough	807A-1H	1.73	805C-1H	1.82	806A-1H	—	−0.09	—	—
A6	Peak	807A-1H	1.85	805C-1H	1.97	806A-1H	2.61	−0.12	−0.76	−0.64
A7	Peak	807A-1H	2.12	805C-1H	2.39	806A-1H	2.93	−0.27	−0.81	−0.54
A8	Trough	807A-1H	2.39	805C-1H	2.54	806A-1H	3.17	−0.15	−0.78	−0.63
A9	Peak	807A-1H	2.54	805C-1H	2.81	806A-1H	3.41	−0.27	−0.87	−0.60
A10	Peak	807A-1H	3.11	805C-1H	3.35	806A-1H	4.40	−0.24	−1.29	−1.05
A11	Peak	807A-1H	3.80	805C-1H	4.04	806A-1H	5.30	−0.24	−1.50	−1.26
A12	Peak	807A-1H	4.58	805C-1H	4.79	806A-1H	6.35	−0.21	−1.77	−1.56
A13	Trough	807A-1H	4.85	805C-1H	4.94	806A-1H	—	−0.09	—	—
A14	Peak	807A-1H	5.48	805C-1H	5.63	806A-1H	—	−0.15	—	—

Note: See Figure 13 for locations of correlative peaks and troughs.

Kroenke, L. W., Berger, W. H., Janecek, T. R , et al., 1991
Proceedings of the Ocean Drilling Program, Initial Reports, Vol. 130

12. INORGANIC GEOCHEMISTRY SUMMARY[1]

M. L. Delaney[2] and Shipboard Scientific Party[3]

INTRODUCTION

We collected a total of 129 interstitial water samples from Sites 803–807, which were drilled on the Ontong-Java Plateau during Ocean Drilling Program (ODP) Leg 130, and analyzed them on board for various dissolved constituents (see "Inorganic Geochemistry" sections in each site chapter, this volume, for detailed descriptions of the results). The sites range in water depths from 2520 to 3861 m and in latitude from 0°19.1′N to 3°36.4′N. Sediment lithology at all sites, with the exception of the deeper sections at Sites 803 and 807, is dominated by nannofossil ooze and chalk with varying abundances of foraminifers. Sedimentation rates vary systematically from site to site, with higher rates for sites at shallower water depths.

The interstitial water gradients at these sites primarily reflect the dominance of biogenic sediment, the paucity of organic carbon supply to the sediments, and the diffusive influence of basalt alteration reactions in the underlying basement. The consistent lithology from site to site with different water depths, distances from the equator, and sedimentation rates makes a comparison of interstitial water chemical gradients from site to site instructive. For the purposes of this comparison, ages were assigned to each interstitial water sample based on its depth and a linear interpolation of age from age-depth control points given in the sedimentation rate sections of the various site reports. In the following, interstitial water chemical profiles are discussed as they reflect three categories of influence on interstitial water chemistry: organic carbon oxidation reactions, biogenic sediment diagenetic reactions, and diffusive influence of basalt alteration reactions.

ORGANIC CARBON OXIDATION REACTIONS

Decreases in sulfate concentration and increases in alkalinity and ammonia concentrations with increasing sub-bottom depths at Sites 803–807 should primarily reflect organic carbon oxidation by sulfate reduction (Fig. 1). The total extent of sulfate depletion ranges over a factor of 2, with the largest total decrease at Site 806, the shallowest site (2520 m) and the closest to the equator. Sulfate depletion is similar in total extent at Sites 803, 805, and 807 (with water depths of 3410, 3188, and 2805 m, respectively), and the lowest at Site 804, the deepest site (3861 m). Sulfate reduction continues to greater sub-bottom depths at sites high on the Ontong Java Plateau, but the age at which the sulfate profile flattens is consistent from site to site because of the inverse correlation between water depth and sedimentation rate. The limited extent of sulfate depletion at all these sites indicates that the supply of organic matter reactive on these time scales limits organic carbon oxidation, not the availability of oxidant.

As is the case for sulfate depletion, the alkalinity gradient is greatest at Site 806 (Fig. 1). The site-to-site differences for alkalinity increases are more complex than the sulfate depletion patterns, however. Controls on alkalinity other than sulfate depletion, such as calcium carbonate precipitation, are important also. The ammonia maximum likewise is greatest at Site 806, intermediate in magnitude at Sites 805 and 807, and smallest at Sites 803 and 804 (Fig. 1). The ammonia increase at each site is much lower than would be predicted based solely on the stoichiometry of organic carbon oxidation, indicating the importance of exchange reactions with clays as a sink for ammonia (Gieskes, 1981).

BIOGENIC SEDIMENT DIAGENETIC REACTIONS

Dissolved silica profiles show similar increases with depth at all five sites. Apparently, these profiles are dominated by biogenic opal dissolution. The increases with age are not consistent from site to site (Fig. 2), suggesting that the controls on the dissolved silica gradients are biogenic opal solubility coupled with diffusion through the sediment-water interface, rather than varying rates of opal dissolution. The deepest samples at Site 803 and 807 show decreases in dissolved silica near or within zones of extensive silicification, superimposed on the general increase with depth.

Increases in dissolved strontium with depth and age reflect biogenic calcite recrystallization to inorganic calcite, which releases Sr to solution (Gieskes, 1981). The dissolved Sr maximum is greatest at Site 806, the shallowest site with the highest sedimentation rates; it is intermediate at Sites 803, 805, and 807, and substantially smaller at Site 804, the deepest site with the lowest sedimentation rates (Fig. 2). Generally, the Sr maximum shallows and occurs in younger sediments if sedimentation rates increase and Sr concentrations are at or near their highest values near the ooze-chalk boundary. This has been previously observed in carbonate-rich sites and ascribed to maximal recrystallization rates there (e.g., Gieskes, 1981).

BASALT ALTERATION: DIFFUSIVE INFLUENCES

The signature of basalt alteration reactions in the underlying basement is present in the profiles of calcium, magnesium, potassium, and rubidium by means of diffusion (e.g., McDuff and Gieskes, 1976; Gieskes, 1981; McDuff, 1981). Typically, the low-temperature, basalt hydrolysis reactions result in the release of Ca to solution and the uptake of Mg; in addition, these reactions typically result in the uptake from solution of the alkali elements potassium and rubidium (McDuff, 1981; Gieskes, 1981). Observed gradients should reflect the integrated flux over time from these alteration reactions and the controls on diffusion in the sediment column.

The gradients of Ca and Mg with depth and the $\Delta Ca/\Delta Mg$ ratio for each site are summarized in Table 1 and are consistent with previous observations. In ocean sediments, if a Ca gradient is present, it averages 8 mM/100 m. The estimated world ocean average gradient (i.e., including areas with thin sediment cover and no Ca depth gradients) is 4 mM/100 m (Gieskes, 1981). The $\Delta Ca/\Delta Mg$ ratios typical for sites located on basaltic basement

---

[1] Kroenke, L. W., Berger, W. H., Janecek, T. R., et al., 1991. *Proc. ODP, Init. Repts.*, 130: College Station, TX (Ocean Drilling Program).

[2] Institute of Marine Sciences, University of California, Santa Cruz, Santa Cruz, CA 95064, U.S.A.

[3] Shipboard Scientific Party is as given in the list of participants preceding the contents.

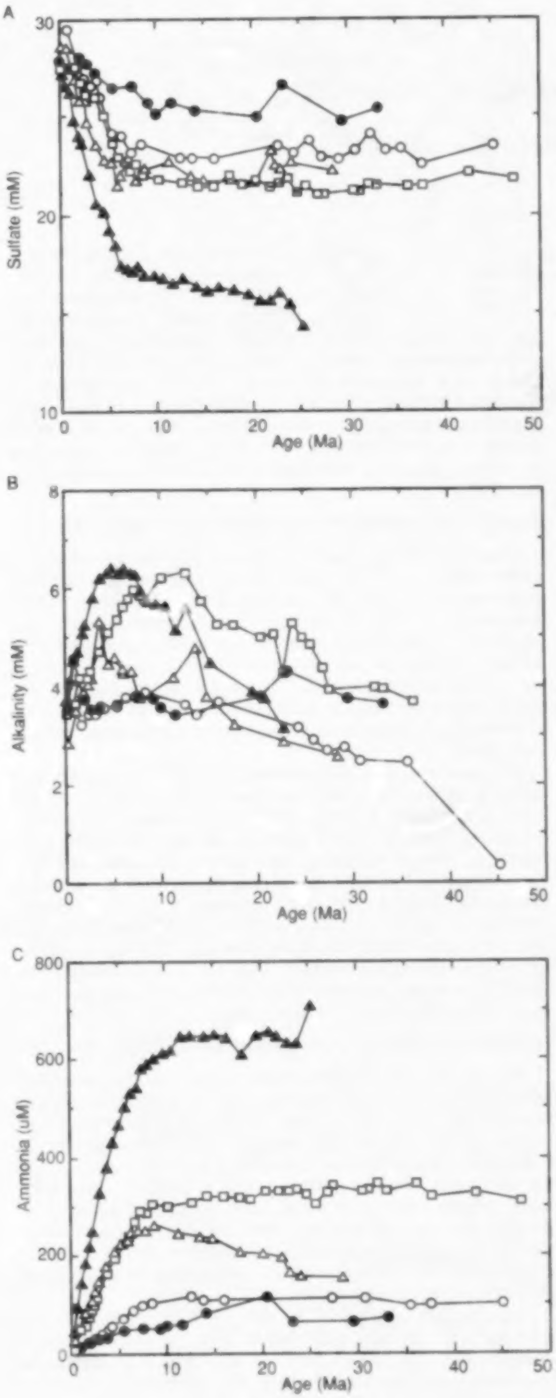

Figure 1. Interstitial water geochemical data for sulfate, alkalinity, and ammonia vs. assigned ages for Sites 803 (open circle), 804 (filled circle), 805 (open triangle), 806 (filled triangle), and 807 (square).

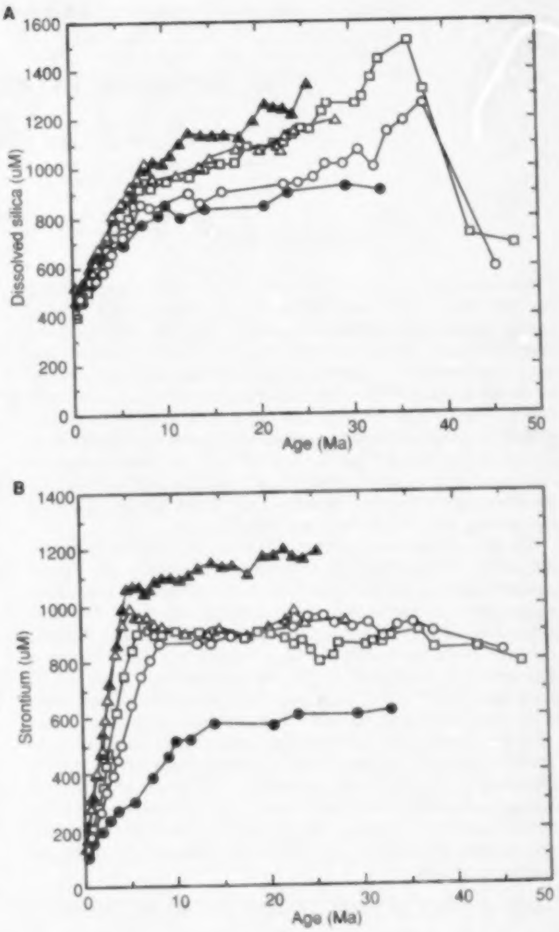

Figure 2. Interstitial water geochemical data for dissolved silica and strontium vs. assigned ages for Sites 803 (open circle), 804 (filled circle), 805 (open triangle), 806 (filled triangle), and 807 (square).

Table 1. Calcium and magnesium depth gradients and $\Delta Ca/\Delta Mg$ ratios for Sites 803-807.

Site	Ca gradient (mM/100 m)	Mg gradient (mM/100 m)	$\Delta Ca/\Delta Mg$
803	6.2	−3.5	−1.8
804	3.7	−3.8	−0.91
805	4.1	−3.4	−1.2
806	2.7	−4.2	−0.71
807	1.1	−1.4	−0.78

average −1.5, with Mg gradients leveling off in magnitude for larger Ca gradients (McDuff, 1981).

Calcium gradients with age are the smallest at Sites 804 and 807 and are the most pronounced at Site 805 (Fig. 3). Magnesium age gradients are the largest at Sites 805 and 806 and are

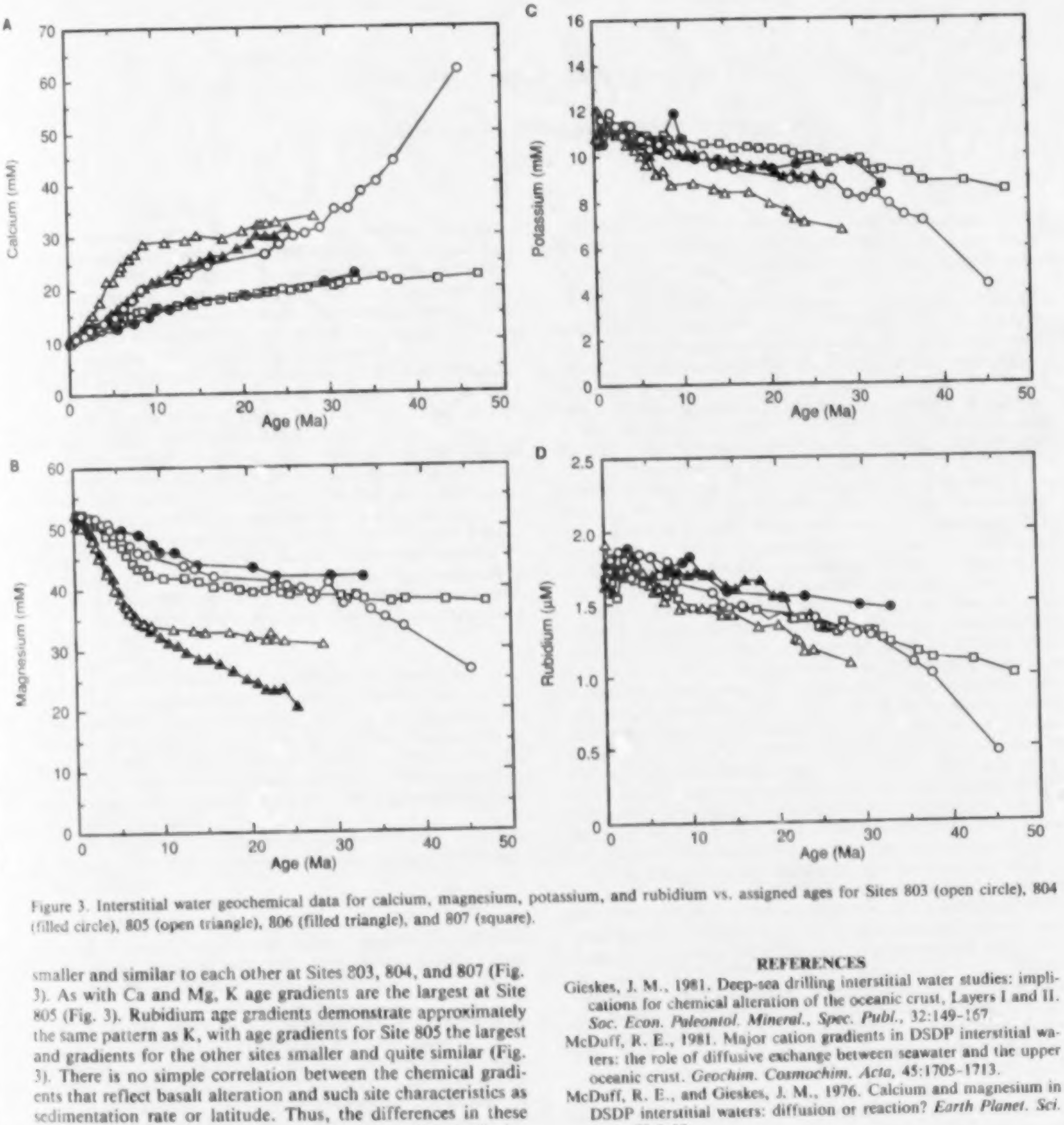

Figure 3. Interstitial water geochemical data for calcium, magnesium, potassium, and rubidium vs. assigned ages for Sites 803 (open circle), 804 (filled circle), 805 (open triangle), 806 (filled triangle), and 807 (square).

smaller and similar to each other at Sites 803, 804, and 807 (Fig. 3). As with Ca and Mg, K age gradients are the largest at Site 805 (Fig. 3). Rubidium age gradients demonstrate approximately the same pattern as K, with age gradients for Site 805 the largest and gradients for the other sites smaller and quite similar (Fig. 3). There is no simple correlation between the chemical gradients that reflect basalt alteration and such site characteristics as sedimentation rate or latitude. Thus, the differences in these gradients from site to site may reflect local variations in the intensity of basalt alteration on the plateau.

REFERENCES

Gieskes, J. M., 1981. Deep-sea drilling interstitial water studies: implications for chemical alteration of the oceanic crust, Layers I and II. *Soc. Econ. Paleontol. Mineral., Spec. Publ.*, 32:149–167.

McDuff, R. E., 1981. Major cation gradients in DSDP interstitial waters: the role of diffusive exchange between seawater and the upper oceanic crust. *Geochim. Cosmochim. Acta*, 45:1705–1713.

McDuff, R. E., and Gieskes, J. M., 1976. Calcium and magnesium in DSDP interstitial waters: diffusion or reaction? *Earth Planet. Sci. Lett.*, 33:1–10.

Ms 130A-112

Kroenke, L. W., Berger, W. H., Janecek, T. R., et al., 1991
Proceedings of the Ocean Drilling Program, Initial Reports, Vol. 130

13. GRAPE DENSITY RECORDS AND DENSITY CYCLICITY[1]

E. Jansen,[2] L. Mayer,[3] and Shipboard Scientific Party[4]

The gamma-ray attenuation porosity evaluator (GRAPE) component of the multisensor track (MST) unit on board the *JOIDES Resolution* measures the saturated bulk density of sediments by relating the attenuation of gamma rays in a core sample to that of a standard with known density (aluminum). After reaching thermal equilibrium, unsplit core sections are routinely run through the MST system. The sampling density chosen for the MST during Ocean Drilling Program (ODP) Leg 130 (about 2-3 cm) provides a near-continuous measurement of sediment density by means of the GRAPE equal to a resolution of 0.5–3 k.y., depending on the sedimentation rate.

Comparisons of GRAPE density values with discrete laboratory density measurements and downhole density logs show that absolute GRAPE density estimates are higher than both laboratory and logging density measurements; however, the downhole trends in the density data are very coherent. The constant offset between the GRAPE data and density measurements made by other means indicates that the offset is a function of the calibration of the GRAPE system. The extremely high sample resolution of the GRAPE makes it possible to use these data for a number of purposes:

1. To perform hole-to-hole correlations at a specific site, evaluating the continuity of the recovered section over core breaks. This provides a rapid method for splicing sections from one hole into missing sections in another hole or, alternatively, to evaluate possible double coring of a particular interval. GRAPE correlations can be made to depths as great as 300 m below seafloor (mbsf), well beyond the depth of useful magnetic susceptibility measurements.
2. To perform fine-scale, site-to-site correlations, especially in intervals with high signal-to-noise ratios or identifiable variability patterns.
3. To provide high-resolution records of environmental variations. Density variations in pelagic sediments are driven by changes in dissolution, winnowing, and dilution of carbonate by terrestrial material and opal; they therefore reflect paleoceanographic and paleoclimatic conditions.

The raw GRAPE data for Sites 803–807 were checked for quality, using the GRAPEFIX routine on the shipboard VAX computer system. Because of the slow passage of the section through the MST system required by magnetic susceptibility measurements, a number of GRAPE density measurements were often performed at a particular level. Multiple measurements were averaged using the program DECIMATE. This program was later transferred to and is now operative on the VAX system. The raw GRAPE data commonly display very low densities in the upper portions of a core. In most cases, these low-density intervals correspond to intervals that contain disturbed and soupy sediments or flow-in.

As a first pass, an additional set of GRAPE data files were produced in which data points that came from intervals described as disturbed by the visual core description were eliminated. This was done for the section cored with the advanced hydraulic piston corer (APC) of at least one hole at each site, and it effectively eliminates most of the apparent variance related to coring disturbance. To increase the signal-to-noise ratio further, these data were smoothed by a 10-point Gaussian filter; the smoothed data sets are displayed in Figures 1 and 2. As is seen in Figure 1, there is no clear evidence of cyclicity at the core length interval (9.5 m), indicating that most of the disturbance signal that results from core breaks has been removed. In some cases, however, the upper parts of some cores still retain anomalously low densities, probably a result of subtle coring disturbances that are not obvious to visual examination.

Despite clear hole-to-hole and site-to-site differences in the GRAPE records, the high-frequency variations in the GRAPE records indicate that there is strong potential for detailed hole-to-hole as well as site-to-site correlations. Preliminary shipboard studies based on the visual correlation of GRAPE records indicate that, in particular, the upper ~100 m of the section are the most promising for correlation as they display the highest amplitudes and have intervals with distinct variability patterns. In Figure 2, we have plotted records from Holes 806B and 807A, which roughly cover the interval from 1 to 2 Ma, based on shipboard biostratigraphy. It is evident from this example that the density variations at the two sites show essentially the same pattern over this interval, with a very regular cyclic appearance.

Using the preliminary shipboard age information, time-series analyses with the SPECMAP program package (Imbrie et al., 1984) were conducted on data from Holes 803B and 806B. These studies document that the GRAPE variance is closely concentrated in narrow frequency bands corresponding to the 100, 41, and 23 ka Milankovitch periodicities, and that the GRAPE signal is coherent with global oxygen isotope records (Imbrie et al., 1984) over the last 1 Ma at each of these frequency bands. An example of these preliminary time-series analyses is shown in Figure 3. The analysis further documents a trend of evolving 100-ka variation at the expense of 41-ka spectral power through the Pleistocene, in the same manner that has previously been documented for oxygen isotope records (Ruddiman et al., 1986). This indicates that the environmental mechanisms that govern sediment density variations are linked with the ice ages and the global climate system and are strongly influenced by orbital forcing.

Shipboard studies were limited to testing the utility of the GRAPE data, and these results need more testing and development during shore-based studies. Of prime importance is the need to arrive at a clear understanding of the specific factors that control the short-term density variations in Ontong Java Plateau sediments. In addition, the more refined and accurate time scales evolving from postcruise studies must be imple-

---

[1] Kroenke, L. W., Berger, W. H., Janecek, T. R., et al., 1991. *Proc. ODP, Init. Repts.*, 130: College Station, TX (Ocean Drilling Program).

[2] Section B, Department of Geology, University of Bergen, Allegaten 41, N-5007 Bergen, Norway.

[3] Department of Oceanography, Dalhousie University, Halifax, Nova Scotia, Canada B3H 4J1.

[4] Shipboard Scientific Party is as given in the list of participants preceding the contents.

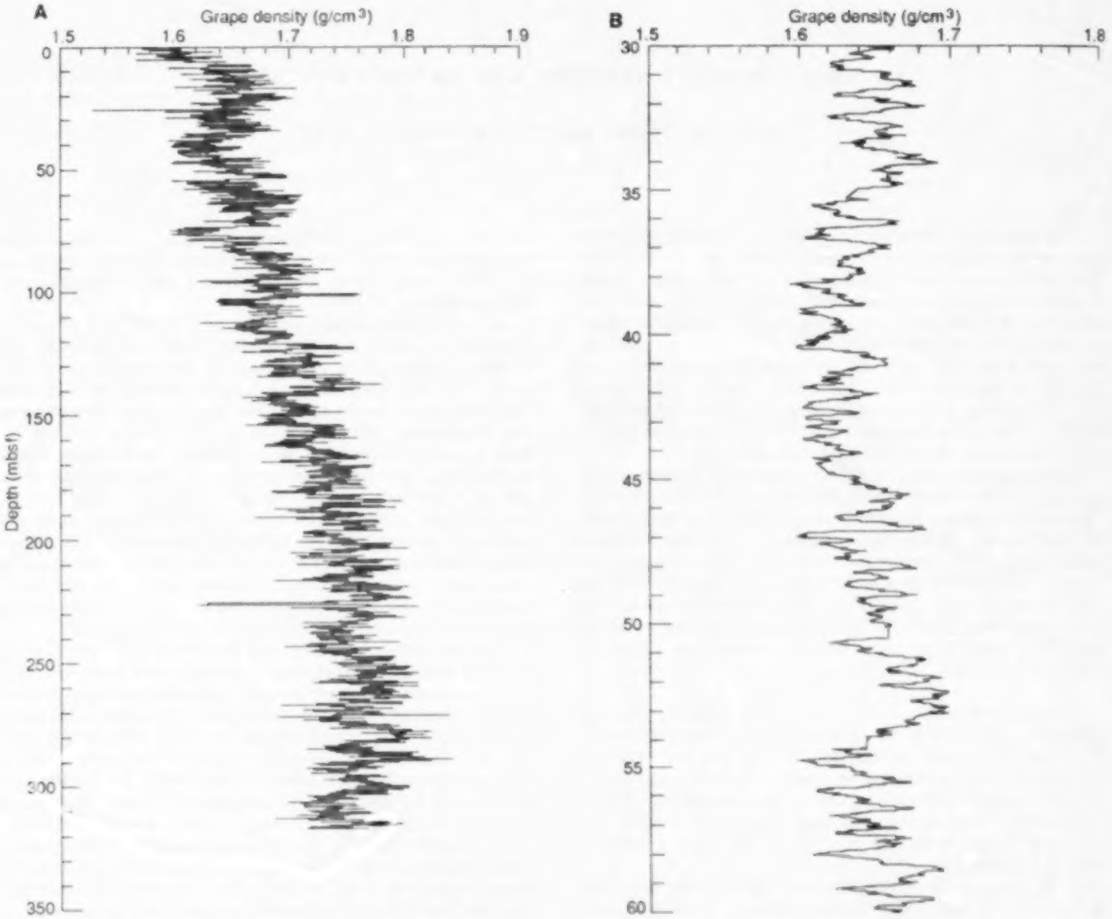

Figure 1. GRAPE density data from Hole 806B plotted vs. sub-bottom depth. **A.** The upper 350 mbsf. **B.** Blown-up section with detail of the interval from 30 to 60 mbsf. The data are smoothed by a 10-pt Gaussian filter.

mented. Shipboard work, however, has already established the large potential for extremely high-resolution records of environmental change that can be extracted from the GRAPE.

REFERENCES

Imbrie, J., Hays, J. D., Martinson, D. G., McIntyre, A., and Mix, A. C., 1984. The orbital theory of Pleistocene climate: support from a revised chronology of the marine $\delta^{18}O$ record. *In* Berger, A., Imbrie, J., Hays, J., Kukla, G., and Salzman, B. (Eds.), *Milankovitch and Climate: Understanding the Response to Astronomical Forcing* (Vol. 1): Dordrecht-Boston-Lancaster (D. Reidel Publ. Co.), 269–305.

Ruddiman, W. R., Raymo, M., and McIntyre, A., 1986. Matuyama 41,000-year cycles: North Atlantic Ocean and Northern Hemisphere ice sheets. *Earth. Planet. Sci. Lett.*, 80:117–129.

Ms 130A-113

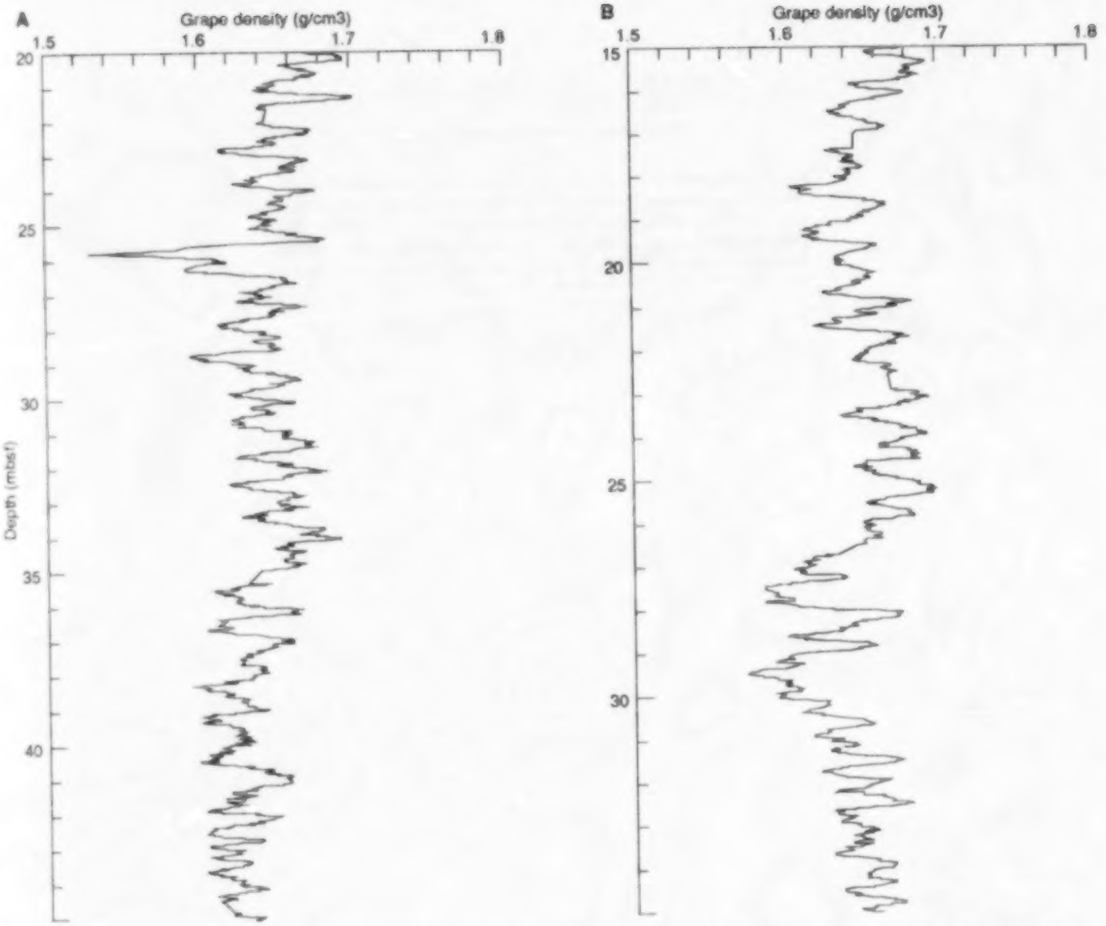

Figure 2. Smoothed GRAPE density data from Holes 806B (**A**) and 807A (**B**) plotted vs. sub-bottom depth. The selected depth intervals roughly cover the period from 1 to 2 Ma in both holes.

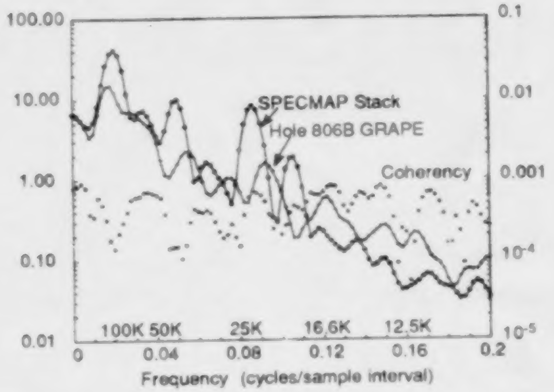

Figure 3. Example of a cross-spectral analysis of the smoothed GRAPE record from the upper 25 mbsf in Hole 806B vs. the global stack of tropical planktonic $\delta^{18}O$ (SPECMAP stack; Imbrie et al., 1984). The GRAPE data used in the analysis were sampled at a constant sampling interval of 2000 yr. The results are preliminary and are based on the shipboard age model for this hole.

SECTION 5: CORES

SITE 803 HOLE A CORE 1H CORED INTERVAL 0.0-0.8 mbsf

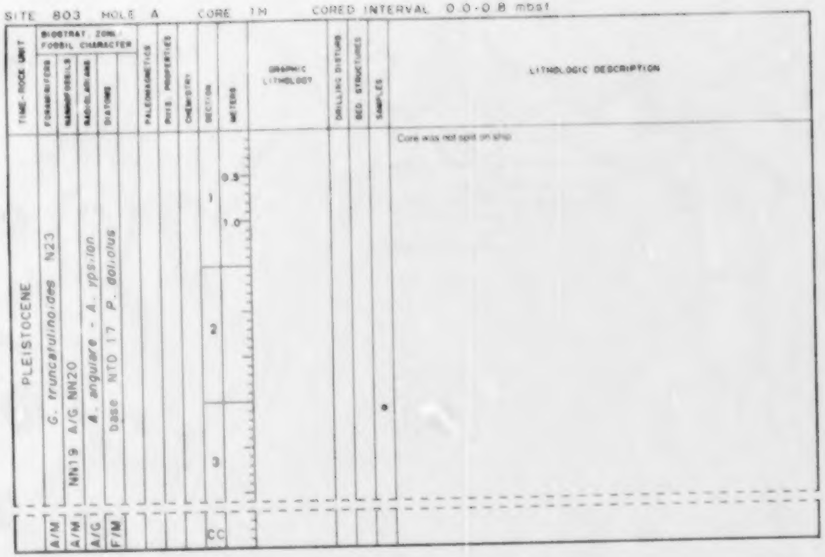
TIME-ROCK UNIT
BIOSTRAT. ZONE/ FOSSIL CHARACTER
FORAMINIFERS
NANNOFOSSILS
RADIOLARIANS
DIATOMS
PALEOMAGNETICS
PHYS. PROPERTIES
CHEMISTRY
SECTION
METERS
GRAPHIC LITHOLOGY
DRILLING DISTURB.
SED. STRUCTURES
SAMPLES
LITHOLOGIC DESCRIPTION
PLEISTOCENE
G. truncatulinoides N23
NN19 A/G NN20
A. angulare - A. ypsilon
base NTD 17 P. doliolus
A/M
A/M
A/G
F/M
1
2
3
CC
0.5
1.0
Core was not split on ship.

SITE 803 HOLE A CORE 2H CORED INTERVAL 8.0-17.5 mbsf

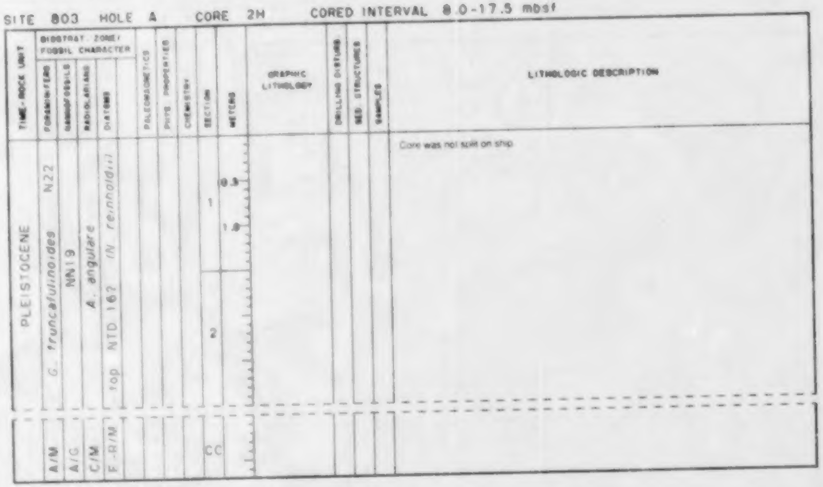
TIME-ROCK UNIT
BIOSTRAT. ZONE/ FOSSIL CHARACTER
FORAMINIFERS
NANNOFOSSILS
RADIOLARIANS
DIATOMS
PALEOMAGNETICS
PHYS. PROPERTIES
CHEMISTRY
SECTION
METERS
GRAPHIC LITHOLOGY
DRILLING DISTURB.
SED. STRUCTURES
SAMPLES
LITHOLOGIC DESCRIPTION
PLEISTOCENE
G. truncatulinoides N22
NN19
A. angulare
top NTD 16? (N. reinholdii)
A/M
A/G
C/M
F-R/M
1
2
CC
0.5
1.0
Core was not split on ship.

SITE 803 HOLE A CORE 3H CORED INTERVAL 17.5-27.0 mbsf

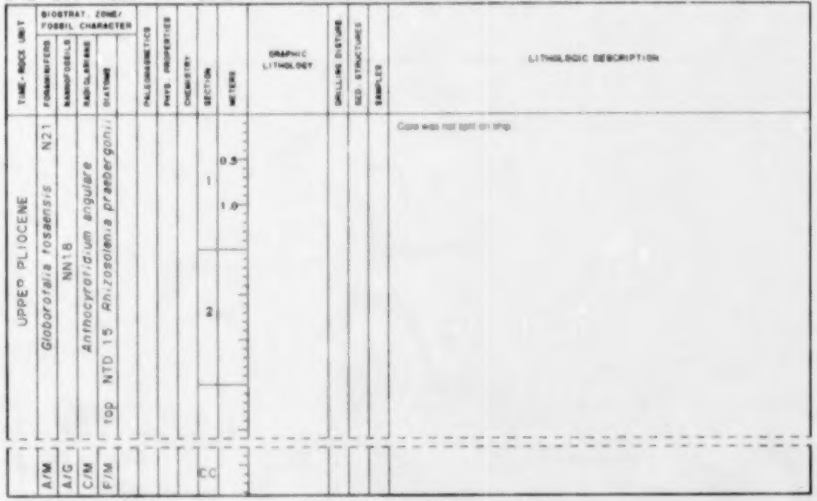
TIME-ROCK UNIT
BIOSTRAT. ZONE/ FOSSIL CHARACTER
FORAMINIFERS
NANNOFOSSILS
RADIOLARIANS
DIATOMS
PALEOMAGNETICS
PHYS. PROPERTIES
CHEMISTRY
SECTION
METERS
GRAPHIC LITHOLOGY
DRILLING DISTURB.
SED. STRUCTURES
SAMPLES
LITHOLOGIC DESCRIPTION
UPPER PLIOCENE
Globorotalia tosaensis N21
NN18
Anthocyrtidium angulare
top NTD 15 Rhizosolenia praebergonii
1
2
CC
0.5
1.0
A/M
A/G
C/M
F/M

Core was not split on ship.

SITE 803 HOLE A CORE 4H CORED INTERVAL 27.0-36.5 mbsf

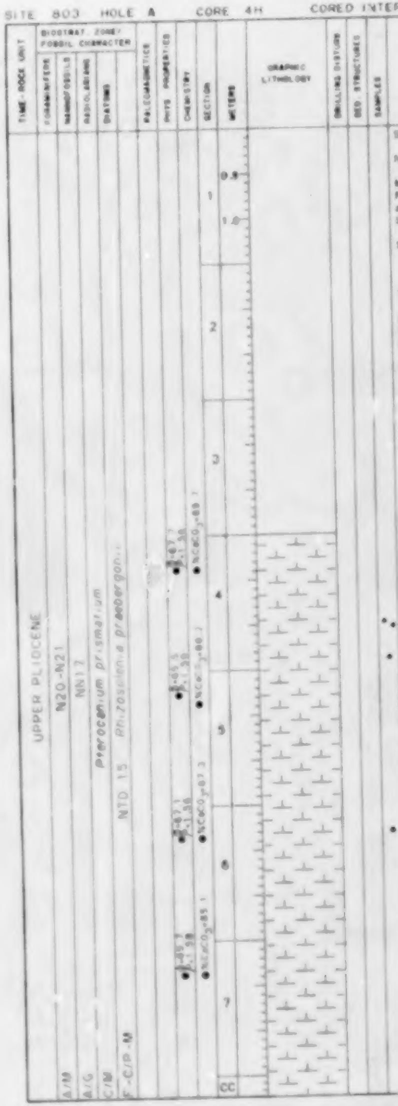
TIME-ROCK UNIT
BIOSTRAT. ZONE/ FOSSIL CHARACTER
FORAMINIFERS
NANNOFOSSILS
RADIOLARIANS
DIATOMS
PALEOMAGNETICS
PHYS. PROPERTIES
CHEMISTRY
SECTION
METERS
GRAPHIC LITHOLOGY
DRILLING DISTURB.
SED. STRUCTURES
SAMPLES
UPPER PLIOCENE
N20-N21
NN17
Pterocanium prismatium
NTD 15 Rhizosolenia praebergonii
A/M
A/G
C/M
F-C/P-M
φ-67.7
γ-1.58
%CaCO3-89.1
φ-65.5
γ-1.58
%CaCO3-90.2
φ-67.1
γ-1.56
%CaCO3-87.3
φ-65.7
γ-1.58
%CaCO3-85.1
1
0.5
1.0
2
3
4
5
6
7
CC

LITHOLOGIC DESCRIPTION

Sections 1 through 3 were not split on ship.

NANNOFOSSIL OOZE and NANNOFOSSIL OOZE with FORAMINIFERS

Major lithology: This core contains NANNOFOSSIL OOZE and NANNOFOSSIL OOZE with FORAMINIFERS. These sediment types grade from white (2.5Y N8/) to light gray (2.5Y N7/), and are slightly to heavily bioturbated. Faint pale green (5G 6/2) color banding occurs in Sections 4 and 5.

SMEAR SLIDE SUMMARY (%):

	4, 101 M	4, 102 M	4, 140 D	6, 30 D
TEXTURE:				
Sand	5	5	—	5
Silt	15	15	5	20
Clay	80	80	95	75
COMPOSITION:				
Foraminifers	10	10	5	20
Nannofossils	90	90	95	80

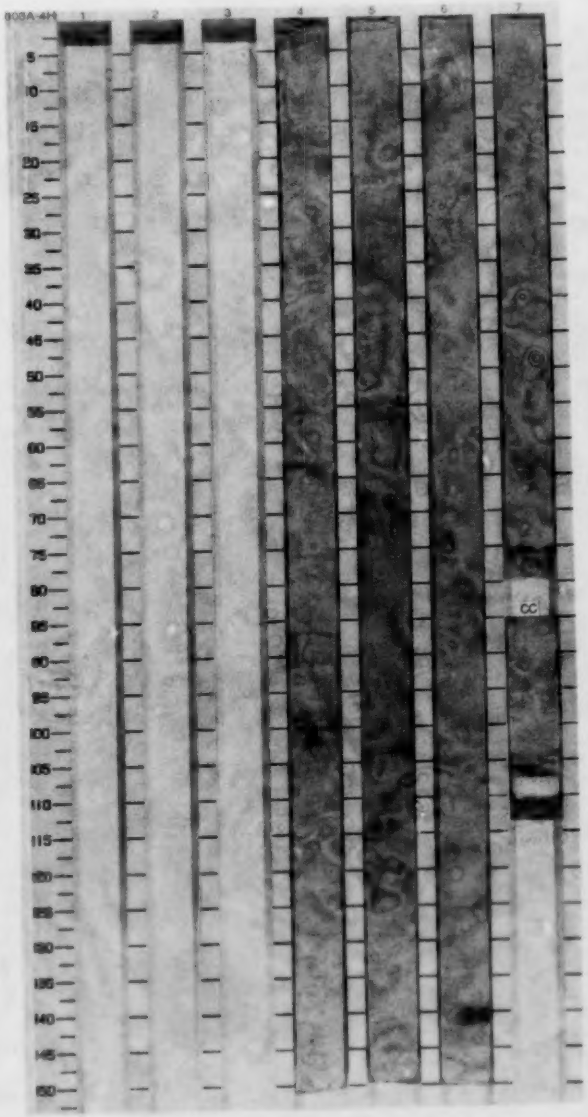
803A-4H
1
2
3
4
5
6
7
CC
5
10
15
20
25
30
35
40
45
50
55
60
65
70
75
80
85
90
95
100
105
110
115
120
125
130
135
140
145
150

SITE 803 HOLE A CORE 5H CORED INTERVAL 36.5-46.0 mbsf

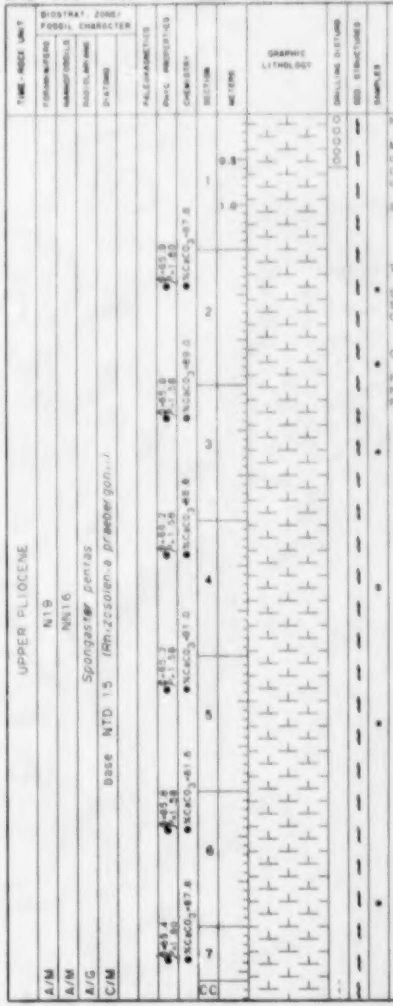
TIME-ROCK UNIT
BIOSTRAT. ZONE/ FOSSIL CHARACTER
FORAMINIFERS
NANNOFOSSILS
RADIOLARIANS
DIATOMS
PALEOMAGNETICS
PHYS. PROPERTIES
CHEMISTRY
SECTION
METERS
GRAPHIC LITHOLOGY
DRILLING DISTURB.
SED. STRUCTURES
SAMPLES
UPPER PLIOCENE
A/M N19
A/M NN16
A/G Spongaster pentas
C/M base NTD 15 (Rhizosolenia praebergonii)
φ-65.9 ρ-1.60
%CaCO₃-87.8
φ-65.0 ρ-1.58
%CaCO₃-89.0
φ-66.2 ρ-1.56
%CaCO₃-88.8
φ-65.3 ρ-1.58
%CaCO₃-81.0
φ-65.8 ρ-1.58
%CaCO₃-81.6
φ-65.4 ρ-1.60
%CaCO₃-87.8
1
2
3
4
5
6
7
CC
0.5
1.0

LITHOLOGIC DESCRIPTION

NANNOFOSSIL OOZE

Major lithology: This core contains slightly to heavily bioturbated NANNOFOSSIL OOZE. Faint color banding is present throughout the core. The primary color of the sediments is white (2.5Y 8/0) to gray (2.5Y 7/0). Color ranges from greenish (10Y 8/1) to purplish (10Y 7/2) in the color bands.

SMEAR SLIDE SUMMARY (%)

	2, 45 D	2, 128 D	3, 75 D	4, 75 D	5, 75 D	6, 125 D
TEXTURE:						
Sand	3	5	1	2	5	5
Silt	3	25	5	3	5	5
Clay	94	70	94	95	90	90
COMPOSITION:						
Foraminifers	5	5	5	5	10	9
Nannofossils	95	95	95	95	90	90
Radiolarians	—	—	—	—	—	1

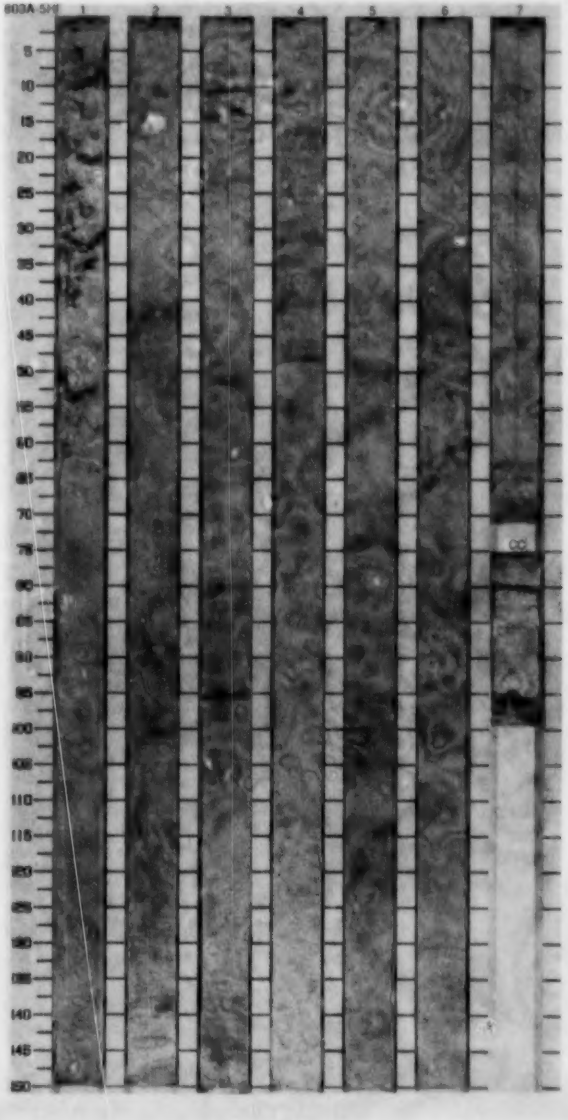
803A-5H
1
2
3
4
5
6
7
CC
5
10
15
20
25
30
35
40
45
50
55
60
65
70
75
80
85
90
95
100
105
110
115
120
125
130
135
140
145
150

SITE 803 HOLE A CORE 6H CORED INTERVAL 46.0-55.5 mbsf

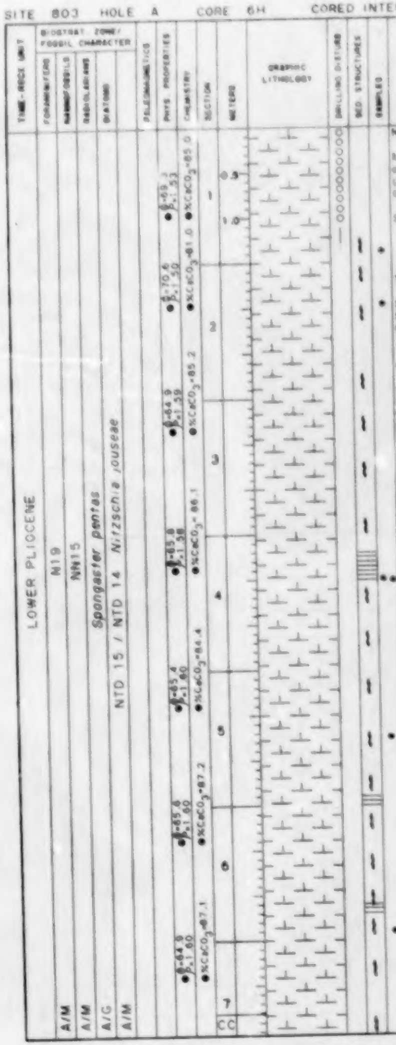
TIME-ROCK UNIT
BIOSTRAT. ZONE/ FOSSIL CHARACTER
FORAMINIFERS
NANNOFOSSILS
RADIOLARIANS
DIATOMS
PALEOMAGNETICS
PHYS. PROPERTIES
CHEMISTRY
SECTION
METERS
GRAPHIC LITHOLOGY
DRILLING DISTURB.
SED. STRUCTURES
SAMPLES
LOWER PLIOCENE
N19
NN15
Spongaster pentas
NTD 15 / NTD 14 Nitzschia jouseae
A/M
A/M
A/G
A/M
φ-69.3 γ-1.53
φ-70.6 γ-1.50
φ-64.9 γ-1.59
φ-65.8 γ-1.58
φ-65.4 γ-1.60
φ-65.6 γ-1.60
φ-64.9 γ-1.60
%CaCO₃-85.0
%CaCO₃-81.0
%CaCO₃-85.2
%CaCO₃-86.1
%CaCO₃-84.4
%CaCO₃-87.2
%CaCO₃-87.1
1
2
3
4
5
6
7
CC
0.5
1.0

LITHOLOGIC DESCRIPTION

NANNOFOSSIL OOZE

Major lithology: This core contains slightly to heavily bioturbated NANNOFOSSIL OOZE. Faint color banding is present throughout the core. The primary color of the sediments is white (2.5Y 8/0) to gray (2.5Y 7/0). Color ranges from olive green (10Y 6/2) to gray-purplish (2.5Y 6/1) in the color bands.

SMEAR SLIDE SUMMARY (%)

	1, 138 D	2, 47 D	4, 49 M	4, 99 D	5, 75 D	6, 140 D
TEXTURE						
Sand	1	1	3	5	3	3
Silt	20	5	5	20	20	20
Clay	79	94	92	75	77	77
COMPOSITION						
Foraminifers	4	5	7	10	15	15
Nannofossils	94	94	92	89	84	80
Radiolarians	—	1	1	1	1	1
Silicoflagellates	1	—	—	—	—	—
Spicules	1	—	—	—	Tr	—

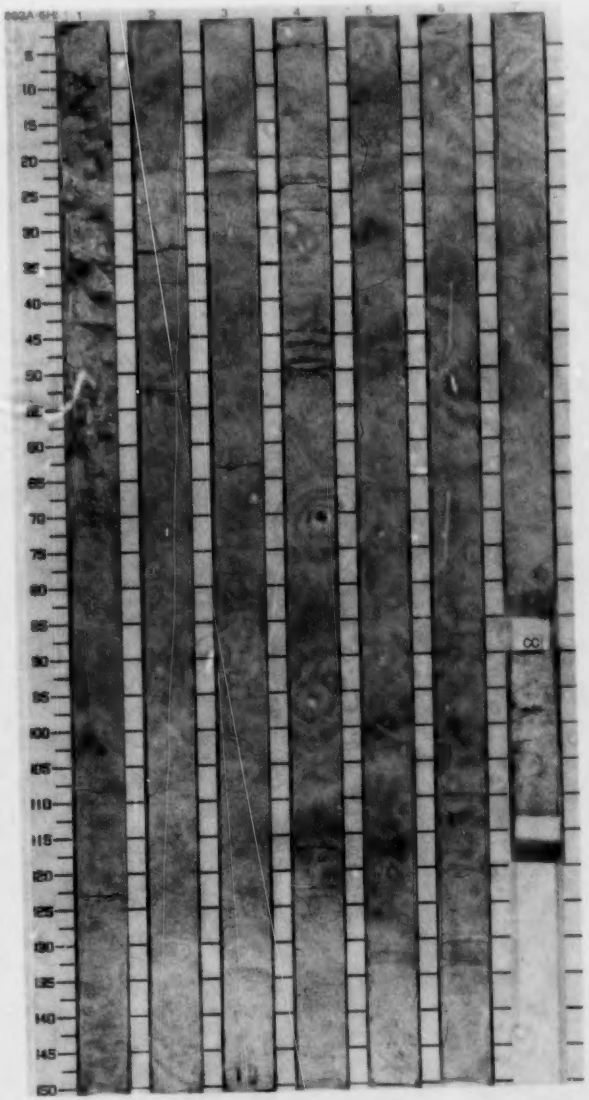
803A-6H
1
2
3
4
5
6
7
CC
5
10
15
20
25
30
35
40
45
50
55
60
65
70
75
80
85
90
95
100
105
110
115
120
125
130
135
140
145
150

SITE 803 HOLE B CORE 1H CORED INTERVAL 0.0-4.3 mbsf

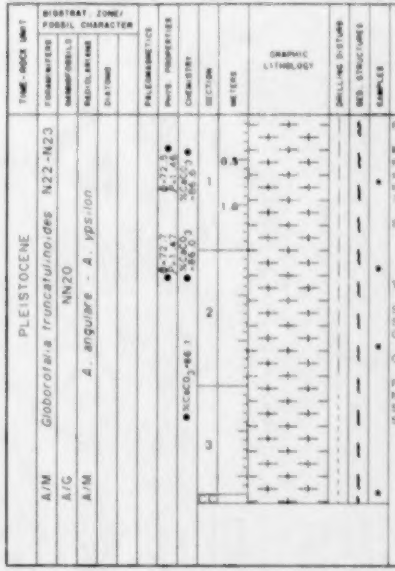
TIME-ROCK UNIT
BIOSTRAT. ZONE/ FOSSIL CHARACTER
FORAMINIFERS
NANNOFOSSILS
RADIOLARIANS
DIATOMS
PALEOMAGNETICS
PHYS. PROPERTIES
CHEMISTRY
SECTION
METERS
GRAPHIC LITHOLOGY
DRILLING DISTURB.
SED. STRUCTURES
SAMPLES
PLEISTOCENE
A/M Globorotalia truncatulinoides N22-N23
A/G NN20
A/M A. angulare - A. ypsilon
ϕ=72.5
γ=1.46
ϕ=72.7
γ=1.47
%CaCO3=86.3
%CaCO3=86.0
%CaCO3=86.1
1
2
3
CC
0.5
1.0

LITHOLOGIC DESCRIPTION

FORAMINIFER NANNOFOSSIL OOZE

Major lithology: This core contains FORAMINIFER NANNOFOSSIL OOZE, with about 25% of the constituents being foraminifers and the remaining majority consisting of nannofossils. The sequence is homogeneous and barren of any structures except mottles, which are attributed to bioturbation. The color of the sediments is pale brown (10YR 6/3) to very pale brown (10YR 7/3 and 10YR 8/3).

SMEAR SLIDE SUMMARY (%):

	1, 75 D	2, 20 D	2, 105 D	3, 118 D
TEXTURE:				
Sand	5	1		2
Silt	40	45	10	39
Clay	55	54	10	59
COMPOSITION:				
Foraminifers	30	10	30	25
Nannofossils	67	86	67	73
Silicoflagellates	1	1	1	1
Spicules	1	1	1	1

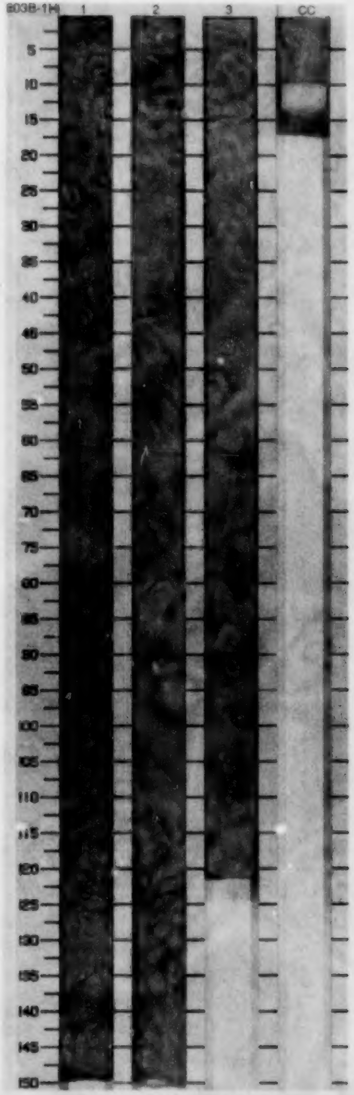
803B-1H
1
2
3
CC
5
10
15
20
25
30
35
40
45
50
55
60
65
70
75
80
85
90
95
100
105
110
115
120
125
130
135
140
145
150

SITE 803 HOLE B CORE 2H CORED INTERVAL 4.3-13.8 mbsf

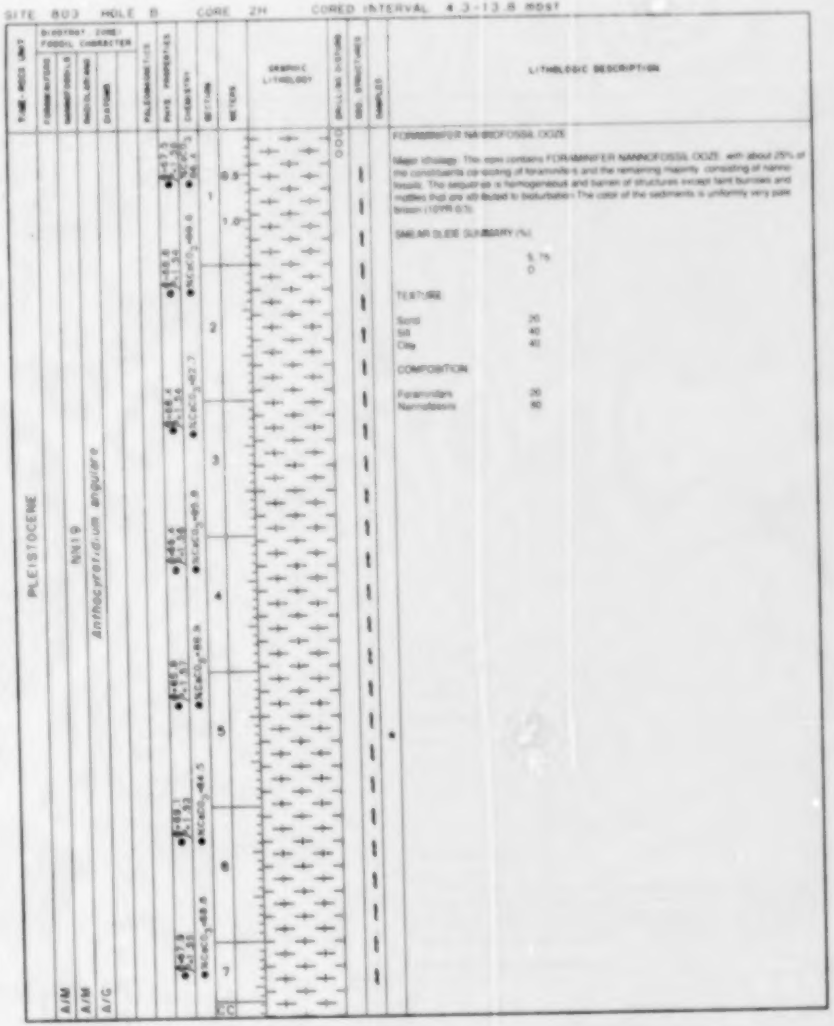
TIME-ROCK UNIT
BIOSTRAT. ZONE/FOSSIL CHARACTER
FORAMINIFERS
NANNOFOSSILS
RADIOLARIANS
DIATOMS
PALEOMAGNETICS
PHYS. PROPERTIES
CHEMISTRY
SECTION
METERS
GRAPHIC LITHOLOGY
DRILLING DISTURB.
SED. STRUCTURES
SAMPLES
LITHOLOGIC DESCRIPTION
PLEISTOCENE
A/M
NN19
A/M
Anthocyrtidium angulare
A/G
0.5
1.0
1
2
3
4
5
6
7
CC

FORAMINIFER NANNOFOSSIL OOZE

Major lithology: The core contains FORAMINIFER NANNOFOSSIL OOZE, with about 25% of the constituents consisting of foraminifers and the remaining majority consisting of nannofossils. The sequence is homogeneous and barren of structures except faint burrows and mottles that are attributed to bioturbation. The color of the sediments is uniformly very pale brown (10YR 8/3).

SMEAR SLIDE SUMMARY (%):

	5, 75
	D
TEXTURE	
Sand	20
Silt	40
Clay	40
COMPOSITION	
Foraminifers	20
Nannofossils	80

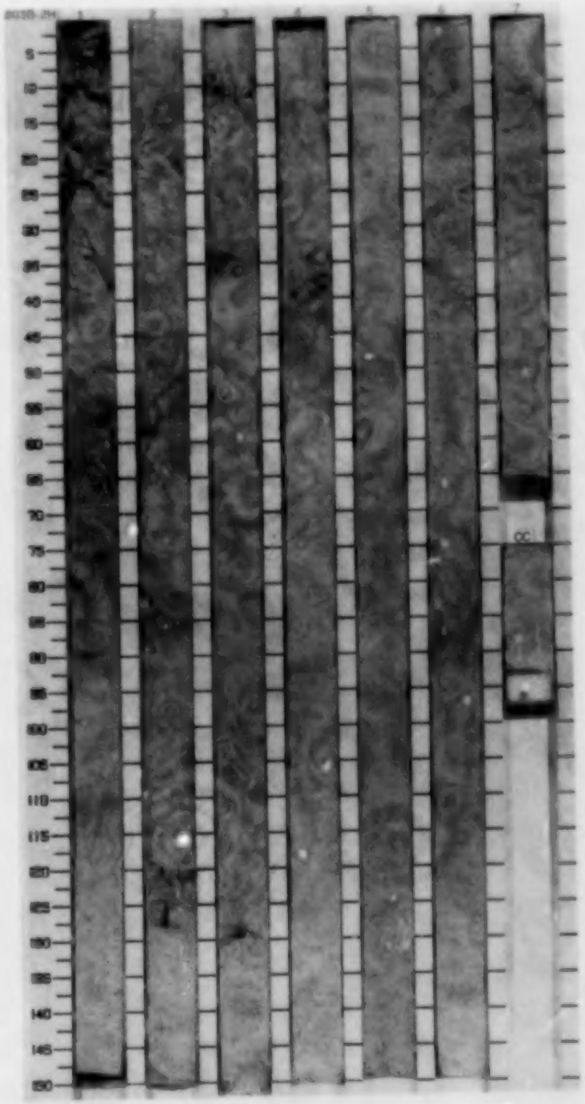
803B-2H
1
2
3
4
5
6
7
CC
5
10
15
20
25
30
35
40
45
50
55
60
65
70
75
80
85
90
95
100
105
110
115
120
125
130
135
140
145
150

SITE 803 HOLE B CORE 3H CORED INTERVAL 13.8-23.3 mbsf

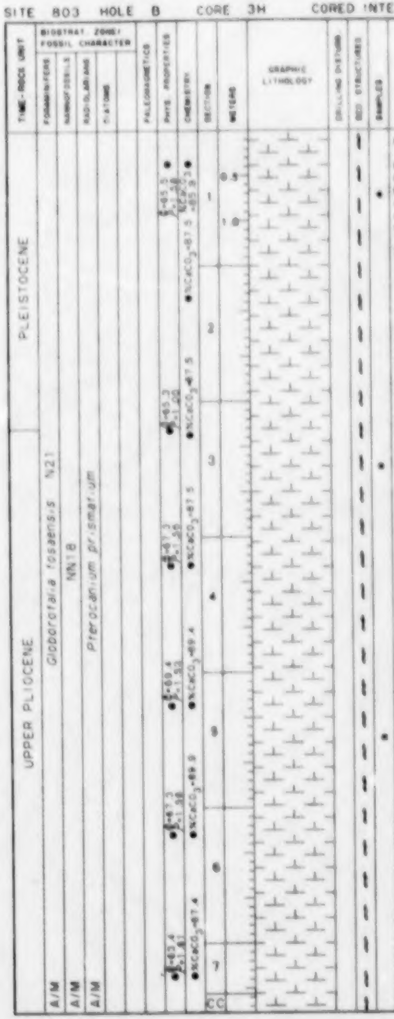
TIME-ROCK UNIT
BIOSTRAT. ZONE/ FOSSIL CHARACTER
FORAMINIFERS
NANNOFOSSILS
RADIOLARIANS
DIATOMS
PALEOMAGNETICS
PHYS. PROPERTIES
CHEMISTRY
SECTION
METERS
GRAPHIC LITHOLOGY
DRILLING DISTURB.
SED. STRUCTURES
SAMPLES
PLEISTOCENE
UPPER PLIOCENE
Globorotalia tosaensis N21
NN18
Pterocanium prismatium
A/M
A/M
A/M
Φ=65.5
γ=1.58
%CaCO3=85.9
%CaCO3=87.5
Φ=65.3
γ=1.60
%CaCO3=87.5
Φ=67.3
γ=1.59
%CaCO3=87.5
Φ=69.4
γ=1.52
%CaCO3=89.4
Φ=67.3
γ=1.58
%CaCO3=89.9
Φ=63.4
γ=1.61
%CaCO3=87.4
0.5
1.0
1
2
3
4
5
6
7
CC

LITHOLOGIC DESCRIPTION

NANNOFOSSIL OOZE with FORAMINIFERS

Major lithology: This core contains NANNOFOSSIL OOZE with FORAMINIFERS. The foraminifer content diminishes downcore, coinciding with a gradational color change from very pale brown (10YR 8/3) to white (5Y 8/1 and 2.5Y 8/0). Faint banding, gray (2.5Y 7/0 and 10Y 5/1) in color, is present in Section 5. Distinct thin and thick planar color bands with sharp contacts are present in Section 6. Bioturbation is apparent throughout this core as trace fossils and mottles.

SMEAR SLIDE SUMMARY (%):

	1, 72 D	3, 72 D	5, 72 D
TEXTURE:			
Sand	3	4	—
Silt	42	31	40
Clay	55	65	60
COMPOSITION:			
Foraminifers	20	10	10
Nannofossils	78	88	89
Siliceous fragments	—	2	1
Silicoflagellates	1	—	—
Spicules	1	—	—

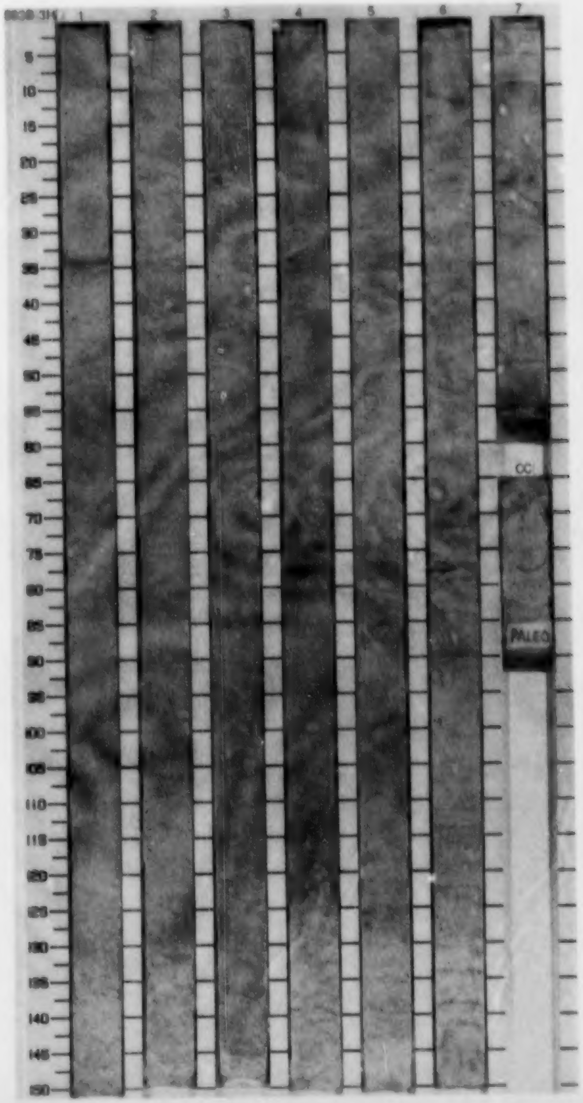
803B-3H
1
2
3
4
5
6
7
CC
PALEO
5
10
15
20
25
30
35
40
45
50
55
60
65
70
75
80
85
90
95
100
105
110
115
120
125
130
135
140
145
150

SITE 803 HOLE B CORE 4H CORED INTERVAL 23.3-32.8 mbsf

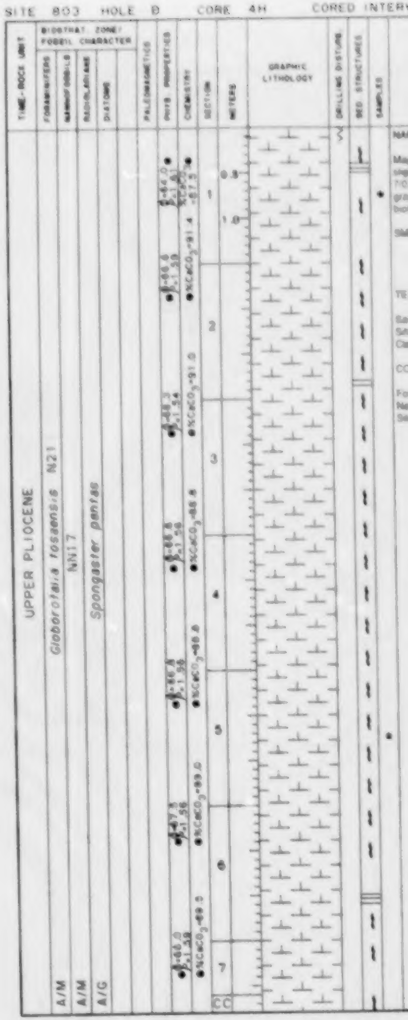
TIME-ROCK UNIT
BIOSTRAT. ZONE/FOSSIL CHARACTER
FORAMINIFERS
NANNOFOSSILS
RADIOLARIANS
DIATOMS
PALEOMAGNETICS
PHYS. PROPERTIES
CHEMISTRY
SECTION
METERS
GRAPHIC LITHOLOGY
DRILLING DISTURB.
SED. STRUCTURES
SAMPLES
UPPER PLIOCENE
Globorotalia tosaensis N21
NN17
Spongaster pentas
A/M
A/M
A/G
φ-64.0
ρ-1.61
%CaCO₃-87.9
%CaCO₃-91.4
φ-66.6
ρ-1.59
%CaCO₃-91.0
φ-68.3
ρ-1.54
%CaCO₃-88.8
φ-66.8
ρ-1.56
%CaCO₃-88.8
φ-66.8
ρ-1.56
%CaCO₃-89.0
φ-67.5
ρ-1.56
%CaCO₃-89.0
φ-66.0
ρ-1.59
0.5
1
1.0
2
3
4
5
6
7
CC

LITHOLOGIC DESCRIPTION

NANNOFOSSIL OOZE

Major lithology: The core contains homogeneous NANNOFOSSIL OOZE characterized by slight to heavy bioturbation. The core is white (2.5Y 8/0 and 5Y 8/1), turning light gray (2.5Y 7/0) in Sections 1, 5 and 6. Zones (between 5 and 20 cm thick) consisting of green and dark gray color banding are found throughout the core. These color bands are not affected by bioturbation.

SMEAR SLIDE SUMMARY (%):

	1, 76 D	5, 75 D
TEXTURE		
Sand	1	3
Silt	29	30
Clay	70	67
COMPOSITION		
Foraminifers	5	5
Nannofossils	93	94
Siliceous fragments	2	1

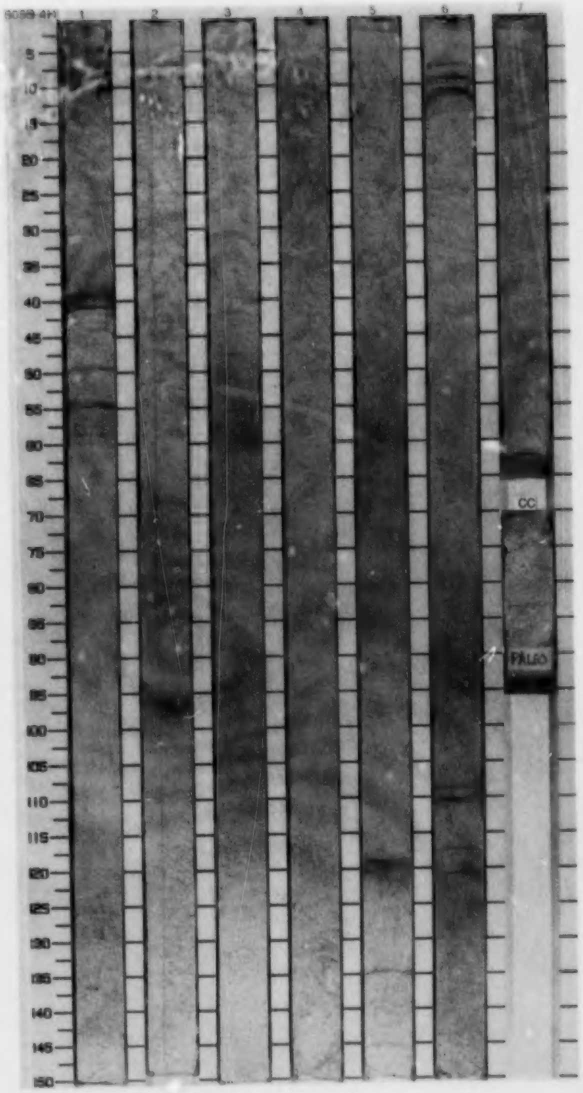
803B-4H
1
2
3
4
5
6
7
CC
PALEO
5
10
15
20
25
30
35
40
45
50
55
60
65
70
75
80
85
90
95
100
105
110
115
120
125
130
135
140
145
150

SITE 803 HOLE B CORE 5H CORED INTERVAL 32.8-42.3 mbsf

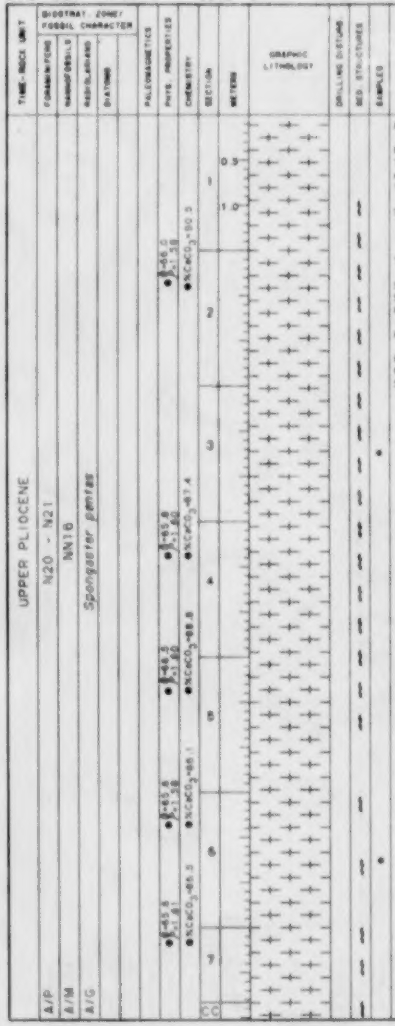
TIME-ROCK UNIT
BIOSTRAT. ZONE/ FOSSIL CHARACTER
FORAMINIFERS
NANNOFOSSILS
RADIOLARIANS
DIATOMS
PALEOMAGNETICS
PHYS. PROPERTIES
CHEMISTRY
SECTION
METERS
GRAPHIC LITHOLOGY
DRILLING DISTURB.
SED. STRUCTURES
SAMPLES
UPPER PLIOCENE
A/P N20 - N21
A/M NN16
A/G Spongaster pentas
φ=66.0 ρ=1.58
%CaCO3=80.5
φ=65.8 ρ=1.60
%CaCO3=87.4
φ=66.5 ρ=1.60
%CaCO3=88.8
φ=65.6 ρ=1.58
%CaCO3=86.1
φ=65.6 ρ=1.61
%CaCO3=85.5
1
2
3
4
5
6
7
CC
0.5
1.0

LITHOLOGIC DESCRIPTION

FORAMINIFER NANNOFOSSIL OOZE

Major lithology: This core contains homogeneous FORAMINIFER NANNOFOSSIL OOZE. The sediments are slightly to heavily bioturbated. Faint color bandings present discontinuously in Sections 3-6. The primary color of the sediments is white (2.5Y 8/0) to gray (2.5Y 7/0). The bands are light gray (5Y 7/1 to 10Y 7/1).

SMEAR SLIDE SUMMARY (%):

	3, 75 D	6, 75 D
TEXTURE:		
Sand	1	1
Silt	40	49
Clay	59	50
COMPOSITION:		
Foraminifers	30	30
Nannofossils	70	69
Siliceous fragments	—	1

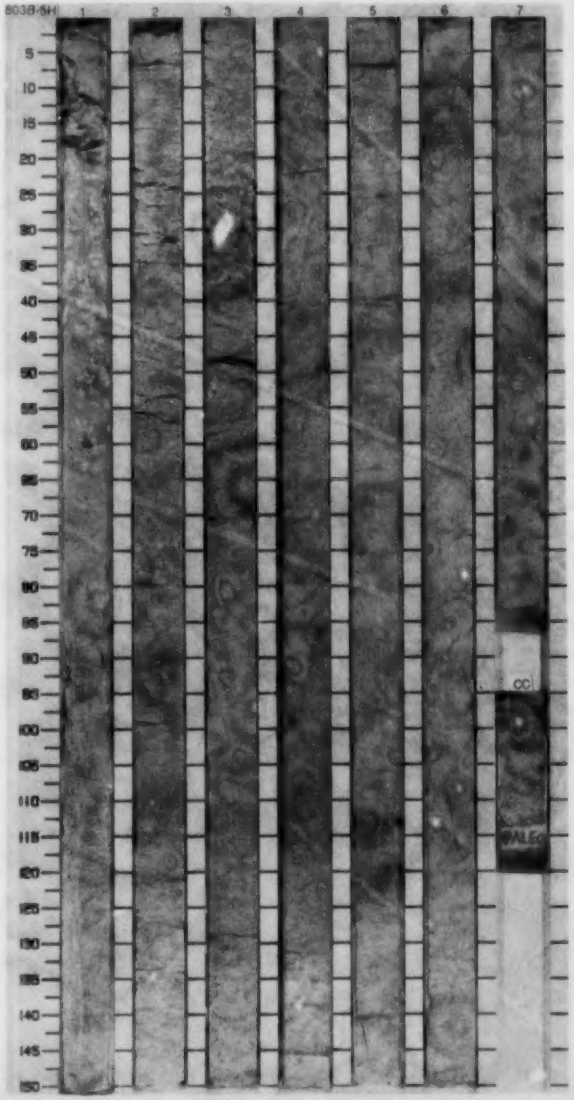
803B-5H
1
2
3
4
5
6
7
5
10
15
20
25
30
35
40
45
50
55
60
65
70
75
80
85
90
95
100
105
110
115
120
125
130
135
140
145
150
CC
PALEO

SITE 803 HOLE B CORE 6H CORED INTERVAL 42.3-51.8 mbsf

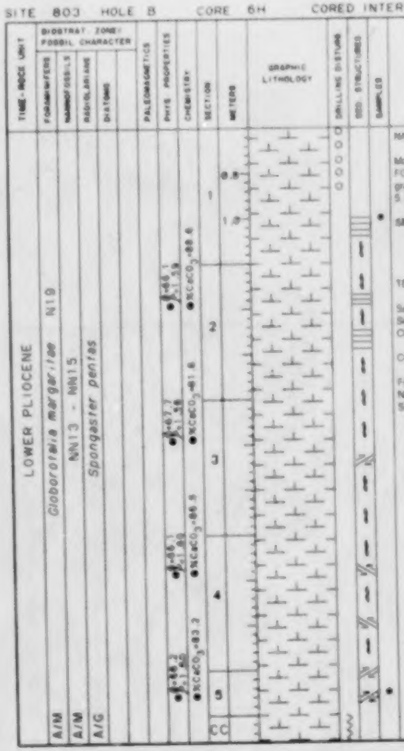
TIME-ROCK UNIT
BIOSTRAT. ZONE/ FOSSIL CHARACTER
FORAMINIFERS
NANNOFOSSILS
RADIOLARIANS
DIATOMS
PALEOMAGNETICS
PHYS. PROPERTIES
CHEMISTRY
SECTION
METERS
GRAPHIC LITHOLOGY
DRILLING DISTURB.
SED. STRUCTURES
SAMPLES
LOWER PLIOCENE
Globorotalia margaritae N19
NN13 - NN15
Spongaster pentas
A/M
A/M
A/G
φ=66.1 ρ=1.59
%CaCO₃=88.6
φ=67.7 ρ=1.56
%CaCO₃=81.6
φ=66.1 ρ=1.60
%CaCO₃=86.5
φ=66.2 ρ=1.60
%CaCO₃=83.2
1
2
3
4
5
CC
0.5
1.0

LITHOLOGIC DESCRIPTION

NANNOFOSSIL OOZE with FORAMINIFERS

Major lithology: This core contains slightly to heavily bioturbated NANNOFOSSIL OOZE with FORAMINIFERS. The primary colors of the sediments are white (5Y 8/1 to 2.5Y 8/0) to light gray (2.5Y 7/0), with zones of gray (10Y 5/1 and 2.5Y 6/0) color banding in Sections 2, 4, and 5. Possible microfaulting, with cm scale offset of color banding, is present in Sections 3-5.

SMEAR SLIDE SUMMARY (%):

	1, 130 D	5, 25 D
TEXTURE:		
Sand	1	3
Silt	60	60
Clay	39	37
COMPOSITION:		
Foraminifers	15	10
Nannofossils	85	90
Siliceous fragments	Tr	Tr

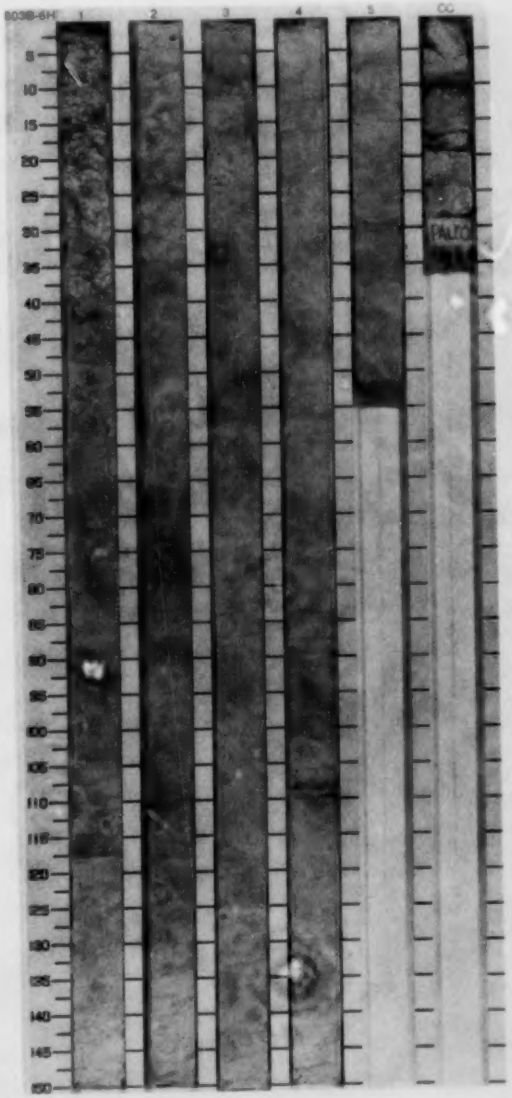
803B-6H
1
2
3
4
5
CC
5
10
15
20
25
30
35
40
45
50
55
60
65
70
75
80
85
90
95
100
105
110
115
120
125
130
135
140
145
150
PALEO

SITE 803 HOLE B CORE 7H CORED INTERVAL 51.8-61.3 mbsf

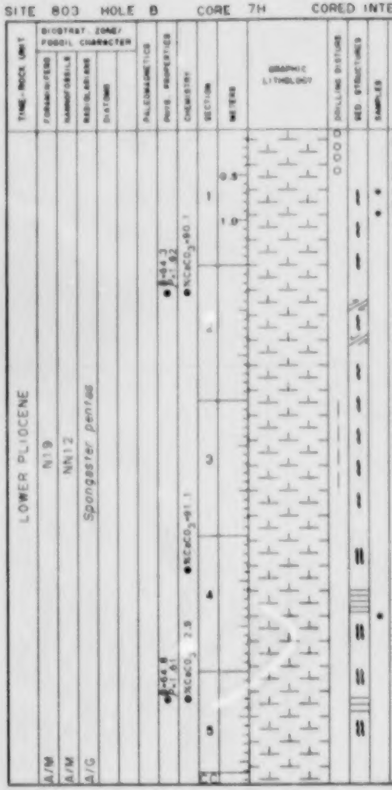
TIME-ROCK UNIT
BIOSTRAT. ZONE/ FOSSIL CHARACTER
FORAMINIFERS
NANNOFOSSILS
RADIOLARIANS
DIATOMS
PALEOMAGNETICS
PHYS. PROPERTIES
CHEMISTRY
SECTION
METERS
GRAPHIC LITHOLOGY
DRILLING DISTURB.
SED. STRUCTURES
SAMPLES
LOWER PLIOCENE
N19
NN12
Spongaster pentas
A/M
A/M
A/G
γ=64.3
ρ=1.82
%CaCO₃=90.1
%CaCO₃=91.1
%CaCO₃ 2.9
γ=64.8
ρ=1.61
%CaCO₃
1
2
3
4
5
CC
0.5
1.0

LITHOLOGIC DESCRIPTION

NANNOFOSSIL OOZE with FORAMINIFERS

Major lithology: This core contains slightly to heavily bioturbated NANNOFOSSIL OOZE with FORAMINIFERS. The primary colors of the sediments are white (5Y 8/1 to 2.5Y 8/0) to light gray (2.5Y 7/0), with zones of faint green (10G 6/2) color banding. Possible microfaulting, with cm scale offset of color bands, is present in Section 2.

SMEAR SLIDE SUMMARY (%):

	1, 99	1, 93	4, 89
	D	M	D
TEXTURE:			
Sand	10	—	—
Silt	90	100	5
Clay	—	—	95
COMPOSITION:			
Foraminifers	10	—	Tr
Inorganic calcite	—	-	2
Nannofossils	90	—	95
Pyrite	—	100	—
Quartz	—	—	3
Volcanic ash	—	—	Tr

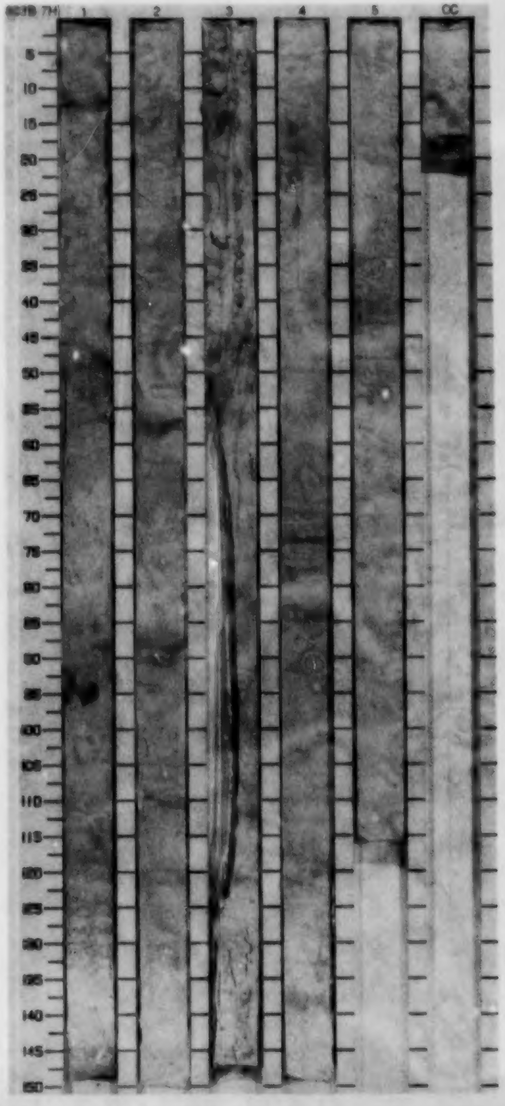
803B 7H
1
2
3
4
5
CC
5
10
15
20
25
30
35
40
45
50
55
60
65
70
75
80
85
90
95
100
105
110
115
120
125
130
135
140
145
150

SITE 803 HOLE C CORE 1H CORED INTERVAL 19.0-28.5 mbsf

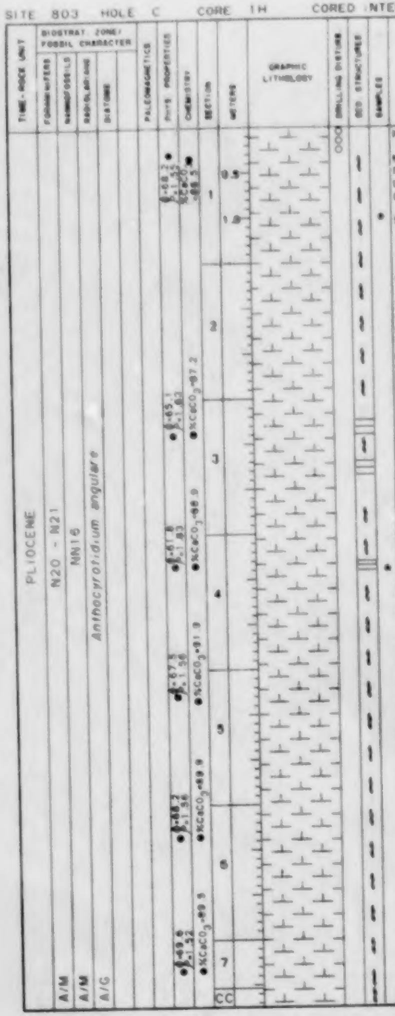
TIME-ROCK UNIT
BIOSTRAT. ZONE/ FOSSIL CHARACTER
FORAMINIFERS
NANNOFOSSILS
RADIOLARIANS
DIATOMS
PALEOMAGNETICS
PHYS. PROPERTIES
CHEMISTRY
SECTION
METERS
GRAPHIC LITHOLOGY
DRILLING DISTURB.
SED. STRUCTURES
SAMPLES
PLIOCENE
N20 - N21
NN16
Anthocyrtidium angulare
A/M
A/M
A/G
φ-68.2
γ-1.55
%CaCO3-88.5
φ-65.1
γ-1.83
%CaCO3-87.2
φ-61.8
γ-1.83
%CaCO3-88.0
φ-67.5
γ-1.56
%CaCO3-91.0
φ-68.2
γ-1.56
%CaCO3-89.9
φ-69.6
γ-1.52
%CaCO3-89.5
1
2
3
4
5
6
7
CC
0.5
1.0

LITHOLOGIC DESCRIPTION

NANNOFOSSIL OOZE with FORAMINIFERS

Major lithology: This core contains partly mottled, slightly to heavily bioturbated NANNOFOSSIL OOZE with FORAMINIFERS. The primary colors of the sediments are white (5Y 8/1 to 2.5Y 8/0) to light gray (2.5Y 7/0). Diffuse to gradational greenish gray (5G 7/1) and light gray (2.5Y 7/1) cm scale color bands are present throughout the core.

SMEAR SLIDE SUMMARY (%)

	1, 100 D	4, 39 M
TEXTURE		
Sand	10	20
Silt	20	10
Clay	70	70
COMPOSITION		
Foraminifers	30	30
Inorganic calcite	Tr	Tr
Nannofossils	70	70
Quartz	Tr	Tr
Volcanic ash	Tr	Tr

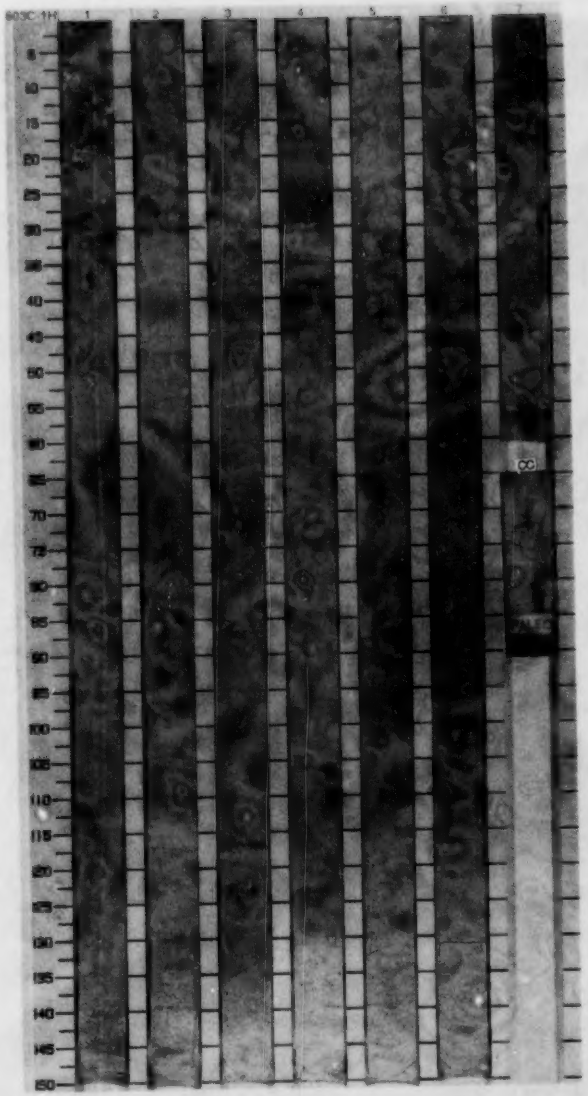
803C-1H
1
2
3
4
5
6
7
CC
5
10
15
20
25
30
35
40
45
50
55
60
65
70
75
80
85
90
95
100
105
110
115
120
125
130
135
140
145
150

SITE 803 HOLE C CORE 2H CORED INTERVAL 28.5-38.0 mbsf

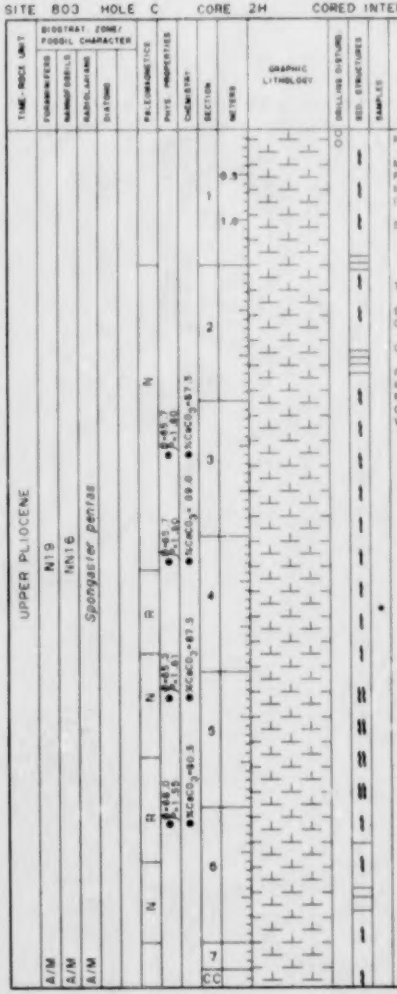

LITHOLOGIC DESCRIPTION

NANNOFOSSIL OOZE with FORAMINIFERS

Major lithology: This core contains partly mottled, slightly to heavily bioturbated NANNOFOSSIL OOZE with FORAMINIFERS. The primary colors of the sediments are white (5Y 8/1 to 2.5Y 8/0) to light gray (2.5Y 7/0). Parts of the core contain faint gray (N6/) and grayish green (10G 4/2) color bands.

SMEAR SLIDE SUMMARY (%):

	4, 80
	D
TEXTURE:	
Sand	10
Clay	90
COMPOSITION:	
Foraminifers	10
Inorganic calcite	Tr
Nannofossils	90
Quartz	Tr
Volcanic ash	Tr

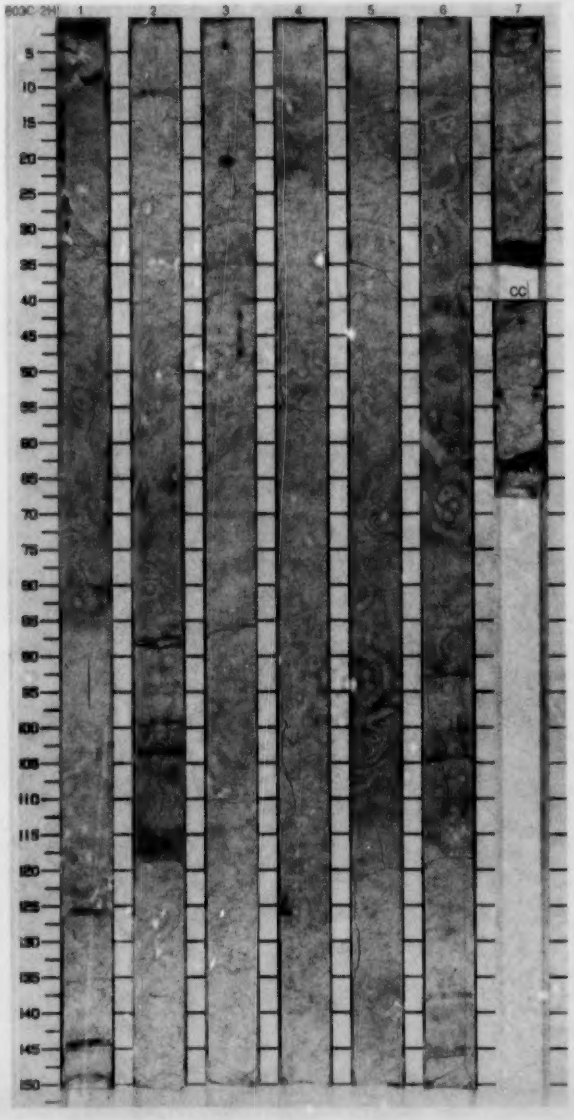
803C-2H
1
2
3
4
5
6
7
CC
5
10
15
20
25
30
35
40
45
50
55
60
65
70
75
80
85
90
95
100
105
110
115
120
125
130
135
140
145
150

SITE 803 HOLE C CORE 3H CORED INTERVAL 38.0-47.5 mbsf

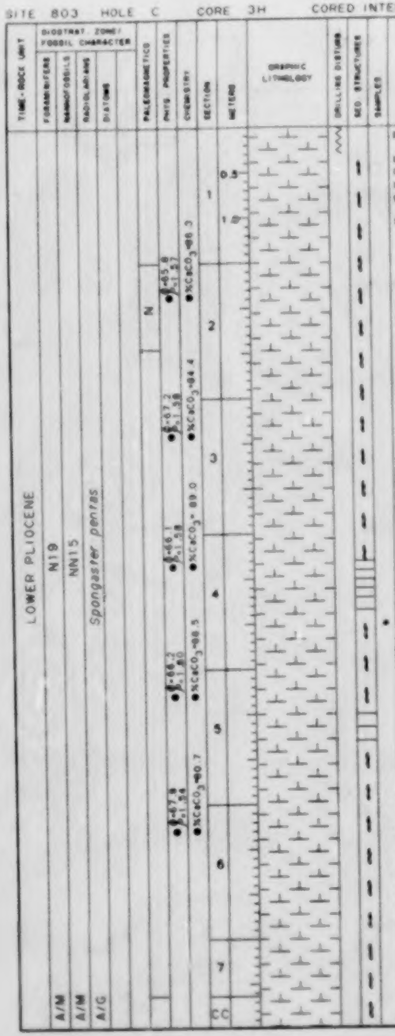
TIME-ROCK UNIT
BIOSTRAT. ZONE/ FOSSIL CHARACTER
FORAMINIFERS
NANNOFOSSILS
RADIOLARIANS
DIATOMS
PALEOMAGNETICS
PHYS. PROPERTIES
CHEMISTRY
SECTION
METERS
GRAPHIC LITHOLOGY
DRILLING DISTURB.
SED. STRUCTURES
SAMPLES
LOWER PLIOCENE
N19
NN15
Spongaster pentas
A/M
A/M
A/G
N
φ=65.8 γ=1.57
φ=67.2 γ=1.58
φ=66.1 γ=1.58
φ=66.2 γ=1.60
φ=67.8 γ=1.54
%CaCO3=86.3
%CaCO3=84.4
%CaCO3= 89.0
%CaCO3=86.5
%CaCO3=90.7
1
2
3
4
5
6
7
CC
0.5
1.0

LITHOLOGIC DESCRIPTION

NANNOFOSSIL OOZE with FORAMINIFERS

Major lithology: This core contains partly mottled, slightly to heavily bioturbated NANNOFOSSIL OOZE with FORAMINIFERS. The primary colors of the sediments are white (5Y 8/1 to 2.5Y 8/0) to light gray (N7/ to 5Y 7/1). Parts of the core contain faint light gray (N7/) and light grayish green (5GY 7/1) color bands.

SMEAR SLIDE SUMMARY (%):

	4, 100
	D
TEXTURE:	
Sand	10
Silt	90
COMPOSITION:	
Accessory minerals	2
Foraminifers	10
Nannofossils	88
Radiolarians	Tr

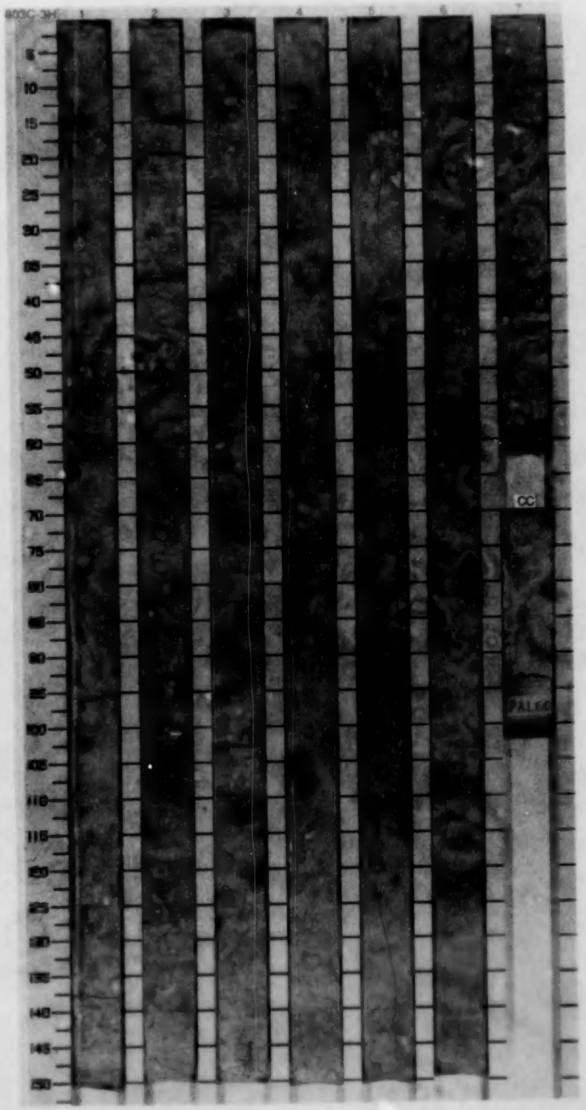
803C-3H
1
2
3
4
5
6
7
CC
PALEO
5
10
15
20
25
30
35
40
45
50
55
60
65
70
75
80
85
90
95
100
105
110
115
120
125
130
135
140
145
150

SITE 803 HOLE C CORE 4H CORED INTERVAL 47.5-57.0 mbsf

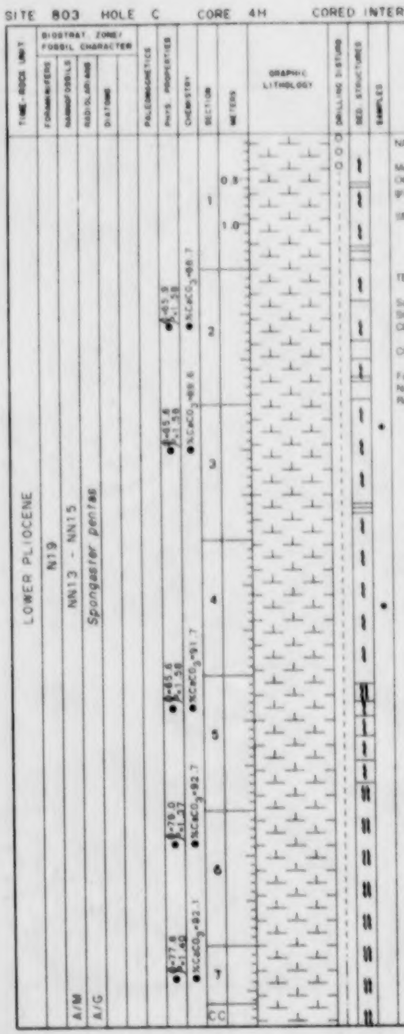
TIME-ROCK UNIT
BIOSTRAT. ZONE/ FOSSIL CHARACTER
FORAMINIFERS
NANNOFOSSILS
RADIOLARIANS
DIATOMS
PALEOMAGNETICS
PHYS. PROPERTIES
CHEMISTRY
SECTION
METERS
GRAPHIC LITHOLOGY
DRILLING DISTURB.
SED. STRUCTURES
SAMPLES
LOWER PLIOCENE
N19
NN13 - NN15
A/M
Spongaster pentas
A/G
ϕ-65.9
γ-1.58
%CaCO₃-88.7
ϕ-65.6
γ-1.58
%CaCO₃-89.6
ϕ-65.6
γ-1.58
%CaCO₃-91.7
ϕ-70.0
γ-1.37
%CaCO₃-92.7
ϕ-77.8
γ-1.40
%CaCO₃-92.1
1
2
3
4
5
6
7
CC
0.5
1.0

LITHOLOGIC DESCRIPTION

NANNOFOSSIL OOZE with FORAMINIFERS

Major lithology: The core contains partly mottled and slightly bioturbated NANNOFOSSIL OOZE with FORAMINIFERS. The primary colors of the sediments are white (2.5Y 8/0) to light gray (2.5Y N7). Parts of the core contain light gray (N7) and pale green (5G 6/2) color bands.

SMEAR SLIDE SUMMARY (%):

	3, 27	4, 74
	M	D
TEXTURE:		
Sand	2	2
Silt	23	23
Clay	75	75
COMPOSITION:		
Foraminifers	4	5
Nannofossils	95	95
Radiolarians	1	—

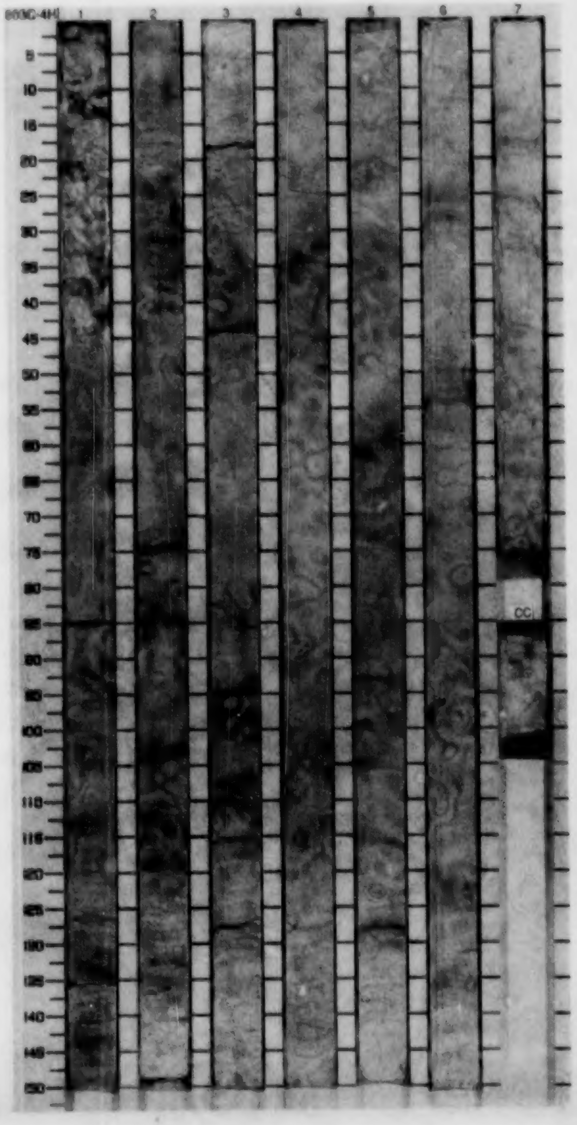
803C-4H
1
2
3
4
5
6
7
CC
5
10
15
20
25
30
35
40
45
50
55
60
65
70
75
80
85
90
95
100
105
110
115
120
125
130
135
140
145
150

SITE 803 HOLE C CORE 5H CORED INTERVAL 57.0-66.5 mbsf

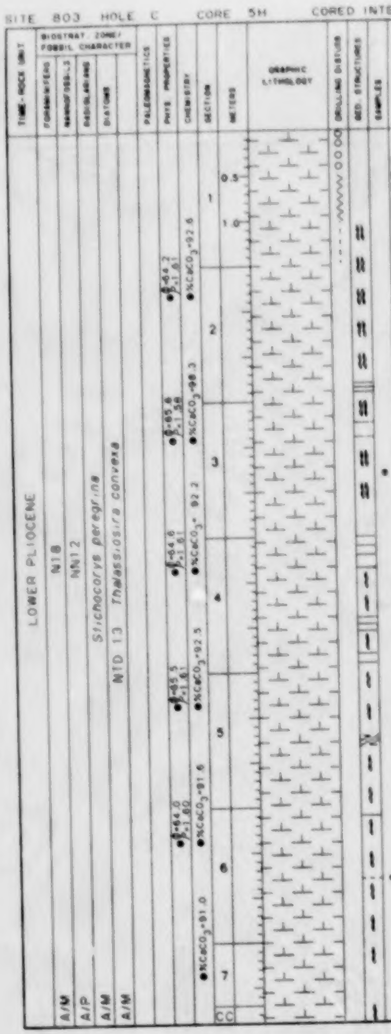
TIME-ROCK UNIT
BIOSTRAT. ZONE/ FOSSIL CHARACTER
FORAMINIFERS
NANNOFOSSILS
RADIOLARIANS
DIATOMS
PALEOMAGNETICS
PHYS. PROPERTIES
CHEMISTRY
SECTION
METERS
GRAPHIC LITHOLOGY
DRILLING DISTURB.
SED. STRUCTURES
SAMPLES
LOWER PLIOCENE
N18
NN12
Stichocorys peregrina
NTD 13 Thalassiosira convexa
A/M
A/M
A/P
A/M
φ=64.2 ρ=1.61
%CaCO3=92.6
φ=65.6 ρ=1.58
%CaCO3=98.3
%CaCO3= 92.2
φ=64.6 ρ=1.61
%CaCO3=92.5
φ=65.5 ρ=1.61
%CaCO3=91.6
φ=64.0 ρ=1.60
%CaCO3=91.0
1
2
3
4
5
6
7
CC
0.5
1.0

LITHOLOGIC DESCRIPTION

NANNOFOSSIL OOZE

Major lithology: This core contains slightly to heavily bioturbated NANNOFOSSIL OOZE. The primary color of the sediment is white (2.5Y 8/0), with light gray (2.5Y 7/0) mottling. Diffuse cm scale color bands of pale green (5G 6/2) and light gray (6N) are present in Sections 3-6. A single microfault is present at Section 5, 70-75 cm.

SMEAR SLIDE SUMMARY (%):

	3, 80 D	6, 80 D
TEXTURE:		
Sand	20	10
Clay	80	90
COMPOSITION:		
Foraminifers	20	5
Nannofossils	80	90
Radiolarians	Tr	5

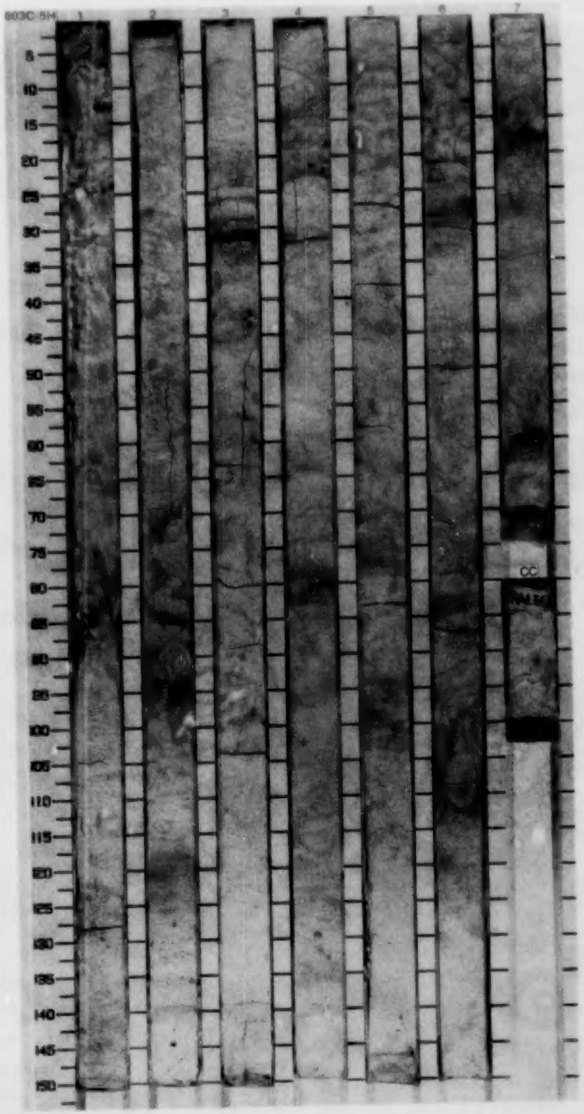
803C-5H
1
2
3
4
5
6
7
CC
5
10
15
20
25
30
35
40
45
50
55
60
65
70
75
80
85
90
95
100
105
110
115
120
125
130
135
140
145
150

SITE 803 HOLE C CORE 6H CORED INTERVAL 66.5-76.0 mbsf

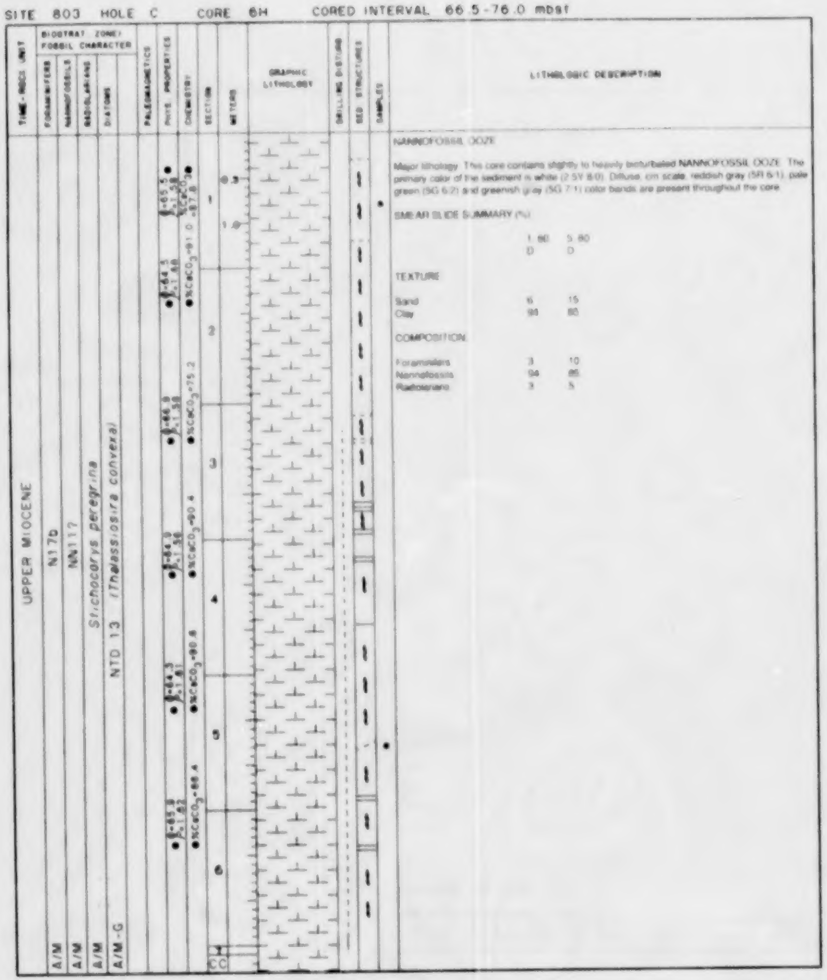
TIME-ROCK UNIT
BIOSTRAT. ZONE/ FOSSIL CHARACTER
FORAMINIFERS
NANNOFOSSILS
RADIOLARIANS
DIATOMS
PALEOMAGNETICS
PHYS. PROPERTIES
CHEMISTRY
SECTION
METERS
GRAPHIC LITHOLOGY
DRILLING DISTURB.
SED. STRUCTURES
SAMPLES
UPPER MIOCENE
N17b
NN11?
Stichocorys peregrina
NTD 13 (Thalassiosira convexa)
A/M
A/M
A/M
A/M-G
φ=65.5 γ=1.58
%CaCO3=91.0
%CaCO3=87.8
φ=64.5 γ=1.60
%CaCO3=75.2
φ=66.9 γ=1.58
%CaCO3=90.4
φ=64.9 γ=1.58
%CaCO3=80.8
φ=64.3 γ=1.61
%CaCO3=88.4
φ=65.8 γ=1.62
1
2
3
4
5
6
CC
0.5
1.0

LITHOLOGIC DESCRIPTION

NANNOFOSSIL OOZE

Major lithology: This core contains slightly to heavily bioturbated NANNOFOSSIL OOZE. The primary color of the sediment is white (2.5Y 8/0). Diffuse, cm scale, reddish gray (5R 6/1), pale green (5G 6/2) and greenish gray (5G 7/1) color bands are present throughout the core.

SMEAR SLIDE SUMMARY (%):

	1, 80 D	5, 80 D
TEXTURE:		
Sand	6	15
Clay	94	85
COMPOSITION:		
Foraminifers	3	10
Nannofossils	94	85
Radiolarians	3	5

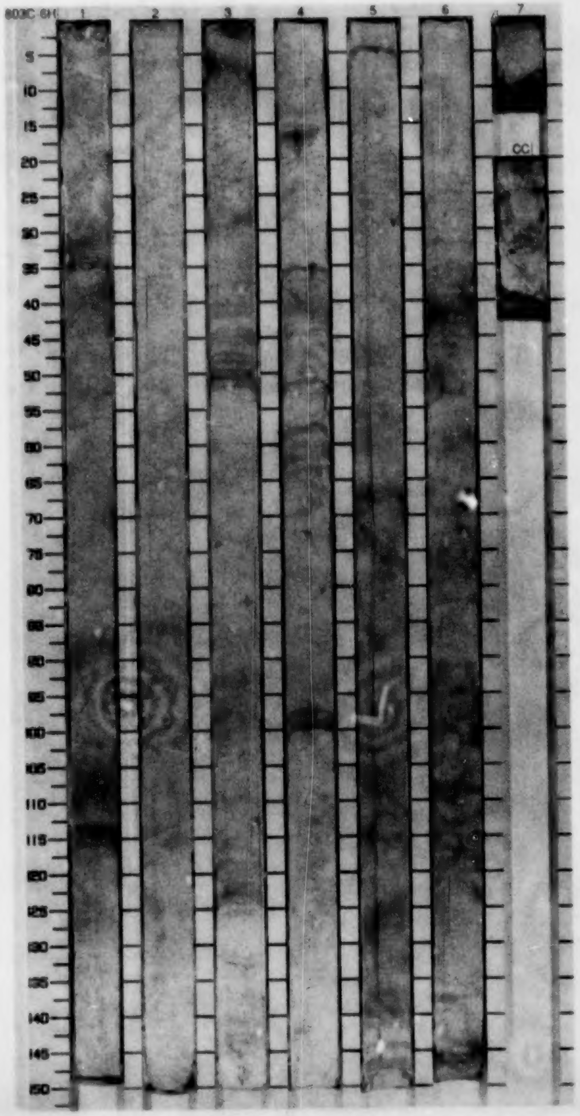
803C 6H
1
2
3
4
5
6
7
CC
5
10
15
20
25
30
35
40
45
50
55
60
65
70
75
80
85
90
95
100
105
110
115
120
125
130
135
140
145
150

SITE 803 HOLE C CORE 7H CORED INTERVAL 76.0-85.5 mbsf

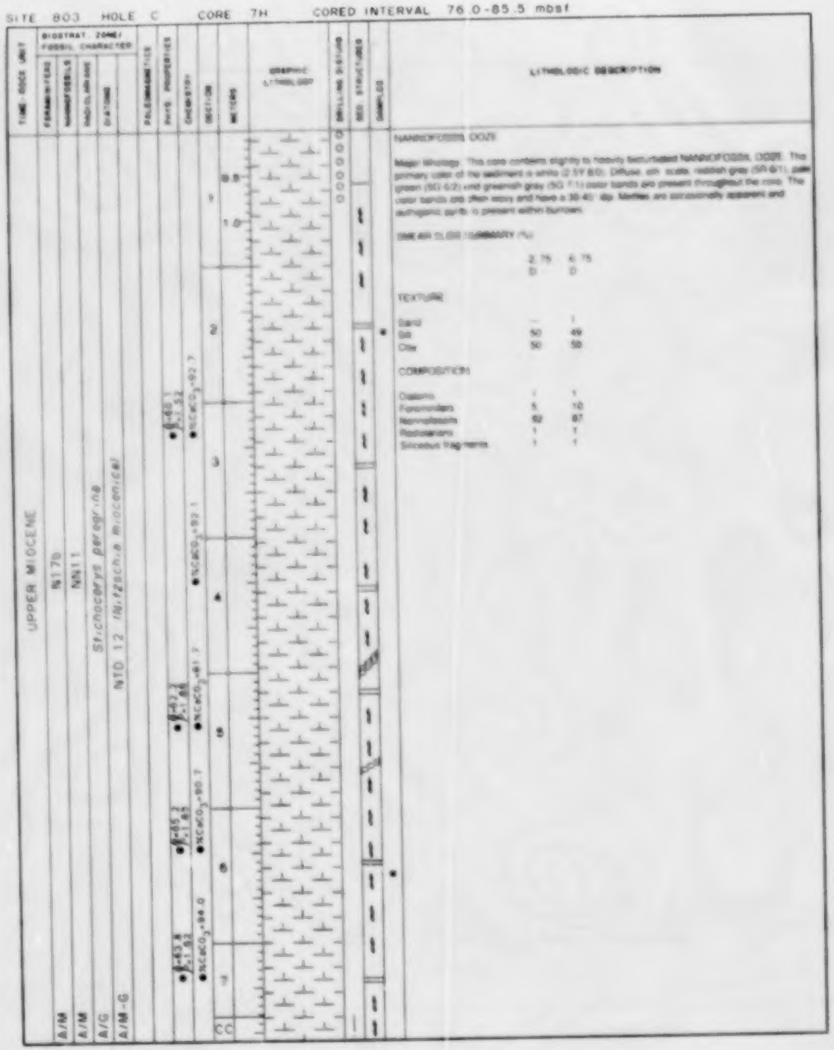

TIME-ROCK UNIT
BIOSTRAT. ZONE/ FOSSIL CHARACTER
FORAMINIFERS
NANNOFOSSILS
RADIOLARIANS
DIATOMS
PALEOMAGNETICS
PHYS. PROPERTIES
CHEMISTRY
SECTION
METERS
GRAPHIC LITHOLOGY
DRILLING DISTURB.
SED. STRUCTURES
SAMPLES
UPPER MIOCENE
A/M N17b
A/M NN11
A/G *Stichocorys peregrina*
A/M-G NTD 12 (*Nitzschia miocenica*)
●ϕ=60.1 γ=1.52
●%CaCO$_3$=92.7
●%CaCO$_3$=92.1
●ϕ=62.2 γ=1.66
●%CaCO$_3$=81.7
●ϕ=65.2 γ=1.65
●%CaCO$_3$=90.7
●ϕ=63.8 γ=1.62
●%CaCO$_3$=94.0
1
2
3
4
5
6
7
CC
0.5
1.0

LITHOLOGIC DESCRIPTION

NANNOFOSSIL OOZE

Major lithology: This core contains slightly to heavily bioturbated NANNOFOSSIL OOZE. The primary color of the sediment is white (2.5Y 8/0). Diffuse, cm-scale, reddish gray (5R 6/1), pale green (5G 6/2) and greenish gray (5G 7/1) color bands are present throughout the core. The color bands are often wavy and have a 30-40° dip. Mottles are occasionally apparent and authigenic pyrite is present within burrows.

SMEAR SLIDE SUMMARY (%):

	2, 75 D	6, 75 D
TEXTURE:		
Sand	—	1
Silt	50	49
Clay	50	50
COMPOSITION:		
Diatoms	1	1
Foraminifers	5	10
Nannofossils	92	87
Radiolarians	1	1
Siliceous fragments	1	1

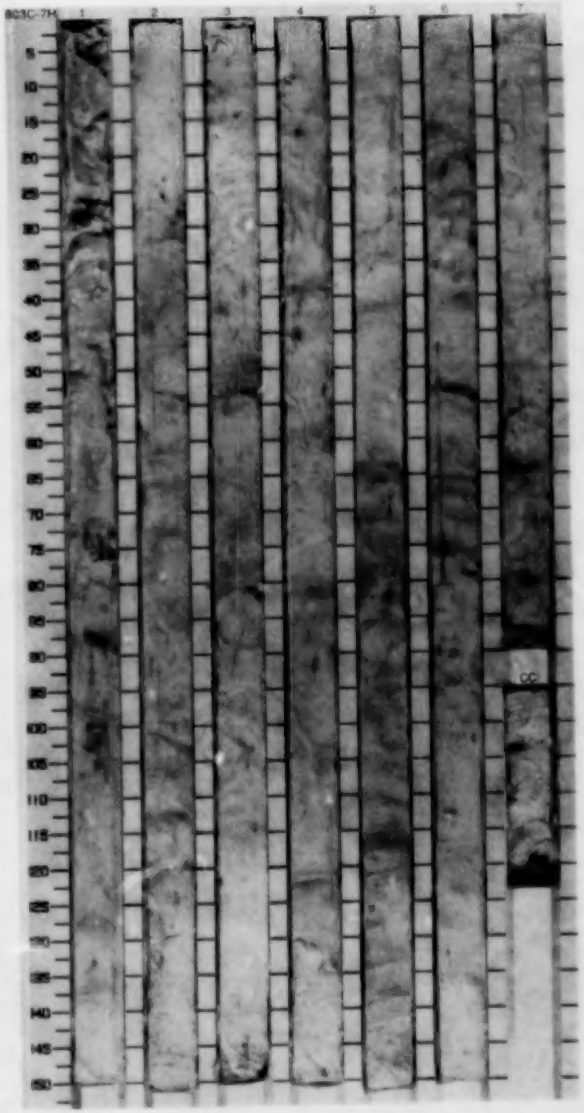

803C-7H
1
2
3
4
5
6
7
CC
5
10
15
20
25
30
35
40
45
50
55
60
65
70
75
80
85
90
95
100
105
110
115
120
125
130
135
140
145
150

SITE 803 HOLE C CORE 8H CORED INTERVAL 85.5-95.0 mbsf

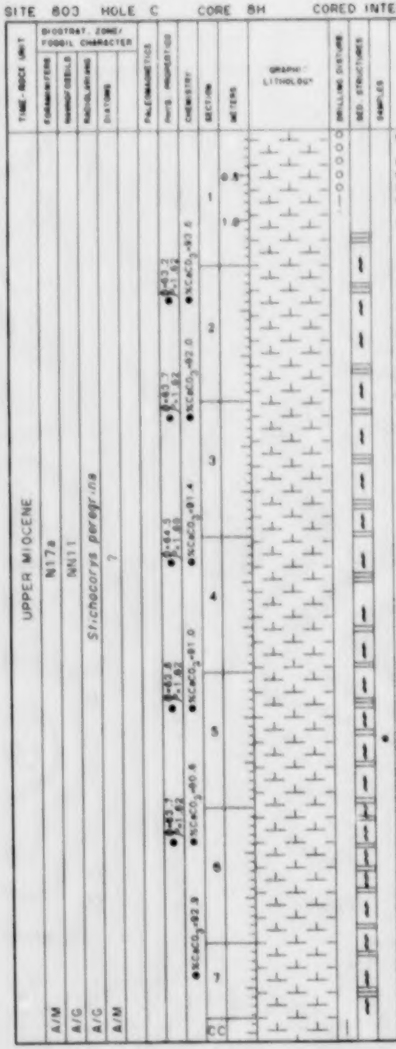
TIME-ROCK UNIT
BIOSTRAT. ZONE/ FOSSIL CHARACTER
FORAMINIFERS
NANNOFOSSILS
RADIOLARIANS
DIATOMS
PALEOMAGNETICS
PHYS. PROPERTIES
CHEMISTRY
SECTION
METERS
GRAPHIC LITHOLOGY
DRILLING DISTURB.
SED. STRUCTURES
SAMPLES
UPPER MIOCENE
N17a
NN11
Stichocorys peregrina
?
A/M
A/G
A/G
A/M
φ=63.2 γ=1.62
φ=63.7 γ=1.62
φ=64.5 γ=1.60
φ=63.8 γ=1.62
φ=63.7 γ=1.62
%CaCO3=93.6
%CaCO3=92.0
%CaCO3=91.4
%CaCO3=91.0
%CaCO3=90.6
%CaCO3=92.9
1
2
3
4
5
6
7
CC
0.5
1.0

LITHOLOGIC DESCRIPTION

NANNOFOSSIL OOZE

Major lithology: This core contains bioturbated NANNOFOSSIL OOZE. The primary color of the sediment is white (2.5Y 8/0). Diffuse, cm scale, reddish gray (5R 6/1), pale green (5G 6/2) and greenish gray (5G 7/1) color bands are present throughout the core. The color bands are often wavy. Some mottling is apparent and authigenic pyrite is present within burrows.

SMEAR SLIDE SUMMARY (%):

	5, 75
	D
TEXTURE:	
Sand	1
Silt	19
Clay	80
COMPOSITION:	
Foraminifers	8
Nannofossils	91
Siliceous fragments	1

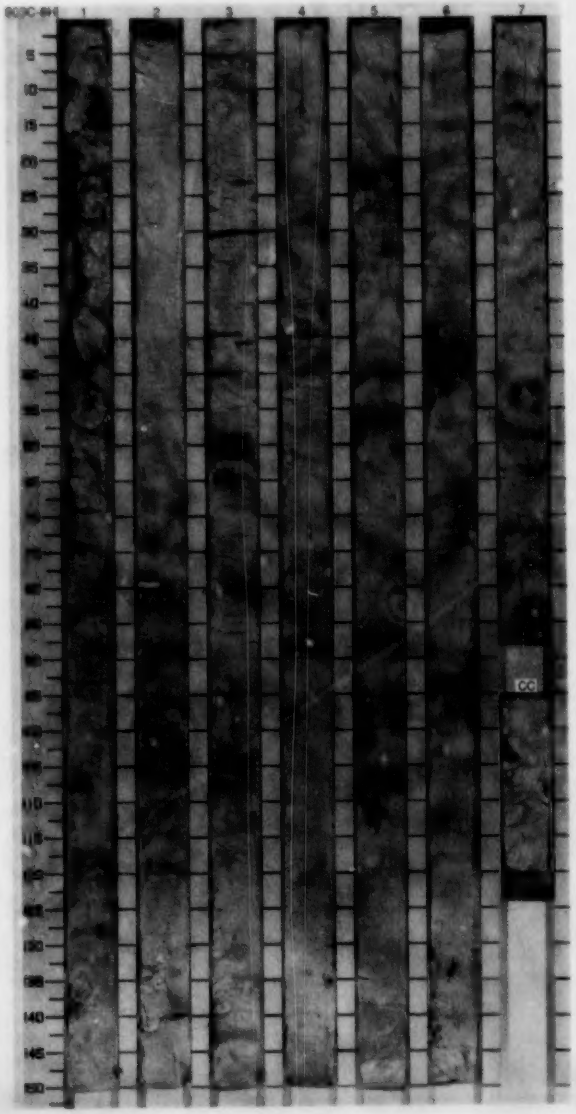
803C-8H
1
2
3
4
5
6
7
CC
5
10
15
20
25
30
35
40
45
50
55
60
65
70
75
80
85
90
95
100
105
110
115
120
125
130
135
140
145
150

SITE 803 HOLE C CORE 9H CORED INTERVAL 95.0-104.5 mbsf

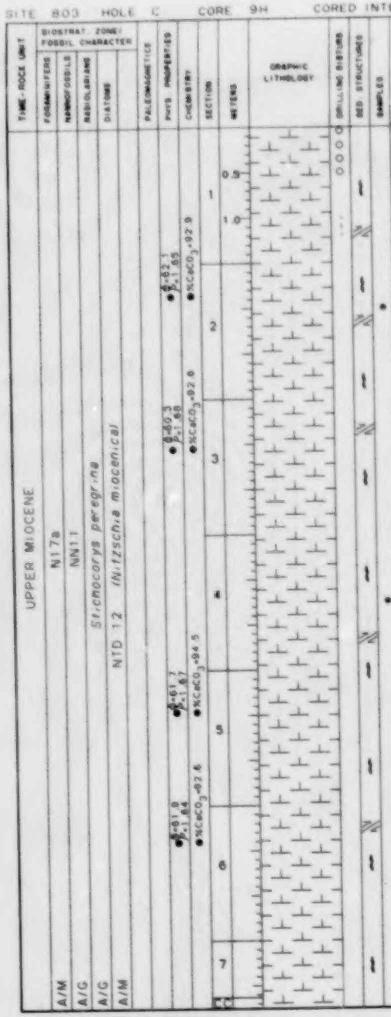
TIME-ROCK UNIT
BIOSTRAT. ZONE/ FOSSIL CHARACTER
FORAMINIFERS
NANNOFOSSILS
RADIOLARIANS
DIATOMS
PALEOMAGNETICS
PHYS. PROPERTIES
CHEMISTRY
SECTION
METERS
GRAPHIC LITHOLOGY
DRILLING DISTURB.
SED. STRUCTURES
SAMPLES
UPPER MIOCENE
N17a
NN11
Stichocorys peregrina
NTD 12 (Nitzschia miocenica)
A/M
A/G
A/G
A/M
φ=62.1
ρ=1.65
%CaCO3=92.9
φ=60.3
ρ=1.68
%CaCO3=92.6
φ=61.7
ρ=1.67
%CaCO3=94.5
φ=61.0
ρ=1.64
%CaCO3=92.6
1
2
3
4
5
6
7
CC
0.5
1.0

LITHOLOGIC DESCRIPTION

NANNOFOSSIL OOZE

Major lithology: This core consists of slightly bioturbated NANNOFOSSIL OOZE. The primary color of the sediment is white (2.5Y 8/0). Color banding is present throughout the entire core. The bands are on a mm to cm scale, pale reddish gray (10R 6/1) and pale green (10Y 6/1) in color, and sometimes smeared. Burrows filled with authigenic pyrite are found in Sections 2 and 3. In Sections 1, 2, 3, 4 and 6, zones of color bands (3-10 cm thick) are offset by microfaulting.

SMEAR SLIDE SUMMARY (%):

	2, 49	4, 75
	D	D
TEXTURE:		
Sand	1	1
Silt	39	14
Clay	60	85
COMPOSITION:		
Foraminifers	5	4
Nannofossils	94	95
Siliceous fragments	1	1

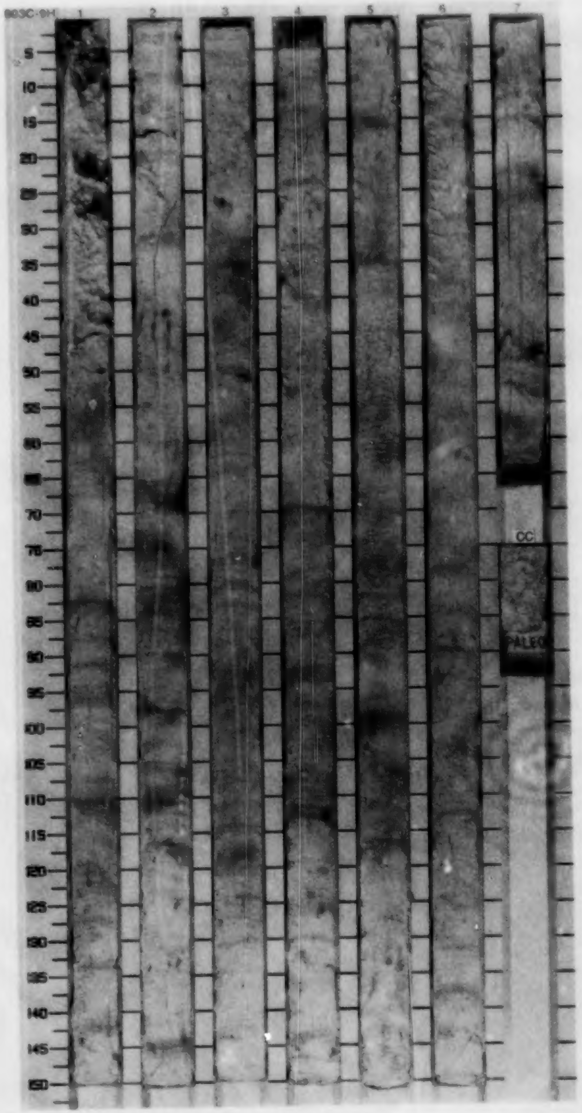
803C-9H
1
2
3
4
5
6
7
CC
PALEO
5
10
15
20
25
30
35
40
45
50
55
60
65
70
75
80
85
90
95
100
105
110
115
120
125
130
135
140
145
150

SITE 803 HOLE C CORE 10H CORED INTERVAL 104.5-114.0 mbsf

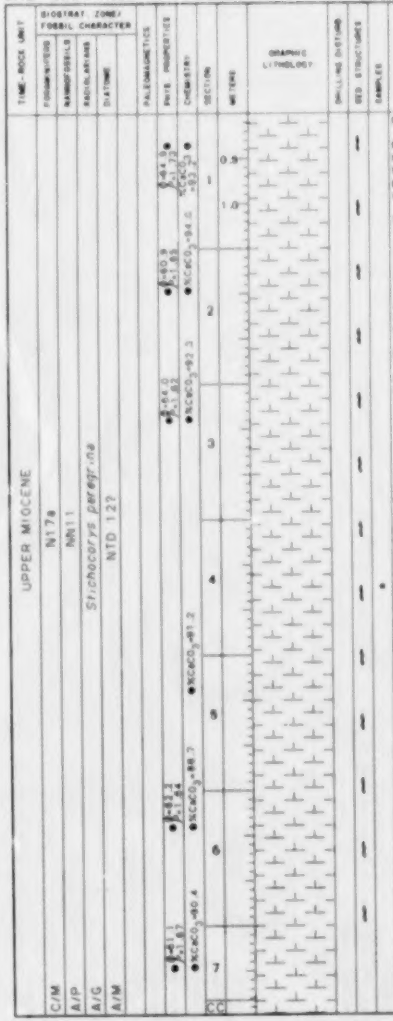
TIME-ROCK UNIT
BIOSTRAT. ZONE/FOSSIL CHARACTER
FORAMINIFERS
NANNOFOSSILS
RADIOLARIANS
DIATOMS
PALEOMAGNETICS
PHYS. PROPERTIES
CHEMISTRY
SECTION
METERS
GRAPHIC LITHOLOGY
DRILLING DISTURB.
SED. STRUCTURES
SAMPLES
UPPER MIOCENE
N17a
NN11
Stichocorys peregrina
NTD 12?
C/M
A/P
A/G
A/M
64.0
1.72
%CaCO3=93.2
60.9
1.85
%CaCO3=94.0
64.0
1.82
%CaCO3=92.3
%CaCO3=91.2
62.2
1.84
%CaCO3=88.7
61.1
1.87
%CaCO3=90.4
0.5
1.0
1
2
3
4
5
6
7
CC

LITHOLOGIC DESCRIPTION

NANNOFOSSIL OOZE

Major lithology: This core consists of bioturbated NANNOFOSSIL OOZE. The primary color of the sediment is white (2.5Y 8/0). Horizontal to sub-horizontal color banding is present throughout the entire core. The bands are up to 2 cm thick, pale reddish gray (10R 6/1) to pale green (10Y 6/1) in color, and commonly smeared. Burrows in Sections 2, 4, and 6 contain authigenic pyrite. White (2.5Y 8/2) mottles are often present.

SMEAR SLIDE SUMMARY (%):

	4, 75
	D
TEXTURE:	
Sand	5
Silt	60
Clay	35
COMPOSITION:	
Foraminifers	5
Nannofossils	95

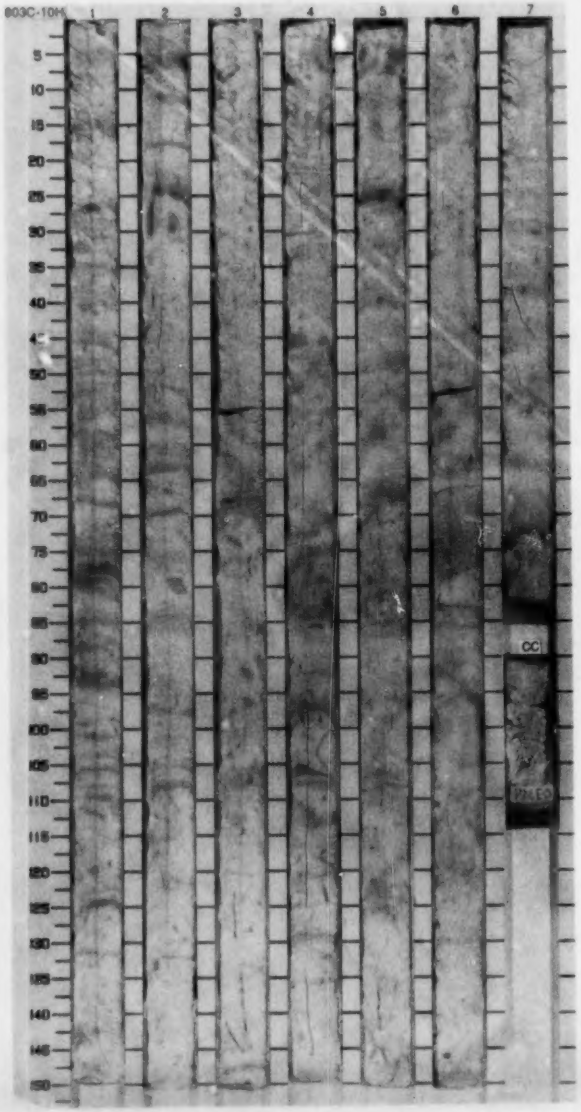
803C-10H
1
2
3
4
5
6
7
CC
PALEO
5
10
15
20
25
30
35
40
45
50
55
60
65
70
75
80
85
90
95
100
105
110
115
120
125
130
135
140
145
150

SITE 803 HOLE C CORE 11H CORED INTERVAL 114.0-123.5 mbsf

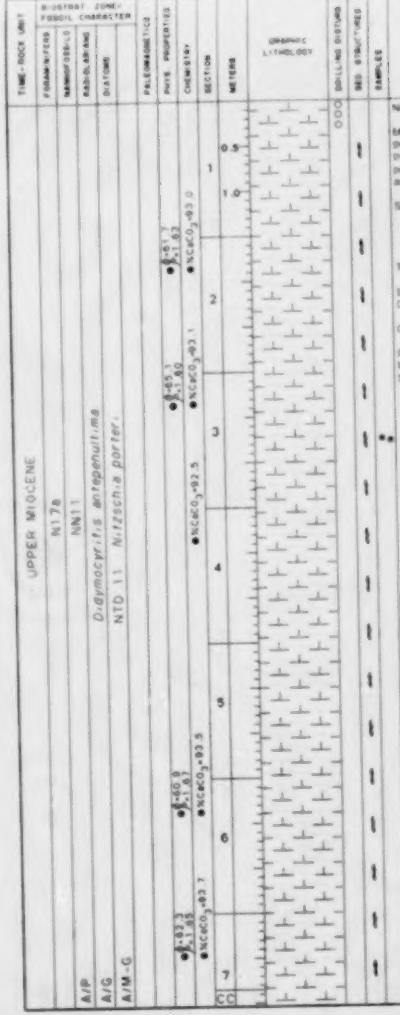
TIME-ROCK UNIT
BIOSTRAT. ZONE/ FOSSIL CHARACTER
FORAMINIFERS
NANNOFOSSILS
RADIOLARIANS
DIATOMS
PALEOMAGNETICS
PHYS. PROPERTIES
CHEMISTRY
SECTION
METERS
GRAPHIC LITHOLOGY
DRILLING DISTURB.
SED. STRUCTURES
SAMPLES
UPPER MIOCENE
N17a
NN11
A/P
Didymocyrtis antepenultima
A/G
NTD 11 Nitzschia porteri
A/M-G
φ-61.7
γ-1.63
%CaCO3-93.0
φ-65.1
γ-1.60
%CaCO3-93.1
%CaCO3-92.5
φ-60.9
γ-1.67
%CaCO3-93.5
φ-62.3
γ-1.65
%CaCO3-93.7
1
2
3
4
5
6
7
CC
0.5
1.0

LITHOLOGIC DESCRIPTION

NANNOFOSSIL OOZE

Major lithology: This core consists of bioturbated NANNOFOSSIL OOZE. The primary color of the sediment is white (2.5Y 8/0). Horizontal to sub-horizontal color banding is present throughout the entire core. The bands are up to 2 cm thick, pale reddish gray (10R 6/1) to pale green (10Y 6/1) in color, and commonly smeared. Burrows in Sections 1, 4, and 7 contain authigenic pyrite. White (2.5Y 8/2) mottles are present discontinuously throughout the core.

SMEAR SLIDE SUMMARY (%)

	3, 74 D	3, 75 D
TEXTURE		
Silt	60	60
Clay	40	40
COMPOSITION		
Foraminifers	5	5
Nannofossils	95	94
Spicules	Tr	1

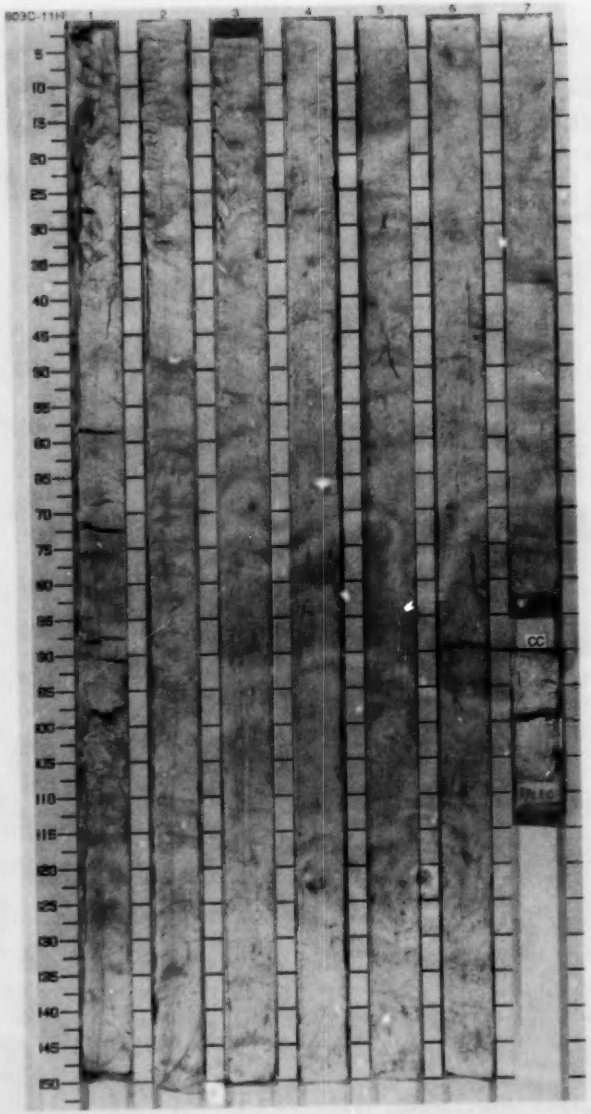
803C-11H
1
2
3
4
5
6
7
5
10
15
20
25
30
35
40
45
50
55
60
65
70
75
80
85
90
95
100
105
110
115
120
125
130
135
140
145
150
CC

SITE 803 HOLE C CORE 12H CORED INTERVAL 123.5-133.0 mbsf

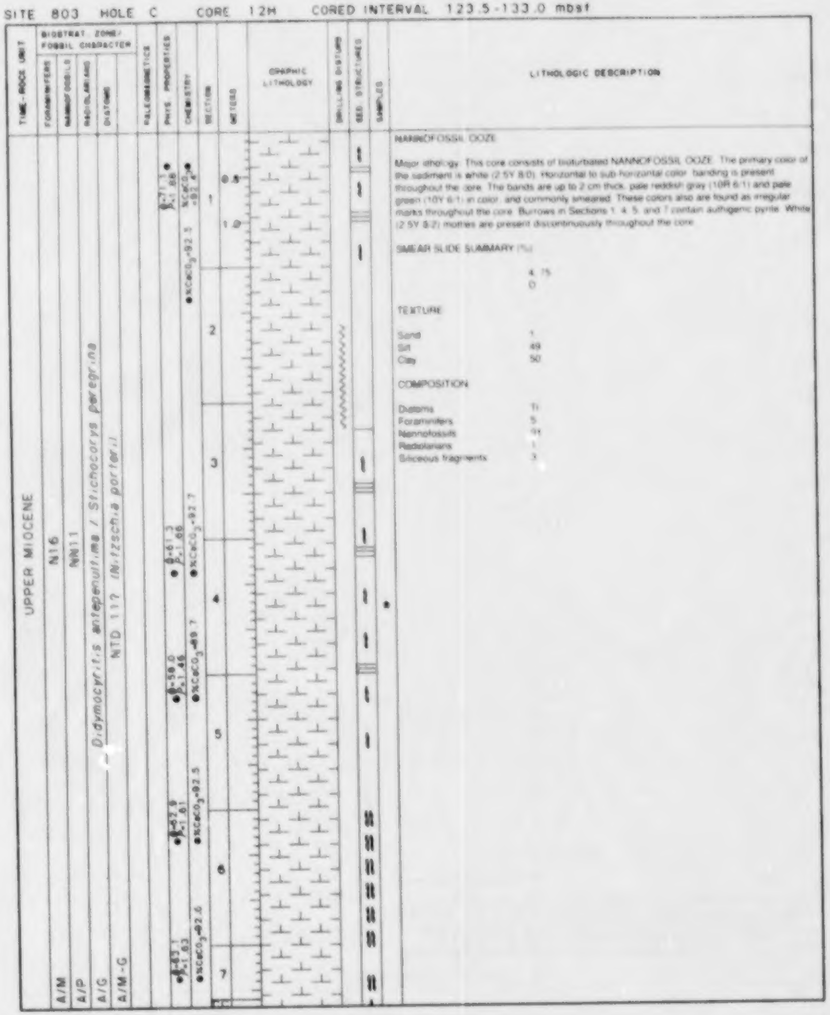
TIME-ROCK UNIT
BIOSTRAT. ZONE/ FOSSIL CHARACTER
FORAMINIFERS
NANNOFOSSILS
RADIOLARIANS
DIATOMS
PALEOMAGNETICS
PHYS. PROPERTIES
CHEMISTRY
SECTION
METERS
GRAPHIC LITHOLOGY
DRILLING DISTURB.
SED. STRUCTURES
SAMPLES
LITHOLOGIC DESCRIPTION
UPPER MIOCENE
A/M N16
A/P NN11
A/G Didymocyrtis antepenultima / Stichocorys peregrina
A/M-G NTD 11? (Nitzschia porteri)
φ-71.1 ρ-1.88
%CaCO3 =92.4
%CaCO3 =92.5
φ-61.3 ρ-1.66
%CaCO3 =92.7
φ-58.0 ρ-1.46
%CaCO3 =89.7
φ-62.9 ρ-1.61
%CaCO3 =92.5
φ-63.1 ρ-1.63
%CaCO3 =92.6
1
2
3
4
5
6
7
0.5
1.0

NANNOFOSSIL OOZE

Major lithology: This core consists of bioturbated NANNOFOSSIL OOZE. The primary color of the sediment is white (2.5Y 8/0). Horizontal to sub-horizontal color banding is present throughout the core. The bands are up to 2 cm thick, pale reddish gray (10R 6/1) and pale green (10Y 6/1) in color, and commonly smeared. These colors also are found as irregular marks throughout the core. Burrows in Sections 1, 4, 5, and 7 contain authigenic pyrite. White (2.5Y 8/2) mottles are present discontinuously throughout the core.

SMEAR SLIDE SUMMARY (%):

	4, 75
	D
TEXTURE:	
Sand	1
Silt	49
Clay	50
COMPOSITION:	
Diatoms	Tr
Foraminifers	5
Nannofossils	91
Radiolarians	1
Siliceous fragments	3

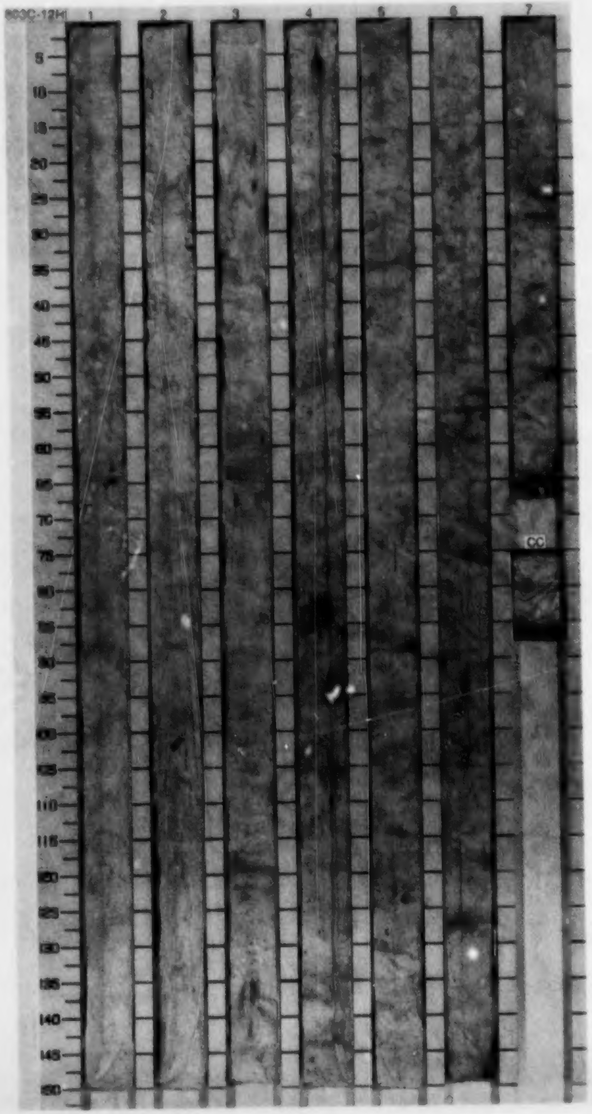
803C-12H
1
2
3
4
5
6
7
CC
5
10
15
20
25
30
35
40
45
50
55
60
65
70
75
80
85
90
95
100
105
110
115
120
125
130
135
140
145
150

SITE 803 HOLE C CORE 13H CORED INTERVAL 133.0-142.5 mbsf

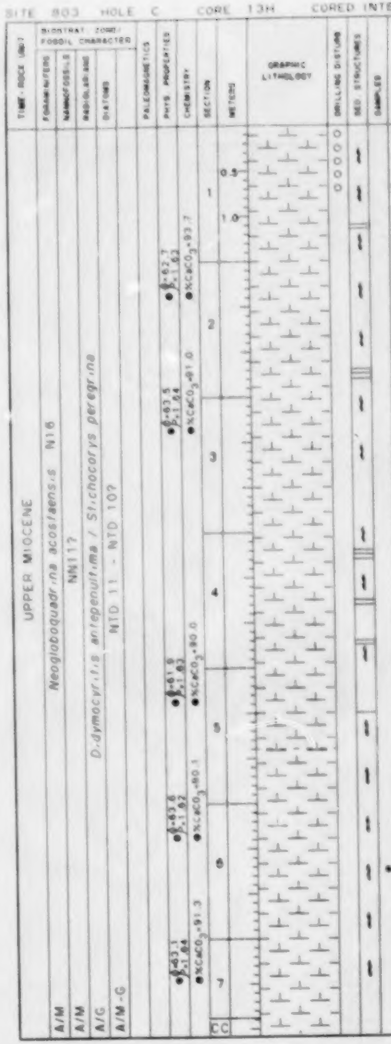
TIME-ROCK UNIT
BIOSTRAT. ZONE/ FOSSIL CHARACTER
FORAMINIFERS
NANNOFOSSILS
RADIOLARIANS
DIATOMS
PALEOMAGNETICS
PHYS. PROPERTIES
CHEMISTRY
SECTION
METERS
GRAPHIC LITHOLOGY
DRILLING DISTURB.
SED. STRUCTURES
SAMPLES
UPPER MIOCENE
A/M
Neogloboquadrina acostaensis N16
A/M
NN11?
A/G
Didymocyrtis antepenultima / Stichocorys peregrina
A/M-G
NTD 11 - NTD 10?
φ=62.7 ρ=1.63
φ=63.5 ρ=1.64
φ=61.9 ρ=1.63
φ=63.6 ρ=1.62
φ=63.1 ρ=1.64
%CaCO3=93.7
%CaCO3=91.0
%CaCO3=90.0
%CaCO3=90.1
%CaCO3=91.3
1
2
3
4
5
6
7
CC
0.5
1.0

LITHOLOGIC DESCRIPTION

NANNOFOSSIL OOZE

Major lithology: This core consists of bioturbated NANNOFOSSIL OOZE. The primary color of the sediment is white (2.5Y 8/0). Faint to distinct horizontal to sub-horizontal color banding is present down to Section 5, 90 cm. The bands are up to 2 cm thick, pale reddish gray (10R 6/1) and pale green (10Y 6/1) in color, and commonly smeared. These colors also are found as irregular marks throughout the core. Burrows also are present throughout the sequence.

Minor lithology: Nannofossil ooze grades into NANNOFOSSIL OOZE with FORAMINIFERS at Section 5, 90 cm. This lithology is structureless, stiffer, coarser in grain size, and exhibits no color banding. Scattered specks of authigenic pyrite are noted.

SMEAR SLIDE SUMMARY (%):

	6, 75
	D
TEXTURE:	
Sand	10
Silt	49
Clay	40
COMPOSITION:	
Diatoms	2
Foraminifers	15
Nannofossils	77
Radiolarians	3
Siliceous fragments	2
Silicoflagellates	1
Spicules	Tr

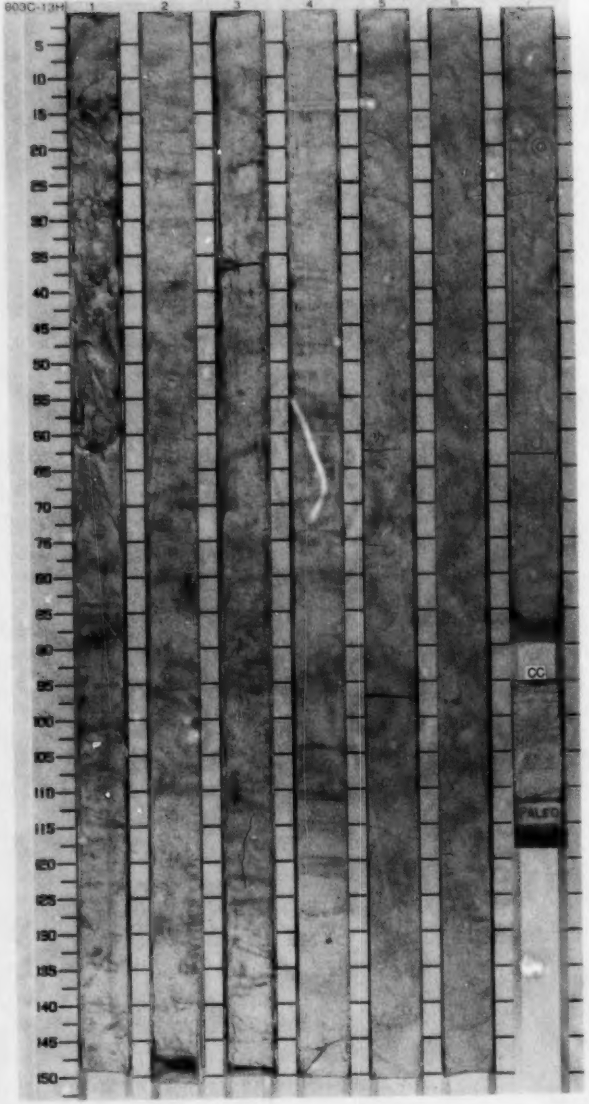
803C-13H
1
2
3
4
5
6
7
CC
PALEO
5
10
15
20
25
30
35
40
45
50
55
60
65
70
75
80
85
90
95
100
105
110
115
120
125
130
135
140
145
150

SITE 803 HOLE C CORE 14H CORED INTERVAL 142.5-152.0 mbsf

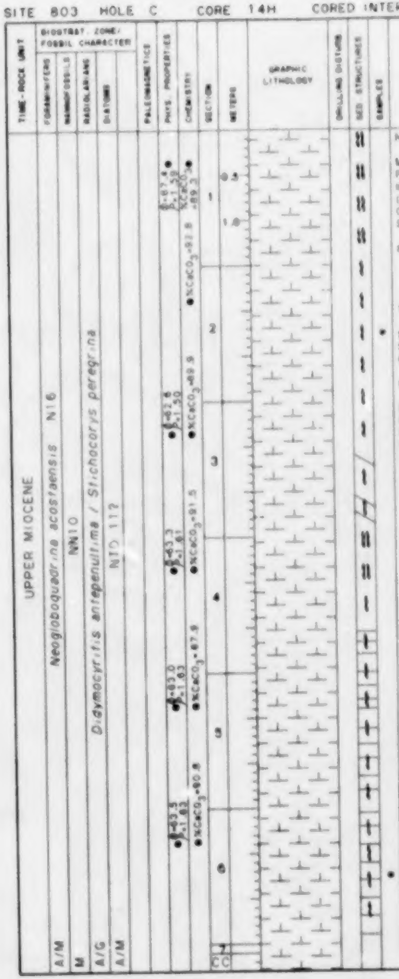
TIME-ROCK UNIT
BIOSTRAT. ZONE/ FOSSIL CHARACTER
FORAMINIFERS
NANNOFOSSILS
RADIOLARIANS
DIATOMS
PALEOMAGNETICS
PHYS. PROPERTIES
CHEMISTRY
SECTION
METERS
GRAPHIC LITHOLOGY
DRILLING DISTURB.
SED. STRUCTURES
SAMPLES
UPPER MIOCENE
Neogloboquadrina acostaensis N16
NN10
Didymocyrtis antepenultima / Stichocorys peregrina
NTD 11?
A/M
M
A/G
A/M
φ=67.4 γ=1.59
%CaCO3=89.3
%CaCO3=92.8
φ=62.6 γ=1.50
%CaCO3=89.9
φ=63.3 γ=1.61
%CaCO3=91.5
φ=63.0 γ=1.63
%CaCO3=87.9
φ=63.5 γ=1.62
%CaCO3=90.8
1
2
3
4
5
6
7
CC
0.5
1.0

LITHOLOGIC DESCRIPTION

NANNOFOSSIL OOZE with FORAMINIFERS and NANNOFOSSIL OOZE

Major lithology: This core contains two major lithologies: NANNOFOSSIL OOZE with FORAMINIFERS above Section 4, 100 cm, and NANNOFOSSIL OOZE below that level. Both lithologies are white (2.5Y 8/0) and bioturbated. Faint pale green (5G 8/2) and reddish gray (5R 6/1) color banding is present in Section 3 and Sections 4, 100 cm, through Section 6. Color banding in Section 3 dips at approximately 35° across the core. Color banding below Section 4, 100 cm, is horizontal.

SMEAR SLIDE SUMMARY (%):

	2, 77 D	6, 75 D
TEXTURE:		
Sand	10	2
Silt	30	23
Clay	60	75
COMPOSITION:		
Diatoms	Tr	Tr
Foraminifers	15	9
Nannofossils	85	90
Radiolarians	Tr	1
Siliceous fragments	Tr	Tr
Silicoflagellates	Tr	Tr
Spicules	Tr	Tr

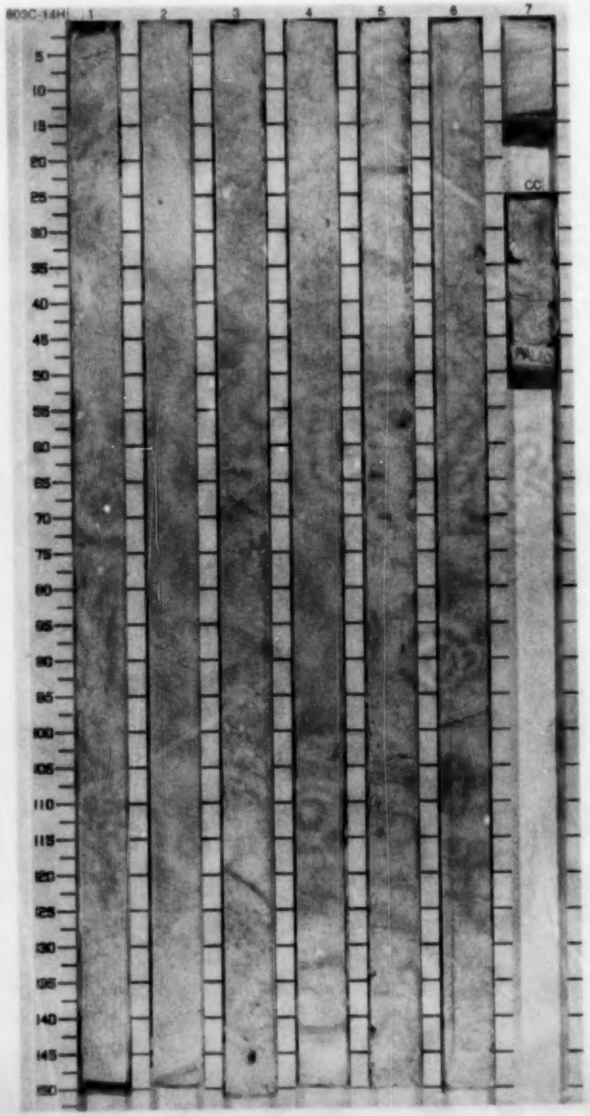
803C-14H
1
2
3
4
5
6
7
CC
PALEO
5
10
15
20
25
30
35
40
45
50
55
60
65
70
75
80
85
90
95
100
105
110
115
120
125
130
135
140
145
150

SITE 803 HOLE C CORE 15H CORED INTERVAL 152.0-161.5 mbsf

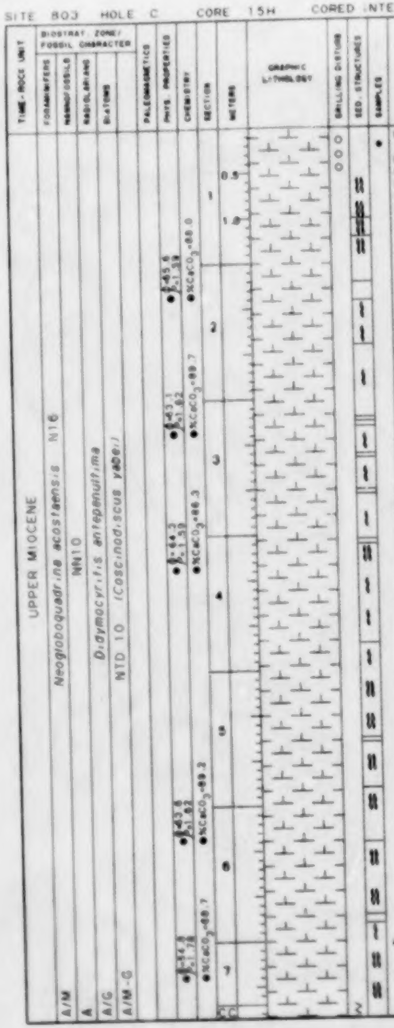
TIME-ROCK UNIT
BIOSTRAT. ZONE/ FOSSIL CHARACTER
FORAMINIFERS
NANNOFOSSILS
RADIOLARIANS
DIATOMS
PALEOMAGNETICS
PHYS. PROPERTIES
CHEMISTRY
SECTION
METERS
GRAPHIC LITHOLOGY
DRILLING DISTURB.
SED. STRUCTURES
SAMPLES
UPPER MIOCENE
Neogloboquadrina acostaensis N16
NN10
Didymocyrtis antepenultima
NTD 10 (Coscinodiscus yabei)
A/M
A
A/G
A/M-G
φ=45.6 γ=1.59
%CaCO3=88.0
φ=43.1 γ=1.62
%CaCO3=89.7
φ=64.3 γ=1.59
%CaCO3=86.3
φ=43.6 γ=1.62
%CaCO3=89.2
φ=54.8 γ=1.78
%CaCO3=88.7
1
2
3
4
5
6
7
CC
0.5
1.0

LITHOLOGIC DESCRIPTION

NANNOFOSSIL OOZE with FORAMINIFERS and NANNOFOSSIL OOZE

Major lithologies: This core contains two major lithologies: NANNOFOSSIL OOZE with FORAMINIFERS which grades into NANNOFOSSIL OOZE in the deeper part of the core. Both lithologies are white (2.5Y 8/0) to light gray (5YR 8/1) and are bioturbated and mottled. Pale green (5G 6/2) and reddish gray (5R 6/1) color banding is present throughout the core.

SMEAR SLIDE SUMMARY (%):

	1, 10	7, 3
	D	D
TEXTURE:		
Sand	10	5
Silt	25	20
Clay	65	75
COMPOSITION:		
Diatoms	Tr	Tr
Foraminifers	10	5
Nannofossils	82	92
Radiolarians	7	3
Spicules	1	Tr

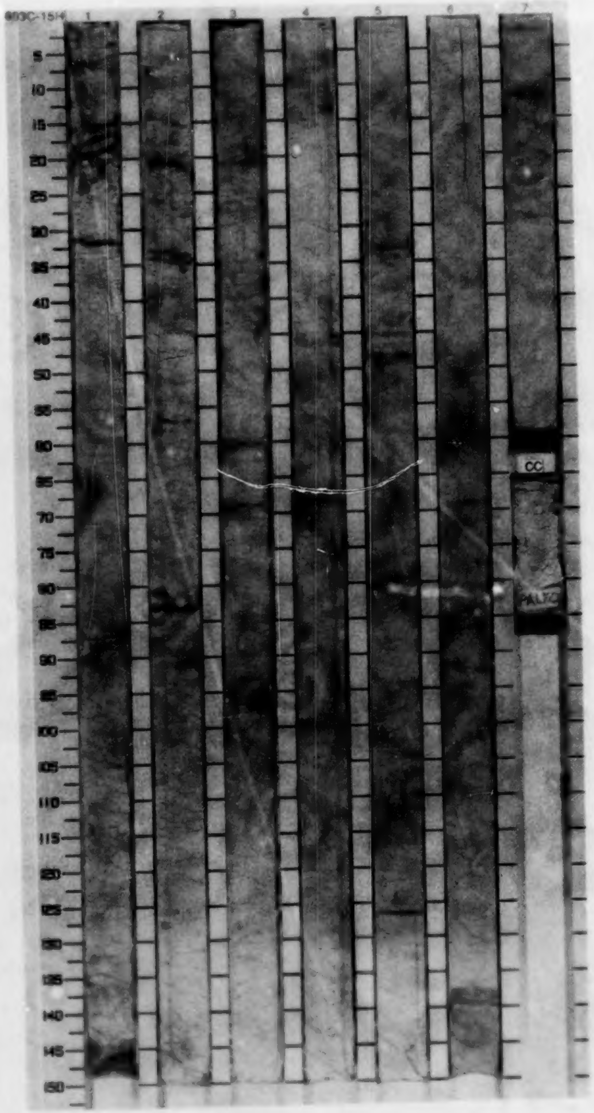
803C-15H
1
2
3
4
5
6
7
CC
PAL/Z
5
10
15
20
25
30
35
40
45
50
55
60
65
70
75
80
85
90
95
100
105
110
115
120
125
130
135
140
145
150

SITE 803 HOLE C CORE 16H CORED INTERVAL 161.5-171.0 mbsf

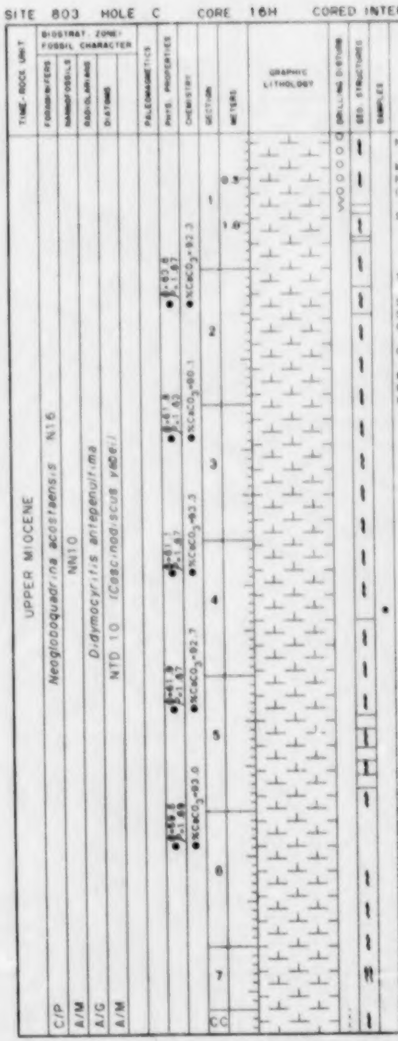
TIME-ROCK UNIT
BIOSTRAT. ZONE/FOSSIL CHARACTER
FORAMINIFERS
NANNOFOSSILS
RADIOLARIANS
DIATOMS
PALEOMAGNETICS
PHYS. PROPERTIES
CHEMISTRY
SECTION
METERS
GRAPHIC LITHOLOGY
DRILLING DISTURB.
SED. STRUCTURES
SAMPLES
UPPER MIOCENE
C/P Neogloboquadrina acostaensis N16
A/M NN10
A/G Didymocyrtis antepenultima
A/M NTD 10 (Coscinodiscus yabei)
63.6
1.67
%CaCO3=92.3
61.8
1.63
%CaCO3=90.1
61.1
1.67
%CaCO3=93.3
61.9
1.67
%CaCO3=92.7
59.6
1.69
%CaCO3=93.0
1
2
3
4
5
6
7
CC
0.5
1.0

LITHOLOGIC DESCRIPTION

NANNOFOSSIL OOZE

Major lithology: This core contains slightly bioturbated and primarily white (2.5Y 8/0) NANNOFOSSIL OOZE. The white color grades into diffuse bands of reddish gray (5R 6/1), light gray (2.5Y 7/1) and light greenish gray (5G 7/1) throughout the core.

SMEAR SLIDE SUMMARY (%):

	4, 79
	D
TEXTURE:	
Sand	5
Silt	15
Clay	80
COMPOSITION:	
Foraminifers	3
Nannofossils	90
Radiolarians	7

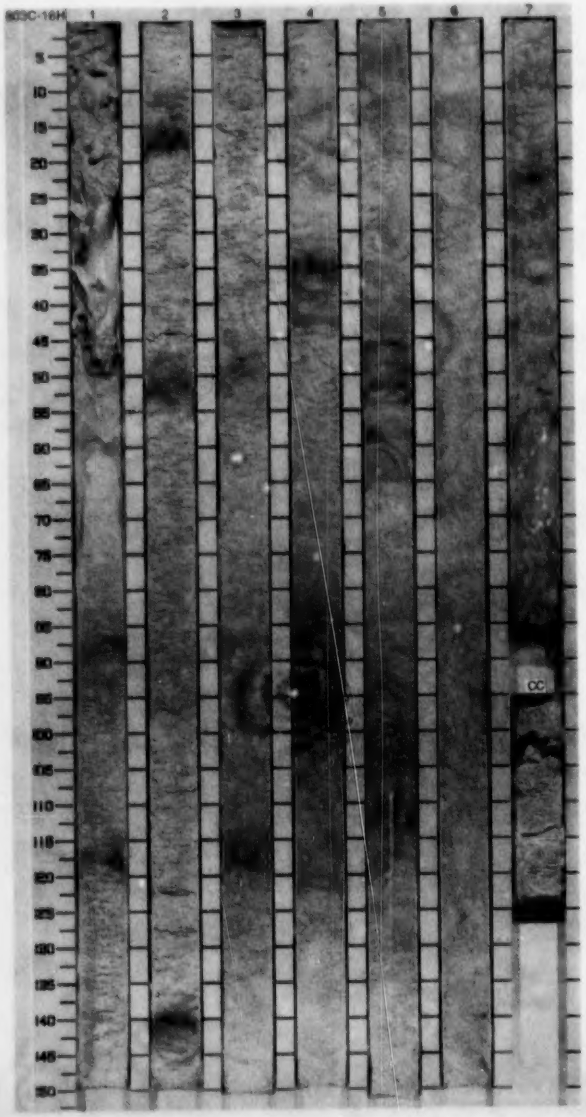
803C-16H
1
2
3
4
5
6
7
CC
5
10
15
20
25
30
35
40
45
50
55
60
65
70
75
80
85
90
95
100
105
110
115
120
125
130
135
140
145
150

SITE 803 HOLE C CORE 17H CORED INTERVAL 171.0-180.5 mbsf

TIME-ROCK UNIT	BIOSTRAT. ZONE/ FOSSIL CHARACTER: FORAMINIFERS	NANNOFOSSILS	RADIOLARIANS	DIATOMS	PALEOMAGNETICS	PHYS. PROPERTIES	CHEMISTRY	SECTION	METERS	DRILLING DISTURB.	SAMPLES
UPPER MIOCENE	*Globorotalia menardii* N15	N19		NTD 10 / NTD 9 (*Actinocyclus moronensis*)				1	0.5 1.0	O O O O O O - - - - -	
						● φ=60.4 ρ=1.88	● %CaCO$_3$=93.0	2			
						● φ=61.6 ρ=1.65	● %CaCO$_3$=91.0	3			*
						● φ=60.0 ρ=1.67	● %CaCO$_3$=93.7	4			
						● φ=60.1 ρ=1.66	● %CaCO$_3$=92.4	5			
						● φ=61.2 ρ=1.66	● %CaCO$_3$=92.0	6			
						● φ=61.7 ρ=1.66	● %CaCO$_3$=92.7	7			
	P	A/M		C/M				CC			

GRAPHIC LITHOLOGY

SED. STRUCTURES

LITHOLOGIC DESCRIPTION

NANNOFOSSIL OOZE

Major lithology: This core contains NANNOFOSSIL OOZE. Section 1, 0-100 cm is soupy, but contains coherent blocks of light greenish gray (5GY 7/1) nannofossil ooze. The remainder of the core is white (2.5Y N8/) with slight to moderate bioturbation.

SMEAR SLIDE SUMMARY (%):

	3, 70
	D
TEXTURE:	
Sand	8
Clay	92
COMPOSITION:	
Nannofossils	92
Radiolarians	8

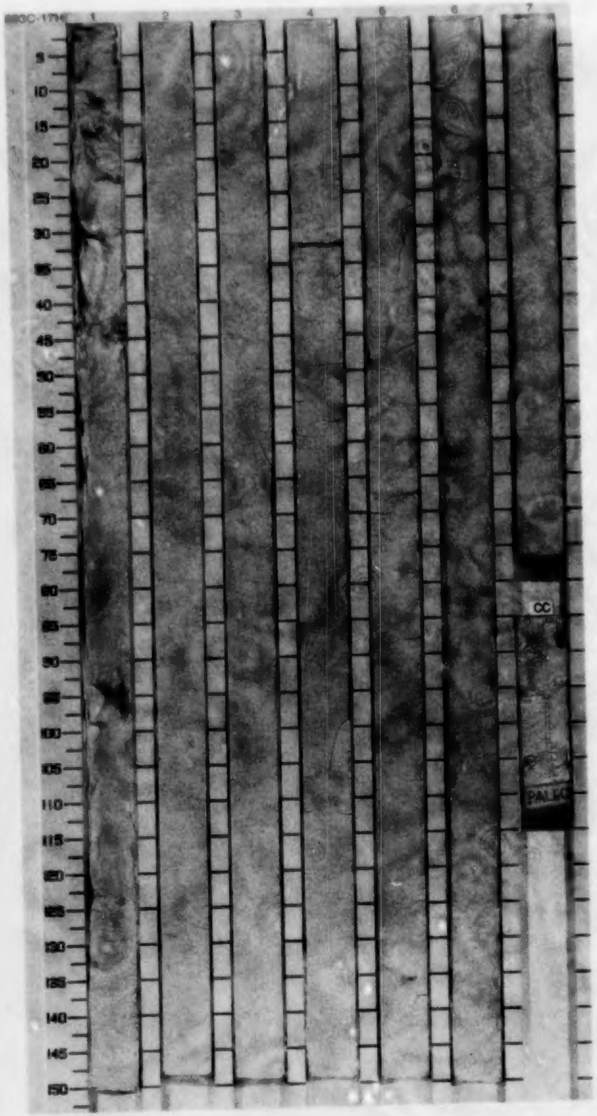
803C-17H
1
2
3
4
5
6
7
5
10
15
20
25
30
35
40
45
50
55
60
65
70
75
80
85
90
95
100
105
110
115
120
125
130
135
140
145
150
CC
PALEO

SITE 803 HOLE C CORE 18H CORED INTERVAL 180.5-190.0 mbsf

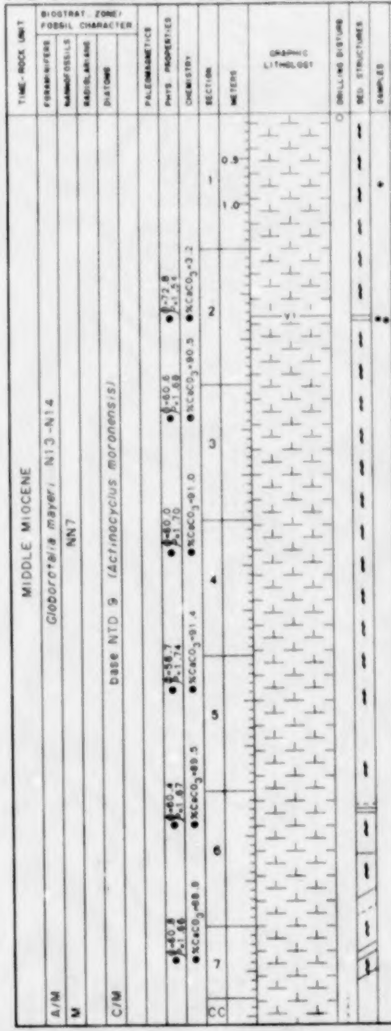
TIME-ROCK UNIT
BIOSTRAT. ZONE/ FOSSIL CHARACTER
FORAMINIFERS
NANNOFOSSILS
RADIOLARIANS
DIATOMS
PALEOMAGNETICS
PHYS. PROPERTIES
CHEMISTRY
SECTION
METERS
GRAPHIC LITHOLOGY
DRILLING DISTURB.
SED. STRUCTURES
SAMPLES
MIDDLE MIOCENE
Globorotalia mayeri N13-N14
NN7
base NTD 9 (Actinocyclus moronensis)
A/M
M
C/M
Φ=72.8 γ=1.54
Φ=60.6 γ=1.68
Φ=60.0 γ=1.70
Φ=58.7 γ=1.74
Φ=60.4 γ=1.67
Φ=60.8 γ=1.68
%CaCO3=3.2
%CaCO3=90.5
%CaCO3=91.0
%CaCO3=91.4
%CaCO3=89.5
%CaCO3=88.8
1
2
3
4
5
6
7
CC
0.5
1.0
V1

LITHOLOGIC DESCRIPTION

NANNOFOSSIL OOZE

Major lithology: This core contains NANNOFOSSIL OOZE. Sections 1-5 are white (2.5Y 8/0 to 10YR 8/1), with light gray (2.5Y 8/0) and reddish gray (5R 6/1) mottles. Sections 6-7 are white (10YR 8/1), bioturbated and contain inclined reddish gray (5R 6/1) color bands, and one irregular reddish gray (5R 6/1) color band, which is possibly a pyritized burrow.

Minor lithology: Section 2 contains a VOLCANIC ASH layer, less than 1 cm thick underlain by a 6 cm thick layer of very dark gray (5Y 3/1) NANNOFOSSIL OOZE.

SMEAR SLIDE SUMMARY (%):

	1, 80 D	2, 79 M	2, 80 M
TEXTURE:			
Sand	10	100	—
Silt	—	—	90
Clay	90	—	10
COMPOSITION:			
Accessory minerals	—	—	15
Foraminifers	3	—	5
Mica	—	—	10
Nannofossils	90	—	30
Radiolarians	7	5	10
Volcanic ash	—	95	—
Zeolite	—	—	30

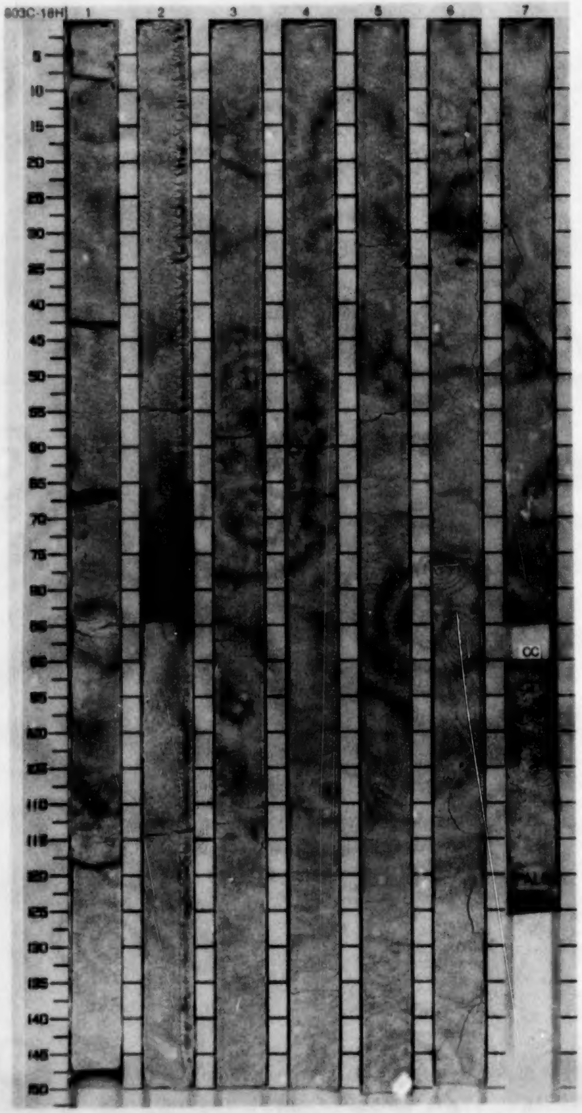
803C-18H
1
2
3
4
5
6
7
5
10
15
20
25
30
35
40
45
50
55
60
65
70
75
80
85
90
95
100
105
110
115
120
125
130
135
140
145
150
CC

SITE 803 HOLE C CORE 19H CORED INTERVAL 190.0-199.5 mbsf

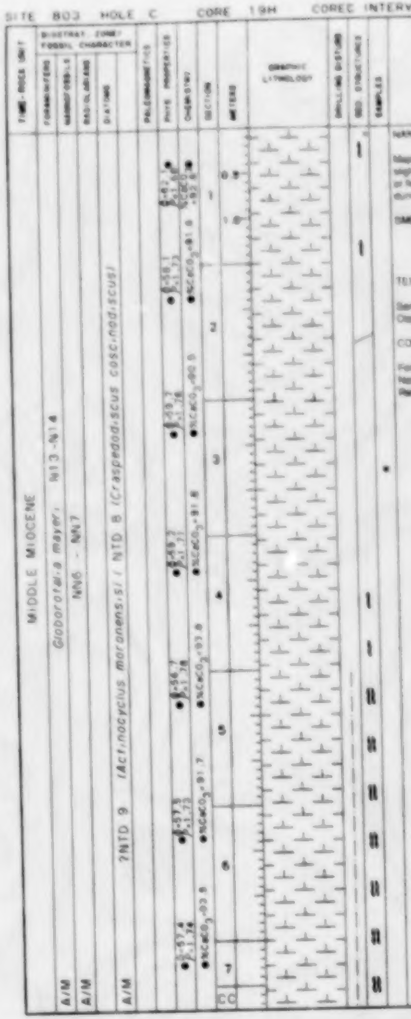
TIME-ROCK UNIT
BIOSTRAT. ZONE/FOSSIL CHARACTER
FORAMINIFERS
NANNOFOSSILS
RADIOLARIANS
DIATOMS
PALEOMAGNETICS
PHYS. PROPERTIES
CHEMISTRY
SECTION
METERS
GRAPHIC LITHOLOGY
DRILLING DISTURB.
SED. STRUCTURES
SAMPLES
MIDDLE MIOCENE
Globorotalia mayeri, N13-N14
NN6 - NN7
?NTD 9 (Actinocyclus moronensis) / NTD 8 (Craspedodiscus coscinodiscus)
A/M
A/M
A/M
%CaCO3=92.6
%CaCO3=91.8
%CaCO3=90.5
%CaCO3=91.8
%CaCO3=93.8
%CaCO3=91.7
%CaCO3=93.8
1
2
3
4
5
6
7
CC
0.5
1.0

LITHOLOGIC DESCRIPTION

NANNOFOSSIL OOZE

Major lithology: This core contains NANNOFOSSIL OOZE. The color is white (7.5YR N8/) with slight, light greenish gray (5G 7/1) and reddish gray (5R 6/1) color mottling/banding. Inclined or flame-shaped color bands are present in Sections 2-4. They may record either disturbance during coring, or the presence of post-depositional slumping/disturbance.

SMEAR SLIDE SUMMARY (%):

	3, 90
	D
TEXTURE:	
Sand	13
Clay	87
COMPOSITION:	
Foraminifers	3
Nannofossils	87
Radiolarians	10

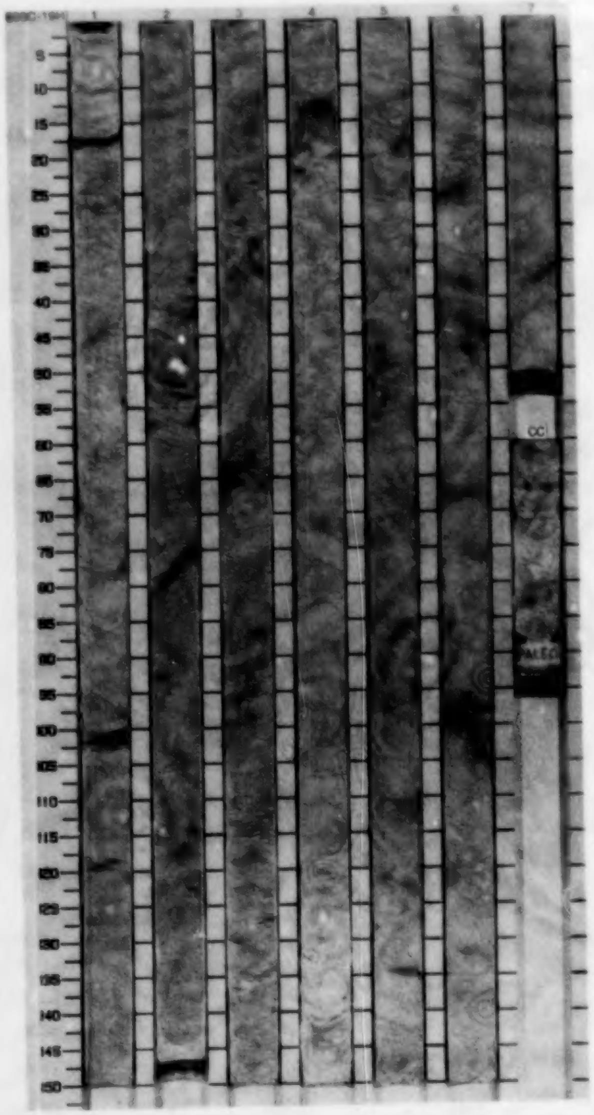
803C-19H
1
2
3
4
5
6
7
CC
PALEO
5
10
15
20
25
30
35
40
45
50
55
60
65
70
75
80
85
90
95
100
105
110
115
120
125
130
135
140
145
150

SITE 803 HOLE C CORE 20H CORED INTERVAL 199.5-209.0 mbsf

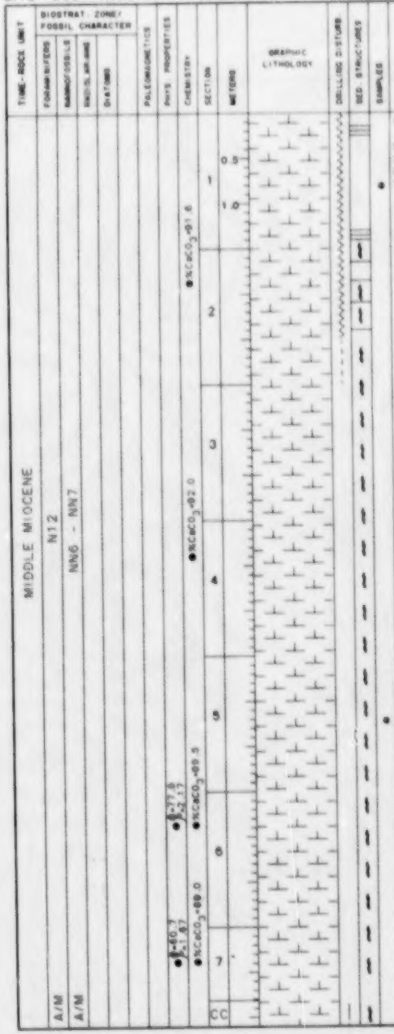

LITHOLOGIC DESCRIPTION

NANNOFOSSIL OOZE with FORAMINIFERS

Major lithology: This core contains NANNOFOSSIL OOZE with FORAMINIFERS. The color of the sediment is (5Y 8/1 grading to 2.5Y N8). Bioturbation is slight to heavy with pyritized burrows present. Convoluted diffuse color bands in [illegible] 1 and the upper 95 cm of Section 2 indicate severe disturbance.

SMEAR SLIDE SUMMARY (%):

	1, 76	5, 72
	D	D
TEXTURE:		
Sand	5	–
Silt	20	30
Clay	75	70
COMPOSITION:		
Foraminifers	Tr	2
Nannofossils	85	98
Radiolarians	15	Tr

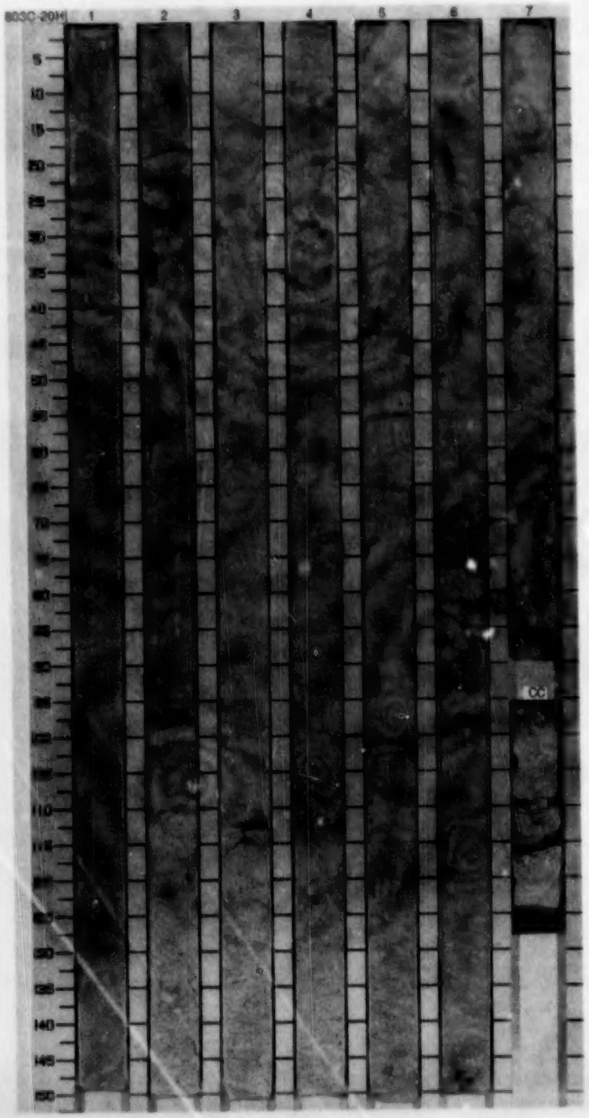
803C-20H
1
2
3
4
5
6
7
CC
5
10
15
20
25
30
35
40
45
50
55
60
65
70
75
80
85
90
95
100
105
110
115
120
125
130
135
140
145
150

SITE 803 HOLE C CORE 21H CORED INTERVAL 209.0-218.5 mbsf

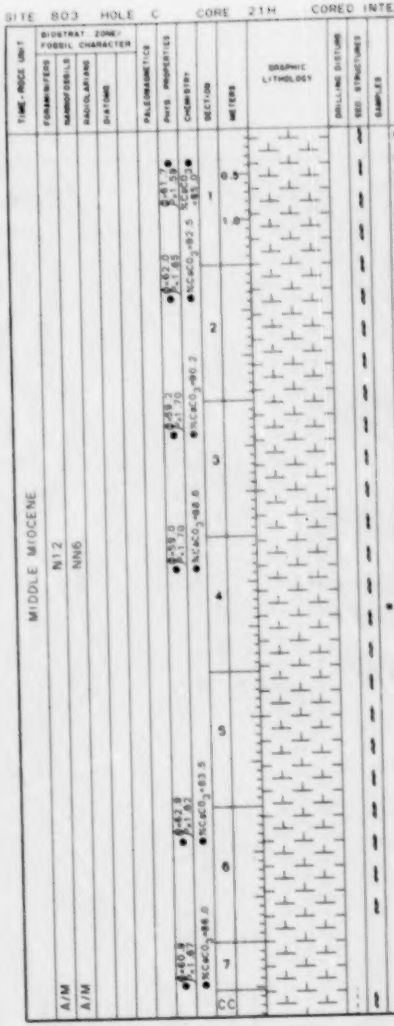
TIME-ROCK UNIT
BIOSTRAT. ZONE/ FOSSIL CHARACTER
FORAMINIFERS
NANNOFOSSILS
RADIOLARIANS
DIATOMS
PALEOMAGNETICS
PHYS. PROPERTIES
CHEMISTRY
SECTION
METERS
GRAPHIC LITHOLOGY
DRILLING DISTURB.
SED. STRUCTURES
SAMPLES
MIDDLE MIOCENE
N12
NN6
A/M
A/M
φ=61.7 γ=1.59
%CaCO3=85.0
φ=62.0 γ=1.63
%CaCO3=92.5
φ=59.2 γ=1.70
%CaCO3=90.2
φ=59.0 γ=1.70
%CaCO3=88.6
φ=62.9 γ=1.62
%CaCO3=83.5
φ=60.9 γ=1.67
%CaCO3=88.0
1
2
3
4
5
6
7
CC
0.5
1.0

LITHOLOGIC DESCRIPTION

NANNOFOSSIL OOZE

Major lithology: This core contains NANNOFOSSIL OOZE. The color is uniformly white (2.5Y 8/1). Slight bioturbation is present over the entire core. Sections 2 and 3 contain minor pyrite mottling.

SMEAR SLIDE SUMMARY (%):

	4, 92
	D
TEXTURE	
Sand	10
Clay	90
COMPOSITION	
Foraminifers	5
Nannofossils	90
Radiolarians	5

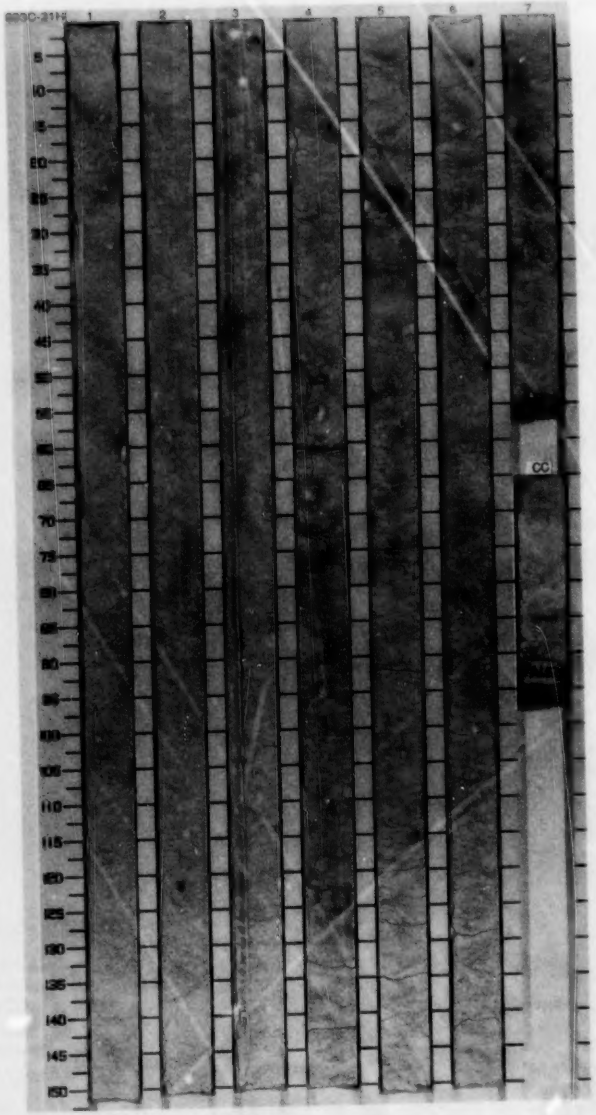
803C-21H
1
2
3
4
5
6
7
CC
5
10
15
20
25
30
35
40
45
50
55
60
65
70
75
80
85
90
95
100
105
110
115
120
125
130
135
140
145
150

SITE 803 HOLE C CORE 22H CORED INTERVAL 218.5-228.0 mbsf

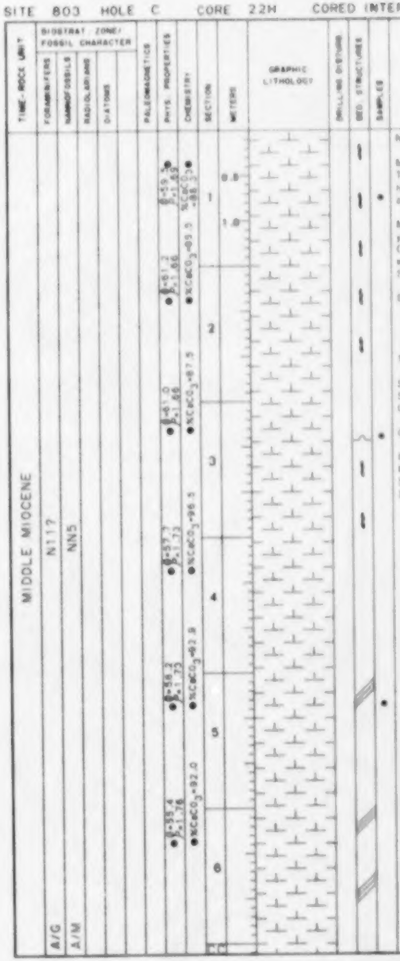
TIME-ROCK UNIT
BIOSTRAT. ZONE/ FOSSIL CHARACTER
FORAMINIFERS
NANNOFOSSILS
RADIOLARIANS
DIATOMS
PALEOMAGNETICS
PHYS. PROPERTIES
CHEMISTRY
SECTION
METERS
GRAPHIC LITHOLOGY
DRILLING DISTURB.
SED. STRUCTURES
SAMPLES
MIDDLE MIOCENE
N11?
NN5
A/G
A/M
φ=59.5 ρ=1.69
%CaCO3 =88.2
%CaCO3=95.5
φ=61.2 ρ=1.66
%CaCO3=87.5
φ=61.0 ρ=1.66
%CaCO3=96.5
φ=57.7 ρ=1.73
%CaCO3=92.8
φ=58.2 ρ=1.73
%CaCO3=92.0
φ=55.4 ρ=1.76
1
2
3
4
5
6
CC
0.5
1.0

LITHOLOGIC DESCRIPTION

NANNOFOSSIL OOZE

Major lithology: The NANNOFOSSIL OOZE is homogeneous, firm, and slightly bioturbated. The color is white (2.5Y 8/0). A few burrows filled with authigenic pyrite are present. Two reddish gray, coarser grained (fine sand and silt), cm thick layers are present in Sections 3 and 6.

Minor lithology: An arcuate shaped shear plane is observed as contact between white and yellowish white colors at Section 3, 100 cm, below which the sediment is NANNOFOSSIL OOZE with FORAMINIFERS. There are color alternations of white (2.5Y 8/0) and yellowish white (5Y 8/2) and the contacts between color alternations are dipping and contorted. In Section 6 and the CC, reddish gray (5R 6/1) color bands dip at 45° and contacts are irregular.

SMEAR SLIDE SUMMARY (%):

	1, 75	3, 99	5, 36
	D	D	D
TEXTURE:			
Sand	—	20	1
Silt	60	60	19
Clay	40	20	80
COMPOSITION:			
Foraminifers	5	40	11
Nannofossils	95	60	88
Siliceous fragments	—	—	1
Spar cement	Tr	—	—

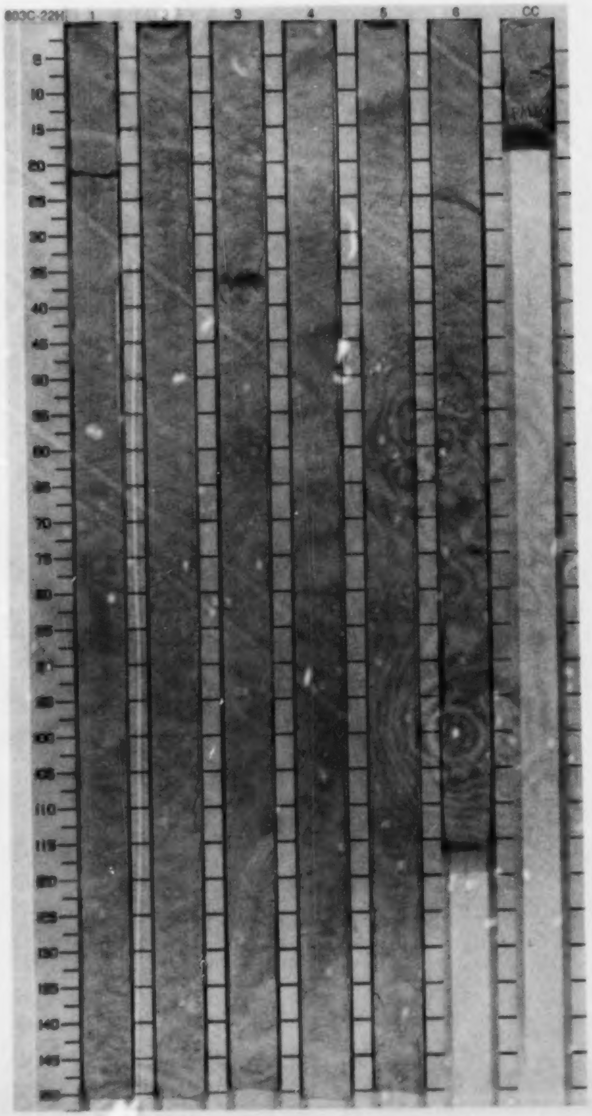
803C-22H
1
2
3
4
5
6
CC
5
10
15
20
25
30
35
40
45
50
55
60
65
70
75
80
85
90
95
100
105
110
115
120
125
130
135
140
145
150

SITE 803 HOLE C CORE 23H CORED INTERVAL 228.0-237.5 mbsf

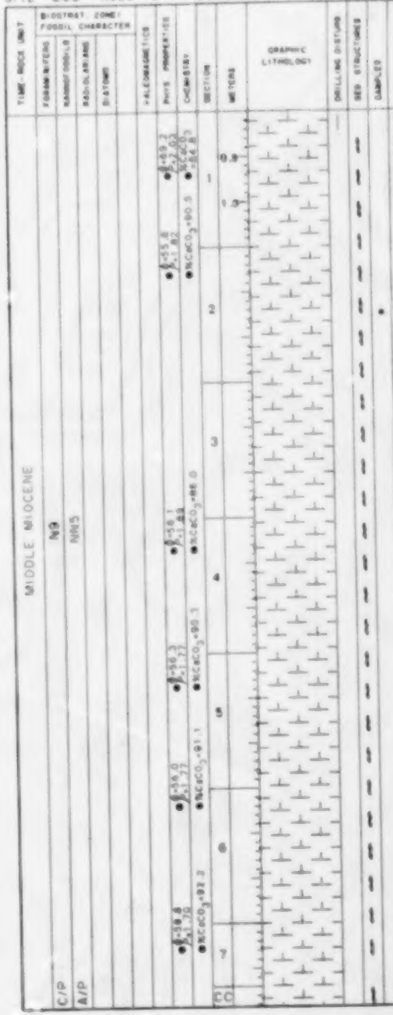
TIME-ROCK UNIT
BIOSTRAT. ZONE/ FOSSIL CHARACTER
FORAMINIFERS
NANNOFOSSILS
RADIOLARIANS
DIATOMS
PALEOMAGNETICS
PHYS. PROPERTIES
CHEMISTRY
SECTION
METERS
GRAPHIC LITHOLOGY
DRILLING DISTURB.
SED. STRUCTURES
SAMPLES
MIDDLE MIOCENE
N9
NN5
C/P
A/P
φ=69.2
γ=2.03
%CaCO3 =84.8
φ=55.8
γ=1.82
%CaCO3=90.5
φ=58.1
γ=1.89
%CaCO3=88.0
φ=56.3
γ=1.77
%CaCO3=90.1
φ=56.0
γ=1.77
%CaCO3=91.1
φ=58.8
γ=1.70
%CaCO3=92.2
1
2
3
4
5
6
7
CC
0.9
1.0

LITHOLOGIC DESCRIPTION

NANNOFOSSIL OOZE

Major lithology: This core contains NANNOFOSSIL OOZE. The color is uniformly white (2.5Y 8/1). Slight bioturbation is seen over the entire core. Mottling is observed as slight discolorations in white (5Y 8/2), representing bioturbation.

SMEAR SLIDE SUMMARY (%):

	2, 74
	D
TEXTURE:	
Sand	1
Silt	9
Clay	90
COMPOSITION:	
Foraminifers	6
Nannofossils	92
Siliceous fragments	1

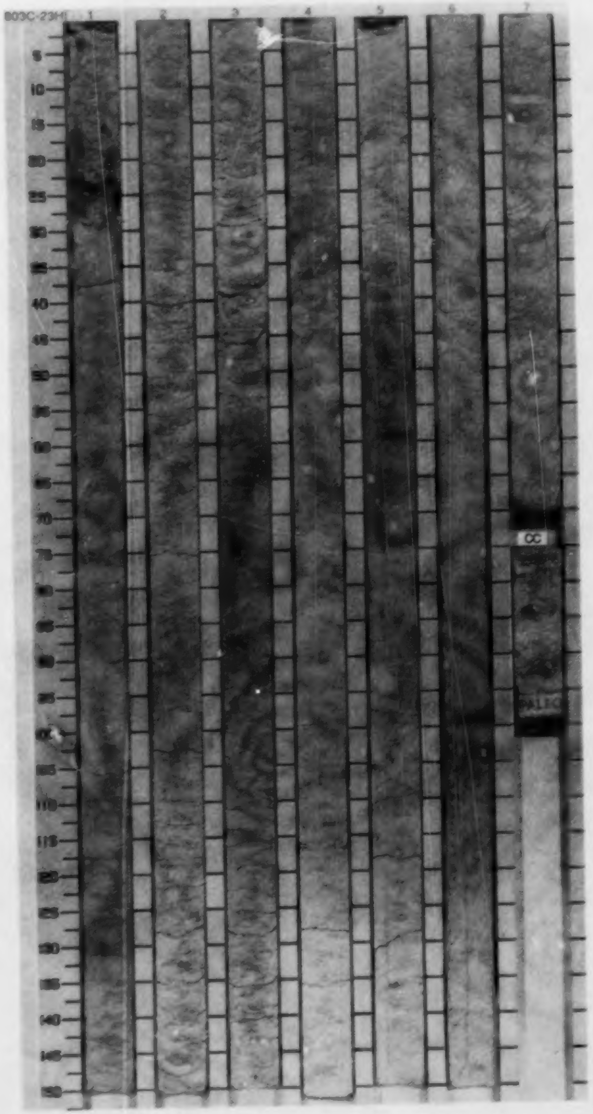
803C-23H
1
2
3
4
5
6
7
CC
5
10
15
20
25
30
35
40
45
50
55
60
65
70
75
80
85
90
95
100
105
110
115
120
125
130
135
140
145
150

SITE 803 HOLE D CORE 1H CORED INTERVAL 0.0-2.5 mbsf

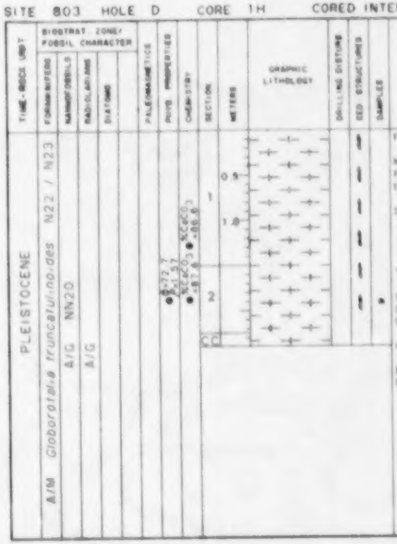
TIME-ROCK UNIT
BIOSTRAT. ZONE/ FOSSIL CHARACTER
FORAMINIFERS
NANNOFOSSILS
RADIOLARIANS
DIATOMS
PALEOMAGNETICS
PHYS. PROPERTIES
CHEMISTRY
SECTION
METERS
GRAPHIC LITHOLOGY
DRILLING DISTURB.
SED. STRUCTURES
SAMPLES
PLEISTOCENE
A/M Globorotalia truncatulinoides N22 / N23
A/G NN20
A/G
φ=72.7
γ=1.57
%CaCO₃ =87.6
%CaCO₃ =86.6
1
2
CC
0.5
1.0

LITHOLOGIC DESCRIPTION

FORAMINIFER NANNOFOSSIL OOZE

Major lithology: This core contains white (2.5Y 8/2) to light yellowish brown (2.5Y 6/4) FORAMINIFER NANNOFOSSIL OOZE. The sediment is uniform, and exhibits slight bioturbation and some mottling.

SMEAR SLIDE SUMMARY (%):

	2, 40
	D
TEXTURE:	
Sand	20
Silt	40
Clay	40
COMPOSITION:	
Foraminifers	25
Nannofossils	75

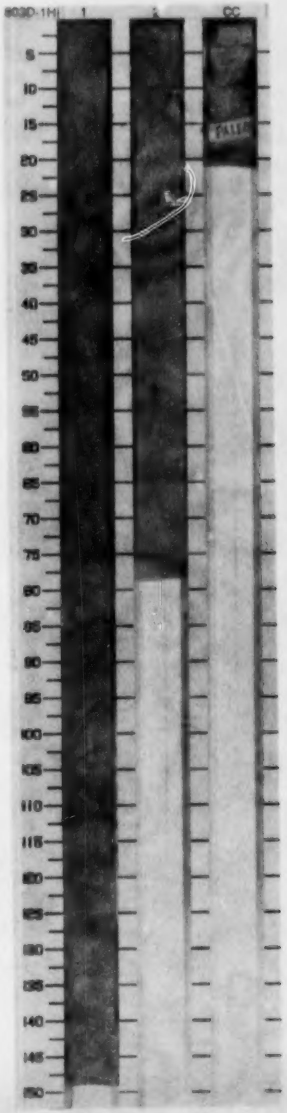
803D-1H
1
2
CC
5
10
15
20
25
30
35
40
45
50
55
60
65
70
75
80
85
90
95
100
105
110
115
120
125
130
135
140
145
150

SITE 803 HOLE D CORE 2H CORED INTERVAL 2.5-12.0 mbsf

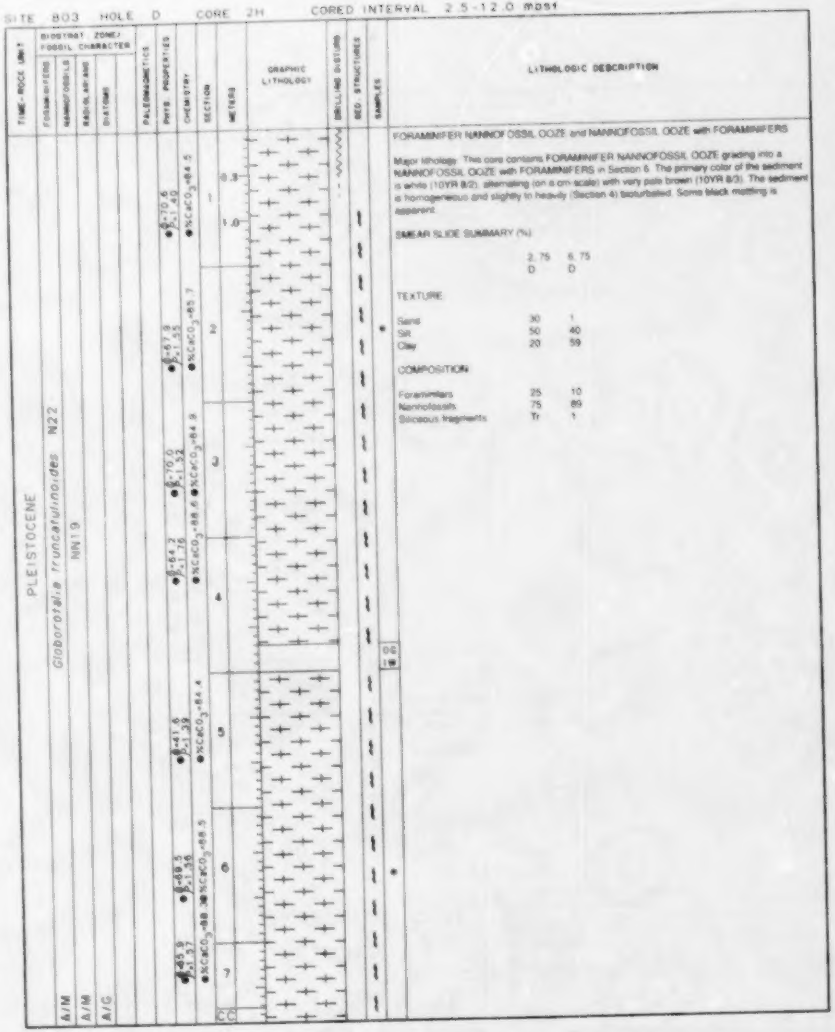
TIME-ROCK UNIT
BIOSTRAT. ZONE/ FOSSIL CHARACTER
FORAMINIFERS
NANNOFOSSILS
RADIOLARIANS
DIATOMS
PALEOMAGNETICS
PHYS. PROPERTIES
CHEMISTRY
SECTION
METERS
GRAPHIC LITHOLOGY
DRILLING DISTURB.
SED. STRUCTURES
SAMPLES
PLEISTOCENE
Globorotalia truncatulinoides N22
NN19
A/M
A/M
A/G
ϕ=70.6 ρ=1.40
%CaCO$_3$=84.5
ϕ=67.9 ρ=1.55
%CaCO$_3$=85.7
ϕ=70.0 ρ=1.52
%CaCO$_3$=84.9
ϕ=64.2 ρ=1.76
%CaCO$_3$=88.6
ϕ=41.6 ρ=1.39
%CaCO$_3$=84.4
ϕ=69.5 ρ=1.56
%CaCO$_3$=88.5
ϕ=65.9 ρ=1.57
%CaCO$_3$=88
1
2
3
4
5
6
7
CC
0.3
1.0
OG
IW

LITHOLOGIC DESCRIPTION

FORAMINIFER NANNOFOSSIL OOZE and NANNOFOSSIL OOZE with FORAMINIFERS

Major lithology: This core contains FORAMINIFER NANNOFOSSIL OOZE grading into a NANNOFOSSIL OOZE with FORAMINIFERS in Section 6. The primary color of the sediment is white (10YR 8/2), alternating (on a cm-scale) with very pale brown (10YR 8/3). The sediment is homogeneous and slightly to heavily (Section 4) bioturbated. Some black mottling is apparent.

SMEAR SLIDE SUMMARY (%):

	2, 75	6, 75
	D	D
TEXTURE:		
Sand	30	1
Silt	50	40
Clay	20	59
COMPOSITION:		
Foraminifers	25	10
Nannofossils	75	89
Siliceous fragments	Tr	1

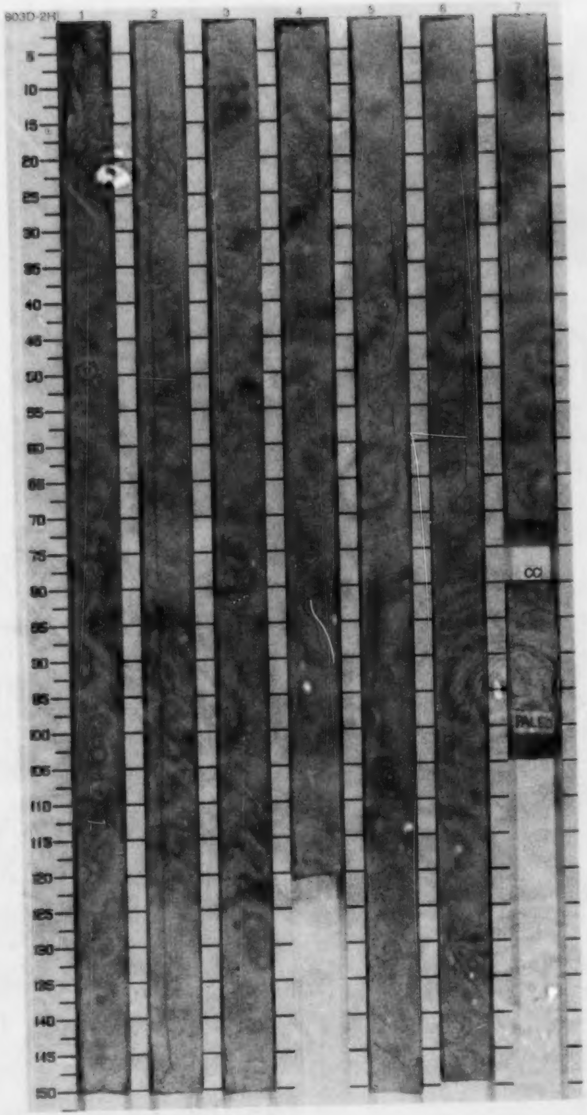
803D-2H
1
2
3
4
5
6
7
5
10
15
20
25
30
35
40
45
50
55
60
65
70
75
80
85
90
95
100
105
110
115
120
125
130
135
140
145
150
CC
PALEO

SITE 803 HOLE D CORE 3H CORED INTERVAL 12.0-21.5 mbsf

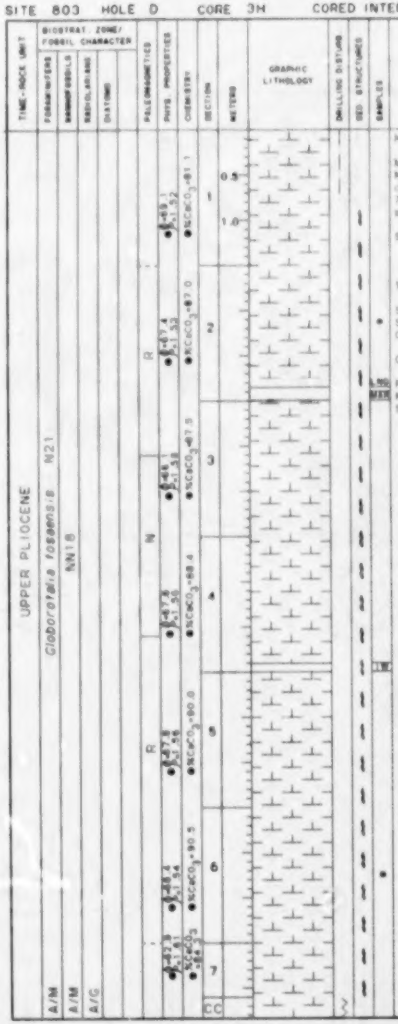

LITHOLOGIC DESCRIPTION

NANNOFOSSIL OOZE with FORAMINIFERS and NANNOFOSSIL OOZE.

Major lithology: This core contains NANNOFOSSIL OOZE with FORAMINIFERS grading into NANNOFOSSIL OOZE in Section 6. The primary color of the sediments is white (10YR 8/1), changing gradually to white (2.5Y 8/0) in Section 4. Beginning in Section 5, faint green (10GY 7/2) and light gray (2.5Y 7/0) color banding is observed. The sediment is homogeneous and shows slight bioturbation. Faint mottling and a few open burrows are observed.

SMEAR SLIDE SUMMARY (%):

	2, 75	6, 75
	D	D
TEXTURE:		
Sand	15	8
Silt	65	55
Clay	20	37
COMPOSITION:		
Foraminifers	12	8
Nannofossils	87	91
Siliceous fragments	1	1

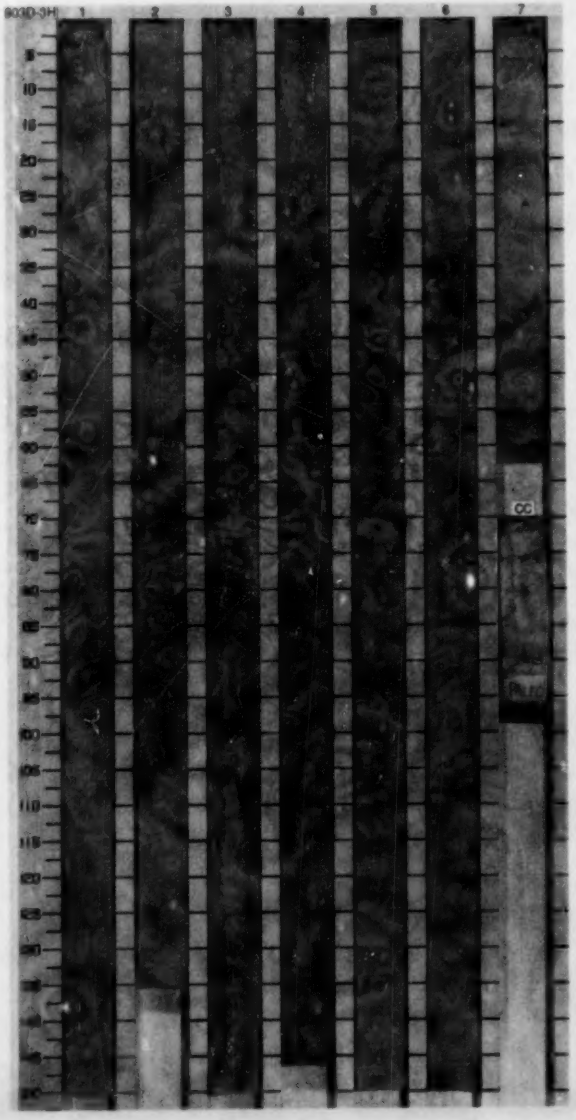
803D-3H
1
2
3
4
5
6
7
CC
5
10
15
20
25
30
35
40
45
50
55
60
65
70
75
80
85
90
95
100
105
110
115
120
125
130
135
140
145
150

SITE 803 HOLE D CORE 4H CORED INTERVAL 21.5-31.0 mbsf

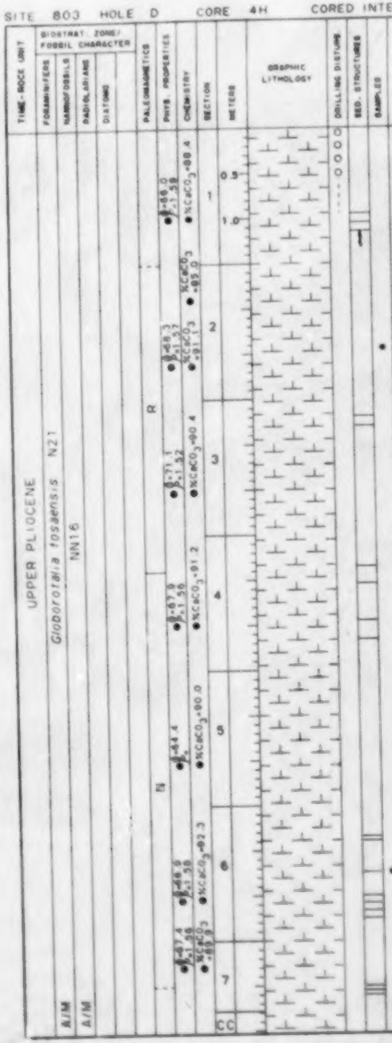

LITHOLOGIC DESCRIPTION

NANNOFOSSIL OOZE with FORAMINIFERS and NANNOFOSSIL OOZE

Major lithology: This core contains NANNOFOSSIL OOZE with FORAMINIFERS grading into NANNOFOSSIL OOZE below Section 2. The sediment is homo- geneous and dominantly white (2.5Y 8/0). Horizontal reddish gray (5R 6/1) and light green (10GY 7/2) color bands spanning intervals of 15- 30 cm are apparent at intervals of 50-100 cm. Mottling of the sediment is common.

SMEAR SLIDE SUMMARY (%):

	2, 94 D	6, 75 D
TEXTURE:		
Sand	30	5
Silt	30	45
Clay	40	50
COMPOSITION:		
Foraminifers	40	5
Nannofossils	60	90
Radiolarians	Tr	—
Zeolite	—	5

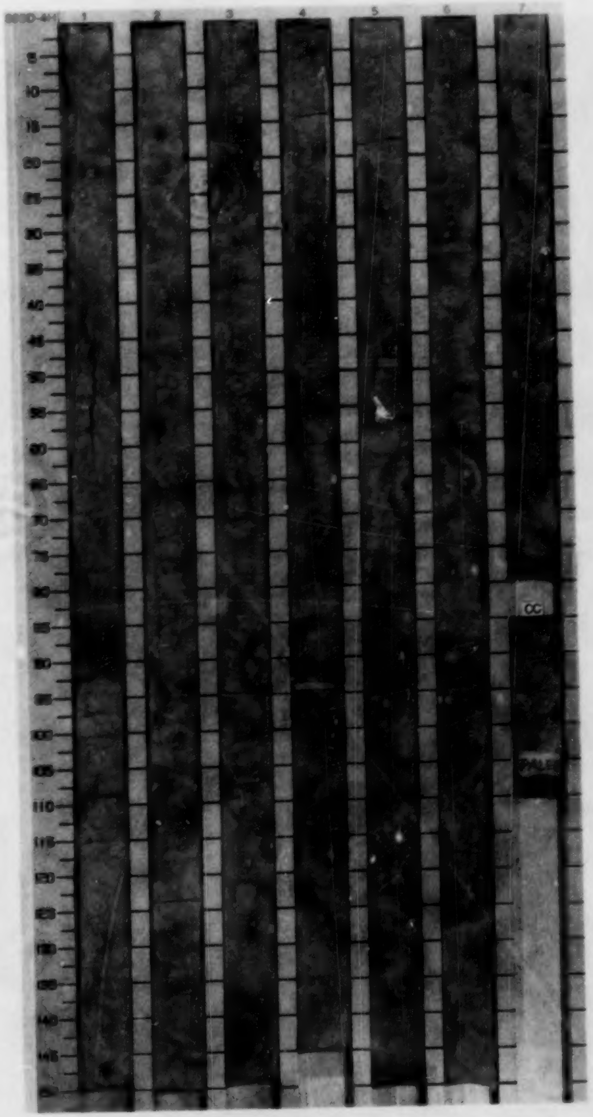
803D-4H
1
2
3
4
5
6
7
CC
5
10
15
20
25
30
35
40
45
50
55
60
65
70
75
80
85
90
95
100
105
110
115
120
125
130
135
140
145
150

SITE 803 HOLE D CORE 5H CORED INTERVAL 31.0-40.5 mbsf

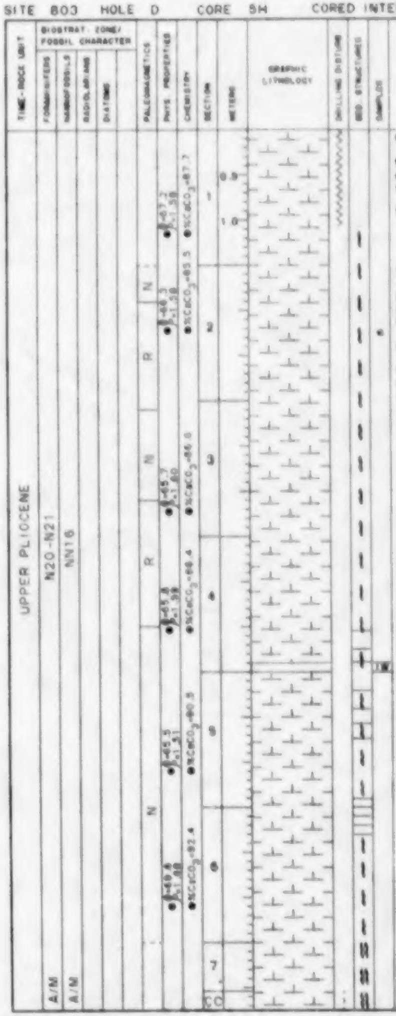
TIME-ROCK UNIT
BIOSTRAT. ZONE/ FOSSIL CHARACTER
FORAMINIFERS
NANNOFOSSILS
RADIOLARIANS
DIATOMS
PALEOMAGNETICS
PHYS. PROPERTIES
CHEMISTRY
SECTION
METERS
GRAPHIC LITHOLOGY
DRILLING DISTURB.
SED. STRUCTURES
SAMPLES
UPPER PLIOCENE
N20-N21
NN16
A/M
A/M
N
R
N
R
N
φ=67.2 γ=1.58
φ=66.3 γ=1.58
φ=65.7 γ=1.60
φ=65.8 γ=1.58
φ=65.5 γ=1.61
φ=69.6 γ=1.60
%CaCO₃=87.7
%CaCO₃=85.5
%CaCO₃=86.0
%CaCO₃=88.4
%CaCO₃=90.5
%CaCO₃=92.4
1
2
3
4
5
6
7
CC
0.5
1.0
IW

LITHOLOGIC DESCRIPTION

NANNOFOSSIL OOZE

Major lithology: This core contains NANNOFOSSIL OOZE. The sediments are homogeneous, bioturbated, mottled and predominantly white (2.5Y 8/0). Horizontal reddish gray (5R 6/1) and light green (10GY 7/2) color bands are present in Sections 4, 5 and 6.

SMEAR SLIDE SUMMARY (%):

	2, 75
	D
TEXTURE:	
Sand	5
Silt	60
Clay	35
COMPOSITION:	
Foraminifers	5
Nannofossils	94
Siliceous fragments	1

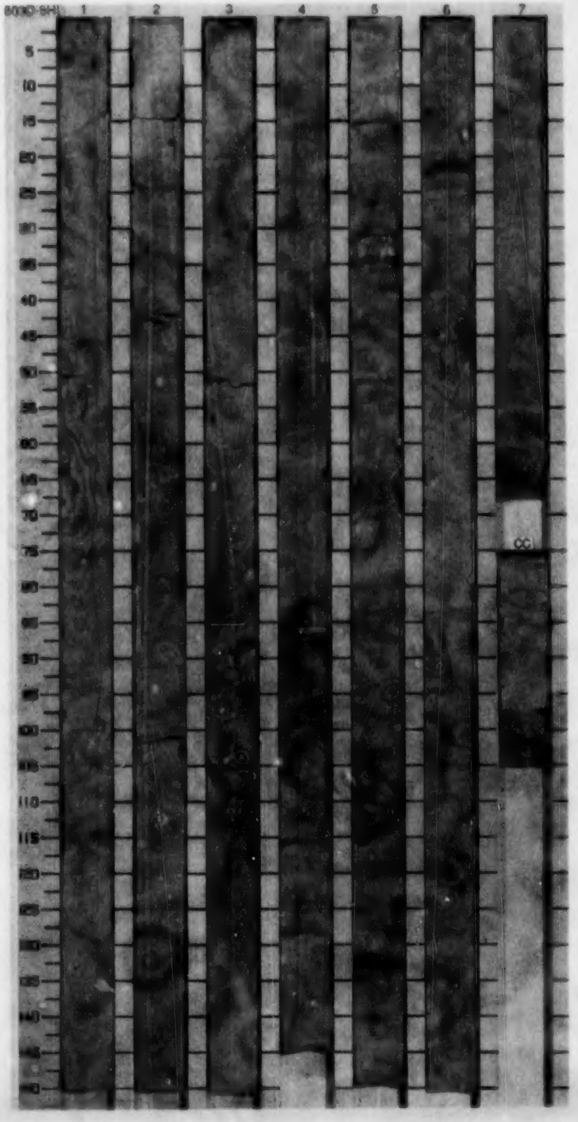
803D-5H
1
2
3
4
5
6
7
CC
5
10
15
20
25
30
35
40
45
50
55
60
65
70
75
80
85
90
95
100
105
110
115
120
125
130
135
140
145
150

SITE 803 HOLE D CORE 6H CORED INTERVAL 40.5-46.1 mbsf

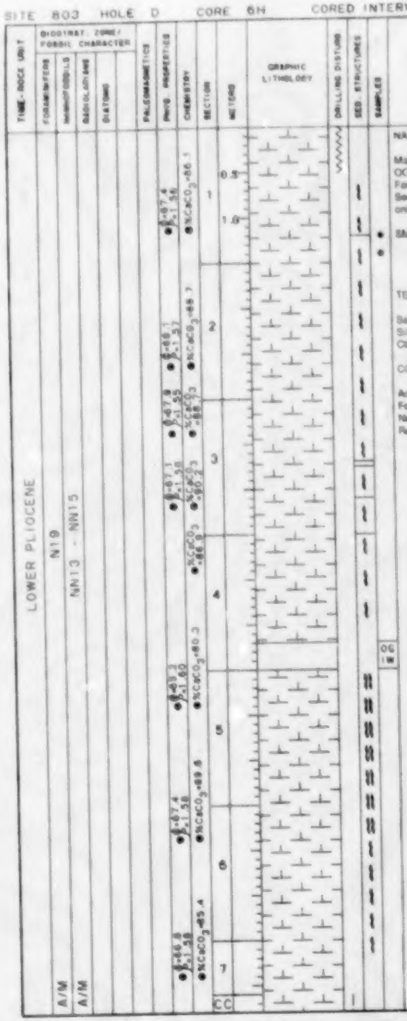
TIME-ROCK UNIT
BIOSTRAT. ZONE/ FOSSIL CHARACTER
FORAMINIFERS
NANNOFOSSILS
RADIOLARIANS
DIATOMS
PALEOMAGNETICS
PHYS. PROPERTIES
CHEMISTRY
SECTION
METERS
GRAPHIC LITHOLOGY
DRILLING DISTURB.
SED. STRUCTURES
SAMPLES
LOWER PLIOCENE
N19
NN13 - NN15
A/M
A/M
γ=67.4 φ=1.56
%CaCO3=86.1
γ=68.1 φ=1.57
%CaCO3=88.7
γ=67.9 φ=1.55
%CaCO3=88.7
γ=67.1 φ=1.58
%CaCO3=90.2
%CaCO3=86.9
%CaCO3=80.3
γ=69.2 φ=1.60
γ=67.4 φ=1.58
%CaCO3=89.8
γ=66.8 φ=1.58
%CaCO3=85.4
1
2
3
4
5
6
7
CC
0.5
1.0
OG
IW

LITHOLOGIC DESCRIPTION

NANNOFOSSIL OOZE

Major lithology: This core contains slightly to heavily bioturbated and mottled NANNOFOSSIL OOZE. The color is mainly white (2.5Y 8/0), but grades into light gray (N7/) downsection. Faint, light greenish gray (5G 7/1) to greenish gray (5G 6/1) color bands are present in Sections 3, 4, 6 and 7. Sections 1 and 2 may not be representative sections, since drilling only advanced 5.6 m while 9.8 m of core were recovered.

SMEAR SLIDE SUMMARY (%):

	1, 130	1, 140
	M	D
TEXTURE:		
Sand	5	5
Silt	20	20
Clay	75	75
COMPOSITION:		
Accessory minerals	10	5
Foraminifers	5	5
Nannofossils	80	85
Radiolarians	5	5

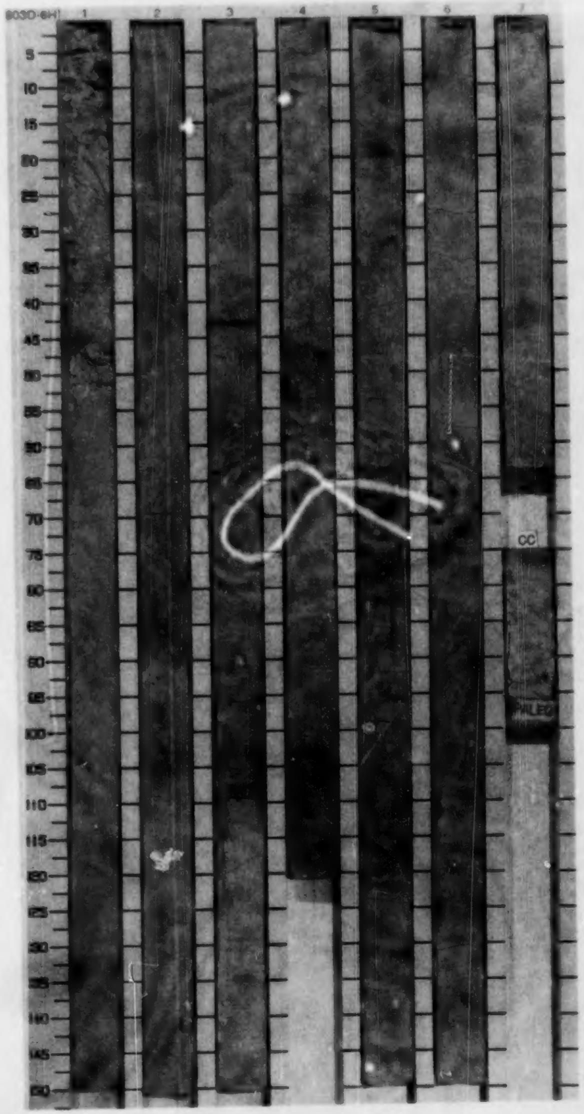
803D-6H
1
2
3
4
5
6
7
CC
PALEO
5
10
15
20
25
30
35
40
45
50
55
60
65
70
75
80
85
90
95
100
105
110
115
120
125
130
135
140
145
150

SITE 803 HOLE D CORE 7H CORED INTERVAL 46.1-56.6 mbsf

TIME-ROCK UNIT	FORAMINIFERS	NANNOFOSSILS	RADIOLARIANS	DIATOMS	PALEOMAGNETICS	PHYS. PROPERTIES	CHEMISTRY	SECTION	METERS
LOWER PLIOCENE	N19	NN13 - NN15				● φ=66.0 γ=1.58	● %CaCO$_3$ =88.0	1	0.5 1.0
						● φ=66.5 γ=1.58	● %CaCO$_3$=85.6	2	
						● φ=67.9 γ=1.56	● %CaCO$_3$=90.5	3	
						● φ=64.5 γ=1.62	● %CaCO$_3$=88.5	4	
						● φ=64.2 γ=1.62	● %CaCO$_3$=91.8	5	
						● φ=64.9 γ=1.60	● %CaCO$_3$=91.9	6	
								7	
	C/M	A/M						CC	

BIOSTRAT. ZONE/ FOSSIL CHARACTER

GRAPHIC LITHOLOGY

DRILLING DISTURB.

SED. STRUCTURES

SAMPLES

LITHOLOGIC DESCRIPTION

NANNOFOSSIL OOZE

Major lithology: This core contains slightly to heavily bioturbated, mottled NANNOFOSSIL OOZE. The color of the sediments is mainly white (2.5Y 8/0). Faint, reddish gray (5R 6/1) to pale green (10G 6/2) color bands are present throughout core.

SMEAR SLIDE SUMMARY (%):

	5, 59 D
TEXTURE:	
Sand	5
Silt	95
COMPOSITION:	
Foraminifers	5
Nannofossils	95

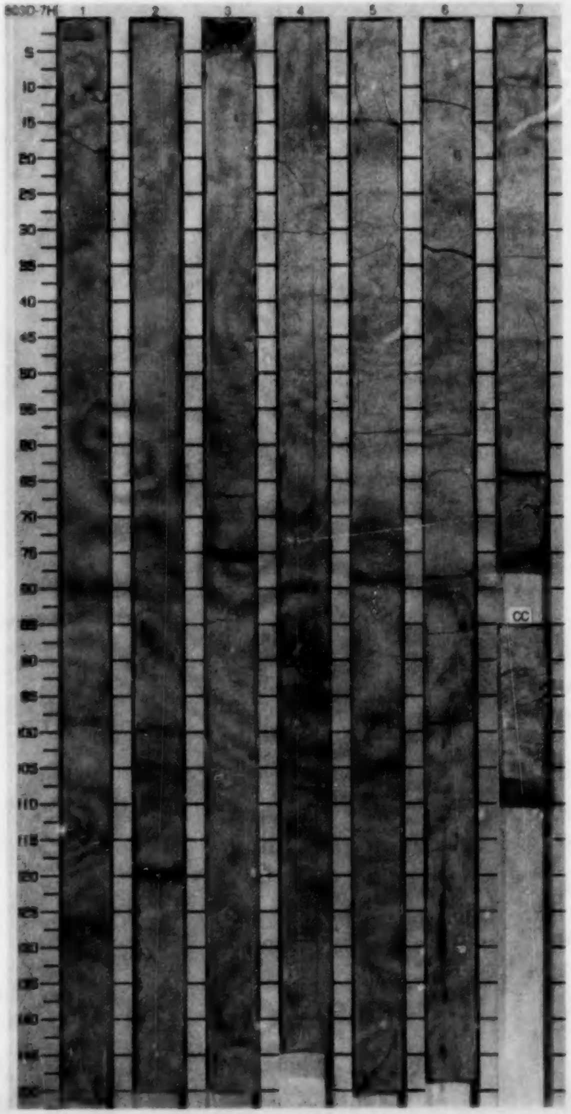
803D-7H
1
2
3
4
5
6
7
CC
5
10
15
20
25
30
35
40
45
50
55
60
65
70
75
80
85
90
95
100
105
110
115
120
125
130
135
140
145
150

SITE 803 HOLE D CORE 8H CORED INTERVAL 58.6-65.1 mbsf

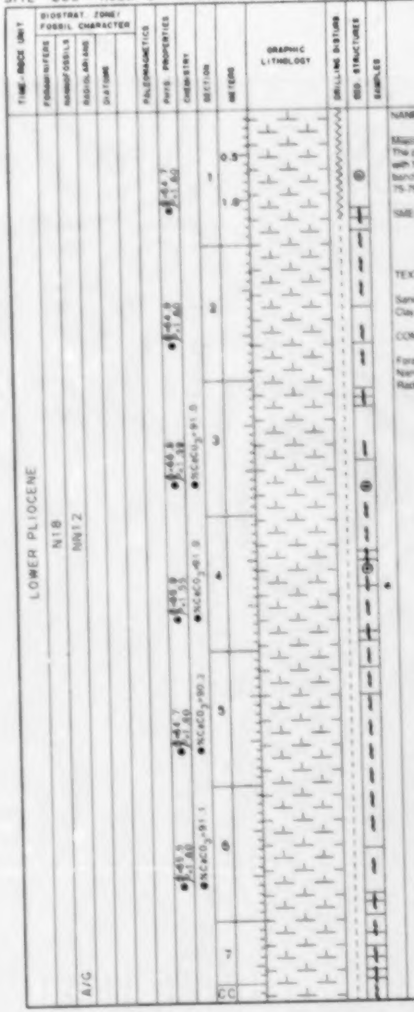
TIME-ROCK UNIT
BIOSTRAT. ZONE/ FOSSIL CHARACTER
FORAMINIFERS
NANNOFOSSILS
RADIOLARIANS
DIATOMS
PALEOMAGNETICS
PHYS. PROPERTIES
CHEMISTRY
SECTION
METERS
GRAPHIC LITHOLOGY
DRILLING DISTURB.
SED. STRUCTURES
SAMPLES
LOWER PLIOCENE
N18
NN12
A/G
φ=64.7 ρ=1.60
φ=64.9 ρ=1.60
φ=66.8 ρ=1.38
φ=65.9 ρ=1.55
φ=64.7 ρ=1.60
φ=65.5 ρ=1.60
%CaCO3=91.0
%CaCO3=91.0
%CaCO3=90.2
%CaCO3=91.1
1
2
3
4
5
6
7
CC
0.5
1.0

LITHOLOGIC DESCRIPTION

NANNOFOSSIL OOZE

Major lithology: This core contains slightly to moderately bioturbated NANNOFOSSIL OOZE. The primary colors of the sediment are white (7.5YR N8 and 10YR 8/1) and light gray (N7) with faint, light blue gray (5B 7/1), light greenish gray (5G 7/1), and reddish gray (5R 6/1) color banding evident throughout the core. Cm-scale pyritized burrow fills are located at Section 1, 75-79 cm, Section 3, 115-118 cm, and Section 4, 56-59 cm.

SMEAR SLIDE SUMMARY (%):

	4, 80
	D
TEXTURE:	
Sand	10
Clay	90
COMPOSITION:	
Foraminifers	5
Nannofossils	90
Radiolarians	5

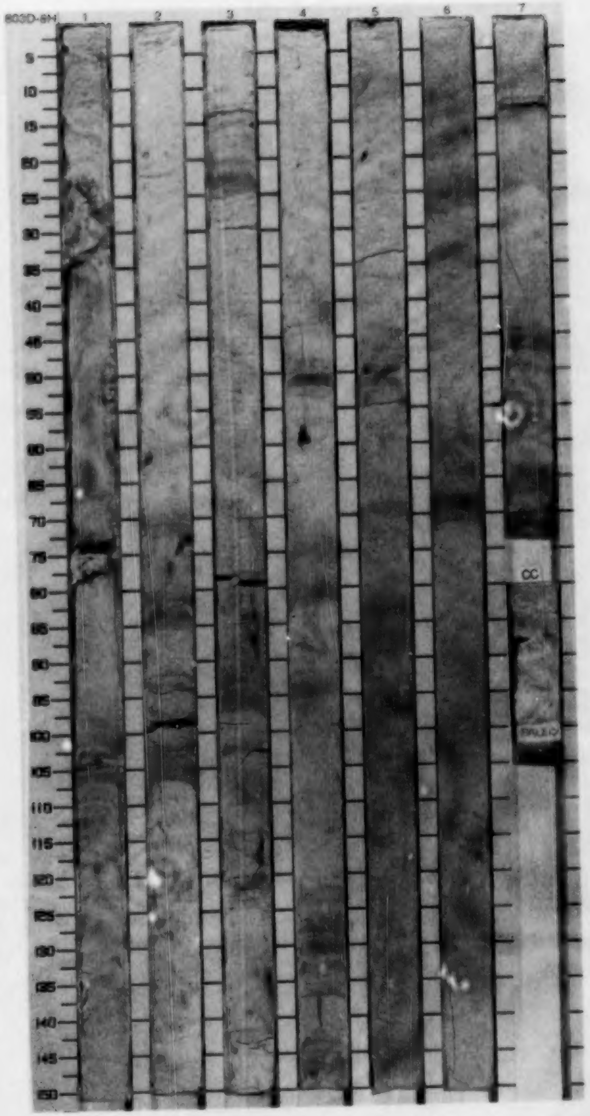
803D-8H
1
2
3
4
5
6
7
5
10
15
20
25
30
35
40
45
50
55
60
65
70
75
80
85
90
95
100
105
110
115
120
125
130
135
140
145
150
CC
PALEO

SITE 803 HOLE D CORE 9H CORED INTERVAL 65.1-74.6 mbsf

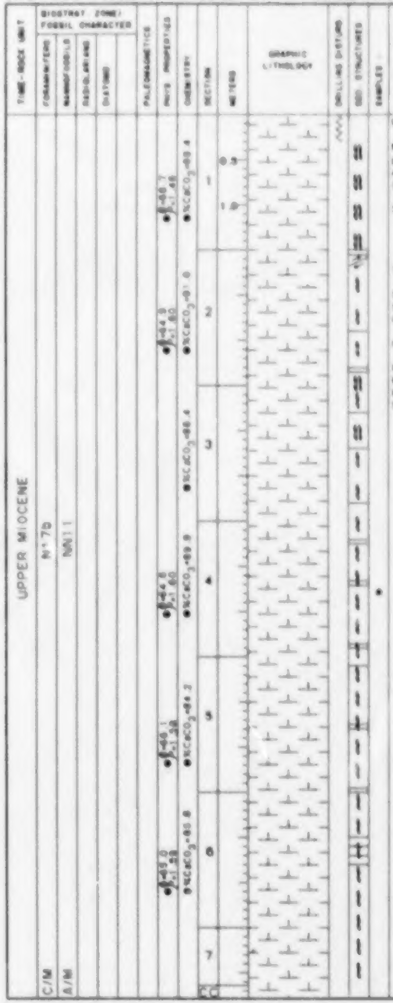
TIME-ROCK UNIT
BIOSTRAT. ZONE/ FOSSIL CHARACTER
FORAMINIFERS
NANNOFOSSILS
RADIOLARIANS
DIATOMS
PALEOMAGNETICS
PHYS. PROPERTIES
CHEMISTRY
SECTION
METERS
GRAPHIC LITHOLOGY
DRILLING DISTURB.
SED. STRUCTURES
SAMPLES
UPPER MIOCENE
N°17b
NN11
C/M
A/M
φ=66.7
γ=1.48
%CaCO3=88.4
φ=64.9
γ=1.60
%CaCO3=91.0
%CaCO3=88.4
φ=64.6
γ=1.60
%CaCO3=89.9
φ=66.1
γ=1.38
%CaCO3=84.2
φ=65.0
γ=1.58
%CaCO3=85.8
1
2
3
4
5
6
7
CC
0.5
1.0

LITHOLOGIC DESCRIPTION

NANNOFOSSIL OOZE

Major lithology: This core contains slightly to heavily bioturbated NANNOFOSSIL OOZE. The primary color of the sediment is white (2.5Y 8/0). Reddish gray (5R 6/1), pale green (10G 6/2) and light gray (N7) color banding and burrow fills are present throughout the core. Microfaults (1-3 cm offset) appear in the upper 25 cm of Section 2.

SMEAR SLIDE SUMMARY (%):

	4, 79
	D
TEXTURE:	
Sand	5
Silt	30
Clay	65
COMPOSITION:	
Foraminifers	1
Nannofossils	89
Radiolarians	5
Spicules	1

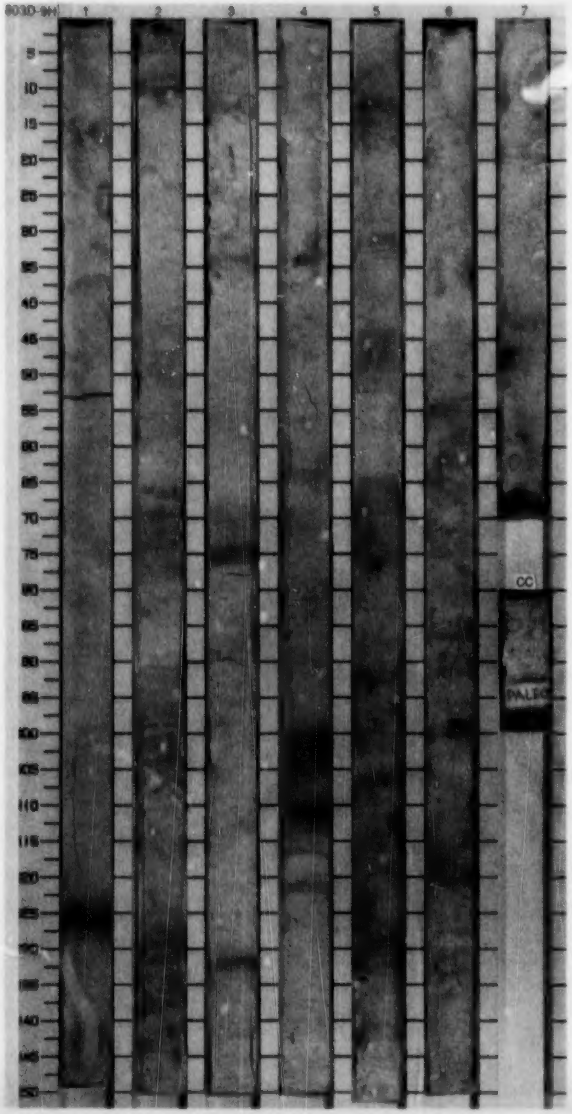
803D-9H
1
2
3
4
5
6
7
5
10
15
20
25
30
35
40
45
50
55
60
65
70
75
80
85
90
95
100
105
110
115
120
125
130
135
140
145
150
CC
PALEO

SITE 803 HOLE D CORE 10H CORED INTERVAL 74.6-84.1 mbsf

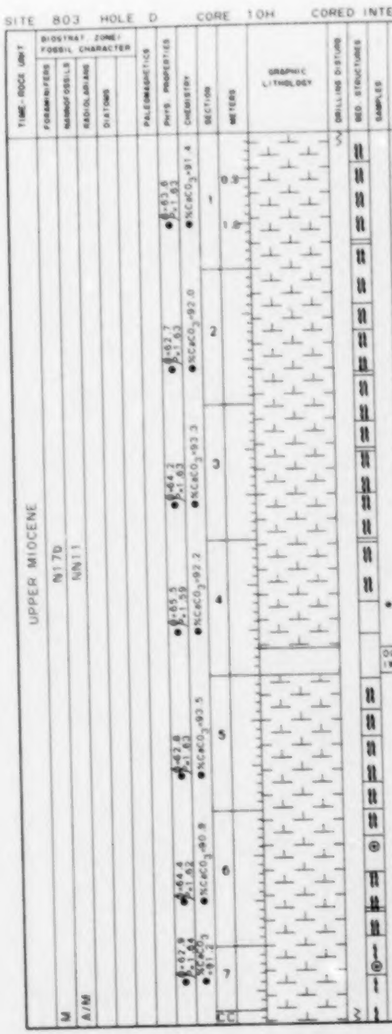
TIME-ROCK UNIT
BIOSTRAT. ZONE/ FOSSIL CHARACTER
FORAMINIFERS
NANNOFOSSILS
RADIOLARIANS
DIATOMS
PALEOMAGNETICS
PHYS. PROPERTIES
CHEMISTRY
SECTION
METERS
GRAPHIC LITHOLOGY
DRILLING DISTURB.
SED. STRUCTURES
SAMPLES
UPPER MIOCENE
N17b
NN11
M
A/M
φ=63.6 γ=1.63
%CaCO₃=91.4
φ=62.7 γ=1.63
%CaCO₃=92.0
φ=64.2 γ=1.63
%CaCO₃=93.3
φ=65.5 γ=1.59
%CaCO₃=92.2
φ=62.8 γ=1.63
%CaCO₃=93.5
φ=64.4 γ=1.62
%CaCO₃=90.8
φ=62.9 γ=1.64
%CaCO₃=91.2
1
2
3
4
5
6
7
CC
0.5
1.0
OG
IW

LITHOLOGIC DESCRIPTION

NANNOFOSSIL OOZE with FORAMINIFERS

Major lithology: This core contains NANNOFOSSIL OOZE with FORAMINIFERS. It is heavily bioturbated and mottled and contains a few pyritized burrow fills. The main color is white (2.5Y 8/0), and burrows are light gray (10YR 7/2) and reddish gray (5R 6/1). Faint light gray (N7/) color bands are present throughout the core.

SMEAR SLIDE SUMMARY (%):

	4, 74
	D
TEXTURE:	
Sand	5
Silt	30
Clay	65
COMPOSITION:	
Diatoms	1
Foraminifers	10
Nannofossils	84
Radiolarians	4
Spicules	1

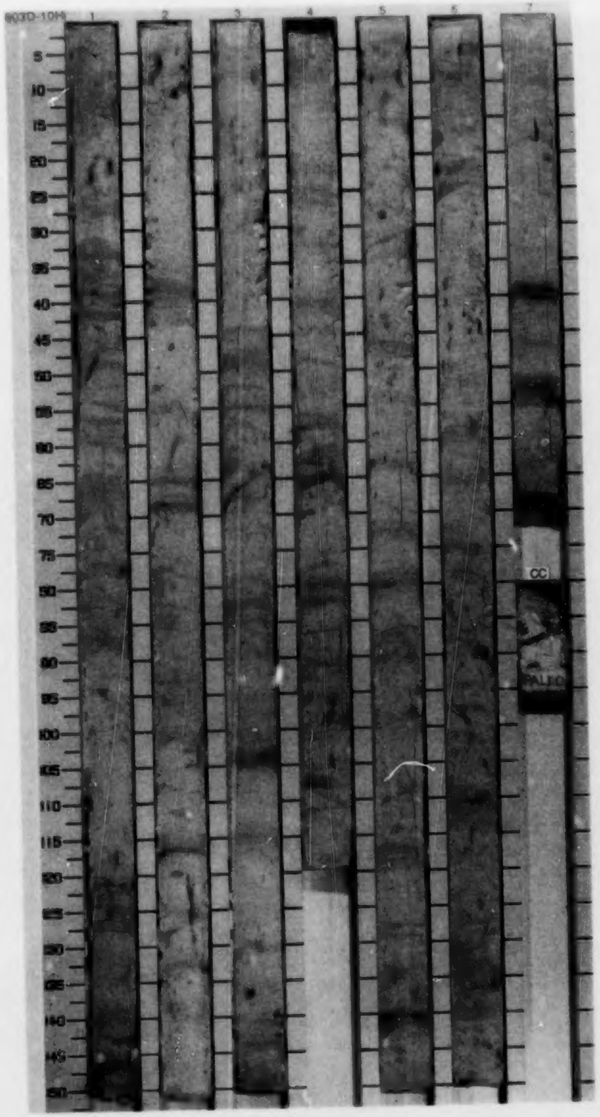
803D-10H
1
2
3
4
5
6
7
CC
PALEO
5
10
15
20
25
30
35
40
45
50
55
60
65
70
75
80
85
90
95
100
105
110
115
120
125
130
135
140
145
150

SITE 803 HOLE D CORE 11H CORED INTERVAL 84.1-93.6 mbsf

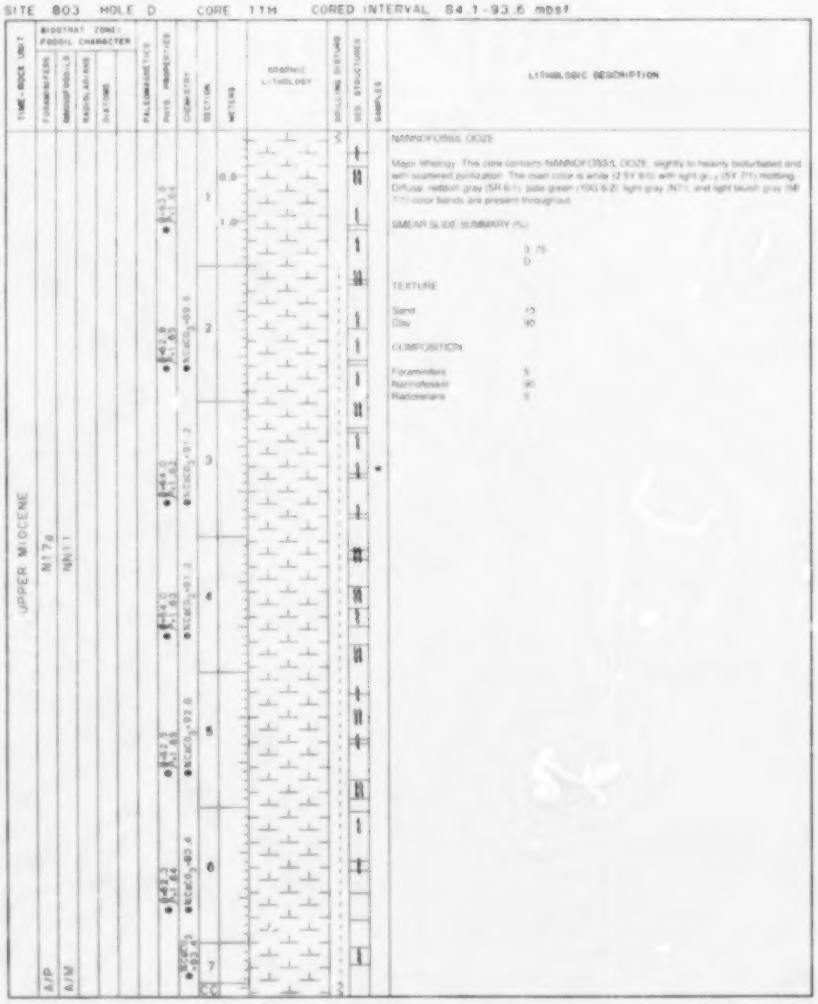
TIME-ROCK UNIT
BIOSTRAT. ZONE/ FOSSIL CHARACTER
FORAMINIFERS
NANNOFOSSILS
RADIOLARIANS
DIATOMS
PALEOMAGNETICS
PHYS. PROPERTIES
CHEMISTRY
SECTION
METERS
GRAPHIC LITHOLOGY
DRILLING DISTURB.
SED. STRUCTURES
SAMPLES
LITHOLOGIC DESCRIPTION
UPPER MIOCENE
N17a
NN11
A/P
A/M
1
2
3
4
5
6
7
CC
0.5
1.0

NANNOFOSSIL OOZE

Major lithology: This core contains NANNOFOSSIL OOZE, slightly to heavily bioturbated and with scattered pyritization. The main color is white (2.5Y 8/0) with light gray (5Y 7/1) mottling. Diffuse, reddish gray (5R 6/1), pale green (10G 6/2), light gray (N7), and light bluish gray (5B 7/1) color bands are present throughout.

SMEAR SLIDE SUMMARY (%):

	3, 75
	D
TEXTURE	
Sand	10
Clay	90
COMPOSITION	
Foraminifers	5
Nannofossils	90
Radiolarians	5

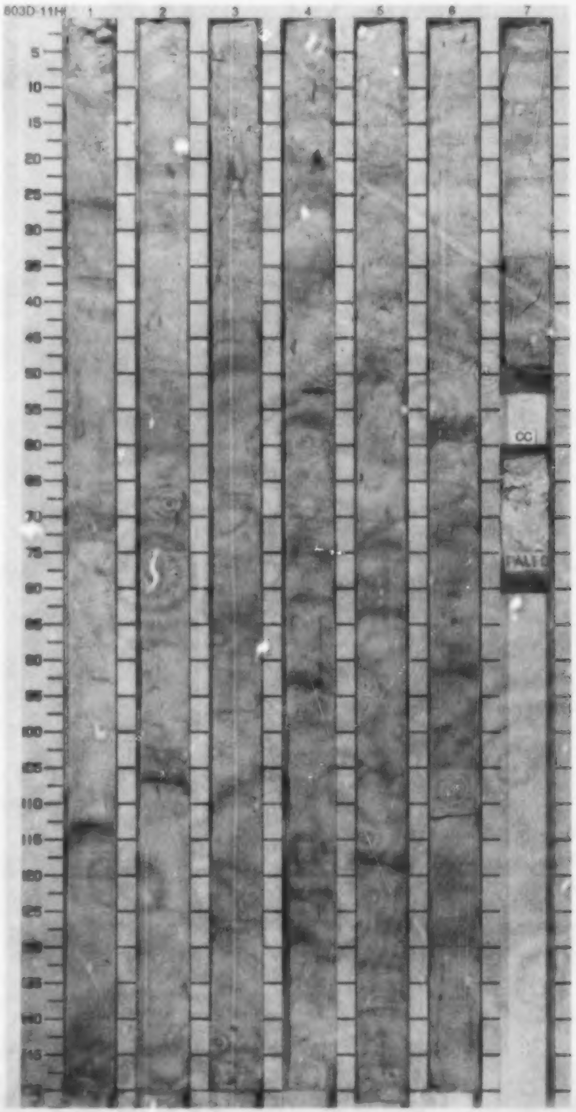
803D-11H
1
2
3
4
5
6
7
5
10
15
20
25
30
35
40
45
50
55
60
65
70
75
80
85
90
95
100
105
110
115
120
125
130
135
140
145
150
CC
PALEO

SITE 803 HOLE D CORE 12H CORED INTERVAL 93.6-103.1 mbsf

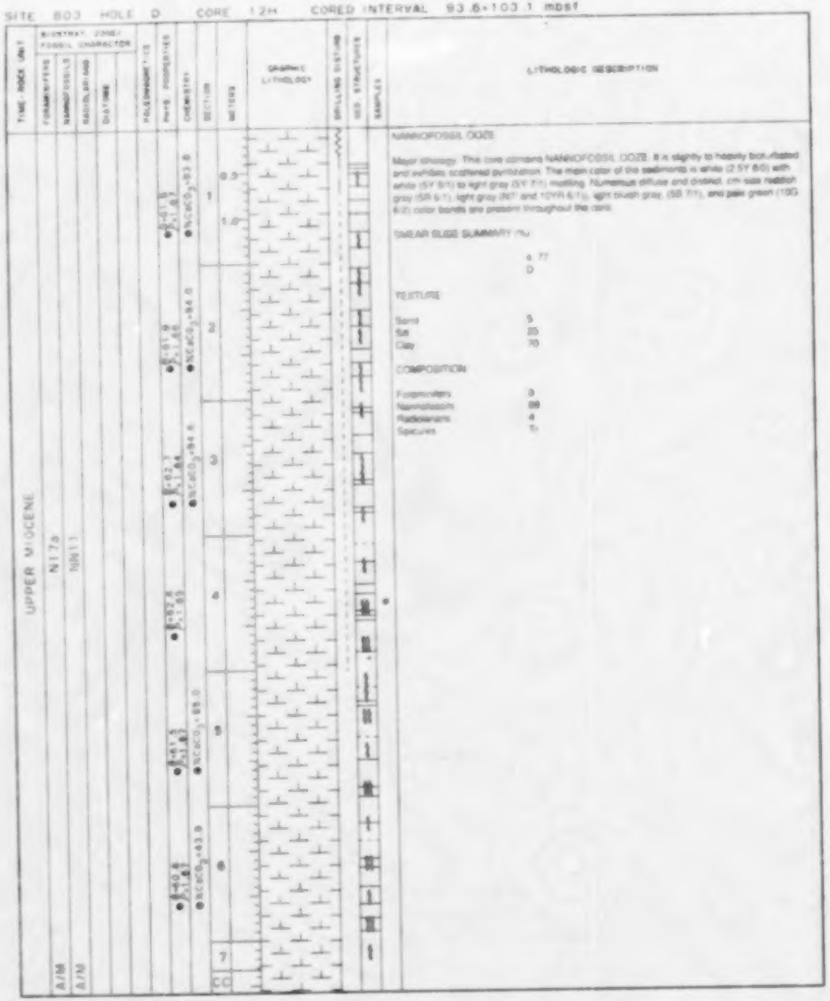
TIME-ROCK UNIT
BIOSTRAT. ZONE/FOSSIL CHARACTER
FORAMINIFERS
NANNOFOSSILS
RADIOLARIANS
DIATOMS
PALEOMAGNETICS
PHYS. PROPERTIES
CHEMISTRY
SECTION
METERS
GRAPHIC LITHOLOGY
DRILLING DISTURB.
SED. STRUCTURES
SAMPLES
LITHOLOGIC DESCRIPTION
UPPER MIOCENE
N17a
NN11
A/M
A/M
●%CaCO3=83.8
●%CaCO3=84.0
●%CaCO3=84.6
●%CaCO3=85.0
●%CaCO3=83.8
1
2
3
4
5
6
7
CC
0.5
1.0

NANNOFOSSIL OOZE

Major lithology: This core contains NANNOFOSSIL OOZE. It is slightly to heavily bioturbated and exhibits scattered pyritization. The main color of the sediments is white (2.5Y 8/0) with white (5Y 8/1) to light gray (5Y 7/1) mottling. Numerous diffuse and distinct, cm-scale reddish gray (5R 6/1), light gray (N7 and 10YR 6/1), light bluish gray (5B 7/1), and pale green (10G 6/2) color bands are present throughout the core.

SMEAR SLIDE SUMMARY (%):

	4, 77
	D
TEXTURE	
Sand	5
Silt	25
Clay	70
COMPOSITION	
Foraminifers	8
Nannofossils	88
Radiolarians	4
Spicules	Tr

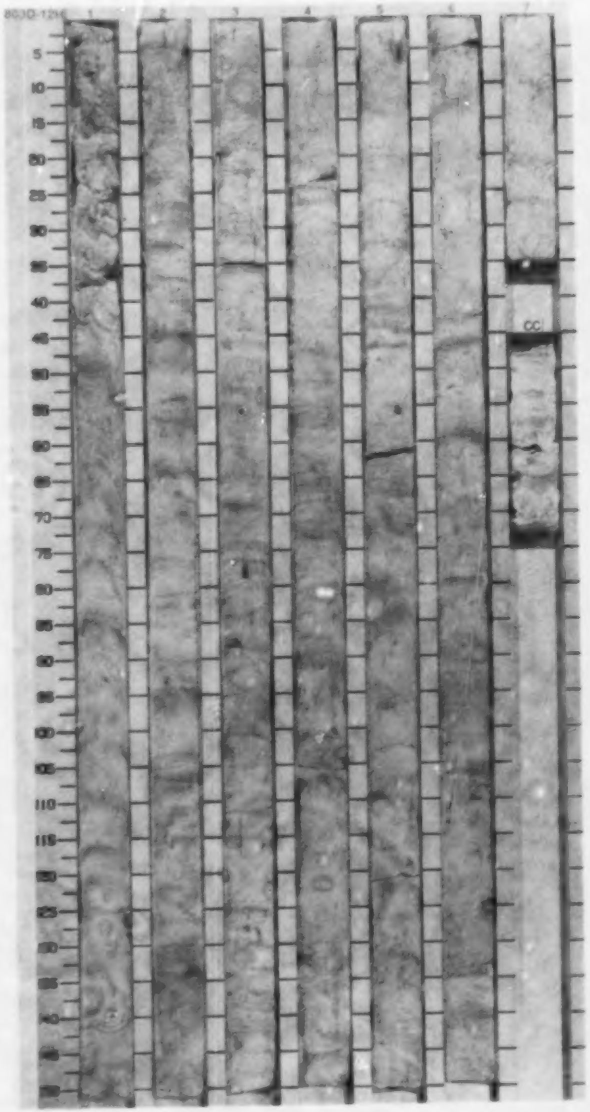
803D-12H
1
2
3
4
5
6
7
CC
5
10
15
20
25
30
35
40
45
50
55
60
65
70
75
80
85
90
95
100
105
110
115
120
125
130
135
140
145
150

SITE 803 HOLE D CORE 13H CORED INTERVAL 103.1-112.6 mbsf

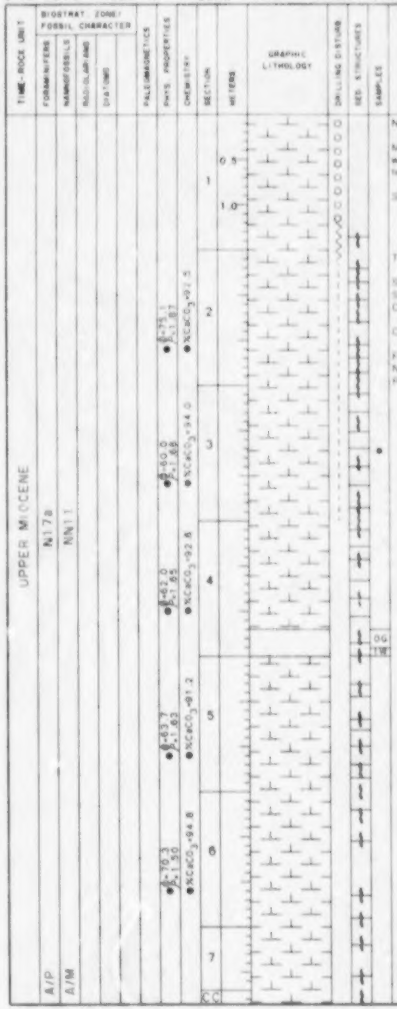
TIME-ROCK UNIT
BIOSTRAT. ZONE/ FOSSIL CHARACTER
FORAMINIFERS
NANNOFOSSILS
RADIOLARIANS
DIATOMS
PALEOMAGNETICS
PHYS. PROPERTIES
CHEMISTRY
SECTION
METERS
GRAPHIC LITHOLOGY
DRILLING DISTURB.
SED. STRUCTURES
SAMPLES
UPPER MIOCENE
N17a
NN11
A/P
A/M
φ=75.1 γ=1.87
φ=60.0 γ=1.68
φ=62.0 γ=1.65
φ=63.7 γ=1.63
φ=70.3 γ=1.50
%CaCO₃=92.5
%CaCO₃=94.0
%CaCO₃=92.8
%CaCO₃=91.2
%CaCO₃=94.8
1
2
3
4
5
6
7
CC
0.5
1.0
OG
IW

LITHOLOGIC DESCRIPTION

NANNOFOSSIL OOZE

Major lithology: This core contains NANNOFOSSIL OOZE. Its primary color is white (2.5Y N8) with abundant pale, light gray (N7, 5Y 7/1, and 10YR 7/1) color bands. Bioturbation is slight to heavy and is expressed as light gray (N7, 5Y 7/1, and 10YR 7/1) mottling.

SMEAR SLIDE SUMMARY (%):

	3, 72
	D
TEXTURE	
Sand	2
Silt	23
Clay	75
COMPOSITION	
Foraminifers	7
Nannofossils	90
Radiolarians	3

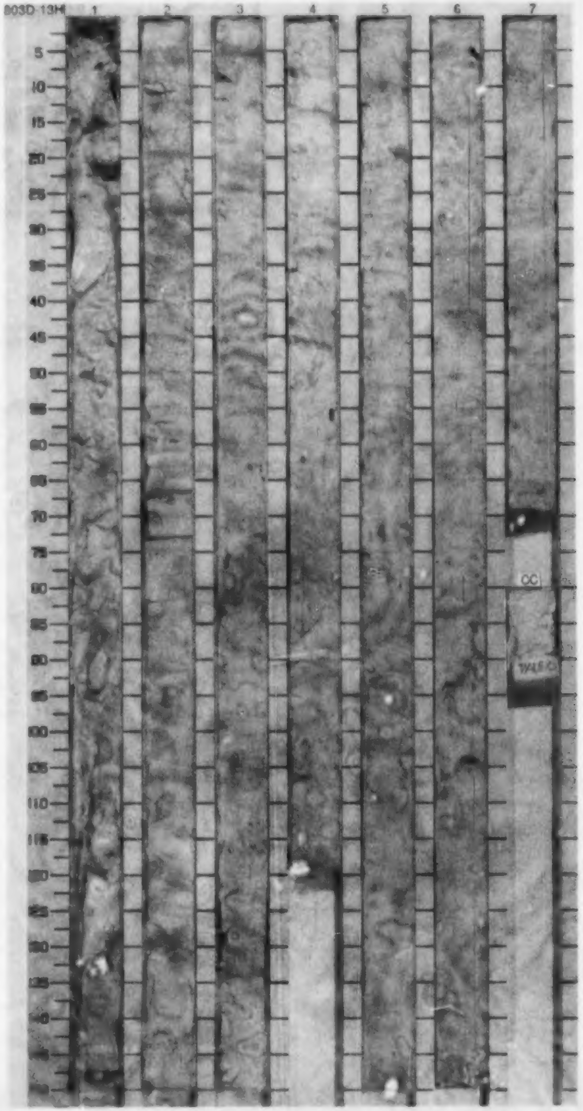
803D-13H
1
2
3
4
5
6
7
5
10
15
20
25
30
35
40
45
50
55
60
65
70
75
80
85
90
95
100
105
110
115
120
125
130
135
140
145
150
CC
TW&G

SITE 803 HOLE D CORE 14H CORED INTERVAL 112.6-122.1 mbsf

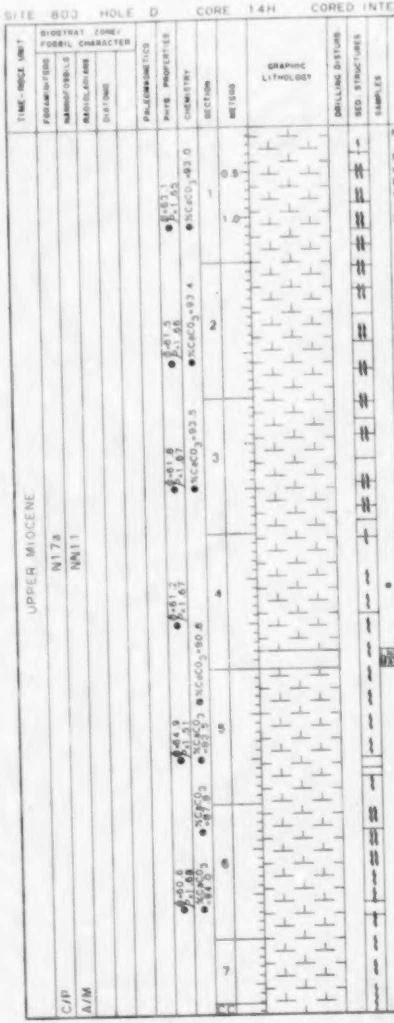
TIME-ROCK UNIT
BIOSTRAT. ZONE/ FOSSIL CHARACTER
FORAMINIFERS
NANNOFOSSILS
RADIOLARIANS
DIATOMS
PALEOMAGNETICS
PHYS. PROPERTIES
CHEMISTRY
SECTION
METERS
GRAPHIC LITHOLOGY
DRILLING DISTURB.
SED. STRUCTURES
SAMPLES
UPPER MIOCENE
N17a
NN11
C/P
A/M
ϕ=63.1 ρ=1.65
%CaCO3=93.0
ϕ=61.5 ρ=1.66
%CaCO3=93.4
ϕ=61.8 ρ=1.67
%CaCO3=93.5
ϕ=61.2 ρ=1.67
%CaCO3=90.8
ϕ=64.9 ρ=1.61
%CaCO3=93.5
%CaCO3=87.8
ϕ=60.6 ρ=1.68
%CaCO3=94.0
1
2
3
4
5
6
7
CC
0.5
1.0

LITHOLOGIC DESCRIPTION

NANNOFOSSIL OOZE

Major lithology: This core contains NANNOFOSSIL OOZE. Its primary color is white (2.5Y N8/), with minor to moderate amounts of pale, light gray (N7/, 5Y 7/1, and 10YR 7/1) color banding. Bioturbation is slight to heavy and is expressed as light gray (N7/, 5Y 7/1, and 10YR 7/1) mottling.

SMEAR SLIDE SUMMARY (%):

	4, 99
	D
TEXTURE:	
Sand	5
Silt	45
Clay	50
COMPOSITION:	
Foraminifers	2
Nannofossils	91
Radiolarians	6
Spicules	1

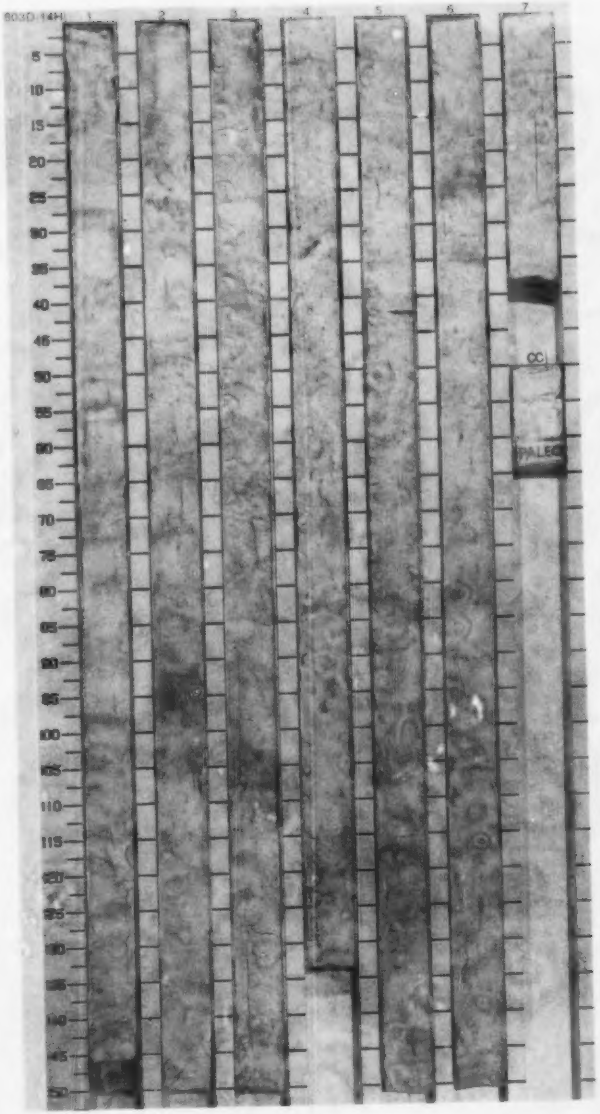
803D-14H
1
2
3
4
5
6
7
CC
PALEO
5
10
15
20
25
30
35
40
45
50
55
60
65
70
75
80
85
90
95
100
105
110
115
120
125
130
135
140
145
150

SITE 803 HOLE D CORE 15H CORED INTERVAL 122.1-131.6 mbsf

TIME-ROCK UNIT	BIOSTRAT. ZONE/ FOSSIL CHARACTER: FORAMINIFERS	NANNOFOSSILS	RADIOLARIANS	DIATOMS	PALEOMAGNETICS	PHYS. PROPERTIES	CHEMISTRY	SECTION	METERS	GRAPHIC LITHOLOGY	DRILLING DISTURB.	SED. STRUCTURES	SAMPLES
UPPER MIOCENE	N17a	NN11				φ=62.2 γ=1.65	%CaCO$_3$=93.5	1	0.5 1.0		○ ○ ○ ○		
						φ=63.0 γ=1.64	%CaCO$_3$=92.4	2					
						φ=63.3 γ=1.63	%CaCO$_3$=96.0	3					
						φ=60.2 γ=1.67	%CaCO$_3$=93.6	4					
						φ=61.5 γ=1.68	%CaCO$_3$=92.4	5					
						φ=63.8 γ=1.63	%CaCO$_3$=94.0	6					●
								7					
	A	A/M						CC					

LITHOLOGIC DESCRIPTION

NANNOFOSSIL OOZE

Major lithology: This core contains NANNOFOSSIL OOZE. Its primary color is white (2.5Y 8/0). Horizontal faint reddish gray (5R 6/1) banding is apparent throughout. Faint greenish (10GY 7/2) bands are less common. Bioturbation is slight to heavy and is expressed in light gray (5Y 7/1, and 10YR 7/1) mottling. Some are pyritized and exhibit a reddish gray (5R [illegible]) halo.

SMEAR SLIDE SUMMARY (%):

	6, 80
	D
TEXTURE:	
Sand	1
Silt	50
Clay	49
COMPOSITION:	
Foraminifers	5
Nannofossils	95

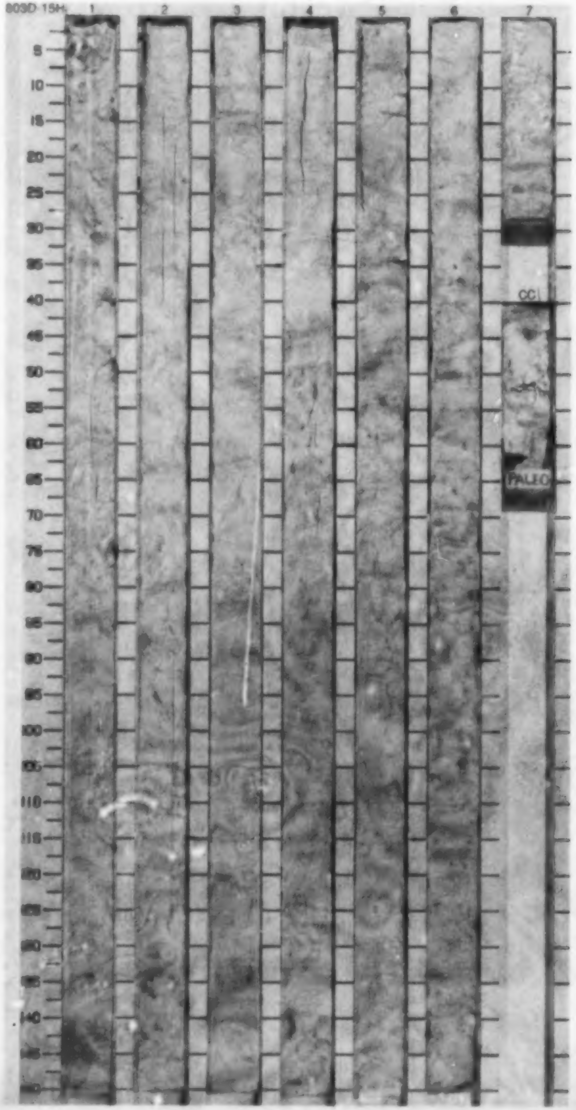
803D-15H
1
2
3
4
5
6
7
5
10
15
20
25
30
35
40
45
50
55
60
65
70
75
80
85
90
95
100
105
110
115
120
125
130
135
140
145
150
CC
PALEO

SITE 803 HOLE D CORE 16H CORED INTERVAL 131.6-141.1 mbsf

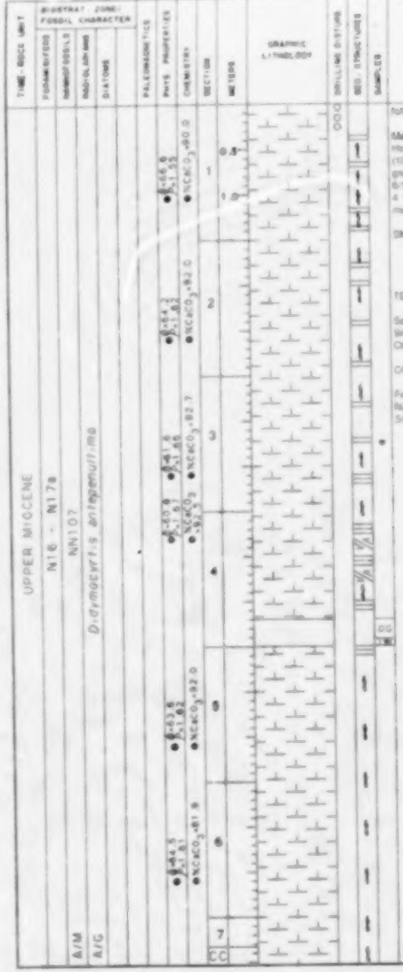
TIME-ROCK UNIT
BIOSTRAT. ZONE/ FOSSIL CHARACTER
FORAMINIFERS
NANNOFOSSILS
RADIOLARIANS
DIATOMS
PALEOMAGNETICS
PHYS. PROPERTIES
CHEMISTRY
SECTION
METERS
GRAPHIC LITHOLOGY
DRILLING DISTURB.
SED. STRUCTURES
SAMPLES
UPPER MIOCENE
N16 - N17a
NN10?
Didymocyrtis antepenultima
A/M
A/G
φ=66.6 ρ=1.55
%CaCO3=90.0
φ=64.2 ρ=1.62
%CaCO3=82.0
φ=60.8 ρ=1.67
%CaCO3=92.5
φ=61.6 ρ=1.66
%CaCO3=82.7
φ=63.6 ρ=1.62
%CaCO3=92.0
φ=64.5 ρ=1.61
%CaCO3=81.8
1
2
3
4
5
6
7
CC
0.5
1.0
OG

LITHOLOGIC DESCRIPTION

NANNOFOSSIL OOZE

Major lithology: This core contains NANNOFOSSIL OOZE. Its primary color is white (2.5Y 8/0). Horizontal reddish gray (5R 6/1) banding is present throughout Sections 1-4. Faint greenish (10GY 7/2) bands are less common. Bioturbation is slight to heavy and is expressed as light gray (5Y7/1 and 10YR 7/1) mottling. Some burrows are pyritized and exhibit a reddish gray (5R 6/1) halo. Microfaulting, expressed as displacement in the color bands, is present in Section 4. The reddish gray (5R 6/1) color is disseminated throughout Sections 5-7, giving a more mixed appearance.

SMEAR SLIDE SUMMARY (%):

	3, 74
	D
TEXTURE	
Sand	5
Silt	60
Clay	35
COMPOSITION	
Foraminifers	5
Nannofossils	94
Siliceous fragments	1

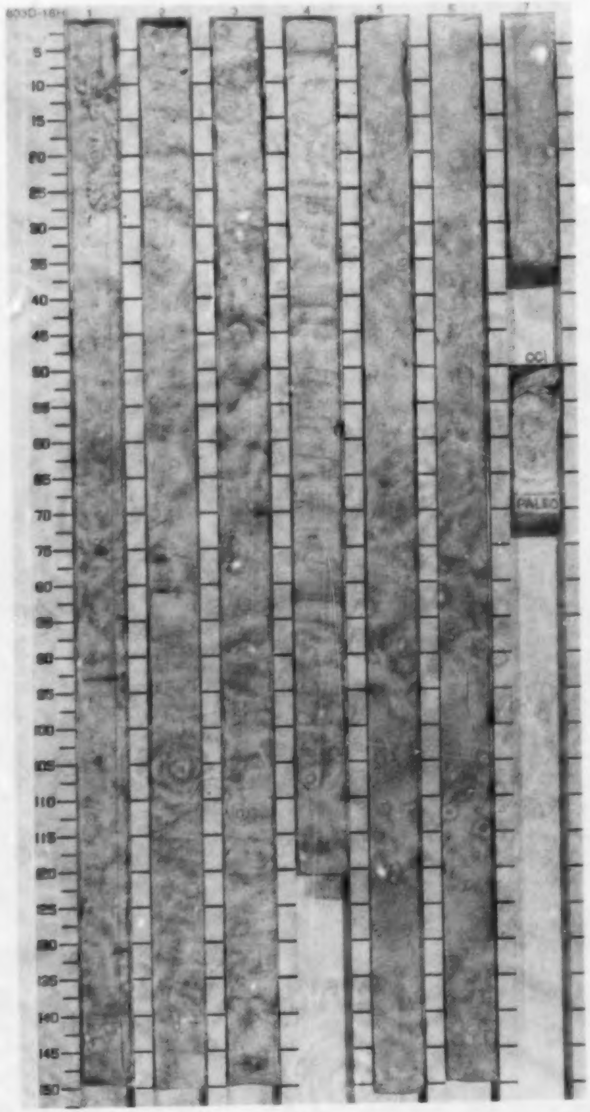
803D-16H
1
2
3
4
5
6
7
5
10
15
20
25
30
35
40
45
50
55
60
65
70
75
80
85
90
95
100
105
110
115
120
125
130
135
140
145
150
OG
PALEO

SITE 803 HOLE D CORE 17H CORED INTERVAL 141.1-150.6 mbsf

TIME-ROCK UNIT	FORAMINIFERS	NANNOFOSSILS	RADIOLARIANS	DIATOMS	PALEOMAGNETICS	PHYS. PROPERTIES	CHEMISTRY	SECTION	METERS
UPPER MIOCENE	N16 - N17a	NN10	*Didymocyrtis antepenultima*			● ϕ=64.0 γ=1.61	● %$CaCO_3$=92.0	1	0.5 1.0
						● ϕ=63.7 γ=1.62	● %$CaCO_3$=93.5	2	
						● ϕ=63.6 γ=1.63	● %$CaCO_3$=92.6	3	
						● ϕ=63.7 γ=1.62	● %$CaCO_3$=90.2	4	
						● ϕ=60.6 γ=1.67	● %$CaCO_3$=93.4	5	
						● ϕ=63.8 γ=1.62	● %$CaCO_3$=90.6	6	
						● ϕ=62.3 γ=1.64	● %$CaCO_3$=94.5	7	
								CC	
	C/P	A/M	A/G						

BIOSTRAT. ZONE/ FOSSIL CHARACTER

GRAPHIC LITHOLOGY

DRILLING DISTURB.

SED. STRUCTURES

SAMPLES

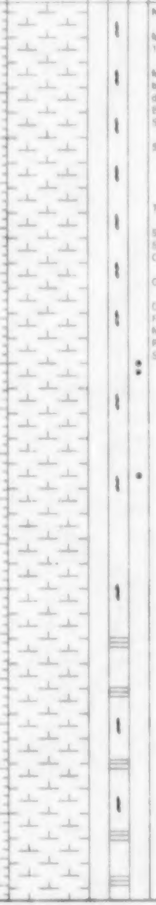

LITHOLOGIC DESCRIPTION

NANNOFOSSIL OOZE with FORAMINIFERS

Major lithology: This core contains NANNOFOSSIL OOZE with FORAMINIFERS in Sections 1-5. It is white (2.5Y 8.0) and homogeneous, though distorted mottles are rarely observed.

Minor lithology: NANNOFOSSIL OOZE is the sediment type from Section 5, 110 cm, to the base of the core. Faint horizontal, reddish gray (5R 6.1)-color banding is apparent in the dominant color of white (2.5Y 8/0). Faint greenish (10GY 7.2) bands are less common. Bioturbation is slight to heavy and is expressed as light gray (5Y 7/1 and 10YR 7/1) mottling. Some burrows are pyritized and exhibit a reddish gray (5R 6.1) halo.

SMEAR SLIDE SUMMARY (%):

	3, 100 D	3, 110 D	4, 75 D
TEXTURE:			
Sand	10	1	3
Silt	45	50	57
Clay	45	49	40
COMPOSITION:			
Diatoms	—	—	2
Foraminifers	10	5	10
Nannofossils	90	95	79
Radiolarians	—	—	1
Siliceous fragments	—	—	8

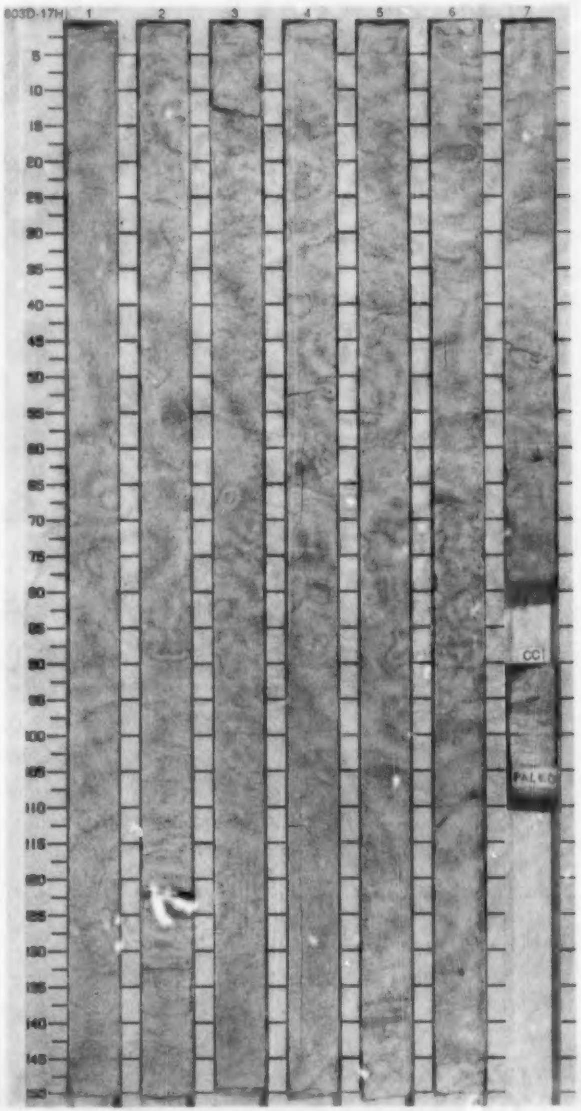

SITE 803 HOLE D CORE 18H CORED INTERVAL 150.6-160.1 mbsf

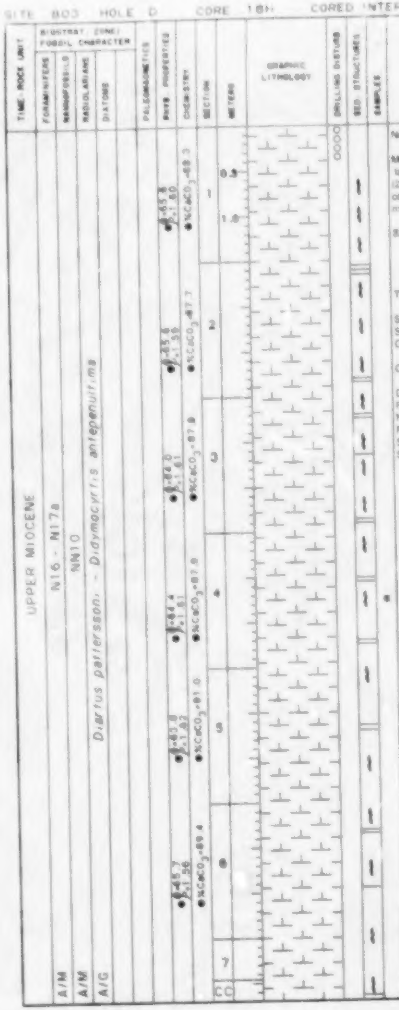
TIME-ROCK UNIT
BIOSTRAT. ZONE/ FOSSIL CHARACTER
FORAMINIFERS
NANNOFOSSILS
RADIOLARIANS
DIATOMS
PALEOMAGNETICS
PHYS. PROPERTIES
CHEMISTRY
SECTION
METERS
GRAPHIC LITHOLOGY
DRILLING DISTURB.
SED. STRUCTURES
SAMPLES
UPPER MIOCENE
N16 - N17a
NN10
Diartus pettersoni - Didymocyrtis antepenultima
A/M
A/M
A/G
φ-65.8 γ-1.60
%CaCO3-88.3
φ-65.6 γ-1.59
%CaCO3-87.7
φ-64.0 γ-1.61
%CaCO3-87.9
φ-64.4 γ-1.61
%CaCO3-87.0
φ-63.8 γ-1.62
%CaCO3-81.0
φ-65.7 γ-1.56
%CaCO3-89.4
1
2
3
4
5
6
7
CC
0.5
1.0

LITHOLOGIC DESCRIPTION

NANNOFOSSIL OOZE with FORAMINIFERS

Major lithology: This core contains NANNOFOSSIL OOZE with FORAMINIFERS. Faint horizontal reddish gray (5R 6/1) color bands are present but not common within the dominant white (2.5Y 8/0) color. Distinct greenish (10GY 7/2) bands with sharp lower contacts are less common. Bioturbation is slight to heavy and is expressed as light gray (5Y 7/1 and 10YR 7/1) mottling. Some burrows are pyritized and exhibit a reddish gray (5R 6/1) halo.

SMEAR SLIDE SUMMARY (%)

	4, 75
	D
TEXTURE	
Sand	1
Silt	59
Clay	40
COMPOSITION	
Diatoms	2
Foraminifers	10
Nannofossils	79
Radiolarians	1
Siliceous fragments	8
Spicules	Tr

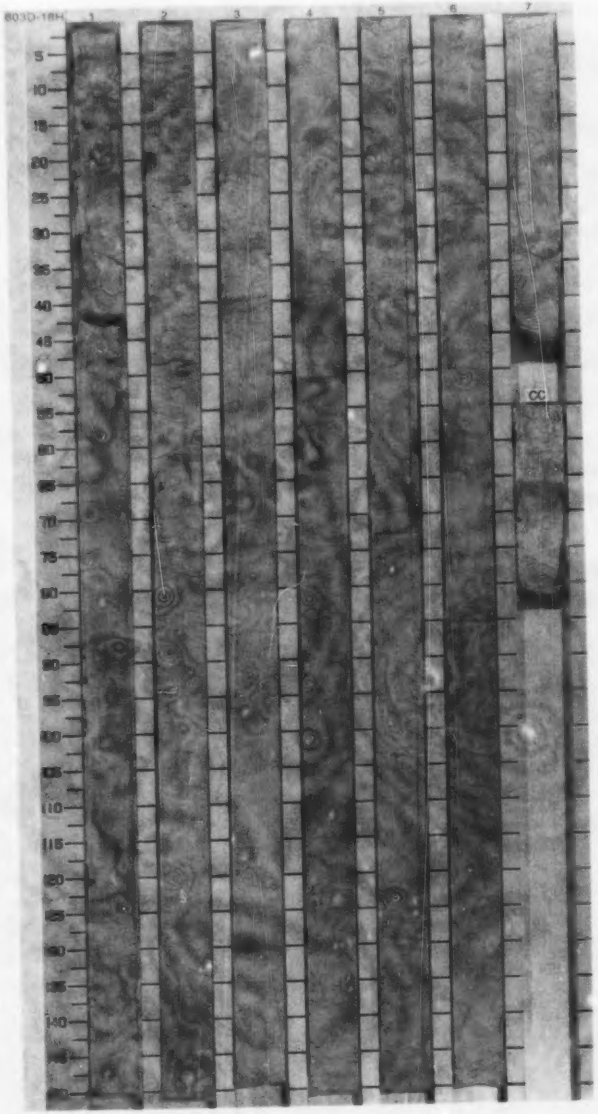
803D-18H
1
2
3
4
5
6
7
CC
5
10
15
20
25
30
35
40
45
50
55
60
65
70
75
80
85
90
95
100
105
110
115
120
125
130
135
140
145
150

SITE 803 HOLE D CORE 19H CORED INTERVAL 160.1-169.6 mbsf

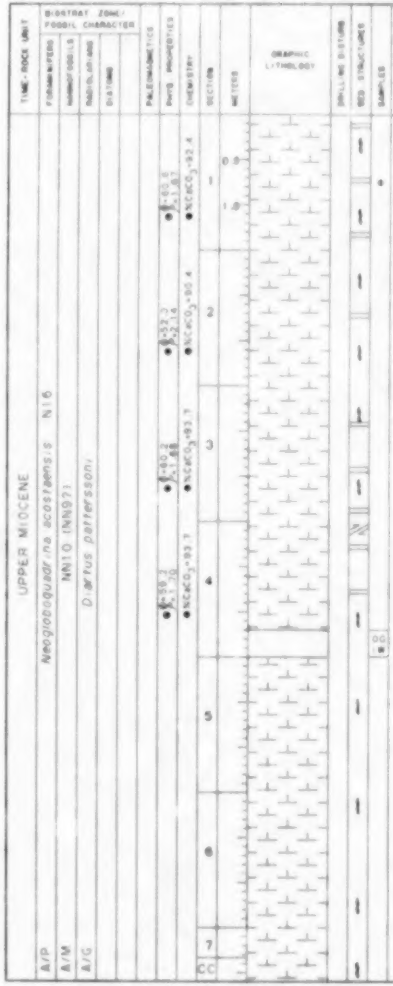
TIME-ROCK UNIT
BIOSTRAT. ZONE/ FOSSIL CHARACTER
FORAMINIFERS
NANNOFOSSILS
RADIOLARIANS
DIATOMS
PALEOMAGNETICS
PHYS. PROPERTIES
CHEMISTRY
SECTION
METERS
GRAPHIC LITHOLOGY
DRILLING DISTURB.
SED. STRUCTURES
SAMPLES
UPPER MIOCENE
A/P Neogloboquadrina acostaensis N16
A/M NN10 (NN9?)
A/G Diartus pettersoni
●φ-60.6 γ-1.87
●%CaCO3-92.4
●φ-52.3 γ-2.14
●%CaCO3-90.4
●φ-60.2 γ-1.88
●%CaCO3-93.7
●φ-58.2 γ-1.70
●%CaCO3-93.7
1
2
3
4
5
6
7
CC
0.5
1.0
OG

LITHOLOGIC DESCRIPTION

NANNOFOSSIL OOZE

Major lithology: This core contains NANNOFOSSIL OOZE. The dominant color is white (2.5Y 8/2) with faint horizontal reddish gray (5R 6/1) intervals at the top of the core. Faint to distinct reddish gray (5R 6/1) color bands are present in Sections 3 and 4. Pale greenish (10GY 7/2) bands with sharp lower contacts are less common. The color is disseminated throughout Sections 5-7. Bioturbation is slight to heavy throughout the core and is expressed as light gray (5Y 7/1 and 10YR 7/1) mottling. Some burrows are pyritized and exhibit a reddish gray (5R 6/1) halo.

SMEAR SLIDE SUMMARY (%):

	1, 75
	D
TEXTURE:	
Sand	3
Silt	67
Clay	30
COMPOSITION:	
Diatoms	1
Foraminifers	5
Nannofossils	94

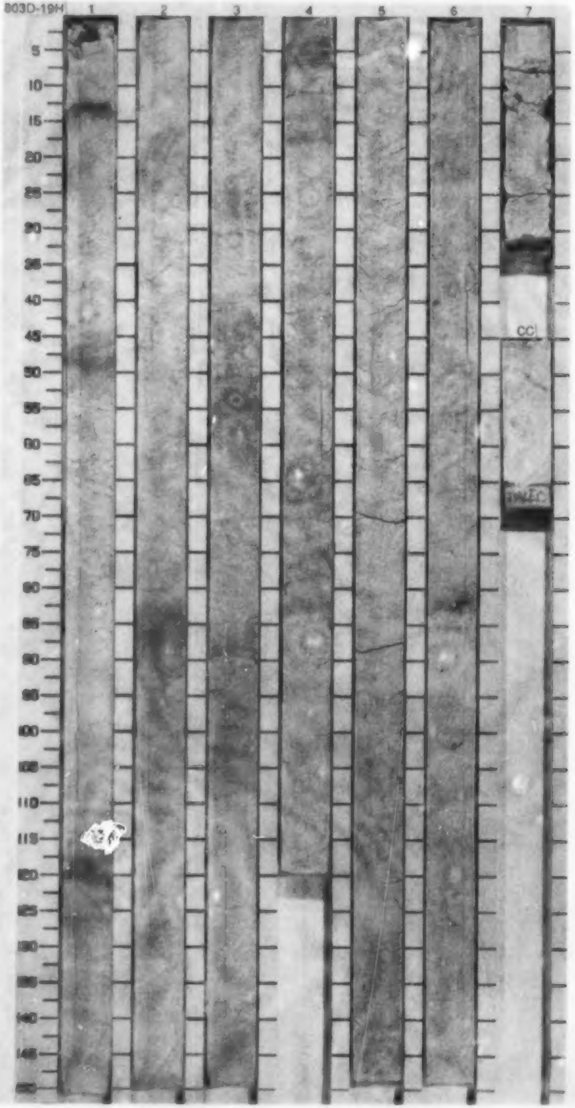
803D-19H
1
2
3
4
5
6
7
5
10
15
20
25
30
35
40
45
50
55
60
65
70
75
80
85
90
95
100
105
110
115
120
125
130
135
140
145
150
CC
19H-CC

SITE 803 HOLE D CORE 20H CORED INTERVAL 169.6-179.1 mbsf

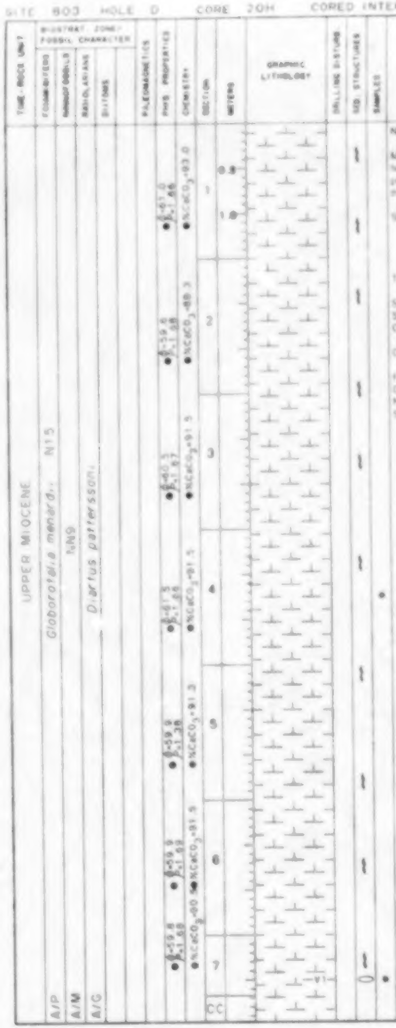
TIME-ROCK UNIT
BIOSTRAT. ZONE/ FOSSIL CHARACTER
FORAMINIFERS
NANNOFOSSILS
RADIOLARIANS
DIATOMS
PALEOMAGNETICS
PHYS. PROPERTIES
CHEMISTRY
SECTION
METERS
GRAPHIC LITHOLOGY
DRILLING DISTURB.
SED. STRUCTURES
SAMPLES
UPPER MIOCENE
Globorotalia menardii N15
NN9
Diartus petterssoni
A/P
A/M
A/G
φ=61.0 γ=1.66
φ=59.6 γ=1.68
φ=60.5 γ=1.67
φ=61.5 γ=1.66
φ=59.9 γ=1.38
φ=59.9 γ=1.69
φ=59.8 γ=1.68
%CaCO3=93.0
%CaCO3=88.3
%CaCO3=91.5
%CaCO3=91.5
%CaCO3=91.3
%CaCO3=91.5
%CaCO3=90.5
0.5
1.0
1
2
3
4
5
6
7
CC
V1

LITHOLOGIC DESCRIPTION

NANNOFOSSIL OOZE

Major lithology: This core contains white (2.5Y 8/0) NANNOFOSSIL OOZE. The sediment is homogeneous and firm. Rare, light gray (2.5Y 7/0) and gray (2.5Y 6/0) mottles and halos are present. A mm-thick, dark gray (2.5Y 4/0) ash layer is observed in Section 7, 50 cm. Above this layer, the color grades into light gray (2.5Y 7/1) and white (2.5Y 8/0).

SMEAR SLIDE SUMMARY (%):

	4, 74	7, 50
	D	M
TEXTURE:		
Sand	2	25
Silt	60	60
Clay	38	15
COMPOSITION:		
Foraminifers	4	5
Glass	—	50
Nannofossils	95	45
Siliceous fragments	1	—

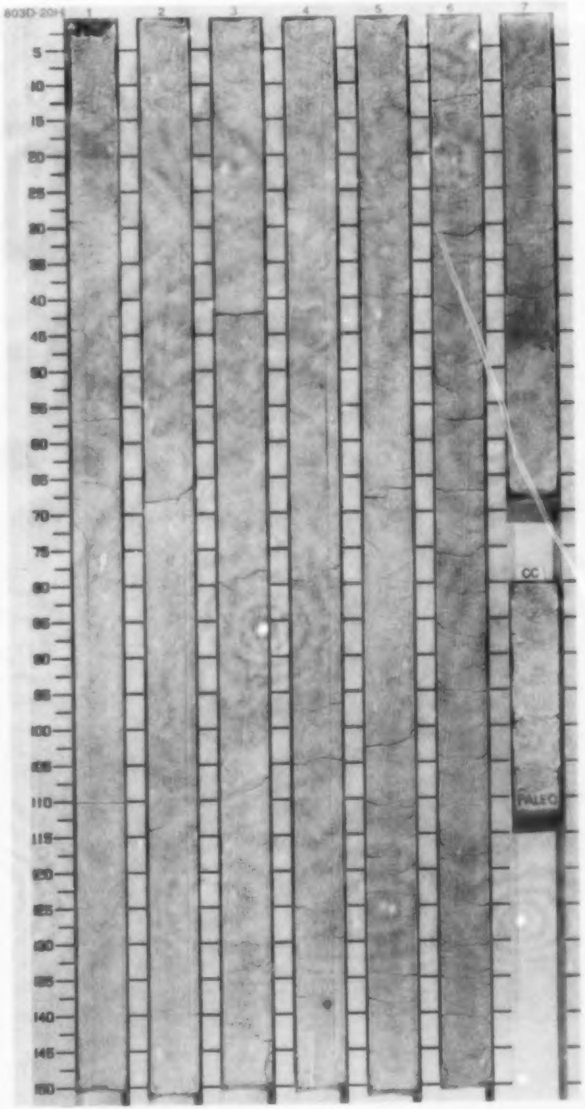
803D-20H
1
2
3
4
5
6
7
CC
PALEO
5
10
15
20
25
30
35
40
45
50
55
60
65
70
75
80
85
90
95
100
105
110
115
120
125
130
135
140
145
150

SITE 803 HOLE D CORE 21H CORED INTERVAL 179.1-188.6 mbsf

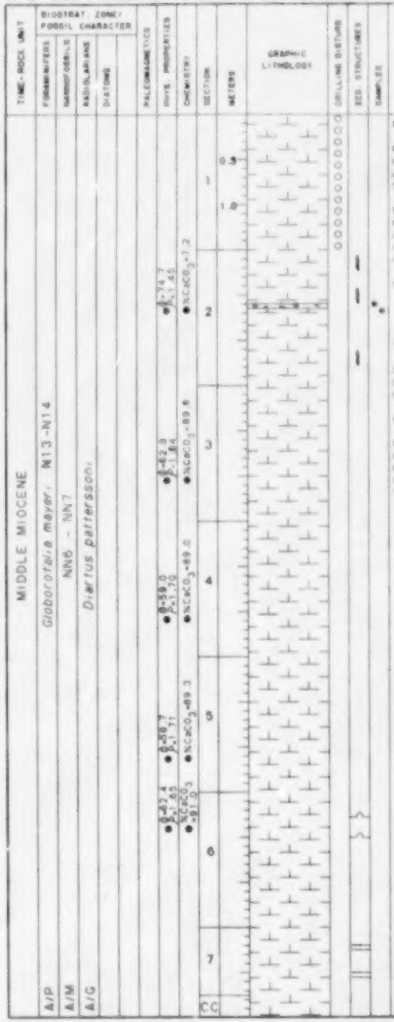

LITHOLOGIC DESCRIPTION

NANNOFOSSIL OOZE

Major lithology: This core contains white (2.5Y 8/0) NANNOFOSSIL OOZE. Reddish gray (5R 6/1) banding is present throughout Sections 6 and 7. Greenish (10GY 7/2) bands and specks are less common. Light gray (2.5Y 7/0) ash is disseminated within the ooze in Section 2, 58-60.5 cm.

Minor lithology: A bed of massive, black (2.5Y 2/0) volcanic ash is present between 60.5 and 62.5 cm in Section 2. The ash is about 0.5 cm thick but is split by a 2-cm coring gap. The upper contact is gradational and the lower one is sharp. This bed is underlain by 9.5 cm of massive, dark gray (2.5Y 4/0) ash-bearing nannofossil ooze, which is bounded by a sharp lower contact.

SMEAR SLIDE SUMMARY (%):

	2, 60	2, 66
	M	M
TEXTURE:		
Sand	80	10
Silt	20	60
Clay	—	30
COMPOSITION:		
Feldspar	5	1
Foraminifers	—	5
Nannofossils	—	60
Rock fragment	—	5
Volcanic ash	90	20

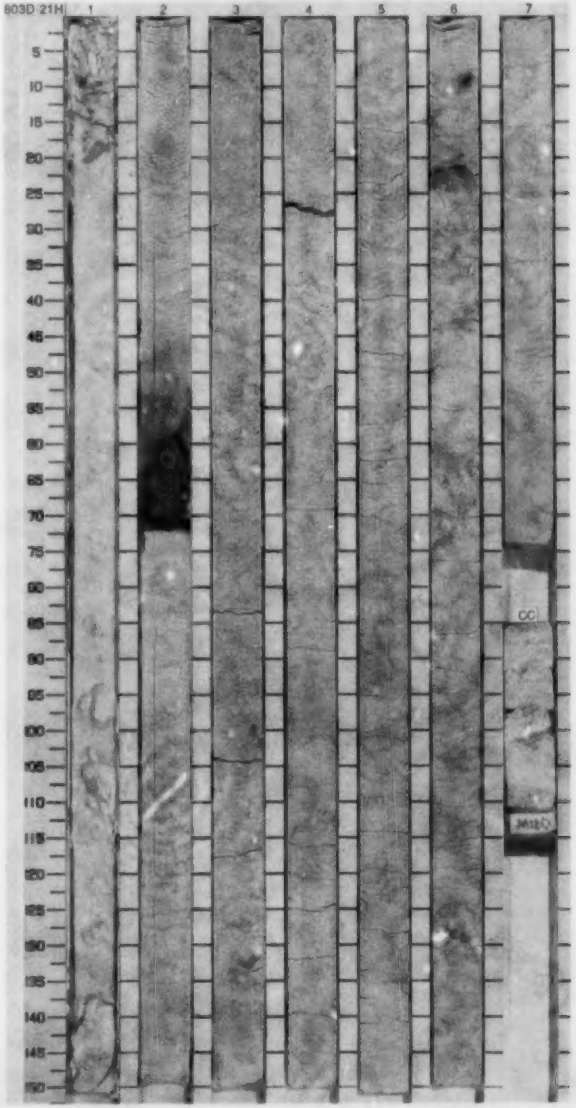
803D 21H
1
2
3
4
5
6
7
CC
5
10
15
20
25
30
35
40
45
50
55
60
65
70
75
80
85
90
95
100
105
110
115
120
125
130
135
140
145
150

SITE 803 HOLE D CORE 22H CORED INTERVAL 188.6-198.1 mbsf

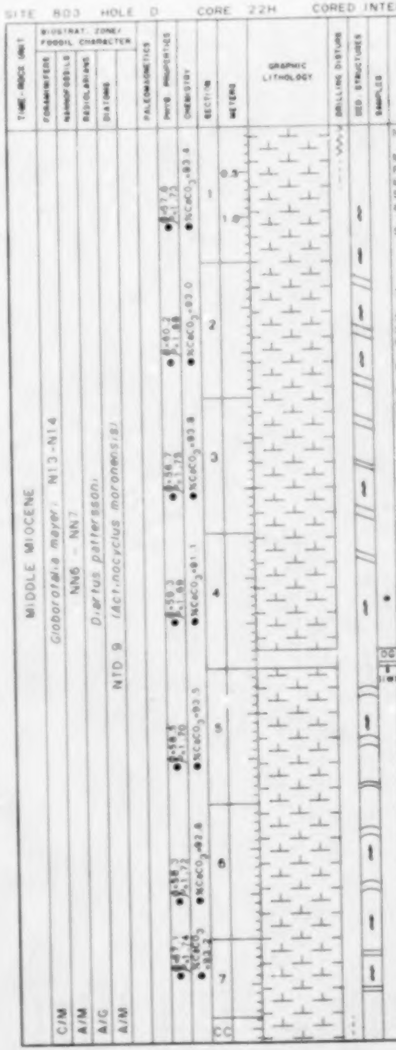
TIME-ROCK UNIT
BIOSTRAT. ZONE/ FOSSIL CHARACTER
FORAMINIFERS
NANNOFOSSILS
RADIOLARIANS
DIATOMS
PALEOMAGNETICS
PHYS. PROPERTIES
CHEMISTRY
SECTION
METERS
GRAPHIC LITHOLOGY
DRILLING DISTURB.
SED. STRUCTURES
SAMPLES
MIDDLE MIOCENE
Globorotalia mayeri N13-N14
NN6 - NN7
Diartus petterssoni
NTD 9 (Actinocyclus moronensis)
C/M
A/M
A/G
A/M
φ=47.8 γ=1.73
%CaCO3=83.4
φ=60.2 γ=1.68
%CaCO3=83.0
φ=56.7 γ=1.75
%CaCO3=83.8
φ=59.3 γ=1.68
%CaCO3=81.1
φ=58.8 γ=1.70
%CaCO3=83.5
φ=58.3 γ=1.72
%CaCO3=82.8
φ=47.1 γ=1.74
%CaCO3=83.2
1
2
3
4
5
6
7
CC
0.5
1.0
OG

LITHOLOGIC DESCRIPTION

NANNOFOSSIL OOZE

Major lithology: This core consists of white (2.5Y 8/0), homogeneous, and firm NANNOFOSSIL OOZE. Beginning in Section 2, color banding is abundant. The bands are mostly light gray (2.5Y 6/1), reddish gray (5R 6/1) and green (10GY 7/2) in color, and wavy. In Sections 2 and 3, the bands dip at a shallow angle, whereas in Sections 4, 5 and 6 they are arcuate. This core is bioturbated throughout.

SMEAR SLIDE SUMMARY (%):

	4, 78
	D
TEXTURE	
Sand	5
Silt	60
Clay	35
COMPOSITION	
Foraminifers	8
Nannofossils	91
Siliceous fragments	1

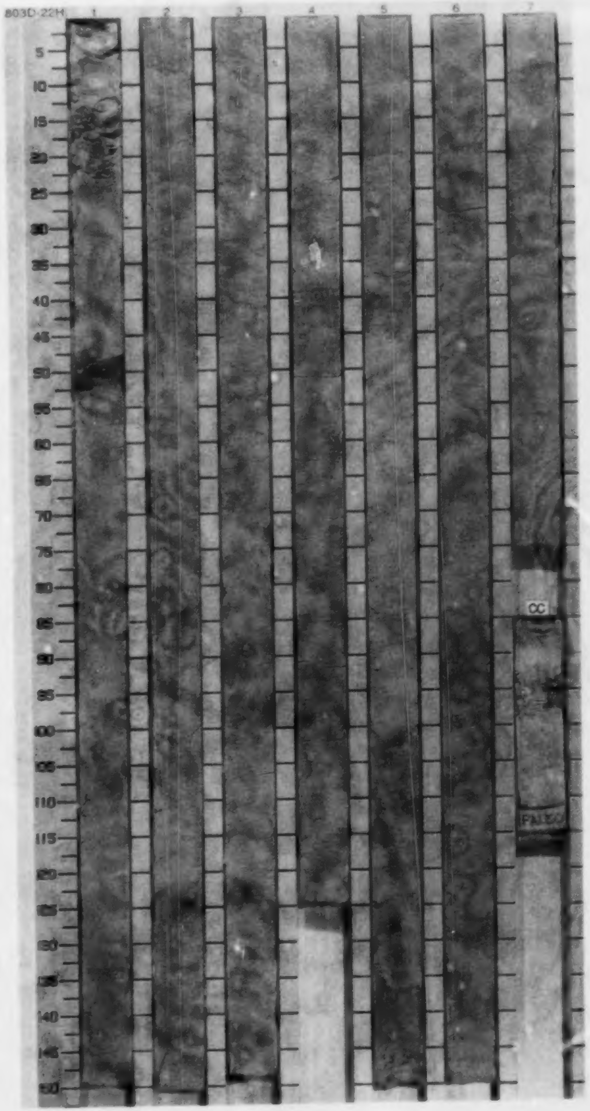
803D-22H
1
2
3
4
5
6
7
CC
5
10
15
20
25
30
35
40
45
50
55
60
65
70
75
80
85
90
95
100
105
110
115
120
125
130
135
140
145
150

SITE 803 HOLE D CORE 23M CORED INTERVAL 198.1-207.6 mbsf

TIME-ROCK UNIT	BIOSTRAT. ZONE/ FOSSIL CHARACTER: FORAMINIFERS	NANNOFOSSILS	RADIOLARIANS	DIATOMS	PALEOMAGNETICS	PHYS. PROPERTIES	CHEMISTRY	SECTION	METERS	DRILLING DISTURB.	SED. STRUCTURES	SAMPLES
MIDDLE MIOCENE	N12	NN6 - NN7	*Diartus petterssoni*	NTD 8 (*Craspedodiscus coscinodiscus*)		●φ=62.6 γ=1.76	●%CaCO$_3$=91.0	1	0.5 1.0			
						●φ=61.2 γ=1.65	●%CaCO$_3$=89.0	2				
								3				
						●φ=61.0 γ=1.69	●%CaCO$_3$=87.5	4				●
								5				
						●φ=61.0 γ=1.65	●%CaCO$_3$=87.3	6				
						●φ=62.4 γ=1.63	●%CaCO$_3$=89.7	7				
	C/M	A/M	A/M	A/M-G				CC				

LITHOLOGIC DESCRIPTION

NANNOFOSSIL OOZE

Major lithology: This core contains soft, structureless and predominantly white (2.5Y 8/0) NANNOFOSSIL OOZE. It is moderately to heavily bioturbated, as evidenced by bioturbation trails infilled with specks of authigenic pyrite and surrounded by purple halos.

SMEAR SLIDE SUMMARY (%):

	4, 75
	D
TEXTURE:	
Sand	5
Silt	65
Clay	30
COMPOSITION:	
Diatoms	3
Foraminifers	5
Nannofossils	88
Radiolarians	1
Siliceous fragments	3

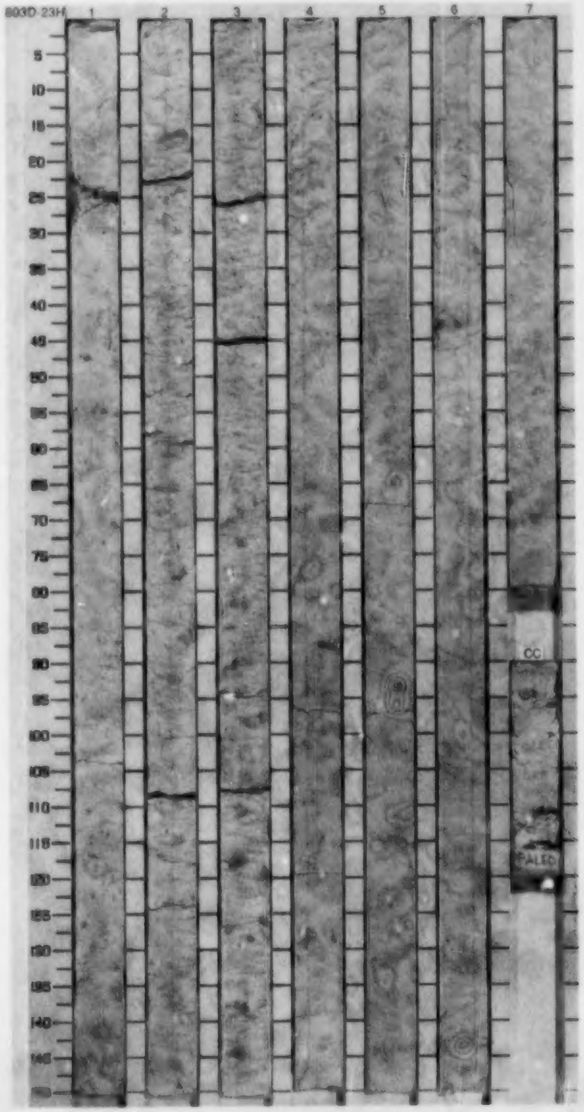
803D-23H
1
2
3
4
5
6
7
5
10
15
20
25
30
35
40
45
50
55
60
65
70
75
80
85
90
95
100
105
110
115
120
125
130
135
140
145
150
CC
PALEO

SITE 803 HOLE D CORE 24H CORED INTERVAL 207.6-217.1 mbsf

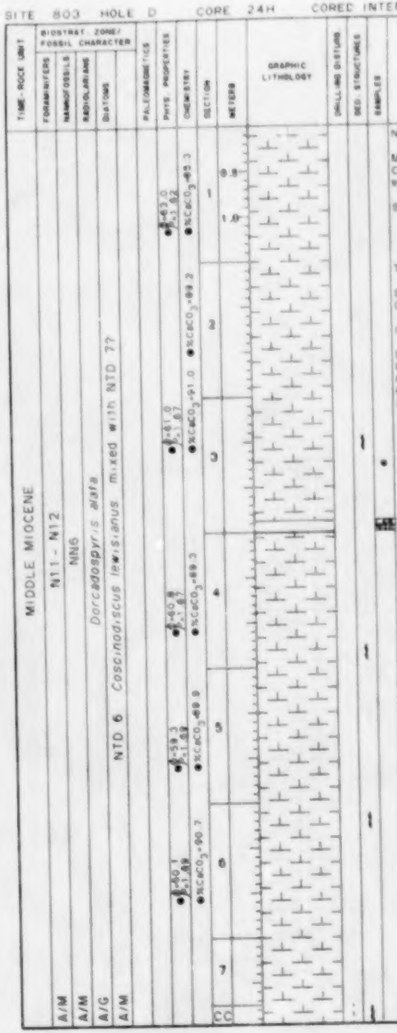
TIME-ROCK UNIT
BIOSTRAT. ZONE/ FOSSIL CHARACTER
FORAMINIFERS
NANNOFOSSILS
RADIOLARIANS
DIATOMS
PALEOMAGNETICS
PHYS. PROPERTIES
CHEMISTRY
SECTION
METERS
GRAPHIC LITHOLOGY
DRILLING DISTURB.
SED. STRUCTURES
SAMPLES
MIDDLE MIOCENE
N11 - N12
NN6
Dorcadospyris alata
NTD 6 Coscinodiscus lewisianus mixed with NTD 7?
A/M
A/M
A/G
A/M
φ=63.0 γ=1.62
φ=61.0 γ=1.67
φ=60.8 γ=1.67
φ=59.3 γ=1.69
φ=60.1 γ=1.69
%CaCO3=85.3
%CaCO3=89.2
%CaCO3=91.0
%CaCO3=89.3
%CaCO3=88.9
%CaCO3=90.7
1
2
3
4
5
6
7
CC
0.5
1.0

LITHOLOGIC DESCRIPTION

NANNOFOSSIL OOZE

Major lithology: This core consists of stiff, structureless and white (2.5Y 8/0) NANNOFOSSIL OOZE. It is slightly bioturbated, as is evident from a few purple halos surrounding bioturbation trails.

SMEAR SLIDE SUMMARY (%):

	3, 75
	D
TEXTURE	
Silt	40
Clay	60
COMPOSITION	
Diatoms	Tr
Foraminifers	5
Nannofossils	95
Radiolarians	Tr
Spicules	Tr

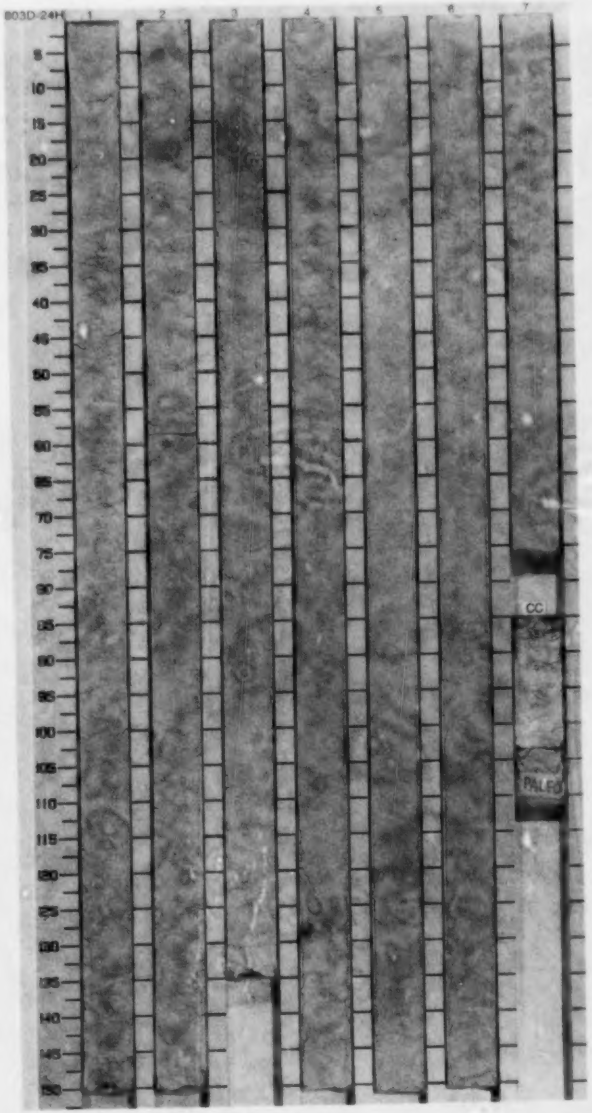
803D-24H
1
2
3
4
5
6
7
5
10
15
20
25
30
35
40
45
50
55
60
65
70
75
80
85
90
95
100
105
110
115
120
125
130
135
140
145
150
CC
PALEO

SITE 803 HOLE D CORE 25X CORED INTERVAL 217.1-226.8 mbsf

TIME-ROCK UNIT	FORAMINIFERS	NANNOFOSSILS	RADIOLARIANS	DIATOMS	PALEOMAGNETICS	PHYS. PROPERTIES	CHEMISTRY	SECTION	METERS	SAMPLES
MIDDLE MIOCENE	N11	NN5	*Dorcadospyris alata*	NTD 6 (*Coscinodiscus lewisianus*)		●ϕ=60.6 ●ρ=1.67	●%$CaCO_3$=88.8	1	0.5 1.0	
						●ϕ=61.5 ●ρ=1.65	●%$CaCO_3$=89.0	2		
						●ϕ=60.6 ●ρ=1.67	●%$CaCO_3$=88.7 ●%$CaCO_3$=92.0	3		OG IW
						●ϕ=59.2 ●ρ=1.69		4		*
								5		
	A/M	A/P	A/M	C/P-M				CC		

LITHOLOGIC DESCRIPTION

NANNOFOSSIL CHALK

Major lithology: This core consists of homogeneous, white (2.5Y 8/0) NANNOFOSSIL CHALK. It is slightly bioturbated, and contains stiff biscuits in a softer matrix. Some light gray (N7/0) mottles are present in the biscuits.

SMEAR SLIDE SUMMARY (%):

	4, 80
	D
TEXTURE:	
Sand	8
Silt	70
Clay	22
COMPOSITION:	
Foraminifers	8
Nannofossils	91
Radiolarians	1

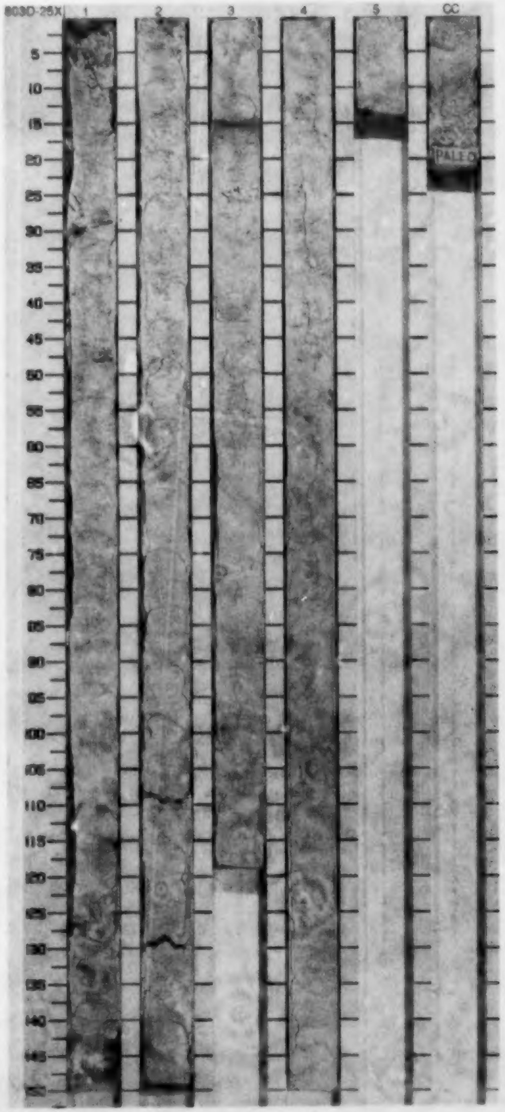
803D-25X
1
2
3
4
5
CC
PALEO
5
10
15
20
25
30
35
40
45
50
55
60
65
70
75
80
85
90
95
100
105
110
115
120
125
130
135
140
145
150

SITE 803 HOLE D CORE 26X CORED INTERVAL 226.8-236.5 mbsf

TIME-ROCK UNIT	FORAMINIFERS	NANNOFOSSILS	RADIOLARIANS	DIATOMS	PALEOMAGNETICS	PHYS. PROPERTIES	CHEMISTRY	SECTION	METERS	DRILLING DISTURB.	SED. STRUCTURES	SAMPLES
MIDDLE MIOCENE	N10	NN5	*Calocycletta costata*			φ=57.1 ρ=2.23	%CaCO$_3$=91.0	1	0.5 1.0			
						φ=55.8 ρ=1.72	%CaCO$_3$=93.1	2				
						φ=57.3 ρ=1.72	%CaCO$_3$=88.9	3				
						φ=59.2 ρ=1.69	%CaCO$_3$=83.5	4				●
						φ=56.7 ρ=1.73	%CaCO$_3$=85.8	5				
						φ=58.2 ρ=1.75	%CaCO$_3$=94.5	6				
	C/M	A/P	A/P	R/P				CC				

LITHOLOGIC DESCRIPTION

NANNOFOSSIL CHALK

Major lithology: This core contains NANNOFOSSIL CHALK. It is homogeneous to slightly bioturbated; drilling disturbance has formed sediment biscuits. The primary color of the sediment is white (2.5Y 8/0 and 5Y 8/1), with minor light gray (N7) mottling.

SMEAR SLIDE SUMMARY (%):

	4, 30 D
TEXTURE	
Sand	2
Silt	18
Clay	80
COMPOSITION	
Foraminifers	3
Nannofossils	94
Radiolarians	3

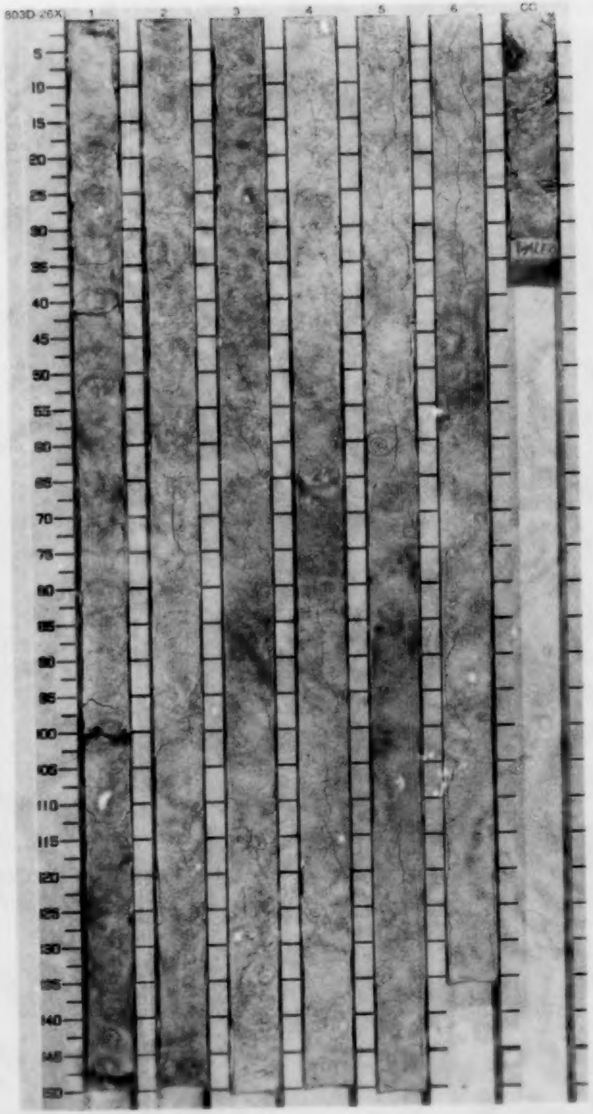
803D-26X
1
2
3
4
5
6
CC
5
10
15
20
25
30
35
40
45
50
55
60
65
70
75
80
85
90
95
100
105
110
115
120
125
130
135
140
145
150

SITE 803 HOLE D CORE 27X CORED INTERVAL 236.5-245.9 mbsf

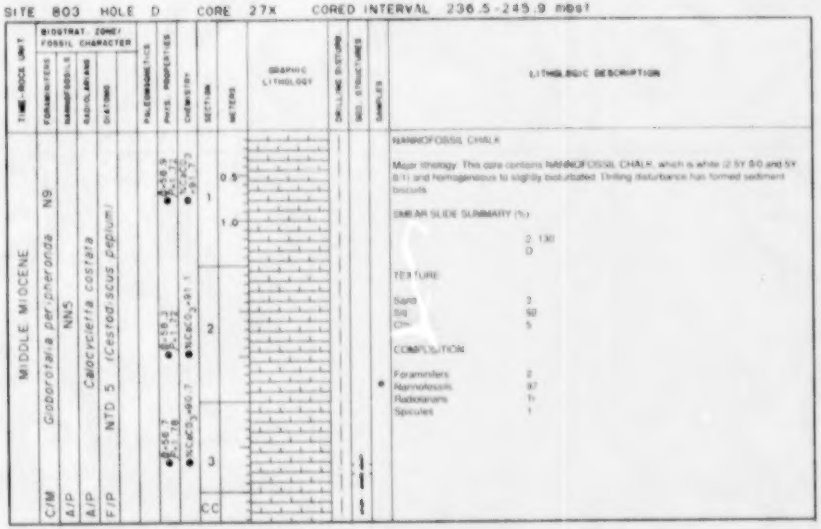
TIME-ROCK UNIT
BIOSTRAT. ZONE/ FOSSIL CHARACTER
FORAMINIFERS
NANNOFOSSILS
RADIOLARIANS
DIATOMS
PALEOMAGNETICS
PHYS. PROPERTIES
CHEMISTRY
SECTION
METERS
GRAPHIC LITHOLOGY
DRILLING DISTURB.
SED. STRUCTURES
SAMPLES
LITHOLOGIC DESCRIPTION
MIDDLE MIOCENE
C/M Globorotalia peripheronda N9
A/P NN5
A/P Calocycletta costata
F/P NTD 5 (Cestodiscus peplum)
φ=58.9 γ=1.73
%CaCO₃ =91.7
φ=58.3 γ=1.72
%CaCO₃=91.1
φ=56.7 γ=1.78
%CaCO₃=90.7
1
2
3
CC
0.5
1.0

NANNOFOSSIL CHALK

Major lithology: This core contains NANNOFOSSIL CHALK, which is white (2.5Y 8/0 and 5Y 8/1) and homogeneous to slightly bioturbated. Drilling disturbance has formed sediment biscuits.

SMEAR SLIDE SUMMARY (%):

	2, 130
	D
TEXTURE:	
Sand	3
Silt	92
Clay	5
COMPOSITION:	
Foraminifers	2
Nannofossils	97
Radiolarians	Tr
Spicules	1

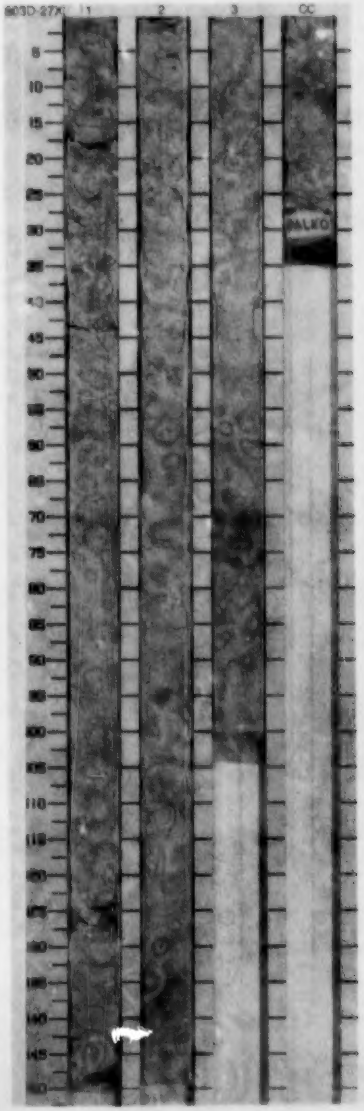
803D-27X
1
2
3
CC
PALEO
5
10
15
20
25
30
35
40
45
50
55
60
65
70
75
80
85
90
95
100
105
110
115
120
125
130
135
140
145
150

SITE 803 HOLE D CORE 28X CORED INTERVAL 245.9-255.5 mbsf

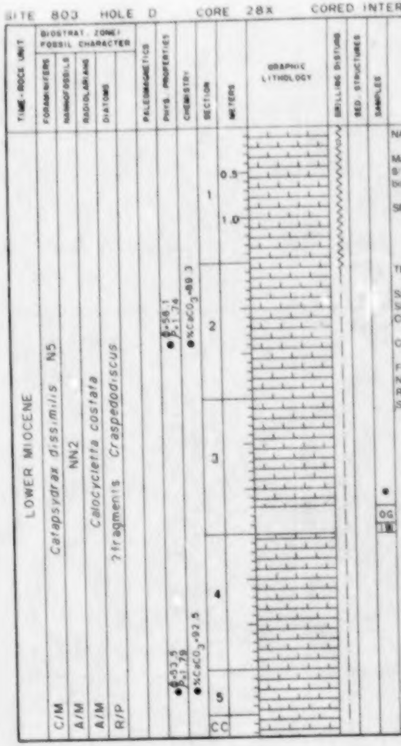
TIME-ROCK UNIT
BIOSTRAT. ZONE/ FOSSIL CHARACTER
FORAMINIFERS
NANNOFOSSILS
RADIOLARIANS
DIATOMS
PALEOMAGNETICS
PHYS. PROPERTIES
CHEMISTRY
SECTION
METERS
GRAPHIC LITHOLOGY
DRILLING DISTURB.
SED. STRUCTURES
SAMPLES
LOWER MIOCENE
C/M Catapsydrax dissimilis N5
A/M NN2
A/M Calocycletta costata
R/P ?fragments Craspedodiscus
● φ=58.1
ρ=1.74
● %CaCO3=89.3
● φ=53.5
ρ=1.79
● %CaCO3=92.5
1
2
3
4
5
CC
0.5
1.0
OG
IW

LITHOLOGIC DESCRIPTION

NANNOFOSSIL CHALK

Major lithology: This core contains NANNOFOSSIL CHALK, which is white (2.5Y 8/0 and 5Y 8/1, grading to 10YR 8/2) and homogeneous. Drilling disturbance has formed sediment biscuits.

SMEAR SLIDE SUMMARY (%):

	3, 106
	D
TEXTURE:	
Sand	5
Silt	90
Clay	5
COMPOSITION:	
Foraminifers	2
Nannofossils	97
Radiolarians	Tr
Spicules	Tr

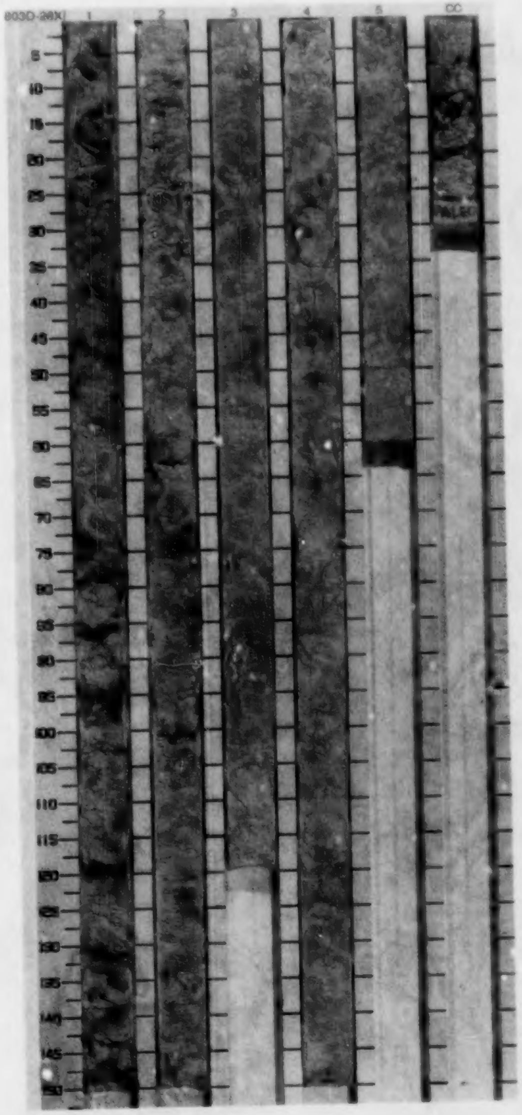
803D-28X
1
2
3
4
5
CC
5
10
15
20
25
30
35
40
45
50
55
60
65
70
75
80
85
90
95
100
105
110
115
120
125
130
135
140
145
150

SITE 803 HOLE D CORE 29X CORED INTERVAL 255.5-265.1 mbsf

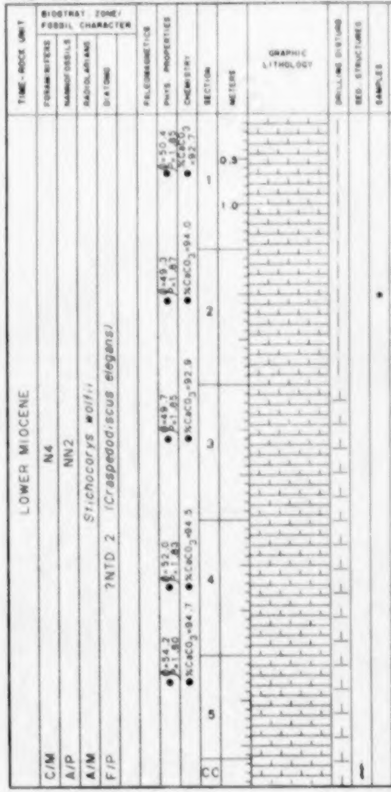
TIME-ROCK UNIT
BIOSTRAT. ZONE/ FOSSIL CHARACTER
FORAMINIFERS
NANNOFOSSILS
RADIOLARIANS
DIATOMS
PALEOMAGNETICS
PHYS. PROPERTIES
CHEMISTRY
SECTION
METERS
GRAPHIC LITHOLOGY
DRILLING DISTURB.
SED. STRUCTURES
SAMPLES
LOWER MIOCENE
N4
NN2
Stichocorys wolffii
?NTD 2 (Craspedodiscus elegans)
C/M
A/P
A/M
F/P
φ=50.4 ρ=1.85
%CaCO₃ =92.7
φ=49.3 ρ=1.87
%CaCO₃=94.0
φ=49.7 ρ=1.85
%CaCO₃=92.9
φ=52.0 ρ=1.83
%CaCO₃=94.5
φ=54.2 ρ=1.80
%CaCO₃=94.7
1
2
3
4
5
CC
0.5
1.0

LITHOLOGIC DESCRIPTION

NANNOFOSSIL CHALK

Major lithology: This core contains NANNOFOSSIL CHALK, which is white (5Y 8/1, grading to 10YR 8/1) and homogeneous. It is moderately fractured by drilling.

SMEAR SLIDE SUMMARY (%):

	2, 50
	D
TEXTURE:	
Silt	60
Clay	40
COMPOSITION:	
Foraminifers	Tr
Nannofossils	100
Radiolarians	Tr
Spicules	Tr

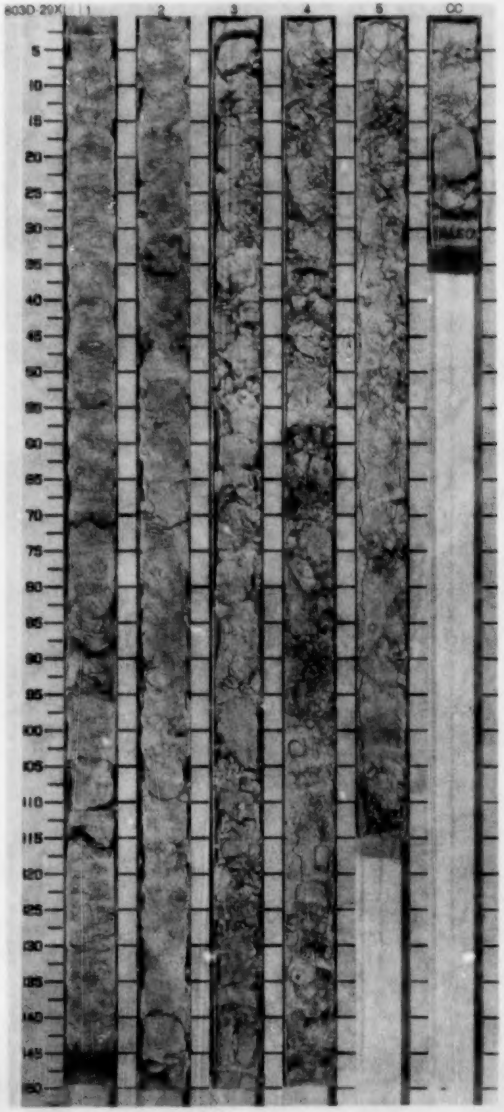
803D-29X
1
2
3
4
5
CC
5
10
15
20
25
30
35
40
45
50
55
60
65
70
75
80
85
90
95
100
105
110
115
120
125
130
135
140
145
150

SITE 803 HOLE D CORE 30X CORED INTERVAL 265.1-274.7 mbsf

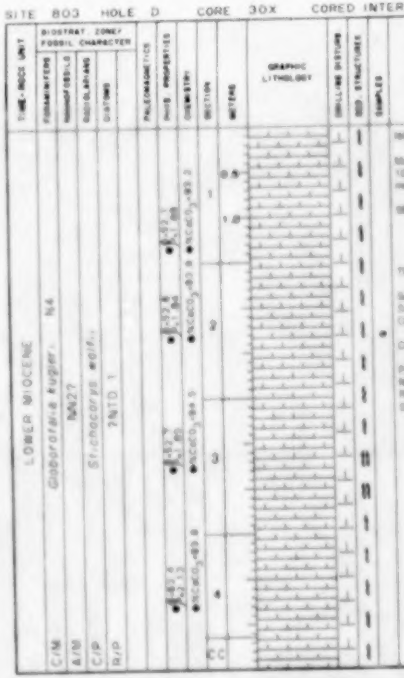
TIME-ROCK UNIT
BIOSTRAT. ZONE/ FOSSIL CHARACTER
FORAMINIFERS
NANNOFOSSILS
RADIOLARIANS
DIATOMS
PALEOMAGNETICS
PHYS. PROPERTIES
CHEMISTRY
SECTION
METERS
GRAPHIC LITHOLOGY
DRILLING DISTURB.
SED. STRUCTURES
SAMPLES
LOWER MIOCENE
Globorotalia kugleri N4
NN2?
Stichocorys wolffii
?NTD 1
C/M
A/M
C/P
R/P
%CaCO3=93.2
%CaCO3=93.8
%CaCO3=94.5
%CaCO3=93.8
1
2
3
4
CC
0.5
1.0

LITHOLOGIC DESCRIPTION

NANNOFOSSIL CHALK

Major lithology: This core contains NANNOFOSSIL CHALK, which is white (5Y 8/1, grading to 10YR 8/1 and 10YR 8/2) and homogeneous. The core is slightly to heavily bioturbated and moderately fractured by drilling.

SMEAR SLIDE SUMMARY (%):

	2, 61
	D
TEXTURE:	
Sand	1
Silt	90
Clay	9
COMPOSITION:	
Foraminifers	1
Nannofossils	99
Radiolarians	Tr
Spicules	Tr

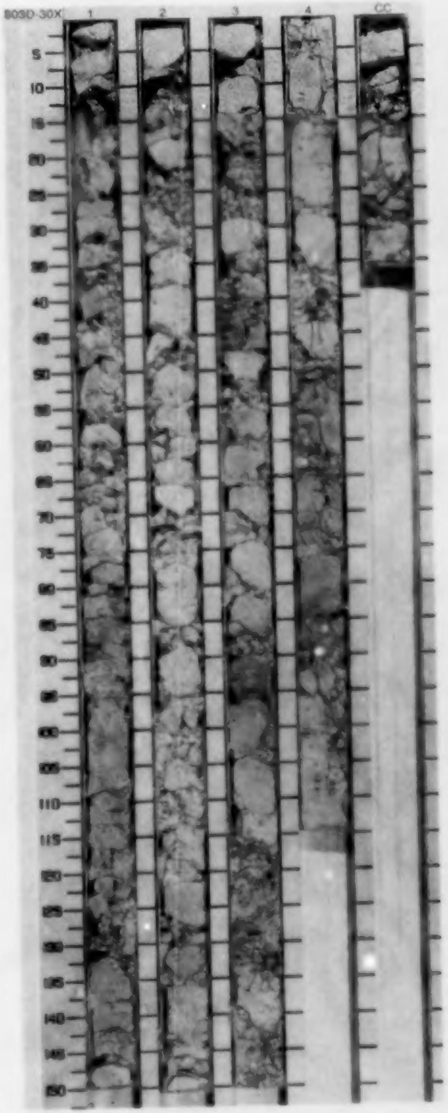
803D-30X
1
2
3
4
CC
5
10
15
20
25
30
35
40
45
50
55
60
65
70
75
80
85
90
95
100
105
110
115
120
125
130
135
140
145
150

SITE 803 HOLE D CORE 31X CORED INTERVAL 274.7-284.3 mbsf

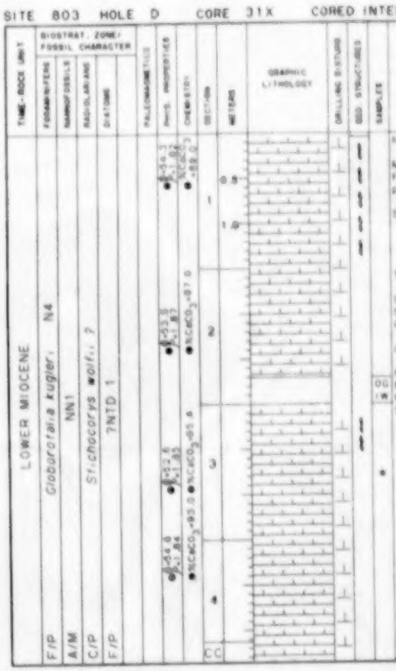
TIME-ROCK UNIT
BIOSTRAT. ZONE/FOSSIL CHARACTER
FORAMINIFERS
NANNOFOSSILS
RADIOLARIANS
DIATOMS
PALEOMAGNETICS
PHYS. PROPERTIES
CHEMISTRY
SECTION
METERS
GRAPHIC LITHOLOGY
DRILLING DISTURB.
SED. STRUCTURES
SAMPLES
LOWER MIOCENE
Globorotalia kugleri, N4
NN1
Stichocorys wolfii ?
?NTD 1
F/P
A/M
C/P
F/P
φ-54.3 γ-1.82
%CaCO3=89.0
φ-53.9 γ-1.87
%CaCO3=87.0
φ-52.6 γ-1.83
%CaCO3=93.0
%CaCO3=85.4
φ-54.6 γ-1.84
%CaCO3=85.4
1
2
3
4
CC
0.5
1.0
OG
IW

LITHOLOGIC DESCRIPTION

NANNOFOSSIL CHALK

Major lithology: This core contains white (5Y 8/1), slightly to moderately bioturbated NANNOFOSSIL CHALK. The core is, in parts, mottled and contains Chondrites. Faint color bands are present in the upper sections of the core. It is moderately fractured by drilling.

SMEAR SLIDE SUMMARY (%):

	3, 78
	D
TEXTURE:	
Sand	1
Silt	90
Clay	9
COMPOSITION:	
Foraminifers	1
Nannofossils	98
Radiolarians	1
Spicules	Tr

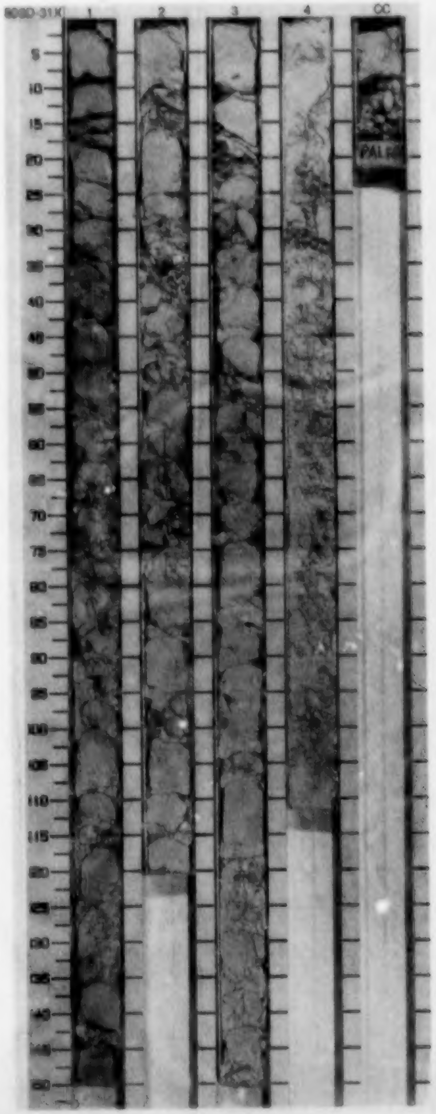
803D-31X
1
2
3
4
CC
PALEO
5
10
15
20
25
30
35
40
45
50
55
60
65
70
75
80
85
90
95
100
105
110
115
120
125
130
135
140
145
150

SITE 803 HOLE D CORE 32X CORED INTERVAL 284.3-294.1 mbsf

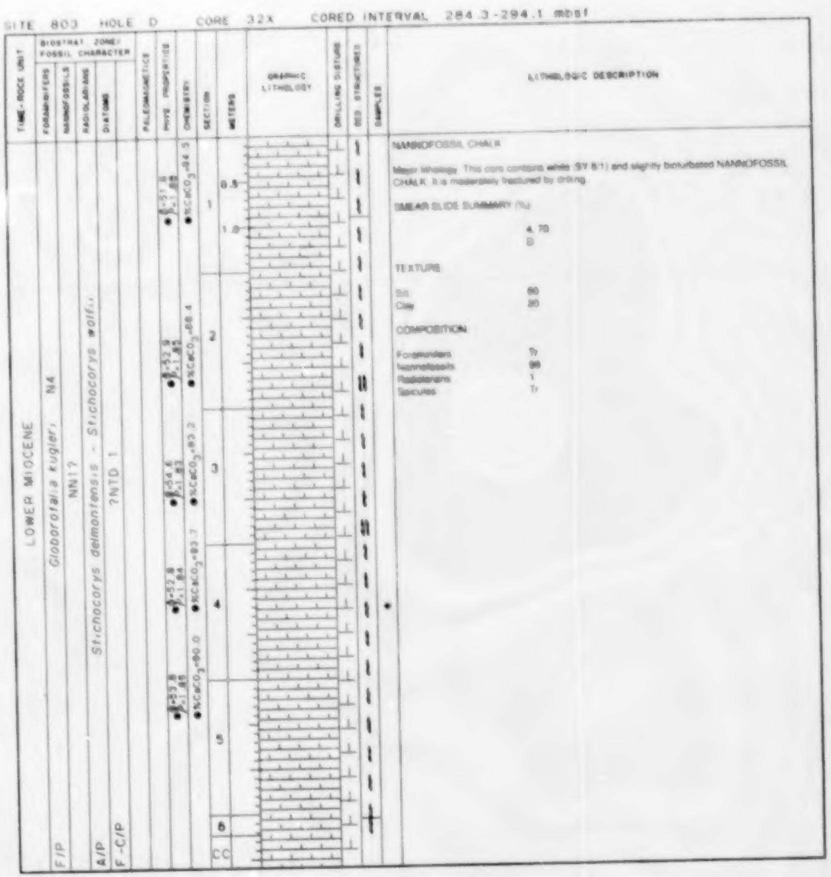
TIME-ROCK UNIT
BIOSTRAT. ZONE/ FOSSIL CHARACTER
FORAMINIFERS
NANNOFOSSILS
RADIOLARIANS
DIATOMS
PALEOMAGNETICS
PHYS. PROPERTIES
CHEMISTRY
SECTION
METERS
GRAPHIC LITHOLOGY
DRILLING DISTURB.
SED. STRUCTURES
SAMPLES
LITHOLOGIC DESCRIPTION
LOWER MIOCENE
F/P Globorotalia kugleri N4
NN1?
A/P Stichocorys delmontensis - Stichocorys wolfii
F-C/P ?NTD 1
●φ=57.8 ρ=1.88
●%CaCO3=84.5
●φ=52.9 ρ=1.85
●%CaCO3=88.4
●φ=54.6 ρ=1.83
●%CaCO3=83.2
●φ=52.8 ρ=1.84
●%CaCO3=83.7
●φ=53.8 ρ=1.85
●%CaCO3=80.0
1
2
3
4
5
6
CC
0.5
1.0

NANNOFOSSIL CHALK

Major lithology: This core contains white (5Y 8/1) and slightly bioturbated NANNOFOSSIL CHALK. It is moderately fractured by drilling.

SMEAR SLIDE SUMMARY (%):

	4, 70
	D
TEXTURE:	
Silt	80
Clay	20
COMPOSITION:	
Foraminifers	Tr
Nannofossils	99
Radiolarians	1
Spicules	Tr

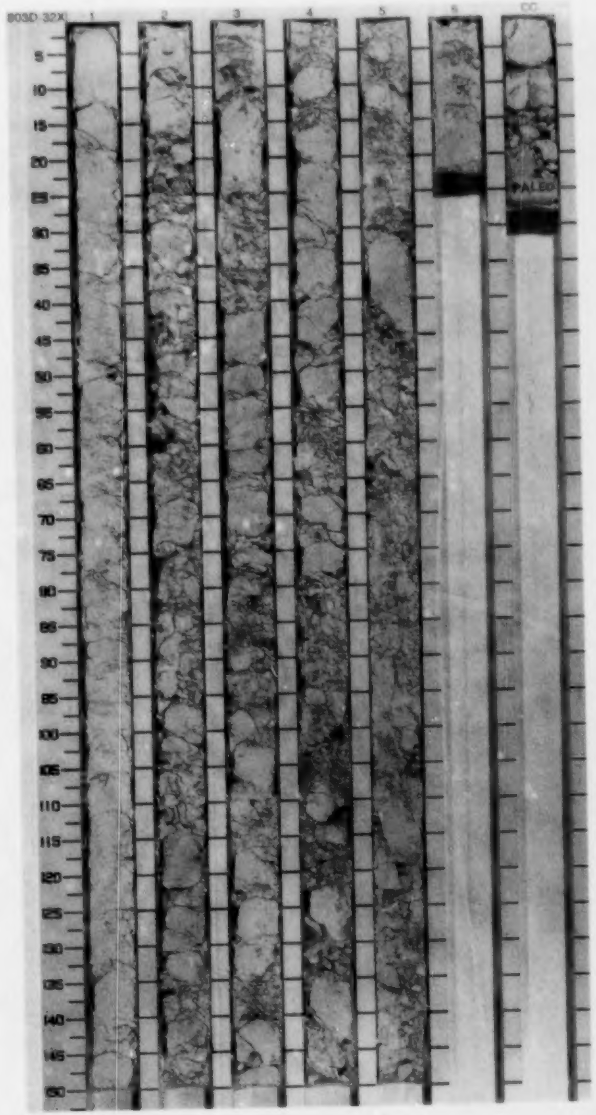
803D 32X
1
2
3
4
5
6
CC
PALEO
5
10
15
20
25
30
35
40
45
50
55
60
65
70
75
80
85
90
95
100
105
110
115
120
125
130
135
140
145
150

SITE 803 HOLE D CORE 33X CORED INTERVAL 294.1-303.3 mbsf

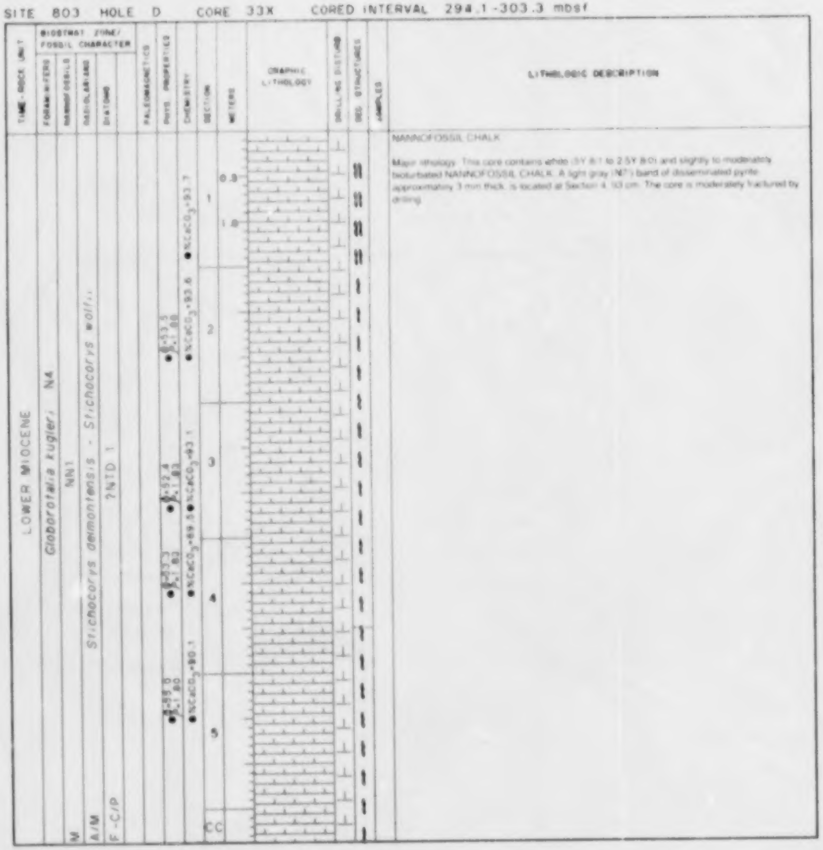
TIME-ROCK UNIT
BIOSTRAT. ZONE/ FOSSIL CHARACTER
FORAMINIFERS
NANNOFOSSILS
RADIOLARIANS
DIATOMS
PALEOMAGNETICS
PHYS. PROPERTIES
CHEMISTRY
SECTION
METERS
GRAPHIC LITHOLOGY
DRILLING DISTURB.
SED. STRUCTURES
SAMPLES
LOWER MIOCENE
Globorotalia kugleri N4
M NN1
A/M Stichocorys delmontensis - Stichocorys wolffii
F-C/P ?NTD 1
φ=53.5 γ=1.80
φ=52.4 γ=1.83
φ=53.3 γ=1.83
φ=55.0 γ=1.80
%CaCO3=93.7
%CaCO3=93.6
%CaCO3=89.5
%CaCO3=93.1
%CaCO3=80.1
1
2
3
4
5
CC
0.5
1.0

LITHOLOGIC DESCRIPTION

NANNOFOSSIL CHALK

Major lithology: This core contains white (5Y 8/1 to 2.5Y 8/0) and slightly to moderately bioturbated NANNOFOSSIL CHALK. A light gray (N7) band of disseminated pyrite approximately 3 mm thick, is located at Section 4, 10 cm. The core is moderately fractured by drilling.

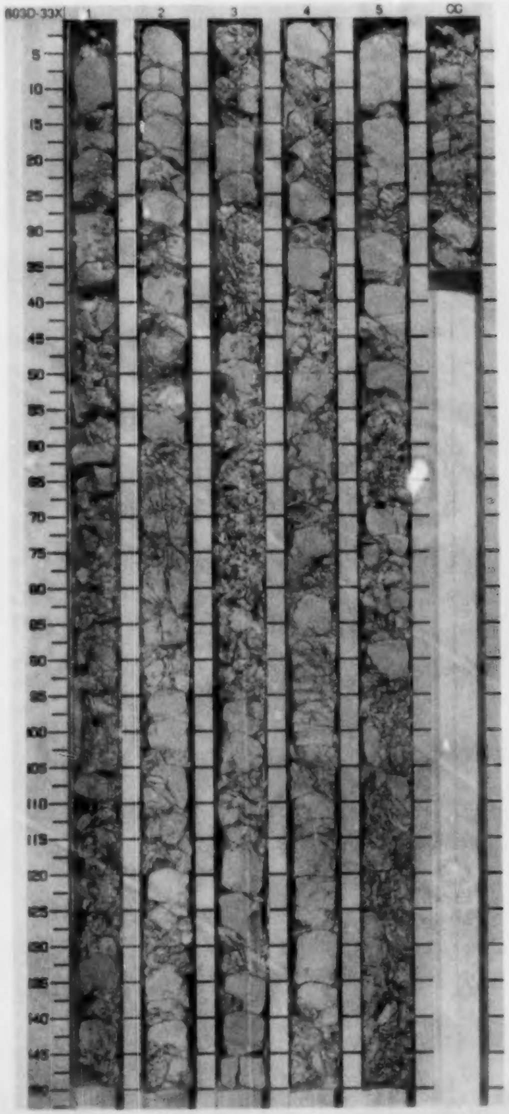
803D-33X
1
2
3
4
5
CC
5
10
15
20
25
30
35
40
45
50
55
60
65
70
75
80
85
90
95
100
105
110
115
120
125
130
135
140
145
150

SITE 803 HOLE D CORE 34X CORED INTERVAL 303.3-313.0 mbsf

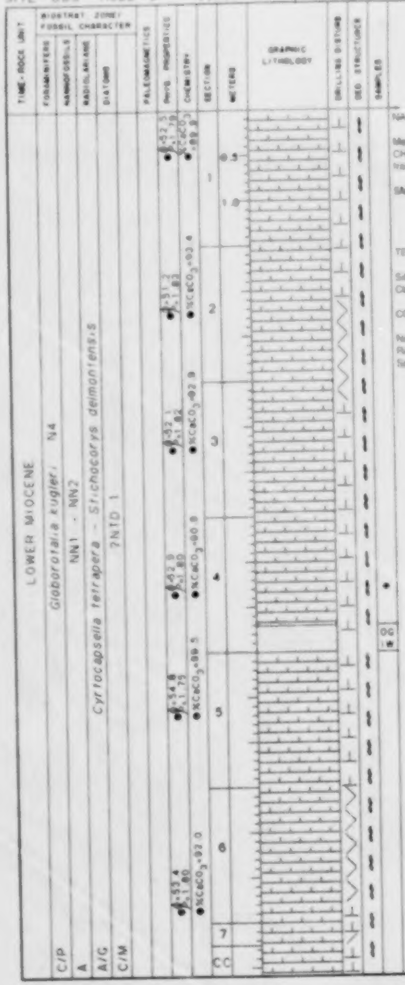
TIME-ROCK UNIT
BIOSTRAT. ZONE/ FOSSIL CHARACTER
FORAMINIFERS
NANNOFOSSILS
RADIOLARIANS
DIATOMS
PALEOMAGNETICS
PHYS. PROPERTIES
CHEMISTRY
SECTION
METERS
GRAPHIC LITHOLOGY
DRILLING DISTURB.
SED. STRUCTURES
SAMPLES
LOWER MIOCENE
Globorotalia kugleri N4
NN1 - NN2
Cyrtocapsella tetrapera - Stichocorys delmontensis
?NTD 1
C/P
A
A/G
C/M
φ=52.5
ρ=1.79
%CaCO3=89.9
φ=51.2
ρ=1.83
%CaCO3=93.4
φ=52.1
ρ=1.82
%CaCO3=92.9
φ=52.9
ρ=1.80
%CaCO3=90.8
φ=54.8
ρ=1.75
%CaCO3=89.5
φ=53.4
ρ=1.80
%CaCO3=92.0
0.5
1.0
1
2
3
4
5
6
7
CC
OG
IW

LITHOLOGIC DESCRIPTION

NANNOFOSSIL CHALK

Major lithology: This core contains white (2.5Y 8/0) and slightly bioturbated NANNOFOSSIL CHALK. It contains small, light gray (2.5Y 7/0) mottles. The core is moderately to highly fractured by drilling.

SMEAR SLIDE SUMMARY (%):

	4, 79
	D
TEXTURE:	
Silt	85
Clay	15
COMPOSITION:	
Nannofossils	95
Radiolarians	5
Spicules	Tr

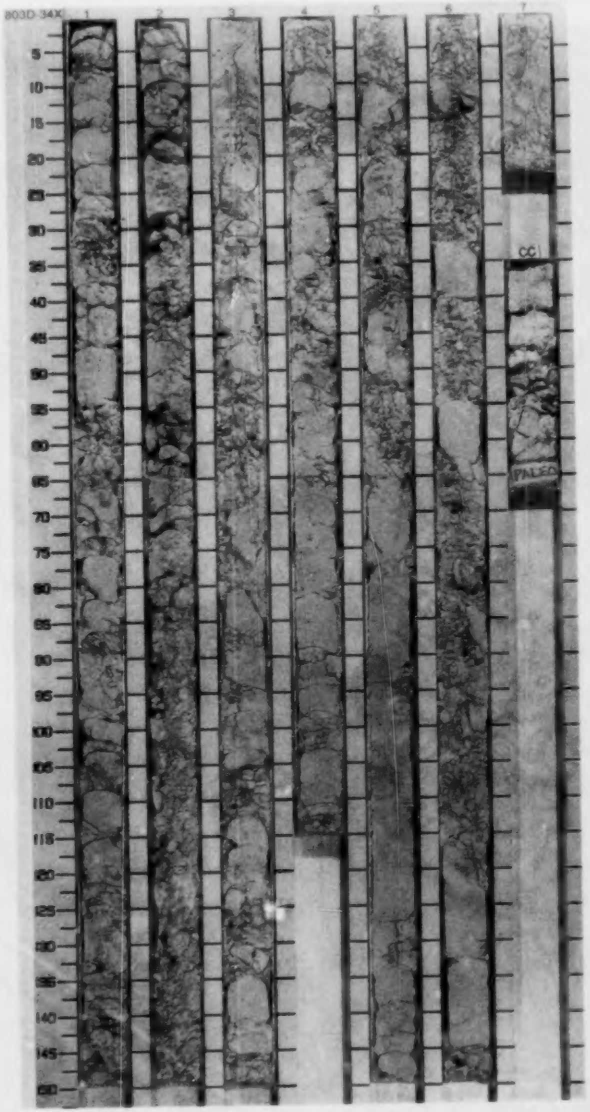
803D-34X
1
2
3
4
5
6
7
CC
PALEO
5
10
15
20
25
30
35
40
45
50
55
60
65
70
75
80
85
90
95
100
105
110
115
120
125
130
135
140
145
150

SITE 803 HOLE D CORE 35X CORED INTERVAL 313.0-322.7 mbsf

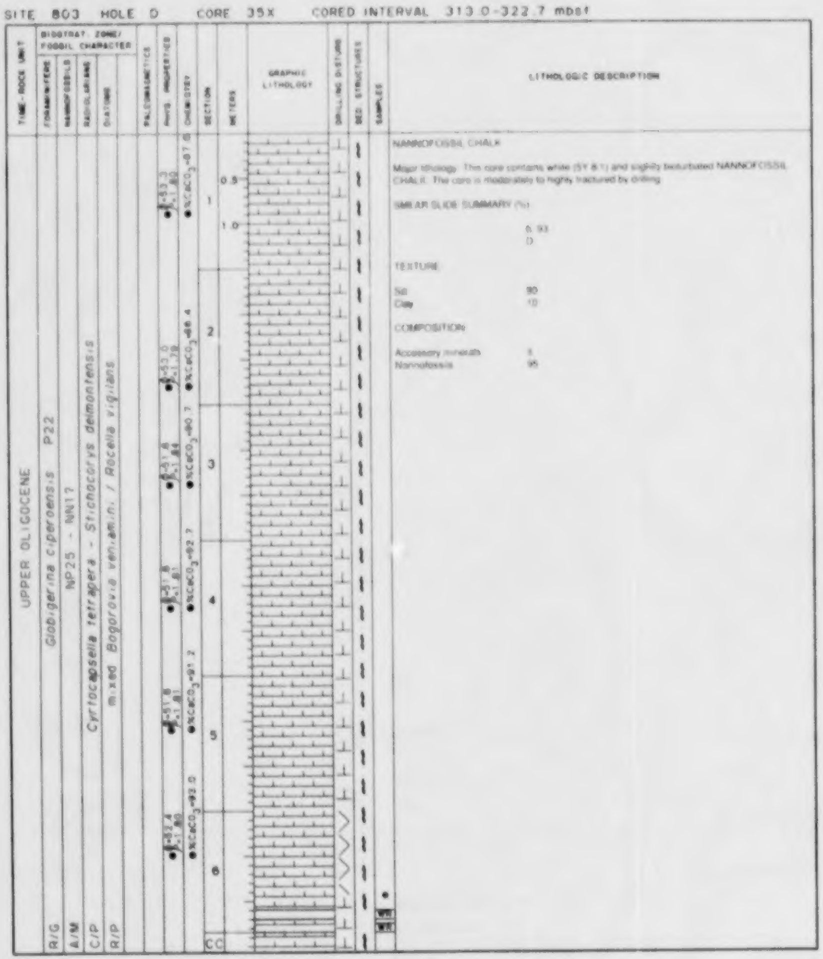
TIME-ROCK UNIT
BIOSTRAT. ZONE/ FOSSIL CHARACTER
FORAMINIFERS
NANNOFOSSILS
RADIOLARIANS
DIATOMS
PALEOMAGNETICS
PHYS. PROPERTIES
CHEMISTRY
SECTION
METERS
GRAPHIC LITHOLOGY
DRILLING DISTURB.
SED. STRUCTURES
SAMPLES
LITHOLOGIC DESCRIPTION
UPPER OLIGOCENE
R/G Globigerina ciperoensis P22
A/M NP25 - NN1?
C/P Cyrtocapsella tetrapera - Stichocorys delmontensis
R/P mixed Bogorovia veniamini / Rocella vigilans
φ=53.3 ρ=1.80
%CaCO3=87.0
φ=53.0 ρ=1.79
%CaCO3=88.4
φ=51.6 ρ=1.84
%CaCO3=90.7
φ=51.8 ρ=1.81
%CaCO3=92.7
φ=51.8 ρ=1.81
%CaCO3=91.2
φ=52.4 ρ=1.80
%CaCO3=93.0
1
2
3
4
5
6
CC
0.5
1.0

NANNOFOSSIL CHALK

Major lithology: This core contains white (5Y 8/1) and slightly bioturbated NANNOFOSSIL CHALK. The core is moderately to highly fractured by drilling.

SMEAR SLIDE SUMMARY (%):

	6, 93
	D
TEXTURE:	
Silt	90
Clay	10
COMPOSITION:	
Accessory minerals	5
Nannofossils	95

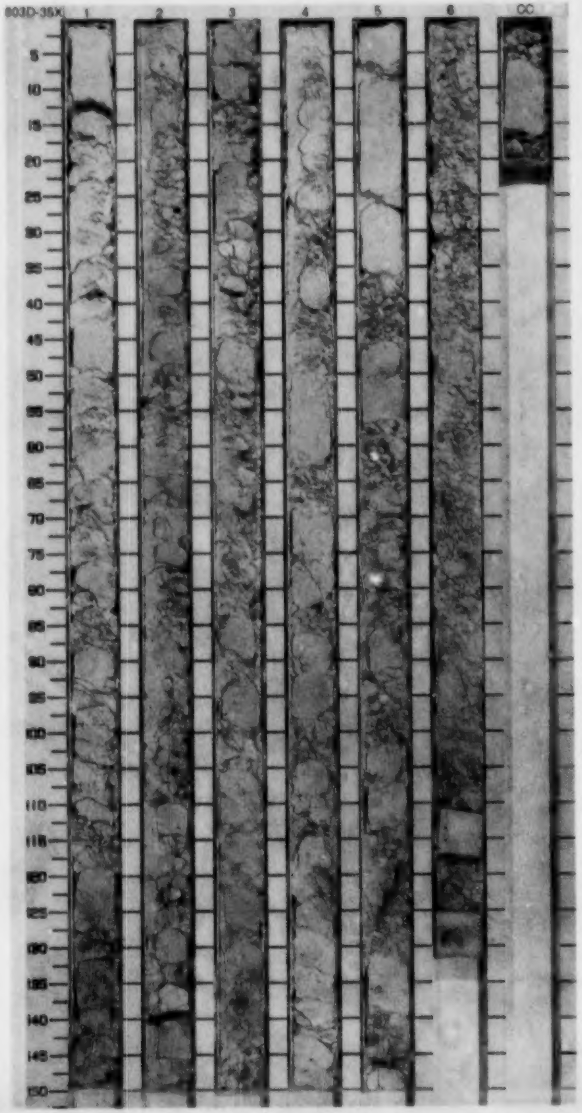
803D-35X
1
2
3
4
5
6
CC
5
10
15
20
25
30
35
40
45
50
55
60
65
70
75
80
85
90
95
100
105
110
115
120
125
130
135
140
145
150

SITE 803 HOLE D CORE 36X CORED INTERVAL 322.7-332.3 mbsf

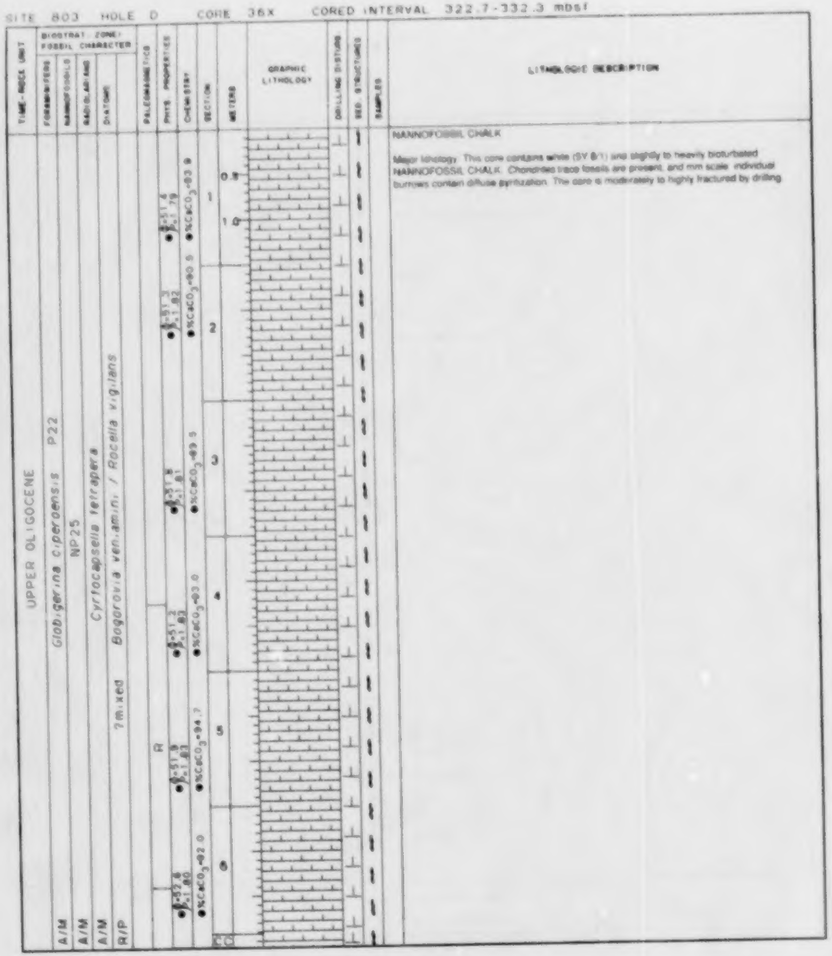

TIME-ROCK UNIT	BIOSTRAT. ZONE/ FOSSIL CHARACTER: FORAMINIFERS	NANNOFOSSILS	RADIOLARIANS	DIATOMS	PALEOMAGNETICS	PHYS. PROPERTIES	CHEMISTRY	SECTION	METERS	GRAPHIC LITHOLOGY	DRILLING DISTURB.	SED. STRUCTURES	SAMPLES	LITHOLOGIC DESCRIPTION
UPPER OLIGOCENE	*Globigerina ciperoensis* P22 A/M	NP25 A/M	*Cyrtocapsella tetrapera* A/M	?mixed *Bogorovia veniamini* / *Rocella vigilans* R/P	R	●ϕ=51.4 γ=1.79	●%CaCO$_3$=83.8	1	0.5 1.0					NANNOFOSSIL CHALK Major lithology: This core contains white (5Y 8/1) and slightly to heavily bioturbated NANNOFOSSIL CHALK. Chondrites trace fossils are present, and mm scale individual burrows contain diffuse pyritization. The core is moderately to highly fractured by drilling.
						●ϕ=51.3 γ=1.82	●%CaCO$_3$=90.5	2						
						●ϕ=51.8 γ=1.81	●%CaCO$_3$=89.5	3						
						●ϕ=51.2 γ=1.83	●%CaCO$_3$=93.0	4						
						●ϕ=51.9 γ=1.83	●%CaCO$_3$=94.7	5						
						●ϕ=52.6 γ=1.80	●%CaCO$_3$=92.0	6						
								CC						

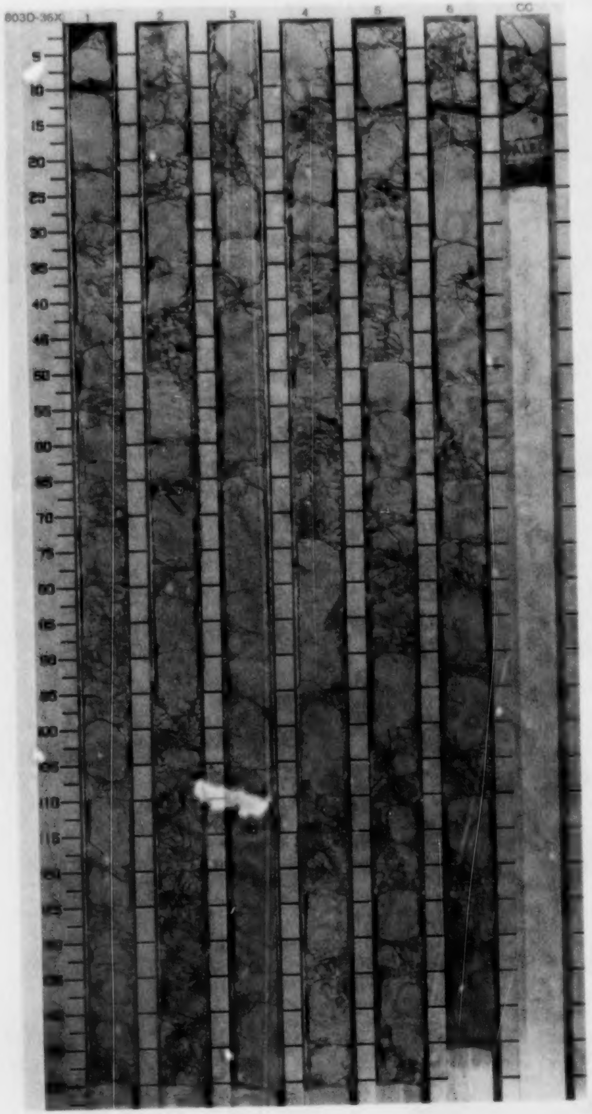

SITE 803 HOLE D CORE 37X CORED INTERVAL 332.3-342.0 mbsf

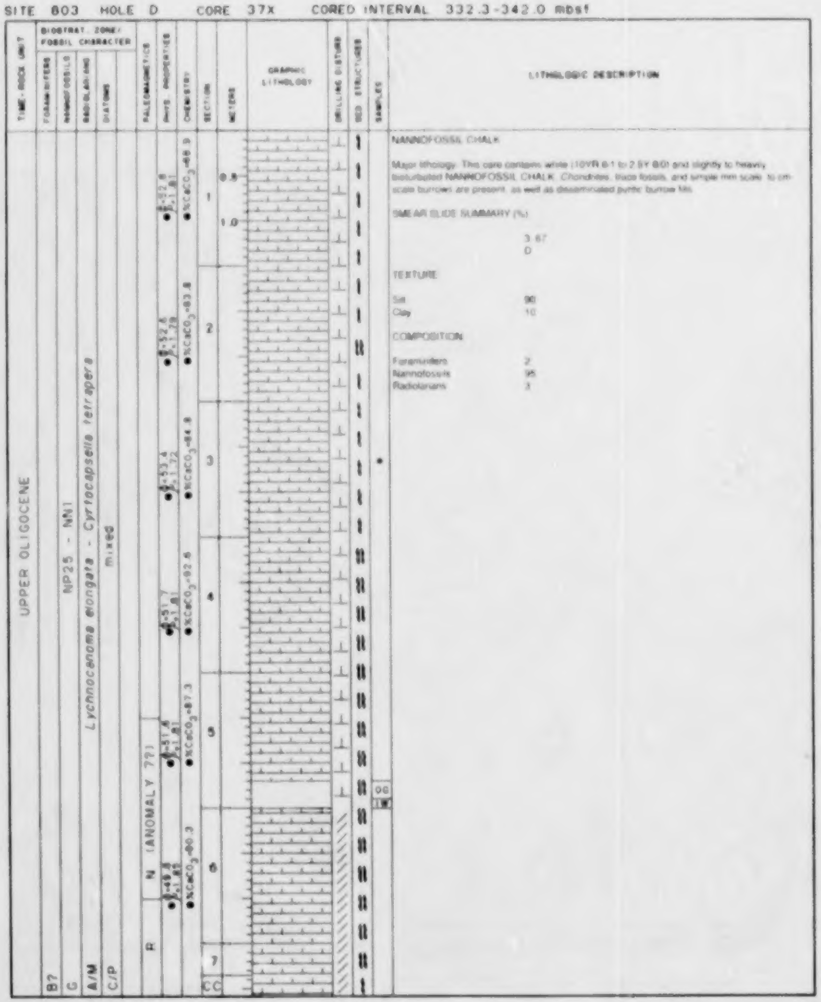
TIME-ROCK UNIT
BIOSTRAT. ZONE/ FOSSIL CHARACTER
FORAMINIFERS
NANNOFOSSILS
RADIOLARIANS
DIATOMS
PALEOMAGNETICS
PHYS. PROPERTIES
CHEMISTRY
SECTION
METERS
GRAPHIC LITHOLOGY
DRILLING DISTURB.
SED. STRUCTURES
SAMPLES
UPPER OLIGOCENE
B?
G
NP25 - NN1
A/M
Lychnocanoma elongata - Cyrtocapsella tetrapera
C/P
mixed
N (ANOMALY 7?)
R
φ=52.8 γ=1.81
%CaCO3=88.9
φ=52.6 γ=1.79
%CaCO3=83.8
φ=53.4 γ=1.72
%CaCO3=84.8
φ=51.7 γ=1.81
%CaCO3=92.6
φ=51.6 γ=1.81
%CaCO3=87.3
φ=49.8 γ=1.85
%CaCO3=80.3
1
2
3
4
5
6
7
CC
0.5
1.0
OG
IW

LITHOLOGIC DESCRIPTION

NANNOFOSSIL CHALK

Major lithology: This core contains white (10YR 8/1 to 2.5Y 8/0) and slightly to heavily bioturbated NANNOFOSSIL CHALK. *Chondrites*, trace fossils, and simple mm-scale to cm-scale burrows are present, as well as disseminated pyritic burrow fills.

SMEAR SLIDE SUMMARY (%):

	3, 67
	D
TEXTURE:	
Silt	90
Clay	10
COMPOSITION:	
Foraminifers	2
Nannofossils	95
Radiolarians	3

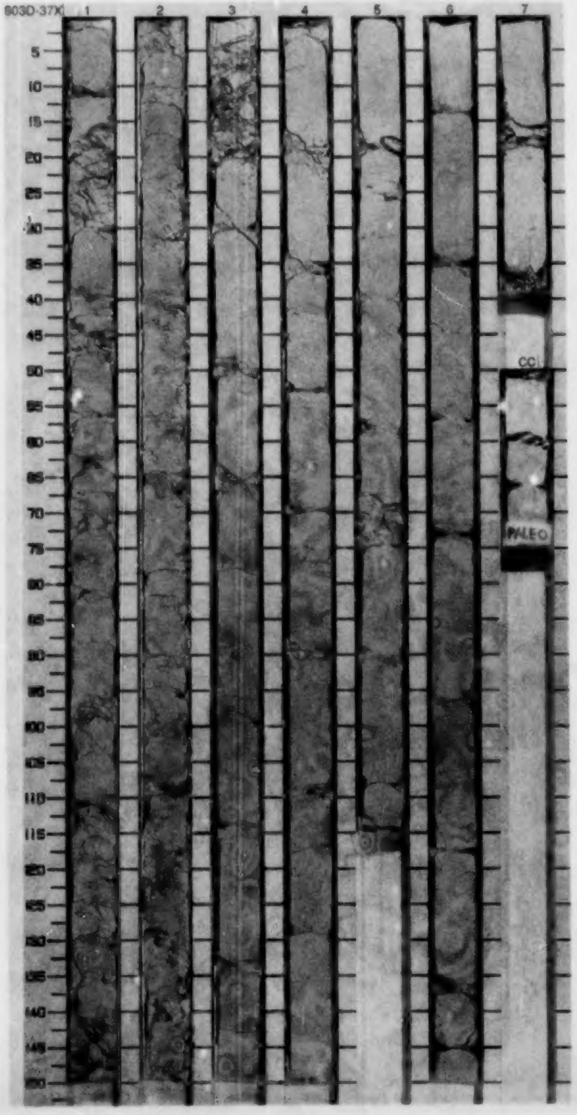
803D-37X
1
2
3
4
5
6
7
CC
PALEO
5
10
15
20
25
30
35
40
45
50
55
60
65
70
75
80
85
90
95
100
105
110
115
120
125
130
135
140
145
150

SITE 803 HOLE D CORE 38X CORED INTERVAL 342.0-351.6 mbsf

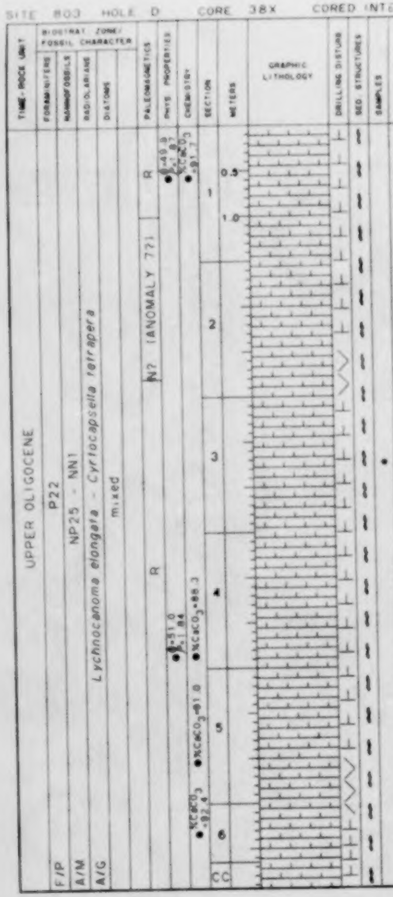
TIME-ROCK UNIT
BIOSTRAT. ZONE/ FOSSIL CHARACTER
FORAMINIFERS
NANNOFOSSILS
RADIOLARIANS
DIATOMS
PALEOMAGNETICS
PHYS. PROPERTIES
CHEMISTRY
SECTION
METERS
GRAPHIC LITHOLOGY
DRILLING DISTURB.
SED. STRUCTURES
SAMPLES
UPPER OLIGOCENE
F/P
P22
A/M
NP25 - NN1
A/G
Lychnocanoma elongata - Cyrtocapsella tetrapera
mixed
R
N? (ANOMALY 7?)
R
ϕ=40.9
γ=1.87
%CaCO$_3$=91.7
ϕ=51.0
γ=1.84
%CaCO$_3$=88.3
%CaCO$_3$=91.0
%CaCO$_3$=92.4
1
2
3
4
5
6
CC
0.5
1.0

LITHOLOGIC DESCRIPTION

NANNOFOSSIL CHALK

Major lithology: This core consists of white (10YR 8/1), homogeneous, moderately fractured and moderately to heavily bioturbated NANNOFOSSIL CHALK. Reddish gray (5R 5/1) pyritic mottles and mm thick, irregular, discontinuous bands are observed throughout the core. Variations in firmness also are observed.

SMEAR SLIDE SUMMARY (%)

	3, 75
	D
TEXTURE	
Silt	40
Clay	60
COMPOSITION	
Nannofossils	100

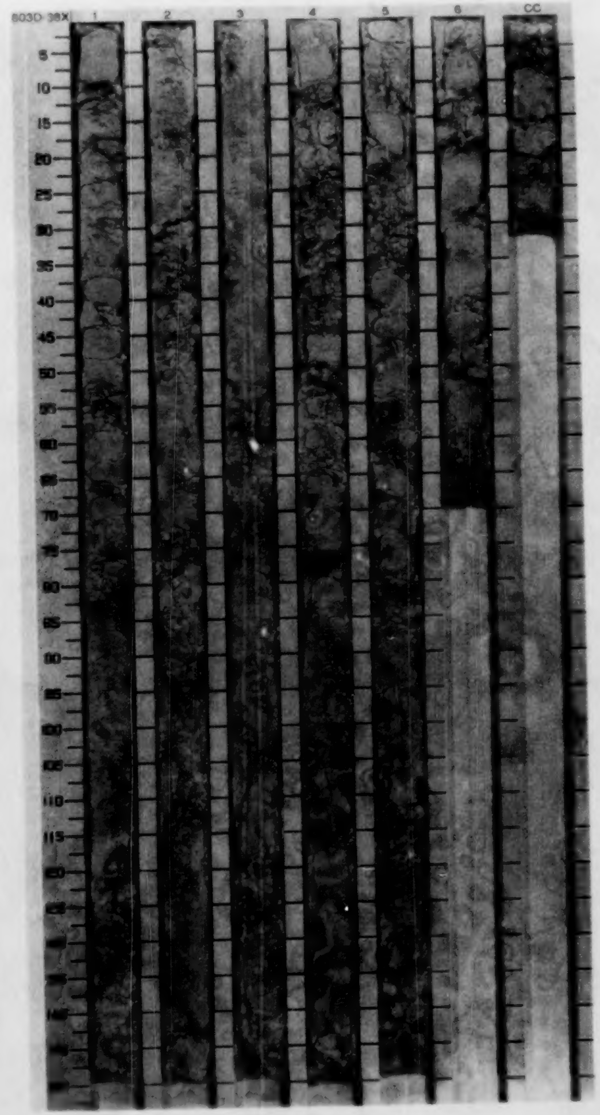
803D-38X
1
2
3
4
5
6
CC
5
10
15
20
25
30
35
40
45
50
55
60
65
70
75
80
85
90
95
100
105
110
115
120
125

SITE 803 HOLE D CORE 39X CORED INTERVAL 351.6-361.3 mbsf

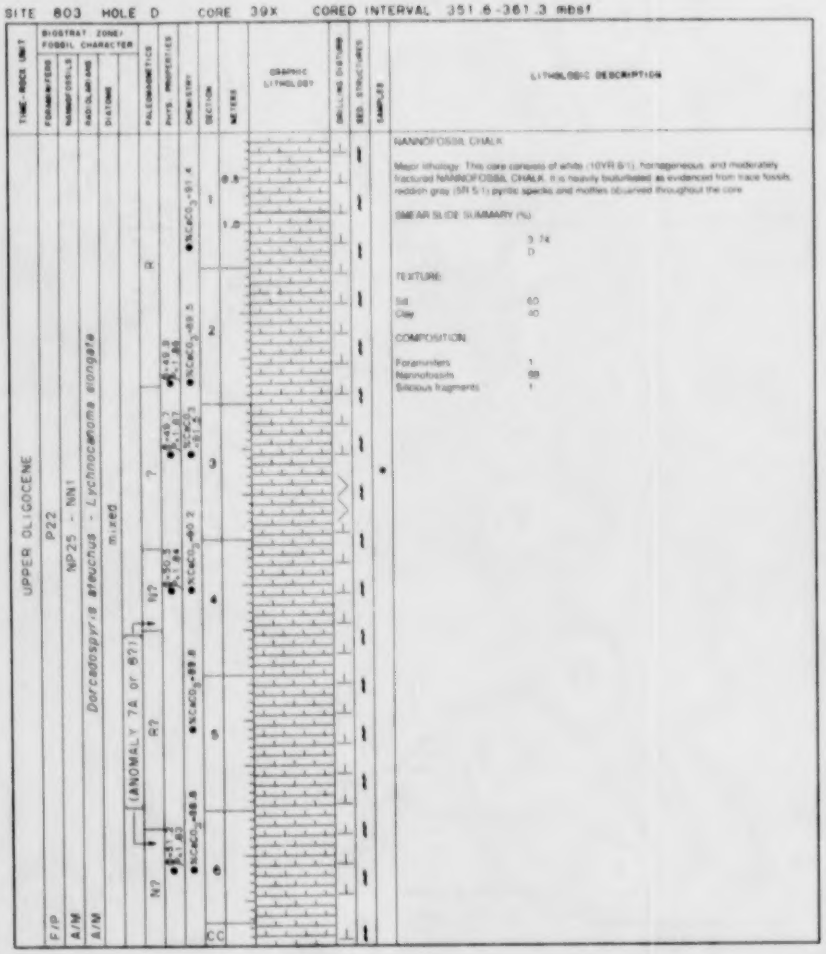
TIME-ROCK UNIT
BIOSTRAT. ZONE/ FOSSIL CHARACTER
FORAMINIFERS
NANNOFOSSILS
RADIOLARIANS
DIATOMS
PALEOMAGNETICS
PHYS. PROPERTIES
CHEMISTRY
SECTION
METERS
GRAPHIC LITHOLOGY
DRILLING DISTURB.
SED. STRUCTURES
SAMPLES
UPPER OLIGOCENE
F/P P22
A/M NP25 - NN1
A/M Dorcadospyris ateuchus - Lychnocanoma elongata
mixed
R
?
N?
R?
N?
(ANOMALY 7A or 8?)
φ=49.9 γ=1.86
φ=49.7 γ=1.87
φ=50.5 γ=1.84
φ=51.2 γ=1.83
%CaCO3=91.4
%CaCO3=89.5
%CaCO3 =91.2
%CaCO3=90.2
%CaCO3=89.8
%CaCO3=88.8
1
2
3
4
5
6
CC
0.5
1.0

LITHOLOGIC DESCRIPTION

NANNOFOSSIL CHALK

Major lithology: This core consists of white (10YR 8/1), homogeneous, and moderately fractured NANNOFOSSIL CHALK. It is heavily bioturbated as evidenced from trace fossils; reddish gray (5R 5/1) pyritic specks and mottles observed throughout the core.

SMEAR SLIDE SUMMARY (%):

	3, 74 D
TEXTURE:	
Silt	60
Clay	40
COMPOSITION:	
Foraminifers	1
Nannofossils	98
Siliceous fragments	1

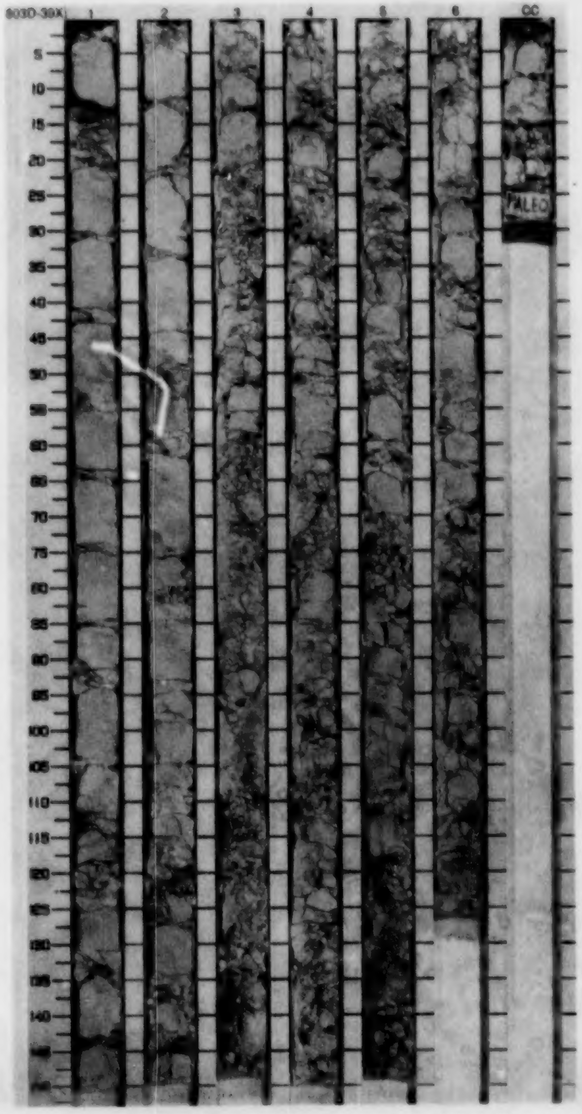
803D-39X
1
2
3
4
5
6
CC
5
10
15
20
25
30
35
40
45
50
55
60
65
70
75
80
85
90
95
100
105
110
115
120
125
130
135
140
145
150
PALEO

SITE 803 HOLE D CORE 40X CORED INTERVAL 361.3-371.0 mbsf

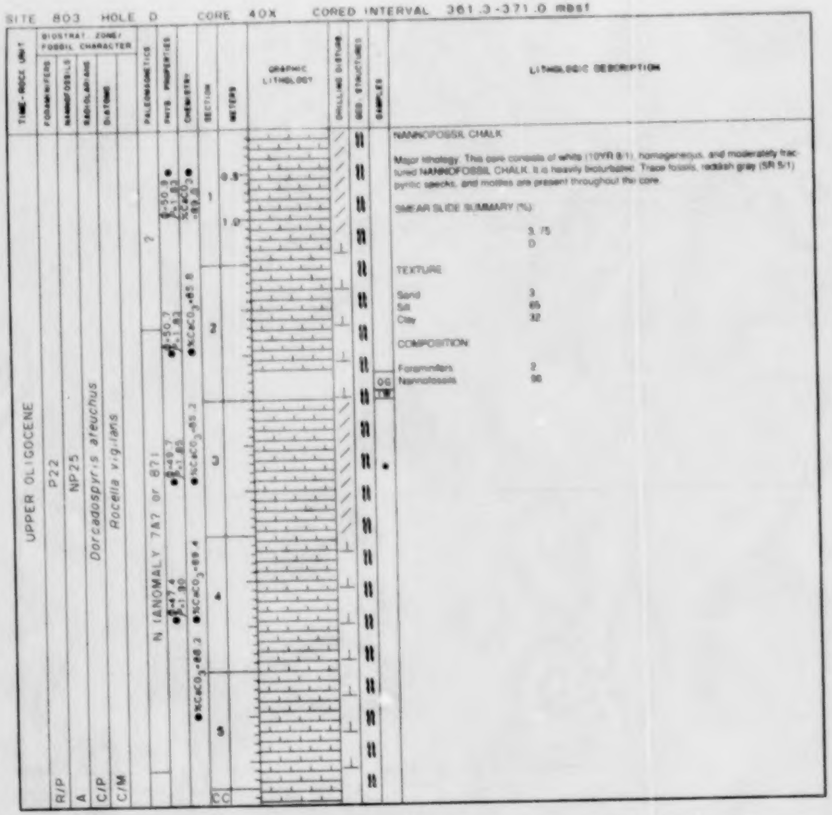
TIME-ROCK UNIT
BIOSTRAT. ZONE/FOSSIL CHARACTER
FORAMINIFERS
NANNOFOSSILS
RADIOLARIANS
DIATOMS
PALEOMAGNETICS
PHYS. PROPERTIES
CHEMISTRY
SECTION
METERS
GRAPHIC LITHOLOGY
DRILLING DISTURB.
SED. STRUCTURES
SAMPLES
UPPER OLIGOCENE
R/P P22
A NP25
C/P Dorcadospyris ateuchus
C/M Rocella vigilans
?
N (ANOMALY 7A? or 8?)
φ=50.9 ρ=1.83
φ=50.7 ρ=1.83
φ=49.7 ρ=1.85
φ=47.4 ρ=1.90
%CaCO₃=89.0
%CaCO₃=85.8
%CaCO₃=85.2
%CaCO₃=89.4
%CaCO₃=88.2
1
2
3
4
5
CC
0.5
1.0
OG
IW

LITHOLOGIC DESCRIPTION

NANNOFOSSIL CHALK

Major lithology: This core consists of white (10YR 8/1), homogeneous, and moderately fractured NANNOFOSSIL CHALK. It is heavily bioturbated. Trace fossils, reddish gray (5R 5/1) pyritic specks, and mottles are present throughout the core.

SMEAR SLIDE SUMMARY (%):

	3, 75
	D
TEXTURE:	
Sand	3
Silt	65
Clay	32
COMPOSITION:	
Foraminifers	2
Nannofossils	98

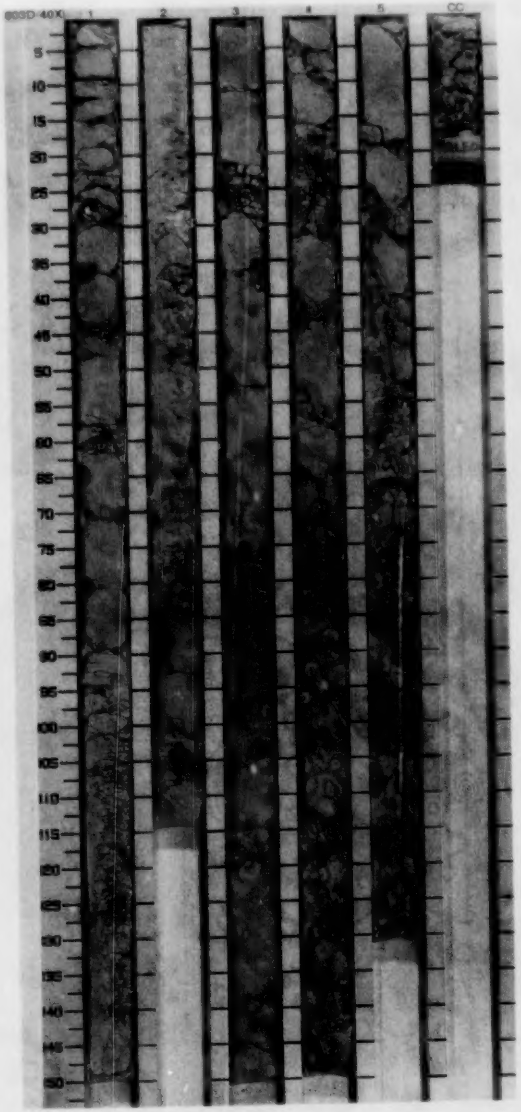
803D-40X
1
2
3
4
5
CC
5
10
15
20
25
30
35
40
45
50
55
60
65
70
75
80
85
90
95
100
105
110
115
120
125
130
135
140
145
150

SITE 803 HOLE D CORE 41X CORED INTERVAL 371.0-380.7 mbsf

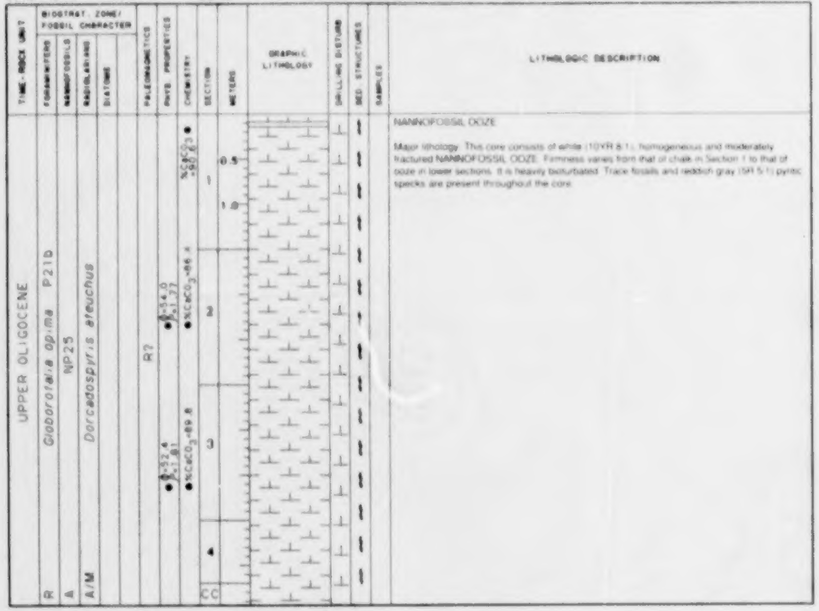
TIME-ROCK UNIT
BIOSTRAT. ZONE/ FOSSIL CHARACTER
FORAMINIFERS
NANNOFOSSILS
RADIOLARIANS
DIATOMS
PALEOMAGNETICS
PHYS. PROPERTIES
CHEMISTRY
SECTION
METERS
GRAPHIC LITHOLOGY
DRILLING DISTURB.
SED. STRUCTURES
SAMPLES
LITHOLOGIC DESCRIPTION
UPPER OLIGOCENE
Globorotalia opima P21b
NP25
Dorcadospyris ateuchus
R
A
A/M
R?
φ=54.0
ρ=1.77
φ=52.4
ρ=1.81
%CaCO3=90.3
%CaCO3=86.4
%CaCO3=89.8
1
2
3
4
CC
0.5
1.0

NANNOFOSSIL OOZE

Major lithology: This core consists of white (10YR 8/1), homogeneous and moderately fractured NANNOFOSSIL OOZE. Firmness varies from that of chalk in Section 1 to that of ooze in lower sections. It is heavily bioturbated. Trace fossils and reddish gray (5R 5/1) pyritic specks are present throughout the core.

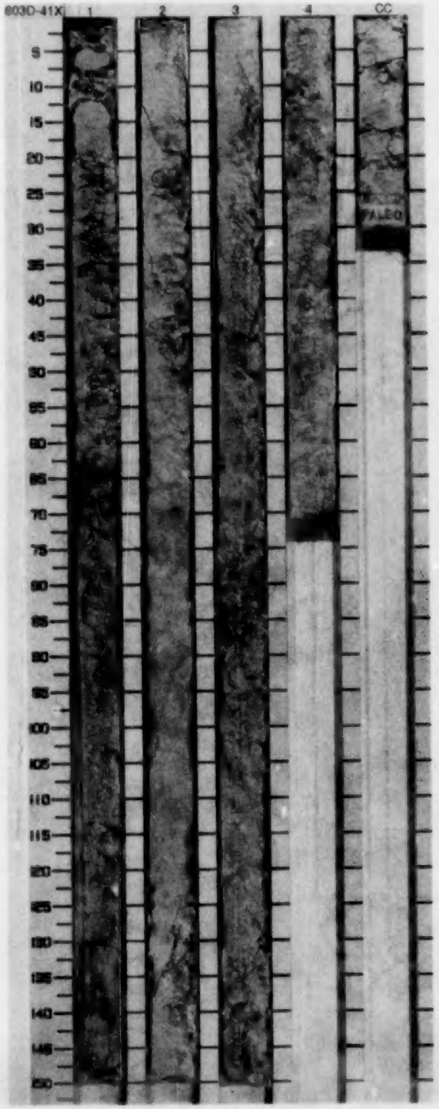
803D-41X
1
2
3
4
CC
5
10
15
20
25
30
35
40
45
50
55
60
65
70
75
80
85
90
95
100
105
110
115
120
125
130
135
140
145
150
PALEO

SITE 803 HOLE D CORE 42X CORED INTERVAL 380.7-390.4 mbsf

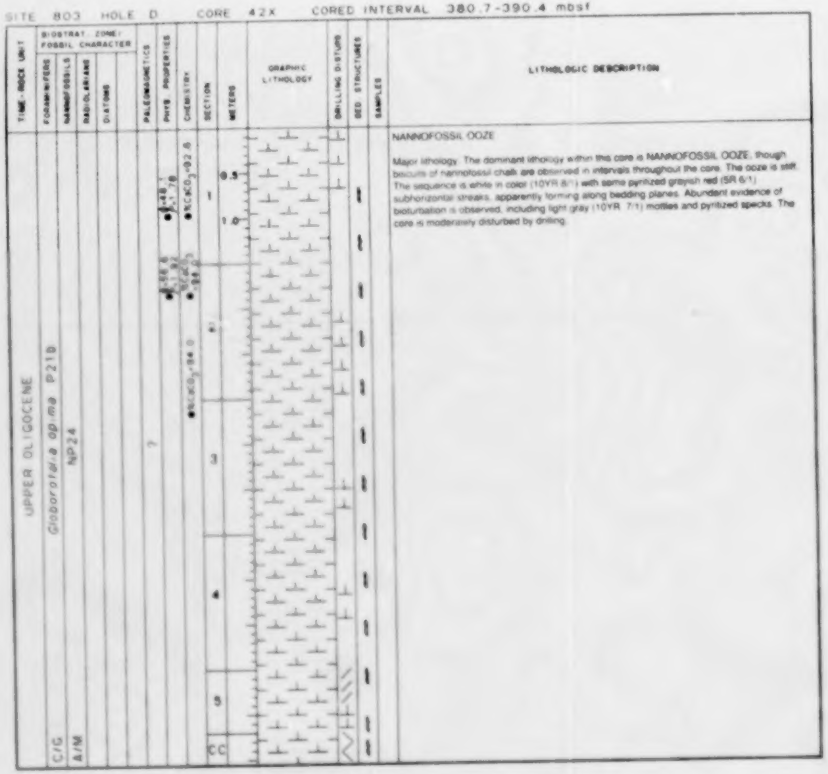
TIME-ROCK UNIT
BIOSTRAT. ZONE/ FOSSIL CHARACTER
FORAMINIFERS
NANNOFOSSILS
RADIOLARIANS
DIATOMS
PALEOMAGNETICS
PHYS. PROPERTIES
CHEMISTRY
SECTION
METERS
GRAPHIC LITHOLOGY
DRILLING DISTURB.
SED. STRUCTURES
SAMPLES
LITHOLOGIC DESCRIPTION
UPPER OLIGOCENE
Globorotalia op.ma P21b
NP24
C/G
A/M
?
%CaCO3=92.6
%CaCO3=94.0
%CaCO3=94.0
0.5
1.0
1
2
3
4
5
CC

NANNOFOSSIL OOZE

Major lithology: The dominant lithology within this core is NANNOFOSSIL OOZE, though biscuits of nannofossil chalk are observed in intervals throughout the core. The ooze is stiff. The sequence is white in color (10YR 8/1) with some pyritized grayish red (5R 6/1) subhorizontal streaks, apparently forming along bedding planes. Abundant evidence of bioturbation is observed, including light gray (10YR 7/1) mottles and pyritized specks. The core is moderately disturbed by drilling.

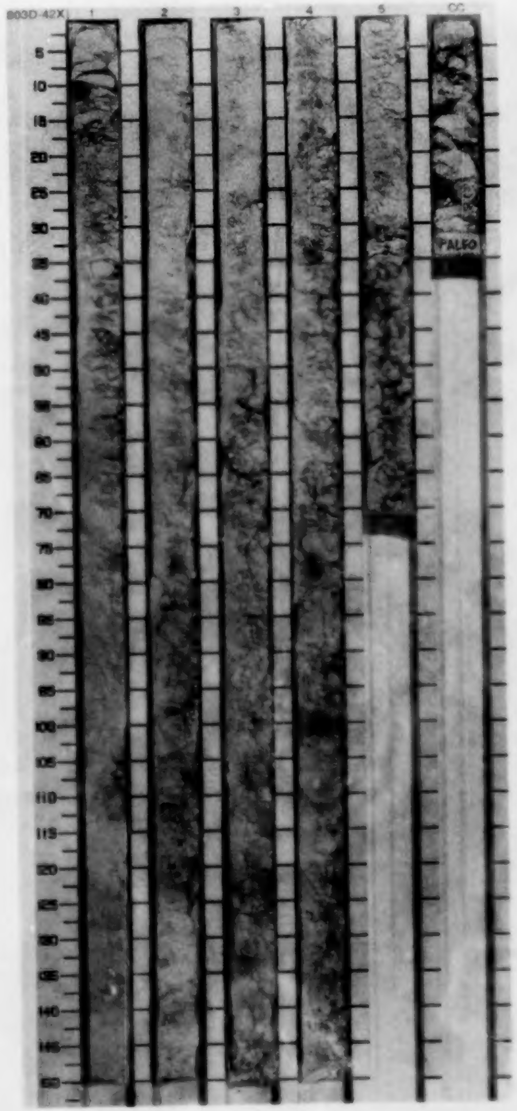
803D-42X
1
2
3
4
5
CC
PALEO
5
10
15
20
25
30
35
40
45
50
55
60
65
70
75
80
85
90
95
100
105
110
115
120
125
130
135
140
145
150

SITE 803 HOLE D CORE 43X CORED INTERVAL 390.4-400.0 mbsf

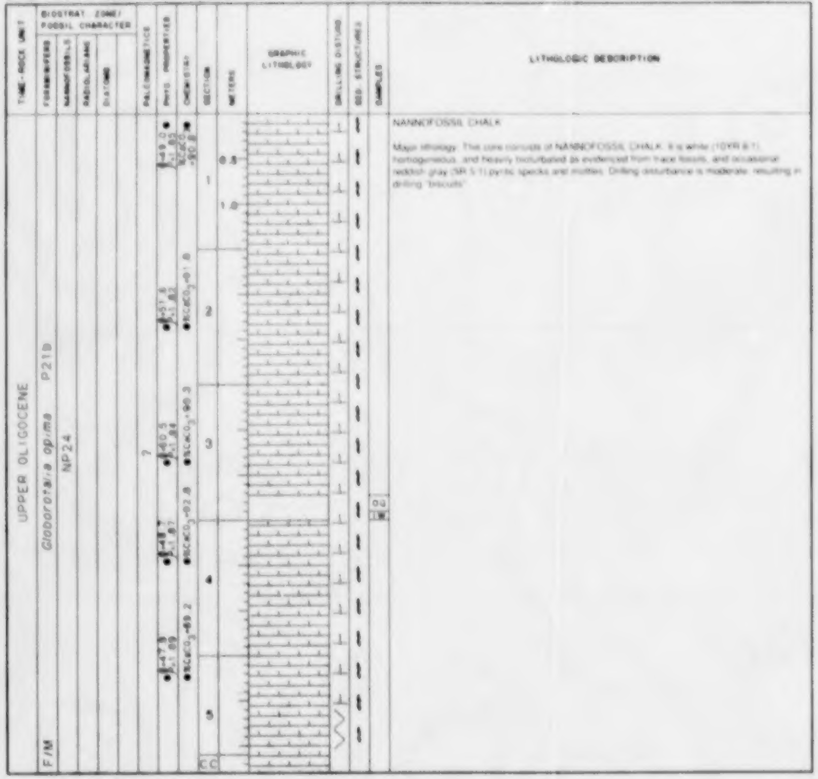
TIME-ROCK UNIT
BIOSTRAT. ZONE/ FOSSIL CHARACTER
FORAMINIFERS
NANNOFOSSILS
RADIOLARIANS
DIATOMS
PALEOMAGNETICS
PHYS. PROPERTIES
CHEMISTRY
SECTION
METERS
GRAPHIC LITHOLOGY
DRILLING DISTURB.
SED. STRUCTURES
SAMPLES
LITHOLOGIC DESCRIPTION
UPPER OLIGOCENE
Globorotalia opima P21b
F/M
NP24
?
φ=49.0 γ=1.93
%CaCO3=90.8
φ=57.6 γ=1.82
%CaCO3=91.8
φ=60.5 γ=1.84
%CaCO3=90.3
φ=48.7 γ=1.87
%CaCO3=92.8
φ=47.5 γ=1.89
%CaCO3=89.2
1
2
3
4
5
CC
0.5
1.0
OG
IW

NANNOFOSSIL CHALK

Major lithology: The core consists of NANNOFOSSIL CHALK. It is white (10YR 8/1), homogeneous, and heavily bioturbated as evidenced from trace fossils, and occasional reddish gray (5R 5/1) pyritic specks and mottles. Drilling disturbance is moderate, resulting in drilling "biscuits".

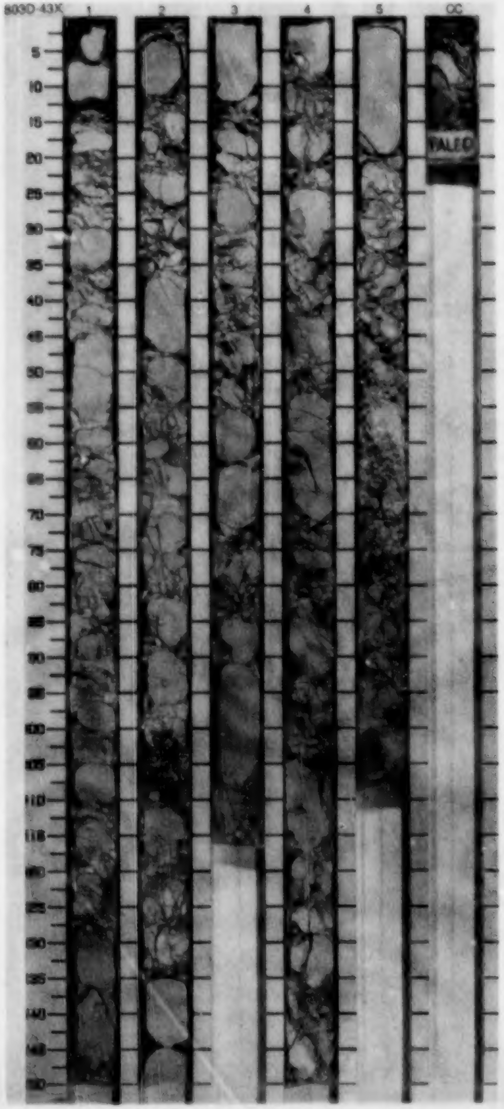
803D-43X
1
2
3
4
5
CC
5
10
15
20
25
30
35
40
45
50
55
60
65
70
75
80
85
90
95
100
105
110
115
120
125
130
135
140
145
150
PALEO

SITE 803 HOLE D CORE 44X CORED INTERVAL 400.0-409.7 mbsf

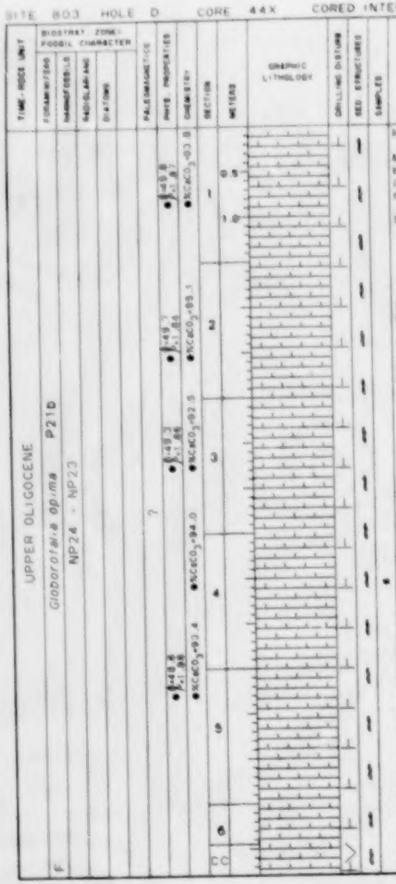
TIME-ROCK UNIT
BIOSTRAT. ZONE/FOSSIL CHARACTER
FORAMINIFERS
NANNOFOSSILS
RADIOLARIANS
DIATOMS
PALEOMAGNETICS
PHYS. PROPERTIES
CHEMISTRY
SECTION
METERS
GRAPHIC LITHOLOGY
DRILLING DISTURB.
SED. STRUCTURES
SAMPLES
UPPER OLIGOCENE
Globorotalia opima P21b
F
NP24 - NP23
?
φ=49.8 γ=1.87
φ=49.7 γ=1.84
φ=49.3 γ=1.86
φ=48.8 γ=1.88
%CaCO3=93.8
%CaCO3=93.1
%CaCO3=92.5
%CaCO3=94.0
%CaCO3=93.4
1
2
3
4
5
6
CC
0.5
1.0

LITHOLOGIC DESCRIPTION

NANNOFOSSIL CHALK

Major lithology: This core consists of white (10YR 8/1), homogeneous, and heavily bioturbated NANNOFOSSIL CHALK. Bioturbation evidence includes numerous reddish gray (5R 5/1) pyritic specks, streaks, and mottles. Drilling disturbance is moderate, resulting in drilling "biscuits".

SMEAR SLIDE SUMMARY (%):

	4, 72
	D
TEXTURE:	
Silt	60
Clay	40
COMPOSITION:	
Diatoms	Tr
Nannofossils	100

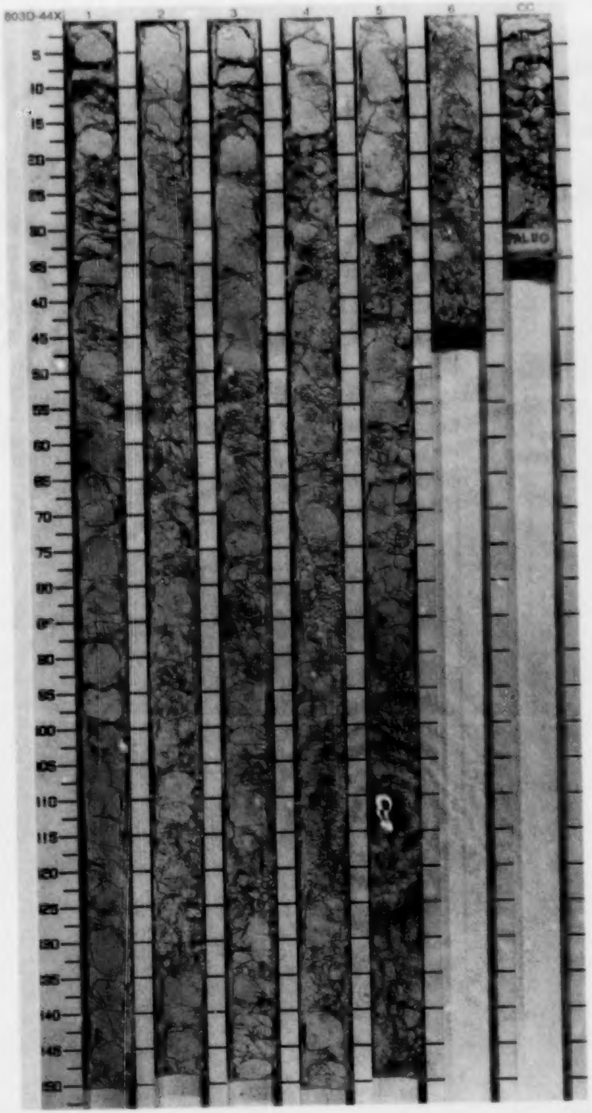
803D-44X
1
2
3
4
5
6
CC
5
10
15
20
25
30
35
40
45
50
55
60
65
70
75
80
85
90
95
100
105
110
115
120
125
130
135
140
145
150
PALEO

SITE 803 HOLE D CORE 45X CORED INTERVAL 409.7-419.3 mbsf

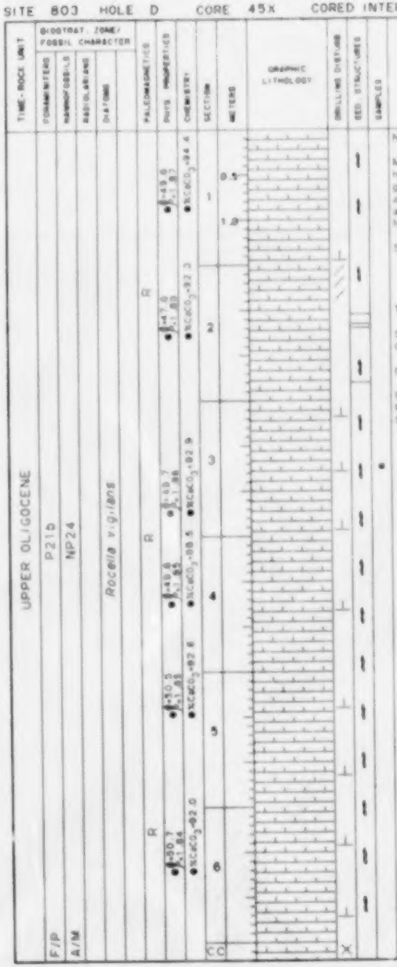
TIME-ROCK UNIT
BIOSTRAT. ZONE/ FOSSIL CHARACTER
FORAMINIFERS
NANNOFOSSILS
RADIOLARIANS
DIATOMS
PALEOMAGNETICS
PHYS. PROPERTIES
CHEMISTRY
SECTION
METERS
GRAPHIC LITHOLOGY
DRILLING DISTURB.
SED. STRUCTURES
SAMPLES
UPPER OLIGOCENE
P21b
NP24
Rocella vigilans
F/P
A/M
R
R
R
φ=49.6 γ=1.87
φ=47.6 γ=1.88
φ=48.7 γ=1.86
φ=49.6 γ=1.85
φ=50.5 γ=1.85
φ=50.7 γ=1.84
%CaCO3=94.4
%CaCO3=92.3
%CaCO3=92.9
%CaCO3=88.5
%CaCO3=92.6
%CaCO3=92.0
1
2
3
4
5
6
CC
0.5
1.0

LITHOLOGIC DESCRIPTION

NANNOFOSSIL CHALK

Major lithology: This core consists of white (10YR 8/0), homogeneous, and moderately to heavily bioturbated NANNOFOSSIL CHALK. Bioturbation evidence includes faint reddish gray (5Y 5/1) mottles, streaks and burrow fills. Throughout the core, intervals of reddish gray and green (10Y 7/2) color bands are observed. The bands are on a mm to cm scale, parallel and have a sharp color contact with the white sequences. A few intervals are moderately fractured.

SMEAR SLIDE SUMMARY (%):

	3, 74
	D
TEXTURE:	
Silt	60
Clay	40
COMPOSITION:	
Foraminifers	1
Nannofossils	98
Siliceous fragments	1

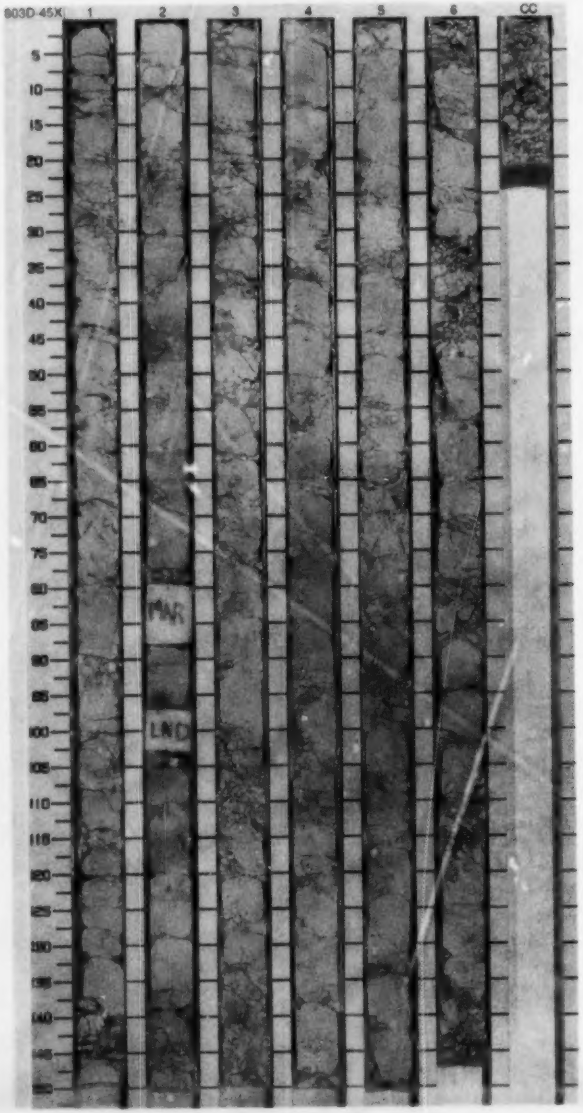
803D-45X
1
2
3
4
5
6
CC
5
10
15
20
25
30
35
40
45
50
55
60
65
70
75
80
85
90
95
100
105
110
115
120
125
130
135
140
145
150
PAL
LND

SITE 803 HOLE D CORE 46X CORED INTERVAL 419.3-429.0 mbsf

TIME-ROCK UNIT	BIOSTRAT. ZONE/ FOSSIL CHARACTER: FORAMINIFERS	NANNOFOSSILS	RADIOLARIANS	DIATOMS	PALEOMAGNETICS	PHYS. PROPERTIES	CHEMISTRY	SECTION	METERS	DRILLING DISTURB.	SED. STRUCTURES	SAMPLES
LOWER OLIGOCENE	*Globorotalia opima* P21a	NP23				● ϕ=48.5 γ=1.87	● %$CaCO_3$=90.4	1	0.5 1.0	⊥	ǀ	
					R	● ϕ=49.8 γ=1.86	● %$CaCO_3$=90.1	2		⊥	ǀ	●
						● ϕ=50.5 γ=1.85	● %$CaCO_3$=88.7	3		⊥	ǀ	
					R			4		⊥	ǀ	OG IW
					R	● ϕ=50.5 γ=1.85	● %$CaCO_3$=89.5	5		⊥	ǀ	
								6		⊥	ǀ	
	F/M	A/P						CC				

LITHOLOGIC DESCRIPTION

NANNOFOSSIL CHALK

Major lithology: This core consists of light gray (10YR 8/1), homogeneous, and moderately to heavily bioturbated NANNOFOSSIL CHALK. Bioturbation evidence includes faint reddish gray (5Y 5/1) mottles, streaks, and burrow fills. Intervals of reddish gray and green (10Y 7/2) color banding are present throughout the core. The bands are on a mm to cm scale, parallel and have sharp contacts.

SMEAR SLIDE SUMMARY (%):

	2, 74
	D
TEXTURE:	
Silt	10
Clay	90
COMPOSITION:	
Diatoms	Tr
Nannofossils	98
Radiolarians	1
Siliceous fragments	1

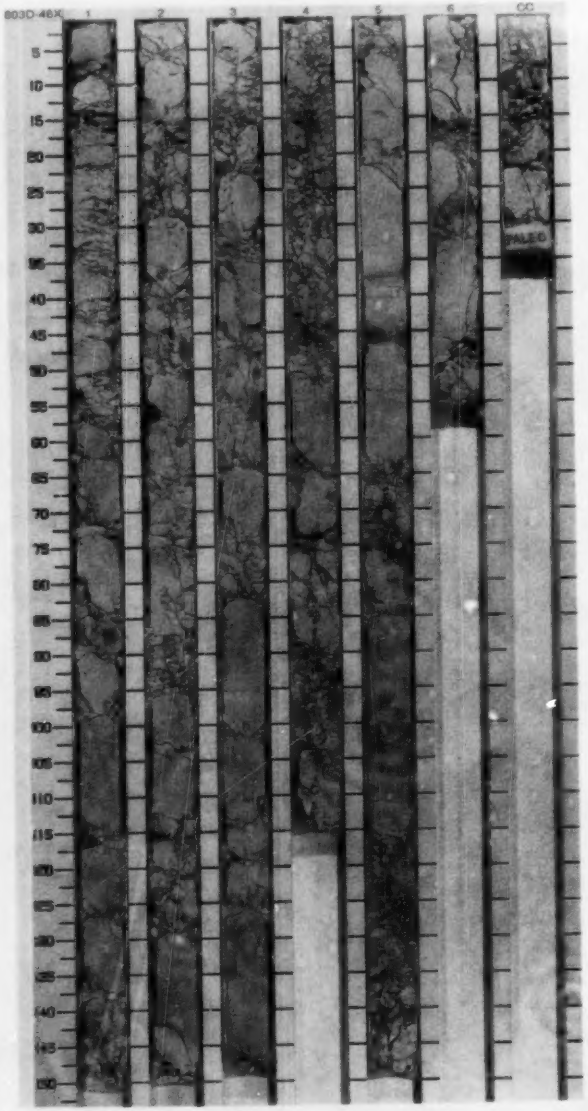

SITE 803 HOLE D CORE 47X CORED INTERVAL 429.0-438.6 mbsf

TIME-ROCK UNIT	BIOSTRAT. ZONE/ FOSSIL CHARACTER: FORAMINIFERS	NANNOFOSSILS	RADIOLARIANS	DIATOMS	PALEOMAGNETICS	PHYS. PROPERTIES	CHEMISTRY	SECTION	METERS
LOWER OLIGOCENE		NP23			?	●φ=50.0 ρ=1.84	●%CaCO3 =92.4	1	0.5 1.0
					N (ANOMALY 11 or 12?)		●%CaCO3=90.7	2	
						●φ=50.0 ρ=1.86	●%CaCO3=90.7	3	
						●φ=51.5 ρ=1.83	●%CaCO3=89.5 ●%CaCO3=81.5	4	
		A/P			?	●φ=48.7 ρ=1.81		5	
								CC	

GRAPHIC LITHOLOGY DRILLING DISTURB. SED. STRUCTURES SAMPLES

LITHOLOGIC DESCRIPTION

NANNOFOSSIL CHALK

Major lithology: This core consists of white (10YR 8/1), homogeneous, and moderately to heavily bioturbated NANNOFOSSIL CHALK. Bioturbation evidence includes mottles and discolored burrow fills. In Sections 1-3, abundant color banding is observed. The bands are mostly faint reddish gray (5R 5/1) although a few green (10GY 7/2) bands are present. All of the color bands are parallel, on a mm scale in thickness, and have sharp color contacts with the white ooze. The core is moderately fractured.

SMEAR SLIDE SUMMARY(%):

	3, 80 D
TEXTURE	
Silt	60
Clay	40
COMPOSITION	
Foraminifers	1
Nannofossils	99
Radiolarians	Tr

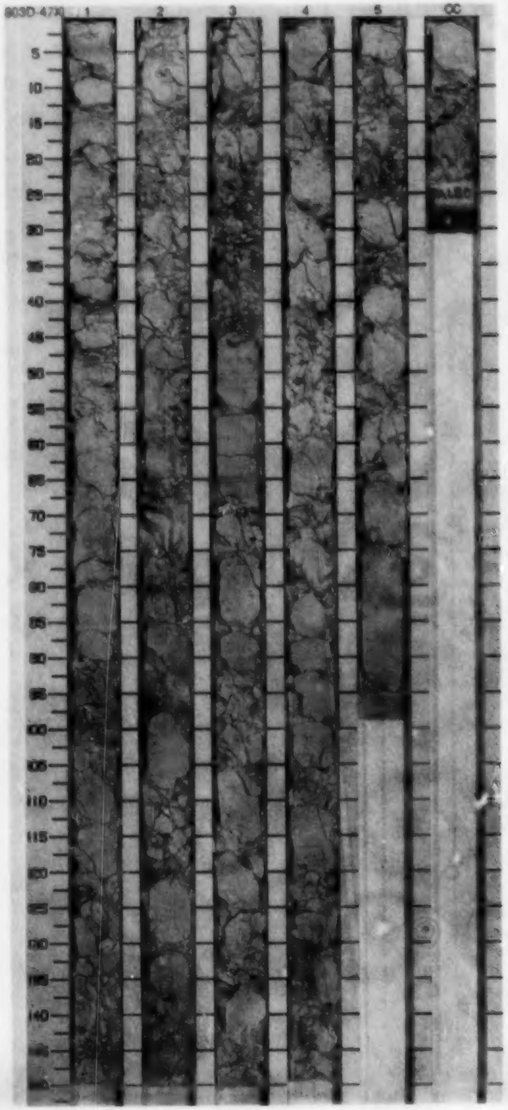

SITE 803 HOLE D CORE 48X CORED INTERVAL 438.6-447.8 mbsf

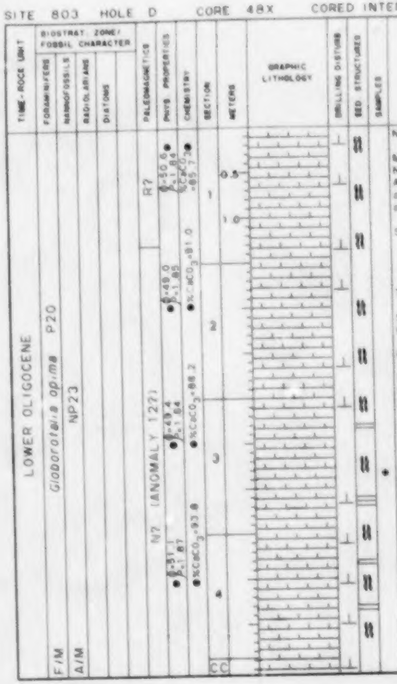
TIME-ROCK UNIT
BIOSTRAT. ZONE/ FOSSIL CHARACTER
FORAMINIFERS
NANNOFOSSILS
RADIOLARIANS
DIATOMS
PALEOMAGNETICS
PHYS. PROPERTIES
CHEMISTRY
SECTION
METERS
GRAPHIC LITHOLOGY
DRILLING DISTURB.
SED. STRUCTURES
SAMPLES
LOWER OLIGOCENE
Globorotalia opima P20
F/M
NP23
A/M
R?
N? (ANOMALY 12?)
φ=50.6 γ=1.84
φ=49.0 γ=1.85
φ=49.4 γ=1.84
φ=51.1 γ=1.87
%CaCO3=85.7
%CaCO3=81.0
%CaCO3=88.2
%CaCO3=93.8
1
2
3
4
CC
0.5
1.0

LITHOLOGIC DESCRIPTION

NANNOFOSSIL CHALK

Major lithology: This core consists of white (10YR 8/1) and moderately to heavily bioturbated NANNOFOSSIL CHALK. Bioturbation evidence includes mottles and discolored burrow fills. A particularly complete and unique trace fossil is observed in Section 4 at 97 cm. In Sections 3 and 4, intervals of fine (< mm thick), parallel and distinct color bands are observed. The bands are mostly reddish gray (5R 5/1) and pale green (10GY 7/2). The core is moderately fractured.

SMEAR SLIDE SUMMARY (%)

	3, 85
	D
TEXTURE:	
Silt	60
Clay	40
COMPOSITION:	
Foraminifers	1
Nannofossils	97
Radiolarians	Tr
Siliceous fragments	1
Zeolite	1

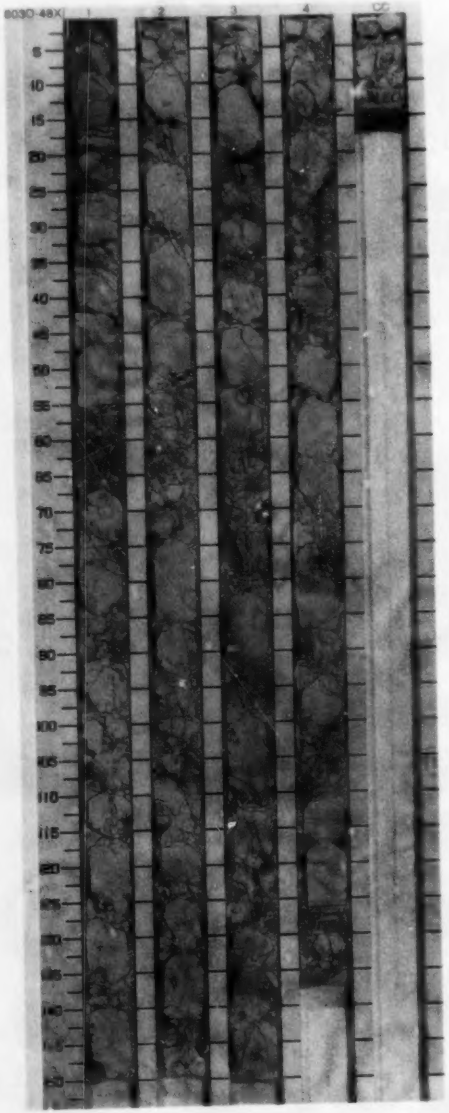
803D-48X
1
2
3
4
CC
5
10
15
20
25
30
35
40
45
50
55
60
65
70
75
80
85
90
95
100
105
110
115
120
125
130
135
140
145
150

SITE 803 HOLE D CORE 49X CORED INTERVAL 447.8-457.5 mbsf

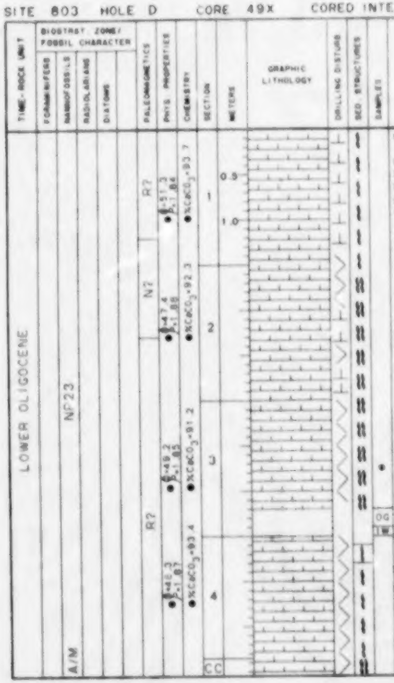
TIME-ROCK UNIT
BIOSTRAT. ZONE/ FOSSIL CHARACTER
FORAMINIFERS
NANNOFOSSILS
RADIOLARIANS
DIATOMS
PALEOMAGNETICS
PHYS. PROPERTIES
CHEMISTRY
SECTION
METERS
GRAPHIC LITHOLOGY
DRILLING DISTURB.
SED. STRUCTURES
SAMPLES
LOWER OLIGOCENE
NP23
A/M
R?
N?
R?
●φ=51.3 ρ=1.84
●φ=47.4 ρ=1.88
●φ=49.2 ρ=1.85
●φ=46.3 ρ=1.87
●%CaCO₃=93.7
●%CaCO₃=92.3
●%CaCO₃=91.2
●%CaCO₃=93.4
1
2
3
4
CC
0.5
1.0
OG
IW

LITHOLOGIC DESCRIPTION

NANNOFOSSIL CHALK

Major lithology: This core consists of white (10YR 8/1) and heavily bioturbated NANNOFOSSIL CHALK. Bioturbation evidence includes mottles and specks. Intervals of fine (< mm thick), parallel, and distinct color bands are observed. The bands are reddish gray (5R 5/1) and pale green (10GY 7/2), and have sharp color contacts with the white ooze. The core is moderately to highly fragmented.

SMEAR SLIDE SUMMARY (%):

	3, 74
	D
TEXTURE:	
Sand	2
Silt	60
Clay	38
COMPOSITION:	
Foraminifers	1
Nannofossils	98
Siliceous fragments	1

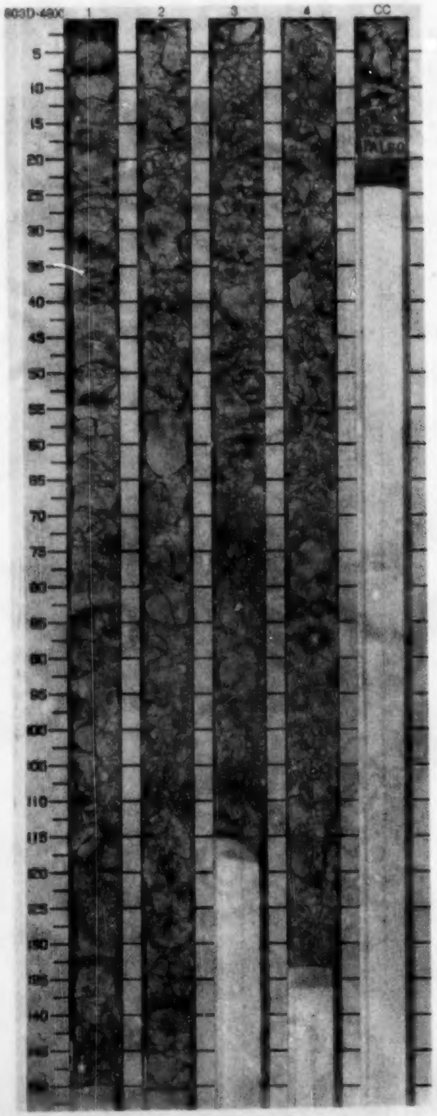
803D-49X
1
2
3
4
CC
PALEO
5
10
15
20
25
30
35
40
45
50
55
60
65
70
75
80
85
90
95
100
105
110
115
120
125
130
135
140
145
150

SITE 803 HOLE D CORE 50X CORED INTERVAL 457.5-467.2 mbsf

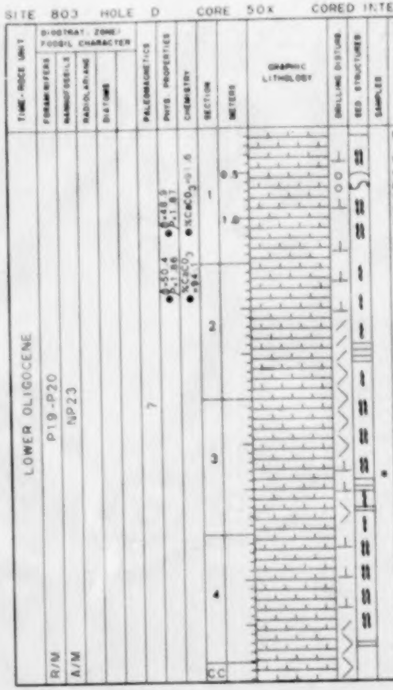

LITHOLOGIC DESCRIPTION

NANNOFOSSIL CHALK

Major lithology: This core consists of NANNOFOSSIL CHALK. It is white (2.5Y 8/0) and moderately to severely fractured by drilling. Drilling biscuits contain fine (mm- to sub-mm scale) parallel dark gray (2.5Y N4/) and light gray (2.5Y 7/0) color bands in Section 1, 60 cm and Section 3, 101-107 and 130-133 cm. Centimeter-scale, reddish gray (5R 6/1), greenish gray (5G 6/1), and light gray (N7/) color bands are located in Section 2, 95-105 cm. Other drilling biscuits are moderately to heavily bioturbated.

SMEAR SLIDE SUMMARY (%):

	3, 87
	D
TEXTURE:	
Sand	3
Silt	90
Clay	7
COMPOSITION:	
Accessory minerals	1
Foraminifers	2
Nannofossils	97

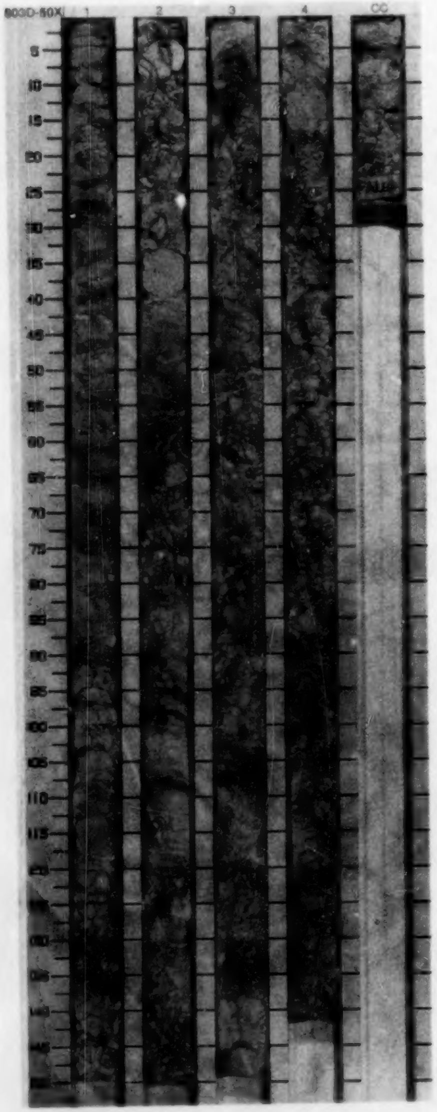
803D-50X
1
2
3
4
CC
5
10
15
20
25
30
35
40
45
50
55
60
65
70
75
80
85
90
95
100
105
110
115
120
125
130
135
140
145
150

SITE 803 HOLE D CORE 51X CORED INTERVAL 467.2-476.9 mbsf

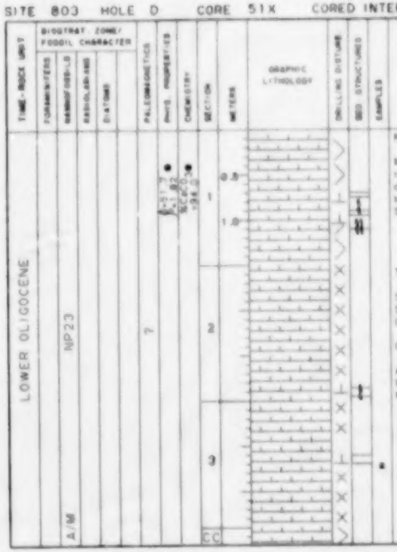
TIME-ROCK UNIT
BIOSTRAT. ZONE/ FOSSIL CHARACTER
FORAMINIFERS
NANNOFOSSILS
RADIOLARIANS
DIATOMS
PALEOMAGNETICS
PHYS. PROPERTIES
CHEMISTRY
SECTION
METERS
GRAPHIC LITHOLOGY
DRILLING DISTURB.
SED. STRUCTURES
SAMPLES
LOWER OLIGOCENE
NP23
A/M
?
0.5
1.0
1
2
3
CC

LITHOLOGIC DESCRIPTION

NANNOFOSSIL CHALK

Major lithology: This core contains NANNOFOSSIL CHALK. It is white (2.5Y 8/0) and moderately to severely fractured in Section 1; the remainder of the core is predominantly drilling breccia. Structures are only visible in the less disturbed pieces and include moderate to intense bioturbation and rare, mm-scale, dark gray (N4) parallel bands (stylolites?).

SMEAR SLIDE SUMMARY (%):

	3, 71
	D
TEXTURE:	
Sand	3
Silt	89
Clay	8
COMPOSITION:	
Accessory minerals	1
Foraminifers	3
Nannofossils	96

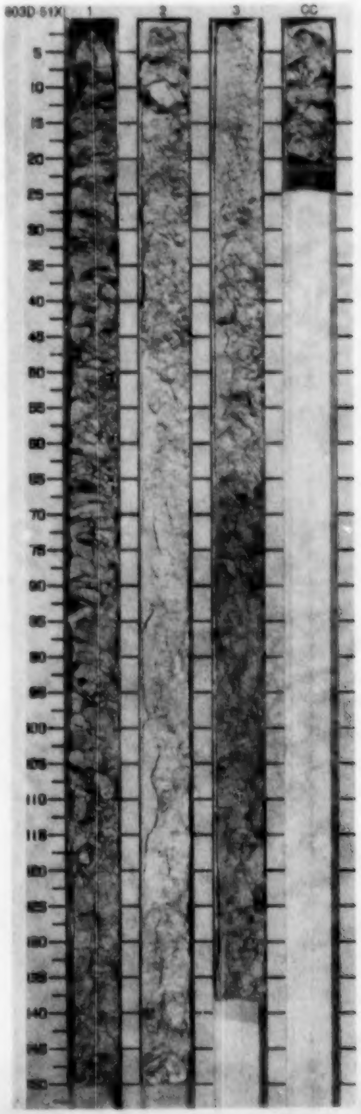
803D-51X
1
2
3
CC
5
10
15
20
25
30
35
40
45
50
55
60
65
70
75
80
85
90
95
100
105
110
115
120
125
130
135
140
145
150

SITE 803 HOLE D CORE 52X CORED INTERVAL 476.9-486.6 mbsf

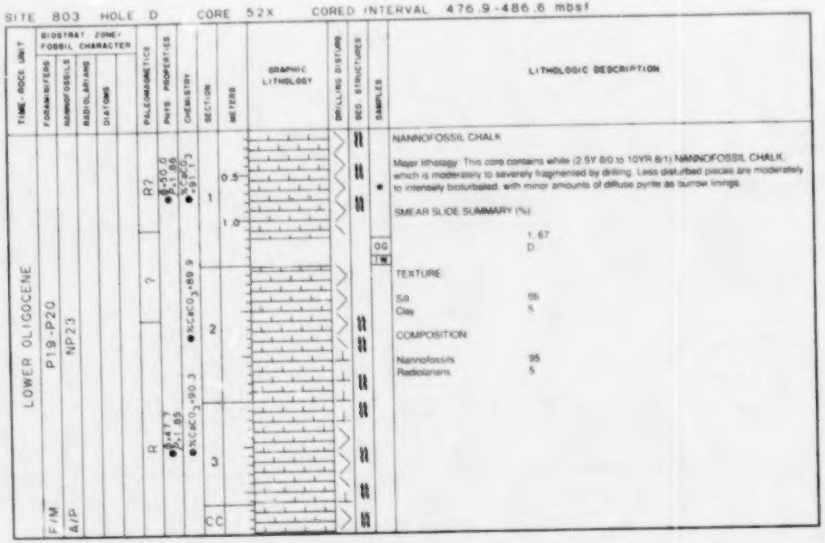
TIME-ROCK UNIT
BIOSTRAT. ZONE/ FOSSIL CHARACTER
FORAMINIFERS
NANNOFOSSILS
RADIOLARIANS
DIATOMS
PALEOMAGNETICS
PHYS. PROPERTIES
CHEMISTRY
SECTION
METERS
GRAPHIC LITHOLOGY
DRILLING DISTURB.
SED. STRUCTURES
SAMPLES
LOWER OLIGOCENE
P19-P20
NP23
F/M
A/P
R?
?
R
●φ-50.0
●γ-1.86
●%CaCO3-91.1
●%CaCO3-89.9
●%CaCO3-90.3
●φ-47.7
●γ-1.85
1
2
3
CC
0.5
1.0
OG
IW

LITHOLOGIC DESCRIPTION

NANNOFOSSIL CHALK

Major lithology: This core contains white (2.5Y 8/0 to 10YR 8/1) NANNOFOSSIL CHALK, which is moderately to severely fragmented by drilling. Less disturbed pieces are moderately to intensely bioturbated, with minor amounts of diffuse pyrite as burrow linings.

SMEAR SLIDE SUMMARY (%):

	1, 67
	D
TEXTURE:	
Silt	95
Clay	5
COMPOSITION:	
Nannofossils	95
Radiolarians	5

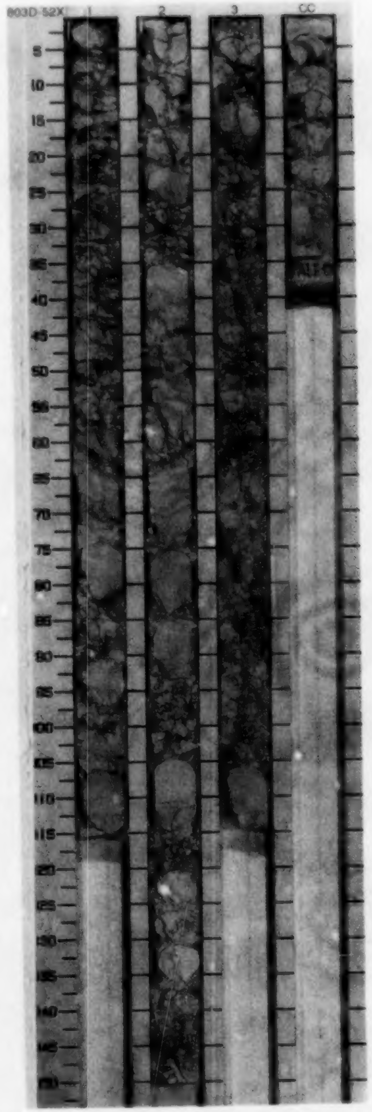
803D-52X
1
2
3
CC
5
10
15
20
25
30
35
40
45
50
55
60
65
70
75
80
85
90
95
100
105
110
115
120
125
130
135
140
145
150

SITE 803 HOLE D CORE 53X CORED INTERVAL 486.6-496.3 mbsf

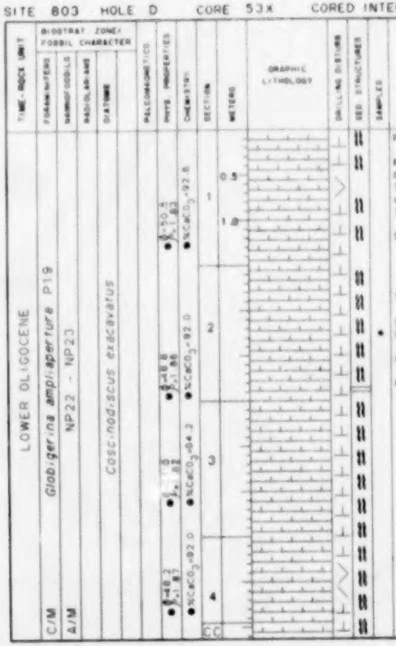
TIME-ROCK UNIT
BIOSTRAT. ZONE/ FOSSIL CHARACTER
FORAMINIFERS
NANNOFOSSILS
RADIOLARIANS
DIATOMS
PALEOMAGNETICS
PHYS. PROPERTIES
CHEMISTRY
SECTION
METERS
GRAPHIC LITHOLOGY
DRILLING DISTURB.
SED. STRUCTURES
SAMPLES
LOWER OLIGOCENE
Globigerina ampliapertura P19
C/M
NP22 - NP23
A/M
Coscinodiscus excavatus
φ=50.5
ρ=1.83
%CaCO₃=92.6
φ=48.8
ρ=1.86
%CaCO₃=92.0
ρ=1.92
%CaCO₃=94.2
φ=48.2
ρ=1.87
%CaCO₃=92.0
1
2
3
4
CC
0.5
1.0

LITHOLOGIC DESCRIPTION

NANNOFOSSIL CHALK

Major lithology: This core contains NANNOFOSSIL CHALK, grading in color from white (10YR 8/1) to white (7.5YR 8/1) as the abundance of disseminated pyritic burrow linings increases. The entire core is moderately to heavily bioturbated with mm-scale, simple burrows. Millimeter scale, parallel color bands of light greenish gray (5GY 7/1) are located in Section 2, 130 and 138 cm.

SMEAR SLIDE SUMMARY (%):

	2, 77
	D
TEXTURE	
Silt	95
Clay	5
COMPOSITION	
Nannofossils	100

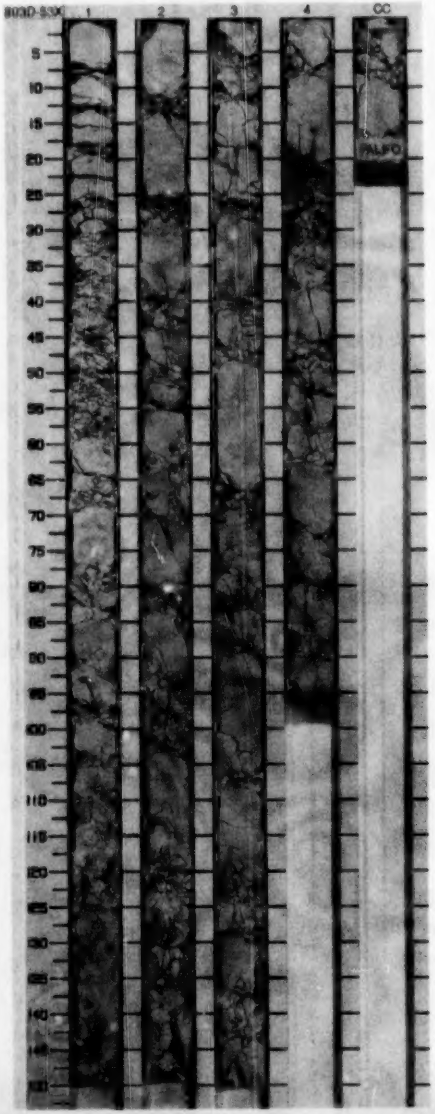
803D-53X
1
2
3
4
CC
PALEO
5
10
15
20
25
30
35
40
45
50
55
60
65
70
75
80
85
90
95
100
105
110
115
120
125
130
135
140
145
150

SITE 803 HOLE D CORE 54X CORED INTERVAL 496.3-506.0 mbsf

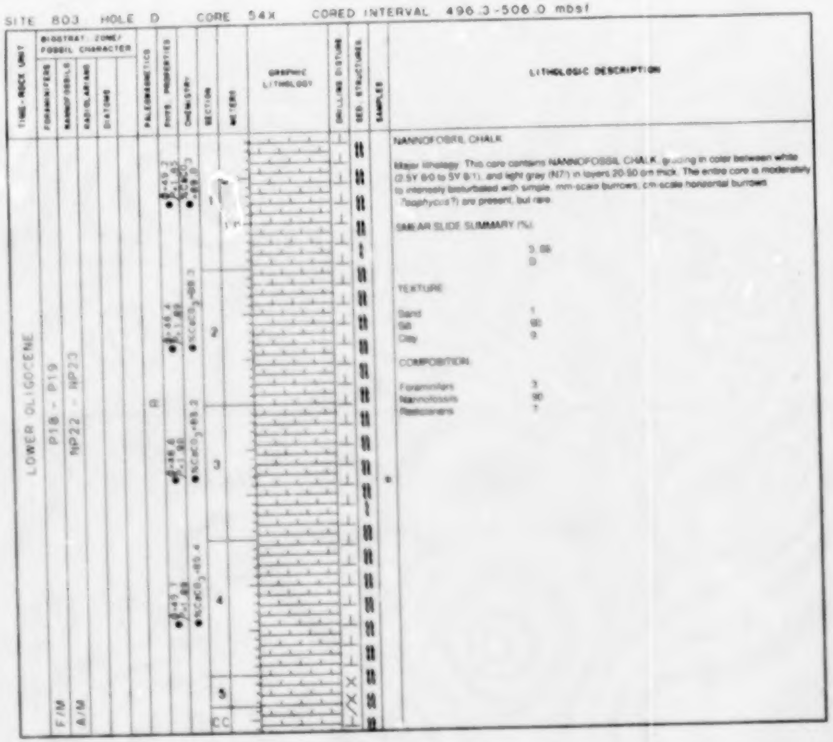
TIME-ROCK UNIT
BIOSTRAT. ZONE/ FOSSIL CHARACTER
FORAMINIFERS
NANNOFOSSILS
RADIOLARIANS
DIATOMS
PALEOMAGNETICS
PHYS. PROPERTIES
CHEMISTRY
SECTION
METERS
GRAPHIC LITHOLOGY
DRILLING DISTURB.
SED. STRUCTURES
SAMPLES
LITHOLOGIC DESCRIPTION
LOWER OLIGOCENE
P18 - P19
NP22 - NP23
F/M
A/M
R
φ=49.2
γ=1.83
%CaCO3=89.0
φ=46.4
γ=1.88
%CaCO3=88.3
φ=48.6
γ=1.90
%CaCO3=89.2
φ=45.1
γ=1.88
%CaCO3=85.4
1
2
3
4
5
CC

NANNOFOSSIL CHALK

Major lithology: This core contains NANNOFOSSIL CHALK, grading in color between white (2.5Y 8/0 to 5Y 8/1), and light gray (N7) in layers 20-50 cm thick. The entire core is moderately to intensely bioturbated with simple, mm-scale burrows; cm-scale horizontal burrows (*Zoophycos*?) are present, but rare.

SMEAR SLIDE SUMMARY (%):

	3, 88
	D
TEXTURE:	
Sand	1
Silt	90
Clay	9
COMPOSITION:	
Foraminifers	3
Nannofossils	90
Radiolarians	7

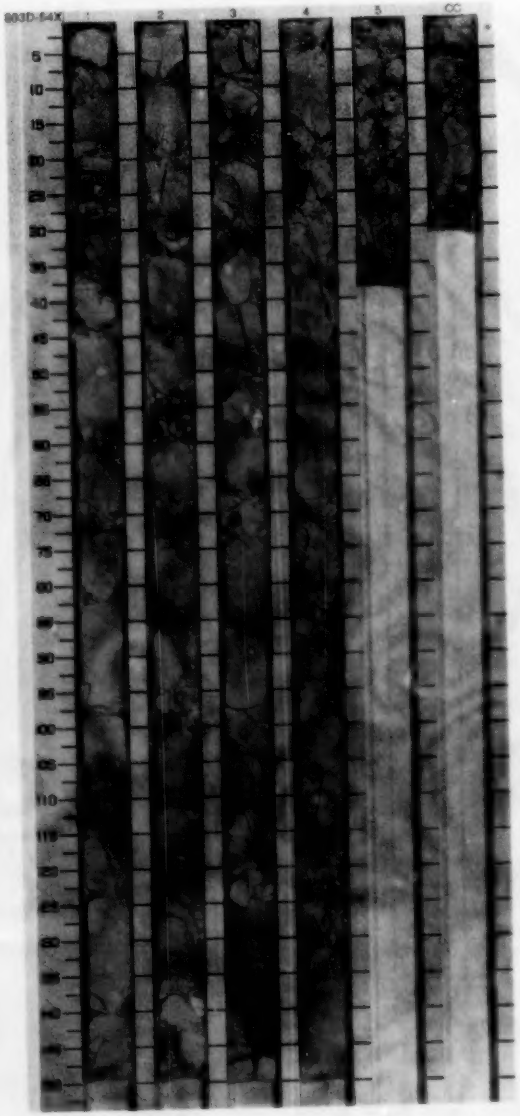
803D-54X
1
2
3
4
5
CC
5
10
15
20
25
30
35
40
45
50
55
60
65
70
75
80
85
90
95
100
105
110
115
120
125
130
135
140
145
150

SITE 803 HOLE D CORE 55X CORED INTERVAL 506.0-515.6 mbsf

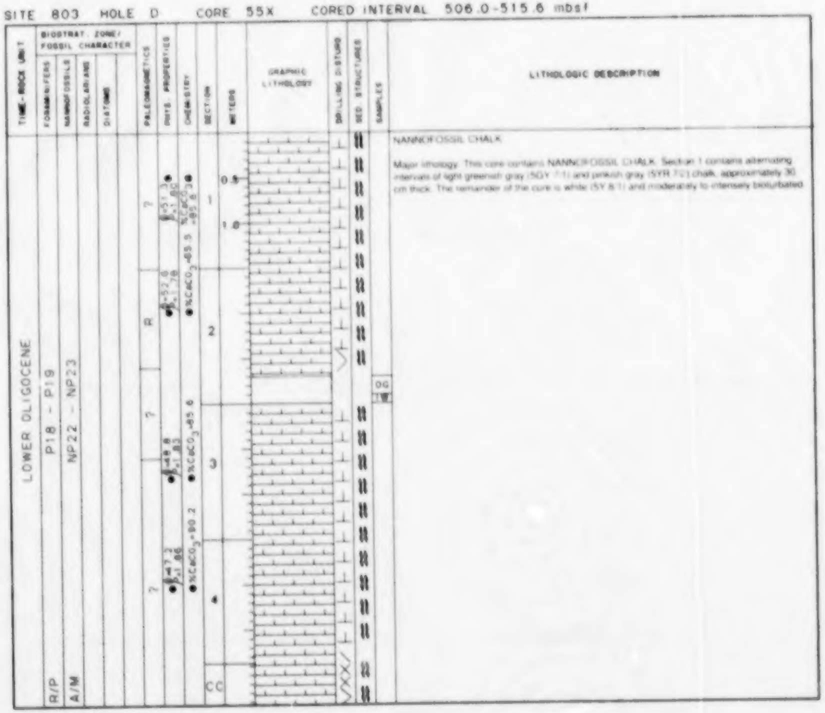
TIME-ROCK UNIT
BIOSTRAT. ZONE/ FOSSIL CHARACTER
FORAMINIFERS
NANNOFOSSILS
RADIOLARIANS
DIATOMS
PALEOMAGNETICS
PHYS. PROPERTIES
CHEMISTRY
SECTION
METERS
GRAPHIC LITHOLOGY
DRILLING DISTURB.
SED. STRUCTURES
SAMPLES
LOWER OLIGOCENE
P18 - P19
NP22 - NP23
R/P
A/M
?
R
?
?
ϕ=51.3
γ=1.80
ϕ=52.6
γ=1.78
ϕ=48.8
γ=1.83
ϕ=47.2
γ=1.86
%CaCO$_3$=85.8
%CaCO$_3$=85.5
%CaCO$_3$=85.6
%CaCO$_3$=90.2
1
2
3
4
CC
0.5
1.0
OG
IW

LITHOLOGIC DESCRIPTION

NANNOFOSSIL CHALK

Major lithology: This core contains NANNOFOSSIL CHALK. Section 1 contains alternating intervals of light greenish gray (5GY 7/1) and pinkish gray (5YR 7/2) chalk, approximately 30 cm thick. The remainder of the core is white (5Y 8/1) and moderately to intensely bioturbated.

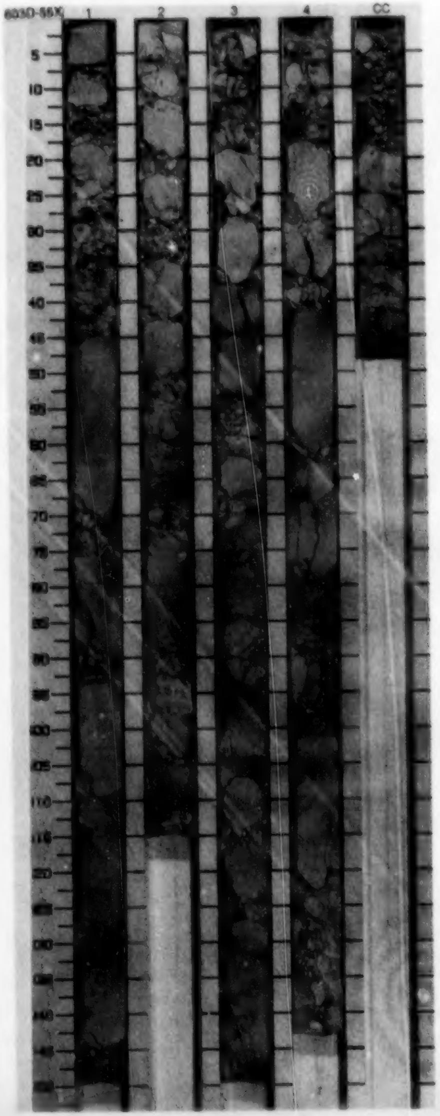
803D-55X
1
2
3
4
CC
5
10
15
20
25
30
35
40
45
50
55
60
65
70
75
80
85
90
95
100
105
110
115
120
125
130
135
140
145
150

SITE 803 HOLE D CORE 56X CORED INTERVAL 515.6-525.3 mbsf

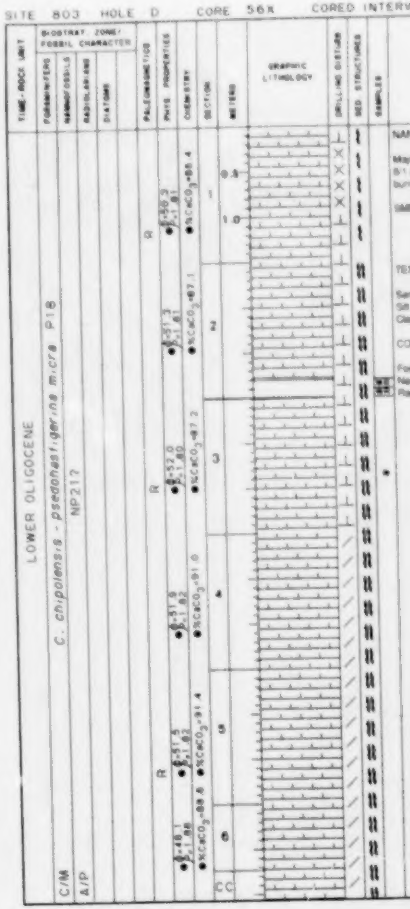
TIME-ROCK UNIT
BIOSTRAT. ZONE/ FOSSIL CHARACTER
FORAMINIFERS
NANNOFOSSILS
RADIOLARIANS
DIATOMS
PALEOMAGNETICS
PHYS. PROPERTIES
CHEMISTRY
SECTION
METERS
GRAPHIC LITHOLOGY
DRILLING DISTURB.
SED. STRUCTURES
SAMPLES
LOWER OLIGOCENE
C. chipolensis - psedohastigerina micra P18
NP21?
C/M
A/P
R
R
R
●φ=50.3 ●γ=1.81
●φ=51.3 ●γ=1.81
●φ=52.0 ●γ=1.80
●φ=51.9 ●γ=1.82
●φ=51.5 ●γ=1.82
●φ=48.1 ●γ=1.86
●%CaCO3=88.4
●%CaCO3=87.1
●%CaCO3=87.2
●%CaCO3=91.0
●%CaCO3=91.4
●%CaCO3=88.6
1
2
3
4
5
6
CC
0.5
1.0

LITHOLOGIC DESCRIPTION

NANNOFOSSIL CHALK

Major lithology: This core contains NANNOFOSSIL CHALK. The core is white (2.5Y 8/0, 5Y 8/1 and 10YR 8/1) to light gray (5YR 7/2) and moderately to intensely bioturbated. The burrows are mainly horizontal.

SMEAR SLIDE SUMMARY (%):

	3, 86
	D
TEXTURE:	
Sand	1
Silt	90
Clay	9
COMPOSITION:	
Foraminifers	3
Nannofossils	90
Radiolarians	7

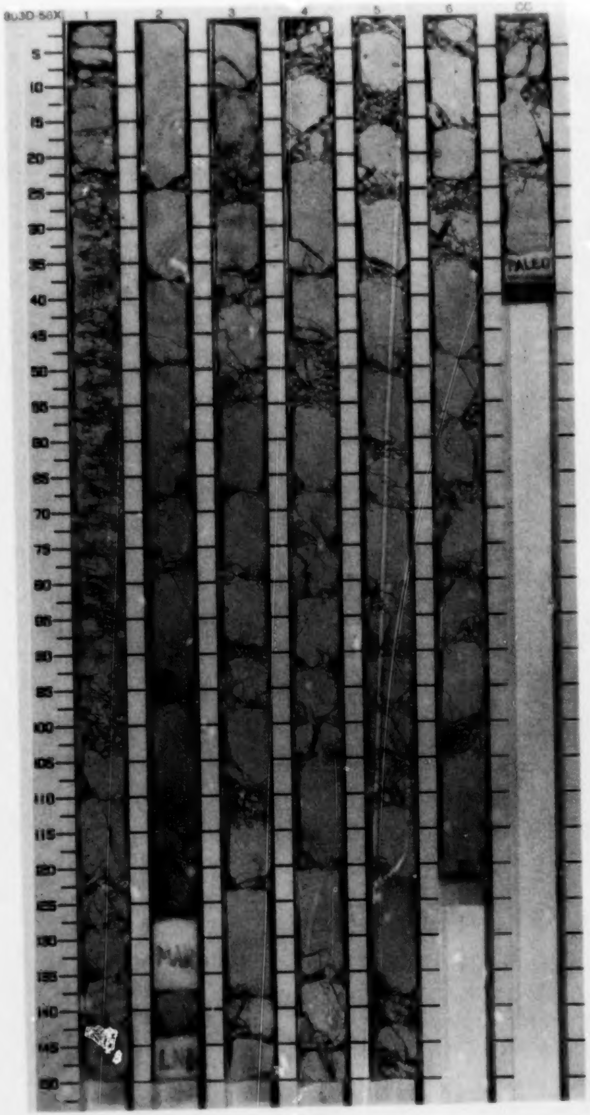
803D-56X
1
2
3
4
5
6
CC
5
10
15
20
25
30
35
40
45
50
55
60
65
70
75
80
85
90
95
100
105
110
115
120
125
130
135
140
145
150
PALEO

SITE 803 HOLE D CORE 57X CORED INTERVAL 525.3-534.6 mbsf

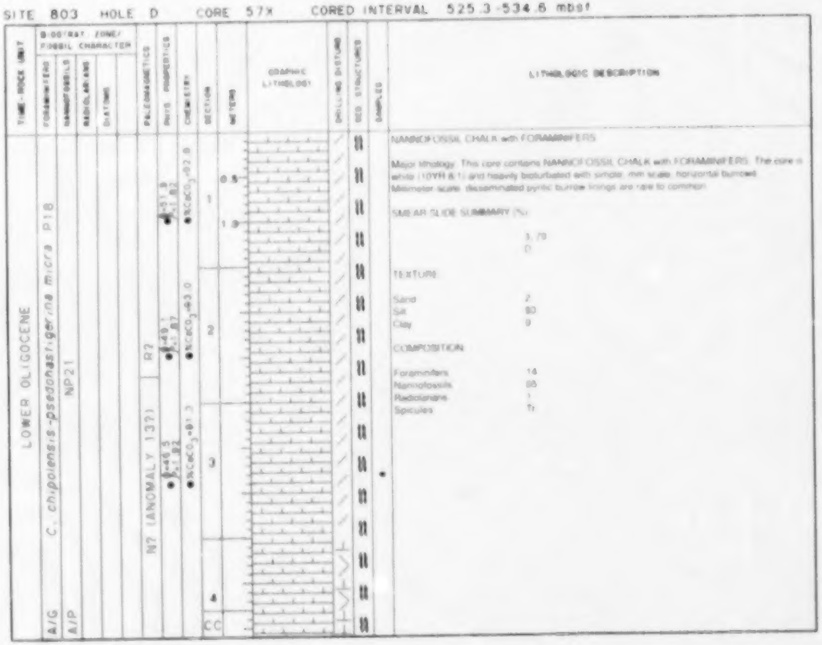
TIME-ROCK UNIT
BIOSTRAT. ZONE/ FOSSIL CHARACTER
FORAMINIFERS
NANNOFOSSILS
RADIOLARIANS
DIATOMS
PALEOMAGNETICS
PHYS. PROPERTIES
CHEMISTRY
SECTION
METERS
GRAPHIC LITHOLOGY
DRILLING DISTURB.
SED. STRUCTURES
SAMPLES
LITHOLOGIC DESCRIPTION
LOWER OLIGOCENE
C. chipolensis-pseudohastigerina micra P18
NP21
A/G
A/P
R?
N? (ANOMALY 13?)
φ=51.8
γ=1.82
φ=49.1
γ=1.87
φ=46.5
γ=1.82
%CaCO3=92.8
%CaCO3=93.0
%CaCO3=91.3
1
2
3
4
CC
0.5
1.0

NANNOFOSSIL CHALK with FORAMINIFERS

Major lithology: This core contains NANNOFOSSIL CHALK with FORAMINIFERS. The core is white (10YR 8/1) and heavily bioturbated with simple, mm scale, horizontal burrows. Millimeter scale, disseminated pyritic burrow linings are rare to common.

SMEAR SLIDE SUMMARY (%):

	3, 70
	D
TEXTURE:	
Sand	2
Silt	90
Clay	8
COMPOSITION:	
Foraminifers	14
Nannofossils	85
Radiolarians	1
Spicules	Tr

SITE 803 HOLE D CORE 58X CORED INTERVAL 534.6-544.3 mbsf

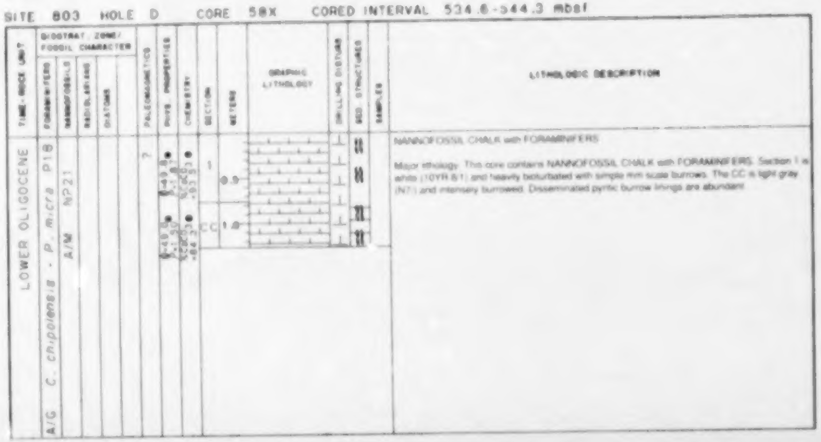
TIME-ROCK UNIT
BIOSTRAT. ZONE/ FOSSIL CHARACTER
FORAMINIFERS
NANNOFOSSILS
RADIOLARIANS
DIATOMS
PALEOMAGNETICS
PHYS. PROPERTIES
CHEMISTRY
SECTION
METERS
GRAPHIC LITHOLOGY
DRILLING DISTURB.
SED. STRUCTURES
SAMPLES
LITHOLOGIC DESCRIPTION
LOWER OLIGOCENE
C. chipolensis - P. micra P18
NP21
A/G
A/M
?
1
CC
0.5
1.0

NANNOFOSSIL CHALK with FORAMINIFERS

Major lithology: This core contains NANNOFOSSIL CHALK with FORAMINIFERS. Section 1 is white (10YR 8/1) and heavily bioturbated with simple mm scale burrows. The CC is light gray (N7) and intensely burrowed. Disseminated pyritic burrow linings are abundant.

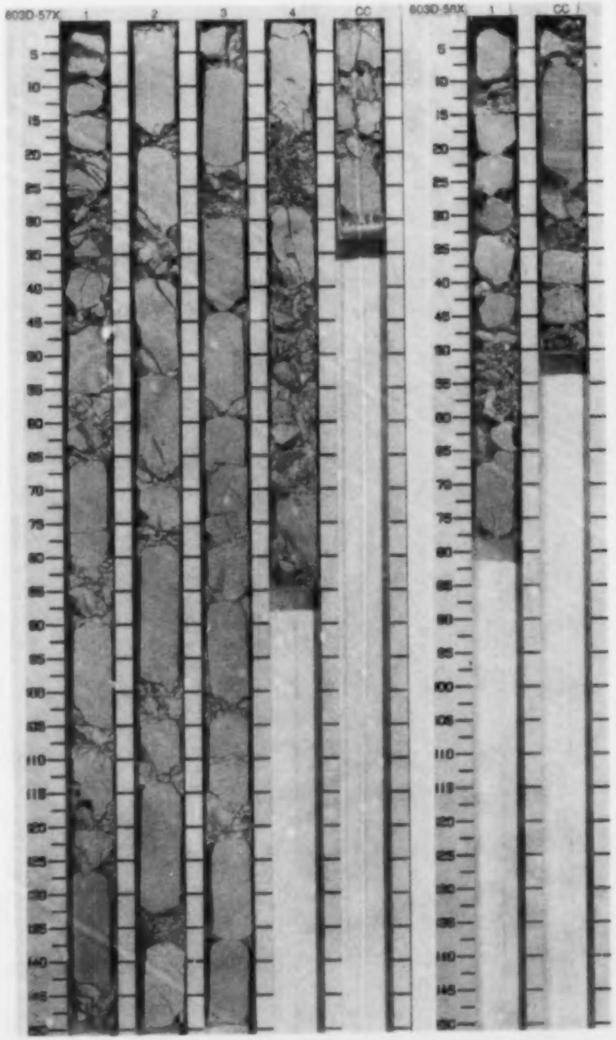
803D-57X
1
2
3
4
CC
803D-58X
1
CC
5
10
15
20
25
30
35
40
45
50
55
60
65
70
75
80
85
90
95
100
105
110
115
120
125
130
135
140
145
150

SITE 803 HOLE D CORE 59X CORED INTERVAL 544.3-554.0 mbsf

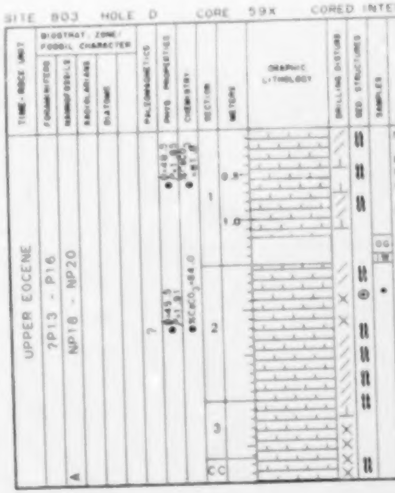
TIME-ROCK UNIT
BIOSTRAT. ZONE/ FOSSIL CHARACTER
FORAMINIFERS
NANNOFOSSILS
RADIOLARIANS
DIATOMS
PALEOMAGNETICS
PHYS. PROPERTIES
CHEMISTRY
SECTION
METERS
GRAPHIC LITHOLOGY
DRILLING DISTURB.
SED. STRUCTURES
SAMPLES
UPPER EOCENE
?P13 - P16
NP18 - NP20
A
?
%CaCO₃=84.0
0.5
1.0
1
2
3
CC
OG
IW

LITHOLOGIC DESCRIPTION

NANNOFOSSIL CHALK with FORAMINIFERS

Major lithology: This core contains white (5Y 8/1 to 10YR 8/1) NANNOFOSSIL CHALK with FORAMINIFERS. It is heavily bioturbated with horizontal burrows. Chert nodules are present in Section 2, 35 cm.

SMEAR SLIDE SUMMARY (%):

	2, 31
	D
TEXTURE:	
Sand	12
Silt	80
Clay	8
COMPOSITION:	
Accessory minerals	2
Foraminifers	10
Nannofossils	88

SITE 803 HOLE D CORE 60X CORED INTERVAL 554.0-563.7 mbsf

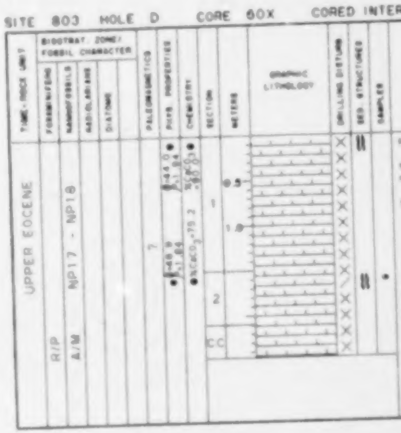
TIME-ROCK UNIT
BIOSTRAT. ZONE/ FOSSIL CHARACTER
FORAMINIFERS
NANNOFOSSILS
RADIOLARIANS
DIATOMS
PALEOMAGNETICS
PHYS. PROPERTIES
CHEMISTRY
SECTION
METERS
GRAPHIC LITHOLOGY
DRILLING DISTURB.
SED. STRUCTURES
SAMPLES
UPPER EOCENE
R/P
A/M
NP17 - NP18
?
%CaCO₃=79.2
0.5
1.0
1
2
CC

LITHOLOGIC DESCRIPTION

NANNOFOSSIL CHALK

Major lithology: This core contains white (2.5Y 8/0 to 10YR 8/1) NANNOFOSSIL CHALK. It is heavily bioturbated and heavily fractured by drilling.

SMEAR SLIDE SUMMARY (%):

	2, 10
	D
TEXTURE:	
Sand	8
Silt	82
Clay	10
COMPOSITION:	
Accessory minerals	1
Foraminifers	2
Nannofossils	92
Spicules	5

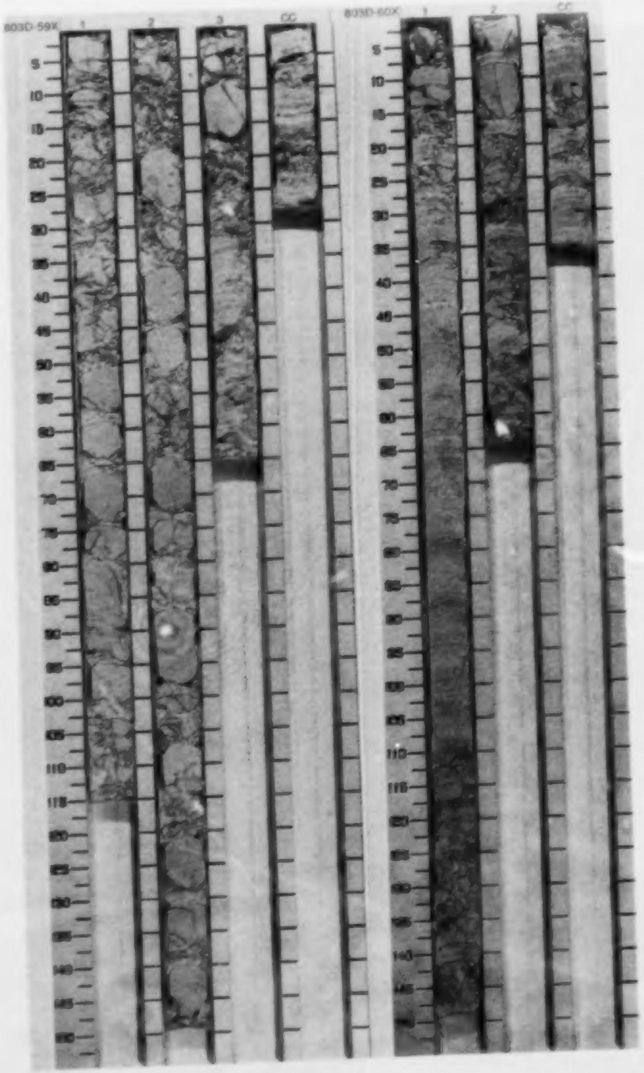
803D-59X
1
2
3
CC
803D-60X
1
2
CC
5
10
15
20
25
30
35
40
45
50
55
60
65
70
75
80
85
90
95
100
105
110
115
120
125
130
135
140
145
150

SITE 803 HOLE D CORE 61X CORED INTERVAL 563.7-573.4 mbsf

TIME-ROCK UNIT	BIOSTRAT. ZONE/ FOSSIL CHARACTER: FORAMINIFERS	NANNOFOSSILS	RADIOLARIANS	DIATOMS		PALEOMAGNETICS	PHYS. PROPERTIES	CHEMISTRY	SECTION	METERS	GRAPHIC LITHOLOGY	DRILLING DISTURB.	SED. STRUCTURES	SAMPLES	LITHOLOGIC DESCRIPTION
UPPER EOCENE	R/P	NP16 - NP18 A				?	● φ=42.4 γ=1.94	● %CaCO3=84.7	1 CC	0.5		X X X X	⌇⌇	•	NANNOFOSSIL CHALK with RADIOLARIANS

Major lithology: This core contains white (2.5Y 8/0) NANNOFOSSIL CHALK with RADIOLARIANS. It is, in parts, heavily bioturbated.

SMEAR SLIDE SUMMARY (%):

	1, 14 D
TEXTURE:	
Sand	1
Silt	94
Clay	5
COMPOSITION:	
Foraminifers	Tr
Nannofossils	90
Radiolarians	10
Spicules	Tr

SITE 803 HOLE D CORE 62X CORED INTERVAL 573.4-583.0 mbsf

TIME-ROCK UNIT	BIOSTRAT. ZONE/ FOSSIL CHARACTER: FORAMINIFERS	NANNOFOSSILS	RADIOLARIANS	DIATOMS		PALEOMAGNETICS	PHYS. PROPERTIES	CHEMISTRY	SECTION	METERS	GRAPHIC LITHOLOGY	DRILLING DISTURB.	SED. STRUCTURES	SAMPLES	LITHOLOGIC DESCRIPTION
UPPER EOCENE	R/P	NP16 - NP18 A							CC			X ⊥		•	NANNOFOSSIL CHALK with RADIOLARIANS

Major lithology: This core contains white, slightly bioturbated (10YR 8/1) NANNOFOSSIL CHALK with RADIOLARIANS.

SMEAR SLIDE SUMMARY (%):

	CC, 19 D
TEXTURE:	
Sand	1
Silt	94
Clay	5
COMPOSITION:	
Foraminifers	Tr
Nannofossils	90
Radiolarians	10
Spicules	Tr

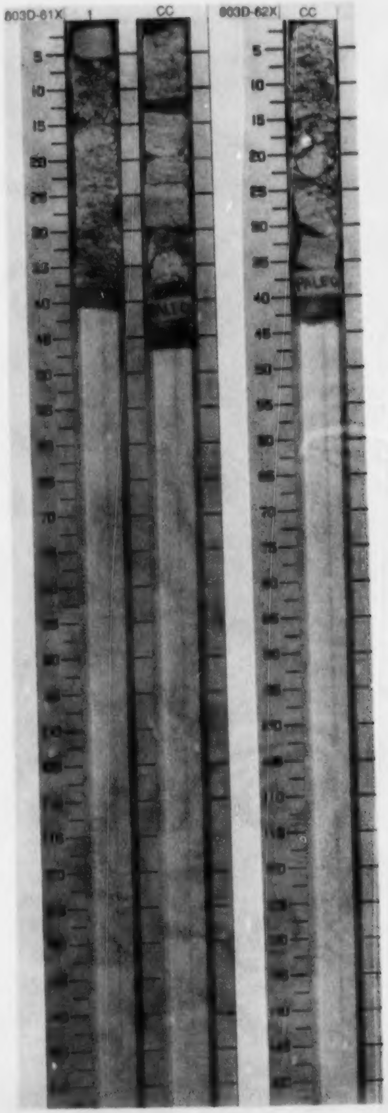

SITE 803 HOLE D CORE 63X CORED INTERVAL 583.0-588.7 mbsf

TIME-ROCK UNIT	BIOSTRAT. ZONE/ FOSSIL CHARACTER				PALEOMAGNETICS	PHYS. PROPERTIES	CHEMISTRY	SECTION	METERS	GRAPHIC LITHOLOGY	DRILLING DISTURB.	SED. STRUCTURES	SAMPLES	LITHOLOGIC DESCRIPTION
	FORAMINIFERS	NANNOFOSSILS	RADIOLARIANS	DIATOMS										
MIDDLE EOCENE	R/P	A/P						CC					*	NANNOFOSSIL CHALK with RADIOLARIANS
		NP16 - NP17												

NANNOFOSSIL CHALK with RADIOLARIANS

Major lithology: This core contains white (10YR 8/1) slightly bioturbated NANNOFOSSIL CHALK with RADIOLARIANS.

SMEAR SLIDE SUMMARY (%):

	CC, 12
	D
TEXTURE:	
Sand	5
Silt	90
Clay	5
COMPOSITION:	
Foraminifers	Tr
Nannofossils	85
Radiolarians	15
Spicules	Tr

SITE 803 HOLE D CORE 64X CORED INTERVAL 588.7-598.4 mbsf

TIME-ROCK UNIT	BIOSTRAT. ZONE/ FOSSIL CHARACTER				PALEOMAGNETICS	PHYS. PROPERTIES	CHEMISTRY	SECTION	METERS	GRAPHIC LITHOLOGY	DRILLING DISTURB.	SED. STRUCTURES	SAMPLES	LITHOLOGIC DESCRIPTION
	FORAMINIFERS	NANNOFOSSILS	RADIOLARIANS	DIATOMS										
MIDDLE EOCENE	F/P	C/P					● $\%CaCO_3$ = 91.6	CC	0.5				*	RADIOLARIAN NANNOFOSSIL CHALK
	P11 - P12	NP16 - NP17												

RADIOLARIAN NANNOFOSSIL CHALK

Major lithology: This core contains RADIOLARIAN NANNOFOSSIL CHALK. The color is white (10YR 8/1 to 10YR 8/2). It is heavily bioturbated.

SMEAR SLIDE SUMMARY (%):

	CC, 24
	D
TEXTURE:	
Sand	10
Silt	85
Clay	5
COMPOSITION:	
Foraminifers	Tr
Nannofossils	75
Radiolarians	25
Spicules	Tr

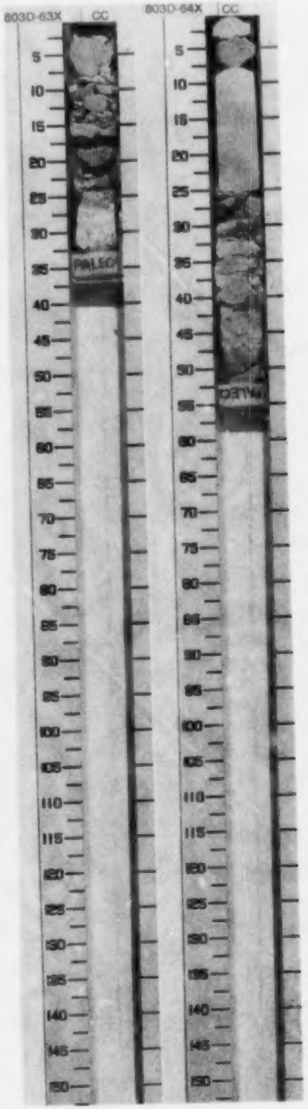

SITE 803 HOLE D CORE 65X CORED INTERVAL 598.4-601.9 mbsf

TIME-ROCK UNIT	BIOSTRAT. ZONE/ FOSSIL CHARACTER: FORAMINIFERS	NANNOFOSSILS	RADIOLARIANS	DIATOMS		PALEOMAGNETICS	PHYS. PROPERTIES	CHEMISTRY	SECTION	METERS	GRAPHIC LITHOLOGY	DRILLING DISTURB.	SED. STRUCTURES	SAMPLES
MIDDLE EOCENE	R/P	A/M NP16					● ϕ=63.7 γ=1.46	● %CaCO$_3$=20.7	CC			X X X	‼ ‼	*

LITHOLOGIC DESCRIPTION

NANNOFOSSIL RADIOLARITE

Major lithology: This core contains NANNOFOSSIL RADIOLARITE. It is white (10YR 8/2) to very pale brown (10YR 7/3), and heavily bioturbated.

SMEAR SLIDE SUMMARY (%):

	CC, 4 D
TEXTURE:	
Sand	20
Silt	75
Clay	5
COMPOSITION:	
Foraminifers	Tr
Nannofossils	35
Radiolarians	65
Spicules	Tr

SITE 803 HOLE D CORE 66X CORED INTERVAL 601.9-612.0 mbsf

TIME-ROCK UNIT	BIOSTRAT. ZONE/ FOSSIL CHARACTER: FORAMINIFERS	NANNOFOSSILS	RADIOLARIANS	DIATOMS		PALEOMAGNETICS	PHYS. PROPERTIES	CHEMISTRY	SECTION	METERS	GRAPHIC LITHOLOGY	DRILLING DISTURB.	SED. STRUCTURES	SAMPLES
MIDDLE EOCENE	R/P	A/M NP16					● ϕ=36.5 γ=2.02	● %CaCO$_3$=84.5	CC			⊥	≋	*

LITHOLOGIC DESCRIPTION

RADIOLARIAN NANNOFOSSIL CHALK

Major lithology: This core contains white (10YR 8/1 to 10YR 8/2) RADIOLARIAN NANNOFOSSIL CHALK. The lowermost part contains fine bands of different shades of white. It is slightly bioturbated.

SMEAR SLIDE SUMMARY (%):

	CC, 4 D
TEXTURE:	
Sand	10
Silt	80
Clay	10
COMPOSITION:	
Foraminifers	Tr
Nannofossils	70
Radiolarians	30
Spicules	Tr

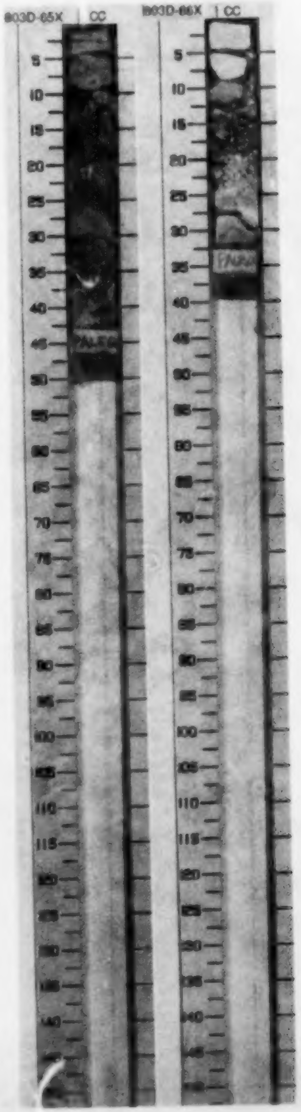

SITE 803 HOLE D CORE 67R CORED INTERVAL 612.0-621.8 mbsf

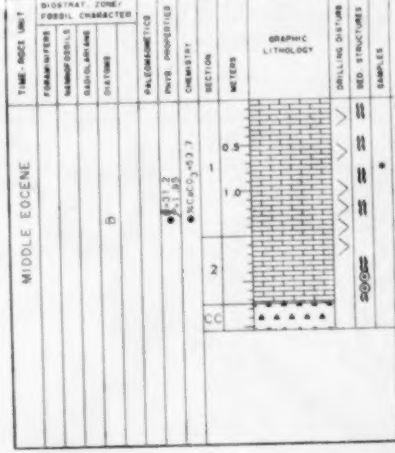
TIME-ROCK UNIT
BIOSTRAT. ZONE/ FOSSIL CHARACTER
FORAMINIFERS
NANNOFOSSILS
RADIOLARIANS
DIATOMS
PALEOMAGNETICS
PHYS. PROPERTIES
CHEMISTRY
SECTION
METERS
GRAPHIC LITHOLOGY
DRILLING DISTURB.
SED. STRUCTURES
SAMPLES
MIDDLE EOCENE
B
φ=31.2
γ=1.95
%CaCO₃=53.7
1
2
CC
0.5
1.0

LITHOLOGIC DESCRIPTION

LIMESTONE with SILICEOUS GRAINS

Major lithology: This core contains very pale brown (10YR 8/3) LIMESTONE with SILICEOUS GRAINS. The sediment is highly bioturbated with burrows ranging in color from white (10YR 8/1) to very pale brown (10YR 7/3). In the lower portion of Section 1, 10 to 20 cm thick intervals of sediment vary between white (10YR 8/1) and very pale brown (10YR 7/3).

Minor lithology: The Core Catcher contains brown (7.5YR 4/4) to pinkish gray (7.5YR 6/2) highly bioturbated CHERT nodules.

SMEAR SLIDE SUMMARY (%):

	1, 75
	D
TEXTURE:	
Sand	5
Silt	55
Clay	40
COMPOSITION:	
Nannofossils	82
Radiolarians	5
Siliceous fragments	10
Zeolite	3

SITE 803 HOLE D CORE 68R CORED INTERVAL 621.8-631.4 mbsf

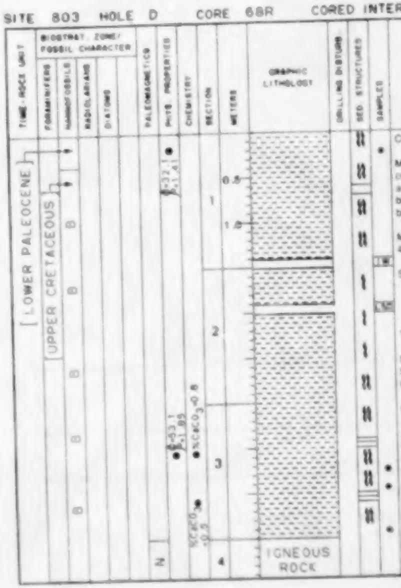
TIME-ROCK UNIT
BIOSTRAT. ZONE/ FOSSIL CHARACTER
FORAMINIFERS
NANNOFOSSILS
RADIOLARIANS
DIATOMS
PALEOMAGNETICS
PHYS. PROPERTIES
CHEMISTRY
SECTION
METERS
GRAPHIC LITHOLOGY
DRILLING DISTURB.
SED. STRUCTURES
SAMPLES
[LOWER PALEOCENE]
[UPPER CRETACEOUS]
B
B
B
B
B
N
φ=32.1
γ=1.41
φ=53.1
γ=1.85
%CaCO₃=0.8
%CaCO₃=0.5
1
2
3
4
0.5
1.0
IGNEOUS ROCK

LITHOLOGIC DESCRIPTION

CLAYSTONE

Major lithology: This core consists of dark brown (7.5YR 4/2) CLAYSTONE. In Section 1, 0-60 cm, brown (7.5YR 5/4) nodules of CLAYSTONE are observed. Section 1, 60-70 cm, contains a brown layer with sharp color contacts; below that, the sediment is dark brown and highly bioturbated with brown burrow fills. In Section 3, intervals with fine, mm to cm thick brown/dark brown (7.5YR 4/4) laminae and layers are noted.

Minor lithology: Section 3 contains four cm thick layers of soft, dark yellowish brown (10YR 4/4) RADIOLARITE.

SMEAR SLIDE SUMMARY (%):

	1, 28	3, 74	3, 95	3, 142
	M	D	M	M
TEXTURE:				
Sand	5	—	60	1
Silt	60	20	30	19
Clay	35	80	10	80
COMPOSITION:				
Accessory minerals	—	7	5	5
Calcispheres	5	—	—	—
Clay	20	90	—	90
Glass	—	3	—	3
Nannofossils	20	—	—	—
Quartz	55	—	—	—
Radiolarians	—	—	95	—
Rock fragment	—	—	—	2

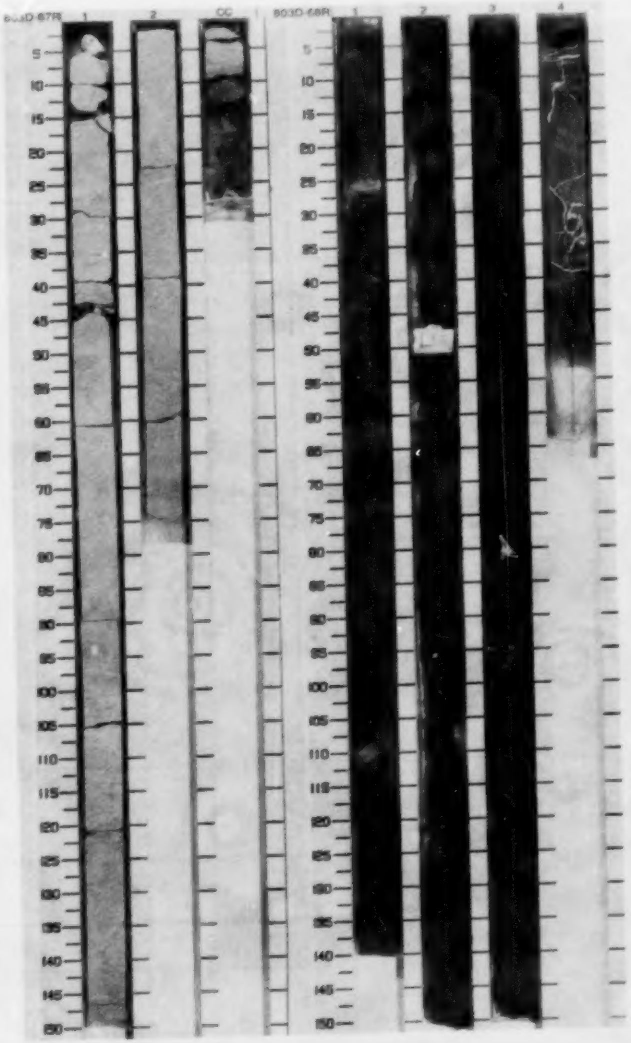
803D-67R
1
2
CC
803D-68R
1
2
3
4
5
10
15
20
25
30
35
40
45
50
55
60
65
70
75
80
85
90
95
100
105
110
115
120
125
130
135
140
145
150

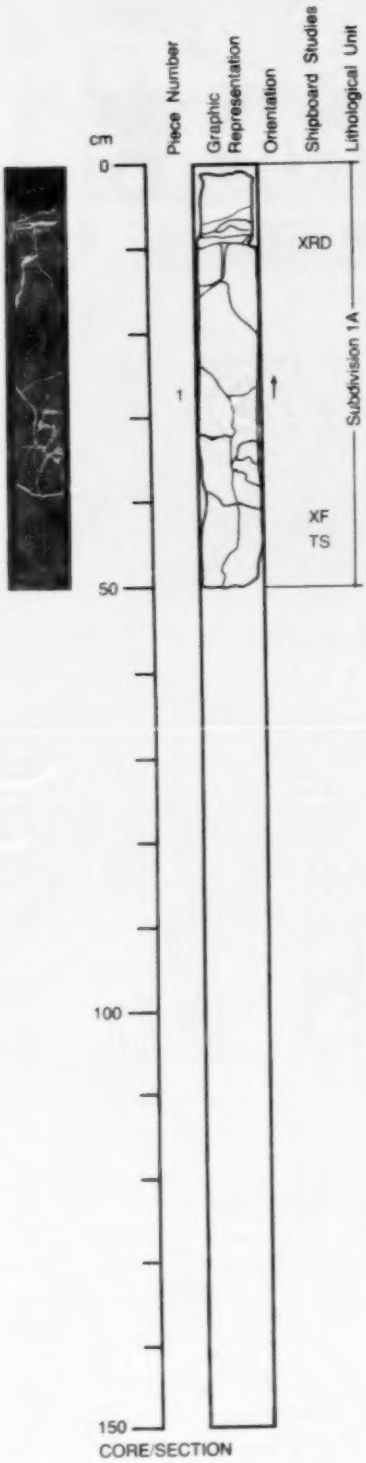
cm
Piece Number
Graphic Representation
Orientation
Shipboard Studies
Lithological Unit
0
50
100
150
1
XRD
XF
TS
Subdivision 1A
CORE/SECTION

130-803D-68R-4

SUBDIVISION 1A: APHYRIC BASALT

Piece 1

CONTACTS: Basalt is overlain by horizontal light-brown clay sediment with intervening 15 mm hydrothermal veins consisting of alternating bands of green and buff colored material.
PHENOCRYSTS: Aphyric.
GROUNDMASS: Fine grained.
VESICLES: Nonvesicular.
COLOR: Dark brown to red/orange-ocher with brown bands.
STRUCTURE: Pillow.
ALTERATION: Very highly altered, with yellow and reddish mottled and banded zones; cross-cut by later calcite veins.
VEINS/FRACTURES: 5%; 0.5-5 mm; vertical and subhorizontal.

130-803D-69R-1

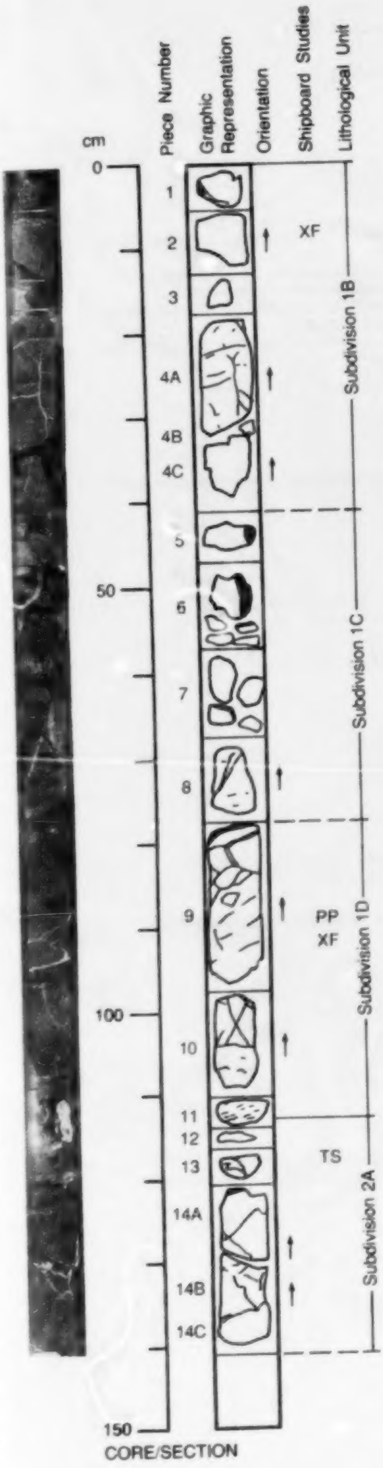
cm
Piece Number
Graphic Representation
Orientation
Shipboard Studies
Lithological Unit
0
50
100
150
1
2
3
4A
4B
4C
5
6
7
8
9
10
11
12
13
14A
14B
14C
XF
PP
XF
TS
Subdivision 1B
Subdivision 1C
Subdivision 1D
Subdivision 2A
CORE/SECTION

SUBDIVISION 1B: APHYRIC BASALT

Pieces 1-4

CONTACTS: None.
PHENOCRYSTS: Aphyric.
GROUNDMASS: Fine grained.
VESICLES: Nonvesicular.
COLOR: Gray to light-medium orange-brown.
STRUCTURE: Pillow.
ALTERATION: Highly altered, mottled appearance with light orange-brown patches.
VEINS/F RACTURES: <5%; 0.2-2 mm; subvertical and subhorizontal; calcite veins in Piece 4.

SUBDIVISION 1C: APHYRIC BASALT

Pieces 5-8

CONTACTS: Top of basalt pillow.
PHENOCRYSTS:
Pyroxene - <1%; ~1 mm; euhedral laths.
GROUNDMASS: Fine grained with glass rims.
VESICLES: Nonvesicular.
COLOR: Gray to dark gray, light-medium orange-brown, black glass rims.
STRUCTURE: Pillow.
ALTERATION: Moderately to highly altered with mottled and banded appearance.
VEINS/FRACTURES: <1-5%; <0.5-5 mm; irregular-subhorizontal; green mineral (celadonite?).

SUBDIVISION 1D: APHYRIC BASALT

Pieces 9, 10

CONTACTS: Margin of pillow.
PHENOCRYSTS: Aphyric.
GROUNDMASS: Fine grained with glassy rims.
VESICLES: Nonvesicular.
COLOR: Gray to dark gray, light-medium orange-brown, black glass rims.
STRUCTURE: Pillow.
ALTERATION: Moderately to highly altered.
VEINS/FRACTURES: <5%; <5 mm; subhorizontal; calcite-filled.

SUBDIVISION 2A: APHYRIC BASALT

Pieces 11-14

CONTACTS: Pieces 11-13 are a mixture of calcite and completely altered green basaltic glass (celadonite, serpentine, chlorite?). Probably the contact between pillow and limestone.
PHENOCRYSTS: Aphyric.
GROUNDMASS: Fine grained, glassy rim to top of Piece 14.
VESICLES: Nonvesicular.
COLOR: Medium gray-brown to light gray-brown/orange-brown.
STRUCTURE: Pillow.
ALTERATION: Very highly altered, mottled and banded appearance.
VEINS/FRACTURES: <5%; 0.5-5 mm; irregular; calcite.

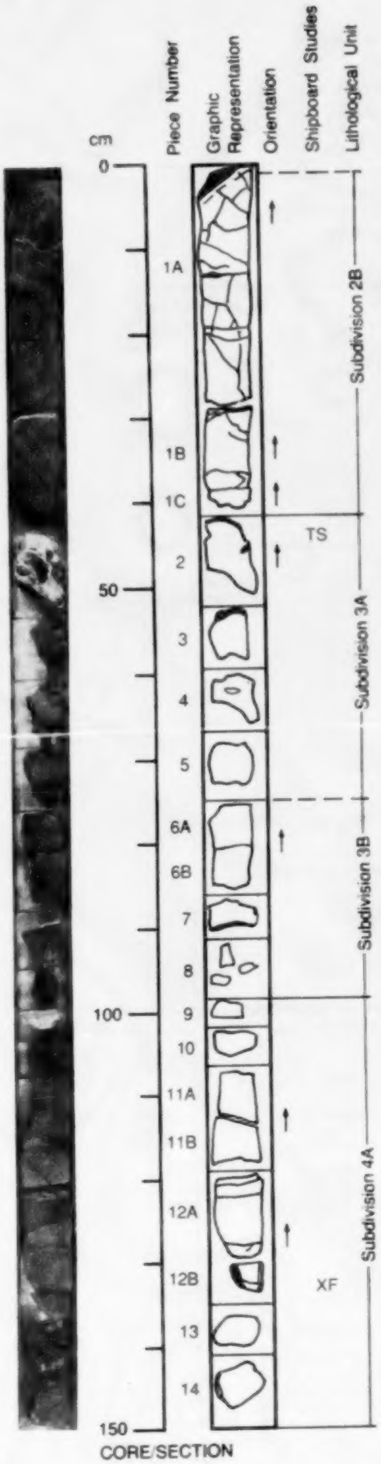
cm
Piece Number
Graphic Representation
Orientation
Shipboard Studies
Lithological Unit
0
50
100
150
1A
1B
1C
2
3
4
5
6A
6B
7
8
9
10
11A
11B
12A
12B
13
14
TS
XF
Subdivision 2B
Subdivision 3A
Subdivision 3B
Subdivision 4A
CORE/SECTION

130-803D-69R-2

SUBDIVISION 2B: APHYRIC BASALT

Piece 1

CONTACTS: Top of basalt pillow.
PHENOCRYSTS: Aphyric.
GROUNDMASS: Fine grained center to glass rim.
VESICLES: Nonvesicular.
COLOR: Black glass rim, dark gray-brown and medium-light gray brown banded and mottled appearance towards the center of the pillow.
STRUCTURE: Piece 1 is an excellent cross section through an individual basalt pillow; concentric and radial cooling fractures (infilled with calcite) are also visible.
ALTERATION: Fresh glass rim to highly altered pillow center, the latter having a gray/dark-light reddish-brown mottled and banded appearance.
VEINS/FRACTURES: ~5%; 0.5-3 mm; radial and concentric to glassy rim; calcite infilling

SUBDIVISION 3A: APHYRIC BASALT

Pieces 2-5

CONTACTS: Top of basalt pillow. Piece 2 is interpillow limestone with dark green altered basaltic glass (celadonite?).
PHENOCRYSTS: Aphyric.
GROUNDMASS: Fine grained.
VESICLES: Nonvesicular.
COLOR: Gray to gray-brown.
STRUCTURE: Pillow.
ALTERATION: Highly altered, mottled and banded appearance.
VEINS/FRACTURES: <1%; up to 2 mm; irregular; calcite.

SUBDIVISION 3B: APHYRIC BASALT

Pieces 6-8

CONTACTS: None.
PHENOCRYSTS: Aphyric.
GROUNDMASS: Fine grained.
VESICLES: Nonvesicular.
COLOR: Gray to gray brown.
STRUCTURE: Pillow.
ALTERATION: Highly altered, mottled and banded appearance.
VEINS/FRACTURES: <1%; up to 2 mm; irregular.

SUBDIVISION 4A: MODERATELY PYROXENE PHYRIC BASALT

Pieces 9-14

CONTACTS: Piece 9 is probably interpillow limestone.
PHENOCRYSTS:
Pyroxene - 5%; 0.5-2 mm; subhedral-euhedral laths.
GROUNDMASS: Fine grained.
VESICLES: Nonvesicular.
COLOR: Gray.
STRUCTURE: Pillow.
ALTERATION: Moderately altered (Pieces 12-14), highly altered (Piece 11).
VEINS/FRACTURES: Top of Piece 12 A has a 10 mm vein composed of calcite and a green mineral.

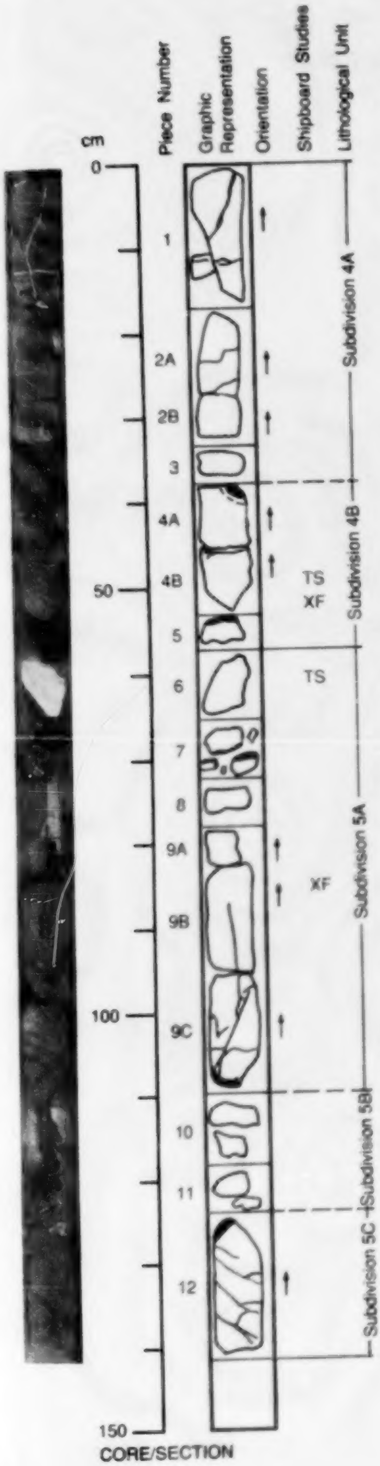
cm
Piece Number
Graphic Representation
Orientation
Shipboard Studies
Lithological Unit
0
50
100
150
1
2A
2B
3
4A
4B
5
6
7
8
9A
9B
9C
10
11
12
TS
XF
TS
XF
Subdivision 4A
Subdivision 4B
Subdivision 5A
Subdivision 5B
Subdivision 5C
CORE/SECTION

130-803D-69R-3

SUBDIVISION 4A: APHYRIC BASALT

Pieces 1-3

CONTACTS: None.
PHENOCRYSTS: Aphyric.
GROUNDMASS: Fine grained.
VESICLES: Nonvesicular.
COLOR: Gray to light red-brown.
STRUCTURE: Pillow.
ALTERATION: Highly altered.
VEINS/FRACTURES: <3%; 0.5-2 mm; horizontal and subvertical; calcite.

SUBDIVISION 4B: SPARSELY PLAGIOCLASE-OLIVINE PHYRIC BASALT

Pieces 4, 5

CONTACTS: Top of basalt pillow.
PHENOCRYSTS:
Plagioclase - 2%; 0.2-0.4 mm; euhedral laths.
Olivine - <1%; 0.2 mm; euhedral-subhedral, altered to iddingsite
GROUNDMASS: Fine grained interior to glassy rims.
VESICLES: Nonvesicular.
COLOR: Black glassy rims, gray/light-brown interior.
STRUCTURE: Pillow.
ALTERATION: Fresh glass rim and highly altered interior.
VEINS/FRACTURES: 2-3%; 0.2-1 mm; none; calcite.

SUBDIVISION 5A: SPARSELY PLAGIOCLASE-OLIVINE PHYRIC BASALT

Pieces 6-9

CONTACTS: Piece 6 is an interpillow limestone.
PHENOCRYSTS:
Plagioclase - 2%; 0.2-0.4 mm; euhedral laths
GROUNDMASS: Fine-grained interior and glassy rims.
VESICLES: Nonvesicular.
COLOR: Black glassy rims to gray/light-brown interior.
STRUCTURE: Pillow.
ALTERATION: Fresh glass rim and highly altered interior.
VEINS/FRACTURES: 2-3%; 0.2-1 mm; none; calcite.

SUBDIVISION 5B: SPARSELY PLAGIOCLASE-PHYRIC BASALT

Pieces 10, 11

CONTACTS: Top of basalt pillow.
PHENOCRYSTS:
Plagioclase - 2%; 0.2-0.4 mm; euhedral laths.
GROUNDMASS: Fine grained interior and glassy rims.
VESICLES: Nonvesicular.
COLOR: Black glassy rims to gray/light-brown interior.
STRUCTURE: Pillow.
ALTERATION: Fresh glass rims and highly altered interior to pillow.
VEINS/FRACTURES: 2-3%; 0.2-2 mm; irregular; calcite.

130-803D-69R-3 (continued)

SUBDIVISION 5C: SPARSELY PLAGIOCLASE-PHYRIC BASALT

Piece 12

CONTACTS: Top of basalt pillow.
PHENOCRYSTS:
Plagioclase - 2%; 0.2-0.4 mm; euhedral laths
GROUNDMASS: Fine grained interior to pillow and glassy rims.
VESICLES: Nonvesicular.
COLOR: Black glassy rims and gray/light-brown interior.
STRUCTURE: Pillow.
ALTERATION: Fresh glass rims and highly altered interior.
VEINS/FRACTURES: ~2-3%; 0.2-1 mm; none; calcite.

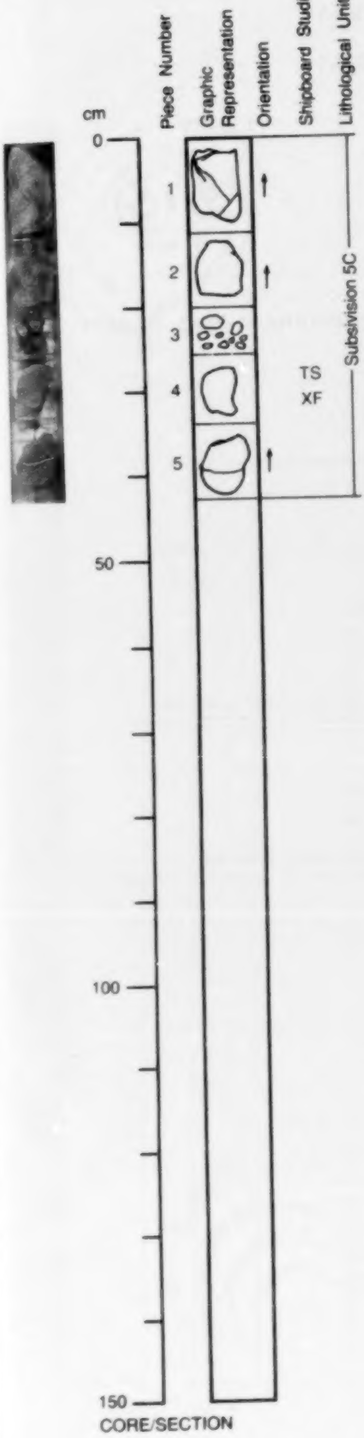
cm
Piece Number
Graphic Representation
Orientation
Shipboard Studies
Lithological Unit
0
1
2
3
4
5
TS
XF
Subdivision 5C
50
100
150
CORE/SECTION

130-803D-69R-4

SUBDIVISION 5C: APHYRIC BASALT

Pieces 1, 2

CONTACTS: None.
PHENOCRYSTS: Aphyric.
GROUNDMASS: Fine-grained.
VESICLES: Nonvesicular.
COLOR: Gray to light red-brown.
STRUCTURE: Pillow.
ALTERATION: Highly altered.
VEINS/FRACTURES: 2-3%; 1-3 mm; none; calcite, brown smectite, celadonite (?).

SUBDIVISION 5C: APHYRIC BASALT

Pieces 3-5

CONTACTS: None.
PHENOCRYSTS: Aphyric.
GROUNDMASS: Medium to fine-grained.
VESICLES: Nonvesicular.
COLOR: Light green-gray.
STRUCTURE: Pillow.
ALTERATION: Moderately altered.
VEINS/FRACTURES: Piece 5 has a single 1-2 mm subhorizontal vein consisting of calcite and brown smectite (?).

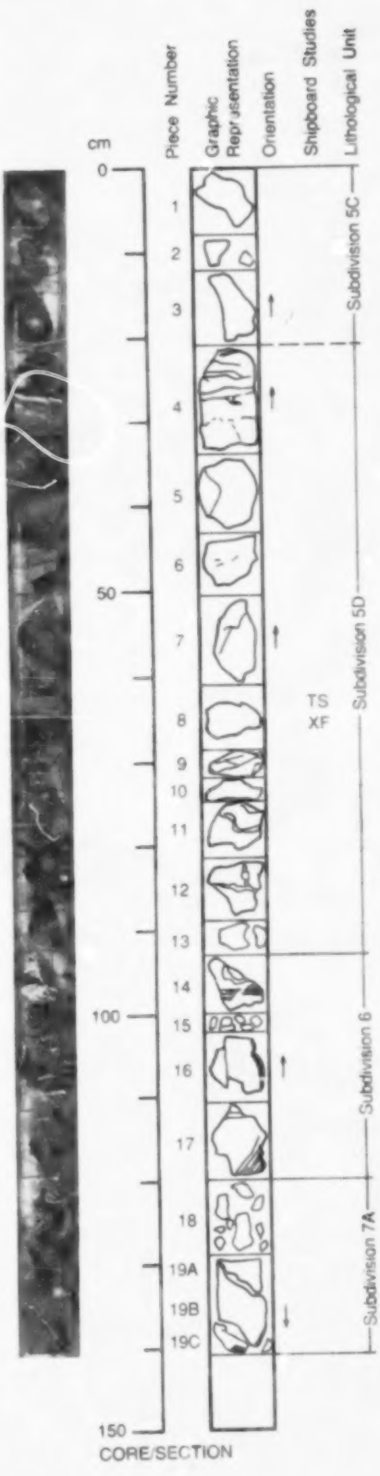
cm
Piece Number
Graphic Representation
Orientation
Shipboard Studies
Lithological Unit
0
50
100
150
1
2
3
4
5
6
7
8
9
10
11
12
13
14
15
16
17
18
19A
19B
19C
TS
XF
Subdivision 5C
Subdivision 5D
Subdivision 6
Subdivision 7A
CORE/SECTION

130-803D-70R-1

SUBDIVISION 5C: APHYRIC BASALT

Pieces 1-3

CONTACTS: None.
PHENOCRYSTS: Aphyric.
GROUNDMASS: Fine grained.
VESICLES: Nonvesicular.
COLOR: Green to brown-gray, mottled appearance.
STRUCTURE: Part of a pillow lava.
ALTERATION: Very highly altered.
VEINS/FRACTURES: None.

SUBDIVISION 5D: SPARSELY PYROXENE-PHYRIC BASALT

Pieces 4-13

CONTACTS: Top of basalt pillow.
PHENOCRYSTS:
Pyroxene - <3%; <0.5 mm; subhedral.
GROUNDMASS: Very fine grained with very altered glassy rim at top of Piece 4.
VESICLES: Nonvesicular.
COLOR: Gray to brown, mottled. Brown to green near some veins.
STRUCTURE: Portions of pillow lava.
ALTERATION: Highly to very highly altered.
VEINS/FRACTURES: 1-10%; <1-7 mm; subhorizontal and subvertical; calcite and smectite(?) vein filling.

SUBDIVISION 6: APHYRIC BASALT

Pieces 14-17

CONTACTS: Piece 14 is an inter-pillow limestone with altered, green basalt glass (celadonite, serpentine?). Piece 15 consists of several very altered fragments with celadonite (?).
PHENOCRYSTS:
Pyroxene - <1%; <0.5 mm; subhedral.
GROUNDMASS: Very fine grained to glassy at margins.
VESICLES: Nonvesicular.
COLOR: Brown interiors to grayish rinds near glassy rims.
STRUCTURE: Pillow.
ALTERATION: Very highly to moderately altered going towards glassy rims.
VEINS/FRACTURES: <5%; 1-4 mm; sub-horizontal; calcite and small amounts of green and brown mineral (smectites?).

SUBDIVISION 7A: APHYRIC BASALT

Pieces 18, 19

CONTACTS: Piece 18 consists of fragments of an inter-pillow limestone, mixed with dark green, totally altered basaltic glass (celadonite?).
PHENOCRYSTS: Aphyric.
GROUNDMASS: Very fine grained to devitrified rim.
VESICLES: Nonvesicular.
COLOR: Gray to brown, mottled.
STRUCTURE: Part of a pillow.
ALTERATION: Very highly altered.
VEINS/FRACTURES: <1%; 1-3 mm; 2 sets at 45°; calcite filled.

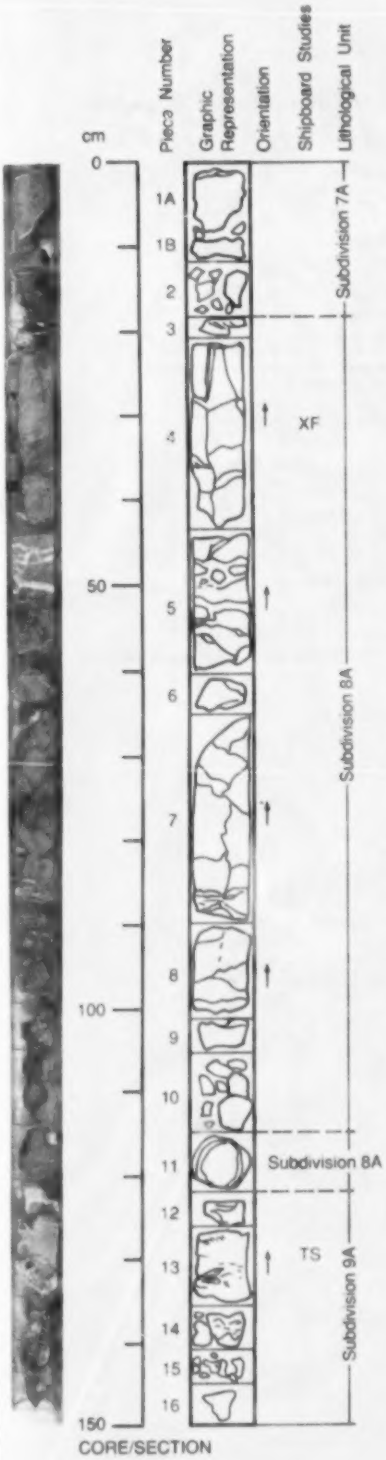
cm
Piece Number
Graphic Representation
Orientation
Shipboard Studies
Lithological Unit
0
50
100
150
1A
1B
2
3
4
5
6
7
8
9
10
11
12
13
14
15
16
XF
TS
Subdivision 7A
Subdivision 8A
Subdivision 8A
Subdivision 9A
CORE/SECTION

130-803D-70R-2

SUBDIVISION 7A: APHYRIC BASALT

Pieces 1, 2

CONTACTS: None.
PHENOCRYSTS: Aphyric.
GROUNDMASS: Very fine grained.
VESICLES: Nonvesicular.
COLOR: Brown to gray with greenish margins.
STRUCTURE: Pillow lava fragments.
ALTERATION: Highly altered interior to moderately altered, near glassy rim.
VEINS/FRACTURES: ~2%; 2-4 mm; subhorizontal; calcite
ADDITIONAL COMMENTS: Piece 3 consists of a dark green mineral (altered basaltic glass) with 0.5-3 mm, subhorizontal, red-white calcite veins.

SUBDIVISION 8A: APHYRIC BASALT

Pieces 3-8

CONTACTS: Piece 3 consists of calcite veins and green altered basalt glass from top of pillow lava.
PHENOCRYSTS:
Pyroxene - <1%; ~0.5 mm; subhedral.
Plagioclase - <1%; ~0.5 mm; euhedral laths.
GROUNDMASS: Very fine grained.
VESICLES: <1%; 1 mm; oval; very rare; infilled with calcite (Piece 8).
COLOR: Gray to brown, blotchy brown-gray, brown near some veins.
STRUCTURE: Massive.
ALTERATION: Very highly to highly altered; blotchy, most pronounced near fractures and veins.
VEINS/FRACTURES: 1-10%; <1-8 mm; mainly subhorizontal; Piece 5 is heavily veined.

SUBDIVISION 8A: APHYRIC BASALT

Pieces 9, 10

CONTACTS: None.
PHENOCRYSTS: Aphyric.
GROUNDMASS: Fine grained.
VESICLES: Nonvesicular.
COLOR: Green-brown to gray-green.
STRUCTURE: Massive.
ALTERATION: Very highly to completely altered.
VEINS/FRACTURES: 3-5%; ~1 mm; none; calcite and green mineral.

SUBDIVISION 8A: APHYRIC BASALT

Piece 11

CONTACTS: None.
PHENOCRYSTS:
Pyroxene - <1%; 0.25-1 mm; equant to prismatic.
GROUNDMASS: Glassy to spherulitic texture.
VESICLES: Nonvesicular.
COLOR: Black to dark gray and green rim.
STRUCTURE: Glassy pillow fragment.
ALTERATION: Highly altered to moderately fresh-small amounts of fresh glass (~1-2%).
VEINS/FRACTURES: 2-3%; 0.5-1 mm; concentric and transverse; calcite.

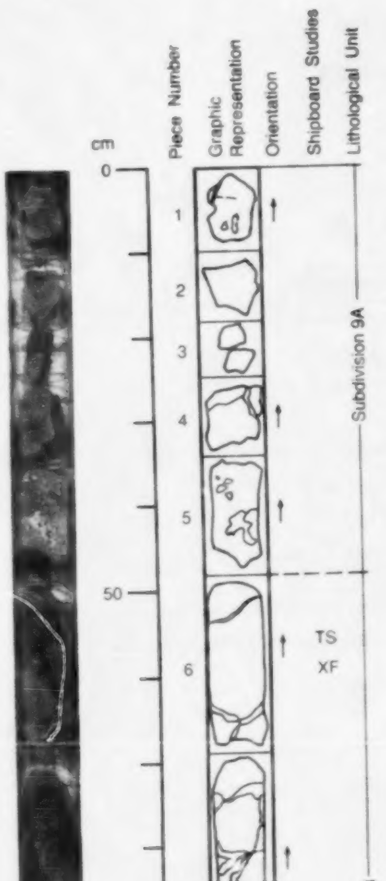
cm
Piece Number
Graphic Representation
Orientation
Shipboard Studies
Lithological Unit
0
50
100
150
1
2
3
4
5
6
7
8
9
10
11
TS
XF
Subdivision 9A
Subdivision 9B
CORE/SECTION

130-803D-70R-3

SUBDIVISION 9A: SPARSELY PYROXENE-PLAGIOCLASE PHYRIC BASALT

Pieces 1-5

CONTACTS: None.
PHENOCRYSTS:
Pyroxene - <2%; 0.5-1 mm; subhedral.
Plagioclase - <2%; 0.5-1 mm; euhedral laths.
GROUNDMASS: Very fine grained.
VESICLES: Nonvesicular.
COLOR: Gray to brown, mottled, greenish near edge.
STRUCTURE: Massive.
ALTERATION: Highly altered, blotchy.
VEINS/FRACTURES: 1-10%; 1 mm; subhorizontal to 45°; calcite and smectite, vugs up to 2 cm in Piece 5.

SUBDIVISION 9B: APHYRIC BASALT

Pieces 6, 7

CONTACTS: None.
PHENOCRYSTS:
Pyroxene - <1%; <1 mm; altered.
GROUNDMASS: Very fine grained.
VESICLES: <1%; 1-4 mm; irregular; rare; calcite-filled with minor green mineral.
COLOR: Gray to brown with greenish patches; mottled.
STRUCTURE: Massive.
ALTERATION: Moderately to very highly altered.
VEINS/FRACTURES: 2-3%; <5 mm; curved, subvertical. Piece 7 highly veined, infilled with calcite and minor smectite.

SUBDIVISION 9B: APHYRIC BASALT

Pieces 8, 9

CONTACTS: None.
PHENOCRYSTS:
Plagioclase - <1%; 1-2 mm; altered.
GROUNDMASS: Very fine grained.
VESICLES: Nonvesicular.
COLOR: Mostly brown, but also gray.
STRUCTURE: Massive.
ALTERATION: Very highly altered, brown patches dominate.
VEINS/FRACTURES: <5%; 0.5-2 mm; subhorizontal and subvertical; calcite.

SUBDIVISION 9B: APHYRIC BASALT

Pieces 10, 11

CONTACTS: None.
PHENOCRYSTS: Aphyric.
GROUNDMASS: Very fine grained.
VESICLES: Nonvesicular.
COLOR: Green-gray to brown.
STRUCTURE: Massive.
ALTERATION: Very highly altered.
VEINS/FRACTURES: <1%; ~0.5 mm; subvertical, calcite.

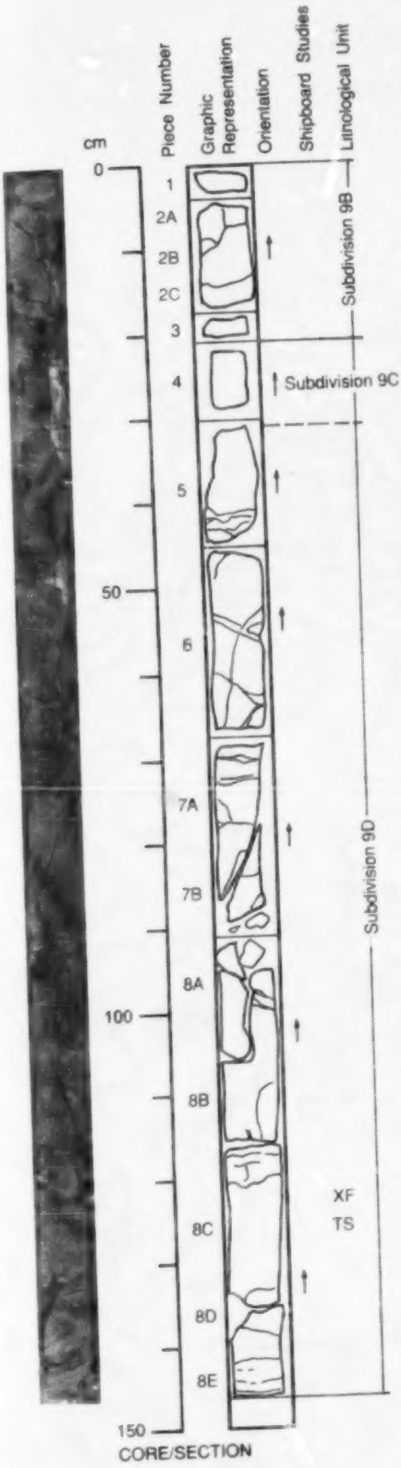
cm
Piece Number
Graphic Representation
Orientation
Shipboard Studies
Lithological Unit
0
50
100
150
1
2A
2B
2C
3
4
5
6
7A
7B
8A
8B
8C
8D
8E
Subdivision 9B
Subdivision 9C
Subdivision 9D
XF
TS
CORE/SECTION

130-803D-71R-1

SUBDIVISION 9B: APHYRIC BASALT

Pieces 1-3

CONTACTS: None.
PHENOCRYSTS: Piece 2 contains rare plagioclase phenocrysts (xenocrysts?).
Pyroxene - <1%; ~0.5 mm; subhedral.
Plagioclase - <<1%; up to 8 mm; euhedral laths.
GROUNDMASS: Very fine grained.
VESICLES: 1%; 1-2 mm; irregular; in Piece 1; calcite filled.
COLOR: Gray to brown, mottled.
STRUCTURE: Massive.
ALTERATION: Highly altered.
VEINS/FRACTURES: 1%; 1-2 mm; subvertical; calcite filled.

SUBDIVISION 9C: APHYRIC BASALT

Piece 4

CONTACTS: None.
PHENOCRYSTS: Aphyric.
GROUNDMASS: Very fine grained.
VESICLES: Nonvesicular.
COLOR: Light gray to brown; spotted appearance.
STRUCTURE: Massive.
ALTERATION: Very highly to highly altered.
VEINS/FRACTURES: 3%; ~1 mm; subvertical and subhorizontal; calcite filled.

SUBDIVISION 9D: APHYRIC BASALT

Piece 5

CONTACTS: None.
PHENOCRYSTS: Aphyric.
GROUNDMASS: Very fine grained.
VESICLES: Nonvesicular.
COLOR: Light gray to brown; spotted appearance.
STRUCTURE: Massive.
ALTERATION: Very highly to highly altered.
VEINS/FRACTURES: 3%; ~1 mm; subvertical and subhorizontal; calcite.

SUBDIVISION 9D: APHYRIC BASALT

Pieces 6-8

CONTACTS: None.
PHENOCRYSTS:
Pyroxene - <1%; 0.5 mm; subhedral.
GROUNDMASS: Very fine grained.
VESICLES: Nonvesicular.
COLOR: Gray to brown; green near fractures.
STRUCTURE: Massive, possible flow band in Piece 8.
ALTERATION: Moderately altered.
VEINS/FRACTURES: 1-3%; 1-3 mm; subvertical and subhorizontal; calcite and green/brown (smectite, celadonite/serpentine?) filling.

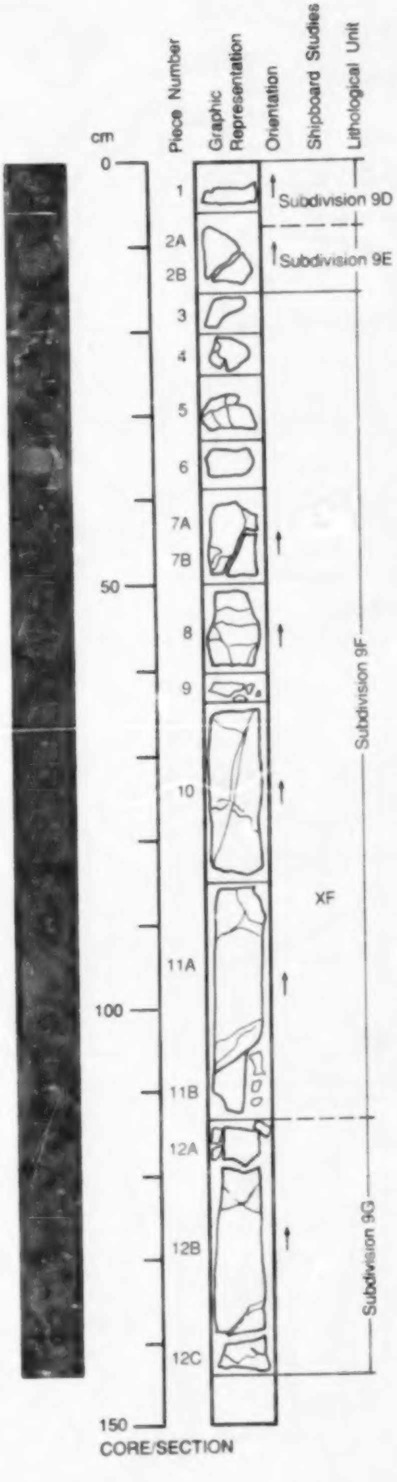
cm
Piece Number
Graphic Representation
Orientation
Shipboard Studies
Lithological Unit
0
50
100
150
1
2A
2B
3
4
5
6
7A
7B
8
9
10
11A
11B
12A
12B
12C
Subdivision 9D
Subdivision 9E
Subdivision 9F
XF
Subdivision 9G
CORE/SECTION

130-803D-71R-2

SUBDIVISION 9D: APHYRIC BASALT

Piece 1

CONTACTS: None.
PHENOCRYSTS: Aphyric.
GROUNDMASS: Fine grained.
VESICLES: Nonvesicular.
COLOR: Green brown.
STRUCTURE: Massive.
ALTERATION: Very highly altered.
VEINS/FRACTURES: <1%; 0.5 mm; subhorizontal, calcite filled.

SUBDIVISION 9E: APHYRIC BASALT

Piece 2

CONTACTS: Top of pillow.
PHENOCRYSTS:
Pyroxene - <1%; <0.5 mm; subhedral.
GROUNDMASS: Very fine grained to glassy rim.
VESICLES: Nonvesicular.
COLOR: Dark gray brown to gray rim.
STRUCTURE: Pillow fragment.
ALTERATION: Very altered (interior) to slightly altered at rim; blotchy.
VEINS/FRACTURES: <2%; 0.5-1 mm; radial; infilled with calcite (greenish).

SUBDIVISION 9F: APHYRIC BASALT

Pieces 3-9

CONTACTS: None.
PHENOCRYSTS:
Plagioclase - <1%; <0.5 mm; euhedral laths.
GROUNDMASS: Very fine grained.
VESICLES: Nonvesicular.
COLOR: Gray with light-dark brown patches.
STRUCTURE: Massive.
ALTERATION: Highly altered, mottled.
VEINS/FRACTURES: <5%; 0.5-2 mm; subhorizontal and subvertical; calcite, green colored in places.

SUBDIVISION 9F: APHYRIC BASALT

Pieces 10, 11

CONTACTS: None.
PHENOCRYSTS: Aphyric.
GROUNDMASS: Fine grained.
VESICLES: Nonvesicular.
COLOR: Gray to brown, mottled.
STRUCTURE: Massive.
ALTERATION: Moderately to highly altered.
VEINS/FRACTURES: <5%; 1-2 mm; irregular; filled with calcite and green mineral.

SUBDIVISION 9G: APHYRIC BASALT

Piece 12

CONTACTS: None.
PHENOCRYSTS: Aphyric.
GROUNDMASS: Fine grained.
VESICLES: Nonvesicular.
COLOR: Gray to brown, mottled.
STRUCTURE: Massive.
ALTERATION: Moderately to highly altered.
VEINS/FRACTURES: <5%; 1-2 mm; irregular; filled with calcite and green minerals.

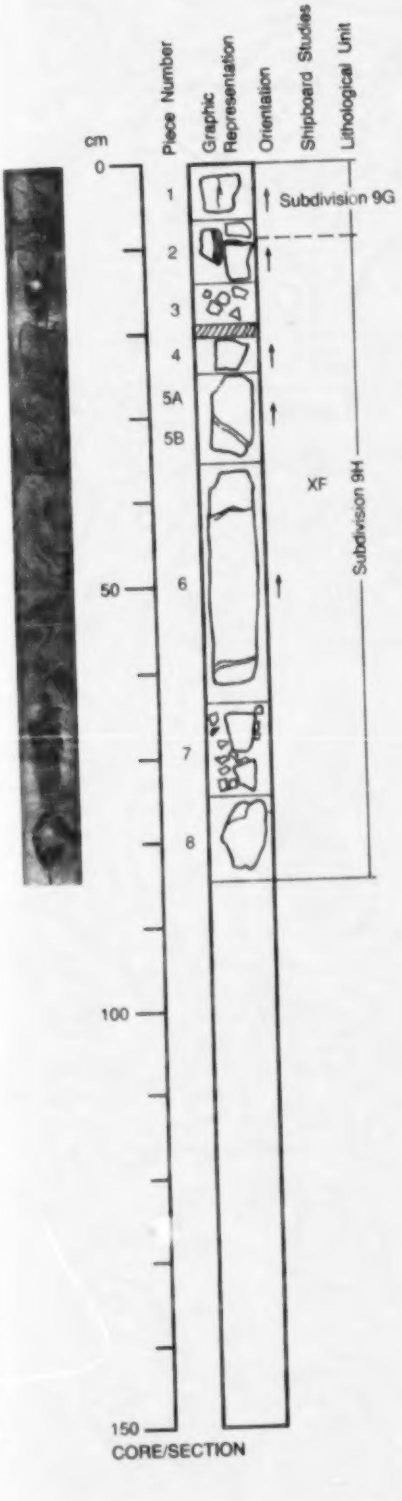
cm
Piece Number
Graphic Representation
Orientation
Shipboard Studies
Lithological Unit
0
1
Subdivision 9G
2
3
4
5A
5B
XF
Subdivision 9H
50
6
7
8
100
150
CORE/SECTION

130-803D-71R-3

SUBDIVISION 9G: APHYRIC BASALT

Piece 1

CONTACTS: None.
PHENOCRYSTS: Aphyric, although Piece 1 contains a 7 mm aggregate (xenolith?) of olivine crystals up to 1 mm.
GROUNDMASS: Very fine grained.
VESICLES: Nonvesicular.
COLOR: Gray to brown, mottled; with red-brown altered zone.
STRUCTURE: Massive.
ALTERATION: Highly altered.
VEINS/FRACTURES: <1%; 1 mm; vertical; calcite.

SUBDIVISION 9H: APHYRIC BASALT

Piece 2

CONTACTS: Top of pillow.
PHENOCRYSTS: Aphyric.
GROUNDMASS: Very fined grained to glassy rim.
VESICLES: Nonvesicular.
COLOR: Gray to blotchy brown.
STRUCTURE: Pillow fragments.
ALTERATION: Moderately to highly altered.
VEINS/FRACTURES: <1%; 0.5-2 mm; vertical; calcite.

SUBDIVISION 9H: APHYRIC BASALT

Pieces 3-8

CONTACTS: None.
PHENOCRYSTS: Aphyric.
GROUNDMASS: Very fine grained.
VESICLES: Nonvesicular.
COLOR: Gray to greenish brown, blotchy to spotty.
STRUCTURE: Massive.
ALTERATION: Moderately to highly altered, mottled patches near veins.
VEINS/FRACTURES: ~1%; 0.5-2 mm; subhorizontal; calcite and brown mineral (smectite?).

130-803D-68R-04 (Piece 1A,45-47 cm) OBSERVER: STO WHERE SAMPLED: Pillow interior

ROCK NAME: Aphyric basalt

GRAIN SIZE: Fine grained

TEXTURE: Intersertal

PRIMARY MINERALOGY	PERCENT PRESENT	PERCENT ORIGINAL	SIZE (mm)	COMPO- SITION	MORPHOLOGY	COMMENTS
PHENOCRYSTS						
Olivine	–	<1	~0.3		Subhedral	Olivine pseudomorphs, replacement mineral consisting of brown smectite and minor green mineral.
GROUNDMASS						
Plagioclase	20	20	0.05-0.5		Thin euhedral laths	Sub-parallel flow alignment, skeletal crystals.
Opaques	5	~5	<0.01		subhedral-anhedral	
Pyroxene (?)	0	10	0.05-0.5		subhedral-euhedral laths	Replaced by dark brown smectites - psudeomorphs exhibit radial arrangement (original quench texture?).

SECONDARY MINERALOGY	PERCENT	REPLACING/ FILLING	COMMENTS
Clays (smectites)	75	Pyroxene, glass.	

VESICLES/ CAVITIES	PERCENT	LOCATION	SIZE (mm)	FILLING	SHAPE
Vesicles	0				

130-803D-69R-04 (Piece 4,28-30 cm) OBSERVER: STO WHERE SAMPLED: Pillow interior

ROCK NAME: Aphyric basalt.

GRAIN SIZE: Fine grained

TEXTURE: Intersertal

PRIMARY MINERALOGY	PERCENT PRESENT	PERCENT ORIGINAL	SIZE (mm)	COMPO- SITION	MORPHOLOGY	COMMENTS
Plagioclase	15	15	0.1-1		Euhedral laths	Skeletal.
Opaques	10	~10	0.02-0.1		Euhedral laths	
Clinopyroxene	2	~2	0.1		Anhedral	Partly replaced by brown smectite.

SECONDARY MINERALOGY	PERCENT	REPLACING/ FILLING	COMMENTS
Brown smectite	75	glass	

VESICLES/ CAVITIES	PERCENT	LOCATION	SIZE (mm)	FILLING	SHAPE
Vesicles	0				

130-803D-70R-01 (Piece 8,62-64 cm) OBSERVER: STO WHERE SAMPLED: Pillow interior

ROCK NAME: Aphyric basalt

GRAIN SIZE: Fine grained to very fine grained.

TEXTURE: Intersertal-intergranular.

PRIMARY MINERALOGY	PERCENT PRESENT	PERCENT ORIGINAL	SIZE (mm)	COMPO-SITION	MORPHOLOGY	COMMENTS
Plagioclase	20	~20	0.1-1		Thin euhedral laths	
Pyroxene	5	~5	0.02-0.1		Anhedral	Partly altered to reddish brown smectite.
Opaques	5	5	0.02-0.1		-	

SECONDARY MINERALOGY	PERCENT	REPLACING/ FILLING	COMMENTS
Clays	70	Mostly glass	Brown smectites.

VESICLES/ CAVITIES	PERCENT	LOCATION	SIZE (mm)	FILLING	SHAPE
Vesicles	0				

130-803D-70R-03 (Piece 6,60-62 cm) OBSERVER: STO WHERE SAMPLED: Pillow interior

ROCK NAME: Clinopyroxene-phyric basalt

GRAIN SIZE: Fine grained

TEXTURE: Intersertal

PRIMARY MINERALOGY	PERCENT PRESENT	PERCENT ORIGINAL	SIZE (mm)	COMPO-SITION	MORPHOLOGY	COMMENTS
PHENOCRYSTS						
Clinopyroxene	5	5	3-5		anhedral-subhedral	Colorless crystals, strongly zoned rims, contains numerous basalt glass inclusions up to 0.05 mm in diameter.
GROUNDMASS						
Plagioclase	25	25	0.1-1.5		Thin euhedral laths	
Clinopyroxene	5	7?	0.1-0.5		Anhedral	Partly altered.

SECONDARY MINERALOGY	PERCENT	REPLACING/ FILLING	COMMENTS
Clays	65	Mostly glass	

VESICLES/ CAVITIES	PERCENT	LOCATION	SIZE (mm)	FILLING	SHAPE
Vesicles	0				

130-803D-71R-01 (Piece 8C,131-137 cm) OBSERVER: STO WHERE SAMPLED: Pillow interior

ROCK NAME: Aphyric basalt

GRAIN SIZE: Fine grained

TEXTURE: Intersertal-intergranular

PRIMARY MINERALOGY	PERCENT PRESENT	PERCENT ORIGINAL	SIZE (mm)	COMPO-SITION	MORPHOLOGY	COMMENTS
Plagioclase	40	~40	0.1-0.5		Thin euhedral laths	
Clinopyroxene	25	~30	0.05-0.1		Anhedral	
Opaques	2	~2	~0.05		Anhedral-subhedral	

SECONDARY MINERALOGY	PERCENT	REPLACING/ FILLING	COMMENTS
Clays	33	Glass (?)	Brown smectite.

VESICLES/ CAVITIES	PERCENT	LOCATION	SIZE (mm)	FILLING	SHAPE
Vesicles	0				

COMMENTS: The specimen is cut by a 1 mm wide green (celadonite?) vein

Reproduced from poor document.

SITE 804 HOLE A CORE 1H CORED INTERVAL 0.0-1.2 mbsf

TIME-ROCK UNIT	BIOSTRAT. ZONE/ FOSSIL CHARACTER: FORAMINIFERS	NANNOFOSSILS	RADIOLARIANS	DIATOMS	PALEOMAGNETICS	PHYS. PROPERTIES	CHEMISTRY	SECTION	METERS	GRAPHIC LITHOLOGY	DRILLING DISTURB.	SED. STRUCTURES	SAMPLES	LITHOLOGIC DESCRIPTION
PLEISTOCENE	*Globorotalia truncatulinoides* N23 A/M	NN20 A/M A/M NN21	*Collosphaera tuberosa* A/G	NTD 17 *Pseudoeunotia doliolus* A/G-C		φ=69 γ=1.51 V=1520 ●	%CaCO3 =80.6 ●	1 CC	0.5				●	NANNOFOSSIL OOZE with FORAMINIFERS

NANNOFOSSIL OOZE with FORAMINIFERS

Major lithology: This core contains heavily bioturbated, mottled, pale brown (10YR 6/3) to light yellowish brown (10YR 6/4) NANNOFOSSIL OOZE with FORAMINIFERS.

SMEAR SLIDE SUMMARY (%):

	1, 14
	D
TEXTURE:	
Sand	10
Silt	80
Clay	10
COMPOSITION:	
Foraminifers	14
Nannofossils	85
Radiolarians	1

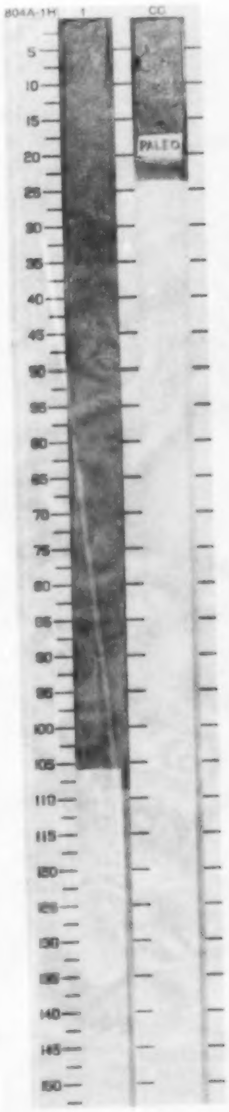
804A-1H
1
CC
PALEO
5
10
15
20
25
30
35
40
45
50
55
60
65
70
75
80
85
90
95
100
105
110
115
120
125
130
135
140
145
150

SITE 804 HOLE A CORE 2H CORED INTERVAL 1.2-10.7 mbsf

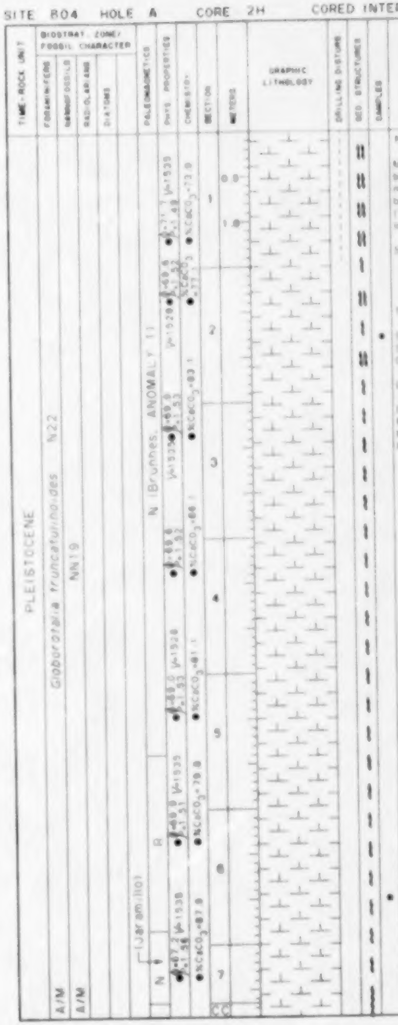
TIME-ROCK UNIT
BIOSTRAT. ZONE/ FOSSIL CHARACTER
FORAMINIFERS
NANNOFOSSILS
RADIOLARIANS
DIATOMS
PALEOMAGNETICS
PHYS. PROPERTIES
CHEMISTRY
SECTION
METERS
GRAPHIC LITHOLOGY
DRILLING DISTURB.
SED. STRUCTURES
SAMPLES
PLEISTOCENE
Globorotalia truncatulinoides N22
NN19
A/M
A/M
N (Brunnes, ANOMALY 1)
R
N
(Jaramillo)
φ=77.1 ρ=1.48 V=1539
%CaCO3=73.0
φ=69.6 ρ=1.52 V=1520
%CaCO3=77.3
φ=60.0 ρ=1.53 V=1535
%CaCO3=83.1
φ=60.6 ρ=1.52
%CaCO3=86.1
φ=60.0 ρ=1.53 V=1528
%CaCO3=81.1
φ=60.9 ρ=1.51 V=1535
%CaCO3=79.8
φ=67.2 ρ=1.56 V=1538
%CaCO3=87.8
1
2
3
4
5
6
7
CC
0.5
1.0

LITHOLOGIC DESCRIPTION

NANNOFOSSIL OOZE

Major lithology: This core contains NANNOFOSSIL OOZE. The first section is heavily bioturbated and is dominantly very pale brown (10YR 7/3) with pale brown (10YR 6/3) mottling. The lower sections are moderately bioturbated. The color varies between pale brown (10YR 6/3) and very pale brown (10YR 7/3) on a 25 cm scale in Section 2, is very brown (10YR 7/3) in Section 3, and is white (10YR 8/2 to 10YR 8/1) to light gray (10YR 7/2) in the lowest part of the core.

SMEAR SLIDE SUMMARY (%):

	2, 79 D	6, 100 D
TEXTURE:		
Sand	1	1
Silt	95	95
Clay	4	4
COMPOSITION:		
Diatoms	Tr	—
Foraminifers	4	4
Nannofossils	95	95
Radiolarians	1	1

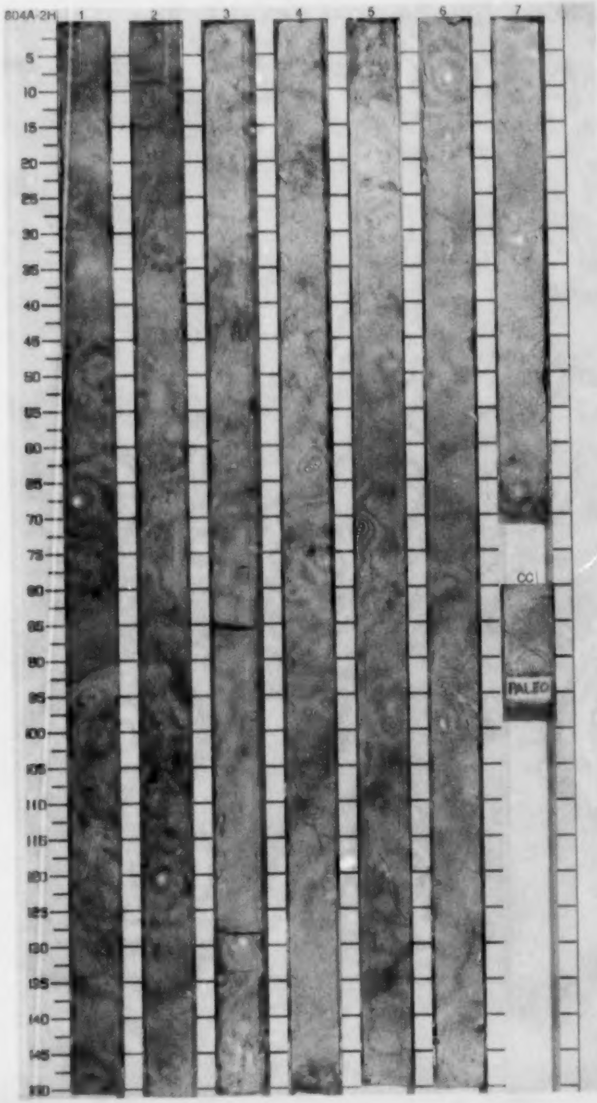
804A-2H
1
2
3
4
5
6
7
CC
PALEO
5
10
15
20
25
30
35
40
45
50
55
60
65
70
75
80
85
90
95
100
105
110
115
120
125
130
135
140
145
150

SITE 804 HOLE A CORE 3H CORED INTERVAL 10.7-20.2 mbsf

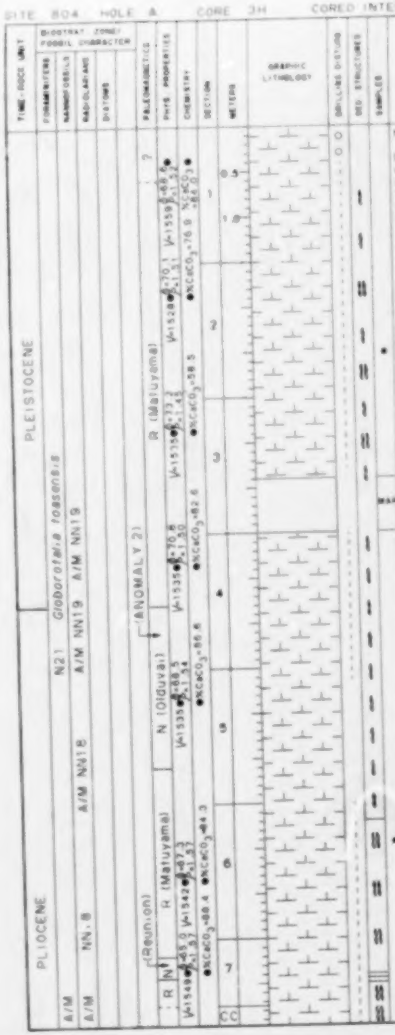
TIME-ROCK UNIT
BIOSTRAT. ZONE/ FOSSIL CHARACTER
FORAMINIFERS
NANNOFOSSILS
RADIOLARIANS
DIATOMS
PALEOMAGNETICS
PHYS. PROPERTIES
CHEMISTRY
SECTION
METERS
GRAPHIC LITHOLOGY
DRILLING DISTURB.
SED. STRUCTURES
SAMPLES
PLEISTOCENE
PLIOCENE
N21 Globorotalia tosaensis
A/M
A/M NN19 A/M NN19
A/M NN18
NN.8
A/M
?
R (Matuyama)
(ANOMALY 2)
N (Olduvai)
R (Matuyama)
(Reunion)
R
N
Vp=1559 φ=68.6 ρ=1.52
φ=70.1 ρ=1.51 Vp=1520
Vp=1515 φ=73.2 ρ=1.45
Vp=1535 φ=70.8 ρ=1.50
Vp=1535 φ=68.5 ρ=1.54
Vp=1542 φ=67.3 ρ=1.57
Vp=1548 φ=65.0 ρ=1.57
%CaCO3=76.9 %CaCO3=84.0
%CaCO3=58.5
%CaCO3=82.6
%CaCO3=86.6
%CaCO3=84.3
%CaCO3=88.4
1
2
3
4
5
6
7
CC
0.5
1.0
IW
OG

LITHOLOGIC DESCRIPTION

NANNOFOSSIL OOZE with FORAMINIFERS

Major lithology: This core contains moderately to heavily bioturbated NANNOFOSSIL OOZE with FORAMINIFERS. Section 1 through Section 6, 25 cm, have colors grading between white (10YR 8/1, 10YR 8/2 and 2.5Y 8/2) and light gray (10YR 7/2, 5Y 7/1, 5Y 7/2 and 2.5Y 7/2) to light brownish gray (2.5Y 6/2) on a 10 to 50 cm scale. Below Section 6, 25 cm, the color is bluish gray (5B 6/1) grading to light gray (5Y 7/1 and 10YR 7/1) and light greenish gray (5G 5/1). Three diffuse mm size light greenish gray (5G 5/1) color bands are present in Section 7.

SMEAR SLIDE SUMMARY (%):

	2, 101	6, 43
	D	D
TEXTURE:		
Sand	10	10
Silt	85	85
Clay	5	5
COMPOSITION:		
Foraminifers	10	10
Nannofossils	90	90

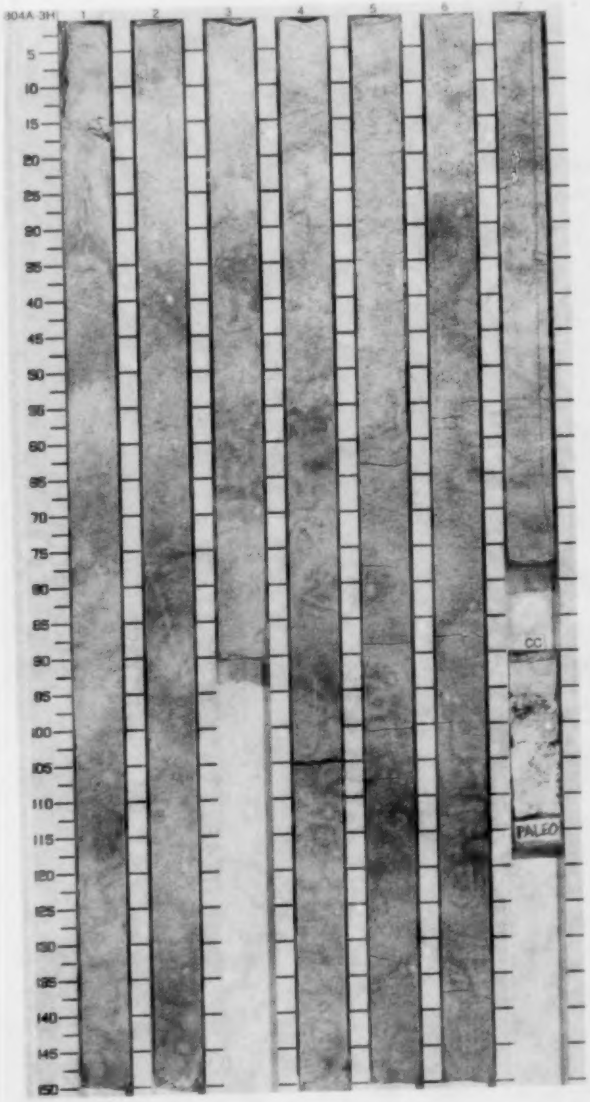
804A-3H
1
2
3
4
5
6
7
CC
PALEO
5
10
15
20
25
30
35
40
45
50
55
60
65
70
75
80
85
90
95
100
105
110
115
120
125
130
135
140
145
150

SITE 804 HOLE A CORE 4H CORED INTERVAL 20.2-29.7 mbsf

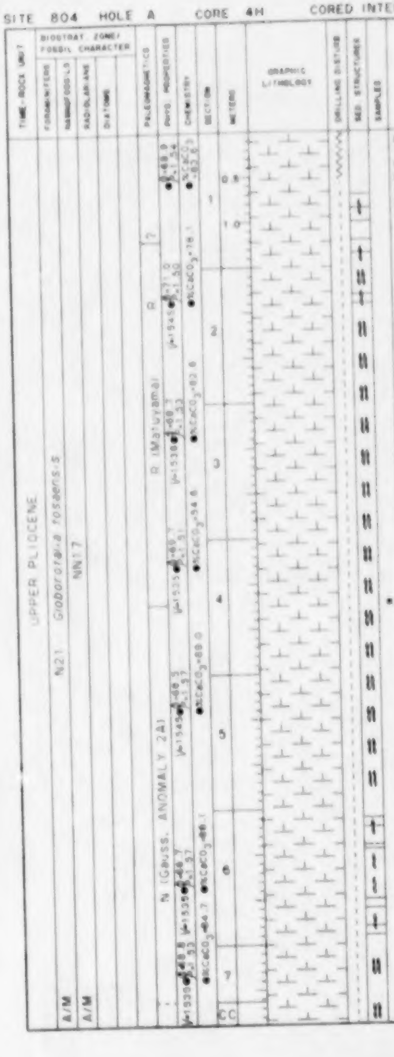

LITHOLOGIC DESCRIPTION

NANNOFOSSIL OOZE

Major lithology: This core contains NANNOFOSSIL OOZE. It is moderately to heavily bioturbated and mottled, with a few mm to cm size pyrite nodules. The dominant color is white (10YR 8/1), with minor intervals of light gray (5Y 7/1). Color bands are light olive gray (5Y 6/2), pale purple (5P 6/2), dusky blue (5PB 3/2), pale yellowish green (10GY 7/2) and medium light gray (5B N6/6).

SMEAR SLIDE SUMMARY (%):

	4, 77
	D
TEXTURE:	
Sand	2
Silt	90
Clay	8
COMPOSITION:	
Foraminifers	4
Nannofossils	95
Radiolarians	1

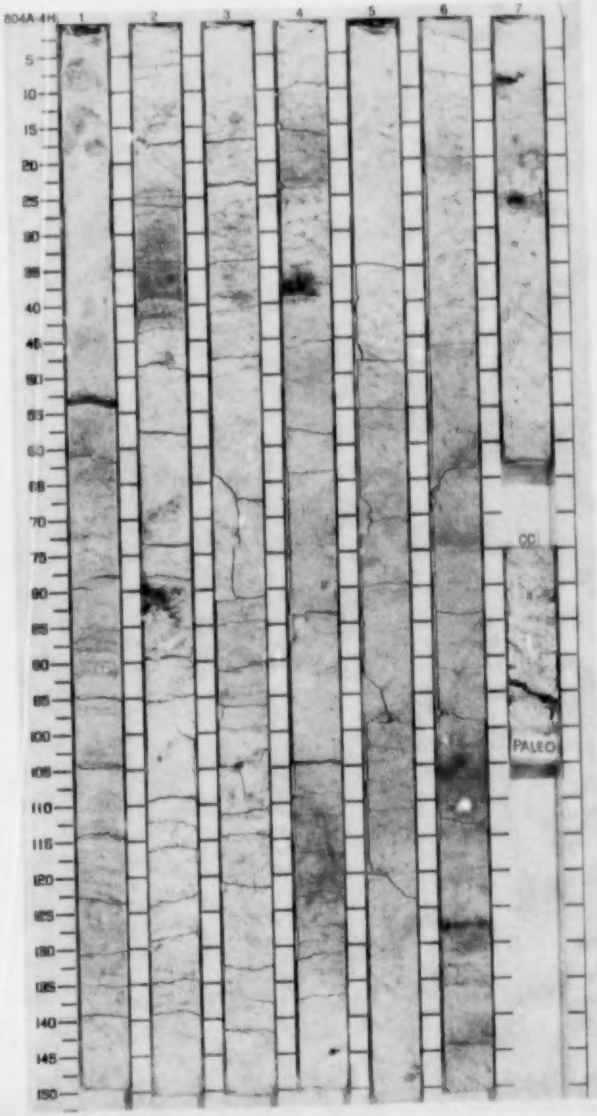
804A-4H
1
2
3
4
5
6
7
CC
PALEO
5
10
15
20
25
30
35
40
45
50
55
60
65
70
75
80
85
90
95
100
105
110
115
120
125
130
135
140
145
150

SITE 804 HOLE A CORE 5H CORED INTERVAL 29.7-39.2 mbsf

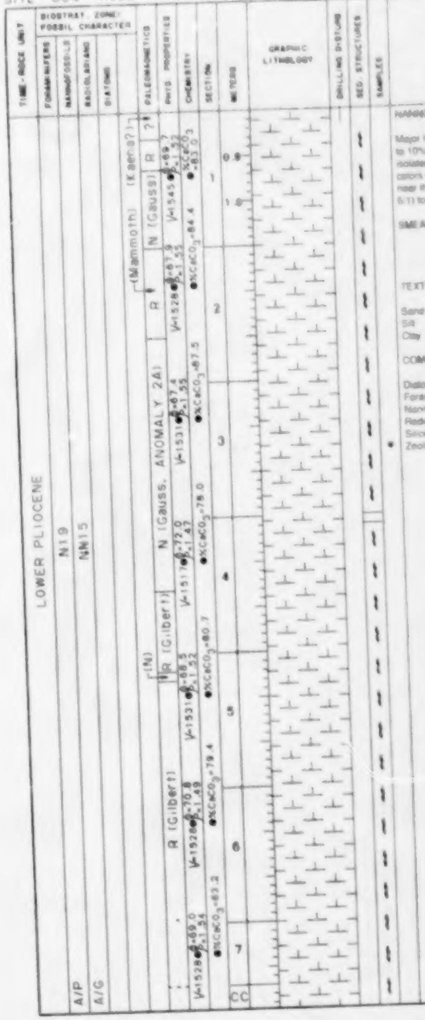
TIME-ROCK UNIT
BIOSTRAT. ZONE/ FOSSIL CHARACTER
FORAMINIFERS
NANNOFOSSILS
RADIOLARIANS
DIATOMS
PALEOMAGNETICS
PHYS. PROPERTIES
CHEMISTRY
SECTION
METERS
GRAPHIC LITHOLOGY
DRILLING DISTURB.
SED. STRUCTURES
SAMPLES
LOWER PLIOCENE
N19
NN15
A/P
A/G
(Mammoth)
(Kaena?)
?
R
N (Gauss)
R
N (Gauss, ANOMALY 2A)
R (Gilbert)
(N)
R (Gilbert)
V=1545 φ=69.7 γ=1.52
V=1528 φ=67.9 γ=1.55
V=1531 φ=67.4 γ=1.55
V=1517 φ=72.0 γ=1.47
V=1531 φ=68.5 γ=1.52
V=1528 φ=70.8 γ=1.49
V=1528 φ=69.0 γ=1.54
%CaCO3=83.0
%CaCO3=84.4
%CaCO3=87.5
%CaCO3=78.0
%CaCO3=80.7
%CaCO3=79.4
%CaCO3=83.2
1
2
3
4
5
6
7
CC
0.5
1.0

LITHOLOGIC DESCRIPTION

NANNOFOSSIL OOZE

Major lithology: This core contains NANNOFOSSIL OOZE. Foraminifers locally constitute up to 10% of the sediment. The sediment is moderately to heavily bioturbated and mottled, with isolated mm to cm size pyrite nodules. The dominant color is light gray (5Y 7/1) and mottle colors range from olive (5Y 5/2) to light gray (5Y 7/1). Color bands vary in thickness from 5 mm near the base of Section 3 to 30 cm in Sections 5, 6, and 7, and range in color from gray (2.5Y 6/1) to reddish gray (5R 6/1) to pale yellowish green (10GY 7/2).

SMEAR SLIDE SUMMARY (%):

	3, 75
	D
TEXTURE:	
Sand	1
Silt	60
Clay	39
COMPOSITION:	
Diatoms	1
Foraminifers	7
Nannofossils	71
Radiolarians	3
Siliceous fragments	3
Zeolite	15

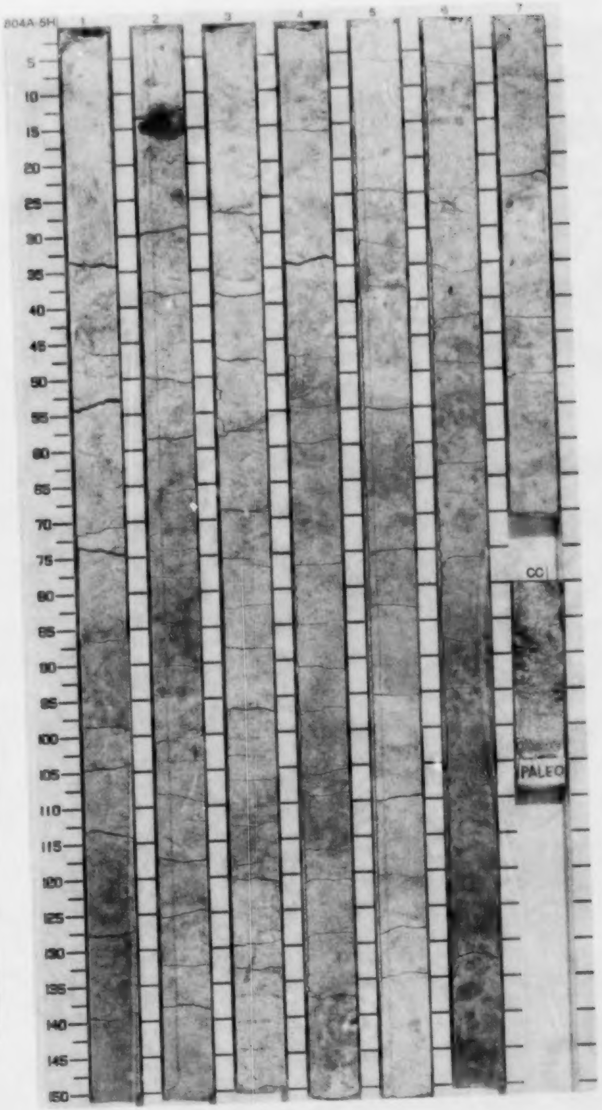
804A-5H
1
2
3
4
5
6
7
CC
PALEO
5
10
15
20
25
30
35
40
45
50
55
60
65
70
75
80
85
90
95
100
105
110
115
120
125
130
135
140
145
150

SITE 804 HOLE A CORE 6H CORED INTERVAL 39.2-48.7 mbsf

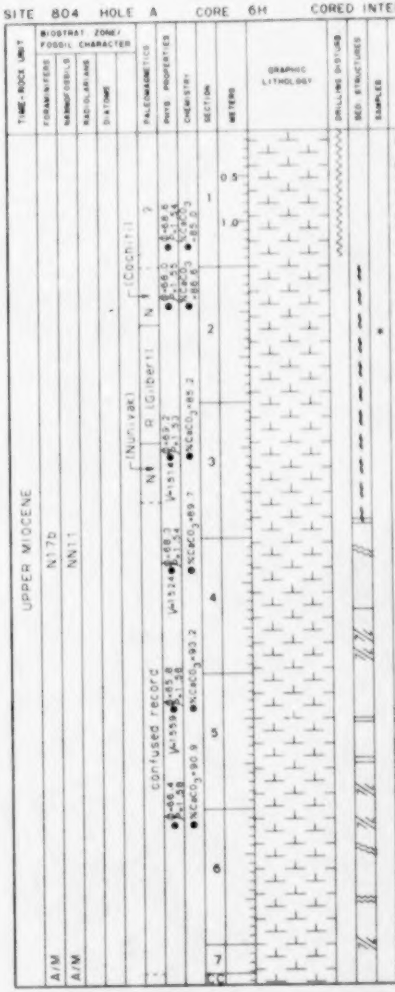

LITHOLOGIC DESCRIPTION

NANNOFOSSIL OOZE

Major lithology: This core contains NANNOFOSSIL OOZE. Section 1, 0-145 cm, is flow in. Sections 2 and 3 are heavily bioturbated as indicated from abundant gray (2.5Y 6/1), light gray (2.5Y 7/0) and white (2.5Y 8/0) mottling. The remainder of the core is primarily white (2.5Y 8/0) with some cm scale color bands of gray (2.5Y 6/1), reddish gray (5R 6/1), and pale yellowish green (10GY 7/2). These color bands are typically faint to smeared in appearance, wavy in form, and show abundant cm scale displacements (microfaulting) in the lower half of the core.

SMEAR SLIDE SUMMARY (%):

	2, 74
	D
TEXTURE:	
Silt	60
Clay	40
COMPOSITION:	
Accessory minerals	7
Diatoms	1
Foraminifers	3
Nannofossils	79
Radiolarians	5
Siliceous fragments	3
Zeolite	3

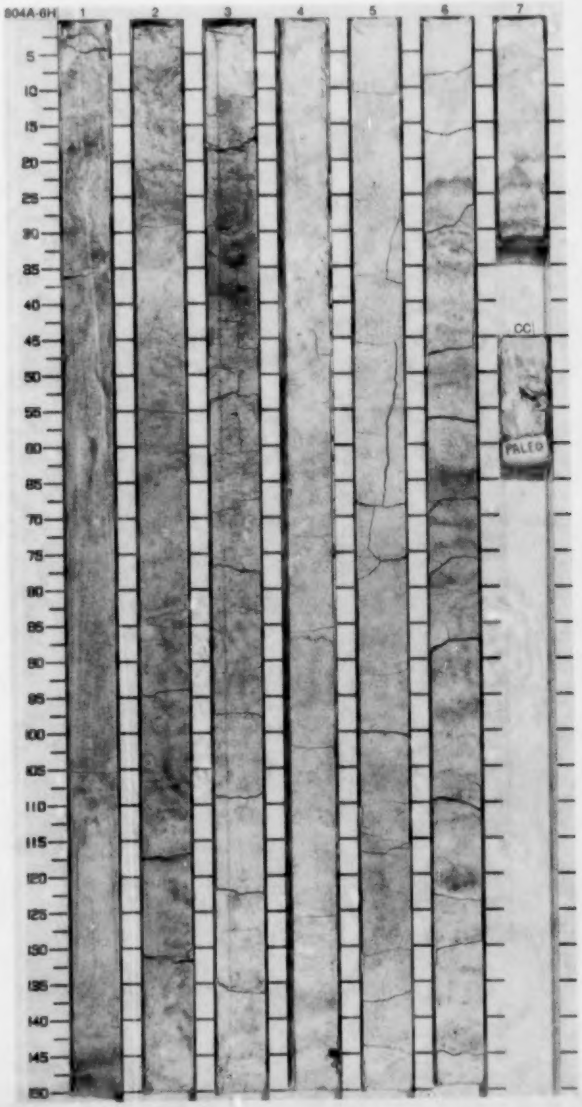
804A-6H
1
2
3
4
5
6
7
CC
PALEO
5
10
15
20
25
30
35
40
45
50
55
60
65
70
75
80
85
90
95
100
105
110
115
120
125
130
135
140
145
150

SITE 804 HOLE B CORE 1H CORED INTERVAL 0.0-4.7 mbsf

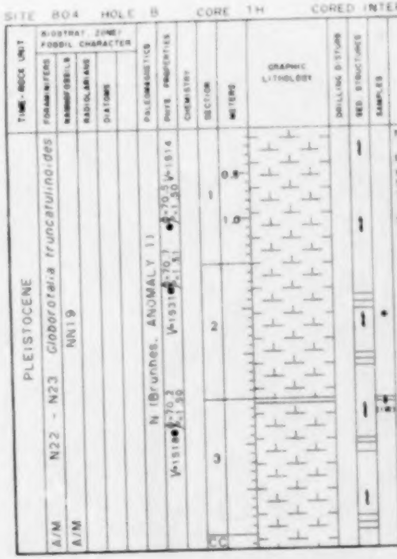
TIME-ROCK UNIT
BIOSTRAT. ZONE/ FOSSIL CHARACTER
FORAMINIFERS
NANNOFOSSILS
RADIOLARIANS
DIATOMS
PALEOMAGNETICS
PHYS. PROPERTIES
CHEMISTRY
SECTION
METERS
GRAPHIC LITHOLOGY
DRILLING DISTURB.
SED. STRUCTURES
SAMPLES
PLEISTOCENE
N22 - N23 Globorotalia truncatulinoides
A/M
NN19
A/M
N (Brunhes, ANOMALY 1)
φ=70.5 γ=1.90 V=1514
φ=70.7 γ=1.81 V=1531
φ=70.2 γ=1.90 V=1518
1
2
3
CC
0.5
1.0

LITHOLOGIC DESCRIPTION

NANNOFOSSIL OOZE with FORAMINIFERS

Major lithology: This core contains heavily bioturbated, mottled, pale yellow (2.5Y 7/4) to light yellowish brown (10YR 6/4) NANNOFOSSIL OOZE with FORAMINIFERS. Color bands in Section 3 are 25 to 35 cm thick and alternate between light gray (2.5Y 8/2) and white (2.5Y 7/2).

SMEAR SLIDE SUMMARY (%):

	2, 58
	D
TEXTURE:	
Sand	5
Silt	55
Clay	40
COMPOSITION:	
Accessory minerals	5
Diatoms	2
Foraminifers	15
Nannofossils	70
Radiolarians	5
Siliceous fragments	3

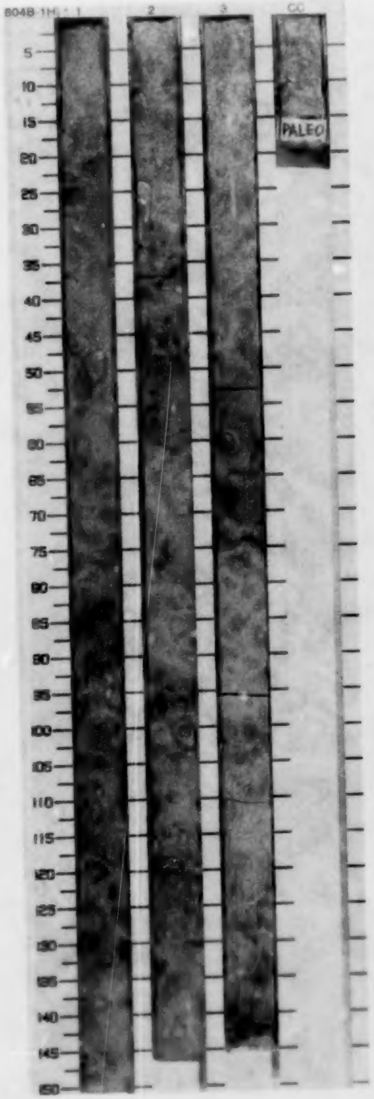
804B-1H
1
2
3
CC
PALEO
5
10
15
20
25
30
35
40
45
50
55
60
65
70
75
80
85
90
95
100
105
110
115
120
125
130
135
140
145
150

SITE 804 HOLE B CORE 2H CORED INTERVAL 4.7-14.2 mbsf

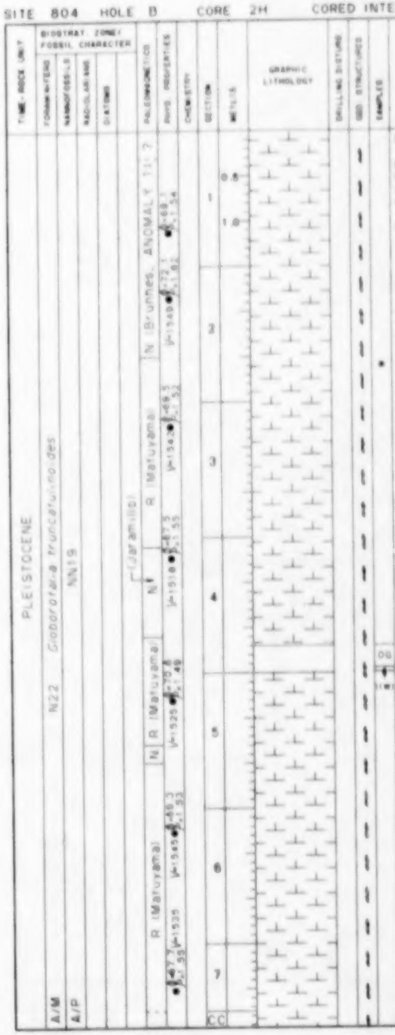

LITHOLOGIC DESCRIPTION

NANNOFOSSIL OOZE with FORAMINIFERS

Major lithology: This core contains white (2.5Y 8/2) to light gray (2.5Y 7/2) NANNOFOSSIL OOZE with FORAMINIFERS. It is heavily bioturbated, as indicated by abundant light gray (2.5Y 7/2) mottles that typically occur in zones 25 to 35 cm thick and approximately 60 to 80 cm apart.

SMEAR SLIDE SUMMARY (%):

	2, 110 D
TEXTURE:	
Sand	5
Silt	60
Clay	35
COMPOSITION:	
Accessory minerals	3
Diatoms	1
Foraminifers	15
Nannofossils	72
Radiolarians	3
Siliceous fragments	3
Silicoflagellates	3

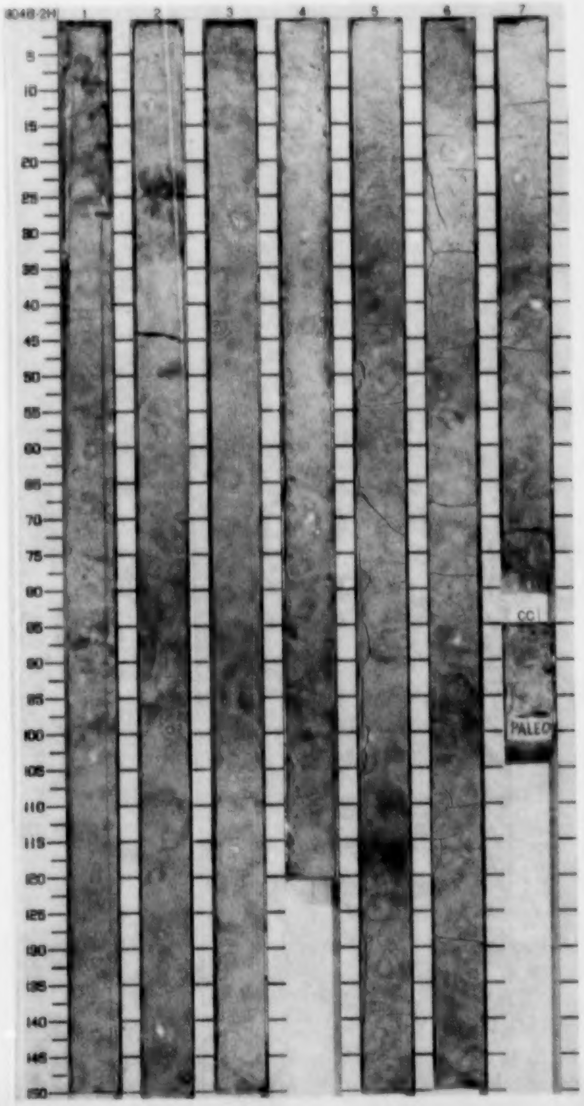
804B-2H
1
2
3
4
5
6
7
CC
PALEO
5
10
15
20
25
30
35
40
45
50
55
60
65
70
75
80
85
90
95
100
105
110
115
120
125
130
135
140
145
150

SITE 804 HOLE B CORE 3H CORED INTERVAL 14.2-23.7 mbsf

TIME-ROCK UNIT	BIOSTRAT. ZONE/ FOSSIL CHARACTER: FORAMINIFERS	NANNOFOSSILS	RADIOLARIANS	DIATOMS	PALEOMAGNETICS	PHYS. PROPERTIES	CHEMISTRY	SECTION	METERS
PLIESTOCENE					?	V=1531 φ=67.7 γ=1.55		1	0.5 1.0
					R (Matuyama)	V=1525 φ=70.4 γ=1.51		2	
UPPER PLIOCENE	N22 (basal) *Globorotalia truncatulinoides*	NN18			N (Olduvai, ANOMALY 2)	V=1535 φ=66.0 γ=1.55		3	
					R (Matuyama)	V=1542 φ=69.0 γ=1.53		4	
					N (Reunion) R (Matuyama)	V=1534 φ=66.6 γ=1.53		5	
					R (Matuyama)	V=1528 φ=66.8 γ=1.56		6	
	A/P	A/M			N?	V=1538 φ=65.7 γ=1.57		7	
								CC	

GRAPHIC LITHOLOGY

DRILLING DISTURB.

SED. STRUCTURES

SAMPLES

IW

LITHOLOGIC DESCRIPTION

NANNOFOSSIL OOZE with FORAMINIFERS

Major lithology: This core contains NANNOFOSSIL OOZE with FORAMINIFERS. It is heavily bioturbated, as indicated by abundant mottles. Between Section 1 and Section 4, 85 cm, the sediment is dominantly white (2.5Y 8/2) to light gray (2.5Y 7/2) and exhibits some banding. From Section 4, 85 cm, to the base, 10 to 20 cm thick color bands alternate between white (5Y 8/1) and light gray (5Y 7/1). Within these bands, 2 to 5 mm thick pale yellowish green (10GY 7/2) and light gray (7.5YR 7/0) bands are common every 2 to 5 cm.

SMEAR SLIDE SUMMARY (%):

	4, 90	4, 130	7, 60
	D	D	D
TEXTURE:			
Sand	—	10	7
Silt	60	55	60
Clay	40	35	33
COMPOSITION:			
Accessory minerals	Tr	Tr	2
Diatoms	—	—	1
Foraminifers	5	25	25
Nannofossils	90	75	68
Radiolarians	Tr	Tr	1
Siliceous fragments	—	—	2

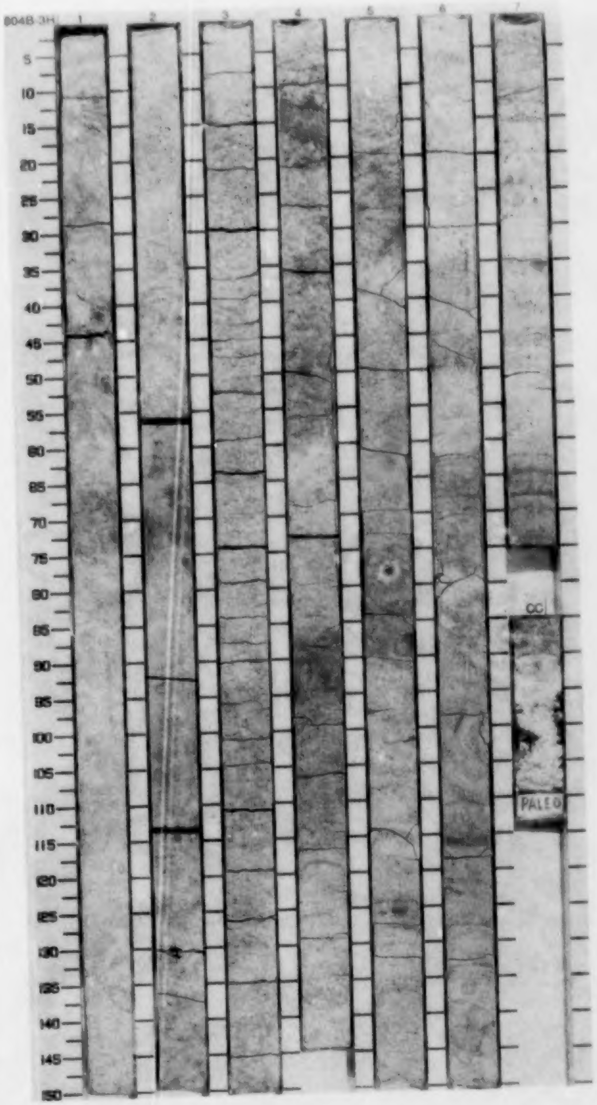

SITE 804 HOLE B CORE 4H CORED INTERVAL 23.7-33.2 mbsf

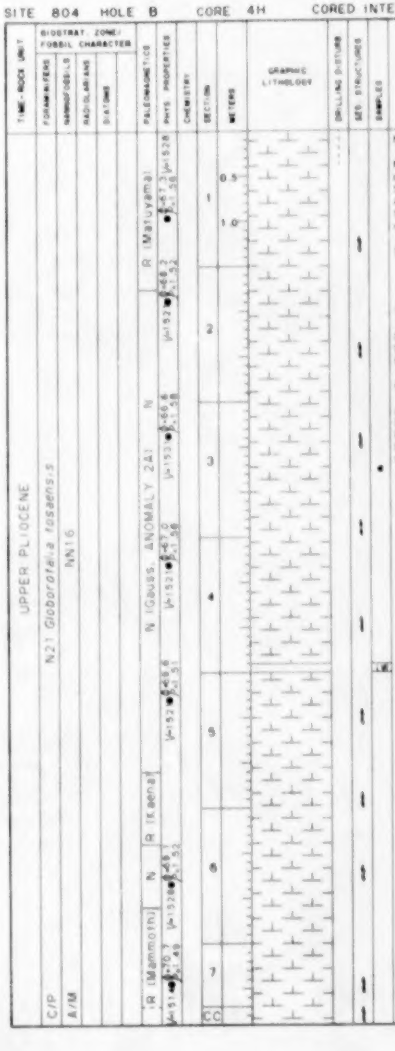
TIME-ROCK UNIT
BIOSTRAT. ZONE/ FOSSIL CHARACTER
FORAMINIFERS
NANNOFOSSILS
RADIOLARIANS
DIATOMS
PALEOMAGNETICS
PHYS. PROPERTIES
CHEMISTRY
SECTION
METERS
GRAPHIC LITHOLOGY
DRILLING DISTURB.
SED. STRUCTURES
SAMPLES
UPPER PLIOCENE
N21 Globorotalia tosaensis
C/P
NN16
A/M
R (Matuyama)
N (Gauss, ANOMALY 2A)
N
R (Kaena)
N
R (Mammoth)
0.5
1.0
1
2
3
4
5
6
7
CC

LITHOLOGIC DESCRIPTION

NANNOFOSSIL OOZE with FORAMINIFERS

Major lithology: This core consists of NANNOFOSSIL OOZE with FORAMINIFERS. The dominant color is white (5Y 8/1), with light gray (5Y 7/1), cm thick intervals 60 to 80 cm apart. In Sections 1 and 4, sharp color contacts between gray (2.5Y 6/0) and white (5Y 8/1) are noted. Also in Section 4, a few pale yellowish green (10GY 7/2) mm to cm thick bands are observed. Slight bioturbation is indicated by mottles, and burrows are filled with softer or pyritized material.

SMEAR SLIDE SUMMARY (%):

	3, 75
	D
TEXTURE:	
Sand	10
Silt	55
Clay	35
COMPOSITION:	
Accessory minerals	Tr
Diatoms	Tr
Foraminifers	15
Nannofossils	85
Radiolarians	Tr

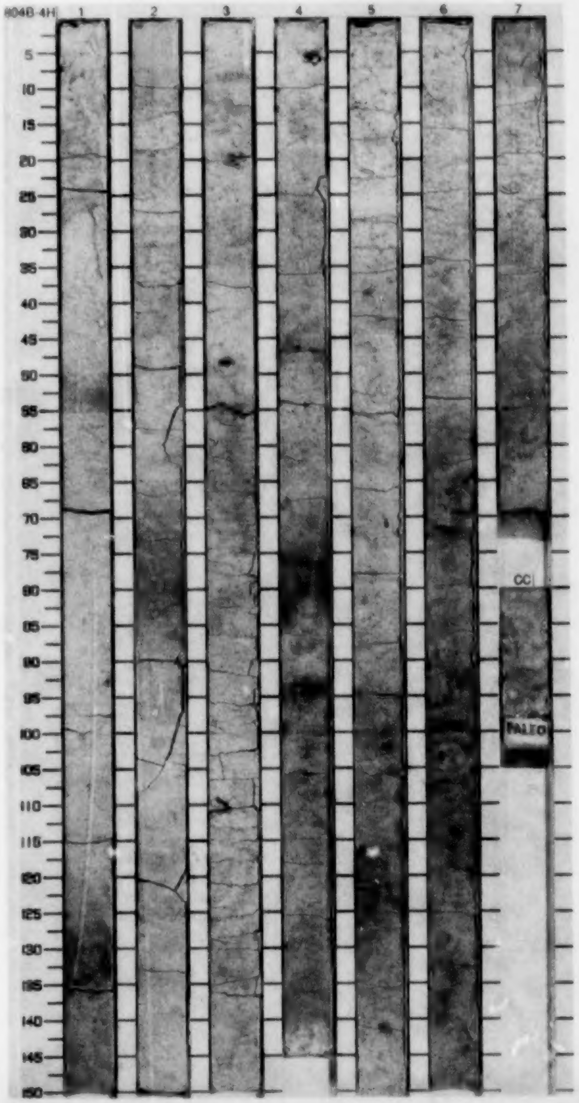
804B-4H
1
2
3
4
5
6
7
5
10
15
20
25
30
35
40
45
50
55
60
65
70
75
80
85
90
95
100
105
110
115
120
125
130
135
140
145
150
CC
PALEO

SITE 804 HOLE B CORE 5H CORED INTERVAL 33.2-42.7 mbsf

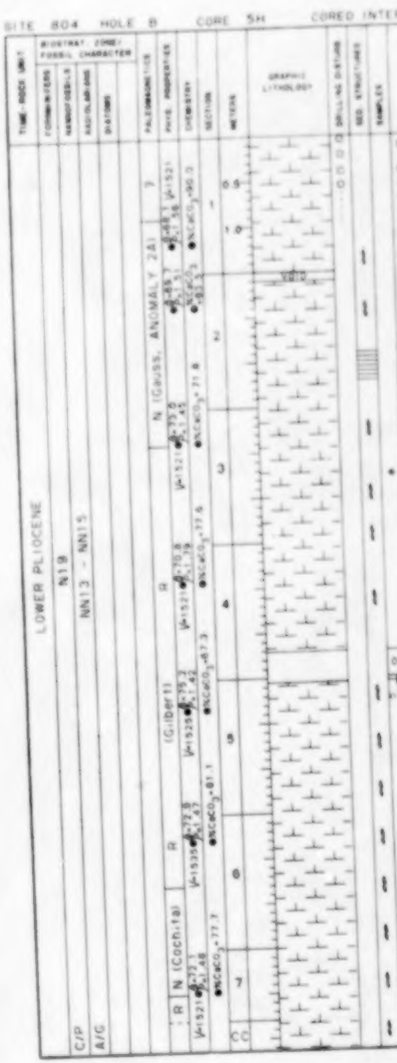
TIME-ROCK UNIT
BIOSTRAT. ZONE/FOSSIL CHARACTER
FORAMINIFERS
NANNOFOSSILS
RADIOLARIANS
DIATOMS
PALEOMAGNETICS
PHYS. PROPERTIES
CHEMISTRY
SECTION
METERS
GRAPHIC LITHOLOGY
DRILLING DISTURB.
SED. STRUCTURES
SAMPLES
LOWER PLIOCENE
N19
NN13 - NN15
C/P
A/G
?
N (Gauss, ANOMALY 2A)
R
(Gilbert)
R
N (Cochiti)
R
γ=1521
γ=1521
γ=1521
γ=1521
γ=1535
γ=1535
γ=1521
φ=72.1
φ=72.8
φ=75.2
φ=70.8
φ=73.6
φ=66.7
φ=68.1
ρ=1.48
ρ=1.47
ρ=1.42
ρ=1.39
ρ=1.45
ρ=1.51
ρ=1.56
●%CaCO$_3$=77.7
●%CaCO$_3$=81.1
●%CaCO$_3$=87.3
●%CaCO$_3$=77.6
●%CaCO$_3$=71.8
●%CaCO$_3$=93.3
●%CaCO$_3$=90.0
1
2
3
4
5
6
7
CC
0.5
1.0
OG

LITHOLOGIC DESCRIPTION

NANNOFOSSIL OOZE with FORAMINIFERS

Major lithology: This core contains NANNOFOSSIL OOZE with FORAMINIFERS. Sections 1, 2 and 6 are mainly white (5Y 8/1), with intervals (up to 70 cm thick) of light gray (5Y 7/1). Sections 3, 4, 5 and 7 are predominantly light gray (5Y 7/1), with intervals of white and gray up to 50 cm thick. Seven very pale green (10GY 7/2) color bands (about 1 cm thick) are present in Section 2, 97-117 cm. The sediment is slightly bioturbated as indicated by mottles and a few pyritized burrow fills.

SMEAR SLIDE SUMMARY (%):

	3, 74
	D
TEXTURE:	
Sand	5
Silt	60
Clay	35
COMPOSITION:	
Accessory minerals	1
Diatoms	2
Foraminifers	20
Nannofossils	75
Radiolarians	1
Spicules	1

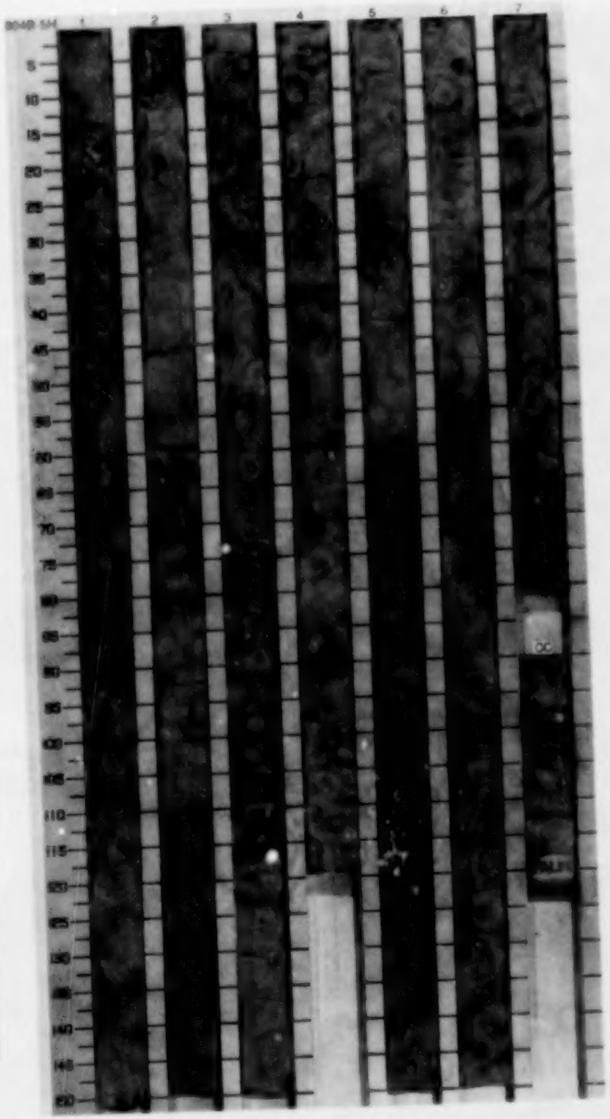
804B 5H
1
2
3
4
5
6
7
5
10
15
20
25
30
35
40
45
50
55
60
65
70
75
80
85
90
95
100
105
110
115
120
125
130
135
140
145
150
CC

SITE 804 HOLE B CORE 6H CORED INTERVAL 42.7-52.2 mbsf

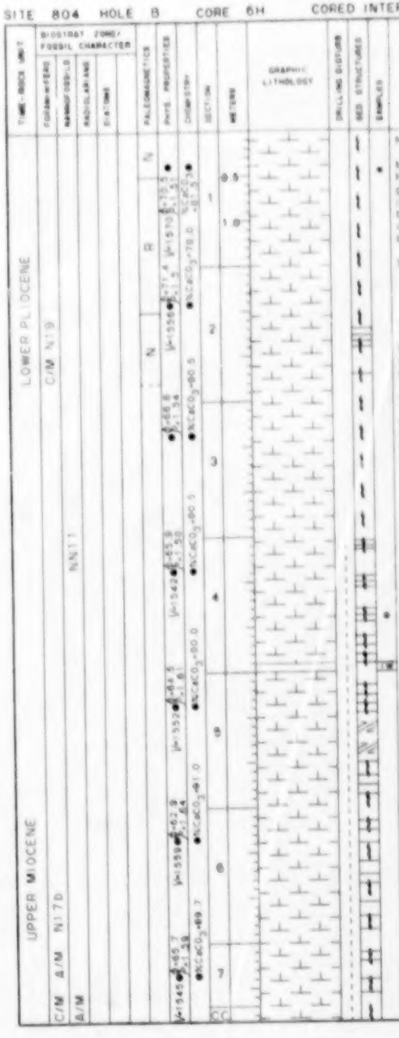
TIME-ROCK UNIT
BIOSTRAT. ZONE/ FOSSIL CHARACTER
FORAMINIFERS
NANNOFOSSILS
RADIOLARIANS
DIATOMS
PALEOMAGNETICS
PHYS. PROPERTIES
CHEMISTRY
SECTION
METERS
GRAPHIC LITHOLOGY
DRILLING DISTURB.
SED. STRUCTURES
SAMPLES
LOWER PLIOCENE
UPPER MIOCENE
C/M N19
C/M A/M N17D
A/M
NN11
N
R
N
0.5
1.0
1
2
3
4
5
6
7
CC
v=1570
v=1556
φ=71.4
φ=68.8 ρ=1.54
%CaCO3=78.0
%CaCO3=80.5
v=1542
φ=65.9 ρ=1.50
%CaCO3=80.9
v=1552
φ=64.5 ρ=1.61
%CaCO3=80.0
v=1559
φ=62.9 ρ=1.64
%CaCO3=81.0
v=1545
φ=65.7 ρ=1.58
%CaCO3=89.7

LITHOLOGIC DESCRIPTION

NANNOFOSSIL OOZE with RADIOLARIANS and NANNOFOSSIL OOZE

Major lithology: This core contains NANNOFOSSIL OOZE with RADIOLARIANS, grading to NANNOFOSSIL OOZE below Section 1. Section 1 is light gray (2.5Y 7/1) and gray (2.5Y 6/1), grading to light gray (7.5YR 7/0) below 128 cm. Colors in Section 2 grade from light gray (7.5YR 7/0) to white (7.5YR N8) downsection. White (7.5YR N8 and 2.5Y 8/0) dominates below Section 2. Faint light greenish gray (5G 7/1) and light gray (N7) color banding is common to abundant in Sections 2 through 7. The entire core is slightly to moderately bioturbated.

SMEAR SLIDE SUMMARY (%):

	1, 44	4, 89
	D	D
TEXTURE:		
Sand	3	1
Silt	90	95
Clay	7	4
COMPOSITION:		
Diatoms	1	Tr
Foraminifers	1	3
Nannofossils	87	95
Radiolarians	10	2
Spicules	1	Tr

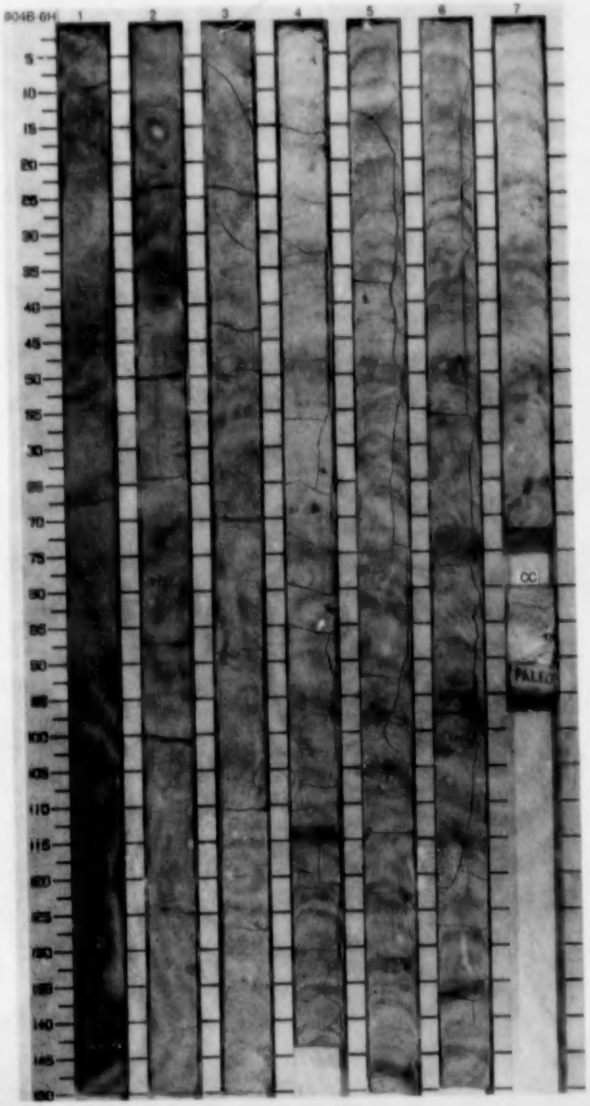
804B-6H
1
2
3
4
5
6
7
5
10
15
20
25
30
35
40
45
50
55
60
65
70
75
80
85
90
95
100
105
110
115
120
125
130
135
140
145
150
CC
PALEO

SITE 804 HOLE B CORE 7H CORED INTERVAL 52.2-61.7 mbsf

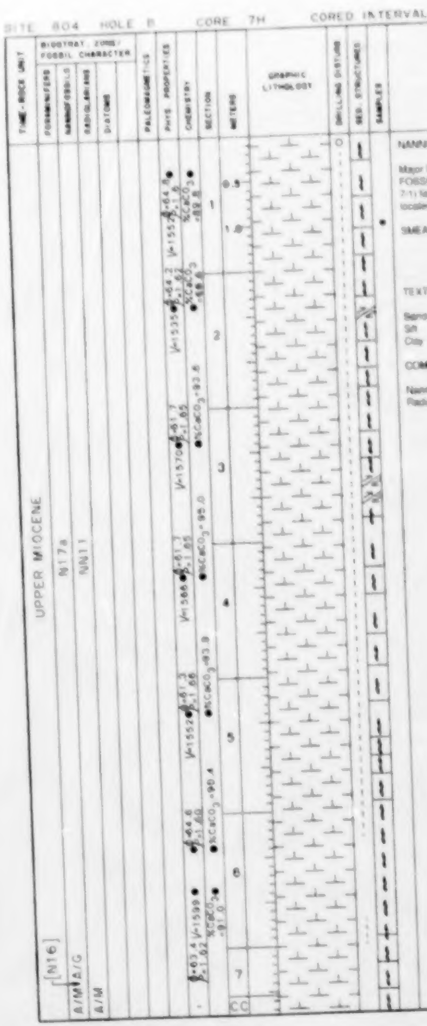

LITHOLOGIC DESCRIPTION

NANNOFOSSIL OOZE

Major lithology: This core contains slightly to heavily bioturbated, white (2.5Y 8/0) NANNOFOSSIL OOZE. Numerous reddish gray (5R 6/1), light gray (N7) and light greenish gray (5G 7/1) faint color bands and mottles are present throughout. Centimeter scale microfaults are located in Section 1, 20-30 cm, Section 2, 40-50 cm and Section 3, 80-107 cm.

SMEAR SLIDE SUMMARY (%):

	1, 100
	D
TEXTURE:	
Sand	5
Silt	90
Clay	5
COMPOSITION:	
Nannofossils	97
Radiolarians	3

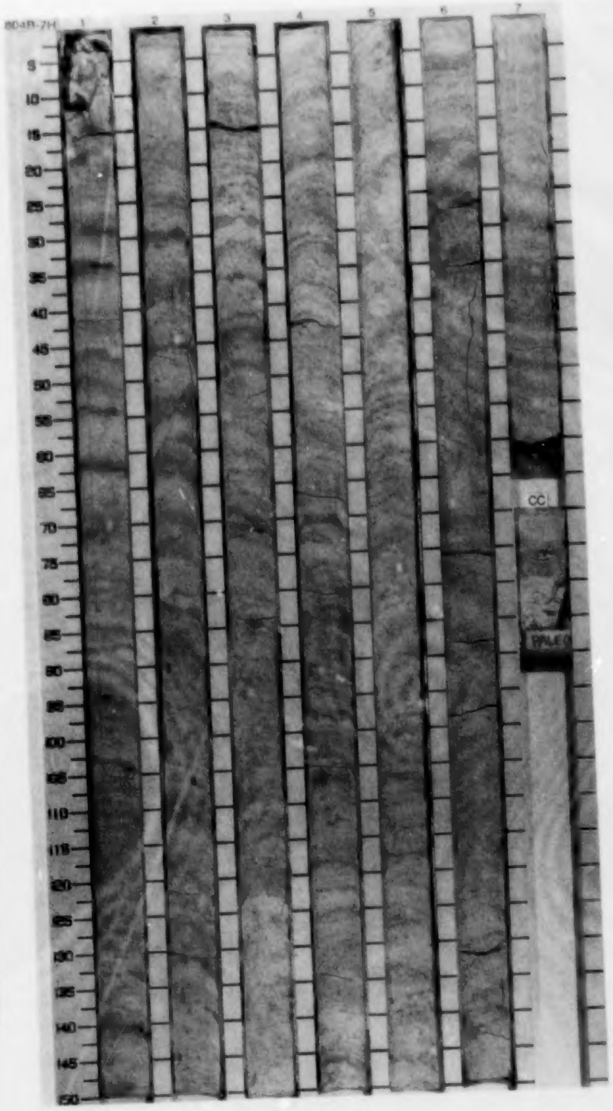
804B-7H
1
2
3
4
5
6
7
CC
PALEO
5
10
15
20
25
30
35
40
45
50
55
60
65
70
75
80
85
90
95
100
105
110
115
120
125
130
135
140
145
150

SITE 804 HOLE B CORE 8H CORED INTERVAL 61.7-71.2 mbsf

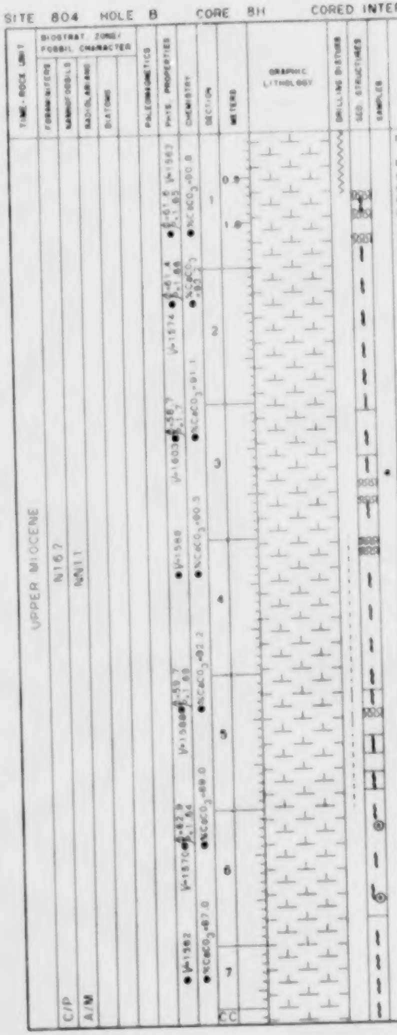
TIME-ROCK UNIT
BIOSTRAT. ZONE/ FOSSIL CHARACTER
FORAMINIFERS
NANNOFOSSILS
RADIOLARIANS
DIATOMS
PALEOMAGNETICS
PHYS. PROPERTIES
CHEMISTRY
SECTION
METERS
GRAPHIC LITHOLOGY
DRILLING DISTURB.
SED. STRUCTURES
SAMPLES
UPPER MIOCENE
N16?
NN11
C/P
A/M
φ=61.6 γ=1.65
V=1562
%CaCO₃=90.8
φ=61.4 γ=1.66
%CaCO₃=92.?
V=1574
%CaCO₃=91.1
φ=58.7 γ=1.7
V=1603
%CaCO₃=90.5
V=1588
φ=59.7 γ=1.68
V=1588
%CaCO₃=92.2
φ=62.9 γ=1.64
V=1570
%CaCO₃=89.0
V=1562
%CaCO₃=87.0
1
2
3
4
5
6
7
CC
0.5
1.0

LITHOLOGIC DESCRIPTION

NANNOFOSSIL OOZE

Major lithology: This core contains NANNOFOSSIL OOZE. The core is white (2.5Y 8/0) and slightly to moderately bioturbated throughout, with abundant light gray (N7; and 5Y 7/1) mottling in Sections 1-4. Sections 5 through CC have a more homogeneous appearance. Color banding is contorted in the following intervals: section 1, 80-115 cm; Section 3, 90-115 cm; Section 4, 0-20 cm; Section 5, 25-44 cm.

SMEAR SLIDE SUMMARY (%):

	3, 80
	D
TEXTURE	
Sand	5
Silt	90
Clay	5
COMPOSITION	
Foraminifers	3
Nannofossils	95
Radiolarians	2

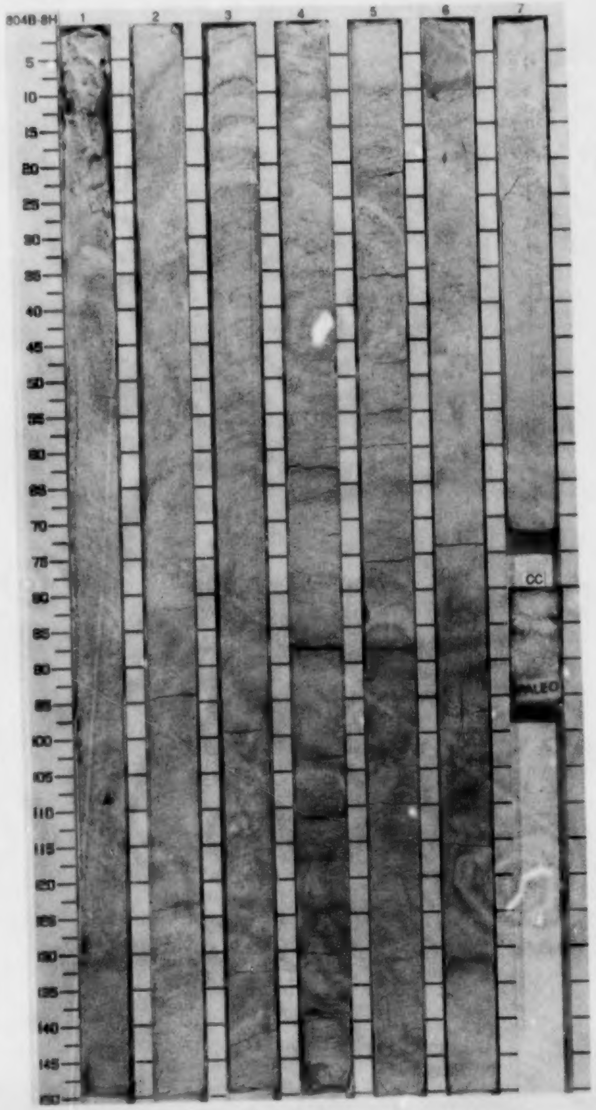
804B-8H
1
2
3
4
5
6
7
CC
PALEO
5
10
15
20
25
30
35
40
45
50
55
60
65
70
75
80
85
90
95
100
105
110
115
120
125
130
135
140
145
150

SITE 804 HOLE B CORE 9H CORED INTERVAL 71.2-80.7 mbsf

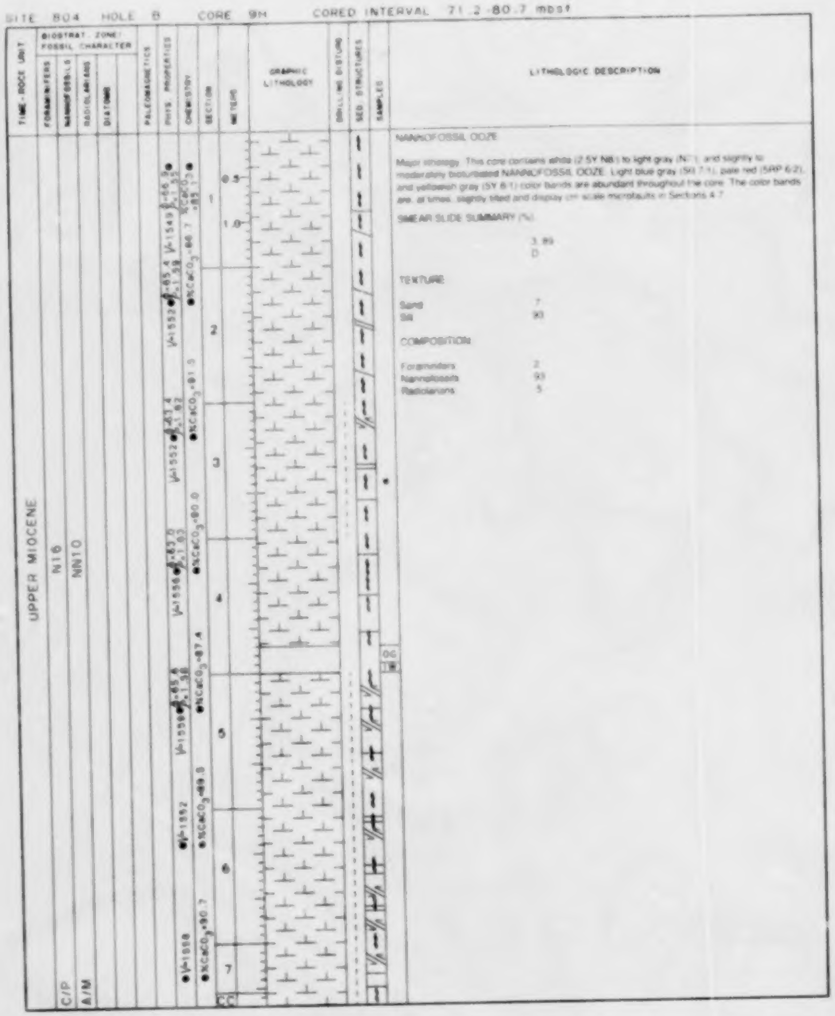
TIME-ROCK UNIT
BIOSTRAT. ZONE/ FOSSIL CHARACTER
FORAMINIFERS
NANNOFOSSILS
RADIOLARIANS
DIATOMS
PALEOMAGNETICS
PHYS. PROPERTIES
CHEMISTRY
SECTION
METERS
GRAPHIC LITHOLOGY
DRILLING DISTURB.
SED. STRUCTURES
SAMPLES
UPPER MIOCENE
N16
NN10
C/P
A/M
V=1549 φ=66.9 γ=1.55
V=1552 φ=65.4 γ=1.58
V=1552 φ=61.4 γ=1.62
V=1556 φ=63.0 γ=1.63
V=1556 φ=65.6 γ=1.58
V=1552
V=1558
%CaCO3=85.1
%CaCO3=86.7
%CaCO3=81.5
%CaCO3=80.0
%CaCO3=87.4
%CaCO3=89.8
%CaCO3=90.7
1
2
3
4
5
6
7
CC
0.5
1.0
OG
IW

LITHOLOGIC DESCRIPTION

NANNOFOSSIL OOZE

Major lithology: This core contains white (2.5Y N8) to light gray (N7), and slightly to moderately bioturbated NANNOFOSSIL OOZE. Light blue gray (5B 7/1), pale red (5RP 6/2), and yellowish gray (5Y 8/1) color bands are abundant throughout the core. The color bands are, at times, slightly tilted and display cm-scale microfaults in Sections 4-7.

SMEAR SLIDE SUMMARY (%):

	3, 89
	D
TEXTURE	
Sand	7
Silt	93
COMPOSITION	
Foraminifers	2
Nannofossils	93
Radiolarians	5

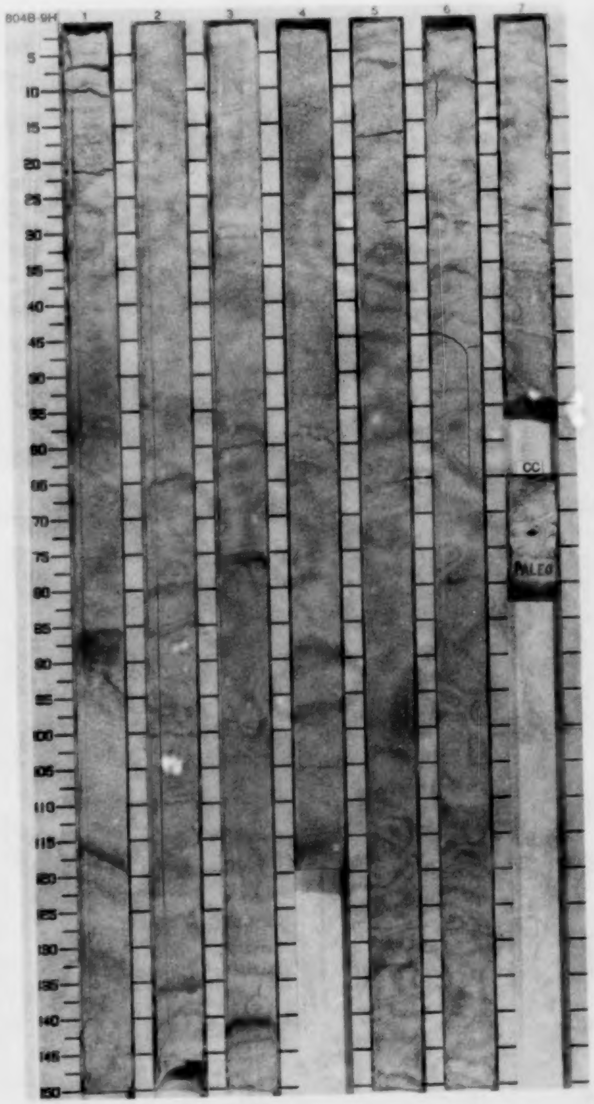
804B-9H
1
2
3
4
5
6
7
5
10
15
20
25
30
35
40
45
50
55
60
65
70
75
80
85
90
95
100
105
110
115
120
125
130
135
140
145
150
CC
PALEO

SITE 804 HOLE B CORE 10H CORED INTERVAL 80.7-90.2 mbsf

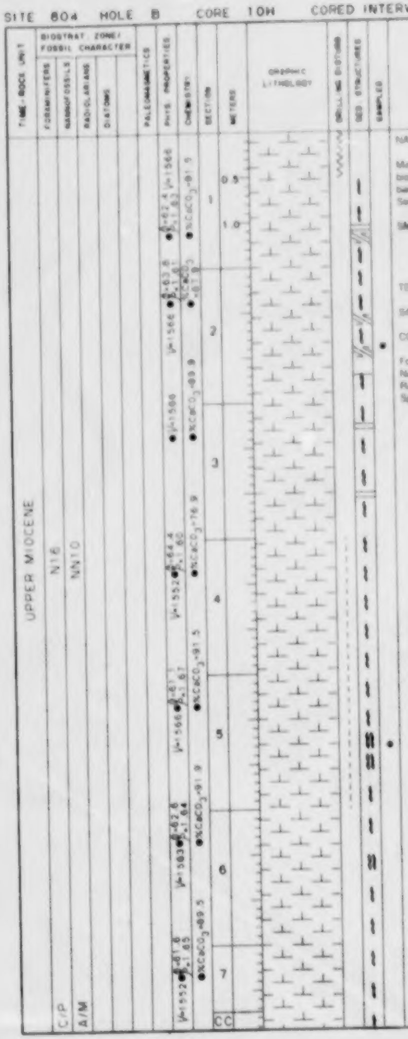
TIME-ROCK UNIT
BIOSTRAT. ZONE/ FOSSIL CHARACTER
FORAMINIFERS
NANNOFOSSILS
RADIOLARIANS
DIATOMS
PALEOMAGNETICS
PHYS. PROPERTIES
CHEMISTRY
SECTION
METERS
GRAPHIC LITHOLOGY
DRILLING DISTURB.
SED. STRUCTURES
SAMPLES
UPPER MIOCENE
N16
NN10
C/P
A/M
φ=62.4 γ=1.63 V=1566
%CaCO3=91.5
φ=63.6 γ=1.61 V=1566
%CaCO3=87.9
V=1566
%CaCO3=89.9
φ=64.4 γ=1.60 V=1552
%CaCO3=76.9
φ=61.1 γ=1.67 V=1566
%CaCO3=91.5
φ=62.6 γ=1.64 V=1563
%CaCO3=91.9
φ=61.6 γ=1.65 V=1552
%CaCO3=89.5
0.5
1.0
1
2
3
4
5
6
7
CC

LITHOLOGIC DESCRIPTION

NANNOFOSSIL OOZE

Major lithology: This core contains white (2.5Y N8) to light gray (N7), slightly to moderately bioturbated NANNOFOSSIL OOZE. Pale green (10G 6/2) and reddish gray (5R 6/1) color bands are common in Sections 3-6. Microfaulting is evident in Section 1, 110-115 cm, and Section 2, 50-110 cm.

SMEAR SLIDE SUMMARY (%):

	2, 89 D	5, 90 D
TEXTURE		
Silt	100	100
COMPOSITION		
Foraminifers	1	1
Nannofossils	95	95
Radiolarians	3	3
Spicules	1	1

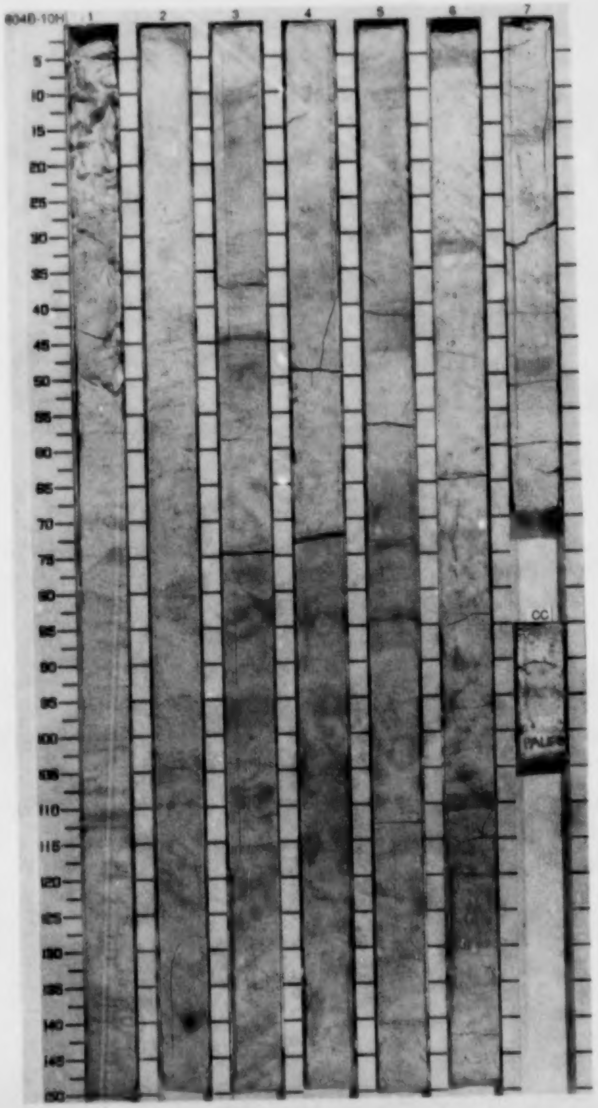
804B-10H
1
2
3
4
5
6
7
CC
PALEO
5
10
15
20
25
30
35
40
45
50
55
60
65
70
75
80
85
90
95
100
105
110
115
120
125
130
135
140
145
150

SITE 804 HOLE B CORE 11H CORED INTERVAL 90.2-99.7 mbsf

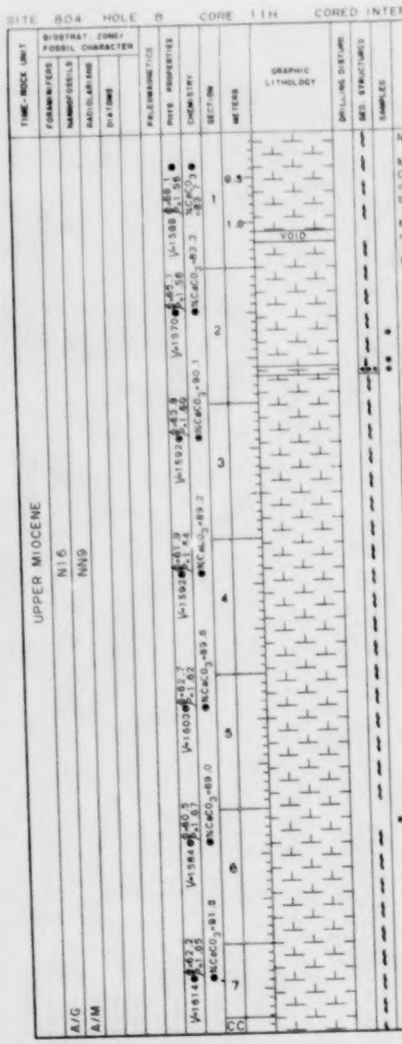
TIME-ROCK UNIT
BIOSTRAT. ZONE/ FOSSIL CHARACTER
FORAMINIFERS
NANNOFOSSILS
RADIOLARIANS
DIATOMS
PALEOMAGNETICS
PHYS. PROPERTIES
CHEMISTRY
SECTION
METERS
GRAPHIC LITHOLOGY
DRILLING DISTURB.
SED. STRUCTURES
SAMPLES
UPPER MIOCENE
N16
NN9
A/G
A/M
φ=66.1
γ=1.56
V=1588
%CaCO3=83.7
%CaCO3=83.3
V=1570
φ=65.1
γ=1.56
%CaCO3=90.1
V=1592
φ=63.9
γ=1.60
%CaCO3=89.2
V=1592
φ=61.9
γ=1.64
%CaCO3=89.8
V=1603
φ=62.7
γ=1.62
%CaCO3=89.0
V=1584
φ=60.5
γ=1.67
%CaCO3=91.8
V=1614
φ=62.2
γ=1.65
1
2
3
4
5
6
7
CC
0.5
1.0
VOID

LITHOLOGIC DESCRIPTION

NANNOFOSSIL OOZE and NANNOFOSSIL OOZE with FORAMINIFERS

Major lithology: This core contains NANNOFOSSIL OOZE, which grades into NANNOFOSSIL OOZE with FORAMINIFERS in Section 2. The core is white (2.5Y N8), faintly mottled and is more uniform and less banded than the overlying cores. Broad pale blue (5PB 7/2) color bands are present in Sections 5-7.

Minor lithology: Section 2, 108-115 cm, contains NANNOFOSSIL FORAMINIFER OOZE. The interval has a sharp base and grades upward into FORAMINIFER NANNOFOSSIL OOZE.

SMEAR SLIDE SUMMARY (%)

	2, 76 D	2, 107 M	2, 115 M	6, 17 M
TEXTURE				
Sand	2	20	30	2
Silt	95	75	65	95
Clay	3	5	5	3
COMPOSITION				
Bioclast	—	10	10	Tr
Diatoms	Tr	Tr	1	Tr
Feldspar	—	—	—	1
Foraminifers	3	30	45	8
Nannofossils	90	55	35	90
Radiolarians	7	5	8	1
Spicules	Tr	Tr	1	Tr

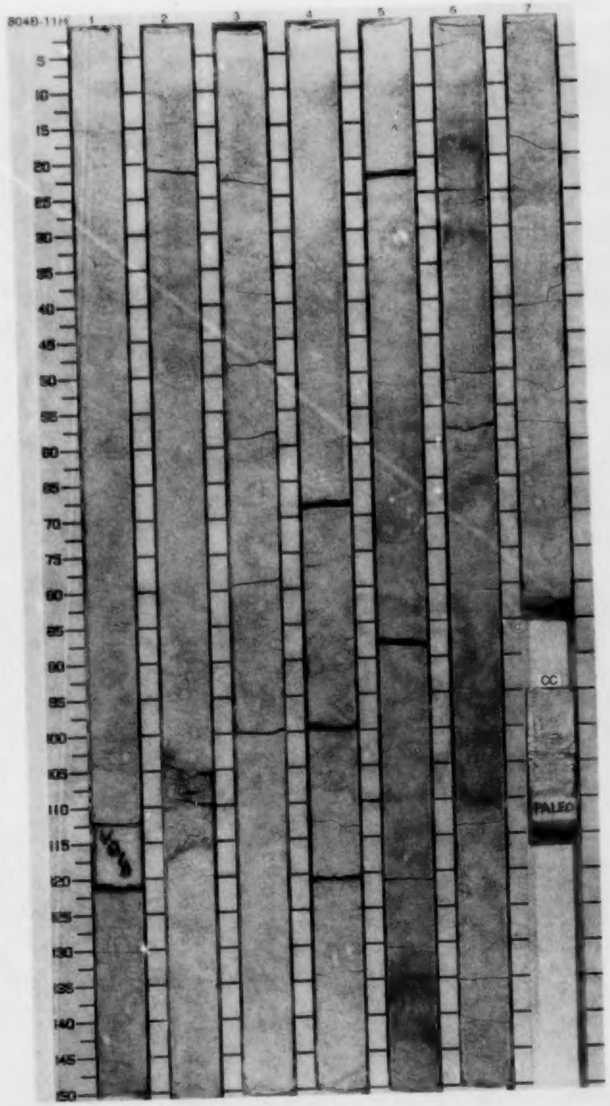
804B-11H
1
2
3
4
5
6
7
5
10
15
20
25
30
35
40
45
50
55
60
65
70
75
80
85
90
95
100
105
110
115
120
125
130
135
140
145
150
VOID
CC
PALEO

SITE 804 HOLE B CORE 12H CORED INTERVAL 99.7-109.2 mbsf

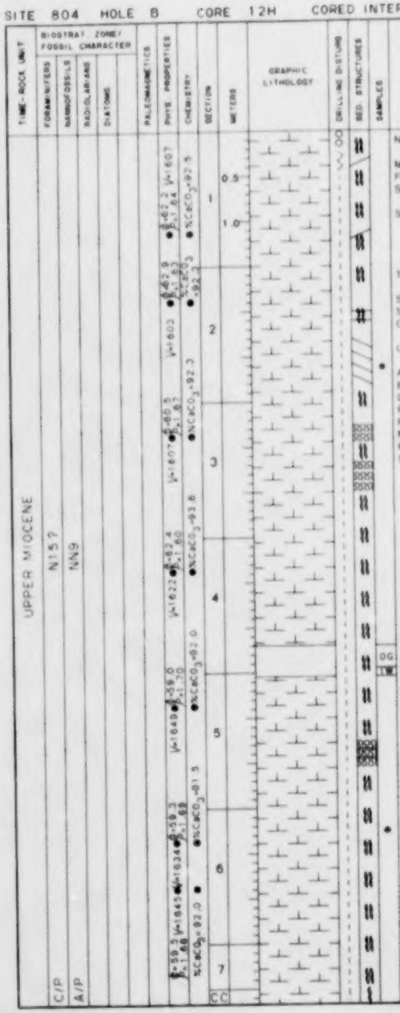
TIME-ROCK UNIT
BIOSTRAT. ZONE/FOSSIL CHARACTER
FORAMINIFERS
NANNOFOSSILS
RADIOLARIANS
DIATOMS
PALEOMAGNETICS
PHYS. PROPERTIES
CHEMISTRY
SECTION
METERS
GRAPHIC LITHOLOGY
DRILLING DISTURB.
SED. STRUCTURES
SAMPLES
UPPER MIOCENE
N15?
NN9
C/P
A/P
φ=62.2 γ=1.64 V=1607
%CaCO3=92.5
φ=62.9 γ=1.63
%CaCO3=92.3
V=1603
%CaCO3=92.3
φ=60.5 γ=1.67
V=1607
%CaCO3=93.6
φ=62.4 γ=1.60
V=1622
%CaCO3=92.0
φ=59.0 γ=1.70
V=1649
%CaCO3=91.5
φ=59.3 γ=1.69
V=1634
V=1645
%CaCO3=92.0
φ=59.5 γ=1.68
1
2
3
4
5
6
7
CC
0.5
1.0
OG
IW

LITHOLOGIC DESCRIPTION

NANNOFOSSIL OOZE

Major lithology: This core contains white (2.5Y N8/), faintly mottled, and uniform NANNOFOSSIL OOZE. Faint pale pink (5RP 8/2) and dusky blue (5BP 3/2) color bands are present in Sections 1-5.

SMEAR SLIDE SUMMARY (%):

	2, 111	6, 24
	D	D
TEXTURE:		
Sand	10	5
Silt	85	90
Clay	5	5
COMPOSITION:		
Accessory minerals	1	Tr
Bioclast	2	2
Diatoms	Tr	1
Feldspar	Tr	Tr
Foraminifers	20	3
Nannofossils	75	90
Radiolarians	2	3
Spicules	Tr	1

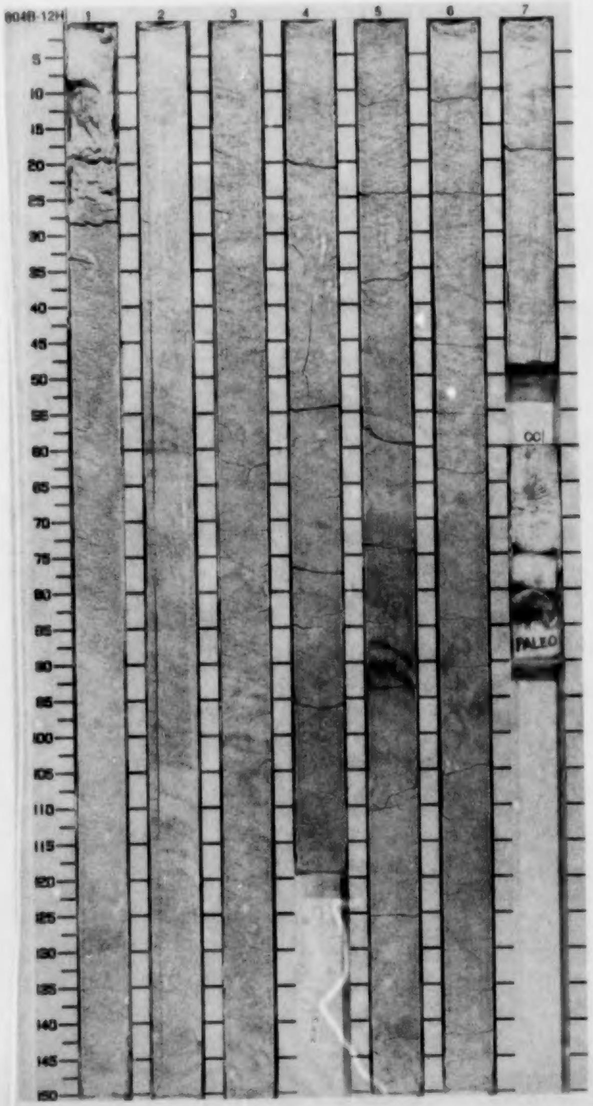
804B-12H
1
2
3
4
5
6
7
5
10
15
20
25
30
35
40
45
50
55
60
65
70
75
80
85
90
95
100
105
110
115
120
125
130
135
140
145
150
OG
PALEO

SITE 804 HOLE B CORE 13H CORED INTERVAL 109.2-118.7 mbsf

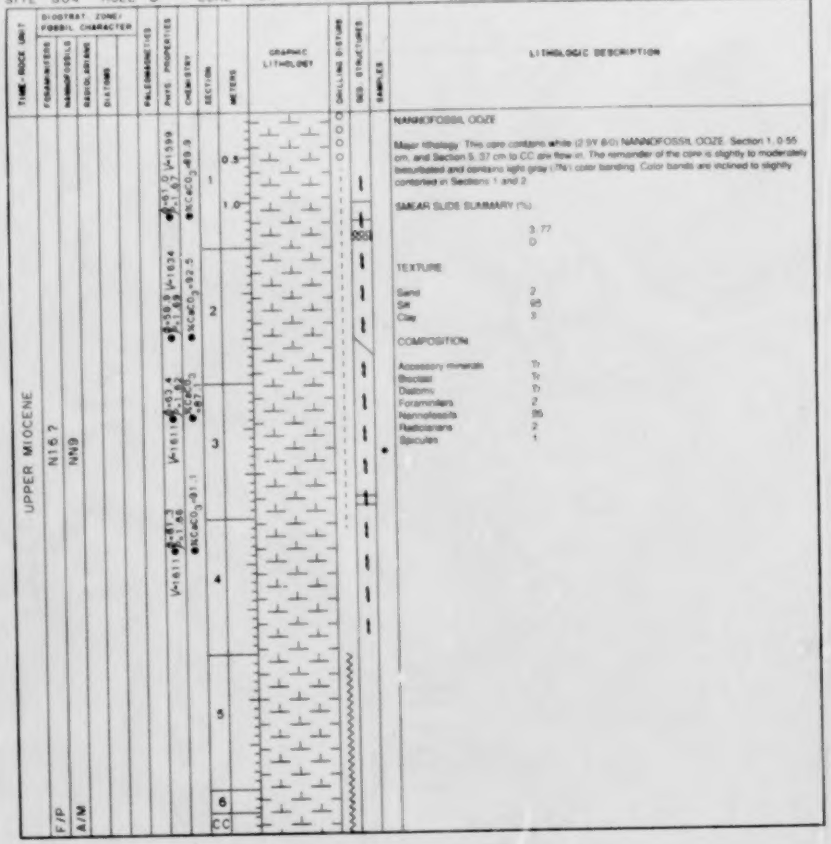
TIME-ROCK UNIT
BIOSTRAT. ZONE/ FOSSIL CHARACTER
FORAMINIFERS
NANNOFOSSILS
RADIOLARIANS
DIATOMS
PALEOMAGNETICS
PHYS. PROPERTIES
CHEMISTRY
SECTION
METERS
GRAPHIC LITHOLOGY
DRILLING DISTURB.
SED. STRUCTURES
SAMPLES
UPPER MIOCENE
N16 ?
NN9
F/P
A/M
φ=61.0 ρ=1.67 V=1599
φ=58.9 ρ=1.69 V=1634
φ=63.4 ρ=1.62 V=1611
V=1611 φ=61.3 ρ=1.66
%CaCO3=89.9
%CaCO3=92.5
%CaCO3=87.1
%CaCO3=91.1
1
2
3
4
5
6
CC
0.5
1.0

LITHOLOGIC DESCRIPTION

NANNOFOSSIL OOZE

Major lithology: This core contains white (2.5Y 8/0) NANNOFOSSIL OOZE. Section 1, 0-55 cm, and Section 5, 37 cm to CC are flow in. The remainder of the core is slightly to moderately bioturbated and contains light gray (7N) color banding. Color bands are inclined to slightly contorted in Sections 1 and 2.

SMEAR SLIDE SUMMARY (%):

	3, 77
	D
TEXTURE	
Sand	2
Silt	95
Clay	3
COMPOSITION	
Accessory minerals	Tr
Bioclast	Tr
Diatoms	Tr
Foraminifers	2
Nannofossils	95
Radiolarians	2
Spicules	1

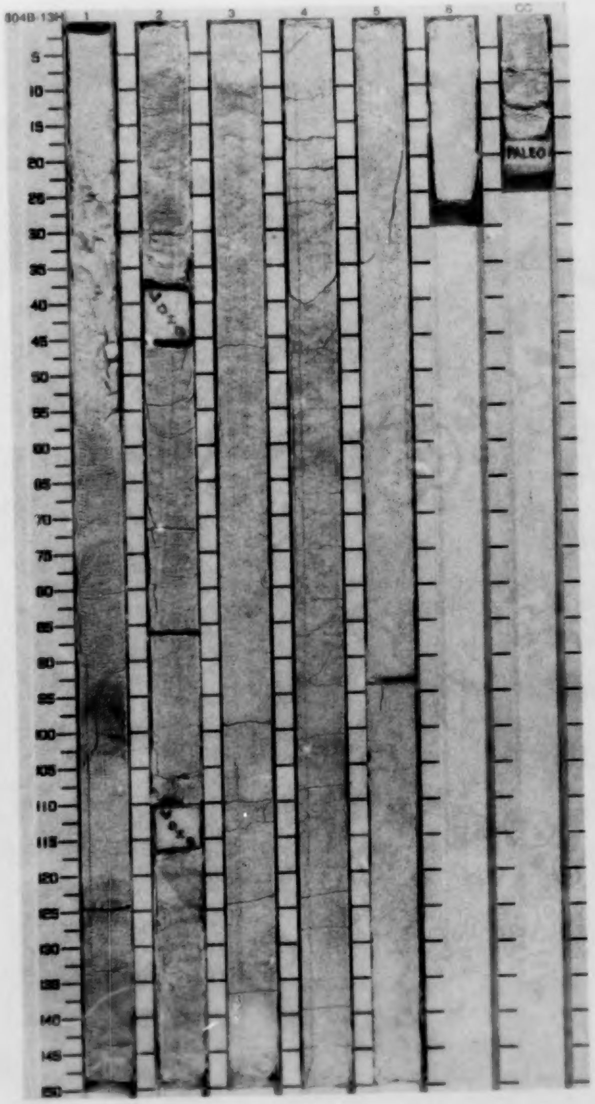
804B-13H
1
2
3
4
5
6
CC
5
10
15
20
25
30
35
40
45
50
55
60
65
70
75
80
85
90
95
100
105
110
115
120
125
130
135
140
145
150
PALEO

SITE 804 HOLE B CORE 14H CORED INTERVAL 118.7-128.2 mbsf

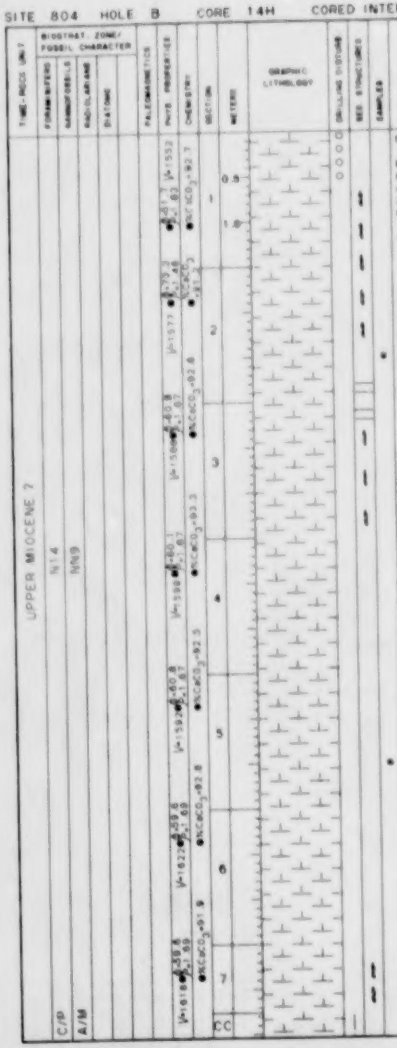
TIME-ROCK UNIT
BIOSTRAT. ZONE/ FOSSIL CHARACTER
FORAMINIFERS
NANNOFOSSILS
RADIOLARIANS
DIATOMS
PALEOMAGNETICS
PHYS. PROPERTIES
CHEMISTRY
SECTION
METERS
GRAPHIC LITHOLOGY
DRILLING DISTURB.
SED. STRUCTURES
SAMPLES
UPPER MIOCENE ?
N14
NN9
C/P
A/M
V=1552
%CaCO3=92.7
%CaCO3=91.2
V=1577
%CaCO3=92.6
V=1588
%CaCO3=93.3
V=1590
%CaCO3=92.5
V=1592
%CaCO3=92.8
V=1622
%CaCO3=91.9
V=1618
0.5
1.0
1
2
3
4
5
6
7
CC

LITHOLOGIC DESCRIPTION

NANNOFOSSIL OOZE

Major lithology: This core contains homogeneous, structureless, and dominantly white (2.5Y 8/0) NANNOFOSSIL OOZE. Two light gray (2.5Y 7/0) intervals (about 10 cm thick) are observed in Sections 2 and 3, both exhibiting sharp color contacts (except the top of Section 2). Also in Section 2, a few cm thick, light gray color bands are noted. The core is slightly bioturbated as indicated by rare pyritized burrows.

SMEAR SLIDE SUMMARY (%):

	2, 100 D	5, 100 D
TEXTURE:		
Silt	60	60
Clay	40	40
COMPOSITION:		
Foraminifers	2	2
Nannofossils	98	98
Quartz	—	Tr
Spicules	Tr	Tr

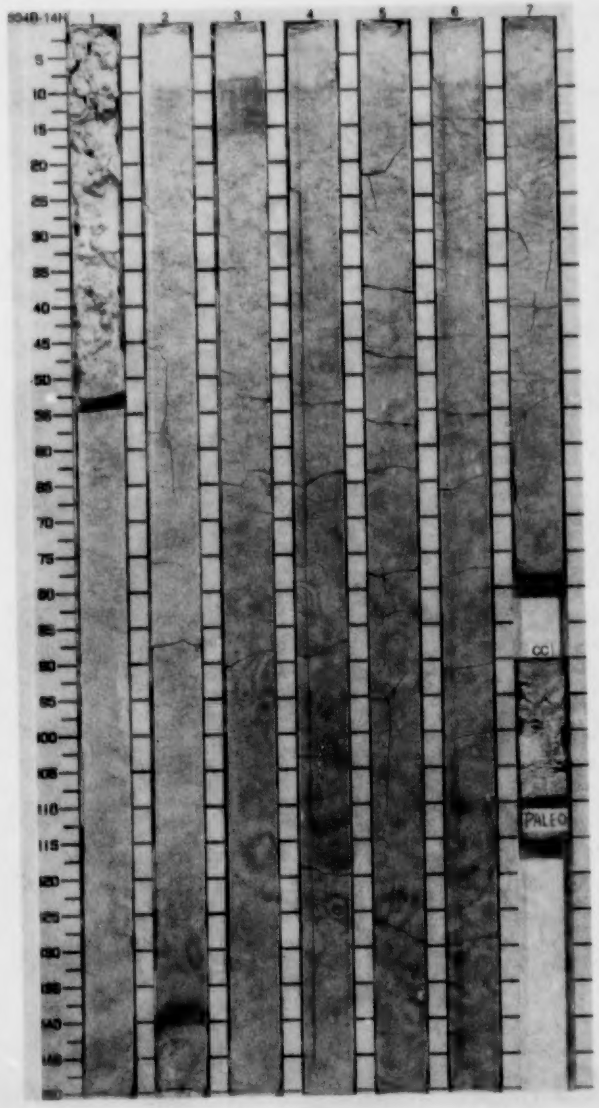
804B-14H
1
2
3
4
5
6
7
CC
PALEO
5
10
15
20
25
30
35
40
45
50
55
60
65
70
75
80
85
90
95
100
105
110
115
120
125
130
135
140
145
150

SITE 804 HOLE B CORE 15H CORED INTERVAL 128.2-137.7 mbsf

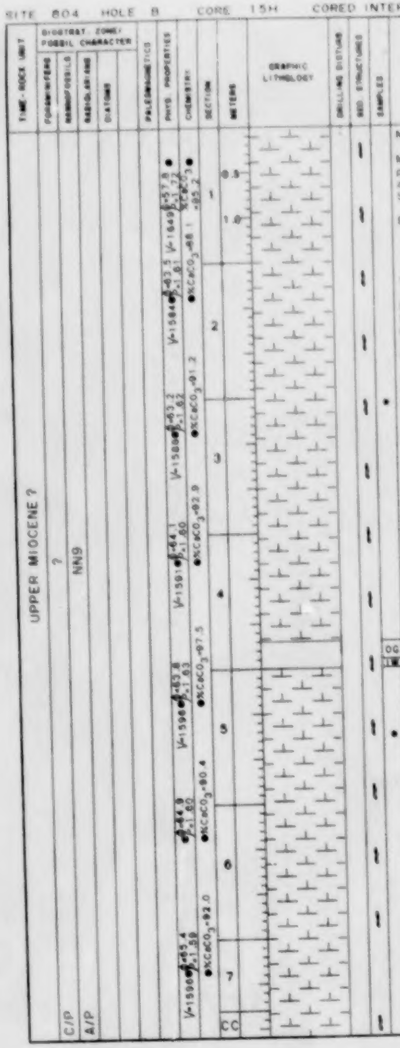

LITHOLOGIC DESCRIPTION

NANNOFOSSIL OOZE

Major lithology: This core contains homogeneous, structureless, bioturbated and predominantly light gray (2.5Y 7/0) to white (2.5Y 8/0) NANNOFOSSIL OOZE. Color changes are gradational. Rare, faint light gray (2.5Y 7/0) and gray (2.5Y 6/0) color bands are apparent in Sections 1, 3 and 6.

SMEAR SLIDE SUMMARY (%):

	3, 8	5, 74
	D	D
TEXTURE:		
Sand	5	5
Silt	65	65
Clay	30	30
COMPOSITION:		
Foraminifers	6	3
Nannofossils	93	95
Siliceous fragments	1	2

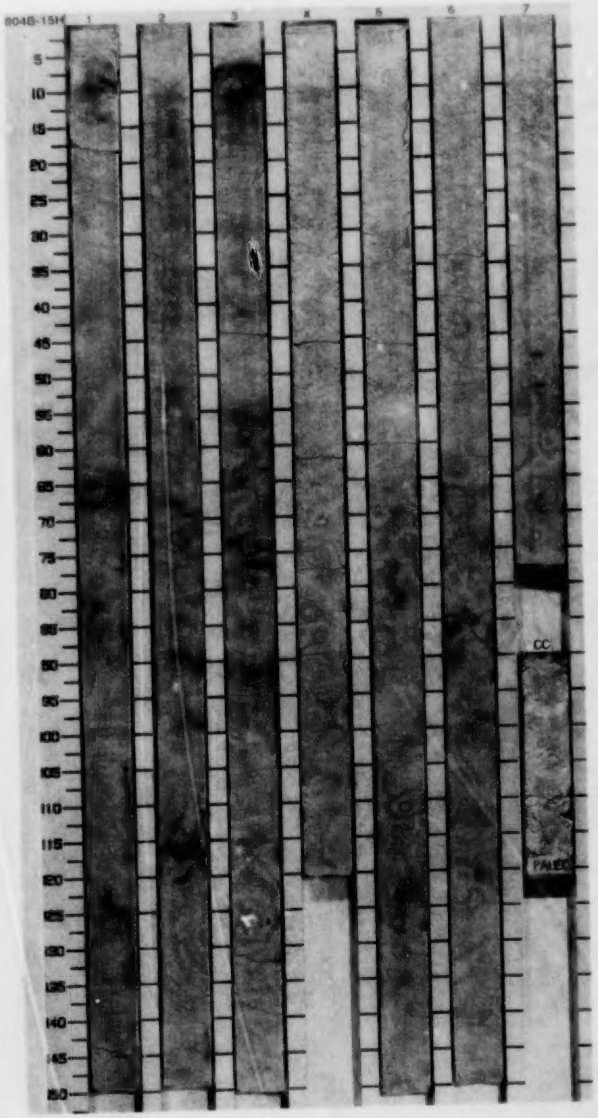
804B-15H
1
2
3
4
5
6
7
5
10
15
20
25
30
35
40
45
50
55
60
65
70
75
80
85
90
95
100
105
110
115
120
125
130
135
140
145
150
CC
PALEO

SITE 804 HOLE C CORE 1H CORED INTERVAL 0.0-6.3 mbsf

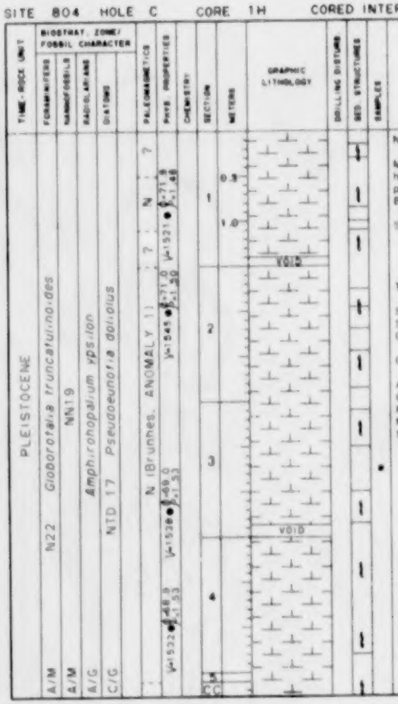
TIME-ROCK UNIT
BIOSTRAT. ZONE/ FOSSIL CHARACTER
FORAMINIFERS
NANNOFOSSILS
RADIOLARIANS
DIATOMS
PALEOMAGNETICS
PHYS. PROPERTIES
CHEMISTRY
SECTION
METERS
GRAPHIC LITHOLOGY
DRILLING DISTURB.
SED. STRUCTURES
SAMPLES
PLEISTOCENE
A/M N22 Globorotalia truncatulinoides
A/M NN19
A/G Amphirhopalum ypsilon
C/G NTD 17 Pseudoeunotia doliolus
?
N
?
N (Brunnes, ANOMALY 1)
V=1521
φ=71.9
γ=1.48
V=1545
φ=71.0
γ=1.50
V=1538
φ=69.0
γ=1.53
V=1532
φ=68.9
γ=1.53
1
2
3
4
5
CC
0.5
1.0
VOID
VOID

LITHOLOGIC DESCRIPTION

NANNOFOSSIL OOZE with FORAMINIFERS

Major lithology: This core contains NANNOFOSSIL OOZE with FORAMINIFERS. It is homogeneous, with abundant color mottling indicative of heavy bioturbation. Alternations of pale brown (10YR 6/3) and light gray (10YR 7/2) colors are present throughout the core. Bioturbation is also evident from zones of disseminated pyrite.

SMEAR SLIDE SUMMARY (%):

	3, 74 D
TEXTURE:	
Sand	3
Silt	65
Clay	32
COMPOSITION:	
Accessory minerals	5
Clay	2
Foraminifers	2
Nannofossils	87
Siliceous fragments	3

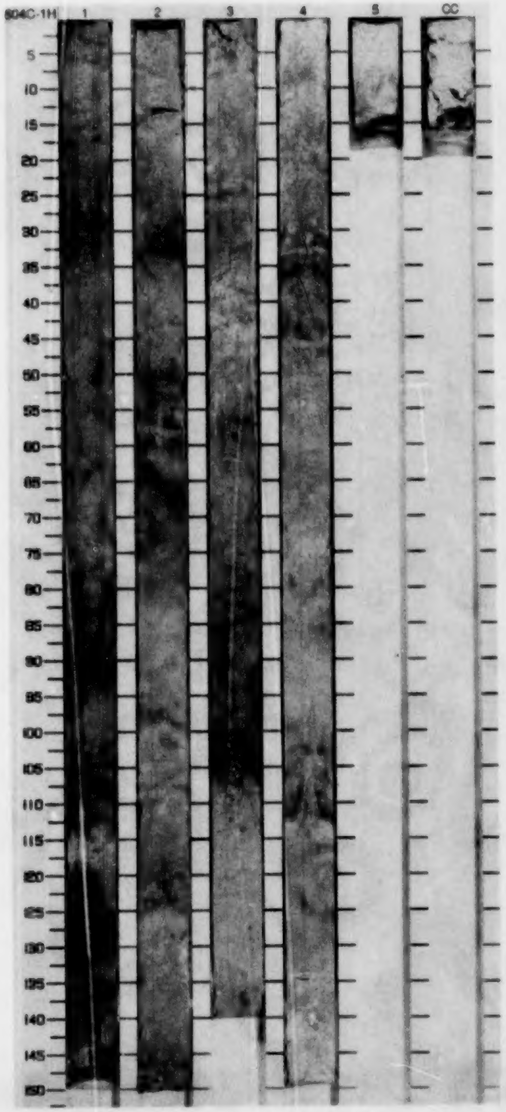
804C-1H
1
2
3
4
5
CC
5
10
15
20
25
30
35
40
45
50
55
60
65
70
75
80
85
90
95
100
105
110
115
120
125
130
135
140
145
150

SITE 804 HOLE C CORE 2H CORED INTERVAL 6.3-15.8 mbsf

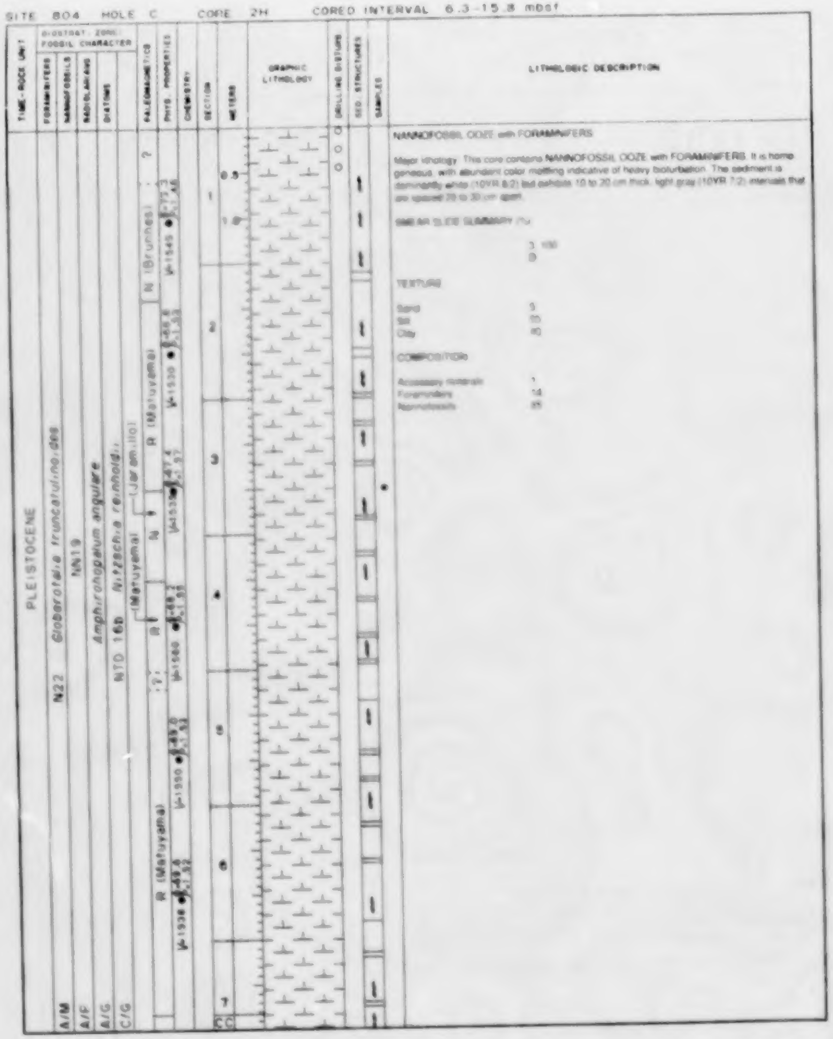
TIME-ROCK UNIT
BIOSTRAT. ZONE/FOSSIL CHARACTER
FORAMINIFERS
NANNOFOSSILS
RADIOLARIANS
DIATOMS
PALEOMAGNETICS
PHYS. PROPERTIES
CHEMISTRY
SECTION
METERS
GRAPHIC LITHOLOGY
DRILLING DISTURB.
SED. STRUCTURES
SAMPLES
LITHOLOGIC DESCRIPTION
PLEISTOCENE
A/M N22 Globorotalia truncatulinoides
A/F NN19
A/G Amphirhopalum angulare
C/G NTD 16b Nitzschia reinholdii
?
N (Brunhes)
R (Matuyama)
(Jaramillo)
(Matuyama)
N
R
R (Matuyama)
γ-1545
γ-1530
γ-1530
γ-1560
γ-1550
γ-1538
0.5
1.0
1
2
3
4
5
6
7
CC

NANNOFOSSIL OOZE with FORAMINIFERS

Major lithology: This core contains NANNOFOSSIL OOZE with FORAMINIFERS. It is homogeneous, with abundant color mottling indicative of heavy bioturbation. The sediment is dominantly white (10YR 8/2) but exhibits 10 to 20 cm thick, light gray (10YR 7/2) intervals that are spaced 20 to 30 cm apart.

SMEAR SLIDE SUMMARY (%):

	3, 100
	D
TEXTURE:	
Sand	5
Silt	35
Clay	60
COMPOSITION:	
Accessory minerals	1
Foraminifers	14
Nannofossils	85

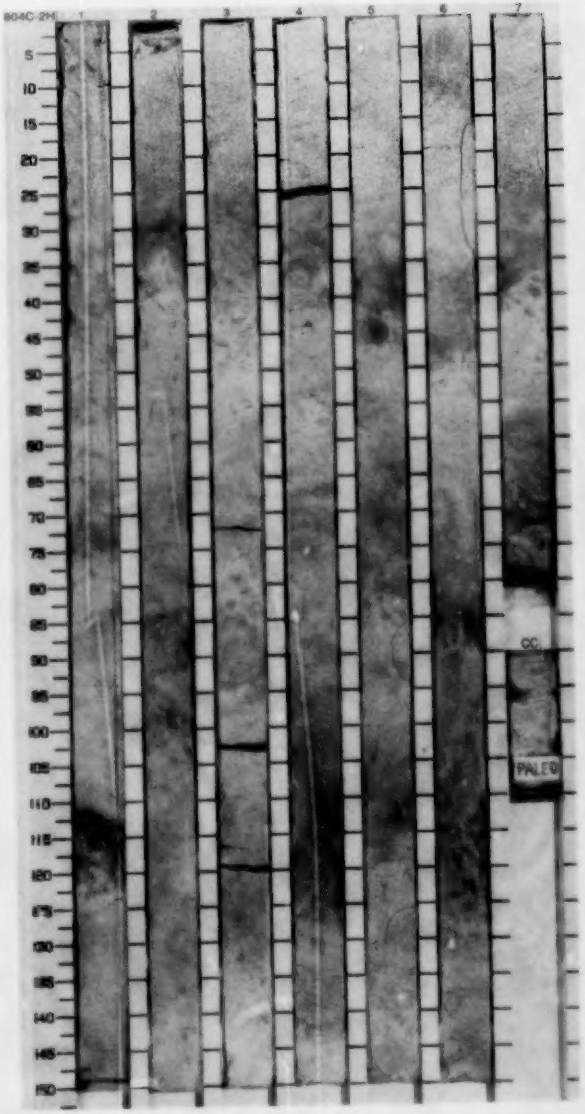
804C-2H
1
2
3
4
5
6
7
5
10
15
20
25
30
35
40
45
50
55
60
65
70
75
80
85
90
95
100
105
110
115
120
125
130
135
140
145
150
CC
PALEO

SITE 804 HOLE C CORE 3H CORED INTERVAL 15.8-25.3 mbsf

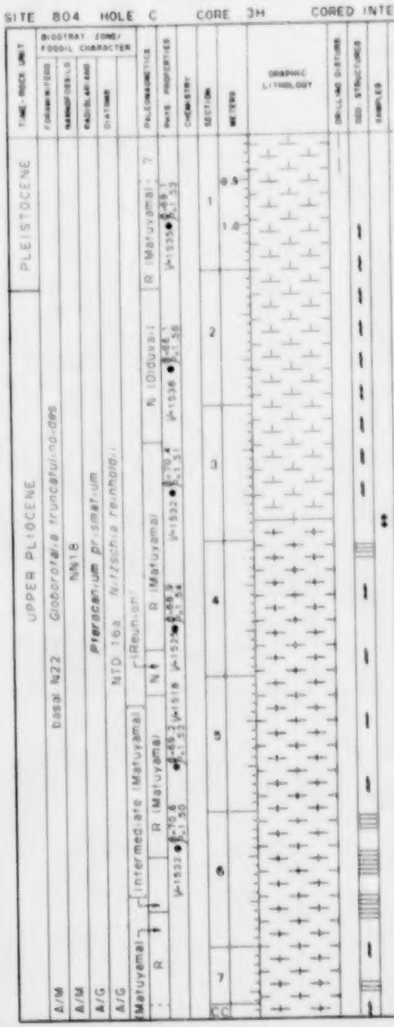
TIME-ROCK UNIT
BIOSTRAT. ZONE/ FOSSIL CHARACTER
FORAMINIFERS
NANNOFOSSILS
RADIOLARIANS
DIATOMS
PALEOMAGNETICS
PHYS. PROPERTIES
CHEMISTRY
SECTION
METERS
GRAPHIC LITHOLOGY
DRILLING DISTURB.
SED. STRUCTURES
SAMPLES
PLEISTOCENE
UPPER PLIOCENE
A/M
basal N22 Globorotalia truncatulinoides
A/M
NN18
A/G
Pterocanium prismatium
A/G
NTD 16a Nitzschia reinholdii
Matuyama
Intermediate (Matuyama)
(Reunion)
R (Matuyama) ?
N (Olduvai)
R (Matuyama)
N
R (Matuyama)
R
γ=1535 ●φ=49.1 ρb=1.53
γ=1538 ●φ=48.1 ρb=1.56
γ=1532 ●φ=70.4 ρb=1.51
γ=1529 ●φ=66.9 ρb=1.54
γ=1516
γ=1518 ●φ=66.2 ρb=1.53
γ=1532 ●φ=70.6 ρb=1.50
0.5
1.0
1
2
3
4
5
6
7
CC

LITHOLOGIC DESCRIPTION

FORAMINIFER NANNOFOSSIL OOZE and NANNOFOSSIL OOZE with FORAMINIFERS

Major lithology: Section 1 to Section 3, 129 cm, contains NANNOFOSSIL OOZE with FORAMINIFERS, which is dominantly white (10YR 8/2) and homogeneous, with abundant color mottling indicative of heavy bioturbation. Section 3, 129 cm to CC is FORAMINIFER NANNOFOSSIL OOZE, which is dominantly white (2.5Y 8/0) with 10 to 20 cm thick, light gray (2.5Y 7/0) intervals that are spaced 20 to 30 cm apart. Pale, 2 to 5 mm thick grayish green bands also are present in the light gray intervals.

SMEAR SLIDE SUMMARY (%):

	3, 127	3, 135
	D	D
TEXTURE:		
Sand	12	15
Silt	53	50
Clay	35	35
COMPOSITION:		
Foraminifers	20	30
Nannofossils	80	70

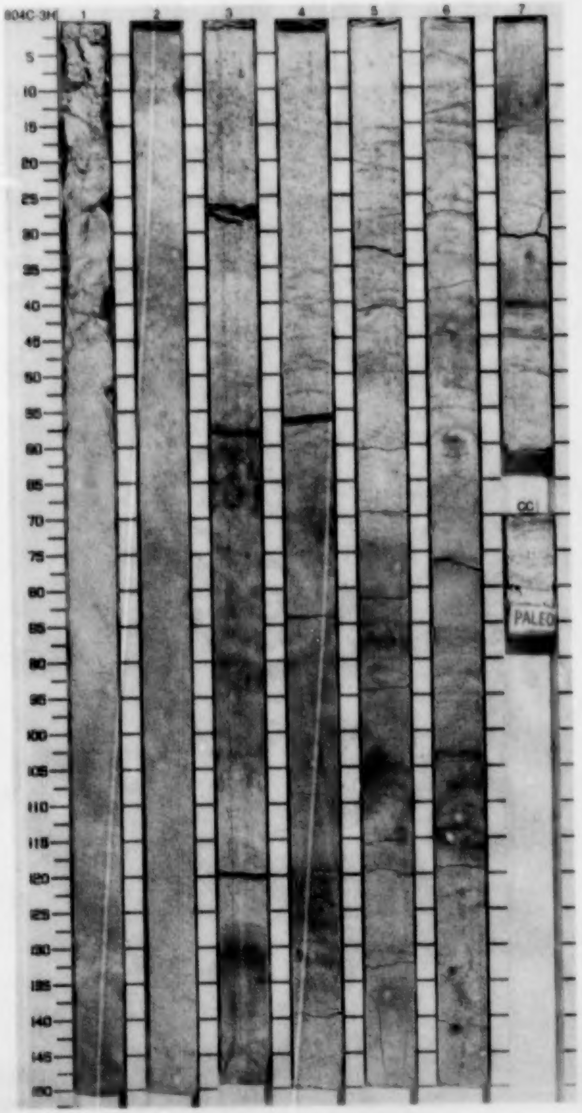
804C-3H
1
2
3
4
5
6
7
CC
PALEO
5
10
15
20
25
30
35
40
45
50
55
60
65
70
75
80
85
90
95
100
105
110
115
120
125
130
135
140
145
150

SITE 804 HOLE C CORE 4H CORED INTERVAL 25.3-34.8 mbsf

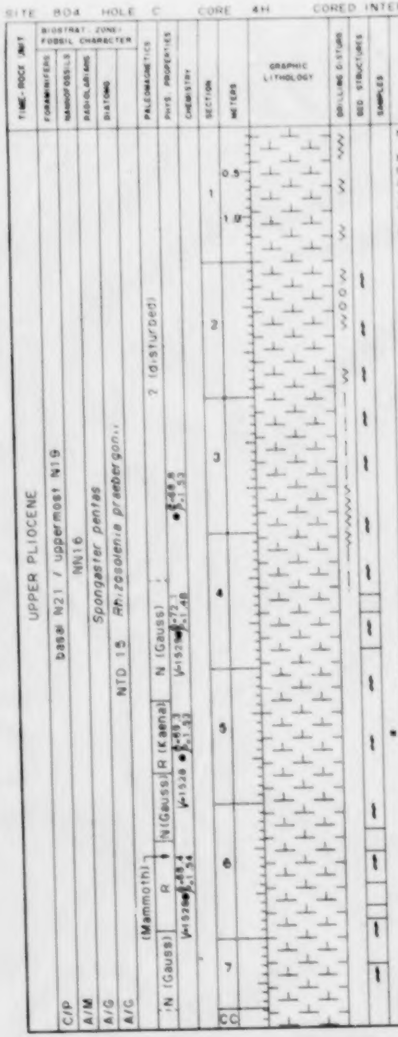
TIME-ROCK UNIT
BIOSTRAT. ZONE/ FOSSIL CHARACTER
FORAMINIFERS
NANNOFOSSILS
RADIOLARIANS
DIATOMS
PALEOMAGNETICS
PHYS. PROPERTIES
CHEMISTRY
SECTION
METERS
GRAPHIC LITHOLOGY
DRILLING DISTURB.
SED. STRUCTURES
SAMPLES
UPPER PLIOCENE
C/P
basal N21 / uppermost N19
A/M
NN16
A/G
Spongaster pentas
A/G
NTD 15 Rhizosolenia praebergonii
? (disturbed)
N (Gauss)
R (Kaena)
N(Gauss)
(Mammoth)
R
N (Gauss)
●φ=69.8 ρ=1.53
V=1528 ●φ=72.1 ρ=1.48
V=1528 ●φ=69.3 ρ=1.53
V=1528 ●φ=68.4 ρ=1.54
1
2
3
4
5
6
7
CC
0.5
1.0

LITHOLOGIC DESCRIPTION

NANNOFOSSIL OOZE with FORAMINIFERS

Major lithology: This core contains NANNOFOSSIL OOZE with FORAMINIFERS. Sections 1 through 4, 40 cm, contain flow in. The remaining sediments alternate between white (5Y 8/1) and light gray (5Y 7/1). Color contacts are gradational and color intervals are approximately of 10 to 35 cm thick and spaced about 40 cm apart. The degree of mottling and pyritized burrow infills suggests that the sediment has been moderately to heavily bioturbated.

SMEAR SLIDE SUMMARY (%):

	5, 75
	D
TEXTURE:	
Sand	10
Silt	50
Clay	40
COMPOSITION:	
Accessory minerals	2
Foraminifers	15
Nannofossils	83

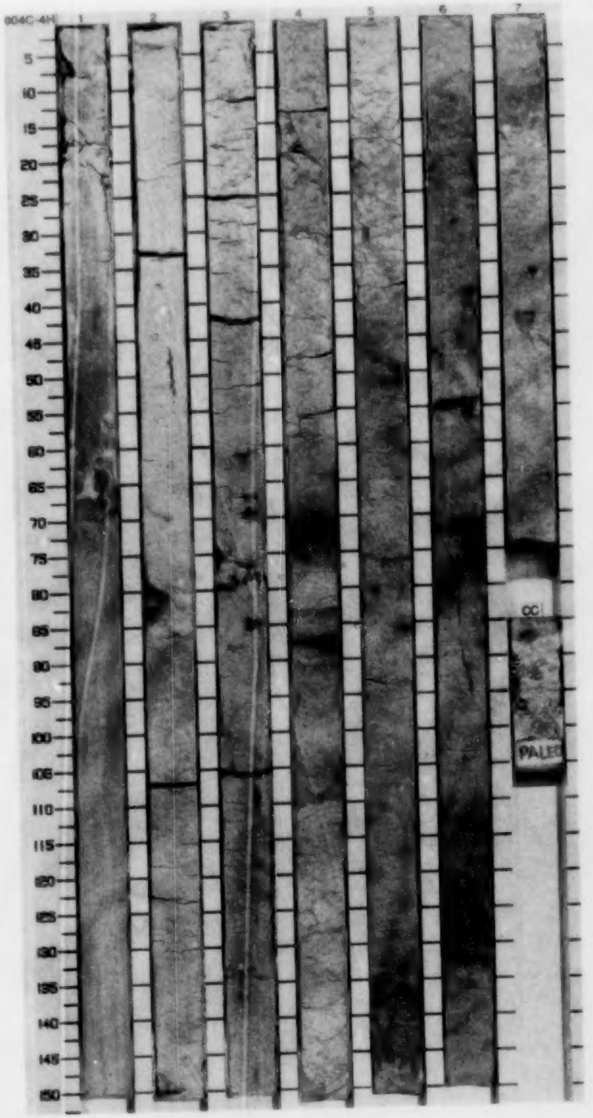
804C-4H
1
2
3
4
5
6
7
5
10
15
20
25
30
35
40
45
50
55
60
65
70
75
80
85
90
95
100
105
110
115
120
125
130
135
140
145
150
CC
PALEO

SITE 804 HOLE C CORE 5H CORED INTERVAL 34.8-44.3 mbsf

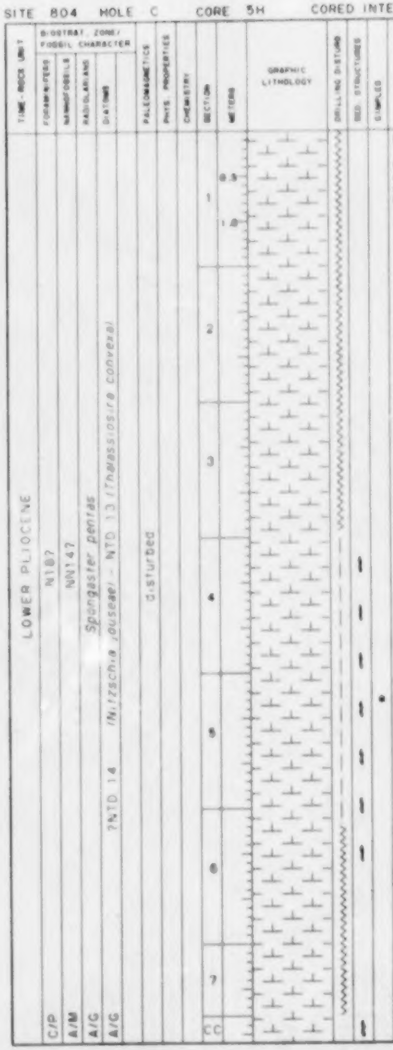
TIME-ROCK UNIT
BIOSTRAT. ZONE/ FOSSIL CHARACTER
FORAMINIFERS
NANNOFOSSILS
RADIOLARIANS
DIATOMS
PALEOMAGNETICS
PHYS. PROPERTIES
CHEMISTRY
SECTION
METERS
GRAPHIC LITHOLOGY
DRILLING DISTURB.
SED. STRUCTURES
SAMPLES
LOWER PLIOCENE
C/P N18?
A/M NN14?
A/G Spongaster pentas
A/G ?NTD 14 (Nitzschia jouseae) - NTD 13 (Thalassiosira convexa)
disturbed
1
2
3
4
5
6
7
CC
0.5
1.0

LITHOLOGIC DESCRIPTION

NANNOFOSSIL OOZE with FORAMINIFERS

Major lithology: This core contains flow-in. Sections 1 through 3 and 6 through 7 are highly disturbed due to flow-in. From Section 4, 35 cm, to Section 6, 60 cm, drilling disturbance is moderate. The lithology within this interval is light gray (5Y 7/1) and heavily bioturbated NANNOFOSSIL OOZE with FORAMINIFERS.

SMEAR SLIDE SUMMARY (%):

	5, 30
	D
TEXTURE	
Sand	5
Silt	65
Clay	30
COMPOSITION	
Accessory minerals	3
Diatoms	2
Foraminifers	15
Nannofossils	74
Radiolarians	3
Siliceous fragments	3

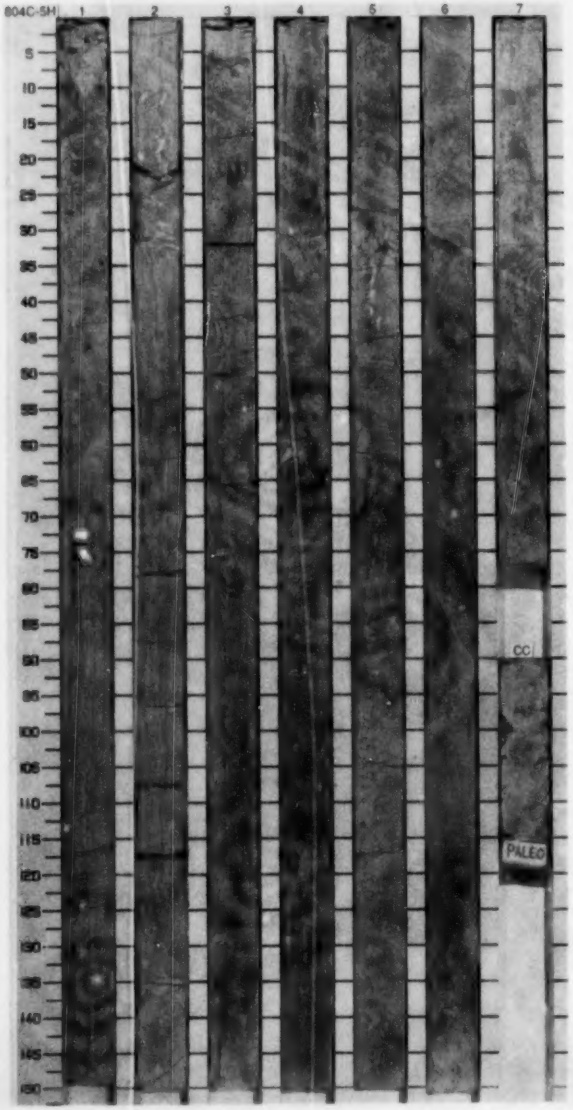
804C-5H
1
2
3
4
5
6
7
CC
PALEO
5
10
15
20
25
30
35
40
45
50
55
60
65
70
75
80
85
90
95
100
105
110
115
120
125
130
135
140
145
150

SITE 804 HOLE C CORE 6H CORED INTERVAL 44.3-53.8 mbsf

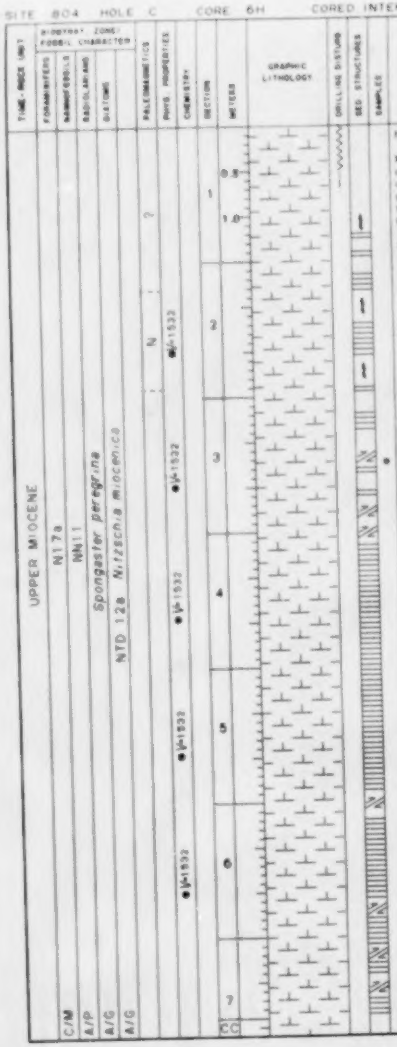
TIME-ROCK UNIT
BIOSTRAT. ZONE/FOSSIL CHARACTER
FORAMINIFERS
NANNOFOSSILS
RADIOLARIANS
DIATOMS
PALEOMAGNETICS
PHYS. PROPERTIES
CHEMISTRY
SECTION
METERS
GRAPHIC LITHOLOGY
DRILLING DISTURB.
SED. STRUCTURES
SAMPLES
UPPER MIOCENE
N17a
NN11
Spongaster peregrina
NTD 12a Nitzschia miocenica
C/M
A/P
A/G
A/G
?
N
●γ=1.532
●γ=1.522
●γ=1.522
●γ=1.532
●γ=1.532
1
2
3
4
5
6
7
CC
0.5
1.0

LITHOLOGIC DESCRIPTION

NANNOFOSSIL OOZE

Major lithology: This core consists of white (2.5Y 8/0) NANNOFOSSIL OOZE (Section 1, 0-50 cm, is flow-in. The core catcher is also highly disturbed). Abundant, irregular and wavy, mm- to cm-thick color bands are noted throughout the core. Most of the bands are gray (7.5R 6/0) or green (10GY 7/2), but a few white (2.5Y 8/2) bands are noted. All show gradational color contacts. Microfaulting was observed in Sections 3, 5, 6 and 7. Moderate bioturbation is indicated by mottles, pyritized burrow fills and disseminated pyrite.

SMEAR SLIDE SUMMARY (%):

	3, 74 D
TEXTURE:	
Sand	5
Silt	60
Clay	35
COMPOSITION:	
Accessory minerals	Tr
Diatoms	Tr
Foraminifers	2
Nannofossils	97
Radiolarians	Tr
Siliceous fragments	1

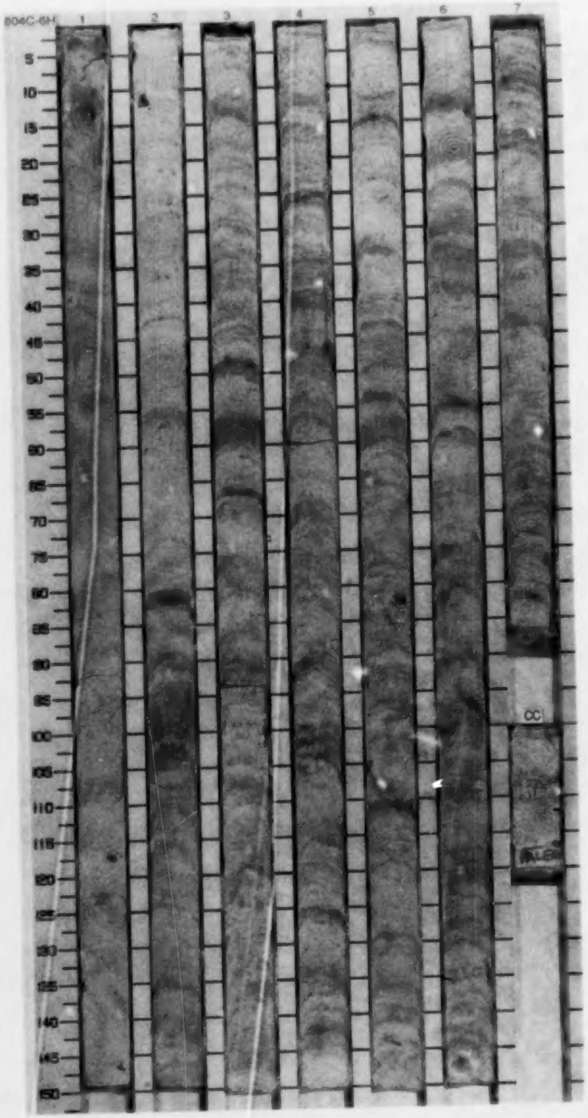
804C-6H
1
2
3
4
5
6
7
5
10
15
20
25
30
35
40
45
50
55
60
65
70
75
80
85
90
95
100
105
110
115
120
125
130
135
140
145
150
CC

SITE 804 HOLE C CORE 7H CORED INTERVAL 53.8-63.3 mbsf

TIME-ROCK UNIT	FORAMINIFERS	NANNOFOSSILS	RADIOLARIANS	DIATOMS	PALEOMAGNETICS	PHYS. PROPERTIES	CHEMISTRY	SECTION	METERS
UPPER MIOCENE	N17a	NN11	*Didymocyrtis penultima*					1	0.5 1.0
						φ=62.1 γ=1.66 V=1521		2	
						φ=61.7 γ=1.65 V=1535		3	
						φ=62.9 γ=1.63 V=1552		4	
						φ=59.4 γ=1.70 V=1550		5	
						φ=60.0 γ=1.70 V=1556		6	
						φ=63.4 γ=1.62 V=1542		7	
	C/M	A/P	A/G					CC	

BIOSTRAT. ZONE/ FOSSIL CHARACTER

GRAPHIC LITHOLOGY

DRILLING DISTURB.

SED. STRUCTURES

SAMPLES

LITHOLOGIC DESCRIPTION

NANNOFOSSIL OOZE

Major lithology: This core contains homogeneous and predominantly white (2.5Y 8/0) NANNOFOSSIL OOZE. Subhorizontal reddish gray (5R 6/1), white (2.5Y 8/2) and pale yellowish green (10GY 7/2) bands are present throughout. The bands are 2 to 10 mm thick and are spaced 1 to 10 cm apart. The sediment is bioturbated and has some pyritized burrow fills.

SMEAR SLIDE SUMMARY (%):

	3, 75 D
TEXTURE:	
Silt	40
Clay	60
COMPOSITION:	
Accessory minerals	2
Diatoms	Tr
Foraminifers	3
Nannofossils	95
Radiolarians	Tr
Siliceous fragments	Tr

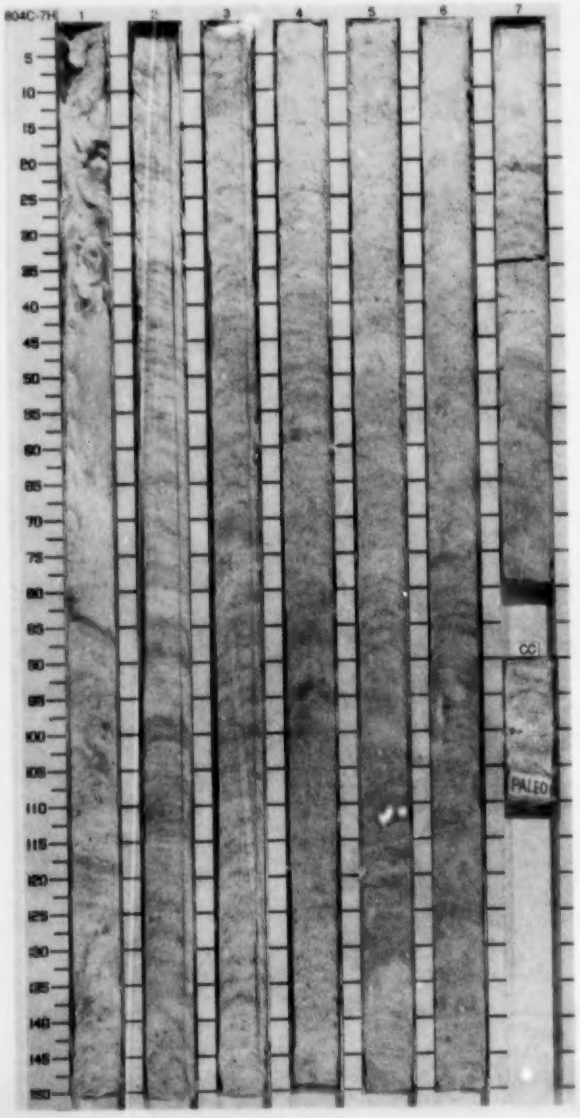

SITE 804 HOLE C CORE 8H CORED INTERVAL 63.3-72.8 mbsf

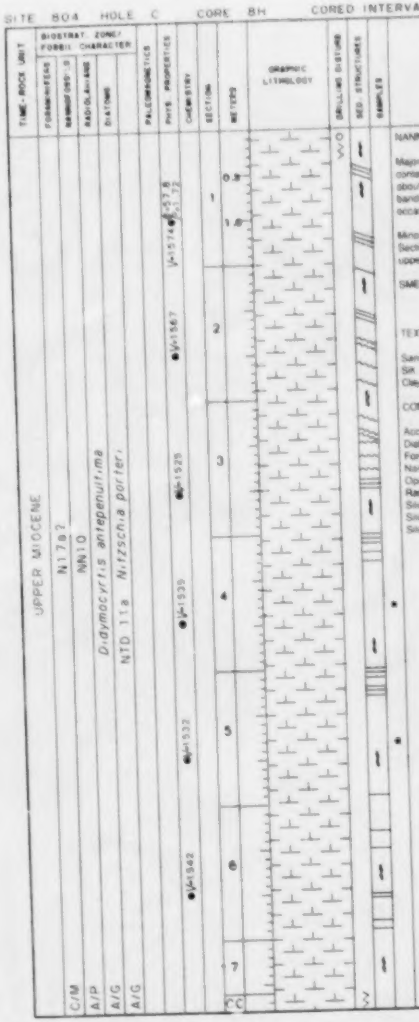
TIME-ROCK UNIT
BIOSTRAT. ZONE/ FOSSIL CHARACTER
FORAMINIFERS
NANNOFOSSILS
RADIOLARIANS
DIATOMS
PALEOMAGNETICS
PHYS. PROPERTIES
CHEMISTRY
SECTION
METERS
GRAPHIC LITHOLOGY
DRILLING DISTURB.
SED. STRUCTURES
SAMPLES
UPPER MIOCENE
N17a?
NN10
C/M
Didymocyrtis antepenultima
A/P
NTD 11a Nitzschia porteri
A/G
A/G
V=1574
●-57.8
◊1.72
●V=1567
●V=1525
●V=1535
●V=1532
●V=1542
1
2
3
4
5
6
7
CC
0.5
1.0
VO

LITHOLOGIC DESCRIPTION

NANNOFOSSIL OOZE

Major lithology: This core contains white (2.5Y 8/0) NANNOFOSSIL OOZE. Sections 1 and 2 contain abundant, tilted and wavy, faint, reddish gray (5R 6/1) color bands. The bands are about 0.5 to 1 cm thick and are separated by about 0.5 to 1 cm of white (2.5Y 8/0) ooze. Color banding is parallel and horizontal from Section 2, 130 cm, to Section 4, 28 cm. Only occasional color banding is observed below this level in the core.

Minor lithology: A thin (3 cm thick) bed of FORAMINIFER NANNOFOSSIL OOZE is noted in Section 5, 78-81 cm. It forms a graded bed with a sharp, irregular lower contact and a distinct upper contact. This bed is very soft in comparison with the surrounding sediment.

SMEAR SLIDE SUMMARY (%):

	4, 80	5, 81
	D	M
TEXTURE:		
Sand	1	20
Silt	59	50
Clay	40	30
COMPOSITION:		
Accessory minerals	2	—
Diatoms	5	2
Foraminifers	8	30
Nannofossils	74	50
Opaques	—	8
Radiolarians	5	2
Siliceous fragments	5	3
Siliceous sponge spicules	—	Tr
Silicoflagellates	1	—

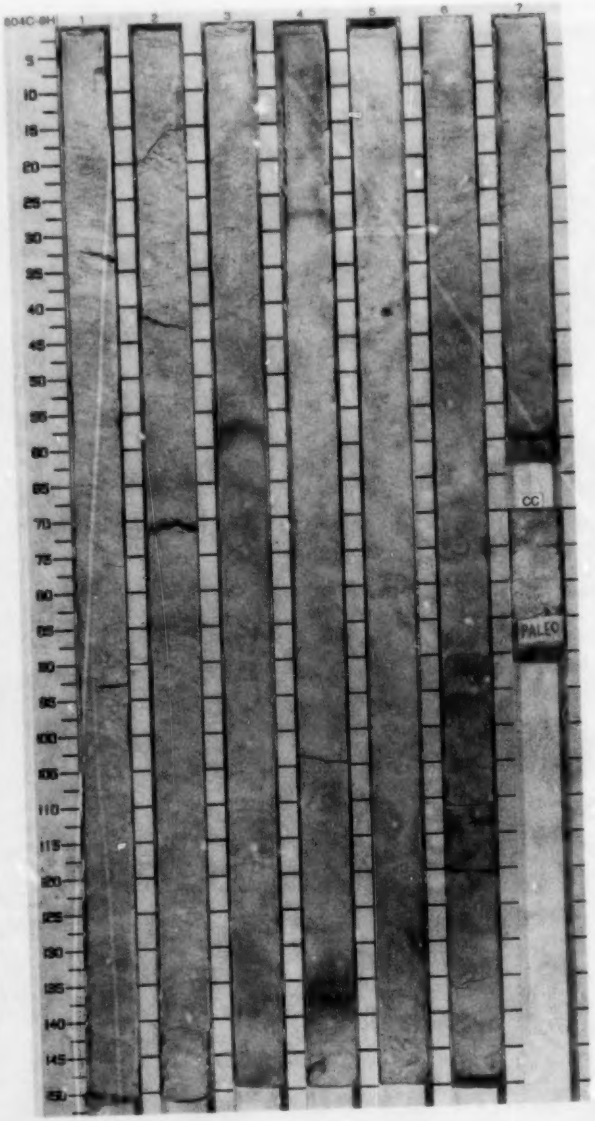
804C-8H
1
2
3
4
5
6
7
5
10
15
20
25
30
35
40
45
50
55
60
65
70
75
80
85
90
95
100
105
110
115
120
125
130
135
140
145
150
CC
PALEO

SITE 804 HOLE C CORE 9H CORED INTERVAL 72.8-82.3 mbsf

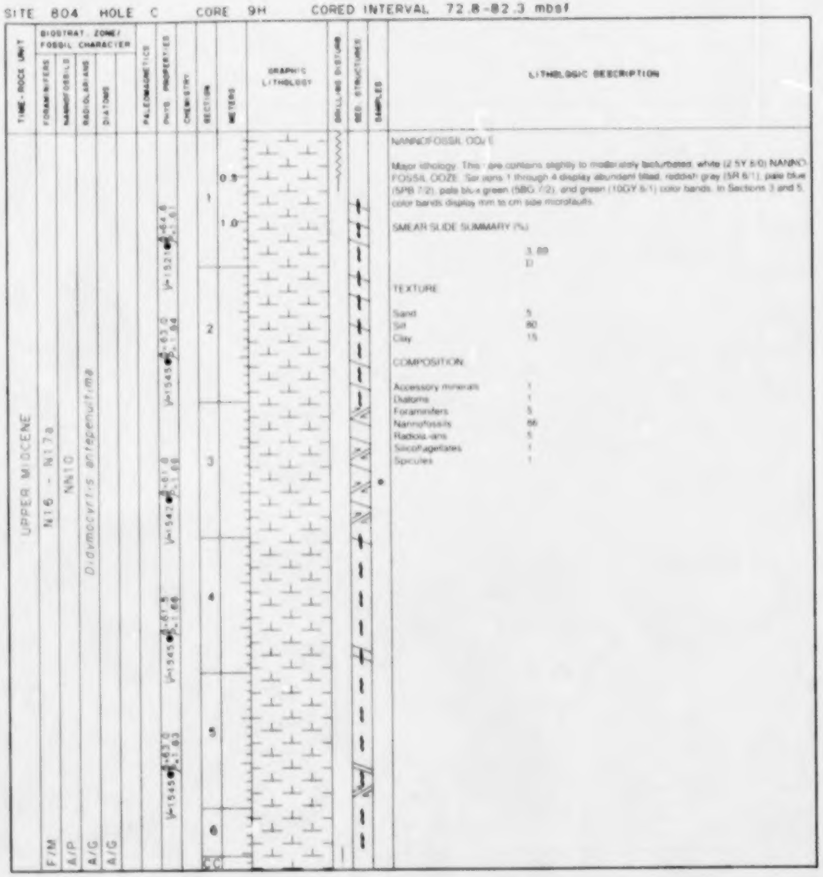
TIME-ROCK UNIT
BIOSTRAT. ZONE/ FOSSIL CHARACTER
FORAMINIFERS
NANNOFOSSILS
RADIOLARIANS
DIATOMS
PALEOMAGNETICS
PHYS. PROPERTIES
CHEMISTRY
SECTION
METERS
GRAPHIC LITHOLOGY
DRILLING DISTURB.
SED. STRUCTURES
SAMPLES
UPPER MIOCENE
F/M N16 - N17a
A/P NN10
A/G Didymocyrtis antepenultima
A/G
V-1521 φ-64.6 γ-1.61
V-1545 φ-63.0 γ-1.64
V-1542 φ-61.0 γ-1.68
V-1545 φ-61.5 γ-1.66
V-1545 φ-63.0 γ-1.63
1
2
3
4
5
6
CC
0.5
1.0

LITHOLOGIC DESCRIPTION

NANNOFOSSIL OOZE

Major lithology: This core contains slightly to moderately bioturbated, white (2.5Y 8/0) NANNOFOSSIL OOZE. Sections 1 through 4 display abundant tilted, reddish gray (5R 6/1), pale blue (5PB 7/2), pale blue green (5BG 7/2), and green (10GY 6/1) color bands. In Sections 3 and 5, color bands display mm to cm size microfaults.

SMEAR SLIDE SUMMARY (%):

	3, 89
	D
TEXTURE:	
Sand	5
Silt	80
Clay	15
COMPOSITION:	
Accessory minerals	1
Diatoms	1
Foraminifers	5
Nannofossils	86
Radiolarians	5
Silicoflagellates	1
Spicules	1

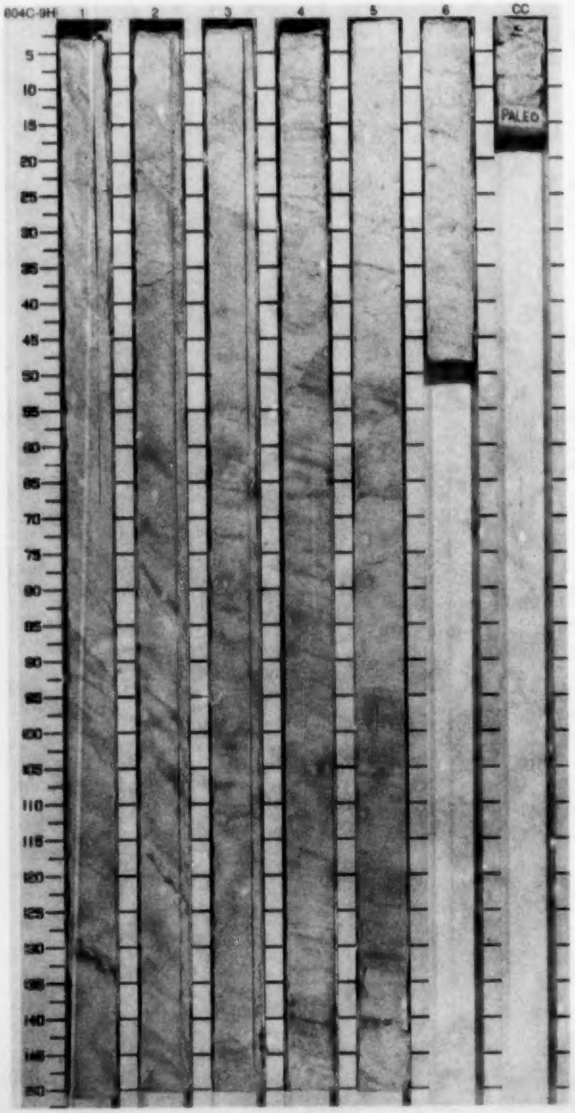
804C-9H
1
2
3
4
5
6
CC
PALEO
5
10
15
20
25
30
35
40
45
50
55
60
65
70
75
80
85
90
95
100
105
110
115
120
125
130
135
140
145
150

SITE 804 HOLE C CORE 10H CORED INTERVAL 82.3-91.8 mbsf

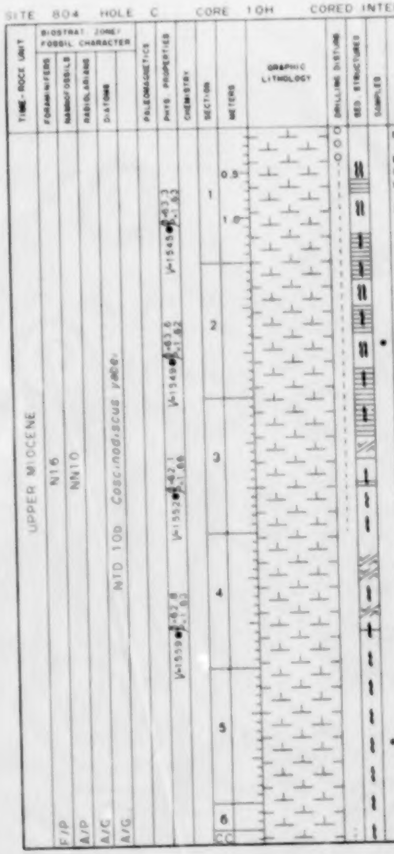
TIME-ROCK UNIT
BIOSTRAT. ZONE/ FOSSIL CHARACTER
FORAMINIFERS
NANNOFOSSILS
RADIOLARIANS
DIATOMS
PALEOMAGNETICS
PHYS. PROPERTIES
CHEMISTRY
SECTION
METERS
GRAPHIC LITHOLOGY
DRILLING DISTURB.
SED. STRUCTURES
SAMPLES
UPPER MIOCENE
N16
NN10
NTD 10b Coscinodiscus yabe.
F/P
A/P
A/C
A/G
V-1545
-63.3
-1.62
V-1549
-63.6
-1.62
V-1552
-62.1
-1.66
V-1559
-62.8
-1.63
1
2
3
4
5
6
CC
0.5
1.0

LITHOLOGIC DESCRIPTION

NANNOFOSSIL OOZE

Major lithology: This core contains slightly to heavily bioturbated white (2.5Y 8/0) NANNOFOSSIL OOZE. Faint pale blue (5PB 7/2), pale purple (5P 6/2), and white (5YR 8/1) color bands are common throughout. Some color bands in Section 3 are heavily bioturbated.

SMEAR SLIDE SUMMARY (%):

	2, 92	5, 84
	D	D
TEXTURE:		
Sand	2	5
Silt	95	90
Clay	3	5
COMPOSITION:		
Accessory minerals	Tr	Tr
Bioclast	—	1
Diatoms	1	Tr
Foraminifers	2	3
Nannofossils	94	93
Radiolarians	2	3
Silicoflagellates	Tr	Tr
Spicules	1	Tr

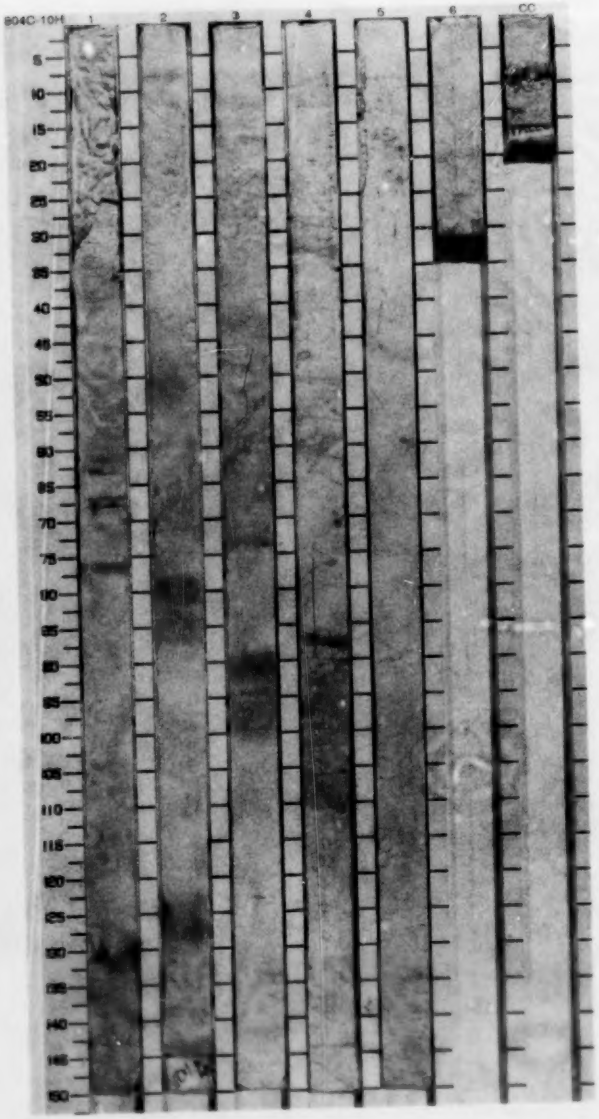
804C-10H
1
2
3
4
5
6
CC
5
10
15
20
25
30
35
40
45
50
55
60
65
70
75
80
85
90
95
100
105
110
115
120
125
130
135
140
145
150

SITE 804 HOLE C CORE 11M CORED INTERVAL 91.8-101.3 mbsf

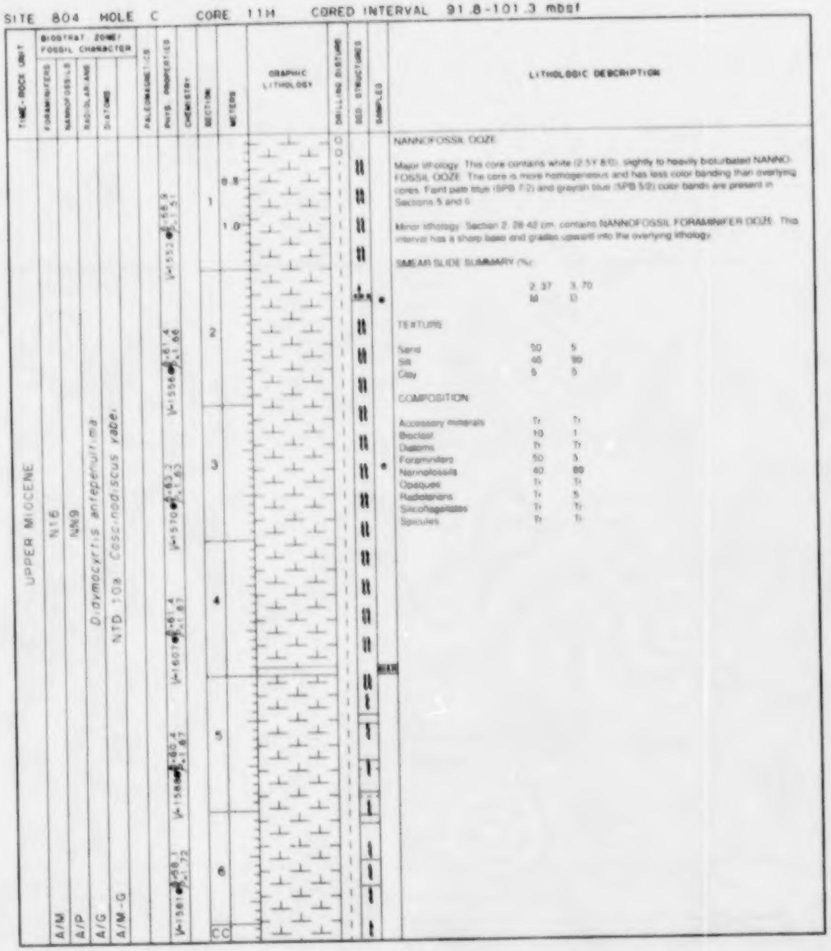
TIME-ROCK UNIT
BIOSTRAT. ZONE/ FOSSIL CHARACTER
FORAMINIFERS
NANNOFOSSILS
RADIOLARIANS
DIATOMS
PALEOMAGNETICS
PHYS. PROPERTIES
CHEMISTRY
SECTION
METERS
GRAPHIC LITHOLOGY
DRILLING DISTURB.
SED. STRUCTURES
SAMPLES
LITHOLOGIC DESCRIPTION
UPPER MIOCENE
N16
NN9
Didymocyrtis antepenultima
NTD 10a Coscinodiscus yabei
A/M
A/P
A/G
A/M-G
V=1552 φ=68.9 γ=1.51
V=1556 φ=61.4 γ=1.66
V=1570 φ=63.2 γ=1.63
V=1607 φ=61.4 γ=1.67
V=1588 φ=60.4 γ=1.67
V=1581 φ=58.1 γ=1.72
1
2
3
4
5
6
CC
0.5
1.0

NANNOFOSSIL OOZE

Major lithology: This core contains white (2.5Y 8/0), slightly to heavily bioturbated NANNOFOSSIL OOZE. The core is more homogeneous and has less color banding than overlying cores. Faint pale blue (5PB 7/2) and grayish blue (5PB 5/2) color bands are present in Sections 5 and 6.

Minor lithology: Section 2, 28-42 cm, contains NANNOFOSSIL FORAMINIFER OOZE. This interval has a sharp base and grades upward into the overlying lithology.

SMEAR SLIDE SUMMARY (%):

	2, 37 M	3, 70 D
TEXTURE:		
Sand	50	5
Silt	45	90
Clay	5	5
COMPOSITION:		
Accessory minerals	Tr	Tr
Bioclast	10	1
Diatoms	Tr	Tr
Foraminifers	50	5
Nannofossils	40	80
Opaques	Tr	Tr
Radiolarians	Tr	5
Silicoflagellates	Tr	Tr
Spicules	Tr	Tr

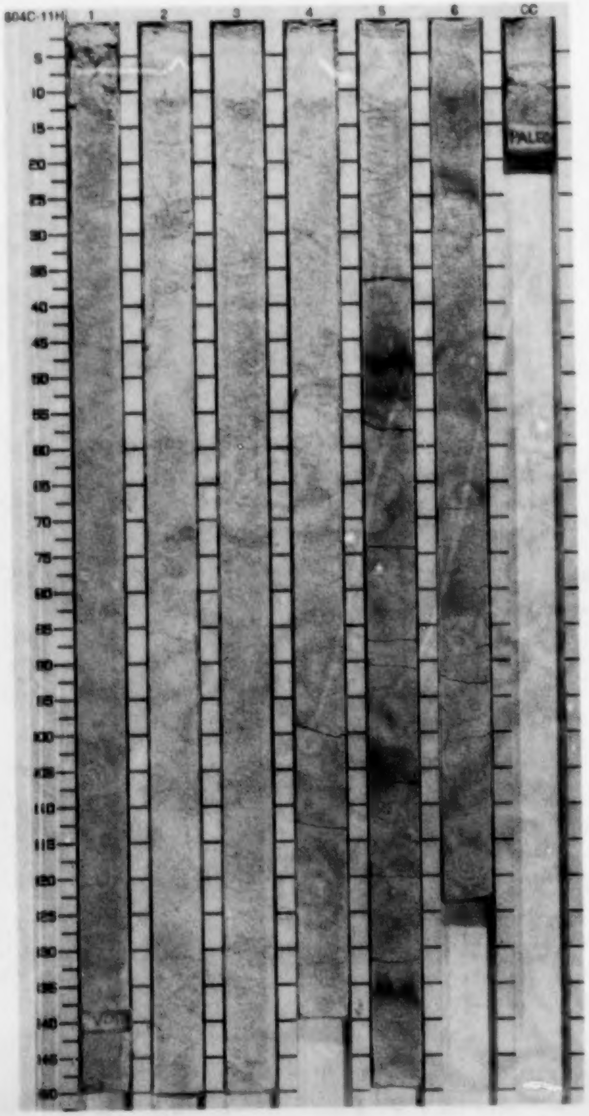
804C-11H
1
2
3
4
5
6
CC
PALEO
5
10
15
20
25
30
35
40
45
50
55
60
65
70
75
80
85
90
95
100
105
110
115
120
125
130
135
140
145
150

SITE 804 HOLE C CORE 12H CORED INTERVAL 101.3-110.8 mbsf

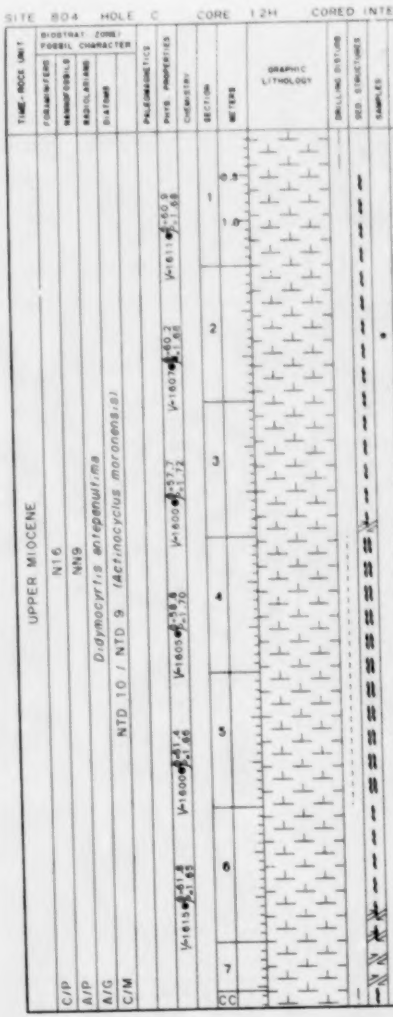
TIME-ROCK UNIT
BIOSTRAT. ZONE/ FOSSIL CHARACTER
FORAMINIFERS
NANNOFOSSILS
RADIOLARIANS
DIATOMS
PALEOMAGNETICS
PHYS. PROPERTIES
CHEMISTRY
SECTION
METERS
GRAPHIC LITHOLOGY
DRILLING DISTURB.
SED. STRUCTURES
SAMPLES
UPPER MIOCENE
N16
NN9
Didymocyrtis antepenultima
NTD 10 / NTD 9 (Actinocyclus moronensis)
C/P
A/P
A/P
A/G
C/M
V-1611 φ-60.9 γ-1.68
V-1607 φ-60.2 γ-1.68
V-1600 φ-57.7 γ-1.72
V-1605 φ-58.8 γ-1.70
V-1600 φ-61.4 γ-1.66
V-1615 φ-61.8 γ-1.65
1
2
3
4
5
6
7
CC
0.5
1.0

LITHOLOGIC DESCRIPTION

NANNOFOSSIL OOZE

Major lithology: This core contains white (2.5Y 8/0), slightly to heavily bioturbated NANNOFOSSIL OOZE. Faint pale blue (5PB 7/2), pale purple (5RP 7/2), and grayish blue (5PB 5/2) color bands are present in Sections 3, 6 and 7. Microfaults are evident in Section 3, 6 and 7.

SMEAR SLIDE SUMMARY (%):

	2, 80 D
TEXTURE:	
Sand	7
Silt	70
Clay	23
COMPOSITION:	
Foraminifers	5
Nannofossils	90
Radiolarians	5
Volcanic ash	Tr

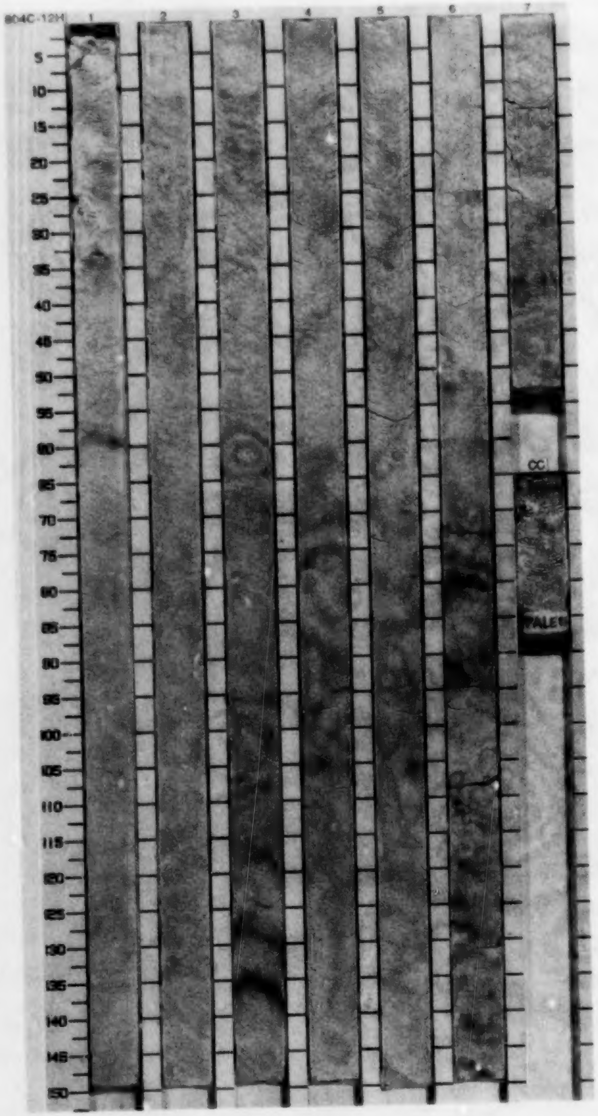
804C-12H
1
2
3
4
5
6
7
CC
5
10
15
20
25
30
35
40
45
50
55
60
65
70
75
80
85
90
95
100
105
110
115
120
125
130
135
140
145
150

SITE 804 HOLE C CORE 13H CORED INTERVAL 110.8-120.3 mbsf

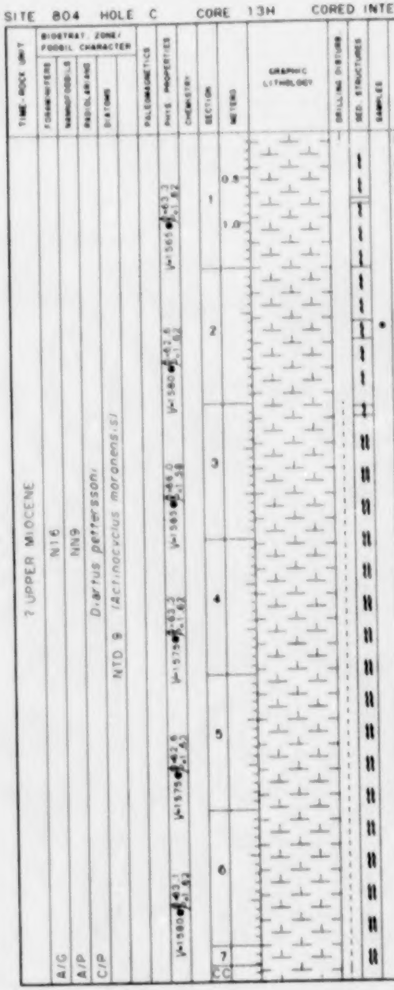
TIME-ROCK UNIT
BIOSTRAT. ZONE/ FOSSIL CHARACTER
FORAMINIFERS
NANNOFOSSILS
RADIOLARIANS
DIATOMS
PALEOMAGNETICS
PHYS. PROPERTIES
CHEMISTRY
SECTION
METERS
GRAPHIC LITHOLOGY
DRILLING DISTURB.
SED. STRUCTURES
SAMPLES
? UPPER MIOCENE
A/G N16
A/P NN9
C/P Diartus petterssoni
NTD 9 (Actinocyclus moronensis)
V=1565 φ=63.3 ρ=1.82
V=1580 φ=62.6 ρ=1.82
V=1585 φ=66.0 ρ=1.58
V=1579 φ=63.2 ρ=1.82
V=1579 φ=62.6 ρ=1.82
V=1580 φ=63.1 ρ=1.82
1
2
3
4
5
6
7
CC
0.5
1.0

LITHOLOGIC DESCRIPTION

NANNOFOSSIL OOZE

Major lithology: This core contains white (2.5Y 8/0), slightly to heavily bioturbated NANNOFOSSIL OOZE. Faint reddish gray (5R 6/1), pale pink (5 RP 8/2), pale blue (5PB 7/2), pale purple (5RP 7/2), and grayish blue (5PB 5/2) color bands are present in Sections 1 through 3.

SMEAR SLIDE SUMMARY (%)

	2, 65
	D
TEXTURE	
Sand	5
Silt	87
Clay	8
COMPOSITION	
Diatoms	1
Foraminifers	5
Nannofossils	92
Radiolarians	1
Silicoflagellates	1

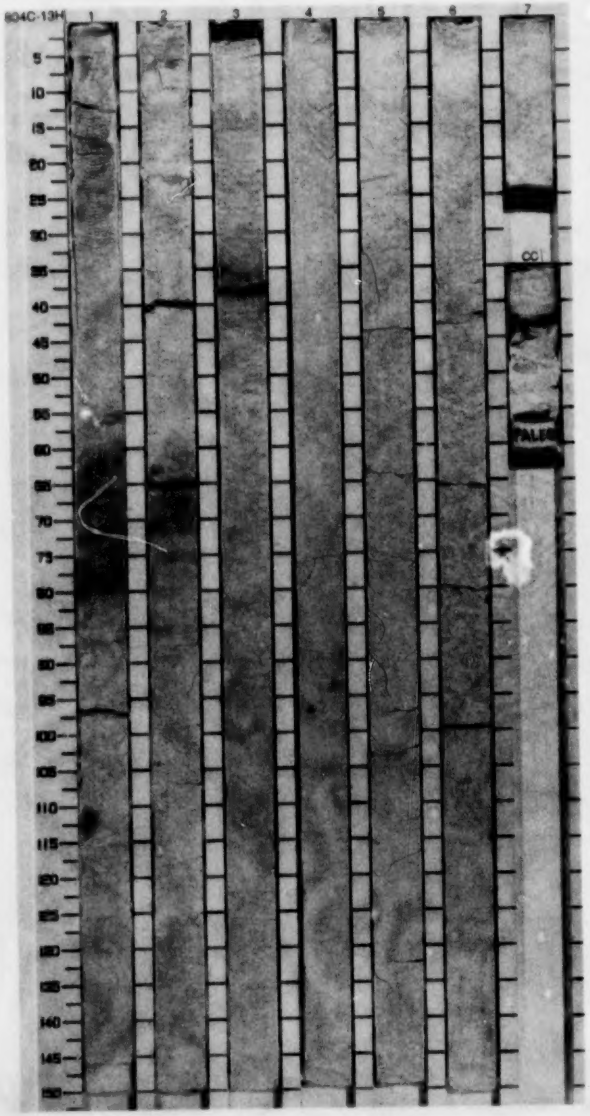
804C-13H
1
2
3
4
5
6
7
CC
PALEO
5
10
15
20
25
30
35
40
45
50
55
60
65
70
75
80
85
90
95
100
105
110
115
120
125
130
135
140
145
150

SITE 804 HOLE C CORE 14X CORED INTERVAL 120.3-129.8 mbsf

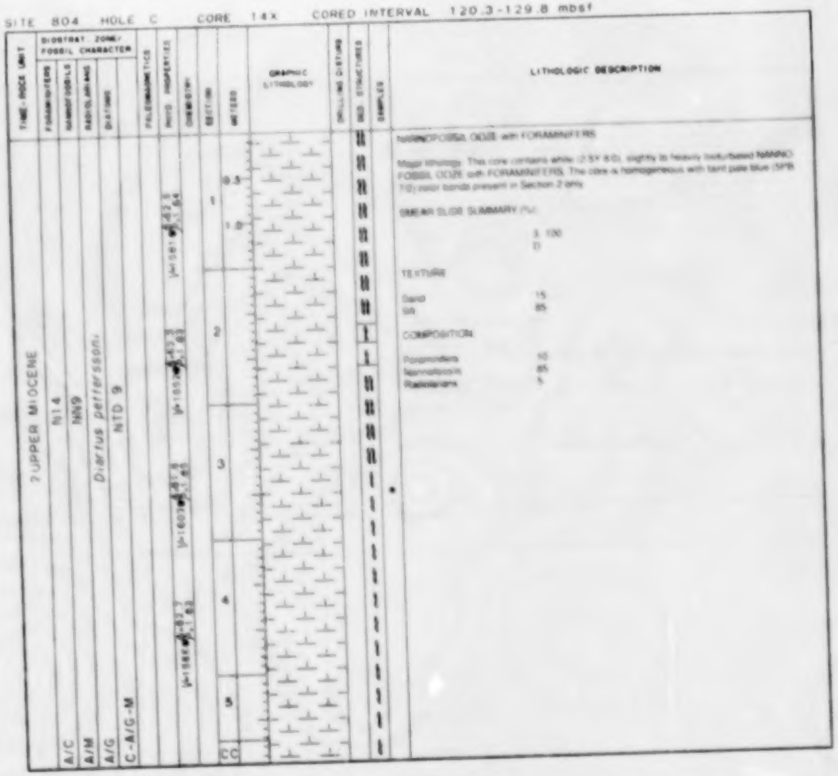
TIME-ROCK UNIT
BIOSTRAT. ZONE/ FOSSIL CHARACTER
FORAMINIFERS
NANNOFOSSILS
RADIOLARIANS
DIATOMS
PALEOMAGNETICS
PHYS. PROPERTIES
CHEMISTRY
SECTION
METERS
GRAPHIC LITHOLOGY
DRILLING DISTURB.
SED. STRUCTURES
SAMPLES
?UPPER MIOCENE
N14
NN9
Diartus petterssoni
NTD 9
A/C
A/M
A/G
C-A/G-M
0.5
1.0
1
2
3
4
5
CC

LITHOLOGIC DESCRIPTION

NANNOFOSSIL OOZE with FORAMINIFERS

Major lithology: This core contains white (2.5Y 8/0), slightly to heavily bioturbated NANNOFOSSIL OOZE with FORAMINIFERS. The core is homogeneous with faint pale blue (5PB 7/2) color bands present in Section 2 only.

SMEAR SLIDE SUMMARY (%):

	3, 100
	D
TEXTURE:	
Sand	15
Silt	85
COMPOSITION:	
Foraminifers	10
Nannofossils	85
Radiolarians	5

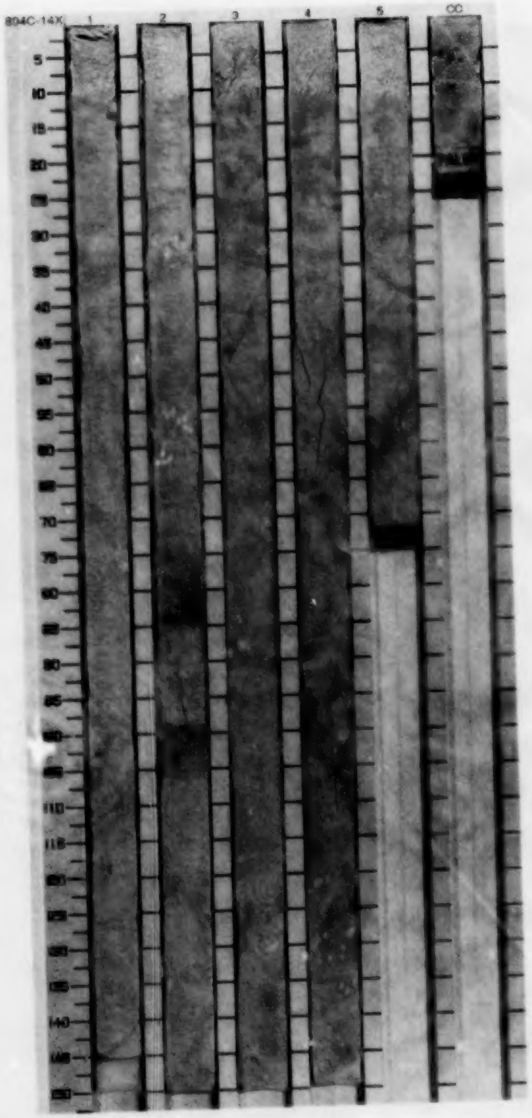
804C-14X
1
2
3
4
5
CC
5
10
15
20
25
30
35
40
45
50
55
60
65
70
75
80
85
90
95
100
105
110
115
120
125
130
135
140
145
150

SITE 804 HOLE C CORE 15X CORED INTERVAL 129.8-139.3 mbsf

TIME-ROCK UNIT	FORAMINIFERS	NANNOFOSSILS	RADIOLARIANS	DIATOMS	PALEOMAGNETICS	PHYS. PROPERTIES	CHEMISTRY	SECTION	METERS	GRAPHIC LITHOLOGY	DRILLING DISTURB.	SED. STRUCTURES	SAMPLES
UPPER MIOCENE?	? F/P	NN9 A/M				V=1607●ϕ=40.6 ρ=1.96 V=1532●ϕ=65.6 ρ=1.58 ●ϕ=45.8 ρ=1.58	●%CaCO$_3$=94.5 ●%CaCO$_3$=88.2 ●%CaCO$_3$=89.8	1 2 3 4 CC	0.5 1.0				●

LITHOLOGIC DESCRIPTION

NANNOFOSSIL OOZE with FORAMINIFERS

Major lithology: This core contains white (2.5Y 8/0), slightly to heavily bioturbated NANNOFOSSIL OOZE with FORAMINIFERS. The core is relatively homogeneous with faint grayish blue (5PB 5/2) color band present only in Section 2.

SMEAR SLIDE SUMMARY (%):

2, 80
D

TEXTURE:

Sand	12
Silt	88

COMPOSITION:

Foraminifers	10
Nannofossils	88
Radiolarians	1
Silicoflagellates	1

SITE 804 HOLE C CORE 16X CORED INTERVAL 139.3-148.8 mbsf

TIME-ROCK UNIT	FORAMINIFERS	NANNOFOSSILS	RADIOLARIANS	DIATOMS	PALEOMAGNETICS	PHYS. PROPERTIES	CHEMISTRY	SECTION	METERS	GRAPHIC LITHOLOGY	DRILLING DISTURB.	SED. STRUCTURES	SAMPLES
UPPER MIOCENE?	A/P	NN9 A/M	D. artus petterssoni A/M	NTD 9 C-A/M		V=1542●ϕ=66.1 ρ=1.58 V=1542●ϕ=67.1 ρ=1.57	●%CaCO$_3$=87.4 ●%CaCO$_3$=88.9	1 2 CC	0.5 1.0				●

LITHOLOGIC DESCRIPTION

NANNOFOSSIL OOZE

Major lithology: This core contains white (2.5Y 8/0), homogeneous, moderately bioturbated NANNOFOSSIL OOZE.

SMEAR SLIDE SUMMARY (%):

1, 70
D

TEXTURE:

Sand	1
Silt	95
Clay	4

COMPOSITION:

Foraminifers	2
Nannofossils	96
Radiolarians	2

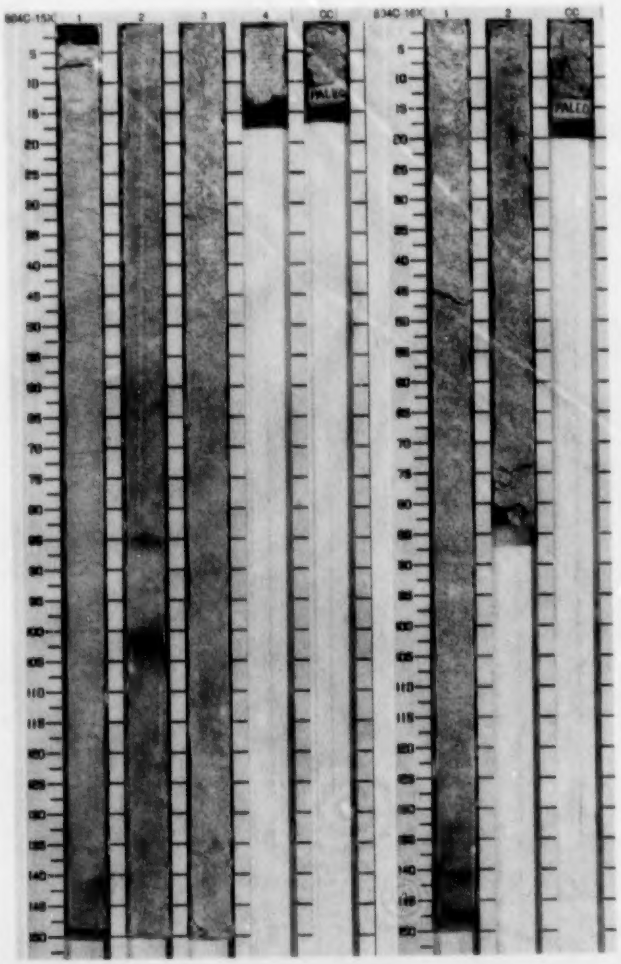

SITE 804 HOLE C CORE 17X CORED INTERVAL 148.8-158.3 mbsf

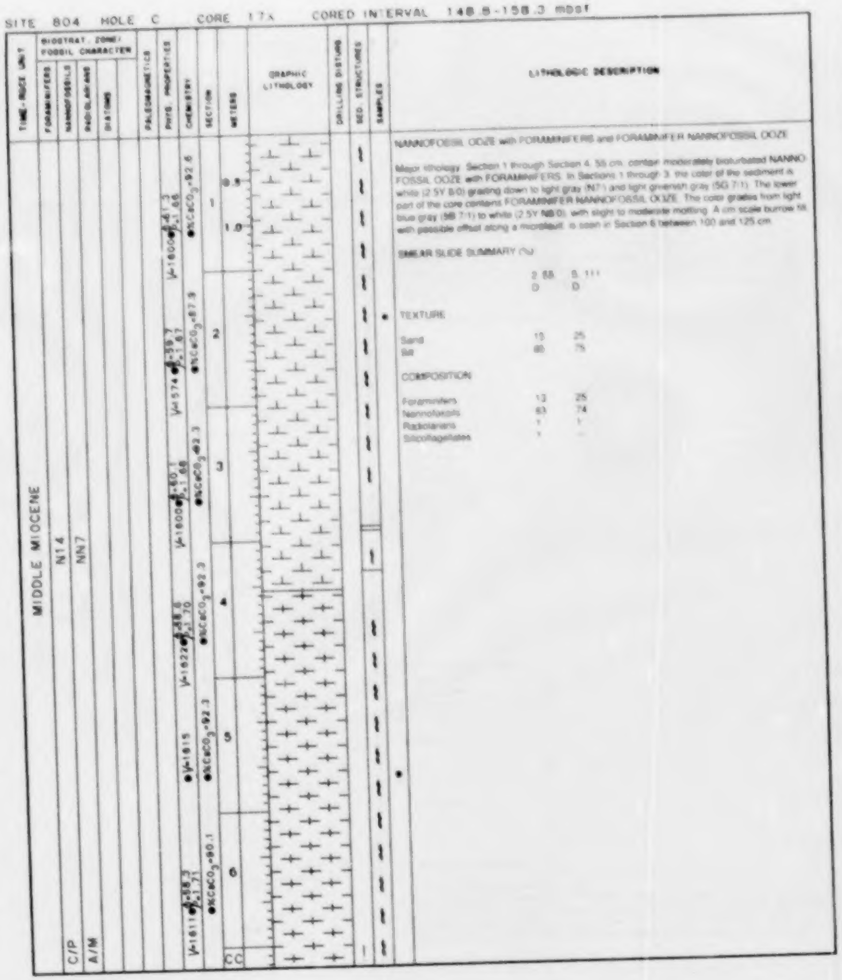
TIME-ROCK UNIT
BIOSTRAT. ZONE/ FOSSIL CHARACTER
FORAMINIFERS
NANNOFOSSILS
RADIOLARIANS
DIATOMS
PALEOMAGNETICS
PHYS. PROPERTIES
CHEMISTRY
SECTION
METERS
GRAPHIC LITHOLOGY
DRILLING DISTURB.
SED. STRUCTURES
SAMPLES
MIDDLE MIOCENE
N14
NN7
C/P
A/M
V=1600 φ=61.3 γ=1.66
%CaCO3=92.6
V=1574 φ=59.7 γ=1.67
%CaCO3=87.9
V=1600 φ=60.1 γ=1.68
%CaCO3=92.3
V=1622 φ=58.6 γ=1.70
%CaCO3=92.3
V=1615
%CaCO3=92.3
V=1611 φ=58.3 γ=1.71
%CaCO3=90.1
1
2
3
4
5
6
CC
0.5
1.0

LITHOLOGIC DESCRIPTION

NANNOFOSSIL OOZE with FORAMINIFERS and FORAMINIFER NANNOFOSSIL OOZE

Major lithology: Section 1 through Section 4, 55 cm, contain moderately bioturbated NANNOFOSSIL OOZE with FORAMINIFERS. In Sections 1 through 3, the color of the sediment is white (2.5Y 8/0) grading down to light gray (N7) and light greenish gray (5G 7/1). The lower part of the core contains FORAMINIFER NANNOFOSSIL OOZE. The color grades from light blue gray (5B 7/1) to white (2.5Y N8/0), with slight to moderate mottling. A cm scale burrow fill with possible offset along a microfault is seen in Section 6 between 100 and 125 cm.

SMEAR SLIDE SUMMARY (%):

	2, 55	5, 111
	D	D
TEXTURE:		
Sand	15	25
Silt	85	75
COMPOSITION:		
Foraminifers	13	25
Nannofossils	83	74
Radiolarians	1	1
Silicoflagellates	1	—

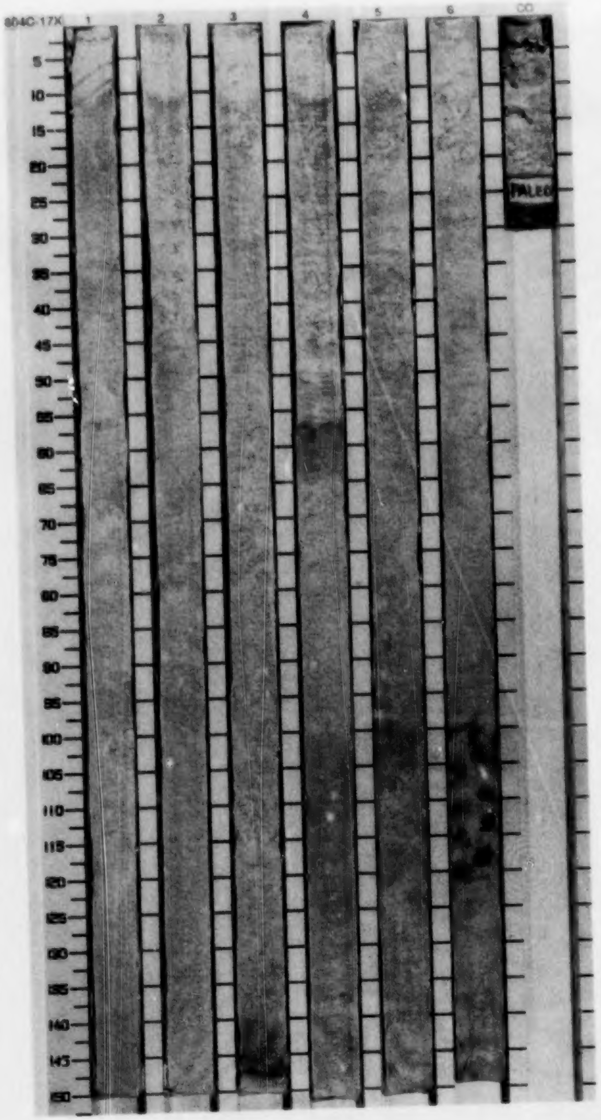
804C-17X
1
2
3
4
5
6
CC
PALEO
5
10
15
20
25
30
35
40
45
50
55
60
65
70
75
80
85
90
95
100
105
110
115
120
125
130
135
140
145
150

SITE 804 HOLE C CORE 18X CORED INTERVAL 158.3-168.0 mbsf

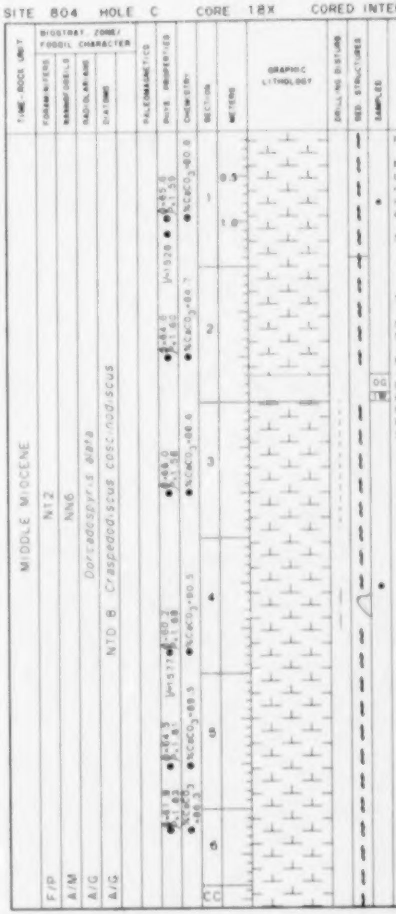
TIME-ROCK UNIT
BIOSTRAT. ZONE/ FOSSIL CHARACTER
FORAMINIFERS
NANNOFOSSILS
RADIOLARIANS
DIATOMS
PALEOMAGNETICS
PHYS. PROPERTIES
CHEMISTRY
SECTION
METERS
GRAPHIC LITHOLOGY
DRILLING DISTURB.
SED. STRUCTURES
SAMPLES
MIDDLE MIOCENE
N12
NN6
Dorcadospyris alata
NTD 8 Craspedodiscus coscinodiscus
F/P
A/M
A/G
A/G
%CaCO3=80.0
%CaCO3=84.7
%CaCO3=88.6
%CaCO3=80.5
%CaCO3=88.5
%CaCO3=88.3
V=1520
V=1577
1
2
3
4
5
6
CC
0.5
1.0
OG
IW

LITHOLOGIC DESCRIPTION

NANNOFOSSIL OOZE with RADIOLARIANS

Major lithology: This core contains slightly bioturbated NANNOFOSSIL OOZE with RADIOLARIANS. Section 1 is light gray (2.5Y 7/0) with a gray (2.5Y 6/0) color band at 140 cm. The remainder of the core is white (2.5Y 8/0). The sediment appears more lithified and harder than in the overlying cores, with relatively hard pieces within a softer matrix. Section 4, 80-95 cm appears disturbed by coring processes.

SMEAR SLIDE SUMMARY (%):

	1, 80	4, 53
	D	D
TEXTURE		
Sand	10	10
Silt	90	90
COMPOSITION		
Diatoms	1	1
Foraminifers	5	3
Nannofossils	82	80
Radiolarians	10	15
Siliceous sponge spicules	2	1

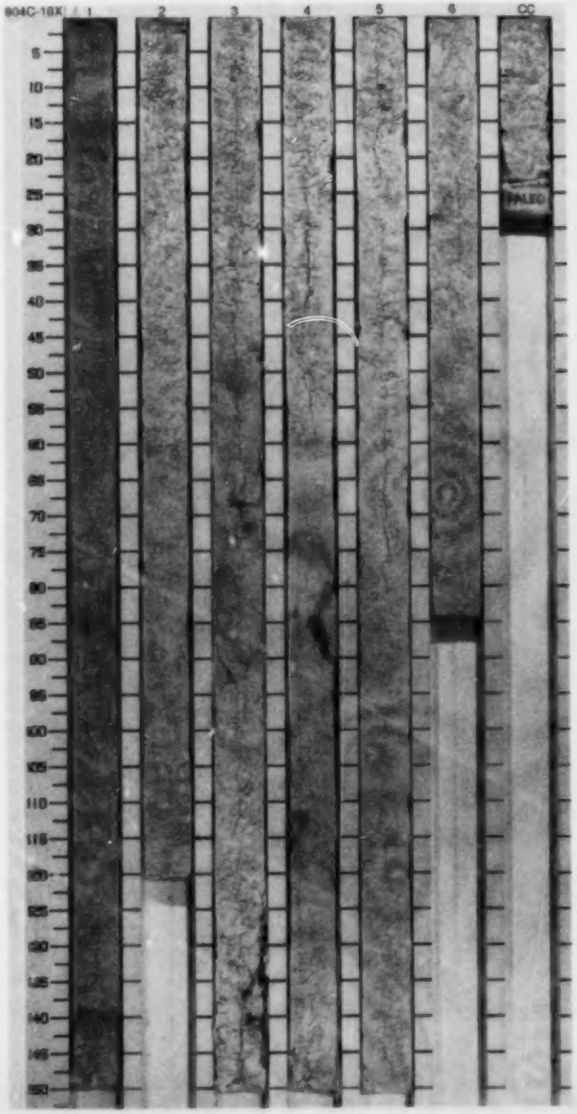
804C-18X 1
2
3
4
5
6
CC
PALEO
5
10
15
20
25
30
35
40
45
50
55
60
65
70
75
80
85
90
95
100
105
110
115
120
125
130
135
140
145
150

SITE 804 HOLE C CORE 19X CORED INTERVAL 168.0-177.7 mbsf

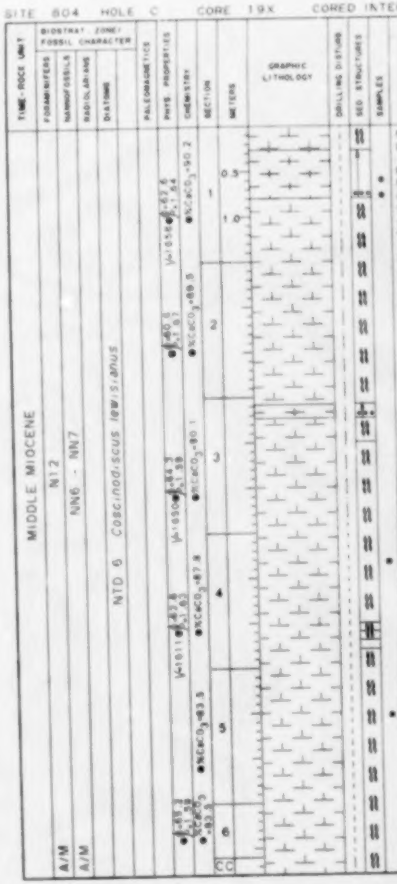
TIME-ROCK UNIT
BIOSTRAT. ZONE/ FOSSIL CHARACTER
FORAMINIFERS
NANNOFOSSILS
RADIOLARIANS
DIATOMS
PALEOMAGNETICS
PHYS. PROPERTIES
CHEMISTRY
SECTION
METERS
GRAPHIC LITHOLOGY
DRILLING DISTURB.
SED. STRUCTURES
SAMPLES
MIDDLE MIOCENE
N12
NN6 - NN7
NTD 6 Coscinodiscus lewisianus
A/M
A/M
γ=1.058 ●φ=67.6 γ=1.64
●%CaCO₃=90.2
●φ=60.0 γ=1.67
●%CaCO₃=89.5
γ=1.050 ●φ=64.3 γ=1.59
●%CaCO₃=90.1
γ=1.011 ●φ=67.8 γ=1.63
●%CaCO₃=87.8
●%CaCO₃=83.5
●φ=65.2 γ=1.59
●%CaCO₃=82.5
1
2
3
4
5
6
CC
0.5
1.0

LITHOLOGIC DESCRIPTION

NANNOFOSSIL OOZE with FORAMINIFERS and NANNOFOSSIL OOZE with RADIOLARIANS

Major lithology: This core contains NANNOFOSSIL OOZE with FORAMINIFERS, grading to NANNOFOSSIL OOZE with RADIOLARIANS in Sections 5 through the Core Catcher. The core is predominantly white (2.5Y 8/0), with minor gradations to light blue gray (5B 7/1) and white (5YR 8/1). Light greenish gray (5GY 8/1), greenish gray (5GY 6/1), pale blue (5PB 7/2) and pale red purple (5RP 6/2) color bands are rare to common throughout the core. The entire core is moderately to heavily bioturbated.

Minor lithology: Two normally graded layers of NANNOFOSSIL FORAMINIFER OOZE are present in this core: the first is at Section 1, 30-80 cm, and the second is at Section 3, 10-22 cm. Both are white (2.5Y 8/0), have sharp top and bottom contacts, and are probably turbidites.

SMEAR SLIDE SUMMARY (%):

	1, 61 M	1, 75 D	4, 32 D	5, 52 D
TEXTURE:				
Sand	80	10	10	15
Silt	20	90	90	85
COMPOSITION:				
Foraminifers	68	12	10	6
Nannofossils	30	85	86	74
Radiolarians	2	2	2	12
Siliceous sponge spicules	—	—	—	5
Silicoflagellates	—	1	1	2

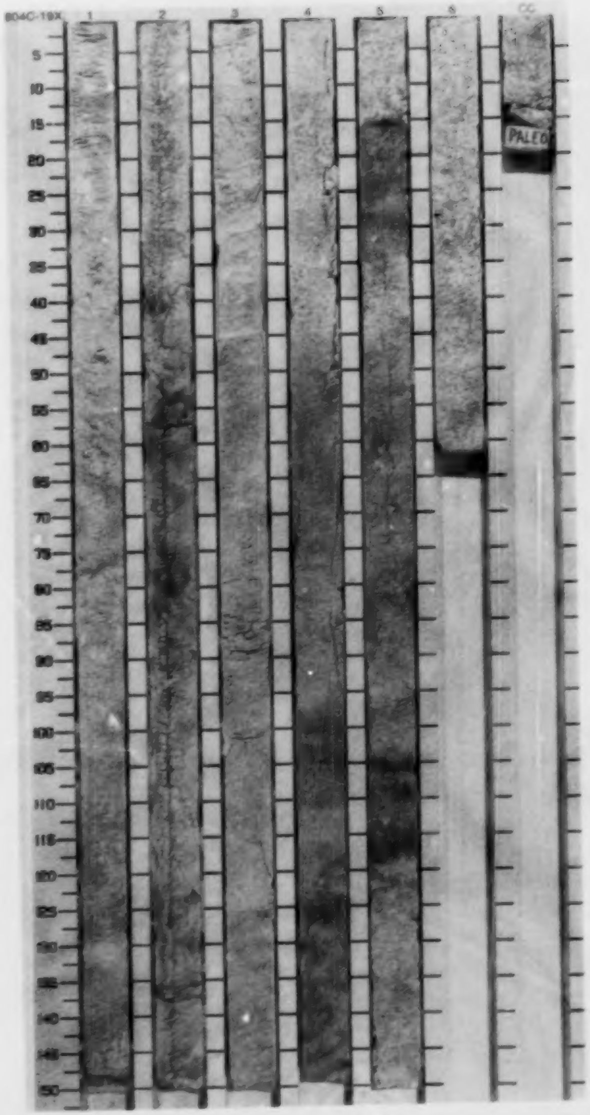
804C-19X
1
2
3
4
5
6
CC
PALEO
5
10
15
20
25
30
35
40
45
50
55
60
65
70
75
80
85
90
95
100
105
110
115
120
125
130
135
140
145
150

SITE 804 HOLE C CORE 20X CORED INTERVAL 177.7-187.4 mbsf

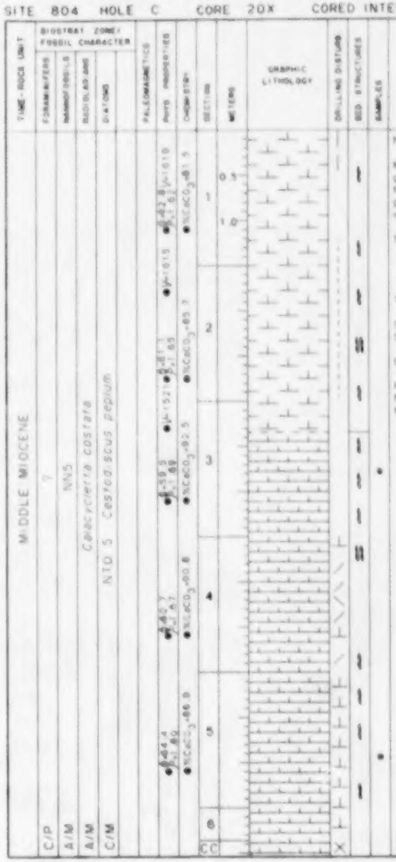
TIME-ROCK UNIT
BIOSTRAT. ZONE/ FOSSIL CHARACTER
FORAMINIFERS
NANNOFOSSILS
RADIOLARIANS
DIATOMS
PALEOMAGNETICS
PHYS. PROPERTIES
CHEMISTRY
SECTION
METERS
GRAPHIC LITHOLOGY
DRILLING DISTURB.
SED. STRUCTURES
SAMPLES
MIDDLE MIOCENE
?
NN5
Calocycletta costata
NTD 5 Cestodiscus peplum
C/P
A/M
A/M
C/M
γ=1.610
φ=42.8
ρ=1.62
%CaCO3=81.5
γ=1.615
φ=41.1
ρ=1.65
%CaCO3=85.7
γ=1.521
%CaCO3=82.5
φ=39.5
ρ=1.69
φ=40.7
ρ=1.67
%CaCO3=80.8
φ=44.4
ρ=1.60
%CaCO3=86.9
1
2
3
4
5
6
CC
0.5
1.0

LITHOLOGIC DESCRIPTION

NANNOFOSSIL OOZE with RADIOLARIANS grading to NANNOFOSSIL CHALK

Major lithology: This core contains bioturbated NANNOFOSSIL OOZE with RADIOLARIANS grading to NANNOFOSSIL CHALK in Section 3, 35 cm. The color of the sediment grades from white (2.5Y 8/0) to white (5Y 8/1 and 5Y 8/2). Light gray (N7 and 5Y 7/1) and light greenish gray (5GY 7/1), 2 to 20 cm thick, heavily burrowed zones are present at 150 cm intervals.

SMEAR SLIDE SUMMARY (%):

	3, 78	5, 94
	D	D
TEXTURE:		
Sand	15	10
Silt	85	90
COMPOSITION:		
Foraminifers	3	5
Nannofossils	87	90
Radiolarians	10	5

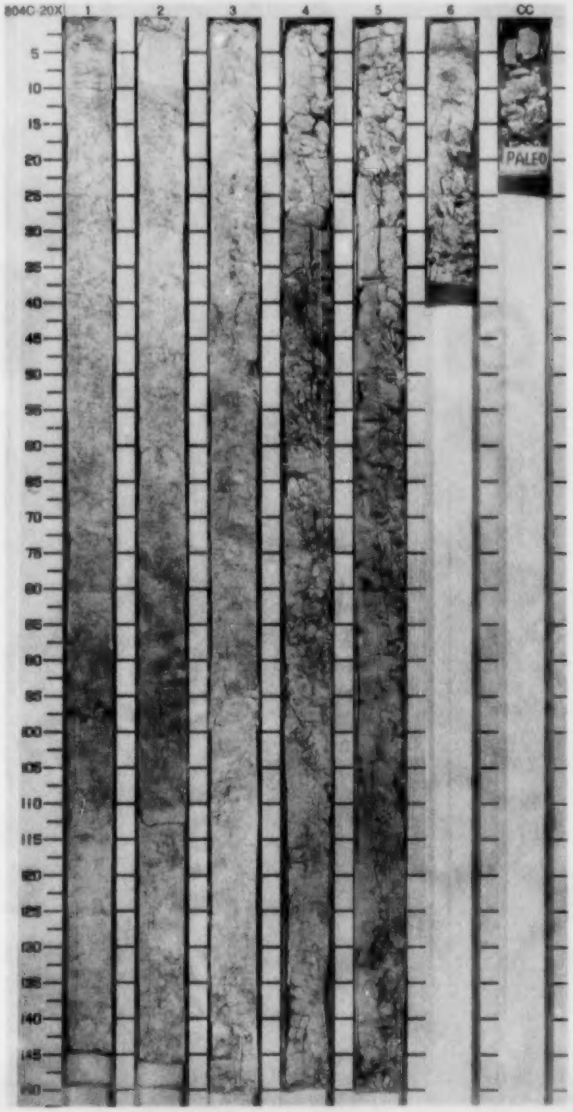
804C-20X
1
2
3
4
5
6
CC
PALEO
5
10
15
20
25
30
35
40
45
50
55
60
65
70
75
80
85
90
95
100
105
110
115
120
125
130
135
140
145
150

SITE 804 HOLE C CORE 21X CORED INTERVAL 187.4-197.1 mbsf

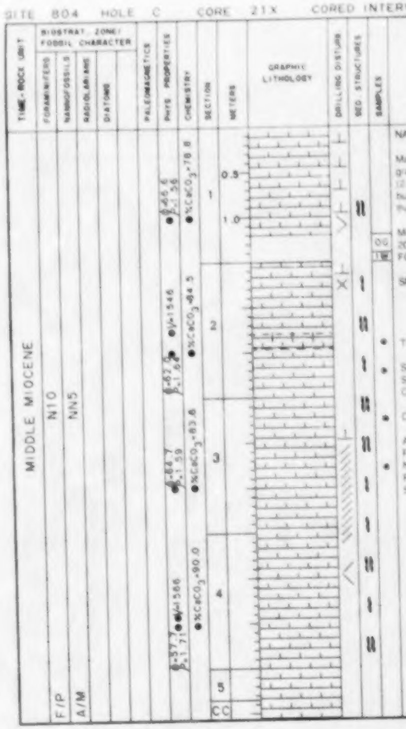

LITHOLOGIC DESCRIPTION

NANNOFOSSIL CHALK

Major lithology: This core contains white (10YR 8/2) NANNOFOSSIL CHALK. One to two light gray intervals (up to 20 cm thick) are observed in each section. The core catcher is light gray (2.5Y 7/2). The sediment is moderately to heavily bioturbated, as seen from mottles and burrow fills. Sections 2 through 4 contain elongate (2-5 cm long) features with faint outlines that may be either burrows or ooze/chalk clasts (SEE MINOR LITHOLOGY).

Minor lithology: The light gray (2.5Y 7/2) intervals in Section 2, 80-97 cm, and Section 3, 20-37 cm, contain FORAMINIFER NANNOFOSSIL CHALK and NANNOFOSSIL CHALK with FORAMINIFERS, respectively.

SMEAR SLIDE SUMMARY (%):

	2, 89 M	2, 122 D	3, 26 M	3, 78 D
TEXTURE:				
Sand	20	8	15	6
Silt	60	80	60	60
Clay	20	12	25	34
COMPOSITION:				
Accessory minerals	1	1	1	3
Foraminifers	27	6	12	5
Nannofossils	70	90	85	90
Radiolarians	Tr	Tr	Tr	Tr
Siliceous fragments	2	3	2	2

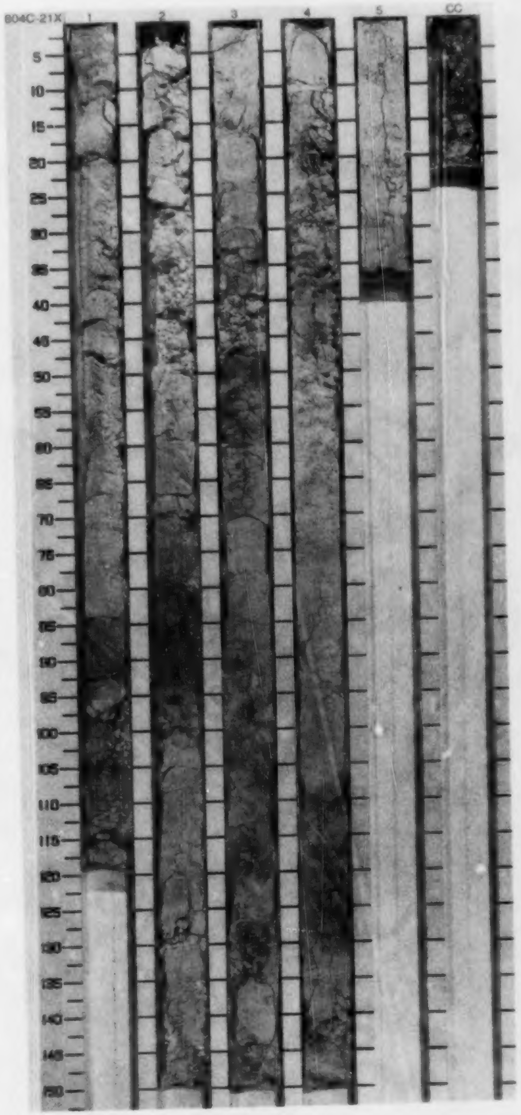

SITE 804 HOLE C CORE 22X CORED INTERVAL 197.1-206.8 mbsf

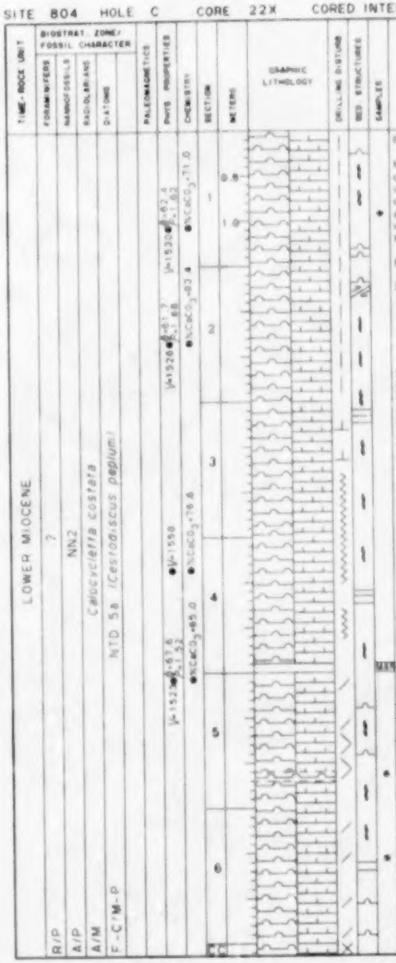
TIME-ROCK UNIT
BIOSTRAT. ZONE/ FOSSIL CHARACTER
FORAMINIFERS
NANNOFOSSILS
RADIOLARIANS
DIATOMS
PALEOMAGNETICS
PHYS. PROPERTIES
CHEMISTRY
SECTION
METERS
GRAPHIC LITHOLOGY
DRILLING DISTURB.
SED. STRUCTURES
SAMPLES
LOWER MIOCENE
R/P ?
A/P NN2
A/M Calocycletta costata
F-C/M-P NTD 5a (Cestodiscus peplum)
V=1530 φ=62.4 ρ=1.82
V=1526 φ=61.7 ρ=1.88
V=1550
V=1523 φ=67.6 ρ=1.52
%CaCO3=71.0
%CaCO3=83.4
%CaCO3=76.8
%CaCO3=65.0
1
2
3
4
5
6
CC
0.5
1.0

LITHOLOGIC DESCRIPTION

RADIOLARIAN NANNOFOSSIL CHALK

Major lithology: This core contains RADIOLARIAN NANNOFOSSIL CHALK. The sediment color varies between very pale brown (10YR 8/4) and white (10YR 8/2). Intense bioturbation is indicated by abundant burrows, trace fossils, and mottling. Most of the bioturbation is highly contorted, swirled, or fractured. Thin color banding or lamination in Section 4, 63-72 cm, appears to be stretched. Thin banding elsewhere exhibits micro faulting, rotation, and irregular contacts. Angular, very pale brown (10YR 7/3) clasts are distributed irregularly through the core.

Minor lithology: A biscuit in Section 5, 115 cm, consists of NANNOFOSSIL RADIOLARITE.

SMEAR SLIDE SUMMARY (%):

	1, 98 D	5, 112 M	6, 57 D
TEXTURE:			
Sand	15	15	15
Silt	60	60	60
Clay	25	25	25
COMPOSITION:			
Nannofossils	60	30	55
Radiolarians	40	70	45
Siliceous sponge spicules	Tr	Tr	Tr

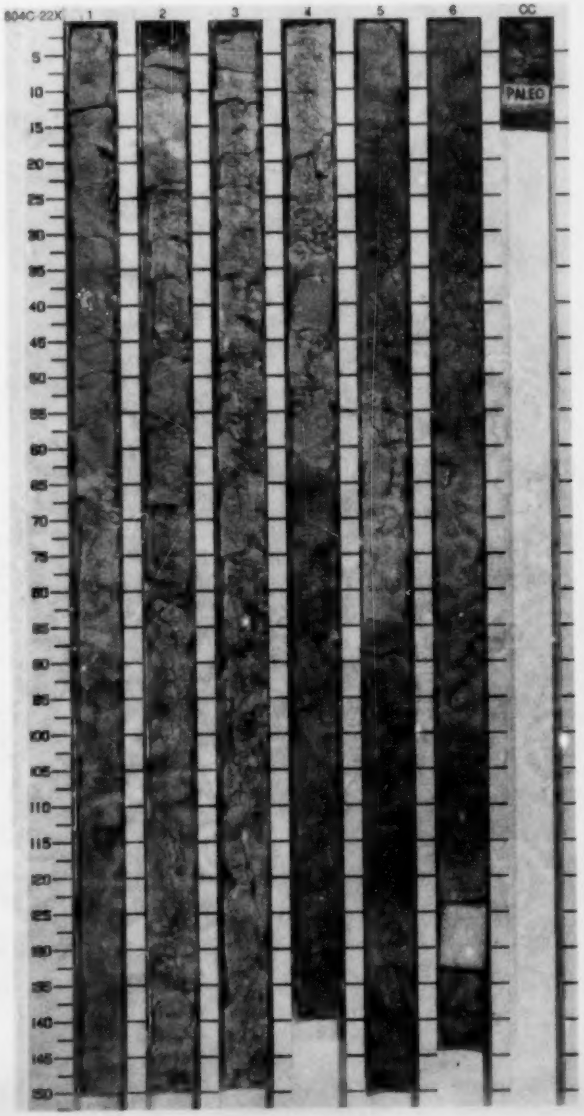
804C-22X
1
2
3
4
5
6
CC
PALEO
5
10
15
20
25
30
35
40
45
50
55
60
65
70
75
80
85
90
95
100
105
110
115
120
125
130
135
140
145
150

SITE 804 HOLE C CORE 23X CORED INTERVAL 206.8-216.5 mbsf

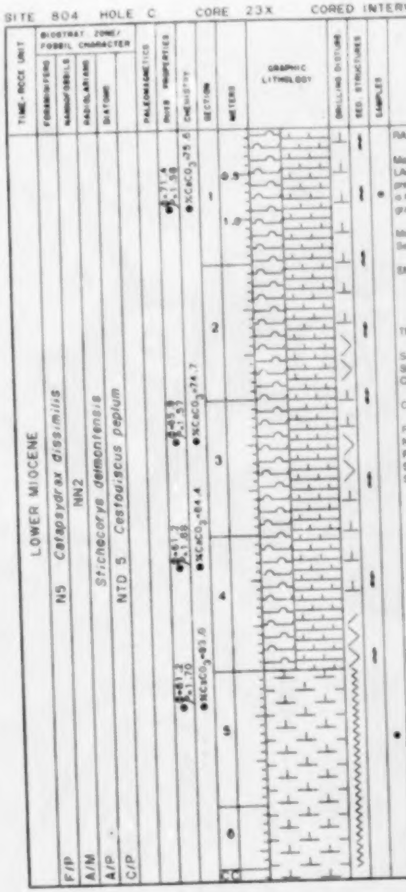
TIME-ROCK UNIT
BIOSTRAT. ZONE/ FOSSIL CHARACTER
FORAMINIFERS
NANNOFOSSILS
RADIOLARIANS
DIATOMS
PALEOMAGNETICS
PHYS. PROPERTIES
CHEMISTRY
SECTION
METERS
GRAPHIC LITHOLOGY
DRILLING DISTURB.
SED. STRUCTURES
SAMPLES
LOWER MIOCENE
F/P N5 Catapsydrax dissimilis
NN2
A/M Stichocorys delmontensis
A/P
C/P NTD 5 Cestodiscus peplum
●φ=71.4
●γ=1.58
●%CaCO₃=75.6
●φ=65.8
●γ=1.57
●%CaCO₃=74.7
●φ=61.2
●γ=1.68
●%CaCO₃=84.4
●φ=61.2
●γ=1.70
●%CaCO₃=93.0
1
2
3
4
5
6
CC
0.5
1.0

LITHOLOGIC DESCRIPTION

RADIOLARIAN NANNOFOSSIL CHALK

Major lithology: Sections 1 through 4 of this core contain pale brown (10YR 7/4) RADIOLARIAN NANNOFOSSIL CHALK. Moderate to heavy bioturbation is evident from well-preserved trace fossils. The sediment is otherwise structureless, although drilling disturbance is heavy. Section 4 grades from very pale brown (10YR 8/3) to white (10YR 8/1). This color gradation marks a transition from radiolarian nannofossil chalk to nannofossil ooze.

Minor lithology: White (10YR 8/1), homogeneous NANNOFOSSIL OOZE is present in Sections 5 and 6 of this core. It is very stiff, structureless, and heavily disturbed by drilling.

SMEAR SLIDE SUMMARY (%):

	1, 75	5, 74
	D	M
TEXTURE:		
Sand	10	5
Silt	55	60
Clay	35	35
COMPOSITION:		
Foraminifers	—	1
Nannofossils	60	89
Radiolarians	40	9
Siliceous fragments	—	1
Siliceous sponge spicules	Tr	—

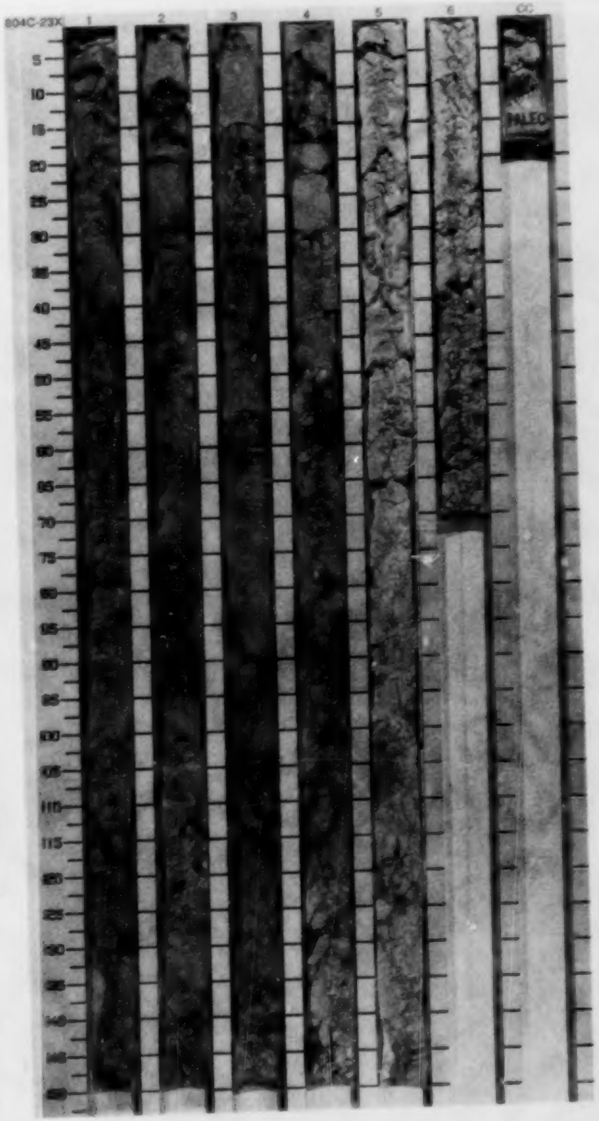
804C-23X
1
2
3
4
5
6
CC
PALEO
5
10
15
20
25
30
35
40
45
50
55
60
65
70
75
80
85
90
95
100
105
110
115
120
125
130
135
140
145
150

SITE 804 HOLE C CORE 24X CORED INTERVAL 216.5-226.2 mbsf

TIME-ROCK UNIT	FORAMINIFERS	NANNOFOSSILS	RADIOLARIANS	DIATOMS		PALEOMAGNETICS	PHYS. PROPERTIES	CHEMISTRY	SECTION	METERS	DRILLING DISTURB.	SED. STRUCTURES	SAMPLES
LOWER MIOCENE	N5 *Catapsydrax dissimilis* F/P	NN2 A/P	*Stichocorys delmontensis* A/P	NTD 2 *Craspedodiscus elegans* C/M			● ϕ=56.8 γ=1.76	● %CaCO$_3$=93.5	1	0.5 1.0	⊥		OG IW
							● ϕ=40.3 γ=1.98	● %CaCO$_3$=92.0	2		⊥ O	~	● ●
									3		V X	~	
									4		X		
									CC		⊥		

LITHOLOGIC DESCRIPTION

NANNOFOSSIL OOZE

Major lithology: This core contains white (2.5Y 8/2), homogeneous, bioturbated NANNOFOSSIL OOZE. The top of Section 2 contains a few pyritized burrow fragments up to 20 mm long. Adjacent to one pyrite fragment is a pod of white (2.5Y 8/0) NANNOFOSSIL OOZE with RADIOLARIANS.

SMEAR SLIDE SUMMARY (%):

	1, 16	2, 75
	M	D
TEXTURE:		
Sand	5	—
Silt	60	40
Clay	35	60
COMPOSITION:		
Foraminifers	1	—
Nannofossils	78	99
Radiolarians	20	Tr
Siliceous fragments	1	1

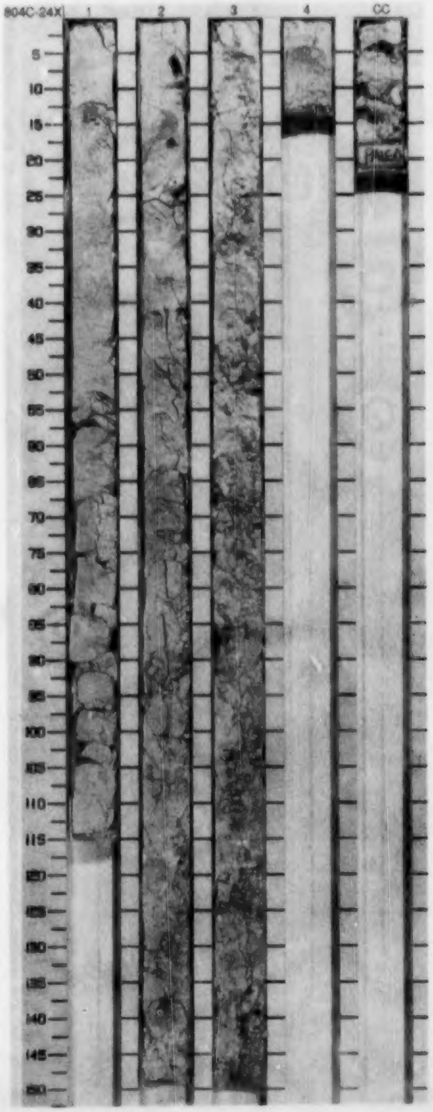
804C-24X
1
2
3
4
CC
5
10
15
20
25
30
35
40
45
50
55
60
65
70
75
80
85
90
95
100
105
110
115
120
125
130
135
140
145
150

SITE 804 HOLE C CORE 25X CORED INTERVAL 226.2-235.8 mbsf

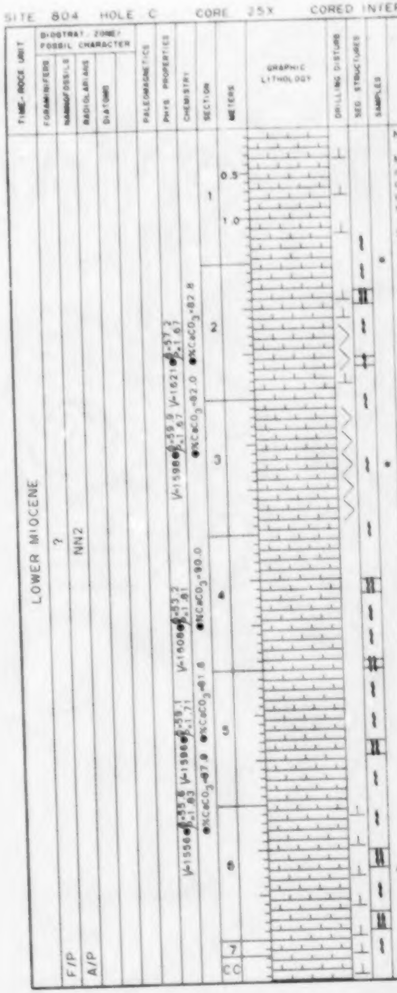
TIME-ROCK UNIT
BIOSTRAT. ZONE/ FOSSIL CHARACTER
FORAMINIFERS
NANNOFOSSILS
RADIOLARIANS
DIATOMS
PALEOMAGNETICS
PHYS. PROPERTIES
CHEMISTRY
SECTION
METERS
GRAPHIC LITHOLOGY
DRILLING DISTURB.
SED. STRUCTURES
SAMPLES
LOWER MIOCENE
?
NN2
F/P
A/P
V=1598● φ=59.9 ρ=1.67
V=1621● φ=57.2 ρ=1.67
V=1508● φ=53.2 ρ=1.81
V=1598● φ=58.1 ρ=1.71
V=1556● φ=55.6 ρ=1.83
●%CaCO3=82.8
●%CaCO3=82.0
●%CaCO3=90.0
●%CaCO3=81.6
●%CaCO3=87.0
1
2
3
4
5
6
7
CC
0.5
1.0

LITHOLOGIC DESCRIPTION

NANNOFOSSIL CHALK

Major lithology: This core contains NANNOFOSSIL CHALK that grades to ooze in a few intervals. In Section 1, the chalk contains a significant percentage of RADIOLARIANS. The chalk is predominantly white (10YR 8/2) with intervals of light gray (10YR 7/2) that are 10 to 30 cm thick. The white colored intervals are slightly bioturbated and the light gray intervals are heavily bioturbated. Color bands (mm scale) in the gray intervals of Section 2 are contorted.

SMEAR SLIDE SUMMARY (%):

	1, 149 M	3, 75 D	6, 75 D
TEXTURE:			
Sand	10	5	5
Silt	60	40	35
Clay	30	55	60
COMPOSITION:			
Accessory minerals	—	—	Tr
Clay	—	—	8
Nannofossils	87	99	90
Radiolarians	12	1	2
Siliceous fragments	1	Tr	Tr
Siliceous sponge spicules	—	Tr	—

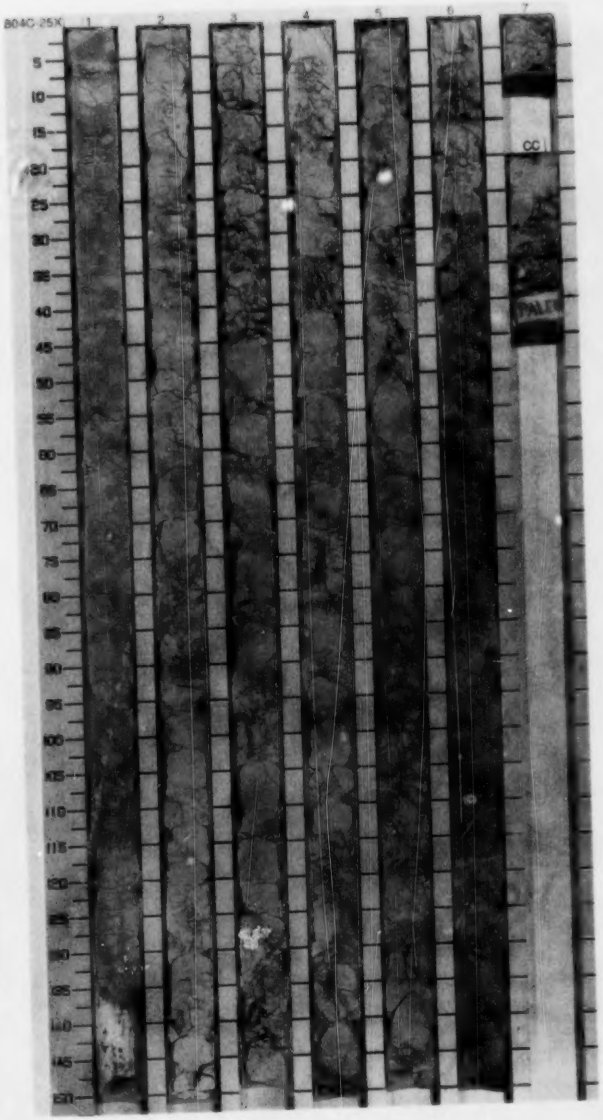
804C-25X
1
2
3
4
5
6
7
CC
PALEO
5
10
15
20
25
30
35
40
45
50
55
60
65
70
75
80
85
90
95
100
105
110
115
120
125
130
135
140
145
150

SITE 804 HOLE C CORE 26X CORED INTERVAL 235.8-245.9 mbsf

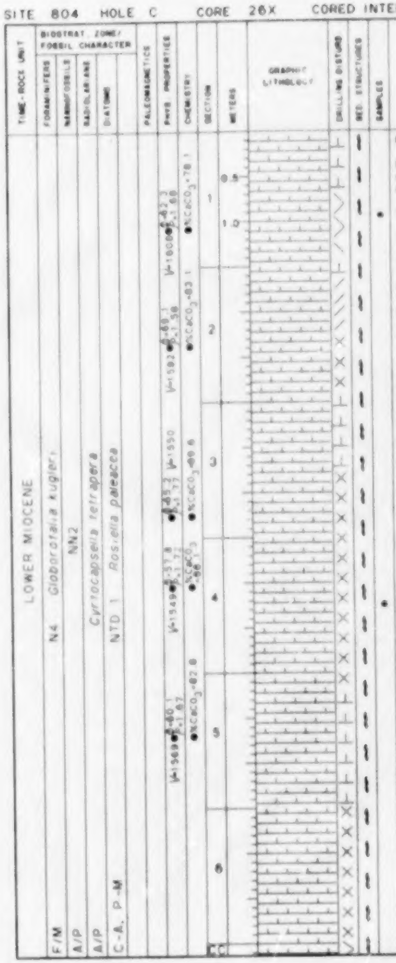
TIME-ROCK UNIT
BIOSTRAT. ZONE/ FOSSIL CHARACTER
FORAMINIFERS
NANNOFOSSILS
RADIOLARIANS
DIATOMS
PALEOMAGNETICS
PHYS. PROPERTIES
CHEMISTRY
SECTION
METERS
GRAPHIC LITHOLOGY
DRILLING DISTURB.
SED. STRUCTURES
SAMPLES
LOWER MIOCENE
F/M N4 Globorotalia kugleri
A/P NN2
A/P Cyrtocapsella tetrapera
C-A, P-M NTD 1 Rossiella paleacea
γ=1000 ϕ=42.3 ρ=1.88
%CaCO3=78.1
γ=1582 ϕ=60.1 ρ=1.58
%CaCO3=83.1
γ=1550
ϕ=45.2 ρ=1.77
%CaCO3=89.6
γ=1549 ϕ=57.8 ρ=1.72
%CaCO3=98.1
γ=1569 ϕ=60.1 ρ=1.67
%CaCO3=82.8
1
2
3
4
5
6
CC
0.5
1.0

LITHOLOGIC DESCRIPTION

NANNOFOSSIL CHALK with RADIOLARIANS

Major lithology: This core contains white (10YR 8/1 and 10YR 8/2) NANNOFOSSIL CHALK with RADIOLARIANS. Heavy bioturbation is indicated by abundant trace fossils. Drilling disturbance is severe, resulting in abundant fragmentation and brecciation of the core.

SMEAR SLIDE SUMMARY (%):

	1, 93	4, 74
	D	D
TEXTURE:		
Sand	15	10
Silt	55	70
Clay	30	20
COMPOSITION:		
Accessory minerals	Tr	Tr
Clay	Tr	Tr
Foraminifers	—	4
Nannofossils	75	71
Radiolarians	20	20
Siliceous fragments	5	5

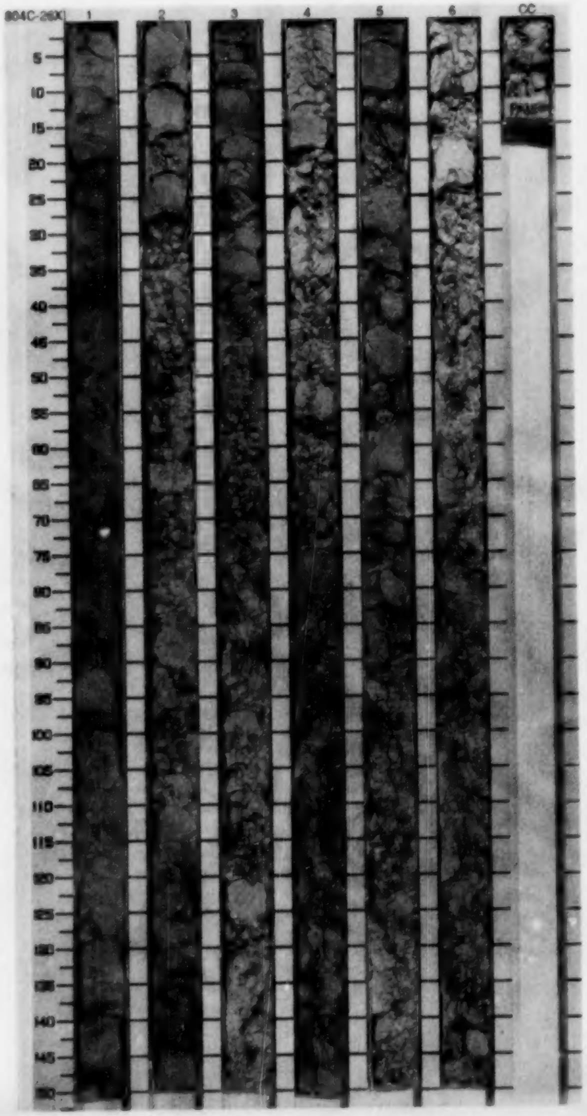
804C-26X
1
2
3
4
5
6
CC
5
10
15
20
25
30
35
40
45
50
55
60
65
70
75
80
85
90
95
100
105
110
115
120
125
130
135
140
145
150

SITE 804 HOLE C CORE 27X CORED INTERVAL 245.9-255.1 mbsf

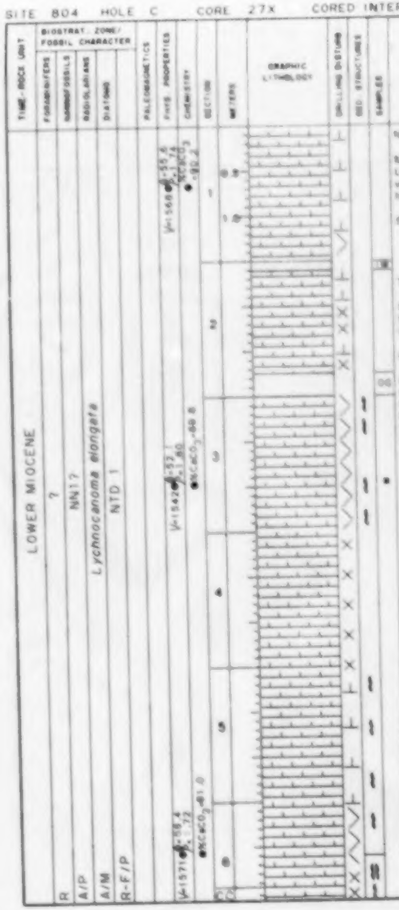
TIME-ROCK UNIT
BIOSTRAT. ZONE/ FOSSIL CHARACTER
FORAMINIFERS
NANNOFOSSILS
RADIOLARIANS
DIATOMS
PALEOMAGNETICS
PHYS. PROPERTIES
CHEMISTRY
SECTION
METERS
GRAPHIC LITHOLOGY
DRILLING DISTURB.
SED. STRUCTURES
SAMPLES
LOWER MIOCENE
?
R
NN17
A/P
Lychnocanoma elongata
A/M
NTD 1
R-F/P
V=1566
φ=55.6
γ=1.74
%CaCO3=90.2
V=1542
φ=52.1
γ=1.80
%CaCO3=88.8
V=1571
φ=56.4
γ=1.72
%CaCO3=81.0
1
2
3
4
5
6
CC
0.5
1.0
IW
OG

LITHOLOGIC DESCRIPTION

NANNOFOSSIL CHALK with RADIOLARIANS

Major lithology: This core consists of white (10YR 8/1) NANNOFOSSIL CHALK with RADIOLARIANS. The color grades from very pale brown (10YR 7/3) in Section 3 to a darker shade of very pale brown (10YR 7/4) in Section 4. Sections 2, 3, 4, 6 and CC are brecciated or highly fragmented into biscuits.

SMEAR SLIDE SUMMARY (%):

	3, 95
	D
TEXTURE	
Sand	7
Silt	60
Clay	33
COMPOSITION	
Accessory minerals	2
Clay	Tr
Foraminifers	2
Nannofossils	80
Radiolarians	11
Siliceous fragments	5

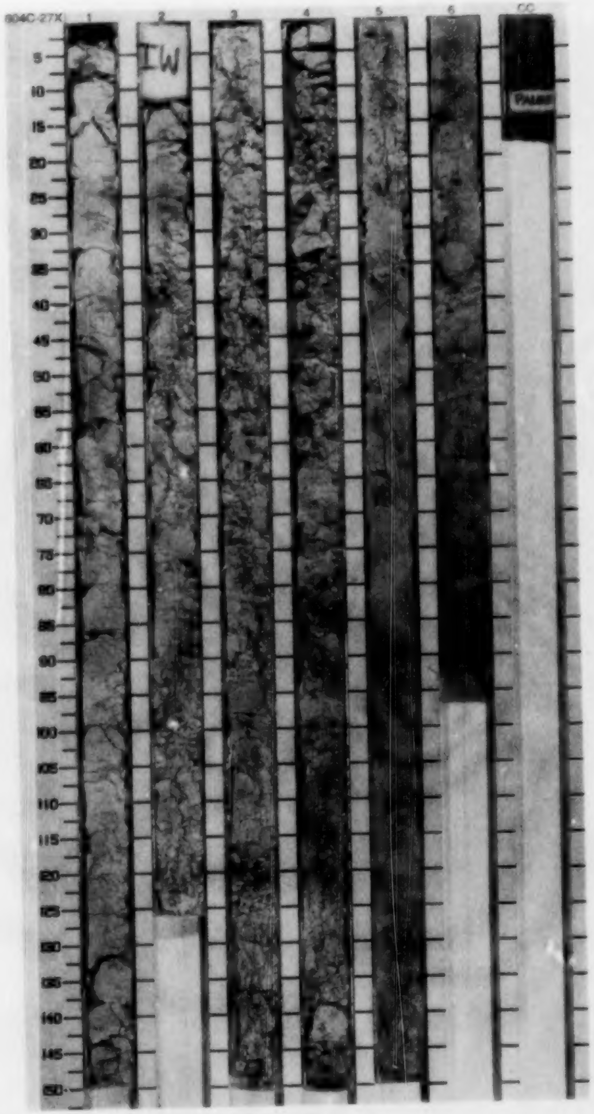
804C-27X
1
2
3
4
5
6
CC
IW
5
10
15
20
25
30
35
40
45
50
55
60
65
70
75
80
85
90
95
100
105
110
115
120
125
130
135
140
145
150

SITE 804 HOLE C CORE 28X CORED INTERVAL 255.1-264.7 mbsf

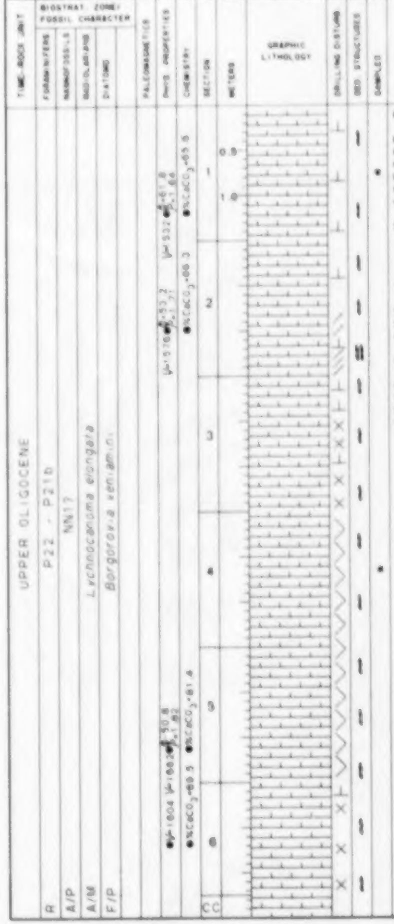
TIME-ROCK UNIT
BIOSTRAT. ZONE/ FOSSIL CHARACTER
FORAMINIFERS
NANNOFOSSILS
RADIOLARIANS
DIATOMS
PALEOMAGNETICS
PHYS. PROPERTIES
CHEMISTRY
SECTION
METERS
GRAPHIC LITHOLOGY
DRILLING DISTURB.
SED. STRUCTURES
SAMPLES
UPPER OLIGOCENE
R
P22 - P21b
A/P
NN17
A/M
Lychnocanoma elongata
F/P
Borgorovia veniamini
V=1532 ●φ=61.8 ρ=1.64
V=1570 ●φ=53.2 ρ=1.77
V=1604 V=1662 ●φ=50.8 ρ=1.82
●%CaCO3=83.6
●%CaCO3=88.3
●%CaCO3=89.5
●%CaCO3=81.4
0.5
1.0
1
2
3
4
5
6
CC

LITHOLOGIC DESCRIPTION

NANNOFOSSIL CHALK and NANNOFOSSIL CHALK with RADIOLARIANS

Major lithology: Sections 1 through 3 are very pale brown (10YR 7/4 to 10YR 8/3) NANNOFOSSIL CHALK with RADIOLARIANS. These sections are heavily bioturbated as evidenced from abundant trace fossils. Below Section 3, the color grades from very pale brown (10YR 8/3) to white (10YR 8/2 and 10YR 8/1). The radiolarian content is reduced in the lower part of the core, where it becomes a NANNOFOSSIL CHALK. Bioturbation is abundant in this interval. Drilling disturbance is moderate to severe throughout the core.

SMEAR SLIDE SUMMARY (%):

	1, 75	4, 63
	D	D
TEXTURE:		
Sand	5	5
Silt	50	55
Clay	45	40
COMPOSITION:		
Clay	5	—
Foraminifers	Tr	3
Nannofossils	85	92
Radiolarians	10	5

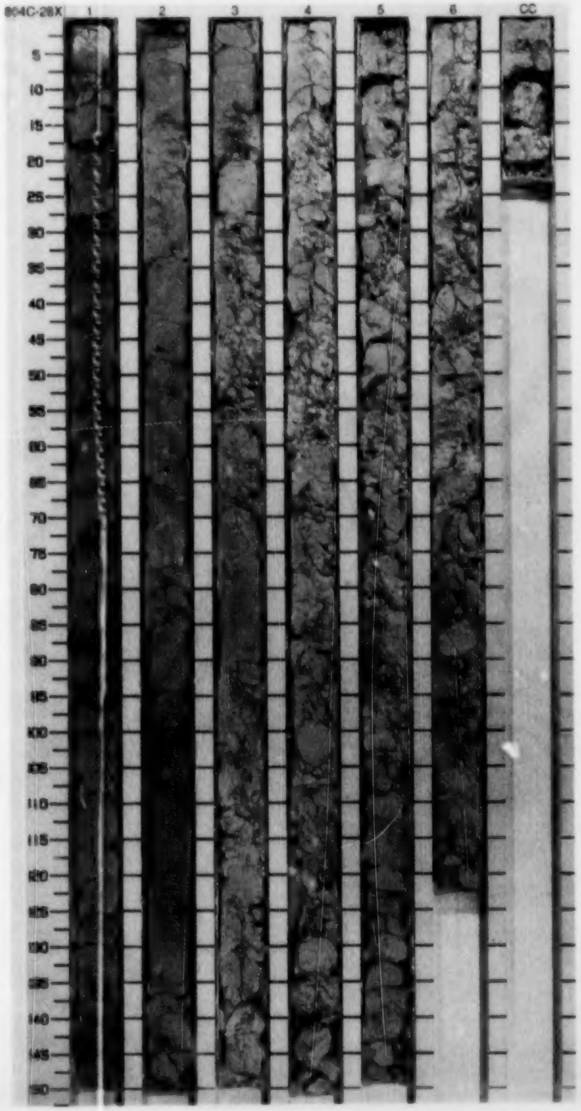
804C-28X
1
2
3
4
5
6
CC
5
10
15
20
25
30
35
40
45
50
55
60
65
70
75
80
85
90
95
100
105
110
115
120
125
130
135
140
145
150

SITE 804 HOLE C CORE 29X CORED INTERVAL 264.7-274.4 mbsf

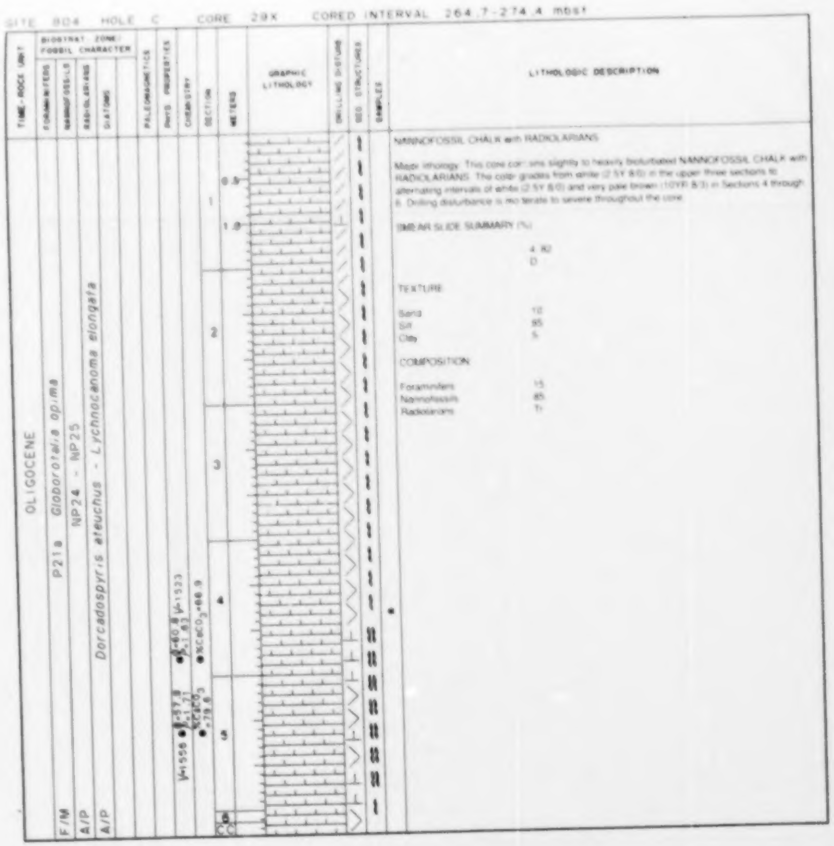
TIME-ROCK UNIT
BIOSTRAT. ZONE/ FOSSIL CHARACTER
FORAMINIFERS
NANNOFOSSILS
RADIOLARIANS
DIATOMS
PALEOMAGNETICS
PHYS. PROPERTIES
CHEMISTRY
SECTION
METERS
GRAPHIC LITHOLOGY
DRILLING DISTURB.
SED. STRUCTURES
SAMPLES
OLIGOCENE
F/M P21a Globorotalia opima
A/P NP24 - NP25
A/P Dorcadospyris ateuchus - Lychnocanoma elongata
φ=60.8 ρ=1.63 V=1523
%CaCO3=88.9
V=1556 φ=57.8 ρ=1.71
%CaCO3 =79.6
1
2
3
4
5
6
CC
0.5
1.0

LITHOLOGIC DESCRIPTION

NANNOFOSSIL CHALK with RADIOLARIANS

Major lithology: This core contains slightly to heavily bioturbated NANNOFOSSIL CHALK with RADIOLARIANS. The color grades from white (2.5Y 8/0) in the upper three sections to alternating intervals of white (2.5Y 8/0) and very pale brown (10YR 8/3) in Sections 4 through 6. Drilling disturbance is moderate to severe throughout the core.

SMEAR SLIDE SUMMARY (%):

	4, 82
	D
TEXTURE:	
Sand	10
Silt	85
Clay	5
COMPOSITION:	
Foraminifers	15
Nannofossils	85
Radiolarians	Tr

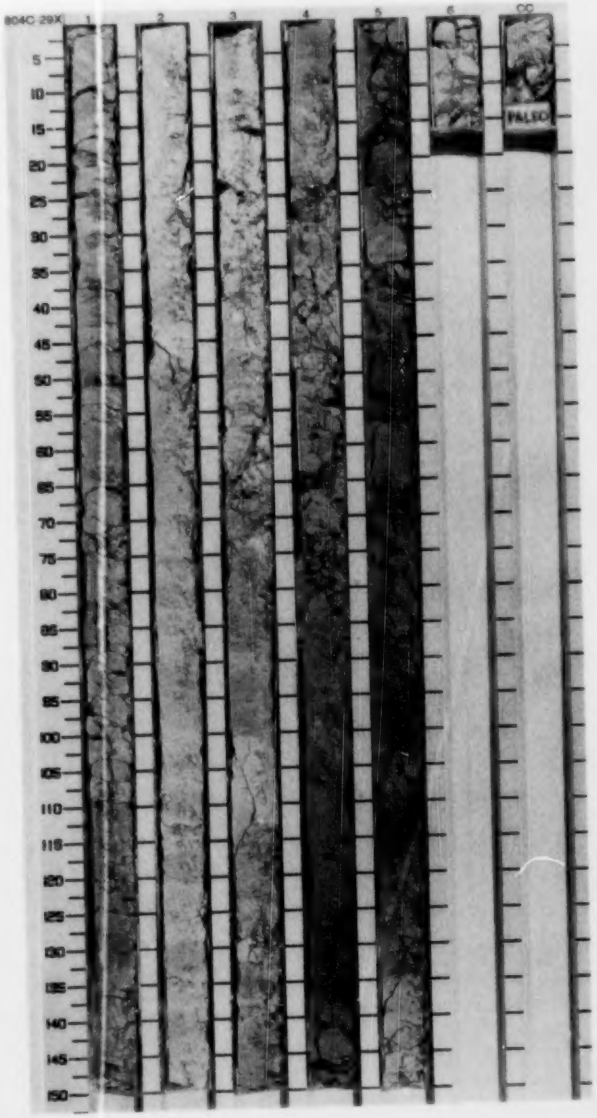
804C-29X
1
2
3
4
5
6
CC
PALEO
5
10
15
20
25
30
35
40
45
50
55
60
65
70
75
80
85
90
95
100
105
110
115
120
125
130
135
140
145
150

SITE 804 HOLE C CORE 30X CORED INTERVAL 274.4-284.0 mbsf

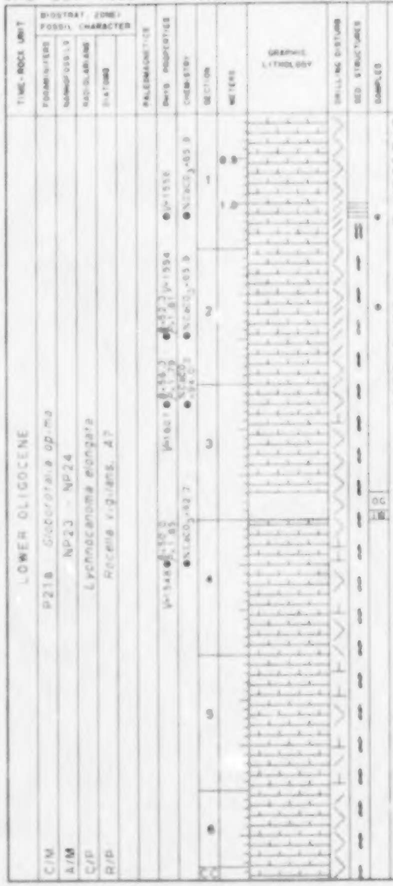
TIME-ROCK UNIT
BIOSTRAT. ZONE/ FOSSIL CHARACTER
FORAMINIFERS
NANNOFOSSILS
RADIOLARIANS
DIATOMS
PALEOMAGNETICS
PHYS. PROPERTIES
CHEMISTRY
SECTION
METERS
GRAPHIC LITHOLOGY
DRILLING DISTURB.
SED. STRUCTURES
SAMPLES
LOWER OLIGOCENE
P21a Globorotalia opima
NP23 - NP24
Lychnocanoma elongata
Rocella vigilans, A?
C/M
A/M
C/P
R/P
●γ=1.556
●γ=1.594
●%CaCO3=93.0
●%CaCO3=93.0
●%CaCO3=92.7
1
2
3
4
5
6
CC
0.5
1.0
OG
IW

LITHOLOGIC DESCRIPTION

NANNOFOSSIL CHALK

Major lithology: This core contains NANNOFOSSIL CHALK. The color varies between shades of white (10YR 8/2, 10YR 8/1) in Section 1 and 2, and is more uniformly white (10YR 8/1) in the remainder of the core. Hard intervals are intermixed with softer ones in Section 1. In Section 1, 100 cm, there is a 5-cm thick section that exhibits discontinuous parallel lamination. The entire core is slightly to heavily bioturbated and is moderately fractured by drilling.

SMEAR SLIDE SUMMARY (%):

	1, 117	2, 67
	D	D
TEXTURE:		
Sand	5	5
Silt	95	95
COMPOSITION:		
Foraminifers	2	2
Nannofossils	91	90
Radiolarians	2	3
Silicoflagellates	5	5

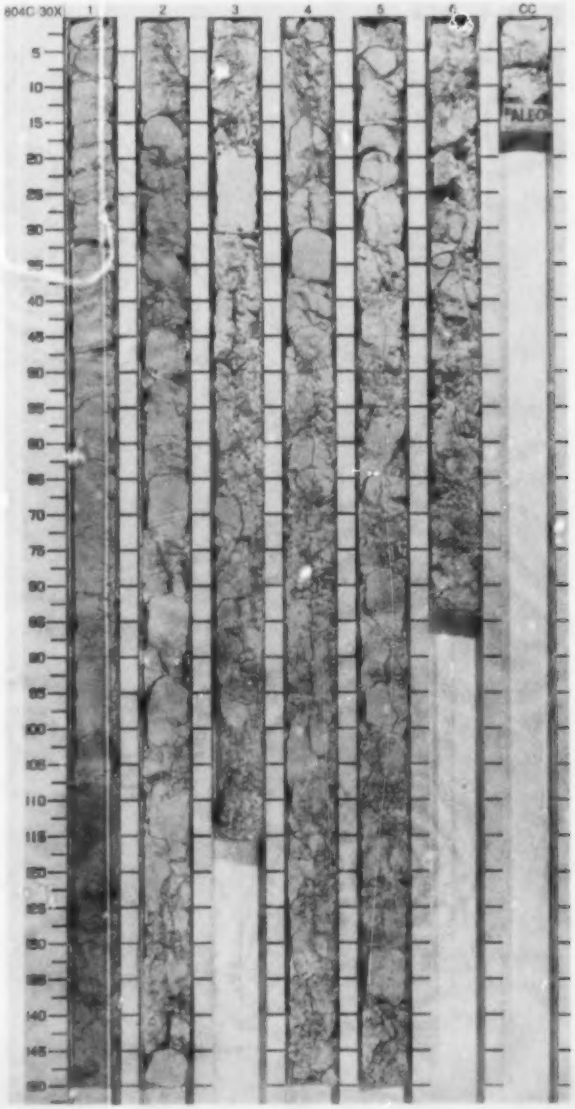
804C 30X
1
2
3
4
5
6
CC
PALEO
5
10
15
20
25
30
35
40
45
50
55
60
65
70
75
80
85
90
95
100
105
110
115
120
125
130
135
140
145
150

SITE 804 HOLE C CORE 31X CORED INTERVAL 284.0-293.7 mbsf

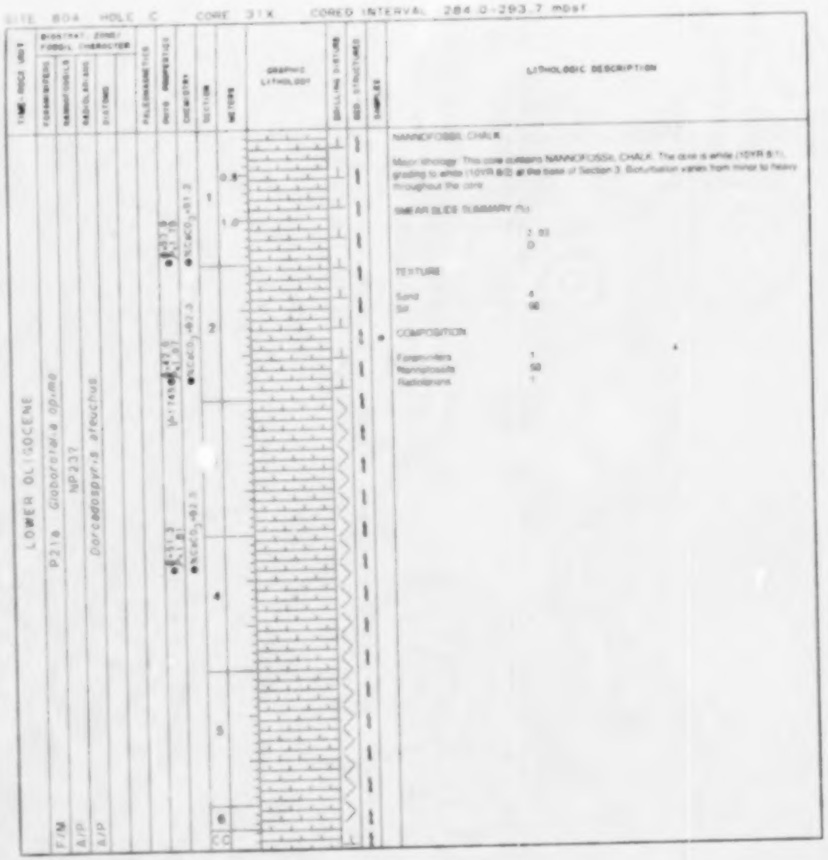
TIME-ROCK UNIT
BIOSTRAT. ZONE/ FOSSIL CHARACTER
FORAMINIFERS
NANNOFOSSILS
RADIOLARIANS
DIATOMS
PALEOMAGNETICS
PHYS. PROPERTIES
CHEMISTRY
SECTION
METERS
GRAPHIC LITHOLOGY
DRILLING DISTURB.
SED. STRUCTURES
SAMPLES
LOWER OLIGOCENE
P21a Globorotalia opima
NP23?
Dorcadospyris ateuchus
F/M
A/P
A/P
●%CaCO3=91.2
●%CaCO3=92.3
●%CaCO3=92.5
0.5
1.0
1
2
3
4
5
6
CC

LITHOLOGIC DESCRIPTION

NANNOFOSSIL CHALK

Major lithology: This core contains NANNOFOSSIL CHALK. The core is white (10YR 8/1), grading to white (10YR 8/2) at the base of Section 3. Bioturbation varies from minor to heavy throughout the core.

SMEAR SLIDE SUMMARY (%):

	2, 93
	D
TEXTURE	
Sand	4
Silt	96
COMPOSITION	
Foraminifers	1
Nannofossils	98
Radiolarians	1

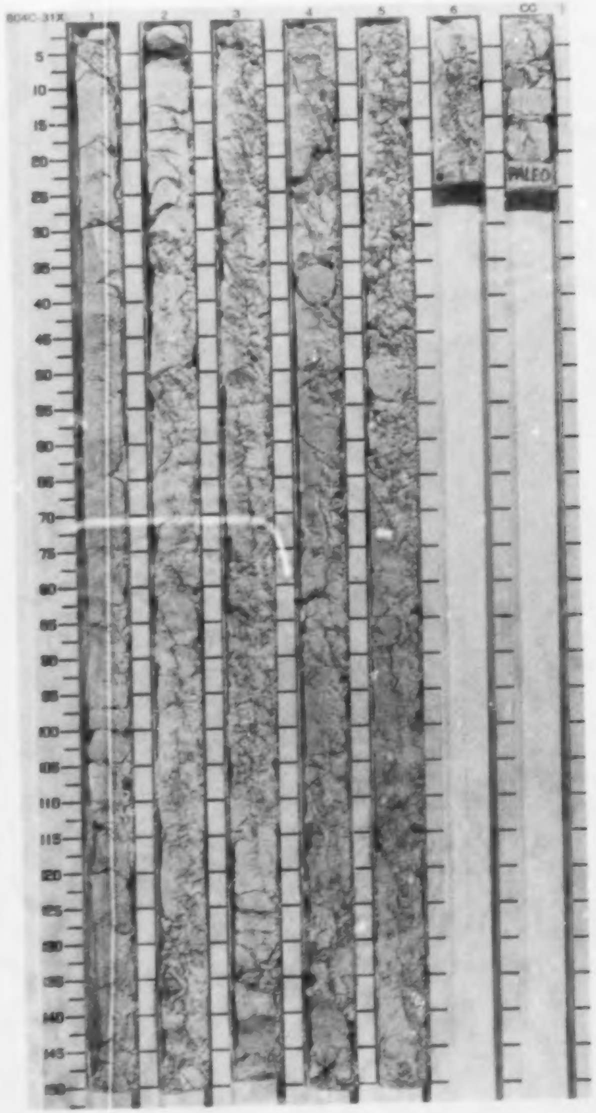
804C-31X
1
2
3
4
5
6
CC
PALEO
5
10
15
20
25
30
35
40
45
50
55
60
65
70
75
80
85
90
95
100
105
110
115
120
125
130
135
140
145
150

SITE 804 HOLE C CORE 32X CORED INTERVAL 293.7-303.3 mbsf

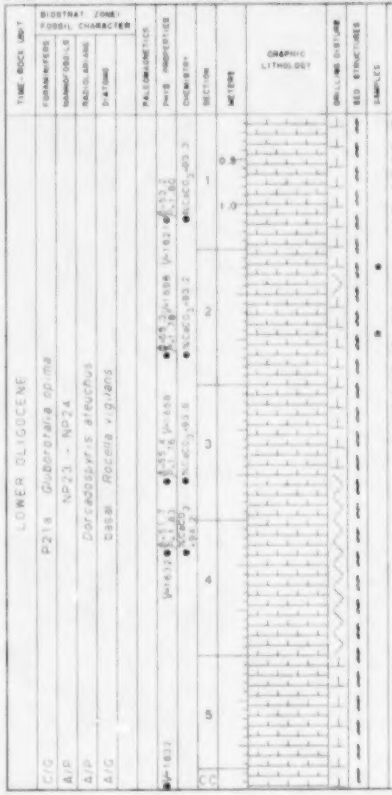

LITHOLOGIC DESCRIPTION

NANNOFOSSIL CHALK to NANNOFOSSIL CHALK with RADIOLARIANS

Major lithology: This core contains NANNOFOSSIL CHALK, grading to NANNOFOSSIL CHALK with RADIOLARIANS. The core is white (10YR 8/1 to 10YR 8/2) in both sediment types. Bioturbation is slight to heavy throughout the core, including well developed *Zoophycos* trace fossils in Section 1.

SMEAR SLIDE SUMMARY (%):

	1, 70	2, 49
	D	D
TEXTURE:		
Sand	8	5
Silt	90	95
Clay	2	—
COMPOSITION:		
Diatoms	1	—
Foraminifers	1	1
Nannofossils	81	94
Quartz	1	—
Radiolarians	10	3
Siliceous sponge spicules	5	2

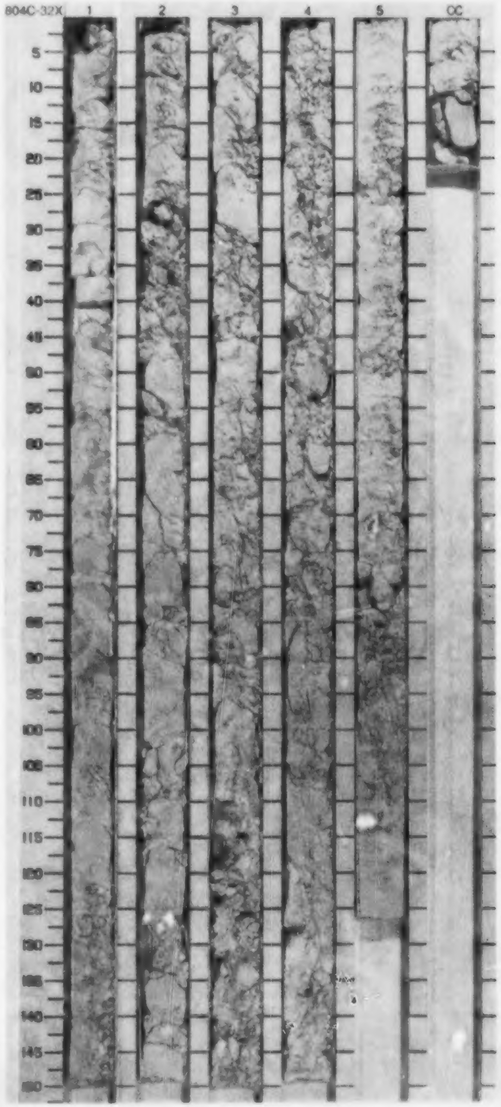
804C-32X
1
2
3
4
5
CC
5
10
15
20
25
30
35
40
45
50
55
60
65
70
75
80
85
90
95
100
105
110
115
120
125
130
135
140
145
150

SITE 804 HOLE C CORE 33X CORED INTERVAL 303.3-312.5 mbsf

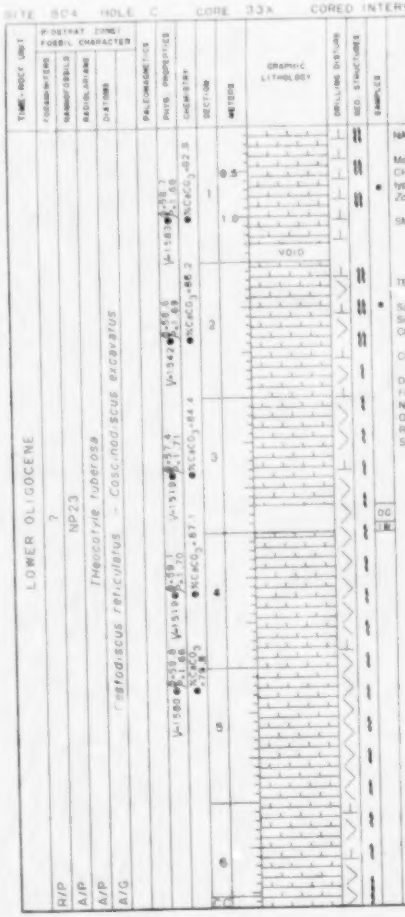
TIME-ROCK UNIT
BIOSTRAT. ZONE/ FOSSIL CHARACTER
FORAMINIFERS
NANNOFOSSILS
RADIOLARIANS
DIATOMS
PALEOMAGNETICS
PHYS. PROPERTIES
CHEMISTRY
SECTION
METERS
GRAPHIC LITHOLOGY
DRILLING DISTURB.
SED. STRUCTURES
SAMPLES
LOWER OLIGOCENE
?
NP23
Theocotyle tuberosa
Cestodiscus reticulatus - Coscinodiscus excavatus
R/P
A/P
A/P
A/G
V=1583 ●φ=58.7 γ=1.60
●%CaCO3=82.9
V=1542 ●φ=58.6 γ=1.69
●%CaCO3=86.2
V=1519 ●φ=57.4 γ=1.71
●%CaCO3=84.4
V=1519 ●φ=58.1 γ=1.70
●%CaCO3=87.1
V=1580 ●φ=58.8 γ=1.66
●%CaCO3=79.8
1
2
3
4
5
6
CC
0.5
1.0
VOID
OG
IW

LITHOLOGIC DESCRIPTION

NANNOFOSSIL CHALK to NANNOFOSSIL CHALK with RADIOLARIANS

Major lithology: This core contains NANNOFOSSIL CHALK, grading to NANNOFOSSIL CHALK with RADIOLARIANS. The core is white (10YR 8/1 to 10YR 8/2) in both sediment types. Bioturbation is slight to heavy throughout the core, including well-developed *Zoophycos* trace fossils in Section 1.

SMEAR SLIDE SUMMARY (%):

	1, 70	2, 49
	D	D
TEXTURE:		
Sand	8	5
Silt	90	95
Clay	2	—
COMPOSITION:		
Diatoms	1	—
Foraminifers	1	1
Nannofossils	81	94
Quartz	1	—
Radiolarians	10	3
Siliceous sponge spicules	5	2

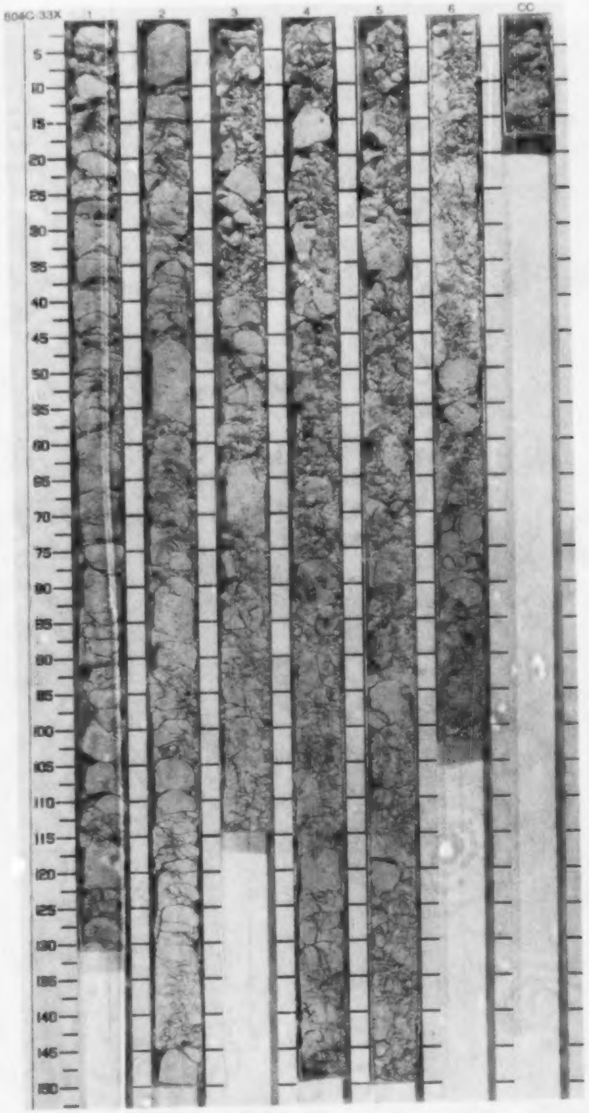
804C-33X
1
2
3
4
5
6
CC
5
10
15
20
25
30
35
40
45
50
55
60
65
70
75
80
85
90
95
100
105
110
115
120
125
130
135
140
145
150

SITE 805 HOLE A CORE 1H CORED INTERVAL 0.0-3.0 mbsf

TIME-ROCK UNIT	BIOSTRAT. ZONE/ FOSSIL CHARACTER				PALEOMAGNETICS	PHYS. PROPERTIES	CHEMISTRY	SECTION	METERS	GRAPHIC LITHOLOGY	DRILLING DISTURB.	SED. STRUCTURES	SAMPLES	LITHOLOGIC DESCRIPTION
	FORAMINIFERS	NANNOFOSSILS	RADIOLARIANS	DIATOMS										
PLEISTOCENE	N22 - N23	NN20 - NN21		NTD 17 *Pseudoeunotia doliolus*				1 2	0.5 1.0					SEDIMENT TYPE This core was not opened on ship
	A/M	A/P		C/P-M				CC						

SITE 805 HOLE A CORE 2H CORED INTERVAL 3.0-12.5 mbsf

TIME-ROCK UNIT	BIOSTRAT. ZONE/ FOSSIL CHARACTER				PALEOMAGNETICS	PHYS. PROPERTIES	CHEMISTRY	SECTION	METERS	GRAPHIC LITHOLOGY	DRILLING DISTURB.	SED. STRUCTURES	SAMPLES	LITHOLOGIC DESCRIPTION
	FORAMINIFERS	NANNOFOSSILS	RADIOLARIANS	DIATOMS										
PLEISTOCENE	N22	NN19		NTD 16 *Nitzschia reinholdii*				1 2	0.5 1.0					SEDIMENT TYPE This core was not opened on ship
	A/M	A		F/P				CC						

SITE 805 HOLE A CORE 3H CORED INTERVAL 12.5-22.0 mbsf

TIME-ROCK UNIT	BIOSTRAT. ZONE/ FOSSIL CHARACTER: FORAMINIFERS	BIOSTRAT. ZONE/ FOSSIL CHARACTER: NANNOFOSSILS	BIOSTRAT. ZONE/ FOSSIL CHARACTER: RADIOLARIANS	BIOSTRAT. ZONE/ FOSSIL CHARACTER: DIATOMS		PALEOMAGNETICS	PHYS. PROPERTIES	CHEMISTRY	SECTION	METERS	GRAPHIC LITHOLOGY	DRILLING DISTURB.	SED. STRUCTURES	SAMPLES	LITHOLOGIC DESCRIPTION
PLEISTOCENE	N22	NN19				R? (Matuyama?)			1	0.5 1.0					SEDIMENT TYPE This core was not opened on ship.
									2						
						N? (Jaramillo?)			3						
						R? (Matuyama?)			4						
					N?	(Cobb?)			5						
						R? (Matuyama?)			6						
	A/M	A/M							CC						

SITE 805 HOLE A CORE 4H CORED INTERVAL 22.0-31.5 mbsf

TIME-ROCK UNIT	BIOSTRAT. ZONE/ FOSSIL CHARACTER				PALEOMAGNETICS	PHYS. PROPERTIES	CHEMISTRY	SECTION	METERS	GRAPHIC LITHOLOGY	DRILLING DISTURB.	SED. STRUCTURES	SAMPLES	LITHOLOGIC DESCRIPTION
	FORAMINIFERS	NANNOFOSSILS	RADIOLARIANS	DIATOMS										
UPPER PLIOCENE	N19 - N21	NN18						1	0.5 1.0					SEDIMENT TYPE This core was not opened on ship
	A/G	A/P						CC						

SITE 805 HOLE A CORE 5H CORED INTERVAL 31.5-41.0 mbsf

TIME-ROCK UNIT	BIOSTRAT. ZONE/ FOSSIL CHARACTER				PALEOMAGNETICS	PHYS. PROPERTIES	CHEMISTRY	SECTION	METERS	GRAPHIC LITHOLOGY	DRILLING DISTURB.	SED. STRUCTURES	SAMPLES	LITHOLOGIC DESCRIPTION
	FORAMINIFERS	NANNOFOSSILS	RADIOLARIANS	DIATOMS										
UPPER PLIOCENE	N21	NN18						1	0.5 1.0					SEDIMENT TYPE This core was not opened on ship
	A/M	A/M						CC						

SITE 805 HOLE A CORE 6H CORED INTERVAL 41.0-50.5 mbsf

TIME-ROCK UNIT	BIOSTRAT. ZONE/ FOSSIL CHARACTER				PALEOMAGNETICS	PHYS. PROPERTIES	CHEMISTRY	SECTION	METERS	GRAPHIC LITHOLOGY	DRILLING DISTURB.	SED. STRUCTURES	SAMPLES	LITHOLOGIC DESCRIPTION
	FORAMINIFERS	NANNOFOSSILS	RADIOLARIANS	DIATOMS										
UPPER PLIOCENE	N19 - N20	NN16						1	0.5 1.0					SEDIMENT TYPE This core was not opened on ship
								2						
	A/P	A/P						CC						

SITE 805 HOLE B CORE 1H CORED INTERVAL 0.0-6.7 mbsf

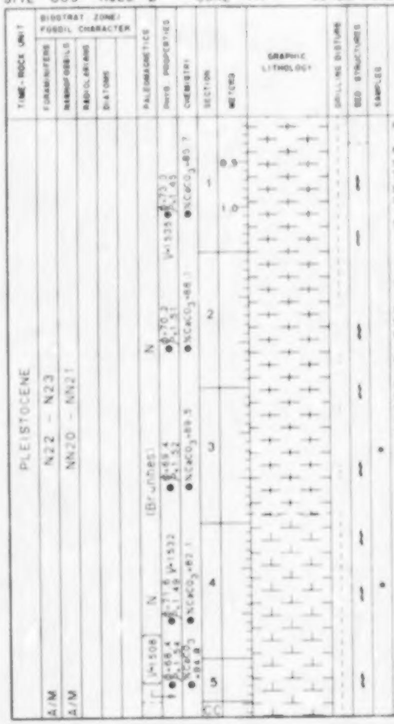
TIME-ROCK UNIT
BIOSTRAT. ZONE/ FOSSIL CHARACTER
FORAMINIFERS
NANNOFOSSILS
RADIOLARIANS
DIATOMS
PALEOMAGNETICS
PHYS. PROPERTIES
CHEMISTRY
SECTION
METERS
GRAPHIC LITHOLOGY
DRILLING DISTURB.
SED. STRUCTURES
SAMPLES
PLEISTOCENE
N22 – N23
NN20 – NN21
A/M
A/M
N
(Brunhes)
N
γ=1.535
γ=1.532
γ=1.508
●NCaCO₃=85.7
●NCaCO₃=88.1
●NCaCO₃=89.5
●NCaCO₃=82.1
●NCaCO₃=84.8
1
2
3
4
5
CC
0.5
1.0

LITHOLOGIC DESCRIPTION

FORAMINIFER NANNOFOSSIL OOZE and NANNOFOSSIL OOZE with FORAMINIFERS

Major lithology: This core contains FORAMINIFER NANNOFOSSIL OOZE in Sections 1 through 3, and grades into NANNOFOSSIL OOZE with FORAMINIFERS in Sections 4 and 5. The color of the sediment grades from pale brown (10YR 6/3) at the top of Section 1 to light gray (10YR 7/2) in Section 2. The remainder of the core is light gray (2.5YR 7/1). The sediments are mottled by slight to heavy bioturbation.

SMEAR SLIDE SUMMARY (%):

	3, 70 D	4, 70 D
TEXTURE:		
Sand	20	12
Silt	78	86
Clay	2	2
COMPOSITION:		
Diatoms	1	—
Foraminifers	25	10
Nannofossils	69	87
Radiolarians	5	2
Siliceous sponge spicules	—	1

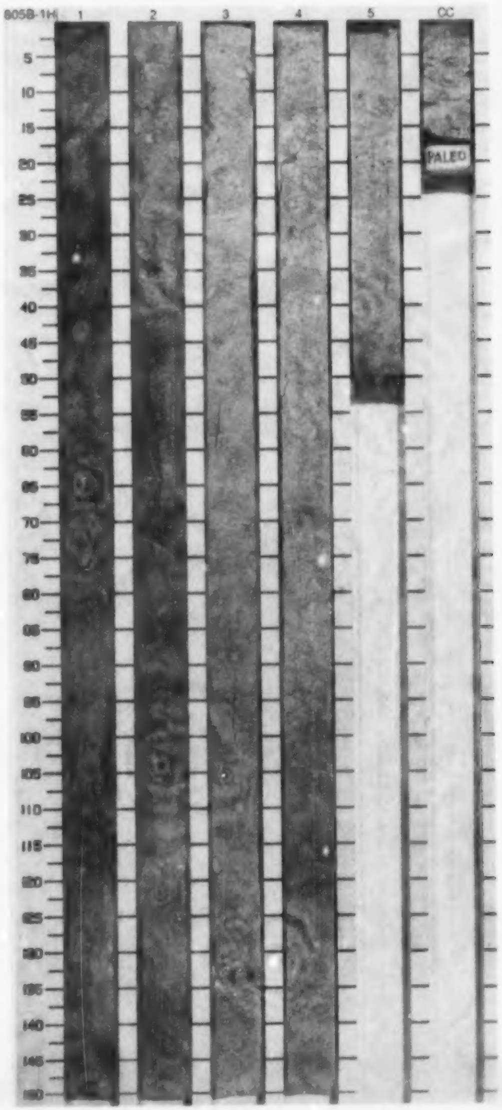
805B-1H
1
2
3
4
5
CC
PALEO
5
10
15
20
25
30
35
40
45
50
55
60
65
70
75
80
85
90
95
100
105
110
115
120
125
130
135
140
145
150

SITE 805 HOLE B CORE 2H CORED INTERVAL 6.7-16.2 mbsf

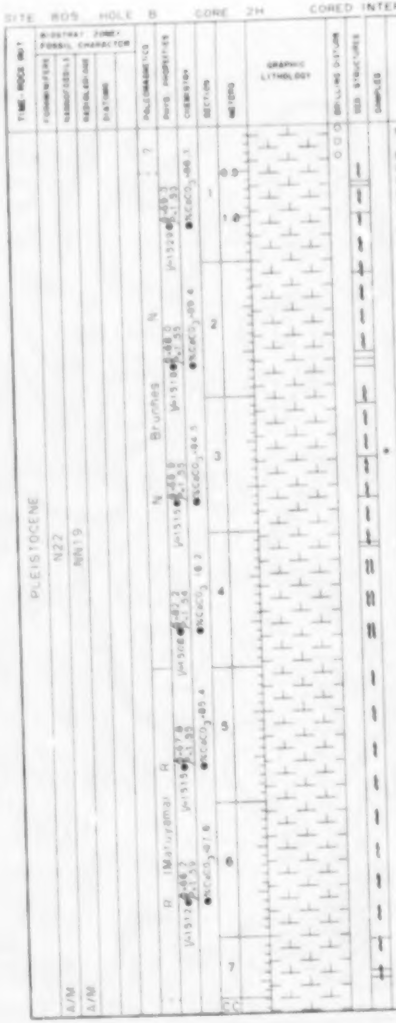
TIME-ROCK UNIT
BIOSTRAT. ZONE/FOSSIL CHARACTER
FORAMINIFERS
NANNOFOSSILS
RADIOLARIANS
DIATOMS
PALEOMAGNETICS
PHYS. PROPERTIES
CHEMISTRY
SECTION
METERS
GRAPHIC LITHOLOGY
DRILLING DISTURB.
SED. STRUCTURES
SAMPLES
PLEISTOCENE
N22
NN19
A/M
A/M
?
N
Brunhes
N
R (Matuyama) R
R
Vp1522 φ=69.3 ρ=1.53
Vp1518 φ=68.0 ρ=1.55
Vp1515 φ=68.8 ρ=1.55
Vp1506 φ=62.2 ρ=1.54
Vp1515 φ=67.8 ρ=1.55
Vp1512 φ=66.2 ρ=1.59
%CaCO3=86.1
%CaCO3=89.4
%CaCO3=84.5
%CaCO3 18.2
%CaCO3=85.4
%CaCO3=87.6
0.5
1.0
1
2
3
4
5
6
7
CC

LITHOLOGIC DESCRIPTION

NANNOFOSSIL OOZE with FORAMINIFERS and NANNOFOSSIL OOZE

Major lithology: This core contains NANNOFOSSIL OOZE with FORAMINIFERS, grading to NANNOFOSSIL OOZE in Section 7. The core is light gray (5Y 7/1, 2.5Y 7/2, and N7), with faint gray (5Y 5/1 and 5Y 6/1), grayish blue (5PB 5/2), pale blue (5PB 7/2), pale purple (5P 6/2) and light greenish gray (5G 7/1) color bands. Bioturbation is slight to heavy throughout the core.

SMEAR SLIDE SUMMARY (%):

	3, 98
	D
TEXTURE:	
Sand	10
Silt	85
Clay	5
COMPOSITION:	
Foraminifers	20
Nannofossils	80
Radiolarians	Tr
Siliceous sponge spicules	Tr

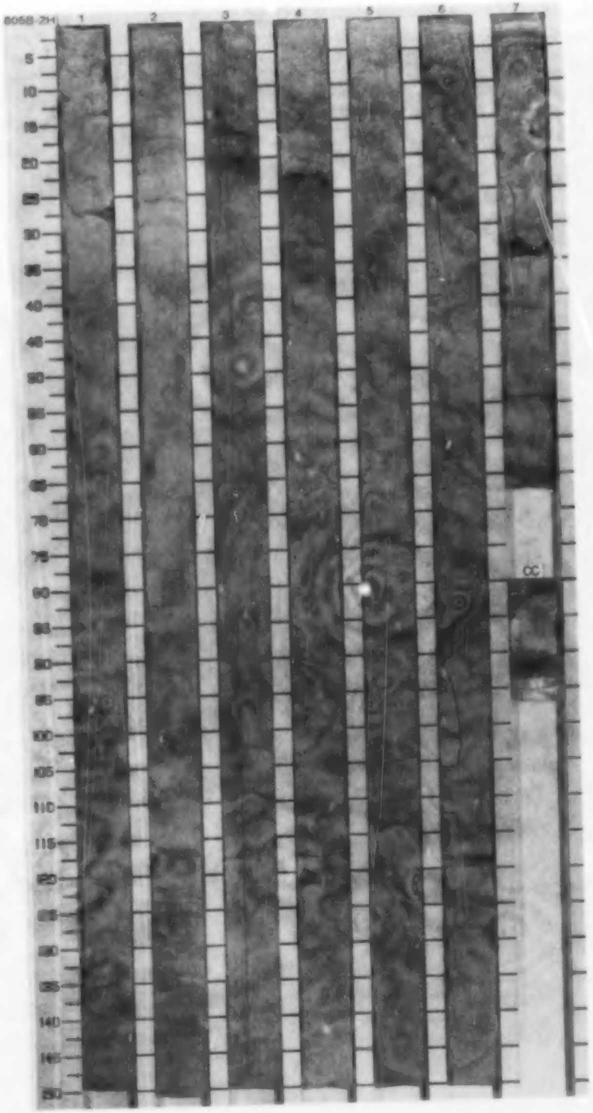
805B-2H
1
2
3
4
5
6
7
CC
5
10
15
20
25
30
35
40
45
50
55
60
65
70
75
80
85
90
95
100
105
110
115
120
125
130
135
140
145
150

SITE 805 HOLE B CORE 3H CORED INTERVAL 16.2-25.7 mbsf

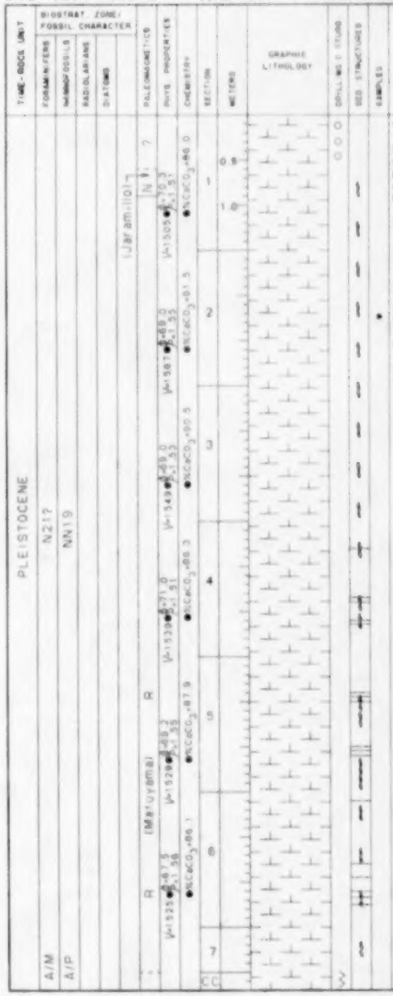
TIME-ROCK UNIT
BIOSTRAT. ZONE/ FOSSIL CHARACTER
FORAMINIFERS
NANNOFOSSILS
RADIOLARIANS
DIATOMS
PALEOMAGNETICS
PHYS. PROPERTIES
CHEMISTRY
SECTION
METERS
GRAPHIC LITHOLOGY
DRILLING DISTURB.
SED. STRUCTURES
SAMPLES
PLEISTOCENE
N21?
NN19
A/M
A/P
(Jaramillo)
N
?
R
(Matuyama)
R
V=1505 φ=70.3 ρ=1.51
V=1507 φ=68.0 ρ=1.55
V=1549 φ=69.0 ρ=1.53
V=1530 φ=71.0 ρ=1.51
V=1520 φ=68.2 ρ=1.55
V=1525 φ=67.5 ρ=1.56
%CaCO3=86.0
%CaCO3=81.5
%CaCO3=90.5
%CaCO3=88.3
%CaCO3=87.9
%CaCO3=86.1
1
2
3
4
5
6
7
CC
0.9
1.0

LITHOLOGIC DESCRIPTION

NANNOFOSSIL OOZE with FORAMINIFERS

Major lithology: This core contains NANNOFOSSIL OOZE with FORAMINIFERS. The sediment is white (5Y 8/1) with light gray mottling due to bioturbation. The burrows are often pyritized. Faint to sharp, cm size, pale purple (5P 6/2), pale green (10G 6/2), gray (N6), bluish gray (5B 6/1) and light greenish gray (5G 7/1) color bands cross and thus postdate bioturbation features.

SMEAR SLIDE SUMMARY (%):

	2, 74
	D
TEXTURE:	
Sand	10
Silt	90
COMPOSITION:	
Foraminifers	12
Nannofossils	88

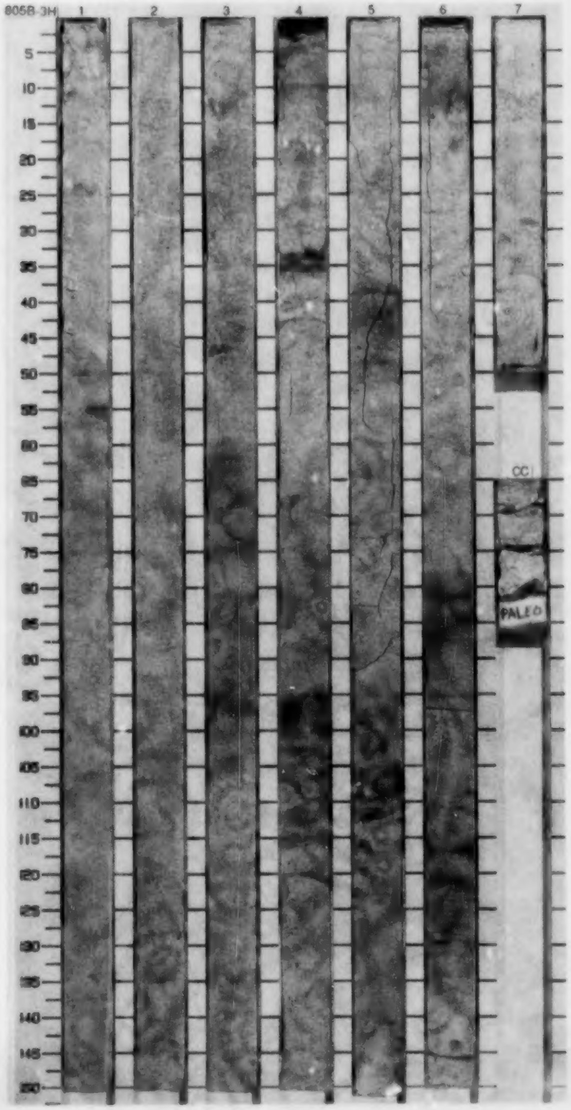
805B-3H
1
2
3
4
5
6
7
5
10
15
20
25
30
35
40
45
50
55
60
65
70
75
80
85
90
95
100
105
110
115
120
125
130
135
140
145
150
CC
PALEO

SITE 805 HOLE B CORE 4H CORED INTERVAL 25.7-35.2 mbsf

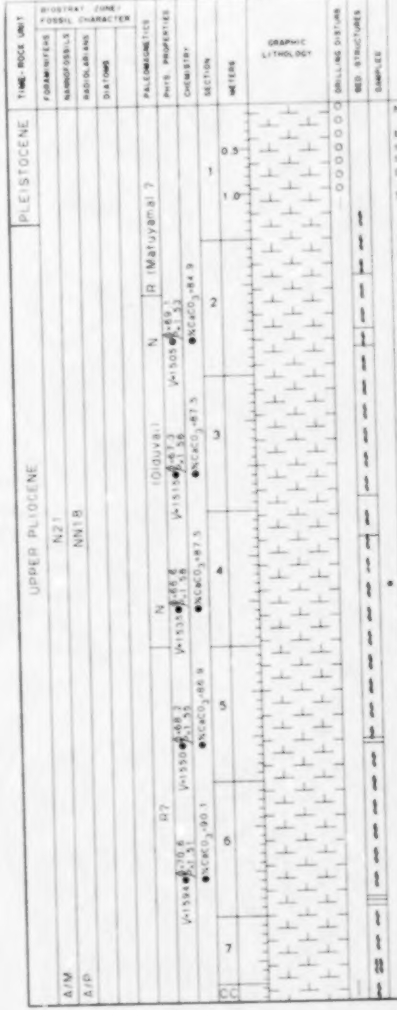
TIME-ROCK UNIT
BIOSTRAT. ZONE/ FOSSIL CHARACTER
FORAMINIFERS
NANNOFOSSILS
RADIOLARIANS
DIATOMS
PALEOMAGNETICS
PHYS. PROPERTIES
CHEMISTRY
SECTION
METERS
GRAPHIC LITHOLOGY
DRILLING DISTURB.
SED. STRUCTURES
SAMPLES
PLEISTOCENE
UPPER PLIOCENE
N21
NN18
A/M
A/P
R (Matuyama) ?
N
(Olduvai)
N
R?
V=1505 ϕ=69.1 ρ=1.53
V=1515 ϕ=67.3 ρ=1.56
V=1535 ϕ=66.6 ρ=1.58
V=1550 ϕ=68.2 ρ=1.55
V=1594 ϕ=70.6 ρ=1.51
%CaCO₃=84.9
%CaCO₃=87.5
%CaCO₃=87.5
%CaCO₃=86.9
%CaCO₃=90.1
1
2
3
4
5
6
7
CC
0.5
1.0

LITHOLOGIC DESCRIPTION

NANNOFOSSIL OOZE with FORAMINIFERS

Major lithology: This core contains NANNOFOSSIL OOZE with FORAMINIFERS. The sediment is white (5Y 8/1 to 2.5Y 8/0) with light gray mottling due to bioturbation. Numerous faint to sharp, pale green (10G 6/2), light greenish gray (5G 7/1), pale purple (5P 6/2), and grayish purple (5P 4/2) color bands are observed throughout the core.

SMEAR SLIDE SUMMARY (%):

	4, 84
	D
TEXTURE:	
Sand	12
Silt	86
Clay	2
COMPOSITION:	
Foraminifers	20
Nannofossils	77
Radiolarians	2
Silicoflagellates	1

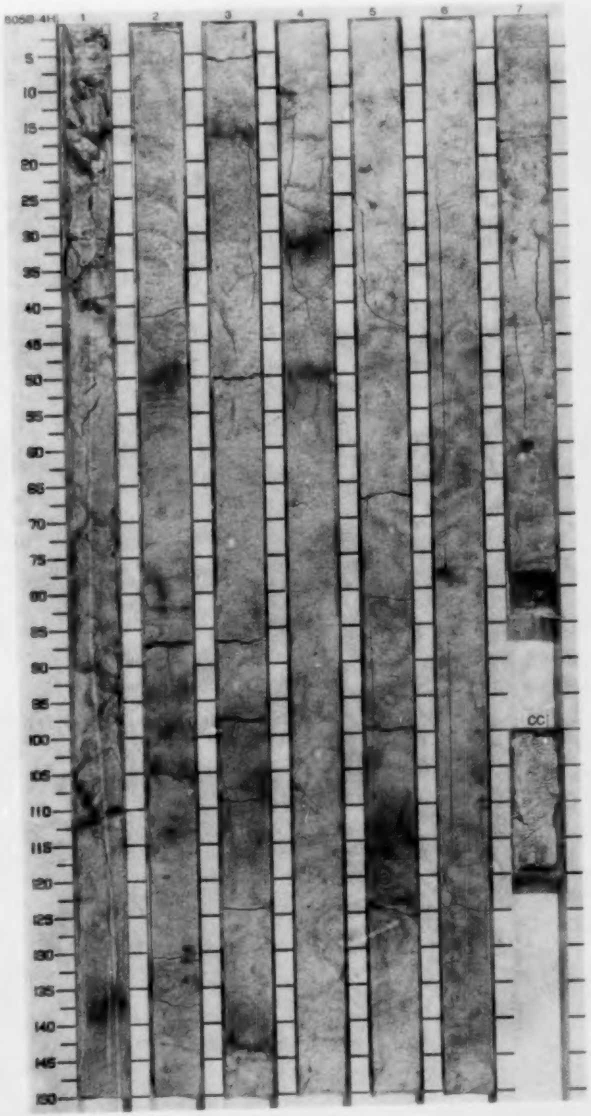
805B-4H
1
2
3
4
5
6
7
CC
5
10
15
20
25
30
35
40
45
50
55
60
65
70
75
80
85
90
95
100
105
110
115
120
125
130
135
140
145
150

SITE 805 HOLE B CORE 5H CORED INTERVAL 35.2-44.7 mbsf

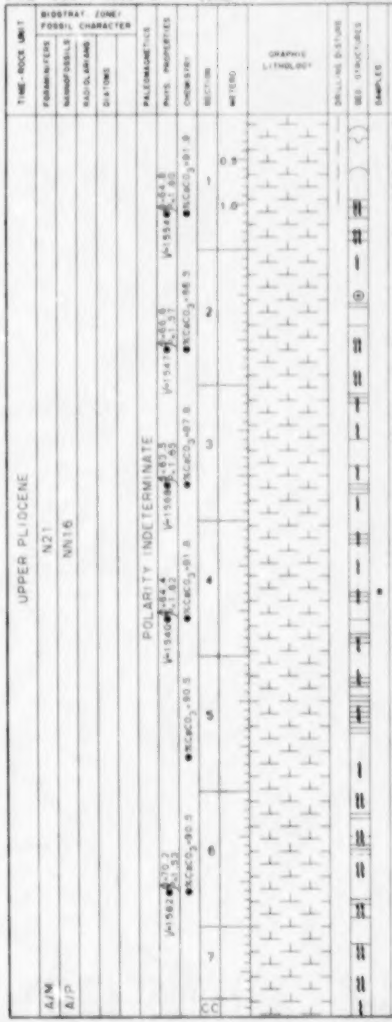
TIME-ROCK UNIT
BIOSTRAT. ZONE/ FOSSIL CHARACTER
FORAMINIFERS
NANNOFOSSILS
RADIOLARIANS
DIATOMS
PALEOMAGNETICS
PHYS. PROPERTIES
CHEMISTRY
SECTION
METERS
GRAPHIC LITHOLOGY
DRILLING DISTURB.
SED. STRUCTURES
SAMPLES
UPPER PLIOCENE
N21
NN16
A/M
A/P
POLARITY INDETERMINATE
V=1554 φ=64.8 γ=1.60
V=1547 φ=66.8 γ=1.57
V=1566 φ=63.5 γ=1.65
V=1540 φ=64.4 γ=1.62
V=1582 φ=70.2 γ=1.53
%CaCO3=91.0
%CaCO3=88.9
%CaCO3=87.0
%CaCO3=91.8
%CaCO3=90.5
%CaCO3=90.5
1
2
3
4
5
6
7
CC
0.5
1.0

LITHOLOGIC DESCRIPTION

NANNOFOSSIL OOZE with FORAMINIFERS

Major lithology: This core contains NANNOFOSSIL OOZE with FORAMINIFERS. The sediment is white (5Y 8/1 to 2.5Y 8/0), with minor to abundant light gray (5Y 7/1) and light olive gray (5Y 6/2) mottling throughout. Diffuse to well defined, light gray (N7), light greenish gray (5G 7/1), greenish gray (5G 6/1), grayish blue (5PB 5/2), and pale blue (5PB 7/2) color bands are common. A pyrite concretion, approximately 0.5 cm in diameter, was recovered in Section 2, 25 cm.

SMEAR SLIDE SUMMARY (%):

	4, 79
	D
TEXTURE:	
Sand	10
Silt	85
Clay	5
COMPOSITION:	
Accessory minerals	1
Diatoms	1
Foraminifers	16
Nannofossils	75
Radiolarians	5
Silicoflagellates	1
Spicules	1

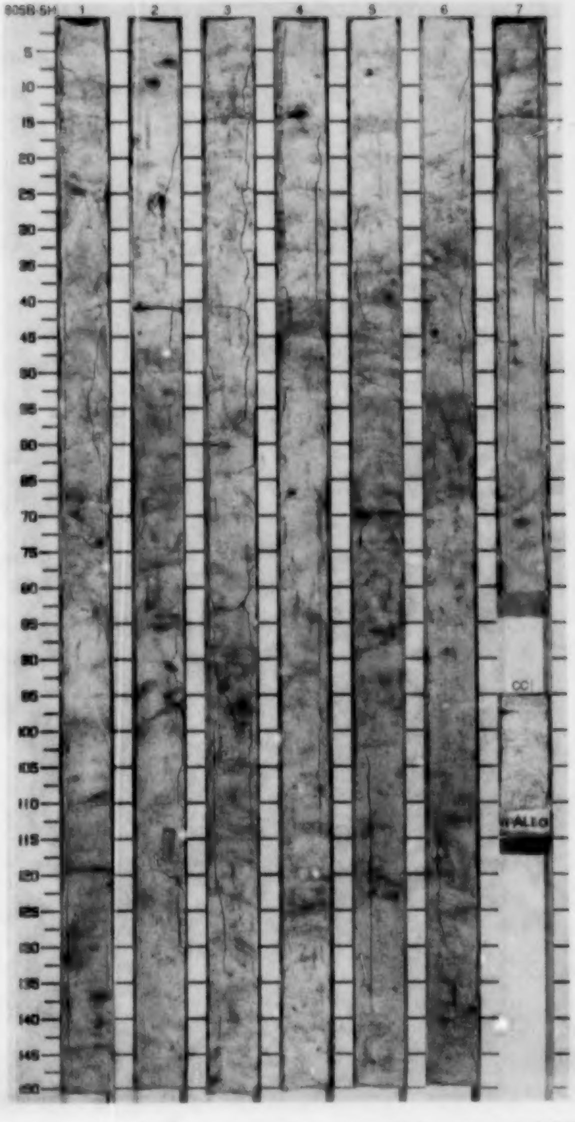
805B-5H
1
2
3
4
5
6
7
CC
PALEO
5
10
15
20
25
30
35
40
45
50
55
60
65
70
75
80
85
90
95
100
105
110
115
120
125
130
135
140
145
150

SITE 805 HOLE B CORE 6H CORED INTERVAL 44.7-54.2 mbsf

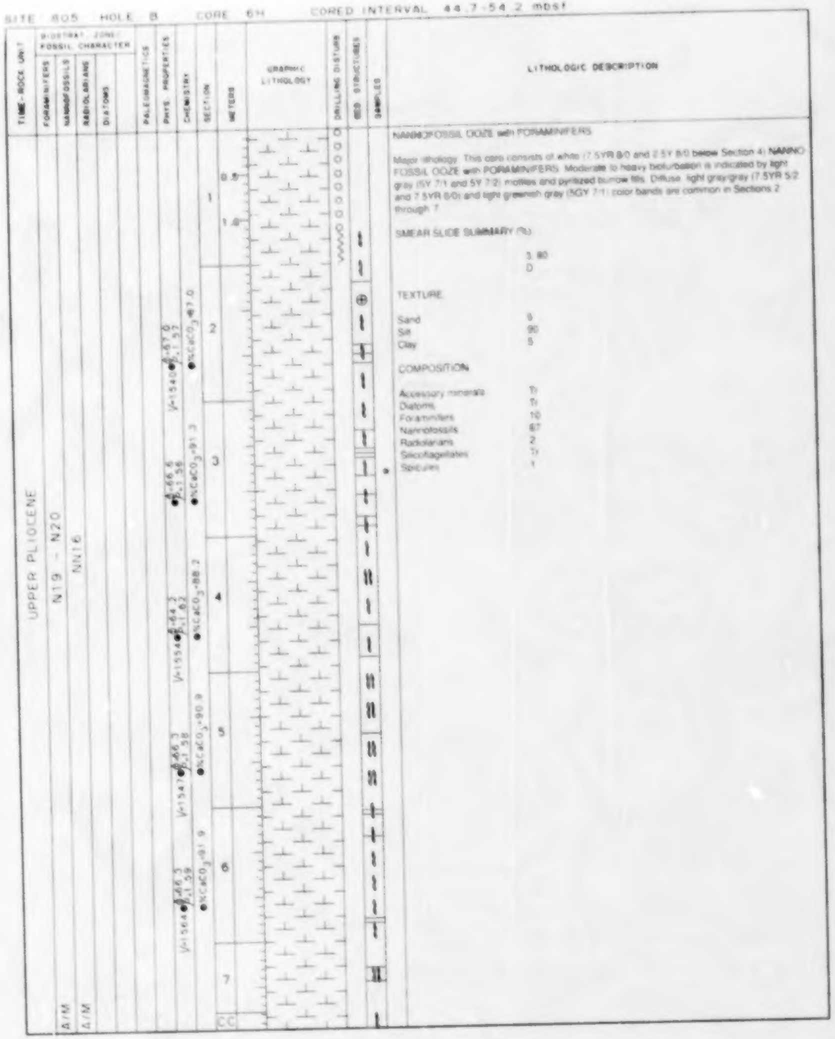

LITHOLOGIC DESCRIPTION

NANNOFOSSIL OOZE with FORAMINIFERS

Major lithology: This core consists of white (7.5YR 8/0 and 2.5Y 8/0 below Section 4) NANNOFOSSIL OOZE with FORAMINIFERS. Moderate to heavy bioturbation is indicated by light gray (5Y 7/1 and 5Y 7/2) mottles and pyritized burrow fills. Diffuse, light gray/gray (7.5YR 5/2 and 7.5YR 6/0) and light greenish gray (5GY 7/1) color bands are common in Sections 2 through 7.

SMEAR SLIDE SUMMARY (%):

	3, 80 D
TEXTURE:	
Sand	5
Silt	90
Clay	5
COMPOSITION:	
Accessory minerals	Tr
Diatoms	Tr
Foraminifers	10
Nannofossils	87
Radiolarians	2
Silicoflagellates	Tr
Spicules	1

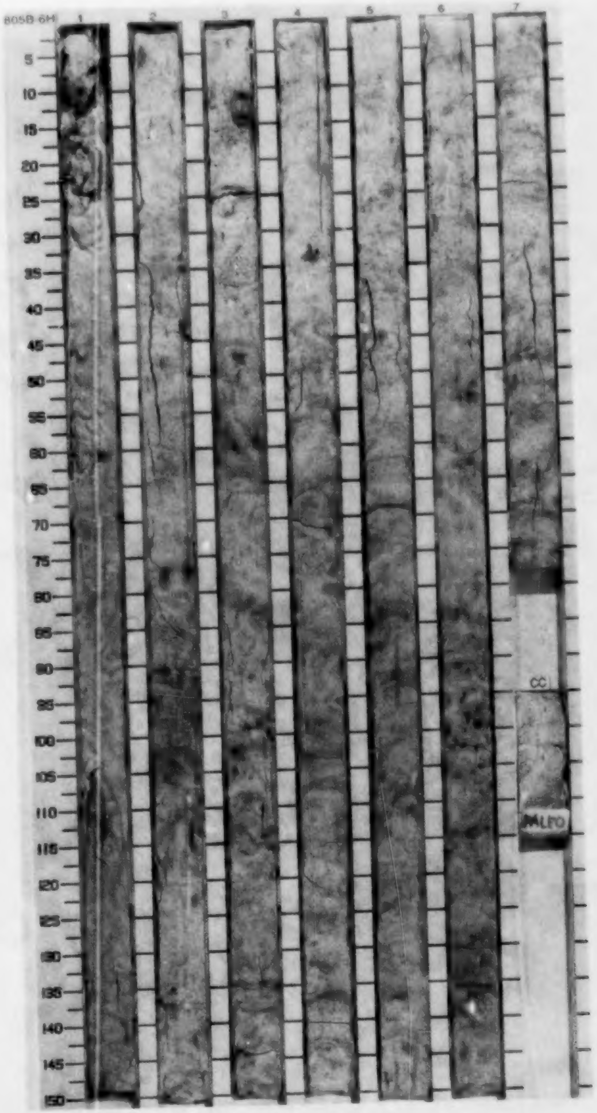
805B-6H
1
2
3
4
5
6
7
CC
PALEO
5
10
15
20
25
30
35
40
45
50
55
60
65
70
75
80
85
90
95
100
105
110
115
120
125
130
135
140
145
150

SITE 805 HOLE B CORE 7H CORED INTERVAL 54.2-63.7 mbsf

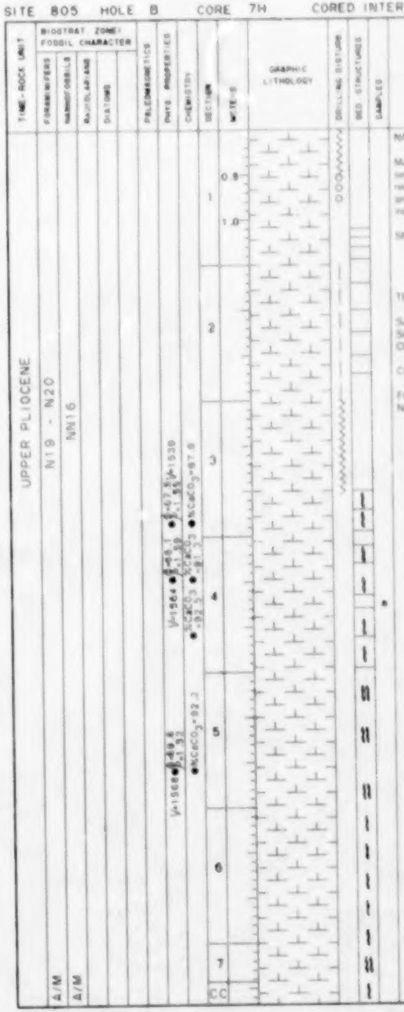
TIME-ROCK UNIT
BIOSTRAT. ZONE/ FOSSIL CHARACTER
FORAMINIFERS
NANNOFOSSILS
RADIOLARIANS
DIATOMS
PALEOMAGNETICS
PHYS. PROPERTIES
CHEMISTRY
SECTION
METERS
GRAPHIC LITHOLOGY
DRILLING DISTURB.
SED. STRUCTURES
SAMPLES
UPPER PLIOCENE
N19 - N20
NN16
A/M
A/M
V=1539
ϕ=67.5
γ=1.55
%CaCO3=87.9
V=1564
ϕ=66.1
γ=1.59
%CaCO3=81.3
%CaCO3=92.5
V=1568
ϕ=69.6
γ=1.52
%CaCO3=92.2
1
2
3
4
5
6
7
CC
0.9
1.0
*

LITHOLOGIC DESCRIPTION

NANNOFOSSIL OOZE with FORAMINIFERS

Major lithology: This core contains NANNOFOSSIL OOZE with FORAMINIFERS. The sediment is predominantly white (2.5Y 8/0) but exhibits extensive color banding in shades of reddish gray (5R 6/1), pale yellowish green (10GY 7/2), and light gray (2.5Y 7/2). The bands are 5 to 15 mm thick and are spaced at intervals of 1 to 3 cm. The sediment is bioturbated, as indicated by mottling and pyritic burrow fills.

SMEAR SLIDE SUMMARY (%):

	4, 75
	D
TEXTURE	
Sand	5
Silt	55
Clay	40
COMPOSITION	
Foraminifers	8
Nannofossils	92

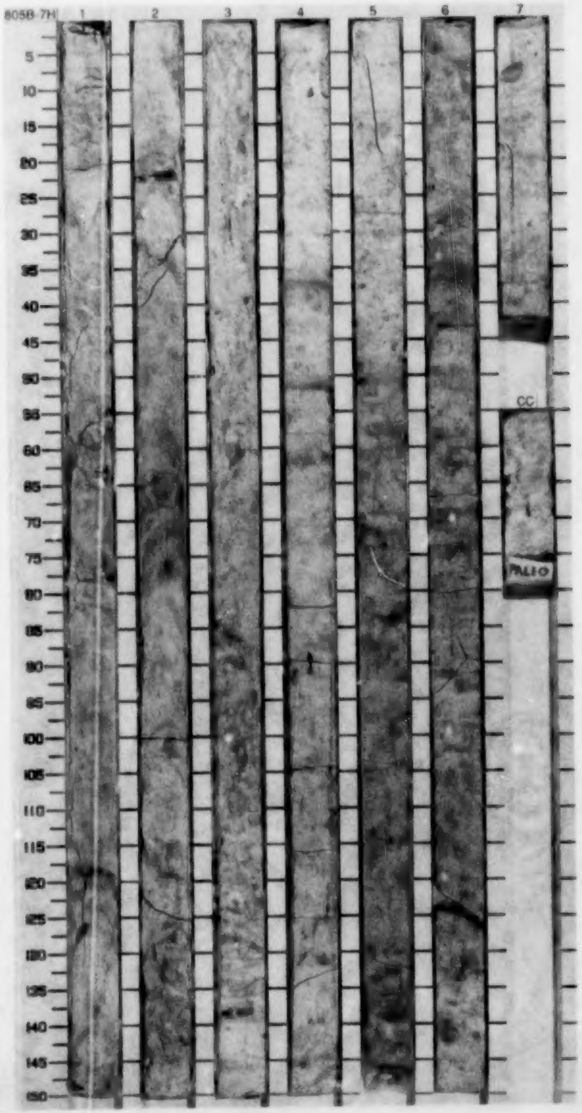
805B-7H
1
2
3
4
5
6
7
CC
PALEO
5
10
15
20
25
30
35
40
45
50
55
60
65
70
75
80
85
90
95
100
105
110
115
120
125
130
135
140
145
150

SITE 805 HOLE B CORE 8H CORED INTERVAL 63.7-73.2 mbsf

TIME-ROCK UNIT	BIOSTRAT. ZONE/ FOSSIL CHARACTER: FORAMINIFERS	NANNOFOSSILS	RADIOLARIANS	DIATOMS	PALEOMAGNETICS	PHYS. PROPERTIES	CHEMISTRY	SECTION	METERS	DRILLING DISTURB.	SED. STRUCTURES	SAMPLES
UPPER PLIOCENE	N19 - N20	NN16						1	0.5 1.0	○ ○ ○ ○		
						V=1539 ● φ=65.9 ρ=1.58	● %CaCO$_3$=92.0	2				
						V=1539 ● φ=66.5 ρ=1.58	● %CaCO$_3$=90.3	3				*
						● φ=65.4 ρ=1.59	● %CaCO$_3$=90.2	4				
						V=1543 ● φ=66.5 ρ=1.59	● %CaCO$_3$=90.5	5				
						V=1536 ● φ=66.1 ρ=1.58	● %CaCO$_3$=90.6	6				
								7				
	A/M	A/M						CC				

LITHOLOGIC DESCRIPTION

NANNOFOSSIL OOZE

Major lithology: This core contains homogeneous, white (2.5YR 8/0) NANNOFOSSIL OOZE. The sediment is moderately to heavily bioturbated as seen in abundant light gray (2.5YR 7/2) mottles and burrow fills as well as pyritized burrow fills. Some pyritized burrows are surrounded by reddish gray (5R 6/1) halos. Centimeter thick, pale yellowish green (10GY 7/2) and reddish gray (5R 6/1) color bands are observed in all sections.

SMEAR SLIDE SUMMARY (%):

	3, 74
	D
TEXTURE:	
Sand	5
Silt	60
Clay	35
COMPOSITION:	
Accessory minerals	1
Foraminifers	7
Nannofossils	90
Siliceous fragments	2

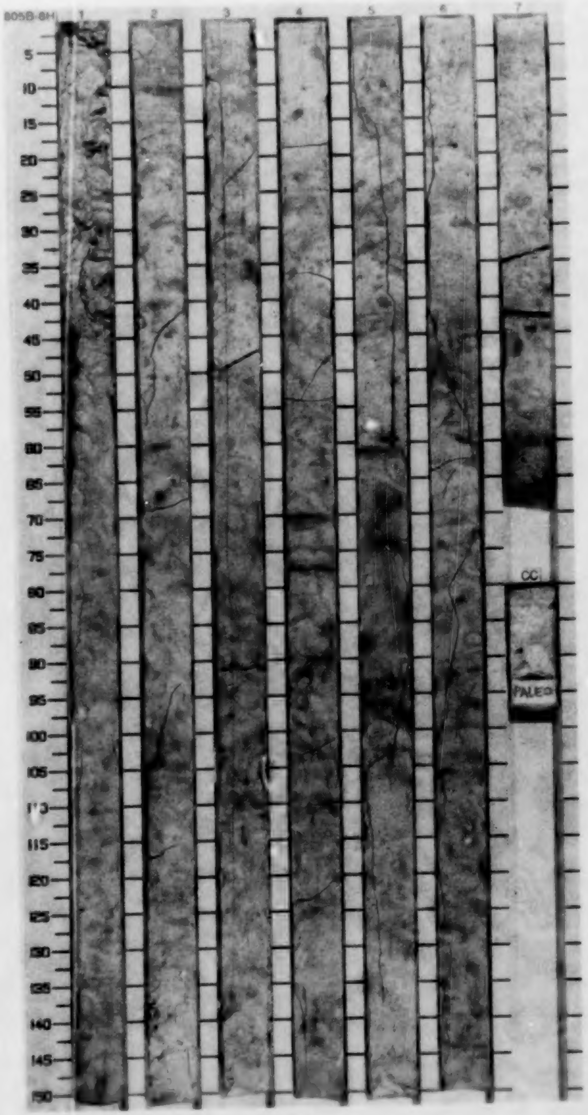

SITE 805 HOLE B CORE 9H CORED INTERVAL 73.2-82.7 mbsf

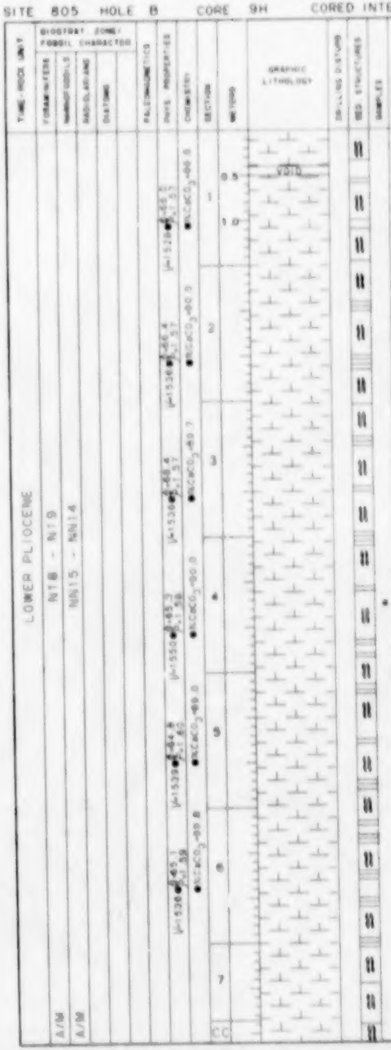
TIME-ROCK UNIT
BIOSTRAT. ZONE/ FOSSIL CHARACTER
FORAMINIFERS
NANNOFOSSILS
RADIOLARIANS
DIATOMS
PALEOMAGNETICS
PHYS. PROPERTIES
CHEMISTRY
SECTION
METERS
GRAPHIC LITHOLOGY
DRILLING DISTURB.
SED. STRUCTURES
SAMPLES
LOWER PLIOCENE
N18 - N19
NN15 - NN14
A/M
A/M
V=1528 φ=66.5 ρ=1.57
V=1536 φ=66.4 ρ=1.57
V=1536 φ=68.4 ρ=1.57
V=1550 φ=65.3 ρ=1.58
V=1539 φ=64.8 ρ=1.60
V=1530 φ=65.1 ρ=1.59
%CaCO3=90.0
%CaCO3=90.0
%CaCO3=89.7
%CaCO3=90.0
%CaCO3=89.0
%CaCO3=89.8
1
2
3
4
5
6
7
CC
0.5
1.0
VOID

LITHOLOGIC DESCRIPTION

NANNOFOSSIL OOZE with FORAMINIFERS

Major lithology: This core contains NANNOFOSSIL OOZE with FORAMINIFERS. The sediment is predominantly white (2.5Y 8/0) but exhibits extensive color banding in shades of reddish gray (5R 6/1) and pale yellowish green (10GY 7/2). The bands are 0.5 to 1.5 cm thick and occur either as individual bands or as packages 3 to 5 cm thick. Large, light gray (2.5Y 7/2) mottles, pyritized burrow fills, and trace fossils with reddish gray halos are indicative of heavy bioturbation. The halos are as much as 3 cm in diameter.

SMEAR SLIDE SUMMARY (%):

	4, 74 D
TEXTURE:	
Sand	7
Silt	60
Clay	33
COMPOSITION:	
Accessory minerals	1
Foraminifers	15
Nannofossils	83
Siliceous fragments	1

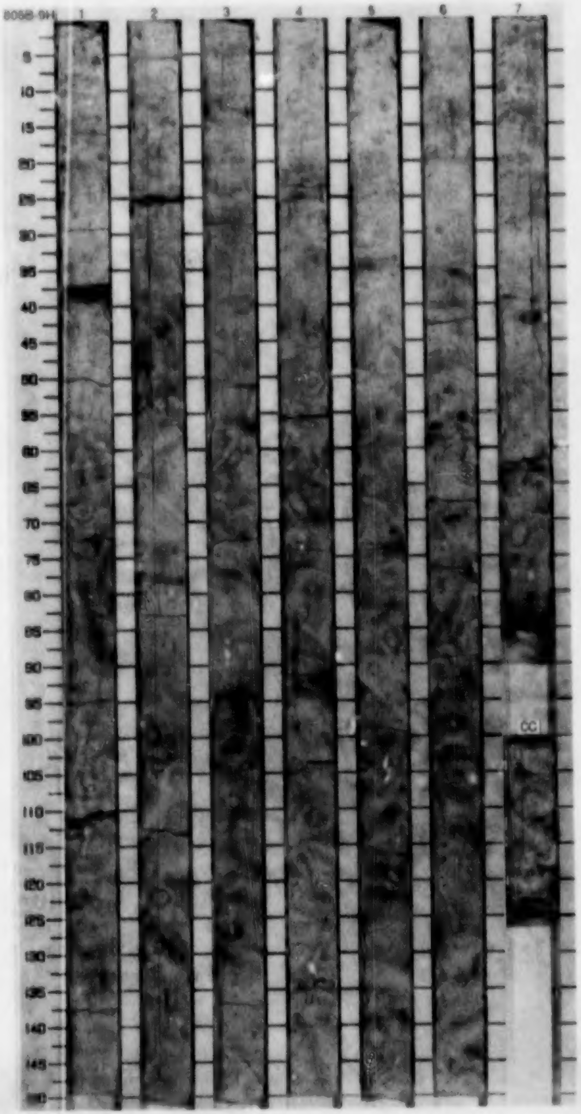
805B-9H
1
2
3
4
5
6
7
CC
5
10
15
20
25
30
35
40
45
50
55
60
65
70
75
80
85
90
95
100
105
110
115
120
125
130
135
140
145
150

SITE 805 HOLE B CORE 10H CORED INTERVAL 82.7-92.2 mbsf

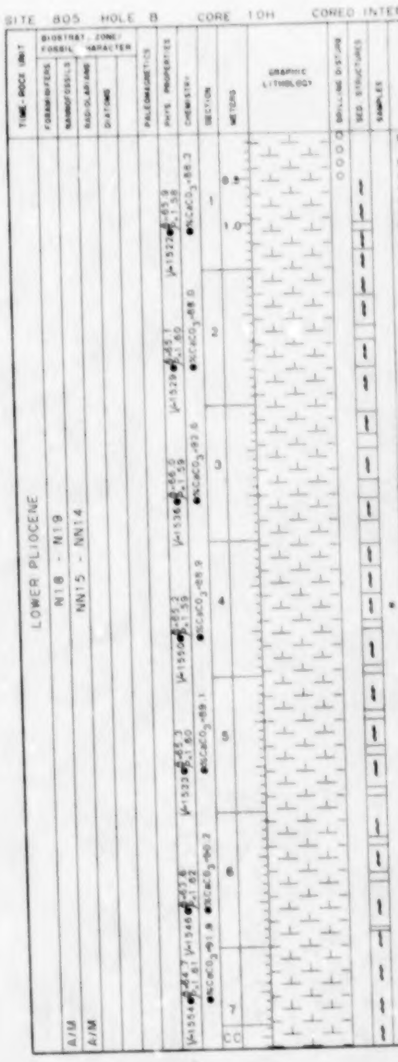

LITHOLOGIC DESCRIPTION

NANNOFOSSIL OOZE with FORAMINIFERS

Major lithology: This core contains NANNOFOSSIL OOZE with FORAMINIFERS. The sediment is predominantly white (2.5Y 8/0) but exhibits extensive color banding in shades of reddish gray (5R 6/1) and pale yellowish green (10GY 7/2). The bands are 0.5 to 1.5 cm thick and spaced up to 10 cm apart. Large, light gray (2.5Y 7/2) mottles, pyritized burrow fills, and trace fossils with reddish gray halos indicate severe bioturbation. The halos are up to 3 cm in diameter.

SMEAR SLIDE SUMMARY (%):

	4, 75
	D
TEXTURE:	
Sand	3
Silt	55
Clay	42
COMPOSITION:	
Accessory minerals	2
Diatoms	3
Foraminifers	15
Nannofossils	70
Radiolarians	3
Siliceous fragments	3
Siliceous sponge spicules	2
Silicoflagellates	2

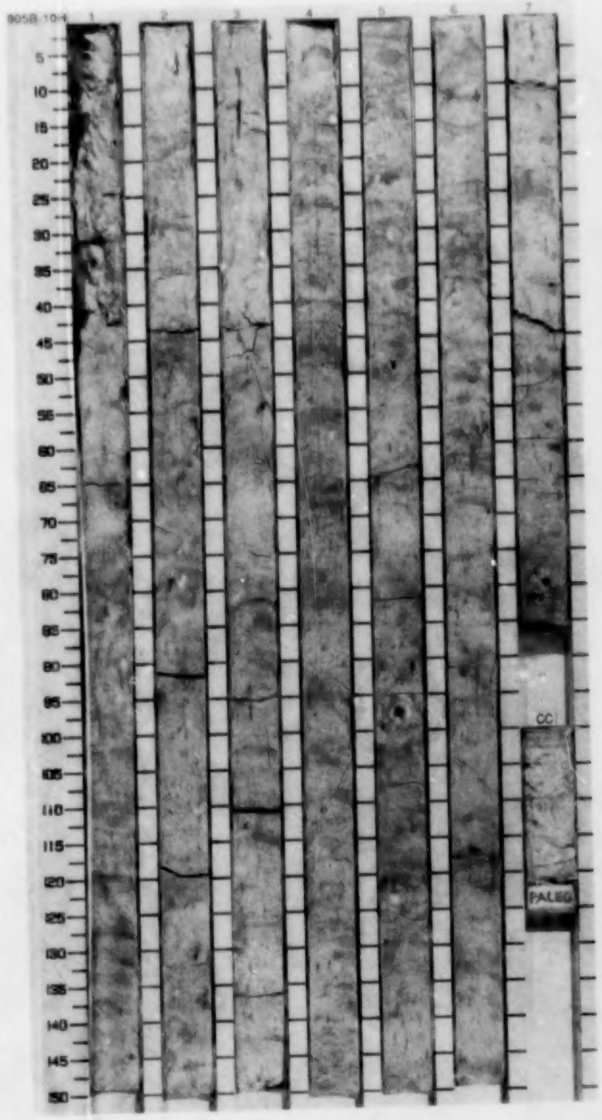
805B-10H
1
2
3
4
5
6
7
CC
PALEO
5
10
15
20
25
30
35
40
45
50
55
60
65
70
75
80
85
90
95
100
105
110
115
120
125
130
135
140
145
150

SITE 805 HOLE B CORE 11H CORED INTERVAL 92.2-101.7 mbsf

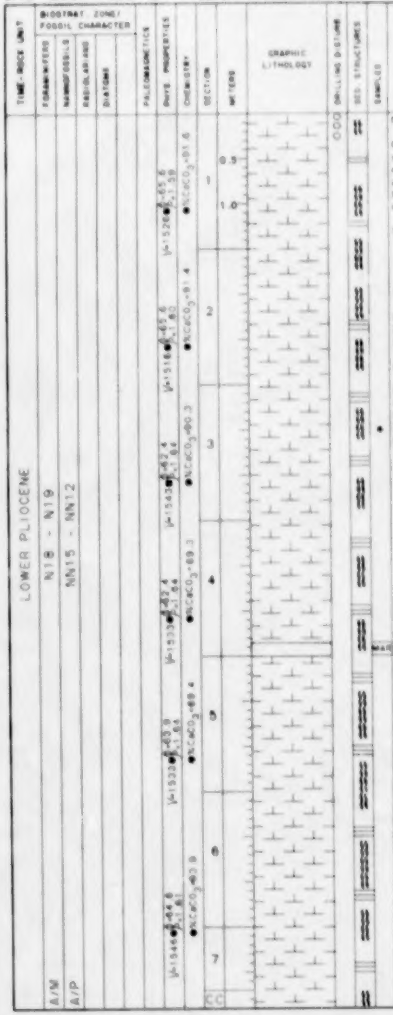
TIME-ROCK UNIT
BIOSTRAT. ZONE/ FOSSIL CHARACTER
FORAMINIFERS
NANNOFOSSILS
RADIOLARIANS
DIATOMS
PALEOMAGNETICS
PHYS. PROPERTIES
CHEMISTRY
SECTION
METERS
GRAPHIC LITHOLOGY
DRILLING DISTURB.
SED. STRUCTURES
SAMPLES
LOWER PLIOCENE
N18 - N19
NN15 - NN12
A/M
A/P
V=1520 φ=65.6 γ=1.59
%CaCO₃=91.6
V=1516 φ=65.6 γ=1.60
%CaCO₃=91.4
V=1543 φ=62.4 γ=1.64
%CaCO₃=90.3
V=1533 φ=62.4 γ=1.64
%CaCO₃=89.3
V=1533 φ=63.9 γ=1.64
%CaCO₃=89.4
V=1546 φ=64.6 γ=1.61
%CaCO₃=93.9
1
2
3
4
5
6
7
CC
0.5
1.0
WAR

LITHOLOGIC DESCRIPTION

NANNOFOSSIL OOZE with FORAMINIFERS

Major lithology: This core contains NANNOFOSSIL OOZE with FORAMINIFERS. The sediment is predominantly white (2.5Y 8.0) but exhibits frequent color banding in shades of reddish gray (5R 6/1) and pale yellowish green (10GY 7/2). The bands are 0.5 to 1.5 cm thick and spaced up to 10 cm apart. Large, light gray (2.5Y 7/2) mottles, pyritized burrow fills, and trace fossils with reddish gray halos indicate severe bioturbation. The halos are up to 3 cm in diameter.

SMEAR SLIDE SUMMARY (%):

	3, 30
	D
TEXTURE:	
Sand	10
Silt	50
Clay	40
COMPOSITION:	
Diatoms	Tr
Foraminifers	20
Nannofossils	80
Radiolarians	Tr
Siliceous sponge spicules	Tr

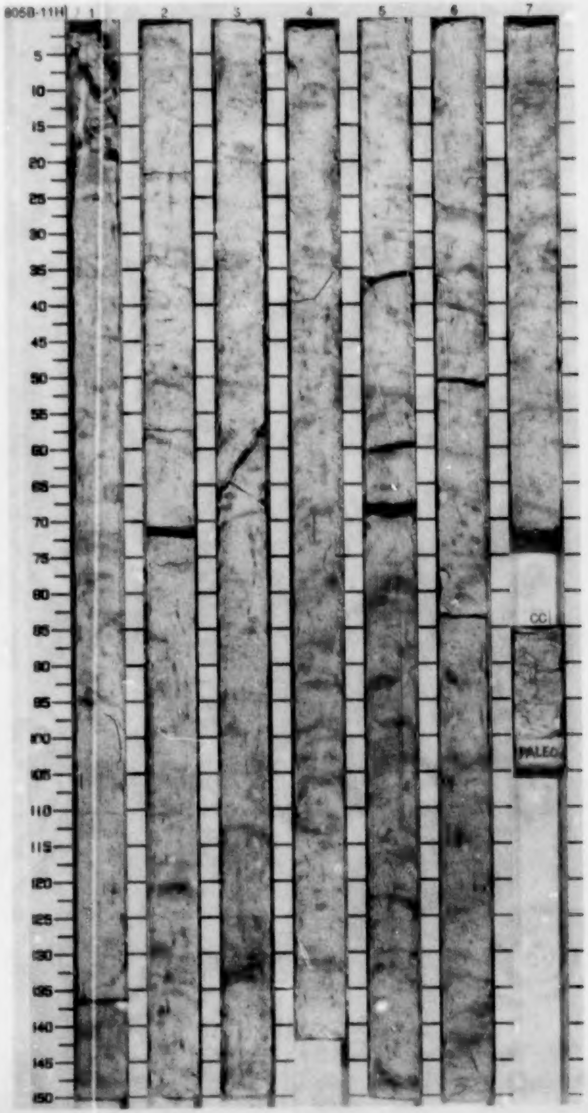
805B-11H
1
2
3
4
5
6
7
CC
PALEO
5
10
15
20
25
30
35
40
45
50
55
60
65
70
75
80
85
90
95
100
105
110
115
120
125
130
135
140
145
150

SITE 805 HOLE B CORE 12H CORED INTERVAL 101.7-111.2 mbsf

TIME-ROCK UNIT	BIOSTRAT. ZONE/ FOSSIL CHARACTER: FORAMINIFERS	NANNOFOSSILS	RADIOLARIANS	DIATOMS	PALEOMAGNETICS	PHYS. PROPERTIES	CHEMISTRY	SECTION	METERS	GRAPHIC LITHOLOGY	DRILLING DISTURB.	SED. STRUCTURES	SAMPLES
LOWER PLIOCENE	N18 - N19	NN12						1	0.5 1.0				
						φ=62.4 γ=1.63	%CaCO$_3$=81.0	2					•
						V=1568 φ=62.4 γ=1.64	%CaCO$_3$=83.1	3					
						V=1581 φ=58.1 γ=1.58	%CaCO$_3$=80.5	4					
						V=1583 φ=56.7 γ=1.61	%CaCO$_3$=80.0	5					
						V=1581 φ=58.1 γ=1.62	%CaCO$_3$=82.2	6					
	A/M	A/M						7					
								CC					

LITHOLOGIC DESCRIPTION

NANNOFOSSIL OOZE with FORAMINIFERS

Major lithology: This core consists of homogeneous, white (2.5Y 8/0) NANNOFOSSIL OOZE with FORAMINIFERS. The sediment is moderately to heavily bioturbated as indicated by mottles and large (cm scale) burrows and pyritized burrow fills. Abundant, faint, cm thick, pale yellowish green (10GY 7/2) and reddish gray (5R 6/1) color bands are noted. In Sections 2, 3, and 4, a few color bands are offset by micro-faulting.

SMEAR SLIDE SUMMARY (%):

	2, 75
	D
TEXTURE:	
Sand	15
Silt	45
Clay	40
COMPOSITION:	
Diatoms	Tr
Foraminifers	20
Nannofossils	78
Radiolarians	2

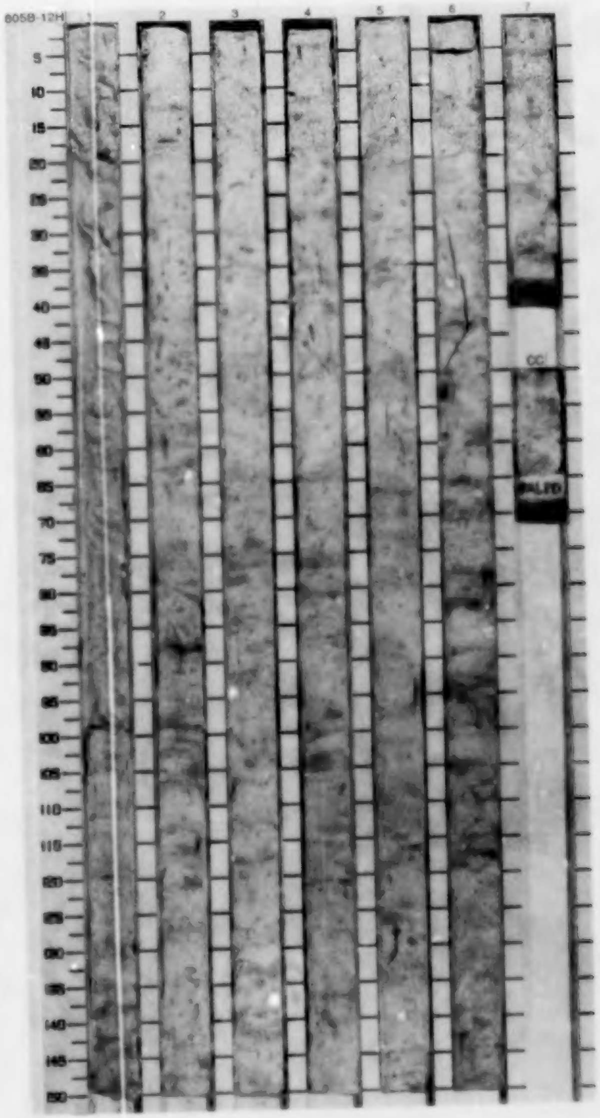

SITE 805 HOLE B CORE 13H CORED INTERVAL 111.2-120.7 mbsf

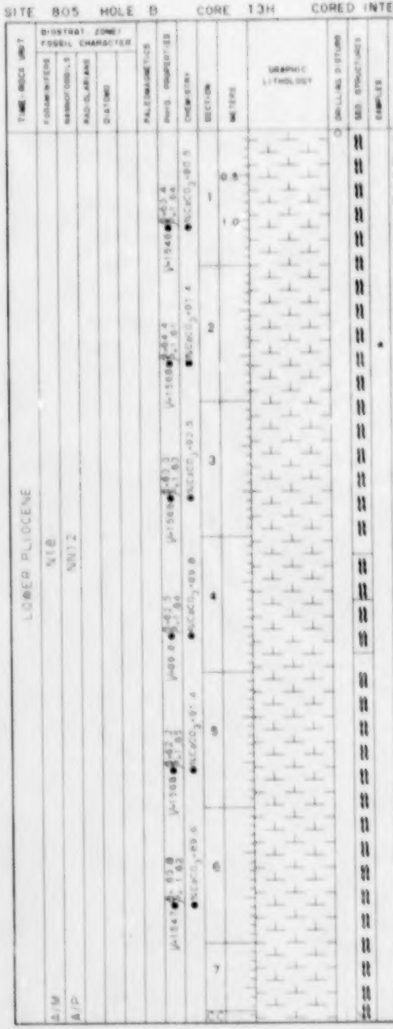

LITHOLOGIC DESCRIPTION

NANNOFOSSIL OOZE with FORAMINIFERS

Major lithology: This core contains homogeneous, white (2.5Y 8/0) NANNOFOSSIL OOZE with FORAMINIFERS. The sediment is heavily bioturbated as indicated by mottles, large (cm-scale) burrows and pyritized burrow fills. Abundant, faint, cm-thick, pale green (10G 6/2), pale purple (5P 6/2) and light gray (2.5Y 7/2) color bands are present throughout the core.

SMEAR SLIDE SUMMARY (%):

	2, 89
	D
TEXTURE:	
Sand	15
Silt	85
COMPOSITION:	
Foraminifers	10
Nannofossils	87
Radiolarians	3

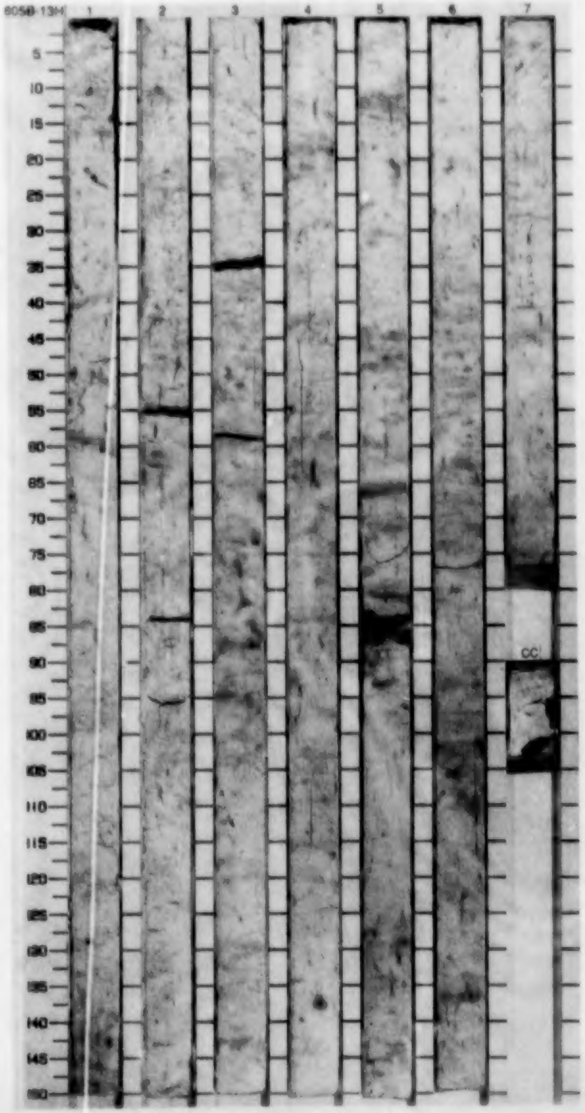
805B-13H
1
2
3
4
5
6
7
CC
5
10
15
20
25
30
35
40
45
50
55
60
65
70
75
80
85
90
95
100
105
110
115
120
125
130
135
140
145
150

SITE 805 HOLE B CORE 14H CORED INTERVAL 120.7-130.2 mbsf

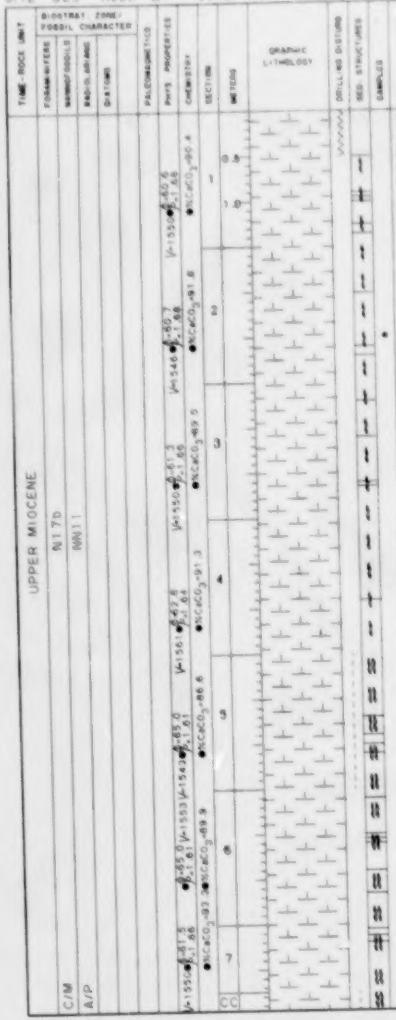

LITHOLOGIC DESCRIPTION

NANNOFOSSIL OOZE with FORAMINIFERS

Major lithology: This core contains homogeneous, white (2.5Y 8/0) NANNOFOSSIL OOZE with FORAMINIFERS. The sediment is heavily bioturbated as indicated by mottles and large (cm scale) burrows with mm size, pyritic linings. Diffuse to sharp, pale green (10G 6/2), pale purple (5P 6/2), pale blue (5PB 7/2), grayish blue (5PB 5/2), light gray (2.5Y 7/2), and light greenish gray (5G 7/1) color bands and mottles are abundant throughout the core.

SMEAR SLIDE SUMMARY (%):

	2, 99
	D
TEXTURE	
Sand	15
Silt	85
COMPOSITION	
Foraminifers	13
Nannofossils	85
Radiolarians	2

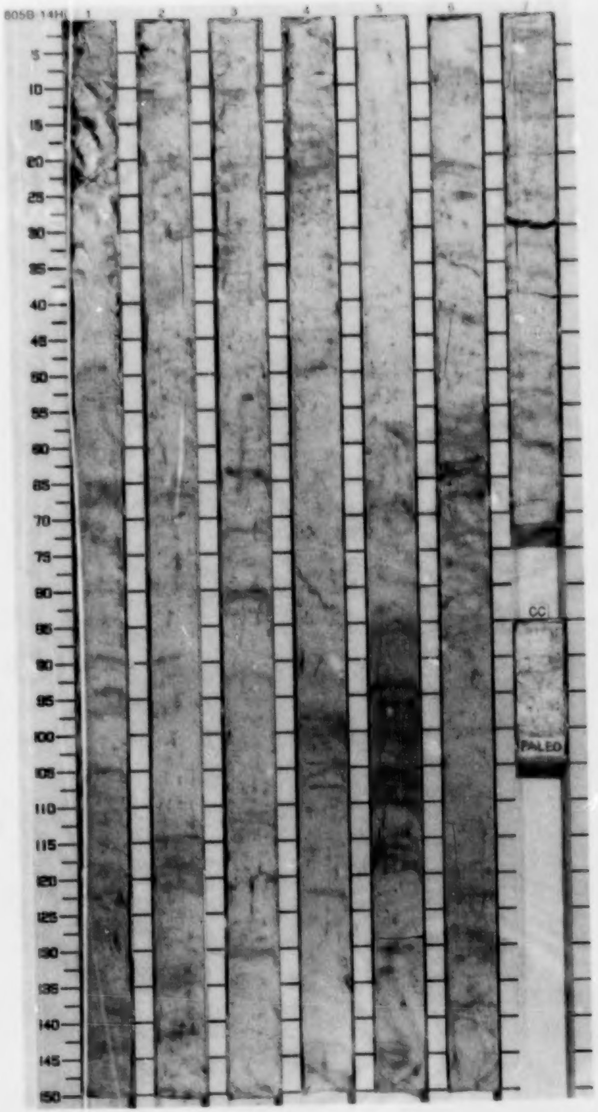
805B 14H
1
2
3
4
5
6
7
CC
PALEO
5
10
15
20
25
30
35
40
45
50
55
60
65
70
75
80
85
90
95
100
105
110
115
120
125
130
135
140
145
150

SITE 805 HOLE B CORE 15H CORED INTERVAL 130.2-139.7 mbsf

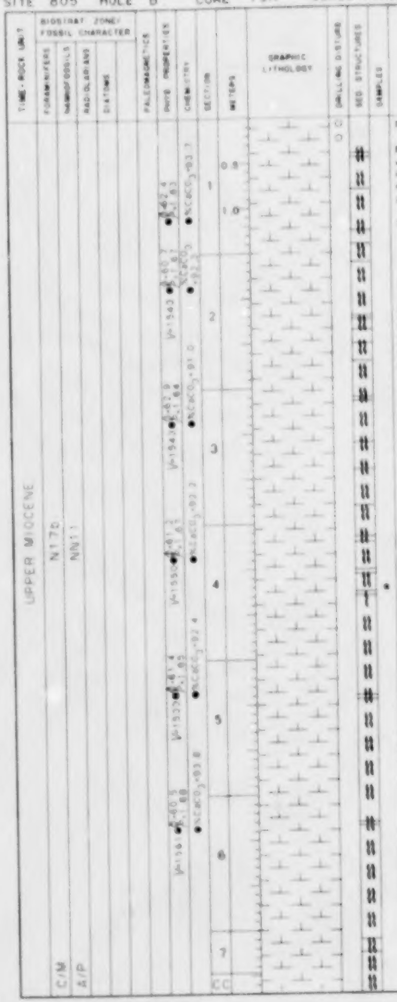

LITHOLOGIC DESCRIPTION

NANNOFOSSIL OOZE with FORAMINIFERS

Major lithology: This core contains homogeneous, white (2.5Y 8/0) NANNOFOSSIL OOZE with FORAMINIFERS. The sediment is heavily bioturbated with abundant cm scale horizontal light gray (5Y 7/1) burrows and common cm scale vertical burrows. Diffuse pale green (10G 6/2), pale purple (5P 6/2), pale blue (5PB 7/2), grayish blue (5PB 5/2), light gray (2.5Y 7/2) and light greenish gray (5G 7/1) color bands and mottles are present throughout the core.

SMEAR SLIDE SUMMARY (%):

	4, 70 D
TEXTURE	
Sand	8
Silt	88
Clay	4
COMPOSITION	
Diatoms	1
Foraminifers	10
Nannofossils	88
Radiolarians	Tr
Siliceous sponge spicules	1

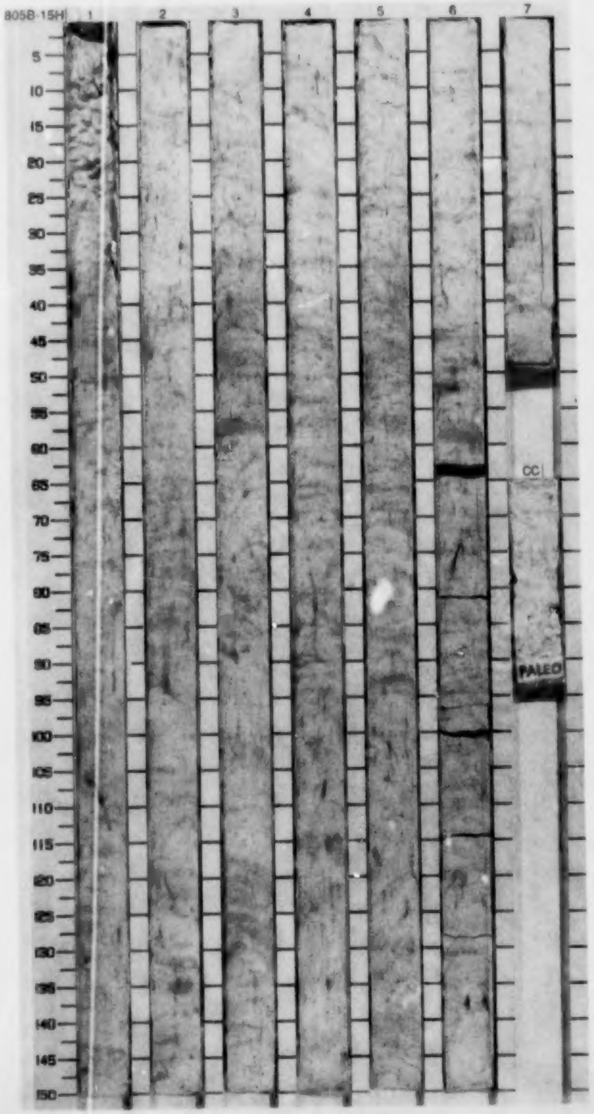
805B-15H
1
2
3
4
5
6
7
5
10
15
20
25
30
35
40
45
50
55
60
65
70
75
80
85
90
95
100
105
110
115
120
125
130
135
140
145
150
CC
PALEO

SITE 805 HOLE B CORE 16H CORED INTERVAL 139.7-149.2 mbsf

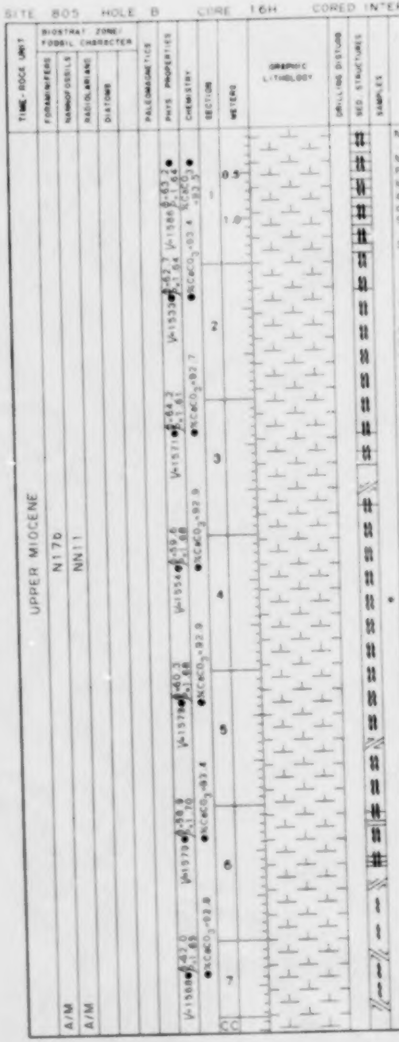
TIME-ROCK UNIT
BIOSTRAT. ZONE/FOSSIL CHARACTER
FORAMINIFERS
NANNOFOSSILS
RADIOLARIANS
DIATOMS
PALEOMAGNETICS
PHYS. PROPERTIES
CHEMISTRY
SECTION
METERS
GRAPHIC LITHOLOGY
DRILLING DISTURB.
SED. STRUCTURES
SAMPLES
UPPER MIOCENE
N17b
NN11
A/M
A/M
V=1586 ϕ=63.2 ρ=1.64
%CaCO3=83.5
%CaCO3=83.4
V=1533 ϕ=62.7 ρ=1.64
%CaCO3=82.7
V=1571 ϕ=64.2 ρ=1.61
%CaCO3=82.9
V=1554 ϕ=59.6 ρ=1.68
%CaCO3=82.9
V=1578 ϕ=60.3 ρ=1.68
%CaCO3=83.4
V=1579 ϕ=58.8 ρ=1.70
%CaCO3=82.8
V=1568 ϕ=42.0 ρ=1.69
1
2
3
4
5
6
7
CC
0.5
1.0

LITHOLOGIC DESCRIPTION

NANNOFOSSIL OOZE with FORAMINIFERS

Major lithology: This core contains white (2.5Y 8/0) NANNOFOSSIL OOZE with FORAMINIFERS. The sediment is moderately to heavily bioturbated with abundant cm scale, horizontal, light gray (5Y 7/1) and pale blue (5PB 7/2) burrow mottles. Millimeter scale, pyritic burrow fills are common. Faint, pale blue (5PB 7/2), pale purple (5P 6/2), and light greenish gray (5G 7/1) color bands are common; microfaulted color bands are present at Section 3, 102 cm, Section 5, 90 cm, Section 6, 87 cm, and Section 7, 20 and 80 cm.

SMEAR SLIDE SUMMARY (%):

	4, 75
	D
TEXTURE:	
Sand	10
Silt	55
Clay	35
COMPOSITION:	
Foraminifers	12
Nannofossils	88
Siliceous sponge spicules	Tr

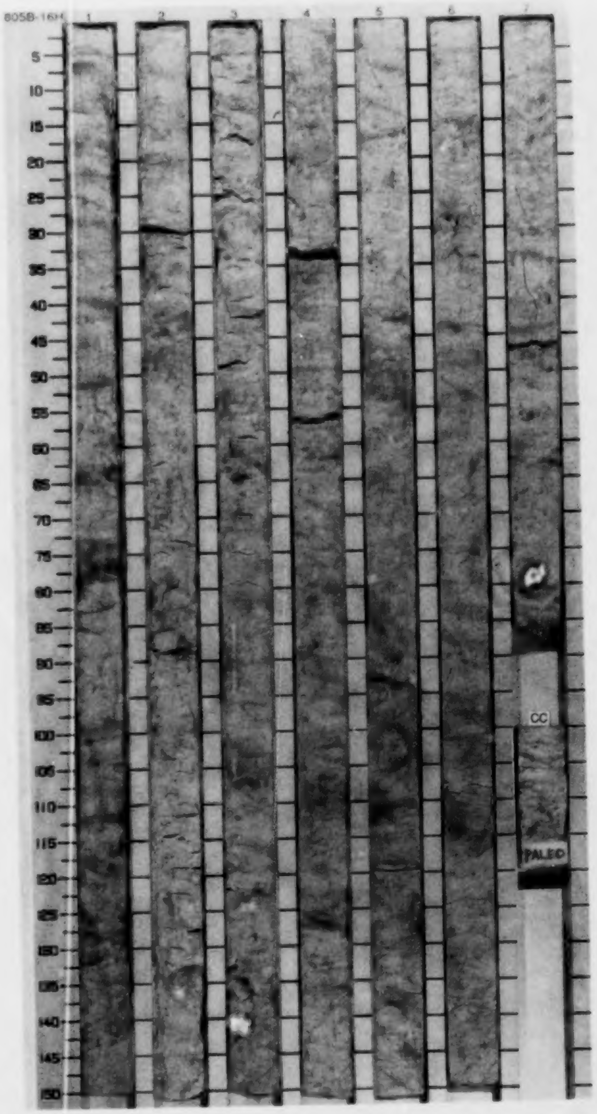
805B-16H
1
2
3
4
5
6
7
5
10
15
20
25
30
35
40
45
50
55
60
65
70
75
80
85
90
95
100
105
110
115
120
125
130
135
140
145
150
CC
PALEO

SITE 805 HOLE B CORE 17H CORED INTERVAL 149.2-158.7 mbsf

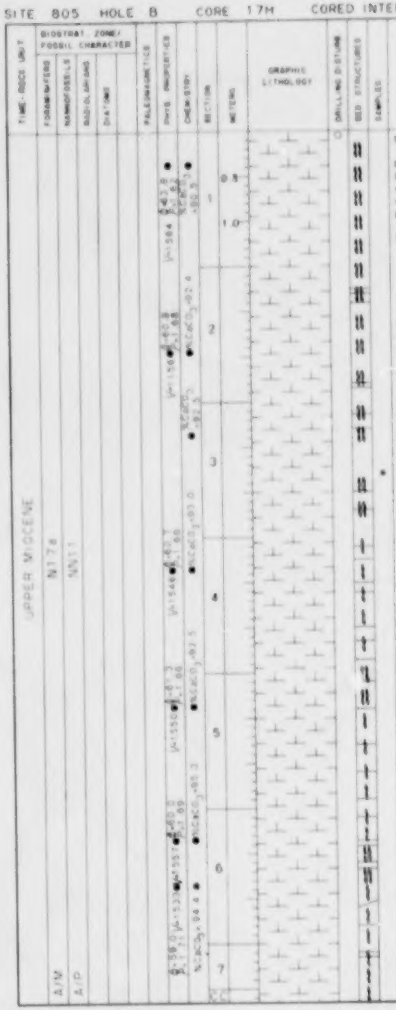
TIME-ROCK UNIT
BIOSTRAT. ZONE/ FOSSIL CHARACTER
FORAMINIFERS
NANNOFOSSILS
RADIOLARIANS
DIATOMS
PALEOMAGNETICS
PHYS. PROPERTIES
CHEMISTRY
SECTION
METERS
GRAPHIC LITHOLOGY
DRILLING DISTURB.
SED. STRUCTURES
SAMPLES
UPPER MIOCENE
N17a
NN11
A/M
A/P
1
2
3
4
5
6
7
CC
0.5
1.0

LITHOLOGIC DESCRIPTION

NANNOFOSSIL OOZE with FORAMINIFERS

Major lithology: This core contains white (2.5Y 8/0) NANNOFOSSIL OOZE with FORAMINIFERS. The sediment is moderately to heavily bioturbated throughout with abundant cm-scale, horizontal, light gray (5Y 7/1), pale purple (5P 6/2) and pale blue (5PB 7/2) burrow mottles. Millimeter scale, pyritic burrow fills are common. Faint pale blue (5PB 7/2), pale purple (5P 6/2), and light greenish gray (5G 7/1) color bands are common.

SMEAR SLIDE SUMMARY (%)

	3, 80
	D
TEXTURE	
Sand	10
Silt	85
Clay	5
COMPOSITION	
Foraminifers	10
Nannofossils	90

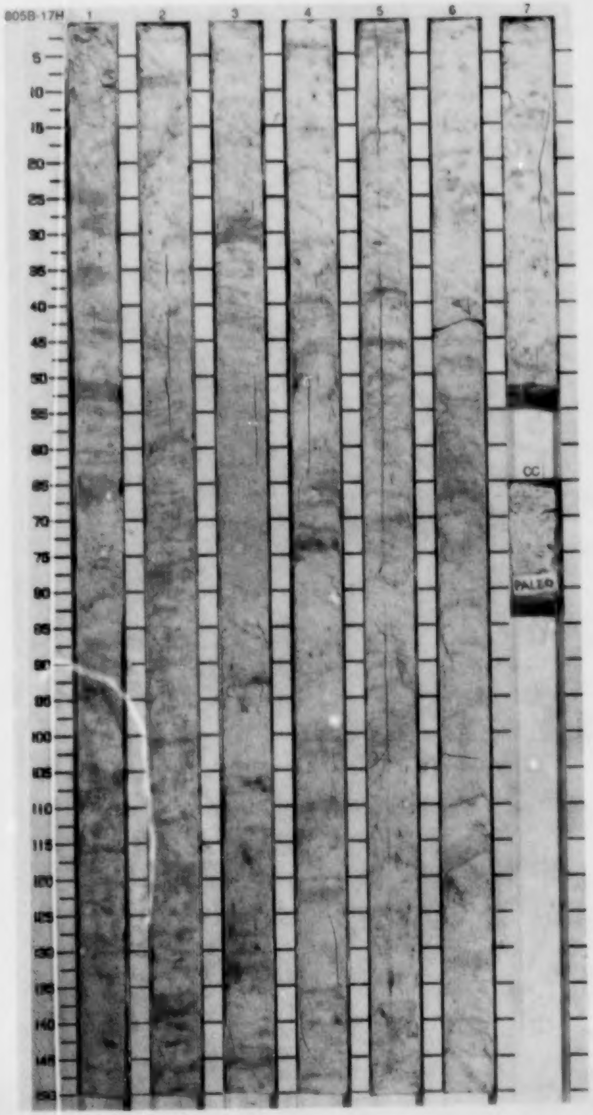
805B-17H
1
2
3
4
5
6
7
CC
PALEO
5
10
15
20
25
30
35
40
45
50
55
60
65
70
75
80
85
90
95
100
105
110
115
120
125
130
135
140
145
150

SITE 805 HOLE B CORE 18H CORED INTERVAL 158.7-168.2 mbsf

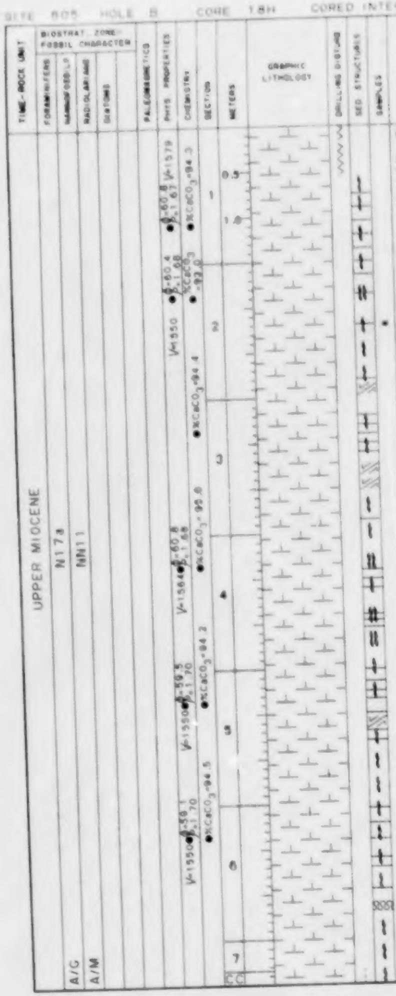
TIME-ROCK UNIT
BIOSTRAT. ZONE/FOSSIL CHARACTER
FORAMINIFERS
NANNOFOSSILS
RADIOLARIANS
DIATOMS
PALEOMAGNETICS
PHYS. PROPERTIES
CHEMISTRY
SECTION
METERS
GRAPHIC LITHOLOGY
DRILLING DISTURB.
SED. STRUCTURES
SAMPLES
UPPER MIOCENE
N17a
NN11
A/G
A/M
φ-60.8 γ-1.67 V-1579
%CaCO3-94.3
φ-60.4 γ-1.68
%CaCO3-93.0
V-1550
%CaCO3-94.4
%CaCO3-95.0
V-1564 φ-60.8 γ-1.68
%CaCO3-94.2
V-1550 φ-59.5 γ-1.70
%CaCO3-94.5
V-1550 φ-58.1 γ-1.70
1
2
3
4
5
6
7
CC
0.5
1.0

LITHOLOGIC DESCRIPTION

NANNOFOSSIL OOZE with FORAMINIFERS

Major lithology: This core contains white (2.5Y 8/0), moderately to heavily bioturbated NANNOFOSSIL OOZE with FORAMINIFERS. Mottling and diffuse, light gray (5Y 7/1, 2.5Y 7/2), pale blue (5PB 7/2), and pale purple (5P 6/2) color bands are common throughout the core. Microfaulted color bands were observed at Section 2, 145 cm, Section 3, 74 and 90 cm and Section 5, 70-85 cm.

SMEAR SLIDE SUMMARY (%):

	2, 70
	D
TEXTURE:	
Sand	10
Silt	86
Clay	4
COMPOSITION:	
Foraminifers	12
Nannofossils	85
Radiolarians	1
Siliceous sponge spicules	2

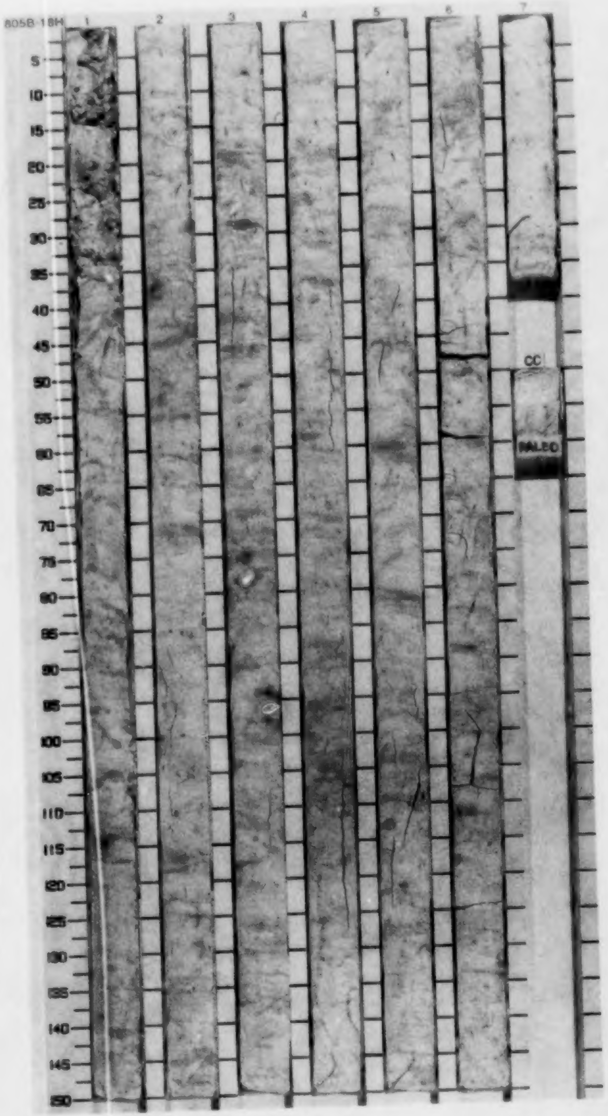
805B-18H
1
2
3
4
5
6
7
CC
PALEO
5
10
15
20
25
30
35
40
45
50
55
60
65
70
75
80
85
90
95
100
105
110
115
120
125
130
135
140
145
150

SITE 805 HOLE B CORE 19H CORED INTERVAL 168.2-177.7 mbsf

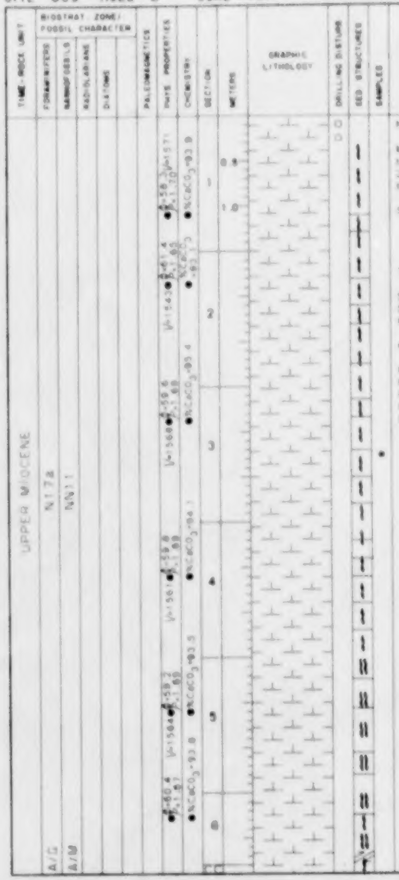

LITHOLOGIC DESCRIPTION

NANNOFOSSIL OOZE

Major lithology: This core contains white (2.5Y 8/0 and 5Y 8/0) moderately to heavily bioturbated NANNOFOSSIL OOZE. Mottling, pyritized burrows and diffuse, light gray (5Y 7/1, 2.5Y 7/2), pale blue (5PB 7/2), and pale purple (5P 6/2) color bands are common throughout the core.

SMEAR SLIDE SUMMARY (%)

	3, 77
	D
TEXTURE	
Sand	5
Silt	90
Clay	5
COMPOSITION	
Foraminifers	7
Nannofossils	90
Pyrite	1
Radiolarians	2
Siliceous sponge spicules	Tr

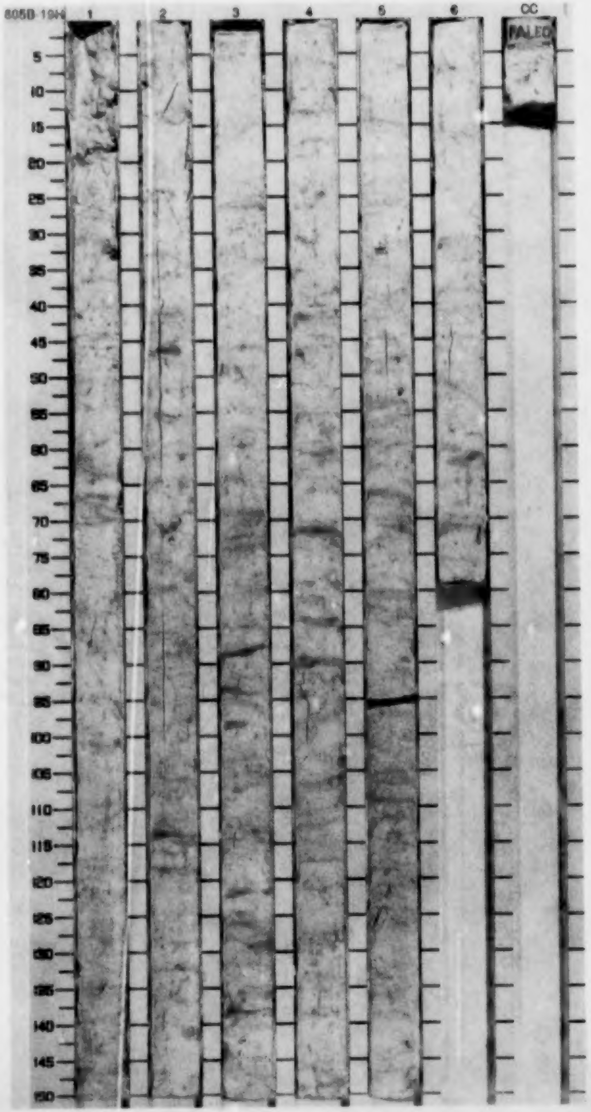
805B-19H
1
2
3
4
5
6
CC
PALEO
5
10
15
20
25
30
35
40
45
50
55
60
65
70
75
80
85
90
95
100
105
110
115
120
125
130
135
140
145
150

SITE 805 HOLE B CORE 20H CORED INTERVAL 177.7-187.2 mbsf

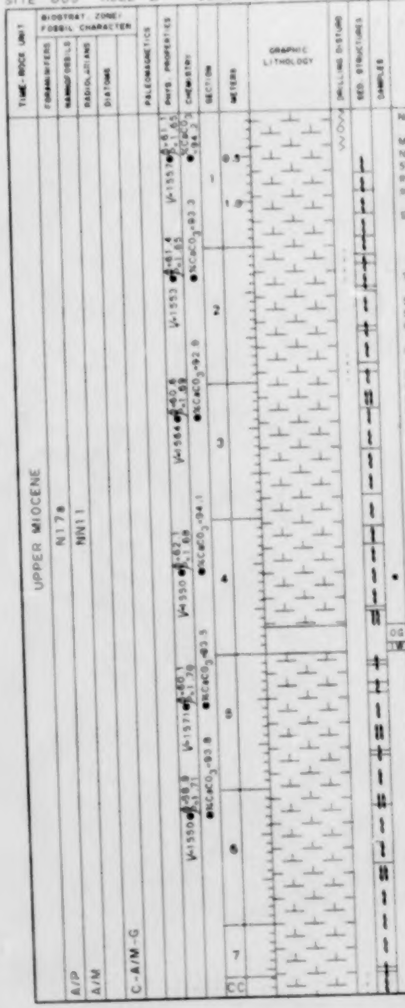

LITHOLOGIC DESCRIPTION

NANNOFOSSIL OOZE

Major lithology: This core contains white (2.5Y 8/0), moderately to heavily bioturbated NANNOFOSSIL OOZE. Mottling, pyritized burrows and diffuse light gray (5Y 7/1, 2.5Y 7/2, 5Y 7/1), pale blue (5PB 7/2), and pale purple (5P 6/2) color bands are common throughout the core. Some color bands in Section 1 are vertical and cross burrows and other horizontal structures.

SMEAR SLIDE SUMMARY (%):

	4, 98
	D
TEXTURE:	
Sand	5
Silt	90
Clay	5
COMPOSITION:	
Diatoms	Tr
Foraminifers	7
Nannofossils	89
Radiolarians	3
Siliceous sponge spicules	1
Silicoflagellates	Tr

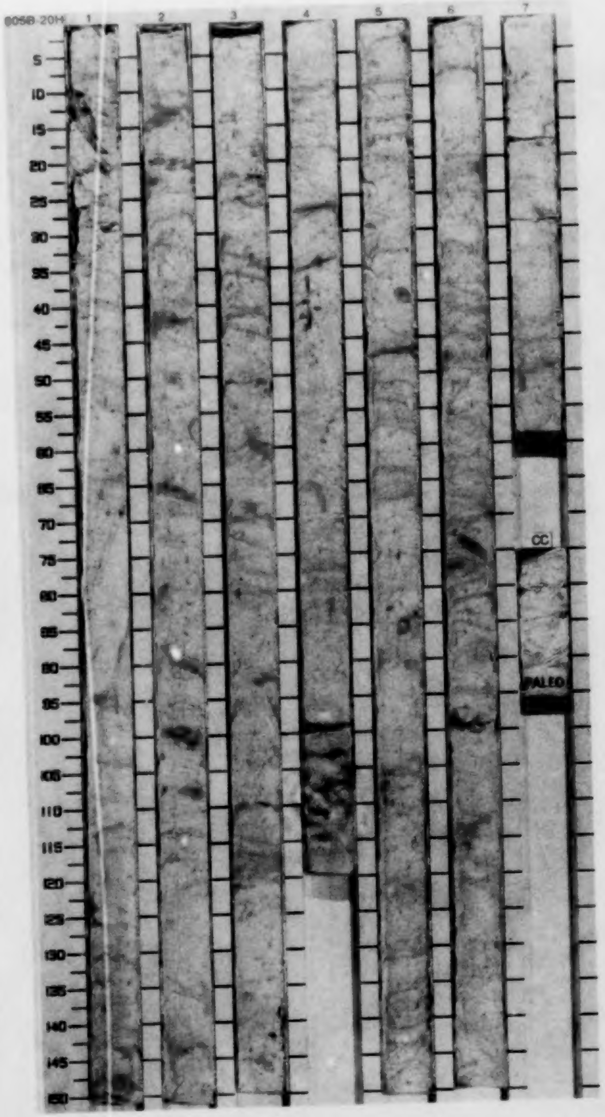
805B-20H
1
2
3
4
5
6
7
CC
PALEO
5
10
15
20
25
30
35
40
45
50
55
60
65
70
75
80
85
90
95
100
105
110
115
120
125
130
135
140
145
150

SITE 805 HOLE B CORE 21H CORED INTERVAL 187.2-196.7 mbsf

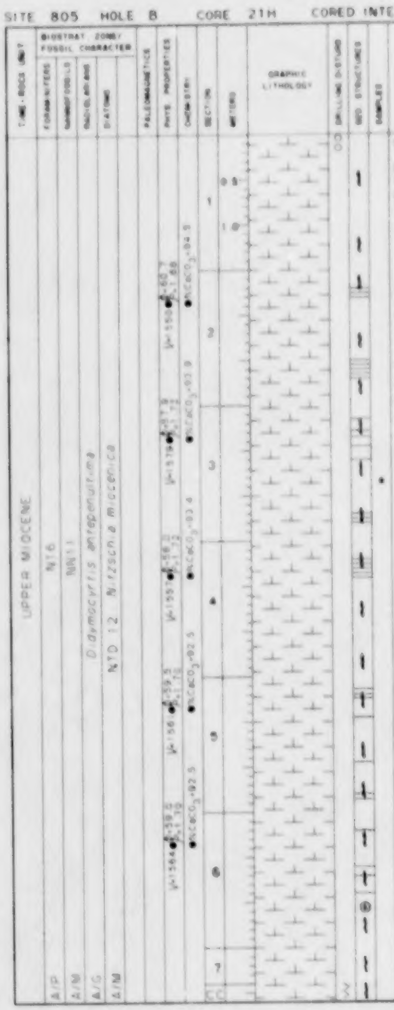
TIME-ROCK UNIT
BIOSTRAT. ZONE/FOSSIL CHARACTER
FORAMINIFERS
NANNOFOSSILS
RADIOLARIANS
DIATOMS
PALEOMAGNETICS
PHYS. PROPERTIES
CHEMISTRY
SECTION
METERS
GRAPHIC LITHOLOGY
DRILLING DISTURB.
SED. STRUCTURES
SAMPLES
UPPER MIOCENE
N16
NN11
Didymocyrtis antepenultima
NTD 12 Nitzschia miocenica
A/P
A/M
A/G
A/M
V=1550 φ=60.7 γ=1.68
V=1537 φ=57.9 γ=1.72
V=1557 φ=56.2 γ=1.72
V=1561 φ=59.5 γ=1.70
V=1564 φ=59.6 γ=1.70
%CaCO3=94.5
%CaCO3=93.9
%CaCO3=93.4
%CaCO3=92.5
%CaCO3=92.5
1
2
3
4
5
6
7
CC
0.5
1.0

LITHOLOGIC DESCRIPTION

NANNOFOSSIL OOZE

Major lithology: This core contains white (2.5Y 8/0), moderately to heavily bioturbated NANNOFOSSIL OOZE. Mottling, pyritized burrows, and faint diffuse light gray (5Y 7/1), pale purple (5P 6/2) and grayish blue (5PB 5/2) color bands are common throughout the core. The pale purple (5P 6/2) color bands generally are horizontal, but a few are inclined.

SMEAR SLIDE SUMMARY (%):

	3, 80
	D
TEXTURE:	
Sand	4
Silt	92
Clay	4
COMPOSITION:	
Foraminifers	5
Nannofossils	94
Radiolarians	1

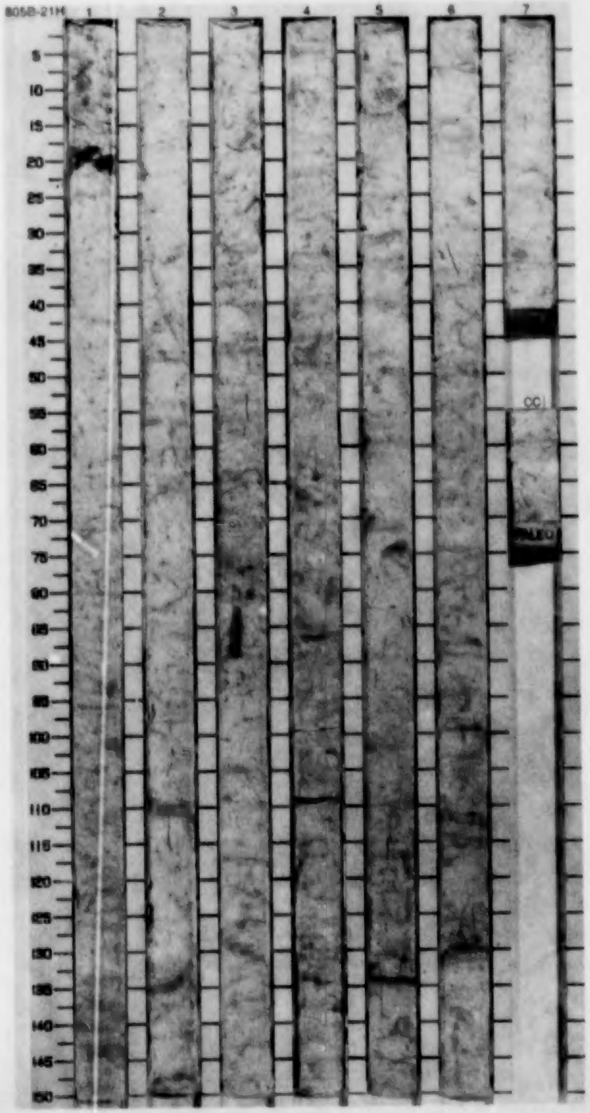
805B-21H
1
2
3
4
5
6
7
5
10
15
20
25
30
35
40
45
50
55
60
65
70
75
80
85
90
95
100
105
110
115
120
125
130
135
140
145
150
CC

SITE 805 HOLE B CORE 22H CORED INTERVAL 196.7-206.2 mbsf

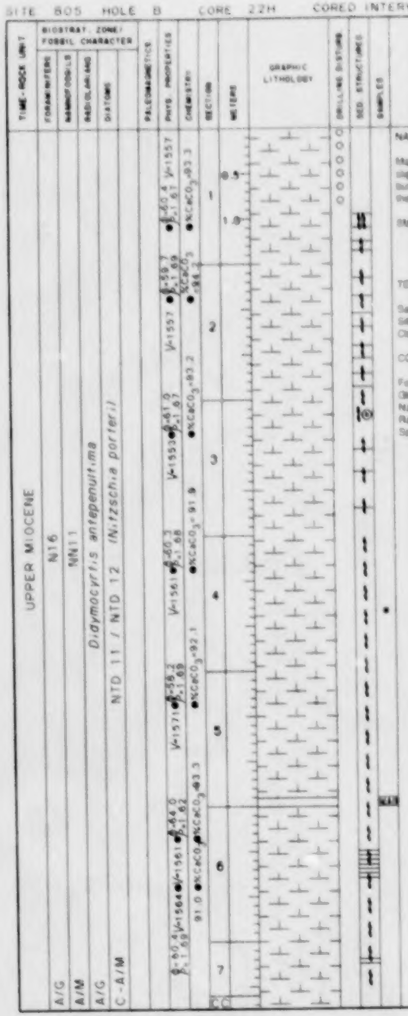

LITHOLOGIC DESCRIPTION

NANNOFOSSIL OOZE

Major lithology: This core contains white (2.5Y 8/0) NANNOFOSSIL OOZE. The sediment is slightly to moderately bioturbated throughout, predominantly indicated by mm scale pyritized burrows. Diffuse, light gray (5Y 7/1) and pale purple (5P 6/2) color bands are present, but their abundance decreases downcore.

SMEAR SLIDE SUMMARY (%):

	4, 83
	D
TEXTURE:	
Sand	5
Silt	90
Clay	5
COMPOSITION:	
Foraminifers	4
Glass	1
Nannofossils	90
Radiolarians	4
Spicules	1

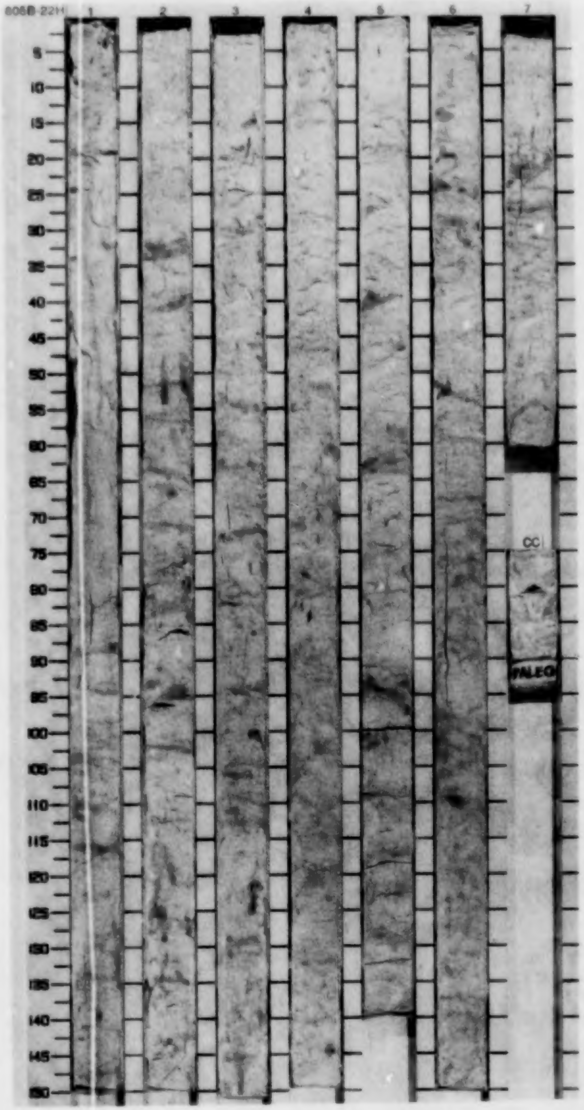
805B-22H
1
2
3
4
5
6
7
5
10
15
20
25
30
35
40
45
50
55
60
65
70
75
80
85
90
95
100
105
110
115
120
125
130
135
140
145
150
CC
PALEO

SITE 805 HOLE B CORE 23H CORED INTERVAL 206.2-215.7 mbsf

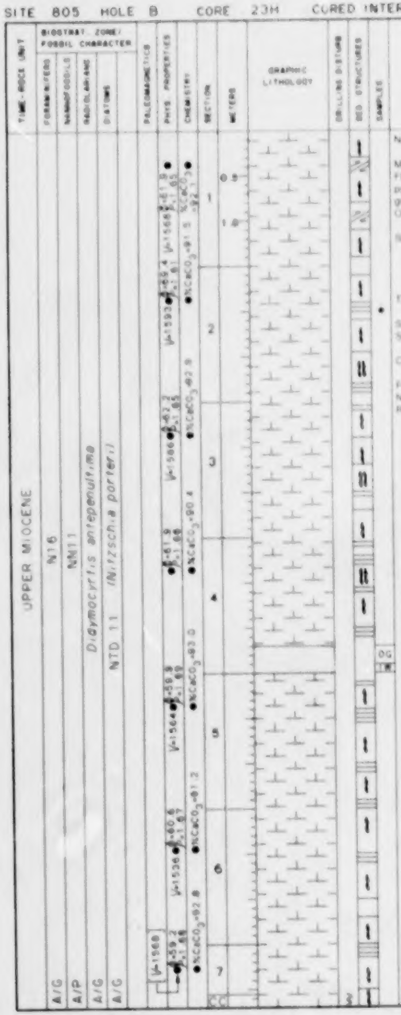
TIME-ROCK UNIT
BIOSTRAT. ZONE/ FOSSIL CHARACTER
FORAMINIFERS
NANNOFOSSILS
RADIOLARIANS
DIATOMS
PALEOMAGNETICS
PHYS. PROPERTIES
CHEMISTRY
SECTION
METERS
GRAPHIC LITHOLOGY
DRILLING DISTURB.
SED. STRUCTURES
SAMPLES
UPPER MIOCENE
N16
NN11
Didymocyrtis antepenultima
NTD 11 (Nitzschia porteri)
A/G
A/P
A/G
A/G
φ=61.9 ρ=1.65
V=1566
%CaCO3=92.1
φ=60.4 ρ=1.61
V=1593
%CaCO3=81.5
%CaCO3=82.9
φ=62.2 ρ=1.65
V=1566
%CaCO3=80.4
φ=61.9 ρ=1.66
%CaCO3=83.0
φ=59.8 ρ=1.69
V=1564
%CaCO3=81.2
φ=60.6 ρ=1.67
V=1536
%CaCO3=82.8
φ=59.2 ρ=1.68
V=1560
1
2
3
4
5
6
7
CC
0.5
1.0
OG
IW

LITHOLOGIC DESCRIPTION

NANNOFOSSIL OOZE with FORAMINIFERS

Major lithology: This core contains white (2.5Y 8/0) NANNOFOSSIL OOZE with FORAMINIFERS. The sediment is moderately to heavily bioturbated throughout, indicated by mm-scale pyritized burrows (with purple halos) and light gray (5Y 7/1) cm-scale mottling. Diffuse light gray (5Y 7/1), pale purple (5P 6/2) and light greenish gray (5G 7/1) color bands are common. Occasional microfaults, shown by displacement in the color bands, are present.

SMEAR SLIDE SUMMARY (%):

	2, 49
	D
TEXTURE:	
Sand	20
Silt	80
COMPOSITION:	
Foraminifers	12
Nannofossils	82
Radiolarians	6

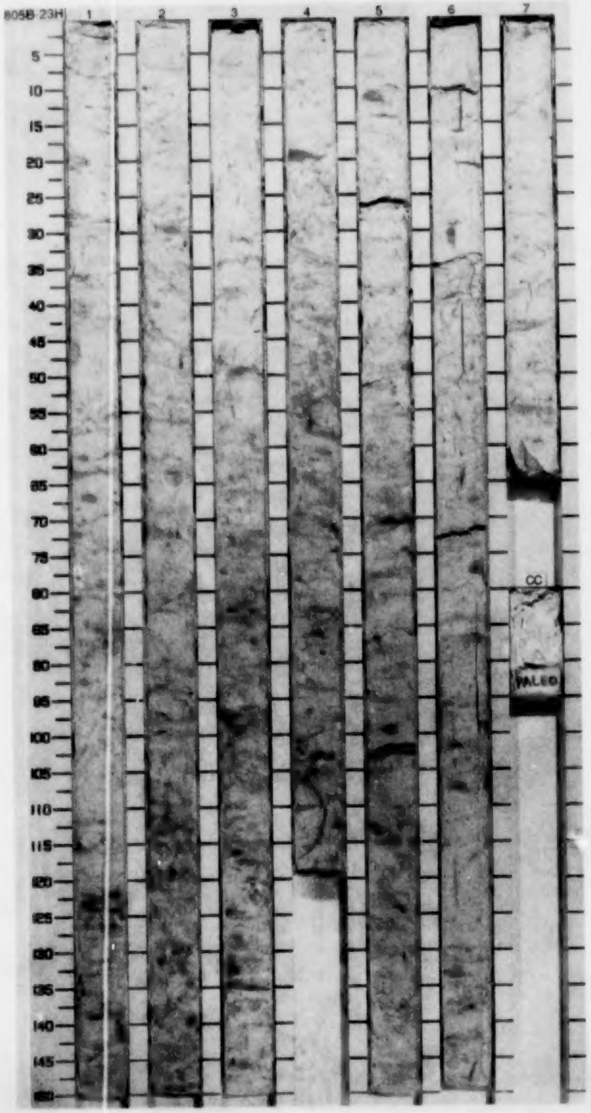
805B-23H
1
2
3
4
5
6
7
5
10
15
20
25
30
35
40
45
50
55
60
65
70
75
80
85
90
95
100
105
110
115
120
125
130
135
140
145
150
CC
PALEO

SITE 805 HOLE B CORE 24H CORED INTERVAL 215.7-225.2 mbsf

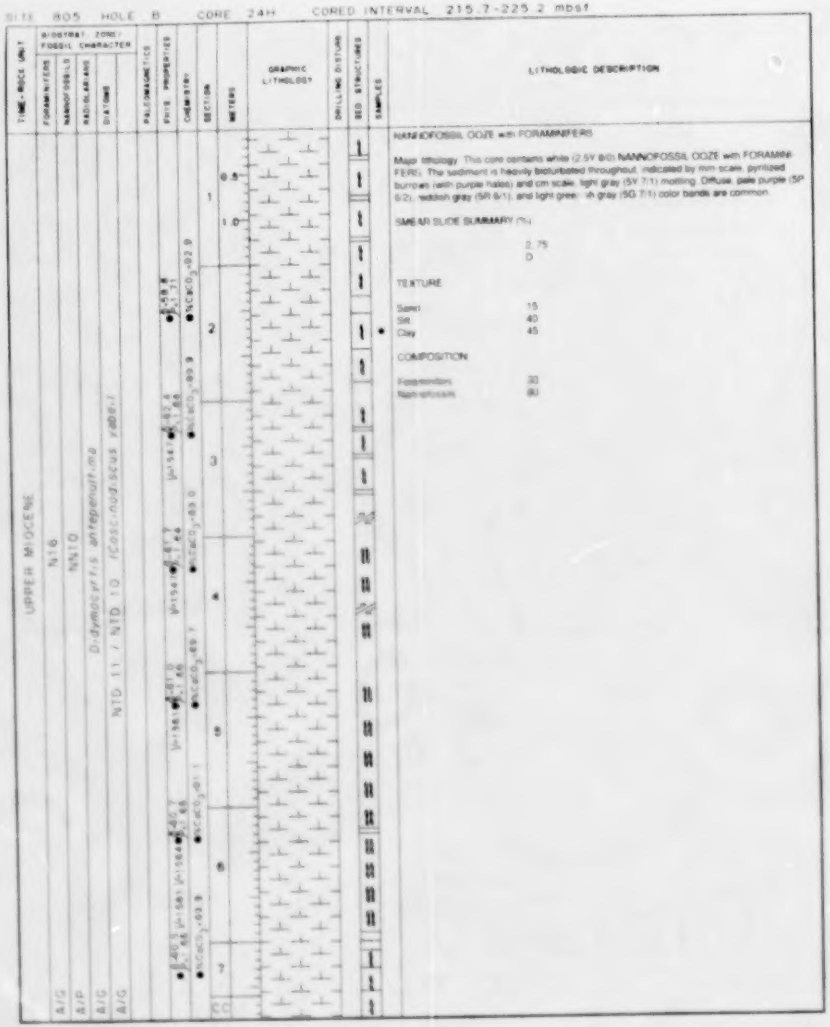
TIME-ROCK UNIT
BIOSTRAT. ZONE/ FOSSIL CHARACTER
FORAMINIFERS
NANNOFOSSILS
RADIOLARIANS
DIATOMS
PALEOMAGNETICS
PHYS. PROPERTIES
CHEMISTRY
SECTION
METERS
GRAPHIC LITHOLOGY
DRILLING DISTURB.
SED. STRUCTURES
SAMPLES
UPPER MIOCENE
N16
NN10
Didymocyrtis antepenultima
NTD 11 / NTD 10 /Coscinodiscus yabei/
A/G
A/P
A/G
A/G
1
2
3
4
5
6
7
CC
0.5
1.0

LITHOLOGIC DESCRIPTION

NANNOFOSSIL OOZE with FORAMINIFERS

Major lithology: This core contains white (2.5Y 8/0) NANNOFOSSIL OOZE with FORAMINIFERS. The sediment is heavily bioturbated throughout, indicated by mm-scale, pyritized burrows (with purple halos) and cm scale, light gray (5Y 7/1) mottling. Diffuse, pale purple (5P 6/2), reddish gray (5R 6/1), and light greenish gray (5G 7/1) color bands are common.

SMEAR SLIDE SUMMARY (%):

	2, 75 D
TEXTURE	
Sand	15
Silt	40
Clay	45
COMPOSITION	
Foraminifers	20
Nannofossils	80

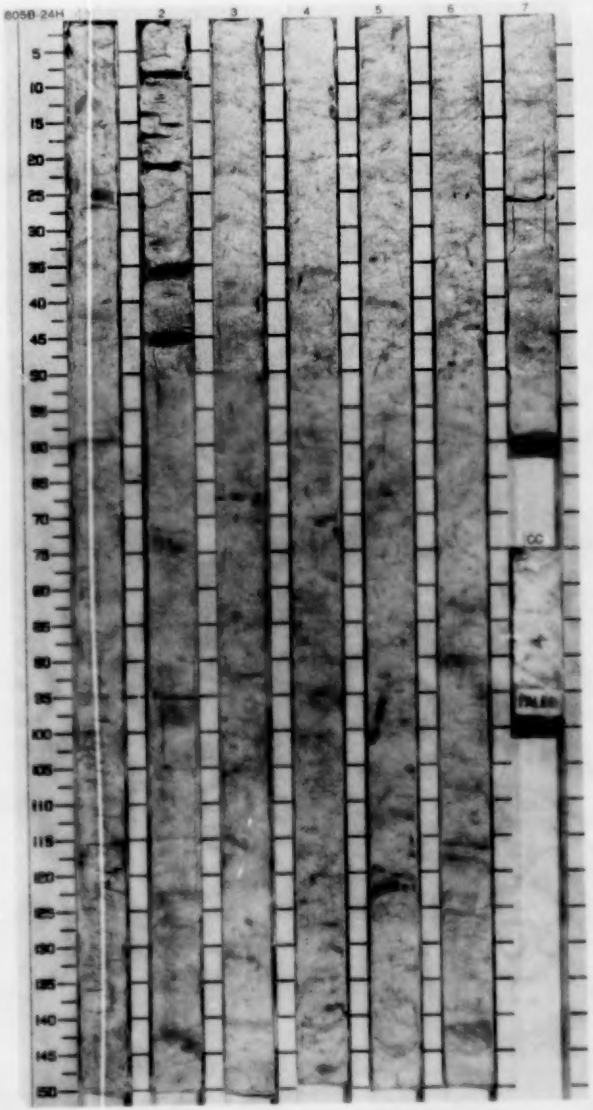
805B-24H
1
2
3
4
5
6
7
CC
5
10
15
20
25
30
35
40
45
50
55
60
65
70
75
80
85
90
95
100
105
110
115
120
125
130
135
140
145
150

SITE 805 HOLE B CORE 25H CORED INTERVAL 225.2-234.7 mbsf

TIME-ROCK UNIT	FORAMINIFERS	NANNOFOSSILS	RADIOLARIANS	DIATOMS	PALEOMAGNETICS	PHYS. PROPERTIES	CHEMISTRY	SECTION	METERS	SED. STRUCTURES	SAMPLES
UPPER MIOCENE	N16	NN10	*Didymocyrtis antepenultima*	NTD 10?		V=1561 ● φ=60.1 γ=1.69	● %CaCO$_3$=90.0	1	0.5 1.0		
						V=1561 ● φ=62.8 γ=1.63	● %CaCO$_3$=88.2	2			*
						V=1571 ● φ=62.4 γ=1.64	● %CaCO$_3$=91.4	3			
						V=1588 ● φ=62.2 γ=1.64	● %CaCO$_3$=92.5	4			
						V=1561 ● φ=60.2 γ=1.66	● %CaCO$_3$=91.0	5			
						● φ=59.5 γ=1.69	● %CaCO$_3$=94.0	6			
								7			
A/G	A/P	A/M						CC			

BIOSTRAT. ZONE/ FOSSIL CHARACTER

GRAPHIC LITHOLOGY

DRILLING DISTURB.

LITHOLOGIC DESCRIPTION

FORAMINIFER NANNOFOSSIL OOZE

Major lithology: This core contains white (2.5Y 8/0) FORAMINIFER NANNOFOSSIL OOZE. Frequent, diffuse, pale purple (5P 6/2), reddish gray (5R 6/1), and light greenish gray (5G 7/1) color bands are present. These color bands are on the order of 1 cm thick and are spaced approximately 5 to 10 cm apart. The sediments are heavily bioturbated, evident from abundant pyrite filled burrows and light gray (5Y 7/1) mottles.

SMEAR SLIDE SUMMARY (%):

	2, 80 D
TEXTURE:	
Sand	10
Silt	50
Clay	40
COMPOSITION:	
Diatoms	1
Foraminifers	25
Nannofossils	70
Radiolarians	2
Siliceous fragments	3

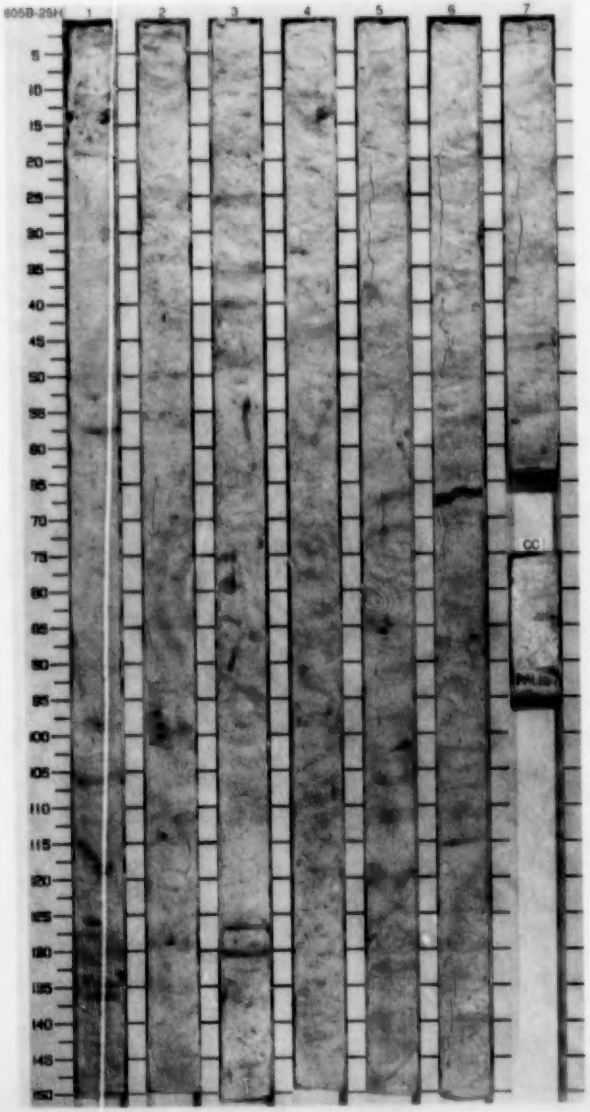

SITE 805 HOLE B CORE 26H CORED INTERVAL 234.7-244.2 mbsf

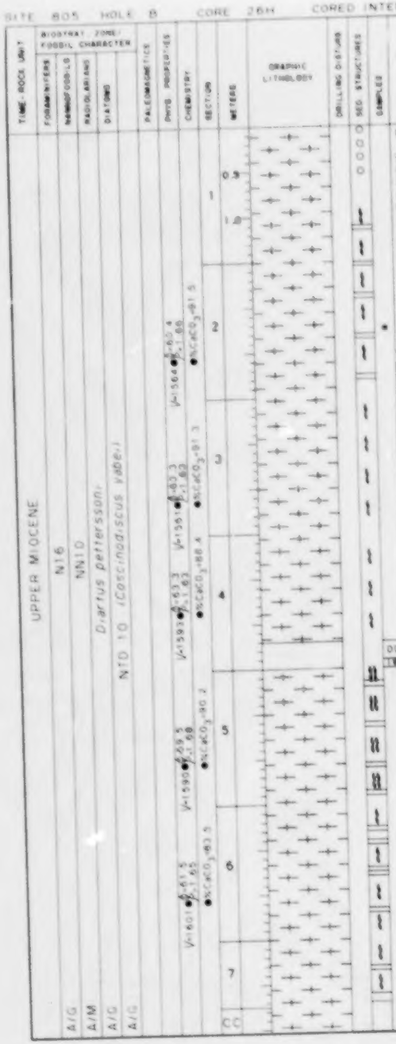
TIME-ROCK UNIT
BIOSTRAT. ZONE/ FOSSIL CHARACTER
FORAMINIFERS
NANNOFOSSILS
RADIOLARIANS
DIATOMS
PALEOMAGNETICS
PHYS. PROPERTIES
CHEMISTRY
SECTION
METERS
GRAPHIC LITHOLOGY
DRILLING DISTURB.
SED. STRUCTURES
SAMPLES
UPPER MIOCENE
N16
NN10
Diartus petterssoni
NTD 10 (Coscinodiscus yabei)
A/G
A/M
A/G
A/G
V=1564
60.4
1.66
V=1561
63.3
1.63
V=1593
63.3
1.63
V=1590
69.5
1.68
V=1601
61.5
1.65
%CaCO3=91.5
%CaCO3=91.3
%CaCO3=88.4
%CaCO3=90.2
%CaCO3=83.5
0.5
1.0
1
2
3
4
5
6
7
CC
OG
IW

LITHOLOGIC DESCRIPTION

FORAMINIFER NANNOFOSSIL OOZE

Major lithology: This core contains white (2.5Y 8/0) FORAMINIFER NANNOFOSSIL OOZE. Pervasive, subhorizontal, faint color bands and streaks of reddish gray (5R 6/1), light gray (2.5Y 7/2), and, to a lesser extent, pale yellowish green (10GY 7/2) occur throughout the core. Mottling, as well as pyrite specks and streaks, attest to extensive bioturbation. Color bands are 5 to 15 mm thick and are spaced at 1- to 10-cm intervals. Some cm thick zones exhibit significant induration.

SMEAR SLIDE SUMMARY (%):

	2, 74 D
TEXTURE:	
Sand	15
Silt	60
Clay	25
COMPOSITION:	
Accessory minerals	1
Diatoms	Tr
Foraminifers	26
Nannofossils	70
Radiolarians	Tr
Siliceous fragments	3

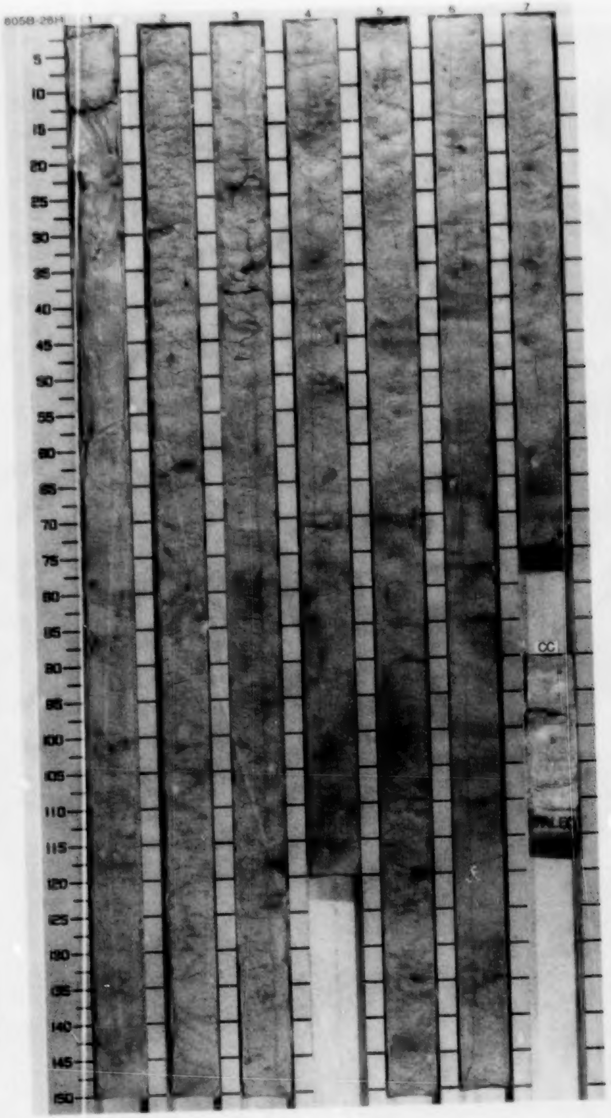
805B-26H
1
2
3
4
5
6
7
CC
5
10
15
20
25
30
35
40
45
50
55
60
65
70
75
80
85
90
95
100
105
110
115
120
125
130
135
140
145
150

SITE 805 HOLE B CORE 27H CORED INTERVAL 244.2-253.7 mbsf

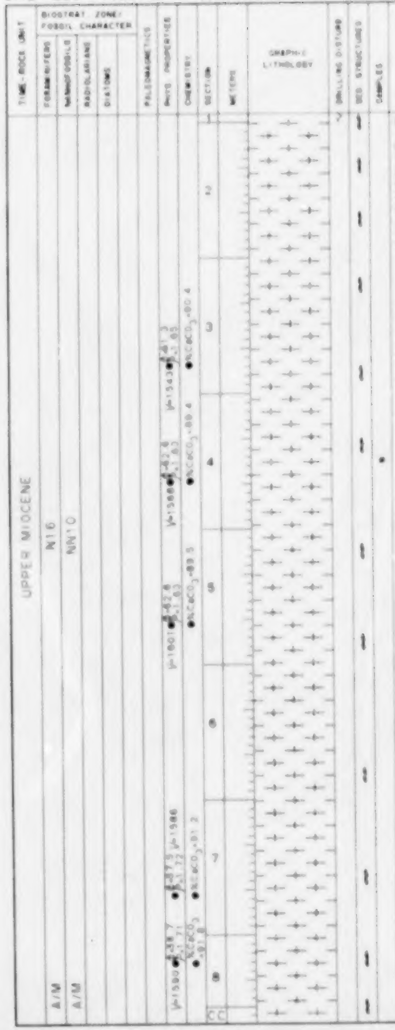

LITHOLOGIC DESCRIPTION

FORAMINIFER NANNOFOSSIL OOZE

Major lithology: This core contains white (2.5Y 8/0) FORAMINIFER NANNOFOSSIL OOZE. Sub-horizontal, faint color bands and streaks of reddish gray (5R 6/1), light gray (2.5Y 7/2) and pale yellowish green (10GY 7/2) are present throughout the core. Green bands are commonly adjacent to, but above, the reddish gray bands. Bands are 5 to 15 mm thick and are spaced at 1 to 10 cm intervals. The mottles and the pyrite specks and streaks are evidence of bioturbation. Some cm-thick zones in the upper 4 sections exhibit significant induration. Sections 5-8 are stiff to hard.

SMEAR SLIDE SUMMARY (%):

	4, 75
	D
TEXTURE:	
Sand	15
Silt	50
Clay	35
COMPOSITION:	
Foraminifers	25
Nannofossils	75
Radiolarians	Tr
Siliceous sponge spicules	Tr

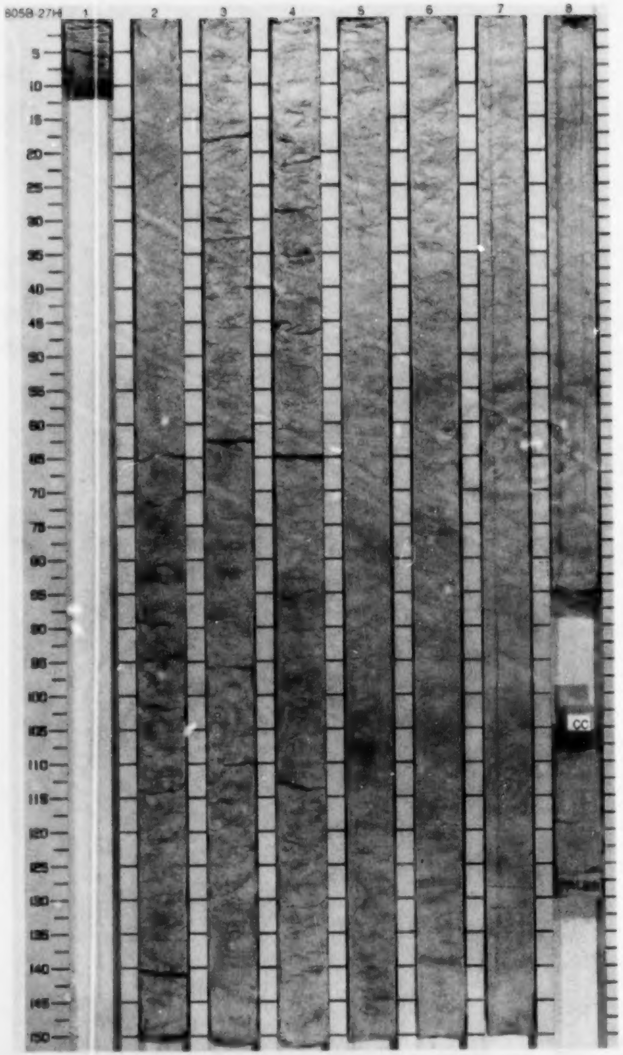
805B-27H
1
2
3
4
5
6
7
8
CC
5
10
15
20
25
30
35
40
45
50
55
60
65
70
75
80
85
90
95
100
105
110
115
120
125
130
135
140
145
150

SITE 805 HOLE B CORE 28H CORED INTERVAL 253.7-263.2 mbsf

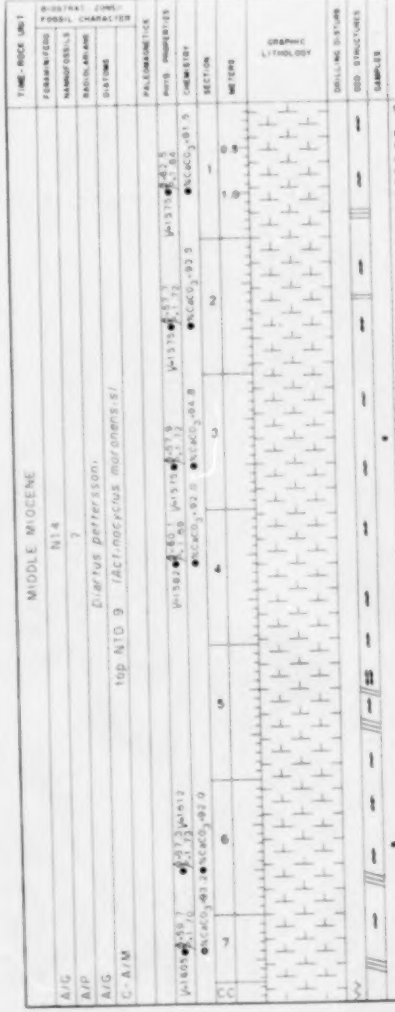

LITHOLOGIC DESCRIPTION

NANNOFOSSIL OOZE with FORAMINIFERS

Major lithology: This core contains white (2.5Y 8/0) NANNOFOSSIL OOZE with FORAMINIFERS. Bioturbation is slight, as indicated by few mottles and pyrite specks. Few faint, cm-thick, reddish gray (5R 6/1) and pale yellowish green (10GY 7/2) color bands are observed. In Sections 5, 6 and 7, some color bands dip at shallow to steep angles. In Section 5 they dip in various directions. Three reddish gray (10GY 7/2) intervals (between 10 and 15 cm thick) are noted in Sections 4, 6 and 7, and have sharp color contacts at the bottom (Sections 4, 7) and the top (Section 7). The sediment is stiff, with cm scale intervals being significantly indurated.

SMEAR SLIDE SUMMARY (%):

	3, 75 D	6, 75 D
TEXTURE		
Sand	5	15
Silt	55	50
Clay	40	35
COMPOSITION		
Foraminifers	10	20
Nannofossils	90	80
Radiolarians	Tr	Tr
Siliceous sponge spicules	Tr	Tr

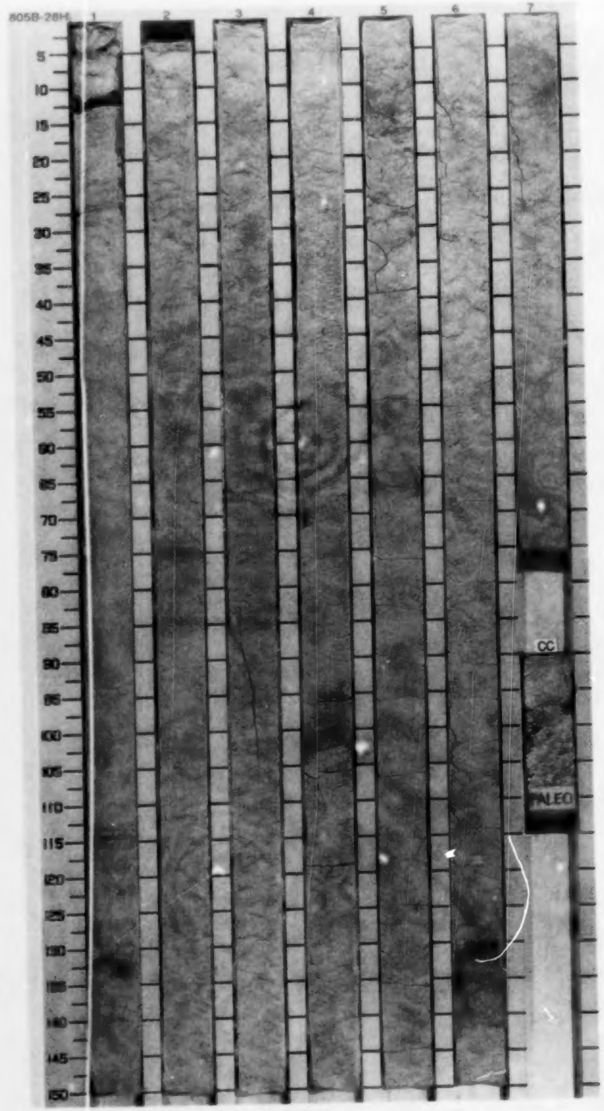
805B-28H
1
2
3
4
5
6
7
CC
PALEO
5
10
15
20
25
30
35
40
45
50
55
60
65
70
75
80
85
90
95
100
105
110
115
120
125
130
135
140
145
150

SITE 805 HOLE B CORE 29X CORED INTERVAL 263.2-272.9 mbsf

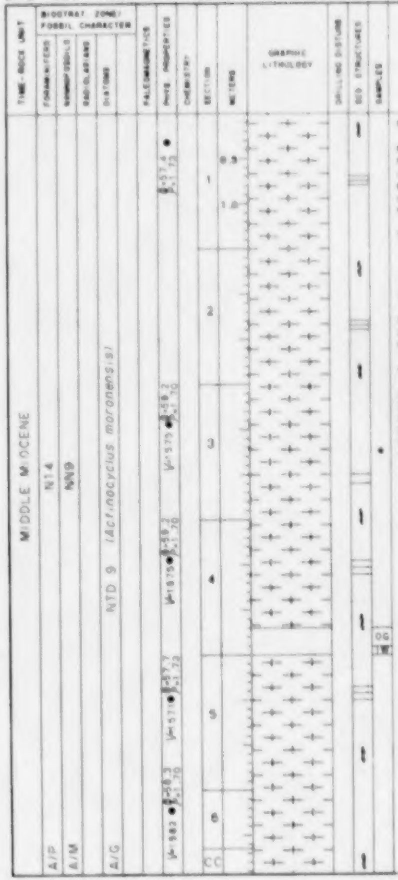
TIME-ROCK UNIT
BIOSTRAT. ZONE/ FOSSIL CHARACTER
FORAMINIFERS
NANNOFOSSILS
RADIOLARIANS
DIATOMS
PALEOMAGNETICS
PHYS. PROPERTIES
CHEMISTRY
SECTION
METERS
GRAPHIC LITHOLOGY
DRILLING DISTURB.
SED. STRUCTURES
SAMPLES
MIDDLE MIOCENE
N14
NN9
NTD 9 (Actinocyclus moronensis)
A/P
A/M
A/G
ϕ=57.4
ρ=1.72
Vp=1575
ϕ=58.2
ρ=1.70
Vp=1575
ϕ=58.2
ρ=1.70
Vp=1571
ϕ=57.7
ρ=1.72
Vp=1582
ϕ=58.3
ρ=1.70
0.5
1.0
1
2
3
4
5
6
CC
OG
IW

LITHOLOGIC DESCRIPTION

FORAMINIFER NANNOFOSSIL OOZE

Major lithology: This core contains white (2.5Y 8/0), slightly bioturbated FORAMINIFER NANNOFOSSIL OOZE. Faint pale yellow green (10GY 7/2), reddish gray (5R 6/1), pale blue (5B 7/2), and pale purple (5P 6/2) color bands are common throughout the core. These color bands are 1-3 cm and are typically horizontal. Within Sections 1 and 2, the color bands sometimes dip in opposite directions. The sediment in this core is very stiff and some thin (1 to 7 cm thick) horizons are hard.

SMEAR SLIDE SUMMARY (%):

	3, 74
	D
TEXTURE:	
Sand	10
Silt	60
Clay	30
COMPOSITION:	
Accessory minerals	3
Diatoms	5
Foraminifers	25
Nannofossils	62
Radiolarians	3
Siliceous fragments	2

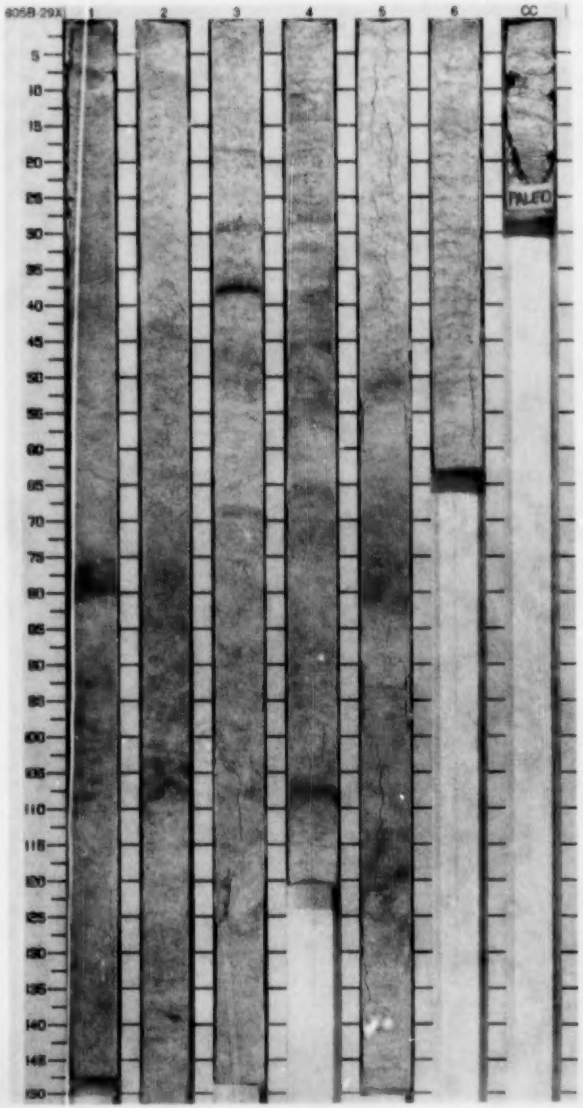
805B-29X
1
2
3
4
5
6
CC
PALEO
5
10
15
20
25
30
35
40
45
50
55
60
65
70
75
80
85
90
95
100
105
110
115
120
125
130
135
140
145
150

SITE 805 HOLE B CORE 30X CORED INTERVAL 272.9-282.5 mbsf

TIME-ROCK UNIT	BIOSTRAT. ZONE/ FOSSIL CHARACTER: FORAMINIFERS	NANNOFOSSILS	RADIOLARIANS	DIATOMS	PALEOMAGNETICS	PHYS. PROPERTIES	CHEMISTRY	SECTION	METERS	GRAPHIC LITHOLOGY	DRILLING DISTURB.	SED. STRUCTURES	SAMPLES	LITHOLOGIC DESCRIPTION
MIDDLE MIOCENE	N14 A/G	NN9 A/P	*Diartus petterssoni* A/G	NTD 9 C-A/G				1	0.5 1.0					NANNOFOSSIL OOZE with FORAMINIFERS Major lithology: This core contains white (2.5Y 8/0) NANNOFOSSIL OOZE with FORAMINIFERS. It is relatively homogeneous, with scattered pyrite specks and streaks indicative of bioturbation. Rare, faint, reddish gray (5R 6/1) and pale yellow green (10GY 7/2) color bands are observed. The ooze is very stiff, with interbedded indurated zones.
								2						
								3						
								4						
						●$V=1582$ ●$\phi=54.5$ $\gamma=1.71$	●%$CaCO_3=93.3$	5						
						●$V=1582$ ●$\phi=59.4$ $\gamma=1.73$	●%$CaCO_3=92.9$	6						
								CC						

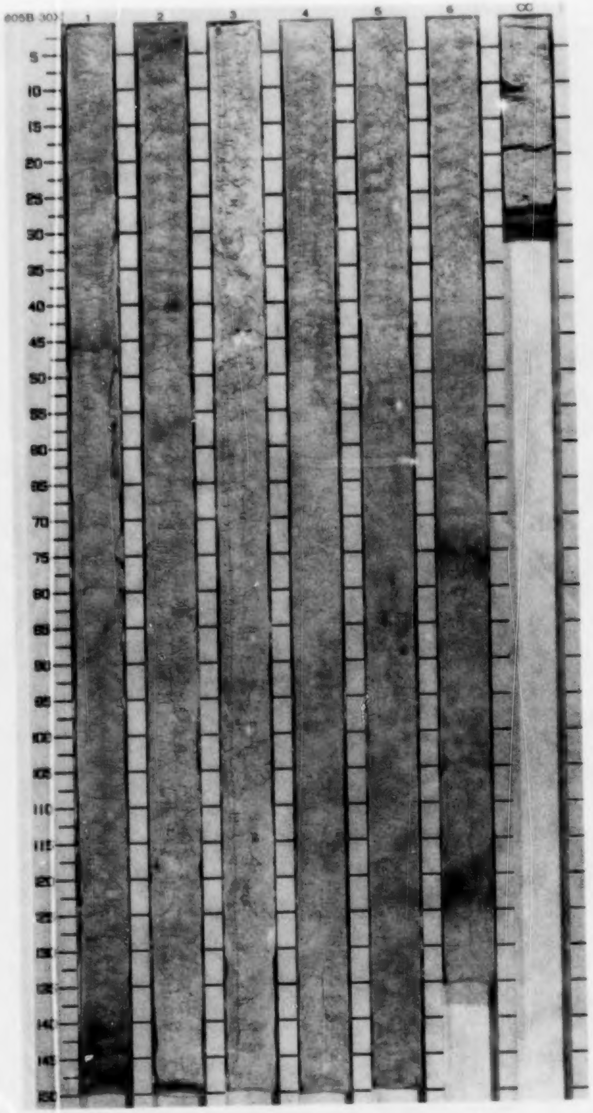
805B-30X
1
2
3
4
5
6
CC
5
10
15
20
25
30
35
40
45
50
55
60
65
70
75
80
85
90
95
100
105
110
115
120
125
130
135
140
145
150

SITE 805 HOLE B CORE 31X CORED INTERVAL 282.5-292.2 mbsf

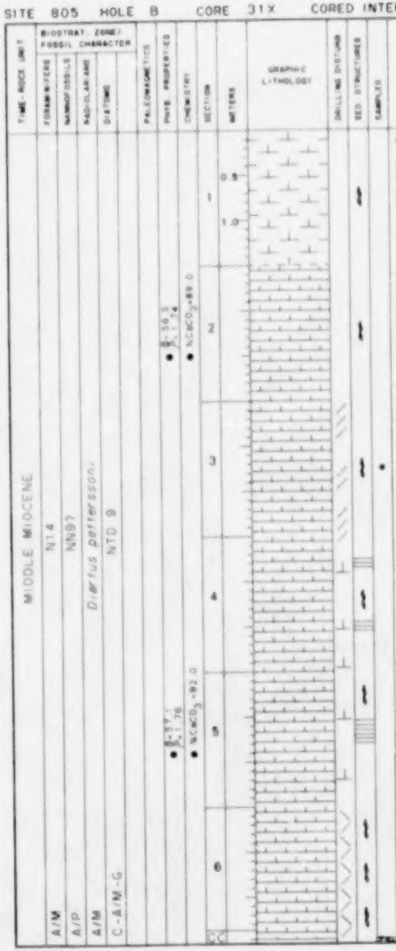
TIME-ROCK UNIT
BIOSTRAT. ZONE/ FOSSIL CHARACTER
FORAMINIFERS
NANNOFOSSILS
RADIOLARIANS
DIATOMS
PALEOMAGNETICS
PHYS. PROPERTIES
CHEMISTRY
SECTION
METERS
GRAPHIC LITHOLOGY
DRILLING DISTURB.
SED. STRUCTURES
SAMPLES
MIDDLE MIOCENE
N14
NN9?
Diartus petterssoni
NTD 9
A/M
A/P
A/M
C-A/M-G
φ=56.5
γ=1.74
%CaCO$_3$=89.0
φ=57.1
γ=1.76
%CaCO$_3$=92.0
1
2
3
4
5
6
CC
0.5
1.0

LITHOLOGIC DESCRIPTION

NANNOFOSSIL CHALK with FORAMINIFERS

Major lithology: This core contains white (2.5Y 8/0), bioturbated and mottled NANNOFOSSIL CHALK with FORAMINIFERS. Intervals of 1 to 5 mm thick, reddish gray (5R 6/2) and pale yellowish green (10GY 7/2) color bands are spaced 10 to 50 cm apart. The sediment is composed of numerous biscuits which are locally interbedded with ooze.

SMEAR SLIDE SUMMARY (%):

	3, 74 D
TEXTURE:	
Sand	10
Silt	60
Clay	30
COMPOSITION:	
Accessory minerals	1
Diatoms	Tr
Foraminifers	15
Nannofossils	82
Radiolarians	Tr
Siliceous fragments	2

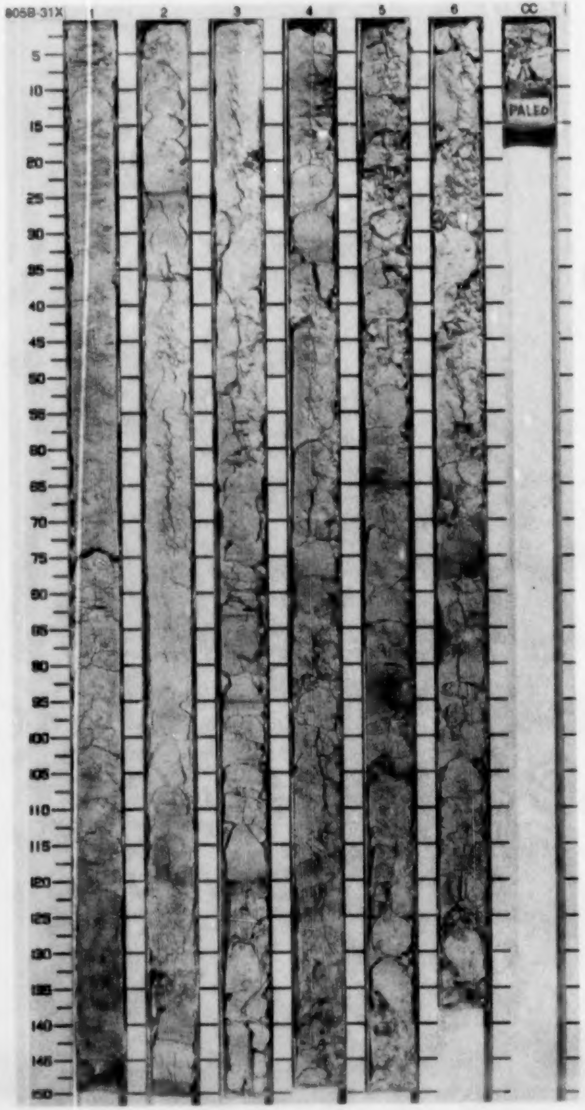
805B-31X
1
2
3
4
5
6
CC
PALEO
5
10
15
20
25
30
35
40
45
50
55
60
65
70
75
80
85
90
95
100
105
110
115
120
125
130
135
140
145
150

SITE 805 HOLE B CORE 32X CORED INTERVAL 292.2-301.4 mbsf

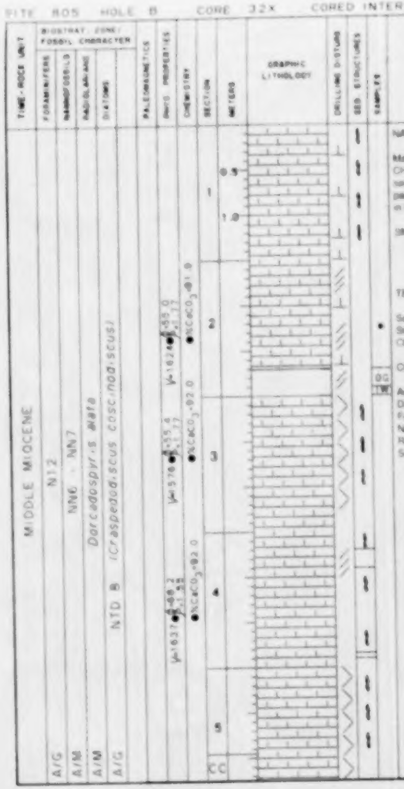
TIME-ROCK UNIT
BIOSTRAT. ZONE/ FOSSIL CHARACTER
FORAMINIFERS
NANNOFOSSILS
RADIOLARIANS
DIATOMS
PALEOMAGNETICS
PHYS. PROPERTIES
CHEMISTRY
SECTION
METERS
GRAPHIC LITHOLOGY
DRILLING DISTURB.
SED. STRUCTURES
SAMPLES
MIDDLE MIOCENE
N12
NN6 - NN7
Dorcadospyris alata
NTD 8 (Craspedodiscus coscinodiscus)
A/G
A/M
A/M
A/G
γ=1.62 ● φ=55.0
γ=1.57 ● φ=55.4
γ=1.63 ● φ=60.2
● %CaCO₃=81.0
● %CaCO₃=92.0
● %CaCO₃=92.0
1
2
3
4
5
CC
0.5
1.0
OG
IW

LITHOLOGIC DESCRIPTION

NANNOFOSSIL CHALK with FORAMINIFERS

Major lithology: This core contains white (2.5Y 8/0), bioturbated and mottled NANNOFOSSIL CHALK with FORAMINIFERS. The percentage of foraminifers increases in Section 5. The sediment exhibits discrete, cm thick zones that contain mm scale, reddish gray (5R 6/2) and pale yellowish green (10GY 7/2) color bands. The core is highly fractured by drilling, resulting in biscuits.

SMEAR SLIDE SUMMARY (%):

	2, 74
	D
TEXTURE:	
Sand	8
Silt	65
Clay	27
COMPOSITION:	
Accessory minerals	2
Diatoms	Tr
Foraminifers	13
Nannofossils	83
Radiolarians	Tr
Siliceous fragments	2

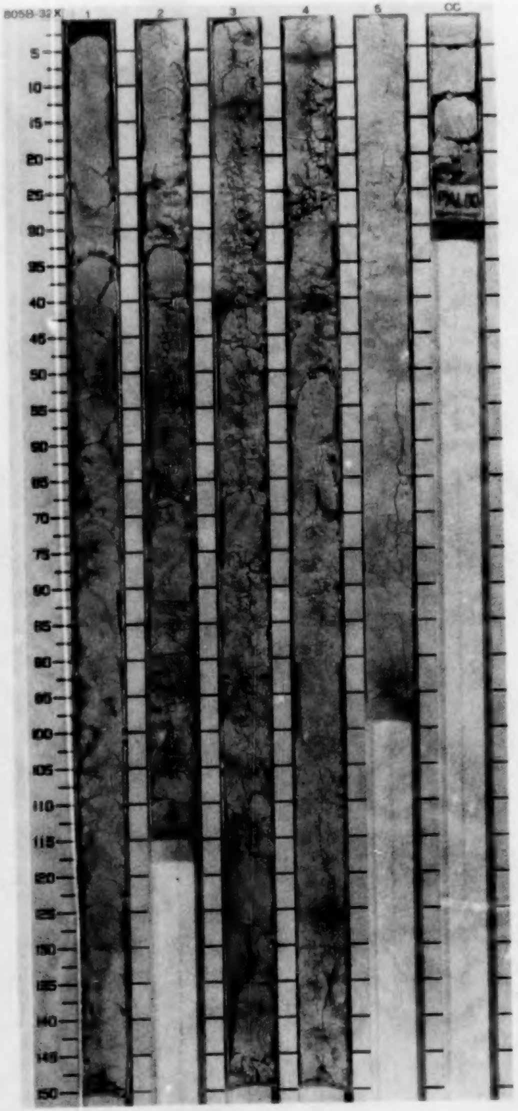
805B-32X
1
2
3
4
5
CC
5
10
15
20
25
30
35
40
45
50
55
60
65
70
75
80
85
90
95
100
105
110
115
120
125
130
135
140
145
150

SITE 805 HOLE B CORE 33X CORED INTERVAL 301.4-311.0 mbsf

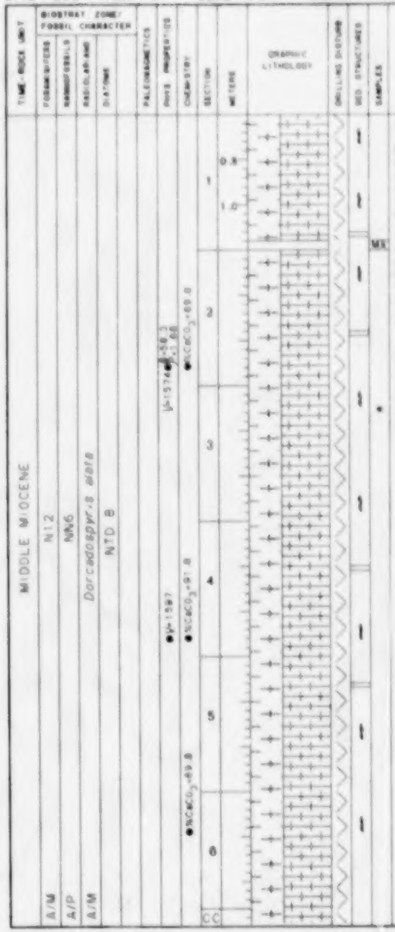
TIME-ROCK UNIT
BIOSTRAT. ZONE/ FOSSIL CHARACTER
FORAMINIFERS
NANNOFOSSILS
RADIOLARIANS
DIATOMS
PALEOMAGNETICS
PHYS. PROPERTIES
CHEMISTRY
SECTION
METERS
GRAPHIC LITHOLOGY
DRILLING DISTURB.
SED. STRUCTURES
SAMPLES
MIDDLE MIOCENE
A/M N12
A/P NN6
A/M Dorcadospyris alata
NTD B
%CaCO3=89.0
%CaCO3=91.8
%CaCO3=89.8
1
2
3
4
5
6
CC
0.8
1.0
MX

LITHOLOGIC DESCRIPTION

Interbedded FORAMINIFER NANNOFOSSIL CHALK and OOZE

Major lithology: About 75% of this core is white (2.5Y 8/0) FORAMINIFER NANNOFOSSIL CHALK. The sediment is sandy as a result of the high percentage of foraminifers in the core. A high degree of drilling disturbance has produced biscuits of chalk that have been rotated and fractured. Occasional distinct, mm to cm scale, reddish gray (5R 6/1) to very dusky purple (5P 2/2) color bands are apparent, although they are often tilted and disrupted in the drilling process. Occasional burrow mottles and pyritized burrows are also obvious.

About 25% of this core is FORAMINIFER NANNOFOSSIL OOZE. The ooze is similar to the chalk, but is not indurated. It is stiff and has been compacted and deformed in the drilling process, but appears to be real and is distinguished from drilling slough by the presence of frequent color bands that are often disturbed. From observations of contact surfaces with the chalk interbeds, it is apparent that drilling has compacted and removed some of the ooze interbeds.

SMEAR SLIDE SUMMARY (%):

	3, 28
	D
TEXTURE:	
Sand	10
Silt	60
Clay	30
COMPOSITION:	
Foraminifers	25
Nannofossils	71
Radiolarians	1
Siliceous fragments	3
Siliceous sponge spicules	Tr

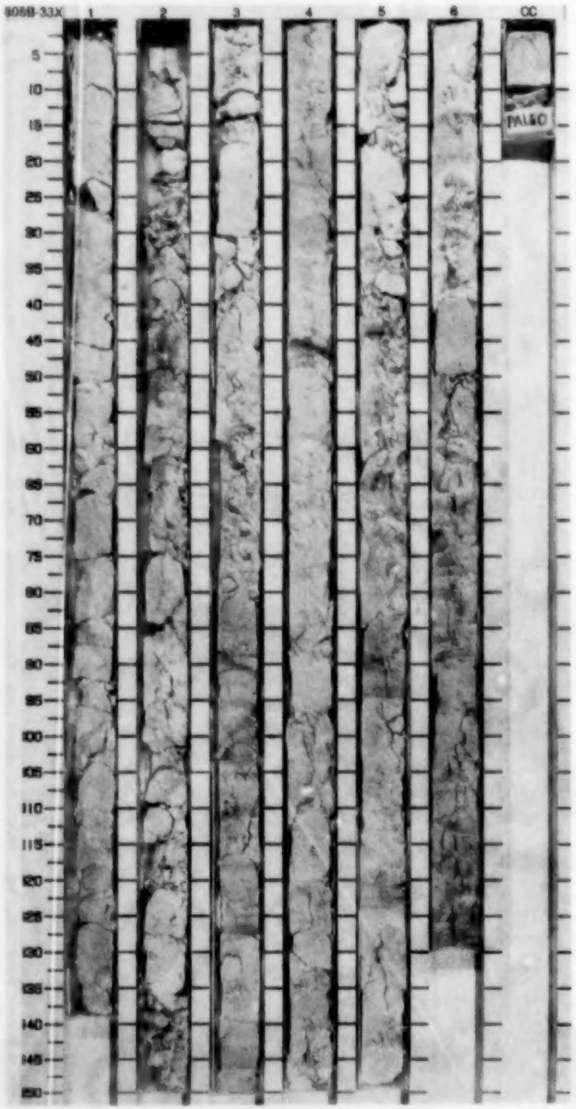
805B-33X
1
2
3
4
5
6
CC
PALEO
5
10
15
20
25
30
35
40
45
50
55
60
65
70
75
80
85
90
95
100
105
110
115
120
125
130
135
140
145
150

SITE 805 HOLE B CORE 34X CORED INTERVAL 311.0-320.5 mbsf

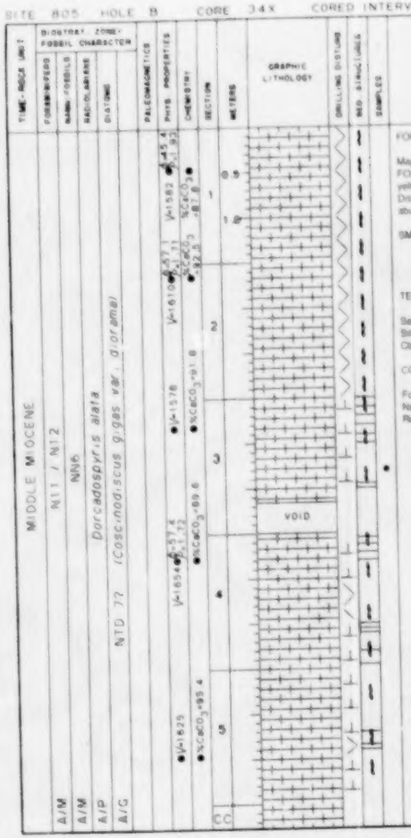
TIME-ROCK UNIT
BIOSTRAT. ZONE/FOSSIL CHARACTER
FORAMINIFERS
NANNOFOSSILS
RADIOLARIANS
DIATOMS
PALEOMAGNETICS
PHYS. PROPERTIES
CHEMISTRY
SECTION
METERS
GRAPHIC LITHOLOGY
DRILLING DISTURB.
SED. STRUCTURES
SAMPLES
MIDDLE MIOCENE
N11 / N12
NN6
Dorcadospyris alata
NTD 7? (Coscinodiscus gigas var. diorama)
A/M
A/M
A/P
A/G
γ=1582 ●φ=45.4 γ=1.93
γ=1610 ●φ=57.1 γ=1.71
●γ=1578
γ=1654 ●φ=57.4 γ=1.72
●γ=1625
%CaCO3 ●=87.8
%CaCO3 ●=92.5
●%CaCO3=91.8
●%CaCO3=89.6
●%CaCO3=95.4
1
2
3
4
5
CC
0.5
1.0
VOID

LITHOLOGIC DESCRIPTION

FORAMINIFER NANNOFOSSIL CHALK

Major lithology: This core contains slightly to moderately bioturbated FORAMINIFER NANNOFOSSIL CHALK, which is predominantly white (2.5Y 8/0), but also has minor zones of pale yellowish green (10GY 7/2), reddish gray (5R 6/1), light gray (N7/), and pale purple (5P 6/2). Distinct mm scale, greenish gray (5G 6/1), gray (N7/), and pale purple (5P 6/2) color bands are abundant and are located in several 10 to 30 cm thick intervals.

SMEAR SLIDE SUMMARY (%):

	3, 80
	D
TEXTURE:	
Sand	20
Silt	78
Clay	2
COMPOSITION:	
Foraminifers	25
Nannofossils	74
Radiolarians	1

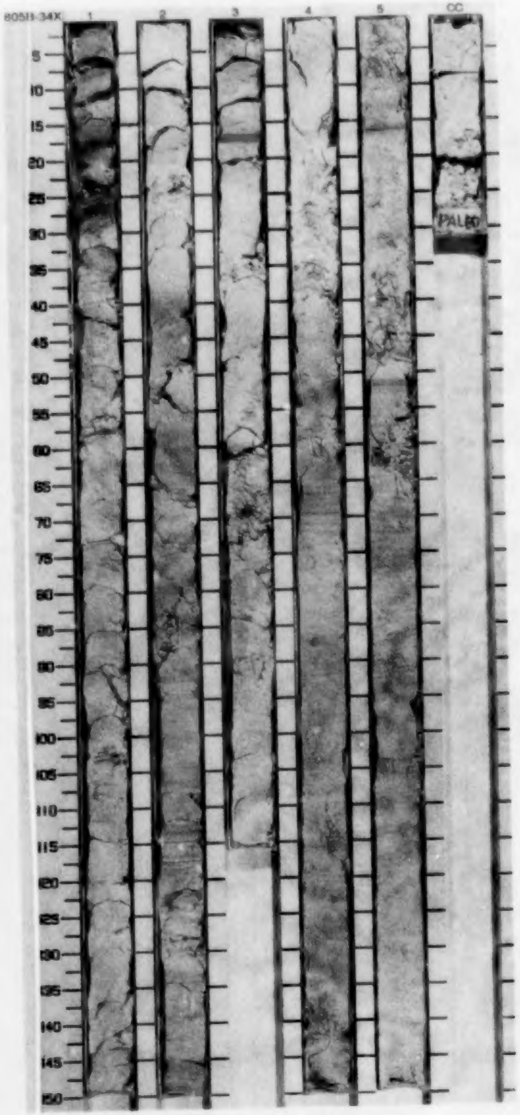
805B-34X
1
2
3
4
5
CC
5
10
15
20
25
30
35
40
45
50
55
60
65
70
75
80
85
90
95
100
105
110
115
120
125
130
135
140
145
150
PALEO

SITE 805 HOLE B CORE 35X CORED INTERVAL 320.5-330.0 mbsf

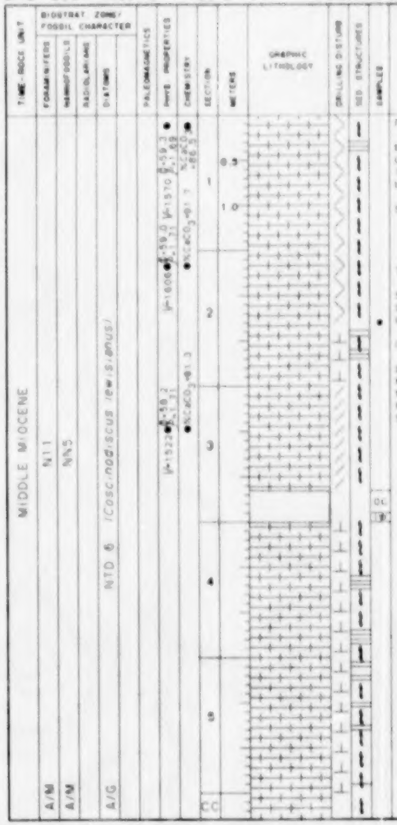
TIME-ROCK UNIT
BIOSTRAT. ZONE/ FOSSIL CHARACTER
FORAMINIFERS
NANNOFOSSILS
RADIOLARIANS
DIATOMS
PALEOMAGNETICS
PHYS. PROPERTIES
CHEMISTRY
SECTION
METERS
GRAPHIC LITHOLOGY
DRILLING DISTURB.
SED. STRUCTURES
SAMPLES
MIDDLE MIOCENE
N11
NN5
NTD 6 (Coscinodiscus lewisianus)
A/M
A/M
A/G
φ-59.3 γ-1.69
V-1570
φ-59.0 γ-1.71
V-1606
φ-58.2 γ-1.71
V-1522
%CaCO3 = 86.5
%CaCO3 = 81.7
%CaCO3 = 81.3
1
2
3
4
5
CC
0.5
1.0
OG
IW

LITHOLOGIC DESCRIPTION

FORAMINIFER NANNOFOSSIL CHALK

Major lithology: This core contains slightly bioturbated FORAMINIFER NANNOFOSSIL CHALK, which is predominantly white (2.5Y 8/0), but also has minor zones of pale blue (5PB 7/1). Distinct, mm scale, greenish gray (5G 6/1), gray (N7), and grayish blue (5PB 7/2) color bands are common in several 10 to 30 cm thick intervals.

SMEAR SLIDE SUMMARY (%):

	2, 80
	D
TEXTURE:	
Sand	15
Silt	83
Clay	2
COMPOSITION:	
Diatoms	2
Foraminifers	26
Nannofossils	70
Radiolarians	1
Siliceous sponge spicules	1

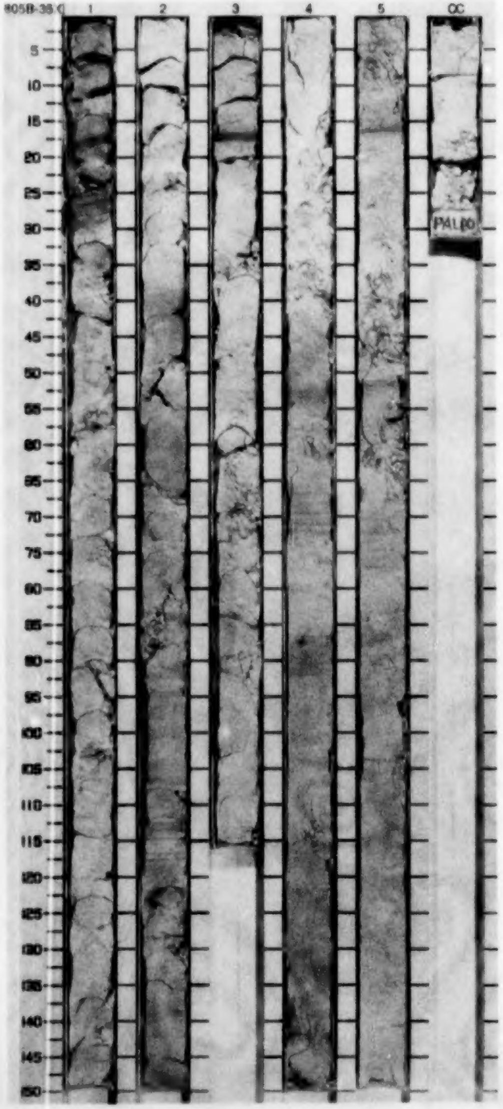
805B-35X
1
2
3
4
5
CC
PALEO
5
10
15
20
25
30
35
40
45
50
55
60
65
70
75
80
85
90
95
100
105
110
115
120
125
130
135
140
145
150

SITE 805 HOLE B CORE 36X CORED INTERVAL 330.0-339.7 mbsf

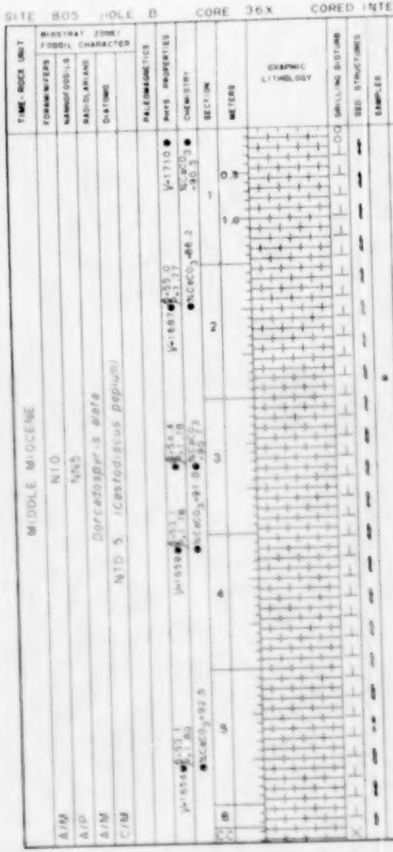
TIME-ROCK UNIT
BIOSTRAT. ZONE/ FOSSIL CHARACTER
FORAMINIFERS
NANNOFOSSILS
RADIOLARIANS
DIATOMS
PALEOMAGNETICS
PHYS. PROPERTIES
CHEMISTRY
SECTION
METERS
GRAPHIC LITHOLOGY
DRILLING DISTURB.
SED. STRUCTURES
SAMPLES
MIDDLE MIOCENE
N10
NN5
Dorcadospyris alata
NTD 5 (Cestodiscus peplum)
A/M
A/P
A/M
C/M
γ=1.710
%CaCO3=90.3
%CaCO3=86.2
%CaCO3=91.0
%CaCO3=92.5
1
2
3
4
5
6
CC
0.5
1.0

LITHOLOGIC DESCRIPTION

FORAMINIFER NANNOFOSSIL CHALK

Major lithology: This core contains white (2.5Y 8/0), slightly bioturbated FORAMINIFER NANNOFOSSIL CHALK. Faint white (5Y 8/1) mottling and specks of dark gray (2.5Y 4/0) are common throughout the core.

SMEAR SLIDE SUMMARY (%):

	2, 131
	D
TEXTURE:	
Sand	10
Silt	85
Clay	5
COMPOSITION:	
Diatoms	Tr
Foraminifers	25
Nannofossils	74
Radiolarians	1
Siliceous sponge spicules	Tr

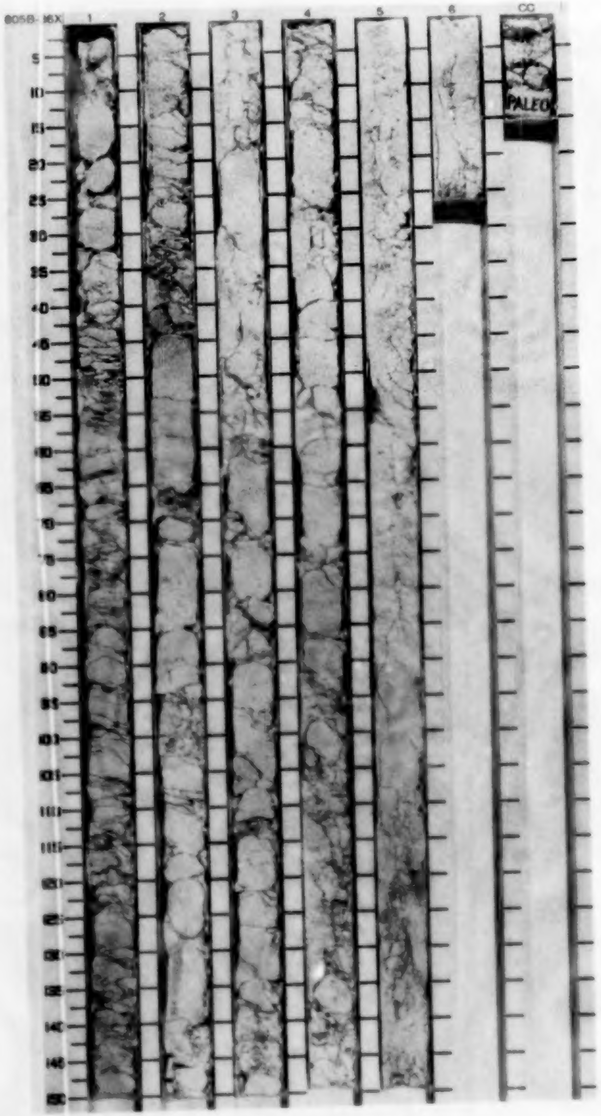
805B-36X
1
2
3
4
5
6
CC
PALEO
5
10
15
20
25
30
35
40
45
50
55
60
65
70
75
80
85
90
95
100
105
110
115
120
125
130
135
140
145
150

SITE 805 HOLE B CORE 37X CORED INTERVAL 339.7-349.4 mbsf

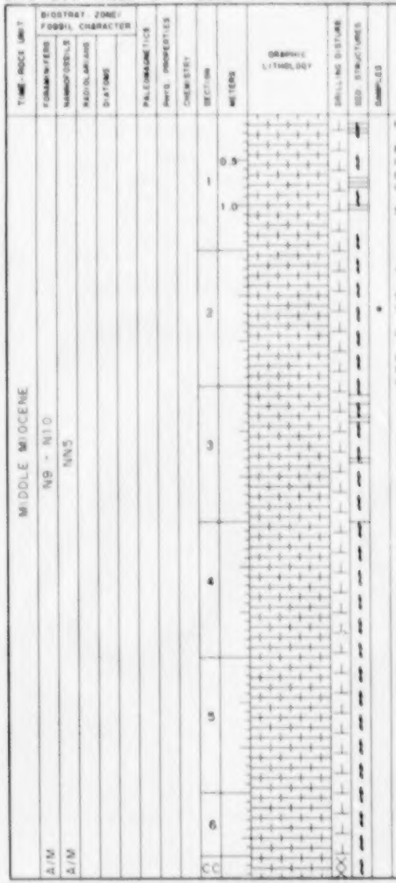
TIME-ROCK UNIT
BIOSTRAT. ZONE/ FOSSIL CHARACTER
FORAMINIFERS
NANNOFOSSILS
RADIOLARIANS
DIATOMS
PALEOMAGNETICS
PHYS. PROPERTIES
CHEMISTRY
SECTION
METERS
GRAPHIC LITHOLOGY
DRILLING DISTURB.
SED. STRUCTURES
SAMPLES
MIDDLE MIOCENE
N9 - N10
NN5
A/M
A/M
0.5
1.0
1
2
3
4
5
6
CC

LITHOLOGIC DESCRIPTION

FORAMINIFER NANNOFOSSIL CHALK

Major lithology: This core contains slightly bioturbated FORAMINIFER NANNOFOSSIL CHALK. It is predominantly white (2.5Y 8/0) in color, but Section 1 has small intervals that grade into pale blue (5PB 7/1). Dusky blue (5PB 3/2) and pale blue (5PB 7/1) color bands are common in Section 3.

SMEAR SLIDE SUMMARY (%):

	2, 66 D
TEXTURE:	
Sand	35
Silt	65
COMPOSITION:	
Foraminifers	25
Nannofossils	72
Radiolarians	3

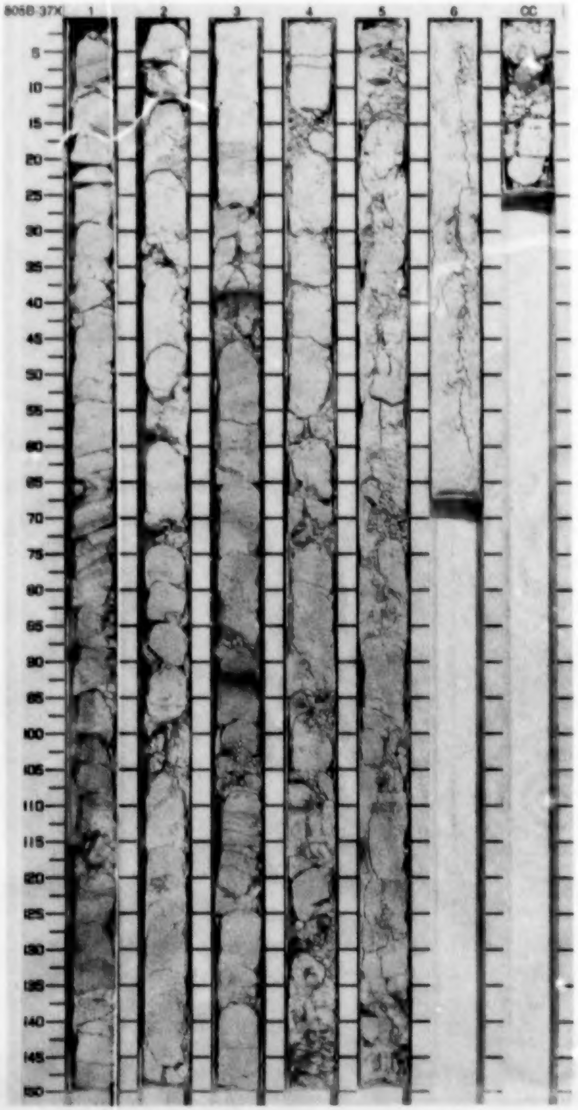
805B-37X
1
2
3
4
5
6
CC
5
10
15
20
25
30
35
40
45
50
55
60
65
70
75
80
85
90
95
100
105
110
115
120
125
130
135
140
145
150

SITE 805 HOLE B CORE 38X CORED INTERVAL 349.4-359.0 mbsf

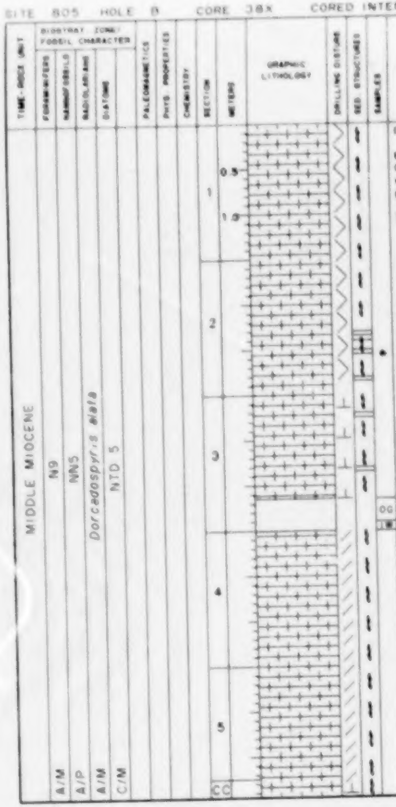
TIME-ROCK UNIT
BIOSTRAT. ZONE/ FOSSIL CHARACTER
FORAMINIFERS
NANNOFOSSILS
RADIOLARIANS
DIATOMS
PALEOMAGNETICS
PHYS. PROPERTIES
CHEMISTRY
SECTION
METERS
GRAPHIC LITHOLOGY
DRILLING DISTURB.
SED. STRUCTURES
SAMPLES
MIDDLE MIOCENE
N9
NN5
Dorcadospyris alata
NTD 5
A/M
A/P
A/M
C/M
0.5
1.0
1
2
3
4
5
CC
OG

LITHOLOGIC DESCRIPTION

FORAMINIFER NANNOFOSSIL CHALK

Major lithology: This core contains slightly bioturbated FORAMINIFER NANNOFOSSIL CHALK. It is predominantly white (2.5Y 8/0), with short intervals which grade into pinkish white (5YR 8/2) in Sections 4 and 5. Sections 1 and 2 are biscuited. Distinct, mm size, light greenish gray (5G 8/1) and pale blue (5PB 7/1) color bands are common in Sections 2 and 3.

SMEAR SLIDE SUMMARY (%):

	2, 105
	D
TEXTURE	
Sand	15
Silt	83
Clay	2
COMPOSITION	
Foraminifers	25
Nannofossils	74
Radiolarians	1

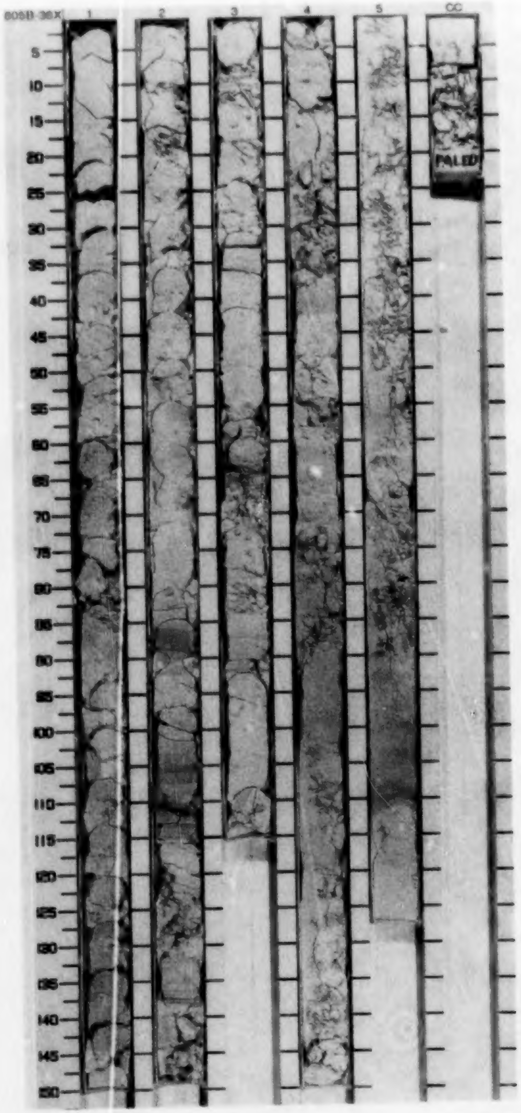
805B-38X
1
2
3
4
5
CC
5
10
15
20
25
30
35
40
45
50
55
60
65
70
75
80
85
90
95
100
105
110
115
120
125
130
135
140
145
150
PALEO

SITE 805 HOLE B CORE 39X CORED INTERVAL 359.0-368.7 mbsf

TIME-ROCK UNIT	BIOSTRAT. ZONE/ FOSSIL CHARACTER: FORAMINIFERS	NANNOFOSSILS	RADIOLARIANS	DIATOMS	PALEOMAGNETICS	PHYS. PROPERTIES	CHEMISTRY	SECTION	METERS
MIDDLE MIOCENE	N9 A/M	NN5 A/P	*Calocycletta costata* A/G	NTD 5 C-A/M				1 2 3 4 5 6 CC	0.5 1.0

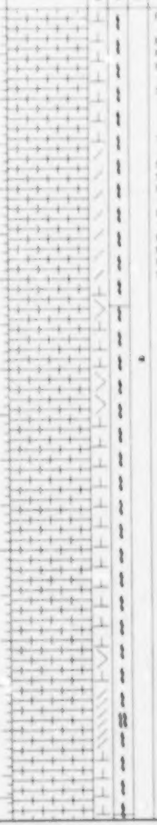
GRAPHIC LITHOLOGY
DRILLING DISTURB.
SED. STRUCTURES
SAMPLES

LITHOLOGIC DESCRIPTION

FORAMINIFER NANNOFOSSIL CHALK

Major lithology: This core contains slightly to moderately bioturbated FORAMINIFER NANNOFOSSIL CHALK. It is predominantly white (2.5Y 8/0), but grades to pale pink (5RP 8/2), white (10Y 8/1), and pale purple (5P 6/2) in intervals 20 to 100 cm long.

SMEAR SLIDE SUMMARY (%):

	3, 90
	D
TEXTURE:	
Sand	20
Silt	78
Clay	2
COMPOSITION:	
Foraminifers	25
Nannofossils	72
Radiolarians	2
Silicoflagellates	1

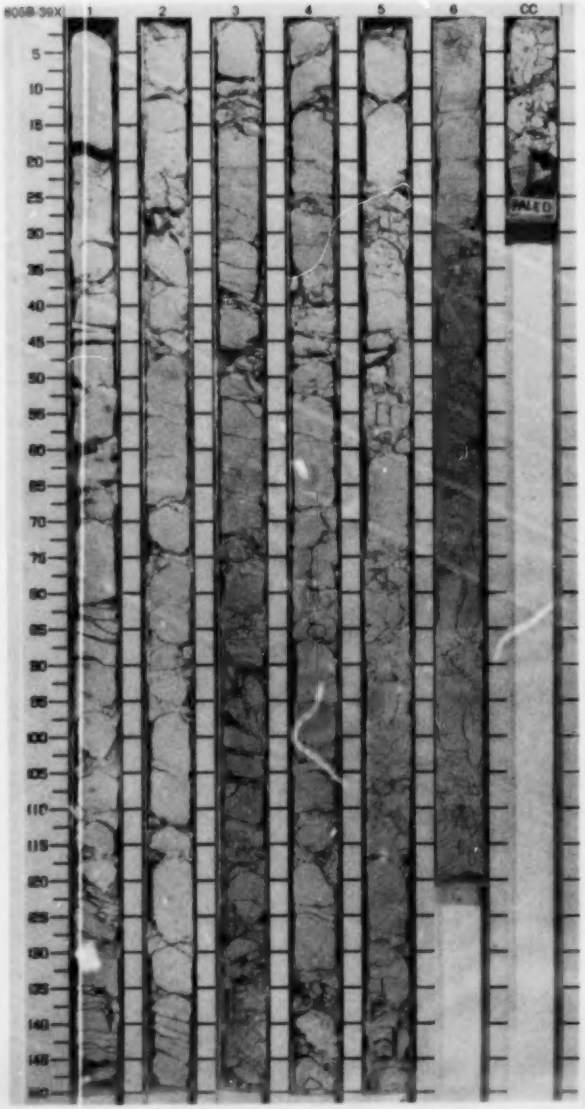
805B-39X
1
2
3
4
5
6
CC
PALEO
5
10
15
20
25
30
35
40
45
50
55
60
65
70
75
80
85
90
95
100
105
110
115
120
125
130
135
140
145
150

SITE 805 HOLE B CORE 40X CORED INTERVAL 368.7-378.3 mbsf

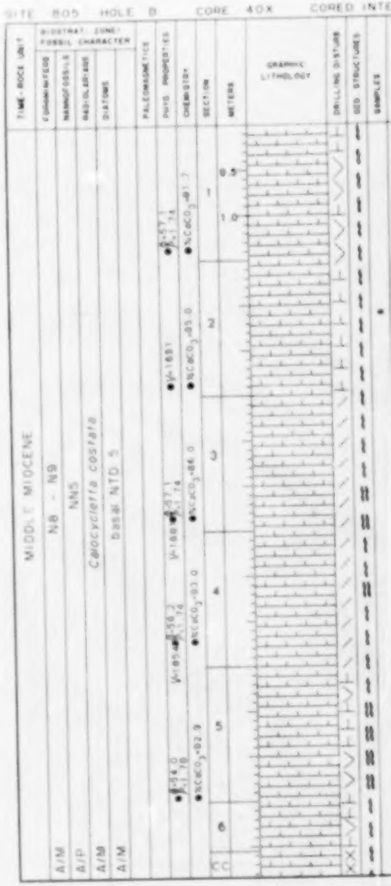
TIME-ROCK UNIT
BIOSTRAT. ZONE/ FOSSIL CHARACTER
FORAMINIFERS
NANNOFOSSILS
RADIOLARIANS
DIATOMS
PALEOMAGNETICS
PHYS. PROPERTIES
CHEMISTRY
SECTION
METERS
GRAPHIC LITHOLOGY
DRILLING DISTURB.
SED. STRUCTURES
SAMPLES
MIDDLE MIOCENE
N8 - N9
NN5
Calocycletta costata
basal NTD 5
A/M
A/P
A/M
A/M
φ-57.1
γ-1.74
V-1681
V-1688
φ-57.1
γ-1.74
V-1654
φ-58.2
γ-1.74
φ-54.0
γ-1.78
%CaCO3-81.7
%CaCO3-85.0
%CaCO3-86.0
%CaCO3-83.0
%CaCO3-82.9
1
2
3
4
5
6
CC
0.5
1.0

LITHOLOGIC DESCRIPTION

NANNOFOSSIL CHALK with FORAMINIFERS

Major lithology: This core contains NANNOFOSSIL CHALK with FORAMINIFERS. It is predominantly white (2.5Y 8/0), but grades to pale blue (5PB 7/2), white (7.5YR 8/0), and light greenish gray (5GY 7/1) over 20 to 40 cm long intervals. The entire core is slightly to heavily bioturbated, with diffuse burrows throughout and cm scale discrete burrows in Section 4.

SMEAR SLIDE SUMMARY (%):

	2, 68
	D
TEXTURE:	
Sand	10
Silt	85
Clay	5
COMPOSITION:	
Foraminifers	20
Glass	1
Nannofossils	77
Radiolarians	2
Silicoflagellates	Tr

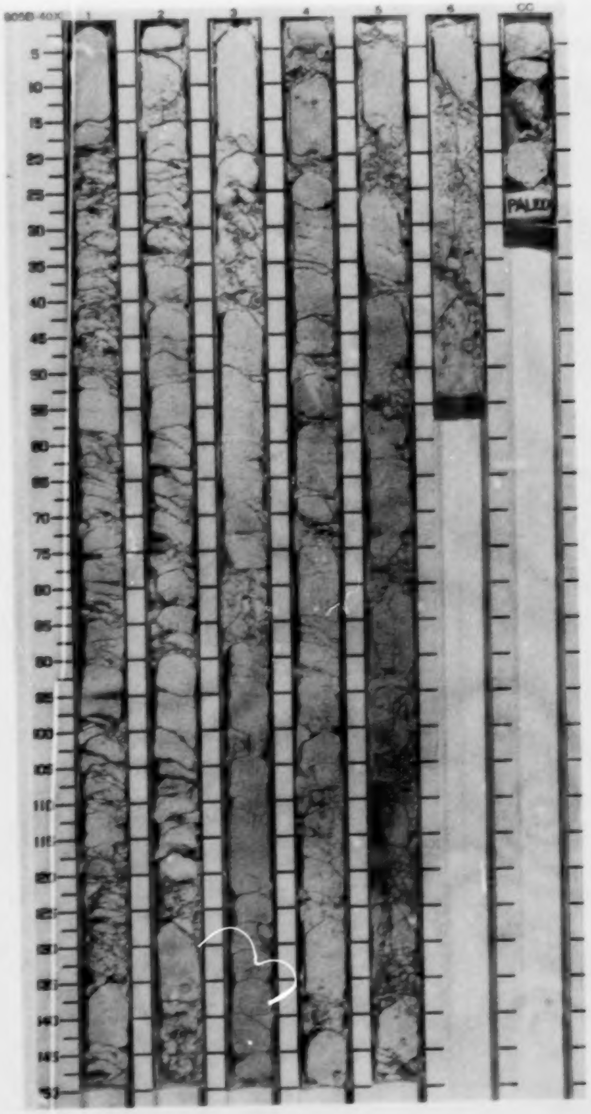
805B-40X
1
2
3
4
5
6
CC
PALEO
5
10
15
20
25
30
35
40
45
50
55
60
65
70
75
80
85
90
95
100
105
110
115
120
125
130
135
140
145
150

SITE 805 HOLE B CORE 41X CORED INTERVAL 378.3-388.0 mbsf

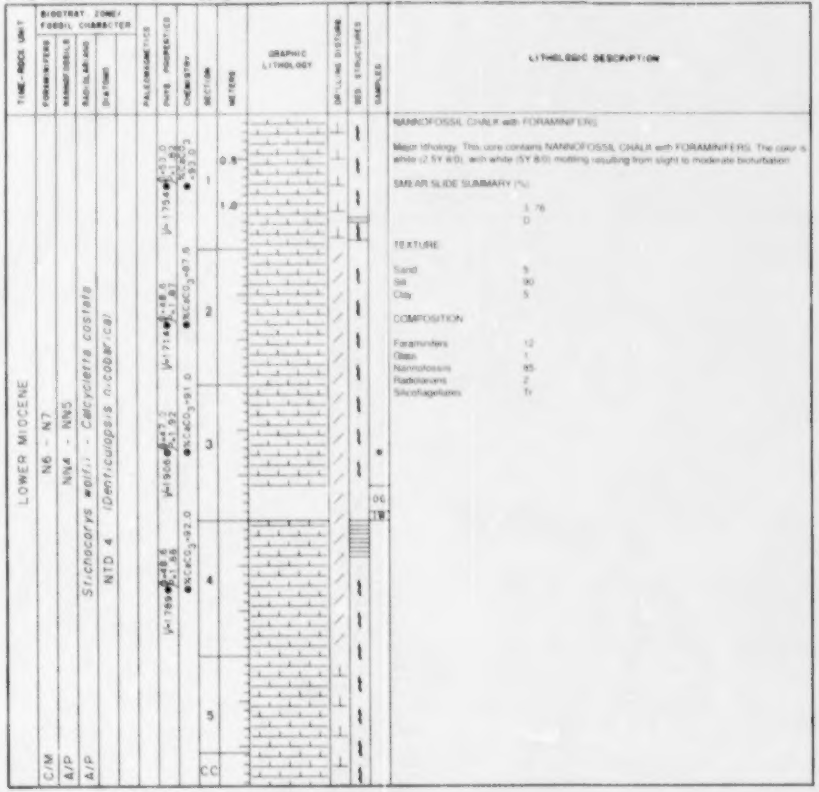

TIME-ROCK UNIT
BIOSTRAT. ZONE/FOSSIL CHARACTER
FORAMINIFERS
NANNOFOSSILS
RADIOLARIANS
DIATOMS
PALEOMAGNETICS
PHYS. PROPERTIES
CHEMISTRY
SECTION
METERS
GRAPHIC LITHOLOGY
DRILLING DISTURB.
SED. STRUCTURES
SAMPLES
LOWER MIOCENE
C/M N6 - N7
A/P NN4 - NN5
A/P Stichocorys wolffii - Calcycletta costata
NTD 4 (Denticulopsis nicobarica)
V=1754 φ=53.0 γ=1.82
%CaCO3=93.0
V=1714 φ=48.6 γ=1.87
%CaCO3=87.6
V=1906 φ=47.2 γ=1.92
%CaCO3=91.0
V=1789 φ=48.6 γ=1.88
%CaCO3=92.0
1
2
3
4
5
CC
0.5
1.0
OG
IW

LITHOLOGIC DESCRIPTION

NANNOFOSSIL CHALK with FORAMINIFERS

Major lithology: This core contains NANNOFOSSIL CHALK with FORAMINIFERS. The color is white (2.5Y 8/0), with white (5Y 8/0) mottling resulting from slight to moderate bioturbation.

SMEAR SLIDE SUMMARY (%):

	3, 76
	D
TEXTURE:	
Sand	5
Silt	90
Clay	5
COMPOSITION:	
Foraminifers	12
Glass	1
Nannofossils	85
Radiolarians	2
Silicoflagellates	Tr

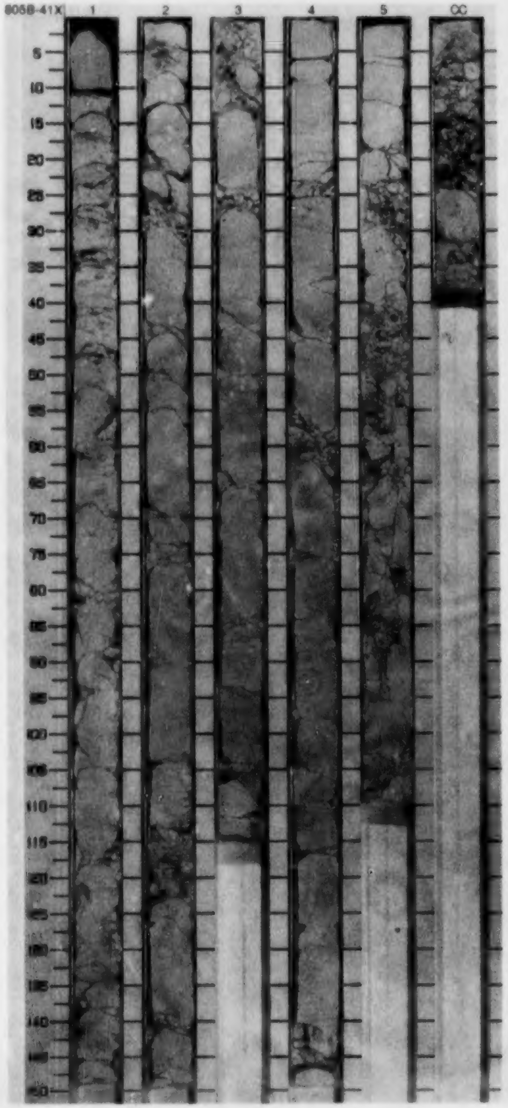

805B-41X
1
2
3
4
5
CC
5
10
15
20
25
30
35
40
45
50
55
60
65
70
75
80
85
90
95
100
105
110
115
120
125
130
135
140
145
150

SITE 805 HOLE B CORE 42X CORED INTERVAL 388.0-397.7 mbsf

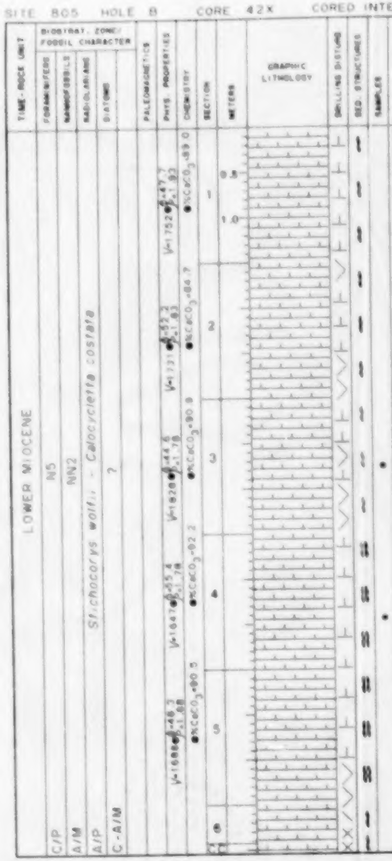
TIME-ROCK UNIT
BIOSTRAT. ZONE/ FOSSIL CHARACTER
FORAMINIFERS
NANNOFOSSILS
RADIOLARIANS
DIATOMS
PALEOMAGNETICS
PHYS. PROPERTIES
CHEMISTRY
SECTION
METERS
GRAPHIC LITHOLOGY
DRILLING DISTURB.
SED. STRUCTURES
SAMPLES
LOWER MIOCENE
N5
NN2
Stichocorys wolffi - Calocycletta costata
?
C/P
A/M
A/P
C-A/M
V=1752
φ=47.7
γ=1.93
%CaCO3=89.0
V=1731
φ=52.2
γ=1.83
%CaCO3=84.7
V=1828
φ=44.6
γ=1.78
%CaCO3=90.8
V=1647
φ=55.4
γ=1.78
%CaCO3=92.2
V=1688
φ=46.3
γ=1.88
%CaCO3=90.5
1
2
3
4
5
6
CC
0.5
1.0

LITHOLOGIC DESCRIPTION

NANNOFOSSIL CHALK with FORAMINIFERS

Major lithology: This core contains NANNOFOSSIL CHALK with FORAMINIFERS. The core is predominantly white in color (10YR 8/1, 10Y 8/1, and 2.5Y 8/0), with a pale blue interval (5PB 7/2) from Section 4, 30 cm, to Section 5, 33 cm. Bioturbation is expressed as mm scale diffuse mottling, and discrete, cm scale vertical and horizontal burrows are present in Section 2.

SMEAR SLIDE SUMMARY (%):

	3, 87	4, 94
	D	D
TEXTURE		
Sand	8	8
Silt	90	90
Clay	2	2
COMPOSITION		
Foraminifers	10	10
Nannofossils	88	88
Radiolarians	2	2
Silicoflagellates	Tr	Tr

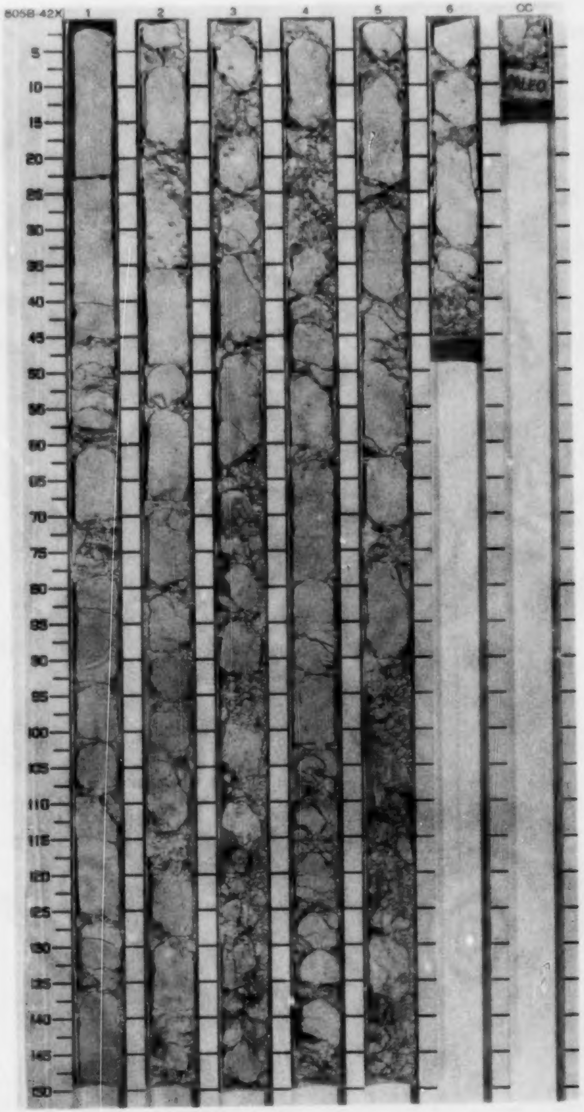
805B-42X
1
2
3
4
5
6
CC
PALEO
5
10
15
20
25
30
35
40
45
50
55
60
65
70
75
80
85
90
95
100
105
110
115
120
125
130
135
140
145
150

SITE 805 HOLE B CORE 43X CORED INTERVAL 397.7-407.3 mbsf

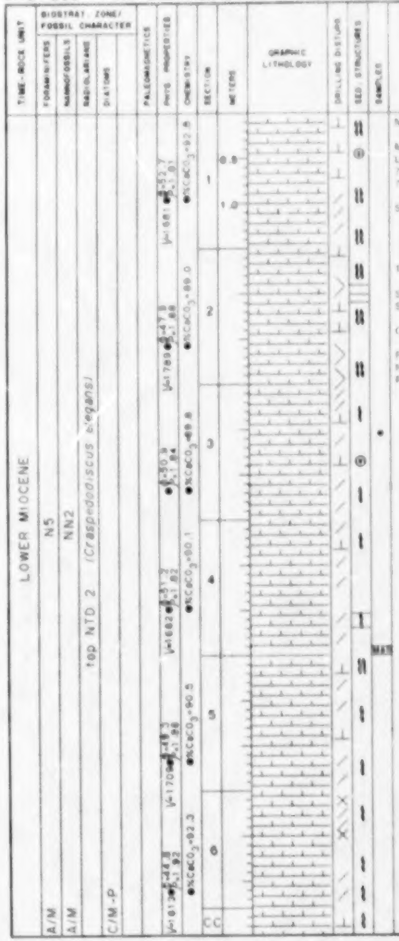
TIME-ROCK UNIT
BIOSTRAT. ZONE/ FOSSIL CHARACTER
FORAMINIFERS
NANNOFOSSILS
RADIOLARIANS
DIATOMS
PALEOMAGNETICS
PHYS. PROPERTIES
CHEMISTRY
SECTION
METERS
GRAPHIC LITHOLOGY
DRILLING DISTURB.
SED. STRUCTURES
SAMPLES
LOWER MIOCENE
N5
NN2
top NTD 2 (Craspedodiscus elegans)
A/M
A/M
C/M-P
V=1681 φ=52.7 γ=1.91
V=1789 φ=47.8 γ=1.88
φ=50.9 γ=1.84
V=1682 φ=51.2 γ=1.82
V=1700 φ=48.3 γ=1.88
V=1613 φ=44.8 γ=1.92
%CaCO3=92.8
%CaCO3=89.0
%CaCO3=89.8
%CaCO3=90.1
%CaCO3=90.5
%CaCO3=92.3
1
2
3
4
5
6
CC
0.5
1.0
MAS

LITHOLOGIC DESCRIPTION

NANNOFOSSIL CHALK with RADIOLARIANS

Major lithology: This core contains white (2.5Y 8/0) NANNOFOSSIL CHALK with RADIOLARIANS. The sediment is bioturbated throughout and several zones have pale blue (5PB 7/2) and pale purple (5P 6/2) mottles. *Zoophycos* trace fossils burrows and pale blue (5PB 7/2) and light gray (N7) color bands are scattered throughout the core.

SMEAR SLIDE SUMMARY (%):

	3, 55
	D
TEXTURE:	
Sand	20
Silt	80
COMPOSITION:	
Foraminifers	7
Nannofossils	83
Radiolarians	10

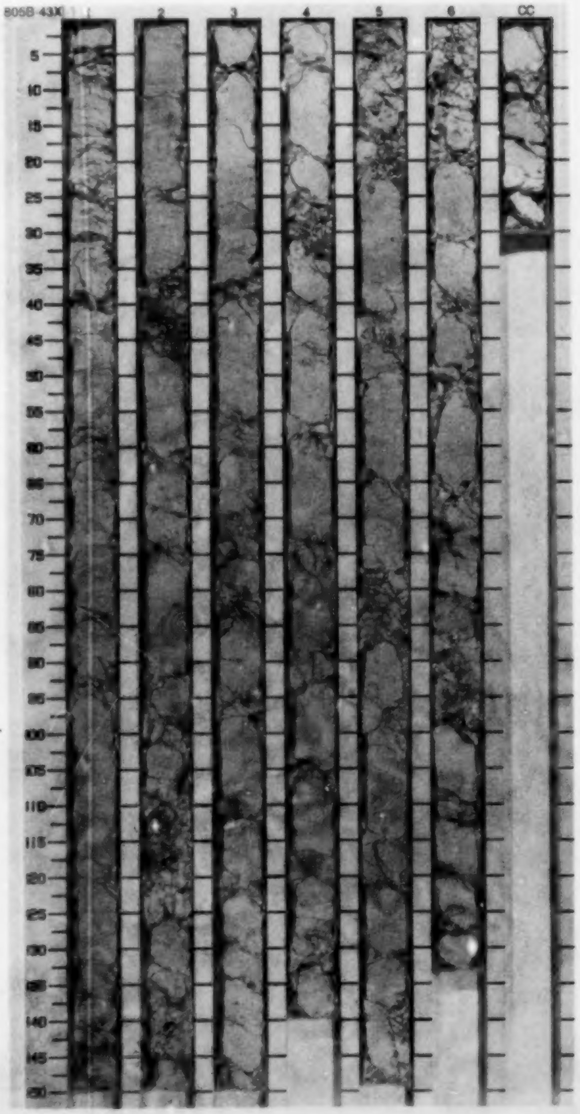
805B-43X
1
2
3
4
5
6
CC
5
10
15
20
25
30
35
40
45
50
55
60
65
70
75
80
85
90
95
100
105
110
115
120
125
130
135
140
145
150

SITE 805 HOLE B CORE 44X CORED INTERVAL 407.3-417.0 mbsf

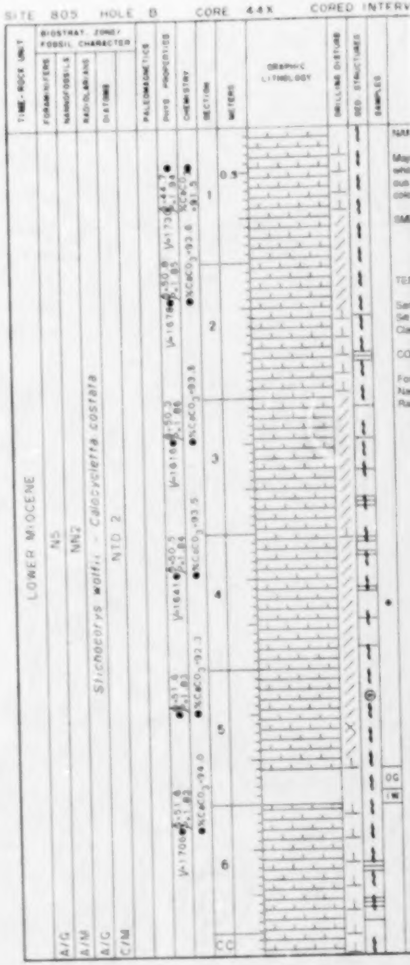
TIME-ROCK UNIT
BIOSTRAT. ZONE/ FOSSIL CHARACTER
FORAMINIFERS
NANNOFOSSILS
RADIOLARIANS
DIATOMS
PALEOMAGNETICS
PHYS. PROPERTIES
CHEMISTRY
SECTION
METERS
GRAPHIC LITHOLOGY
DRILLING DISTURB.
SED. STRUCTURES
SAMPLES
LOWER MIOCENE
N5
NN2
Stichocorys wolffi - Calocycletta costata
NTD 2
A/G
A/M
A/G
C/M
V=1730 φ=44.7 ρ=1.94
%CaCO3=91.5
V=1678 φ=50.8 ρ=1.85
%CaCO3=93.8
V=1616 φ=50.3 ρ=1.86
%CaCO3=93.8
V=1641 φ=50.5 ρ=1.84
%CaCO3=93.5
φ=51.6 ρ=1.83
%CaCO3=92.3
V=1700 φ=51.8 ρ=1.82
%CaCO3=94.0
0.5
1
2
3
4
5
6
CC
OG
IW

LITHOLOGIC DESCRIPTION

NANNOFOSSIL CHALK

Major lithology: This core contains NANNOFOSSIL CHALK. The sediment is predominantly white (2.5Y 8/0 and 5Y 8/1), but several zones contain pale blue (5PB 7/2) mottles. Numerous distinct, mm-sized, gray (N5), light greenish gray (5G 7/1), and grayish green (5G 5/2) color bands are evident throughout the core.

SMEAR SLIDE SUMMARY (%):

	4, 79
	D
TEXTURE:	
Sand	4
Silt	90
Clay	6
COMPOSITION:	
Foraminifers	5
Nannofossils	94
Radiolarians	1

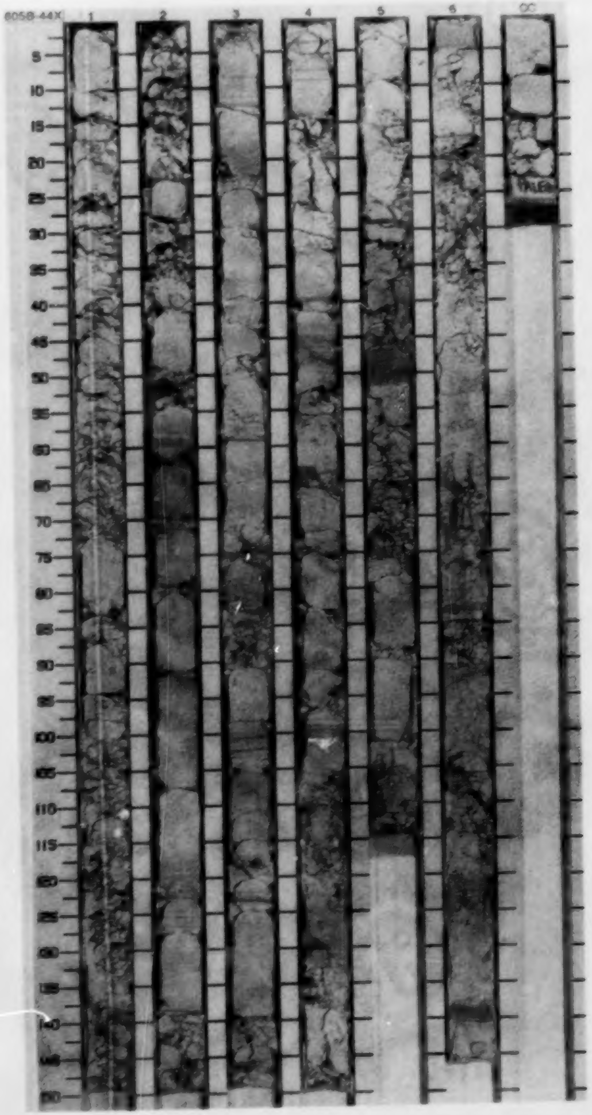
805B-44X
1
2
3
4
5
6
CC
5
10
15
20
25
30
35
40
45
50
55
60
65
70
75
80
85
90
95
100
105
110
115
120
125
130
135
140
145
150

SITE 805 HOLE B CORE 45X CORED INTERVAL 417.0-426.5 mbsf

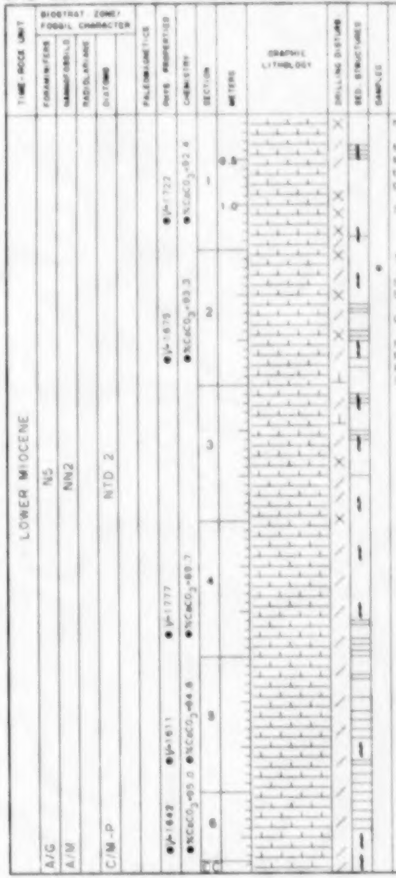
TIME-ROCK UNIT
BIOSTRAT. ZONE/ FOSSIL CHARACTER
FORAMINIFERS
NANNOFOSSILS
RADIOLARIANS
DIATOMS
PALEOMAGNETICS
PHYS. PROPERTIES
CHEMISTRY
SECTION
METERS
GRAPHIC LITHOLOGY
DRILLING DISTURB.
SED. STRUCTURES
SAMPLES
LOWER MIOCENE
N5
NN2
NTD 2
A/G
A/M
C/M-P
●γ=1.722
●γ=1.679
●γ=1.777
●γ=1.611
●γ=1.642
●%CaCO3=92.4
●%CaCO3=93.3
●%CaCO3=89.7
●%CaCO3=94.8
●%CaCO3=95.0
1
2
3
4
5
6
CC
0.5
1.0

LITHOLOGIC DESCRIPTION

NANNOFOSSIL CHALK with FORAMINIFERS

Major lithology: This core contains slightly bioturbated NANNOFOSSIL CHALK with FORAMINIFERS. The sediment is predominantly white (2.5Y 8/0), but several zones contain pale blue (5PB 7/2) mottles. Centimeter to mm sized intervals contain numerous distinct, mm size greenish gray (5G 6/1), gray (N5), and white (2.5Y 8/0) color bands.

SMEAR SLIDE SUMMARY (%):

	2, 20
	D
TEXTURE:	
Sand	25
Silt	75
COMPOSITION:	
Foraminifers	14
Nannofossils	78
Radiolarians	7
Silicoflagellates	1

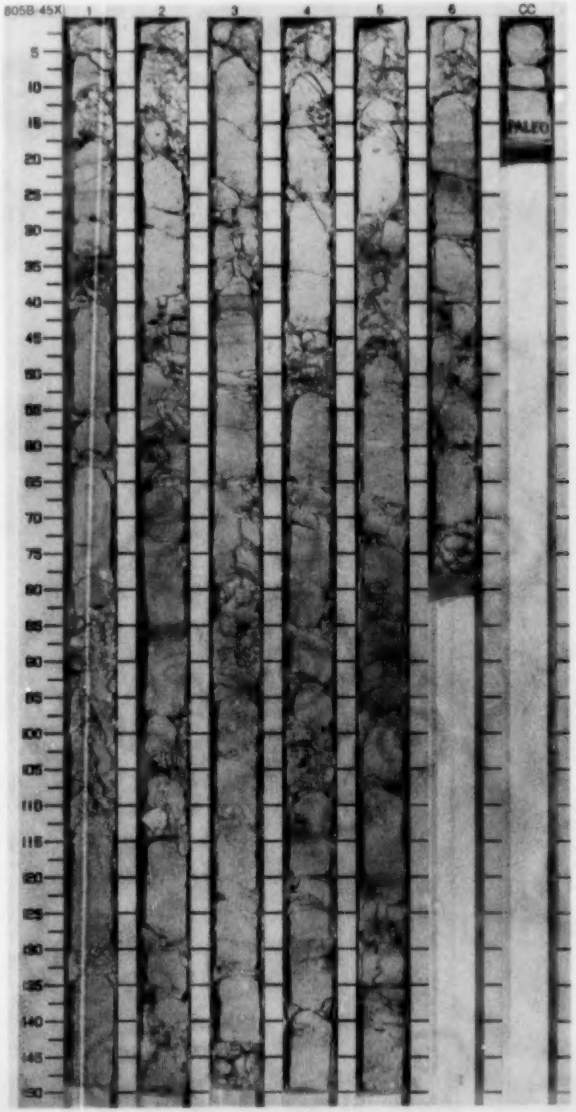
805B-45X
1
2
3
4
5
6
CC
PALEO
5
10
15
20
25
30
35
40
45
50
55
60
65
70
75
80
85
90
95
100
105
110
115
120
125
130
135
140
145
150

SITE 805 HOLE B CORE 46X CORED INTERVAL 426.5-436.0 mbsf

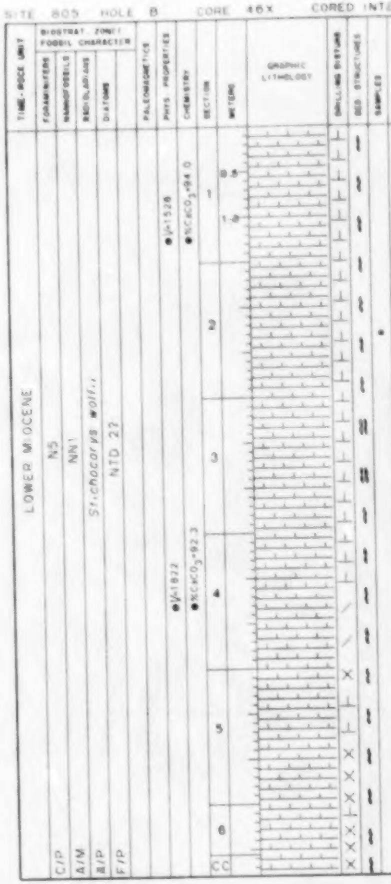
TIME-ROCK UNIT
BIOSTRAT. ZONE/ FOSSIL CHARACTER
FORAMINIFERS
NANNOFOSSILS
RADIOLARIANS
DIATOMS
PALEOMAGNETICS
PHYS. PROPERTIES
CHEMISTRY
SECTION
METERS
GRAPHIC LITHOLOGY
DRILLING DISTURB.
SED. STRUCTURES
SAMPLES
LOWER MIOCENE
N5
NN1
Stichocorys wolffi
NTD 22
C/P
A/M
R/P
F/P
●V=1526
●V=1822
●%CaCO3=94.0
●%CaCO3=92.3
1
2
3
4
5
6
CC
0.5
1.0

LITHOLOGIC DESCRIPTION

NANNOFOSSIL CHALK

Major lithology: This core contains white (2.5Y 8/0, 10Y 8/1 and 5Y 8/1), slightly to heavily bioturbated NANNOFOSSIL CHALK. A few pale purple halos are seen around burrows in Section 1. Section 3 contains a zone of extensive, diffuse pale blue (5PB 7/2) mottling. In Sections 4 through 6, light gray (5Y 7/1), zones ca. 10 cm thick with distinct burrows are spaced about 60 cm apart.

SMEAR SLIDE SUMMARY (%):

	2, 80
	D
TEXTURE	
Sand	6
Silt	64
Clay	30
COMPOSITION	
Foraminifers	4
Nannofossils	94
Radiolarians	2
Silicoflagellates	Tr
Spicules	Tr

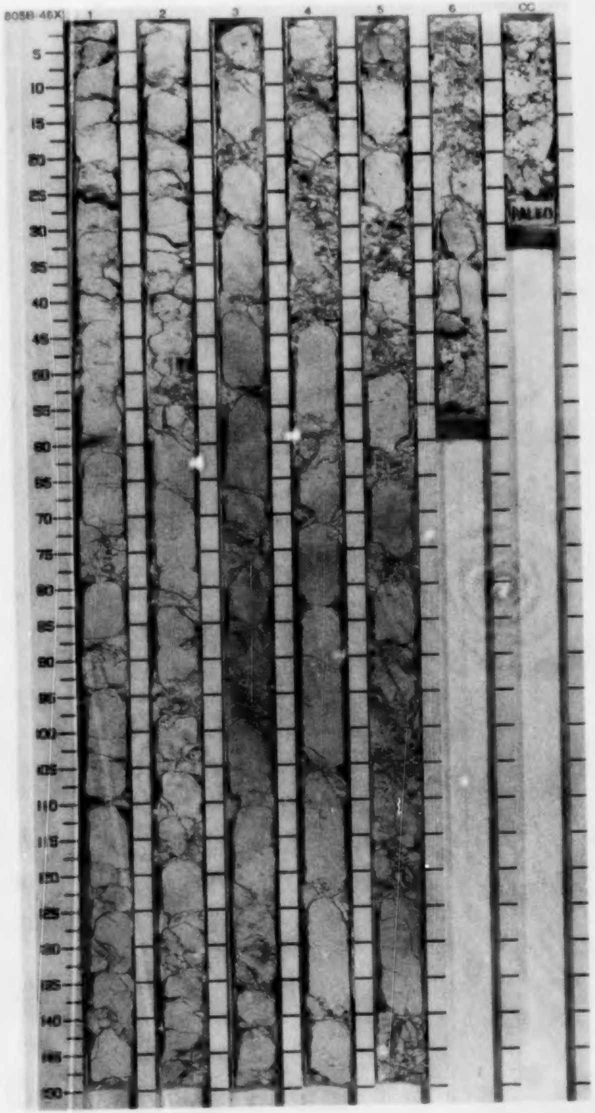
805B-46X
1
2
3
4
5
6
CC
5
10
15
20
25
30
35
40
45
50
55
60
65
70
75
80
85
90
95
100
105
110
115
120
125
130
135
140
145
150

SITE 805 HOLE B CORE 47X CORED INTERVAL 436.0-445.5 mbsf

TIME-ROCK UNIT	BIOSTRAT. ZONE/ FOSSIL CHARACTER: FORAMINIFERS	NANNOFOSSILS	RADIOLARIANS	DIATOMS		PALEOMAGNETICS	PHYS. PROPERTIES	CHEMISTRY	SECTION	METERS	GRAPHIC LITHOLOGY	DRILLING DISTURB.	SED. STRUCTURES	SAMPLES	LITHOLOGIC DESCRIPTION
LOWER MIOCENE	N4 A/M	NN1? A		? F/P			● φ=45.9 [illegible] Vp=1824	● [illegible]	1 CC					*	NANNOFOSSIL CHALK Major lithology: This core contains white (2.5Y 8/0), moderately to heavily bioturbated NANNOFOSSIL CHALK. SMEAR SLIDE SUMMARY (%): 1, 27 D TEXTURE: Sand 10 Silt 90 COMPOSITION: Foraminifers 5 Nannofossils 90 Radiolarians 5

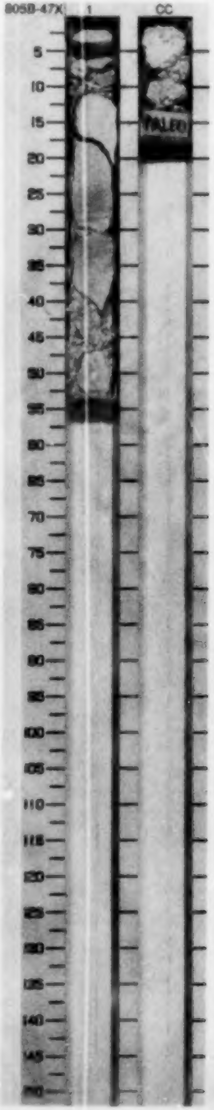
805B-47X
1
CC
5
10
15
20
25
30
35
40
45
50
55
60
65
70
75
80
85
90
95
100
105
110
115
120
125
130
135
140
145
150
PALEO

SITE 805 HOLE B CORE 48X CORED INTERVAL 445.5-455.1 mbsf

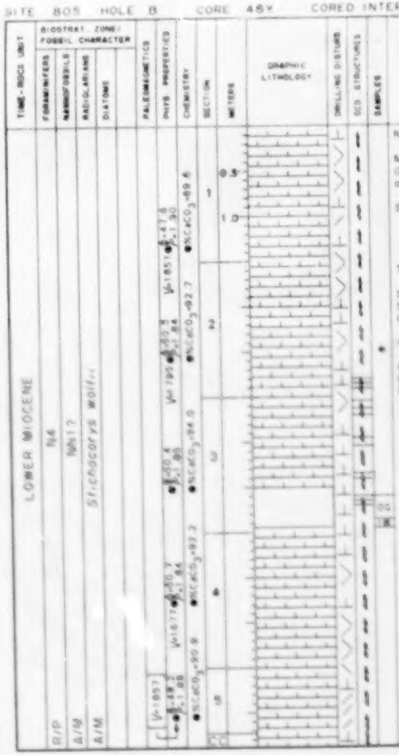
TIME-ROCK UNIT
BIOSTRAT. ZONE/ FOSSIL CHARACTER
FORAMINIFERS
NANNOFOSSILS
RADIOLARIANS
DIATOMS
PALEOMAGNETICS
PHYS. PROPERTIES
CHEMISTRY
SECTION
METERS
GRAPHIC LITHOLOGY
DRILLING DISTURB.
SED. STRUCTURES
SAMPLES
LOWER MIOCENE
N4
NN1?
Stichocorys wolffii
R/P
A/M
A/M
V=1851 φ=47.6 γ=1.90
%CaCO3=89.6
V=1795 φ=50.5 γ=1.84
%CaCO3=92.7
φ=50.4 γ=1.85
%CaCO3=94.0
V=1677 φ=50.7 γ=1.84
%CaCO3=92.2
V=1857 φ=48.2 γ=1.88
%CaCO3=90.9
1
2
3
4
5
CC
0.5
1.0
OG
IW

LITHOLOGIC DESCRIPTION

NANNOFOSSIL CHALK

Major lithology: This core contains NANNOFOSSIL CHALK, which is predominantly white (2.5Y 8/0), but grades to pale blue (5PB 7/2), greenish gray (5GY 6/1), and light gray (N7) over intervals of 10 cm or less. The entire core is slightly to moderately bioturbated.

SMEAR SLIDE SUMMARY (%):

	2, 98
	D
TEXTURE:	
Sand	10
Silt	85
Clay	5
COMPOSITION:	
Foraminifers	8
Nannofossils	90
Radiolarians	2

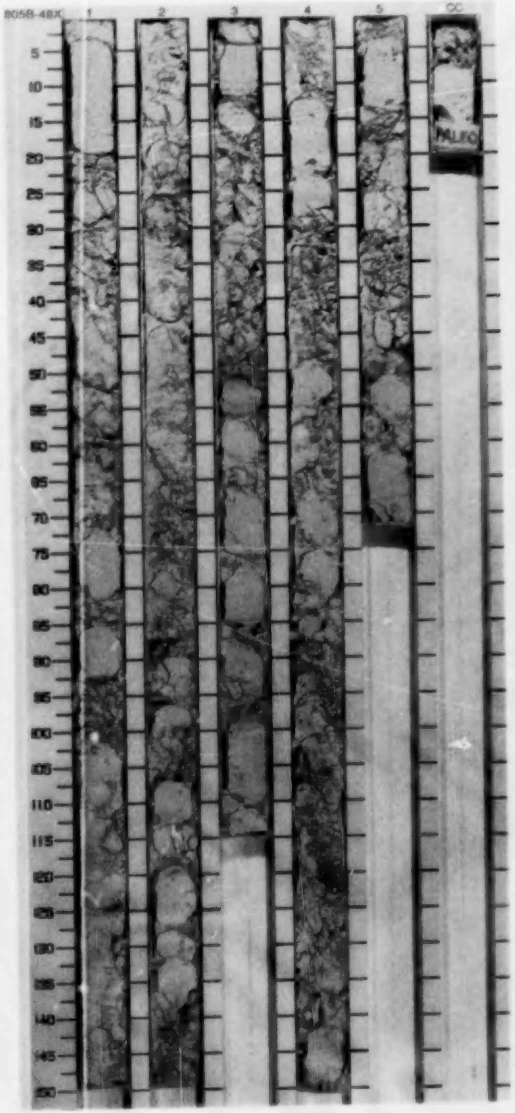
805B-48X
1
2
3
4
5
CC
5
10
15
20
25
30
35
40
45
50
55
60
65
70
75
80
85
90
95
100
105
110
115
120
125
130
135
140
145
150
PALEO

SITE 805 HOLE B CORE 49X CORED INTERVAL 455.1-464.8 mbsf

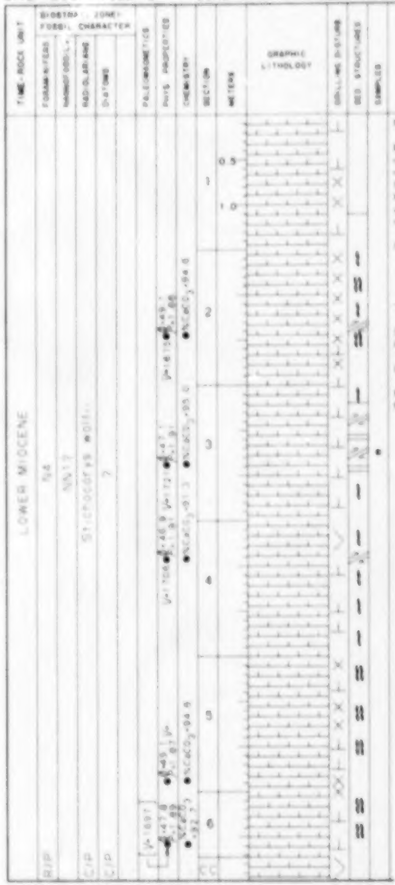
TIME-ROCK UNIT
BIOSTRAT. ZONE/ FOSSIL CHARACTER
FORAMINIFERS
NANNOFOSSILS
RADIOLARIANS
DIATOMS
PALEOMAGNETICS
PHYS. PROPERTIES
CHEMISTRY
SECTION
METERS
GRAPHIC LITHOLOGY
DRILLING DISTURB.
SED. STRUCTURES
SAMPLES
LOWER MIOCENE
N4
NN17
Stichocorys wolffi
?
R/P
C/P
C/P
●%CaCO3=94.0
●%CaCO3=95.0
●%CaCO3=91.3
●%CaCO3=94.6
1
2
3
4
5
6
CC
0.5
1.0

LITHOLOGIC DESCRIPTION

NANNOFOSSIL CHALK

Major lithology: This core consists of white (2.5Y 8/0) NANNOFOSSIL CHALK. The color is reddish gray (5R 6/1) from the bottom of Section 1 through most of Section 2. Distinct reddish gray (5R 6/1) and pale yellowish green color bands (mm thick) are abundant in Sections 2 and 3. The sediment is moderately to highly bioturbated as indicated by trace fossils and a few pyritized burrow fills. Most of the core is moderately to highly fragmented with intervals containing drilling breccia. Biscuits of chalk generally are imbedded in a stiff matrix of ooze and breccia.

SMEAR SLIDE SUMMARY (%):

	3, 75
	D
TEXTURE:	
Silt	60
Clay	40
COMPOSITION:	
Foraminifers	2
Nannofossils	98

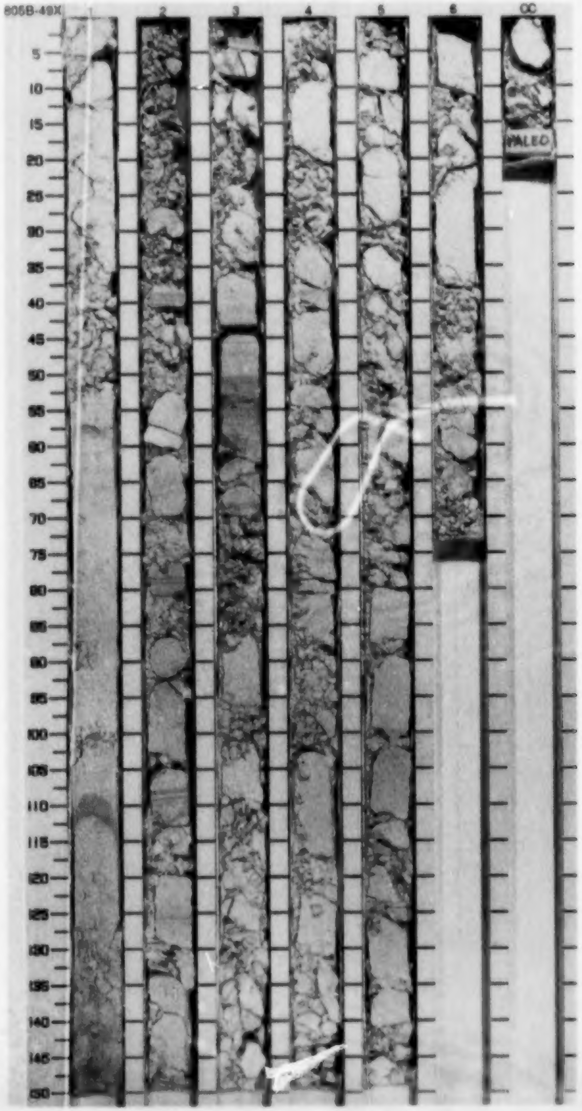
805B-49X
1
2
3
4
5
6
CC
PALEO
5
10
15
20
25
30
35
40
45
50
55
60
65
70
75
80
85
90
95
100
105
110
115
120
125
130
135
140
145
150

SITE 805 HOLE B CORE 50X CORED INTERVAL 464.8-473.3 mbsf

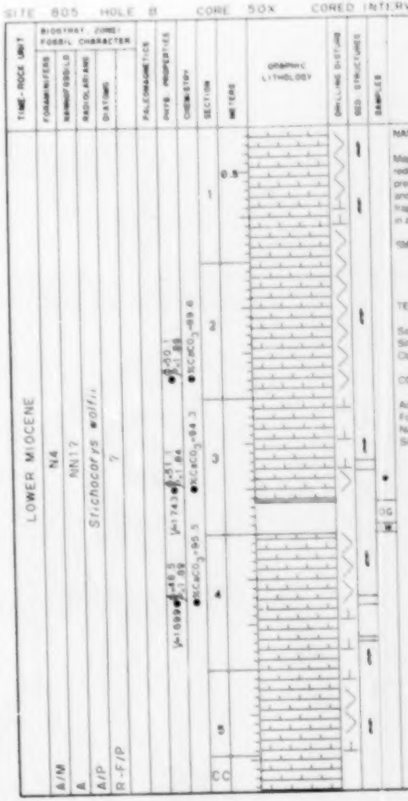
TIME-ROCK UNIT
BIOSTRAT. ZONE/ FOSSIL CHARACTER
FORAMINIFERS
NANNOFOSSILS
RADIOLARIANS
DIATOMS
PALEOMAGNETICS
PHYS. PROPERTIES
CHEMISTRY
SECTION
METERS
GRAPHIC LITHOLOGY
DRILLING DISTURB.
SED. STRUCTURES
SAMPLES
LOWER MIOCENE
N4
NN12
Stichocorys wolffi
?
A/M
A
A/P
R-F/P
γ=1743
φ=51.1
γ=1.84
γ=1699
φ=48.5
γ=1.89
φ=50.1
γ=1.88
%CaCO3=89.6
%CaCO3=84.3
%CaCO3=95.5
0.5
1
2
3
4
5
CC
OG

LITHOLOGIC DESCRIPTION

NANNOFOSSIL CHALK

Major lithology: This core consists of white (2.5Y 8/0) NANNOFOSSIL CHALK. Distinct reddish gray (5R 6/1) and pale yellowish green (10GY 7/2) color bands (mm thickness) are present in Sections 2 through 4. The sediment is bioturbated, as indicated by trace fossils and a few pyritized burrow fills, some with halos. Most of the core is moderately to highly fragmented, with intervals containing drilling breccia. Biscuits of chalk are generally imbedded in a stiff matrix of ooze and breccia.

SMEAR SLIDE SUMMARY (%):

	3, 68
	D
TEXTURE	
Sand	7
Silt	60
Clay	33
COMPOSITION	
Accessory minerals	1
Foraminifers	8
Nannofossils	90
Siliceous fragments	1

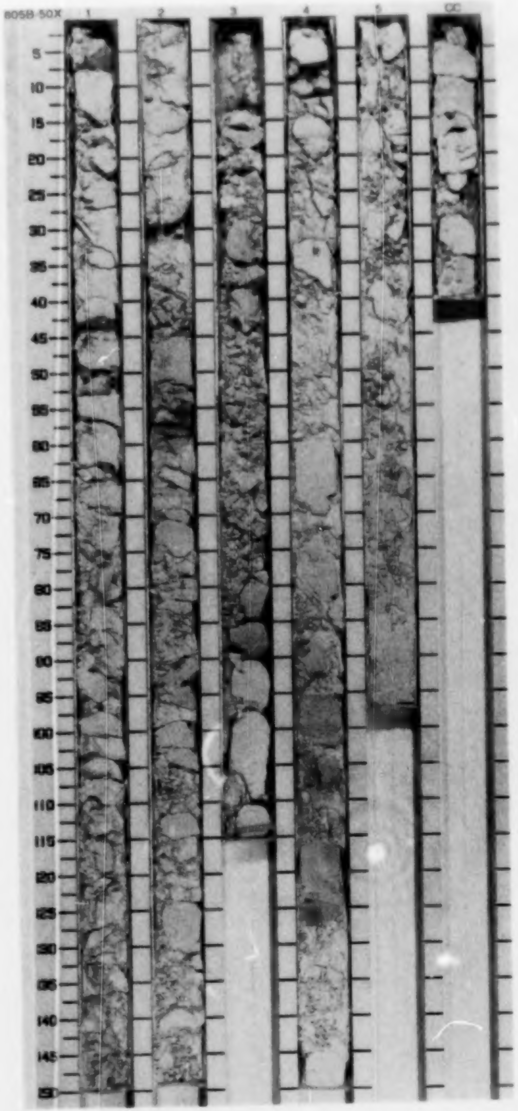
805B-50X
1
2
3
4
5
CC
5
10
15
20
25
30
35
40
45
50
55
60
65
70
75
80
85
90
95
100
105
110
115
120
125
130
135
140
145
150

SITE 805 HOLE C CORE 1H CORED INTERVAL 0.0-7.8 mbsf

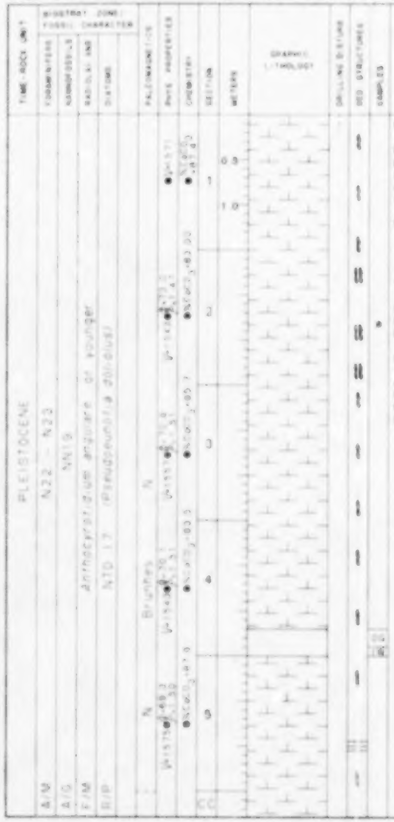
TIME-ROCK UNIT
BIOSTRAT. ZONE/ FOSSIL CHARACTER
FORAMINIFERS
NANNOFOSSILS
RADIOLARIANS
DIATOMS
PALEOMAGNETICS
PHYS. PROPERTIES
CHEMISTRY
SECTION
METERS
GRAPHIC LITHOLOGY
DRILLING DISTURB.
SED. STRUCTURES
SAMPLES
PLEISTOCENE
N22 - N23
NN19
Anthocyrtidium angulare or younger
NTD 17 (Pseudoeunotia doliolus)
A/M
A/G
F/M
R/P
N
Brunhes
N
1
2
3
4
5
CC
0.5
1.0
OG
IW

LITHOLOGIC DESCRIPTION

NANNOFOSSIL OOZE with FORAMINIFERS

Major lithology: This core contains NANNOFOSSIL OOZE with FORAMINIFERS. The ooze is pale brown (10YR 6/3) in Sections 1 and 2, white (2.5Y 8/2) in Section 3, 0-110 cm, and white (2.5Y 8/1) from Section 3, 110 cm to the base of the core. The ooze is bioturbated and contains several vertical burrows. From Sections 3 to the base, 3 to 10 cm thick reddish gray (5R 6/2) color bands are spaced at 40 to 60 cm intervals.

SMEAR SLIDE SUMMARY (%):

	2, 82 D
TEXTURE:	
Sand	20
Silt	50
Clay	30
COMPOSITION:	
Accessory minerals	1
Foraminifers	20
Nannofossils	77
Siliceous fragments	2

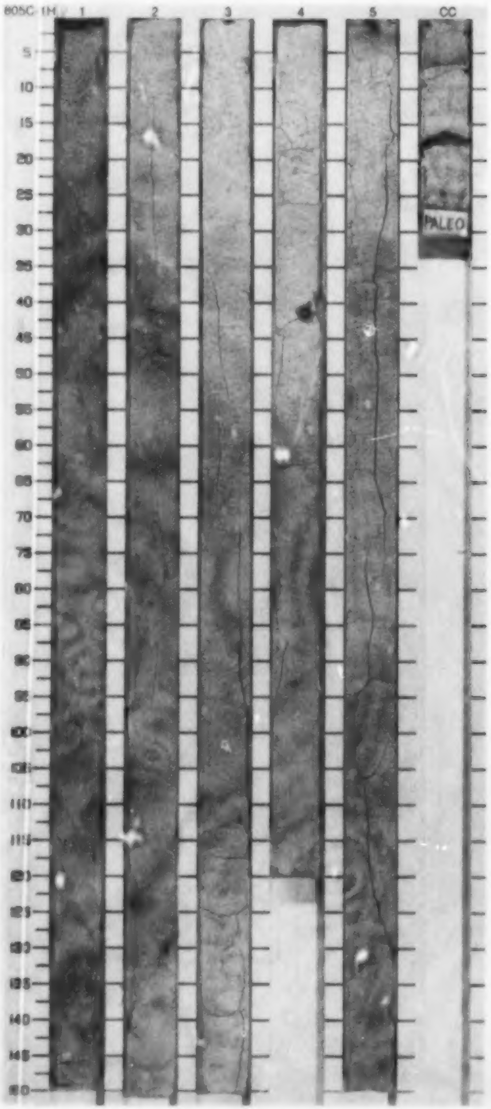
805C-1H
1
2
3
4
5
CC
PALEO
5
10
15
20
25
30
35
40
45
50
55
60
65
70
75
80
85
90
95
100
105
110
115
120
125
130
135
140
145
150

SITE 805 HOLE C CORE 2H CORED INTERVAL 7.8-17.3 mbsf

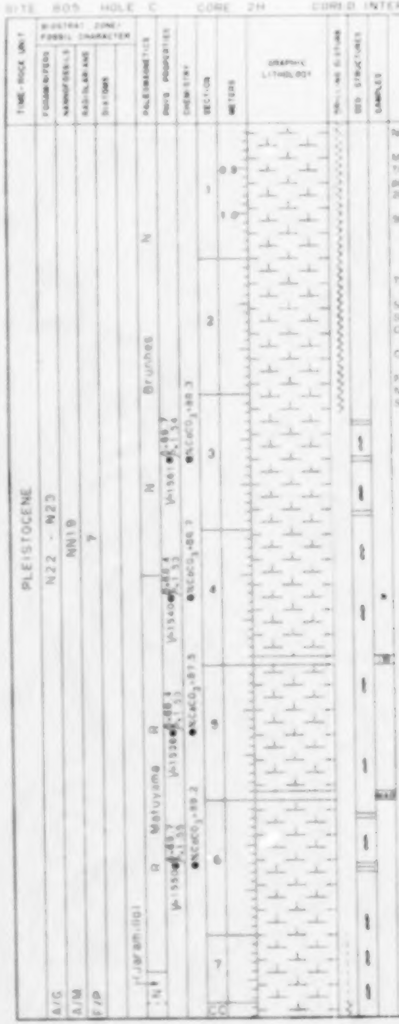
TIME-ROCK UNIT
BIOSTRAT. ZONE/ FOSSIL CHARACTER
FORAMINIFERS
NANNOFOSSILS
RADIOLARIANS
DIATOMS
PALEOMAGNETICS
PHYS. PROPERTIES
CHEMISTRY
SECTION
METERS
GRAPHIC LITHOLOGY
DRILLING DISTURB.
SED. STRUCTURES
SAMPLES
PLEISTOCENE
N22 - N23
NN19
?
A/G
A/M
F/P
N
Brunhes
N
R
Matuyama
R
(Jaramillo)
N
V=1561 ●φ=66.7 γ=1.54
V=1540 ●φ=66.4 γ=1.53
V=1536 ●φ=66.4 γ=1.53
V=1550 ●φ=65.7 γ=1.55
●%CaCO3=88.3
●%CaCO3=86.7
●%CaCO3=87.5
●%CaCO3=88.2
1
2
3
4
5
6
7
CC
0.5
1.0

LITHOLOGIC DESCRIPTION

NANNOFOSSIL OOZE with FORAMINIFERS

Major lithology: This core contains bioturbated NANNOFOSSIL OOZE with FORAMINIFERS. The ooze is predominantly white (5Y 8/1) but contains numerous reddish gray (5R 6/1) and pale yellowish green (10GY 7/2) color bands. The bands are 5 to 15 mm thick and are spaced 20 to 30 cm apart. Sections 1 and 2 contain flow-in.

SMEAR SLIDE SUMMARY (%):

	4, 75
	D
TEXTURE:	
Sand	20
Silt	40
Clay	40
COMPOSITION:	
Foraminifers	10
Nannofossils	87
Siliceous fragments	3

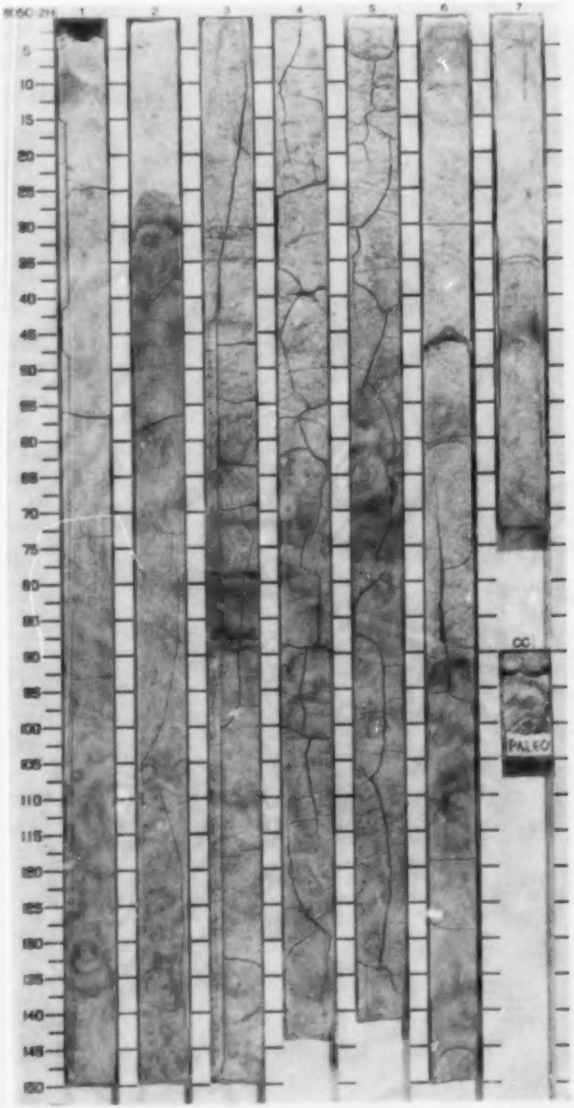
805C-2H
1
2
3
4
5
6
7
CC
PALEO
5
10
15
20
25
30
35
40
45
50
55
60
65
70
75
80
85
90
95
100
105
110
115
120
125
130
135
140
145
150

SITE 805 HOLE C CORE 3H CORED INTERVAL 17.3-26.8 mbsf

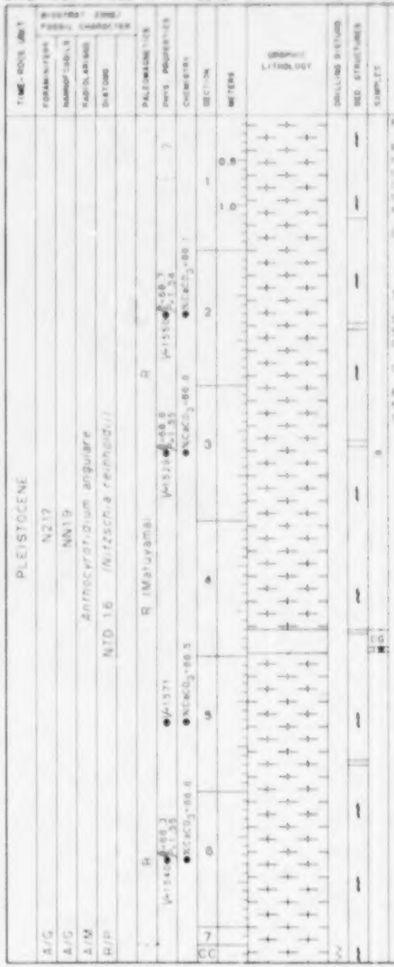
TIME-ROCK UNIT
BIOSTRAT. ZONE/ FOSSIL CHARACTER
FORAMINIFERS
NANNOFOSSILS
RADIOLARIANS
DIATOMS
PALEOMAGNETICS
PHYS. PROPERTIES
CHEMISTRY
SECTION
METERS
GRAPHIC LITHOLOGY
DRILLING DISTURB.
SED. STRUCTURES
SAMPLES
PLEISTOCENE
A/G N21?
A/G NN19
A/M Anthocyrtidium angulare
R/P NTD 16 (Nitzschia reinholdii)
R
R (Matuyama)
R
γ=1556 φ=60.7 ρ=1.34
γ=1519 φ=60.8 ρ=1.35
γ=1571
γ=1540 φ=60.2 ρ=1.35
%CaCO₃=80.1
%CaCO₃=86.0
%CaCO₃=88.5
%CaCO₃=86.6
1 2 3 4 5 6 7 CC
0.5
1.0
OG

LITHOLOGIC DESCRIPTION

FORAMINIFER NANNOFOSSIL OOZE

Major lithology: This core contains FORAMINIFER NANNOFOSSIL OOZE. The ooze is homogeneous and predominantly white (2.5Y 8/0). Intervals of faint, reddish gray (5R 6/2) color bands, 10 to 20 cm thick, are spaced 30 to 40 cm apart. The color bands contain thinner (5 to 15 mm thick) reddish gray and pale yellowish green (10GY 7/2) intervals. The sediment is bioturbated, with some of the burrow fill distinctly coarser than the surrounding ooze. Pyrite specks and streaks also are present.

SMEAR SLIDE SUMMARY (%):

	3, 74
	D
TEXTURE:	
Sand	15
Silt	60
Clay	25
COMPOSITION:	
Foraminifers	[illegible]
Nannofossils	71
Siliceous fragments	2

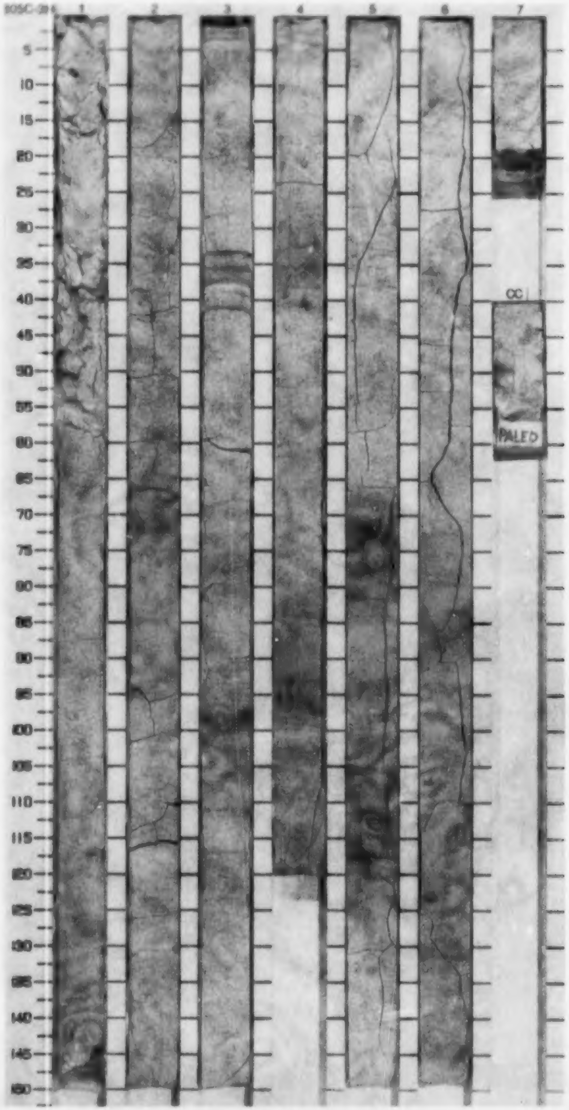
805C-3H
1
2
3
4
5
6
7
CC
PALEO
5
10
15
20
25
30
35
40
45
50
55
60
65
70
75
80
85
90
95
100
105
110
115
120
125
130
135
140
145
150

SITE 805 HOLE C CORE 4H CORED INTERVAL 26.8-36.3 mbsf

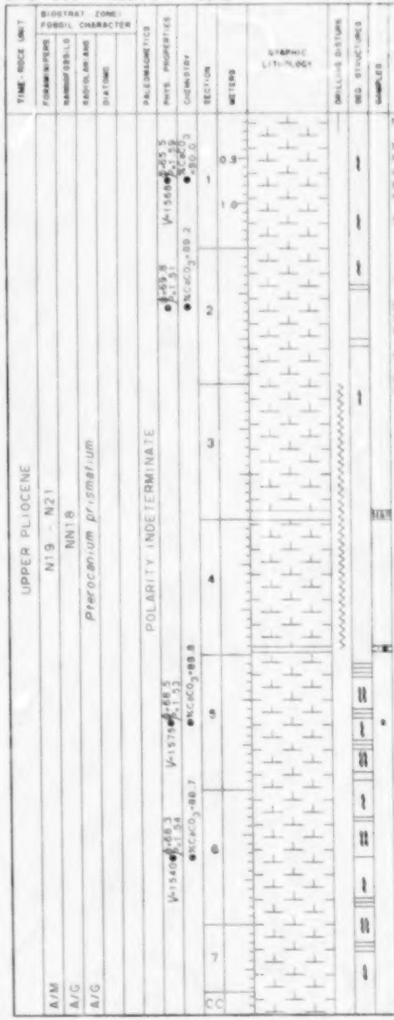
TIME-ROCK UNIT
BIOSTRAT. ZONE/ FOSSIL CHARACTER
FORAMINIFERS
NANNOFOSSILS
RADIOLARIANS
DIATOMS
PALEOMAGNETICS
PHYS. PROPERTIES
CHEMISTRY
SECTION
METERS
GRAPHIC LITHOLOGY
DRILLING DISTURB.
SED. STRUCTURES
SAMPLES
UPPER PLIOCENE
N19 - N21
NN18
Pterocanium prismatium
A/M
A/G
A/G
POLARITY INDETERMINATE
V=1568
ϕ=65.5
γ=1.59
%CaCO3 =90.0
ϕ=69.8
γ=1.51
%CaCO3=89.2
V=1575
ϕ=68.5
γ=1.53
%CaCO3=88.8
V=1540
ϕ=66.3
γ=1.54
%CaCO3=88.7
1
2
3
4
5
6
7
CC
0.5
1.0

LITHOLOGIC DESCRIPTION

NANNOFOSSIL OOZE with FORAMINIFERS

Major lithology: This core consists of white (2.5Y 8/0) NANNOFOSSIL OOZE with FORAMINIFERS. Sections 3 and 4 contain flow in. The sediment is moderately to heavily bioturbated as indicated by light gray (2.5Y 7/2) mottles, burrow fills and pyritized burrow fills. Reddish gray (5R 6/1) and pale yellowish green (10GY 7/2) color bands (mm- to cm-scale) are common in Sections 1 and 2, and abundant in Sections 5, 6, and 7.

SMEAR SLIDE SUMMARY (%):

	5, 75 D
TEXTURE:	
Sand	10
Silt	60
Clay	30
COMPOSITION:	
Foraminifers	10
Nannofossils	90

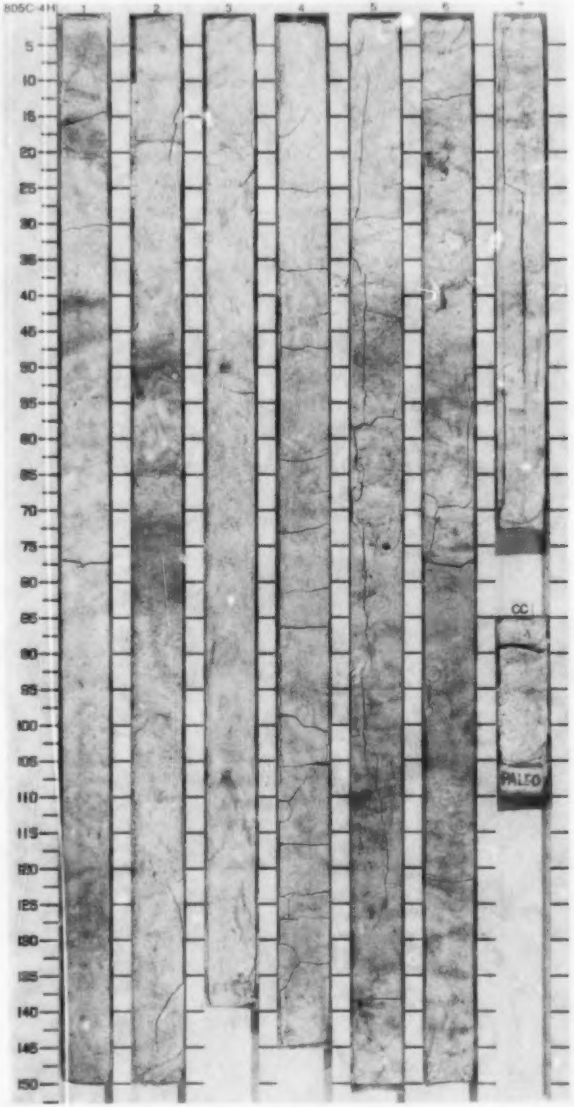
805C-4H
1
2
3
4
5
6
7
5
10
15
20
25
30
35
40
45
50
55
60
65
70
75
80
85
90
95
100
105
110
115
120
125
130
135
140
145
150
CC
PALEO

SITE 805 HOLE C CORE 5H CORED INTERVAL 36.3-45.8 mbsf

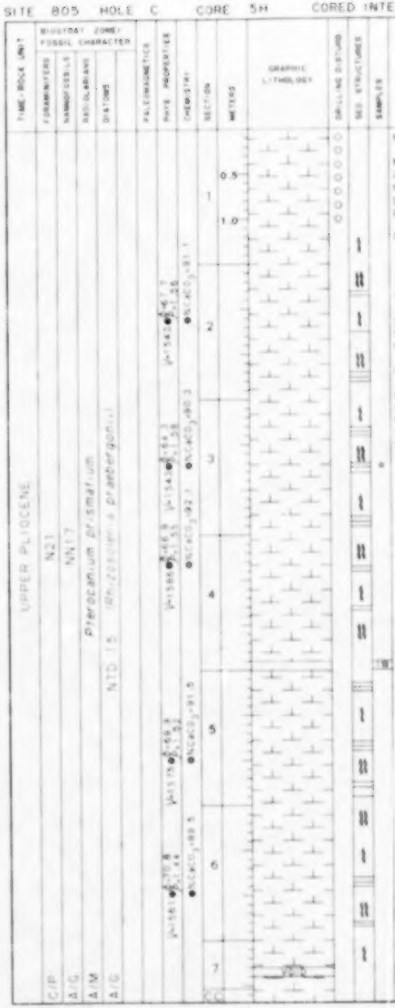
TIME-ROCK UNIT
BIOSTRAT. ZONE/ FOSSIL CHARACTER
FORAMINIFERS
NANNOFOSSILS
RADIOLARIANS
DIATOMS
PALEOMAGNETICS
PHYS. PROPERTIES
CHEMISTRY
SECTION
METERS
GRAPHIC LITHOLOGY
DRILLING DISTURB.
SED. STRUCTURES
SAMPLES
UPPER PLIOCENE
N21
NN17
Pterocanium prismatium
NTD 15 (Rhizosolenia praebergonii)
C/P
A/G
A/M
A/G
V=1543 ●φ=67.7 γ=1.56
●%CaCO3=81.1
V=1543 ●φ=64.3 γ=1.58
●%CaCO3=90.3
V=1588 ●φ=66.8 γ=1.55
●%CaCO3=92.1
V=1578 ●φ=69.8 γ=1.52
●%CaCO3=91.5
V=1581 ●φ=70.8 γ=1.44
●%CaCO3=89.5
1
2
3
4
5
6
7
CC
0.5
1.0
IW

LITHOLOGIC DESCRIPTION

NANNOFOSSIL OOZE

Major lithology: This core contains NANNOFOSSIL OOZE. The sediment is white (5Y 8/1 to 2.5Y 8/0), with minor to abundant light gray (5Y 7/1) and light olive gray (5Y 6/2) mottling throughout. Diffuse to well defined light gray (N7), light greenish gray (5G 7/1), greenish gray (5G 6/1), grayish blue (5PB 5/2), and pale blue (5PB 7/7) color bands are common. A pyrite concretion, approximately 0.5 cm in diameter, was recovered at Section 2, 25 cm.

SMEAR SLIDE SUMMARY (%):

	3, 75
	D
TEXTURE:	
Sand	5
Silt	60
Clay	35
COMPOSITION:	
Diatoms	3
Foraminifers	8
Nannofossils	83
Radiolarians	3
Siliceous fragments	3

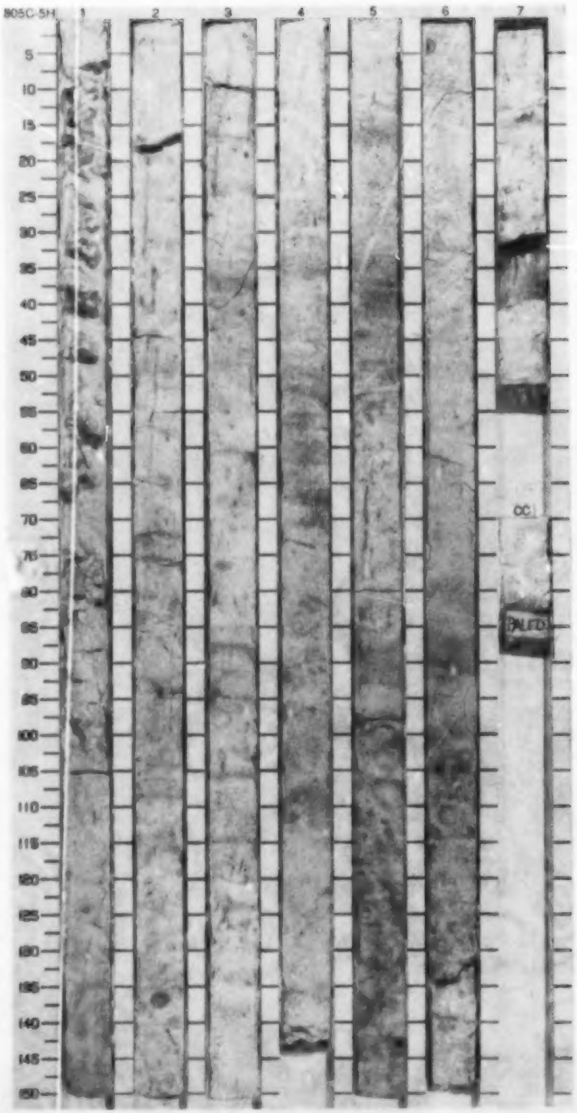
805C-5H
1
2
3
4
5
6
7
5
10
15
20
25
30
35
40
45
50
55
60
65
70
75
80
85
90
95
100
105
110
115
120
125
130
135
140
145
150
CC
PALEO

SITE 805 HOLE C CORE 6H CORED INTERVAL 45.6-55.3 mbsf

TIME-ROCK UNIT	BIOSTRAT. ZONE / FOSSIL CHARACTER: FORAMINIFERS	NANNOFOSSILS	RADIOLARIANS	DIATOMS
UPPER PLIOCENE	A/M N21	A/M NN16	A/G *Spongaster pentas*	A/G NTD 15 / NTD 14 *Nitzschia jouseae*

SECTION	PHYS. PROPERTIES	CHEMISTRY
1	Vp=1540 ●φ=64.6 γ=1.60	●%CaCO$_3$=89.9
2	Vp=1... ●φ=60.7 γ=1.53	●%CaCO$_3$=90.0
3	Vp=1529 ●φ=64.8 γ=1.61	●%CaCO$_3$=91.1
4	Vp=1547 ●φ=66.0 γ=1.58	●%CaCO$_3$=90.3
5	Vp=1528 ●φ=67.4 γ=1.55	●%CaCO$_3$=88.6
6	Vp=1540 ●φ=68.0 γ=1.58	●%CaCO$_3$=89.5
7		
CC		

GRAPHIC LITHOLOGY: VOID

LITHOLOGIC DESCRIPTION

NANNOFOSSIL OOZE

Major lithology: This core consists of white (5Y 8/1) NANNOFOSSIL OOZE. Moderate to heavy bioturbation is indicated by light gray (5Y 7/1 and 5Y 7/2) mottles and pyritized burrow fills. Diffuse light gray-gray (7.5YR 5/2 and 7.5YR 6/0) and light greenish gray (5GY 7/1) color bands are common throughout.

SMEAR SLIDE SUMMARY (%):

	4, 80
	D
TEXTURE	
Sand	5
Silt	90
Clay	5
COMPOSITION	
Diatoms	1
Foraminifers	5
Nannofossils	90
Radiolarians	1
Silicoflagellates	1
Spicules	1

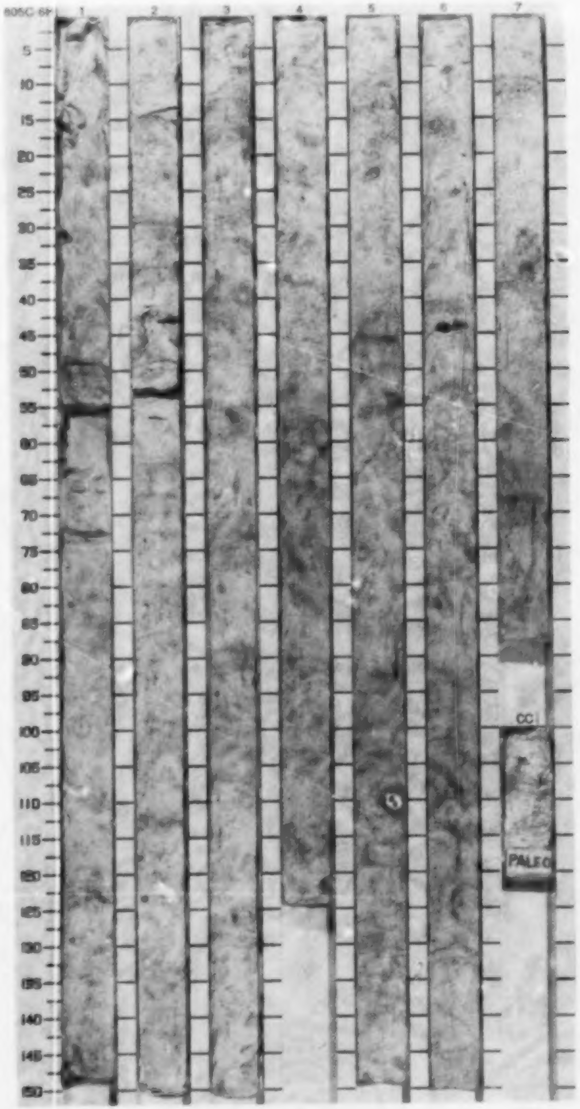
805C-6H
1
2
3
4
5
6
7
CC
PALEO
5
10
15
20
25
30
35
40
45
50
55
60
65
70
75
80
85
90
95
100
105
110
115
120
125
130
135
140
145
150

SITE 805 HOLE C CORE 7H CORED INTERVAL 55.3-64.8 mbsf

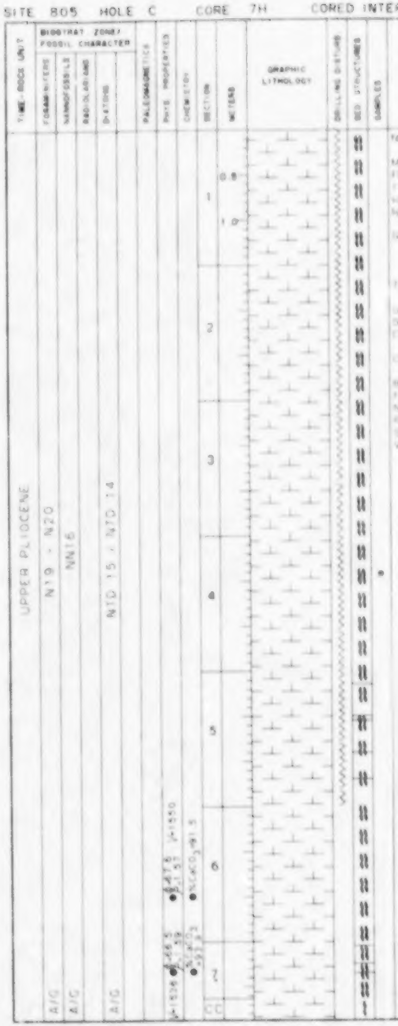
TIME-ROCK UNIT
BIOSTRAT. ZONE/ FOSSIL CHARACTER
FORAMINIFERS
NANNOFOSSILS
RADIOLARIANS
DIATOMS
PALEOMAGNETICS
PHYS. PROPERTIES
CHEMISTRY
SECTION
METERS
GRAPHIC LITHOLOGY
DRILLING DISTURB.
SED. STRUCTURES
SAMPLES
UPPER PLIOCENE
N19 - N20
NN16
NTD 15 / NTD 14
A/G
A/G
A/G
0.5
1.0
1
2
3
4
5
6
7
CC
φ47.6 ρ1.57 V=1550
φ48.5 ρ1.59 V=1536
%CaCO3=91.5
%CaCO3=93.3

LITHOLOGIC DESCRIPTION

NANNOFOSSIL OOZE with FORAMINIFERS

Major lithology: This core contains white (2.5Y 8/0) NANNOFOSSIL OOZE with FORAMINIFERS. Sections 1 through 5 are flow in. In Section 1, the intervals 13-44 cm, 87-91 cm and 115-122 cm may be coherent. The distortion is less in Section 5, with vertical displacements varying between 3 and 10 cm. The remainder of the core is undisturbed. Light gray (N7) and light greenish gray (5GY 7/1) mottling is common throughout the core.

SMEAR SLIDE SUMMARY (%):

	4, 42
	D
TEXTURE:	
Sand	13
Silt	60
Clay	27
COMPOSITION:	
Bioclast	Tr
Foraminifers	10
Nannofossils	87
Radiolarians	3
Spicules	Tr
Volcanic ash	Tr

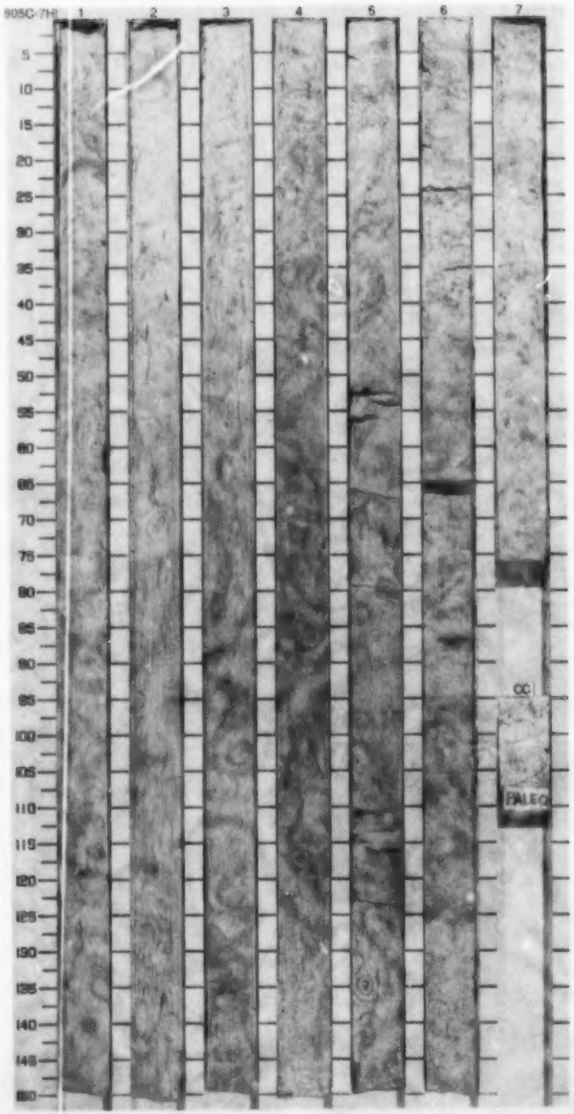
805C-7H
1
2
3
4
5
6
7
5
10
15
20
25
30
35
40
45
50
55
60
65
70
75
80
85
90
95
100
105
110
115
120
125
130
135
140
145
150
CC
PALEO

SITE 805 HOLE C CORE 8H CORED INTERVAL 64.8-74.3 mbsf

TIME-ROCK UNIT	BIOSTRAT. ZONE/FOSSIL CHARACTER: FORAMINIFERS	NANNOFOSSILS	RADIOLARIANS	DIATOMS	PALEOMAGNETICS	PHYS. PROPERTIES	CHEMISTRY	SECTION	METERS	GRAPHIC LITHOLOGY	DRILLING DISTURB.	SED. STRUCTURES	SAMPLES
UPPER PLIOCENE	N19 - N20	NN16	*Spongaster pentas*					1 2 3 4 5 6 7 CC	0.5 1.0				●
	A/G	A/G	A/G										

LITHOLOGIC DESCRIPTION

NANNOFOSSIL OOZE with FORAMINIFERS

Major lithology: This core contains white (2.5Y 8/0) NANNOFOSSIL OOZE with FORAMINIFERS. The whole core is flow in. Burrow mottles and remnants of light gray (5Y 7/2), light greenish gray (5GY 7/1) and light gray (N7/1) color bands are visible.

SMEAR SLIDE SUMMARY (%):

	2, 97
	D
TEXTURE:	
Sand	15
Silt	85
COMPOSITION:	
Foraminifers	10
Nannofossils	88
Radiolarians	2

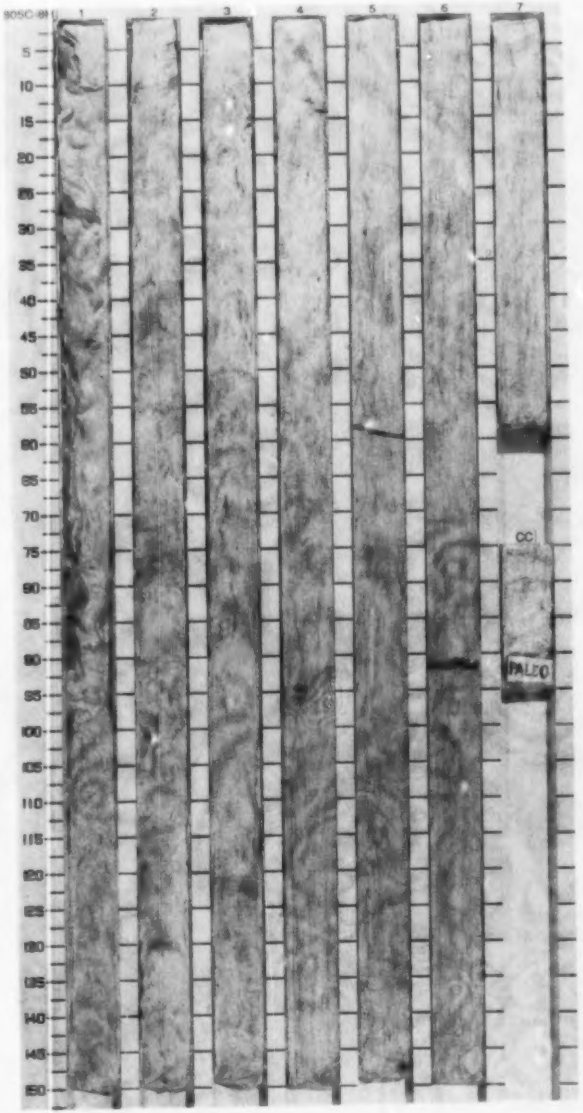
805C-8H
1
2
3
4
5
6
7
CC
PALEO
5
10
15
20
25
30
35
40
45
50
55
60
65
70
75
80
85
90
95
100
105
110
115
120
125
130
135
140
145
150

SITE 805 HOLE C CORE 9H CORED INTERVAL 74.3-83.8 mbsf

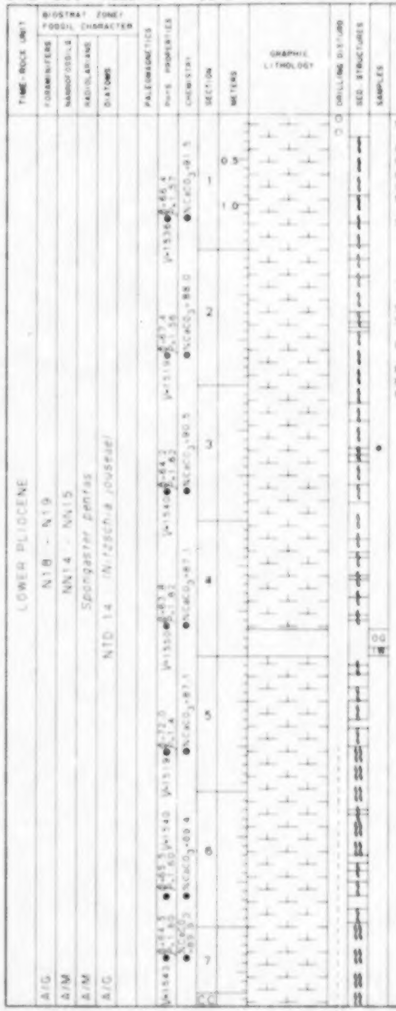
TIME-ROCK UNIT
BIOSTRAT. ZONE/ FOSSIL CHARACTER
FORAMINIFERS
NANNOFOSSILS
RADIOLARIANS
DIATOMS
PALEOMAGNETICS
PHYS. PROPERTIES
CHEMISTRY
SECTION
METERS
GRAPHIC LITHOLOGY
DRILLING DISTURB.
SED. STRUCTURES
SAMPLES
LOWER PLIOCENE
N18 - N19
NN14 - NN15
Spongaster pentas
NTD 14 (Nitzschia jouseae)
A/G
A/M
A/M
A/G
V=1536● φ=66.4 γ=1.57
V=1519● φ=67.4 γ=1.56
V=1540● φ=64.2 γ=1.62
V=1550● φ=67.8 γ=1.62
V=1519● φ=72.0 γ=1.4
V=1540● φ=65.5 γ=1.60 V=1540
V=1543● φ=64.5 γ=1.60
●%CaCO3=81.5
●%CaCO3=88.0
●%CaCO3=90.5
●%CaCO3=87.1
●%CaCO3=87.1
●%CaCO3=89.4
●%CaCO3=89.3
1
2
3
4
5
6
7
CC
0.5
1.0
OG
IW

LITHOLOGIC DESCRIPTION

NANNOFOSSIL OOZE

Major lithology: The core consists of white (2.5Y 8/0) to light gray (5Y 7/1) NANNOFOSSIL OOZE. The sediments are heavily to moderately bioturbated as indicated by abundant light gray (2.5Y 7/2 and 5Y 7/1) and grayish blue (5PB 5/2) mottling. Faint pale yellowish green (10GY 7/2), light gray (N7) and light greenish gray (5GY 7/1) color bands are common throughout the core.

SMEAR SLIDE SUMMARY (%):

	3, 70
	D
TEXTURE:	
Sand	15
Silt	85
COMPOSITION:	
Foraminifers	8
Nannofossils	90
Radiolarians	2

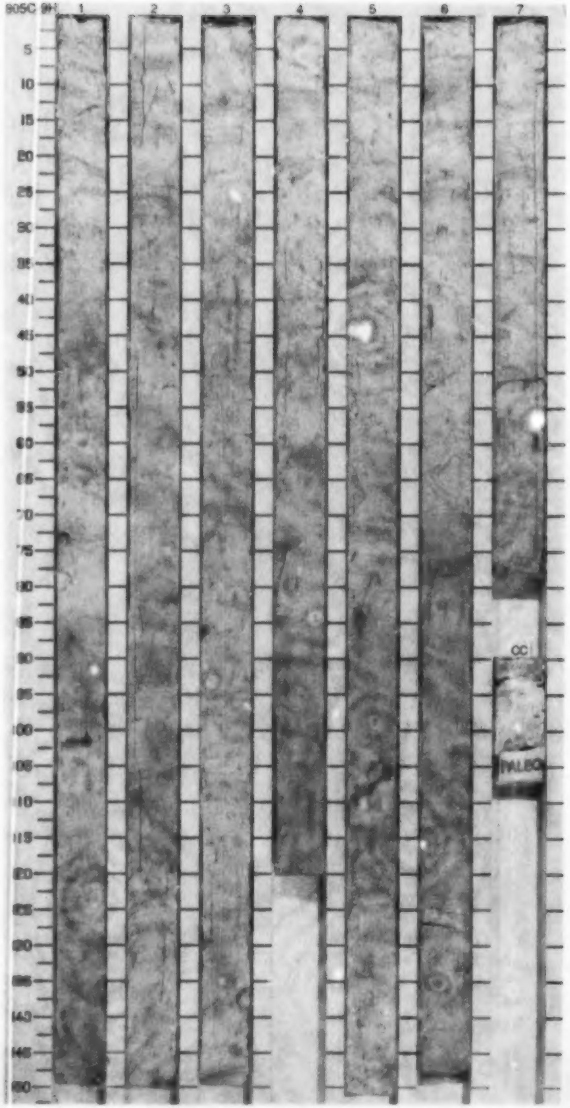
805C 9H
1
2
3
4
5
6
7
5
10
15
20
25
30
35
40
45
50
55
60
65
70
75
80
85
90
95
100
105
110
115
120
125
130
135
140
145
150
CC
PALEO

SITE 805 HOLE C CORE 10H CORED INTERVAL 83.8-93.3 mbsf

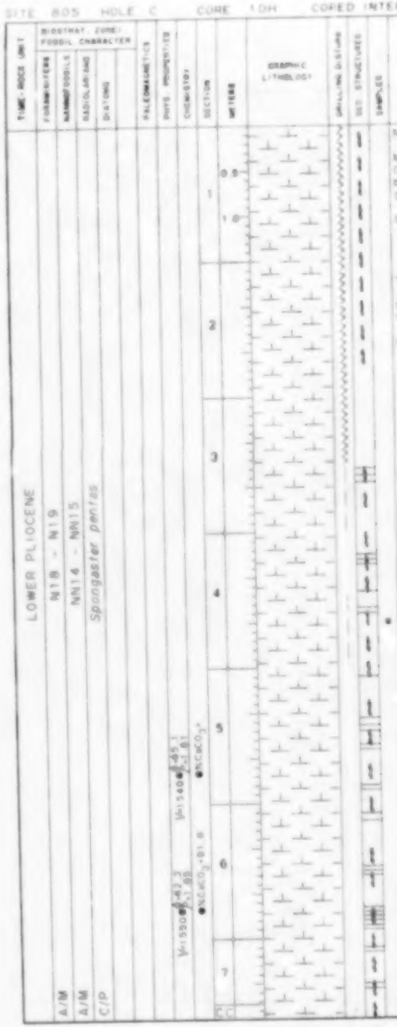
TIME-ROCK UNIT
BIOSTRAT. ZONE/ FOSSIL CHARACTER
FORAMINIFERS
NANNOFOSSILS
RADIOLARIANS
DIATOMS
PALEOMAGNETICS
PHYS. PROPERTIES
CHEMISTRY
SECTION
METERS
GRAPHIC LITHOLOGY
DRILLING DISTURB.
SED. STRUCTURES
SAMPLES
LOWER PLIOCENE
N18 - N19
NN14 - NN15
Spongaster pentas
A/M
A/M
C/P
V=1540● φ-65.1 ρ-1.61
●%CaCO₃-*
V=1550● φ-62.3 ρ-1.65
●%CaCO₃-81.6
1
2
3
4
5
6
7
CC
0.5
1.0

LITHOLOGIC DESCRIPTION

NANNOFOSSIL OOZE with FORAMINIFERS

Major lithology: This core contains white (2.5Y 8/0) to light gray (2.5Y 7/1) NANNOFOSSIL OOZE with FORAMINIFERS, with cm-scale, light gray (5Y 7/1) mottling. Additional bioturbation is indicated by mm to cm scale pyritic burrow fillings and burrow "halos". Diffuse light gray (N7) and light greenish gray (5GY 7/1) color bands are common.

SMEAR SLIDE SUMMARY (%):

	4, 100
	D
TEXTURE	
Sand	18
Silt	82
COMPOSITION	
Foraminifers	15
Nannofossils	82
Radiolarians	3

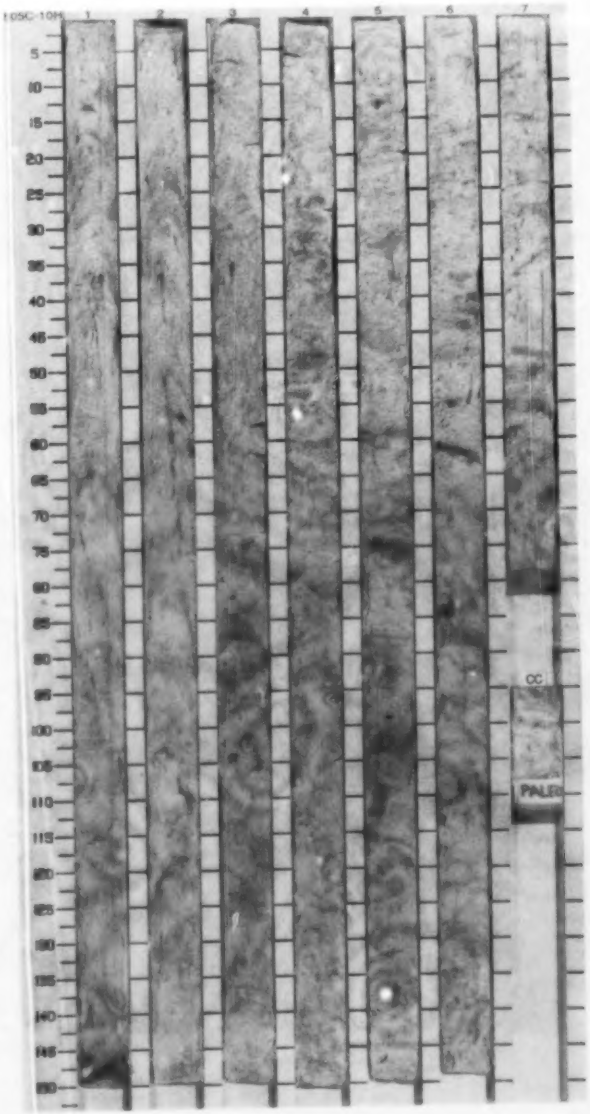
805C-10H
1
2
3
4
5
6
7
CC
PALEO
5
10
15
20
25
30
35
40
45
50
55
60
65
70
75
80
85
90
95
100
105
110
115
120
125
130
135
140
145
150

SITE 805 HOLE C CORE 11H CORED INTERVAL 93.3-102.8 mbsf

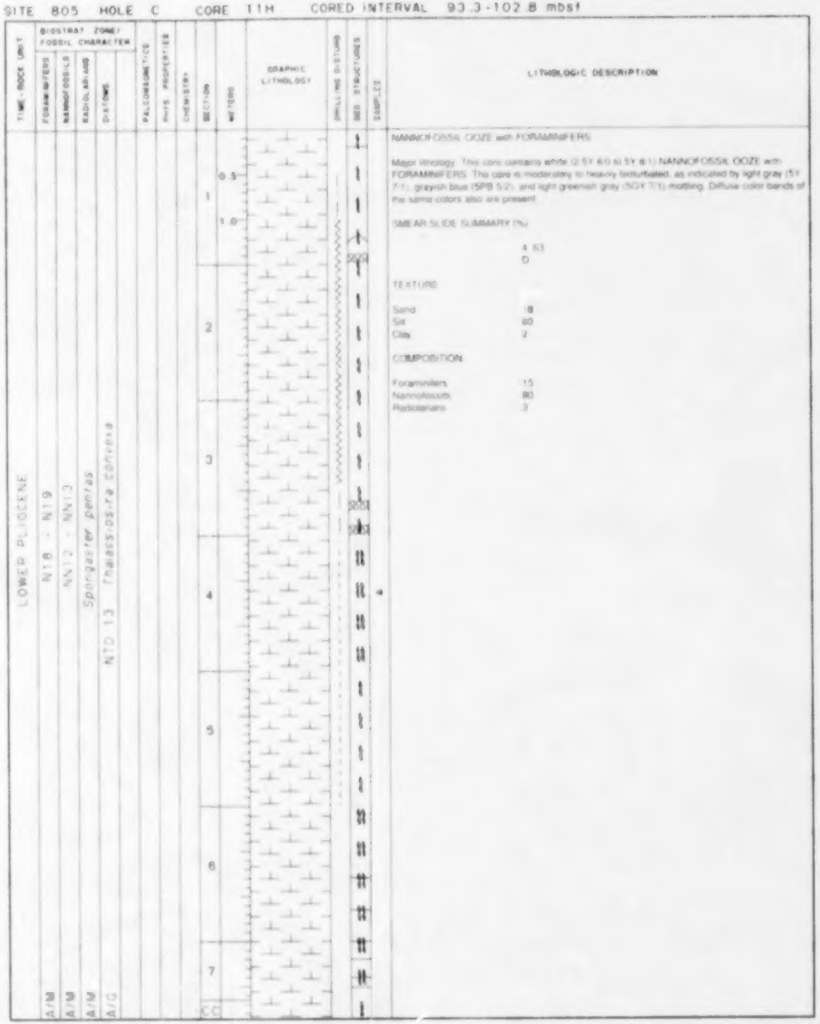
TIME-ROCK UNIT
BIOSTRAT. ZONE/ FOSSIL CHARACTER
FORAMINIFERS
NANNOFOSSILS
RADIOLARIANS
DIATOMS
PALEOMAGNETICS
PHYS. PROPERTIES
CHEMISTRY
SECTION
METERS
GRAPHIC LITHOLOGY
DRILLING DISTURB.
SED. STRUCTURES
SAMPLES
LOWER PLIOCENE
N18 - N19
NN12 - NN13
Spongaster pentas
NTD 13 Thalassiosira convexa
A/M
A/M
A/M
A/G
0.5
1.0
1
2
3
4
5
6
7
CC

LITHOLOGIC DESCRIPTION

NANNOFOSSIL OOZE with FORAMINIFERS

Major lithology: This core contains white (2.5Y 8/0 to 5Y 8/1) NANNOFOSSIL OOZE with FORAMINIFERS. The core is moderately to heavily bioturbated, as indicated by light gray (5Y 7/1), grayish blue (5PB 5/2), and light greenish gray (5GY 7/1) mottling. Diffuse color bands of the same colors also are present.

SMEAR SLIDE SUMMARY (%):

	4, 63
	D
TEXTURE:	
Sand	18
Silt	80
Clay	2
COMPOSITION:	
Foraminifers	15
Nannofossils	80
Radiolarians	3

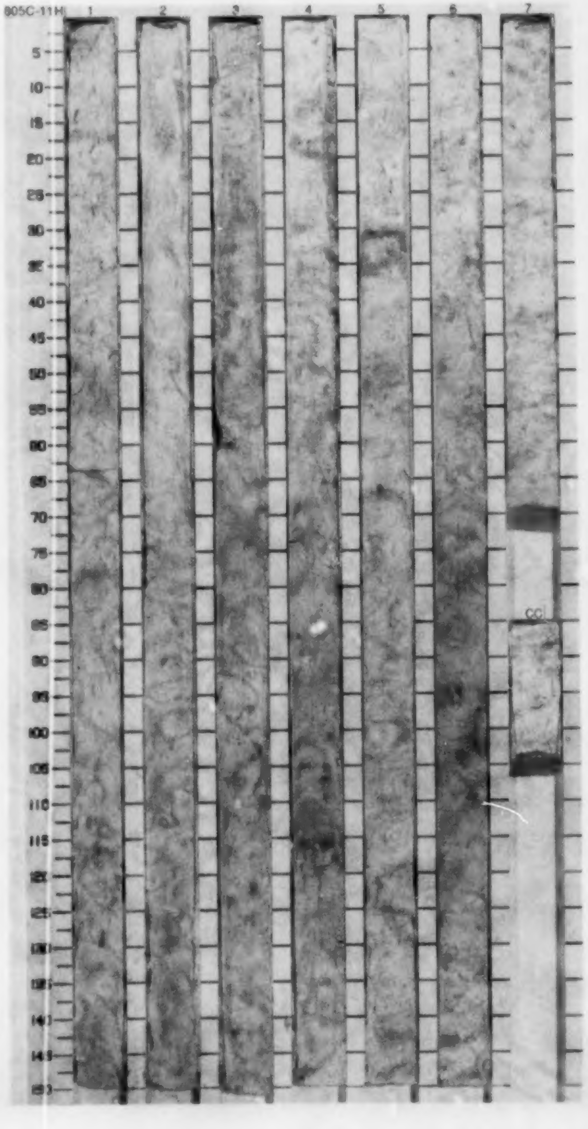
805C-11H
1
2
3
4
5
6
7
CC
5
10
15
20
25
30
35
40
45
50
55
60
65
70
75
80
85
90
95
100
105
110
115
120
125
130
135
140
145
150

SITE 805 HOLE C CORE 12H CORED INTERVAL 102.8-112.3 mbsf

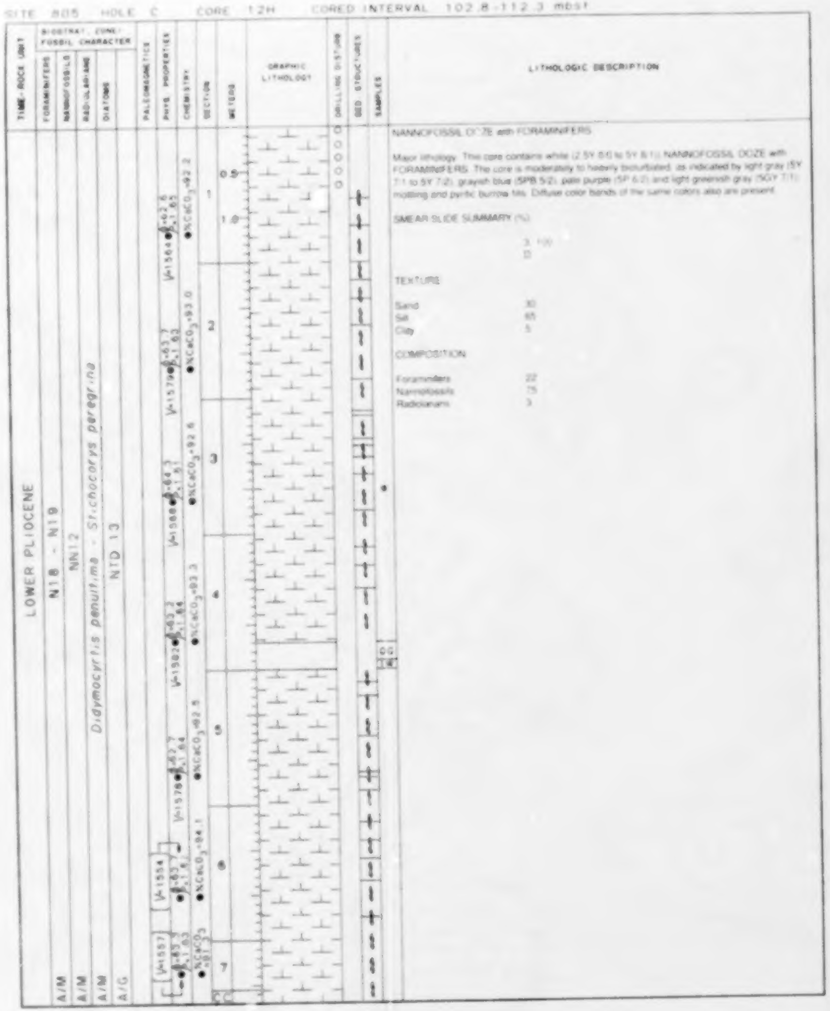
TIME-ROCK UNIT
BIOSTRAT. ZONE/FOSSIL CHARACTER
FORAMINIFERS
NANNOFOSSILS
RADIOLARIANS
DIATOMS
PALEOMAGNETICS
PHYS. PROPERTIES
CHEMISTRY
SECTION
METERS
GRAPHIC LITHOLOGY
DRILLING DISTURB.
SED. STRUCTURES
SAMPLES
LOWER PLIOCENE
N18 - N19
NN12
Didymocyrtis penultima - Stichocorys peregrina
NTD 13
A/M
A/M
A/M
A/G
V=1564 ●φ=62.6 γ=1.65
●%CaCO₃=92.2
V=1579 ●φ=63.7 γ=1.63
●%CaCO₃=93.0
V=1588 ●φ=64.3 γ=1.61
●%CaCO₃=92.6
V=1582 ●φ=63.2 γ=1.64
●%CaCO₃=93.3
V=1578 ●φ=62.7 γ=1.64
●%CaCO₃=92.5
V=1554 ●φ=63 γ=1.62
●%CaCO₃=94.1
V=1557 ●φ=63.3 γ=1.63
●%CaCO₃=91.3
1
2
3
4
5
6
7
CC
0.5
1.0
OG
PAL

LITHOLOGIC DESCRIPTION

NANNOFOSSIL OOZE with FORAMINIFERS

Major lithology: This core contains white (2.5Y 8/0 to 5Y 8/1) NANNOFOSSIL OOZE with FORAMINIFERS. The core is moderately to heavily bioturbated, as indicated by light gray (5Y 7/1 to 5Y 7/2), grayish blue (5PB 5/2), pale purple (5P 6/2) and light greenish gray (5GY 7/1) mottling and pyritic burrow fills. Diffuse color bands of the same colors also are present.

SMEAR SLIDE SUMMARY (%):

	3, 100
	D
TEXTURE:	
Sand	30
Silt	65
Clay	5
COMPOSITION:	
Foraminifers	22
Nannofossils	75
Radiolarians	3

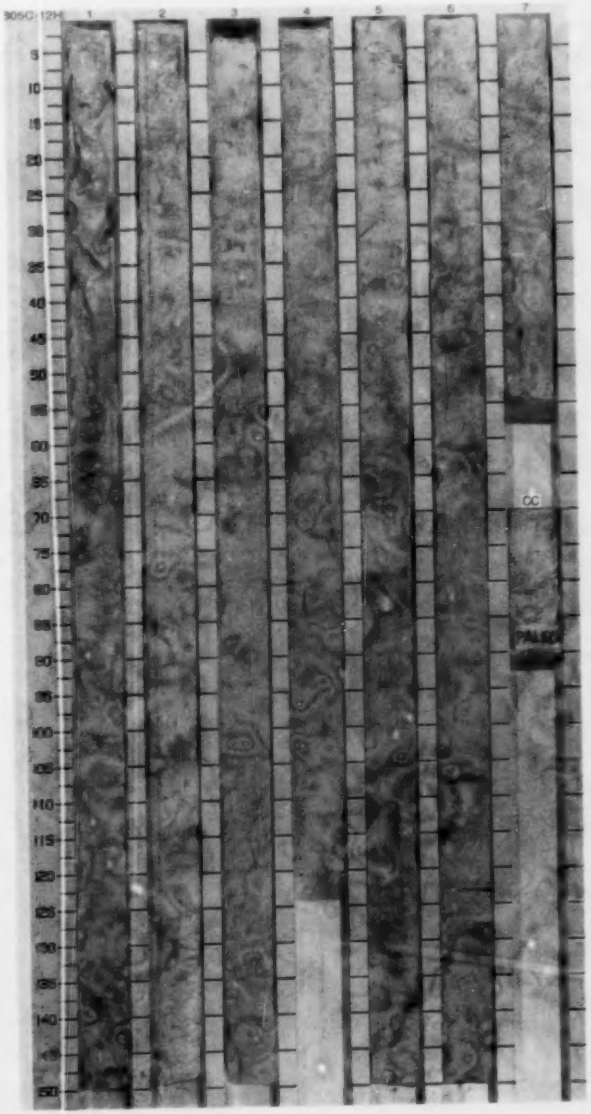
805C-12H
1
2
3
4
5
6
7
5
10
15
20
25
30
35
40
45
50
55
60
65
70
75
80
85
90
95
100
105
110
115
120
125
130
135
140
145
150
OC
PALEO

SITE 805 HOLE C CORE 13H CORED INTERVAL 112.3-121.8 mbsf

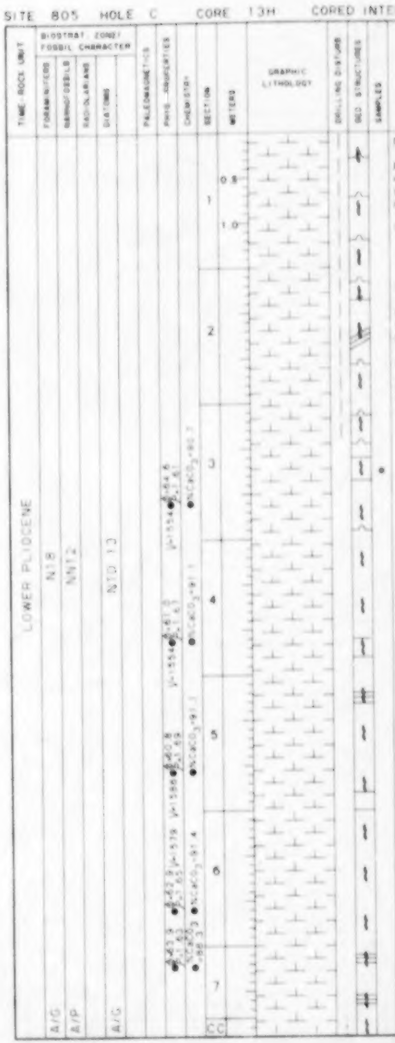
TIME-ROCK UNIT
BIOSTRAT. ZONE/ FOSSIL CHARACTER
FORAMINIFERS
NANNOFOSSILS
RADIOLARIANS
DIATOMS
PALEOMAGNETICS
PHYS. PROPERTIES
CHEMISTRY
SECTION
METERS
GRAPHIC LITHOLOGY
DRILLING DISTURB.
SED. STRUCTURES
SAMPLES
LOWER PLIOCENE
N18
NN12
NTD 13
A/G
A/P
A/G
V=1554 φ=64.6 γ=1.61
%CaCO3=90.7
V=1554 φ=61.0 γ=1.67
%CaCO3=91.1
V=1586 φ=60.8 γ=1.69
%CaCO3=91.1
φ=62.9 γ=1.65 V=1579
%CaCO3=91.4
φ=63.9 γ=1.63
%CaCO3=88.3
1
2
3
4
5
6
7
CC
0.5
1.0

LITHOLOGIC DESCRIPTION

NANNOFOSSIL OOZE

Major lithology: This core contains white (2.5Y 8/0) NANNOFOSSIL OOZE. The core is moderately bioturbated, as indicated by pale purple (5P 6/2), light gray (5Y 7/2) and grayish blue (5PB 5/2) mottling and burrow fill. Diffuse pale purple (5P 6/2), light gray (5Y 7/2), and light greenish gray (5G 7/1) color bands also are present.

SMEAR SLIDE SUMMARY (%)

	3, 75
	D
TEXTURE	
Sand	1
Silt	95
Clay	4
COMPOSITION	
Foraminifers	5
Nannofossils	94
Spicules	1

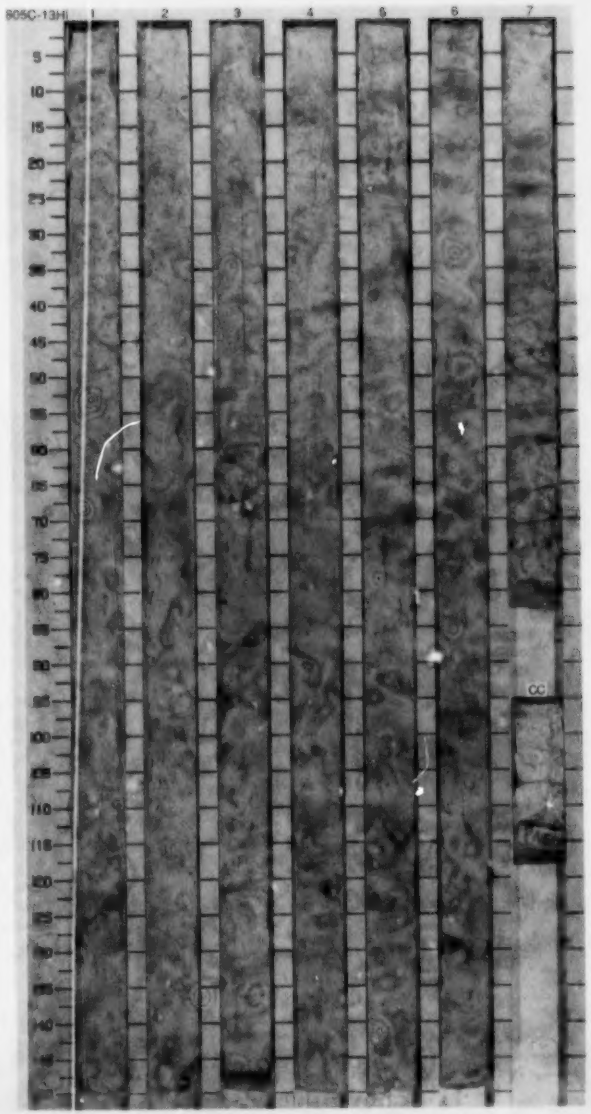
805C-13H
1
2
3
4
5
6
7
CC
5
10
15
20
25
30
35
40
45
50
55
60
65
70
75
80
85
90
95
100
105
110
115
120
125
130
135
140
145

SITE 805 HOLE C CORE 14H CORED INTERVAL 121.8-131.3 mbsf

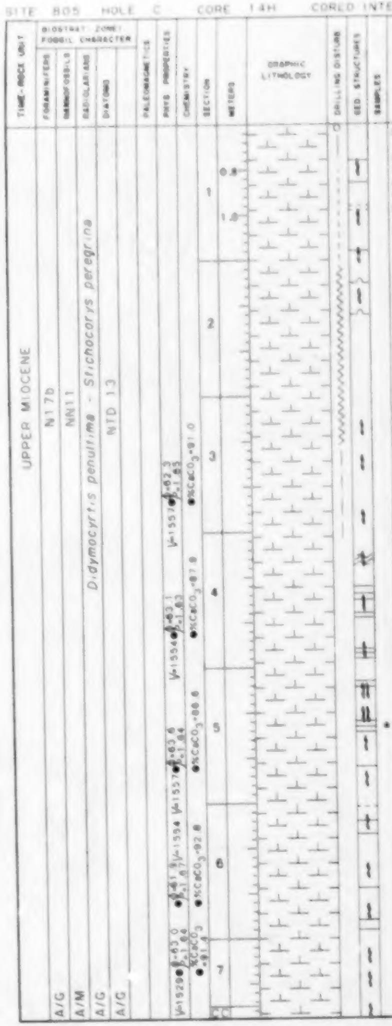
TIME-ROCK UNIT
BIOSTRAT. ZONE/ FOSSIL CHARACTER
FORAMINIFERS
NANNOFOSSILS
RADIOLARIANS
DIATOMS
PALEOMAGNETICS
PHYS. PROPERTIES
CHEMISTRY
SECTION
METERS
GRAPHIC LITHOLOGY
DRILLING DISTURB.
SED. STRUCTURES
SAMPLES
UPPER MIOCENE
N17b
NN11
Didymocyrtis penultima - Stichocorys peregrina
NTD 13
A/G
A/M
A/G
A/G
V=1557 φ=62.3 ρ=1.85
%CaCO3=91.0
V=1554 φ=63.1 ρ=1.83
%CaCO3=87.8
V=1557 φ=63.6 ρ=1.84
%CaCO3=88.6
V=1554 φ=61.9 ρ=1.87
%CaCO3=92.8
V=1520 φ=63.0 ρ=1.84
%CaCO3=91.4
1
2
3
4
5
6
7
CC
0.5
1.0
O

LITHOLOGIC DESCRIPTION

NANNOFOSSIL OOZE

Major lithology: This core contains white (2.5Y 8/0) NANNOFOSSIL OOZE. Section 2 to Section 3, 55 cm, is flow-in. Microfaulted color bands are present in Section 4, 20-40 cm. The core is moderately bioturbated, as indicated by pale purple (5P 6/2) and light gray (5Y 7/2) mottling and burrow fills. Diffuse pale purple (5P 6/2), light gray (5Y 7/2), and light greenish gray (5G 7/1) color bands are also present.

SMEAR SLIDE SUMMARY (%):

	5, 57
	D
TEXTURE:	
Sand	5
Silt	90
Clay	5
COMPOSITION:	
Foraminifers	5
Nannofossils	94
Radiolarians	1
Silicoflagellates	Tr

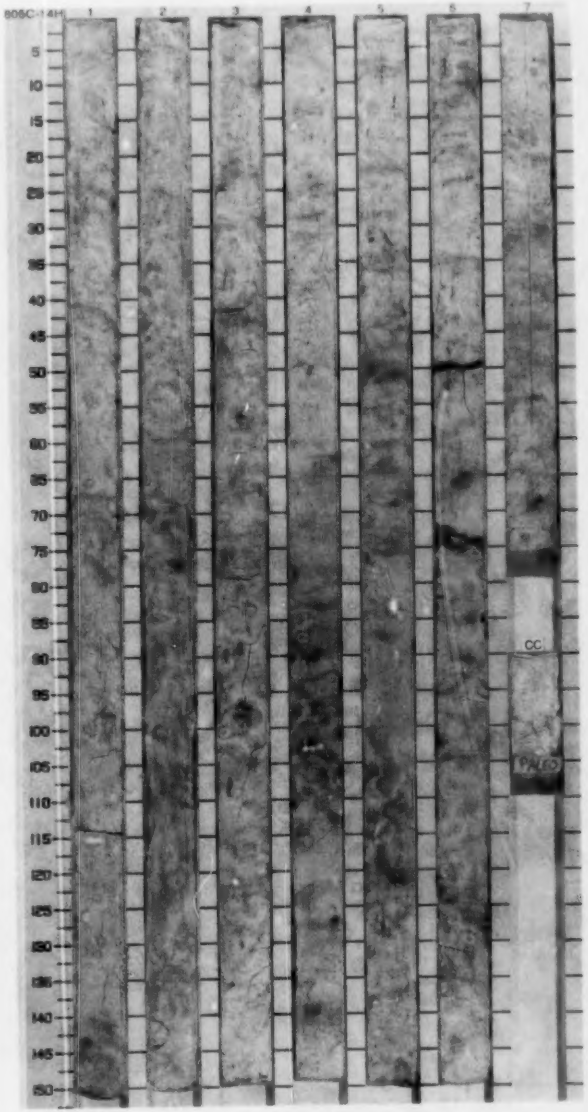
805C-14H
1
2
3
4
5
6
7
CC
PALEO
5
10
15
20
25
30
35
40
45
50
55
60
65
70
75
80
85
90
95
100
105
110
115
120
125
130
135
140
145
150

SITE 805 HOLE C CORE 15H CORED INTERVAL 131.3-140.8 mbsf

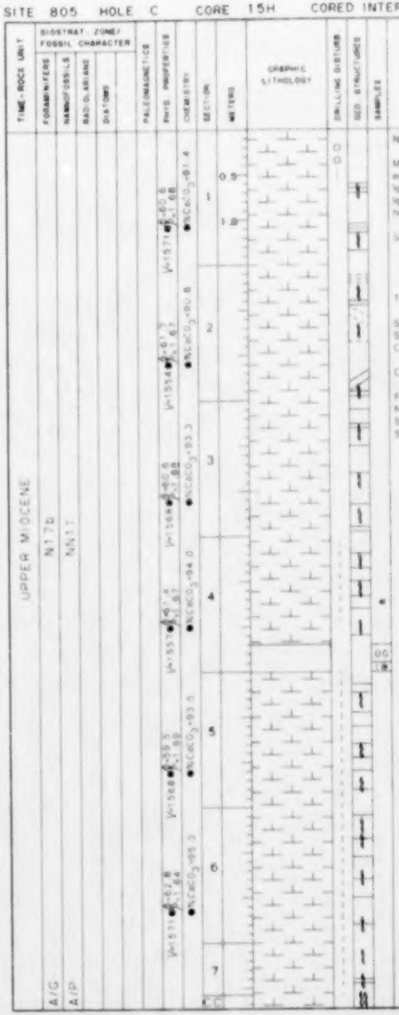

LITHOLOGIC DESCRIPTION

NANNOFOSSIL OOZE

Major lithology: This core contains white (2.5Y 8/0) NANNOFOSSIL OOZE. The core is moderately to heavily bioturbated, as indicated by pale purple (5P 6/2), pale yellow (2.5Y 7/4) and light gray (5Y 7/2) mottling and burrow fills. Diffuse pale purple (5P 6/2), light gray (5Y 7/2) and light greenish gray (5G 7/1) color bands, a few of which are steeply inclined and cross horizontal structures, are common.

SMEAR SLIDE SUMMARY (%):

	4, 78
	D
TEXTURE:	
Sand	1
Silt	95
Clay	4
COMPOSITION:	
Foraminifers	5
Nannofossils	94
Silicoflagellates	Tr
Spicules	1

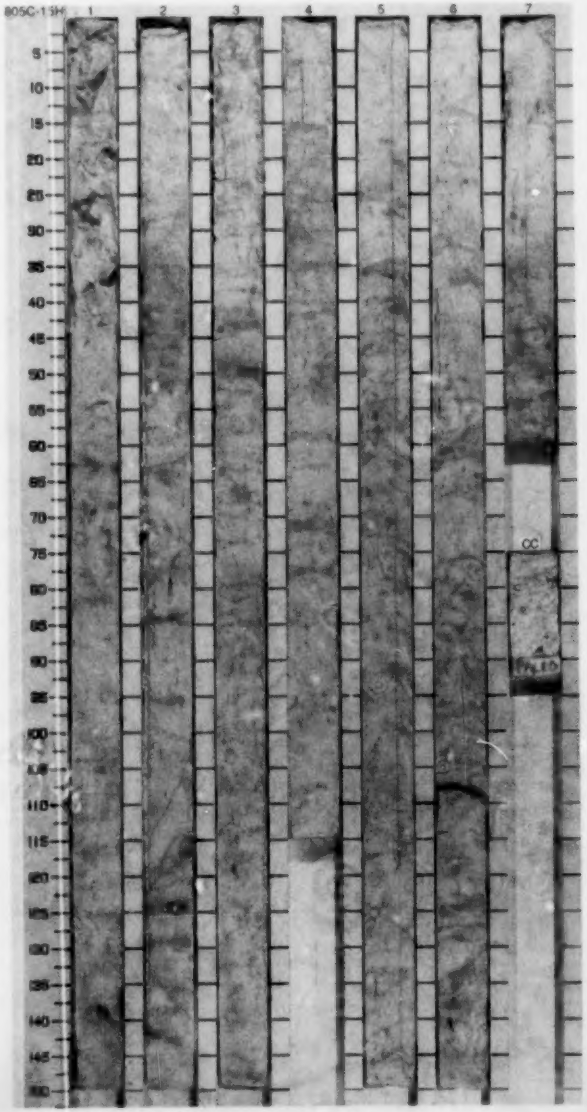
805C-15H
1
2
3
4
5
6
7
CC
5
10
15
20
25
30
35
40
45
50
55
60
65
70
75
80
85
90
95
100
105
110
115
120
125
130
135
140
145
150

SITE 805 HOLE C CORE 16H CORED INTERVAL 140.8-150.3 mbsf

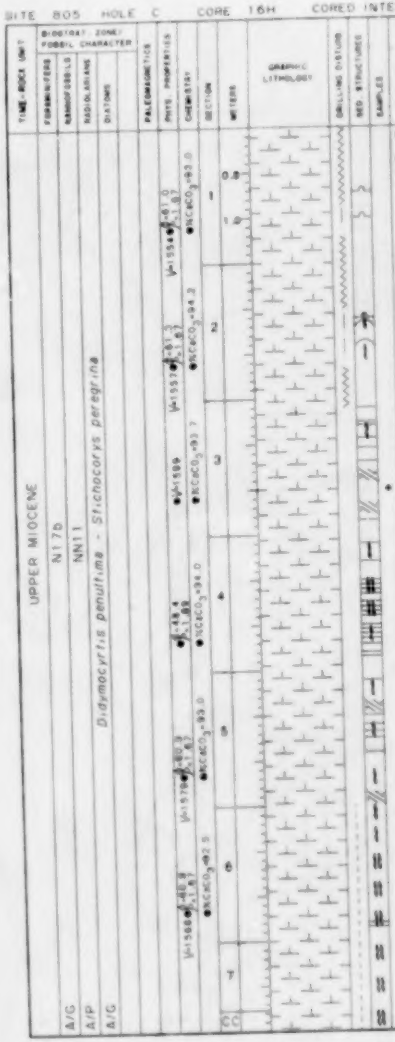
TIME-ROCK UNIT
BIOSTRAT. ZONE/ FOSSIL CHARACTER
FORAMINIFERS
NANNOFOSSILS
RADIOLARIANS
DIATOMS
PALEOMAGNETICS
PHYS. PROPERTIES
CHEMISTRY
SECTION
METERS
GRAPHIC LITHOLOGY
DRILLING DISTURB.
SED. STRUCTURES
SAMPLES
UPPER MIOCENE
N17b
NN11
Didymocyrtis penultima - Stichocorys peregrina
A/G
A/P
A/G
V=1554● φ=61.0 γ=1.87
●%CaCO3=93.0
V=1557● φ=61.3 γ=1.87
●%CaCO3=94.2
●V=1599
●%CaCO3=93.7
● φ=48.4 γ=1.88
●%CaCO3=94.0
V=1578● φ=60.9 γ=1.87
●%CaCO3=93.0
V=1560● φ=60.8 γ=1.87
●%CaCO3=92.5
1
2
3
4
5
6
7
CC
0.5
1.0

LITHOLOGIC DESCRIPTION

NANNOFOSSIL OOZE with FORAMINIFERS

Major lithology: This core contains white (2.5Y 8/0) NANNOFOSSIL OOZE with FORAMINIFERS. The sediment is moderately to heavily bioturbated, as indicated by light gray (5Y 7/2) and pale purple (5P 6/2) mottling and burrow fills. Pyritization of single burrows, and pale purple (5P 6/2) halos around burrows are seen. Diffuse pale purple (5P 6/2), light gray (5Y 7/2), light greenish gray (5G 7/1), and pale blue green (5BG 7/2) color bands are common. Microfaults often offset color bands.

SMEAR SLIDE SUMMARY (%):

	3, 100
	D
TEXTURE:	
Sand	15
Silt	80
Clay	5
COMPOSITION:	
Foraminifers	10
Nannofossils	85
Radiolarians	3
Silicoflagellates	2

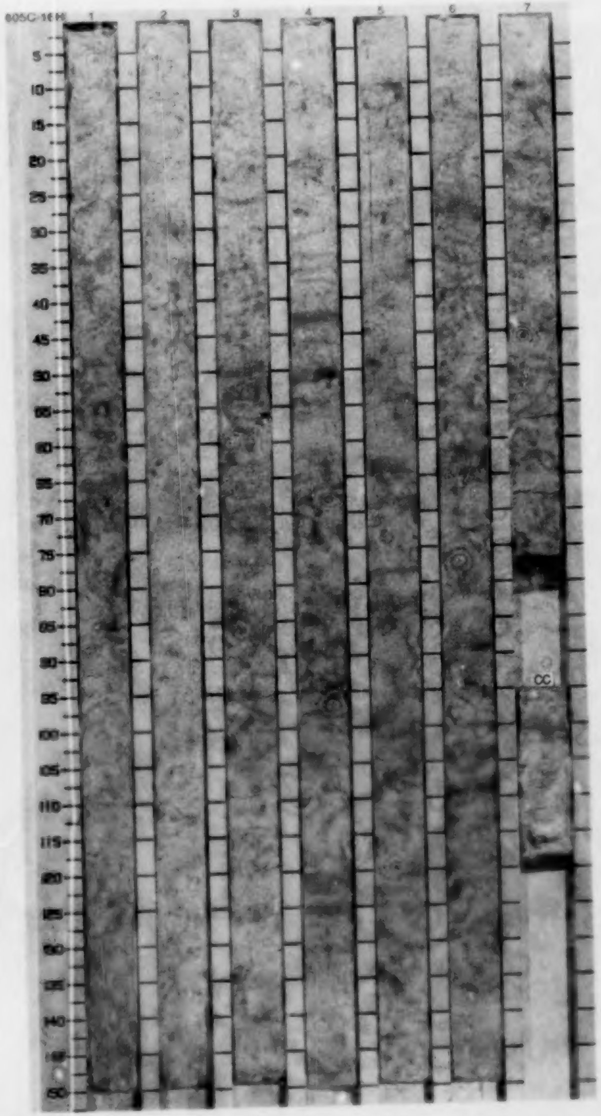
805C-16H
1
2
3
4
5
6
7
CC
5
10
15
20
25
30
35
40
45
50
55
60
65
70
75
80
85
90
95
100
105
110
115
120
125
130
135
140
145
150

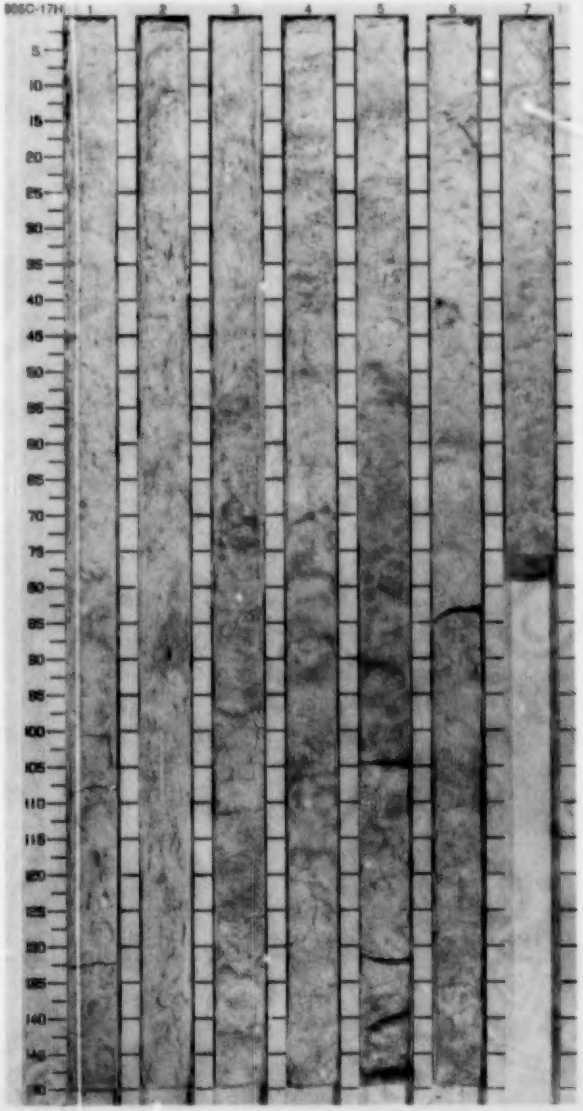
805C-17H
1
2
3
4
5
6
7
5
10
15
20
25
30
35
40
45
50
55
60
65
70
75
80
85
90
95
100
105
110
115
120
125
130
135
140
145
150

SITE 805 HOLE C CORE 17H CORED INTERVAL 150.3-159.8 mbsf

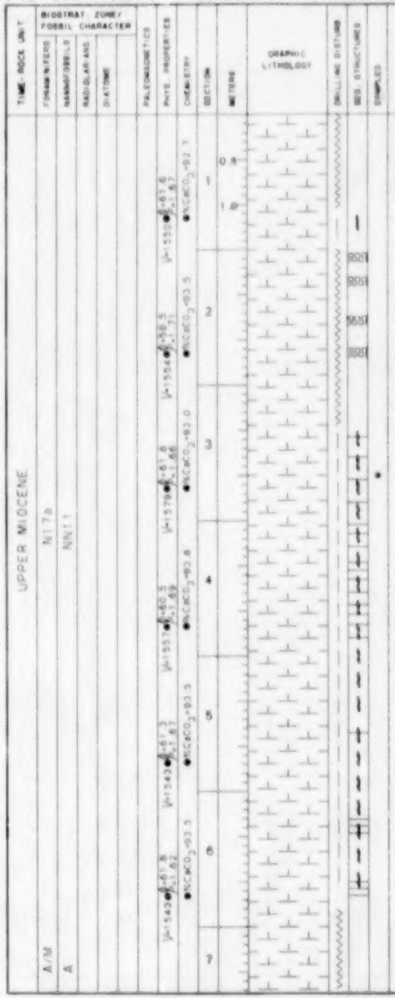
TIME-ROCK UNIT
BIOSTRAT. ZONE/ FOSSIL CHARACTER
FORAMINIFERS
NANNOFOSSILS
RADIOLARIANS
DIATOMS
PALEOMAGNETICS
PHYS. PROPERTIES
CHEMISTRY
SECTION
METERS
GRAPHIC LITHOLOGY
DRILLING DISTURB.
SED. STRUCTURES
SAMPLES
UPPER MIOCENE
N17a
NN11
A/M
A
0.5
1.0

SECTION	PHYS. PROPERTIES	CHEMISTRY
1	V=1550 φ=61.6 γ=1.67	%CaCO$_3$=92.7
2	V=1554 φ=58.5 γ=1.71	%CaCO$_3$=93.5
3	V=1579 φ=61.8 γ=1.66	%CaCO$_3$=93.0
4	V=1557 φ=60.5 γ=1.69	%CaCO$_3$=93.6
5	V=1543 φ=61.3 γ=1.67	%CaCO$_3$=93.5
6	V=1543 φ=61.8 γ=1.62	%CaCO$_3$=93.5
7		

LITHOLOGIC DESCRIPTION

NANNOFOSSIL OOZE with FORAMINIFERS

Major lithology: This core contains white (2.5Y 8/0) NANNOFOSSIL OOZE with FORAMINIFERS. The sediment is slightly to heavily bioturbated and has light gray (5Y 7/2) and pale purple (5P 6/2) mottling. Diffuse pale purple (5P 6/2), very pale blue (5B 8/2), and grayish blue (5PB 5/2) color bands are present throughout the core and abundant in Section 4. Some color bands are microfaulted, but they may have been distorted during drilling.

SMEAR SLIDE SUMMARY (%):

	3, 100
	D
TEXTURE:	
Sand	30
Silt	65
Clay	5
COMPOSITION:	
Foraminifers	23
Nannofossils	73
Radiolarians	3
Silicoflagellates	1

SITE 805 HOLE C CORE 18H CORED INTERVAL 159.8-169.3 mbsf

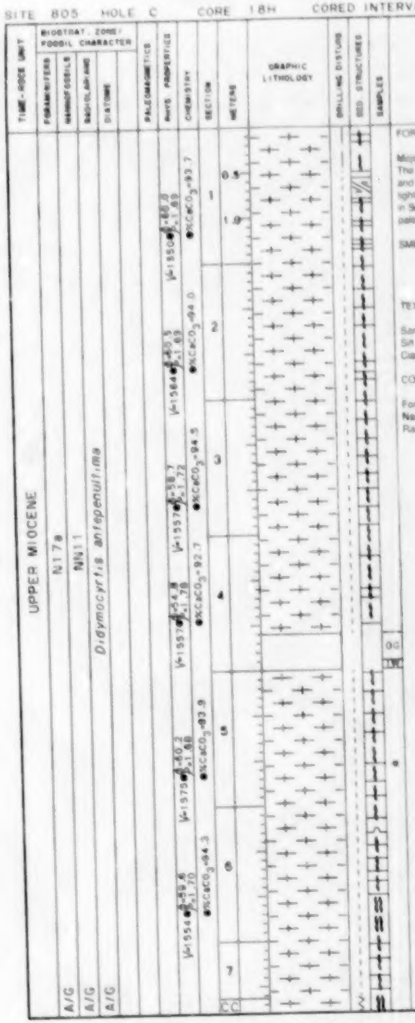

LITHOLOGIC DESCRIPTION

FORAMINIFERAL NANNOFOSSIL OOZE

Major lithology: This core contains white (2.5Y 8/0) FORAMINIFERAL NANNOFOSSIL OOZE. The sediment is slightly to heavily bioturbated and has light gray (5Y 7/2), pale purple (5P 6/2) and light olive brown (2.5Y 5/4) mottles. Diffuse pale purple (5P 6/2), pale blue (5PB 7/2), and light greenish gray (5G 7/1) color bands are present throughout the core. Some color bands in Section 1, 60-80 cm, are micro faulted. In Section 3, several large (about 7 cm in diameter), pale purple burrow halos are present.

SMEAR SLIDE SUMMARY (%):

	5, 107
	D
TEXTURE:	
Sand	30
Silt	68
Clay	2
COMPOSITION:	
Foraminifers	25
Nannofossils	70
Radiolarians	5

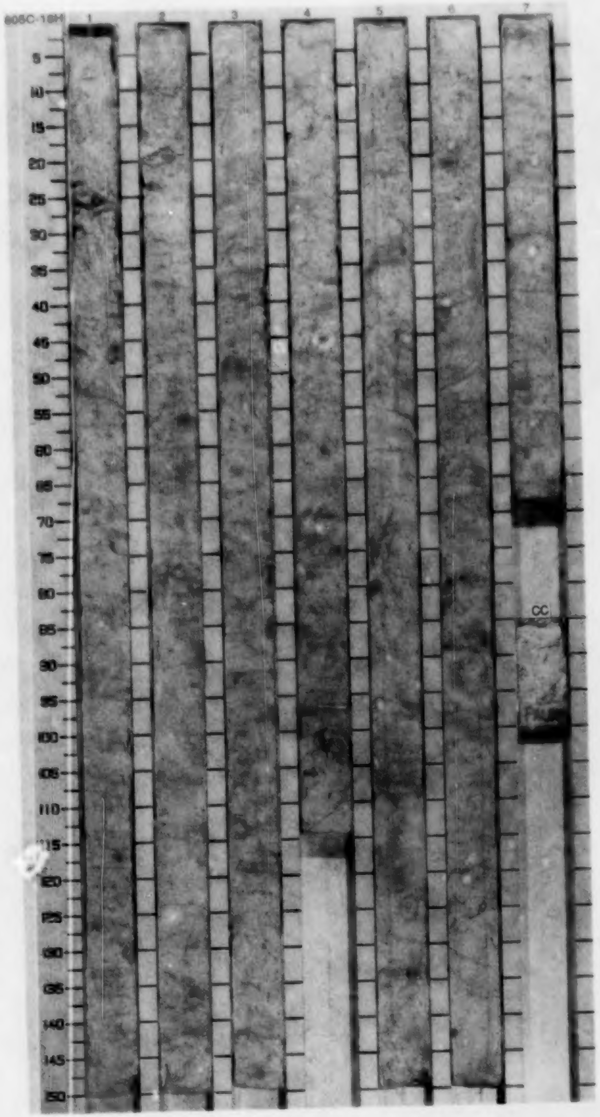
805C-18H
1
2
3
4
5
6
7
CC
5
10
15
20
25
30
35
40
45
50
55
60
65
70
75
80
85
90
95
100
105
110
115
120
125
130
135
140
145
150

SITE 805 HOLE C CORE 19H CORED INTERVAL 169.3-178.8 mbsf

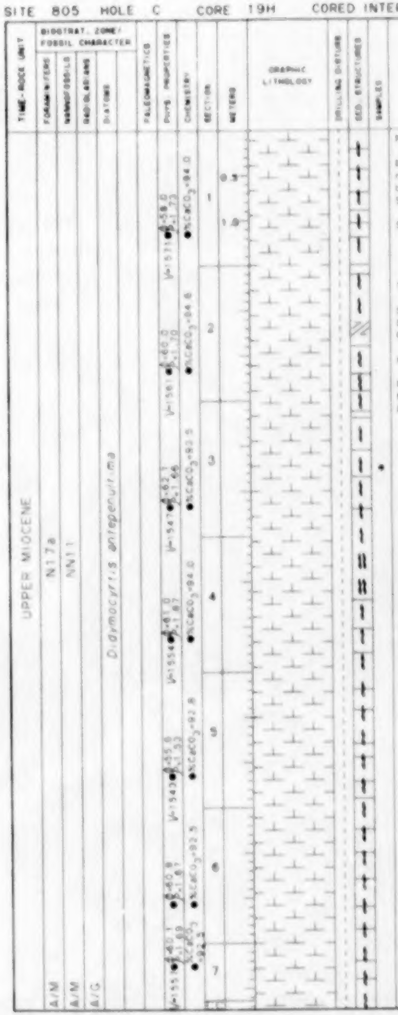
TIME-ROCK UNIT
BIOSTRAT. ZONE/ FOSSIL CHARACTER
FORAMINIFERS
NANNOFOSSILS
RADIOLARIANS
DIATOMS
PALEOMAGNETICS
PHYS. PROPERTIES
CHEMISTRY
SECTION
METERS
GRAPHIC LITHOLOGY
DRILLING DISTURB.
SED. STRUCTURES
SAMPLES
UPPER MIOCENE
N17a
NN11
Didymocyrtis antepenultima
A/M
A/M
A/G
V=1571 58.0 1.73
%CaCO3=94.0
V=1561 60.0 1.70
%CaCO3=94.6
V=1547 62.1 1.66
%CaCO3=93.5
V=1554 61.0 1.67
%CaCO3=94.0
V=1543 55.6 1.53
%CaCO3=92.8
60.8 1.67
%CaCO3=93.5
V=1553 60.1 1.69
%CaCO3=92.3
1
2
3
4
5
6
7
0.5
1.0

LITHOLOGIC DESCRIPTION

NANNOFOSSIL OOZE

Major lithology: This core contains white (2.5Y 8/0) NANNOFOSSIL OOZE. Bioturbation is moderate to heavy as indicated by abundant pale purple (5P 6/2) and light gray (5Y 7/2) burrow mottles. Diffuse pale purple (5P 6/2) color bands are present throughout the core. In Section 2, some of the bands are microfaulted.

SMEAR SLIDE SUMMARY (%):

	3, 75
	D
TEXTURE:	
Sand	7
Silt	68
Clay	25
COMPOSITION:	
Foraminifers	2
Nannofossils	93
Radiolarians	5

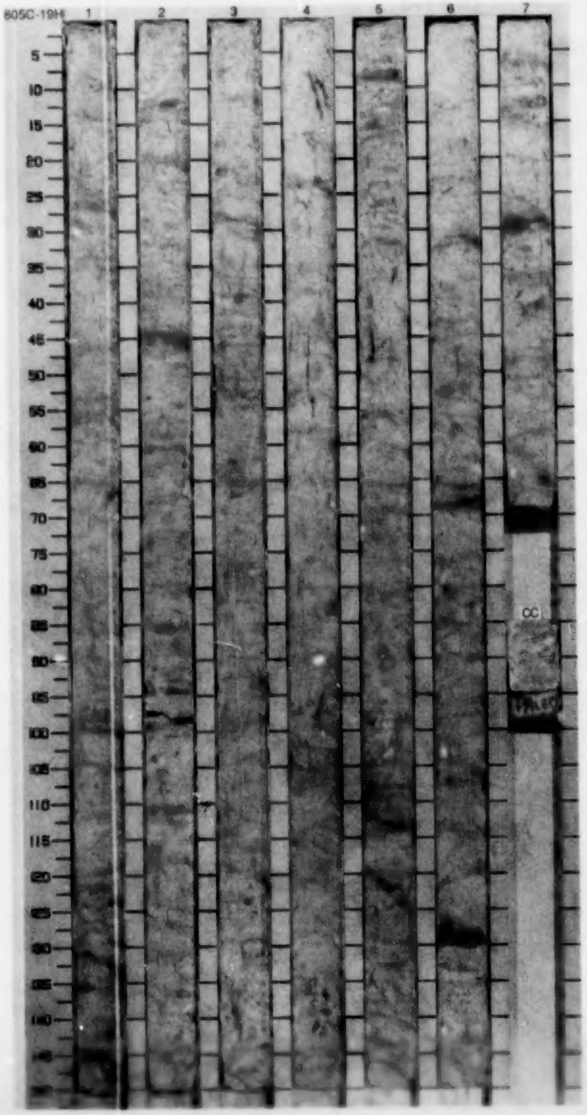
805C-19H
1
2
3
4
5
6
7
5
10
15
20
25
30
35
40
45
50
55
60
65
70
75
80
85
90
95
100
105
110
115
120
125
130
135
140
145
150
CC

SITE 805 HOLE C CORE 20H CORED INTERVAL 178.8-188.3 mbsf

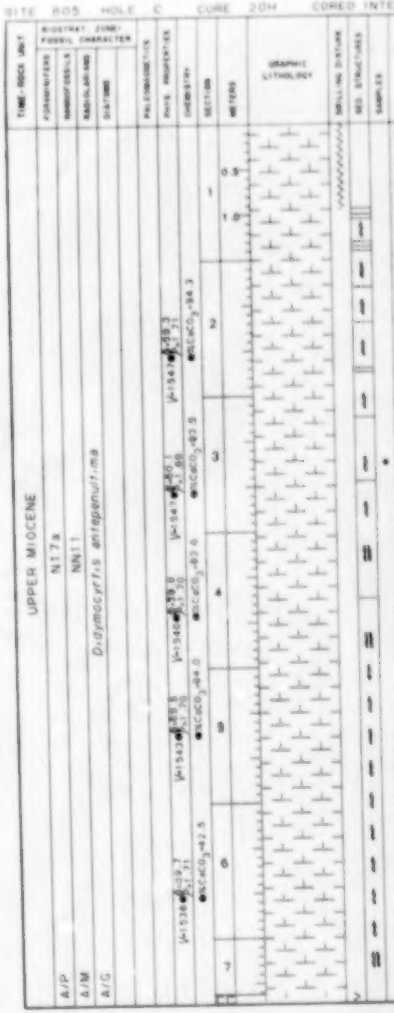
TIME-ROCK UNIT
BIOSTRAT. ZONE/ FOSSIL CHARACTER
FORAMINIFERS
NANNOFOSSILS
RADIOLARIANS
DIATOMS
PALEOMAGNETICS
PHYS. PROPERTIES
CHEMISTRY
SECTION
METERS
GRAPHIC LITHOLOGY
DRILLING DISTURB.
SED. STRUCTURES
SAMPLES
UPPER MIOCENE
N17a
NN11
Didymocyrtis antepenultima
A/P
A/M
A/G
Vp=1547 φ=58.3 γ=1.71
Vp=1547 φ=60.1 γ=1.69
Vp=1540 φ=59.8 γ=1.70
Vp=1543 φ=58.8 γ=1.70
Vp=1536 φ=59.7 γ=1.71
%CaCO3=94.3
%CaCO3=93.5
%CaCO3=93.0
%CaCO3=94.0
%CaCO3=92.5
0.5
1.0
1
2
3
4
5
6
7
CC

LITHOLOGIC DESCRIPTION

NANNOFOSSIL OOZE

Major lithology: This core contains homogeneous white (2.5Y 8/0) NANNOFOSSIL OOZE. Reddish gray (5R 6/2) specks, streaks, and subhorizontal, 5 to 15 mm thick, color bands are abundant. The ooze is bioturbated and contains pyritic burrow fills.

SMEAR SLIDE SUMMARY (%):

	3, 75
	D
TEXTURE	
Sand	3
Silt	47
Clay	50
COMPOSITION	
Diatoms	3
Foraminifers	5
Nannofossils	89
Radiolarians	1
Siliceous fragments	2

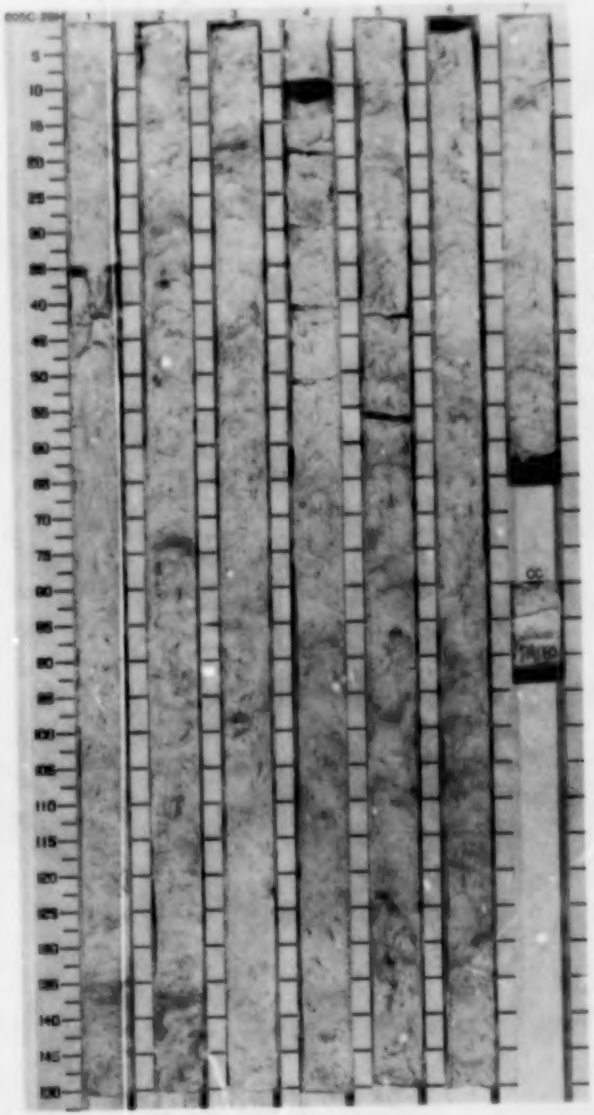
805C-20H
1
2
3
4
5
6
7
CC
5
10
15
20
25
30
35
40
45
50
55
60
65
70
75
80
85
90
95
100
105
110
115
120
125
130
135
140
145
150

SITE 805 HOLE C CORE 21H CORED INTERVAL 188.3-197.8 mbsf

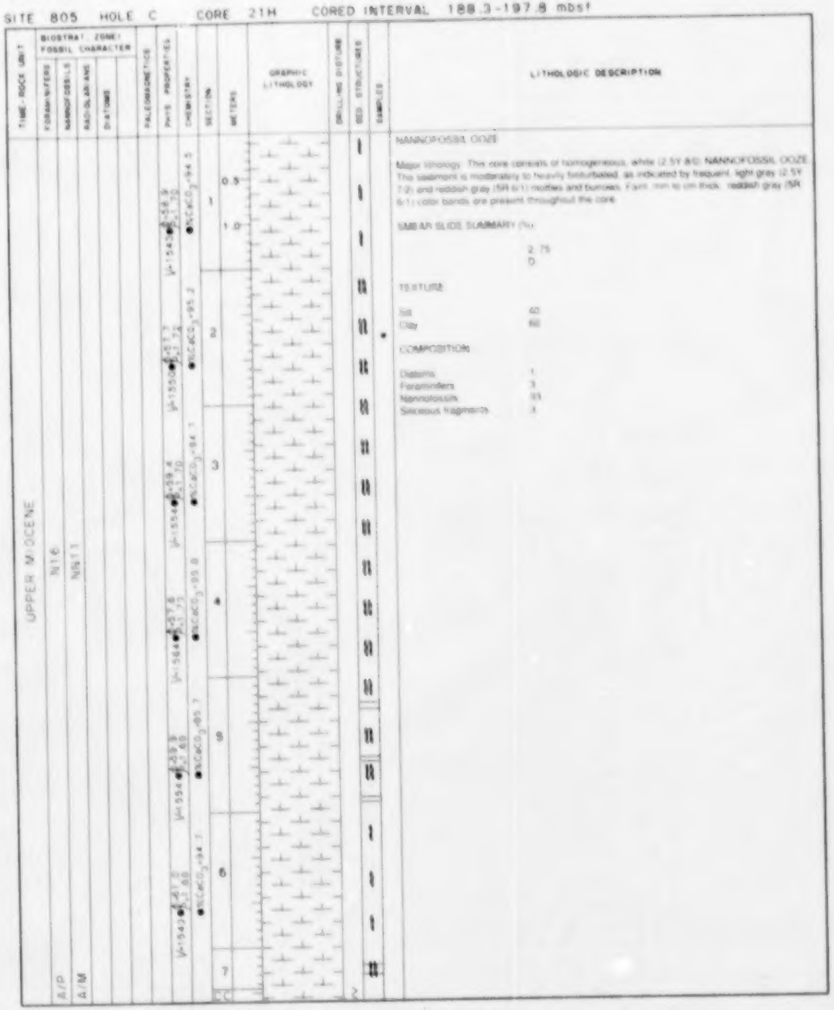
TIME-ROCK UNIT
BIOSTRAT. ZONE/ FOSSIL CHARACTER
FORAMINIFERS
NANNOFOSSILS
RADIOLARIANS
DIATOMS
PALEOMAGNETICS
PHYS. PROPERTIES
CHEMISTRY
SECTION
METERS
GRAPHIC LITHOLOGY
DRILLING DISTURB.
SED. STRUCTURES
SAMPLES
UPPER MIOCENE
N16
NN11
A/P
A/M
V=1543 φ=58.9 γ=1.70
%CaCO3=94.5
V=1550 φ=61.7 γ=1.72
%CaCO3=95.2
V=1554 φ=59.4 γ=1.70
%CaCO3=94.1
V=1564 φ=57.6 γ=1.73
%CaCO3=95.0
V=1554 φ=59.9 γ=1.68
%CaCO3=95.7
V=1543 φ=61.0 γ=1.68
%CaCO3=94.7
1
2
3
4
5
6
7
CC
0.5
1.0

LITHOLOGIC DESCRIPTION

NANNOFOSSIL OOZE

Major lithology: This core consists of homogeneous, white (2.5Y 8/0) NANNOFOSSIL OOZE. The sediment is moderately to heavily bioturbated, as indicated by frequent, light gray (2.5Y 7/2) and reddish gray (5R 6/1) mottles and burrows. Faint, mm to cm thick, reddish gray (5R 6/1) color bands are present throughout the core.

SMEAR SLIDE SUMMARY (%):

	2, 75
	D
TEXTURE:	
Silt	40
Clay	60
COMPOSITION:	
Diatoms	1
Foraminifers	3
Nannofossils	93
Siliceous fragments	3

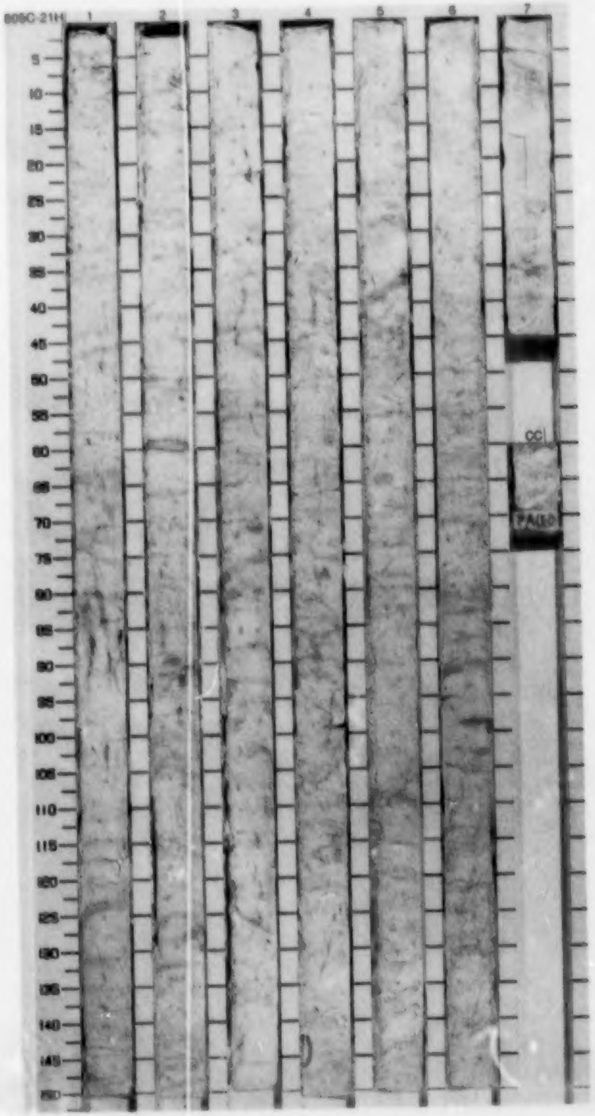
805C-21H
1
2
3
4
5
6
7
CC
PAL(L)
5
10
15
20
25
30
35
40
45
50
55
60
65
70
75
80
85
90
95
100
105
110
115
120
125
130
135
140
145
150

SITE 805 HOLE C CORE 22H CORED INTERVAL 197.8-207.3 mbsf

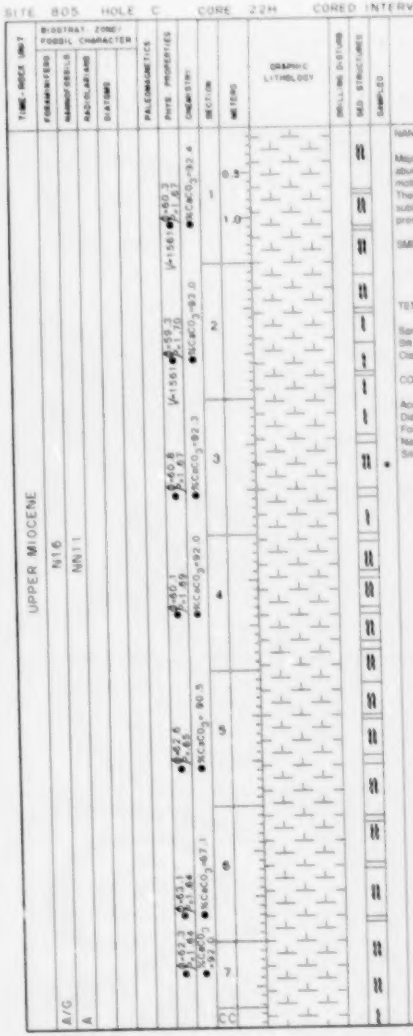

LITHOLOGIC DESCRIPTION

NANNOFOSSIL OOZE

Major lithology: This core consists of homogeneous, white, NANNOFOSSIL OOZE with abundant reddish gray (5R 6/1) and pale purple (5P 6/2) mottling. Light gray (2.5Y 7/2) mottles, up to several cm in diameter, and pyritized specks and trace fossils are also evident. These features are indicative of moderate to heavy bioturbation. Some faint, cm scale subhorizontal, pale purple (5P 6/2) and pale yellowish green (10GY 7/2) color banding is present.

SMEAR SLIDE SUMMARY (%):

	3, 74
	D
TEXTURE:	
Sand	0
Silt	60
Clay	32
COMPOSITION:	
Accessory minerals	1
Diatoms	Tr
Foraminifers	8
Nannofossils	89
Siliceous fragments	2

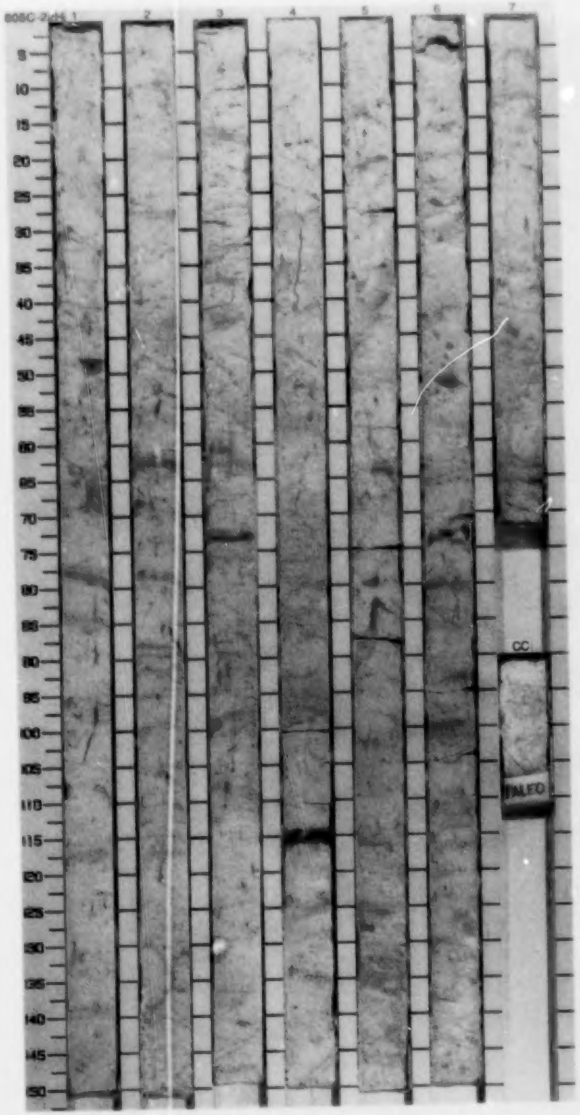
805C-22H 1
2
3
4
5
6
7
CC
PALEO
5
10
15
20
25
30
35
40
45
50
55
60
65
70
75
80
85
90
95
100
105
110
115
120
125
130
135
140
145
150

SITE 805 HOLE C CORE 23H CORED INTERVAL 207.3-216.8 mbsf

TIME-ROCK UNIT	BIOSTRAT. ZONE/ FOSSIL CHARACTER					PALEOMAGNETICS	PHYS. PROPERTIES	CHEMISTRY	SECTION	METERS	GRAPHIC LITHOLOGY	DRILLING DISTURB.	SED. STRUCTURES	SAMPLES	LITHOLOGIC DESCRIPTION
	FORAMINIFERS	NANNOFOSSILS	RADIOLARIANS	DIATOMS											
UPPER MIOCENE	N16 A/M	NN11 A/M					● ϕ-62.3 γ-1.65 V_p-1580 V_p-1569 ● ϕ-64.5 γ-1.59	● %CaCO$_3$-93.9 ● %CaCO$_3$-87.2	1 2	0.5 1.0			‖ ‖ ‖	●	NANNOFOSSIL OOZE with FORAMINIFERS

Major lithology: The core consists of homogeneous, white NANNOFOSSIL OOZE with FORAMINIFERS. Abundant reddish gray (5R 6/1) and pale purple (5P 6/2) mottling is present. Some mottles are semi-lithified.

SMEAR SLIDE SUMMARY (%):

	2, 31 D
TEXTURE:	
Sand	10
Silt	60
Clay	30
COMPOSITION:	
Accessory minerals	1
Diatoms	Tr
Foraminifers	15
Nannofossils	82
Siliceous fragments	2

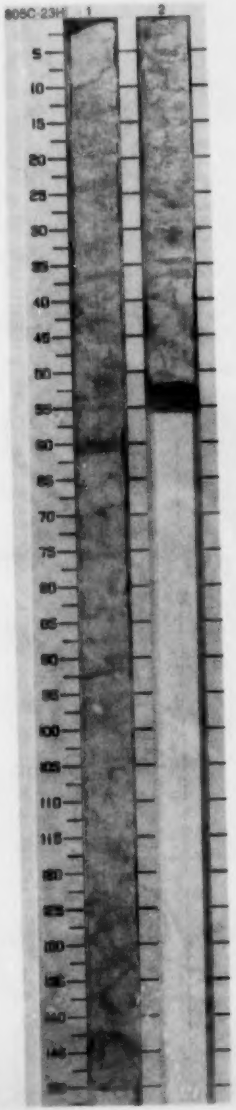
805C-23H
1
2
5
10
15
20
25
30
35
40
45
50
55
60
65
70
75
80
85
90
95
100
105
110
115
120
125
130
135
140
145
150

SITE 805 HOLE C CORE 24H CORED INTERVAL 216.8-226.3 mbsf

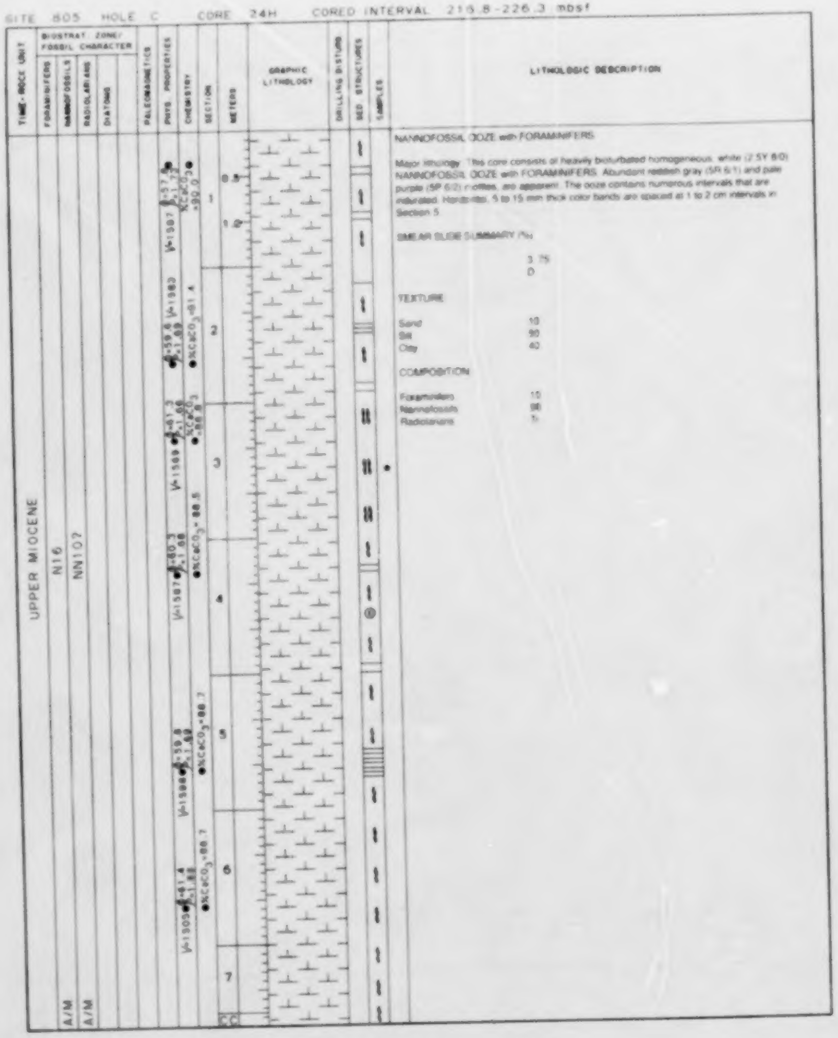
TIME-ROCK UNIT
BIOSTRAT. ZONE/ FOSSIL CHARACTER
FORAMINIFERS
NANNOFOSSILS
RADIOLARIANS
DIATOMS
PALEOMAGNETICS
PHYS. PROPERTIES
CHEMISTRY
SECTION
METERS
GRAPHIC LITHOLOGY
DRILLING DISTURB.
SED. STRUCTURES
SAMPLES
UPPER MIOCENE
N16
NN10?
A/M
A/M
V=1507
φ=57.?
γ=1.72
%CaCO3 =90.0
φ=59.6
γ=1.69
V=1983
%CaCO3=91.4
V=1569
φ=61.3
γ=1.66
%CaCO3 =88.8
%CaCO3=88.5
V=1587
φ=60.3
γ=1.68
V=1588
φ=59.8
γ=1.69
%CaCO3=88.7
V=1505
φ=61.4
γ=1.68
%CaCO3=88.7
1
2
3
4
5
6
7
CC
0.5
1.0

LITHOLOGIC DESCRIPTION

NANNOFOSSIL OOZE with FORAMINIFERS

Major lithology: This core consists of heavily bioturbated homogeneous, white (2.5Y 8/0) NANNOFOSSIL OOZE with FORAMINIFERS. Abundant reddish gray (5R 6/1) and pale purple (5P 6/2) mottles, are apparent. The ooze contains numerous intervals that are indurated. Horizontal, 5 to 15 mm thick color bands are spaced at 1 to 2 cm intervals in Section 5.

SMEAR SLIDE SUMMARY (%):

	3, 75
	D
TEXTURE:	
Sand	10
Silt	50
Clay	40
COMPOSITION:	
Foraminifers	10
Nannofossils	90
Radiolarians	Tr

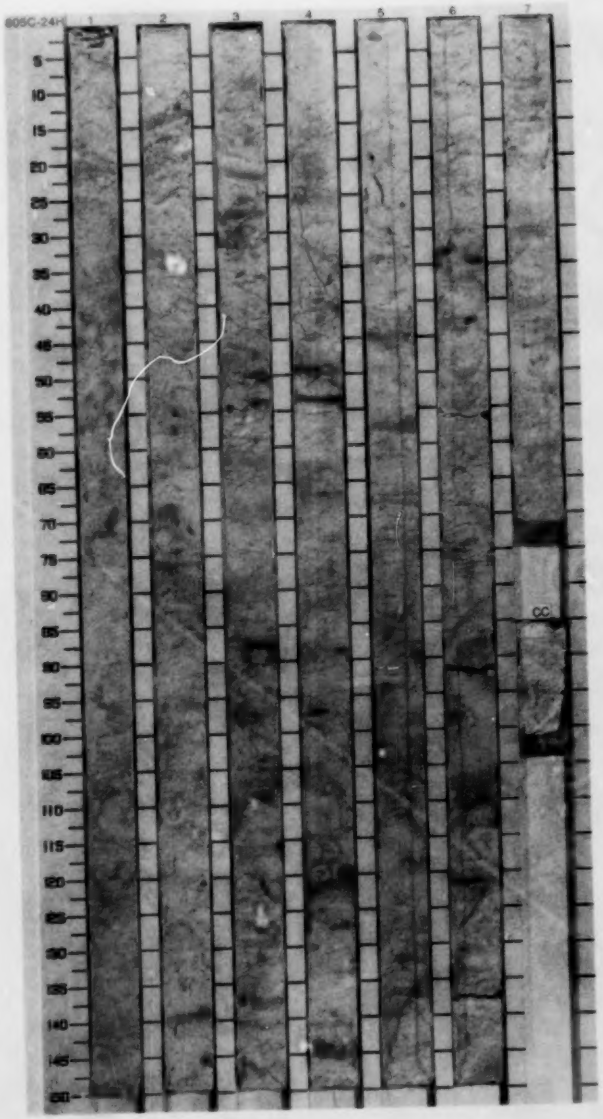
805C-24H
1
2
3
4
5
6
7
CC
5
10
15
20
25
30
35
40
45
50
55
60
65
70
75
80
85
90
95
100
105
110
115
120
125
130
135
140
145
150

SITE 805 HOLE C CORE 25H CORED INTERVAL 226.3-235.8 mbsf

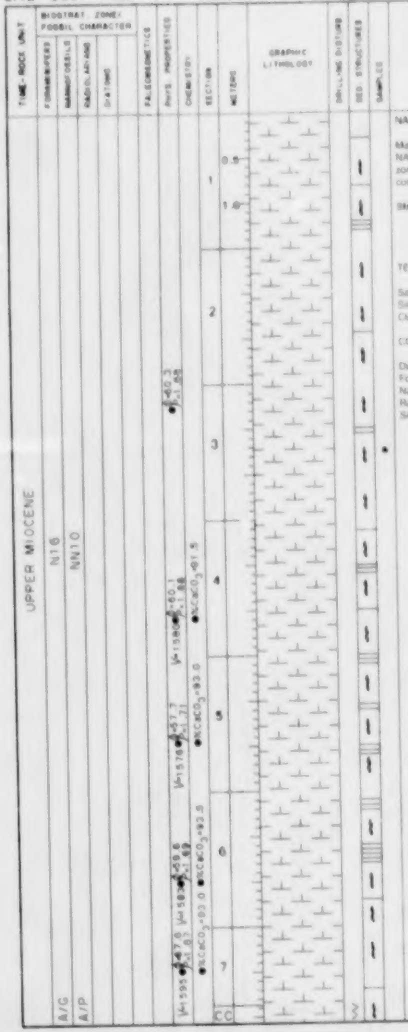
TIME-ROCK UNIT
BIOSTRAT. ZONE/ FOSSIL CHARACTER
FORAMINIFERS
NANNOFOSSILS
RADIOLARIANS
DIATOMS
PALEOMAGNETICS
PHYS. PROPERTIES
CHEMISTRY
SECTION
METERS
GRAPHIC LITHOLOGY
DRILLING DISTURB.
SED. STRUCTURES
SAMPLES
UPPER MIOCENE
N16
NN10
A/G
A/P
φ=60.3
γ=1.88
V=1580
φ=60.1
γ=1.88
V=1578
φ=57.7
γ=1.71
V=1583
φ=59.6
γ=1.69
V=1595
φ=47.6
γ=1.87
%CaCO3=91.5
%CaCO3=93.0
%CaCO3=93.5
%CaCO3=93.0
1
2
3
4
5
6
7
CC
0.5
1.0

LITHOLOGIC DESCRIPTION

NANNOFOSSIL OOZE with FORAMINIFERS

Major lithology: This core consists of heavily bioturbated, homogeneous, white (2.5Y 8/0) NANNOFOSSIL OOZE with FORAMINIFERS. The ooze contains numerous semi-lithified zones that commonly take the form of nodules. Reddish gray (5R 6/2) color bands are common.

SMEAR SLIDE SUMMARY (%):

	3, 75
	D
TEXTURE:	
Sand	3
Silt	57
Clay	40
COMPOSITION:	
Diatoms	3
Foraminifers	10
Nannofossils	85
Radiolarians	Tr
Siliceous fragments	2

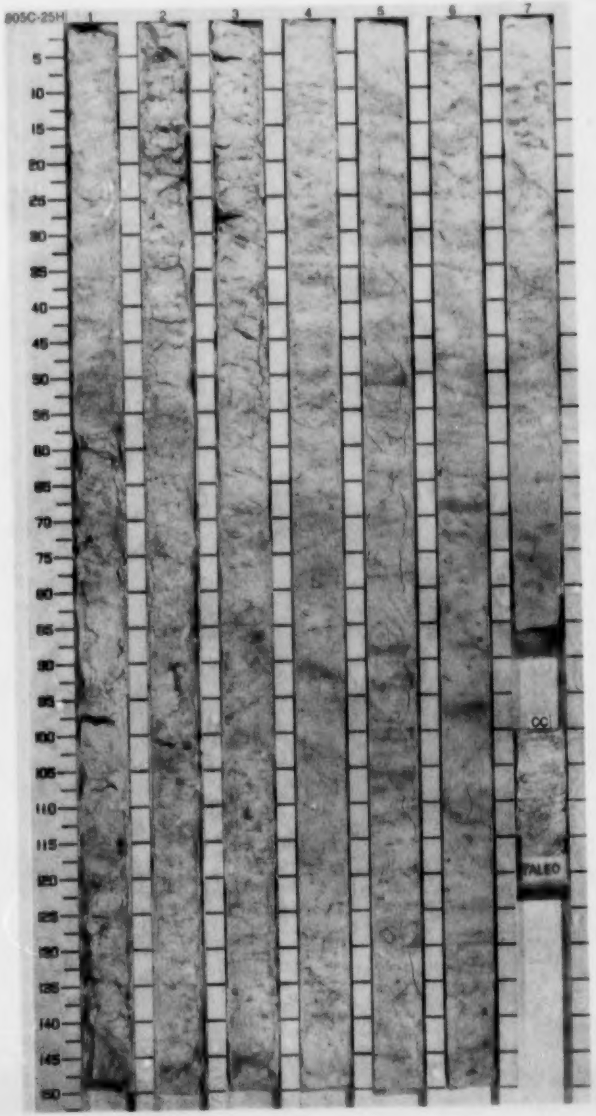
805C-25H
1
2
3
4
5
6
7
5
10
15
20
25
30
35
40
45
50
55
60
65
70
75
80
85
90
95
100
105
110
115
120
125
130
135
140
145
150
CC
PALEO

SITE 805 HOLE C CORE 26X CORED INTERVAL 235.8-245.4 mbsf

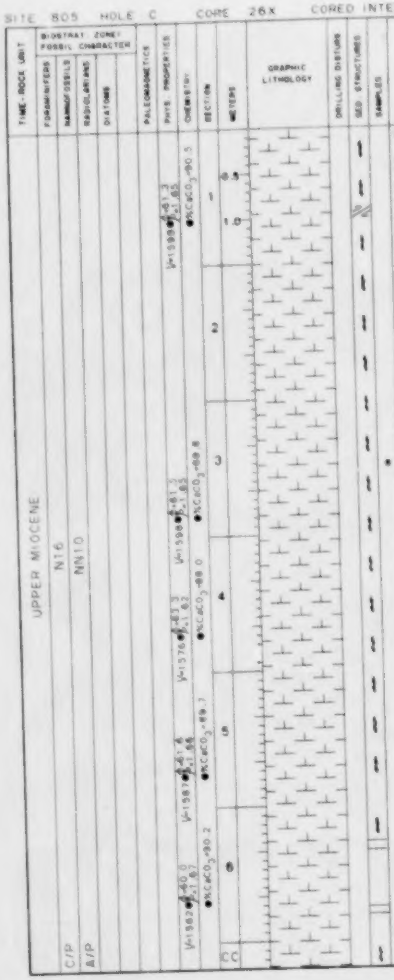
TIME-ROCK UNIT
BIOSTRAT. ZONE/ FOSSIL CHARACTER
FORAMINIFERS
NANNOFOSSILS
RADIOLARIANS
DIATOMS
PALEOMAGNETICS
PHYS. PROPERTIES
CHEMISTRY
SECTION
METERS
GRAPHIC LITHOLOGY
DRILLING DISTURB.
SED. STRUCTURES
SAMPLES
UPPER MIOCENE
N16
NN10
C/P
A/P
V=1599 φ=61.3 γ=1.85
%CaCO3=90.5
V=1598 φ=61.5 γ=1.85
%CaCO3=89.8
V=1576 φ=63.3 γ=1.82
%CaCO3=88.0
V=1587 φ=61.6 γ=1.86
%CaCO3=89.7
V=1562 φ=60.0 γ=1.87
%CaCO3=90.2
1
2
3
4
5
6
CC
0.5
1.0

LITHOLOGIC DESCRIPTION

NANNOFOSSIL OOZE with FORAMINIFERS

Major lithology: This core contains white (2.5Y 8/0) NANNOFOSSIL OOZE with FORAMINIFERS. The ooze consists of semi-lithified nodules, each several cm thick, intercalated with softer sediment. No lithologic difference between the semi-lithified nodules and the softer sediment is noticeable, and color bands often pass continuously between the two. Color bands are apparent as diffuse zones of reddish gray (5R 6/1) and pale purple (5P 6/2). Light gray (2.5Y 7/2) pyritized burrows and mottles indicate pervasive bioturbation.

SMEAR SLIDE SUMMARY (%):

	3, 75 D
TEXTURE:	
Sand	10
Silt	55
Clay	35
COMPOSITION:	
Diatoms	2
Foraminifers	12
Nannofossils	86
Radiolarians	Tr
Siliceous fragments	Tr

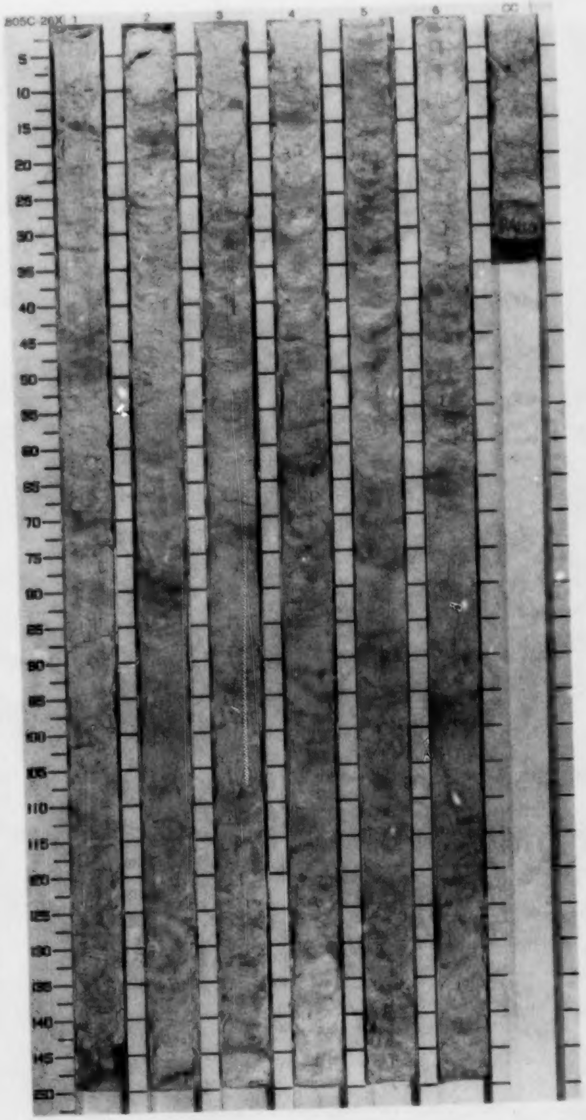
805C-26X
1
2
3
4
5
6
CC
5
10
15
20
25
30
35
40
45
50
55
60
65
70
75
80
85
90
95
100
105
110
115
120
125
130
135
140
145
150

SITE 805 HOLE C CORE 27x CORED INTERVAL 245.4-255.1 mbsf

TIME-ROCK UNIT	BIOSTRAT. ZONE/ FOSSIL CHARACTER					PALEOMAGNETICS	PHYS. PROPERTIES	CHEMISTRY	SECTION	METERS	GRAPHIC LITHOLOGY	DRILLING DISTURB.	SED. STRUCTURES	SAMPLES	LITHOLOGIC DESCRIPTION
	FORAMINIFERS	NANNOFOSSILS	RADIOLARIANS	DIATOMS											
UPPER MIOCENE	A/M N16	A/P NN10					● ϕ=59.6 V=1578 γ=1.68	● %CaCO$_3$=90.3	1 CC	0.5 1.0					NANNOFOSSIL OOZE with FORAMINIFERS Major lithology: This core contains white (2.5Y 8/0) NANNOFOSSIL OOZE with FORAMINIFERS. The ooze is composed of semi-lithified, nodules or beds, each several cm thick, intercalated with stiff ooze. Diffuse pale purple (5P6/2) color banding is common. Mottles indicate heavy bioturbation.

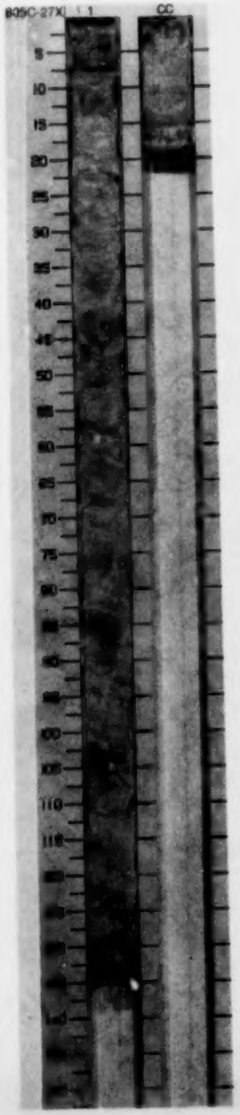

SITE 805 HOLE C CORE 28X CORED INTERVAL 255.1-264.7 mbsf

TIME-ROCK UNIT	BIOSTRAT. ZONE/ FOSSIL CHARACTER: FORAMINIFERS	NANNOFOSSILS	RADIOLARIANS	DIATOMS	PALEOMAGNETICS	PHYS. PROPERTIES	CHEMISTRY	SECTION	METERS	GRAPHIC LITHOLOGY	DRILLING DISTURB.	SED. STRUCTURES	SAMPLES
UPPER MIOCENE	N16	NN10				●φ-62.3 γ-1.58 V-1565		1	0.5 1.0				
						●φ-60.4 γ-1.67 V-1573	●%CaCO$_3$-93.4	2					
						●φ-41.0 γ-1.88 V-1570	●%CaCO$_3$-94.5	3					●
	C/M					●φ-56.7 γ-1.88 V-1583	●%CaCO$_3$-93.4	4					●
MIDDLE MIOCENE	N14							5					
	A/M	A				●φ-58.1 γ-1.72 V-1555	●%CaCO$_3$-91.6	6					
								CC					

LITHOLOGIC DESCRIPTION

NANNOFOSSIL OOZE

Major lithology: This core contains white (2.5Y 8/0), stiff to semi-lithified NANNOFOSSIL OOZE. The semi-lithified sediments dominate the sequence and appear as nodules or interbeds. The sediment is relatively homogeneous although some indistinct pale purple (5P 6/2) color banding is present. Rare mottles (light gray 2.5Y 7/2) and disseminated pyrite specks also are present. A bioturbated ash layer is located at Section 4, 68-71 cm.

SMEAR SLIDE SUMMARY (%):

	3, 74	4, 69
	D	M
TEXTURE		
Sand	5	25
Silt	65	50
Clay	30	25
COMPOSITION		
Accessory minerals	1	Tr
Diatoms	Tr	Tr
Foraminifers	6	3
Glass	—	55
Nannofossils	85	40
Radiolarians	5	Tr
Siliceous fragments	2	2

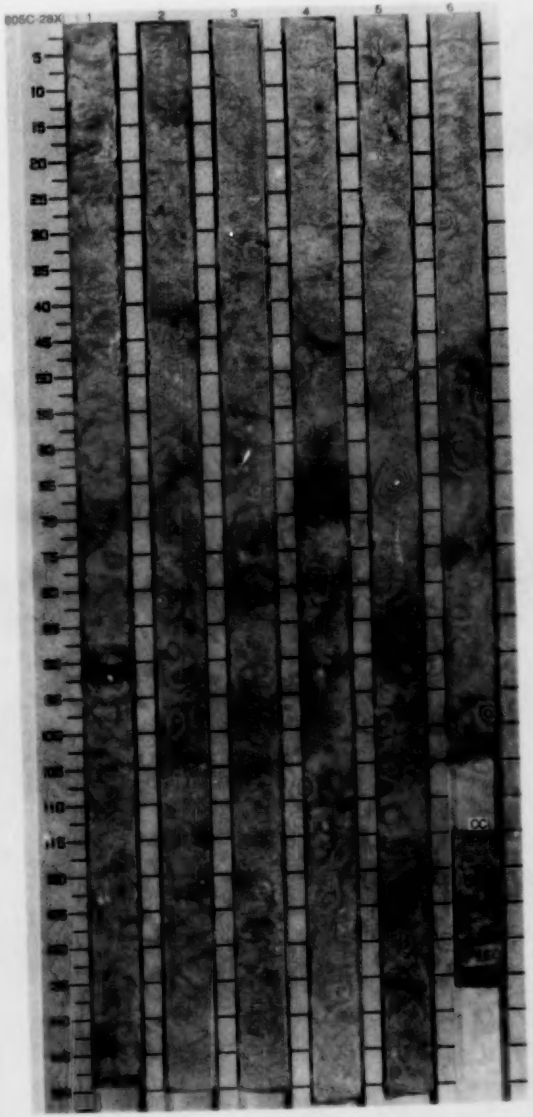

SITE 805 HOLE C CORE 29X CORED INTERVAL 264.7-274.4 mbsf

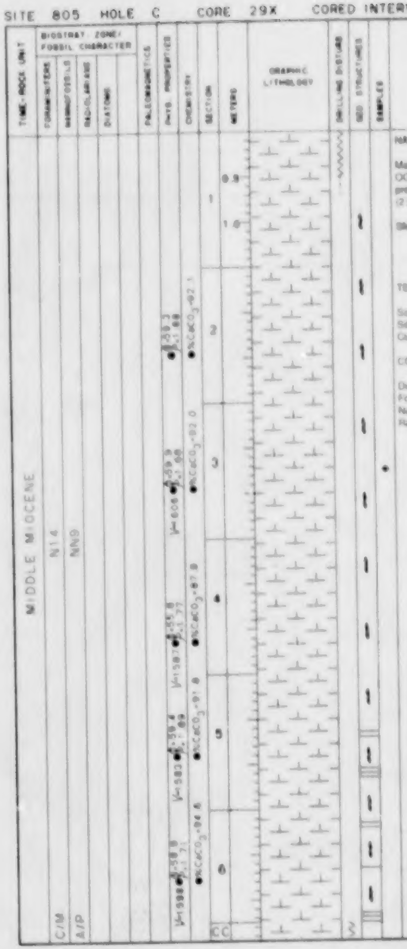
TIME-ROCK UNIT
BIOSTRAT. ZONE/ FOSSIL CHARACTER
FORAMINIFERS
NANNOFOSSILS
RADIOLARIANS
DIATOMS
PALEOMAGNETICS
PHYS. PROPERTIES
CHEMISTRY
SECTION
METERS
GRAPHIC LITHOLOGY
DRILLING DISTURB.
SED. STRUCTURES
SAMPLES
MIDDLE MIOCENE
N14
NN9
C/M
A/P
φ=59.3
γ=1.88
%CaCO3=92.1
V=1606
φ=59.9
γ=1.88
%CaCO3=92.0
V=1587
φ=55.8
γ=1.77
%CaCO3=87.8
V=1583
φ=59.4
γ=1.89
%CaCO3=91.8
V=1588
φ=58.8
γ=1.71
%CaCO3=94.6
0.9
1.0
1
2
3
4
5
6
CC

LITHOLOGIC DESCRIPTION

NANNOFOSSIL OOZE with FORAMINIFERS

Major lithology: This core contains white (2.5Y 8/0), stiff to semi-lithified NANNOFOSSIL OOZE with FORAMINIFERS. Reddish gray (5R 6/1) color bands, 2 to 5 cm in thickness, are present throughout the core. The ooze is strongly bioturbated, as indicated by light gray (2.5Y 7/2) mottling and pyrite burrow fillings.

SMEAR SLIDE SUMMARY (%):

	3, 74
	D
TEXTURE	
Sand	12
Silt	50
Clay	38
COMPOSITION	
Diatoms	Tr
Foraminifers	15
Nannofossils	80
Radiolarians	5

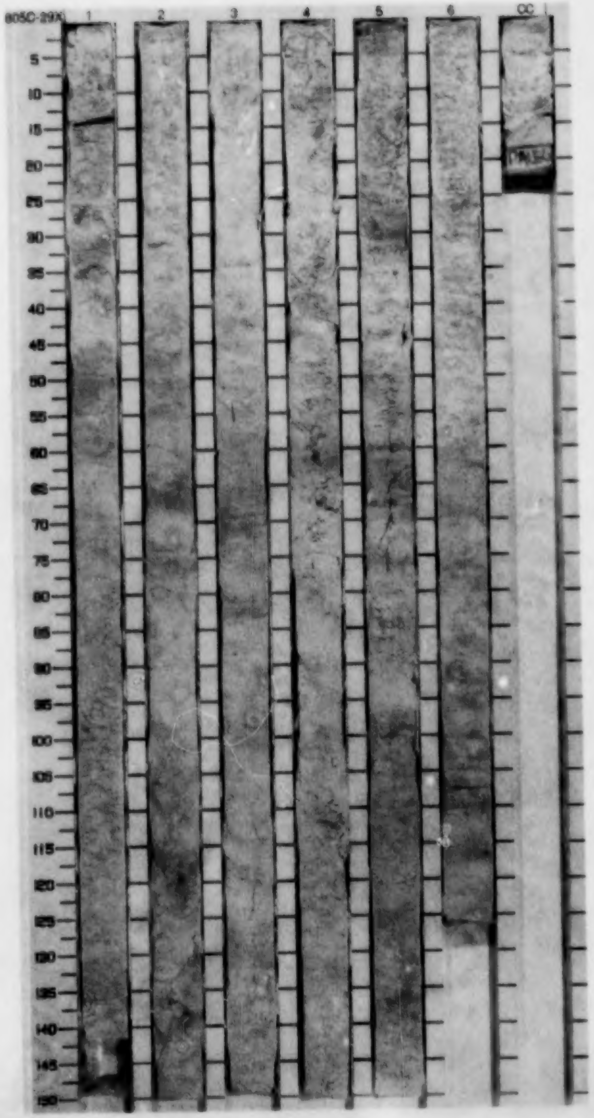
805C-29X
1
2
3
4
5
6
CC
5
10
15
20
25
30
35
40
45
50
55
60
65
70
75
80
85
90
95
100
105
110
115
120
125
130
135
140
145
150

SITE 805 HOLE C CORE 30X CORED INTERVAL 274.4-284.0 mbsf

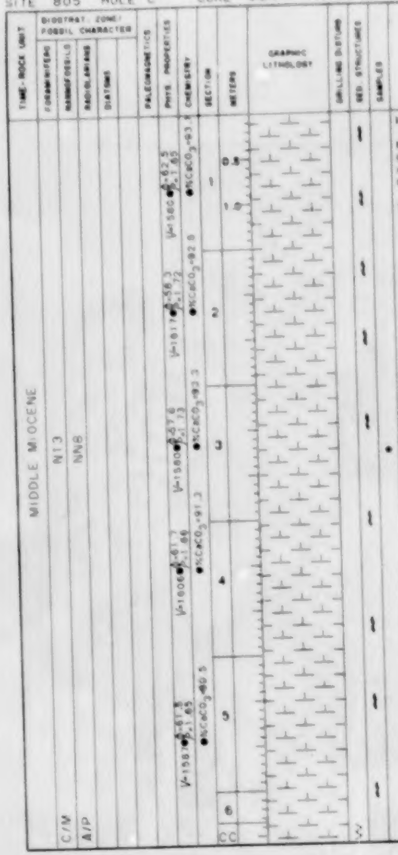

LITHOLOGIC DESCRIPTION

NANNOFOSSIL OOZE

Major lithology: This core contains white (2.5Y 8/0), stiff to semi-lithified NANNOFOSSIL OOZE. The sediment is slightly bioturbated, as indicated by a few reddish gray (5R 6/1) mottles. Several reddish gray zones (several cm to several tens of cm thick) and pale green bands (mm to cm thick) are noted throughout the core.

SMEAR SLIDE SUMMARY (%):

	3, 74
	D
TEXTURE	
Sand	8
Silt	62
Clay	30
COMPOSITION	
Accessory minerals	1
Diatoms	2
Foraminifers	8
Nannofossils	82
Radiolarians	5
Siliceous fragments	2

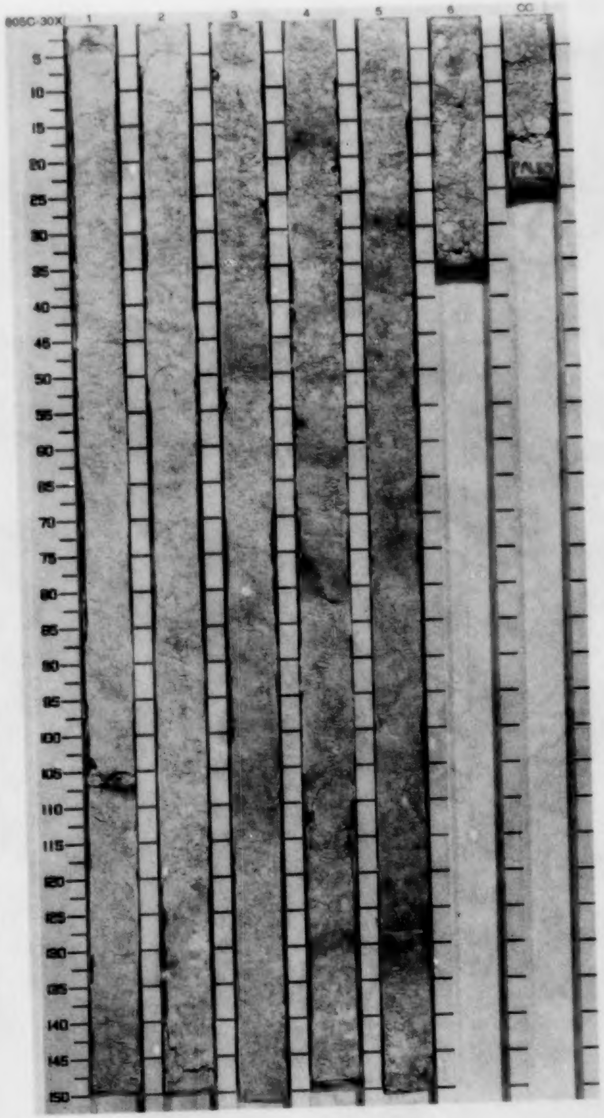
805C-30X
1
2
3
4
5
6
CC
5
10
15
20
25
30
35
40
45
50
55
60
65
70
75
80
85
90
95
100
105
110
115
120
125
130
135
140
145
150

SITE 805 HOLE C CORE 31X CORED INTERVAL 284.0-293.7 mbsf

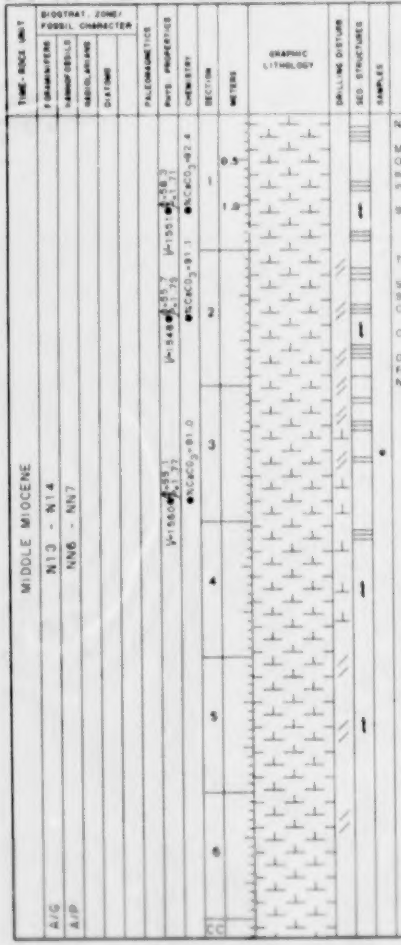
TIME-ROCK UNIT
BIOSTRAT. ZONE/ FOSSIL CHARACTER
FORAMINIFERS
NANNOFOSSILS
RADIOLARIANS
DIATOMS
PALEOMAGNETICS
PHYS. PROPERTIES
CHEMISTRY
SECTION
METERS
GRAPHIC LITHOLOGY
DRILLING DISTURB.
SED. STRUCTURES
SAMPLES
MIDDLE MIOCENE
N13 - N14
NN6 - NN7
A/G
A/P
V=1551 φ=58.3 γ=1.71
V=1548 φ=55.7 γ=1.79
V=1560 φ=55.1 γ=1.77
%CaCO3=82.4
%CaCO3=81.1
%CaCO3=81.0
1
2
3
4
5
6
CC
0.5
1.0

LITHOLOGIC DESCRIPTION

NANNOFOSSIL OOZE

Major lithology: This core contains white (2.5Y 8/0), stiff to semi-lithified NANNOFOSSIL OOZE. Faint, reddish gray (5R 6/2), 20 to 30 cm thick zones, spaced 40 to 50 cm apart exhibit mm thick banding. Some mm thick bands are also pale yellowish green (10GY 7/2) in color. The sediment is strongly bioturbated, especially in the reddish gray zones.

SMEAR SLIDE SUMMARY (%):

	3, 75
	D
TEXTURE:	
Sand	1
Silt	60
Clay	39
COMPOSITION:	
Diatoms	1
Foraminifers	7
Nannofossils	89

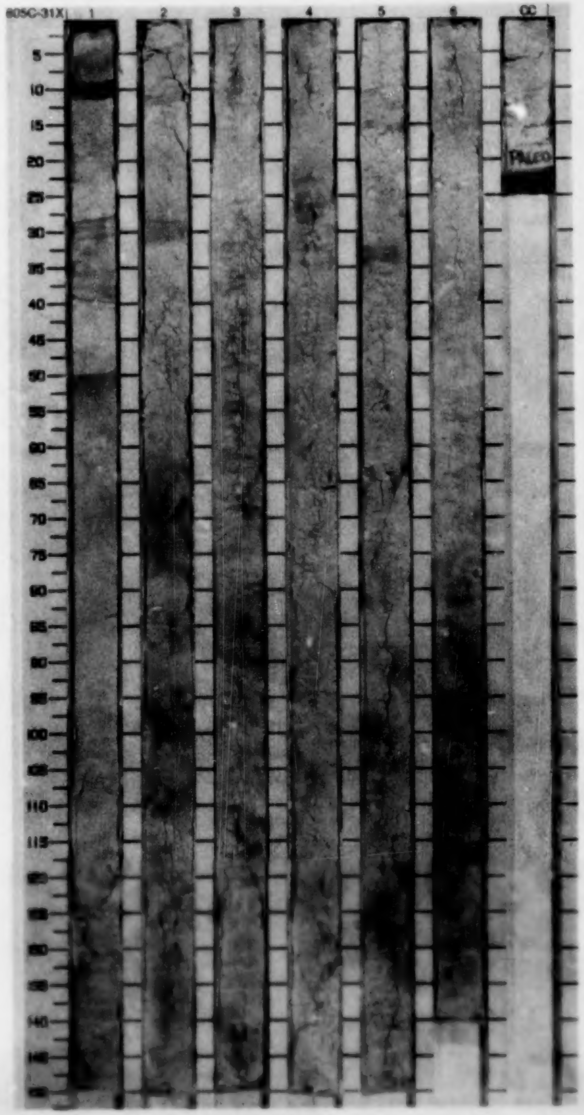
805C-31X
1
2
3
4
5
6
CC
PALEO
5
10
15
20
25
30
35
40
45
50
55
60
65
70
75
80
85
90
95
100
105
110
115
120
125
130
135
140
145
150

SITE 805 HOLE C CORE 32X CORED INTERVAL 293.7-302.9 mbsf

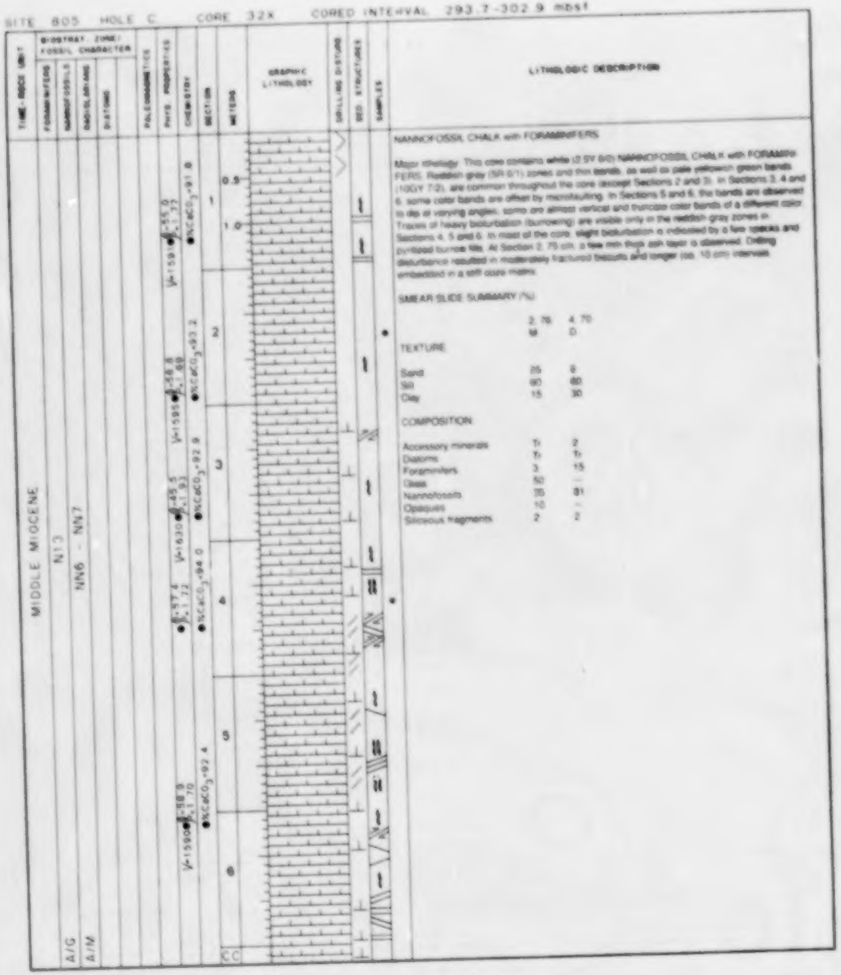
TIME-ROCK UNIT
BIOSTRAT. ZONE/ FOSSIL CHARACTER
FORAMINIFERS
NANNOFOSSILS
RADIOLARIANS
DIATOMS
PALEOMAGNETICS
PHYS. PROPERTIES
CHEMISTRY
SECTION
METERS
GRAPHIC LITHOLOGY
DRILLING DISTURB.
SED. STRUCTURES
SAMPLES
MIDDLE MIOCENE
N13
NN6 - NN7
A/G
A/M
V-1591 φ-55.0 γ-1.77
V-1595 φ-58.8 γ-1.69
V-1630 φ-45.5 γ-1.93
φ-57.4 γ-1.72
V-1590 φ-58.9 γ-1.70
%CaCO3-91.8
%CaCO3-93.2
%CaCO3-92.9
%CaCO3-94.0
%CaCO3-92.4
1
2
3
4
5
6
CC
0.5
1.0

LITHOLOGIC DESCRIPTION

NANNOFOSSIL CHALK with FORAMINIFERS

Major lithology: This core contains white (2.5Y 8/0) NANNOFOSSIL CHALK with FORAMINIFERS. Reddish gray (5R 6/1) zones and thin bands, as well as pale yellowish green bands (10GY 7/2), are common throughout the core (except Sections 2 and 3). In Sections 3, 4 and 6, some color bands are offset by microfaulting. In Sections 5 and 6, the bands are observed to dip at varying angles; some are almost vertical and truncate color bands of a different color. Traces of heavy bioturbation (burrowing) are visible only in the reddish gray zones in Sections 4, 5 and 6. In most of the core, slight bioturbation is indicated by a few specks and pyritized burrow fills. At Section 2, 75 cm, a few mm thick ash layer is observed. Drilling disturbance resulted in moderately fractured biscuits and longer (ca. 10 cm) intervals embedded in a stiff ooze matrix.

SMEAR SLIDE SUMMARY (%):

	2, 75 M	4, 70 D
TEXTURE:		
Sand	25	5
Silt	60	60
Clay	15	30
COMPOSITION:		
Accessory minerals	Tr	2
Diatoms	Tr	Tr
Foraminifers	3	15
Glass	50	—
Nannofossils	35	81
Opaques	10	—
Siliceous fragments	2	2

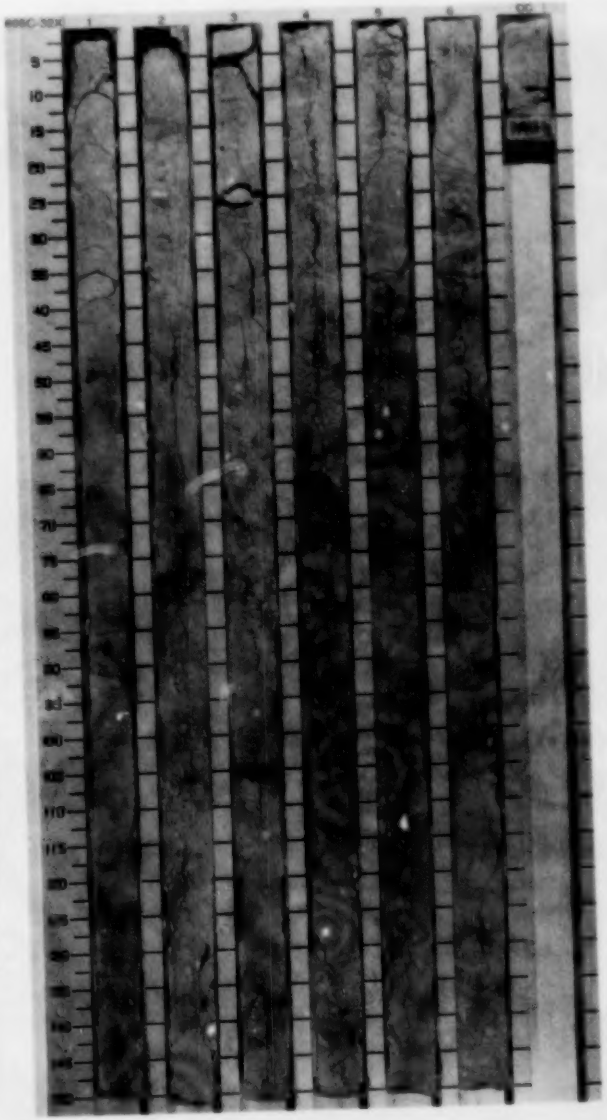
805C-32X
1
2
3
4
5
6
CC
5
10
15
20
25
30
35
40
45
50
55
60
65
70
75
80
85
90
95
100
105
110
115
120
125
130
135
140
145
150

SITE 805 HOLE C CORE 33X CORED INTERVAL 302.9-312.6 mbsf

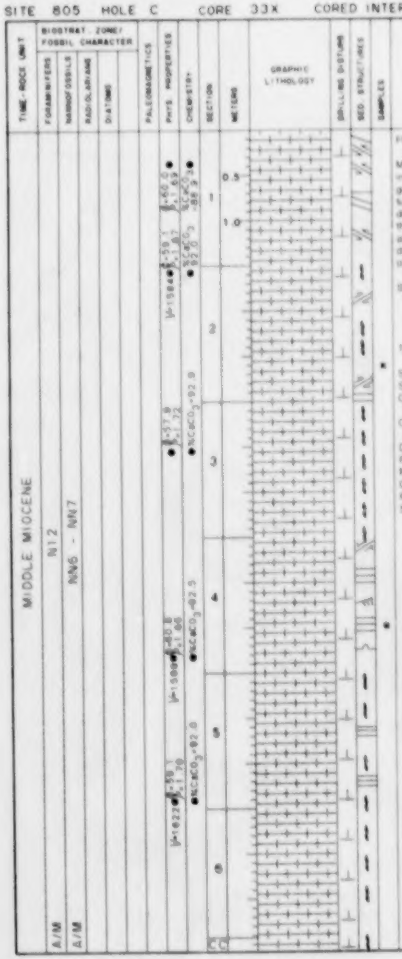
TIME-ROCK UNIT
BIOSTRAT. ZONE/ FOSSIL CHARACTER
FORAMINIFERS
NANNOFOSSILS
RADIOLARIANS
DIATOMS
PALEOMAGNETICS
PHYS. PROPERTIES
CHEMISTRY
SECTION
METERS
GRAPHIC LITHOLOGY
DRILLING DISTURB.
SED. STRUCTURES
SAMPLES
MIDDLE MIOCENE
N12
NN6 - NN7
A/M
A/M
Φ-60.0 γ-1.69
%CaCO3-88.9
V-1584 Φ-59.1 γ-1.67
%CaCO3-92.0
%CaCO3-92.0
Φ-57.9 γ-1.72
%CaCO3-92.5
V-1508 Φ-60.8 γ-1.66
V-1622 Φ-58.1 γ-1.70
%CaCO3-92.0
1
2
3
4
5
6
CC
0.5
1.0

LITHOLOGIC DESCRIPTION

FORAMINIFER NANNOFOSSIL CHALK

Major lithology: This core contains FORAMINIFER NANNOFOSSIL CHALK. It is predominantly white (2.5Y 8/0), but frequent, mm-thick, distinct, pale purple (5P6/2), pale yellow green (10GY 7/2) and dark gray (2.5Y 4/0) color banding is present. Intervals of heavy bioturbation are also evident, shown by abundant burrows, trails and traces. Microfaulting, dipping color banding, contorted color banding and smeared burrow structures in Sections 1 through 4 are noted. Section 4, 57-94 cm, contains very fine laminae that are wispy in nature and possibly form cross laminae. Section 5 has zones (about 2 cm thick) that contain very distinct horizontal or near horizontal color bands. These zones are separated by about 30 cm of heavily bioturbated sediment.

SMEAR SLIDE SUMMARY (%):

	2, 111 M	4, 102 D
TEXTURE:		
Sand	20	15
Silt	40	40
Clay	40	45
COMPOSITION:		
Diatoms	2	1
Foraminifers	15	30
Nannofossils	68	65
Opaques	10	—
Radiolarians	2	1
Siliceous fragments	3	3

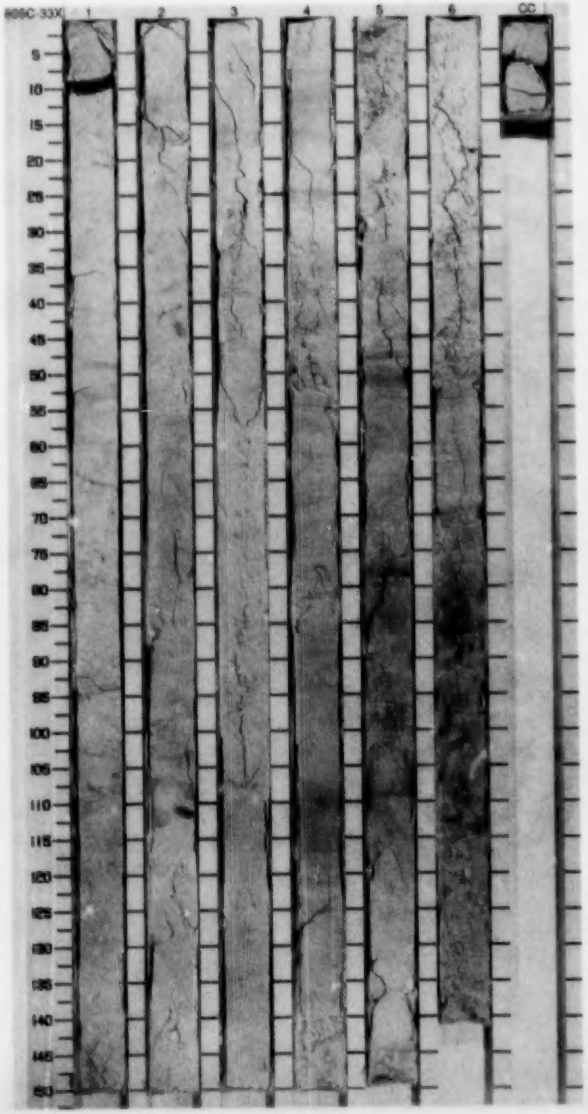
805C-33X
1
2
3
4
5
6
CC
5
10
15
20
25
30
35
40
45
50
55
60
65
70
75
80
85
90
95
100
105
110
115
120
125
130
135
140
145
150

SITE 805 HOLE C CORE 34X CORED INTERVAL 312.6-322.3 mbsf

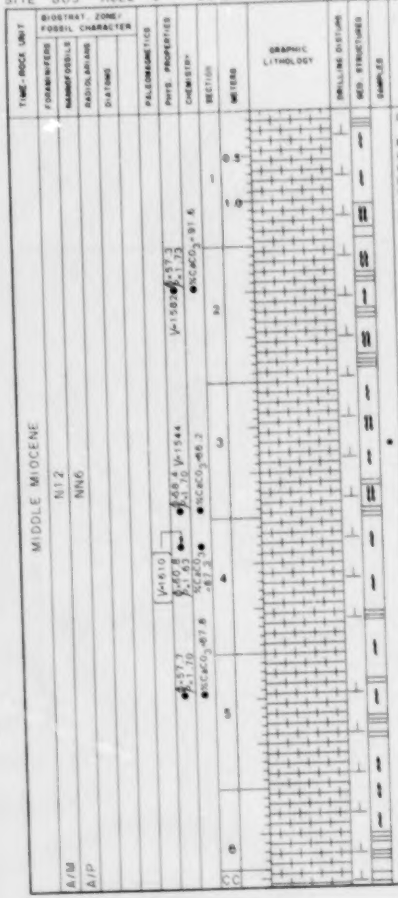
TIME-ROCK UNIT
BIOSTRAT. ZONE/ FOSSIL CHARACTER
FORAMINIFERS
NANNOFOSSILS
RADIOLARIANS
DIATOMS
PALEOMAGNETICS
PHYS. PROPERTIES
CHEMISTRY
SECTION
METERS
GRAPHIC LITHOLOGY
DRILLING DISTURB.
SED. STRUCTURES
SAMPLES
MIDDLE MIOCENE
N12
NN6
A/M
A/P
V-1582 ϕ-57.3 ρ-1.73
%CaCO3-91.6
ϕ-68.4 ρ-1.70 V-1544
%CaCO3-88.2
V-1610
ϕ-60.8 ρ-1.63
%CaCO3-87.2
ϕ-57.7 ρ-1.70
%CaCO3-87.8
0.5
1.0
1
2
3
4
5
6
CC

LITHOLOGIC DESCRIPTION

FORAMINIFER NANNOFOSSIL CHALK

Major lithology: This core contains FORAMINIFER NANNOFOSSIL CHALK. It is predominantly white (2.5Y 8/0), but grades into thinner pale pink (5RP 8/2) intervals. Millimeter-thick distinct pale purple (5P 6/2), pale blue (5PB 7/2), pale yellowish green (10GY 7/2), reddish gray (5R 6/1) and dark gray (2.5Y 4/0) color banding is common. Intervals of moderate to heavy bioturbation are common.

SMEAR SLIDE SUMMARY (%):

	3, 70
	D
TEXTURE:	
Sand	10
Silt	50
Clay	40
COMPOSITION:	
Diatoms	1
Foraminifers	25
Nannofossils	69
Radiolarians	2
Siliceous fragments	3

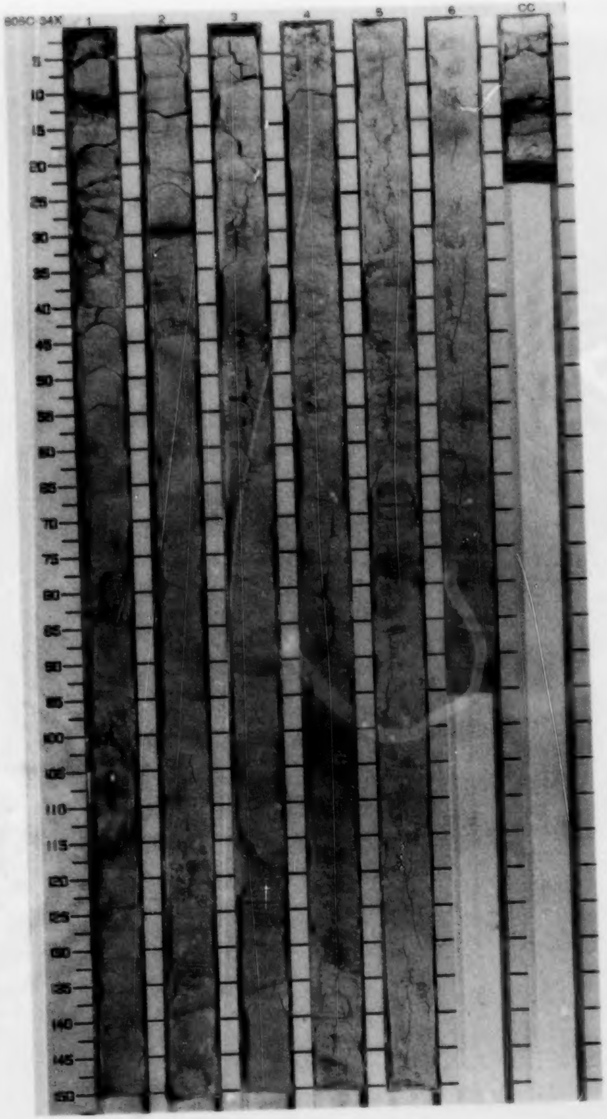
805C-34X
1
2
3
4
5
6
CC
5
10
15
20
25
30
35
40
45
50
55
60
65
70
75
80
85
90
95
100
105
110
115
120
125
130
135
140
145
150

SITE 805 HOLE C CORE 35X CORED INTERVAL 322.3-331.8 mbsf

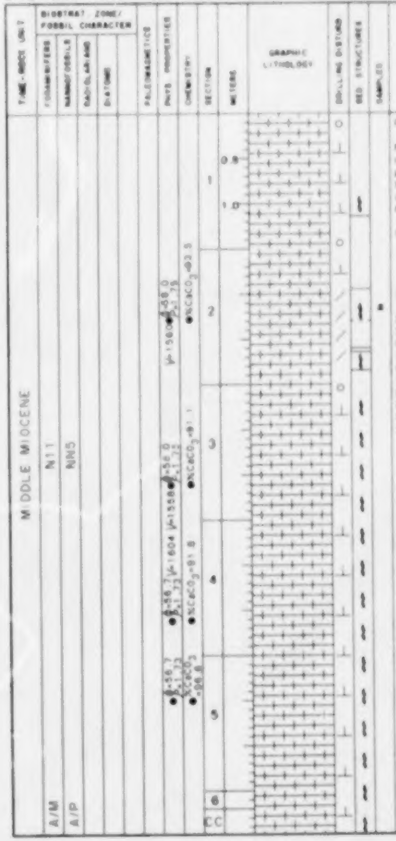

LITHOLOGIC DESCRIPTION

FORAMINIFER NANNOFOSSIL CHALK

Major lithology: This core contains FORAMINIFER NANNOFOSSIL CHALK. It is predominantly white (2.5Y 8/0), but grades into thinner pale blue (5PB 7/2) intervals. Distinct pale purple (5P 6/2), pale blue (5PB 7/2) and grayish green (5G 5/2) color banding is common. Intervals of moderate to heavy bioturbation also are common, documented mostly by horizontal burrows, grayish blue (5PB 5/2) and light gray (2.5Y 7/2) mottles and a few *Zoophycos* trace fossils.

SMEAR SLIDE SUMMARY (%):

	2, 67
	D
TEXTURE:	
Sand	35
Silt	60
Clay	5
COMPOSITION:	
Foraminifers	30
Nannofossils	65
Radiolarians	3
Silicoflagellates	2

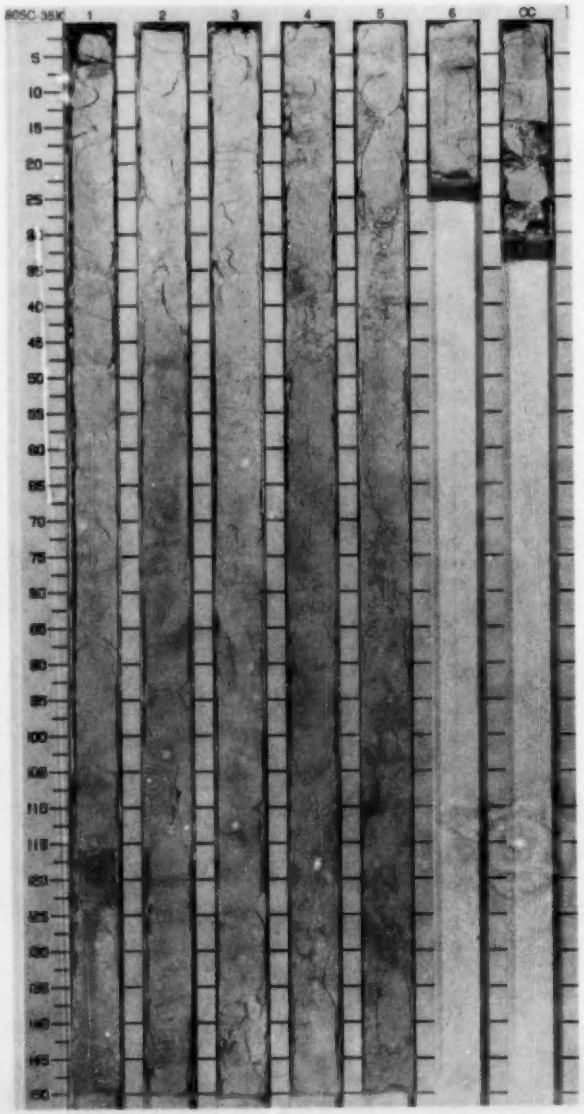
805C-35X
1
2
3
4
5
6
CC
5
10
15
20
25
30
35
40
45
50
55
60
65
70
75
80
85
90
95
100
105
110
115
120
125
130
135
140
145
150

SITE 805 HOLE C CORE 36X CORED INTERVAL 331.8-341.5 mbsf

TIME-ROCK UNIT	BIOSTRAT. ZONE/ FOSSIL CHARACTER: FORAMINIFERS	NANNOFOSSILS	RADIOLARIANS	DIATOMS	PALEOMAGNETICS	PHYS. PROPERTIES	CHEMISTRY	SECTION	METERS	GRAPHIC LITHOLOGY	DRILLING DISTURB.	SED. STRUCTURES	SAMPLES
MIDDLE MIOCENE	N11 A/M	NN5 A/P				●ϕ=54.5 γ=1.79	●%CaCO$_3$=90.5	1	0.5 1.0				
						V=1710●ϕ=57.9 γ=1.72	●%CaCO$_3$=93.8	2					
						V=1625●ϕ=55.4 γ=1.75	●%CaCO$_3$=94.0	3					*
						V=1643●ϕ=54.9 γ=1.78	●%CaCO$_3$=92.2	4					
						V=1701●ϕ=53.5 γ=1.80	●%CaCO$_3$=90.5	5					
						V=1653●ϕ=56.4 γ=1.74	●%CaCO$_3$=93.0	6					
								CC					

LITHOLOGIC DESCRIPTION

NANNOFOSSIL CHALK with FORAMINIFERS

Major lithology: The core contains NANNOFOSSIL CHALK with FORAMINIFERS. It is predominantly white (2.5Y 8/2) but grades into a pale blue (5PB 7/2) color in short zones of Section 5 and 6. The sediments are slightly bioturbated and are faintly mottled in pale purple (5PB 7/2). Distinct grayish green (5G 5/2), grey (N5/) and grayish blue (5PB 5/2) color bands are present in Sections 5 and 6.

SMEAR SLIDE SUMMARY (%):

	3, 100
	D
TEXTURE	
Sand	18
Silt	60
Clay	22
COMPOSITION	
Foraminifers	12
Nannofossils	80
Radiolarians	6
Spicules	Tr

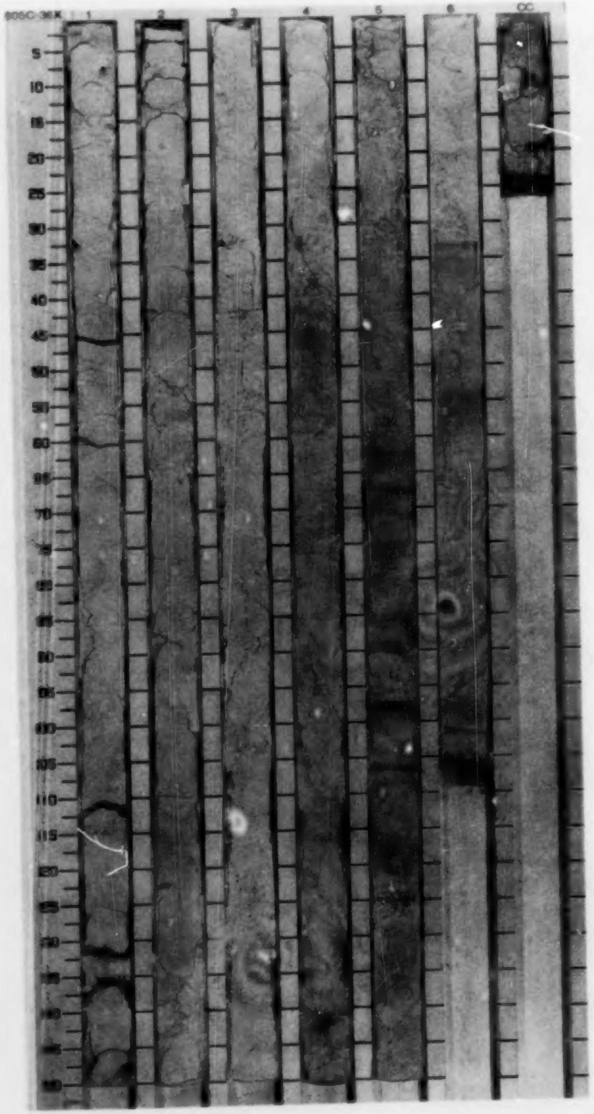

SITE 805 HOLE C CORE 37X CORED INTERVAL 341.5-351.2 mbsf

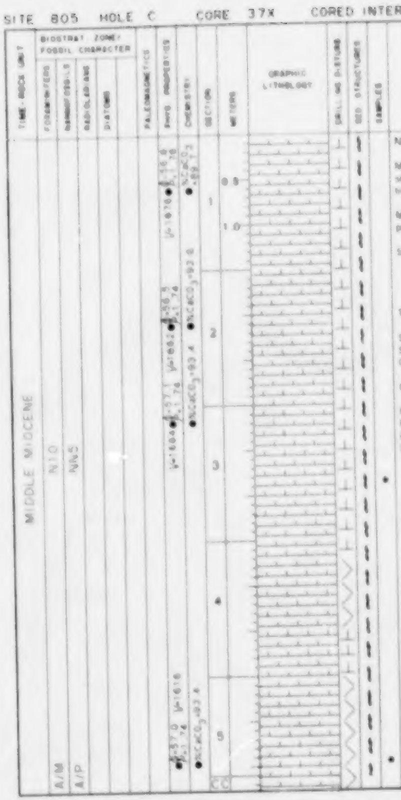
TIME-ROCK UNIT
BIOSTRAT. ZONE/ FOSSIL CHARACTER
FORAMINIFERS
NANNOFOSSILS
RADIOLARIANS
DIATOMS
PALEOMAGNETICS
PHYS. PROPERTIES
CHEMISTRY
SECTION
METERS
GRAPHIC LITHOLOGY
DRILLING DISTURB.
SED. STRUCTURES
SAMPLES
MIDDLE MIOCENE
N10
NN5
A/M
A/P
γ=1676
φ=56.6
%CaCO3=89.7
%CaCO3=93.0
γ=1682
φ=56.5
%CaCO3=93.4
γ=1684
φ=57.1
%CaCO3=93.4
γ=1616
φ=57.0
1
2
3
4
5
CC
0.5
1.0

LITHOLOGIC DESCRIPTION

NANNOFOSSIL CHALK with FORAMINIFERS

Major lithology: This core contains NANNOFOSSIL CHALK with FORAMINIFERS. The sediment is predominantly white (2.5Y 8/0), but is mixed with a diffuse pale purple (5P 6/2) tint in the upper half of Section 1. Bioturbation is light throughout the core.

Minor lithology: A 2 cm thick interval of CHERT is present at Section 2, 135-137 cm. This piece may be a fragment of a chert nodule.

SMEAR SLIDE SUMMARY (%):

	3, 87	5, 95
	D	D
TEXTURE:		
Sand	7	12
Silt	88	85
Clay	5	3
COMPOSITION:		
Foraminifers	10	12
Nannofossils	87	86
Radiolarians	2	2
Spicules	1	—

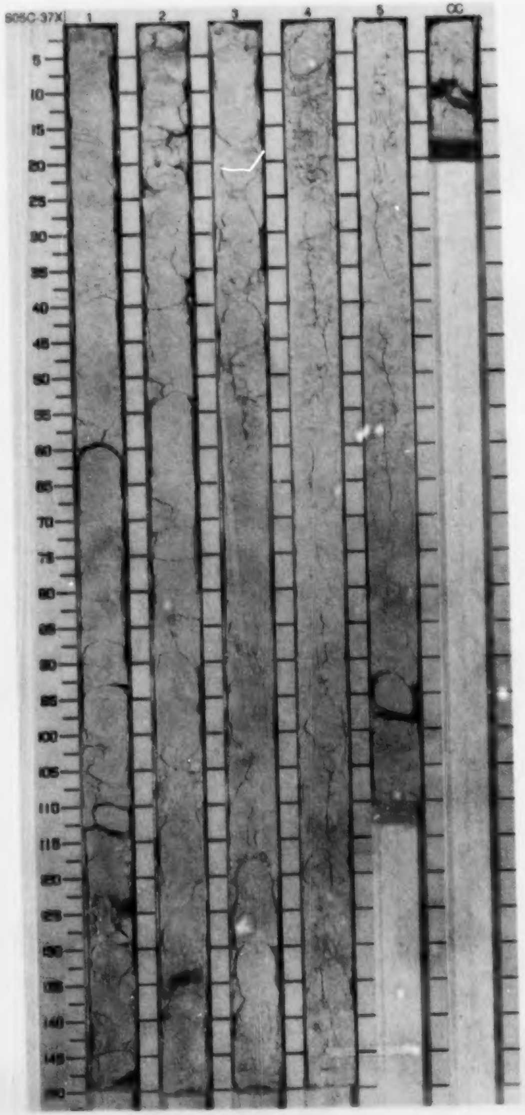
805C-37X
1
2
3
4
5
CC
5
10
15
20
25
30
35
40
45
50
55
60
65
70
75
80
85
90
95
100
105
110
115
120
125
130
135
140
145
150

SITE 805 HOLE C CORE 38X CORED INTERVAL 351.2-360.9 mbsf

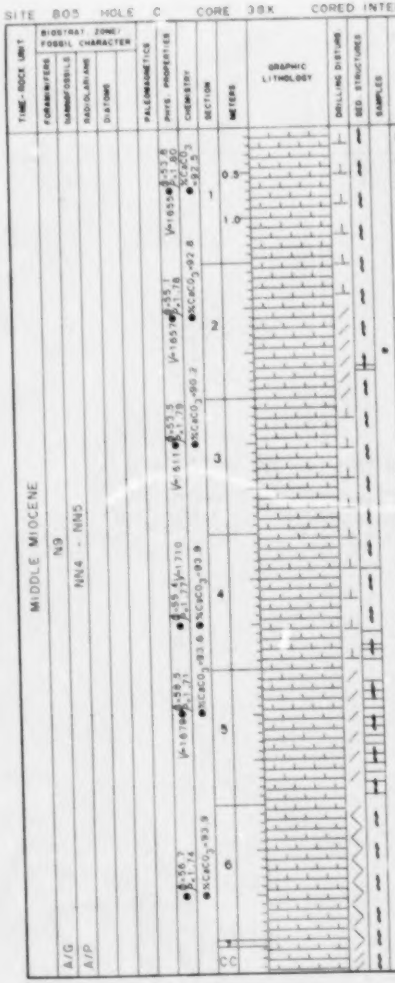
TIME-ROCK UNIT
BIOSTRAT. ZONE/ FOSSIL CHARACTER
FORAMINIFERS
NANNOFOSSILS
RADIOLARIANS
DIATOMS
PALEOMAGNETICS
PHYS. PROPERTIES
CHEMISTRY
SECTION
METERS
GRAPHIC LITHOLOGY
DRILLING DISTURB.
SED. STRUCTURES
SAMPLES
MIDDLE MIOCENE
N9
NN4 - NN5
A/G
A/P
V=1655 φ=53.8 ρ=1.80
%CaCO3 =92.5
%CaCO3=92.8
V=1657 φ=55.1 ρ=1.78
%CaCO3=90.2
V=1611 φ=53.5 ρ=1.79
φ=55.4 ρ=1.77 V=1710
%CaCO3=93.9
%CaCO3=93.6
V=1678 φ=58.5 ρ=1.71
φ=56.7 ρ=1.74
%CaCO3=93.9
1
2
3
4
5
6
CC
0.5
1.0

LITHOLOGIC DESCRIPTION

NANNOFOSSIL CHALK with FORAMINIFERS

Major lithology: This core contains NANNOFOSSIL CHALK with FORAMINIFERS. The dominant color is white (2.5Y 8/0), occasionally grading to pale blue (5PB 7/2). In Sections 1 through 4, the following sequence is common: the pale blue sediments have a sharp base and grade to white over intervals of 5-10 cm, and are then overlain by 5-50 cm of white chalk. Pale purple (5P 6/2) and very pale green (10G 8/2), mm scale pale purple (5P 6/2) to white (2.5Y 8/0) color bands are present throughout Section 5. Bioturbation is slight to common throughout the core.

SMEAR SLIDE SUMMARY (%)

	2, 100
	D
TEXTURE	
Sand	20
Silt	80
COMPOSITION	
Foraminifers	15
Nannofossils	83
Radiolarians	2

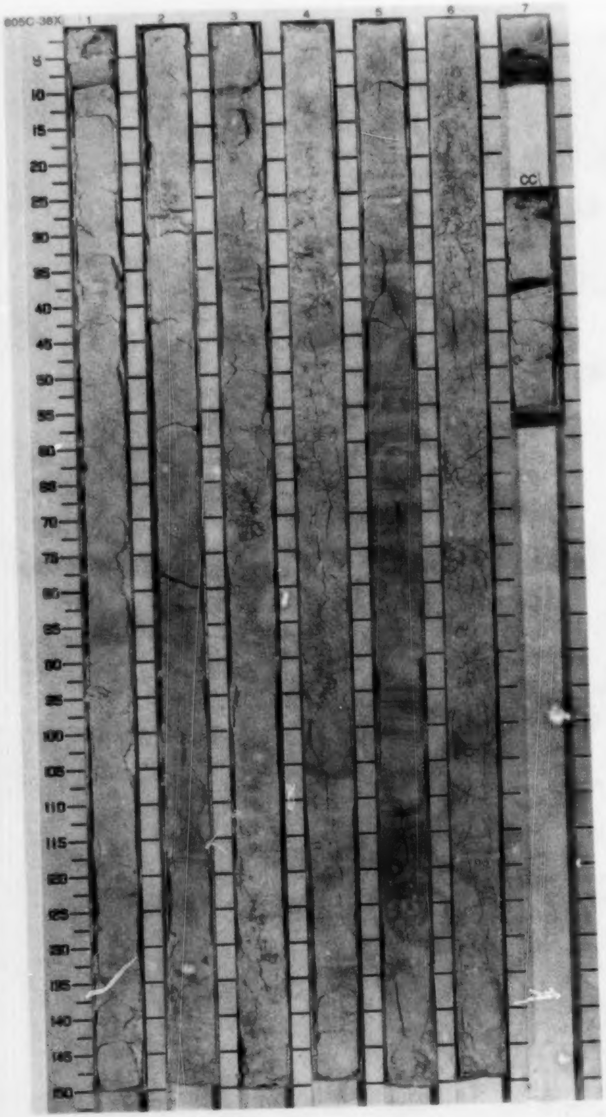
805C-38X
1
2
3
4
5
6
7
CC
5
10
15
20
25
30
35
40
45
50
55
60
65
70
75
80
85
90
95
100
105
110
115
120
125
130
135
140
145
150

SITE 805 HOLE C CORE 39X CORED INTERVAL 360.9-370.6 mbsf

TIME-ROCK UNIT	FORAMINIFERS	NANNOFOSSILS	RADIOLARIANS	DIATOMS	PALEOMAGNETICS	PHYS. PROPERTIES	CHEMISTRY	SECTION	METERS	SAMPLES
MIDDLE MIOCENE	N8 - N9 A/M	NN4 - NN5 A/P		NTD 5 / NTD 4 C/M		● $\phi=52.6$ $\gamma=1.81$	● $\%CaCO_3=90.2$	1	0.5 1.0	
								2		
						$V=1622$ ● $\phi=55.4$ $\gamma=1.74$	● $\%CaCO_3=86.7$	3		•
						$V=1640$ ● $\phi=58.1$ $\gamma=1.72$	● $\%CaCO_3=89.1$	4		
						$V=1680$ ● $\phi=52.7$ $\gamma=1.79$	● $\%CaCO_3=88.0$	5		
						$V=1748$ ● $\phi=57.1$ $\gamma=1.73$	● $\%CaCO_3=92.8$	6		
								CC		

GRAPHIC LITHOLOGY

DRILLING DISTURB.

SED. STRUCTURES

LITHOLOGIC DESCRIPTION

NANNOFOSSIL CHALK with FORAMINIFERS

Major lithology: This core contains NANNOFOSSIL CHALK with FORAMINIFERS, grading between white (2.5Y 8/0), light gray (5YR 7/1), light greenish gray (5GY 7/1), pale blue (5PB 7/2), and pale purple (5P 6/2). Bioturbation is moderate to heavy throughout the core and includes discrete, cm scale, horizontal burrows.

SMEAR SLIDE SUMMARY (%):

	3, 78
	D
TEXTURE	
Sand	30
Silt	65
Clay	5
COMPOSITION	
Foraminifers	20
Nannofossils	70
Radiolarians	8
Silicoflagellates	2

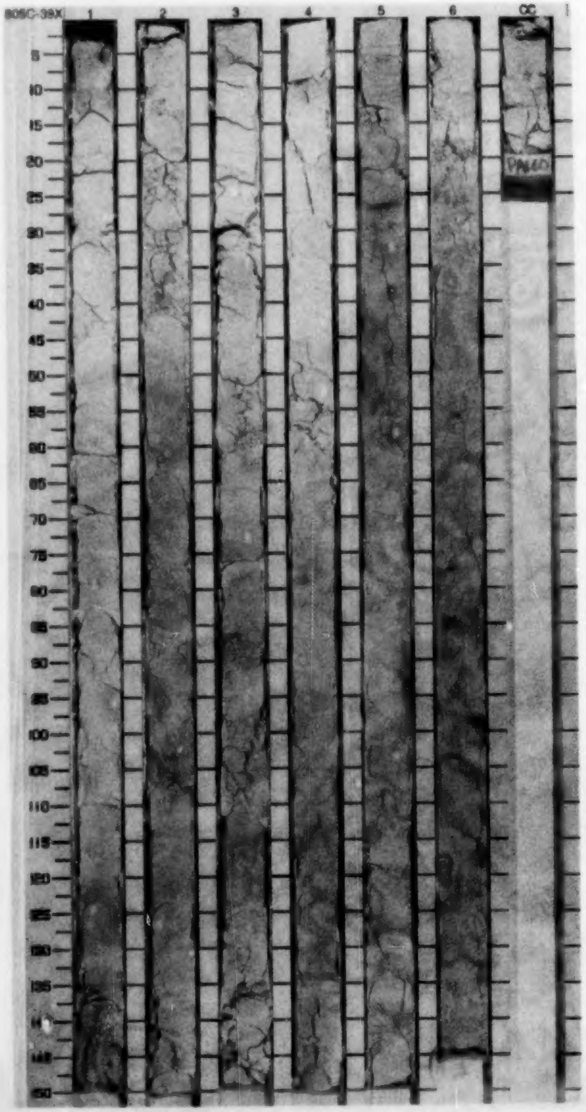
805C-39X
1
2
3
4
5
6
CC
5
10
15
20
25
30
35
40
45
50
55
60
65
70
75
80
85
90
95
100
105
110
115
120
125
130
135
140
145
150
PALEO

SITE 805 HOLE C CORE 40X CORED INTERVAL 370.6-380.3 mbsf

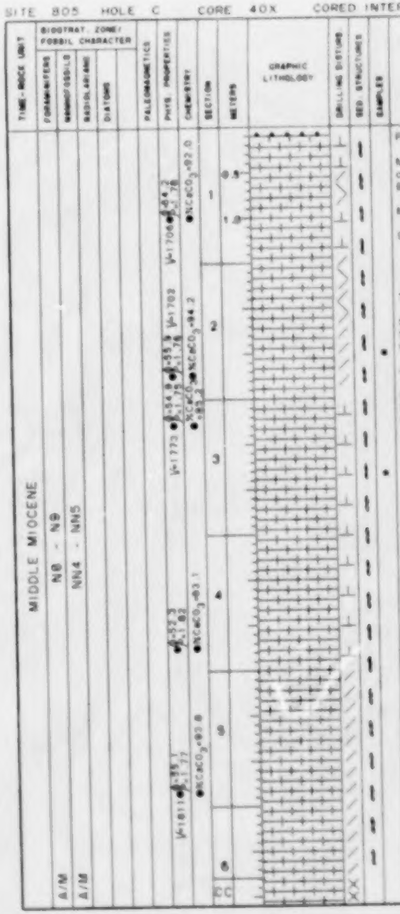
TIME-ROCK UNIT
BIOSTRAT. ZONE/ FOSSIL CHARACTER
FORAMINIFERS
NANNOFOSSILS
RADIOLARIANS
DIATOMS
PALEOMAGNETICS
PHYS. PROPERTIES
CHEMISTRY
SECTION
METERS
GRAPHIC LITHOLOGY
DRILLING DISTURB.
SED. STRUCTURES
SAMPLES
MIDDLE MIOCENE
N8 - N9
NN4 - NN5
A/M
A/M
ϕ=64.2
γ=1.78
V=1706
V=1702
ϕ=55.5
γ=1.76
ϕ=54.8
γ=1.75
V=1773
ϕ=52.3
γ=1.82
ϕ=55.1
γ=1.77
V=1811
%CaCO3=92.0
%CaCO3=94.2
%CaCO3=93.2
%CaCO3=93.1
%CaCO3=93.8
1
2
3
4
5
6
CC
0.5
1.0

LITHOLOGIC DESCRIPTION

FORAMINIFER NANNOFOSSIL CHALK

Major lithology: This core contains FORAMINIFER NANNOFOSSIL CHALK, which grades in color between white (2.5Y 8/... 5Y 8/1), light gray (5YR 7/1), and pale pink (5RP 8/2). Bioturbation is moderate to heavy throughout the core.

Minor Lithology: Section 1, 0-10 cm, contains light gray (N7) CHERT fragments.

SMEAR SLIDE SUMMARY (%):

	2, 100 D	3, 83 D
TEXTURE:		
Sand	35	25
Silt	60	70
Clay	5	4
COMPOSITION:		
Foraminifers	25	20
Nannofossils	70	75
Radiolarians	5	5

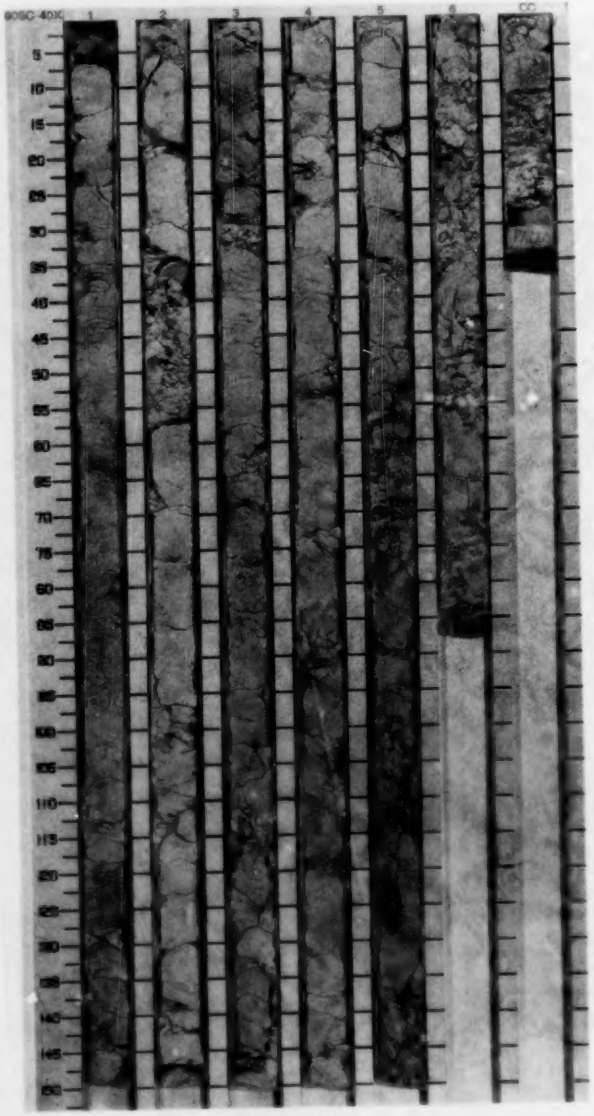
805C-40X
1
2
3
4
5
6
CC
5
10
15
20
25
30
35
40
45
50
55
60
65
70
75
80
85
90
95
100
105
110
115
120
125
130
135
140
145
150

SITE 805 HOLE C CORE 41X CORED INTERVAL 380.3-389.9 mbsf

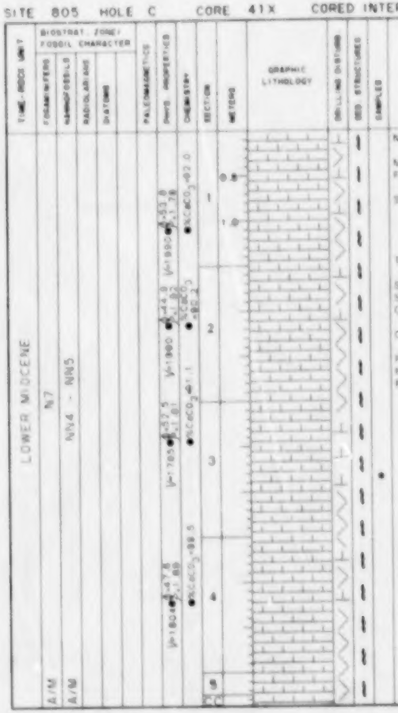
TIME-ROCK UNIT
BIOSTRAT. ZONE/ FOSSIL CHARACTER
FORAMINIFERS
NANNOFOSSILS
RADIOLARIANS
DIATOMS
PALEOMAGNETICS
PHYS. PROPERTIES
CHEMISTRY
SECTION
METERS
GRAPHIC LITHOLOGY
DRILLING DISTURB.
SED. STRUCTURES
SAMPLES
LOWER MIOCENE
N7
NN4 - NN5
A/M
A/M
V=1990
φ=53.8
γ=1.78
%CaCO3=92.0
V=1980
φ=44.0
γ=1.92
%CaCO3=90.2
V=1785
φ=52.5
γ=1.81
%CaCO3=91.1
V=1804
φ=47.8
γ=1.88
%CaCO3=88.5
1
2
3
4
5
CC
0.8
1.0

LITHOLOGIC DESCRIPTION

NANNOFOSSIL CHALK with FORAMINIFERS

Major lithology: This core contains white (5Y 8/1 to 10YR 8/1), slightly bioturbated NANNOFOSSIL CHALK with FORAMINIFERS.

SMEAR SLIDE SUMMARY (%):

	3, 83
	D
TEXTURE:	
Sand	25
Silt	70
Clay	5
COMPOSITION:	
Foraminifers	20
Nannofossils	75
Radiolarians	5

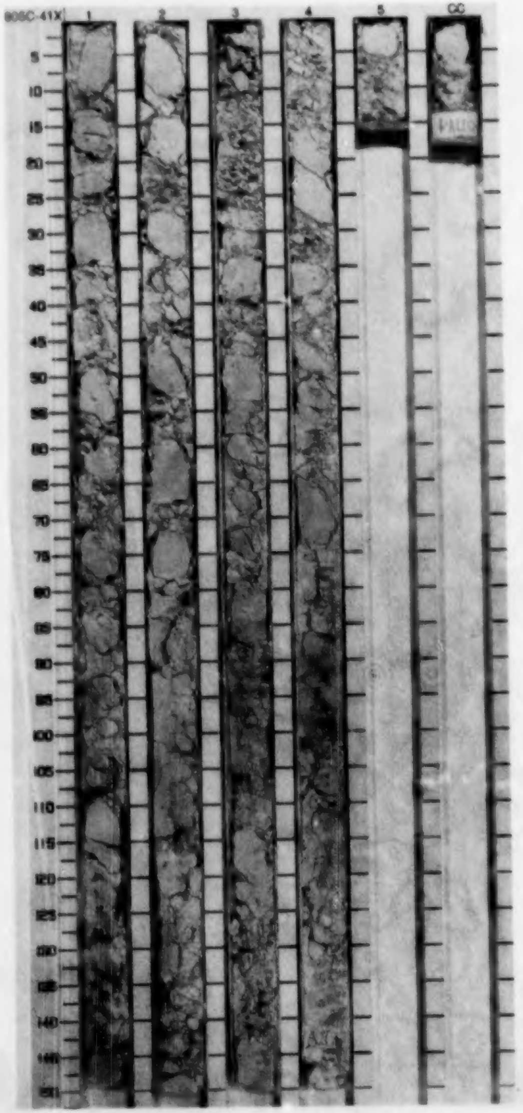
805C-41X
1
2
3
4
5
CC
5
10
15
20
25
30
35
40
45
50
55
60
65
70
75
80
85
90
95
100
105
110
115
120
125
130
135
140
145
150

SITE 805 HOLE C CORE 42X CORED INTERVAL 389.9-399.5 mbsf

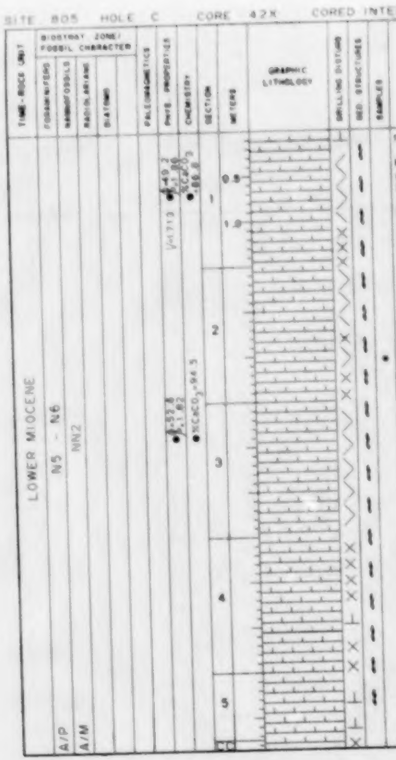
TIME-ROCK UNIT
BIOSTRAT. ZONE/ FOSSIL CHARACTER
FORAMINIFERS
NANNOFOSSILS
RADIOLARIANS
DIATOMS
PALEOMAGNETICS
PHYS. PROPERTIES
CHEMISTRY
SECTION
METERS
GRAPHIC LITHOLOGY
DRILLING DISTURB.
SED. STRUCTURES
SAMPLES
LOWER MIOCENE
N5 - N6
NN2
A/P
A/M
φ=49.2
γ=1.86
Vp=1713
%CaCO3=86.8
φ=52.8
γ=1.82
%CaCO3=94.5
0.5
1.0
1
2
3
4
5
CC

LITHOLOGIC DESCRIPTION

NANNOFOSSIL CHALK

Major lithology: This core contains NANNOFOSSIL CHALK, which is predominantly white (10YR 8/1 and 2.5Y 8/0 to 5Y 8/1). Diffuse pale blue (5PB 7/2) mottling is present in Sections 3 and 5. The entire core is slightly bioturbated.

SMEAR SLIDE SUMMARY (%):

	2, 105
	D
TEXTURE:	
Sand	15
Silt	80
Clay	5
COMPOSITION:	
Foraminifers	9
Nannofossils	90
Radiolarians	1

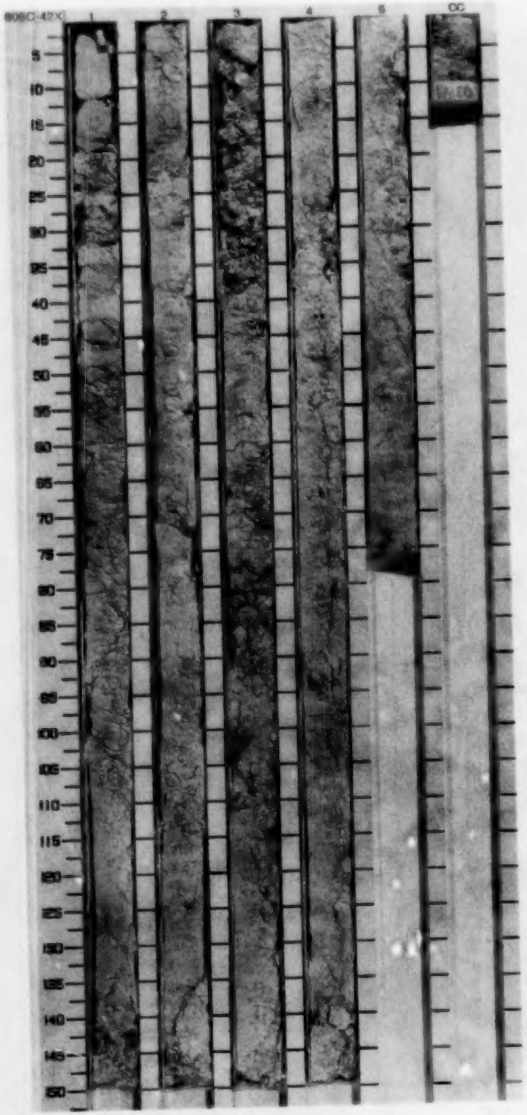
805C-42X
1
2
3
4
5
CC
5
10
15
20
25
30
35
40
45
50
55
60
65
70
75
80
85
90
95
100
105
110
115
120
125
130
135
140
145
150

SITE 805 HOLE C CORE 43X CORED INTERVAL 399.5-409.1 mbsf

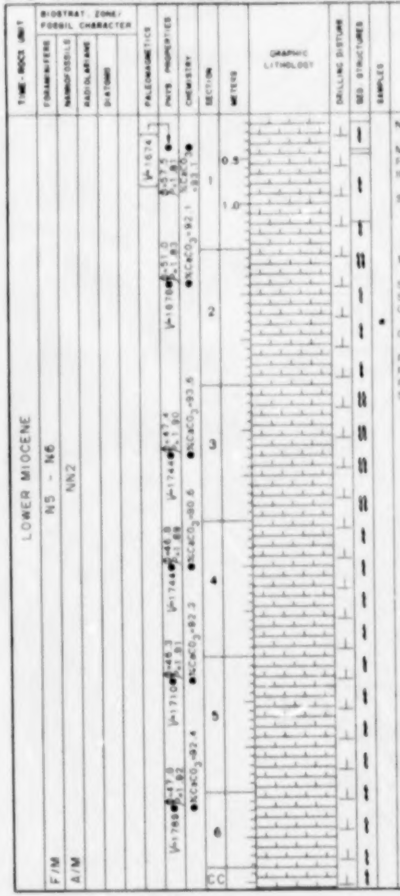
TIME-ROCK UNIT
BIOSTRAT. ZONE/ FOSSIL CHARACTER
FORAMINIFERS
NANNOFOSSILS
RADIOLARIANS
DIATOMS
PALEOMAGNETICS
PHYS. PROPERTIES
CHEMISTRY
SECTION
METERS
GRAPHIC LITHOLOGY
DRILLING DISTURB.
SED. STRUCTURES
SAMPLES
LOWER MIOCENE
N5 - N6
NN2
F/M
A/M
V=1674
φ=57.5
γ=1.81
%CaCO3=83.1
%CaCO3=92.1
V=1870
φ=51.0
γ=1.83
%CaCO3=93.6
V=1744
φ=47.4
γ=1.90
%CaCO3=90.6
V=1744
φ=46.8
γ=1.88
%CaCO3=82.3
V=1710
φ=46.3
γ=1.91
%CaCO3=92.4
V=1780
φ=47.0
γ=1.92
1
2
3
4
5
6
CC
0.5
1.0

LITHOLOGIC DESCRIPTION

NANNOFOSSIL CHALK with FORAMINIFERS

Major lithology: This core contains white (10YR 8/1 to 5Y 8/1) NANNOFOSSIL CHALK with FORAMINIFERS. Diffuse pale blue (5PB 7/2) and pale purple (5P 6/2) mottling is common throughout. The entire core is slightly bioturbated.

SMEAR SLIDE SUMMARY (%):

	2, 81
	D
TEXTURE	
Sand	7
Silt	90
Clay	3
COMPOSITION	
Foraminifers	10
Nannofossils	88
Radiolarians	1
Spicules	1

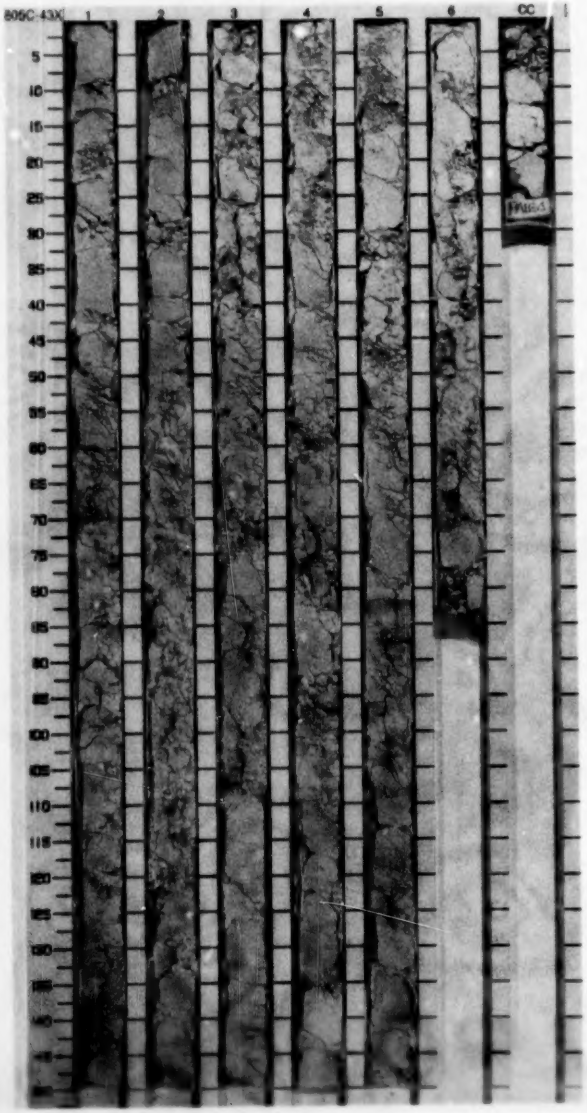
805C-43X
1
2
3
4
5
6
CC
5
10
15
20
25
30
35
40
45
50
55
60
65
70
75
80
85
90
95
100
105
110
115
120
125
130
135
140
145
150

SITE 805 HOLE C CORE 44X CORED INTERVAL 409.1-418.7 mbsf

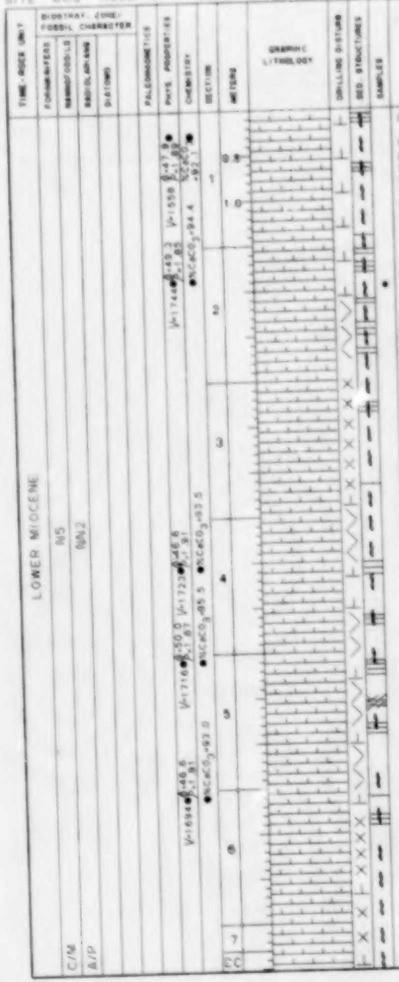
TIME-ROCK UNIT
BIOSTRAT. ZONE/ FOSSIL CHARACTER
FORAMINIFERS
NANNOFOSSILS
RADIOLARIANS
DIATOMS
PALEOMAGNETICS
PHYS. PROPERTIES
CHEMISTRY
SECTION
METERS
GRAPHIC LITHOLOGY
DRILLING DISTURB.
SED. STRUCTURES
SAMPLES
LOWER MIOCENE
N5
NN2
C/M
A/P
Φ=47.9
ρ=1.89
V=1558
%CaCO3
=92.1
%CaCO3=94.4
Φ=49.3
ρ=1.85
V=1744
%CaCO3=93.5
Φ=50.0
ρ=1.87
V=1716
%CaCO3=95.5
Φ=46.6
ρ=1.91
V=1723
Φ=46.6
ρ=1.91
V=1694
%CaCO3=93.0
1
2
3
4
5
6
7
CC
0.5
1.0

LITHOLOGIC DESCRIPTION

NANNOFOSSIL CHALK with FORAMINIFERS

Major lithology: This core contains NANNOFOSSIL CHALK with FORAMINIFERS. It is predominantly white (10YR 8/1 to 2.5Y 8/0) and grades into shorter intervals of pale blue (5PB 7/2). Well developed greenish gray (5G 6/1) and gray (N5) color bands are common. Color bands in Section 5 are microfaulted. Five to ten cm thick, pale blue, intervals underlie most color bands. In addition to pyritized burrows and *Zoophycos* trace fossils, diffuse pale blue (5PB 7/2) and pale purple (5P 6/2) color mottling is common. The entire core is slightly bioturbated.

SMEAR SLIDE SUMMARY (%):

	2, 45 D
TEXTURE:	
Sand	20
Silt	75
Clay	5
COMPOSITION:	
Foraminifers	15
Nannofossils	80
Radiolarians	3
Spicules	2

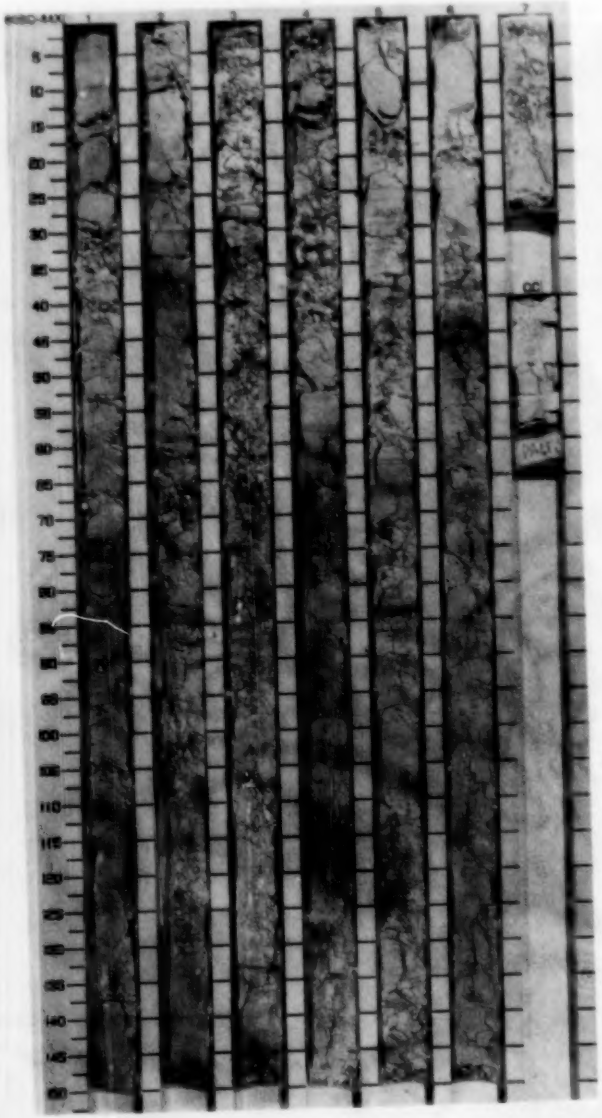
805C-44X
1
2
3
4
5
6
7
CC
5
10
15
20
25
30
35
40
45
50
55
60
65
70
75
80
85
90
95
100
105
110
115
120
125
130
135
140
145
150

SITE 805 HOLE C CORE 45X CORED INTERVAL 418.7-428.4 mbsf

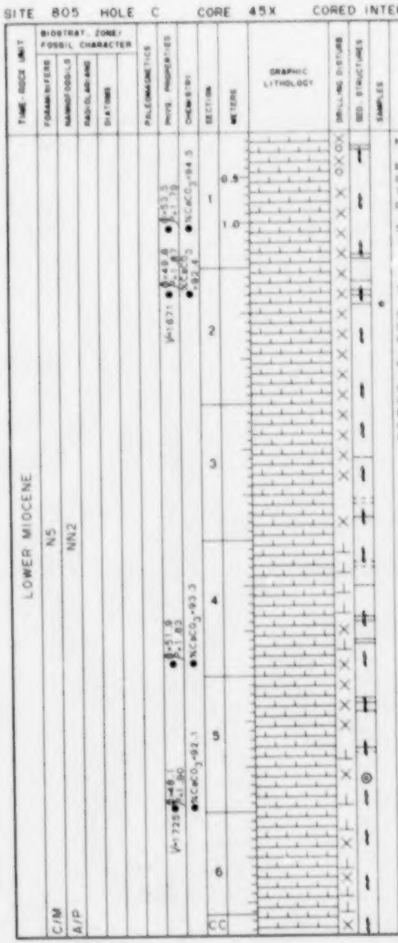
TIME-ROCK UNIT
BIOSTRAT. ZONE/ FOSSIL CHARACTER
FORAMINIFERS
NANNOFOSSILS
RADIOLARIANS
DIATOMS
PALEOMAGNETICS
PHYS. PROPERTIES
CHEMISTRY
SECTION
METERS
GRAPHIC LITHOLOGY
DRILLING DISTURB.
SED. STRUCTURES
SAMPLES
LOWER MIOCENE
N5
NN2
C/M
A/P
φ=53.5
γ=1.79
φ=49.6
γ=1.87
Vp=1671
φ=51.9
γ=1.83
φ=48.1
γ=1.90
Vp=1725
%CaCO$_3$=94.5
%CaCO$_3$=92.4
%CaCO$_3$=93.3
%CaCO$_3$=92.1
1
2
3
4
5
6
CC
0.5
1.0

LITHOLOGIC DESCRIPTION

NANNOFOSSIL CHALK

Major lithology: The core contains NANNOFOSSIL CHALK. It is predominantly white (2.5Y 8/0), but grades into mottled pale blue (5PB 7/2) over short intervals. Distinct pale blue (5PB 7/2), gray (N5/) and light greenish gray (5GY 7/1) color bands are common. Mottling and pyritized burrows are evidence of slight to moderate bioturbation throughout the core.

SMEAR SLIDE SUMMARY (%):

	2, 40
	D
TEXTURE:	
Sand	7
Silt	60
Clay	33
COMPOSITION:	
Foraminifers	5
Glass	Tr
Nannofossils	93
Quartz	Tr
Radiolarians	2

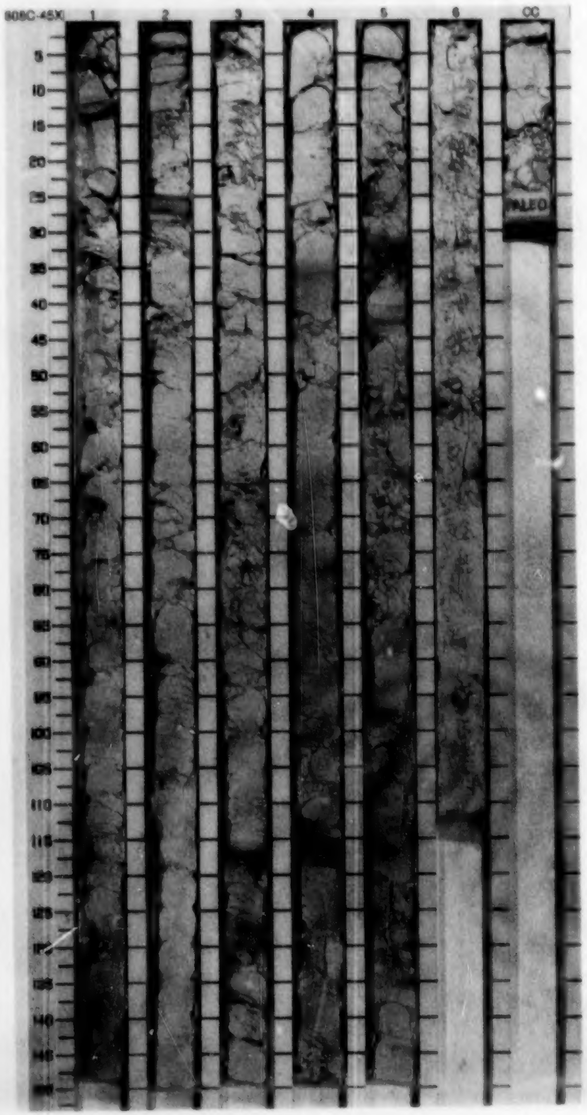
805C-45X
1
2
3
4
5
6
CC
PALEO
5
10
15
20
25
30
35
40
45
50
55
60
65
70
75
80
85
90
95
100
105
110
115
120
125
130
135
140
145
150

SITE 805 HOLE C CORE 46X CORED INTERVAL 428.4-438.1 mbsf

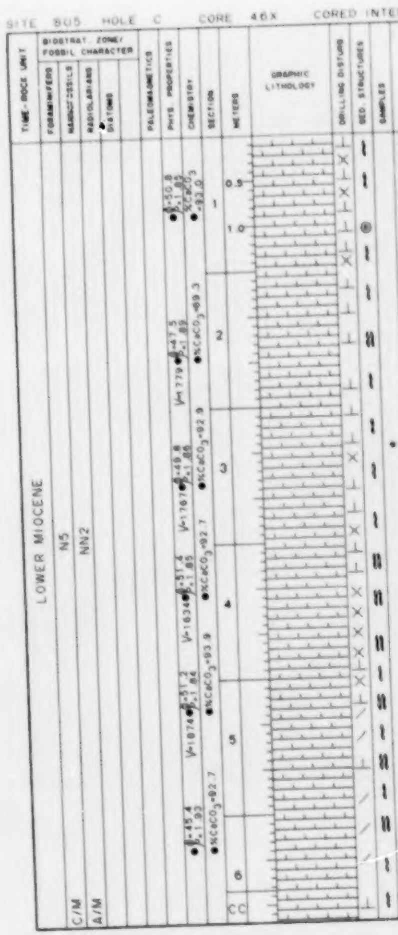
TIME-ROCK UNIT
BIOSTRAT. ZONE/ FOSSIL CHARACTER
FORAMINIFERS
NANNOFOSSILS
RADIOLARIANS
DIATOMS
PALEOMAGNETICS
PHYS. PROPERTIES
CHEMISTRY
SECTION
METERS
GRAPHIC LITHOLOGY
DRILLING DISTURB.
SED. STRUCTURES
SAMPLES
LOWER MIOCENE
N5
NN2
C/M
A/M
φ=50.8
ρ=1.85
%CaCO3 =93.0
V=1779 φ=47.5
ρ=1.89
%CaCO3=89.3
V=1767 φ=49.8
ρ=1.86
%CaCO3=92.9
%CaCO3=92.7
V=1634 φ=51.4
ρ=1.85
%CaCO3=93.9
V=1874 φ=51.2
ρ=1.84
φ=45.4
ρ=1.93
%CaCO3=92.7
1
2
3
4
5
6
CC
0.5
1.0

LITHOLOGIC DESCRIPTION

NANNOFOSSIL CHALK

Major lithology: The core contains moderately to heavily bioturbated NANNOFOSSIL CHALK. It is predominantly white (2.5Y 8/0) in color but grades into pale purple (5P 6/2) between 60 and 135 cm in Section 1 and between 20 and 60 cm in Section 4. Heavily burrowed, light gray (5Y 7/1), 5- to 10-cm-thick intervals of sediment are noted throughout the core.

SMEAR SLIDE SUMMARY (%):

	3, 45
	D
TEXTURE:	
Sand	15
Silt	80
Clay	5
COMPOSITION:	
Foraminifers	8
Nannofossils	90
Radiolarians	2

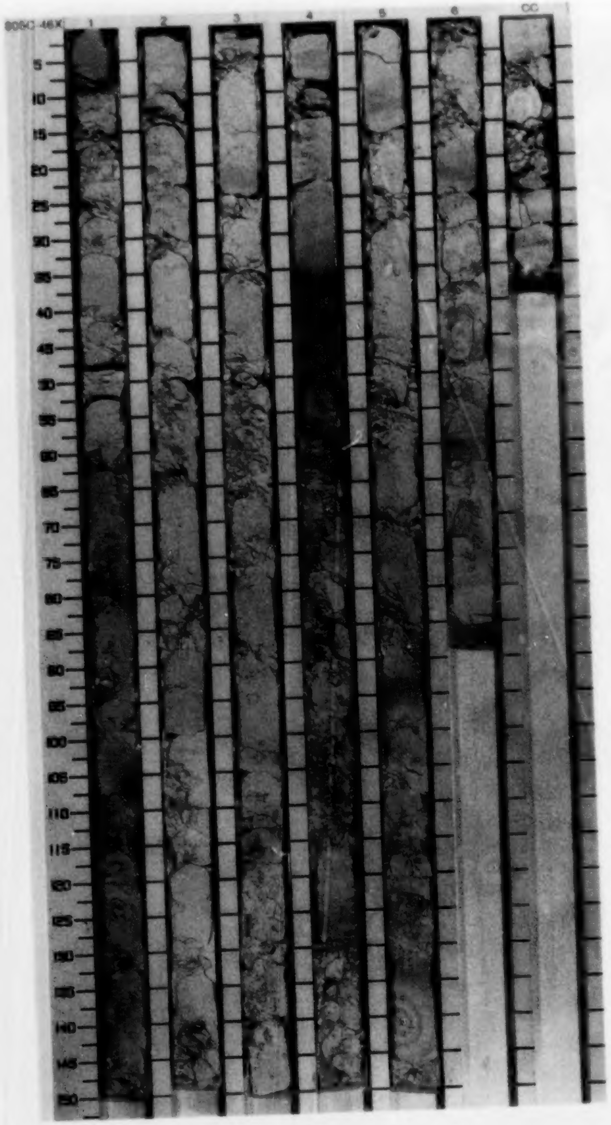
805C-46X
1
2
3
4
5
6
CC
5
10
15
20
25
30
35
40
45
50
55
60
65
70
75
80
85
90
95
100
105
110
115
120
125
130
135
140
145
150

SITE 805 HOLE C CORE 47X CORED INTERVAL 438.1-447.7 mbsf

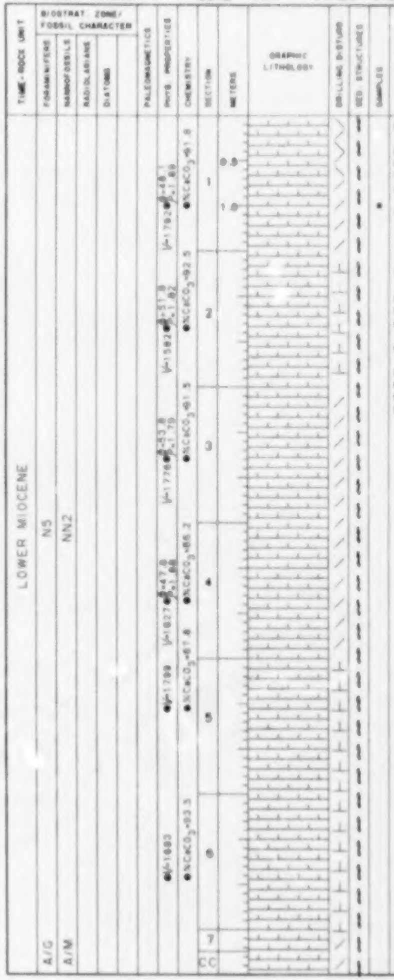
TIME-ROCK UNIT
BIOSTRAT. ZONE/ FOSSIL CHARACTER
FORAMINIFERS
NANNOFOSSILS
RADIOLARIANS
DIATOMS
PALEOMAGNETICS
PHYS. PROPERTIES
CHEMISTRY
SECTION
METERS
GRAPHIC LITHOLOGY
DRILLING DISTURB.
SED. STRUCTURES
SAMPLES
LOWER MIOCENE
N5
NN2
A/G
A/M
V=1792 φ=48.1 γ=1.89
V=1582 φ=51.8 γ=1.82
V=1776 φ=53.8 γ=1.70
V=1827 φ=47.8 γ=1.88
V=1799
V=1883
●%CaCO3=91.8
●%CaCO3=92.5
●%CaCO3=91.5
●%CaCO3=86.2
●%CaCO3=87.6
●%CaCO3=93.5
1
2
3
4
5
6
7
CC
0.5
1.0

LITHOLOGIC DESCRIPTION

NANNOFOSSIL CHALK

Major lithology: The core contains moderately to heavily bioturbated NANNOFOSSIL CHALK. It is predominantly white (2.5Y 8/0) in color but grades into pale purple in the upper portion of Section 3. A faint, light gray (5Y 7/1) color band is visible at Section 1, 82 cm. A grayish purple (5P 4/2) halo is present in Section 7.

SMEAR SLIDE SUMMARY (%):

	1, 99
	D
TEXTURE:	
Sand	10
Silt	85
Clay	2
COMPOSITION:	
Foraminifers	8
Nannofossils	85
Radiolarians	2
Silicoflagellates	1

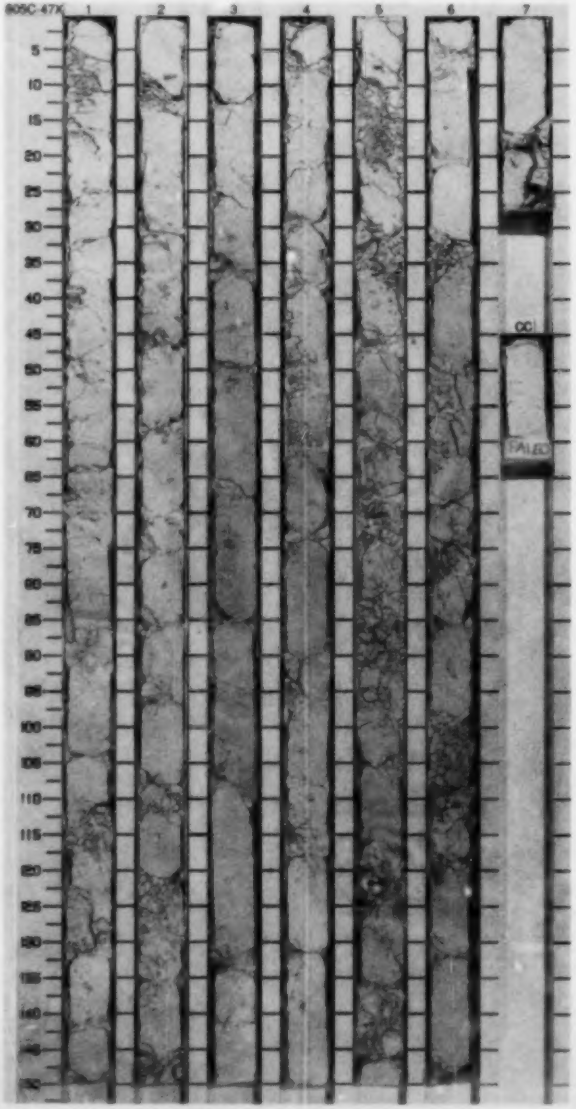
805C-47X
1
2
3
4
5
6
7
CC
PALEO
5
10
15
20
25
30
35
40
45
50
55
60
65
70
75
80
85
90
95
100
105
110
115
120
125
130
135
140
145
150

SITE 805 HOLE C CORE 48X CORED INTERVAL 447.7-457.4 mbsf

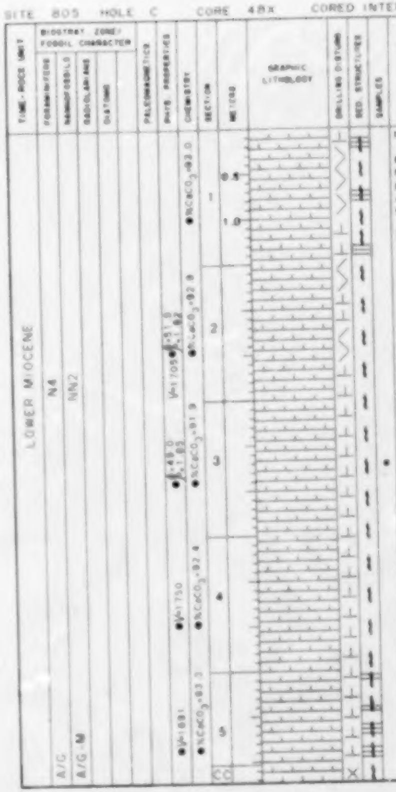

LITHOLOGIC DESCRIPTION

NANNOFOSSIL CHALK

Major lithology: The core contains NANNOFOSSIL CHALK. It is predominantly white (2.5 Y 8/0) in color but grades into pale blue (5P 7/2) in the lower part of Section 4 and into very pale purple (5RP 8/2) in Section 5. The sediment is moderately bioturbated with well-developed *Zoophycos* trace fossils. Faint to distinct, mm-size, light gray (5Y 7/1), gray (N 6/1) and greenish gray (5G 6/1) color bands are common.

SMEAR SLIDE SUMMARY (%):

	3, 71
	D
TEXTURE:	
Sand	10
Silt	85
Clay	5
COMPOSITION:	
Foraminifers	8
Nannofossils	90
Radiolarians	2

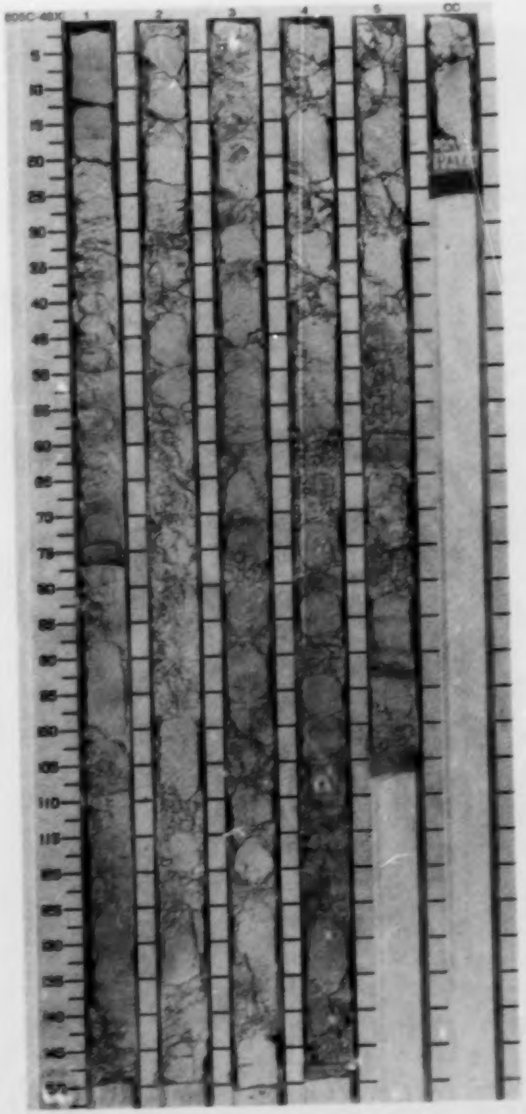
805C-48X
1
2
3
4
5
CC
5
10
15
20
25
30
35
40
45
50
55
60
65
70
75
80
85
90
95
100
105
110
115
120
125
130
135
140
145
150

SITE 805 HOLE C CORE 49X CORED INTERVAL 457.4-467.0 mbsf

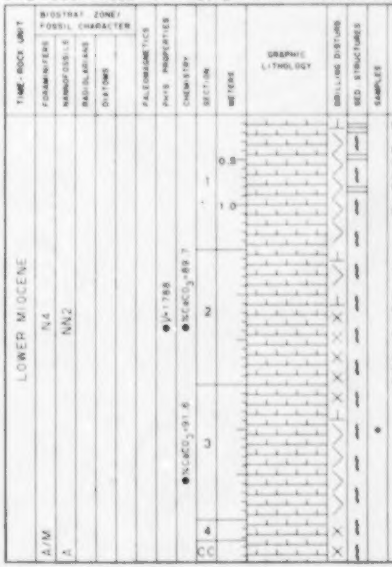
TIME-ROCK UNIT
BIOSTRAT. ZONE/ FOSSIL CHARACTER
FORAMINIFERS
NANNOFOSSILS
RADIOLARIANS
DIATOMS
PALEOMAGNETICS
PHYS. PROPERTIES
CHEMISTRY
SECTION
METERS
GRAPHIC LITHOLOGY
DRILLING DISTURB.
SED. STRUCTURES
SAMPLES
LOWER MIOCENE
N4
NN2
A/M
A
●γ=1.788
●%CaCO3=89.7
●%CaCO3=91.6
1
2
3
4
CC
0.5
1.0

LITHOLOGIC DESCRIPTION

NANNOFOSSIL CHALK

Major lithology: The core contains slightly to moderately bioturbated NANNOFOSSIL CHALK. It is predominantly white (2.5Y 8/0, 5Y 8/1 and 10YR 8/1) in color with a 10-cm thick, light gray zone in Section 2. Distinct, mm size, grayish green (5G 5/2) color bands are seen in Section 1, and mm to cm size, diffuse pale blue (5PB 7/2) bands are present throughout the core.

SMEAR SLIDE SUMMARY (%):

	3, 50
	D
TEXTURE:	
Silt	95
Clay	5
COMPOSITION:	
Foraminifers	1
Nannofossils	99
Radiolarians	Tr

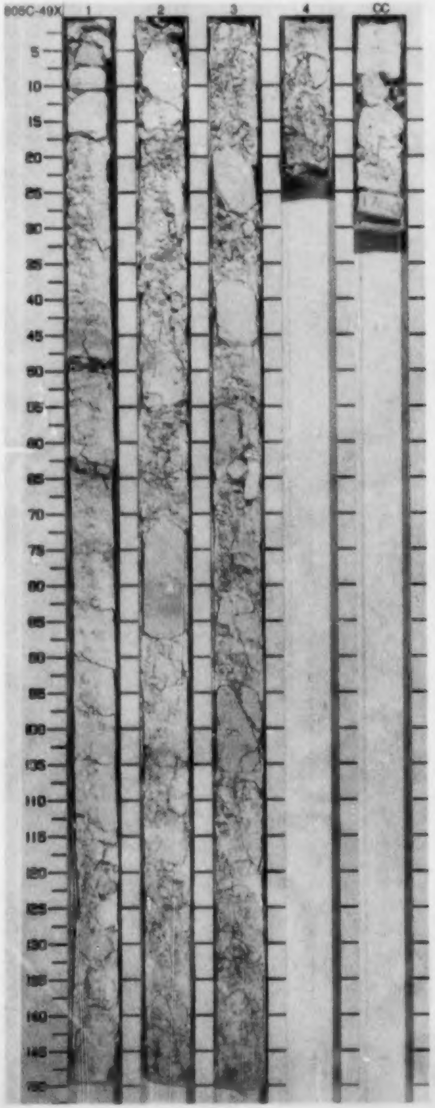
805C-49X
1
2
3
4
CC
5
10
15
20
25
30
35
40
45
50
55
60
65
70
75
80
85
90
95
100
105
110
115
120
125
130
135
140
145
150

SITE 805 HOLE C CORE 50X CORED INTERVAL 467.0-475.5 mbsf

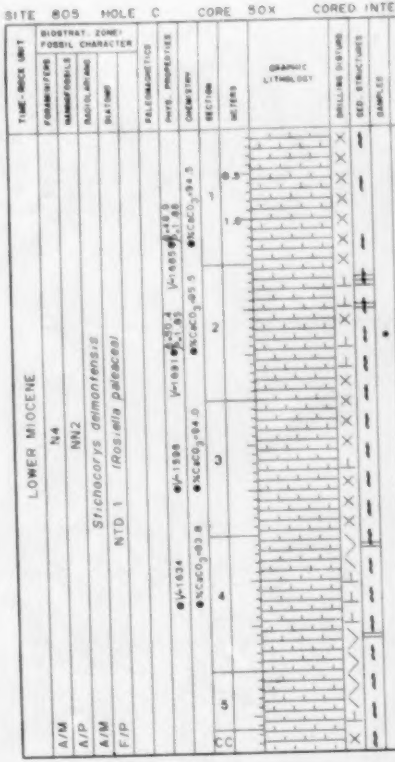

LITHOLOGIC DESCRIPTION

NANNOFOSSIL CHALK

Major lithology: This core contains NANNOFOSSIL CHALK, which is predominantly white (2.5Y 8/0) but grades to pale blue (5PB 7/2) and pale pink (5RP 8/2) in 10 to 40 cm thick intervals of Sections 1, 2, and 3. Well defined, mm scale, greenish gray (5GY 6/1), pale blue (5PB 7/2), and gray (N5/) bands are present in Sections 2 and 4. The entire core is slightly to moderately bioturbated.

SMEAR SLIDE SUMMARY (%):

	2, 80
	D
TEXTURE	
Sand	8
Silt	60
Clay	32
COMPOSITION	
Foraminifers	5
Nannofossils	92
Radiolarians	3

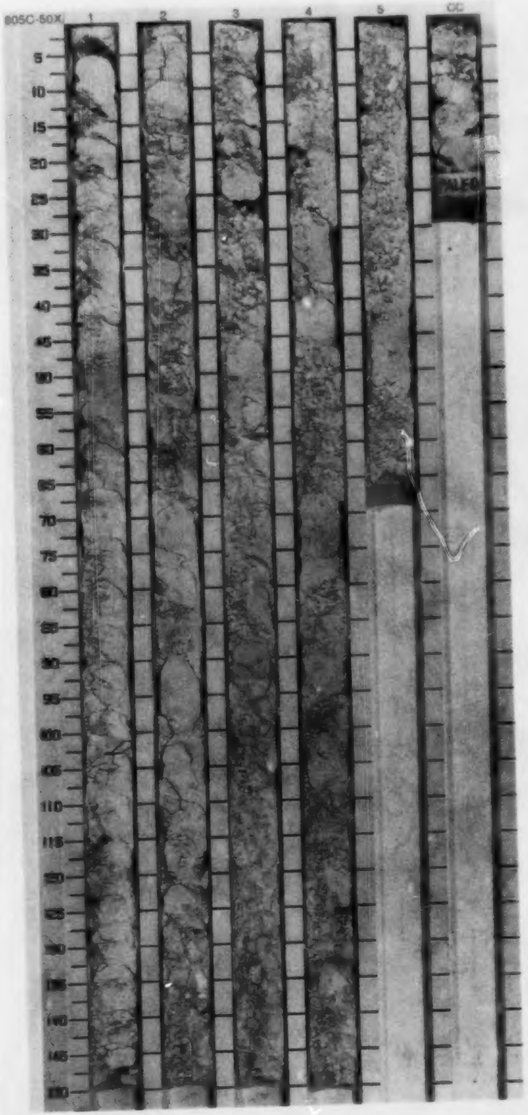
805C-50X
1
2
3
4
5
CC
PALEO
5
10
15
20
25
30
35
40
45
50
55
60
65
70
75
80
85
90
95
100
105
110
115
120
125
130
135
140
145
150

SITE 805 HOLE C CORE 51X CORED INTERVAL 475.5-485.2 mbsf

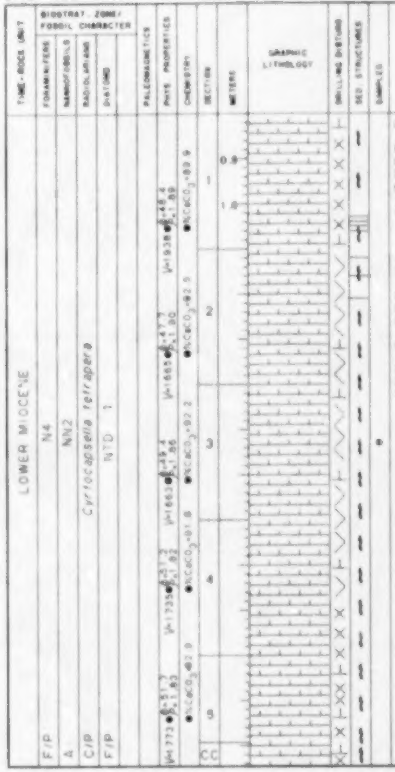
TIME-ROCK UNIT
BIOSTRAT. ZONE/ FOSSIL CHARACTER
FORAMINIFERS
NANNOFOSSILS
RADIOLARIANS
DIATOMS
PALEOMAGNETICS
PHYS. PROPERTIES
CHEMISTRY
SECTION
METERS
GRAPHIC LITHOLOGY
DRILLING DISTURB.
SED. STRUCTURES
SAMPLES
LOWER MIOCENE
N4
NN2
Cyrtocapsella tetrapera
NTD 1
F/P
A
C/P
F/P
V=1938 ϕ=48.4 γ=1.89
V=1665 ϕ=47.7 γ=1.90
V=1663 ϕ=49.4 γ=1.86
V=1735 ϕ=51.2 γ=1.82
V=1773 ϕ=51.7 γ=1.83
%CaCO₃=89.9
%CaCO₃=92.5
%CaCO₃=92.2
%CaCO₃=91.8
%CaCO₃=92.0
1
2
3
4
5
CC
0.8
1.0

LITHOLOGIC DESCRIPTION

NANNOFOSSIL CHALK

Major lithology: This core contains moderately bioturbated NANNOFOSSIL CHALK. The core is predominantly white (2.5Y 8/0) in color, but the lower part of Section 1 and the upper part of Section 2 are pale purple (5P 6/2). Light gray (5Y 7/1), cm-size color band with mm-size grayish green sub-bands, are present in Sections 1 and 2.

SMEAR SLIDE SUMMARY (%):

	3, 84
	D
TEXTURE:	
Sand	2
Silt	95
Clay	3
COMPOSITION:	
Foraminifers	5
Nannofossils	92
Radiolarians	3

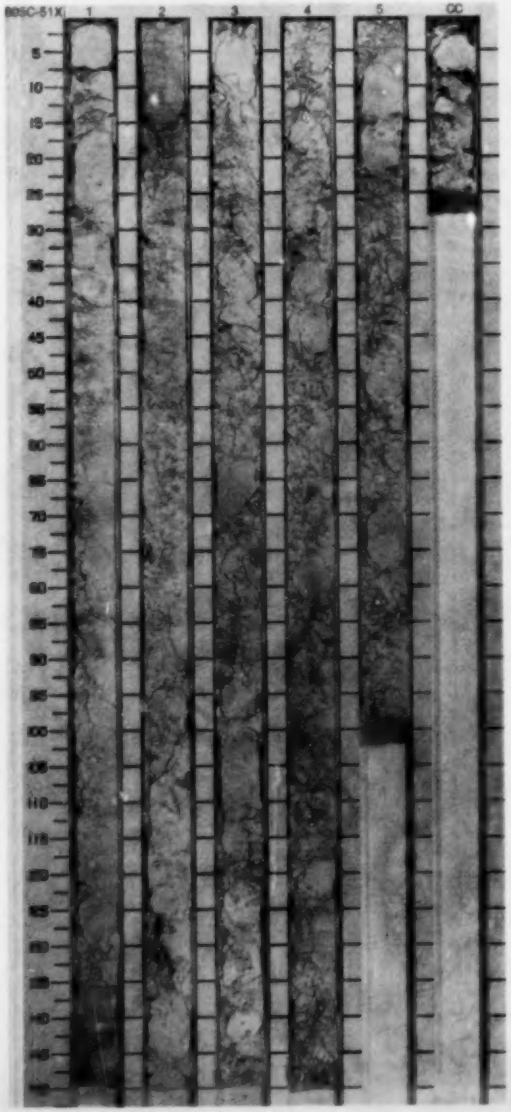
805C-51X
1
2
3
4
5
CC
5
10
15
20
25
30
35
40
45
50
55
60
65
70
75
80
85
90
95
100
105
110
115
120
125
130
135
140
145
150

SITE 805 HOLE C CORE 52X CORED INTERVAL 485.2-494.9 mbsf

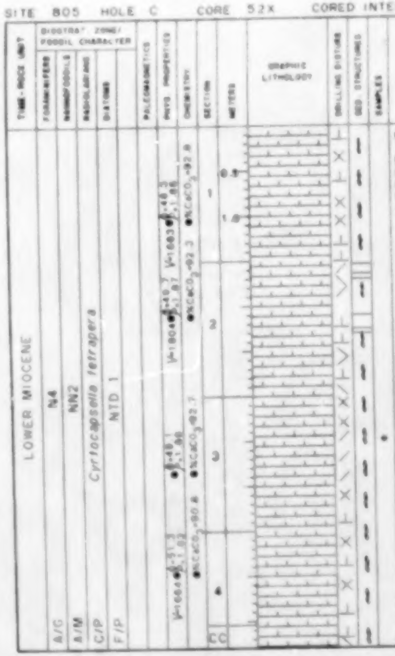
TIME-ROCK UNIT
BIOSTRAT. ZONE/ FOSSIL CHARACTER
FORAMINIFERS
NANNOFOSSILS
RADIOLARIANS
DIATOMS
PALEOMAGNETICS
PHYS. PROPERTIES
CHEMISTRY
SECTION
METERS
GRAPHIC LITHOLOGY
DRILLING DISTURB.
SED. STRUCTURES
SAMPLES
LOWER MIOCENE
N4
NN2
Cyrtocapsella tetrapera
NTD 1
A/G
A/M
C/P
F/P
V=1663
φ=48.3
γ=1.86
V=1804
φ=40.7
γ=1.97
φ=49.1
γ=1.86
V=1664
φ=51.3
γ=1.82
%CaCO₃=92.8
%CaCO₃=92.3
%CaCO₃=92.7
%CaCO₃=90.8
1
2
3
4
CC
0.5
1.0

LITHOLOGIC DESCRIPTION

NANNOFOSSIL CHALK

Major lithology: This core contains white (2.5Y 8/0) NANNOFOSSIL CHALK, which grades into pale pink (5RP 8/2) in the lower half of Section 1, the top half of Section 2, and a 30 cm interval in the middle of Section 3. The core is moderately fragmented to highly fractured. Bioturbation is slight to moderate. In Section 2, white and pale blue (5PB 7/2) color bands and well-defined, mm scale, greenish gray (5G 6/1) color bands are noted.

SMEAR SLIDE SUMMARY (%):

	3, 40 D
TEXTURE	
Sand	2
Silt	95
Clay	3
COMPOSITION	
Foraminifers	4
Nannofossils	95
Radiolarians	1

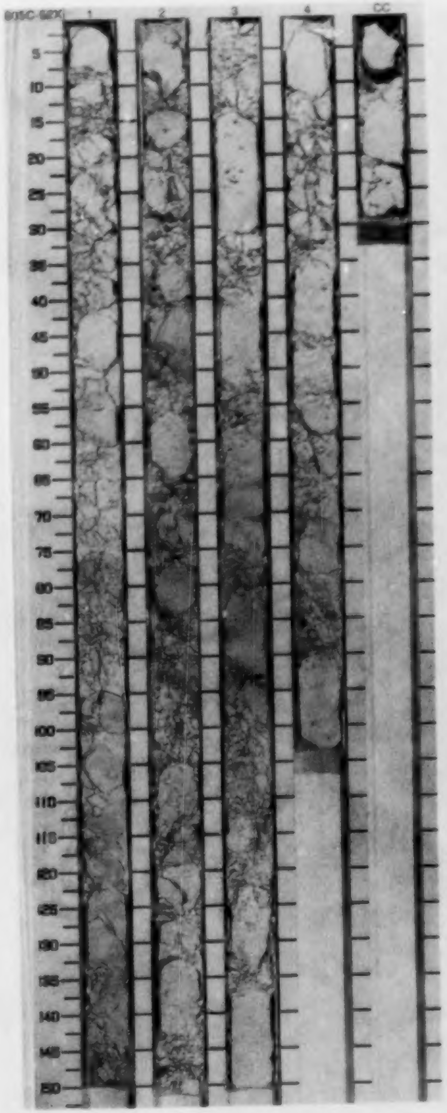
805C-52X
1
2
3
4
CC
5
10
15
20
25
30
35
40
45
50
55
60
65
70
75
80
85
90
95
100
105
110
115
120
125
130
135
140
145
150

SITE 805 HOLE C CORE 53X CORED INTERVAL 494.9-504.8 mbsf

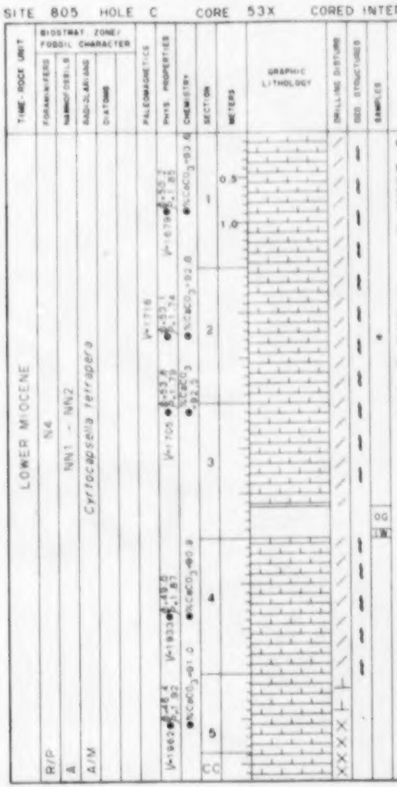
TIME-ROCK UNIT
BIOSTRAT. ZONE/ FOSSIL CHARACTER
FORAMINIFERS
NANNOFOSSILS
RADIOLARIANS
DIATOMS
PALEOMAGNETICS
PHYS. PROPERTIES
CHEMISTRY
SECTION
METERS
GRAPHIC LITHOLOGY
DRILLING DISTURB.
SED. STRUCTURES
SAMPLES
LOWER MIOCENE
N4
NN1 - NN2
Cyrtocapsella tetrapera
R/P
A
A/M
V=1716
V=1679 ϕ=50.2 ρ=1.85
ϕ=53.1 ρ=1.74
V=1705 ϕ=53.8 ρ=1.79
V=1933 ϕ=49.0 ρ=1.87
V=1962 ϕ=48.4 ρ=1.92
%CaCO3=93.6
%CaCO3=92.8
%CaCO3=92.5
%CaCO3=90.9
%CaCO3=91.0
1
2
3
4
5
CC
0.5
1.0
OG
IW

LITHOLOGIC DESCRIPTION

NANNOFOSSIL CHALK

Major lithology: This core contains moderately to highly bioturbated, homogeneous, white (2.5Y 8/0) NANNOFOSSIL CHALK. The core is pale purple (5P 6/2) from the lower part of Section 2 through the middle of Section 3. Sections 1 through 4 are slightly fractured, while Sections 5 and CC are moderately fractured to brecciated.

SMEAR SLIDE SUMMARY (%):

	2, 79
	D
TEXTURE	
Sand	10
Silt	85
Clay	5
COMPOSITION	
Foraminifers	8
Nannofossils	90
Radiolarians	2

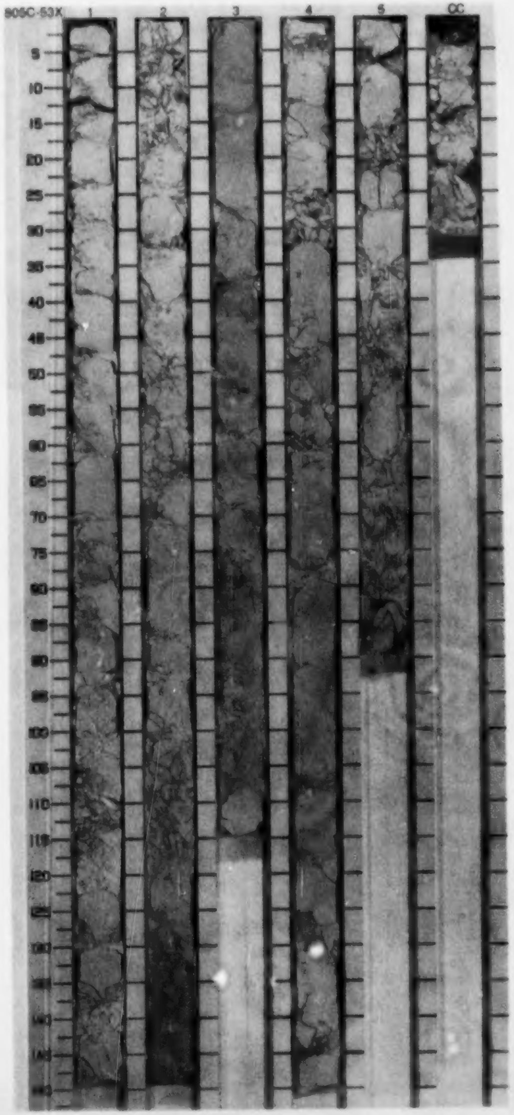
805C-53X
1
2
3
4
5
CC
5
10
15
20
25
30
35
40
45
50
55
60
65
70
75
80
85
90
95
100
105
110
115
120
125
130
135
140
145
150

SITE 805 HOLE C CORE 54X CORED INTERVAL 504.6-514.2 mbsf

TIME-ROCK UNIT	FORAMINIFERS	NANNOFOSSILS	RADIOLARIANS	DIATOMS	PALEOMAGNETICS	PHYS. PROPERTIES	CHEMISTRY	SECTION	METERS
LOWER MIOCENE	R/P N4	A/G NN1 - NN2	A/M *Dorcadospyris ateuchus - Lychnocanoma elongata*	R-F/P-M NDT 1?		●φ=51.8 ρ=1.85	●%CaCO₃ =93.6	1	0.9 1.0
						V=1748●φ=51.8 ρ=1.92	●%CaCO₃=94.3	2	
						V=1825●φ=46.3 ρ=1.93	●%CaCO₃=92.0	3	
						V=1733●φ=48.0 ρ=1.92	●%CaCO₃=85.6	4	
								5	
								CC	

LITHOLOGIC DESCRIPTION

NANNOFOSSIL CHALK

Major lithology: This core contains heavily bioturbated, homogeneous, white (2.5Y 8/0) NANNOFOSSIL CHALK. From Section 2, 37 cm to Section 3, 73 cm, the chalk is pale pink (5RP 8/2) in color.

SMEAR SLIDE SUMMARY (%):

	2, 75
	D
TEXTURE:	
Sand	1
Silt	49
Clay	50
COMPOSITION:	
Foraminifers	8
Nannofossils	90
Siliceous fragments	2

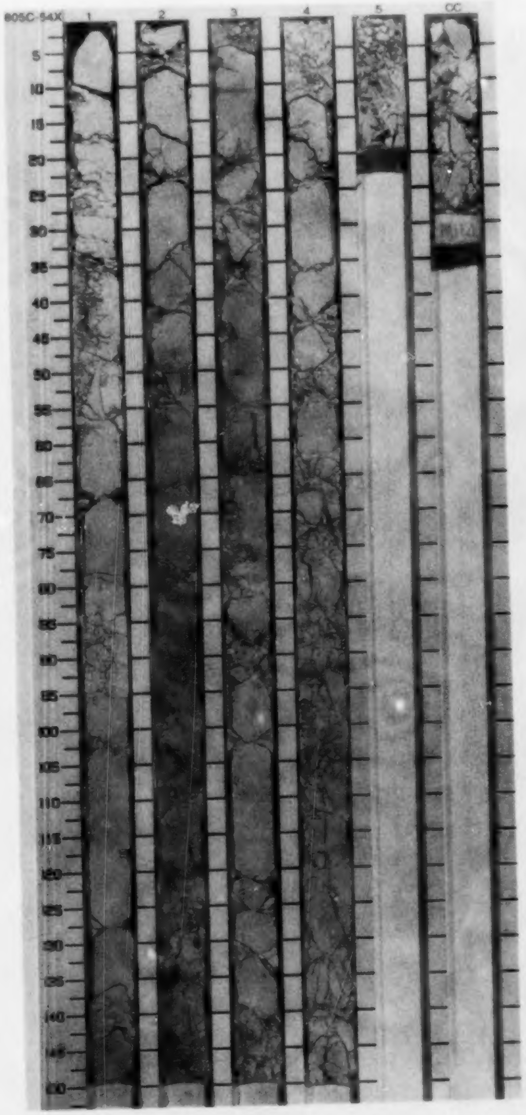
805C-54X
1
2
3
4
5
CC
5
10
15
20
25
30
35
40
45
50
55
60
65
70
75
80
85
90
95
100
105
110
115
120
125
130
135
140
145
150

SITE 805 HOLE C CORE 55X CORED INTERVAL 514.2-523.9 mbsf

TIME-ROCK UNIT	BIOSTRAT. ZONE/ FOSSIL CHARACTER: FORAMINIFERS	NANNOFOSSILS	RADIOLARIANS	DIATOMS	PALEOMAGNETICS	PHYS. PROPERTIES	CHEMISTRY	SECTION	METERS	GRAPHIC LITHOLOGY	DRILLING DISTURB.	SED. STRUCTURES	SAMPLES
LOWER MIOCENE	N4	NN1 - NN2	D. ateuchus - L. elongata	?		V=1855 ●φ=48.7 ρ=1.89	●%CaCO3=92.8	1	0.5 1.0				
						V=1807 ●φ=46.1 ρ=1.91	●%CaCO3=94.5	2					●
						V=1890 ●φ=44.1 ρ=1.93	●%CaCO3=89.5	3					
	R/P	A	A/P	F/P-M				CC					

LITHOLOGIC DESCRIPTION

NANNOFOSSIL CHALK

Major lithology: This core contains homogeneous, white (2.5Y 8/0) NANNOFOSSIL CHALK. The sediment has abundant burrows and trace fossils, indicative of heavy bioturbation. These structures appear to be compacted and possibly smeared. The sediment at Section 2, 125 to 140 cm, shows evidence of cracks that have rehealed.

SMEAR SLIDE SUMMARY (%):

	2, 70
	D
TEXTURE:	
Sand	10
Silt	60
Clay	30
COMPOSITION:	
Foraminifers	Tr
Nannofossils	100
Siliceous fragments	Tr

SITE 805 HOLE C CORE 56X CORED INTERVAL 523.9-533.5 mbsf

TIME-ROCK UNIT	BIOSTRAT. ZONE/ FOSSIL CHARACTER: FORAMINIFERS	NANNOFOSSILS	RADIOLARIANS	DIATOMS	PALEOMAGNETICS	PHYS. PROPERTIES	CHEMISTRY	SECTION	METERS	GRAPHIC LITHOLOGY	DRILLING DISTURB.	SED. STRUCTURES	SAMPLES
UPPER OLIGOCENE	P22	NN1 - NN2	Dorcadospyris ateuchus?	Bogorovia veniamini				1					
	F/P	A/M	A/M	F/P-M				CC					

LITHOLOGIC DESCRIPTION

NANNOFOSSIL CHALK

Major lithology: This core contains homogeneous, white (2.5Y 8/0) NANNOFOSSIL CHALK. The chalk has abundant bioturbation structures that appear to be compacted and possibly smeared (tectonized).

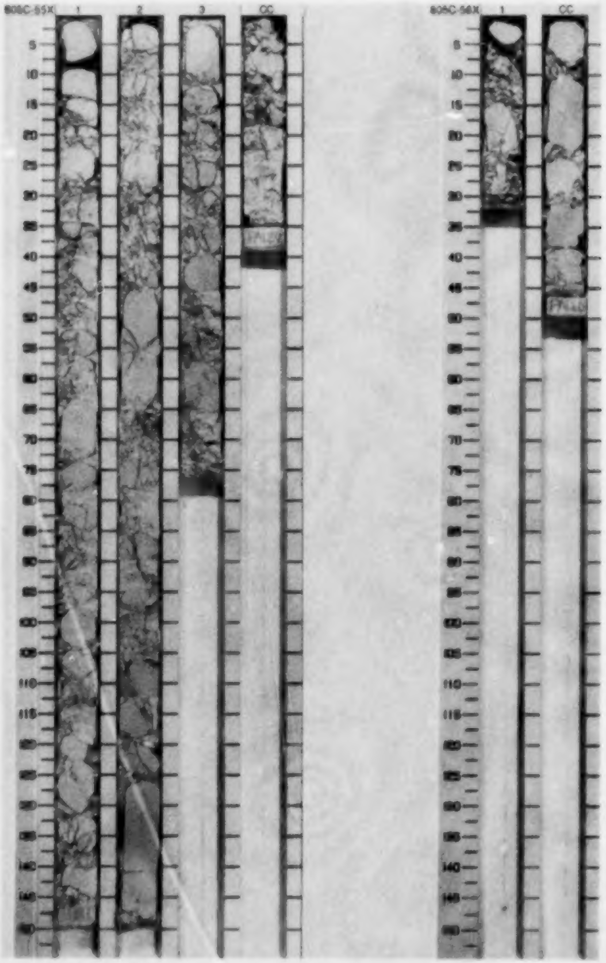

SITE 805 HOLE C CORE 57X CORED INTERVAL 533.5-543.2 mbsf

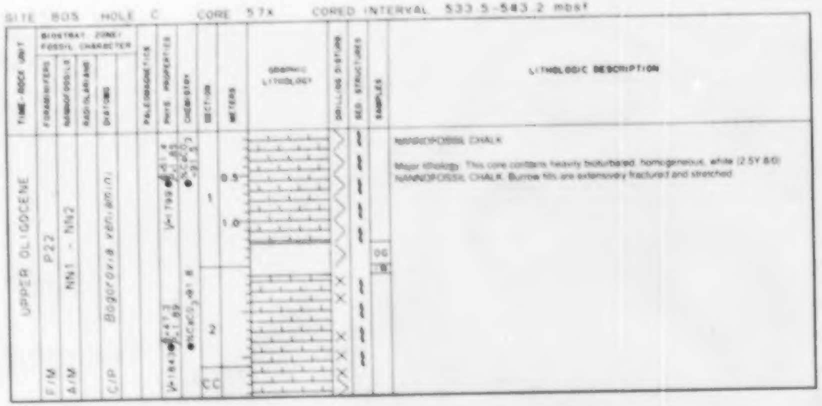
TIME-ROCK UNIT
BIOSTRAT. ZONE/ FOSSIL CHARACTER
FORAMINIFERS
NANNOFOSSILS
RADIOLARIANS
DIATOMS
PALEOMAGNETICS
PHYS. PROPERTIES
CHEMISTRY
SECTION
METERS
GRAPHIC LITHOLOGY
DRILLING DISTURB.
SED. STRUCTURES
SAMPLES
LITHOLOGIC DESCRIPTION
UPPER OLIGOCENE
P22
F/M
NN1 - NN2
A/M
Bogorovia veniamini
C/P
V=1843
%CaCO₃=91.8
1
2
CC
0.5
1.0
OG
IW

NANNOFOSSIL CHALK

Major lithology: This core contains heavily bioturbated, homogeneous, white (2.5Y 8/0) NANNOFOSSIL CHALK. Burrow fills are extensively fractured and stretched.

SITE 805 HOLE C CORE 58X CORED INTERVAL 543.2-552.9 mbsf

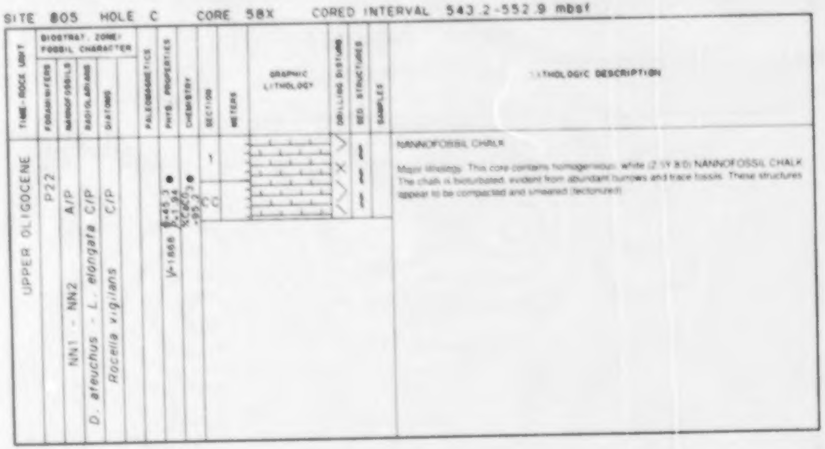
TIME-ROCK UNIT
BIOSTRAT. ZONE/ FOSSIL CHARACTER
FORAMINIFERS
NANNOFOSSILS
RADIOLARIANS
DIATOMS
PALEOMAGNETICS
PHYS. PROPERTIES
CHEMISTRY
SECTION
METERS
GRAPHIC LITHOLOGY
DRILLING DISTURB.
SED. STRUCTURES
SAMPLES
LITHOLOGIC DESCRIPTION
UPPER OLIGOCENE
P22
NN1 - NN2
A/P
D. ateuchus - L. elongata C/P
Rocella vigilans
C/P
V=1866 φ=45.3 ρ=1.94
%CaCO₃=95.2
1
CC

NANNOFOSSIL CHALK

Major lithology: This core contains homogeneous, white (2.5Y 8/0) NANNOFOSSIL CHALK. The chalk is bioturbated, evident from abundant burrows and trace fossils. These structures appear to be compacted and smeared (tectonized).

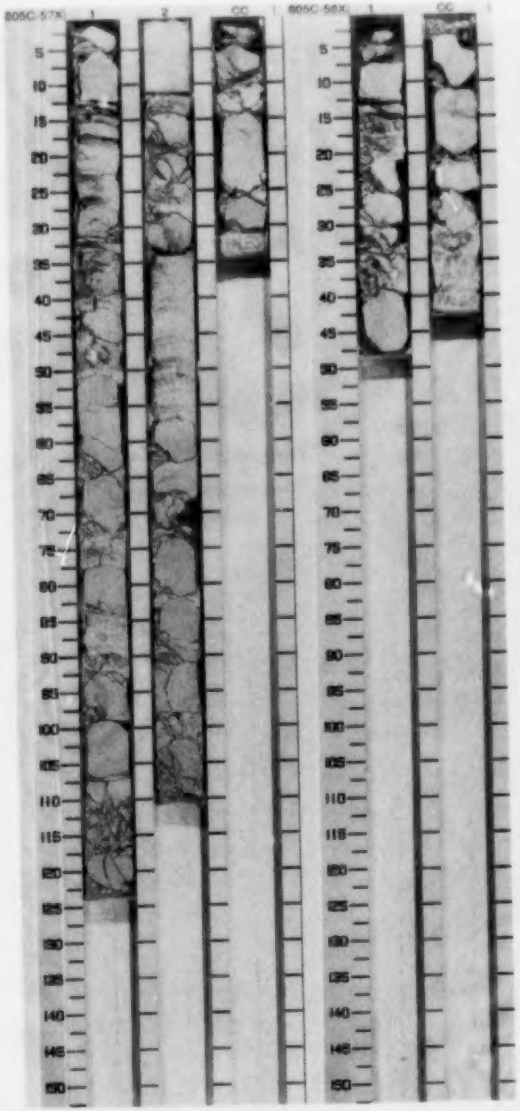
805C-57X
1
2
CC
805C-58X
1
CC
5
10
15
20
25
30
35
40
45
50
55
60
65
70
75
80
85
90
95
100
105
110
115
120
125
130
135
140
145
150

SITE 805 HOLE C CORE 59X CORED INTERVAL 552.9-562.6 mbsf

TIME-ROCK UNIT	FORAMINIFERS	NANNOFOSSILS	RADIOLARIANS	DIATOMS	PALEOMAGNETICS	PHYS. PROPERTIES	CHEMISTRY	SECTION	METERS	GRAPHIC LITHOLOGY	DRILLING DISTURB.	SED. STRUCTURES	SAMPLES
UPPER OLIGOCENE	P22 F/M	NP25? A/M				● [illegible] ● [illegible]	● %CaCO₃=[illegible] ● %CaCO₃=89.3	1 2 CC	0.5 1.0		⊥ ⊥ X X ⊥ ⊥ ⊥ ⊥ ⊥		●

LITHOLOGIC DESCRIPTION

NANNOFOSSIL CHALK

Major lithology: This core contains homogeneous, white (2.5Y 8/0) NANNOFOSSIL CHALK. Bioturbation is apparent from abundant trace fossils. The core is highly disturbed by the coring process.

SMEAR SLIDE SUMMARY (%):

	CC, 10
	D
TEXTURE:	
Sand	5
Silt	65
Clay	30
COMPOSITION:	
Foraminifers	3
Nannofossils	95
Siliceous fragments	2

SITE 805 HOLE C CORE 60X CORED INTERVAL 562.6-572.3 mbsf

TIME-ROCK UNIT	FORAMINIFERS	NANNOFOSSILS	RADIOLARIANS	DIATOMS	PALEOMAGNETICS	PHYS. PROPERTIES	CHEMISTRY	SECTION	METERS	GRAPHIC LITHOLOGY	DRILLING DISTURB.	SED. STRUCTURES	SAMPLES
UPPER OLIGOCENE	P22 F/M	NP25 A/M	*D. ateuchus - L. elongata* C/P	*Rocella vigilans* A/P		● [illegible]	● %CaCO₃=[illegible]	1 CC	0.5		X X X ╱X		

LITHOLOGIC DESCRIPTION

NANNOFOSSIL CHALK

Major lithology: This core contains homogeneous, white (2.5Y 8/0) NANNOFOSSIL CHALK.

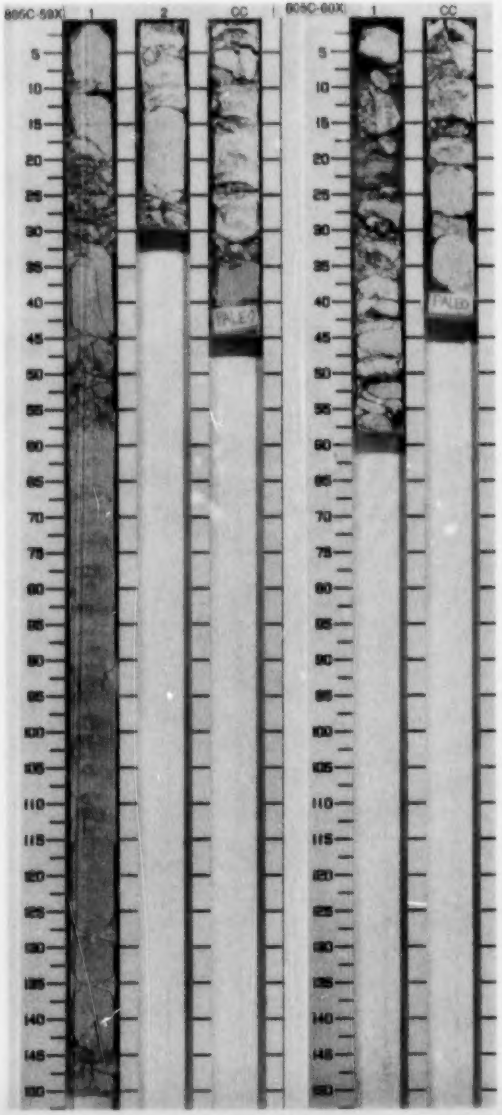

SITE 805 HOLE C CORE 61X CORED INTERVAL 572.3-582.0 mbsf

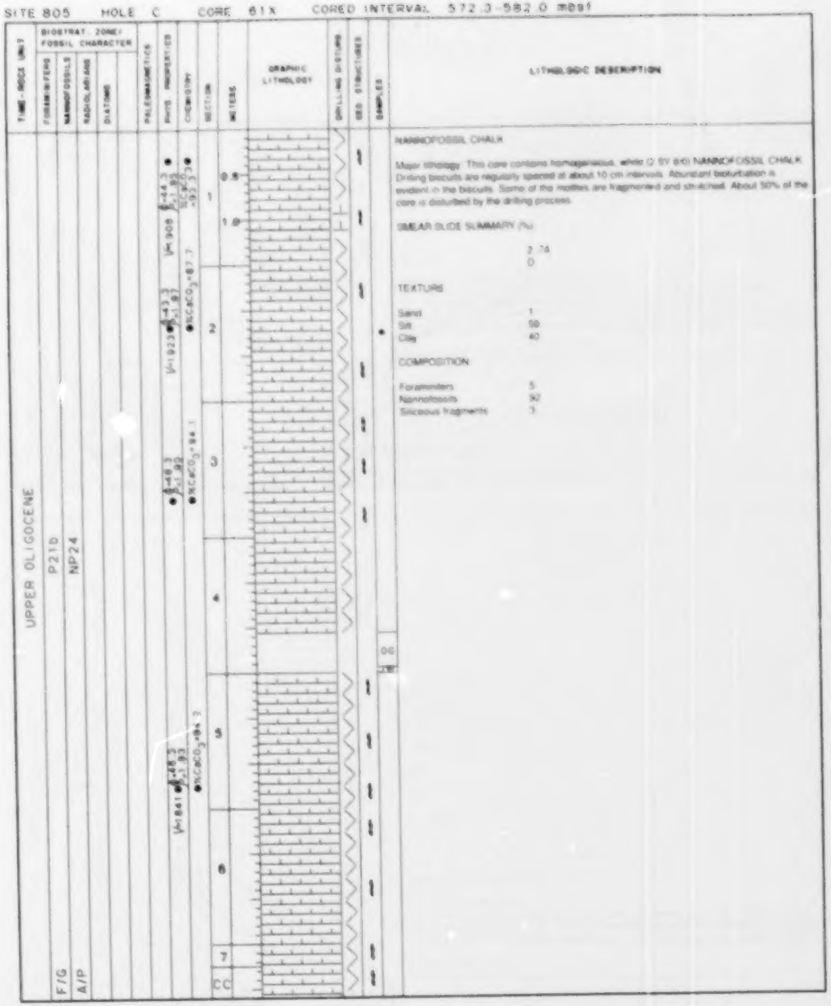
TIME-ROCK UNIT
BIOSTRAT. ZONE/ FOSSIL CHARACTER
FORAMINIFERS
NANNOFOSSILS
RADIOLARIANS
DIATOMS
PALEOMAGNETICS
PHYS. PROPERTIES
CHEMISTRY
SECTION
METERS
GRAPHIC LITHOLOGY
DRILLING DISTURB.
SED. STRUCTURES
SAMPLES
LITHOLOGIC DESCRIPTION
UPPER OLIGOCENE
P21b
NP24
F/G
A/P
V=1908
φ=44.3
γ=1.85
%CaCO3=93.3
V=1923
φ=43.3
γ=1.97
%CaCO3=87.7
φ=46.3
γ=1.92
%CaCO3=94.1
V=1841
φ=46.3
γ=1.93
%CaCO3=94.3
0.5
1.0
1
2
3
4
5
6
7
CC
OG

NANNOFOSSIL CHALK

Major lithology: This core contains homogeneous, white (2.5Y 8/0) NANNOFOSSIL CHALK. Drilling biscuits are regularly spaced at about 10 cm intervals. Abundant bioturbation is evident in the biscuits. Some of the mottles are fragmented and stretched. About 50% of the core is disturbed by the drilling process.

SMEAR SLIDE SUMMARY (%):

	2, 74
	D
TEXTURE:	
Sand	1
Silt	59
Clay	40
COMPOSITION:	
Foraminifers	5
Nannofossils	92
Siliceous fragments	3

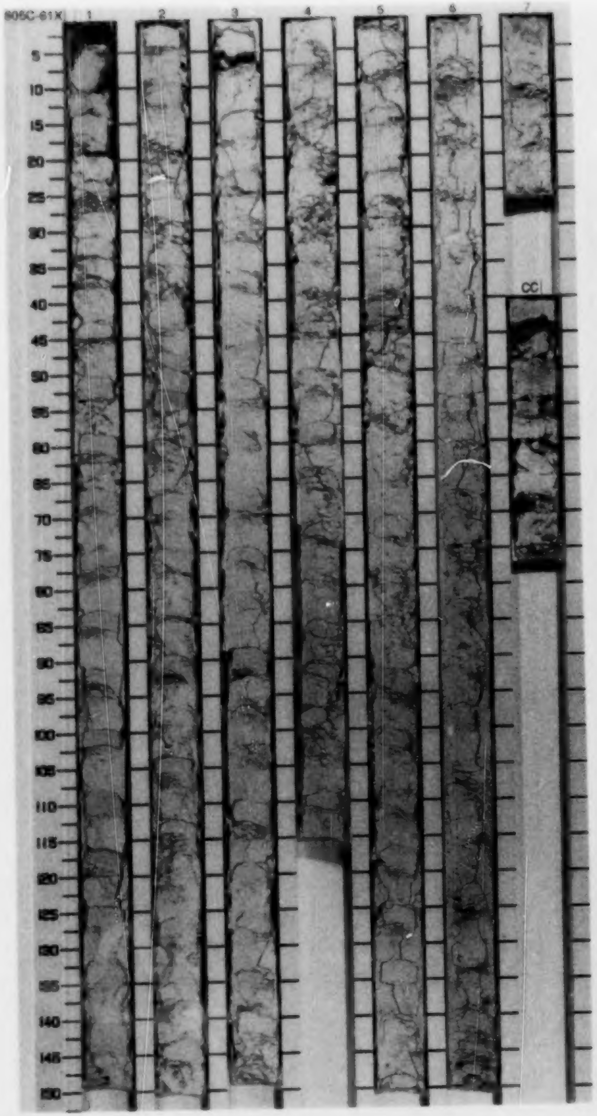
805C-61X
1
2
3
4
5
6
7
CC
5
10
15
20
25
30
35
40
45
50
55
60
65
70
75
80
85
90
95
100
105
110
115
120
125
130
135
140
145
150

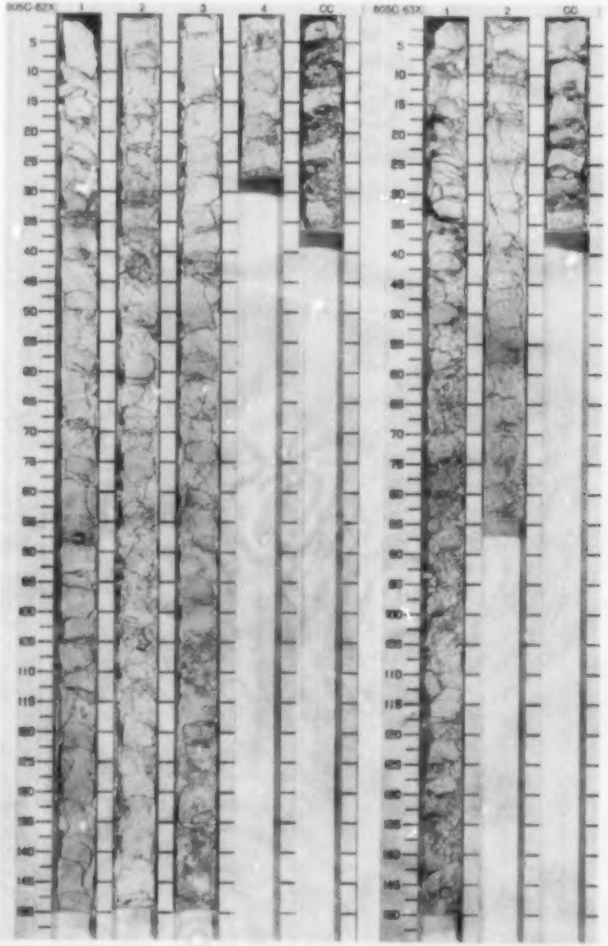
805C-62X
1
2
3
4
CC
805C-63X
1
2
CC
5
10
15
20
25
30
35
40
45
50
55
60
65
70
75
80
85
90
95
100
105
110
115
120
125
130
135
140
145
150

SITE 805 HOLE C CORE 62X CORED INTERVAL 582.0-591.7 mbsf

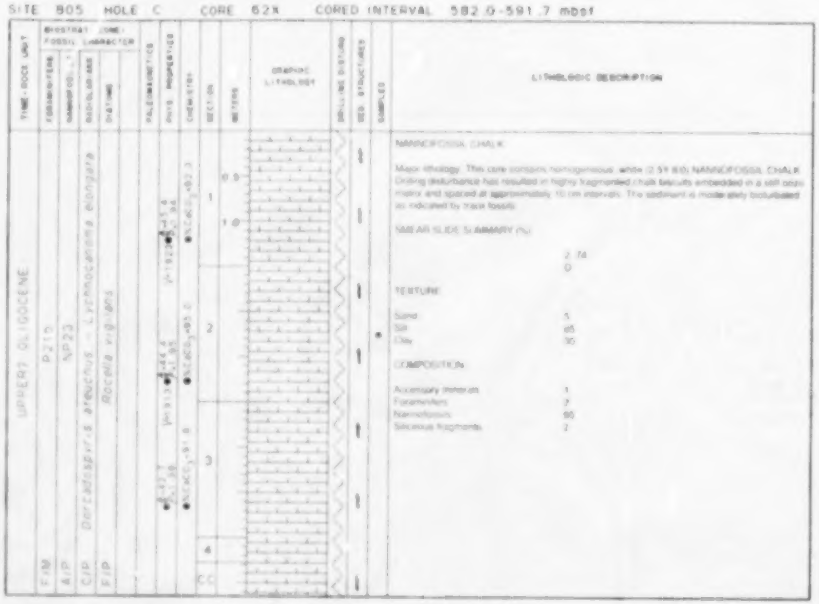
TIME-ROCK UNIT
BIOSTRAT. ZONE/FOSSIL CHARACTER
FORAMINIFERS
NANNOFOSSILS
RADIOLARIANS
DIATOMS
PALEOMAGNETICS
PHYS. PROPERTIES
CHEMISTRY
SECTION
METERS
GRAPHIC LITHOLOGY
DRILLING DISTURB.
SED. STRUCTURES
SAMPLES
UPPER? OLIGOCENE
P21b
NP23
Dorcadospyris ateuchus - Lychnocanoma elongata
Rocella vigilans
F/M
A/P
C/P
F/P
φ=45.4
γ=1.94
Vp=1623
%CaCO3=92.3
φ=44.4
γ=1.95
Vp=1613
%CaCO3=95.0
φ=43.7
γ=1.98
%CaCO3=91.8
0.5
1.0
1
2
3
4
CC

LITHOLOGIC DESCRIPTION

NANNOFOSSIL CHALK

Major lithology: This core contains homogeneous white (2.5Y 8/0) NANNOFOSSIL CHALK. Drilling disturbance has resulted in highly fragmented chalk biscuits embedded in a stiff ooze matrix and spaced at approximately 10 cm intervals. The sediment is moderately bioturbated as indicated by trace fossils.

SMEAR SLIDE SUMMARY (%):

	2, 74
	D
TEXTURE:	
Sand	5
Silt	65
Clay	30
COMPOSITION:	
Accessory minerals	1
Foraminifers	7
Nannofossils	90
Siliceous fragments	2

SITE 805 HOLE C CORE 63X CORED INTERVAL 591.7-601.3 mbsf

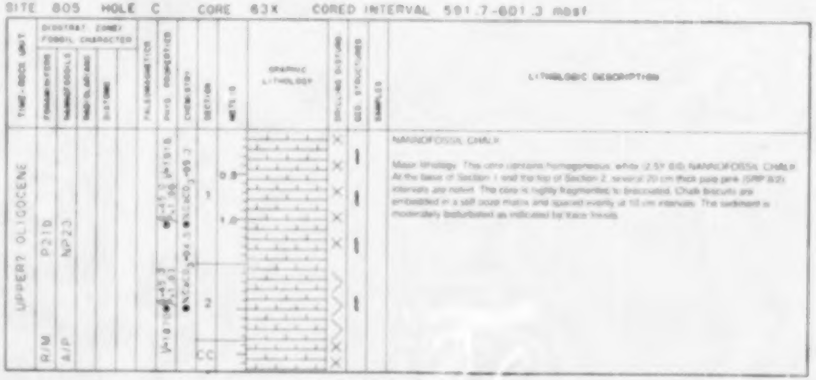
TIME-ROCK UNIT
BIOSTRAT. ZONE/FOSSIL CHARACTER
FORAMINIFERS
NANNOFOSSILS
RADIOLARIANS
DIATOMS
PALEOMAGNETICS
PHYS. PROPERTIES
CHEMISTRY
SECTION
METERS
GRAPHIC LITHOLOGY
DRILLING DISTURB.
SED. STRUCTURES
SAMPLES
UPPER? OLIGOCENE
P21b
NP23
R/M
A/P
Vp=1610
φ=45.2
γ=1.90
%CaCO3=93.3
%CaCO3=94.5
φ=45.3
γ=1.91
Vp=1670
0.5
1.0
1
2
CC

LITHOLOGIC DESCRIPTION

NANNOFOSSIL CHALK

Major lithology: This core contains homogeneous white (2.5Y 8/0) NANNOFOSSIL CHALK. At the base of Section 1 and the top of Section 2, several 20 cm thick pale pink (5RP 8/2) intervals are noted. The core is highly fragmented to brecciated. Chalk biscuits are embedded in a stiff ooze matrix and spaced evenly at 10 cm intervals. The sediment is moderately bioturbated as indicated by trace fossils.

SITE 805 HOLE C CORE 64X CORED INTERVAL 601.3-611.0 mbsf

TIME-ROCK UNIT	BIOSTRAT. ZONE/ FOSSIL CHARACTER: FORAMINIFERS	NANNOFOSSILS	RADIOLARIANS	DIATOMS		PALEOMAGNETICS	PHYS. PROPERTIES	CHEMISTRY	SECTION	METERS	GRAPHIC LITHOLOGY	DRILLING DISTURB.	SED. STRUCTURES	SAMPLES	LITHOLOGIC DESCRIPTION
UPPER OLIGOCENE	P21b R/M	NP23 A/P	D. ateuchus - L. elongata A/M	? F/P			● [illegible] 43.0 [illegible] V=1898	● [illegible]	1 CC	0.5				●	NANNOFOSSIL CHALK Major lithology: This core contains homogeneous, white (2.5Y 8/0) NANNOFOSSIL CHALK. The few chalk biscuits are bioturbated. SMEAR SLIDE SUMMARY (%): 1, 15 D TEXTURE: Sand 5 Silt 50 Clay 40 COMPOSITION: Nannofossils 100

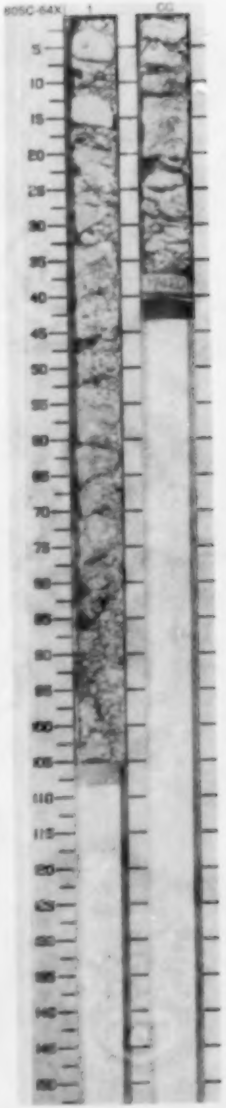
805C-64X
1
CC
5
10
15
20
25
30
35
40
45
50
55
60
65
70
75
80
85
90
95
100
105
110
115
120
125
130
135
140
145
150

SITE 806 HOLE A CORE 1H CORED INTERVAL 0.0-7.7 mbsf

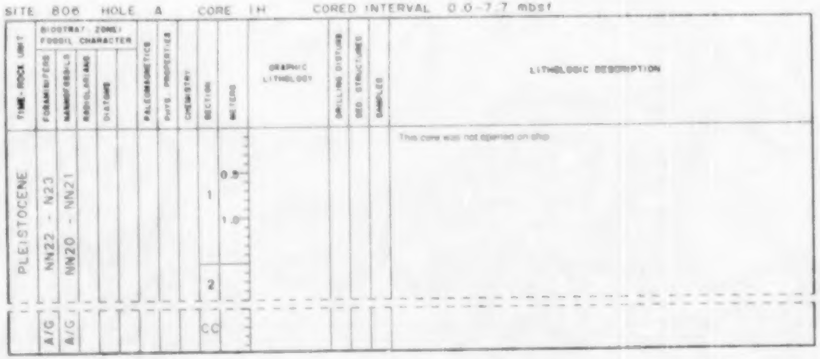
TIME-ROCK UNIT
BIOSTRAT. ZONE/ FOSSIL CHARACTER
FORAMINIFERS
NANNOFOSSILS
RADIOLARIANS
DIATOMS
PALEOMAGNETICS
PHYS. PROPERTIES
CHEMISTRY
SECTION
METERS
GRAPHIC LITHOLOGY
DRILLING DISTURB.
SED. STRUCTURES
SAMPLES
LITHOLOGIC DESCRIPTION
PLEISTOCENE
NN22 - N23
NN20 - NN21
A/G
A/G
1
2
CC
0.5
1.0

This core was not opened on ship

SITE 806 HOLE A CORE 2H CORED INTERVAL 7.7-17.2 mbsf

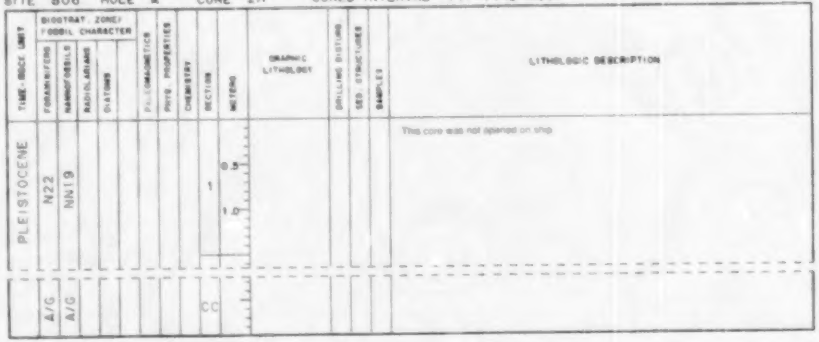
TIME-ROCK UNIT
BIOSTRAT. ZONE/ FOSSIL CHARACTER
FORAMINIFERS
NANNOFOSSILS
RADIOLARIANS
DIATOMS
PALEOMAGNETICS
PHYS. PROPERTIES
CHEMISTRY
SECTION
METERS
GRAPHIC LITHOLOGY
DRILLING DISTURB.
SED. STRUCTURES
SAMPLES
LITHOLOGIC DESCRIPTION
PLEISTOCENE
N22
NN19
A/G
A/G
1
CC
0.5
1.0

This core was not opened on ship

SITE 806 HOLE A CORE 3H CORED INTERVAL 17.2-26.7 mbsf

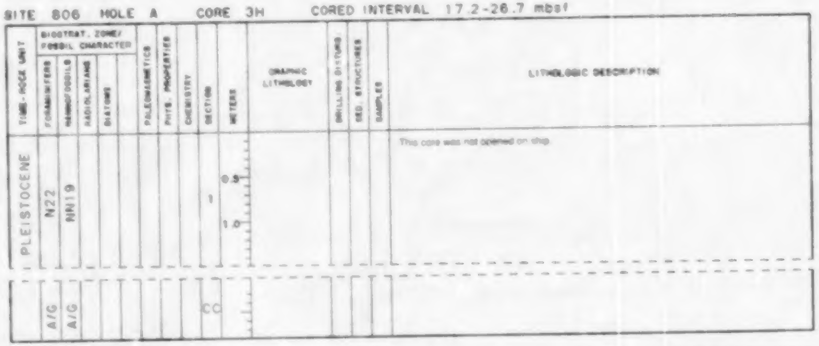
TIME-ROCK UNIT
BIOSTRAT. ZONE/ FOSSIL CHARACTER
FORAMINIFERS
NANNOFOSSILS
RADIOLARIANS
DIATOMS
PALEOMAGNETICS
PHYS. PROPERTIES
CHEMISTRY
SECTION
METERS
GRAPHIC LITHOLOGY
DRILLING DISTURB.
SED. STRUCTURES
SAMPLES
LITHOLOGIC DESCRIPTION
PLEISTOCENE
N22
NN19
A/G
A/G
1
CC
0.5
1.0

This core was not opened on ship

SITE 806 HOLE A CORE 4H CORED INTERVAL 26.7-36.2 mbsf

TIME-ROCK UNIT	BIOSTRAT. ZONE/ FOSSIL CHARACTER				PALEOMAGNETICS	PHYS. PROPERTIES	CHEMISTRY	SECTION	METERS	GRAPHIC LITHOLOGY	DRILLING DISTURB.	SED. STRUCTURES	SAMPLES	LITHOLOGIC DESCRIPTION
	FORAMINIFERS	NANNOFOSSILS	RADIOLARIANS	DIATOMS										
PLEISTOCENE	N21?	NN19						1	0.5 1.0					This core was not opened on ship
	A/G	A/M						CC						

SITE 806 HOLE A CORE 5H CORED INTERVAL 36.2-45.7 mbsf

TIME-ROCK UNIT	BIOSTRAT. ZONE/ FOSSIL CHARACTER				PALEOMAGNETICS	PHYS. PROPERTIES	CHEMISTRY	SECTION	METERS	GRAPHIC LITHOLOGY	DRILLING DISTURB.	SED. STRUCTURES	SAMPLES	LITHOLOGIC DESCRIPTION
	FORAMINIFERS	NANNOFOSSILS	RADIOLARIANS	DIATOMS										
UPPER PLIOCENE	N21	NN18						1 2	0.5 1.0					This core was not opened on ship
	A/G	A						CC						

SITE 806 HOLE A CORE 6H CORED INTERVAL 45.7-55.2 mbsf

TIME-ROCK UNIT	BIOSTRAT. ZONE/ FOSSIL CHARACTER				PALEOMAGNETICS	PHYS. PROPERTIES	CHEMISTRY	SECTION	METERS	GRAPHIC LITHOLOGY	DRILLING DISTURB.	SED. STRUCTURES	SAMPLES	LITHOLOGIC DESCRIPTION
	FORAMINIFERS	NANNOFOSSILS	RADIOLARIANS	DIATOMS										
UPPER PLIOCENE	N21	NN17						1	0.5 1.0					This core was not opened on ship
	A/G	A						CC						

SITE 806 HOLE A CORE 7H CORED INTERVAL 55.2-64.7 mbsf

TIME-ROCK UNIT	BIOSTRAT. ZONE/ FOSSIL CHARACTER				PALEOMAGNETICS	PHYS. PROPERTIES	CHEMISTRY	SECTION	METERS	GRAPHIC LITHOLOGY	DRILLING DISTURB.	SED. STRUCTURES	SAMPLES	LITHOLOGIC DESCRIPTION
	FORAMINIFERS	NANNOFOSSILS	RADIOLARIANS	DIATOMS										
UPPER PLIOCENE	N19 - N20	NN16						1	0.5 1.0					This core was not opened on ship
	A/P	A/M						2						

SITE 806 HOLE A CORE 8H CORED INTERVAL 64.7-74.2 mbsf

TIME-ROCK UNIT	BIOSTRAT. ZONE/ FOSSIL CHARACTER				PALEOMAGNETICS	PHYS. PROPERTIES	CHEMISTRY	SECTION	METERS	GRAPHIC LITHOLOGY	DRILLING DISTURB.	SED. STRUCTURES	SAMPLES	LITHOLOGIC DESCRIPTION
	FORAMINIFERS	NANNOFOSSILS	RADIOLARIANS	DIATOMS										
UPPER PLIOCENE	N19 - N20	NN16						1	0.5 1.0					This core was not opened on ship
	A/P	A/M						CC						

SITE 806 HOLE A CORE 9H CORED INTERVAL 74.2-83.7 mbsf

TIME-ROCK UNIT	BIOSTRAT. ZONE/ FOSSIL CHARACTER				PALEOMAGNETICS	PHYS. PROPERTIES	CHEMISTRY	SECTION	METERS	GRAPHIC LITHOLOGY	DRILLING DISTURB.	SED. STRUCTURES	SAMPLES	LITHOLOGIC DESCRIPTION
	FORAMINIFERS	NANNOFOSSILS	RADIOLARIANS	DIATOMS										
UPPER PLIOCENE	N19 - N20	NN16						1	0.5 1.0					This core was not opened on ship
	A/G	A/G						CC						

SITE 806 HOLE B CORE 1H CORED INTERVAL 0.0-6.5 mbsf

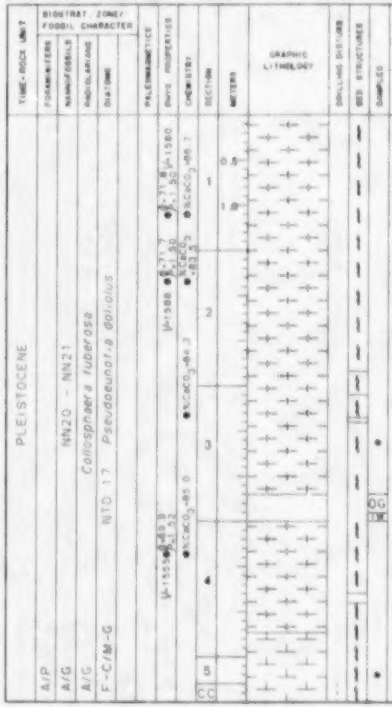
TIME-ROCK UNIT
BIOSTRAT. ZONE/ FOSSIL CHARACTER
FORAMINIFERS
NANNOFOSSILS
RADIOLARIANS
DIATOMS
PALEOMAGNETICS
PHYS. PROPERTIES
CHEMISTRY
SECTION
METERS
GRAPHIC LITHOLOGY
DRILLING DISTURB.
SED. STRUCTURES
SAMPLES
PLEISTOCENE
A/P
A/G
NN20 - NN21
A/G
Collosphaera tuberosa
F-C/M-G
NTD 17 Pseudoeunotia doliolus
γ=71.8 γ=1.50 V=1580
V=1588 φ=71.7 γ=1.50
V=1555 φ=69.9 γ=1.52
%CaCO3=86.7
%CaCO3=83.5
%CaCO3=84.2
%CaCO3=85.0
1
2
3
4
5
CC
0.5
1.0
OG
IW

LITHOLOGIC DESCRIPTION

FORAMINIFER NANNOFOSSIL OOZE and NANNOFOSSIL OOZE with FORAMINIFERS

Major lithology: This core contains FORAMINIFER NANNOFOSSIL OOZE which grades into NANNOFOSSIL OOZE with FORAMINIFERS in Section 4 at 122 cm. Section 1 grades from very pale brown (10YR 7/3) into light gray (10YR 7/2 to 5Y 7/1). Below Section 1, 108 cm, the dominant color is light gray (5Y 7/1) with short intervals of light gray (10YR 7/1) and gray (2.5Y 6/0). Section 5 and Core Catcher are predominantly white (2.5Y 8/0). The sediments are moderately bioturbated with common grayish blue 5/2) and light olive gray (5Y 6/2) mottling. Faint greenish gray (10GY 5/2 and 5G 6/1) and grayish blue (5PB 5/2) color bands are sporadically present in Sections 2 through 4.

SMEAR SLIDE SUMMARY (%)

	3, 62 D	5, 20 D
TEXTURE		
Sand	40	30
Silt	60	70
COMPOSITION		
Foraminifers	40	23
Nannofossils	55	72
Radiolarians	5	5

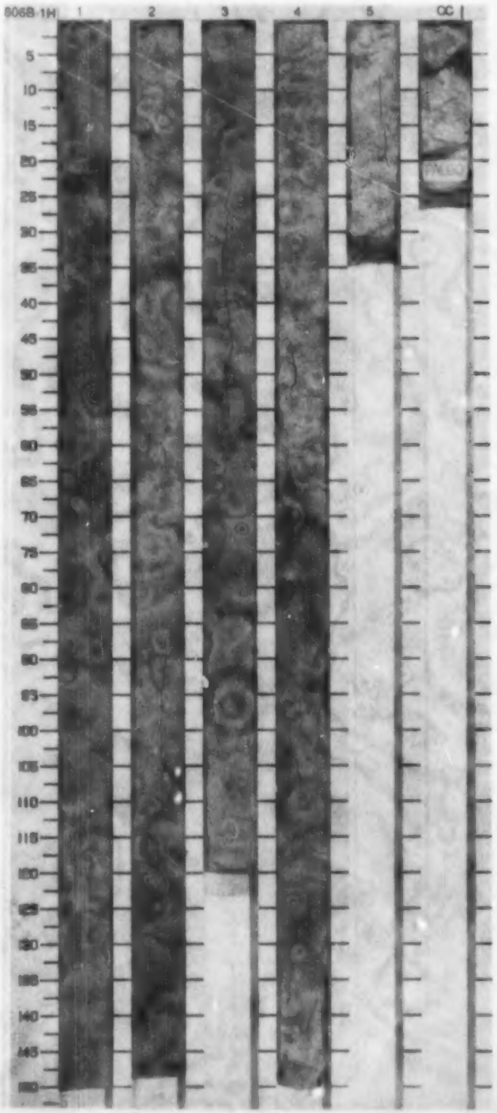
806B-1H
1
2
3
4
5
CC
5
10
15
20
25
30
35
40
45
50
55
60
65
70
75
80
85
90
95
100
105
110
115
120
125
130
135
140
145
150

SITE 806 HOLE B CORE 2H CORED INTERVAL 6.5-16.0 mbsf

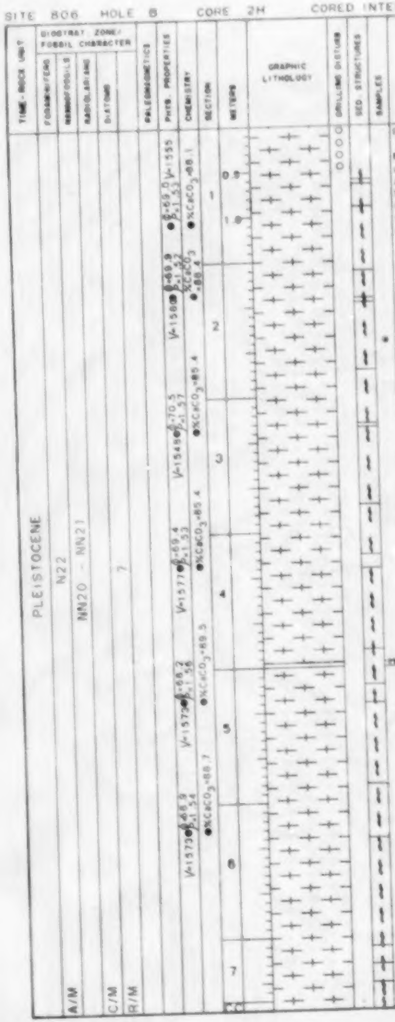
TIME-ROCK UNIT
BIOSTRAT. ZONE/ FOSSIL CHARACTER
FORAMINIFERS
NANNOFOSSILS
RADIOLARIANS
DIATOMS
PALEOMAGNETICS
PHYS. PROPERTIES
CHEMISTRY
SECTION
METERS
GRAPHIC LITHOLOGY
DRILLING DISTURB.
SED. STRUCTURES
SAMPLES
PLEISTOCENE
N22
NN20 - NN21
?
A/M
C/M
R/M
φ=69.0 γ=1.53 V=1555
%CaCO3=88.1
φ=69.9 γ=1.52 V=1580
%CaCO3=88.4
φ=70.5 γ=1.57 V=1548
%CaCO3=85.4
φ=69.4 γ=1.53 V=1577
%CaCO3=85.4
φ=68.2 γ=1.56 V=1573
%CaCO3=89.5
φ=68.9 γ=1.54 V=1573
%CaCO3=88.7
1
2
3
4
5
6
7
CC
0.5
1.0
*
IW

LITHOLOGIC DESCRIPTION

FORAMINIFER NANNOFOSSIL OOZE

Major lithology: The core contains FORAMINIFER NANNOFOSSIL OOZE. The dominant color alternates in 10 to 30 cm thick intervals between light gray (5Y 7/1), 10YR 7/1 to 10Y 7/1) and white (2.5Y 8/0). The white and lightest gray intervals are less sandy and contain fewer foraminifers than the darker ones, which are more heavily mottled. The sediments are moderately bioturbated with common, grayish blue (5PB 5/2) and light olive gray (5Y 6/2) mottling. Faint and sharp, greenish gray (5G 6/1) and grayish blue (5PB 5/2) color bands also are common.

SMEAR SLIDE SUMMARY (%):

	2, 80 D
TEXTURE:	
Sand	25
Silt	71
Clay	4
COMPOSITION:	
Foraminifers	30
Nannofossils	68
Radiolarians	1
Silicoflagellates	1

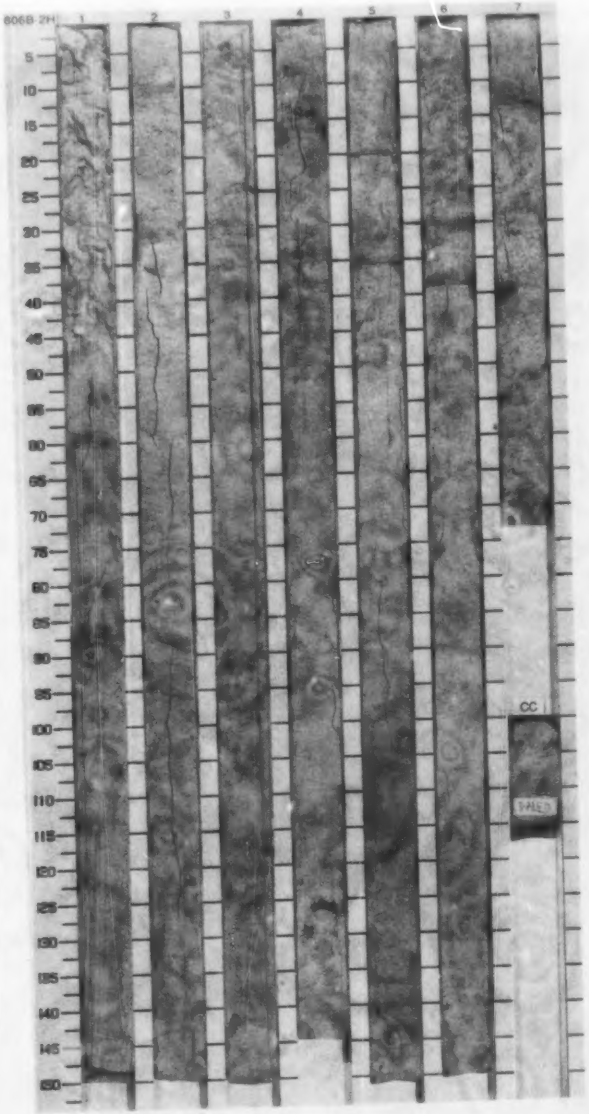
806B-2H
1
2
3
4
5
6
7
CC
5
10
15
20
25
30
35
40
45
50
55
60
65
70
75
80
85
90
95
100
105
110
115
120
125
130
135
140
145
150

SITE 806 HOLE B CORE 3H CORED INTERVAL 16.0-25.5 mbsf

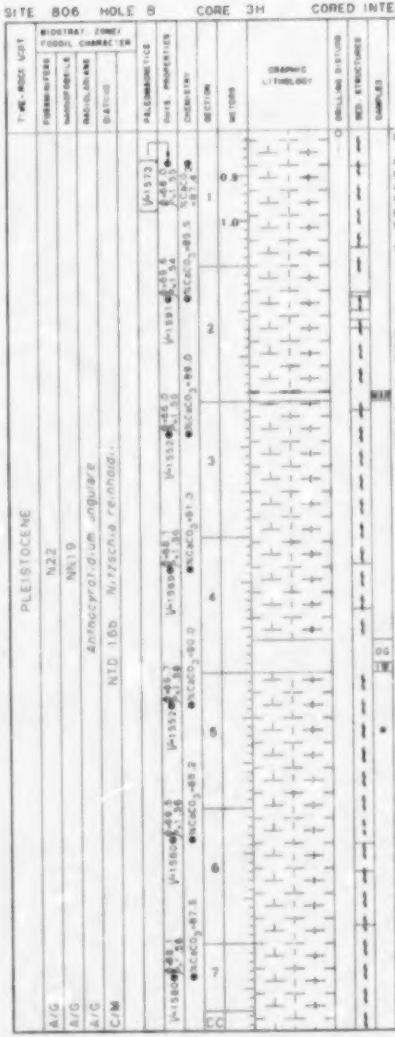
TIME-ROCK UNIT
BIOSTRAT. ZONE/ FOSSIL CHARACTER
FORAMINIFERS
NANNOFOSSILS
RADIOLARIANS
DIATOMS
PALEOMAGNETICS
PHYS. PROPERTIES
CHEMISTRY
SECTION
METERS
GRAPHIC LITHOLOGY
DRILLING DISTURB.
SED. STRUCTURES
SAMPLES
PLEISTOCENE
N22
NN19
Anthocyrtidium angulare
NTD 16b Nitzschia reinholdii
A/G
A/G
A/G
C/M
V=1573
φ=66.0
γ=1.55
%CaCO3=87.4
φ=68.6
γ=1.54
V=1591
%CaCO3=85.5
φ=66.0
γ=1.50
V=1552
%CaCO3=88.0
φ=68.1
γ=1.38
V=1580
%CaCO3=91.3
φ=66.7
γ=1.38
V=1552
%CaCO3=90.0
φ=69.5
γ=1.38
V=1580
%CaCO3=89.2
φ=68.1
γ=1.38
V=1580
%CaCO3=87.8
1
2
3
4
5
6
7
CC
0.5
1.0
OG
IW

LITHOLOGIC DESCRIPTION

FORAMINIFER NANNOFOSSIL OOZE AND NANNOFOSSIL OOZE with FORAMINIFERS

Major lithology: This core contains 10 to 70 cm thick, gradational interbeds of FORAMINIFER NANNOFOSSIL OOZE and NANNOFOSSIL OOZE with FORAMINIFERS. The primary colors are white (2.5Y 8/0) for the nannofossil ooze with foraminifers and light gray (5Y 7/1) for the foraminifer nannofossil ooze. The entire core is slightly to moderately bioturbated, with light gray (5Y 7/1), light olive gray (5Y 6/2), and grayish blue (5PB 5/2) mottling. Light greenish gray (5G 7/1) and grayish blue (5PB 5/2) color bands are common.

SMEAR SLIDE SUMMARY (%):

	5, 64
	D
TEXTURE:	
Sand	3
Silt	90
Clay	7
COMPOSITION:	
Foraminifers	15
Nannofossils	85
Radiolarians	Tr
Silicoflagellates	Tr

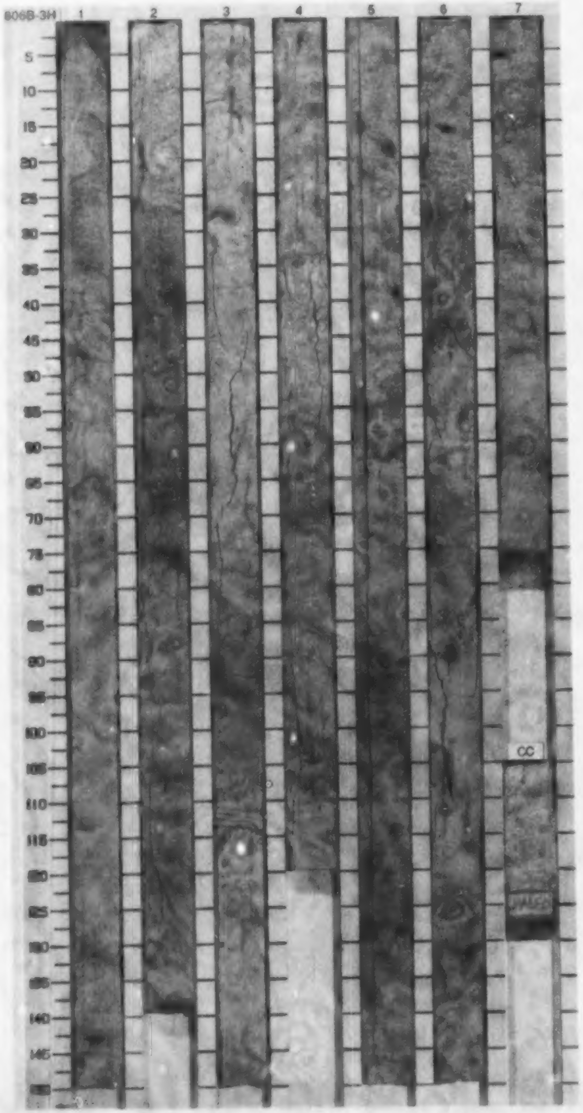
806B-3H
1
2
3
4
5
6
7
5
10
15
20
25
30
35
40
45
50
55
60
65
70
75
80
85
90
95
100
105
110
115
120
125
130
135
140
145
150
CC

SITE 806 HOLE B CORE 4H CORED INTERVAL 25.5-35.0 mbsf

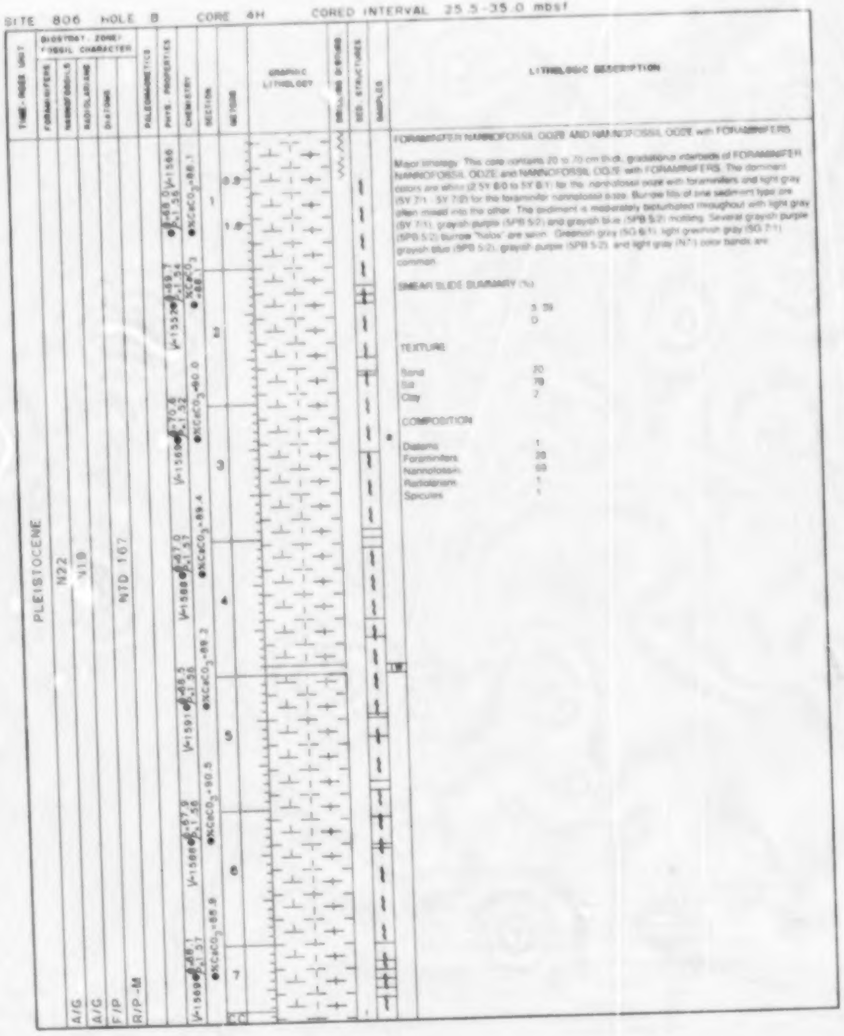
TIME-ROCK UNIT
BIOSTRAT. ZONE/ FOSSIL CHARACTER
FORAMINIFERS
NANNOFOSSILS
RADIOLARIANS
DIATOMS
PALEOMAGNETICS
PHYS. PROPERTIES
CHEMISTRY
SECTION
METERS
GRAPHIC LITHOLOGY
DRILLING DISTURB.
SED. STRUCTURES
SAMPLES
PLEISTOCENE
N22
NN19
NTD 167
A/G
A/G
F/P
R/P-M
Φ=68.0 ρ=1.56 V=1588
%CaCO3=88.1
Φ=69.7 ρ=1.54 V=1552
%CaCO3=88.1
Φ=70.6 ρ=1.52 V=1569
%CaCO3=90.0
Φ=67.0 ρ=1.57 V=1588
%CaCO3=89.4
Φ=68.5 ρ=1.56 V=1591
%CaCO3=89.2
Φ=67.9 ρ=1.56 V=1588
%CaCO3=90.5
Φ=68.1 ρ=1.57 V=1589
%CaCO3=88.9
1
2
3
4
5
6
7
CC
0.5
1.0
IW

LITHOLOGIC DESCRIPTION

FORAMINIFER NANNOFOSSIL OOZE AND NANNOFOSSIL OOZE with FORAMINIFERS

Major lithology: This core contains 20 to 70 cm thick, gradational interbeds of FORAMINIFER NANNOFOSSIL OOZE and NANNOFOSSIL OOZE with FORAMINIFERS. The dominant colors are white (2.5Y 8/0 to 5Y 8/1) for the nannofossil ooze with foraminifers and light gray (5Y 7/1 - 5Y 7/2) for the foraminifer nannofossil ooze. Burrow fills of one sediment type are often mixed into the other. The sediment is moderately bioturbated throughout with light gray (5Y 7/1), grayish purple (5PB 5/2) and grayish blue (5PB 5/2) mottling. Several grayish purple (5PB 5/2) burrow "halos" are seen. Greenish gray (5G 6/1), light greenish gray (5G 7/1), grayish blue (5PB 5/2), grayish purple (5PB 5/2), and light gray (N7) color bands are common.

SMEAR SLIDE SUMMARY (%):

	3, 39
	D
TEXTURE:	
Sand	20
Silt	78
Clay	2
COMPOSITION:	
Diatoms	1
Foraminifers	20
Nannofossils	69
Radiolarians	1
Spicules	1

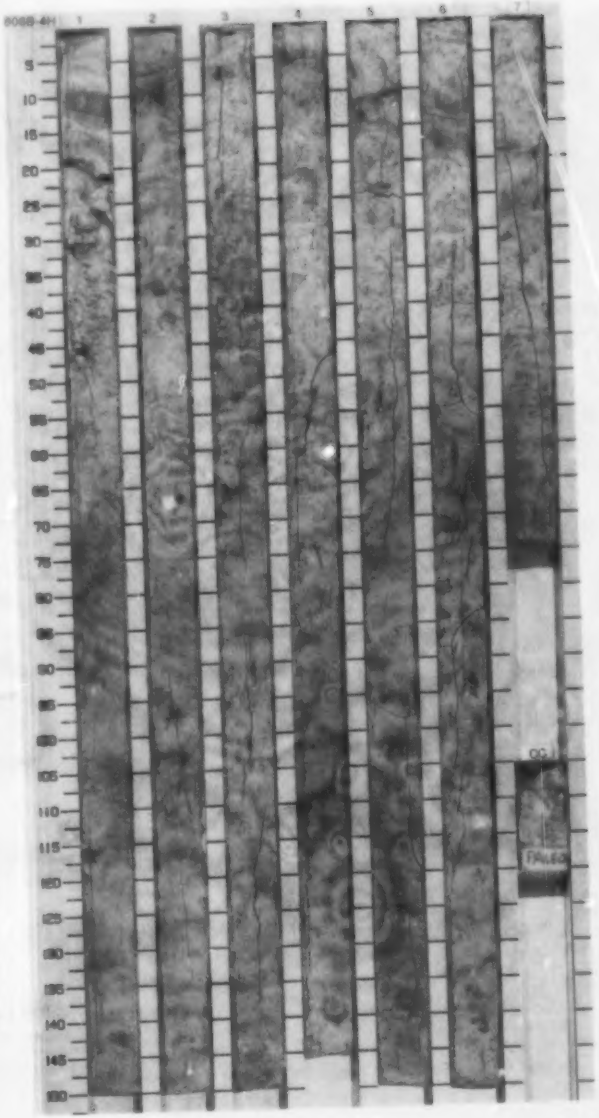
806B-4H
1
2
3
4
5
6
7
5
10
15
20
25
30
35
40
45
50
55
60
65
70
75
80
85
90
95
100
105
110
115
120
125
130
135
140
145
150
CC
PALEO

SITE 806 HOLE B CORE 5H CORED INTERVAL 35.0-44.5 mbsf

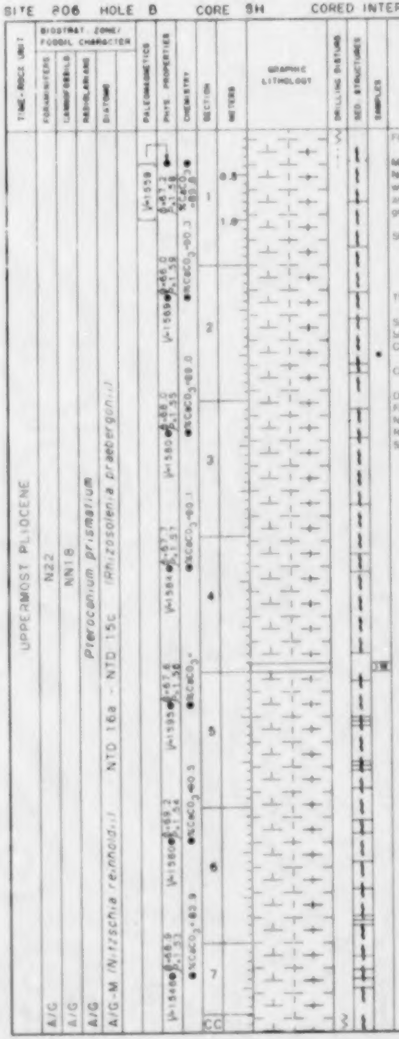
TIME-ROCK UNIT
BIOSTRAT. ZONE/ FOSSIL CHARACTER
FORAMINIFERS
CALCAREOUS NANNOFOSSILS
RADIOLARIANS
DIATOMS
PALEOMAGNETICS
PHYS. PROPERTIES
CHEMISTRY
SECTION
METERS
GRAPHIC LITHOLOGY
DRILLING DISTURB.
SED. STRUCTURES
SAMPLES
UPPERMOST PLIOCENE
A/G N22
A/G NN18
A/G Pterocanium prismatium
A/G-M (Nitzschia reinholdii) NTD 16a - NTD 15c (Rhizosolenia praebergonii)
V=1558
γ=67.2 ρ=1.48
%CaCO3=80.8
V=1569 γ=66.0 ρ=1.58
%CaCO3=80.3
V=1580 γ=68.0 ρ=1.55
%CaCO3=88.0
V=1584 γ=67.7 ρ=1.57
%CaCO3=80.1
V=1593 γ=67.6 ρ=1.56
%CaCO3=
V=1580 γ=69.2 ρ=1.54
%CaCO3=80.5
V=1546 γ=68.9 ρ=1.53
%CaCO3=83.9
1
2
3
4
5
6
7
CC
0.5
1.0
IW

LITHOLOGIC DESCRIPTION

FORAMINIFER NANNOFOSSIL OOZE to NANNOFOSSIL OOZE with FORAMINIFERS

Major lithology: This core contains FORAMINIFER NANNOFOSSIL OOZE, grading to NANNOFOSSIL OOZE with FORAMINIFERS. The dominant sediment colors range from white (5Y 8/1) to light gray (5Y 7/1 and 5Y 7/2), with light gray (5Y 7/1), grayish purple (5P 4/2) and grayish blue (5PB 5/2) mottling. Bioturbation is moderate throughout the core. Light greenish gray (5G 7/1) and light gray (N7) color bands are common throughout the core.

SMEAR SLIDE SUMMARY (%)

	2, 100
	D
TEXTURE	
Sand	25
Silt	70
Clay	5
COMPOSITION	
Diatoms	1
Foraminifers	33
Nannofossils	65
Radiolarians	1
Spicules	Tr

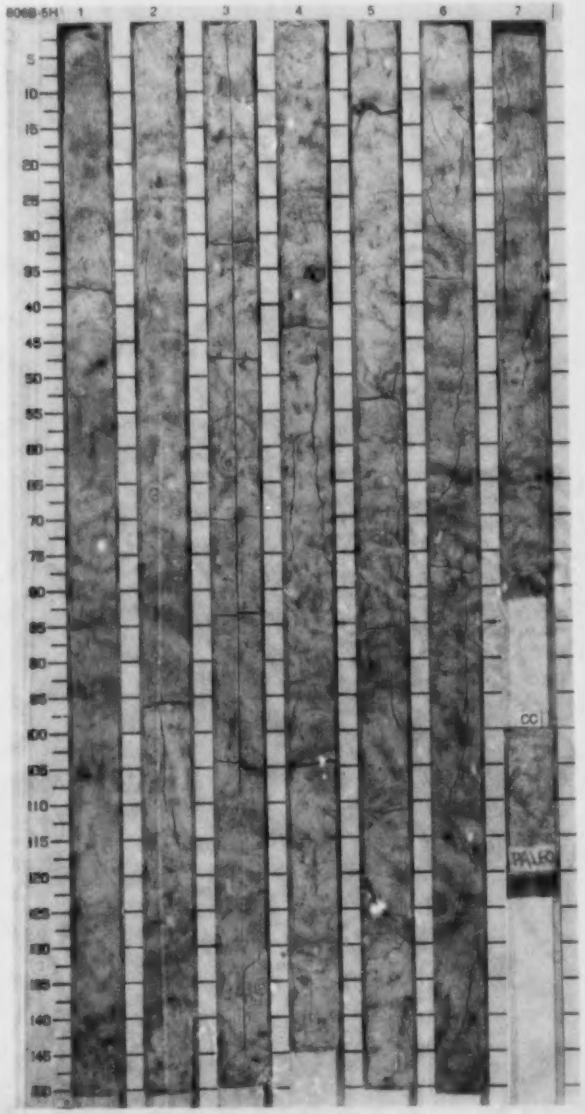
806B-5H
1
2
3
4
5
6
7
5
10
15
20
25
30
35
40
45
50
55
60
65
70
75
80
85
90
95
100
105
110
115
120
125
130
135
140
145
150
CC
PALEO

SITE 806 HOLE B CORE 6H CORED INTERVAL 44.5-54.0 mbsf

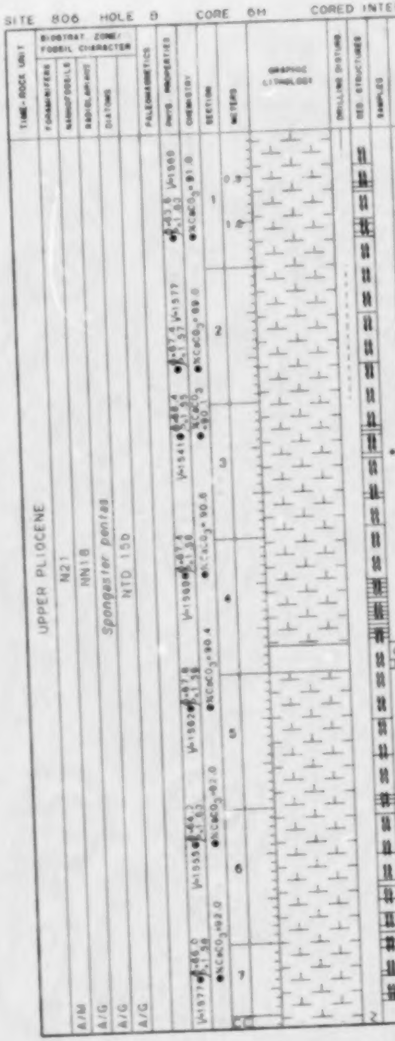
TIME-ROCK UNIT
BIOSTRAT. ZONE/ FOSSIL CHARACTER
FORAMINIFERS
NANNOFOSSILS
RADIOLARIANS
DIATOMS
PALEOMAGNETICS
PHYS. PROPERTIES
CHEMISTRY
SECTION
METERS
GRAPHIC LITHOLOGY
DRILLING DISTURB.
SED. STRUCTURES
SAMPLES
UPPER PLIOCENE
N21
NN18
Spongaster pentas
NTD 15b
A/M
A/G
A/G
A/G
%CaCO3=91.0
%CaCO3=89.0
%CaCO3=90.1
%CaCO3=90.6
%CaCO3=90.4
%CaCO3=92.0
%CaCO3=92.0
Vp=1560
Vp=1577
Vp=1541
Vp=1560
Vp=1562
Vp=1555
Vp=1577
1
2
3
4
5
6
7
CC
0.5
1.0
OG
IW

LITHOLOGIC DESCRIPTION

NANNOFOSSIL OOZE with FORAMINIFERS

Major lithology: This core contains white (5Y 8/1), light gray (5Y 7/1), and light greenish gray (5G 7/1) NANNOFOSSIL OOZE with FORAMINIFERS, which is heavily bioturbated and mottled. Diffuse greenish gray (5G 6/1) and light gray (N7) color bands are present to abundant throughout this core.

SMEAR SLIDE SUMMARY (%):

	3, 60
	D
TEXTURE:	
Sand	10
Silt	85
Clay	5
COMPOSITION:	
Diatoms	Tr
Foraminifers	20
Nannofossils	78
Radiolarians	1
Silicoflagellates	1
Spicules	Tr

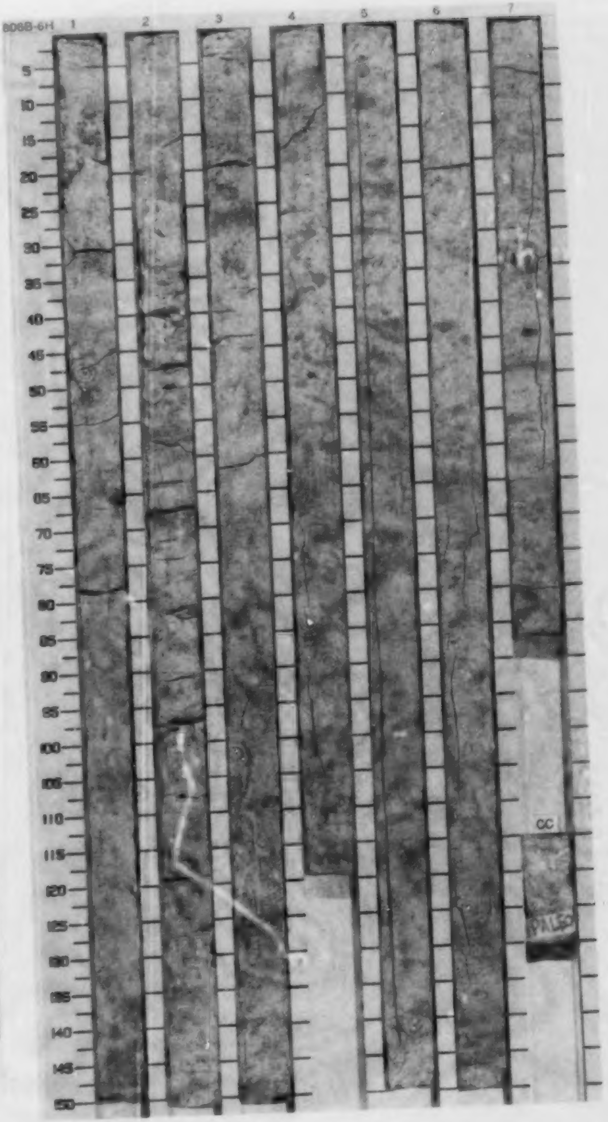
806B-6H
1
2
3
4
5
6
7
5
10
15
20
25
30
35
40
45
50
55
60
65
70
75
80
85
90
95
100
105
110
115
120
125
130
135
140
145
150
CC
PALEO

SITE 806 HOLE B CORE 7H CORED INTERVAL 54.0-63.5 mbsf

TIME-ROCK UNIT	FORAMINIFERS	NANNOFOSSILS	RADIOLARIANS	DIATOMS
UPPER PLIOCENE	N21	NN16	*Spongaster pentas*	NTD 15b
	A/G	A/G	A/G	A-C/M

SECTION	METERS	PHYS. PROPERTIES	CHEMISTRY
1	0.9 1.0	φ=70.3 ρ=1.52 V=1591	%CaCO$_3$=88.1
2		φ=68.0 ρ=1.55 V=1562	%CaCO$_3$=89.7
2			%CaCO$_3$=89.6
3		φ=64.6 ρ=1.62 V=1534	
3			%CaCO$_3$=90.9
4		φ=66.4 ρ=1.58 V=1559	
4			%CaCO$_3$=90.9
5		φ=66.5 ρ=1.58 V=1566	
5			%CaCO$_3$=92.2
6		φ=65.8 ρ=1.59 V=1580	
6			%CaCO$_3$=90.5
7		φ=66.2 ρ=1.60 V=1559	
CC			

LITHOLOGIC DESCRIPTION

NANNOFOSSIL OOZE with FORAMINIFERS interbedded with FORAMINIFER NANNOFOSSIL OOZE

Major lithology: This core contains white (5Y 8/1) to light gray (5Y 7/1) NANNOFOSSIL OOZE with FORAMINIFERS interbedded with FORAMINIFER NANNOFOSSIL OOZE. It is heavily bioturbated, evident from abundant mottles (light gray, 5Y 7/2) and pyrite-filled burrows. Occasional to common, diffuse, cm-scale, pale yellowish green (10GY 7/2), greenish gray (5G 6/1), and pale purple (5P 6/2) color bands are present. A slight odor of H_2S was noticed when the core was split.

SMEAR SLIDE SUMMARY (%):

	4, 74
	D
TEXTURE:	
Sand	12
Silt	60
Clay	28
COMPOSITION:	
Diatoms	Tr
Foraminifers	30
Nannofossils	60
Radiolarians	Tr
Siliceous fragments	2
Spicules	Tr

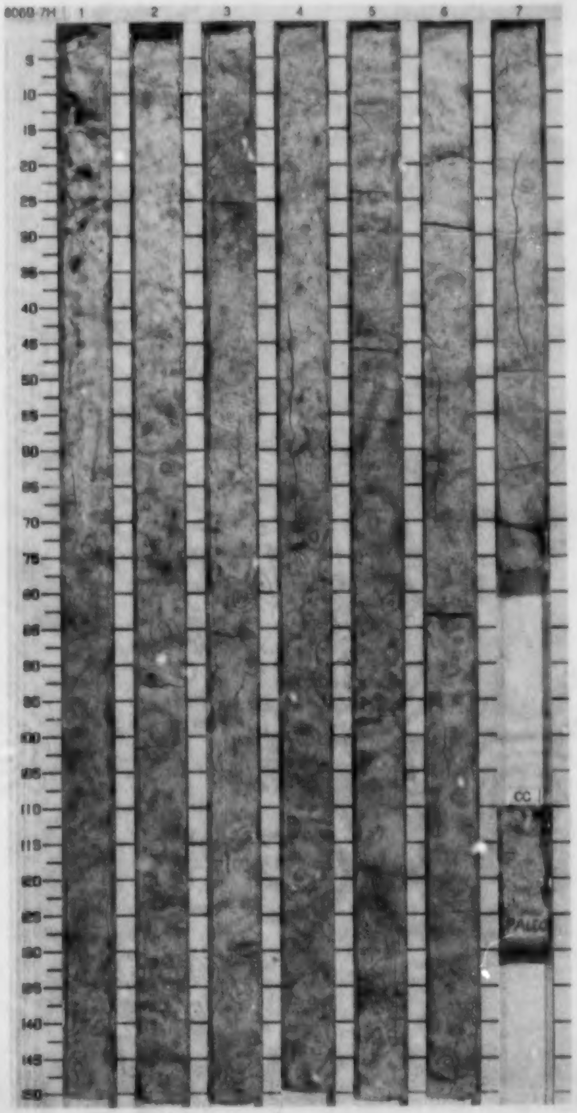

SITE 806 HOLE B CORE 8H CORED INTERVAL 63.5-73.0 mbsf

TIME-ROCK UNIT: UPPER PLIOCENE

BIOSTRAT. ZONE/FOSSIL CHARACTER

FORAMINIFERS: N21

NANNOFOSSILS: NN16 A/G

RADIOLARIANS: *Spongaster pentas* A/G

DIATOMS: NTD 15 A/G

PALEOMAGNETICS: C/M

PHYS. PROPERTIES:
- Section 1: V-1558●
- Section 2: V-1555● ϕ-67.1 ρ-1.56
- Section 3: V-1562● ϕ-67.0 ρ-1.58
- Section 4: V-1559● ϕ-68.1 ρ-1.56
- Section 5: V-1555● ϕ-67.4 ρ-1.57
- Section 6: V-1562● ϕ-69.0 ρ-1.54; V-1562
- Section 7: ● ϕ-67.4 ρ-1.67

CHEMISTRY:
- Section 1: %CaCO$_3$=90.0●
- Section 2: ●%CaCO$_3$=86.0
- Section 3: ●%CaCO$_3$=90.7
- Section 4: ●%CaCO$_3$=90.5
- Section 5: ●%CaCO$_3$=89.6
- Section 6: ●%CaCO$_3$=92.1
- Section 7: ●%CaCO$_3$=91.5

SECTION: 1, 2, 3, 4, 5, 6, 7, CC

METERS: 0.5, 1.0

GRAPHIC LITHOLOGY

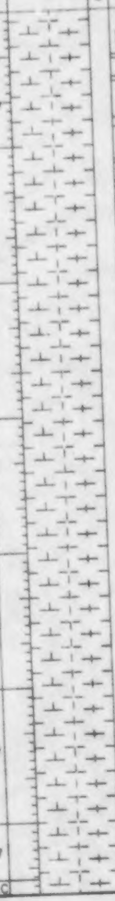

DRILLING DISTURB.

SED. STRUCTURES

SAMPLES

LITHOLOGIC DESCRIPTION

NANNOFOSSIL OOZE with FORAMINIFERS interbedded with FORAMINIFER NANNOFOSSIL OOZE

Major lithology: This core contains white (5Y 8/1) to light gray (5Y 7/1) NANNOFOSSIL OOZE with FORAMINIFERS interbedded with FORAMINIFER NANNOFOSSIL OOZE. It is heavily bioturbated, evident from abundant light gray (5Y 7/2) mottles, pyritization of burrows, and large pale purple (5P 6/2) color "halos". Horizontal, diffuse, 2 to 3 cm thick, pale yellowish green 10GY 7/2) color bands, spaced about 10-20 cm apart, are noted. Pale purple (5P 6/2) to reddish gray (5R 6/1) color bands, about 0.5 cm wide, are also common. These bands are often inclined.

SMEAR SLIDE SUMMARY (%):

	3, 75
	D
TEXTURE:	
Sand	10
Silt	50
Clay	40
COMPOSITION:	
Diatoms	1
Foraminifers	30
Nannofossils	66
Radiolarians	Tr
Siliceous fragments	3

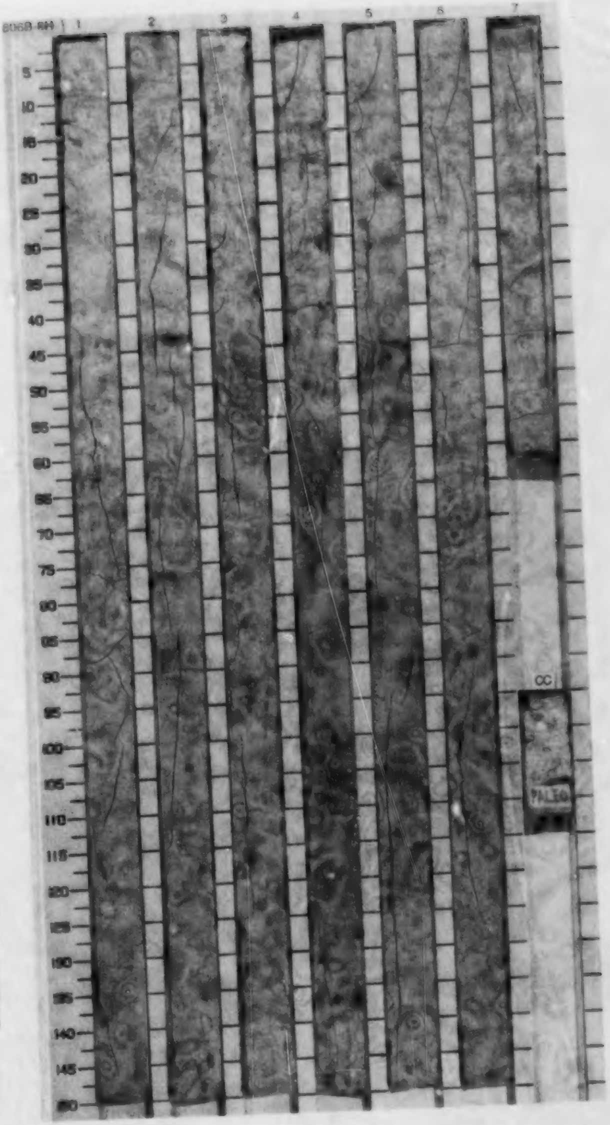

SITE 806 HOLE B CORE 9H CORED INTERVAL 73.0-82.5 mbsf

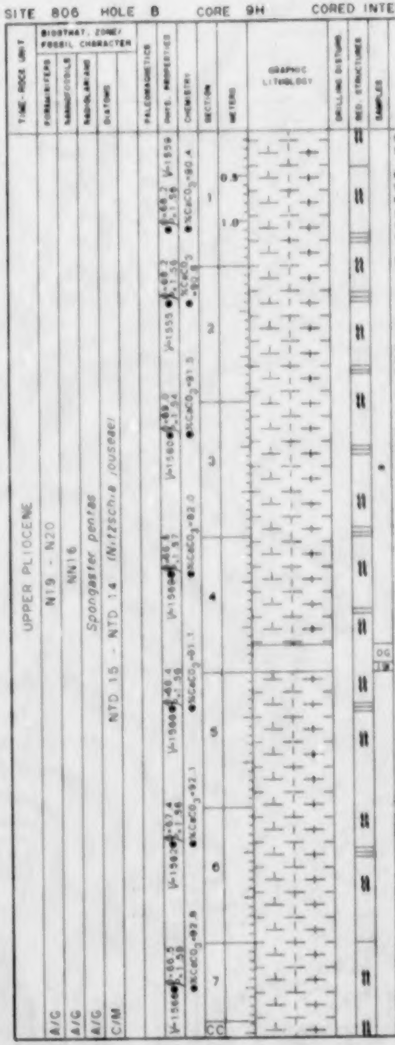
TIME-ROCK UNIT
BIOSTRAT. ZONE/ FOSSIL CHARACTER
FORAMINIFERS
NANNOFOSSILS
RADIOLARIANS
DIATOMS
PALEOMAGNETICS
PHYS. PROPERTIES
CHEMISTRY
SECTION
METERS
GRAPHIC LITHOLOGY
DRILLING DISTURB.
SED. STRUCTURES
SAMPLES
UPPER PLIOCENE
N19 - N20
NN16
Spongaster pentas
NTD 15 - NTD 14 (Nitzschia jouseae)
A/G
A/G
A/G
C/M
V-1559
ϕ-68.2 γ-1.56
V-1555
ϕ-68.2 γ-1.56
V-1560
ϕ-69.0 γ-1.54
V-1560
ϕ-66.6 γ-1.57
V-1560
ϕ-66.4 γ-1.58
V-1562
ϕ-67.4 γ-1.56
V-1560
ϕ-66.5 γ-1.58
%CaCO3-90.4
%CaCO3-92.8
%CaCO3-91.5
%CaCO3-92.0
%CaCO3-91.1
%CaCO3-92.1
%CaCO3-92.8
1
2
3
4
5
6
7
CC
0.5
1.0
OG
IW

LITHOLOGIC DESCRIPTION

NANNOFOSSIL OOZE with FORAMINIFERS interbedded with FORAMINIFER NANNOFOSSIL OOZE

Major lithology: This core contains white (5Y 8/1) NANNOFOSSIL OOZE with FORAMINIFERS interbedded with FORAMINIFER NANNOFOSSIL OOZE. The sediment is heavily bioturbated, with light gray (5Y 7/1) mottles throughout. Horizontal, 1 to 2 cm thick, pale yellowish green (10GY 7/2) color bands are common. Pale purple (5P 6/2) streaks and specks also are common, especially around burrows. Vertical pale purple streaks in some instances overprint green bands.

SMEAR SLIDE SUMMARY (%):

	3, 75 D
TEXTURE:	
Sand	10
Silt	50
Clay	40
COMPOSITION:	
Diatoms	1
Foraminifers	25
Nannofossils	70
Radiolarians	1
Siliceous fragments	2

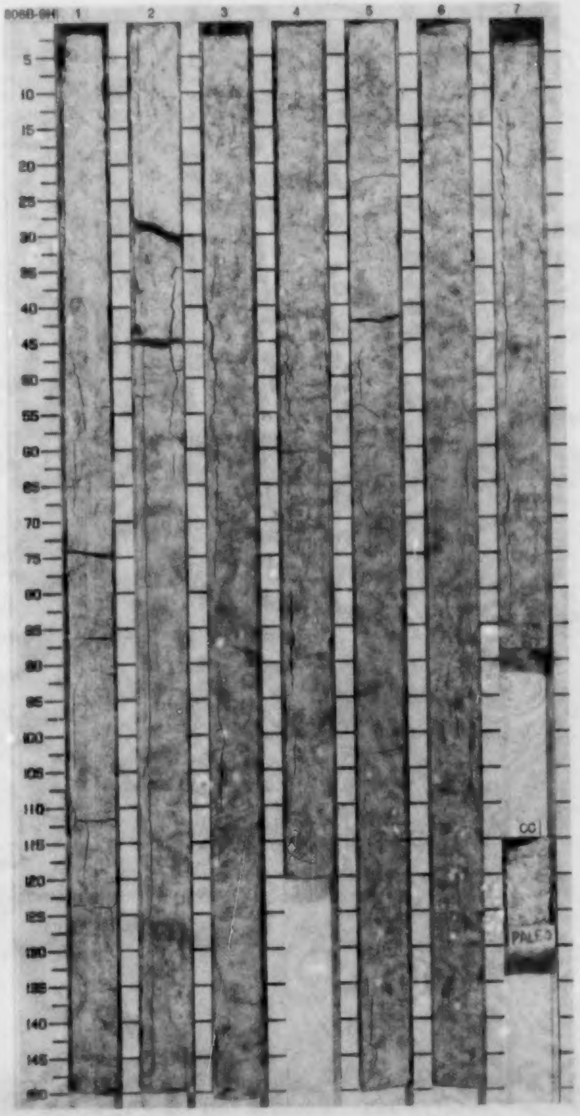
806B-9H
1
2
3
4
5
6
7
5
10
15
20
25
30
35
40
45
50
55
60
65
70
75
80
85
90
95
100
105
110
115
120
125
130
135
140
145
150
CC
PALE 3

SITE 806 HOLE B CORE 10H CORED INTERVAL 82.5-92.0 mbsf

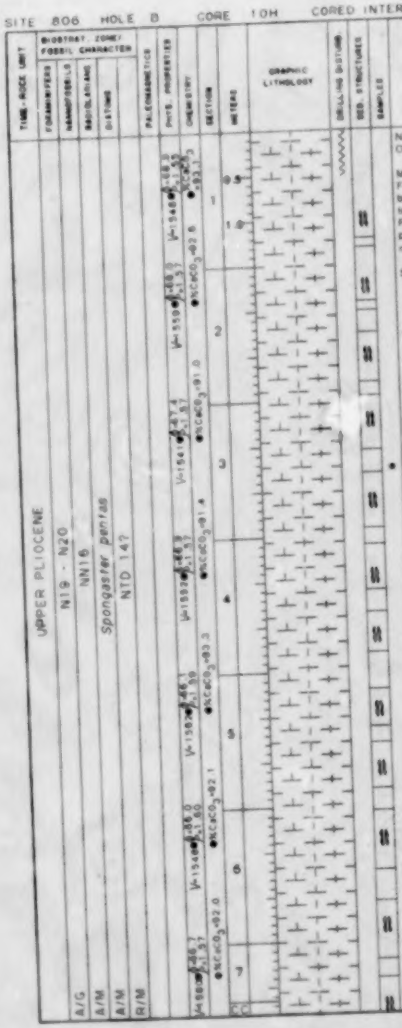
TIME-ROCK UNIT
BIOSTRAT. ZONE/ FOSSIL CHARACTER
FORAMINIFERS
NANNOFOSSILS
RADIOLARIANS
DIATOMS
PALEOMAGNETICS
PHYS. PROPERTIES
CHEMISTRY
SECTION
METERS
GRAPHIC LITHOLOGY
DRILLING DISTURB.
SED. STRUCTURES
SAMPLES
UPPER PLIOCENE
N19 - N20
NN16
Spongaster pentas
NTD 14?
A/G
A/M
A/M
R/M
V=1548 φ=66.3 γ=1.53
%CaCO3=93.1
%CaCO3=92.6
V=1550 φ=66.0 γ=1.57
%CaCO3=91.0
V=1541 φ=67.4 γ=1.57
%CaCO3=91.4
V=1592 φ=66.9 γ=1.57
%CaCO3=93.3
V=1502 φ=66.1 γ=1.59
%CaCO3=92.1
V=1546 φ=66.0 γ=1.60
%CaCO3=92.0
V=1580 φ=66.7 γ=1.57
0.5
1.0
1
2
3
4
5
6
7
CC

LITHOLOGIC DESCRIPTION

NANNOFOSSIL OOZE with FORAMINIFERS interbedded FORAMINIFER NANNOFOSSIL OOZE

Major lithology: This core contains white (5Y 8/1) NANNOFOSSIL OOZE with FORAMINIFERS interbedded with FORAMINIFER NANNOFOSSIL OOZE. The sediment is heavily bioturbated, with light gray (5Y 7/1) mottles and burrows throughout. Horizontal, diffuse, 1 to 2 cm thick, pale yellowish green (10GY 7/2) color bands are present throughout the core. Pale purple (5P 6/2) streaks and specks are common, especially around burrows. Vertical pale purple streaks, in some instances, overprint many green bands. A slight H_2S odor was noticed when the core was split.

SMEAR SLIDE SUMMARY (%):

	3, 75
	D
TEXTURE	
Sand	20
Silt	45
Clay	35
COMPOSITION	
Diatoms	Tr
Foraminifers	35
Nannofossils	65
Radiolarians	Tr

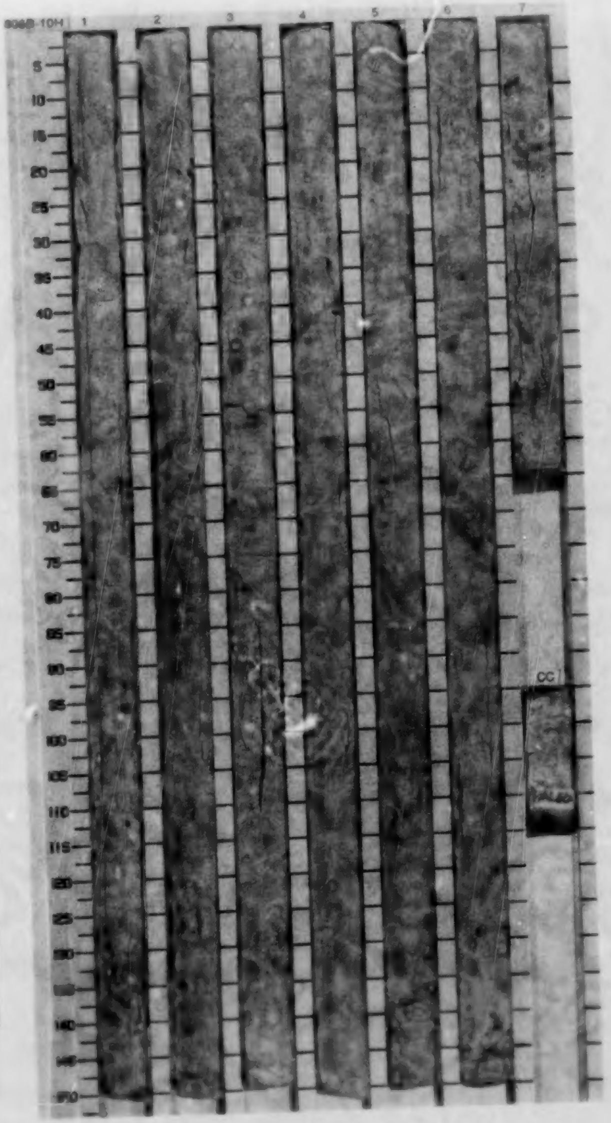
806B-10H
1
2
3
4
5
6
7
CC
5
10
15
20
25
30
35
40
45
50
55
60
65
70
75
80
85
90
95
100
105
110
115
120
125
130
135
140
145
150

SITE 806 HOLE B CORE 11H CORED INTERVAL 92.0-101.5 mbsf

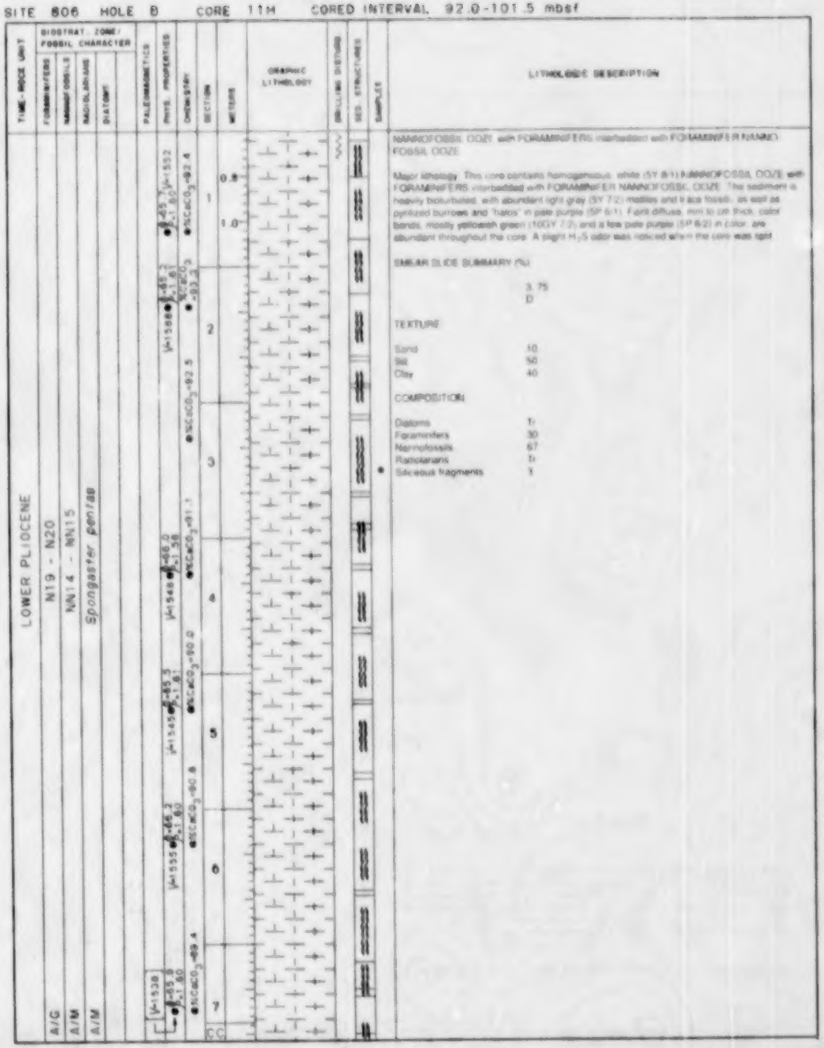

TIME-ROCK UNIT	FORAMINIFERS	NANNOFOSSILS	RADIOLARIANS	DIATOMS	PALEOMAGNETICS	PHYS. PROPERTIES	CHEMISTRY	SECTION	METERS
LOWER PLIOCENE	N19 - N20	NN14 - NN15	*Spongaster pentas*			ϕ=65.7 γ=1.60 V=1552	%CaCO$_3$=92.4	1	0.5, 1.0
						V=1568 ϕ=66.2 γ=1.61	%CaCO$_3$=93.2	2	
							%CaCO$_3$=92.5	3	
						V=1548 ϕ=66.0 γ=1.58	%CaCO$_3$=91.1	4	
						V=1545 ϕ=65.5 γ=1.61	%CaCO$_3$=90.0	5	
						V=1555 ϕ=66.2 γ=1.60	%CaCO$_3$=90.8	6	
						V=1538 ϕ=65.8 γ=1.60	%CaCO$_3$=89.4	7	
	A/G	A/M	A/M					CC	

BIOSTRAT. ZONE/ FOSSIL CHARACTER
GRAPHIC LITHOLOGY
DRILLING DISTURB.
SED. STRUCTURES
SAMPLES

LITHOLOGIC DESCRIPTION

NANNOFOSSIL OOZE with FORAMINIFERS interbedded with FORAMINIFER NANNOFOSSIL OOZE

Major lithology: This core contains homogeneous, white (5Y 8/1) NANNOFOSSIL OOZE with FORAMINIFERS interbedded with FORAMINIFER NANNOFOSSIL OOZE. The sediment is heavily bioturbated, with abundant light gray (5Y 7/2) mottles and trace fossils, as well as pyritized burrows and "halos" in pale purple (5P 6/1). Faint diffuse, mm to cm thick, color bands, mostly yellowish green (10GY 7/2) and a few pale purple (5P 6/2) in color, are abundant throughout the core. A slight H_2S odor was noticed when the core was split.

SMEAR SLIDE SUMMARY (%):

	3, 75
	D
TEXTURE:	
Sand	10
Silt	50
Clay	40
COMPOSITION:	
Diatoms	Tr
Foraminifers	30
Nannofossils	67
Radiolarians	Tr
Siliceous fragments	3

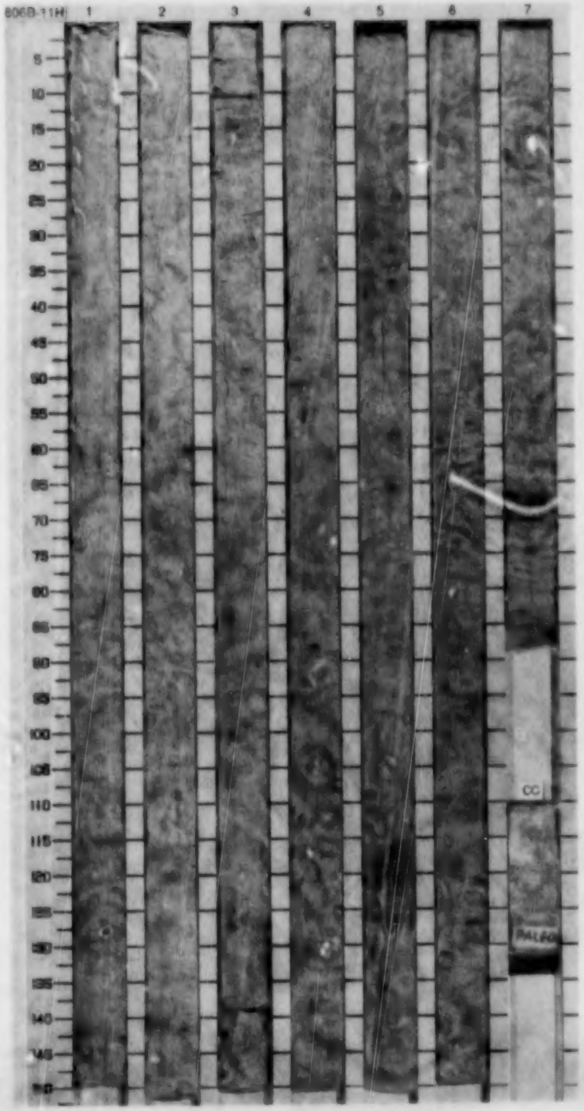
806B-11H
1
2
3
4
5
6
7
5
10
15
20
25
30
35
40
45
50
55
60
65
70
75
80
85
90
95
100
105
110
115
120
125
130
135
140
145
150
CC
PALEO

SITE 806 HOLE B CORE 12H CORED INTERVAL 101.5-111.0 mbsf

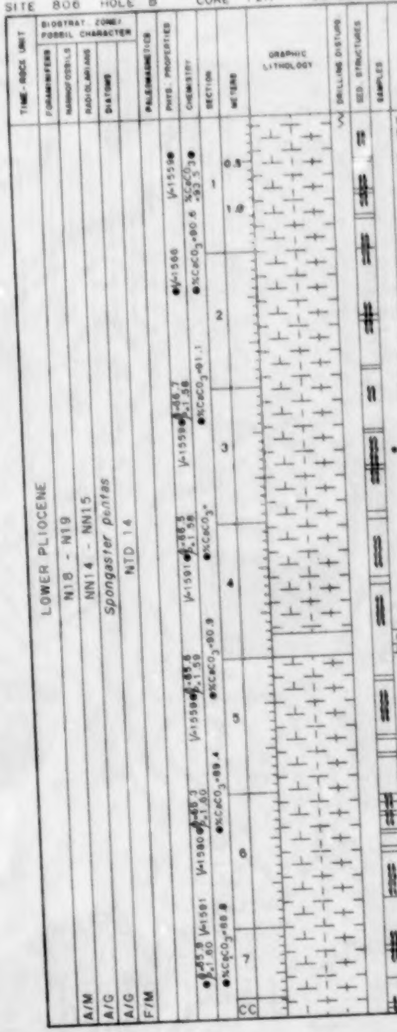
TIME-ROCK UNIT
BIOSTRAT. ZONE/ FOSSIL CHARACTER
FORAMINIFERS
NANNOFOSSILS
RADIOLARIANS
DIATOMS
PALEOMAGNETICS
PHYS. PROPERTIES
CHEMISTRY
SECTION
METERS
GRAPHIC LITHOLOGY
DRILLING DISTURB.
SED. STRUCTURES
SAMPLES
LOWER PLIOCENE
N18 - N19
NN14 - NN15
Spongaster pentas
NTD 14
A/M
A/G
A/G
F/M
V=1559
V=1566
V=1559 φ=66.7 ρ=1.58
V=1591 φ=66.5 ρ=1.58
V=1559 φ=65.6 ρ=1.59
V=1580 φ=66.3 ρ=1.60
V=1581
φ=65.8 ρ=1.60
%$CaCO_3$=93.5
%$CaCO_3$=90.6
%$CaCO_3$=91.1
%$CaCO_3$*
%$CaCO_3$=90.9
%$CaCO_3$=89.4
%$CaCO_3$=88.8
1
2
3
4
5
6
7
CC
0.5
1.0
OG
IW

LITHOLOGIC DESCRIPTION

NANNOFOSSIL OOZE with FORAMINIFERS interbedded with FORAMINIFER NANNOFOSSIL OOZE

Major lithology: This core contains white (5Y 8/1) to light gray (5Y 7/1) NANNOFOSSIL OOZE with FORAMINIFERS interbedded with FORAMINIFER NANNOFOSSIL OOZE. It is heavily bioturbated with abundant light gray (5Y 7/2) mottles and pyritized burrow. Pale purple (5P 6/2) "halos" and mottles also are associated with this bioturbation. Faint horizontal, thin (0.5 cm thick) pale purple color band and thicker (1 to 2 cm thick) pale yellow green (10GY 7/2) color bands are observed. A slight H_2S odor was noted upon splitting the core.

SMEAR SLIDE SUMMARY (%):

	3, 75
	D
TEXTURE	
Sand	5
Silt	50
Clay	45
COMPOSITION	
Foraminifers	35
Nannofossils	63
Radiolarians	Tr
Siliceous fragments	2

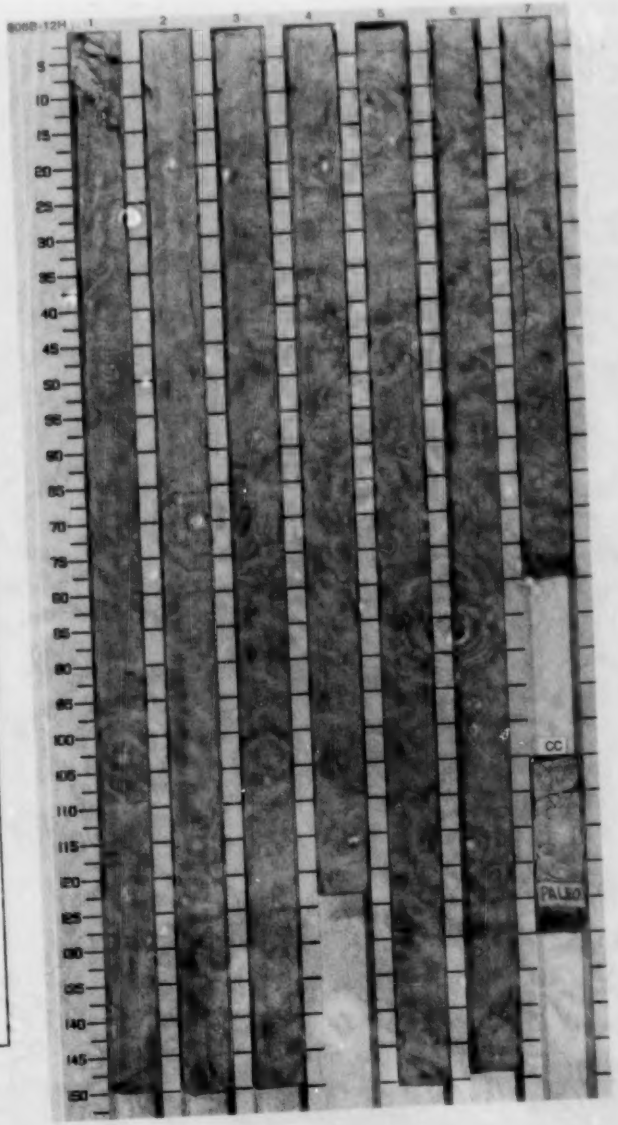
806B-12H
1
2
3
4
5
6
7
5
10
15
20
25
30
35
40
45
50
55
60
65
70
75
80
85
90
95
100
105
110
115
120
125
130
135
140
145
150
CC
PALEO

SITE 806 HOLE B CORE 13H CORED INTERVAL 111.0-120.5 mbsf

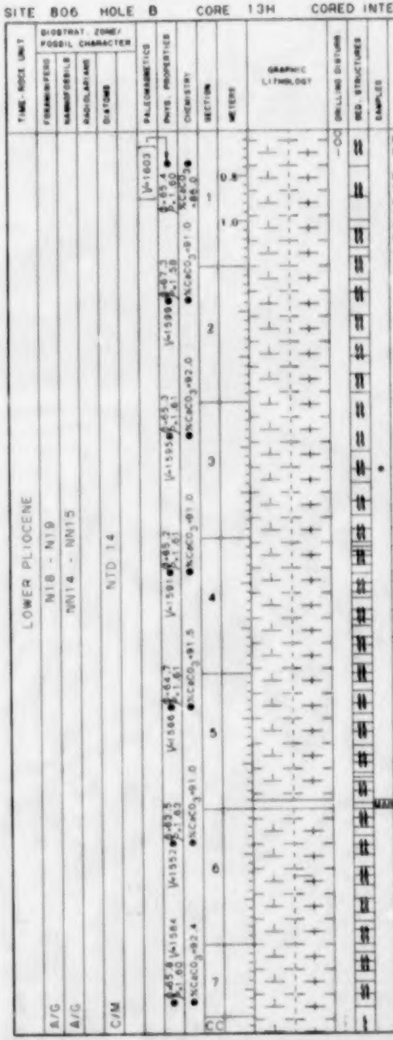
TIME-ROCK UNIT
BIOSTRAT. ZONE/ FOSSIL CHARACTER
FORAMINIFERS
NANNOFOSSILS
RADIOLARIANS
DIATOMS
PALEOMAGNETICS
PHYS. PROPERTIES
CHEMISTRY
SECTION
METERS
GRAPHIC LITHOLOGY
DRILLING DISTURB.
SED. STRUCTURES
SAMPLES
LOWER PLIOCENE
N18 - N19
NN14 - NN15
NTD 14
A/G
A/G
C/M
V=1603
φ=65.4 γ=1.60
%CaCO3=86.0
%CaCO3=91.0
φ=67.3 γ=1.58 V=1599
%CaCO3=92.0
φ=65.3 γ=1.61 V=1595
%CaCO3=91.0
φ=65.2 γ=1.61 V=1591
%CaCO3=91.5
φ=64.7 γ=1.61 V=1586
%CaCO3=91.0
φ=63.5 γ=1.63 V=1552
φ=65.8 γ=1.60 V=1584
%CaCO3=92.4
0.5
1.0
1
2
3
4
5
6
7
CC
OG
IW

LITHOLOGIC DESCRIPTION

NANNOFOSSIL OOZE with FORAMINIFERS interbedded with FORAMINIFER NANNOFOSSIL OOZE

Major lithology: This core contains white (5Y 8/1) NANNOFOSSIL OOZE with FORAMINIFERS interbedded with FORAMINIFER NANNOFOSSIL OOZE, both of which are moderately to heavily bioturbated throughout. Light gray (5Y 7/1 and N7), light greenish gray (5G 7/1), and grayish blue (5PB 5/2) mottles and light gray (N7) to grayish blue (5PB 5/2) burrow halos are common to abundant. Diffuse light gray (N7) and light greenish gray (5G 7/1) color bands are common. Inclined color bands appear to be parts of large burrow halos intersected by the core.

SMEAR SLIDE SUMMARY (%):

	2, 75
	D
TEXTURE:	
Sand	26
Silt	50
Clay	24
COMPOSITION:	
Diatoms	Tr
Foraminifers	25
Nannofossils	74
Radiolarians	Tr
Volcanic ash	1

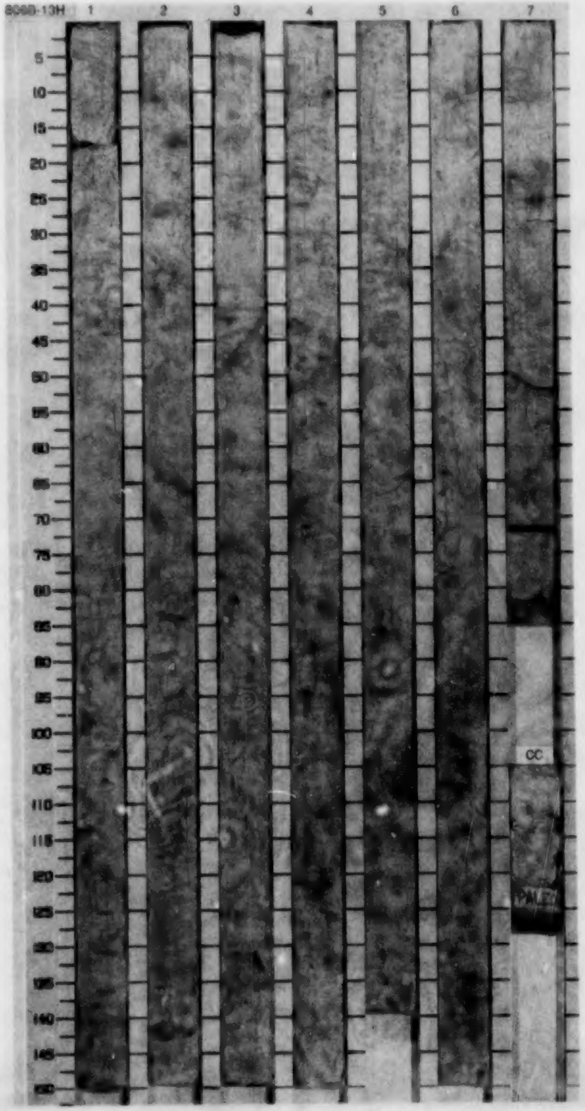
806B-13H
1
2
3
4
5
6
7
5
10
15
20
25
30
35
40
45
50
55
60
65
70
75
80
85
90
95
100
105
110
115
120
125
130
135
140
145
150
CC

SITE 806 HOLE B CORE 14H CORED INTERVAL 120.5-130.0 mbsf

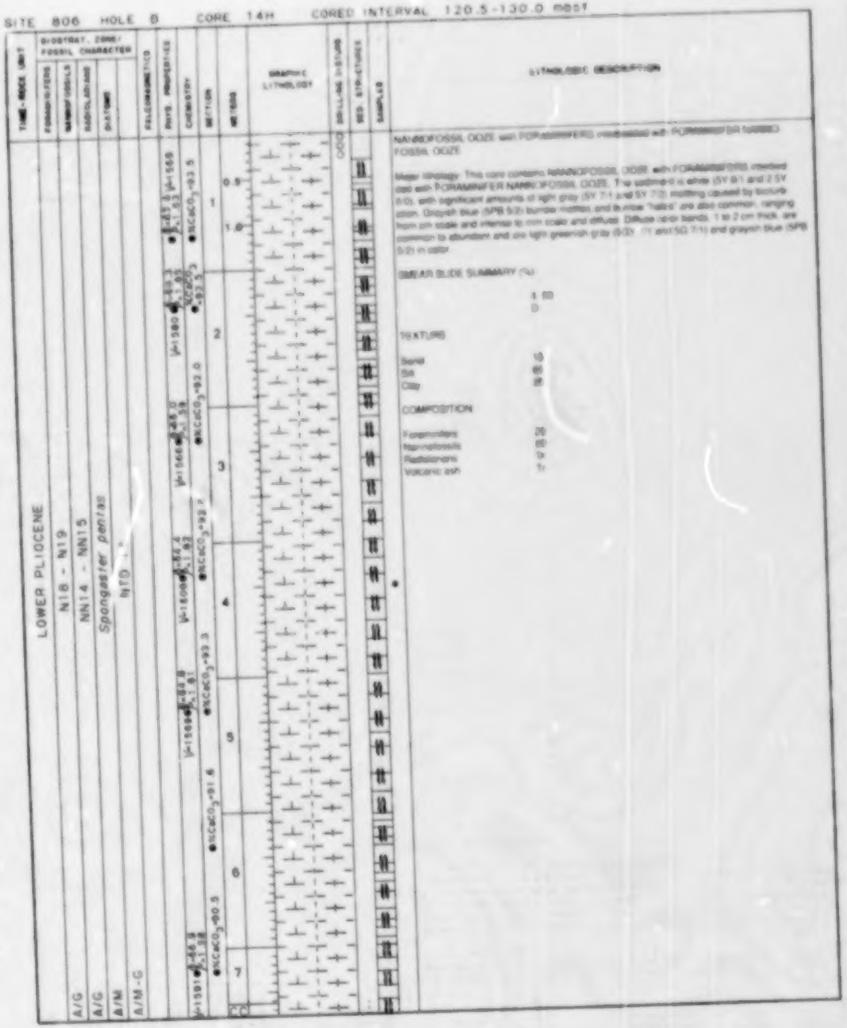

TIME-ROCK UNIT	FORAMINIFERS	NANNOFOSSILS	RADIOLARIANS	DIATOMS	PALEOMAGNETICS	PHYS. PROPERTIES	CHEMISTRY	SECTION	METERS	DRILLING DISTURB.	SAMPLES
LOWER PLIOCENE	A/G N18 - N19	A/G NN14 - NN15	A/M *Spongaster pentas*	A/M-G NTD		φ=63.0 ρ=1.63 V=1568	●%CaCO₃=93.5	1	0.5 1.0	OOO	
						φ=60.3 ρ=1.65 V=1580	●%CaCO₃=93.5 ●%CaCO₃=92.0	2			
						φ=48.0 ρ=1.59 V=1566	●%CaCO₃=92.?	3			
						φ=64.4 ρ=1.62 V=1600	●%CaCO₃=93.3	4			●
						φ=64.8 ρ=1.61 V=1589	●%CaCO₃=91.6	5			
							●%CaCO₃=90.5	6			
						φ=66.8 ρ=1.58 V=1591		7			
								CC			

LITHOLOGIC DESCRIPTION

NANNOFOSSIL OOZE with FORAMINIFERS interbedded with FORAMINIFER NANNOFOSSIL OOZE

Major lithology: This core contains NANNOFOSSIL OOZE with FORAMINIFERS interbedded with FORAMINIFER NANNOFOSSIL OOZE. The sediment is white (5Y 8/1 and 2.5Y 8/0), with significant amounts of light gray (5Y 7/1 and 5Y 7/2) mottling caused by bioturbation. Grayish blue (5PB 5/2) burrow mottles and burrow "halos" are also common, ranging from cm scale and intense to mm scale and diffuse. Diffuse color bands, 1 to 2 cm thick, are common to abundant and are light greenish gray (5GY 7/1 and 5G 7/1) and grayish blue (5PB 5/2) in color.

SMEAR SLIDE SUMMARY (%):

	4, 80
	D
TEXTURE:	
Sand	[illegible]
Silt	[illegible]
Clay	[illegible]
COMPOSITION:	
Foraminifers	[illegible]
Nannofossils	[illegible]
Radiolarians	[illegible]
Volcanic ash	Tr

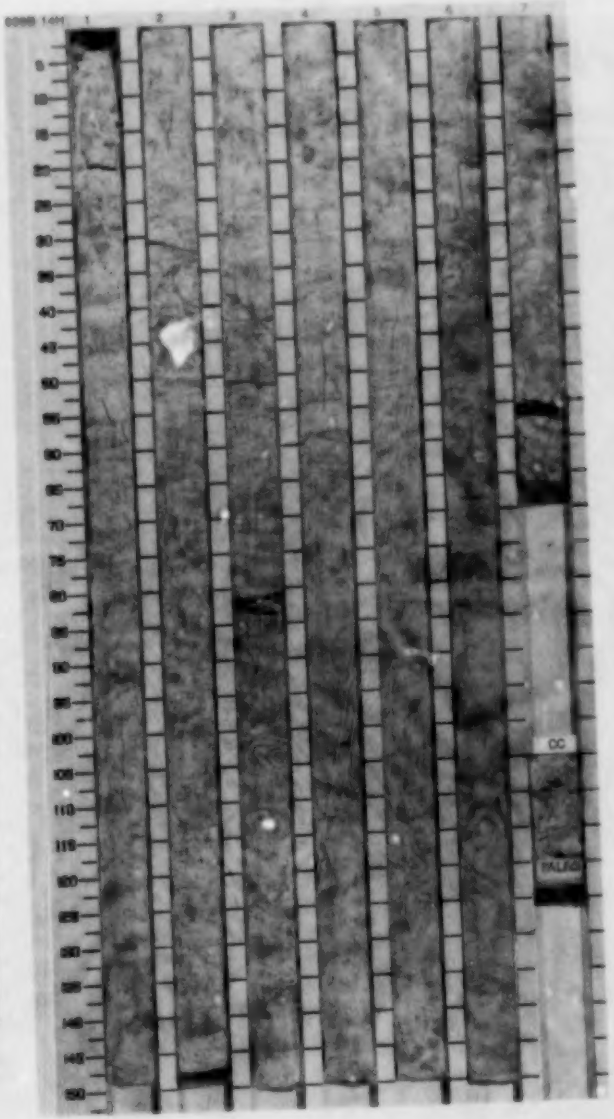

SITE 806 HOLE B CORE 15H CORED INTERVAL 130.0-139.5 mbsf

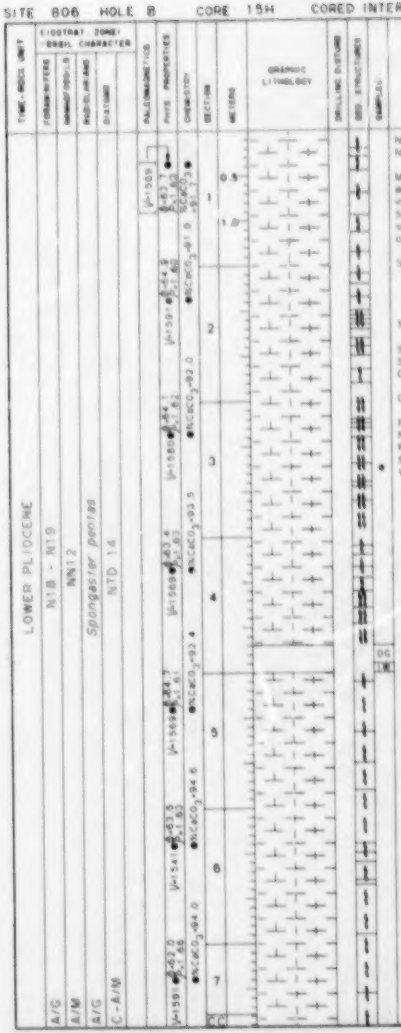
TIME-ROCK UNIT
BIOSTRAT. ZONE/ FOSSIL CHARACTER
FORAMINIFERS
NANNOFOSSILS
RADIOLARIANS
DIATOMS
PALEOMAGNETICS
PHYS. PROPERTIES
CHEMISTRY
SECTION
METERS
GRAPHIC LITHOLOGY
DRILLING DISTURB.
SED. STRUCTURES
SAMPLES
LOWER PLIOCENE
N18 - N19
NN12
Spongaster pentas
NTD 14
A/G
A/M
A/G
C-A/M
V=1509
φ=63.7
ρ=1.62
%CaCO3=91.7
%CaCO3=91.0
V=1591 φ=64.9 ρ=1.60
%CaCO3=92.0
V=1580 φ=64.1 ρ=1.62
%CaCO3=93.5
V=1569 φ=63.4 ρ=1.63
%CaCO3=92.4
V=1569 φ=64.7 ρ=1.61
%CaCO3=94.6
V=1541 φ=63.5 ρ=1.63
%CaCO3=94.0
V=1591 φ=62.0 ρ=1.66
1
0.5
1.0
2
3
4
5
6
7
CC
OG
IW

LITHOLOGIC DESCRIPTION

NANNOFOSSIL OOZE with FORAMINIFERS interbedded with FORAMINIFER NANNOFOSSIL OOZE

Major lithology: This core contains NANNOFOSSIL OOZE with FORAMINIFERS interbedded with FORAMINIFER NANNOFOSSIL OOZE. The sediment is white (2.5Y 8/0), with intervals of light gray (5Y 7/1 and 5Y 7/2) mottling caused by bioturbation. Grayish blue (5PB 5/2) mottles and burrow "halos" are also common, ranging from cm scale and intense to mm scale and diffuse. Diffuse light greenish gray (5GY 7/1 and 5G 8/1) and grayish blue (5PB 5/2) color bands, 1 to 2 cm thick, are present throughout the core.

SMEAR SLIDE SUMMARY (%):

	3, 75
	D
TEXTURE:	
Sand	15
Silt	82
Clay	3
COMPOSITION:	
Foraminifers	30
Nannofossils	65
Radiolarians	3
Silicoflagellates	1
Volcanic ash	1

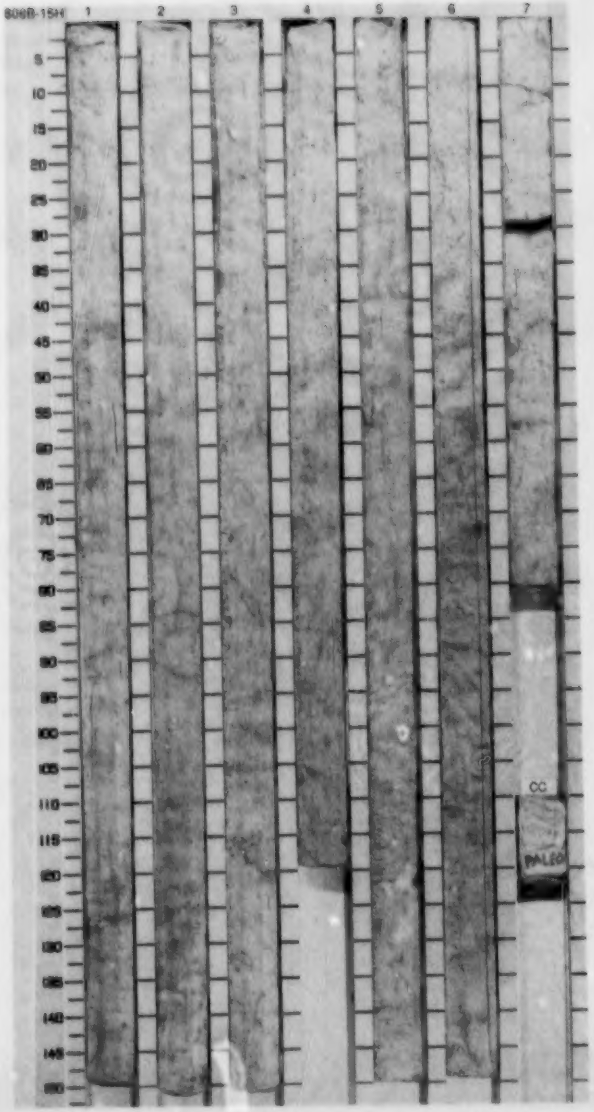
806B-15H
1
2
3
4
5
6
7
5
10
15
20
25
30
35
40
45
50
55
60
65
70
75
80
85
90
95
100
105
110
115
120
125
130
135
140
145
150
CC
PALEO

SITE 806 HOLE B CORE 16H CORED INTERVAL 139.5-149.0 mbsf

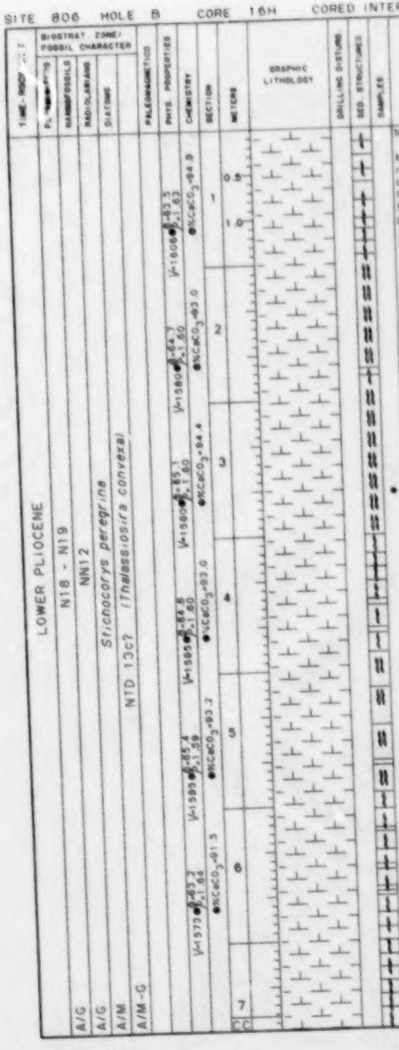
TIME-ROCK UNIT
BIOSTRAT. ZONE/ FOSSIL CHARACTER
FORAMINIFERS
NANNOFOSSILS
RADIOLARIANS
DIATOMS
PALEOMAGNETICS
PHYS. PROPERTIES
CHEMISTRY
SECTION
METERS
GRAPHIC LITHOLOGY
DRILLING DISTURB.
SED. STRUCTURES
SAMPLES
LOWER PLIOCENE
A/G N18 - N19
A/G NN12
A/M Stichocorys peregrina
A/M-G NTD 13c? (Thalassiosira convexa)
V=1606 63.5 1.63
%CaCO3=94.9
V=1580 64.7 1.60
%CaCO3=93.0
V=1580 65.1 1.60
%CaCO3=94.4
V=1585 64.8 1.60
%CaCO3=93.0
V=1593 65.4 1.59
%CaCO3=93.2
V=1573 63.2 1.64
%CaCO3=91.5
1
2
3
4
5
6
7
CC
0.5
1.0

LITHOLOGIC DESCRIPTION

NANNOFOSSIL OOZE with FORAMINIFERS

Major lithology: This core contains NANNOFOSSIL OOZE with FORAMINIFERS. The sediment is white (2.5Y 8/0), with intervals of light gray (5Y 7/1 and 5Y 7/2) mottling caused by bioturbation. Grayish blue (5PB 5/2) mottles and burrow "halos" also are common, ranging from cm scale and intense to mm scale and diffuse. Diffuse light greenish gray (5GY 7/1 and 5G 8/1), pale purple (5P 6/2), and grayish blue (5PB 5/2) color bands, 1 to 2 cm thick, are present throughout the core.

SMEAR SLIDE SUMMARY (%):

	3, 102
	D
TEXTURE:	
Sand	20
Silt	75
Clay	5
COMPOSITION:	
Foraminifers	20
Nannofossils	77
Radiolarians	3

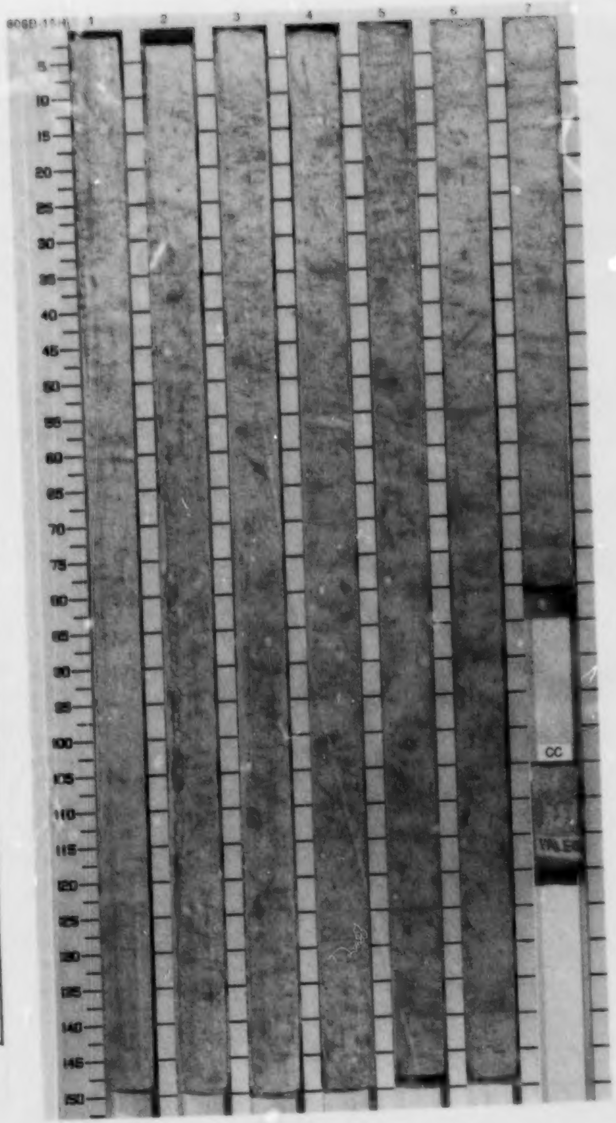
806B-16H
1
2
3
4
5
6
7
CC
5
10
15
20
25
30
35
40
45
50
55
60
65
70
75
80
85
90
95
100
105
110
115
120
125
130
135
140
145
150

SITE 806 HOLE B CORE 17H CORED INTERVAL 149.0-158.5 mbsf

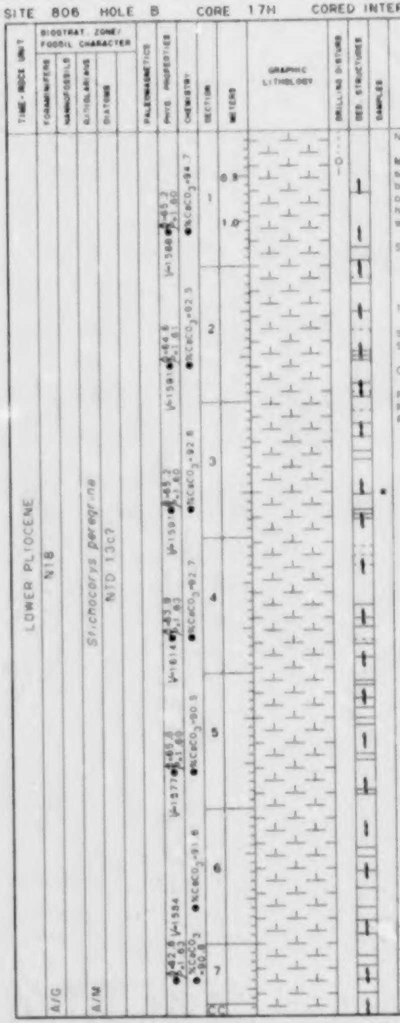

LITHOLOGIC DESCRIPTION

NANNOFOSSIL OOZE with FORAMINIFERS

Major lithology: This core contains NANNOFOSSIL OOZE with FORAMINIFERS. The sediment is white (5Y 8/1 and 2.5Y 8/0), with light gray (5Y 7/1 and 5Y 7/2) mottling caused by bioturbation. Grayish blue (5PB 5/2) to pale purple (5P 6/2) mottles and burrow "halos" are common. Steeply inclined and horizontal color bands and diffuse 0.5 to 2 cm thick horizontal, light greenish gray (5G 7/1) color bands are present throughout the core. The steep grayish blue bands may cross the greenish bands.

SMEAR SLIDE SUMMARY (%)

	3, 98
	D
TEXTURE	
Sand	20
Silt	80
COMPOSITION	
Foraminifers	15
Nannofossils	82
Radiolarians	3

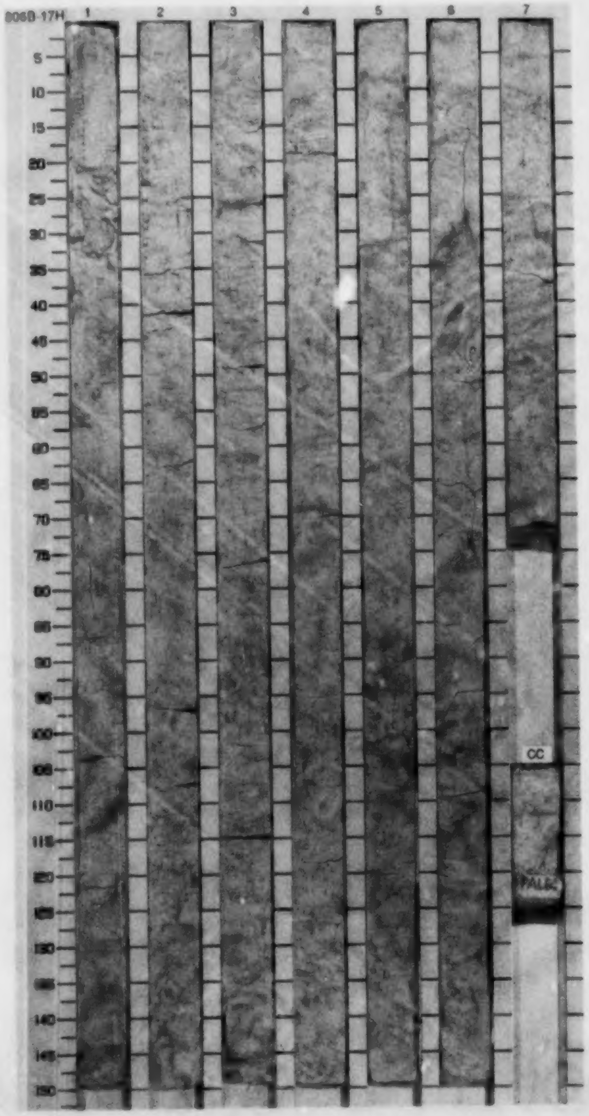
806B-17H
1
2
3
4
5
6
7
CC
PALEO
5
10
15
20
25
30
35
40
45
50
55
60
65
70
75
80
85
90
95
100
105
110
115
120
125
130
135
140
145
150

SITE 806 HOLE B CORE 18H CORED INTERVAL 158.5-168.0 mbsf

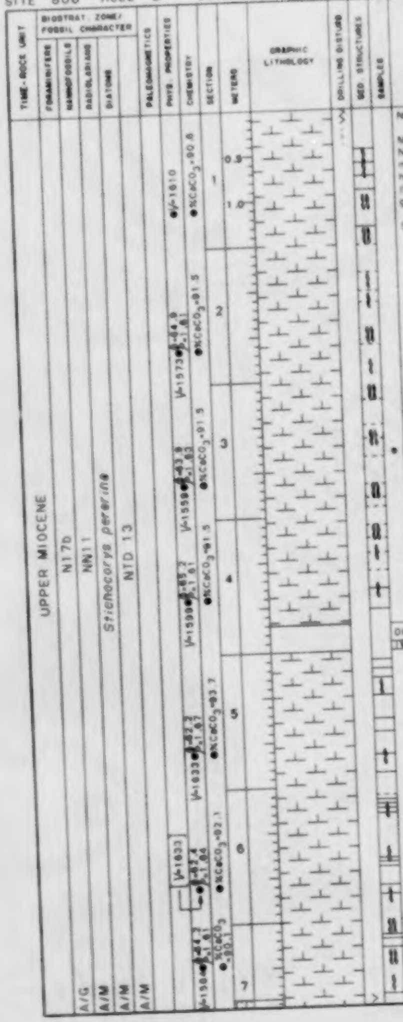
TIME-ROCK UNIT
BIOSTRAT. ZONE/ FOSSIL CHARACTER
FORAMINIFERS
NANNOFOSSILS
RADIOLARIANS
DIATOMS
PALEOMAGNETICS
PHYS. PROPERTIES
CHEMISTRY
SECTION
METERS
GRAPHIC LITHOLOGY
DRILLING DISTURB.
SED. STRUCTURES
SAMPLES
UPPER MIOCENE
N17b
NN11
Stichocorys peregrina
NTD 13
A/G
A/M
A/M
A/M
V-1610
%CaCO3=90.6
V-1573 -64.9 ,1.61
%CaCO3=91.5
V-1559 -63.9 ,1.63
%CaCO3=91.5
V-1599 -65.2 ,1.61
%CaCO3=91.5
V-1633 -62.2 ,1.67
%CaCO3=93.7
V-1633
-62.4 ,1.64
%CaCO3=92.1
V-1584 -64.2 ,1.61
%CaCO3 =90.1
0.5
1.0
1
2
3
4
5
6
7
OG
IW

LITHOLOGIC DESCRIPTION

NANNOFOSSIL OOZE with FORAMINIFERS

Major lithology: This core contains moderately to heavily bioturbated, white (5Y 8/1) NANNOFOSSIL OOZE with FORAMINIFERS, with light gray (5Y 7/2) color bands and mottling. Grayish blue (5PB 5/2) mottles and burrow "halos", and steeply inclined to horizontal color bands, are common. Diffuse 0.5 to 1 cm thick, horizontal, light greenish gray (5G 7/1) color bands are noted throughout. The steep grayish blue bands may cross the greenish bands.

SMEAR SLIDE SUMMARY (%):

	3, 80
	D
TEXTURE	
Sand	12
Silt	85
Clay	3
COMPOSITION	
Foraminifers	20
Nannofossils	77
Radiolarians	1

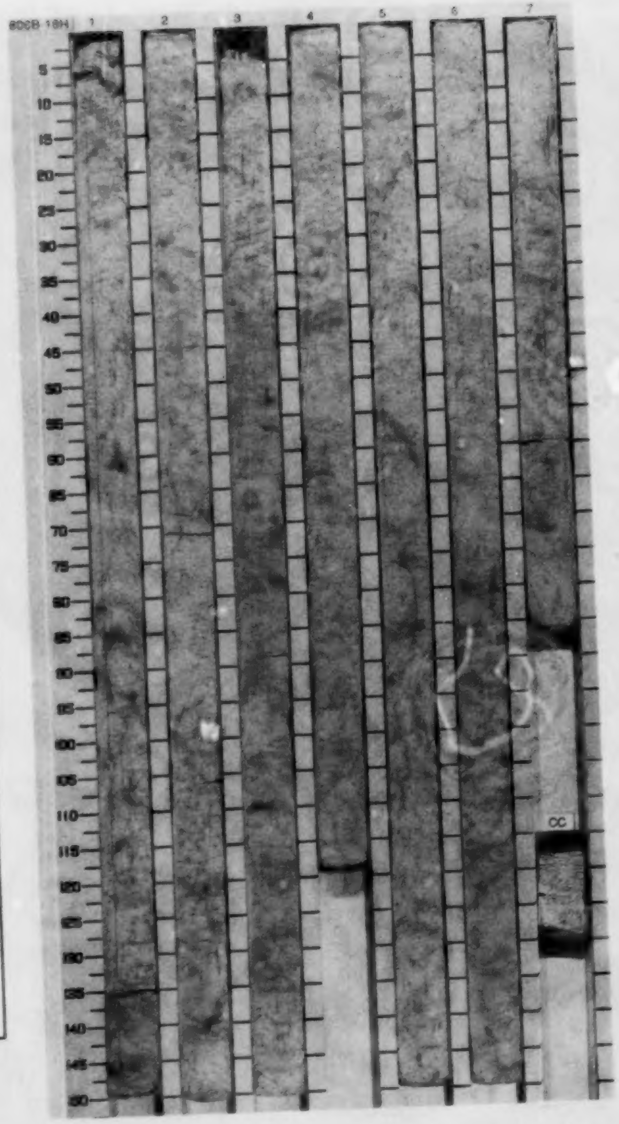
806B 18H
1
2
3
4
5
6
7
5
10
15
20
25
30
35
40
45
50
55
60
65
70
75
80
85
90
95
100
105
110
115
120
125
130
135
140
145
150
CC

SITE 806 HOLE B CORE 19H CORED INTERVAL 168.0-177.5 mbsf

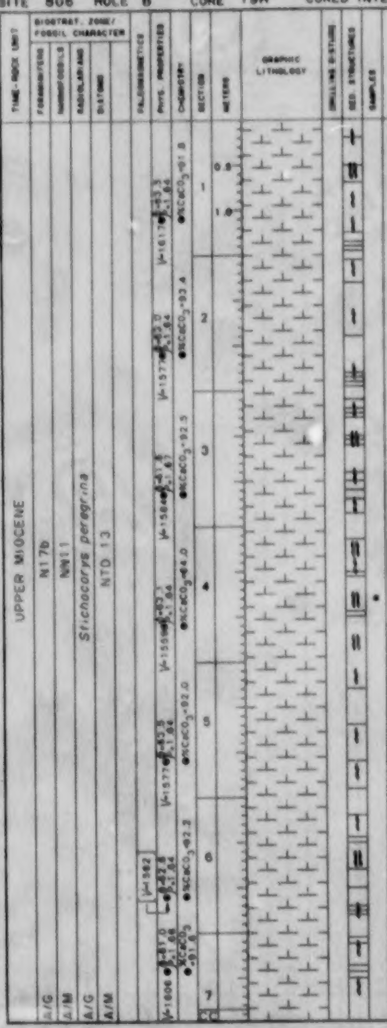
TIME-ROCK UNIT
BIOSTRAT. ZONE/FOSSIL CHARACTER
FORAMINIFERS
NANNOFOSSILS
RADIOLARIANS
DIATOMS
PALEOMAGNETICS
PHYS. PROPERTIES
CHEMISTRY
SECTION
METERS
GRAPHIC LITHOLOGY
DRILLING DISTURB.
SED. STRUCTURES
SAMPLES
UPPER MIOCENE
A/G N17b
A/M NN11
A/G Stichocorys peregrina
A/M NTD 13
V=1617 γ=53.3 ρ=1.84
V=1577 γ=53.0 ρ=1.84
V=1584 γ=51.8 ρ=1.87
V=1559 γ=53.1 ρ=1.84
V=1577 γ=53.8 ρ=1.84
V=1582
γ=52.8 ρ=1.84
V=1606 γ=51.0 ρ=1.88
%CaCO3=91.8
%CaCO3=93.4
%CaCO3=92.5
%CaCO3=94.0
%CaCO3=92.0
%CaCO3=92.2
%CaCO3=91.6
1
2
3
4
5
6
7
CC
0.5
1.0

LITHOLOGIC DESCRIPTION

NANNOFOSSIL OOZE with FORAMINIFERS

Major lithology: This core contains white (5Y 8/1 to 2.5Y 8/0) NANNOFOSSIL OOZE with FORAMINIFERS. Bioturbation is moderate to heavy throughout the core, with cm scale light gray (5Y 7/1 and 5Y 7/2) mottling and mm to cm scale grayish purple (5PB 5/2) mottling and burrow "halos". Very faint, light greenish gray (5G 7/1) and diffuse grayish purple (5PB 5/2) color bands are present to common.

SMEAR SLIDE SUMMARY (%):

	3, 74
	D
TEXTURE	
Sand	15
Silt	50
Clay	35
COMPOSITION	
Accessory minerals	1
Foraminifers	22
Nannofossils	75
Siliceous fragments	2

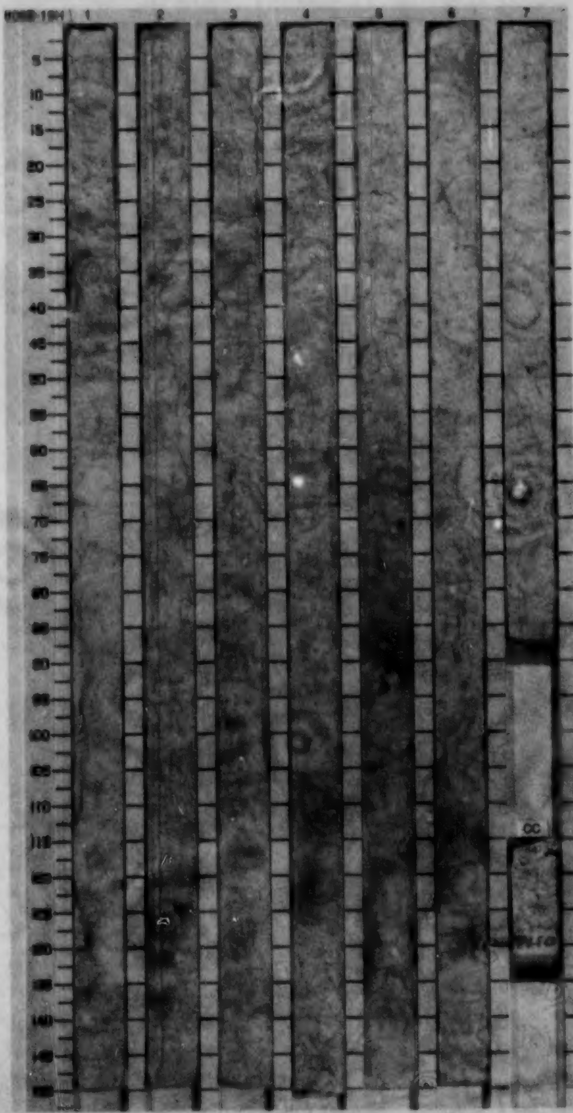
806B-19H
1
2
3
4
5
6
7
CC
5
10
15
20
25
30
35
40
45
50
55
60
65
70
75
80
85
90
95
100
105
110
115
120
125
130
135
140
145
150

SITE 806 HOLE D CORE 20H CORED INTERVAL 177.5-187.0 mbsf

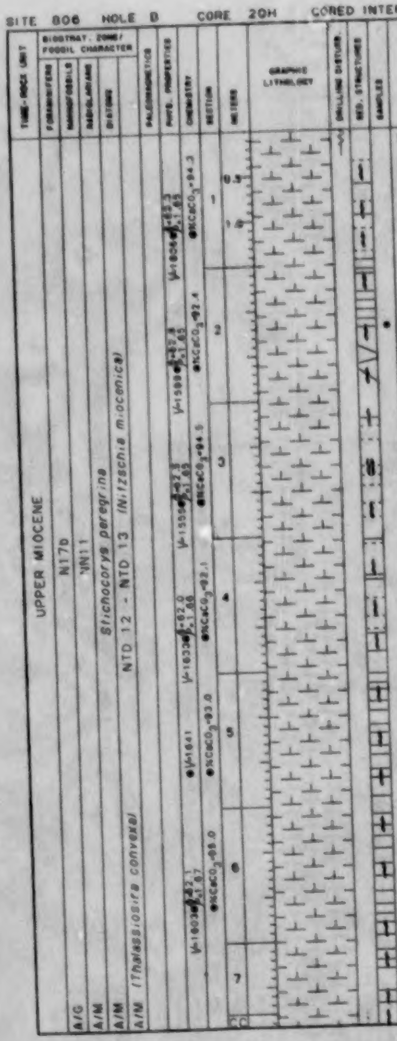
TIME-ROCK UNIT
BIOSTRAT. ZONE/ FOSSIL CHARACTER
FORAMINIFERS
NANNOFOSSILS
RADIOLARIANS
DIATOMS
PALEOMAGNETICS
PHYS. PROPERTIES
CHEMISTRY
SECTION
METERS
GRAPHIC LITHOLOGY
DRILLING DISTURB.
SED. STRUCTURES
SAMPLES
UPPER MIOCENE
A/G N17b
A/M NN11
A/M Stichocorys peregrina
A/M NTD 12 - NTD 13 (Nitzschia miocenica) (Thalassiosira convexa)
V=1606 ϕ=63.3 ρ=1.63
V=1598 ϕ=62.8 ρ=1.65
V=1555 ϕ=62.8 ρ=1.65
V=1633 ϕ=62.0 ρ=1.66
V=1641
V=1603 ϕ=62.1 ρ=1.67
%CaCO3=94.3
%CaCO3=92.4
%CaCO3=94.5
%CaCO3=92.1
%CaCO3=93.0
%CaCO3=88.0
1
2
3
4
5
6
7
CC
0.5
1.0

LITHOLOGIC DESCRIPTION

NANNOFOSSIL OOZE with FORAMINIFERS

Major lithology: This core contains white (2.5Y 8/0) NANNOFOSSIL OOZE with FORAMINIFERS. Bioturbation is moderate, with cm scale, light gray (5Y 7/1) and white (5Y 8/0) mottling and mm to cm scale, grayish blue (5PB 5/2) to pale purple (5P 6/2) mottling and burrow "halos". Very faint, light greenish gray (5G 7/1) and diffuse grayish blue (5PB 5/2) to pale purple (5P 6/2) color bands are present to common throughout the core.

SMEAR SLIDE SUMMARY (%):

	2, 90
	D
TEXTURE:	
Sand	25
Silt	75
COMPOSITION:	
Foraminifers	20
Nannofossils	75
Radiolarians	5

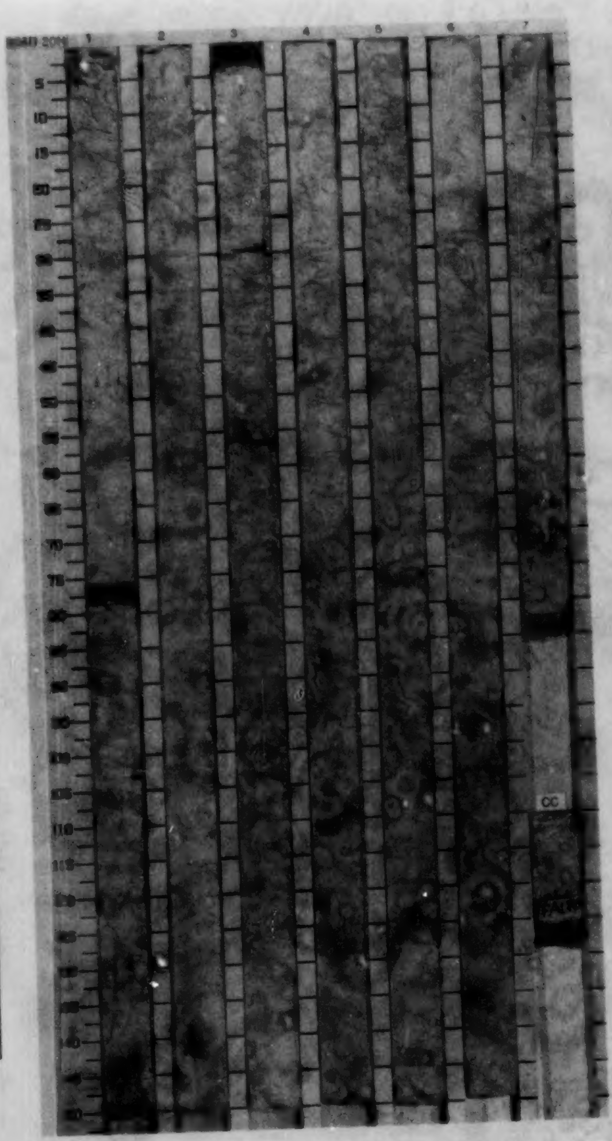
806D 20H
1
2
3
4
5
6
7
CC
5
10
15
20
25
30
35
40
45
50
55
60
65
70
75
80
85
90
95
100
105
110
115
120
125
130
135
140
145
150

SITE 806 HOLE B CORE 21H CORED INTERVAL 187.0-196.5 mbsf

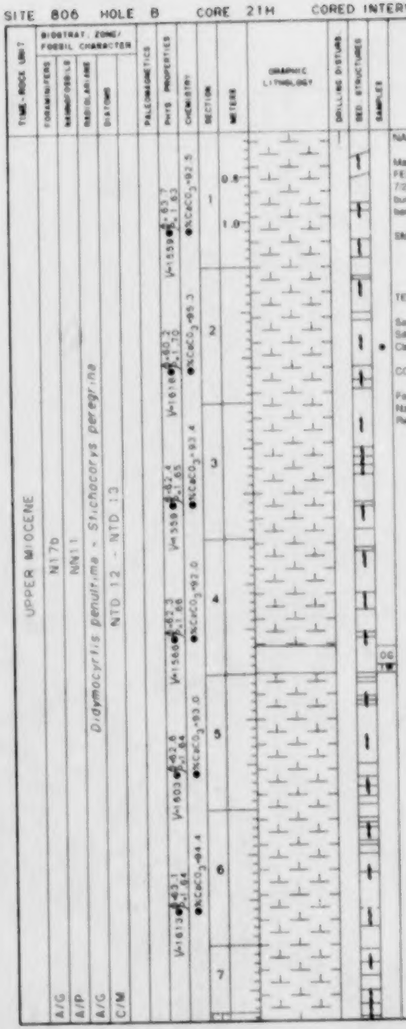
TIME-ROCK UNIT
BIOSTRAT. ZONE/ FOSSIL CHARACTER
FORAMINIFERS
NANNOFOSSILS
RADIOLARIANS
DIATOMS
PALEOMAGNETICS
PHYS. PROPERTIES
CHEMISTRY
SECTION
METERS
GRAPHIC LITHOLOGY
DRILLING DISTURB.
SED. STRUCTURES
SAMPLES
UPPER MIOCENE
A/G N17b
A/P NN11
A/G Didymocyrtis penultima - Stichocorys peregrina
C/M NTD 12 - NTD 13
V=1559 ● φ=63.7 γ=1.63
V=1618 ● φ=60.2 γ=1.70
V=1558 ● φ=62.4 γ=1.65
V=1560 ● φ=62.3 γ=1.66
V=1603 ● φ=62.6 γ=1.64
V=1613 ● φ=63.1 γ=1.64
● %CaCO3=92.5
● %CaCO3=95.3
● %CaCO3=93.4
● %CaCO3=92.0
● %CaCO3=93.0
● %CaCO3=94.4
1
2
3
4
5
6
7
0.5
1.0
OG
IW

LITHOLOGIC DESCRIPTION

NANNOFOSSIL OOZE with FORAMINIFERS

Major lithology: This core contains white (2.5Y 8/0) NANNOFOSSIL OOZE with FORAMINIFERS. Bioturbation is moderate throughout the core with cm scale, light gray (5Y 7/1 and 5Y 7/2) and olive (5Y 5/3) mottling and mm to cm scale grayish blue (5PB 5/2) mottling and burrow "halos". Very faint, light greenish gray (5G 7/1) and diffuse grayish blue 5PB 5/2) color bands are present to common throughout the core.

SMEAR SLIDE SUMMARY (%):

	2, 90
	D
TEXTURE:	
Sand	20
Silt	75
Clay	5
COMPOSITION:	
Foraminifers	20
Nannofossils	75
Radiolarians	5

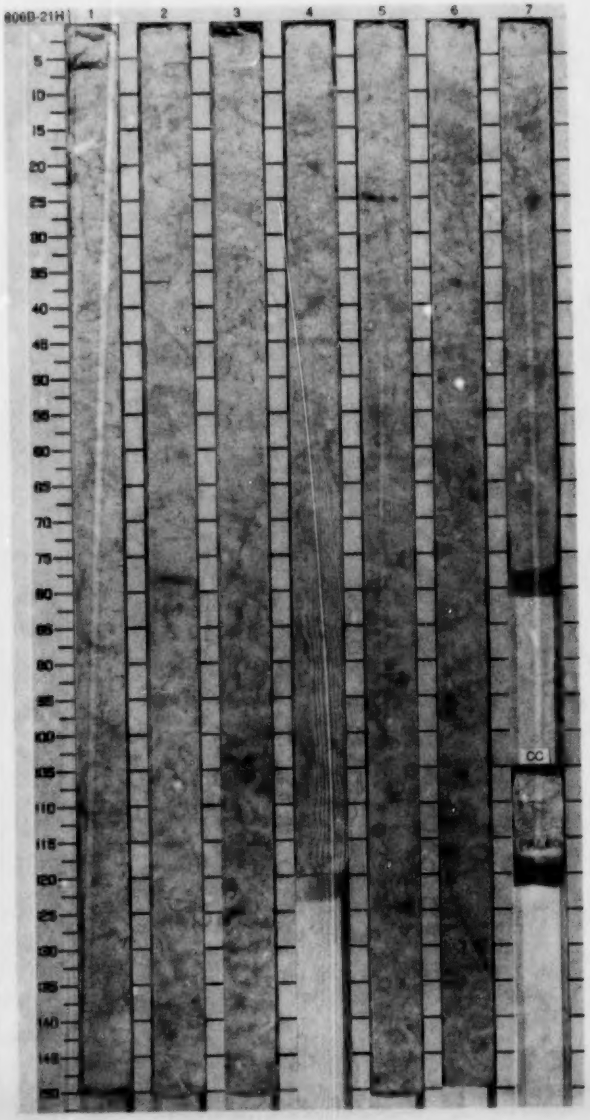
806B-21H
1
2
3
4
5
6
7
5
10
15
20
25
30
35
40
45
50
55
60
65
70
75
80
85
90
95
100
105
110
115
120
125
130
135
140
145
150
CC

SITE 806 HOLE B CORE 22H CORED INTERVAL 196.5-206.0 mbsf

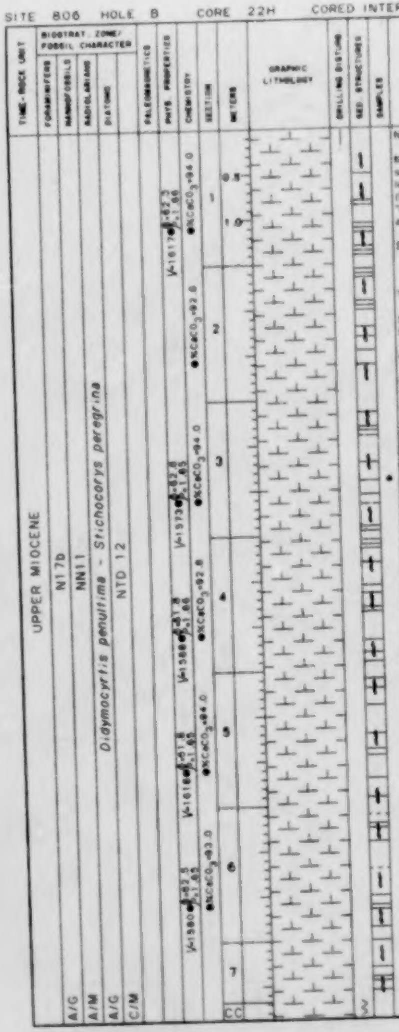
TIME-ROCK UNIT
BIOSTRAT. ZONE/ FOSSIL CHARACTER
FORAMINIFERS
NANNOFOSSILS
RADIOLARIANS
DIATOMS
PALEOMAGNETICS
PHYS. PROPERTIES
CHEMISTRY
SECTION
METERS
GRAPHIC LITHOLOGY
DRILLING DISTURB.
SED. STRUCTURES
SAMPLES
UPPER MIOCENE
N17b
NN11
Didymocyrtis penultima - Stichocorys peregrina
NTD 12
A/G
A/M
A/G
C/M
V=1617 φ=62.3 γ=1.66
%CaCO3=94.0
%CaCO3=92.0
V=1573 φ=62.8 γ=1.65
%CaCO3=94.0
V=1588 φ=61.8 γ=1.66
%CaCO3=92.8
V=1618 φ=61.6 γ=1.65
%CaCO3=94.0
V=1590 φ=62.5 γ=1.65
%CaCO3=93.0
1
2
3
4
5
6
7
CC
0.5
1.0

LITHOLOGIC DESCRIPTION

NANNOFOSSIL OOZE with FORAMINIFERS

Major lithology: This core contains NANNOFOSSIL OOZE with FORAMINIFERS. The sediment is predominantly white (2.5Y 8/0 to 5Y 8/1) with a single diffuse, 25 cm thick zone of light gray (5Y 7/1). The sediment is slightly to moderately bioturbated with cm scale, light gray (5Y 7/1 and 5Y 7/2) mottling and mm to cm scale, grayish blue (5PB 5/2) mottling and burrow "halos". Very faint, light greenish gray (5G 7/1) and diffuse grayish blue (5PB 5/2) color bands are present to abundant throughout the core.

SMEAR SLIDE SUMMARY (%):

	3, 69
	D
TEXTURE:	
Sand	20
Silt	80
COMPOSITION:	
Foraminifers	15
Nannofossils	80
Radiolarians	5

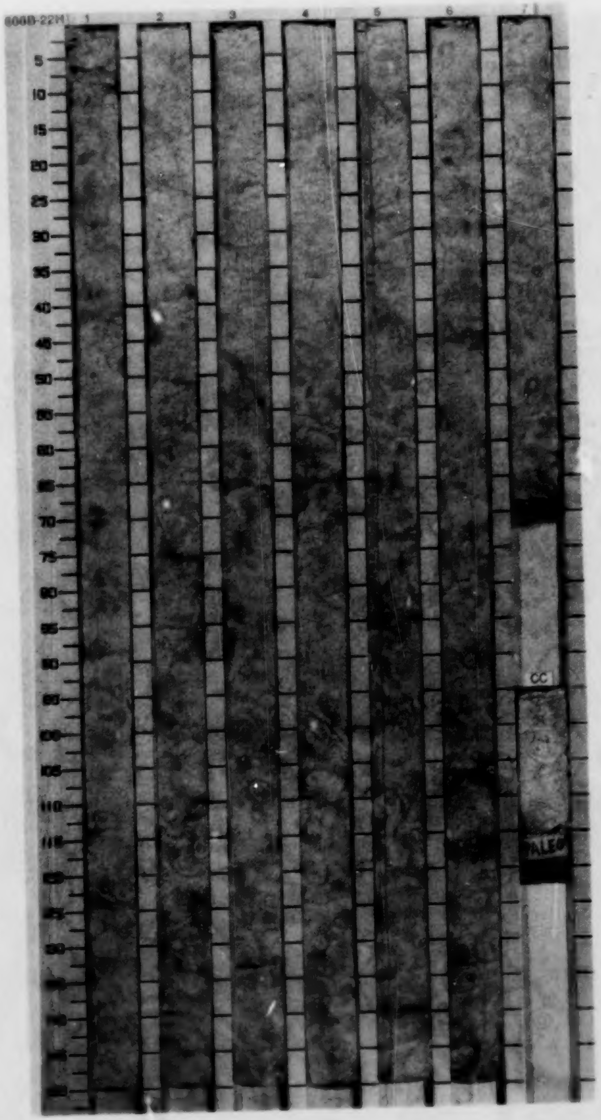
806B-22H
1
2
3
4
5
6
7
5
10
15
20
25
30
35
40
45
50
55
60
65
70
75
80
85
90
95
100
105
110
115
120
125
130
135
140
145
150
CC
PALEO

SITE 806 HOLE B CORE 23H CORED INTERVAL 206.0-215.5 mbsf

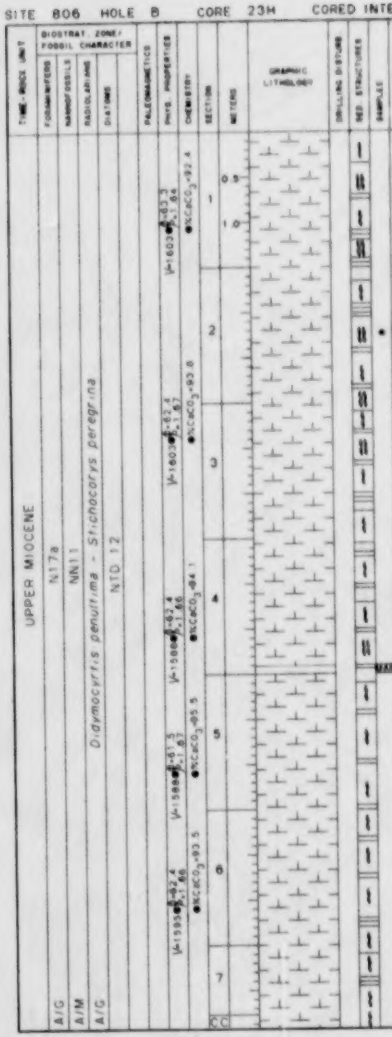
TIME-ROCK UNIT
BIOSTRAT. ZONE/ FOSSIL CHARACTER
FORAMINIFERS
NANNOFOSSILS
RADIOLARIANS
DIATOMS
PALEOMAGNETICS
PHYS. PROPERTIES
CHEMISTRY
SECTION
METERS
GRAPHIC LITHOLOGY
DRILLING DISTURB.
SED. STRUCTURES
SAMPLES
UPPER MIOCENE
N17a
NN11
Didymocyrtis penultima - Stichocorys peregrina
NTD 12
A/G
A/M
A/G
V=1603 φ=63.3 ρ=1.64
%CaCO3=92.4
V=1603 φ=62.4 ρ=1.67
%CaCO3=93.8
V=1588 φ=62.4 ρ=1.66
%CaCO3=94.1
V=1588 φ=61.5 ρ=1.67
%CaCO3=95.5
V=1593 φ=62.4 ρ=1.66
%CaCO3=93.5
1
2
3
4
5
6
7
CC
0.5
1.0
MAX

LITHOLOGIC DESCRIPTION

NANNOFOSSIL OOZE with FORAMINIFERS

Major lithology: This core contains moderately to heavily bioturbated, homogeneous, white (2.5Y 8/0) NANNOFOSSIL OOZE with FORAMINIFERS. Predominantly horizontal, cm scale light gray (5Y 7/1) and grayish blue (5PB 5/2) burrow mottles are abundant, and mm scale grayish blue pyritic burrow fills are common. In Section 2, the outlines of large burrow "halos" are observed as dipping grayish blue color bands. Faint light greenish gray (5G 7/1) and diffuse grayish blue (5PB 5/2) color bands are present. Rare, cm thick, stiffer intervals are spaced irregularly throughout the core.

SMEAR SLIDE SUMMARY (%):

	2, 72
	D
TEXTURE:	
Sand	10
Silt	85
Clay	5
COMPOSITION:	
Foraminifers	20
Nannofossils	79
Radiolarians	1

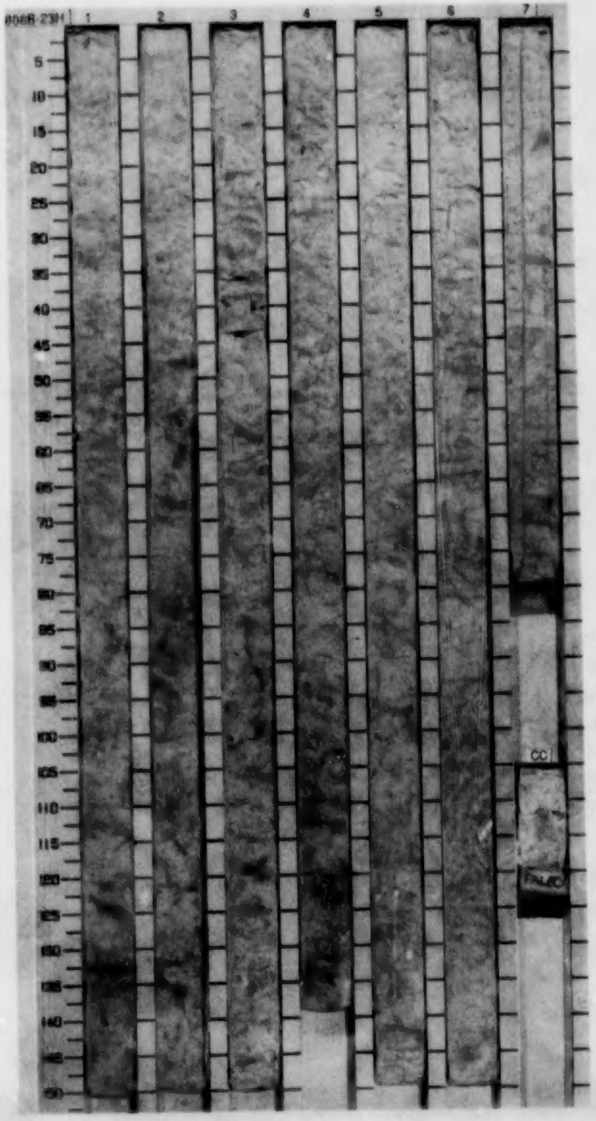
806B-23H
1
2
3
4
5
6
7
CC
PALEO
5
10
15
20
25
30
35
40
45
50
55
60
65
70
75
80
85
90
95
100
105
110
115
120
125
130
135
140
145
150

SITE 806 HOLE B CORE 24H CORED INTERVAL 215.5-225.0 mbsf

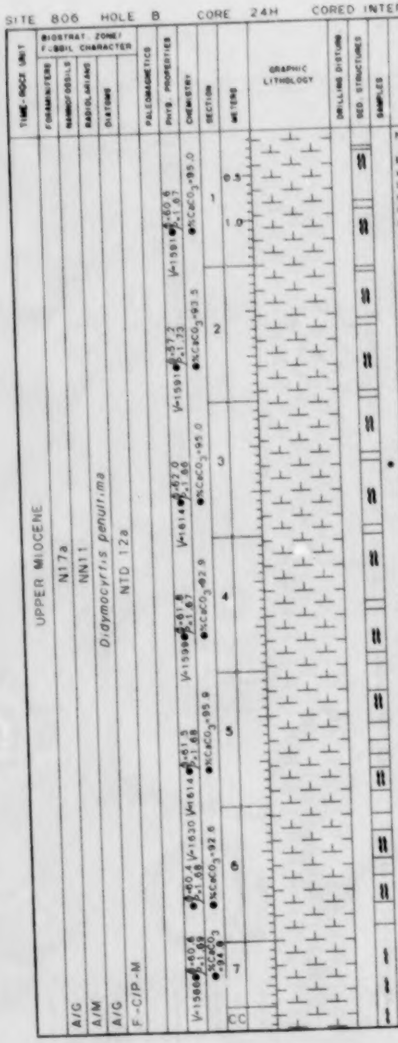
TIME-ROCK UNIT
BIOSTRAT. ZONE/ FOSSIL CHARACTER
FORAMINIFERS
NANNOFOSSILS
RADIOLARIANS
DIATOMS
PALEOMAGNETICS
PHYS. PROPERTIES
CHEMISTRY
SECTION
METERS
GRAPHIC LITHOLOGY
DRILLING DISTURB.
SED. STRUCTURES
SAMPLES
UPPER MIOCENE
N17a
NN11
Didymocyrtis penultima
NTD 12a
A/G
A/M
A/G
F-C/P-M
V-1591 ϕ-60.6 ρ-1.67
%CaCO3=95.0
V-1591 ϕ-57.2 ρ-1.73
%CaCO3=93.5
V-1614 ϕ-62.0 ρ-1.66
%CaCO3=95.0
V-1599 ϕ-61.8 ρ-1.67
%CaCO3=92.9
V-1614 ϕ-61.5 ρ-1.68
%CaCO3=95.9
V-1630 ϕ-60.4 ρ-1.68
%CaCO3=92.6
V-1566 ϕ-60.6 ρ-1.69
%CaCO3 =94.9
0.5
1.0
1
2
3
4
5
6
7
CC

LITHOLOGIC DESCRIPTION

NANNOFOSSIL OOZE with FORAMINIFERS

Major lithology: This core contains homogeneous, white (2.5Y 8/0) NANNOFOSSIL OOZE with FORAMINIFERS. The sediments are moderately to heavily bioturbated, with abundant light gray (5Y 7/1) mottles and pale purple (5P 6/2) pyritized burrows an "halos." Faint diffuse, mm to cm thick, greenish gray (5G 7/1) color bands are abundant. Rare cm thick, stiffer intervals are spaced irregularly throughout the core. A slight H_2S odor was noted when the core was split.

SMEAR SLIDE SUMMARY (%)

	3, 75 D
TEXTURE	
Sand	10
Silt	50
Clay	40
COMPOSITION	
Foraminifers	20
Nannofossils	77
Radiolarians	1
Siliceous fragments	2

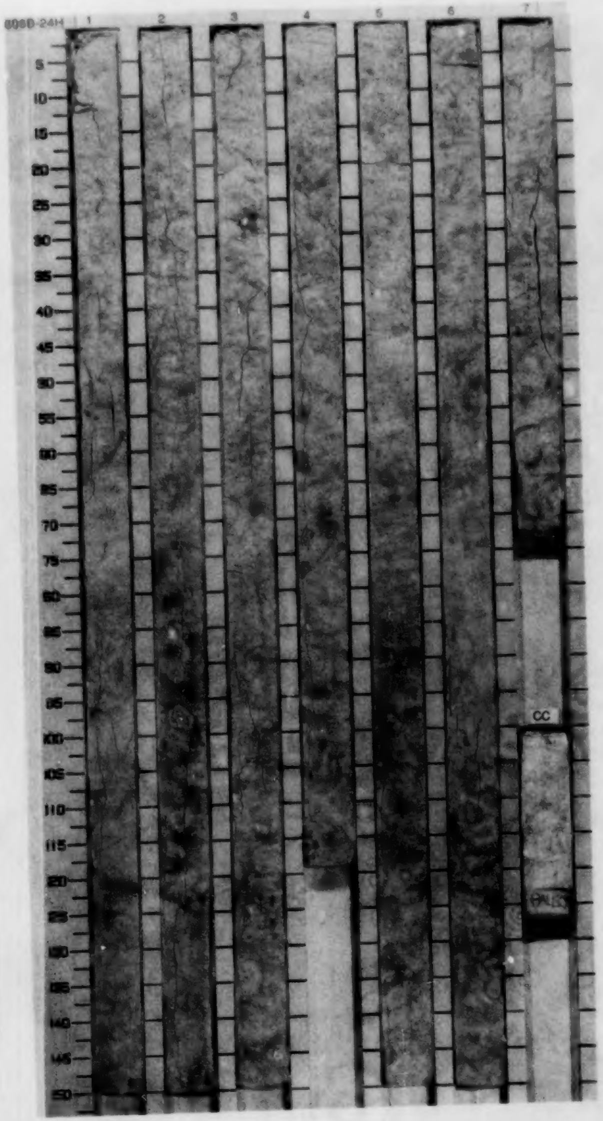
806B-24H
1
2
3
4
5
6
7
CC
5
10
15
20
25
30
35
40
45
50
55
60
65
70
75
80
85
90
95
100
105
110
115
120
125
130
135
140
145
150

SITE 806 HOLE B CORE 25H CORED INTERVAL 225.0-234.5 mbsf

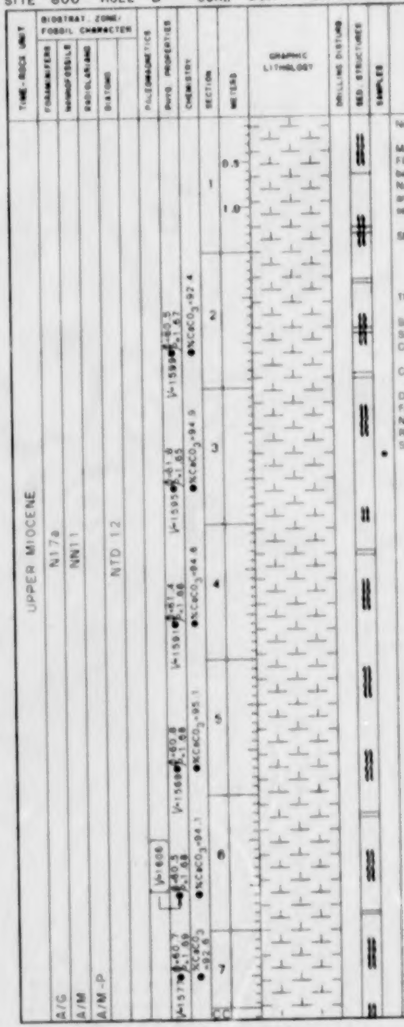
TIME-ROCK UNIT
BIOSTRAT. ZONE/ FOSSIL CHARACTER
FORAMINIFERS
NANNOFOSSILS
RADIOLARIANS
DIATOMS
PALEOMAGNETICS
PHYS. PROPERTIES
CHEMISTRY
SECTION
METERS
GRAPHIC LITHOLOGY
DRILLING DISTURB.
SED. STRUCTURES
SAMPLES
UPPER MIOCENE
N17a
NN11
NTD 12
A/G
A/M
A/M-P
V-1599 γ-60.5 ρ-1.67
%CaCO3-92.4
V-1595 γ-61.6 ρ-1.65
%CaCO3-94.9
V-1591 γ-61.4 ρ-1.66
%CaCO3-94.6
V-1568 γ-60.8 ρ-1.68
%CaCO3-95.1
V-1606
γ-60.5 ρ-1.68
%CaCO3-94.1
V-1577 γ-60.7 ρ-1.69
%CaCO3-92.6
1
2
3
4
5
6
7
CC
0.5
1.0

LITHOLOGIC DESCRIPTION

NANNOFOSSIL OOZE with FORAMINIFERS

Major lithology: This core contains white (2.5Y 8/0) NANNOFOSSIL OOZE with FORAMINIFERS. Abundant thin (0.2 to 0.5 cm) pale purple (5P 6/2) and reddish gray (5R 6/1) color bands and streaks are observed. These colors appear to be related to bioturbation patterns. Numerous light gray (2.5Y 7/2) mottles, mostly subhorizontal, are also noted, although a few are vertical. Some very faint, pale yellowish green (10GY 7/2) color zones are also visible. The sediment is firm to stiff. A slight odor of H_2S was apparent when the core was split.

SMEAR SLIDE SUMMARY (%)

	3, 75
	D
TEXTURE	
Sand	10
Silt	50
Clay	40
COMPOSITION	
Diatoms	Tr
Foraminifers	20
Nannofossils	78
Radiolarians	Tr
Siliceous fragments	2

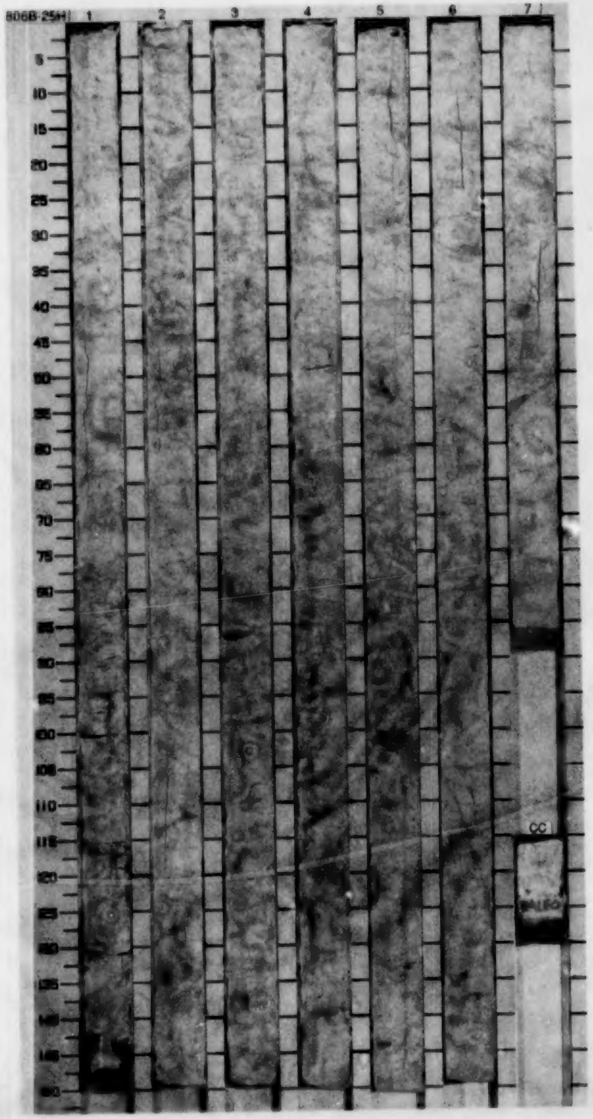
806B-25H
1
2
3
4
5
6
7
CC
5
10
15
20
25
30
35
40
45
50
55
60
65
70
75
80
85
90
95
100
105
110
115
120
125
130
135
140
145
150

SITE 806 HOLE B CORE 26H CORED INTERVAL 234.5-244.0 mbsf

TIME-ROCK UNIT	BIOSTRAT. ZONE/FOSSIL CHARACTER: FORAMINIFERS	NANNOFOSSILS	RADIOLARIANS	DIATOMS	PALEOMAGNETICS	PHYS. PROPERTIES	CHEMISTRY	SECTION	METERS	GRAPHIC LITHOLOGY	DRILLING DISTURB.	SED. STRUCTURES	SAMPLES	LITHOLOGIC DESCRIPTION
UPPER MIOCENE	N17a A/G	NN11 A	*Didymocyrtis penultima* A/G	NTD 12 C-A/P-M		V_p=1572 ● ϕ=60.7 γ=1.67 V_p=1599 ● ϕ=62.0 γ=1.63 V_p=1610 ● ϕ=61.4 γ=1.66 V_p=1598 ● ϕ=61.4 γ=1.66 V_p=1603 ● ϕ=61.4 γ=1.66 V_p=1595 ● ϕ=61.0 γ=1.65	● %$CaCO_3$=93.1 ● %$CaCO_3$=93.3 ● %$CaCO_3$=94.2 ● %$CaCO_3$=94.4 ● %$CaCO_3$=93.5 ● %$CaCO_3$=93.6 ● %$CaCO_3$=92.3	1 2 3 4 5 6 7 CC	0.5 1.0				*	see below

NANNOFOSSIL OOZE with FORAMINIFERS

Major lithology: This core contains NANNOFOSSIL OOZE with FORAMINIFERS. The sediment is white (7.5YR 8/0) with numerous pale purple (5P 6/2) and light gray (2.5Y 7/0) mottles. A few, very faint, pale yellow green (10GY 7/2) color bands are discernable. The core is stiff, with thin (1 cm) zones of hard to semi-lithified material irregularly distributed throughout the core, especially in Sections 5 and 6. A slight H_2S odor was noticed when the core was split.

SMEAR SLIDE SUMMARY (%):

	4, 76
	D
TEXTURE	
Sand	10
Silt	65
Clay	25
COMPOSITION	
Accessory minerals	2
Foraminifers	15
Nannofossils	8
Siliceous fragments	3

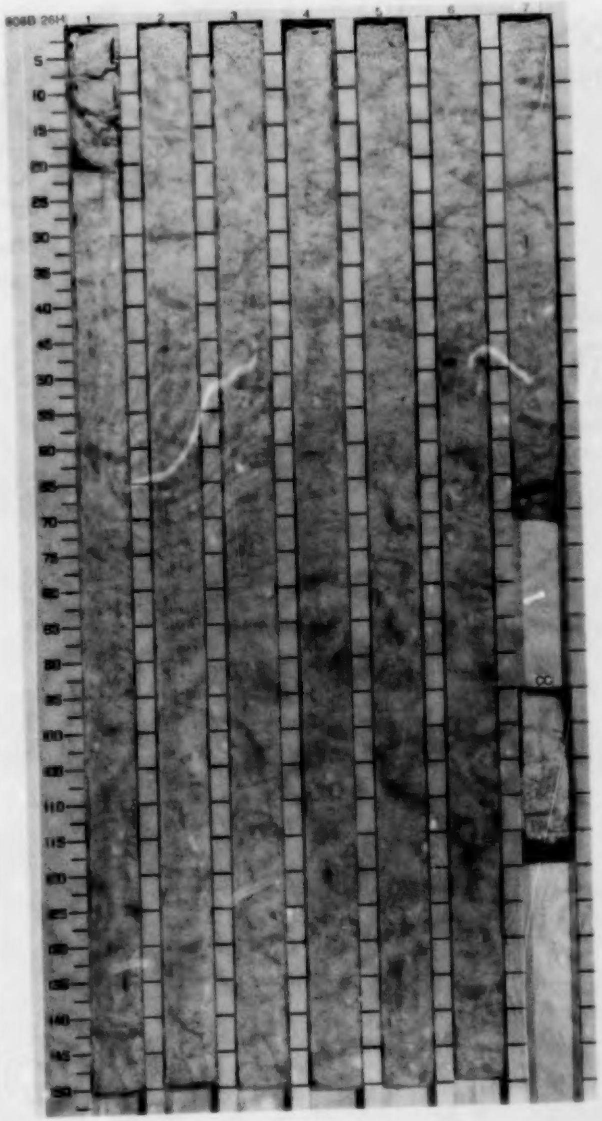

SITE 806 HOLE B CORE 27H CORED INTERVAL 244.0-253.5 mbsf

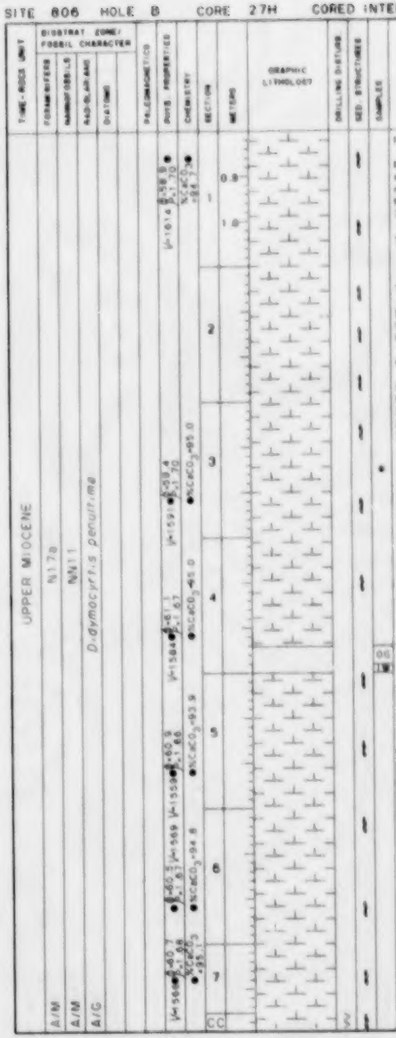
TIME-ROCK UNIT
BIOSTRAT. ZONE/ FOSSIL CHARACTER
FORAMINIFERS
NANNOFOSSILS
RADIOLARIANS
DIATOMS
PALEOMAGNETICS
PHYS. PROPERTIES
CHEMISTRY
SECTION
METERS
GRAPHIC LITHOLOGY
DRILLING DISTURB.
SED. STRUCTURES
SAMPLES
UPPER MIOCENE
N17a
NN11
D. dymocyrtis penultima
A/M
A/M
A/G
V=1614 φ=58.8 ρ=1.70
%CaCO3=84.7
V=1591 φ=58.4 ρ=1.70
%CaCO3=85.0
V=1584 φ=61.1 ρ=1.67
%CaCO3=85.0
V=1559 φ=60.9 ρ=1.66
%CaCO3=93.9
V=1569 φ=60.5 ρ=1.67
%CaCO3=94.8
V=1566 φ=60.7 ρ=1.66
%CaCO3=85.1
1
2
3
4
5
6
7
CC
0.8
1.0
OG
IW

LITHOLOGIC DESCRIPTION

NANNOFOSSIL OOZE with FORAMINIFER

Major lithology: This core contains NANNOFOSSIL OOZE with FORAMINIFERS. The sediment is white (7.5YR 8/0) with numerous pale purple (5P 6/2) and light gray (2.5Y 7/2) mottles. Pale purple bands are predominantly sub horizontal and arcuate halo segments. A few pieces of the sediment are markedly indurated. Some small pale yellowish green (10GY 7/2) specks are apparent. The sediment has a slight H_2S odor.

SMEAR SLIDE SUMMARY (%)

	3, 75
	D
TEXTURE	
Sand	10
Silt	50
Clay	40
COMPOSITION	
Foraminifers	10
Nannofossils	85
Radiolarians	Tr
Siliceous fragments	Tr
Siliceous sponge spicules	Tr

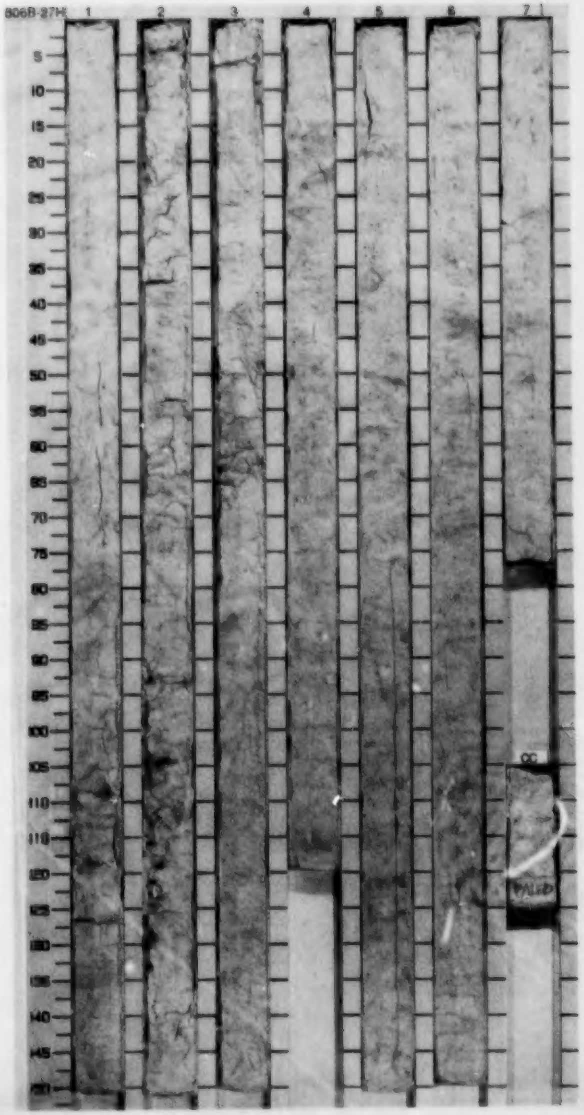
806B-27H
1
2
3
4
5
6
7
5
10
15
20
25
30
35
40
45
50
55
60
65
70
75
80
85
90
95
100
105
110
115
120
125
130
135
140
145
150
CC

SITE 806 HOLE B CORE 28H CORED INTERVAL 253.5-263.0 mbsf

TIME-ROCK UNIT	FORAMINIFERS	NANNOFOSSILS	RADIOLARIANS	DIATOMS	PALEOMAGNETICS	PHYS. PROPERTIES	CHEMISTRY	SECTION	METERS	GRAPHIC LITHOLOGY	DRILLING DISTURB.	SED. STRUCTURES	SAMPLES
UPPER MIOCENE	N17a	NN11	*Didymocyrtis antepenultima*	NTD 11b - NTD 11b (*Nitzschia porteri*)		V=1591 ● φ=60.3 γ=1.68	● %CaCO$_3$=94.9	1	0.5 1.0				
						V=1595 ● φ=60.2 γ=1.67	● %CaCO$_3$=94.8	2					*
						V=1588 ● φ=59.3 γ=1.70	● %CaCO$_3$=95.5	3					
						V=1618 ● φ=59.2 γ=1.69	● %CaCO$_3$=95.2	4					
						V=1603 ● φ=60.7 γ=1.67	● %CaCO$_3$=94.8	5					
						V=1588 ● φ=61.0 γ=1.66	● %CaCO$_3$=94.5	6					
								7					
	A/M	A/P	A/G	C-A/M									

LITHOLOGIC DESCRIPTION

NANNOFOSSIL OOZE with FORAMINIFERS

Major lithology: This core contains white (7.5YR 8/0) NANNOFOSSIL OOZE with FORAMINIFERS. The ooze is firm with some irregular semi-lithified areas. Abundant white (2.5Y 8/2) burrow fills and mottles indicate significant bioturbation. Pale purple (5P 6/2) streaks, "halos", and, to a lesser extent, bands that are up to 1 cm thick are present throughout. Horizontal bands are particularly prominent in Section 6, 25 cm to 62 cm. There are a few pale yellowish green (10GY 7/2) specks in this core. The sediment has a slight H_2S odor.

SMEAR SLIDE SUMMARY (%):

	2, 75 D
TEXTURE:	
Sand	10
Silt	50
Clay	40
COMPOSITION:	
Foraminifers	12
Nannofossils	88
Radiolarians	Tr
Siliceous fragments	Tr
Siliceous sponge spicules	Tr

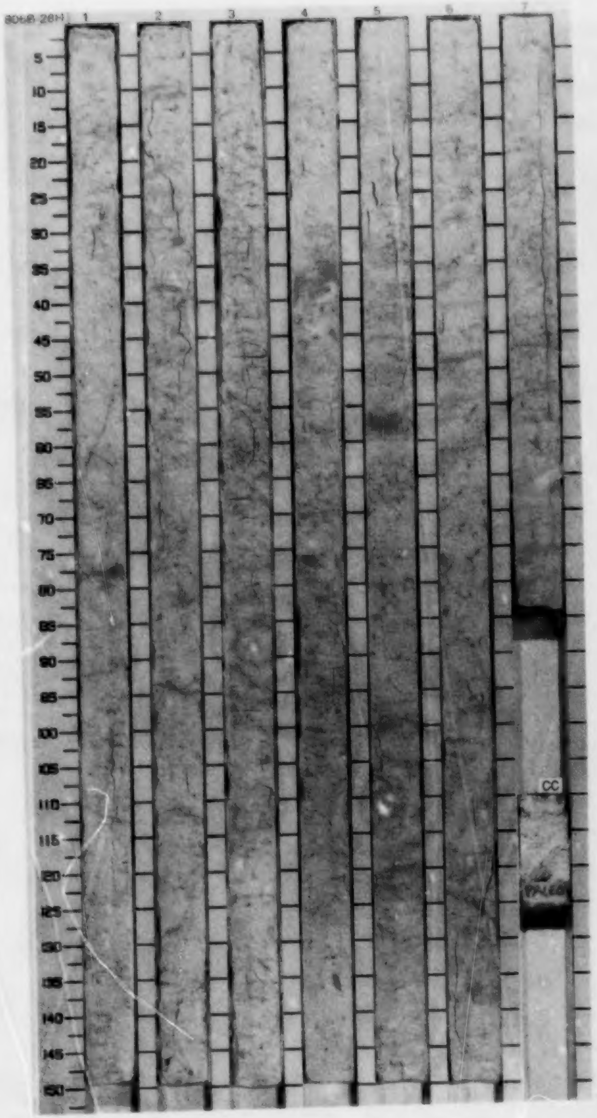

SITE 806 HOLE B CORE 29H CORED INTERVAL 263.0-272.5 mbsf

TIME-ROCK UNIT	BIOSTRAT. ZONE/ FOSSIL CHARACTER: FORAMINIFERS	NANNOFOSSILS	RADIOLARIANS	DIATOMS	PALEOMAGNETICS	PHYS. PROPERTIES	CHEMISTRY	SECTION	METERS	GRAPHIC LITHOLOGY	DRILLING DISTURB.	SED. STRUCTURES	SAMPLES
UPPER MIOCENE	N16 A/M	NN11 A/M	*Didymocyrtis antepenultima* A/G	NTD 11 A/M		V=1603 ● φ=61.7 γ=1.66	● %CaCO$_3$=93.5	1	0.5 1.0				
						V=1599 ● φ=60.4 γ=1.68	● %CaCO$_3$=93.8	2					
						V=1622 ● φ=63.7 γ=1.62	● %CaCO$_3$=93.0	3					●
						V=1580 ● φ=62.1 γ=1.63	● %CaCO$_3$=94.0	4					
						V=1603 ● φ=62.9 γ=1.63	● %CaCO$_3$=93.7	5					
						V=1603 ● φ=63.7 γ=1.61	● %CaCO$_3$=93.8	6					
								7					
								CC					

LITHOLOGIC DESCRIPTION

NANNOFOSSIL OOZE with FORAMINIFERS

Major lithology: This core contains white (7.5YR 8/0) NANNOFOSSIL OOZE with FORAMINIFERS. It is moderately to heavily bioturbated, with abundant light gray (2.5Y 7/2) and pale purple (5P 6/2) mottles and pyrite-filled burrows. Very faint, pale purple (5P 6/2) and greenish gray (5G 7/2) color bands occasionally are present. Hard and semi-lithified intervals, 1 cm thick and closely spaced, are distributed throughout the core.

SMEAR SLIDE SUMMARY (%):

	3, 74
	D
TEXTURE:	
Sand	10
Silt	60
Clay	30
COMPOSITION:	
Foraminifers	15
Nannofossils	80
Siliceous fragments	5

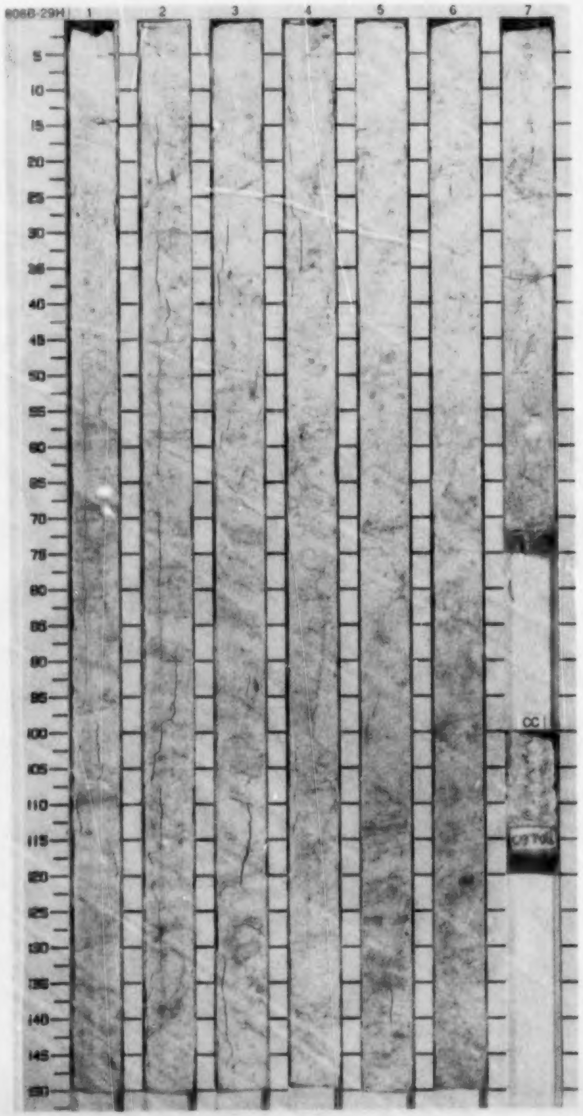

SITE 806 HOLE B CORE 30H CORED INTERVAL 272.5-282.0 mbsf

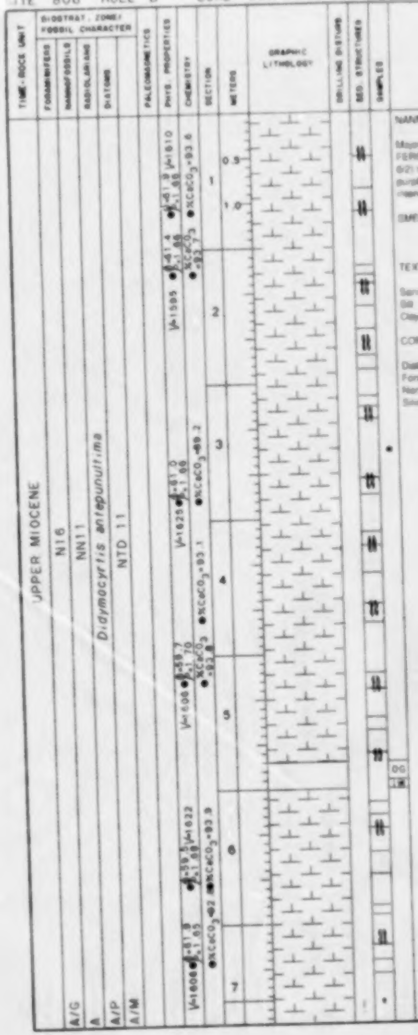
TIME-ROCK UNIT
BIOSTRAT. ZONE/ FOSSIL CHARACTER
FORAMINIFERS
NANNOFOSSILS
RADIOLARIANS
DIATOMS
PALEOMAGNETICS
PHYS. PROPERTIES
CHEMISTRY
SECTION
METERS
GRAPHIC LITHOLOGY
DRILLING DISTURB.
SED. STRUCTURES
SAMPLES
UPPER MIOCENE
N16
NN11
Didymocyrtis antepenultima
NTD 11
A/G
A
A/P
A/M
γ=1610
φ=61.9
γ=1.68
%CaCO3=93.6
γ=1595
φ=41.4
γ=1.86
%CaCO3=93.7
γ=1625
φ=61.0
γ=1.66
%CaCO3=89.2
%CaCO3=93.1
γ=1600
φ=59.7
γ=1.70
%CaCO3=93.8
γ=1622
φ=59.5
γ=1.68
%CaCO3=93.9
γ=1608
φ=61.8
γ=1.65
%CaCO3=92
0.5
1.0
1
2
3
4
5
6
7
OG
IW

LITHOLOGIC DESCRIPTION

NANNOFOSSIL OOZE with FORAMINIFERS

Major lithology: This core contains white (7.5YR 8/0) NANNOFOSSIL OOZE with FORAMINIFERS. It is moderately to heavily bioturbated, with light gray (2.5Y 7/2) and pale purple (5P 6/2) mottles (0.5-1 cm in diameter) and fewer pyrite-filled burrows. Occasional, very faint, pale purple (5P 7/2) and greenish gray (5G 7/2) color bands are noted. Hard and semi-lithified intervals, about 1 cm thick and closely spaced, are distributed throughout the core.

SMEAR SLIDE SUMMARY (%):

	3, 75
	D
TEXTURE:	
Sand	10
Silt	50
Clay	40
COMPOSITION:	
Diatoms	1
Foraminifers	20
Nannofossils	77
Siliceous fragments	2

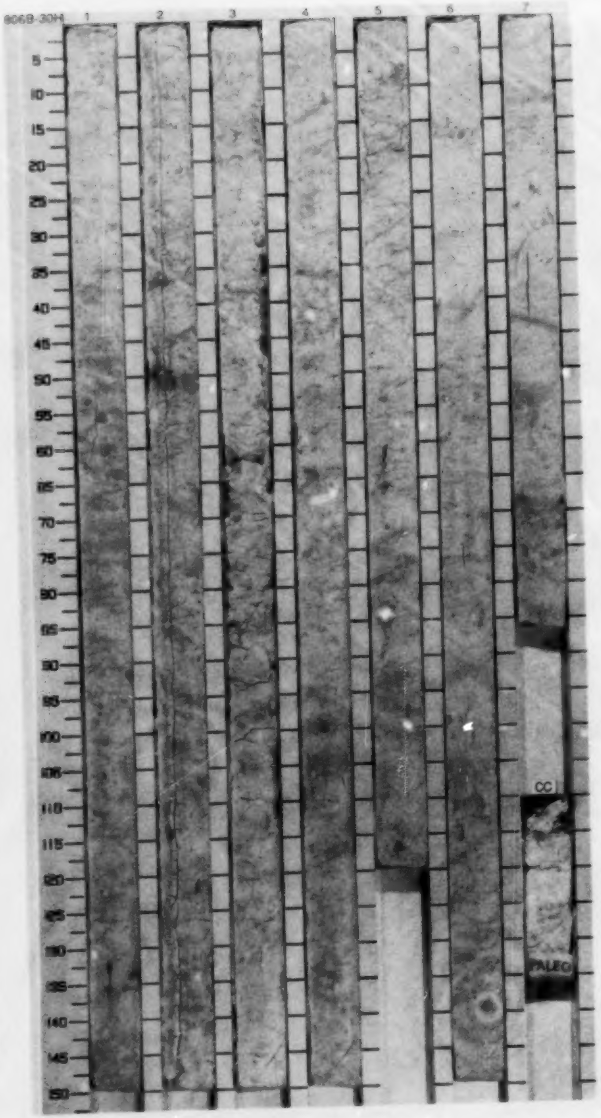
806B-30H
1
2
3
4
5
6
7
5
10
15
20
25
30
35
40
45
50
55
60
65
70
75
80
85
90
95
100
105
110
115
120
125
130
135
140
145
150
CC
PALEO

SITE 806 HOLE B CORE 31H CORED INTERVAL 282.0-291.5 mbsf

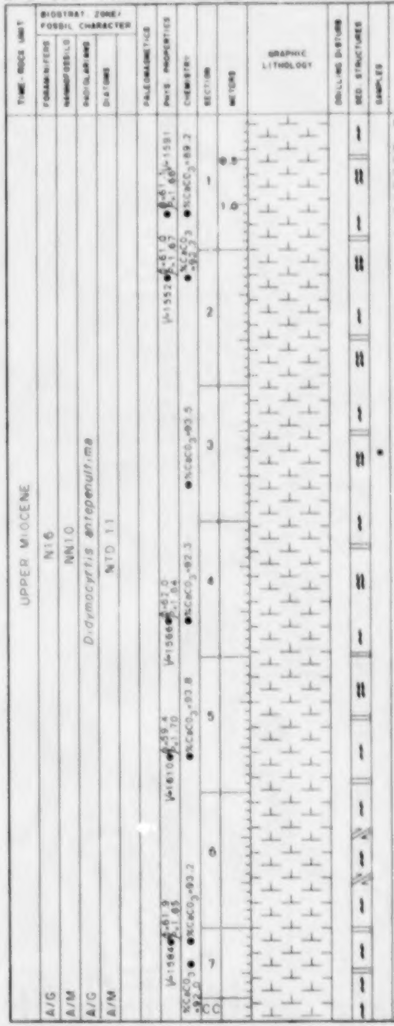

LITHOLOGIC DESCRIPTION

NANNOFOSSIL OOZE with FORAMINIFERS

Major lithology: This core contains white (7.5YR 8/0) NANNOFOSSIL OOZE with FORAMINIFERS. It is moderately to heavily bioturbated, with abundant pyrite filled burrows and frequent light gray (2.5Y 7/2) and pale purple (5P 6/2) burrow mottles. Faint banding is common, with colors of pale purple (5P 6/2), reddish gray (5R 6/1) and pale yellowish green (10GY 7/2). The ooze alternates between stiff and semi-lithified intervals on a scale of several cm. Several microfaults, displacing color bands, were observed in Section 6.

SMEAR SLIDE SUMMARY (%):

	3, 75
	D
TEXTURE:	
Sand	8
Silt	60
Clay	32
COMPOSITION:	
Diatoms	1
Foraminifers	20
Nannofossils	76
Radiolarians	Tr
Siliceous fragments	3

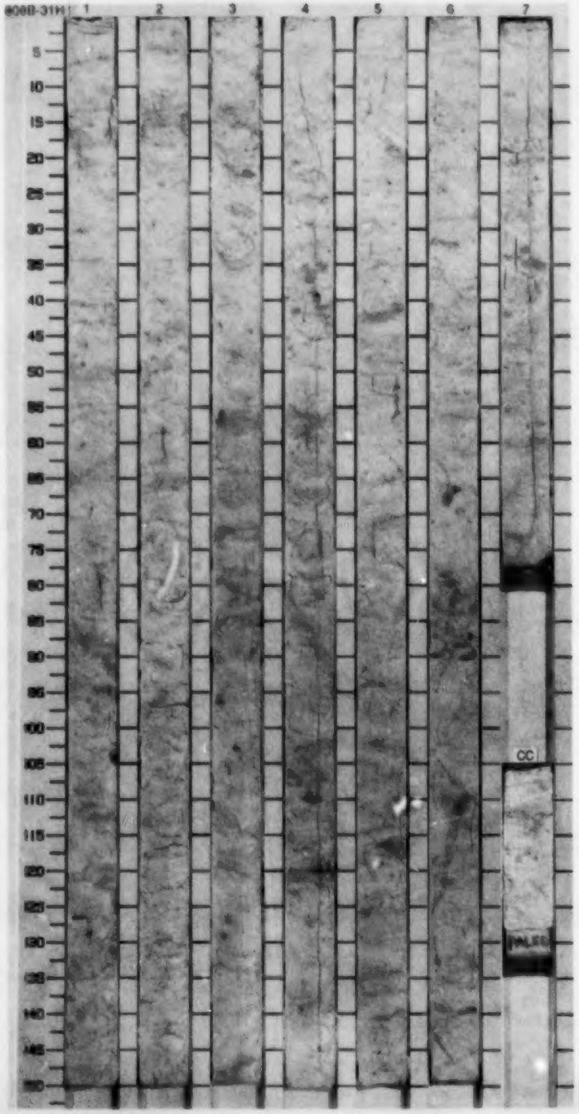
806B-31H
1
2
3
4
5
6
7
5
10
15
20
25
30
35
40
45
50
55
60
65
70
75
80
85
90
95
100
105
110
115
120
125
130
135
140
145
150
CC
PALEO

SITE 806 HOLE B CORE 32H CORED INTERVAL 291.5-301.0 mbsf

TIME-ROCK UNIT	BIOSTRAT. ZONE/ FOSSIL CHARACTER: FORAMINIFERS	NANNOFOSSILS	RADIOLARIANS	DIATOMS	PALEOMAGNETICS	PHYS. PROPERTIES	CHEMISTRY	SECTION	METERS	GRAPHIC LITHOLOGY	DRILLING DISTURB.	SED. STRUCTURES	SAMPLES
UPPER MIOCENE	N16	NN10	*Didymocyrtis antepenultima*	NTD 11		V=1603 φ=61.5 γ=1.66 V=1595 φ=63.8 γ=1.63 V=1637 φ=61.7 γ=1.66 V=1618 φ=60.2 γ=1.68	%CaCO$_3$=92.8 %CaCO$_3$=93.9 %CaCO$_3$=93.5 %CaCO$_3$=92.2 %CaCO$_3$=93.5 %CaCO$_3$=93.7 %CaCO$_3$=95.6	1 2 3 4 5 6 7 CC	0.5 1.0				●
	A/G	A/M	A/G	A/M									

LITHOLOGIC DESCRIPTION

NANNOFOSSIL OOZE with FORAMINIFERS

Major lithology: This core contains NANNOFOSSIL OOZE with FORAMINIFERS. It is predominantly white (7.5YR 8/0) with frequent, faint, pale purple (5P 6/2) and pale yellowish green (10GY 7/2) color bands. Bioturbation is moderate to heavy, with mottles and pyritic burrow fills. These mottles are either light gray (2.5Y 7/2) or pale purple in color. A few burrows in Sections 6 and 7 are up to 5 cm in diameter and up to 10 cm long. The ooze is very stiff to hard, with abundant semi-lithified zones several cm thick.

SMEAR SLIDE SUMMARY (%):

	3, 75
	D
TEXTURE:	
Sand	5
Silt	50
Clay	45
COMPOSITION:	
Diatoms	3
Foraminifers	20
Nannofossils	73
Radiolarians	1
Siliceous fragments	3

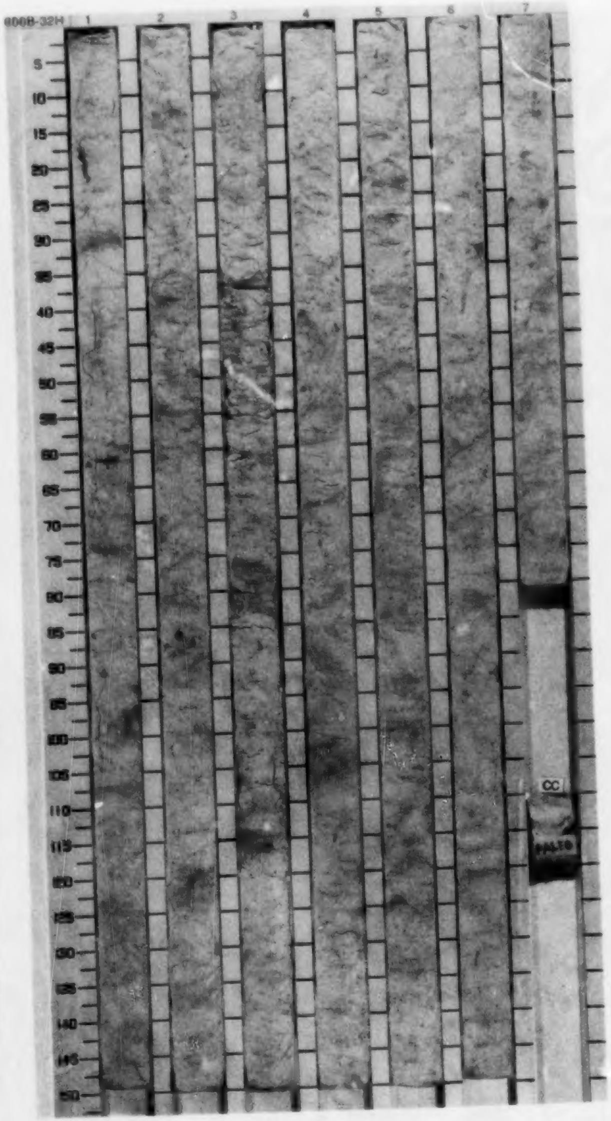

SITE 806 HOLE B CORE 33H CORED INTERVAL 301.0-310.5 mbsf

TIME-ROCK UNIT	BIOSTRAT. ZONE/ FOSSIL CHARACTER: FORAMINIFERS	NANNOFOSSILS	RADIOLARIANS	DIATOMS
UPPER MIOCENE	N16	NN10	Didymocyrtis antepenultima	top NTD 10b? - NTD 11a (Coscinodiscus yabei)
	A/G	A	A/G	A/M

SECTION	METERS	PHYS. PROPERTIES	CHEMISTRY
1	0.5 1.0	V=1614 φ=60.4 γ=1.69	●%CaCO$_3$=93.9
2		V=1625 φ=61.1 γ=1.66	●%CaCO$_3$=93.2
3		V=1599 φ=61.8 γ=1.65	●%CaCO$_3$=92.9
4		V=1603 φ=63.3 γ=1.63	●%CaCO$_3$=90.0
5		V=1610 φ=60.6 γ=1.67	●%CaCO$_3$=92.5
6		V=1618 φ=62.3 γ=1.64	●%CaCO$_3$=91.2
7			
CC			

PALEOMAGNETICS | GRAPHIC LITHOLOGY | DRILLING DISTURB. | SED. STRUCTURES | SAMPLES

OG

LITHOLOGIC DESCRIPTION

NANNOFOSSIL OOZE with FORAMINIFERS

Major lithology: This core contains NANNOFOSSIL OOZE with FORAMINIFERS. It is stiff with semi-indurated intervals. The color is white (2.5Y 8/0) with white (5Y 8/1), light gray (5Y 7/2), very dark gray (2.5Y 3/0), grayish blue (5PB 5/2), and light greenish gray (5G 7/1) mottling due to slight to moderate bioturbation. Several mm scale, grayish blue (5PB 5/2) pyritic burrow fills, a single intense grayish green (5G 5/2) trace fossil and grayish blue burrow "halos" are observed. A chert nodule (5 cm x 2 cm x 3 cm) is located in Section 3, 95-97 cm. Faint horizontal, pale purple (5P 6/2), grayish blue (5PB 5/2), and light greenish gray (5G 7/1) color bands, up to 2 cm thick, are present throughout the core.

SMEAR SLIDE SUMMARY (%):

	3, 50
	D
TEXTURE	
Sand	5
Silt	90
Clay	5
COMPOSITION	
Diatoms	Tr
Foraminifers	22
Nannofossils	75
Radiolarians	1
Siliceous fragments	2

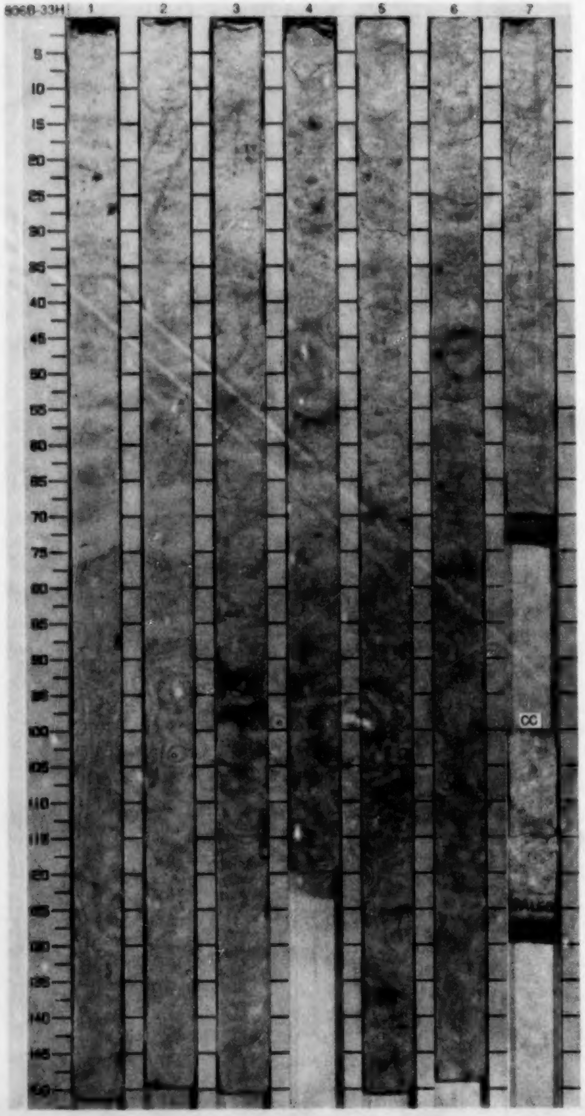

SITE 806 HOLE B CORE 34H CORED INTERVAL 310.5-320.0 mbsf

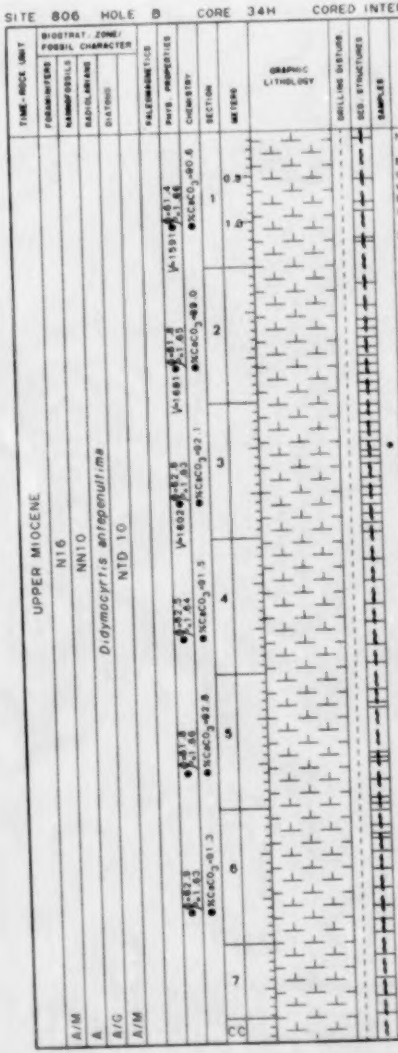
TIME-ROCK UNIT
BIOSTRAT. ZONE/ FOSSIL CHARACTER
FORAMINIFERS
NANNOFOSSILS
RADIOLARIANS
DIATOMS
PALEOMAGNETICS
PHYS. PROPERTIES
CHEMISTRY
SECTION
METERS
GRAPHIC LITHOLOGY
DRILLING DISTURB.
SED. STRUCTURES
SAMPLES
UPPER MIOCENE
N16
NN10
Didymocyrtis antepenultima
NTD 10
A/M
A
A/G
A/M
V-1591 φ-61.4 γ-1.66
V-1681 φ-61.8 γ-1.65
V-1602 φ-62.6 γ-1.63
φ-62.5 γ-1.64
φ-61.8 γ-1.66
φ-62.5 γ-1.63
●%CaCO3-90.6
●%CaCO3-89.0
●%CaCO3-92.1
●%CaCO3-91.5
●%CaCO3-92.8
●%CaCO3-91.3
1
2
3
4
5
6
7
CC
0.5
1.0

LITHOLOGIC DESCRIPTION

NANNOFOSSIL OOZE with FORAMINIFERS

Major lithology: This core consists of NANNOFOSSIL OOZE with FORAMINIFERS. The sediment is stiff and slightly biscuited, with alternating hard and soft intervals. The color is white (2.5Y 8/0) with light gray (5Y 7/1), white (10YR 8/0), dusky blue (5PB 3/2), and grayish blue (5PB 5/2) mottling. Bioturbation is slight to moderate. Faint to diffuse, light greenish gray (5G 7/1), grayish blue (5PB 5/2), and pale pink (5RP 8/2) color bands are common.

SMEAR SLIDE SUMMARY (%):

	3, 50
	D
TEXTURE:	
Sand	15
Silt	82
Clay	3
COMPOSITION:	
Diatoms	1
Foraminifers	20
Nannofossils	72
Radiolarians	5
Spicules	1

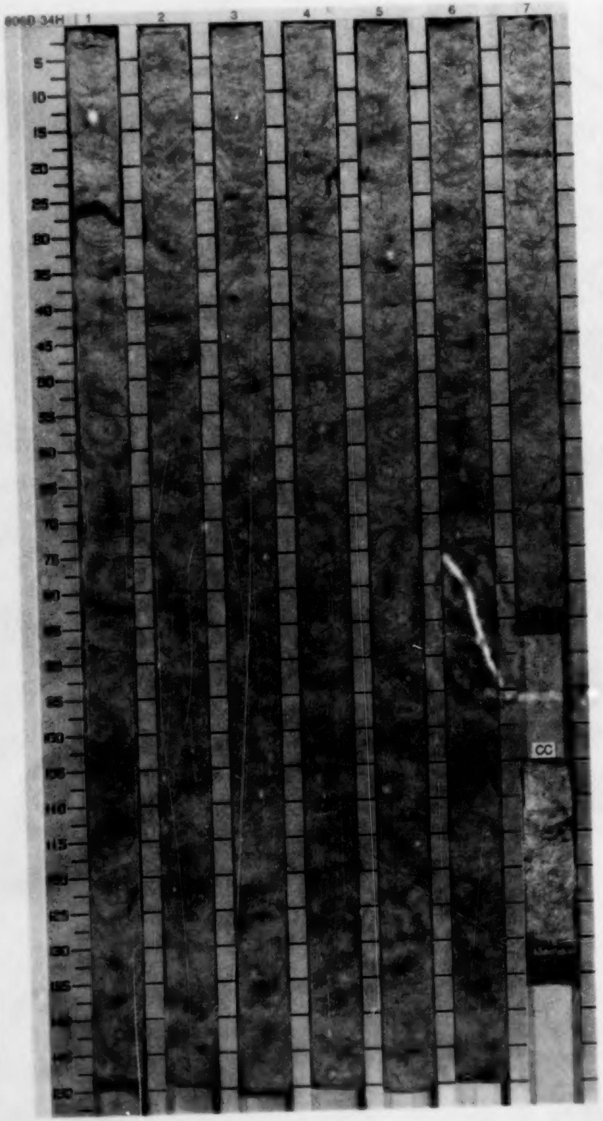
806B-34H
1
2
3
4
5
6
7
CC
5
10
15
20
25
30
35
40
45
50
55
60
65
70
75
80
85
90
95
100
105
110
115
120
125
130
135
140
145
150

SITE 806 HOLE B CORE 35X CORED INTERVAL 320.0-329.7 mbsf

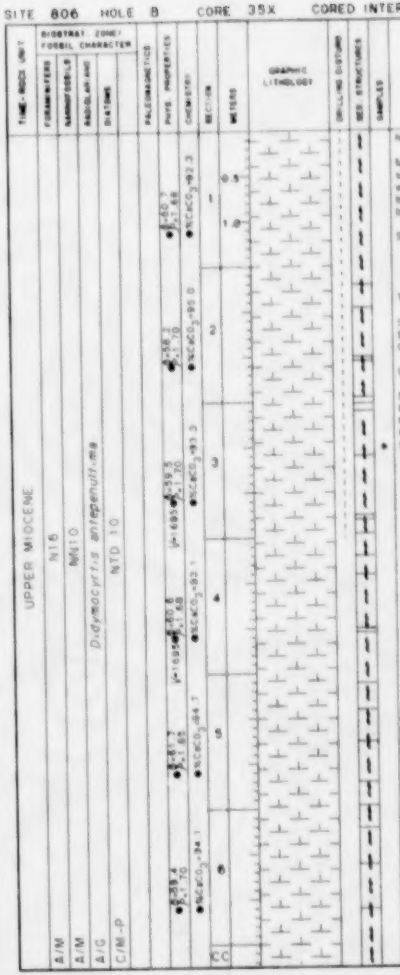
TIME-ROCK UNIT
BIOSTRAT. ZONE/ FOSSIL CHARACTER
FORAMINIFERS
NANNOFOSSILS
RADIOLARIANS
DIATOMS
PALEOMAGNETICS
PHYS. PROPERTIES
CHEMISTRY
SECTION
METERS
GRAPHIC LITHOLOGY
DRILLING DISTURB.
SED. STRUCTURES
SAMPLES
UPPER MIOCENE
N16
NN10
Didymocyrtis antepenultima
NTD 10
A/M
A/M
A/G
C/M-P
φ=60.7 γ=1.68
%CaCO3=92.3
φ=58.2 γ=1.70
%CaCO3=95.0
V=1695 φ=59.5 γ=1.70
%CaCO3=93.3
V=1695 φ=60.6 γ=1.68
%CaCO3=93.1
φ=61.7 γ=1.65
%CaCO3=84.7
φ=58.4 γ=1.70
%CaCO3=94.1
1
2
3
4
5
6
CC
0.5
1.0

LITHOLOGIC DESCRIPTION

NANNOFOSSIL OOZE with FORAMINIFERS

Major lithology: This core consists of NANNOFOSSIL OOZE with FORAMINIFERS. The sediment is stiff and slightly biscuited, with alternating hard and soft intervals. The color is white (2.5Y 8/0), with light gray (5Y 7/1), white (10YR 8/0), dusky blue (5PB 3/2) and grayish blue (5PB 5/2) mottling. Bioturbation is slight. Diffuse light greenish gray (5G 7/1), grayish blue (5PB 5/2), and pale purple (5P 6/2) color bands are common.

SMEAR SLIDE SUMMARY (%):

	3, 90
	D
TEXTURE:	
Sand	12
Silt	60
Clay	28
COMPOSITION:	
Diatoms	Tr
Foraminifers	15
Nannofossils	83
Radiolarians	2
Spicules	Tr

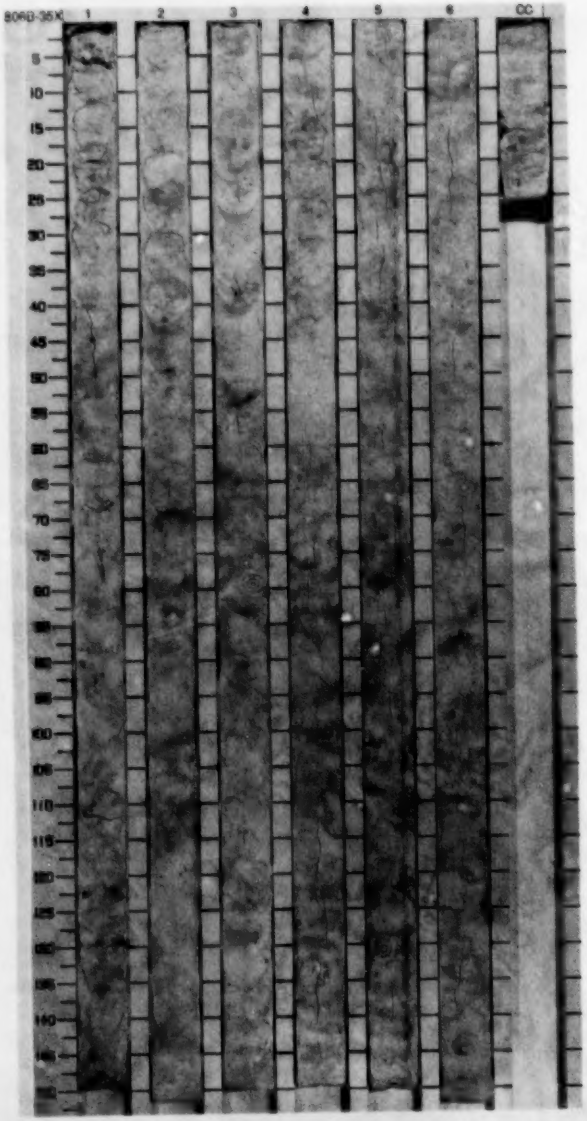
806B-35X
1
2
3
4
5
6
CC
5
10
15
20
25
30
35
40
45
50
55
60
65
70
75
80
85
90
95
100
105
110
115
120
125
130
135
140
145
150

SITE 806 HOLE B CORE 36X CORED INTERVAL 329.7-339.4 mbsf

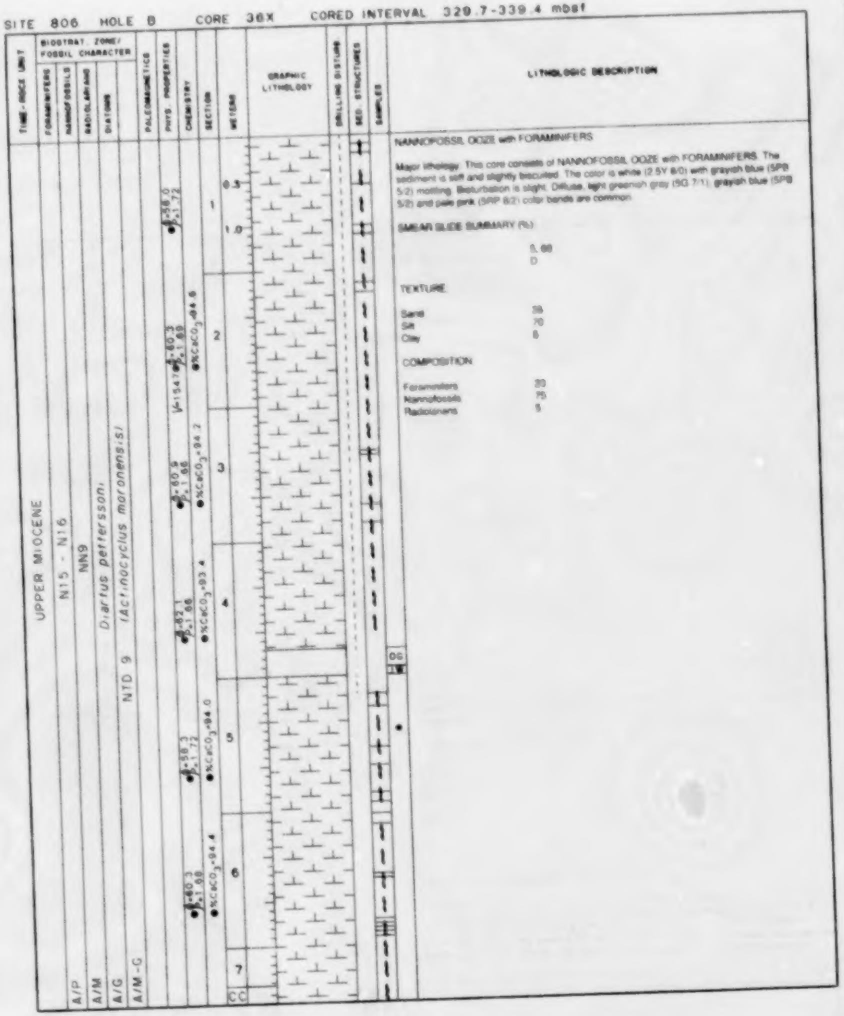
TIME-ROCK UNIT
BIOSTRAT. ZONE/ FOSSIL CHARACTER
FORAMINIFERS
NANNOFOSSILS
RADIOLARIANS
DIATOMS
PALEOMAGNETICS
PHYS. PROPERTIES
CHEMISTRY
SECTION
METERS
GRAPHIC LITHOLOGY
DRILLING DISTURB.
SED. STRUCTURES
SAMPLES
UPPER MIOCENE
N15 - N16
NN9
Diartus petterssoni
NTD 9 (Actinocyclus moronensis)
A/P
A/M
A/G
A/M-G
φ=58.0
ρ=1.72
φ=60.3
ρ=1.69
V=1547
φ=60.9
ρ=1.66
φ=62.1
ρ=1.66
φ=58.3
ρ=1.72
φ=60.3
ρ=1.68
%CaCO3=94.6
%CaCO3=94.2
%CaCO3=93.4
%CaCO3=94.0
%CaCO3=94.4
0.5
1.0
1
2
3
4
5
6
7
CC
OG
IW

LITHOLOGIC DESCRIPTION

NANNOFOSSIL OOZE with FORAMINIFERS

Major lithology: This core consists of NANNOFOSSIL OOZE with FORAMINIFERS. The sediment is stiff and slightly biscuited. The color is white (2.5Y 8/0) with grayish blue (5PB 5/2) mottling. Bioturbation is slight. Diffuse, light greenish gray (5G 7/1), grayish blue (5PB 5/2) and pale pink (5RP 8/2) color bands are common.

SMEAR SLIDE SUMMARY (%):

	5, 88
	D
TEXTURE:	
Sand	25
Silt	70
Clay	5
COMPOSITION:	
Foraminifers	20
Nannofossils	75
Radiolarians	5

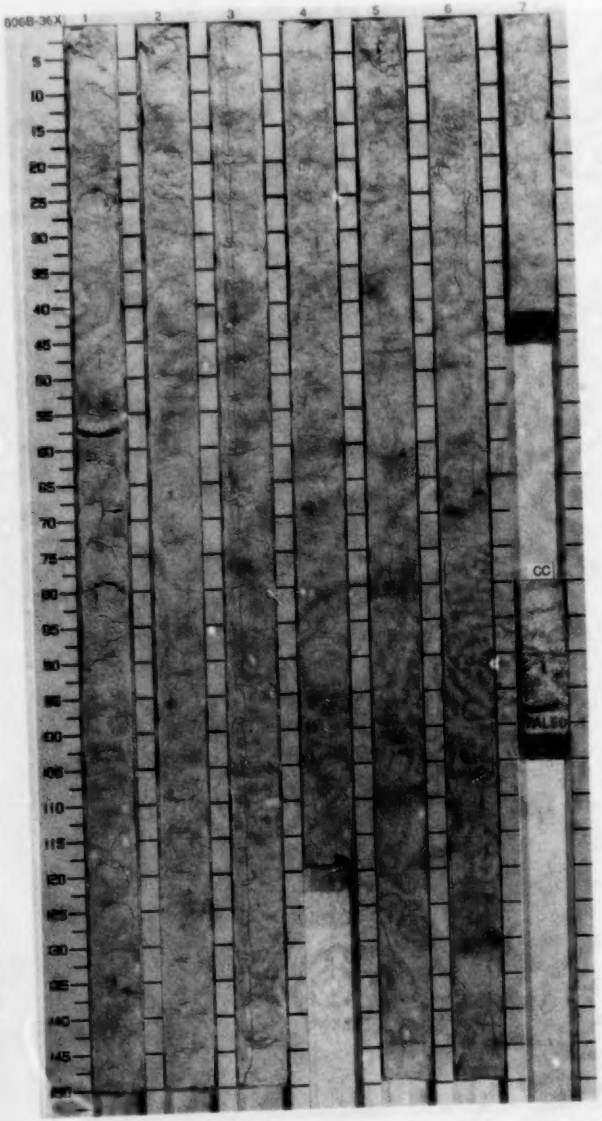
806B-36X
1
2
3
4
5
6
7
CC
5
10
15
20
25
30
35
40
45
50
55
60
65
70
75
80
85
90
95
100
105
110
115
120
125
130
135
140
145
150

SITE 806 HOLE B CORE 37X CORED INTERVAL 339.4-349.1 mbsf

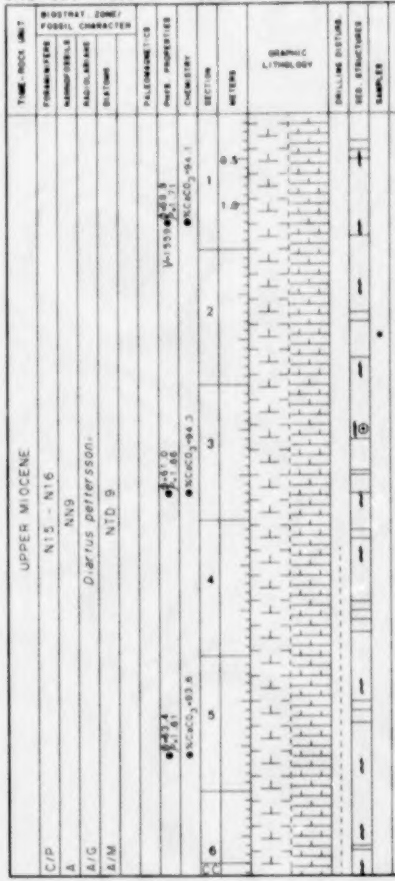
TIME-ROCK UNIT
BIOSTRAT. ZONE/ FOSSIL CHARACTER
FORAMINIFERS
NANNOFOSSILS
RADIOLARIANS
DIATOMS
PALEOMAGNETICS
PHYS. PROPERTIES
CHEMISTRY
SECTION
METERS
GRAPHIC LITHOLOGY
DRILLING DISTURB.
SED. STRUCTURES
SAMPLES
UPPER MIOCENE
C/P N15 - N16
A NN9
A/G Diartus petterssoni
A/M NTD 9
V=1559
γ=1.71
%CaCO$_3$=94.1
γ=1.66
%CaCO$_3$=94.3
γ=1.61
%CaCO$_3$=93.6
1
2
3
4
5
6
CC
0.5
1.0

LITHOLOGIC DESCRIPTION

NANNOFOSSIL OOZE/CHALK with FORAMINIFERS

Major lithology: This core contains white (2.5Y 8/0) NANNOFOSSIL OOZE/ CHALK with FORAMINIFERS. The stiffness of the sediment varies on a scale of cm. Slight bioturbation is indicated by faint mottling and individual pyritized burrows with associated pale purple mottling. Pale purple (5P 6/2), 4 cm thick color bands are present every 1.2 to 2 m. Light greenish gray (5G 7/1), 1 cm thick color bands are present in all sections.

SMEAR SLIDE SUMMARY (%):

	2, 96
	D
TEXTURE:	
Sand	20
Silt	75
Clay	5
COMPOSITION:	
Foraminifers	15
Nannofossils	80
Radiolarians	5

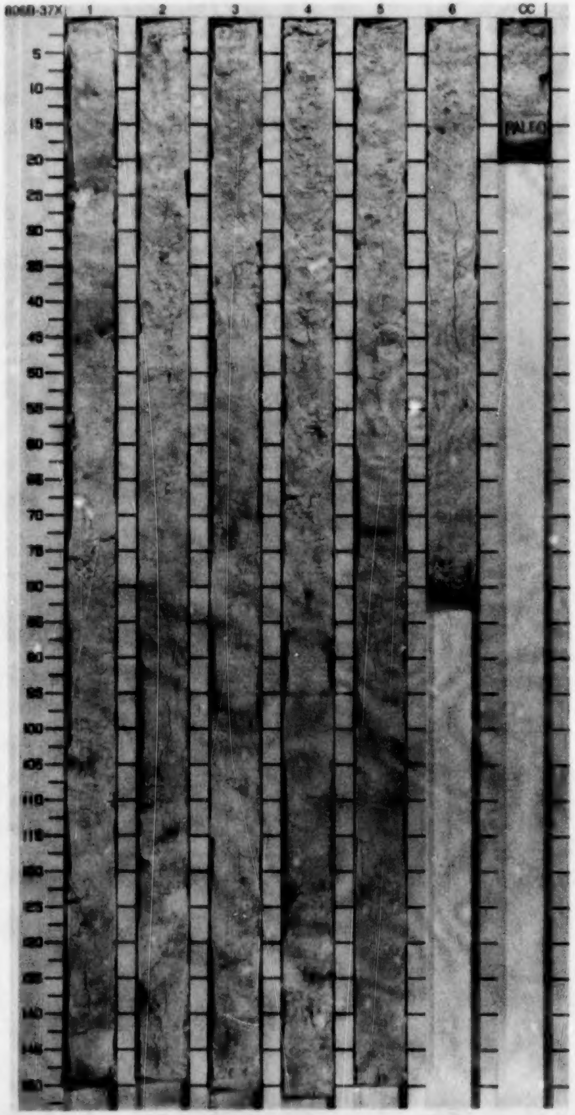
806B-37X
1
2
3
4
5
6
CC
PALEO
5
10
15
20
25
30
35
40
45
50
55
60
65
70
75
80
85
90
95
100
105
110
115
120
125
130
135
140
145
150

SITE 806 HOLE B CORE 38X CORED INTERVAL 349.1-358.8 mbsf

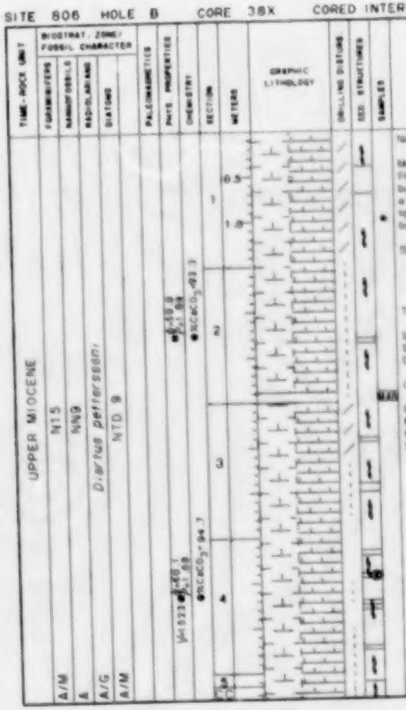
TIME-ROCK UNIT
BIOSTRAT. ZONE/ FOSSIL CHARACTER
FORAMINIFERS
NANNOFOSSILS
RADIOLARIANS
DIATOMS
PALEOMAGNETICS
PHYS. PROPERTIES
CHEMISTRY
SECTION
METERS
GRAPHIC LITHOLOGY
DRILLING DISTURB.
SED. STRUCTURES
SAMPLES
UPPER MIOCENE
N15
NN9
Diartus petterssoni
NTD 9
A/M
A
A/G
A/M
1
2
3
4
0.5
1.0
%CaCO3=93.3
%CaCO3=94.7
MAN

LITHOLOGIC DESCRIPTION

NANNOFOSSIL OOZE/CHALK with FORAMINIFERS

Major lithology: This core contains white (2.5Y 8/0) NANNOFOSSIL OOZE/CHALK with FORAMINIFERS. Bioturbation is slight as indicated by faint mottling and scattered pyritized burrows with associated grayish blue (5PB 5/2) color mottling. In the first three sections, only a few scattered light greenish gray (5G 7/1) color bands are seen. In Section 4, 1 cm thick light greenish gray (5G 7/1) bands, pale purple bands (5P 6/2) and grayish blue (5PB 5/2) bands are present.

SMEAR SLIDE SUMMARY (%):

	1, 98
	D
TEXTURE	
Sand	15
Silt	80
Clay	5
COMPOSITION	
Foraminifers	10
Nannofossils	85
Radiolarians	4
Silicoflagellates	1

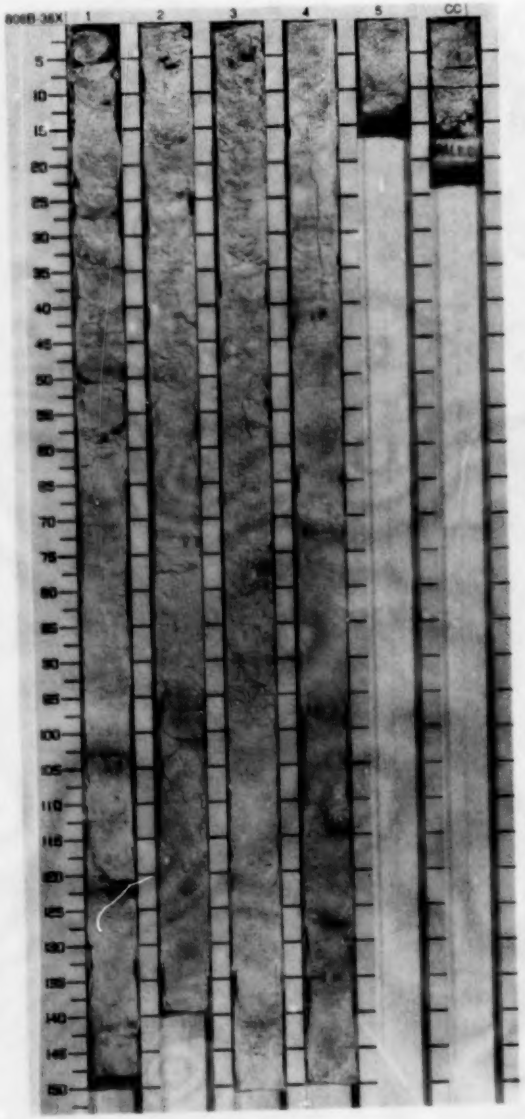
806B-38X
1
2
3
4
5
CC
5
10
15
20
25
30
35
40
45
50
55
60
65
70
75
80
85
90
95
100
105
110
115
120
125
130
135
140
145
150

SITE 806 HOLE B CORE 39X CORED INTERVAL 358.8-368.5 mbsf

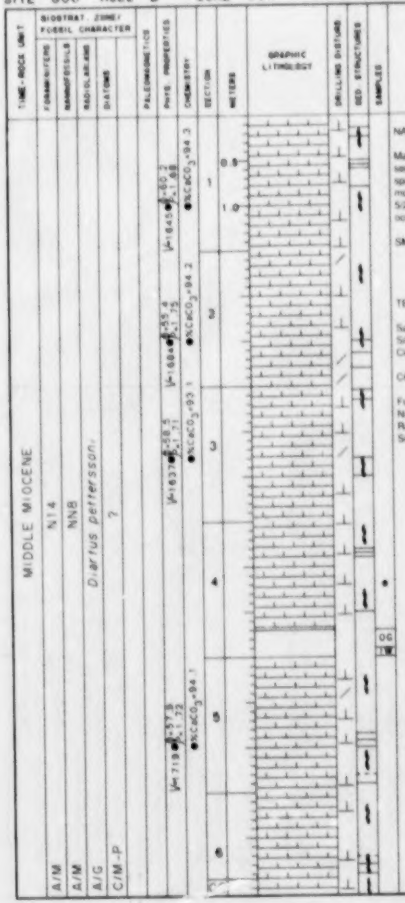
TIME-ROCK UNIT
BIOSTRAT. ZONE/ FOSSIL CHARACTER
FORAMINIFERS
NANNOFOSSILS
RADIOLARIANS
DIATOMS
PALEOMAGNETICS
PHYS. PROPERTIES
CHEMISTRY
SECTION
METERS
GRAPHIC LITHOLOGY
DRILLING DISTURB.
SED. STRUCTURES
SAMPLES
MIDDLE MIOCENE
N14
NN8
Diartus petterssoni
?
A/M
A/M
A/G
C/M-P
V=1645● φ=60.2 γ=1.88
V=1684● φ=55.4 γ=1.75
V=1637● φ=58.5 γ=1.71
V=7190● φ=57.8 γ=1.72
●%CaCO3=94.3
●%CaCO3=94.2
●%CaCO3=93.1
●%CaCO3=94.1
1
2
3
4
5
6
0.5
1.0
OG
IW

LITHOLOGIC DESCRIPTION

NANNOFOSSIL CHALK with FORAMINIFERS

Major lithology: This core contains NANNOFOSSIL CHALK with FORAMINIFERS. The sediment is white (2.5Y 8/0 grading to 5Y 8/1) with pale purple (5P 6/2), 4 to 5 cm thick bands spaced at irregular intervals. The sediment is slightly bioturbated with light gray (2.5Y 7/2) mottled and by pyritized grayish purple (5P 4/2) burrows. Distinct mm size, grayish green (5G 5/2) to light grayish green (5G 7/1), pale purple (5P 6/2) and gray (N6/ to N8/) color bands occur in zones or as single bands.

SMEAR SLIDE SUMMARY (%):

	4, 70
	D
TEXTURE:	
Sand	5
Silt	90
Clay	5
COMPOSITION:	
Foraminifers	14
Nannofossils	85
Radiolarians	Tr
Siliceous fragments	1

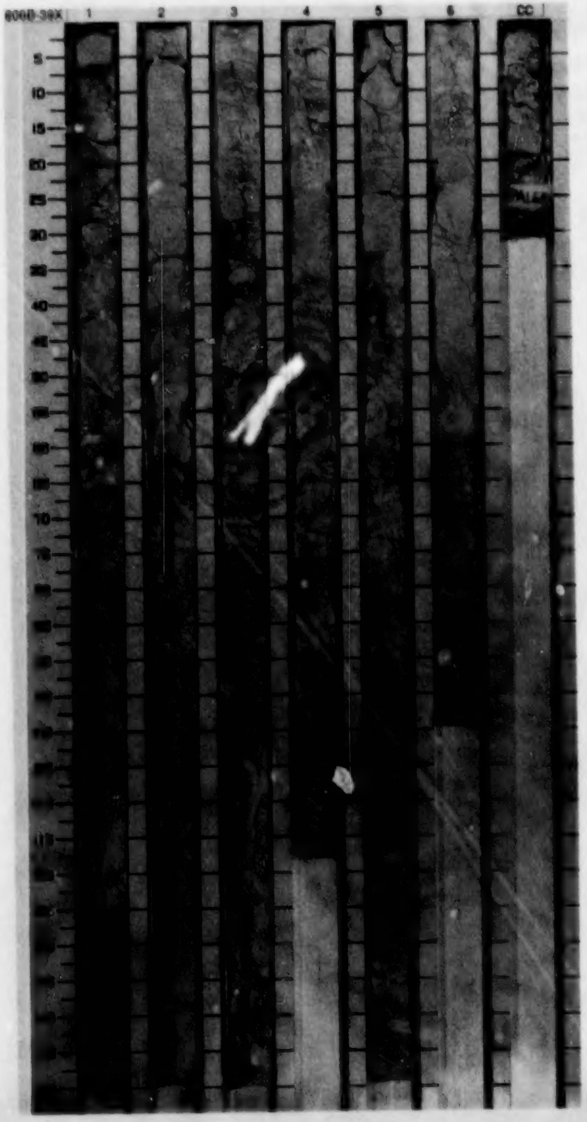
806B-39X
1
2
3
4
5
6
CC
5
10
15
20
25
30
35
40
45
50
55
60
65
70
75

SITE 806 HOLE B CORE 40X CORED INTERVAL 368.5-378.2 mbsf

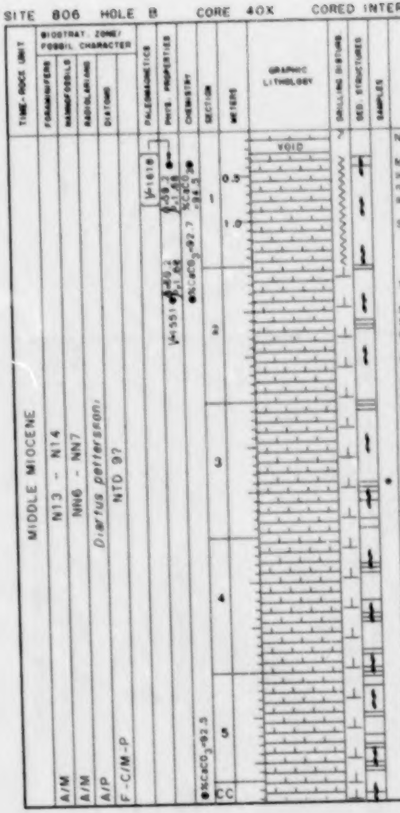
TIME-ROCK UNIT
BIOSTRAT. ZONE/ FOSSIL CHARACTER
FORAMINIFERS
NANNOFOSSILS
RADIOLARIANS
DIATOMS
PALEOMAGNETICS
PHYS. PROPERTIES
CHEMISTRY
SECTION
METERS
GRAPHIC LITHOLOGY
DRILLING DISTURB.
SED. STRUCTURES
SAMPLES
MIDDLE MIOCENE
N13 - N14
NN6 - NN7
Diartus petterssoni
NTD 9?
A/M
A/M
A/P
F-C/M-P
V=1618
φ=59.2 γ=1.68
V=1551 φ=60.2 γ=1.66
%CaCO3=94.5
%CaCO3=92.7
%CaCO3=92.5
1
2
3
4
5
CC
0.5
1.0
VOID

LITHOLOGIC DESCRIPTION

NANNOFOSSIL CHALK

Major lithology: This core contains white (2.5Y 8/0 and 5Y 8/1) NANNOFOSSIL CHALK. The sediment is slightly to moderately bioturbated, with pyritized burrows and white (10YR 8/1) mottles. Millimeter scale grayish blue (5PB 5/2), pale purple (5P 6/2), greenish gray (5G 6/1) and light greenish gray (5G 7/1) color bands are common.

SMEAR SLIDE SUMMARY (%):

	3, 90
	D
TEXTURE:	
Sand	1
Silt	90
Clay	9
COMPOSITION:	
Foraminifers	7
Nannofossils	91
Radiolarians	1
Siliceous fragments	1

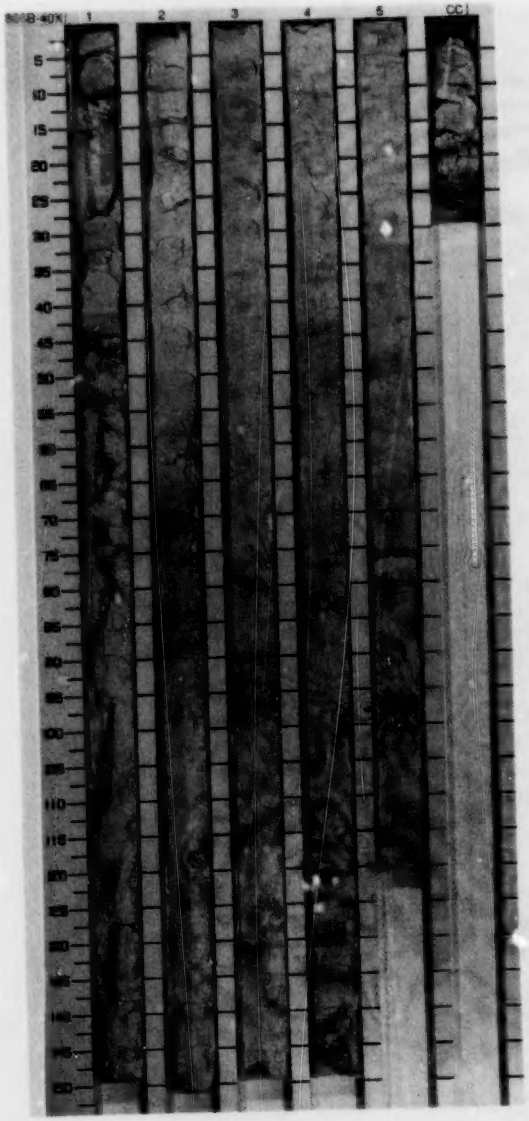
806B-40X
1
2
3
4
5
CC
5
10
15
20
25
30
35
40
45
50
55
60
65
70
75
80
85
90
95
100
105
110
115
120
125
130
135
140
145
150

SITE 806 HOLE B CORE 41X CORED INTERVAL 378.2-387.9 mbsf

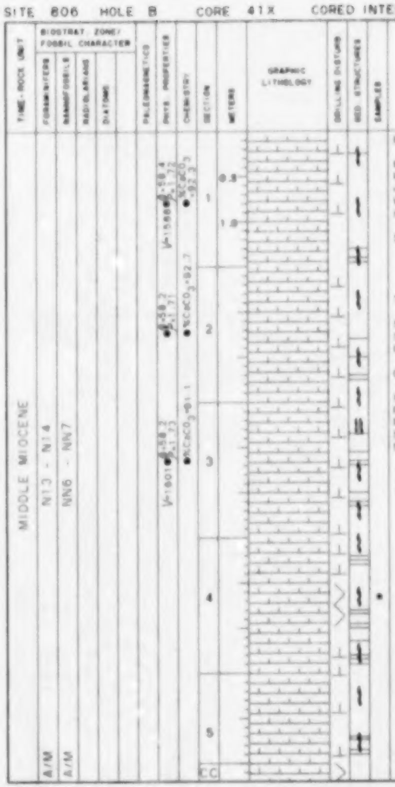
TIME-ROCK UNIT
BIOSTRAT. ZONE/ FOSSIL CHARACTER
FORAMINIFERS
NANNOFOSSILS
RADIOLARIANS
DIATOMS
PALEOMAGNETICS
PHYS. PROPERTIES
CHEMISTRY
SECTION
METERS
GRAPHIC LITHOLOGY
DRILLING DISTURB.
SED. STRUCTURES
SAMPLES
MIDDLE MIOCENE
N13 - N14
NN6 - NN7
A/M
A/M
V=1588
φ=58.4
γ=1.72
%CaCO3=92.3
φ=58.2
γ=1.71
%CaCO3=92.7
V=1601
φ=58.2
γ=1.73
%CaCO3=91.1
1
2
3
4
5
CC
0.5
1.0

LITHOLOGIC DESCRIPTION

NANNOFOSSIL OOZE with FORAMINIFERS

Major lithology: This core contains white (5Y 8/1) NANNOFOSSIL CHALK with FORAMINIFERS. The color grades to pale blue (5PB 7/2) or light greenish gray (5G 7/1) over short intervals. The sediment is slightly to heavily bioturbated, with sand-size pyritic burrow fills. Well-defined, mm scale, greenish gray (5G 6/1), light greenish gray (5G 7/1) and grayish blue (5PB 5/2) color bands are present.

SMEAR SLIDE SUMMARY (%)

	4, 67
	D
TEXTURE	
Sand	7
Silt	90
Clay	3
COMPOSITION	
Foraminifers	15
Nannofossils	82
Radiolarians	1
Siliceous fragments	1
Silicoflagellates	1

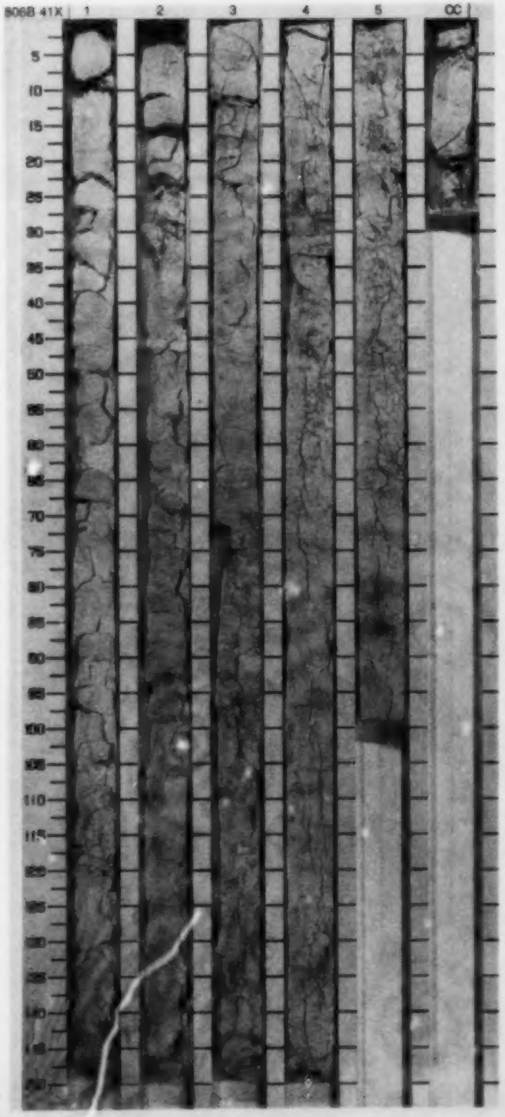
806B 41X
1
2
3
4
5
CC
5
10
15
20
25
30
35
40
45
50
55
60
65
70
75
80
85
90
95
100
105
110
115
120
125
130
135
140
145
150

SITE 806 HOLE B CORE 42X CORED INTERVAL 387.9-397.5 mbsf

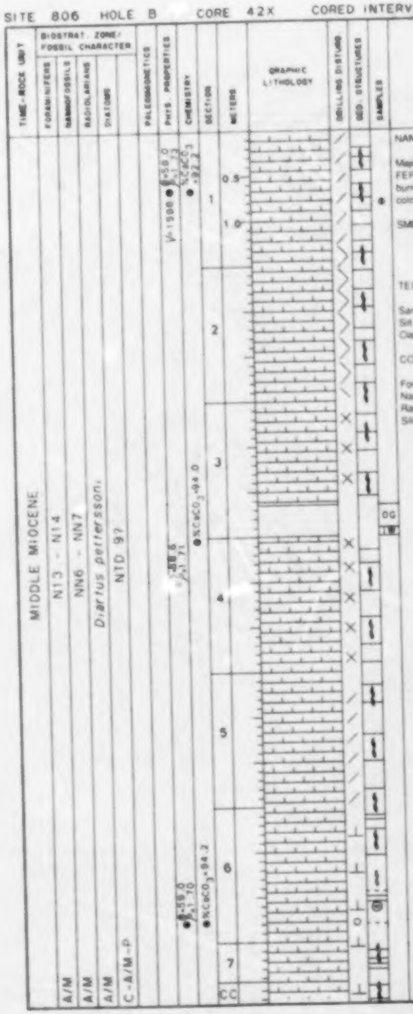
TIME-ROCK UNIT
BIOSTRAT. ZONE/ FOSSIL CHARACTER
FORAMINIFERS
NANNOFOSSILS
RADIOLARIANS
DIATOMS
PALEOMAGNETICS
PHYS. PROPERTIES
CHEMISTRY
SECTION
METERS
GRAPHIC LITHOLOGY
DRILLING DISTURB.
SED. STRUCTURES
SAMPLES
MIDDLE MIOCENE
N13 - N14
NN6 - NN7
Diartus petterssoni
NTD 9?
A/M
A/M
A/M
C-A/M-P
V=1588
φ=58.0
ρ=1.73
%CaCO3=92.2
φ=58.6
ρ=1.71
%CaCO3=94.0
φ=59.0
ρ=1.70
%CaCO3=94.2
1
2
3
4
5
6
7
CC
0.5
1.0
OG
IW

LITHOLOGIC DESCRIPTION

NANNOFOSSIL CHALK with FORAMINIFERS

Major lithology: This core contains white (2.5Y 8/0) NANNOFOSSIL CHALK with FORAMINIFERS. The sediment is slightly to moderately bioturbated, with light gray (5Y 7/1) pyritized burrows. Millimeter size light greenish gray (5G 7/1), light gray (N 6/) and pale purple (5P 6/2) color bands are present throughout the core.

SMEAR SLIDE SUMMARY (%):

	1, 80
	D
TEXTURE:	
Sand	15
Silt	80
Clay	5
COMPOSITION:	
Foraminifers	10
Nannofossils	88
Radiolarians	2
Silicoflagellates	Tr

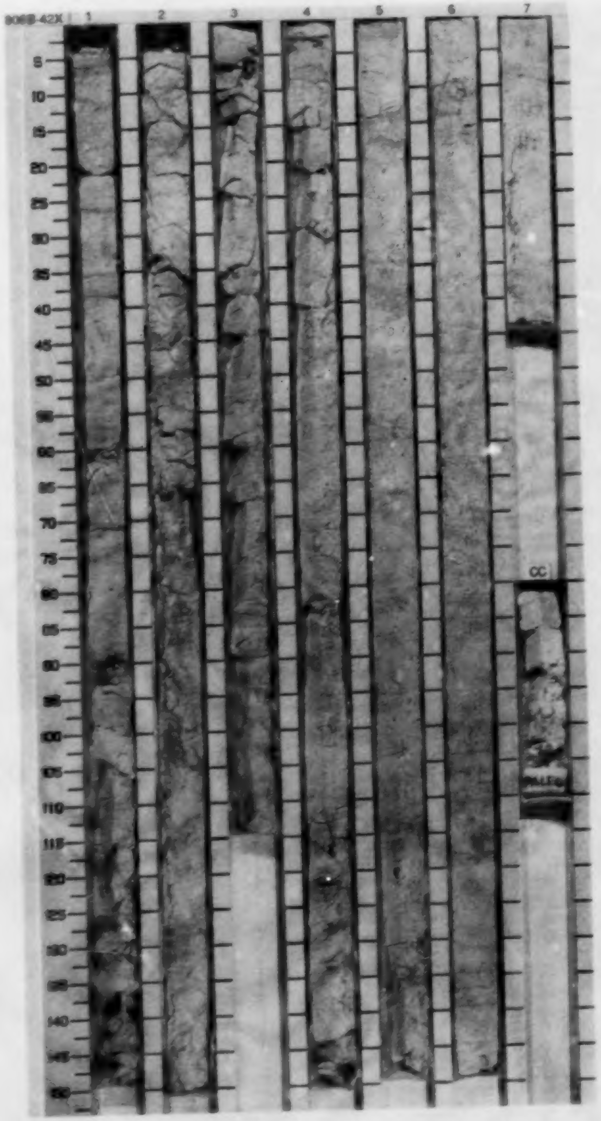
806B-42X
1
2
3
4
5
6
7
CC
5
10
15
20
25
30
35
40
45
50
55
60
65
70
75
80
85
90
95
100
105
110
115
120
125
130
135
140
145
150

SITE 806 HOLE B CORE 43X CORED INTERVAL 397.5-407.2 mbsf

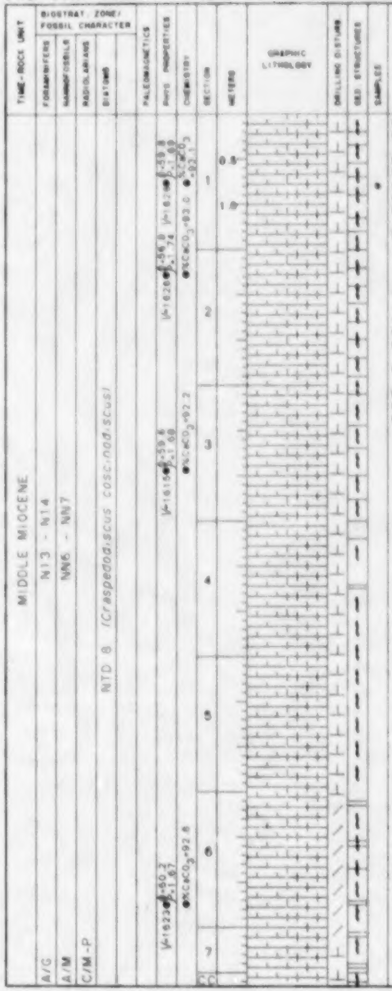
TIME-ROCK UNIT
BIOSTRAT. ZONE/ FOSSIL CHARACTER
FORAMINIFERS
NANNOFOSSILS
RADIOLARIANS
DIATOMS
PALEOMAGNETICS
PHYS. PROPERTIES
CHEMISTRY
SECTION
METERS
GRAPHIC LITHOLOGY
DRILLING DISTURB.
SED. STRUCTURES
SAMPLES
MIDDLE MIOCENE
N13 - N14
NN6 - NN7
NTD 8 (Craspedodiscus coscinodiscus)
A/G
A/M
C/M-P
V-1620 φ-59.8 γ-1.69
%CaCO3=93.0
%CaCO3=92.1
V-1626 φ-56.8 γ-1.74
V-1615 φ-59.6 γ-1.68
%CaCO3=92.2
V-1623 φ-60.2 γ-1.67
%CaCO3=92.8
1
2
3
4
5
6
7
CC
0.5
1.0

LITHOLOGIC DESCRIPTION

NANNOFOSSIL CHALK with FORAMINIFERS interbedded with FORAMINIFER NANNOFOSSIL CHALK

Major lithology: This core contains white (2.5Y 8/0) NANNOFOSSIL CHALK with FORAMINIFERS interbedded with FORAMINIFER NANNOFOSSIL CHALK. The sediment is slightly to moderately bioturbated, with light gray (5Y 7/1) pyritized burrows. Millimeter size, light greenish gray (5G 7/1), light gray (N 6), grayish blue (5PB 5/2) and pale purple (5P 6/2) color bands are common throughout the core.

SMEAR SLIDE SUMMARY (%):

	1, 80
	D
TEXTURE:	
Sand	20
Silt	75
Clay	5
COMPOSITION:	
Foraminifers	17
Nannofossils	80
Radiolarians	3

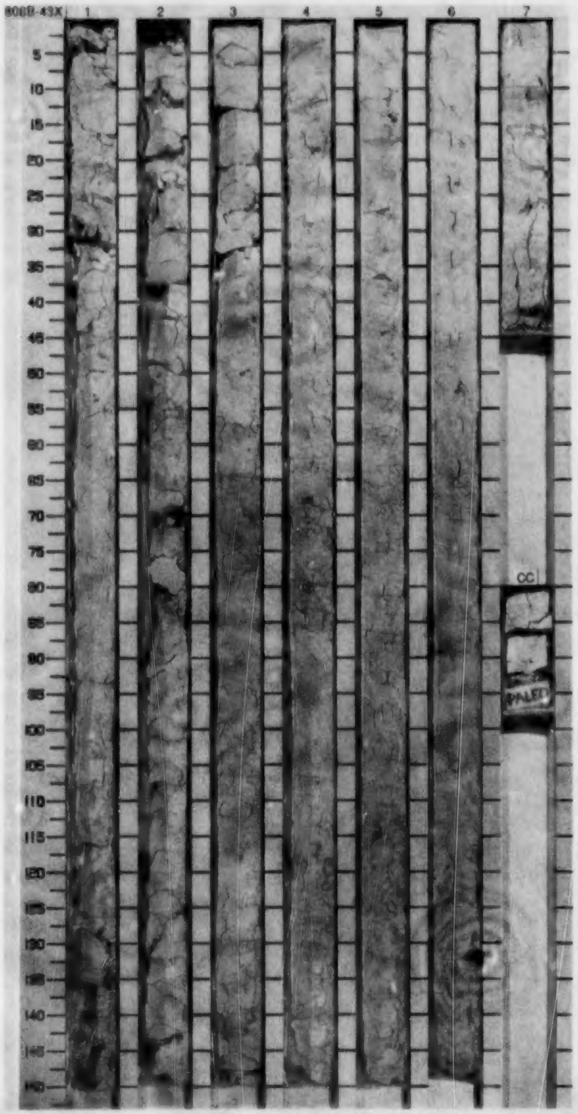
806B-43X
1
2
3
4
5
6
7
CC
PALEO
5
10
15
20
25
30
35
40
45
50
55
60
65
70
75
80
85
90
95
100
105
110
115
120
125
130
135
140
145
150

SITE 806 HOLE B CORE 44X CORED INTERVAL 407.2-416.9 mbsf

TIME-ROCK UNIT	BIOSTRAT. ZONE/ FOSSIL CHARACTER: FORAMINIFERS	NANNOFOSSILS	RADIOLARIANS	DIATOMS	PALEOMAGNETICS	PHYS. PROPERTIES	CHEMISTRY	SECTION	METERS
MIDDLE MIOCENE	N12	NN6 - NN7	*Dorcadospyris alata*	NTD 8 - NTD 7		V=1655 ● ϕ=59.8 ρ=1.88	● %CaCO$_3$ =91.3	1	0.5 1.0
						V=1863 ● ϕ=58.2 ρ=1.71	● %CaCO$_3$=91.2	2	
						V=1612 ● ϕ=52.8 ρ=1.80	● %CaCO$_3$=91.5	3	
								4	
						● ϕ=58.0 ρ=1.71	● %CaCO$_3$=92.6	5	
						V=1711 ● ϕ=57.3 ρ=1.73	● %CaCO$_3$=92.0	6	
								7	
								CC	
	A/M	A/M	A/G	A/M					

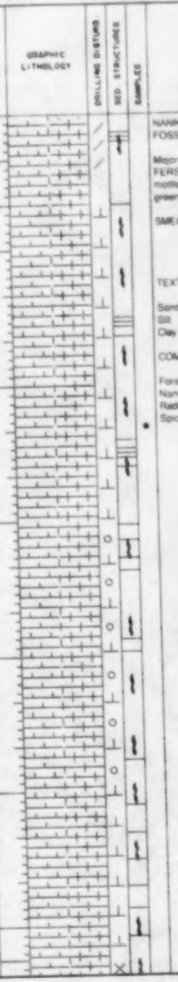
GRAPHIC LITHOLOGY
DRILLING DISTURB.
SED. STRUCTURES
SAMPLES

LITHOLOGIC DESCRIPTION

NANNOFOSSIL CHALK with FORAMINIFERS interbedded with FORAMINIFER NANNOFOSSIL CHALK

Major lithology: This core contains white (5Y 8/1) NANNOFOSSIL CHALK with FORAMINIFERS interbedded with FORAMINIFER NANNOFOSSIL CHALK. The sediment is slightly mottled due to bioturbation, and single pyritized burrows are seen. Millimeter-size light greenish gray (5G 7/1), light gray (N 5/1) and pale purple (5P 6/2) color bands are visible.

SMEAR SLIDE SUMMARY (%):

	3, 46
	D
TEXTURE:	
Sand	15
Silt	82
Clay	3
COMPOSITION:	
Foraminifers	20
Nannofossils	77
Radiolarians	2
Spicules	1

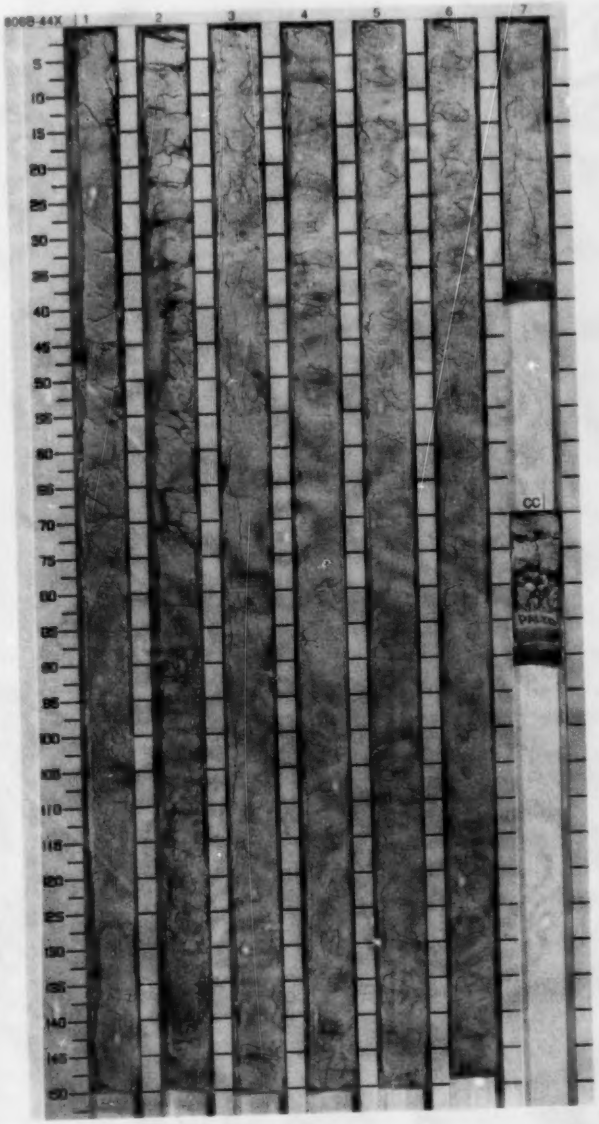
806B-44X
1
2
3
4
5
6
7
5
10
15
20
25
30
35
40
45
50
55
60
65
70
75
80
85
90
95
100
105
110
115
120
125
130
135
140
145
150
CC

SITE 806 HOLE B CORE 45X CORED INTERVAL 416.9-426.5 mbsf

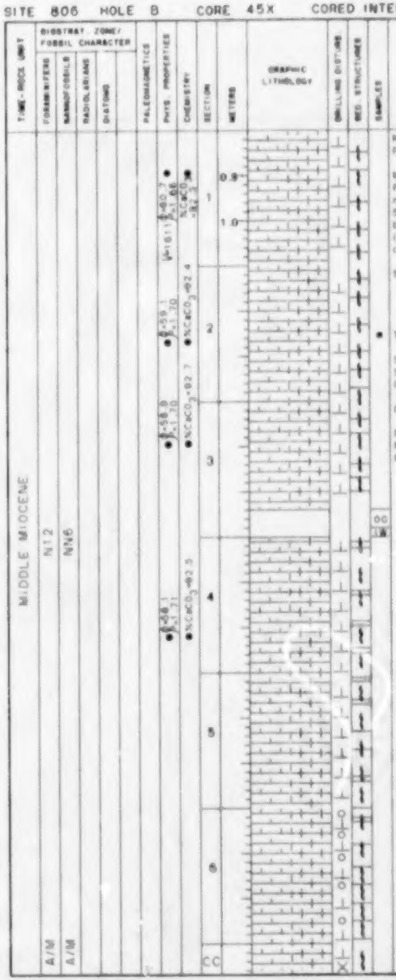

LITHOLOGIC DESCRIPTION

NANNOFOSSIL CHALK with FORAMINIFERS interbedded with FORAMINIFER NANNOFOSSIL CHALK

Major lithology: This core contains white (2.5Y 8/0) NANNOFOSSIL CHALK with FORAMINIFERS interbedded with FORAMINIFER NANNOFOSSIL CHALK. The sediment is slightly to moderately bioturbated as reflected by cm scale, light gray (5Y 7/2) and grayish blue (5PB 5/2) mottling and mm scale pyritic burrow fills. Several large (6 to 10 cm in diameter) grayish blue (5PB 5/2) burrow "halos" are seen. Faint to well defined color bands, light greenish gray (5G 7/1) to gray (N6/) and diffuse grayish blue (5G 7/1) in color, are common throughout the core.

SMEAR SLIDE SUMMARY (%):

	2, 78
	D
TEXTURE:	
Sand	40
Silt	55
Clay	5
COMPOSITION:	
Foraminifers	35
Nannofossils	60
Radiolarians	5

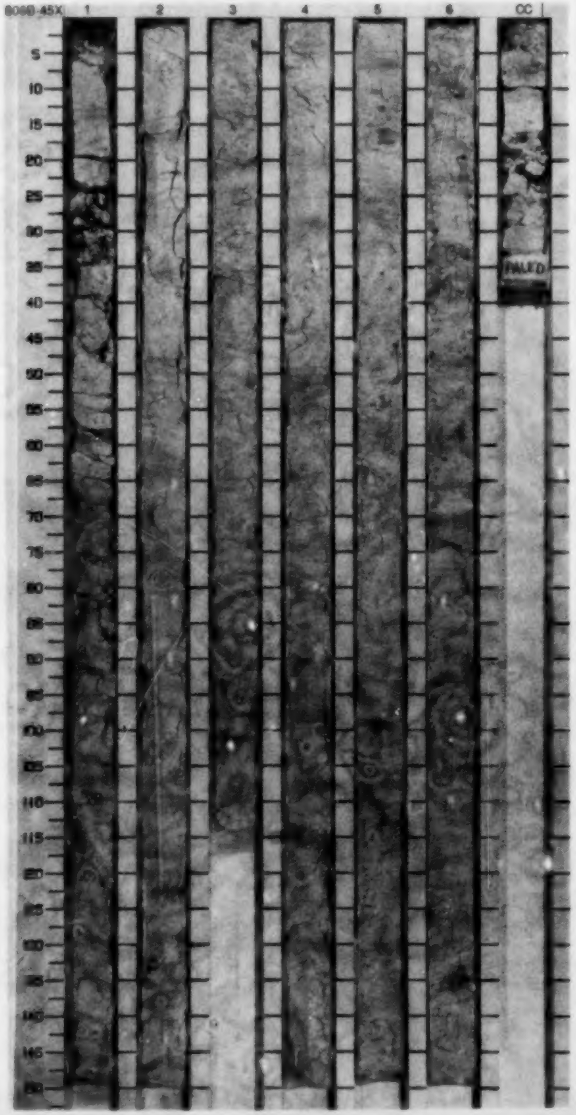
806B-45X
1
2
3
4
5
6
CC
5
10
15
20
25
30
35
40
45
50
55
60
65
70
75
80
85
90
95
100
105
110
115
120
125
130
135
140
145
150
FAILED

SITE 806 HOLE B CORE 46X CORED INTERVAL 426.5-436.1 mbsf

TIME-ROCK UNIT	BIOSTRAT. ZONE/ FOSSIL CHARACTER: FORAMINIFERS	NANNOFOSSILS	RADIOLARIANS	DIATOMS	PALEOMAGNETICS	PHYS. PROPERTIES	CHEMISTRY	SECTION	METERS
MIDDLE MIOCENE	N12	NN6	*Dorcadospyris alata*	top NTD 67 (*Coscinodiscus lewisianus*)		● ϕ=58.9 ρ=1.70	● %CaCO$_3$ =94.5	1	0.5 1.0
						● ϕ=57.8 ρ=1.72	● %CaCO$_3$=94.3	2	
						● ϕ=57.8 ρ=1.72	● %CaCO$_3$=93.5	3	
						● ϕ=56.9 ρ=1.74	● %CaCO$_3$=95.2	4	
						● ϕ=56.6 ρ=1.71	● %CaCO$_3$=94.8	5	
						● ϕ=58.5 ρ=1.71	● %CaCO$_3$=92.1	6	
								7	
	A/M	A/M	A/G	A/M				CC	

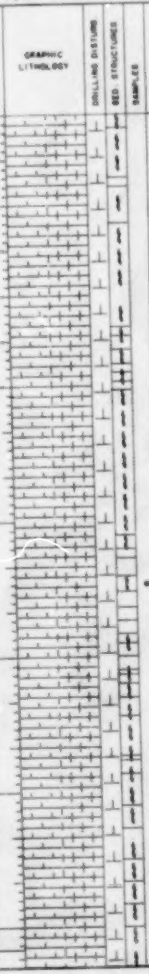
GRAPHIC LITHOLOGY
DRILLING DISTURB.
SED. STRUCTURES
SAMPLES

LITHOLOGIC DESCRIPTION

NANNOFOSSIL CHALK with FORAMINIFERS interbedded with FORAMINIFER NANNOFOSSIL CHALK

Major lithology: This core contains white (2.5Y 8/0) NANNOFOSSIL CHALK with FORAMINIFERS interbedded with FORAMINIFER NANNOFOSSIL CHALK. The sediment is slightly to moderately bioturbated as reflected by light gray (5Y 7/2), cm scale mottles and grayish blue (5PB 5/2), cm scale and mm scale mottles and pyritic burrow fills. Well developed *Zoophycos* trace fossils are seen, as well as several grayish blue (5PB 5/2) burrow "halos". Diffuse light greenish gray (5G 7/1) and pale purple (5P 6/2) color bands are present throughout the core.

SMEAR SLIDE SUMMARY (%)

	4, 70 D
TEXTURE	
Sand	35
Silt	60
Clay	5
COMPOSITION	
Foraminifers	25
Nannofossils	70
Radiolarians	4
Silicoflagellates	1

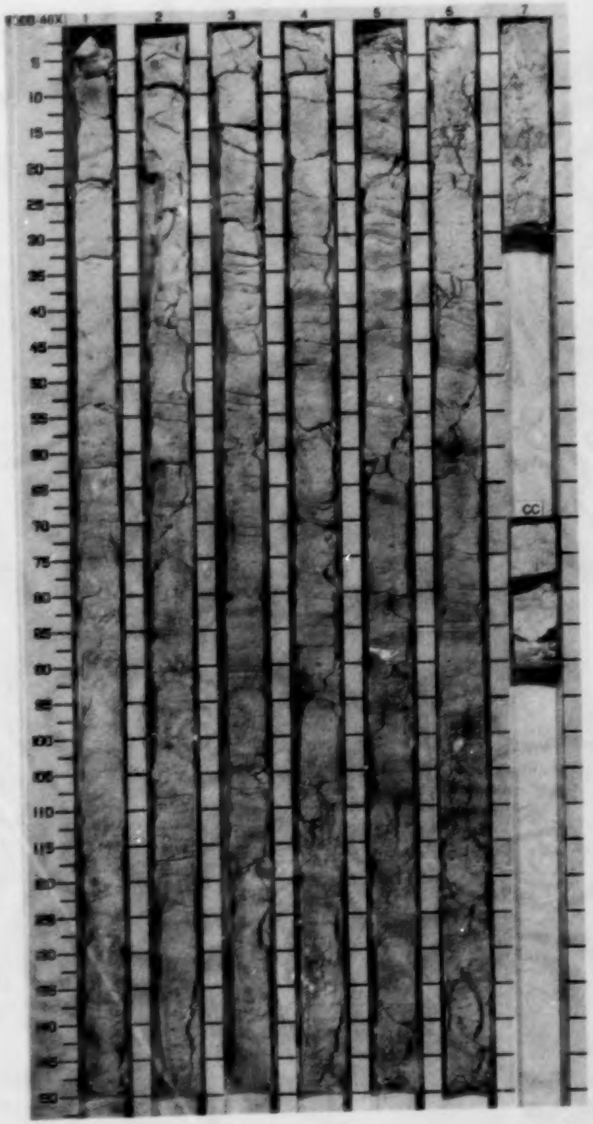
806B-46X
1
2
3
4
5
6
7
CC
5
10
15
20
25
30
35
40
45
50
55
60
65
70
75
80
85
90
95
100
105
110
115
120
125
130
135
140
145
150

SITE 806 HOLE B CORE 47X CORED INTERVAL 436.1-445.8 mbsf

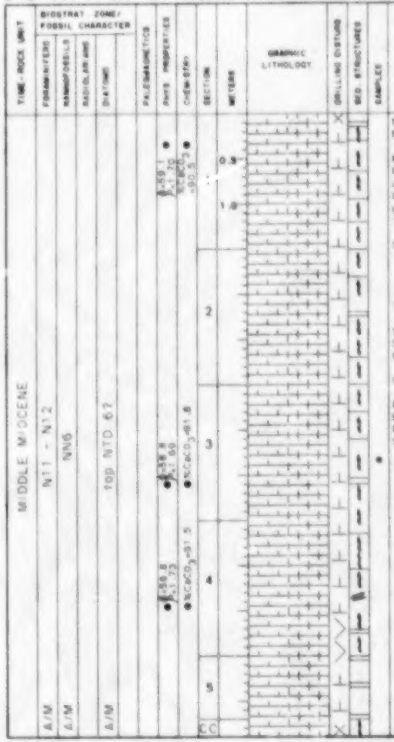
TIME-ROCK UNIT
BIOSTRAT. ZONE/ FOSSIL CHARACTER
FORAMINIFERS
NANNOFOSSILS
RADIOLARIANS
DIATOMS
PALEOMAGNETICS
PHYS. PROPERTIES
CHEMISTRY
SECTION
METERS
GRAPHIC LITHOLOGY
DRILLING DISTURB.
SED. STRUCTURES
SAMPLES
MIDDLE MIOCENE
N11 - N12
NN6
top NTD 67
A/M
A/M
A/M
φ=59.1
γ=1.70
%CaCO3=90.5
φ=58.8
γ=1.69
%CaCO3=91.6
φ=56.8
γ=1.73
%CaCO3=91.5
1
2
3
4
5
CC
0.5
1.0

LITHOLOGIC DESCRIPTION

NANNOFOSSIL CHALK with FORAMINIFERS interbedded with FORAMINIFER NANNOFOSSIL CHALK

Major lithology: This core contains white (2.5Y 8/0 to 10YR 8/1) NANNOFOSSIL CHALK with FORAMINIFERS interbedded with FORAMINIFER NANNOFOSSIL CHALK. Slight to moderate bioturbation is indicated by light gray (2.5Y 7/2 to 10YR 7/1) mottling, mm scale pyritic burrow fills and well developed *Zoophycos* trace fossils. Millimeter to cm size, diffuse light greenish gray (5G 7/1), and grayish blue (5PB 5/2) color bands occur in intervals about 5 to 10 cm thick.

SMEAR SLIDE SUMMARY (%):

	3, 68
	D
TEXTURE:	
Sand	30
Silt	65
Clay	5
COMPOSITION:	
Foraminifers	20
Nannofossils	74
Radiolarians	4
Silicoflagellates	2

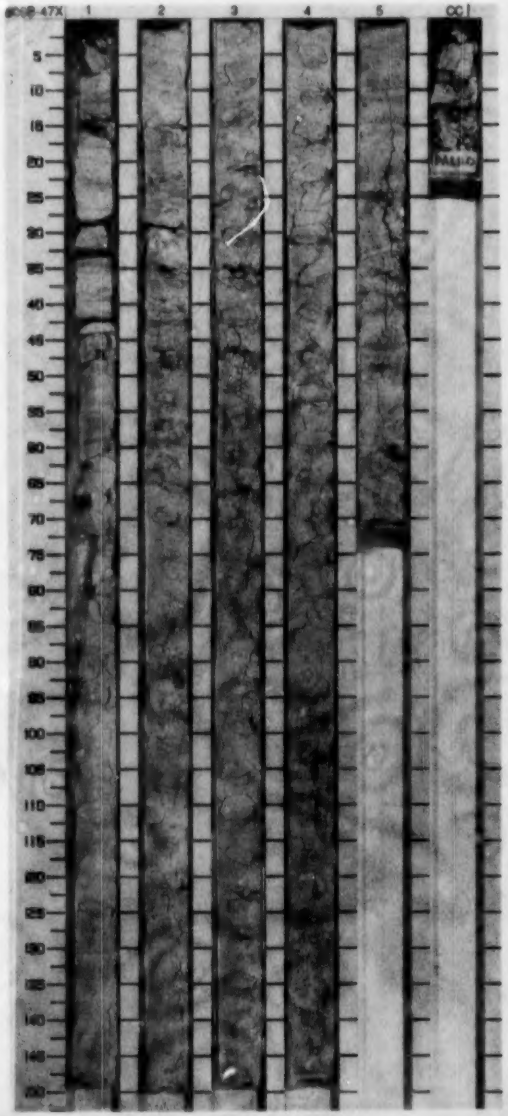
806B-47X
1
2
3
4
5
CC
5
10
15
20
25
30
35
40
45
50
55
60
65
70
75
80
85
90
95
100
105
110
115
120
125
130
135
140
145
150

SITE 806 HOLE D CORE 48X CORED INTERVAL 445.8-455.5 mbsf

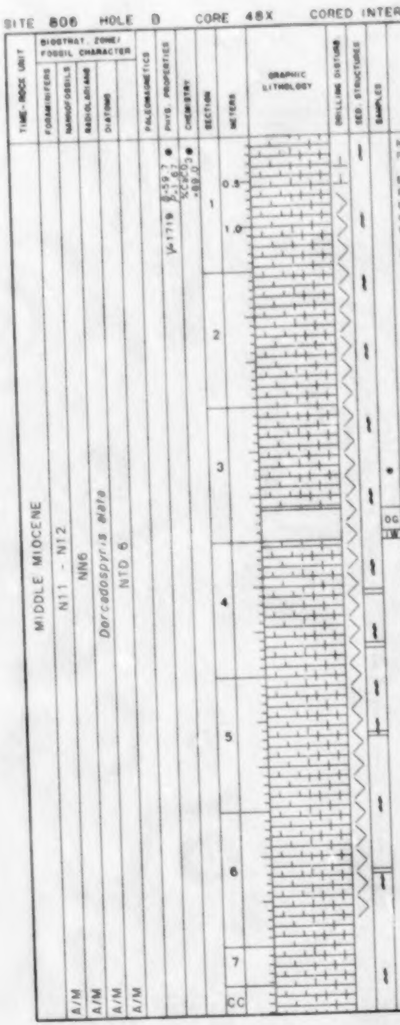
TIME-ROCK UNIT
BIOSTRAT. ZONE/ FOSSIL CHARACTER
FORAMINIFERS
NANNOFOSSILS
RADIOLARIANS
DIATOMS
PALEOMAGNETICS
PHYS. PROPERTIES
CHEMISTRY
SECTION
METERS
GRAPHIC LITHOLOGY
DRILLING DISTURB.
SED. STRUCTURES
SAMPLES
MIDDLE MIOCENE
N11 - N12
NN6
Dorcadospyris alata
NTD 6
A/M
A/M
A/M
A/M
V-1719
ϕ-59.7
ρ-1.67
%CaCO3
=89.0
0.5
1.0
1
2
3
4
5
6
7
CC
OG
IW

LITHOLOGIC DESCRIPTION

NANNOFOSSIL CHALK with FORAMINIFERS interbedded with FORAMINIFER NANNOFOSSIL CHALK

Major lithology: This core contains white (10YR 8/0) NANNOFOSSIL CHALK with FORAMINIFERS interbedded with FORAMINIFER NANNOFOSSIL CHALK. It is slightly to moderately bioturbated with cm scale, light gray mottles and some pyrite infilling of burrows. Faint to distinct, mm scale, greenish gray (5G 6/1) color banding is common only in specific intervals throughout the core.

SMEAR SLIDE SUMMARY (%):

	3, 75
	D
TEXTURE	
Sand	10
Silt	60
Clay	30
COMPOSITION	
Diatoms	2
Foraminifers	25
Nannofossils	70
Radiolarians	Tr
Siliceous fragments	3

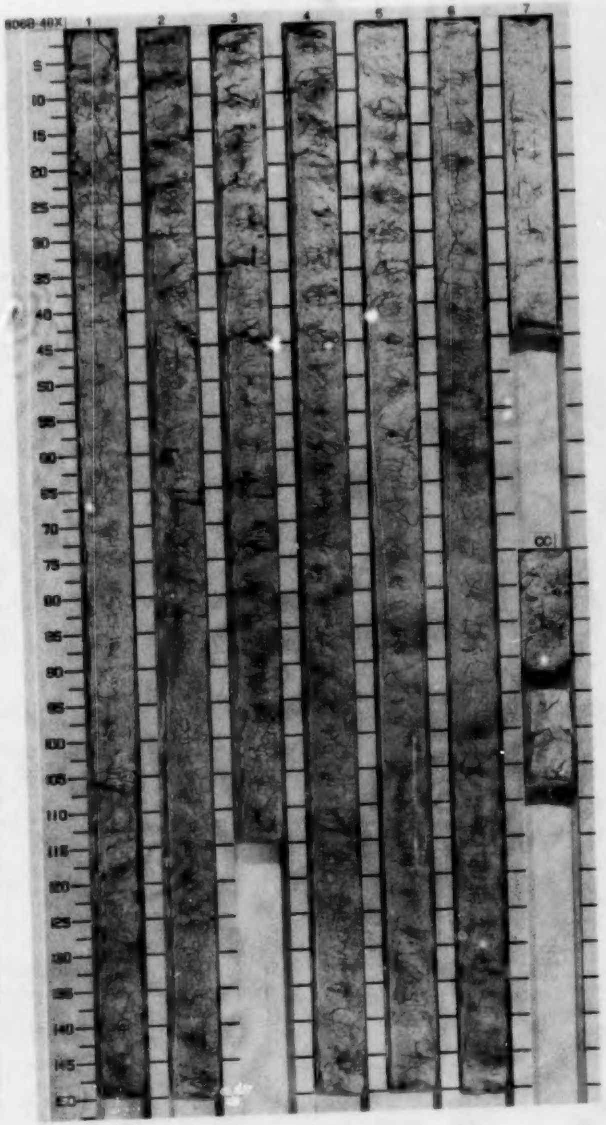
806B-48X
1
2
3
4
5
6
7
CC
5
10
15
20
25
30
35
40
45
50
55
60
65
70
75
80
85
90
95
100
105
110
115
120
125
130
135
140
145
150

SITE 806 HOLE B CORE 49X CORED INTERVAL 455.0-463.6 mbsf

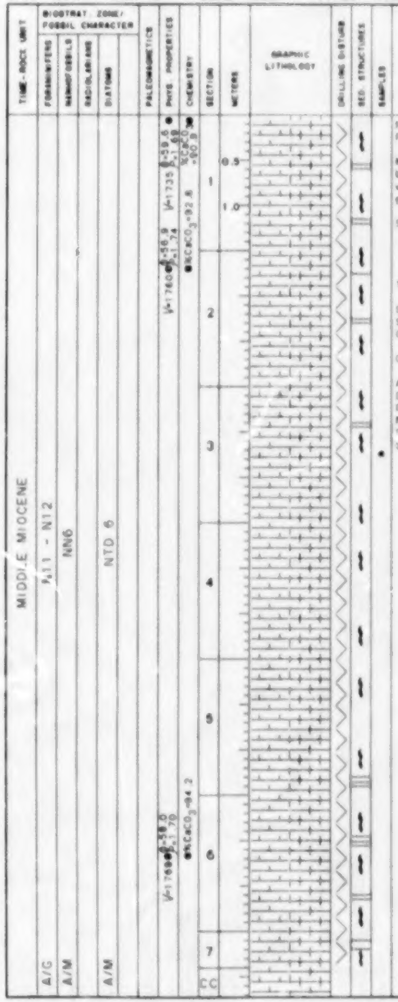
TIME-ROCK UNIT
BIOSTRAT. ZONE/ FOSSIL CHARACTER
FORAMINIFERS
NANNOFOSSILS
RADIOLARIANS
DIATOMS
PALEOMAGNETICS
PHYS. PROPERTIES
CHEMISTRY
SECTION
METERS
GRAPHIC LITHOLOGY
DRILLING DISTURB.
SED. STRUCTURES
SAMPLES
MIDDLE MIOCENE
N11 - N12
NN6
NTD 6
A/G
A/M
A/M
●φ=59.6
●γ=1.69
V=1735
%CaCO3=90.8
●%CaCO3=92.8
V=1760●φ=56.9
γ=1.74
V=1768●φ=58.0
γ=1.70
●%CaCO3=94.2
1
2
3
4
5
6
7
CC
0.5
1.0

LITHOLOGIC DESCRIPTION

NANNOFOSSIL CHALK with FORAMINIFERS interbedded with FORAMINIFER NANNOFOSSIL CHALK

Major lithology: This core contains NANNOFOSSIL CHALK with FORAMINIFERS interbedded with FORAMINIFER NANNOFOSSIL CHALK. It is predominantly white (7.5YR 8/0) with distinct greenish gray (5GY 7/2) color bands. A few light gray (2.5Y 7/2) to light brownish gray (2.5Y 6/2) burrows were noted. Some pyritization streaks were also observed.

SMEAR SLIDE SUMMARY (%):

	3, 74
	D
TEXTURE:	
Sand	10
Silt	60
Clay	30
COMPOSITION:	
Accessory minerals	2
Diatoms	Tr
Foraminifers	18
Nannofossils	77
Radiolarians	Tr
Siliceous fragments	3

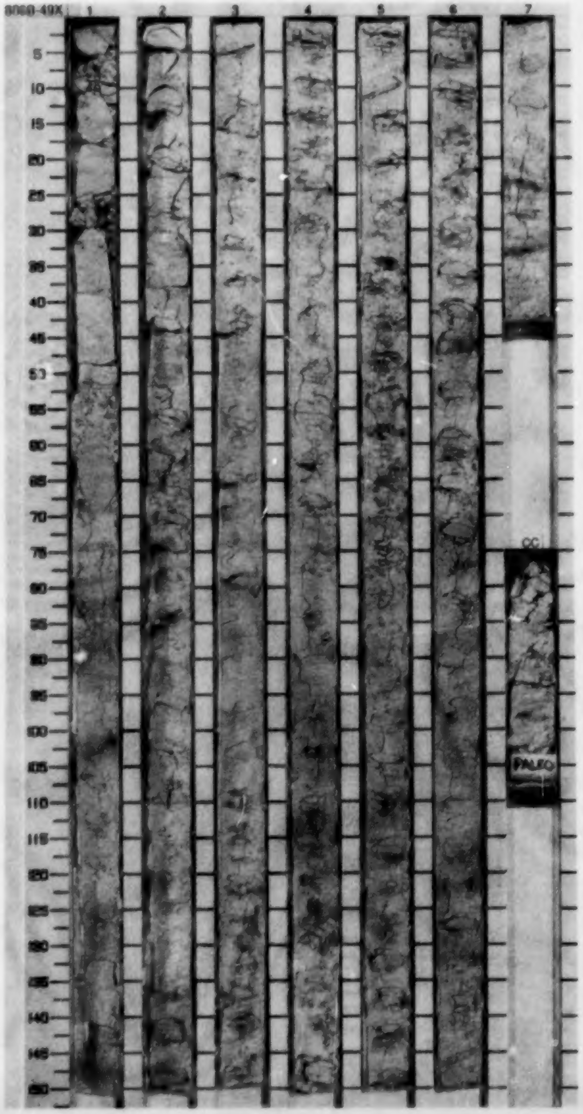
806B-49X
1
2
3
4
5
6
7
CC
PALEO
5
10
15
20
25
30
35
40
45
50
55
60
65
70
75
80
85
90
95
100
105
110
115
120
125
130
135
140
145
150

SITE 806 HOLE B CORE 50X CORED INTERVAL 463.6-473.3 mbsf

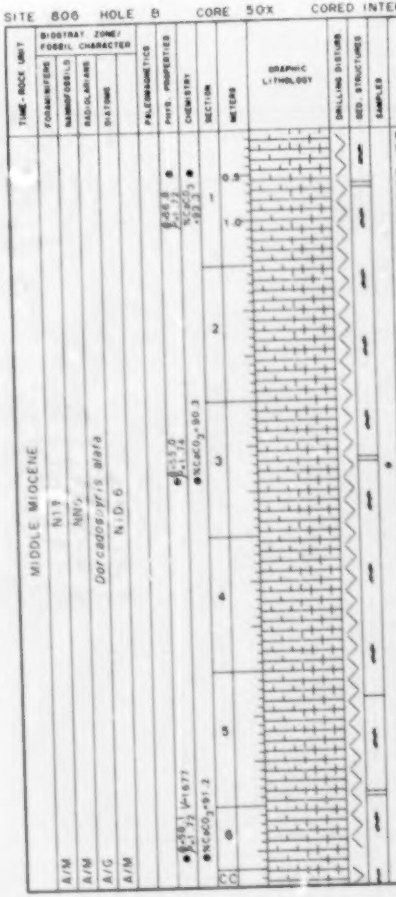
TIME-ROCK UNIT
BIOSTRAT. ZONE/ FOSSIL CHARACTER
FORAMINIFERS
NANNOFOSSILS
RADIOLARIANS
DIATOMS
PALEOMAGNETICS
PHYS. PROPERTIES
CHEMISTRY
SECTION
METERS
GRAPHIC LITHOLOGY
DRILLING DISTURB.
SED. STRUCTURES
SAMPLES
MIDDLE MIOCENE
N11
NN5
Dorcadospyris alata
N.D. 6
A/M
A/M
A/G
A/M
%CaCO3=92.3
%CaCO3=90.3
%CaCO3=91.2
V=1677
1
2
3
4
5
6
CC
0.5
1.0

LITHOLOGIC DESCRIPTION

NANNOFOSSIL CHALK with FORAMINIFERS interbedded with FORAMINIFER NANNOFOSSIL CHALK

Major lithology: This core contains white (7.5YR 8/0) NANNOFOSSIL CHALK with FORAMINIFERS interbedded with FORAMINIFER NANNOFOSSIL CHALK. Numerous borrows and mottles indicate significant bioturbation. Many drilling biscuits contain 1 mm thick, subhorizontal bands, light greenish gray (5GY 7/1) and, to a lesser extent, pale purple (5P 6/2) in color. The biscuits are spaced at 5 to 10 cm intervals. The top of Section 1 contains calcite concretion, which probably represents a burrow fill.

SMEAR SLIDE SUMMARY (%):

	3, 75
	D
TEXTURE:	
Sand	15
Silt	50
Clay	35
COMPOSITION:	
Diatoms	3
Foraminifers	25
Nannofossils	68
Radiolarians	1
Siliceous fragments	3

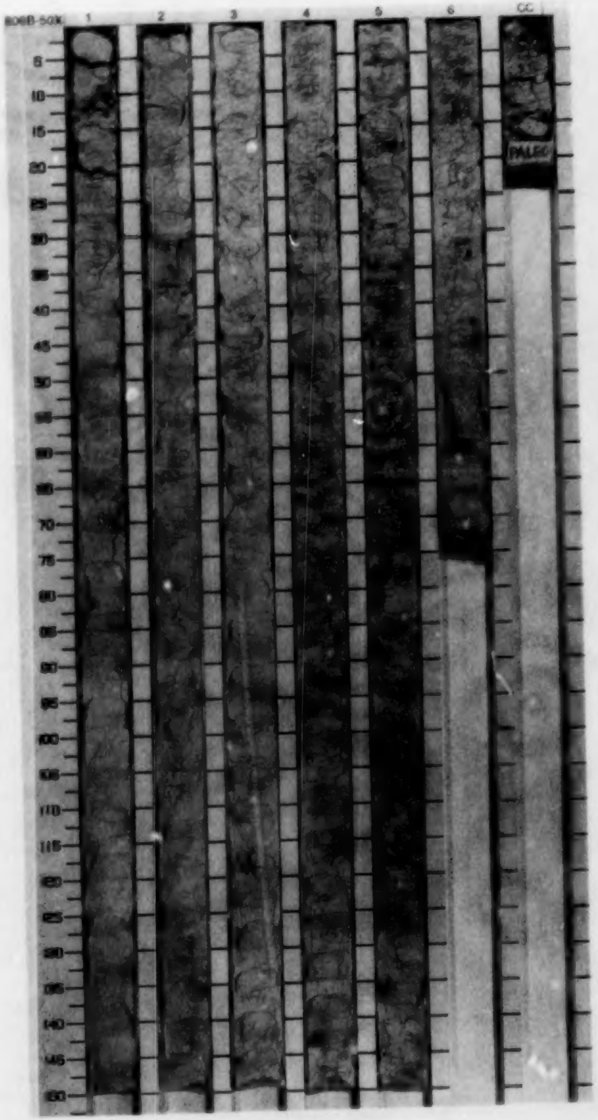
806B-50X
1
2
3
4
5
6
CC
PALEO
5
10
15
20
25
30
35
40
45
50
55
60
65
70
75
80
85
90
95
100
105
110
115
120
125
130
135
140
145
150

SITE 806 HOLE B CORE 51X CORED INTERVAL 473.3-482.6 mbsf

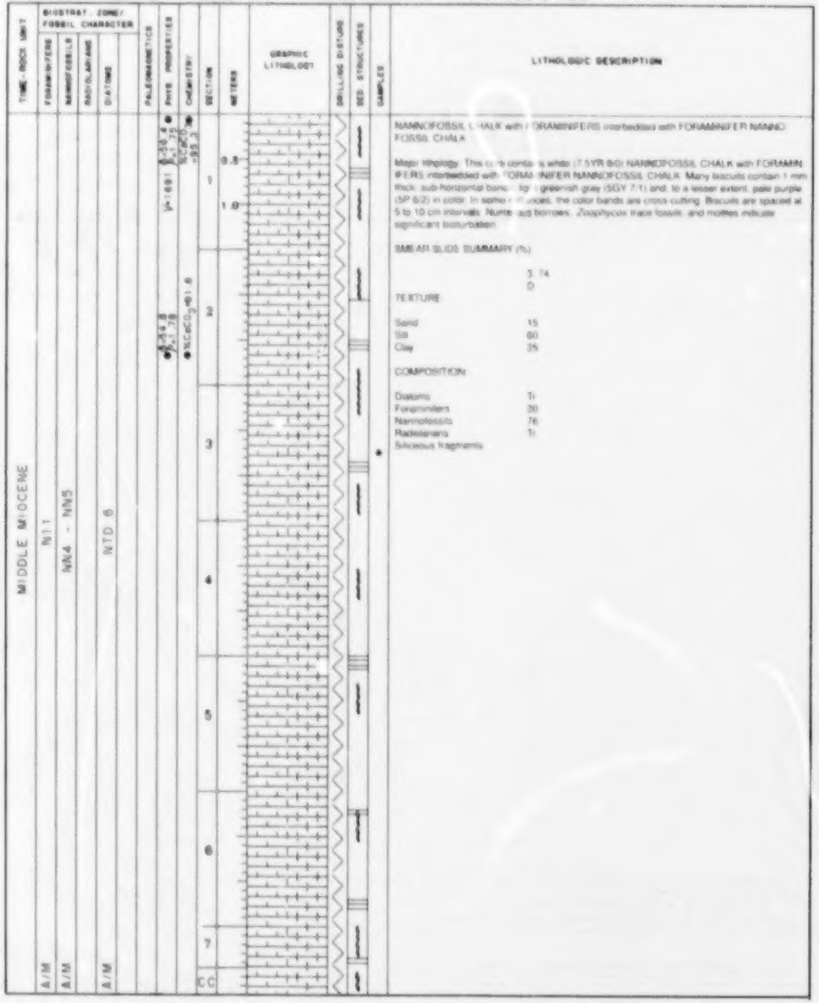
TIME-ROCK UNIT
BIOSTRAT. ZONE/ FOSSIL CHARACTER
FORAMINIFERS
NANNOFOSSILS
RADIOLARIANS
DIATOMS
PALEOMAGNETICS
PHYS. PROPERTIES
CHEMISTRY
SECTION
METERS
GRAPHIC LITHOLOGY
DRILLING DISTURB.
SED. STRUCTURES
SAMPLES
MIDDLE MIOCENE
N11
NN4 - NN5
NTD 6
A/M
A/M
A/M
φ=50.4
γ=1.75
V=1691
φ=54.8
γ=1.78
%CaCO3=95.2
%CaCO3=91.6
1
2
3
4
5
6
7
CC
0.5
1.0

LITHOLOGIC DESCRIPTION

NANNOFOSSIL CHALK with FORAMINIFERS interbedded with FORAMINIFER NANNOFOSSIL CHALK

Major lithology: This core contains white (7.5YR 8/0) NANNOFOSSIL CHALK with FORAMINIFERS interbedded with FORAMINIFER NANNOFOSSIL CHALK. Many biscuits contain 1 mm thick, sub-horizontal bands, light greenish gray (5GY 7/1) and, to a lesser extent, pale purple (5P 6/2) in color. In some instances, the color bands are cross-cutting. Biscuits are spaced at 5 to 10 cm intervals. Numerous burrows, *Zoophycos* trace fossils, and mottles indicate significant bioturbation.

SMEAR SLIDE SUMMARY (%):

	3, 74
	D
TEXTURE:	
Sand	15
Silt	60
Clay	25
COMPOSITION:	
Diatoms	Tr
Foraminifers	20
Nannofossils	76
Radiolarians	Tr
Siliceous fragments	

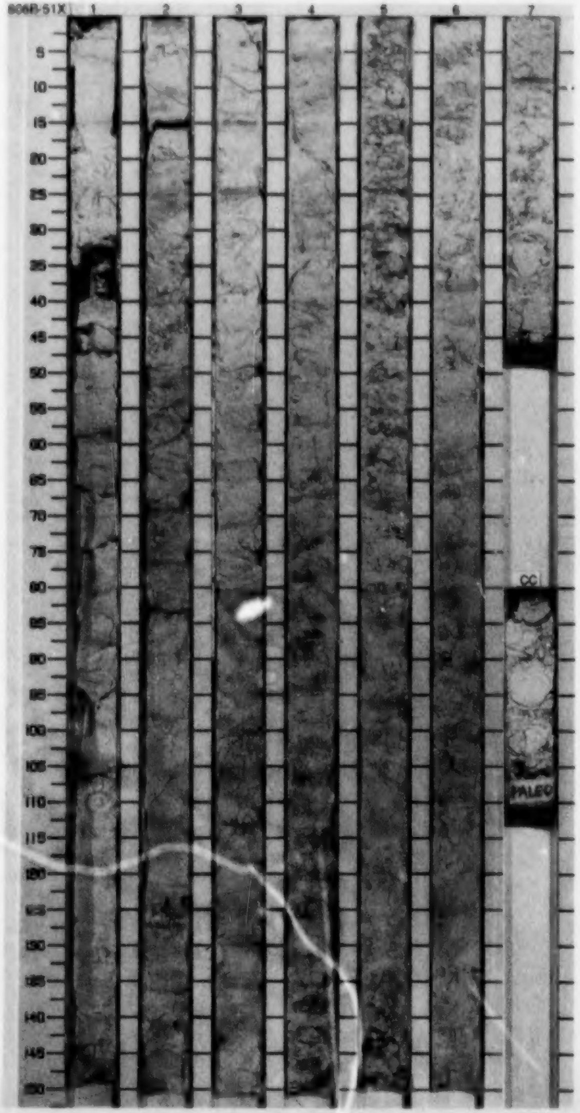
806B-51X
1
2
3
4
5
6
7
CC
PALEO
5
10
15
20
25
30
35
40
45
50
55
60
65
70
75
80
85
90
95
100
105
110
115
120
125
130
135
140
145
150

SITE 806 HOLE B CORE 52X CORED INTERVAL 482.6-492.3 mbsf

TIME-ROCK UNIT	FORAMINIFERS	NANNOFOSSILS	RADIOLARIANS	DIATOMS	PALEOMAGNETICS	PHYS. PROPERTIES	CHEMISTRY	SECTION	METERS
MIDDLE MIOCENE	A/M N10	A/P NN4 - NN5	A/M *Dorcadospyris alata*	F-C/P-M NTD 67		V=1856 ϕ=56.2 γ=1.75 V=1793 ϕ=56.4 γ=1.75 V=1728 ϕ=55.5 γ=1.76 V=1825 ϕ=57.9 γ=1.71	%CaCO$_3$=92.9 %CaCO$_3$=94.0 %CaCO$_3$=93.5 %CaCO$_3$=92.7	1 2 3 4 5 CC	0.5 1.0

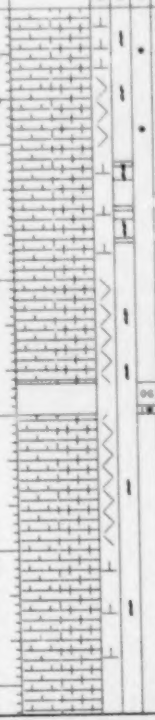
GRAPHIC LITHOLOGY
DRILLING DISTURB.
SED. STRUCTURES
SAMPLES
OG
IW

LITHOLOGIC DESCRIPTION

NANNOFOSSIL CHALK with FORAMINIFERS interbedded with FORAMINIFER NANNOFOSSIL CHALK

Major lithology: This core contains nearly equal proportions of white (7.5YR 8/0) NANNOFOSSIL CHALK with FORAMINIFERS interbedded with FORAMINIFER NANNOFOSSIL CHALK. From Section 2, 93 cm, through Section 5, 50 cm, the chalk is uniformly white. Above and below this interval, 10 to 15 cm thick, faint pale purple (5P 6/2) bands are separated by white intervals. The purplish bands contain 1 mm thick, sub-horizontal, light greenish gray (5GY 7/1) and pale purple (5P 6/2) color bands. Numerous burrows, *Zoophycos* trace fossils, and mottles indicate significant bioturbation.

SMEAR SLIDE SUMMARY (%):

	1, 48	1, 134
	M	D
TEXTURE:		
Sand	15	30
Silt	60	50
Clay	25	20
COMPOSITION:		
Foraminifers	20	40
Nannofossils	80	60
Radiolarians	Tr	—
Siliceous sponge spicules	—	Tr

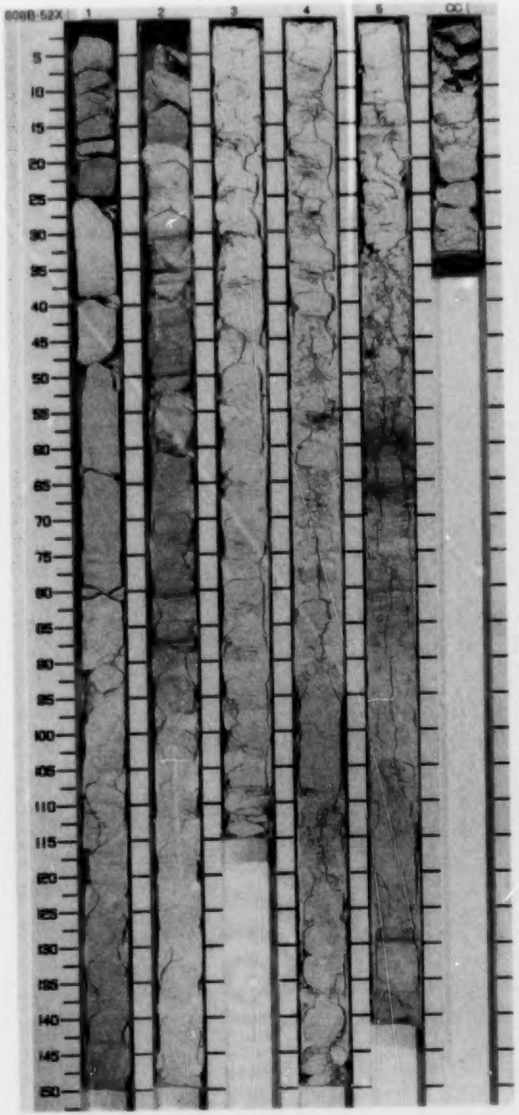
806B-52X
1
2
3
4
5
CC
5
10
15
20
25
30
35
40
45
50
55
60
65
70
75
80
85
90
95
100
105
110
115
120
125
130
135
140
145
150

SITE 806 HOLE B CORE 53X CORED INTERVAL 492.3-501.9 mbsf

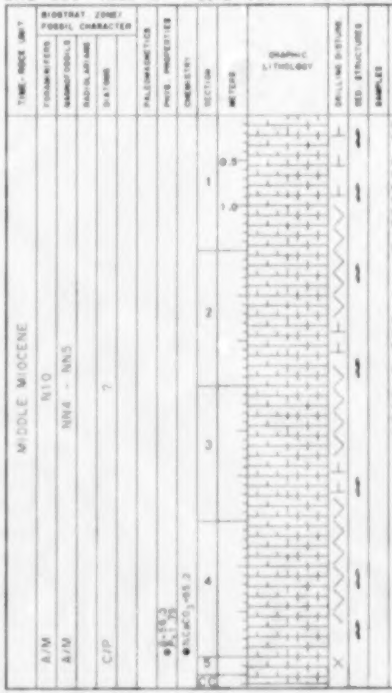
TIME-ROCK UNIT
BIOSTRAT. ZONE/ FOSSIL CHARACTER
FORAMINIFERS
NANNOFOSSILS
RADIOLARIANS
DIATOMS
PALEOMAGNETICS
PHYS. PROPERTIES
CHEMISTRY
SECTION
METERS
GRAPHIC LITHOLOGY
DRILLING DISTURB.
SED. STRUCTURES
SAMPLES
MIDDLE MIOCENE
N10
A/M
NN4 - NN5
A/M
?
C/P
●φ-58.3
●γ-1.75
●%CaCO₃-85.2
1
2
3
4
5
CC
0.5
1.0

LITHOLOGIC DESCRIPTION

NANNOFOSSIL CHALK with FORAMINIFERS interbedded with FORAMINIFER NANNOFOSSIL CHALK

Major lithology: This core contains subequal amounts of NANNOFOSSIL CHALK with FORAMINIFERS and FORAMINIFER NANNOFOSSIL CHALK. The sediment is predominantly white (7.5YR 8/0) and contacts between sediment types are gradational. The coarser foraminifer nannofossil chalk tends to be softer and more prone to drilling disturbance. A few intervals contain very fine, distinct grayish green (10GY 5/2) color banding. Mottles and distinct burrows are common.

SMEAR SLIDE SUMMARY (%):

	2, 64 D
TEXTURE:	
Sand	12
Silt	60
Clay	28
COMPOSITION:	
Accessory minerals	2
Foraminifers	12
Nannofossils	83
Siliceous fragments	3

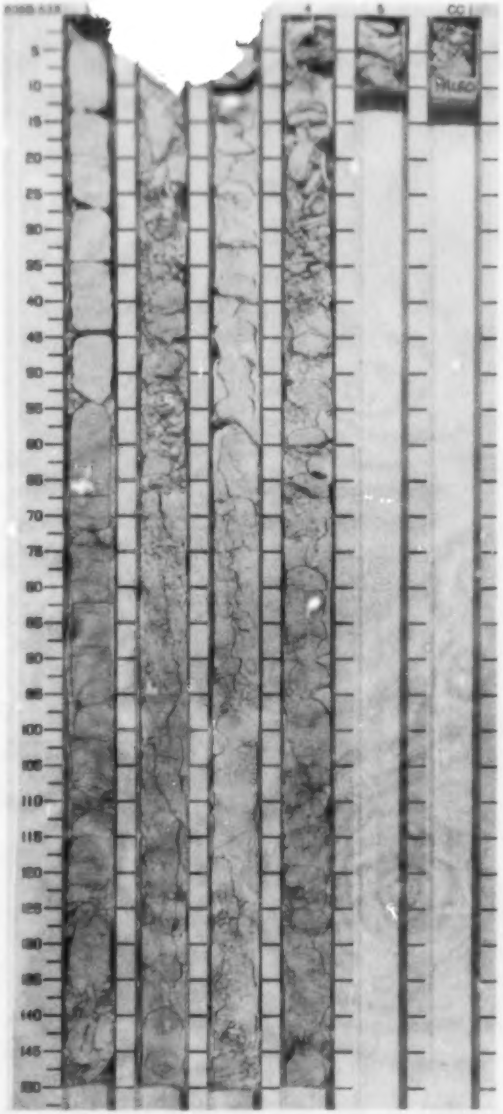
806B-53X
4
5
CC
5
10
15
20
25
30
35
40
45
50
55
60
65
70
75
80
85
90
95
100
105
110
115
120
125
130
135
140
145
150

SITE 806 HOLE B CORE 54X CORED INTERVAL 501.9-511.6 mbsf

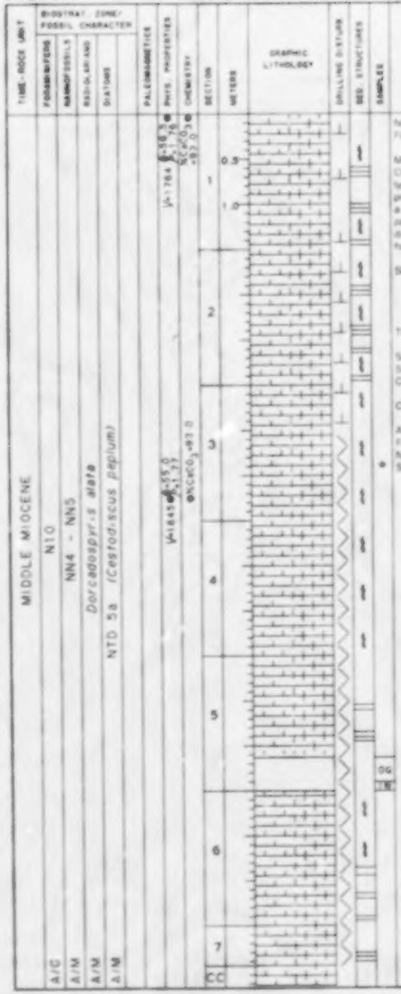
TIME-ROCK UNIT
BIOSTRAT. ZONE/ FOSSIL CHARACTER
FORAMINIFERS
NANNOFOSSILS
RADIOLARIANS
DIATOMS
PALEOMAGNETICS
PHYS. PROPERTIES
CHEMISTRY
SECTION
METERS
GRAPHIC LITHOLOGY
DRILLING DISTURB.
SED. STRUCTURES
SAMPLES
MIDDLE MIOCENE
N10
NN4 - NN5
Dorcadospyris alata
NTD 5a (Cestodiscus peplum)
A/G
A/M
A/M
A/M
γA=1.764
γA=1.845
%CaCO3=87.0
0.5
1.0
1
2
3
4
5
6
7
CC
OG
IW

LITHOLOGIC DESCRIPTION

NANNOFOSSIL CHALK with FORAMINIFERS interbedded with FORAMINIFER NANNOFOSSIL CHALK

Major lithology: This core contains subequal amounts of FORAMINIFER NANNOFOSSIL CHALK and NANNOFOSSIL CHALK with FORAMINIFERS. Contacts between the sediment types are gradational. The predominant color is white (7.5YR 8/0), with 20 to 50 cm thick, pale pink (5RP 8/2) intervals in Sections 1 and 5. Bioturbation is slight to moderate as indicated by a few pyritized or disseminated burrow fills. Distinct, mm thick, greenish gray (5G 7/1) and pale purple (5P 6/2) color bands are common in Sections 1, 2, 5, 6 and 7. A small (1 cm in diameter) calcite concretion is found at the bottom of Section 5. Severe drilling disturbance has resulted in heavily fragmented biscuits embedded in a stiff paste matrix.

SMEAR SLIDE SUMMARY (%):

	3, 69
	D
TEXTURE	
Sand	12
Silt	55
Clay	33
COMPOSITION	
Accessory minerals	1
Foraminifers	15
Nannofossils	81
Siliceous fragments	3

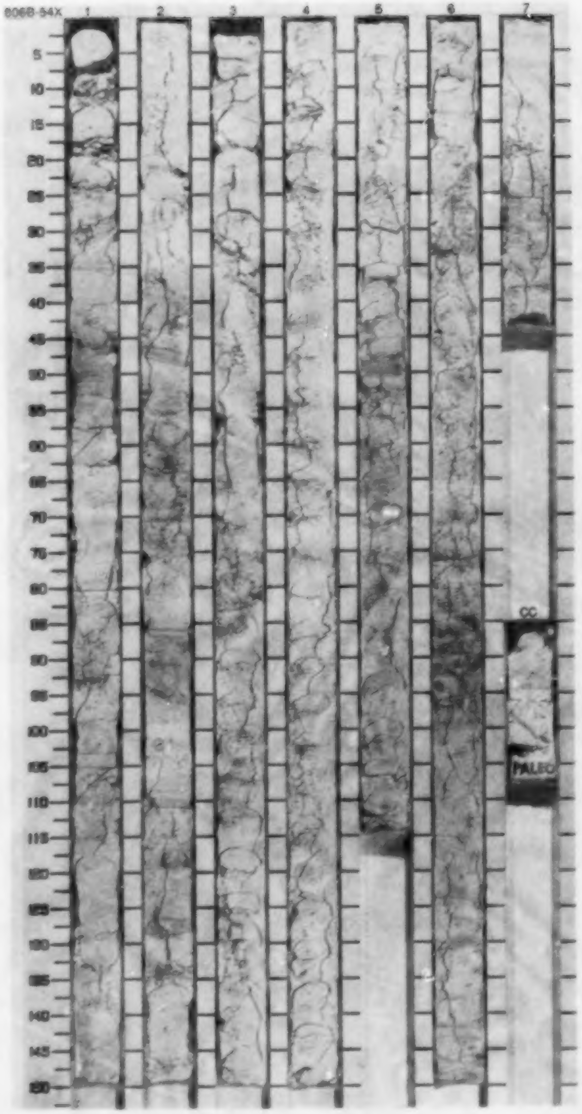
806B-54X
1
2
3
4
5
6
7
5
10
15
20
25
30
35
40
45
50
55
60
65
70
75
80
85
90
95
100
105
110
115
120
125
130
135
140
145
150
CC
PALEO

SITE 806 HOLE B CORE 55X CORED INTERVAL 511.6-521.3 mbsf

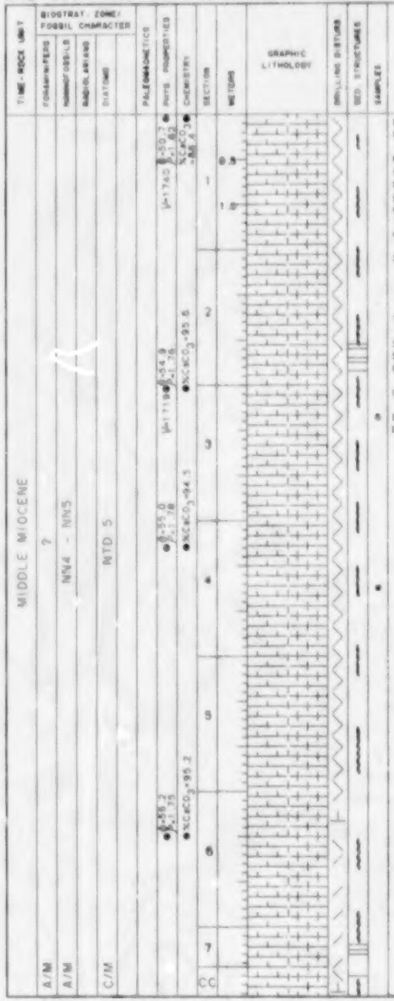
TIME-ROCK UNIT
BIOSTRAT. ZONE/ FOSSIL CHARACTER
FORAMINIFERS
NANNOFOSSILS
RADIOLARIANS
DIATOMS
PALEOMAGNETICS
PHYS. PROPERTIES
CHEMISTRY
SECTION
METERS
GRAPHIC LITHOLOGY
DRILLING DISTURB.
SED. STRUCTURES
SAMPLES
MIDDLE MIOCENE
?
NN4 - NN5
NTD 5
A/M
A/M
C/M
φ=50.7
γ=1.82
ν=1740
%CaCO3=88.4
φ=54.9
γ=1.76
ν=1719
%CaCO3=95.6
φ=55.0
γ=1.78
%CaCO3=94.5
φ=56.2
γ=1.75
%CaCO3=95.2
1
2
3
4
5
6
7
CC
0.5
1.0

LITHOLOGIC DESCRIPTION

NANNOFOSSIL CHALK with FORAMINIFERS interbedded with FORAMINIFER NANNOFOSSIL CHALK

Major lithology: This core contains subequal amounts of FORAMINIFER NANNOFOSSIL CHALK and NANNOFOSSIL CHALK with FORAMINIFERS. Contacts between the sediment types are gradational and the dominant color is white (7.5YR 8/0). Most of the core is homogeneous, with some evidence of bioturbation in the form of burrows and mottles. Very thin, distinct color banding is observed in Sections 2 and 7. These color bands are less than 1 mm thick and are either pale purple (5P 6/1) or grayish green (10GY 5/2) in color. Some disseminated pyrite is also noted. A calcite concretion was observed at Section 2, 89 cm.

SMEAR SLIDE SUMMARY (%):

	3, 36	4, 73
	D	D
TEXTURE:		
Sand	30	15
Silt	50	60
Clay	20	25
COMPOSITION:		
Foraminifers	50	15
Nannofossils	50	85

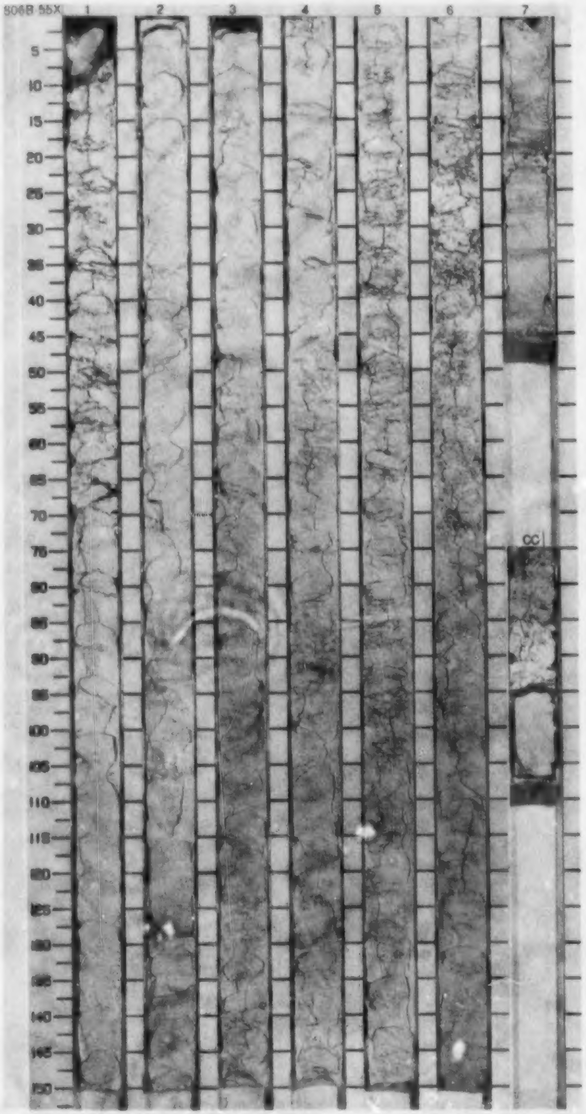
806B 55X
1
2
3
4
5
6
7
CC
5
10
15
20
25
30
35
40
45
50
55
60
65
70
75
80
85
90
95
100
105
110
115
120
125
130
135
140
145
150

SITE 806 HOLE B CORE 56X CORED INTERVAL 521.3-530.9 mbsf

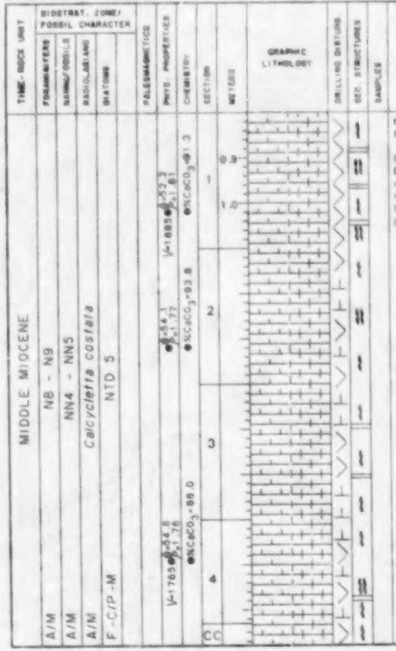
TIME-ROCK UNIT
BIOSTRAT. ZONE/ FOSSIL CHARACTER
FORAMINIFERS
NANNOFOSSILS
RADIOLARIANS
DIATOMS
PALEOMAGNETICS
PHYS. PROPERTIES
CHEMISTRY
SECTION
METERS
GRAPHIC LITHOLOGY
DRILLING DISTURB.
SED. STRUCTURES
SAMPLES
MIDDLE MIOCENE
A/M N8 - N9
A/M NN4 - NN5
A/M Calcycletta costata
F-C/P-M NTD 5
V=1885 ●φ=52.2 ρ=1.81
●φ=54.1 ρ=1.77
V=1765 ●φ=54.8 ρ=1.76
●%CaCO3=91.3
●%CaCO3=93.8
●%CaCO3=88.0
1
2
3
4
CC
0.5
1.0

LITHOLOGIC DESCRIPTION

NANNOFOSSIL CHALK with FORAMINIFERS interbedded with FORAMINIFER NANNOFOSSIL CHALK

Major lithology: This core contains subequal amounts of NANNOFOSSIL CHALK with FORAMINIFERS and FORAMINIFER NANNOFOSSIL CHALK. The predominant sediment color is white (7.5YR 8/0) but grades into pale pink for most of Section 1. Bioturbation is moderate to heavy as seen from abundant burrows. A well-preserved *Zoophycos* trace fossil trail is observed in Section 1. A few zones with mm-thick, distinct, pale purple (5P 6/2) and greenish gray (5G 7/1) color bands are noted in Sections 1, 3 and 4.

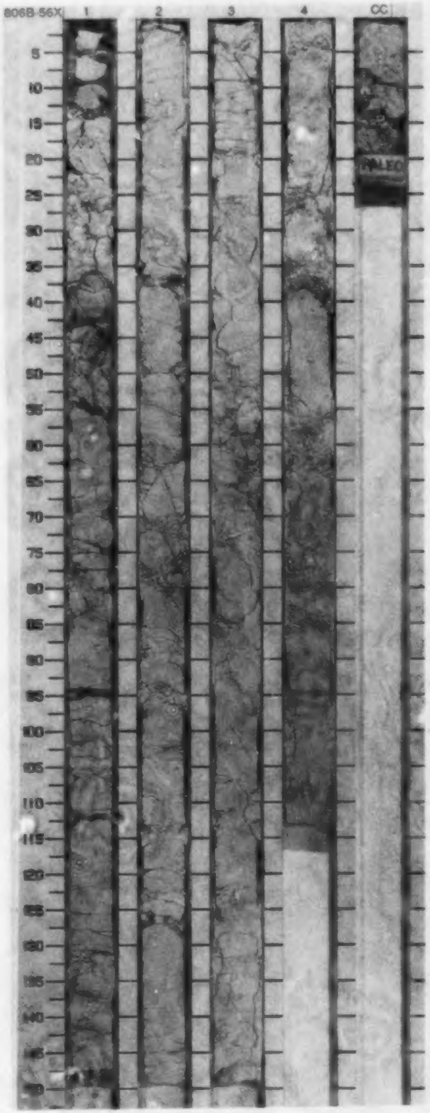
806B-56X
1
2
3
4
CC
PALEO
5
10
15
20
25
30
35
40
45
50
55
60
65
70
75
80
85
90
95
100
105
110
115
120
125
130
135
140
145
150

SITE 806 HOLE B CORE 57X CORED INTERVAL 530.9-540.5 mbsf

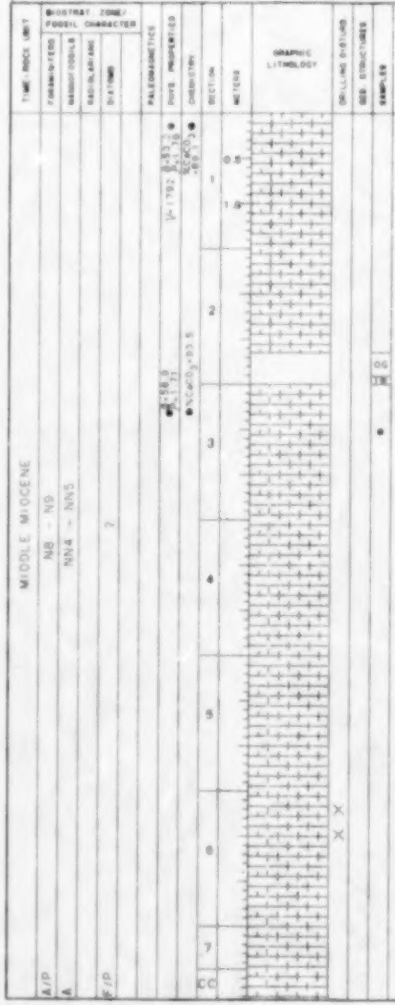
TIME-ROCK UNIT
BIOSTRAT. ZONE/ FOSSIL CHARACTER
FORAMINIFERS
NANNOFOSSILS
RADIOLARIANS
DIATOMS
PALEOMAGNETICS
PHYS. PROPERTIES
CHEMISTRY
SECTION
METERS
GRAPHIC LITHOLOGY
DRILLING DISTURB.
SED. STRUCTURES
SAMPLES
MIDDLE MIOCENE
N8 - N9
NNN4 - NN5
?
A/P
A
F/P
γ=1.78 φ=53.2
γ=1.77 φ=58.8
%CaCO3=89.2
%CaCO3=93.5
0.5
1.0
1
2
3
4
5
6
7
CC
OG
IW

LITHOLOGIC DESCRIPTION

NANNOFOSSIL CHALK with FORAMINIFERS interbedded with FORAMINIFER NANNOFOSSIL CHALK

Major lithology: This core contains interbedded FORAMINIFER NANNOFOSSIL CHALK (75%) and NANNOFOSSIL CHALK with FORAMINIFERS (25%). Contacts between the two sediment types are gradational. Some very fine (<1 mm thick) distinct color banding is obvious. A few trace fossils are noted. The core is highly drilling disturbed and, in some cases, brecciated.

SMEAR SLIDE SUMMARY (%)

	3, 51
	D
TEXTURE	
Sand	20
Silt	50
Clay	30
COMPOSITION	
Diatoms	1
Foraminifers	25
Nannofossils	72
Siliceous fragments	2

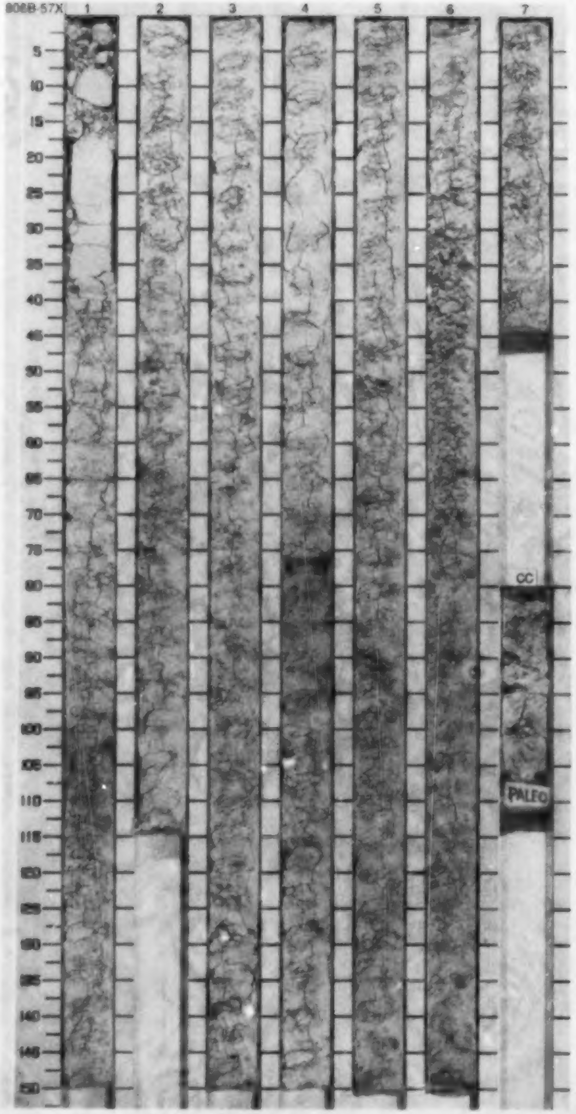
806B-57X
1
2
3
4
5
6
7
5
10
15
20
25
30
35
40
45
50
55
60
65
70
75
80
85
90
95
100
105
110
115
120
125
130
135
140
145
150
CC
PALEO

SITE 806 HOLE B CORE 58X CORED INTERVAL 540.5-550.2 mbsf

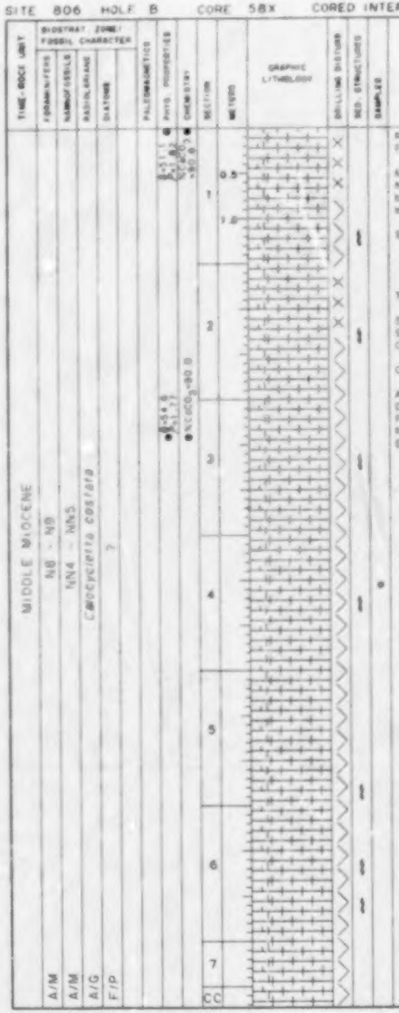
TIME-ROCK UNIT
BIOSTRAT. ZONE/ FOSSIL CHARACTER
FORAMINIFERS
NANNOFOSSILS
RADIOLARIANS
DIATOMS
PALEOMAGNETICS
PHYS. PROPERTIES
CHEMISTRY
SECTION
METERS
GRAPHIC LITHOLOGY
DRILLING DISTURB.
SED. STRUCTURES
SAMPLES
MIDDLE MIOCENE
N8 - N9
NN4 - NN5
Calocycletta costata
?
A/M
A/M
A/G
F/P
%CaCO$_3$=90.0
1
2
3
4
5
6
7
CC
0.5
1.0

LITHOLOGIC DESCRIPTION

NANNOFOSSIL CHALK with FORAMINIFERS interbedded with FORAMINIFER NANNOFOSSIL CHALK

Major lithology: This core contains interbedded FORAMINIFER NANNOFOSSIL CHALK and NANNOFOSSIL CHALK with FORAMINIFERS. The chalk is predominantly white (7.5YR 8/0) but grades to pale pink (5P 8/2) in some intervals. Trace fossils and burrows indicate bioturbation.

SMEAR SLIDE SUMMARY (%):

	4, 55
	D
TEXTURE:	
Sand	15
Silt	60
Clay	25
COMPOSITION:	
Accessory minerals	1
Diatoms	Tr
Foraminifers	20
Nannofossils	70
Siliceous fragments	9

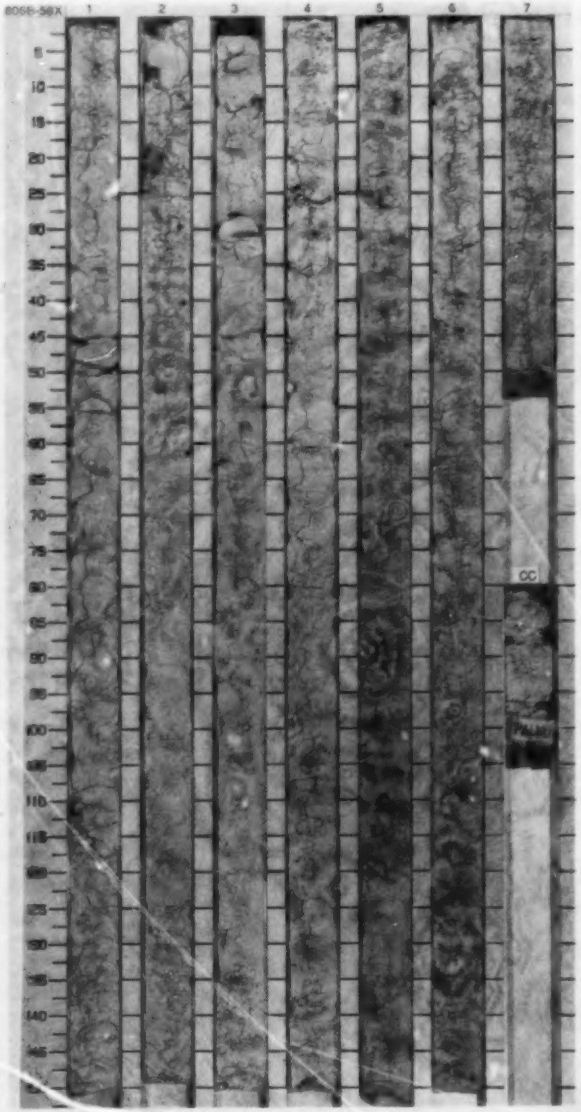
806B-58X
1
2
3
4
5
6
7
CC
5
10
15
20
25
30
35
40
45
50
55
60
65
70
75
80
85
90
95
100
105
110
115
120
125
130
135
140
145
150

SITE 806 HOLE B CORE 59X CORED INTERVAL 550.2-559.9 mbsf

TIME-ROCK UNIT	FORAMINIFERS	NANNOFOSSILS	RADIOLARIANS	DIATOMS	PALEOMAGNETICS	PHYS. PROPERTIES	CHEMISTRY	SECTION	METERS	GRAPHIC LITHOLOGY	DRILLING DISTURB.	SED. STRUCTURES	SAMPLES
MIDDLE MIOCENE	N8 - N9	NN4 - NN5		NTD 4 - NTD 5 (*Denticulopsis nicobarica*)		● φ=51.1 γ=1.84 V=1896	● %CaCO$_3$ =90.3	1	0.5 1.0				
						● φ=55.0 γ=1.77	● %CaCO$_3$=83.0	2					
						● φ=55.4 γ=1.78	● %CaCO$_3$ =81.1	3					●
								4					
								5					
								6					
								7					
								CC					
	A/M	A/P		C/P									

LITHOLOGIC DESCRIPTION

FORAMINIFER NANNOFOSSIL CHALK

Major lithology: This core contains homogeneous, white (7.5YR 8/0) FORAMINIFERAL CHALK. Drilling disturbance is extensive, resulting in drilling biscuits.

SMEAR SLIDE SUMMARY (%):

	3, 81
	D
TEXTURE:	
Sand	25
Silt	50
Clay	25
COMPOSITION:	
Foraminifers	50
Nannofossils	50
Radiolarians	Tr

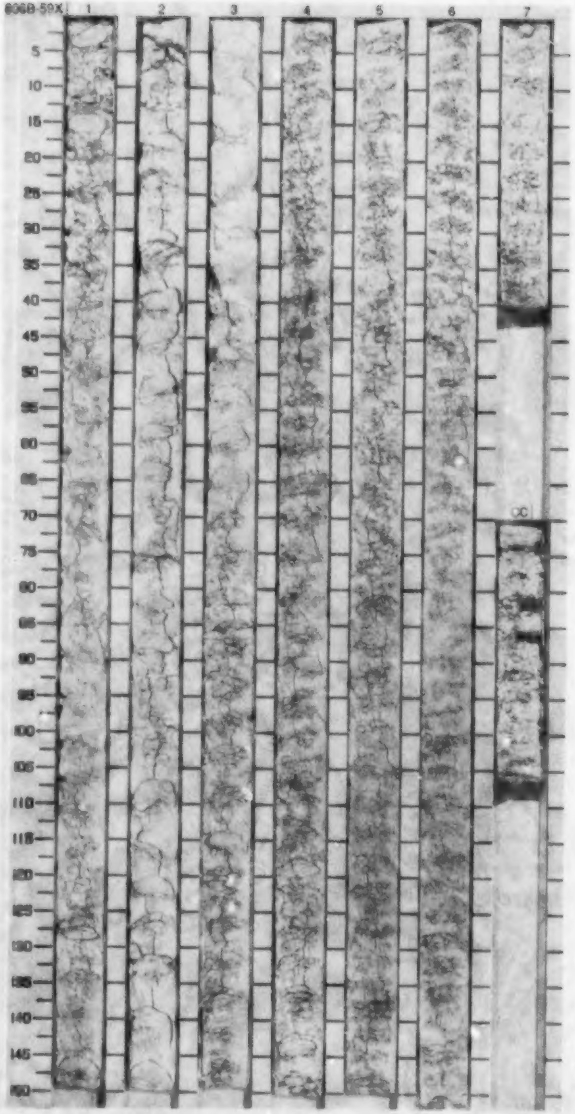
806B-59X
1
2
3
4
5
6
7
CC
5
10
15
20
25
30
35
40
45
50
55
60
65
70
75
80
85
90
95
100
105
110
115
120
125
130
135
140
145
150

SITE 806 HOLE B CORE 60X CORED INTERVAL 559.9-569.6 mbsf

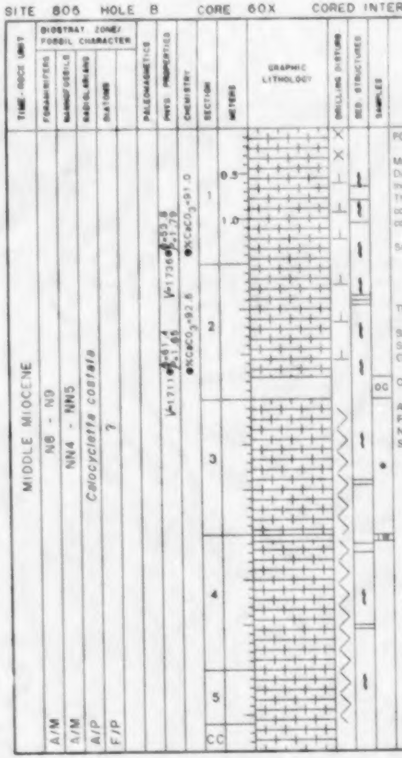
TIME-ROCK UNIT
BIOSTRAT. ZONE/ FOSSIL CHARACTER
FORAMINIFERS
NANNOFOSSILS
RADIOLARIANS
DIATOMS
PALEOMAGNETICS
PHYS. PROPERTIES
CHEMISTRY
SECTION
METERS
GRAPHIC LITHOLOGY
DRILLING DISTURB.
SED. STRUCTURES
SAMPLES
MIDDLE MIOCENE
A/M N8 - N9
A/M NN4 - NN5
A/P Calocycletta costata
F/P ?
V=1736 ● φ=53.8 γ=1.79
V=1711 ● φ=61.4 γ=1.85
●%CaCO3=91.0
●%CaCO3=92.6
1
2
3
4
5
CC
0.5
1.0
OG

LITHOLOGIC DESCRIPTION

FORAMINIFER NANNOFOSSIL CHALK

Major lithology: This core contains well-drilled FORAMINIFER NANNOFOSSIL CHALK. Disseminated purple-colored specks throughout the core give a pale pink (5RP 8/2) hue to the sediment. It is moderately to heavily bioturbated, with fine-scale mottling and trace fossils. These structures appear to be stretched in the horizontal direction, possibly as a result of compaction. A few very fine (< 1 mm thick), distinct, gray color bands are observed within this core.

SMEAR SLIDE SUMMARY (%):

	3, 74 D
TEXTURE:	
Sand	15
Silt	55
Clay	30
COMPOSITION:	
Accessory minerals	2
Foraminifers	25
Nannofossils	70
Siliceous fragments	3

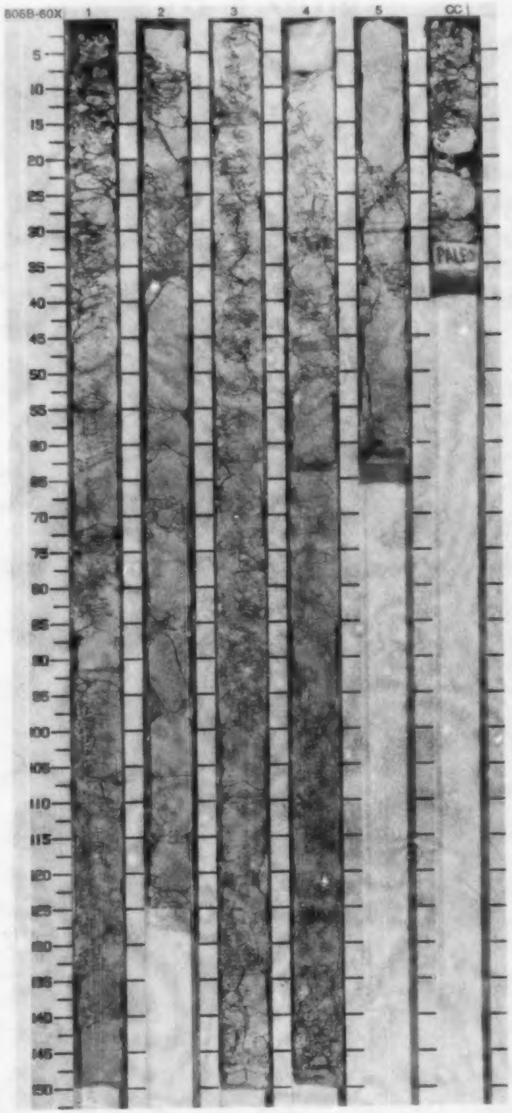
806B-60X
1
2
3
4
5
CC
PALEO
5
10
15
20
25
30
35
40
45
50
55
60
65
70
75
80
85
90
95
100
105
110
115
120
125
130
135
140
145
150

SITE 806 HOLE B CORE 61X CORED INTERVAL 569.9-579.3 mbsf

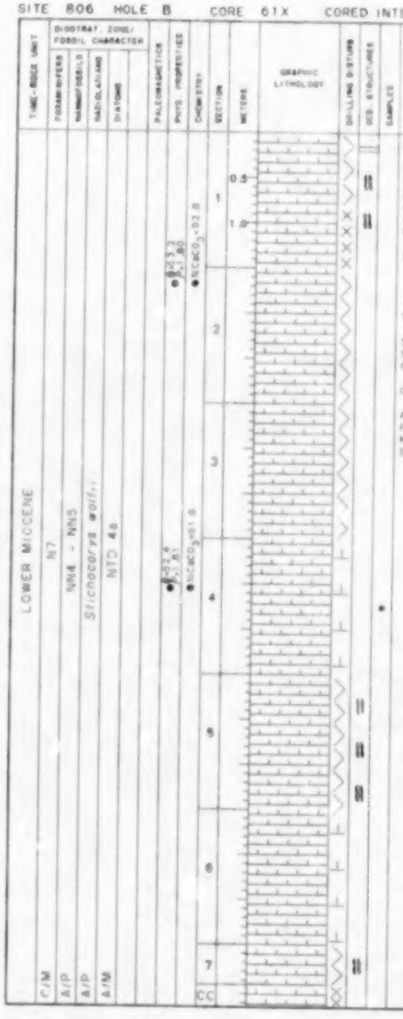

LITHOLOGIC DESCRIPTION

NANNOFOSSIL CHALK with FORAMINIFERS

Major lithology: This core contains well lithified NANNOFOSSIL CHALK with FORAMINIFERS. The dominant color is white (7.5YR 8/0), with long intervals (60 and 120 cm) of pale pink (5RP 8/2) in Sections 1 and 5. Signs of heavy bioturbation are visible only in the pink intervals and Section 7. They include faint mottles and burrows. A few distinct, very thin (<1 mm), gray (2.5Y 5/0) color bands are noted in Section 1. Drilling disturbance has resulted in moderately fractured to highly fragmented biscuits in a stiff paste matrix.

SMEAR SLIDE SUMMARY (%):

	4, 74
	D
TEXTURE	
Sand	10
Silt	50
Clay	40
COMPOSITION	
Accessory minerals	1
Foraminifers	12
Nannofossils	85
Siliceous fragments	2

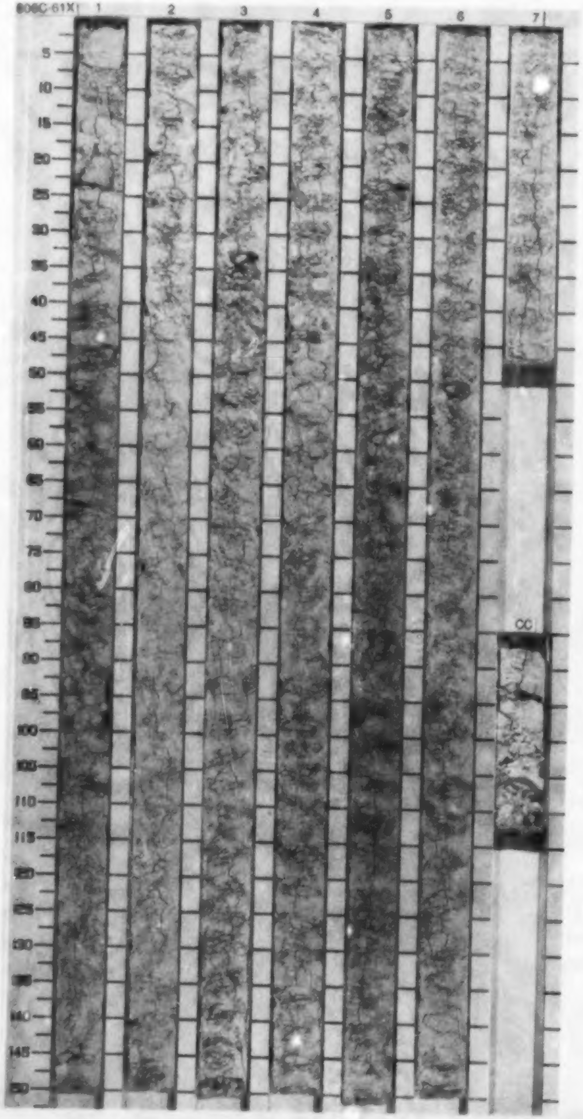
806B-61X
1
2
3
4
5
6
7
CC
5
10
15
20
25
30
35
40
45
50
55
60
65
70
75
80
85
90
95
100
105
110
115
120
125
130
135
140
145
150

SITE 806 HOLE B CORE 62X CORED INTERVAL 579.3-589.0 mbsf

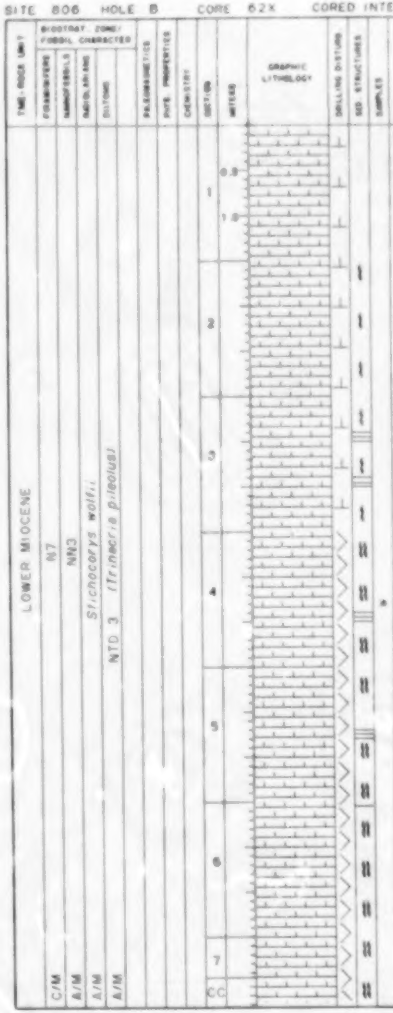

LITHOLOGIC DESCRIPTION

NANNOFOSSIL CHALK WITH FORAMINIFERS

Major lithology: This core contains predominantly white (7.5YR 8/0) NANNOFOSSIL CHALK with FORAMINIFERS. Sections 3 through 5 contain a few pale pink (5RP 8/2), 10 to 20 cm thick intervals. Distinct greenish gray (5GY 6/1) bands, about 1 mm thick, are commonly associated with the pale pink intervals. Some intervals are strongly bioturbated.

SMEAR SLIDE SUMMARY (%):

	4, 80
	D
TEXTURE	
Sand	5
Silt	50
Clay	45
COMPOSITION	
Diatoms	1
Foraminifers	12
Nannofossils	84
Radiolarians	1
Siliceous fragments	2

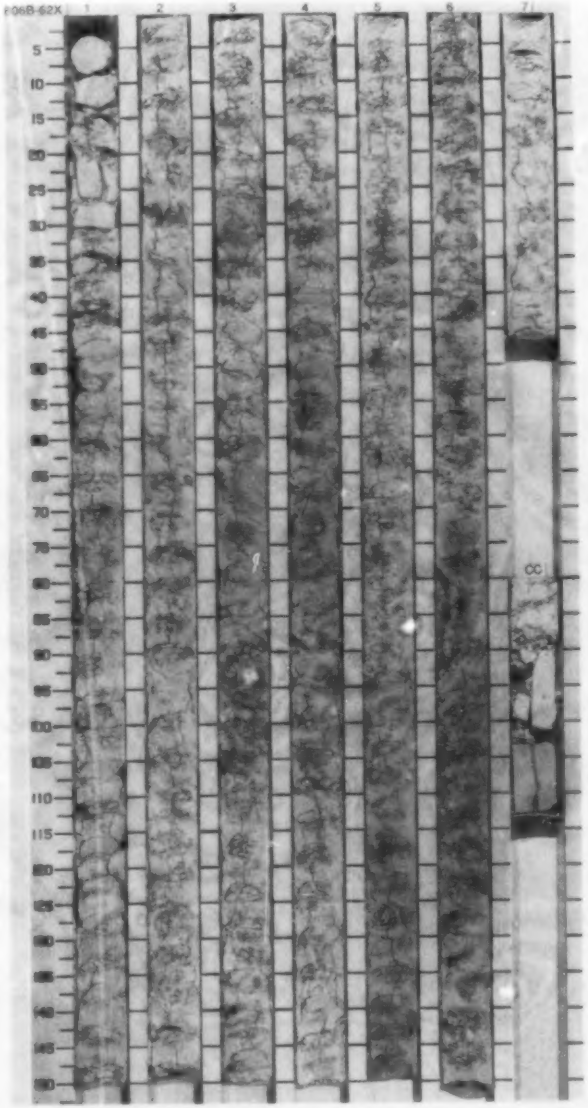
806B-62X
1
2
3
4
5
6
7
CC
5
10
15
20
25
30
35
40
45
50
55
60
65
70
75
80
85
90
95
100
105
110
115
120
125
130
135
140
145
150

SITE 806 HOLE B CORE 63X CORED INTERVAL 589.0-598.6 mbsf

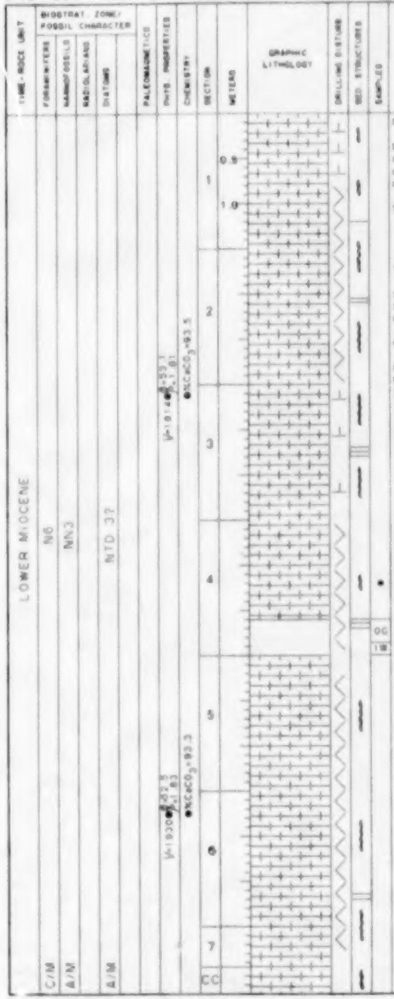
TIME-ROCK UNIT
BIOSTRAT. ZONE/ FOSSIL CHARACTER
FORAMINIFERS
NANNOFOSSILS
RADIOLARIANS
DIATOMS
PALEOMAGNETICS
PHYS. PROPERTIES
CHEMISTRY
SECTION
METERS
GRAPHIC LITHOLOGY
DRILLING DISTURB.
SED. STRUCTURES
SAMPLES
LOWER MIOCENE
N6
NN3
NTD 3?
C/M
A/M
A/M
V=1814 φ=53.1 γ=1.81
%CaCO3=93.5
V=1930 φ=52.5 γ=1.83
%CaCO3=93.3
1
2
3
4
5
6
7
CC
0.5
1.0
OG
IW

LITHOLOGIC DESCRIPTION

FORAMINIFER NANNOFOSSIL CHALK

Major lithology: This core contains white (7.5YR 8/0) FORAMINIFER NANNOFOSSIL CHALK. It is moderately bioturbated, with numerous burrows and trace fossils. Scattered occurrences of very thin (< 1 mm), distinct, gray (2.5Y 5/0) and greenish gray (5GY 7/2) color bands are noted. The core is predominantly composed of drilling biscuits.

SMEAR SLIDE SUMMARY (%):

	4, 77
	D
TEXTURE:	
Sand	10
Silt	60
Clay	30
COMPOSITION:	
Foraminifers	25
Nannofossils	73
Siliceous fragments	2

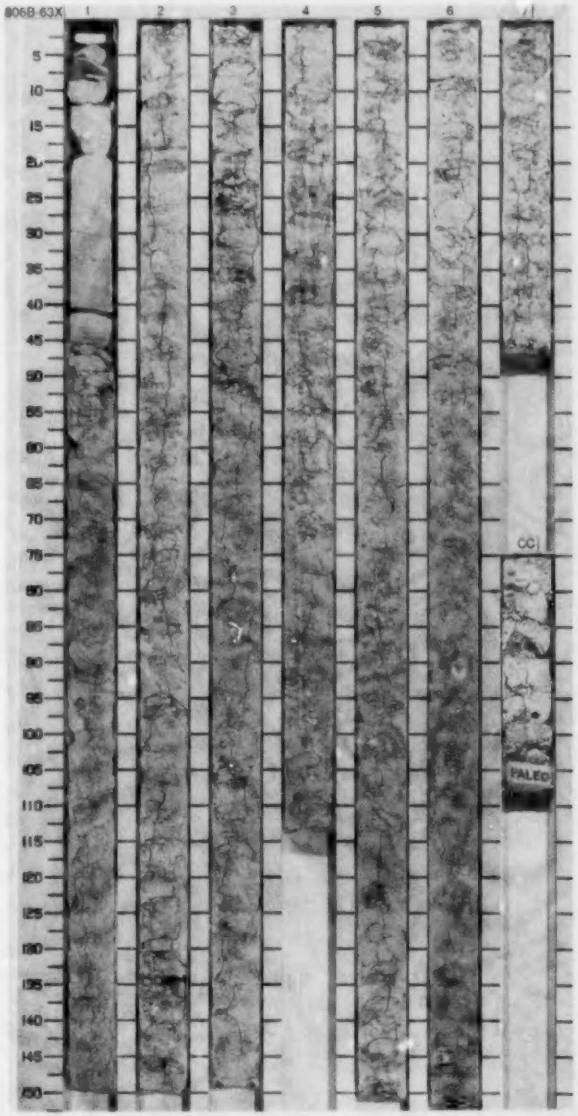
806B-63X
1
2
3
4
5
6
7
5
10
15
20
25
30
35
40
45
50
55
60
65
70
75
80
85
90
95
100
105
110
115
120
125
130
135
140
145
150
CC
PALEO

SITE 806 HOLE B CORE 64X CORED INTERVAL 598.6-608.3 mbsf

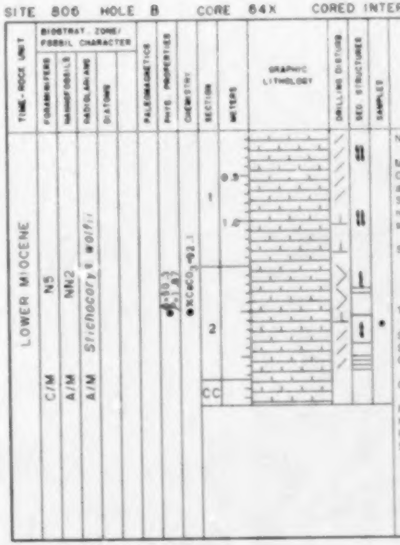
TIME-ROCK UNIT
BIOSTRAT. ZONE/ FOSSIL CHARACTER
FORAMINIFERS
NANNOFOSSILS
RADIOLARIANS
DIATOMS
PALEOMAGNETICS
PHYS. PROPERTIES
CHEMISTRY
SECTION
METERS
GRAPHIC LITHOLOGY
DRILLING DISTURB.
SED. STRUCTURES
SAMPLES
LOWER MIOCENE
C/M N5
A/M NN2
A/M Stichocorys wolffi
φ=50.3
γ=1.87
●%CaCO₃=92.1
1
2
CC
0.5
1.0

LITHOLOGIC DESCRIPTION

NANNOFOSSIL CHALK with FORAMINIFERS

Major lithology: This core contains white (7.5YR 8/0) and pink (5RP 8/2) NANNOFOSSIL CHALK with FORAMINIFERS. The sediment is moderately to heavily bioturbated with abundant and trace fossils. Thin (<1 mm), distinct, gray (2.5Y 5/0) color bands are common in Section 2. Two thin color bands are discontinuous and appear to be intersected and reworked by a burrow. Drilling disturbance has resulted in slightly to moderately fractured segments (ca. 10 cm long) and biscuits.

SMEAR SLIDE SUMMARY (%):

	2, 66
	D
TEXTURE:	
Sand	5
Silt	60
Clay	35
COMPOSITION:	
Foraminifers	15
Nannofossils	83
Radiolarians	1
Siliceous fragments	1

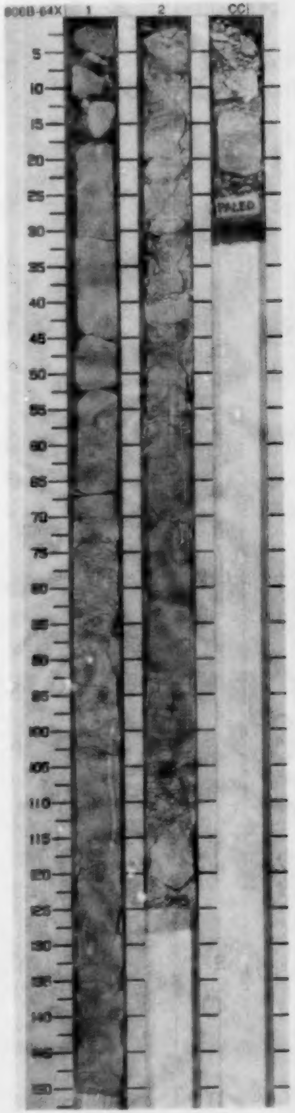
806B-64X
1
2
CC
VOID
5
10
15
20
25
30
35
40
45
50
55
60
65
70
75
80
85
90
95
100
105
110
115
120
125
130
135
140
145
150

SITE 806 HOLE B CORE 65X CORED INTERVAL 608.3-617.9 mbsf

TIME-ROCK UNIT	FORAMINIFERS	NANNOFOSSILS	RADIOLARIANS	DIATOMS	PALEOMAGNETICS	PHYS. PROPERTIES	CHEMISTRY	SECTION	METERS	SAMPLES
LOWER MIOCENE	N5 C/M	NN2 A/M	*Stichocorys wolffii* A/M	NTD 2 - NTD 3 (*Craspedodiscus elegans*) A/M		γ=1.887 ●		1 2 3 4 5 6 CC	0.5 1.0	●

BIOSTRAT. ZONE/ FOSSIL CHARACTER

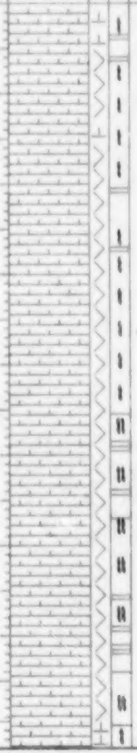
GRAPHIC LITHOLOGY
DRILLING DISTURB.
SED. STRUCTURES

LITHOLOGIC DESCRIPTION

NANNOFOSSIL CHALK with FORAMINIFERS

Major lithology: This core is predominantly white (7.5YR 8/0) NANNOFOSSIL CHALK WITH FORAMINIFERS. Abundant subhorizontal and a few vertical trace fossils are evident, most of which are on the scale of 0.5 cm in diameter. Some pyritized specks and burrow fills are apparent. A few very thin, distinct, gray (2.5Y 5/0), grayish green (5GY 7/2), and pale to grayish purple (5P 6/2 - 5P 4/2) color bands are noted. Much of the core is composed of drilling biscuits.

SMEAR SLIDE SUMMARY (%):

	3, 65
	D
TEXTURE:	
Sand	15
Silt	60
Clay	25
COMPOSITION:	
Foraminifers	20
Nannofossils	80

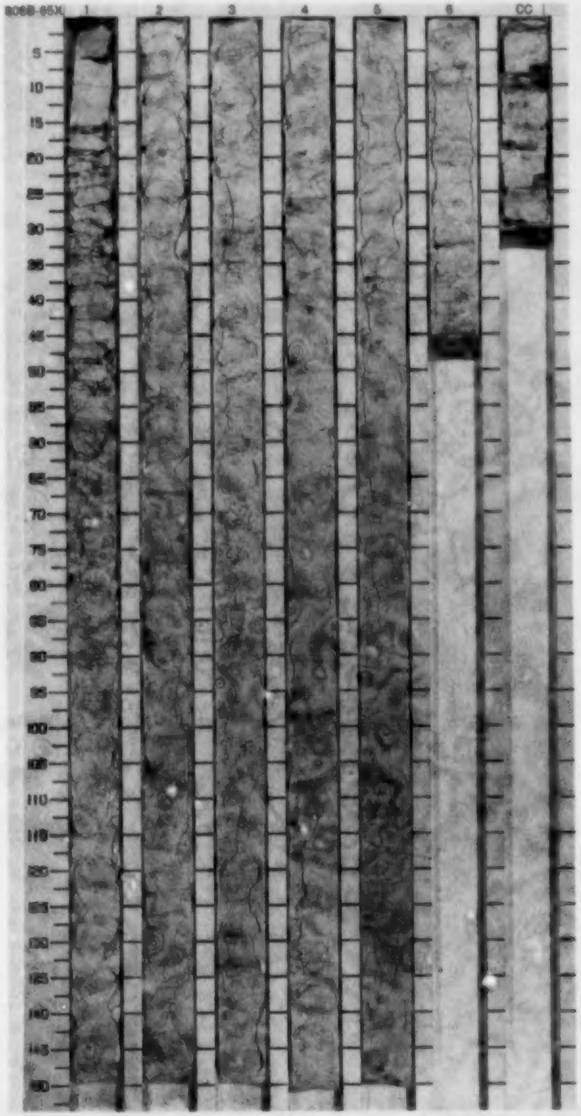
806B-65X
1
2
3
4
5
6
CC
5
10
15
20
25
30
35
40
45
50
55
60
65
70
75
80
85
90
95
100
105
110
115
120
125
130
135
140
145
150

SITE 806 HOLE B CORE 66X CORED INTERVAL 617.9-627.5 mbsf

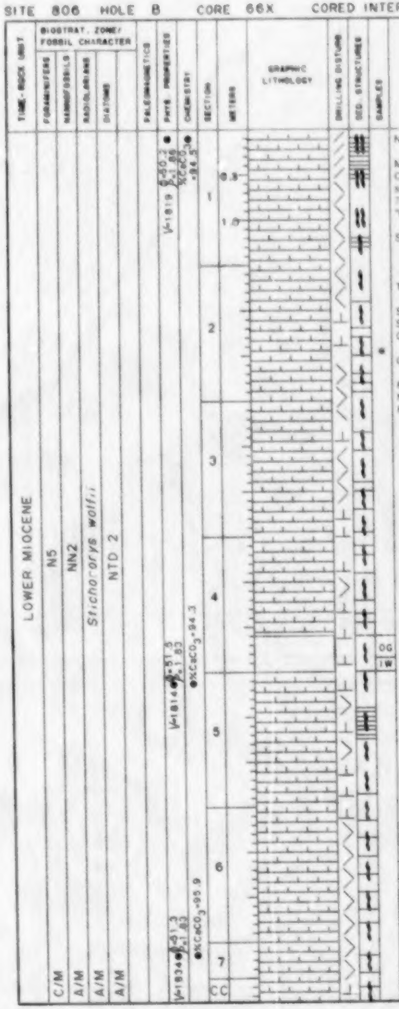
TIME-ROCK UNIT
BIOSTRAT. ZONE/ FOSSIL CHARACTER
FORAMINIFERS
NANNOFOSSILS
RADIOLARIANS
DIATOMS
PALEOMAGNETICS
PHYS. PROPERTIES
CHEMISTRY
SECTION
METERS
GRAPHIC LITHOLOGY
DRILLING DISTURB.
SED. STRUCTURES
SAMPLES
LOWER MIOCENE
N5
NN2
Stichocorys wolffi
NTD 2
C/M
A/M
A/M
A/M
V=1819 φ=50.2 ρ=1.86
%CaCO3=94.5
V=1814 φ=51.3 ρ=1.83
%CaCO3=94.3
V=1834 φ=51.3 ρ=1.83
%CaCO3=95.9
1
2
3
4
5
6
7
CC
0.5
1.0
OG
IW

LITHOLOGIC DESCRIPTION

NANNOFOSSIL CHALK with FORAMINIFERS

Major lithology: This core contains white (7.5YR 8/0, 5YR 8/1, and 2.5Y 8/0) NANNOFOSSIL CHALK with FORAMINIFERS. Section 1 is heavily bioturbated; the remainder of the core is slightly bioturbated. Millimeter scale, distinct greenish gray (5G 6/1), light greenish gray (5G 7/1), and light gray (N7) color bands are present in approximately 30-60% of the drilling "biscuits".

SMEAR SLIDE SUMMARY (%)

	2, 96
TEXTURE	
Sand	20
Silt	75
Clay	
COMPOSITION	
Foraminifers	12
Nannofossils	85
Radiolarians	3

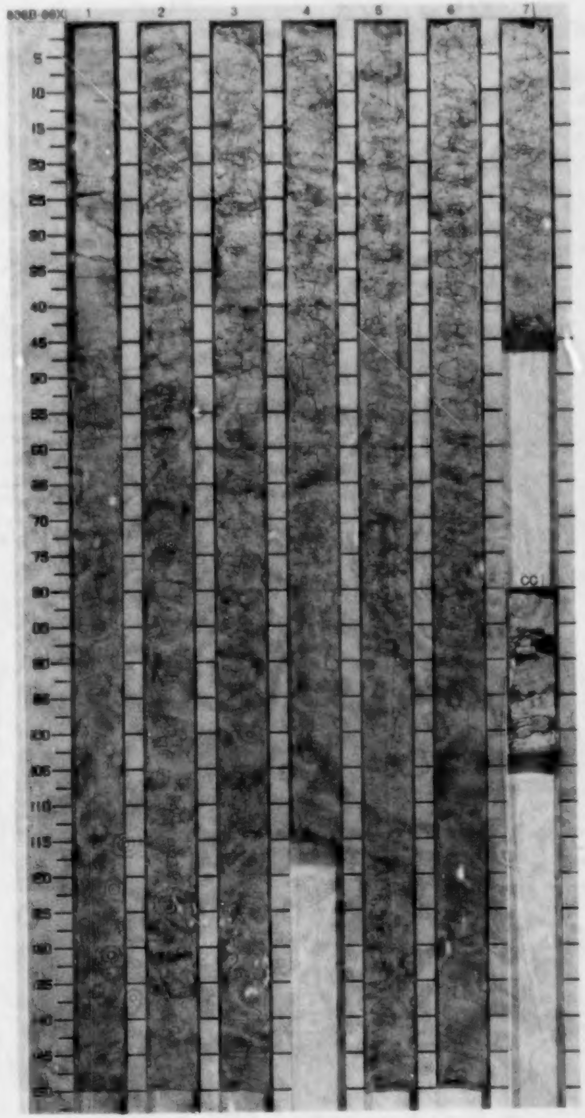
806B-66X
1
2
3
4
5
6
7
CC
5
10
15
20
25
30
35
40
45
50
55
60
65
70
75
80
85
90
95
100
105
110
115
120
125
130
135
140
145
150

SITE 806 HOLE B CORE 67X CORED INTERVAL 627.5-637.2 mbsf

TIME-ROCK UNIT	BIOSTRAT. ZONE/ FOSSIL CHARACTER: FORAMINIFERS	NANNOFOSSILS	RADIOLARIANS	DIATOMS	PALEOMAGNETICS	PHYS. PROPERTIES	CHEMISTRY	SECTION	METERS
LOWER MIOCENE	N5 C/M	NN2 A/P	*Stichocorys delmontensis* A/G	NTD 2 C/M - P		●γ-1940 φ-51.0 γ-1.83 ●γ-1882 φ-50.7 γ-1.84	●%CaCO₃-94.5 ●%CaCO₃-94.7	1 2 CC	0.5 1.0

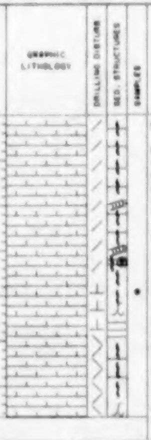
GRAPHIC LITHOLOGY
DRILLING DISTURB.
SED. STRUCTURES
SAMPLES

LITHOLOGIC DESCRIPTION

NANNOFOSSIL CHALK

Major lithology: This core contains white (5Y 8/1 and 2.5Y 8/0) NANNOFOSSIL CHALK. It is slightly to moderately bioturbated throughout, including *Zoophycos* spreiten, mm scale grayish blue (5PB 5/2) mottling, and a 5 mm diameter pyritic burrow fill. Thin, distinct, greenish gray (5G 6/1) and faint light gray (N7) color bands are present throughout; some light gray color bands have microstylolitic waving. Several 4 cm thick zones of with flaser structures are seen in Sections 2 and CC.

SMEAR SLIDE SUMMARY (%):

	2, 48 D
TEXTURE	
Sand	2
Silt	90
Clay	8
COMPOSITION	
Foraminifers	7
Nannofossils	92
Radiolarians	1

SITE 806 HOLE B CORE 68X CORED INTERVAL 637.2-646.5 mbsf

TIME-ROCK UNIT	BIOSTRAT. ZONE/ FOSSIL CHARACTER: FORAMINIFERS	NANNOFOSSILS	RADIOLARIANS	DIATOMS	PALEOMAGNETICS	PHYS. PROPERTIES	CHEMISTRY	SECTION	METERS
LOWER MIOCENE	N5 C/M	NN2 A/P	*Stichocorys delmontensis* A/M	NTD 2 F/P		●φ-47.5 γ-1.89	●%CaCO₃-94.6	1 CC	0.5

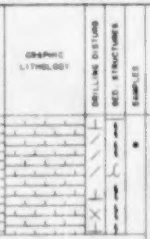
GRAPHIC LITHOLOGY
DRILLING DISTURB.
SED. STRUCTURES
SAMPLES

LITHOLOGIC DESCRIPTION

NANNOFOSSIL CHALK with FORAMINIFERS

Major lithology: This core contains NANNOFOSSIL CHALK with FORAMINIFERS. The color is pale blue (5PB 7/2) in the upper 30 cm of Section 1, with a sharp contact to the underlying white (2.5Y 8/0). Slight to moderate bioturbation is represented by well-developed *Zoophycos* trace fossils. A 4 cm thick zone of with flaser structures is seen, as well as single light gray (N7) color bands/microstylolites.

SMEAR SLIDE SUMMARY (%):

	1, 32 D
TEXTURE	
Sand	5
Silt	90
Clay	5
COMPOSITION	
Foraminifers	20
Nannofossils	79
Radiolarians	Tr
Siliceous fragments	1

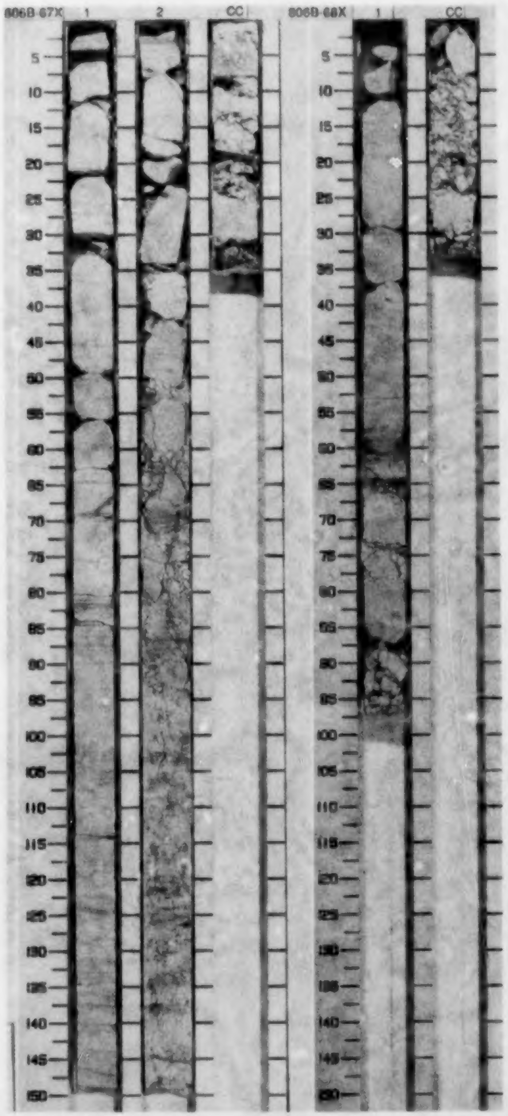
806B-67X
1
2
CC
806B-68X
1
CC
5
10
15
20
25
30
35
40
45
50
55
60
65
70
75
80
85
90
95
100
105
110
115
120
125
130
135
140
145
150

SITE 806 HOLE B CORE 69X CORED INTERVAL 646.5-656.2 mbsf

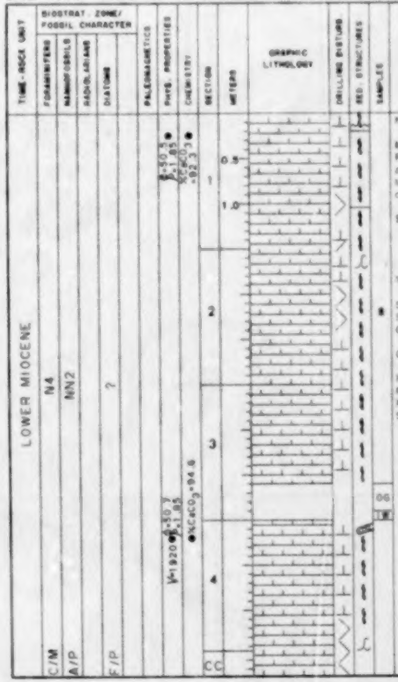
TIME-ROCK UNIT
BIOSTRAT. ZONE/ FOSSIL CHARACTER
FORAMINIFERS
NANNOFOSSILS
RADIOLARIANS
DIATOMS
PALEOMAGNETICS
PHYS. PROPERTIES
CHEMISTRY
SECTION
METERS
GRAPHIC LITHOLOGY
DRILLING DISTURB.
SED. STRUCTURES
SAMPLES
LOWER MIOCENE
N4
NN2
?
C/M
A/P
F/P
φ=50.5
γ=1.85
%CaCO₃=92.3
Vp=1920
φ=50.7
γ=1.85
%CaCO₃=94.6
1
2
3
4
CC
0.5
1.0
OG
IW

LITHOLOGIC DESCRIPTION

NANNOFOSSIL CHALK WITH FORAMINIFERS

Major lithology: This core contains white (5YR 8/1, 2.5Y 8/0) NANNOFOSSIL CHALK with FORAMINIFERS. In Section 4, gradational changes to pale purple (5PB 7/2) at 40 to 46 cm and light gray (N7) at 135 to 143 cm are observed. The sediment is slightly to moderately bioturbated throughout. Well developed *Zoophycos* trace fossils are present in Section 4, 10 cm. Flaser structures, wavy color bands and microstylolites are seen throughout the core.

SMEAR SLIDE SUMMARY (%):

	2, 70
	D
TEXTURE:	
Sand	35
Silt	60
Clay	5
COMPOSITION:	
Foraminifers	20
Nannofossils	75
Radiolarians	4
Silicoflagellates	1

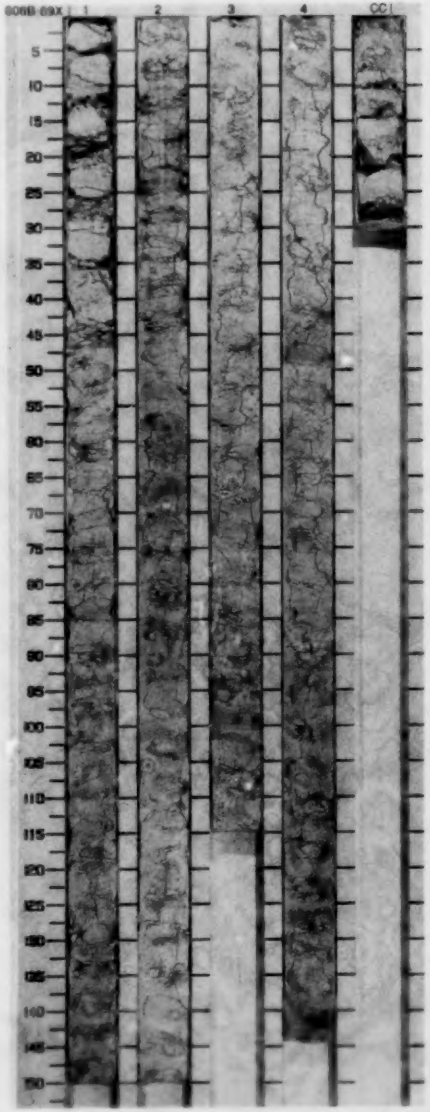
806B 69X
1
2
3
4
CC
5
10
15
20
25
30
35
40
45
50
55
60
65
70
75
80
85
90
95
100
105
110
115
120
125
130
135
140
145
150

SITE 806 HOLE B CORE 70X CORED INTERVAL 656.2-665.8 mbsf

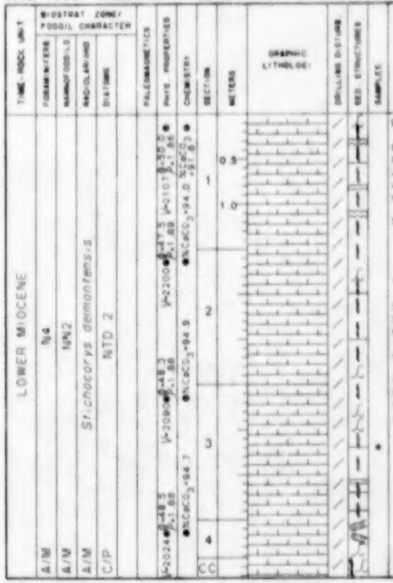
TIME-ROCK UNIT
BIOSTRAT. ZONE/ FOSSIL CHARACTER
FORAMINIFERS
NANNOFOSSILS
RADIOLARIANS
DIATOMS
PALEOMAGNETICS
PHYS. PROPERTIES
CHEMISTRY
SECTION
METERS
GRAPHIC LITHOLOGY
DRILLING DISTURB.
SED. STRUCTURES
SAMPLES
LOWER MIOCENE
N4
NN2
Stichocorys delmontensis
NTD 2
A/M
A/M
A/M
C/P
γ=2024 ● φ=48.5 ρ=1.88
γ=2090 ● φ=48.3 ρ=1.88
γ=2200 ● φ=47.5 ρ=1.89
γ=2107 φ=50.0 ρ=1.86 ●
● %CaCO3=94.7
● %CaCO3=94.9
● %CaCO3=94.0 %CaCO3=91.0 ●
1
2
3
4
CC
0.5
1.0

LITHOLOGIC DESCRIPTION

NANNOFOSSIL CHALK with FORAMINIFERS

Major lithology: This core contains white (5YR 8/1, 2.5Y 8/0) NANNOFOSSIL CHALK with FORAMINIFERS. The sediment is slightly to moderately bioturbated throughout. A vertical *Zoophycos* trace fossil appears in Section 1, 51 to 63 cm. Flaserstructures, wavy color bands and microstylolites are observed. Faint to discrete greenish gray (5G 6/1) to light gray (N7) color bands are common throughout the core.

SMEAR SLIDE SUMMARY (%):

	3, 70
	D
TEXTURE:	
Sand	25
Silt	70
Clay	5
COMPOSITION:	
Foraminifers	15
Nannofossils	80
Radiolarians	4
Silicoflagellates	1

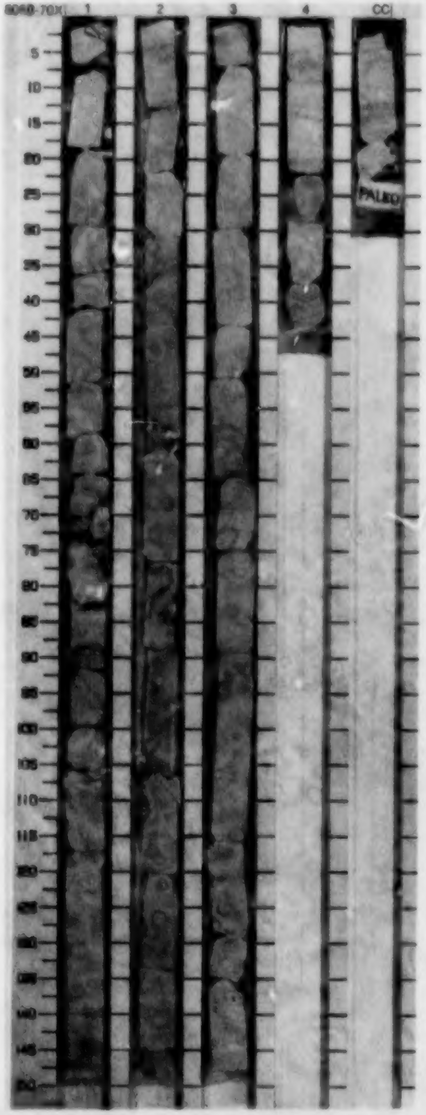
806B-70X
1
2
3
4
CC
PALEO
5
10
15
20
25
30
35
40
45
50
55
60
65
70
75
80
85
90
95
100
105
110
115
120
125
130
135
140
145
150

SITE 806 HOLE B CORE 71X CORED INTERVAL 665.8-675.5 mbsf

TIME-ROCK UNIT	BIOSTRAT. ZONE/ FOSSIL CHARACTER: FORAMINIFERS	NANNOFOSSILS	RADIOLARIANS	DIATOMS	PALEOMAGNETICS	PHYS. PROPERTIES	CHEMISTRY	SECTION	METERS
LOWER MIOCENE	N4 A/M	NN2 M	Stichocorys delmontensis A/M	? F-C/M-P		V=2086 ● Φ=47.2 ρ=1.89	● %CaCO$_3$ =92.0	1 2 3 CC	0.5 1.0

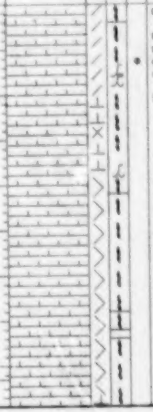
GRAPHIC LITHOLOGY
DRILLING DISTURB.
SED. STRUCTURES
SAMPLES

LITHOLOGIC DESCRIPTION

NANNOFOSSIL CHALK

Major lithology: This core contains white (5YR 8/1, 2.5Y 8/0), slightly to moderately bioturbated NANNOFOSSIL CHALK. Flaser structures, wavy color bands, and microstylolites are observed. Faint to intense, well-defined, mm scale, greenish gray (5G 6/1) to light gray (N7/) color bands are common throughout.

SMEAR SLIDE SUMMARY (%):

	1, 63 D
TEXTURE:	
Sand	20
Silt	75
Clay	5
COMPOSITION:	
Foraminifers	8
Nannofossils	87
Radiolarians	4
Silicoflagellates	1

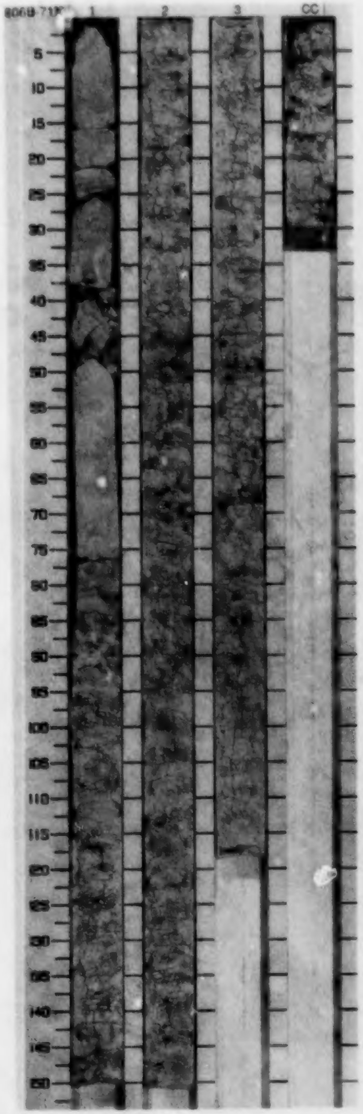
806B-71X
1
2
3
CC
5
10
15
20
25
30
35
40
45
50
55
60
65
70
75
80
85
90
95
100
105
110
115
120
125
130
135
140
145
150

SITE 806 HOLE B CORE 72X CORED INTERVAL 675.5-685.2 mbsf

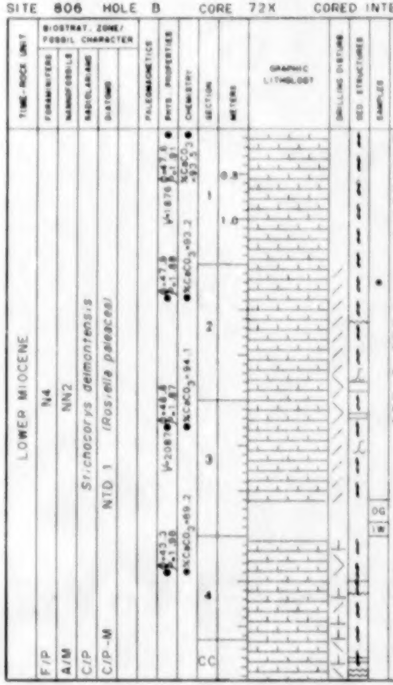
TIME-ROCK UNIT
BIOSTRAT. ZONE/FOSSIL CHARACTER
FORAMINIFERS
NANNOFOSSILS
RADIOLARIANS
DIATOMS
PALEOMAGNETICS
PHYS. PROPERTIES
CHEMISTRY
SECTION
METERS
GRAPHIC LITHOLOGY
DRILLING DISTURB.
SED. STRUCTURES
SAMPLES
LOWER MIOCENE
F/P N4
A/M NN2
C/P Stichocorys delmontensis
C/P-M NTD 1 (Rosiella paleacea)
φ=47.6 ρ=1.91
V=1876
%CaCO3=93.5
%CaCO3=93.2
φ=47.9 ρ=1.88
%CaCO3=94.1
φ=48.8 ρ=1.87
V=2087
%CaCO3=89.2
φ=43.3 ρ=1.98
1
2
3
4
CC
0.5
1.0
OG
IW

LITHOLOGIC DESCRIPTION

NANNOFOSSIL CHALK with FORAMINIFERS

Major lithology: This core contains slightly to moderately bioturbated NANNOFOSSIL CHALK with FORAMINIFERS. The color is predominantly white (5YR 8/1, 2.5Y 8/0), with short intervals of light gray (N7). Flaser structures, wavy color bands and possible microstylolites are observed. Faint to well-developed greenish gray (5G 6/1) to light gray (N7) color bands are common.

SMEAR SLIDE SUMMARY (%):

	2, 20
	D
TEXTURE	
Sand	30
Silt	65
Clay	5
COMPOSITION	
Foraminifers	22
Nannofossils	75
Radiolarians	3

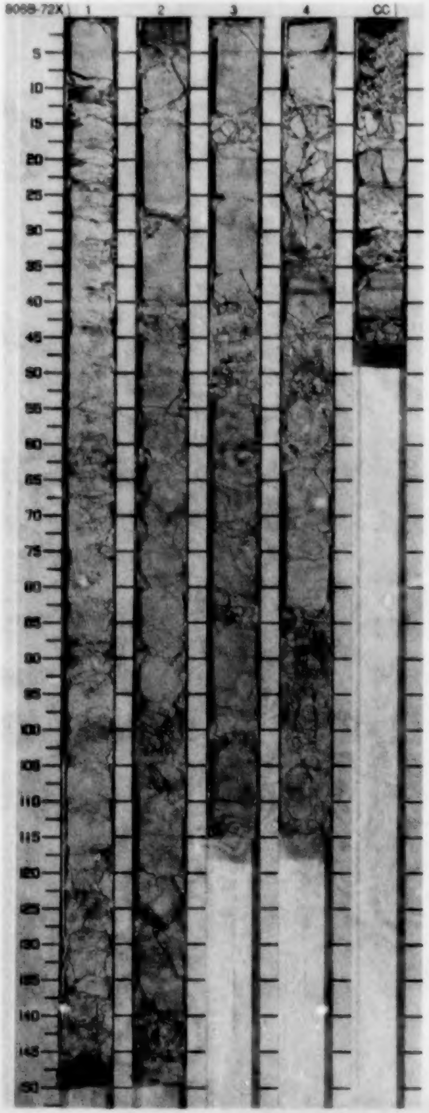
806B-72X
1
2
3
4
CC
5
10
15
20
25
30
35
40
45
50
55
60
65
70
75
80
85
90
95
100
105
110
115
120
125
130
135
140
145
150

SITE 806 HOLE B CORE 73X CORED INTERVAL 685.2-694.8 mbsf

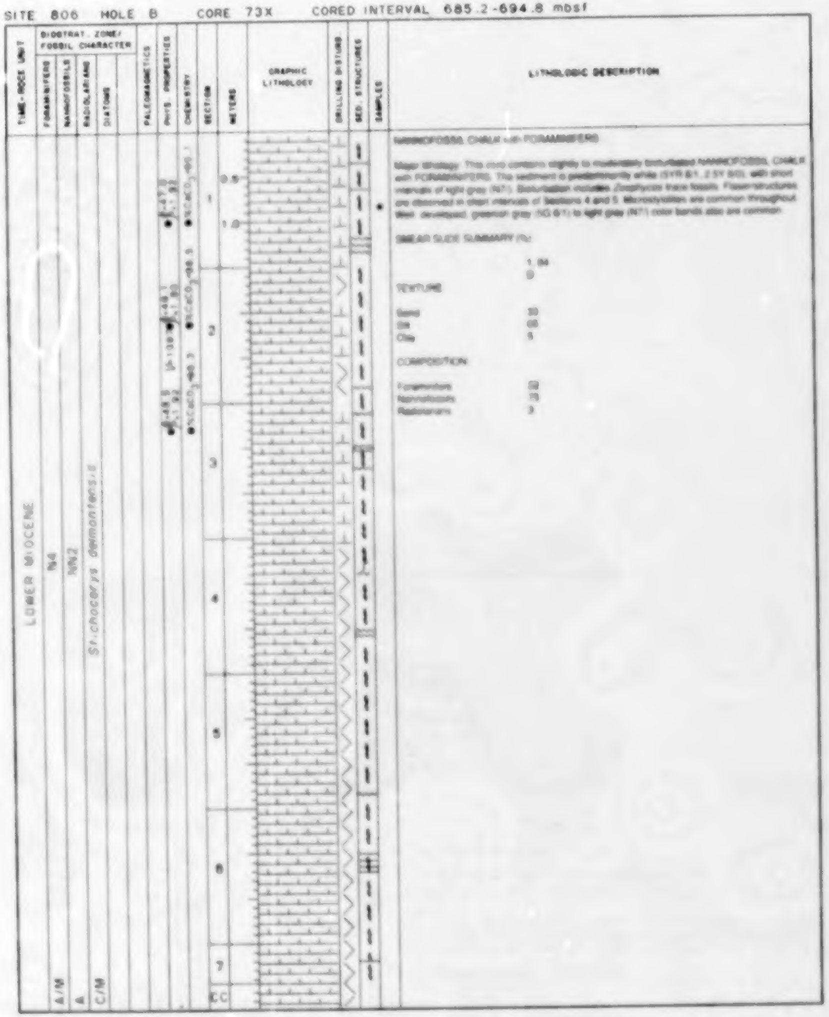
TIME-ROCK UNIT
BIOSTRAT. ZONE/ FOSSIL CHARACTER
FORAMINIFERS
NANNOFOSSILS
RADIOLARIANS
DIATOMS
PALEOMAGNETICS
PHYS. PROPERTIES
CHEMISTRY
SECTION
METERS
GRAPHIC LITHOLOGY
DRILLING DISTURB.
SED. STRUCTURES
SAMPLES
LITHOLOGIC DESCRIPTION
LOWER MIOCENE
N4
NN2
St. chocerys wemontensis
A/M
A
C/M
φ-47.0 γ-1.92
%CaCO3-90.1
%CaCO3-88.5
φ-48.1 γ-1.90
Vp-1900
%CaCO3-88.3
φ-48.5 γ-1.92
1
2
3
4
5
6
7
CC
0.5
1.0

NANNOFOSSIL CHALK with FORAMINIFERS

Major lithology: This core contains slightly to moderately bioturbated NANNOFOSSIL CHALK with FORAMINIFERS. The sediment is predominantly white (5YR 8/1, 2.5Y 8/0), with short intervals of light gray (N7). Bioturbation includes *Zoophycos* trace fossils. Flaser structures are observed in short intervals of Sections 4 and 5. Microstylolites are common throughout. Well developed, greenish gray (5G 6/1) to light gray (N7) color bands also are common.

SMEAR SLIDE SUMMARY (%):

	1, 84
	D
TEXTURE	
Sand	10
Silt	85
Clay	5
COMPOSITION	
Foraminifers	22
Nannofossils	75
Radiolarians	3

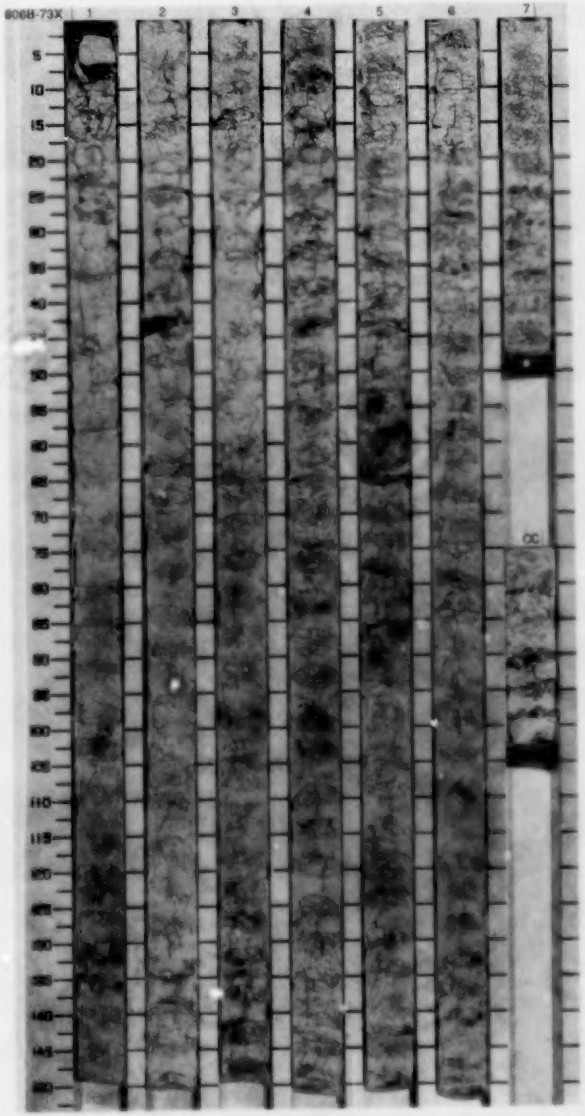
806B-73X
1
2
3
4
5
6
7
CC
5
10
15
20
25
30
35
40
45
50
55
60
65
70
75
80
85
90
95
100
105
110
115
120
125
130
135
140
145
150

SITE 806 HOLE B CORE 74X CORED INTERVAL 694.8-704.5 mbsf

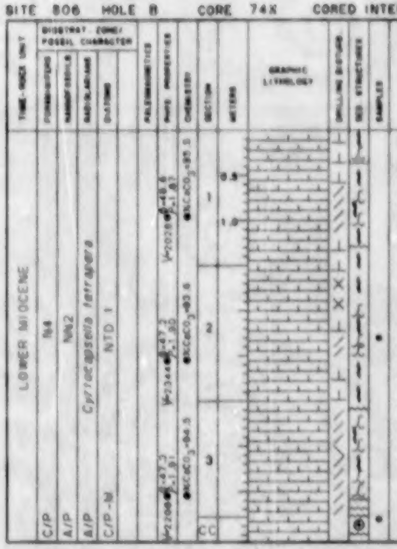
TIME-ROCK UNIT
BIOSTRAT. ZONE/ FOSSIL CHARACTER
FORAMINIFERS
NANNOFOSSILS
RADIOLARIANS
DIATOMS
PALEOMAGNETICS
PHYS. PROPERTIES
CHEMISTRY
SECTION
METERS
GRAPHIC LITHOLOGY
DRILLING DISTURB.
SED. STRUCTURES
SAMPLES
LOWER MIOCENE
N4
NN2
Cyrtocapsella tetrapera
NTD 1
C/P
A/P
A/P
C/P-M
V=2028
Φ=48.6
ρ=1.87
V=2344
Φ=47.2
ρ=1.90
V=2208
Φ=47.3
ρ=1.91
%CaCO3=85.5
%CaCO3=83.6
%CaCO3=84.5
1
2
3
CC
0.5
1.0

LITHOLOGIC DESCRIPTION

NANNOFOSSIL CHALK WITH FORAMINIFERS

Major lithology: This core contains slightly to moderately bioturbated, white (2.5Y 8/0) NANNOFOSSIL CHALK WITH FORAMINIFERS. Flaser structures are present throughout the core, becoming more abundant toward the base. Individual microstylolites are present to common.

Minor lithology: Two nodules of CHERT are present in the Core Catcher, 1 to 3 cm. Each nodule is approximately 1 cm in diameter and light gray (N7) in color.

SMEAR SLIDE SUMMARY (%):

	2, 80 D	CC, 1 M
TEXTURE:		
Sand	30	—
Silt	65	70
Clay	5	30
COMPOSITION:		
Foraminifers	23	—
Nannofossils	75	30
Radiolarians	2	—
Silica	—	70

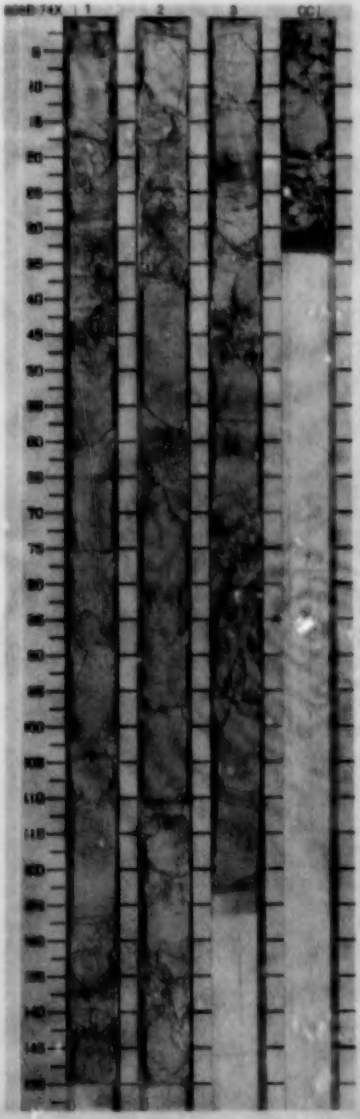
806B-74X
1
2
3
CC
5
10
15
20
25
30
35
40
45
50
55
60
65
70
75
80
85
90
95
100
105
110
115
120
125
130
135
140
145
150

SITE 806 HOLE B CORE 75X CORED INTERVAL 704.5-714.1 mbsf

TIME-ROCK UNIT	BIOSTRAT. ZONE/ FOSSIL CHARACTER: FORAMINIFERS	NANNOFOSSILS	RADIOLARIANS	DIATOMS	PALEOMAGNETICS	PHYS. PROPERTIES	CHEMISTRY	SECTION	METERS
LOWER MIOCENE	N4	NN2		NTD 1		●Φ=48.1 ρ=1.88	●%CaCO3=93.7	1	0.5 1.0
								2	
								3	
						V=2071●Φ=47.3 ρ=1.88	●%CaCO3=89.0	4	
								5	
								6	
								CC	
	R/P	A/M		C/M					

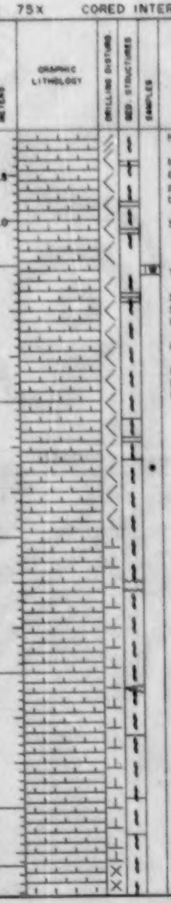
GRAPHIC LITHOLOGY
DRILLING DISTURB.
SED. STRUCTURES
SAMPLES
SW

LITHOLOGIC DESCRIPTION

NANNOFOSSIL CHALK with FORAMINIFERS

Major lithology: This core contains moderately to heavily bioturbated, white (2.5Y 8/0 and 5Y 8/1) NANNOFOSSIL CHALK with FORAMINIFERS. Planar structures and microstylolites are present throughout the core. Minor grayish green (5G 5/2) and grayish blue (5PB 5/2) color banding is present in Section 5.

SMEAR SLIDE SUMMARY (%):

	3, 73
	D
TEXTURE:	
Sand	35
Silt	60
Clay	5
COMPOSITION:	
Foraminifers	22
Nannofossils	75
Radiolarians	3

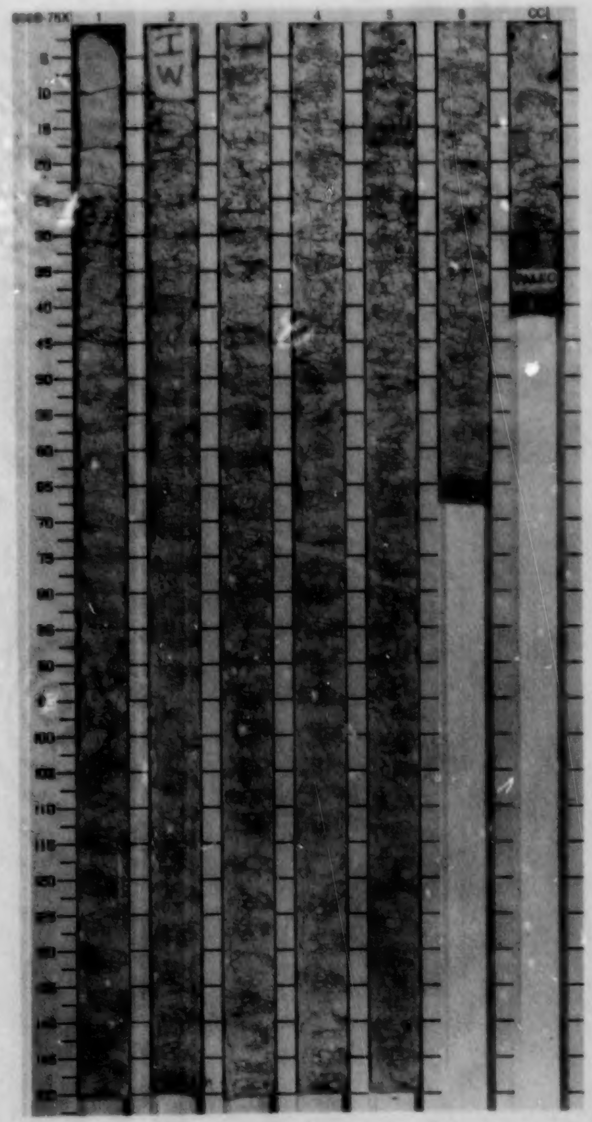
806B-75X
1
2
3
4
5
6
CC
HW
PALEO
5
10
15
20
25
30
35
40
45
50
55
60
65
70
75
80
85
90
95
100
105
110
115
120
125
130
135
140
145
150

SITE 806 HOLE B CORE 76X CORED INTERVAL 714.1-723.7 mbsf

TIME-ROCK UNIT	FORAMINIFERS	NANNOFOSSILS	RADIOLARIANS	DIATOMS	PALEOMAGNETICS	PHYS. PROPERTIES	CHEMISTRY	SECTION	METERS	SAMPLES
LOWER MIOCENE	N4	NN2	*Cyrtocapsella tetrapera*	NTD 1		● φ=48.8 γ=1.86	● %CaCO3=88.0	1	0.5 1.0	
						● φ=48.0 γ=1.90 Vp=2166	● %CaCO3=94.1	2		● OG IW
						● φ=46.3 γ=1.92	● %CaCO3=95.1	3		
	F/P	A/M	A/M	C/P-M				CC		

LITHOLOGIC DESCRIPTION

NANNOFOSSIL CHALK with FORAMINIFERS

Major lithology: This core contains moderately to heavily bioturbated, white (2.5Y 8/0) NANNOFOSSIL CHALK with FORAMINIFERS. Well developed *Zoophycos* trace fossils are common. Microstylolites and flaser structures also are common.

SMEAR SLIDE SUMMARY (%):

	2, 87 D
TEXTURE:	
Sand	30
Silt	65
Clay	5
COMPOSITION:	
Foraminifers	20
Nannofossils	78
Radiolarians	2

SITE 806 HOLE B CORE 77X CORED INTERVAL 723.7-733.4 mbsf

TIME-ROCK UNIT	FORAMINIFERS	NANNOFOSSILS	RADIOLARIANS	DIATOMS	PALEOMAGNETICS	PHYS. PROPERTIES	CHEMISTRY	SECTION	METERS	SAMPLES
LOWER MIOCENE		NN2	*Cyrtocapsella tetrapera*	NTD 1?						
		A/M	C/P	C/P				CC		●

LITHOLOGIC DESCRIPTION

NANNOFOSSIL CHALK with FORAMINIFERS

Major lithology: This core contains heavily mottled white (5YR 8/1) NANNOFOSSIL CHALK with FORAMINIFERS. Microstylolites are present.

SMEAR SLIDE SUMMARY (%):

	CC, 18 D
TEXTURE:	
Sand	30
Silt	65
Clay	5
COMPOSITION:	
Foraminifers	20
Nannofossils	78
Radiolarians	2

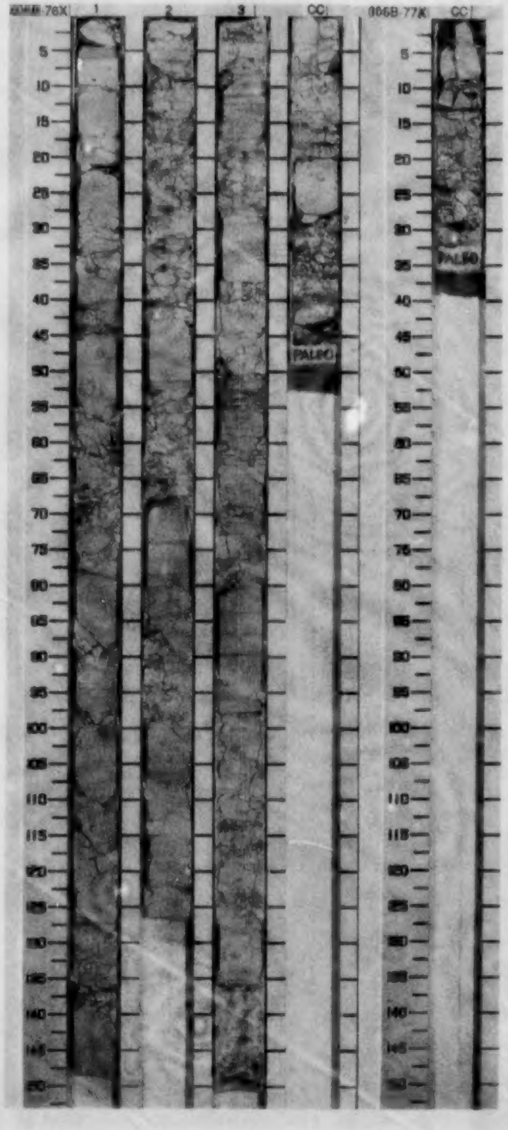

SITE 806 HOLE B CORE 78X CORED INTERVAL 733.4-743.1 mbsf

TIME-ROCK UNIT	BIOSTRAT. ZONE/ FOSSIL CHARACTER					PALEOMAGNETICS	PHYS. PROPERTIES	CHEMISTRY	SECTION	METERS	GRAPHIC LITHOLOGY	DRILLING DISTURB.	SED. STRUCTURES	SAMPLES
	FORAMINIFERS	NANNOFOSSILS	RADIOLARIANS	DIATOMS										
LOWER MIOCENE	N4 A/M	NN1 - NN2 A/P	D. stauchus - C. tetrapera C/P	? (almost Barren) R-B/P			● ϕ=48.0 γ=1.84 V-2235	● %CaCO$_3$ =83.0	1	0.5	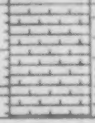	⊥ ⊥ ⊥ X X X		●
									CC					

LITHOLOGIC DESCRIPTION

NANNOFOSSIL CHALK with FORAMINIFERS

Major lithology: This core contains moderately bioturbated, white (5YR 8/1 and 5Y 8/1) NANNOFOSSIL CHALK with FORAMINIFERS. Gray (N6) microstylolites and flaser structures are present but not abundant.

SMEAR SLIDE SUMMARY (%):

	1, 45
	D
TEXTURE	
Sand	30
Silt	65
Clay	5
COMPOSITION	
Foraminifers	20
Nannofossils	78
Radiolarians	20

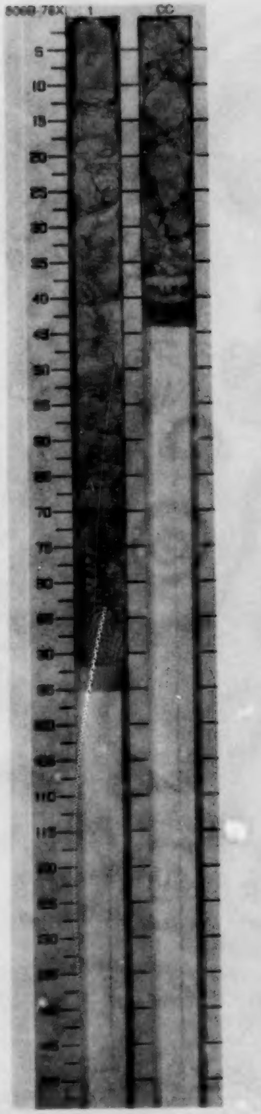
806B-78X
1
CC
5
10
15
20
25
30
35
40
45
50
55
60
65
70
75
80
85
90
95
100
105
110
115
120
125
130
135
140
145
150

SITE 806 HOLE C CORE 1H CORED INTERVAL 0.0-5.6 mbsf

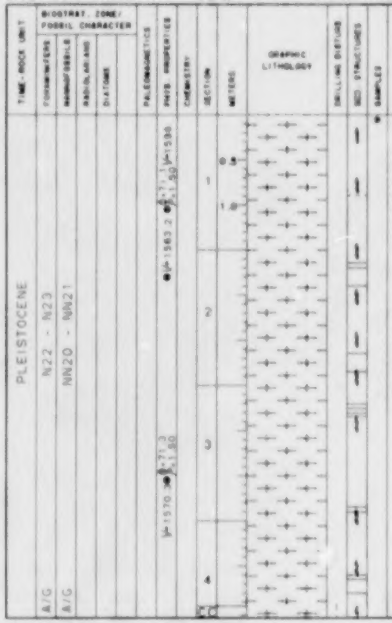

LITHOLOGIC DESCRIPTION

FORAMINIFER NANNOFOSSIL OOZE

Major lithology: This core contains FORAMINIFER NANNOFOSSIL OOZE, which grades from light gray (10YR 7/2) and very pale brown (10YR 7/3) to light gray (5Y 7/1) within Section 1. The remainder of the core is light gray (5Y 7/1 to 2.5Y 7/0) in color, with minor intervals of light olive gray (5Y 6/2). The entire core is moderately to heavily bioturbated, with grayish red purple (5RP 4/2) mottling. Diffuse cm scale, gray (N6), greenish gray (5G 6/1 and 5BG 5/1), and pale purple (5P 6/2) color bands are present.

SMEAR SLIDE SUMMARY (%):

	1, 7 D
TEXTURE:	
Sand	25
Silt	70
Clay	5
COMPOSITION:	
Foraminifers	45
Nannofossils	55

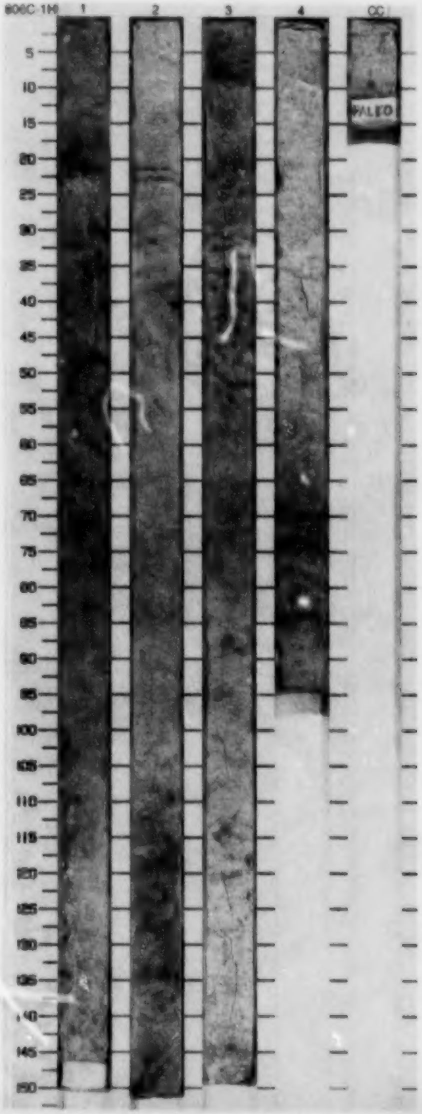
806C-1H
1
2
3
4
CC
PALEO
5
10
15
20
25
30
35
40
45
50
55
60
65
70
75
80
85
90
95
100
105
110
115
120
125
130
135
140
145
150

SITE 806 HOLE C CORE 2H CORED INTERVAL 5.6-15.1 mbsf

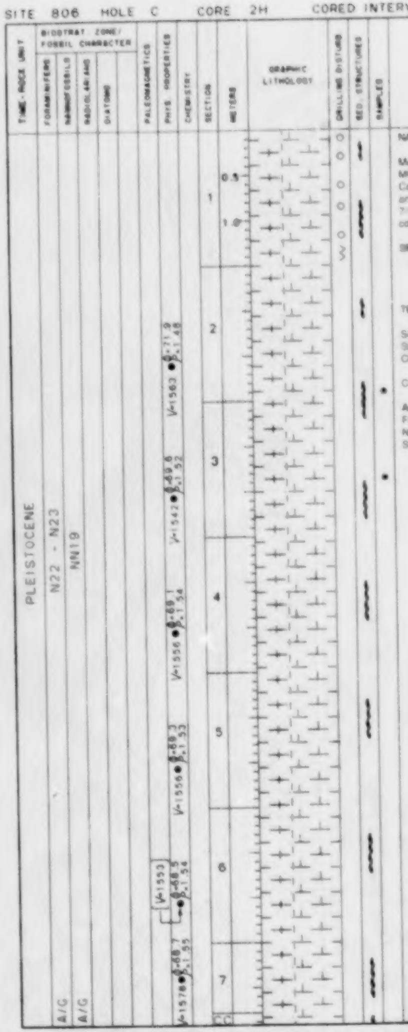
TIME-ROCK UNIT
BIOSTRAT. ZONE/ FOSSIL CHARACTER
FORAMINIFERS
NANNOFOSSILS
RADIOLARIANS
DIATOMS
PALEOMAGNETICS
PHYS. PROPERTIES
CHEMISTRY
SECTION
METERS
GRAPHIC LITHOLOGY
DRILLING DISTURB.
SED. STRUCTURES
SAMPLES
PLEISTOCENE
N22 - N23
NN19
A/G
A/G
V-1563 ● φ-71.9 ρ-1.48
V-1542 ● φ-69.6 ρ-1.52
V-1556 ● φ-68.1 ρ-1.54
V-1556 ● φ-68.3 ρ-1.53
V-1553
● φ-68.5 ρ-1.54
V-1578 ● φ-68.7 ρ-1.55
1
2
3
4
5
6
7
CC
0.5
1.0

LITHOLOGIC DESCRIPTION

NANNOFOSSIL OOZE with FORAMINIFERS and FORAMINIFER NANNOFOSSIL OOZE

Major lithology: This core contains 60% light gray (5Y 7/1) NANNOFOSSIL OOZE with FORAMINIFERS interbedded with 40% light gray (5Y 7/1) FORAMINIFER NANNOFOSSIL OOZE. Contacts between the two sediment types are graded. Evidence of bioturbation is abundant, including light gray (2.5Y 7/2) mottles and pyrite-filled burrows. Light greenish gray (5G 7/1) color bands, approximately 0.5 to 1 cm thick, are common. A few pale purple (5P 6/2) color bands are present.

SMEAR SLIDE SUMMARY (%):

	2, 140 D	3, 65 D
TEXTURE:		
Sand	25	6
Silt	60	60
Clay	15	34
COMPOSITION:		
Accessory minerals	—	2
Foraminifers	38	15
Nannofossils	60	80
Siliceous fragments	2	3

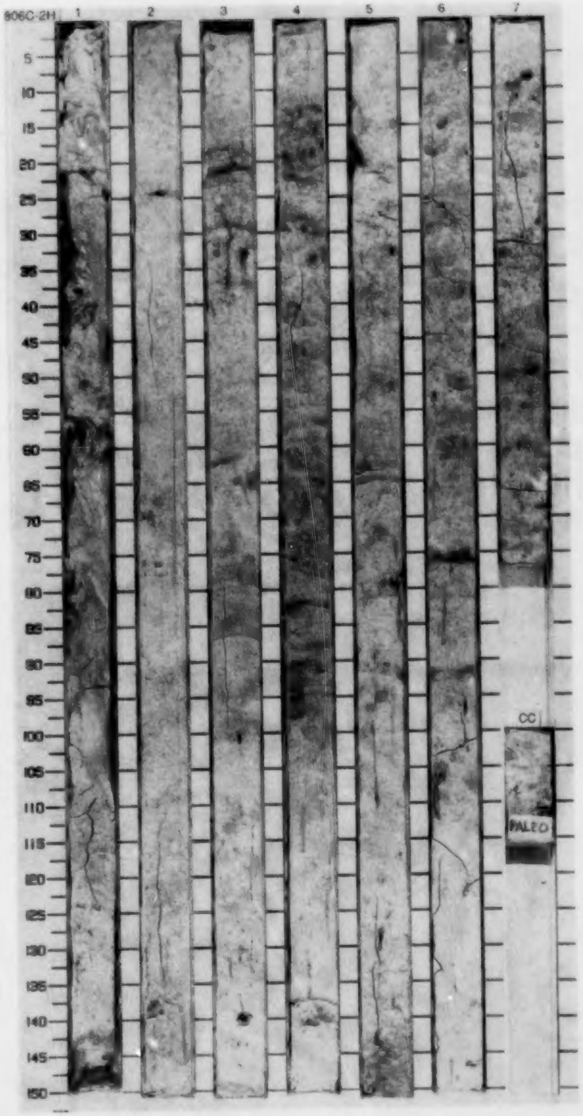
806C-2H
1
2
3
4
5
6
7
CC
PALEO
5
10
15
20
25
30
35
40
45
50
55
60
65
70
75
80
85
90
95
100
105
110
115
120
125
130
135
140
145
150

SITE 806 HOLE C CORE 3H CORED INTERVAL 15.1-24.6 mbsf

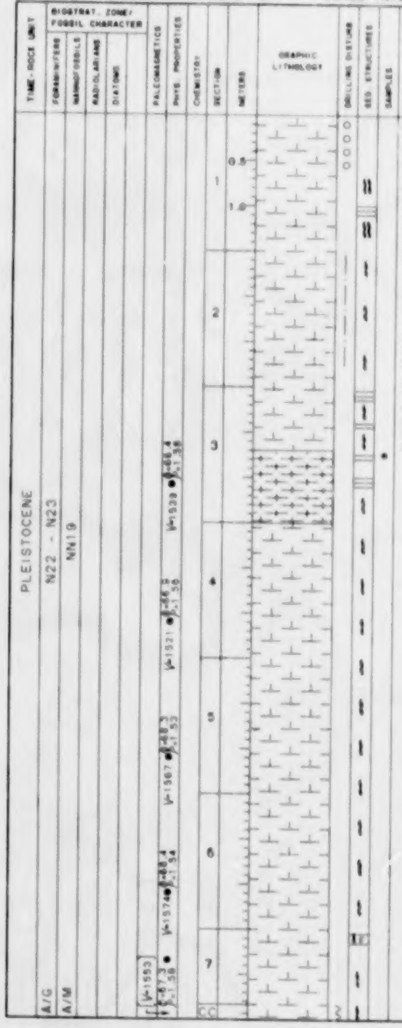
TIME-ROCK UNIT
BIOSTRAT. ZONE/ FOSSIL CHARACTER
FORAMINIFERS
NANNOFOSSILS
RADIOLARIANS
DIATOMS
PALEOMAGNETICS
PHYS. PROPERTIES
CHEMISTRY
SECTION
METERS
GRAPHIC LITHOLOGY
DRILLING DISTURB.
SED. STRUCTURES
SAMPLES
PLEISTOCENE
N22 - N23
NN19
A/G
A/M
V-1530
Φ-66.4
γ-1.58
V-1521
Φ-66.9
γ-1.56
V-1567
Φ-68.3
γ-1.53
V-1574
Φ-68.4
γ-1.54
V-1550
Φ-67.3
γ-1.58
1
2
3
4
5
6
7
CC
0.5
1.0

LITHOLOGIC DESCRIPTION

NANNOFOSSIL OOZE with FORAMINIFERS

Major lithology: This core contains NANNOFOSSIL OOZE with FORAMINIFERS. The ooze is predominantly white (2.5Y 8.0 to 2.5Y 8.2). Abundant burrow fills and light gray (2.5Y 7/1) mottles indicate extensive bioturbation. Some of the burrows contain pyrite or pale purple (5P 6/2) ooze. Pale purple (5P 6/2) streaks are associated with some burrows. Light greenish gray (5GY 7/1) bands, 1 cm thick, are common. The ooze has a slight H_2S odor.

Minor Lithology: The nannofossil ooze with foraminifers grades into a heavily bioturbated FORAMINIFER NANNOFOSSIL OOZE in Section 3, 70 to 150 cm.

SMEAR SLIDE SUMMARY (%):

	3, 75
	D
TEXTURE:	
Sand	15
Silt	60
Clay	25
COMPOSITION:	
Foraminifers	20
Nannofossils	77
Radiolarians	1
Siliceous fragments	2

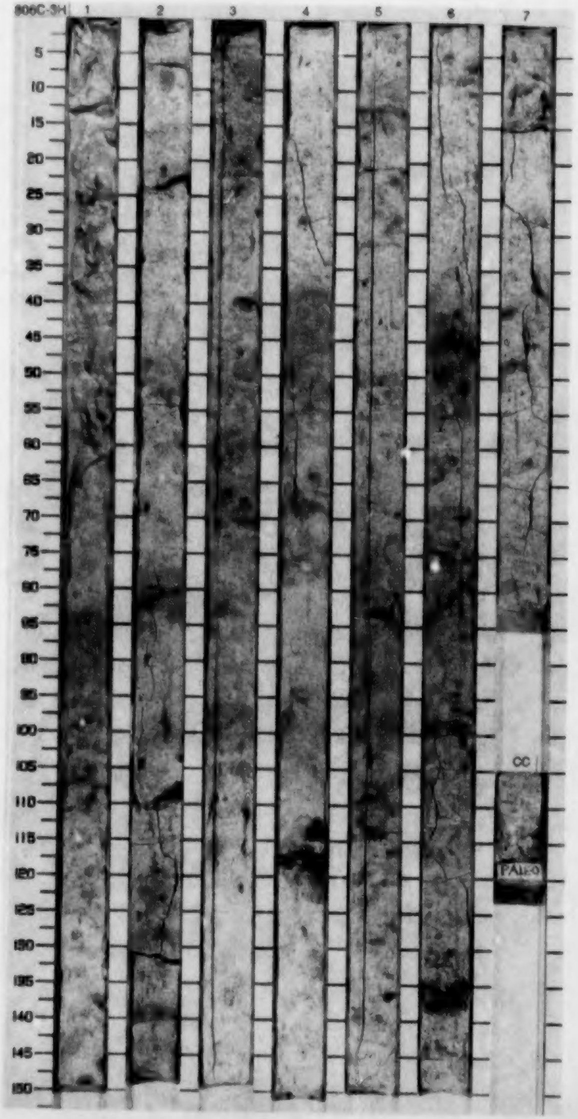
806C-3H
1
2
3
4
5
6
7
CC
PALEO
5
10
15
20
25
30
35
40
45
50
55
60
65
70
75
80
85
90
95
100
105
110
115
120
125
130
135
140
145
150

SITE 806 HOLE C CORE 4H CORED INTERVAL 24.6-34.1 mbsf

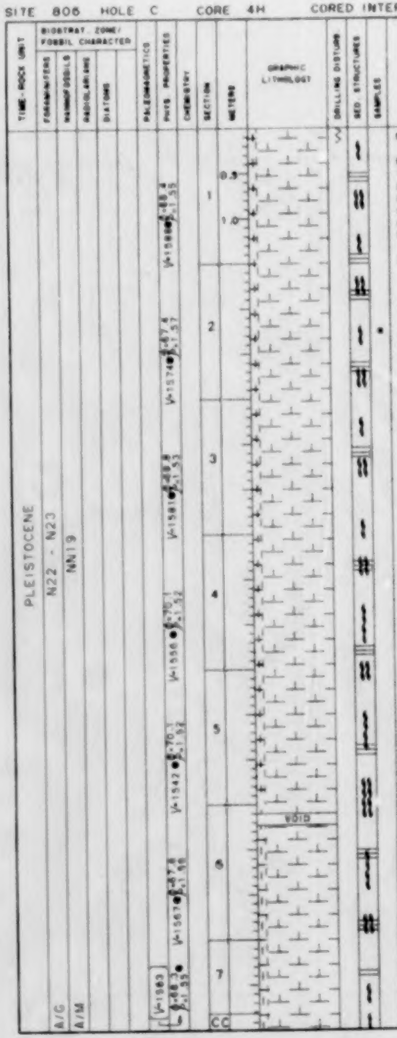

LITHOLOGIC DESCRIPTION

NANNOFOSSIL OOZE with FORAMINIFERS and FORAMINIFER NANNOFOSSIL OOZE

Major lithology: This core contains 90% NANNOFOSSIL OOZE with FORAMINIFERS and 10% FORAMINIFER NANNOFOSSIL OOZE, both of which are white (2.5Y 8/0) in color. The sediment is moderately to heavily bioturbated, as indicated by abundant light gray (5Y 7/2) mottles and burrows, disseminated pyritic pale purple (5P 6/2) burrows, and burrows filled with pyritized, dark gray (2.5Y 4/0) material that is coarser and softer than the surrounding sediment. Diffuse faint, greenish gray (5G 7/2) color bands (cm scale) are frequent throughout the core.

SMEAR SLIDE SUMMARY (%):

	2, 75
	D
TEXTURE:	
Sand	10
Silt	60
Clay	30
COMPOSITION:	
Foraminifers	10
Nannofossils	90
Radiolarians	Tr
Siliceous fragments	Tr

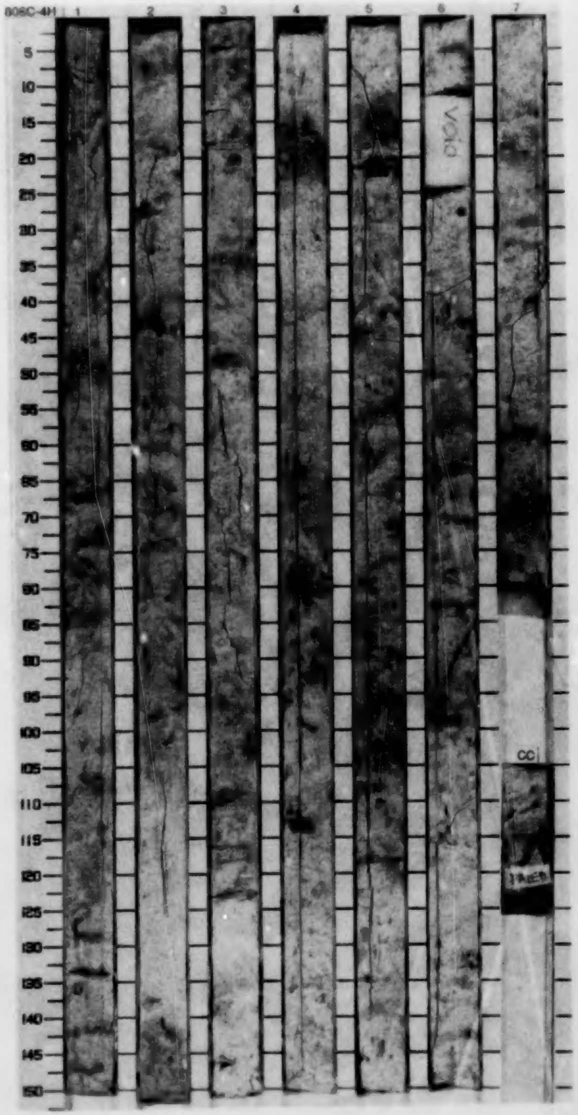
806C-4H
1
2
3
4
5
6
7
5
10
15
20
25
30
35
40
45
50
55
60
65
70
75
80
85
90
95
100
105
110
115
120
125
130
135
140
145
150
VOID
CC

SITE 806 HOLE C CORE 5H CORED INTERVAL 34.1-43.6 mbsf

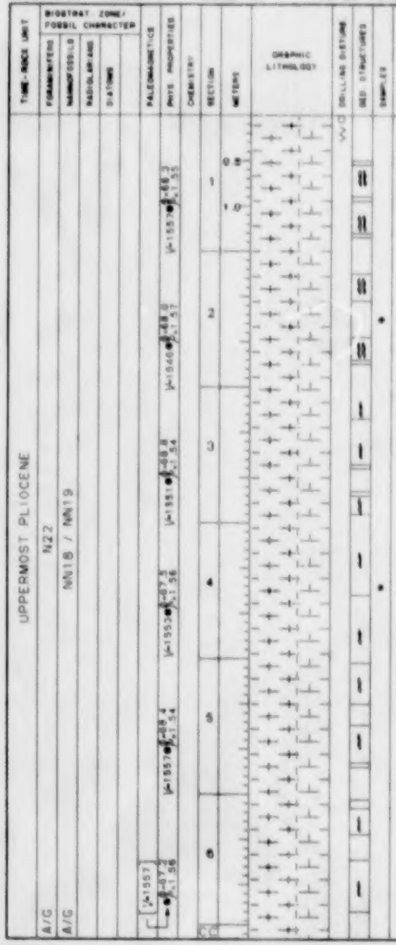
TIME-ROCK UNIT
BIOSTRAT. ZONE/FOSSIL CHARACTER
FORAMINIFERS
NANNOFOSSILS
RADIOLARIANS
DIATOMS
PALEOMAGNETICS
PHYS. PROPERTIES
CHEMISTRY
SECTION
METERS
GRAPHIC LITHOLOGY
DRILLING DISTURB.
SED. STRUCTURES
SAMPLES
UPPERMOST PLIOCENE
N22
NN18 / NN19
A/G
A/G
V=1553 ●-68.3 γ1.55
V=1546 ●-68.0 γ1.57
V=1551 ●-68.8 γ1.54
V=1553 ●-67.5 γ1.56
V=1557 ●-68.4 γ1.54
V=1557 ●-67.2 γ1.56
1
2
3
4
5
6
CC
0.5
1.0
VOID

LITHOLOGIC DESCRIPTION

FORAMINIFER NANNOFOSSIL OOZE and NANNOFOSSIL OOZE with FORAMINIFER

Major lithology: This core contains 60% FORAMINIFER NANNOFOSSIL OOZE interbedded with 40% NANNOFOSSIL OOZE with FORAMINIFERS, both white (2.5Y 8/0) in color. The ooze is heavily bioturbated with light gray (2.5Y 7/1) mottles, and pale purple (5P 6/2) pyrite specks. The ooze exhibits 1 cm thick, greenish gray (5G 7/2) and pale purple (5P 6/2) bands.

Minor lithology: Section 4, 83 cm, contains a thin, well sorted bed of FORAMINIFER OOZE.

SMEAR SLIDE SUMMARY (%):

	2, 75 D	4, 70 D
TEXTURE:		
Sand	10	15
Silt	50	60
Clay	40	25
COMPOSITION:		
Foraminifers	25	20
Nannofossils	72	78
Radiolarians	1	—
Siliceous fragments	2	2

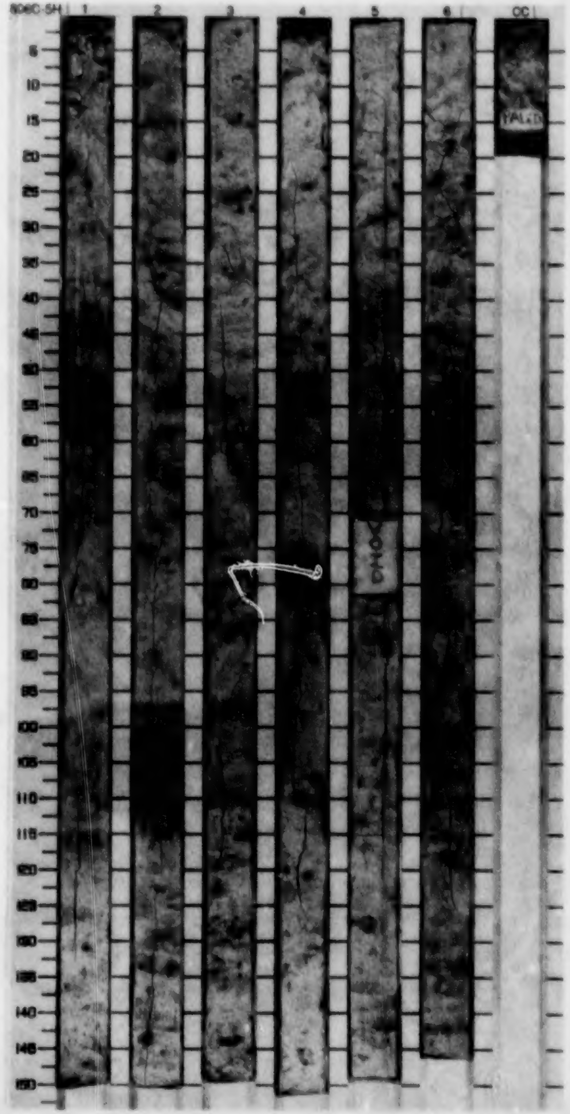
806C-5H
1
2
3
4
5
6
CC
5
10
15
20
25
30
35
40
45
50
55
60
65
70
75
80
85
90
95
100
105
110
115
120
125
130
135
140
145
150
PALEO
OHOX

SITE 806 HOLE C CORE 6H CORED INTERVAL 43.6-53.1 mbsf

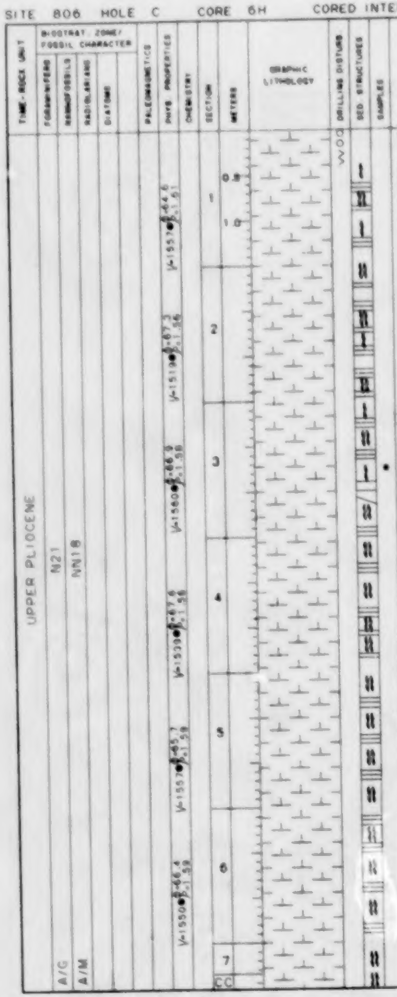
TIME-ROCK UNIT
BIOSTRAT. ZONE/ FOSSIL CHARACTER
FORAMINIFERS
NANNOFOSSILS
RADIOLARIANS
DIATOMS
PALEOMAGNETICS
PHYS. PROPERTIES
CHEMISTRY
SECTION
METERS
GRAPHIC LITHOLOGY
DRILLING DISTURB.
SED. STRUCTURES
SAMPLES
UPPER PLIOCENE
N21
NN18
A/G
A/M
V=1557 64.6 1.61
V=1519 67.3 1.56
V=1560 66.9 1.58
V=1539 67.6 1.58
V=1557 65.7 1.59
V=1550 66.4 1.59
1
2
3
4
5
6
7
CC
0.5
1.0

LITHOLOGIC DESCRIPTION

NANNOFOSSIL OOZE with FORAMINIFERS

Major lithology: This core contains white (2.5Y 8/0) NANNOFOSSIL OOZE with FORAMINIFERS. The ooze is heavily bioturbated, with light gray (2.5Y 7/1) mottles and pale purple (5P 6/2) pyrite specks and "halos". One cm thick, greenish gray (5G 7/2) and pale purple (5P 6/2) bands are common. Section 2, 2 to 4 cm, has a thin graded bed.

SMEAR SLIDE SUMMARY (%):

	3, 75
	D
TEXTURE:	
Sand	5
Silt	70
Clay	25
COMPOSITION:	
Diatoms	1
Foraminifers	20
Nannofossils	70
Radiolarians	3
Siliceous fragments	5

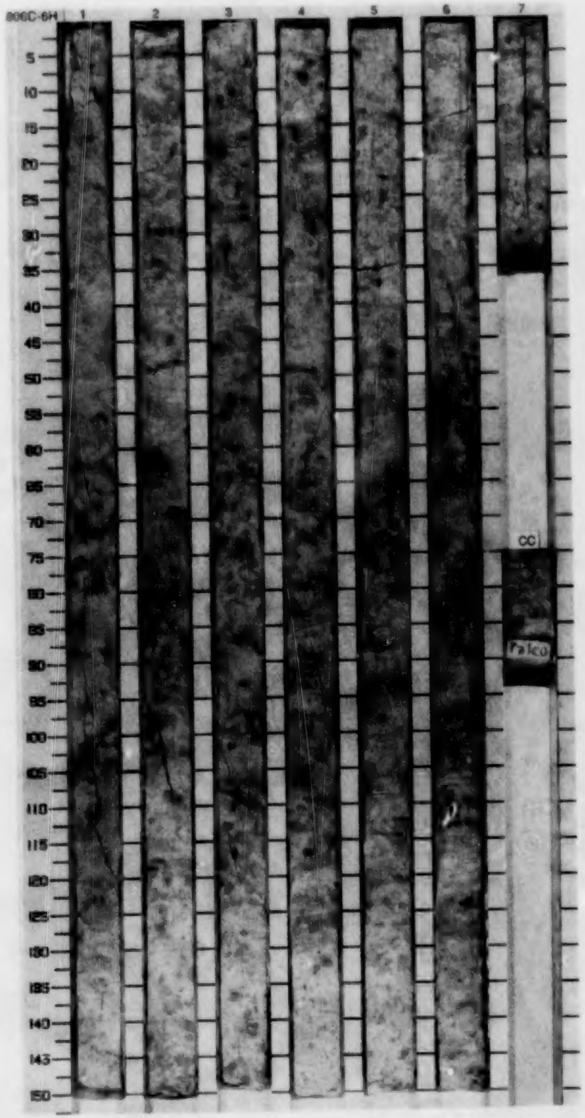
806C-6H
1
2
3
4
5
6
7
5
10
15
20
25
30
35
40
45
50
55
60
65
70
75
80
85
90
95
100
105
110
115
120
125
130
135
140
145
150
CC
Paleo

SITE 806 HOLE C CORE 7H CORED INTERVAL 53.1-62.6 mbsf

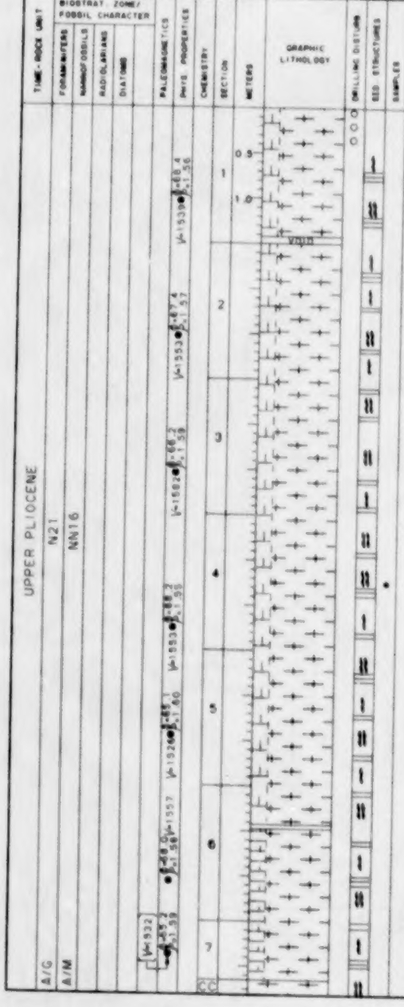
TIME-ROCK UNIT
BIOSTRAT. ZONE/ FOSSIL CHARACTER
FORAMINIFERS
NANNOFOSSILS
RADIOLARIANS
DIATOMS
PALEOMAGNETICS
PHYS. PROPERTIES
CHEMISTRY
SECTION
METERS
GRAPHIC LITHOLOGY
DRILLING DISTURB.
SED. STRUCTURES
SAMPLES
UPPER PLIOCENE
N21
NN16
A/G
A/M
V-1539
68.4
1.56
V-1553
67.4
1.57
V-1582
66.2
1.59
V-1553
68.2
1.55
V-1526
65.1
1.60
V-1557
68.0
1.58
V-1532
65.2
1.59
0.5
1.0
1
2
3
4
5
6
7
CC
VOID

LITHOLOGIC DESCRIPTION

NANNOFOSSIL OOZE with FORAMINIFERS interbedded with FORAMINIFER NANNOFOSSIL OOZE

Major lithology: This core contains about 75% FORAMINIFER NANNOFOSSIL OOZE interbedded with 25% NANNOFOSSIL OOZE with FORAMINIFERS. It is predominantly white (2.5Y 8/0) in color, with abundant light gray (5Y 7/2) and pale purple (5P 6/2) mottles and pyrite specks. These features indicate slight to moderate bioturbation. Several diffuse faint greenish gray (5G 7/1) and fewer pale purple (5P 6/2) color bands were observed. A 2 cm diameter pumice pebble was observed in Section 3, 52 to 54 cm. Trace amounts of volcanic glass were noted in the smear slide from Section 4.

SMEAR SLIDE SUMMARY (%):

	4, 75
	D
TEXTURE:	
Sand	20
Silt	50
Clay	30
COMPOSITION:	
Diatoms	Tr
Foraminifers	30
Glass	Tr
Nannofossils	70
Radiolarians	Tr

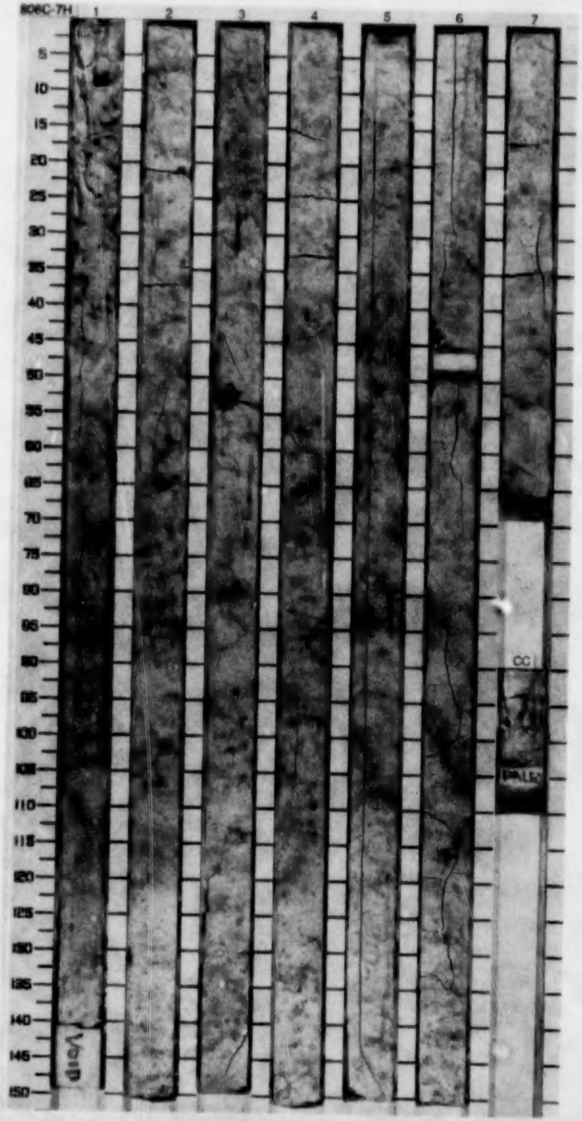
806C-7H
1
2
3
4
5
6
7
5
10
15
20
25
30
35
40
45
50
55
60
65
70
75
80
85
90
95
100
105
110
115
120
125
130
135
140
145
150
CC
PALEO
VOID

SITE 806 HOLE C CORE 8H CORED INTERVAL 62.6-72.1 mbsf

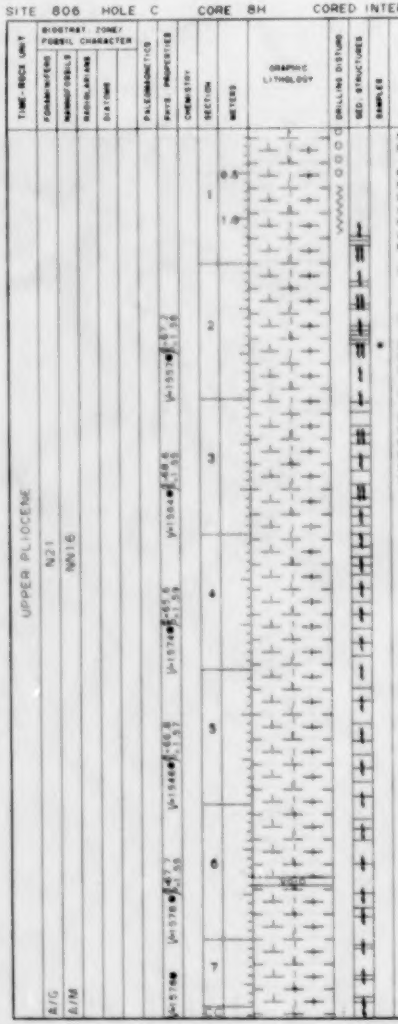
TIME-ROCK UNIT
BIOSTRAT. ZONE/ FOSSIL CHARACTER
FORAMINIFERS
NANNOFOSSILS
RADIOLARIANS
DIATOMS
PALEOMAGNETICS
PHYS. PROPERTIES
CHEMISTRY
SECTION
METERS
GRAPHIC LITHOLOGY
DRILLING DISTURB.
SED. STRUCTURES
SAMPLES
UPPER PLIOCENE
N21
NN16
A/G
A/M
V=1557● 67.2 1.56
V=1564● 68.6 1.55
V=1574● 65.6 1.59
V=1546● 66.8 1.57
V=1578● 67.7 1.55
V=1578●
1
2
3
4
5
6
7
CC
0.5
1.0
VOID

LITHOLOGIC DESCRIPTION

NANNOFOSSIL OOZE with FORAMINIFERS interbedded with FORAMINIFER NANNOFOSSIL OOZE

Major lithology: This core contains predominantly white (2.5Y 8/0 and 10YR 8/2) NANNOFOSSIL OOZE with FORAMINIFERS interbedded with FORAMINIFER NANNOFOSSIL OOZE, but the color often grades between white (2.5Y 8/0) and light gray (5Y 7/1). The sediment is moderately to heavily bioturbated, with light gray (5Y 7/2), and pale purple (5P 6/2) mottling common throughout. Faint grayish green (5G 7/2), light greenish gray (5G 7/1), and grayish blue (5PB 5/2) color bands are evident. Long (>10 cm), dipping, grayish blue bands appear in Sections 3 and 4, possibly as parts of burrow "holes".

SMEAR SLIDE SUMMARY (%):

	2, 91
	D
TEXTURE:	
Sand	15
Silt	81
Clay	4
COMPOSITION:	
Diatoms	1
Foraminifers	20
Nannofossils	73
Radiolarians	3
Silicoflagellates	2
Spicules	1

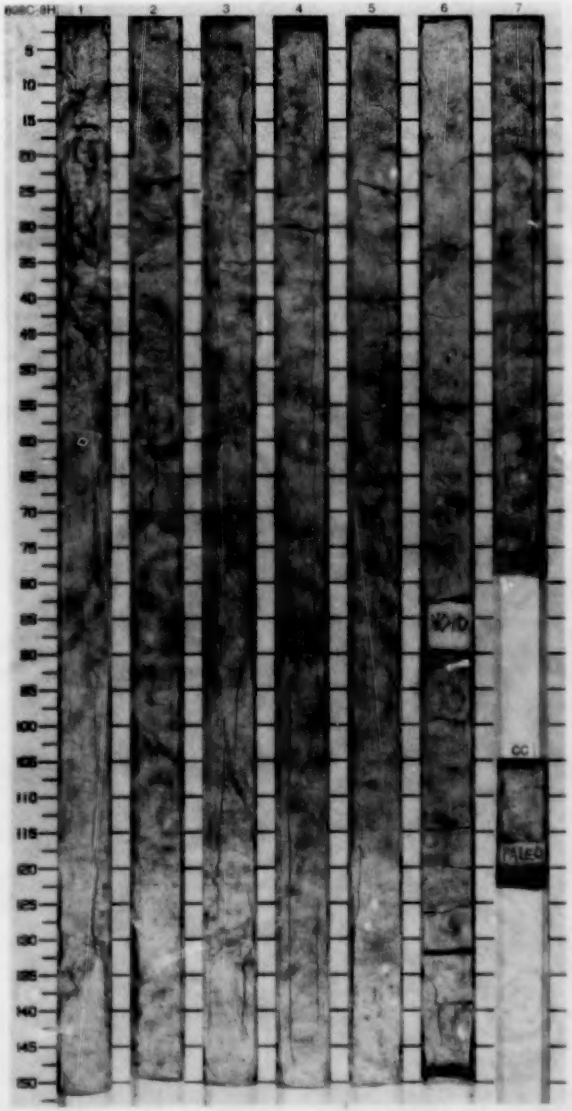
806C-8H
1
2
3
4
5
6
7
5
10
15
20
25
30
35
40
45
50
55
60
65
70
75
80
85
90
95
100
105
110
115
120
125
130
135
140
145
150
IW/OD
CC
PALEO

SITE 806 HOLE C CORE 9H CORED INTERVAL 72.1-81.6 mbsf

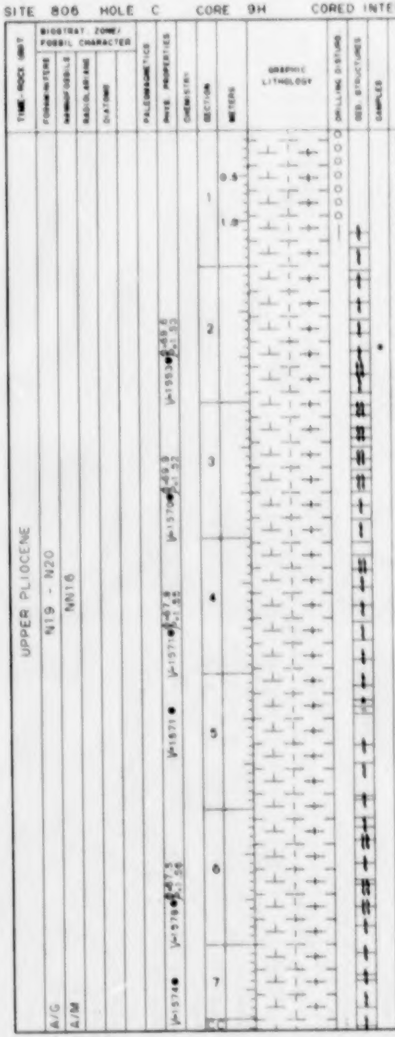
TIME-ROCK UNIT
BIOSTRAT. ZONE/ FOSSIL CHARACTER
FORAMINIFERS
NANNOFOSSILS
RADIOLARIANS
DIATOMS
PALEOMAGNETICS
PHYS. PROPERTIES
CHEMISTRY
SECTION
METERS
GRAPHIC LITHOLOGY
DRILLING DISTURB.
SED. STRUCTURES
SAMPLES
UPPER PLIOCENE
N19 - N20
NN16
A/G
A/M
0.5
1.0
1
2
3
4
5
6
7
CC

LITHOLOGIC DESCRIPTION

NANNOFOSSIL OOZE with FORAMINIFERS interbedded with FORAMINIFER NANNOFOSSIL OOZE

Major lithology: This core contains white (2.5Y 8/0 and 10YR 8/2) NANNOFOSSIL OOZE FORAMINIFERS interbedded with FORAMINIFER NANNOFOSSIL OOZE. The sediment is moderately to heavily bioturbated, with light gray (5Y 7/2) and grayish blue (5PB 5/2) mottles. Faint and diffuse, grayish green (5G 7/2), light greenish gray (5G 7/1), and grayish blue (5PB 5/2) color bands are present throughout.

SMEAR SLIDE SUMMARY (%):

	2, 90
	D
TEXTURE:	
Sand	15
Silt	80
Clay	5
COMPOSITION:	
Foraminifers	11
Nannofossils	85
Radiolarians	3
Silicoflagellates	1

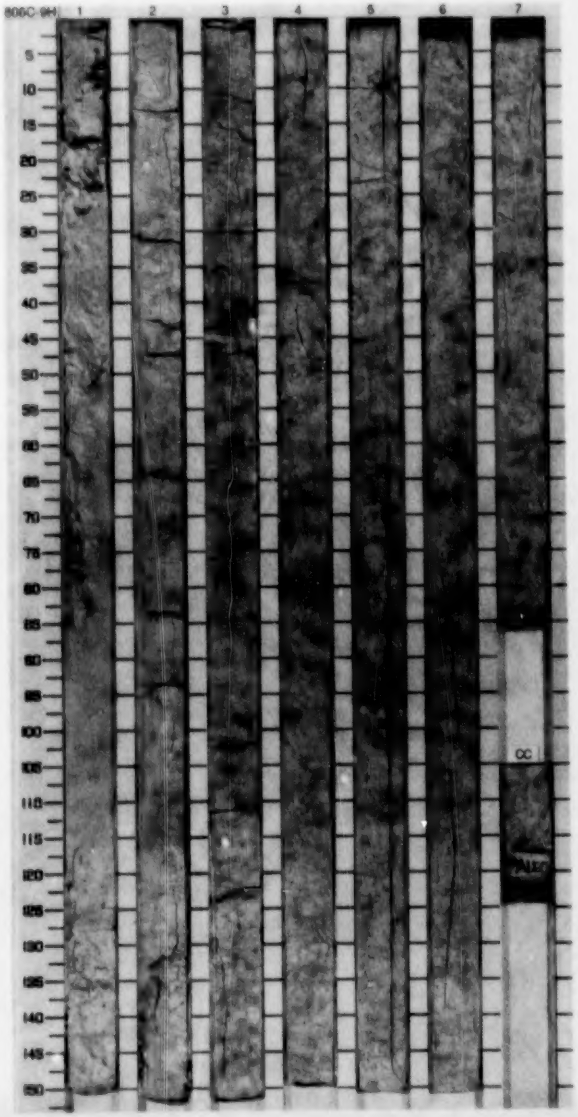
806C-9H
1
2
3
4
5
6
7
CC
PALEO
5
10
15
20
25
30
35
40
45
50
55
60
65
70
75
80
85
90
95
100
105
110
115
120
125
130
135
140
145
150

SITE 806 HOLE C CORE 10H CORED INTERVAL 81.6-91.1 mbsf

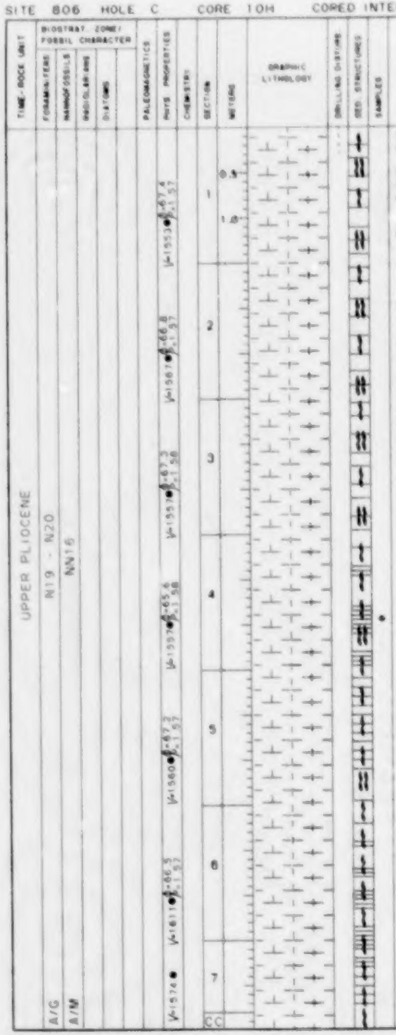
TIME-ROCK UNIT
BIOSTRAT. ZONE/ FOSSIL CHARACTER
FORAMINIFERS
NANNOFOSSILS
RADIOLARIANS
DIATOMS
PALEOMAGNETICS
PHYS. PROPERTIES
CHEMISTRY
SECTION
METERS
GRAPHIC LITHOLOGY
DRILLING DISTURB.
SED. STRUCTURES
SAMPLES
UPPER PLIOCENE
N19 - N20
NN16
A/G
A/M
V=1553● φ=67.4 ρ=1.57
V=1567● φ=66.8 ρ=1.57
V=1557● φ=67.3 ρ=1.58
V=1557● φ=65.6 ρ=1.58
V=1560● φ=67.2 ρ=1.57
V=1611● φ=66.5 ρ=1.57
V=1574●
1
2
3
4
5
6
7
CC
0.5
1.0

LITHOLOGIC DESCRIPTION

NANNOFOSSIL OOZE with FORAMINIFERS interbedded with FORAMINIFER NANNOFOSSIL OOZE

Major lithology: This core contains white (2.5Y 8/0 and 5Y 8/1) NANNOFOSSIL OOZE with FORAMINIFERS interbedded with FORAMINIFER NANNOFOSSIL OOZE, which have light gray (5Y 7/2) and grayish blue (5PB 5/2) mottles. The sediment is moderately to heavily bioturbated. Numerous faint and diffuse, grayish green (5G 7/2), light greenish gray (5G 7/1), and grayish blue (5PB 5/2) color bands are present throughout. Inclined, grayish blue color bands in Section 1 may be part of burrow "halos."

SMEAR SLIDE SUMMARY (%):

	4, 96
	D
TEXTURE:	
Sand	20
Silt	75
Clay	5
COMPOSITION:	
Foraminifers	15
Nannofossils	82
Radiolarians	2
Silicoflagellates	1

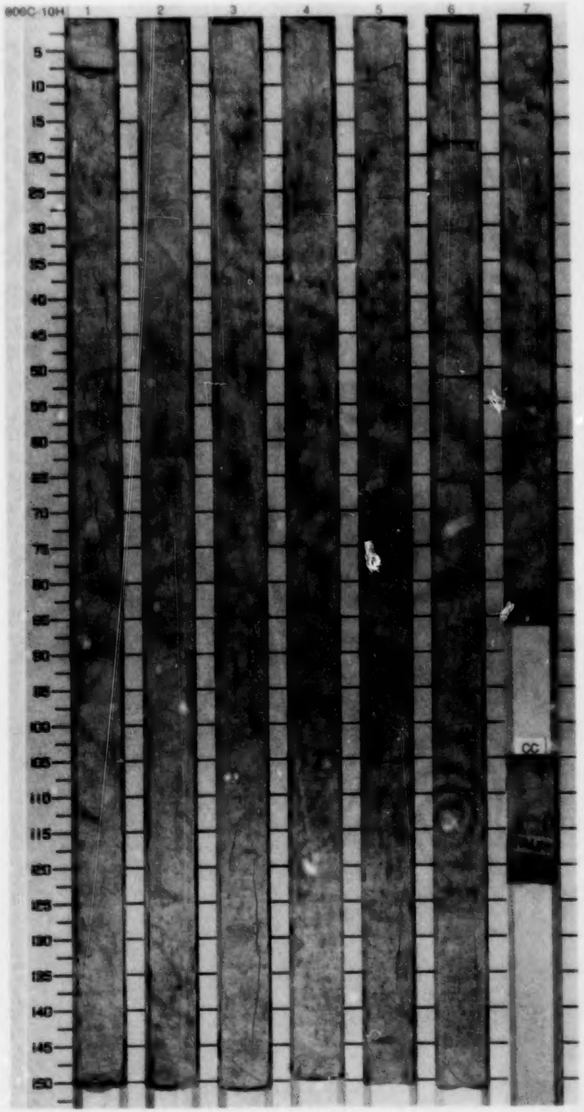
806C-10H
1
2
3
4
5
6
7
5
10
15
20
25
30
35
40
45
50
55
60
65
70
75
80
85
90
95
100
105
110
115
120
125
130
135
140
145
150
CC

SITE 806 HOLE C CORE 11H CORED INTERVAL 91.1-100.6 mbsf

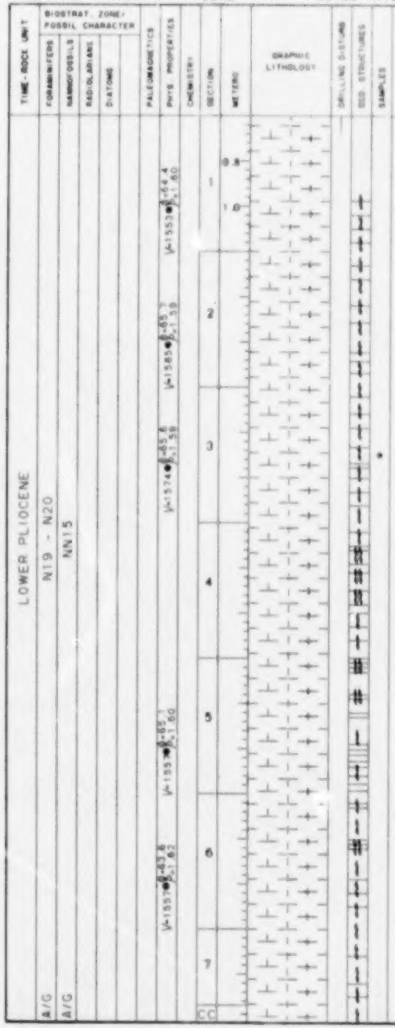
TIME-ROCK UNIT
BIOSTRAT. ZONE/ FOSSIL CHARACTER
FORAMINIFERS
NANNOFOSSILS
RADIOLARIANS
DIATOMS
PALEOMAGNETICS
PHYS. PROPERTIES
CHEMISTRY
SECTION
METERS
GRAPHIC LITHOLOGY
DRILLING DISTURB.
SED. STRUCTURES
SAMPLES
LOWER PLIOCENE
N19 - N20
NN15
A/G
A/G
V=1553 64.4 1.60
V=1585 65.7 1.59
V=1574 65.6 1.59
V=155 65.1 1.60
V=1557 63.6 1.62
1
2
3
4
5
6
7
CC
0.5
1.0

LITHOLOGIC DESCRIPTION

NANNOFOSSIL OOZE with FORAMINIFERS interbedded with FORAMINIFER NANNOFOSSIL OOZE

Major lithology: This core contains white (2.5Y 8/0) to light gray (5Y 7/1) NANNOFOSSIL OOZE with FORAMINIFERS interbedded with FORAMINIFER NANNOFOSSIL OOZE. The sediment is moderately to heavily bioturbated, with light gray (5Y 7/2) and grayish blue (5PB 5/2) mottles. Numerous faint and diffuse, grayish green (5G 7/2), light greenish gray (5G 7/1) and grayish blue (5PB 5/2) color bands, as well as burrow "halos", are present throughout.

SMEAR SLIDE SUMMARY (%):

	3, 75
	D
TEXTURE:	
Sand	5
Silt	90
Clay	5
COMPOSITION:	
Foraminifers	15
Nannofossils	84
Radiolarians	1

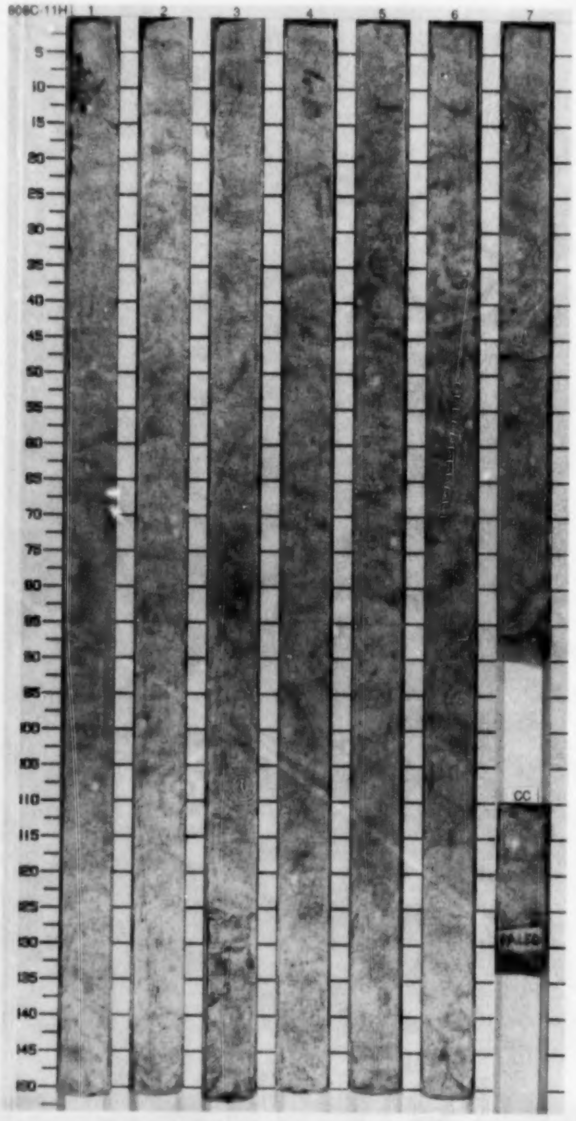
806C-11H
1
2
3
4
5
6
7
CC
5
10
15
20
25
30
35
40
45
50
55
60
65
70
75
80
85
90
95
100
105
110
115
120
125
130
135
140
145
150

SITE 806 HOLE C CORE 12H CORED INTERVAL 100.6-110.1 mbsf

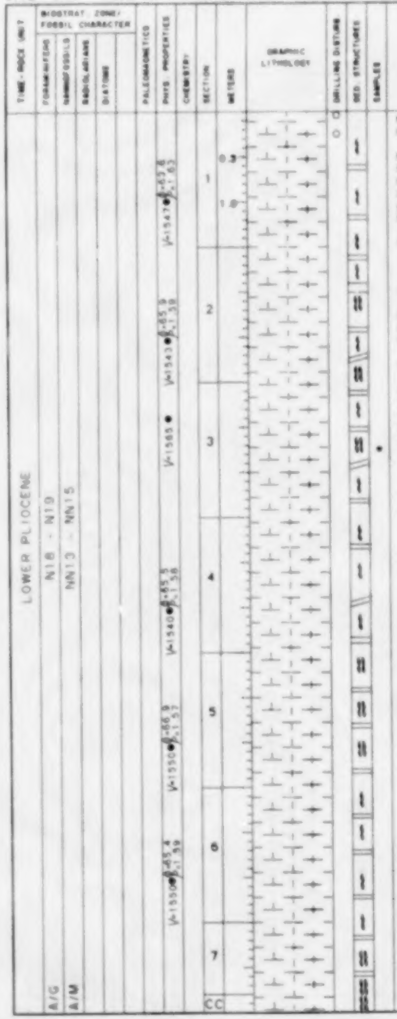
TIME-ROCK UNIT
BIOSTRAT. ZONE/ FOSSIL CHARACTER
FORAMINIFERS
NANNOFOSSILS
RADIOLARIANS
DIATOMS
PALEOMAGNETICS
PHYS. PROPERTIES
CHEMISTRY
SECTION
METERS
GRAPHIC LITHOLOGY
DRILLING DISTURB.
SED. STRUCTURES
SAMPLES
LOWER PLIOCENE
N18 - N19
NN13 - NN15
A/G
A/M
V=1547 ● φ=65.8 γ=1.63
V=1543 ● φ=65.9 γ=1.58
V=1565 ●
V=1540 ● φ=65.5 γ=1.56
V=1550 ● φ=66.9 γ=1.57
V=1550 ● φ=65.4 γ=1.59
1
2
3
4
5
6
7
CC
0.5
1.0

LITHOLOGIC DESCRIPTION

NANNOFOSSIL OOZE with FORAMINIFERS interbedded with FORAMINIFER NANNOFOSSIL OOZE

Major lithology: This core contains white (5Y 8/1) NANNOFOSSIL OOZE with FORAMINIFERS interbedded with FORAMINIFER NANNOFOSSIL OOZE. Moderate to heavy bioturbation is evident from abundant light gray (5Y 7/2) mottles, and pyritized burrow fills and specks. Some burrows exhibit pale purple (5P 6/2) halos. Diffuse, faint, cm thick, greenish gray (5G 7/1) color bands are frequently present; pale purple bands are less frequent throughout the core. In Sections 2, 3 and 4, a few dipping color bands were observed.

SMEAR SLIDE SUMMARY (%):

	3, 74
	D
TEXTURE	
Sand	12
Silt	55
Clay	33
COMPOSITION	
Accessory minerals	2
Foraminifers	26
Nannofossils	69
Radiolarians	Tr
Siliceous fragments	3

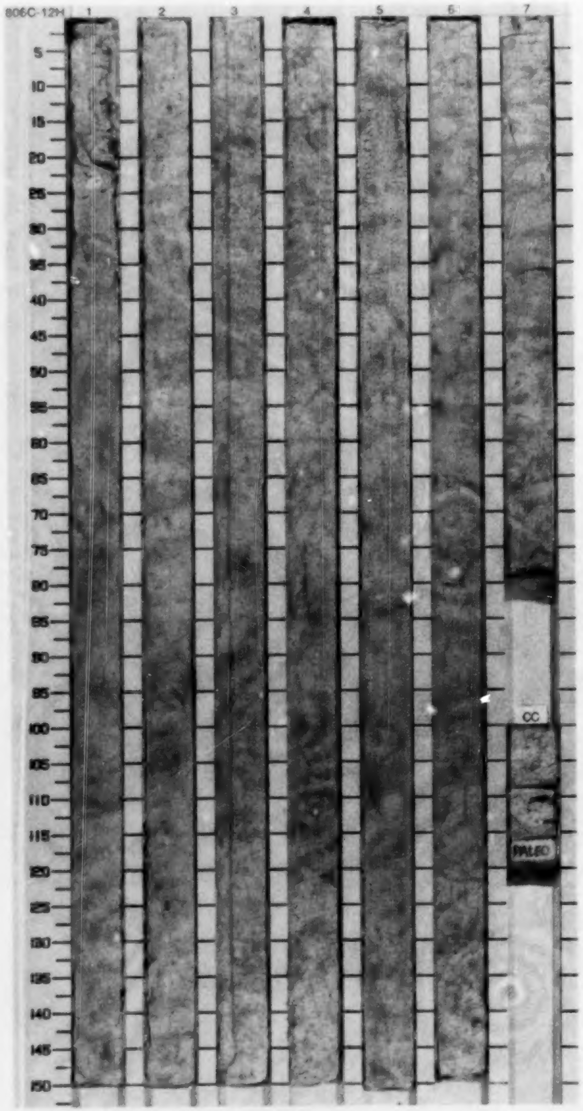
806C-12H
1
2
3
4
5
6
7
5
10
15
20
25
30
35
40
45
50
55
60
65
70
75
80
85
90
95
100
105
110
115
120
125
130
135
140
145
150
CC
PALEO

SITE 806 HOLE C CORE 13H CORED INTERVAL 110.1-119.6 mbsf

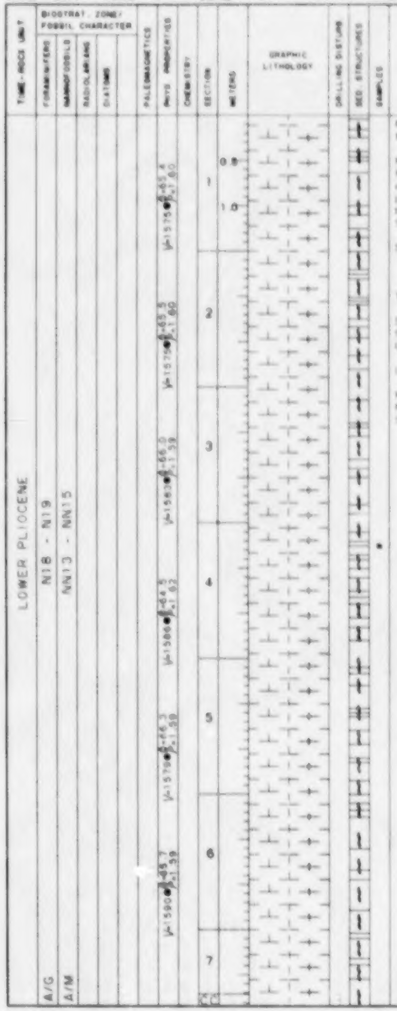
TIME-ROCK UNIT
BIOSTRAT. ZONE/ FOSSIL CHARACTER
FORAMINIFERS
NANNOFOSSILS
RADIOLARIANS
DIATOMS
PALEOMAGNETICS
PHYS. PROPERTIES
CHEMISTRY
SECTION
METERS
GRAPHIC LITHOLOGY
DRILLING DISTURB.
SED. STRUCTURES
SAMPLES
LOWER PLIOCENE
N18 - N19
NN13 - NN15
A/G
A/M
V=1575 φ=65.4 γ=1.60
V=1575 φ=65.5 γ=1.60
V=1583 φ=66.0 γ=1.59
V=1586 φ=64.5 γ=1.62
V=1579 φ=66.3 γ=1.59
V=1590 φ=65.7 γ=1.59
1
2
3
4
5
6
7
CC
0.8
1.0

LITHOLOGIC DESCRIPTION

NANNOFOSSIL OOZE with FORAMINIFERS interbedded with FORAMINIFER NANNOFOSSIL OOZE

Major lithology: This core contains white (5Y 8/1) NANNOFOSSIL OOZE with FORAMINIFERS interbedded with FORAMINIFER NANNOFOSSIL OOZE. Moderate bioturbation is evident from abundant light gray (5Y 7/1 to 5Y 7/2) mottles and grayish blue (5PB 5/2) pyritized burrow fills and specks. Diffuse, cm thick, light greenish gray (5G 7/1) and grayish blue (5PB 5/2) color bands are frequently observed. Long (10 to 20 cm) grayish blue (5PB 5/2) vertical bands and burrow "halos" are noted.

SMEAR SLIDE SUMMARY (%):

	4, 27
	D
TEXTURE:	
Sand	5
Silt	90
Clay	5
COMPOSITION:	
Foraminifers	12
Nannofossils	87
Silicoflagellates	1

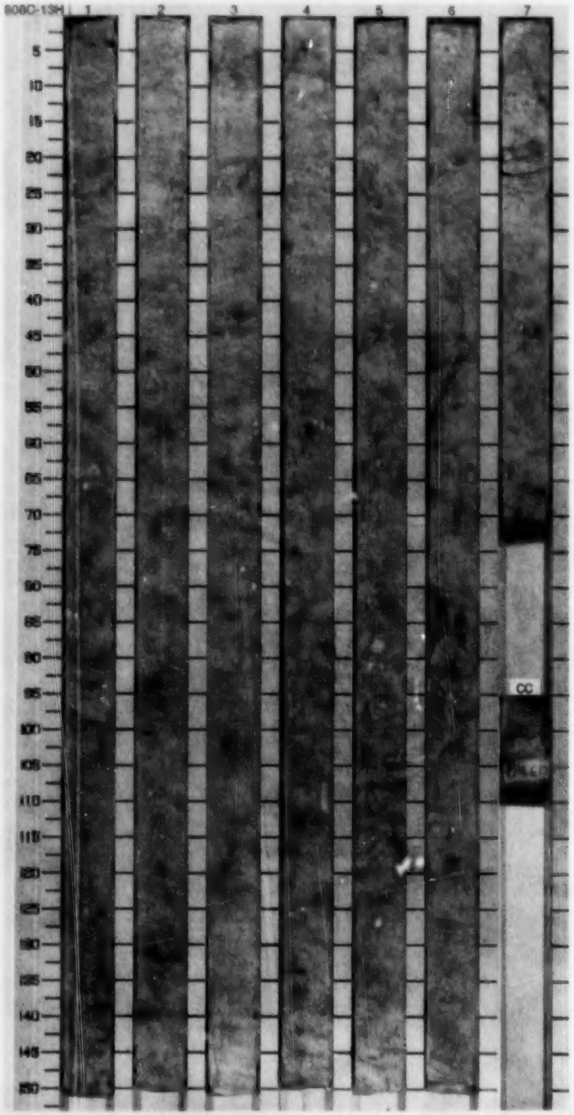
806C-13H
1
2
3
4
5
6
7
CC
5
10
15
20
25
30
35
40
45
50
55
60
65
70
75
80
85
90
95
100
105
110
115
120
125
130
135
140
145
150

SITE 806 HOLE C CORE 14H CORED INTERVAL 119.6-129.1 mbsf

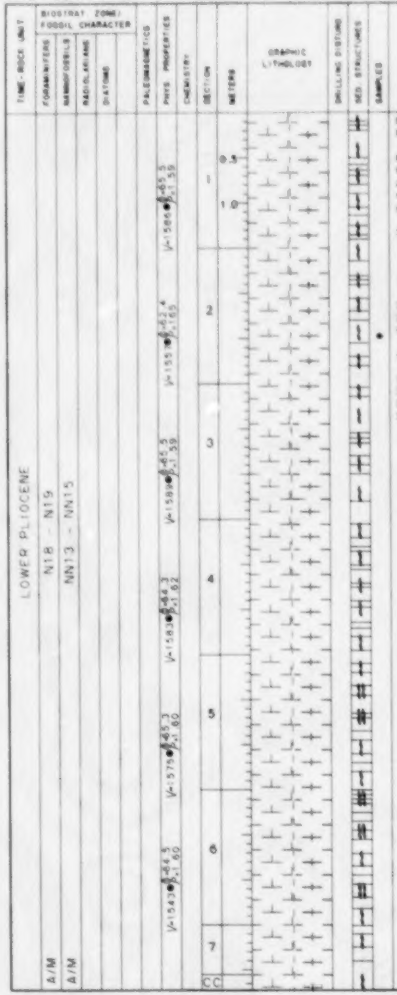
TIME-ROCK UNIT
BIOSTRAT. ZONE/ FOSSIL CHARACTER
FORAMINIFERS
NANNOFOSSILS
RADIOLARIANS
DIATOMS
PALEOMAGNETICS
PHYS. PROPERTIES
CHEMISTRY
SECTION
METERS
GRAPHIC LITHOLOGY
DRILLING DISTURB.
SED. STRUCTURES
SAMPLES
LOWER PLIOCENE
N18 - N19
NN13 - NN15
A/M
A/M
V=1586 ● φ=65.5 ρ=1.59
V=1551 ● φ=62.4 ρ=1.65
V=1589 ● φ=65.5 ρ=1.59
V=1583 ● φ=64.3 ρ=1.62
V=1575 ● φ=65.3 ρ=1.60
V=1543 ● φ=64.5 ρ=1.60
1
2
3
4
5
6
7
CC
0.5
1.0

LITHOLOGIC DESCRIPTION

NANNOFOSSIL OOZE with FORAMINIFERS interbedded with FORAMINIFER NANNOFOSSIL OOZE

Major lithology: This core contains white (5Y 8/1) NANNOFOSSIL OOZE with FORAMINIFERS interbedded with FORAMINIFER NANNOFOSSIL OOZE. The sediments are moderately to heavily bioturbated, with light gray (5Y 7/1, 5Y 7/2 and N7) and grayish blue (5PB 5/2) mottling and pyritized burrow linings common throughout. Diffuse, cm thick, light greenish gray (5G 7/1) and grayish blue (5PB 5/2) color bands also are common.

SMEAR SLIDE SUMMARY (%):

	2, 98
	D
TEXTURE:	
Sand	15
Silt	80
Clay	5
COMPOSITION:	
Foraminifers	10
Nannofossils	87
Radiolarians	2
Silicoflagellates	1

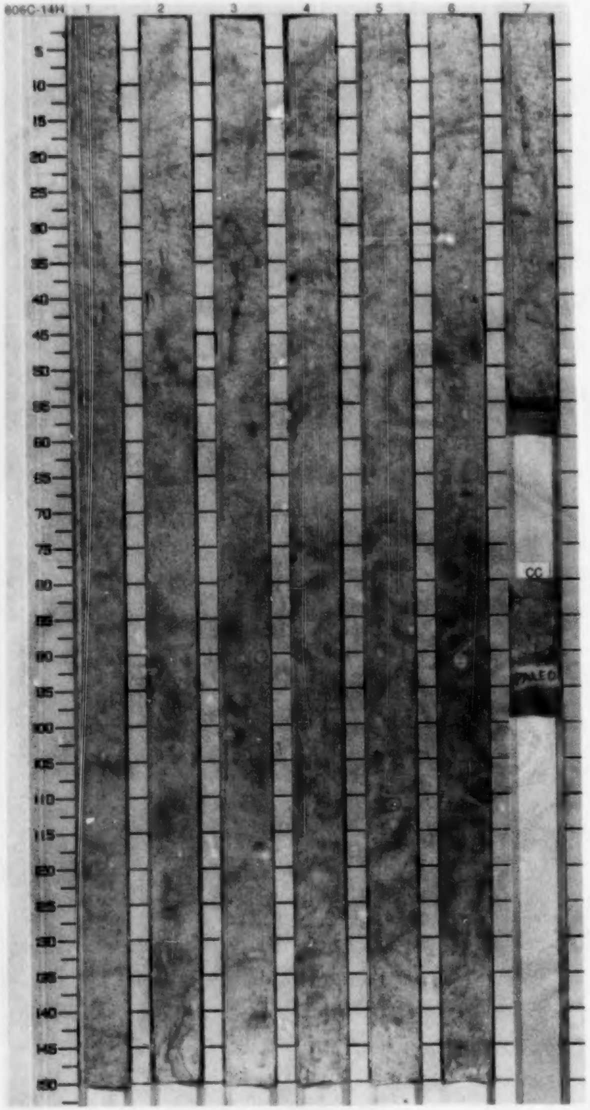
806C-14H
1
2
3
4
5
6
7
5
10
15
20
25
30
35
40
45
50
55
60
65
70
75
80
85
90
95
100
105
110
115
120
125
130
135
140
145
150
CC
PALEO

SITE 806 HOLE C CORE 15H CORED INTERVAL 129.1-138.6 mbsf

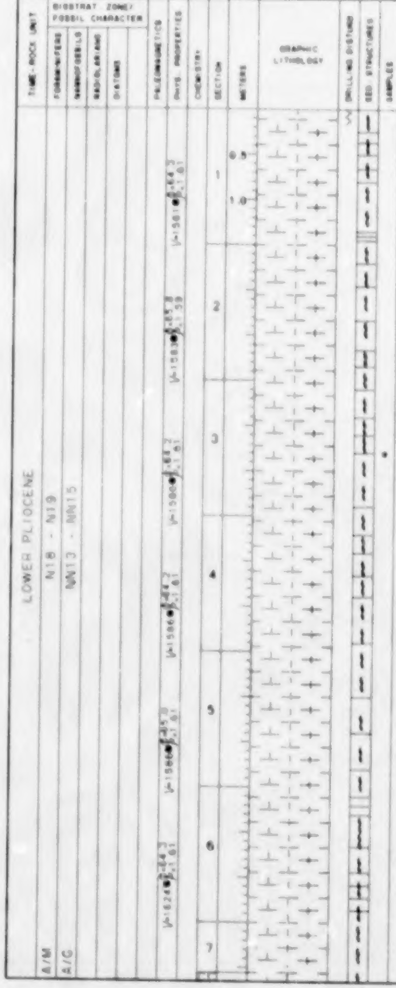

LITHOLOGIC DESCRIPTION

NANNOFOSSIL OOZE with FORAMINIFERS interbedded with FORAMINIFER NANNOFOSSIL OOZE

Major lithology: This core contains white (5Y 8/1 and 2.5Y 8/0) NANNOFOSSIL OOZE with FORAMINIFERS interbedded with FORAMINIFER NANNOFOSSIL OOZE. The sediments are moderately to heavily bioturbated, with light gray (5Y 7/1, 5Y 7/2 and N7/), cm scale (mainly horizontal) mottles. Grayish blue (5PB 5/2) and pale purple (5P 6/2) mottling and pyritized burrow linings appear frequently throughout the core. Diffuse, cm thick, light greenish gray (5G 7/1), pale purple (5P 6/2) and grayish blue (5PB 5/2) color bands are common.

SMEAR SLIDE SUMMARY (%)

	3, 77 D
TEXTURE	
Sand	5
Silt	90
Clay	5
COMPOSITION	
Foraminifers	12
Nannofossils	85
Radiolarians	1
Siliceous fragments	1
Silicoflagellates	1

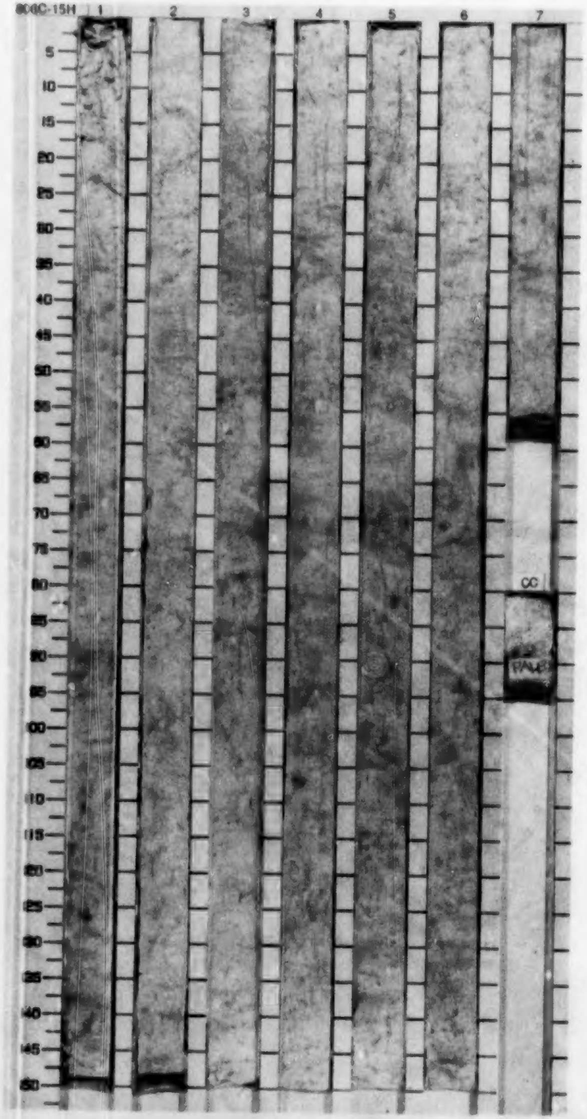
806C-15H
1
2
3
4
5
6
7
CC
PALEO
5
10
15
20
25
30
35
40
45
50
55
60
65
70
75
80
85
90
95
100
105
110
115
120
125
130
135
140
145
150

SITE 806 HOLE C CORE 16H CORED INTERVAL 138.6-148.1 mbsf

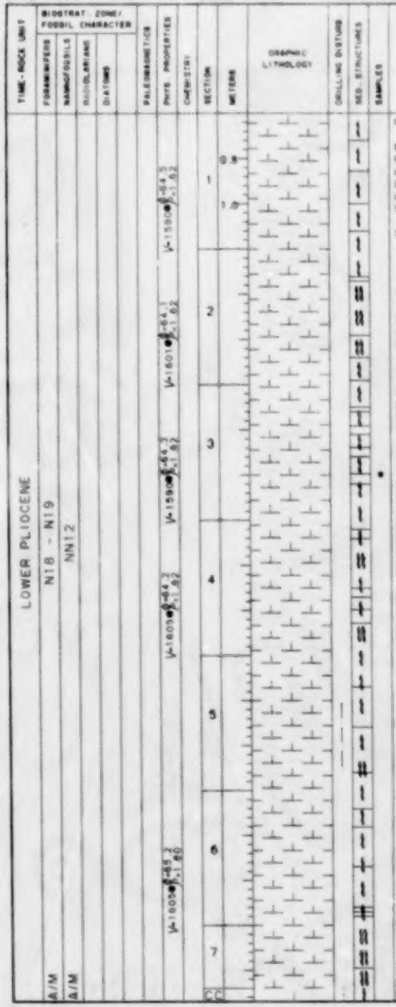
TIME-ROCK UNIT
BIOSTRAT. ZONE/ FOSSIL CHARACTER
FORAMINIFERS
NANNOFOSSILS
RADIOLARIANS
DIATOMS
PALEOMAGNETICS
PHYS. PROPERTIES
CHEMISTRY
SECTION
METERS
GRAPHIC LITHOLOGY
DRILLING DISTURB.
SED. STRUCTURES
SAMPLES
LOWER PLIOCENE
N18 - N19
NN12
A/M
A/M
V-1590 φ-64.5 γ-1.62
V-1601 φ-64.1 γ-1.62
V-1590 φ-64.3 γ-1.62
V-1605 φ-64.2 γ-1.62
V-1605 φ-65.2 γ-1.60
1
2
3
4
5
6
7
CC
0.5
1.0

LITHOLOGIC DESCRIPTION

NANNOFOSSIL OOZE with FORAMINIFERS

Major lithology: This core contains white (10YR 8/1) NANNOFOSSIL OOZE with FORAMINIFERS. The sediments are slightly to heavily bioturbated, with light gray (5Y 7/1 and 5Y 7/2) cm scale (mainly horizontal) mottles and grayish blue (5PB 5/2), mm scale, pyritic burrow fills. Diffuse light greenish gray (5G 7/1) and grayish blue (5PB 5/2), cm thick color bands are common. Short (cm size), more indurated intervals are present in Sections 6 and 7. Section 5, 61-124 cm, is stretched and moderately disturbed by coring.

SMEAR SLIDE SUMMARY (%):

	3, 99
	D
TEXTURE:	
Sand	15
Silt	82
Clay	3
COMPOSITION:	
Foraminifers	10
Nannofossils	86
Radiolarians	3
Silicoflagellates	1

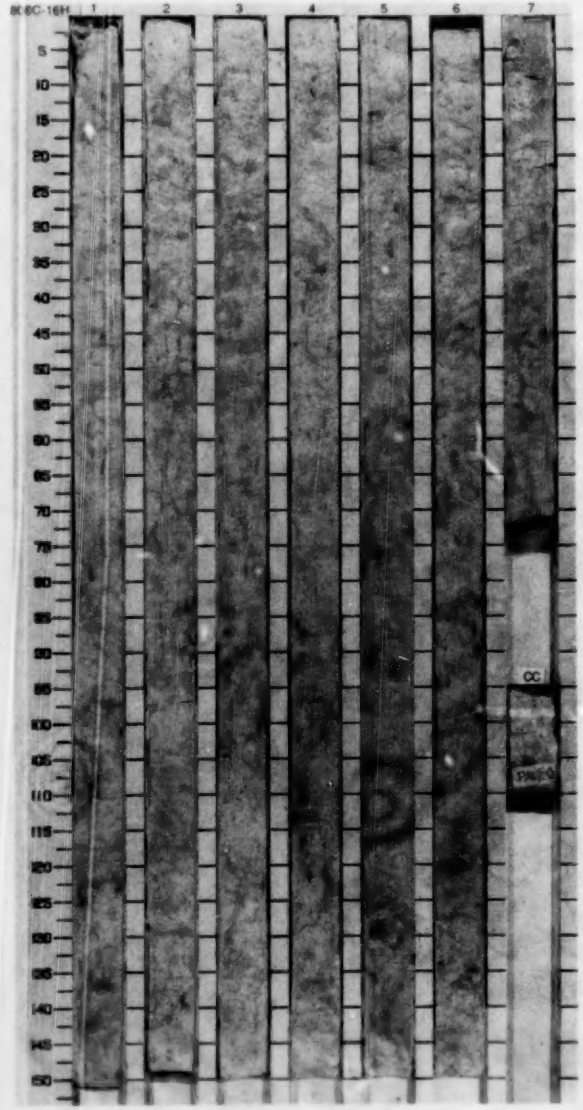
806C-16H
1
2
3
4
5
6
7
5
10
15
20
25
30
35
40
45
50
55
60
65
70
75
80
85
90
95
100
105
110
115
120
125
130
135
140
145
150
CC
PALEO

SITE 806 HOLE C CORE 17H CORED INTERVAL 148.1-157.6 mbsf

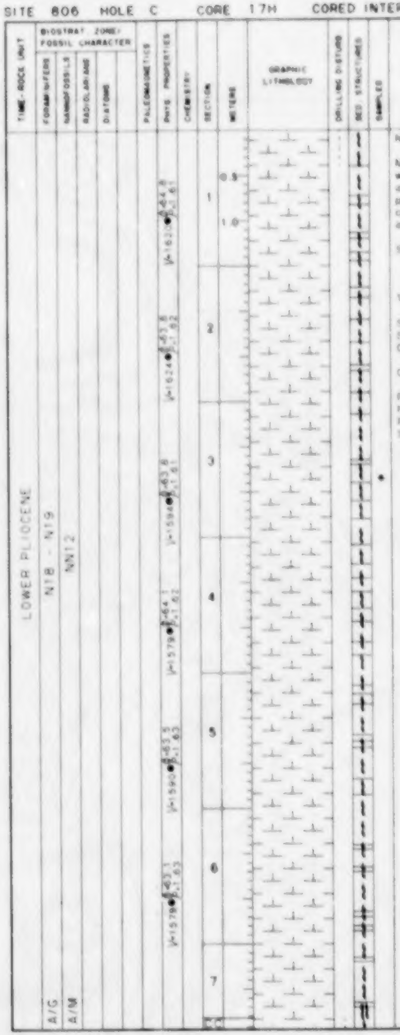
TIME-ROCK UNIT
BIOSTRAT. ZONE/ FOSSIL CHARACTER
FORAMINIFERS
NANNOFOSSILS
RADIOLARIANS
DIATOMS
PALEOMAGNETICS
PHYS. PROPERTIES
CHEMISTRY
SECTION
METERS
GRAPHIC LITHOLOGY
DRILLING DISTURB.
SED. STRUCTURES
SAMPLES
LOWER PLIOCENE
N18 - N19
NN12
A/G
A/M
V=1620 φ=64.8 γ=1.61
V=1624 φ=63.8 γ=1.62
V=1594 φ=63.6 γ=1.61
V=1579 φ=64.1 γ=1.62
V=1590 φ=63.5 γ=1.63
V=1579 φ=63.1 γ=1.63
1
2
3
4
5
6
7
CC
0.5
1.0

LITHOLOGIC DESCRIPTION

NANNOFOSSIL OOZE with FORAMINIFERS

Major lithology: This core contains white (7.5YR 8/0 and 10YR 8/1) NANNOFOSSIL OOZE with FORAMINIFERS. The sediments are slightly to heavily bioturbated, with light gray (5Y 7/1 and 5Y 7/2), cm scale (mainly horizontal) mottles and grayish blue (5PB 5/2), cm to mm scale pyritic burrow fills. Diffuse, light greenish gray (5G 7/1) and grayish blue (5PB 5/2), cm thick color bands and "halos", and vertical to steeply inclined grayish blue (5PB 5/2) color bands are common.

SMEAR SLIDE SUMMARY (%):

	3, 87
	D
TEXTURE:	
Sand	25
Silt	70
Clay	5
COMPOSITION:	
Foraminifers	20
Nannofossils	75
Radiolarians	4
Silicoflagellates	1

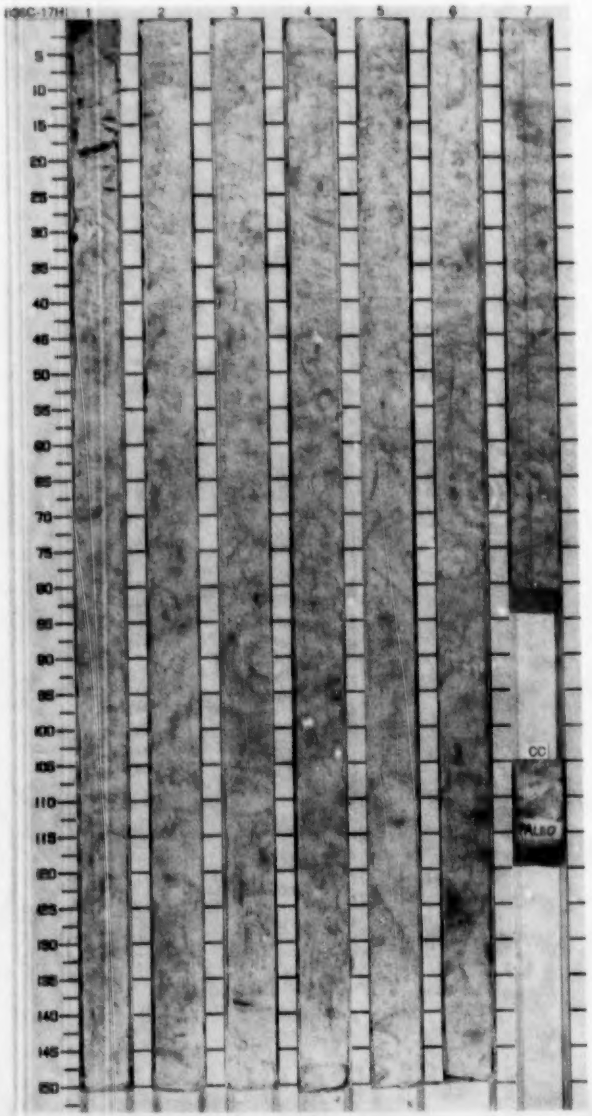
806C-17H
1
2
3
4
5
6
7
5
10
15
20
25
30
35
40
45
50
55
60
65
70
75
80
85
90
95
100
105
110
115
120
125
130
135
140
145
150
CC
PALEO

SITE 806 HOLE C CORE 18H CORED INTERVAL 157.6-167.1 mbsf

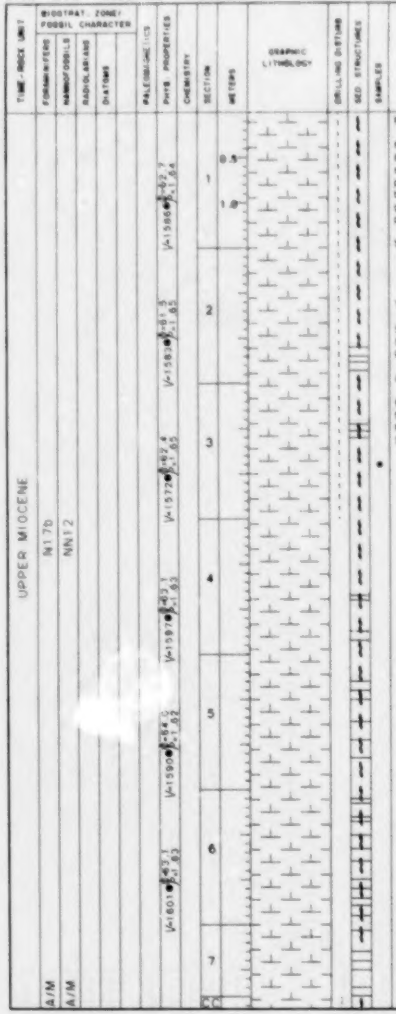
TIME-ROCK UNIT
BIOSTRAT. ZONE/ FOSSIL CHARACTER
FORAMINIFERS
NANNOFOSSILS
RADIOLARIANS
DIATOMS
PALEOMAGNETICS
PHYS. PROPERTIES
CHEMISTRY
SECTION
METERS
GRAPHIC LITHOLOGY
DRILLING DISTURB.
SED. STRUCTURES
SAMPLES
UPPER MIOCENE
N17b
NN12
A/M
A/M
V=1586 φ=62.7 γ=1.64
V=1583 φ=61.5 γ=1.65
V=1572 φ=62.4 γ=1.65
V=1597 φ=63.1 γ=1.63
V=1590 φ=64.0 γ=1.62
V=1601 φ=63.1 γ=1.63
1
2
3
4
5
6
7
CC
0.5
1.0

LITHOLOGIC DESCRIPTION

NANNOFOSSIL OOZE with FORAMINIFERS

Major lithology: This core contains slightly to heavily bioturbated, white)7/5YR 8/0 and 2.5Y 8/0) NANNOFOSSIL OOZXE with FORAMINIFERS. Evidence for burrowing includes cm scale, light gray (5Y 7/1 and 2.5Y 7/2) mottling and mm scale, grayish blue (5PB 5/2) and pale purple (5P 6/2), pyritic burrow fills. Irregular, vertical, grayish blue (5PB 5/2) and pale purple bands (5P 6/2) are probably parts of large burrow "halos". Diffuse, horizontal, light greenish gray (5G 7/1 and 5GY 7/1) and pale purple (5P 6/2) to grayish blue (5PB 5/2) color bands are present throughout the core, anc become more abundant downcore.

SMEAR SLIDE SUMMARY (%):

	3, 90
	D
TEXTURE:	
Sand	15
Silt	83
Clay	2
COMPOSITION:	
Foraminifers	10
Nannofossils	87
Radiolarians	2
Silicoflagellates	1

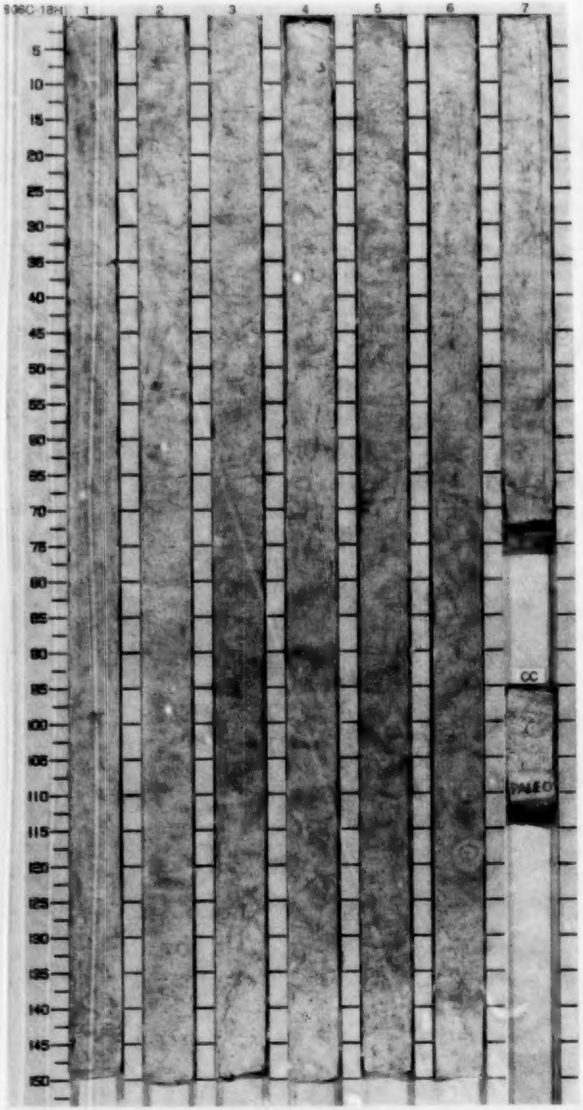
806C-18H
1
2
3
4
5
6
7
CC
PALEO
5
10
15
20
25
30
35
40
45
50
55
60
65
70
75
80
85
90
95
100
105
110
115
120
125
130
135
140
145
150

SITE 806 HOLE C CORE 19H CORED INTERVAL 167.1-176.6 mbsf

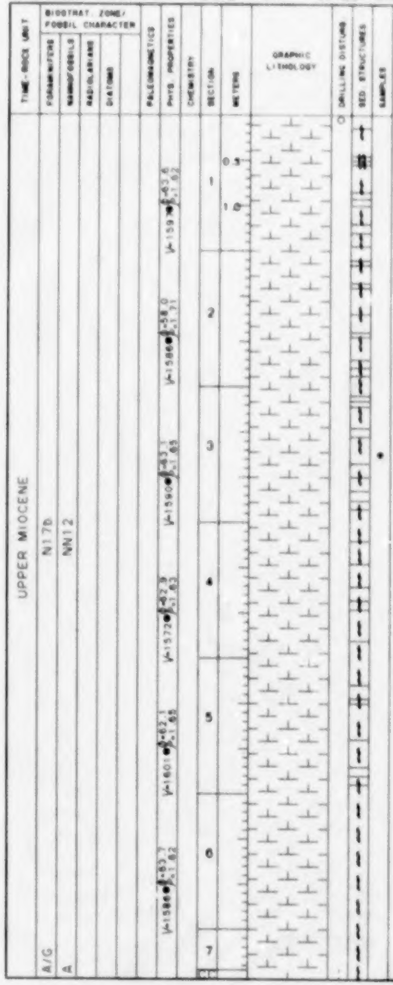
TIME-ROCK UNIT
BIOSTRAT. ZONE/ FOSSIL CHARACTER
FORAMINIFERS
NANNOFOSSILS
RADIOLARIANS
DIATOMS
PALEOMAGNETICS
PHYS. PROPERTIES
CHEMISTRY
SECTION
METERS
GRAPHIC LITHOLOGY
DRILLING DISTURB.
SED. STRUCTURES
SAMPLES
UPPER MIOCENE
N17b
NN12
A/G
A
V-1597 φ-63.6 ρ-1.62
V-1586 φ-58.0 ρ-1.71
V-1590 φ-63.1 ρ-1.65
V-1572 φ-62.9 ρ-1.63
V-1601 φ-62.1 ρ-1.65
V-1586 φ-63.7 ρ-1.62
1
2
3
4
5
6
7
CC
0.5
1.0

LITHOLOGIC DESCRIPTION

NANNOFOSSIL OOZE with FORAMINIFERS

Major lithology: This core contains slightly to heavily bioturbated, predominantly white (7.5YR 8/0 and 2.5Y 8/0) NANNOFOSSIL OOZE with FORAMINIFERS. Heavily bioturbated intervals are light gray (5Y 7/1) to light brownish gray (2.5Y 6/2). Evidence for burrowing includes cm scale, light gray (5Y 7/1 and 2.5Y 7/2) to light brownish gray (2.5Y 6/2) mottling and mm scale grayish blue (5PB 5/2) and pale purple (5P 6/2) pyritic burrow fills. Irregular vertical, grayish blue (5PB 5/2) and pale purple (5P 6/2) bands are probably parts of large burrow "halos". Diffuse, horizontal, light greenish gray (5G 7/1 and 5GY 7/1) and pale purple (5P 6/2) to grayish blue (5PB 5/2) color bands are present throughout the core.

SMEAR SLIDE SUMMARY (%):

	3, 75
	D
TEXTURE:	
Sand	15
Silt	83
Clay	2
COMPOSITION:	
Foraminifers	20
Nannofossils	78
Radiolarians	1
Silicoflagellates	1

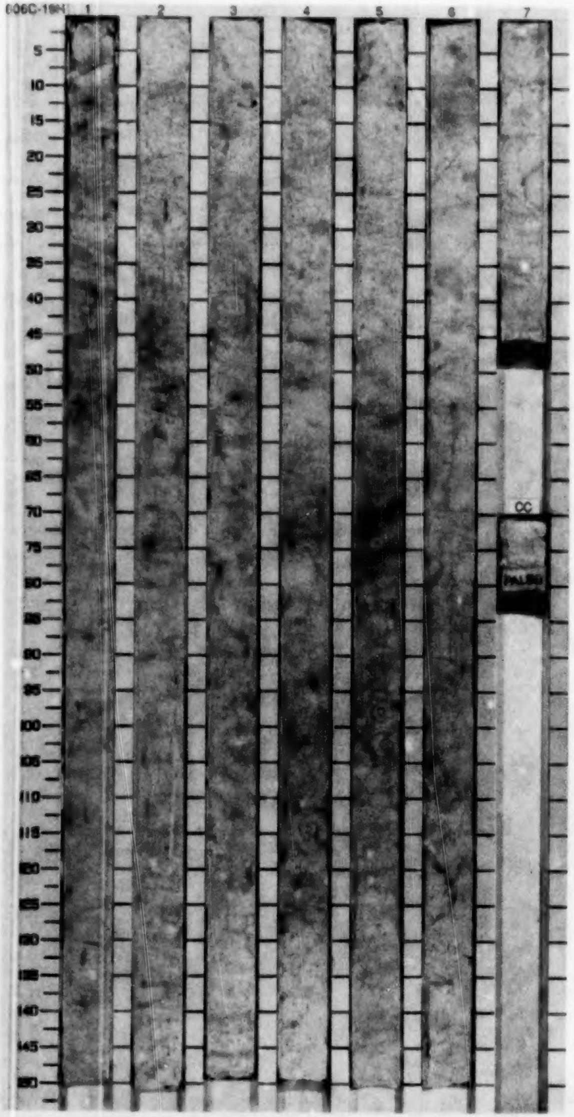
806C-19H
1
2
3
4
5
6
7
CC
PALEO
5
10
15
20
25
30
35
40
45
50
55
60
65
70
75
80
85
90
95
100
105
110
115
120
125
130
135
140
145
150

SITE 806 HOLE C CORE 20H CORED INTERVAL 176.6-186.1 mbsf

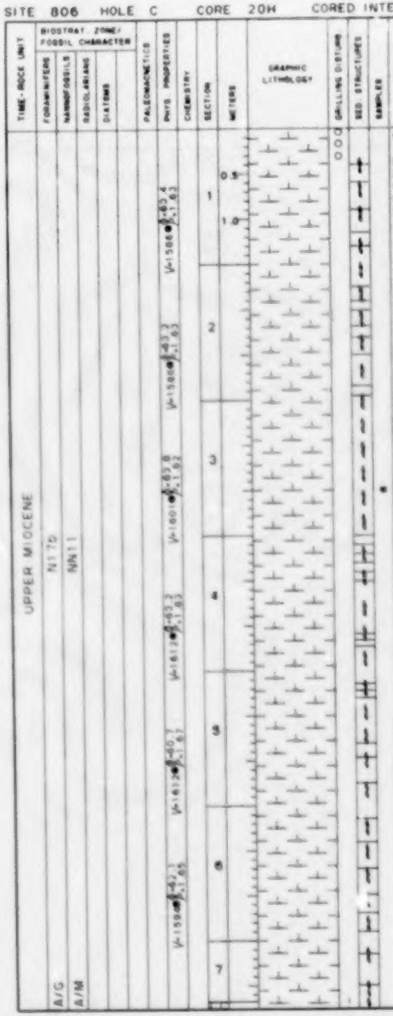
TIME-ROCK UNIT
BIOSTRAT. ZONE/ FOSSIL CHARACTER
FORAMINIFERS
NANNOFOSSILS
RADIOLARIANS
DIATOMS
PALEOMAGNETICS
PHYS. PROPERTIES
CHEMISTRY
SECTION
METERS
GRAPHIC LITHOLOGY
DRILLING DISTURB.
SED. STRUCTURES
SAMPLES
UPPER MIOCENE
N17b
NN11
A/G
A/M
V=1586 φ=63.4 γ=1.63
V=1580 φ=63.2 γ=1.63
V=1601 φ=63.8 γ=1.62
V=1612 φ=63.2 γ=1.63
V=1612 φ=60.7 γ=1.67
V=1594 φ=62.1 γ=1.65
1
2
3
4
5
6
7
0.5
1.0

LITHOLOGIC DESCRIPTION

NANNOFOSSIL OOZE with FORAMINIFERS

Major lithology: This core contains white (5Y 8/1 and 2.5Y 8/0) NANNOFOSSIL OOZE with FORAMINIFERS and is moderately bioturbated as indicated by light gray (5Y 7/1 and N8/) mottling. Pyritic burrow fills (mm size) are present, with associated grayish blue (5PB 5/2) mottling and "halos". Diffuse horizontal, light greenish gray (5G 7/1), pale purple (5P 6/2) and grayish blue (5PB 5/2) color bands are present throughout the core.

SMEAR SLIDE SUMMARY (%):

	3, 100
	D
TEXTURE:	
Sand	10
Silt	65
Clay	25
COMPOSITION:	
Diatoms	1
Foraminifers	10
Nannofossils	85
Radiolarians	Tr

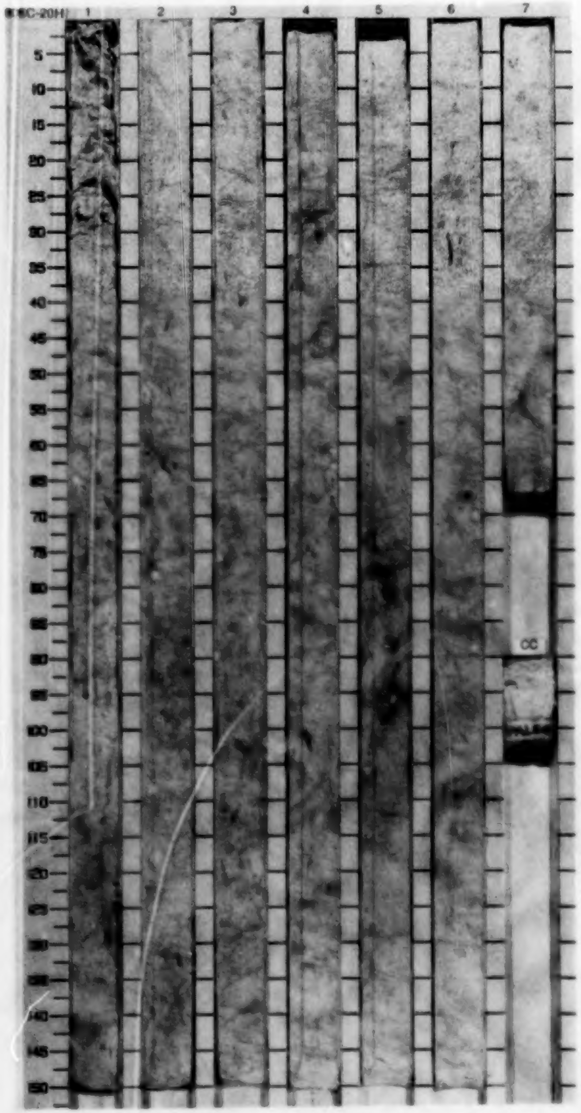
806C-20H
1
2
3
4
5
6
7
CC
5
10
15
20
25
30
35
40
45
50
55
60
65
70
75
80
85
90
95
100
105
110
115
120
125
130
135
140
145
150

SITE 806 HOLE C CORE 21H CORED INTERVAL 186.1-195.6 mbsf

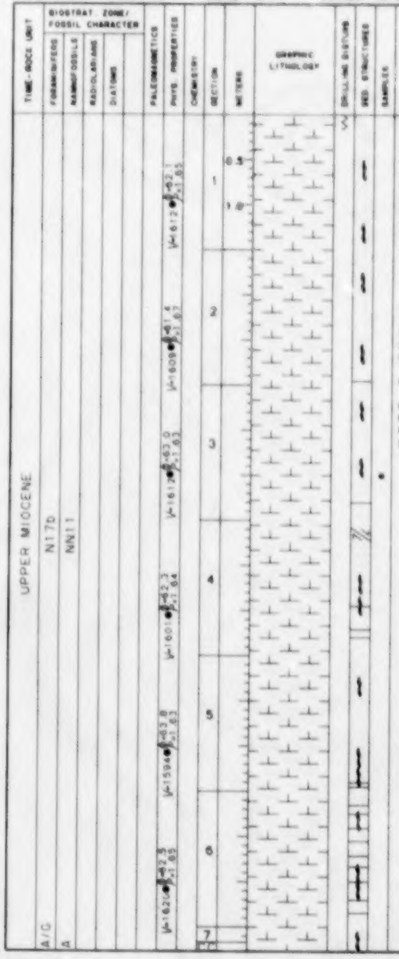
TIME-ROCK UNIT
BIOSTRAT. ZONE/ FOSSIL CHARACTER
FORAMINIFERS
NANNOFOSSILS
RADIOLARIANS
DIATOMS
PALEOMAGNETICS
PHYS. PROPERTIES
CHEMISTRY
SECTION
METERS
GRAPHIC LITHOLOGY
DRILLING DISTURB.
SED. STRUCTURES
SAMPLES
UPPER MIOCENE
N17b
NN11
A/G
A
γ=1612 φ=62.1 ρ=1.65
γ=1609 φ=61.4 ρ=1.67
γ=1612 φ=63.0 ρ=1.63
γ=1601 φ=62.3 ρ=1.64
γ=1594 φ=63.8 ρ=1.63
γ=1620 φ=62.5 ρ=1.65
1
2
3
4
5
6
7
CC
0.5
1.0

LITHOLOGIC DESCRIPTION

NANNOFOSSIL OOZE with FORAMINIFERS

Major lithology: This core contains white (2.5Y 8/0 and 7.5YR 8/0) NANNOFOSSIL OOZE with FORAMINIFERS. Bioturbation is slight to moderate throughout the core, and is expressed as light gray (5Y 7/1 and 2.5Y 7/2), pale purple (5P 6/2), and grayish blue (5PB 5/2) cm-scale mottling. Vertical pale purple (5P 6/2) and grayish blue (5PB 5/2) color bands are probably portions of large burrow "halos". Diffuse horizontal, light greenish gray (5G 7/1 and 5GY 7/1) and pale purple (5P 5/2) color bands are common in Sections 4 and 6, but rare in the remainder of the core. A microfault is present in Section 4, 5-15 cm.

SMEAR SLIDE SUMMARY (%):

	3, 100
	D
TEXTURE:	
Sand	10
Silt	87
Clay	3
COMPOSITION:	
Foraminifers	10
Nannofossils	88
Radiolarians	1
Silic. oflagellates	1

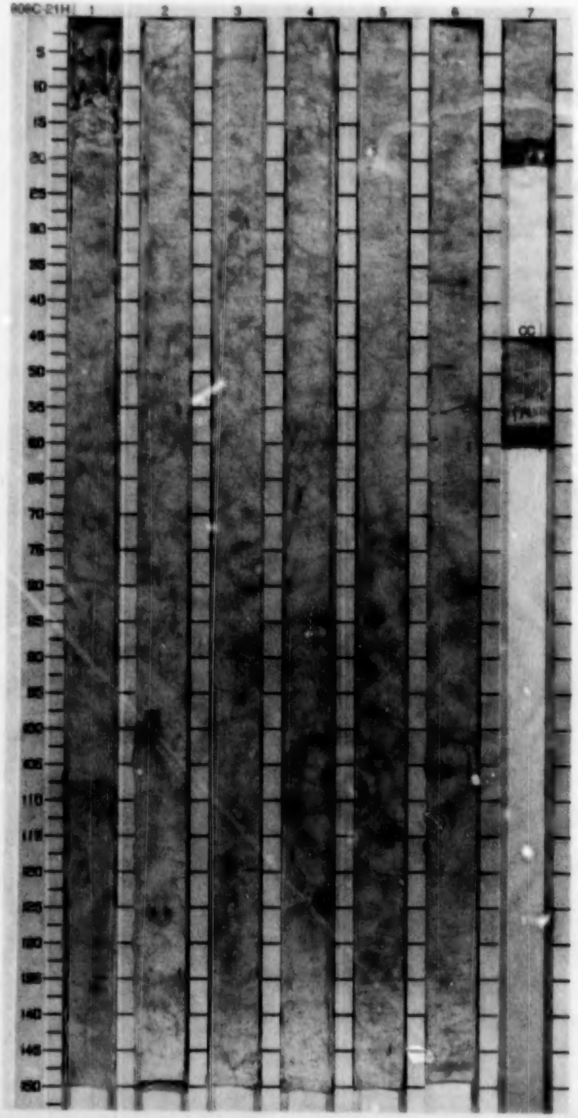
806C-21H
1
2
3
4
5
6
7
CC
5
10
15
20
25
30
35
40
45
50
55
60
65
70
75
80
85
90
95
100
105
110
115
120
125
130
135
140
145
150

SITE 806 HOLE C CORE 22H CORED INTERVAL 195.6-205.1 mbsf

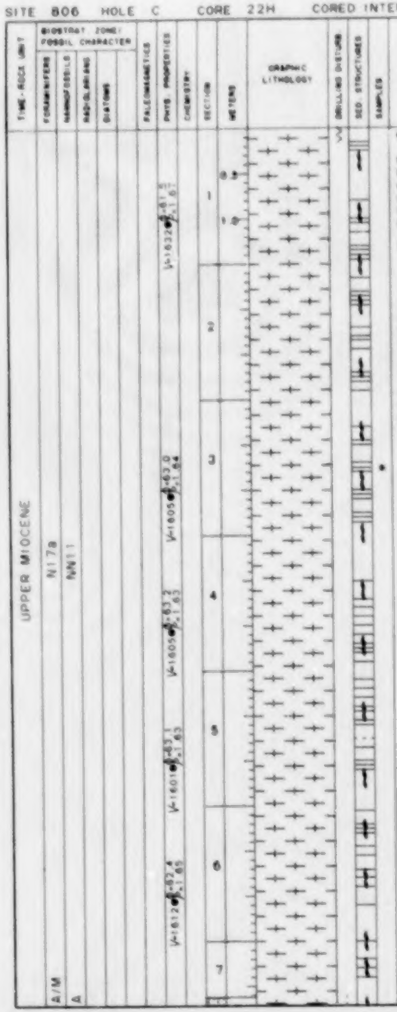
TIME-ROCK UNIT
BIOSTRAT. ZONE/ FOSSIL CHARACTER
FORAMINIFERS
NANNOFOSSILS
RADIOLARIANS
DIATOMS
PALEOMAGNETICS
PHYS. PROPERTIES
CHEMISTRY
SECTION
METERS
GRAPHIC LITHOLOGY
DRILLING DISTURB.
SED. STRUCTURES
SAMPLES
UPPER MIOCENE
N17a
NN11
A/M
A
V=1632
V=1605
V=1605
V=1601
V=1612
1
2
3
4
5
6
7
0.5
1.0

LITHOLOGIC DESCRIPTION

FORAMINIFER NANNOFOSSIL OOZE

Major lithology: This core contains white (7.5YR 8/0) FORAMINIFER NANNOFOSSIL OOZE. Bioturbation is light to moderate and is expressed as cm scale, light gray (5Y 7/1), predominantly horizontal burrows, mm scale, grayish blue (5PB 5/2) pyritic burrow fills, and cm scale, horizontal grayish blue (5PB 5/2) burrows. Large grayish blue (5PB 5/2) "halos" also are present, as are grayish green (5G 5/2) mottles. Diffuse light greenish gray (5G 7/1) and pale purple (5P 6/2) color bands are common.

SMEAR SLIDE SUMMARY (%)

	3, 77
	D
TEXTURE	
Sand	15
Silt	83
Clay	2
COMPOSITION	
Foraminifers	25
Nannofossils	73
Radiolarians	1
Silicoflagellates	1

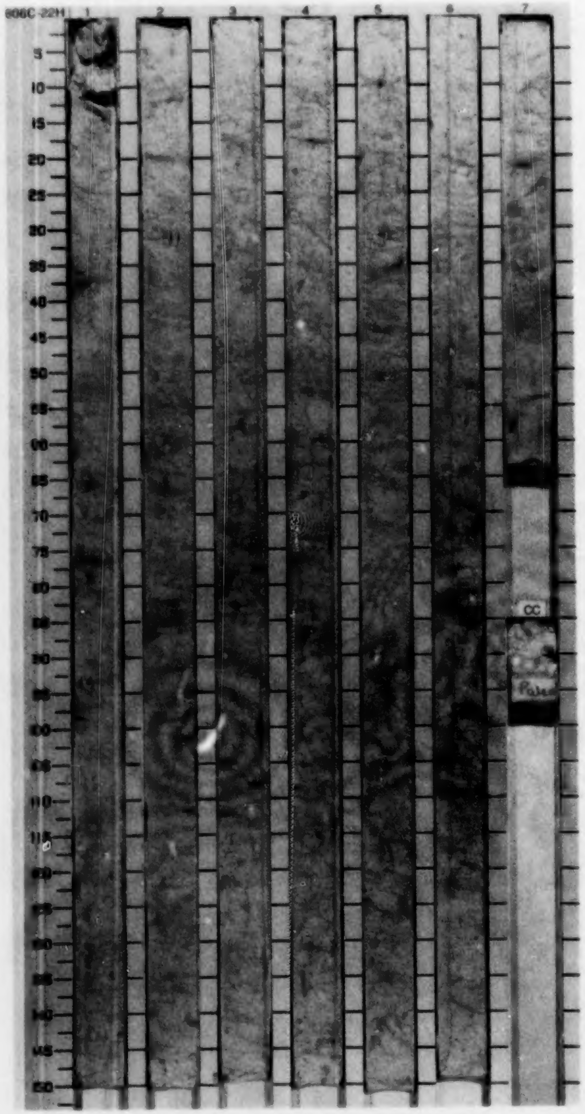
806C-22H
1
2
3
4
5
6
7
5
10
15
20
25
30
35
40
45
50
55
60
65
70
75
80
85
90
95
100
105
110
115
120
125
130
135
140
145
150
CC
Paleo

SITE 806 HOLE C CORE 23H CORED INTERVAL 205.1-214.6 mbsf

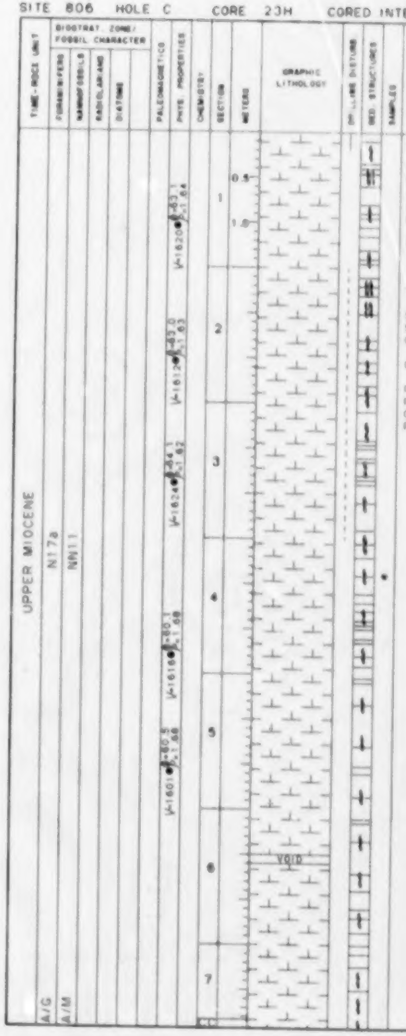
TIME-ROCK UNIT
BIOSTRAT. ZONE/ FOSSIL CHARACTER
FORAMINIFERS
NANNOFOSSILS
RADIOLARIANS
DIATOMS
PALEOMAGNETICS
PHYS. PROPERTIES
CHEMISTRY
SECTION
METERS
GRAPHIC LITHOLOGY
DRILLING DISTURB.
SED. STRUCTURES
SAMPLES
UPPER MIOCENE
N17a
NN11
A/G
A/M
V-1620 φ-63.1 γ-1.64
V-1612 φ-63.0 γ-1.63
V-1624 φ-64.1 γ-1.62
V-1616 φ-60.1 γ-1.68
V-1601 φ-60.5 γ-1.68
1
2
3
4
5
6
7
CC
0.5
1.0
VOID

LITHOLOGIC DESCRIPTION

NANNOFOSSIL OOZE with FORAMINIFERS

Major lithology: This core contains white (7.5YR 8/0 and 5Y 8/0) NANNOFOSSIL OOZE with FORAMINIFERS. Bioturbation is moderate to heavy and is expressed as cm scale, light gray (5Y 7/1), predominantly horizontal burrows, mm scale, pyritic grayish blue (5PB 5/2) burrows and cm scale, horizontal grayish blue (5PB 5/2) burrows. Diffuse horizontal, light greenish gray (5G 7/1) and pale purple (5P 6/2) color bands are common.

SMEAR SLIDE SUMMARY (%):

	4, 50
	D
TEXTURE:	
Sand	10
Silt	70
Clay	20
COMPOSITION:	
Foraminifers	12
Nannofossils	87
Quartz	Tr
Radiolarians	1

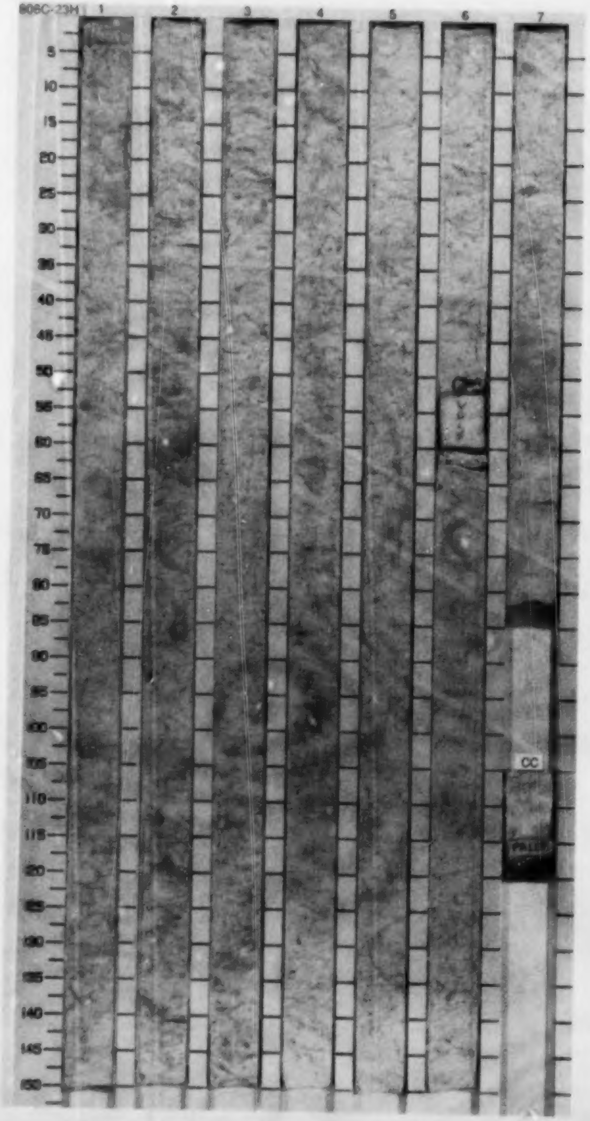
806C-23H
1
2
3
4
5
6
7
5
10
15
20
25
30
35
40
45
50
55
60
65
70
75
80
85
90
95
100
105
110
115
120
125
130
135
140
145
150
CC

SITE 806 HOLE C CORE 24H CORED INTERVAL 214.6-224.1 mbsf

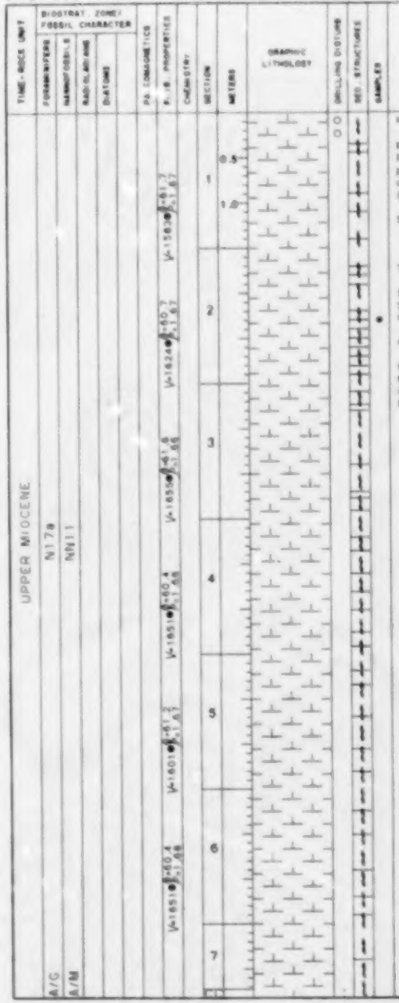
TIME-ROCK UNIT
BIOSTRAT. ZONE/ FOSSIL CHARACTER
FORAMINIFERS
NANNOFOSSILS
RADIOLARIANS
DIATOMS
PALEOMAGNETICS
PHYS. PROPERTIES
CHEMISTRY
SECTION
METERS
GRAPHIC LITHOLOGY
DRILLING DISTURB.
SED. STRUCTURES
SAMPLES
UPPER MIOCENE
N17a
NN11
A/G
A/M
V=1583 φ=61.7 γ=1.67
V=1624 φ=60.7 γ=1.67
V=1655 φ=61.6 γ=1.66
V=1651 φ=60.4 γ=1.68
V=1601 φ=61.2 γ=1.67
V=1651 φ=60.4 γ=1.68
1
2
3
4
5
6
7
0.5
1.0

LITHOLOGIC DESCRIPTION

NANNOFOSSIL OOZE with FORAMINIFERS

Major lithology: This core contains white (7.5YR 8/0 and 5Y 8/0) NANNOFOSSIL OOZE with FORAMINIFERS. Bioturbation is moderate and is expressed as cm scale, light gray (5Y 7/2) predominantly horizontal burrows, mm scale, pyritic, grayish blue (5PB 5/2) burrow fills, and cm scale, horizontal, grayish blue (5PB 5/2) burrows. Diffuse horizontal, light greenish gray (5G 7/1), grayish blue (5PB 5/2), and pale purple (5P 6/2) color bands are common.

SMEAR SLIDE SUMMARY (%):

	2, 80
	D
TEXTURE:	
Sand	20
Silt	75
Clay	5
COMPOSITION:	
Foraminifers	10
Nannofossils	86
Quartz	1
Radiolarians	3

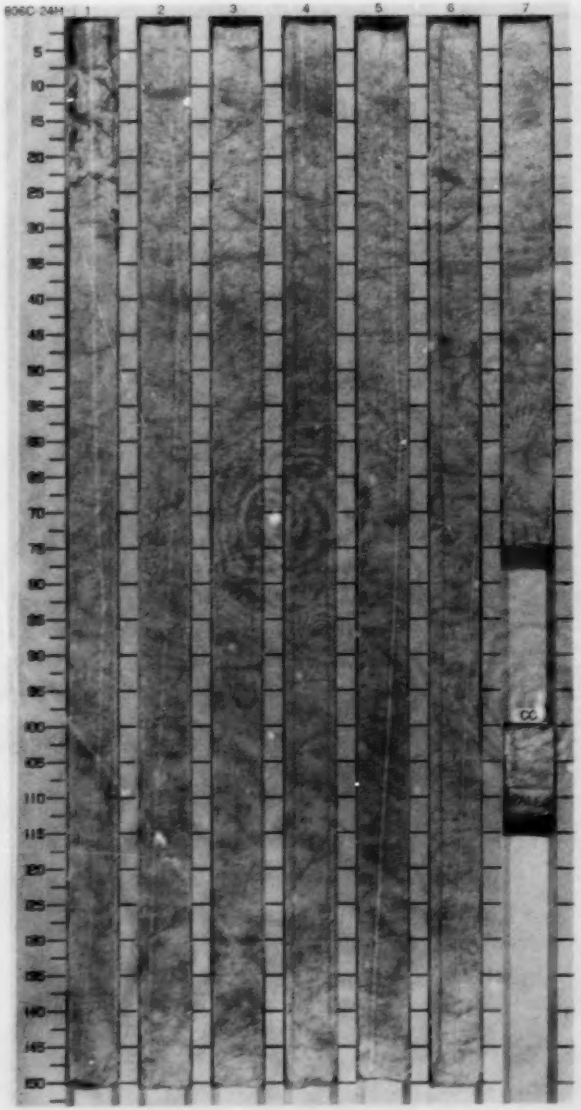
806C-24H
1
2
3
4
5
6
7
CC
5
10
15
20
25
30
35
40
45
50
55
60
65
70
75
80
85
90
95
100
105
110
115
120
125
130
135
140
145
150

SITE 806 HOLE C CORE 25H CORED INTERVAL 224.1-233.6 mbsf

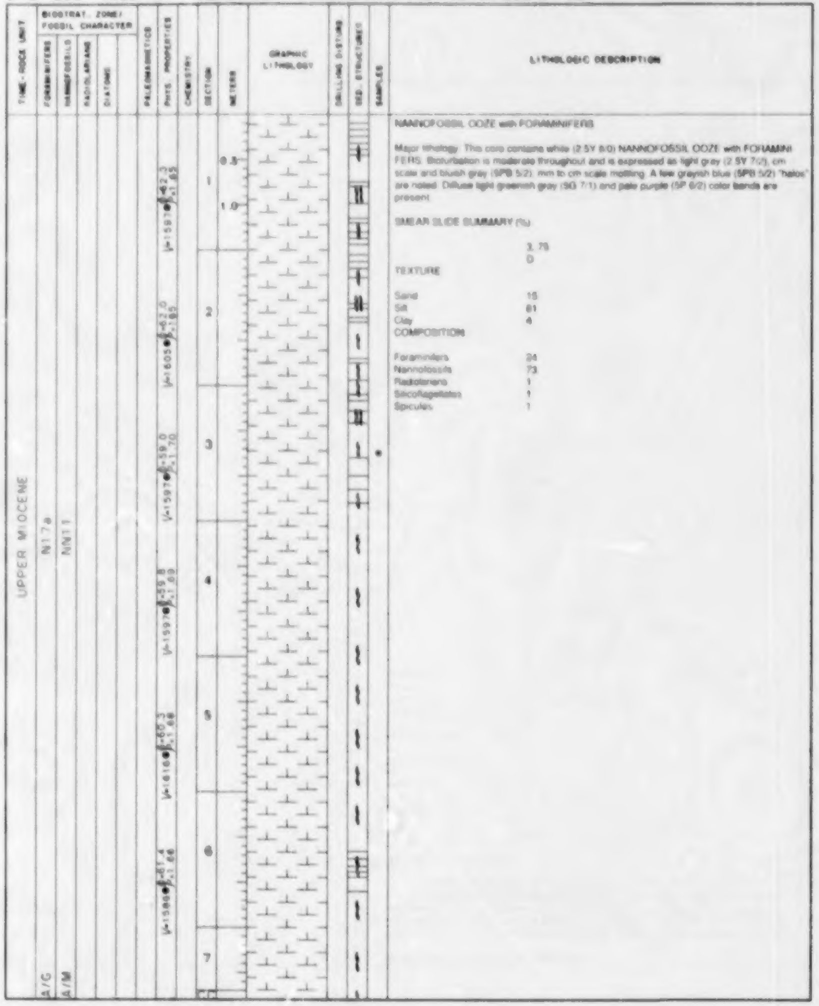
TIME-ROCK UNIT
BIOSTRAT. ZONE/ FOSSIL CHARACTER
FORAMINIFERS
NANNOFOSSILS
RADIOLARIANS
DIATOMS
PALEOMAGNETICS
PHYS. PROPERTIES
CHEMISTRY
SECTION
METERS
GRAPHIC LITHOLOGY
DRILLING DISTURB.
SED. STRUCTURES
SAMPLES
UPPER MIOCENE
N17a
NN11
A/G
A/M
V=1597 φ=62.3 ρ=1.85
V=1605 φ=62.0 ρ=1.85
V=1597 φ=59.0 ρ=1.70
V=1597 φ=59.8 ρ=1.69
V=1616 φ=60.3 ρ=1.68
V=1586 φ=61.4 ρ=1.66
1
2
3
4
5
6
7
CC
0.5
1.0

LITHOLOGIC DESCRIPTION

NANNOFOSSIL OOZE with FORAMINIFERS

Major lithology: This core contains white (2.5Y 8/0) NANNOFOSSIL OOZE with FORAMINIFERS. Bioturbation is moderate throughout and is expressed as light gray (2.5Y 7/2), cm scale and bluish gray (5PB 5/2) mm to cm scale mottling. A few grayish blue (5PB 5/2) "halos" are noted. Diffuse light greenish gray (5G 7/1) and pale purple (5P 6/2) color bands are present.

SMEAR SLIDE SUMMARY (%):

	3, 75
	D
TEXTURE:	
Sand	15
Silt	81
Clay	4
COMPOSITION:	
Foraminifers	24
Nannofossils	73
Radiolarians	1
Silicoflagellates	1
Spicules	1

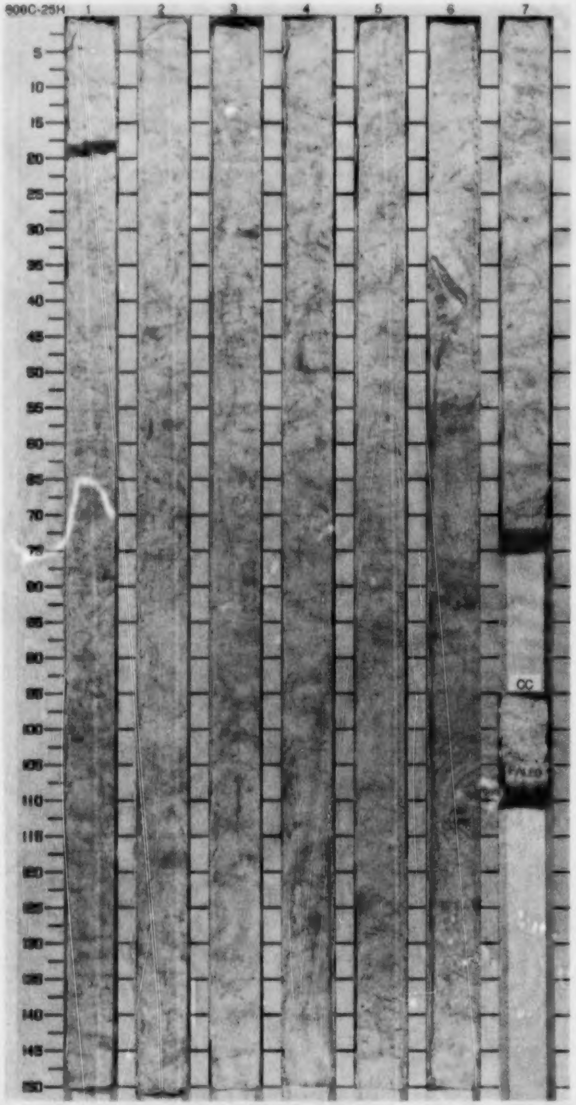
806C-25H
1
2
3
4
5
6
7
CC
5
10
15
20
25
30
35
40
45
50
55
60
65
70
75
80
85
90
95
100
105
110
115
120
125
130
135
140
145
150

SITE 806 HOLE C CORE 26H CORED INTERVAL 233.6-243.1 mbsf

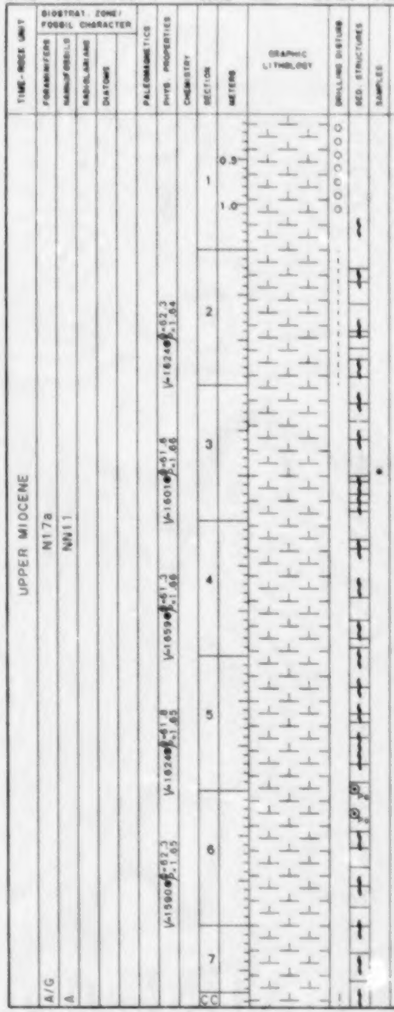
TIME-ROCK UNIT
BIOSTRAT. ZONE/ FOSSIL CHARACTER
FORAMINIFERS
NANNOFOSSILS
RADIOLARIANS
DIATOMS
PALEOMAGNETICS
PHYS. PROPERTIES
CHEMISTRY
SECTION
METERS
GRAPHIC LITHOLOGY
DRILLING DISTURB.
SED. STRUCTURES
SAMPLES
UPPER MIOCENE
N17a
NN11
A/G
A
V-1624●-62.3 γ-1.64
V-1601●-61.6 γ-1.66
V-1659●-61.3 γ-1.66
V-1624●-61.8 γ-1.65
V-1590●-62.3 γ-1.65
1
2
3
4
5
6
7
CC
0.5
1.0

LITHOLOGIC DESCRIPTION

NANNOFOSSIL OOZE with FORAMINIFERS

Major lithology: This core contains slightly to moderately bioturbated, white (2.5Y 8/0) NANNOFOSSIL OOZE with FORAMINIFERS. Bioturbation includes light gray (5Y 7/1), cm scale mottles, and mm to cm scale, grayish blue (5PB 5/2) mottles and pyritic burrow linings. Minor large burrow "halos" are present. Diffuse light greenish gray (5G 7/1) and pale purple (5P 6/2), horizontal color bands are present, but rare and poorly developed.

Minor lithology: Nodules of PORCELLANITE are present at Section 5, 140 cm and Section 6, 25 cm. These nodules are light gray (N7/) and each is approximately 2 cm in diameter.

SMEAR SLIDE SUMMARY (%):

	3, 97
	D
TEXTURE:	
Sand	22
Silt	74
Clay	4
COMPOSITION:	
Foraminifers	22
Nannofossils	74
Radiolarians	3
Silicoflagellates	1

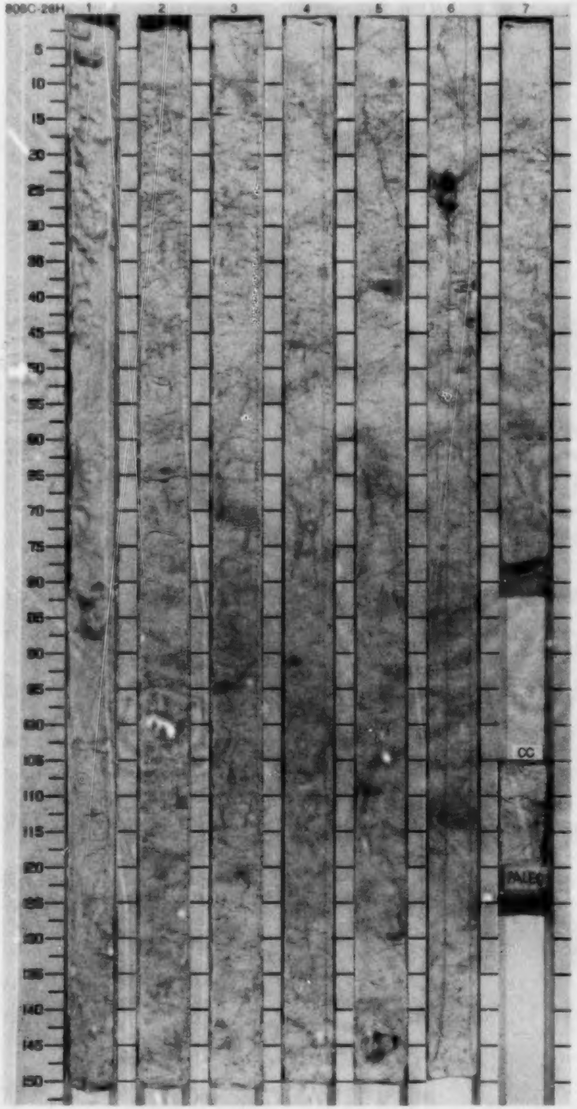
806C-26H
1
2
3
4
5
6
7
CC
PALEO
5
10
15
20
25
30
35
40
45
50
55
60
65
70
75
80
85
90
95
100
105
110
115
120
125
130
135
140
145
150

SITE 806 HOLE C CORE 27H CORED INTERVAL 243.1-252.6 mbsf

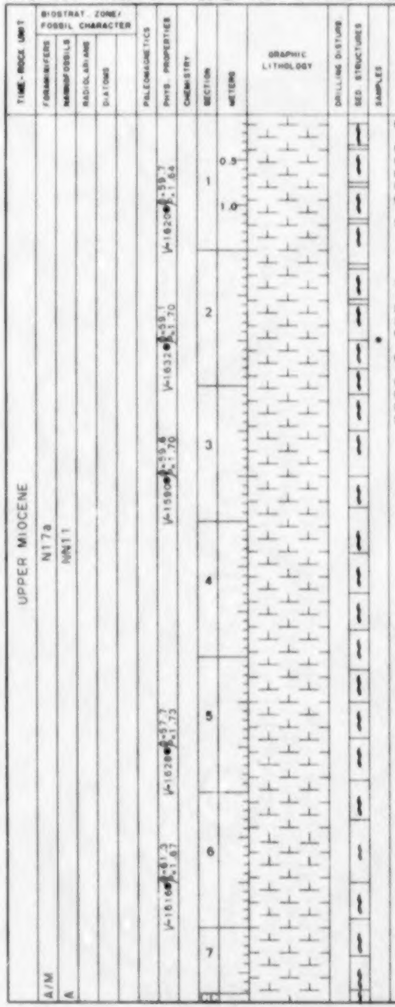
TIME-ROCK UNIT
BIOSTRAT. ZONE/ FOSSIL CHARACTER
FORAMINIFERS
NANNOFOSSILS
RADIOLARIANS
DIATOMS
PALEOMAGNETICS
PHYS. PROPERTIES
CHEMISTRY
SECTION
METERS
GRAPHIC LITHOLOGY
DRILLING DISTURB.
SED. STRUCTURES
SAMPLES
UPPER MIOCENE
N17a
NN11
A/M
A
V-1620 ● φ-59.7 γ-1.64
V-1632 ● φ-59.1 γ-1.70
V-1590 ● φ-59.6 γ-1.70
V-1620 ● φ-57.7 γ-1.73
V-1616 ● φ-61.3 γ-1.67
1
2
3
4
5
6
7
CC
0.5
1.0

LITHOLOGIC DESCRIPTION

NANNOFOSSIL OOZE with FORAMINIFERS

Major lithology: This core contains slightly to moderately bioturbated, white (2.5Y 8/0) NANNOFOSSIL OOZE with FORAMINIFERS. Bioturbation is seen as cm scale, light gray (5Y 7/1) burrows, with minor mm to cm scale grayish blue (5PB 5/2) mottling. Pale purple (5P 6/2) and light greenish gray (5G 7/1), 0.5 to 1 cm thick color bands are present, but rare. Long, vertical grayish blue (5PB 5/2) color bands may represent parts of large burrow "halos".

SMEAR SLIDE SUMMARY (%):

	2, 99 D
TEXTURE:	
Sand	20
Silt	75
Clay	5
COMPOSITION:	
Foraminifers	15
Nannofossils	82
Radiolarians	2
Silicoflagellates	1

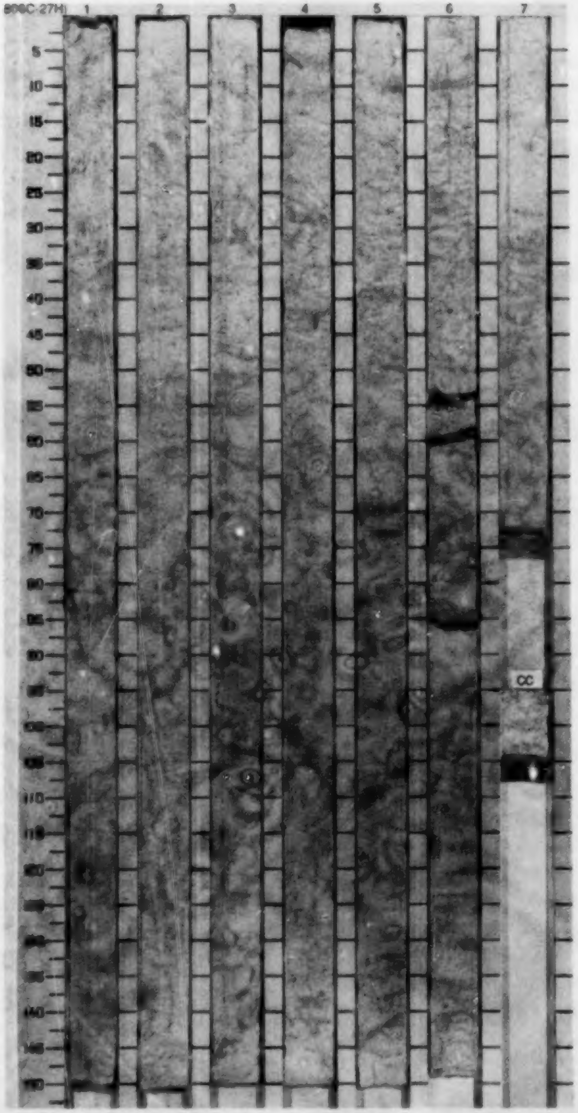
806C-27H
1
2
3
4
5
6
7
CC
5
10
15
20
25
30
35
40
45
50
55
60
65
70
75
80
85
90
95
100
105
110
115
120
125
130
135
140
145
150

SITE 806 HOLE C CORE 28H CORED INTERVAL 252.6-262.1 mbsf

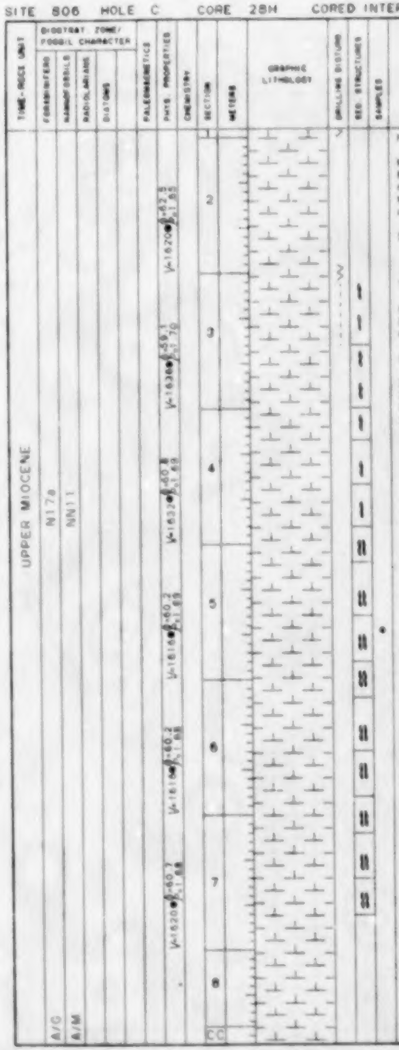
TIME-ROCK UNIT
BIOSTRAT. ZONE/ FOSSIL CHARACTER
FORAMINIFERS
NANNOFOSSILS
RADIOLARIANS
DIATOMS
PALEOMAGNETICS
PHYS. PROPERTIES
CHEMISTRY
SECTION
METERS
GRAPHIC LITHOLOGY
DRILLING DISTURB.
SED. STRUCTURES
SAMPLES
UPPER MIOCENE
N17a
NN11
A/G
A/M
V-1620 ϕ-62.5 ρ-1.85
V-1636 ϕ-59.1 ρ-1.70
V-1632 ϕ-60.8 ρ-1.69
V-1616 ϕ-60.2 ρ-1.69
V-1616 ϕ-60.2 ρ-1.68
V-1620 ϕ-60.7 ρ-1.68
1
2
3
4
5
6
7
8
CC

LITHOLOGIC DESCRIPTION

NANNOFOSSIL OOZE with FORAMINIFERS

Major lithology: This core contains white (7.5YR 8/0) NANNOFOSSIL OOZE with FORAMINIFERS. The sediment is moderately to heavily bioturbated, with abundant light gray (5Y 7/1) mottles, pyritic burrow fills, and specks. Some burrows have pale purple (5P 6/2) "halos". A few diffuse, pale purple and greenish gray (5G 7/1) color bands are observed throughout the core.

SMEAR SLIDE SUMMARY (%):

	5, 97
	D
TEXTURE:	
Sand	20
Silt	75
Clay	5
COMPOSITION:	
Foraminifers	12
Nannofossils	85
Radiolarians	2
Silicoflagellates	1

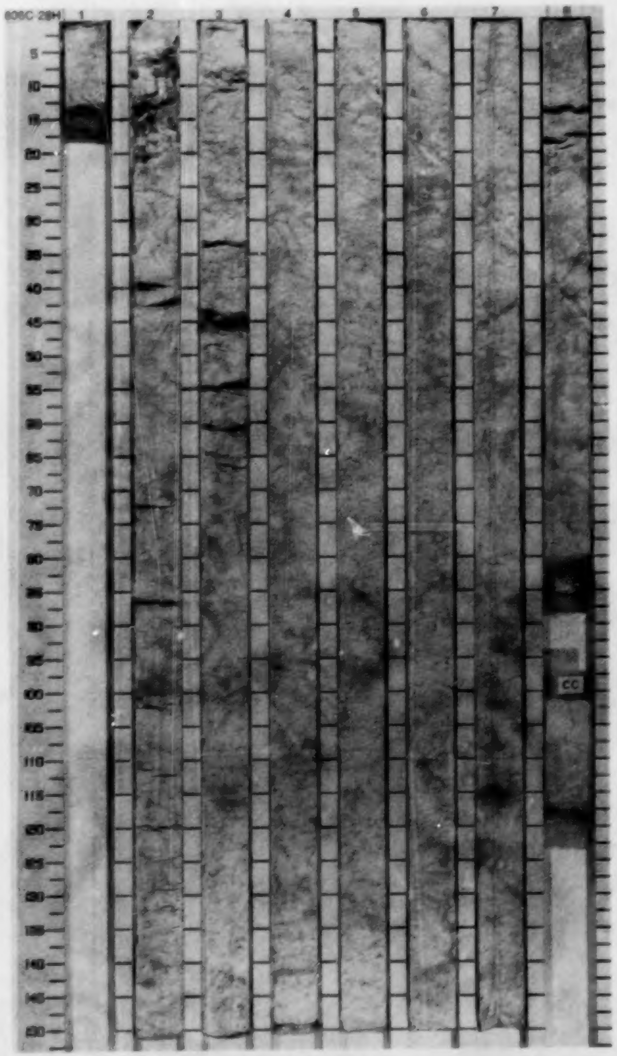
806C 28H
1
2
3
4
5
6
7
8
CC
5
10
15
20
25
30
35
40
45
50
55
60
65
70
75
80
85
90
95
100
105
110
115
120
125
130
135
140
145
150

SITE 806 HOLE C CORE 29H CORED INTERVAL 262.1-271.6 mbsf

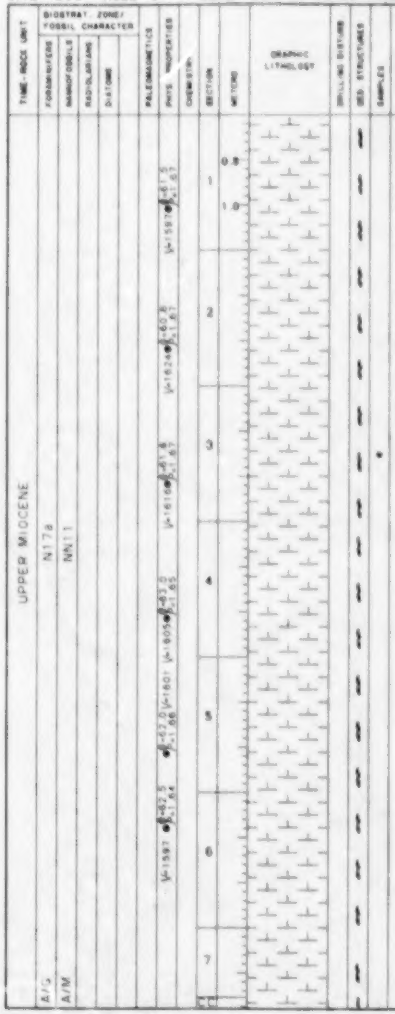
TIME-ROCK UNIT
BIOSTRAT. ZONE/ FOSSIL CHARACTER
FORAMINIFERS
NANNOFOSSILS
RADIOLARIANS
DIATOMS
PALEOMAGNETICS
PHYS. PROPERTIES
CHEMISTRY
SECTION
METERS
GRAPHIC LITHOLOGY
DRILLING DISTURB.
SED. STRUCTURES
SAMPLES
UPPER MIOCENE
N17a
NN11
A/G
A/M
V=1597 φ=61.5 γ=1.67
V=1624 φ=60.8 γ=1.67
V=1616 φ=61.6 γ=1.67
V=1605 φ=63.0 γ=1.65
V=1601 φ=62.0 γ=1.66
V=1597 φ=62.5 γ=1.64
1
2
3
4
5
6
7
CC
0.5
1.0

LITHOLOGIC DESCRIPTION

NANNOFOSSIL OOZE with FORAMINIFERS

Major lithology: This core contains white (7.5YR 8/0) NANNOFOSSIL OOZE with FORAMINIFERS. The ooze is bioturbated, with pale purple (5P 6/2) specks, streaks, and "halo" segments. Further evidence of bioturbation is provided by white (2.5Y 8/2) mottles. Several 4 to 5 cm thick intervals are more consolidated than the surrounding sections. The consolidated ooze commonly has a nodular shape. Section 2, 40 cm, contains one porcellanite concretion.

SMEAR SLIDE SUMMARY (%):

	3, 75
	D
TEXTURE:	
Sand	10
Silt	50
Clay	40
COMPOSITION:	
Foraminifers	15
Nannofossils	82
Siliceous fragments	3

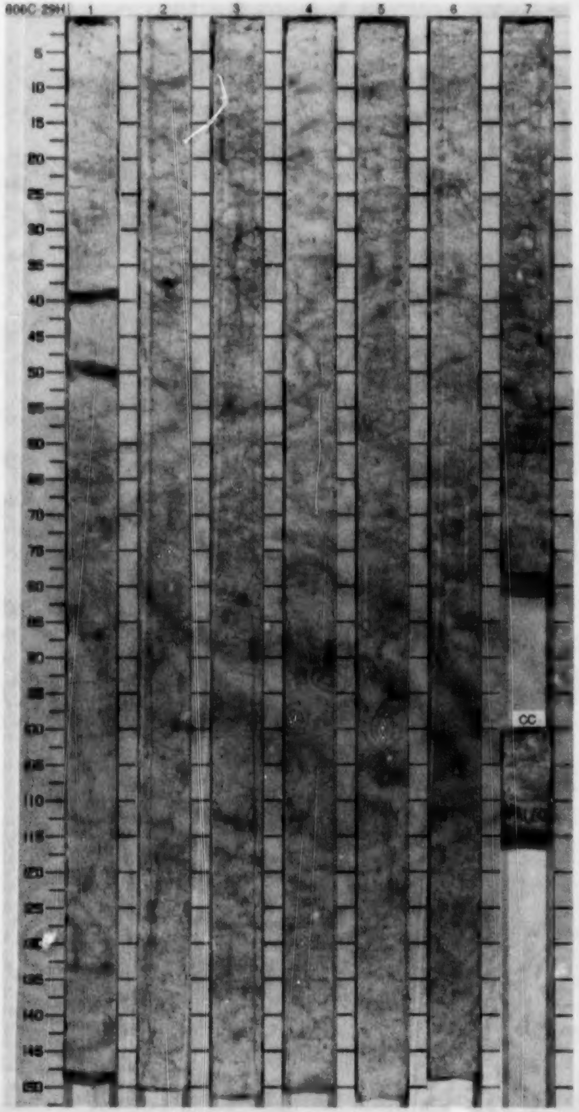
806C-29H
1
2
3
4
5
6
7
CC
5
10
15
20
25
30
35
40
45
50
55
60
65
70
75
80
85
90
95
100
105
110
115
120
125
130
135
140
145
150

SITE 806 HOLE C CORE 30H CORED INTERVAL 271.6-281.1 mbsf

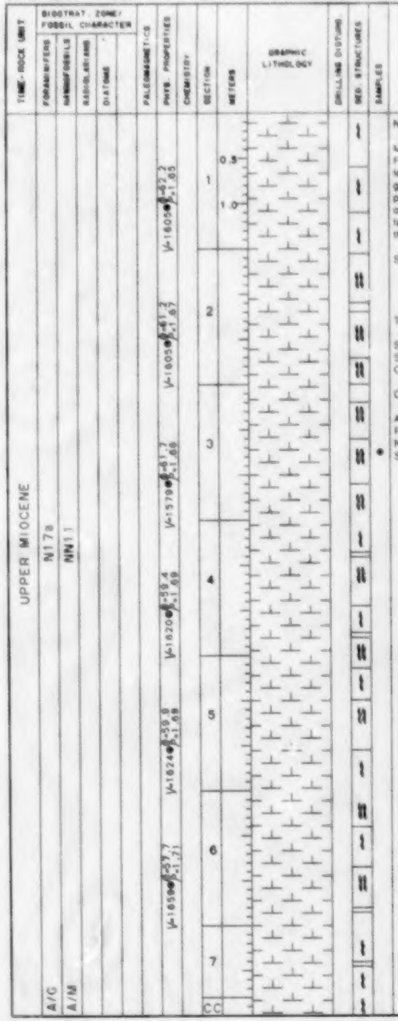
TIME-ROCK UNIT
BIOSTRAT. ZONE/FOSSIL CHARACTER
FORAMINIFERS
NANNOFOSSILS
RADIOLARIANS
DIATOMS
PALEOMAGNETICS
PHYS. PROPERTIES
CHEMISTRY
SECTION
METERS
GRAPHIC LITHOLOGY
DRILLING DISTURB.
SED. STRUCTURES
SAMPLES
UPPER MIOCENE
N17a
NN11
A/G
A/M
V-1605 φ-62.2 γ-1.65
V-1605 φ-61.2 γ-1.67
V-1579 φ-61.7 γ-1.66
V-1620 φ-59.4 γ-1.69
V-1624 φ-59.8 γ-1.68
V-1650 φ-57.7 γ-1.71
1
2
3
4
5
6
7
CC
0.5
1.0

LITHOLOGIC DESCRIPTION

NANNOFOSSIL OOZE with FORAMINIFERS

Major lithology: This core contains white (7.5YR 8/0) NANNOFOSSIL OOZE with FORAMINIFERS. The sequence appears to become coarser, with a higher concentration of foraminifers, towards the base of the core. The ooze is bioturbated as indicated by abundant light gray (2.5Y 7/2) mottles (1 to 3 cm in diameter), abundant pale purple (5P 6/2) mottles, and pyritized infillings of burrow. A number of cm scale, stiff to hard intervals are noticed within the ooze sequence. These intervals are spaced about 10 cm apart throughout the core. Some faint, diffuse pale yellowish green (10GY 7/2) color bands, about 1 cm thick, are scattered throughout the core.

SMEAR SLIDE SUMMARY (%):

	3, 78
	D
TEXTURE:	
Sand	10
Silt	55
Clay	33
COMPOSITION:	
Accessory minerals	2
Foraminifers	18
Nannofossils	77
Siliceous fragments	3

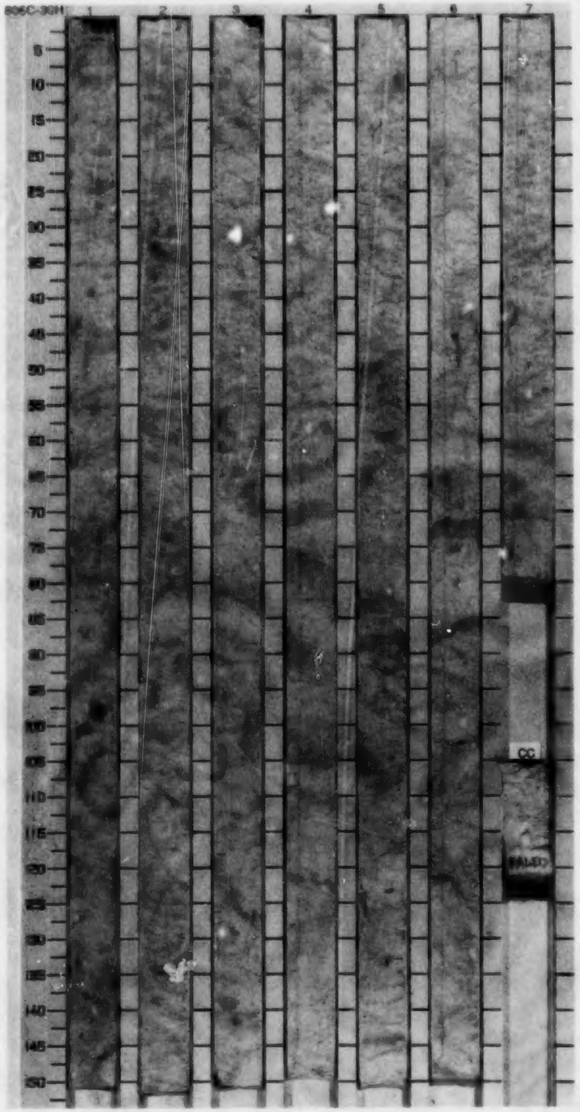
806C-30H
1
2
3
4
5
6
7
5
10
15
20
25
30
35
40
45
50
55
60
65
70
75
80
85
90
95
100
105
110
115
120
125
130
135
140
145
150
CC
PALEO

SITE 806 HOLE C CORE 31H CORED INTERVAL 281.1-290.6 mbsf

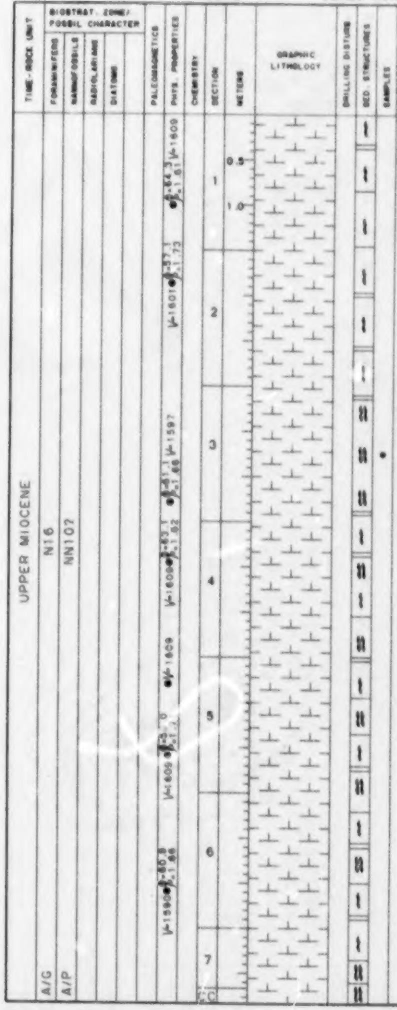

LITHOLOGIC DESCRIPTION

NANNOFOSSIL OOZE with FORAMINIFERS

Major lithology: This core contains white (7.5YR 8/0) NANNOFOSSIL OOZE with FORAMINIFERS. Light gray (2.5Y 7/2) mottles, 0.5 to 4 cm in diameter, are abundant. Numerous mottles, and pale purple (5P 6/2) halo structures also are present. Some traces of pyrite infilling are noticeable. Pale yellowish green (10GY 7/2) and pale purple (5P 6/2) color banding is sometimes recognizable. Semi-indurated (stiff) to semi-lithified (hard) layers are intercalated with the softer ooze throughout the core. These layers may represent nodules, 1 to several cm thick, and occur every 5 to 10 cm.

SMEAR SLIDE SUMMARY (%):

	3, 74
	D
TEXTURE:	
Sand	8
Silt	60
Clay	32
COMPOSITION:	
Accessory minerals	2
Foraminifers	10
Nannofossils	85
Siliceous fragments	3

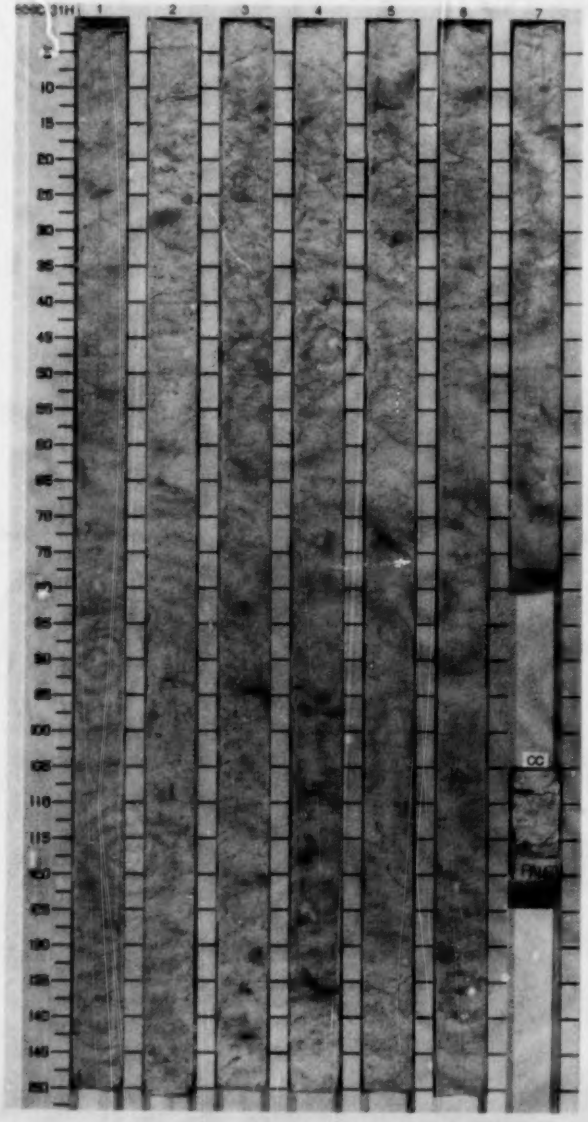
806C 31H
1
2
3
4
5
6
7
CC
0
10
15
20
25
30
35
40
45
50
55
60
65
70
75
80
85
90
95
100
105
110
115
120
125
130
135
140
145
150

SITE 806 HOLE C CORE 32H CORED INTERVAL 290.8-300.1 mbsf

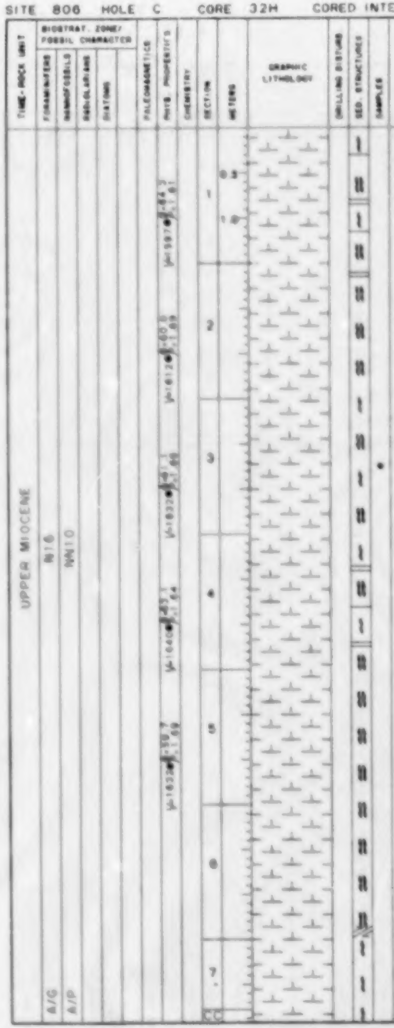
TIME-ROCK UNIT
BIOSTRAT. ZONE/ FOSSIL CHARACTER
FORAMINIFERS
NANNOFOSSILS
RADIOLARIANS
DIATOMS
PALEOMAGNETICS
PHYS. PROPERTIES
CHEMISTRY
SECTION
METERS
GRAPHIC LITHOLOGY
DRILLING DISTURB.
SED. STRUCTURES
SAMPLES
UPPER MIOCENE
N16
NN10
A/G
A/P
1
2
3
4
5
6
7
CC
0.5
1.0

LITHOLOGIC DESCRIPTION

NANNOFOSSIL OOZE with FORAMINIFERS

Major lithology: This core contains white (7.5YR 8/0) NANNOFOSSIL OOZE with FORAMINIFERS. The ooze is bioturbated with pale purple (5P 6/2) halos, and streaks, and light gray (5Y 7/2) burrow fills. Some intervals (3 to 5 cm thick) are stiffer than the surrounding sections. Faint pale purple (5P 6/2) and, less commonly, pale yellowish green (10GY 7/2), 1 to 2 cm thick bands are present throughout. The base of Section 6 exhibits minor microfaulting.

SMEAR SLIDE SUMMARY (%)

	3, 75
	D
TEXTURE:	
Sand	15
Silt	60
Clay	25
COMPOSITION:	
Diatoms	1
Foraminifers	20
Nannofossils	77
Radiolarians	1
Siliceous fragments	1

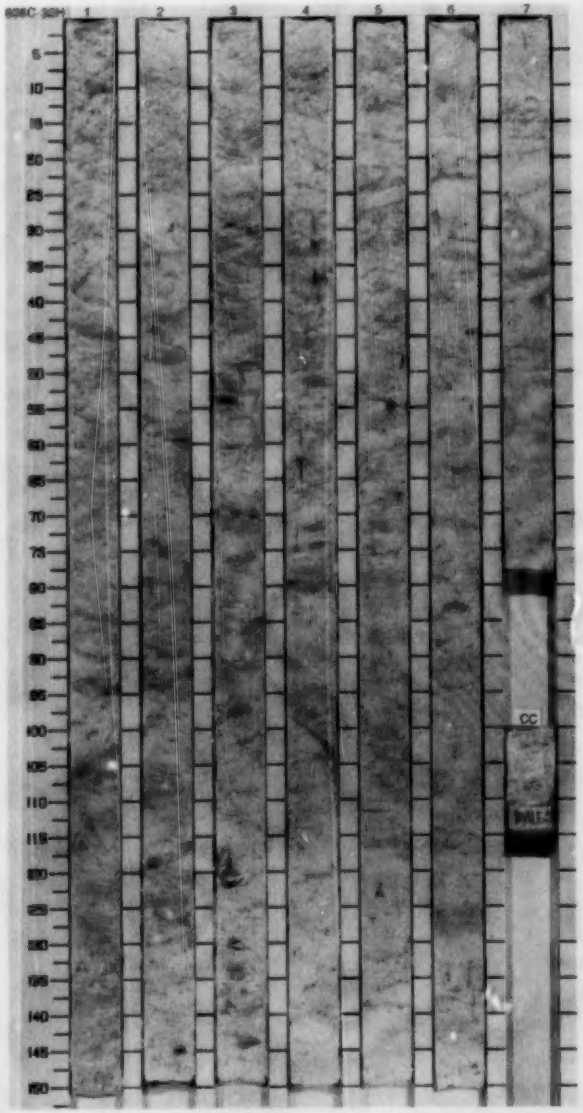
806C-32H
1
2
3
4
5
6
7
CC
5
10
15
20
25
30
35
40
45
50
55
60
65
70
75
80
85
90
95
100
105
110
115
120
125
130
135
140
145
150

SITE 806 HOLE C CORE 33H CORED INTERVAL 300.1-309.6 mbsf

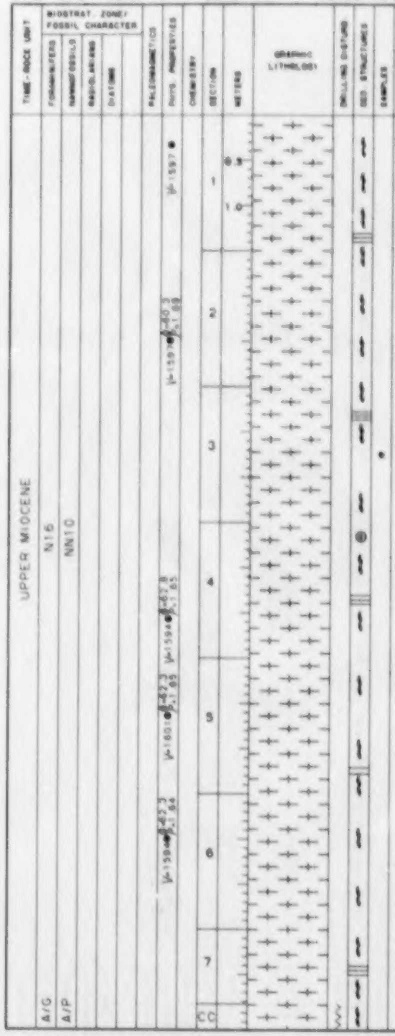
TIME-ROCK UNIT
BIOSTRAT. ZONE/ FOSSIL CHARACTER
FORAMINIFERS
NANNOFOSSILS
RADIOLARIANS
DIATOMS
PALEOMAGNETICS
PHYS. PROPERTIES
CHEMISTRY
SECTION
METERS
GRAPHIC LITHOLOGY
DRILLING DISTURB.
SED. STRUCTURES
SAMPLES
UPPER MIOCENE
N16
NN10
A/G
A/P
1
2
3
4
5
6
7
CC
0.5
1.0

LITHOLOGIC DESCRIPTION

NANNOFOSSIL OOZE with FORAMINIFERS

Major lithology: This core contains white (7.5YR 8/0) NANNOFOSSIL OOZE with FORAMINIFERS. Many 3 to 5 cm thick intervals are semi-consolidated. The ooze is bioturbated with light gray (5Y 7/2) mottles and pale purple (5P 6/2) streaks. The top of Section 4 contains a large porcellanite nodule. Faint pale purple (5P 6/2) and pale yellowish green (10GY 7/2), 1 to 2 cm thick bands are present throughout the core.

SMEAR SLIDE SUMMARY (%):

	3, 75
	D
TEXTURE:	
Sand	10
Silt	60
Clay	30
COMPOSITION:	
Diatoms	2
Foraminifers	25
Nannofossils	69
Radiolarians	1
Siliceous fragments	3
Siliceous sponge spicules	Tr

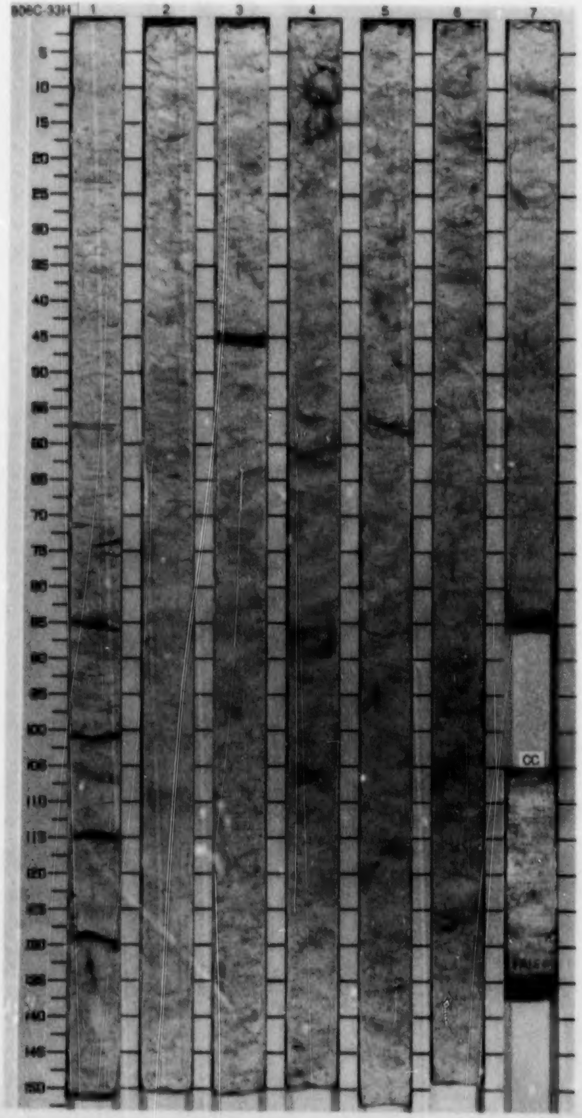
806C-33H
1
2
3
4
5
6
7
CC
5
10
15
20
25
30
35
40
45
50
55
60
65
70
75
80
85
90
95
100
105
110
115
120
125
130
135
140
145
150

SITE 806 HOLE C CORE 34X CORED INTERVAL 309.6-319.3 mbsf

TIME-ROCK UNIT	BIOSTRAT. ZONE/ FOSSIL CHARACTER				PALEOMAGNETICS	PHYS. PROPERTIES	CHEMISTRY	SECTION	METERS	GRAPHIC LITHOLOGY	DRILLING DISTURB.	SED. STRUCTURES	SAMPLES	LITHOLOGIC DESCRIPTION
	FORAMINIFERS	NANNOFOSSILS	RADIOLARIANS	DIATOMS										
UPPER MIOCENE	A/M N16	A/M NN10						CC						All recovery went to the paleontology laboratory. SMEAR SLIDE SUMMARY (%): CC, 1 D TEXTURE: Silt 70 Clay 30 COMPOSITION: Nannofossils 30 Silica 70

SITE 806 HOLE C CORE 35X CORED INTERVAL 319.3-328.9 mbsf

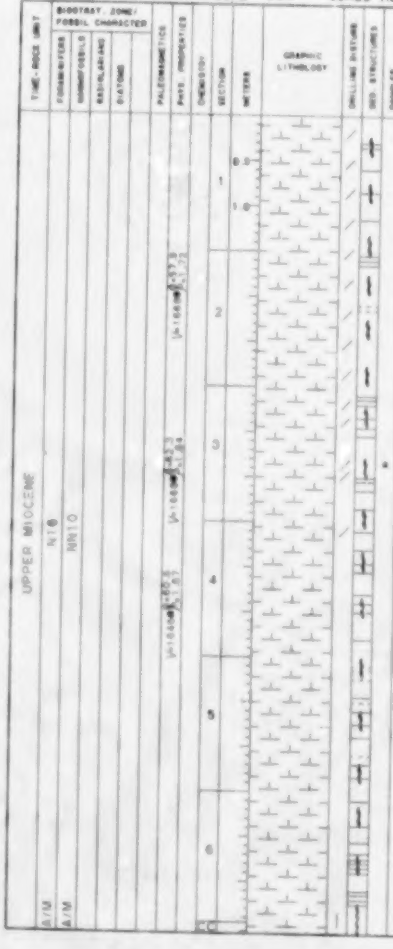
TIME-ROCK UNIT
BIOSTRAT. ZONE/ FOSSIL CHARACTER
FORAMINIFERS
NANNOFOSSILS
RADIOLARIANS
DIATOMS
PALEOMAGNETICS
PHYS. PROPERTIES
CHEMISTRY
SECTION
METERS
GRAPHIC LITHOLOGY
DRILLING DISTURB.
SED. STRUCTURES
SAMPLES
UPPER MIOCENE
N18
NN10
A/M
A/M
1
2
3
4
5
6
CC
0.5
1.0

LITHOLOGIC DESCRIPTION

NANNOFOSSIL OOZE

Major lithology: This core contains white (2.5Y 8/0) NANNOFOSSIL OOZE. The softer ooze is interbedded with 5 cm thick indurated sections. The entire core is moderately bioturbated with pyritized burrows and faint grayish blue (5PB 5/2) to pale purple (5P [illegible]/2) and dark gray (5Y 4/1) to light gray (2.5Y 7/2) mottling. Diffuse light greenish gray (5G [illegible]/1) and grayish blue (5PB 5/2) color bands are widespread.

SMEAR SLIDE SUMMARY (%):

	3, 80
	D
TEXTURE:	
Sand	2
Silt	90
Clay	8
COMPOSITION:	
Foraminifers	6
Nannofossils	92
Radiolarians	1
Siliceous fragments	1

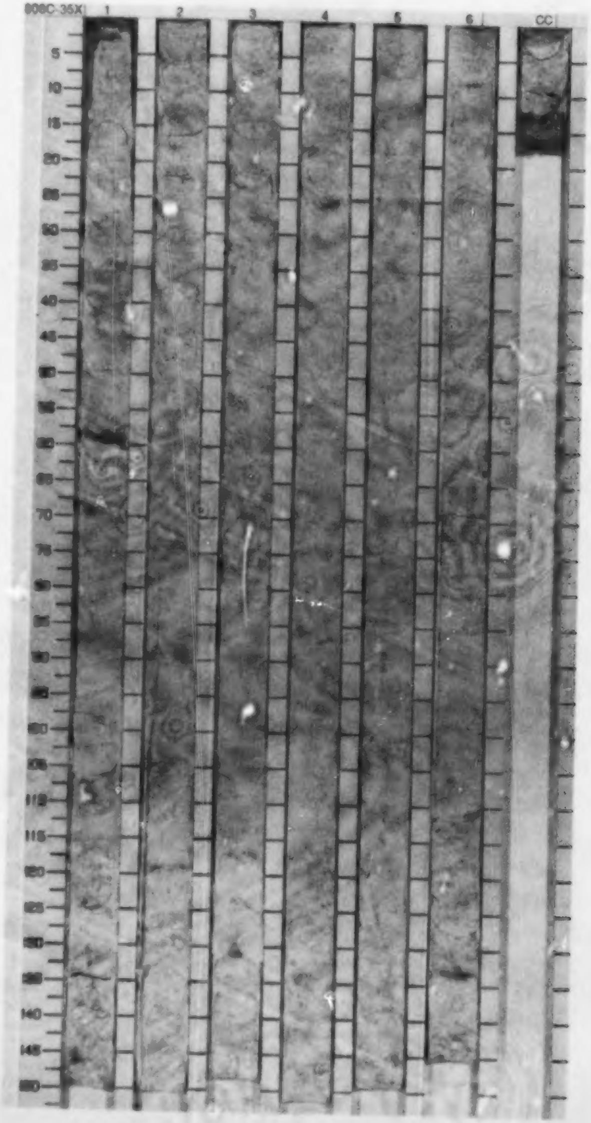
806C-35X
1
2
3
4
5
6
CC
5
10
15
20
25
30
35
40
45
50
55
60
65
70
75
80
85
90
95
100
105
110
115
120
125
130
135
140
145
150

SITE 806 HOLE C CORE 36X CORED INTERVAL 328.9-338.5 mbsf

TIME-ROCK UNIT	FORAMINIFERS	NANNOFOSSILS	RADIOLARIANS	DIATOMS	PALEOMAGNETICS	PHYS. PROPERTIES	CHEMISTRY	SECTION	METERS	DRILLING DISTURB.	SED. STRUCTURES	SAMPLES
UPPER MIOCENE	N16	NN9				V=1662 φ=59.9 γ=1.72		1	0.5 1.0			*
						V=1627 φ=57.8 γ=1.64		2				
						V=1580 φ=60.6 γ=1.66		3				
						V=1550 φ=57.5 γ=1.63		4				
						V=1519		5				
						V=1555 φ=60.4 γ=1.67		6				
	A/M	A/M						7 CC				

GRAPHIC LITHOLOGY

LITHOLOGIC DESCRIPTION

NANNOFOSSIL OOZE

Major lithology: This core contains white (2.5Y 8/0) NANNOFOSSIL OOZE. The softer ooze is interbedded with 5 to 10 cm thick, indurated sections. The entire core is moderately bioturbated with pyritized burrows and faint, grayish blue (5PB 5/2) to pale purple (5P 6/2) and dark gray (5Y 4/1) to light gray (2.5Y 7/2) mottling. Diffuse light greenish gray (5G 7/1) and grayish blue (5PB 5/2) color bands appear throughout.

SMEAR SLIDE SUMMARY (%):

	1, 80
	D
TEXTURE:	
Sand	10
Silt	85
Clay	5
COMPOSITION:	
Foraminifers	8
Nannofossils	91
Radiolarians	1

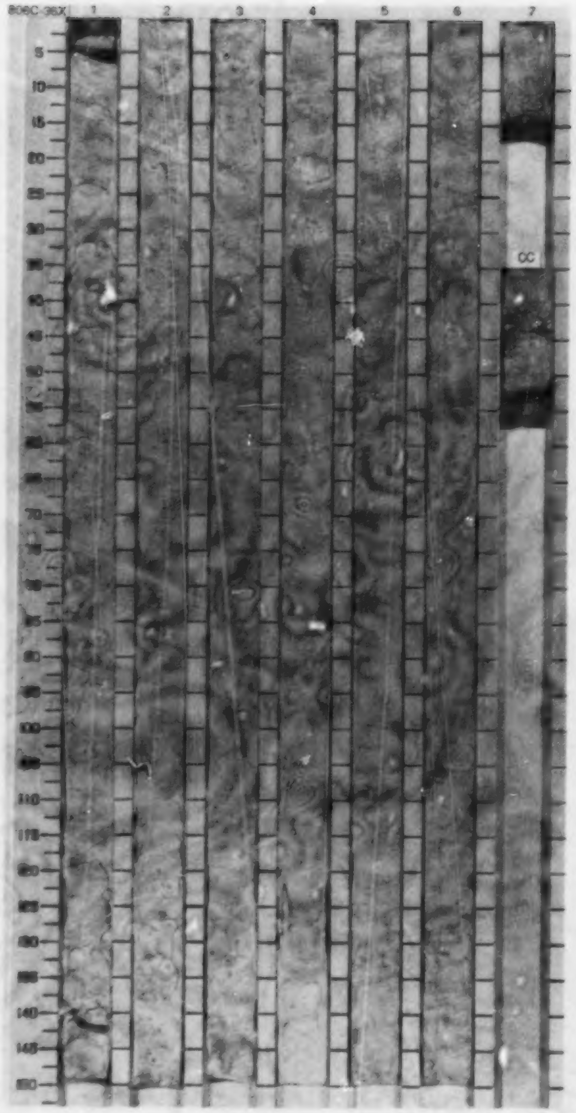
806C-36X
1
2
3
4
5
6
7
CC
5
10
15
20
25
30
35
40
45
50
55
60
65
70
75
80
85
90
95
100
105
110
115
120
125
130
135
140
145
150

SITE 806 HOLE C CORE 37X CORED INTERVAL 338.5-348.2 mbsf

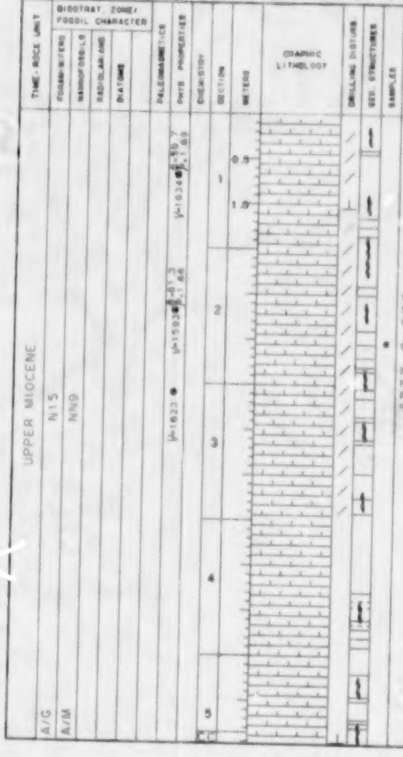
TIME-ROCK UNIT
BIOSTRAT. ZONE/ FOSSIL CHARACTER
FORAMINIFERS
NANNOFOSSILS
RADIOLARIANS
DIATOMS
PALEOMAGNETICS
PHYS. PROPERTIES
CHEMISTRY
SECTION
METERS
GRAPHIC LITHOLOGY
DRILLING DISTURB.
SED. STRUCTURES
SAMPLES
UPPER MIOCENE
N15
NN9
A/G
A/M
V=1634
φ=59.7
γ=1.60
V=1593
φ=61.3
γ=1.64
V=1623
1
2
3
4
5
CC
0.5
1.0

LITHOLOGIC DESCRIPTION

NANNOFOSSIL CHALK

Major lithology: This core contains white (2.5Y 8/0) NANNOFOSSIL CHALK. It is slightly to moderately fragmented. Slight to moderate bioturbation is represented by pyritized burrows and grayish blue (5PB 5/2) mottling. Faint and sharp, pale pink (5RP 5/2), light greenish gray (5G 7/1) and pale purple (5P 6/2) color bands are present through this core.

SMEAR SLIDE SUMMARY (%):

	2, 102 D
TEXTURE:	
Sand	15
Silt	80
Clay	5
COMPOSITION:	
Foraminifers	8
Nannofossils	90
Radiolarians	1
Silicoflagellates	1

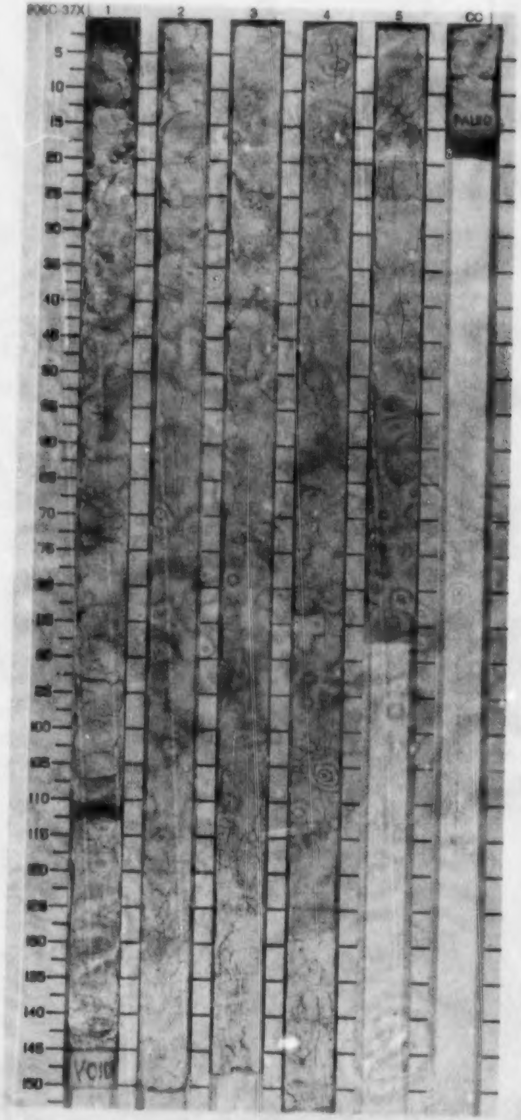
806C-37X
1
2
3
4
5
CC
PALEO
VOID
5
10
15
20
25
30
35
40
45
50
55
60
65
70
75
80
85
90
95
100
105
110
115
120
125
130
135
140
145
150

SITE 806 HOLE C CORE 38X CORED INTERVAL 248.2-357.9 mbsf

TIME-ROCK UNIT	BIOSTRAT. ZONE/ FOSSIL CHARACTER FORAMINIFERS	NANNOFOSSILS	RADIOLARIANS	DIATOMS	PALEOMAGNETICS	PHYS. PROPERTIES	CHEMISTRY	SECTION	METERS	GRAPHIC LITHOLOGY	DRILLING DISTURB.	SED. STRUCTURES	SAMPLES
UPPER MIOCENE	N15	NN9				V-1593● φ-58.1 γ-1.72		1	0.5 1.0				*
						V-1623● φ-63.3 γ-1.62		2					
						V-1670● φ-63.4 γ-1.62		3					
						V-1666● φ-58.6 γ-1.70		4					
						V-1703● φ-62.8 γ-1.63		5					
	A/M	A/M						CC					

LITHOLOGIC DESCRIPTION

NANNOFOSSIL CHALK

Major lithology: This core contains white (2.5Y 8/0 and 10YR 8/0) NANNOFOSSIL CHALK. Bioturbation is slight to moderate as indicated by mottling. Centimeter size chert nodules are present in Sections 1 and 2. Distinct mm size, gray (N6), greenish gray (5G 6/1) to grayish green (5G 5/2) bands and diffuse, cm scale, light greenish gray (5G 7/1), pale purple (5P 6/2) and grayish blue (5PB 5/2) bands are common.

SMEAR SLIDE SUMMARY (%):

	1, 96 D
TEXTURE:	
Sand	15
Silt	80
Clay	5
COMPOSITION:	
Foraminifers	8
Nannofossils	90
Radiolarians	2

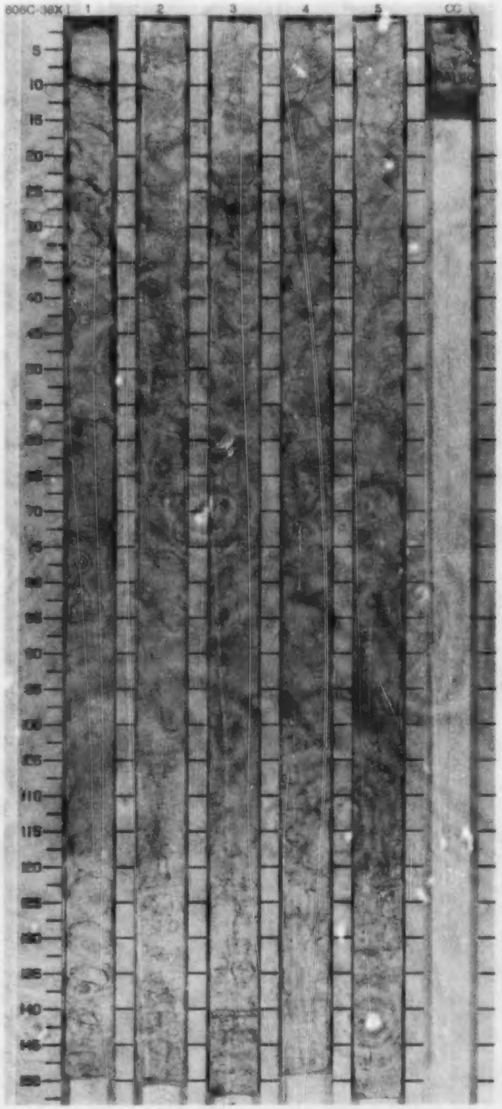

SITE 806 HOLE C CORE 39X CORED INTERVAL 357.9-367.6 mbsf

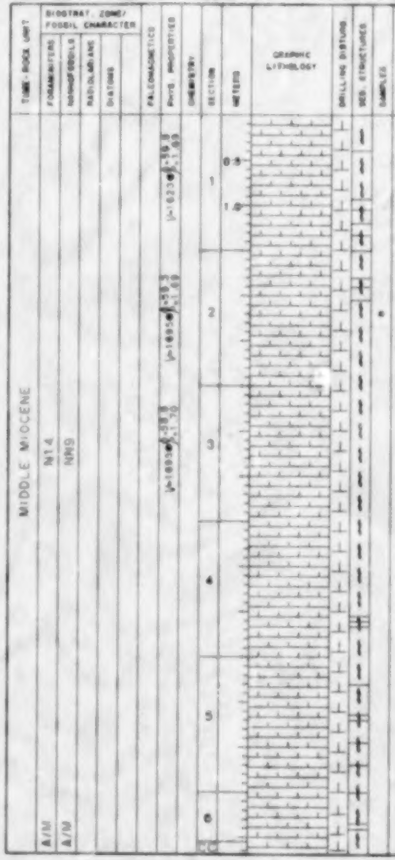
TIME-ROCK UNIT
BIOSTRAT. ZONE/ FOSSIL CHARACTER
FORAMINIFERS
NANNOFOSSILS
RADIOLARIANS
DIATOMS
PALEOMAGNETICS
PHYS. PROPERTIES
CHEMISTRY
SECTION
METERS
GRAPHIC LITHOLOGY
DRILLING DISTURB.
SED. STRUCTURES
SAMPLES
MIDDLE MIOCENE
N14
NN9
A/M
A/M
V=1623 ● φ=59.8 γ=1.83
V=1695 ● φ=59.3 γ=1.69
V=1695 ● φ=58.9 γ=1.70
1
2
3
4
5
6
CC
0.5
1.0

LITHOLOGIC DESCRIPTION

NANNOFOSSIL CHALK with FORAMINIFERS

Major lithology: This core contains slightly to moderately bioturbated, white (2.5Y 8/0) NANNOFOSSIL CHALK with FORAMINIFERS. The color grades locally to pale pink (5RP 8/2) and pale purple (5P 6/2) for intervals of 1 to 3 cm. Minor mm scale, grayish blue (5 PB 5/2) pyritic burrow fills are present, as are mm to cm thick, light greenish gray (5G 7/1) and light grayish green (5G 8/2) color bands.

SMEAR SLIDE SUMMARY (%):

	2, 70
	D
TEXTURE:	
Sand	20
Silt	75
Clay	5
COMPOSITION:	
Foraminifers	12
Nannofossils	83
Radiolarians	5

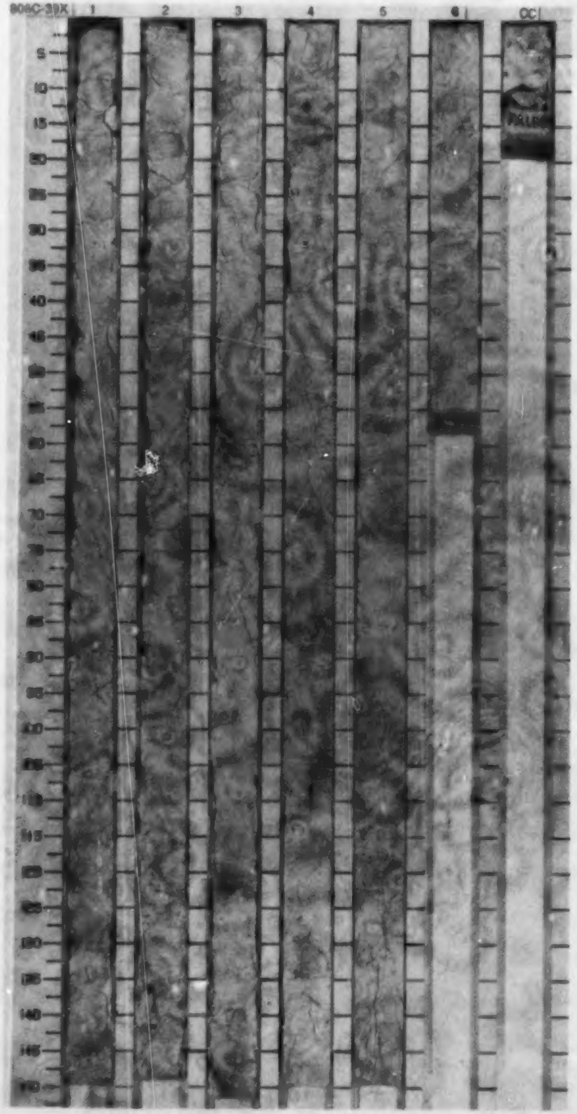
806C-39X
1
2
3
4
5
6
CC
5
10
15
20
25
30
35
40
45
50
55
60
65
70
75
80
85
90
95
100
105
110
115
120
125
130
135
140
145
150

SITE 806 HOLE C CORE 40X CORED INTERVAL 367.6-377.3 mbsf

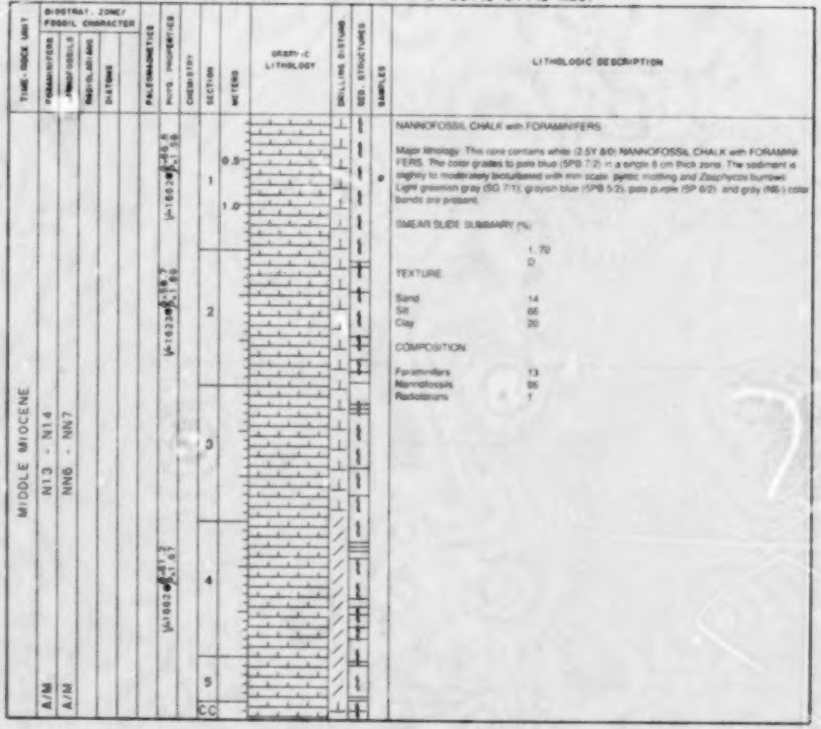
TIME-ROCK UNIT
BIOSTRAT. ZONE/ FOSSIL CHARACTER
FORAMINIFERS
NANNOFOSSILS
RADIOLARIANS
DIATOMS
PALEOMAGNETICS
PHYS. PROPERTIES
CHEMISTRY
SECTION
METERS
GRAPHIC LITHOLOGY
DRILLING DISTURB.
SED. STRUCTURES
SAMPLES
MIDDLE MIOCENE
N13 - N14
NN6 - NN7
A/M
A/M
0.5
1.0
1
2
3
4
5
CC

LITHOLOGIC DESCRIPTION

NANNOFOSSIL CHALK with FORAMINIFERS

Major lithology: This core contains white (2.5Y 8/0) NANNOFOSSIL CHALK with FORAMINIFERS. The color grades to pale blue (5PB 7/2) in a single 8 cm thick zone. The sediment is slightly to moderately bioturbated with mm scale, pyritic mottling and *Zoophycos* burrows. Light greenish gray (5G 7/1), grayish blue (5PB 5/2), pale purple (5P 6/2), and gray (N6) color bands are present.

SMEAR SLIDE SUMMARY (%):

	1, 70
	D
TEXTURE:	
Sand	14
Silt	66
Clay	20
COMPOSITION:	
Foraminifers	13
Nannofossils	86
Radiolarians	1

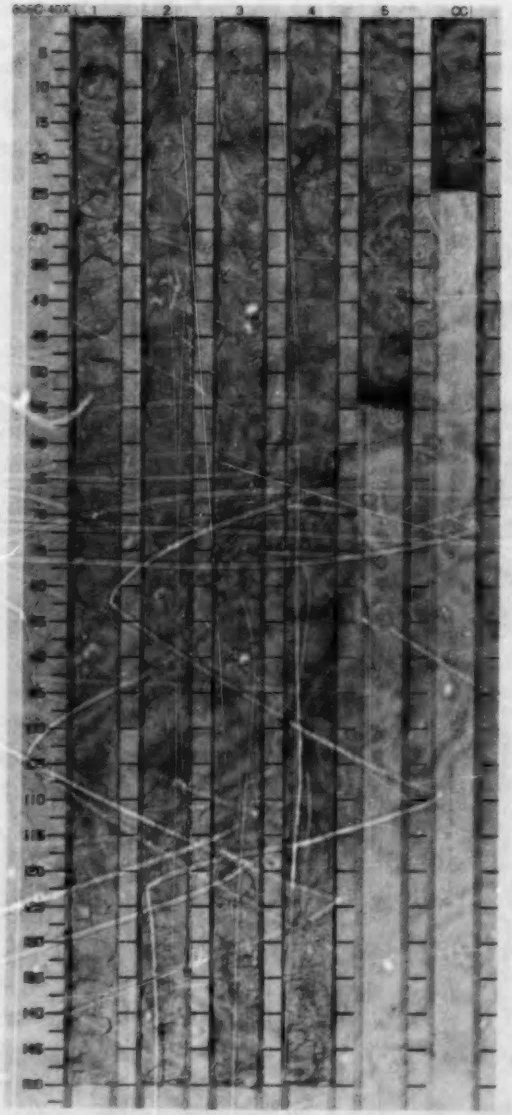
806C-40X
1
2
3
4
5
CC
5
10
15
20
25
30
35
40
45
50
55
60
65
70
75
80
85
90
95
100
105
110
115
120
125
130
135
140
145
150

SITE 806 HOLE C CORE 41X CORED INTERVAL 377.3-387.0 mbsf

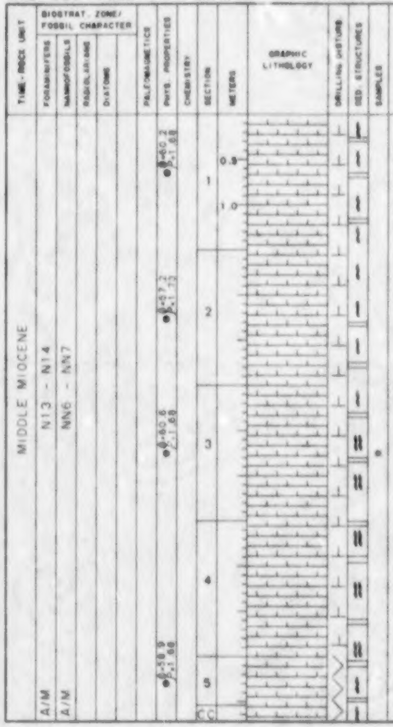
TIME-ROCK UNIT
BIOSTRAT. ZONE/ FOSSIL CHARACTER
FORAMINIFERS
NANNOFOSSILS
RADIOLARIANS
DIATOMS
PALEOMAGNETICS
PHYS. PROPERTIES
CHEMISTRY
SECTION
METERS
GRAPHIC LITHOLOGY
DRILLING DISTURB.
SED. STRUCTURES
SAMPLES
MIDDLE MIOCENE
N13 - N14
NN6 - NN7
A/M
A/M
60.2
1.68
67.2
1.73
60.6
1.68
58.9
1.68
1
2
3
4
5
CC
0.5
1.0

LITHOLOGIC DESCRIPTION

NANNOFOSSIL CHALK with FORAMINIFERS

Major lithology: This core contains white (10YR 8/1) NANNOFOSSIL CHALK with FORAMINIFERS. The sediment is moderately to heavily bioturbated, evident from disseminated pyritic burrow fills. Distinct and faint, mm to cm scale, greenish gray (5G 7/1) and pale purple (5P 6/2) color bands are common.

SMEAR SLIDE SUMMARY (%):

	3, 75
	D
TEXTURE	
Sand	15
Silt	60
Clay	20
COMPOSITION	
Diatoms	Tr
Foraminifers	20
Nannofossils	80
Siliceous fragments	Tr

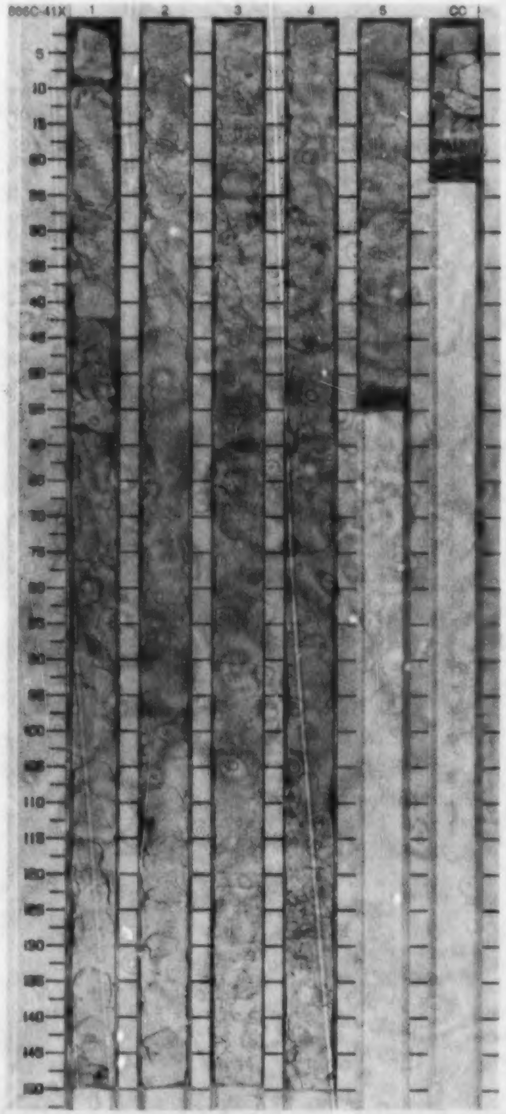
806C-41X
1
2
3
4
5
CC
5
10
15
20
25
30
35
40
45
50
55
60
65
70
75
80
85
90
95
100
105
110
115
120
125
130
135
140
145
150

SITE 806 HOLE C CORE 42X CORED INTERVAL 387.0-396.7 mbsf

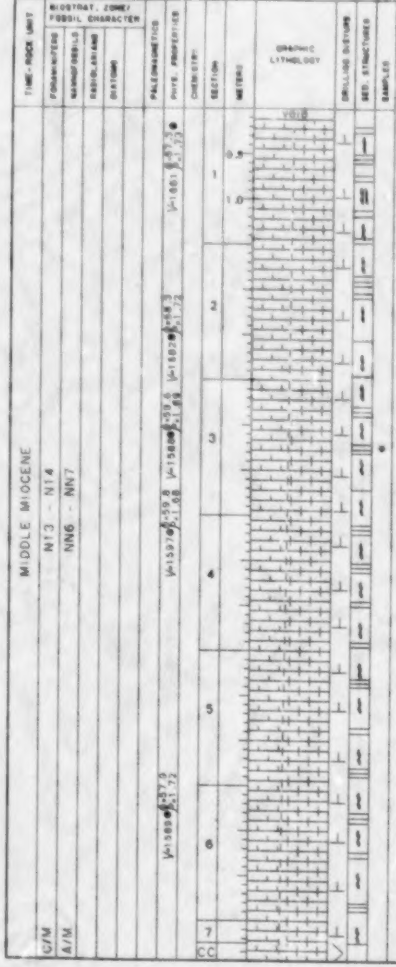
TIME-ROCK UNIT
BIOSTRAT. ZONE/ FOSSIL CHARACTER
FORAMINIFERS
NANNOFOSSILS
RADIOLARIANS
DIATOMS
PALEOMAGNETICS
PHYS. PROPERTIES
CHEMISTRY
SECTION
METERS
GRAPHIC LITHOLOGY
DRILLING DISTURB.
SED. STRUCTURES
SAMPLES
MIDDLE MIOCENE
N13 - N14
NN6 - NN7
C/M
A/M
V-1661 ϕ-57.3 •1.73
V-1582 ϕ-58.3 •1.72
V-1588 ϕ-59.6 •1.69
V-1597 ϕ-59.8 •1.68
V-1580 ϕ-57.9 •1.72
1
2
3
4
5
6
7
CC
0.5
1.0
VOID

LITHOLOGIC DESCRIPTION

NANNOFOSSIL CHALK with FORAMINIFERS interbedded with FORAMINIFER NANNOFOSSIL CHALK

Major lithology: This core contains white (10YR 8/1) NANNOFOSSIL CHALK with FORAMINIFERS interbedded with FORAMINIFER NANNOFOSSIL CHALK. Disseminated pyrite burrow fills, pyrite concretions, and trace fossils are indicative of moderate bioturbation. Abundant distinct, very thin (mm scale), pale yellowish green (10GY 7/2) and grayish green (5GY 7/1) color bands are present throughout the core. Pale purple (5P 6/2) color bands are less abundant.

SMEAR SLIDE SUMMARY (%):

	3, 75
	D
TEXTURE:	
Sand	20
Silt	55
Clay	25
COMPOSITION:	
Foraminifers	30
Nannofossils	70
Siliceous sponge spicules	Tr

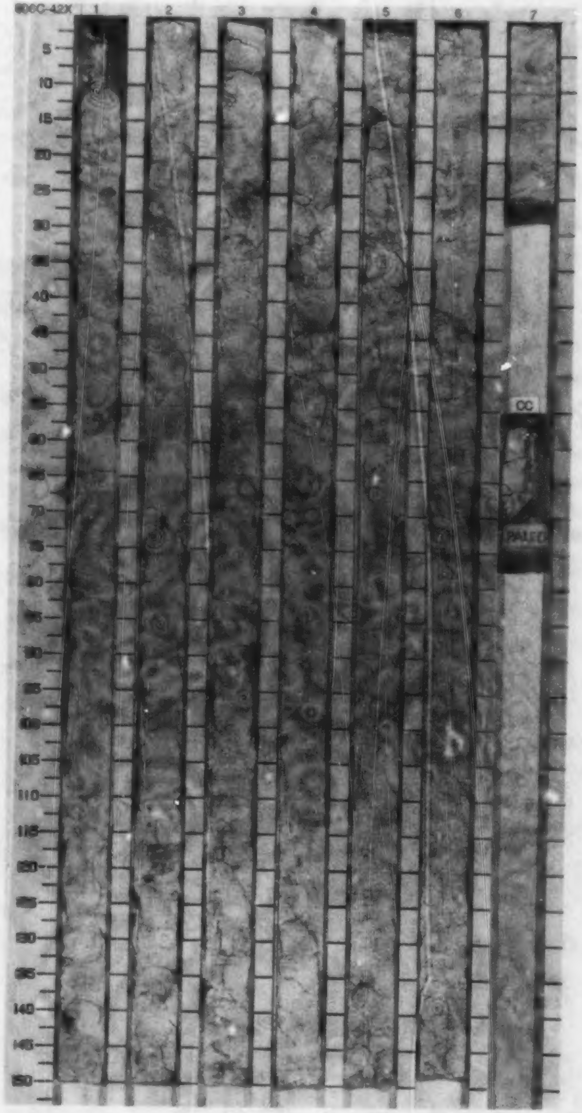
806C-42X
1
2
3
4
5
6
7
CC
PALEO
5
10
15
20
25
30
35
40
45
50
55
60
65
70
75
80
85
90
95
100
105
110
115
120
125
130
135
140
145
150

SITE 806 HOLE C CORE 43X CORED INTERVAL 396.7-406.3 mbsf

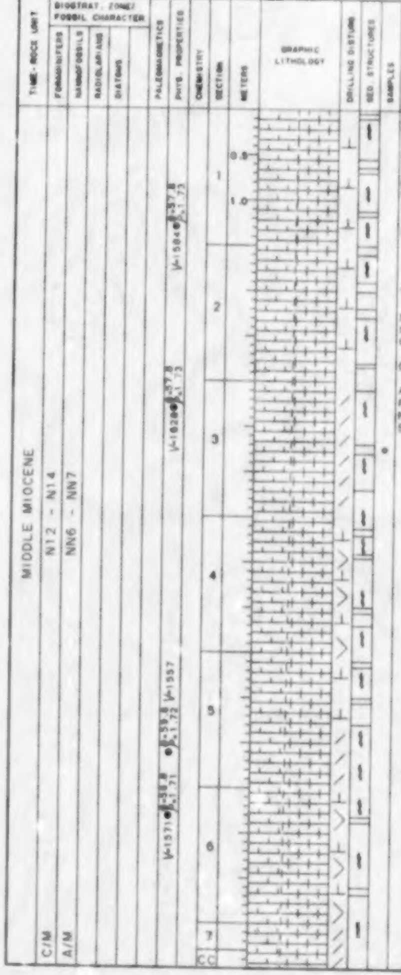
TIME-ROCK UNIT
BIOSTRAT. ZONE/ FOSSIL CHARACTER
FORAMINIFERS
NANNOFOSSILS
RADIOLARIANS
DIATOMS
PALEOMAGNETICS
PHYS. PROPERTIES
CHEMISTRY
SECTION
METERS
GRAPHIC LITHOLOGY
DRILLING DISTURB.
SED. STRUCTURES
SAMPLES
MIDDLE MIOCENE
N12 - N14
NN6 - NN7
C/M
A/M
γ-1504
φ-57.8
γ-1.73
γ-1628
φ-57.8
γ-1.73
γ-1571
φ-58.8
γ-1.71
φ-59.8
γ-1.72
γ-1557
1
2
3
4
5
6
7
CC
0.5
1.0

LITHOLOGIC DESCRIPTION

NANNOFOSSIL CHALK with FORAMINIFERS interbedded with FORAMINIFER NANNOFOSSIL CHALK

Major lithology: This core contains white (10YR 8/1) NANNOFOSSIL CHALK with FORAMINIFERS interbedded with FORAMINIFER NANNOFOSSIL CHALK. Horizontal, 1 to 2 mm thick pale yellowish green (10GY 7/2) and grayish green (5GY 7/1) bands are present throughout the core. Disseminated pyrite burrow fills and pyrite concretions, and trace fossils indicate moderate bioturbation.

SMEAR SLIDE SUMMARY (%):

	3, 74
	D
TEXTURE	
Sand	10
Silt	60
Clay	30
COMPOSITION	
Accessory minerals	2
Foraminifers	20
Nannofossils	75
Siliceous fragments	3

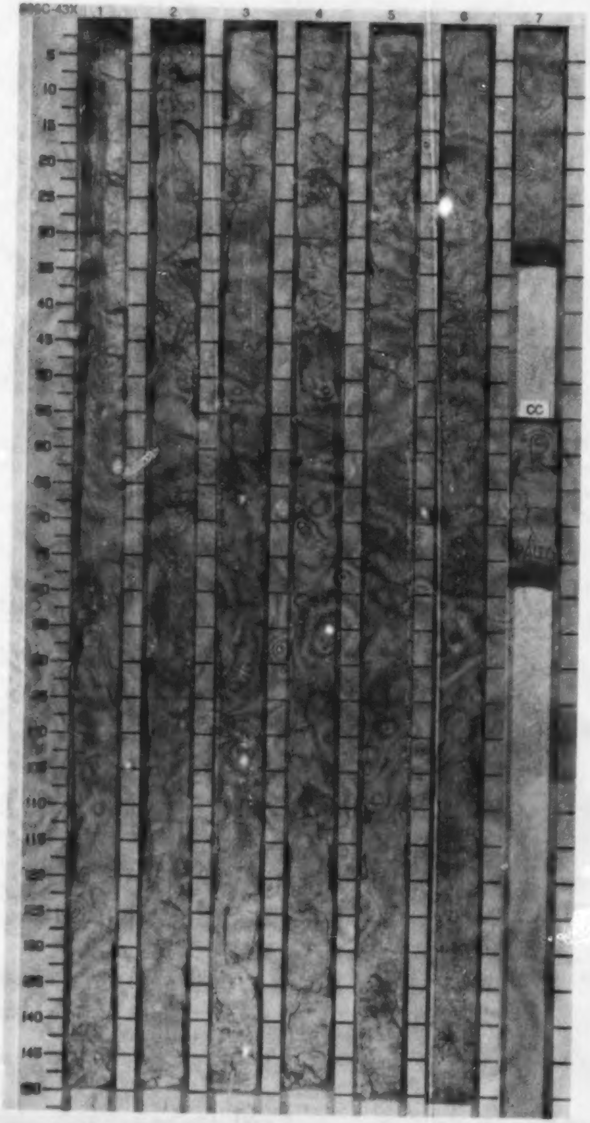
806C-43X
1
2
3
4
5
6
7
5
10
15
20
25
30
35
40
45
50
55
60
65
70
75
80
85
90
95
100
105
110
115
120
125
130
135
140
145
150
CC

SITE 806 HOLE C CORE 44X CORED INTERVAL 406.3-415.9 mbsf

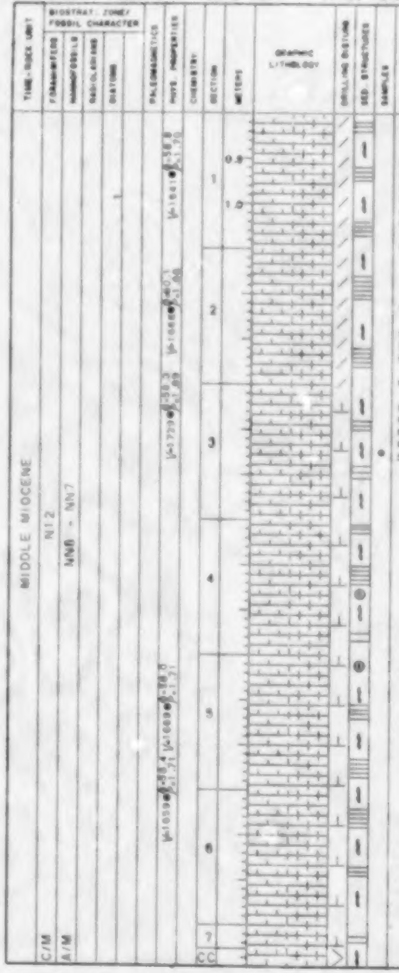

LITHOLOGIC DESCRIPTION

NANNOFOSSIL CHALK with FORAMINIFERS interbedded with FORAMINIFER NANNOFOSSIL CHALK

Major lithology: The core contains white (10YR 8/1) NANNOFOSSIL CHALK with FORAMINIFERS interbedded with FORAMINIFER NANNOFOSSIL CHALK. Light gray (2.5Y 7/2) cm-scale burrow mottles, disseminated pyrite-filled burrows, and calcite nodules are indicative of moderate bioturbation. Thin (mm scale), distinct and faint, greenish gray (5G 7/1) and pale yellowish green (10GY 7/2) color bands are common. Pale purple (5P 6/2) color bands are less common. Section 7 and the Core Catcher are characterized by faint color bands.

SMEAR SLIDE SUMMARY (%):

	3, 75
	D
TEXTURE:	
Sand	10
Silt	60
Clay	30
COMPOSITION:	
Diatoms	3
Foraminifers	25
Nannofossils	64
Radiolarians	3
Siliceous fragments	5

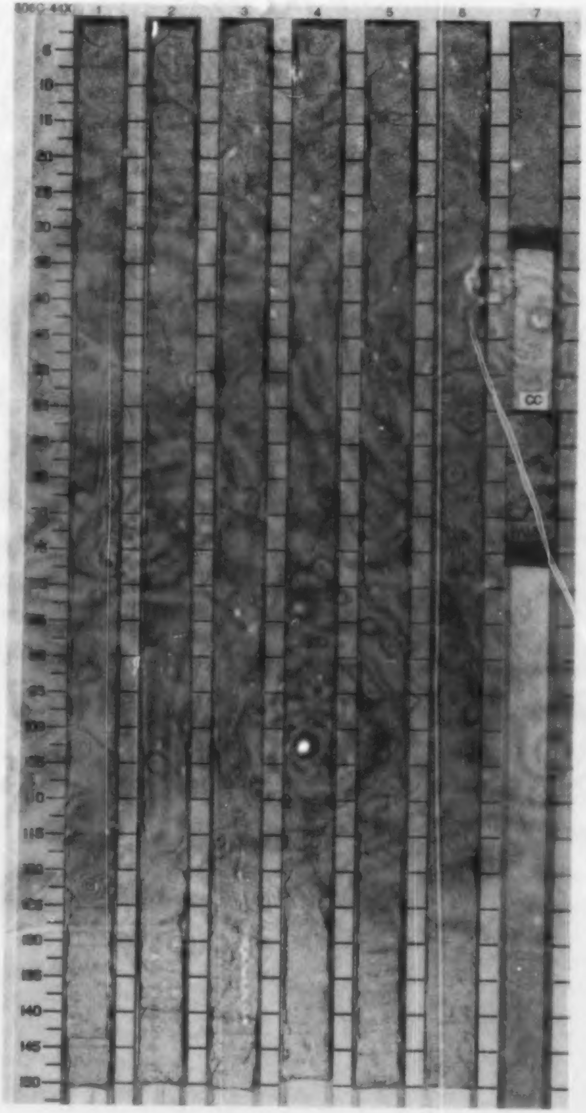
806C-44X
1
2
3
4
5
6
7
CC
5
10
15
20
25
30
35
40
45
50
55
60
65
70
75
80
85
90
95
100
105
110
115
120
125
130
135
140
145
150

SITE 806 HOLE C CORE 45X CORED INTERVAL 415.9-425.6 mbsf

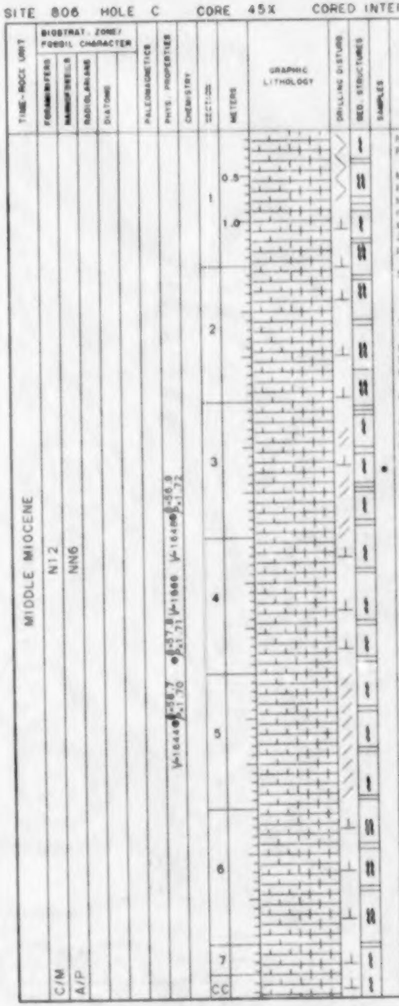

LITHOLOGIC DESCRIPTION

NANNOFOSSIL CHALK with FORAMINIFERS interbedded with FORAMINIFER NANNOFOSSIL CHALK

Major lithology: This core contains white (10YR 8/0) NANNOFOSSIL CHALK with FORAMINIFERS interbedded with FORAMINIFER NANNOFOSSIL CHALK, both of which are slightly to moderately fractured (heavily fragmented in top of Section 1) by drilling. The sediment is moderately bioturbated as indicated by light gray (2.5Y 7/2) mottles, pyritized burrow fills and specks. Some pyritic burrows are disseminated and others exhibit halos. In Section 7, a *Zoophycos* burrow is observed. Faint, distinct, mm thick, greenish gray (5G 7/1) and pale purple (5P 6/2) color bands are abundant throughout the core.

SMEAR SLIDE SUMMARY (%):

	3, 75
	D
TEXTURE:	
Sand	10
Silt	65
Clay	25
COMPOSITION:	
Diatoms	1
Foraminifers	28
Nannofossils	67
Radiolarians	1
Siliceous fragments	3

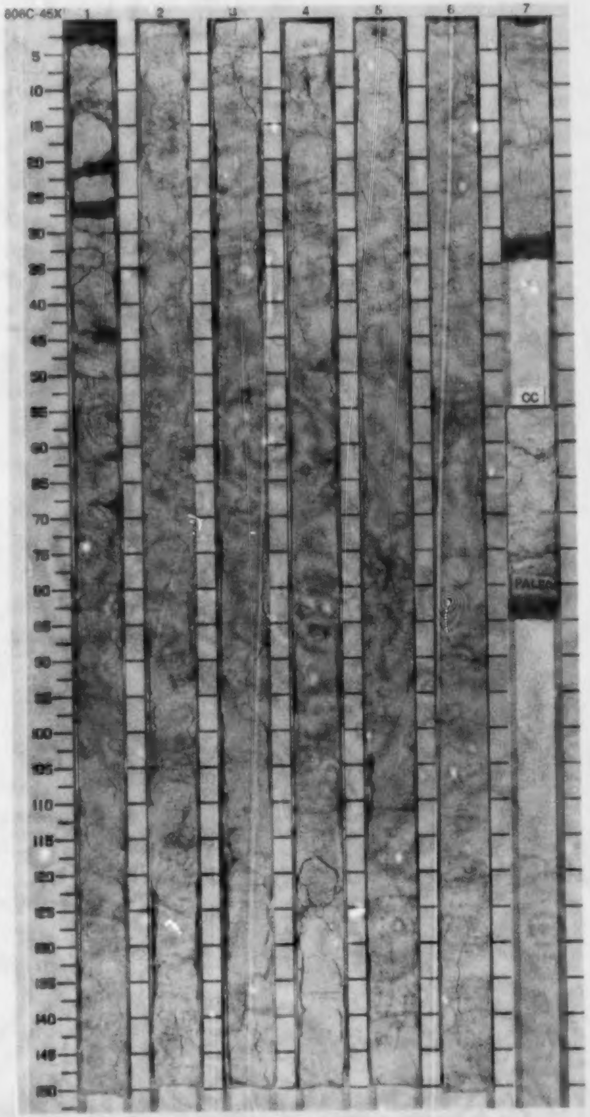
806C-45X
1
2
3
4
5
6
7
CC
PALEO
5
10
15
20
25
30
35
40
45
50
55
60
65
70
75
80
85
90
95
100
105
110
115
120
125
130
135
140
145
150

SITE 806 HOLE C CORE 46X CORED INTERVAL 425.6-435.2 mbsf

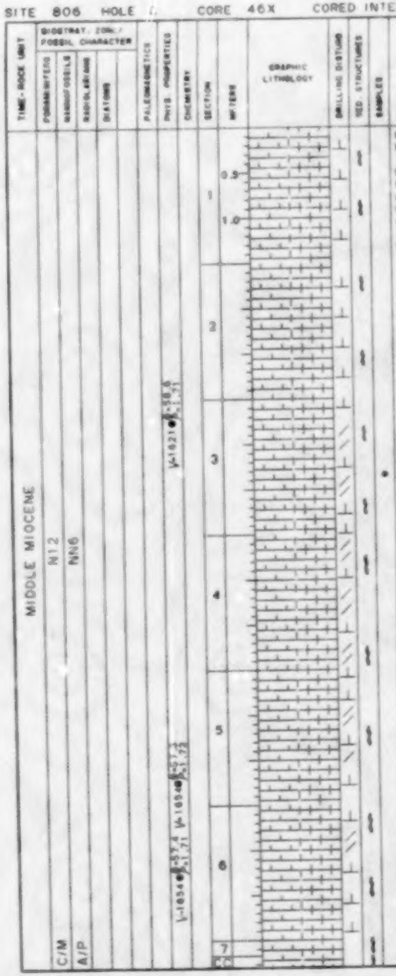
TIME-ROCK UNIT
BIOSTRAT. ZONE/ FOSSIL CHARACTER
FORAMINIFERS
NANNOFOSSILS
RADIOLARIANS
DIATOMS
PALEOMAGNETICS
PHYS. PROPERTIES
CHEMISTRY
SECTION
METERS
GRAPHIC LITHOLOGY
DRILLING DISTURB.
SED. STRUCTURES
SAMPLES
MIDDLE MIOCENE
N12
NN6
C/M
A/P
V-1621
φ-58.6
γ-1.71
V-1654
φ-57.4
γ-1.71
V-1654
φ-57.2
γ-1.72
1
2
3
4
5
6
7
CC
0.5
1.0

LITHOLOGIC DESCRIPTION

NANNOFOSSIL CHALK with FORAMINIFERS interbedded with FORAMINIFER NANNOFOSSIL CHALK

Major lithology: This core contains white (10YR 8/0) NANNOFOSSIL CHALK with FORAMINIFERS interbedded with FORAMINIFER NANNOFOSSIL CHALK. The chalk is bioturbated as indicated by light gray (2.5Y 7/2) burrows, pyrite specks, pale purple (5P 6/2) streaks, and trace fossils. Faint greenish gray (5G 7/1) and pale purple (5P 6/2) bands, between 0.1 and 1 cm thick, are apparent throughout. Microfaulting is present at the base of Section 5.

SMEAR SLIDE SUMMARY (%):

	3, 84
	D
TEXTURE:	
Sand	15
Silt	50
Clay	35
COMPOSITION:	
Diatoms	Tr
Foraminifers	27
Nannofossils	67
Radiolarians	2
Siliceous fragments	3

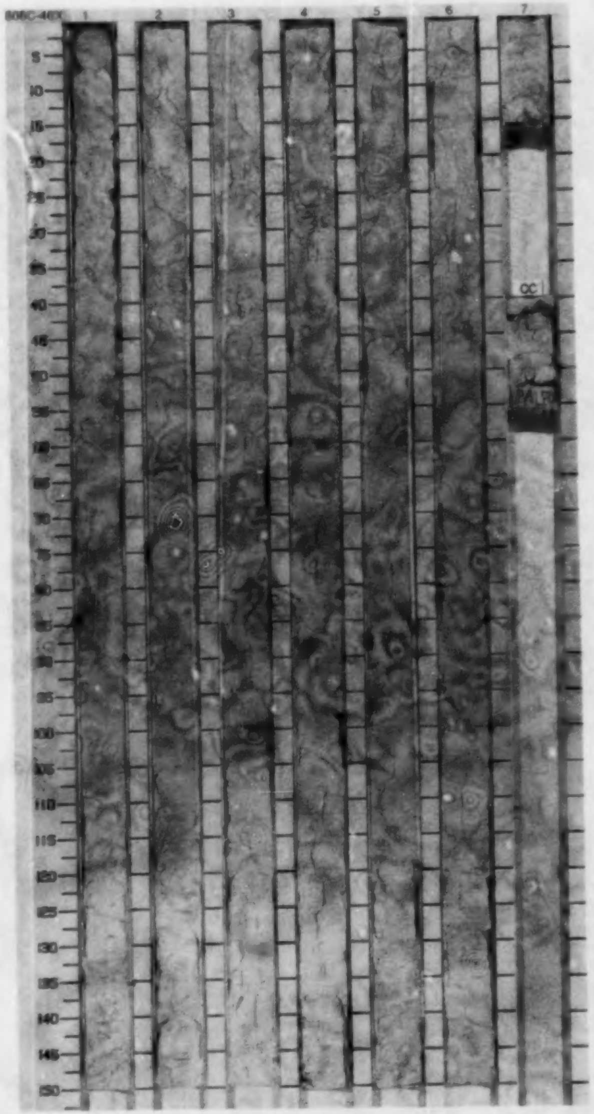
806C-46X
1
2
3
4
5
6
7
CC
PAL
5
10
15
20
25
30
35
40
45
50
55
60
65
70
75
80
85
90
95
100
105
110
115
120
125
130
135
140
145
150

SITE 806 HOLE C CORE 47X CORED INTERVAL 435.2-444.9 mbsf

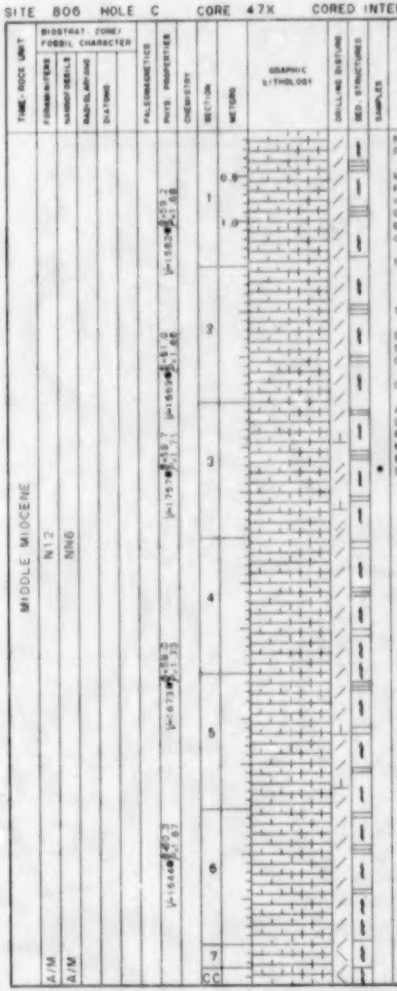

LITHOLOGIC DESCRIPTION

NANNOFOSSIL CHALK with FORAMINIFERS interbedded with FORAMINIFER NANNOFOSSIL CHALK

Major lithology: This core contains white (10YR 8/2) NANNOFOSSIL CHALK with FORAMINIFERS interbedded with FORAMINIFER NANNOFOSSIL CHALK. The chalk is bioturbated as indicated by light gray (2.5Y 7/2) burrows (*Zoophycos*), and pyrite specks, pale purple (5P 6/2) streaks, and trace fossils. Faint pale yellowish green (10GY 7/2) and pale purple (5P 6/2) bands, between 0.1 and 1 cm thick, are apparent throughout the core. The color bands are commonly grouped in 5 to 10 cm thick, pale purple zones.

SMEAR SLIDE SUMMARY (%):

	3, 74 D
TEXTURE:	
Sand	17
Silt	50
Clay	33
COMPOSITION:	
Accessory minerals	1
Diatoms	Tr
Foraminifers	25
Nannofossils	70
Radiolarians	Tr
Siliceous fragments	3

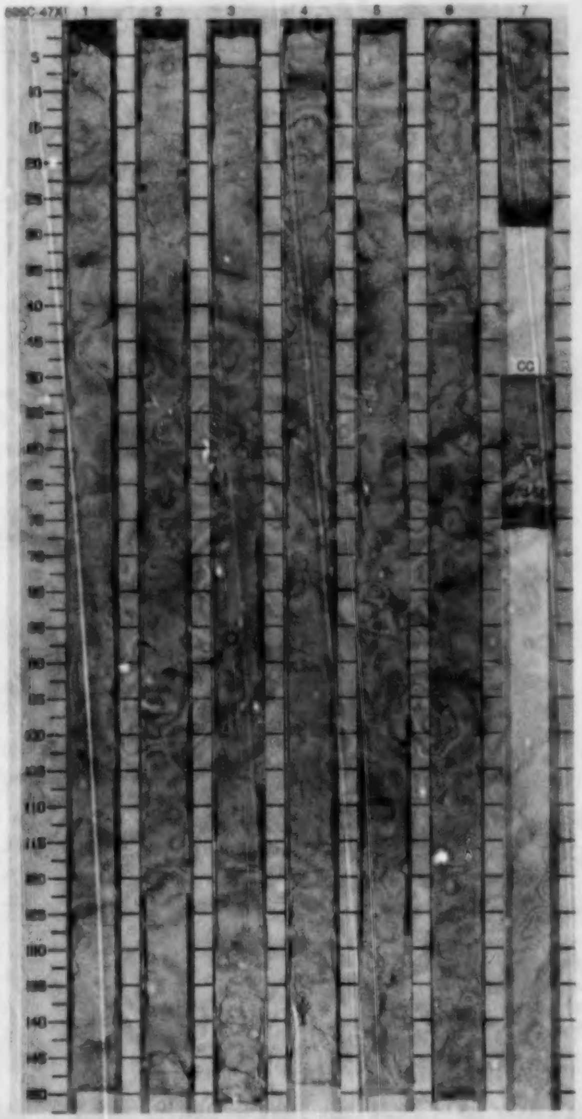
806C-47X
1
2
3
4
5
6
7
CC
5
10
15
20
25
30
35
40
45
50
55
60
65
70
75
80
85
90
95
100
105
110
115
120
125
130
135
140
145
150

SITE 806 HOLE C CORE 48X CORED INTERVAL 444.9-454.6 mbsf

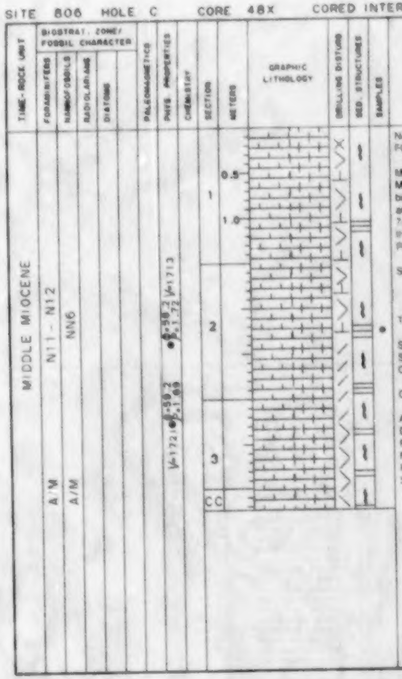
TIME-ROCK UNIT
BIOSTRAT. ZONE/ FOSSIL CHARACTER
FORAMINIFERS
NANNOFOSSILS
RADIOLARIANS
DIATOMS
PALEOMAGNETICS
PHYS. PROPERTIES
CHEMISTRY
SECTION
METERS
GRAPHIC LITHOLOGY
DRILLING DISTURB.
SED. STRUCTURES
SAMPLES
MIDDLE MIOCENE
N11 - N12
A/M
NN6
A/M
●φ=58.2 γ=1.72 V=1713
V=1721●φ=59.2 γ=1.69
1
2
3
CC
0.5
1.0

LITHOLOGIC DESCRIPTION

NANNOFOSSIL CHALK with FORAMINIFERS interbedded with FORAMINIFER NANNOFOSSIL CHALK

Major lithology: The core contains white (10YR 8/0) NANNOFOSSIL CHALK with FORAMINIFERS interbedded with FORAMINIFER NANNOFOSSIL CHALK. The chalk is bioturbated as indicated by light gray (2.5Y 7/2) burrows (*Zoophycos*) and pyrite specks and pale purple (5P 6/2) streaks. Faint pale yellowish green (10GY 7/2), greenish gray (5G 7/1) and pale purple (5P 6/2) color bands, between 0.1 and 1 cm thick, are apparent throughout. The color bands are commonly located in 5 to 10 cm thick, pale purple zones. Porcellanite concretions/nodules are abundant at the top of Section 1.

SMEAR SLIDE SUMMARY (%):

	2, 74
	D
TEXTURE:	
Sand	15
Silt	55
Clay	30
COMPOSITION:	
Accessory minerals	2
Diatoms	Tr
Foraminifers	28
Nannofossils	69
Radiolarians	Tr
Siliceous fragments	3

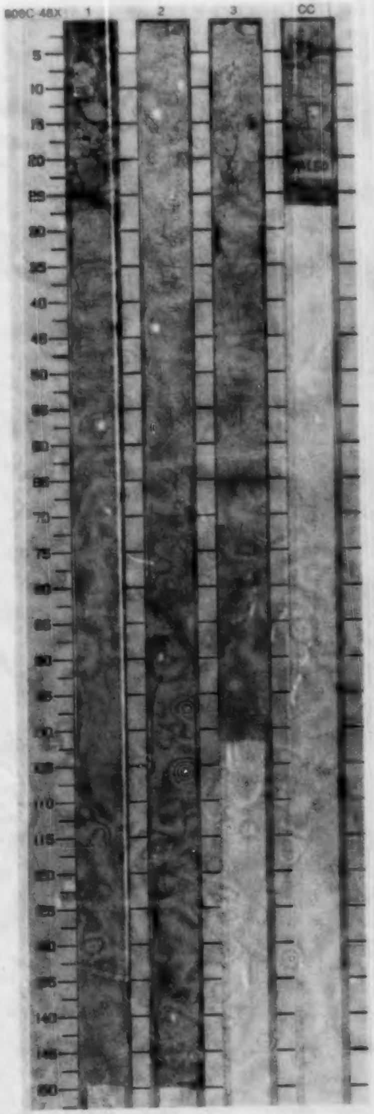
806C-48X
1
2
3
CC
5
10
15
20
25
30
35
40
45
50
55
60
65
70
75
80
85
90
95
100
105
110
115
120
125
130
135
140
145
150
PALEO

SITE 806 HOLE C CORE 49X CORED INTERVAL 454.6-464.5 mbsf

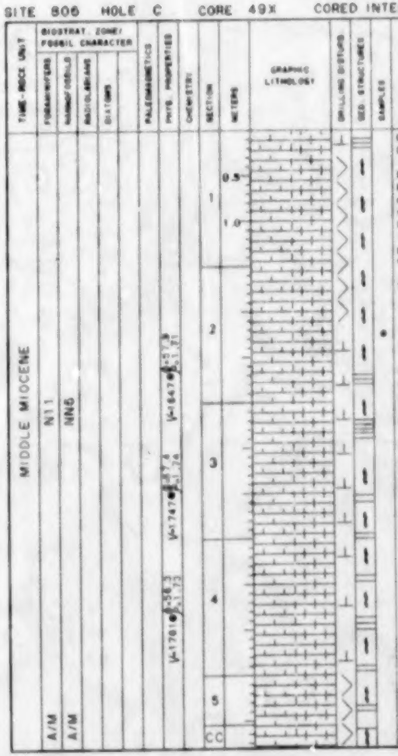
TIME-ROCK UNIT
BIOSTRAT. ZONE/ FOSSIL CHARACTER
FORAMINIFERS
NANNOFOSSILS
RADIOLARIANS
DIATOMS
PALEOMAGNETICS
PHYS. PROPERTIES
CHEMISTRY
SECTION
METERS
GRAPHIC LITHOLOGY
DRILLING DISTURB.
SED. STRUCTURES
SAMPLES
MIDDLE MIOCENE
N11
NN6
A/M
A/M
V=1847 φ=57.9 γ=1.71
V=1747 φ=57.4 γ=1.74
V=1701 φ=56.3 γ=1.73
1
2
3
4
5
CC
0.5
1.0

LITHOLOGIC DESCRIPTION

NANNOFOSSIL CHALK with FORAMINIFERS interbedded with FORAMINIFER NANNOFOSSIL CHALK

Major lithology: This core contains white (10YR 8/0) NANNOFOSSIL CHALK with FORAMINIFERS interbedded with FORAMINIFER NANNOFOSSIL CHALK. Drilling disturbance resulted in moderately fractured to heavily fragmented biscuits in a stiff ooze matrix. The sediment is moderately bioturbated as indicated by light gray (2.5Y 7/2) mottles and pyritic burrow fills. A *Zoophycos* burrow is noted in Section 4. Distinct mm thick, greenish gray (5G7/1) color bands are frequent throughout the core, and a few diffuse, cm thick, pale purple (5P 6/2) color zones are observed. A few porcellanous concretions are present at the top of Section 1.

SMEAR SLIDE SUMMARY (%):

	2, 75
	D
TEXTURE:	
Sand	30
Silt	50
Clay	20
COMPOSITION:	
Diatoms	Tr
Foraminifers	40
Nannofossils	60
Radiolarians	Tr

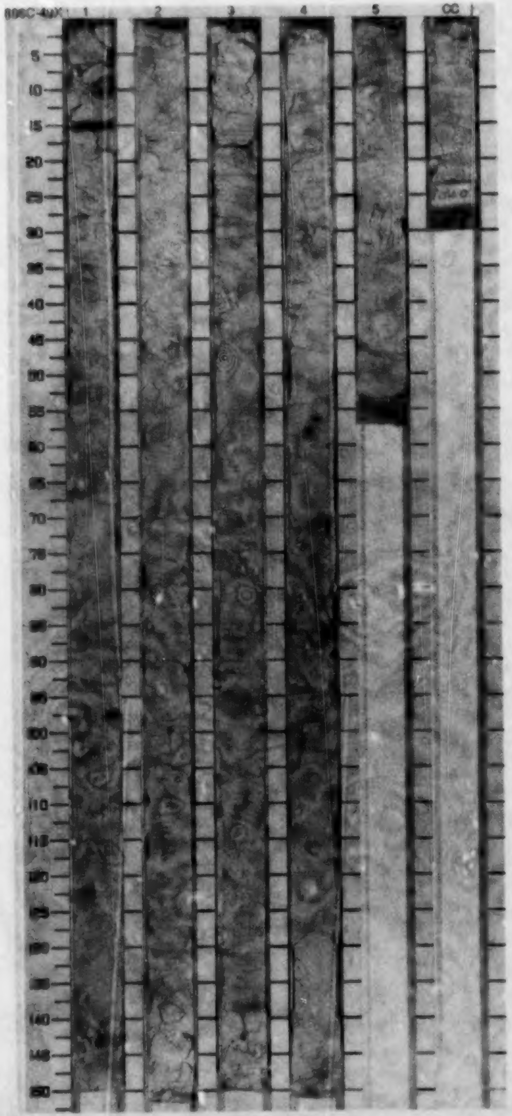
806C-49X
1
2
3
4
5
CC
5
10
15
20
25
30
35
40
45
50
55
60
65
70
75
80
85
90
95
100
105
110
115
120
125
130
135
140
145
150

SITE 806 HOLE C CORE 50X CORED INTERVAL 464.5-474.3 mbsf

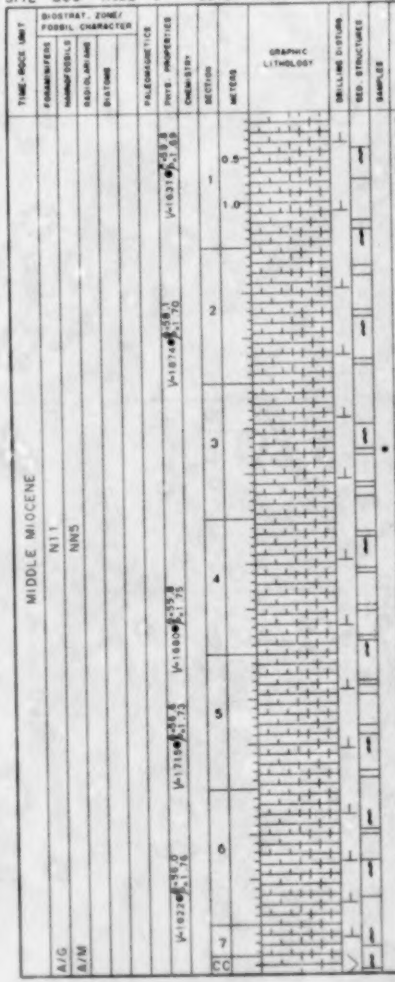
TIME-ROCK UNIT
BIOSTRAT. ZONE/ FOSSIL CHARACTER
FORAMINIFERS
NANNOFOSSILS
RADIOLARIANS
DIATOMS
PALEOMAGNETICS
PHYS. PROPERTIES
CHEMISTRY
SECTION
METERS
GRAPHIC LITHOLOGY
DRILLING DISTURB.
SED. STRUCTURES
SAMPLES
MIDDLE MIOCENE
N11
NN5
A/G
A/M
V=1631 φ=59.8 ρ=1.69
V=1874 φ=58.1 ρ=1.70
V=1680 φ=55.8 ρ=1.75
V=1715 φ=56.6 ρ=1.73
V=1622 φ=56.0 ρ=1.76
1
2
3
4
5
6
7
CC
0.5
1.0

LITHOLOGIC DESCRIPTION

NANNOFOSSIL CHALK with FORAMINIFERS interbedded with FORAMINIFER NANNOFOSSIL CHALK

Major lithology: The core contains white (10YR 8/1) NANNOFOSSIL CHALK with FORAMINIFERS interbedded with FORAMINIFER NANNOFOSSIL CHALK. The sediment is moderately bioturbated as indicated by light gray (2.5Y 7/2) mottles and pyritic burrow fills. Distinct, mm thick, greenish gray (5G 7/1) color bands are frequently present throughout the core, and a few diffuse, cm thick, pale purple (5P 6/2) color zones are observed.

SMEAR SLIDE SUMMARY (%):

	3, 75
	D
TEXTURE:	
Sand	15
Silt	60
Clay	25
COMPOSITION:	
Diatoms	1
Foraminifers	20
Nannofossils	79
Radiolarians	Tr

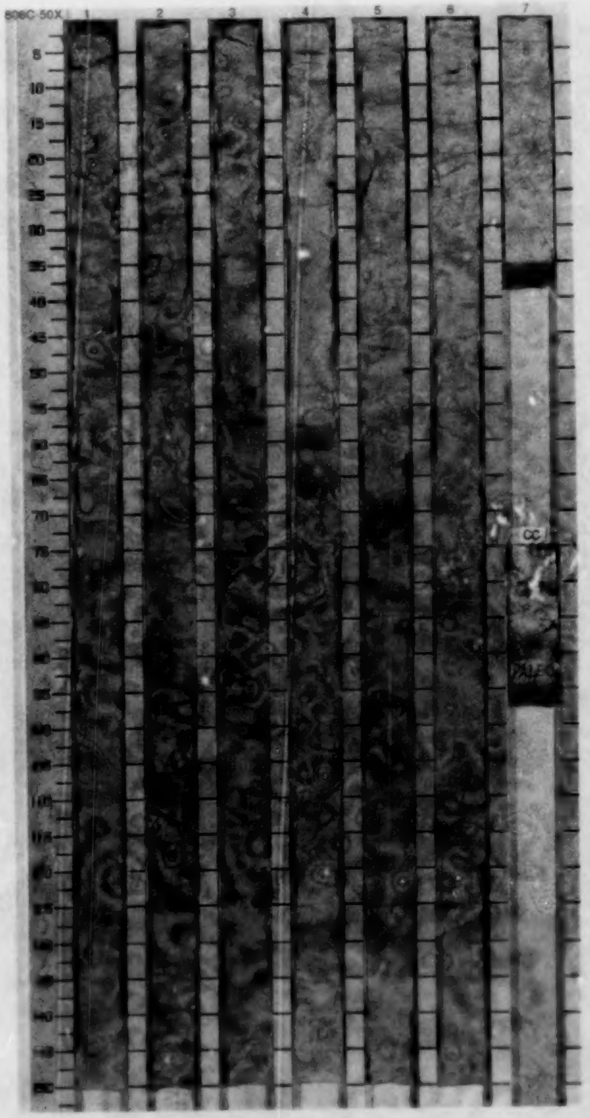
806C-50X
1
2
3
4
5
6
7
5
10
15
20
25
30
35
40
45
50
55
60
65
70
75
80
85
90
95
100
105
110
115
120
125
130
135
140
145
150
CC
PALEO

SITE 806 HOLE C CORE 51X CORED INTERVAL 474.3-483.7 mbsf

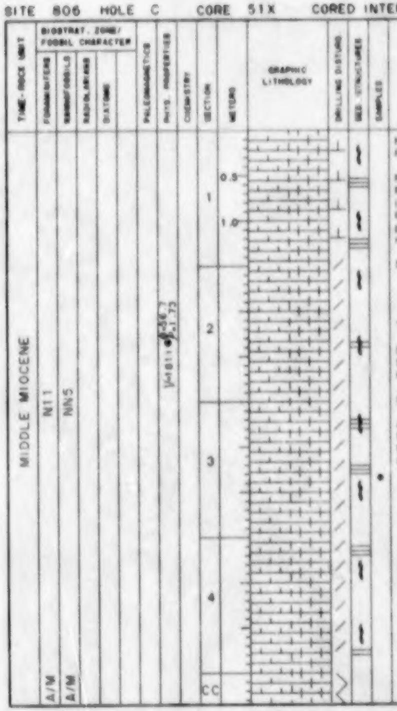
TIME-ROCK UNIT
BIOSTRAT. ZONE/ FOSSIL CHARACTER
FORAMINIFERS
NANNOFOSSILS
RADIOLARIANS
DIATOMS
PALEOMAGNETICS
PHYS. PROPERTIES
CHEMISTRY
SECTION
METERS
GRAPHIC LITHOLOGY
DRILLING DISTURB.
SED. STRUCTURES
SAMPLES
MIDDLE MIOCENE
N11
NN5
A/M
A/M
γ=1.81
φ=56.7
ρ=1.73
1
2
3
4
CC
0.5
1.0

LITHOLOGIC DESCRIPTION

NANNOFOSSIL CHALK with FORAMINIFERS interbedded with FORAMINIFER NANNOFOSSIL CHALK

Major lithology: This core contains white (10YR 8/1) NANNOFOSSIL CHALK with FORAMINIFERS interbedded with FORAMINIFER NANNOFOSSIL CHALK. Pale yellowish green (10GY 7/2), very thin color bands are common to frequent. Some cm scale, pale purple (5P 6/2) color bands are also present. Numerous burrow mottles, burrows (*Zoophycos*), and pyritized specks are indicative of moderate bioturbation. A few porcellanite concretions/nodules are observed.

SMEAR SLIDE SUMMARY (%)

	3, 84
	D
TEXTURE	
Sand	15
Silt	55
Clay	30
COMPOSITION	
Accessory minerals	2
Diatoms	Tr
Nannofossils	98
Radiolarians	Tr

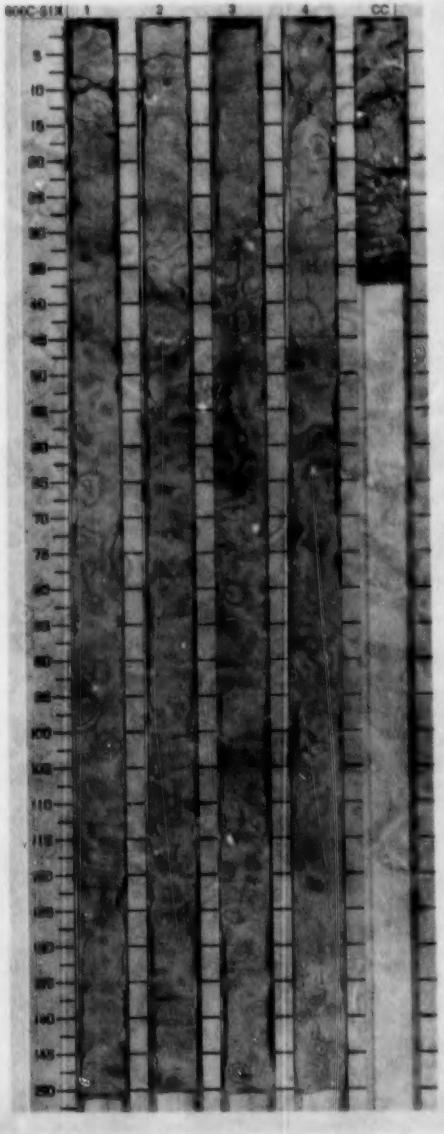
806C-51X
1
2
3
4
CC
5
10
15
20
25
30
35
40
45
50
55
60
65
70
75
80
85
90
95
100
105
110
115
120
125
130
135
140
145
150

SITE 806 HOLE C CORE 52X CORED INTERVAL 483.7-493.3 mbsf

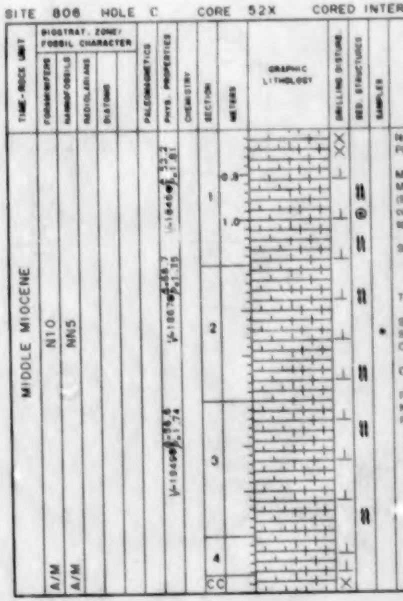
TIME-ROCK UNIT
BIOSTRAT. ZONE/ FOSSIL CHARACTER
FORAMINIFERS
NANNOFOSSILS
RADIOLARIANS
DIATOMS
PALEOMAGNETICS
PHYS. PROPERTIES
CHEMISTRY
SECTION
METERS
GRAPHIC LITHOLOGY
DRILLING DISTURB.
SED. STRUCTURES
SAMPLES
MIDDLE MIOCENE
N10
NN5
A/M
A/M
V=1846
55.2
1.91
V=1867
58.7
1.35
V=1946
56.6
1.74
1
2
3
4
CC
0.5
1.0

LITHOLOGIC DESCRIPTION

NANNOFOSSIL CHALK with FORAMINIFERS interbedded with FORAMINIFER NANNOFOSSIL CHALK

Major lithology: This core contains white (10YR 8/1) NANNOFOSSIL CHALK with FORAMINIFERS interbedded with FORAMINIFER NANNOFOSSIL CHALK. Zones of pale pink (5RP 8/2), between 20 and 40 cm thick, are present in Sections 1 and 2. These zones contain sets of thin (1 mm) greenish gray (5BG 5/1) and pale purple (5P 6/2) bands that are spaced about 5 cm apart. The chalk is bioturbated with *Zoophycos* trace fossils.

SMEAR SLIDE SUMMARY (%):

	2, 75
	D
TEXTURE:	
Sand	20
Silt	60
Clay	20
COMPOSITION:	
Foraminifers	25
Nannofossils	75
Radiolarians	Tr

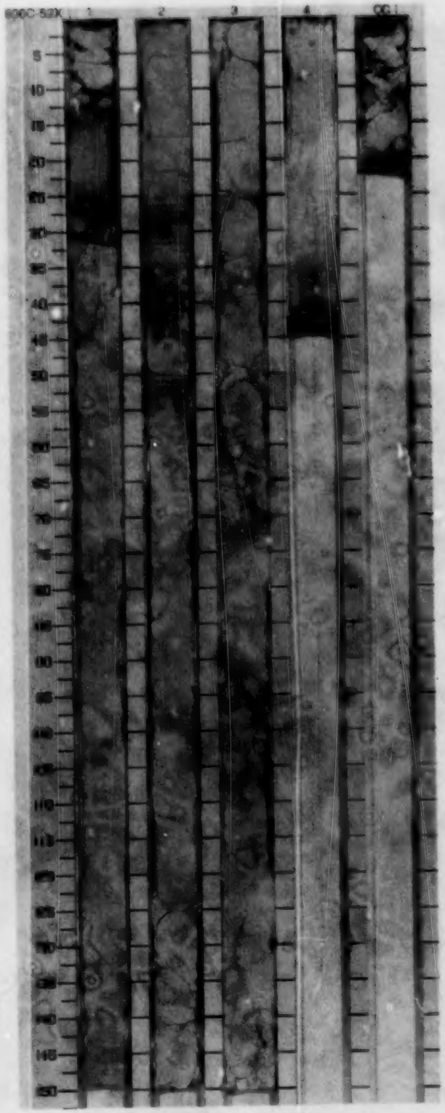
806C-52X
1
2
3
4
CC
5
10
15
20
25
30
35
40
45
50
55
60
65
70
75
80
85
90
95
100
105
110
115
120
125
130
135
140
145
150

SITE 806 HOLE C CORE 53X CORED INTERVAL 493.3-503.0 mbsf

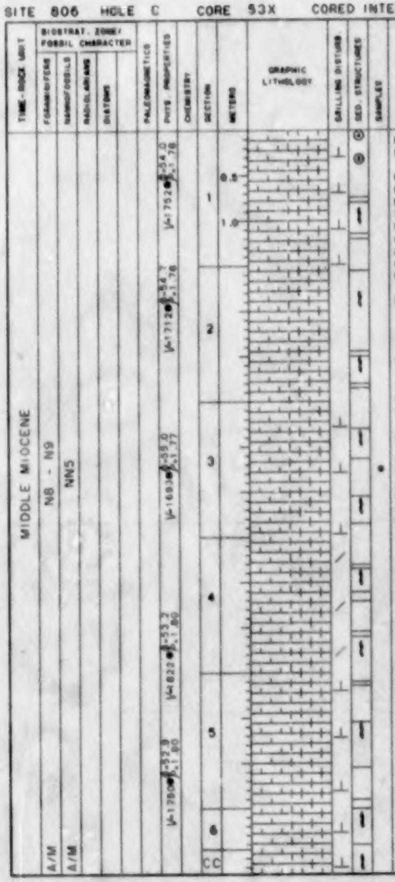
TIME-ROCK UNIT
BIOSTRAT. ZONE/ FOSSIL CHARACTER
FORAMINIFERS
NANNOFOSSILS
RADIOLARIANS
DIATOMS
PALEOMAGNETICS
PHYS. PROPERTIES
CHEMISTRY
SECTION
METERS
GRAPHIC LITHOLOGY
DRILLING DISTURB.
SED. STRUCTURES
SAMPLES
MIDDLE MIOCENE
N8 - N9
NN5
A/M
A/M
V-1752 φ-54.0 γ-1.78
V-1712 φ-54.7 γ-1.76
V-1693 φ-55.0 γ-1.77
V-1822 φ-53.2 γ-1.80
V-1780 φ-52.9 γ-1.80
1
2
3
4
5
6
CC
0.5
1.0

LITHOLOGIC DESCRIPTION

NANNOFOSSIL CHALK with FORAMINIFERS interbedded with FORAMINIFER NANNOFOSSIL CHALK

Major lithology: This core contains white (10YR 8/1) NANNOFOSSIL CHALK with FORAMINIFERS interbedded with FORAMINIFER NANNOFOSSIL CHALK. Only a few color bands were observed. These bands are distinct, very thin (<1 mm) and greenish gray (5G 7/1) and pale purple (5P 6/2) in color. In Section 3, they are observed in intervals 5-10 cm thick. Bioturbation appears to be moderate, as indicated by a few light gray (2.5Y 7/2) mottles, pyritized burrow fills, and *Zoophycos* trace fossils in Section 4. Bioturbation appears to be heavy in a few darker intervals. At the top of Section 1, several calcite nodules (ca. 1 cm in diameter) are found. The concentration of these nodules at the top of the core may indicate that they are washed in.

SMEAR SLIDE SUMMARY (%):

	3, 75
	D
TEXTURE	
Sand	15
Silt	70
Clay	15
COMPOSITION	
Diatoms	1
Foraminifers	30
Nannofossils	66
Radiolarians	1
Siliceous fragments	2
Siliceous sponge spicules	Tr

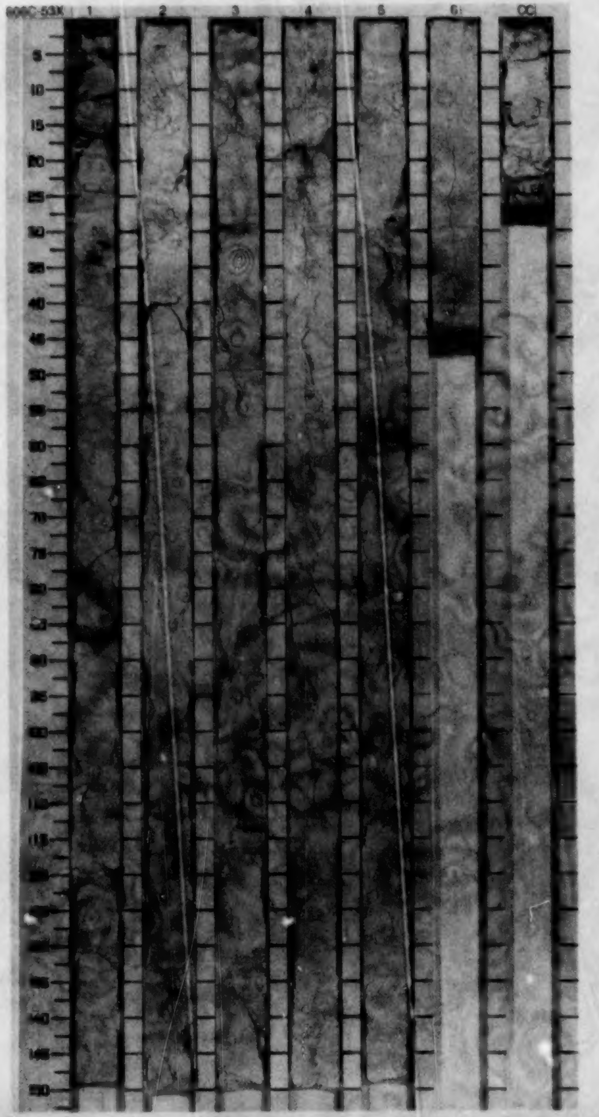
806C-53X
1
2
3
4
5
6
CC
5
10
15
20
25
30
35
40
45
50
55
60
65
70
75
80
85
90
95
100
105
110
115
120
125
130
135
140
145
150

SITE 806 HOLE C CORE 54X CORED INTERVAL 503.0-512.7 mbsf

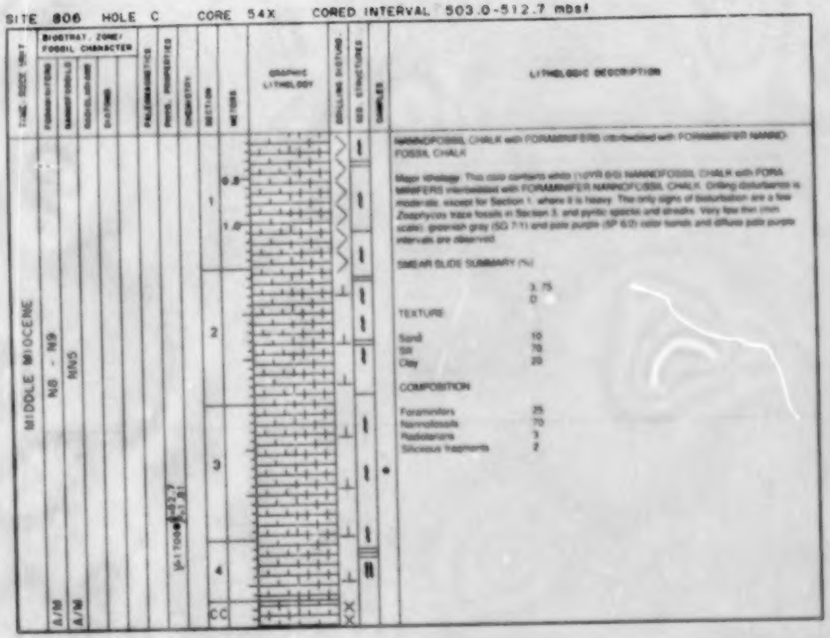
TIME-ROCK UNIT
BIOSTRAT. ZONE/ FOSSIL CHARACTER
FORAMINIFERS
NANNOFOSSILS
RADIOLARIANS
DIATOMS
PALEOMAGNETICS
PHYS. PROPERTIES
CHEMISTRY
SECTION
METERS
GRAPHIC LITHOLOGY
DRILLING DISTURB.
SED. STRUCTURES
SAMPLES
MIDDLE MIOCENE
N8 - N9
NN5
A/M
A/M
0.5
1.0
1
2
3
4
CC

LITHOLOGIC DESCRIPTION

NANNOFOSSIL CHALK with FORAMINIFERS interbedded with FORAMINIFER NANNOFOSSIL CHALK

Major lithology: This core contains white (10YR 8/2) NANNOFOSSIL CHALK with FORAMINIFERS interbedded with FORAMINIFER NANNOFOSSIL CHALK. Drilling disturbance is moderate, except for Section 1, where it is heavy. The only signs of bioturbation are a few *Zoophycos* trace fossils in Section 3, and pyritic specks and streaks. Very few thin (mm scale), greenish gray (5G 7/1) and pale purple (5P 6/2) color bands and diffuse pale purple intervals are observed.

SMEAR SLIDE SUMMARY (%)

	3, 75 D
TEXTURE:	
Sand	10
Silt	70
Clay	20
COMPOSITION:	
Foraminifers	25
Nannofossils	70
Radiolarians	3
Siliceous fragments	2

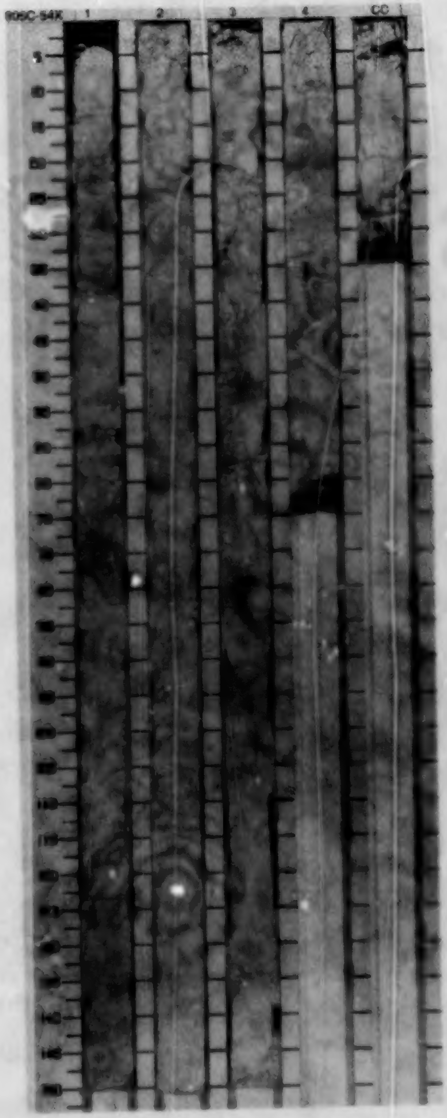
806C-54X
1
2
3
4
CC

SITE 806 HOLE C CORE 55X CORED INTERVAL 512.7-522.4 mbsf

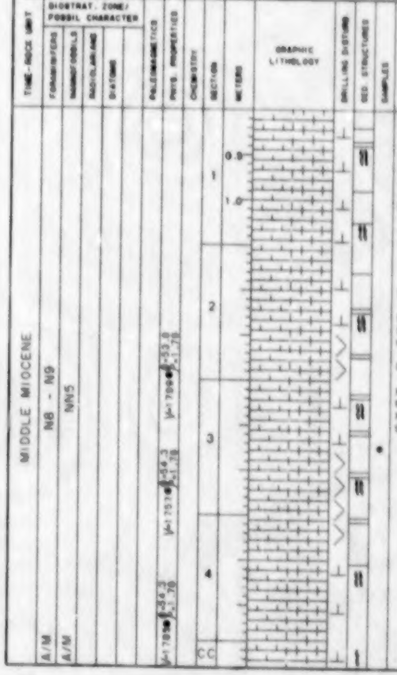
TIME-ROCK UNIT
BIOSTRAT. ZONE/ FOSSIL CHARACTER
FORAMINIFERS
NANNOFOSSILS
RADIOLARIANS
DIATOMS
PALEOMAGNETICS
PHYS. PROPERTIES
CHEMISTRY
SECTION
METERS
GRAPHIC LITHOLOGY
DRILLING DISTURB.
SED. STRUCTURES
SAMPLES
MIDDLE MIOCENE
N8 - N9
NN5
A/M
A/M
1
2
3
4
CC
0.5
1.0

LITHOLOGIC DESCRIPTION

NANNOFOSSIL CHALK with FORAMINIFERS interbedded with FORAMINIFER NANNOFOSSIL CHALK

Major lithology: This core contains white (10YR 8/0) NANNOFOSSIL CHALK with FORAMINIFERS interbedded with FORAMINIFER NANNOFOSSIL CHALK. The chalk is moderately bioturbated as indicated by burrows, trace fossils, and pyrite specks. The chalk is characterized by 5 to 10 cm thick, pale pink (5RP 8/2) zones, which contain fine (1 mm) bluish gray (5B 5/1) bands. A porcellanite nodule is noted at the top of Section 4.

SMEAR SLIDE SUMMARY (%):

	3, 75
	D
TEXTURE:	
Sand	10
Silt	70
Clay	20
COMPOSITION:	
Foraminifers	30
Nannofossils	64
Radiolarians	3
Siliceous fragments	3

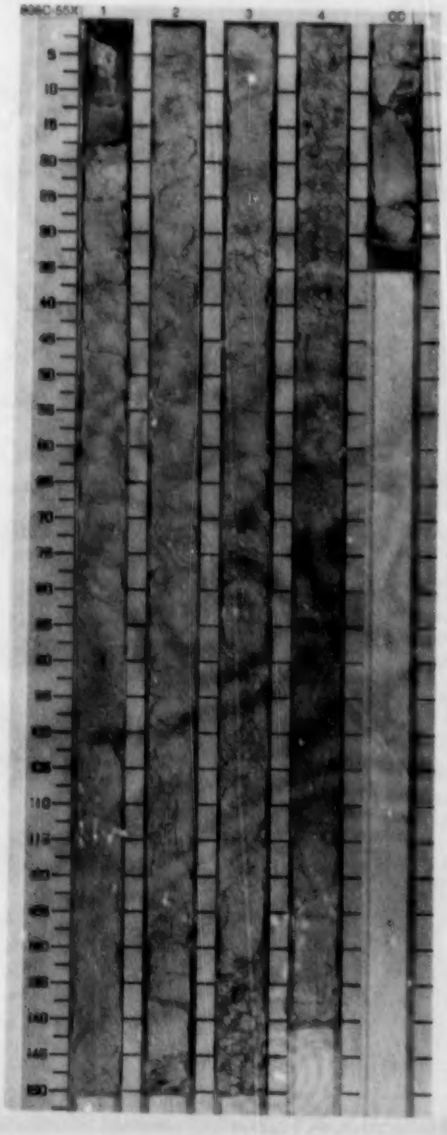
806C-55X
1
2
3
4
CC
5
10
15
20
25
30
35
40
45
50
55
60
65
70
75
80
85
90
95
100
105
110
115
120
125
130
135
140
145
150

SITE 806 HOLE C CORE 56X CORED INTERVAL 522.4-532.0 mbsf

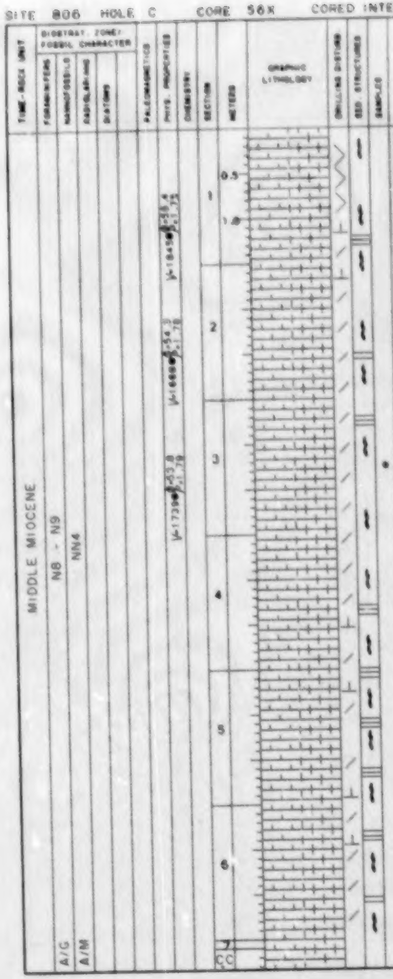
TIME-ROCK UNIT
BIOSTRAT. ZONE/ FOSSIL CHARACTER
FORAMINIFERS
NANNOFOSSILS
RADIOLARIANS
DIATOMS
PALEOMAGNETICS
PHYS. PROPERTIES
CHEMISTRY
SECTION
METERS
GRAPHIC LITHOLOGY
DRILLING DISTURB.
SED. STRUCTURES
SAMPLES
MIDDLE MIOCENE
N8 - N9
NN4
A/G
A/M
V=1845 φ=58.4 γ=1.75
V=1666 φ=54.2 γ=1.78
V=1739 φ=53.8 γ=1.79
1
2
3
4
5
6
7
CC
0.5
1.0

LITHOLOGIC DESCRIPTION

NANNOFOSSIL CHALK with FORAMINIFERS interbedded with FORAMINIFER NANNOFOSSIL CHALK

Major lithology: This core contains white (10YR 8/1) NANNOFOSSIL CHALK with FORAMINIFERS interbedded with FORAMINIFER NANNOFOSSIL CHALK. It is moderately bioturbated, as is evident from mottles, trace fossils (*Zoophycos*), and pyrite-filled burrows. Distinct mm thick, dark gray (2.5Y 4/0) and greenish gray (5G 6/1) color bands, and cm thick, pale purple (5P 6/2) zones are common. The pale purple zones have distinct, horizontal mm thick, white (10YR 8/1) bands within them.

SMEAR SLIDE SUMMARY (%):

	3, 74 D
TEXTURE	
Sand	15
Silt	50
Clay	35
COMPOSITION	
Accessory minerals	2
Foraminifers	28
Nannofossils	67
Radiolarians	Tr
Siliceous fragments	3

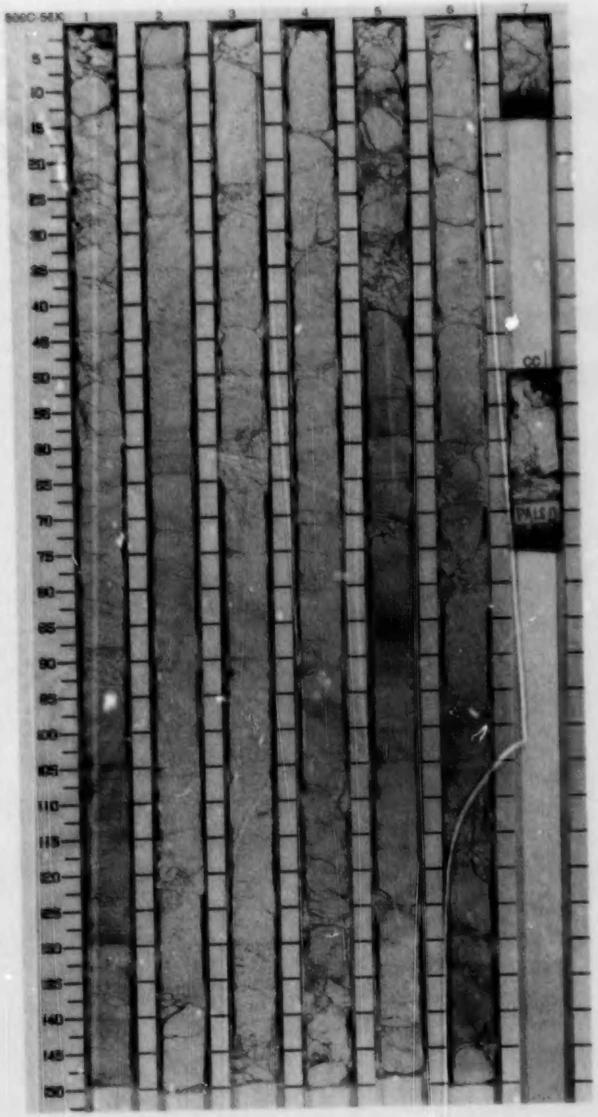
806C-56X
1
2
3
4
5
6
7
CC
PALEO
5
10
15
20
25
30
35
40
45
50
55
60
65
70
75
80
85
90
95
100
105
110
115
120
125
130
135
140
145
150

SITE 806 HOLE C CORE 57X CORED INTERVAL 532.0-541.7 mbsf

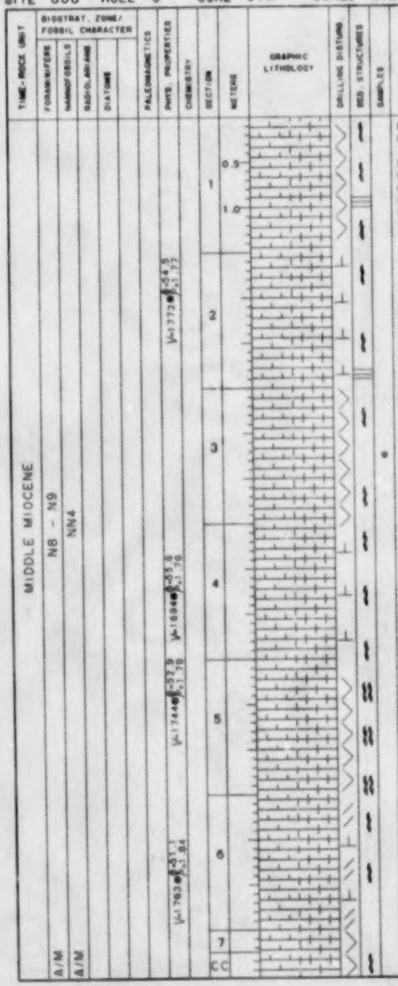
TIME-ROCK UNIT
BIOSTRAT. ZONE/ FOSSIL CHARACTER
FORAMINIFERS
NANNOFOSSILS
RADIOLARIANS
DIATOMS
PALEOMAGNETICS
PHYS. PROPERTIES
CHEMISTRY
SECTION
METERS
GRAPHIC LITHOLOGY
DRILLING DISTURB.
SED. STRUCTURES
SAMPLES
MIDDLE MIOCENE
N8 - N9
NN4
A/M
A/M
V-1773● ϕ-54.5 γ-1.77
V-1694● ϕ-55.6 γ-1.76
V-1744● ϕ-52.9 γ-1.79
V-1762● ϕ-51.1 γ-1.84
1
2
3
4
5
6
7
CC
0.5
1.0

LITHOLOGIC DESCRIPTION

NANNOFOSSIL CHALK with FORAMINIFERS interbedded with FORAMINIFER NANNOFOSSIL CHALK

Major lithology: This core contains white (10YR 8/1) NANNOFOSSIL CHALK with FORAMINIFERS interbedded with FORAMINIFER NANNOFOSSIL CHALK. It is moderately bioturbated and has numerous trace fossils, including *Zoophycos*, and pyrite infillings of burrows. Trace fossils are especially abundant in several 10 to 20 cm thick pale pink (5RP 8/2) zones. A few, very distinct, thin (<1 mm) dark gray (2.5Y 4/0) and greenish gray (5G 7/1) color bands are noted. The chalk is well lithified in this core.

SMEAR SLIDE SUMMARY (%):

	3, 74
	D
TEXTURE:	
Sand	8
Silt	65
Clay	27
COMPOSITION:	
Accessory minerals	2
Foraminifers	27
Nannofossils	68
Radiolarians	Tr
Siliceous fragments	3

WASH CORE: 541.7 to 599.0 mbsf

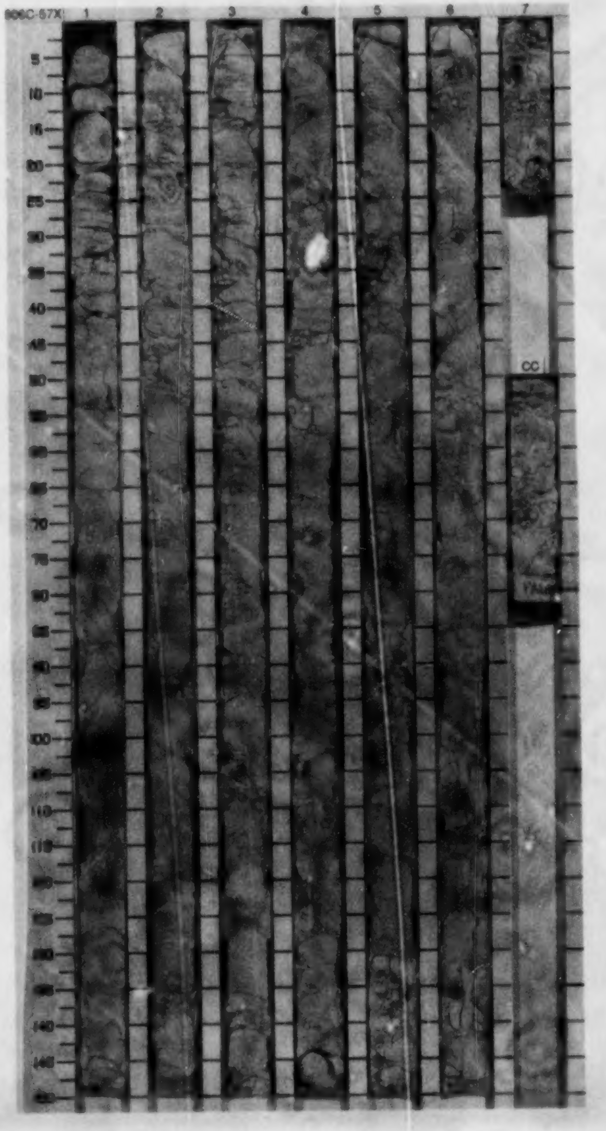
806C-57X
1
2
3
4
5
6
7
CC
5
10
15
20
25
30
35
40
45
50
55
60
65
70
75
80
85
90
95
100
105
110
115
120
125
130
135
140
145
150

SITE 806 HOLE C CORE 58X CORED INTERVAL 599.0-608.5 mbsf

TIME-ROCK UNIT	BIOSTRAT. ZONE/ FOSSIL CHARACTER				PALEOMAGNETICS	PHYS. PROPERTIES	CHEMISTRY	SECTION	METERS	GRAPHIC LITHOLOGY	DRILLING DISTURB.	SED. STRUCTURES	SAMPLES
	FORAMINIFERS	NANNOFOSSILS	RADIOLARIANS	DIATOMS									
LOWER MIOCENE	N5	NN2						1	0.5 1.0				
								2					
						V=1965 ● Φ=40.5 γ=1.88		3					●
						V=1995 ● Φ=40.0 γ=1.88		4					
								5					
								6					
	C/M	A/M						CC					

LITHOLOGIC DESCRIPTION

NANNOFOSSIL CHALK with FORAMINIFERS

Major lithology: This core contains NANNOFOSSIL CHALK with FORAMINIFERS. It is white (10YR 8/1) at the top of Section 1, in all of Sections 3 and 4, and most of Section 5; the remainder of the core is pale pink (5RP 8/2) in color. The sediment is moderately bioturbated, as indicated by faint mottles, and a few disseminated, pyritic burrow fills. In Section 4, *Zoophycos* trace fossils are noted. Very few distinct, mm thick, greenish gray (5G 7/1) and dark gray (2.5Y 4/0) color bands are present throughout the core. Drilling disturbance has resulted in highly fragmented biscuits in a stiff ooze matrix.

SMEAR SLIDE SUMMARY (%):

	3, 77 D
TEXTURE:	
Sand	10
Silt	60
Clay	30
COMPOSITION:	
Diatoms	Tr
Foraminifers	12
Nannofossils	82
Radiolarians	Tr
Siliceous fragments	3

WASH CORE: 608.5 to 740.0 mbsf

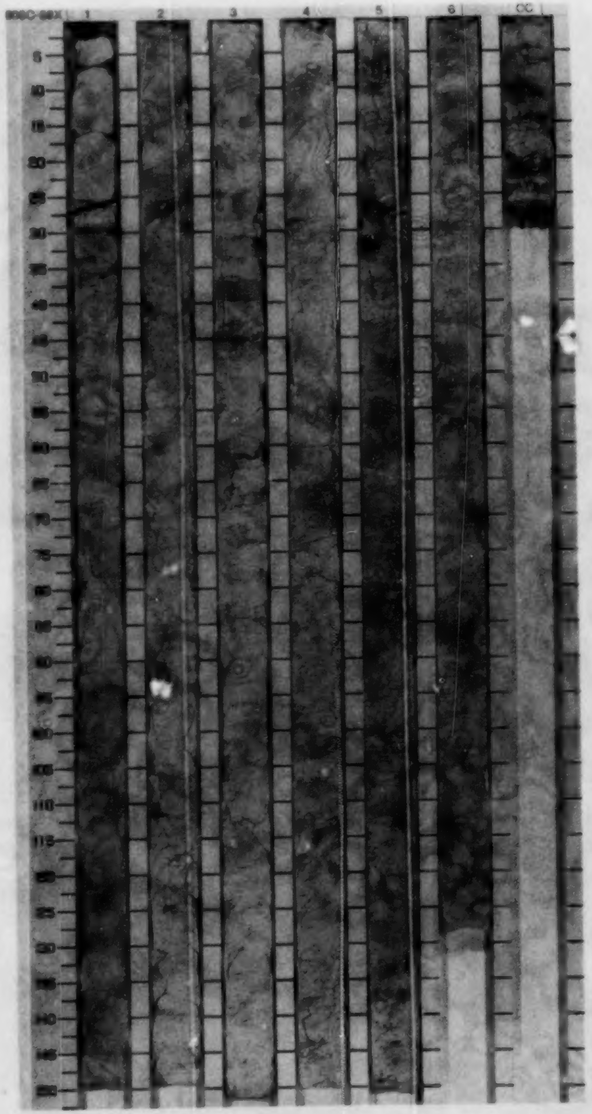

SITE 806 HOLE C CORE 59X CORED INTERVAL 740.0-749.5 mbsf

TIME-ROCK UNIT	BIOSTRAT. ZONE/ FOSSIL CHARACTER					PALEOMAGNETICS	PHYS. PROPERTIES	CHEMISTRY	SECTION	METERS	GRAPHIC LITHOLOGY	DRILLING DISTURB.	SED. STRUCTURES	SAMPLES
	FORAMINIFERS	NANNOFOSSILS	RADIOLARIANS	DIATOMS										
UPPER OLIGOCENE	P22 C/P	NN1 - NN2 A/M	*Dorcadospyris ateuchus - Lychnocanoma elongata* A/P	*Bergerovia veniamini* F-C/P			● φ=46.3 γ=1.91 V=1960		1					•
									CC					

LITHOLOGIC DESCRIPTION

NANNOFOSSIL CHALK with FORAMINIFERS

Major lithology: This core contains white (10YR 8/1) NANNOFOSSIL CHALK with FORAMINIFERS. Bioturbation is moderate, as indicated by faint mottles and burrow traces. A few distinct, mm thick, gray (10YR 6/1) color bands are noted. Drilling disturbance has resulted in highly fragmented biscuits in a stiff ooze matrix.

SMEAR SLIDE SUMMARY (%):

	1, 14
	D
TEXTURE:	
Sand	5
Silt	80
Clay	15
COMPOSITION:	
Diatoms	Tr
Foraminifers	15
Nannofossils	82
Radiolarians	1
Siliceous fragments	2

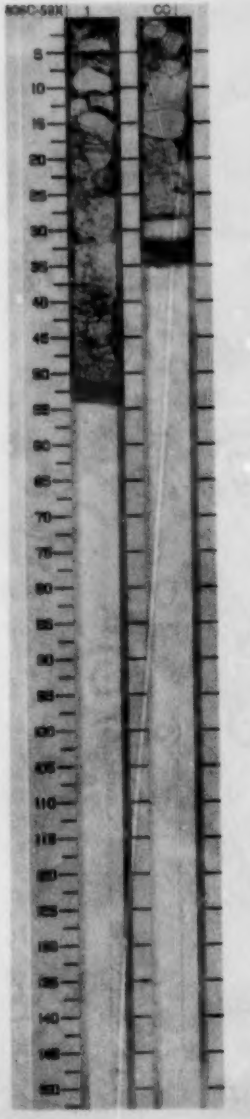

SITE 806 HOLE C CORE 60X CORED INTERVAL 749.5-759.2 mbsf

TIME-ROCK UNIT	BIOSTRAT. ZONE/ FOSSIL CHARACTER					PALEOMAGNETICS	PHYS. PROPERTIES	CHEMISTRY	SECTION	METERS	GRAPHIC LITHOLOGY	DRILLING DISTURB.	SED. STRUCTURES	SAMPLES	LITHOLOGIC DESCRIPTION
	FORAMINIFERS	NANNOFOSSILS	RADIOLARIANS	DIATOMS											
UPPER OLIGOCENE	P22 C/P	NN1 - NN2 A/P	*Dorcadospyris ateuchus* - *Lychnocanoma elongata* A/P	? F-C/P			γ-2113 ●		1						NANNOFOSSIL CHALK with FORAMINIFERS Major lithology: This core contains white (5Y 8/1) NANNOFOSSIL CHALK with FORAMINIFERS. The sediment is heavily bioturbated, as indicated by abundant burrows and trace fossils. Numerous thin, wavy, greenish gray (5G 7/1) color bands are observed. Drilling disturbance has resulted in highly fragmented biscuits in a stiff ooze matrix.
									CC						

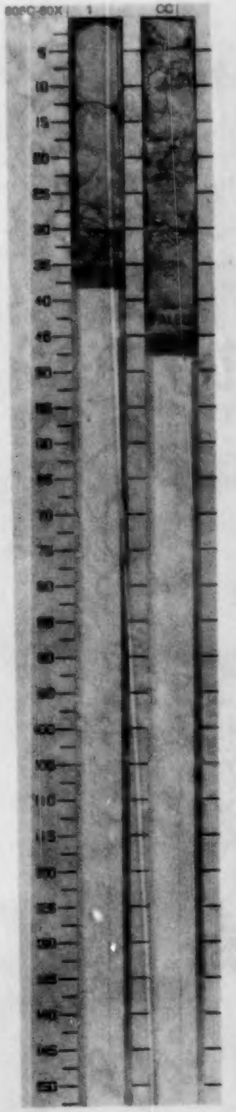
806C-60X
1
CC
5
10
15
20
25
30
35
40
45
50
55
60
65
70
75
80
85
90
95
100
105
110
115
120
125
130
135
140
145
150

SITE 806 HOLE C CORE 61X CORED INTERVAL 759.2-766.7 mbsf

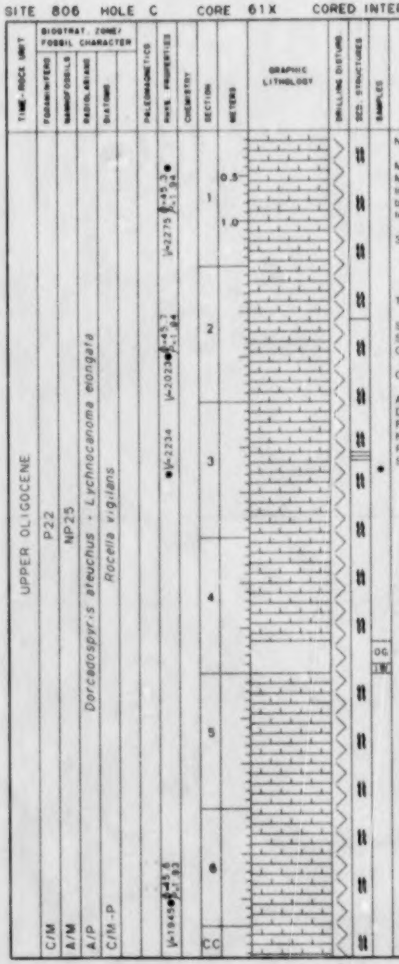
TIME-ROCK UNIT
BIOSTRAT. ZONE/ FOSSIL CHARACTER
FORAMINIFERS
NANNOFOSSILS
RADIOLARIANS
DIATOMS
PALEOMAGNETICS
PHYS. PROPERTIES
CHEMISTRY
SECTION
METERS
GRAPHIC LITHOLOGY
DRILLING DISTURB.
SED. STRUCTURES
SAMPLES
UPPER OLIGOCENE
C/M
P22
A/M
NP25
A/P
Dorcadospyris ateuchus - Lychnocanoma elongata
C/M-P
Rocella vigilans
V-2275
φ-45.3
γ-1.94
V-2023
φ-45.7
γ-1.94
V-2234
V-1945
φ-45.6
γ-1.93
1
2
3
4
5
6
CC
0.5
1.0
OG
IW

LITHOLOGIC DESCRIPTION

NANNOFOSSIL CHALK with FORAMINIFERS

Major lithology: This core contains white (10YR 8/1) NANNOFOSSIL CHALK with FORAMINIFERS. The sediment is heavily bioturbated, as evident from abundant burrows and trace fossils. Numerous ultra-thin (<1 mm), wavy greenish gray to gray (5G 7/1 to N7/) color bands and zones of color bands (cm's thick) are apparent. Much of the core consists of fragmented biscuits in a stiff ooze matrix, which formed during the drilling process.

SMEAR SLIDE SUMMARY (%)

	3, 74 D
TEXTURE	
Sand	8
Silt	60
Clay	32
COMPOSITION	
Accessory minerals	2
Diatoms	Tr
Foraminifers	10
Nannofossils	85
Radiolarians	Tr
Siliceous fragments	3

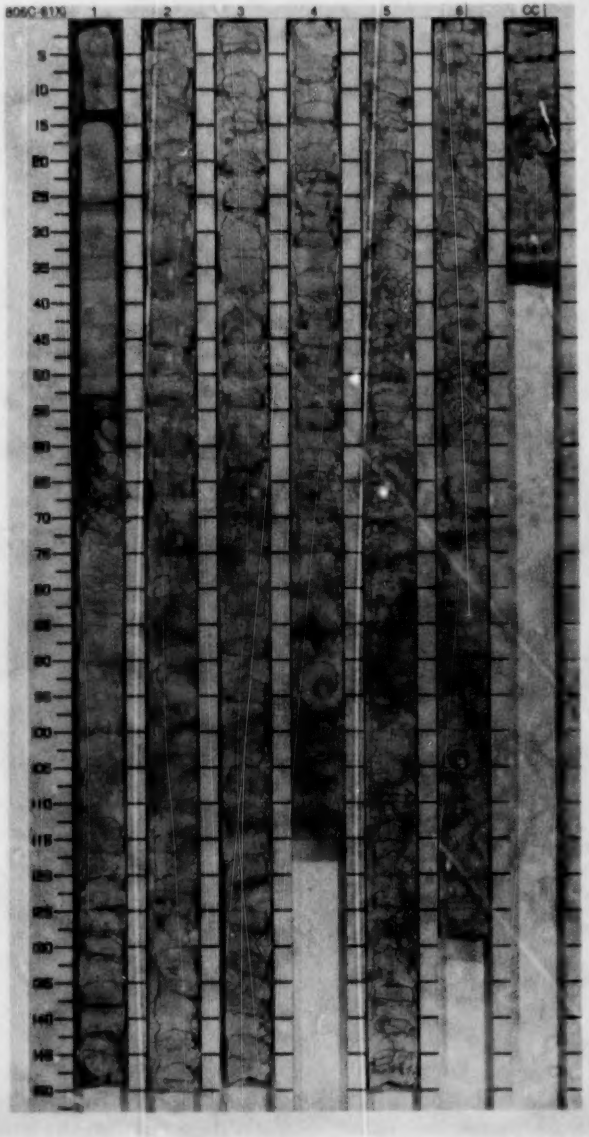
806C-61X
1
2
3
4
5
6
CC
5
10
15
20
25
30
35
40
45
50
55
60
65
70
75
80
85
90
95
100
105
110
115
120
125
130
135
140
145
150

SITE 806 HOLE C CORE 62X CORED INTERVAL 766.7-776.4 mbsf

TIME-ROCK UNIT	FORAMINIFERS	NANNOFOSSILS	RADIOLARIANS	DIATOMS	PALEOMAGNETICS	PHYS. PROPERTIES	CHEMISTRY	SECTION	METERS	GRAPHIC LITHOL. 3Y	DRILLING DISTURB.	SED. STRUCTURES	SAMPLES
UPPER OLIGOCENE	P22	NP25 A/G	*Dorcadospyris ateuchus* - *Lychnocanoma elongata* A/P	*Rocella vigilans* C/P-M		● φ=43.4 γ=1.96 Vp=1780		1	0.5		⊥	≀≀	●
								CC			⊥	≀≀	

LITHOLOGIC DESCRIPTION

NANNOFOSSIL CHALK with FORAMINIFERS

Major lithology: This core contains white (5Y 8/1) NANNOFOSSIL CHALK with FORAMINIFERS. The chalk is bioturbated with burrows and trace fossils. Distinct, very thin (<1 mm), gray (5Y 6/1) bands that form a braided pattern are present over intervals of 1 to 3 cm.

SMEAR SLIDE SUMMARY (%):

	1, 43
	D
TEXTURE	
Sand	5
Silt	75
Clay	20
COMPOSITION	
Accessory minerals	1
Diatoms	1
Foraminifers	10
Nannofossils	86
Radiolarians	Tr
Siliceous fragments	2

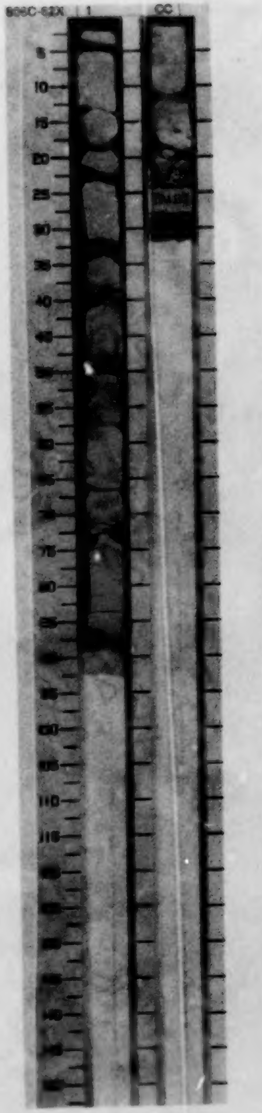
806C-62X
1
CC
5
10
15
20
25
30
35
40
45
50
55
60
65
70
75
80
85
90
95
100
105
110
115
120
125
130
135
140
145
150

SITE 807 HOLE A CORE 1H CORED INTERVAL 0.0-7.4 mbsf

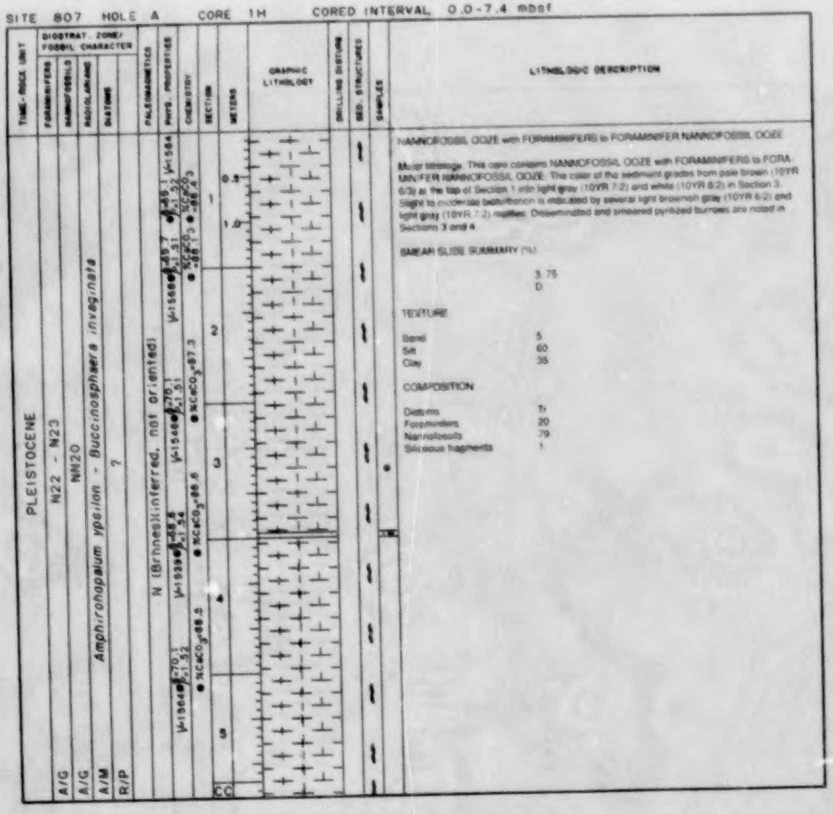
TIME-ROCK UNIT
BIOSTRAT. ZONE/ FOSSIL CHARACTER
FORAMINIFERS
NANNOFOSSILS
RADIOLARIANS
DIATOMS
PALEOMAGNETICS
PHYS. PROPERTIES
CHEMISTRY
SECTION
METERS
GRAPHIC LITHOLOGY
DRILLING DISTURB.
SED. STRUCTURES
SAMPLES
PLEISTOCENE
A/G N22 - N23
A/G NN20
A/M Amphirhopalum ypsilon - Buccinosphaera invaginata
R/P ?
N (Brhnes)(inferred, not oriented)
V=1584
φ=69.1 ρ=1.52
V=1566 φ=69.7 ρ=1.51
%CaCO3=88.4
%CaCO3=88.1
V=1546 φ=70.1 ρ=1.51
%CaCO3=87.3
V=1539 φ=68.6 ρ=1.54
%CaCO3=88.6
V=1564 φ=70.1 ρ=1.52
%CaCO3=88.5
0.5
1.0
1
2
3
4
5
CC

LITHOLOGIC DESCRIPTION

NANNOFOSSIL OOZE with FORAMINIFERS to FORAMINIFER NANNOFOSSIL OOZE

Major lithology: This core contains NANNOFOSSIL OOZE with FORAMINIFERS to FORAMINIFER NANNOFOSSIL OOZE. The color of the sediment grades from pale brown (10YR 6/3) at the top of Section 1 into light gray (10YR 7/2) and white (10YR 8/2) in Section 3. Slight to moderate bioturbation is indicated by several light brownish gray (10YR 6/2) and light gray (10YR 7/2) mottles. Disseminated and smeared pyritized burrows are noted in Sections 3 and 4.

SMEAR SLIDE SUMMARY (%):

	3, 75 D
TEXTURE:	
Sand	5
Silt	60
Clay	35
COMPOSITION:	
Diatoms	Tr
Foraminifers	20
Nannofossils	79
Siliceous fragments	1

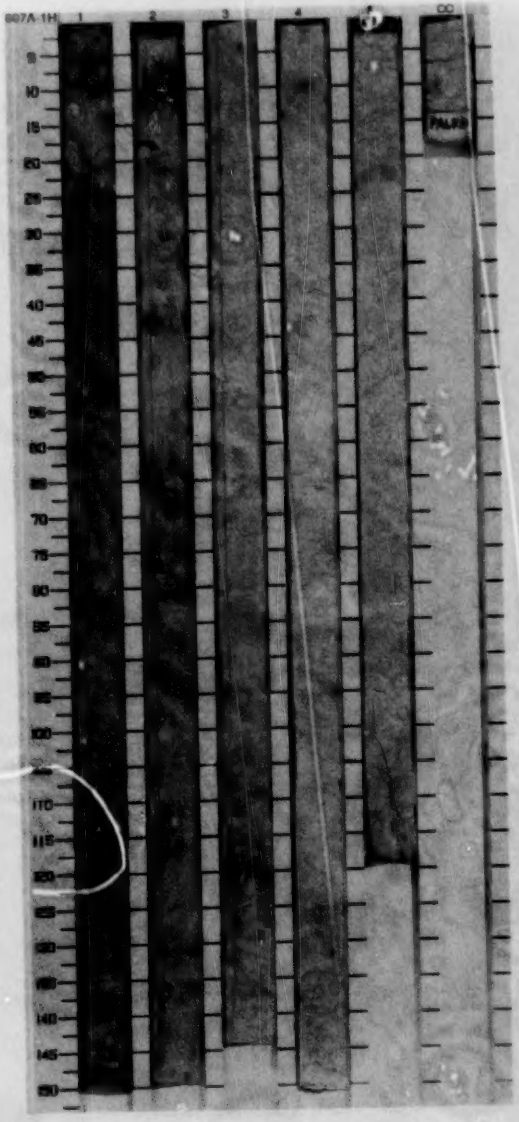
807A-1H
1
2
3
4
5
CC
PALEO
5
10
15
20
25
30
35
40
45
50
55
60
65
70
75
80
85
90
95
100
105
110
115
120
125
130
135
140
145
150

SITE 807 HOLE A CORE 2H CORED INTERVAL 7.4-16.9 mbsf

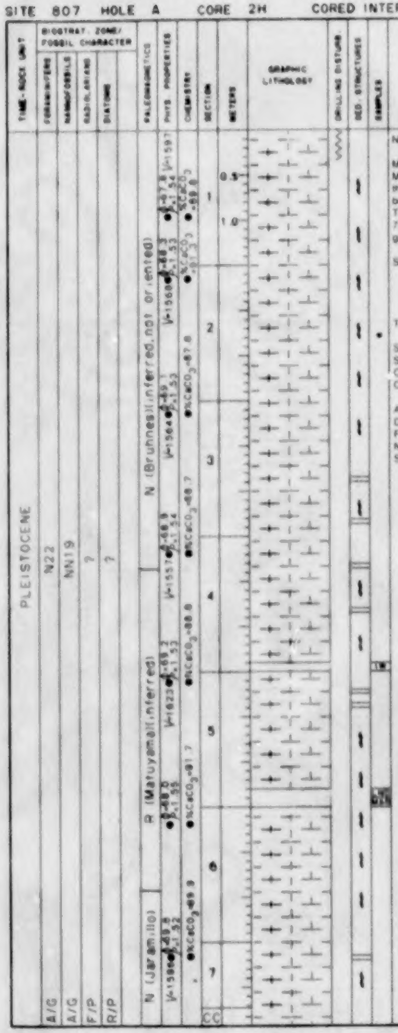
TIME-ROCK UNIT
BIOSTRAT. ZONE/ FOSSIL CHARACTER
FORAMINIFERS
NANNOFOSSILS
RADIOLARIANS
DIATOMS
PALEOMAGNETICS
PHYS. PROPERTIES
CHEMISTRY
SECTION
METERS
GRAPHIC LITHOLOGY
DRILLING DISTURB.
SED. STRUCTURES
SAMPLES
PLEISTOCENE
N22
NN19
?
?
A/G
A/G
F/P
R/P
N (Brunhes)(inferred, not oriented)
R (Matuyama)(inferred)
N (Jaramillo)
φ=67.8
ρ=1.54
V=1597
φ=68.3
ρ=1.53
V=1566
φ=69.1
ρ=1.53
V=1564
φ=68.9
ρ=1.54
V=1557
φ=69.2
ρ=1.53
V=1623
φ=68.0
ρ=1.55
φ=69.5
ρ=1.52
V=1580
%CaCO3=89.0
%CaCO3=81.3
%CaCO3=87.8
%CaCO3=88.7
%CaCO3=88.8
%CaCO3=81.7
%CaCO3=89.9
1
2
3
4
5
6
7
CC
0.5
1.0
IW
OG
PALEO

LITHOLOGIC DESCRIPTION

NANNOFOSSIL OOZE with FORAMINIFERS to FORAMINIFER NANNOFOSSIL OOZE

Major lithology: This core contains NANNOFOSSIL OOZE with FORAMINIFERS to FORAMINIFER NANNOFOSSIL OOZE. Bioturbation is evident throughout the core. In Section 1, the ooze grades from yellowish white (10YR 8/1) above 43 cm to grayish white (7.5YR 8/0) below 43 cm. From the top of Section 2 downcore, the ooze exhibits cyclic color changes. The typical cycle is white (7.5YR 8/0), grading downward into a pale yellowish green (10GY 7/2) interval bounded by a sharp base. White bands are between 5 and 100 cm thick. Light gray bands are between 5 and 20 cm thick. Pale yellowish green bands are 1 to 5 cm thick.

SMEAR SLIDE SUMMARY (%):

	2, 74
	D
TEXTURE:	
Sand	10
Silt	60
Clay	30
COMPOSITION:	
Accessory minerals	2
Diatoms	Tr
Foraminifers	20
Nannofossils	75
Siliceous fragments	3

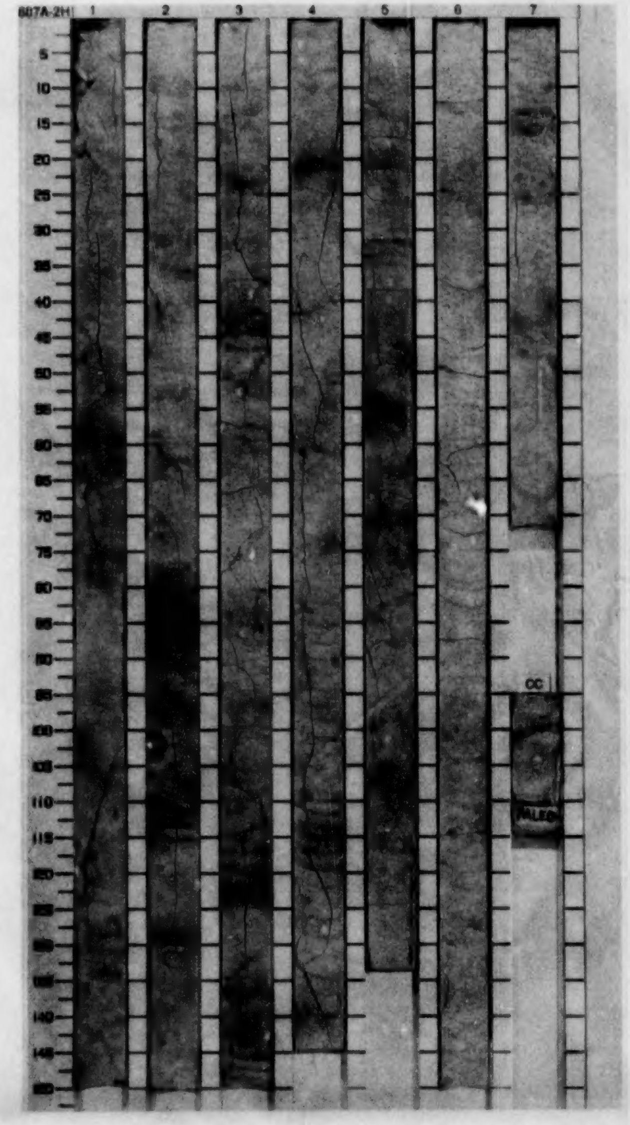
807A-2H
1
2
3
4
5
6
7
5
10
15
20
25
30
35
40
45
50
55
60
65
70
75
80
85
90
95
100
105
110
115
120
125
130
135
140
145
150
CC
PALEO

SITE 807 HOLE A CORE 3H CORED INTERVAL 16.9-26.4 mbsf

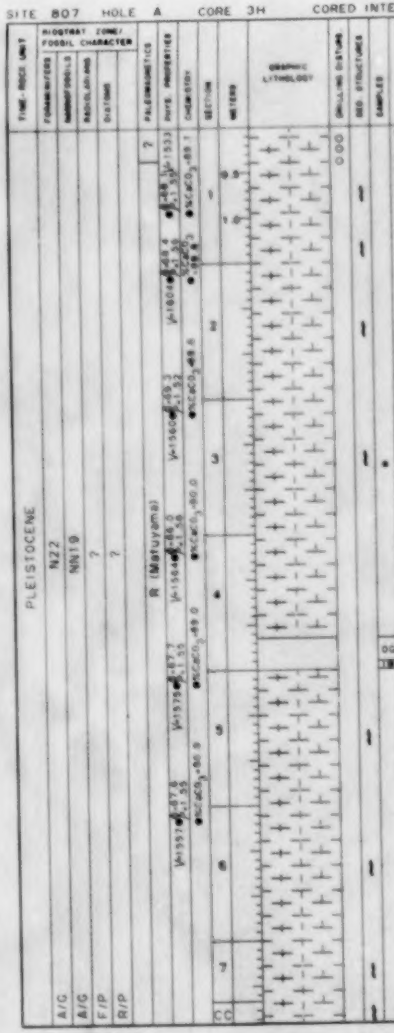
TIME-ROCK UNIT
BIOSTRAT. ZONE/ FOSSIL CHARACTER
FORAMINIFERS
NANNOFOSSILS
RADIOLARIANS
DIATOMS
PALEOMAGNETICS
PHYS. PROPERTIES
CHEMISTRY
SECTION
METERS
GRAPHIC LITHOLOGY
DRILLING DISTURB.
SED. STRUCTURES
SAMPLES
PLEISTOCENE
A/G N22
A/G NN19
F/P ?
R/P ?
?
R (Matuyama)
γ=1533 φ=68.1 γ=1.55
%CaCO3=88.1
Vp=1604 φ=68.4 γ=1.58
%CaCO3=88.8
Vp=1560 φ=69.3 γ=1.52
%CaCO3=88.6
Vp=1564 φ=68.0 γ=1.58
%CaCO3=90.0
Vp=1575 φ=67.7 γ=1.55
%CaCO3=89.0
Vp=1557 φ=67.8 γ=1.55
%CaCO3=90.9
1
2
3
4
5
6
7
CC
0.5
1.0
OG
IW

LITHOLOGIC DESCRIPTION

FORAMINIFER NANNOFOSSIL OOZE to NANNOFOSSIL OOZE with FORAMINIFERS

Major lithology: This core contains FORAMINIFER NANNOFOSSIL OOZE to NANNOFOSSIL OOZE with FORAMINIFERS. The sediment is slightly bioturbated, homogeneous, and white (7.5YR 8/0). The few burrows present are filled with softer material. Slightly gritty zones, approximately 20 cm in length, are observed throughout the core (about one per section).

SMEAR SLIDE SUMMARY (%):

	3, 74
	D
TEXTURE:	
Sand	15
Silt	60
Clay	25
COMPOSITION:	
Accessory minerals	2
Diatoms	Tr
Foraminifers	28
Nannofossils	67
Siliceous fragments	3

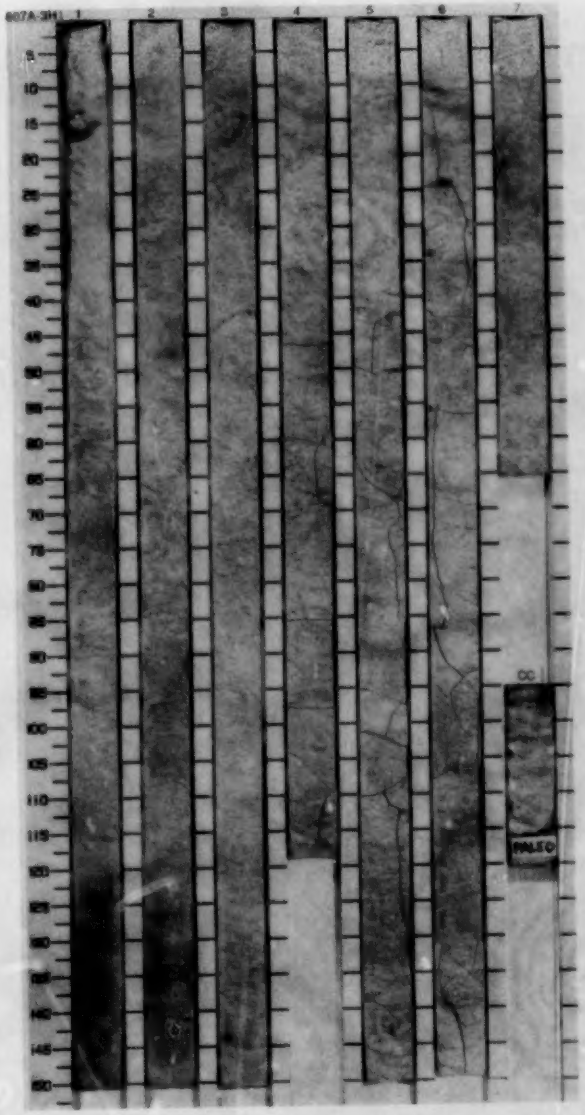
807A-3H
1
2
3
4
5
6
7
5
10
15
20
25
30
35
40
45
50
55
60
65
70
75
80
85
90
95
100
105
110
115
120
125
130
135
140
145
150
CC
PALEO

SITE 807 HOLE A CORE 4H CORED INTERVAL 26.4-35.9 mbsf

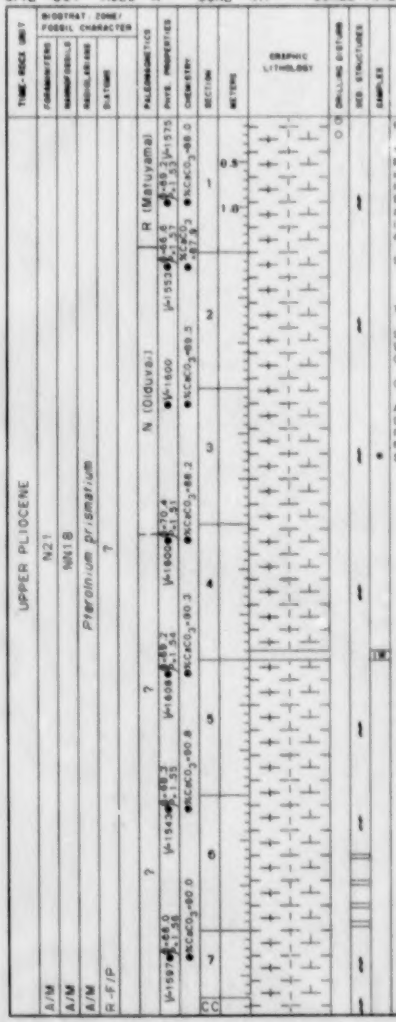

LITHOLOGIC DESCRIPTION

FORAMINIFER NANNOFOSSIL OOZE to NANNOFOSSIL OOZE with FORAMINIFERS

Major lithology: This core contains homogeneous FORAMINIFER NANNOFOSSIL OOZE to NANNOFOSSIL OOZE with FORAMINIFERS. The sediment is white (7.5YR 8/0 grading into 10YR 8/1 in Section 6) and slightly bioturbated, as indicated by a few watery, pyrite filled burrows and by gray (10YR 6/1) and light gray (10YR 7/2) mottles below Section 6. In Sections 2 through 5, several diffuse cm scale, gray (7.5YR 6/0) and bluish gray (5B 6/1) zones are present. In Sections 6 and 7, a few diffuse, cm scale, bluish gray, reddish gray (10R 6/1) and greenish gray (5G 7/1) zones, as well as greenish gray color bands (cm scale) are noted.

SMEAR SLIDE SUMMARY (%):

	3, 74 D
TEXTURE:	
Sand	15
Silt	60
Clay	25
COMPOSITION:	
Accessory minerals	2
Diatoms	Tr
Foraminifers	28
Nannofossils	67
Siliceous fragments	3

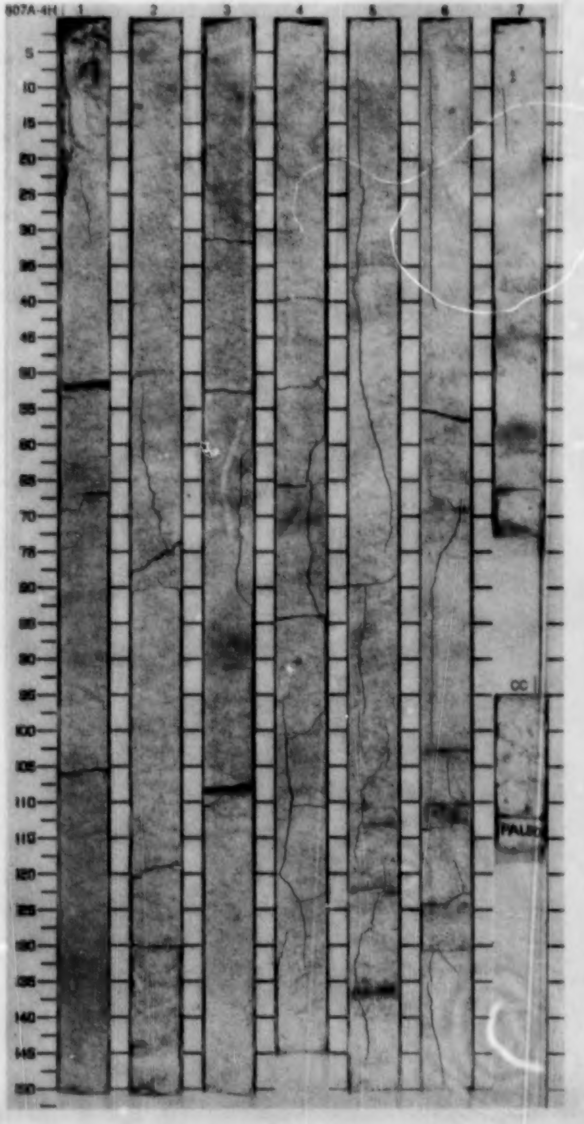
807A-4H
1
2
3
4
5
6
7
CC
PALEO
5
10
15
20
25
30
35
40
45
50
55
60
65
70
75
80
85
90
95
100
105
110
115
120
125
130
135
140
145
150

SITE 807 HOLE A CORE 5H CORED INTERVAL 35.9-45.4 mbsf

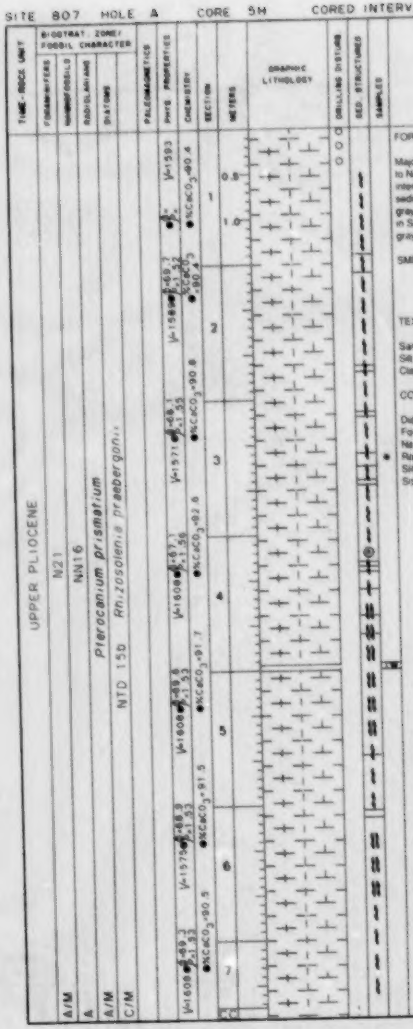

LITHOLOGIC DESCRIPTION

FORAMINIFER NANNOFOSSIL OOZE to NANNOFOSSIL OOZE with FORAMINIFERS

Major lithology: This core contains white (7.5YR 8/0) FORAMINIFER NANNOFOSSIL OOZ to NANNOFOSSIL OOZE with FORAMINIFERS, which grades into a 5 cm thick gray (N7/) interval at Section 1, 145 cm and a pale purple (5P 6/2) interval at Section 5, 95 cm. The sediment is slightly to heavily bioturbated, and contains watery pyrite-filled burrows and lig gray (5Y 7/1) and light olive gray (5Y 6/2) mottling. A 2 cm long pyrite concretion is present in Section 4, 15 cm. Faint to sharp, pale blue (5PB 7/2), pale purple (5P 6/2), light greenis gray (5G 7/1), and pale green (5G 6/2) color bands are common throughout the core.

SMEAR SLIDE SUMMARY (%):

	3, 98
	D
TEXTURE:	
Sand	14
Silt	80
Clay	6
COMPOSITION:	
Diatoms	Tr
Foraminifers	25
Nannofossils	70
Radiolarians	2
Silicoflagellates	2
Spicules	1

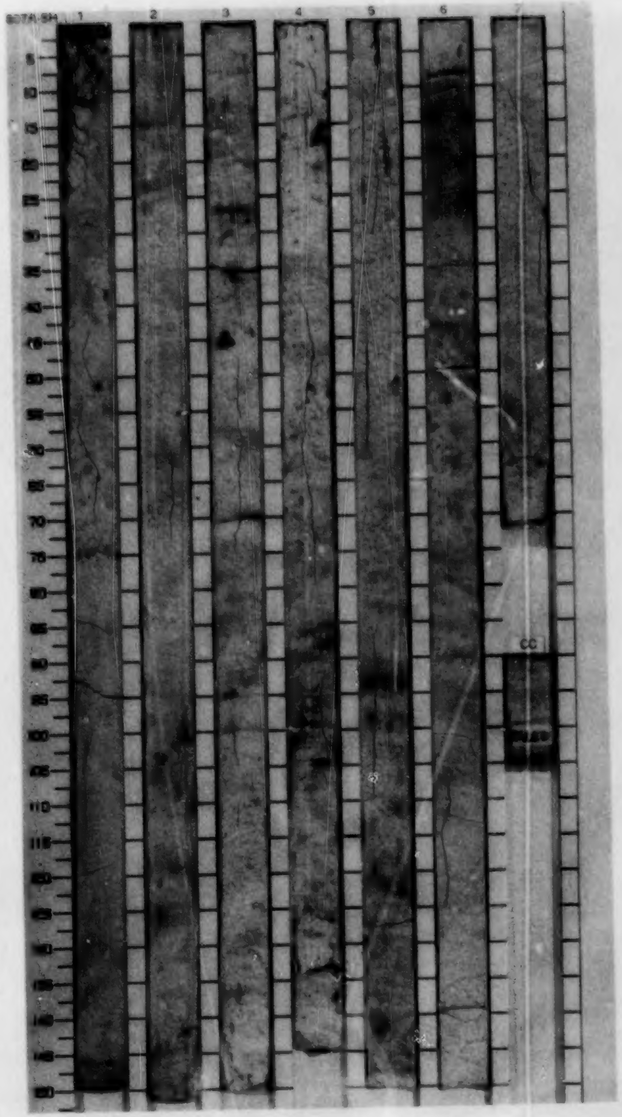
807A-5H
1
2
3
4
5
6
7
CC
5
10
15
20
25
30
35
40
45
50
55
60
65
70
75
80
85
90
95
100
105
110
115
120
125
130
135
140
145
150

SITE 807 HOLE A CORE 6H CORED INTERVAL 45.4-54.9 mbsf

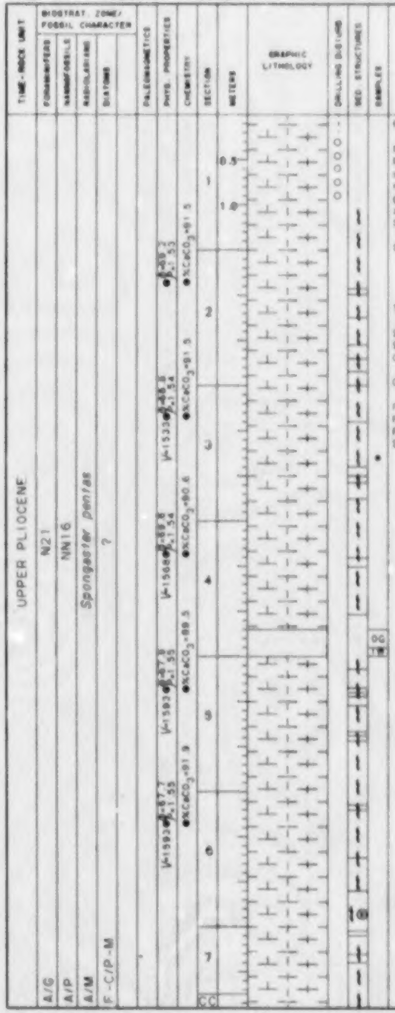
TIME-ROCK UNIT
BIOSTRAT. ZONE/ FOSSIL CHARACTER
FORAMINIFERS
NANNOFOSSILS
RADIOLARIANS
DIATOMS
PALEOMAGNETICS
PHYS. PROPERTIES
CHEMISTRY
SECTION
METERS
GRAPHIC LITHOLOGY
DRILLING DISTURB.
SED. STRUCTURES
SAMPLES
UPPER PLIOCENE
N21
NN16
Spongaster pentas
?
A/G
A/P
A/M
F-C/P-M
φ=69.2
γ=1.53
V=1533
φ=68.8
γ=1.54
V=1568
φ=69.8
γ=1.54
V=1593
φ=67.8
γ=1.55
V=1593
φ=67.7
γ=1.55
%CaCO3=91.5
%CaCO3=91.5
%CaCO3=80.6
%CaCO3=89.5
%CaCO3=91.9
1
2
3
4
5
6
7
CC
0.5
1.0
OG
IW

LITHOLOGIC DESCRIPTION

NANNOFOSSIL OOZE with FORAMINIFERS to FORAMINIFER NANNOFOSSIL OOZE

Major lithology: This core contains NANNOFOSSIL OOZE with FORAMINIFERS to FORAMINIFER NANNOFOSSIL OOZE. The sediment is white (7.5YR 8/0 and 2.5Y 8/0) and slightly to moderately bioturbated, as indicated by light gray (5Y 7/1 and 5Y 7/2) mottles and mm to cm scale, pyrite filled burrows. Light greenish gray (5G 7/1), pale blue (5PB 7/2), and grayish blue (5 PB 5/2) color bands are present throughout the core and form concentrated zones at Section 3, 90-105 cm, Section 5, 35-60 and 80-100 cm, Section 6, 22-27 cm, and Section 7, 0-36 cm.

SMEAR SLIDE SUMMARY (%):

	3, 80
	D
TEXTURE	
Sand	25
Silt	70
Clay	5
COMPOSITION	
Foraminifers	15
Nannofossils	82
Radiolarians	2
Silicoflagellates	1

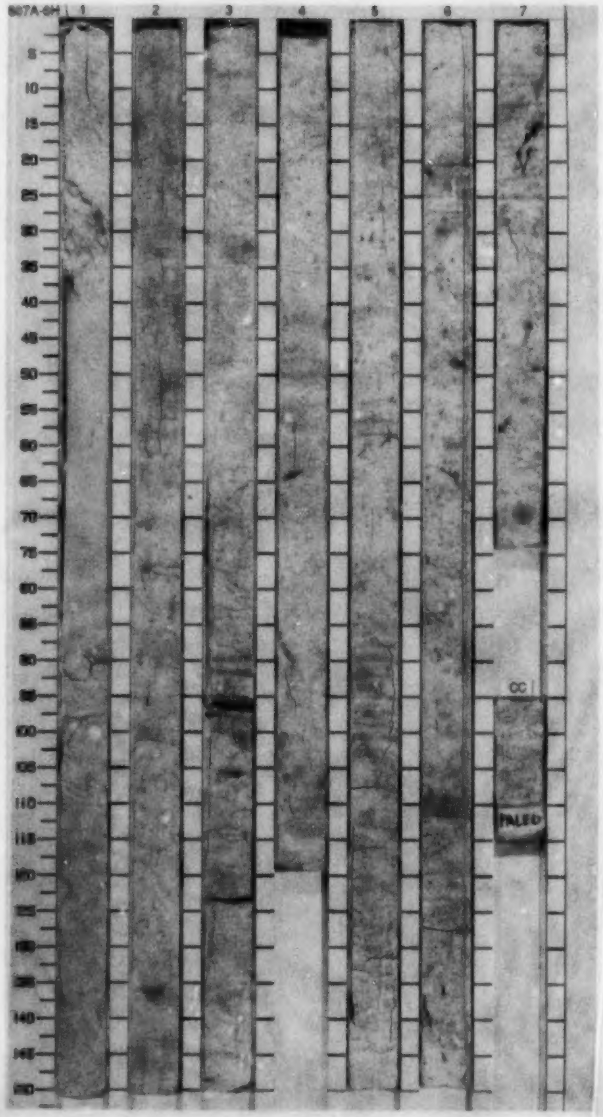
807A-6H
1
2
3
4
5
6
7
5
10
15
20
25
30
35
40
45
50
55
60
65
70
75
80
85
90
95
100
105
110
115
120
125
130
135
140
145
150
CC
PALEO

SITE 807 HOLE A CORE 7H CORED INTERVAL 54.9-64.4 mbsf

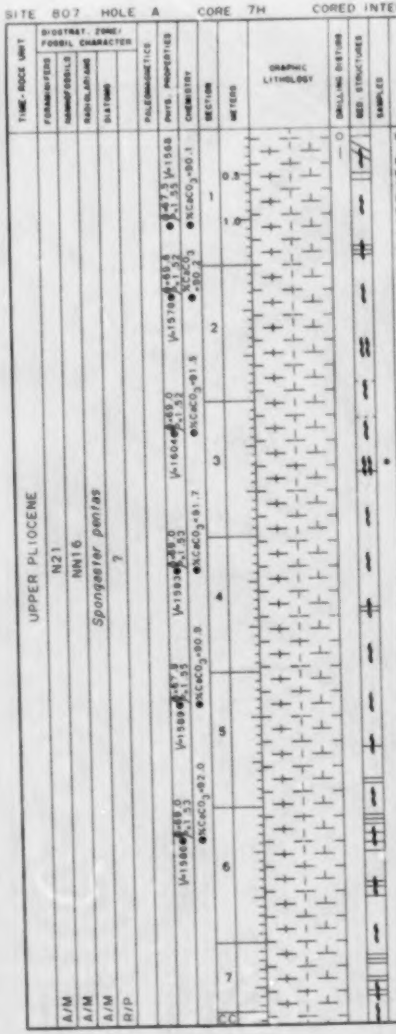

LITHOLOGIC DESCRIPTION

NANNOFOSSIL OOZE with FORAMINIFERS to FORAMINIFER NANNOFOSSIL OOZE

Major lithology: This core contains NANNOFOSSIL OOZE with FORAMINIFERS to FORAMINIFER NANNOFOSSIL OOZE. The sediment is white (2.5Y 8/0), grading to light gray (5Y 7/1) in the lower part of Section 7. Diffuse pale blue (5PB 7/2), light gray (N7), and light bluish gray (5B 7/1) zones, 3 to 10 cm wide, are present in Sections 3 through 5. Moderate to heavy bioturbation is indicated by light gray (5Y 7/2) and grayish blue (5PB 5/2) mottling. Very fine-grained pyrite-filled burrows are seen in all sections. A 4 cm diameter burrow "halo" is noted in Section 6. Diffuse to distinct, light greenish gray (5G 7/1), pale purple (5P 6/2), and grayish blue (5PB 5/2), 0.5 to 1 cm wide color bands are present.

SMEAR SLIDE SUMMARY (%):

	3, 70
	D
TEXTURE:	
Sand	10
Silt	86
Clay	4
COMPOSITION:	
Foraminifers	12
Nannofossils	83
Radiolarians	2
Silicoflagellates	2
Spicules	1

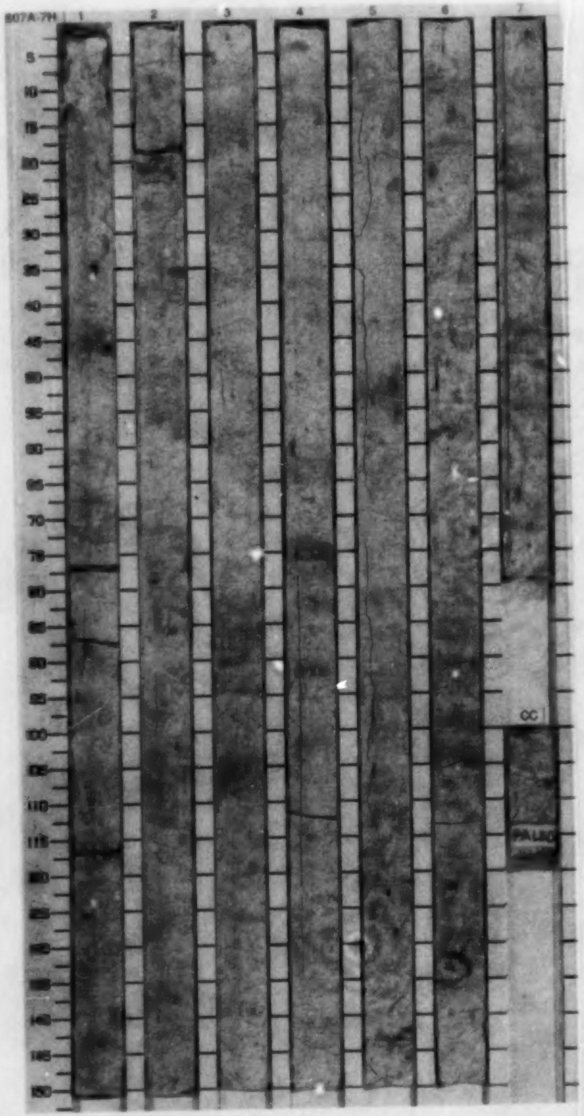
807A-7H
1
2
3
4
5
6
7
5
10
15
20
25
30
35
40
45
50
55
60
65
70
75
80
85
90
95
100
105
110
115
120
125
130
135
140
145
150
CC
PALEO

SITE 807 HOLE A CORE 8H CORED INTERVAL 64.4-73.9 mbsf

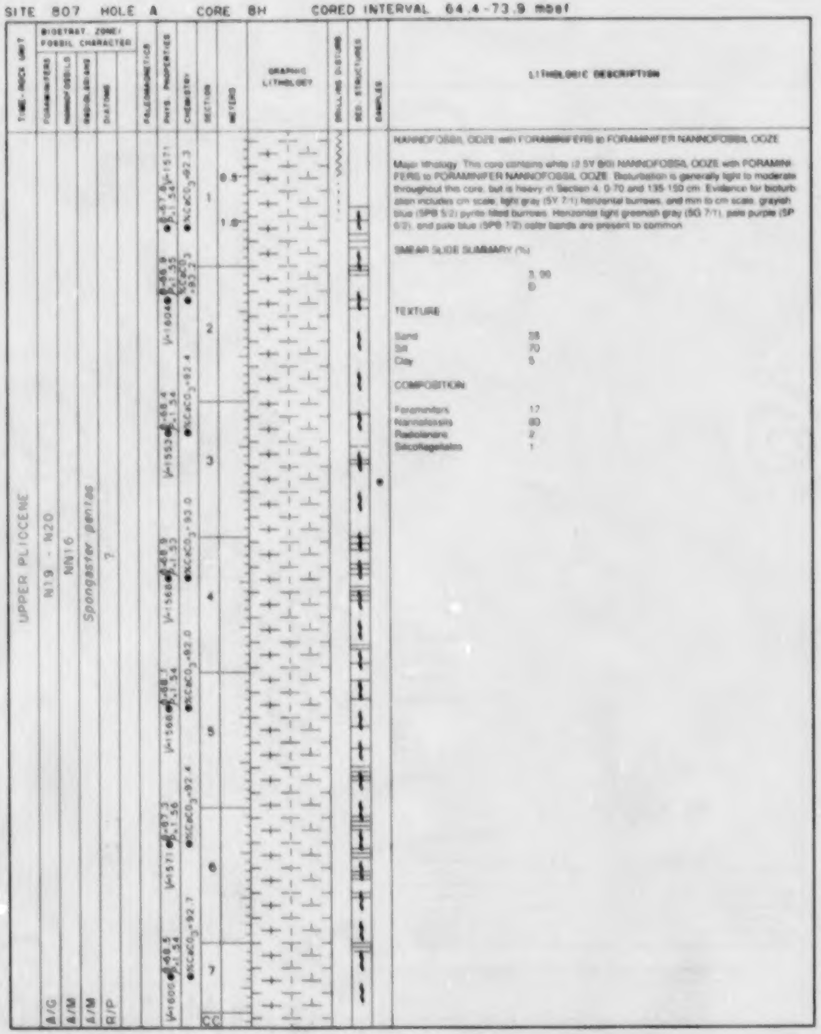
TIME-ROCK UNIT
BIOSTRAT. ZONE/ FOSSIL CHARACTER
FORAMINIFERS
NANNOFOSSILS
RADIOLARIANS
DIATOMS
PALEOMAGNETICS
PHYS. PROPERTIES
CHEMISTRY
SECTION
METERS
GRAPHIC LITHOLOGY
DRILLING DISTURB.
SED. STRUCTURES
SAMPLES
UPPER PLIOCENE
A/G
N19 - N20
A/M
NN16
A/M
Spongaster pentas
R/P
?
φ=67.6 ρ=1.54 V=1571
%CaCO$_3$=92.3
φ=66.9 ρ=1.55
%CaCO$_3$=93.2
V=1604
φ=68.4 ρ=1.54 V=1553
%CaCO$_3$=92.4
φ=68.9 ρ=1.53 V=1568
%CaCO$_3$=93.0
φ=68.1 ρ=1.54 V=1568
%CaCO$_3$=92.0
φ=67.3 ρ=1.56 V=1571
%CaCO$_3$=92.4
φ=68.5 ρ=1.54 V=1600
%CaCO$_3$=92.7
1
2
3
4
5
6
7
CC
0.5
1.0

LITHOLOGIC DESCRIPTION

NANNOFOSSIL OOZE with FORAMINIFERS to FORAMINIFER NANNOFOSSIL OOZE

Major lithology: This core contains white (2.5Y 8/0) NANNOFOSSIL OOZE with FORAMINIFERS to FORAMINIFER NANNOFOSSIL OOZE. Bioturbation is generally light to moderate throughout this core, but is heavy in Section 4, 0-70 and 135-150 cm. Evidence for bioturbation includes cm scale, light gray (5Y 7/1) horizontal burrows, and mm to cm scale, grayish blue (5PB 5/2) pyrite filled burrows. Horizontal light greenish gray (5G 7/1), pale purple (5P 6/2), and pale blue (5PB 7/2) color bands are present to common.

SMEAR SLIDE SUMMARY (%):

	3, 90
	D
TEXTURE:	
Sand	25
Silt	70
Clay	5
COMPOSITION:	
Foraminifers	17
Nannofossils	80
Radiolarians	2
Silicoflagellates	1

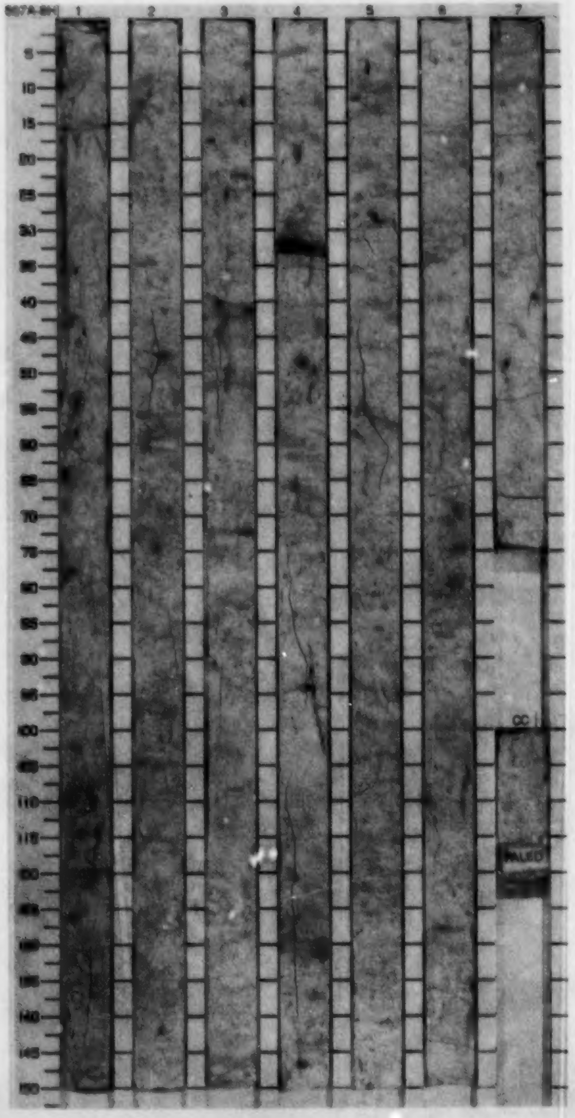
807A-8H
1
2
3
4
5
6
7
5
10
15
20
25
30
35
40
45
50
55
60
65
70
75
80
85
90
95
100
105
110
115
120
125
130
135
140
145
150
CC
PALEO

SITE 807 HOLE A CORE 9H CORED INTERVAL 73.9-83.4 mbsf

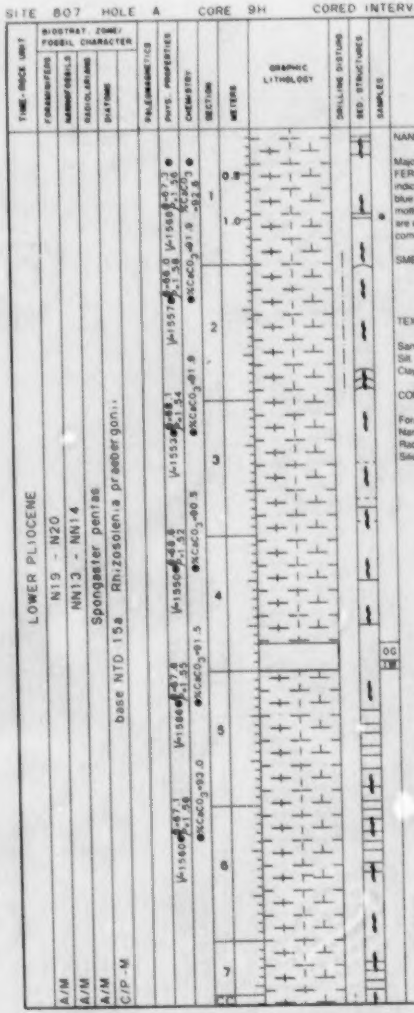
TIME-ROCK UNIT
BIOSTRAT. ZONE/ FOSSIL CHARACTER
FORAMINIFERS
NANNOFOSSILS
RADIOLARIANS
DIATOMS
PALEOMAGNETICS
PHYS. PROPERTIES
CHEMISTRY
SECTION
METERS
GRAPHIC LITHOLOGY
DRILLING DISTURB.
SED. STRUCTURES
SAMPLES
LOWER PLIOCENE
A/M N19 - N20
A/M NN13 - NN14
A/M Spongaster pentas
C/P-M base NTD 15a Rhizosolenia praebergonii
V=1568 φ=67.3 ρ=1.56
%CaCO3 =92.6
V=1557 φ=66.0 ρ=1.58
%CaCO3=91.9
%CaCO3=91.9
V=1553 φ=68.1 ρ=1.54
%CaCO3=90.5
V=1550 φ=68.8 ρ=1.52
%CaCO3=91.5
V=1566 φ=67.6 ρ=1.55
%CaCO3=93.0
V=1560 φ=67.1 ρ=1.56
0.5
1.0
1
2
3
4
5
6
7
CC
OG
IW

LITHOLOGIC DESCRIPTION

NANNOFOSSIL OOZE with FORAMINIFERS to FORAMINIFER NANNOFOSSIL OOZE

Major lithology: This core contains white (2.5Y 8/0) NANNOFOSSIL OOZE with FORAMINIFERS to FORAMINIFER NANNOFOSSIL OOZE. Slight to moderate bioturbation is indicated by pyritized, commonly vertical, dark gray (N4) burrows and associated grayish blue (5PB 5/2) mottling and "halos". Several cm scale, light gray (5Y 7/1) burrows and mottles are present. Distinct and diffuse, cm size, light greenish gray (5G 7/1) color bands are common throughout the core. Grayish blue (5PB 5/2) bands are present but less common.

SMEAR SLIDE SUMMARY (%):

	1, 99
	D
TEXTURE:	
Sand	25
Silt	70
Clay	5
COMPOSITION:	
Foraminifers	20
Nannofossils	76
Radiolarians	3
Silicoflagellates	1

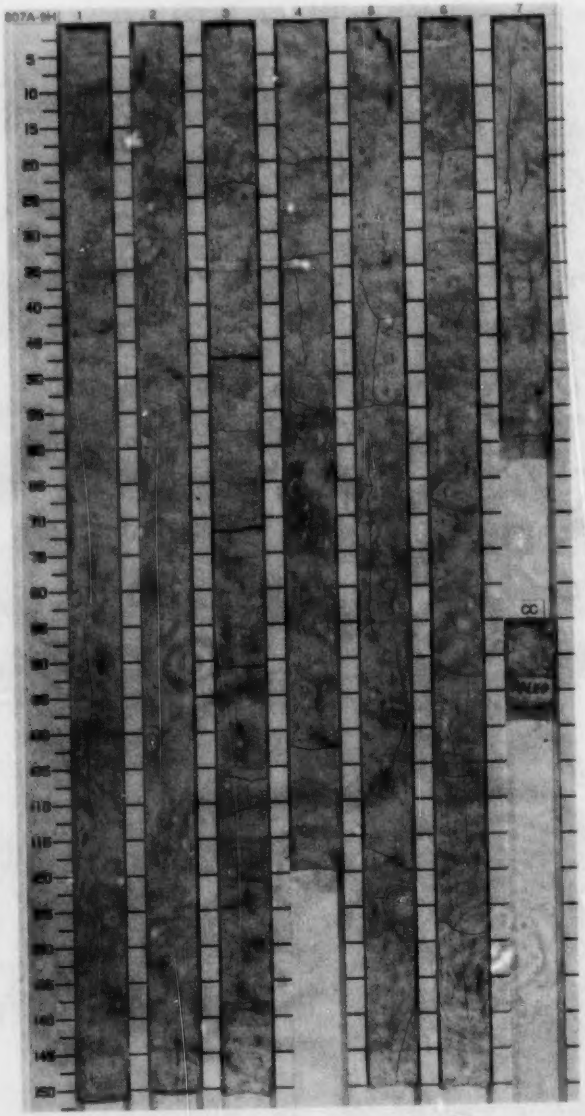
807A-9H
1
2
3
4
5
6
7
5
10
15
20
25
30
35
40
45
50
55
60
65
70
75
80
85
90
95
100
105
110
115
120
125
130
135
140
145
150
CC

SITE 807 HOLE A CORE 10H CORED INTERVAL 83.4-92.9 mbsf

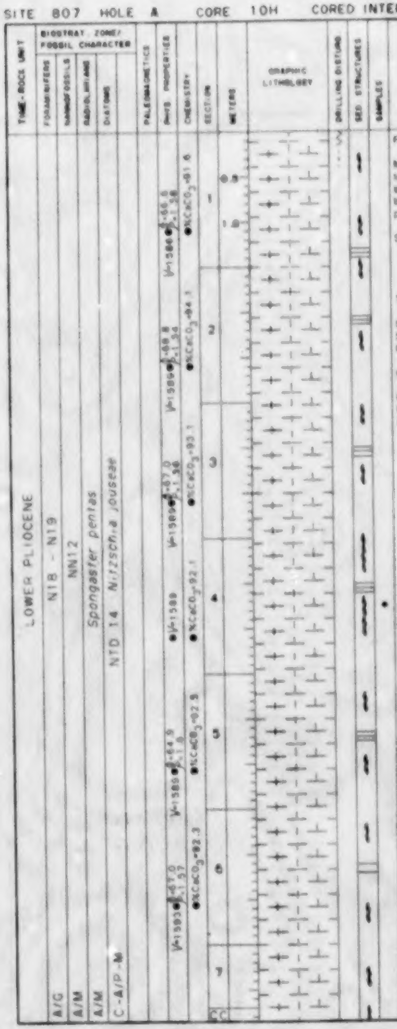
TIME-ROCK UNIT
BIOSTRAT. ZONE/ FOSSIL CHARACTER
FORAMINIFERS
NANNOFOSSILS
RADIOLARIANS
DIATOMS
PALEOMAGNETICS
PHYS. PROPERTIES
CHEMISTRY
SECTION
METERS
GRAPHIC LITHOLOGY
DRILLING DISTURB.
SED. STRUCTURES
SAMPLES
LOWER PLIOCENE
N18 - N19
NN12
Spongaster pentas
NTD 14 Nitzschia jouseae
A/G
A/M
A/M
C-A/P-M
V=1586●φ=66.6 γ=1.58
●%CaCO3=91.6
V=1589●φ=68.8 γ=1.54
●%CaCO3=94.1
V=1589●φ=67.0 γ=1.56
●%CaCO3=93.1
●V=1588
●%CaCO3=92.1
V=1589●φ=64.9 γ=1.6
●%CaCO3=92.5
V=1593●φ=67.0 γ=1.57
●%CaCO3=92.3
1
2
3
4
5
6
7
CC
0.5
1.0

LITHOLOGIC DESCRIPTION

FORAMINIFER NANNOFOSSIL OOZE to NANNOFOSSIL OOZE with FORAMINIFERS

Major lithology: This core contains white (2.5Y 8/0) FORAMINIFER NANNOFOSSIL OOZE to NANNOFOSSIL OOZE with FORAMINIFERS. Moderate bioturbation is evident as cm scale, light gray (5Y 7/1) mottles and mm to cm scale, grayish blue (5PB 5/2) pyrite filled burrows and halos. Diffuse light greenish gray (5G 7/1) color banding is common, and pale purple (5P 6/2) bands are present, but rare.

SMEAR SLIDE SUMMARY (%):

	4, 75
	D
TEXTURE:	
Sand	15
Silt	65
Clay	20
COMPOSITION:	
Foraminifers	25
Nannofossils	75
Radiolarians	Tr

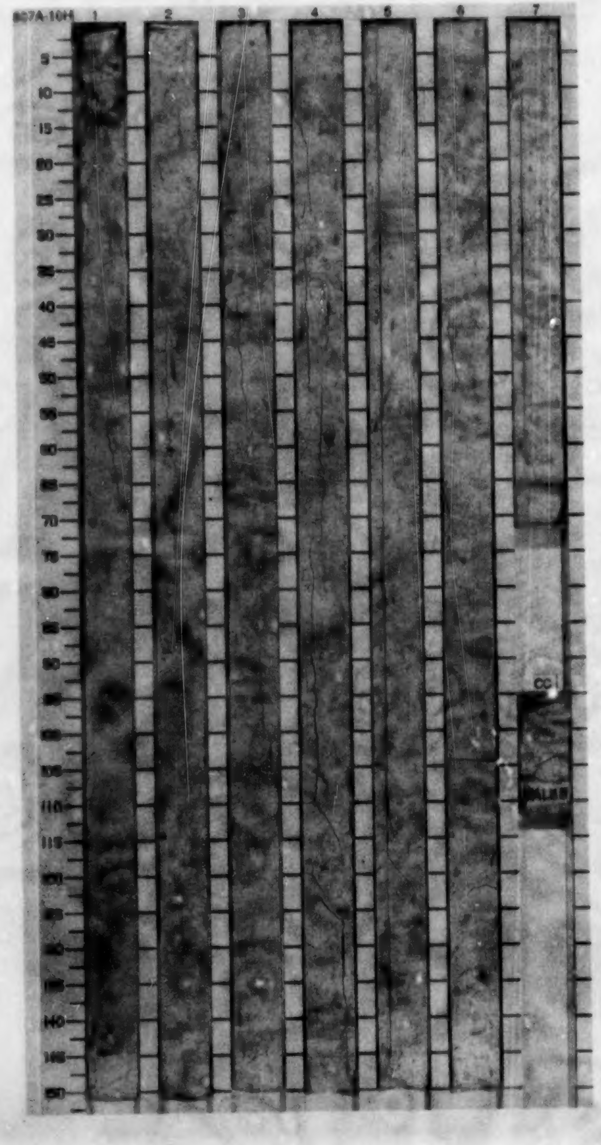
807A-10H
1
2
3
4
5
6
7
5
10
15
20
25
30
35
40
45
50
55
60
65
70
75
80
85
90
95
100
105
110
115
120
125
130
135
140
145
150
CC

SITE 807 HOLE A CORE 11H CORED INTERVAL 92.9-102.4 mbsf

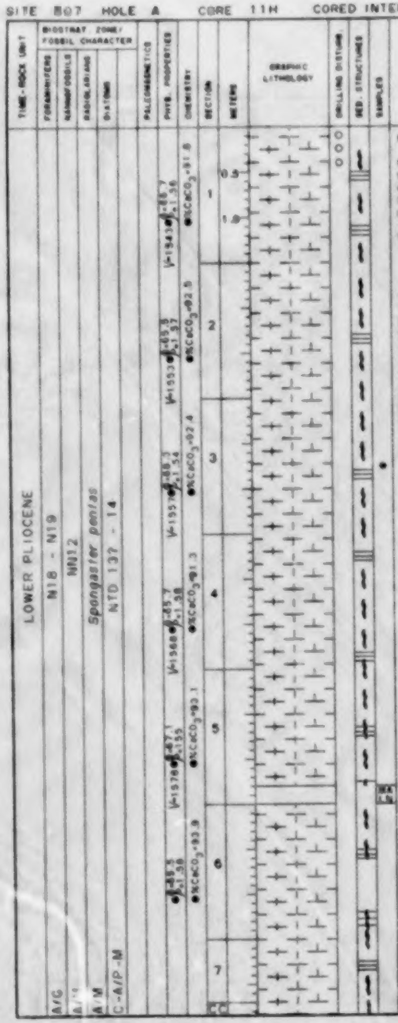
TIME-ROCK UNIT
BIOSTRAT. ZONE/ FOSSIL CHARACTER
FORAMINIFERS
NANNOFOSSILS
RADIOLARIANS
DIATOMS
PALEOMAGNETICS
PHYS. PROPERTIES
CHEMISTRY
SECTION
METERS
GRAPHIC LITHOLOGY
DRILLING DISTURB.
SED. STRUCTURES
SAMPLES
LOWER PLIOCENE
N18 - N19
NN12
Spongaster pentas
NTD 13? - 14
A/G
A/?
A/M
C-A/P-M
V=1543 65.7 1.56
%CaCO3=91.8
V=1553 65.5 1.57
%CaCO3=92.5
V=1557 68.3 1.54
%CaCO3=92.4
V=1566 65.7 1.58
%CaCO3=91.3
V=1578 67.1 1.55
%CaCO3=93.1
65.5 1.58
%CaCO3=93.9
1
2
3
4
5
6
7
CC
0.5
1.0

LITHOLOGIC DESCRIPTION

FORAMINIFER NANNOFOSSIL OOZE to NANNOFOSSIL OOZE with FORAMINIFERS

Major lithology: This core contains white (2.5Y 8/0) FORAMINIFER NANNOFOSSIL OOZE to NANNOFOSSIL OOZE with FORAMINIFERS. Common to abundant, 1 m thick intervals of color banding are evident. The color bands are mostly pale yellowish green (10GY 7/2). Slight to moderate bioturbation is indicated by mottles (2.5Y 8/2) and burrow infillings of pyrite with pale purple (5P 7/2) borders and streaks.

SMEAR SLIDE SUMMARY (%):

	3, 75
	D
TEXTURE:	
Sand	10
Silt	70
Clay	20
COMPOSITION:	
Diatoms	1
Foraminifers	25
Nannofossils	71
Radiolarians	1
Siliceous fragments	2

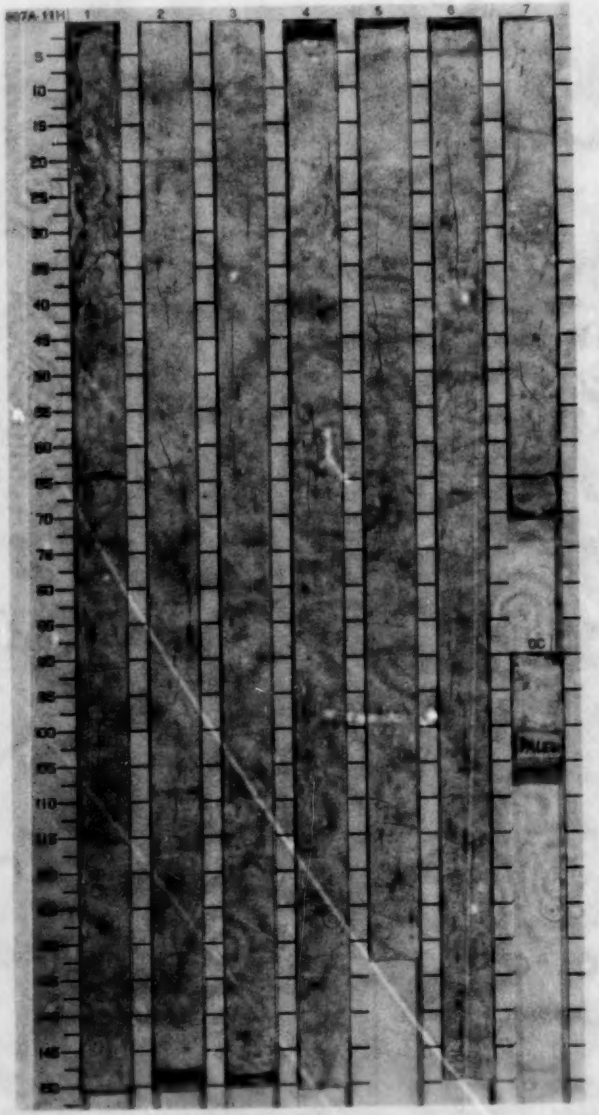
807A-11H
1
2
3
4
5
6
7
5
10
15
20
25
30
35
40
45
50
55
60
65
70
75
80
85
90
95
100
105
110
115
120
125
130
135
140
145
150
CC
PALEO

SITE 807 HOLE A CORE 12H CORED INTERVAL 102.4-111.9 mbsf

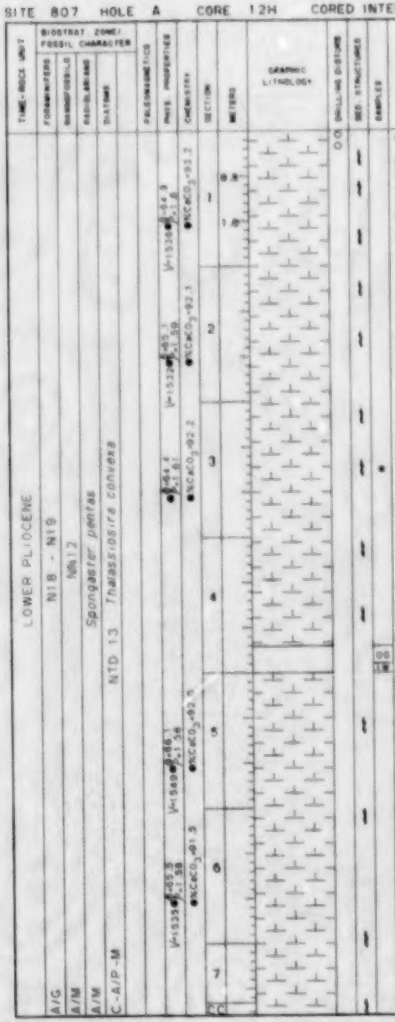

LITHOLOGIC DESCRIPTION

NANNOFOSSIL OOZE with FORAMINIFERS

Major lithology: This core contains white (2.5Y 8/0) NANNOFOSSIL OOZE with FORAMINIFERS. Greenish gray (5G 7/1), pale yellowish green (10GY 7/2), and pale purple (5P 6/2) color banding is common. Moderate to heavy bioturbation is evident from abundant cm-scale, light gray (2.5Y 7/2) mottles, pyrite-filled burrows, disseminated pyrite specks and pale purple (5P 6/2) mottles.

SMEAR SLIDE SUMMARY (%):

	3, 70 D
TEXTURE	
Sand	10
Silt	70
Clay	20
COMPOSITION	
Diatoms	Tr
Foraminifers	20
Nannofossils	78
Radiolarians	Tr
Siliceous fragments	2

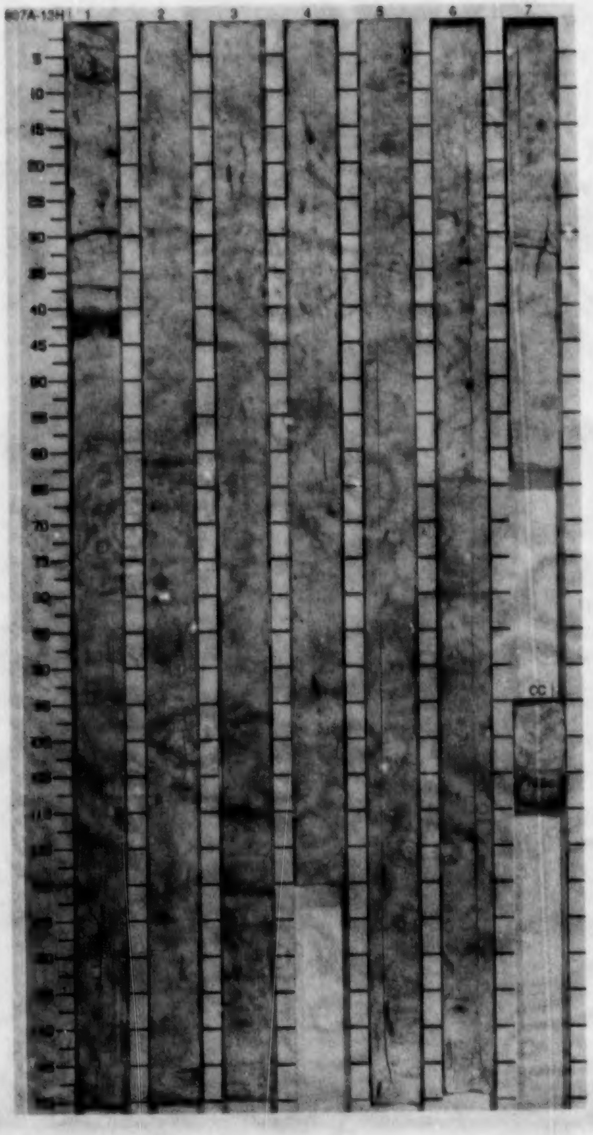
807A-12H
1
2
3
4
5
6
7
CC
5
10
15
20
25
30
35
40
45
50
55
60
65
70
75
80
85
90
95
100
105
110
115
120
125
130
135
140
145
150

SITE 807 HOLE A CORE 13H CORED INTERVAL 111.9-121.4 mbsf

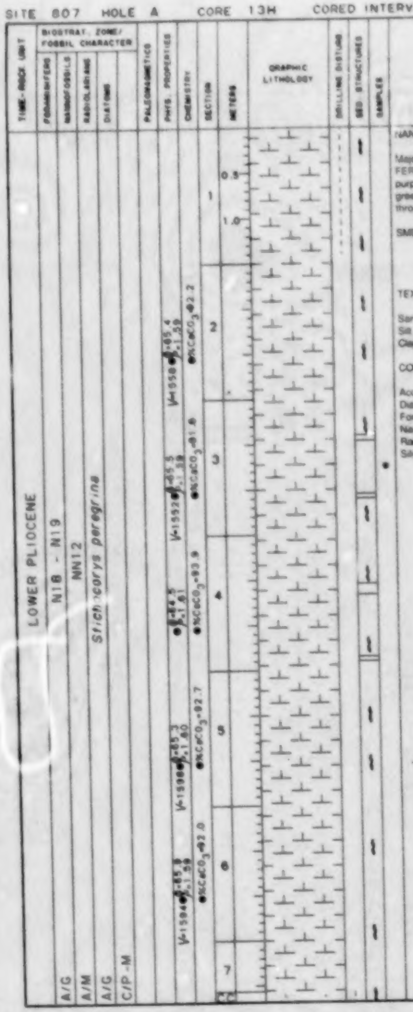

LITHOLOGIC DESCRIPTION

NANNOFOSSIL OOZE with FORAMINIFERS

Major lithology: This core contains white (2.5Y 8/0) NANNOFOSSIL OOZE with FORAMINIFERS. The sediment is moderately bioturbated, as indicated by white (2.5Y 8/2) and pale purple (5P 6/2) mottles, pyrite filled burrows, and "halos". Very few diffuse cm thick greenish gray (5G 7/1) and pale purple (5P 6/2) color bands and zones are present throughout the core.

SMEAR SLIDE SUMMARY (%):

	3, 74
	D
TEXTURE	
Sand	12
Silt	55
Clay	33
COMPOSITION	
Accessory minerals	2
Diatoms	Tr
Foraminifers	14
Nannofossils	81
Radiolarians	Tr
Siliceous fragments	3

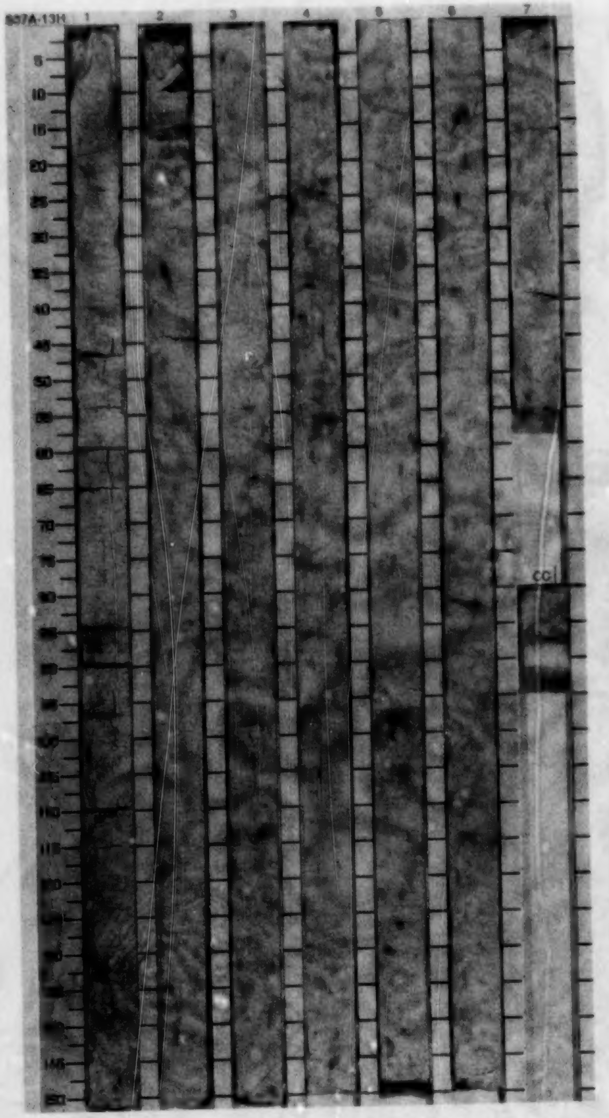
807A-13H
1
2
3
4
5
6
7
CC
5
10
15
20
25
30
35
40
45
50
55
60
65
70
75
80
85
90
95
100
105
110
115
120
125
130
135
140
145
150

SITE 807 HOLE A CORE 14H CORED INTERVAL 121.4-130.9 mbsf

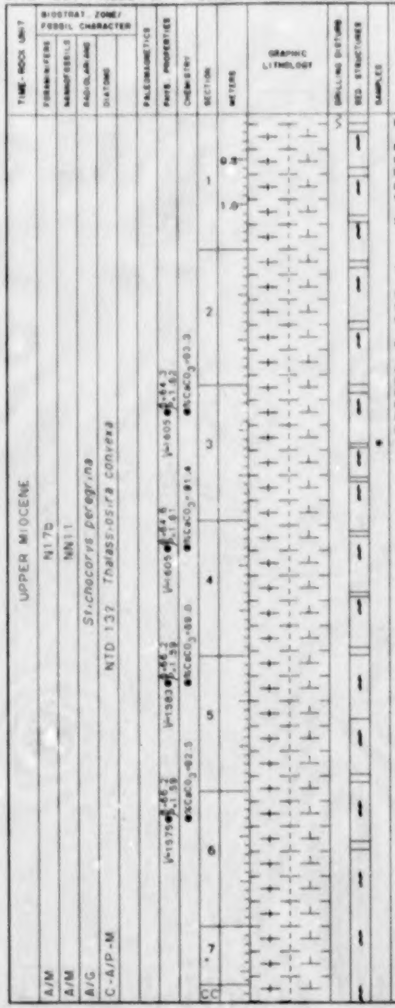
TIME-ROCK UNIT
BIOSTRAT. ZONE/ FOSSIL CHARACTER
FORAMINIFERS
NANNOFOSSILS
RADIOLARIANS
DIATOMS
PALEOMAGNETICS
PHYS. PROPERTIES
CHEMISTRY
SECTION
METERS
GRAPHIC LITHOLOGY
DRILLING DISTURB.
SED. STRUCTURES
SAMPLES
UPPER MIOCENE
N17b
NN11
Stichocorys peregrina
NTD 132 Thalassiosira convexa
A/M
A/M
A/G
C-A/P-M
V=1575 φ=66.2 γ=1.59
V=1583 φ=66.2 γ=1.59
V=1605 φ=64.6 γ=1.61
V=1605 φ=64.3 γ=1.62
%CaCO3=92.5
%CaCO3=88.0
%CaCO3=91.4
%CaCO3=93.3
1
2
3
4
5
6
7
CC
0.5
1.0

LITHOLOGIC DESCRIPTION

FORAMINIFER NANNOFOSSIL OOZE to NANNOFOSSIL OOZE with FORAMINIFERS

Major lithology: This core contains white (2.5Y 8/0) FORAMINIFER NANNOFOSSIL OOZE to NANNOFOSSIL OOZE with FORAMINIFERS. The sediment is moderately to heavily bioturbated, as indicated by light gray (2.5Y 7/2) and pale purple (5P 6/2) mottles and pyrite-filled burrows and specks. A few diffuse cm scale, faint greenish gray (5G 7/1) and very few pale purple (5P 6/2) color bands are noted throughout the core.

SMEAR SLIDE SUMMARY (%):

	3, 74
	D
TEXTURE:	
Sand	15
Silt	55
Clay	30
COMPOSITION:	
Accessory minerals	1
Diatoms	Tr
Foraminifers	27
Nannofossils	69
Radiolarians	Tr
Siliceous fragments	3

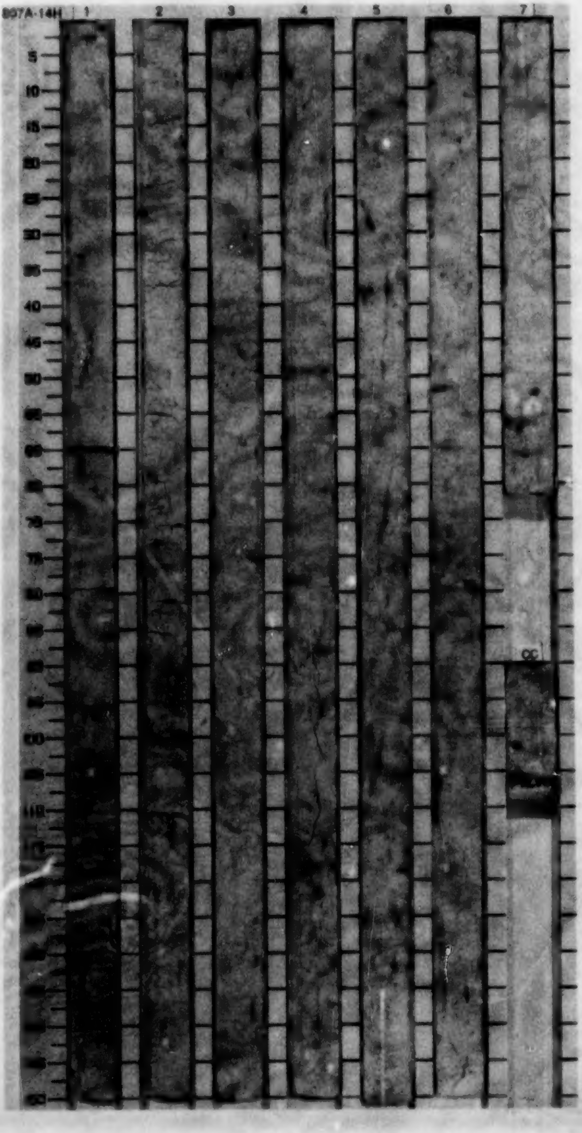
807A-14H
1
2
3
4
5
6
7
CC
5
10
15
20
25
30
35
40
45
50
55
60
65
70
75
80
85
90
95
100
105
110
115
120
125
130
135
140
145
150

SITE 807 HOLE A CORE 15H CORED INTERVAL 130.9-140.4 mbsf

TIME-ROCK UNIT	BIOSTRAT. ZONE/ FOSSIL CHARACTER: FORAMINIFERS	NANNOFOSSILS	RADIOLARIANS	DIATOMS	PALEOMAGNETICS	PHYS. PROPERTIES	CHEMISTRY	SECTION	METERS	GRAPHIC LITHOLOGY	DRILLING DISTURB.	SED. STRUCTURES	SAMPLES
UPPER MIOCENE	N17b	NN11						1			○		
								2			○ ○ ○ ○		
						V=1561 ●68.6 1.59	●%CaCO$_3$=93.0	3					
						V=1578 ●67.0 1.57	●%CaCO$_3$=91.1	4					●
						V=1554 ●63.2 1.63	●%CaCO$_3$=91.5	5					OG
						V=1550 ●63.2 1.62	●%CaCO$_3$=92.8	6					
						V=1569 ●62.8 1.63	●%CaCO$_3$=92.8	7		VOID			
								8					
	A/M	A/M		C-A/P-M				CC					

LITHOLOGIC DESCRIPTION

NANNOFOSSIL OOZE with FORAMINIFERS to NANNOFOSSIL OOZE

Major lithology: This core contains white (2.5Y 8/0) NANNOFOSSIL OOZE with FORAMINIFERS to NANNOFOSSIL OOZE. The sediment is moderately bioturbated, as indicated by light gray (2.5Y 7/2) and pale purple (5P 6/2) mottles, pyrite-filled burrows, and halos. Diffuse faint greenish gray (5G 7/1) and pale purple (5P 6/2) color bands (cm scale) are noted throughout the core.

SMEAR SLIDE SUMMARY (%):

	4, 74
	D
TEXTURE:	
Sand	15
Silt	55
Clay	30
COMPOSITION:	
Accessory minerals	2
Diatoms	Tr
Foraminifers	14
Nannofossils	80
Radiolarians	1
Siliceous fragments	3

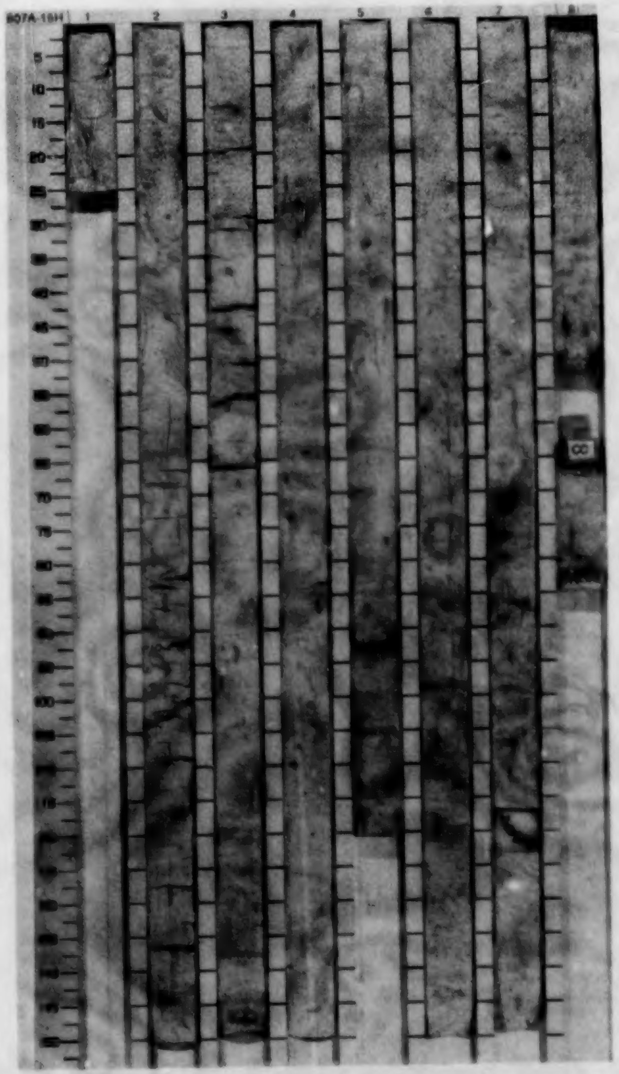

SITE 807 HOLE A CORE 16H CORED INTERVAL 140.4-149.9 mbsf

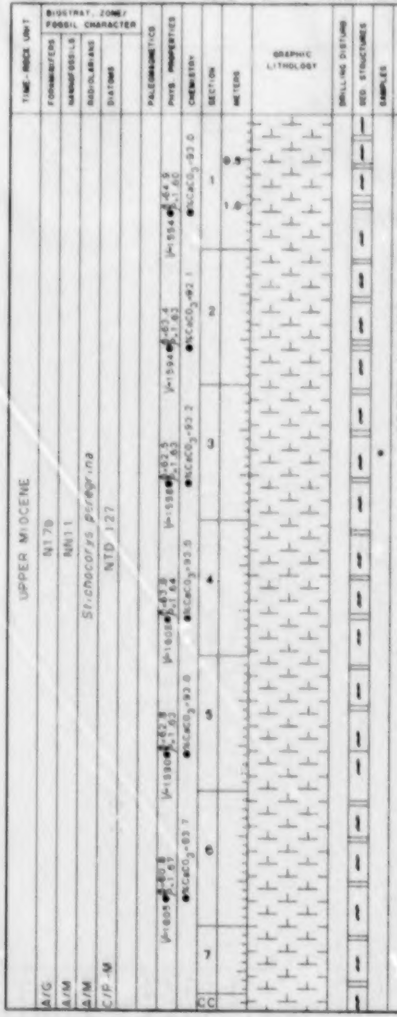
TIME-ROCK UNIT
BIOSTRAT. ZONE/ FOSSIL CHARACTER
FORAMINIFERS
NANNOFOSSILS
RADIOLARIANS
DIATOMS
PALEOMAGNETICS
PHYS. PROPERTIES
CHEMISTRY
SECTION
METERS
GRAPHIC LITHOLOGY
DRILLING DISTURB.
SED. STRUCTURES
SAMPLES
UPPER MIOCENE
N17b
NN11
Stichocorys peregrina
NTD 127
A/G
A/M
A/M
C/P-M
V=1554 φ=64.9 γ=1.60
%CaCO3=93.0
V=1594 φ=63.4 γ=1.63
%CaCO3=92.1
V=1598 φ=62.5 γ=1.63
%CaCO3=93.2
V=1605 φ=63.8 γ=1.64
%CaCO3=93.5
V=1590 φ=62.8 γ=1.63
%CaCO3=93.0
V=1605 φ=60.8 γ=1.67
%CaCO3=93.7
1
2
3
4
5
6
7
CC
0.5
1.0

LITHOLOGIC DESCRIPTION

NANNOFOSSIL OOZE with FORAMINIFERS to NANNOFOSSIL OOZE

Major lithology: This core contains white (2.5Y 8/0) NANNOFOSSIL OOZE with FORAMINIFERS to NANNOFOSSIL OOZE. Bioturbation is indicated by extensive white (2.5Y 8/2) mottles, burrow fills, pyrite specks, pale purple streaks, and purple "halos". Horizontal, 1 to 2 cm thick, faint pale purple (5P 6/2) and pale yellowish green (10GY 7/2) color bands are noted throughout the core.

SMEAR SLIDE SUMMARY (%):

	3, 74
	D
TEXTURE:	
Sand	15
Silt	55
Clay	30
COMPOSITION:	
Accessory minerals	1
Foraminifers	22
Nannofossils	75
Radiolarians	Tr
Siliceous fragments	2

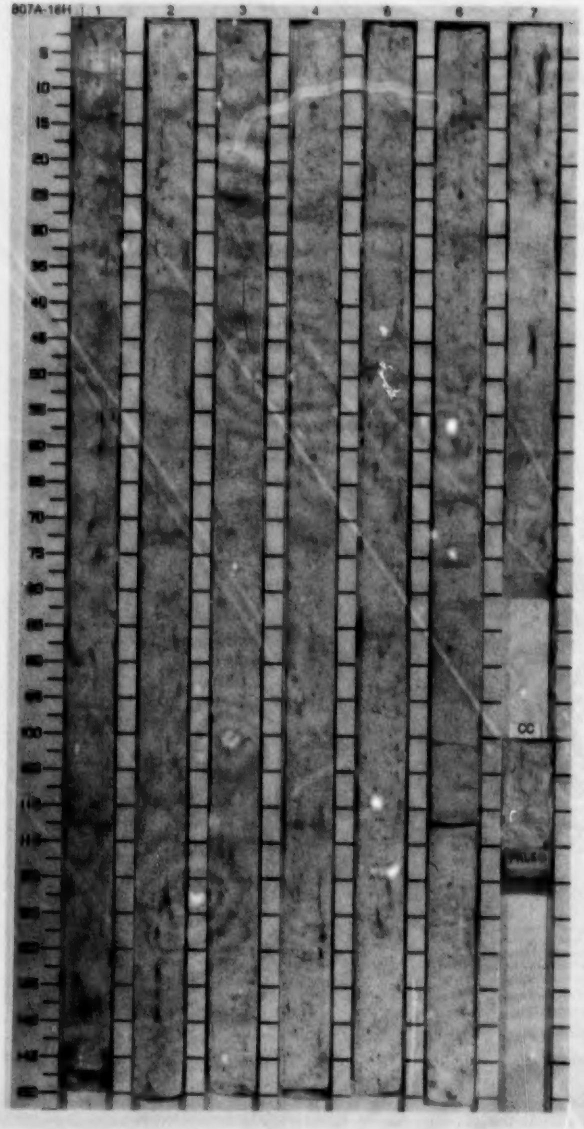
807A-16H
1
2
3
4
5
6
7
5
10
15
20
25
30
35
40
45
50
55
60
65
70
75
80
85
90
95
100
105
110
115
120
125
130
135
140
145
150
CC

SITE 807 HOLE A CORE 17H CORED INTERVAL 149.9-159.4 mbsf

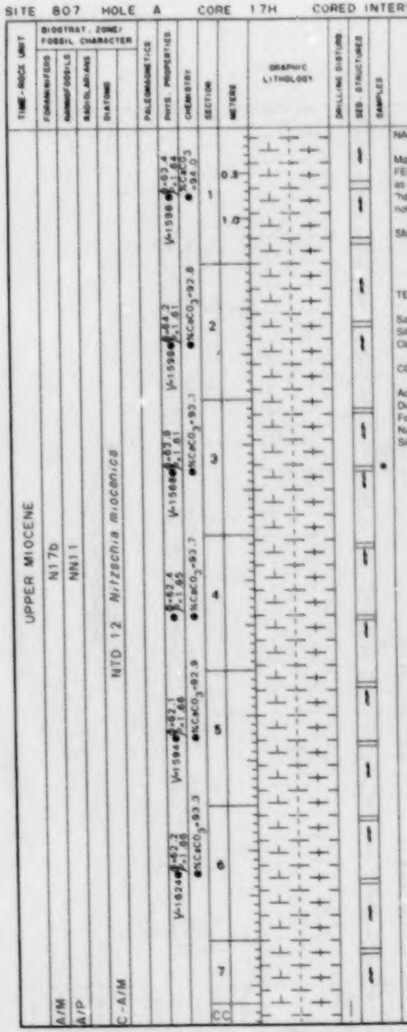
TIME-ROCK UNIT
BIOSTRAT. ZONE/ FOSSIL CHARACTER
FORAMINIFERS
NANNOFOSSILS
RADIOLARIANS
DIATOMS
PALEOMAGNETICS
PHYS. PROPERTIES
CHEMISTRY
SECTION
METERS
GRAPHIC LITHOLOGY
DRILLING DISTURB.
SED. STRUCTURES
SAMPLES
UPPER MIOCENE
N17b
NN11
NTD 12 Nitzschia miocenica
A/M
A/P
C-A/M
V=1598 φ=63.4 ρ=1.64
%CaCO3=94.0
%CaCO3=92.8
V=1598 φ=64.2 ρ=1.61
%CaCO3=93.1
V=1568 φ=63.8 ρ=1.61
φ=62.4 ρ=1.65
%CaCO3=93.7
V=1594 φ=62.1 ρ=1.66
%CaCO3=92.9
V=1624 φ=62.2 ρ=1.66
%CaCO3=93.3
1
2
3
4
5
6
7
CC
0.5
1.0

LITHOLOGIC DESCRIPTION

NANNOFOSSIL OOZE with FORAMINIFERS to FORAMINIFER NANNOFOSSIL OOZE

Major lithology: This core contains white (2.5Y 8/0) NANNOFOSSIL OOZE with FORAMINIFERS to FORAMINIFER NANNOFOSSIL OOZE. The sediment is moderately bioturbated as indicated by light gray (2.5Y 7/2) mottles, pyrite filled burrows and pale purple (5P 6/2) "halos." Diffuse faint greenish gray (5G 7/1) and pale purple color bands (cm scale) are noted throughout the core.

SMEAR SLIDE SUMMARY (%):

	3, 75
	D
TEXTURE:	
Sand	10
Silt	75
Clay	15
COMPOSITION:	
Accessory minerals	Tr
Diatoms	Tr
Foraminifers	25
Nannofossils	74
Siliceous fragments	1

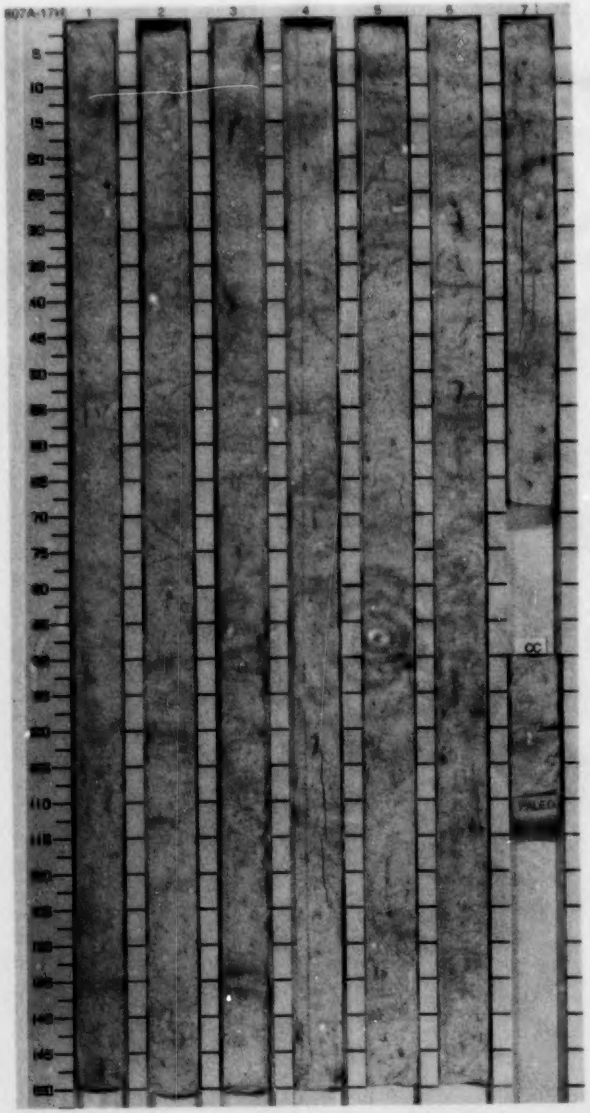
807A-17H
1
2
3
4
5
6
7
CC
PALEO
5
10
15
20
25
30
35
40
45
50
55
60
65
70
75
80
85
90
95
100
105
110
115
120
125
130
135
140
145
150

SITE 807 HOLE A CORE 18H CORED INTERVAL 159.4-168.9 mbsf

TIME-ROCK UNIT	BIOSTRAT. ZONE/FOSSIL CHARACTER: FORAMINIFERS	NANNOFOSSILS	RADIOLARIANS	DIATOMS
UPPER MIOCENE	N17a	NN11	*Stichocorys peregrina*	NTD 12 *Nitzschia miocenica*
	A/G	A/M	A/G	A/M

SECTION	PHYS. PROPERTIES	CHEMISTRY
1	V=1605 φ=63.6 ρ=1.62	%CaCO$_3$=93.0
2	V=1590 φ=63.4 ρ=1.63	%CaCO$_3$=93.0
3	V=1601 φ=65.2 ρ=1.61	%CaCO$_3$=92.5
4	V=1554 φ=62.8 ρ=1.63	%CaCO$_3$=93.0
5	V=1575 φ=63.8 ρ=1.63	%CaCO$_3$=93.5
6	V=1598 φ=63.6 ρ=1.63	%CaCO$_3$=93.3
7		

METERS: 0.5, 1.0

SAMPLES: OG, IW

LITHOLOGIC DESCRIPTION

NANNOFOSSIL OOZE with FORAMINIFERS to FORAMINIFER NANNOFOSSIL OOZE

Major lithology: This core contains NANNOFOSSIL OOZE with FORAMINIFERS to FORAMINIFER NANNOFOSSIL OOZE. Some intervals are coarser than others, suggesting intergradational bedding. The sediment is predominantly white (2.5Y 8/0) and commonly contains faint pale greenish gray (5G 7/1) color bands, about 1 cm in diameter, and pale purple (5P 6/2) to reddish gray (5R 6/1) color bands, several cm in diameter. Bioturbation is evident from abundant pyrite-filled burrows (very dusky purple (5P 2/2) in the center with borders of pale purple (5P 6/2)), and common light gray (2.5Y 7/2) burrow mottles, about 1 cm in diameter.

SMEAR SLIDE SUMMARY (%):

	3, 75
	D
TEXTURE:	
Sand	15
Silt	60
Clay	25
COMPOSITION:	
Foraminifers	25
Nannofossils	75
Radiolarians	Tr
Siliceous sponge spicules	Tr

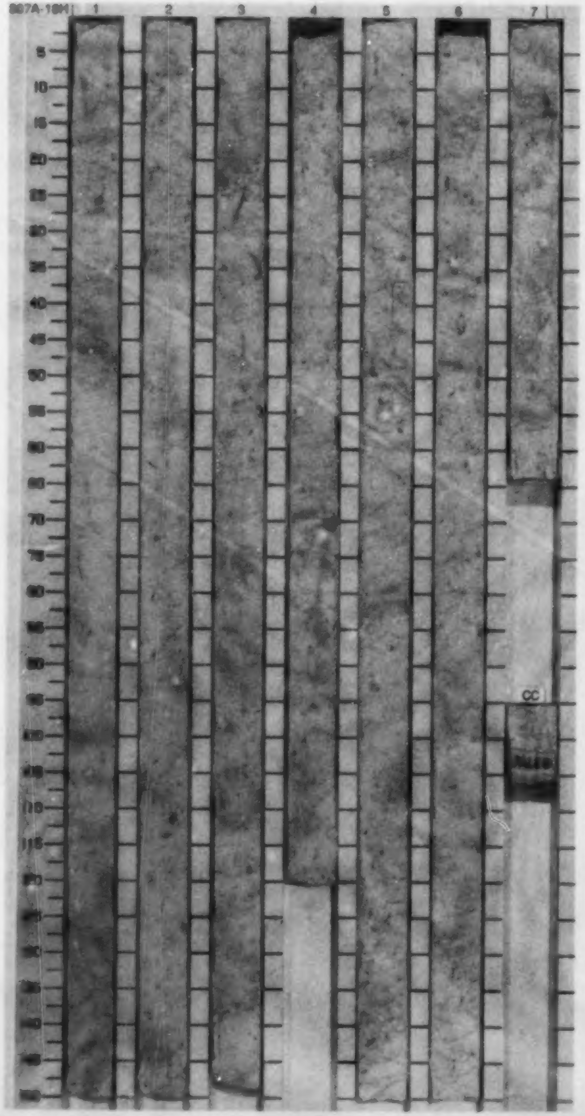

SITE 807 HOLE A CORE 19H CORED INTERVAL 168.9-178.4 mbsf

TIME-ROCK UNIT	BIOSTRAT. ZONE/ FOSSIL CHARACTER				PALEOMAGNETICS	PHYS. PROPERTIES	CHEMISTRY	SECTION	METERS	GRAPHIC LITHOLOGY	DRILLING DISTURB.	SED. STRUCTURES	SAMPLES
	FORAMINIFERS	NANNOFOSSILS	RADIOLARIANS	DIATOMS									
UPPER MIOCENE	N17a	NN11	Didymocyrtis penultima	NTD 12 Nitzschia miocenica		V=1570 ● φ=62.8 γ=1.63	●%CaCO₃ =94.4	1	0.5 1.0				
						V=1570 ● φ=62.7 γ=1.65	●%CaCO₃=93.5	2					
						V=1588 ● φ=62.6 γ=1.65	●%CaCO₃=93.2	3					*
						V=1568 ● φ=63.1 γ=1.64	●%CaCO₃=94.5	4					
						V=1605 ● φ=63.6 γ=1.64	●%CaCO₃=92.2	5					
						V=1609 ● φ=63.6 γ=1.64	●%CaCO₃=93.5	6					
								7					
	A/G	A/P	A/M	C-A/M				CC					

LITHOLOGIC DESCRIPTION

NANNOFOSSIL OOZE with FORAMINIFERS to FORAMINIFER NANNOFOSSIL OOZE

Major lithology: This core contains white (2.5Y 8/1) NANNOFOSSIL OOZE with FORAMINIFERS interbedded with FORAMINIFER NANNOFOSSIL OOZE. Very faint pale greenish gray (5G 7/1), 0.5 cm thick color bands are common throughout. Pale purple (5P 6/2) to reddish gray (5R 6/1), 1 to 2 cm thick, color bands are also present. There are abundant pyrite-filled burrows and light gray (2.5Y 7/2) mottles suggesting moderate to heavy bioturbation. The pyrite-filled trace structures are very dusky purple (5P 2/2) in the center with borders of pale purple (5P 6/2) and occur as specks, patches and vertical traces. Pale purple (5P 6/2) color migration fronts, which form "halo"-like structures, are also present.

SMEAR SLIDE SUMMARY (%):

	3, 75
	D
TEXTURE:	
Sand	10
Silt	60
Clay	30
COMPOSITION:	
Accessory minerals	Tr
Foraminifers	25
Nannofossils	75
Siliceous fragments	Tr

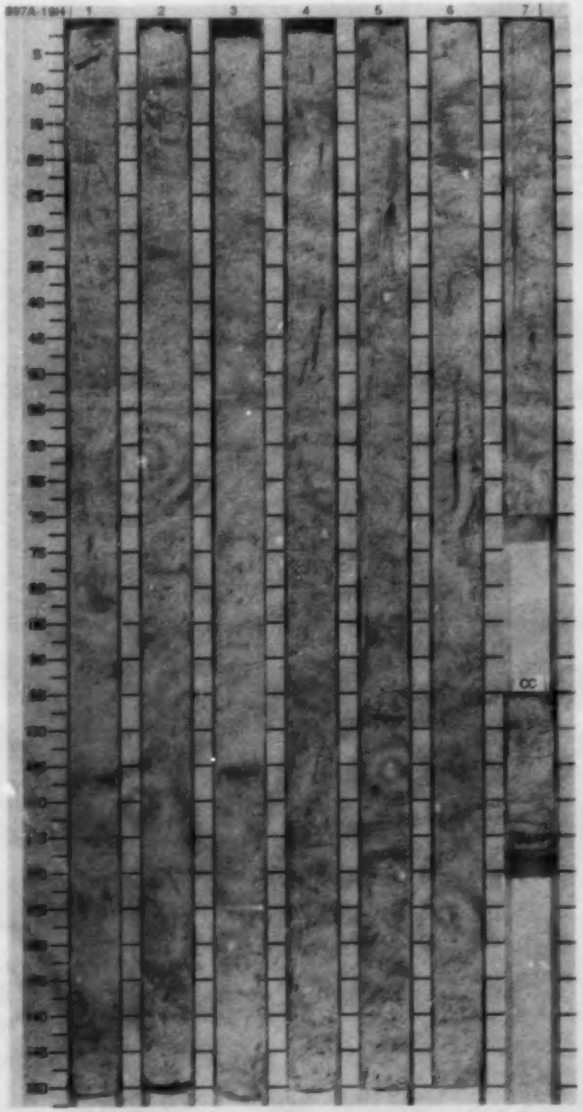

SITE 807 HOLE A CORE 20H CORED INTERVAL 178.4-187.9 mbsf

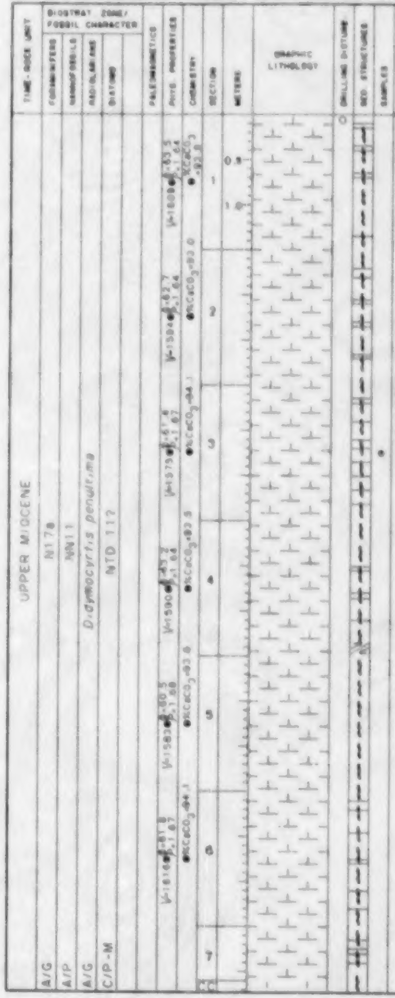

LITHOLOGIC DESCRIPTION

NANNOFOSSIL OOZE with FORAMINIFERS

Major lithology: This core contains white (2.5 7/2) NANNOFOSSIL OOZE with FORAMINIFERS. Pyritized burrows and light gray (2.5Y 7/2) mottles are abundant. Very faint greenish gray (5G 7/1) 0.5 cm thick color bands are common. Microfaults are observed at 140-150 cm in Sections 4 and 6. A large pale purple (5P 7/1) swirl is observed between 95 and 135 cm in Section 5, possibly indicating that the color, in this case, is related to fluid migration.

SMEAR SLIDE SUMMARY (%):

	3, 75
	D
TEXTURE:	
Sand	10
Silt	70
Clay	20
COMPOSITION:	
Diatoms	Tr
Foraminifers	20
Nannofossils	79
Radiolarians	Tr
Siliceous fragments	1

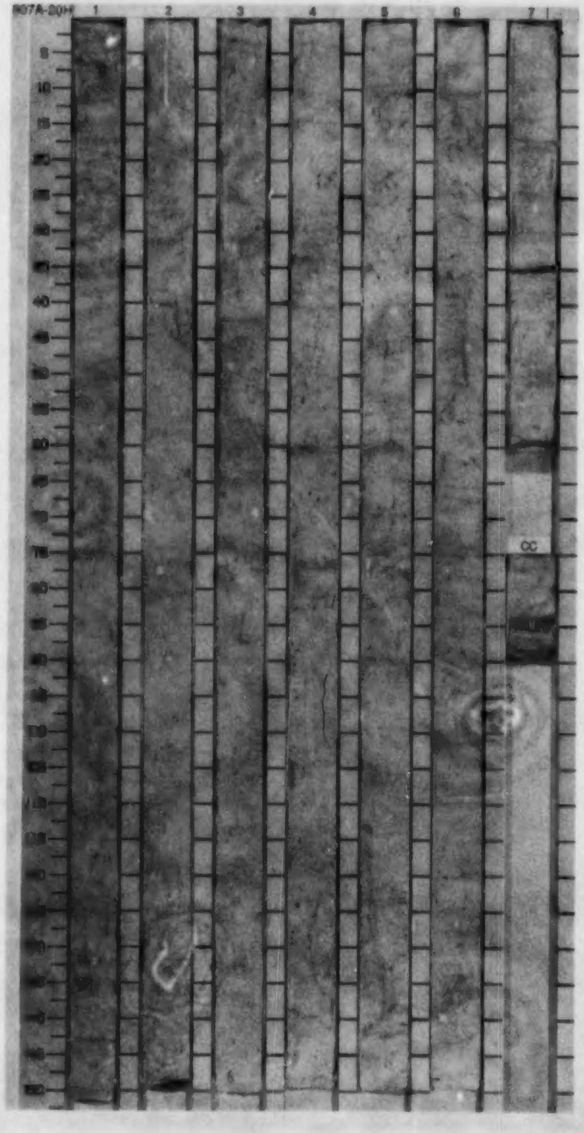

SITE 807 HOLE A CORE 21H CORED INTERVAL 187.9-197.4 mbsf

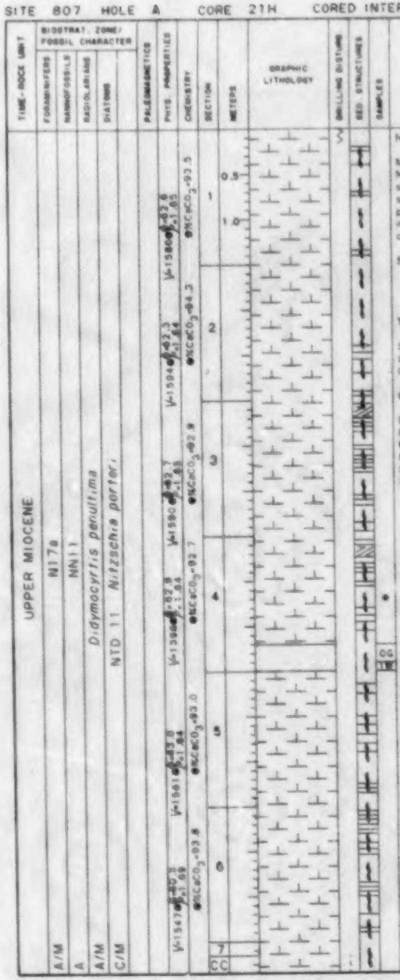
TIME-ROCK UNIT
BIOSTRAT. ZONE/ FOSSIL CHARACTER
FORAMINIFERS
NANNOFOSSILS
RADIOLARIANS
DIATOMS
PALEOMAGNETICS
PHYS. PROPERTIES
CHEMISTRY
SECTION
METERS
GRAPHIC LITHOLOGY
DRILLING DISTURB.
SED. STRUCTURES
SAMPLES
UPPER MIOCENE
N17a
NN11
Didymocyrtis penultima
NTD 11 Nitzschia porteri
A/M
A
A/M
C/M
V=1580
φ=62.6
γ=1.65
%CaCO3=93.5
V=1594
φ=62.3
γ=1.84
%CaCO3=94.3
V=1590
φ=62.7
γ=1.88
%CaCO3=92.9
V=1590
φ=62.8
γ=1.84
%CaCO3=93.7
V=1561
φ=63.8
γ=1.84
%CaCO3=93.0
V=1547
φ=60.9
γ=1.69
%CaCO3=93.8
1
2
3
4
5
6
7
CC
0.5
1.0
OG
IW

LITHOLOGIC DESCRIPTION

NANNOFOSSIL OOZE with FORAMINIFERS

Major lithology: This core contains slightly to moderately bioturbated, white (2.5Y 8/0) NANNOFOSSIL OOZE with FORAMINIFERS. The bioturbation structures include mm to cm scale, grayish blue (5PB 5/2) pyrite-filled burrows. In Sections 3 and 6, these fills outline the spreiten in individual *Zoophycos* trace fossils. Diffuse light greenish gray (5G 7/1), pale purple (5PB 7/2), and grayish blue (5PB 5/2) color bands are common to abundant, ranging in thickness from 0.5 cm to several cm. Individual color bands are microfaulted near the tops of Sections 3 and 4.

SMEAR SLIDE SUMMARY (%):

	4, 89
	D
TEXTURE	
Sand	14
Silt	82
Clay	4
COMPOSITION	
Diatoms	1
Foraminifers	15
Nannofossils	78
Radiolarians	2
Silicoflagellates	3
Spicules	1

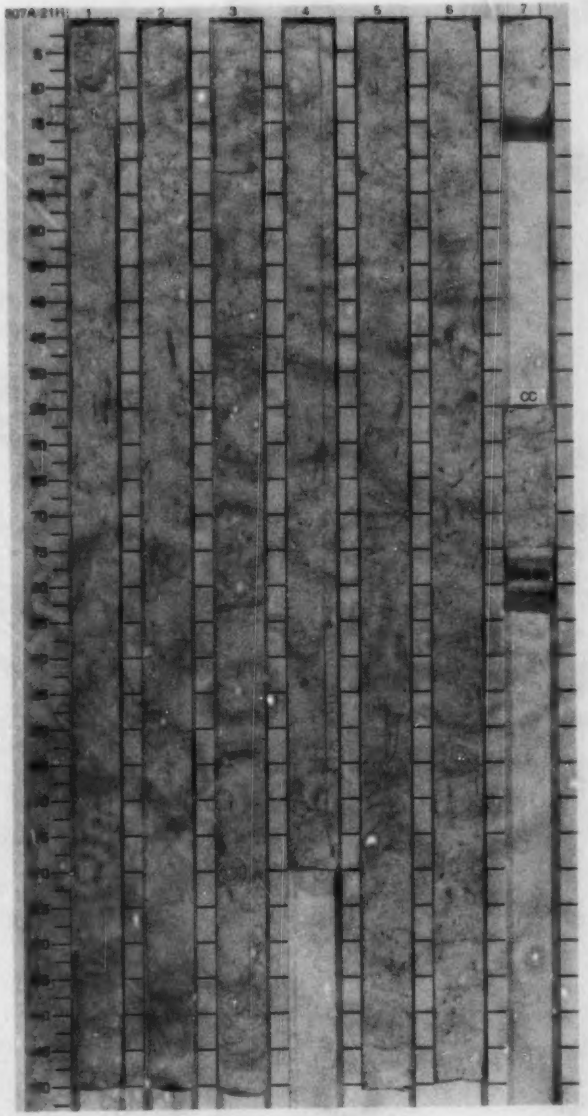
807A-21H
1
2
3
4
5
6
7
CC

SITE 807 HOLE A CORE 22H CORED INTERVAL 197.4-206.9 mbsf

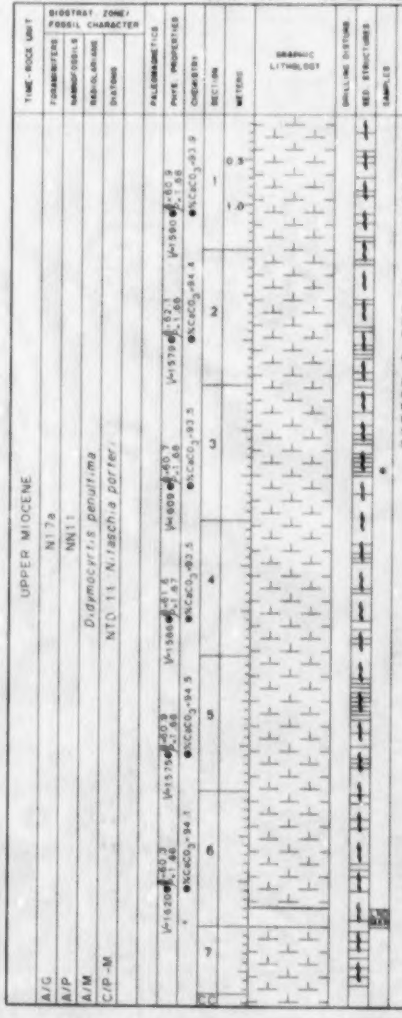

LITHOLOGIC DESCRIPTION

NANNOFOSSIL OOZE with FORAMINIFERS

Major lithology: This core contains moderately bioturbated, white (2.5Y 8/0) NANNOFOSSIL OOZE with FORAMINIFERS. Bioturbation structures include mm to cm scale grayish blue (5PB 5/2) pyrite-filled burrows, and light gray (2.5Y 7/2 and 5Y 7/1) mottling. Light greenish gray (5G 7/1), grayish blue (5PB 5/2), and pale purple (5PB 7/2) diffuse color banding is present to abundant.

SMEAR SLIDE SUMMARY (%):

	3, 92
	D
TEXTURE	
Sand	10
Silt	86
Clay	4
COMPOSITION	
Diatoms	1
Foraminifers	12
Nannofossils	81
Radiolarians	3
Silicoflagellates	2
Spicules	1

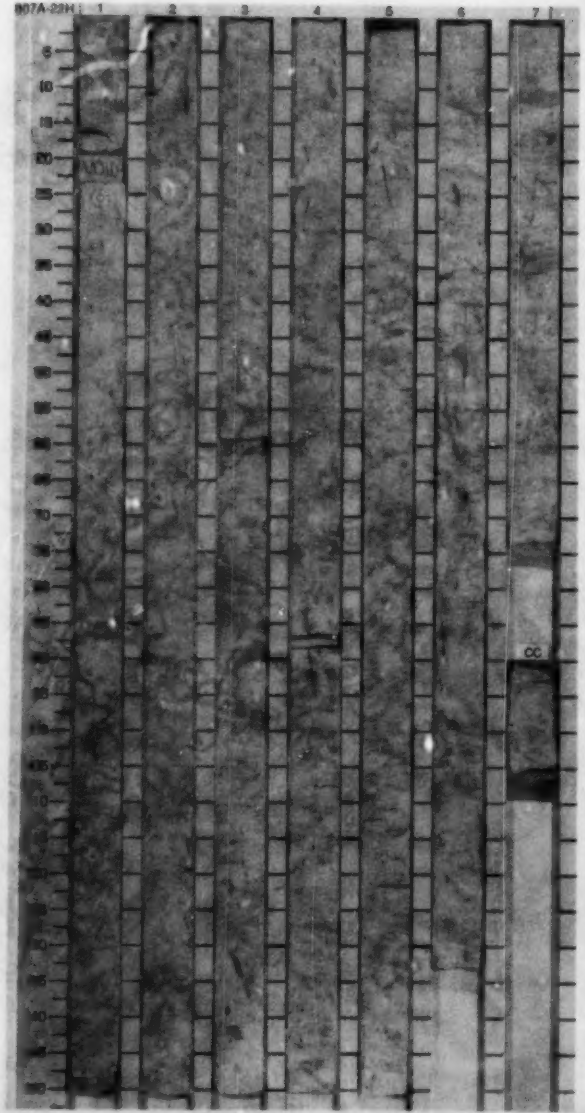

SITE 807 HOLE A CORE 23H CORED INTERVAL 206.9-216.4 mbsf

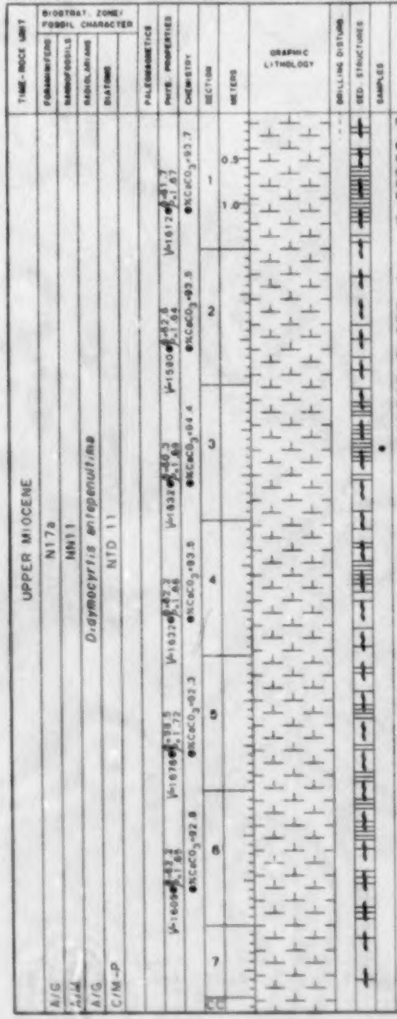
TIME-ROCK UNIT
BIOSTRAT. ZONE/ FOSSIL CHARACTER
FORAMINIFERS
NANNOFOSSILS
RADIOLARIANS
DIATOMS
PALEOMAGNETICS
PHYS. PROPERTIES
CHEMISTRY
SECTION
METERS
GRAPHIC LITHOLOGY
DRILLING DISTURB.
SED. STRUCTURES
SAMPLES
UPPER MIOCENE
N17a
NN11
Didymocyrtis antepenultima
NTD 11
A/G
A/M
A/G
C/M-P
V=1612 φ=61.7 ρ=1.67
V=1580 φ=62.6 ρ=1.64
V=1632 φ=60.3 ρ=1.69
V=1632 φ=62.2 ρ=1.66
V=1676 φ=59.5 ρ=1.72
V=1609 φ=62.2 ρ=1.65
●%CaCO3=93.7
●%CaCO3=93.5
●%CaCO3=94.4
●%CaCO3=93.5
●%CaCO3=92.3
●%CaCO3=92.8
1
2
3
4
5
6
7
CC
0.5
1.0

LITHOLOGIC DESCRIPTION

NANNOFOSSIL OOZE with FORAMINIFERS

Major lithology: This core contains moderately bioturbated, white (2.5Y 8/0) NANNOFOSSIL OOZE with FORAMINIFERS. Bioturbation structures include mm to cm scale grayish blue (5PB 5/2), pyrite-filled burrows and light gray (2.5Y 7/2 and 5Y 7/2) mottling. Light greenish gray (5G 7/1), grayish blue (5PB 5/2), and pale purple (5PB 7/2) diffuse color banding is present to abundant.

SMEAR SLIDE SUMMARY (%):

	3, 71
	D
TEXTURE:	
Sand	10
Silt	86
Clay	4
COMPOSITION:	
Diatoms	Tr
Foraminifers	10
Nannofossils	86
Radiolarians	2
Silicoflagellates	1
Spicules	1

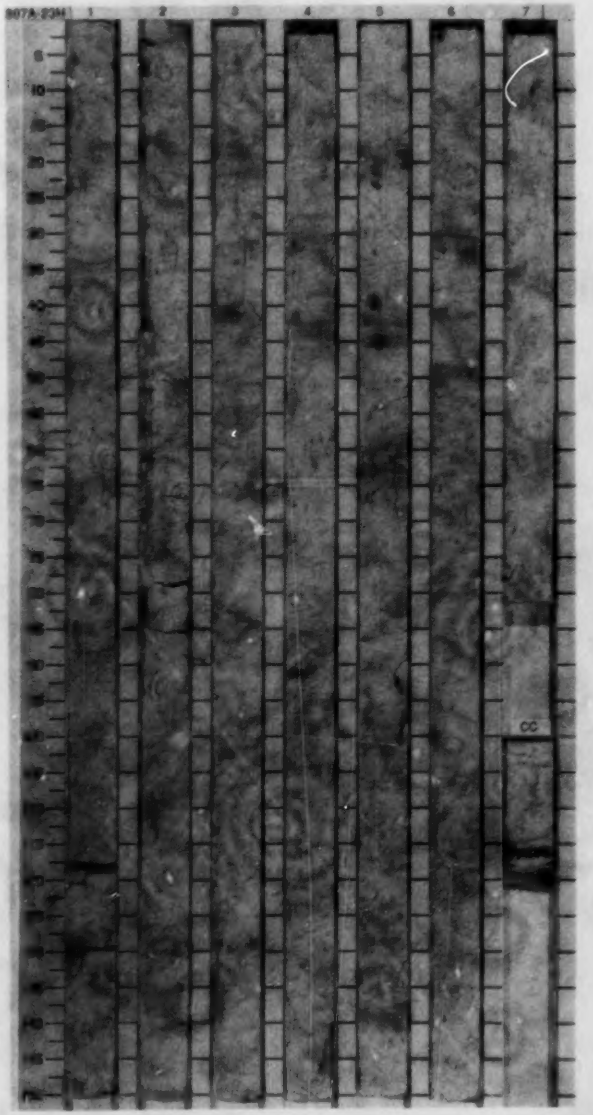
807A-23H
1
2
3
4
5
6
7
CC

SITE 807 HOLE A CORE 24H CORED INTERVAL 216.4-225.9 mbsf

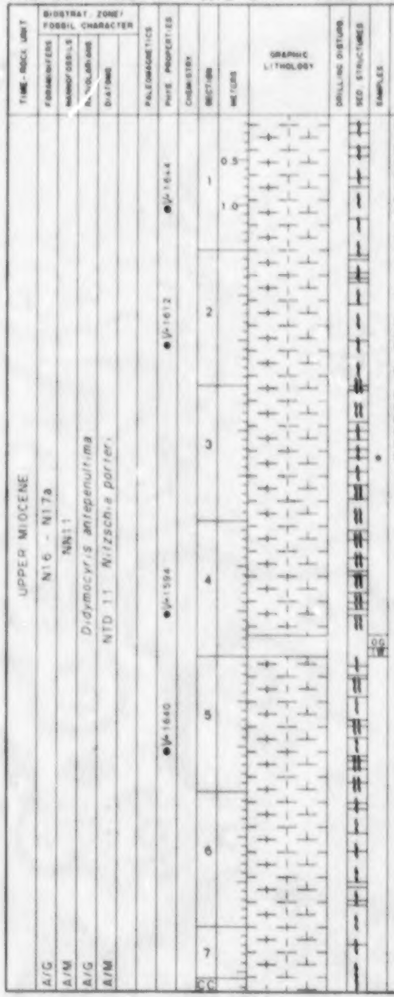
TIME-ROCK UNIT
BIOSTRAT. ZONE/ FOSSIL CHARACTER
FORAMINIFERS
NANNOFOSSILS
RADIOLARIANS
DIATOMS
PALEOMAGNETICS
PHYS. PROPERTIES
CHEMISTRY
SECTION
METERS
GRAPHIC LITHOLOGY
DRILLING DISTURB.
SED. STRUCTURES
SAMPLES
UPPER MIOCENE
A/G N16 - N17a
A/M NN11
A/G Didymocyrtis antepenultima
A/M NTD 11 Nitzschia porteri
●Vp-1644
●Vp-1612
●Vp-1594
●Vp-1640
1
2
3
4
5
6
7
CC
0.5
1.0
OG
IW

LITHOLOGIC DESCRIPTION

NANNOFOSSIL OOZE with FORAMINIFERS to FORAMINIFER NANNOFOSSIL OOZE

Major lithology: This core contains moderately to heavily bioturbated, white (2.5Y 8/0) NANNOFOSSIL OOZE with FORAMINIFERS to FORAMINIFER NANNOFOSSIL OOZE. Bioturbation structures include mm to cm scale, grayish blue (5PB 5/2), pyrite filled burrows and light gray (2.5Y 7/2 and 5Y 7/2) mottling. The heavily bioturbated intervals are dominated by the light gray mottling. Light greenish gray (5G 7/1), grayish blue (5PB 5/2), and pale purple (5PB 7/2) diffuse color banding is present to abundant.

SMEAR SLIDE SUMMARY (%):

	3, 80
	D
TEXTURE:	
Sand	15
Silt	81
Clay	4
COMPOSITION:	
Diatoms	1
Foraminifers	25
Nannofossils	69
Radiolarians	2
Silicoflagellates	2
Spicules	1

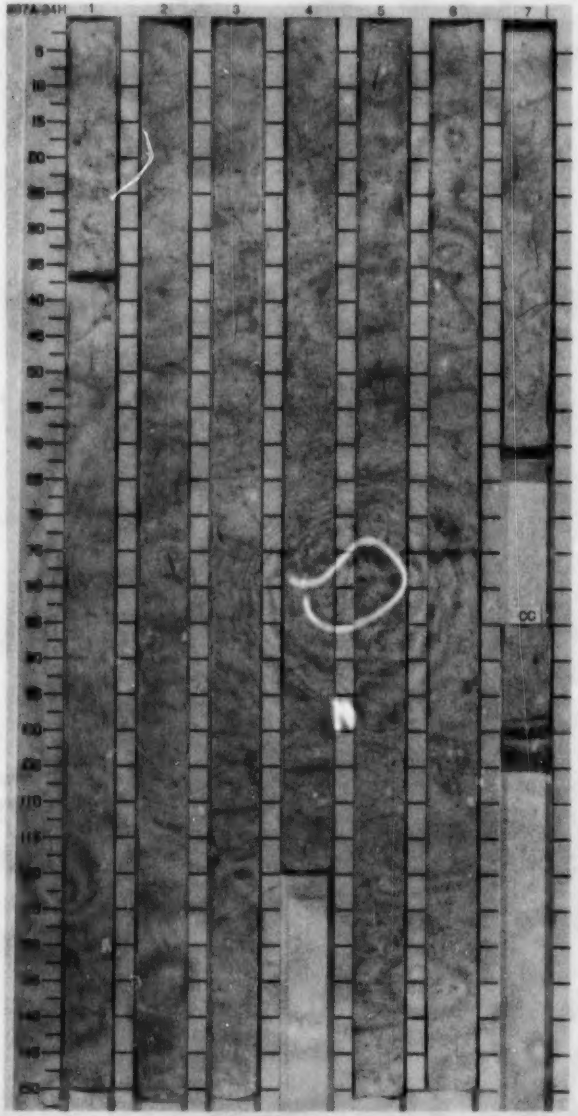
807A-24H
1
2
3
4
5
6
7
CC
5
10
15
20
25
30
35
40
45
50
55
60
65
70
75
80
85
90
95
100
105
110
115
120
125
130
135
140
145
150

SITE 807 HOLE A CORE 25H CORED INTERVAL 225.9-235.4 mbsf

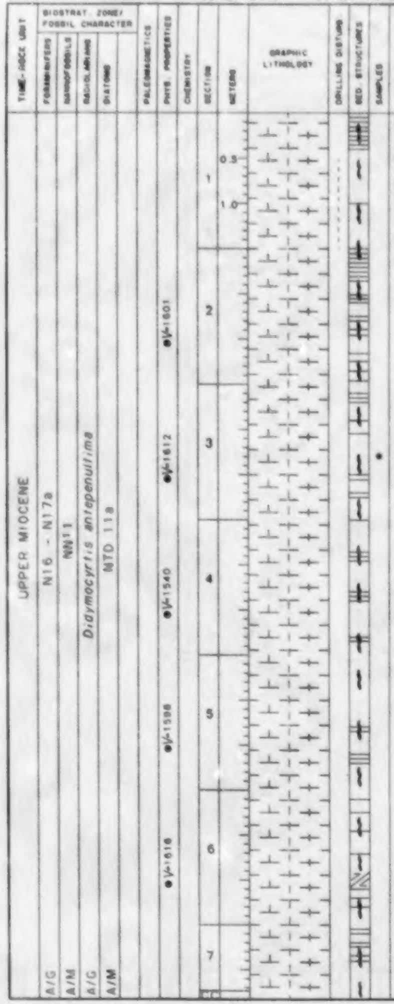
TIME-ROCK UNIT
BIOSTRAT. ZONE/ FOSSIL CHARACTER
FORAMINIFERS
NANNOFOSSILS
RADIOLARIANS
DIATOMS
PALEOMAGNETICS
PHYS. PROPERTIES
CHEMISTRY
SECTION
METERS
GRAPHIC LITHOLOGY
DRILLING DISTURB.
SED. STRUCTURES
SAMPLES
UPPER MIOCENE
A/G N16 - N17a
A/M NN11
A/G Didymocyrtis antepenultima
A/M NTD 11a
•V-1601
•V-1612
•V-1540
•V-1598
•V-1618
1
2
3
4
5
6
7
CC
0.5
1.0

LITHOLOGIC DESCRIPTION

NANNOFOSSIL OOZE with FORAMINIFERS to FORAMINIFER NANNOFOSSIL OOZE

Major lithology: This core contains white (2.5Y 8/0) NANNOFOSSIL OOZE with FORAMINIFERS to FORAMINIFER NANNOFOSSIL OOZE, with alternating soft and semi-indurated intervals. The color grades locally to light gray (N7). The sediment is slightly to moderately bioturbated, as indicated by cm scale, light gray (5Y 7/2) mottling and mm scale, grayish blue (5PB 5/2) pyrite-filled burrows. A 10 cm long vertical pyritized burrow was observed in Section 1. Diffuse light greenish gray (5G 7/1), grayish blue (5PB 5/2), and pale purple (5P 6/2) color bands are common. In Section 2, a halo encircling a pyritized burrow apparently causes grayish blue (5PB 5/2) color bands to "fade" and leaves them greenish gray inside the halo. A light gray (N7), 15 cm long patch in Section 5 may represent mottling or fluid migration.

SMEAR SLIDE SUMMARY (%):

	3, 79
	D
TEXTURE:	
Sand	15
Silt	80
Clay	5
COMPOSITION:	
Diatoms	Tr
Foraminifers	25
Nannofossils	71
Radiolarians	2
Silicoflagellates	1
Spicules	1

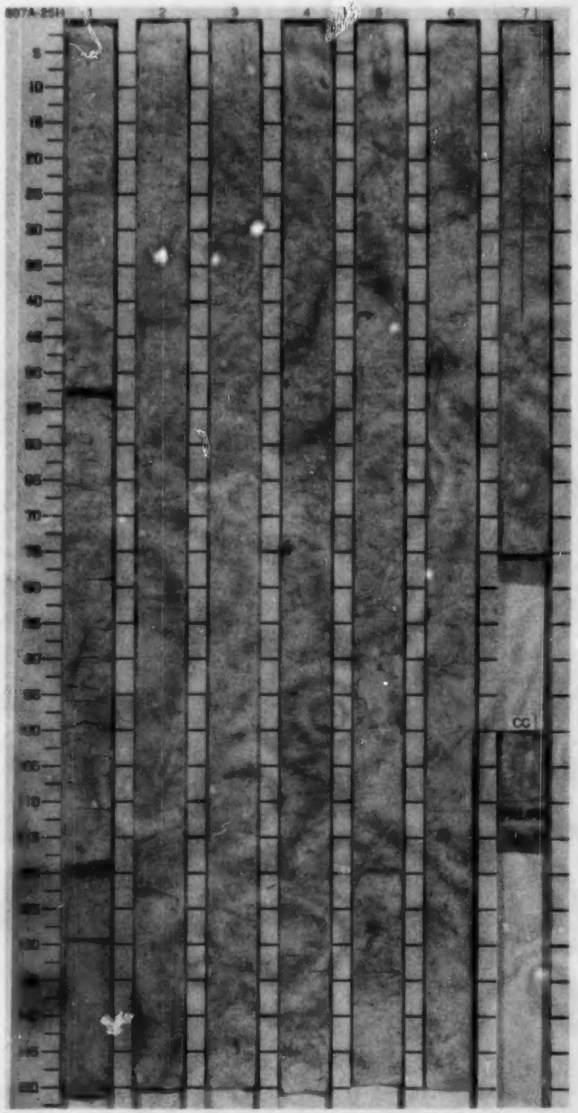
807A-25H
1
2
3
4
5
6
7
CC
5
10
15
20
25
30
35
40
45
50
55
60
65
70
75
80
85
90
95
100
105
110
115
120
125
130
135
140
145
150

SITE 807 HOLE A CORE 26H CORED INTERVAL 235.4-244.9 mbsf

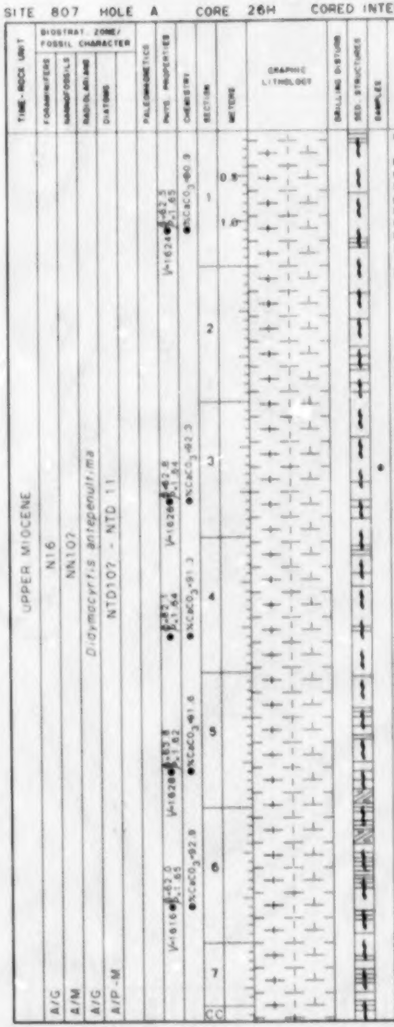
TIME-ROCK UNIT
BIOSTRAT. ZONE/ FOSSIL CHARACTER
FORAMINIFERS
NANNOFOSSILS
RADIOLARIANS
DIATOMS
PALEOMAGNETICS
PHYS. PROPERTIES
CHEMISTRY
SECTION
METERS
GRAPHIC LITHOLOGY
DRILLING DISTURB.
SED. STRUCTURES
SAMPLES
UPPER MIOCENE
N16
NN10?
Didymocyrtis antepenultima
NTD10? - NTD 11
A/G
A/M
A/G
A/P-M
V=1624 φ=62.5 γ=1.65
%CaCO3=90.9
V=1626 φ=62.8 γ=1.64
%CaCO3=92.3
φ=62.1 γ=1.64
%CaCO3=91.3
V=1620 φ=63.8 γ=1.62
%CaCO3=91.6
V=1616 φ=62.0 γ=1.65
%CaCO3=92.8
1
2
3
4
5
6
7
CC
0.5
1.0

LITHOLOGIC DESCRIPTION

FORAMINIFER NANNOFOSSIL OOZE to NANNOFOSSIL OOZE with FORAMINIFERS

Major lithology: This core contains white (2.5Y 8/0) FORAMINIFER NANNOFOSSIL OOZE to NANNOFOSSIL OOZE with FORAMINIFERS, which has [illegible] drilling "biscuits" in Sections 1 through 3. The sediment is slightly to moderately bioturbated, with mm scale grayish blue (5PB 5/2), pyrite filled burrows common throughout the core. The more heavily bioturbated intervals also contain cm scale, light gray (5Y 7/1 and 2.5Y 7/2) mottling. Diffuse light greenish gray (5G 7/1), pale purple (5P 6/2), and pale blue (5PB 6/2) color bands generally become more abundant downcore. Microfaulted color bands are present at Section 5, 130 cm, and Section 6, 37 cm.

SMEAR SLIDE SUMMARY (%):

	3, 84 D
TEXTURE:	
Sand	18
Silt	78
Clay	4
COMPOSITION:	
Foraminifers	36
Nannofossils	62
Radiolarians	1
Silicoflagellates	1
Spicules	1

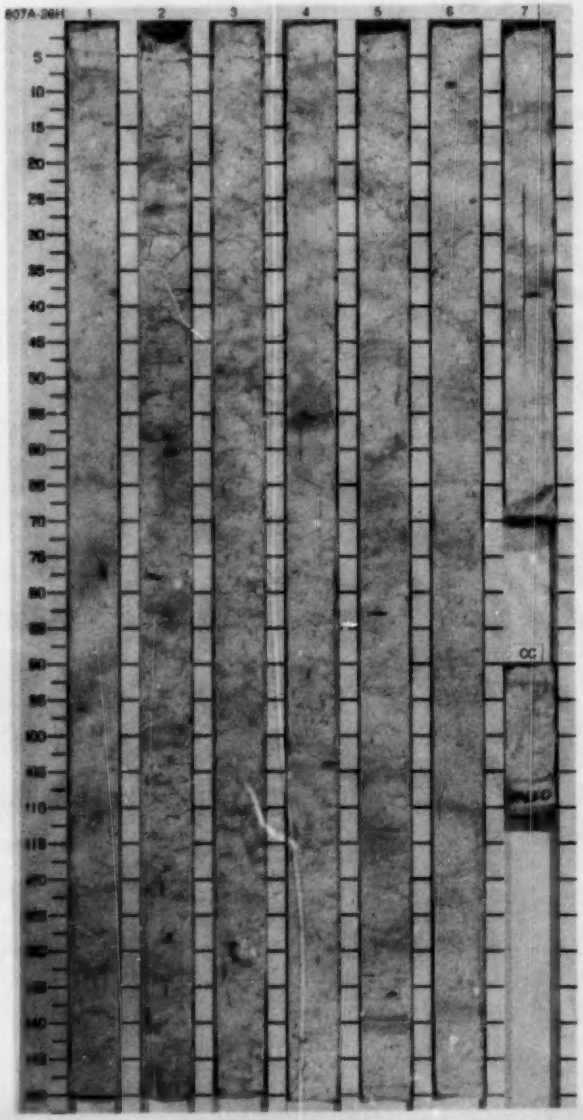
807A-26H
1
2
3
4
5
6
7
CC
5
10
15
20
25
30
35
40
45
50
55
60
65
70
75
80
85
90
95
100
105
110
115
120
125
130
135
140
145
150

SITE 807 HOLE A CORE 27H CORED INTERVAL 244.9-254.4 mbsf

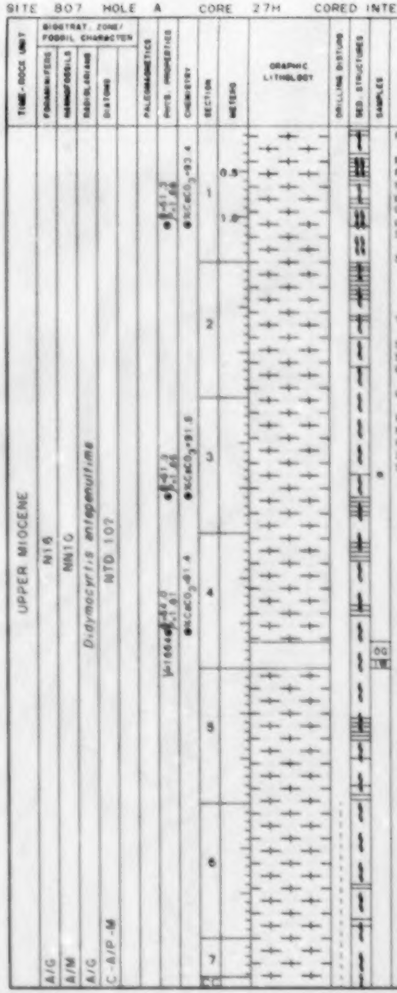
TIME-ROCK UNIT
BIOSTRAT. ZONE/ FOSSIL CHARACTER
FORAMINIFERS
NANNOFOSSILS
RADIOLARIANS
DIATOMS
PALEOMAGNETICS
PHYS. PROPERTIES
CHEMISTRY
SECTION
METERS
GRAPHIC LITHOLOGY
DRILLING DISTURB.
SED. STRUCTURES
SAMPLES
UPPER MIOCENE
N16
NN10
Didymocyrtis antepenultima
NTD 107
A/G
A/M
A/G
C-A/P-M
%CaCO3=93.4
%CaCO3=91.8
%CaCO3=91.4
1
2
3
4
5
6
7
CC
0.5
1.0
OG
IW

LITHOLOGIC DESCRIPTION

FORAMINIFER NANNOFOSSIL OOZE

Major lithology: This core contains white (2.5Y 8/0 to 10YR 8/1) FORAMINIFER NANNOFOSSIL OOZE, which becomes more uniform in appearance downcore. Sections 1 through 5 are slightly to moderately bioturbated, with grayish blue (5PB 5/2) mm scale pyrite filled burrows and light gray (2.5Y 7/2) cm scale mottling. Sections 6 through Core Catcher are slightly bioturbated, with few distinct mottles. Faint light greenish gray (5G 7/1), pale purple (5P 6/2), and pale blue (5PB 7/2) color bands are present to abundant in Sections 1 through 6.

SMEAR SLIDE SUMMARY (%):

	3, 85
	D
TEXTURE:	
Sand	15
Silt	81
Clay	4
COMPOSITION:	
Foraminifers	30
Nannofossils	65
Radiolarians	2
Silicoflagellates	2
Spicules	1

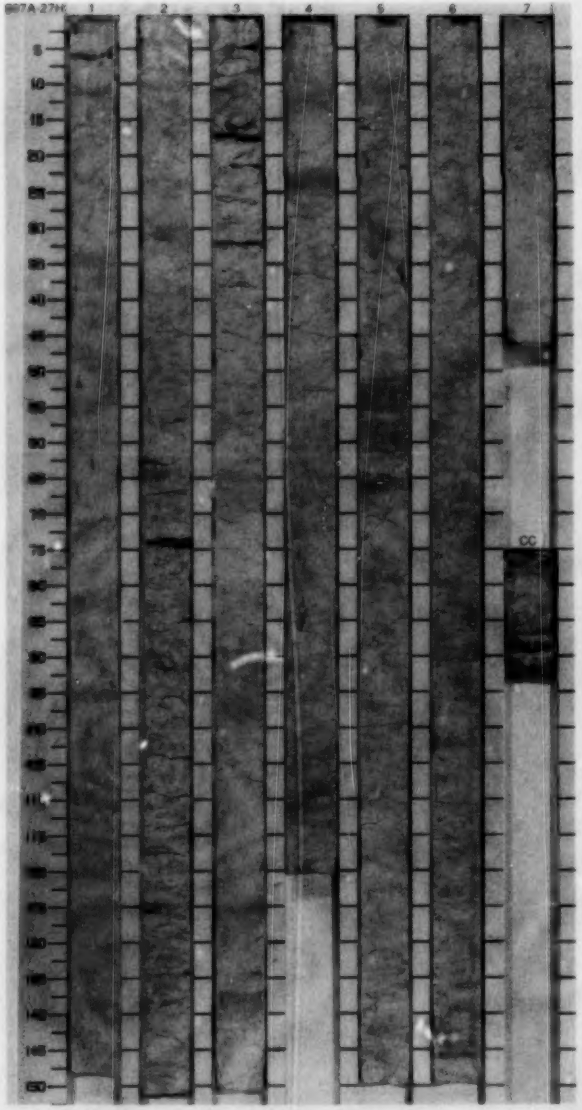
807A-27H
1
2
3
4
5
6
7
CC
5
10
15
20
25
30
35
40
45
50
55
60
65
70
75
80
85
90
95
100
105
110
115
120
125
130
135
140
145
150

SITE 807 HOLE A CORE 28X CORED INTERVAL 254.4-264.1 mbsf

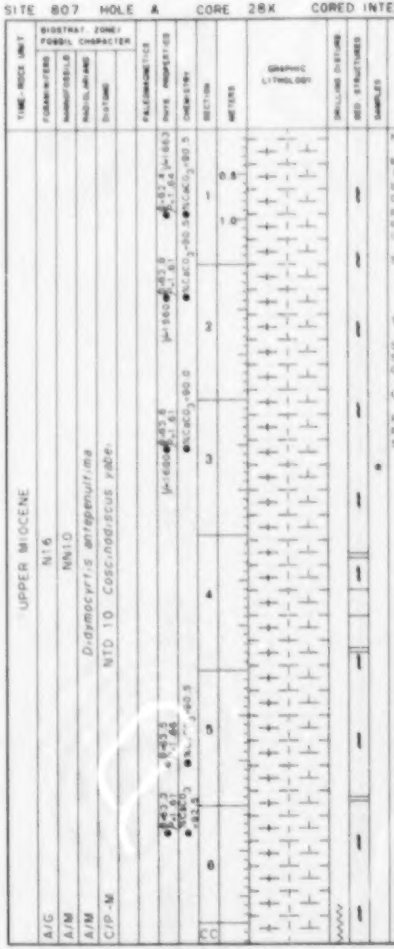
TIME-ROCK UNIT
BIOSTRAT. ZONE/ FOSSIL CHARACTER
FORAMINIFERS
NANNOFOSSILS
RADIOLARIANS
DIATOMS
PALEOMAGNETICS
PHYS. PROPERTIES
CHEMISTRY
SECTION
METERS
GRAPHIC LITHOLOGY
DRILLING DISTURB.
SED. STRUCTURES
SAMPLES
UPPER MIOCENE
N16
NN10
Didymocyrtis antepenultima
NTD 10 Coscinodiscus yabei
A/G
A/M
A/M
C/P-M
0.5
1.0
1
2
3
4
5
6
CC

LITHOLOGIC DESCRIPTION

NANNOFOSSIL OOZE with FORAMINIFERS to FORAMINIFER NANNOFOSSIL OOZE

Major lithology: This core contains white (7.5YR 8/0) NANNOFOSSIL OOZE with FORAMINIFERS to FORAMINIFER NANNOFOSSIL OOZE. The sediment is very stiff to hard and is biscuited by the drilling process. The core is relatively homogeneous, with infrequent 0.2 to 0.5 cm thick, greenish gray (5G 7/1), pale blue (5PB 7/2), pale purple (5P 6/2), and pale pink (5RP 8/2) color bands. Only a few signs of bioturbation are evident in the form of occasional pyrite-filled traces with purple borders, and small (0.5 to 1 cm thick), light gray (2.5Y 7/2) mottles.

SMEAR SLIDE SUMMARY (%):

	3, 75
	D
TEXTURE:	
Sand	15
Silt	60
Clay	25
COMPOSITION:	
Foraminifers	23
Nannofossils	77
Siliceous sponge spicules	Tr

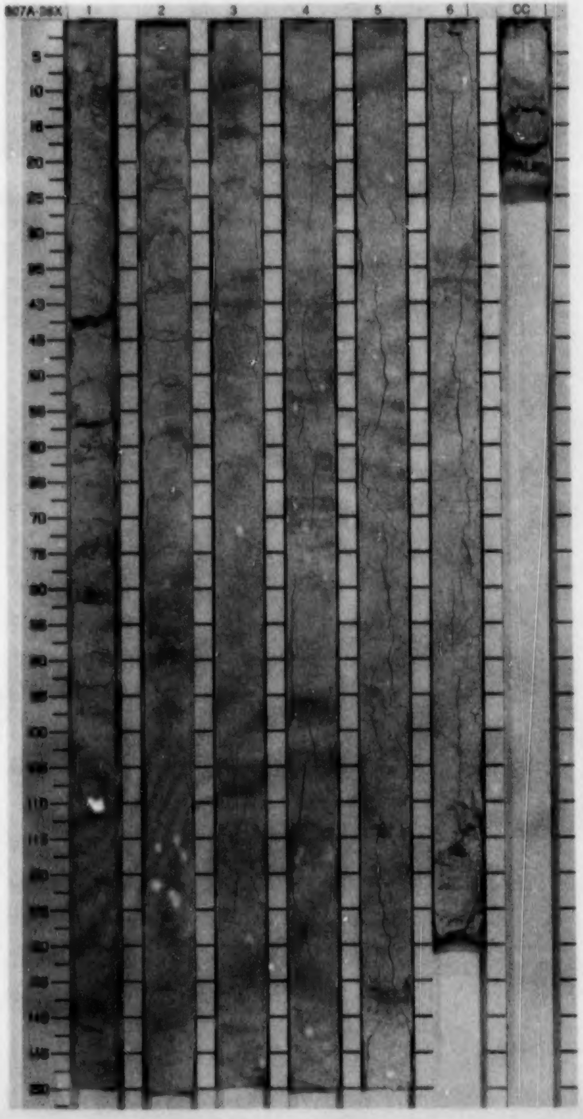
807A-28X
1
2
3
4
5
6
CC
5
10
15
20
25
30
35
40
45
50
55
60
65
70
75
80
85
90
95
100
105
110
115
120
125
130
135
140
145
150

SITE 807 HOLE A CORE 29X CORED INTERVAL 264.1-273.8 mbsf

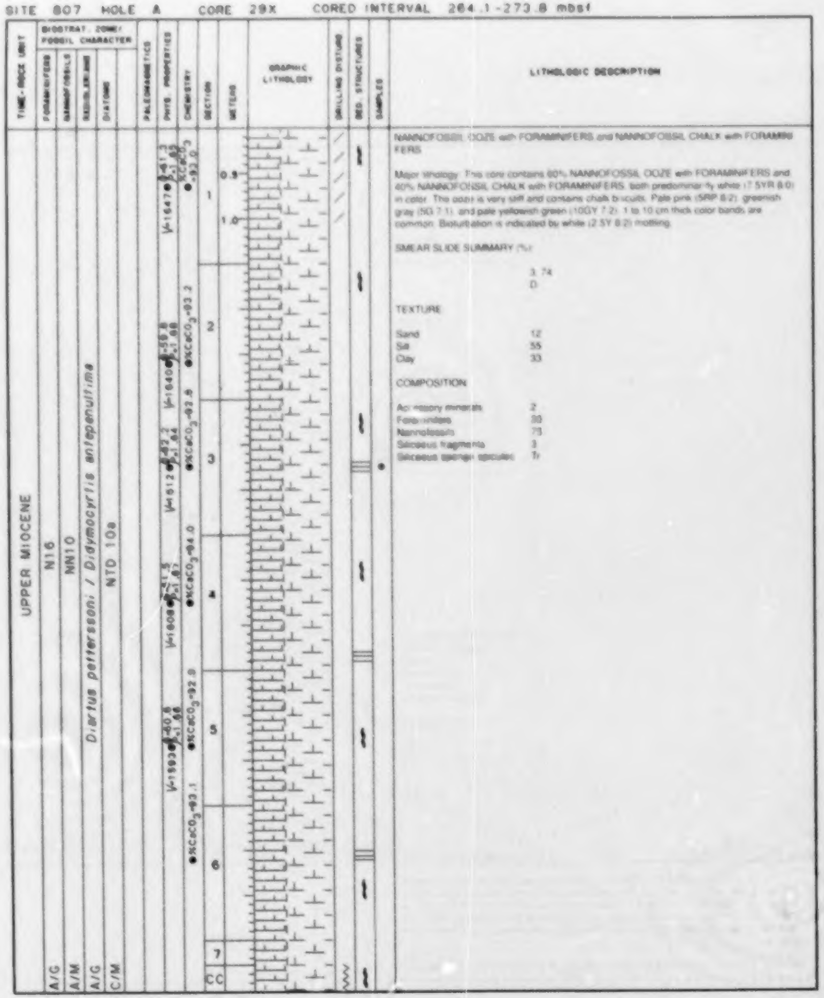
TIME-ROCK UNIT
BIOSTRAT. ZONE/ FOSSIL CHARACTER
FORAMINIFERS
NANNOFOSSILS
RADIOLARIANS
DIATOMS
PALEOMAGNETICS
PHYS. PROPERTIES
CHEMISTRY
SECTION
METERS
GRAPHIC LITHOLOGY
DRILLING DISTURB.
SED. STRUCTURES
SAMPLES
UPPER MIOCENE
N16
NN10
Diartus petterssoni / Didymocyrtis antepenultima
NTD 10a
A/G
A/M
A/G
C/M
V=1647 ● φ=41.3 γ=1.83
%CaCO3 ● =93.0
V=1640 ● φ=58.8 γ=1.68
● %CaCO3=93.2
● %CaCO3=92.8
V=1612 ● φ=42.2 γ=1.84
● %CaCO3=94.0
V=1608 ● φ=41.5 γ=1.87
● %CaCO3=92.8
V=1593 ● φ=50.6 γ=1.66
● %CaCO3=93.1
0.5
1.0
1
2
3
4
5
6
7
CC

LITHOLOGIC DESCRIPTION

NANNOFOSSIL OOZE with FORAMINIFERS and NANNOFOSSIL CHALK with FORAMINIFERS

Major lithology: This core contains 60% NANNOFOSSIL OOZE with FORAMINIFERS and 40% NANNOFOSSIL CHALK with FORAMINIFERS, both predominantly white (7.5YR 8/0) in color. The ooze is very stiff and contains chalk biscuits. Pale pink (5RP 8/2), greenish gray (5G 7/1), and pale yellowish green (10GY 7/2) 1 to 10 cm thick color bands are common. Bioturbation is indicated by white (2.5Y 8/2) mottling.

SMEAR SLIDE SUMMARY (%):

	3, 74
	D
TEXTURE:	
Sand	12
Silt	55
Clay	33
COMPOSITION:	
Accessory minerals	2
Foraminifers	20
Nannofossils	75
Siliceous fragments	3
Siliceous sponge spicules	Tr

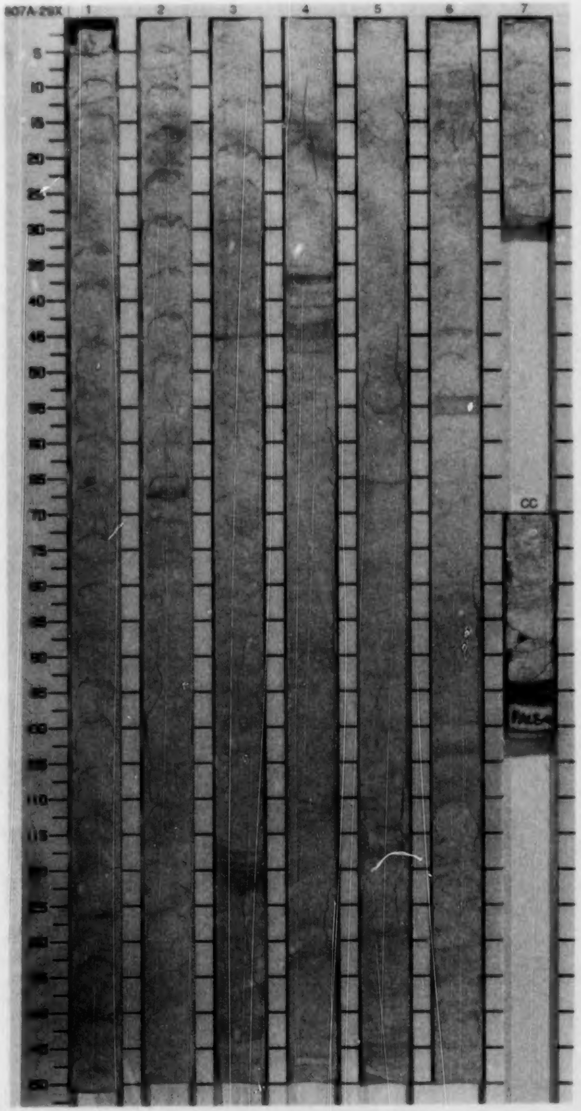
807A-29X
1
2
3
4
5
6
7
CC
5
10
15
20
25
30
35
40
45
50
55
60
65
70
75
80
85
90
95
100
105
110
115
120
125
130
135
140
145
150

SITE 807 HOLE A CORE 30X CORED INTERVAL 273.8-283.5 mbsf

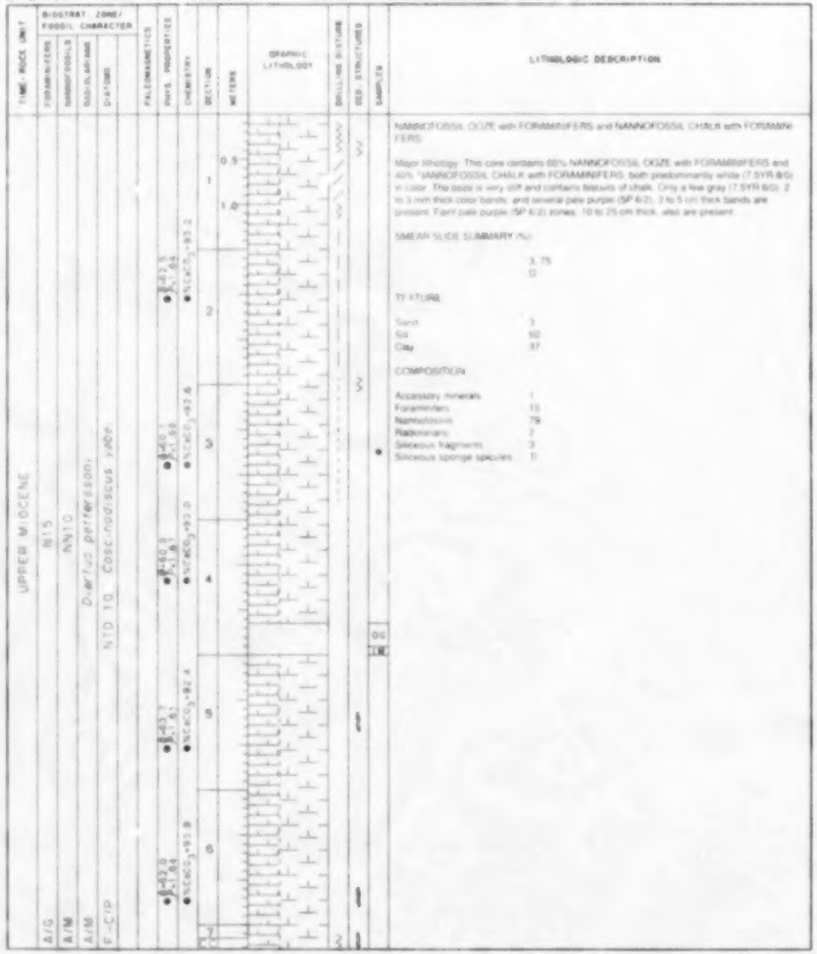
TIME-ROCK UNIT
BIOSTRAT. ZONE/ FOSSIL CHARACTER
FORAMINIFERS
NANNOFOSSILS
RADIOLARIANS
DIATOMS
PALEOMAGNETICS
PHYS. PROPERTIES
CHEMISTRY
SECTION
METERS
GRAPHIC LITHOLOGY
DRILLING DISTURB.
SED. STRUCTURES
SAMPLES
UPPER MIOCENE
N15
NN10
Diartus petterssoni
NTD 10 Coscinodiscus yabei
A/G
A/M
A/M
F-C/P
%CaCO3=93.2
%CaCO3=92.6
%CaCO3=93.0
%CaCO3=92.4
%CaCO3=93.8
1
2
3
4
5
6
7
0.5
1.0
OG
IW

LITHOLOGIC DESCRIPTION

NANNOFOSSIL OOZE with FORAMINIFERS and NANNOFOSSIL CHALK with FORAMINIFERS.

Major lithology: This core contains 60% NANNOFOSSIL OOZE with FORAMINIFERS and 40% NANNOFOSSIL CHALK with FORAMINIFERS, both predominantly white (7.5YR 8/0) in color. The ooze is very stiff and contains biscuits of chalk. Only a few gray (7.5YR 6/0), 2 to 3 mm thick color bands, and several pale purple (5P 6/2), 2 to 5 cm thick bands are present. Faint pale purple (5P 6/2) zones, 10 to 25 cm thick, also are present.

SMEAR SLIDE SUMMARY (%):

	3, 75 D
TEXTURE	
Sand	3
Silt	60
Clay	37
COMPOSITION	
Accessory minerals	1
Foraminifers	15
Nannofossils	78
Radiolarians	2
Siliceous fragments	3
Siliceous sponge spicules	Tr

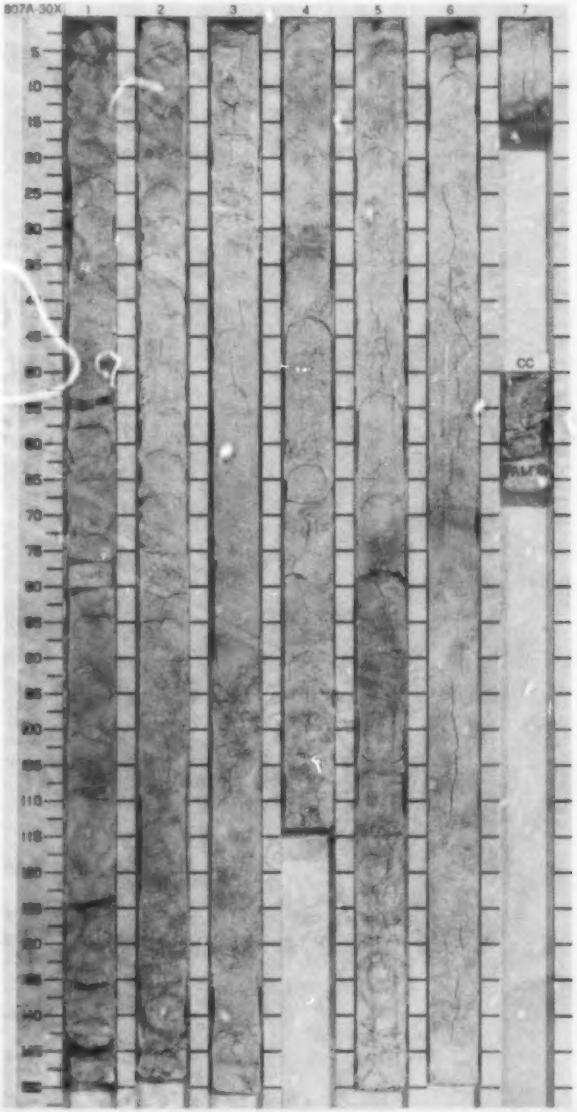
807A-30X
1
2
3
4
5
6
7
CC
5
10
15
20
25
30
35
40
45
50
55
60
65
70
75
80
85
90
95
100
105
110
115
120
125
130
135
140
145
150

SITE 807 HOLE A CORE 31X CORED INTERVAL 283.5-292.7 mbsf

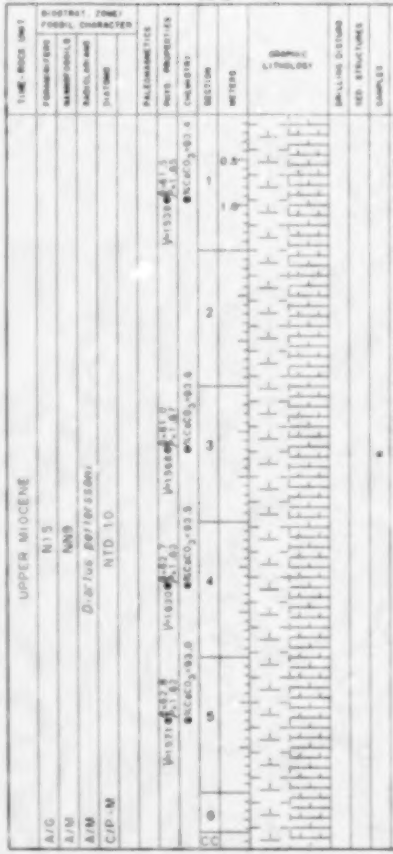
TIME-ROCK UNIT
BIOSTRAT. ZONE/ FOSSIL CHARACTER
FORAMINIFERS
NANNOFOSSILS
RADIOLARIANS
DIATOMS
PALEOMAGNETICS
PHYS. PROPERTIES
CHEMISTRY
SECTION
METERS
GRAPHIC LITHOLOGY
DRILLING DISTURB.
SED. STRUCTURES
SAMPLES
UPPER MIOCENE
N15
NN9
D. arius pentas
NTD 10
A/G
A/M
A/M
C/P-M
%CaCO3=93.4
%CaCO3=93.0
%CaCO3=93.5
%CaCO3=93.0
0.5
1.0
1
2
3
4
5
6
CC

LITHOLOGIC DESCRIPTION

NANNOFOSSIL OOZE with FORAMINIFERS and NANNOFOSSIL CHALK with FORAMINIFERS

Major lithology: This core contains white (7.5YR 8.0) NANNOFOSSIL OOZE with FORAMINIFERS and NANNOFOSSIL CHALK with FORAMINIFERS. A 45-cm-thick, pale purple (5P 6/2) interval is present at the top of Section 3. The sediment is hard, and chalky intervals occur primarily as biscuits within Sections 1 through 4. Sections 5 and 6 are very stiff ooze. There is a noticeable lack of bioturbation structures; only a few small pyrite-filled burrows are present.

SMEAR SLIDE SUMMARY (%):

	3, 75
	D
TEXTURE:	
Sand	5
Silt	70
Clay	25
COMPOSITION:	
Accessory minerals	1
Foraminifers	15
Nannofossils	82
Radiolarians	1
Siliceous fragments	1

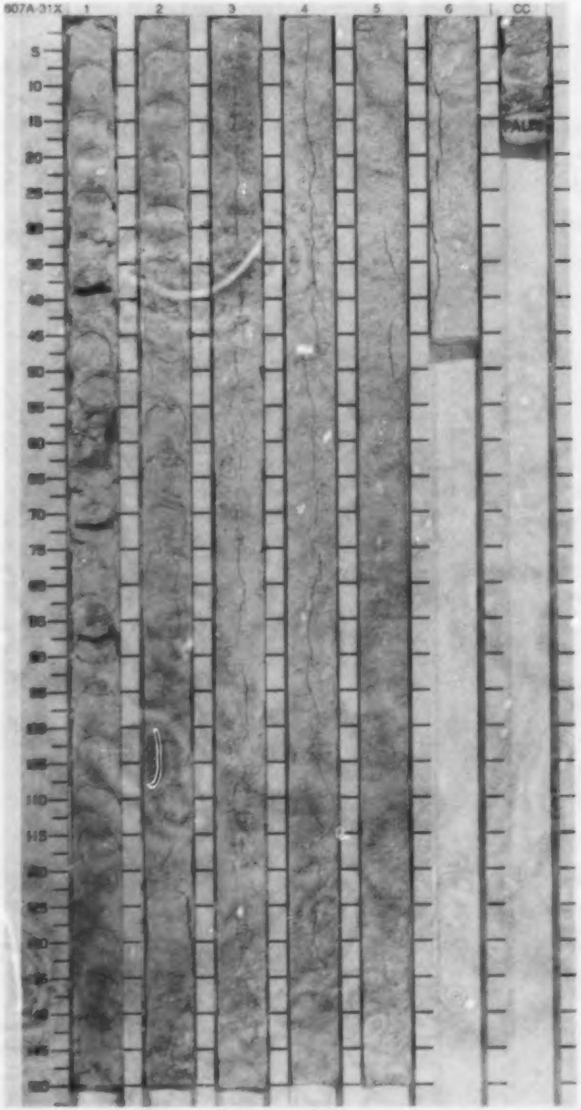
807A-31X
1
2
3
4
5
6
CC
5
10
15
20
25
30
35
40
45
50
55
60
65
70
75
80
85
90
95
100
105
110
115
120
125
130
135
140
145
150
PAL

SITE 807 HOLE A CORE 32X CORED INTERVAL 292.7-302.3 mbsl

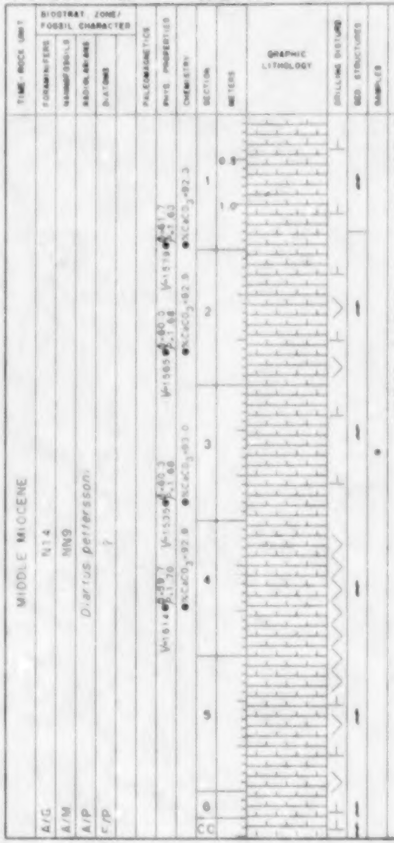
TIME-ROCK UNIT
BIOSTRAT. ZONE/ FOSSIL CHARACTER
FORAMINIFERS
NANNOFOSSILS
RADIOLARIANS
DIATOMS
PALEOMAGNETICS
PHYS. PROPERTIES
CHEMISTRY
SECTION
METERS
GRAPHIC LITHOLOGY
DRILLING DISTURB.
SED. STRUCTURES
SAMPLES
MIDDLE MIOCENE
N14
NN9
Diartus petterssoni
?
A/G
A/M
A/P
F/P
V=1579 ●ϕ=61.7 ρ=1.63
●%CaCO$_3$=92.3
V=1565 ●ϕ=60.5 ρ=1.68
●%CaCO$_3$=92.9
V=1535 ●ϕ=60.3 ρ=1.68
●%CaCO$_3$=93.0
V=1614 ●ϕ=59.7 ρ=1.70
●%CaCO$_3$=92.8
1
2
3
4
5
6
CC
0.5
1.0

LITHOLOGIC DESCRIPTION

NANNOFOSSIL CHALK with FORAMINIFERS

Major lithology: This core contains white (2.5Y 8/0) NANNOFOSSIL CHALK with FORAMINIFERS. Slight bioturbation is indicated by very few mottles, pyrite filled burrows, and specks. The drilling process has resulted in moderately fractured to highly fragmented biscuits in a stiff ooze matrix.

SMEAR SLIDE SUMMARY (%):

	3, 74
	D
TEXTURE:	
Sand	7
Silt	55
Clay	37
COMPOSITION:	
Accessory minerals	2
Foraminifers	15
Nannofossils	80
Radiolarians	Tr
Siliceous fragments	3

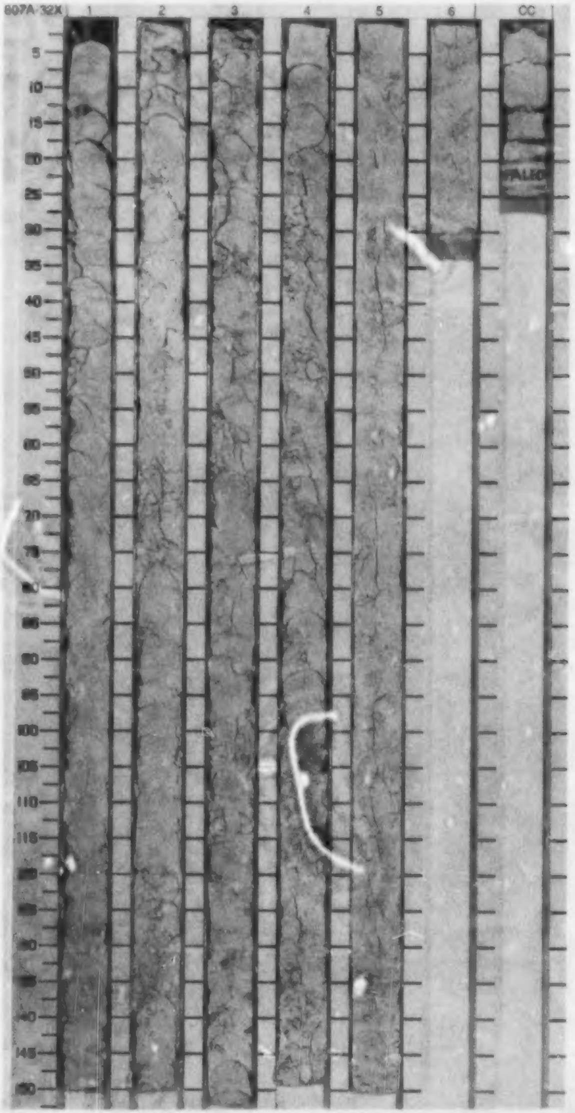
807A-32X
1
2
3
4
5
6
CC
5
10
15
20
25
30
35
40
45
50
55
60
65
70
75
80
85
90
95
100
105
110
115
120
125
130
135
140
145
150
PALEO

SITE 807 HOLE A CORE 33X CORED INTERVAL 302.3-312.0 mbsf

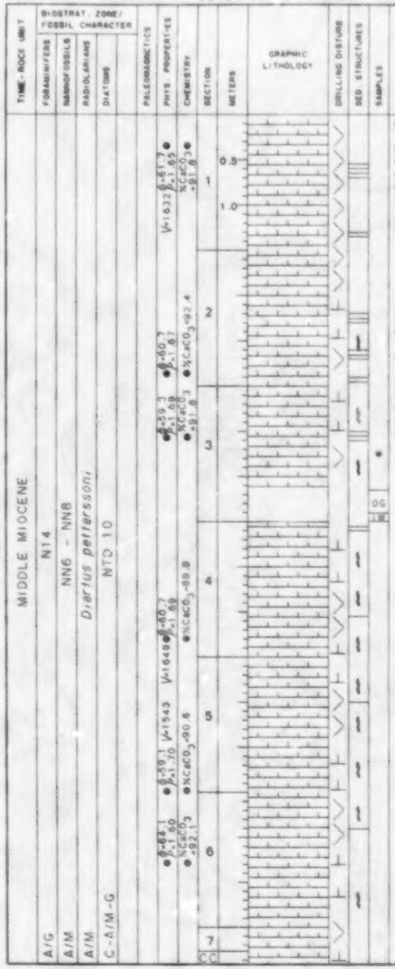
TIME-ROCK UNIT
BIOSTRAT. ZONE/ FOSSIL CHARACTER
FORAMINIFERS
NANNOFOSSILS
RADIOLARIANS
DIATOMS
PALEOMAGNETICS
PHYS. PROPERTIES
CHEMISTRY
SECTION
METERS
GRAPHIC LITHOLOGY
DRILLING DISTURB.
SED. STRUCTURES
SAMPLES
MIDDLE MIOCENE
A/G
N14
A/M
NN6 - NN8
A/M
Diartus petterssoni
C-A/M-G
NTD 10
ϕ=61.7 ρ=1.65 V=1632
%CaCO3 =91.9
ϕ=60.7 ρ=1.67
%CaCO3=92.4
ϕ=59.3 ρ=1.69
%CaCO3 =91.8
V=1649 ϕ=60.7 ρ=1.69
%CaCO3=89.8
ϕ=59.1 ρ=1.70 V=1543
%CaCO3=90.6
ϕ=64.1 ρ=1.60
%CaCO3 =92.1
1
2
3
4
5
6
7
CC
0.5
1.0
OG
IW

LITHOLOGIC DESCRIPTION

NANNOFOSSIL CHALK with FORAMINIFERS

Major lithology: This core contains NANNOFOSSIL CHALK with FORAMINIFERS. The predominant color is white, with a few 10 cm thick, pale purple (5P 6/2) intervals. Thin (<1 mm) distinct, white color bands are abundant within these intervals. A few greenish gray (5G 7/1) color bands, 1 mm to 1 cm thick, also are present. Slight bioturbation is indicated by small (<1 cm thick) faint mottles and trace fossils.

SMEAR SLIDE SUMMARY (%):

	3, 74
	D
TEXTURE:	
Sand	15
Silt	70
Clay	15
COMPOSITION:	
Accessory minerals	Tr
Foraminifers	15
Nannofossils	85
Radiolarians	Tr
Siliceous fragments	Tr

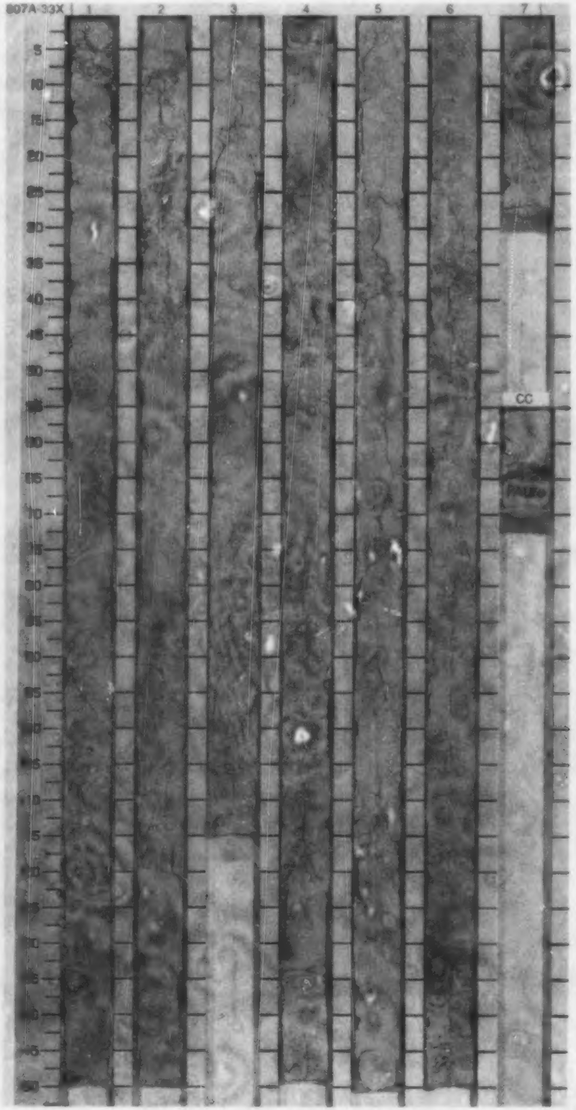
807A-33X
1
2
3
4
5
6
7
CC
PALEO
5
10
15
20
25
30
35
40
45
50
55
60
65
70
75
80
85
90
95
100
105
110
115
120
125
130
135
140
145
150

SITE 807 HOLE A CORE 34X CORED INTERVAL 312.0-321.2 mbsf

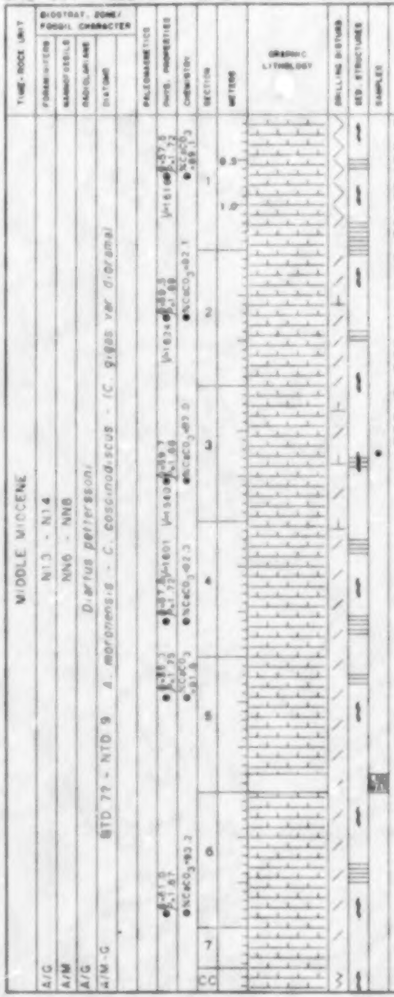

LITHOLOGIC DESCRIPTION

NANNOFOSSIL CHALK with FORAMINIFERS

Major lithology: This core contains white (2.5Y 8/0) NANNOFOSSIL CHALK with FORAMINIFERS. Distinct mm thick, irregular, wavy, pale purple (5P 6/2) color bands are abundant in 10 to 50 cm thick intervals in Sections 1, 4, 6 and 7. In the remaining sections, a few pale purple color bands are observed and several greenish gray (5G 5/2) color bands are noted throughout the core. The white sediment shows signs of bioturbation, including mottles and pyritic specks. In some of the pale purple intervals, bioturbation is heavy as indicated by abundant burrows. The drilling process has resulted in moderately fractured biscuits in a stiff ooze matrix.

SMEAR SLIDE SUMMARY (%):

	3, 75
	D
TEXTURE:	
Sand	15
Silt	65
Clay	20
COMPOSITION:	
Foraminifers	20
Nannofossils	80
Radiolarians	Tr

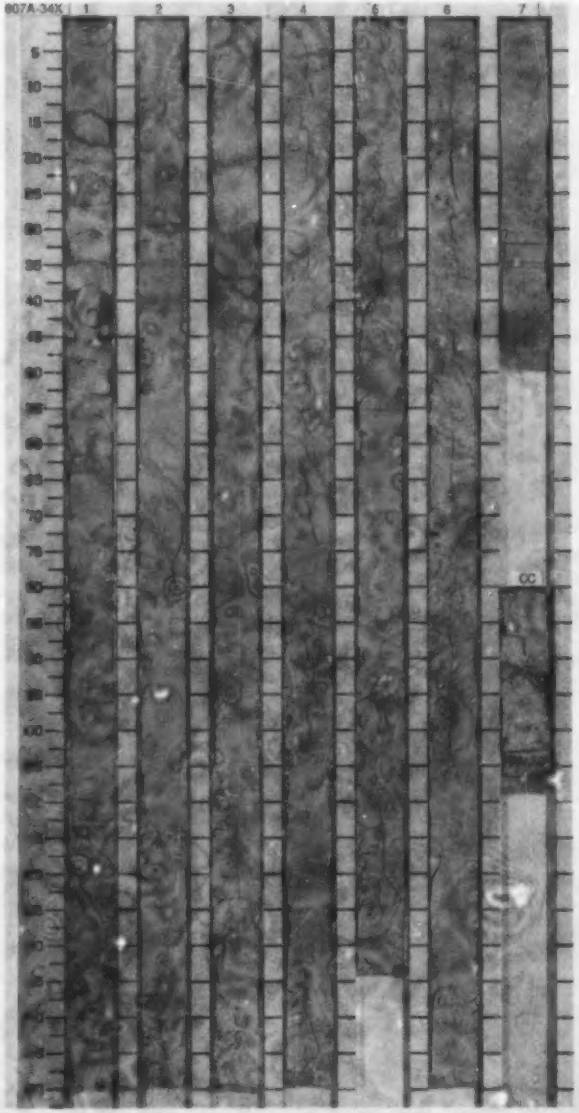
807A-34X
1
2
3
4
5
6
7
CC
5
10
15
20
25
30
35
40
45
50
55
60
65
70
75
80
85
90
95
100
105
110
115
120
125
130
135
140
145
150

SITE 807 HOLE A CORE 35X CORED INTERVAL 321.2-330.9 mbsf

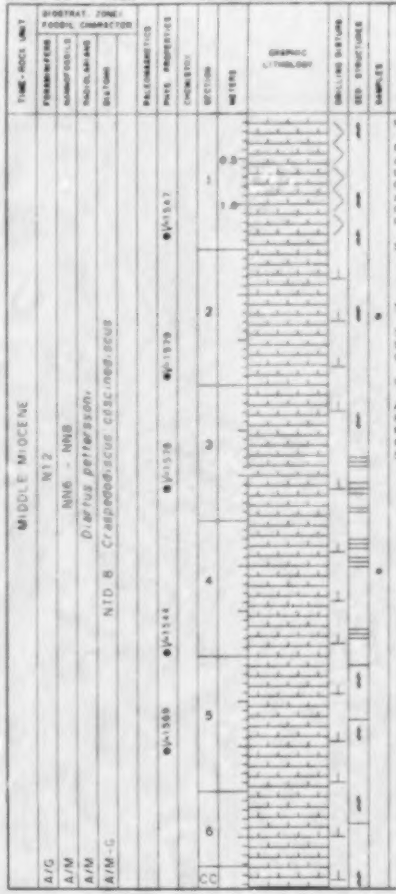
TIME-ROCK UNIT
BIOSTRAT. ZONE/ FOSSIL CHARACTER
FORAMINIFERS
NANNOFOSSILS
RADIOLARIANS
DIATOMS
PALEOMAGNETICS
PHYS. PROPERTIES
CHEMISTRY
SECTION
METERS
GRAPHIC LITHOLOGY
DRILLING DISTURB.
SED. STRUCTURES
SAMPLES
MIDDLE MIOCENE
N12
NN6 - NN8
Diartus petterssoni
NID 8 Craspedodiscus coscinodiscus
A/G
A/M
A/M
A/M-G
●γ=1.547
●γ=1.970
●γ=1.578
●γ=1.544
●γ=1.569
0.5
1.0
1
2
3
4
5
6
CC

LITHOLOGIC DESCRIPTION

NANNOFOSSIL CHALK

Major lithology: This core contains white (7.5YR 8/0) NANNOFOSSIL CHALK. Sections 4 and 5 each have two pale pink (5RP 8/2) intervals (10-50 cm long). The sediment is slightly bioturbated as indicated by a few pyrite-filled mottles and specks. Distinct pale purple (5P 6/2) and greenish gray (5G 5/2), mm-scale color bands and a few cm-scale, pale purple zones are noted in Sections 3, 5 and 6. Drilling disturbance has resulted in moderately fractured biscuits in a stiff paste matrix, except for Section 1, where the biscuits are highly fragmented.

SMEAR SLIDE SUMMARY (%)

	2, 76	4, 57
	D	D
TEXTURE		
Sand	10	6
Silt	70	60
Clay	20	34
COMPOSITION		
Accessory minerals	—	2
Foraminifers	8	6
Nannofossils	92	87
Radiolarians	Tr	Tr
Siliceous fragments	—	5

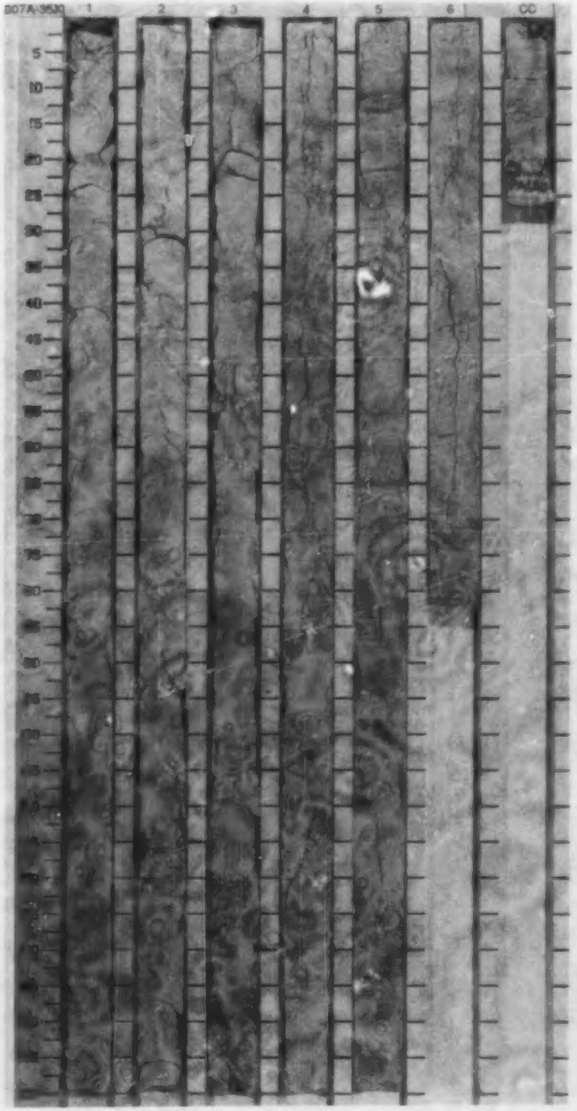
807A-35X
1
2
3
4
5
6
CC
5
10
15
20
25
30
35
40
45
50
55
60
65
70
75
80
85
90
95
100
105
110
115
120
125
130
135
140
145
150

SITE 807 HOLE A CORE 36X CORED INTERVAL 330.9-340.6 mbsf

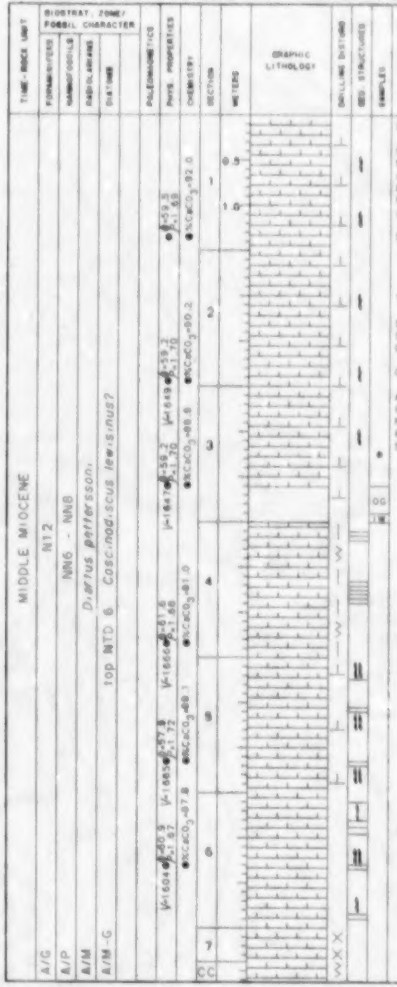
TIME-ROCK UNIT
BIOSTRAT. ZONE/ FOSSIL CHARACTER
FORAMINIFERS
NANNOFOSSILS
RADIOLARIANS
DIATOMS
PALEOMAGNETICS
PHYS. PROPERTIES
CHEMISTRY
SECTION
METERS
GRAPHIC LITHOLOGY
DRILLING DISTURB.
SED. STRUCTURES
SAMPLES
MIDDLE MIOCENE
A/G N12
A/P NN6 - NN8
A/M Didymus pettersson.
A/M-G top NTD 6 Cosc.nod.scus lew.s.nus?
φ=59.5 ρ=1.68
%CaCO3=92.0
V=1649 φ=59.2 ρ=1.70
%CaCO3=90.2
V=1647 φ=58.2 ρ=1.70
%CaCO3=88.8
V=1666 φ=61.6 ρ=1.66
%CaCO3=81.0
V=1665 φ=57.8 ρ=1.72
%CaCO3=88.1
V=1604 φ=60.9 ρ=1.67
%CaCO3=87.8
1
2
3
4
5
6
7
CC
0.5
1.0
OG
IW

LITHOLOGIC DESCRIPTION

NANNOFOSSIL CHALK with FORAMINIFERS

Major lithology: This core contains white (7.5YR 8/0) NANNOFOSSIL CHALK with FORAMINIFERS. Sections 1 through 3 are white and homogeneous. From Section 4 to the base of the core, there are a few 20 to 30 cm thick intervals that exhibit fine-scale color banding that is primarily pale purple (5P 6/2) and, to a lesser extent, pale yellowish green (10GY 7/2). Fine-scale color banding imparts a pale pink (5RP 8/2) color to some intervals. A few pink intervals exhibit significant traces of bioturbation.

SMEAR SLIDE SUMMARY (%):

	3, 75
	D
TEXTURE:	
Sand	12
Silt	56
Clay	32
COMPOSITION:	
Accessory minerals	1
Foraminifers	12
Nannofossils	84
Radiolarians	5
Siliceous fragments	3

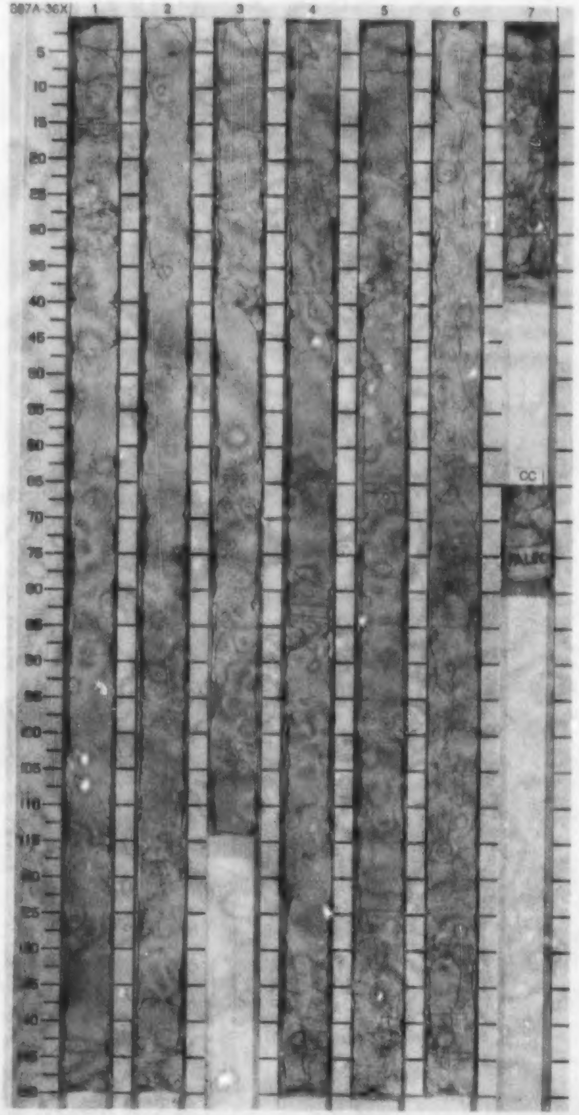
807A-36X
1
2
3
4
5
6
7
CC
PALEO
5
10
15
20
25
30
35
40
45
50
55
60
65
70
75
80
85
90
95
100
105
110
115
120
125
130
135
140
145
150

SITE 807 HOLE A CORE 37X CORED INTERVAL 340.6-350.2 mbsf

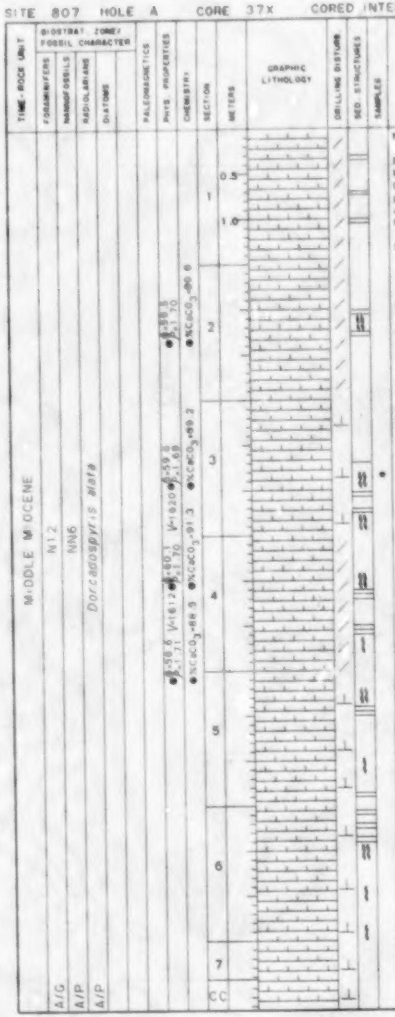
TIME-ROCK UNIT
BIOSTRAT. ZONE/ FOSSIL CHARACTER
FORAMINIFERS
NANNOFOSSILS
RADIOLARIANS
DIATOMS
PALEOMAGNETICS
PHYS. PROPERTIES
CHEMISTRY
SECTION
METERS
GRAPHIC LITHOLOGY
DRILLING DISTURB.
SED. STRUCTURES
SAMPLES
MIDDLE MIOCENE
N12
NN6
Dorcadospyris alata
A/G
A/P
A/P
●φ=58.5 ●γ=1.70
●%CaCO3=90.6
●φ=60.1 ●γ=1.70 V=1612
●%CaCO3=88.9
●φ=59.8 ●γ=1.69 V=1620
●%CaCO3=91.3
●%CaCO3=89.2
●φ=58.6 ●γ=1.71
1
2
3
4
5
6
7
CC
0.5
1.0

LITHOLOGIC DESCRIPTION

NANNOFOSSIL CHALK with FORAMINIFERS

Major lithology: This core contains white (7.5YR 8/0) NANNOFOSSIL CHALK with FORAMINIFERS. Pale pink (5P 8/2), dm-scale intervals are observed in Sections 2-6. Signs of bioturbation are rare in the white intervals, but heavy bioturbation is observed in the pale pink parts of the core. A few zones of distinct mm scale, greenish gray (5G 7/1) color bands are noted throughout the core. The drilling process has resulted in slightly to moderately fractured biscuits in a stiff ooze matrix.

SMEAR SLIDE SUMMARY (%)

	3, 82 D
TEXTURE	
Sand	10
Silt	55
Clay	35
COMPOSITION	
Accessory minerals	1
Foraminifers	12
Nannofossils	83
Radiolarians	Tr
Siliceous fragments	4

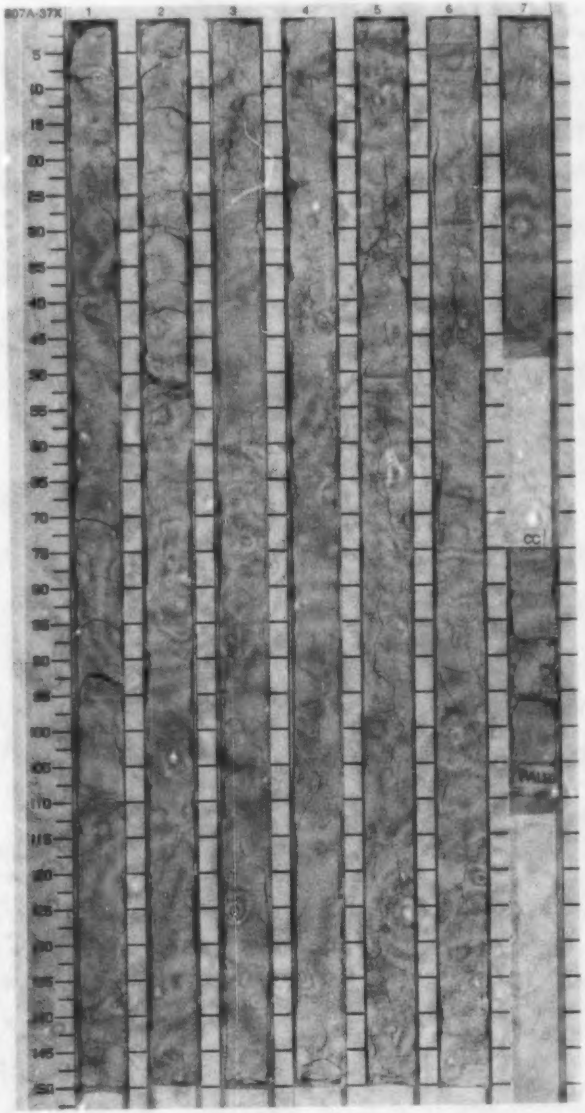
807A-37X
1
2
3
4
5
6
7
CC
PALEO
5
10
15
20
25
30
35
40
45
50
55
60
65
70
75
80
85
90
95
100
105
110
115
120
125
130
135
140
145
150

SITE 807 HOLE A CORE 38X CORED INTERVAL 350.2-359.9 mbsf

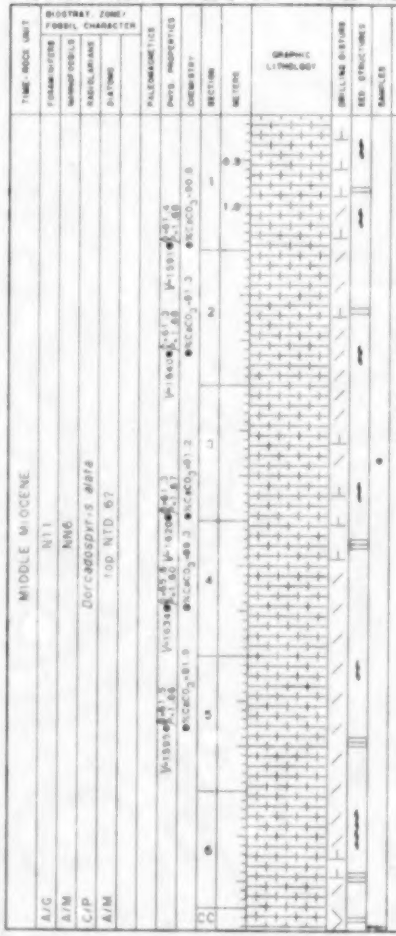
TIME-ROCK UNIT
BIOSTRAT. ZONE/ FOSSIL CHARACTER
FORAMINIFERS
NANNOFOSSILS
RADIOLARIANS
DIATOMS
PALEOMAGNETICS
PHYS. PROPERTIES
CHEMISTRY
SECTION
METERS
GRAPHIC LITHOLOGY
DRILLING DISTURB.
SED. STRUCTURES
SAMPLES
MIDDLE MIOCENE
A/G
N11
A/M
NN6
C/P
Dorcadospyris alata
A/M
top NTD 6?
V=1591 φ=61.4 γ=1.88
V=1640 φ=61.2 γ=1.88
V=1620 φ=61.3 γ=1.87
V=1634 φ=65.6 γ=1.80
V=1593 φ=61.3 γ=1.88
%CaCO3=90.8
%CaCO3=91.3
%CaCO3=91.2
%CaCO3=89.3
%CaCO3=91.0
1
2
3
4
5
6
CC
0.5
1.0

LITHOLOGIC DESCRIPTION

FORAMINIFER NANNOFOSSIL CHALK

Major lithology: This core contains white (7.5YR 8/0) FORAMINIFER NANNOFOSSIL CHALK. Thin (0.1-1 cm), pale yellowish green (10GY 7/2), greenish gray (5G 7/1), grayish blue (5PB 5/2), and dark gray (N5) color bands are common. At Section 5, 145 cm, gray bands begin to resemble flaser structures. Moderate bioturbation is evident from faint mottles and a few pyrite-filled burrows.

SMEAR SLIDE SUMMARY (%)

	3, 82
	D
TEXTURE	
Sand	15
Silt	50
Clay	35
COMPOSITION	
Foraminifers	25
Nannofossils	74
Radiolarians	Tr
Siliceous fragments	1
Siliceous sponge spicules	Tr

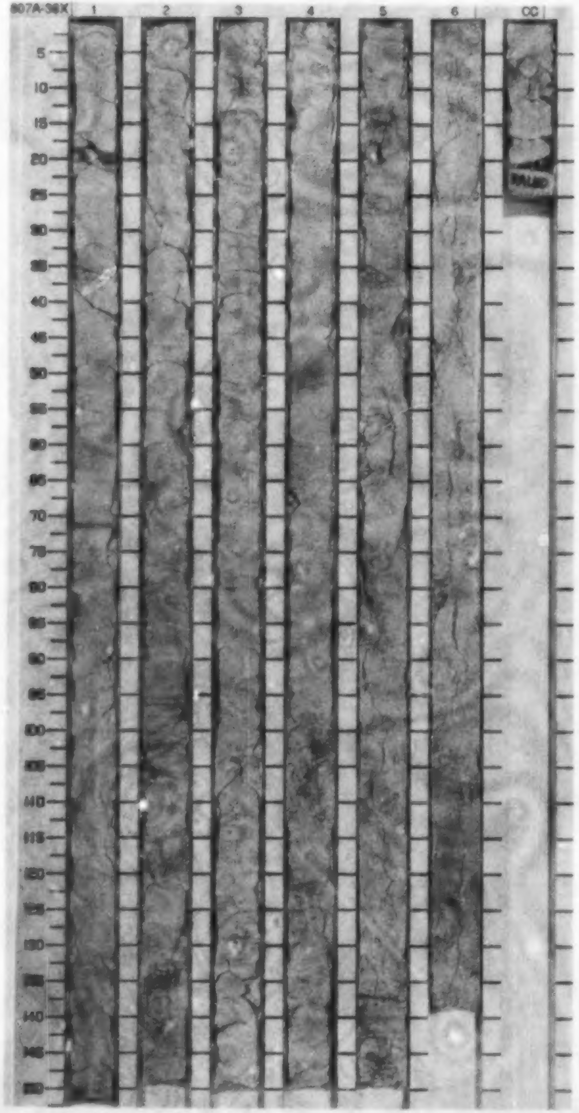
807A-38X
1
2
3
4
5
6
CC
5
10
15
20
25
30
35
40
45
50
55
60
65
70
75
80
85
90
95
100
105
110
115
120
125
130
135
140
145
150

SITE 807 HOLE A CORE 39X CORED INTERVAL 359.8-369.7 mbsf

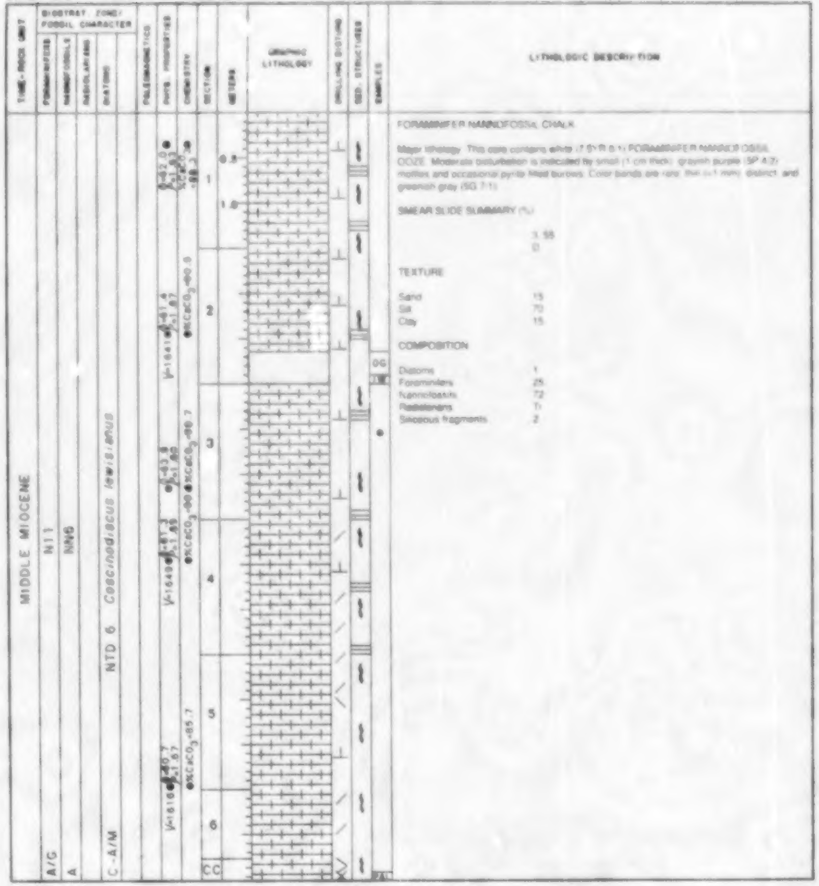
TIME-ROCK UNIT
BIOSTRAT. ZONE/ FOSSIL CHARACTER
FORAMINIFERS
NANNOFOSSILS
RADIOLARIANS
DIATOMS
PALEOMAGNETICS
PHYS. PROPERTIES
CHEMISTRY
SECTION
METERS
GRAPHIC LITHOLOGY
DRILLING DISTURB.
SED. STRUCTURES
SAMPLES
MIDDLE MIOCENE
N11
A/G
NN6
A
NTD 6 Coscinodiscus lewisianus
C-A/M
γ=62.0
V=1641
γ=61.4
ρ=1.67
V=1640
γ=61.2
ρ=1.65
γ=63.8
ρ=1.60
V=1610
γ=60.7
ρ=1.67
%CaCO3=80.0
%CaCO3=80
%CaCO3=80.7
%CaCO3=85.7
1
2
3
4
5
6
CC
0.5
1.0
OG

LITHOLOGIC DESCRIPTION

FORAMINIFER NANNOFOSSIL CHALK

Major lithology: This core contains white (7.5YR 8/1) FORAMINIFER NANNOFOSSIL OOZE. Moderate bioturbation is indicated by small (1 cm thick) grayish purple (5P 4/2) mottles and occasional pyrite filled burrows. Color bands are rare, thin (<1 mm), distinct, and greenish gray (5G 7/1).

SMEAR SLIDE SUMMARY (%):

	3, 55
	D
TEXTURE	
Sand	15
Silt	70
Clay	15
COMPOSITION	
Diatoms	1
Foraminifers	25
Nannofossils	72
Radiolarians	Tr
Siliceous fragments	2

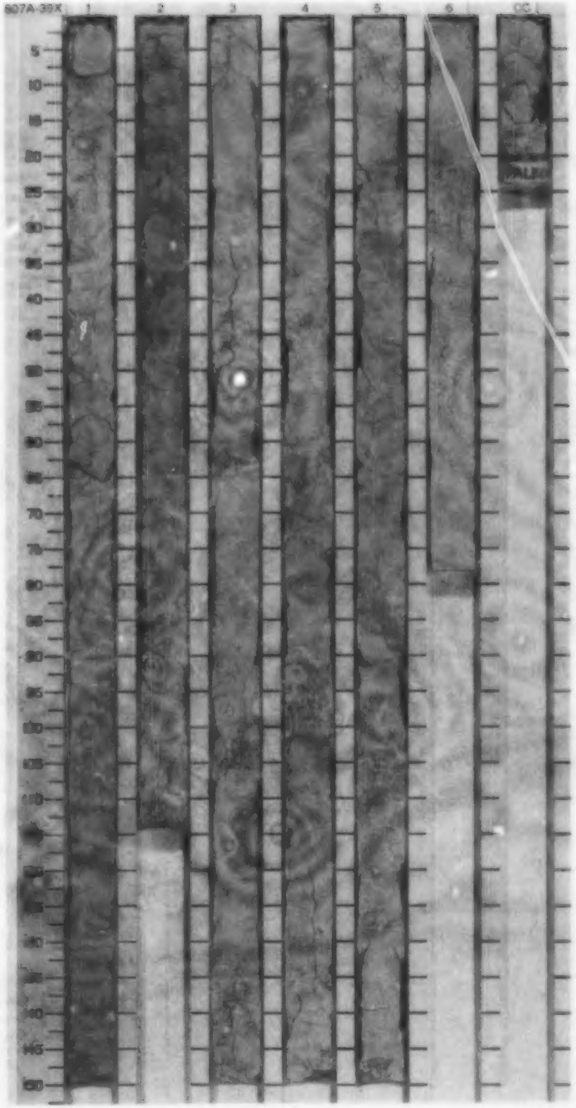
807A-39X
1
2
3
4
5
6
CC
5
10
15
20
25
30
35
40
45
50
55
60
65
70
75
80
85
90
95
100
105
110
115
120
125
130
135
140
145
150

SITE 807 HOLE A CORE 40X CORED INTERVAL 369.7-379.5 mbsf

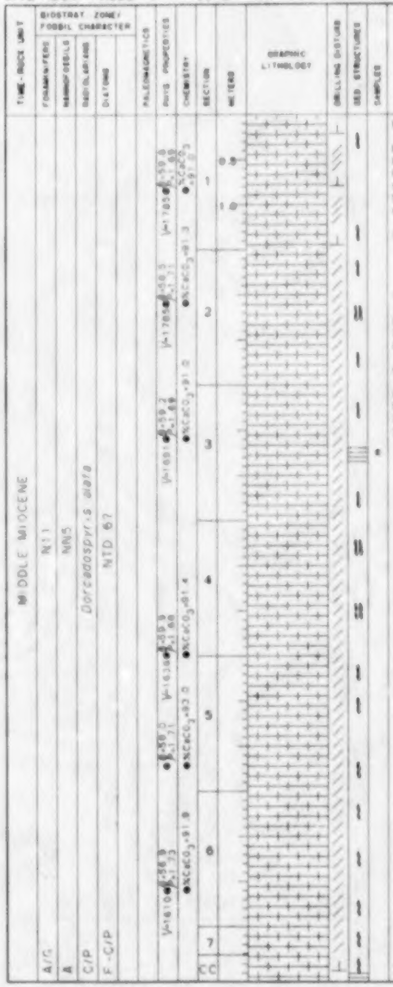
TIME-ROCK UNIT
BIOSTRAT. ZONE/ FOSSIL CHARACTER
FORAMINIFERS
NANNOFOSSILS
RADIOLARIANS
DIATOMS
PALEOMAGNETICS
PHYS. PROPERTIES
CHEMISTRY
SECTION
METERS
GRAPHIC LITHOLOGY
DRILLING DISTURB.
SED. STRUCTURES
SAMPLES
MIDDLE MIOCENE
N11
NN5
Dorcadospyris alata
NTD 67
A/G
A
C/P
F-C/P
0.5
1.0
1
2
3
4
5
6
7
CC

LITHOLOGIC DESCRIPTION

FORAMINIFER NANNOFOSSIL CHALK

Major lithology: This core contains white (7.5YR 8/0) FORAMINIFER NANNOFOSSIL CHALK with pale purple (5P 6/2) intervals present in Sections 2 and 3. In the white parts of the core, bioturbation is slight to moderate, as indicated by several pyrite-filled burrows and specks. Signs of heavy bioturbation, however, are noted in the pale purple intervals. In Sections 3 and CC, a few distinct, mm-thick, greenish gray (5G 7/1) color bands are observed. Drilling disturbance is slight throughout the core.

SMEAR SLIDE SUMMARY (%):

	3, 75
	D
TEXTURE:	
Sand	20
Silt	65
Clay	15
COMPOSITION:	
Foraminifers	25
Nannofossils	74
Radiolarians	Tr
Siliceous sponge spicules	1

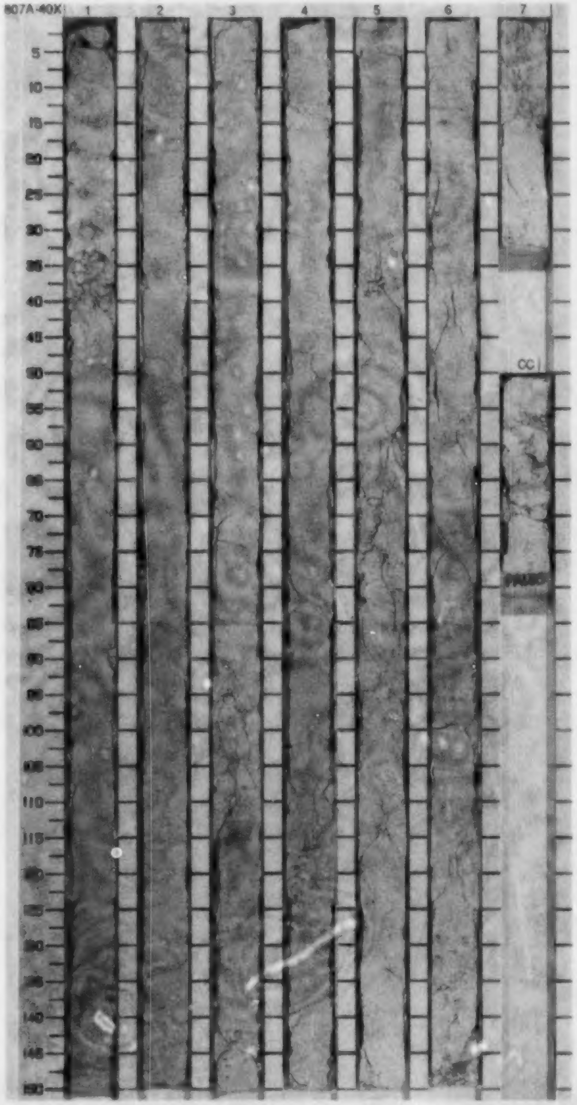
807A-40X
1
2
3
4
5
6
7
CC
5
10
15
20
25
30
35
40
45
50
55
60
65
70
75
80
85
90
95
100
105
110
115
120
125
130
135
140
145
150

SITE 807 HOLE A CORE 4 X CORED INTERVAL 379.5-389.2 mbsf

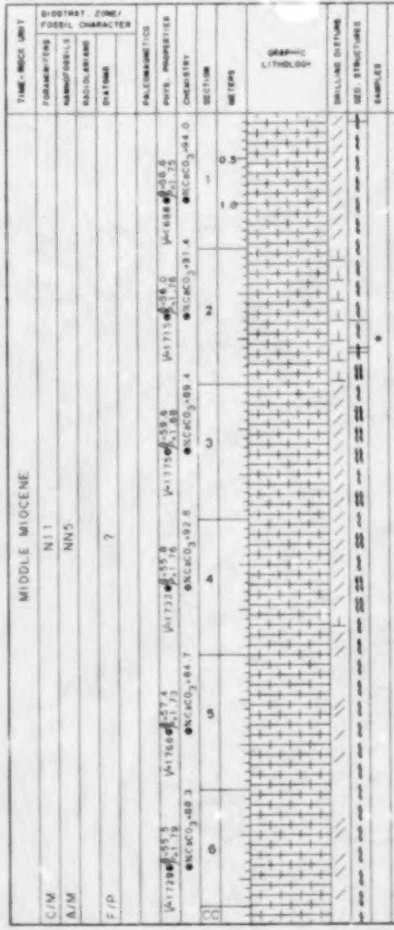
TIME-ROCK UNIT
BIOSTRAT. ZONE/ FOSSIL CHARACTER
FORAMINIFERS
NANNOFOSSILS
RADIOLARIANS
DIATOMS
PALEOMAGNETICS
PHYS. PROPERTIES
CHEMISTRY
SECTION
METERS
GRAPHIC LITHOLOGY
DRILLING DISTURB.
SED. STRUCTURES
SAMPLES
MIDDLE MIOCENE
N11
NN5
?
C/M
A/M
F/P
V=1688 φ=60.6 γ=1.75
V=1715 φ=56.0 γ=1.78
V=1775 φ=59.6 γ=1.68
V=1732 φ=55.8 γ=1.76
V=1766 φ=57.4 γ=1.73
V=1729 φ=55.5 γ=1.79
%CaCO3=94.0
%CaCO3=91.4
%CaCO3=89.4
%CaCO3=92.8
%CaCO3=84.7
%CaCO3=88.3
1
2
3
4
5
6
CC
0.5
1.0

LITHOLOGIC DESCRIPTION

FORAMINIFER NANNOFOSSIL CHALK

Major lithology: This core contains moderately to highly bioturbated, white (7.5YR 8/0) FORAMINIFER NANNOFOSSIL CHALK. Disseminated pyrite filled burrows are present but not abundant. Minor intervals of light greenish gray (5G 7/1) color bands are present in Section 2.

SMEAR SLIDE SUMMARY (%):

	2, 100
	D
TEXTURE:	
Sand	35
Silt	60
Clay	5
COMPOSITION:	
Foraminifers	32
Nannofossils	65
Radiolarians	2
Silicoflagellates	1

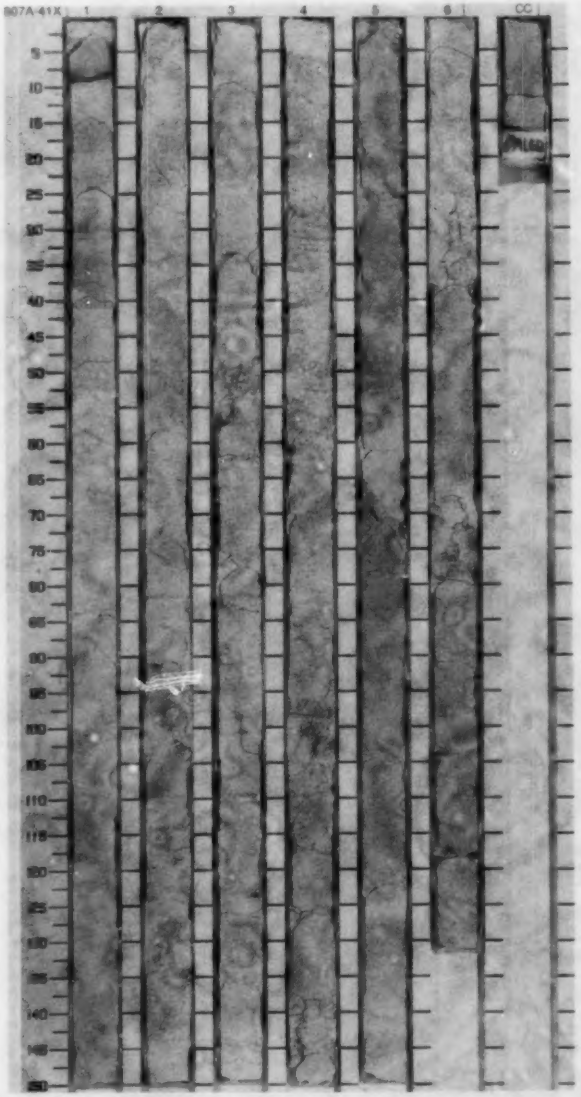
807A-41X
1
2
3
4
5
6
CC
5
10
15
20
25
30
35
40
45
50
55
60
65
70
75
80
85
90
95
100
105
110
115
120
125
130
135
140
145
150
PALEO

SITE 807 HOLE A CORE 42X CORED INTERVAL 389.2-398.9 mbsf

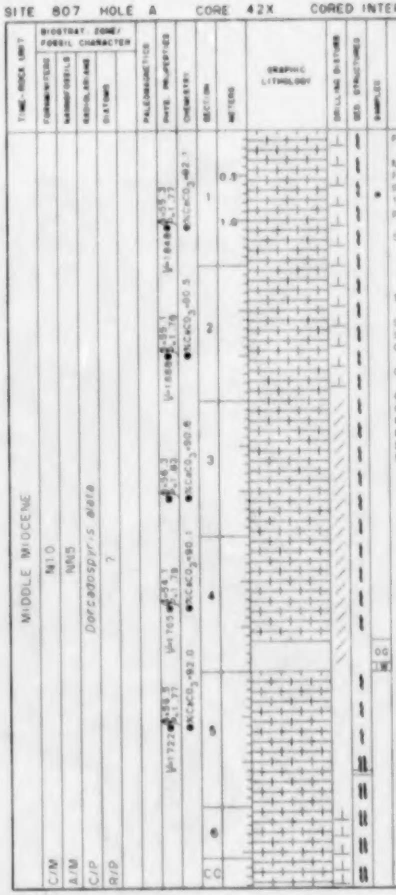
TIME-ROCK UNIT
BIOSTRAT. ZONE/ FOSSIL CHARACTER
FORAMINIFERS
NANNOFOSSILS
RADIOLARIANS
DIATOMS
PALEOMAGNETICS
PHYS. PROPERTIES
CHEMISTRY
SECTION
METERS
GRAPHIC LITHOLOGY
DRILLING DISTURB.
SED. STRUCTURES
SAMPLES
MIDDLE MIOCENE
N10
NN5
Dorcadospyris alata
?
C/M
A/M
C/P
R/P
φ=55.3
γ=1.77
Vp=1848
φ=55.1
γ=1.76
Vp=1888
φ=56.3
γ=1.82
φ=54.1
γ=1.78
Vp=1705
φ=56.5
γ=1.77
Vp=1722
%CaCO3=92.1
%CaCO3=90.5
%CaCO3=90.8
%CaCO3=90.1
%CaCO3=92.0
1
2
3
4
5
6
CC
0.5
1.0
OG
IW

LITHOLOGIC DESCRIPTION

FORAMINIFER NANNOFOSSIL CHALK

Major lithology: This core contains white (7.5YR 8/0), moderately to highly bioturbated FORAMINIFER NANNOFOSSIL CHALK. Indistinct burrow mottles are present in Sections 1 through 5. An interval of light greenish gray (5G 7/1) color bands is present at Section 5, 110 cm. Below this level, the sediments are extensively stained with grayish blue (5PB 5/2) pyrite filled burrows.

SMEAR SLIDE SUMMARY (%):

	1, 72 D
TEXTURE	
Sand	15
Silt	81
Clay	4
COMPOSITION	
Foraminifers	30
Glass	Tr
Nannofossils	67
Radiolarians	1
Silicoflagellates	1
Spicules	1

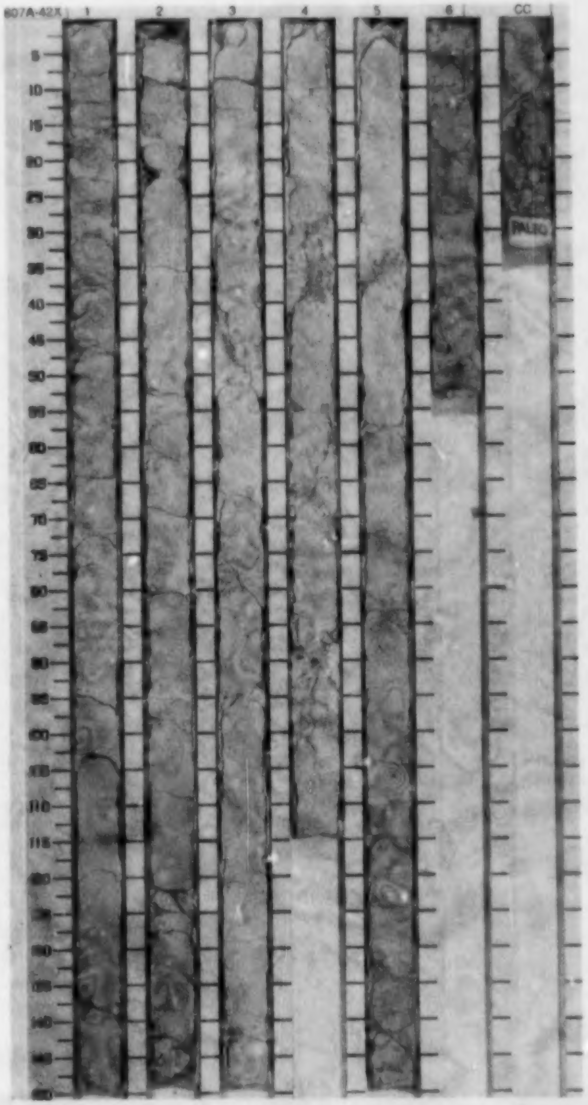
807A-42X
1
2
3
4
5
6
CC
5
10
15
20
25
30
35
40
45
50
55
60
65
70
75
80
85
90
95
100
105
110
115
120
125
130
135
140
145
150
PALEO

SITE 807 HOLE A CORE 43X CORED INTERVAL 398.9-408.6 mbsf

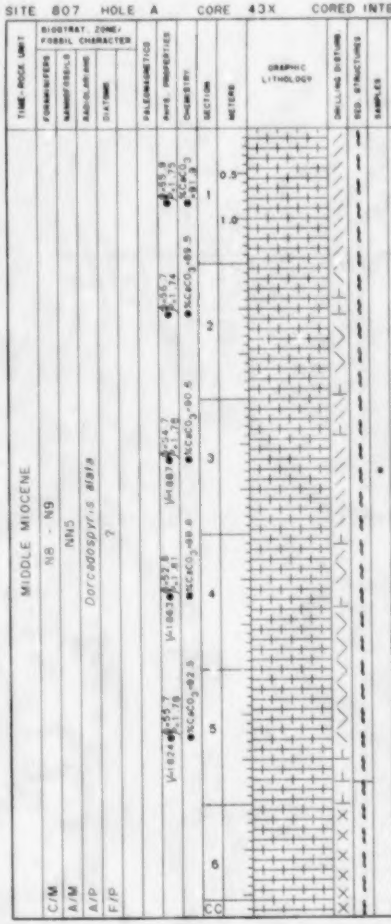
TIME-ROCK UNIT
BIOSTRAT. ZONE/ FOSSIL CHARACTER
FORAMINIFERS
NANNOFOSSILS
RADIOLARIANS
DIATOMS
PALEOMAGNETICS
PHYS. PROPERTIES
CHEMISTRY
SECTION
METERS
GRAPHIC LITHOLOGY
DRILLING DISTURB.
SED. STRUCTURES
SAMPLES
MIDDLE MIOCENE
N8 - N9
NN5
Dorcadospyris alata
?
C/M
A/M
A/P
F/P
ϕ-55.9
ρ-1.75
%CaCO3 -91.8
ϕ-56.7
ρ-1.74
%CaCO3-89.5
V-1887
ϕ-54.7
ρ-1.78
%CaCO3-90.6
V-1863
ϕ-52.8
ρ-1.81
%CaCO3-88.8
V-1824
ϕ-55.7
ρ-1.78
%CaCO3-92.5
1
2
3
4
5
6
CC
0.5
1.0

LITHOLOGIC DESCRIPTION

FORAMINIFER NANNOFOSSIL CHALK

Major lithology: This core contains white (7.5YR 8/0 and 5Y 8/1) FORAMINIFER NANNOFOSSIL CHALK. The chalk is slightly to moderately bioturbated throughout, and Section 1 is stained by moderate amounts of grayish blue (5PB 5/2) pyrite filled burrows. Several light gray (N7), thin (mm scale) color bands are present at Section 5, 130 cm.

SMEAR SLIDE SUMMARY (%):

	3, 80 D
TEXTURE	
Sand	20
Silt	75
Clay	5
COMPOSITION	
Foraminifers	25
Nannofossils	70
Radiolarians	4
Silicoflagellates	1

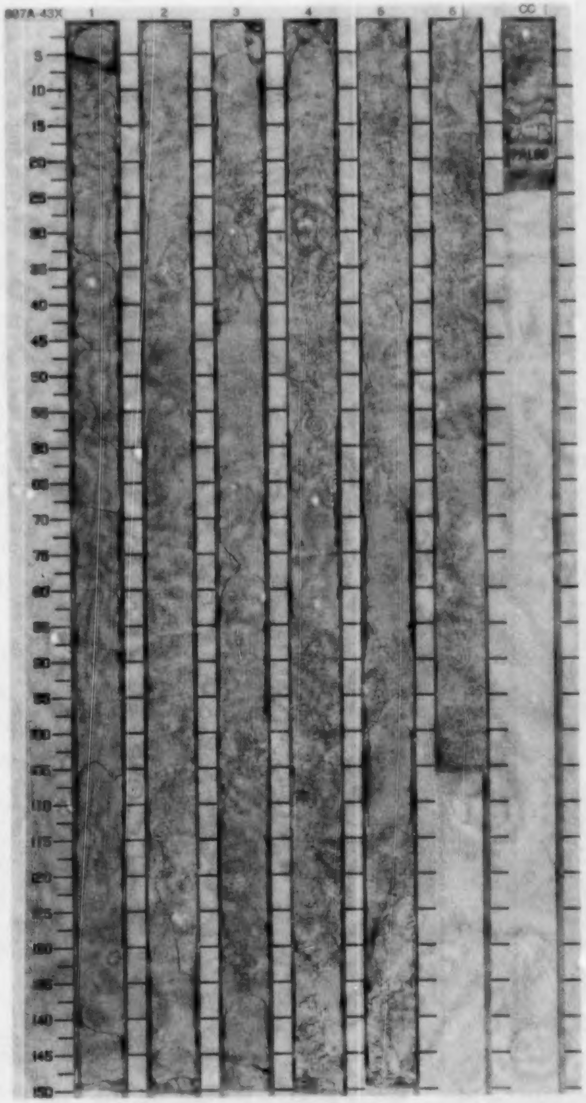
807A-43X
1
2
3
4
5
6
CC
5
10
15
20
25
30
35
40
45
50
55
60
65
70
75
80
85
90
95
100
105
110
115
120
125
130
135
140
145
150

SITE 807 HOLE A CORE 44X CORED INTERVAL 408.6-418.3 mbsf

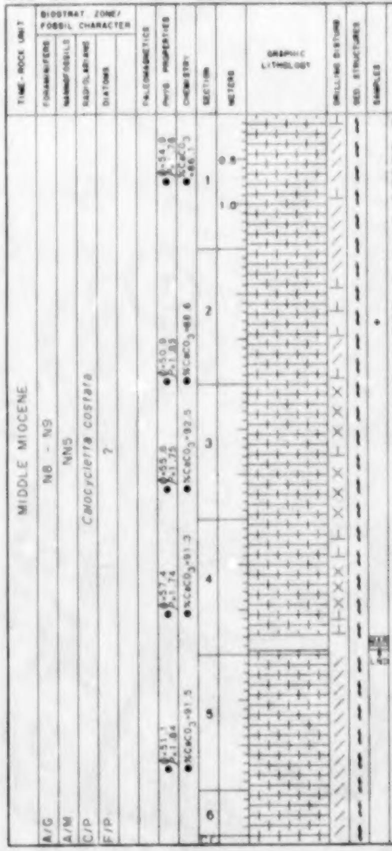
TIME-ROCK UNIT
BIOSTRAT. ZONE/ FOSSIL CHARACTER
FORAMINIFERS
NANNOFOSSILS
RADIOLARIANS
DIATOMS
PALEOMAGNETICS
PHYS. PROPERTIES
CHEMISTRY
SECTION
METERS
GRAPHIC LITHOLOGY
DRILLING DISTURB.
SED. STRUCTURES
SAMPLES
MIDDLE MIOCENE
N8 - N9
NN5
Calocycletta costata
?
A/G
A/M
C/P
F/P
φ=54.0
γ=1.78
%CaCO3=86.1
φ=50.0
γ=1.85
%CaCO3=88.6
φ=55.6
γ=1.75
%CaCO3=92.5
φ=57.4
γ=1.74
%CaCO3=91.3
φ=51.1
γ=1.84
%CaCO3=91.5
1
2
3
4
5
6
CC
0.5
1.0
PAL
IW
LND

LITHOLOGIC DESCRIPTION

FORAMINIFER NANNOFOSSIL CHALK

Major lithology: This core contains white (7.5YR 8/0, 2.5Y 8/0, and 5Y 8/1) FORAMINIFER NANNOFOSSIL CHALK. The sediments are slightly to moderately bioturbated, with indistinct mottling and minor staining by grayish blue (5PB 5/2), pyrite-filled burrows. Several light gray (5Y 7/1) color bands are present in Sections 1 and 5, and dip at angles of 10-30° across the core surface. These may represent sediment deformation zones.

SMEAR SLIDE SUMMARY (%)

	2, 79 D
TEXTURE	
Sand	30
Silt	65
Clay	5
COMPOSITION	
Foraminifers	26
Nannofossils	70
Radiolarians	4
Silicoflagellates	Tr

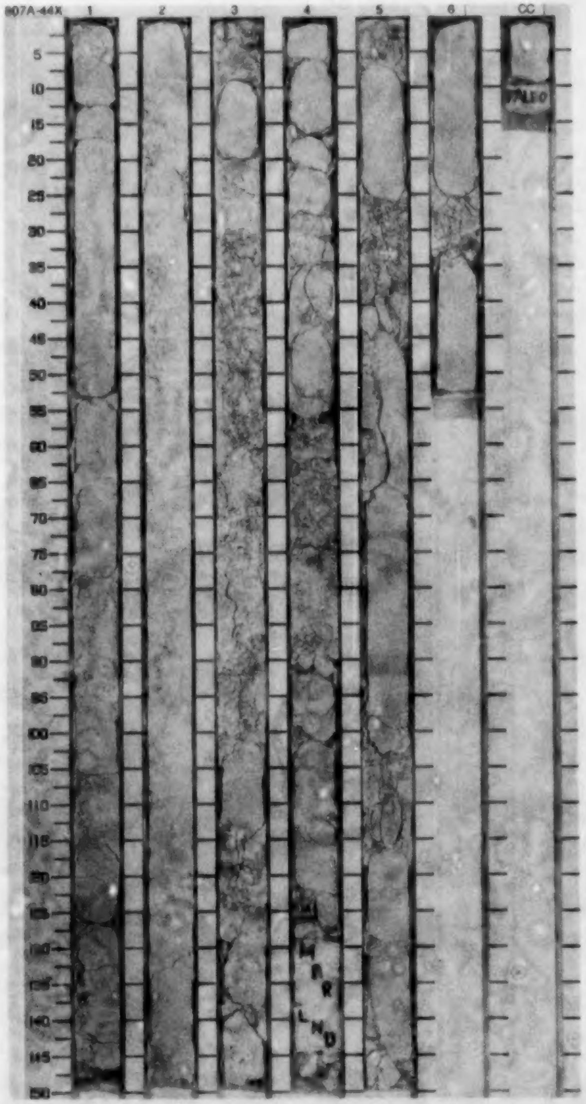
807A-44X
1
2
3
4
5
6
CC
5
10
15
20
25
30
35
40
45
50
55
60
65
70
75
80
85
90
95
100
105
110
115
120
125
130
135
140
145
150
PALEO
W.R.
LND

SITE 807 HOLE A CORE 45X CORED INTERVAL 418.3-427.8 mbsf

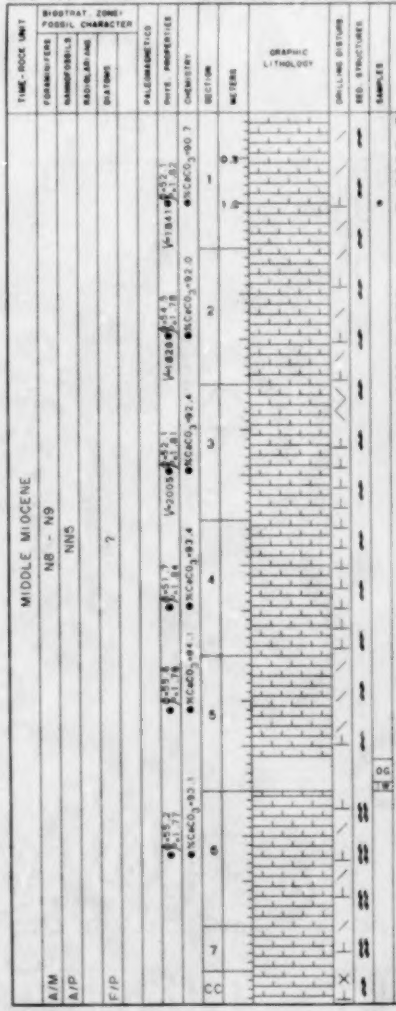
TIME-ROCK UNIT
BIOSTRAT. ZONE/ FOSSIL CHARACTER
FORAMINIFERS
NANNOFOSSILS
RADIOLARIANS
DIATOMS
PALEOMAGNETICS
PHYS. PROPERTIES
CHEMISTRY
SECTION
METERS
GRAPHIC LITHOLOGY
DRILLING DISTURB.
SED. STRUCTURES
SAMPLES
MIDDLE MIOCENE
N8 - N9
NN5
?
A/M
A/P
F/P
V=1841 φ=52.1 γ=1.82
V=1828 φ=54.5 γ=1.78
V=2005 φ=52.1 γ=1.81
φ=51.7 γ=1.84
φ=55.8 γ=1.78
φ=55.2 γ=1.77
%CaCO3=90.7
%CaCO3=92.0
%CaCO3=92.4
%CaCO3=93.4
%CaCO3=94.1
%CaCO3=93.1
1
2
3
4
5
6
7
CC
0.5
1.0
OG
IW

LITHOLOGIC DESCRIPTION

NANNOFOSSIL CHALK with FORAMINIFERS

Major lithology: This core contains white (5Y 8/1 and 10YR 8/1) NANNOFOSSIL CHALK with FORAMINIFERS. Moderate to heavy bioturbation is indicated by horizontal 0.5 cm wide burrows and mottling, minor grayish blue (5PB 5/2) mottling, and pyrite filled burrows. No color bands were seen.

SMEAR SLIDE SUMMARY (%):

	1, 100
	D
TEXTURE	
Sand	25
Silt	70
Clay	5
COMPOSITION	
Foraminifers	18
Nannofossils	80
Radiolarians	2

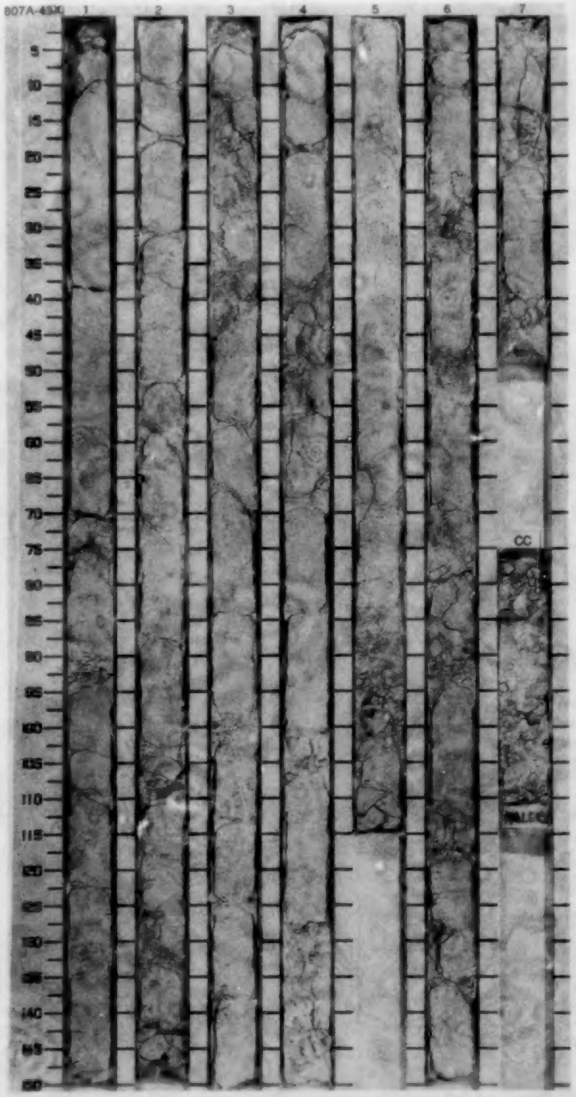
807A-45X
1
2
3
4
5
6
7
CC
5
10
15
20
25
30
35
40
45
50
55
60
65
70
75
80
85
90
95
100
105
110
115
120
125
130
135
140
145
150

SITE 807 HOLE A CORE 46X CORED INTERVAL 427.8-437.5 mbsf

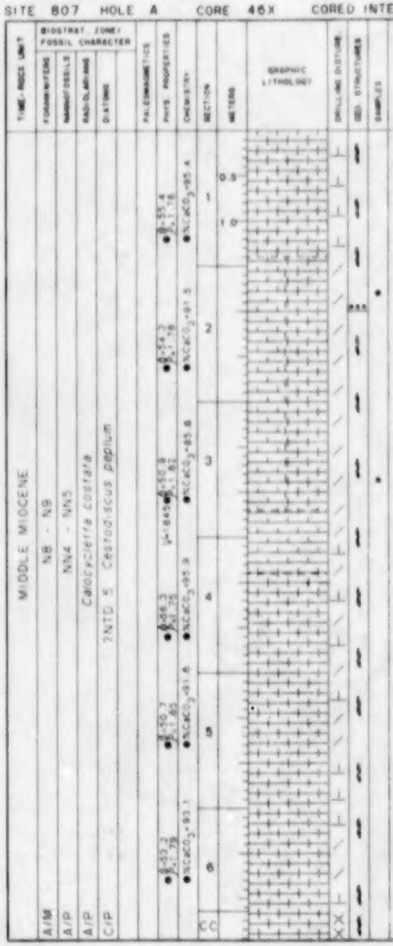
TIME-ROCK UNIT
BIOSTRAT. ZONE/ FOSSIL CHARACTER
FORAMINIFERS
NANNOFOSSILS
RADIOLARIANS
DIATOMS
PALEOMAGNETICS
PHYS. PROPERTIES
CHEMISTRY
SECTION
METERS
GRAPHIC LITHOLOGY
DRILLING DISTURB.
SED. STRUCTURES
SAMPLES
MIDDLE MIOCENE
A/M N8 - N9
A/P NN4 - NN5
A/P Calocycletta costata
C/P ?NTD 5 Cestodiscus peplum
φ=55.4 γ=1.76
φ=54.3 γ=1.78
Vp=1845 φ=50.9 γ=1.82
φ=56.3 γ=1.75
φ=50.7 γ=1.85
φ=53.2 γ=1.79
%CaCO3=95.4
%CaCO3=97.5
%CaCO3=85.6
%CaCO3=95.9
%CaCO3=91.6
%CaCO3=93.1
1
2
3
4
5
6
CC
0.5
1.0

LITHOLOGIC DESCRIPTION

FORAMINIFER NANNOFOSSIL CHALK

Major lithology: The predominant lithology in this core is white (2.5Y 8/0 and 5Y 8/1) FORAMINIFER NANNOFOSSIL CHALK, with a 7 cm thick, coarse grained, reddish gray (10R 6/1), graded bed located in Section 2. Heavy to slight bioturbation is indicated by white mottling on a 2 to 3 mm scale, and by single spots associated with pyritized burrows.

Minor lithology: Sections 2, 3 and 4 contain 10 to 50 cm thick beds of NANNOFOSSIL CHALK which grade into the major lithology. The sediment is white (2.5Y 8/0 and 5Y 8/1) and moderately bioturbated as indicated by white mottles and burrows, and by diffuse burrow associated pyritization.

SMEAR SLIDE SUMMARY (%):

	2, 30	3, 99
	D	D
TEXTURE:		
Sand	2	15
Silt	94	81
Clay	4	4
COMPOSITION:		
Foraminifers	4	35
Nannofossils	93	61
Radiolarians	1	2
Silicoflagellates	—	1
Spicules	2	1

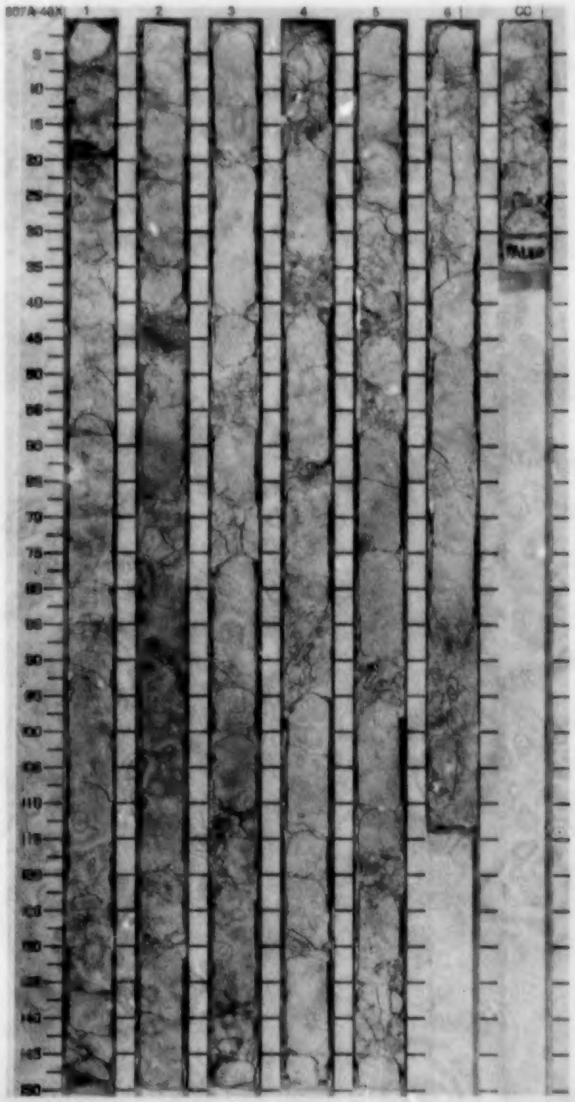
807A-46X
1
2
3
4
5
6
CC
5
10
15
20
25
30
35
40
45
50
55
60
65
70
75
80
85
90
95
100
105
110
115
120
125
130
135
140
145
150
PALEO

SITE 807 HOLE A CORE 47X CORED INTERVAL 437.5-447.1 mbsf

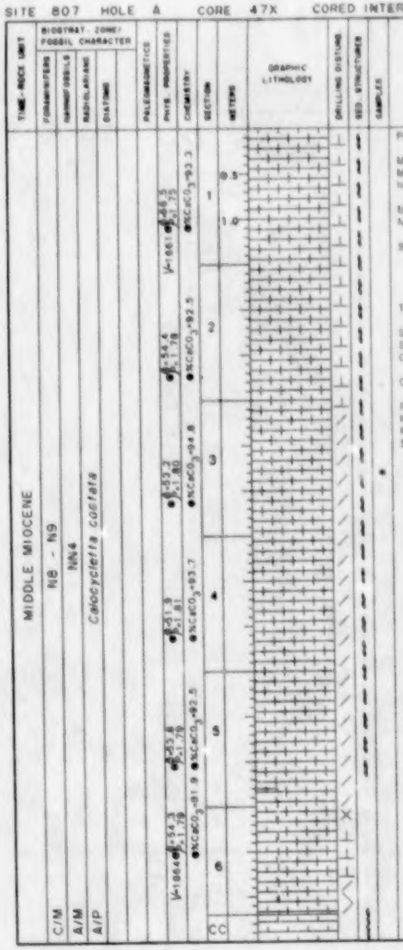
TIME-ROCK UNIT
BIOSTRAT. ZONE/ FOSSIL CHARACTER
FORAMINIFERS
NANNOFOSSILS
RADIOLARIANS
DIATOMS
PALEOMAGNETICS
PHYS. PROPERTIES
CHEMISTRY
SECTION
METERS
GRAPHIC LITHOLOGY
DRILLING DISTURB.
SED. STRUCTURES
SAMPLES
MIDDLE MIOCENE
N8 - N9
NN4
Calocycletta costata
C/M
A/M
A/P
γ-54.4
φ-56.5
ρ-1.75
V-1661
%CaCO3=93.3
%CaCO3=92.5
γ-54.4
ρ-1.76
γ-53.2
ρ-1.80
%CaCO3=94.8
γ-51.9
ρ-1.81
%CaCO3=93.7
γ-53.8
ρ-1.79
%CaCO3=92.5
%CaCO3=81.9
V-1864
γ-54.3
ρ-1.79
1
2
3
4
5
6
CC
0.5
1.0

LITHOLOGIC DESCRIPTION

FORAMINIFER NANNOFOSSIL CHALK

Major lithology: The major portion of the core contains white (10YR 8/0 and 5Y 8/1) FORAMINIFER NANNOFOSSIL CHALK. The upper 4 sections are homogeneous with minor horizontal, pyrite filled burrows. The entire core is moderately bioturbated.

Minor lithology: Below Section 5, 121 cm, 10 to 30 cm thick, white (5Y 8/1) intervals NANNOFOSSIL CHALK with FORAMINIFERS are interbedded with the major lithology.

SMEAR SLIDE SUMMARY (%):

	3, 80 D
TEXTURE:	
Sand	20
Silt	76
Clay	4
COMPOSITION:	
Foraminifers	35
Nannofossils	62
Radiolarians	1
Spicules	2

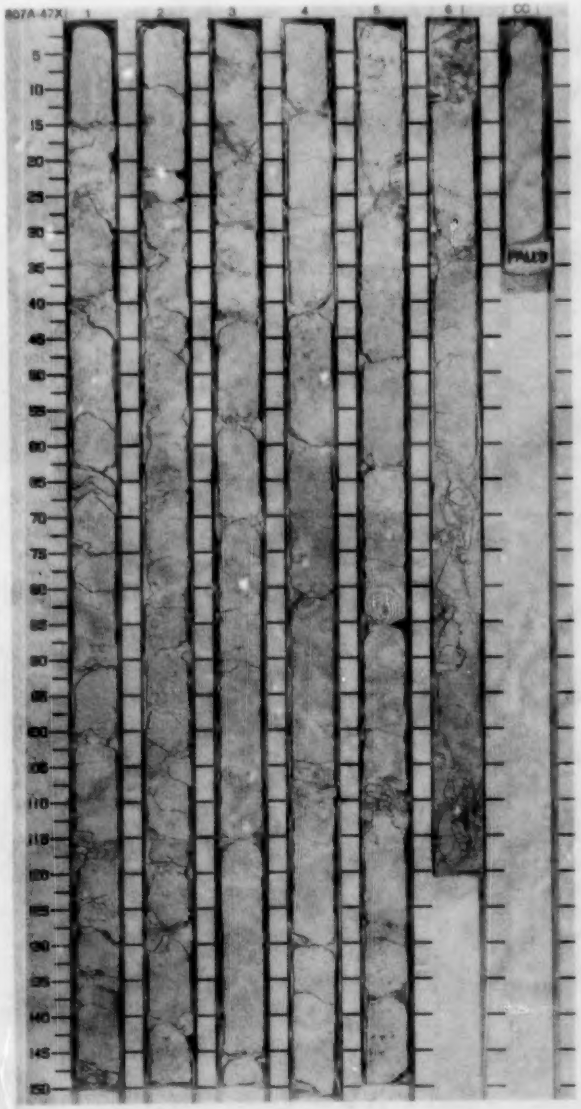
807A-47X
1
2
3
4
5
6
CC
5
10
15
20
25
30
35
40
45
50
55
60
65
70
75
80
85
90
95
100
105
110
115
120
125
130
135
140
145
150
PAL

SITE 807 HOLE A CORE 48X CORED INTERVAL 447.1-456.8 mbsf

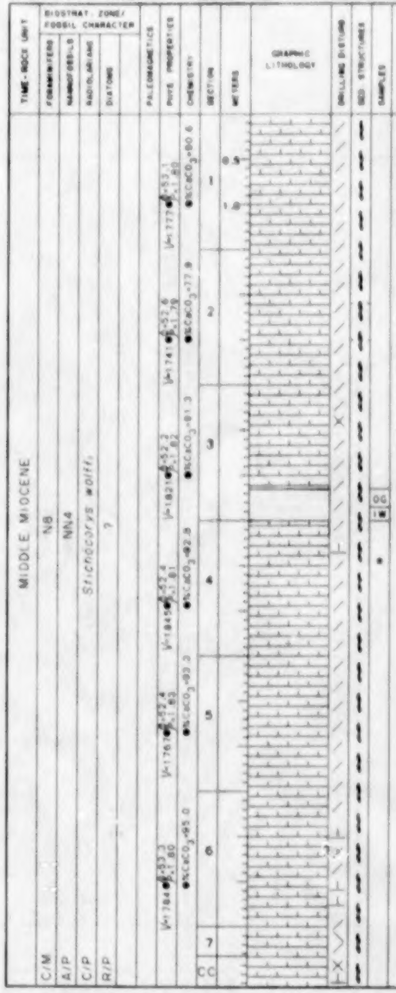
TIME-ROCK UNIT
BIOSTRAT. ZONE/ FOSSIL CHARACTER
FORAMINIFERS
NANNOFOSSILS
RADIOLARIANS
DIATOMS
PALEOMAGNETICS
PHYS. PROPERTIES
CHEMISTRY
SECTION
METERS
GRAPHIC LITHOLOGY
DRILLING DISTURB.
SED. STRUCTURES
SAMPLES
MIDDLE MIOCENE
N8
NN4
Stichocorys wolffi
?
C/M
A/P
C/P
R/P
V=1777 ●φ=53.1 γ=1.80
●%CaCO3=80.6
V=1741 ●φ=52.6 γ=1.79
●%CaCO3=77.8
V=1821 ●φ=52.2 γ=1.82
●%CaCO3=81.3
V=1845 ●φ=52.4 γ=1.81
●%CaCO3=82.8
V=1767 ●φ=52.4 γ=1.83
●%CaCO3=83.3
V=1784 ●φ=53.3 γ=1.80
●%CaCO3=85.0
1
2
3
4
5
6
7
CC
0.5
1.0
OG
IW
*

LITHOLOGIC DESCRIPTION

NANNOFOSSIL CHALK with FORAMINIFERS

Major lithology: This core contains white (5Y 8/1 and 10YR 8/1) NANNOFOSSIL CHALK with FORAMINIFERS. Bioturbation is heavy to slight throughout the core and decreases in intensity downcore. The bioturbation is generally expressed as simple horizontal burrow mottling, although a *Zoophycos* trace fossil is present in Section 1, and *Chondrites* is present in Section 4.

SMEAR SLIDE SUMMARY (%):

	4, 44
	D
TEXTURE	
Sand	10
Silt	86
Clay	4
COMPOSITION	
Foraminifers	15
Nannofossils	82
Radiolarians	1
Silicoflagellates	1
Spicules	1

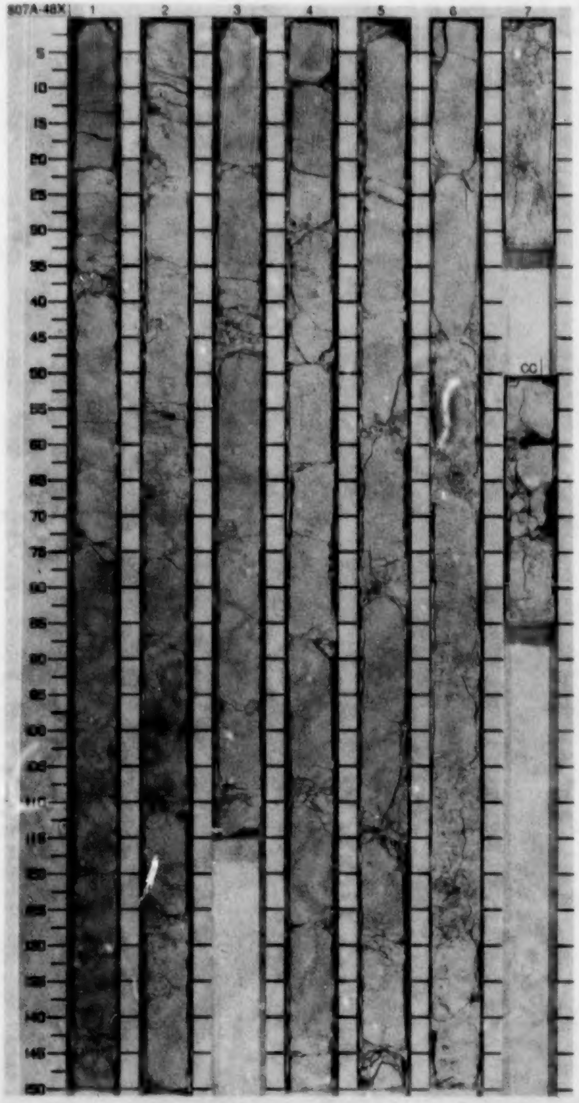
807A-48X
1
2
3
4
5
6
7
CC
5
10
15
20
25
30
35
40
45
50
55
60
65
70
75
80
85
90
95
100
105
110
115
120
125
130
135
140
145
150

SITE 807 HOLE A CORE 49X CORED INTERVAL 456.8-466.4 mbsf

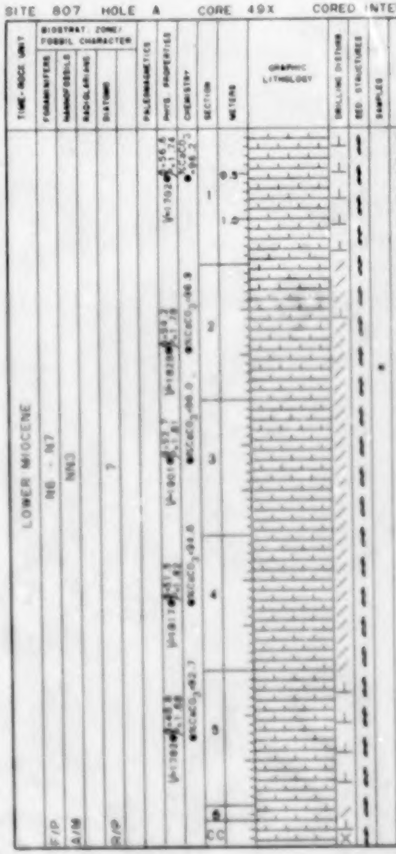
TIME-ROCK UNIT
BIOSTRAT. ZONE/ FOSSIL CHARACTER
FORAMINIFERS
NANNOFOSSILS
RADIOLARIANS
DIATOMS
PALEOMAGNETICS
PHYS. PROPERTIES
CHEMISTRY
SECTION
METERS
GRAPHIC LITHOLOGY
DRILLING DISTURB.
SED. STRUCTURES
SAMPLES
LOWER MIOCENE
N6 - N7
NN3
?
F/P
A/M
R/P
Vp=1702 ●φ=56.6 γ=1.74
%CaCO3 ●=96.2
●%CaCO3=96.9
●%CaCO3=90.0
●%CaCO3=94.6
●%CaCO3=92.7
1
2
3
4
5
6
CC
0.5
1.0

LITHOLOGIC DESCRIPTION

NANNOFOSSIL CHALK with FORAMINIFERS

Major lithology: This core contains white (10YR 8/1), moderately to heavily bioturbated NANNOFOSSIL CHALK with FORAMINIFERS.

SMEAR SLIDE SUMMARY (%):

	2, 116
	D
TEXTURE:	
Sand	9
Silt	85
Clay	6
COMPOSITION:	
Foraminifers	14
Nannofossils	85
Radiolarians	Tr
Siliceous fragments	1
Silicoflagellates	Tr

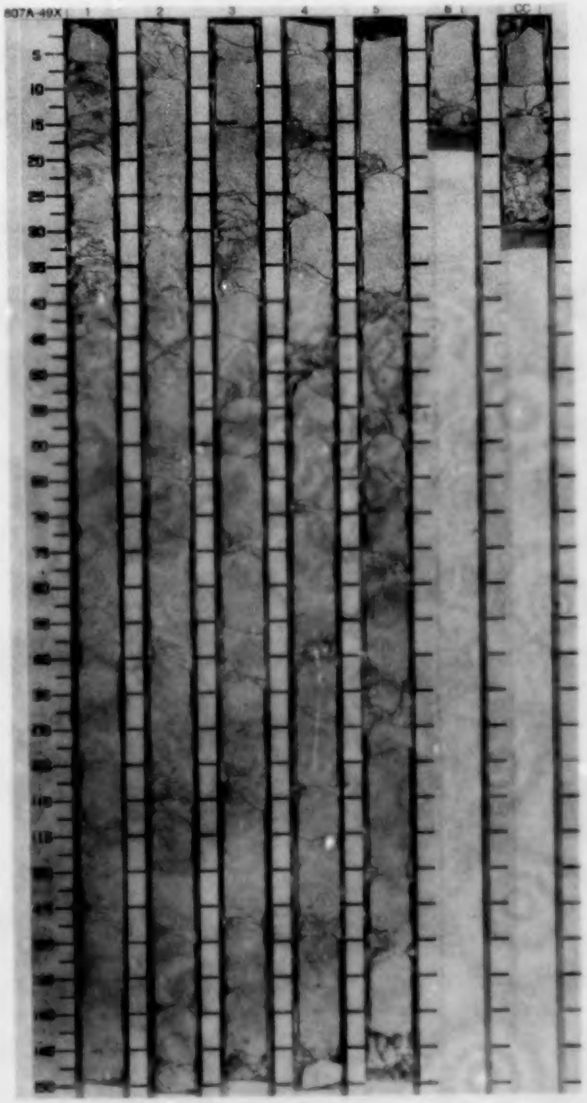
807A-49X
1
2
3
4
5
6
CC
5
10
15
20
25
30
35
40
45
50
55
60
65
70
75
80
85
90
95
100
105
110
115
120
125
130
135
140
145
150

SITE 807 HOLE A CORE 50X CORED INTERVAL 466.4-476.1 mbsf

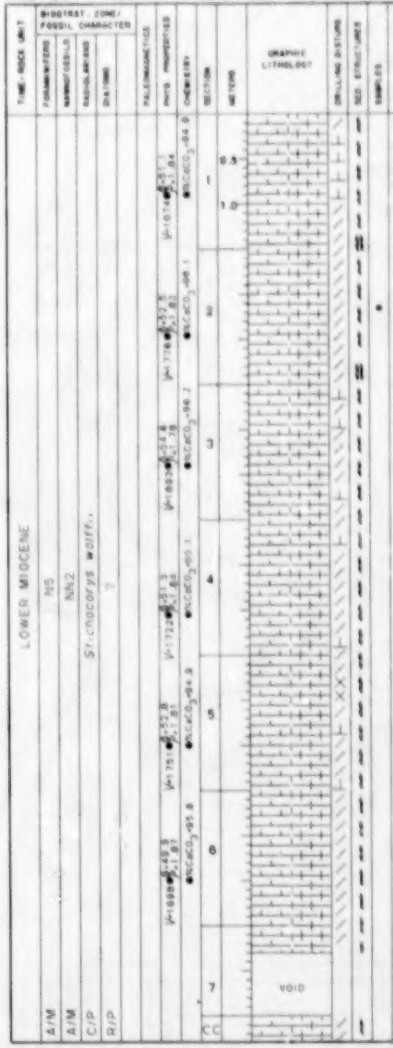
TIME-ROCK UNIT
BIOSTRAT. ZONE/ FOSSIL CHARACTER
FORAMINIFERS
NANNOFOSSILS
RADIOLARIANS
DIATOMS
PALEOMAGNETICS
PHYS. PROPERTIES
CHEMISTRY
SECTION
METERS
GRAPHIC LITHOLOGY
DRILLING DISTURB.
SED. STRUCTURES
SAMPLES
LOWER MIOCENE
A/M
N5
A/M
NN2
C/P
Stichocorys wolffii
R/P
?
γ=1074 φ=61.1 ρ=1.84
%CaCO3=84.9
γ=1778 φ=52.5 ρ=1.82
%CaCO3=86.1
γ=1603 φ=54.4 ρ=1.78
%CaCO3=86.2
γ=1722 φ=51.3 ρ=1.84
%CaCO3=85.1
γ=1751 φ=52.8 ρ=1.81
%CaCO3=84.9
γ=1688 φ=48.5 ρ=1.87
%CaCO3=85.8
1
2
3
4
5
6
7
CC
0.5
1.0
VOID

LITHOLOGIC DESCRIPTION

NANNOFOSSIL CHALK with FORAMINIFERS to FORAMINIFER NANNOFOSSIL CHALK

Major lithology: This core contains white (2.5Y 8/0, 5Y 8/1 and 10YR 8/0) NANNOFOSSIL CHALK with FORAMINIFERS to FORAMINIFER NANNOFOSSIL CHALK. It is moderately bioturbated with faint white mottling, mm to cm size burrows, and a few pale purple (5P 6/2) pyritized burrows.

SMEAR SLIDE SUMMARY (%):

	2, 88
	D
TEXTURE:	
Sand	15
Silt	80
Clay	5
COMPOSITION:	
Foraminifers	25
Nannofossils	73
Radiolarians	1
Siliceous fragments	1
Silicoflagellates	Tr

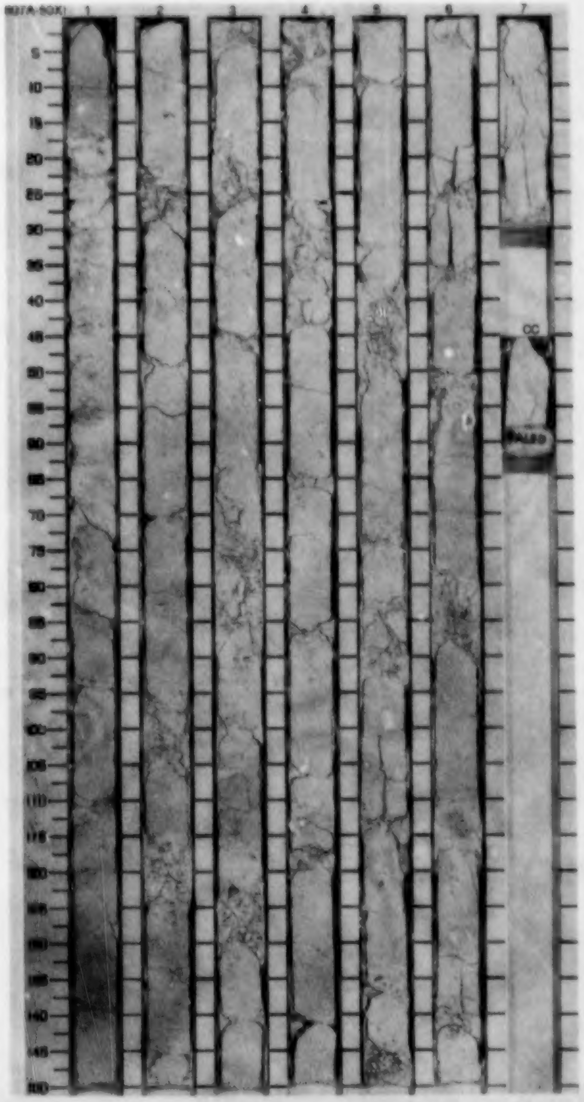
807A-50X
1
2
3
4
5
6
7
CC
PALEO
5
10
15
20
25
30
35
40
45
50
55
60
65
70
75
80
85
90
95
100
105
110
115
120
125
130
135
140
145
150

SITE 807 HOLE A CORE 51X CORED INTERVAL 476.1-485.8 mbsf

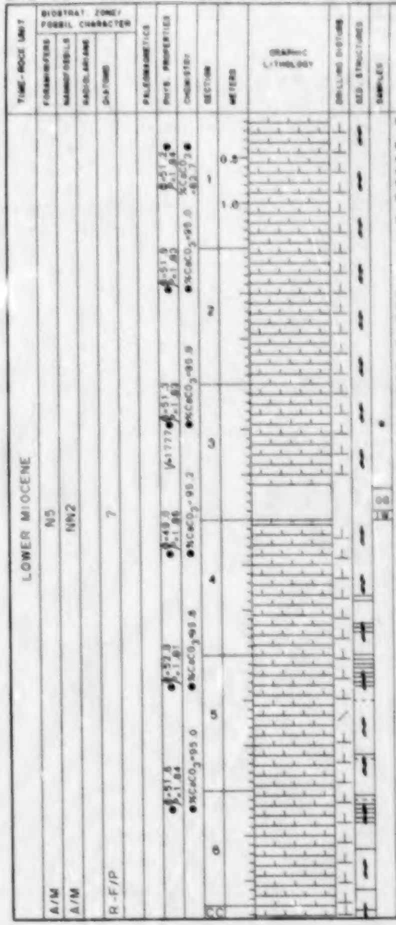
TIME-ROCK UNIT
BIOSTRAT. ZONE/ FOSSIL CHARACTER
FORAMINIFERS
NANNOFOSSILS
RADIOLARIANS
DIATOMS
PALEOMAGNETICS
PHYS. PROPERTIES
CHEMISTRY
SECTION
METERS
GRAPHIC LITHOLOGY
DRILLING DISTURB.
SED. STRUCTURES
SAMPLES
LOWER MIOCENE
N5
NN2
?
A/M
A/M
R-F/P
φ=51.2
ρ=1.84
%CaCO3=83.7
%CaCO3=95.0
φ=51.8
ρ=1.83
%CaCO3=95.9
Vp=1777
φ=51.3
ρ=1.83
%CaCO3=95.2
φ=48.8
ρ=1.86
%CaCO3=95.8
φ=52.8
ρ=1.81
%CaCO3=95.0
φ=51.6
ρ=1.84
1
2
3
4
5
6
CC
0.5
1.0
OG
IW

LITHOLOGIC DESCRIPTION

NANNOFOSSIL CHALK with FORAMINIFERS

Major lithology: This core contains white (10YR 8/0 and 2.5Y 8/0) NANNOFOSSIL CHALK with FORAMINIFERS. Moderate bioturbation is indicated by faint mottling in various shades of white. Single, small (mm size) grayish blue (5PB 5/2) pyritized burrows are present. From the lower half of Section 4 to the base of the core, mm-size distinct, and cm-size diffuse light gray (N7) to gray (N5) color bands are common.

SMEAR SLIDE SUMMARY (%):

	3, 44
	D
TEXTURE:	
Sand	25
Silt	70
Clay	5
COMPOSITION:	
Foraminifers	22
Nannofossils	75
Radiolarians	3

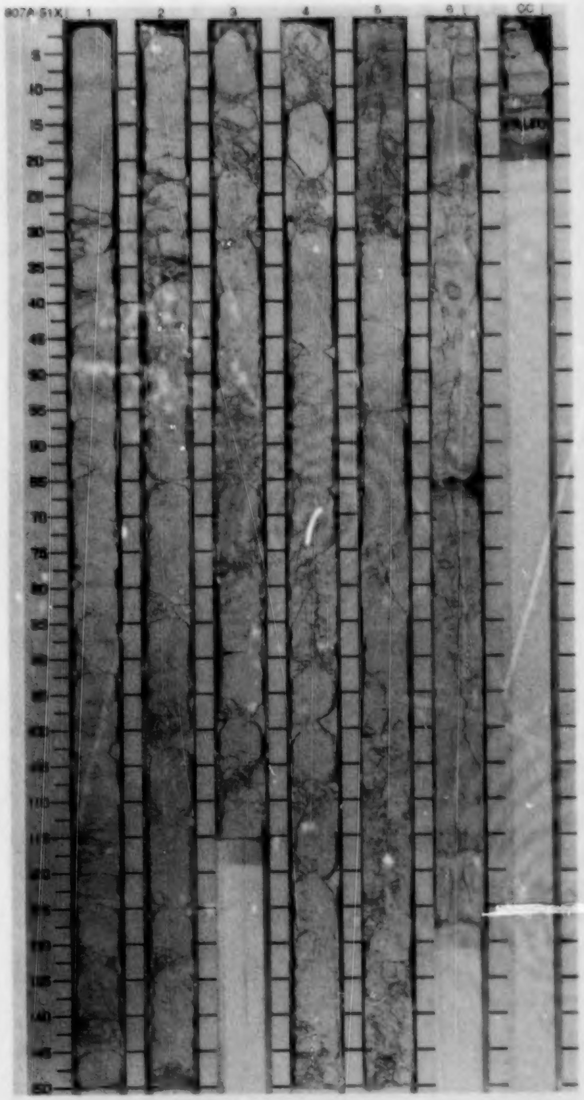
807A 51X
1
2
3
4
5
6
CC
5
10
15
20
25
30
35
40
45
50
55
60
65
70
75
80
85
90
95
100
105
110
115
120
125
130
135
140
145
150

SITE 807 HOLE A CORE 52X CORED INTERVAL 485.8-495.4 mbsf

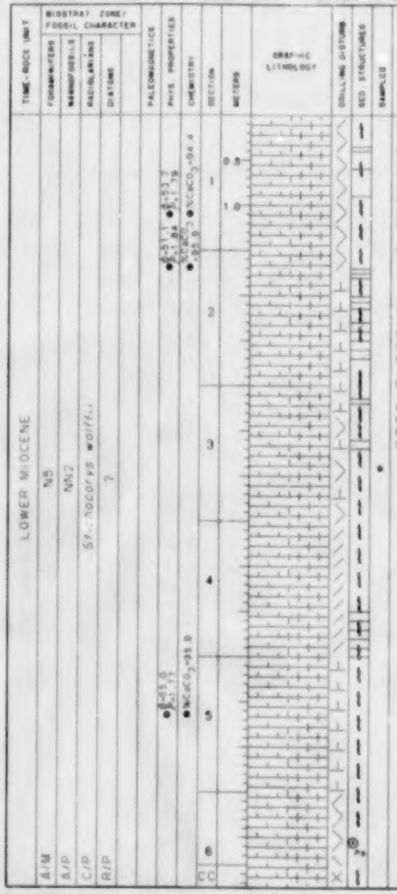
TIME-ROCK UNIT
BIOSTRAT. ZONE/ FOSSIL CHARACTER
FORAMINIFERS
NANNOFOSSILS
RADIOLARIANS
DIATOMS
PALEOMAGNETICS
PHYS. PROPERTIES
CHEMISTRY
SECTION
METERS
GRAPHIC LITHOLOGY
DRILLING DISTURB.
SED. STRUCTURES
SAMPLES
LOWER MIOCENE
N5
NN2
St. nocorys wolffii
?
A/M
A/P
C/P
R/P
φ=51.1
ρ=1.84
φ=53.7
ρ=1.79
%CaCO3=95.8
%CaCO3=94.4
φ=53.0
ρ=1.77
%CaCO3=95.8
1
2
3
4
5
6
CC
0.5
1.0
Pg

LITHOLOGIC DESCRIPTION

NANNOFOSSIL CHALK with FORAMINIFERS to FORAMINIFER NANNOFOSSIL CHALK

Major lithology: This core contains slightly to heavily bioturbated, white (2.5Y 8/0 and 10YR 8/0) NANNOFOSSIL CHALK with FORAMINIFERS to FORAMINIFER NANNOFOSSIL CHALK. Pyrite-filled burrows give rise to a grayish blue (5PB 5/2) hue for the lower 10 cm of Section 2 and to a pale purple (5PB 7/2) hue in the lower 40 cm of Section 3. A single distinct, greenish gray (5G 6/1) color band and several mm to cm size diffuse light greenish gray (5G 7/1) bands are present. A 2 to 3 cm diameter porcellanite nodule is located in Section 6, 60 cm.

SMEAR SLIDE SUMMARY (%):

	3, 91
	D
TEXTURE	
Sand	10
Silt	85
Clay	5
COMPOSITION	
Foraminifers	25
Nannofossils	73
Radiolarians	1
Silicoflagellates	1

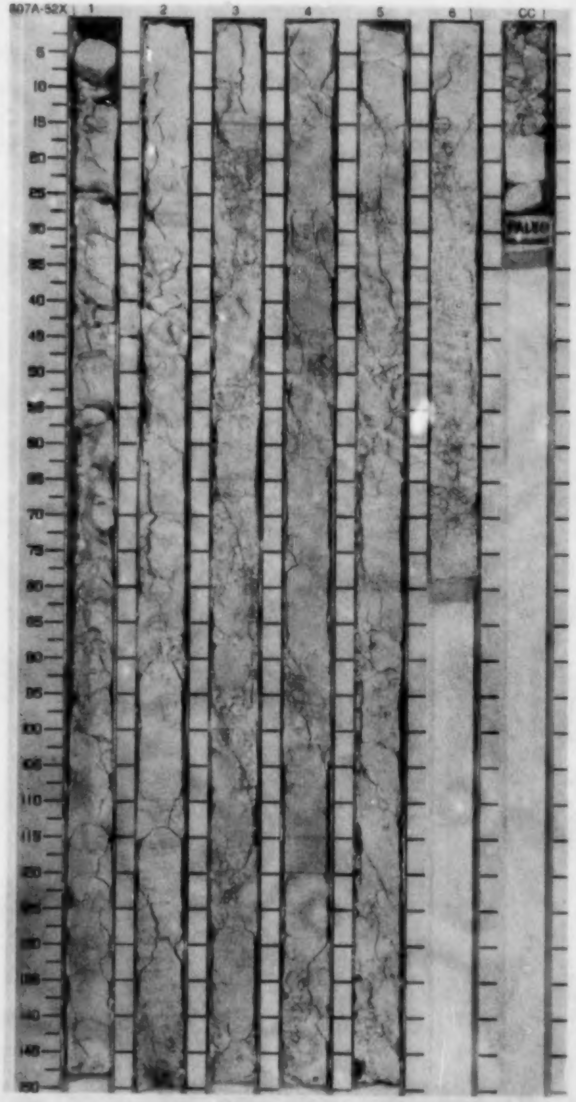
807A-52X
1
2
3
4
5
6
CC
5
10
15
20
25
30
35
40
45
50
55
60
65
70
75
80
85
90
95
100
105
110
115
120
125
130
135
140
145
150
PALEO

SITE 807 HOLE A CORE 53X CORED INTERVAL 495.4-505.1 mbsf

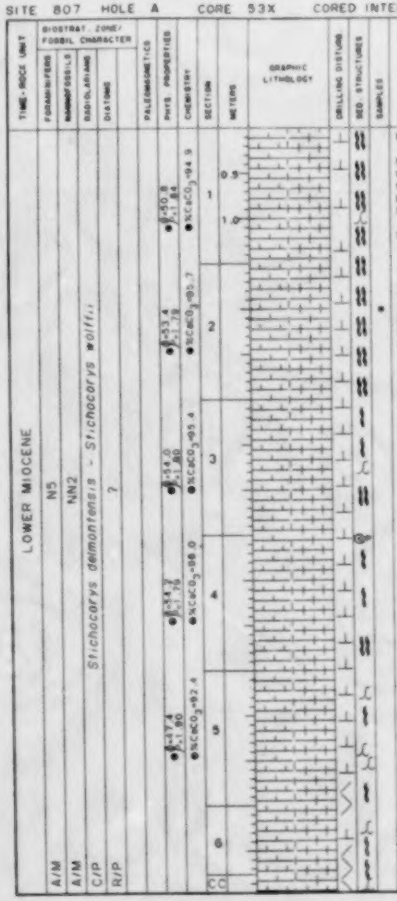
TIME-ROCK UNIT
BIOSTRAT. ZONE/ FOSSIL CHARACTER
FORAMINIFERS
NANNOFOSSILS
RADIOLARIANS
DIATOMS
PALEOMAGNETICS
PHYS. PROPERTIES
CHEMISTRY
SECTION
METERS
GRAPHIC LITHOLOGY
DRILLING DISTURB.
SED. STRUCTURES
SAMPLES
LOWER MIOCENE
N5
NN2
Stichocorys delmontensis - Stichocorys wolffii
?
A/M
A/M
C/P
R/P
φ=50.8
γ=1.84
φ=53.4
γ=1.79
φ=54.0
γ=1.80
φ=54.2
γ=1.76
φ=47.4
γ=1.90
%CaCO3=94.9
%CaCO3=95.7
%CaCO3=95.4
%CaCO3=98.0
%CaCO3=92.4
1
2
3
4
5
6
CC
0.5
1.0

LITHOLOGIC DESCRIPTION

FORAMINIFER NANNOFOSSIL CHALK to NANNOFOSSIL CHALK with FORAMINIFERS

Major lithology: This core contains white (2.5Y 8/0) FORAMINIFER NANNOFOSSIL CHALK to NANNOFOSSIL CHALK with FORAMINIFERS. In Sections 1 through 4, moderate to heavy bioturbation is indicated by abundant mottles and grayish blue (5PB 5/2) pyrite filled burrows. In Sections 5 through CC, only a few signs of bioturbation are visible. Sections 3, 5, 6 and CC have several zones (a few cm thick) of light gray (5Y 7/1) flaser structures.

SMEAR SLIDE SUMMARY (%):

	2, 90 D
TEXTURE:	
Sand	30
Silt	65
Clay	5
COMPOSITION:	
Foraminifers	25
Nannofossils	70
Radiolarians	4
Silicoflagellates	Tr
Spicules	Tr

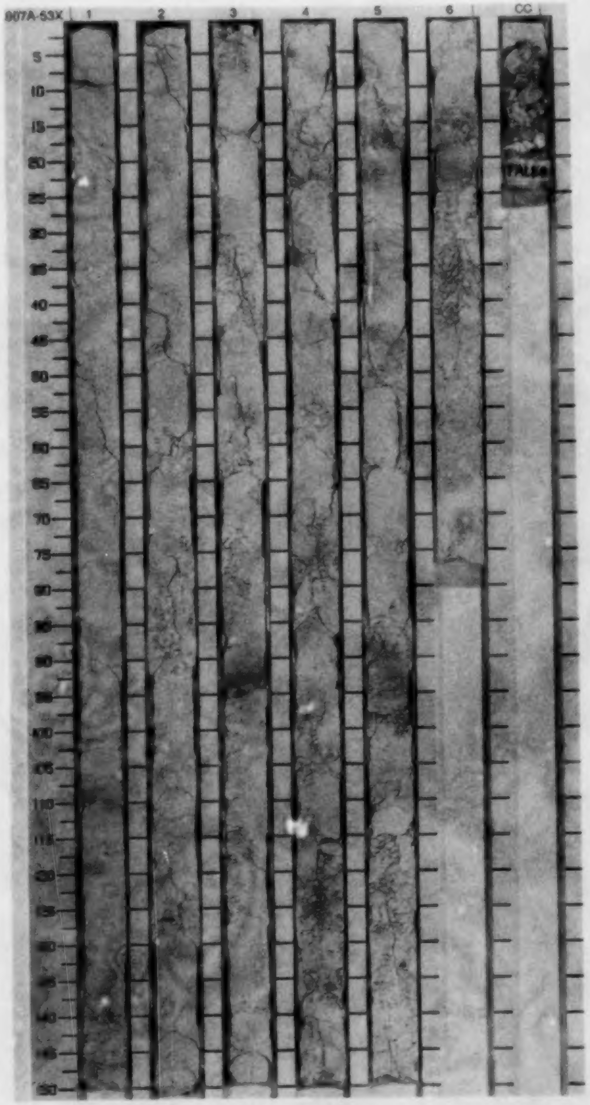
807A-53X
1
2
3
4
5
6
CC
5
10
15
20
25
30
35
40
45
50
55
60
65
70
75
80
85
90
95
100
105
110
115
120
125
130
135
140
145
150

SITE 807 HOLE A CORE 54X CORED INTERVAL 505.1-514.8 mbsf

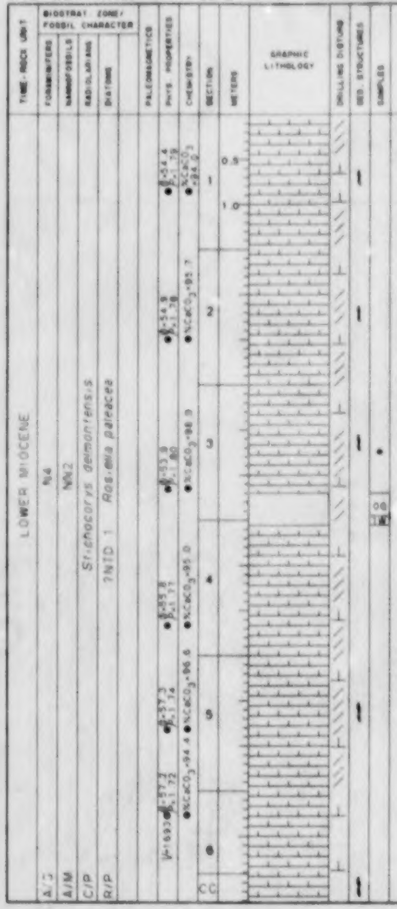
TIME-ROCK UNIT
BIOSTRAT. ZONE/ FOSSIL CHARACTER
FORAMINIFERS
NANNOFOSSILS
RADIOLARIANS
DIATOMS
PALEOMAGNETICS
PHYS. PROPERTIES
CHEMISTRY
SECTION
METERS
GRAPHIC LITHOLOGY
DRILLING DISTURB.
SED. STRUCTURES
SAMPLES
LOWER MIOCENE
N4
NN2
Stichocorys delmontensis
?NTD 1 Rossiella paleacea
A/G
A/M
C/P
R/P
ϕ=54.4 γ=1.79
%CaCO3=94.0
ϕ=54.9 γ=1.78
%CaCO3=95.7
ϕ=53.9 γ=1.80
%CaCO3=98.0
ϕ=55.8 γ=1.77
%CaCO3=95.0
ϕ=57.3 γ=1.74
%CaCO3=96.6
V=1693 ϕ=57.2 γ=1.72
%CaCO3=94.4
1
2
3
4
5
6
CC
0.5
1.0
OG

LITHOLOGIC DESCRIPTION

NANNOFOSSIL CHALK with FORAMINIFERS

Major lithology: This core contains white (2.5Y 8/0) NANNOFOSSIL CHALK with FORAMINIFERS. There are occasional faser structures observed as braided color bands. Bioturbation is slight, with only a few disseminated pyrite specks in the core; otherwise the core is structureless.

SMEAR SLIDE SUMMARY (%):

	3, 74
	D
TEXTURE:	
Sand	12
Silt	60
Clay	28
COMPOSITION:	
Accessory minerals	2
Foraminifers	20
Nannofossils	75
Radiolarians	Tr
Siliceous fragments	3
Silicoflagellates	Tr

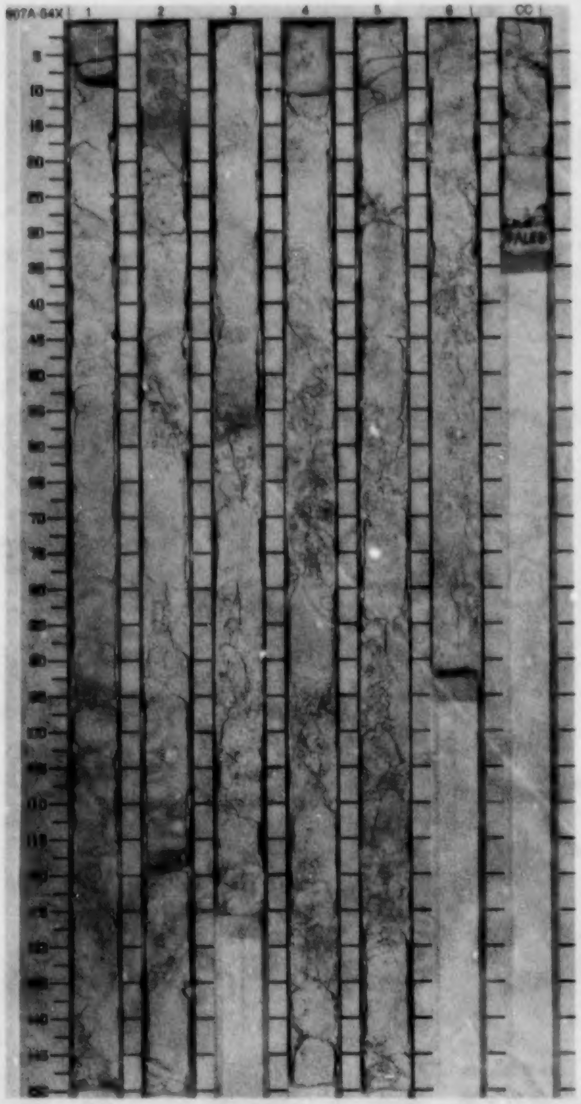
807A-54X
1
2
3
4
5
6
CC
5
10
15
20
25
30
35
40
45
50
55
60
65
70
75
80
85
90
95
100
105
110
115
120
125
130
135
140
145
150
PALEO

SITE 807 HOLE A CORE 55X CORED INTERVAL 514.8-524.0 mbsf

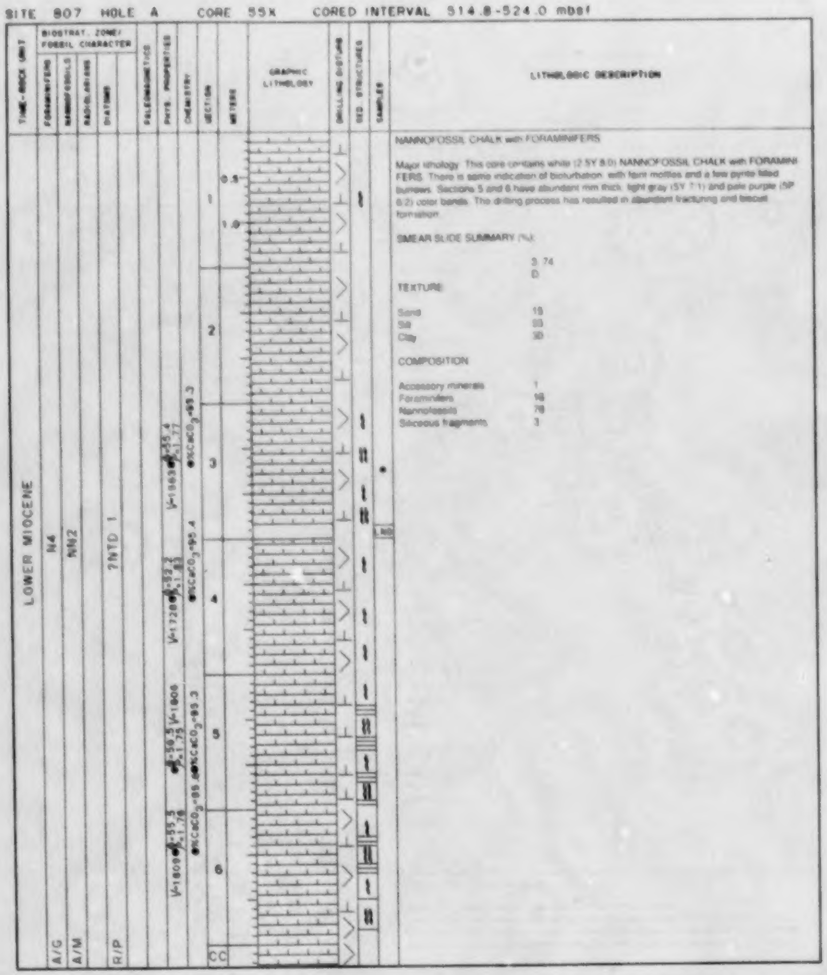
TIME-ROCK UNIT
BIOSTRAT. ZONE/FOSSIL CHARACTER
FORAMINIFERS
NANNOFOSSILS
RADIOLARIANS
DIATOMS
PALEOMAGNETICS
PHYS. PROPERTIES
CHEMISTRY
SECTION
METERS
GRAPHIC LITHOLOGY
DRILLING DISTURB.
SED. STRUCTURES
SAMPLES
LOWER MIOCENE
N4
A/G
NN2
A/M
?NTD 1
R/P
V=1863 φ=55.4 ρ=1.77
V=1720 φ=53.2 ρ=1.83
V=1806 φ=56.5 ρ=1.75
V=1808 φ=55.5 ρ=1.76
%CaCO3=93.3
%CaCO3=95.4
%CaCO3=88.8 %CaCO3=93.3
1
2
3
4
5
6
CC
0.5
1.0
LAG

LITHOLOGIC DESCRIPTION

NANNOFOSSIL CHALK with FORAMINIFERS

Major lithology: This core contains white (2.5Y 8.0) NANNOFOSSIL CHALK with FORAMINIFERS. There is some indication of bioturbation, with faint mottles and a few pyrite filled burrows. Sections 5 and 6 have abundant mm thick, light gray (5Y 7/1) and pale purple (5P 6/2) color bands. The drilling process has resulted in abundant fracturing and biscuit formation.

SMEAR SLIDE SUMMARY (%):

	3, 74
	D
TEXTURE	
Sand	15
Silt	55
Clay	30
COMPOSITION	
Accessory minerals	1
Foraminifers	16
Nannofossils	78
Siliceous fragments	3

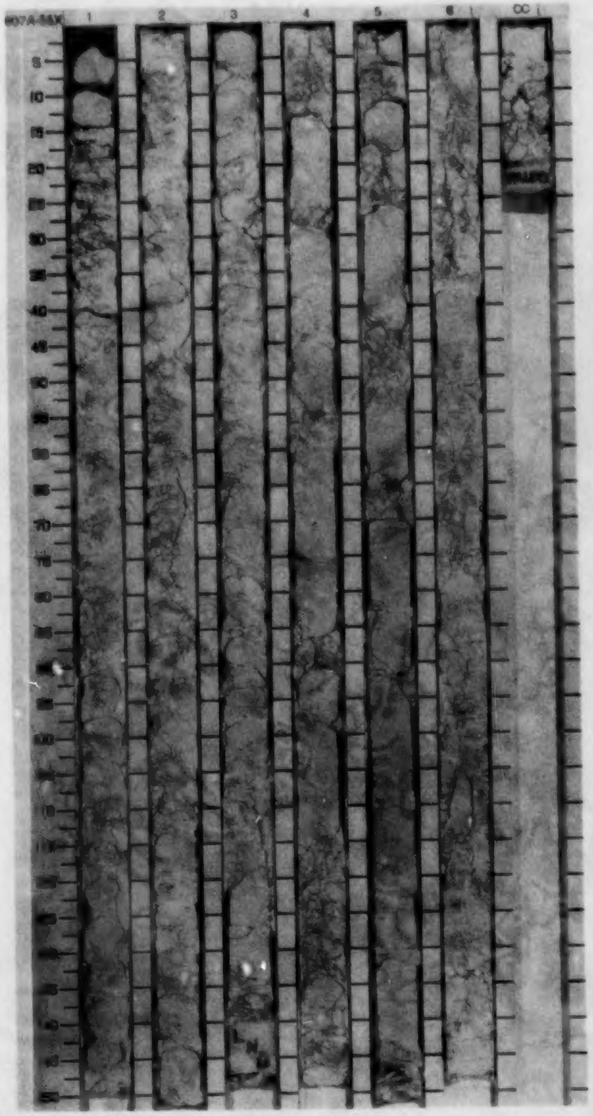
807A-55X
1
2
3
4
5
6
CC
5
10
15
20
25
30
35
40
45
50
55
60
65
70
75
80
85
90
95
100
105
110
115
120
125
130
135
140
145
150

SITE 807 HOLE A CORE 56X CORED INTERVAL 524.0-533.7 mbsf

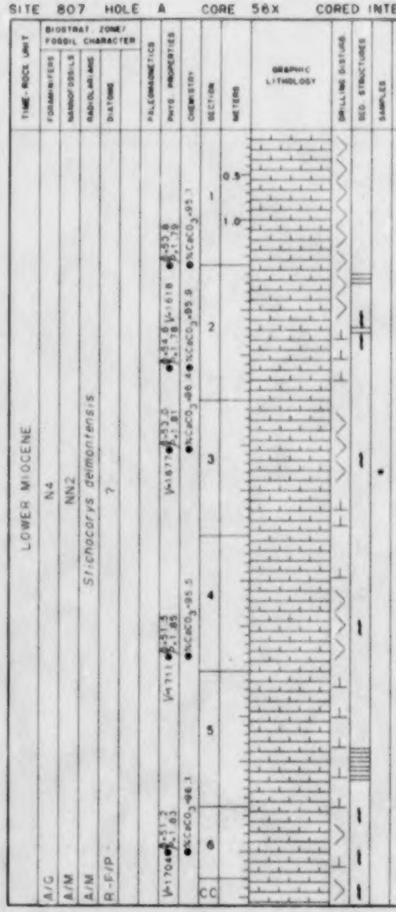
TIME-ROCK UNIT
BIOSTRAT. ZONE/ FOSSIL CHARACTER
FORAMINIFERS
NANNOFOSSILS
RADIOLARIANS
DIATOMS
PALEOMAGNETICS
PHYS. PROPERTIES
CHEMISTRY
SECTION
METERS
GRAPHIC LITHOLOGY
DRILLING DISTURB.
SED. STRUCTURES
SAMPLES
LOWER MIOCENE
A/G
N4
A/M
NN2
A/M
Stichocorys delmontensis
R-F/P
?
φ=53.8
ρ=1.79
V=1618
φ=54.6
ρ=1.78
V=1677
φ=53.0
ρ=1.81
V=1711
φ=51.3
ρ=1.85
V=1704
φ=51.2
ρ=1.83
%CaCO3=95.1
%CaCO3=95.9
%CaCO3=96.4
%CaCO3=95.5
%CaCO3=96.1
1
2
3
4
5
6
CC
0.5
1.0

LITHOLOGIC DESCRIPTION

NANNOFOSSIL CHALK

Major lithology: This core contains white (2.5Y 8/0) NANNOFOSSIL CHALK. It is relatively structureless with only a few intervals showing bioturbation structures (mottles and pyrite filled burrows), and some pale pink (5RP 8/2) intervals with frequent, fine scale (< 1 mm) white color banding. Drilling disturbance is moderate to heavy.

SMEAR SLIDE SUMMARY (%):

	3, 79
	D
TEXTURE	
Sand	5
Silt	75
Clay	20
COMPOSITION	
Foraminifers	5
Nannofossils	95
Radiolarians	Tr
Siliceous fragments	Tr

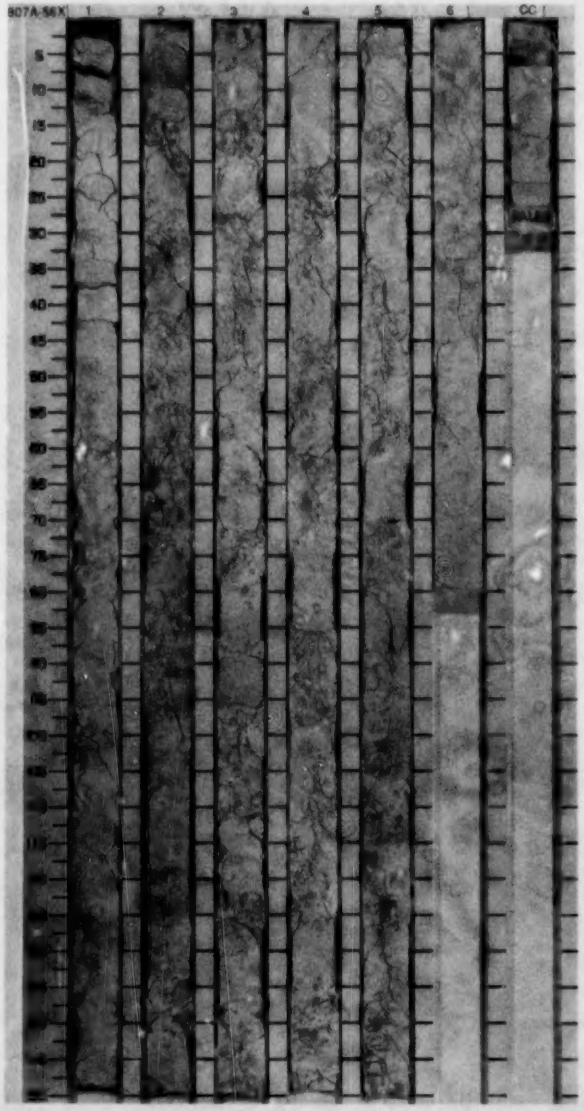
807A-56X
1
2
3
4
5
6
CC

SITE 807 HOLE A CORE 57X CORED INTERVAL 533.7-543.4 mbsf

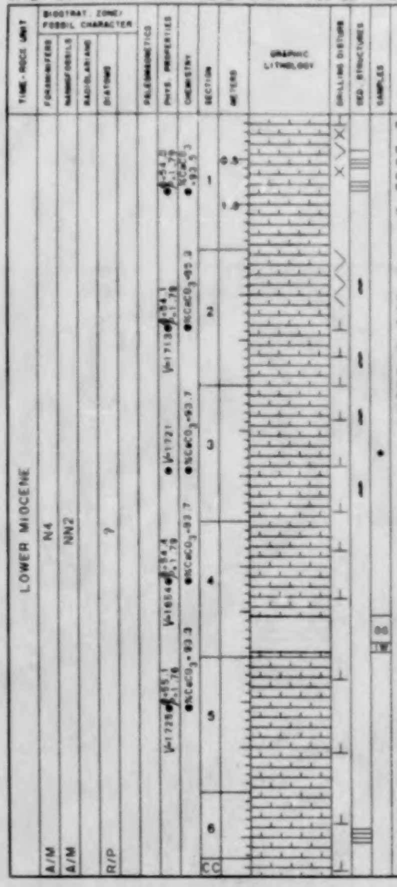
TIME-ROCK UNIT
BIOSTRAT. ZONE/ FOSSIL CHARACTER
FORAMINIFERS
NANNOFOSSILS
RADIOLARIANS
DIATOMS
PALEOMAGNETICS
PHYS. PROPERTIES
CHEMISTRY
SECTION
METERS
GRAPHIC LITHOLOGY
DRILLING DISTURB.
SED. STRUCTURES
SAMPLES
LOWER MIOCENE
N4
NN2
?
A/M
A/M
R/P
φ-54.2
γ-1.79
%CaCO3-93.5
φ-54.1
γ-1.78
Vp-1713
%CaCO3-93.3
Vp-1721
%CaCO3-93.7
φ-54.4
γ-1.79
Vp-1654
%CaCO3-93.7
φ-55.1
γ-1.76
Vp-1728
%CaCO3-93.3
1
2
3
4
5
6
CC
0.5
1.0
OG
IW

LITHOLOGIC DESCRIPTION

NANNOFOSSIL CHALK with FORAMINIFERS

Major lithology: This core contains white (2.5Y 8/0) NANNOFOSSIL CHALK with FORAMINIFERS. The chalk is predominantly homogeneous. A few 20 to 40 cm thick intervals are pale pink (5RP 8/2) and exhibit very fine-scale (1 mm) greenish gray (5G 7/1), pale purple (5P 8/2), and white (2.5Y 8/0) color bands. Bioturbation appears to be minor.

SMEAR SLIDE SUMMARY (%):

	3, 75
	D
TEXTURE:	
Sand	5
Silt	80
Clay	15
COMPOSITION:	
Diatoms	Tr
Foraminifers	20
Nannofossils	77
Siliceous fragments	3

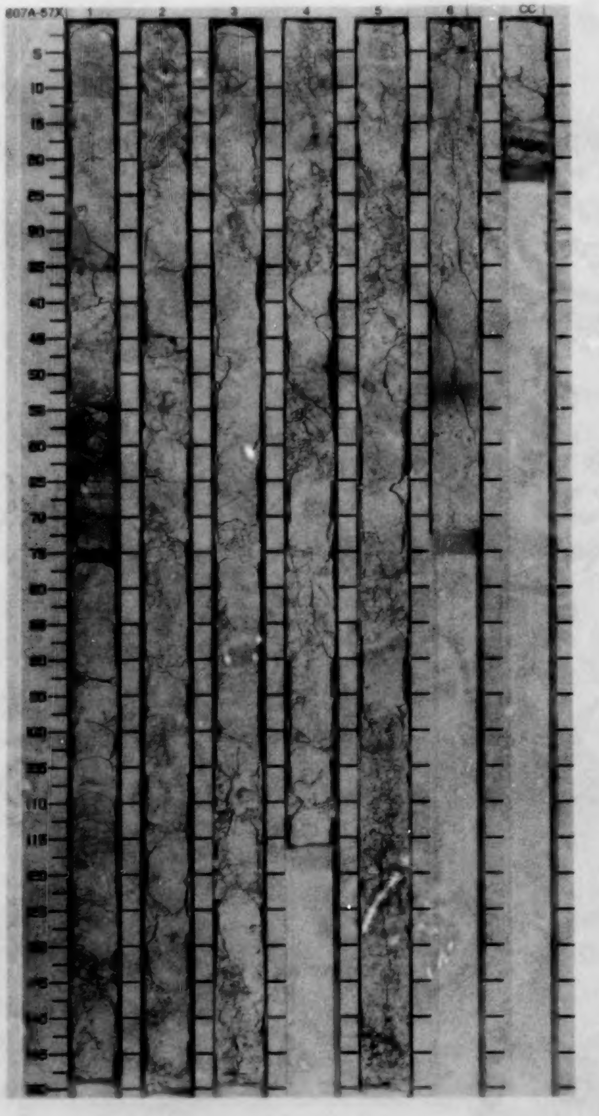
807A-57X
1
2
3
4
5
6
CC
5
10
15
20
25
30
35
40
45
50
55
60
65
70
75
80
85
90
95
100
105
110
115
120
125
130
135
140
145
150

SITE 807 HOLE A CORE 58X CORED INTERVAL 543.4-553.0 mbsf

TIME-ROCK UNIT	BIOSTRAT. ZONE/ FOSSIL CHARACTER FORAMINIFERS	NANNOFOSSILS	RADIOLARIANS	DIATOMS		PALEOMAGNETICS	PHYS. PROPERTIES	CHEMISTRY	SECTION	METERS	GRAPHIC LITHOLOGY	DRILLING DISTURB.	SED. STRUCTURES	SAMPLES
LOWER MIOCENE	N4	NN2	*Stichocorys delmontensis*	?			γ=1.71 ●ϕ=53.8 P=1.79	●%$CaCO_3$=96.0	1	0.5 1.0			⊙	
							γ=1.71 ●ϕ=55.2 P=1.79	●%$CaCO_3$=96.0	2					
							γ=1.69 ●ϕ=55.1 P=1.79	●%$CaCO_3$=95.5	3					●
							γ=1.68 ●ϕ=54.5 P=1.80	●%$CaCO_3$=95.0	4					
									5					
	A/G	A/M	C/P	F-C/P					CC					

LITHOLOGIC DESCRIPTION

NANNOFOSSIL CHALK with FORAMINIFERS

Major lithology: This core contains homogeneous, white (2.5Y 8/0) NANNOFOSSIL CHALK with FORAMINIFERS. The basal 10 cm of Sections 4 and 5 are pale pink (5RP 6/2) in color. One thin (1 mm) bluish gray color band is present above the pale pink interval in Section 5. There is very little evidence of bioturbation.

SMEAR SLIDE SUMMARY (%):

	3, 75 D
TEXTURE:	
Sand	10
Silt	60
Clay	30
COMPOSITION:	
Foraminifers	12
Nannofossils	88
Radiolarians	Tr
Siliceous fragments	Tr

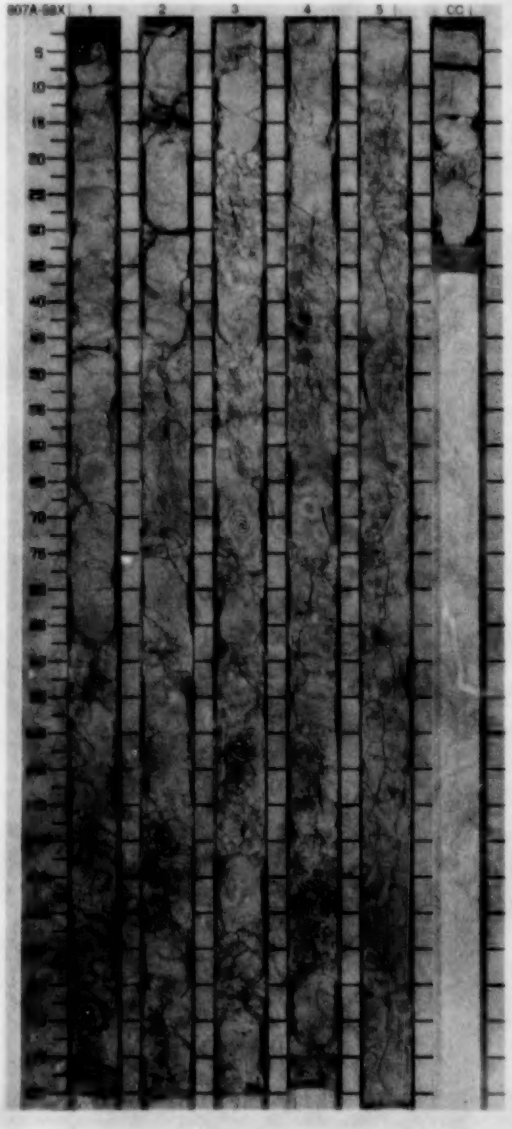

SITE 807 HOLE A CORE 59X CORED INTERVAL 553.0-562.8 mbsf

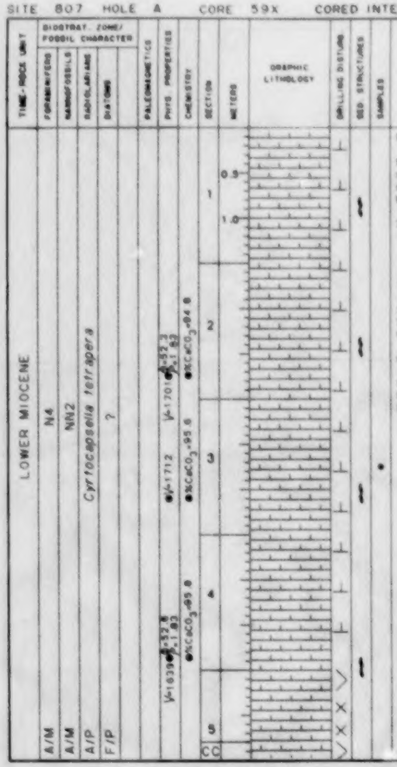
TIME-ROCK UNIT
BIOSTRAT. ZONE/ FOSSIL CHARACTER
FORAMINIFERS
NANNOFOSSILS
RADIOLARIANS
DIATOMS
PALEOMAGNETICS
PHYS. PROPERTIES
CHEMISTRY
SECTION
METERS
GRAPHIC LITHOLOGY
DRILLING DISTURB.
SED. STRUCTURES
SAMPLES
LOWER MIOCENE
N4
NN2
Cyrtocapsella tetrapera
?
A/M
A/M
A/P
F/P
V=1701
φ=52.3
γ=1.82
V=1712
V=1639
φ=52.8
γ=1.83
%CaCO3=84.8
%CaCO3=95.6
%CaCO3=95.8
0.5
1.0
1
2
3
4
5
CC

LITHOLOGIC DESCRIPTION

NANNOFOSSIL CHALK with FORAMINIFERS

Major lithology: This core contains homogeneous white (2.5Y 8/0) NANNOFOSSIL CHALK with FORAMINIFERS. A few intervals of pale pink (5RP 8/2) and light gray (2.5Y 7/0) sediment are noted. Evidence of bioturbation is scarce and consists of a few pyritized burrows.

SMEAR SLIDE SUMMARY (%):

	3, 75 D
TEXTURE:	
Sand	5
Silt	75
Clay	20
COMPOSITION:	
Foraminifers	10
Nannofossils	89
Siliceous fragments	1

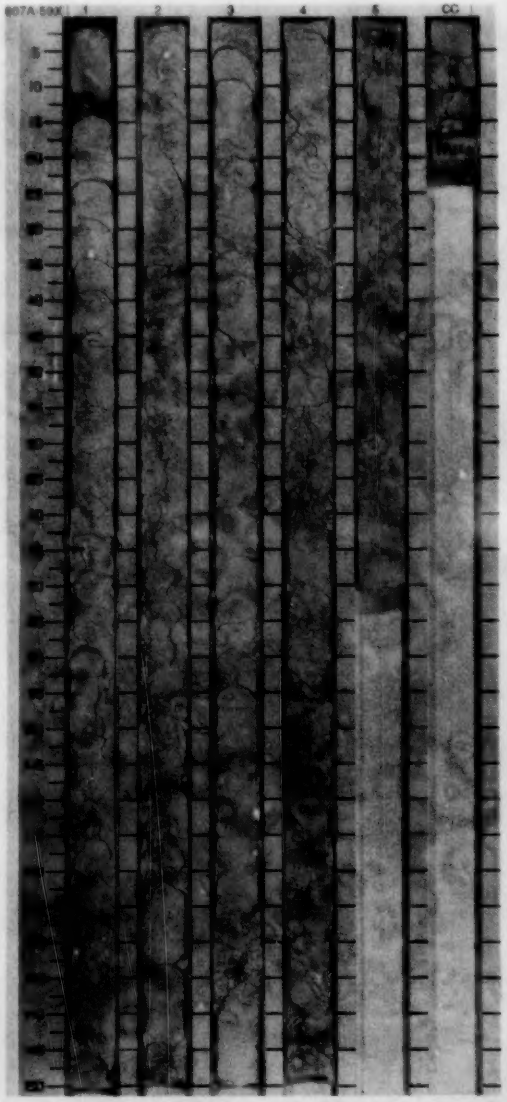
807A-59X
1
2
3
4
5
CC

SITE 807 HOLE A CORE 60X CORED INTERVAL 562.6-572.3 mbsf

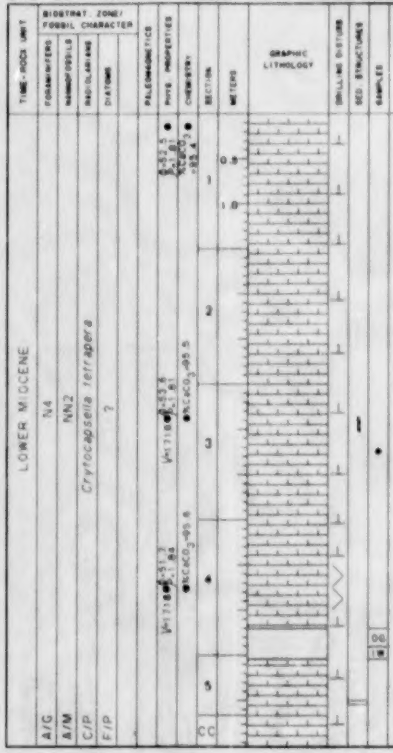
TIME-ROCK UNIT
BIOSTRAT. ZONE/ FOSSIL CHARACTER
FORAMINIFERS
NANNOFOSSILS
RADIOLARIANS
DIATOMS
PALEOMAGNETICS
PHYS. PROPERTIES
CHEMISTRY
SECTION
METERS
GRAPHIC LITHOLOGY
DRILLING DISTURB.
SED. STRUCTURES
SAMPLES
LOWER MIOCENE
N4
NN2
Crytocapsella tetrapera
?
A/G
A/M
C/P
F/P
φ-52.5
γ-1.81
%CaCO3
=95.4
%CaCO3=95.5
Vp=1718
φ-53.6
γ-1.81
%CaCO3=95.6
Vp=1718
φ-51.7
γ-1.84
0.5
1.0
1
2
3
4
5
CC
OG
IW

LITHOLOGIC DESCRIPTION

NANNOFOSSIL CHALK with FORAMINIFERS

Major lithology: This core contains homogeneous, white (2.5Y 8/0) NANNOFOSSIL CHALK with FORAMINIFERS. A 1 cm thick interval, at the base of Section 5, has very thin, grayish blue (5PB 5/2) bands. Bioturbation structures are not seen.

SMEAR SLIDE SUMMARY (%):

	3, 74
	D
TEXTURE:	
Sand	10
Silt	55
Clay	35
COMPOSITION:	
Accessory minerals	1
Foraminifers	13
Nannofossils	84
Siliceous fragments	2

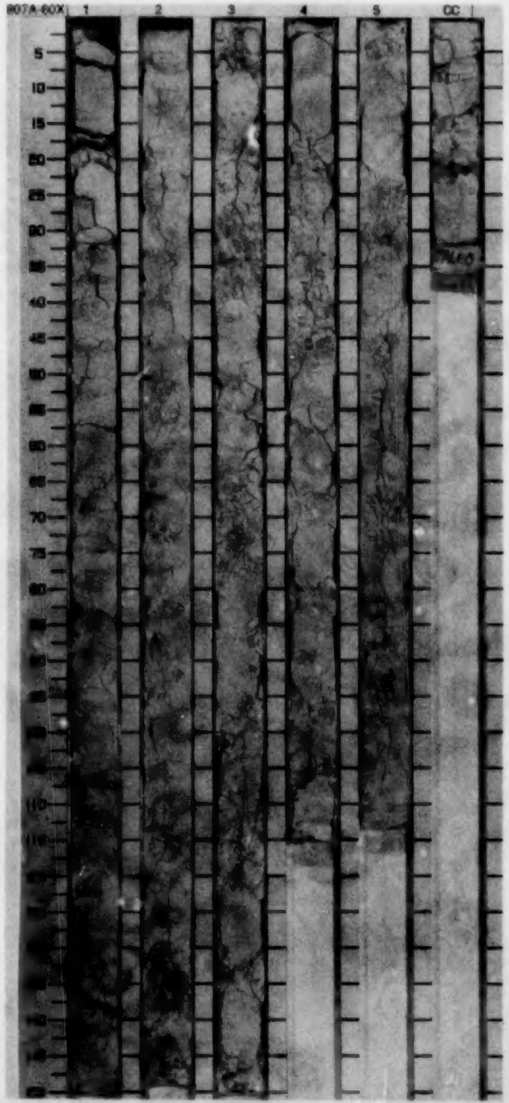
807A-60X
1
2
3
4
5
CC
5
10
15
20
25
30
35
40
45
50
55
60
65
70
75
80
85
90
95
100
105
110
115
120
125
130
135
140
145
150

SITE 807 HOLE A CORE 61X CORED INTERVAL 572.3-581.9 mbsf

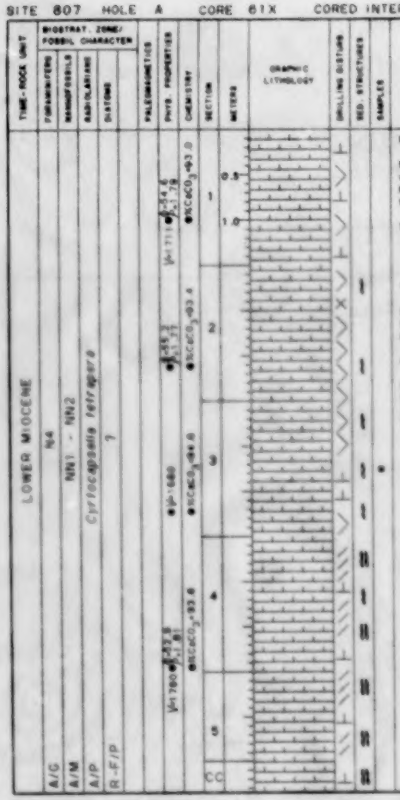
TIME-ROCK UNIT
BIOSTRAT. ZONE/ FOSSIL CHARACTER
FORAMINIFERS
NANNOFOSSILS
RADIOLARIANS
DIATOMS
PALEOMAGNETICS
PHYS. PROPERTIES
CHEMISTRY
SECTION
METERS
GRAPHIC LITHOLOGY
DRILLING DISTURB.
SED. STRUCTURES
SAMPLES
LOWER MIOCENE
A/G
N4
A/M
NN1 - NN2
A/P
Cyrtocapsella tetrapera
R-F/P
?
φ=54.6
γ=1.78
Vp=1711
φ=55.2
γ=1.77
Vp=1680
φ=52.8
γ=1.81
Vp=1780
%CaCO3=93.0
%CaCO3=93.4
%CaCO3=94.6
%CaCO3=93.8
1
2
3
4
5
CC
0.5
1.0

LITHOLOGIC DESCRIPTION

NANNOFOSSIL CHALK with FORAMINIFERS

Major lithology: This core contains white (2.5Y 8/0), homogeneous NANNOFOSSIL CHALK with FORAMINIFERS. The drilling process has resulted in abundant fracturing and biscuiting in the top three sections. Bioturbation is apparent on clean split faces as mottles that are compacted in the vertical direction.

SMEAR SLIDE SUMMARY (%):

	3, 75
	D
TEXTURE:	
Sand	5
Silt	60
Clay	35
COMPOSITION:	
Foraminifers	10
Nannofossils	89
Siliceous fragments	1
Siliceous sponge spicules	Tr

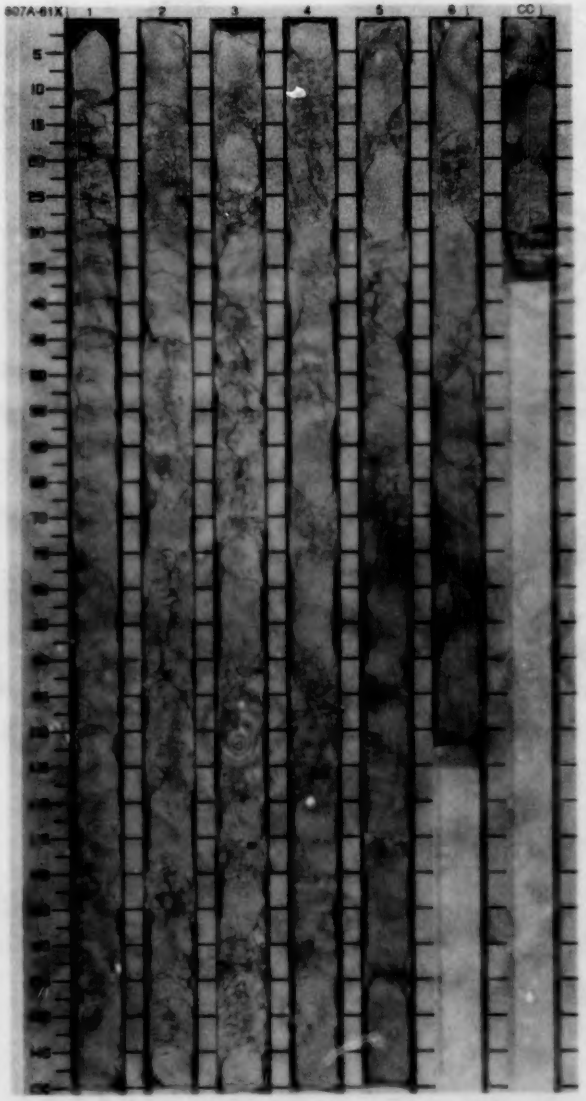
807A-61X
1
2
3
4
5
6
CC
5
10
15

SITE 807 HOLE A CORE 62X CORED INTERVAL 581.9-591.6 mbsf

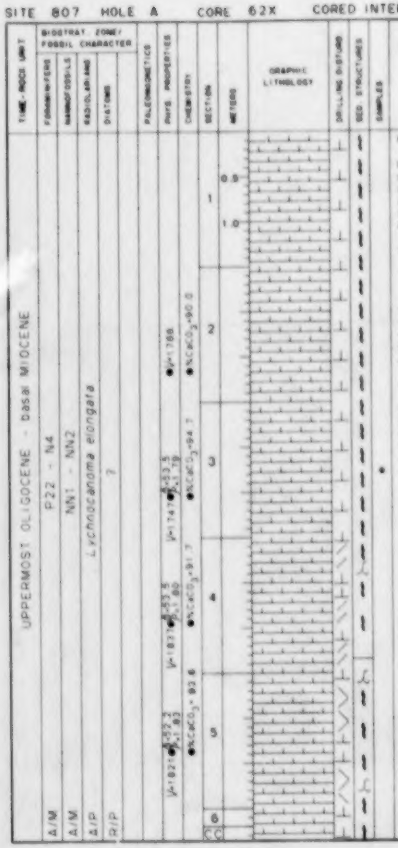
TIME-ROCK UNIT
BIOSTRAT. ZONE/ FOSSIL CHARACTER
FORAMINIFERS
NANNOFOSSILS
RADIOLARIANS
DIATOMS
PALEOMAGNETICS
PHYS. PROPERTIES
CHEMISTRY
SECTION
METERS
GRAPHIC LITHOLOGY
DRILLING DISTURB.
SED. STRUCTURES
SAMPLES
UPPERMOST OLIGOCENE - basal MIOCENE
A/M P22 - N4
A/M NN1 - NN2
A/P Lychnocanoma elongata
R/P ?
●γ=1788
●%CaCO₃=90.0
γ=1747●ϕ=53.5 ρ=1.79
●%CaCO₃=94.7
γ=1837●ϕ=53.5 ρ=1.80
●%CaCO₃=91.7
γ=1821●ϕ=52.2 ρ=1.83
●%CaCO₃=93.6
1
2
3
4
5
6
CC
0.5
1.0

LITHOLOGIC DESCRIPTION

NANNOFOSSIL CHALK with FORAMINIFERS

Major lithology: This core contains white (10YR 8/0 and 10YR 8/1) NANNOFOSSIL CHALK with FORAMINIFERS. Bioturbation is apparent on clean split faces as predominantly horizontal mottles. The lower part of Sections 4 through CC are slightly tinted with grayish blue (5PB 5/2); pyrite filled burrows. Poorly developed, gray (N6) flaser structures and light gray (N7) color bands appear in Section 4, 25-30 cm, in Section 5, 9 and 132 cm, and in Section 6, 9 cm.

SMEAR SLIDE SUMMARY (%)

	3, 78
	D
TEXTURE	
Sand	8
Silt	85
Clay	7
COMPOSITION	
Foraminifers	15
Nannofossils	83
Radiolarians	1
Siliceous fragments	1

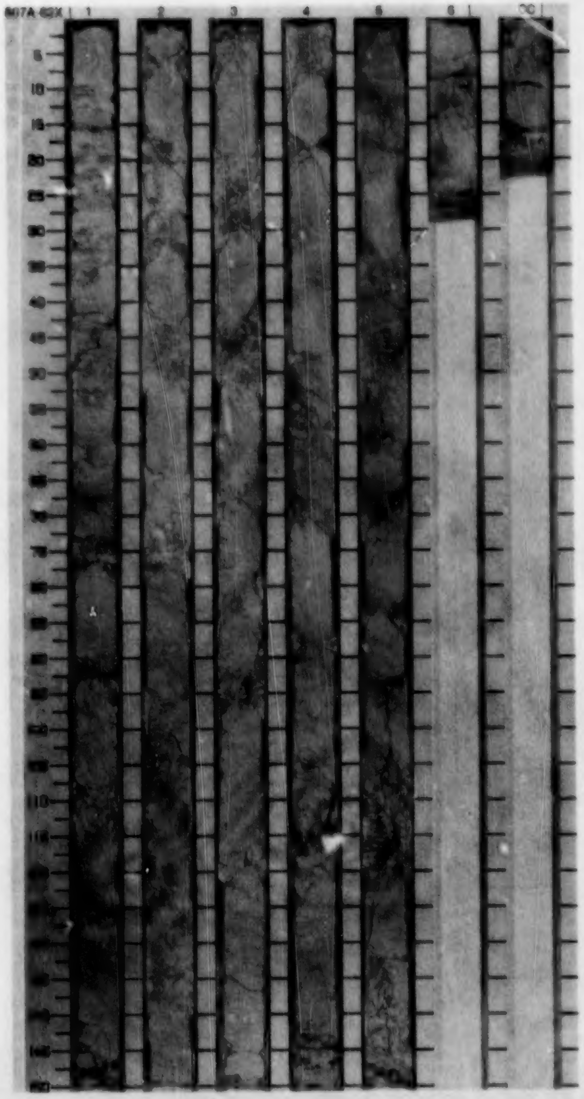
807A-62X
1
2
3
4
5
6
CC
5
10
15
20
25
30
35
40
45
50
55
60
65
70
75
80
85
90
95
100
105
110
115
120
125
130
135
140
145
150

SITE 807 HOLE A CORE 63X CORED INTERVAL 591.6-601.3 mbsf

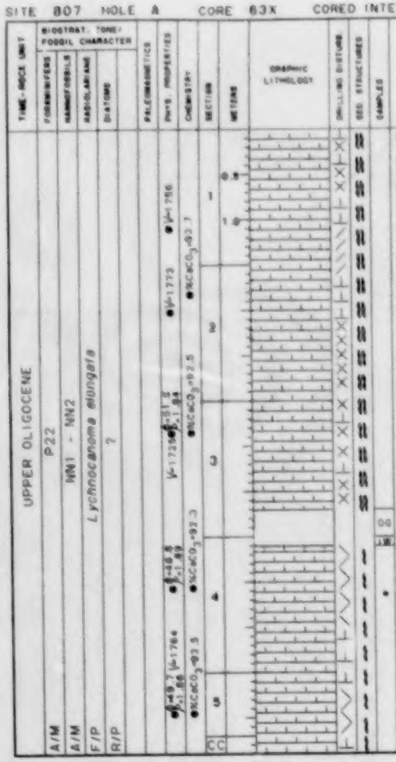
TIME-ROCK UNIT
BIOSTRAT. ZONE/ FOSSIL CHARACTER
FORAMINIFERS
NANNOFOSSILS
RADIOLARIANS
DIATOMS
PALEOMAGNETICS
PHYS. PROPERTIES
CHEMISTRY
SECTION
METERS
GRAPHIC LITHOLOGY
DRILLING DISTURB.
SED. STRUCTURES
SAMPLES
UPPER OLIGOCENE
A/M P22
A/M NN1 - NN2
F/P Lychnocanoma elongata
R/P ?
φ=1756
φ=1773
φ=61.2 γ=1.84 V=1725
φ=48.8 γ=1.89
φ=49.7 γ=1.88 V=1764
%CaCO3=93.7
%CaCO3=92.5
%CaCO3=92.3
%CaCO3=93.5
1
2
3
4
5
CC
0.5
1.0
OG
IW

LITHOLOGIC DESCRIPTION

NANNOFOSSIL CHALK with FORAMINIFERS

Major lithology: This core contains heavily to moderately bioturbated, white (10YR 8/0 and 10YR 8/1) NANNOFOSSIL CHALK with FORAMINIFERS. Bioturbation appears as predominantly horizontal mottles. Sections 1, 2 and 3 are tinted slightly with pale blue (5PB 7/2) and grayish blue (5PB 5/2) pyrite filled burrows.

SMEAR SLIDE SUMMARY (%):

	4, 60
	D
TEXTURE:	
Sand	30
Silt	65
Clay	5
COMPOSITION:	
Foraminifers	15
Nannofossils	80
Radiolarians	4
Siliceous fragments	Tr
Silicoflagellates	Tr

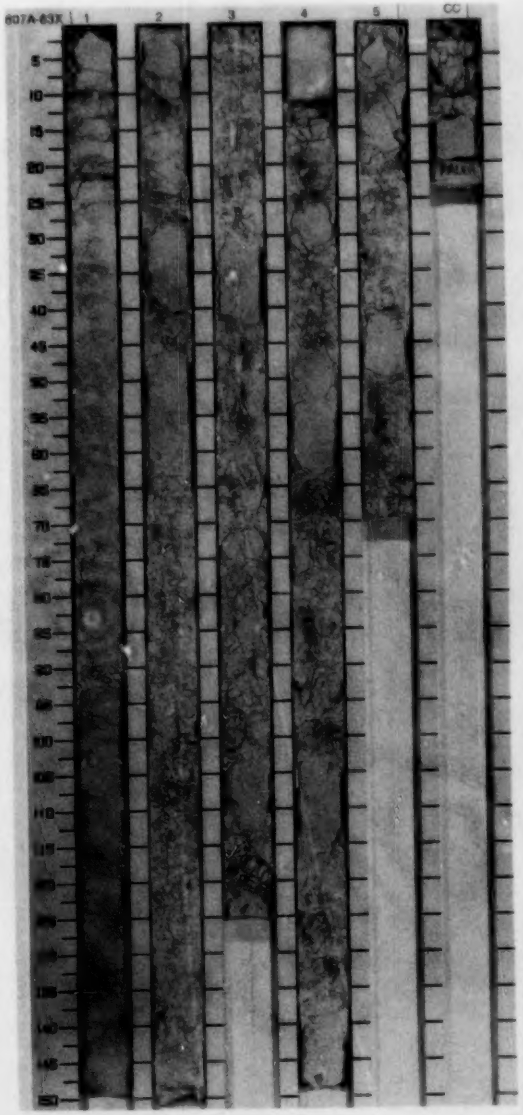
807A-63X
1
2
3
4
5
CC
5
10
15
20
25
30
35
40
45
50
55
60
65
70
75
80
85
90
95
100
105
110
115
120
125
130
135
140
145
150

SITE 807 HOLE A CORE 64X CORED INTERVAL 601.3-611.0 mbsf

TIME-ROCK UNIT	FORAMINIFERS	NANNOFOSSILS	RADIOLARIANS	DIATOMS	PALEOMAGNETICS	PHYS. PROPERTIES	CHEMISTRY	SECTION	METERS	SAMPLES
UPPER OLIGOCENE	P22	NN1 - NN2	*Lychnocanoma elongata*	?		V=1767 ● φ=51.0 ρ=1.84	● %CaCO$_3$=93.5	1	0.5 1.0	
						V=1935 ● φ=46.6 ρ=1.91	● %CaCO$_3$=89.6	2		
						V=1816 ● φ=49.2 ρ=1.87	● %CaCO$_3$=91.5	3		●
							● %CaCO$_3$=91.5	4		
						V=1832 ● φ=51.9 ρ=1.84		5		
	A/M	A/P	A/P	R/P				CC		

LITHOLOGIC DESCRIPTION

NANNOFOSSIL CHALK with FORAMINIFERS

Major lithology: This core contains slightly to moderately bioturbated, white (10YR 8/1 and 2.5Y 8/0) NANNOFOSSIL CHALK with FORAMINIFERS. Bioturbation structures appear predominantly as horizontal mottles. The interval from 120 to 135 cm in Section 4 is composed of gray (5YR 6/1) burrowed sediment, with probable *Teichichnus*-type burrows.

SMEAR SLIDE SUMMARY (%):

	3, 90 D
TEXTURE:	
Sand	8
Silt	88
Clay	4
COMPOSITION:	
Foraminifers	10
Nannofossils	86
Radiolarians	1
Silicoflagellates	1
Spicules	2

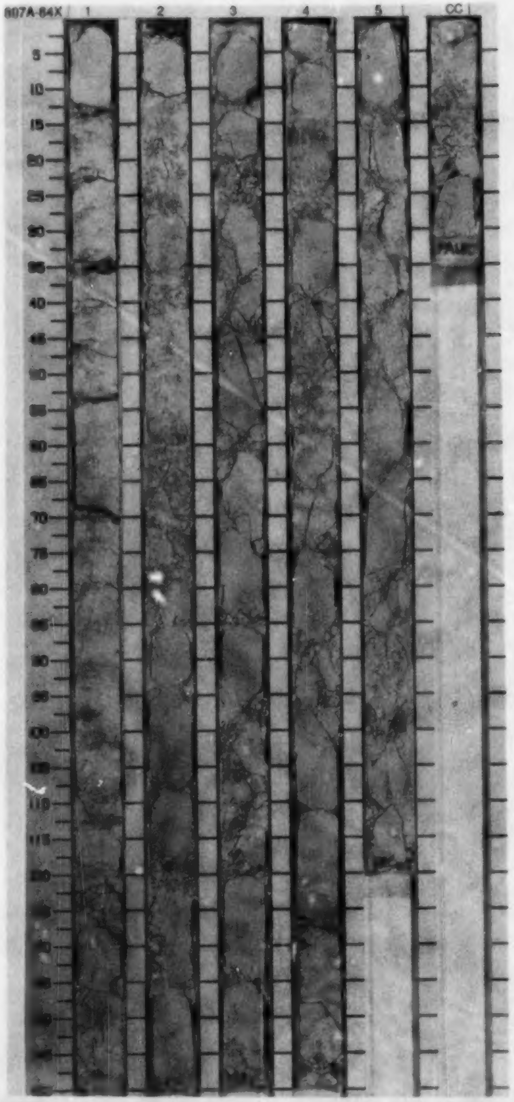

SITE 807 HOLE A CORE 65X CORED INTERVAL 611.0-620.6 mbsf

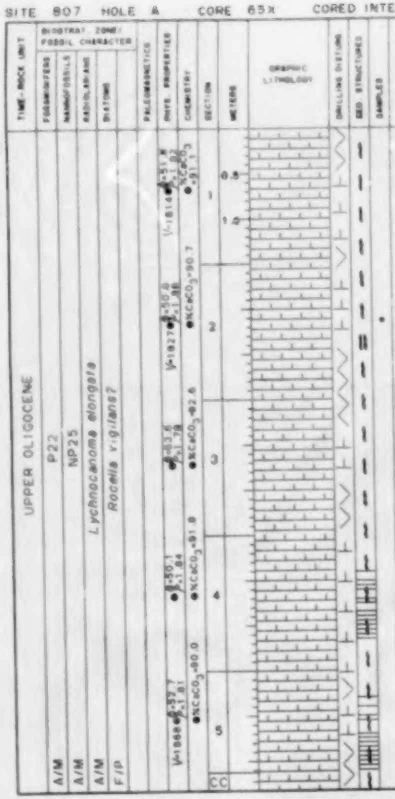
TIME-ROCK UNIT
BIOSTRAT. ZONE/ FOSSIL CHARACTER
FORAMINIFERS
NANNOFOSSILS
RADIOLARIANS
DIATOMS
PALEOMAGNETICS
PHYS. PROPERTIES
CHEMISTRY
SECTION
METERS
GRAPHIC LITHOLOGY
DRILLING DISTURB.
SED. STRUCTURES
SAMPLES
UPPER OLIGOCENE
A/M P22
A/M NP25
A/M Lychnocanoma elongata
F/P Rocella vigilans?
V=1814
ϕ=51.8
γ=1.82
%CaCO3 =91.1
%CaCO3=90.7
V=1827
ϕ=50.6
γ=1.86
ϕ=53.6
γ=1.78
%CaCO3=92.6
ϕ=50.1
γ=1.84
%CaCO3=91.8
V=1866
ϕ=52.7
γ=1.81
%CaCO3=80.0
1
2
3
4
5
CC
0.5
1.0

LITHOLOGIC DESCRIPTION

NANNOFOSSIL CHALK with FORAMINIFERS

Major lithology: This core contains moderately to heavily bioturbated, white (10YR 8/1 to 2.5Y 8/0 and 7.5YR 8/1) NANNOFOSSIL CHALK with FORAMINIFERS. Faint color banding is present in Section 4, 37-122 cm and Section 5, 35-112 cm, and results from a combination of abundant, semi-continuous horizontal burrows across the core surface and very faint, grayish blue (5PB 5/2) color banding. Well-developed, mm-scale, light gray (N7) and grayish blue (5PB 5/2) color bands are present at Section 4, 47-49 cm.

SMEAR SLIDE SUMMARY (%):

	2, 58
	D
TEXTURE:	
Sand	25
Silt	70
Clay	5
COMPOSITION:	
Foraminifers	10
Nannofossils	85
Radiolarians	3
Silicoflagellates	Tr
Spicules	Tr

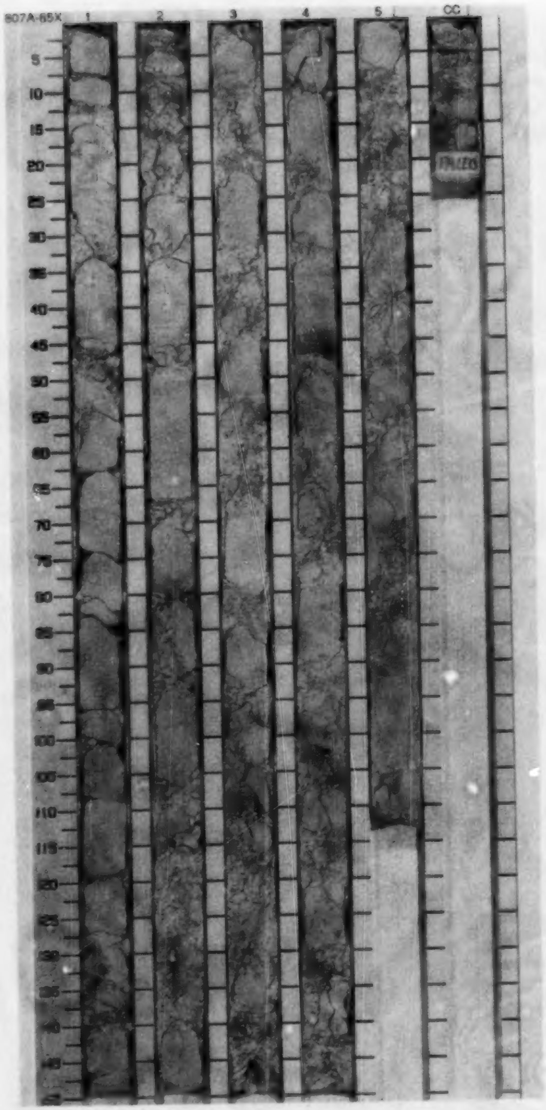
807A-65X
1
2
3
4
5
CC
PALEO
5
10
15
20
25
30
35
40
45
50
55
60
65
70
75
80
85
90
95
100
105
110
115
120
125
130
135
140
145
150

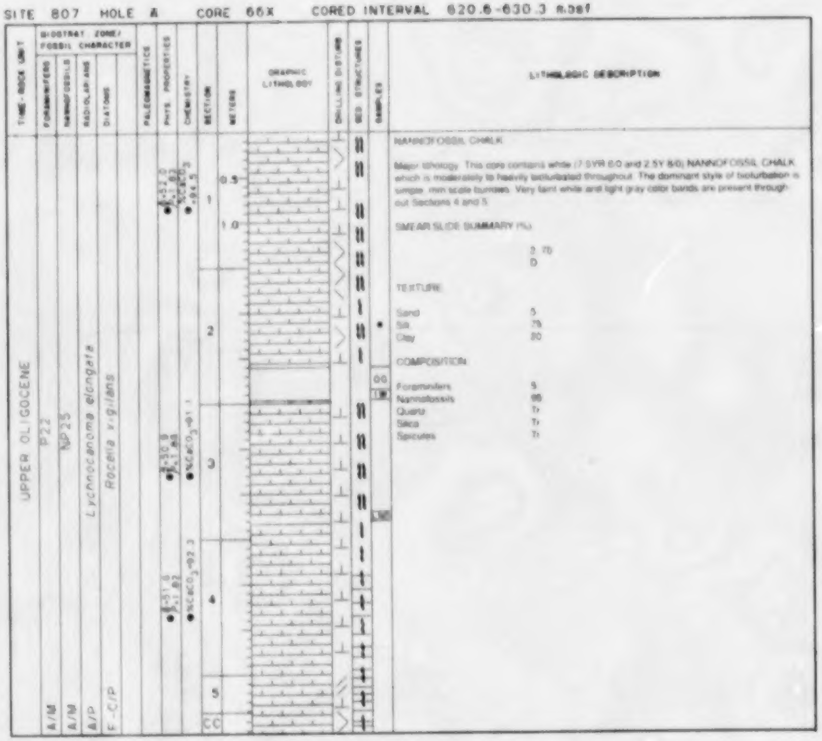
SITE 807 HOLE A CORE 66X CORED INTERVAL 620.6-630.3 mbsf
TIME-ROCK UNIT
BIOSTRAT. ZONE/ FOSSIL CHARACTER
FORAMINIFERS
NANNOFOSSILS
RADIOLARIANS
DIATOMS
PALEOMAGNETICS
PHYS. PROPERTIES
CHEMISTRY
SECTION
METERS
GRAPHIC LITHOLOGY
DRILLING DISTURB.
SED. STRUCTURES
SAMPLES
LITHOLOGIC DESCRIPTION
UPPER OLIGOCENE
P22
NP25
Lychnocanoma elongata
Rocella vigilans
A/M
A/M
A/P
F-C/P
φ=52.0
γ=1.82
%CaCO3=94.5
φ=50.9
γ=1.88
%CaCO3=91.1
φ=51.6
γ=1.82
%CaCO3=92.3
1
2
3
4
5
CC
0.5
1.0
OG
IW
PAL

NANNOFOSSIL CHALK

Major lithology: This core contains white (7.5YR 8/0 and 2.5Y 8/0) NANNOFOSSIL CHALK which is moderately to heavily bioturbated throughout. The dominant style of bioturbation is simple, mm-scale burrows. Very faint white and light gray color bands are present throughout Sections 4 and 5.

SMEAR SLIDE SUMMARY (%):

	2, 70
	D
TEXTURE:	
Sand	5
Silt	75
Clay	20
COMPOSITION:	
Foraminifers	5
Nannofossils	95
Quartz	Tr
Silica	Tr
Spicules	Tr

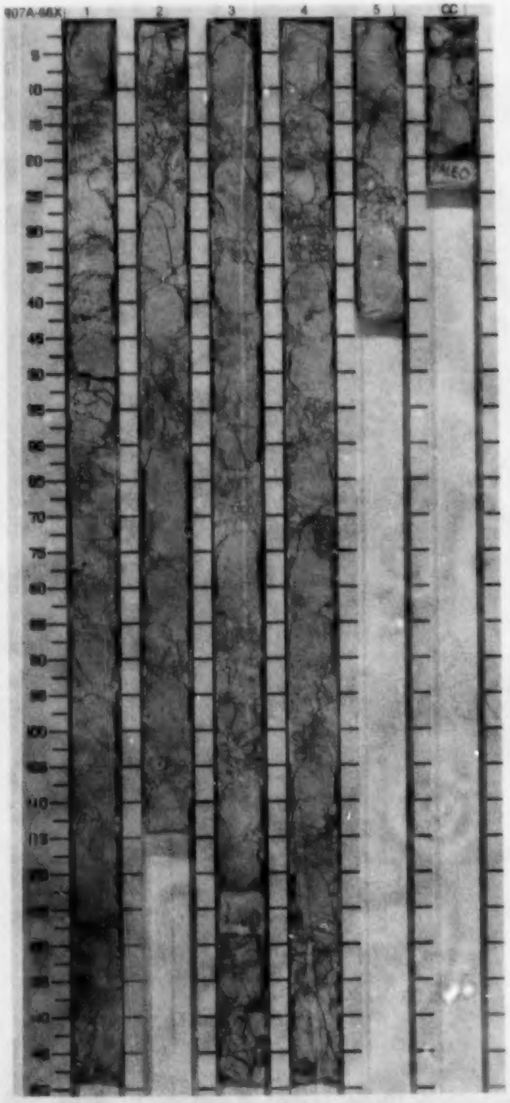
807A-66X
1
2
3
4
5
CC
5
10
15
20
25
30
35
40
45
50
55
60
65
70
75
80
85
90
95
100
105
110
115
120
125
130
135
140
145
150

SITE 807 HOLE A CORE 67X CORED INTERVAL 630.3-639.9 mbsf

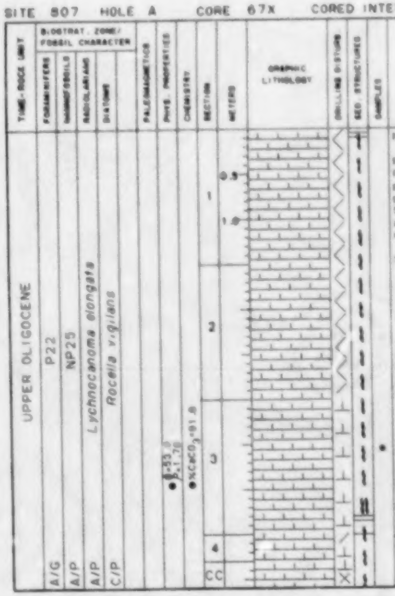
TIME-ROCK UNIT
BIOSTRAT. ZONE/ FOSSIL CHARACTER
FORAMINIFERS
NANNOFOSSILS
RADIOLARIANS
DIATOMS
PALEOMAGNETICS
PHYS. PROPERTIES
CHEMISTRY
SECTION
METERS
GRAPHIC LITHOLOGY
DRILLING DISTURB.
SED. STRUCTURES
SAMPLES
UPPER OLIGOCENE
P22
NP25
Lychnocanoma elongata
Rocella vigilans
A/G
A/P
A/P
C/P
●φ=53.0
●γ=1.70
●%CaCO$_3$=91.8
1
2
3
4
CC
0.5
1.0

LITHOLOGIC DESCRIPTION

NANNOFOSSIL CHALK with FORAMINIFERS

Major lithology: This core contains white (2.5Y 8/0) NANNOFOSSIL CHALK with FORAMINIFERS, which is slightly to moderately bioturbated throughout. Zones with minor tints of pale purple (5P 6/2) are present in Sections 1 and 2. Gray (N6/) mm scale color bands are present at Section 3, 133-137 cm, and light gray (N7/) mm scale color bands are present at Section 4, 7-9 cm. A sample from the Core Catcher that was processed for paleontologic analyses contained abundant volcanic ash; the volcanic ash was not obvious during inspection of the core itself.

SMEAR SLIDE SUMMARY (%):

	3, 98 D
TEXTURE:	
Sand	30
Silt	65
Clay	5
COMPOSITION:	
Foraminifers	15
Nannofossils	80
Quartz	Tr
Silica	Tr
Silicoflagellates	1
Spicules	Tr

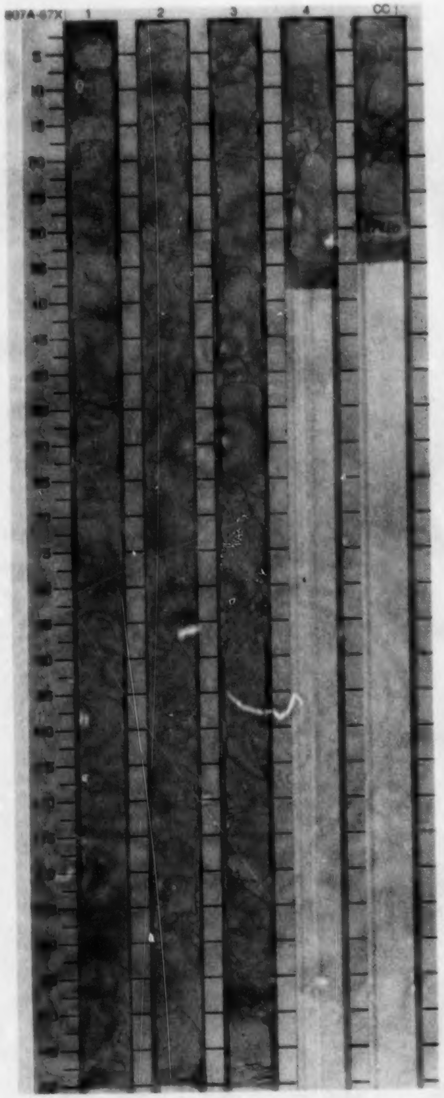
807A-67X
1
2
3
4
CC

SITE 807 HOLE A CORE 68X CORED INTERVAL 639.9-649.6 mbsf

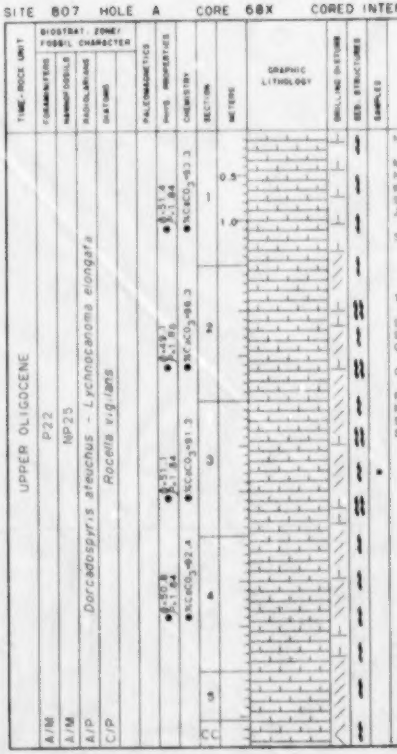
TIME-ROCK UNIT
BIOSTRAT. ZONE/FOSSIL CHARACTER
FORAMINIFERS
NANNOFOSSILS
RADIOLARIANS
DIATOMS
PALEOMAGNETICS
PHYS. PROPERTIES
CHEMISTRY
SECTION
METERS
GRAPHIC LITHOLOGY
DRILLING DISTURB.
SED. STRUCTURES
SAMPLES
UPPER OLIGOCENE
A/M P22
A/M NP25
A/P Dorcadospyris ateuchus - Lychnocanoma elongata
C/P Rocella vigilans
φ=51.4 γ=1.84
%CaCO3=93.3
φ=49.1 γ=1.86
%CaCO3=88.3
φ=51.1 γ=1.84
%CaCO3=91.3
φ=50.8 γ=1.84
%CaCO3=92.4
1
2
3
4
5
CC
0.5
1.0

LITHOLOGIC DESCRIPTION

NANNOFOSSIL CHALK with FORAMINIFERS

Major lithology: This core contains white (2.5Y 8/0 to 7.5YR 8/0) to light gray (2.5Y 7/0) NANNOFOSSIL CHALK with FORAMINIFERS. Bioturbation is moderate to heavy throughout the core, and is expressed as diffuse color mottling and simple burrows. Section 2, 62-68 cm is gray (N6) in color and contains discontinuous burrows and a distinct *Zoophycos* trace fossil.

SMEAR SLIDE SUMMARY (%):

	3, 80
	D
TEXTURE	
Sand	10
Silt	86
Clay	4
COMPOSITION	
Foraminifers	12
Nannofossils	84
Silicoflagellates	1
Spicules	2

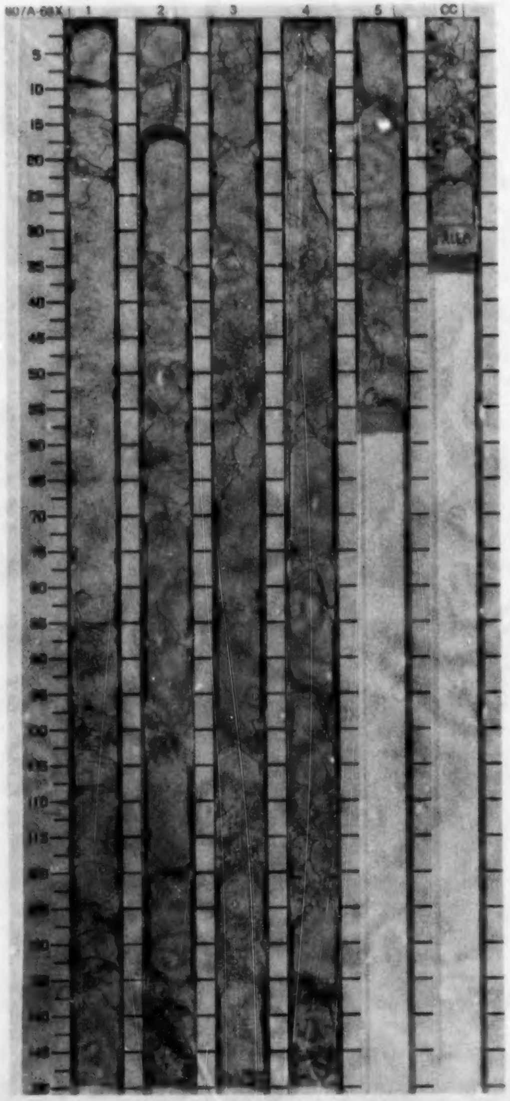
807A-68X
1
2
3
4
5
CC
5
10
15
20
25
30
35
40
45
50
55
60
65
70
75
80
85
90
95
100
105
110
115
120
125
130
135
140
145
150

SITE 807 HOLE A CORE 69X CORED INTERVAL 649.6-659.2 mbsf

TIME-ROCK UNIT	BIOSTRAT. ZONE/ FOSSIL CHARACTER: FORAMINIFERS	NANNOFOSSILS	RADIOLARIANS	DIATOMS	PALEOMAGNETICS	PHYS. PROPERTIES	CHEMISTRY	SECTION	METERS	GRAPHIC LITHOLOGY	DRILLING DISTURB.	SED. STRUCTURES	SAMPLES	LITHOLOGIC DESCRIPTION
UPPER OLIGOCENE	A/G P22	A/P NP25	*D. ateuchus - L. elongata* C/P	*Rocella vigilans* C-A/P				1 CC	0.5 1.0		⊥	≀≀	●	NANNOFOSSIL CHALK with FORAMINIFERS

NANNOFOSSIL CHALK with FORAMINIFERS

Major lithology: This core contains white (5YR 8/1) to light gray (5YP 7/1), heavily bioturbated NANNOFOSSIL CHALK with FORAMINIFERS. The sediments are relatively homogeneous, except for two cm scale, grayish red purple (5RP 4/2) burrow "halos" present in the Core Catcher.

SMEAR SLIDE SUMMARY (%):

	1, 54
	D
TEXTURE	
Sand	14
Silt	82
Clay	4
COMPOSITION	
Diatoms	Tr
Foraminifers	15
Nannofossils	80
Silicoflagellates	1
Spicules	2

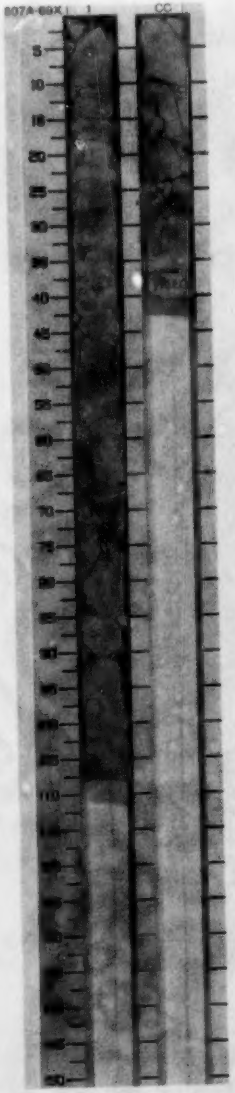

SITE 807 HOLE A CORE 70X CORED INTERVAL 659.2-668.9 mbsf

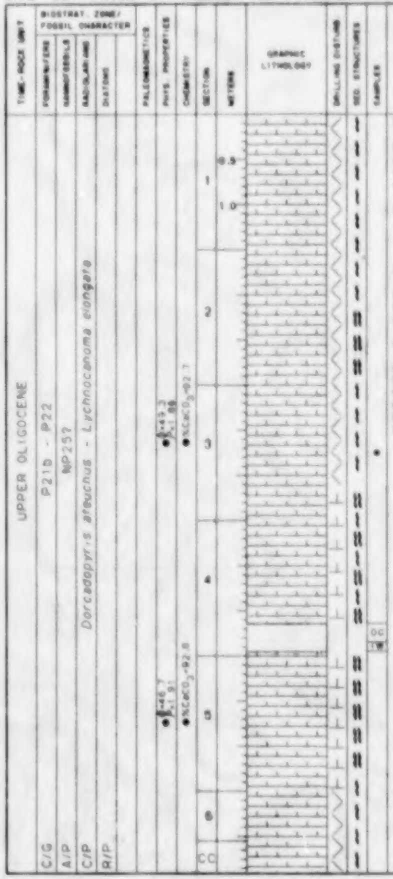
TIME-ROCK UNIT
BIOSTRAT. ZONE/ FOSSIL CHARACTER
FORAMINIFERS
NANNOFOSSILS
RADIOLARIANS
DIATOMS
PALEOMAGNETICS
PHYS. PROPERTIES
CHEMISTRY
SECTION
METERS
GRAPHIC LITHOLOGY
DRILLING DISTURB.
SED. STRUCTURES
SAMPLES
UPPER OLIGOCENE
P21b - P22
NP25?
Dorcadopyris ateuchus - Lychnocanoma elongata
C/G
A/P
C/P
R/P
=49.3
=1.88
●%CaCO3=92.7
=46.7
=1.91
●%CaCO3=92.8
1
2
3
4
5
6
CC
0.5
1.0
OG
IW

LITHOLOGIC DESCRIPTION

NANNOFOSSIL CHALK with FORAMINIFERS

Major lithology: This core contains white (2.5Y 8/0 to 10YR 8/1) NANNOFOSSIL CHALK with FORAMINIFERS. The entire core is moderately to heavily bioturbated with simple, mm-scale, horizontal burrows. Section 5, 109-116 cm, contains white (2.5Y 8/0) and gray (N6) chalk, extensively mixed by burrowing.

SMEAR SLIDE SUMMARY (%):

	3, 77
	D
TEXTURE:	
Sand	20
Silt	75
Clay	5
COMPOSITION:	
Diatoms	Tr
Foraminifers	15
Nannofossils	80
Radiolarians	2
Silicoflagellates	Tr
Spicules	Tr

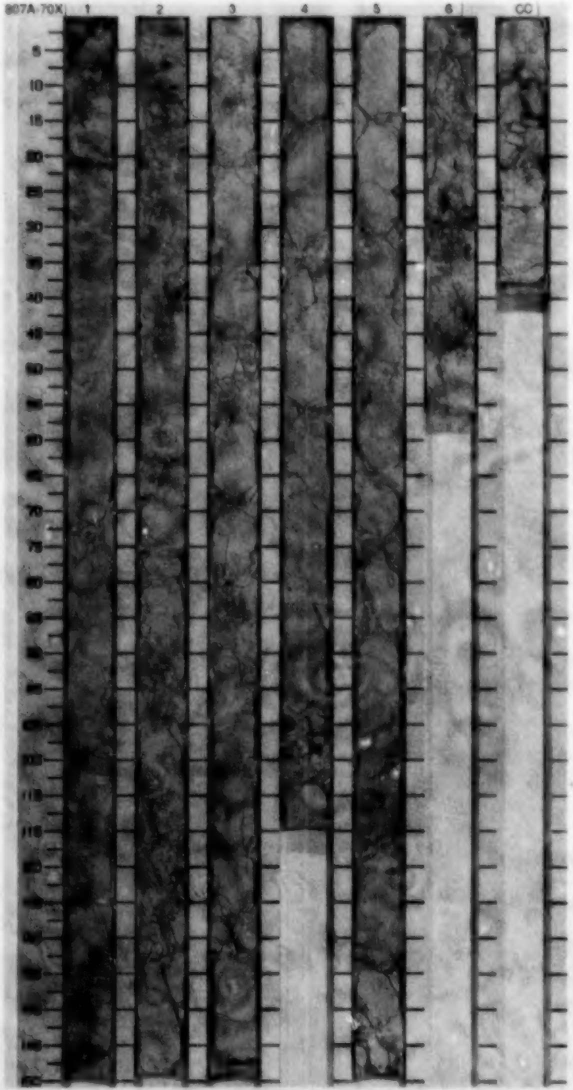
807A-70X
1
2
3
4
5
6
CC
5
10
15
20
25
30
35
40
45
50
55
60
65
70
75
80
85
90
95
100
105
110
115
120
125
130
135
140
145
150

SITE 807 HOLE A CORE 71X CORED INTERVAL 668.9-678.2 mbsf

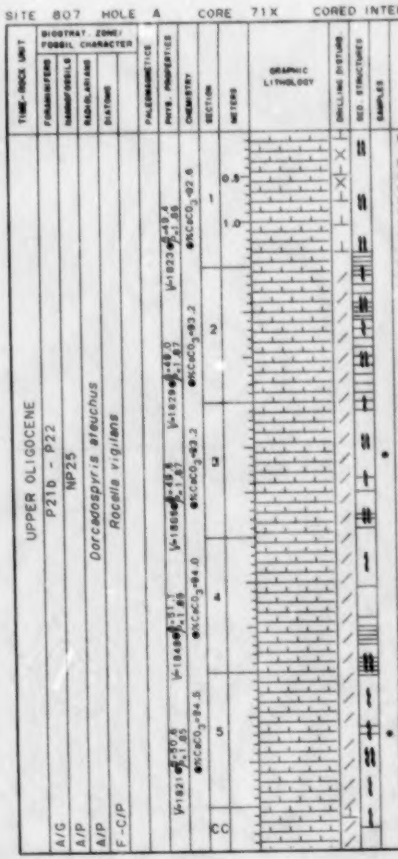
TIME-ROCK UNIT
BIOSTRAT. ZONE/ FOSSIL CHARACTER
FORAMINIFERS
NANNOFOSSILS
RADIOLARIANS
DIATOMS
PALEOMAGNETICS
PHYS. PROPERTIES
CHEMISTRY
SECTION
METERS
GRAPHIC LITHOLOGY
DRILLING DISTURB.
SED. STRUCTURES
SAMPLES
UPPER OLIGOCENE
A/G
P21b - P22
A/P
NP25
A/P
Dorcadospyris ateuchus
F-C/P
Rocella vigilans
V=1823 φ=49.4 ρ=1.89
%CaCO3=92.6
V=1829 φ=48.0 ρ=1.87
%CaCO3=93.2
V=1808 φ=48.8 ρ=1.87
%CaCO3=93.2
V=1848 φ=51.1 ρ=1.88
%CaCO3=94.0
V=1821 φ=50.6 ρ=1.85
%CaCO3=94.5
1
2
3
4
5
CC
0.5
1.0

LITHOLOGIC DESCRIPTION

NANNOFOSSIL CHALK

Major lithology: This core is predominantly NANNOFOSSIL CHALK. The color is white (7.5YR 8.0) but grades to pale blue (5PB 7.2) in the lower parts of Section 2 and Section 5 and to grayish blue (5BP 5.2) over 5 cm intervals in Sections 3 and 4. Bioturbation is moderate to heavy and dominated by *Zoophycos* burrows. White and grayish blue (5PB 5.2) mottles and cm scale pyritized specks are also present. Section 2 and parts of Sections 1, 3 and 4 contain densely spaced white and grayish blue (5PB 5.2) color bands. Single greenish gray (5GY 6.1) bands are wispy and 2 to 3 mm wide.

Minor lithology: NANNOFOSSIL CHALK with ASH is found in Section 5 between 63 and 70 cm. The color grades from light gray (N7) at 63 cm to dark gray (N 4) near 70 cm. The layer is moderately bioturbated, including *Chondrites* burrows.

SMEAR SLIDE SUMMARY (%):

	3, 80 D	5, 70 M
TEXTURE:		
Sand	5	6
Silt	70	74
Clay	25	20
COMPOSITION:		
Diatoms	Tr	—
Foraminifers	8	Tr
Nannofossils	94	89
Radiolarians	1	—
Spicules	Tr	Tr
Volcanic ash	Tr	10

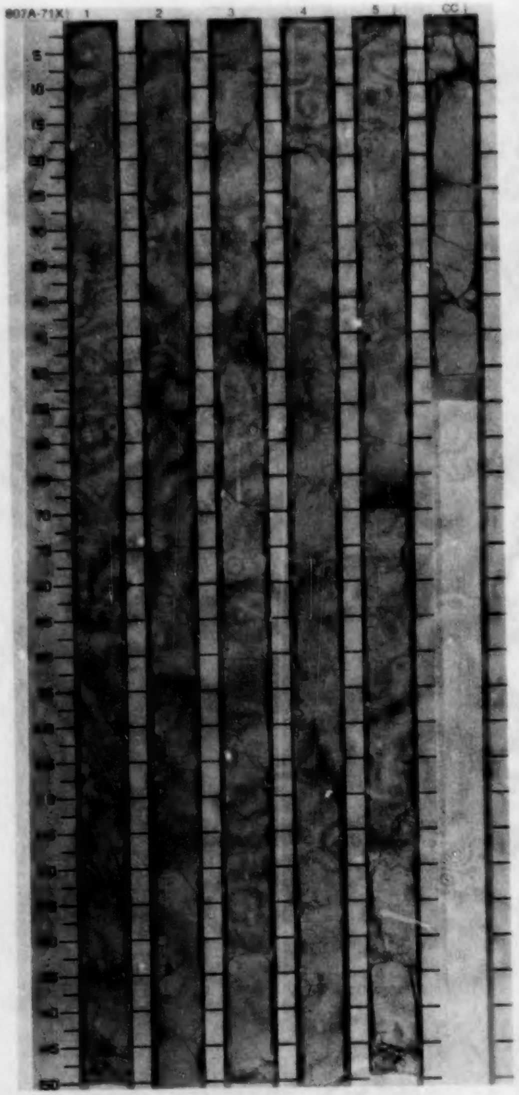
807A-71X
1
2
3
4
5
CC
5
10
15
20
25
30
35
40
45
50
55
60
65
70
75
80
85
90
95
100
105
110
115
120
125
130
135
140
145
150

SITE 807 HOLE A CORE 72X CORED INTERVAL 678.2-687.8 mbsf

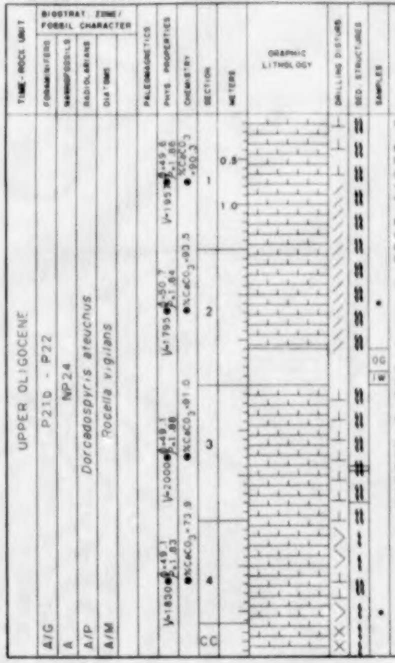
TIME-ROCK UNIT
BIOSTRAT. ZONE/ FOSSIL CHARACTER
FORAMINIFERS
NANNOFOSSILS
RADIOLARIANS
DIATOMS
PALEOMAGNETICS
PHYS. PROPERTIES
CHEMISTRY
SECTION
METERS
GRAPHIC LITHOLOGY
DRILLING DISTURB.
SED. STRUCTURES
SAMPLES
UPPER OLIGOCENE
A/G P21b - P22
A NP24
A/P Dorcadospyris ateuchus
A/M Rocella vigilans
V=1953 ф=49.6 ρ=1.86
%CaCO3 =90.3
V=1795 ф=50.7 ρ=1.84
%CaCO3=93.5
V=2000 ф=48.1 ρ=1.88
%CaCO3=81.0
V=1830 ф=49.1 ρ=1.83
%CaCO3=73.9
1
2
3
4
CC
0.5
1.0
OG
IW

LITHOLOGIC DESCRIPTION

NANNOFOSSIL CHALK with FORAMINIFERS

Major lithology: This core contains white (2.5Y 8.0), moderately to heavily bioturbated NANNOFOSSIL CHALK with FORAMINIFERS. Horizontal, mm to cm scale, white to light gray (N8) burrows are common throughout. Intervals of light gray (N6) flaser structures and wavy color bands are observed throughout. A few grayish blue (5PB 5/2), pyritized burrows were observed in Section 3.

Minor lithology: NANNOFOSSIL CHALK with ASH is found in Section 4 between 66 and 69 cm and between 94 and 98 cm. The color is gray (N6) in the upper ash layer and grades between gray (N6) and dark gray (N 3) in the lower ash zone. Both ash layers are bioturbated.

SMEAR SLIDE SUMMARY (%):

	2, 60	4, 96
	D	M
TEXTURE:		
Sand	12	16
Silt	65	60
Clay	23	24
COMPOSITION:		
Diatoms	—	Tr
Foraminifers	10	5
Nannofossils	67	74
Radiolarians	2	1
Spicules	Tr	Tr
Volcanic ash	1	20

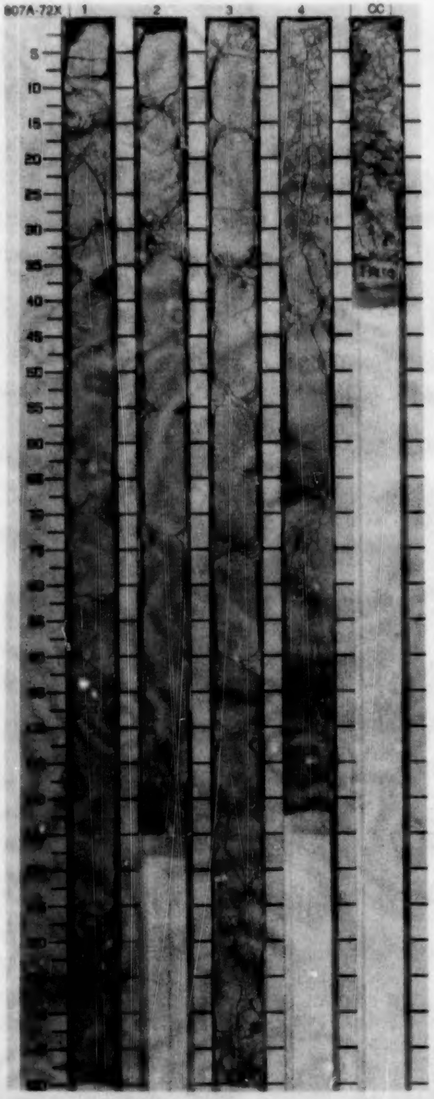
807A-72X
1
2
3
4
CC
5
10
15
20
25
30
35
40
45
50
55
60

SITE 807 HOLE A CORE 73X CORED INTERVAL 687.8-697.5 mbsf

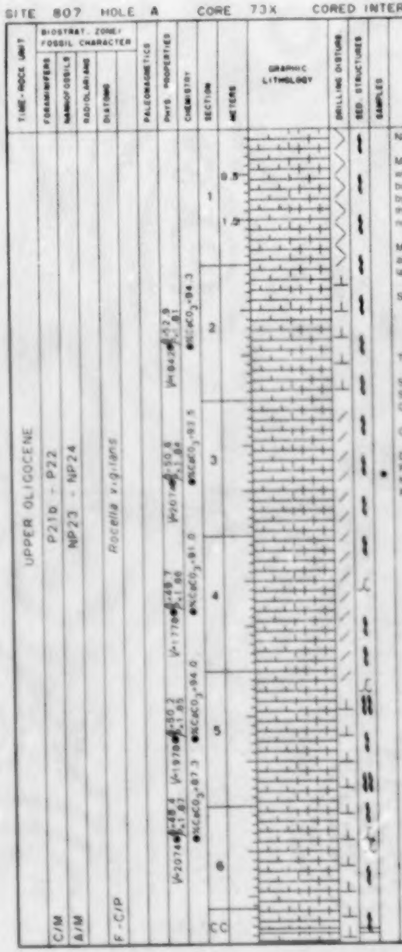
TIME-ROCK UNIT
BIOSTRAT. ZONE/ FOSSIL CHARACTER
FORAMINIFERS
NANNOFOSSILS
RADIOLARIANS
DIATOMS
PALEOMAGNETICS
PHYS. PROPERTIES
CHEMISTRY
SECTION
METERS
GRAPHIC LITHOLOGY
DRILLING DISTURB.
SED. STRUCTURES
SAMPLES
UPPER OLIGOCENE
P21b - P22
C/M
NP23 - NP24
A/M
Rocella vigilans
F-C/P
V=1842 φ=52.9 γ=1.81
%CaCO3=84.3
V=2017 φ=50.6 γ=1.84
%CaCO3=93.5
V=1770 φ=48.7 γ=1.86
%CaCO3=91.0
V=1970 φ=50.2 γ=1.85
%CaCO3=94.0
V=2074 φ=48.4 γ=1.87
%CaCO3=87.3
1
2
3
4
5
6
CC
0.5
1.0
1.5
*

LITHOLOGIC DESCRIPTION

NANNOFOSSIL CHALK with FORAMINIFERS and FORAMINIFER NANNOFOSSIL CHALK

Major lithology: This core contains white (10YR 8/1 and 2.5Y 8/0) NANNOFOSSIL CHALK with FORAMINIFERS and FORAMINIFER NANNOFOSSIL CHALK. Moderate to heavy bioturbation is indicated by white to light gray (N7/) mottling, by subhorizontal burrows, and by a single, 2 cm diameter, grayish purple (5P 4/2) "halo". Several intervals, up to 20 cm thick, contain wispy flaser structures. A single color-banded, pale blue (5PB 7/2) zone is noted in Section 5.

Minor lithology: NANNOFOSSIL CHALK with ASH is found in the Core Catcher between 27 and 34 cm. The color grades from light gray (N7/) near 27 cm to dark gray (N4/) near 34. The layer is bioturbated.

SMEAR SLIDE SUMMARY (%):

	3, 82
	D
TEXTURE:	
Sand	30
Silt	65
Clay	5
COMPOSITION:	
Diatoms	Tr
Foraminifers	25
Nannofossils	70
Radiolarians	Tr

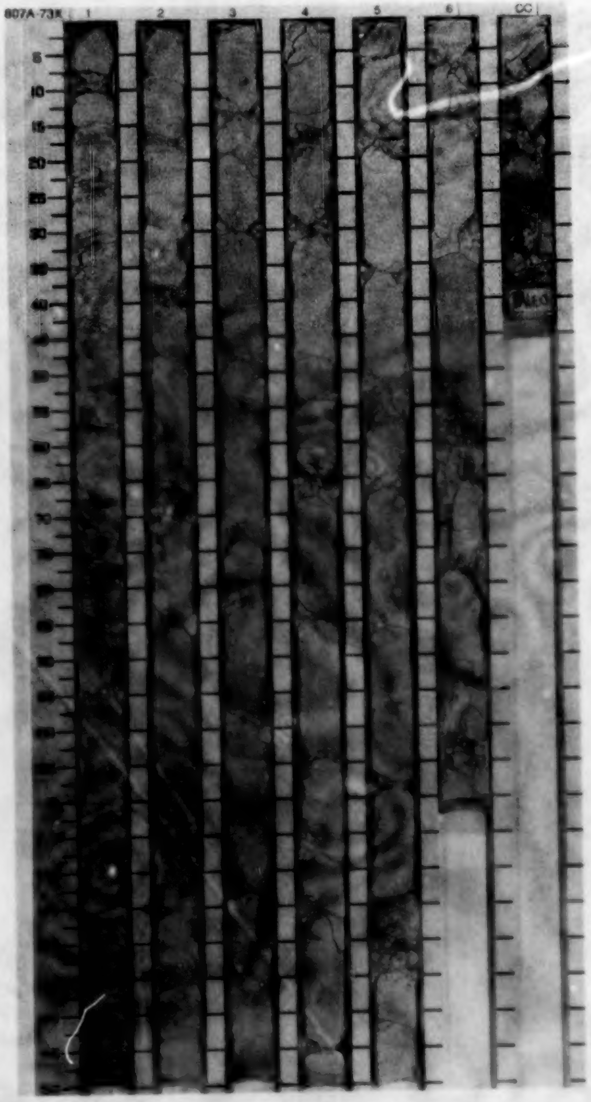
807A-73X
1
2
3
4
5
6
CC
5
10
15
20
25
30
35
40
45
50
55
60
65
70
75
80
85
90
95
100
105
110
115
120
125
130
135
140
145
150

SITE 807 HOLE A CORE 74X CORED INTERVAL 697.5-707.2 mbsf

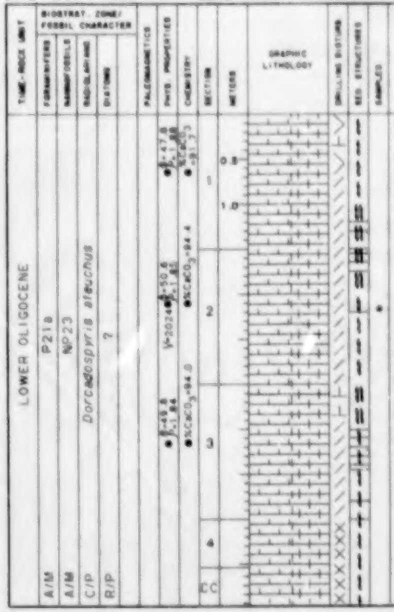
TIME-ROCK UNIT
BIOSTRAT. ZONE/ FOSSIL CHARACTER
FORAMINIFERS
NANNOFOSSILS
RADIOLARIANS
DIATOMS
PALEOMAGNETICS
PHYS. PROPERTIES
CHEMISTRY
SECTION
METERS
GRAPHIC LITHOLOGY
DRILLING DISTURB.
SED. STRUCTURES
SAMPLES
LOWER OLIGOCENE
P21a
NP23
Dorcadospyris ateuchus
?
A/M
A/M
C/P
R/P
φ=47.8
γ=1.88
%CaCO3=91.7
φ=50.6
γ=1.85
V=2024
%CaCO3=94.4
φ=49.6
γ=1.84
%CaCO3=94.0
1
2
3
4
CC
0.5
1.0

LITHOLOGIC DESCRIPTION

NANNOFOSSIL CHALK with FORAMINIFERS and FORAMINIFER NANNOFOSSIL CHALK

Major lithology: This core contains NANNOFOSSIL CHALK with FORAMINIFERS and FORAMINIFER NANNOFOSSIL CHALK. The sediment is white (2.5Y 8/0), with 5 to 15 cm thick intervals grading into light gray (2.5Y 7/0) in Section 2. The base of a light gray interval is often sharp. Moderate to heavy bioturbation is indicated by abundant mottling and sub horizontal burrows. Thin (mm size), gray (N6/), wispy color bands with flaser structures are common in conjunction with microstylolites.

SMEAR SLIDE SUMMARY (%)

	2, 67 D
TEXTURE:	
Sand	30
Silt	65
Clay	5
COMPOSITION:	
Diatoms	Tr
Foraminifers	25
Nannofossils	70
Quartz	Tr
Radiolarians	Tr
Silicoflagellates	Tr

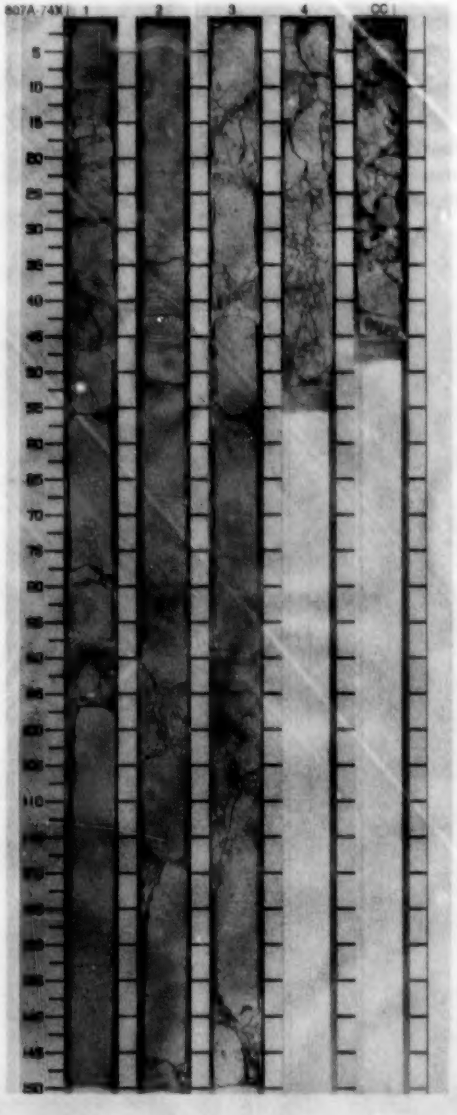
807A-74X
1
2
3
4
CC
5
10
15
20
25
30
35
40
45
50
55
60
65
70
75
80
85
90
95
100
105
110
115
120
125
130
135
140
145
150

SITE 807 HOLE A CORE 75X CORED INTERVAL 707.2-716.9 mbsf

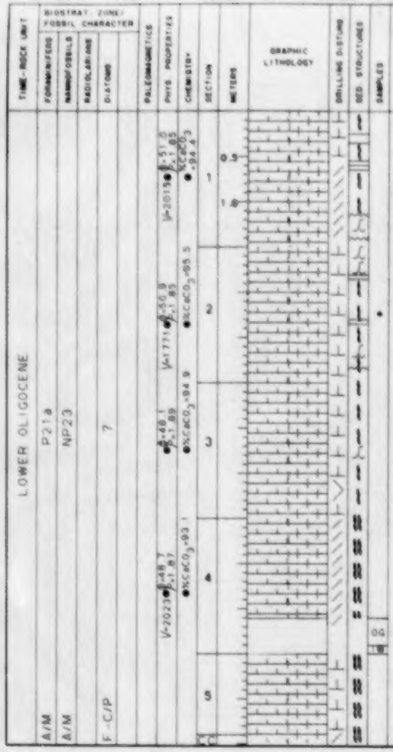
TIME-ROCK UNIT
BIOSTRAT. ZONE/ FOSSIL CHARACTER
FORAMINIFERS
NANNOFOSSILS
RADIOLARIANS
DIATOMS
PALEOMAGNETICS
PHYS. PROPERTIES
CHEMISTRY
SECTION
METERS
GRAPHIC LITHOLOGY
DRILLING DISTURB.
SED. STRUCTURES
SAMPLES
LOWER OLIGOCENE
P21a
NP23
?
A/M
A/M
F-C/P
V=2015 φ=51.0 γ=1.85
%CaCO3 =94.4
V=1771 φ=50.9 γ=1.85
%CaCO3=95.5
φ=48.1 γ=1.89
%CaCO3=94.9
V=2023 φ=48.7 γ=1.87
%CaCO3=93.1
1
2
3
4
5
CC
0.5
1.0
OG

LITHOLOGIC DESCRIPTION

NANNOFOSSIL CHALK with FORAMINIFERS AND FORAMINIFER NANNOFOSSIL CHALK

Major lithology: This core contains white (2.5Y 8/0) NANNOFOSSIL CHALK with FORAMINIFERS and FORAMINIFER NANNOFOSSIL CHALK, which becomes more uniform in appearance downcore. Gray (N6) stylolites and distinct, mm thick, greenish gray (5G 6/1) color bands are common in Sections 1 and 2, whereas light gray (N7) intervals of flaser structures with microstylolites are common in Sections 1 and 2, and present in Section 3. Sections 1 through 3 are slightly to moderately bioturbated. Sections 4 through Core Catcher are moderately to heavily bioturbated.

SMEAR SLIDE SUMMARY (%):

	2, 66
	D
TEXTURE:	
Sand	30
Silt	65
Clay	5
COMPOSITION:	
Diatoms	Tr
Foraminifers	25
Nannofossils	70
Quartz	Tr
Radiolarians	Tr
Silicoflagellates	Tr

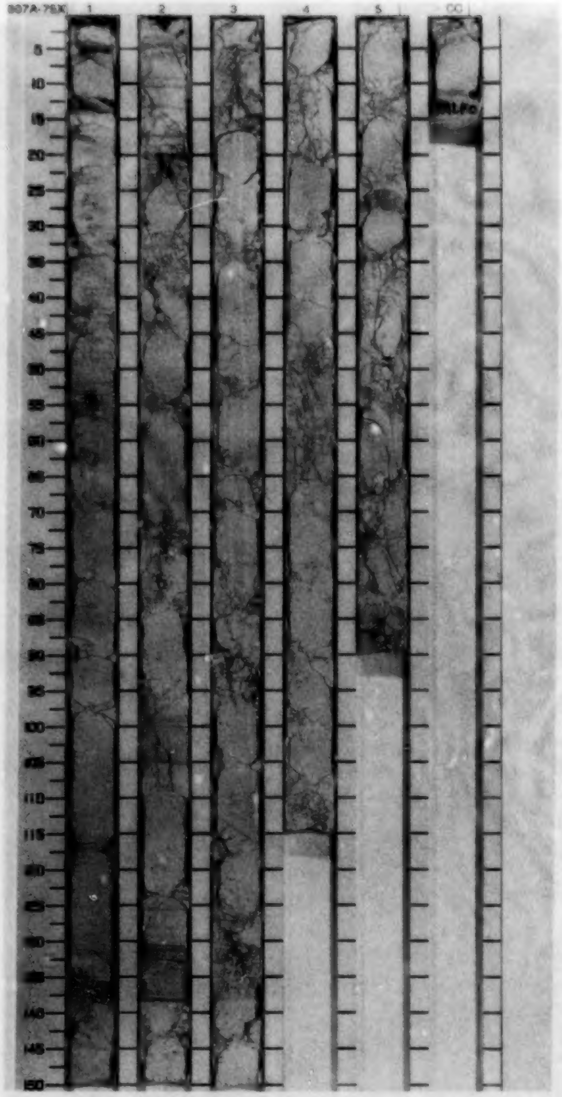
807A-75X
1
2
3
4
5
CC
5
10
15
20
25
30
35
40
45
50
55
60
65
70
75
80
85
90
95
100
105
110
115
120
125
130
135
140
145
150

SITE 807 HOLE A CORE 76X CORED INTERVAL 716.9-726.5 mbsf

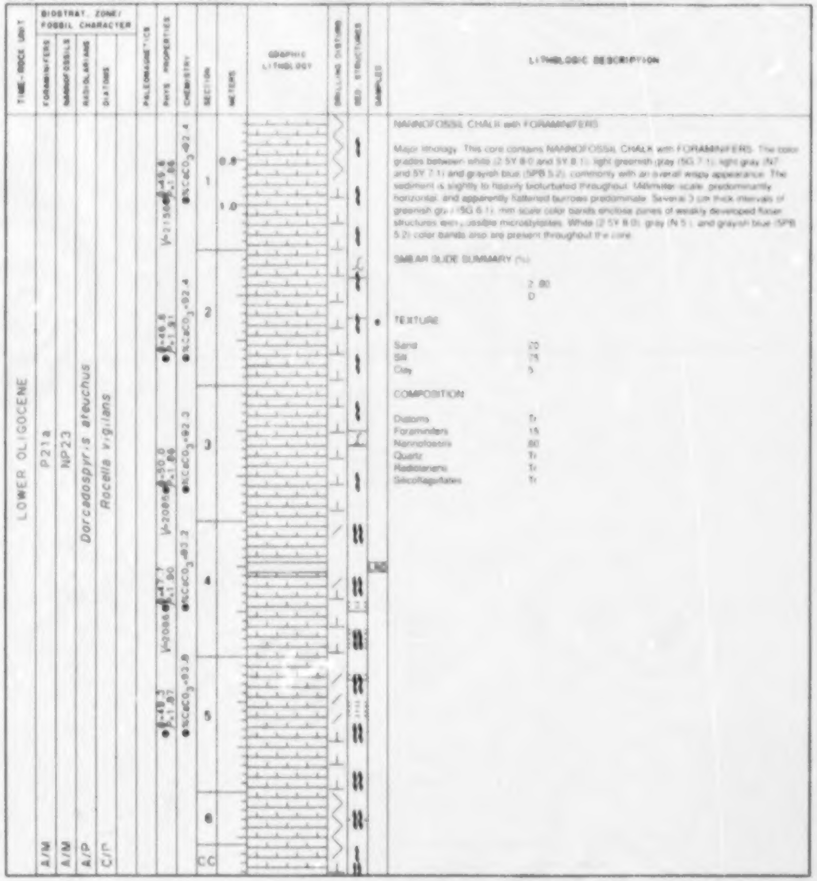
TIME-ROCK UNIT
BIOSTRAT. ZONE/ FOSSIL CHARACTER
FORAMINIFERS
NANNOFOSSILS
RADIOLARIANS
DIATOMS
PALEOMAGNETICS
PHYS. PROPERTIES
CHEMISTRY
SECTION
METERS
GRAPHIC LITHOLOGY
DRILLING DISTURB.
SED. STRUCTURES
SAMPLES
LITHOLOGIC DESCRIPTION
LOWER OLIGOCENE
A/M P21a
A/M NP23
A/P Dorcadospyris ateuchus
C/P Rocella vigilans
Vp=2150 φ=49.8 ρ=1.96
φ=46.8 ρ=1.91
Vp=2085 φ=50.0 ρ=1.86
Vp=2086 φ=47.7 ρ=1.90
φ=49.3 ρ=1.87
%CaCO3=92.4
%CaCO3=92.4
%CaCO3=92.3
%CaCO3=93.2
%CaCO3=93.8
1
2
3
4
5
6
CC
0.5
1.0
IW

NANNOFOSSIL CHALK with FORAMINIFERS

Major lithology: This core contains NANNOFOSSIL CHALK with FORAMINIFERS. The color grades between white (2.5Y 8/0 and 5Y 8/1), light greenish gray (5G 7/1), light gray (N7 and 5Y 7/1) and grayish blue (5PB 5/2), commonly with an overall wispy appearance. The sediment is slightly to heavily bioturbated throughout. Millimeter-scale, predominantly horizontal, and apparently flattened burrows predominate. Several 3 cm thick intervals of greenish gray (5G 6/1), mm-scale color bands enclose zones of weakly developed flaser structures with possible microstylolites. White (2.5Y 8/0), gray (N 5), and grayish blue (5PB 5/2) color bands also are present throughout the core.

SMEAR SLIDE SUMMARY (%):

	2, 80 D
TEXTURE:	
Sand	20
Silt	75
Clay	5
COMPOSITION:	
Diatoms	Tr
Foraminifers	15
Nannofossils	80
Quartz	Tr
Radiolarians	Tr
Silicoflagellates	Tr

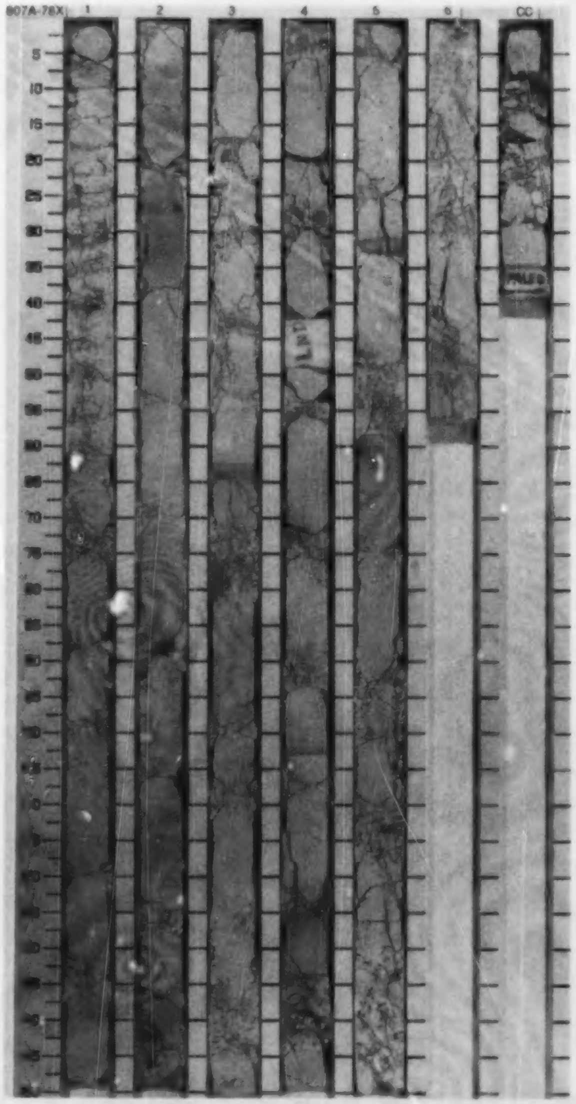
807A-76X
1
2
3
4
5
6
CC
5
10
15
20
25
30
35
40
45
50
55
60
65
70
75
80
85
90
95
100
105
110
115
120
125
130
135
140
145
150
LNT
PALEO

SITE 807 HOLE A CORE 77X CORED INTERVAL 726.5-736.2 mbsf

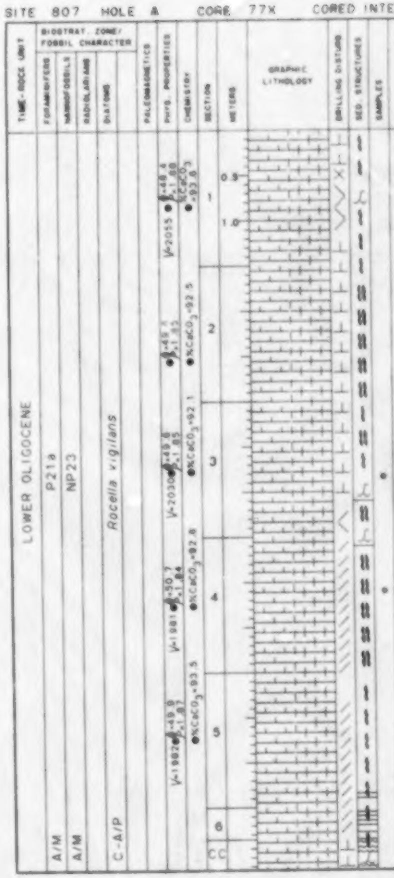
TIME-ROCK UNIT
BIOSTRAT. ZONE/ FOSSIL CHARACTER
FORAMINIFERS
NANNOFOSSILS
RADIOLARIANS
DIATOMS
PALEOMAGNETICS
PHYS. PROPERTIES
CHEMISTRY
SECTION
METERS
GRAPHIC LITHOLOGY
DRILLING DISTURB.
SED. STRUCTURES
SAMPLES
LOWER OLIGOCENE
P21a
NP23
Rocella vigilans
A/M
A/M
C-A/P
V=2055 ● ∅=48.4 γ=1.88
%CaCO3 =93.6
● ∅=49.1 γ=1.83
●%CaCO3=92.5
V=2030 ● ∅=48.6 γ=1.85
●%CaCO3=92.1
V=1981 ● ∅=50.7 γ=1.84
●%CaCO3=92.8
V=1982 ● ∅=49.0 γ=1.87
●%CaCO3=93.5
1
2
3
4
5
6
CC
0.5
1.0

LITHOLOGIC DESCRIPTION

NANNOFOSSIL CHALK with FORAMINIFERS AND FORAMINIFER NANNOFOSSIL CHALK

Major lithology: This core contains NANNOFOSSIL CHALK with FORAMINIFERS and FORAMINIFER NANNOFOSSIL CHALK. The color grades between white (2.5Y 8.0, 5Y 8.1, and 7.5YR 8.0) and light gray (7.5YR 7.0). The sediment is quite uniform and moderately to heavily bioturbated, predominantly with subhorizontal, mm-scale, simple burrows. Discrete cm-scale, horizontal burrows also are present in Section 1. Flaser structures with microstylolites are seen in Sections 1 and 3. Millimeter-scale, faint color bands occur in Section 5 and throughout Section 6. Section 4, 56-61 cm, contains a heavily bioturbated, gray (2.5Y 6.0) layer, which contains about 5% volcanic ash.

SMEAR SLIDE SUMMARY (%):

	3, 92 D	4, 60 M
TEXTURE:		
Sand	30	10
Silt	65	70
Clay	5	20
COMPOSITION:		
Diatoms	Tr	—
Foraminifers	25	7
Nannofossils	70	86
Quartz	Tr	Tr
Radiolarians	Tr	2
Silicoflagellates	Tr	—
Volcanic ash	—	5

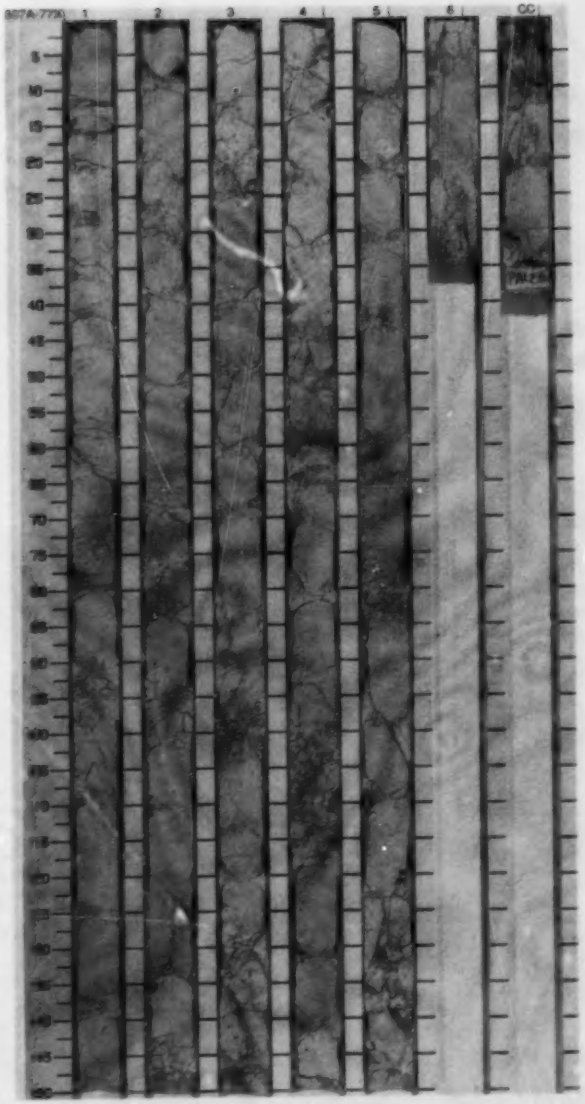
807A-77X
1
2
3
4
5
6
CC
5
10
15
20
25
30
35
40
45
50
55
60
65
70
75
80
85
90
95
100
105
110
115
120
125
130
135
140
145
150

SITE 807 HOLE A CORE 78X CORED INTERVAL 736.2-745.5 mbsf

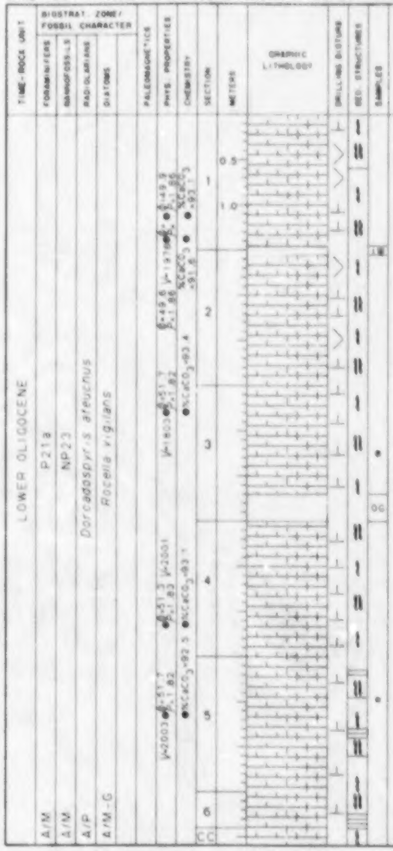
TIME-ROCK UNIT
BIOSTRAT. ZONE/ FOSSIL CHARACTER
FORAMINIFERS
NANNOFOSSILS
RADIOLARIANS
DIATOMS
PALEOMAGNETICS
PHYS. PROPERTIES
CHEMISTRY
SECTION
METERS
GRAPHIC LITHOLOGY
DRILLING DISTURB.
SED. STRUCTURES
SAMPLES
LOWER OLIGOCENE
P21a
NP23
Dorcadospyris ateuchus
Rocella vigilans
A/M
A/M
A/P
A/M-G
φ=49.9 ρ=1.86
ν=1978
%CaCO3 =93.1
φ=49.6 ρ=1.86
%CaCO3 =91.6
φ=51.7 ρ=1.82
ν=1803
%CaCO3=93.4
φ=51.3 ρ=1.83
ν=2001
%CaCO3=93.1
ν=2003
φ=51.7 ρ=1.82
%CaCO3=92.5
1
2
3
4
5
6
CC
0.5
1.0
OG

LITHOLOGIC DESCRIPTION

NANNOFOSSIL CHALK with FORAMINIFERS and FORAMINIFER NANNOFOSSIL CHALK

Major lithology: This core contains bioturbated NANNOFOSSIL CHALK with FORAMINIFERS and FORAMINIFER NANNOFOSSIL CHALK in equal percentages. The chalk is predominantly white (2.5Y 8/0), with minor pale pink (5RP 8/2) intervals. The chalk has two styles of color banding: 5 to 15 cm thick, pale pink bands and 1 to 2 mm thick, dark gray (2.5Y 4/) bands that exhibit flaser structures.

Minor lithology: Section 5, 45-47 cm, contains a heavily bioturbated dark gray (2.5Y 4/0) NANNOFOSSIL CHALK with ASH.

SMEAR SLIDE SUMMARY (%):

	3, 75	5, 45
	D	M
TEXTURE:		
Sand	10	10
Silt	60	60
Clay	30	30
COMPOSITION:		
Accessory minerals	—	5
Diatoms	Tr	—
Foraminifers	25	—
Nannofossils	73	60
Opaques	—	15
Radiolarians	1	8
Siliceous fragments	1	—
Siliceous sponge spicules	—	Tr
Volcanic ash	Tr	12

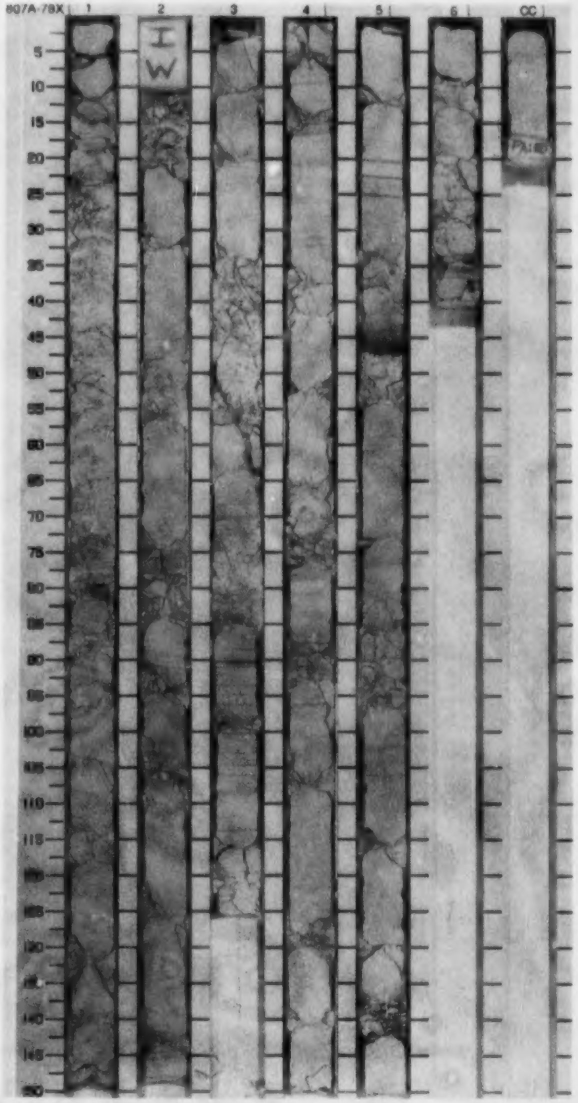
807A-78X
1
2
3
4
5
6
CC
5
10
15
20
25
30
35
40
45
50
55
60
65
70
75
80
85
90
95
100
105
110
115
120
125
130
135
140
145
150
IW
PAL

SITE 807 HOLE A CORE 79X CORED INTERVAL 745.5-755.2 mbsf

TIME-ROCK UNIT	BIOSTRAT. ZONE/ FOSSIL CHARACTER: FORAMINIFERS	NANNOFOSSILS	RADIOLARIANS	DIATOMS	PALEOMAGNETICS	PHYS. PROPERTIES	CHEMISTRY	SECTION	METERS	GRAPHIC LITHOLOGY	DRILLING DISTURB.	SED. STRUCTURES	SAMPLES
LOWER OLIGOCENE	P21a A/M	NP23 A/M		Rocella vigilans A/M-G		V=1595 φ=51.5 γ=1.83	%CaCO3=94.0	1 2 CC	0.5 1.0				*

LITHOLOGIC DESCRIPTION

NANNOFOSSIL CHALK with FORAMINIFERS

Major lithology: This core contains white (2.5Y 8.0) NANNOFOSSIL CHALK with FORAMINIFERS. Several 10 cm thick, pale pink (5RP 8.2) to pale purple (5P 6/2) intervals are present and contain numerous distinct, sharp, thin (<1 mm) white color bands. Heavy bioturbation is indicated by numerous trace fossils. These structures appear to be compacted. A *Zoophycos* trace is present in Section 1, 98 cm. There are a few gray, wavy and braided color bands that may be flaser structures.

SMEAR SLIDE SUMMARY (%):

	2, 20 D
TEXTURE:	
Sand	10
Silt	75
Clay	15
COMPOSITION:	
Diatoms	1
Foraminifers	20
Nannofossils	79
Siliceous fragments	1

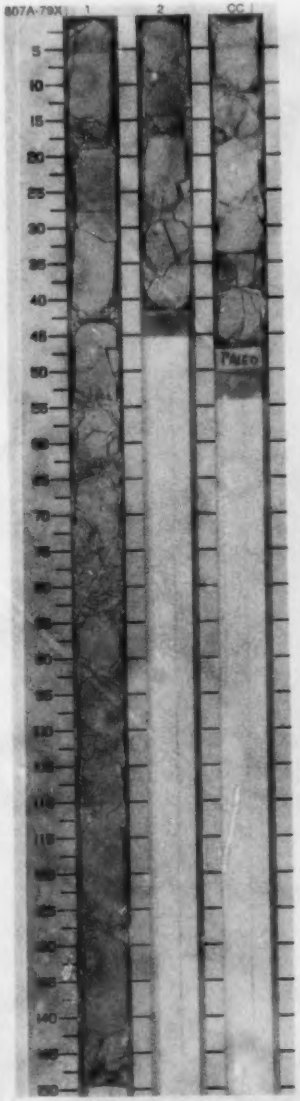

SITE 807 HOLE A CORE 80X CORED INTERVAL 755.2-764.9 mbsf

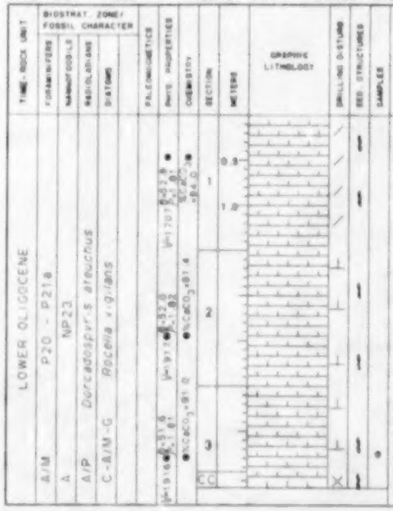
TIME-ROCK UNIT
BIOSTRAT. ZONE/ FOSSIL CHARACTER
FORAMINIFERS
NANNOFOSSILS
RADIOLARIANS
DIATOMS
PALEOMAGNETICS
PHYS. PROPERTIES
CHEMISTRY
SECTION
METERS
GRAPHIC LITHOLOGY
DRILLING DISTURB.
SED. STRUCTURES
SAMPLES
LOWER OLIGOCENE
A/M P20 - P21a
A NP23
A/P Dorcadospyris ateuchus
C-A/M-G Rocella vigilans
γ=1.70 ϕ=52.8
γ=1.91 ϕ=52.0
γ=1.91 ϕ=51.6
%CaCO3=84.0
%CaCO3=81.4
%CaCO3=81.0
1
2
3
CC
0.5
1.0

LITHOLOGIC DESCRIPTION

NANNOFOSSIL CHALK

Major lithology: This core contains white (2.5Y 8/0) NANNOFOSSIL CHALK. Heavy bioturbation is evident from numerous trace fossils. A few thin (<1 mm) horizontal, wispy, braided color bands are present. Several pale pink (5RP 6/2) zones, with thin (<1 mm) white distinct, horizontal bands are also present.

Minor lithology: Section 3, 48-50 cm contains a heavily bioturbated, dark gray (2.5Y 4/0) NANNOFOSSIL CHALK with ASH.

SMEAR SLIDE SUMMARY (%):

	3, 74
	M
TEXTURE:	
Sand	10
Silt	55
Clay	35
COMPOSITION:	
Diatoms	Tr
Foraminifers	4
Glass	20
Nannofossils	68
Opaques	6
Siliceous fragments	2

SITE 807 HOLE A CORE 81X CORED INTERVAL 764.9-774.5 mbsf

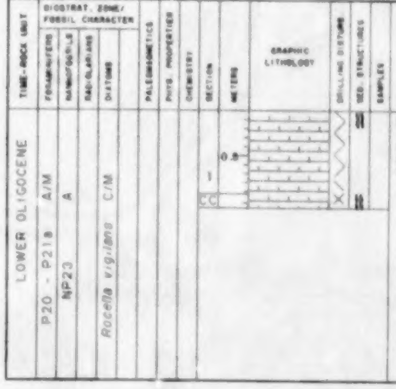
TIME-ROCK UNIT
BIOSTRAT. ZONE/ FOSSIL CHARACTER
FORAMINIFERS
NANNOFOSSILS
RADIOLARIANS
DIATOMS
PALEOMAGNETICS
PHYS. PROPERTIES
CHEMISTRY
SECTION
METERS
GRAPHIC LITHOLOGY
DRILLING DISTURB.
SED. STRUCTURES
SAMPLES
LOWER OLIGOCENE
P20 - P21a A/M
NP23 A
Rocella vigilans C/M
1
CC
0.5

LITHOLOGIC DESCRIPTION

NANNOFOSSIL CHALK

Major lithology: This core contains white NANNOFOSSIL CHALK. Heavy bioturbation is indicated by numerous mottles and trace fossils. The core is highly fractured by drilling and contains a large amount of drilling breccia.

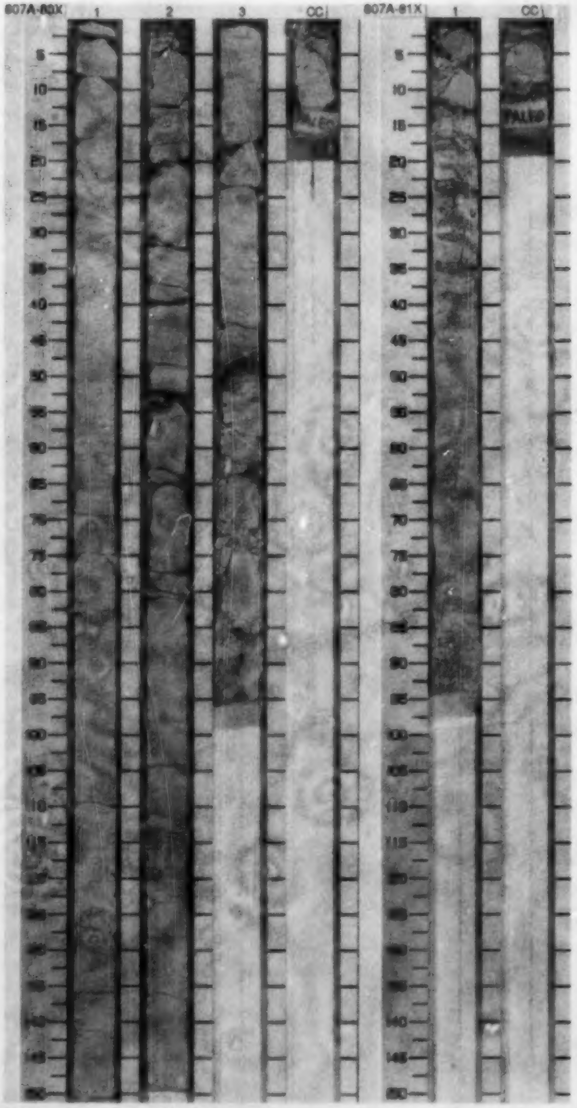
807A-80X
1
2
3
CC
807A-81X
1
CC
5
10
15
20
25
30
35
40
45
50
55
60
65
70
75
80
85
90
95
100
105
110
115
120
125
130
135
140
145
150

SITE 807 HOLE A CORE 82X CORED INTERVAL 774.5-784.2 mbsf

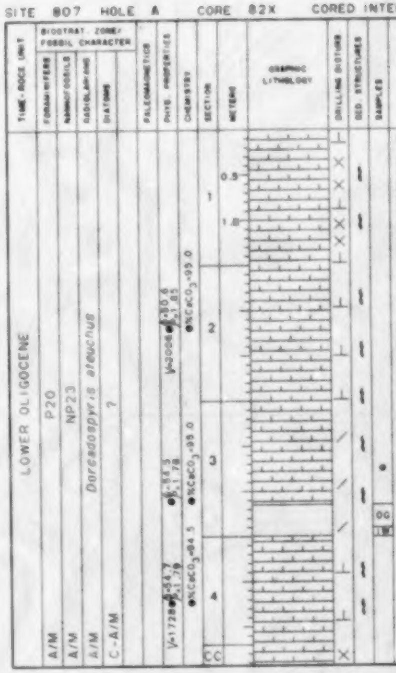
TIME-ROCK UNIT
BIOSTRAT. ZONE/ FOSSIL CHARACTER
FORAMINIFERS
NANNOFOSSILS
RADIOLARIANS
DIATOMS
PALEOMAGNETICS
PHYS. PROPERTIES
CHEMISTRY
SECTION
METERS
GRAPHIC LITHOLOGY
DRILLING DISTURB.
SED. STRUCTURES
SAMPLES
LOWER OLIGOCENE
P20
NP23
Dorcadospyris ateuchus
?
A/M
A/M
A/M
C-A/M
V=1728● φ=54.7 ρ=1.79
● φ=54.3 ρ=1.78
V=2008● φ=50.6 ρ=1.85
●%CaCO3=94.5
●%CaCO3=95.0
●%CaCO3=95.0
1
2
3
4
CC
0.5
1.0
OG
IW

LITHOLOGIC DESCRIPTION

NANNOFOSSIL CHALK with FORAMINIFERS

Major lithology: This core contains NANNOFOSSIL CHALK with FORAMINIFERS. The sediment is white (2.5Y 8/0) with some pale pink (5RP 8/2) zones. Heavy bioturbation is evident from numerous trace fossils. Numerous very thin (<<1mm), dark gray (2.5Y 4/0), horizontal, wavy, and braided bands are evident throughout the core. Fracturing occurs readily along these surfaces, possibly indicative of micro-stylolitization.

SMEAR SLIDE SUMMARY (%)

	3, 75
	D
TEXTURE:	
Sand	10
Silt	55
Clay	35
COMPOSITION:	
Accessory minerals	2
Diatoms	Tr
Foraminifers	15
Nannofossils	80
Siliceous fragments	3

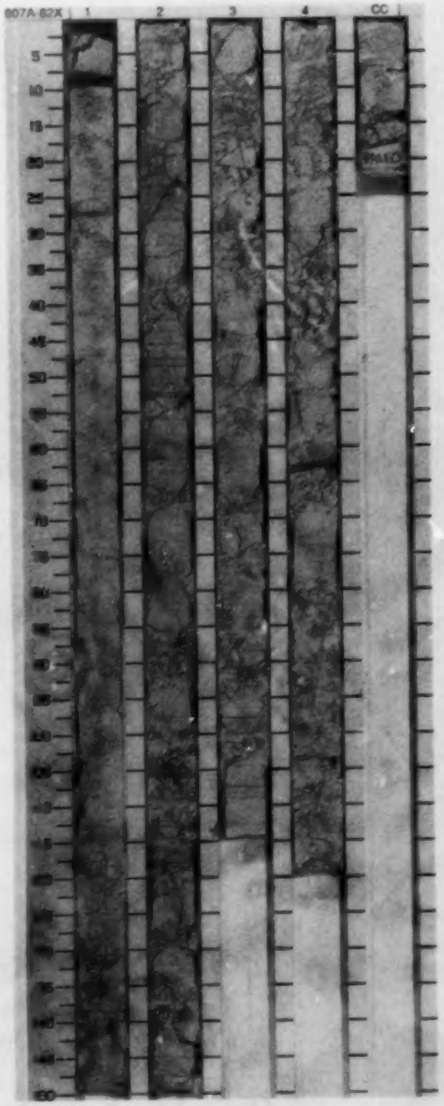
807A-82X
1
2
3
4
CC
5
10
15
20
25
30
35
40
45
50
55
60
65
70
75
80
85
90
95
100
105
110
115
120
125
130
135
140
145
150

SITE 807 HOLE A CORE 83X CORED INTERVAL 784.2-793.9 mbsf

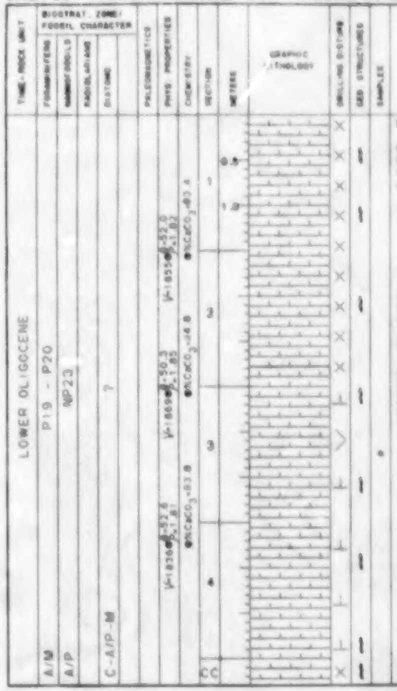
TIME-ROCK UNIT
BIOSTRAT. ZONE/ FOSSIL CHARACTER
FORAMINIFERS
NANNOFOSSILS
RADIOLARIANS
DIATOMS
PALEOMAGNETICS
PHYS. PROPERTIES
CHEMISTRY
SECTION
METERS
GRAPHIC LITHOLOGY
DRILLING DISTURB.
SED. STRUCTURES
SAMPLES
LOWER OLIGOCENE
P19 - P20
A/M
NP23
A/P
?
C-A/P-M
V=1855 ●Φ=52.0 γ=1.82
V=1869 ●Φ=50.3 γ=1.85
V=1830 ●Φ=52.6 γ=1.81
●%CaCO3=83.4
●%CaCO3=84.8
●%CaCO3=83.8
1
2
3
4
CC
0.5
1.0

LITHOLOGIC DESCRIPTION

NANNOFOSSIL CHALK with FORAMINIFERS

Major lithology: This core contains white (2.5Y 8.0) to pale pink (5RP 8/2) NANNOFOSSIL CHALK with FORAMINIFERS. Abundant bioturbation can be observed as trace fossils. Ultra thin dark gray (2.5Y 4/0) bands are evident throughout the core and fracturing occurs readily along them (possible microstylolites).

SMEAR SLIDE SUMMARY (%):

	3, 74
	D
TEXTURE:	
Sand	11
Silt	49
Clay	40
COMPOSITION:	
Accessory minerals	2
Diatoms	Tr
Foraminifers	15
Nannofossils	80
Siliceous fragments	3

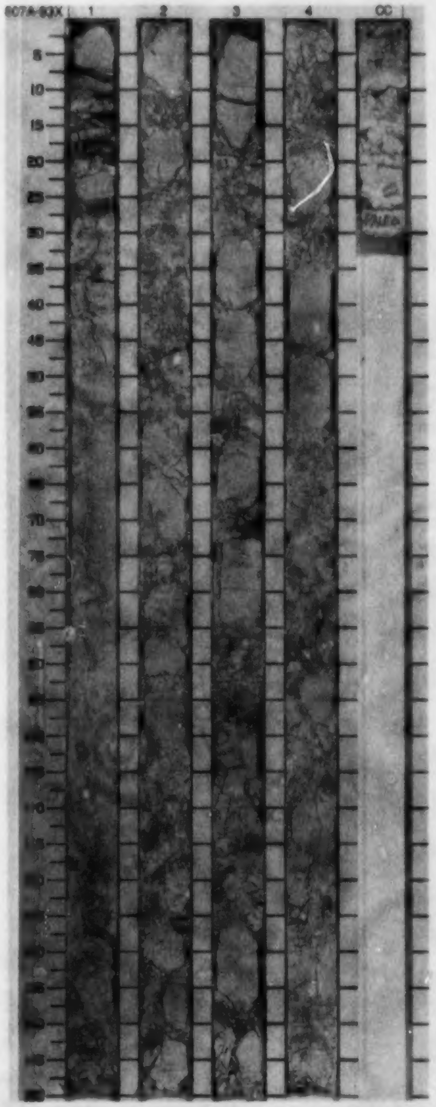
807A-83X
1
2
3
4
CC
5
10
15
20
25
30
35
40
45
50
55
60
65
70
75
80
85
90
95
100
105
110
115
120
125
130
135
140
145
150

SITE 807 HOLE A CORE 84X CORED INTERVAL 793.9-803.6 mbsf

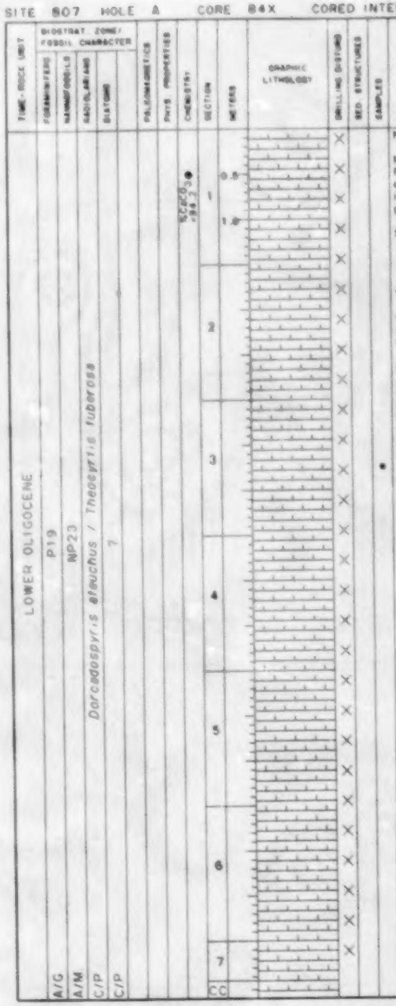
TIME-ROCK UNIT
BIOSTRAT. ZONE/ FOSSIL CHARACTER
FORAMINIFERS
NANNOFOSSILS
RADIOLARIANS
DIATOMS
PALEOMAGNETICS
PHYS. PROPERTIES
CHEMISTRY
SECTION
METERS
GRAPHIC LITHOLOGY
DRILLING DISTURB.
SED. STRUCTURES
SAMPLES
LOWER OLIGOCENE
P19
NP23
Dorcadospyris ateuchus / Theocyrtis tuberosa
?
A/G
A/M
C/P
C/P
%CaCO3 =94.2
1
2
3
4
5
6
7
CC
0.5
1.0

LITHOLOGIC DESCRIPTION

NANNOFOSSIL CHALK/OOZE with FORAMINIFERS

Major lithology: This core contains white (2.5Y 8/0) NANNOFOSSIL CHALK/OOZE with FORAMINIFERS. The core consists of highly fractured drilling biscuits and breccia in an ooze matrix. As a result, the *in-situ* state of lithification is not known. Structures are impossible to see as a result of this disturbance, though evidence for some of the ultra thin gray bands (microstylolites?) can be seen.

SMEAR SLIDE SUMMARY (%):

	3, 74
	D
TEXTURE:	
Sand	12
Silt	55
Clay	33
COMPOSITION:	
Accessory minerals	2
Diatoms	Tr
Foraminifers	15
Nannofossils	80
Siliceous fragments	3

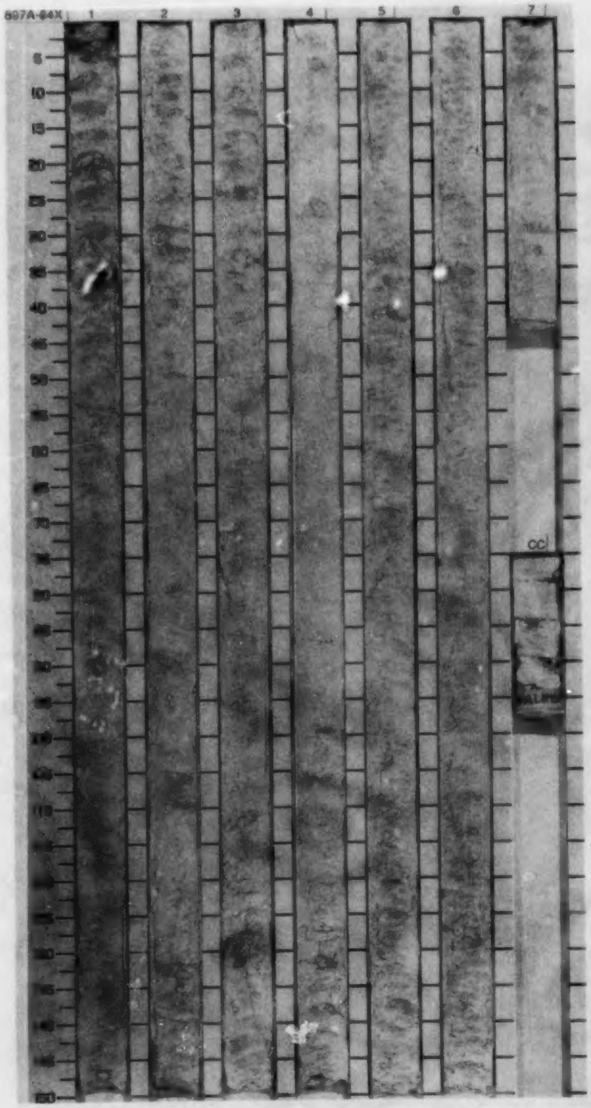
807A-84X
1
2
3
4
5
6
7
CC
5
10
15
20
25
30
35
40
45
50
55
60
65
70
75
80
85
90
95
100
105
110
115
120
125
130
135
140
145
150

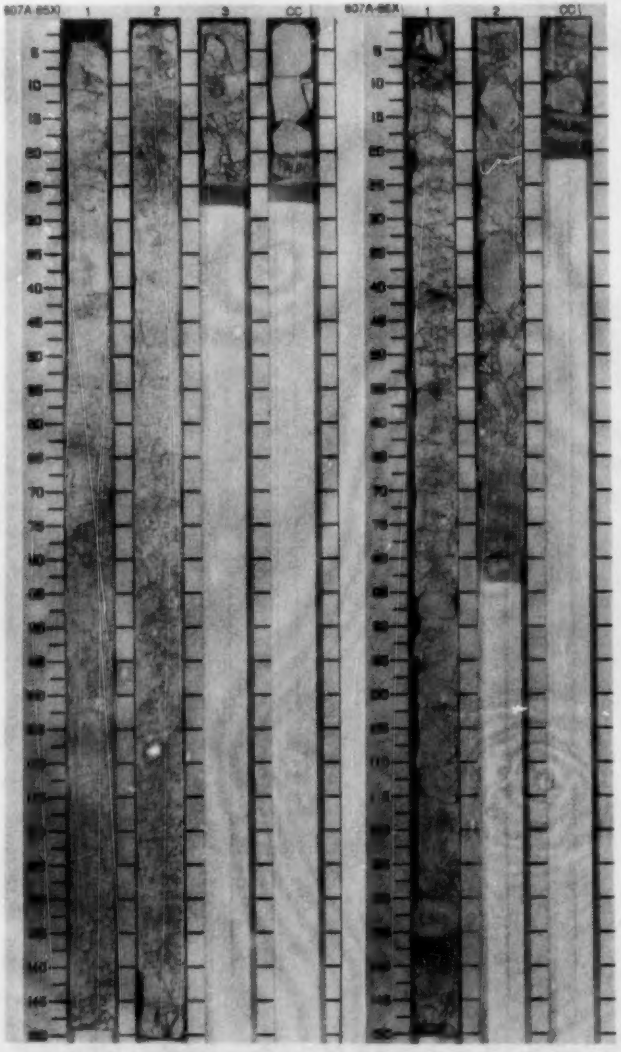

SITE 807 HOLE A CORE 85X CORED INTERVAL 803.6-813.2 mbsf

TIME-ROCK UNIT	FORAMINIFERS	NANNOFOSSILS	RADIOLARIANS	DIATOMS	PALEOMAGNETICS	PHYS. PROPERTIES	CHEMISTRY	SECTION	METERS	DRILLING DISTURB.	SAMPLES
LOWER OLIGOCENE	P19 A/G	NP23 A/M	*Theocyrtis tuberosa* A/P	? A/P-M				1 2 3 CC	0.5 1.0	× × × × × × ⊥	•

LITHOLOGIC DESCRIPTION

NANNOFOSSIL CHALK/OOZE

Major lithology: This core contains white (2.5Y 8/0) NANNOFOSSIL CHALK/OOZE. The entire core consists of highly fragmented drilling biscuits and breccia in an ooze matrix. A few signs of bioturbation are visible, such as *Zoophycos* trace fossils (Section 1), and faint mottles and pyritic specks. Fine [illegible] dark gray (2.5Y 4/0), straight and braided bands are observed in Section 2. Both Sections 1 and 2 contain several mm thick layers of pyrite.

SMEAR SLIDE SUMMARY (%):

	2, 70 D
TEXTURE:	
Sand	5
Silt	60
Clay	3
COMPOSITION:	
Foraminifers	8
Nannofossils	92

SITE 807 HOLE A CORE 86X CORED INTERVAL 813.2-822.9 mbsf

TIME-ROCK UNIT	FORAMINIFERS	NANNOFOSSILS	RADIOLARIANS	DIATOMS	PALEOMAGNETICS	PHYS. PROPERTIES	CHEMISTRY	SECTION	METERS	DRILLING DISTURB.	SAMPLES
LOWER OLIGOCENE	P19 A/M	NP23 A/M	*Theocyrtis tuberosa* A/P	*Coscinodiscus excavatus* C-A/M				1 2 CC	0.5 1.0		IW •

LITHOLOGIC DESCRIPTION

NANNOFOSSIL CHALK with FORAMINIFERS

Major lithology: This core contains white (2.5Y 8/0) NANNOFOSSIL CHALK with FORAMINIFERS. Sections 2 and 3 grade to pale blue (5B 8/2) at their bottoms. Traces of heavy bioturbation, such as faint mottles, are seen in intact biscuits. Drilling disturbance has produced highly fragmented biscuits in an ooze matrix.

SMEAR SLIDE SUMMARY (%):

	2, 13 D
TEXTURE:	
Sand	11
Silt	55
Clay	34
COMPOSITION:	
Accessory minerals	2
Foraminifers	15
Nannofossils	80
Radiolarians	1
Siliceous fragments	2

SITE 807 HOLE B CORE 1H CORED INTERVAL 0.0-3.1 mbsf

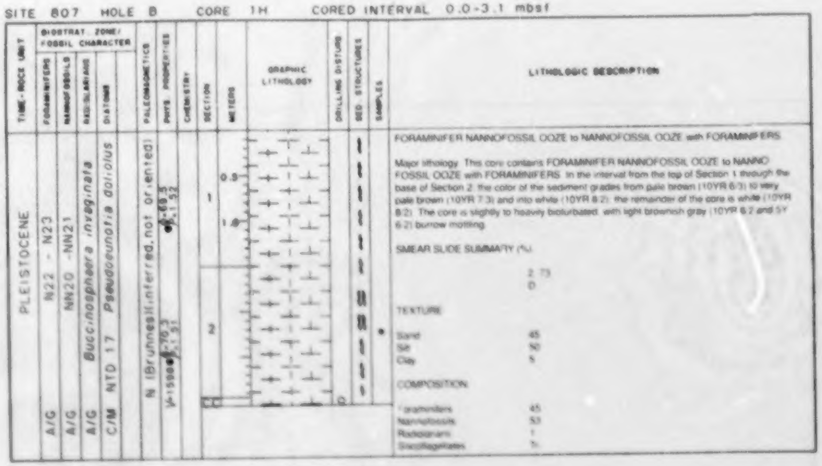

TIME-ROCK UNIT
BIOSTRAT. ZONE/ FOSSIL CHARACTER
FORAMINIFERS
NANNOFOSSILS
RADIOLARIANS
DIATOMS
PALEOMAGNETICS
PHYS. PROPERTIES
CHEMISTRY
SECTION
METERS
GRAPHIC LITHOLOGY
DRILLING DISTURB.
SED. STRUCTURES
SAMPLES
PLEISTOCENE
A/G N22 - N23
A/G NN20 -NN21
A/G Buccinosphaera invaginata
C/M NTD 17 Pseudoeunotia doliolus
N (Brunhes)(inferred, not oriented)
φ-69.5
γ-1.52
V-1590
φ-76.3
γ-1.51
1
2
CC
0.5
1.0

LITHOLOGIC DESCRIPTION

FORAMINIFER NANNOFOSSIL OOZE to NANNOFOSSIL OOZE with FORAMINIFERS

Major lithology: This core contains FORAMINIFER NANNOFOSSIL OOZE to NANNOFOSSIL OOZE with FORAMINIFERS. In the interval from the top of Section 1 through the base of Section 2, the color of the sediment grades from pale brown (10YR 6/3) to very pale brown (10YR 7/3) and into white (10YR 8/2); the remainder of the core is white (10YR 8/2). The core is slightly to heavily bioturbated, with light brownish gray (10YR 6/2 and 5Y 6/2) burrow mottling.

SMEAR SLIDE SUMMARY (%):

	2, 73
	D
TEXTURE:	
Sand	45
Silt	50
Clay	5
COMPOSITION:	
Foraminifers	45
Nannofossils	53
Radiolarians	1
Silicoflagellates	Tr

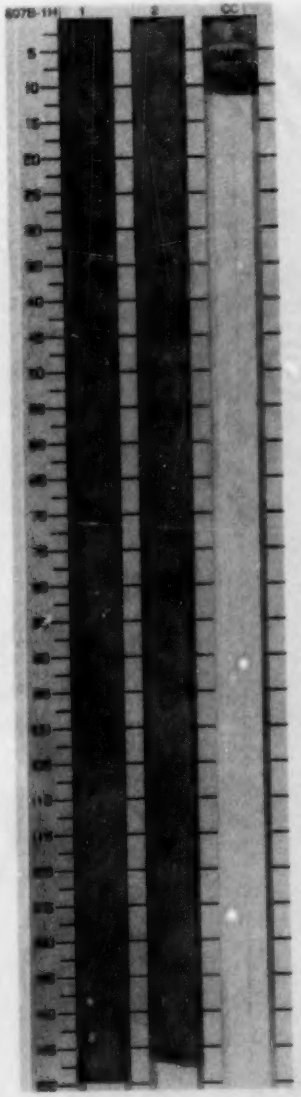

807B-1H
1
2
CC
5
10
15
20
25
30
35
40
45
50
55
60
65
70
75
80
85
90
95
100
105
110
115
120
125
130
135
140
145
150

SITE 807 HOLE B CORE 2H CORED INTERVAL 3.1-12.6 mbsf

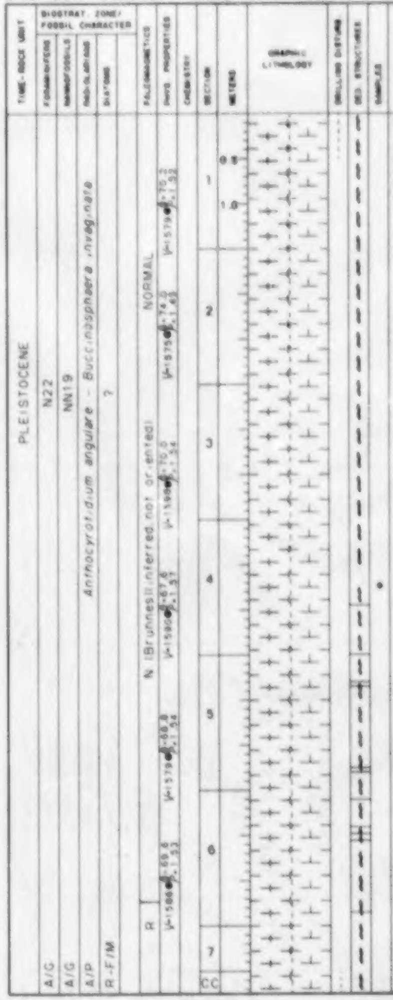
TIME-ROCK UNIT
BIOSTRAT. ZONE/ FOSSIL CHARACTER
FORAMINIFERS
NANNOFOSSILS
RADIOLARIANS
DIATOMS
PALEOMAGNETICS
PHYS. PROPERTIES
CHEMISTRY
SECTION
METERS
GRAPHIC LITHOLOGY
DRILLING DISTURB.
SED. STRUCTURES
SAMPLES
PLEISTOCENE
N22
NN19
Anthocyrtidium angulare - Buccinosphaera invaginata
?
A/G
A/G
A/P
R-F/M
NORMAL
N (Brunnes)(inferred not oriented)
R
V=1579 φ=70.2 γ=1.92
V=1575 φ=74.0 γ=1.63
V=1566 φ=70.0 γ=1.54
V=1590 φ=67.6 γ=1.57
V=1579 φ=68.8 γ=1.54
V=1586 φ=69.6 γ=1.53
1
2
3
4
5
6
7
CC
0.5
1.0

LITHOLOGIC DESCRIPTION

FORAMINIFER NANNOFOSSIL OOZE to NANNOFOSSIL OOZE with FORAMINIFERS

Major lithology: This core contains slightly to moderately bioturbated FORAMINIFER NANNOFOSSIL OOZE to NANNOFOSSIL OOZE with FORAMINIFERS. The color from the top of Section 1 to Section 2, 120 cm, is white (10YR 8/2); the rest of the core alternates between white (2.5Y 8/0 and 7.5YR 8/0) and light gray (2.5Y 7/0). Below Section 4, light gray (5Y 7/1) cm scale mottles were observed. Light greenish gray (5G 7/1) color bands and rarer grayish blue (5PB 5/2) color bands are present in Sections 4 through 7.

SMEAR SLIDE SUMMARY (%):

	4, 72 D
TEXTURE:	
Sand	40
Silt	55
Clay	5
COMPOSITION:	
Foraminifers	30
Nannofossils	65
Radiolarians	3
Silicoflagellates	Tr

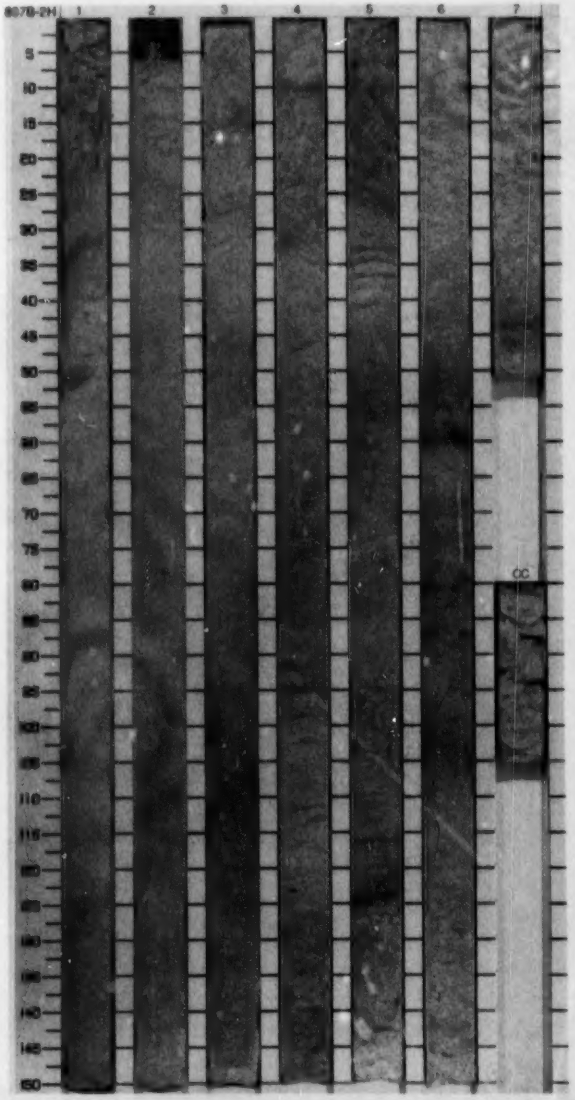
807B-2H
1
2
3
4
5
6
7
CC
5
10
15
20
25
30
35
40
45
50
55
60
65
70
75
80
85
90
95
100
105
110
115
120
125
130
135
140
145
150

SITE 807 HOLE B CORE 3H CORED INTERVAL 12.6-22.1 mbsf

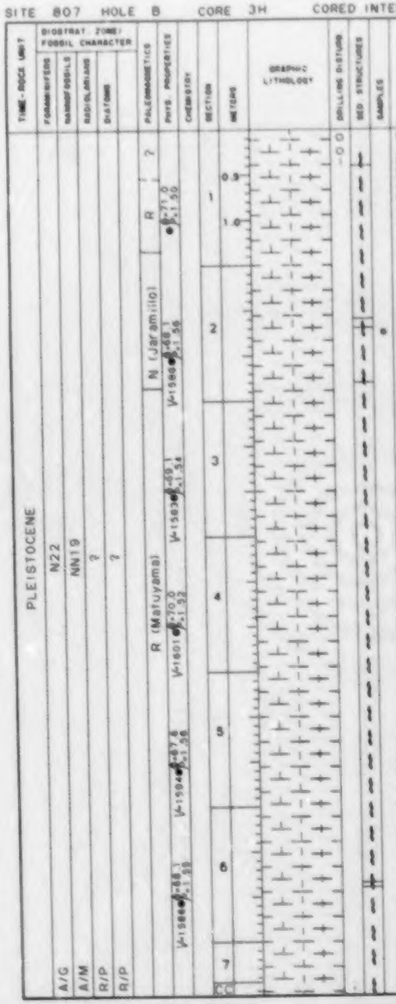
TIME-ROCK UNIT
BIOSTRAT. ZONE/ FOSSIL CHARACTER
FORAMINIFERS
NANNOFOSSILS
RADIOLARIANS
DIATOMS
PALEOMAGNETICS
PHYS. PROPERTIES
CHEMISTRY
SECTION
METERS
GRAPHIC LITHOLOGY
DRILLING DISTURB.
SED. STRUCTURES
SAMPLES
PLEISTOCENE
N22
NN19
?
?
A/G
A/M
R/P
R/P
?
R
N (Jaramillo)
R (Matuyama)
φ=71.0
γ=1.50
V=1586
φ=68.1
γ=1.56
V=1583
φ=69.1
γ=1.54
V=1601
φ=70.0
γ=1.52
V=1594
φ=67.8
γ=1.56
V=1586
φ=68.1
γ=1.55
1
2
3
4
5
6
7
CC
0.5
1.0

LITHOLOGIC DESCRIPTION

FORAMINIFER NANNOFOSSIL OOZE to NANNOFOSSIL OOZE with FORAMINIFERS

Major lithology: This core contains interbedded FORAMINIFER NANNOFOSSIL OOZE to NANNOFOSSIL OOZE with FORAMINIFERS. The color grades from light gray (N7) to white (2.5Y 8.0). Diffuse intervals of gray (N6) with a slight purplish tint are observed. Slight bioturbation is documented by grayish blue (5PB 5.2), pyrite filled burrows and minor light gray (2.5Y 7.1) and gray (N6) mottling. Diffuse light greenish gray (5G 7.10) color bands are evident in Sections 1, 2 and 6.

SMEAR SLIDE SUMMARY (%):

	2, 75
	D
TEXTURE:	
Sand	25
Silt	70
Clay	5
COMPOSITION:	
Foraminifers	25
Nannofossils	70
Quartz	Tr
Radiolarians	2
Silicoflagellates	Tr

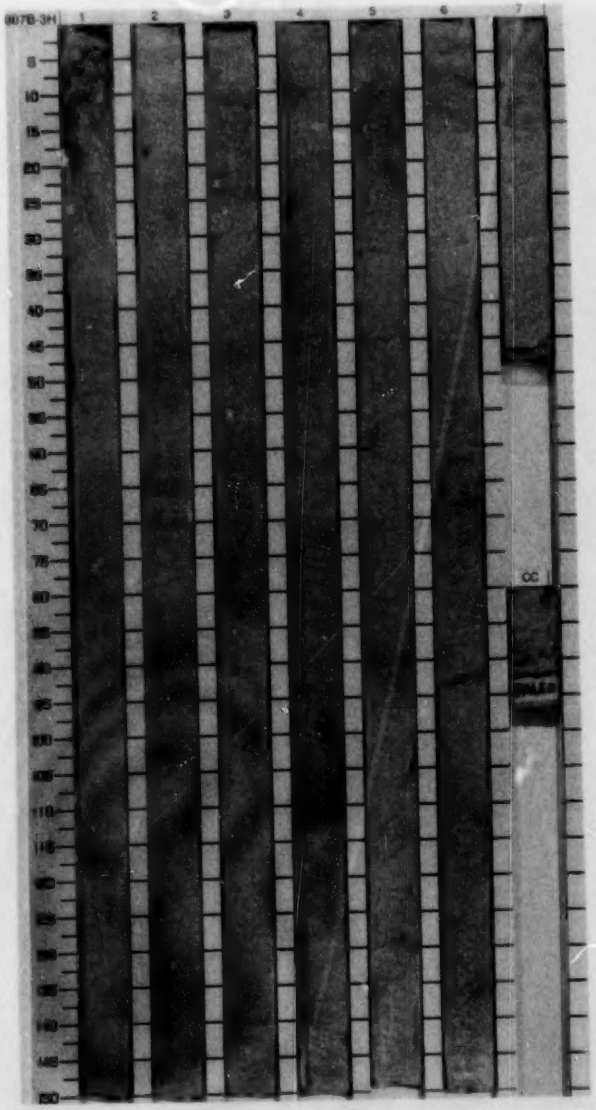
807B-3H
1
2
3
4
5
6
7
CC
5
10
15
20
25
30
35
40
45
50
55
60
65
70
75
80
85
90
95
100
105
110
115
120
125
130
135
140
145
150

SITE 807 HOLE B CORE 4H CORED INTERVAL 22.1-31.6 mbsf

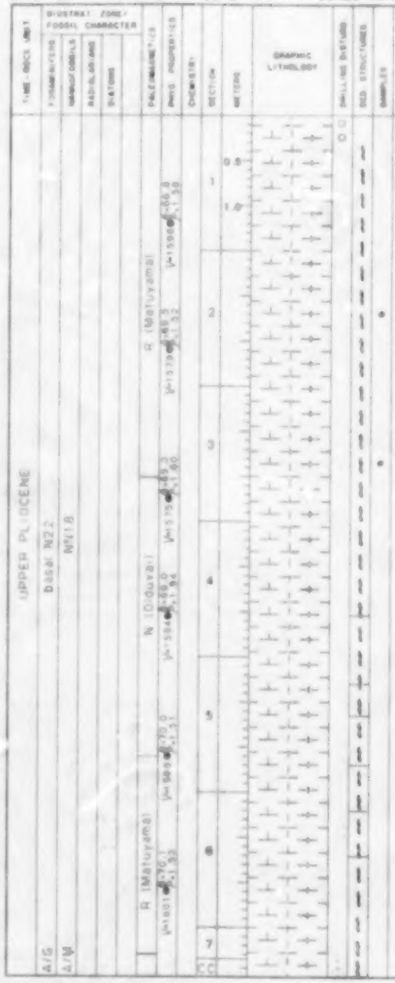
TIME-ROCK UNIT
BIOSTRAT. ZONE/ FOSSIL CHARACTER
FORAMINIFERS
NANNOFOSSILS
RADIOLARIANS
DIATOMS
PALEOMAGNETICS
PHYS. PROPERTIES
CHEMISTRY
SECTION
METERS
GRAPHIC LITHOLOGY
DRILLING DISTURB.
SED. STRUCTURES
SAMPLES
UPPER PLIOCENE
A/G
Basal N22
A/M
NN18
R (Matuyama)
N (Olduvai)
R (Matuyama)
1
2
3
4
5
6
7
CC
0.5
1.0

LITHOLOGIC DESCRIPTION

FORAMINIFER NANNOFOSSIL OOZE to NANNOFOSSIL OOZE with FORAMINIFERS

Major lithology: This core contains interbedded FORAMINIFER NANNOFOSSIL OOZE to NANNOFOSSIL OOZE with FORAMINIFERS. The color of the sediment is gradational between light gray (N7) and white (2.5Y 8/0). The sediment is slightly to moderately bioturbated with light gray (N7) mottling. Faint light greenish gray (5G 7/1) color bands are observed in Sections 4 through 6.

SMEAR SLIDE SUMMARY (%):

	2, 70 D	3, 74 D
TEXTURE:		
Sand	48	15
Silt	50	60
Clay	2	25
COMPOSITION:		
Accessory minerals	—	2
Diatoms	—	Tr
Foraminifers	40	28
Nannofossils	55	67
Quartz	Tr	—
Radiolarians	2	—
Siliceous fragments	—	3
Silicoflagellates	Tr	—

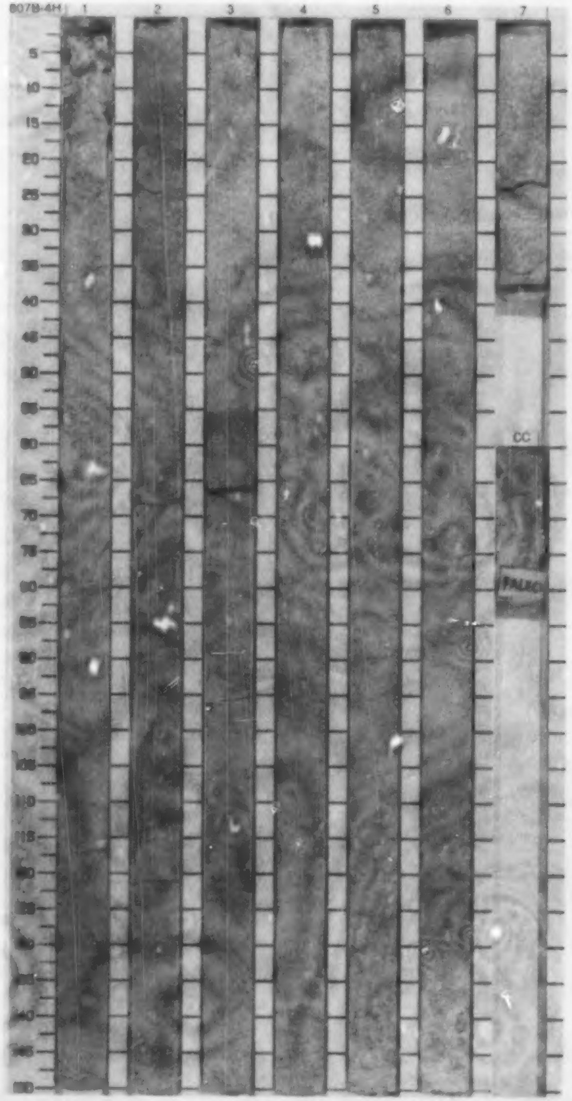
807B-4H
1
2
3
4
5
6
7
CC
PALEO
5
10
15
20
25
30
35
40
45
50
55
60
65
70
75
80
85
90
95
100
105
110
115
120
125
130
135
140
145
150

SITE 807 HOLE B CORE 5H CORED INTERVAL 31.6-41.1 mbsf

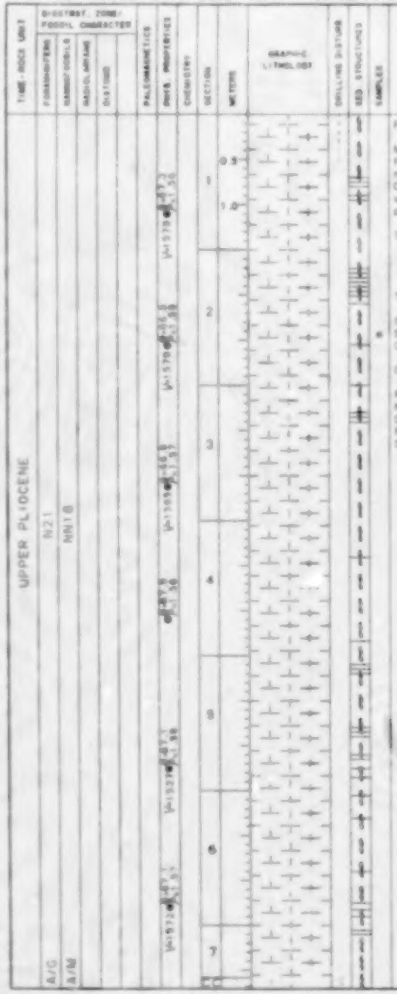
TIME-ROCK UNIT
BIOSTRAT. ZONE/ FOSSIL CHARACTER
FORAMINIFERS
NANNOFOSSILS
RADIOLARIANS
DIATOMS
PALEOMAGNETICS
PHYS. PROPERTIES
CHEMISTRY
SECTION
METERS
GRAPHIC LITHOLOGY
DRILLING DISTURB.
SED. STRUCTURES
SAMPLES
UPPER PLIOCENE
N21
NN18
A/G
A/M
0.5
1.0
1
2
3
4
5
6
7
CC

LITHOLOGIC DESCRIPTION

FORAMINIFER NANNOFOSSIL OOZE to NANNOFOSSIL OOZE with FORAMINIFERS

Major lithology: This core consists white (2.5Y 8/0) bioturbated FORAMINIFER NANNOFOSSIL OOZE to NANNOFOSSIL OOZE with FORAMINIFERS. Bioturbation is slight to moderate in Sections 1 through 5, and moderate to heavy in Sections 6 through Core Catcher. Bioturbation is expressed as both cm-scale light gray (2.5Y 7/2) mottling and cm-scale dark gray (N5) pyrite-filled burrows. Light greenish gray (5G 7/1), light gray (N7), pale purple (5P 6/2), and grayish blue (5PB 5/2) color banding is present to abundant core.

SMEAR SLIDE SUMMARY (%):

	2, 92
	D
TEXTURE:	
Sand	35
Silt	60
Clay	5
COMPOSITION:	
Foraminifers	38
Nannofossils	57
Quartz	Tr
Radiolarians	2
Silicoflagellates	Tr

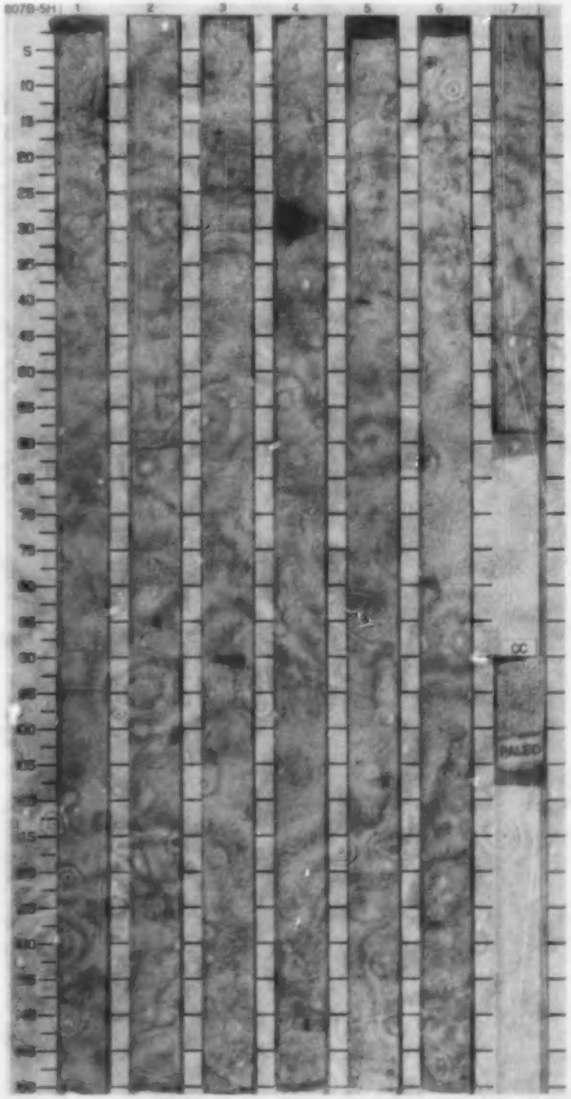
807B-5H
1
2
3
4
5
6
7
5
10
15
20
25
30
35
40
45
50
55
60
65
70
75
80
85
90
95
100
105
110
115
120
125
130
135
140
145
150
CC
PALEO

SITE 807 HOLE B CORE 6H CORED INTERVAL 41.1-50.6 mbsf

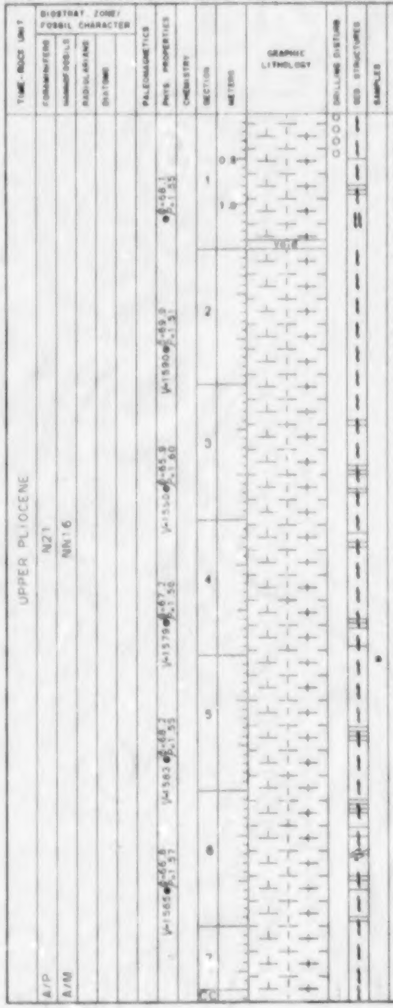
TIME-ROCK UNIT
BIOSTRAT. ZONE/ FOSSIL CHARACTER
FORAMINIFERS
NANNOFOSSILS
RADIOLARIANS
DIATOMS
PALEOMAGNETICS
PHYS. PROPERTIES
CHEMISTRY
SECTION
METERS
GRAPHIC LITHOLOGY
DRILLING DISTURB.
SED. STRUCTURES
SAMPLES
UPPER PLIOCENE
N21
NN16
A/P
A/M
φ-68.1 γ-1.55
V-1590 φ-69.0 γ-1.51
V-1550 φ-65.9 γ-1.60
V-1579 φ-67.2 γ-1.50
V-1583 φ-68.2 γ-1.55
V-1565 φ-66.8 γ-1.57
1
2
3
4
5
6
7
CC
0.5
1.0
VOID

LITHOLOGIC DESCRIPTION

FORAMINIFER NANNOFOSSIL OOZE to NANNOFOSSIL OOZE with FORAMINIFERS

Major lithology: This core contains white (2.5Y 8/0 to 10YR 8/1) and pale pink (5RP 8/2) interbedded FORAMINIFER NANNOFOSSIL OOZE to NANNOFOSSIL OOZE with FORAMINIFERS. Core is slightly to heavily bioturbated, with cm scale light gray (5Y 7/2) mottles and grayish blue (5PB 5/2), pyrite filled burrows. Grayish blue (5PB 5/2), light greenish gray (5G 7/1), and pale purple (5P 6/2) to light gray (N7) color bands are present to abundant. A microfault at Section _, 60 cm, offsets color bands.

SMEAR SLIDE SUMMARY (%):

	5, 5
	D
TEXTURE	
Sand	15
Silt	80
Clay	5
COMPOSITION	
Foraminifers	10
Nannofossils	85
Quartz	Tr
Radiolarians	2
Silicoflagellates	Tr

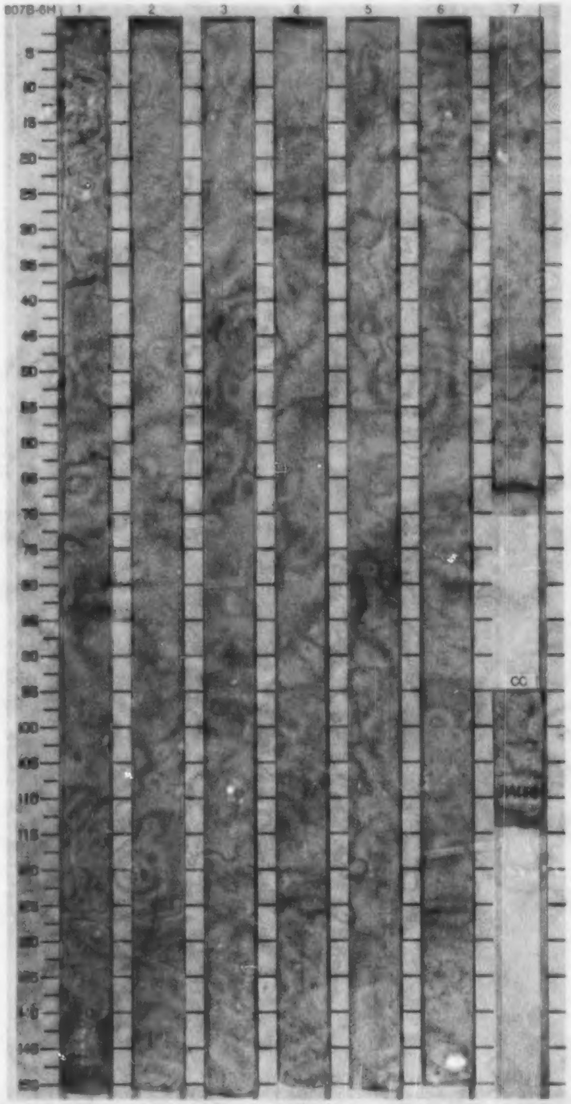
807B-6H
1
2
3
4
5
6
7
CC
VOID
5
10
15
20
25
30
35
40
45
50
55
60
65
70
75
80
85
90
95
100
105
110
115
120
125
130
135
140
145
150

SITE 807 HOLE B CORE 7H CORED INTERVAL 50.6-60.1 mbsf

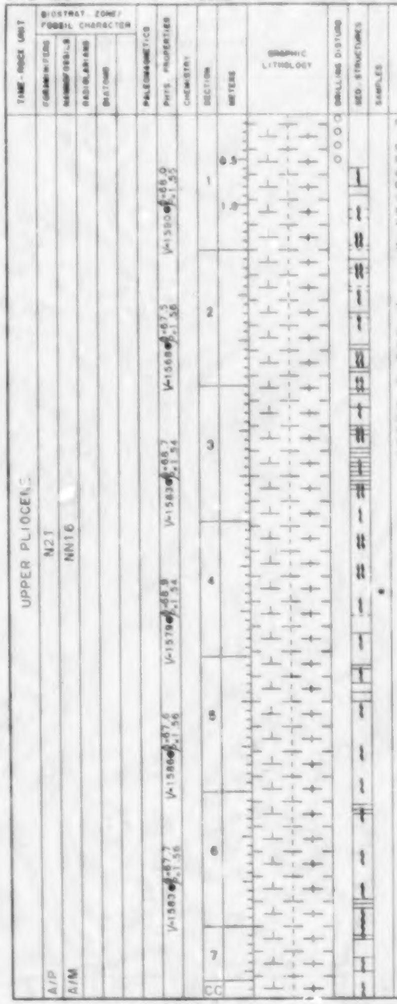
TIME-ROCK UNIT
BIOSTRAT. ZONE/ FOSSIL CHARACTER
FORAMINIFERS
NANNOFOSSILS
RADIOLARIANS
DIATOMS
PALEOMAGNETICS
PHYS. PROPERTIES
CHEMISTRY
SECTION
METERS
GRAPHIC LITHOLOGY
DRILLING DISTURB.
SED. STRUCTURES
SAMPLES
UPPER PLIOCENE
N21
NN16
A/P
A/M
V-1590 φ-68.0 γ-1.55
V-1568 φ-67.5 γ-1.56
V-1583 φ-66.7 γ-1.54
V-1579 φ-68.8 γ-1.54
V-1586 φ-67.6 γ-1.56
V-1583 φ-67.7 γ-1.56
1
2
3
4
5
6
7
CC
0.5
1.0

LITHOLOGIC DESCRIPTION

FORAMINIFER NANNOFOSSIL OOZE to NANNOFOSSIL OOZE with FORAMINIFERS

Major lithology: This core contains white (2.5Y 8.0) interbedded FORAMINIFER NANNOFOSSIL OOZE to NANNOFOSSIL OOZE with FORAMINIFERS. The sediment is moderately to heavily bioturbated, with cm-scale light gray (5Y 7/2), vertical and horizontal burrows. The burrow fills are often sandier than the surrounding sediment. Grayish blue (5PB 5/2), commonly vertical, mm-size, pyrite burrows are less common. Light greenish gray (5G 7/1), and pale purple (5P 6/2) to grayish blue (PB 5/2) color bands are present to abundant.

SMEAR SLIDE SUMMARY (%):

	4, 79
	D
TEXTURE	
Sand	30
Silt	65
Clay	5
COMPOSITION	
Foraminifers	35
Nannofossils	60
Quartz	Tr
Radiolarians	2
Silicoflagellates	Tr

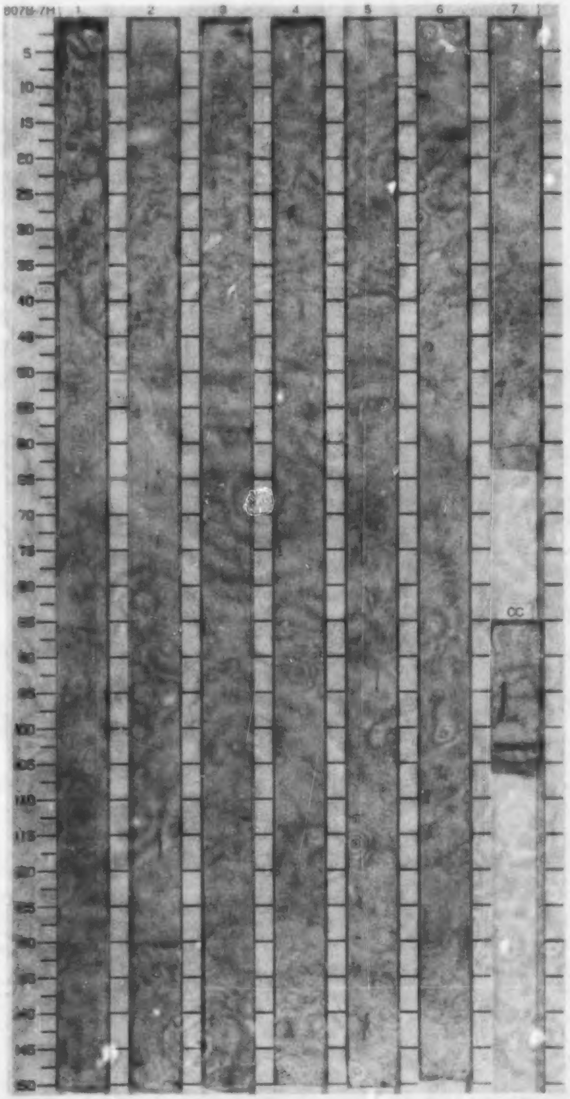
807B-7H
1
2
3
4
5
6
7
CC
5
10
15
20
25
30
35
40
45
50
55
60
65
70
75
80
85
90
95
100
105
110
115
120
125
130
135
140
145
150

SITE 807 HOLE B CORE 8H CORED INTERVAL 60.1-69.6 mbsf

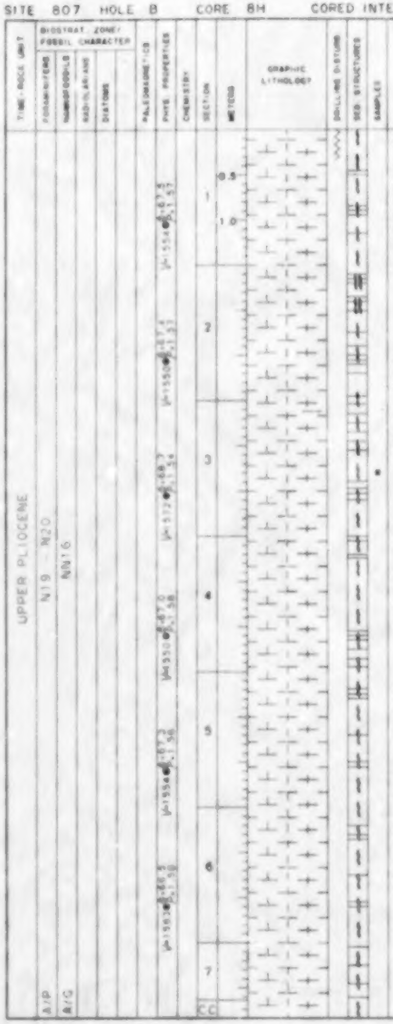
TIME-ROCK UNIT
BIOSTRAT. ZONE/ FOSSIL CHARACTER
FORAMINIFERS
NANNOFOSSILS
RADIOLARIANS
DIATOMS
PALEOMAGNETICS
PHYS. PROPERTIES
CHEMISTRY
SECTION
METERS
GRAPHIC LITHOLOGY
DRILLING DISTURB.
SED. STRUCTURES
SAMPLES
UPPER PLIOCENE
N19 - N20
NN16
A/P
A/G
0.5
1.0
1
2
3
4
5
6
7
CC

LITHOLOGIC DESCRIPTION

FORAMINIFER NANNOFOSSIL OOZE to NANNOFOSSIL OOZE with FORAMINIFERS

Major lithology: This core contains white (2.5Y 8/0) interbedded FORAMINIFER NANNOFOSSIL OOZE and NANNOFOSSIL OOZE with FORAMINIFERS. Slight to heavy bioturbation is indicated by cm scale, light gray (2.5Y 7/2) and grayish blue (5PB 5/2) pyritized burrows. Light greenish gray (5G 7/1) color bands are present to abundant throughout the core. Pale purple (5P 6/2) to grayish blue (PB 5/2) color bands are less common and are present in Sections 1 through 5.

SMEAR SLIDE SUMMARY (%):

	3, 80 D
TEXTURE:	
Sand	35
Silt	60
Clay	5
COMPOSITION:	
Foraminifers	35
Nannofossils	60
Quartz	Tr
Radiolarians	2
Silicoflagellates	Tr

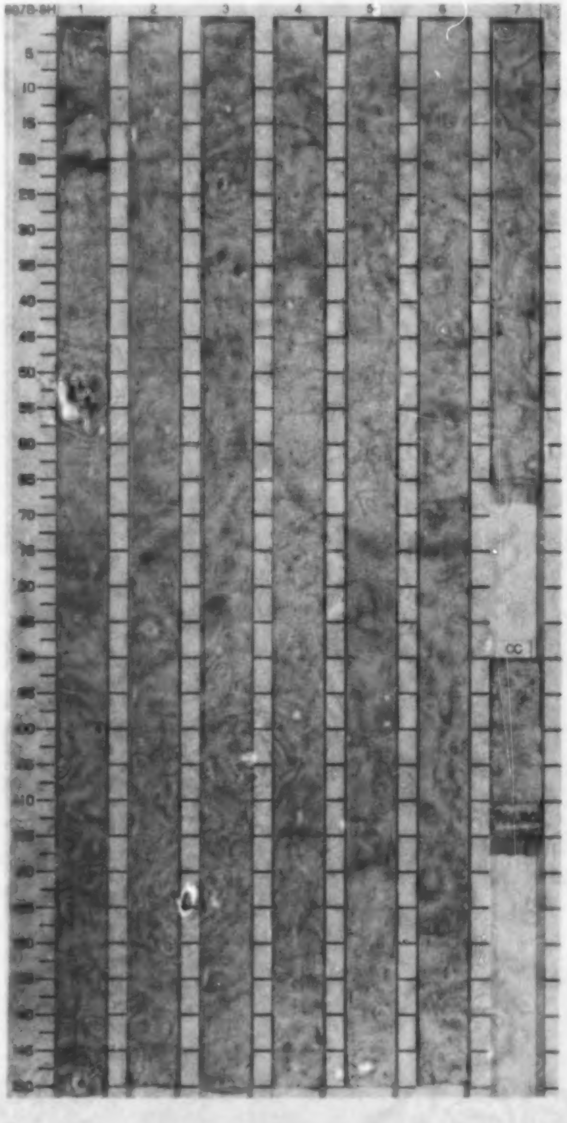
807B-8H
1
2
3
4
5
6
7
CC
5
10
15
20
25
30
35
40
45
50
55
60
65
70
75
80
85
90
95
100
105
110
115
120
125
130
135
140
145
150

SITE 807 HOLE B CORE 9H CORED INTERVAL 69.6-79.1 mbsf

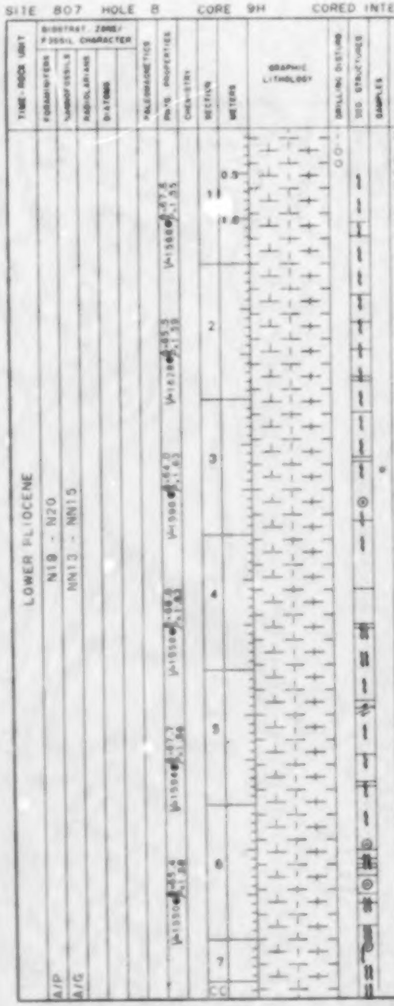
TIME-ROCK UNIT
BIOSTRAT. ZONE/ FOSSIL CHARACTER
FORAMINIFERS
NANNOFOSSILS
RADIOLARIANS
DIATOMS
PALEOMAGNETICS
PHYS. PROPERTIES
CHEMISTRY
SECTION
METERS
GRAPHIC LITHOLOGY
DRILLING DISTURB.
SED. STRUCTURES
SAMPLES
LOWER PLIOCENE
N18 - N20
NN13 - NN15
A/P
A/G
0.5
1.0
1
2
3
4
5
6
7
CC

LITHOLOGIC DESCRIPTION

FORAMINIFER NANNOFOSSIL OOZE to NANNOFOSSIL OOZE with FORAMINIFERS

Major lithology: This core contains white (2.5Y 8.0) interbedded FORAMINIFER NANNOFOSSIL OOZE to NANNOFOSSIL OOZE with FORAMINIFERS. Slight to heavy bioturbation is indicated by cm-scale light gray (2.5Y 7.2 and 5Y7.1) mottling and grayish blue (5PB 5.2) pyritized burrows. Light greenish gray (5G 7.1) color bands are present to abundant throughout the core; white pale purple (5P 6.2) to grayish blue (PB 5.2) color bands are less common. A color band at 52-55 cm in Section 5 is microfaulted. Pyrite nodules are present in Sections 3 and 6.

SMEAR SLIDE SUMMARY (%):

	3, 79 D
TEXTURE:	
Sand	25
Silt	70
Clay	5
COMPOSITION:	
Foraminifers	30
Nannofossils	69
Siliceous fragments	1

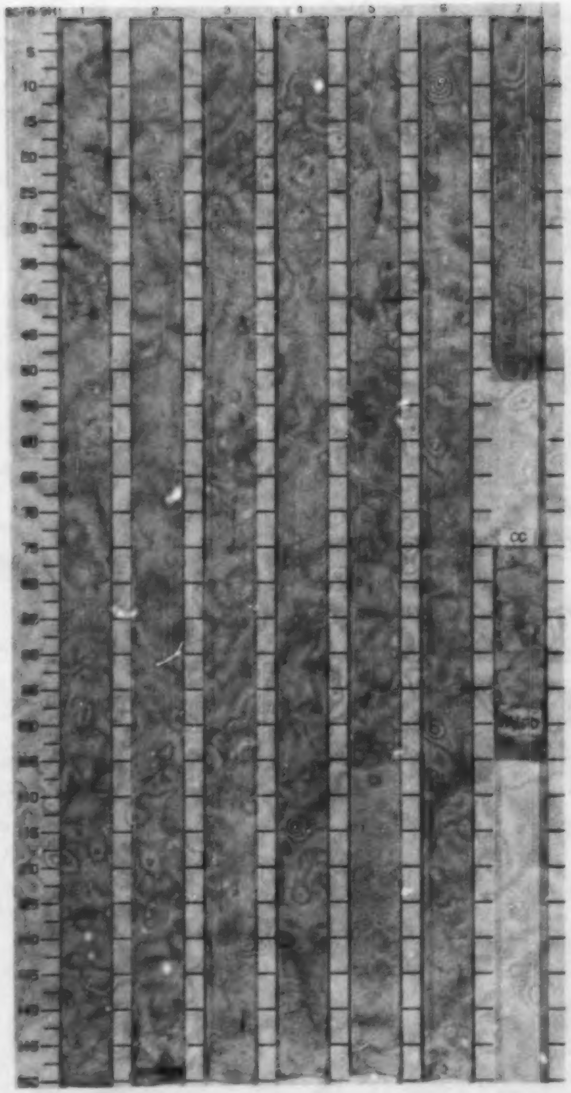
807B 9H
1
2
3
4
5
6
7
CC

SITE 807 HOLE B CORE 10H CORED INTERVAL 79.1-88.6 mbsf

TIME-ROCK UNIT	FORAMINIFERS	NANNOFOSSILS	RADIOLARIANS	DIATOMS	PALEOMAGNETICS	PHYS. PROPERTIES	CHEMISTRY	SECTION	METERS	GRAPHIC LITHOLOGY	DRILLING DISTURB.	SED. STRUCTURES	SAMPLES
LOWER PLIOCENE	N18 - N19	NN13 - NN15				V-1561 ● φ-66.3 γ-1.59		1	0.5 1.0				
						V-1558 ● φ-66.3 γ-1.59		2					
						V-1554 ● φ-65.9 γ-1.58		3					●
						V-1565 ● φ-67.1 γ-1.58		4					
						● φ-65.4 γ-1.60		5					
						V-1550 ● φ-65.7 γ-1.59		6					
								7					
	A/P	A/M						CC					

LITHOLOGIC DESCRIPTION

FORAMINIFER NANNOFOSSIL OOZE to NANNOFOSSIL OOZE with FORAMINIFERS

Major lithology: This core contains white (2.5Y 8/0), interbedded FORAMINIFER NANNOFOSSIL OOZE and NANNOFOSSIL OOZE with FORAMINIFERS. Slight to heavy bioturbation is indicated by cm-scale, light gray (2.5Y 7/2) mottling, by individual, vertical and horizontal burrows, and by grayish blue (5PB 6/2), pyritized, commonly vertical, burrows. Light greenish gray (5G 7/1) color bands are common to abundant throughout this core, while pale purple (5P 6/2) to grayish blue (PB 5/2) color bands are present but less common.

SMEAR SLIDE SUMMARY (%):

	3, 88
	D
TEXTURE:	
Sand	30
Silt	65
Clay	5
COMPOSITION:	
Foraminifers	28
Nannofossils	67
Radiolarians	2
Siliceous fragments	Tr
Silicoflagellates	Tr

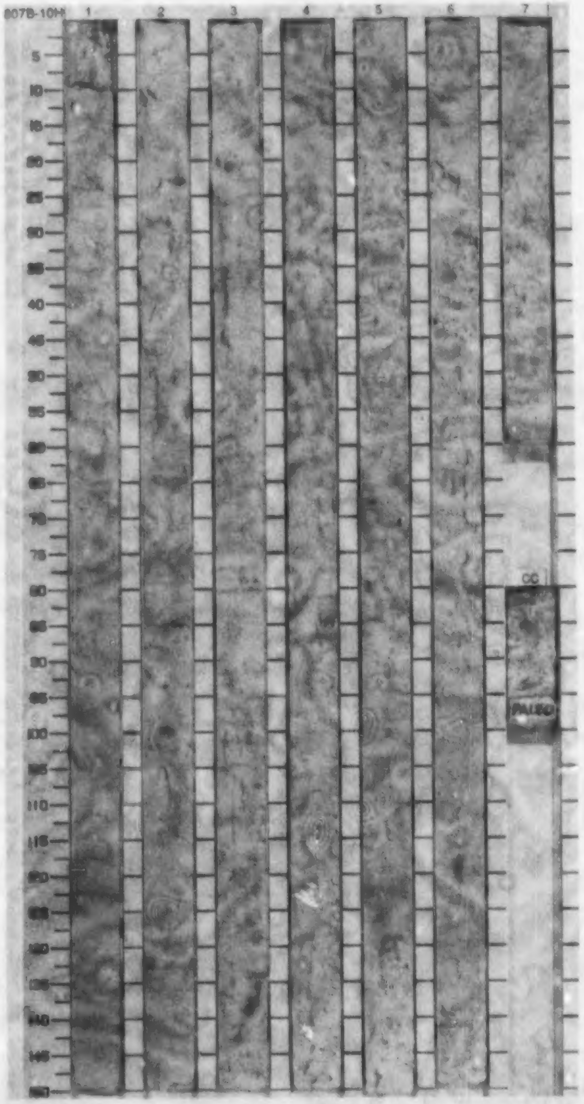

SITE 807 HOLE B CORE 11H CORED INTERVAL 88.6-98.1 mbsf

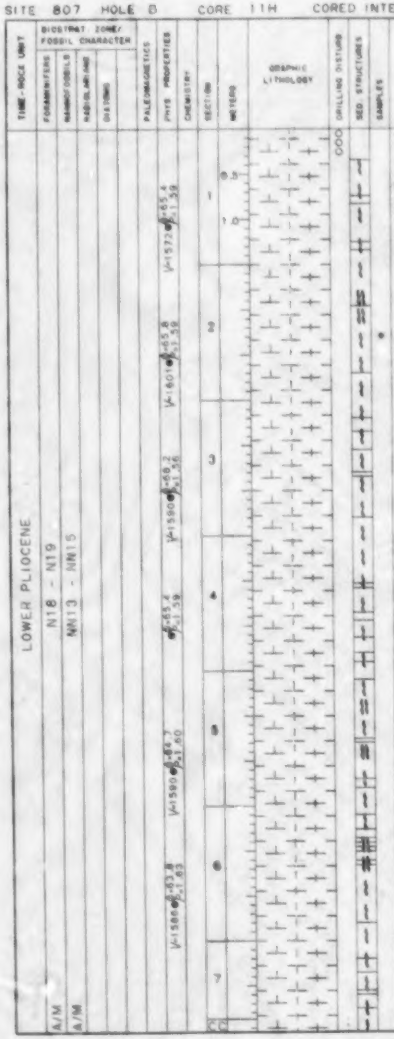

LITHOLOGIC DESCRIPTION

FORAMINIFER NANNOFOSSIL OOZE to NANNOFOSSIL OOZE with FORAMINIFERS

Major lithology: This core contains white (2.5Y 8/0) interbedded FORAMINIFER NANNOFOSSIL OOZE and NANNOFOSSIL OOZE with FORAMINIFERS. Slight to heavy bioturbation is indicated by cm-scale, light gray (2.5Y 7/2) mottling, by individual, vertical and horizontal burrows, and by grayish blue (5PB 5/2) pyritized, commonly vertical burrows. Light greenish gray (5G 7/1) color bands are common to abundant throughout this core, while pale purple (5P 6/2) to grayish blue (PB 5/2) color bands are present but less common.

SMEAR SLIDE SUMMARY (%):

	2, 79
	D
TEXTURE	
Sand	30
Silt	65
Clay	5
COMPOSITION	
Foraminifers	35
Nannofossils	60
Radiolarians	2
Siliceous fragments	Tr
Silicoflagellates	Tr

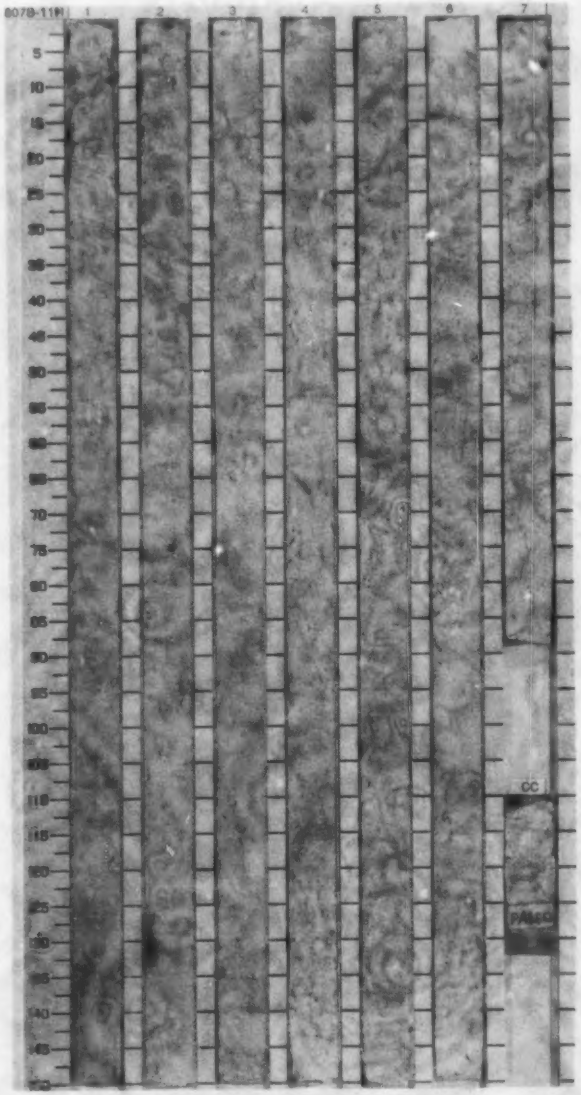
807B-11H
1
2
3
4
5
6
7
5
10
15
20
25
30
35
40
45
50
55
60
65
70
75
80
85
90
95
100
105
110
115
120
125
130
135
140
145
150
CC
PALEO

SITE 807 HOLE B CORE 12H CORED INTERVAL 98.1-107.6 mbsf

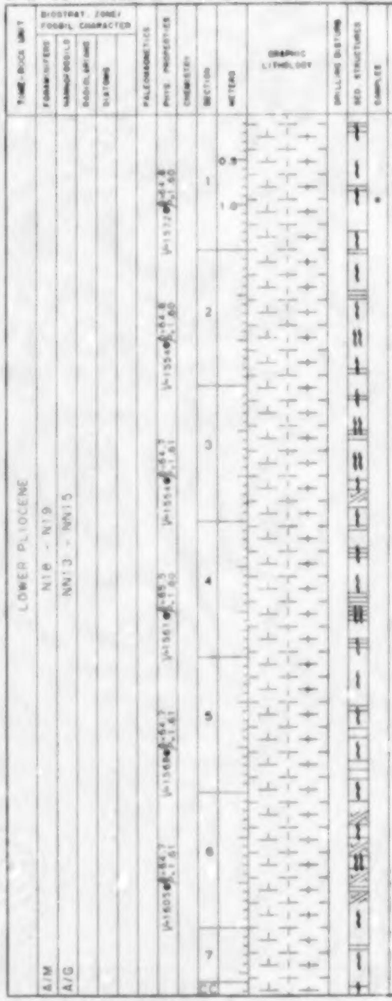
TIME-ROCK UNIT
BIOSTRAT. ZONE/ FOSSIL CHARACTER
FORAMINIFERS
NANNOFOSSILS
RADIOLARIANS
DIATOMS
PALEOMAGNETICS
PHYS. PROPERTIES
CHEMISTRY
SECTION
METERS
GRAPHIC LITHOLOGY
DRILLING DISTURB.
SED. STRUCTURES
SAMPLES
LOWER PLIOCENE
N18 - N19
NN13 - NN15
A/M
A/G
V=1572 φ=64.8 ρ=1.60
V=1554 φ=64.8 ρ=1.60
V=1554 φ=64.7 ρ=1.61
V=1561 φ=65.3 ρ=1.60
V=1568 φ=64.7 ρ=1.61
V=1605 φ=64.7 ρ=1.61
1
2
3
4
5
6
7
CC
0.5
1.0

LITHOLOGIC DESCRIPTION

FORAMINIFER NANNOFOSSIL OOZE to NANNOFOSSIL OOZE with FORAMINIFERS

Major lithology: This core contains white (2.5Y 8/0) microbedded FORAMINIFER NANNOFOSSIL OOZE to NANNOFOSSIL OOZE with FORAMINIFERS. Slight to heavy bioturbation is represented by cm scale, light gray (2.5Y 7/2) mottling and grayish blue (5PB 5/2) pyritized, commonly vertical burrows. Light greenish gray (5G 7/1) color bands are common to abundant through this core, while pale purple (5P 6/2) to grayish blue (PB 5/2) color bands are present but less common. Microfaults are observed in Section 3, 135 cm, and in Section 6, 35 cm, 70 cm, 95 cm 100 cm, 112 cm, and 121 cm.

SMEAR SLIDE SUMMARY (%):

	1, 97 D
TEXTURE:	
Sand	10
Silt	86
Clay	4
COMPOSITION:	
Diatoms	1
Foraminifers	20
Nannofossils	76
Radiolarians	2
Silicoflagellates	1

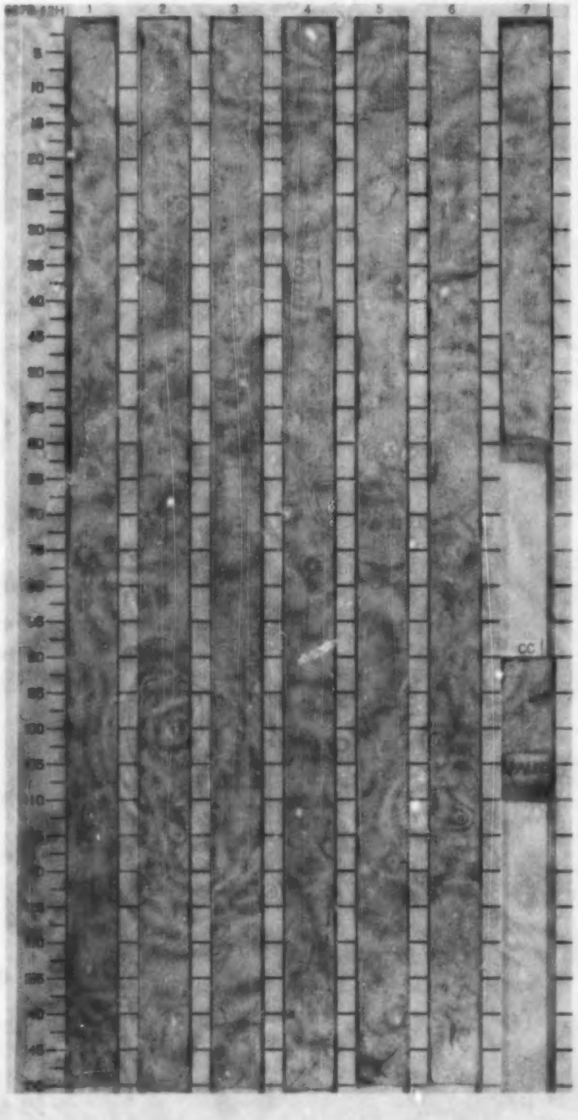
807B-12H
1
2
3
4
5
6
7
CC
5
10
15
20
25
30
35
40
45
50
55
60
65
70
75
80
85
90
95
100
105
110
115
120
125
130
135
140
145
150

SITE 807 HOLE B CORE 13H CORED INTERVAL 107.6-117.1 mbsf

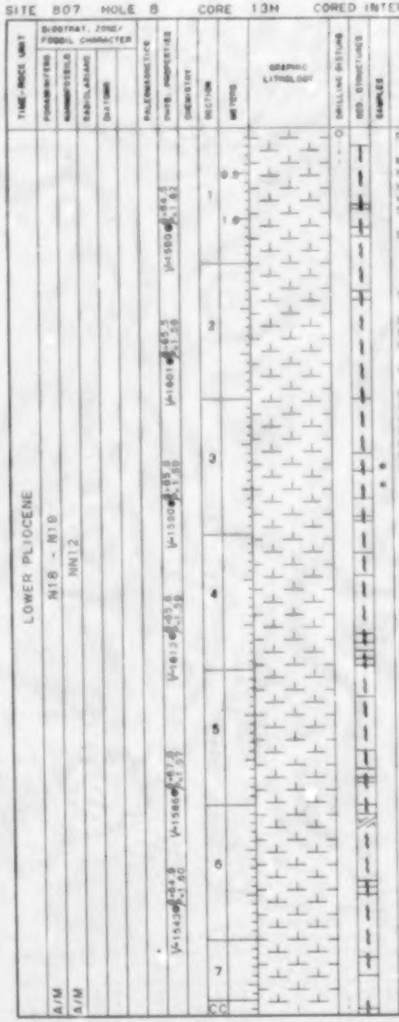
TIME-ROCK UNIT
BIOSTRAT. ZONE/ FOSSIL CHARACTER
FORAMINIFERS
NANNOFOSSILS
RADIOLARIANS
DIATOMS
PALEOMAGNETICS
PHYS. PROPERTIES
CHEMISTRY
SECTION
METERS
GRAPHIC LITHOLOGY
DRILLING DISTURB.
SED. STRUCTURES
SAMPLES
LOWER PLIOCENE
N18 - N19
NN12
A/M
A/M
V=1580
64.6
1.62
V=1601
65.5
1.59
V=1580
65.8
1.60
V=1613
65.6
1.58
V=1586
67.7
1.57
V=1543
64.8
1.60
1
2
3
4
5
6
7
CC
0.5
1.0

LITHOLOGIC DESCRIPTION

NANNOFOSSIL OOZE with FORAMINIFERS

Major lithology: This core contains slightly to moderately bioturbated, white (2.5Y 8/0) NANNOFOSSIL OOZE with FORAMINIFERS. Bioturbation is represented by cm-scale light gray (2.5Y 7/2 and 5Y 7/1) mottling and grayish blue (5PB 5/2) pyritized, commonly vertical, burrows. Light greenish gray (5G 7/1) and pale purple (5P 6/2) to grayish blue (PB 5/2) color bands are common. Microfaults are observed at Section 6, 10-15 cm.

SMEAR SLIDE SUMMARY (%):

	3, 74	3, 98
	D	D
TEXTURE:		
Sand	17	10
Silt	63	65
Clay	20	25
COMPOSITION:		
Feldspar	—	Tr
Foraminifers	20	15
Glass	Tr	Tr
Nannofossils	80	84
Quartz	Tr	Tr
Radiolarians	Tr	1
Siliceous sponge spicules	Tr	Tr

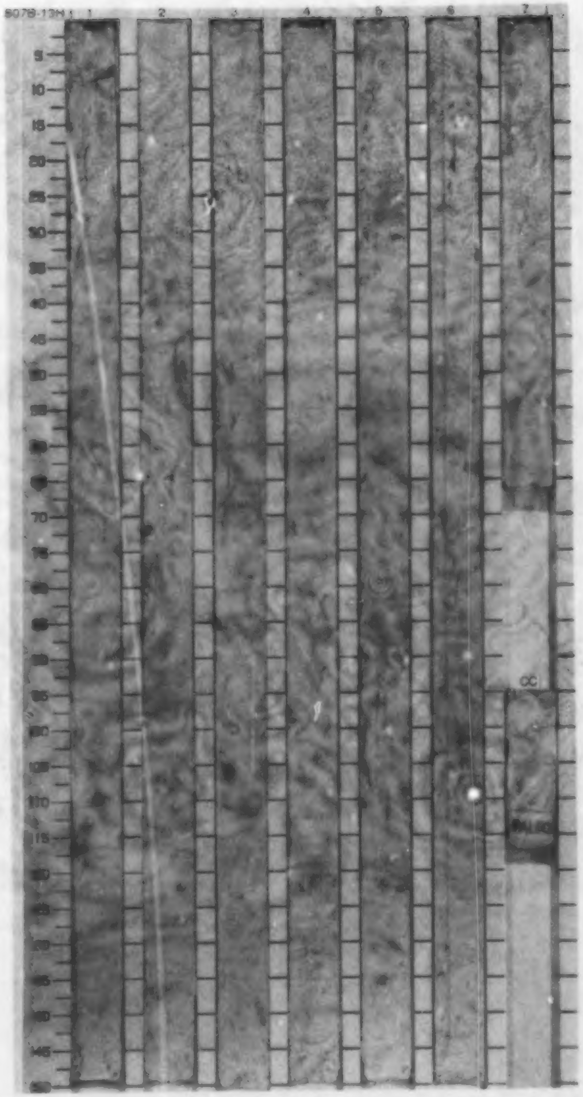
807B-13H
1
2
3
4
5
6
7
CC
5
10
15
20
25
30
35
40
45
50
55
60
65
70
75
80
85
90
95
100
105
110
115
120
125
130
135
140
145
150

SITE 807 HOLE B CORE 14H CORED INTERVAL 117.1-126.6 mbsf

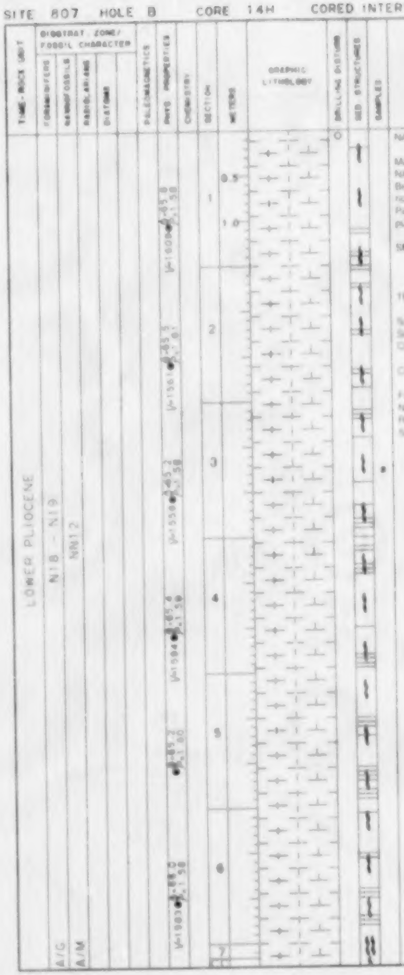
TIME-ROCK UNIT
BIOSTRAT. ZONE/ FOSSIL CHARACTER
FORAMINIFERS
NANNOFOSSILS
RADIOLARIANS
DIATOMS
PALEOMAGNETICS
PHYS. PROPERTIES
CHEMISTRY
SECTION
METERS
GRAPHIC LITHOLOGY
DRILLING DISTURB.
SED. STRUCTURES
SAMPLES
LOWER PLIOCENE
N18 - N19
NN12
A/G
A/M
V=1600 ●Φ=65.8 γ=1.58
V=1561 ●Φ=65.5 γ=1.61
V=1558 ●Φ=65.2 γ=1.58
V=1584 ●Φ=65.4 γ=1.59
●Φ=65.2 γ=1.60
V=1583 ●Φ=68.0 γ=1.58
1
2
3
4
5
6
7
0.5
1.0

LITHOLOGIC DESCRIPTION

NANNOFOSSIL OOZE with FORAMINIFERS to FORAMINIFER NANNOFOSSIL OOZE

Major lithology: This core contains slightly to moderately bioturbated, white (2.5Y 8/0) NANNOFOSSIL OOZE with FORAMINIFERS to FORAMINIFER NANNOFOSSIL OOZE. Bioturbation is represented by cm scale, light gray (2.5Y 7/2 and 5Y 7/1), commonly horizontal burrows, and by grayish blue (5PB 5/2) pyritized, commonly vertical, burrows. Pale purple (5P 6/2) burrow "halos" are also present. Light greenish gray (5G 7/1) and pale purple (5P 6/2) to grayish blue (PB 5/2) color bands are common.

SMEAR SLIDE SUMMARY (%):

	3, 78
	D
TEXTURE:	
Sand	5
Silt	90
Clay	5
COMPOSITION:	
Foraminifers	15
Nannofossils	83
Radiolarians	2
Siliceous sponge spicules	Tr

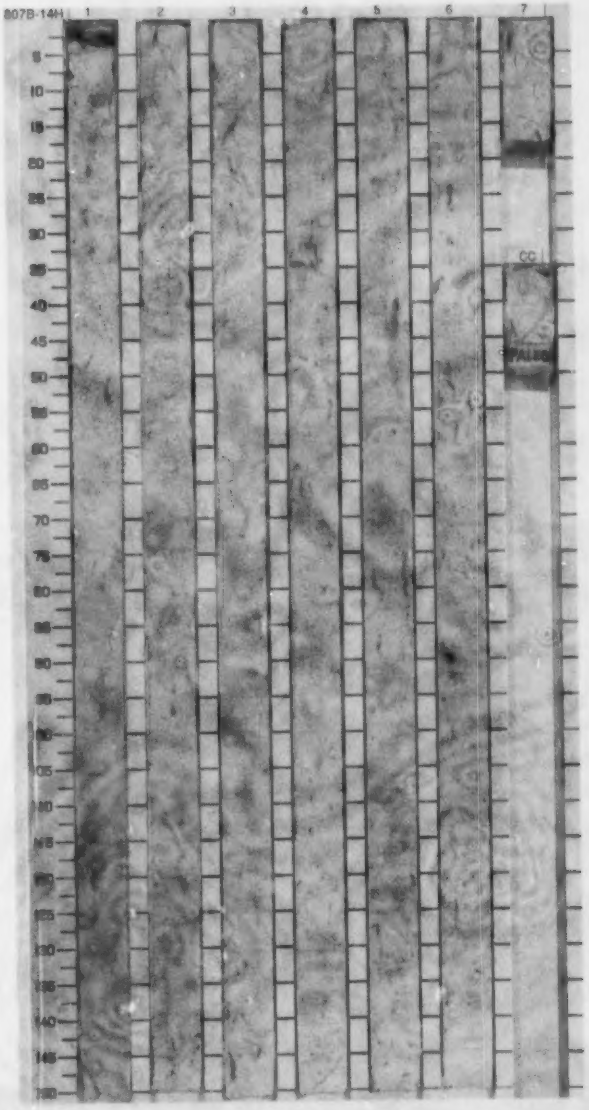
807B-14H
1
2
3
4
5
6
7
CC
PAL
5
10
15
20
25
30
35
40
45
50
55
60
65
70
75
80
85
90
95
100
105
110
115
120
125
130
135
140
145
150

SITE 807 HOLE B CORE 15H CORED INTERVAL 126.6-136.1 mbsf

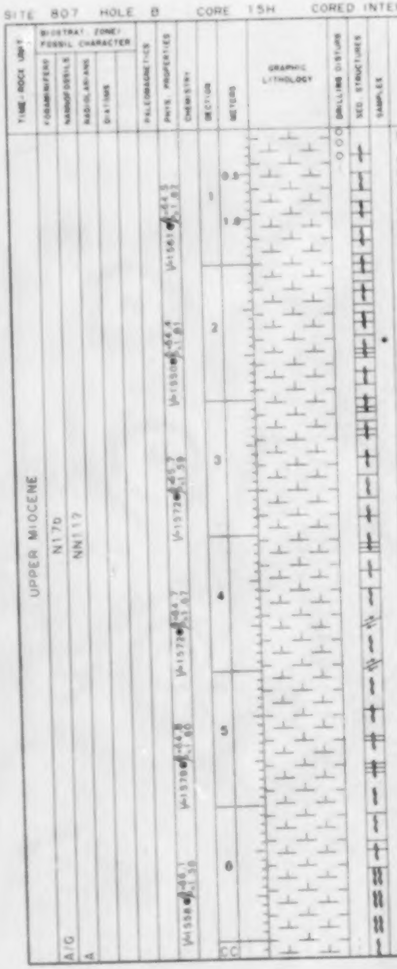

LITHOLOGIC DESCRIPTION

NANNOFOSSIL OOZE to NANNOFOSSIL OOZE with FORAMINIFERS

Major lithology: This core contains slightly to moderately bioturbated, white (2.5Y 8/0) NANNOFOSSIL OOZE to NANNOFOSSIL OOZE with FORAMINIFERS. Bioturbation is represented by cm-scale, light gray (2.5Y 7/2 and 5Y 7/1), commonly horizontal burrows and by grayish blue (5PB 5/2) pyritized, mm-scale, vertical burrows. Pale purple (5P 6/2) burrow "halos" are also present. Light greenish gray (5G 7/1) and pale purple (5P 6/2) to grayish blue (PB 5/2) color bands are common throughout. In Section 4, some of color bands are microfaulted.

SMEAR SLIDE SUMMARY (%):

	2, 87
	D
TEXTURE:	
Sand	10
Silt	85
Clay	5
COMPOSITION:	
Foraminifers	8
Nannofossils	90
Radiolarians	Tr
Siliceous sponge spicules	Tr
Silicoflagellates	Tr

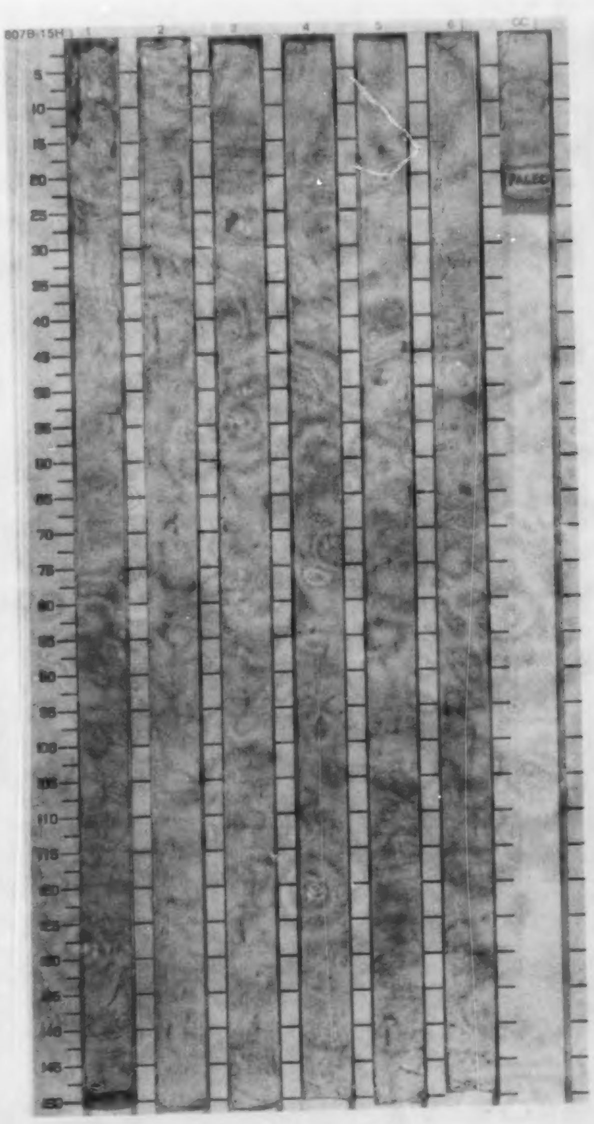
807B-15H
1
2
3
4
5
6
CC
PALEO
5
10
15
20
25
30
35
40
45
50
55
60
65
70
75
80
85
90
95
100
105
110
115
120
125
130
135
140
145
150

SITE 807 HOLE B CORE 16H CORED INTERVAL 136.1-145.6 mbsf

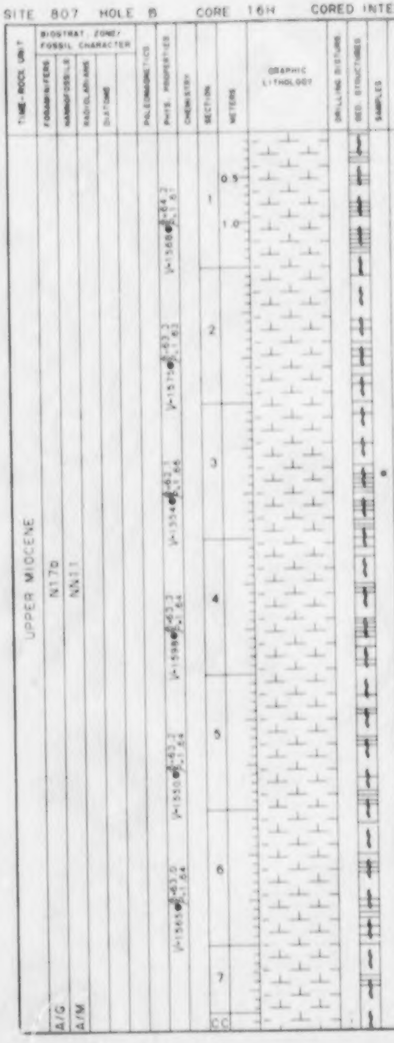
TIME-ROCK UNIT
BIOSTRAT. ZONE/ FOSSIL CHARACTER
FORAMINIFERS
NANNOFOSSILS
RADIOLARIANS
DIATOMS
PALEOMAGNETICS
PHYS. PROPERTIES
CHEMISTRY
SECTION
METERS
GRAPHIC LITHOLOGY
DRILLING DISTURB.
SED. STRUCTURES
SAMPLES
UPPER MIOCENE
N17b
NN11
A/G
A/M
V=1568 φ=64.2 γ=1.61
V=1575 φ=63.3 γ=1.63
V=1554 φ=62.1 γ=1.66
V=1598 φ=63.3 γ=1.64
V=1550 φ=63.2 γ=1.64
V=1565 φ=63.0 γ=1.64
1
2
3
4
5
6
7
CC
0.5
1.0

LITHOLOGIC DESCRIPTION

NANNOFOSSIL OOZE to NANNOFOSSIL OOZE with FORAMINIFERS

Major lithology: This core contains slightly to moderately bioturbated, white (2.5Y 8/0) NANNOFOSSIL OOZE to NANNOFOSSIL OOZE with FORAMINIFERS. Bioturbation is expressed as cm scale, light gray (2.5Y 7/2) mottles and mm to cm scale grayish blue (5PB 5/2), pyrite filled burrows. Faint, light greenish gray (5G 7/1) and pale purple (5P 6/2) color bands are present to abundant through this core. Grayish blue (5PB 5/2) color bands are less common.

SMEAR SLIDE SUMMARY (%):

	3, 80
	D
TEXTURE:	
Sand	10
Silt	85
Clay	5
COMPOSITION:	
Foraminifers	8
Nannofossils	90
Radiolarians	Tr
Siliceous sponge spicules	Tr
Silicoflagellates	Tr

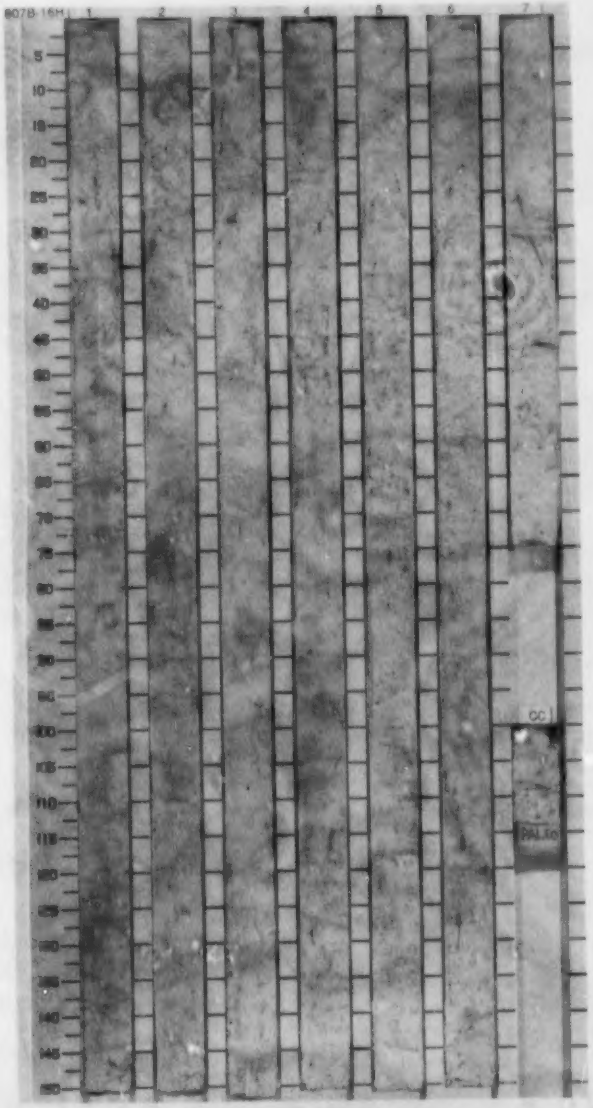
807B-16H
1
2
3
4
5
6
7
CC
PALEO
5
10
15
20
25
30
35
40
45
50
55
60
65
70
75
80
85
90
95
100
105
110
115
120
125
130
135
140
145
150

SITE 807 HOLE B CORE 17H CORED INTERVAL 145.6-155.1 mbsf

TIME-ROCK UNIT	BIOSTRAT. ZONE/ FOSSIL CHARACTER: FORAMINIFERS	NANNOFOSSILS	RADIOLARIANS	DIATOMS	PALEOMAGNETICS	PHYS. PROPERTIES	CHEMISTRY	SECTION	METERS	GRAPHIC LITHOLOGY	DRILLING DISTURB.	SED. STRUCTURES	SAMPLES
UPPER MIOCENE	N17b	NN11				V-1594 ● φ-64.3 γ-1.64		1	0.5 1.0				
						V-1605 ● φ-62.7 γ-1.64		2					
						V-1628 ● φ-63.5 γ-1.63		3					
						V-1601 ● φ-64.5 γ-1.61		4					●
						V-1620 ● φ-62.9 γ-1.64		5					
						V-1565 ● φ-63.5 γ-1.63		6					
								7					
	A/G							CC					

LITHOLOGIC DESCRIPTION

NANNOFOSSIL OOZE with FORAMINIFERS

Major lithology: This core contains moderately to heavily bioturbated, white (2.5Y 8.0) NANNOFOSSIL OOZE with FORAMINIFERS. Bioturbation is expressed as light gray (2.5Y 7.2) mottling and grayish blue (5PB 5.2) to pale purple (5P 6.2), pyrite filled burrows and mottling. Diffuse light greenish gray (5G 7.1) and pale purple (5P 6.2) color bands are present to abundant.

SMEAR SLIDE SUMMARY (%):

	4, 81
	D
TEXTURE:	
Sand	16
Silt	64
Clay	20
COMPOSITION:	
Foraminifers	15
Glass	Tr
Nannofossils	84
Quartz	Tr
Radiolarians	1
Siliceous sponge spicules	Tr

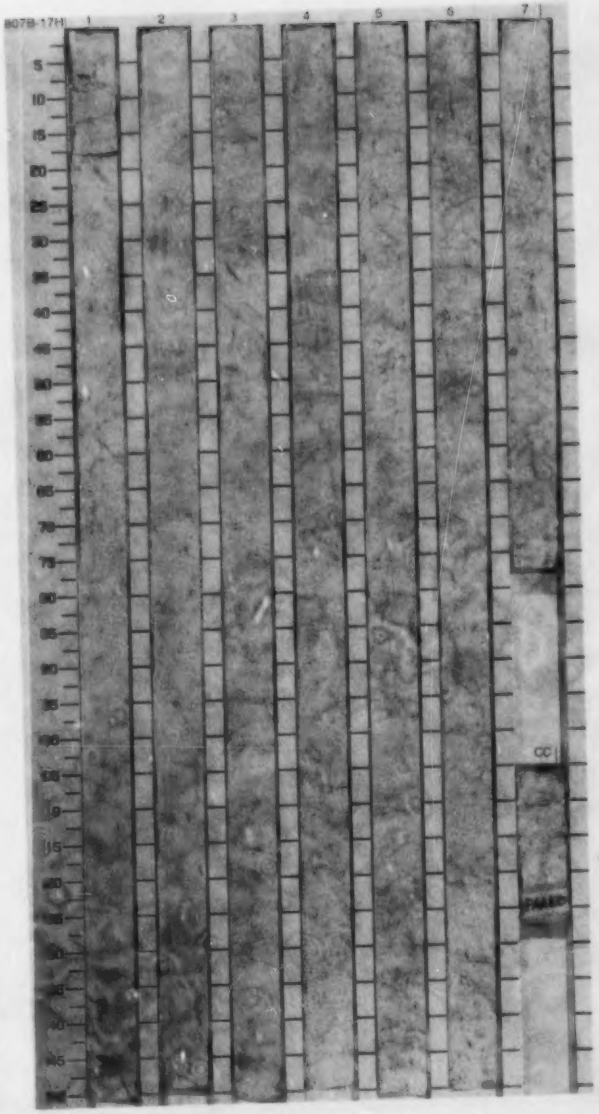

SITE 807 HOLE B CORE 18H CORED INTERVAL 1551.-164.6 mbsf

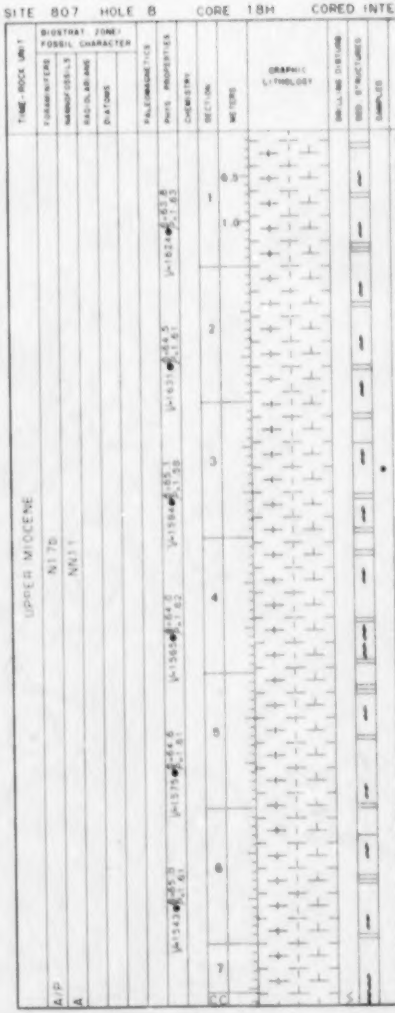
TIME-ROCK UNIT
BIOSTRAT. ZONE/ FOSSIL CHARACTER
FORAMINIFERS
NANNOFOSSILS
RADIOLARIANS
DIATOMS
PALEOMAGNETICS
PHYS. PROPERTIES
CHEMISTRY
SECTION
METERS
GRAPHIC LITHOLOGY
DRILLING DISTURB.
SED. STRUCTURES
SAMPLES
UPPER MIOCENE
N17b
NN11
A/P
A
V=1624 ● φ=63.8 γ=1.63
V=1631 ● φ=64.5 γ=1.61
V=1594 ● φ=65.1 γ=1.59
V=1565 ● φ=64.0 γ=1.62
V=1575 ● φ=64.6 γ=1.61
V=1543 ● φ=65.0 γ=1.61
1
2
3
4
5
6
7
CC
0.5
1.0

LITHOLOGIC DESCRIPTION

NANNOFOSSIL OOZE with FORAMINIFERS to FORAMINIFER NANNOFOSSIL OOZE

Major lithology: This core contains white (2.5Y 8/0) NANNOFOSSIL OOZE with FORAMINIFERS to FORAMINIFER NANNOFOSSIL OOZE. Moderate to heavy bioturbation is evident from abundant pyrite filled burrows, and light gray (2.5Y 7/2) mottles. Pale purple (5P 6/2), greenish gray (5G 7/1), and reddish gray (5R 6/1) color bands, about 1 cm in width, are common, usually occurring together in pairs and triplets. The color bands are usually faint.

SMEAR SLIDE SUMMARY (%):

	3, 74
	D
TEXTURE:	
Sand	12
Silt	55
Clay	33
COMPOSITION:	
Accessory minerals	1
Foraminifers	21
Nannofossils	75
Siliceous fragments	3

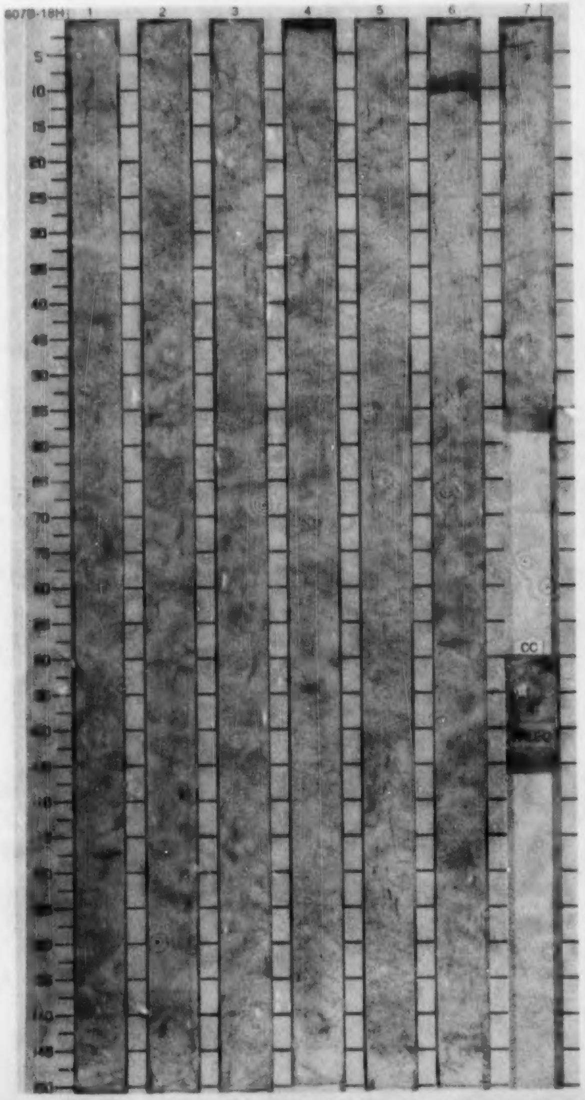
807B-18H
1
2
3
4
5
6
7
CC
5
10
15
20
25
30
35
40
45
50
55
60
65
70
75
80
85
90
95
100
105
110
115
120
125
130
135
140
145
150

SITE 807 HOLE B CORE 19H CORED INTERVAL 164.6-174.1 mbsf

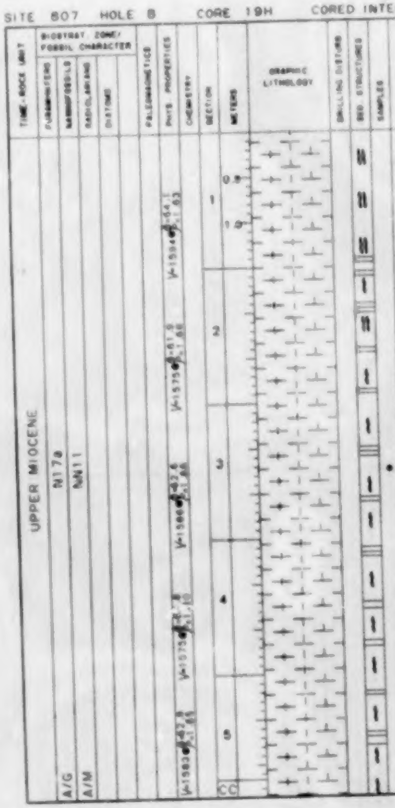
TIME-ROCK UNIT
BIOSTRAT. ZONE/ FOSSIL CHARACTER
FORAMINIFERS
NANNOFOSSILS
RADIOLARIANS
DIATOMS
PALEOMAGNETICS
PHYS. PROPERTIES
CHEMISTRY
SECTION
METERS
GRAPHIC LITHOLOGY
DRILLING DISTURB.
SED. STRUCTURES
SAMPLES
UPPER MIOCENE
N17a
NN11
A/G
A/M
V=1594 Φ=64.1 γ=1.63
V=1575 Φ=61.9 γ=1.68
V=1586 Φ=62.6 γ=1.66
V=1575 Φ=62.8 γ=1.10
V=1583 Φ=62.8 γ=1.65
1
2
3
4
5
CC
0.5
1.0

LITHOLOGIC DESCRIPTION

NANNOFOSSIL OOZE with FORAMINIFERS to FORAMINIFER NANNOFOSSIL OOZE

Major lithology: This core contains white (2.5Y 8/0) NANNOFOSSIL OOZE with FORAMINIFERS to FORAMINIFER NANNOFOSSIL OOZE. Light gray (2.5Y 7/2) burrows and pale purple (5P 6/2) mottles and pyrite fragments indicate extensive bioturbation. Pale green (5G 7/1) and pale purple (5P 6/2) horizontal, 1 to 3 cm thick color bands are present throughout. A few intervals (< 1 cm thick) are stiffer than the rest of the sediment. There is a slight H_2S odor to the core. The base of Section 1 is microfaulted.

SMEAR SLIDE SUMMARY (%):

	3, 74
	D
TEXTURE	
Sand	15
Silt	55
Clay	30
COMPOSITION	
Accessory minerals	1
Foraminifers	22
Nannofossils	75
Siliceous fragments	2

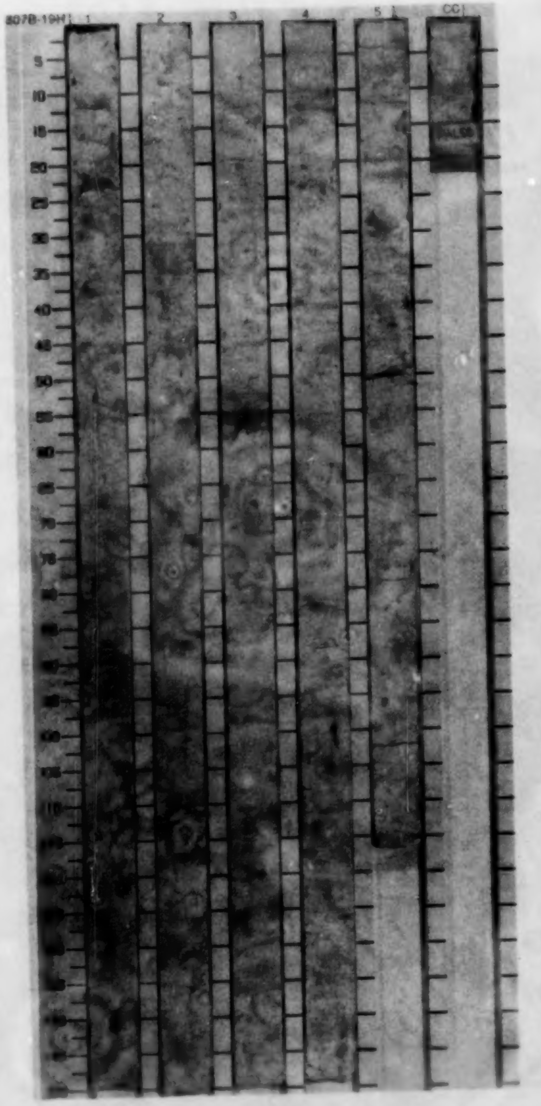
807B-19H
1
2
3
4
5
CC
5
10
15
20
25
30
35
40
45
50
55
60
65
70
75

SITE 807 HOLE B CORE 20H CORED INTERVAL 174.1-183.6 mbsf

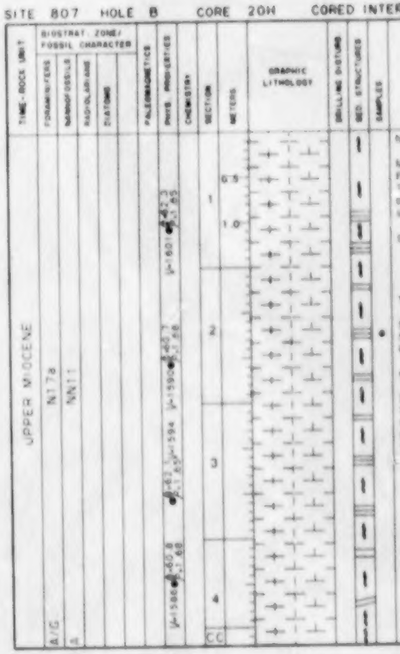
TIME-ROCK UNIT
BIOSTRAT. ZONE/ FOSSIL CHARACTER
FORAMINIFERS
NANNOFOSSILS
RADIOLARIANS
DIATOMS
PALEOMAGNETICS
PHYS. PROPERTIES
CHEMISTRY
SECTION
METERS
GRAPHIC LITHOLOGY
DRILLING DISTURB.
SED. STRUCTURES
SAMPLES
UPPER MIOCENE
N17a
NN11
A/G
A
φ=62.3
γ=1.65
V=1601
φ=60.7
γ=1.68
V=1590
V=1594
φ=62.1
γ=1.65
φ=60.8
γ=1.68
V=1586
1
2
3
4
CC
0.5
1.0

LITHOLOGIC DESCRIPTION

NANNOFOSSIL OOZE with FORAMINIFERS to FORAMINIFER NANNOFOSSIL OOZE

Major lithology: This core contains white (2.5Y 8/0) NANNOFOSSIL OOZE with FORAMINIFERS to FORAMINIFER NANNOFOSSIL OOZE. Abundant cm-thick, greenish gray (5G 7/1), pale purple (5P 6/2), and reddish gray (5R 6/1) color banding is noted. Pyrite-filled burrows with purple borders also are abundant and indicative of heavy bioturbation. A slight H_2S odor was noted upon splitting the core.

SMEAR SLIDE SUMMARY (%):

	2, 75
	D
TEXTURE:	
Sand	10
Silt	80
Clay	10
COMPOSITION:	
Diatoms	Tr
Foraminifers	15
Nannofossils	85
Radiolarians	Tr
Siliceous fragments	Tr

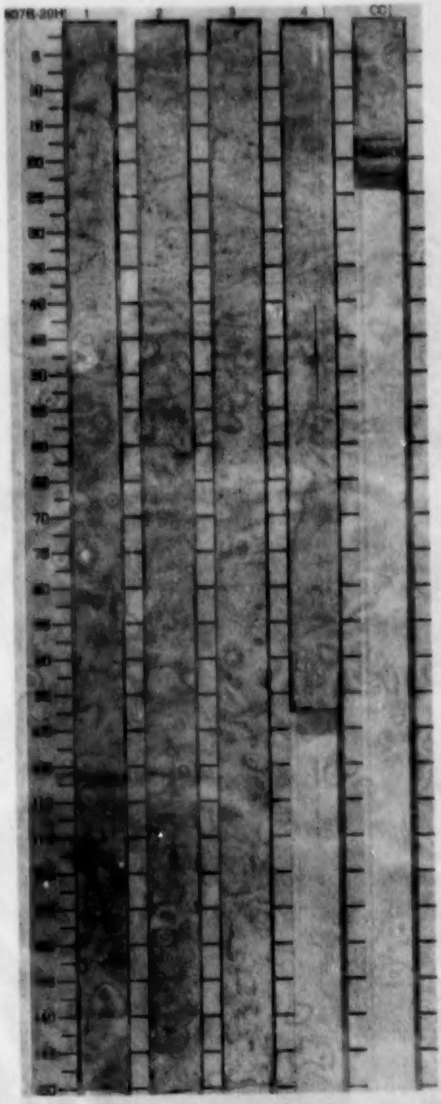
807B-20H
1
2
3
4
CC

SITE 807 HOLE B CORE 21H CORED INTERVAL 183.6-193.1 mbsf

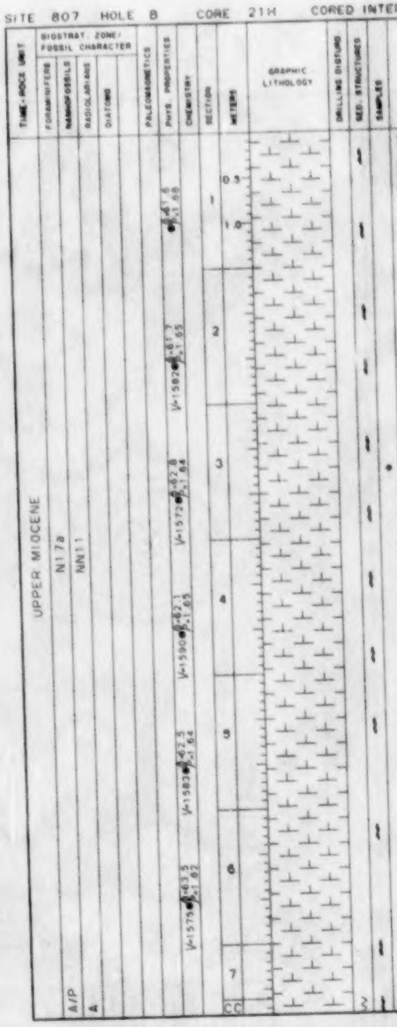
TIME-ROCK UNIT
BIOSTRAT. ZONE/ FOSSIL CHARACTER
FORAMINIFERS
NANNOFOSSILS
RADIOLARIANS
DIATOMS
PALEOMAGNETICS
PHYS. PROPERTIES
CHEMISTRY
SECTION
METERS
GRAPHIC LITHOLOGY
DRILLING DISTURB.
SED. STRUCTURES
SAMPLES
UPPER MIOCENE
N17a
NN11
A/P
A
ϕ-61.6 γ-1.66
V-1582 ϕ-61.7 γ-1.65
V-1572 ϕ-62.8 γ-1.64
V-1590 ϕ-62.1 γ-1.65
V-1583 ϕ-62.5 γ-1.64
V-1579 ϕ-63.5 γ-1.62
1
2
3
4
5
6
7
CC
0.5
1.0

LITHOLOGIC DESCRIPTION

NANNOFOSSIL OOZE with FORAMINIFERS

Major lithology: This core contains white (2.5Y 8/0) NANNOFOSSIL OOZE with FORAMINIFERS. Centimeter-scale greenish gray (5G 7/1), pale purple (5P 6/2) and reddish gray (5R 6/1) color banding is common. The color bands are typically faint, though some are distinct. A few gray (2.5Y 6/1) color bands are also noted. Heavy bioturbation is indicated by abundant pyrite filled burrows. Some pale purple swirls and halo structures were observed that appear to be related to fluid migration vents. These features overprint the horizontal color bands. Centimeter-scale, slightly stiffer intervals were noted, often corresponding to intervals of color banding.

SMEAR SLIDE SUMMARY (%):

	3, 75 D
TEXTURE	
Sand	5
Silt	75
Clay	20
COMPOSITION	
Diatoms	Tr
Foraminifers	10
Nannofossils	90
Radiolarians	Tr
Siliceous fragments	Tr

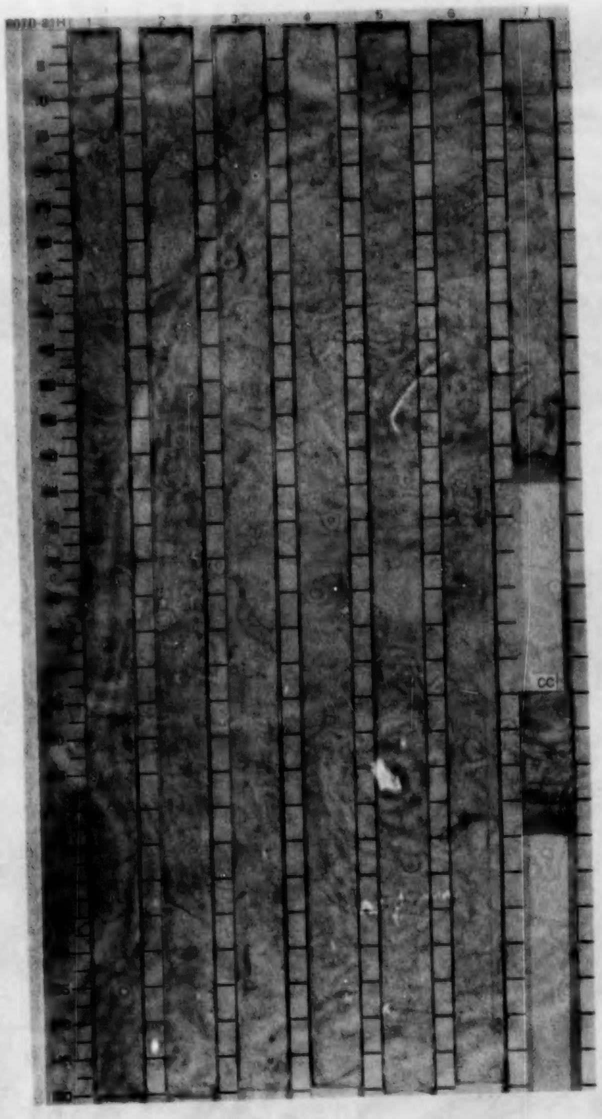
807B-21H
1
2
3
4
5
6
7
CC

SITE 807 HOLE B CORE 22H CORED INTERVAL 193.1-202.6 mbsf

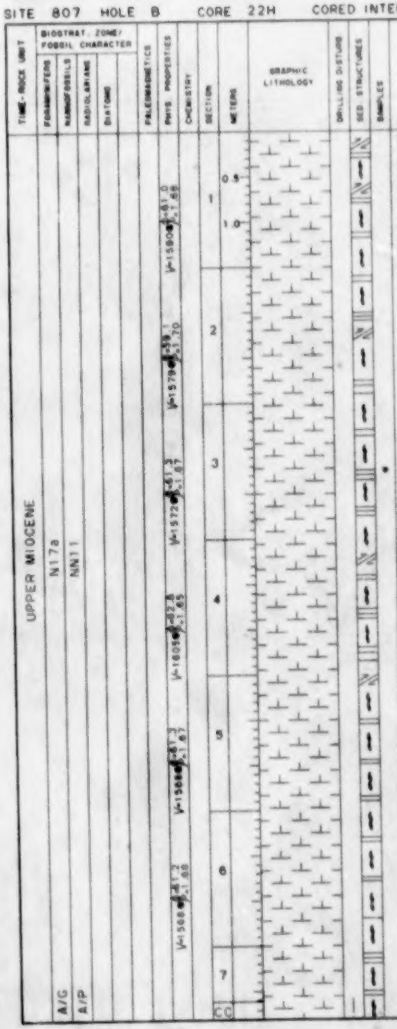

LITHOLOGIC DESCRIPTION

NANNOFOSSIL OOZE with FORAMINIFERS

Major lithology: This core contains intensely bioturbated, white (2.5Y 8.0) NANNOFOSSIL OOZE with FORAMINIFERS. Evidence for bioturbation consists of light gray (2.5Y 7.2) burrow fills, and pyrite fragments, as well as pale purple (5P 6.2) halos, and mottles. Horizontal 1 to 3 cm thick color bands are present throughout the core and are either pale purple (5P 6.2) or pale green (5G 7.2) in color. The bands are often overprinted by the pale purple mottles. A few microfaults are present in the top two sections. Some of the color bands are distinctly stiffer than the surrounding ooze.

SMEAR SLIDE SUMMARY (%):

	3, 74
	D
TEXTURE	
Sand	13
Silt	55
Clay	32
COMPOSITION	
Accessory minerals	1
Diatoms	Tr
Foraminifers	18
Nannofossils	79
Siliceous fragments	2

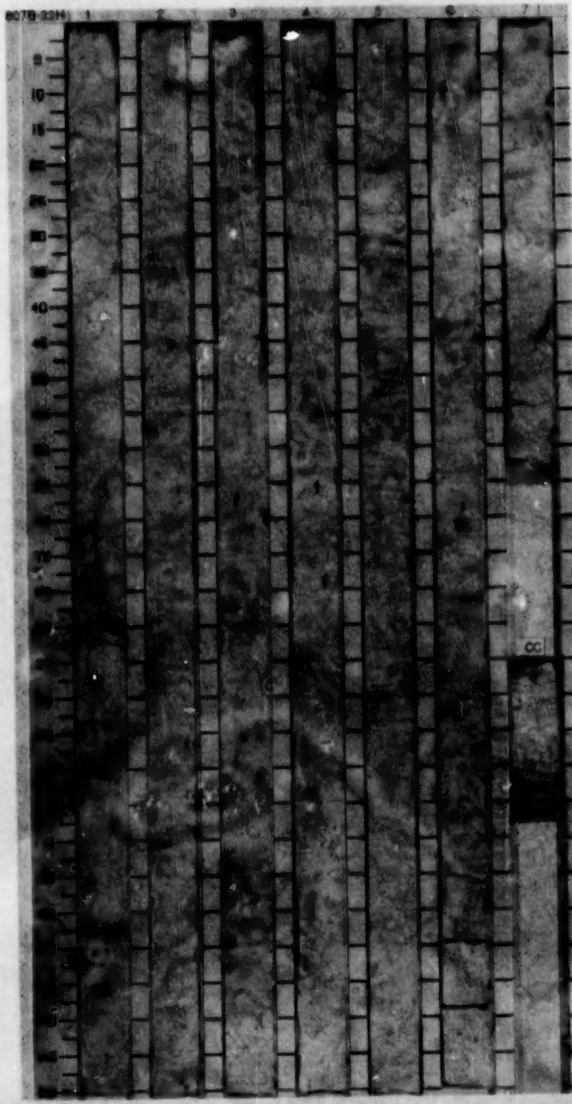

SITE 807 HOLE B CORE 23H CORED INTERVAL 202.6-212.1 mbsf

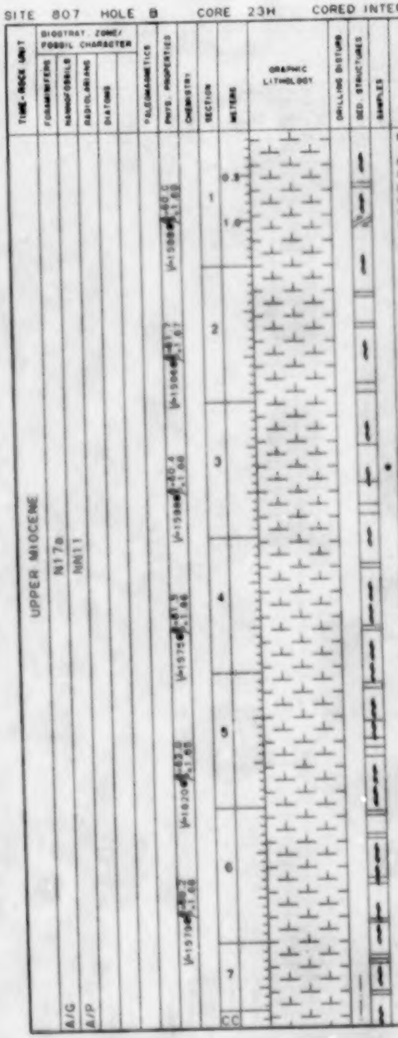
TIME-ROCK UNIT
BIOSTRAT. ZONE/ FOSSIL CHARACTER
FORAMINIFERS
NANNOFOSSILS
RADIOLARIANS
DIATOMS
PALEOMAGNETICS
PHYS. PROPERTIES
CHEMISTRY
SECTION
METERS
GRAPHIC LITHOLOGY
DRILLING DISTURB.
SED. STRUCTURES
SAMPLES
UPPER MIOCENE
N17a
NN11
A/G
A/P
V=1508
V=1506
V=1508
V=1575
V=1620
V=1570
1
2
3
4
5
6
7
CC
0.5
1.0

LITHOLOGIC DESCRIPTION

NANNOFOSSIL OOZE with FORAMINIFERS

Major lithology: This core contains white (2.5Y 8.0) NANNOFOSSIL OOZE with FORAMINIFERS. Faint horizontal color bands appear throughout. The bands are predominantly pale purple (5P 6.2) and pale green (5G 7.2) in color. Evidence for bioturbation includes light gray (2.5Y 7.2) mottles and pyrite specks, as well as pale purple (5P 6.2) mottles. These mottles commonly overprint the faint color bands. Some of the color bands are slightly stiffer than the white ooze.

SMEAR SLIDE SUMMARY (%):

	3, 74
	D
TEXTURE:	
Sand	15
Silt	50
Clay	35
COMPOSITION:	
Accessory minerals	1
Diatoms	1
Foraminifers	20
Nannofossils	77
Siliceous fragments	2

807B-23H
1
2
3
4
5
6
7
CC

SITE 807 HOLE B CORE 24H CORED INTERVAL 212.1-221.6 mbsf

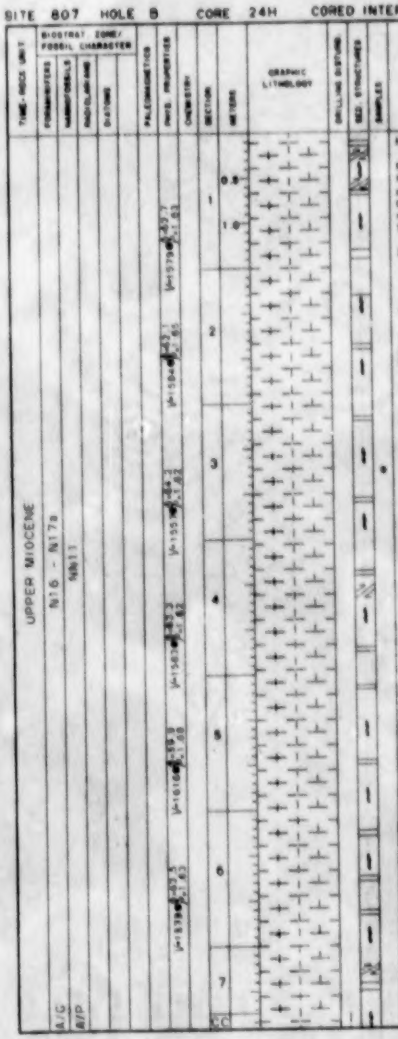
TIME-ROCK UNIT
BIOSTRAT. ZONE/ FOSSIL CHARACTER
FORAMINIFERS
NANNOFOSSILS
RADIOLARIANS
DIATOMS
PALEOMAGNETICS
PHYS. PROPERTIES
CHEMISTRY
SECTION
METERS
GRAPHIC LITHOLOGY
DRILLING DISTURB.
SED. STRUCTURES
SAMPLES
UPPER MIOCENE
N16 - N17a
NN11
A/G
A/P
0.5
1.0
1
2
3
4
5
6
7
CC

LITHOLOGIC DESCRIPTION

NANNOFOSSIL OOZE with FORAMINIFERS to NANNOFOSSIL OOZE

Major lithology: This core contains white (2.5Y 8/0) NANNOFOSSIL OOZE with FORAMINIFERS to FORAMINIFER NANNOFOSSIL OOZE. The sediment has faint, horizontal, pale purple (5P 6/2) and pale green (5G 7/2) color bands throughout. Bioturbation is indicated by abundant light gray (2.5Y 7/2) and pale purple (5P 6/2) mottles. These mottles commonly overprint the faint color bands. Microfaults are apparent in sections 1,2 and 4. Some of the color bands are slightly stiffer than white ooze.

SMEAR SLIDE SUMMARY (%):

	3, 74
	D
TEXTURE:	
Sand	15
Silt	55
Clay	30
COMPOSITION:	
Accessory minerals	1
Diatoms	Tr
Foraminifers	21
Nannofossils	75
Siliceous fragments	3

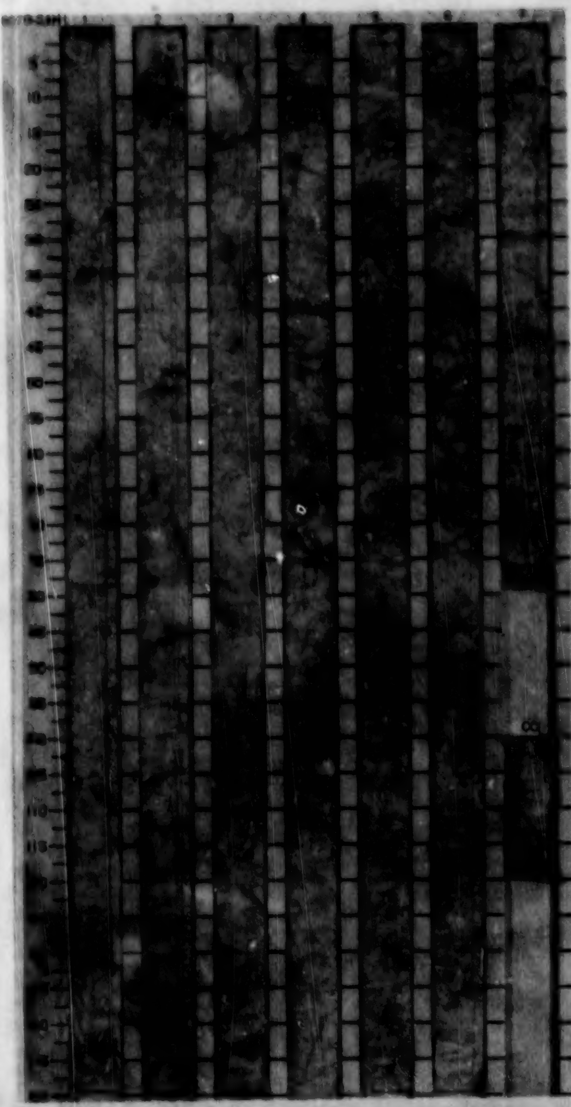

SITE 807 HOLE B CORE 25H CORED INTERVAL 221.6-231.1 mbsf

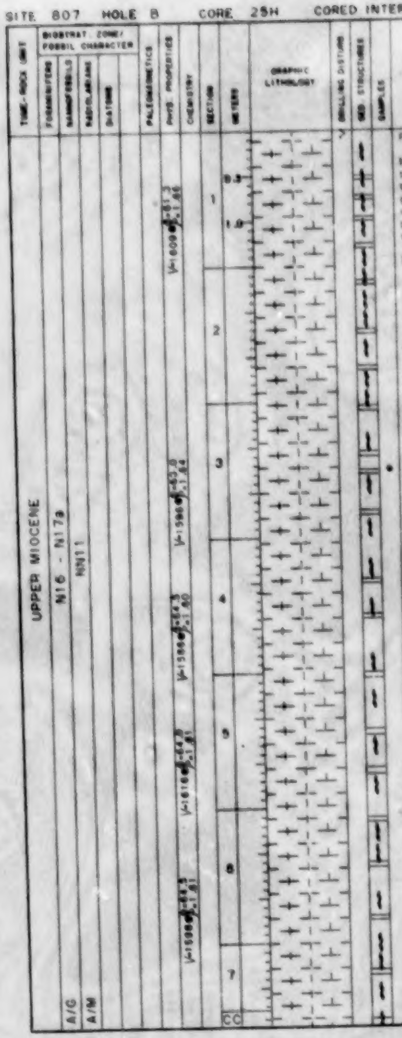

LITHOLOGIC DESCRIPTION

FORAMINIFER NANNOFOSSIL OOZE to NANNOFOSSIL OOZE with FORAMINIFERS

Major lithology: This core contains white (2.5Y 8/0) FORAMINIFER NANNOFOSSIL OOZE to NANNOFOSSIL OOZE with FORAMINIFERS. The sediment has sub horizontal, 1 to 2 cm thick, color bands throughout. The bands are predominantly pale purple (5P 6/2), pale green (5G 7/2) and, to a lesser extent, pale greenish gray (5G 7/1) and dark gray (2.5Y 5/0) in color. Intense bioturbation is indicated by abundant light gray (5Y 7/2) mottles, and pale purple halos. Some intervals (1-2 cm thick) are quite stiff to hard. A porcellanite nodule was found in Section 1, 85 cm.

SMEAR SLIDE SUMMARY (%):

	3, 75 D
TEXTURE:	
Sand	15
Silt	60
Clay	25
COMPOSITION:	
Diatoms	1
Foraminifers	30
Nannofossils	65
Radiolarians	Tr
Siliceous fragments	3
Siliceous sponge spicules	Tr

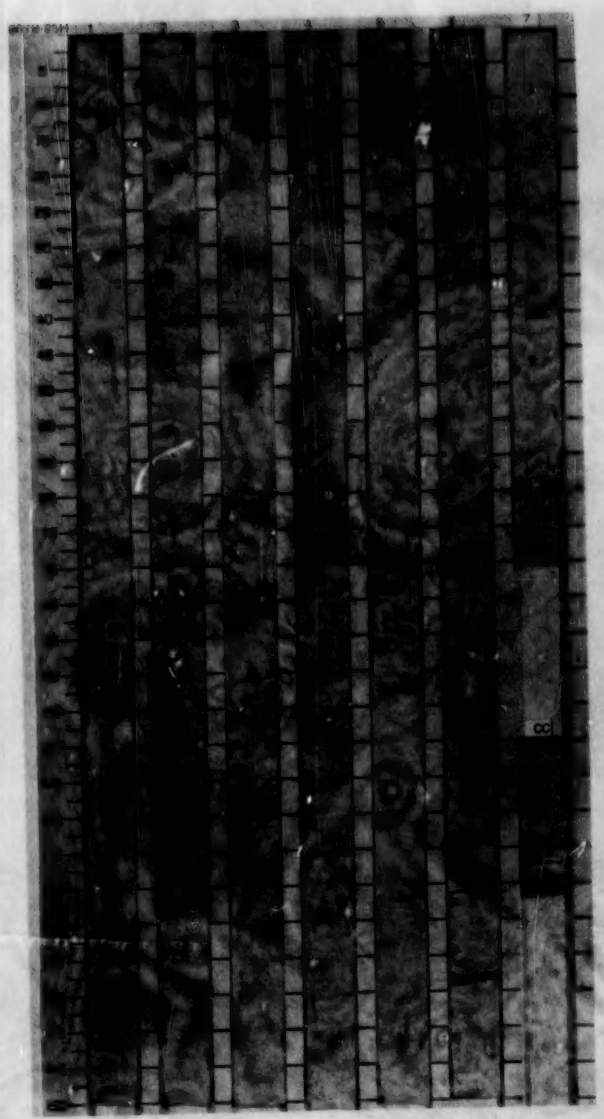

SITE 807 HOLE B CORE 26H CORED INTERVAL 231.1-240.6 mbsf

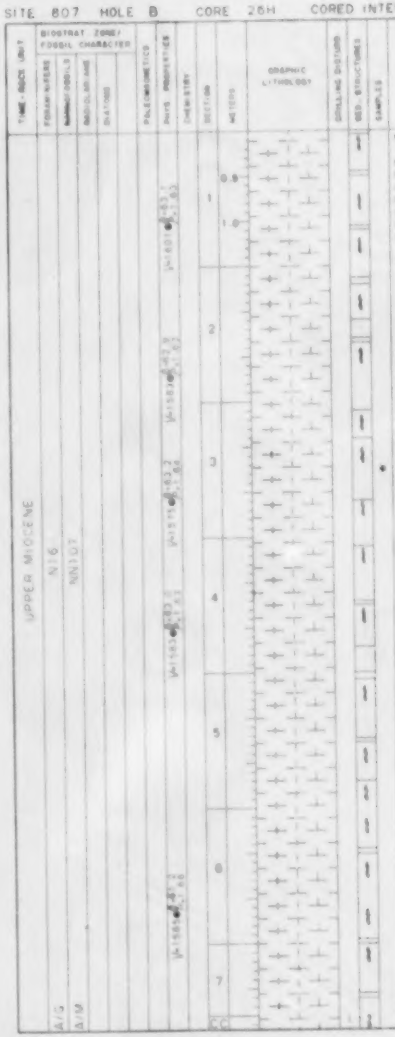
TIME-ROCK UNIT
BIOSTRAT. ZONE/ FOSSIL CHARACTER
FORAMINIFERS
NANNOFOSSILS
RADIOLARIANS
DIATOMS
PALEOMAGNETICS
PHYS. PROPERTIES
CHEMISTRY
SECTION
METERS
GRAPHIC LITHOLOGY
DRILLING DISTURB.
SED. STRUCTURES
SAMPLES
UPPER MIOCENE
N16
NN10?
A/G
A/M
0.5
1.0
1
2
3
4
5
6
7
CC

LITHOLOGIC DESCRIPTION

NANNOFOSSIL OOZE with FORAMINIFERS to FORAMINIFER NANNOFOSSIL OOZE

Major lithology: This core contains white (2.5Y 8/0) NANNOFOSSIL OOZE with FORAMINIFERS to FORAMINIFER NANNOFOSSIL OOZE. Moderate to heavy bioturbation is indicated by light gray (2.5Y 7/2) mottles, pale purple (5P 6/2) halos and pyrite filled burrows, traces, and specks. Diffuse irregular color bands, greenish gray (5G7/1) and, less commonly, pale purple in color, are observed throughout the core. Some bands are subhorizontal. Very stiff, 1 to 2 cm thick intervals are distributed irregularly spaced at 5-15 cm intervals throughout the core.

SMEAR SLIDE SUMMARY (%):

	3, 74
	D
TEXTURE:	
Sand	15
Silt	55
Clay	30
COMPOSITION:	
Accessory minerals	1
Diatoms	Tr
Foraminifers	22
Nannofossils	75
Radiolarians	Tr
Siliceous fragments	2

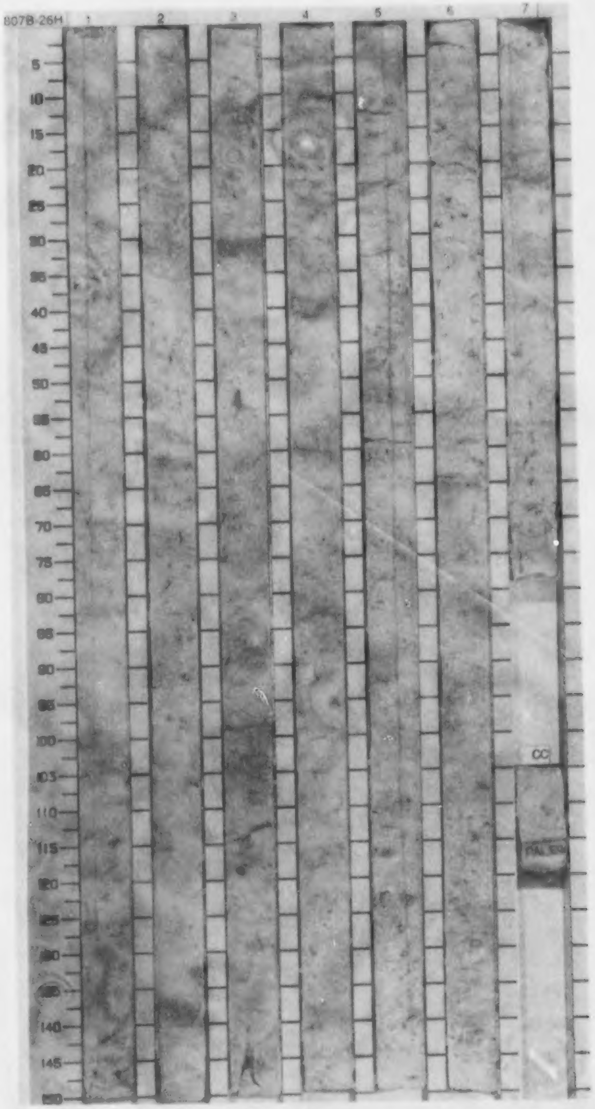
807B-26H
1
2
3
4
5
6
7
5
10
15
20
25
30
35
40
45
50
55
60
65
70
75
80
85
90
95
100
105
110
115
120
125
130
135
140
145
150
CC
PALEO

SITE 807 HOLE B CORE 27H CORED INTERVAL 240.6-250.1 mbsf

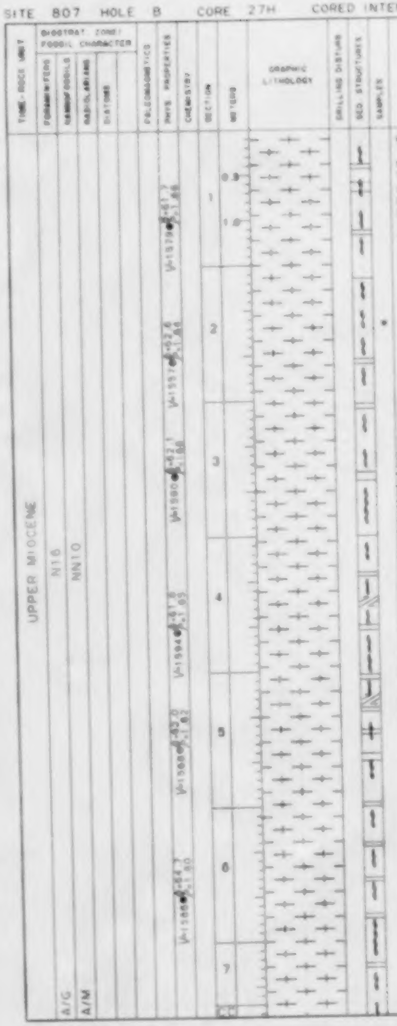
TIME-ROCK UNIT
BIOSTRAT. ZONE/ FOSSIL CHARACTER
FORAMINIFERS
NANNOFOSSILS
RADIOLARIANS
DIATOMS
PALEOMAGNETICS
PHYS. PROPERTIES
CHEMISTRY
SECTION
METERS
GRAPHIC LITHOLOGY
DRILLING DISTURB.
SED. STRUCTURES
SAMPLES
UPPER MIOCENE
N16
NN10
A/G
A/M
Vp-1578 φ-61.7 ρ-1.66
Vp-1557 φ-62.6 ρ-1.64
Vp-1590 φ-62.1 ρ-1.66
Vp-1594 φ-61.8 ρ-1.65
Vp-1588 φ-63.0 ρ-1.62
Vp-1588 φ-64.7 ρ-1.60
1
2
3
4
5
6
7
0.5
1.0
CC

LITHOLOGIC DESCRIPTION

FORAMINIFER NANNOFOSSIL OOZE

Major lithology: This core contains white (2.5Y 8.0) FORAMINIFER NANNOFOSSIL OOZE. There are faint and distinct, 1-cm-thick, greenish gray (5G 7/1) and pale purple (5P 6/2) color bands. Abundant evidence for bioturbation includes mottles and pyrite-filled burrows. Frequent, stiff to hard 1- to 2-cm-thick intervals are present every 3 to 4 cm. Microfaults are noted in Sections 4 and 5.

SMEAR SLIDE SUMMARY (%):

	2, 75
	D
TEXTURE:	
Sand	20
Silt	60
Clay	20
COMPOSITION:	
Diatoms	Tr
Foraminifers	30
Nannofossils	70
Radiolarians	Tr

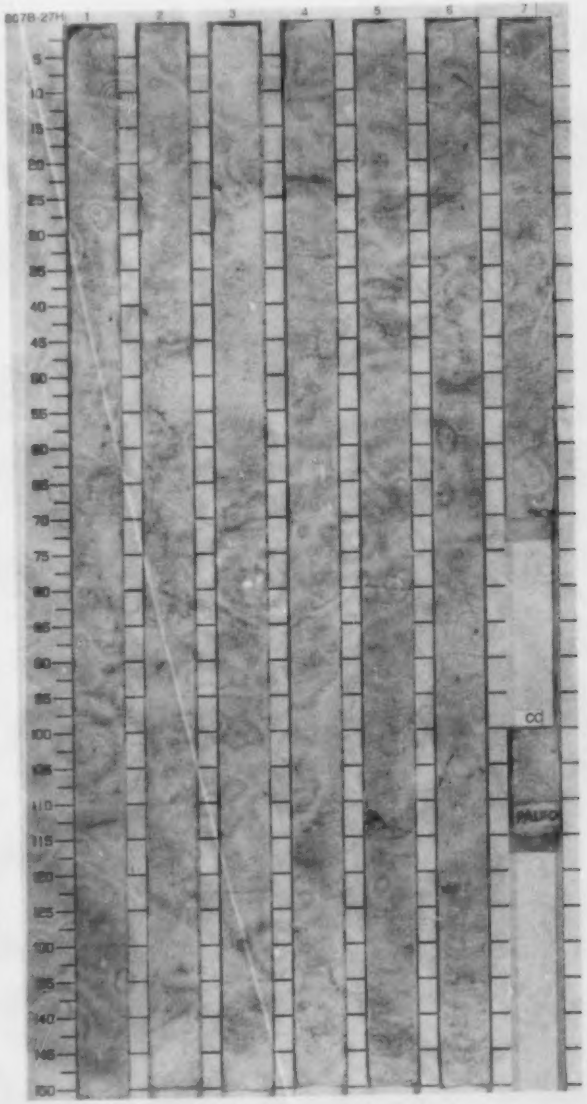
807B-27H
1
2
3
4
5
6
7
5
10
15
20
25
30
35
40
45
50
55
60
65
70
75
80
85
90
95
100
105
110
115
120
125
130
135
140
145
150
CC
PALEO

SITE 807 HOLE B CORE 28H CORED INTERVAL 250.1-259.6 mbsf

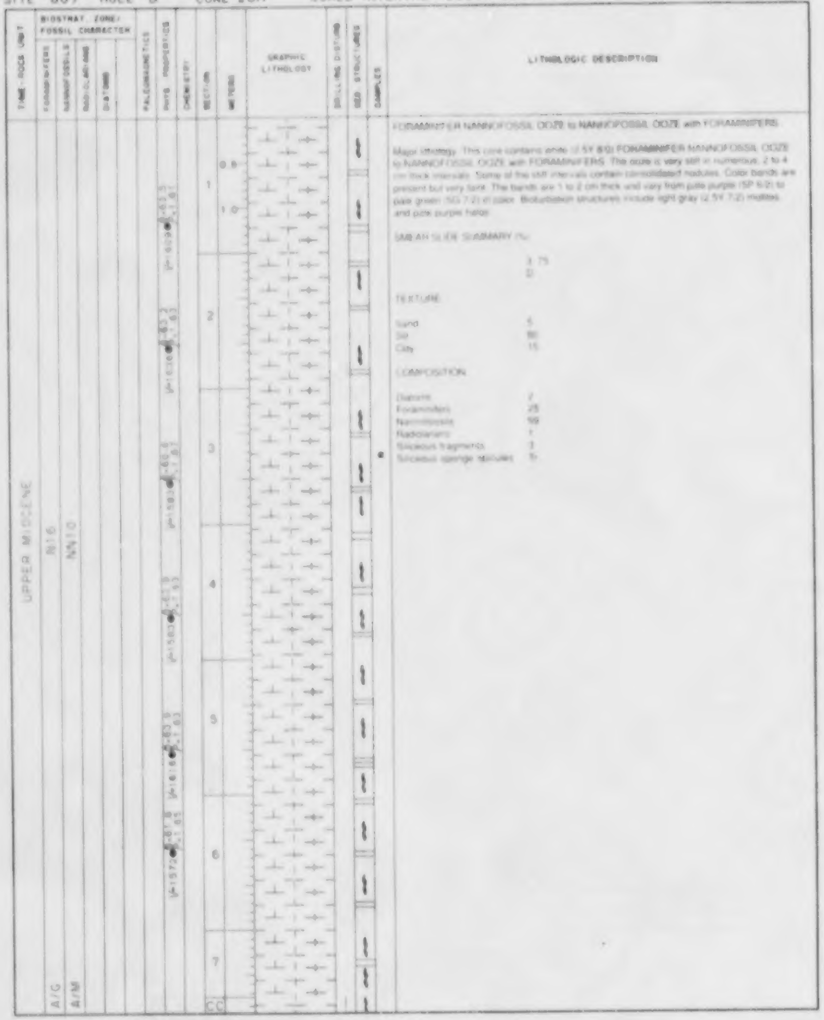

FORAMINIFER NANNOFOSSIL OOZE to NANNOFOSSIL OOZE with FORAMINIFERS.

Major lithology: This core contains white (2.5Y 8/0) FORAMINIFER NANNOFOSSIL OOZE to NANNOFOSSIL OOZE with FORAMINIFERS. The ooze is very stiff in numerous, 2 to 4 cm thick intervals. Some of the stiff intervals contain consolidated nodules. Color bands are present but very faint. The bands are 1 to 2 cm thick and vary from pale purple (5P 6/2) to pale green (5G 7/2) in color. Bioturbation structures include light gray (2.5Y 7/2) mottles and pale purple halos.

SMEAR SLIDE SUMMARY (%):

	3, 75
	D
TEXTURE:	
Sand	5
Silt	80
Clay	15
COMPOSITION:	
Diatoms	2
Foraminifers	25
Nannofossils	69
Radiolarians	1
Siliceous fragments	3
Siliceous sponge spicules	Tr

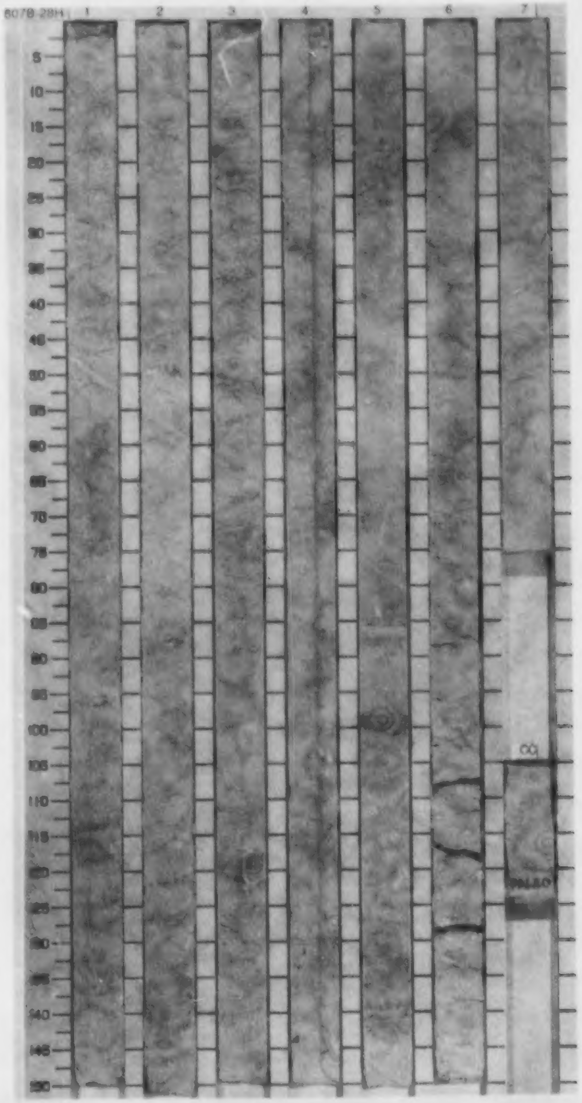
807B-28H
1
2
3
4
5
6
7
5
10
15
20
25
30
35
40
45
50
55
60
65
70
75
80
85
90
95
100
105
110
115
120
125
130
135
140
145
150
CC
PALEO

SITE 807 HOLE B CORE 29H CORED INTERVAL 259.6-269.1 mbsf

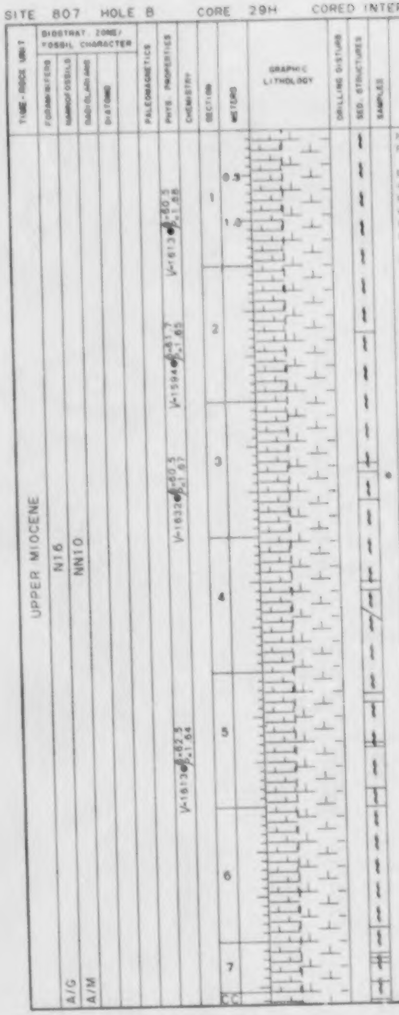
TIME-ROCK UNIT
BIOSTRAT. ZONE/ FOSSIL CHARACTER
FORAMINIFERS
NANNOFOSSILS
RADIOLARIANS
DIATOMS
PALEOMAGNETICS
PHYS. PROPERTIES
CHEMISTRY
SECTION
METERS
GRAPHIC LITHOLOGY
DRILLING DISTURB.
SED. STRUCTURES
SAMPLES
UPPER MIOCENE
N16
NN10
A/G
A/M
V-1613 ●ϕ-60.5 ρ-1.88
V-1594 ●ϕ-61.7 ρ-1.65
V-1632 ●ϕ-60.5 ρ-1.67
V-1613 ●ϕ-62.5 ρ-1.64
1
2
3
4
5
6
7
CC
0.5
1.0

LITHOLOGIC DESCRIPTION

NANNOFOSSIL OOZE with FORAMINIFERS and NANNOFOSSIL CHALK with FORAMINIFERS.

Major lithology: This core contains 60% NANNOFOSSIL OOZE with FORAMINIFERS and 40% NANNOFOSSIL CHALK with FORAMINIFERS, both of white (2.5Y 8.0) color. Slightly to moderately fractured drilling "biscuits" are embedded in a stiff ooze matrix. The sediment is slightly to moderately bioturbated and relatively uniform in appearance. Minor pale blue (5PB 7.2), light greenish gray (5G 7.1), and pale purple (5P 6.2) color bands are present and become more abundant from Section 5 through the Core Catcher.

SMEAR SLIDE SUMMARY (%):

	3, 84
	D
TEXTURE:	
Sand	20
Silt	75
Clay	5
COMPOSITION:	
Foraminifers	12
Nannofossils	83
Radiolarians	2
Siliceous fragments	Tr
Siliceous sponge spicules	Tr

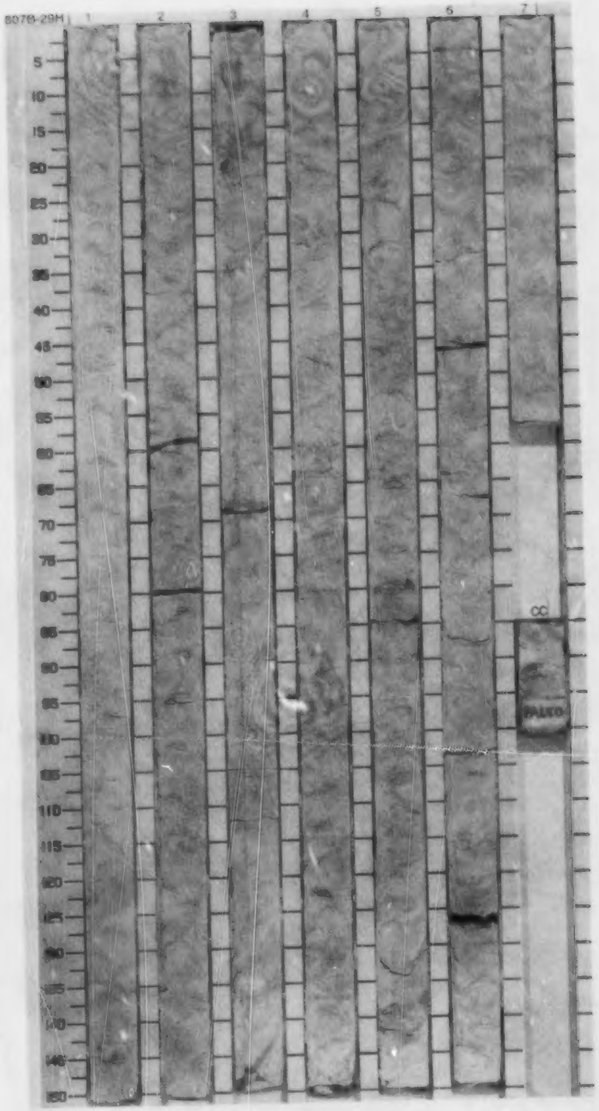
807B-29H
1
2
3
4
5
6
7
CC
PALEO
5
10
15
20
25
30
35
40
45
50
55
60
65
70
75
80
85
90
95
100
105
110
115
120
125
130
135
140
145
150

SITE 807 HOLE B CORE 30H CORED INTERVAL 269.1-278.6 mbsf

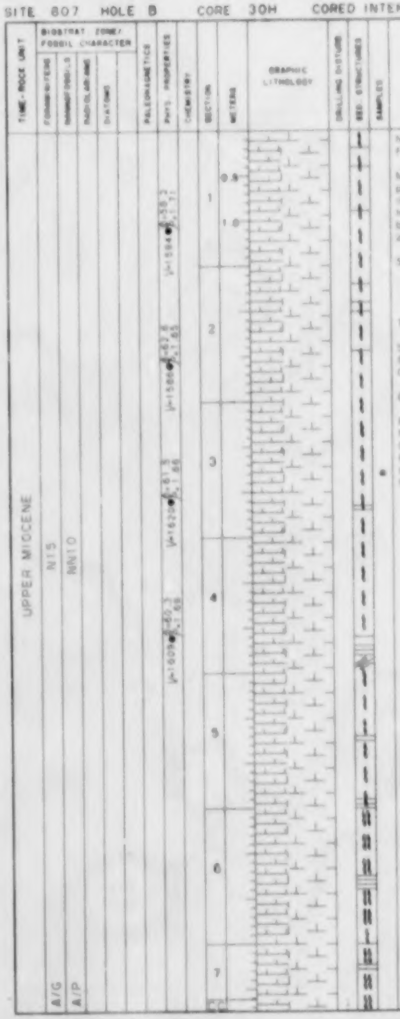
TIME-ROCK UNIT
BIOSTRAT. ZONE/ FOSSIL CHARACTER
FORAMINIFERS
NANNOFOSSILS
RADIOLARIANS
DIATOMS
PALEOMAGNETICS
PHYS. PROPERTIES
CHEMISTRY
SECTION
METERS
GRAPHIC LITHOLOGY
DRILLING DISTURB.
SED. STRUCTURES
SAMPLES
UPPER MIOCENE
N15
NN10
A/G
A/P
V=1594 φ=58.2 γ=1.71
V=1586 φ=62.8 γ=1.65
V=1620 φ=61.5 γ=1.66
V=1609 φ=60.2 γ=1.66
0.5
1.0
1
2
3
4
5
6
7
CC

LITHOLOGIC DESCRIPTION

NANNOFOSSIL OOZE with FORAMINIFERS and NANNOFOSSIL CHALK with FORAMINIFERS

Major lithology: This core contains slightly to moderately bioturbated, white (2.5Y 8/0) to pale purple (5Y 6/2) and pale pink (5RP 8/2) NANNOFOSSIL OOZE with FORAMINIFERS (60%) and NANNOFOSSIL CHALK with FORAMINIFERS (40%). The sediment ranges from uniformly stiff ooze to moderately fractured biscuits. Faint pale purple (5P 6/2), grayish blue (5PB 5/2), light gray (N7), and light greenish gray (5G 7/1) color bands are present and locally abundant. A color band at Section 4, 140 cm is microfaulted.

SMEAR SLIDE SUMMARY (%):

	3, 40
	D
TEXTURE:	
Sand	20
Silt	75
Clay	5
COMPOSITION:	
Foraminifers	15
Nannofossils	80
Quartz	Tr
Radiolarians	2
Siliceous fragments	Tr
Siliceous sponge spicules	Tr

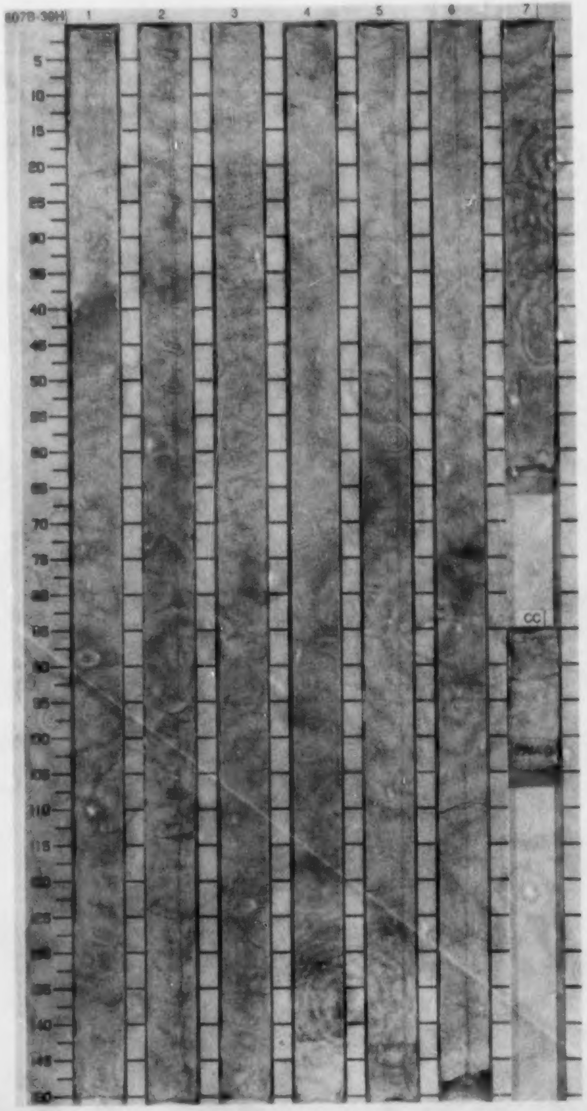
807B-30H
1
2
3
4
5
6
7
CC
5
10
15
20
25
30
35
40
45
50
55
60
65
70
75
80
85
90
95
100
105
110
115
120
125
130
135
140
145
150

SITE 807 HOLE C CORE 1R CORED INTERVAL 780.0-789.7 mbsf

TIME-ROCK UNIT	BIOSTRAT. ZONE/ FOSSIL CHARACTER: FORAMINIFERS	NANNOFOSSILS	RADIOLARIANS	DIATOMS	PALEOMAGNETICS	PHYS. PROPERTIES	CHEMISTRY	SECTION	METERS	GRAPHIC LITHOLOGY	DRILLING DISTURB.	SED. STRUCTURES	SAMPLES
LOWER OLIGOCENE	A/M P19	A/M NP23	Dorcadospyris ateuchus A/M	A/M Rocella vigilans				CC					●

LITHOLOGIC DESCRIPTION

NANNOFOSSIL CHALK with FORAMINIFERS

Major lithology: This core contains slightly bioturbated, highly fragmented, white (2.5Y 8/0) NANNOFOSSIL CHALK with FORAMINIFERS.

SMEAR SLIDE SUMMARY (%):

	CC, 5
	D
TEXTURE:	
Sand	20
Silt	75
Clay	5
COMPOSITION:	
Foraminifers	12
Nannofossils	80
Quartz	Tr
Radiolarians	3
Silicoflagellates	Tr

SITE 807 HOLE C CORE 2R CORED INTERVAL 789.7-799.3 mbsf

TIME-ROCK UNIT	BIOSTRAT. ZONE/ FOSSIL CHARACTER: FORAMINIFERS	NANNOFOSSILS	RADIOLARIANS	DIATOMS	PALEOMAGNETICS	PHYS. PROPERTIES	CHEMISTRY	SECTION	METERS	GRAPHIC LITHOLOGY	DRILLING DISTURB.	SED. STRUCTURES	SAMPLES
LOWER OLIGOCENE	A/M P19	A/M NP23	A/M Dorcadospyris ateuchus / Theocotyle tuberosa	A/M Rocella vigilans?		● ϕ=51.6 γ=1.87 V=1791 ● ϕ=51.0 γ=1.85	● %CaCO$_3$=93.0 ● %CaCO$_3$=96.1	1 2	0.5 1.0				●

LITHOLOGIC DESCRIPTION

NANNOFOSSIL CHALK with FORAMINIFERS

Major lithology: This core contains heavily bioturbated, white (2.5Y 8/0) to pale pink (5RP 8/2) NANNOFOSSIL CHALK with FORAMINIFERS. A well-developed *Zoophycos* trace fossil is present in Section 1, 110-130 cm. Gray (N4/) microstylolites are common below Section 2, 30 cm.

SMEAR SLIDE SUMMARY (%):

	2, 39
	D
TEXTURE:	
Sand	20
Silt	75
Clay	5
COMPOSITION:	
Foraminifers	15
Nannofossils	82
Quartz	Tr
Radiolarians	3
Silicoflagellates	Tr

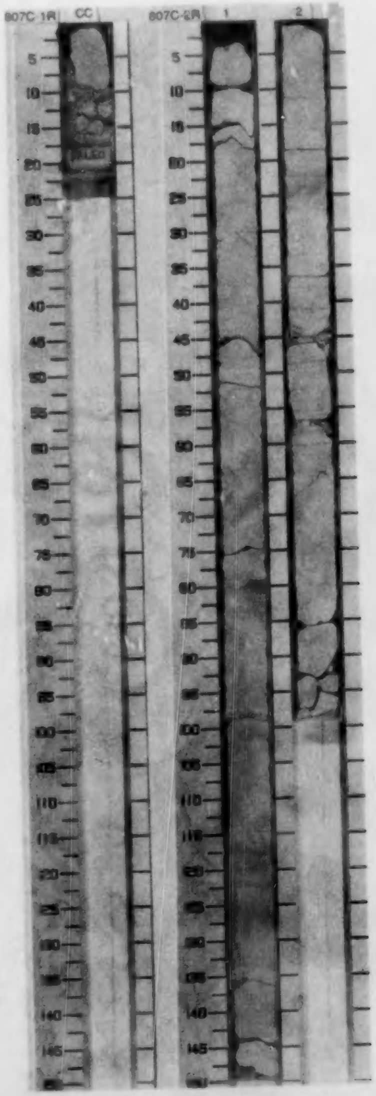

SITE 807 HOLE C CORE 3R CORED INTERVAL 799.3-809.0 mbsf

TIME-ROCK UNIT	BIOSTRAT. ZONE/ FOSSIL CHARACTER				PALEOMAGNETICS	PHYS. PROPERTIES	CHEMISTRY	SECTION	METERS	GRAPHIC LITHOLOGY	DRILLING DISTURB.	SED. STRUCTURES	SAMPLES	LITHOLOGIC DESCRIPTION
	FORAMINIFERS	NANNOFOSSILS	RADIOLARIANS	DIATOMS										
LOWER OLIGOCENE	A/M P19	A/M NP23	A/M *Theocotyle tuberosa*	C/M *Rocella vigilans?*										THE ENTIRE CORE CATCHER (3 cm) WAS USED FOR PALEONTOLOGICAL ANALYSIS

SITE 807 HOLE C CORE 4R CORED INTERVAL 809.0-818.6 mbsf

TIME-ROCK UNIT	BIOSTRAT. ZONE/ FOSSIL CHARACTER				PALEOMAGNETICS	PHYS. PROPERTIES	CHEMISTRY	SECTION	METERS	GRAPHIC LITHOLOGY	DRILLING DISTURB.	SED. STRUCTURES	SAMPLES	LITHOLOGIC DESCRIPTION
	FORAMINIFERS	NANNOFOSSILS	RADIOLARIANS	DIATOMS										
LOWER OLIGOCENE	C/P P19	A/M NP23	A/M *Theocotyle tuberosa*	C/M *Rocella vigilans?*		V=1837 ● φ=52.0 γ=1.82	● %CaCO$_3$=93.0	1	0.5 1.0				OG IW	NANNOFOSSIL CHALK with FORAMINIFERS
						V=1809 ● φ=48.5 γ=1.87	● %CaCO$_3$=90.5	2					●	
								CC						

Major lithology: This core contains heavily to moderately bioturbated, white (2.5Y 8/0) NANNOFOSSIL CHALK with FORAMINIFERS. Diffuse and discontinuous, wavy, light gray (N7) color bands (<1 mm thick) are observed in Section 1. Gray (N6) microstylolites are common in Section 2.

SMEAR SLIDE SUMMARY (%):

	2, 80
	D
TEXTURE:	
Sand	30
Silt	70
Clay	0
COMPOSITION:	
Foraminifers	15
Nannofossils	80
Quartz	Tr
Radiolarians	3
Silicoflagellates	Tr

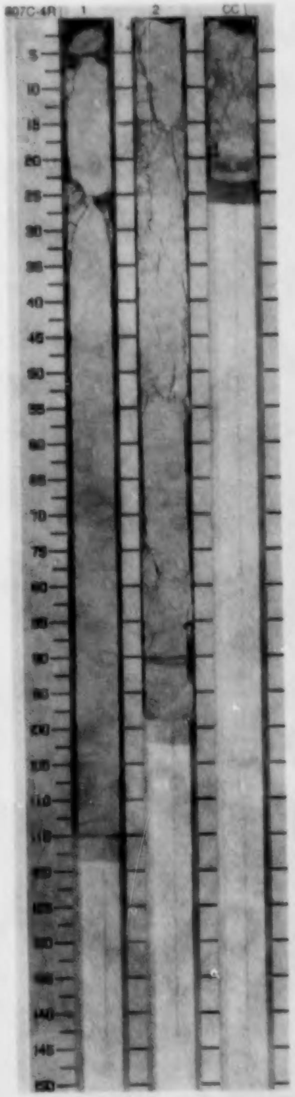

SITE 807 HOLE C CORE 5R CORED INTERVAL 818.6-828.3 mbsf

TIME-ROCK UNIT	BIOSTRAT. ZONE/ FOSSIL CHARACTER					PALEOMAGNETICS	PHYS. PROPERTIES	CHEMISTRY	SECTION	METERS	GRAPHIC LITHOLOGY	DRILLING DISTURB.	SED. STRUCTURES	SAMPLES	LITHOLOGIC DESCRIPTION
	FORAMINIFERS	NANNOFOSSILS	RADIOLARIANS	DIATOMS											
LOWER OLIGOCENE	A/M P19	A/M NP23		A/M *Coscinodiscus excavatus*											THE ENTIRE CORE CATCHER (2 cm) WAS USED FOR PALEONTOLOGICAL ANALYSIS

SITE 807 HOLE C CORE 6R CORED INTERVAL 828.3-838.0 mbsf

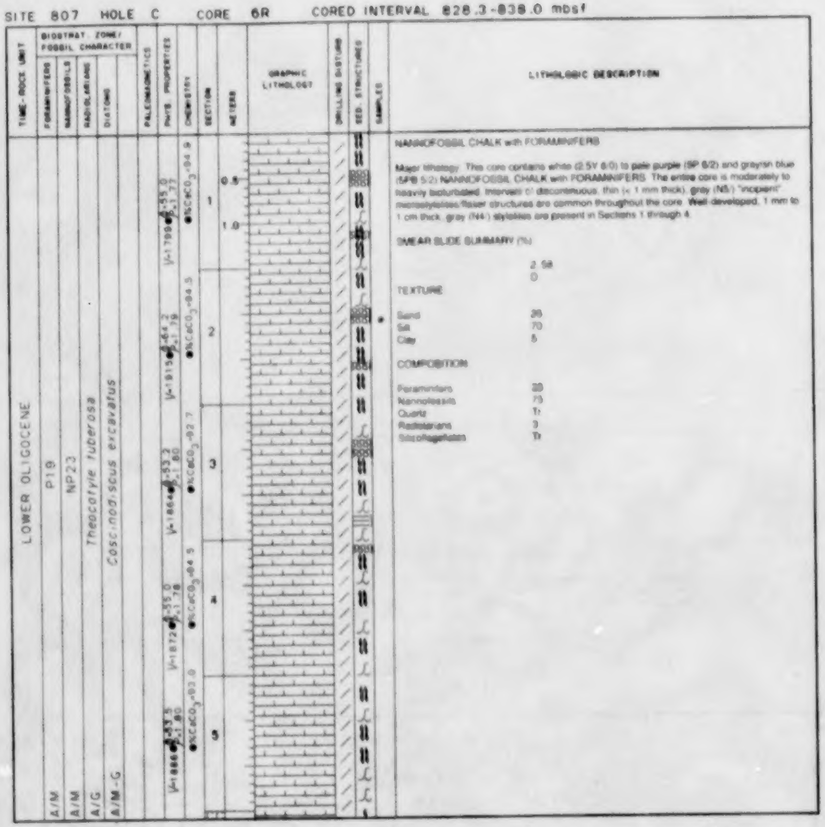
TIME-ROCK UNIT
BIOSTRAT. ZONE/ FOSSIL CHARACTER
FORAMINIFERS
NANNOFOSSILS
RADIOLARIANS
DIATOMS
PALEOMAGNETICS
PHYS. PROPERTIES
CHEMISTRY
SECTION
METERS
GRAPHIC LITHOLOGY
DRILLING DISTURB.
SED. STRUCTURES
SAMPLES
LITHOLOGIC DESCRIPTION
LOWER OLIGOCENE
A/M P19
A/M NP23
A/G Theocotyle tuberosa
A/M-G Coscinodiscus excavatus
V-1799 φ-55.0 ρ-1.77
%CaCO3-94.9
V-1915 φ-64.2 ρ-1.79
%CaCO3-94.5
V-1864 φ-53.2 ρ-1.80
%CaCO3-92.7
V-1872 φ-55.0 ρ-1.78
%CaCO3-94.5
V-1886 φ-53.5 ρ-1.80
%CaCO3-93.0
1
2
3
4
5
0.5
1.0

NANNOFOSSIL CHALK with FORAMINIFERS

Major lithology: This core contains white (2.5Y 8/0) to pale purple (5P 6/2) and grayish blue (5PB 5/2) NANNOFOSSIL CHALK with FORAMINIFERS. The entire core is moderately to heavily bioturbated. Intervals of discontinuous, thin (< 1 mm thick), gray (N5/) "incipient" microstylolites/flaser structures are common throughout the core. Well-developed, 1 mm to 1 cm thick, gray (N4/) stylolites are present in Sections 1 through 4.

SMEAR SLIDE SUMMARY (%):

	2, 58
	D
TEXTURE:	
Sand	25
Silt	70
Clay	5
COMPOSITION:	
Foraminifers	20
Nannofossils	75
Quartz	Tr
Radiolarians	3
Silicoflagellates	Tr

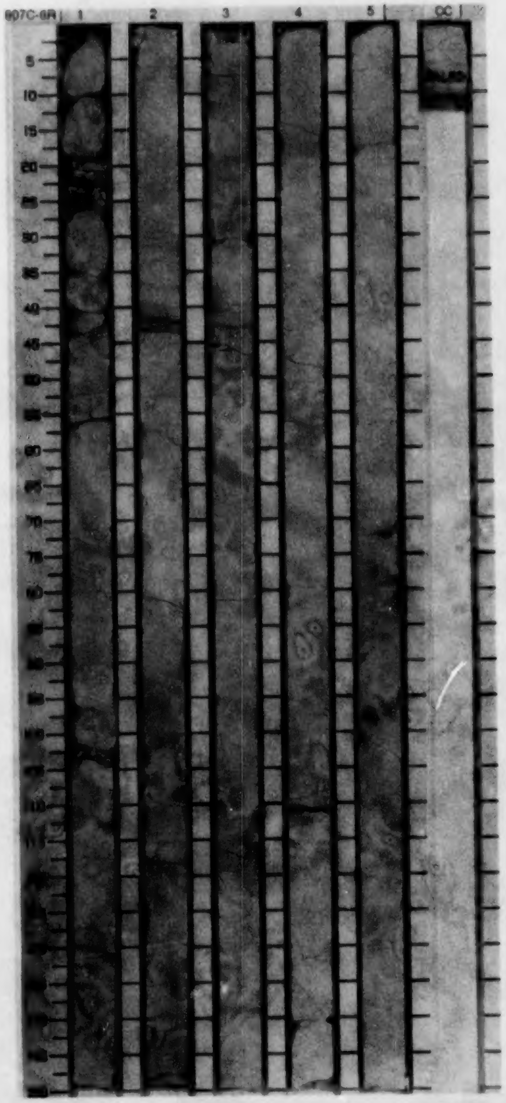
807C-6R
1
2
3
4
5
CC
5
10
15
20
25
30
35
40
45
50
55
60
65
70
75
80
85
90
95
100
105
110
115
120
125
130
135
140
145
150

SITE 807 HOLE C CORE 7R CORED INTERVAL 838.0-847.7 mbsf

TIME-ROCK UNIT	BIOSTRAT. ZONE/ FOSSIL CHARACTER: FORAMINIFERS	NANNOFOSSILS	RADIOLARIANS	DIATOMS	PALEOMAGNETICS	PHYS. PROPERTIES	CHEMISTRY	SECTION	METERS	GRAPHIC LITHOLOGY	DRILLING DISTURB.	SED. STRUCTURES	SAMPLES	LITHOLOGIC DESCRIPTION
LOWER OLIGOCENE	A/M P19	A/M NP23		A/M *Coscinodiscus excavatus*				CC					*	NANNOFOSSIL CHALK with FORAMINIFERS

Major lithology: This core contains white (2.5Y 8/0), highly fragmented NANNOFOSSIL CHALK with FORAMINIFERS.

SMEAR SLIDE SUMMARY (%):

	CC, 5
	D
TEXTURE:	
Sand	20
Silt	75
Clay	5
COMPOSITION:	
Foraminifers	20
Nannofossils	75
Quartz	Tr
Radiolarians	2
Silicoflagellates	Tr

SITE 807 HOLE C CORE 8R CORED INTERVAL 847.7-857.4 mbsf

TIME-ROCK UNIT	BIOSTRAT. ZONE/ FOSSIL CHARACTER: FORAMINIFERS	NANNOFOSSILS	RADIOLARIANS	DIATOMS	PALEOMAGNETICS	PHYS. PROPERTIES	CHEMISTRY	SECTION	METERS	GRAPHIC LITHOLOGY	DRILLING DISTURB.	SED. STRUCTURES	SAMPLES	LITHOLOGIC DESCRIPTION
LOWER OLIGOCENE	C/M P19	A/M NP23	A/M *Theocotyle tuberosa*	A/M *Coscinodiscus excavatus*										THE ENTIRE CORE CATCHER (1 cm) WAS USED FOR PALEONTOLOGICAL ANALYSIS.

807C-7R, CC
5
10
15
20
25
30
35
40
45
50
55
60
65
70
75
80
85
90
95
100
105
110
115
120
125
130
135
140
145
150

SITE 807 HOLE C CORE 9R CORED INTERVAL 857.4-867.1 mbsf

TIME-ROCK UNIT	BIOSTRAT. ZONE/ FOSSIL CHARACTER: FORAMINIFERS	BIOSTRAT. ZONE/ FOSSIL CHARACTER: NANNOFOSSILS	BIOSTRAT. ZONE/ FOSSIL CHARACTER: RADIOLARIANS	BIOSTRAT. ZONE/ FOSSIL CHARACTER: DIATOMS	PALEOMAGNETICS	PHYS. PROPERTIES	CHEMISTRY	SECTION	METERS	GRAPHIC LITHOLOGY	DRILLING DISTURB.	SED. STRUCTURES	SAMPLES
LOWER OLIGOCENE	P19 A/M	NP22 A/M		Coscinodiscus excavatus A/M		● φ=53.2 ρ=1.80 V=1853	● %CaCO3=91.7	1 CC					●

LITHOLOGIC DESCRIPTION

NANNOFOSSIL CHALK

Major lithology: This core contains moderately to heavily bioturbated, white (2.5Y 8/0) to light greenish gray (5G 7/1) NANNOFOSSIL CHALK. Thin (< 1 mm thick) light greenish gray (5G 7/1) flaser structures are common in the lower portion of Section 1 and throughout the CC.

SMEAR SLIDE SUMMARY (%):

	1, 32
	D
TEXTURE	
Sand	7
Silt	90
Clay	3
COMPOSITION	
Foraminifers	9
Nannofossils	88
Quartz	Tr
Radiolarians	3
Silicoflagellates	Tr

807 C 10R NO RECOVERY

807 C 11R NO RECOVERY

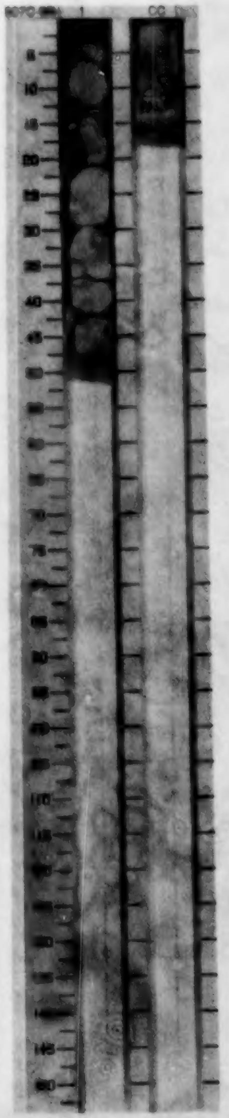

SITE 807 HOLE C CORE 12R CORED INTERVAL 876.6-881.9 mbsf

TIME-ROCK UNIT	BIOSTRAT. ZONE/ FOSSIL CHARACTER FORAMINIFERS	NANNOFOSSILS	RADIOLARIANS	DIATOMS	PALEOMAGNETICS	PHYS. PROPERTIES	CHEMISTRY	SECTION	METERS	GRAPHIC LITHOLOGY	DRILLING DISTURB.	SED. STRUCTURES	SAMPLES
LOWER OLIGOCENE	P18 C/M	NP22 A/M	*Theocotyle tuberosa* A/M	*Coscinodiscus excavatus* A/M		● φ=52.5 γ=1.83 Vp=1771	● %CaCO$_3$ =95.0	1			⊥	≋	●

LITHOLOGIC DESCRIPTION

NANNOFOSSIL CHALK with FORAMINIFERS

Major lithology: This core contains white (2.5Y 8/0) NANNOFOSSIL CHALK with FORAMINIFERS. Heavy bioturbation is evident from faint mottles, burrows and disseminated pyrite specks. Ultra thin (<<1 mm) wavy and braided color bands are present throughout the core.

SMEAR SLIDE SUMMARY (%):

	1, 30 D
TEXTURE:	
Sand	8
Silt	80
Clay	12
COMPOSITION:	
Diatoms	Tr
Foraminifers	12
Nannofossils	87
Radiolarians	Tr
Siliceous fragments	Tr

SITE 807 HOLE C CORE 13R CORED INTERVAL 881.9-888.9 mbsf

TIME-ROCK UNIT	BIOSTRAT. ZONE/ FOSSIL CHARACTER FORAMINIFERS	NANNOFOSSILS	RADIOLARIANS	DIATOMS	PALEOMAGNETICS	PHYS. PROPERTIES	CHEMISTRY	SECTION	METERS	GRAPHIC LITHOLOGY	DRILLING DISTURB.	SED. STRUCTURES	SAMPLES
LOWER OLIGOCENE	P18 C/M	NP21 A/P	*Theocotyle tuberosa* A/M	*Coscinodiscus excavatus*				CC			☒	⊥	●

LITHOLOGIC DESCRIPTION

NANNOFOSSIL CHALK with FORAMINIFERS

Major lithology: This core contains bioturbated, white (2.5Y 8/0) NANNOFOSSIL CHALK with FORAMINIFERS. A few specks of an opaque mineral are scattered over the few chert nodules in the core.

SMEAR SLIDE SUMMARY (%):

	1, 9 D
TEXTURE:	
Sand	5
Silt	60
Clay	35
COMPOSITION:	
Accessory minerals	1
Foraminifers	20
Nannofossils	78
Siliceous fragments	1

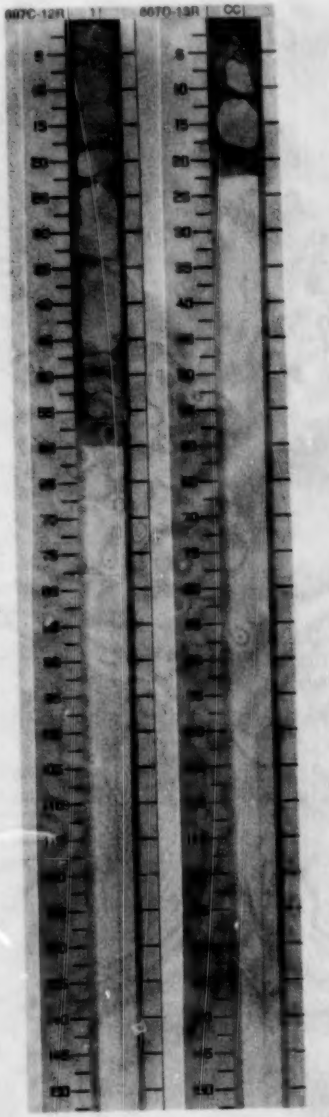

SITE 807 HOLE C CORE 14R CORED INTERVAL 888.9-893.9 mbsf

TIME-ROCK UNIT	BIOSTRAT. ZONE/ FOSSIL CHARACTER: FORAMINIFERS	NANNOFOSSILS	RADIOLARIANS	DIATOMS	PALEOMAGNETICS	PHYS. PROPERTIES	CHEMISTRY	SECTION	METERS	GRAPHIC LITHOLOGY	DRILLING DISTURB.	SED. STRUCTURES	SAMPLES
LOWER OLIGOCENE	P18 C/M	NP21 A/P	*Theocotyle tuberosa* A/P	*Coscinodiscus excavatus* A/M-G				CC			×		●

LITHOLOGIC DESCRIPTION

NANNOFOSSIL CHALK with FORAMINIFERS

Major lithology: This core contains bioturbated white (2.5Y 8/0) NANNOFOSSIL CHALK with FORAMINIFERS. A few specks of an opaque mineral are scattered over the few chert nodules in the core.

SMEAR SLIDE SUMMARY (%):

	CC, 5
	D
TEXTURE:	
Sand	8
Silt	65
Clay	27
COMPOSITION:	
Accessory minerals	1
Foraminifers	15
Nannofossils	80
Siliceous fragments	1

SITE 807 HOLE C CORE 15R CORED INTERVAL 893.9-898.9 mbsf

TIME-ROCK UNIT	BIOSTRAT. ZONE/ FOSSIL CHARACTER: FORAMINIFERS	NANNOFOSSILS	RADIOLARIANS	DIATOMS	PALEOMAGNETICS	PHYS. PROPERTIES	CHEMISTRY	SECTION	METERS	GRAPHIC LITHOLOGY	DRILLING DISTURB.	SED. STRUCTURES	SAMPLES
LOWER OLIGOCENE	P18 A/M	NP21 A/M	*Theocotyle tuberosa* A/G					1 CC	0.5				

LITHOLOGIC DESCRIPTION

NANNOFOSSIL CHALK

Major lithology: This core contains white (2.5Y 8/0) NANNOFOSSIL CHALK. Moderate to heavy bioturbation is evident from burrows and abundant trace fossils that appear compacted. One thin zone (1 cm thick) of broken, ultra-thin light blue gray (5Y 6/2) color bands is present in Section 1, 34 cm. Stylolites are noted throughout the core.

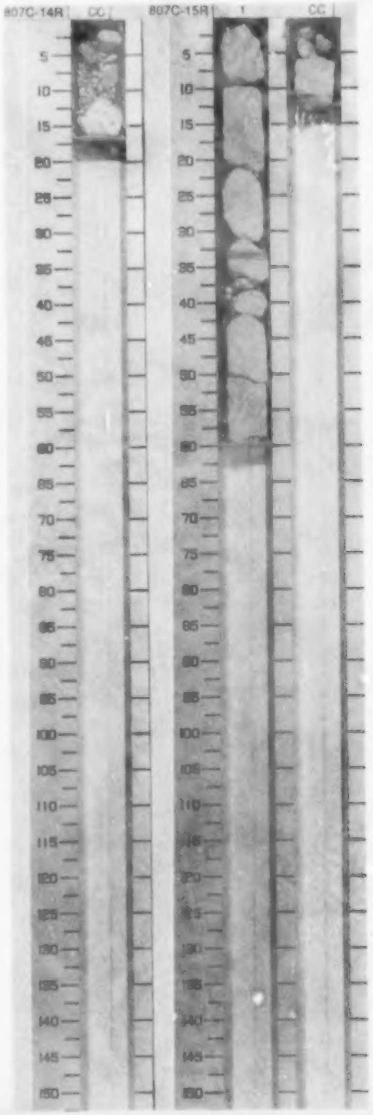

SITE 807 HOLE C CORE 16R CORED INTERVAL 898.9-903.9 mbsf

TIME-ROCK UNIT	FORAMINIFERS	NANNOFOSSILS	RADIOLARIANS	DIATOMS	PALEOMAGNETICS	PHYS. PROPERTIES	CHEMISTRY	SECTION	METERS
LOWERMOST OLIGOCENE	F/P P18?	A/P NP21	A/M *Theocotyle tuberosa*	A/V-C basal *Coscinodiscus excavatus*		V=2005 ●	●	1	0.5 1.0

LITHOLOGIC DESCRIPTION

NANNOFOSSIL CHALK with FORAMINIFERS

Major lithology: This core contains white (2.5Y 8/0) NANNOFOSSIL CHALK with FORAMINIFERS. Numerous ultra thin, braided, light olive gray (5Y 6/2) color bands/stylolites are located in Section 1 at 65-78 cm and 109-115 cm. Heavy bioturbation is indicated by trace fossils that appear to have been compacted.

SMEAR SLIDE SUMMARY (%):

	1, 85 D
TEXTURE:	
Sand	3
Silt	75
Clay	22
COMPOSITION:	
Foraminifers	10
Nannofossils	89
Radiolarians	Tr
Siliceous fragments	1
Siliceous sponge spicules	Tr

SITE 807 HOLE C CORE 17R CORED INTERVAL 903.9-908.9 mbsf

TIME-ROCK UNIT	FORAMINIFERS	NANNOFOSSILS	RADIOLARIANS	DIATOMS	PALEOMAGNETICS	PHYS. PROPERTIES	CHEMISTRY	SECTION	METERS
LOWERMOST OLIGOCENE	R/P P18?	A NP21	A/M *Cryptopora ornata* • upper *Thyrsocyrtis bromia*	C-A/G *Bacteriopsis brunii*		● V=1752 ● V=1639	● %CaCO₃=92.0 ● %CaCO₃=92.0	1 2 3	0.5 1.0

LITHOLOGIC DESCRIPTION

NANNOFOSSIL CHALK with FORAMINIFERS to FORAMINIFER NANNOFOSSIL CHALK

Major lithology: This core contains white (2.5Y 8/0) NANNOFOSSIL CHALK with FORAMINIFERS to FORAMINIFER NANNOFOSSIL CHALK. There are several 5 to 10 cm thick zones of braided, light olive gray (5Y 6/2) color bands. Several gray bands are very distinct. Bioturbation structures are common and include mottles and trace fossils. The lowermost part of the core contains abundant faint, pale purple (5P 6/2) to greenish gray (5G 6/1) color bands. The base of the core has a 5 cm thick interval of very distinct, thin (<=1 mm), horizontal, straight color bands.

SMEAR SLIDE SUMMARY (%):

	2, 75 D
TEXTURE:	
Sand	10
Silt	80
Clay	10
COMPOSITION:	
Diatoms	Tr
Foraminifers	25
Nannofossils	69
Radiolarians	1
Siliceous fragments	4
Siliceous sponge spicules	Tr

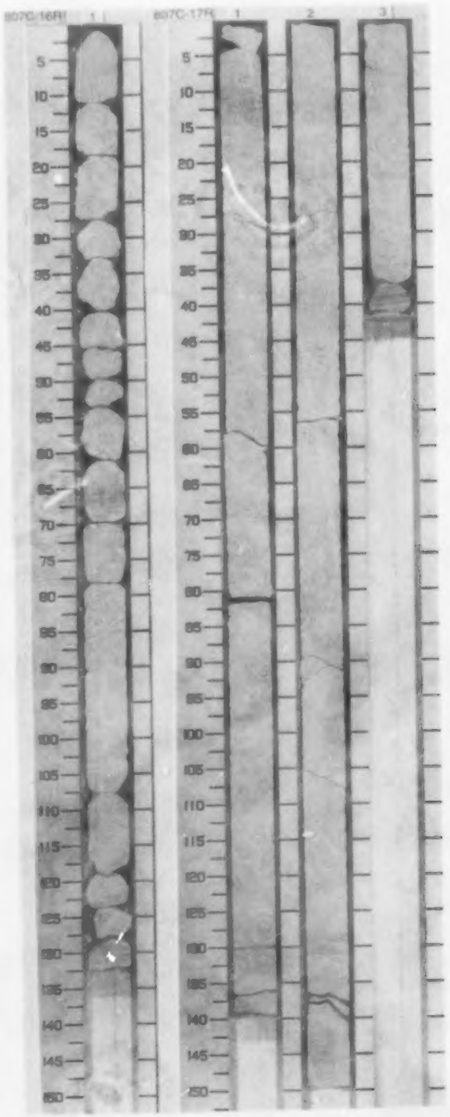

SITE 807 HOLE C CORE 18R CORED INTERVAL 908.9-913.9 mbsf

TIME-ROCK UNIT	BIOSTRAT. ZONE/ FOSSIL CHARACTER: FORAMINIFERS	NANNOFOSSILS	RADIOLARIANS	DIATOMS	PALEOMAGNETICS	PHYS. PROPERTIES	CHEMISTRY	SECTION	METERS	GRAPHIC LITHOLOGY	DRILLING DISTURB.	SED. STRUCTURES	SAMPLES	LITHOLOGIC DESCRIPTION
UPPER EOCENE	C/M P17	A NP19 - NP20	A/G Cryptopora ornata | upper Thyrsocyrtis bromia	C-A/M-G Baxteriopsis brunii		●	●	CC					*	NANNOFOSSIL CHALK with FORAMINIFERS

NANNOFOSSIL CHALK with FORAMINIFERS

Major lithology: This core contains white (2.5Y 8/0), moderately bioturbated NANNOFOSSIL CHALK with FORAMINIFERS. Gray (N6) microstylolites and flaser structures are common.

SMEAR SLIDE SUMMARY (%):

	CC, 15
	D
TEXTURE:	
Sand	15
Silt	81
Clay	4
COMPOSITION:	
Foraminifers	15
Nannofossils	81
Radiolarians	1
Siliceous sponge spicules	1

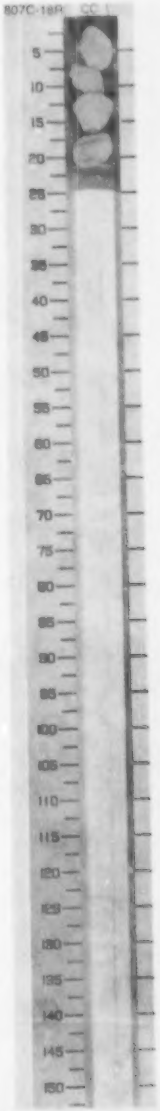
807C-18R CC
5
10
15
20
25
30
35
40
45
50
55
60
65
70
75
80
85
90
95
100
105
110
115
120
125
130
135
140
145
150

SITE 807 HOLE C CORE 19R CORED INTERVAL 913.9-918.9 mbsf

TIME-ROCK UNIT	BIOSTRAT. ZONE/ FOSSIL CHARACTER: FORAMINIFERS	NANNOFOSSILS	RADIOLARIANS	DIATOMS	PALEOMAGNETICS	PHYS. PROPERTIES	CHEMISTRY	SECTION	METERS	GRAPHIC LITHOLOGY	DRILLING DISTURB.	SED. STRUCTURES	SAMPLES
UPPER EOCENE	P17 A/M	upper *Thyrosocyrtis bromia* NP19 - NP20 A/P	*Cryptopora ornata* / =upper *Thyrosocyrtis bromia* A/M	*Baxteriopsis brunii* C-A/M		● φ=51.7 γ=1.83 Vp=1824	● %CaCO3=92.0	1	0.5				●

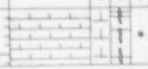

LITHOLOGIC DESCRIPTION

NANNOFOSSIL CHALK

Major lithology: This core contains white (2.5Y 8/0), moderately bioturbated NANNOFOSSIL CHALK. Gray (N6) microstylolites and color bands with flaser structures are common.

SMEAR SLIDE SUMMARY (%):

	1, 30 D
TEXTURE:	
Sand	10
Silt	85
Clay	5
COMPOSITION:	
Diatoms	1
Foraminifers	5
Nannofossils	87
Radiolarians	3
Siliceous sponge spicules	2
Silicoflagellates	2

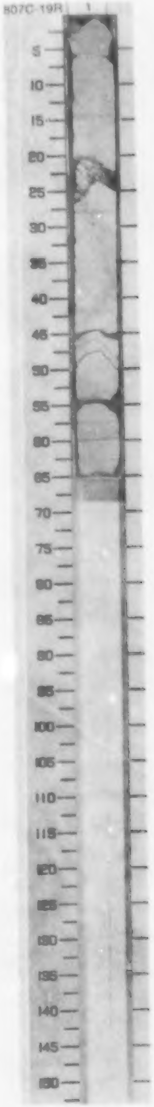
807C-19R
1
5
10
15
20
25
30
35
40
45
50
55
60
65
70
75
80
85
90
95
100
105
110
115
120
125
130
135
140
145
150

SITE 807 HOLE C CORE 20R CORED INTERVAL 918.9-923.9 mbsf

TIME-ROCK UNIT	BIOSTRAT. ZONE/ FOSSIL CHARACTER					PALEOMAGNETICS	PHYS. PROPERTIES	CHEMISTRY	SECTION	METERS	GRAPHIC LITHOLOGY	DRILLING DISTURB.	SED. STRUCTURES	SAMPLES	LITHOLOGIC DESCRIPTION
	FORAMINIFERS	NANNOFOSSILS	RADIOLARIANS	DIATOMS											
UPPER EOCENE	P17 A/M	NP19 - NP20 A/P	*Cryptopora ornata* *upper Thyrsocyrtis bromia* A/M	*Baxteriopsis brunii* C-A/M					1					●	NANNOFOSSIL CHALK

NANNOFOSSIL CHALK

Major lithology: This core contains white (2.5Y 8/0), moderately bioturbated NANNOFOSSIL CHALK. Stylolites are present in Section 1 at 12-15 cm.

SMEAR SLIDE SUMMARY (%):

	1, 10
	D
TEXTURE:	
Sand	10
Silt	8
Clay	5
COMPOSITION:	
Diatoms	1
Foraminifers	8
Nannofossils	87
Radiolarians	2
Siliceous sponge spicules	2

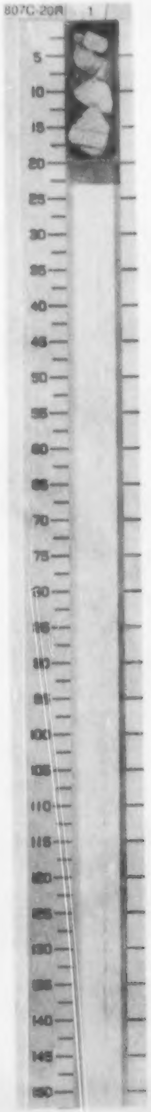
807C-20R
1
5
10
15
20
25
30
35
40
45
50
55
60
65
70
75
80
85
90
95
100
105
110
115
120
125
130
135
140
145
150

SITE 807 HOLE C CORE 21R CORED INTERVAL 923.9-933.7 mbsf

TIME-ROCK UNIT	BIOSTRAT. ZONE/ FOSSIL CHARACTER: FORAMINIFERS	NANNOFOSSILS	RADIOLARIANS	DIATOMS	PALEOMAGNETICS	PHYS. PROPERTIES	CHEMISTRY	SECTION	METERS	GRAPHIC LITHOLOGY	DRILLING DISTURB.	SED. STRUCTURES	SAMPLES	LITHOLOGIC DESCRIPTION
UPPER EOCENE	P16 - P17 A/M	NP19 - NP20 A/P	A/M Cryptopora ornata -upper Thyrsocyrtis bromia	C/P-M Baxteriopsis brunii		● [illegible] γ=1.838	● [illegible] 91.9	1					●	

NANNOFOSSIL CHALK

Major lithology: This core contains white (2.5Y 8/0), moderately bioturbated NANNOFOSSIL CHALK. A gray (N6) color band with fissure structure is noted at 17-20 cm.

SMEAR SLIDE SUMMARY (%):

	1, 20
	D
TEXTURE:	
Sand	10
Silt	86
Clay	4
COMPOSITION:	
Diatoms	1
Foraminifers	7
Nannofossils	82
Radiolarians	5
Siliceous sponge spicules	3
Silicoflagellates	2

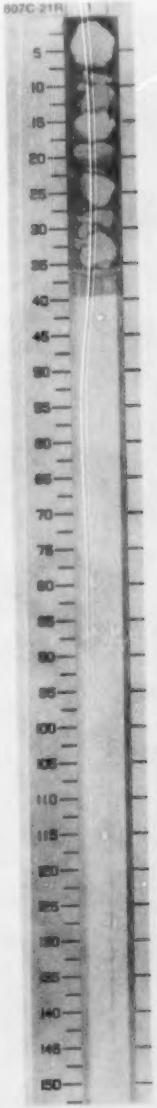
807C-21R
1
5
10
15
20
25
30
35
40
45
50
55
60
65
70
75
80
85
90
95
100
105
110
115
120
125
130
135
140
145
150

SITE 807 HOLE C CORE 22R CORED INTERVAL 933.7-938.7 mbsf

TIME-ROCK UNIT	BIOSTRAT. ZONE/ FOSSIL CHARACTER: FORAMINIFERS	NANNOFOSSILS	RADIOLARIANS	DIATOMS	PALEOMAGNETICS	PHYS. PROPERTIES	CHEMISTRY	SECTION	METERS	GRAPHIC LITHOLOGY	DRILLING DISTURB.	SED. STRUCTURES	SAMPLES
UPPER EOCENE	P14 - P17 C/P	NP17 - NP19 A/P	*Cryptopora ornata* -upper *Thyrsocyrtis bromia* A/P	*Asterolampra marylandica?* F-C/P-M				1			⊥	SS	●

LITHOLOGIC DESCRIPTION

NANNOFOSSIL CHALK with FORAMINIFERS

Major lithology: This core contains white (2.5Y 8/0) NANNOFOSSIL CHALK with FORAMINIFERS. Moderate to heavy bioturbation is indicated by mottling and mm-scale pyrite-filled burrows.

SMEAR SLIDE SUMMARY (%):

	1, 19 D
TEXTURE:	
Sand	15
Silt	81
Clay	4
COMPOSITION:	
Diatoms	1
Foraminifers	10
Nannofossils	76
Radiolarians	4
Siliceous sponge spicules	5
Silicoflagellates	2

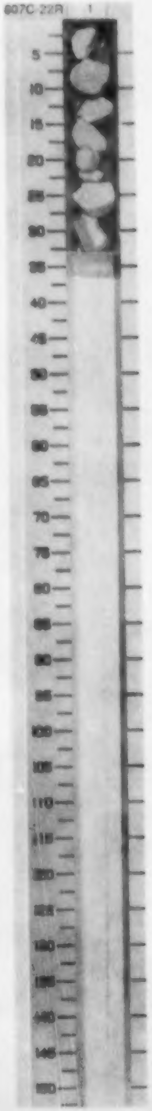
807C-22R
1
5
10
15
20
25
30
35
40
45
50
55
60
65
70
75
80
85
90
95
100
105
110
115
120
125
130
135
140
145
150

SITE 807 HOLE C CORE 23R CORED INTERVAL 938.7-943.7 mbsf

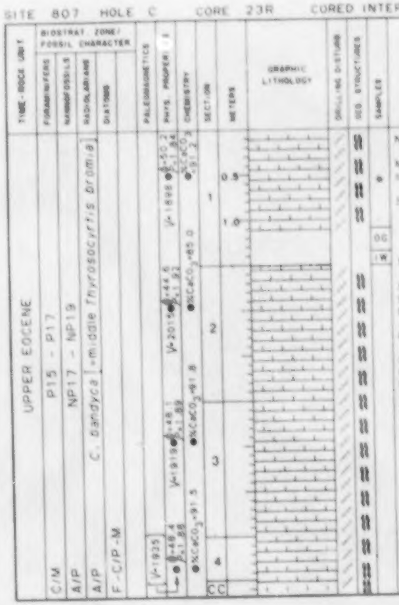
TIME-ROCK UNIT
BIOSTRAT. ZONE/ FOSSIL CHARACTER
FORAMINIFERS
NANNOFOSSILS
RADIOLARIANS
DIATOMS
PALEOMAGNETICS
PHYS. PROPERTIES
CHEMISTRY
SECTION
METERS
GRAPHIC LITHOLOGY
DRILLING DISTURB.
SED. STRUCTURES
SAMPLES
UPPER EOCENE
C/M P15 - P17
A/P NP17 - NP19
A/P C. bandyca =middle Thyrsocyrtis bromia
F-C/P-M
V=1898 ● φ=50.2 ρ=1.84
●%CaCO3=91.2
V=2015 ● φ=44.6 ρ=1.92
●%CaCO3=85.0
V=1919 ● φ=48.1 ρ=1.89
●%CaCO3=91.8
V=1935
● φ=48.4 ρ=1.88
●%CaCO3=91.5
1
2
3
4
CC
0.5
1.0
OG
IW

LITHOLOGIC DESCRIPTION

NANNOFOSSIL CHALK

Major lithology: This core contains white (2.5Y 8.0) NANNOFOSSIL CHALK. It is moderately to heavily bioturbated with mm to cm scale, generally horizontal and compacted burrows.

SMEAR SLIDE SUMMARY (%):

	1, 50
	D
TEXTURE:	
Sand	10
Silt	86
Clay	4
COMPOSITION:	
Diatoms	1
Foraminifers	8
Nannofossils	80
Radiolarians	4
Siliceous sponge spicules	6
Silicoflagellates	1

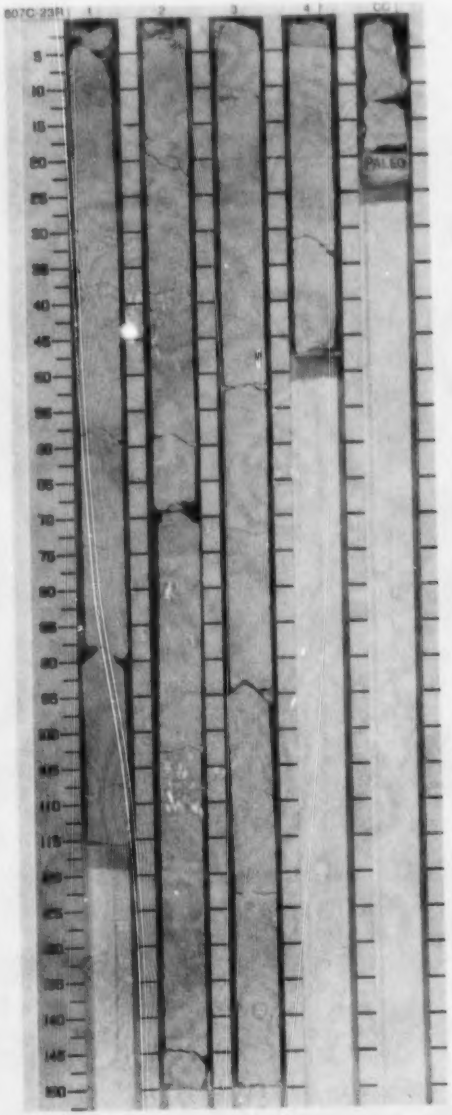
807C-23R
1
2
3
4
CC
PALEO
5
10
15
20
25
30
35
40
45
50
55
60
65
70
75
80
85
90
95
100
105
110
115
120
125
130
135
140
145
150

SITE 807 HOLE C CORE 24R CORED INTERVAL 943.7-948.4 mbsf

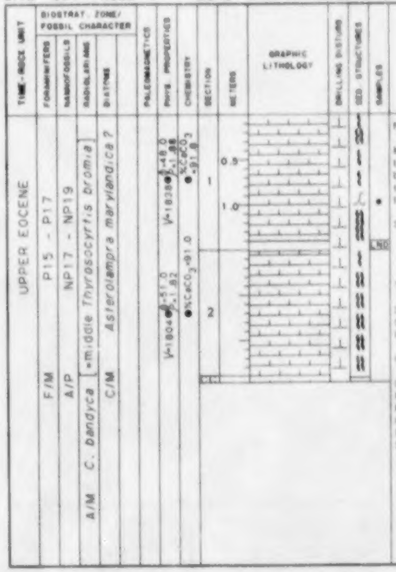
TIME-ROCK UNIT
BIOSTRAT. ZONE/ FOSSIL CHARACTER
FORAMINIFERS
NANNOFOSSILS
RADIOLARIANS
DIATOMS
PALEOMAGNETICS
PHYS. PROPERTIES
CHEMISTRY
SECTION
METERS
GRAPHIC LITHOLOGY
DRILLING DISTURB.
SED. STRUCTURES
SAMPLES
UPPER EOCENE
P15 - P17
F/M
NP17 - NP19
A/P
=middle Thyrsocyrtis bromia
C. bandyca
A/M
Asterolampra marylandica ?
C/M
V=1838
φ=48.0
ρ=1.88
%CaCO3 =91.8
V=1804
φ=51.0
ρ=1.82
%CaCO3=91.0
1
2
CC
0.5
1.0
END

LITHOLOGIC DESCRIPTION

NANNOFOSSIL CHALK

Major lithology: This core contains white (2.5Y 8/0) NANNOFOSSIL CHALK. It is moderately to heavily bioturbated with mm to cm scale, flattened burrows and mm scale pyrite filled burrows. Burrows, grading into flaser structures, are noted in Section 1, 90-105 cm, and a single, 1 cm thick light gray (N7) color band with only slight flaser structure is observed in the CC.

SMEAR SLIDE SUMMARY (%):

	1, 100
	D
TEXTURE:	
Sand	10
Silt	85
Clay	5
COMPOSITION:	
Diatoms	Tr
Foraminifers	4
Nannofossils	90
Quartz	Tr
Radiolarians	4
Siliceous sponge spicules	Tr

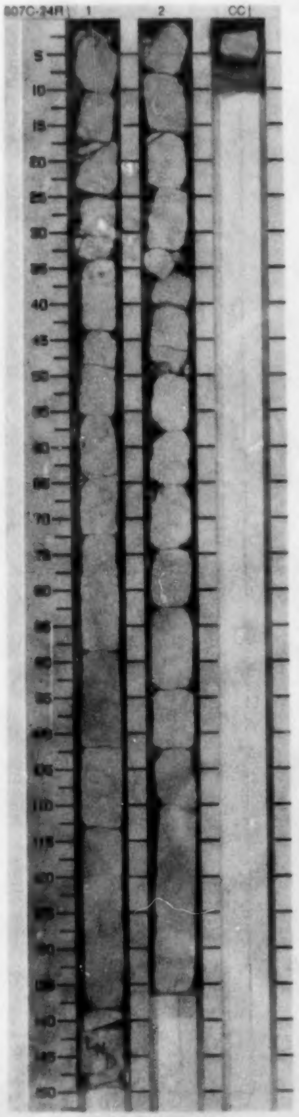
807C-24R
1
2
CC
5
10
15
20
25
30
35
40
45
50
55
60
65
70
75
80
85
90
95
100
105
110
115
120
125
130
135
140
145
150

SITE 807 HOLE C CORE 25R CORED INTERVAL 948.4-958.1 mbsf

TIME-ROCK UNIT	BIOSTRAT. ZONE/ FOSSIL CHARACTER: FORAMINIFERS	NANNOFOSSILS	RADIOLARIANS	DIATOMS		PALEOMAGNETICS	PHYS. PROPERTIES	CHEMISTRY	SECTION	METERS	GRAPHIC LITHOLOGY	DRILLING DISTURB.	SED. STRUCTURES	SAMPLES	LITHOLOGIC DESCRIPTION
UPPER EOCENE	F/M P15 - P17	A/M NP17 - NP19	A/M C. bandyca – m.ddle ? T. bromia	F/P-M Asterolampra marylandica?			● ϕ=47.1 ρ=1.90 V=1902	● %CaCO$_3$ =87.5	1 CC	0.5 1.0				●	NANNOFOSSIL CHALK

NANNOFOSSIL CHALK

Major lithology: This core contains white (2.5Y 8/0) NANNOFOSSIL CHALK. Moderate to heavy bioturbation is indicated by mottling in shades of white.

SMEAR SLIDE SUMMARY (%):

	1, 100
	D
TEXTURE:	
Sand	10
Silt	85
Clay	5
COMPOSITION:	
Diatoms	Tr
Foraminifers	2
Nannofossils	90
Quartz	Tr
Radiolarians	8
Siliceous sponge spicules	Tr

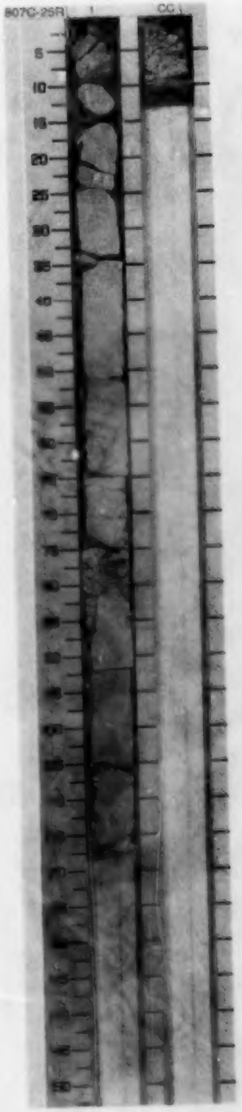

SITE 807 HOLE C CORE 26R CORED INTERVAL 958.1-967.8 mbsf

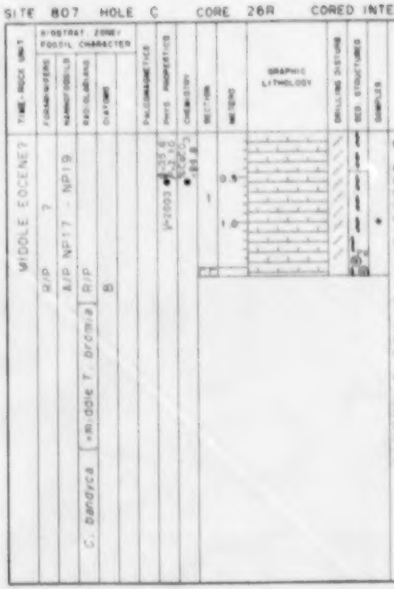
TIME-ROCK UNIT
BIOSTRAT. ZONE/ FOSSIL CHARACTER
FORAMINIFERS
NANNOFOSSILS
RADIOLARIANS
DIATOMS
PALEOMAGNETICS
PHYS. PROPERTIES
CHEMISTRY
SECTION
METERS
GRAPHIC LITHOLOGY
DRILLING DISTURB.
SED. STRUCTURES
SAMPLES
MIDDLE EOCENE?
R/P ?
A/P NP17 - NP19
R/P
C. bandyca
middle T. bromia
B
1
0.5
1.0
CC

LITHOLOGIC DESCRIPTION

NANNOFOSSIL CHALK

Major lithology: This core contains white (2.5Y 8/0) NANNOFOSSIL CHALK. Moderate to heavy bioturbation is indicated by mottling in shades of white. A single stylolite is present in Section 1, 45 cm, and zones with flaser structures are noted in Section 1, 50-57 cm and 78-85 cm. Chert nodules surrounded by thin, partly silicified rims are found near the bottom of the core.

SMEAR SLIDE SUMMARY (%):

	1, 100
	D
TEXTURE:	
Sand	10
Silt	85
Clay	5
COMPOSITION:	
Diatoms	Tr
Foraminifers	8
Nannofossils	85
Quartz	Tr
Radiolarians	3
Siliceous sponge spicules	Tr

SITE 807 HOLE C CORE 27R CORED INTERVAL 967.8-977.5 mbsf

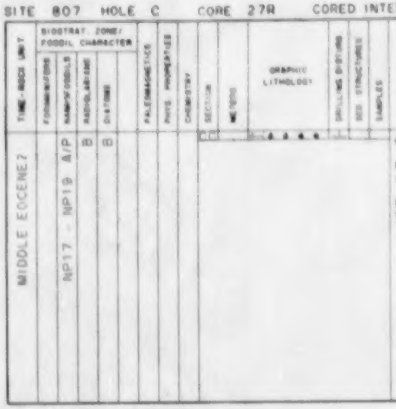
TIME-ROCK UNIT
BIOSTRAT. ZONE/ FOSSIL CHARACTER
FORAMINIFERS
NANNOFOSSILS
RADIOLARIANS
DIATOMS
PALEOMAGNETICS
PHYS. PROPERTIES
CHEMISTRY
SECTION
METERS
GRAPHIC LITHOLOGY
DRILLING DISTURB.
SED. STRUCTURES
SAMPLES
MIDDLE EOCENE?
NP17 - NP19 A/P
B
B
CC

LITHOLOGIC DESCRIPTION

CHERT

Major lithology: The core contains two fragments of gray (N5) CHERT, probably of nodular origin. The larger fragment is 6 cm in diameter. The smaller fragment is 3 cm in diameter.

Minor lithology: White (2.5Y 8/0) NANNOFOSSIL CHALK occurs around the perimeter of the chert and is present as 5 mm wide inclusions in the chert.

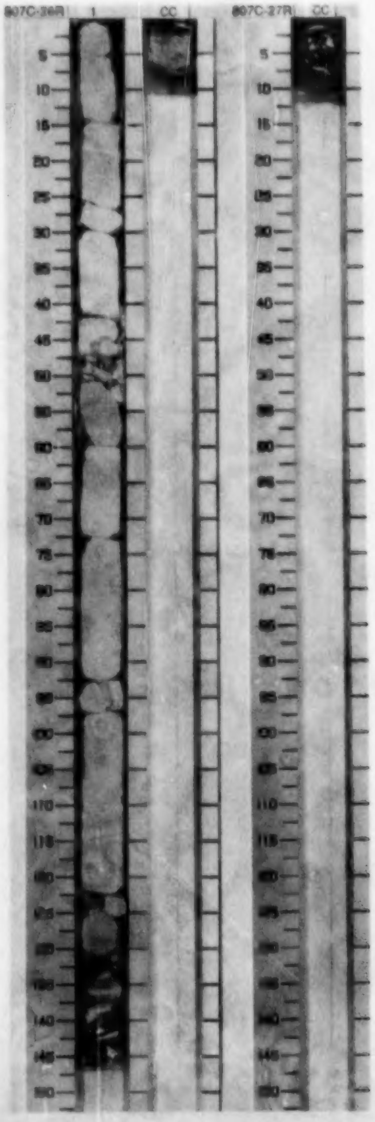
807C-26R
1
CC
807C-27R
CC
5
10
15
20
25
30
35
40
45
50
55
60
65
70
75
80
85
90
95
100
105
110
115
120
125
130
135
140
145
150

SITE 807 HOLE C CORE 28R CORED INTERVAL 977.5-987.1 mbsf

TIME-ROCK UNIT	BIOSTRAT. ZONE/ FOSSIL CHARACTER: FORAMINIFERS	NANNOFOSSILS	RADIOLARIANS	DIATOMS	PALEOMAGNETICS	PHYS. PROPERTIES	CHEMISTRY	SECTION	METERS	GRAPHIC LITHOLOGY	DRILLING DISTURB.	SED. STRUCTURES	SAMPLES	LITHOLOGIC DESCRIPTION
MIDDLE EOCENE?		NP17 - NP19 A/P	B					CC						CHERT Major lithology: The majority of the recovered core is gray (N5) CHERT, probably of nodular origin. The fragments are 2 to 5 cm in diameter. Minor lithology: White (2.5Y 8/0) NANNOFOSSIL CHALK occurs around the perimeter of the chert and as inclusions in the chert.

SITE 807 HOLE C CORE 29R CORED INTERVAL 987.1-996.8 mbsf

TIME-ROCK UNIT	BIOSTRAT. ZONE/ FOSSIL CHARACTER: FORAMINIFERS	NANNOFOSSILS	RADIOLARIANS	DIATOMS	PALEOMAGNETICS	PHYS. PROPERTIES	CHEMISTRY	SECTION	METERS	GRAPHIC LITHOLOGY	DRILLING DISTURB.	SED. STRUCTURES	SAMPLES	LITHOLOGIC DESCRIPTION
MIDDLE EOCENE		NP16 A/P	MIDDLE - UPPER EOCENE R/P	B				1 CC					•	NANNOFOSSIL CHALK and CHERT

Major lithology: The dominant lithology of the core is white (2.5Y 8/0) NANNOFOSSIL CHALK. It is slightly to moderately bioturbated with flattened horizontal burrows. Flaser structures and microstylolites are observed in Section 1, 13-15 cm. Gray (N5) CHERT, probably of nodular origin, constitutes the second major lithology. The chert has a horizontal contact with the chalk and contains mm-scale chalk inclusions.

SMEAR SLIDE SUMMARY (%):

	1, 10
	D
TEXTURE:	
Sand	10
Silt	85
Clay	5
COMPOSITION:	
Diatoms	Tr
Foraminifers	6
Nannofossils	90
Quartz	Tr
Radiolarians	2
Siliceous sponge spicules	Tr

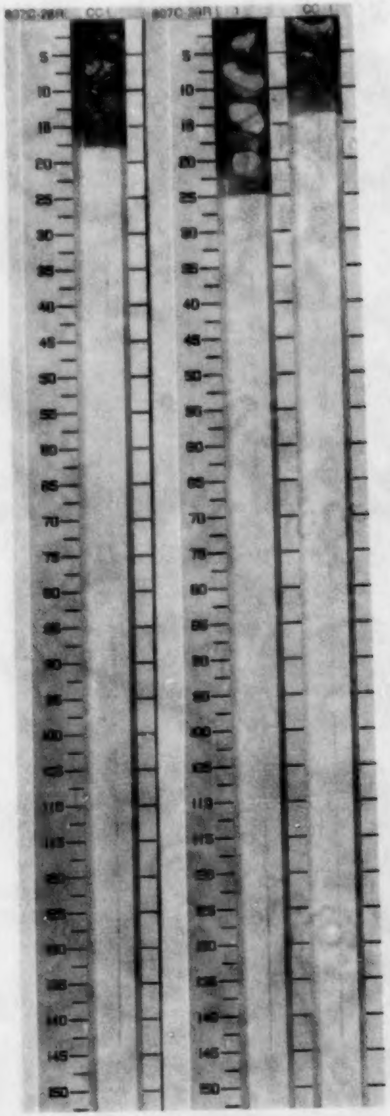

SITE 807 HOLE C CORE 30R CORED INTERVAL 996.8-1006.5 mbsf

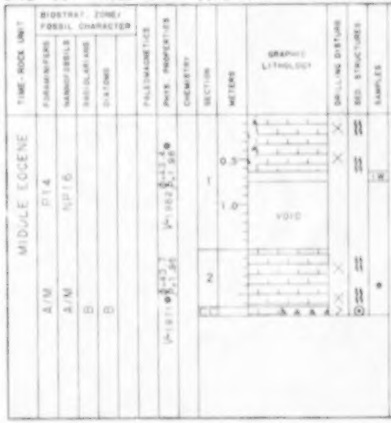
TIME-ROCK UNIT
BIOSTRAT. ZONE/ FOSSIL CHARACTER
FORAMINIFERS
NANNOFOSSILS
RADIOLARIANS
DIATOMS
PALEOMAGNETICS
PHYS. PROPERTIES
CHEMISTRY
SECTION
METERS
GRAPHIC LITHOLOGY
DRILLING DISTURB.
SED. STRUCTURES
SAMPLES
MIDDLE EOCENE
P14
A/M
NP16
A/M
B
B
Vp=1982 φ=43.4 ρ=1.96
Vp=1911 φ=43.7 ρ=1.96
1
2
CC
0.5
1.0
VOID
IW

LITHOLOGIC DESCRIPTION

NANNOFOSSIL CHALK with FORAMINIFERS.

Major lithology: This core contains white (5Y 8/1) NANNOFOSSIL CHALK with FORAMINIFERS. There are abundant, very thin (<1 mm), wavy, braided gray (5Y 5/1) color bands that appear as flaser structures. Abundant faint burrows have been compacted.

Minor lithology: Dark gray (5Y 4/1) CHERT is present as cobbles within the core.

SMEAR SLIDE SUMMARY (%):

	2, 40
	D
TEXTURE:	
Sand	4
Silt	86
Clay	10
COMPOSITION:	
Foraminifers	10
Nannofossils	90

SITE 807 HOLE C CORE 31R CORED INTERVAL 1006.5-1016.1 mbsf

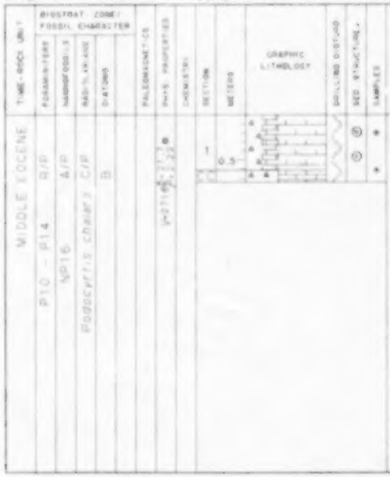
TIME-ROCK UNIT
BIOSTRAT. ZONE/ FOSSIL CHARACTER
FORAMINIFERS
NANNOFOSSILS
RADIOLARIANS
DIATOMS
PALEOMAGNETICS
PHYS. PROPERTIES
CHEMISTRY
SECTION
METERS
GRAPHIC LITHOLOGY
DRILLING DISTURB.
SED. STRUCTURES
SAMPLES
MIDDLE EOCENE
P10 - P14
R/P
NP16
A/P
Podocyrtis chalara
C/P
B
Vp=2716
1
CC
0.5

LITHOLOGIC DESCRIPTION

NANNOFOSSIL CHALK with FORAMINIFERS.

Major lithology: This core contains numerous cobbles of NANNOFOSSIL CHALK with FORAMINIFERS. It is white (2.5Y 8/0) and greenish gray (5G 7/1) in color. The greenish gray color comes from abundant flaser structures/color bands, which occur in cm-scale zones. The chalks are extremely well-cemented.

Minor lithology: This core also contains several cobbles of white (2.5Y 8/0) LIMESTONE and several cobbles of CHERT. Bands of chert run through some of the limestone cobbles.

SMEAR SLIDE SUMMARY (%):

	1, 20	1, 61
	D	M
TEXTURE:		
Sand	2	—
Silt	80	70
Clay	18	30
COMPOSITION:		
Accessory minerals	—	Tr
Foraminifers	10	4
Nannofossils	89	96
Radiolarians	Tr	—
Siliceous fragments	Tr	—

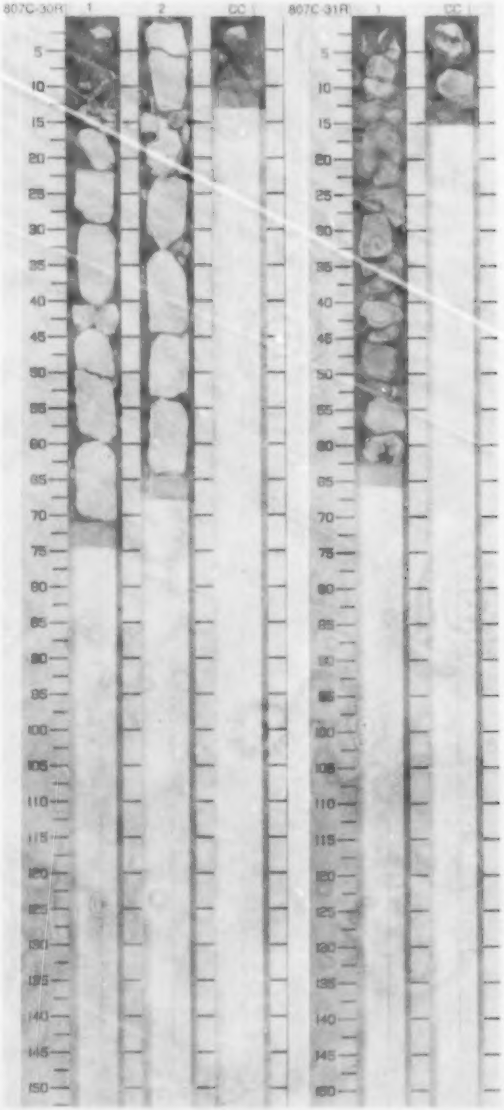
807C-30R
1
2
CC
807C-31R
1
CC
5
10
15
20
25
30
35
40
45
50
55
60
65
70
75
80
85
90
95
100
105
110
115
120
125
130
135
140
145
150

SITE 807 HOLE C CORE 32R CORED INTERVAL 1016.1-1025.4 mbsf

TIME-ROCK UNIT	FORAMINIFERS	NANNOFOSSILS	RADIOLARIANS	DIATOMS	PALEOMAGNETICS	PHYS. PROPERTIES	CHEMISTRY	SECTION	METERS	GRAPHIC LITHOLOGY	DRILLING DISTURB.	SED. STRUCTURES	SAMPLES	LITHOLOGIC DESCRIPTION
MIDDLE EOCENE	P12 - P14 C/P	NP15 - NP16 A/M	B	B				1			×	◎		NANNOFOSSIL CHALK, LIMESTONE, and CHERT Major lithology: This core contains several cobbles of CHALK, LIMESTONE, and CHERT. The chalk and limestone are white (2.5Y 8/0), and the chert is mostly gray to dark gray (5Y 6/1).

SITE 807 HOLE C CORE 33R CORED INTERVAL 1025.4-1034.6 mbsf

TIME-ROCK UNIT	FORAMINIFERS	NANNOFOSSILS	RADIOLARIANS	DIATOMS	PALEOMAGNETICS	PHYS. PROPERTIES	CHEMISTRY	SECTION	METERS	GRAPHIC LITHOLOGY	DRILLING DISTURB.	SED. STRUCTURES	SAMPLES	LITHOLOGIC DESCRIPTION
MIDDLE EOCENE		NP15 - NP16 F/P	T. triacantha - T. bromia R/P	B				1				◎		CHERT, LIMESTONE, and CHALK Major lithology: This core contains several cobbles of CHERT, LIMESTONE, and CHALK. The limestone and chalk are mostly white (2.5Y 8/0). The chert is gray to dark gray (5Y 6/1). The limestone cobbles have inclusions of chert.

SITE 807 HOLE C CORE 34R CORED INTERVAL 1034.6-1044.3 mbsf

TIME-ROCK UNIT	FORAMINIFERS	NANNOFOSSILS	RADIOLARIANS	DIATOMS	PALEOMAGNETICS	PHYS. PROPERTIES	CHEMISTRY	SECTION	METERS	GRAPHIC LITHOLOGY	DRILLING DISTURB.	SED. STRUCTURES	SAMPLES	LITHOLOGIC DESCRIPTION
MIDDLE EOCENE	P10 - P14 F/P	NP15 - NP16 A/P	B	B				1 CC			× ×	◎ ◎		CHERT and LIMESTONE Major lithology: This core contains pebbles of LIMESTONE and CHERT. The limestone is light gray (5Y 7/1) and bioturbated. The chert is very dark gray (5Y 3/1). The limestone pebbles contain pieces of chert.

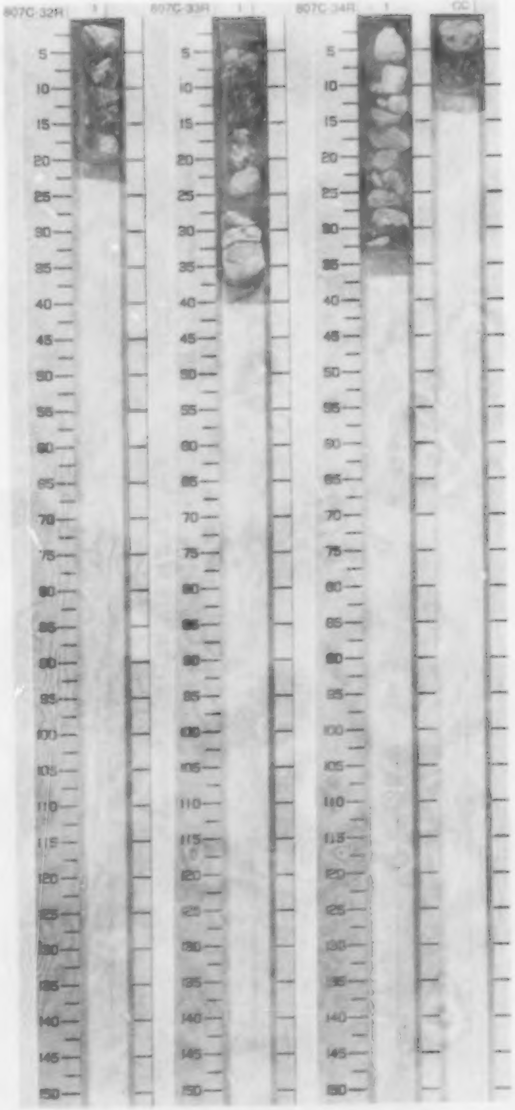

SITE 807 HOLE C CORE 35R CORED INTERVAL 1044.3-1054.0 mbsf

TIME-ROCK UNIT	FORAMINIFERS	NANNOFOSSILS	RADIOLARIANS	DIATOMS	PALEOMAGNETICS	PHYS. PROPERTIES	CHEMISTRY	SECTION	METERS	GRAPHIC LITHOLOGY	DRILLING DISTURB.	SED. STRUCTURES	SAMPLES
MIDDLE EOCENE	P10 - P14 A/M	NP15 - NP16 A/M	B	B		[illegible]		1 CC	0.5				●

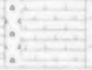

LITHOLOGIC DESCRIPTION

NANNOFOSSIL CHALK with FORAMINIFERS

Major lithology: This core contains white (2.5Y 8/0) NANNOFOSSIL CHALK with FORAMINIFERS. Moderate bioturbation is indicated from abundant compacted mottles. Steeply dipping stylolites are observed in Section 6, 10 cm. It is not clear if the dip is natural or the result of drilling disturbance. Several mottles appear to be aligned with the dipping stylolites.

Minor lithology: Several pieces of dark gray (2.5Y 4/0) CHERT are present at the top of Section 1 and in the CC.

SMEAR SLIDE SUMMARY (%):

	1, 25 D
TEXTURE:	
Silt	80
Clay	20
COMPOSITION:	
Accessory minerals	Tr
Foraminifers	20
Nannofossils	80

SITE 807 HOLE C CORE 36R CORED INTERVAL 1054.0-1063.7 mbsf

TIME-ROCK UNIT	FORAMINIFERS	NANNOFOSSILS	RADIOLARIANS	DIATOMS	PALEOMAGNETICS	PHYS. PROPERTIES	CHEMISTRY	SECTION	METERS	GRAPHIC LITHOLOGY	DRILLING DISTURB.	SED. STRUCTURES	SAMPLES
MIDDLE EOCENE	P10 - P14 A/M	NP15 - NP16 R/P	*Podocyrtis chalara* R/P	B				1 CC					

LITHOLOGIC DESCRIPTION

NANNOFOSSIL CHALK with FORAMINIFERS and CHERT

Major lithology: This core contains white (5Y 8/1) NANNOFOSSIL CHALK with FORAMINIFERS and dark gray (7.5Y 4/0) CHERT. Drilling has brecciated the section.

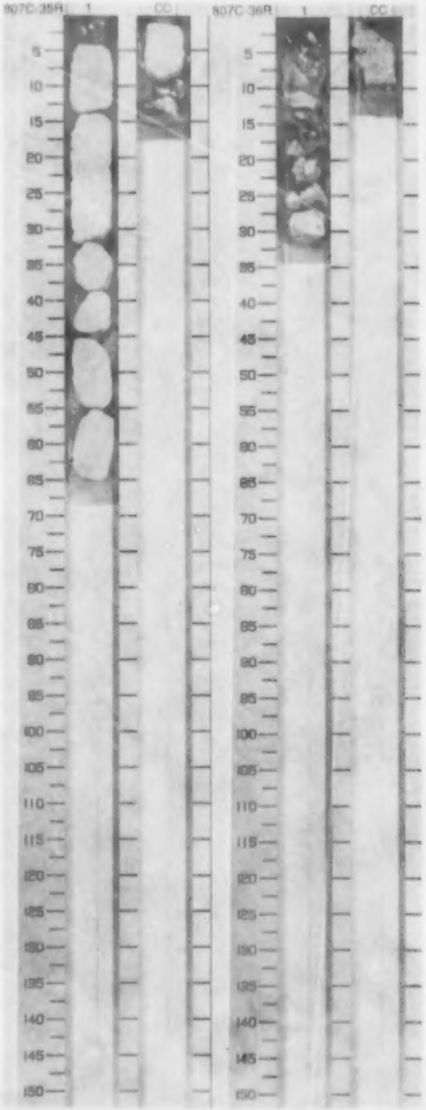

SITE 807 HOLE C CORE 37R CORED INTERVAL 1063.7-1073.2 mbsf

TIME-ROCK UNIT	BIOSTRAT. ZONE/ FOSSIL CHARACTER: FORAMINIFERS	NANNOFOSSILS	RADIOLARIANS	DIATOMS	PALEOMAGNETICS	PHYS. PROPERTIES	CHEMISTRY	SECTION	METERS	GRAPHIC LITHOLOGY	DRILLING DISTURB.	SED. STRUCTURES	SAMPLES	LITHOLOGIC DESCRIPTION
MIDDLE EOCENE	? R/P	NP15 - NP16 C/P	T. triacantha - T. bromia R/P	B		● [illegible]		1					●	NANNOFOSSIL LIMESTONE to CHALK Major lithology: The recovered material contains white (2.5Y 8/0) NANNOFOSSIL LIMESTONE to CHALK. Moderate bioturbation is indicated by compacted horizontal burrows. The hardness probably varies with silica content. Minor lithology: A piece of reddish gray (10R 5/1) CHERT is present in Section 1, 25-29 cm. It has a sharp contact with the chalk and also contains cm-scale inclusions of chalk. SMEAR SLIDE SUMMARY (%): 1, 15 D TEXTURE: Sand 10 Silt 86 Clay 4 COMPOSITION: Carbonate particles 42 Foraminifers 8 Nannofossils 50

SITE 807 HOLE C CORE 38R CORED INTERVAL 1073.2-1082.4 mbsf

TIME-ROCK UNIT	BIOSTRAT. ZONE/ FOSSIL CHARACTER: FORAMINIFERS	NANNOFOSSILS	RADIOLARIANS	DIATOMS	PALEOMAGNETICS	PHYS. PROPERTIES	CHEMISTRY	SECTION	METERS	GRAPHIC LITHOLOGY	DRILLING DISTURB.	SED. STRUCTURES	SAMPLES	LITHOLOGIC DESCRIPTION
MIDDLE EOCENE	P11 C/M	NP15 A/P	B	B				1	0.5				●	NANNOFOSSIL CHALK to SILICIFIED LIMESTONE Major lithology: This core contains white (2.5Y 8/0) NANNOFOSSIL CHALK to SILICIFIED LIMESTONE. It is moderately bioturbated with common compacted burrows. Minor lithology: The core also contains gray (N6) CHERT, which may be nodular in origin and which contains cm-scale burrows and inclusions of chalk/limestone. SMEAR SLIDE SUMMARY (%): 1, 30 D TEXTURE: Sand 10 Silt 86 Clay 4 COMPOSITION: Carbonate particles 45 Foraminifers 5 Nannofossils 50

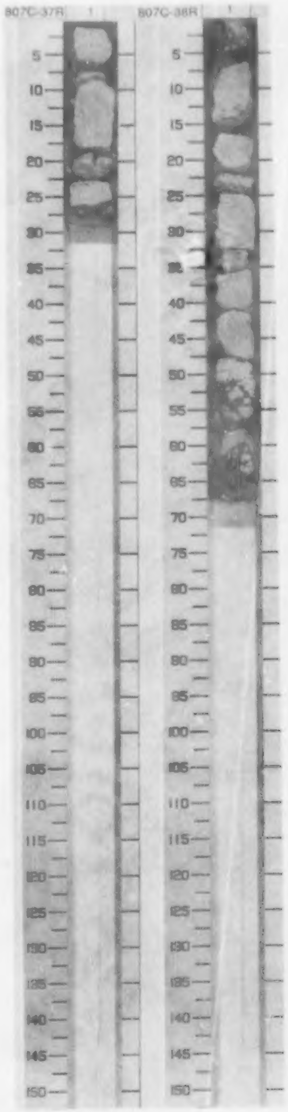

SITE 807 HOLE C CORE 39R CORED INTERVAL 1082.4-1092.0 mbsf

TIME-ROCK UNIT	BIOSTRAT. ZONE/ FOSSIL CHARACTER					PALEOMAGNETICS	PHYS. PROPERTIES	CHEMISTRY	SECTION	METERS	GRAPHIC LITHOLOGY	DRILLING DISTURB.	SED. STRUCTURES	SAMPLES	LITHOLOGIC DESCRIPTION
	FORAMINIFERS	NANNOFOSSILS	RADIOLARIANS	DIATOMS											
MIDDLE EOCENE	R/M ?	A/P NP15	A/M *Thyrsocyrtis triacantha*	B					1			X X		●	CHERT and SILICIFIED LIMESTONE Major lithology: The recovered material is dominated by CHERT, which may be nodular and contain up to cm-size inclusions of limestone. The chert pieces are gray (N5 and 5YR 5/1) and dark reddish gray (5YR 4/2), and have chalk along some of the outer rims. The chert pieces vary between 1 cm and 5 cm in diameter. The remainder of the recovered material is slightly bioturbated, white (2.5Y 8/0) SILICIFIED LIMESTONE. SMEAR SLIDE SUMMARY (%): 1, 23 D TEXTURE: Silt 95 Clay 5 COMPOSITION: Carbonate particles 44 Foraminifers 1 Nannofossils 50 Siliceous fragments 5

SITE 807 HOLE C CORE 40R CORED INTERVAL 1092.0-1097.7 mbsf

TIME-ROCK UNIT	BIOSTRAT. ZONE/ FOSSIL CHARACTER					PALEOMAGNETICS	PHYS. PROPERTIES	CHEMISTRY	SECTION	METERS	GRAPHIC LITHOLOGY	DRILLING DISTURB.	SED. STRUCTURES	SAMPLES	LITHOLOGIC DESCRIPTION
	FORAMINIFERS	NANNOFOSSILS	RADIOLARIANS	DIATOMS											
MIDDLE EOCENE	R/P ?	A/P NP14 - NP15	F/P *Theocotyle cryptocephala - Ptero. adon ampla*	B		[illegible] ●		1 2	0.5 1.0				●	NANNOFOSSIL CHALK to SILICEOUS NANNOFOSSIL LIMESTONE and CHERT Major lithology: The recovered material contains white (2.5Y 8/0 and 5Y 8/1) and moderately bioturbated NANNOFOSSIL CHALK to SILICEOUS NANNOFOSSIL LIMESTONE. Compacted horizontal burrows are common. The core also contains reddish gray (10R 5/1) to gray (N6) CHERT, possibly of nodular origin. It has thin layers and inclusions of chalk. Some of the chalk pieces contain layers and cm-scale inclusions of chert. SMEAR SLIDE SUMMARY (%): 1, 38 D TEXTURE: Silt 95 Clay 5 COMPOSITION: Carbonate particles 34 Foraminifers 4 Nannofossils 60 Siliceous fragments 2

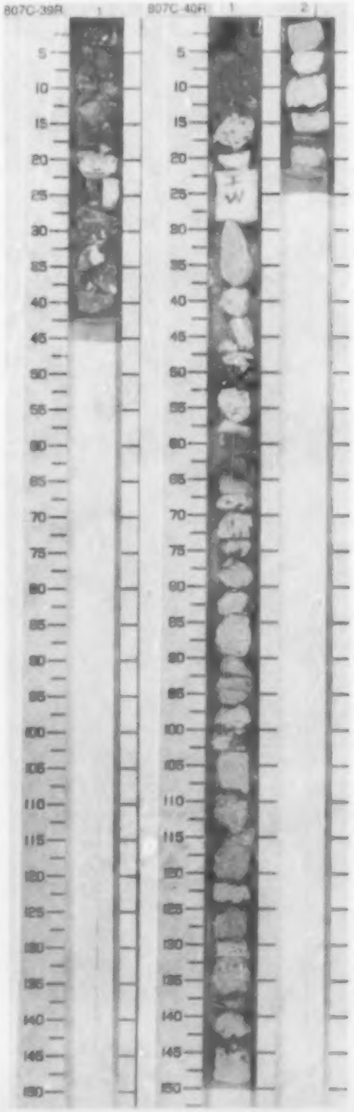

SITE 807 HOLE C CORE 41R CORED INTERVAL 1097.7-1102.4 mbsf

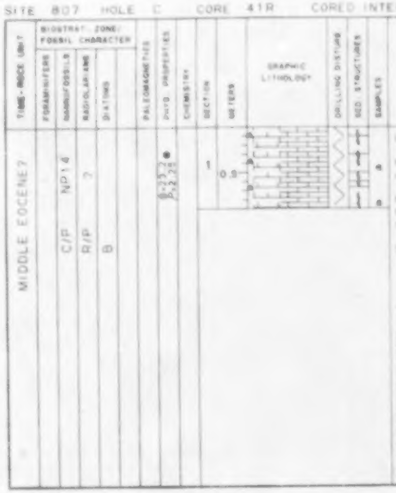
TIME-ROCK UNIT
BIOSTRAT. ZONE/ FOSSIL CHARACTER
FORAMINIFERS
NANNOFOSSILS
RADIOLARIANS
DIATOMS
PALEOMAGNETICS
PHYS. PROPERTIES
CHEMISTRY
SECTION
METERS
GRAPHIC LITHOLOGY
DRILLING DISTURB.
SED. STRUCTURES
SAMPLES
MIDDLE EOCENE?
NP14
C/P
?
R/P
B
1
0.5

LITHOLOGIC DESCRIPTION

LIMESTONE

Major lithology: This core contains white (2.5Y 8/0) LIMESTONE with flaser structures and relict bioturbation structures.

Minor lithology: The limestone pieces have 0.5 cm thick rims of light greenish gray (5GY 7/1) CHALK. Gray (5Y 5/1) and reddish gray (5YR 5/2) CHERT nodules (up to 2 cm thick) with mm-size inclusions of limestone comprise about 5% of the recovered material.

SMEAR SLIDE SUMMARY (%):

	1, 47 D	1, 84 D
TEXTURE:		
Sand	5	—
Silt	90	95
Clay	5	5
COMPOSITION:		
Accessory minerals	—	1
Carbonate particles	—	47
Foraminifers	5	Tr
Micrite	95	—
Nannofossils	—	50
Siliceous fragments	—	2

SITE 807 HOLE C CORE 42R CORED INTERVAL 1102.4-1106.4 mbsf

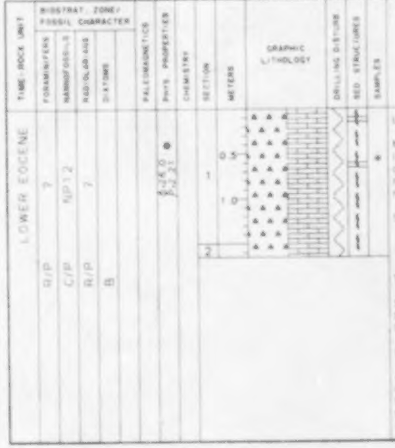
TIME-ROCK UNIT
BIOSTRAT. ZONE/ FOSSIL CHARACTER
FORAMINIFERS
NANNOFOSSILS
RADIOLARIANS
DIATOMS
PALEOMAGNETICS
PHYS. PROPERTIES
CHEMISTRY
SECTION
METERS
GRAPHIC LITHOLOGY
DRILLING DISTURB.
SED. STRUCTURES
SAMPLES
LOWER EOCENE
?
R/P
NP12
C/P
?
R/P
B
1
2
0.5
1.0

LITHOLOGIC DESCRIPTION

LIMESTONE and CHERT

Major lithology: This core contains white (5Y 8/1) LIMESTONE and light brownish gray (10YR 6/2) and gray (2.5YR 5/0) CHERT. The limestone is moderately bioturbated with compacted horizontal burrows and faint flaser structures. The limestone pieces contain as much as 50% chert in the form of thin stringers and inclusions. The chert is present as nodules (ca. 3 cm in diameter) with cm scale chalk/limestone inclusions.

SMEAR SLIDE SUMMARY (%):

	1, 57 D
TEXTURE:	
Sand	30
Silt	65
Clay	5
COMPOSITION:	
Accessory minerals	Tr
Carbonate particles	35
Foraminifers	Tr
Nannofossils	60
Siliceous fragments	Tr

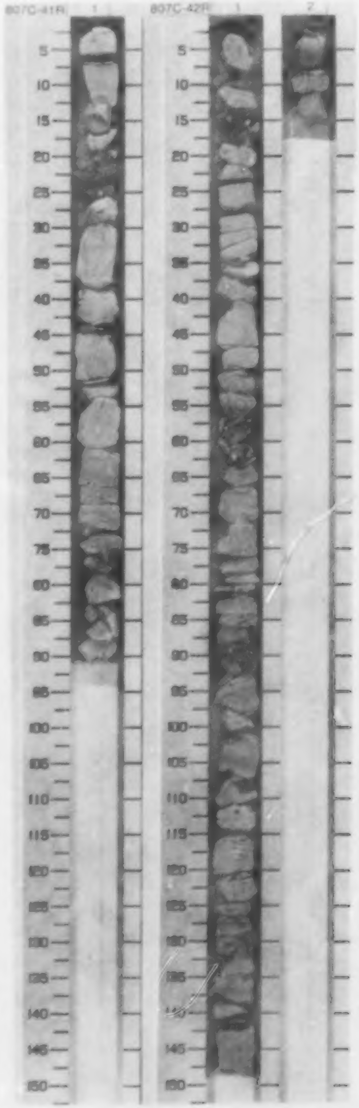
807C-41R
1
807C-42R
1
2
5
10
15
20
25
30
35
40
45
50
55
60
65
70
75
80
85
90
95
100
105
110
115
120
125
130
135
140
145
150

SITE 807 HOLE C CORE 43R CORED INTERVAL 1106.4-1116.0 mbsf

TIME-ROCK UNIT	FORAMINIFERS	NANNOFOSSILS	RADIOLARIANS	DIATOMS	PALEOMAGNETICS	PHYS. PROPERTIES	CHEMISTRY	SECTION	METERS
LOWER EOCENE	?	? R/P	? R/P	B		● ϕ=61.7 γ=2.28		1	0.5 1.0

LITHOLOGIC DESCRIPTION

LIMESTONE and CHERT

Major lithology: This core contains white (5Y 8/1) LIMESTONE and gray (2.5Y 5/0) CHERT. The limestone exhibits compacted burrows and wispy horizontal laminations. The chert is present as stringers and cm-scale inclusions, as well as pieces up to 4 cm thick.

Minor lithology: A piece of white (10YR 8/1) RADIOLARITE is present in Section 1, 106 cm.

SMEAR SLIDE SUMMARY (%):

	1, 99 D	1, 110 M
TEXTURE:		
Sand	5	80
Silt	60	15
Clay	35	5
COMPOSITION:		
Calcareous fragments	39	—
Diatoms	Tr	—
Foraminifers	1	—
Nannofossils	60	—
Quartz	—	Tr
Radiolarians	1	93
Siliceous fragments	—	Tr
Siliceous sponge spicules	Tr	—
Silicoflagellates	—	Tr

SITE 807 HOLE C CORE 44R CORED INTERVAL 1116.0-1125.6 mbsf

TIME-ROCK UNIT	FORAMINIFERS	NANNOFOSSILS	RADIOLARIANS	DIATOMS	PALEOMAGNETICS	PHYS. PROPERTIES	CHEMISTRY	SECTION	METERS
LOWER EOCENE	? R/P	NP12 C/P	B	B		● ϕ=30.2 γ=2.20 Vp=2520		1	0.5

LITHOLOGIC DESCRIPTION

LIMESTONE

Major lithology: This core contains white (2.5Y 8/0) LIMESTONE. Very thin, wavy greenish gray (5GY 7/1) color bands are common throughout the core. Stylolites are common in Section 1, at 40 and 67 cm, and a few pebbles of chalk are noted in Section 1, 22-25 cm. The limestone has very compacted, mm-size burrows.

Minor lithology: Gray (2.5Y 5/0) CHERT pebbles are found at the top of the Section 1 and between 94-106 cm.

SMEAR SLIDE SUMMARY (%):

	1, 29 D	1, 46 D	1, 101 M
TEXTURE:			
Sand	0	2	5
Silt	90	50	75
Clay	1	48	20
COMPOSITION:			
Calcareous fragments	—	90	80
Foraminifers	10	—	—
Micrite	90	—	—
Nannofossils	—	—	10
Siliceous fragments	—	10	10

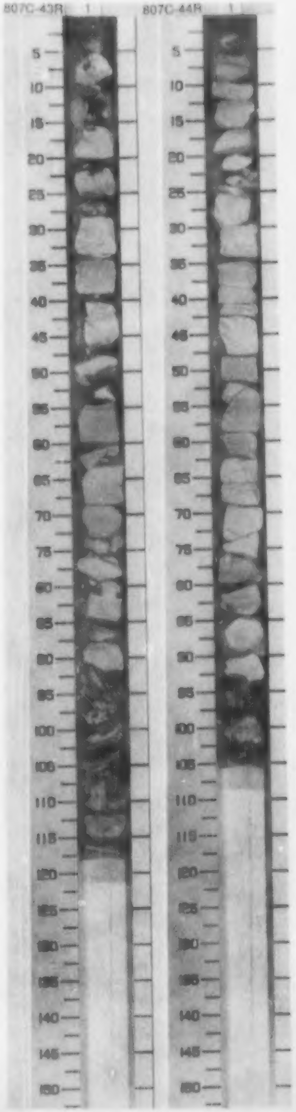

SITE 807 HOLE C CORE 45R CORED INTERVAL 1125.6-1135.2 mbsf

TIME-ROCK UNIT	FORAMINIFERS	NANNOFOSSILS	RADIOLARIANS	DIATOMS	PHYS. PROPERTIES	SECTION	METERS
LOWER EOCENE? [P4 - P5	C/M	C/P F/P NP12	NP9		ø-23.4 γ-2.29	1	0.5 1.0
	R/P ?				ø-16.8 γ-2.38 V=3280	2	
			B	B		CC	

LITHOLOGIC DESCRIPTION

LIMESTONE

Major lithology: This core contains LIMESTONE. It is white (2.5Y 8/0) to light gray (5Y 7/1) in color. The light gray color is found in zones composed of abundant wispy color bands, such as at Section 1, 86-150 cm, and Section 2, 73-82 cm. Several well formed chert nodules and chert bands are apparent (e.g. nodules at 3 cm and 52 cm in Section 1). A thin interval (2 cm) of fine, wavy, dark gray, purple, and light gray, flaser-like color bands is present at Section 1, 116-118 cm. A stylolite is observed at Section 1, at 132 cm. Section 1, 0-87 cm contains numerous small clasts.

SMEAR SLIDE SUMMARY (%):

	1, 46 D	2, 51 D	2, 70 M
TEXTURE:			
Sand	20	1	5
Silt	80	50	60
Clay	—	49	35
COMPOSITION:			
Accessory minerals	—	Tr	Tr
Calcareous fragments	—	30	95
Foraminifers	20	10	Tr
Micrite	80	—	—
Nannofossils	—	60	Tr
Radiolarians	—	Tr	Tr
Siliceous fragments	—	3	5

SITE 807 HOLE C CORE 46R CORED INTERVAL 1135.2-1140.2 mbsf

TIME-ROCK UNIT	FORAMINIFERS	NANNOFOSSILS	RADIOLARIANS	DIATOMS	PHYS. PROPERTIES	SECTION	METERS
LOWER EOCENE	P5	R/P NP11			V=4263	1	0.5 1.0
		R/P NP11			V=3520	2	
	A/C	R/P		B		3	
						CC	

LITHOLOGIC DESCRIPTION

LIMESTONE

Major lithology: This core contains white (2.5Y 8/0 and 5Y 8/1) to light gray (5Y 7/1) LIMESTONE. Moderate to heavy bioturbation is indicated by elongate, compacted burrow traces. Faint, small-scale flaser structures are observed in the light gray (5Y 7/1) zones. Rare and thin (<2 mm thick) stylolites are present in Section 3.

Minor lithology: Dark gray (5YR 5/1), gray (N5/) and light gray (N6/) CHERT is observed in three forms: 1) horizontally discontinuous 1 to 2 mm thick layers 2) continuous horizontal layers, up to 1 cm thick, and 3) irregularly shaped masses in limestone, up to 2 cm in diameter.

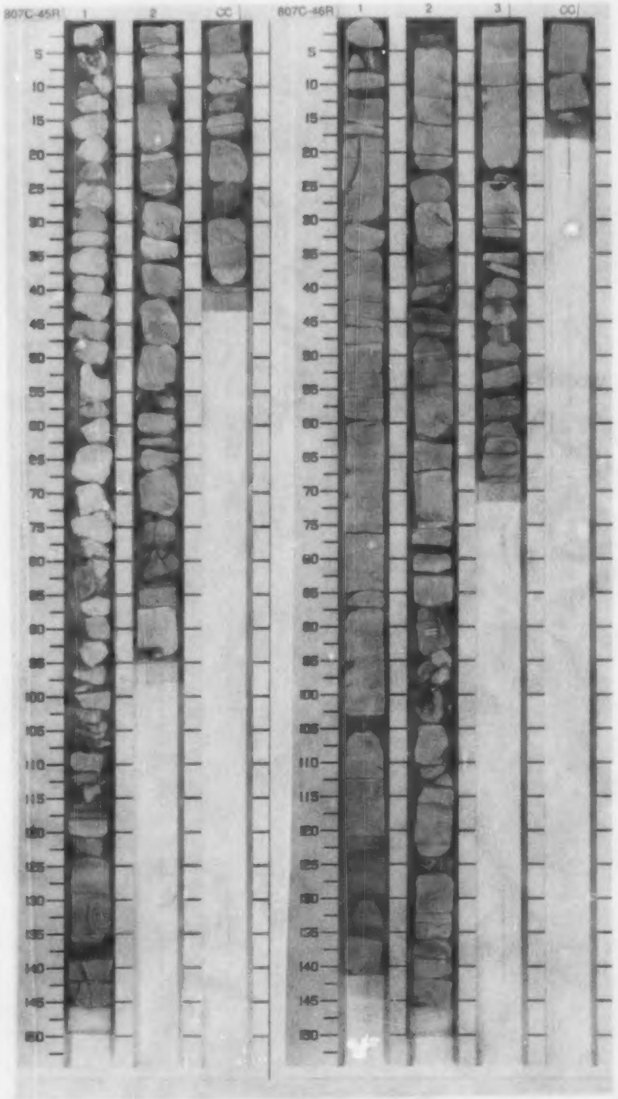

SITE 807 HOLE C CORE 47R CORED INTERVAL 1140.2-1145.2 mbsf

TIME-ROCK UNIT	FORAMINIFERS	NANNOFOSSILS	RADIOLARIANS	DIATOMS		PALEOMAGNETICS	PHYS. PROPERTIES	CHEMISTRY	SECTION	METERS	GRAPHIC LITHOLOGY	DRILLING DISTURB.	SED. STRUCTURES	SAMPLES
UPPER PALEOCENE	R?	NP9 C/P	B	B			V=3799 ●φ=18.5 γ=2.44 V=4305 ●V=4772		1 2 CC	0.5 1.0				● ●

LITHOLOGIC DESCRIPTION

LIMESTONE

Major lithology: This core contains white (2.5Y 8/0 and 5Y 8/1) LIMESTONE. Moderate bioturbation is evident as elongate, compacted burrow traces. Faint, small-scale flaser structures are abundant. Thin (<1 mm thick) stylolites are present to abundant.

Minor lithology: Dark gray (5YR 5/1), gray (N5), and light gray (N6) CHERT is observed in three forms: 1) horizontally discontinuous 1 to 2 mm thick layers, 2) continuous horizontal layers, up to 12 cm thick, and 3) irregularly shaped masses in limestone, up to 2 cm in diameter. A layer of gray (N4), finely laminated VOLCANIC ASH, approximately 1 cm thick is present at Section 1, 40 cm.

SMEAR SLIDE SUMMARY (%):

	1, 37 M	1, 40 M
TEXTURE:		
Sand	—	5
Silt	90	93
Clay	10	2
COMPOSITION:		
Calcareous fragments	55	3
Nannofossils	—	2
Volcanic ash	45	95

SITE 807 HOLE C CORE 48R CORED INTERVAL 1145.2-1150.2 mbsf

TIME-ROCK UNIT	FORAMINIFERS	NANNOFOSSILS	RADIOLARIANS	DIATOMS		PALEOMAGNETICS	PHYS. PROPERTIES	CHEMISTRY	SECTION	METERS	GRAPHIC LITHOLOGY	DRILLING DISTURB.	SED. STRUCTURES	SAMPLES
UPPER PALEOCENE	? R	NP9 F/P	B	B			●V=4158 V=3726 ●φ=18.8 γ=2.46		1 2 CC	0.5 1.0				

LITHOLOGIC DESCRIPTION

LIMESTONE

Major lithology: This core contains white (2.5Y 8/0 and 5Y 8/1) LIMESTONE. Moderate bioturbation is evident as elongate compacted burrows. Faint, small-scale flaser structures are present in Section 2. Thin (<1 mm thick) stylolites are common throughout the core.

Minor lithology: Gray (N5) and brownish gray (5YR 6/1) CHERT is observed in Sections 1 as horizontally discontinuous layers (1-2 cm thick) or in continuous horizontal layers up to 5 cm thick. The chert appears spotty with light gray (N7) and very light gray (N8) cm-scale inclusions. In Section 2, limestone inclusions are present in the chert layer.

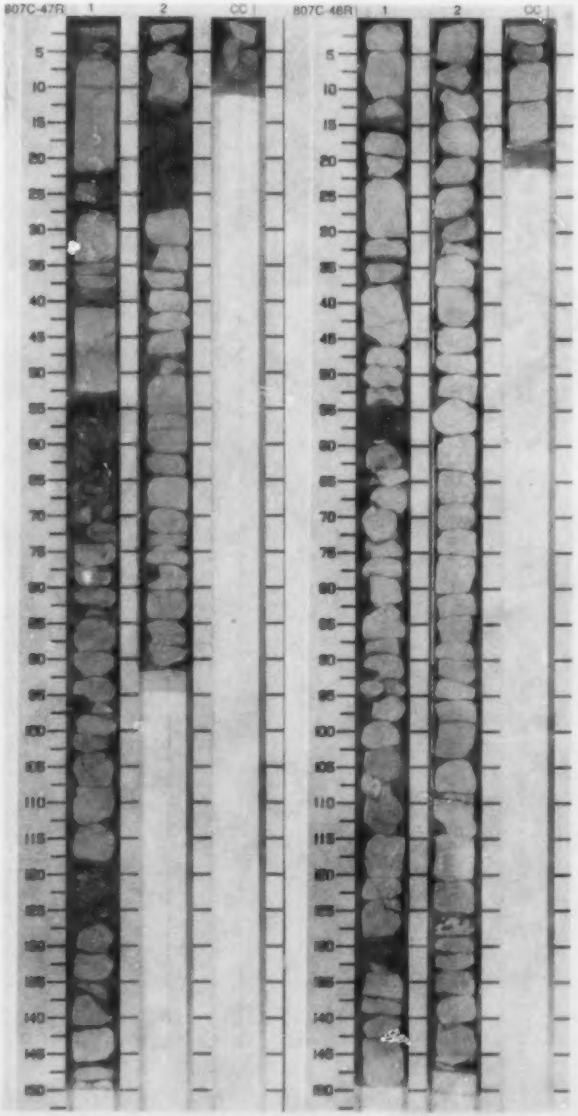

SITE 807 HOLE C CORE 49R CORED INTERVAL 1150.2-1155.2 mbsf

TIME-ROCK UNIT	BIOSTRAT. ZONE/ FOSSIL CHARACTER: FORAMINIFERS	NANNOFOSSILS	RADIOLARIANS	DIATOMS	PALEOMAGNETICS	PHYS. PROPERTIES	CHEMISTRY	SECTION	METERS	GRAPHIC LITHOLOGY	DRILLING DISTURB.	SED. STRUCTURES	SAMPLES	LITHOLOGIC DESCRIPTION
UPPER PALEOCENE	R/P P3 - P4	F/P NP9	B	B		●φ=13.0 ●γ=2.31	●%CaCO3 =98.1	1	0.5 1.0					LIMESTONE Major lithology: This core contains white (2.5Y 8/0) LIMESTONE. Moderate bioturbation is evident as elongate compacted burrows. Faint, small-scale flaser structures are present in minor intervals. Thin (<1 mm thick) stylolites are present to abundant. Minor lithology: Gray chert (N5) is present as a thin band and as a nodule 3 cm in diameter in the interval between 100 and 104 cm. The chert band has a sharp contact with the limestone.

SITE 807 HOLE C CORE 50R CORED INTERVAL 1155.2-1160.2 mbsf

TIME-ROCK UNIT	BIOSTRAT. ZONE/ FOSSIL CHARACTER: FORAMINIFERS	NANNOFOSSILS	RADIOLARIANS	DIATOMS	PALEOMAGNETICS	PHYS. PROPERTIES	CHEMISTRY	SECTION	METERS	GRAPHIC LITHOLOGY	DRILLING DISTURB.	SED. STRUCTURES	SAMPLES	LITHOLOGIC DESCRIPTION
UPPER PALEOCENE	R/P P2 - P4	A/M-P NP9	B	B		●φ=11.7 ●γ=2.29	●%CaCO3 =99.9	1 2	0.5 1.0				● ●	LIMESTONE Major lithology: This core contains white (2.5Y 8/0) LIMESTONE. Moderate bioturbation is indicated by mm-scale horizontal and compacted burrows. Stylolites are present in Section 1, 42 and 44 cm. Minor lithology: Gray (N5), 2 to 5 cm thick pods of CHERT with limestone inclusions are common. Section 1, 12-15 cm contains 100% VOLCANIC ASH, composed of abundant clear ash particles and common brown particles.

SMEAR SLIDE SUMMARY (%):

	1, 12 M	1, 20 D
TEXTURE:		
Sand	—	5
Silt	90	90
Clay	10	5
COMPOSITION:		
Calcareous fragments	Tr	100
Nannofossils	Tr	—
Volcanic ash	100	—

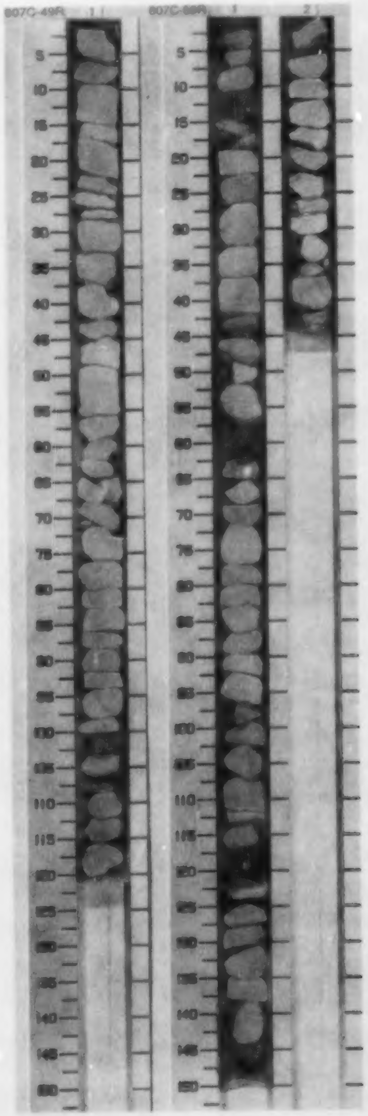

SITE 807 HOLE C CORE 51R CORED INTERVAL 1160.2-1169.9 mbsf

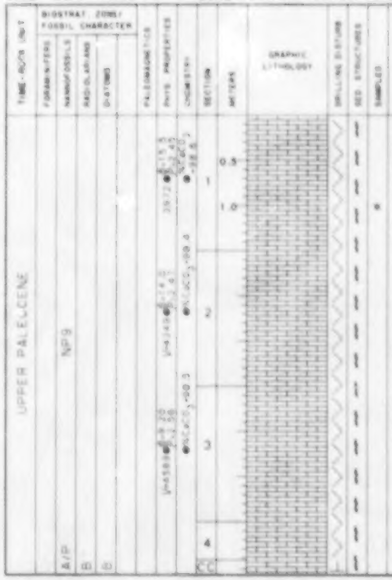
TIME-ROCK UNIT
BIOSTRAT. ZONE/ FOSSIL CHARACTER
FORAMINIFERS
NANNOFOSSILS
RADIOLARIANS
DIATOMS
PALEOMAGNETICS
PHYS. PROPERTIES
CHEMISTRY
SECTION
METERS
GRAPHIC LITHOLOGY
DRILLING DISTURB.
SED. STRUCTURES
SAMPLES
UPPER PALEOCENE
NP9
A/P
B
B
3972
$CaCO_3$=98.8
$CaCO_3$=99.4
$CaCO_3$=99.3
1
2
3
4
CC
0.5
1.0

LITHOLOGIC DESCRIPTION

LIMESTONE

Major lithology: This core contains white (5Y 8/1) LIMESTONE, with slight to moderate amounts of bioturbation indicated by mm scale mottling. Millimeter-scale, disseminated grayish blue (5PB 5/2) pyrite-filled burrows are abundant below Section 3, 57 cm. Stylolites are not common in the fragments recovered, but features on the tops and bottoms of the core fragments suggest that stylolites are abundant in the original section.

Minor lithology: Gray (N5) to light gray (N7) CHERT is present as fragments of layers and/or nodules in Section 1, 0-10 cm, Section 2, 106-110 cm, and Section 3, 16-20 cm.

SMEAR SLIDE SUMMARY (%)

	1, 101
	D
TEXTURE	
Sand	10
Silt	85
Clay	5
COMPOSITION	
Calcareous fragments	88
Nannofossils	10

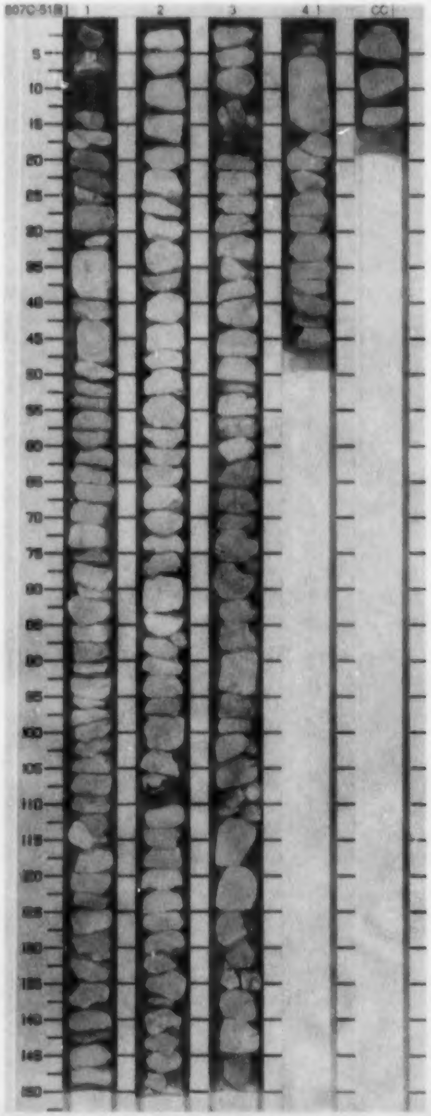
807C-51R
1
2
3
4
CC
5
10
15
20
25
30
35
40
45
50
55
60
65
70
75
80
85
90
95
100
105
110
115
120
125
130
135
140
145
150

SITE 807 HOLE C CORE 52R CORED INTERVAL 1169.8-1179.4 mbsf

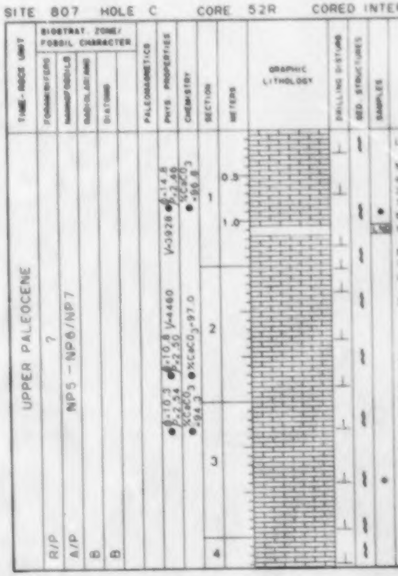
TIME-ROCK UNIT
BIOSTRAT. ZONE/ FOSSIL CHARACTER
FORAMINIFERS
NANNOFOSSILS
RADIOLARIANS
DIATOMS
PALEOMAGNETICS
PHYS. PROPERTIES
CHEMISTRY
SECTION
METERS
GRAPHIC LITHOLOGY
DRILLING DISTURB.
SED. STRUCTURES
SAMPLES
UPPER PALEOCENE
?
NP5 – NP6/NP7
R/P
A/P
B
B
φ=14.8
ρ=2.40
V=3928
%CaCO3 =90.8
φ=10.8
ρ=2.50
V=4460
%CaCO3=97.0
φ=10.3
ρ=2.54
%CaCO3 =94.3
1
2
3
4
0.5
1.0

LITHOLOGIC DESCRIPTION

LIMESTONE

Major lithology: This core contains white (2.5Y 8/0) LIMESTONE. Moderate bioturbation is evident from abundant discolored mottles, as well as zones of disseminated pyrite. Section 2 contains a zone of black bands exhibiting flaser and lenticular structures (microstylolites?). The core in Section 3, 67-100 cm is white (5Y 8/1), with abundant mm-thick, gray (5Y 5/1) bands (ash?). The remainder of the core has light gray (5Y 7/1) burrows and very thin flaser structures. At Section 3, 177 cm, stylolites displace a burrow.

Minor lithology: CHERT pieces, several cm in diameter, are present in Sections 1 and 2. The color varies from reddish brown (4YR 4/2) to grayish blue (5PB 5/2). Section 3 contains a piece of gray (5Y 6/1) chert or highly siliceous limestone.

SMEAR SLIDE SUMMARY (%):

	1, 91 D	3, 89 M
TEXTURE:		
Silt	50	30
Clay	50	70
COMPOSITION:		
Calcareous fragments	100	70
Glass		30

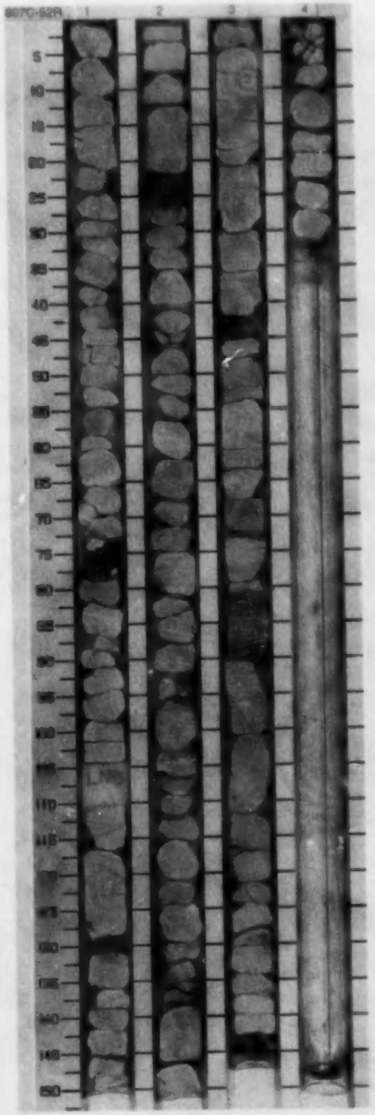
807C-52R
1
2
3
4
5
10
15
20
25
30
35
40
45
50
55
60
65
70
75
80
85
90
95
100
105
110
115
120
125
130
135
140
145
150

SITE 807 HOLE C CORE 53R CORED INTERVAL 1179.4-1188.8 mbsf

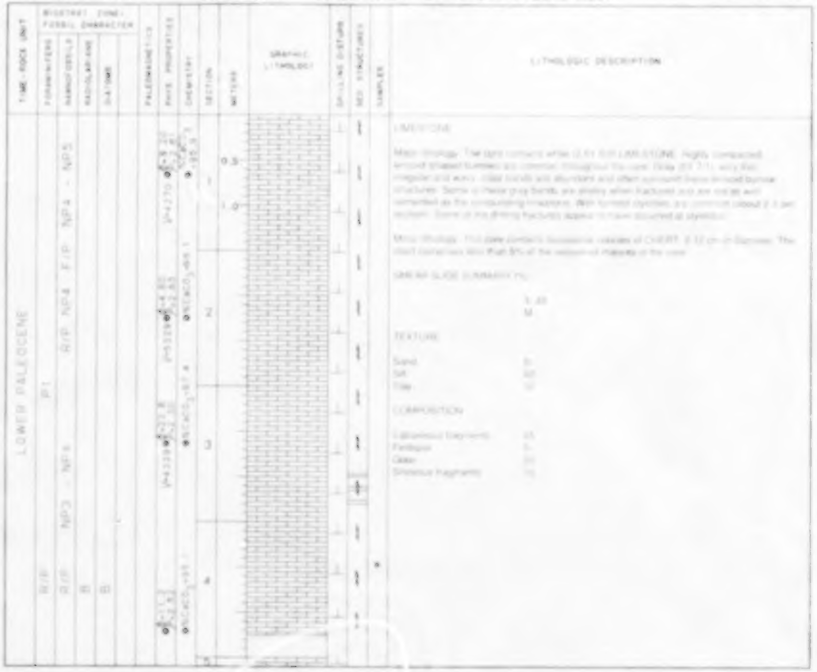
TIME-ROCK UNIT
BIOSTRAT. ZONE/FOSSIL CHARACTER
FORAMINIFERS
NANNOFOSSILS
RADIOLARIANS
DIATOMS
PALEOMAGNETICS
PHYS. PROPERTIES
CHEMISTRY
SECTION
METERS
GRAPHIC LITHOLOGY
DRILLING DISTURB.
SED. STRUCTURES
SAMPLES
LOWER PALEOCENE
P1
R/P
R/P NP4 F/P NP4 - NP5
NP3 - NP4
R/P
B
B
γ=4270
γ=5339
γ=4339
%CaCO$_3$=95.1
%CaCO$_3$=87.4
%CaCO$_3$=95
0.5
1.0
1
2
3
4
5

LITHOLOGIC DESCRIPTION

LIMESTONE

Major lithology: The core contains white (2.5Y 8/0) LIMESTONE. Highly compacted, lenticel-shaped burrows are common throughout the core. Gray (5Y 7/1), very thin, irregular and wavy, color bands are abundant and often surround these lenticel burrow structures. Some of these gray bands are shaley when fractured and are not as well cemented as the surrounding limestone. Well formed stylolites are common (about 2-3 per section). Some of the drilling fractures appear to have occurred at stylolites.

Minor lithology: This core contains occasional nodules of CHERT, 8-12 cm in diameter. The chert comprises less than 5% of the volume of material in the core.

SMEAR SLIDE SUMMARY (%):

	3, 48
	M
TEXTURE:	
Sand	[illegible]
Silt	60
Clay	[illegible]
COMPOSITION:	
Calcareous fragments	65
Feldspar	5
Clay	20
Siliceous fragments	10

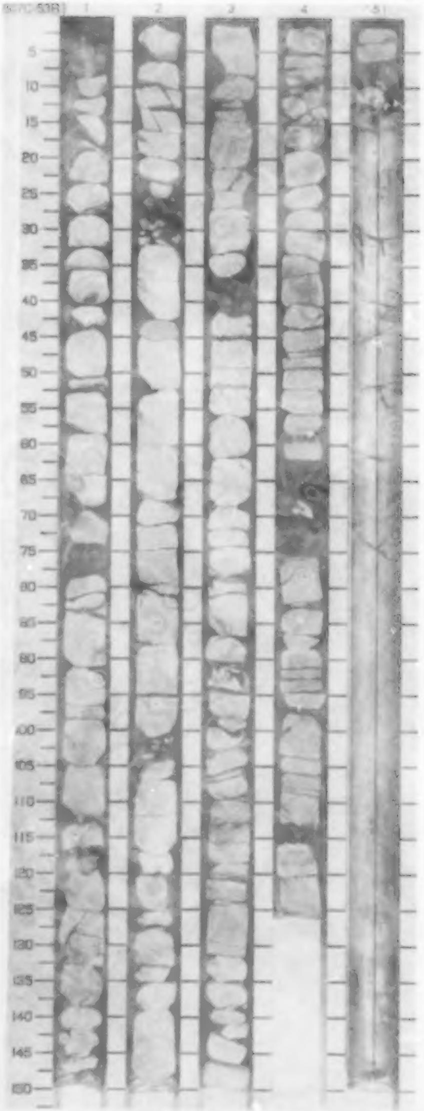
807C-53R
1
2
3
4
5
5
10
15
20
25
30
35
40
45
50
55
60
65
70
75
80
85
90
95
100
105
110
115
120
125
130
135
140
145
150

SITE 807 HOLE C CORE 54R CORED INTERVAL 1188.5-1198.9 mbsf

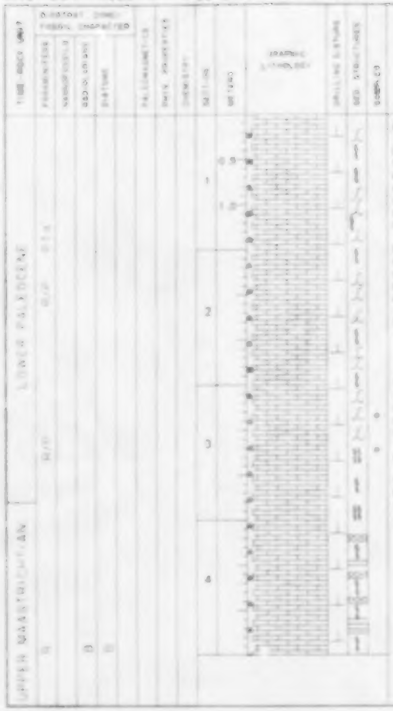
TIME-ROCK UNIT
BIOSTRAT. ZONE/FOSSIL CHARACTER
FORAMINIFERS
NANNOFOSSILS
RADIOLARIANS
DIATOMS
PALEOMAGNETICS
PHYS. PROPERTIES
CHEMISTRY
SECTION
METERS
GRAPHIC LITHOLOGY
DRILLING DISTURB.
SED. STRUCTURES
SAMPLES
LOWER PALEOCENE
UPPER MAASTRICHTIAN
G/P P1a
B/P
B
B
B
1
2
3
4
0.5
1.0

LITHOLOGIC DESCRIPTION

LIMESTONE

Major lithology: This core contains white (2.5Y 8/2 and 10YR 8/1) to light gray (N7) LIMESTONE, with variable amounts of silica cement. The sediment is moderately to highly bioturbated with mm to cm scale subhorizontal, compacted burrows. Faint, light gray (N7) submm-scale flaser structures are present to abundant in Sections 1 through 3. Faint, light gray (10YR 7/2) color bands are common in Section 4. Stylolites are common in Section 4, and evidence for stylolites is present in Section 1 as gray coatings and irregular ends on limestone pieces.

Minor lithologies: Dark reddish gray (5YR 4/2) CHERT is present as fragments of continuous layers up to 5 cm thick and as irregularly shaped masses in limestone pieces. Thin intervals (<1 cm thick) of gray (N5) LIMESTONE WITH VOLCANIC ASH are present at Section 1, 40, 65, and 138 cm; and Section 2, 13, 16, 40, 70, 83, and 115 cm; and Section 3, 27 and 134 cm.

SMEAR SLIDE SUMMARY (%):

	2, 34 M	3, 71 D
TEXTURE:		
Sand	15	—
Silt	80	95
Clay	5	5
COMPOSITION:		
Calcareous fragments	85	100
Nannofossils	5	—
Volcanic ash	5	—

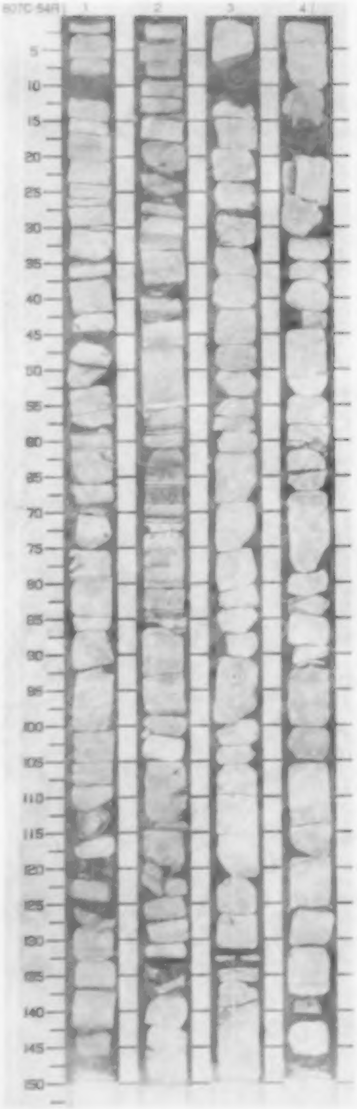
807C-54R
1
2
3
4
5
10
15
20
25
30
35
40
45
50
55
60
65
70
75
80
85
90
95
100
105
110
115
120
125
130
135
140
145
150

SITE 807 HOLE C CORE 55R CORED INTERVAL 1196.9-1206.6 mbsf

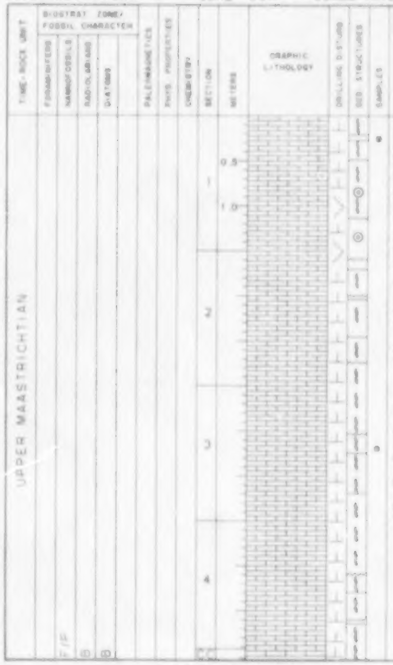
TIME-ROCK UNIT
BIOSTRAT. ZONE/ FOSSIL CHARACTER
FORAMINIFERS
NANNOFOSSILS
RADIOLARIANS
DIATOMS
PALEOMAGNETICS
PHYS. PROPERTIES
CHEMISTRY
SECTION
METERS
GRAPHIC LITHOLOGY
DRILLING DISTURB.
SED. STRUCTURES
SAMPLES
UPPER MAASTRICHTIAN
F/P
B
B
1
2
3
4
CC
0.5
1.0

LITHOLOGIC DESCRIPTION

LIMESTONE

Major lithology: This core contains white (5Y 8/1 and 10YR 8/1) LIMESTONE. The color grades to light gray (5Y 7/1) in the lower part of Section 1. Slight to heavy bioturbation is indicated by white and light gray mottling. Less bioturbated intervals are homogeneous, 5-10 cm thick and interbedded with 10-20 cm thick intervals containing numerous, flattened burrows. Burrows are predominantly mm scale, but rare cm scale ones are observed. Millimeter-scale, white and light gray (10YR 7/1) color banding is found in Section 1, 0 and 50 cm; in Section 3, 22 and 96 cm; and in Section 4, 93 and 108 cm. The banding in Section 1 is partly due to grain size variations and may represent primary lamination. Dusky blue (5PB 3/2) mottling is present in Sections 1 and 2 and may represent very finely disseminated pyritic material. Stylolites are found in all sections.

Minor lithology: Pieces of reddish brown (5YR 4/3) CHERT, up to 7 cm diameter, are present in Section 1, 93 cm and 140 cm and in Section 2, 140 cm. The single pieces may represent nodules or thin chert layers. Dark gray (5Y 4/1) layers of LIMESTONE with less than 10% volcanic ash are found in Section 1, 27 cm and 67 cm.

SMEAR SLIDE SUMMARY (%):

	1, 75	3, 70
	M	D
TEXTURE:		
Sand	15	15
Silt	80	80
Clay	5	5
COMPOSITION:		
Calcareous fragments	90	95
Volcanic ash	5	—

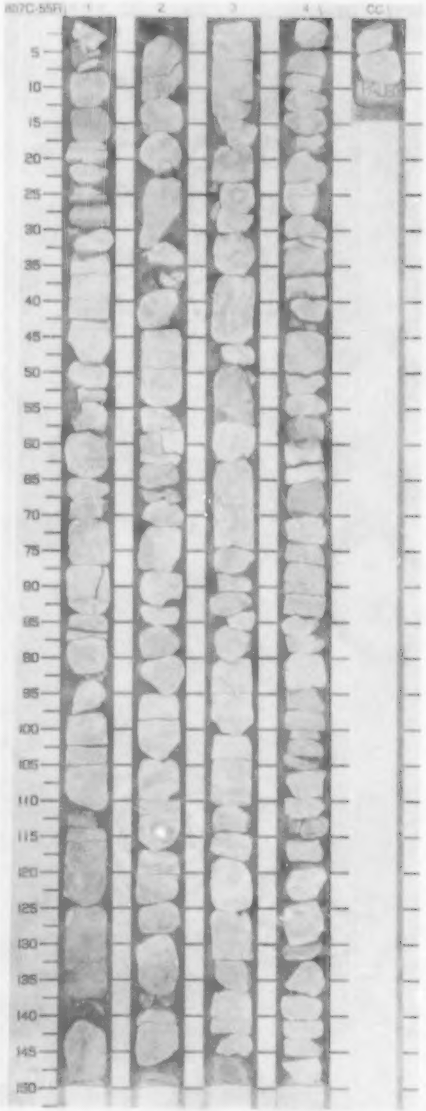
807C-55R
1
2
3
4
CC
5
10
15
20
25
30
35
40
45
50
55
60
65
70
75
80
85
90
95
100
105
110
115
120
125
130
135
140
145
150

SITE 807 HOLE C CORE 56R CORED INTERVAL 1206.0-1216.3 mbsf

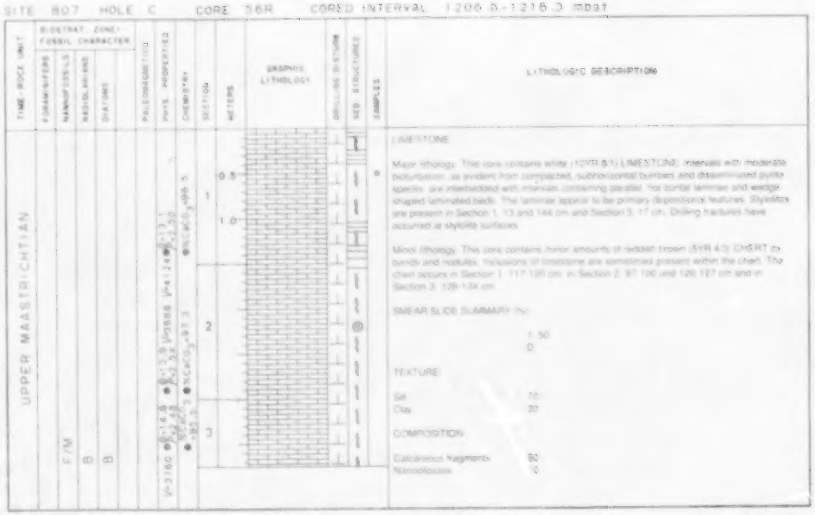

TIME-ROCK UNIT	FORAMINIFERS	NANNOFOSSILS	RADIOLARIANS	DIATOMS	PALEOMAGNETICS	PHYS. PROPERTIES	CHEMISTRY	SECTION	METERS	GRAPHIC LITHOLOGY	DRILLING DISTURB.	SED. STRUCTURES	SAMPLES	LITHOLOGIC DESCRIPTION
UPPER MAASTRICHTIAN		F/M	B	B		V=4124 ●φ=13.1 γ=2.50	●%CaCO$_3$=98.5	1	0.5 1.0				●	
						●φ=13.9 γ=2.34 V=3888	●%CaCO$_3$=97.3	2						
						V=3160 ●φ=16.8 γ=2.48	●%CaCO$_3$=95.3	3						

LIMESTONE

Major lithology: This core contains white (10YR 8/1) LIMESTONE. Intervals with moderate bioturbation, as evident from compacted, subhorizontal burrows and disseminated pyrite specks, are interbedded with intervals containing parallel, horizontal laminae and wedge-shaped laminated beds. The laminae appear to be primary depositional features. Stylolites are present in Section 1, 13 and 144 cm and Section 3, 17 cm. Drilling fractures have occurred at stylolite surfaces.

Minor lithology: This core contains minor amounts of reddish brown (5YR 4/3) CHERT as bands and nodules. Inclusions of limestone are sometimes present within the chert. The chert occurs in Section 1, 117-120 cm, in Section 2, 97-100 and 120-127 cm and in Section 3, 128-134 cm.

SMEAR SLIDE SUMMARY (%):

	1, 50
	D
TEXTURE:	
Silt	70
Clay	30
COMPOSITION:	
Calcareous fragments	90
Nannofossils	10

SITE 807 HOLE C CORE 57R CORED INTERVAL 1216.3-1222.5 mbsf

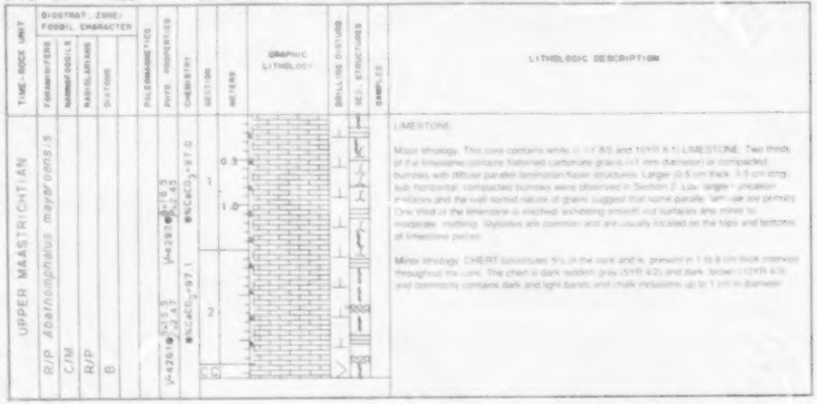

TIME-ROCK UNIT	FORAMINIFERS	NANNOFOSSILS	RADIOLARIANS	DIATOMS	PALEOMAGNETICS	PHYS. PROPERTIES	CHEMISTRY	SECTION	METERS	GRAPHIC LITHOLOGY	DRILLING DISTURB.	SED. STRUCTURES	SAMPLES	LITHOLOGIC DESCRIPTION
UPPER MAASTRICHTIAN	R/P *Abathomphalus mayaroensis*	C/M	R/P	B		V=4293 ●φ=16.5 γ=2.45	●%CaCO$_3$=97.0	1	0.5 1.0					
						V=4261 ●φ=15.5 γ=2.47	●%CaCO$_3$=97.1	2						
								CC						

LIMESTONE

Major lithology: This core contains white (2.5Y 8/0 and 10YR 8/1) LIMESTONE. Two thirds of the limestone contains flattened carbonate grains (<1 mm diameter) or compacted burrows with diffuse parallel lamination/flaser structures. Larger (0.5 cm thick, 3.5 cm long) sub-horizontal, compacted burrows were observed in Section 2. Low angle [illegible] truncations and the well sorted nature of grains suggest that some parallel laminae are primary. One third of the limestone is silicified, exhibiting smooth cut surfaces and minor to moderate mottling. Stylolites are common and are usually located on the tops and bottoms of limestone pieces.

Minor lithology: CHERT constitutes 5% of the core and is present in 1 to 8 cm thick intervals throughout the core. The chert is dark reddish gray (5YR 4/2) and dark brown (10YR 4/3) and commonly contains dark and light bands and chalk inclusions up to 1 cm in diameter.

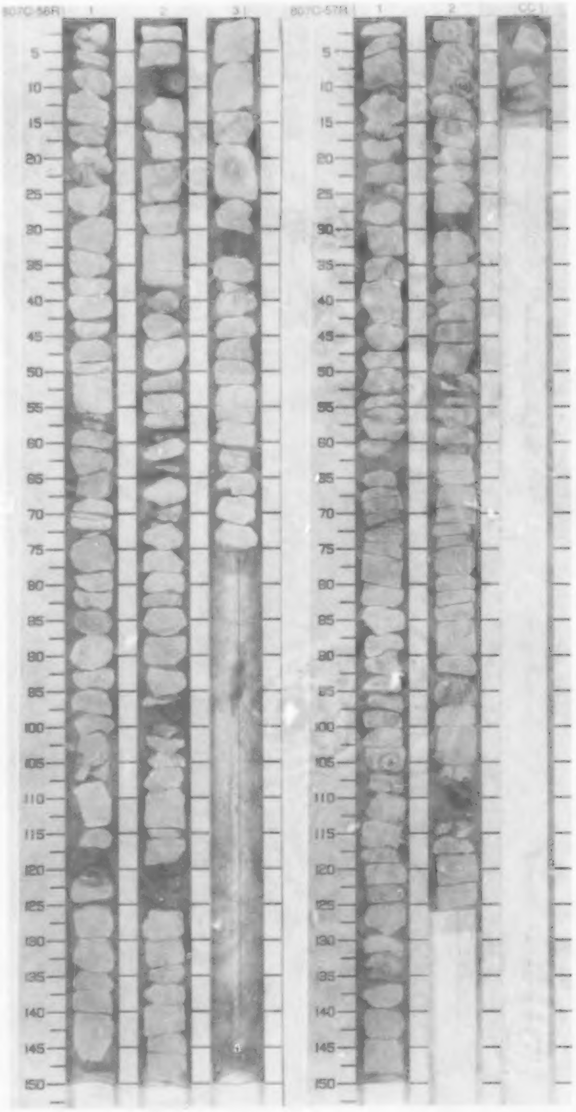

SITE 807 HOLE C CORE 58R CORED INTERVAL 1222.5-1232.2 mbsf

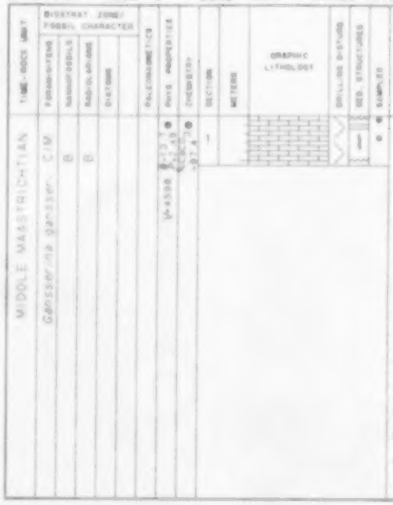
TIME-ROCK UNIT
BIOSTRAT. ZONE/ FOSSIL CHARACTER
FORAMINIFERS
NANNOFOSSILS
RADIOLARIANS
DIATOMS
PALEOMAGNETICS
PHYS. PROPERTIES
CHEMISTRY
SECTION
METERS
GRAPHIC LITHOLOGY
DRILLING DISTURB.
SED. STRUCTURES
SAMPLES
MIDDLE MAASTRICHTIAN
Gansserina gansseri C/M
B
B
V=4598
1

LITHOLOGIC DESCRIPTION

LIMESTONE

Major lithology: This core contains white (10YR 8/1) LIMESTONE, generally in rounded pieces between 1 and 4 cm in thick. In Section 1, 0-5 cm and 28-52 cm, carbonate particles, possibly representing overgrown or recrystallized foraminifers are present as "spots" on the core. Slight banding in various shades of white is seen in Section 1, 9-15 cm. This banding may be of depositional or of diagenetic origin. In the relatively homogeneous interval at Section 1, 17 to 41 cm, slight bioturbation is indicated by [illegible] mottling. Stylolites with dark greenish gray drapes are found at Section 1, 3 cm and 49 cm.

Minor lithology: Dark gray (5YR 4/1) CHERT is found in Section 1 at 30-32 cm and 41-45 cm. The pieces are homogeneous, have broken surfaces, and may represent nodules or continuous layers.

SMEAR SLIDE SUMMARY (%):

	1, 3	1, 20
	M	D
TEXTURE:		
Sand	10	5
Silt	85	90
Clay	5	5
COMPOSITION:		
Calcareous fragments	90	95
Nannofossils	10	5

SITE 807 HOLE C CORE 59R CORED INTERVAL 1232.2-1241.8 mbsf

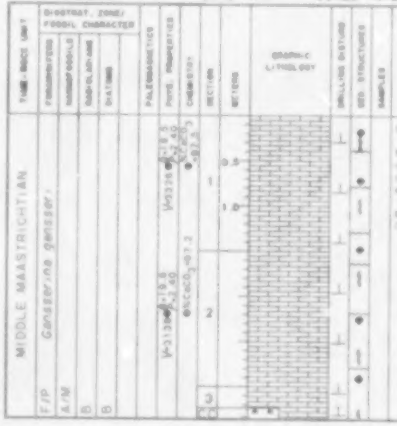
TIME-ROCK UNIT
BIOSTRAT. ZONE/ FOSSIL CHARACTER
FORAMINIFERS
NANNOFOSSILS
RADIOLARIANS
DIATOMS
PALEOMAGNETICS
PHYS. PROPERTIES
CHEMISTRY
SECTION
METERS
GRAPHIC LITHOLOGY
DRILLING DISTURB.
SED. STRUCTURES
SAMPLES
MIDDLE MAASTRICHTIAN
Gansserina gansseri
F/P
A/M
B
B
V=3326
V=3136
%CaCO3=97.2
1
2
3
CC
0.5
1.0

LITHOLOGIC DESCRIPTION

LIMESTONE

Major lithology: This core contains white (10YR 8/1) LIMESTONE. Specks of pyrite are disseminated throughout the core. White (2.5Y 8/0), mm-size, slightly compacted clasts, which are finer grained than the matrix, are common. Stylolites are well developed and some exhibit tension cracks.

Minor lithology: Dark reddish gray (5YR 4/2) CHERT comprises about 40% of the Core Catcher.

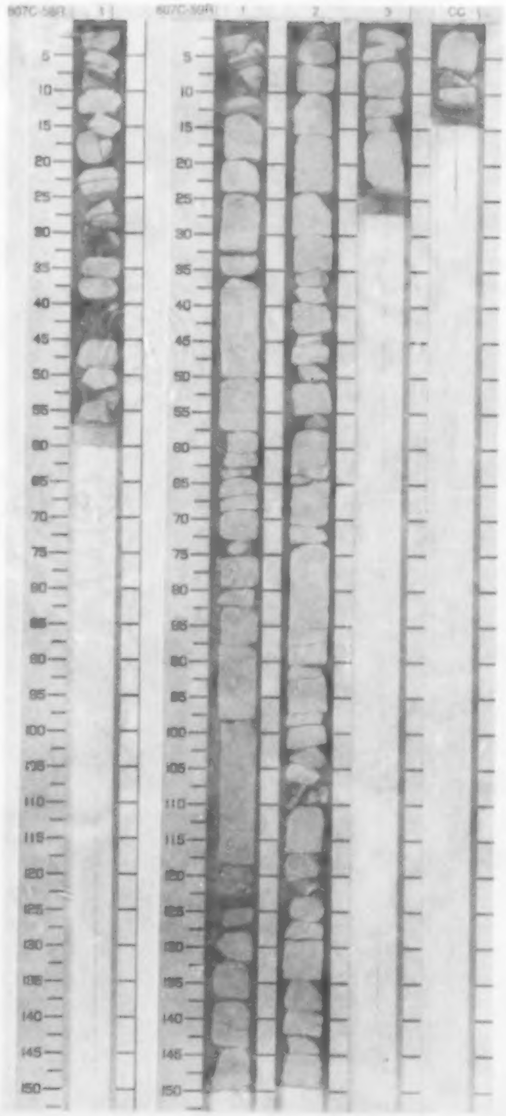
807C-58R
1
807C-59R
1
2
3
CC
5
10
15
20
25
30
35
40
45
50
55
60
65
70
75
80
85
90
95
100
105
110
115
120
125
130
135
140
145
150

SITE 807 HOLE C CORE 60R CORED INTERVAL 1241.8-1251.5 mbsf

TIME-ROCK UNIT	FORAMINIFERS	NANNOFOSSILS	RADIOLARIANS	DIATOMS	PALEOMAGNETICS	PHYS. PROPERTIES	CHEMISTRY	SECTION	METERS	GRAPHIC LITHOLOGY	DRILLING DISTURB.	SED. STRUCTURES	SAMPLES	LITHOLOGIC DESCRIPTION
MIDDLE MAASTRICHTIAN	R/P	A/P	B	B				CC						LIMESTONE Major lithology: This core contains white (10YR 8/0) LIMESTONE. The limestone has a few elongate, mm-scale, white (2.5Y 8/0) clasts. Tiny dark specks of pyrite(?) are abundant throughout. Minor lithology: Chert comprises about 40% of the CC.

SITE 807 HOLE C CORE 61R CORED INTERVAL 1251.5-1261.2 mbsf

TIME-ROCK UNIT	FORAMINIFERS	NANNOFOSSILS	RADIOLARIANS	DIATOMS	PALEOMAGNETICS	PHYS. PROPERTIES	CHEMISTRY	SECTION	METERS	GRAPHIC LITHOLOGY	DRILLING DISTURB.	SED. STRUCTURES	SAMPLES	LITHOLOGIC DESCRIPTION
UPPER CAMPANIAN - LOWER MAASTRICHTIAN	B/P	B	B			[illegible] ● V=3073 [illegible] ● V=3005	● %CaCO$_3$=97.2 ● %CaCO$_3$=97.3	1 2	0.5 1.0					LIMESTONE Major lithology: This core contains white (10YR 8/0) to gray (2.5Y 6/0) LIMESTONE. Disseminated pyrite specks are abundant throughout the core. Small (<1-mm) compacted clasts appear to have a parallel alignment. A few trace fossils are apparent. Well-developed stylolites are also present. Minor lithology: CHERT occurs as three concretions in Section 1 and dusky blue (5PB 3/2) and dark brown (7.5YR 4/2) in color.

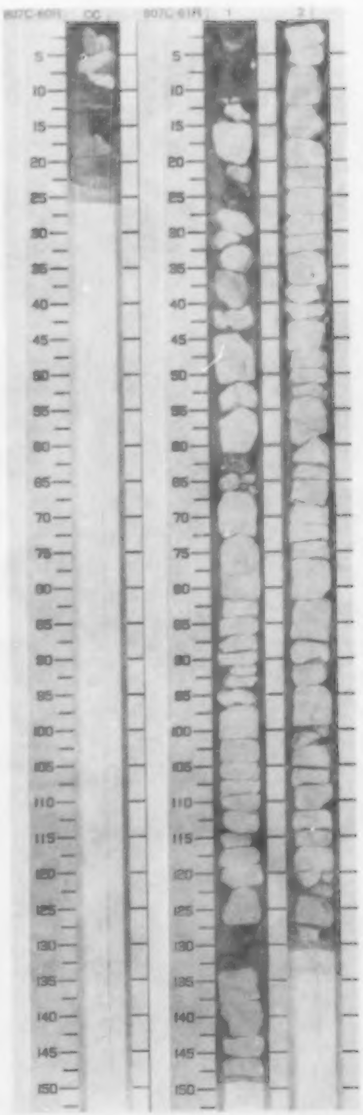

SITE 807 HOLE C CORE 62R CORED INTERVAL 1261.2-1270.8 mbsf

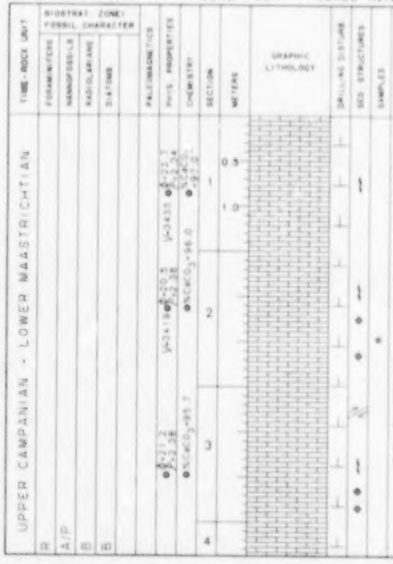
TIME-ROCK UNIT
BIOSTRAT. ZONE/ FOSSIL CHARACTER
FORAMINIFERS
NANNOFOSSILS
RADIOLARIANS
DIATOMS
PALEOMAGNETICS
PHYS. PROPERTIES
CHEMISTRY
SECTION
METERS
GRAPHIC LITHOLOGY
DRILLING DISTURB.
SED. STRUCTURES
SAMPLES
UPPER CAMPANIAN - LOWER MAASTRICHTIAN
R
A/P
B
B
φ=23.1
ρ=2.34
γ=3435
%CaCO3=97.0
%CaCO3=96.0
φ=20.6
ρ=2.38
γ=3419
φ=21.2
ρ=2.38
%CaCO3=95.7
1
2
3
4
0.5
1.0

LITHOLOGIC DESCRIPTION

LIMESTONE

Major lithology: This core contains white (7.5YR 8/0) LIMESTONE. White and light gray clasts, 1 to 5 mm in diameter and normally graded, are abundant at Section 2, 57 to 150 cm. The clasts are slightly compacted and oriented subhorizontally. Stylolites are common and sometimes truncate the clasts. Patches of purple-colored specks (pyrite) and disseminated specks of an unknown dark mineral are observed throughout. In Section 3, 7 to 10 cm, load structures are apparent in two separate pieces of limestone, which are underlain by a piece with a microfault. The microfault is apparent from the displacement of disseminated purple specks (pyrite?).

Minor lithology: Several 2 to 15 cm thick intervals of dark brown (7.5YR 4/2) CHERT are present within the core.

SMEAR SLIDE SUMMARY (%):

	2, 100
	D
TEXTURE:	
Sand	1
Silt	99
COMPOSITION:	
Foraminifers	1
Micrite	99

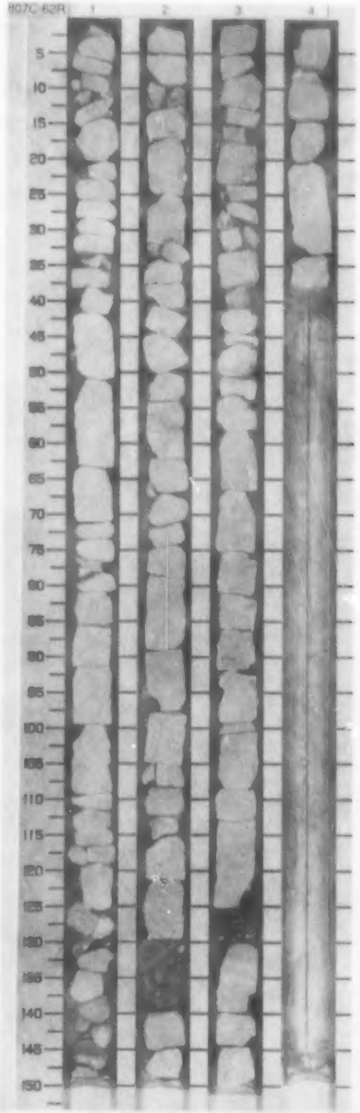
807C-62R
1
2
3
4
5
10
15
20
25
30
35
40
45
50
55
60
65
70
75
80
85
90
95
100
105
110
115
120
125
130
135
140
145
150

SITE 807 HOLE C CORE 63R CORED INTERVAL 1270.8-1280.5 mbsf

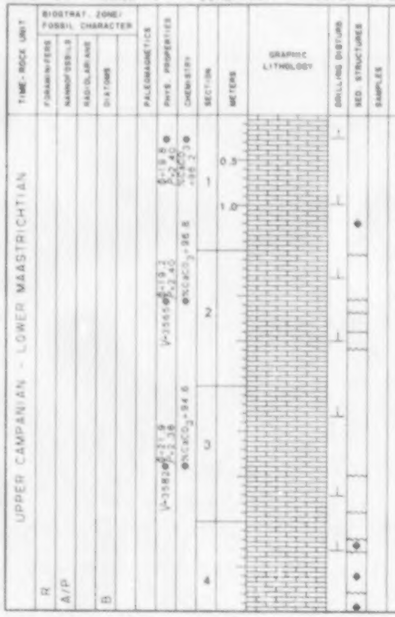
TIME-ROCK UNIT
BIOSTRAT. ZONE/ FOSSIL CHARACTER
FORAMINIFERS
NANNOFOSSILS
RADIOLARIANS
DIATOMS
PALEOMAGNETICS
PHYS. PROPERTIES
CHEMISTRY
SECTION
METERS
GRAPHIC LITHOLOGY
DRILLING DISTURB.
SED. STRUCTURES
SAMPLES
UPPER CAMPANIAN - LOWER MAASTRICHTIAN
R
A/P
B
φ=19.6
ρ=2.40
%CaCO3=98.2
V=3565
φ=19.2
ρ=2.40
%CaCO3=96.8
V=3582
φ=21.9
ρ=2.38
%CaCO3=94.6
1
2
3
4
0.5
1.0

LITHOLOGIC DESCRIPTION

LIMESTONE

Major lithology: This core contains white (7.5YR 8/0) LIMESTONE. Intervals of disseminated grayish blue (5PB 5/2) specks (pyrite?), possibly representing bioturbation, are common. Thin, intervals of horizontal, parallel swirls, possibly representing flow structures, are located in Section 1, 73-86 cm and 94-103 cm and in numerous intervals in Section 2. Very thin laminae (1 grain thick) of material that is coarser than the surrounding matrix are noted in Section 2, 79-80 cm. These laminae are distinct, horizontal, and parallel. Below the laminae are the subhorizontal swirl features. Several intervals of small (<= 1 mm) bright white and gray clasts are seen in Section 4, 7-15 cm and 40-95 cm.

Minor lithology: Dark brown (7.5YR 4/2) to weak red (2.5YR 4/2) CHERT is present as 2 to 10 cm thick pieces in the core at a spacing of one per section.

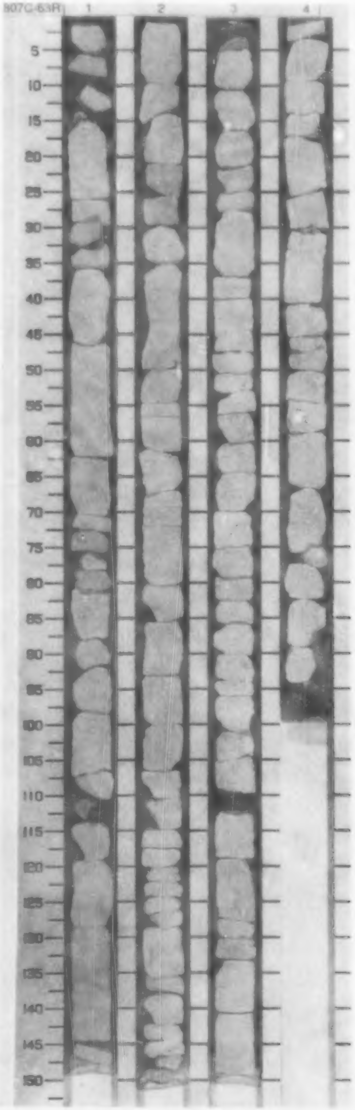
807C-63R
1
2
3
4
5
10
15
20
25
30
35
40
45
50
55
60
65
70
75
80
85
90
95
100
105
110
115
120
125
130
135
140
145
150

SITE 807 HOLE C CORE 64R CORED INTERVAL 1280.5-1290.1 mbsf

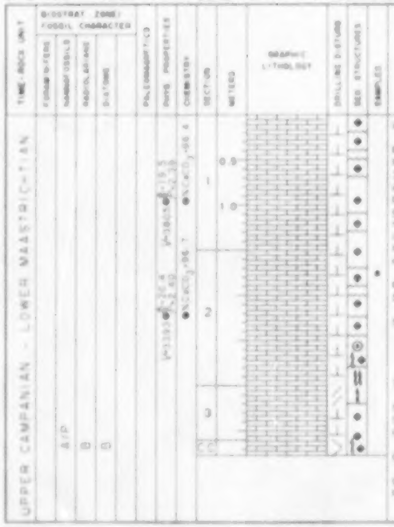
TIME-ROCK UNIT
BIOSTRAT. ZONE/ FOSSIL CHARACTER
FORAMINIFERS
NANNOFOSSILS
RADIOLARIANS
DIATOMS
PALEOMAGNETICS
PHYS. PROPERTIES
CHEMISTRY
SECTION
METERS
GRAPHIC LITHOLOGY
DRILLING DISTURB.
SED. STRUCTURES
SAMPLES
UPPER CAMPANIAN - LOWER MAASTRICHTIAN
A/P
B
B
%CaCO3=96.4
%CaCO3=96.1
1
2
3
CC
0.5
1.0

LITHOLOGIC DESCRIPTION

LIMESTONE

Major lithology: This core contains white (2.5Y 8/0) LIMESTONE. White, rounded to slightly flattened chalk clasts are common to abundant in Section 1, Section 2, 0-120 cm, Section 3, 15-59 cm, and Core Catcher. These clasts form parallel to subparallel horizontal bands and range up to approximately 4 mm in diameter. Several of the largest clasts contain burrows that terminate at the clast edge. Fewer than 1% of the clasts are gray (N5) to light gray (N7) in color and are composed of isotropic to slightly birefringent noncalcareous material. These clasts may be redeposited and variably altered volcanic ash. Section 2, 120 cm to Section 3, 15 cm contains flaser structures and moderate amounts of bioturbation; the presence of elongated burrow outlines suggests that this interval may have been deformed slightly. Stylolites are common to abundant in Sections 1 and 2.

Minor lithology: A 2 cm thick fragment of dark reddish gray (5YR 4/2) CHERT is present at Section 2, 113-115 cm.

SMEAR SLIDE SUMMARY (%):

	2, 25
	D
TEXTURE:	
Sand	10
Silt	85
Clay	5
COMPOSITION:	
Calcareous fragments	95
Nannofossils	5

SITE 807 HOLE C CORE 65R CORED INTERVAL 1290.1-1299.8 mbsf

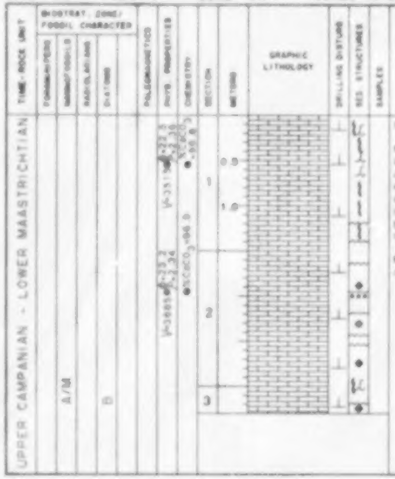
TIME-ROCK UNIT
BIOSTRAT. ZONE/ FOSSIL CHARACTER
FORAMINIFERS
NANNOFOSSILS
RADIOLARIANS
DIATOMS
PALEOMAGNETICS
PHYS. PROPERTIES
CHEMISTRY
SECTION
METERS
GRAPHIC LITHOLOGY
DRILLING DISTURB.
SED. STRUCTURES
SAMPLES
UPPER CAMPANIAN - LOWER MAASTRICHTIAN
A/M
B
%CaCO3=96.0
1
2
3
0.5
1.0

LITHOLOGIC DESCRIPTION

LIMESTONE

Major lithology: This core contains white (2.5Y 8/0 and 10YR 8/1) LIMESTONE. The limestone alternates between intervals of uniform, slightly bioturbated stratified (?) limestone and limestone with common to abundant, rounded to slightly elongate, 1 to 5 mm diameter white limestone clasts. A minor portion (<5%) of the clasts are light gray (N7). The clasts are arranged in parallel to sub-parallel intervals. Section 3, 20-30 cm also contains angular clasts of dusky blue green (5BG 3/2) color. Flaser structures were observed Section 1. Inverse graded bedding is present in Section 2, 51-57 cm. Stylolites are common throughout the core.

Minor lithology: Section 1, 77-85 cm, contains dark reddish gray (5YR 4/2) CHERT. The chert contains chalk/limestone inclusions up to 1 cm in diameter.

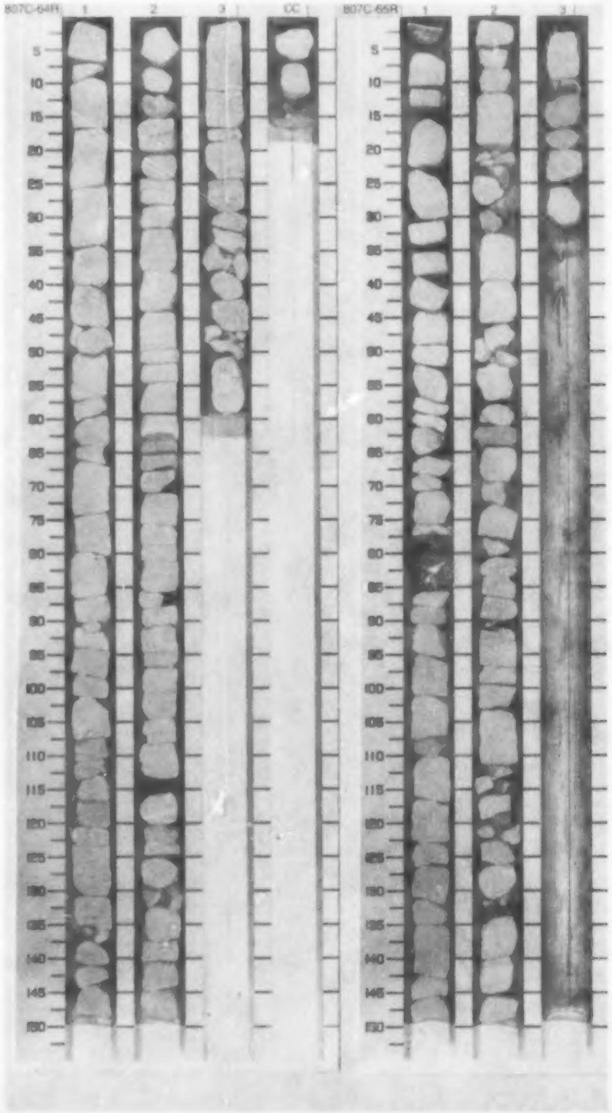
807C-64R
1
2
3
CC
807C-65R
1
2
3
5
10
15
20
25
30
35
40
45
50
55
60
65
70
75
80
85
90
95
100
105
110
115
120
125
130
135
140
145
150

SITE 807 HOLE C CORE 66R CORED INTERVAL 1299.8-1309.5 mbsf

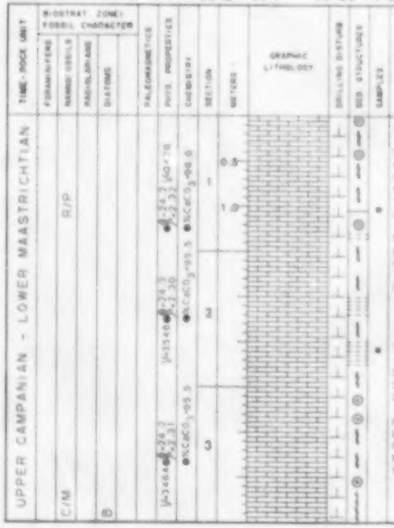
TIME-ROCK UNIT
BIOSTRAT. ZONE/ FOSSIL CHARACTER
FORAMINIFERS
NANNOFOSSILS
RADIOLARIANS
DIATOMS
PALEOMAGNETICS
PHYS. PROPERTIES
CHEMISTRY
SECTION
METERS
GRAPHIC LITHOLOGY
DRILLING DISTURB.
SED. STRUCTURES
SAMPLES
UPPER CAMPANIAN - LOWER MAASTRICHTIAN
R/P
C/M
B
γ-2.32
φ-24.2
Vp=2270
%CaCO3=96.6
%CaCO3=95.5
γ-2.30
φ-24.3
Vp=3540
%CaCO3=95.5
γ-2.31
φ-24.2
Vp=3464
1
2
3
0.5
1.0

LITHOLOGIC DESCRIPTION

LIMESTONE

Major lithology: This core contains white (2.5Y 8/0 and 10YR 8/1) LIMESTONE. The limestone alternates in composition between uniform, moderately to heavily bioturbated limestone, and limestone with faint horizontal laminae or fossil structures. Both vertical and horizontal burrows are visible. A dark gray (N3), 1 cm thick ash layer is noted in Section 1, 102 cm. White, mm scale limestone clasts are observed in Section 2, 124-125 cm. Stylolites are present throughout the core.

Minor lithology: Dark reddish brown (5YR 3/3) and reddish brown (5YR 4/3) CHERT is present as nodules or in 1 to 5 cm thick layers. The chert contains chalk limestone inclusions up to 1 cm in diameter.

SMEAR SLIDE SUMMARY (%):

	1, 102	2, 105
	M	D
TEXTURE		
Sand	20	—
Silt	75	90
Clay	5	10
COMPOSITION		
Carbonate particles	—	95
Foraminifers	Tr	—
Nannofossils	Tr	5
Volcanic ash	95	—

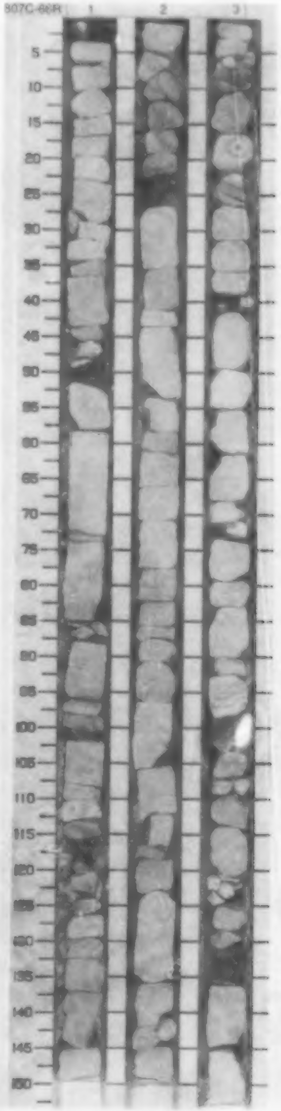
807C-66R
1
2
3
5
10
15
20
25
30
35
40
45
50
55
60
65
70
75
80
85
90
95
100
105
110
115
120
125
130
135
140
145
150

SITE 807 HOLE C CORE 67R CORED INTERVAL 1309.5-1319.1 mbsf

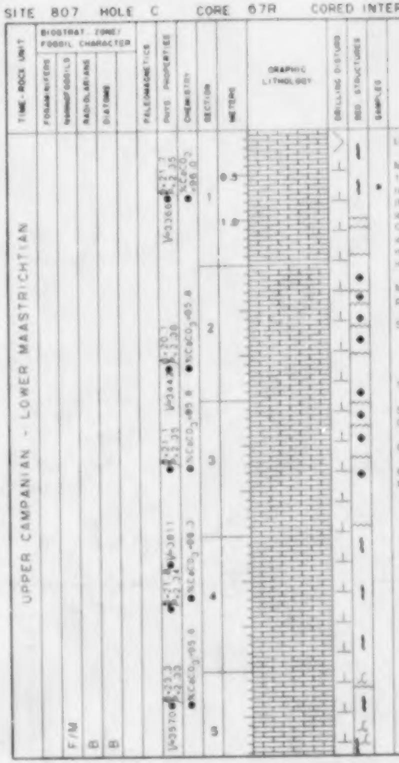
TIME-ROCK UNIT
BIOSTRAT. ZONE/ FOSSIL CHARACTER
FORAMINIFERS
NANNOFOSSILS
RADIOLARIANS
DIATOMS
PALEOMAGNETICS
PHYS. PROPERTIES
CHEMISTRY
SECTION
METERS
GRAPHIC LITHOLOGY
DRILLING DISTURB.
SED. STRUCTURES
SAMPLES
UPPER CAMPANIAN - LOWER MAASTRICHTIAN
F/M
B
B
%CaCO3=86.0
%CaCO3=85.8
%CaCO3=85.8
%CaCO3=88.3
%CaCO3=85.6
1
2
3
4
5
0.5
1.0

LITHOLOGIC DESCRIPTION

LIMESTONE

Major lithology: This core contains white (5YR 8/1 to 2.5Y 8/0) LIMESTONE. From Section 1, 120 cm to Section 3, 107 cm, the limestone contains common to abundant, mm-scale, rounded to slightly flattened clasts of three types: white (2.5Y 8/0) limestone, light gray (N7) limestone?, and greenish gray (5G 5/1), more angular ?clay or glauconite?. The clasts are aligned in parallel to subparallel, horizontal bands. From Section 3, 107 cm to Core Catcher, the sediment is slightly to heavily bioturbated; the more heavily burrowed zones are mottled and contain flaser structures, whereas the less heavily burrowed intervals are more homogenous in appearance. Stylolites are present in Sections 1 and 3, and common in Section 2.

Minor lithology: CHERT: dark reddish gray (5YR 4/2) to dusky red (10R 3/3) CHERT is present as 2 to 3 cm thick fragments at Section 1, 5-15 cm and Section 4, 80-83 cm.

SMEAR SLIDE SUMMARY (%):

	1, 86
	D
TEXTURE	
Silt	90
Clay	10
COMPOSITION	
Carbonate particles	90
Nannofossils	10

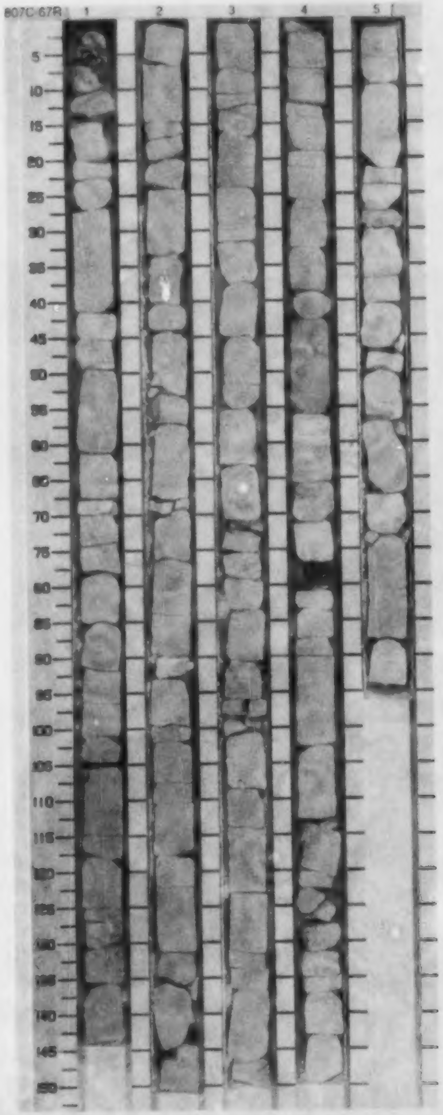
807C-67R
1
2
3
4
5
5
10
15
20
25
30
35
40
45
50
55
60
65
70
75
80
85
90
95
100
105
110
115
120
125
130
135
140
145
150

SITE 807 HOLE C CORE 68R CORED INTERVAL 1319.1-1328.8 mbsf

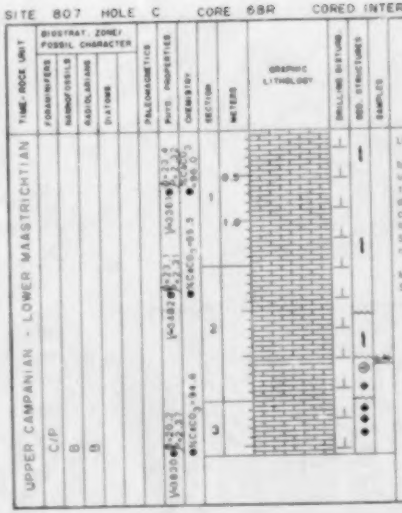
TIME-ROCK UNIT
BIOSTRAT. ZONE/ FOSSIL CHARACTER
FORAMINIFERS
NANNOFOSSILS
RADIOLARIANS
DIATOMS
PALEOMAGNETICS
PHYS. PROPERTIES
CHEMISTRY
SECTION
METERS
GRAPHIC LITHOLOGY
DRILLING DISTURB.
SED. STRUCTURES
SAMPLES
UPPER CAMPANIAN - LOWER MAASTRICHTIAN
C/P
B
B
Vp3301 ● φ=23.4 γ=2.32
●%CaCO3=96.0
Vp4582 ● φ=23.1 γ=2.31
●%CaCO3=95.9
Vp4830 ● φ=20.2 γ=2.37
●%CaCO3=94.6
1
2
3
0.5
1.0

LITHOLOGIC DESCRIPTION

LIMESTONE

Major lithology: This core contains white (7.5YR 8/0 to 5YR 8/0) LIMESTONE. The limestone is strongly bioturbated, particularly in Section 1, 34-43 cm, 63-67 cm, and 130-140 cm. Some 10 to 20 cm thick intervals are structureless. White clasts, up to 5 mm in diameter and elongated in a horizontal direction, are abundant below Section 2, 80 cm. The clast-rich interval does not have a graded texture. Dark brown (7.5YR 3/2) clay layers and flattened clasts are present below Section 2, 123 cm. Clay minerals are more abundant in Section 3, where the limestone is pinkish gray (5YR 6/1). Clay layers are the locus of numerous stylolites.

Minor lithology: Dark reddish gray (5YR 4/2) to dusky red (10R 3/3) CHERT is present in Section 1, 0-2 cm and in Section 2, 125 cm.

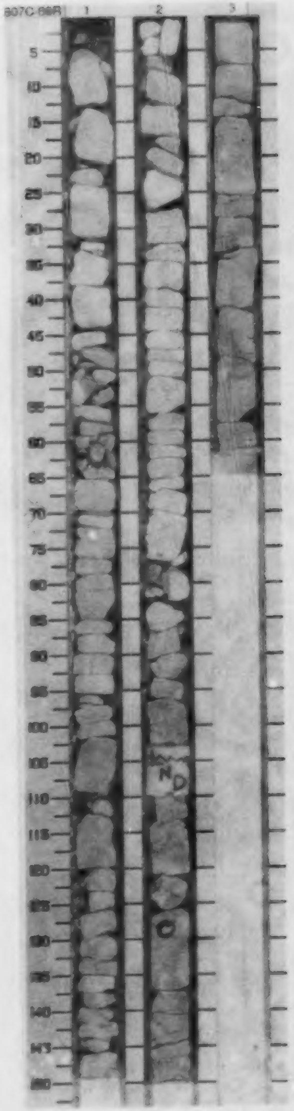
807C-68R
1
2
3
5
10
15
20
25
30
35
40
45
50
55
60
65
70
75
80
85
90
95
100
105
110
115
120
125
130
135
140
145
150
ND
O

SITE 807 HOLE C CORE 69R CORED INTERVAL 1328.8-1338.4 mbsf

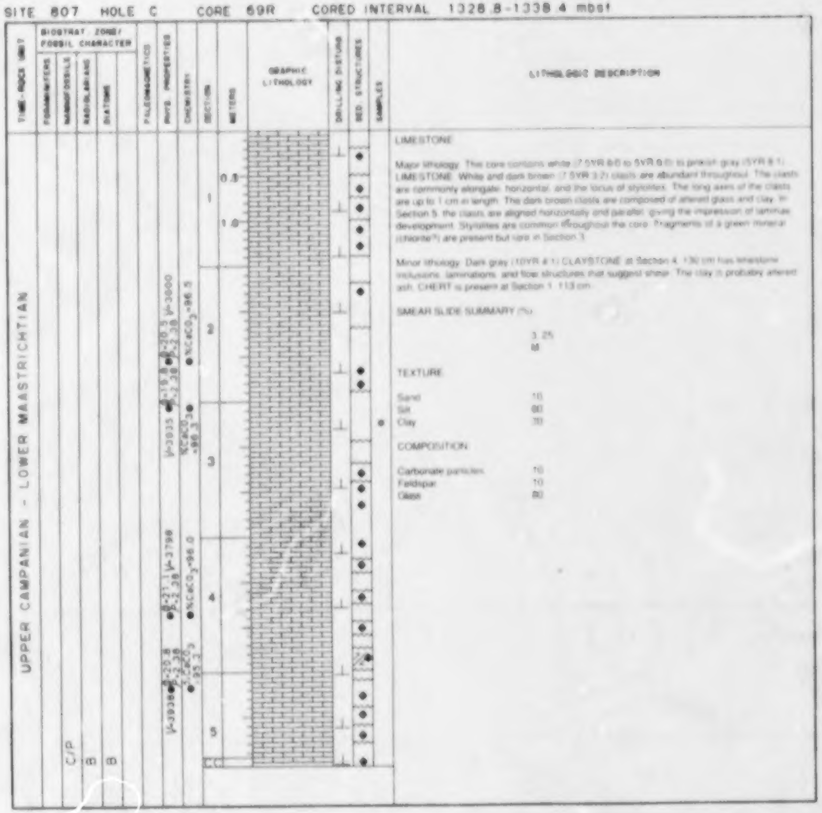
TIME-ROCK UNIT
BIOSTRAT. ZONE/ FOSSIL CHARACTER
FORAMINIFERS
NANNOFOSSILS
RADIOLARIANS
DIATOMS
PALEOMAGNETICS
PHYS. PROPERTIES
CHEMISTRY
SECTION
METERS
GRAPHIC LITHOLOGY
DRILLING DISTURB.
SED. STRUCTURES
SAMPLES
LITHOLOGIC DESCRIPTION
UPPER CAMPANIAN - LOWER MAASTRICHTIAN
C/P
B
B
φ=20.5 γ=2.38 V=3000
φ=19.8 γ=2.38 V=3035
φ=21.1 γ=2.38 V=3798
φ=20.8 γ=2.38 V=3938
%CaCO3=96.5
%CaCO3=96.3
%CaCO3=96.0
%CaCO3=95.3
1
2
3
4
5
CC
0.5
1.0

LIMESTONE

Major lithology: This core contains white (7.5YR 8/0 to 5YR 8/0) to pinkish gray (5YR 8/1) LIMESTONE. White and dark brown (7.5YR 3/2) clasts are abundant throughout. The clasts are commonly elongate, horizontal, and the locus of stylolites. The long axes of the clasts are up to 1 cm in length. The dark brown clasts are composed of altered glass and clay. In Section 5, the clasts are aligned horizontally and parallel, giving the impression of laminae development. Stylolites are common throughout the core. Fragments of a green mineral (chlorite?) are present but rare in Section 3.

Minor lithology: Dark gray (10YR 4/1) CLAYSTONE at Section 4, 130 cm has limestone inclusions, laminations, and flow structures that suggest shear. The clay is probably altered ash. CHERT is present at Section 1, 113 cm.

SMEAR SLIDE SUMMARY (%):

	3, 25
	M
TEXTURE:	
Sand	10
Silt	60
Clay	30
COMPOSITION:	
Carbonate particles	10
Feldspar	10
Glass	80

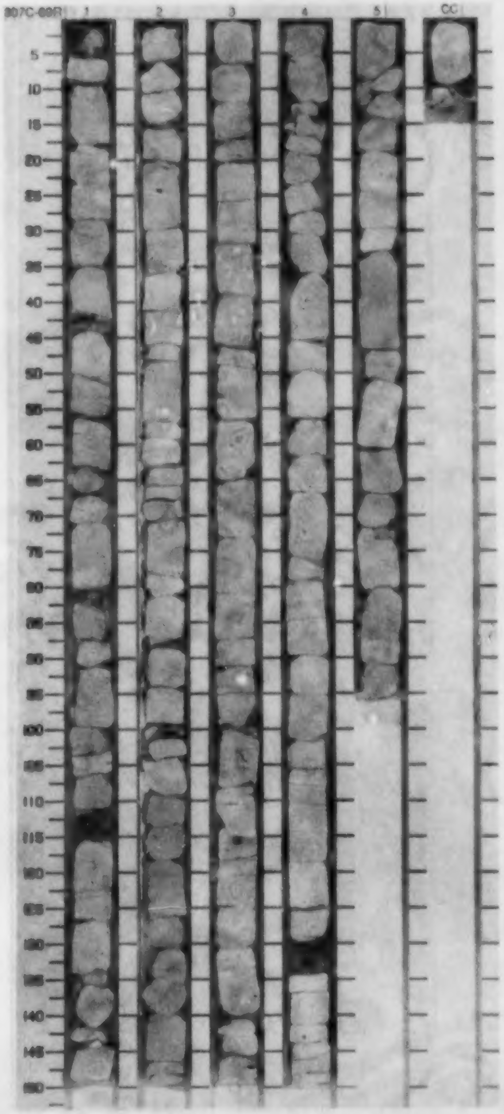
807C-69R
1
2
3
4
5
CC
5
10
15
20
25
30
35
40
45
50
55
60
65
70
75
80
85
90
95
100
105
110
115
120
125
130
135
140
145
150

SITE 807 HOLE C CORE 70R CORED INTERVAL 1338.4-1348.0 mbsf

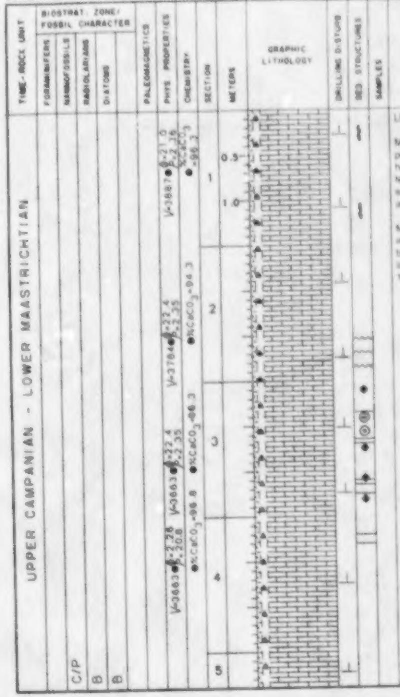
TIME-ROCK UNIT
BIOSTRAT. ZONE/ FOSSIL CHARACTER
FORAMINIFERS
NANNOFOSSILS
RADIOLARIANS
DIATOMS
PALEOMAGNETICS
PHYS. PROPERTIES
CHEMISTRY
SECTION
METERS
GRAPHIC LITHOLOGY
DRILLING DISTURB.
SED. STRUCTURES
SAMPLES
UPPER CAMPANIAN - LOWER MAASTRICHTIAN
C/P
B
B
V=3887 φ=21.0 γ=2.36
%CaCO3=96.3
V=3784 φ=22.4 γ=2.35
%CaCO3=94.3
V=3663 φ=22.4 γ=2.35
%CaCO3=96.3
V=3663 γ=2.28 φ=20.8
%CaCO3=96.8
1
2
3
4
5
0.5
1.0

LITHOLOGIC DESCRIPTION

LIMESTONE

Major lithology: This core contains white (10YR 8/1) LIMESTONE. Much of the core is composed of intervals of marbled brown, light gray, and white colors. This marbling is subhorizontal in orientation and possibly represents sheared sedimentary and bioturbation features, with a diagenetic overprinting. Small clasts (<1 mm) in the limestone matrix are scattered throughout Section 3. These clasts are especially evident in Section 3, 0-20 cm and are underlain by a fold structure. Only a few, poorly developed stylolites are present.

Minor lithology: Thin beds (1-15 cm) of CLAYSTONE are interbedded within the limestone in Sections 3, 4, and 5 (11 beds total). The claystone is dark brown (10YR 3/3) in color. The beds are laminated and typically wavy or even braided in appearance. They may represent layers of altered ash beds. CHERT is also present in small amounts in this core (several 1- to 2-cm thick intervals).

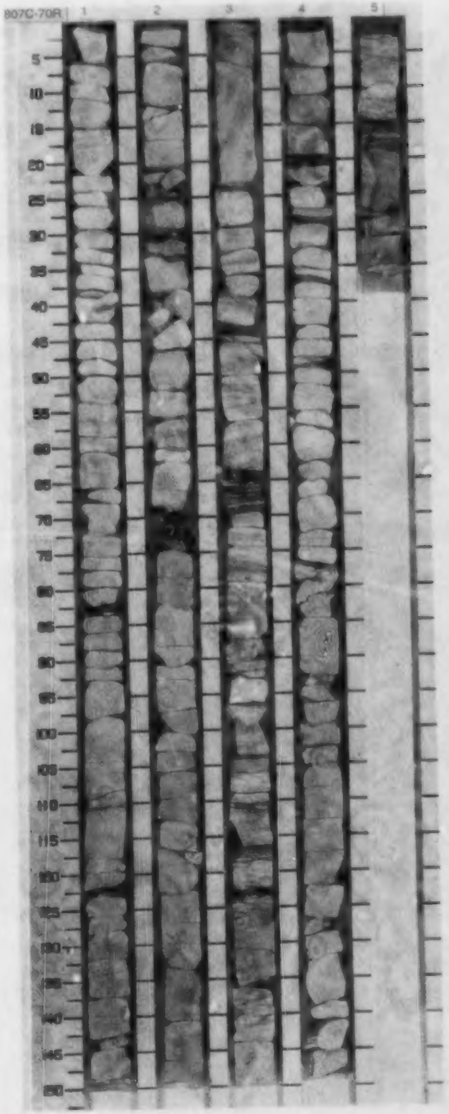
807C-70R
1
2
3
4
5
5
10
15
20
25
30
35
40
45
50
55
60
65
70
75
80
85
90
95
100
105
110
115
120
125
130
135
140
145
150

SITE 807 HOLE C CORE 71R CORED INTERVAL 1348.0-1357.7 mbsf

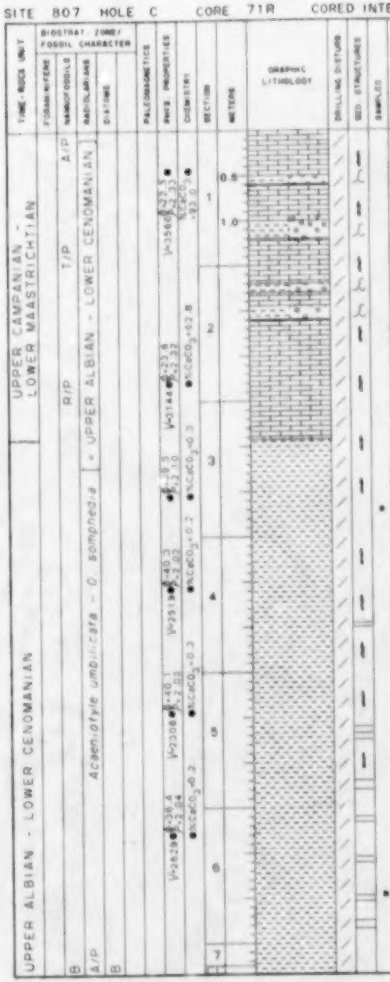
TIME-ROCK UNIT
BIOSTRAT. ZONE/ FOSSIL CHARACTER
FORAMINIFERS
NANNOFOSSILS
RADIOLARIANS
DIATOMS
PALEOMAGNETICS
PHYS. PROPERTIES
CHEMISTRY
SECTION
METERS
GRAPHIC LITHOLOGY
DRILLING DISTURB.
SED. STRUCTURES
SAMPLES
UPPER CAMPANIAN - LOWER MAASTRICHTIAN
UPPER ALBIAN - LOWER CENOMANIAN
B
A/P
T/P
R/P
A/P
B
Acaeniotyle umbilicata - D. somphedia
= UPPER ALBIAN - LOWER CENOMANIAN
B
V=3560
φ=27.5
γ=2.33
%CaCO3=93.0
V=3144
φ=23.6
γ=2.32
%CaCO3=62.8
φ=38.5
γ=2.10
%CaCO3=0.3
V=2519
φ=40.3
γ=2.02
%CaCO3=0.2
V=2308
φ=40.1
γ=2.03
%CaCO3=0.3
V=2428
φ=38.4
γ=2.04
%CaCO3=0.2
1
2
3
4
5
6
7
CC
0.5
1.0

LITHOLOGIC DESCRIPTION

LIMESTONE AND CLAYSTONE

Major lithology: This core contains white (7.5YR 8/0) and light gray (10YR 7/2) to very pale green (10G 8/2) LIMESTONE in Sections 1 through 3, 45 cm. The limestone is slightly to moderately bioturbated and contains 10 to 20 cm thick intervals of volcanic ash-rich CLAYSTONE characterized by heavy bioturbation, compaction, and/or shearing. The claystone is dark grayish brown (10YR 4/2), light gray (5Y 7/1), and grayish green (5G 5/2), and its abundance increases from Section 1 to Section 3, 45 cm. CLAYSTONE is predominant below Section 3, 45 cm, and is very dark grayish brown (10YR 3/2) to reddish brown (5YR 4/4) in Section 3, 45 cm to Section 5, 95 cm, and Section 6 to Core Catcher. Section 5, 95-150 cm is black (10YR 2/1). Moderate bioturbation is expressed in the grayish brown to reddish brown claystone by mm scale specks and cm scale burrows. Minor color banding is present in the black claystone.

Minor lithology: SILTSTONE WITH RADIOLARIANS is present in abundant, 0.5 to 4 cm thick, pale blue green (5BG 7/2), reddish brown (5YR 4/4), and pink (7.5YR 7/4) beds, from Section 6, 10 cm to Core Catcher.

SMEAR SLIDE SUMMARY (%):

	3, 120 D	6, 97 M
TEXTURE:		
Sand	—	15
Silt	9	80
Clay	91	5
COMPOSITION:		
Accessory minerals	5	—
Chert	5	—
Clay	90	—
Opaques	—	1
Radiolarians	—	15
Siliceous fragments	—	84

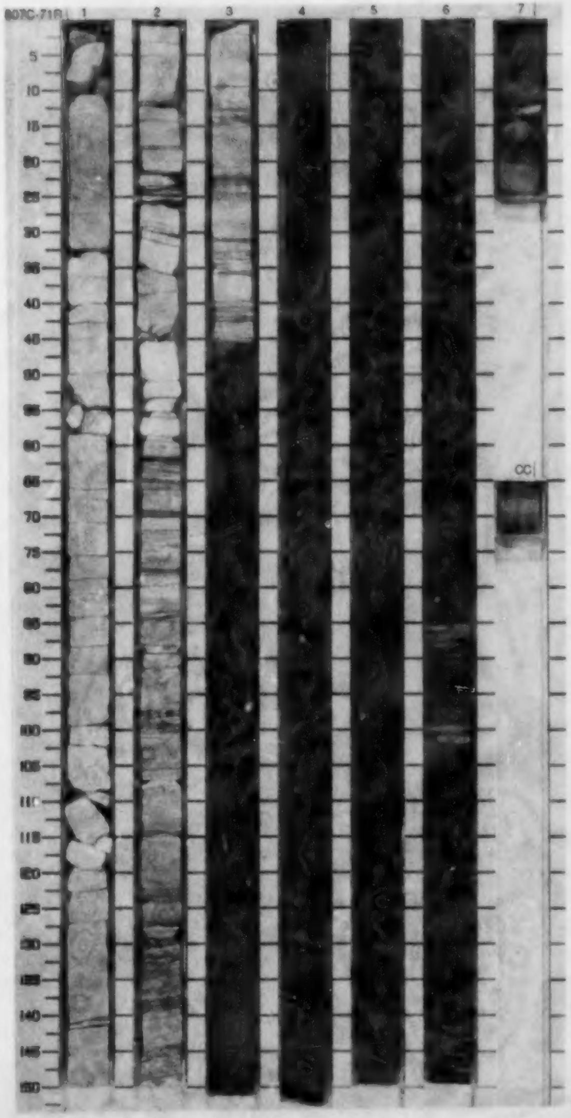
807C-71R
1
2
3
4
5
6
7
CC
5
10
15
20
25
30
35
40
45
50
55
60
65
70
75
80
85
90
95
100
105
110
115
120
125
130
135
140
145
150

SITE 807 HOLE C CORE 72R CORED INTERVAL 1357.7-1367.4 mbsf

TIME-ROCK UNIT: UPPER ALBIAN - LOWER CENOMANIAN

BIOSTRAT. ZONE/ FOSSIL CHARACTER

FORAMINIFERS	NANNOFOSSILS	RADIOLARIANS	DIATOMS
		A/P A/P C/P A/P A/P	
		UPPER ALBIAN - LOWER CENOMANIAN	*Acaeniotyle umbilicata - O. somphedia*
	B	B	B

PALEOMAGNETICS

PHYS. PROPERTIES: V=2269 ● ϕ=44.5 γ=1.60

CHEMISTRY: ●%CaCO$_3$=0.2

SECTION: 1, 2, 3

METERS: 0.5, 1.0

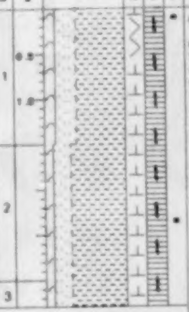

LITHOLOGIC DESCRIPTION

CLAYSTONE and RADIOLARIAN SILTSTONE

Major lithology: Approximately 65% of the core consists of dark brown (10YR 3/2) CLAYSTONE. The rock is interbedded with RADIOLARIAN SILTSTONE. Slight bioturbation is indicated by faint mm to cm scale burrows in some layers. Flaser structures and wavy discontinuous thin layers are common. The interbeds display either sharp contacts or normal grading with fine scale lamination. Evidence of microfaulting is observed in Section 1, 135 cm. Scouring and flow structures are observed in Section 2, 122 cm. Approximately 35% of the core is composed of pinkish gray (7.5YR 7/2) and light gray (N7) RADIOLARIAN SILTSTONE. This lithology is interbedded with the claystone and forms mm to 5 cm thick beds. Individual beds are partially laminated, and often stretched and discontinuous. A few beds display weak normal grading. Faint burrowing indicates slight bioturbation. Smear slide analysis indicates that the non-radiolarian fragments are fine-grained silicic particles of undetermined origin.

SMEAR SLIDE SUMMARY (%):

	1, 10 M	2, 87 D
TEXTURE:		
Sand	20	10
Silt	75	70
Clay	5	20
COMPOSITION:		
Accessory minerals	Tr	Tr
Clay	—	99
Glass	—	1
Quartz	—	Tr
Radiolarians	30	Tr
Siliceous fragments	70	—

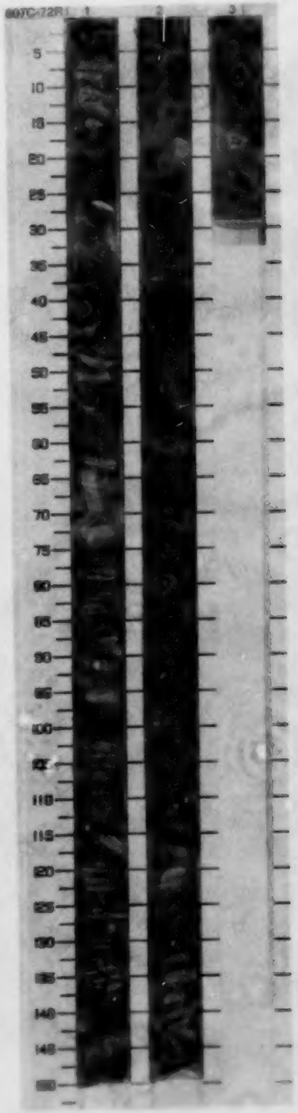

SITE 807 HOLE C CORE 73R CORED INTERVAL 1367.4-1375.4 mbsf

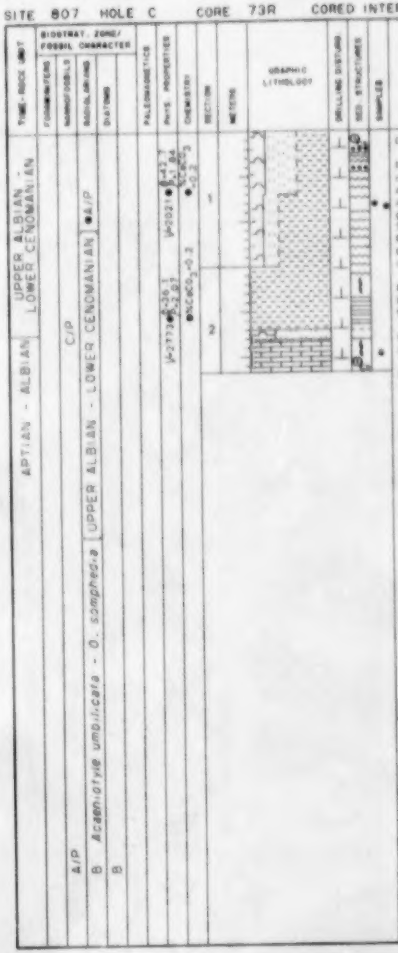
TIME-ROCK UNIT
BIOSTRAT. ZONE/ FOSSIL CHARACTER
FORAMINIFERS
NANNOFOSSILS
RADIOLARIANS
DIATOMS
PALEOMAGNETICS
PHYS. PROPERTIES
CHEMISTRY
SECTION
METERS
GRAPHIC LITHOLOGY
DRILLING DISTURB.
SED. STRUCTURES
SAMPLES
UPPER ALBIAN - LOWER CENOMANIAN
APTIAN - ALBIAN
C/P
A/P
UPPER ALBIAN - LOWER CENOMANIAN ●A/P
B Acaeniotyle umbilicata - O. somphedia
B
1
2
●%CaCO3=0.2

LITHOLOGIC DESCRIPTION

CLAYSTONE and RADIOLARIAN SANDY SILTSTONE overlying LIMESTONE

Major lithology: Approximately 60% of this core is very dark gray (10YR 3/1) CLAYSTONE. It is interbedded on a 2 mm to 2 cm scale with grayish brown (10YR 5/2) to gray (10YR 6/1) and light brownish gray (10YR 6/2) RADIOLARIAN SANDY SILTSTONE, which comprises about 35% of the core. The contacts between the two sediment types are mostly gradational but sharp contacts are also common. Graded bedding is seen in upper part of Section 1. Wavy interfaces are common, and not all layers are continuous across the core. No clear evidence of scouring or load structures was found. Very dark gray (10YR 3/1) and brown (7.5YR 5/4) burrows occur in Section 2 between 27 and 34 cm. Flattened burrows can be discerned in some of the laminated sequences.

Minor lithology: Below Section 2, 82 cm, the core is moderately bioturbated gray (10YR 6/1) LIMESTONE. Steeply dipping, very fine anastomosing fractures are seen below Section 2, 98 cm.

Black (2.5YR 2.5/0) cm scale CHERT nodules are seen in Section 1, 10 cm and in Section 2, 105 cm.

SMEAR SLIDE SUMMARY (%):

	1, 81 D	1, 83 D	2, 98 D
TEXTURE:			
Sand	2	35	—
Silt	20	60	30
Clay	78	5	70
COMPOSITION:			
Accessory minerals	—	—	3
Carbonate grains	—	—	96
Chert	—	2	—
Clay	93	5	—
Glass	1	—	Tr
Nannofossils	—	—	1
Oxide	5	—	—
Radiolarians	1	35	—
Siliceous fragments	—	58	—

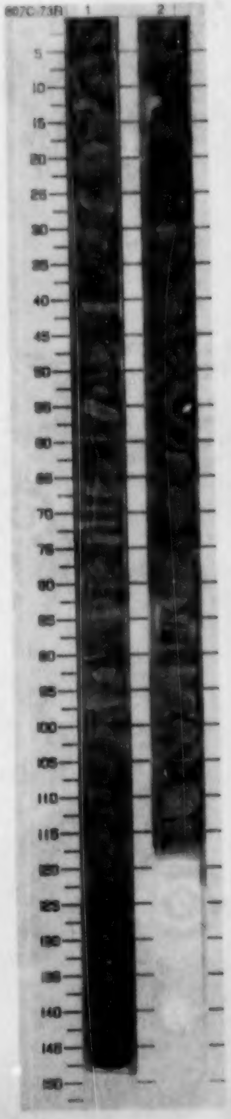
807C-73R
1
2
5
10
15
20
25
30
35
40
45
50
55
60
65
70
75
80
85
90
95
100
105
110
115
120
125
130
135
140
145
150

SITE 807 HOLE C CORE 74R CORED INTERVAL 1375.4-1385.2 mbsf

TIME-ROCK UNIT	BIOSTRAT. ZONE/ FOSSIL CHARACTER FORAMINIFERS	NANNOFOSSILS	RADIOLARIANS	DIATOMS	PALEOMAGNETICS	PHYS. PROPERTIES	CHEMISTRY	SECTION	METERS	GRAPHIC LITHOLOGY	DRILLING DISTURB.	SED. STRUCTURES	SAMPLES	LITHOLOGIC DESCRIPTION
APTIAN - ALBIAN		A/P	R/P APTIAN - CENOMANIAN ?	R ?				1 2 3 4 CC	0.5 1.0	BASALT			●	LIMESTONE AND CHERT

LIMESTONE AND CHERT

Major lithology: This core contains 25 cm of moderately fragmented, dark gray (N5) CHERT and dark grayish brown (10YR 4/2) to light gray (10YR 7/2) LIMESTONE. The chert contains limestone inclusions, brecciated fragments, and external coatings, and appears to have formed post depositionally as nodules. The limestone exhibits pervasive flaser structures on a scale of 5 mm to 3 cm. The largest piece of limestone, which is located at Section 1, 19-25 cm, contains three major microfaults and abundant healed tensional cracks.

SMEAR SLIDE SUMMARY (%):

	1, 14
	D
TEXTURE:	
Silt	50
Clay	50
COMPOSITION:	
Carbonate grains	92
Chert	2
Glass	1
Nannofossils	5

807 C 75R HARD ROCK

807 C 76R HARD ROCK

807 C 77R HARD ROCK

807 C 78R HARD ROCK

807 C 79R HARD ROCK

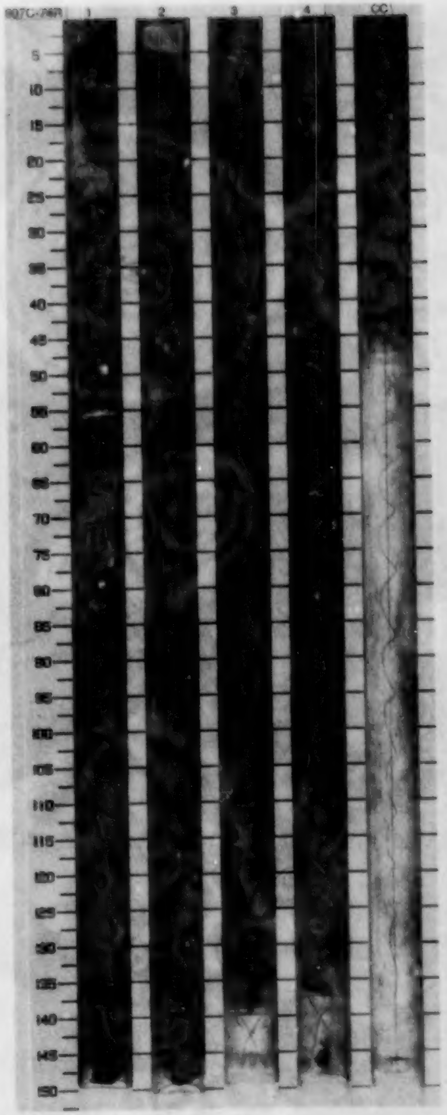

SITE 807 HOLE C CORE 80R CORED INTERVAL 1423.9-1433.6 mbsf

TIME-ROCK UNIT	BIOSTRAT. ZONE/ FOSSIL CHARACTER: FORAMINIFERS	NANNOFOSSILS	RADIOLARIANS	DIATOMS	PALEOMAGNETICS	PHYS. PROPERTIES	CHEMISTRY	SECTION	METERS	GRAPHIC LITHOLOGY	DRILLING DISTURB.	SED. STRUCTURES	SAMPLES	LITHOLOGIC DESCRIPTION
LOWER CRETACEOUS								1 2 3 4	0.5 1.0	BASALT BASALT			● ●	see below

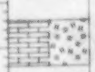

LIMESTONE and CLAYEY VITRIC TUFF with OXIDES

Major lithology: Brecciated pieces of LIMESTONE interbedded with CLAYEY VITRIC TUFF with OXIDES comprise the material in Section 1, 70-120 cm. The limestone is white (10YR 8/1 to 10YR 8/2) and contains angular fragments and clasts of vitric tuff and basaltic glass. Rounded fragments of altered vitric tuff, 1 to 2 mm thick concentrations of carbonate, and lensoid concentrations of sand-sized grains, including vitric tuff and basaltic clasts, are also observed. Some pieces have fracture fills of sparry calcite. The clayey vitric tuff is dark reddish brown (5YR 3/3) to reddish brown (5YR 4/3). The clays are probably smectite. One piece of the tuff contains long, vertical and horizontal, carbonate-filled fractures, up to 1 cm wide, and angular vitric tuff clasts.

SMEAR SLIDE SUMMARY (%):

	1, 80 D	1, 90 D
TEXTURE:		
Silt	80	60
Clay	20	40
COMPOSITION:		
Carbonate grains	100	—
Clay	—	30
Diatoms	Tr	—
Glass	Tr	60
Nannofossils	Tr	—
Oxide	—	10

807 C 81R HARD ROCK

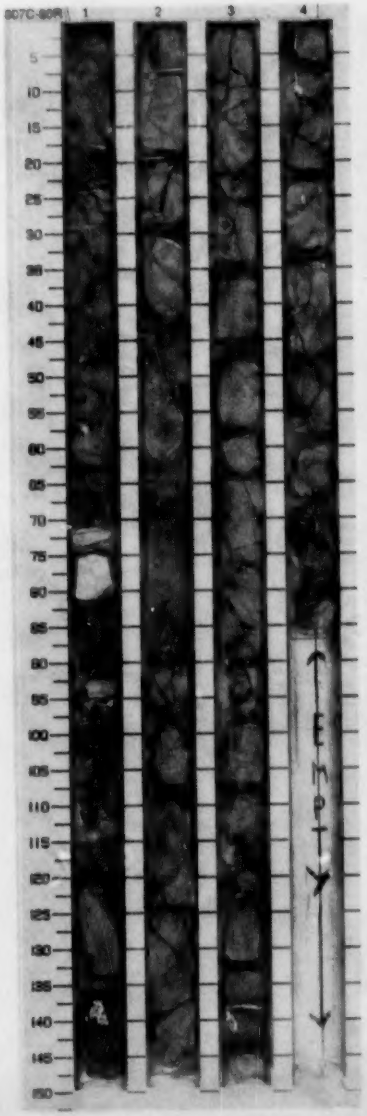

SITE 807 HOLE C CORE 82R CORED INTERVAL 1438.2-1447.2 mbsf

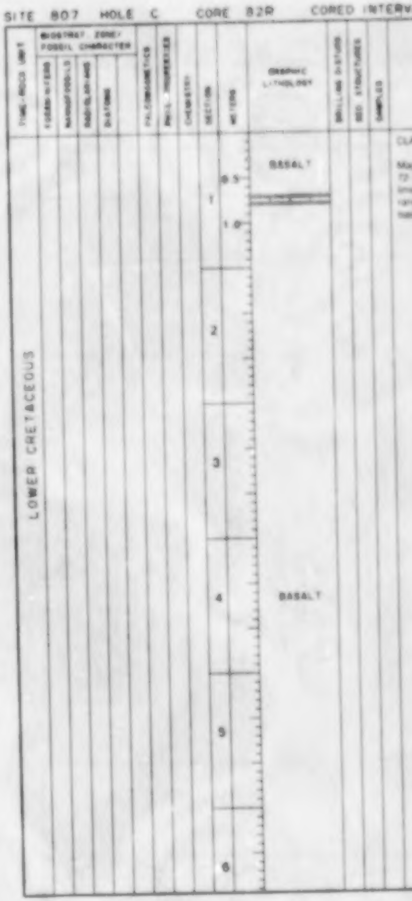
TIME-ROCK UNIT
BIOSTRAT. ZONE/ FOSSIL CHARACTER
FORAMINIFERS
NANNOFOSSILS
RADIOLARIANS
DIATOMS
PALEOMAGNETICS
PHYS. PROPERTIES
CHEMISTRY
SECTION
METERS
GRAPHIC LITHOLOGY
DRILLING DISTURB.
SED. STRUCTURES
SAMPLES
LOWER CRETACEOUS
1
2
3
4
5
6
0.5
1.0
BASALT
BASALT

LITHOLOGIC DESCRIPTION

CLAYEY LIMESTONE

Major lithology: One piece of olive brown CLAYEY LIMESTONE is present in Section 3, 72-79 cm. The clay is probably smectite, and iron oxides are common to abundant. The limestone contains 5-10% grayish green (5G 5/2) clasts that are 2-3 mm in diameter and range in shape from elongate and angular to pelletal. These clasts could be glauconite or basaltic debris.

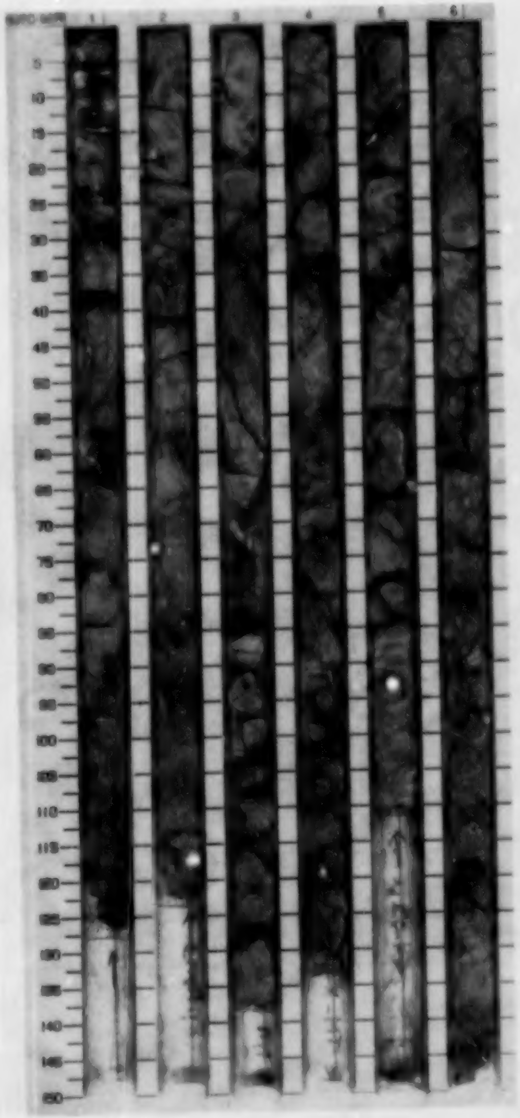
1
2
3
4
5
6
0
5
10
15
20
25
30
35
40
45
50
55
60
65
70
75
80
85
90
95
100
105
110
115
120
125
130
135
140
145
150

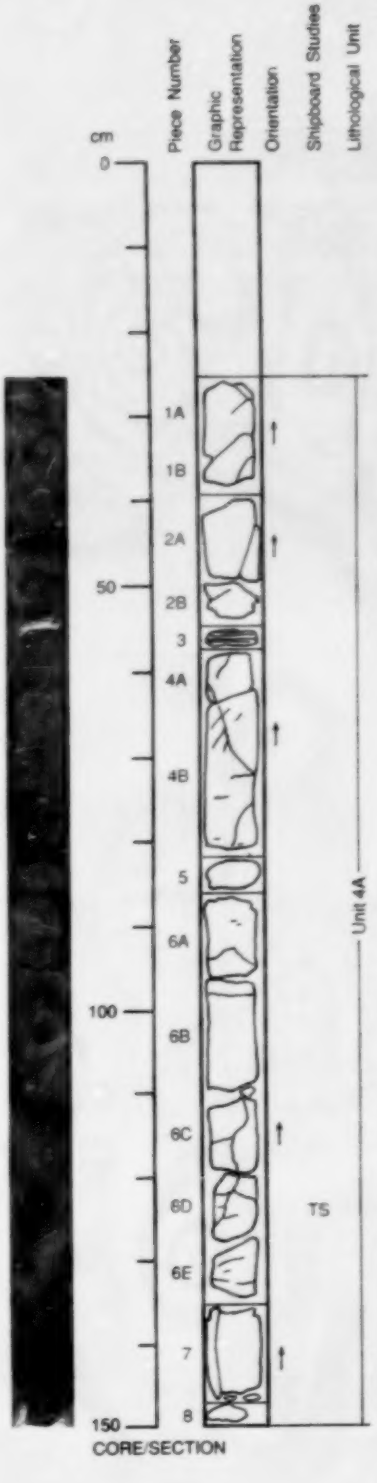

130-807C-74R-1

UNIT 4A: APHYRIC BASALT

Pieces 1, 2

CONTACTS: Pillow margin.
PHENOCRYSTS:
Pyroxene - ~1%; 1 mm; euhedral.
GROUNDMASS: Fine grained.
VESICLES: Nonvesicular.
COLOR: Gray to red-brown.
STRUCTURE: Pillow.
ALTERATION: Highly altered, mottled and banded appearance.
VEINS/FRACTURES: ~1%; 0.5-2 mm; subvertical to subhorizontal; calcite filled.

UNIT 4A: APHYRIC BASALT

Pieces 3, 4

CONTACTS: None.
PHENOCRYSTS:
Plagioclase - <1%; 1-2 mm; subhedral to euhedral.
GROUNDMASS: Fine grained.
VESICLES: Nonvesicular.
COLOR: Gray with red-brown patches.
STRUCTURE: Pillow lava.
ALTERATION: Moderate to high, mottled appearance near top.
VEINS/FRACTURES: 2-3%; 0.2-2 mm; subvertical to subhorizontal; brown and green clay vein filling, blue-green mineral present.
ADDITIONAL COMMENTS: Piece 3 is an inter-pillow breccia consisting of green altered glass (celadonite?) and calcite.

UNIT 4A: APHYRIC BASALT

Piece 5

CONTACTS: None.
PHENOCRYSTS: Aphyric.
GROUNDMASS: Fine grained.
VESICLES: Nonvesicular.
COLOR: Gray.
STRUCTURE: Pillow lava.
ALTERATION: Moderate to high.
VEINS/FRACTURES: ~1%; 0.2-1 mm; varied orientations; calcite.

UNIT 4A: APHYRIC BASALT

Piece 6

CONTACTS: None.
PHENOCRYSTS: Piece 6D contains 5 mm aggregate of plagioclase phenocrysts.
Plagioclase - <1%; 1-3 mm; euhedral.
GROUNDMASS: Fine grained to glassy.
VESICLES: Nonvesicular.
COLOR: Medium to dark gray.
STRUCTURE: Pillow lava.
ALTERATION: Slight to high.
VEINS/FRACTURES: ~3%; 0.5-1 mm; subvertical to subhorizontal; calcite, green and brown clay.

UNIT 4A: APHYRIC BASALT

Pieces 7, 8

CONTACTS: None.
PHENOCRYSTS: Aphyric.
GROUNDMASS: Fine grained.
VESICLES: Nonvesicular.
COLOR: Gray.
STRUCTURE: None.
ALTERATION: Moderate.
VEINS/FRACTURES: <1%; 0.2-1 mm; subvertical; calcite.

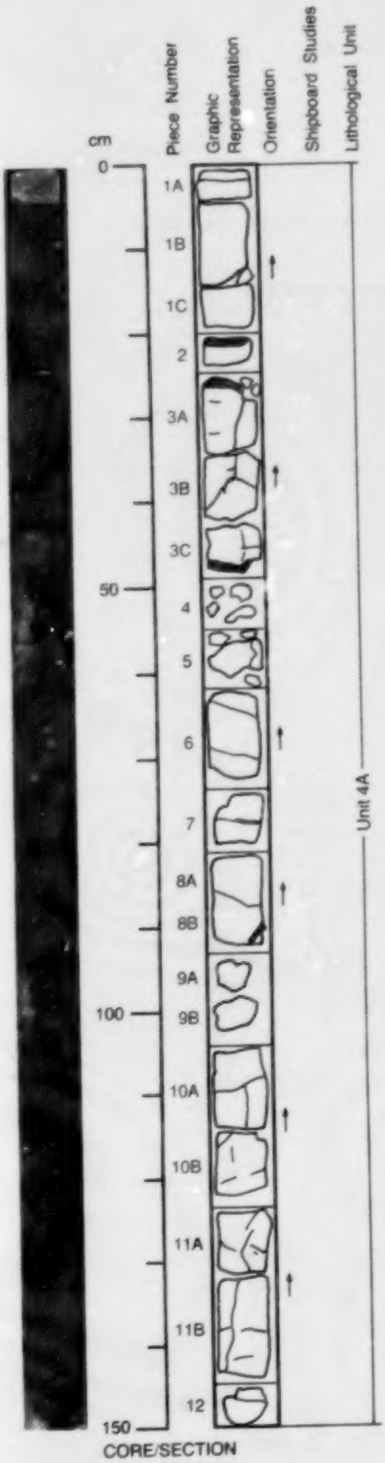
cm
Piece Number
Graphic Representation
Orientation
Shipboard Studies
Lithological Unit
0
50
100
150
1A
1B
1C
2
3A
3B
3C
4
5
6
7
8A
8B
9A
9B
10A
10B
11A
11B
12
Unit 4A
CORE/SECTION

130-807C-74R-2

UNIT 4A: APHYRIC BASALT

Pieces 1-3

CONTACTS: None.
PHENOCRYSTS: Aphyric.
GROUNDMASS: Fine grained with glass margins.
VESICLES: Nonvesicular.
COLOR: Dark gray to medium gray.
STRUCTURE: Pillow lava.
ALTERATION: Slightly altered near margin to moderately altered interior.
VEINS/FRACTURES: <1%; 0.5-2 mm; subvertical and subhorizontal; calcite filled with minor clays and/or iron oxides.
ADDITIONAL COMMENTS: Piece 1A is a banded limestone vein filling. The upper 1-1.5 cm contains a green mineral (epidote?). It shows a sharp contact with a light brownish band (~2.5 cm thick), very fine grained at top, coarser (~1 mm grain size) at bottom.

UNIT 4A: APHYRIC BASALT

Pieces 4-8

CONTACTS: None.
PHENOCRYSTS: Aphyric.
GROUNDMASS: Fine grained to glassy at margins.
VESICLES: Nonvesicular.
COLOR: Dark to medium gray with blotchy appearance in interior.
STRUCTURE: Pillow lava.
ALTERATION: Slight to moderate, some brown-red Fe-oxide staining.
VEINS/FRACTURES: <1%; 1-2 mm; several at 30°-45°; calcite and brown clay and/or Fe-oxides; glass altered to celadonite (?) and brown clay.

UNIT 4A: APHYRIC BASALT

Pieces 9-12

CONTACTS: None.
PHENOCRYSTS:
Plagioclase - <1%; 3 mm; very rare subhedral laths.
GROUNDMASS: Fine grained to glassy at margins.
VESICLES: Nonvesicular.
COLOR: Medium gray to dark gray.
STRUCTURE: Pillow lava.
ALTERATION: Slight to moderate, blotchy alteration in Piece 10A.
VEINS/FRACTURES: <1%; 0.5-2 mm; near vertical; calcite filled, small amounts of green mineral and dark brown Fe-oxides and/or clay.

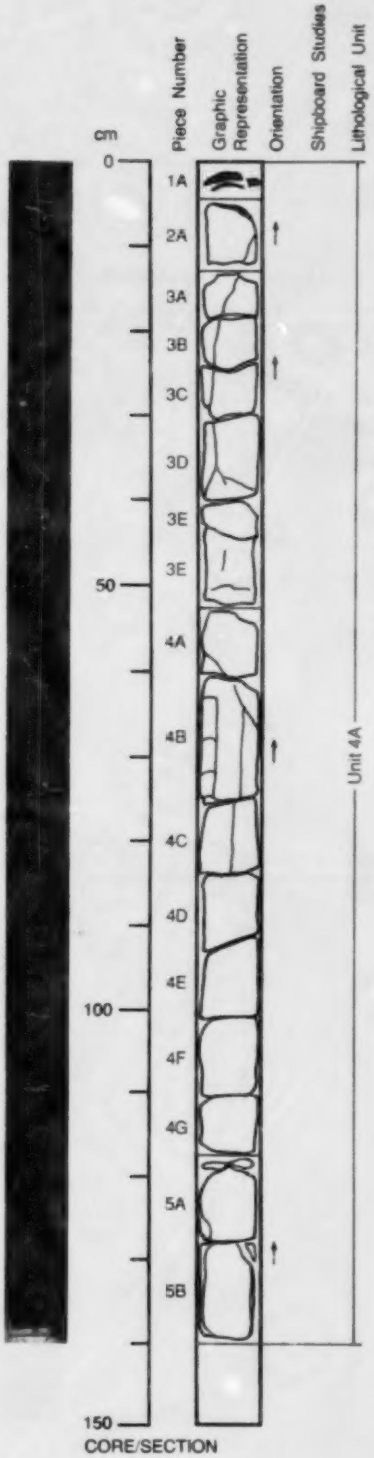
cm
Piece Number
Graphic Representation
Orientation
Shipboard Studies
Lithological Unit
0
50
100
150
1A
2A
3A
3B
3C
3D
3E
3E
4A
4B
4C
4D
4E
4F
4G
5A
5B
Unit 4A
CORE/SECTION

130-807C-74R-3

UNIT 4A: APHYRIC BASALT

Pieces 1-5

CONTACTS: Top of pillow.
PHENOCRYSTS: Aphyric.
GROUNDMASS: Fine grained with glassy top margin, coarsening towards bottom.
VESICLES: Nonvesicular.
COLOR: Medium to dark gray.
STRUCTURE: Pillow top, massive, interior.
ALTERATION: Slight to moderate, staining near vertical fractures.
VEINS/FRACTURES: <1%; 1-3 mm; vertical and at ~ 60°; calcite and olive green mineral.

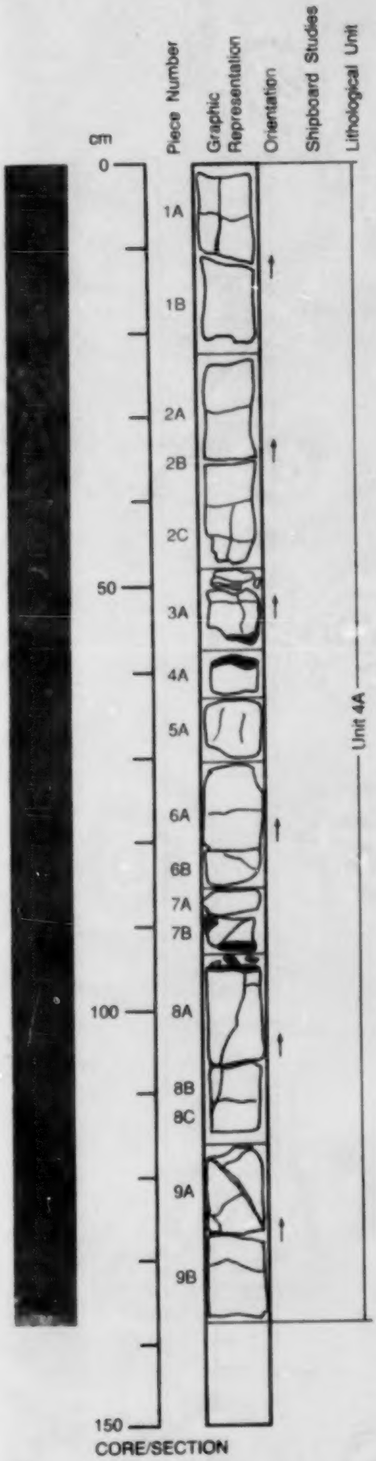
cm
Piece Number
Graphic Representation
Orientation
Shipboard Studies
Lithological Unit
0
1A
1B
2A
2B
2C
50
3A
4A
5A
6A
6B
7A
7B
100
8A
8B
8C
9A
9B
150
Unit 4A
CORE/SECTION

130-807C-74R-4

UNIT 4A: APHYRIC BASALT

Pieces 1-3

CONTACTS: None.
PHENOCRYSTS: Aphyric.
GROUNDMASS: Fine grained with glassy margin at bottom.
VESICLES: Nonvesicular.
COLOR: Dark gray.
STRUCTURE: Massive top, chilled bottom.
ALTERATION: Slight to moderate, gray staining near veins.
VEINS/FRACTURES: <1%; 0.5-5 mm; mostly subhorizontal; calcite, celadonite (?), brown clay and/or Fe-oxides.

UNIT 4A: APHYRIC BASALT

Pieces 4-7

CONTACTS: None.
PHENOCRYSTS: Aphyric.
GROUNDMASS: Fine grained with glassy margins.
VESICLES: Nonvesicular.
COLOR: Medium gray.
STRUCTURE: Pillow lava.
ALTERATION: Slight to moderate.
VEINS/FRACTURES: <1%; up to 2 mm; subvertical to subhorizontal; calcite.

UNIT 4A: APHYRIC BASALT

Pieces 8, 9

CONTACTS: None.
PHENOCRYSTS:
Plagioclase - <1%; up to 3 mm; euhedral laths.
GROUNDMASS: Fine grained, glassy top.
VESICLES: Nonvesicular.
COLOR: Medium gray.
STRUCTURE: Pillow to massive.
ALTERATION: Slight to moderate.
VEINS/FRACTURES: <1%; 2-3 mm; subvertical to 45°; calcite.

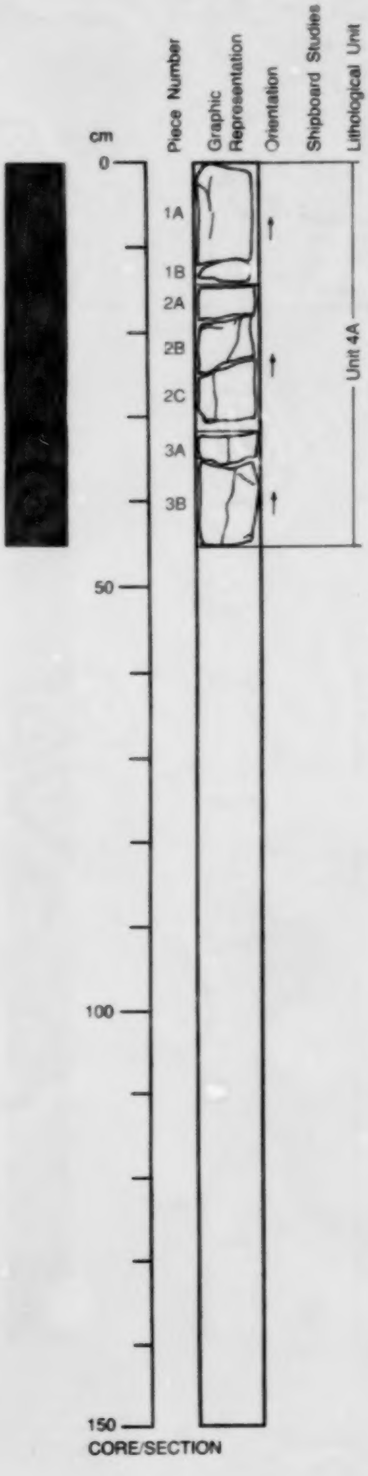
cm
Piece Number
Graphic Representation
Orientation
Shipboard Studies
Lithological Unit
0
1A
1B
2A
2B
2C
3A
3B
Unit 4A
50
100
150
CORE/SECTION

130-807C-74R-5

UNIT 4A: APHYRIC BASALT

Pieces 1-3

CONTACTS: None.
PHENOCRYSTS:
Plagioclase - <1%; 2 mm; euhedral laths.
GROUNDMASS: Fine grained.
VESICLES: Nonvesicular.
COLOR: Medium gray.
STRUCTURE: Massive.
ALTERATION: Slight.
VEINS/FRACTURES: <1%; ~0.5 mm; subvertical; calcite

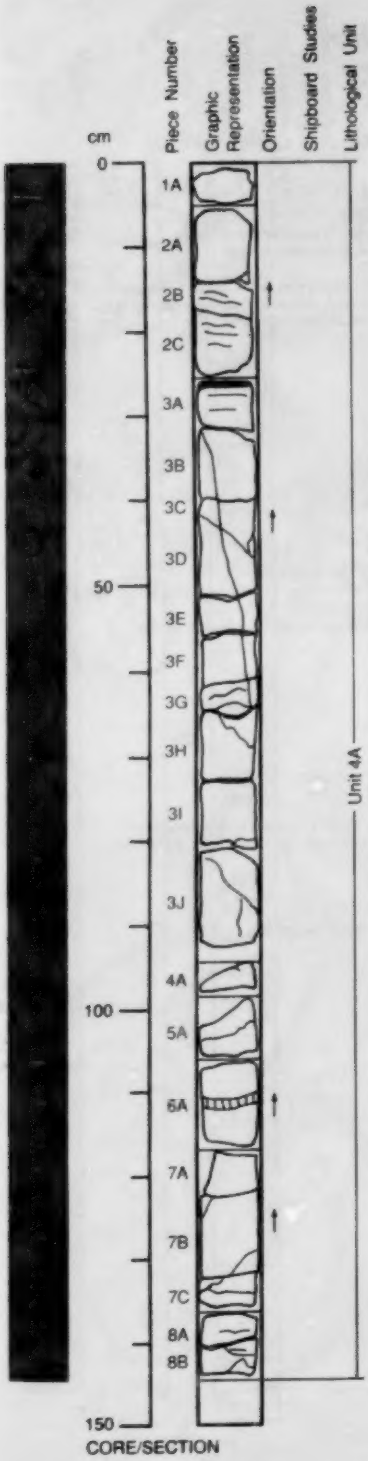
cm
Piece Number
Graphic Representation
Orientation
Shipboard Studies
Lithological Unit
0
50
100
150
1A
2A
2B
2C
3A
3B
3C
3D
3E
3F
3G
3H
3I
3J
4A
5A
6A
7A
7B
7C
8A
8B
Unit 4A
CORE/SECTION

130-807C-75R-1

UNIT 4A: APHYRIC BASALT

Pieces 1, 2

CONTACTS: None.
PHENOCRYSTS: Aphyric.
GROUNDMASS: Fine grained, horizontal flow banding in Pieces 2B and 2C.
VESICLES: Nonvesicular.
COLOR: Medium gray.
STRUCTURE: Massive.
ALTERATION: Slight to moderate.
VEINS/FRACTURES: <1%; <0.5 mm; irregular; calcite, clay and or Fe-oxides.

UNIT 4A: APHYRIC BASALT

Pieces 3-8

CONTACTS: None.
PHENOCRYSTS: Aphyric.
GROUNDMASS: Glassy at top of Piece 3, otherwise fine grained.
VESICLES: Nonvesicular.
COLOR: Medium gray.
STRUCTURE: Massive.
ALTERATION: Slight to moderate.
VEINS/FRACTURES: <1%; ~1-2 mm; subhorizontal to subvertical; calcite with minor clay and chlorite (?).

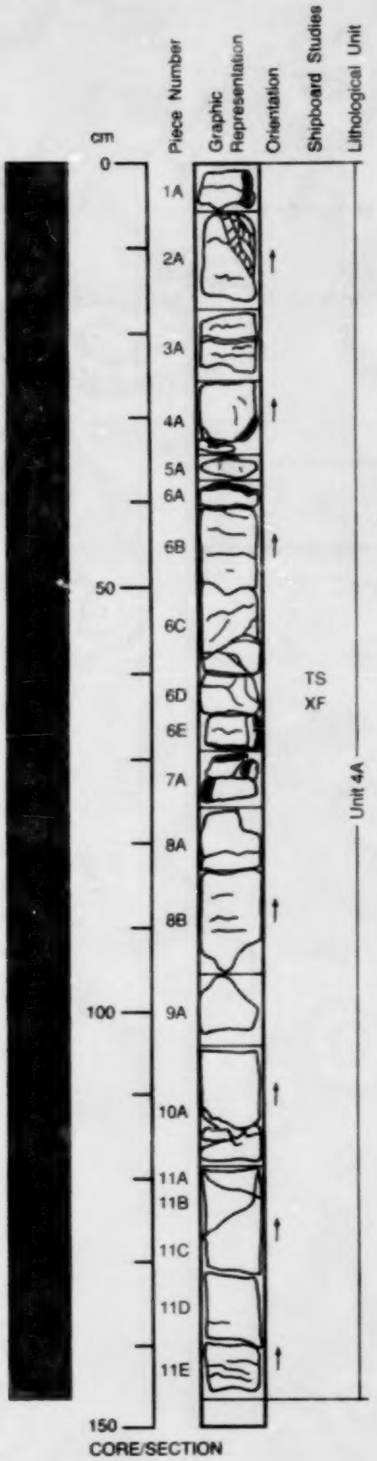
cm
Piece Number
Graphic Representation
Orientation
Shipboard Studies
Lithological Unit
0
50
100
150
1A
2A
3A
4A
5A
6A
6B
6C
6D
6E
7A
8A
8B
9A
10A
11A
11B
11C
11D
11E
TS
XF
Unit 4A
CORE/SECTION

130-807C-75R-2

UNIT 4A: APHYRIC BASALT

Pieces 1-4

CONTACTS: None.
PHENOCRYSTS: Aphyric.
GROUNDMASS: Fine grained to glassy at margins.
VESICLES: Piece 3 contains 3 mm calcite, chlorite (?) and clays filled vesicle.
COLOR: Medium gray with slight brown-red staining in a few patches.
STRUCTURE: Pillow.
ALTERATION: Moderate; glass altered to bright blue-green and dark green minerals.
VEINS/FRACTURES: <1%; 0.5-1 mm; subhorizontal; calcite and dark green and brown clays and/or Fe-oxides; Piece 2 has 5 mm calcite vein in glass.

UNIT 4A: APHYRIC BASALT

Pieces 5, 6

CONTACTS: None.
PHENOCRYSTS:
Plagioclase - <1%; ~1 mm; euhedral.
GROUNDMASS: Fine grained, glass at margins.
VESICLES: Nonvesicular.
COLOR: Medium gray.
STRUCTURE: Pillow.
ALTERATION: Slight to moderate, freshest near glassy margins.
VEINS/FRACTURES: <1%; 0.5- 1 mm; various; brown clay or Fe-oxide, dark blue-green clay; one vug filled with olive-green mineral (epidote?).
ADDITIONAL COMMENTS: Piece 5 is inter-pillow calcite with a greenish mineral (chlorite?, smectite?).

UNIT 4A: APHYRIC BASALT

Pieces 7-11

CONTACTS: None.
PHENOCRYSTS:
Plagioclase - <<1%; ~ 1; euhedral.
GROUNDMASS: Fine grained near glassy top of Piece 7; coarser in interior of flow.
VESICLES: Nonvesicular, but one ~5 mm amygdule filled with calcite, dark green clay and olive-green mineral (epidote?).
COLOR: Medium gray.
STRUCTURE: Massive.
ALTERATION: Moderate.
VEINS/FRACTURES: <1%; 0.5-2 mm; subhorizontal; green clay.

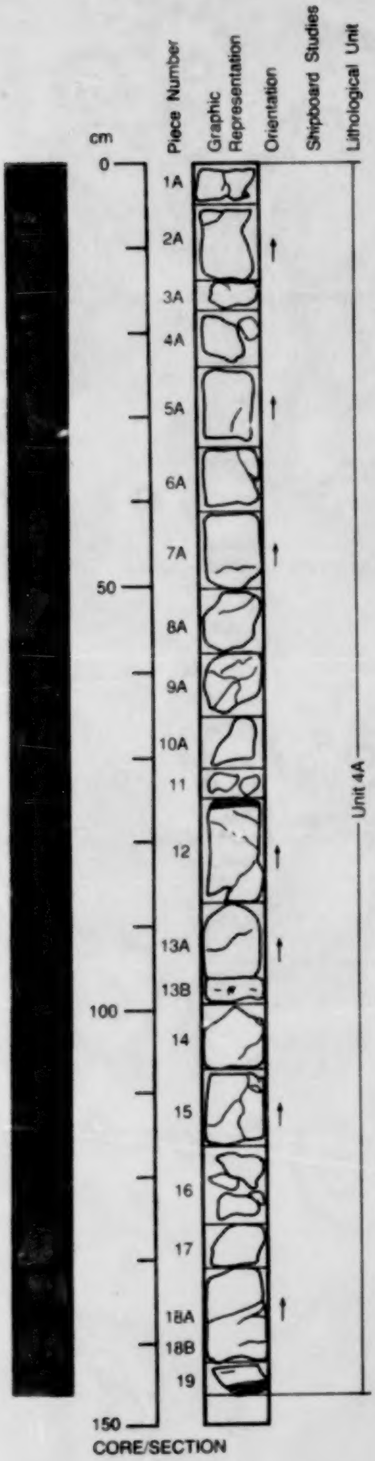
cm
Piece Number
Graphic Representation
Orientation
Shipboard Studies
Lithological Unit
0
50
100
150
1A
2A
3A
4A
5A
6A
7A
8A
9A
10A
11
12
13A
13B
14
15
16
17
18A
18B
19
Unit 4A
CORE/SECTION

130-807C-75R-3

UNIT 4A: APHYRIC BASALT

Pieces 1-3

CONTACTS: None.
PHENOCRYSTS: Aphyric.
GROUNDMASS: Fine grained.
VESICLES: Nonvesicular.
COLOR: Medium gray with green and brown blotches.
STRUCTURE: Pillow?
ALTERATION: Moderate to high.
VEINS/FRACTURES: <1%; up to 5 mm; varied orientation; calcite and minor dark green mineral.

UNIT 4A: APHYRIC BASALT

Pieces 4-11

CONTACTS: None.
PHENOCRYSTS:
Plagioclase - <<1%; ~1 mm; cluster of euhedral laths.
GROUNDMASS: Fine grained.
VESICLES: Nonvesicular.
COLOR: Medium to dark gray, mottled in places.
STRUCTURE: Massive.
ALTERATION: Moderate.
VEINS/FRACTURES: <1%; ~0.5 mm; varied orientation; calcite with lesser brown clay and/or Fe-oxides.

UNIT 4A: APHYRIC BASALT

Pieces 12-19

CONTACTS: None.
PHENOCRYSTS:
Plagioclase - <1%; 1-3 mm; euhedral.
GROUNDMASS: Fine grained with glassy top and bottom.
VESICLES: Nonvesicular.
COLOR: Medium gray.
STRUCTURE: Pillow to massive.
ALTERATION: Slight to moderate.
VEINS/FRACTURES: <1%; 0.5-1 mm; varied orientation; calcite and minor green clay.

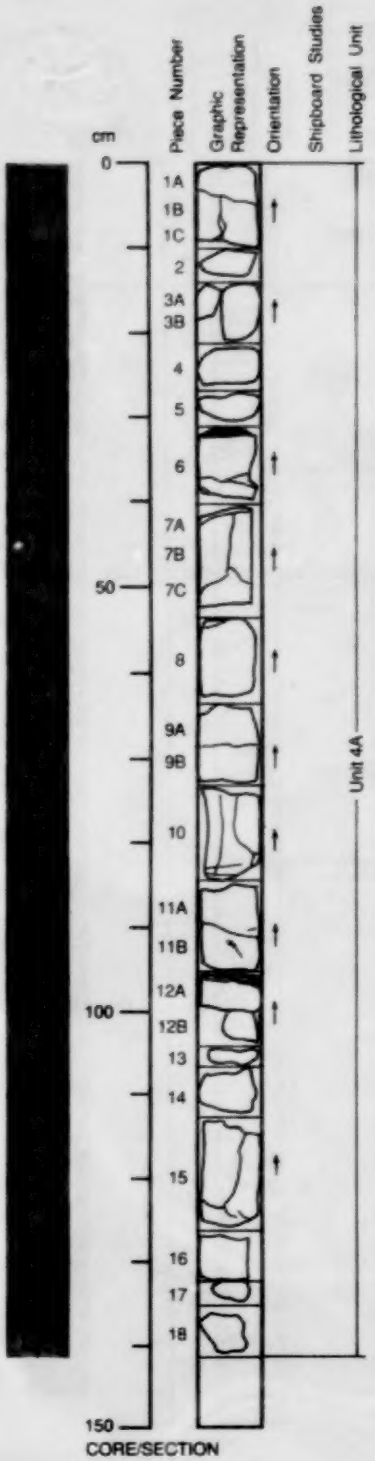
cm
Piece Number
Graphic Representation
Orientation
Shipboard Studies
Lithological Unit
0
50
100
150
1A
1B
1C
2
3A
3B
4
5
6
7A
7B
7C
8
9A
9B
10
11A
11B
12A
12B
13
14
15
16
17
18
Unit 4A
CORE/SECTION

130-807C-75R-4

UNIT 4A: APHYRIC BASALT

Pieces 1-5

CONTACTS: None.
PHENOCRYSTS: Aphyric.
GROUNDMASS: Fine grained.
VESICLES: Nonvesicular.
COLOR: Medium gray.
STRUCTURE: Massive.
ALTERATION: Slight to moderate.
VEINS/FRACTURES: <<1%; 0.5 mm; vertical; calcite, brown clay and/or Fe oxide.

UNIT 4A: APHYRIC BASALT

Pieces 6-11

CONTACTS: None.
PHENOCRYSTS: Very rare.
Plagioclase - <<1%; 1-2 by 0.5-1 mm; euhedral.
GROUNDMASS: Fine grained, glassy at top of Piece 6.
VESICLES: Nonvesicular.
COLOR: Medium gray.
STRUCTURE: Pillow lava.
ALTERATION: Slight to moderate.
VEINS/FRACTURES: <1%; 0.5-1 mm; subvertical to subhorizontal; calcite veins.

UNIT 4A: APHYRIC BASALT

Pieces 12-18

CONTACTS: None.
PHENOCRYSTS: Very rare.
Plagioclase - <<1%; 1-2 by 0.5 mm; euhedral.
GROUNDMASS: Fine grained, glassy at top of Piece 12.
VESICLES: Nonvesicular.
COLOR: Medium to dark gray, mottled in upper part.
STRUCTURE: Massive.
ALTERATION: Slight to moderate, some blotchy alteration.
VEINS/FRACTURES: <<1%; 0.5-1 mm; varied orientation; calcite and clay filled.

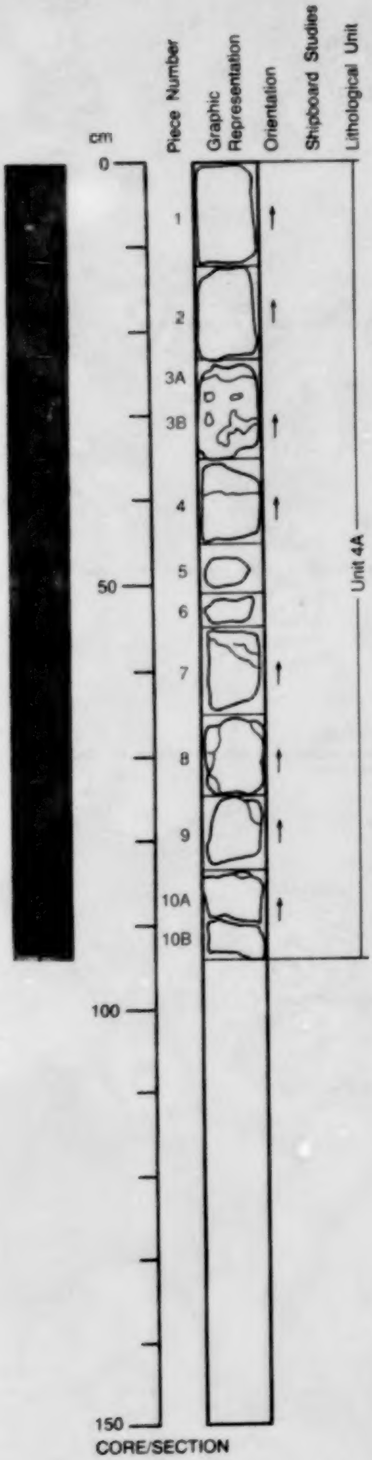
cm
Piece Number
Graphic Representation
Orientation
Shipboard Studies
Lithological Unit
0
50
100
150
1
2
3A
3B
4
5
6
7
8
9
10A
10B
Unit 4A
CORE/SECTION

130-807C-75R-5

UNIT 4A: APHYRIC BASALT

Pieces 1-10

CONTACTS: None.
PHENOCRYSTS: Rare.
Plagioclase - <<1%; 1-2 by 4 - 2 mm; euhedral to subhedral.
GROUNDMASS: Fine grained.
VESICLES: Irregular amygdules filled with calcite and green clay in Pieces 3 and 4.
COLOR: Medium gray.
STRUCTURE: Massive.
ALTERATION: Slight to moderate.
VEINS/FRACTURES: <<1%; 0.5 mm; subhorizontal; calcite and light green clay.

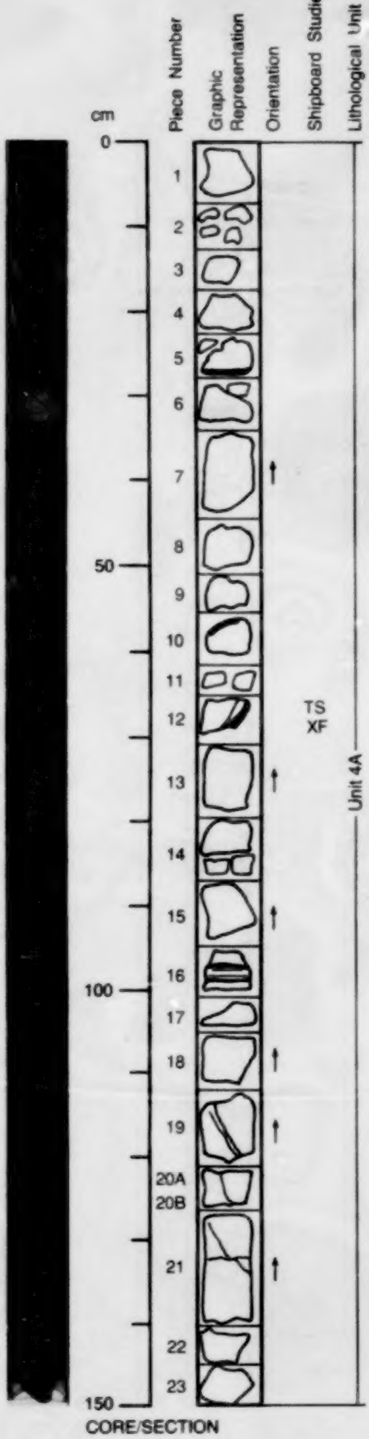
cm
Piece Number
Graphic Representation
Orientation
Shipboard Studies
Lithological Unit
0
50
100
150
1
2
3
4
5
6
7
8
9
10
11
12
13
14
15
16
17
18
19
20A
20B
21
22
23
TS
XF
Unit 4A
CORE/SECTION

130-807C-76R-1

UNIT 4A: APHYRIC BASALT

Pieces 1-5

CONTACTS: None.
PHENOCRYSTS: Sparse.
Plagioclase - <<1%; 2 mm; subhedral.
GROUNDMASS: Fine grained.
VESICLES: Nonvesicular.
COLOR: Medium gray.
STRUCTURE: Pillow lava.
ALTERATION: Moderate, slightly blotchy.
VEINS/FRACTURES: <<1%; 0.5 mm; varied orientation; calcite and clay filled.

UNIT 4A: APHYRIC BASALT

Pieces 6-9

CONTACTS: None.
PHENOCRYSTS: Aphyric.
GROUNDMASS: Fine grained.
VESICLES: Nonvesicular.
COLOR: Medium gray.
STRUCTURE: Pillow lava.
ALTERATION: Moderate.
VEINS/FRACTURES: <<1%; 0.5-1 mm; varied orientation; calcite, clay and/or Fe-oxide.

UNIT 4A: APHYRIC BASALT

Pieces 10-15

CONTACTS: None.
PHENOCRYSTS: Aphyric.
GROUNDMASS: Fine grained, glassy at top and bottom.
VESICLES: In Pieces 13 and 14 sparse, irregular amygdules (1-5 mm), calcite and clay filled.
COLOR: Medium gray, slight blotchy texture lower down.
STRUCTURE: Pillow lava.
ALTERATION: Slight to moderate.
VEINS/FRACTURES: Sparse, radial fractures.

UNIT 4A: APHYRIC BASALT

Pieces 16-23

CONTACTS: None.
PHENOCRYSTS: Aphyric.
GROUNDMASS: Fine grained, glassy upper margin on Piece 16.
VESICLES: Nonvesicular.
COLOR: Medium gray.
STRUCTURE: Pillow lava.
ALTERATION: Slight to moderate.
VEINS/FRACTURES: Mostly unfractured, a little clay filling.

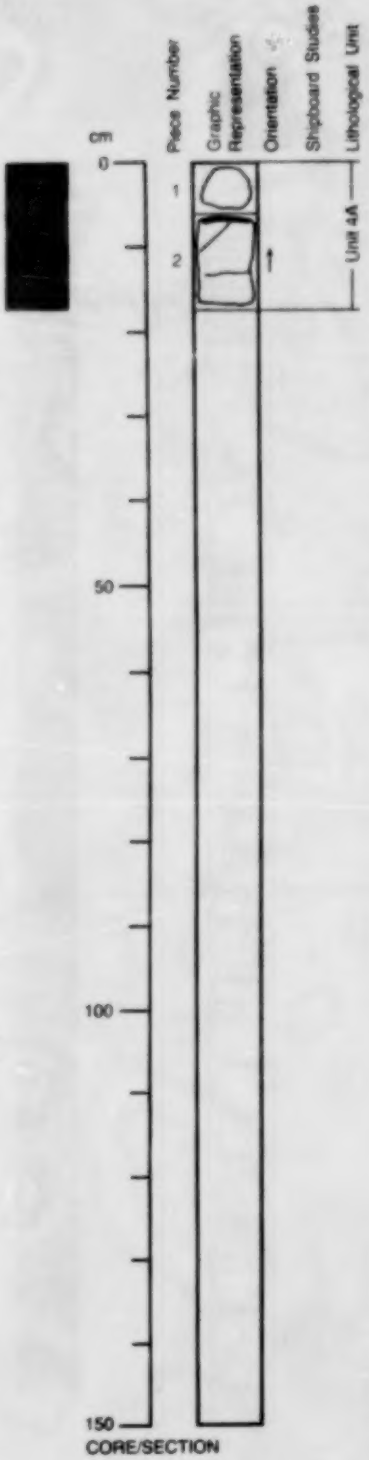
cm
Piece Number
Graphic Representation
Orientation
Shipboard Studies
Lithological Unit
0
1
2
Unit 4A
50
100
150
CORE/SECTION

130-807C-76R-2

UNIT 4A: APHYRIC BASALT

Pieces 1-2

CONTACTS: Glassy on one margin.
PHENOCRYSTS: Aphyric.
GROUNDMASS: Fine grained, glassy margin on Piece 2.
VESICLES: Nonvesicular.
COLOR: Medium gray.
STRUCTURE: Pillow lava fragments.
ALTERATION: Moderate.
VEINS/FRACTURES: <<1%; ~0.5 mm; varied orientation; calcite with some brown and dark green clay.

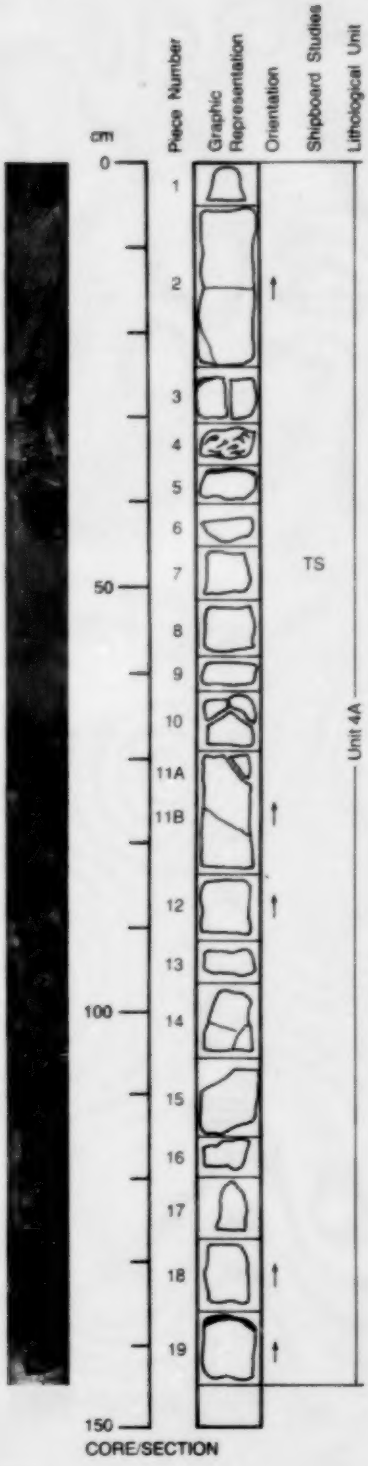
cm
Piece Number
Graphic Representation
Orientation
Shipboard Studies
Lithological Unit
0
50
100
150
1
2
3
4
5
6
7
8
9
10
11A
11B
12
13
14
15
16
17
18
19
TS
Unit 4A
CORE/SECTION

130-807C-77R-1

UNIT 4A: APHYRIC BASALT

Pieces 1-3

CONTACTS: None.
PHENOCRYSTS: Aphyric.
GROUNDMASS: Fine grained.
VESICLES: Nonvesicular.
COLOR: Medium gray.
STRUCTURE: Pillow lava.
ALTERATION: Slight to moderate.
VEINS/FRACTURES: <<1%; 1-2 mm thick; varied orientation; calcite and minor dark green and brown clay.

UNIT 4A: APHYRIC BASALT

Pieces 4-18

CONTACTS: Glass.
PHENOCRYSTS: Very sparse.
Plagioclase - <<1%; ~1 mm; subhedral.
Clinopyroxene - <<1%; ~1 mm; subhedral.
GROUNDMASS: Fine grained, glass at top.
VESICLES: Nonvesicular.
COLOR: Medium to dark gray.
STRUCTURE: Pillow lava.
ALTERATION: Slight to moderate.
VEINS/FRACTURES: <<1%; 0.5-2 mm thick; varied; calcite with minor clay.
ADDITIONAL COMMENTS: Piece 4 is an inter-pillow breccia of glass shards (pillow rim), ~1.5 cm long, moderately fresh to very altered, in calcite matrix.

UNIT 4A: APHYRIC BASALT

Piece 19

CONTACTS: Glass.
PHENOCRYSTS: Aphyric.
GROUNDMASS: Glassy to fine grained.
VESICLES: Nonvesicular.
COLOR: Medium gray.
STRUCTURE: Pillow top.
ALTERATION: Slight.
VEINS/FRACTURES: <<1%; ~0.5 mm thick; varied orientation; calcite with minor clay.

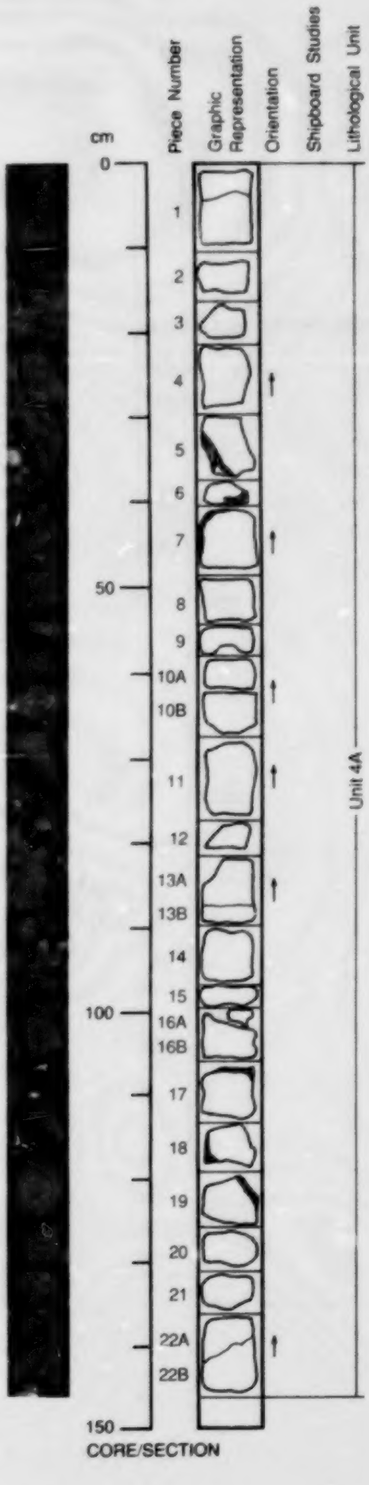
cm
Piece Number
Graphic Representation
Orientation
Shipboard Studies
Lithological Unit
0
50
100
150
1
2
3
4
5
6
7
8
9
10A
10B
11
12
13A
13B
14
15
16A
16B
17
18
19
20
21
22A
22B
Unit 4A
CORE/SECTION

130-807C-77R-2

UNIT 4A: APHYRIC BASALT

Pieces 1-6

CONTACTS: None.
PHENOCRYSTS: Aphyric.
GROUNDMASS: Fine grained to glassy margins (Pieces 5 and 6).
VESICLES: Nonvesicular.
COLOR: Medium gray with brown-green color patches.
STRUCTURE: Pillow lava.
ALTERATION: Slight to moderate.
VEINS/FRACTURES: <<1%; 1-2 mm thick; varied orientation; minor clay and calcite filling.

UNIT 4A: APHYRIC BASALT

Pieces 7-16

CONTACTS: Glass.
PHENOCRYSTS: Aphyric.
GROUNDMASS: Fine grained, glassy rim on Piece 7.
VESICLES: Nonvesicular.
COLOR: Medium to light gray, slight amount of greenish staining.
STRUCTURE: Pillow lava.
ALTERATION: Slight to moderate.
VEINS/FRACTURES: <<1%; <0.5 mm; varied orientation; fractures with minor clay; calcite near glass on Piece 7.

UNIT 4A: APHYRIC BASALT

Pieces 17-22

CONTACTS: Glass.
PHENOCRYSTS: Aphyric.
GROUNDMASS: Fine grained to glassy at the rims.
VESICLES: Nonvesicular.
COLOR: Light to medium gray.
STRUCTURE: Pillow lava.
ALTERATION: Slight to moderate.
VEINS/FRACTURES: <<1%; <0.5 mm; varied orientation; fractures with minor calcite and brown clay; calcite matrix invades glassy rims on Pieces 17, 18, 19.

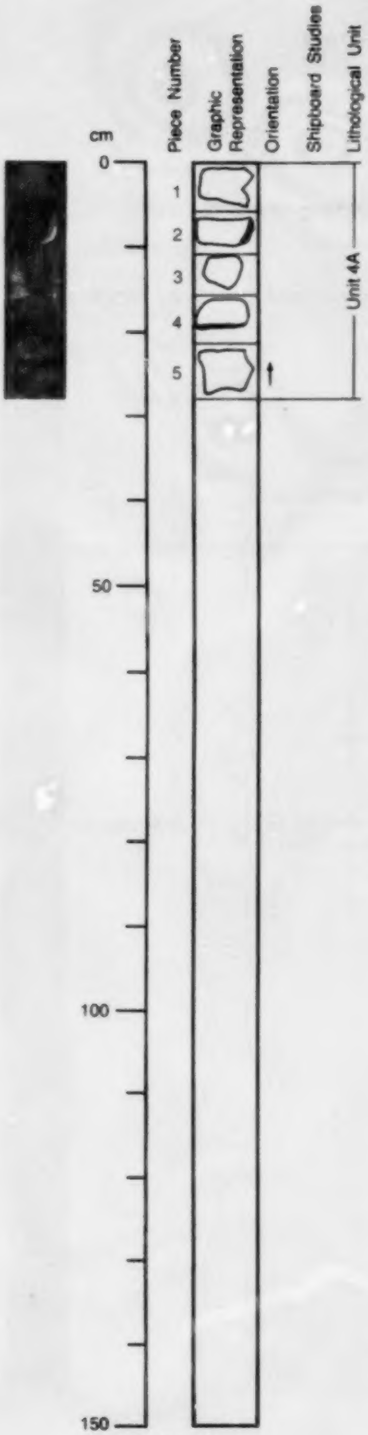
cm
Piece Number
Graphic Representation
Orientation
Shipboard Studies
Lithological Unit
0
1
2
3
4
5
Unit 4A
50
100
150
CORE/SECTION

130-807C-77R-3

UNIT 4A: APHYRIC BASALT

Pieces 1-5

CONTACTS: None.
PHENOCRYSTS: Sparse.
Plagioclase - <1%; 2-3 mm; euhedral.
GROUNDMASS: Glassy to fine grained.
VESICLES: Nonvesicular.
COLOR: Medium to light gray.
STRUCTURE: Pillow.
ALTERATION: Slight to moderate.
VEINS/FRACTURES: <<1%; 0.5 mm or less; varied orientation; calcite veins with minor clay; inter-pillow calcite on glass rim of Piece 2.

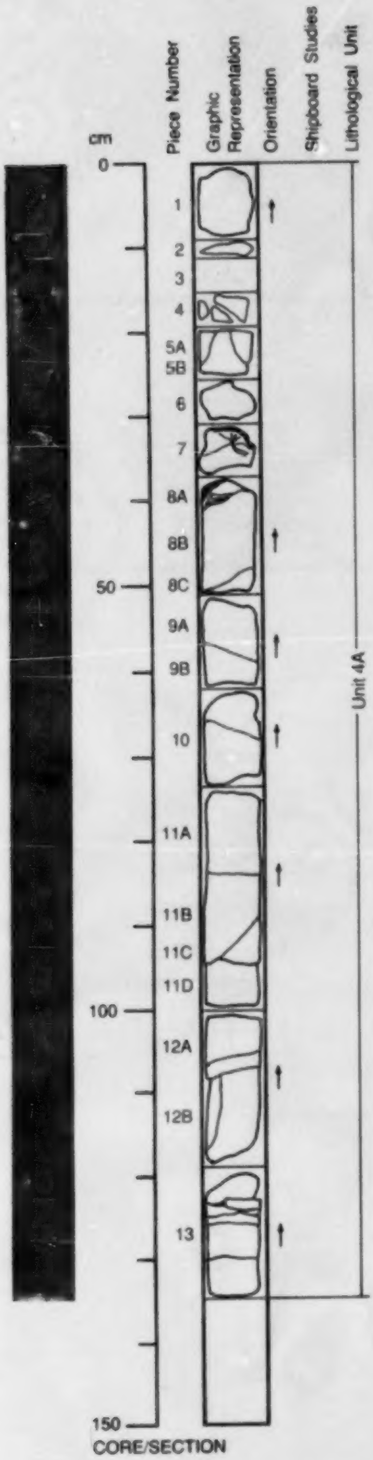
cm
Piece Number
Graphic Representation
Orientation
Shipboard Studies
Lithological Unit
0
50
100
150
1
2
3
4
5A
5B
6
7
8A
8B
8C
9A
9B
10
11A
11B
11C
11D
12A
12B
13
Unit 4A
CORE/SECTION

130-807C-78R-1

UNIT 4A: APHYRIC BASALT

Pieces 1-6

CONTACTS: None.
PHENOCRYSTS: Aphyric.
GROUNDMASS: Fine grained.
VESICLES: Nonvesicular.
COLOR: Medium gray.
STRUCTURE: Thick pillow or massive flow.
ALTERATION: Slight to moderate.
VEINS/FRACTURES: <<1%; <0.5 mm; subvertical.

UNIT 4A: APHYRIC BASALT

Pieces 7-13

CONTACTS: Glass.
PHENOCRYSTS: Very rare.
Plagioclase - <<1%; ~1 mm; subhedral.
GROUNDMASS: Fine grained, glassy at top.
VESICLES: Nonvesicular.
COLOR: Medium gray.
STRUCTURE: Massive.
ALTERATION: Slight to moderate.
VEINS/FRACTURES: <<1%; ~1-3 mm thick; varied orientation; calcite near glassy top, contains minor green clays; fractures sparse, with minor brown clay and/or iron oxide.

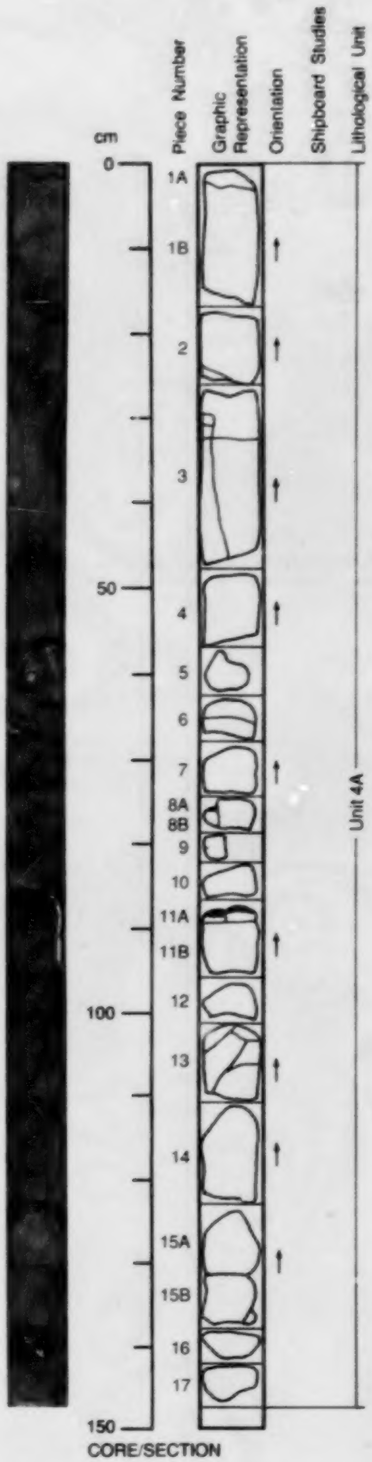
cm
Piece Number
Graphic Representation
Orientation
Shipboard Studies
Lithological Unit
0
50
100
150
1A
1B
2
3
4
5
6
7
8A
8B
9
10
11A
11B
12
13
14
15A
15B
16
17
Unit 4A
CORE/SECTION

130-807C-78R-2

UNITS 4A: APHYRIC BASALT

Pieces 1-10

CONTACTS: None.
PHENOCRYSTS: Aphyric.
GROUNDMASS: Fine grained.
VESICLES: Nonvesicular.
COLOR: Medium gray.
STRUCTURE: Massive.
ALTERATION: Slight to moderate.
VEINS/FRACTURES: <<1%; <0.5 mm; subvertical to subhorizontal; fractures with minor clay.

UNITS 4A: APHYRIC BASALT

Pieces 11-17

CONTACTS: Glass.
PHENOCRYSTS: Aphyric.
GROUNDMASS: Fine grained.
VESICLES: Nonvesicular.
COLOR: Medium gray.
STRUCTURE: Massive.
ALTERATION: Slight.
VEINS/FRACTURES: <<1%; <0.5 mm thick; varied orientation; fractures with minor clay and calcite.

130-807C-78R-3

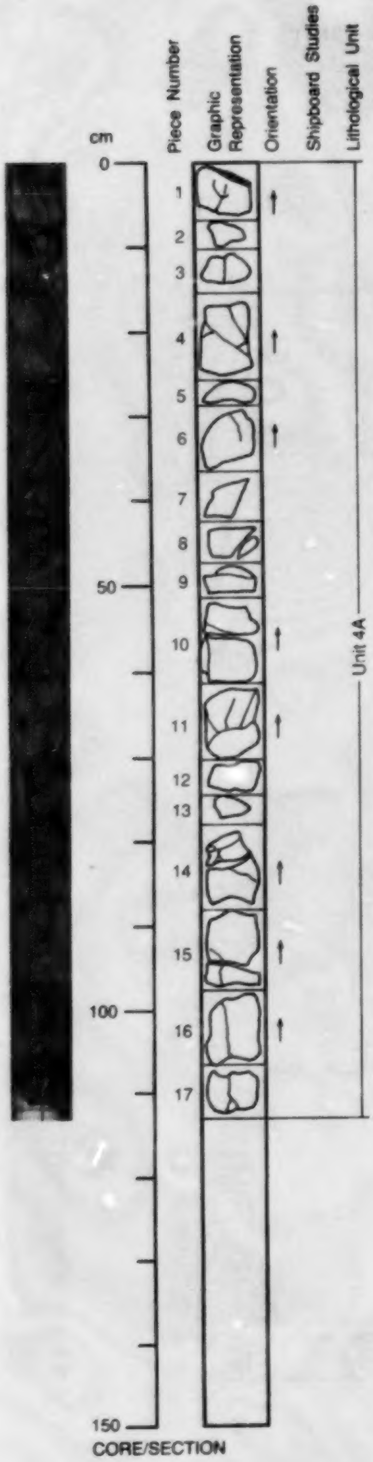
cm
Piece Number
Graphic Representation
Orientation
Shipboard Studies
Lithological Unit
0
50
100
150
1
2
3
4
5
6
7
8
9
10
11
12
13
14
15
16
17
Unit 4A
CORE/SECTION

UNITS 4A: APHYRIC BASALT

Pieces 1-17

CONTACTS: Glass.
PHENOCRYSTS: Very sparse.
Plagioclase - <<1%; ~2 mm across; euhedral.
GROUNDMASS: Fine grained.
VESICLES: Nonvesicular.
COLOR: Light to medium gray
STRUCTURE: Massive with pillow top.
ALTERATION: Slight to moderate.
VEINS/FRACTURES: <<1%; 1-2 mm thick; horizontal and vertical; calcite and clay veins, one horizontal 0.5-mm-thick red-brown Fe-oxide or clay (?) vein.

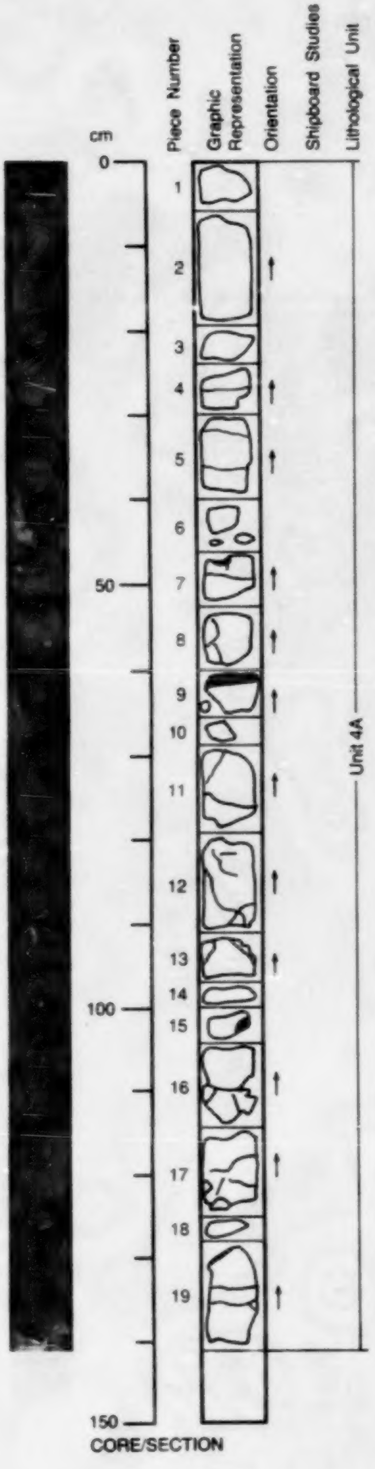
cm
0
50
100
150
Piece Number
Graphic Representation
Orientation
Shipboard Studies
Lithological Unit
1
2
3
4
5
6
7
8
9
10
11
12
13
14
15
16
17
18
19
Unit 4A
CORE/SECTION

130-807C-79R-1

UNIT 4A: APHYRIC BASALT

Pieces 1-6

CONTACTS: None.
PHENOCRYSTS: Aphyric.
GROUNDMASS: Fine grained.
VESICLES: Nonvesicular.
COLOR: Medium gray.
STRUCTURE: Massive.
ALTERATION: Slight.
VEINS/FRACTURES: <<1%; 1-2 mm; varied orientation; calcite.

UNIT 4A: APHYRIC BASALT

Pieces 7,8

CONTACTS: Glass.
PHENOCRYSTS: Aphyric.
GROUNDMASS: Fine grained to glassy (Piece 7).
VESICLES: Nonvesicular.
COLOR: Medium to dark gray.
STRUCTURE: Pillow.
ALTERATION: Slight.
VEINS/FRACTURES: None.

UNIT 4A: APHYRIC BASALT

Pieces 9-14

CONTACTS: Glass.
PHENOCRYSTS: Aphyric.
GROUNDMASS: Fine grained to glassy (Piece 9).
VESICLES: Nonvesicular.
COLOR: Medium to dark gray.
STRUCTURE: Pillow to massive.
ALTERATION: Slight.
VEINS/FRACTURES: 2%; 0.5 - 2 mm; varied orientation; calcite and green and brown clay.

UNIT 4A: APHYRIC BASALT

Pieces 15-17

CONTACTS: Glass.
PHENOCRYSTS: Aphyric.
GROUNDMASS: Fine grained.
VESICLES: Nonvesicular.
COLOR: Light to medium gray.
STRUCTURE: Pillow.
ALTERATION: Moderate.
VEINS/FRACTURES: 2-3%; 1-2 mm; varied orientation; calcite and clay.

UNIT 4A: APHYRIC BASALT

Pieces 18,19

CONTACTS: Glass.
PHENOCRYSTS: Aphyric.
GROUNDMASS: Fine grained to glassy.
VESICLES: Nonvesicular.
COLOR: Light to dark gray.
STRUCTURE: Pillow.
ALTERATION: Slight to moderate.
VEINS/FRACTURES: ~1%; 0.5 mm; varied orientation; green clay.
ADDITIONAL COMMENTS: Piece 18 is a breccia consisting of green altered basalt fragments in a calcite and clay matrix.

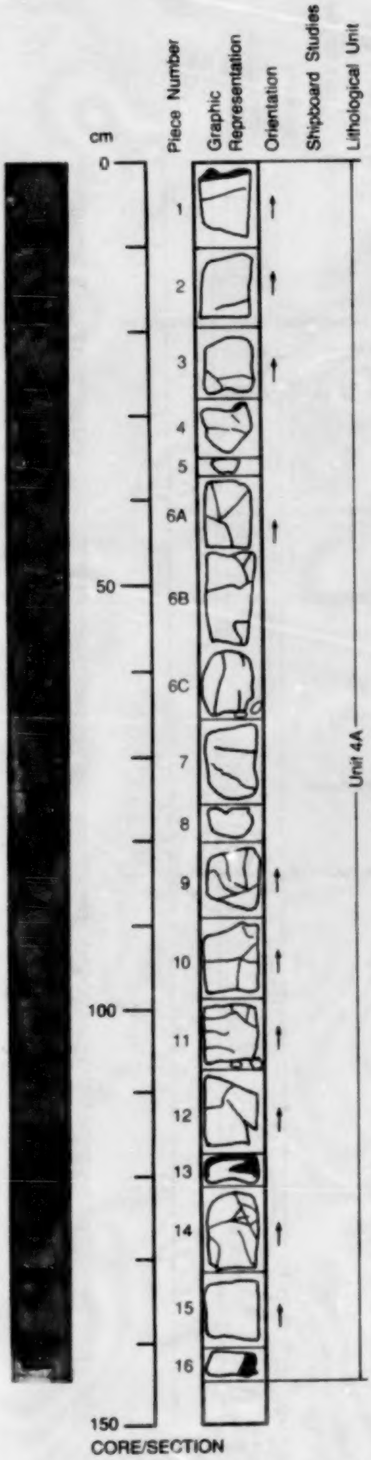
cm
0
50
100
150
Piece Number
Graphic Representation
Orientation
Shipboard Studies
Lithological Unit
1
2
3
4
5
6A
6B
6C
7
8
9
10
11
12
13
14
15
16
Unit 4A
CORE/SECTION

130-807C-79R-2

UNIT 4A: APHYRIC BASALT

Pieces 1-7

CONTACTS: Glass.
PHENOCRYSTS: Aphyric.
GROUNDMASS: Fine grained; Piece 1 has a glassy rim.
VESICLES: Nonvesicular.
COLOR: Medium gray.
STRUCTURE: Massive with pillow top.
ALTERATION: Slight to moderate.
VEINS/FRACTURES: <1%; 0.5-4 mm; varied orientation; calcite and clay.

UNIT 4A: APHYRIC BASALT

Pieces 8-12

CONTACTS: Glass.
PHENOCRYSTS: Very rare.
Plagioclase - <1%; 1-2 mm; euhedral laths.
GROUNDMASS: Fine grained; Piece 8 has glassy rim.
VESICLES: Nonvesicular.
COLOR: Light to dark gray.
STRUCTURE: Massive with pillow top.
ALTERATION: Moderate.
VEINS/FRACTURES: 2-3%; 0.5-4 mm; varied orientation; calcite and clay.

UNIT 4A: APHYRIC BASALT

Pieces 13-15

CONTACTS: Glass.
PHENOCRYSTS: Aphyric.
GROUNDMASS: Fine grained.
VESICLES: Nonvesicular.
COLOR: Medium gray.
STRUCTURE: Pillow.
ALTERATION: Moderate.
VEINS/FRACTURES: 2-3%; 0.3-3 mm; varied orientation; calcite, green and brown clay.

UNIT 4A: APHYRIC BASALT

Piece 16

CONTACTS: None.
PHENOCRYSTS: Very rare.
Plagioclase - <1%; 1 mm; euhedral laths.
GROUNDMASS: Fine grained, glassy rim.
VESICLES: Nonvesicular.
COLOR: Medium to dark gray.
STRUCTURE: Pillow.
ALTERATION: Moderate.
VEINS/FRACTURES: <1%; 0.5-1 mm; varied orientation; calcite and clay.

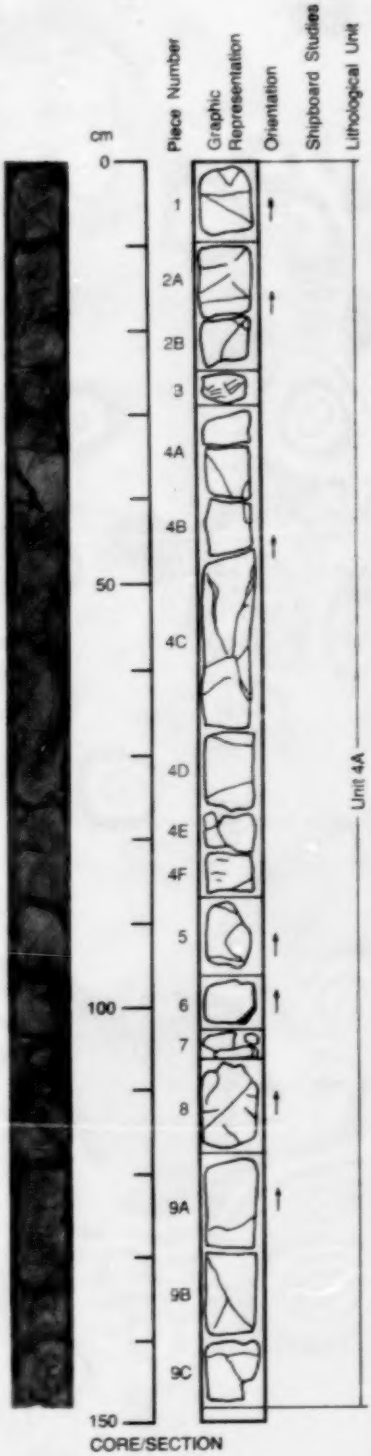
cm
Piece Number
Graphic Representation
Orientation
Shipboard Studies
Lithological Unit
0
50
100
150
1
2A
2B
3
4A
4B
4C
4D
4E
4F
5
6
7
8
9A
9B
9C
Unit 4A
CORE/SECTION

130-807C-79R-3

UNIT 4A: APHYRIC BASALT

Pieces 1,2

CONTACTS: None.
PHENOCRYSTS: Very rare.
Plagioclase - <1%; 1 mm; euhedral.
GROUNDMASS: Fine grained.
VESICLES: Nonvesicular.
COLOR: Gray green, purplish gray.
STRUCTURE: Massive.
ALTERATION: Moderate to high.
VEINS/FRACTURES: 2-3%; 0.3-1 mm; mostly subhorizontal; green and brown clays.

UNIT 4A: APHYRIC BASALT

Pieces 3-5

CONTACTS: None.
PHENOCRYSTS: Very rare.
Plagioclase - <<1%; ~1 mm; euhedral laths.
GROUNDMASS: Fine grained, fining towards top of Piece 3.
VESICLES: Nonvesicular.
COLOR: Medium gray.
STRUCTURE: Massive.
ALTERATION: Moderate.
VEINS/FRACTURES: 2-3%; 0.3-4 mm; mostly subhorizontal; mainly clay.

UNIT 4A: APHYRIC BASALT

Pieces 6-9

CONTACTS: None.
PHENOCRYSTS: Very rare.
Plagioclase - <1%; 1-2 mm; euhedral laths.
GROUNDMASS: Fine grained. Piece 6 has glassy margin.
VESICLES: Nonvesicular.
COLOR: Medium gray.
STRUCTURE: Massive.
ALTERATION: Slight to moderate.
VEINS/FRACTURES: 1%; 0.5-1 mm; varied orientation; green and brown clay.
ADDITIONAL COMMENTS: Piece 8 contains a 10 mm aggregate of plagioclase phenocrysts.

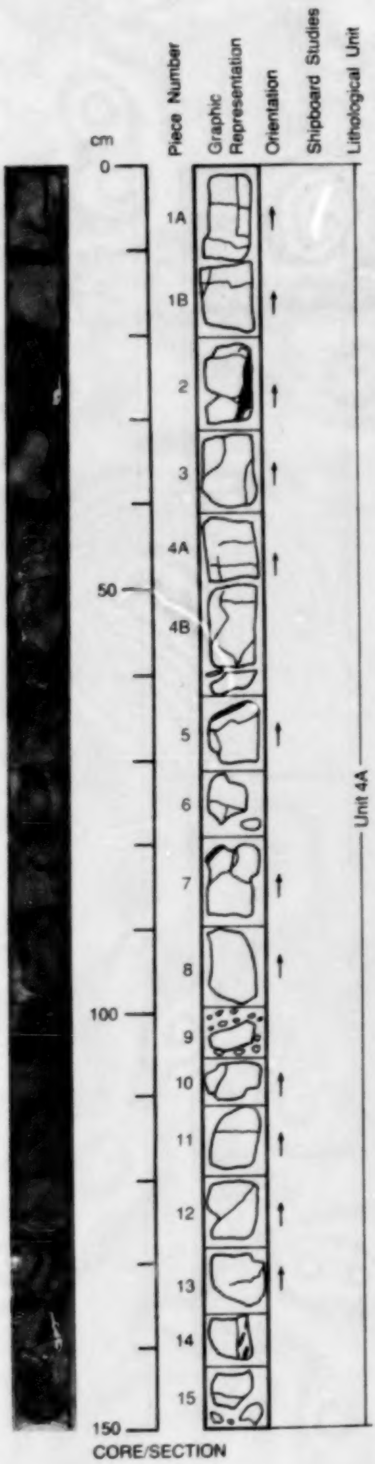
cm
0
50
100
150
Piece Number
Graphic Representation
Orientation
Shipboard Studies
Lithological Unit
1A
1B
2
3
4A
4B
5
6
7
8
9
10
11
12
13
14
15
Unit 4A
CORE/SECTION

130-807C-79R-4

UNIT 4A: APHYRIC BASALT

Pieces 1-4

CONTACTS: None.
PHENOCRYSTS: Very rare.
Plagioclase - <<1%; 1-2 mm; euhedral laths.
GROUNDMASS: Fine grained to glassy (Piece 2).
VESICLES: Nonvesicular.
COLOR: Medium to dark gray.
STRUCTURE: Pillow lava.
ALTERATION: Slight to moderate.
VEINS/FRACTURES: 1-2%; 0.5-10 mm; varied orientation; clay and calcite

UNIT 4A: APHYRIC BASALT

Pieces 5-13

CONTACTS: Glass.
PHENOCRYSTS: Aphyric.
GROUNDMASS: Fine grained to glassy (Pieces 5, 6, and 7).
VESICLES: Nonvesicular.
COLOR: Medium to dark gray.
STRUCTURE: Massive.
ALTERATION: Slight to moderate.
VEINS/FRACTURES: <1%; 0.5-1 mm; varied orientation; clays.

UNIT 4A: APHYRIC BASALT

Pieces 14, 15

CONTACTS: None.
PHENOCRYSTS: Aphyric.
GROUNDMASS: Fine grained, glassy margin.
VESICLES: Nonvesicular.
COLOR: Gray.
STRUCTURE: Pillow margin fragments.
ALTERATION: Slight to moderate.
VEINS/FRACTURES: <1%; <0.5 mm; varied orientation; Piece 14 has breccia margin of altered glass shards up to 1.5 cm long in calcite matrix.

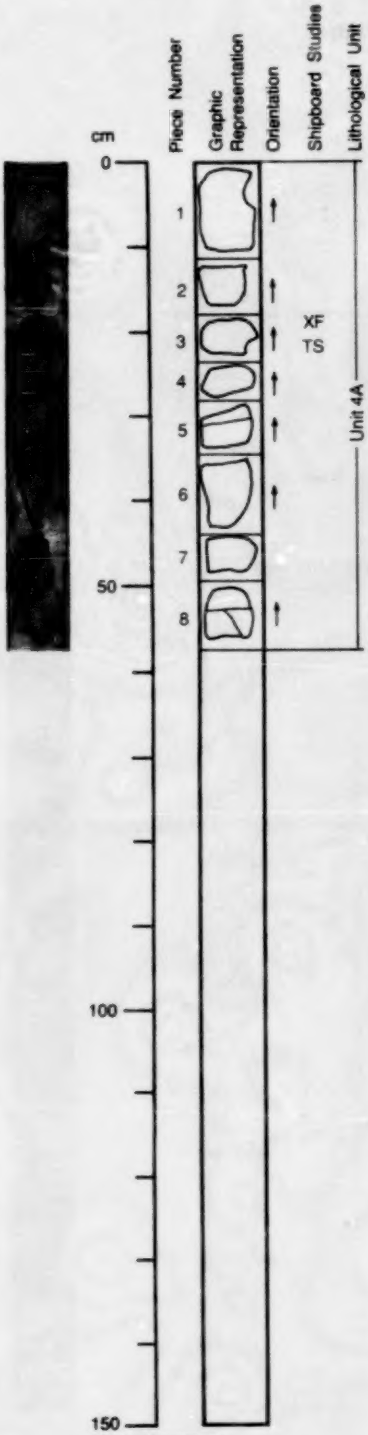
cm
Piece Number
Graphic Representation
Orientation
Shipboard Studies
Lithological Unit
0
50
100
150
1
2
3
4
5
6
7
8
XF
TS
Unit 4A
CORE/SECTION

130-807C-79R-5

UNIT 4A: APHYRIC BASALT

Pieces 1-8

CONTACTS: None.
PHENOCRYSTS: Aphyric.
GROUNDMASS: Fine grained.
VESICLES: Nonvesicular.
COLOR: Medium to dark gray.
STRUCTURE: Massive.
ALTERATION: Slight to moderate.
VEINS/FRACTURES: <1%; up to 2 mm; subhorizontal; calcite and clay.

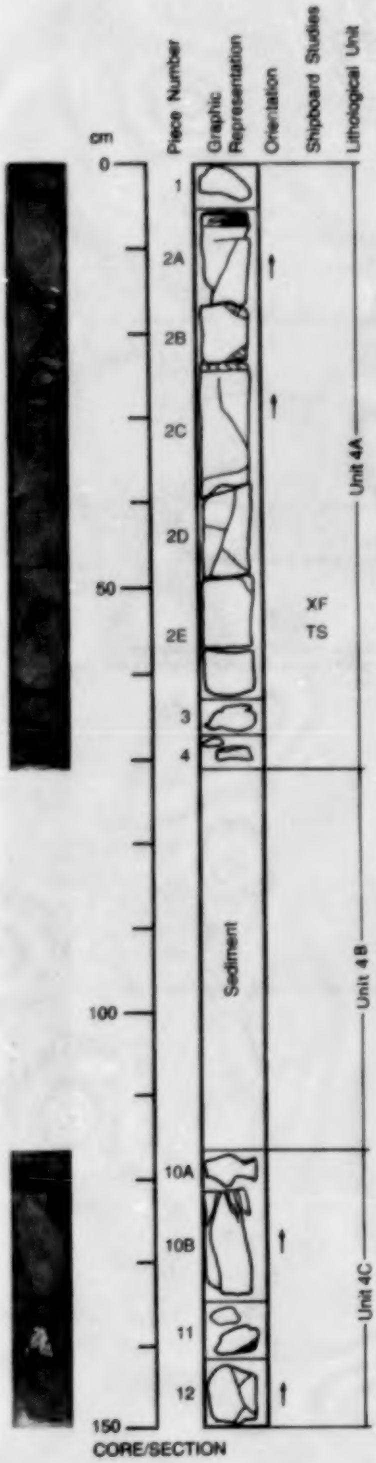

130-807C-80R-1

SUBDIVISION 4A: APHYRIC BASALT

Piece 1

CONTACTS: None.
PHENOCRYSTS: Aphyric.
GROUNDMASS: Fine grained.
VESICLES: Nonvesicular.
COLOR: Medium gray.
STRUCTURE: Massive.
ALTERATION: Slight.
VEINS/FRACTURES: <1%; 0.3 mm; varied orientation; brown clay.

UNIT 4A: APHYRIC BASALT

Pieces 2-4

CONTACTS: Glass.
PHENOCRYSTS: Aphyric.
Plagioclase - <1%; up to 3 mm; euhedral laths.
GROUNDMASS: Fine grained, glassy at top of Piece 2A.
VESICLES: Nonvesicular.
COLOR: Medium gray.
STRUCTURE: Massive.
ALTERATION: Slight to moderate.
VEINS/FRACTURES: 2-3%; up to 2 mm; varied orientation; calcite and clay filled. Pieces 2B and 2C contain irregular vugs up to 4 cm in width, infilled with calcite, quartz, zeolites(?), green mineral. Rim of vug consists of 5-mm-thick dark-green clay

UNIT 4B: SEDIMENT

COMMENTS: Major lithology: Breccia pieces of LIMESTONE interbedded with CLAYEY VITRIC TUFF with OXIDES comprise the material in section 1, 70-120 cm. The limestone is white (10YR 8/1 to 10YR 8/2) and contains angular fragments and clasts of altered vitric tuff and basaltic glass. Rounded fragments of altered vitric tuff, 1-2 mm thick concentrations of carbonate, and lensoid concentrations of sandsized grains, including vitric tuff and basaltic clasts, are also obsereved. Some pieces have have fracture fills of sparry calcite. The clayey vitric tuff is dark reddish brown (5YR 3/3) to reddish brown (5YR 4/3). The clays are probably smectite. One piece of the tuff contains long, vertical and horizontal, corbonate-filled fractures, up to 1 cm wide, and angular vitric tuff clasts.

UNIT 4C: APHYRIC BASALT

Pieces 10-12

CONTACTS: None.
PHENOCRYSTS:
Olivine - ~1%; up to 1 mm; subhedral to euhedral.
Clinopyroxene? - <1%; ~1 mm; subhedral to euhedral.
GROUNDMASS: Fine grained.
VESICLES: Nonvesicular.
COLOR: Ligh[illegible]o medium gray; top 1-2 cm of Piece 10B is yellow-brown.
STRUCTURE: Massive.
ALTERATION: Moderate; top of Piece 10B is highly altered to highly weathered, top of flow.
VEINS/FRACTURES: 1-2%; 0.5-3 mm; subvertical to subhorizontal; calcite, brown clay, red-brown mineral (Fe-oxides?) stains on some fracture surfaces.

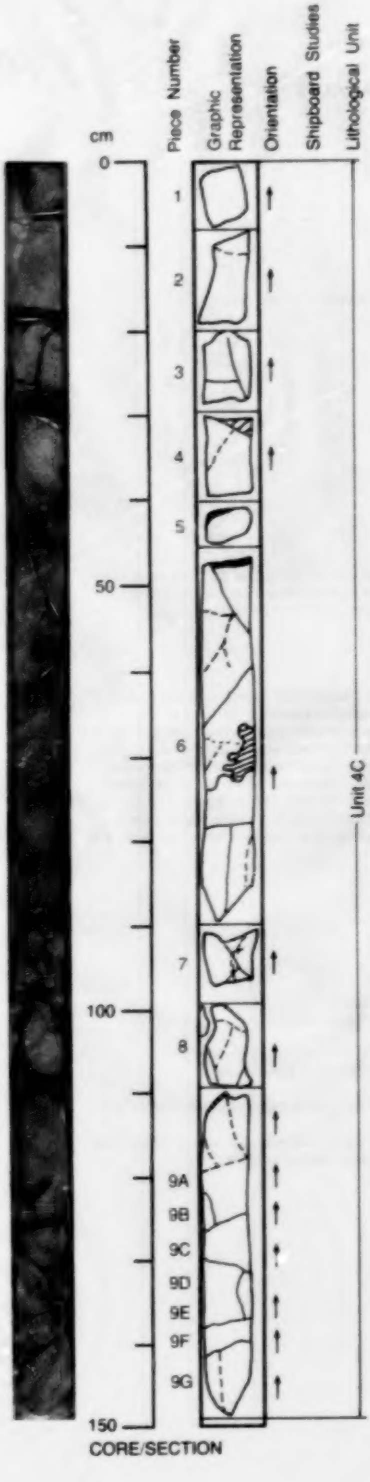
cm
Piece Number
Graphic Representation
Orientation
Shipboard Studies
Lithological Unit
0
50
100
150
1
2
3
4
5
6
7
8
9A
9B
9C
9D
9E
9F
9G
Unit 4C
CORE/SECTION

130-807C-80R-2

UNIT 4C: APHYRIC BASALT

Pieces 1-4

CONTACTS: None.
PHENOCRYSTS:
Olivine? - ~1%; 0.5-1.5 mm; subhedral.
GROUNDMASS: Fine grained.
VESICLES: Nonvesicular.
COLOR: Medium gray.
STRUCTURE: Massive.
ALTERATION: Slight to high (in vicinity of veins).
VEINS/FRACTURES: 1-2%; 0.2-6 mm; subvertical to subhorizontal; calcite center, thin brown clay margin.

UNIT 4C: APHYRIC BASALT

Pieces 5-8

CONTACTS: Glass.
PHENOCRYSTS:
Plagioclase - <1%; ~0.5 mm; euhedral to subhedral.
Olivine? - ~1%; 0.5-1 mm; subhedral.
Clinopyroxene? - <1%; 0.5-1 mm; subhedral.
GROUNDMASS: Fine grained; Pieces 5 and 6 have glassy margins at top.
VESICLES: Nonvesicular.
COLOR: Medium gray.
STRUCTURE: Massive.
ALTERATION: Slight to high (in vicinity of veins).
VEINS/FRACTURES: 2-3%; 0.2-2 mm; subvertical to subhorizontal; conjugate set of veins at 60° in Piece 7. Piece 6 contains irregular shaped vugs up to 1.5 cm in width containing calcite and red-brown mineral (clay?).

UNIT 4C: APHYRIC BASALT

Piece 9

CONTACTS: Glass.
PHENOCRYSTS:
Plagioclase - <1%; up to 1 mm; subhedral.
Olivine? - ~1%; 0.3-1 mm; subhedral.
Clinopyroxene? - <1%; 0.3-1 mm; subhedral.
GROUNDMASS: Fine grained, glassy margin at top.
VESICLES: Nonvesicular.
COLOR: Medium gray.
STRUCTURE: Massive.
ALTERATION: Slight to moderate.
VEINS/FRACTURES: 1%; 0.5-2 mm; subvertical to subhorizontal; calcite and green-brown clay.

130-807C-80R-3

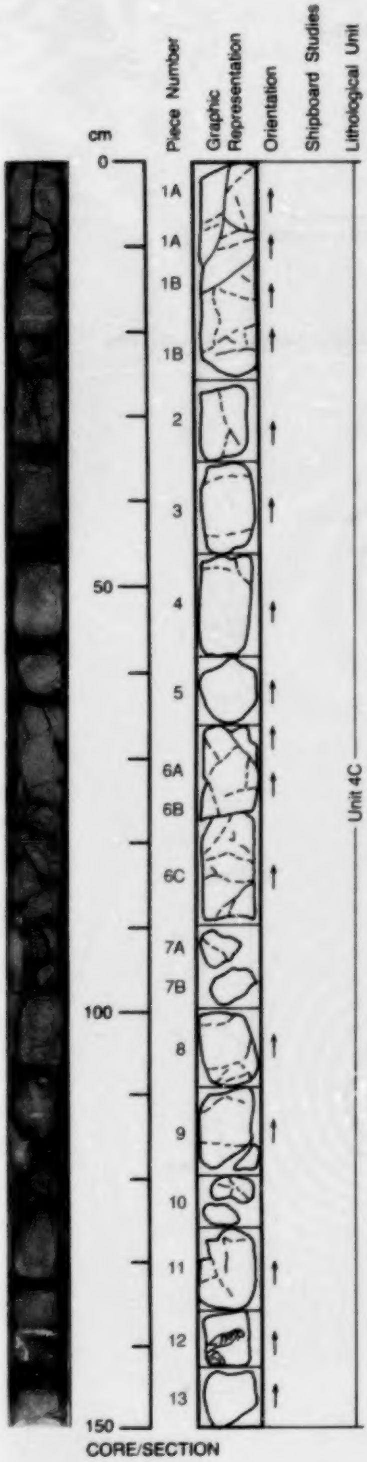
cm
Piece Number
Graphic Representation
Orientation
Shipboard Studies
Lithological Unit
0
50
100
150
1A
1A
1B
1B
2
3
4
5
6A
6B
6C
7A
7B
8
9
10
11
12
13
Unit 4C
CORE/SECTION

UNIT 4C: APHYRIC BASALT

Pieces 1-13

CONTACTS: None.
PHENOCRYSTS:
Plagioclase - <1%; up to 1 mm; subhedral to euhedral.
Olivine? - 1-3%; 0.3-1 mm; subhedral.
Clinopyroxene? - <1%; 0.3-1 mm; subhedral.
GROUNDMASS: Fine grained.
VESICLES: Nonvesicular.
COLOR: Medium to light gray, gray-green.
STRUCTURE: Massive.
ALTERATION: Slight to high.
VEINS/FRACTURES: <1-4%; <0.5-5 mm; varied orientation; mostly green-brown clay with some calcite. Piece 12 has ~2-cm-thick horizontal vein mainly consisting of calcite with dark green and brown-red minerals at vein/basalt contact. Pieces 1 and 6 have 3-4% veins.

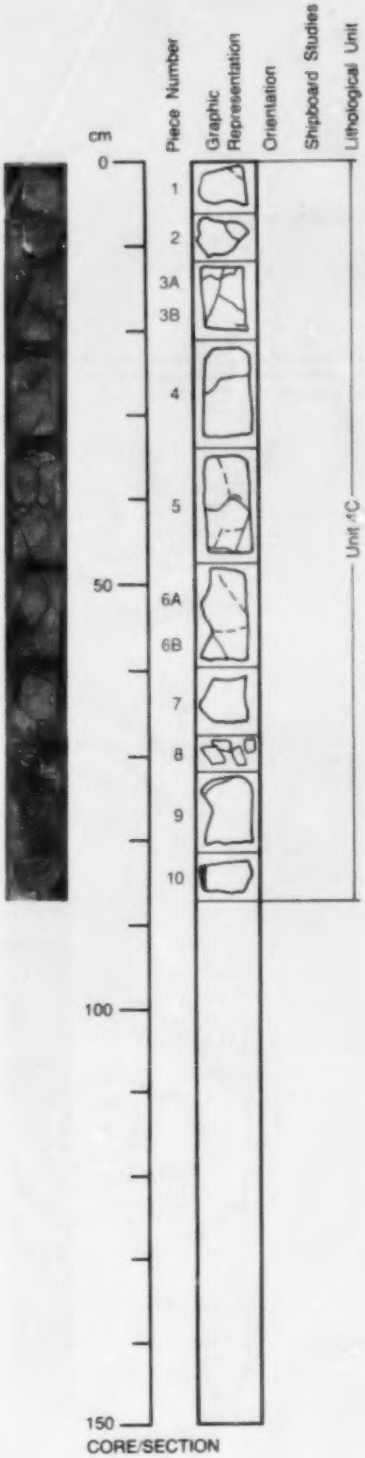
cm
Piece Number
Graphic Representation
Orientation
Shipboard Studies
Lithological Unit
0
50
100
150
1
2
3A
3B
4
5
6A
6B
7
8
9
10
Unit 4C
CORE/SECTION

130-807C-80R-4

UNIT 4C: APHYRIC BASALT

Pieces 1-9

CONTACTS: None.
PHENOCRYSTS:
- Plagioclase - <1%; up to 1 mm; subhedral.
- Olivine? - ~1%; up to 1 mm; subhedral to euhedral laths.
- Clinopyroxene? - <1%; up to 1 mm; subhedral to euhedral laths.

GROUNDMASS: Fine grained.
VESICLES: Nonvesicular.
COLOR: Medium to light gray.
STRUCTURE: Massive.
ALTERATION: Slight to high.
VEINS/FRACTURES: <1-5%; <2 mm; varied orientation, calcite and brown clay, some fracture surfaces stained by green mineral.

UNIT 4C: APHYRIC BASALT

Piece 10

CONTACTS: None.
PHENOCRYSTS:
- Plagioclase - <1%; up to 1 mm; subhedral to euhedral.
- Olivine? - ~1%; up to 1 mm; subhedral.
- Clinopyroxene? - <1%; up to 1 mm; subhedral.

GROUNDMASS: Fine grained with glassy margin.
VESICLES: Nonvesicular.
COLOR: Medium gray.
STRUCTURE: Part of pillow?
ALTERATION: Slight.
VEINS/FRACTURES: None.

130-807C-81R-1

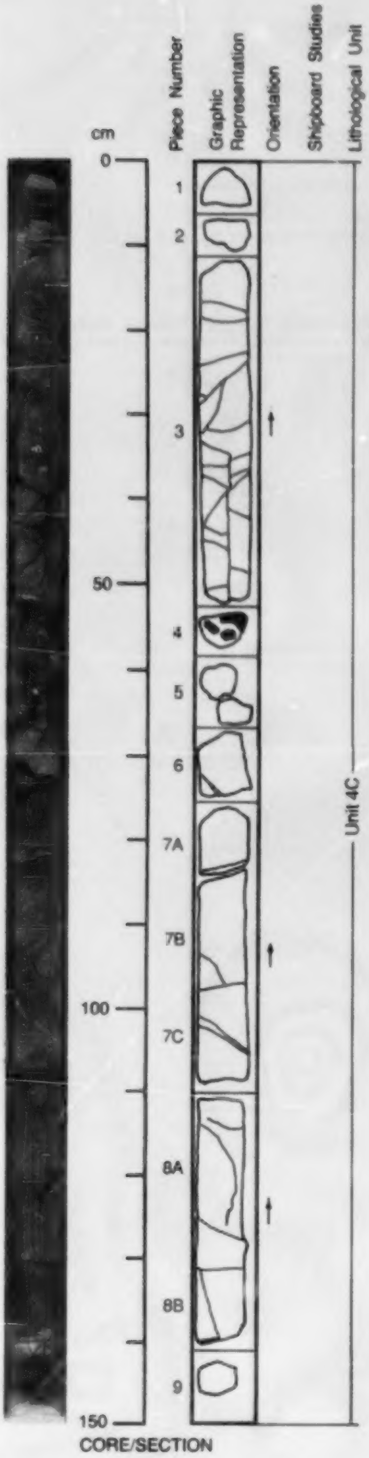
cm
Piece Number
Graphic Representation
Orientation
Shipboard Studies
Lithological Unit
0
50
100
150
1
2
3
4
5
6
7A
7B
7C
8A
8B
9
Unit 4C
CORE/SECTION

UNIT 4C: APHYRIC BASALT

Pieces 1-3

CONTACTS: None.
PHENOCRYSTS:
Plagioclase - <1%; 1 mm; subhedral to euhedral laths.
Olivine? - ~1%; 1 mm; subhedral to euhedral laths.
Clinopyroxene? - <1%; 1 mm; subhedral.
GROUNDMASS: Fine grained.
VESICLES: Nonvesicular.
COLOR: Medium to light gray to gray-green.
STRUCTURE: Massive.
ALTERATION: Slight to high.
VEINS/FRACTURES: Piece 3 heavily fractured (5%), subvertical to subhorizontal, filled with calcite and brown clay.

UNIT 4C: APHYRIC BASALT

Pieces 4-9

CONTACTS: None.
PHENOCRYSTS:
Plagioclase - <1%; 0.5-1 mm; subhedral to euhedral.
Olivine? - ~1%; 1 mm; subhedral.
Clinopyroxene? - <1%; 1 mm; subhedral.
GROUNDMASS: Fine grained to glassy (bottom of Piece 8B).
VESICLES: Non-vesicular.
COLOR: Medium to light gray.
STRUCTURE: Massive.
ALTERATION: Slight to moderate.
VEINS/FRACTURES: <5%; <0.5-6 mm; varied orientation; up to 5% in Pieces 7 and 8, filled by calcite with some clay and/or Fe-oxide.
ADDITIONAL COMMENTS: Piece 4 is a breccia consisting of angular, green altered glass fragments (celadonite?) up to 2 cm, in matrix of calcite and clay.

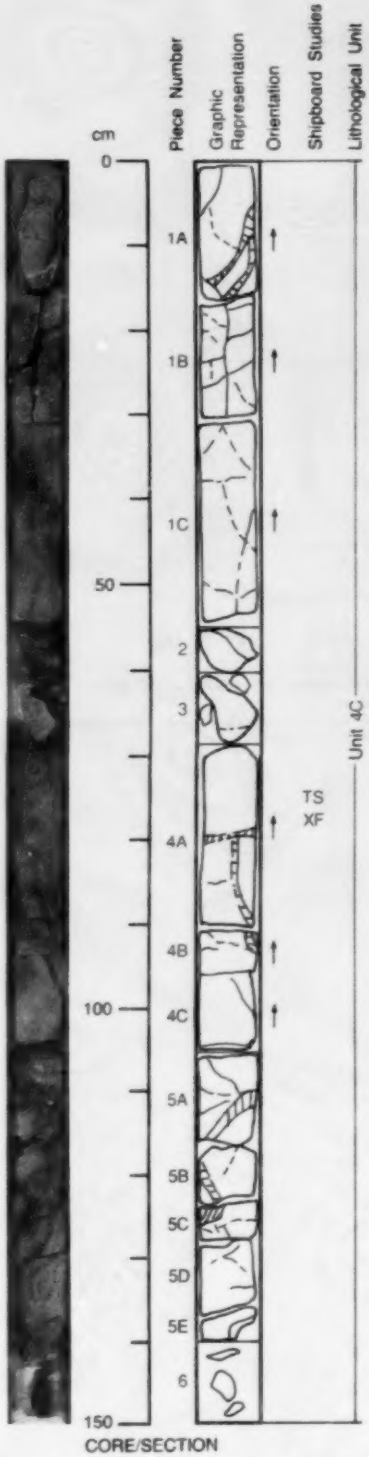
cm
Piece Number
Graphic Representation
Orientation
Shipboard Studies
Lithological Unit
0
50
100
150
1A
1B
1C
2
3
4A
4B
4C
5A
5B
5C
5D
5E
6
TS
XF
Unit 4C
CORE/SECTION

130-807C-81R-2

UNIT 4C: APHYRIC BASALT

Pieces 1-6

CONTACTS: None.
PHENOCRYSTS: Plagioclase - <1%; <1 mm; subhedral to euhedral laths.
Olivine? - ~1%; 0.2-1 mm; subhedral.
Clinopyroxene? - <1%; 0.2-1 mm; subhedral.
GROUNDMASS: Fine grained to glassy (top of Piece 1A, bottom of Pieces 5E and 6).
VESICLES: Nonvesicular.
COLOR: Dark to light gray.
STRUCTURE: Massive.
ALTERATION: Slight to high.
VEINS/FRACTURES: <1-7%; 0.2 - 8 mm; varied orientation; up to 7% in Piece 1B. Mostly calcite with some green and red-brown clay. Piece 5A has 8 mm red-brown clay vein.
ADDITIONAL COMMENTS: Section through a thick pillow?

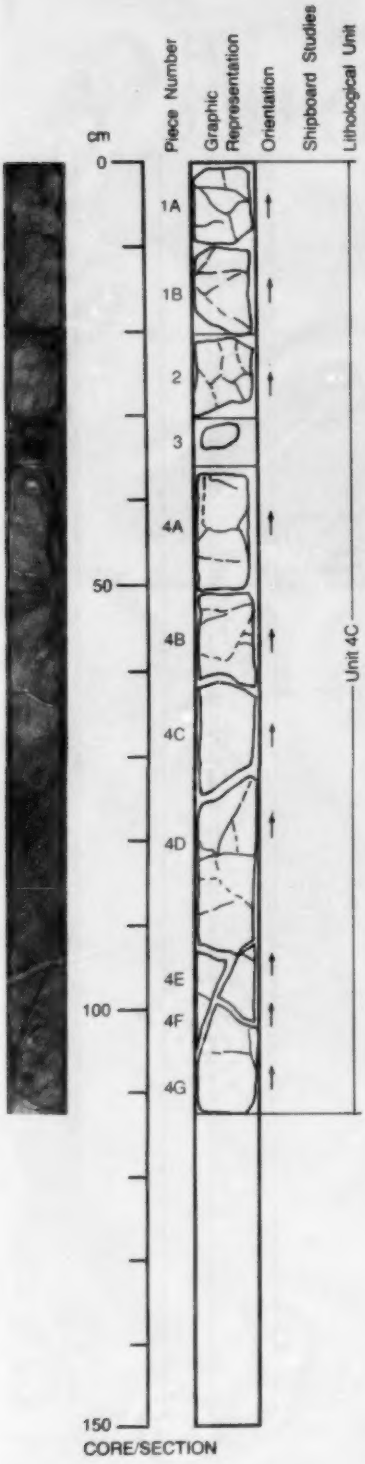
cm
Piece Number
Graphic Representation
Orientation
Shipboard Studies
Lithological Unit
0
50
100
150
1A
1B
2
3
4A
4B
4C
4D
4E
4F
4G
Unit 4C
CORE/SECTION

130-807C-81R-3

UNIT 4C: APHYRIC BASALT.

Pieces 1-4

CONTACTS: None
PHENOCRYSTS: Glomeroporphyritic texture.
  Plagioclase - ~1%; 0.5 mm; subhedral to euhedral.
  Clinopyroxene? - <1%; <0.2-1 mm; subhedral.
  Olivine? - ~1%; 0.2-1 mm; subhedral.
GROUNDMASS: Fine grained.
VESICLES: Nonvesicular.
COLOR: Dark to medium gray.
STRUCTURE: Massive.
ALTERATION: Slight to moderate.
VEINS/FRACTURES: 2-3%; <0.3-3 mm; varied orientation; filled with calcite and green-gray to brown clay.

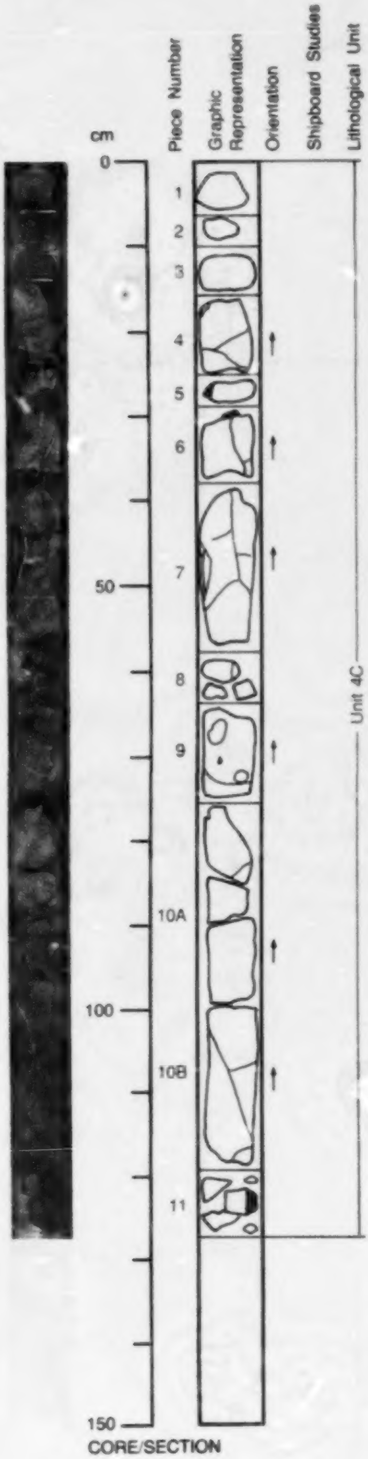
cm
Piece Number
Graphic Representation
Orientation
Shipboard Studies
Lithological Unit
0
50
100
150
1
2
3
4
5
6
7
8
9
10A
10B
11
Unit 4C
CORE/SECTION

130-807C-82R-1

UNIT 4C: APHYRIC BASALT

Pieces 1-4

CONTACTS: None.
PHENOCRYSTS:
  Plagioclase - <1%; 1 mm; euhedral.
  Olivine - ~1%; 0.2-1 mm; subhedral.
GROUNDMASS: Fine grained, coarsest in Pieces 2 and 3.
VESICLES: Nonvesicular.
COLOR: Gray to gray-green.
STRUCTURE: Massive.
ALTERATION: Slight to moderate.
VEINS/FRACTURES: <2-3%; 0.5-3 mm; varied orientation; filled with calcite, green and brown clay.

UNIT 4C: APHYRIC BASALT

Pieces 5-11

CONTACTS: None.
PHENOCRYSTS:
  Plagioclase - <1%; 0.2-0.75 mm; subhedral to euhedral.
  Olivine? - ~1%; 0.2-0.75 mm; subhedral.
  Clinopyroxene? - <1%; 0.2-0.75 mm; subhedral.
GROUNDMASS: Fine grained with glassy rinds (Pieces 5 and 11).
VESICLES: Nonvesicular. Piece 9 has several irregular vugs up to 1 cm wide containing calcite and brown clay.
COLOR: Medium to light gray.
STRUCTURE: Massive.
ALTERATION: Slight to moderate.
VEINS/FRACTURES: <5%; 0.5-4 mm; varied orientation; up to 5% in Pieces 7 and 10A, mostly calcite filled but also red-brown and dark gray-green clay.

130-807C-82R-2

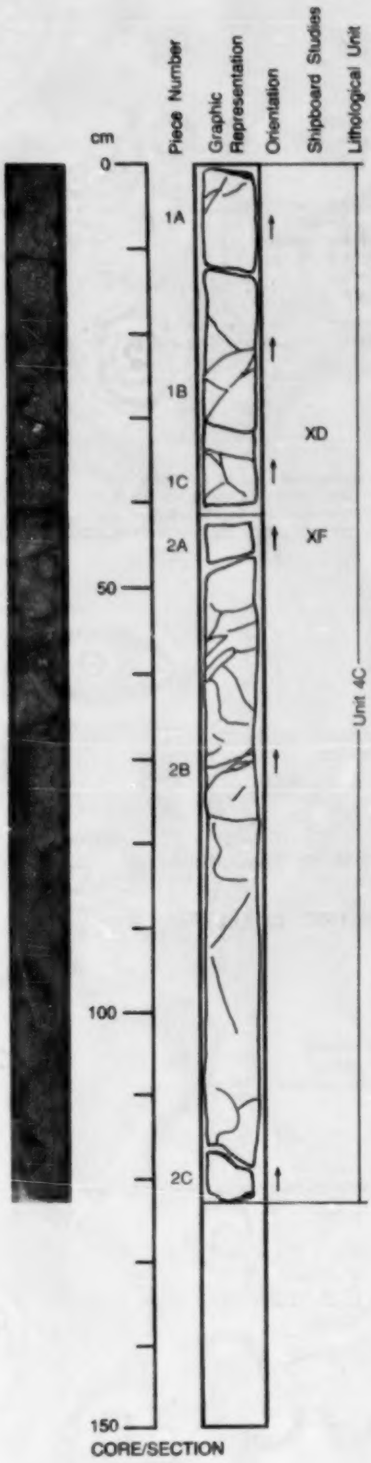
cm
Piece Number
Graphic Representation
Orientation
Shipboard Studies
Lithological Unit
0
50
100
150
1A
1B
1C
2A
2B
2C
XD
XF
Unit 4C
CORE/SECTION

UNIT 4C: APHYRIC BASALT

Pieces 1, 2

CONTACTS: None.
PHENOCRYSTS: Glomeroporphyritic texture, aggregates up to approximately 3 mm.
Plagioclase - <1%; <0.2-0.75 mm; euhedral to subhedral.
Olivine? - ~1-2%; <0.2-0.75 mm; euhedral to subhedral.
Clinopyroxene? - ~1-2%; 0.2-0.75 mm; euhedral to subhedral.
GROUNDMASS: Fine-grained to glassy (rims of Pieces 1A and 2C).
VESICLES: Nonvesicular.
COLOR: Medium gray.
STRUCTURE: Massive.
ALTERATION: Slight to moderate.
VEINS/FRACTURES: <5%; <0.2-10 mm; varied orientation; most are subvertical or subhorizontal and are infilled with calcite, brown and green-blue clays (?). Brown clay (?) fillings at 40 and 58 cm contain small (0.5 to 1.0 mm) pieces of native copper.

130-807C-82R-3

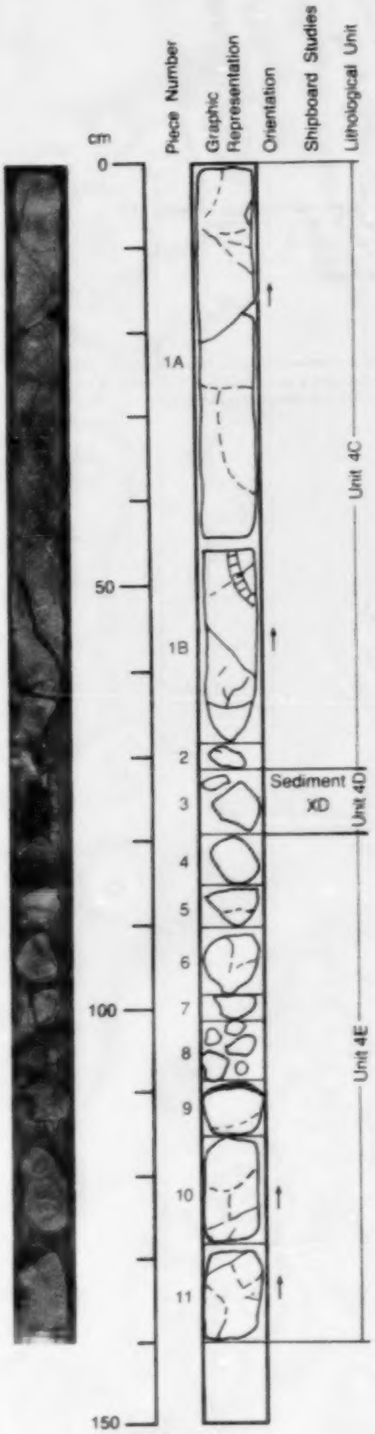

UNIT 4C: APHYRIC BASALT

Pieces 1, 2

CONTACTS: None.
PHENOCRYSTS:
Plagioclase - <1%; <0.2-0.75 mm; subhedral to euhedral laths.
Olivine? - ~1%; <0.2-0.75 mm; anhedral to subhedral.
Clinopyroxene? - <1%; 0.2-0.75 mm; anhedral to subhedral.
GROUNDMASS: Fine grained to glassy (top of Piece 1A).
VESICLES: Nonvesicular.
COLOR: Medium gray.
STRUCTURE: Massive.
ALTERATION: Slight to moderate.
VEINS/FRACTURES: <2-3%; <3 mm; varied orientation; calcite and brown clay fill.

UNIT 4D: SEDIMENT

Piece 3

COMMENTS: 72-79 cm: Olive brown (2.5YR 4/4) clayey limestone; clay is probably smectite and iron oxides are common to abundant. Limestone contains ~ 5-10% clasts that are 2-3 mm in diameter, range in shape from elongate and angular to pelletal, and are grayish green (5G 5/2) in color. There appears to be glauconite, although there may also be basaltic debris.

UNIT 4E: APHYRIC BASALT

Pieces 4-8

CONTACTS: None.
PHENOCRYSTS: Glomeroporphyritic texture.
Plagioclase - ~1%; <0.2-1.0 mm; anhedral-euhedral.
Olivine? - ~1-2%; <0.2-1.0 mm; anhedral-subhedral.
GROUNDMASS: Fine grained.
VESICLES: Nonvesicular.
COLOR: Medium gray.
STRUCTURE: Massive.
ALTERATION: Slight.
VEINS/FRACTURES: Thin (0.5 mm) vein in Piece 5A, filled with green-brown clay.

UNIT 4E: SPARSELY OLIVINE-PHYRIC BASALT

Pieces 9, 10, 11

CONTACTS: None.
PHENOCRYSTS:
Plagioclase - <1%; <0.2-1.0 mm; anhedral to euhedral.
Olivine? - ~2%; <0.2-1.0 mm; anhedral to subhedral.
Clinopyroxene? - <1%; 0.2 to 1 mm; anhedral to subhedral.
GROUNDMASS: Fine grained.
VESICLES: Nonvesicular.
COLOR: Medium gray.
STRUCTURE: Massive.
ALTERATION: Slight.
VEINS/FRACTURES: 1%; 0.2-1.0 mm; varied orientation; filled with calcite and green and brown clays.

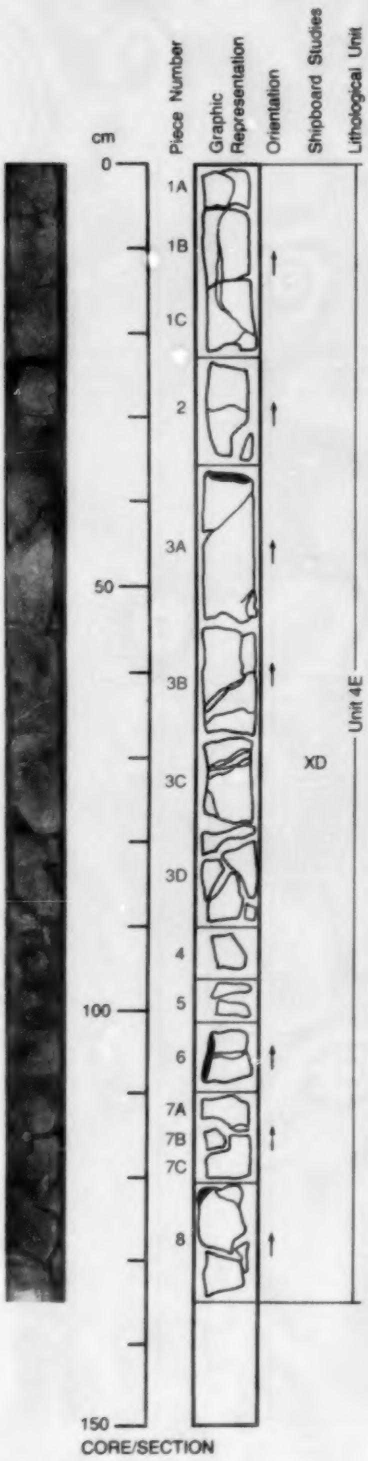
cm
Piece Number
Graphic Representation
Orientation
Shipboard Studies
Lithological Unit
0
50
100
150
1A
1B
1C
2
3A
3B
3C
3D
4
5
6
7A
7B
7C
8
XD
Unit 4E
CORE/SECTION

130-807C-82R-4

UNIT 4E: APHYRIC BASALT

Pieces 1, 2

CONTACTS: None.
PHENOCRYSTS:
Plagioclase - <<1%; <0.5 mm; subhedral to anhedral.
Olivine? - 1%; 0.2-0.5 mm; subhedral.
Clinopyroxene? - <1%; 0.2-0.5 mm; subhedral.
GROUNDMASS: Fine grained.
VESICLES: Nonvesicular.
COLOR: Medium gray.
STRUCTURE: Massive.
ALTERATION: Moderate; greater near veins with Fe-oxide staining.
VEINS/FRACTURES: <1%; 0.3-2 mm; varied orientations; calcite with minor green clay and reddish Fe-oxide.

UNIT 4E: APHYRIC BASALT

Pieces 3-6

CONTACTS: None.
PHENOCRYSTS:
Plagioclase - <1%; <0.5 mm; anhedral to subhedral.
Olivine? - ~1%; 0.2-1.0 mm; subhedral.
Clinopyroxene? - <1%; 0.2-1.0 mm; subhedral.
GROUNDMASS: Fine grained with glassy top and bottom.
VESICLES: Nonvesicular.
COLOR: Medium gray.
STRUCTURE: Massive (could be a thick pillow).
ALTERATION: Slight to moderate.
VEINS/FRACTURES: 2%; 0.5-8 mm; subhorizontal; calcite filling. One vein has a 2-3-mm-thick red zone (Fe-oxide rich?), another has interior zone of dark green clay.

UNIT 4E: APHYRIC BASALT

Pieces 7, 8

CONTACTS: None.
PHENOCRYSTS:
Plagioclase - <<1%; <0.5 mm; subhedral.
Olivine? - ~1%; 0.2-0.5 mm; subhedral.
GROUNDMASS: Fine grained with glassy margin.
VESICLES: Nonvesicular.
COLOR: Medium gray.
STRUCTURE: Massive.
ALTERATION: Slight to moderate.
VEINS/FRACTURES: <1%; 0.5-2 mm; varied orientation; calcite filled.

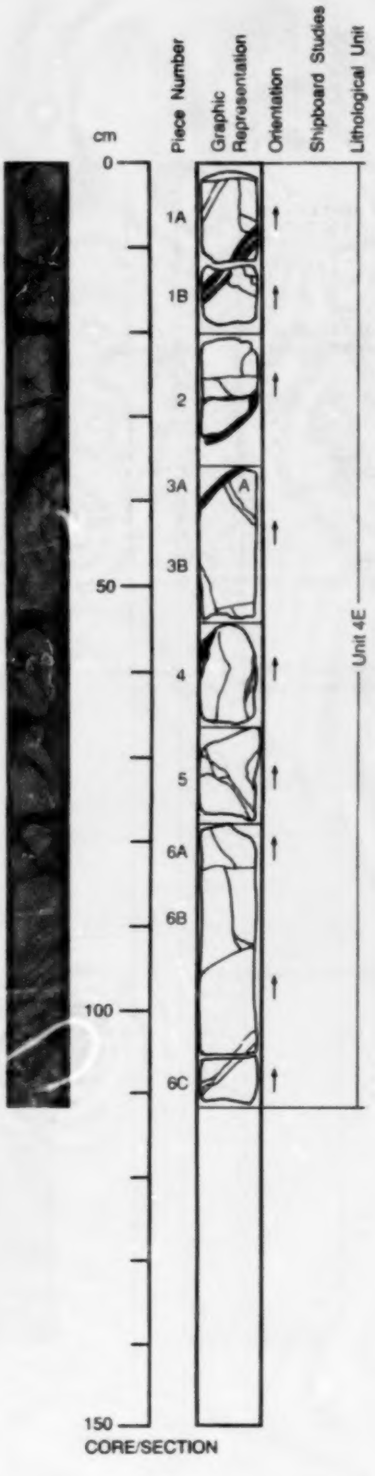
cm
Piece Number
Graphic Representation
Orientation
Shipboard Studies
Lithological Unit
0
50
100
150
1A
1B
2
3A
3B
4
5
6A
6B
6C
A
Unit 4E
CORE/SECTION

130-807C-82R-5

UNIT 4E: APHYRIC BASALT

Pieces 1, 2

CONTACTS: None.
PHENOCRYSTS:
  Plagioclase - <<1%; 0.2-0.3 mm; anhedral.
  Olivine? - ~1%; 0.3-0.5 mm; subhedral.
GROUNDMASS: Fine grained to glassy at margins.
VESICLES: Nonvesicular.
COLOR: Medium gray.
STRUCTURE: Pillow lava.
ALTERATION: Slight to moderate.
VEINS/FRACTURES: 2%; <1 - 6 mm; varied orientation; calcite between glass rims; brown clay with calcite elsewhere; minor dark green clay.

UNIT 4E: APHYRIC BASALT

Pieces 3-6

CONTACTS: None.
PHENOCRYSTS:
  Plagioclase - <<1%; 0.2-0.5 mm; anhedral.
  Olivine? - ~1%; 0.25-1.0 mm; subhedral to anhedral.
  Clinopyroxene? - <1%; 0.25-1.0 mm; subhedral to anhedral.
GROUNDMASS: Fine grained with glassy margins.
VESICLES: Nonvesicular.
COLOR: Medium gray.
STRUCTURE: Massive pillow lava.
ALTERATION: Slight to moderate.
VEINS/FRACTURES: <1%; <0.5-3 mm; varied orientation; filled with calcite and lesser amounts of dark green clay. Two brown clay and/or Fe-oxide veins in Piece 6.

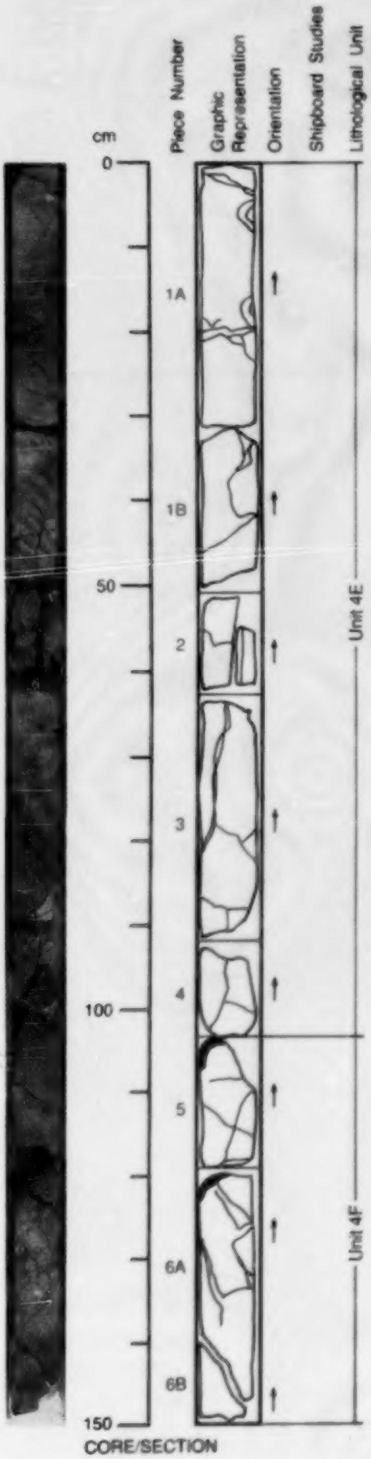
cm
Piece Number
Graphic Representation
Orientation
Shipboard Studies
Lithological Unit
0
50
100
150
1A
1B
2
3
4
5
6A
6B
Unit 4E
Unit 4F
CORE/SECTION

130-807C-82R-6

UNIT 4E: APHYRIC BASALT

Pieces 1-4

CONTACTS: None.
PHENOCRYSTS:
Plagioclase - <<1%; <0.5 mm; subhedral, mostly associated with olivine/clinopyroxene.
Olivine? - 1%; 0.25-1 mm; euhedral to subhedral.
GROUNDMASS: Fine grained.
VESICLES: Nonvesicular.
COLOR: Medium gray, slight greenish to darker gray mottling.
STRUCTURE: Massive.
ALTERATION: Slight to moderate (in coarser grained areas).
VEINS/FRACTURES: 2%; <1-6 mm; varied orientation; dark brown clay and/or oxide veins in Pieces 1 and 2, one with dark blue-green clay edges and secondary veinlets (earlier, non-crosscutting). Also calcite with greenish clay and reddish Fe-oxide(?).

UNIT 4F: APHYRIC BASALT

Pieces 5, 6

CONTACTS: None.
PHENOCRYSTS:
Plagioclase - <1%; 0.2-0.5 mm; subhedral.
Olivine? - 1%; 0.25-1.0 mm; subhedral to euhedral.
GROUNDMASS: Fine grained, glassy at top.
VESICLES: Nonvesicular.
COLOR: Medium gray.
STRUCTURE: Pillow to massive.
ALTERATION: Slight to moderate.
VEINS/FRACTURES: <1%; 0.5-1.0 mm; varied orientation; dark green clay and calcite; minor dark brown clay and green clay in Piece 6.

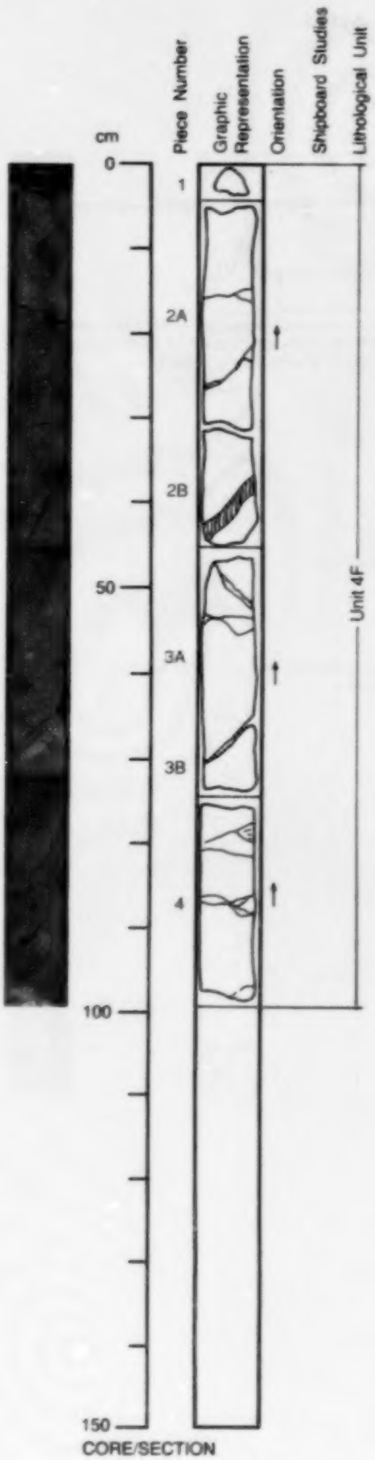
cm
Piece Number
Graphic Representation
Orientation
Shipboard Studies
Lithological Unit
0
50
100
150
1
2A
2B
3A
3B
4
Unit 4F
CORE/SECTION

130-807C-83R-1

UNIT 4F: APHYRIC BASALT

Pieces 1-4

CONTACTS: None.
PHENOCRYSTS:
    Plagioclase - <<1%; 0.2-0.5 mm; subhedral.
    Olivine? - 1%; 0.2-1.0 mm; subhedral.
    Clinopyroxene? - <1%; 0.2-1.0 mm; subhedral.
GROUNDMASS: Fine grained.
VESICLES: Nonvesicular.
COLOR: Medium gray.
STRUCTURE: Massive.
ALTERATION: Slight.
VEINS/FRACTURES: 1%; 0.5-6 mm; horizontal to 45°; calcite with and brown clays, some dark green clay.

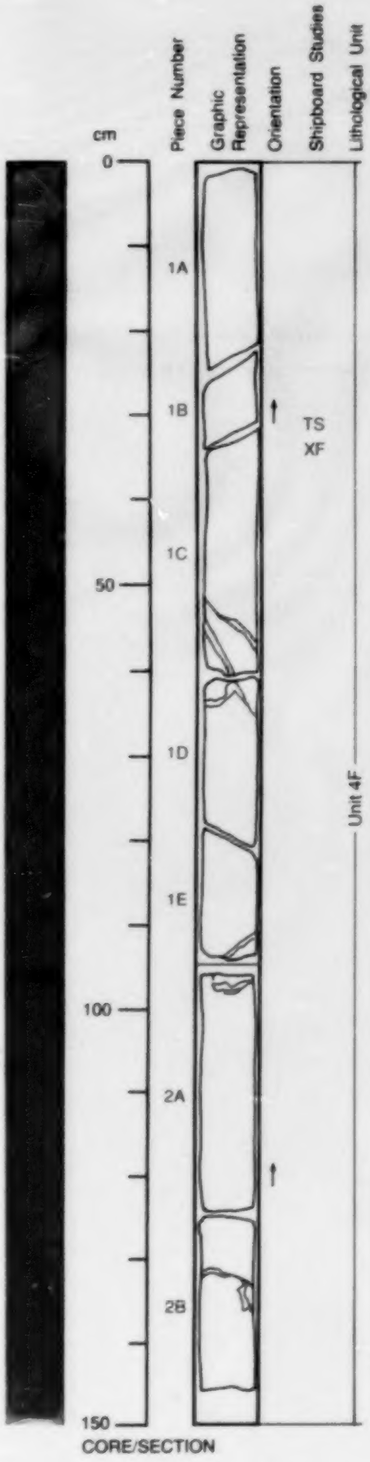
cm
Piece Number
Graphic Representation
Orientation
Shipboard Studies
Lithological Unit
0
50
100
150
1A
1B
1C
1D
1E
2A
2B
TS
XF
Unit 4F
CORE/SECTION

130-807C-83R-2

UNIT 4F: APHYRIC BASALT

Pieces 1, 2

CONTACTS: None.
PHENOCRYSTS:
Olivine? - ~1%; 0.5-1.0 mm; subhedral.
GROUNDMASS: Fine grained.
VESICLES: Nonvesicular.
COLOR: Medium gray.
STRUCTURE: Massive.
ALTERATION: Slight, moderate in places (blotches).
VEINS/FRACTURES: <1%; 0.5-3 mm; varied orientation; calcite with lesser brown or green clay.

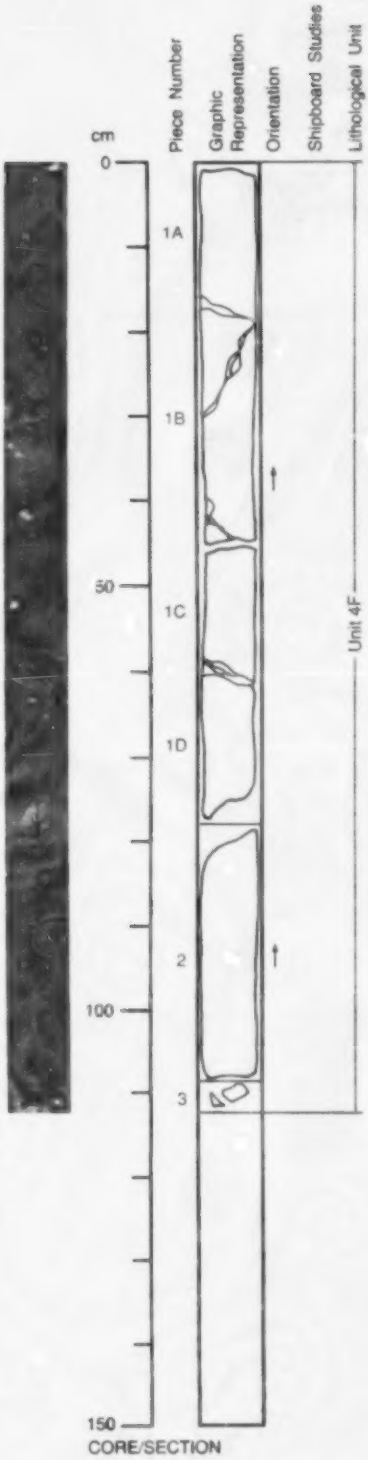
cm
Piece Number
Graphic Representation
Orientation
Shipboard Studies
Lithological Unit
0
50
100
150
1A
1B
1C
1D
2
3
Unit 4F
CORE/SECTION

130-807C-83R-3

SUBDIVISION 4F: APHYRIC BASALT

Pieces 1-3

CONTACTS: None.
PHENOCRYSTS:
Olivine? - <1%; 0.5-1.0 mm; subhedral.
GROUNDMASS: Fine grained.
VESICLES: Nonvesicular.
COLOR: Medium gray.
STRUCTURE: Massive.
ALTERATION: Slight.
VEINS/FRACTURES: <1%; <0.5-5 mm; horizontal and at 45°; calcite and nearly black to dark brown clays.
ADDITIONAL COMMENTS: Piece 3 consists of two vein fragments; one a brown clay, the other a dark green-gray clay with calcite.

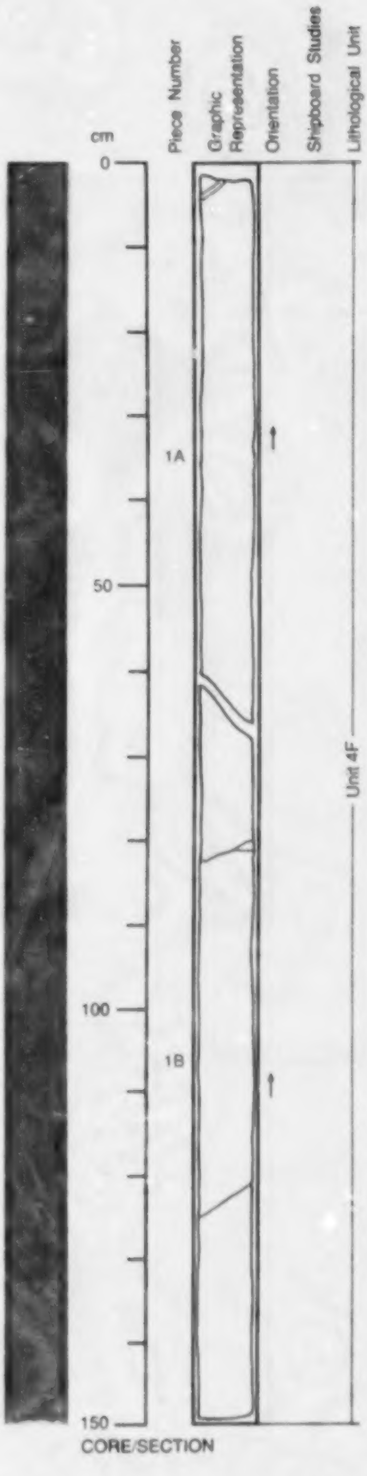
cm
Piece Number
Graphic Representation
Orientation
Shipboard Studies
Lithological Unit
0
50
100
150
1A
1B
Unit 4F
CORE/SECTION

130-807C-83R-4

UNIT 4F: APHYRIC BASALT

Piece 1

CONTACTS: None.
PHENOCRYSTS:
Olivine? - <1%; 0.5-1.0 mm; subhedral to anhedral.
GROUNDMASS: Fine grained (coarser than Core 83R-3).
VESICLES: Nonvesicular.
COLOR: Medium gray.
STRUCTURE: Massive.
ALTERATION: Relatively fresh to slightly altered.
VEINS/FRACTURES: <<1%; 0.5-2mm; horizontal and at 45°; calcite filled.

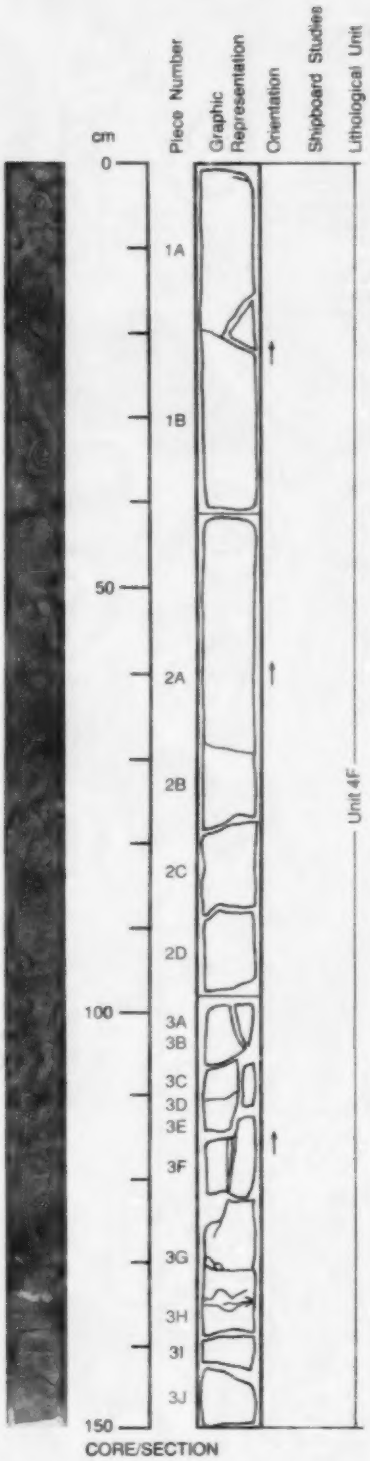
cm
Piece Number
Graphic Representation
Orientation
Shipboard Studies
Lithological Unit
0
50
100
150
1A
1B
2A
2B
2C
2D
3A
3B
3C
3D
3E
3F
3G
3H
3I
3J
Unit 4F
CORE/SECTION

130-807C-83R-5

UNIT 4F: APHYRIC BASALT

Pieces 1, 2, 3

CONTACTS: None.
PHENOCRYSTS:
Olivine? - <1%; up to 1 mm; subhedral.
GROUNDMASS: Fine grained
VESICLES: Nonvesicular.
COLOR: Medium gray
STRUCTURE: Massive.
ALTERATION: Slight.
VEINS/FRACTURES: <1%, 0.5-10 mm, subhorizontal to subvertical; calcite with lesser black and olive green clay.

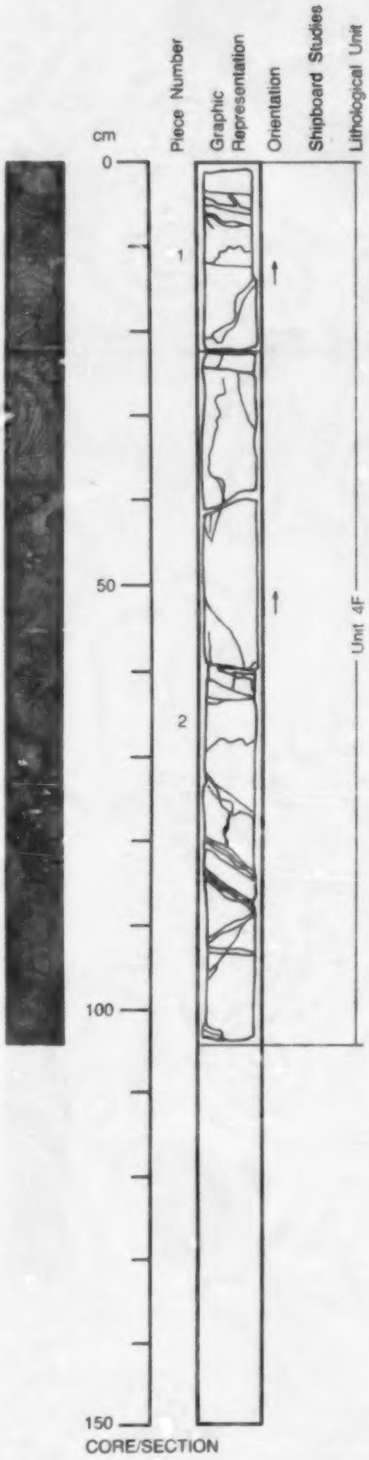
cm
Piece Number
Graphic Representation
Orientation
Shipboard Studies
Lithological Unit
0
1
50
2
100
150
Unit 4F
CORE/SECTION

130-807C-83R-6

UNIT 4F: APHYRIC BASALT

Pieces 1, 2

CONTACTS: None.
PHENOCRYSTS:
Olivine? - 1%; 0.3-1 mm; subhedral.
GROUNDMASS: Fine grained.
VESICLES: Nonvesicular.
COLOR: Light to medium gray with dark gray and greenish patches toward the bottom.
STRUCTURE: Massive.
ALTERATION: Slight to high (near large veins).
VEINS/FRACTURES: 5%; <1-25 mm; varied orientation; large vein (~2.5 mm thick) at 45° (at interval 75-87 cm) consisting of outer zone of black clay with an inner zone of a yellow-brown mineral containing angular black clay clasts. Other veins of black clay, yellow brown clay, and minor calcite. Sediment injected into fracture?

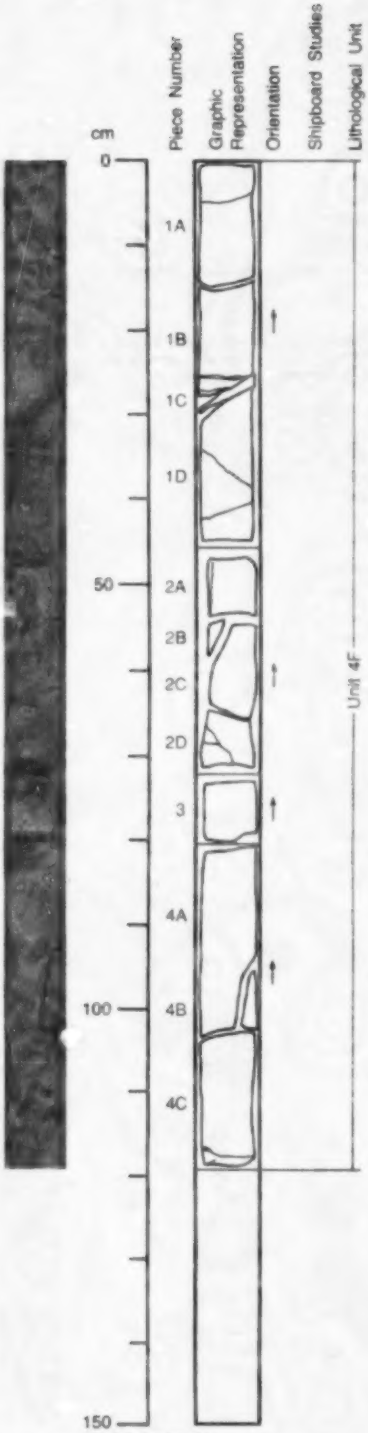
cm
Piece Number
Graphic Representation
Orientation
Shipboard Studies
Lithological Unit
0
50
100
150
1A
1B
1C
1D
2A
2B
2C
2D
3
4A
4B
4C
Unit 4F
CORE/SECTION

130-807C-83R-7

UNIT 4F: APHYRIC BASALT

Pieces 1-4

CONTACTS: None.
PHENOCRYSTS:
  Plagioclase - <1%; 0.5-0.8 mm; euhedral.
  Olivine? - 1%; 0.5-1.0 mm; subhedral.
GROUNDMASS: Fine grained.
VESICLES: Nonvesicular.
COLOR: Medium gray.
STRUCTURE: Massive.
ALTERATION: Slight.
VEINS/FRACTURES: <1%; <0.5-7 mm; subhorizontal and at 45°; calcite with black clay. One 7-mm-thick vein with light brown clay interior and outer zone of dark gray to black clay.

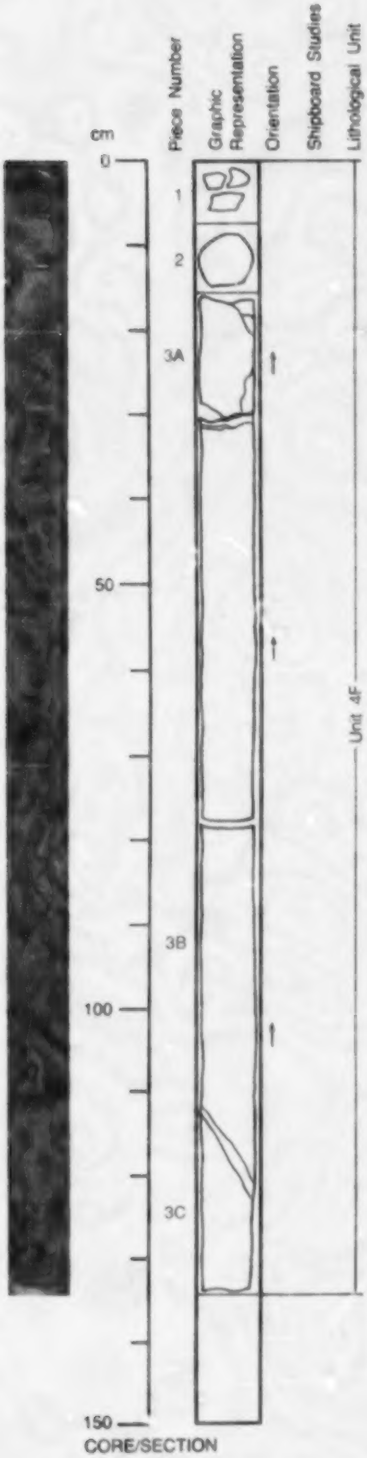
cm
Piece Number
Graphic Representation
Orientation
Shipboard Studies
Lithological Unit
0
1
2
3A
50
3B
100
3C
150
Unit 4F
CORE/SECTION

130-807C-84R-1

UNIT 4F: APHYRIC BASALT

Pieces 1-3

CONTACTS: None.
PHENOCRYSTS:
Olivine? - <1%; 0.5-1 mm; subhedral.
GROUNDMASS: Fine grained.
VESICLES: Nonvesicular.
COLOR: Medium gray.
STRUCTURE: Massive.
ALTERATION: Slight.
VEINS/FRACTURES: <<1%; <1-5 mm; varied orientation; calcite with minor black and green clay.
ADDITIONAL COMMENTS: Piece 1 contains 3 fragments: (i) chert, probably washed downhole; (ii) brown clay vein; (iii) fine-grained basalt.

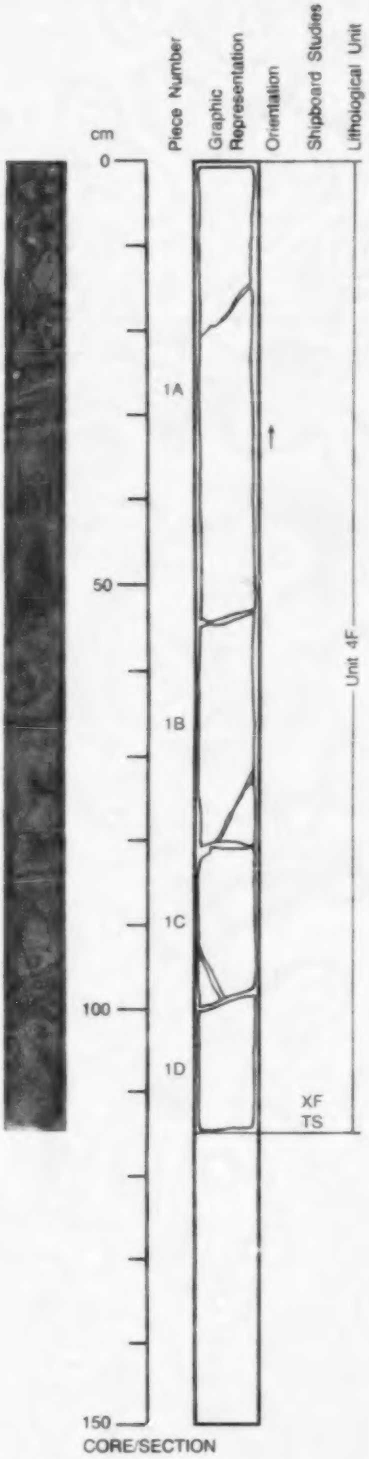
cm
Piece Number
Graphic Representation
Orientation
Shipboard Studies
Lithological Unit
0
50
100
150
1A
1B
1C
1D
XF
TS
Unit 4F
CORE/SECTION

130-807C-84R-2

UNIT 4F: APHYRIC BASALT

Piece 1

CONTACTS: None.
PHENOCRYSTS:
  Olivine? - <1%; 0.5-1mm; subhedral.
  Plagioclase - <1%; 0.5-1mm; euhedral to subhedral.
GROUNDMASS: Fine grained.
VESICLES: Nonvesicular.
COLOR: Medium gray.
STRUCTURE: Massive.
ALTERATION: Slight.
VEINS/FRACTURES: <1%; 0.2-4 mm; subhorizontal and at ~60°, calcite and dark gray clay(?).

130-807C-84R-3

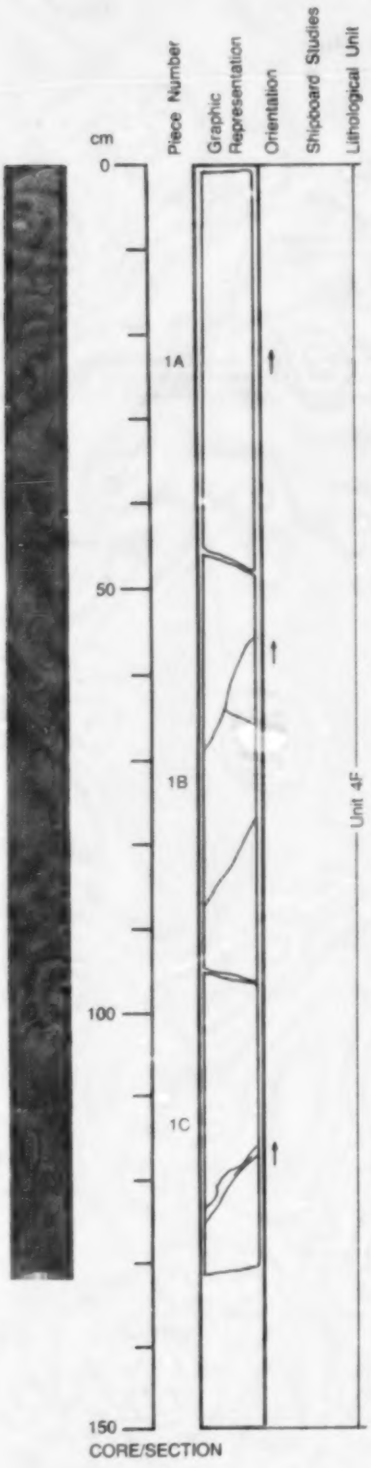
cm
0
50
100
150
CORE/SECTION
Piece Number
Graphic Representation
Orientation
Shipboard Studies
Lithological Unit
1A
1B
1C
Unit 4F

UNIT 4F: APHYRIC BASALT

Piece 1

CONTACTS: None.
PHENOCRYSTS:
- Olivine? - ~1%; 0.5-1 mm; subhedral to euhedral.
- Clinopyroxene? - <1%; 0.5-1 mm; subhedral to euhedral.
- Plagioclase - <1%; 0.5-1 mm; subhedral to euhedral.

GROUNDMASS: Fine grained.
VESICLES: Nonvesicular.
COLOR: Medium gray.
STRUCTURE: Massive.
ALTERATION: Slight.
VEINS/FRACTURES: <<1%; 0.5-4 mm; varied orientation; mostly dark gray clay, thin (1 mm) pyrite vein near bottom of Piece 1C.

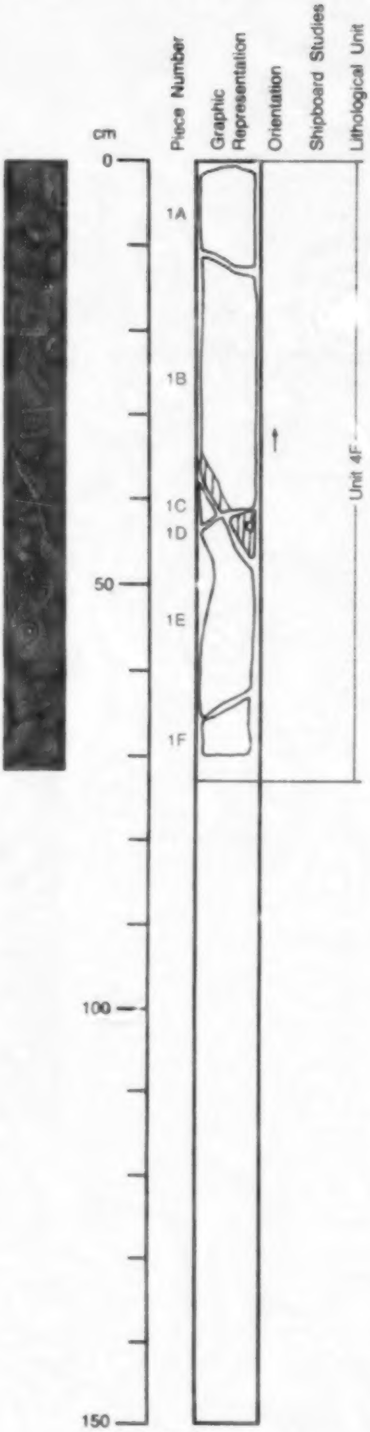
cm
Piece Number
Graphic Representation
Orientation
Shipboard Studies
Lithological Unit
0
50
100
150
1A
1B
1C
1D
1E
1F
Unit 4F
CORE/SECTION

130-807C-84R-4

UNIT 4F: APHYRIC BASALT

Piece 1

CONTACTS: None.
PHENOCRYSTS:
- Olivine? - ~1%; 0.5- 1 mm; subhedral to euhedral.
- Clinopyroxene? - <1%; 0.5-1 mm; subhedral to euhedral.
- Plagioclase - <1%; 0.5-1 mm; subhedral to euhedral.

GROUNDMASS: Fine grained.
VESICLES: Nonvesicular.
COLOR: Medium gray.
STRUCTURE: Massive.
ALTERATION: Slight.
VEINS/FRACTURES: <1%, 1-10 mm; varied orientation; dark gray-green clay. From the bottom of Piece 1B and continuing into Piece 1D is a 10 mm thick composite vein, the bottom half consisting of calcite with minor pyrite and clays, and the top half of a ~5 mm thick basalt dike.

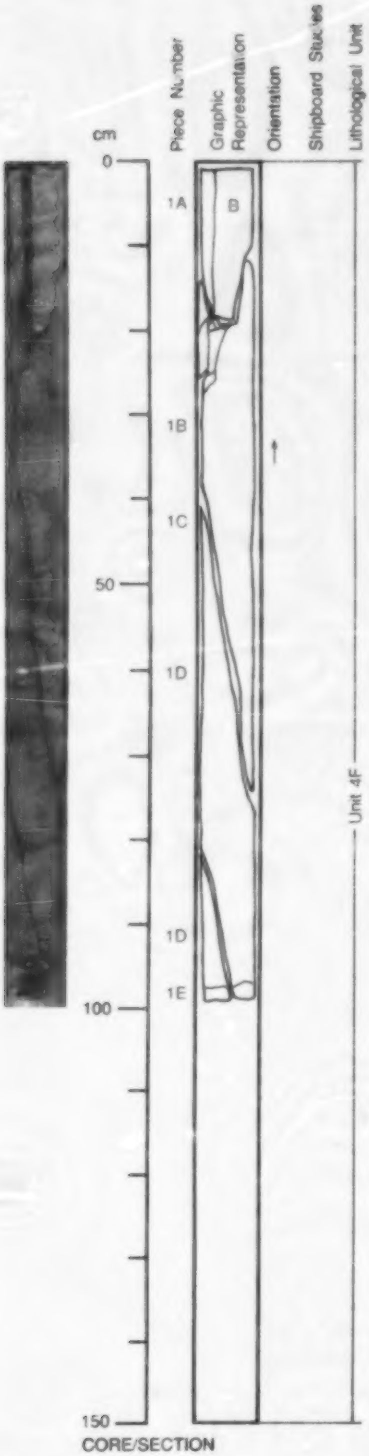
cm
0
50
100
150
Piece Number
Graphic Representation
Orientation
Shipboard Studies
Lithological Unit
1A
B
1B
1C
1D
1D
1E
Unit 4F
CORE/SECTION

130-807C-84R-5

UNIT 4F: APHYRIC BASALT

Piece 1

CONTACTS: None.
PHENOCRYSTS:
- Olivine? - 1-2%; 0.5-1 mm; subhedral to euhedral.
- Clinopyroxene? - <1%; 0.5-1 mm; subhedral to euhedral.
- Plagioclase - <1%; 0.5-1 mm; subhedral to euhedral.

GROUNDMASS: Fine grained.
VESICLES: Nonvesicular.
COLOR: Medium gray.
STRUCTURE: Massive.
ALTERATION: Slight.
VEINS/FRACTURES: <<1%; 0.2-2 mm; subvertical; gray-green clays, heavily fractured.

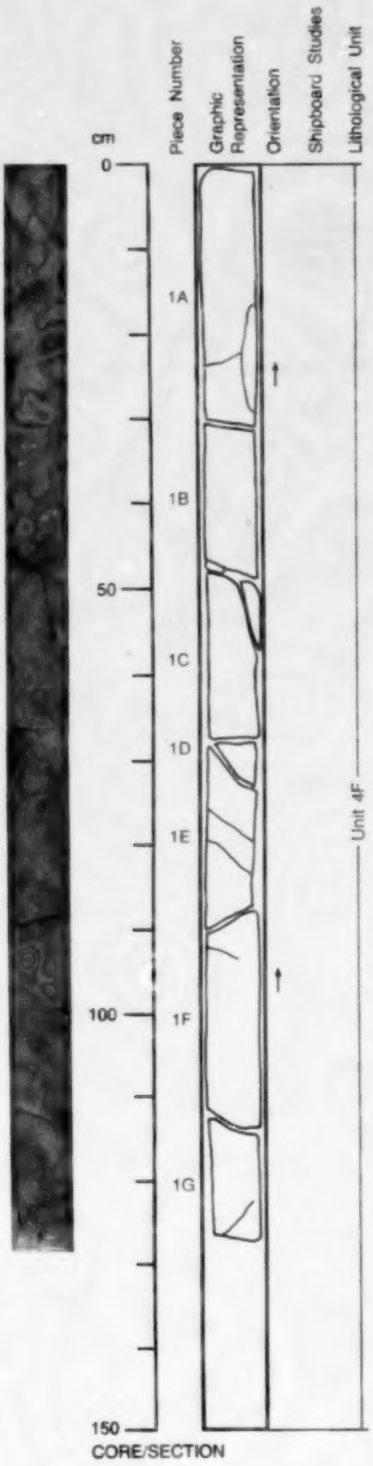
cm
Piece Number
Graphic Representation
Orientation
Shipboard Studies
Lithological Unit
0
50
100
150
1A
1B
1C
1D
1E
1F
1G
Unit 4F
CORE/SECTION

130-807C-84R-6

UNIT 4F: APHYRIC BASALT

Piece 1

CONTACTS: None.
PHENOCRYSTS: Glomeroporphyritic texture.
  Olivine? - ~1%; 0.3-1 mm; subhedral to euhedral.
  Clinopyroxene? - <1%; up to 1 mm; subhedral to euhedral.
  Plagioclase - <1%; up to 1 mm; subhedral to euhedral.
GROUNDMASS: Fine grained.
VESICLES: Nonvesicular.
COLOR: Medium gray.
STRUCTURE: Massive.
ALTERATION: Slight.
VEINS/FRACTURES: <<1%; 0.2-1 mm; varied orientation; dark gray clay, calcite.

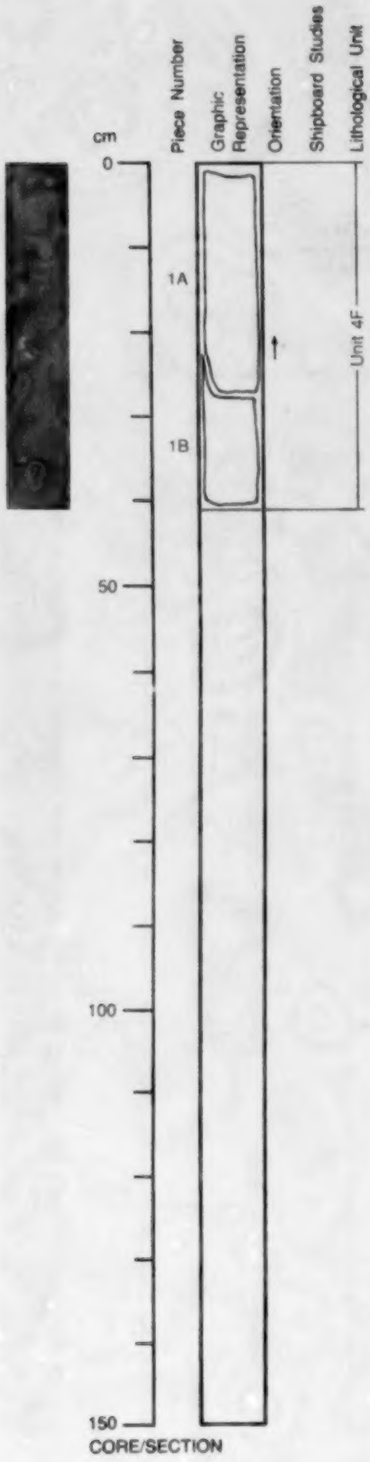
cm
Piece Number
Graphic Representation
Orientation
Shipboard Studies
Lithological Unit
0
50
100
150
1A
1B
Unit 4F
CORE/SECTION

130-807C-84R-7

UNIT 4F: APHYRIC BASALT

Piece 1

CONTACTS: None.
PHENOCRYSTS:
- Olivine? - ~1%; 0.5-1 mm; subhedral to euhedral.
- Clinopyroxene? - <1%; 0.5-1 mm; subhedral to euhedral.
- Plagioclase - <1%; up to 1 mm; subhedral.

GROUNDMASS: Fine grained.
VESICLES: Nonvesicular.
COLOR: Medium gray.
STRUCTURE: Massive.
ALTERATION: Slight.
VEINS/FRACTURES: <<1%; ~0.5 mm; subvertical; dark gray clay.

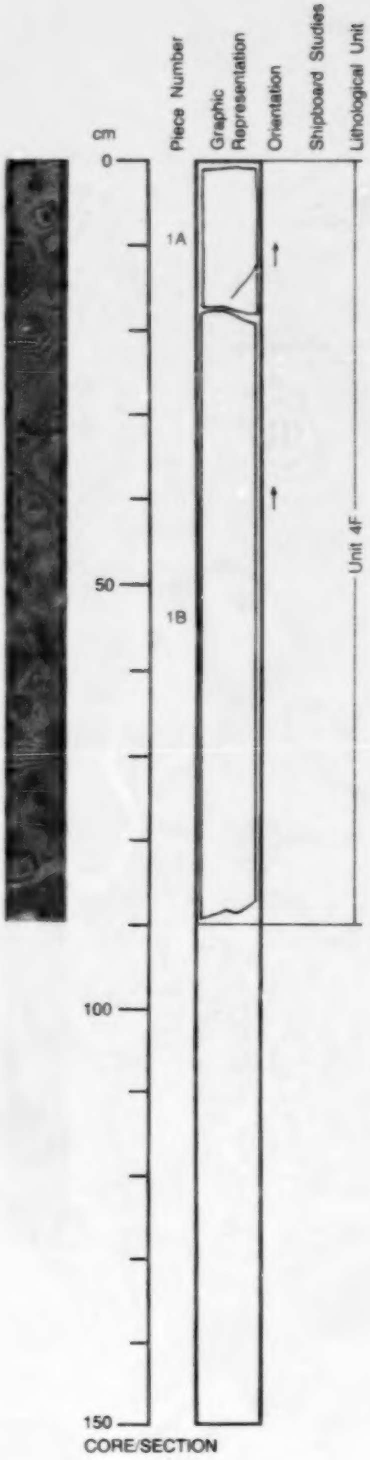
cm
Piece Number
Graphic Representation
Orientation
Shipboard Studies
Lithological Unit
0
50
100
150
1A
1B
Unit 4F
CORE/SECTION

130-807C-85R-1

UNIT 4F: APHYRIC BASALT

Piece 1

CONTACTS: None.
PHENOCRYSTS:
  Olivine? - ~1%; 0.5-1 mm; subhedral to euhedral.
  Clinopyroxene? - <1%; 0.5-1 mm; subhedral to euhedral.
  Plagioclase - <1%; 0.5-1 mm; subhedral to euhedral.
GROUNDMASS: Fine grained.
VESICLES: Nonvesicular.
COLOR: Medium gray.
STRUCTURE: Massive.
ALTERATION: Slight.
VEINS/FRACTURES: <<1%; 0.5 mm; high angles; gray clay filled vein in Piece 1A.

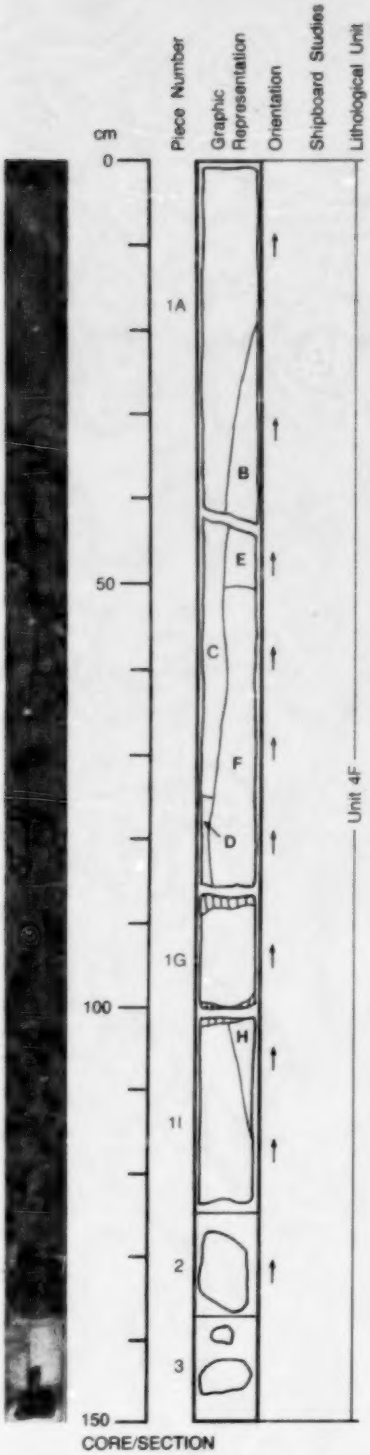
cm
Piece Number
Graphic Representation
Orientation
Shipboard Studies
Lithological Unit
0
50
100
150
1A
B
E
C
F
D
1G
H
1I
2
3
Unit 4F
CORE/SECTION

130-807C-85R-2

UNIT 4F: APHYRIC BASALT

Pieces 1-3

CONTACTS: None.
PHENOCRYSTS:
Olivine? - ~1%; 0.5-1 mm; subhedral to euhedral.
Clinopyroxene? - <1%; 0.5-1 mm; subhedral to euhedral.
Plagioclase - <1%; 0.5-1 mm; subhedral to euhedral.
GROUNDMASS: Fine grained.
VESICLES: Nonvesicular.
COLOR: Medium gray.
STRUCTURE: Massive.
ALTERATION: Slight.
VEINS/FRACTURES: ~1%; 0.5-5 mm; subvertical to subhorizontal; filled with dark gray-green clay.

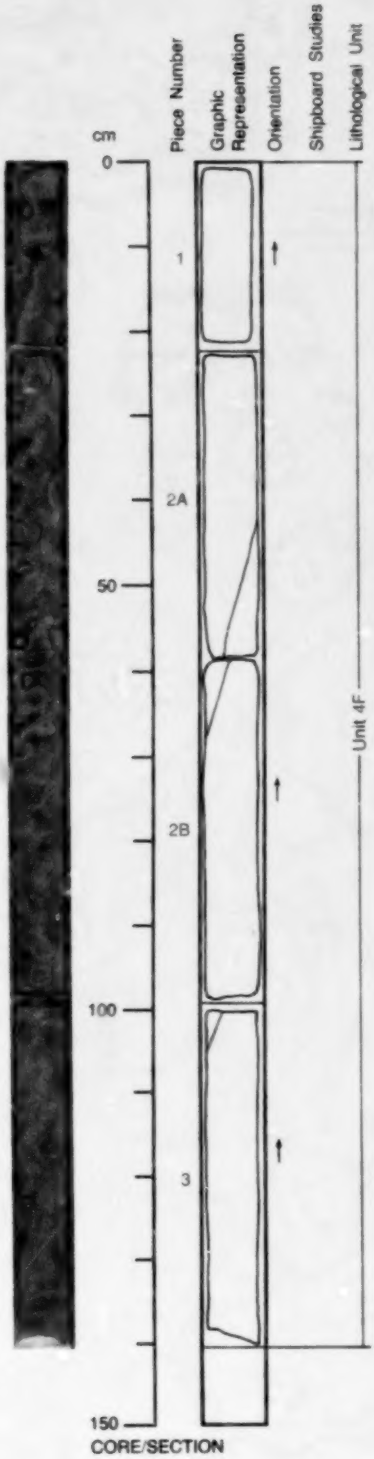
cm
Piece Number
Graphic Representation
Orientation
Shipboard Studies
Lithological Unit
0
1
2A
50
2B
100
3
150
Unit 4F
CORE/SECTION

130-807C-85R-3

UNIT 4F: APHYRIC BASALT

Pieces 1-3

CONTACTS: None.
PHENOCRYSTS:
  Olivine? - ~1%; 0.5-1 mm; subhedral to euhedral.
  Clinopyroxene? - <1%; 0.5-1 mm; subhedral to euhedral.
  Plagioclase - <1%; 0.5-1 mm; subhedral to euhedral.
GROUNDMASS: Fine grained.
VESICLES: Nonvesicular.
COLOR: Medium gray.
STRUCTURE: Massive.
ALTERATION: Slight.
VEINS/FRACTURES: <<1%; 0.5-1 mm; subvertical; filled with dark gray clay.

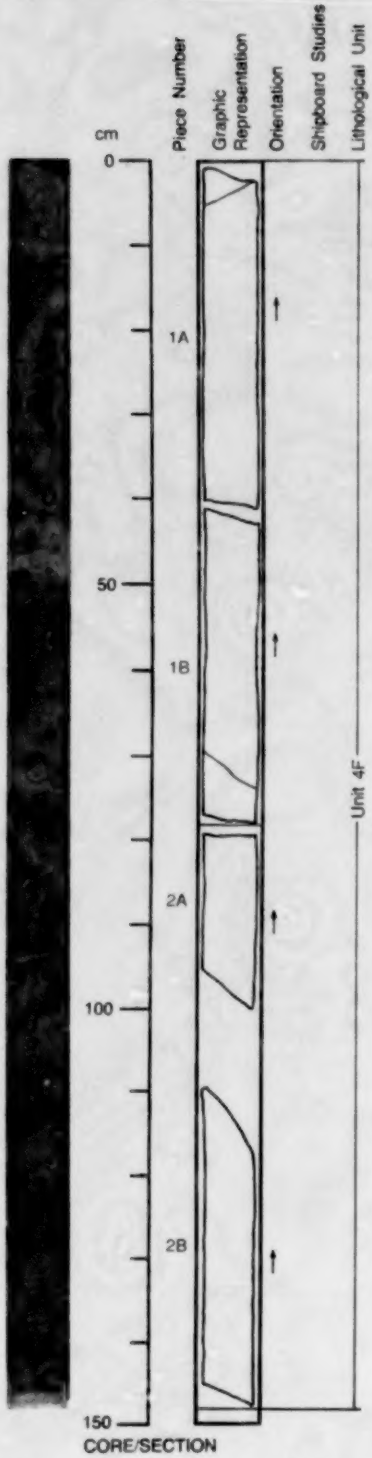
cm
Piece Number
Graphic Representation
Orientation
Shipboard Studies
Lithological Unit
0
50
100
150
1A
1B
2A
2B
Unit 4F
CORE/SECTION

130-807C-85R-4

UNIT 4F: APHYRIC BASALT

Pieces 1, 2

CONTACTS: None.
PHENOCRYSTS:
- Olivine? - ~1%; 0.5-1 mm; subhedral to euhedral.
- Clinopyroxene? - <1%; 0.5-1 mm; subhedral to euhedral.
- Plagioclase - <1%; 0.5-1 mm; subhedral to euhedral.

GROUNDMASS: Fine grained.
VESICLES: Nonvesicular.
COLOR: Medium gray.
STRUCTURE: Massive.
ALTERATION: Slight.
VEINS/FRACTURES: <<1%, 0.2-1 mm, varied orientation; filled with dark gray clay.

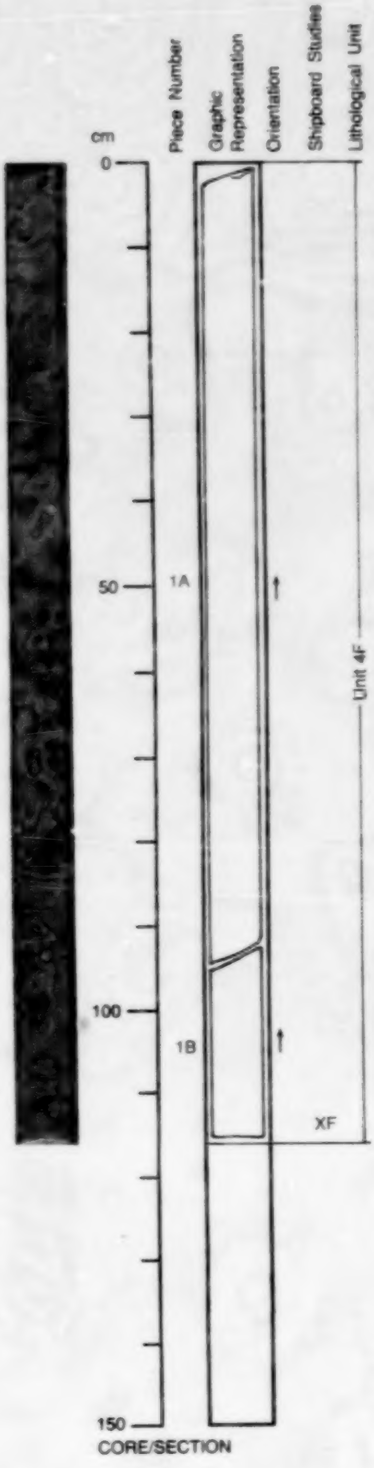
cm
Piece Number
Graphic Representation
Orientation
Shipboard Studies
Lithological Unit
0
50
100
150
1A
1B
Unit 4F
XF
CORE/SECTION

130-807C-85R-5

UNIT 4F: APHYRIC BASALT

Piece 1

CONTACTS: None.
PHENOCRYSTS:
  Olivine? - ~1%; 0.5-1 mm; subhedral to euhedral.
  Clinopyroxene? - <1%; 0.5-1 mm; subhedral to euhedral.
  Plagioclase - <1%; 0.5-1 mm; subhedral to euhedral.
GROUNDMASS: Fine grained.
VESICLES: Nonvesicular.
COLOR: Medium gray.
STRUCTURE: Massive.
ALTERATION: Slight.
VEINS/FRACTURES: None.

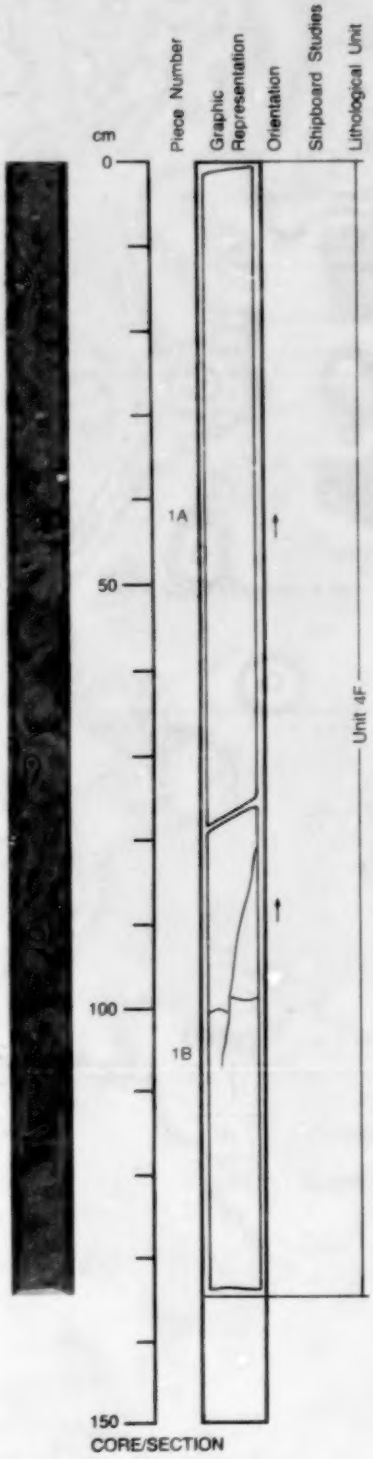
cm
Piece Number
Graphic Representation
Orientation
Shipboard Studies
Lithological Unit
0
50
100
150
1A
1B
Unit 4F
CORE/SECTION

130-807C-85R-6

UNIT 4F: APHYRIC BASALT

Piece 1

CONTACTS: None.
PHENOCRYSTS:
Olivine? - ~1%; 0.5-1 mm; subhedral to euhedral.
Clinopyroxene? - <1%; 0.5-1 mm; subhedral to euhedral.
Plagioclase - <1%; 0.5-1 mm; subhedral to euhedral.
GROUNDMASS: Fine grained.
VESICLES: Nonvesicular.
COLOR: Medium gray.
STRUCTURE: Massive.
ALTERATION: Slight.
VEINS/FRACTURES: ~1%; 0.2-3 mm; subvertical to subhorizontal; filled with calcite and dark green-gray clay.

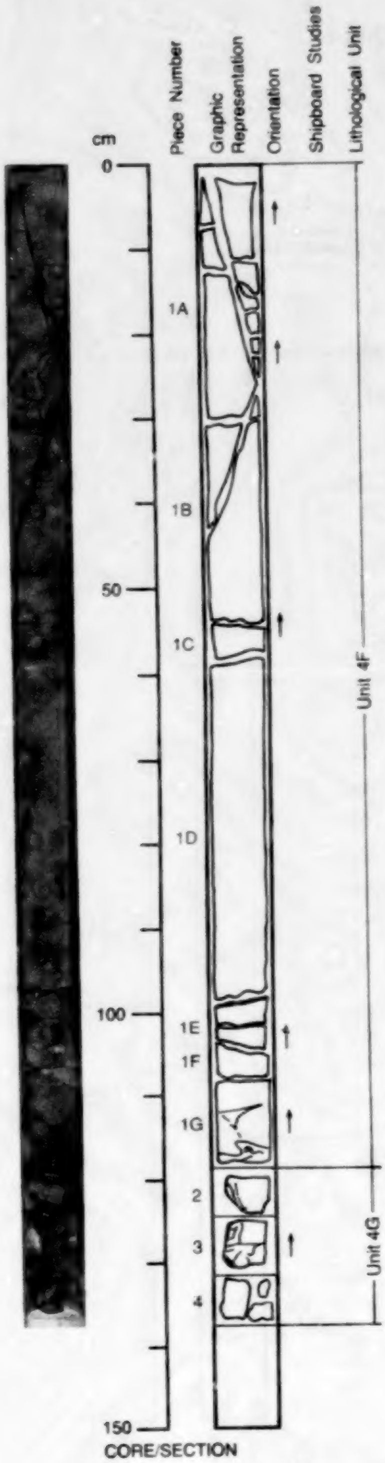
cm
Piece Number
Graphic Representation
Orientation
Shipboard Studies
Lithological Unit
0
50
100
150
1A
1B
1C
1D
1E
1F
1G
2
3
4
Unit 4F
Unit 4G
CORE/SECTION

130-807C-85R-7

UNIT 4F: APHYRIC BASALT

Piece 1

CONTACTS: Piece 1G is the base of this flow.
PHENOCRYSTS: Glomeroporphyritic texture, crystal aggregates up to 3 mm.
  Olivine? - ~1%; 0.5-1 mm; subhedral to euhedral.
  Clinopyroxene? - <1%; 0.5-1 mm; subhedral to euhedral.
  Plagioclase - <1%; 0.5-1 mm; subhedral to euhedral.
GROUNDMASS: Fine grained, becoming finer grained in Pieces 1F and 1G.
VESICLES: Nonvesicular.
COLOR: Medium gray.
STRUCTURE: Massive, base of flow slightly brecciated (Piece 1G).
ALTERATION: Slight, moderate in Piece 1G.
VEINS/FRACTURES: <1%; 0.2-2 mm; horizontal and high angle; filled with calcite and dark clays; irregularly orientated vein in Piece 1G contains calcite and brown clay and/or Fe-oxide (?).

UNIT 4G: APHYRIC BASALT

Pieces 2-4

CONTACTS: Fine-grained to glassy flow margin.
PHENOCRYSTS:
  Olivine? - ~1%; 0.5-1 mm; subhedral to euhedral.
  Clinopyroxene? - <1%; 0.5-1 mm; subhedral.
  Plagioclase - <1%; 0.5-1 mm; subhedral to euhedral, associated with livine and/or clinopyroxene phenocrysts.
GROUNDMASS: Fine grained to glassy.
VESICLES: Nonvesicular.
COLOR: Medium to dark gray.
STRUCTURE: Flow margin, slightly brecciated.
ALTERATION: Slight to moderate.
VEINS/FRACTURES: 2-3%; 0.2-5 mm; varied orientation; mainly calcite with green and brown clays; veins concentrated in the very fine grained to glassy margins of Pieces 2 and 3.

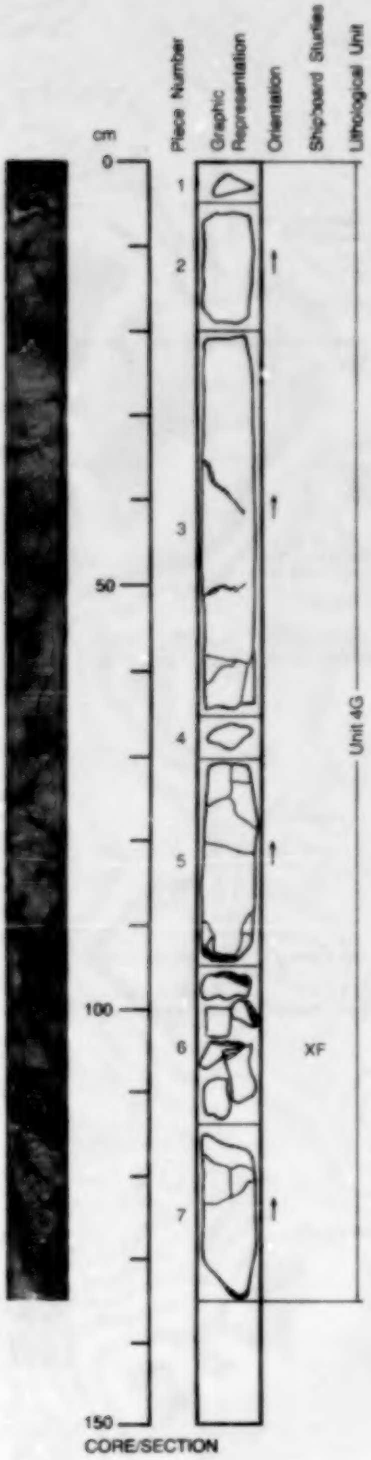
cm
Piece Number
Graphic Representation
Orientation
Shipboard Studies
Lithological Unit
0
50
100
150
1
2
3
4
5
6
7
XF
Unit 4G
CORE/SECTION

130-807C 96R-1

UNIT 4G: APHYRIC BASALT

Pieces 1-5

CONTACTS: None.
PHENOCRYSTS:
Plagioclase - ~1%; 0.5-1 mm; euhedral to subhedral.
Olivine? - ~1%; 0.3-1 mm; euhedral to subhedral.
Clinopyroxene? - <1%, 0.3-1 mm; euhedral to subhedral.
GROUNDMASS: Fine grained to glassy, at bottom.
VESICLES: Nonvesicular.
COLOR: Medium gray.
STRUCTURE: Massive.
ALTERATION: Slight to moderate.
VEINS/FRACTURES: ~1%; <1-3 mm; varied orientation; filled with brown clay and/or Fe-oxide, some calcite. Highly fractured.

UNIT 4G: APHYRIC BASALT

Pieces 6,7

CONTACTS: Glassy.
PHENOCRYSTS:
Plagioclase - <1%; 0.2-0.5 mm; subhedral.
Olivine? - ~1%; 0.3-1 mm; subhedral.
Clinopyroxene? - <1%; up to 1 mm; subhedral.
GROUNDMASS: Fine grained with glassy margins.
VESICLES: Nonvesicular.
COLOR: Medium gray.
STRUCTURE: Pillow lava.
ALTERATION: Slight to moderate.
VEINS/FRACTURES: ~2%; 0.5-2 mm; varied orientation; filled with calcite and brown and greenish clays, highly fractured.

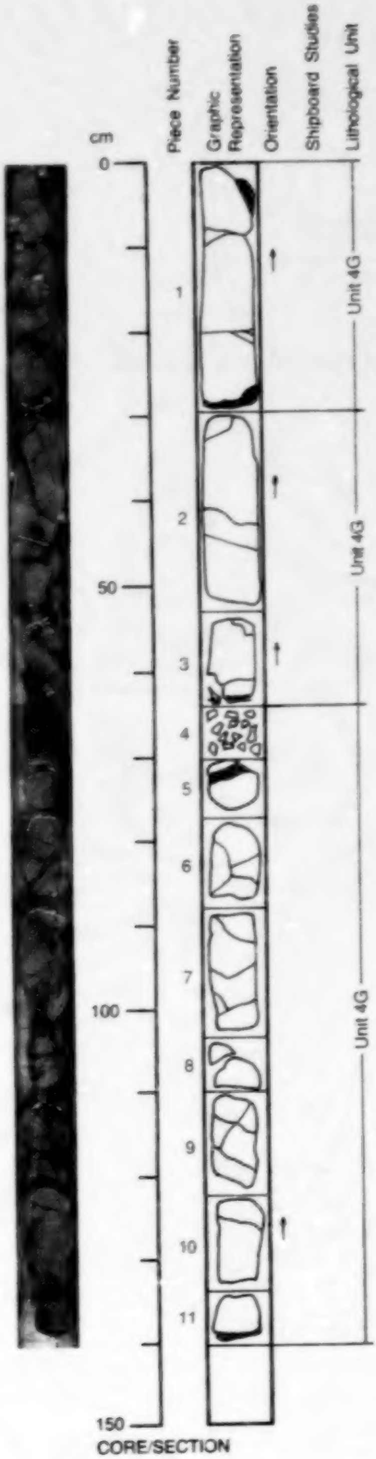
cm
0
50
100
150
Piece Number
Graphic Representation
Orientation
Shipboard Studies
Lithological Unit
1
2
3
4
5
6
7
8
9
10
11
Unit 4G
Unit 4G
Unit 4G
CORE/SECTION

130-807C-86R-2

UNIT 4G: APHYRIC BASALT

Piece 1

CONTACTS: Glassy.
PHENOCRYSTS:
Plagioclase - <1%; 0.3-0.5 mm; euhedral to subhedral.
Olivine? - ~1%; 0.3-1 mm; euhedral to subhedral.
GROUNDMASS: Fine grained to glassy at margins.
VESICLES: Nonvesicular.
COLOR: Medium gray.
STRUCTURE: Pillow lava.
ALTERATION: Slight.
VEINS/FRACTURES: <1%; 0.5-2 mm; varied orientation; filled with calcite and red-brown clay and/or Fe-oxide, some black clay.

UNIT 4G: APHYRIC BASALT

Pieces 2,3

CONTACTS: None.
PHENOCRYSTS:
Plagioclase - <1%; 0.2-0.5 mm; subhedral.
Clinopyroxene - ~1%; 0.2-0.8 mm; subhedral to euhedral.
GROUNDMASS: Very fine grained with glassy lower margin.
VESICLES: Nonvesicular.
COLOR: Medium gray.
STRUCTURE: Pillow lava.
ALTERATION: Slight.
VEINS/FRACTURES: <<1%; <0.5 mm; varied; one calcite vein (~2 mm) at glass margin.

UNIT 4G: APHYRIC BASALT

Pieces 4-11

CONTACTS: None.
PHENOCRYSTS:
Plagioclase - <1%; 0.3-0.5 mm; subhedral to euhedral.
Olivine? - ~1%; 0.3-1 mm; euhedral.
Clinopyroxene? - <1%; 0.3-1 mm; subhedral to euhedral.
GROUNDMASS: Fine grained with glassy margins.
VESICLES: Nonvesicular.
COLOR: Medium gray.
STRUCTURE: Pillow lava.
ALTERATION: Slight to moderate.
VEINS/FRACTURES: <1%; <0.5-2 mm; varied orientation; filled with calcite and dark green clay.
ADDITIONAL COMMENTS: Piece 4 consists of small chips of altered glass and basalt; Piece 5 has top of inter-pillow calcite breccia with glass clasts totally altered to green clay.

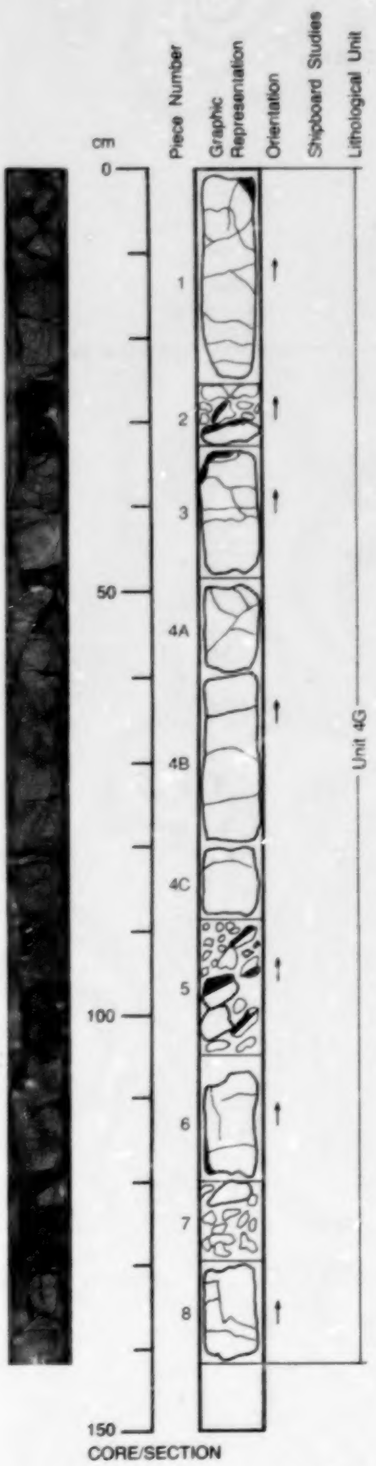

130-807C-86R-3

UNIT 4G: APHYRIC BASALT

Pieces 1,2

CONTACTS: Glassy.
PHENOCRYSTS: Some plagioclase is associated with olivine and/or clinopyroxene.
Plagioclase - <1%; 0.3-0.5 mm; euhedral to subhedral.
Olivine? - ~1%; 0.3-0.8 mm; euhedral to subhedral.
Clinopyroxene? - <1%; 0.3-0.8 mm; euhedral to subhedral.
GROUNDMASS: Fine grained
VESICLES: Nonvesicular.
COLOR: Medium gray.
STRUCTURE: Pillow lava.
ALTERATION: Slight.
VEINS/FRACTURES: ~2%; <0.5-2 mm; varied orientation; filled with brown and green clay, calcite.

UNIT 4G: APHYRIC BASALT

Pieces 3,4

CONTACTS: Glassy
PHENOCRYSTS:
Plagioclase - <1%; 0.3-0.8 mm; subhedral to euhedral.
Olivine? - ~1%; 0.3-1 mm; subhedral to euhedral.
Clinopyroxene? - <1%; 0.3-0.8 mm; subhedral to euhedral.
GROUNDMASS: Fine grained, glassy at top margin.
VESICLES: Nonvesicular.
COLOR: Medium gray.
STRUCTURE: Pillow lava.
ALTERATION: Slight to moderate.
VEINS/FRACTURES: <1%; <1 mm; subhorizontal to about 45°; a few radial pillow cracks. Filled with brown and green clays.

UNIT 4G: APHYRIC BASALT

Pieces 5-8

CONTACTS: Glassy.
Plagioclase - <1%; 0.2-1 mm, euhedral to subhedral.
Olivine - ~1%; 0.2-0.8 mm; subhedral to euhedral.
GROUNDMASS: Fine grained to glass (highly altered) in Piece 5.
VESICLES: Nonvesicular.
COLOR: Medium gray.
STRUCTURE: Pillow lava.
ALTERATION: Slight to moderate, high in chips from Pieces 5 and 7.
VEINS/FRACTURES: ~1%; <1 mm; varied orientation; highly fractured; filled with brown clay, minor calcite.

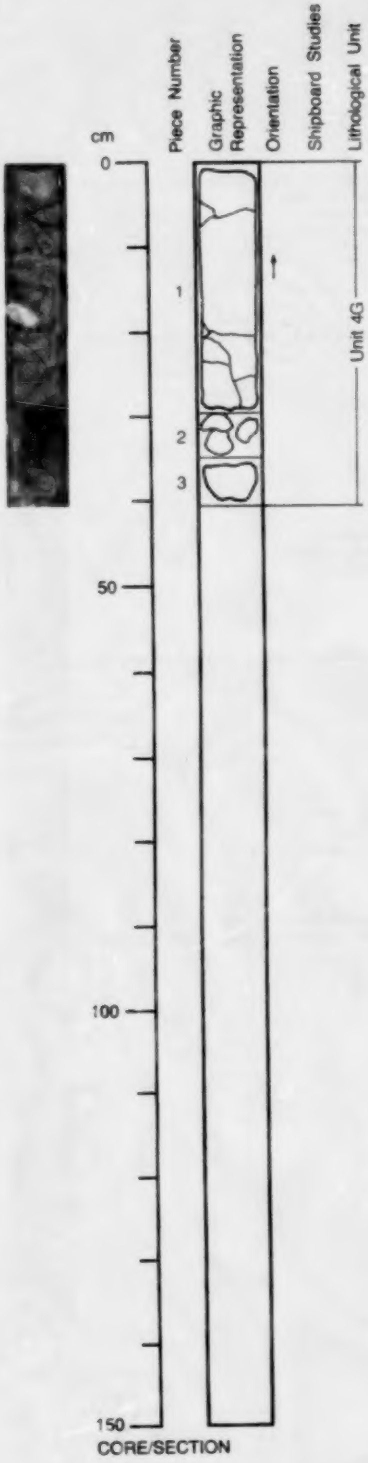
cm
Piece Number
Graphic Representation
Orientation
Shipboard Studies
Lithological Unit
0
50
100
150
1
2
3
Unit 4G
CORE/SECTION

130-807C-86R-4

UNIT 4G: APHYRIC BASALT

Pieces 1-3

CONTACTS: None.
PHENOCRYSTS:
  Plagioclase - <1%; 0.2-0.5 mm; euhedral.
  Olivine? - ~1%; 0.2-0.8 mm; euhedral.
GROUNDMASS: Fine grained.
VESICLES: Nonvesicular.
COLOR: Medium gray.
STRUCTURE: Massive, probably pillow.
ALTERATION: Slight to moderate.
VEINS/FRACTURES: <1%; <0.5-2 mm; subvertical to subhorizontal; filled with brown clay and minor calcite.

130-807C-87R-1

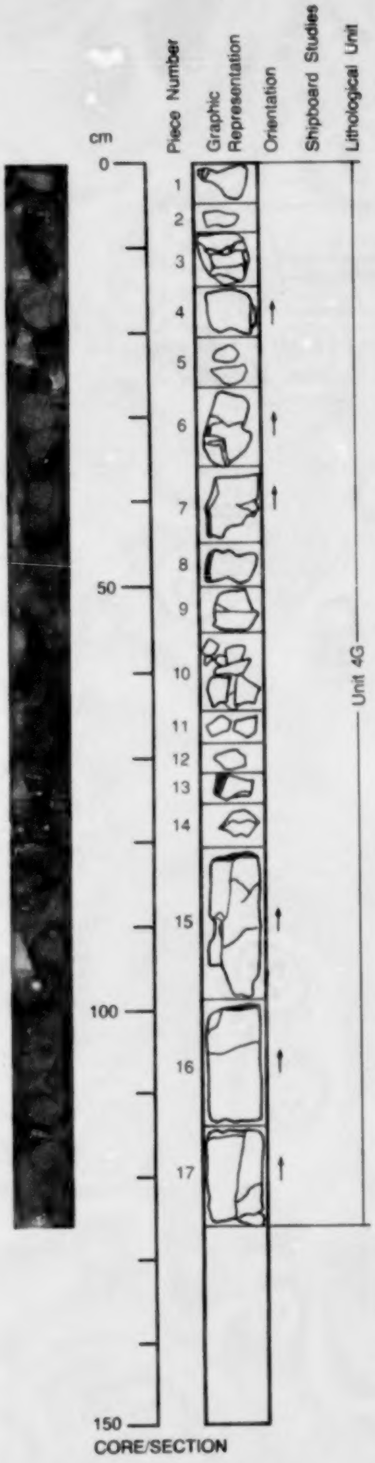
cm
Piece Number
Graphic Representation
Orientation
Shipboard Studies
Lithological Unit
0
50
100
150
1
2
3
4
5
6
7
8
9
10
11
12
13
14
15
16
17
Unit 4G
CORE/SECTION

UNIT 4G: APHYRIC BASALT

Pieces 1-17

CONTACTS: None.
PHENOCRYSTS:
Plagioclase - <<1%; 0.3-0.5 mm; subhedral.
Olivine? - ~1%; 0.3-0.8 mm; euhedral to subhedral.
GROUNDMASS: Fine grained with glassy margins.
VESICLES: Nonvesicular.
COLOR: Medium gray.
STRUCTURE: Pillow fragments.
ALTERATION: Slight to moderate.
VEINS/FRACTURES: <1%; <1 mm; varied orientation; filled with black clay and minor calcite.

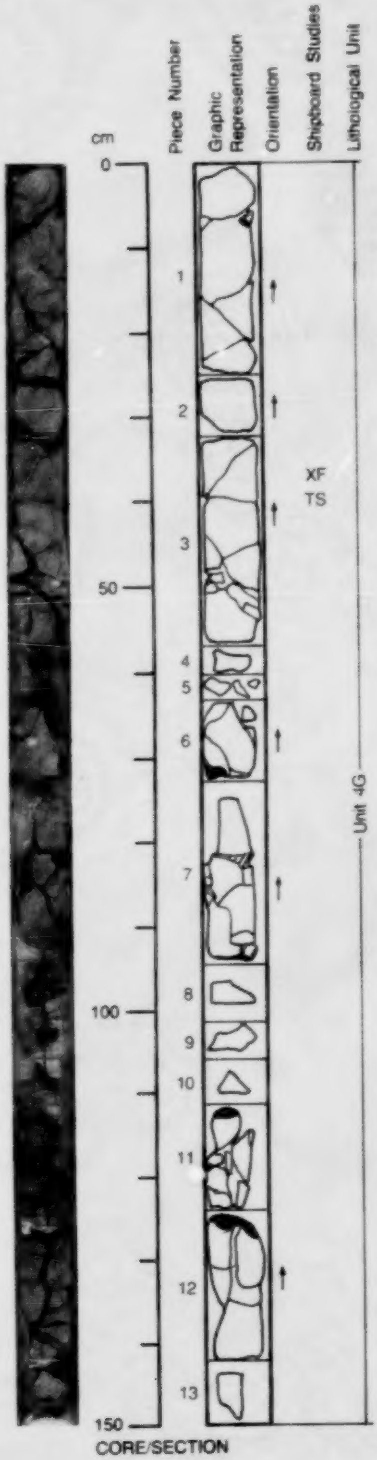
cm
Piece Number
Graphic Representation
Orientation
Shipboard Studies
Lithological Unit
0
50
100
150
1
2
3
4
5
6
7
8
9
10
11
12
13
XF
TS
Unit 4G
CORE/SECTION

130-807C-87R-2

UNIT 4G: APHYRIC BASALT

Pieces 1-13

CONTACTS: Glassy rim fragments.

PHENOCRYSTS:

Plagioclase - <1%; 0.3-0.8 mm; subhedral, some in association with olivine and/or clinopyroxene.

Olivine? - ~1%; 0.3-1 mm; subhedral to euhedral.

Clinopyroxene? - <1%; 0.3-1 mm; subhedral to euhedral.

GROUNDMASS: Fine grained to glassy near several rims.

VESICLES: Nonvesicular.

COLOR: Medium gray with blotchy, black areas of alteration in Piece 1.

STRUCTURE: Pillow lava fragments.

ALTERATION: Slight to high in Piece 1, irregular blotches of black to dark green clay up to 3 cm across in Piece 1.

VEINS/FRACTURES: ~1%; <0.5-2 mm; varied; highly fractured; veins filled with dark green to black clay, some Fe-oxide (?), minor calcite.

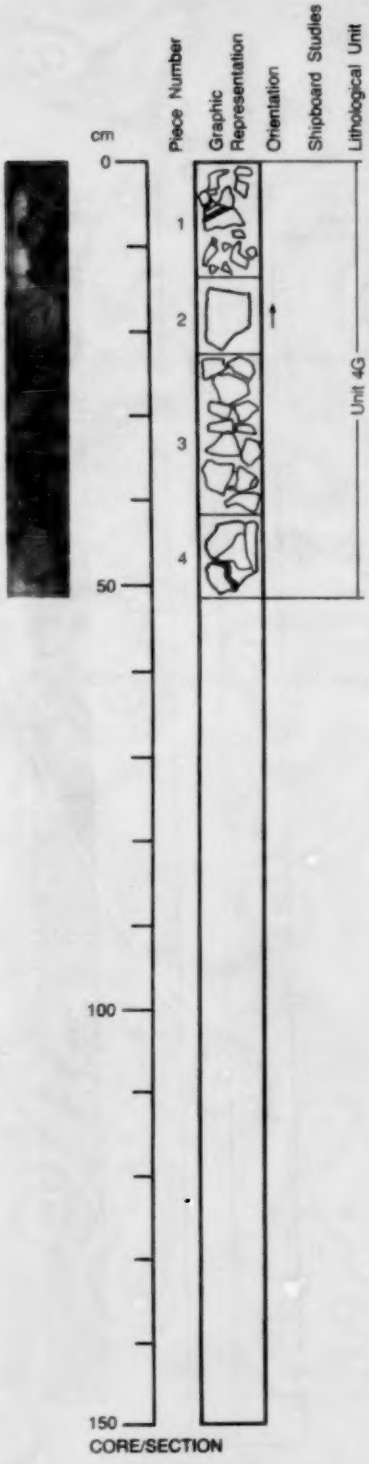
cm
Piece Number
Graphic Representation
Orientation
Shipboard Studies
Lithological Unit
0
1
2
3
4
50
Unit 4G
100
150
CORE/SECTION

130-807C-87R-3

UNIT 4G: APHYRIC BASALT

Pieces 1-4

CONTACTS: None.
Plagioclase - <<1%; 0.3-0.5 mm; subhedral.
Olivine? - ~1%; 0.3-1 mm; euhedral to subhedral.
GROUNDMASS: Fine grained; some very altered glass in Piece 1.
VESICLES: Nonvesicular.
COLOR: Medium gray.
STRUCTURE: Pillows.
ALTERATION: Slight in Pieces 2 and 4.
VEINS/FRACTURES: ~3%; <0.5-3 mm; original orientation unknown; filled with brown clay and/or Fe-oxide.

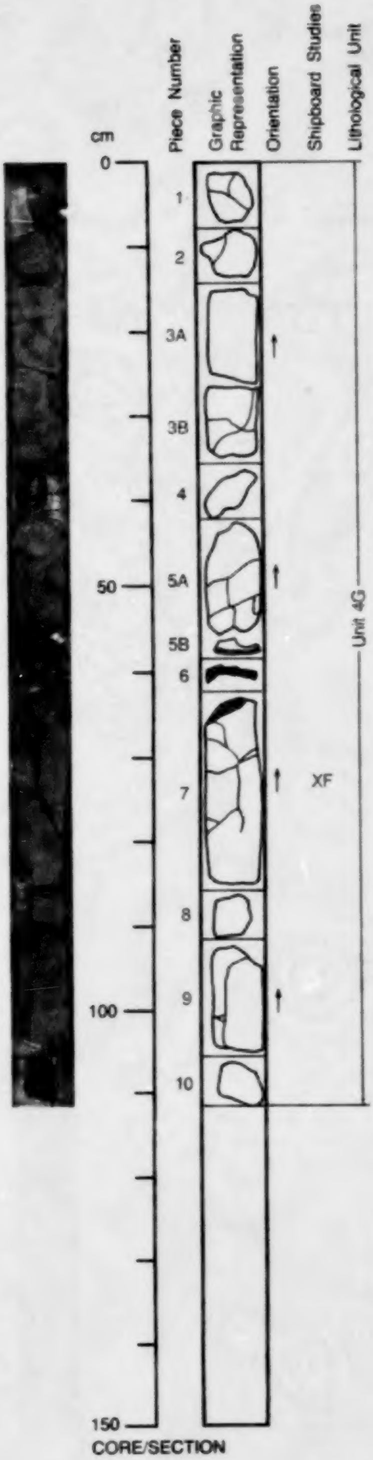
cm
Piece Number
Graphic Representation
Orientation
Shipboard Studies
Lithological Unit
0
50
100
150
1
2
3A
3B
4
5A
5B
6
7
8
9
10
XF
Unit 4G
CORE/SECTION

130-807C-88R-1

UNIT 4G: APHYRIC BASALT.

Pieces 1-5

CONTACTS: None.
PHENOCRYSTS:
Olivine? - ~1%; 0.2-0.8 mm; subhedral to euhedral.
Clinopyroxene? - <<1%; 0.2-0.8 mm; subhedral to euhedral.
Plagioclase - <<1%; 0.2-0.8 mm; euhedral.
GROUNDMASS: Fine grained.
VESICLES: Nonvesicular.
COLOR: Medium gray.
STRUCTURE: Massive, probably thick pillow lava.
ALTERATION: Slight.
VEINS/FRACTURES: <1%; 0.5-1 mm; varied orientation; filled with brown clay and/or oxide.

UNIT 4G: APHYRIC BASALT

Pieces 6-10

CONTACTS: None.
PHENOCRYSTS:
Olivine? - ~1%; 0.2-1 mm; subhedral to euhedral.
Clinopyroxene? - <<1%; up to 1 mm; subhedral.
Plagioclase - <<1%; up to 0.5 mm; subhedral.
GROUNDMASS: Fine grained, glassy upper margin.
VESICLES: Nonvesicular.
COLOR: Medium gray.
STRUCTURE: Massive, probably thick pillow lava flow.
ALTERATION: Slight.
VEINS/FRACTURES: <1%; ~0.5 mm; varied orientation; filled with dark green clay.

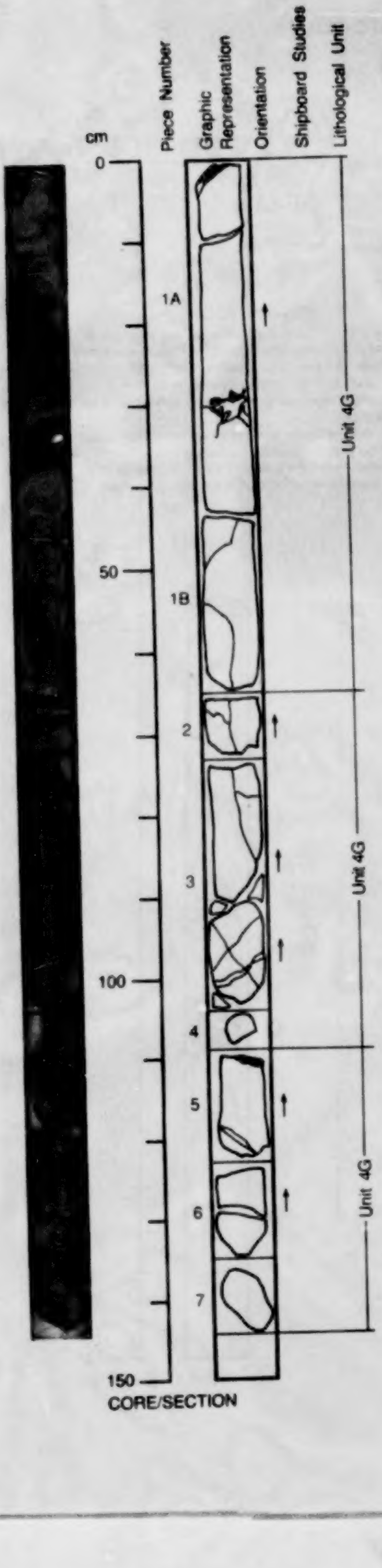
cm
Piece Number
Graphic Representation
Orientation
Shipboard Studies
Lithological Unit
0
50
100
150
1A
1B
2
3
4
5
6
7
Unit 4G
Unit 4G
Unit 4G
CORE/SECTION

130-807C-88R-2

UNIT 4G: APHYRIC BASALT

Piece 1

CONTACTS: Glass at top and bottom.
PHENOCRYSTS:
Olivine? - <1%; 0.2-0.8 mm; subhedral.
Clinopyroxene? - <<1%; 0.2-0.5 mm; subhedral.
Plagioclase - <<1%; 0.2-0.5 mm; subhedral.
GROUNDMASS: Fine grained, coarser in interior.
VESICLES: Nonvesicular.
COLOR: Medium gray.
STRUCTURE: Massive, thick pillow (?).
ALTERATION: Slight except near vein at 34 cm.
VEINS/FRACTURES: <1%; <0.5-3 mm; subhorizontal; irregular brown and black blotches up to 6 mm across.

UNIT 4G: APHYRIC BASALT

Pieces 2-4

CONTACTS: Upper glassy margin.
PHENOCRYSTS:
Clinopyroxene? - <1%; 0.2-1 mm; subhedral.
Olivine? - <1%; 0.2 mm; subhedral.
GROUNDMASS: Fine grained to glassy at top of Piece 2.
VESICLES: Nonvesicular.
COLOR: Medium gray to dark gray and brown in altered patches.
STRUCTURE: Massive.
ALTERATION: Slight to high in central portion.
VEINS/FRACTURES: 2%; <0.5-3.0 mm; varied orientation; one subhorizontal calcite vein; one subvertical dark brown oxide and/or clay vein.

UNIT 4G: APHYRIC BASALT

Pieces 5-7

CONTACTS: Piece 5 has glassy margin.
PHENOCRYSTS:
Olivine? - ~1%; 0.2-1 mm; euhedral to subhedral.
Clinopyroxene? - <1%; 0.2-1 mm; euhedral to subhedral.
GROUNDMASS: Fine grained to glassy at top.
VESICLES: Nonvesicular.
COLOR: Medium gray.
STRUCTURE: Pillow lava.
ALTERATION: Slight.
VEINS/FRACTURES: <1%; ~1 mm; minor radial fractures' calcite in glass (Piece 5).

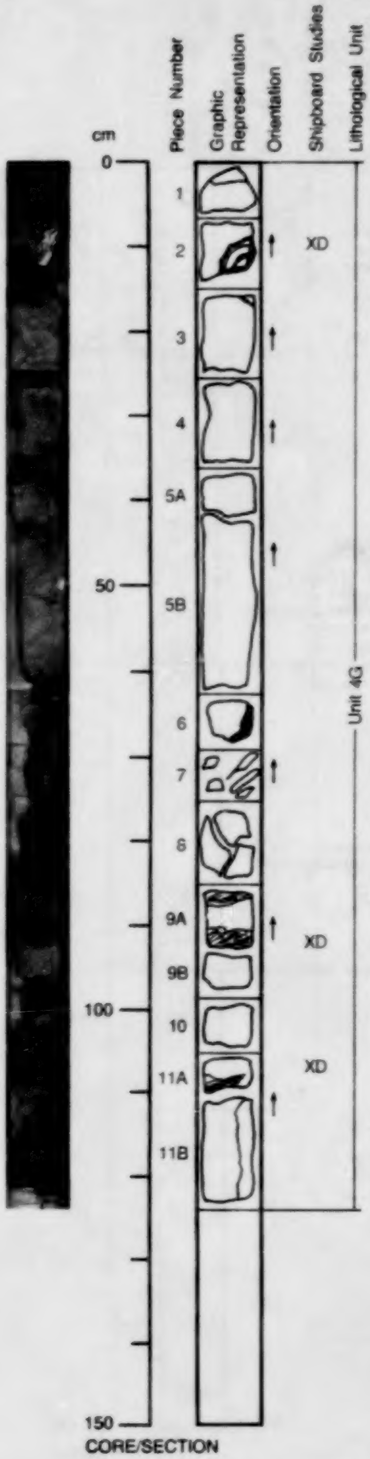
cm
Piece Number
Graphic Representation
Orientation
Shipboard Studies
Lithological Unit
0
50
100
150
1
2
3
4
5A
5B
6
7
8
9A
9B
10
11A
11B
XD
XD
XD
Unit 4G
CORE/SECTION

130-807C-88R-3

UNIT 4G: APHYRIC BASALT

Pieces 1-11

CONTACTS: Glassy margins in Pieces 2, 3, and 6.
PHENOCRYSTS:
Olivine? - ~1%; 0.2-1 mm; subhedral to euhedral.
Clinopyroxene? - <<1%; 0.2-1 mm; subhedral.
Plagioclase - <<1%; 0.2-0.5 mm; subhedral.
GROUNDMASS: Fine grained to glassy margins.
VESICLES: Nonvesicular.
COLOR: Medium gray to dark gray in patches.
STRUCTURE: Pillow to massive.
ALTERATION: Slight to high.
VEINS/FRACTURES: Piece 2 has part of a vein ~1-3 cm thick between two inter-pillow glass and calcite rims. The vein material is light gray-green, hard, and effervesces only slightly in HCl (baked sediment?). Pieces 3-6 have <1% veins/fractures, <0.5 mm-1.5 mm, varied orientations between horizontal and 45°, infilled by orange-brown mineral; Piece 9 has 2 veins (one 3 cm wide) of a blue-green mineral with blebs of an orange-brown mineral, along with black clay.
ADDITIONAL COMMENTS: Piece 11 has veins at upper and lower contacts with basalt. Vein material nearest the contact with the basalt consists of a dark-green to blue-green mineral, 0.5-1 cm thick. The material which forms the center of the vein consists of a dark blue-gray mineral with patches of a red-brown mineral that has a slight metallic to waxy luster on fresh cut surfaces.

130-807C-88R-4

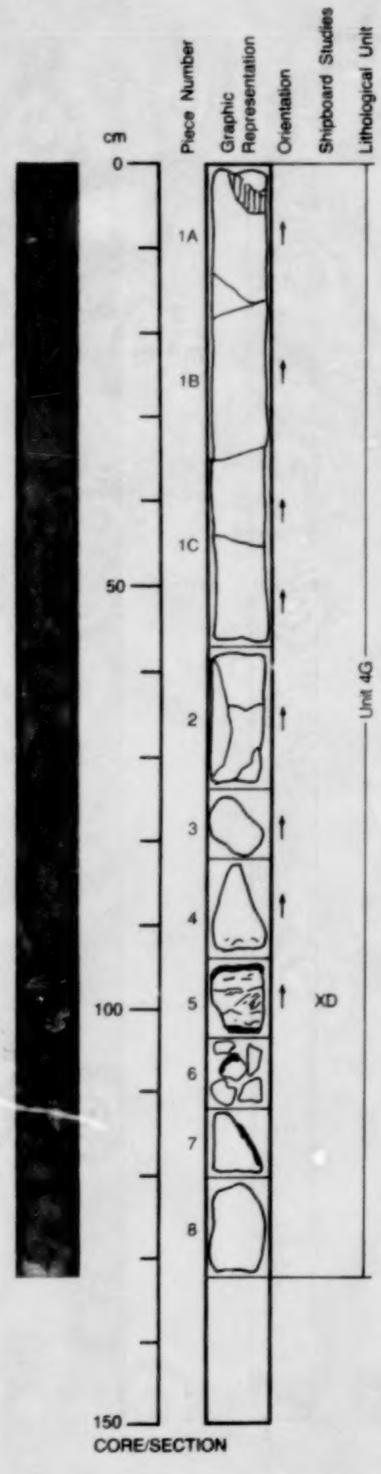

UNIT 4G: APHYRIC BASALT

Pieces 1-4

CONTACTS: None.
PHENOCRYSTS:
Olivine? - ~1%; 0.2-0.8 mm; subhedral to euhedral.
Clinopyroxene? - <<1%; 0.2-0.8 mm; subhedral.
Plagioclase - <<1%; 0.2-0.8 mm; subhedral.
GROUNDMASS: Fine grained.
VESICLES: Nonvesicular.
COLOR: Medium gray to bluish or greenish gray in altered patches.
STRUCTURE: Massive.
ALTERATION: Slight to high, especially top of Piece 1.
VEINS/FRACTURES: ~3%; <0.5 mm to >3 cm; varied orientation; thin veins consist of green and brown minerals;one thick vein at the top with ~ 6-10 mm dark green mineral (clay?) in layer nearest basalt, top 1.5 cm contains dark-gray and reddish-brown minerals.

UNIT 4G: APHYRIC BASALT

Pieces 5-8

CONTACTS: Glass on Piece 7 (pillow margin).
PHENOCRYSTS:
Olivine? - ~1%; 0.2-1 mm; subhedral.
Clinopyroxene? - <<1%; 0.2-0.5 mm; subhedral.
Plagioclase - <<1%; 0.2-0.5 mm; subhedral.
GROUNDMASS: Fine grained to glassy at margin of Piece 7.
VESICLES: Nonvesicular.
COLOR: Medium gray.
STRUCTURE: Massive-pillow.
ALTERATION: Slight.
VEINS/FRACTURES: <1%; <1 mm; varied orientation; filled with brown clay.
ADDITIONAL COMMENTS: Piece 5 is an interflow limestone breccia with green altered glass shards on either side of a 2.5-4 cm thick vein with irregular margins. Vein filling is light brown on top, non-effervescing in HCl, darker brown in middle, with calcite and light green mineral on bottom.

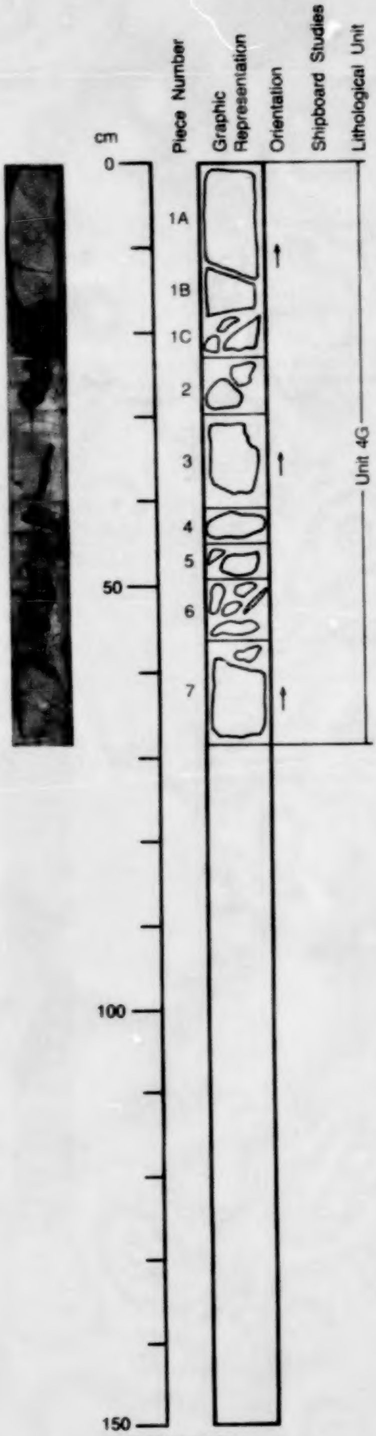
cm
Piece Number
Graphic Representation
Orientation
Shipboard Studies
Lithological Unit
0
50
100
150
1A
1B
1C
2
3
4
5
6
7
Unit 4G
CORE/SECTION

130-807C-88R-5

UNIT 4G: APHYRIC BASALT

Pieces 1-7

CONTACTS: None.
PHENOCRYSTS:
Olivine? - ~1%; 0.2-0.8 mm; subhedral.
Clinopyroxene? - <<1%; 0.2-0.5 mm; subhedral.
Plagioclase - <<1%; 0.2-0.5 mm; subhedral.
GROUNDMASS: Fine grained.
VESICLES: Nonvesicular.
COLOR: Medium gray.
STRUCTURE: Massive in Piece 1.
ALTERATION: Slight.
VEINS/FRACTURES: <1%; <0.5 to 1 mm; varied orientation; filled with brown clay (?), lesser calcite.

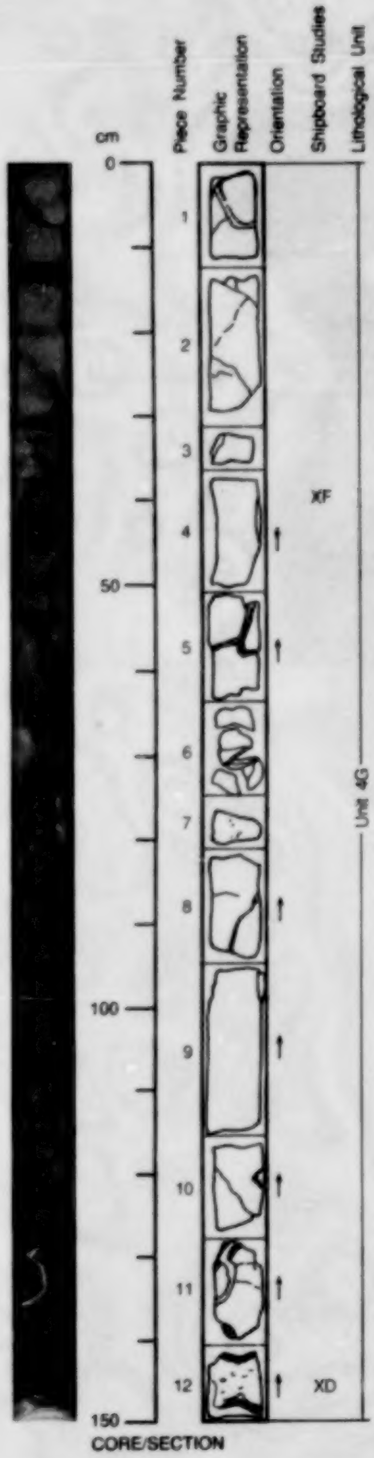
cm
Piece Number
Graphic Representation
Orientation
Shipboard Studies
Lithological Unit
0
50
100
150
1
2
3
4
5
6
7
8
9
10
11
12
XF
XD
Unit 4G
CORE/SECTION

130-807C-89R-1

UNIT 4G: APHYRIC BASALT

Pieces 1-10

CONTACTS: None.
PHENOCRYSTS:
Olivine? - <1%; 0.2-0.8 mm; euhedral to subhedral.
Clinopyroxene? - <<1%; 0.2-0.8 mm; subhedral.
GROUNDMASS: Fine grained.
VESICLES: Nonvesicular.
COLOR: Medium gray, bluish tinge in altered zone near veins.
STRUCTURE: Massive.
ALTERATION: Slight, moderate in a few small patches, minor pyrite in groundmass.
VEINS/FRACTURES: <<1%; <0.5-1 mm; varied orientation; dark blue clay, calcite and pyrite (fracture in Piece 5).

UNIT 4G: APHYRIC BASALT

Pieces 11,12

CONTACTS: Glassy upper and lower margins.
PHENOCRYSTS:
Olivine? - ~1%; 0.2-0.8 mm; euhedral to subhedral.
Clinopyroxene? - <1%; 0.2-1 mm; subhedral.
Plagioclase - <1%; 0.2-1 mm; subhedral.
GROUNDMASS: Fine grained to glassy at margins.
VESICLES: Nonvesicular.
COLOR: Medium gray.
STRUCTURE: Small pillow.
ALTERATION: Slight.
VEINS/FRACTURES: ~5%; 2-5 mm; varied orientation; calcite vein; <0.5 mm brown clay and/or Fe-oxide (?) vein.
ADDITIONAL COMMENTS: Piece 12 is a vein of a dark-olive green mineral, as in Piece 2, Core 130-807C-88R. Non-effervescent in HCl. Contains 0.5-2 mm clasts (?) of calcite which look like subhedral pseudomorphs of another mineral. Upper and lower portions of this piece are glassy-calcite inter-pillow breccias. Could be baked clay sediment.

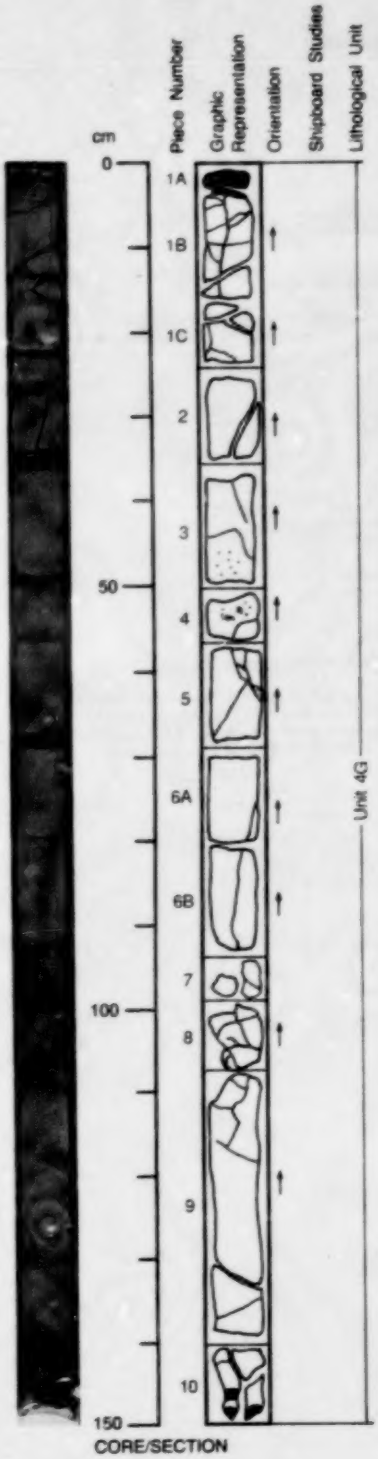
cm
Piece Number
Graphic Representation
Orientation
Shipboard Studies
Lithological Unit
0
50
100
150
1A
1B
1C
2
3
4
5
6A
6B
7
8
9
10
Unit 4G
CORE/SECTION

130-807C-89R-2

UNIT 4G: APHYRIC BASALT

Pieces 1-6

CONTACTS: Glassy top.
PHENOCRYSTS:
Olivine? - ~1%; 0.2-1 mm; euhedral to subhedral.
Clinopyroxene? - <<1%; 0.2-0.5 mm; subhedral.
Plagioclase - <<1%; 0.2-0.5 mm; subhedral, associated with olivine and/or clinopyroxene.
GROUNDMASS: Fine grained, glassy at top margin.
VESICLES: Nonvesicular.
COLOR: Medium gray; bluish gray in altered patches.
STRUCTURE: Massive.
ALTERATION: Slight to moderate; bluish patches in Pieces 1 and 2.
VEINS/FRACTURES: ~1%; <0.5-2 mm; varied orientation; mostly in Piece 1; filled with brown clay and dark brown to dark blue-gray clay; minor calcite.

UNIT 4G: APHYRIC BASALT

Pieces 7-10

CONTACTS: Lower glassy margin.
PHENOCRYSTS:
Olivine? - ~1%; 0.2-0.5 mm; euhedral to subhedral.
GROUNDMASS: Fine grained, glassy at bottom.
VESICLES: Nonvesicular.
COLOR: Medium gray.
STRUCTURE: Pillow or thin, massive, flow.
ALTERATION: Slight to moderate.
VEINS/FRACTURES: <1%; <1 mm wide; varied orientation; filled with brown or dark blue-green clays.

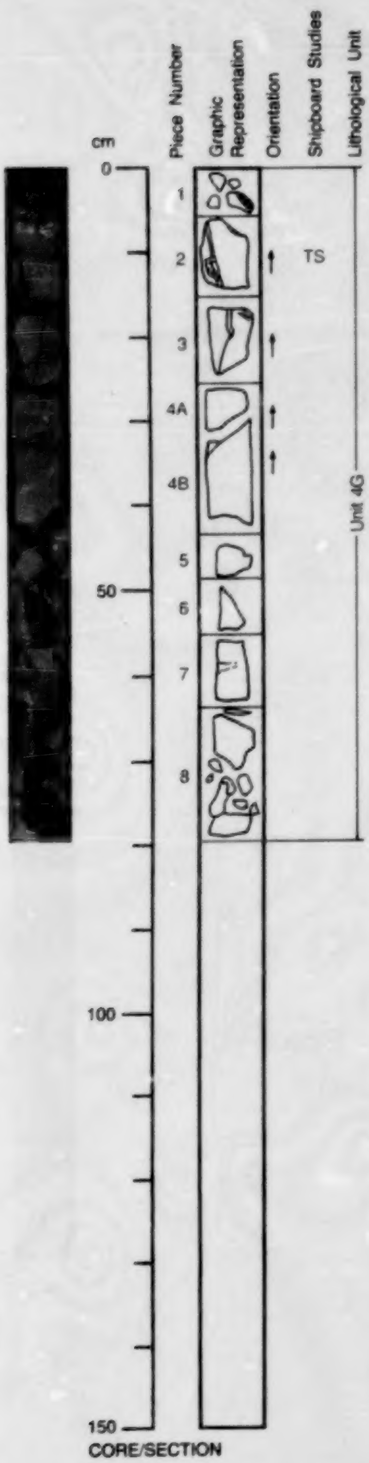
cm
Piece Number
Graphic Representation
Orientation
Shipboard Studies
Lithological Unit
0
50
100
150
1
2
3
4A
4B
5
6
7
8
TS
Unit 4G
CORE/SECTION

130-807C-89R-3

UNIT 4G: APHYRIC BASALT

Pieces 1-8

CONTACTS: None.
PHENOCRYSTS:
  Plagioclase - <<1%; 0.2-0.8 mm; subhedral.
  Olivine? - ~1%; 0.2-0.8 mm; subhedral to euhedral.
  Clinopyroxene? - <1%; 0.2-0.8 mm; subhedral to euhedral.
GROUNDMASS: Fine grained.
VESICLES: Nonvesicular.
COLOR: Medium gray.
STRUCTURE: Massive or thick pillow lava.
ALTERATION: Slight.
VEINS/FRACTURES: ~2%; <1-3 mm; subvertical; Pieces 2 and 3 have brownish mineral and dark blue-green to black clays.

130-807C-90R-1

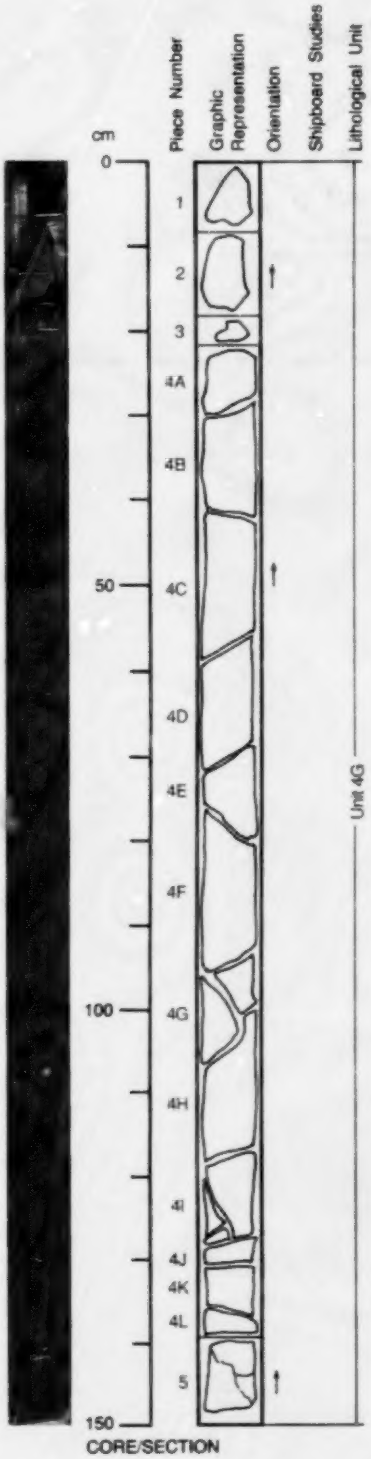
cm
Piece Number
Graphic Representation
Orientation
Shipboard Studies
Lithological Unit
0
50
100
150
1
2
3
4A
4B
4C
4D
4E
4F
4G
4H
4I
4J
4K
4L
5
Unit 4G
CORE/SECTION

UNIT 4G: APHYRIC BASALT

Pieces 1-5

CONTACTS: None.
PHENOCRYSTS:
Olivine? - <<1%; ~1 mm; subhedral.
GROUNDMASS: Fine grained.
VESICLES: Nonvesicular.
COLOR: Medium gray.
STRUCTURE: Massive flow.
ALTERATION: Slight.
VEINS/FRACTURES: <<1%; <1 mm; varied orientation; small amounts of calcite, dark smectite and traces of pyrite.

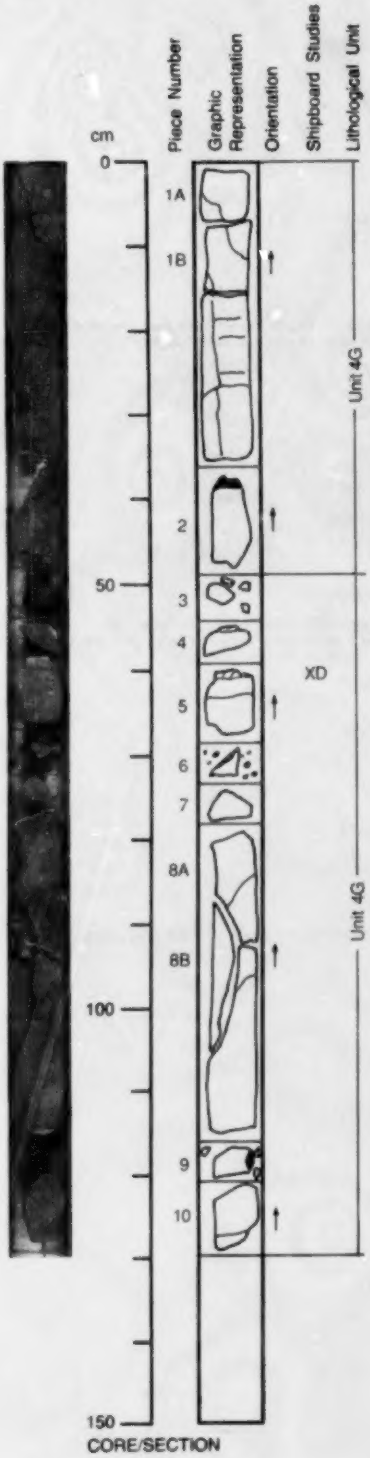

130-807C-90R-2

UNIT 4G: APHYRIC BASALT

Pieces 1, 2

CONTACTS: Glassy pillow margin, Piece 2.
PHENOCRYSTS: Olivine mainly altered to dark green clay.
Olivine - ~1%; 0.2-0.6 mm; subhedral to eudedral.
Plagioclase - <1%; 0.2-1 mm; subhedral to euhedral.
GROUNDMASS: Fine grained to glassy (margin of Piece 2).
VESICLES: Nonvesicular.
COLOR: Medium gray
STRUCTURE: Pillow.
ALTERATION: Slight to moderate.
VEINS/FRACTURES: 1%; 0.5-3 mm; subvertical to subhorizontal; calcite, green blue (clay?) mineral, orange-brown mineral (goethite).

UNIT 4G: APHYRIC BASALT

Pieces 3-8

CONTACTS: None.
PHENOCRYSTS:
Olivine - <1%; 0.2-0.6 mm; subhedral to euhedral.
Plagioclase - <<1%; 0.2-1 mm; subhedral to euhedral.
GROUNDMASS: Fine grained.
VESICLES: ~1%; up to 4 mm; oval to irregular; top of Piece 8A; infilled with green/brown clays.
COLOR: Medium gray.
STRUCTURE: Pillow.
ALTERATION: Moderate.
VEINS/FRACTURES: ~1%; 1-3 mm; varied orientation; infilled with calcite, green-blue clay (?), an orange-brown mineral (goethite?). Piece 4 and 5 have a subhorizontal 1 cm vein containing calcite and a light green mineral, with lesser amounts of orange-brown mineral. The margin of the vein consists of very dark gray-green mineral (0.5 mm thick). Veins also are located in Pieces 1B and 8B.

UNIT 4G: APHYRIC BASALT

Pieces 9, 10

CONTACTS: None.
PHENOCRYSTS:
Olivine - ~1%; 0.2-0.5 mm; subhedral to euhedral.
Plagioclase - <1%; 0.2-1mm; subhedral to euhedral.
GROUNDMASS: Fine grained to glassy (margin Piece 9).
VESICLES: Nonvesicular.
COLOR: Medium gray.
STRUCTURE: Pillow.
ALTERATION: Slight to moderate.
VEINS/FRACTURES: <1%; 0.5-1 mm; varied orientation; filled with calcite, clays and orange-brown mineral (goethite?).

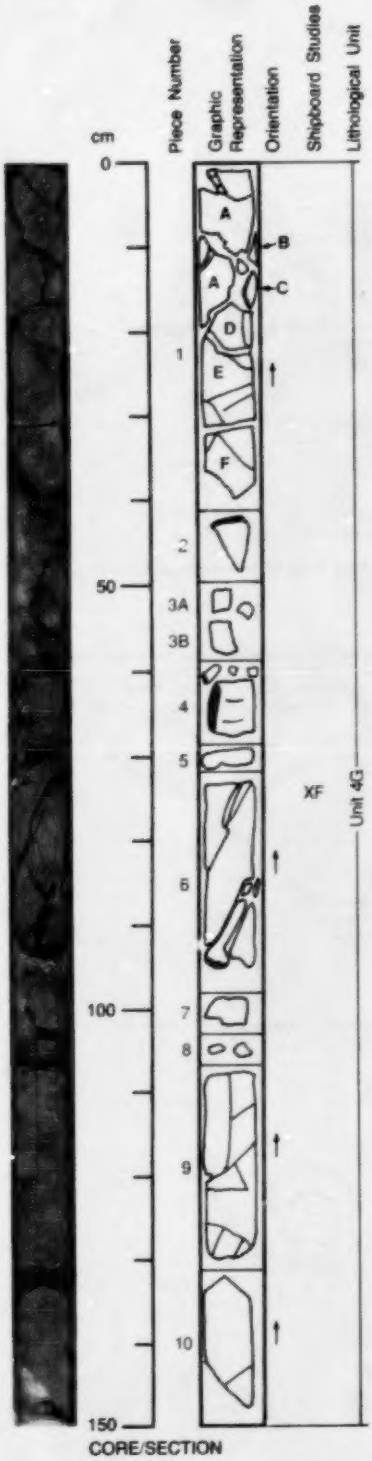
cm
Piece Number
Graphic Representation
Orientation
Shipboard Studies
Lithological Unit
0
50
100
150
1
2
3A
3B
4
5
6
7
8
9
10
A
B
A
C
D
E
F
XF
Unit 4G
CORE/SECTION

130-807C-90R-3

UNIT 4G: APHYRIC BASALT

Piece 1

CONTACTS: None.
PHENOCRYSTS:
Olivine - ~1%; 0.3-0.8 mm; subhedral to euhedral.
GROUNDMASS: Fine grained.
VESICLES: Nonvesicular.
COLOR: Medium gray.
STRUCTURE: Pillow.
ALTERATION: Slight to moderate.
VEINS/FRACTURES: ~1%; 0.5-5 mm; varied orientation; calcite, filled with dark gray-blue clay (?), pyrite, a light orange-brown mineral, with semi-metallic luster (goethite?).

UNIT 4G: APHYRIC BASALT

Pieces 2-6

CONTACTS: Glassy pillow margin (Pieces 2, 4, and 6).
PHENOCRYSTS:
Olivine? - ~1%; 0.3-1 mm; subhedral to euhedral.
GROUNDMASS: Fine grained to glassy.
VESICLES: Nonvesicular.
COLOR: Medium to dark gray.
STRUCTURE: Pillow.
ALTERATION: Slight to moderate.
VEINS/FRACTURES: <1%; 0.5-4 mm; varied orientation; glass margin on Piece 4 is heavily calcite veined. Piece 6 has 1 mm thick vein at top consisting of a dark gray-green mineral with small (~0.2 mm) blebs of a orange-brown mineral (goethite?).

UNIT 4G: APHYRIC BASALT

Pieces 7-10

CONTACTS: None.
PHENOCRYSTS:
Olivine - <1%; 0.3-1 mm; subhedral to euhedral.
GROUNDMASS: Fine grained.
VESICLES: Nonvesicular.
COLOR: Medium gray.
STRUCTURE: Massive.
ALTERATION: Slight.
VEINS/FRACTURES: ~1%; 0.5-2 mm; vertical, subhorizontal and ~ 45°; dark gray-green clay, minor pyrite.

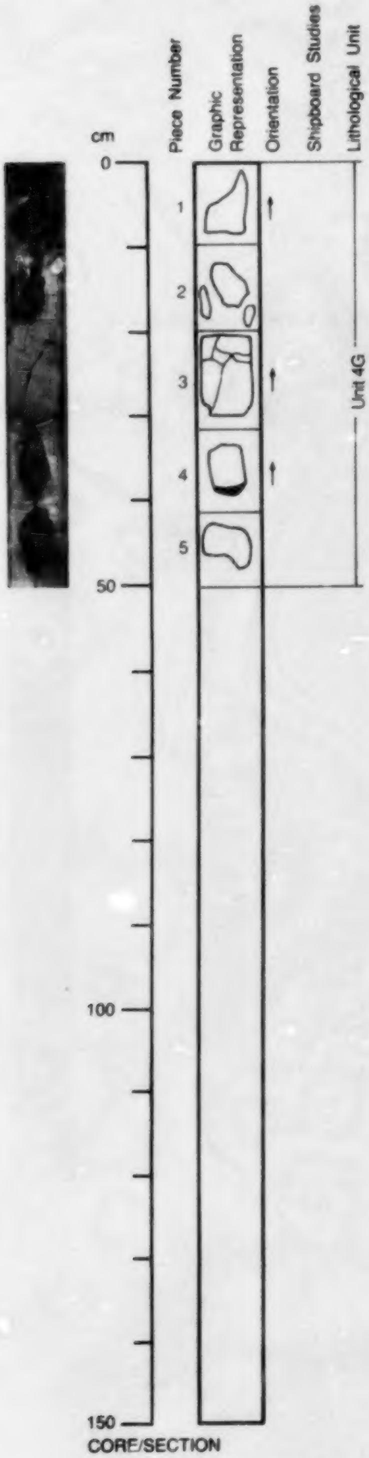
cm
Piece Number
Graphic Representation
Orientation
Shipboard Studies
Lithological Unit
0
1
2
3
4
5
50
100
150
Unit 4G
CORE/SECTION

130-807C-90R-4

UNIT 4G: APHYRIC BASALT

Pieces 1-5

CONTACTS: Glassy pillow margin (Piece 4).
PHENOCRYSTS:
  Olivine - ~1%; 0.2-0.8 mm; subhedral to euhedral.
  Plagioclase - <<1%; 0.2-0.8 mm; subhedral to euhedral.
GROUNDMASS: Fine grained.
VESICLES: Nonvesicular.
COLOR: Medium to dark gray.
STRUCTURE: Pillow.
ALTERATION: Slight to moderate.
VEINS/FRACTURES: <1%; ~0.5 mm; varied orientation; fracture surfaces stained black (manganese?), yellow-brown (Fe-oxides?) and/or dark green.

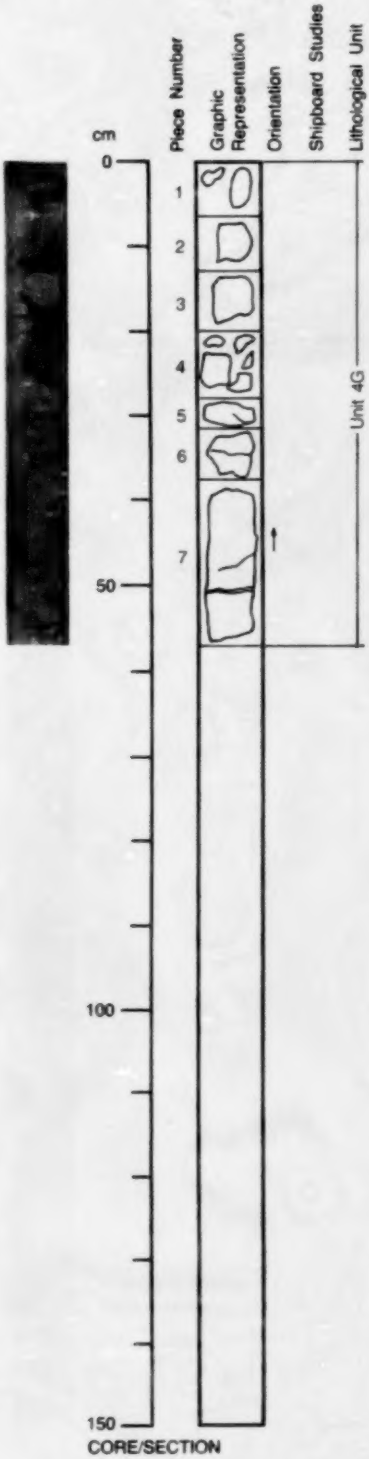
cm
Piece Number
Graphic Representation
Orientation
Shipboard Studies
Lithological Unit
0
1
2
3
4
5
6
7
50
100
150
Unit 4G
CORE/SECTION

130-807C-91R-1

UNIT 4G: APHYRIC BASALT

Pieces 1-7

CONTACTS: None.
PHENOCRYSTS:
Olivine - <1%; 0.3-1 mm; subhedral to euhedral.
GROUNDMASS: Fine grained.
VESICLES: Nonvesicular.
COLOR: Medium gray.
STRUCTURE: Massive.
ALTERATION: Slight to moderate.
VEINS/FRACTURES: <1%; 0.5-1 mm; subhorizontal; filled with dark gray clay, minor pyrite.

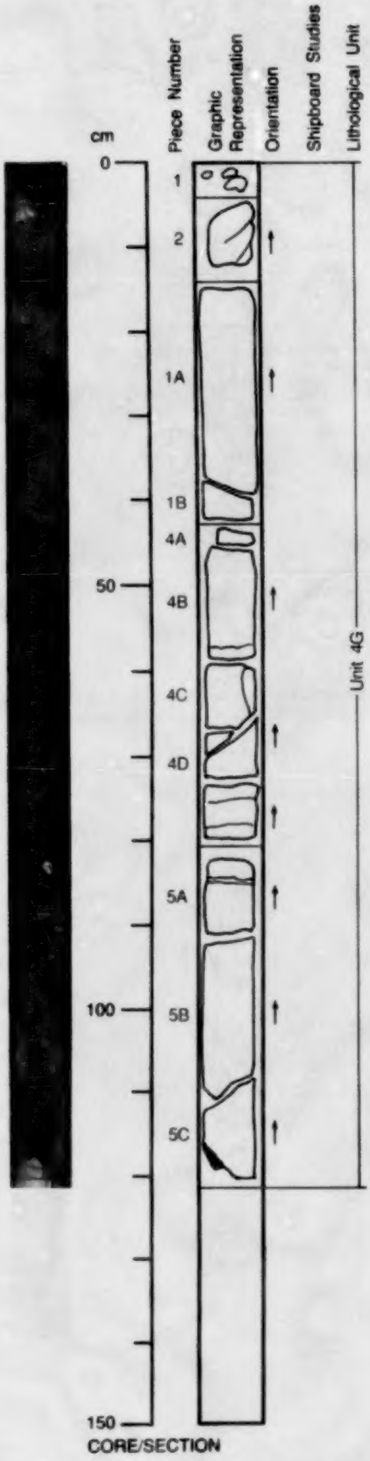
cm
Piece Number
Graphic Representation
Orientation
Shipboard Studies
Lithological Unit
0
50
100
150
1
2
1A
1B
4A
4B
4C
4D
5A
5B
5C
Unit 4G
CORE/SECTION

130-807C-92R-1

UNIT 4G: APHYRIC BASALT

Pieces 1-5

CONTACTS: Glassy flow margin, bottom of Piece 5C.
PHENOCRYSTS:
Olivine - ~1%; 0.2-1 mm; subhedral to euhedral.
GROUNDMASS: Fine grained to glassy (bottom of Piece 5C).
VESICLES: Nonvesicular.
COLOR: Medium to dark gray.
STRUCTURE: Massive.
ALTERATION: Slight.
VEINS/FRACTURES: <<1%; <1 mm; subhorizontal and 45°; filled with clay and calcite.

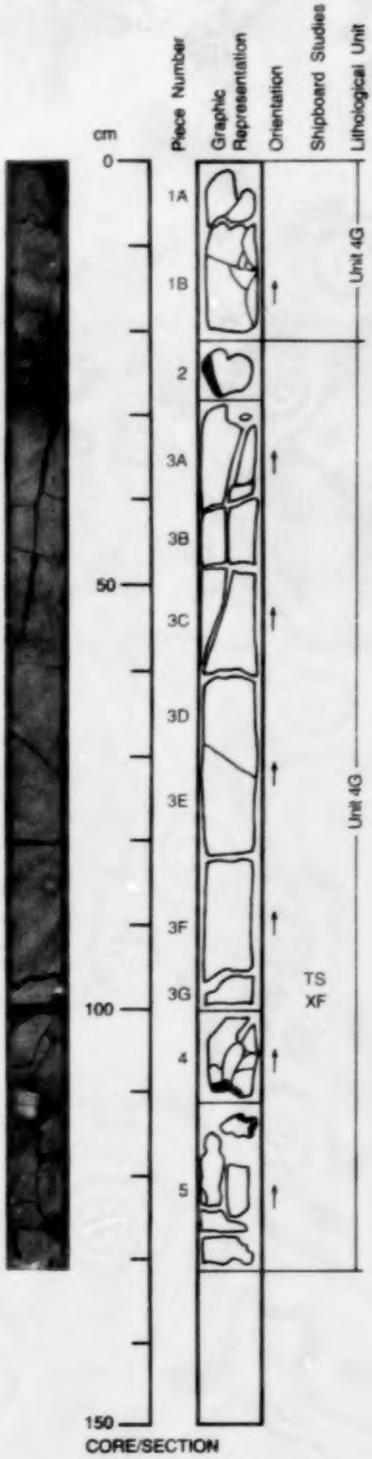
cm
Piece Number
Graphic Representation
Orientation
Shipboard Studies
Lithological Unit
0
50
100
150
1A
1B
2
3A
3B
3C
3D
3E
3F
3G
4
5
TS
XF
Unit 4G
Unit 4G
CORE/SECTION

130-807C-92R-2

UNIT 4G: APHYRIC BASALT

Piece 1

CONTACTS: None.
PHENOCRYSTS:
 Olivine - <1%; 0.2-0.8 mm; anhedral to euhedral.
 Plagioclase - <<1%; 0.2-1mm; subhedral to euhedral.
GROUNDMASS: Fine grained.
VESICLES: Nonvesicular.
COLOR: Medium gray.
STRUCTURE: Pillow.
ALTERATION: Slight to moderate.
VEINS/FRACTURES: 1%; <0.5-2 mm; varied orientation; infilled by an orange-brown mineral (goethite?), minor calcite, and green clays.

UNIT 4G: APHYRIC BASALT

Pieces 2-5

CONTACTS: Glassy flow margins, Pieces 2, 4, and 5.
PHENOCRYSTS:
 Olivine - <1%; 0.2-0.8 mm; subhedral to euhedral.
 Plagioclase - <<1%; 0.2-1 mm; subhedral to euhedral.
GROUNDMASS: Fine grained to glassy (Pieces 2, 4, and 5).
VESICLES: Nonvesicular.
COLOR: Medium gray to gray-black.
STRUCTURE: Thick pillow or massive.
ALTERATION: Slight to moderate.
VEINS/FRACTURES: ~1%; <0.5-2 mm; mostly subvertical and subhorizontal; infilled by blue-gray clays, and an orange-brown mineral. Glass in Piece 4 heavily veined by calcite.

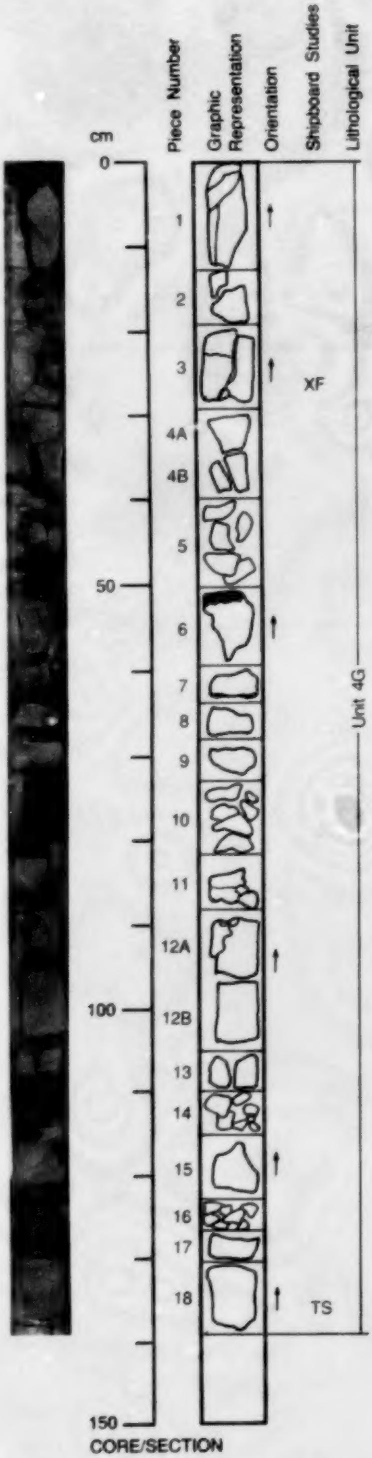
cm
Piece Number
Graphic Representation
Orientation
Shipboard Studies
Lithological Unit
0
50
100
150
1
2
3
4A
4B
5
6
7
8
9
10
11
12A
12B
13
14
15
16
17
18
XF
TS
Unit 4G
CORE/SECTION

130-807C-93R-1

UNIT 4G: APHYRIC BASALT

Pieces 1-18

CONTACTS: Glassy rims on Pieces 6 and 7.
PHENOCRYSTS:
Olivine - ~1%; 0.2-0.8 mm; subhedral to euhedral.
Plagioclase - <<1%; 0.2-0.5 mm; subhedral.
GROUNDMASS: Fine grained to glassy (rims of Pieces 6 and 7).
VESICLES: Nonvesicular.
COLOR: Medium gray.
STRUCTURE: Fragments of pillow lava.
ALTERATION: Slight, to moderate in Pieces 11 and 12 (near veins).
VEINS/FRACTURES: ~1%; <1->6 mm; varied orientation; filled with clay and small amounts of pyrite; 1 mm thick calcite veins in glass on Piece 6.

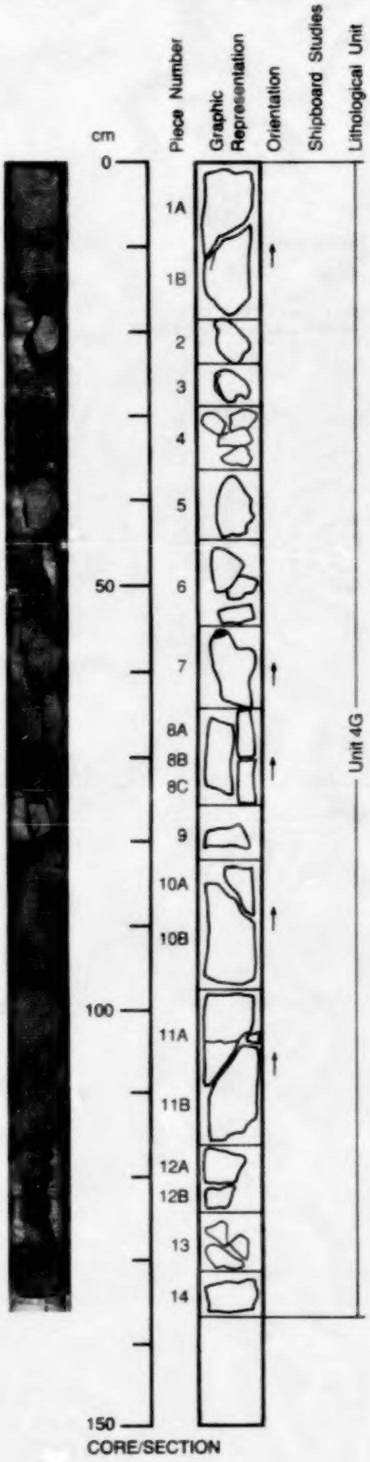
cm
Piece Number
Graphic Representation
Orientation
Shipboard Studies
Lithological Unit
0
1A
1B
2
3
4
5
50
6
7
8A
8B
8C
9
10A
10B
100
11A
11B
12A
12B
13
14
150
Unit 4G
CORE/SECTION

130-807C-93R-2

UNIT 4G: APHYRIC BASALT

Pieces 1-14

CONTACTS: None.
Olivine - ~1%; 0.2-1 mm; euhedral to subhedral.
Plagioclase - <<1%; 0.2-1 mm; subhedral.
GROUNDMASS: Fine grained.
VESICLES: Nonvesicular.
COLOR: Medium gray.
STRUCTURE: Pillow lava fragments; Pieces 7-14 are possibly fragments of more massive flow.
ALTERATION: Slight to moderate in a few patches.
VEINS/FRACTURES: <<1%; <1 mm; varied orientation; filled with dark gray clay and minor pyrite.

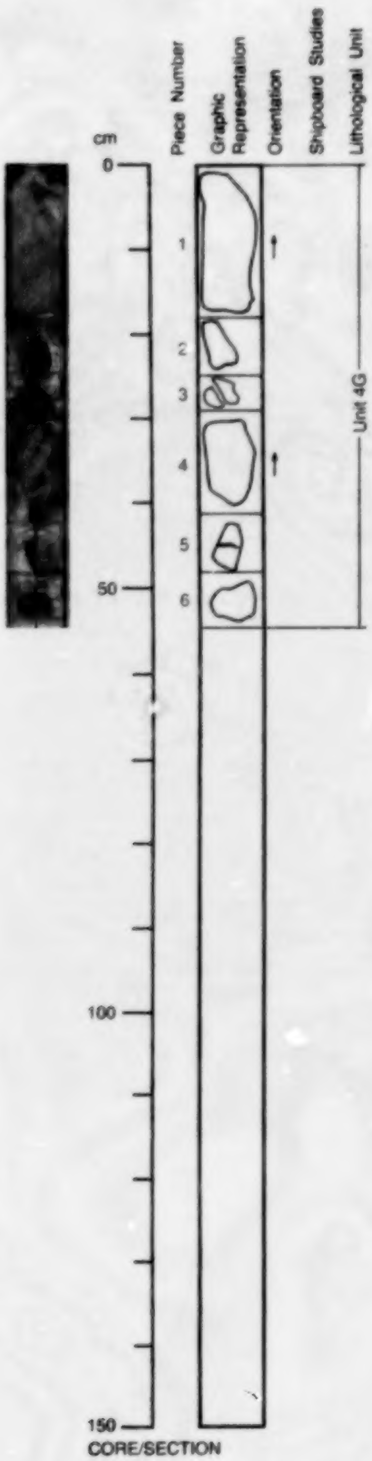
cm
Piece Number
Graphic Representation
Orientation
Shipboard Studies
Lithological Unit
0
50
100
150
1
2
3
4
5
6
Unit 4G
CORE/SECTION

130-807C-93R-3

UNIT 4G: APHYRIC BASALT

Pieces 1-6

CONTACTS: None.
PHENOCRYSTS:
Olivine - ~1%; 0.2-1 mm; subhedral to euhedral.
GROUNDMASS: Fine grained; dark band (1-5 mm wide) of mafic minerals in Piece 5.
VESICLES: Nonvesicular.
COLOR: Medium gray.
STRUCTURE: Massive. lava fragments.
ALTERATION: Slight to moderate.
VEINS/FRACTURES: None; filled with minor clays and calcite.

130-807C-74R-01 (Piece 6D,124-127 cm)   OBSERVER: JJM   WHERE SAMPLED: Pillow

ROCK NAME: Aphyric basalt

GRAIN SIZE: Fine grained

TEXTURE: Intersertal

PRIMARY MINERALOGY	PERCENT PRESENT	PERCENT ORIGINAL	SIZE (mm)	COMPO-SITION	MORPHOLOGY	COMMENTS
PHENOCRYSTS						
Plagioclase	<1	<1	0.3-1		euhedral	
Clinopyroxene	<1	<1	~0.3		subhedral	
GROUNDMASS						
Plagioclase	40	40	<0.5-0.1		laths	
Clinopyroxene	15	20	<0.1		anhedral	
Opaques	5	5	<0.05		anhedral	

SECONDARY MINERALOGY	PERCENT	REPLACING/ FILLING	COMMENTS
Clays	35	glass	Brownish.
Clays	5	clinopyroxene	Greenish to brown.
Clays	<1	vein	Bright green celadonite and black clay.

VESICLES/ CAVITIES	PERCENT	LOCATION	SIZE (mm)	FILLING	SHAPE
Vesicles	0				

130-807C-75R-02 (Piece 6D,60-61 cm)   OBSERVER: STO   WHERE SAMPLED: Pillow interior

ROCK NAME: Aphyric basalt

GRAIN SIZE: Fine grained

TEXTURE: Intergranular

PRIMARY MINERALOGY	PERCENT PRESENT	PERCENT ORIGINAL	SIZE (mm)	COMPO-SITION	MORPHOLOGY	COMMENTS
Plagioclase	30	30	0.05-0.5		subhedral to euhedral	
Clinopyroxene	10	10	~0.05		anhedral	

SECONDARY MINERALOGY	PERCENT	REPLACING/ FILLING	COMMENTS
Clays	50		

VESICLES/ CAVITIES	PERCENT	LOCATION	SIZE (mm)	FILLING	SHAPE
Vesicles	0				

```
130-807C-77R-01 (Piece 7,46-48 cm)          OBSERVER: JJM         WHERE SAMPLED: Pillow interior

ROCK NAME: Aphyric basalt

GRAIN SIZE: Fine grained

TEXTURE: Intersertal

-----------------------------------------------------------------------------------------------------------------------------

PRIMARY          PERCENT PERCENT  SIZE        COMPO-
MINERALOGY       PRESENT ORIGINAL (mm)        SITION              MORPHOLOGY                    COMMENTS

 PHENOCRYSTS
Plagioclase       <1      <1      0.5-1                          euhedral
Clinopyroxene     <<1     <<1     0.3-0.5                        anhedral

 GROUNDMASS
Plagioclase       30      30      ?                              subhedral
Clinopyroxene     10      20      ?                              anhedral
Glass             10      47      ?                              ?
Opaques           3       3       ?                              ?

SECONDARY                  REPLACING/
MINERALOGY       PERCENT    FILLING                                                     COMMENTS
Clays and         10      clinopyroxene                              Red-brown.
oxides
Clays             37      glass                                      Dark brown.
-----------------------------------------------------------------------------------------------------------------------------
VESICLES/                              SIZE
CAVITIES         PERCENT  LOCATION     (mm)                   FILLING                          SHAPE
Vesicles          0
-----------------------------------------------------------------------------------------------------------------------------

130-807C-78R-02 (Piece 7,72-73 cm)          OBSERVER: STO         WHERE SAMPLED: Part of massive flow

ROCK NAME: Aphyric basalt

GRAIN SIZE: Fine grained

TEXTURE: Subophitic

-----------------------------------------------------------------------------------------------------------------------------

PRIMARY          PERCENT PERCENT  SIZE        COMPO-
MINERALOGY       PRESENT ORIGINAL (mm)        SITION              MORPHOLOGY                    COMMENTS

 PHENOCRYSTS
Plagioclase       <1      <1      ~0.5                           euhedral laths
Clinopyroxene     <1      <1      ~0.4                           anhedral

 GROUNDMASS
Plagioclase       40      40      0.1-0.4                        thin euhedral laths
Clinopyroxene     40      40      0.05-0.3                       anhedral
Opaques           10      10      0.01-0.1                       anhedral           Some thin skeletal grains (ilmenite?).

SECONDARY                  REPLACING/
MINERALOGY       PERCENT    FILLING                                                     COMMENTS
Clays             10      glass?
-----------------------------------------------------------------------------------------------------------------------------
VESICLES/                              SIZE
CAVITIES         PERCENT  LOCATION     (mm)                   FILLING                          SHAPE
Vesicles          0
-----------------------------------------------------------------------------------------------------------------------------
```

Reproduced from poor document.

130-807C-79R-05 (Piece 3,28-30 cm)   OBSERVER: STO   WHERE SAMPLED: Part of massive flow

ROCK NAME: Aphyric basalt

GRAIN SIZE: Fine grained

TEXTURE: Intergranular

PRIMARY MINERALOGY	PERCENT PRESENT	PERCENT ORIGINAL	SIZE (mm)	COMPOSITION	MORPHOLOGY	COMMENTS
PHENOCRYSTS						
Plagioclase	<1	<1	~1		euhedral laths	
GROUNDMASS						
Plagioclase	60	60	0.1-0.5		thin euhedral laths	
Opaques	5	5	0.02-0.1		anhedral-subhedral	
Clinopyroxene	20	20	0.02-0.2		anhedral-subhedral	

SECONDARY MINERALOGY	PERCENT	REPLACING/ FILLING	COMMENTS
Clays	15	glass?	

VESICLES/ CAVITIES	PERCENT	LOCATION	SIZE (mm)	FILLING	SHAPE
Vesicles	0				

130-807C-80R-01 (Piece 6,49-51 cm)   OBSERVER: STO   WHERE SAMPLED: Near flow top

ROCK NAME: Aphyric basalt

GRAIN SIZE: Fine grained

TEXTURE: Intergranular

PRIMARY MINERALOGY	PERCENT PRESENT	PERCENT ORIGINAL	SIZE (mm)	COMPOSITION	MORPHOLOGY	COMMENTS
Plagioclase	35	35	0.1-0.5		euhedral thin laths	
Clinopyroxene	30	30	0.02-0.1		anhedral	
Opaques	5	5	0.01-0.1		equant and skeletal	

SECONDARY MINERALOGY	PERCENT	REPLACING/ FILLING	COMMENTS
Clays	30	glass	Green smectite.

VESICLES/ CAVITIES	PERCENT	LOCATION	SIZE (mm)	FILLING	SHAPE
Vesicles	0				

130-807C-81R-02 (Piece 4A,74-77 cm)   OBSERVER: STO   WHERE SAMPLED: Part of massivu flow

ROCK NAME: Aphyric basalt

GRAIN SIZE: Fine grained

TEXTURE: Intergranular-subophitic

PRIMARY MINERALOGY	PERCENT PRESENT	PERCENT ORIGINAL	SIZE (mm)	COMPOSITION	MORPHOLOGY	COMMENTS
PHENOCRYSTS						
? Clinopyroxene	<1	<1	up to 0.8		euhedral-subhedral	Altered to smectite.
GROUNDMASS						
Plagioclase	55	55	?		?	
Clinopyroxene	10	10	?		?	
Opaques	3	3	?		subhedral-anhedral	Equant and skeletal.

SECONDARY MINERALOGY	PERCENT	REPLACING/ FILLING	COMMENTS
Clays	32	mainly glass	Green and yellow-green smectites.

VESICLES/ CAVITIES	PERCENT	LOCATION	SIZE (mm)	FILLING	SHAPE
Vesicles	0				

130-807C-83R-02 (Piece 1B,28-30 cm) OBSERVER: STO WHERE SAMPLED: Part of massive flow

ROCK NAME: Aphyric basalt

GRAIN SIZE: Fine grained

TEXTURE: ??

PRIMARY MINERALOGY	PERCENT PRESENT	PERCENT ORIGINAL	SIZE (mm)	COMPO-SITION	MORPHOLOGY	COMMENTS
PHENOCRYSTS						
Olivine	<1	<1	~0.6		subhedral-euhedral	Completely replaced by olive-green mineral.
Plagioclase	<1	<1	~1		euhedral	
Clinopyroxene	<1	<1	~0.8		subhedral	
GROUNDMASS						
Plagioclase	40	40	0.1-1		thin euhedral laths	
Clinopyroxene	40	40	0.1-0.3		anhedral-subhedral	
Opaques	7	7	0.05-0.2		anhedral-subhedral	

SECONDARY MINERALOGY	PERCENT	REPLACING/ FILLING	COMMENTS
Clays	13	glass?	

VESICLES/ CAVITIES	PERCENT	LOCATION	SIZE (mm)	FILLING	SHAPE
Vesicles	0				

Reproduced from poor document.

SECTION 6: POLICY

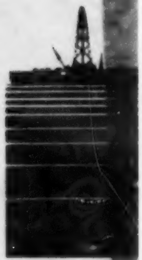

JOIDES ADVISORY GROUPS*

Executive Committee (EXCOM)

Charles E. Helsley
University of Hawaii

Roger N. Anderson (Wireline Logging Services liaison)
Columbia University

D. James Baker, Jr. (JOI liaison)
Joint Oceanographic Institutions, Inc.

Bernard Biju-Duval
IFREMER (France)

James C. Briden
Natural Environment Research Council (U.K.)

Douglas R. Caldwell
Oregon State University

Craig E. Dorman
Woods Hole Oceanographic Institution

Robert A. Duce
University of Rhode Island

Hans-J. Dürbaum
Bundesanstalt für Geowissenschaften und Rohstoffe

David Falvey
Bureau of Mineral Resources, Geology and Geophysics (Australia)

Edward A. Frieman
University of California, San Diego

G. Ross Heath
University of Washington

Donald F. Heinrichs (NSF liaison)
National Science Foundation (U.S.)

Dennis V. Kent
Columbia University

Arthur E. Maxwell
University of Texas at Austin

William J. Merrell, Jr.
Texas A&M University at Galveston

Ralph Moberly (PCOM liaison)
University of Hawaii

Takahisa Nemoto
University of Tokyo

Philip D. Rabinowitz (Science Operator liaison)
Texas A&M University

Bruce R. Rosendahl
University of Miami

Leif Westgaard
Norwegian Research Council for Science and Humanities

Planning Committee (PCOM)

Ralph Moberly
University of Hawaii

James A. Austin, Jr.
University of Texas at Austin

Garrett W. Brass
University of Miami

Maria Bianca Cita-Sironi
Università degli Studi di Milano

Darrel S. Cowan
University of Washington

Robert A. Duncan
Oregon State University

Louis E. Garrison (Science Operator liaison)
Texas A&M University

Richard D. Jarrard (Wireline Logging Services liaison)
Columbia University

Hugh C. Jenkyns
University of Oxford

Yves P. Lancelot
Université Pierre et Marie Curie

Marcus G. Langseth
Columbia University

Margaret Leinen
University of Rhode Island

Bruce Malfait (NSF liaison)
National Science Foundation (U.S.)

John Malpas
Memorial University

James Natland
University of California, San Diego

Thomas E. Pyle (JOI liaison)
Joint Oceanographic Institutions, Inc.

Asahiko Taira
University of Tokyo

Brian E. Tucholke
Woods Hole Oceanographic Institution

Ulrich von Rad
Bundesanstalt für Geowissenschaften und Rohstoffe

Joel Watkins
Texas A&M University

Budget Committee (BCOM)

Brian T.R. Lewis
University of Washington

James A. Austin, Jr.
University of Texas at Austin

James C. Briden
Natural Environment Research Council (U.K.)

Hans-J. Dürbaum
Bundesanstalt für Geowissenschaften und Rohstoffe

Ralph Moberly
University of Hawaii

Central and Eastern Pacific Detailed Planning Group (CEPDPG)

David K. Rea
University of Michigan

Helmut Beiersdorf
Bundesanstalt für Geowissenschaften und Rohstoffe

Earl E. Davis
Geological Survey of Canada

André W. Droxler (OHP liaison)
Rice University

Martin F.J. Flower
University of Illinois, Chicago

Peter A. Floyd
University of Keele

Jean Francheteau
Université Pierre et Marie Curie

Loren W. Kroenke
University of Hawaii

Margaret Leinen (PCOM liaison)
University of Rhode Island

Ralph Moberly (PCOM liaison)
University of Hawaii

Hakuyu Okada
Kyushu University

Robin P. Riddihough
Geological Survey of Canada

Constance A. Sancetta
Columbia University

Seymour O. Schlanger
Northwestern University

Hans Joachim Schrader
University of Bergen

---

* Membership at time of cruise.

William V. Sliter
U.S. Geological Survey

Roy H. Wilkens (DMP liaison)
University of Hawaii

Downhole Measurements Panel (DMP)

Paul F. Worthington
British Petroleum Company, Ltd.

Keir Becker (LITHP liaison)
University of Miami

Bobb Carson
Lehigh University

Darrel S. Cowan (PCOM liaison)
University of Washington

Hugh Crocker
Crocker Data Processing Pty., Ltd.

Andrew Fisher (Science Operator liaison)
Texas A&M University

Jean-Paul Foucher
IFREMER (France)

Joris M. Gieskes
University of California, San Diego

Xenia Golovchenko (Wireline Logging Services liaison)
Columbia University

Eddie P. Howell
Arco Oil and Gas Company

Mark W. Hutchinson
Ponca City, Oklahoma

Daniel E. Karig
Cornell University

Hajimu Kinoshita
Chiba University

Marcus G. Langseth (PCOM liaison)
Columbia University

Peter Lysne
Sandia National Laboratories

Jürgen Mienert (SGPP liaison)
GEOMAR (F.R.G.)

Roger H. Morin
U.S. Geological Survey

Carl Sondergeld
Amoco Production Company

Ove Stephansson
University of Luleå

Heinrich Villinger
Alfred Wegener Institute for Polar and Marine Research

Roy H. Wilkens
University of Hawaii

Fluid Processes in Accretionary Prisms Working Group (FPAPWG)

Graham K. Westbrook
University of Birmingham

Keir Becker
University of Miami

Joris M. Gieskes
University of California, San Diego

Roy D. Hyndman
Pacific Geoscience Centre (Canada)

Daniel E. Karig
Cornell University

Xavier Le Pichon
Ecole Normale Supérieure

J. Casey Moore
University of California, Santa Cruz

E. Nuti
Istituto Internationale de Geotermia

Thomas H. Shipley
University of Texas at Austin

Erwin Suess
GEOMAR (F.R.G.)

Roland von Huene
GEOMAR (F.R.G.)

Information Handling Panel (IHP)

Ted C. Moore, Jr.
University of Michigan

James A. Austin, Jr. (PCOM liaison)
University of Texas at Austin

Cristina Broglia (Wireline Logging Services liaison)
Columbia University

Brian M. Funnell
University of East Anglia

Raymond V. Ingersoll
University of California, Los Angeles

Yves P. Lancelot (PCOM liaison)
Université Pierre et Marie Curie

Chao-Shing Lee
Bureau of Mineral Resources, Geology and Geophysics (Australia)

Michael S. Loughridge
National Geophysical Data Center (U.S.)

Russell B. Merrill (Science Operator liaison)
Texas A&M University

William R. Riedel
University of California, San Diego

William W. Sager
Texas A&M University

John B. Saunders
Naturhistorisches Museum (Basel, Switzerland)

André Schaaf
Université Claude Bernard

Henry Spall
U.S. Geological Survey

Volkhard Spiess
Universität Bremen

Kensaku Tamaki
University of Tokyo

Lithosphere Panel (LITHP)

Rodey Batiza
University of Hawaii

Keir Becker
University of Miami

Thomas Brocher
U.S. Geological Survey

Roger Buck (TECP liaison)
Columbia University

Lawrence M. Cathles
Cornell University

Sierd Cloetingh
Vrije Universiteit

Robert A. Duncan (PCOM liaison)
Oregon State University

Jörg Erzinger
Universität Giessen

James M. Franklin
Geological Survey of Canada

Toshitsugu Fujii
University of Tokyo

Martin B. Goldhaber (SGPP liaison)
U.S. Geological Survey

Susan E. Humphris
Woods Hole Oceanographic Institution

John Malpas (PCOM liaison)
Memorial University

James S. McClain
University of California, Davis

Catherine Mevel
Université Pierre et Marie Curie

John C. Mutter
Columbia University

James Natland (PCOM liaison)
University of California, San Diego

Julian A. Pearce
University of Durham

Michael R. Perfit
University of Florida

W. Jason Phipps-Morgan
Massachusetts Institute of Technology

Guy M. Smith
St. Louis University

Ocean History Panel (OHP)

Nicholas J. Shackleton
University of Cambridge

Eric J. Barron
Pennsylvania State University

Wolfgang H. Berger
University of California, San Diego

William A. Berggren
Woods Hole Oceanographic Institution

Timothy J. Bralower
Florida International University

Garrett W. Brass (PCOM liaison)
University of Miami

Peter J. Davies
Bureau of Mineral Resources, Geology and Geophysics (Australia)

Margaret Lois Delaney
University of California, Santa Cruz

André W. Droxler
Rice University

Philip N. Froelich (SGPP liaison)
Columbia University

Eystein Jansen
University of Bergen

Hugh C. Jenkyns (PCOM liaison)
University of Oxford

Dennis V. Kent
Columbia University

Tom S. Loutit
Exxon Production Research Company

Lawrence Mayer
Dalhousie University

Alan C. Mix
Oregon State University

Tsunemasa Saito
Yamagata University

Guy M. Smith (LITHP liaison)
St. Louis University

Ruediger Stein
Universität Giessen

Edith Vincent
Université Pierre et Marie Curie

Pollution Prevention and Safety Panel (PPSP)

Mahlon M. Ball
U.S. Geological Survey

Yutaka Aoki
Japex Geoscience Institute, Inc.

Carl Brenner (Databank liaison)
Columbia University

Emanuela Cassano
AGIP S.p.A. (Italy)

George E. Claypool
Mobil Oil Company

Claude Delas
Total Compagnie Française des Pétroles

Mimi Fortier
Canadian Oil & Gas Lands Administration

Louis E. Garrison (Science Operator liaison)
Texas A&M University

Arthur R. Green
Exxon Production Research Company

Paul Haseldonckx
Deminex (F.R.G.)

Barry J. Katz
Texaco, Inc.

Stephen D. Lewis (SSP liaison)
U.S. Geological Survey

David B. MacKenzie
Littleton, Colorado

Ralph Moberly (PCOM liaison)
University of Hawaii

David G. Roberts
British Petroleum Exploration, Inc. (Houston, Texas)

Sedimentary and Geochemical Processes Panel (SGPP)

Erwin Suess
GEOMAR (F.R.G.)

Jeffrey C. Alt
University of Michigan

Jacques J. Boulègue
Université Pierre et Marie Curie

Lawrence M. Cathles (LITHP liaison)
Cornell University

Nicholas Christie-Blick
Columbia University

Shirley Dreiss
University of California, Santa Cruz

André W. Droxler (OHP liaison)
Rice University

Henry Elderfield
University of Cambridge

Roger D. Flood
State University of New York, Stony Brook

Philip N. Froelich
Columbia University

Martin B. Goldhaber
U.S. Geological Survey

William W. Hay
University of Colorado

Makoto Ito
Chiba University

Stephen A. Macko
Université du Québec à Montréal

Judith A. McKenzie
Eidgenossische Technische Hochschule

Jürgen Mienert
GEOMAR (F.R.G.)

Frederick Prahl
Oregon State University

Dorrik A.V. Stow
University of Southampton

Ulrich von Rad (PCOM liaison)
Bundesanstalt für Geowissenschaften und Rohstoffe

Graham K. Westbrook (TECP liaison)
University of Birmingham

Shipboard Measurements Panel (SMP)

Kate Moran
Bedford Institute of Oceanography

Maria Bianca Cita-Sironi (PCOM liaison)
Università degli Studi di Milano

Ian L. Gibson
University of Waterloo

Joris M. Gieskes (DMP liaison)
University of California, San Diego

John W. King
University of Rhode Island

Margaret Leinen (PCOM liaison)
University of Rhode Island

Audrey W. Meyer (Science Operator liaison)
Texas A&M University

Michael J. Mottl
University of Hawaii

J. Michael Rhodes
University of Massachusetts

Adrian F. Richards
Adrian Richards Company (Netherlands)

Ellen Thomas
Wesleyan University

Hidekazu Tokuyama
University of Tokyo

Jean-Pierre Valet
Université Pierre et Marie Curie

Robert B. Whitmarsh
Institute of Oceanographic Sciences (U.K.)

Site Survey Panel (SSP)

Robert B. Kidd
University College of Swansea

Mahlon M. Ball (PPSP liaison)
U.S. Geological Survey

Carl Brenner (Databank liaison)
Columbia University

Frederick K. Duennebier
University of Hawaii

James D. Hedberg
Exxon Exploration, Inc.

Kim A. Kastens
Columbia University

Yves P. Lancelot (PCOM liaison)
Université Pierre et Marie Curie

Birger Larsen
Danmarks Geologiske Undersogelse

Stephen D. Lewis
U.S. Geological Survey

Keith E. Louden
Dalhousie University

Audrey W. Meyer (Science Operator liaison)
Texas A&M University

Heinrich Meyer
Bundesanstalt für Geowissenschaften und Rohstoffe

Kate Moran (SMP liaison)
Bedford Institute of Oceanography

Guy Pautot
IFREMER (France)

Thomas E. Pyle (JOI liaison)
Joint Oceanographic Institutions, Inc.

Kiyoshi Suyehiro
University of Tokyo

Richard P. Von Herzen
Woods Hole Oceanographic Institution

Joel Watkins (PCOM liaison)
Texas A&M University

Technology and Engineering Development Committee (TEDCOM)

Charles Sparks
Institut Français du Pétrole

Jean Bonnasse-Gahot
Elf-Aquitaine

Garrett W. Brass (PCOM liaison)
University of Miami

William R. Cotten
Chevron Services Company

Hiromi Fujimoto
University of Tokyo

David D. Grassick
Enterprise Oil, plc

Barry W. Harding (Science Operator liaison)
Texas A&M University

Keith Manchester
Bedford Institute of Oceanography

Claus Marx
Institut für Tiefbohrkunde und Erdölgewinnung

Keith Millheim
Amoco Production Company

Heinrich Rischmüller
Bundesanstalt für Geowissenschaften und Rohstoffe

Frank J. Schuh
Intertech Operations Technology, Inc.

F. Earl Shanks
Mobil Oil Company, Inc.

Howard L. Shatto
Houston, Texas

Paul N. Stanton
Exxon Production Research Company

Harald Strand
Norsk Hydro

Walter W. Svendsen
Longyear Company

Paul F. Worthington (DMP liaison)
British Petroleum Company, Ltd.

Tectonics Panel (TECP)

Ian W.D. Dalziel
University of Texas at Austin

Tanya M. Atwater
University of California, Santa Barbara

Jacques Bourgois
Université Pierre et Marie Curie

Roger Buck
Columbia University

Shirley Dreiss (SGPP liaison)
University of California, Santa Cruz

David C. Engebretson
Western Washington University

Michael A. Etheridge
Australian National University

Karl Hinz
Bundesanstalt für Geowissenschaften und Rohstoffe

Kim D. Klitgord
U.S. Geological Survey

Hans-Christian Larsen
Greenland Geological Survey

Catherine Mevel (LITHP liaison)
Université Pierre et Marie Curie

J. Casey Moore
University of California, Santa Cruz

E. M. Moores
University of California, Davis

Yujiro Ogawa
Kyushu University

G. Michael Purdy
Woods Hole Oceanographic Institution

Dale S. Sawyer
Rice University

Asahiko Taira (PCOM liaison)
University of Tokyo

Brian E. Tucholke (PCOM liaison)
Woods Hole Oceanographic Institution

Graham K. Westbrook
University of Birmingham

Western Pacific Detailed Planning Group (WPDPG)

James B. Gill
University of California, Santa Cruz

Kent Brooks
Kobenhavns Universitet

David S. Cronan
University of London, Imperial College

James V. Eade
CCOP/SOPAC (Fiji)

Neville Exon
Bureau of Mineral Resources, Geology and Geophysics (Australia)

Philippe Huchon
Ecole Normale Supérieure

Roy D. Hyndman
Pacific Geoscience Centre (Canada)

H. R. Kudrass
Bundesanstalt für Geowissenschaften und Rohstoffe

Gregory F. Moore
University of Hawaii

James Natland
University of California, San Diego

Steven D. Scott
University of Toronto

Asahiko Taira (PCOM liaison)
University of Tokyo

Kensaku Tamaki
University of Tokyo

Brian Taylor
University of Hawaii

SAMPLE-DISTRIBUTION POLICY[1]

Distribution of Ocean Drilling Program (ODP) and Deep Sea Drilling Project (DSDP) samples is undertaken in order to (1) provide support to shipboard scientists in achieving the scientific objectives of their cruise and to support shore-based investigators who are preparing contributions to ODP reports, (2) provide individual investigators with materials to conduct detailed studies beyond the scope of ODP reports, (3) provide micropaleontological reference centers with samples for reference and comparison purposes, and (4) provide educators with samples for teaching purposes.

Funding for sample-related activities must be secured by the investigator independently of requesting the samples.

The Ocean Drilling Program Curator is responsible for distributing samples and for preserving and conserving core material. The Curator, who may accept advice from chairmen of the appropriate JOIDES advisory panels, is responsible for enforcing the provisions of this Sample-Distribution Policy. He is responsible for maintaining a record of all samples that have been distributed, both on board ship and subsequently from the repositories, indicating the recipients and the nature of investigations proposed. This information is available to interested investigators on request.

Every sample distributed from the ship or from a repository is labeled with a standard identifier, which includes leg number, hole number, core and section numbers, and interval within the section from which the sample was removed. It is imperative that this standard identifier be associated with all data reported in the literature, and that residues of the sample remain labeled throughout their lives, so that later workers can relate the data to the cores.

Distribution of sample materials is made directly from the repositories (Lamont-Doherty Geological Observatory, Scripps Institution of Oceanography, and Texas A&M University) by the Curator or his designated representative.

1. *Distribution of Samples for Research Leading to Contributions to ODP Reports*

Any investigator who wishes to contribute to the reports of a scheduled cruise may write to the Curator, Ocean Drilling Program, 1000 Discovery Drive, College Station, Texas 77845-9547, U.S.A., in order to request samples from that cruise. Requests for a specific cruise must be received by the Curator at least TWO MONTHS in advance of the departure of that cruise, in order to allow time for review of the request in conjunction with other requests, so that a suitable shipboard sampling program can be assembled. The request should include a statement of the nature of the proposed research, the size and approximate number of samples required to complete the study, and any particular sampling technique or equipment which may be required. Requests will be reviewed by the Staff Representative and co-chief scientists of the cruise and by the Curator. Approval/disapproval will be based on the scientific requirements of the cruise as determined by the appropriate JOIDES advisory panel(s). The scope of a request must be such that samples can be processed, that proposed research can be completed, and that the paper can be written in time for submission to the relevant ODP cruise report.

Except for rare, specific instances involving ephemeral properties, the total volume of samples removed during a cruise-related sampling program will not exceed one-quarter of the volume of core recovered, and no interval will be depleted. One-half of all recovered materials will be retained in the archives in as pristine a condition as is practicable. Investigators requesting shipboard samples of igneous materials may receive a maximum of 100 igneous samples per cruise.

Because many sample requests are received for shipboard work and because the time of the shipboard party is at a premium, co-chief scientists are strongly urged to limit shipboard sampling to the minimum necessary to accomplish the cruise objectives. Shore-based investigators whose requests for cruise-related samples are approved should expect that they will receive the samples after the cores are returned to the repository, and should schedule research activities accordingly.

Co-chief scientists may invite investigators who are not cruise participants to perform special studies of selected core samples in direct support of shipboard activities. If this occurs, the names and addresses of these investigators and details of all samples loaned or distributed to them must be forwarded to the Curator, via the ODP Staff Representative to that cruise, immediately after the cruise. These investigators are expected to contribute to the cruise reports as though they had been cruise participants. All requirements of the Sample-Distribution Policy apply.

Any publication of results other than in ODP reports within twelve (12) months of completion of the cruise must be approved and authored by the whole shipboard party and, where appropriate, shore-based investigators. After twelve (12) months, individual investigators may submit related papers for open publication, provided they have already submitted their contributions to ODP reports and had them accepted. Investigations which are not completed in time for inclusion in the ODP reports for a specific cruise may be published in a later edition of the ODP reports; however, they may not appear in another journal until the report for which they were intended has been published.

2. *Distribution of Samples for Research Leading to Publication Outside of the ODP Reports*

   A. Researchers who wish to use samples for studies beyond the scope of the ODP reports should obtain sample-request forms from the Curator, Ocean Drilling Program, 1000 Discovery Drive, College Station, Texas 77845-9547, U.S.A. Requestors are required to specify the quantities and intervals of core required, to make a clear statement of the nature of the proposed research, to state the time which will be required to complete the work and to submit results for publication, and to specify funding status and the availability of equipment and space for the research.

   Additionally, if the requestor has received samples from ODP or from DSDP previously, he/she will be required to account for the disposition of those samples by citing published works, four (4) copies of which must be sent to the Curator. If no report has been published, this requirement can be fulfilled by sending a brief (two- or three-page) report of the status of the research.

   If the requestor has never before received samples from ODP or DSDP, he/she will be required to show that the samples will be used for responsible research. This requirement can be met by providing the Curator with a copy of the requestor's résumé and bibliography. If the requestor is a student working on a higher degree, he/she can meet this requirement by sending a copy of his/her dissertation or research proposal endorsed by the student's advisor.

   Unused and residual samples should be returned and data should be sent to the Curator if the project has terminated. Paleontological materials may be returned either to the Curator at ODP or to one of the designated micropaleontological reference centers. If material is returned to a reference center, notify the Curator when it is sent.

   Requests for samples from researchers in industrial laboratories will be honored in the same manner as those from academic organizations. Industrial investigators have the same obligations as other investigators to publish all results promptly in the open literature and to provide the Curator with copies of all reports published and of all data acquired in their research.

   In order to ensure that all requests for highly desirable but limited samples can be considered together, approval of requests and distribution of samples will be delayed until twelve (12) months after completion of the cruise or two (2) months after official publication of the core descriptions, whichever occurs earlier. The only exceptions to this policy will be made for specific requests involving ephemeral properties. Requests for samples may be based on core descriptions published in ODP reports produced by the shipboard party, copies of which are on file at various institutions throughout the world. Copies of original core logs and data are kept on open file at ODP, and at the repositories at Lamont-Doherty Geological Observatory and Scripps Institution of Oceanography.

---

[1] Revised October 1988.

B. Most investigations can be accomplished handily with sample volumes of 10 mL or less. Investigators must provide explicit justification of requests for larger sample sizes or for frequent intervals within a core. Requests which exceed reasonable size or frequency limits will require more time to process and are unlikely to be granted in their entirety.

Requests for samples from thin layers, from stratigraphically important boundaries, or from sections which are badly depleted or in unusually high demand may be delayed in order to coordinate requests from several investigators or while the Curator seeks advice from the community. Investigators who submit such requests may expect to receive suggestions for alternative sampling programs or for joining with a research consortium which will share the samples. In any event, such exceptional requests will require more time for processing than will more routine requests.

Investigators who wish to study ephemeral properties may request a waiver of the twelve-month waiting period; however, such requests will be referred automatically to the relevant co-chiefs. If such a request is approved, the investigator will join the shore-based contributors to the shipboard science effort, and will incur the obligations thereof (see section 1).

C. Samples will not be provided until the requestor assures the Curator that funding for the proposed research is available or unnecessary. If a sample request is dependent in any way on proposed funding, the Curator is prepared to provide the proposed funding organization with information on the availability (or potential availability) of suitable samples.

D. Investigators who receive samples incur the following obligations:

(1) To publish significant results promptly; however, no contribution may be submitted for publication prior to twelve (12) months following the termination of the relevant leg unless it is approved and authored by the entire shipboard party.

(2) To acknowledge in all publications that the samples were supplied through the assistance of the international Ocean Drilling Program and others as appropriate.

(3) To submit four (4) copies of reprints of all published works to the Curator, Ocean Drilling Program, 1000 Discovery Drive, College Station, Texas 77845-9547, U.S.A. These reprints will be distributed to the repositories and to the ship. All reprints received will be logged in an on-line bibliographic data base.

(4) To submit all final analytical data obtained from the samples to the Data Librarian, Ocean Drilling Program, 1000 Discovery Drive, College Station, Texas 77845-9547, U.S.A. Please consult announcements in the *JOIDES Journal* or call (409–845-2673) for information on acceptable data formats. Investigators should be aware that they may have other data obligations under the National Science Foundation's Ocean Science Data Policy or under relevant policies of other funding agencies which require submission of data to national data centers.

(5) To return all unused or residual samples, in good condition and with a detailed explanation of any processing they may have undergone, upon termination of the proposed research. In particular, all thin sections and smear slides manufactured on board the vessel or in the repositories are to be returned to the Curator. Paleontological materials may be returned either to the Curator at ODP or to one of the designated micropaleontological reference centers.

Failure to honor these obligations will prejudice future applications for samples.

E. Cores are available for examination by interested parties at the repositories. Investigators are welcome to visit the repositories in order to inspect cores and to specify sample locations when that is required for their research; however, time and space in the workrooms are limited, so advance appointments are required. Occasionally, the space may be fully booked several weeks in advance, so investigators are urged to call for appointments well ahead in order to avoid disappointment. Only the Curator or his delegate may actually remove samples from the cores.

F. A reference library of thin sections, smear slides, and archive photographs is maintained in the repositories for the use of visiting investigators. All thin sections and smear slides produced on board the ship or in repositories belong to this library.

3. *Distribution of Samples to Micropaleontological Reference Centers*

As a separate and special category of repository activity, selected samples are distributed to micropaleontological reference centers, where the prepared material may be studied by visitors. Foraminifers, calcareous nannofossils, and diatoms can be viewed; radiolarians will be prepared in the future. The present centers are (1) U.S. East Coast: Lamont-Doherty Geological Observatory, Palisades, NY 10964 (Ms. Rusty Lotti; telephone, 914–359-2900; telex, 7105762653 LAMONTGEO); (2) U.S. National Museum: Smithsonian Institution, Washington, D.C. 20560 (Dr. Martin Buzas; telephone, 202–357-1390; telex, 264729); (3) U.S. Gulf Coast: Texas A&M University, Department of Oceanography, College Station, TX 77843 (Dr. Stefan Gartner; telephone, 409–845-8479; telex, 792779/ODP TAMU); (4) U.S. West Coast: Scripps Institution of Oceanography, La Jolla, CA 92093 (Dr. William Riedel; telephone, 619–534-4386); telex, 910337127 IUC WWD SIOSDG); (5) Western Europe: Natural History Museum, CH-4001 Basel, Switzerland (Mr. J. B. Saunders; telephone, 061-29-55-64); (6) U.S.S.R.: Institute of the Lithosphere, Staromonet 22, Moscow 109180, U.S.S.R. (Dr. Ivan Basov; telephone, 231-48-[illegible]6); (7) Japan: National Science Museum, Department of Geology, 3-23-1 Hyakunin-cho, Shinjuku-ku, Tokyo 160, Japan (Dr. Y. Tanimura; telephone, 03-364-2311; telemail, 03-364-2316); (8) New Zealand: New Zealand Geological Survey, P.O Box 30368, Lower Hutt, New Zealand (Dr. Tony Edwards; telephone, (04) 699059).

Further details concerning the micropaleontological reference centers are reported periodically in the *JOIDES Journal*.

4. *Distribution of Samples for Educational Purposes*

Samples may be available in limited quantities to college-level educators for teaching purposes. Interested educators should request application forms from the Curator, Ocean Drilling Program, 1000 Discovery Drive, College Station, Texas 77845-9547, U.S.A. Requestors are required to specify preferred sample size and location, to make a very clear statement of the nature of the course work in which the samples will be used, to explain how the samples will be prepared and how they will be used in the classroom, to explain in detail why similar materials derived from outcrops or dredge hauls cannot be used (it is NOT acceptable to argue that it requires less effort for the requestor to obtain samples from ODP than to assemble them from other sources), and to certify that funds are available to prepare the materials for classroom use. In general, only samples of materials which are abundant in the collection and which are in little demand for research purposes should be requested for educational purposes. The Curator will not approve requests for materials which are limited in supply or for which demand (real or potential) is great, including most paleontological materials.

5. *Distribution of Data*

The Deep Sea Drilling Project and the Ocean Drilling Program have routinely captured much of the data generated on board ship and published in Program reports. Additionally, data supplied by investigators who have received samples are incorporated into the data bases, so data sets which are larger than can be published are available to investigators. Magnetic, downhole-logging, seismic-reflection, bathymetric, and other data collected by the drilling vessel become available for distribution to investigators at the same time as core samples.

Requests for ODP and DSDP data should be addressed to the Data Librarian, Ocean Drilling Program, 1000 Discovery Drive, College Station, Texas 77845-9547, U.S.A. Many varieties of DSDP data are included in ODP data bases. Information on sources of DSDP data is available from the ODP Data Librarian.

A charge will be made to recover material expenses greater than $25.00 incurred in filling individual requests. If required, estimates of charges can be furnished before the work is performed.

Chart Transposed to

End of Volume.

Drilling Locations

Leg	Location	Rep.	Sites
Phase 1	**1968–1970**		
1	North Atlantic	E	1–7
2	North Atlantic	E	8–12
3	South Atlantic	E	13–22
4	Central Atlantic	E	23–31
5	North Pacific	W	32–43
6	North Pacific	W	44–60
7	Central Pacific	W	61–67
8	Central Pacific	W	68–75
9	Central Pacific	W	76–84
Phase 2	**1970–1972**		
10	Gulf of Mexico	E	85–97
11	North Atlantic	E	98–108
Re-entry trials		E	109–110
12	North Atlantic	E	111–119
13	Mediterranean	E	120–134
14	Central Atlantic	E	135–144
15	Caribbean	E	144–154
16	Central Pacific	W	155–163
17	Central Pacific	W	164–171
18	North Pacific	W	172–182
19	North Pacific	W	183–193
20	North Pacific	W	194–202
21	Coral Sea	W	203–210
22	Indian Ocean	W	211–218
23	Arabian Sea	W	219–230
24	Indian Ocean	W	231–238
25	Indian Ocean	W	239–249
Phase 3	**1972–1975**		
26	Indian Ocean	W	250–258
27	Indian Ocean	W	259–263
28	Antarctic	E	264–274
29	Tasman Sea	E	275–284
30	South Pacific	W	285–289
31	North Pacific	W	290–302
32	North Pacific	W	303–313
33	North Pacific	W	314–318
34	South Pacific	W	319–321
35	South Pacific	E	322–325
36	South Atlantic	E	326–331
37	North Atlantic	E	332–335
38	Arctic	E	336–352
39	Atlantic	E	353–359
40	South Atlantic	E	360–365
41	South Atlantic	E	366–370
42A	Mediterranean	E	371–378
42B	Black Sea	E	379–381
43	North Atlantic	E	382–387
44	North Atlantic	E	388–392
44A	North Atlantic	E	393–394
IPOD 1	**1975–1983**		
45	North Atlantic	E	395–396
46	North Atlantic	E	396A–396B
47	North Atlantic	E	397–398
48	North Atlantic	E	399–406
49	North Atlantic	E	407–414
50	North Atlantic	E	415–416
51A	North Atlantic	E	417–417A
51B	North Atlantic	E	417B–417D
52	North Atlantic	E	417D–418A
53	North Atlantic	E	418A–418B
54	Central Pacific	E	419–429
55	North Pacific	W	430–433
56	North Pacific	W	434–437
57	North Pacific	W	438–441
58	North Pacific	W	442–446
59	North Pacific	W	447–451
60	North Pacific	W	452–461
61	Central Pacific	W	462
62	North Pacific	W	463–466
63	North Pacific	W	467–473
64	Gulf of California	W	474–481
65	Gulf of California	W	482–485
66	Central Pacific	W	486–493
67	Central Pacific	W	494–500
68	Central Pacific	W	502–503
69	Central Pacific	W	504–505, 501
70	Central Pacific	W	506–510, 504B
71	South Atlantic	E	511–514
72	South Atlantic	E	515–518
73	South Atlantic	E	519–524
74	South Atlantic	E	525–529
75	South Atlantic	E	530–532
76	North Atlantic	E	533–534
77	Caribbean	E	535–540
78	North Atlantic	E	541–543, 395A&B
79	North Atlantic	E	544–547
80	North Atlantic	E	548–551
81	North Atlantic	E	552–555
82	North Atlantic	E	556–564
83	Central Pacific	W	504B
84	Central Pacific	W	565–570
85	Central Pacific	W	571–575
86	North Pacific	W	576–58
87	North Pacific	W	582–584
88	North Pacific	W	581
89	Central Pacific	W	585–586, 462A
90	South Pacific	W	587–594
91	Central Pacific	W	595–596
92	Central Pacific	W	597–602, 504B
93	North Atlantic	E	603–605
94	North Atlantic	E	606–611
95	North Atlantic	E	612–613, 603
96	Gulf of Mexico	E	614–624

Core Storage:
E - East Coast Repository
W - West Coast Repository

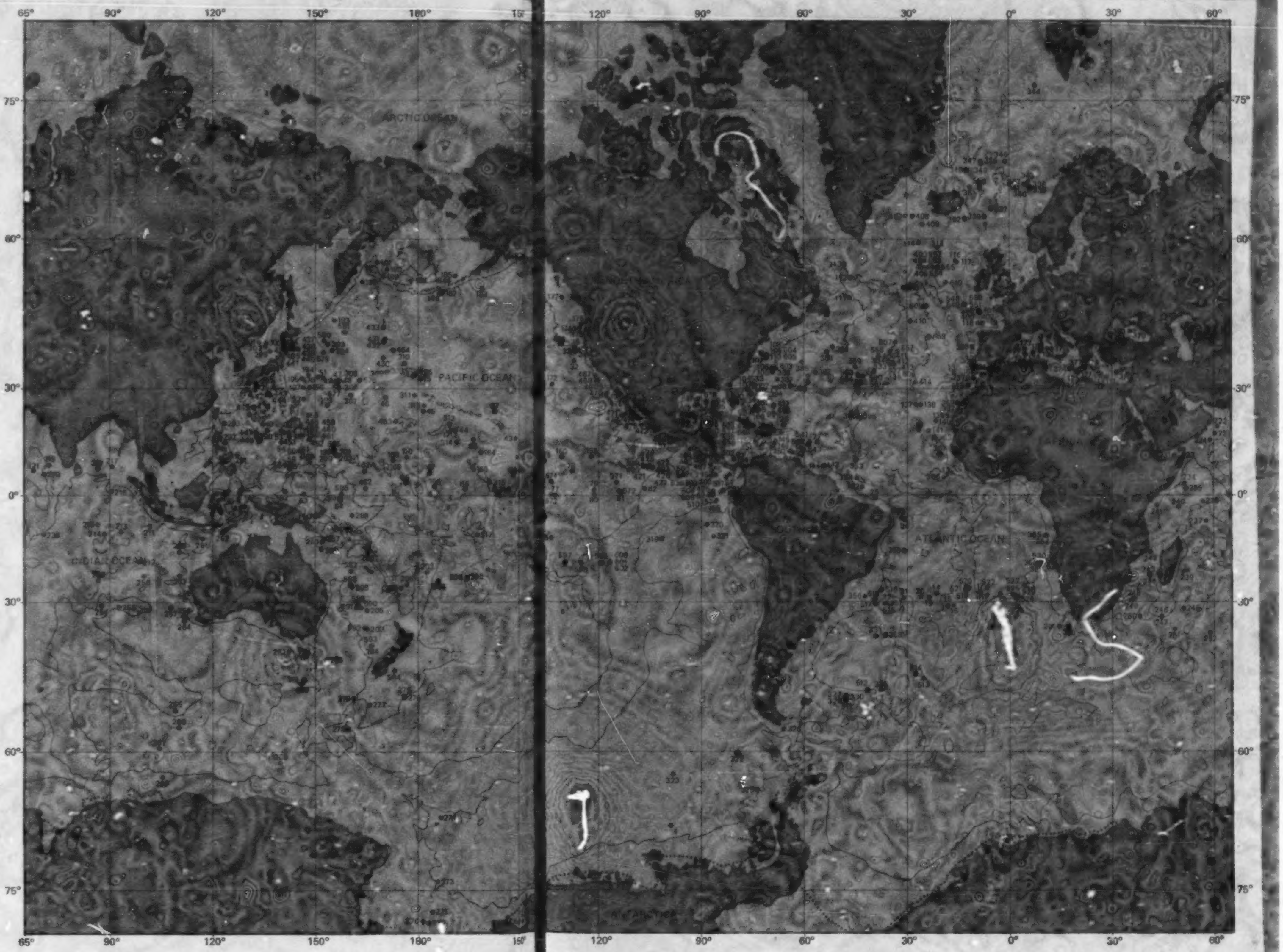

DEE A DRILLING PROJECT

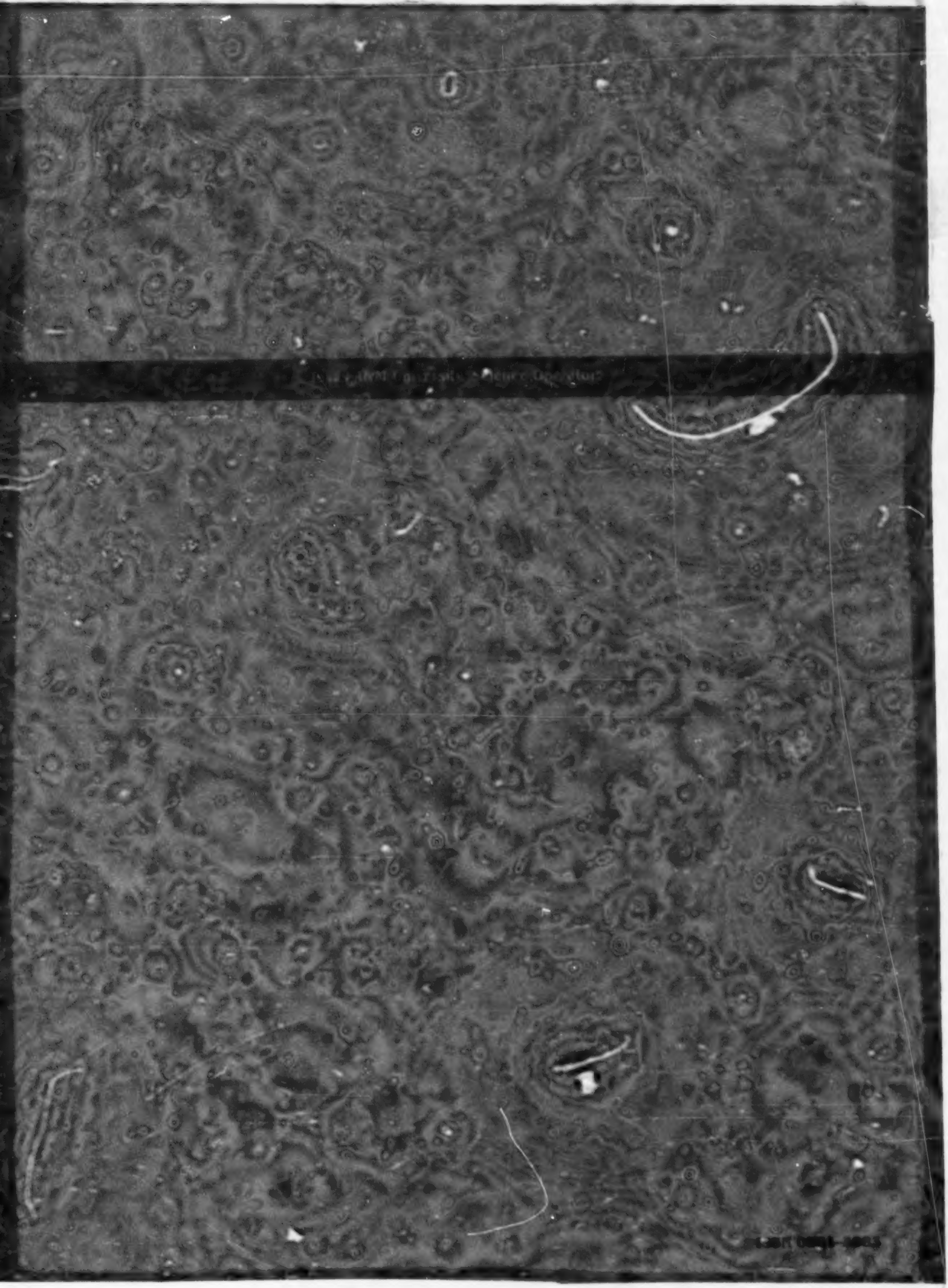

Initial Reports Volume 130, Chapter 11, Figure 1. Whole-core magnetic susceptibility data from Holes 805A, 806A, and 807A to 35 mbsf using a 80-mm Bartington MS2C sensor. Magnetic susceptibility values decrease rapidly at a sub-bottom depth that is common to the offset APC cores at a single site but different between sites. The decrease occurs at approximately 26 mbsf for Hole 805A, 11 mbsf for Hole 806A, and 32 mbsf for Hole 807A.

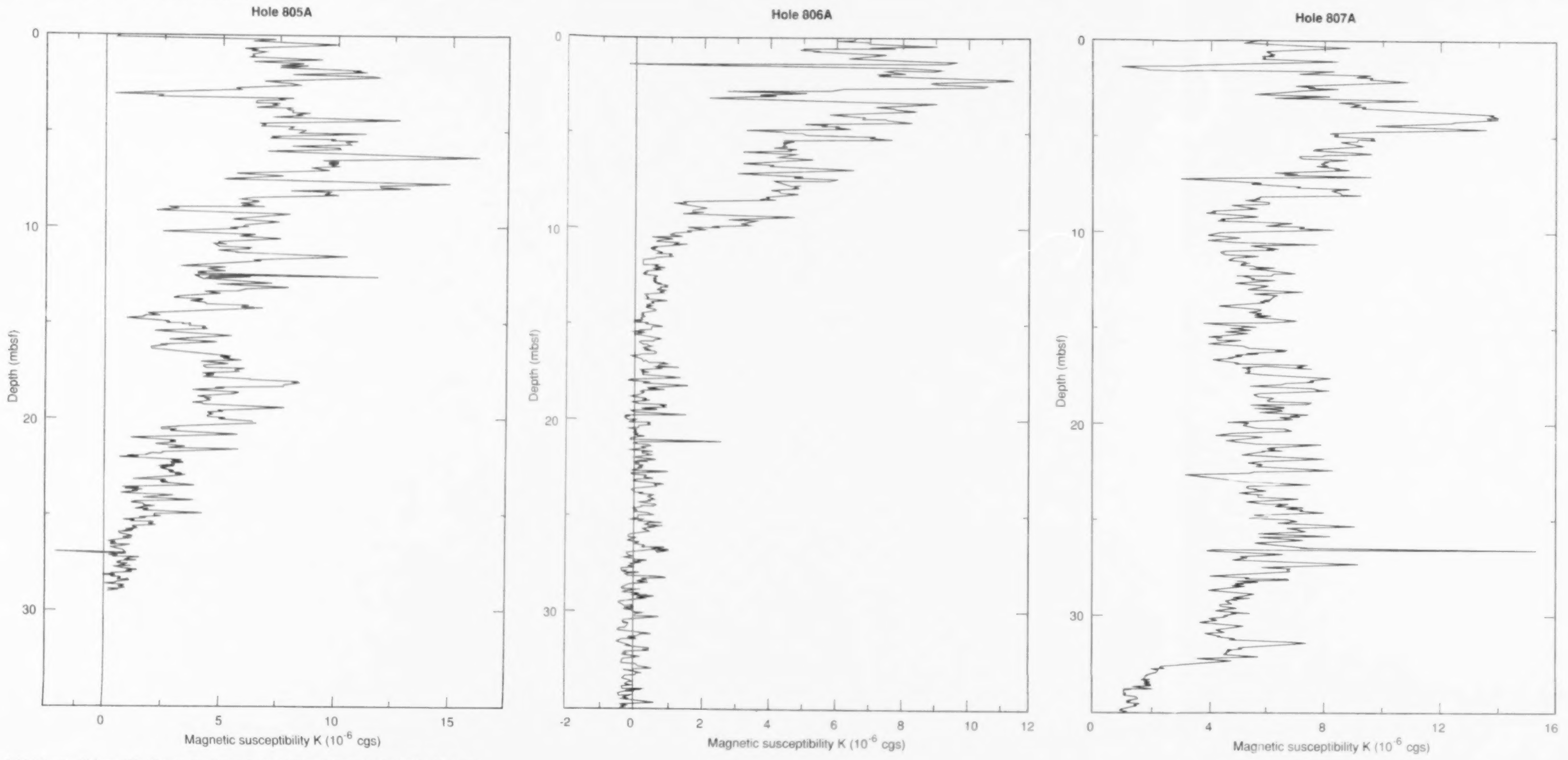

Initial Reports Volume 130, Chapter 11, Figure 3. Correlation between Holes 806A, 806B, and 806C to 15.0 mbsf using whole-core magnetic susceptibility data. Data for Holes 806A and 806C were obtained using a 80-mm MS2C Bartington sensor; data for Hole 806B were obtained using a 100-mm MS1C Bartington sensor. Note the prominent drop in magnetic susceptibility values at 10.48 mbsf in Hole 806A and 10.6 mbsf in Hole 806C.

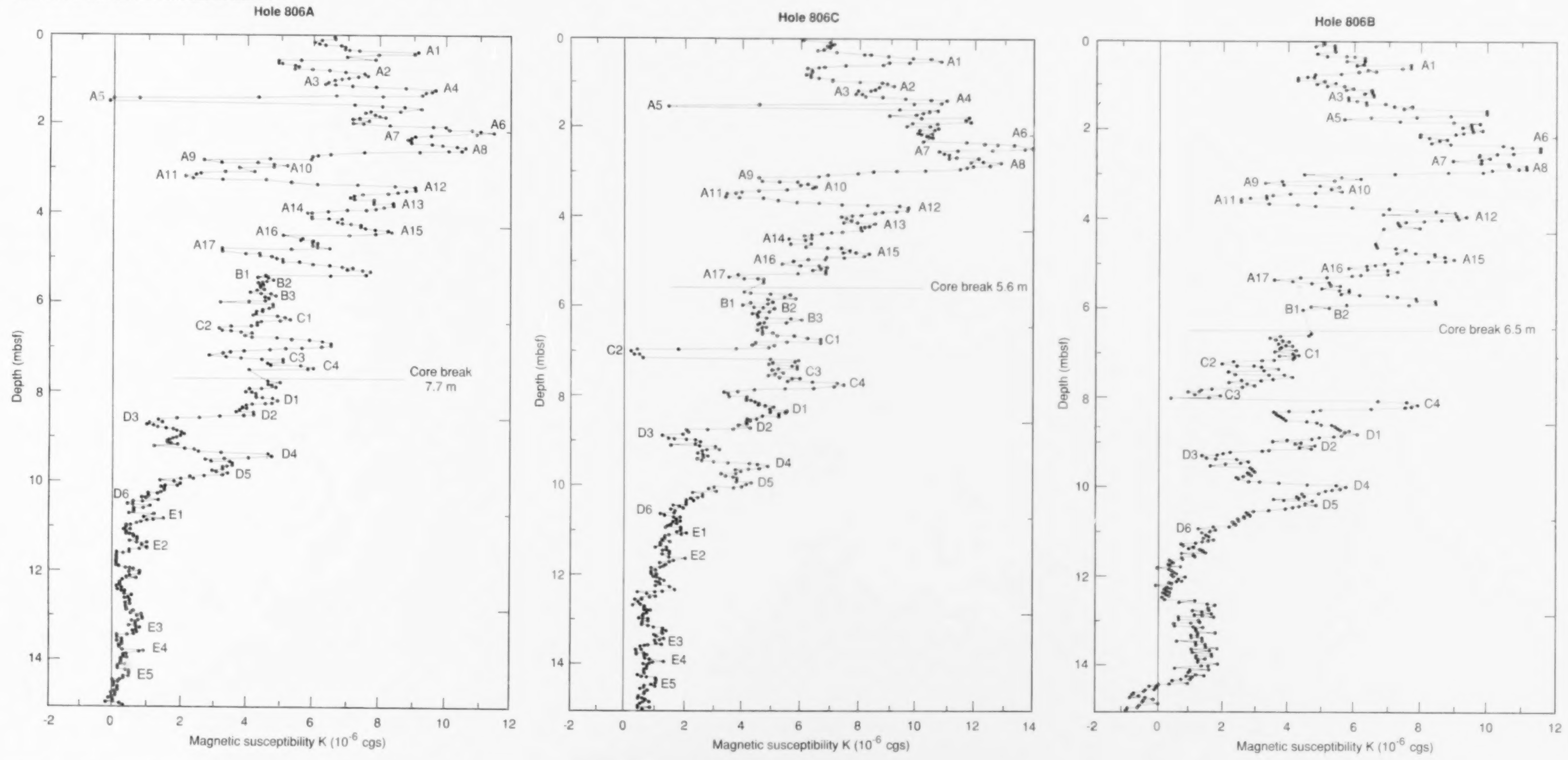

Initial Reports Volume 130, Chapter 11, Figure 4. Comparison of whole-core magnetic susceptibility data for Site 806A using a 80-mm MS2C Bartington sensor and a 100-mm MS1C Bartington sensor. Also shown are data from Hole 806C, using a 80-mm MS2C Bartington sensor.

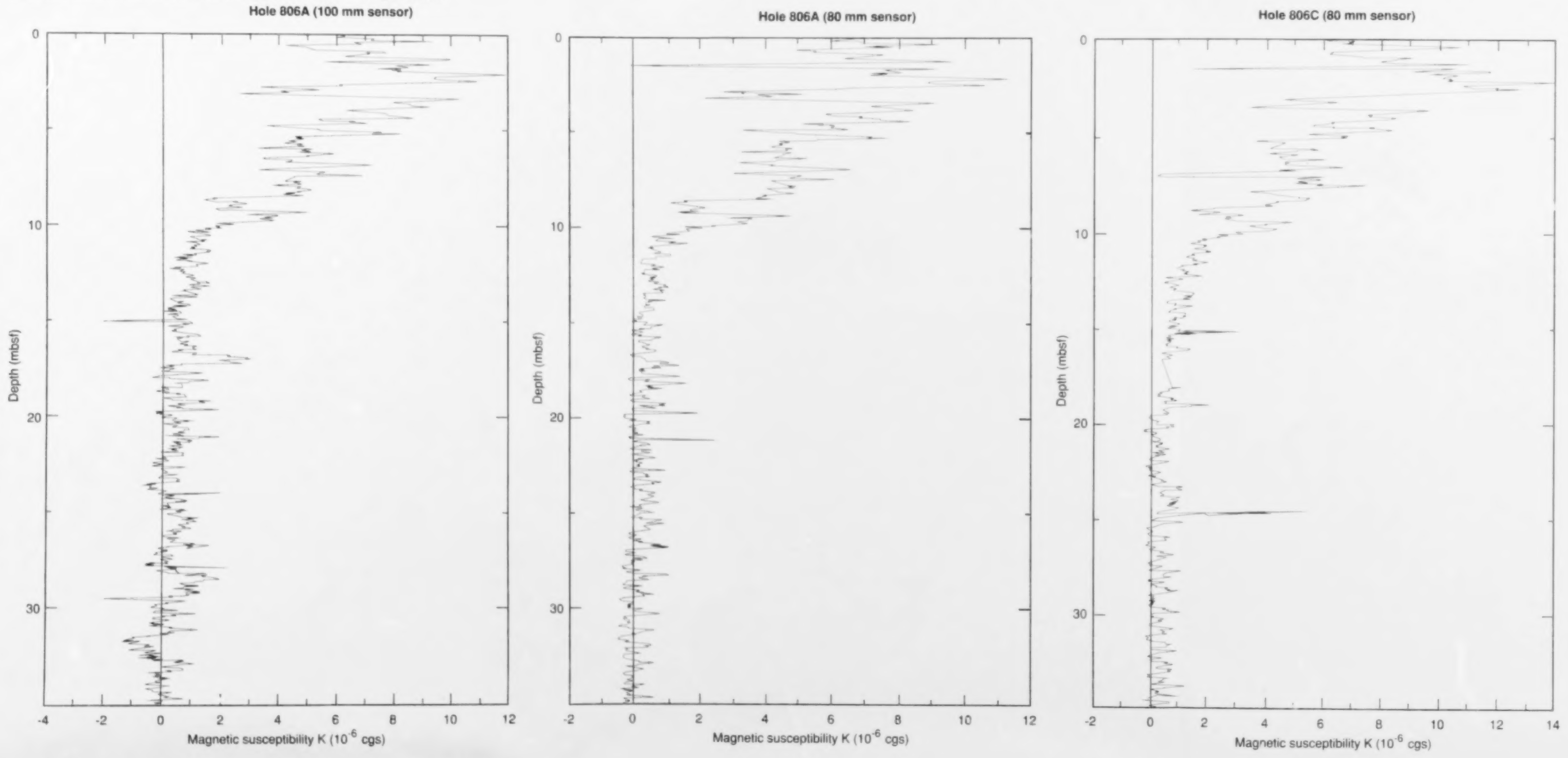

Initial Reports Volume 130, Chapter 11, Figure 13. Correlation between Holes 807A, 805C, and 806A down to 7.0 mbsf using whole-core magnetic susceptibility data.

Hole 807A

Hole 805C

Hole 806A

Initial Reports Volume 130, Chapter 11, Figure 2. Correlation between Holes 805A and 805C using whole-core magnetic susceptibility data.

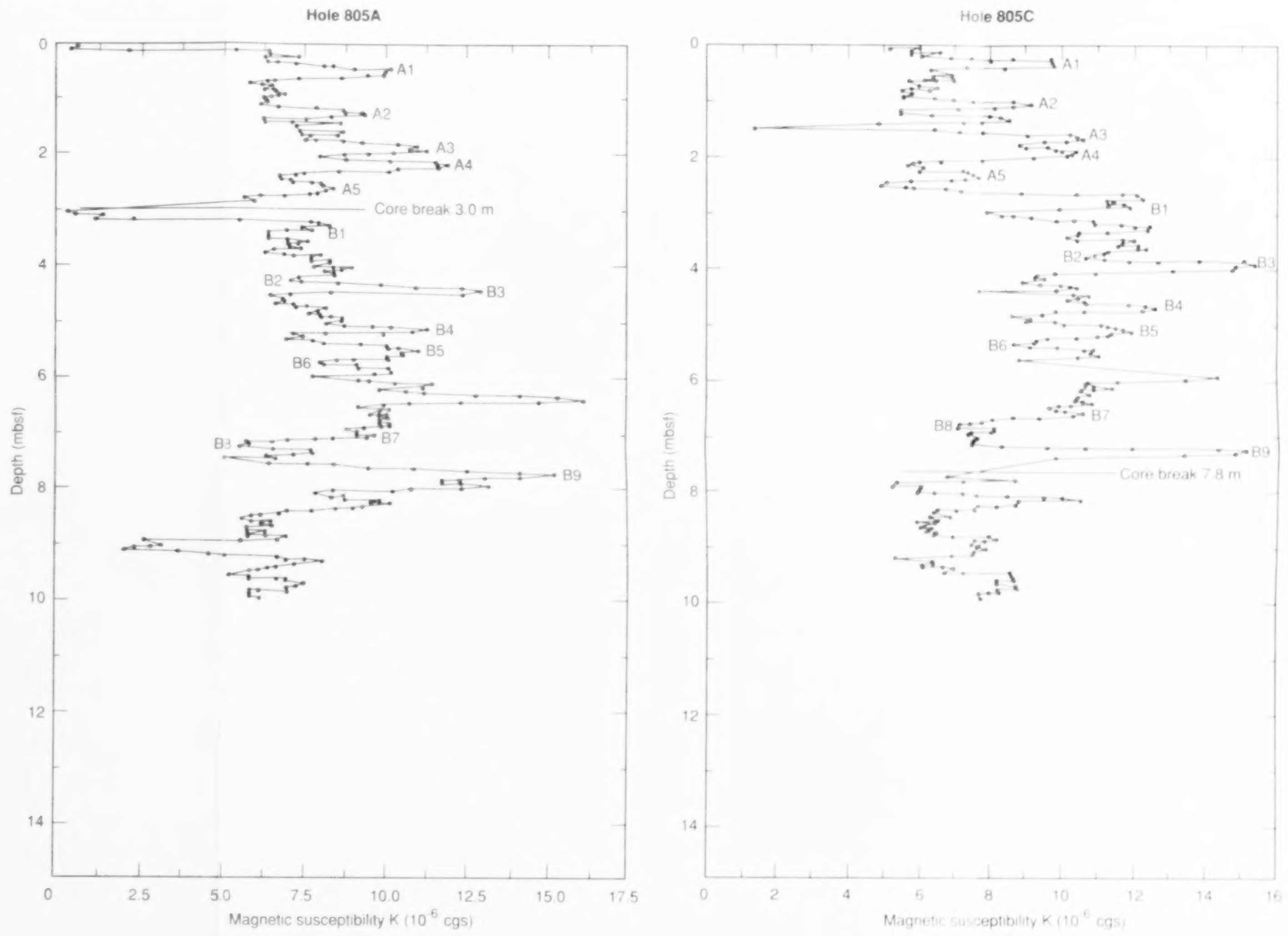

Initial Reports Volume 130, Chapter 11, Figure 11. Correlation between Holes 807A and 807B using whole-core magnetic susceptibility data.

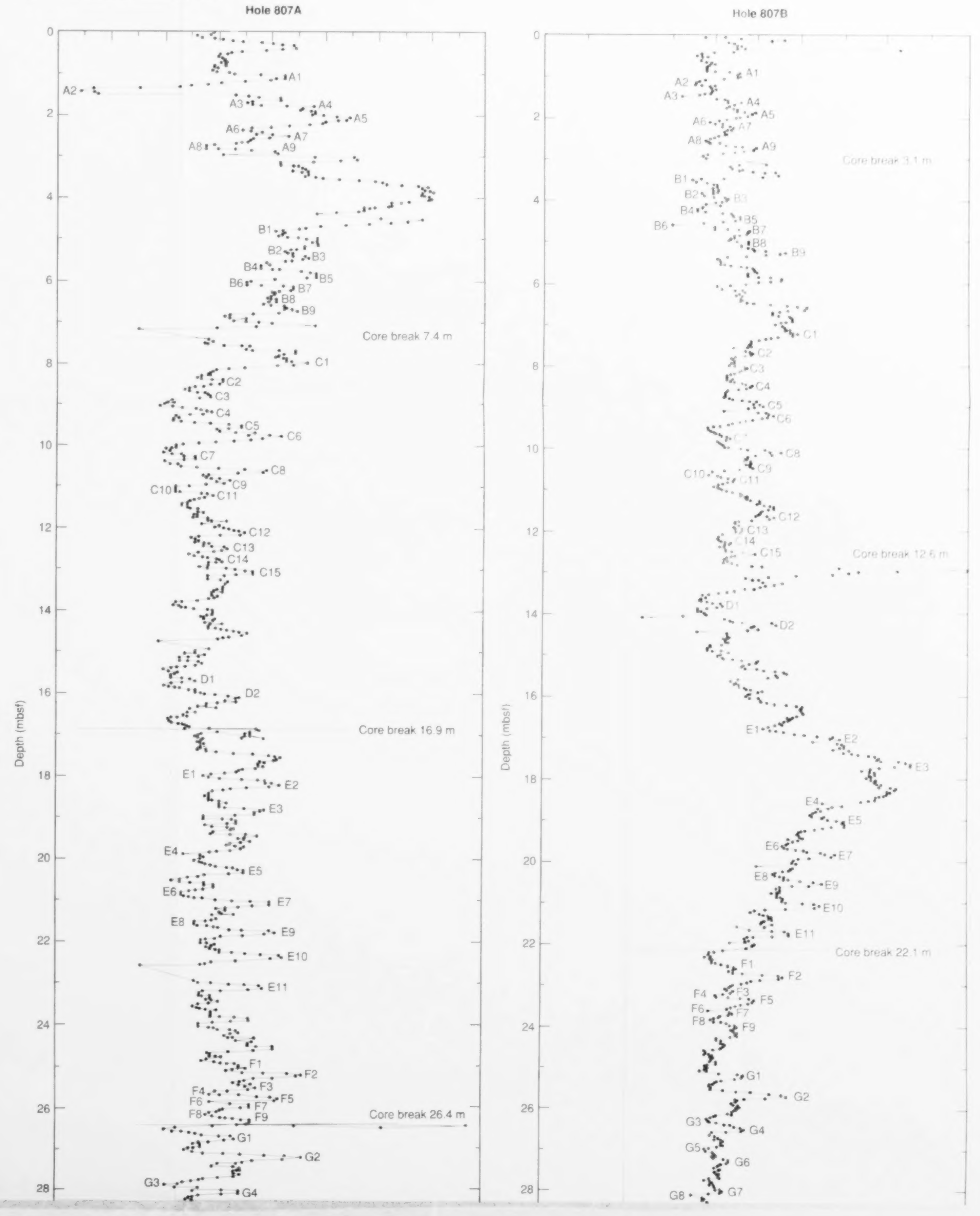

best copy available

Magnetic susceptibility K (10^-6 cgs)
Magnetic susceptibility K (10^-6 cgs)
Magnetic susceptibility K (10^-6 cgs)

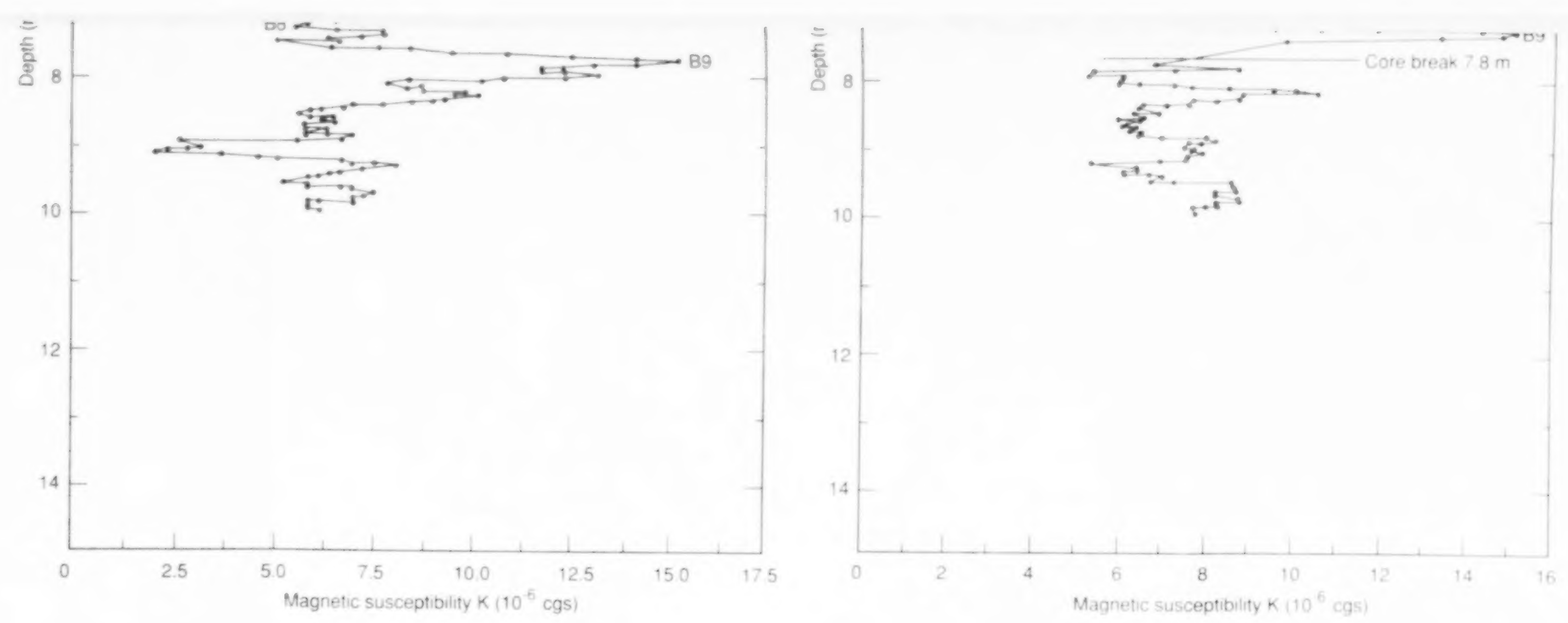

Initial Reports Volume 130, Chapter 11, Figure 3. Correlation between Holes 806A, 806B, and 806C to 15.0 mbsf using whole-core magnetic susceptibility data. Data for Holes 806A and 806C were obtained using a 80-mm MS2C Bartington sensor; data for Hole 806B were obtained using a 100-mm MS1C Bartington sensor. Note the prominent drop in magnetic susceptibility values at 10.48 mbsf in Hole 806A and 10.6 mbsf in Hole 806C.

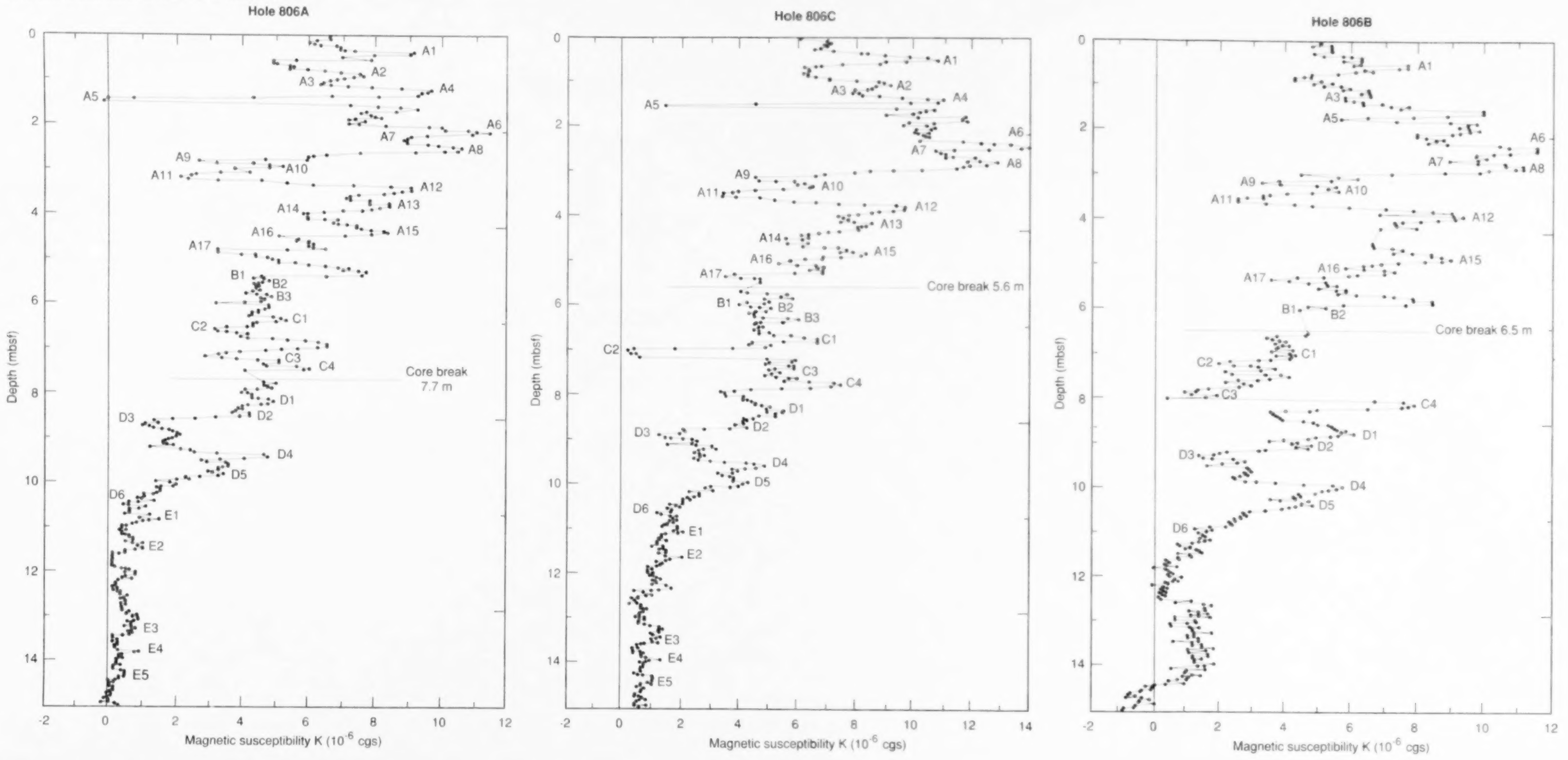

Initial Reports Volume 130, Chapter 11, Figure 4. Comparison of whole-core magnetic susceptibility data for Site 806A using a 80-mm MS2C Bartington sensor and a 100-mm MS1C Bartington sensor. Also shown are data from Hole 806C, using a 80-mm MS2C Bartington sensor.

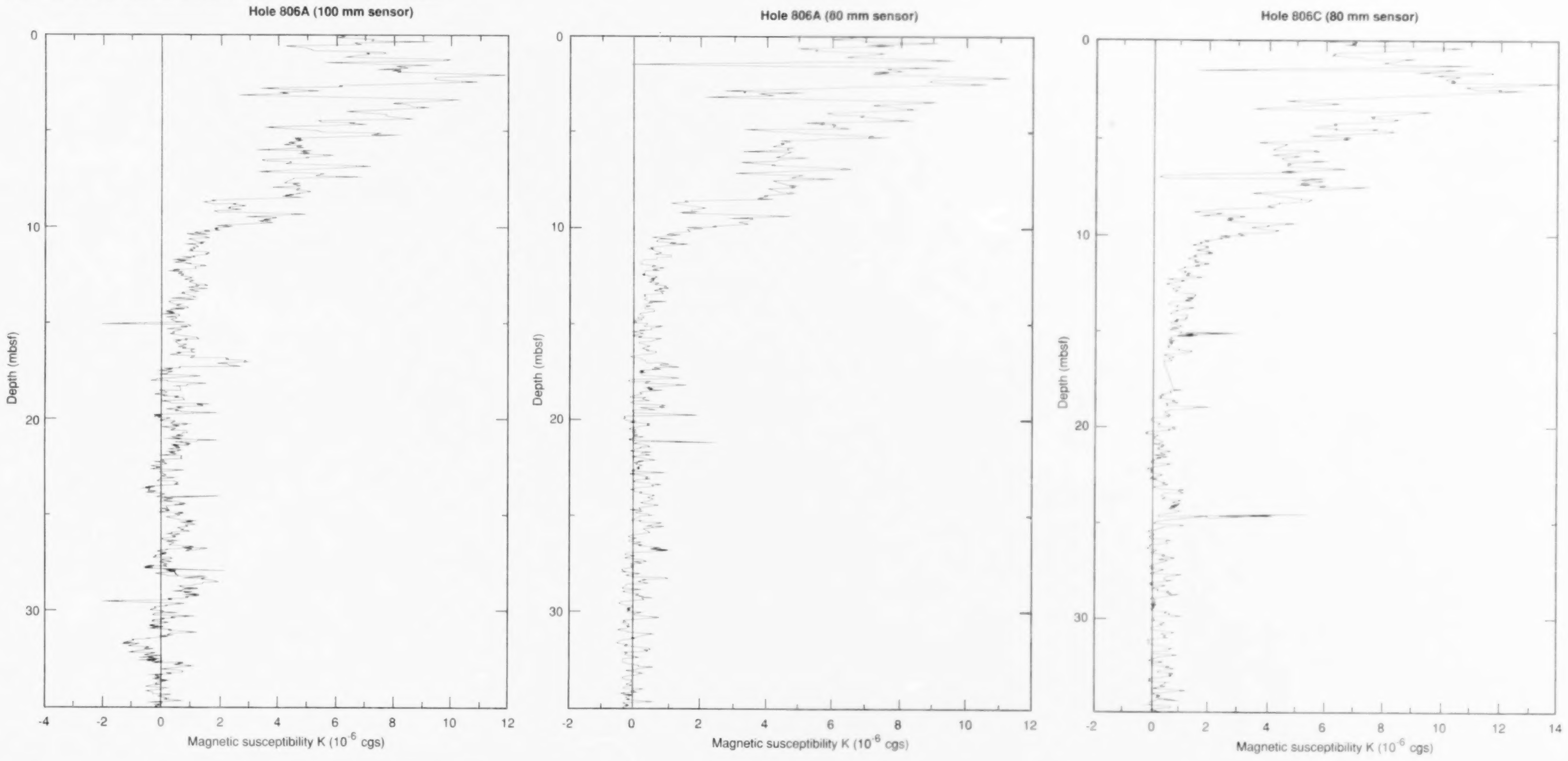

Initial Reports Volume 130, Chapter 11, Figure 13. Correlation between Holes 807A, 805C, and 806A down to 7.0 mbsf using whole-core magnetic susceptibility data.

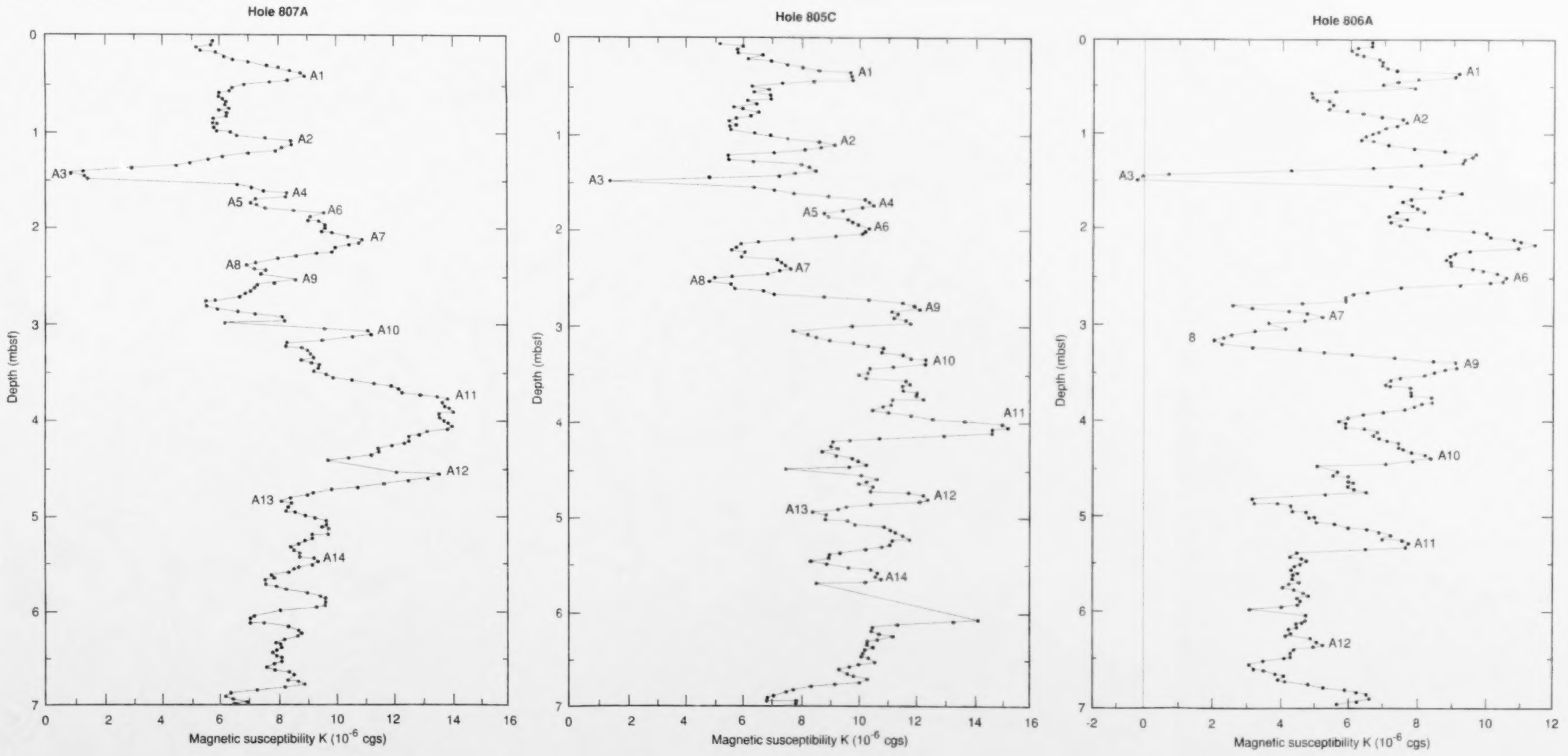

Initial Reports Volume 130, Chapter 11, Figure 11. Correlation between Holes 807A and 807B using whole-core magnetic susceptibility data.

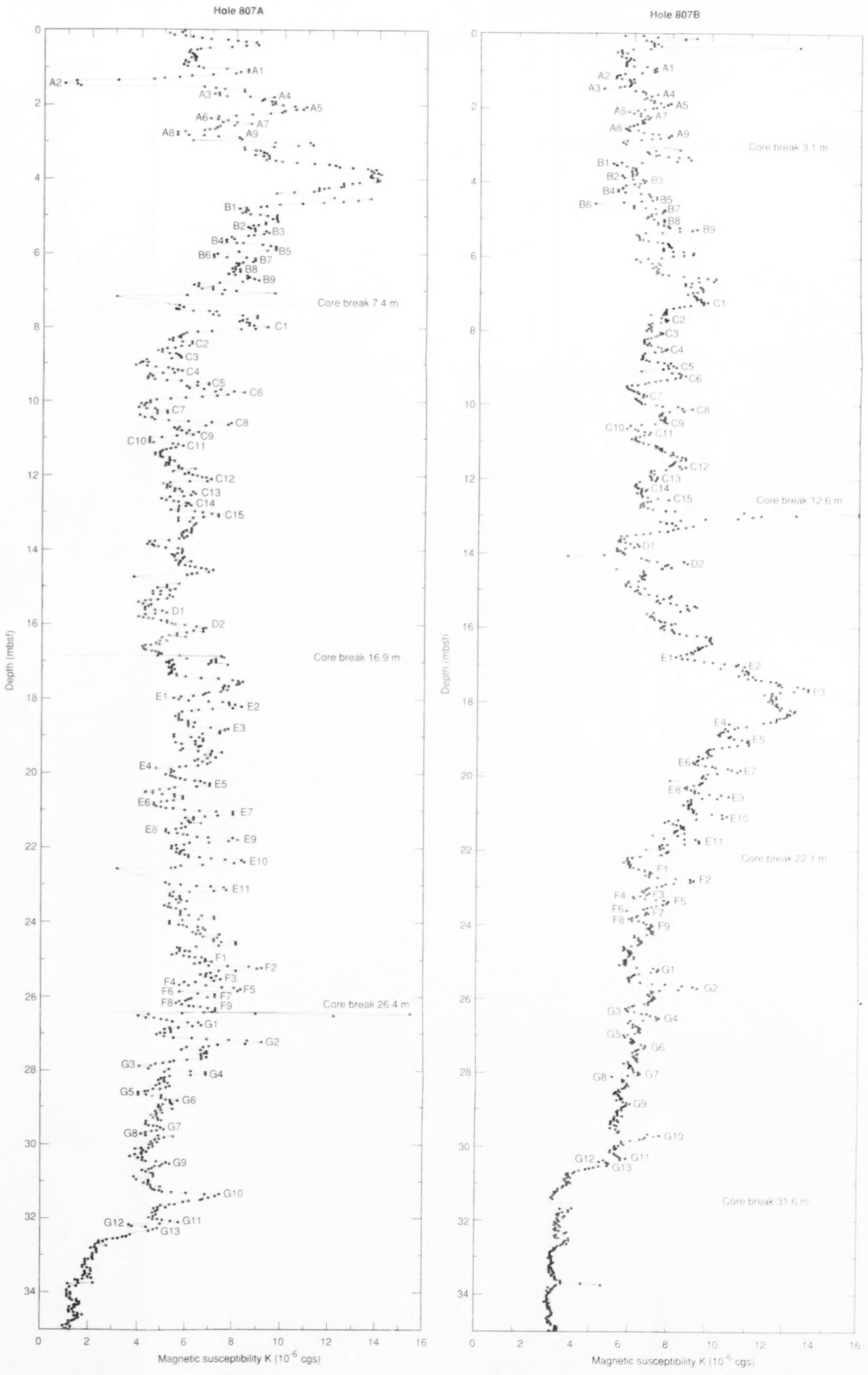

INDEX

LEG 130 MICROFICHE

803-D	
MAIN LOG (PASS2)	92-306 MBSF
MAIN LOG (PASS1)	299-611 MBSF
807-C	
MAIN LOG (PASS2)	1097-1504 MBSF

Leg 130 FMS Images:

Two Holes on Leg 130, 803D and 807C, were logged by the Formation MicroScanner.

Two passes are presented for site 803D. Pass 2 is from 92 meters below sea floor to 306 mbsf; Pass 1 is from 299 to 611 mbsf. The hole was often wider than the caliper holding the FMS resistivity pads to the borehole wall, and as a result much of the data is low in quality, especially above 300 mbsf.

At Hole 807C, two FMS passes were made, the first from 947 mbsf to 1504 mbsf, and the second from 1097 mbsf to 1504 mbsf. We present the second pass in this microfiche because most of the upper section in Pass 1 is of poor quality due to wide hole conditions. Pass 1 also contains significantly more noise from a minor tool malfunction. In this hole, sediments are shown from 1097 to 1379 mbsf, while the basement section is 1379 to 1504 mbsf.

803-D
MAIN LOG
(PASS 2)

92 - 306
MBSF

Advanced Images, INC.
Rt 22 West Round Valley Plaza
Lebanon, N.J. 08833

SCHLUMBERGER

FMS
BOREHOLE
IMAGING

COMPANY	LAMONT DOHERTY
WELL	ODP HOLE 803D
FIELD	ONTONG JAVA PLATEAU
COUNTRY	LEG 130
RUN	2
DATE LOGGED	05 - FEB 90
REFERENCE	STATIC PS 2 92 120

STATIC NORMALIZATION

PASS 2

FILE : MEST.002

ZONE FROM 120.0 M TO 92.0 M

DEPTH SCALE = 1/ 5

IMAGE SCALE = 1/ 5

BITSIZE = 9.88

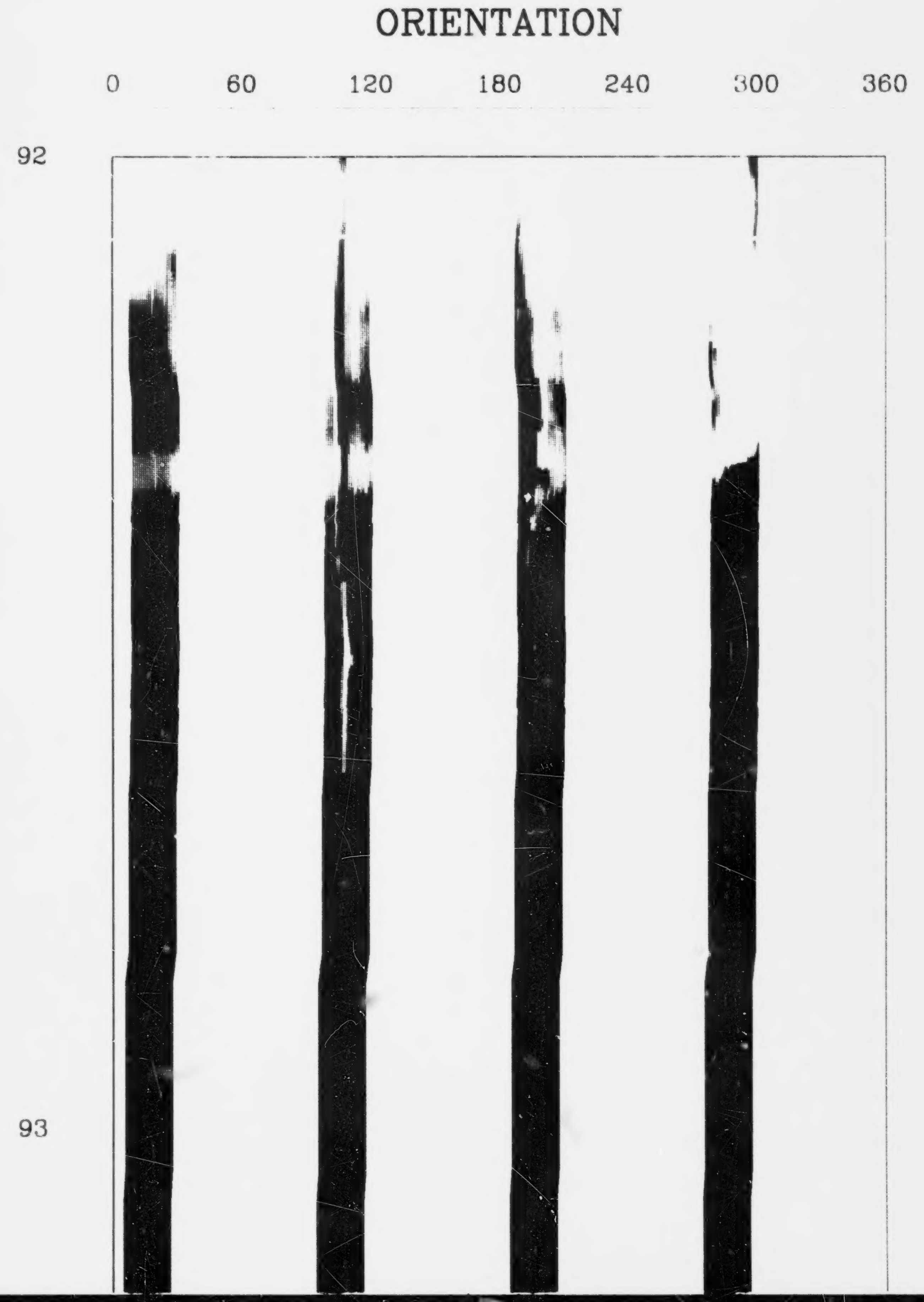

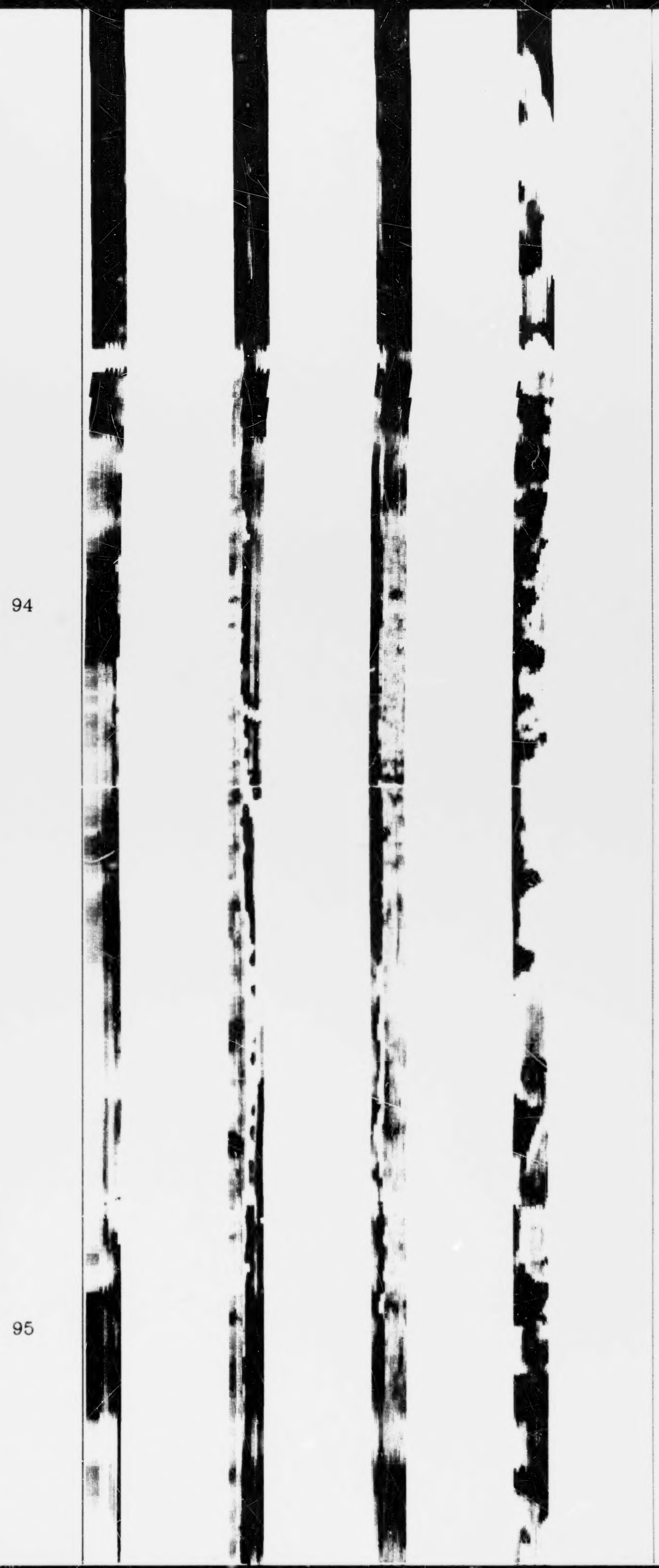
94
95

[illegible]

[illegible]

98

99

[redacted]

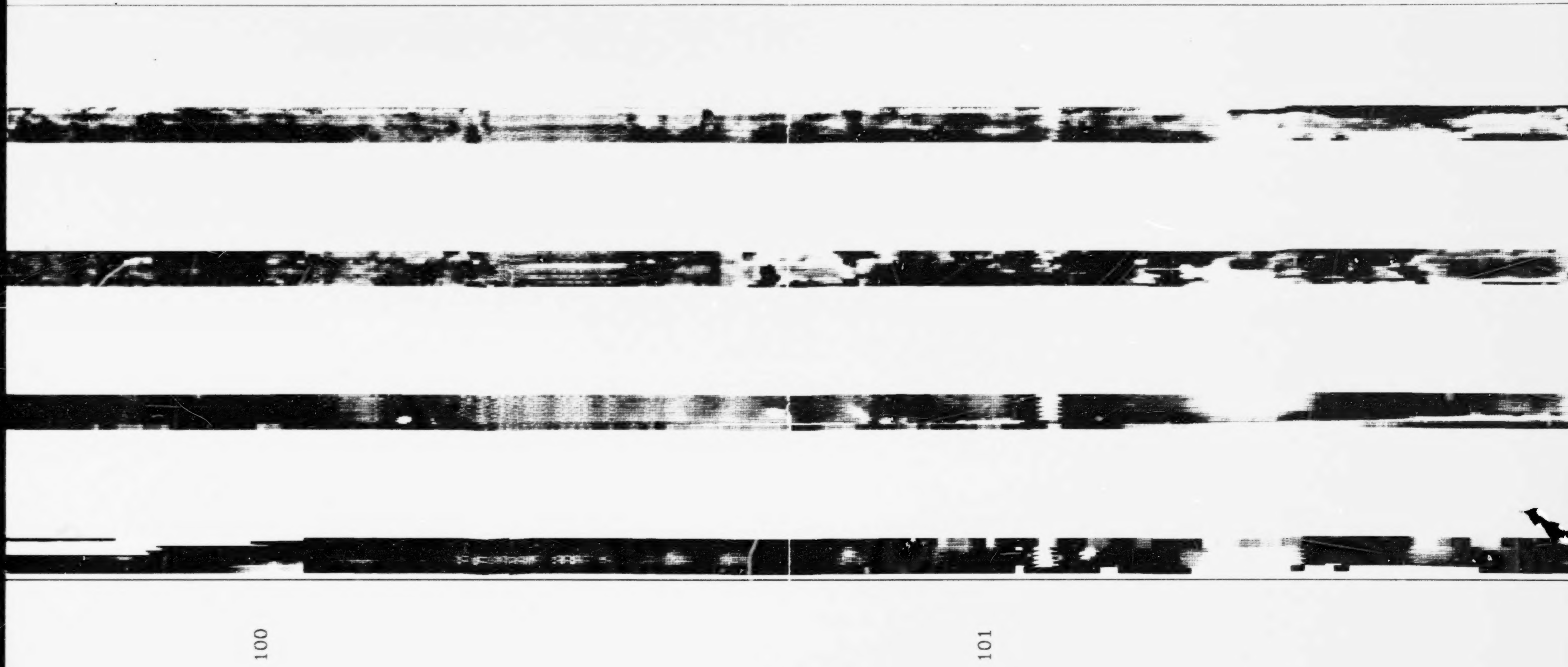
100
101

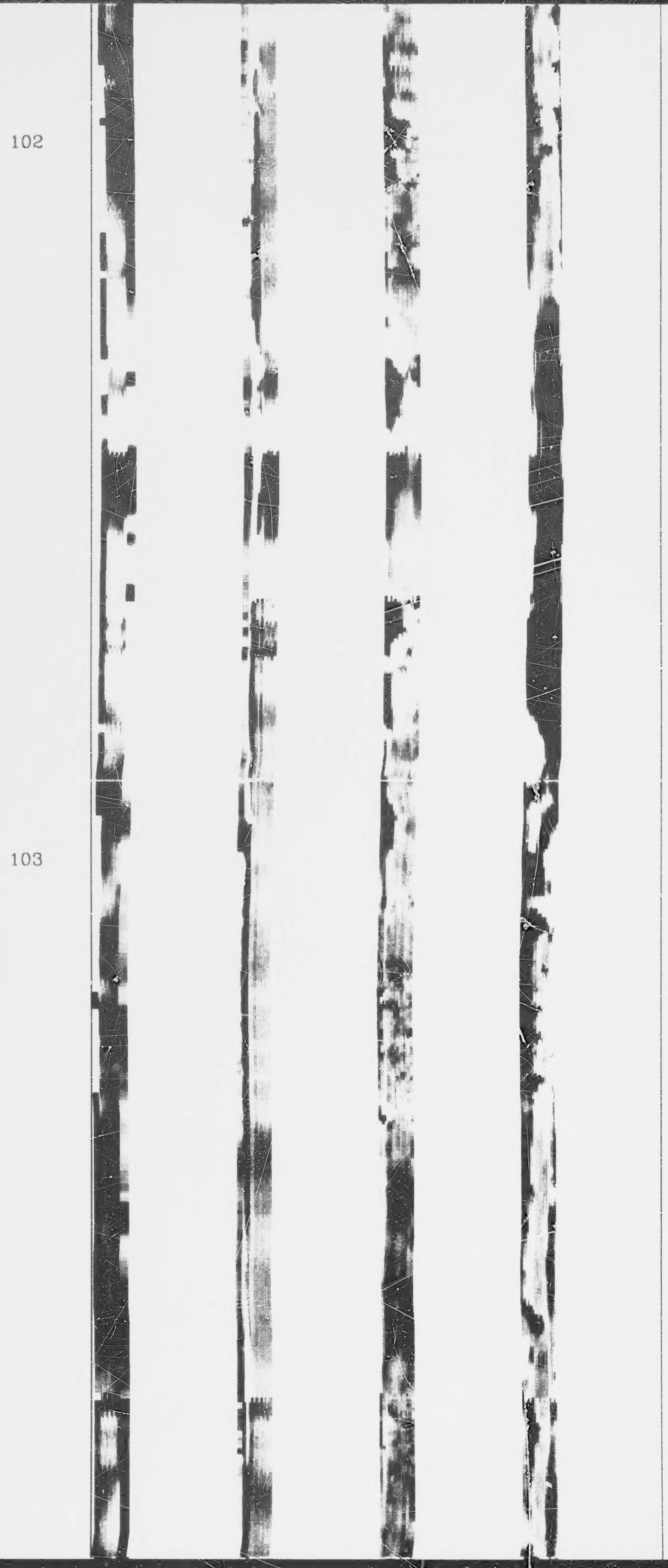
102
103

104
105
106

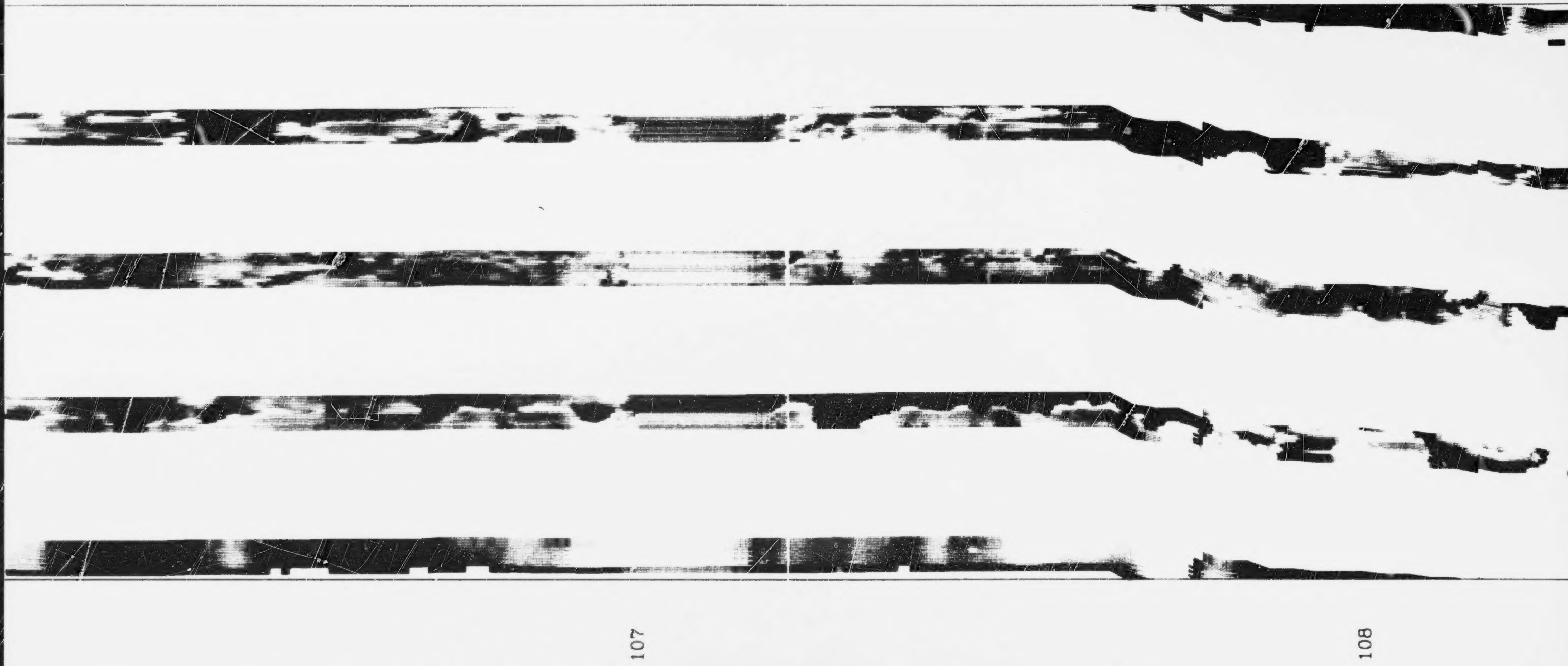
107
108

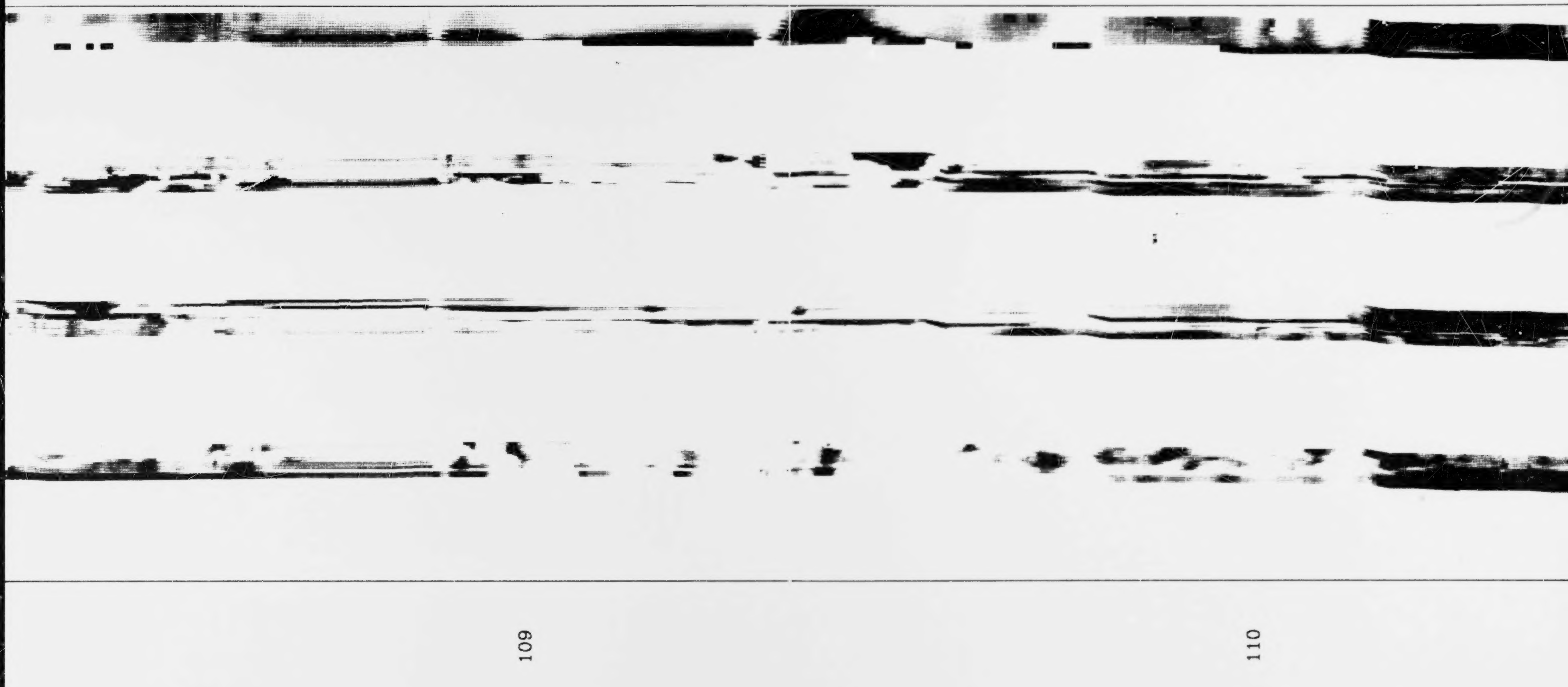
109
110

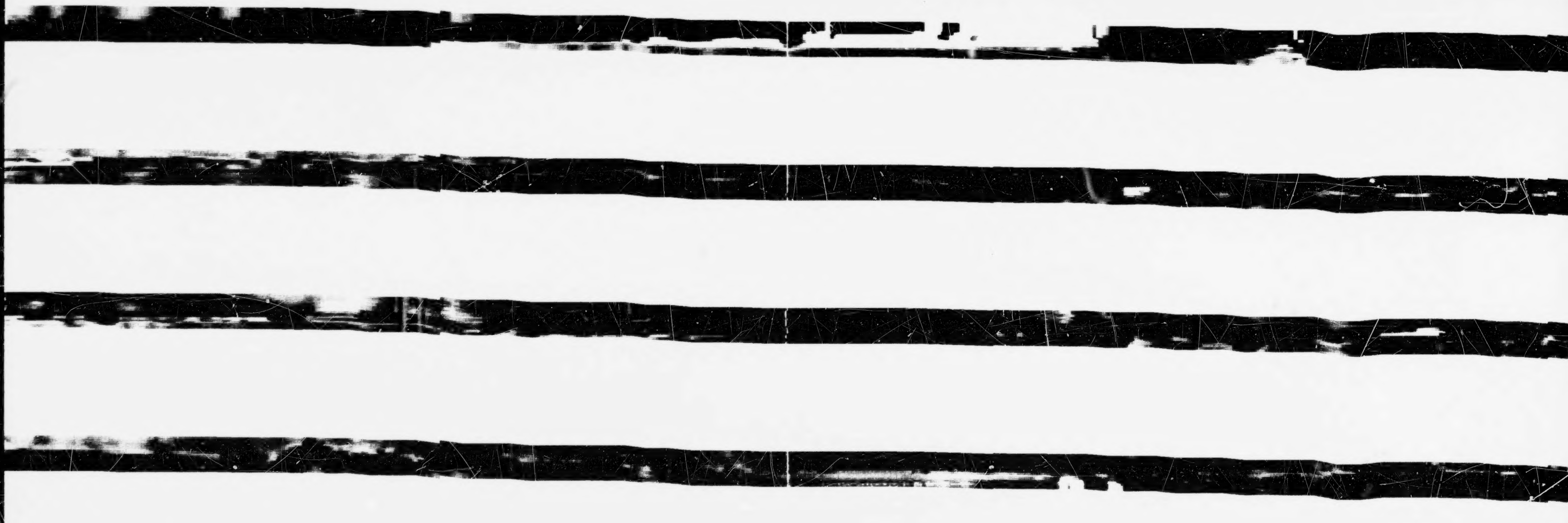
111
112

[redacted]

[redacted]

115 [illegible]

116 [illegible]

117
118
119

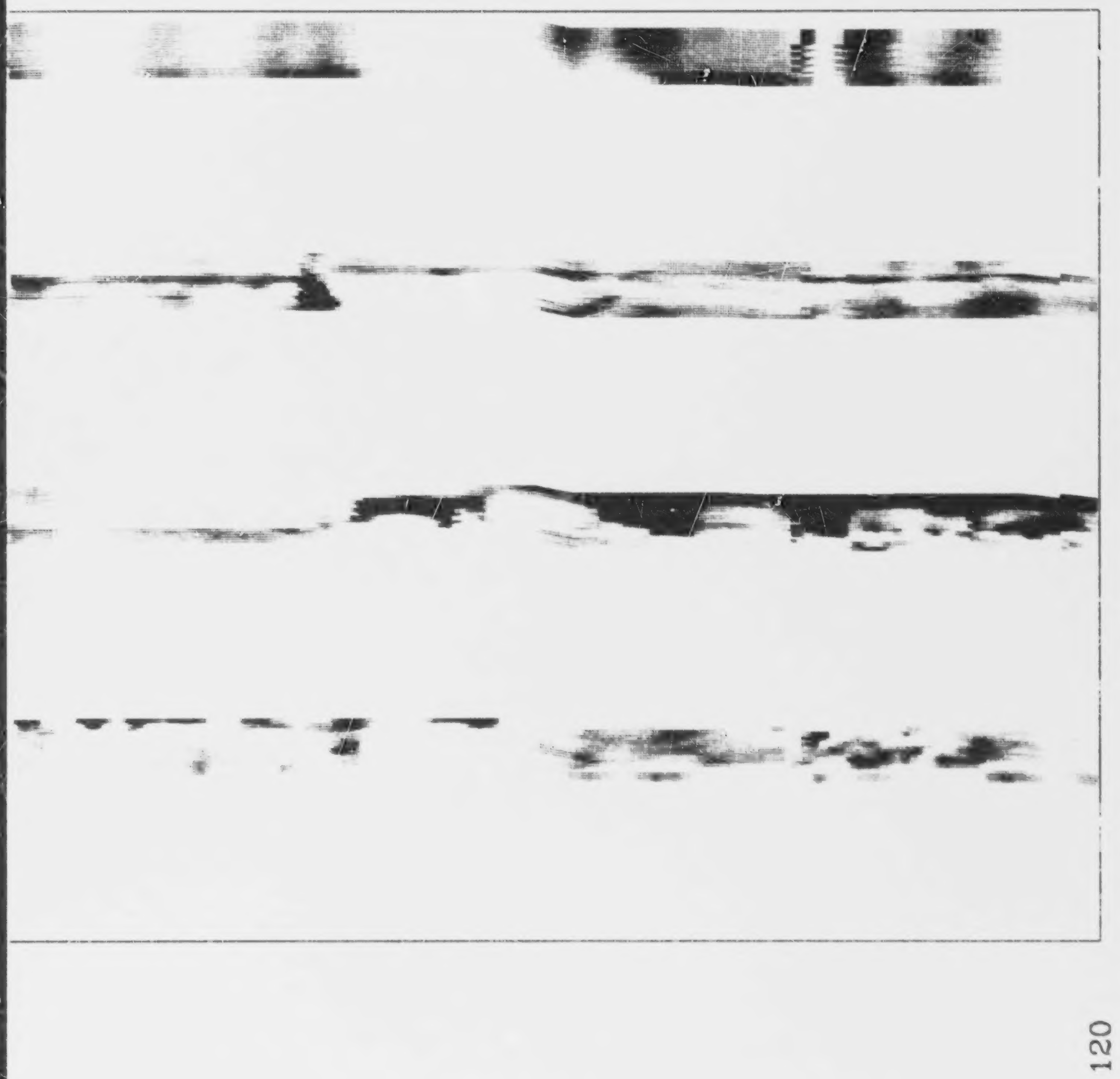

SCHLUMBERGER

FMS
BOREHOLE
IMAGING

COMPANY	LAMONT DOHERTY
WELL	ODP HOLE 803D
FIELD	ONTONG JAVA PLATEAU
COUNTRY	LEG 130
RUN	2
DATE LOGGED	05 - FEB - 90
REFERENCE	STATIC PS 2 120 160

```
STATIC  NORMALIZATION

PASS 2

FILE : MEST.002



            ZONE FROM  160.0      M   TO  120.0      M

            DEPTH SCALE = 1/    5

            IMAGE SCALE = 1/    5

            BITSIZE         =     9.88
```

ORIENTATION

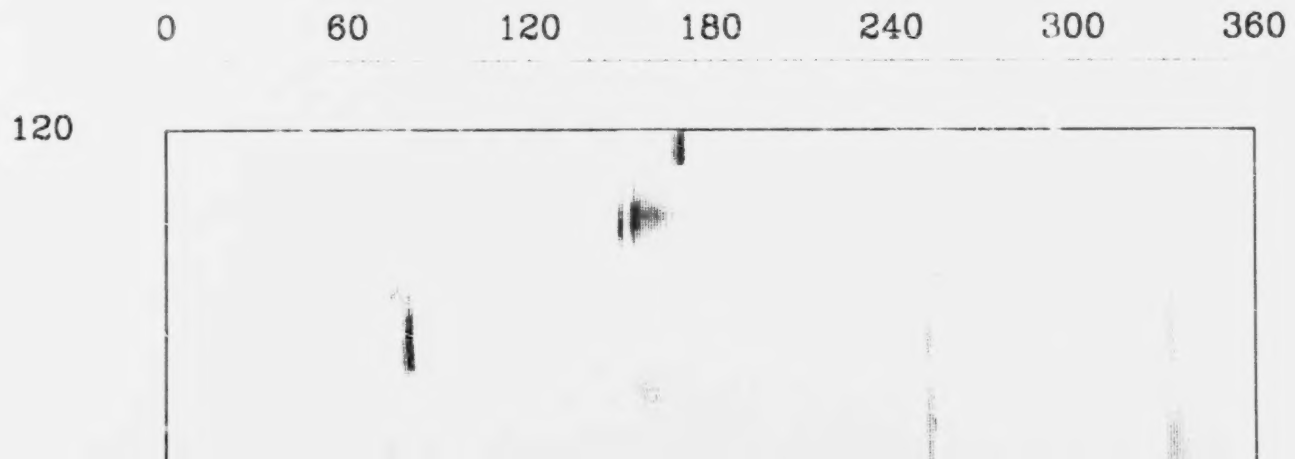

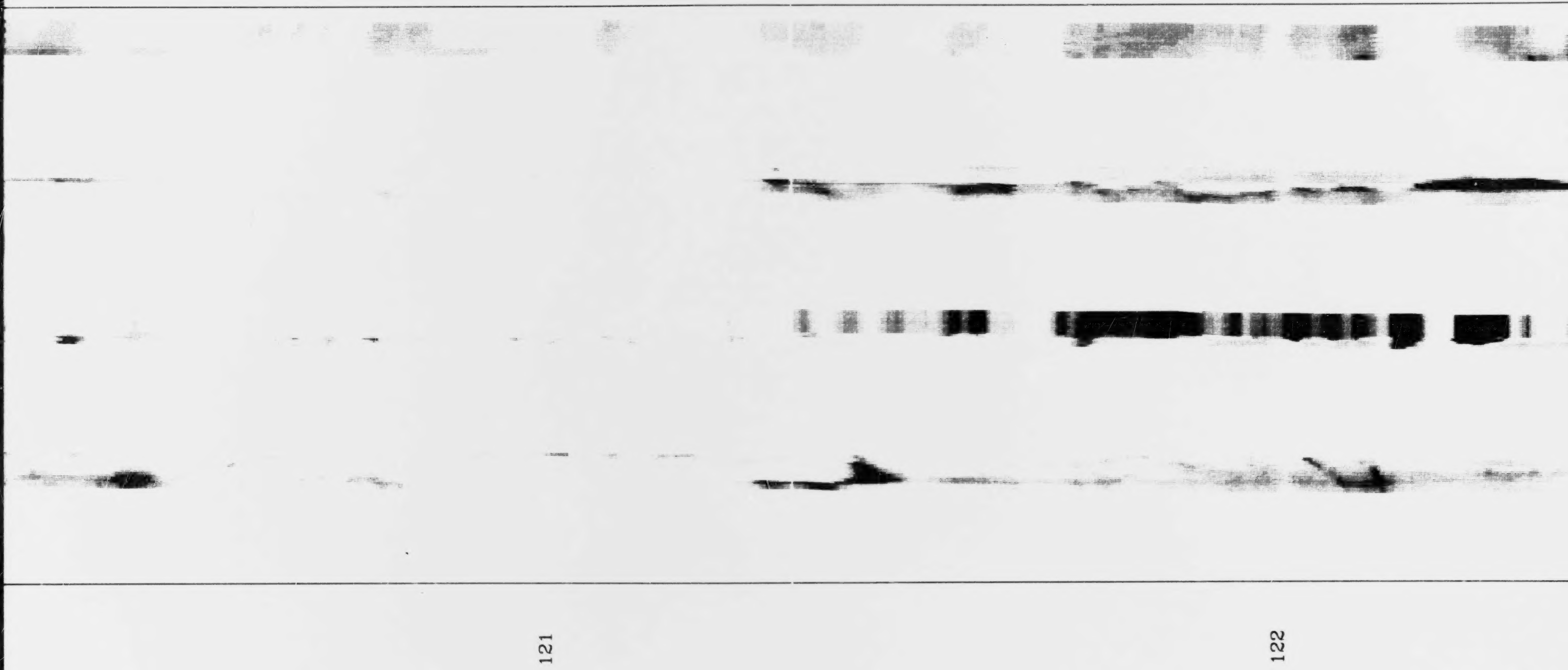
121
122

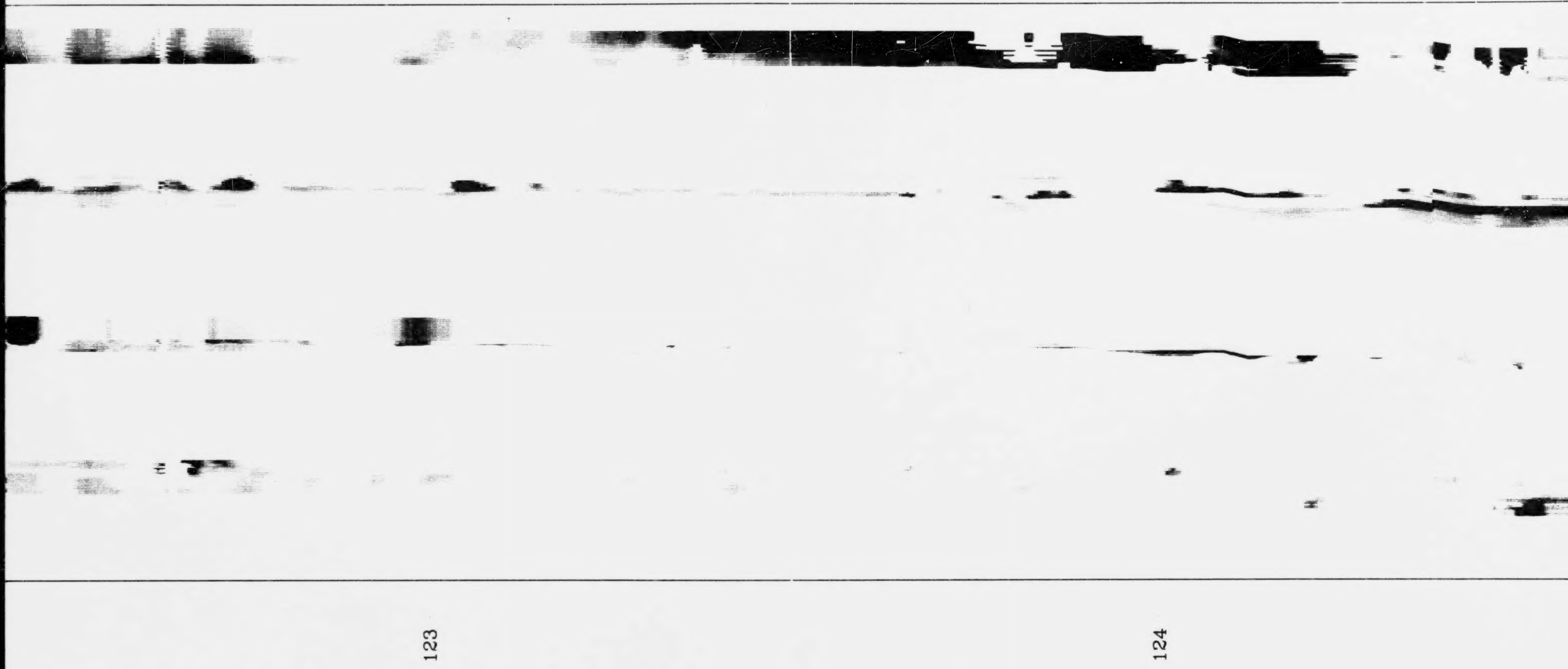
123
124

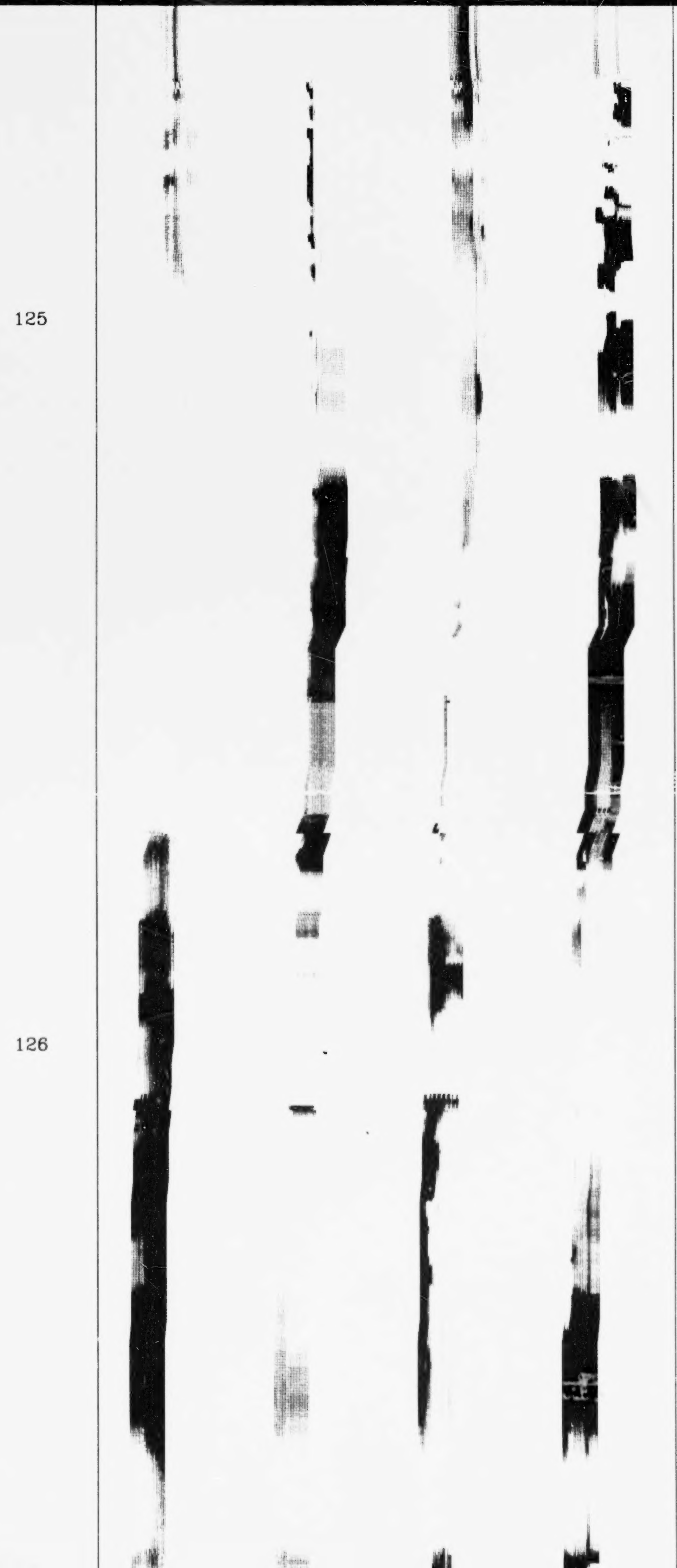
125
126

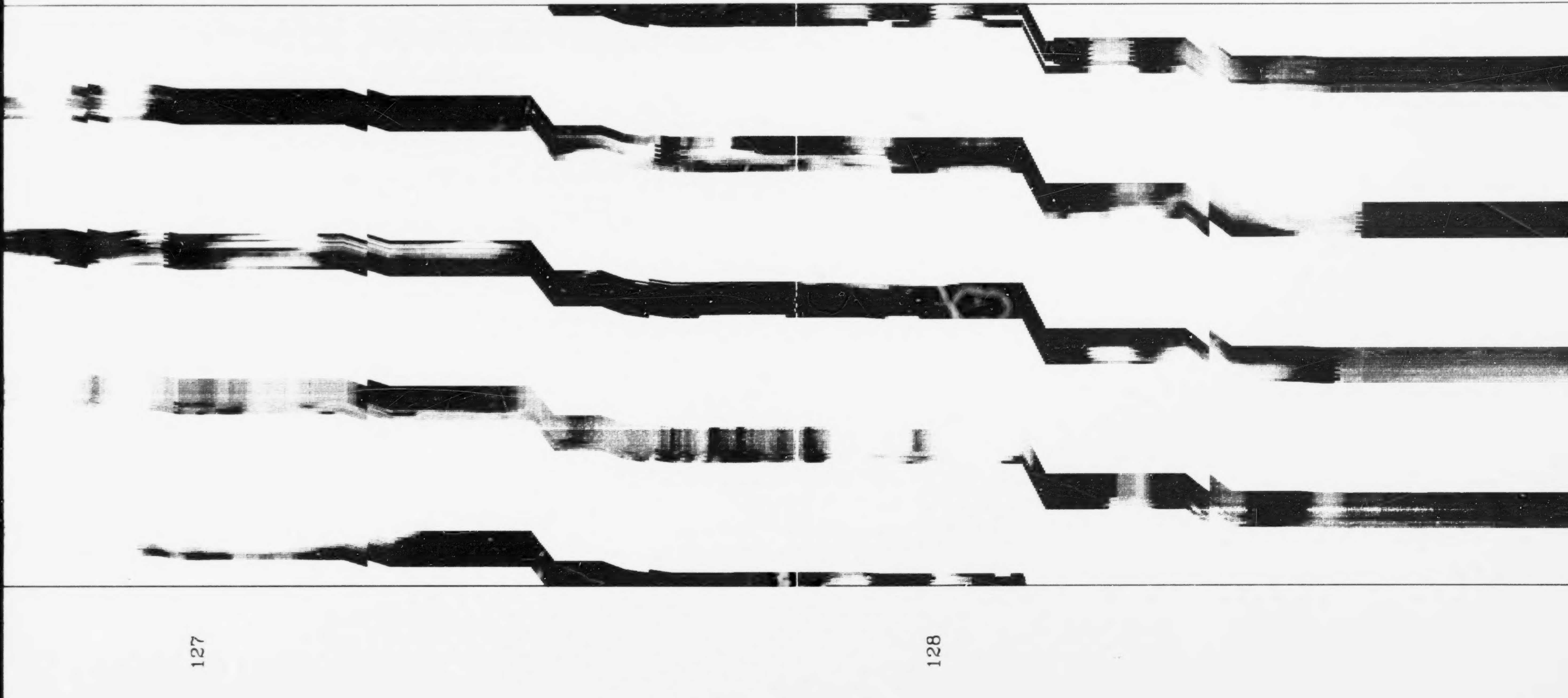
127
128

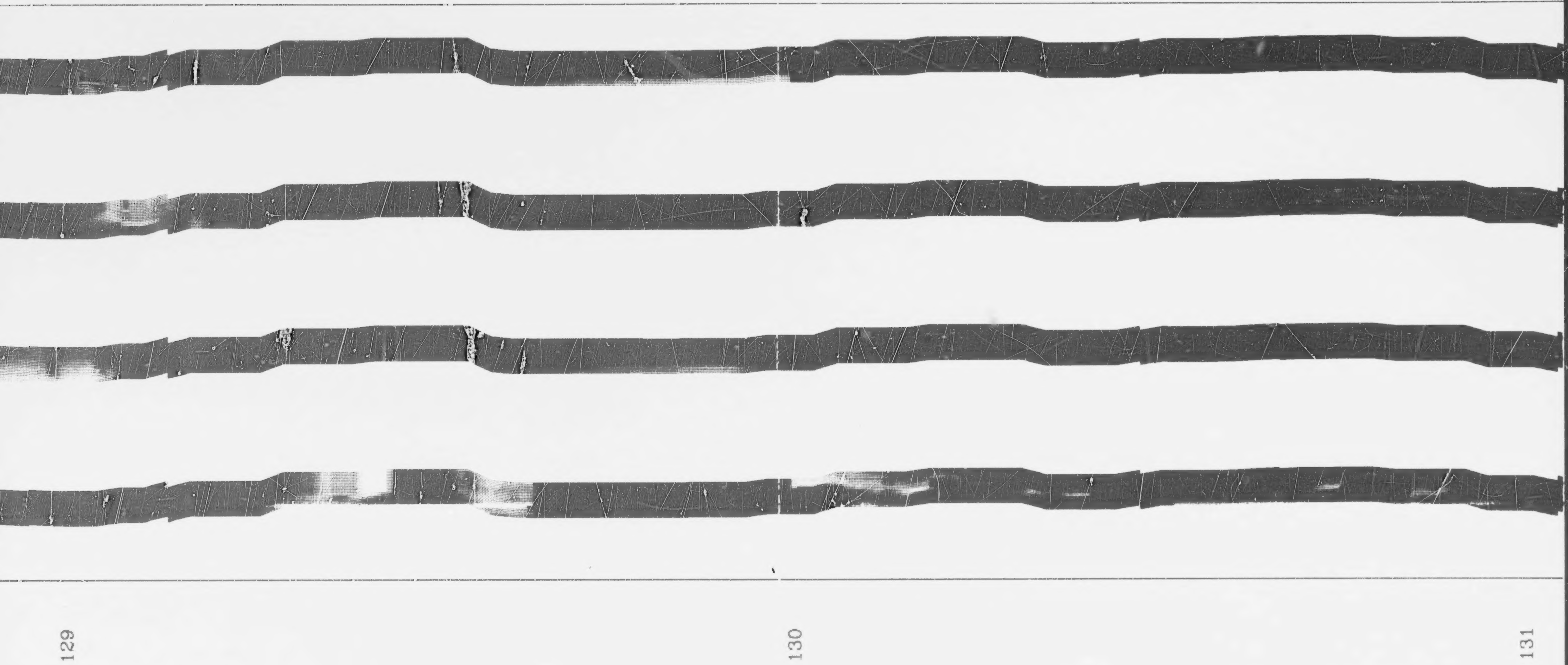
129
130
131

132
133

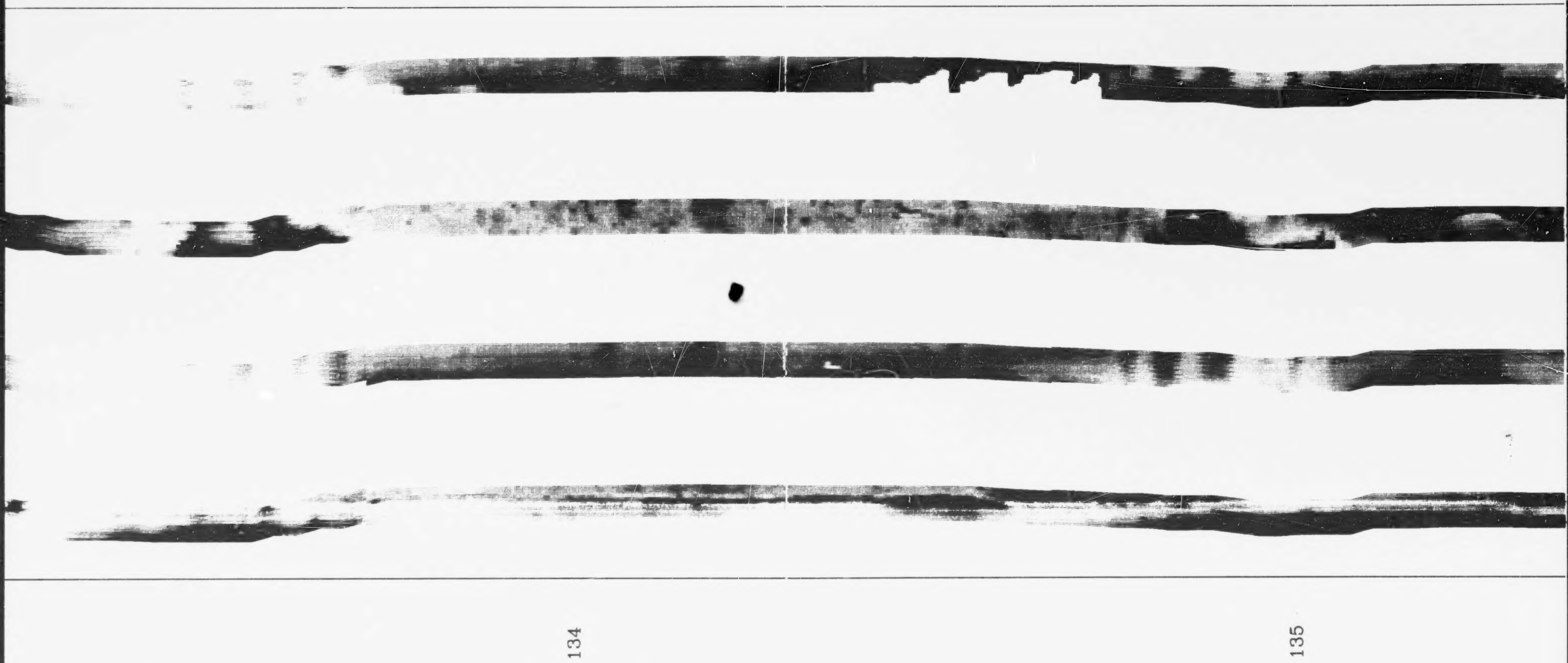
134
135

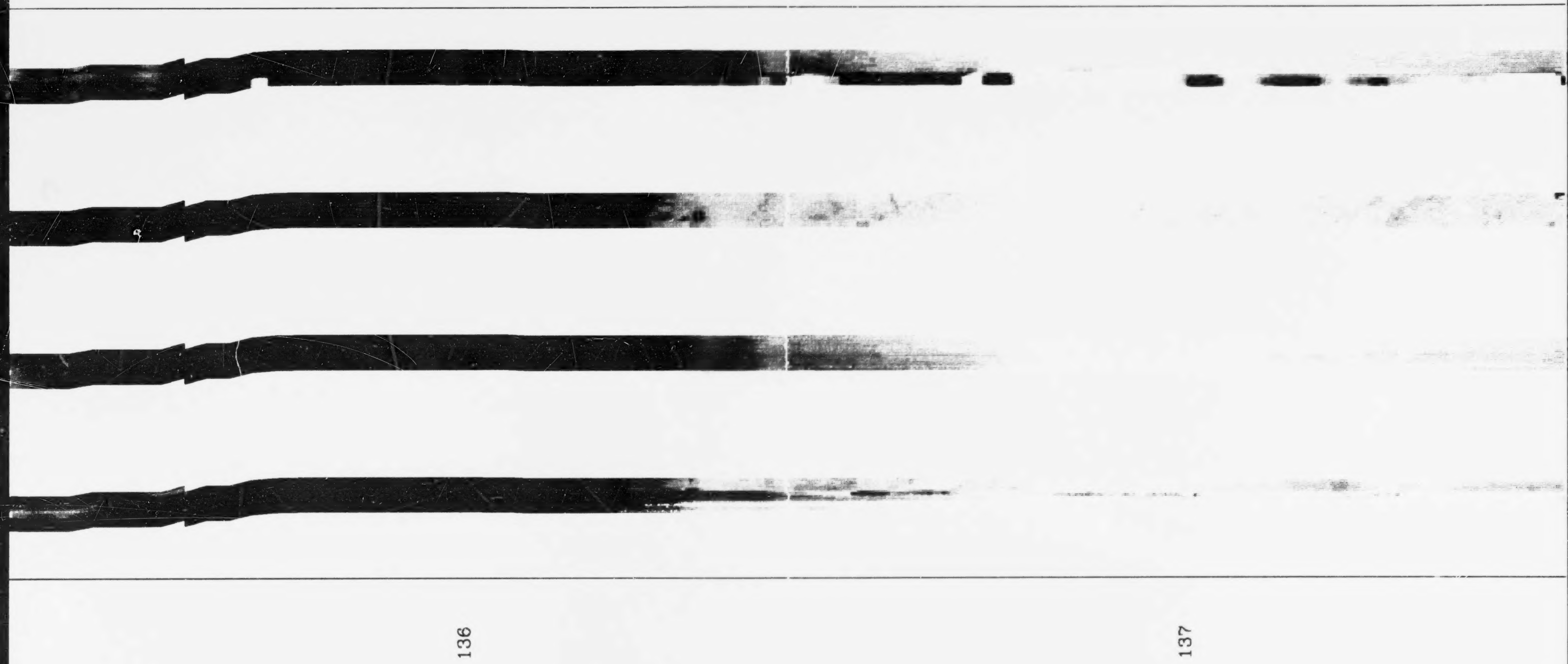
136
137

138

139

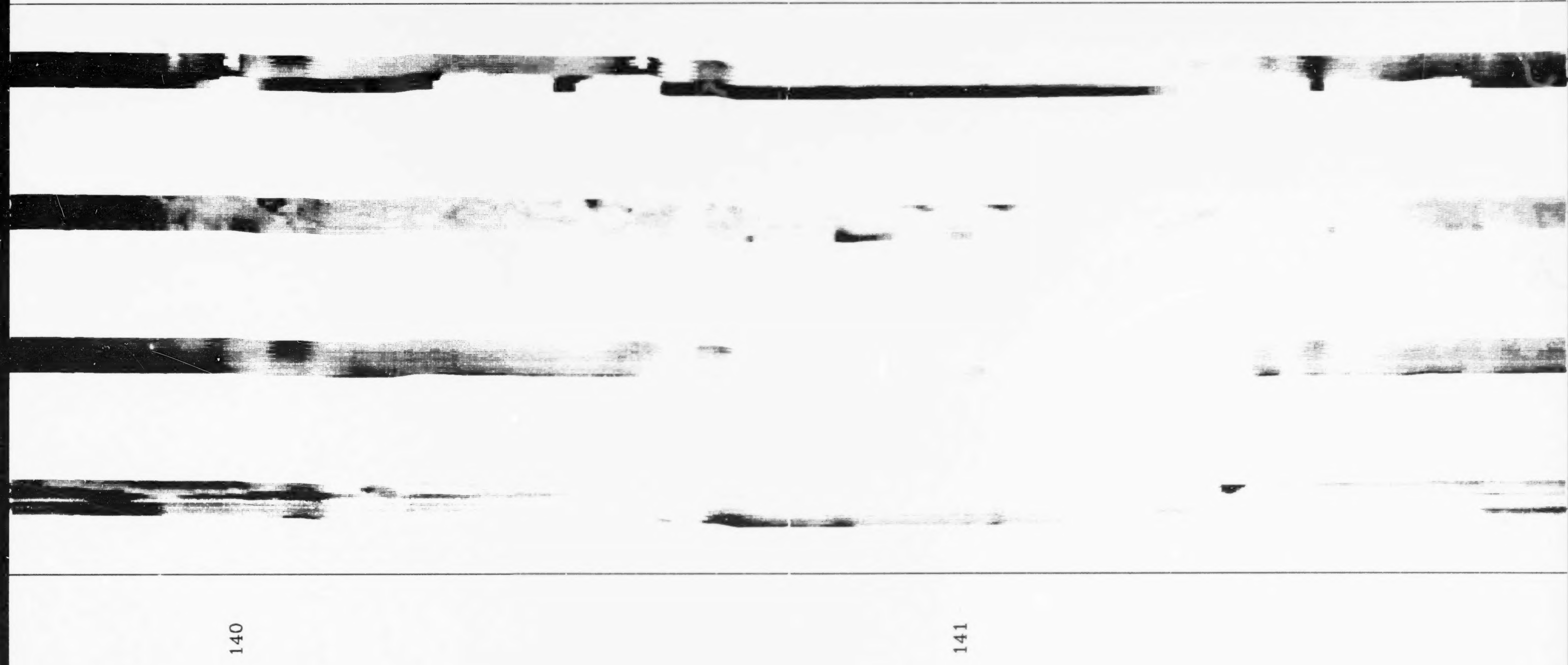
140
141

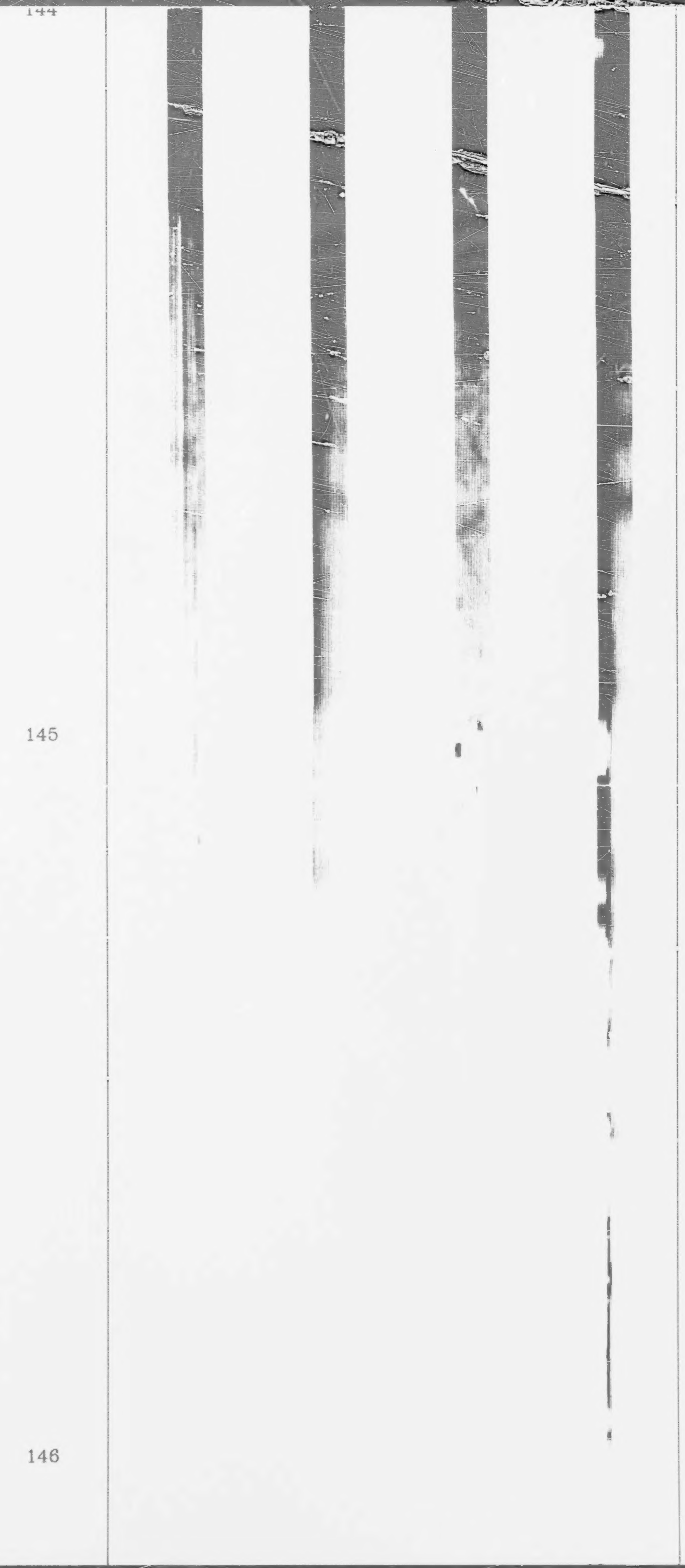
144
145
146

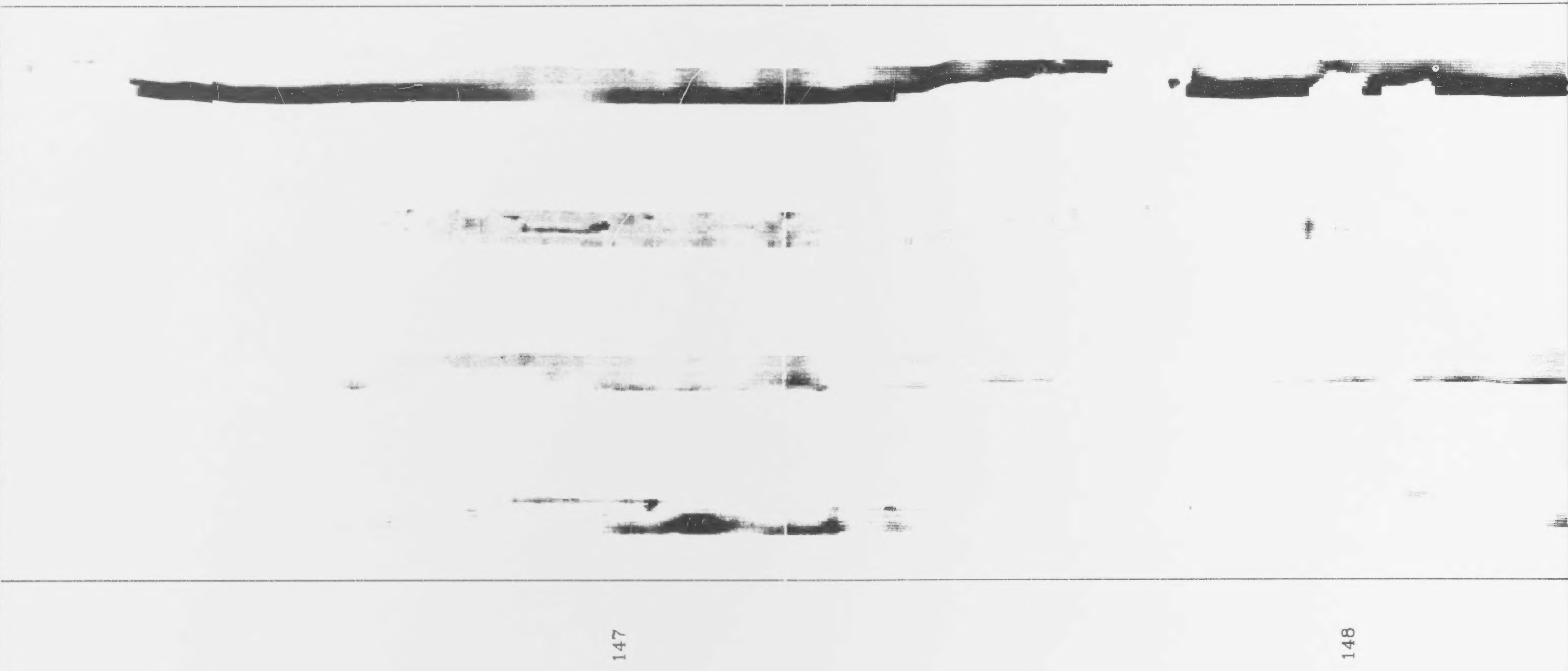
147
148

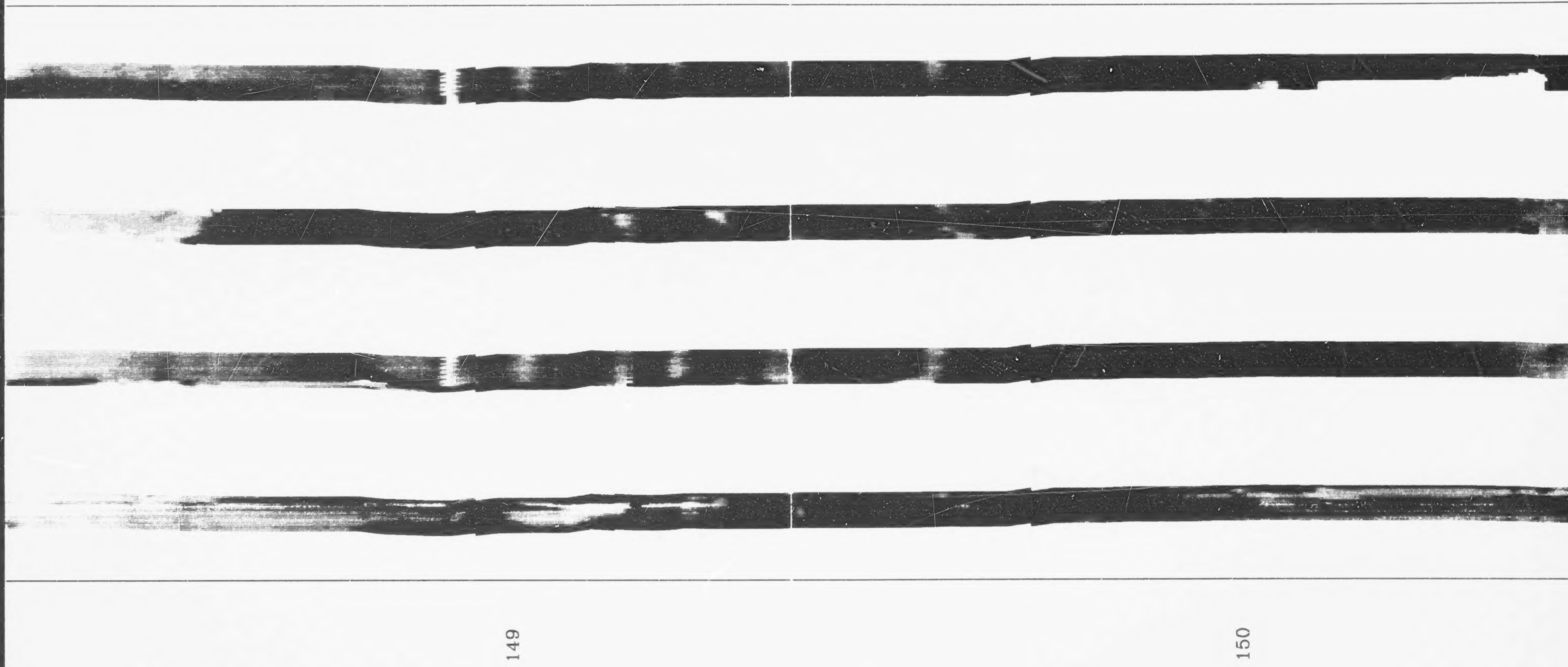
149
150

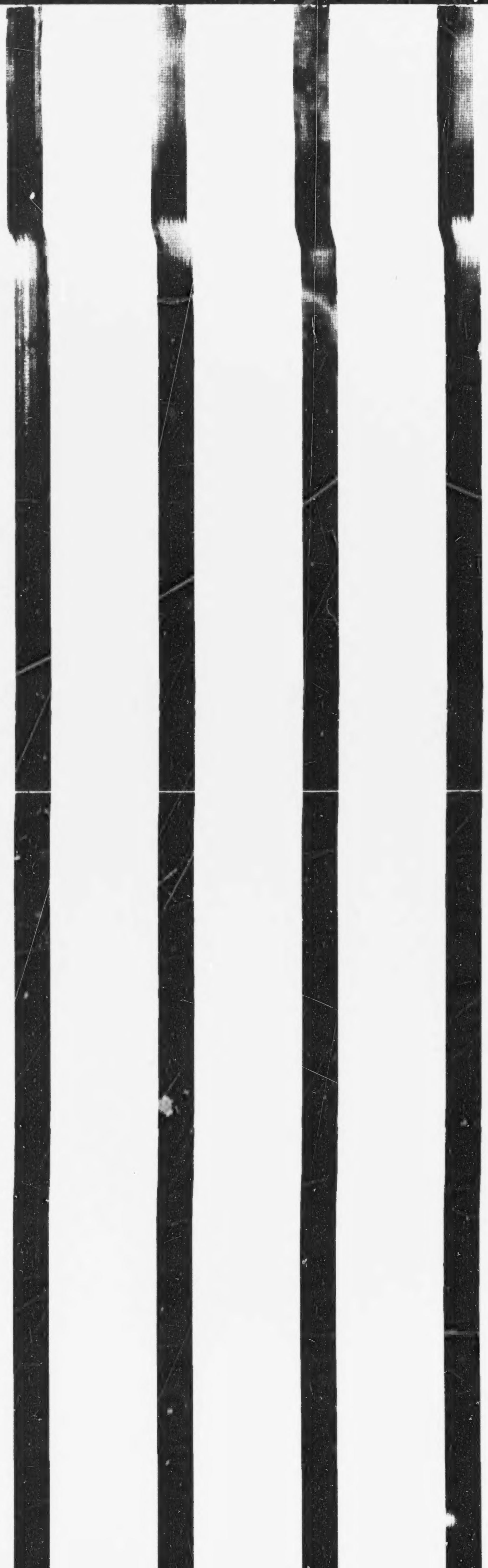

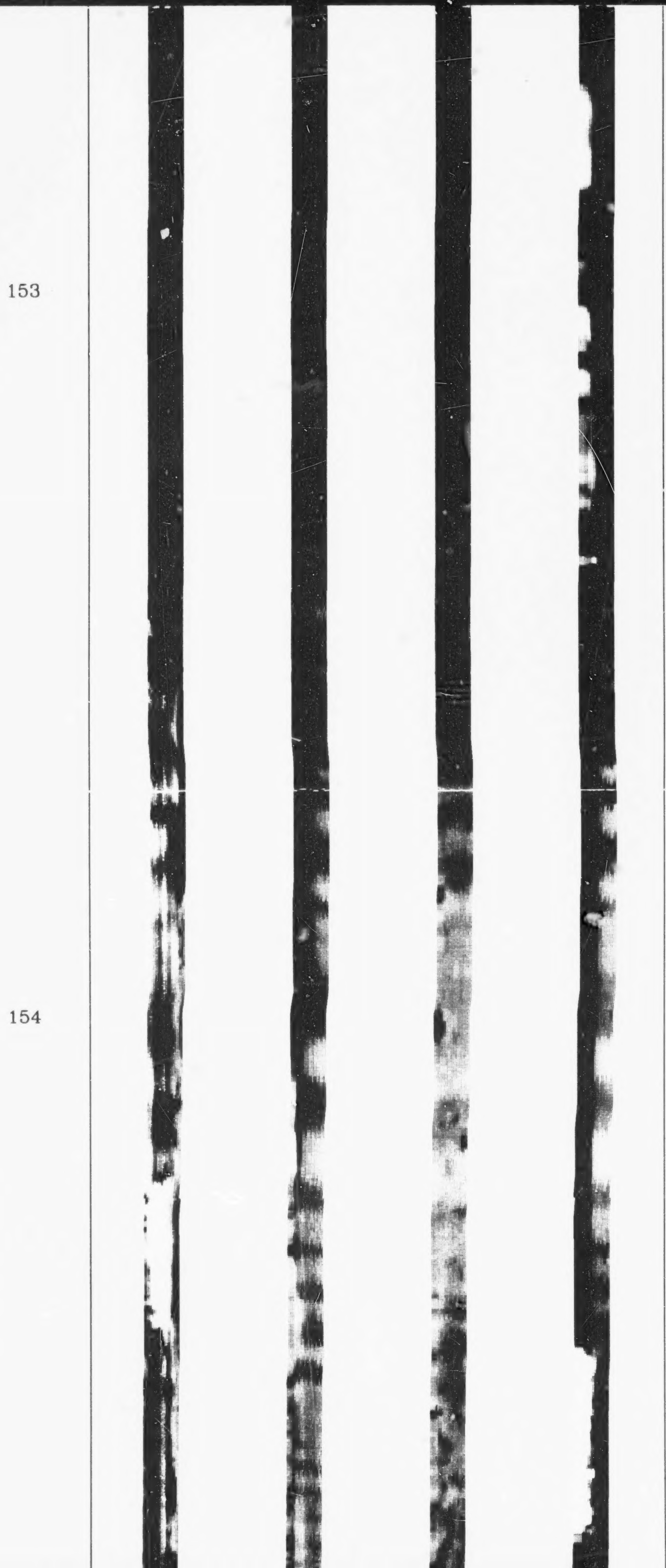
153
154

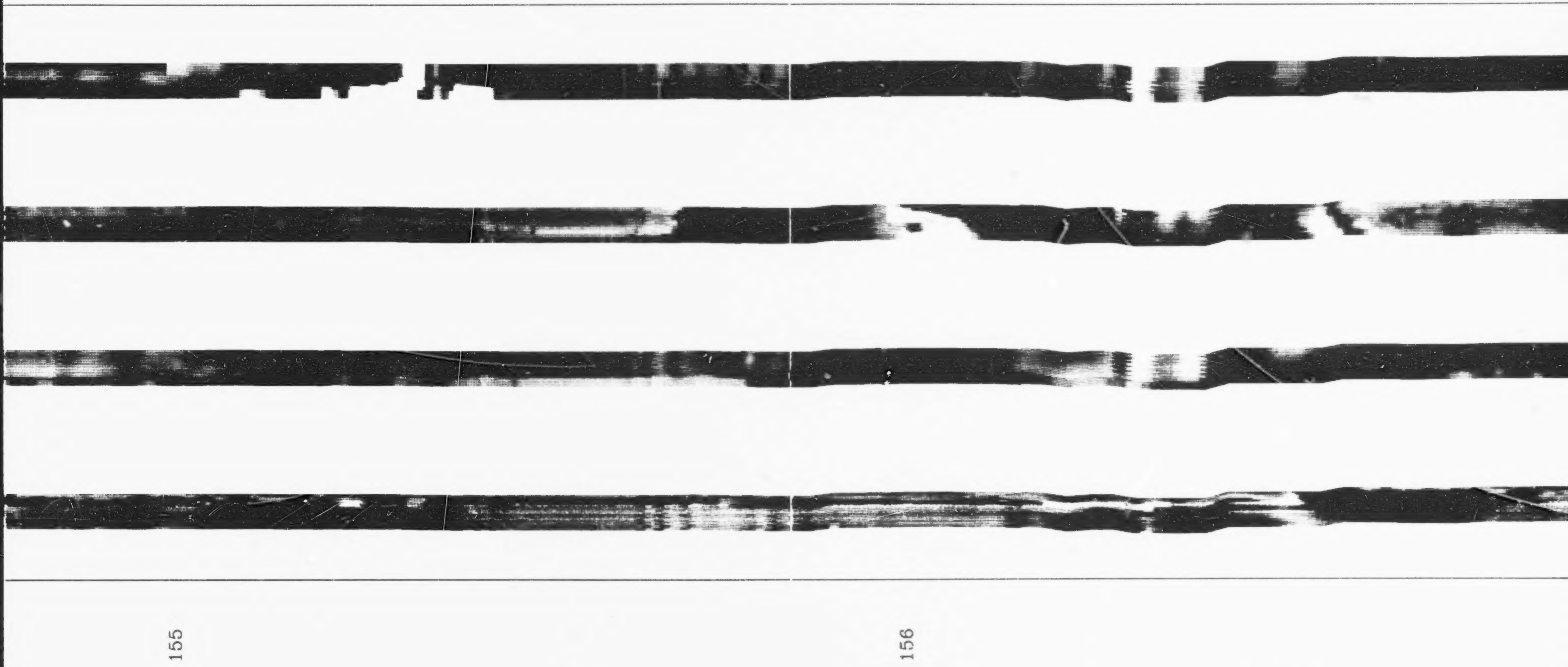
155
156

157
158
159

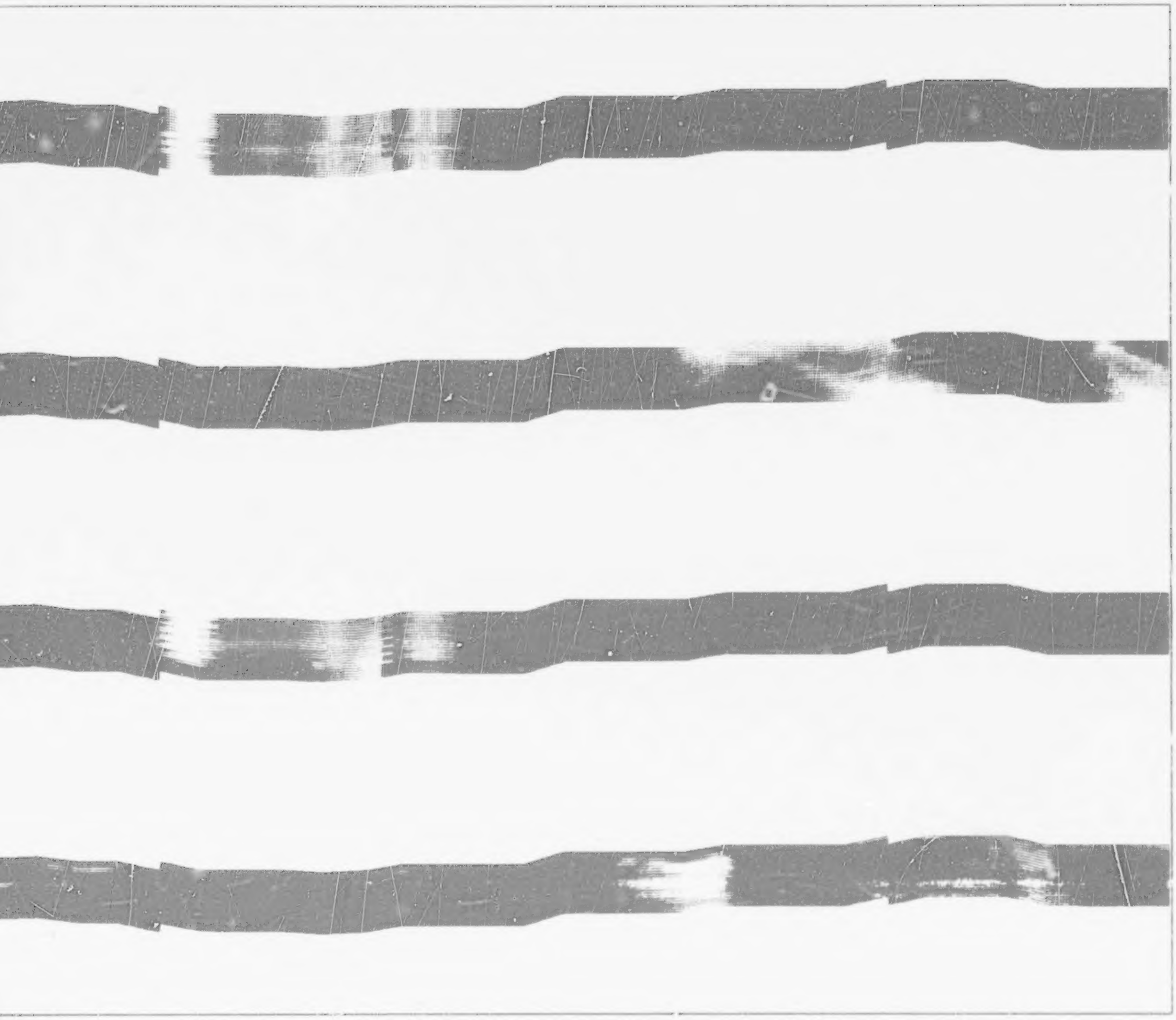

SCHLUMBERGER

FMS
BOREHOLE
IMAGING

COMPANY	LAMONT DOHERTY
WELL	ODP HOLE 803D
FIELD	ONTONG JAVA PLATEAU
COUNTRY	LEG 130
RUN	2
DATE LOGGED	05 – FEB – 90
REFERENCE	STATIC PS-2 160-200

STATIC NORMALIZATION

PASS 2

FILE : MEST.002

ZONE FROM 200.0 M TO 160.0 M

DEPTH SCALE = 1/ 5

IMAGE SCALE = 1/ 5

BITSIZE = 9.88

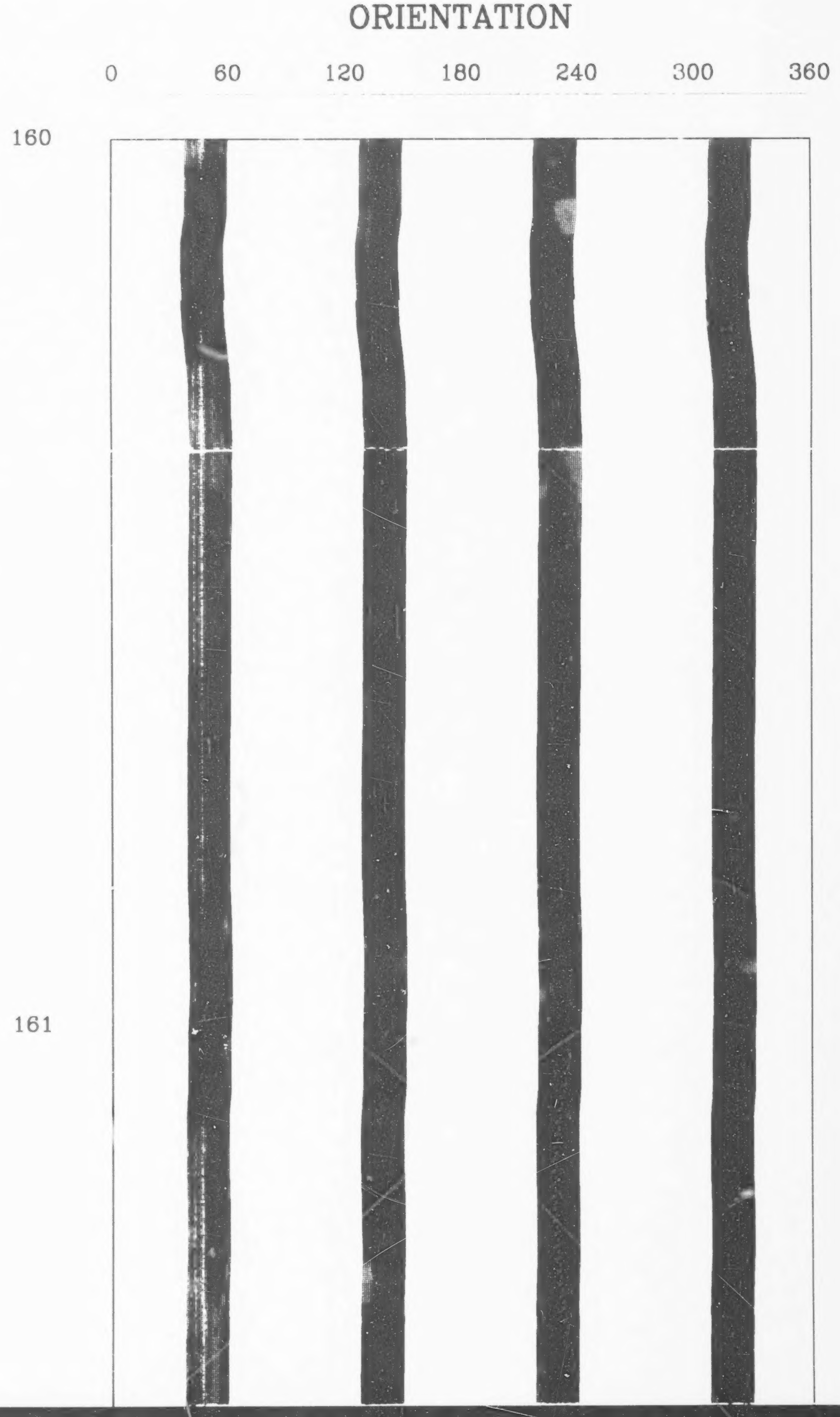

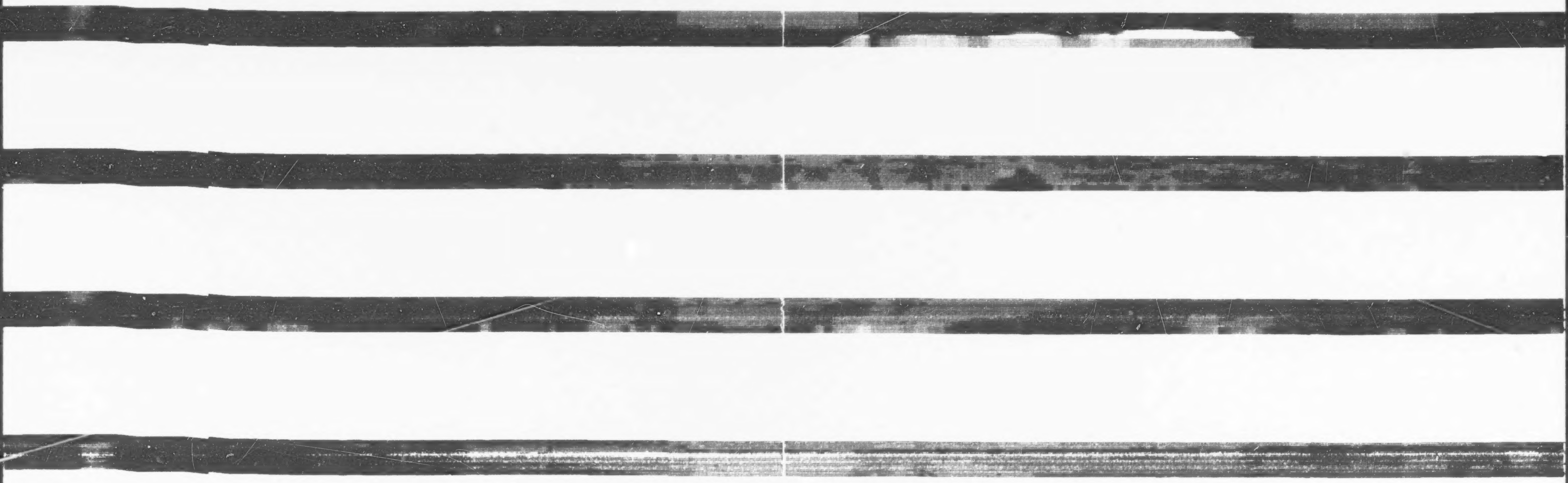

162
163

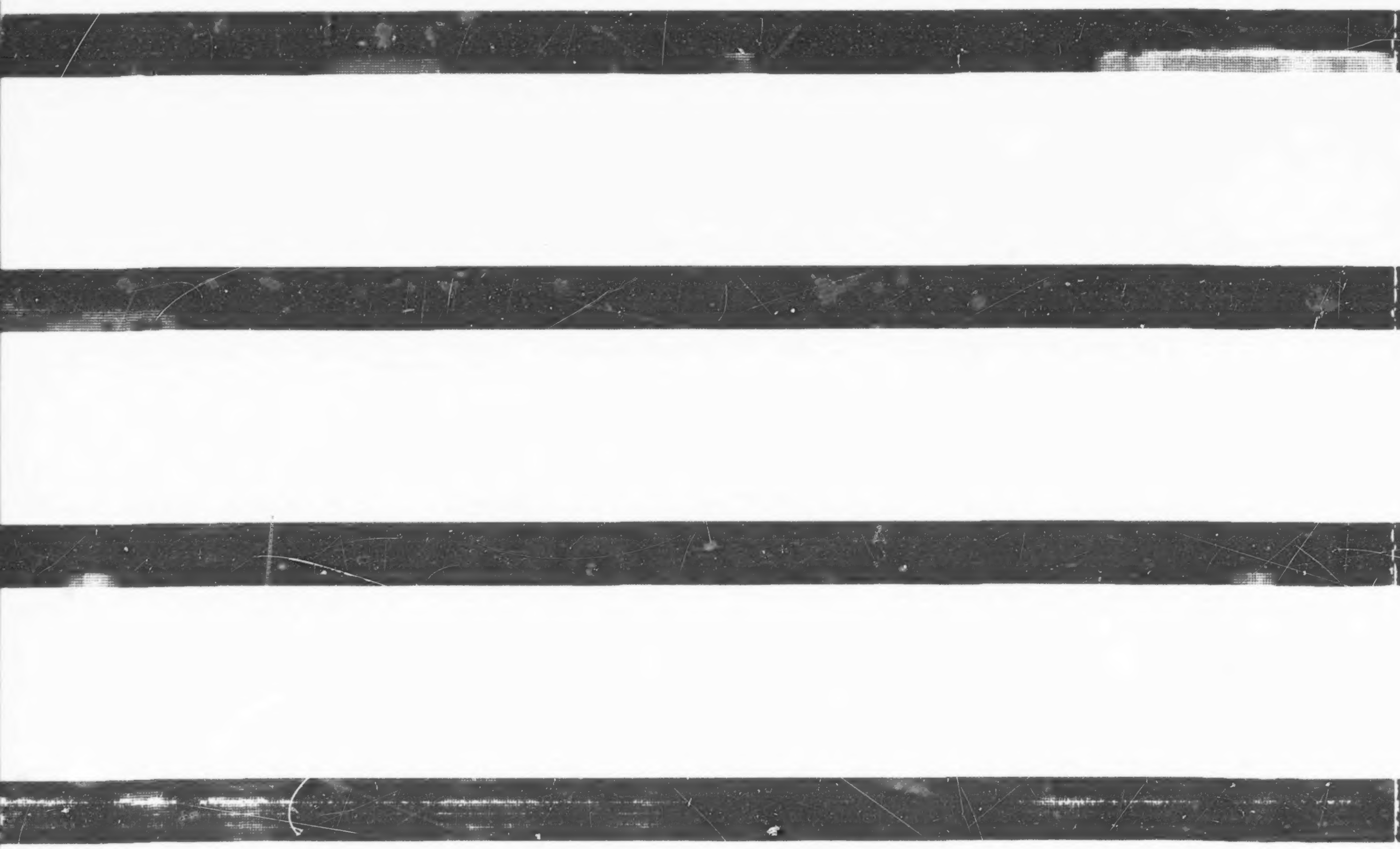

164

165

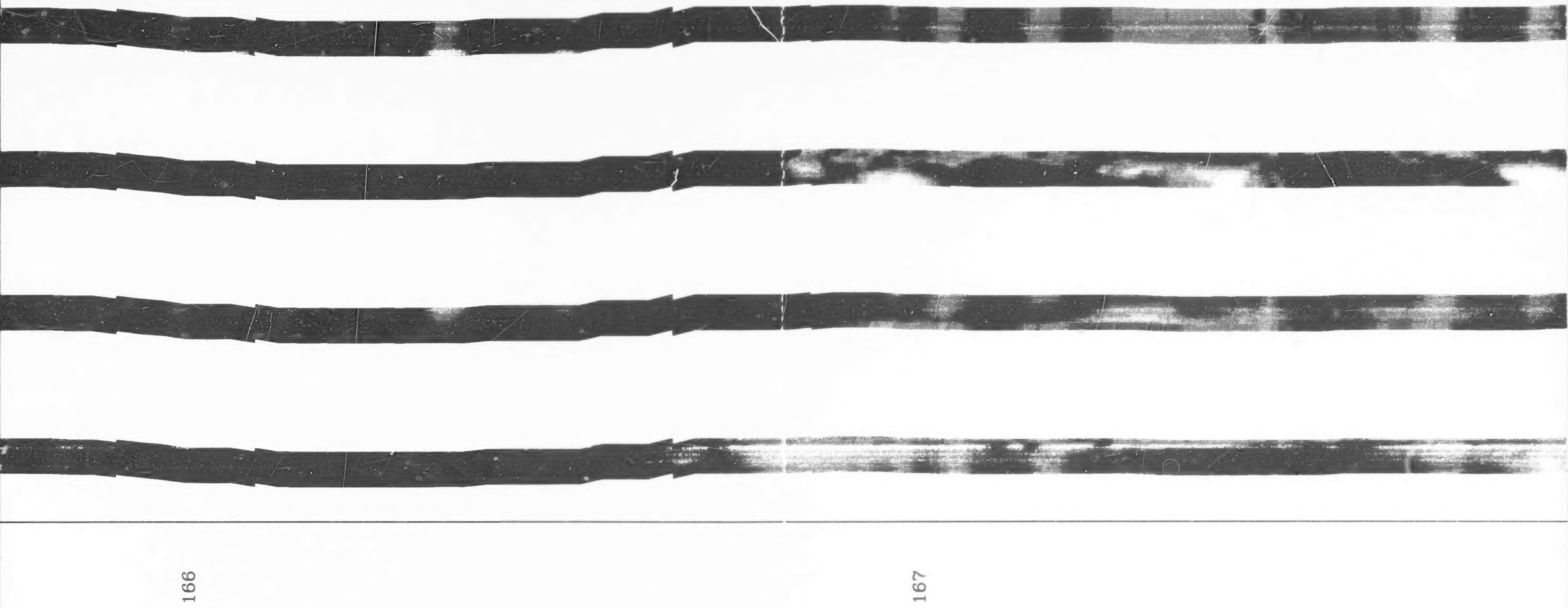
166
167

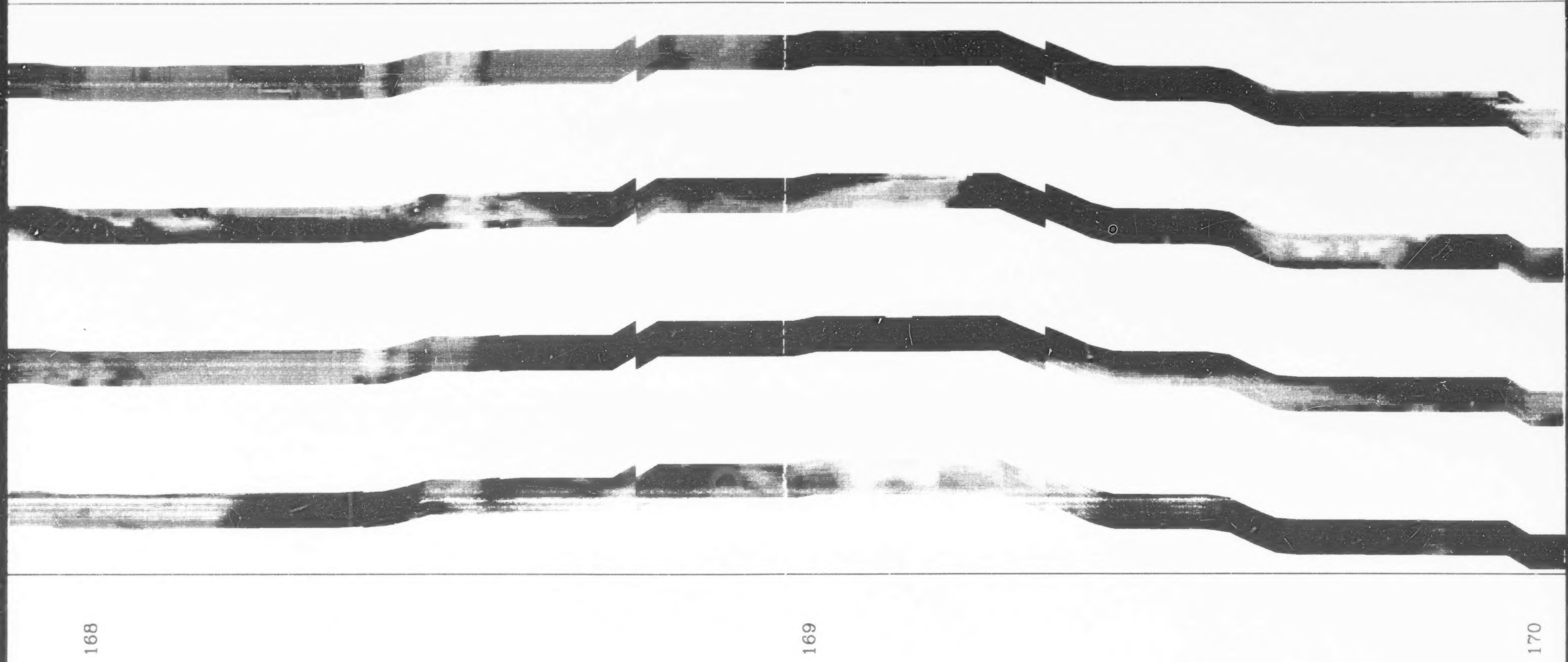
168
169
170

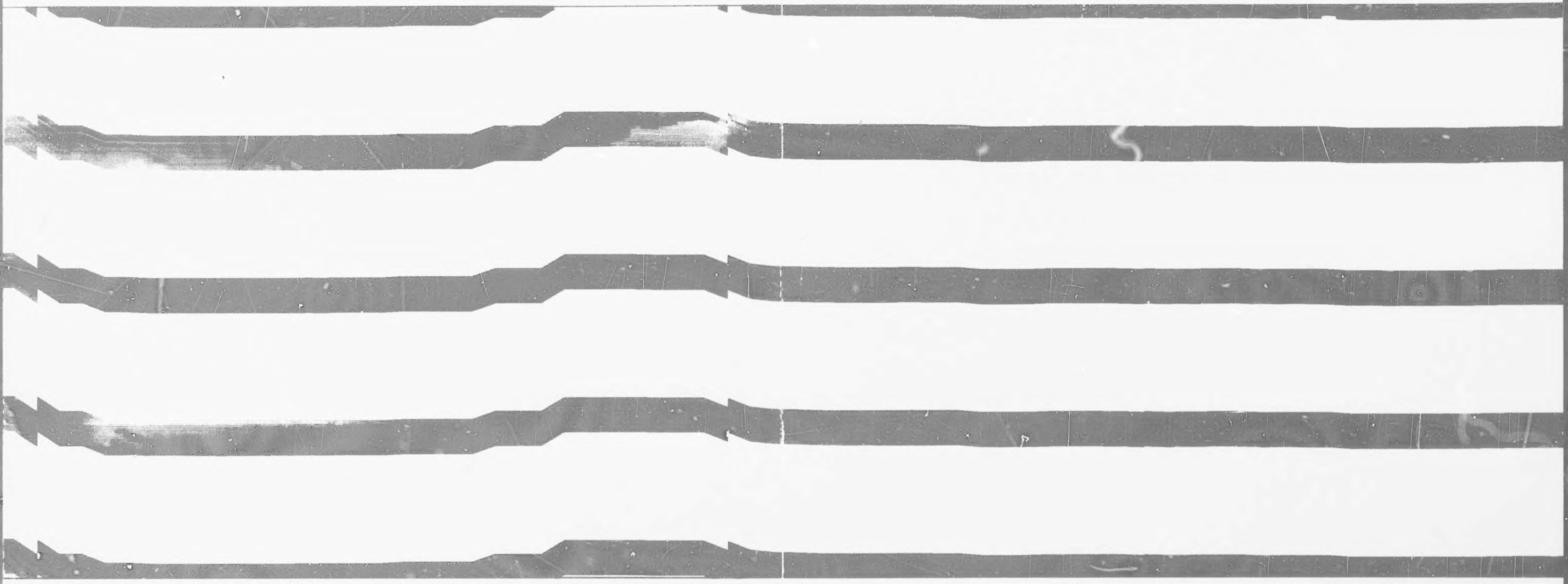
171
172

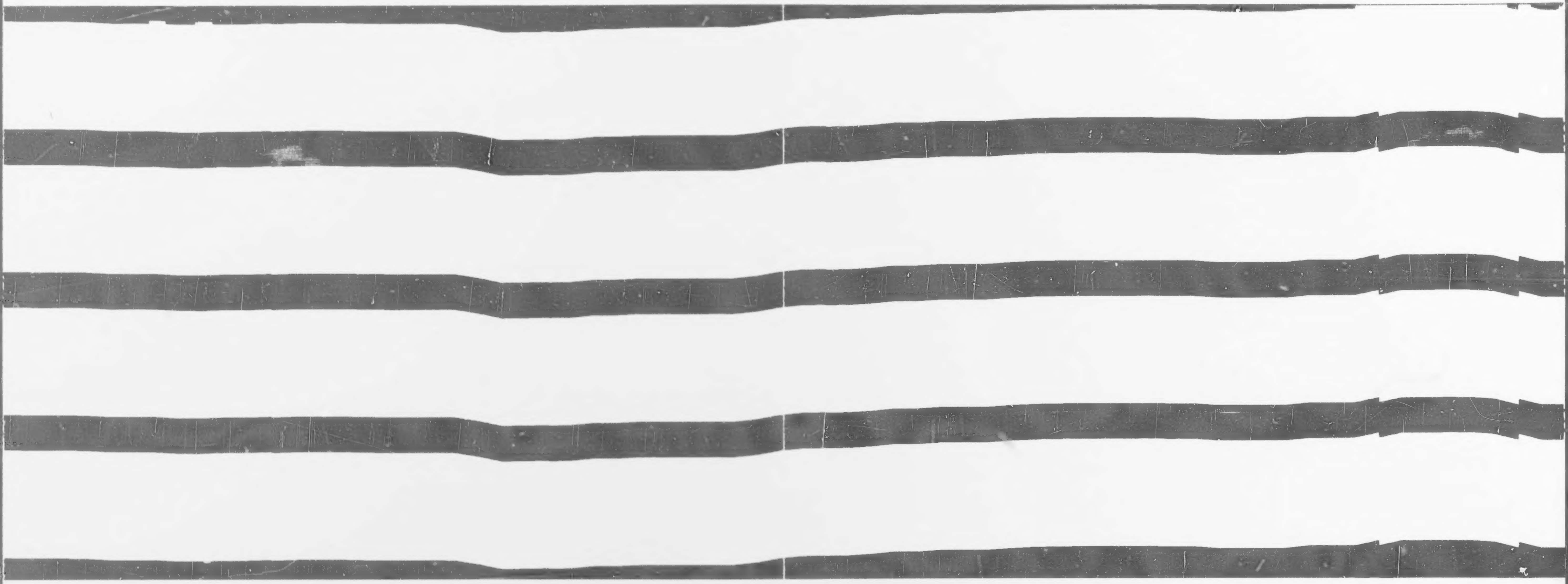

173

174

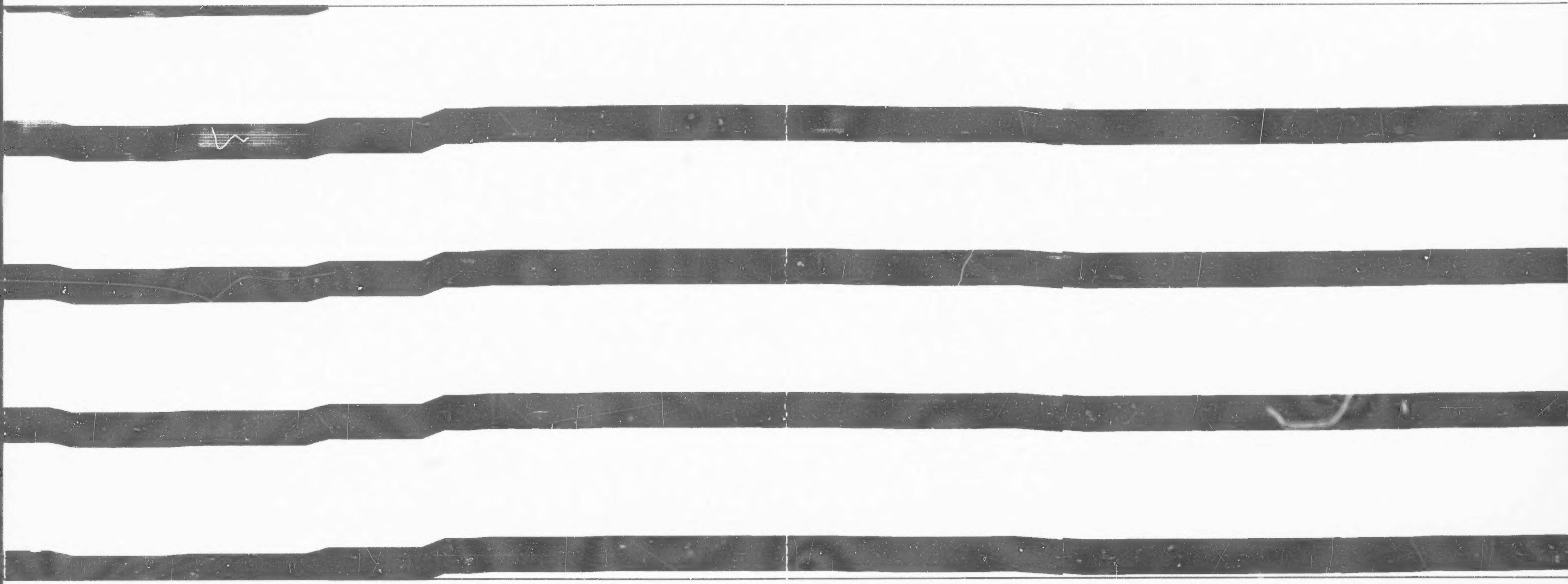

175
176

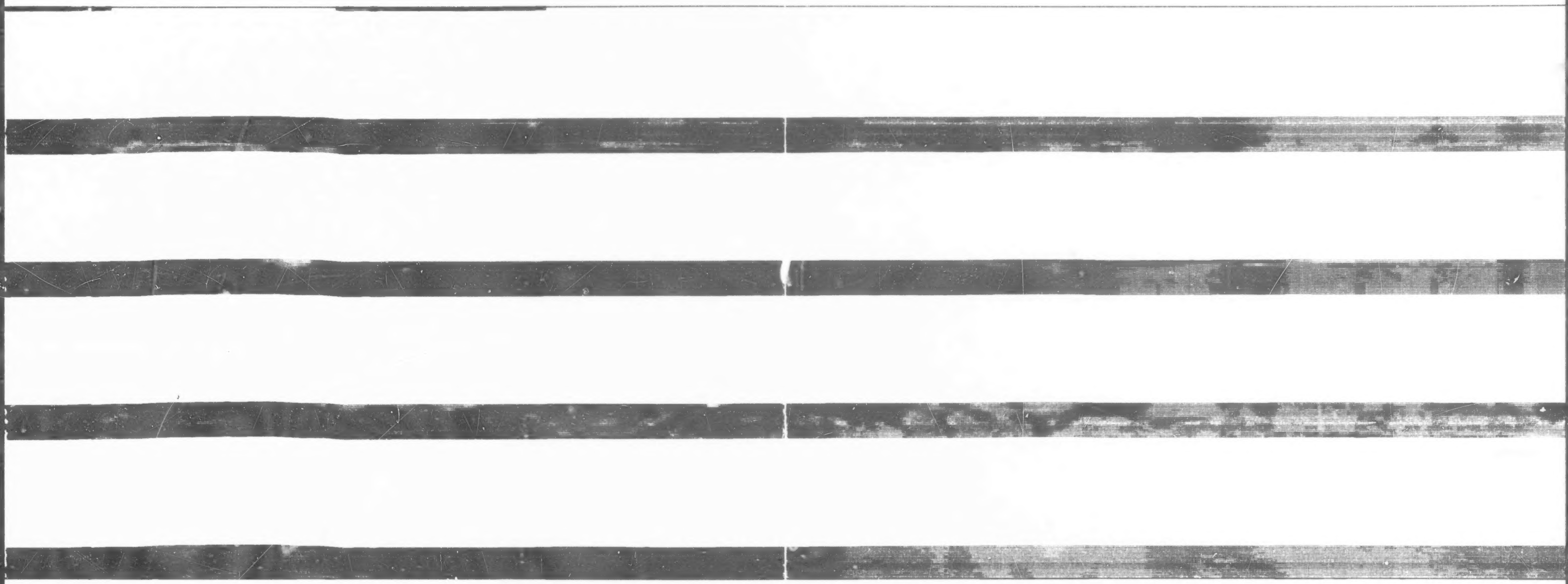

181

182

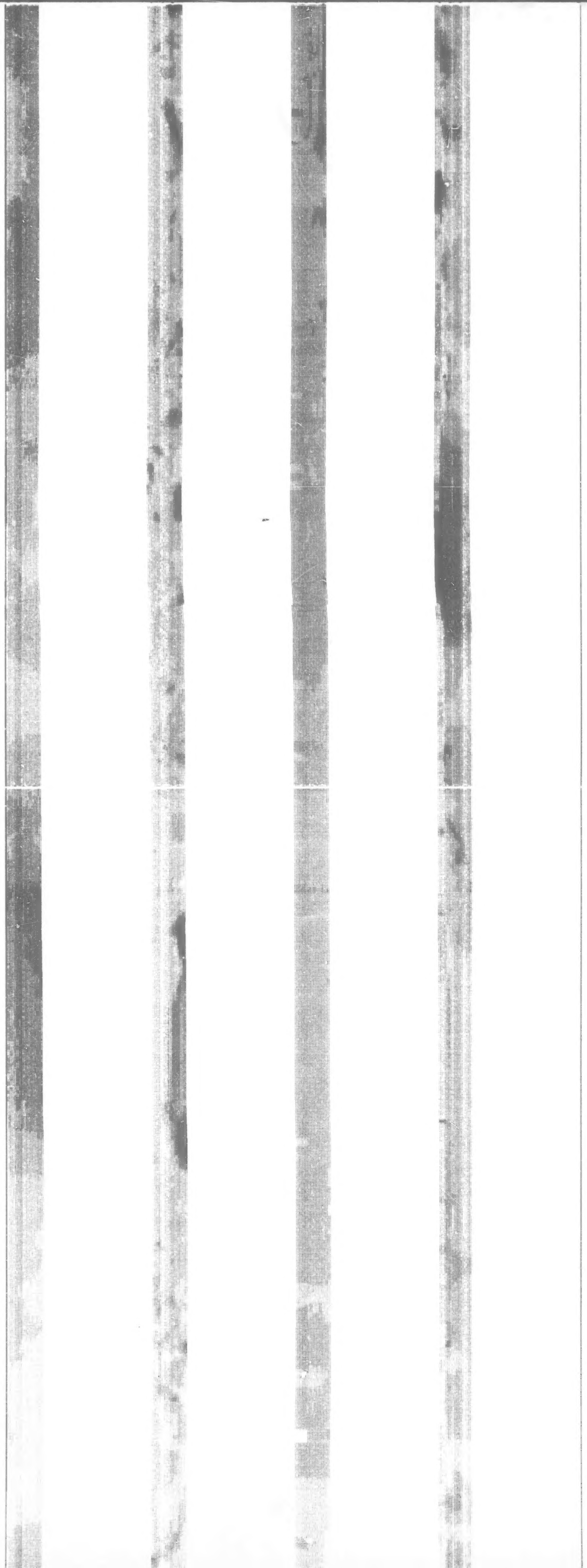
183
184
185

188

189

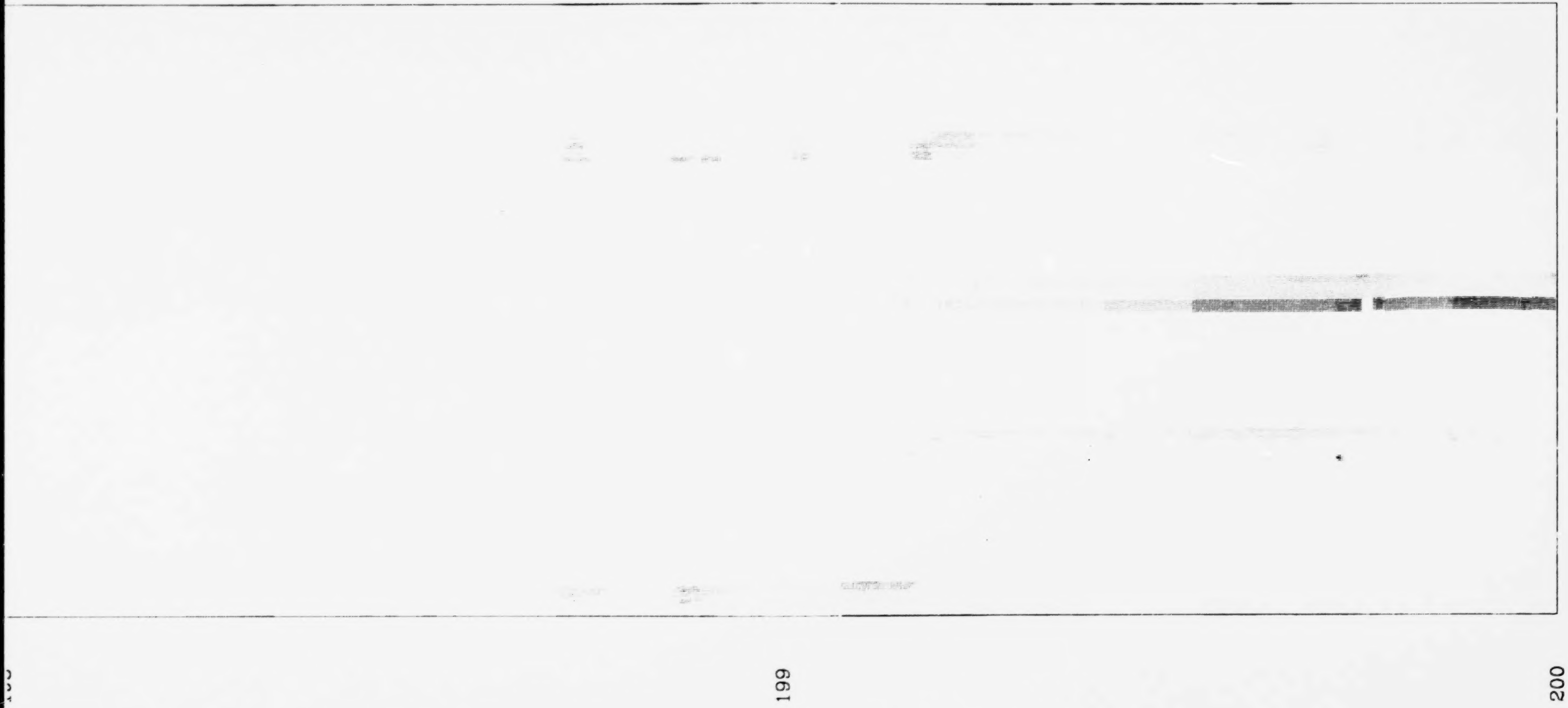
199
200

SCHLUMBERGER

FMS
BOREHOLE
IMAGING

COMPANY	LAMONT DOHERTY
WELL	ODP HOLE 803D
FIELD	ONTONG JAVA PLATEAU
COUNTRY	LEG 130
RUN	2
DATE LOGGED	05 - FEB - 90
REFERENCE	STATIC PS 2 200 240

STATIC NORMALIZATION

PASS 2

FILE : MEST.002

ZONE FROM 240.0 M TO 200.0 M

DEPTH SCALE = 1/ 5

IMAGE SCALE = 1/ 5

BITSIZE = 9.88

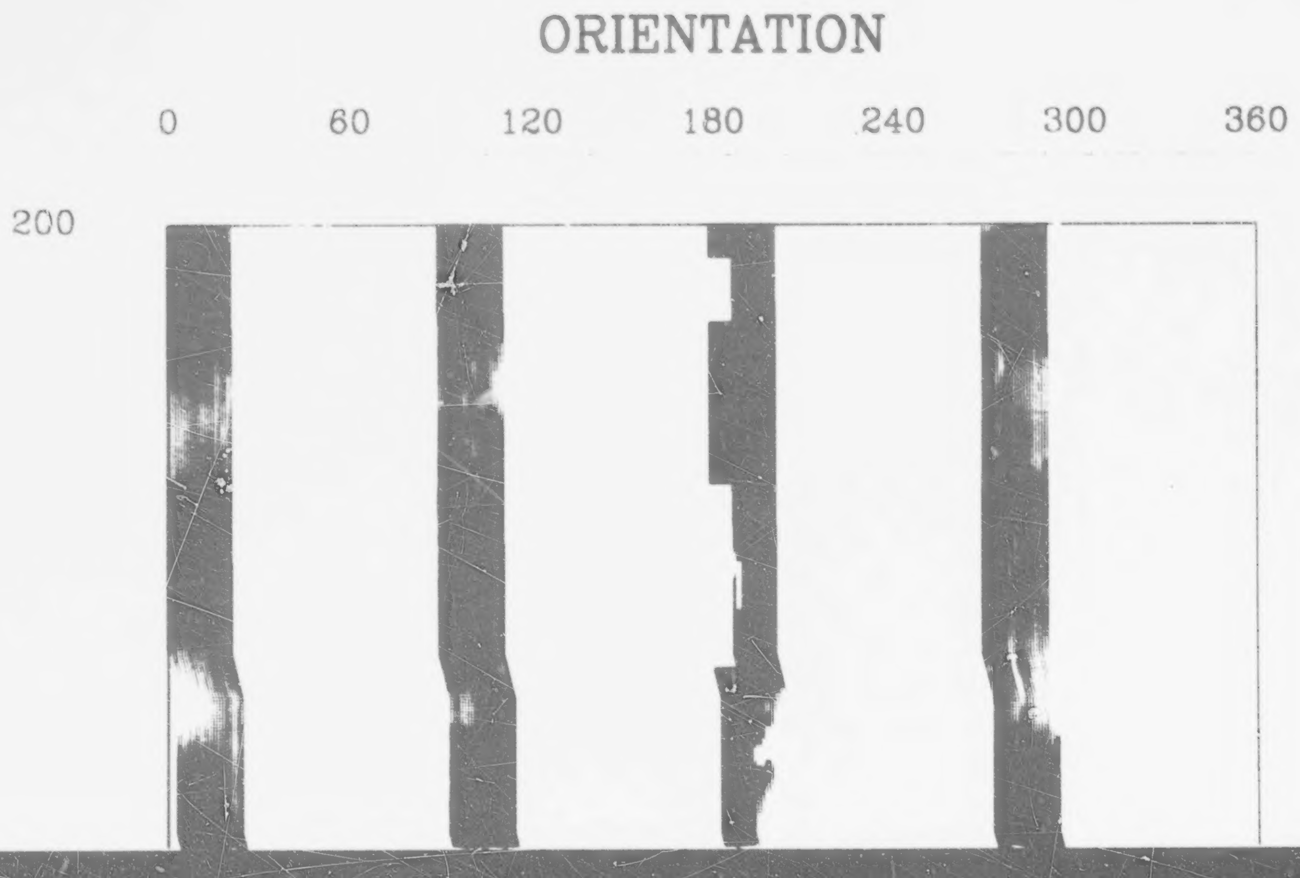

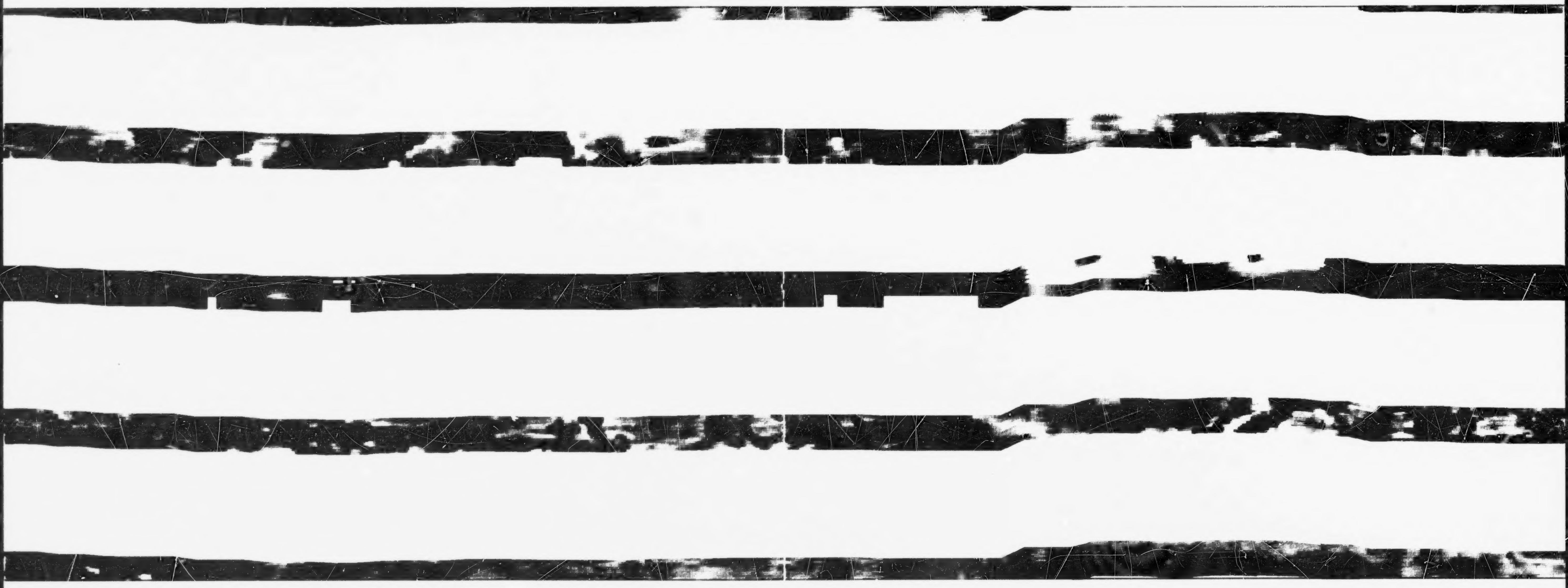

205
206

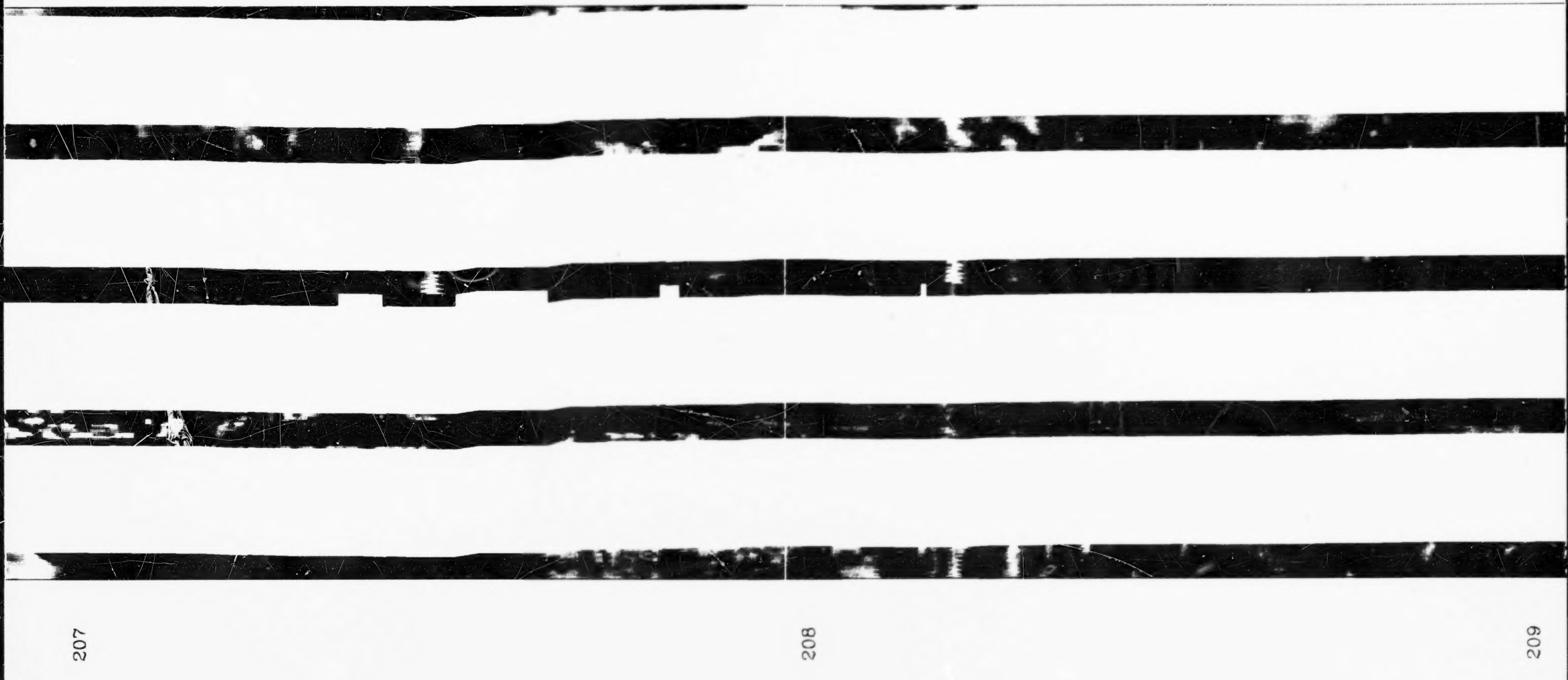

207
208
209

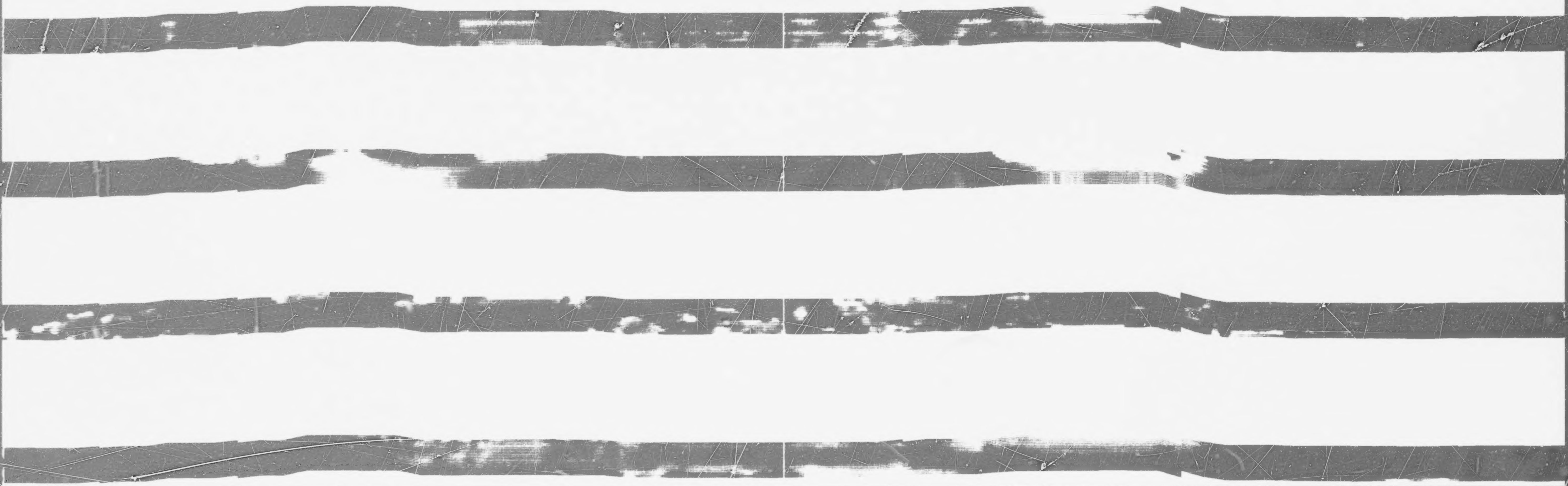

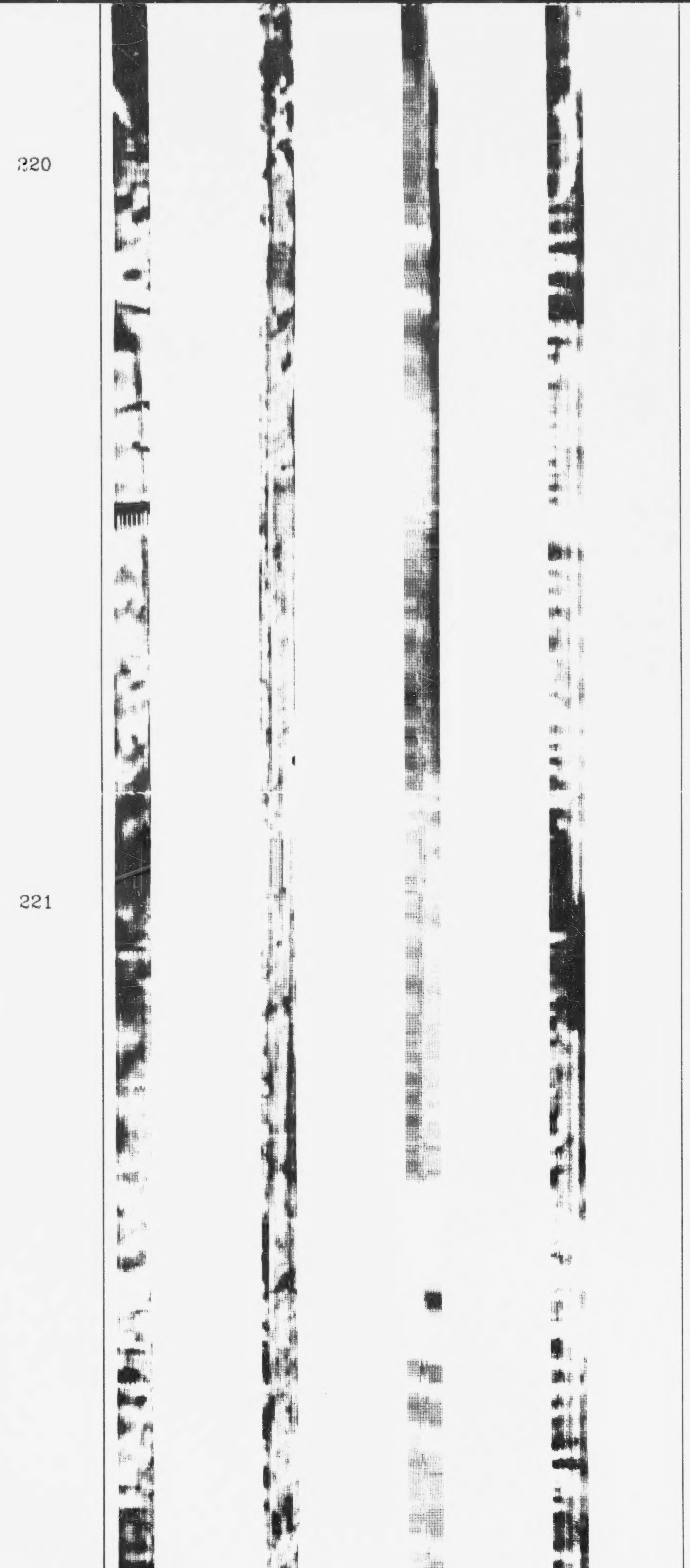
220
221

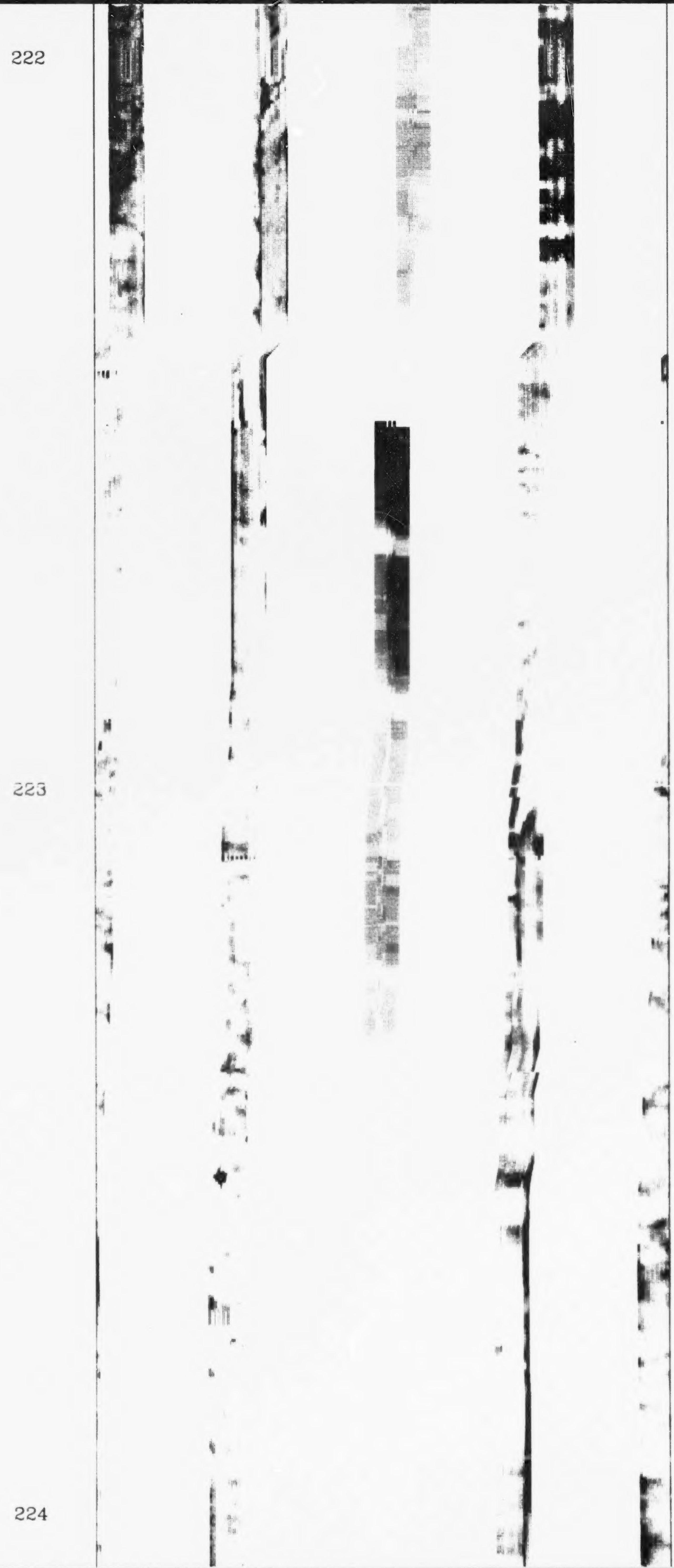
222
223
224

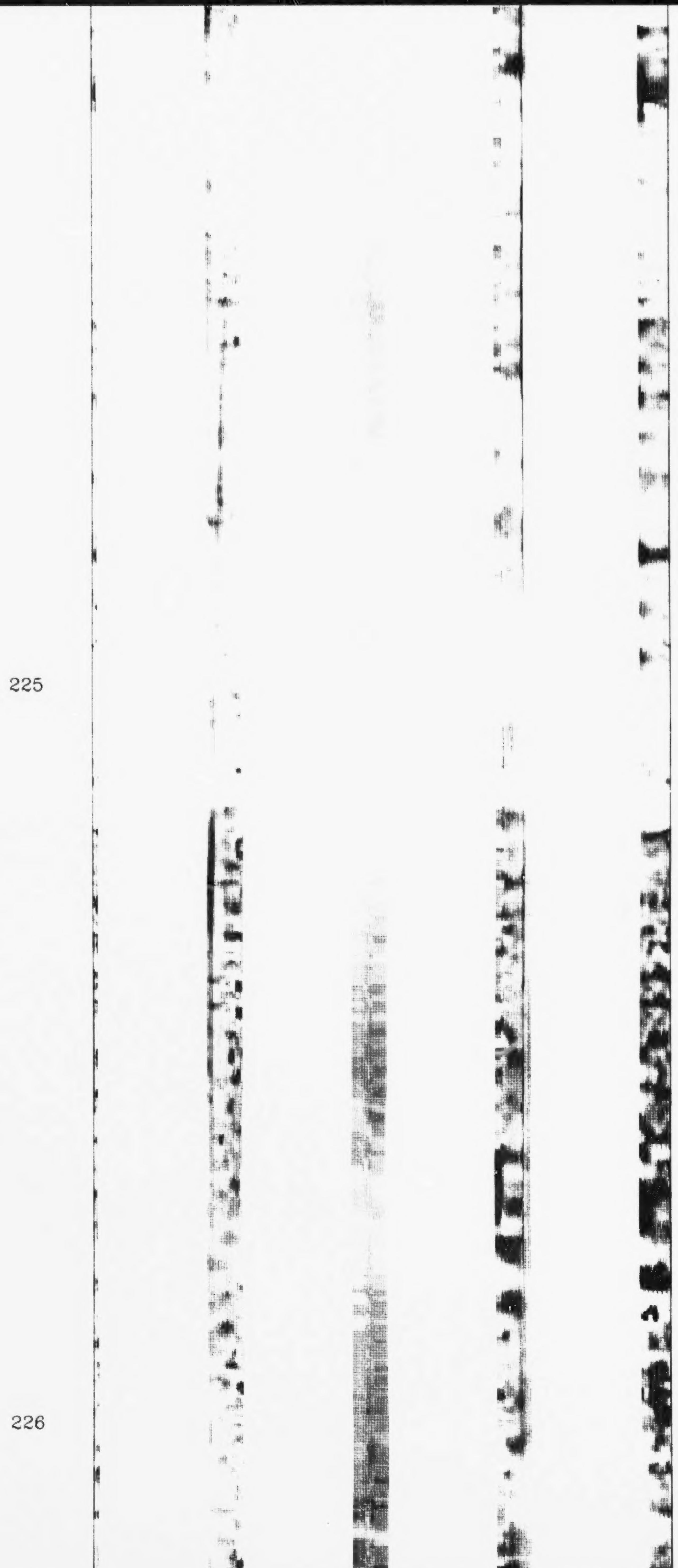
225
226

229
230

231

232

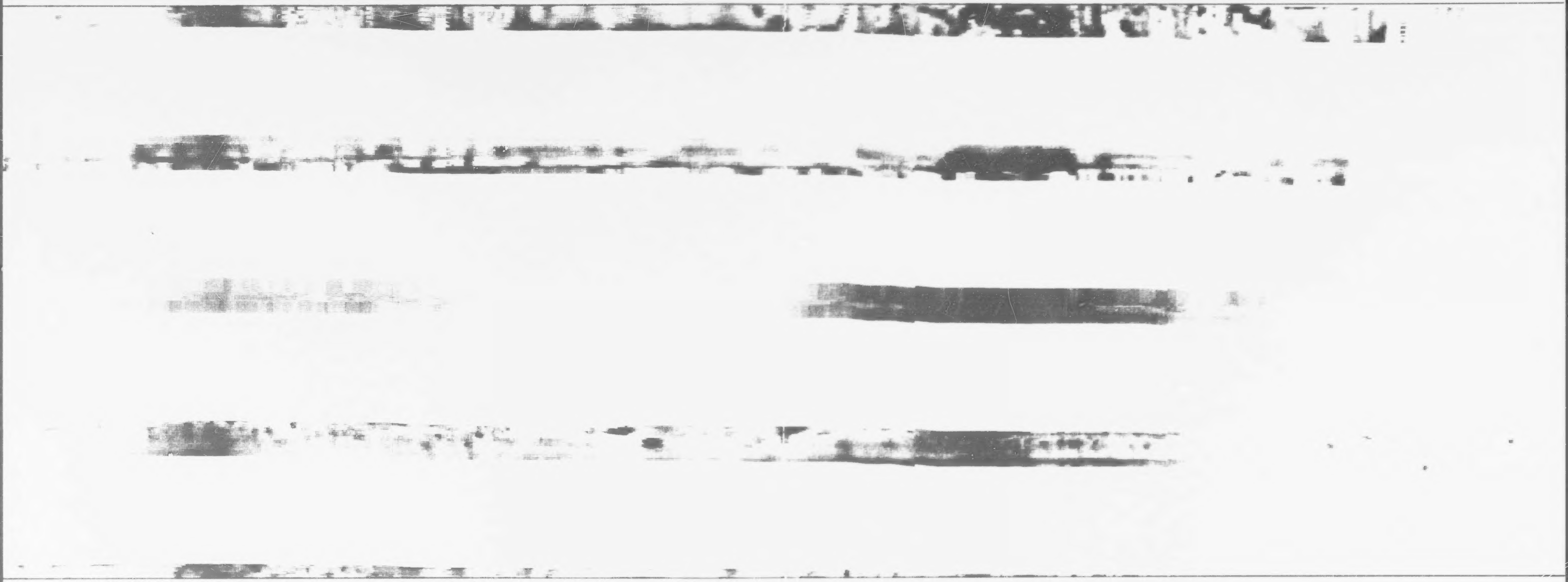
233
234

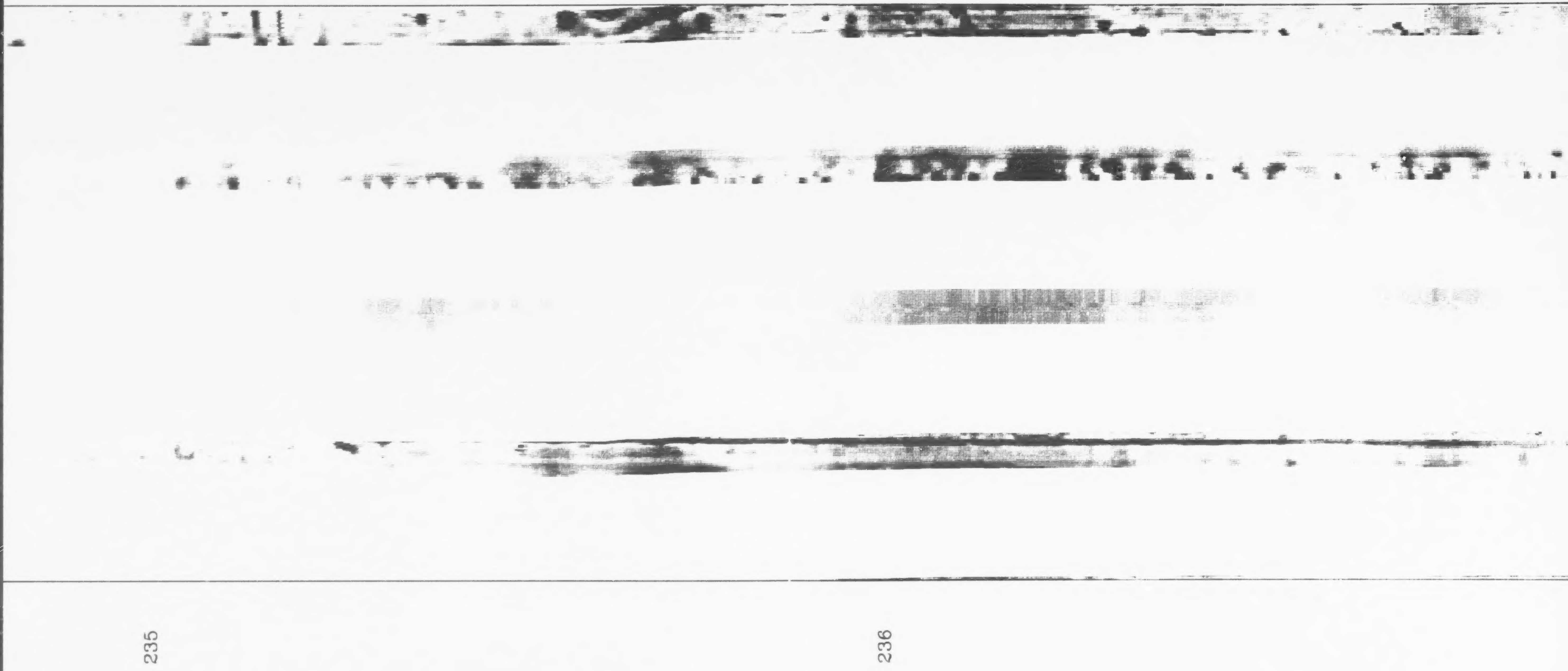
235
236

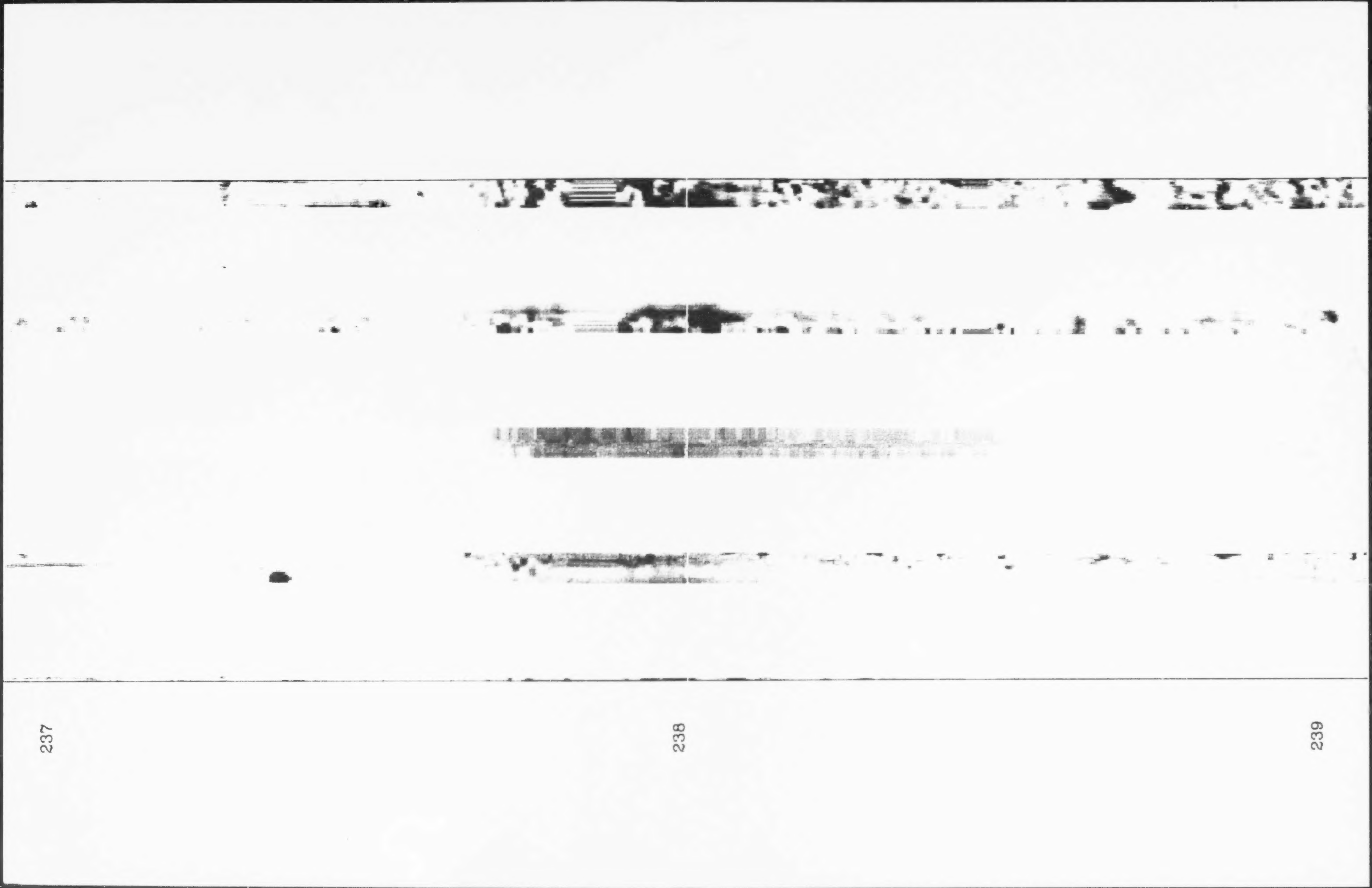
237
238
239

SCHLUMBERGER

FMS
BOREHOLE
IMAGING

COMPANY	LAMONT DOHERTY
WELL	ODP HOLE 803D
FIELD	ONTONG JAVA PLATEAU
COUNTRY	LEG 130
RUN	2
DATE LOGGED	05 – FEB – 90
REFERENCE	STATIC PS 2 240 280

STATIC NORMALIZATION

PASS 2

FILE : MEST.002

ZONE FROM 280.0 M TO 240.0 M

DEPTH SCALE = 1/ 5

IMAGE SCALE = 1/ 5

BITSIZE = 9.88

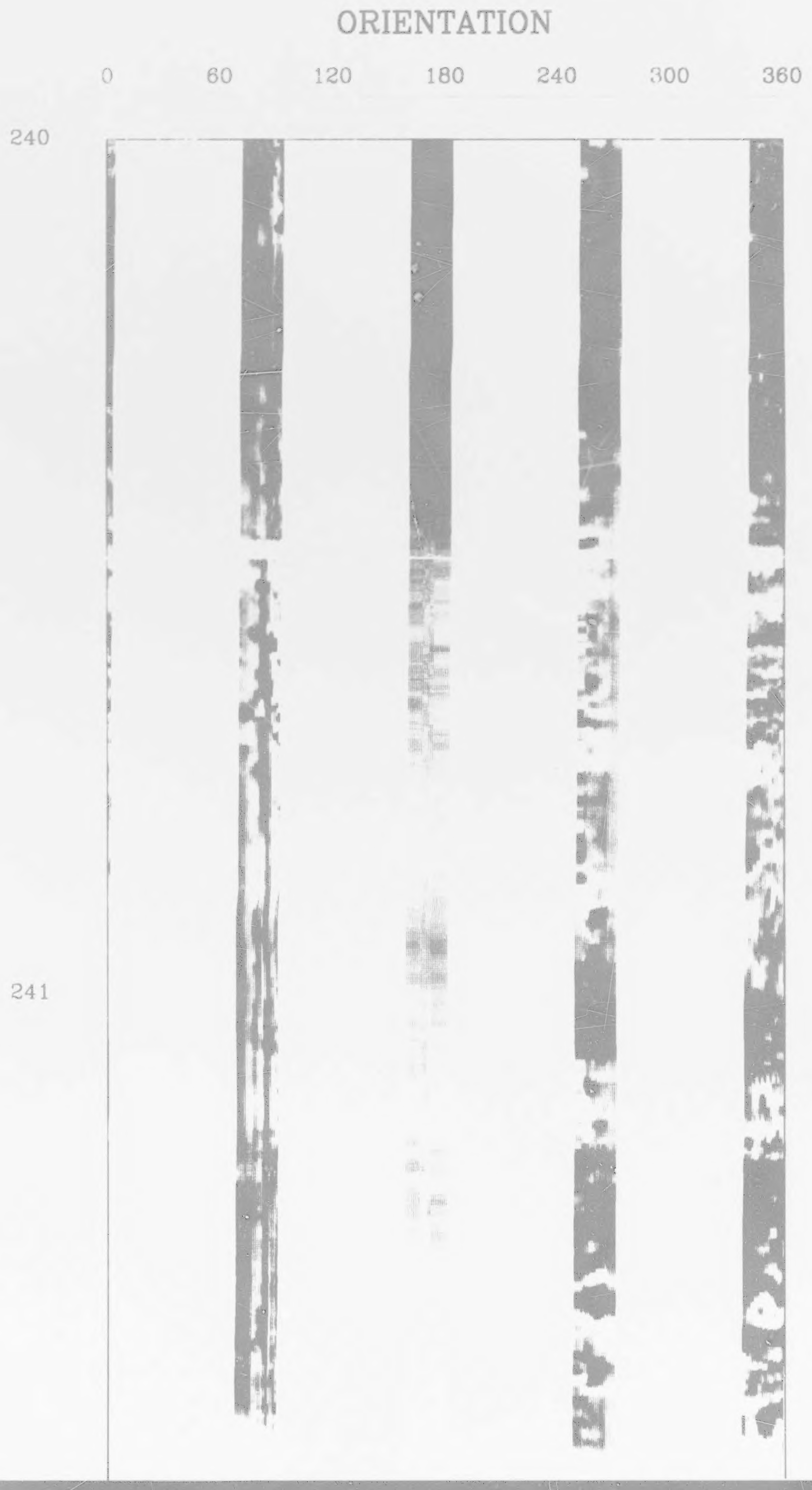

[redacted]

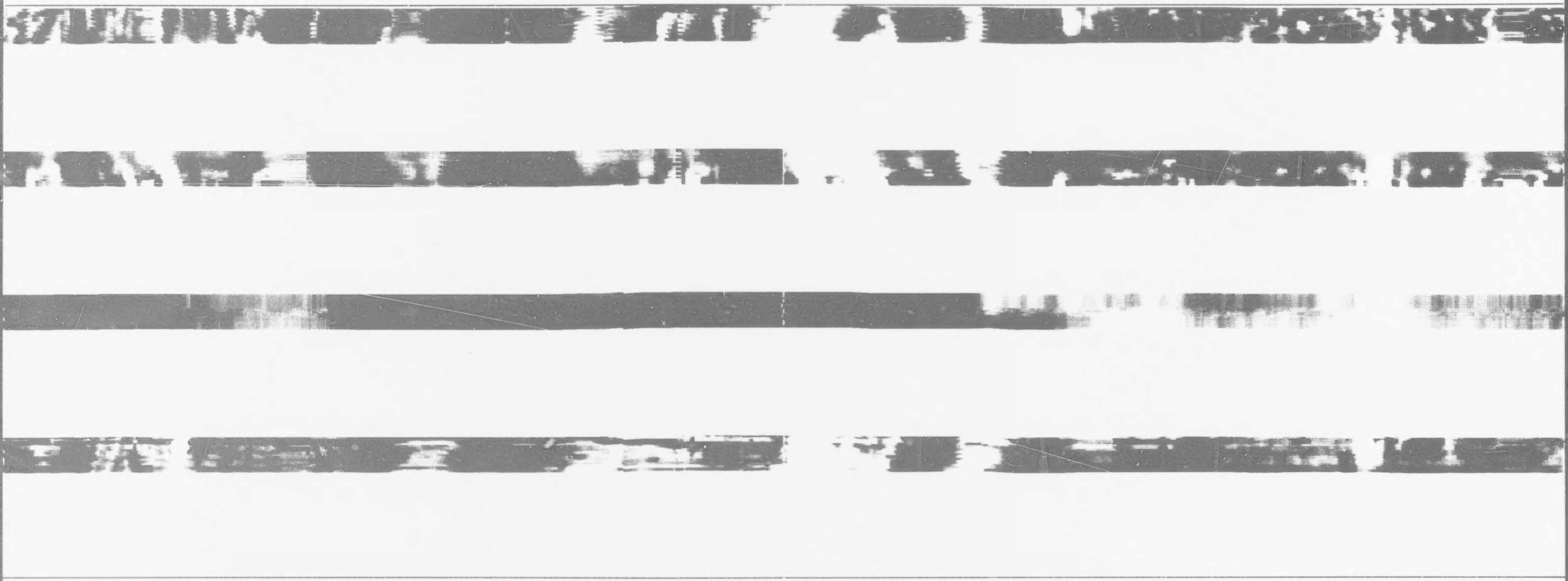

244
245

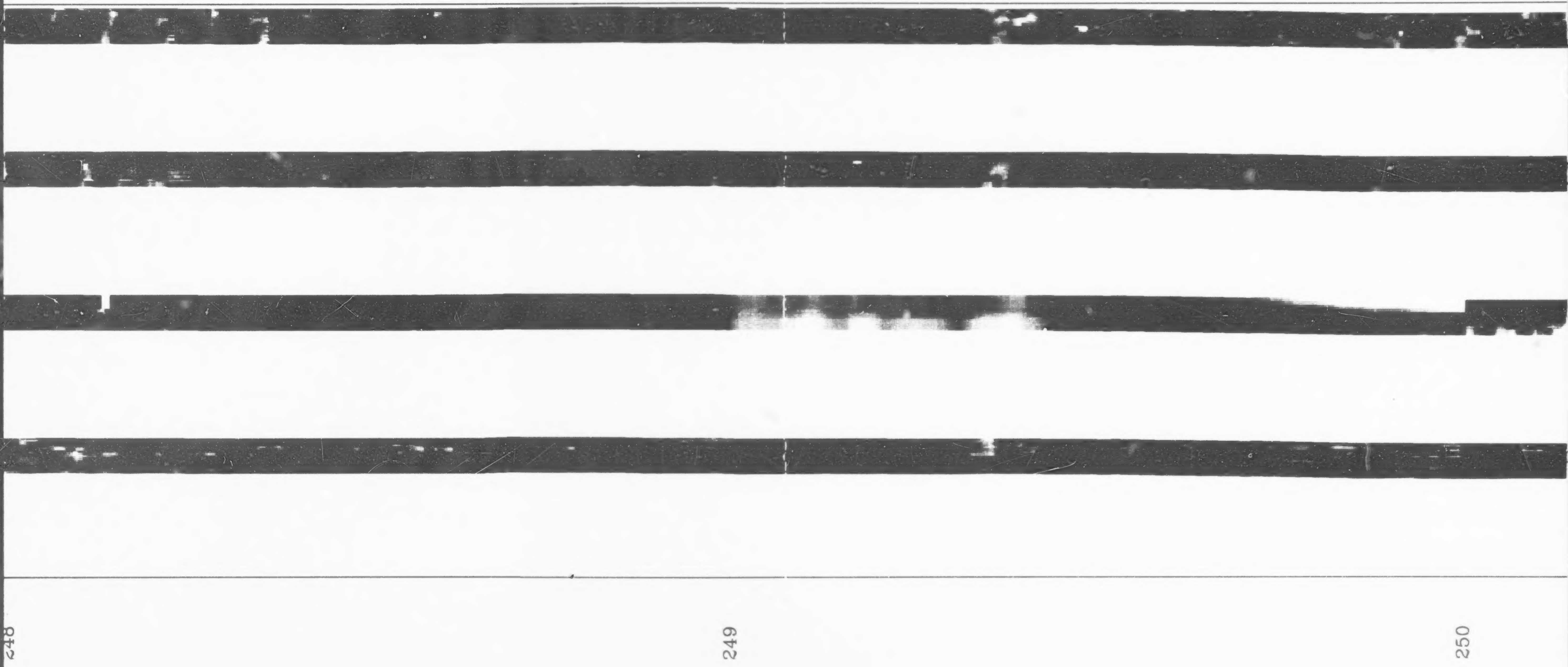
248
249
250

253

254

[redacted]

[redacted]

[redacted]

[redacted]

[redacted]

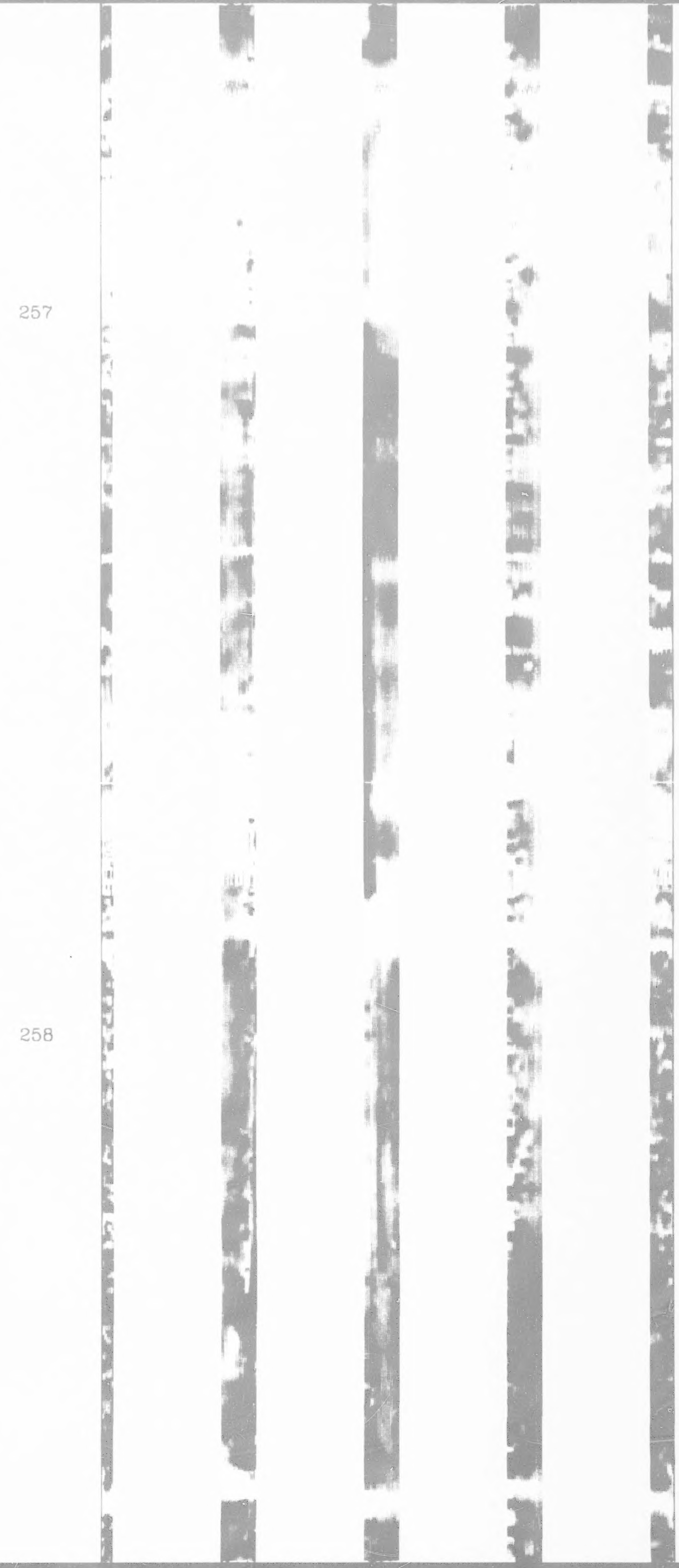
257
258

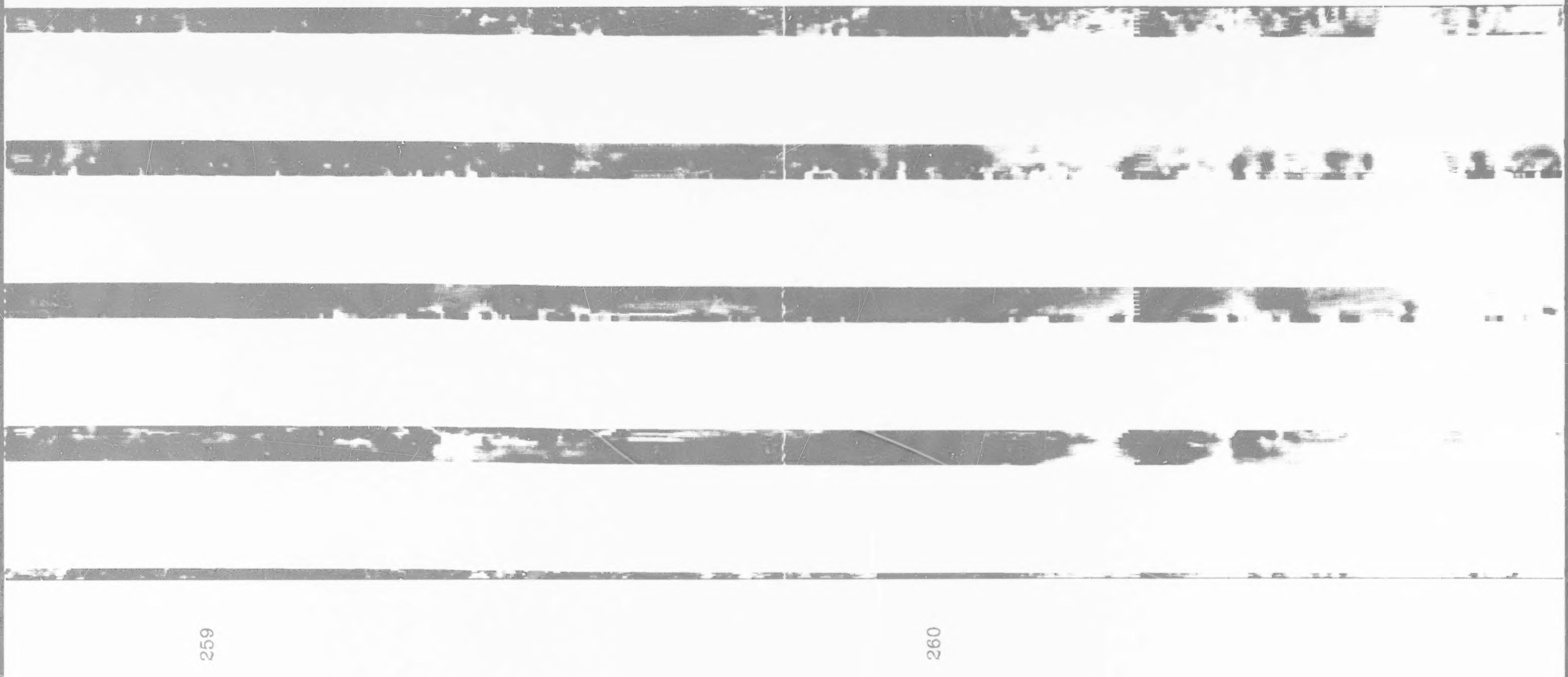
259
260

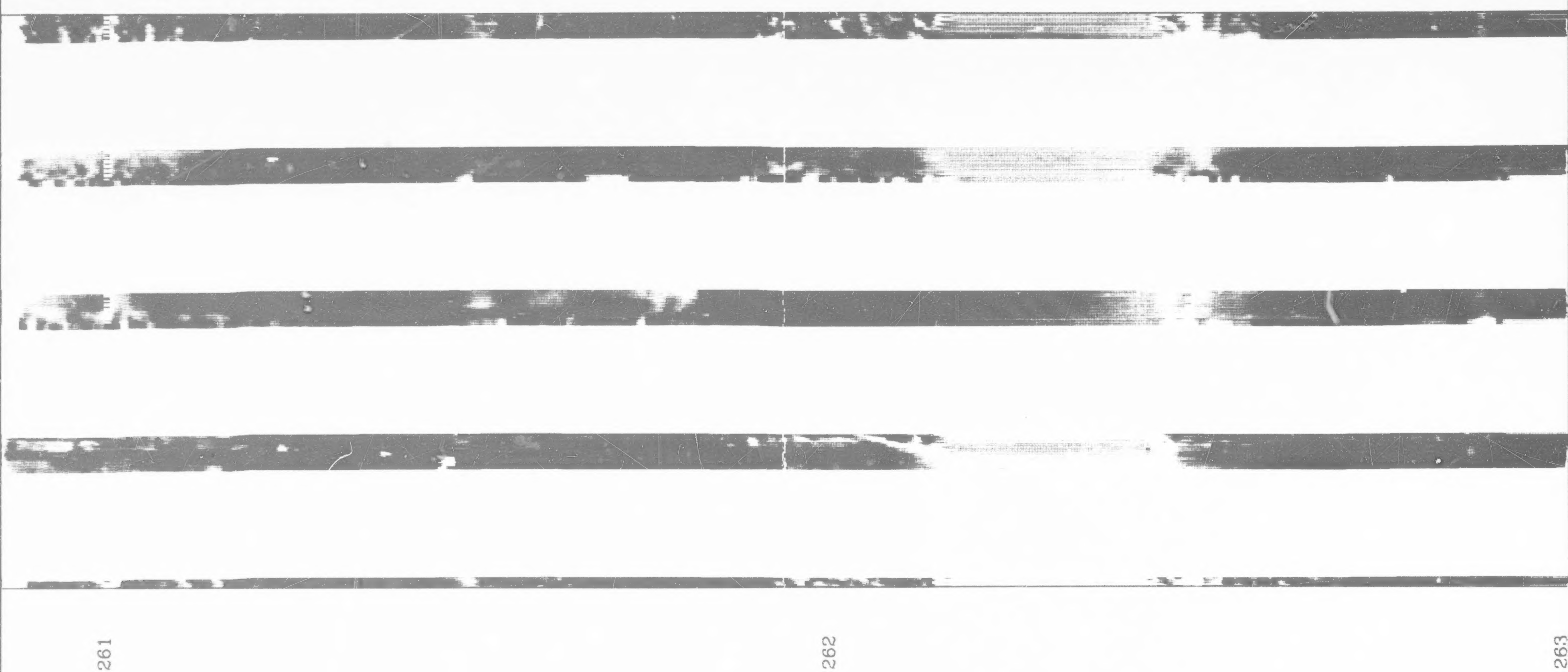
261
262
263

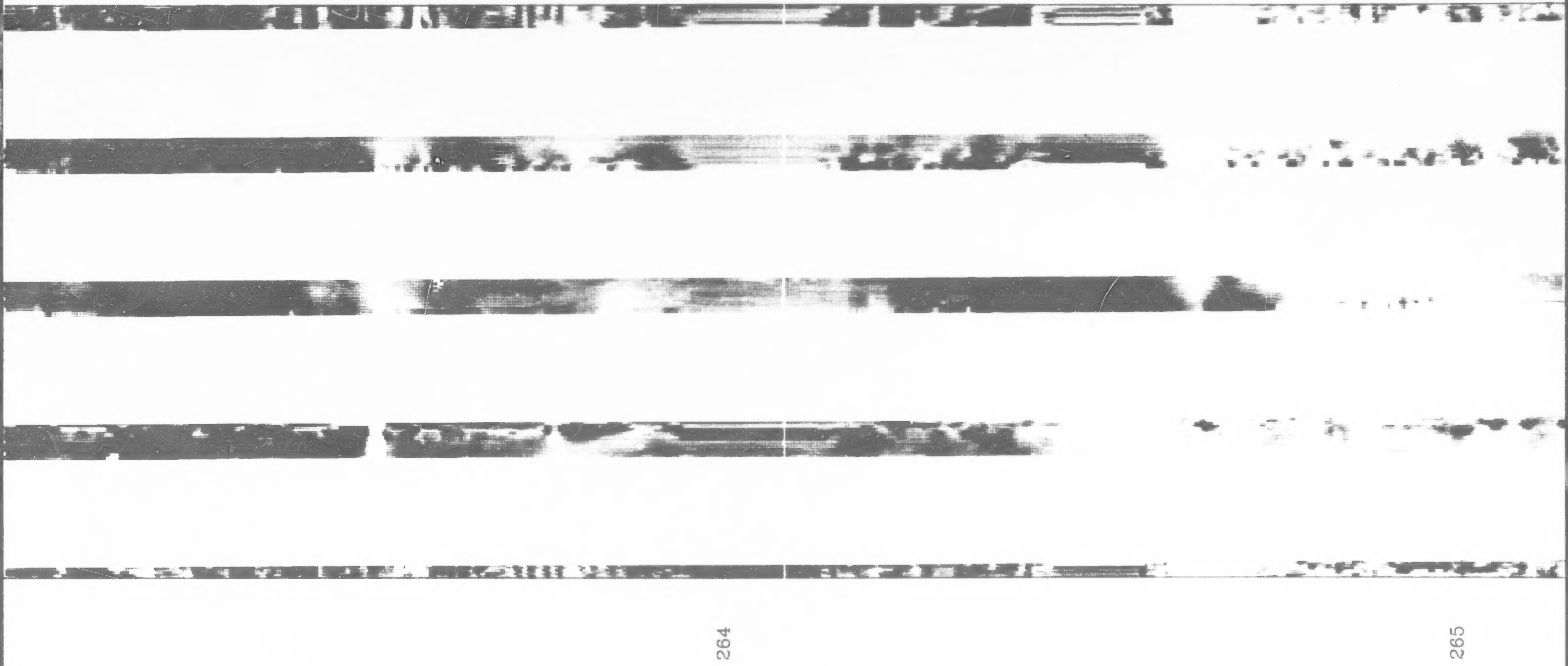
264
265

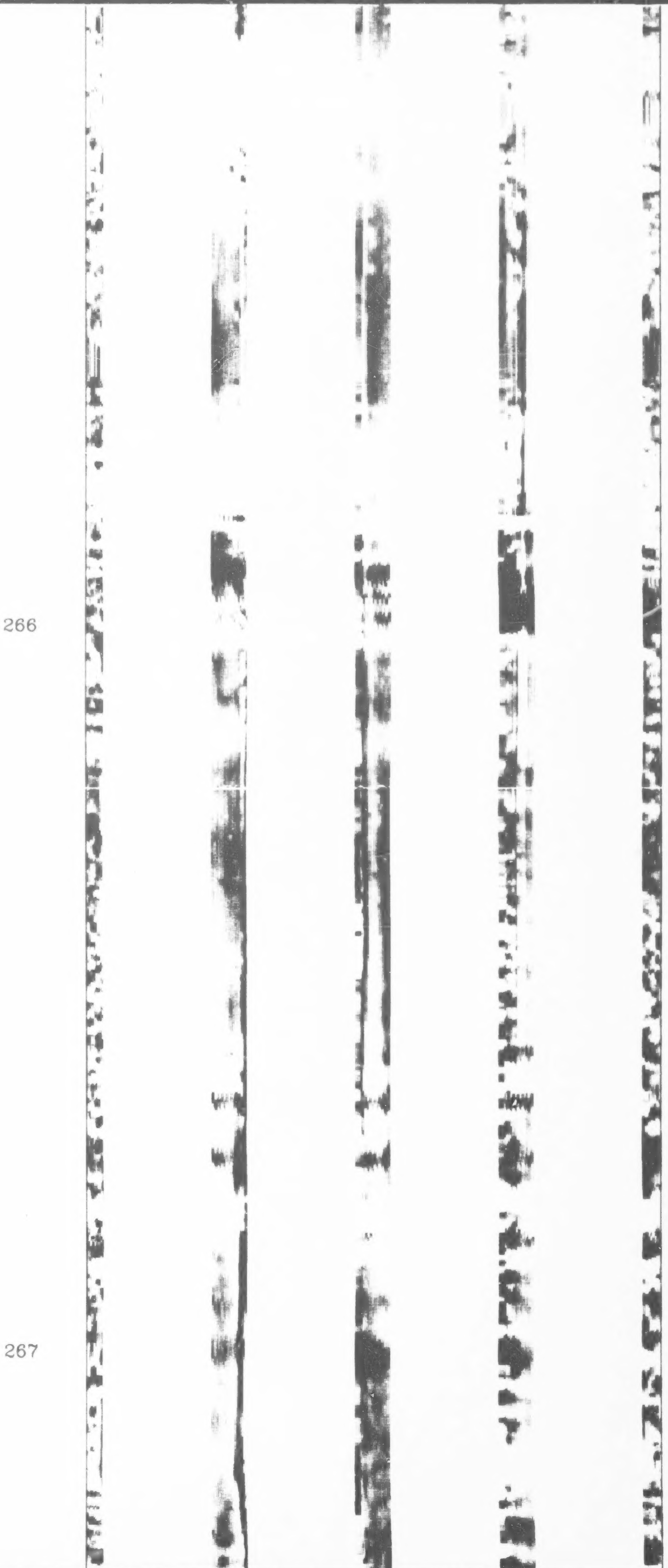
266
267

270
271

272

273

274

[illegible]

275

[illegible]

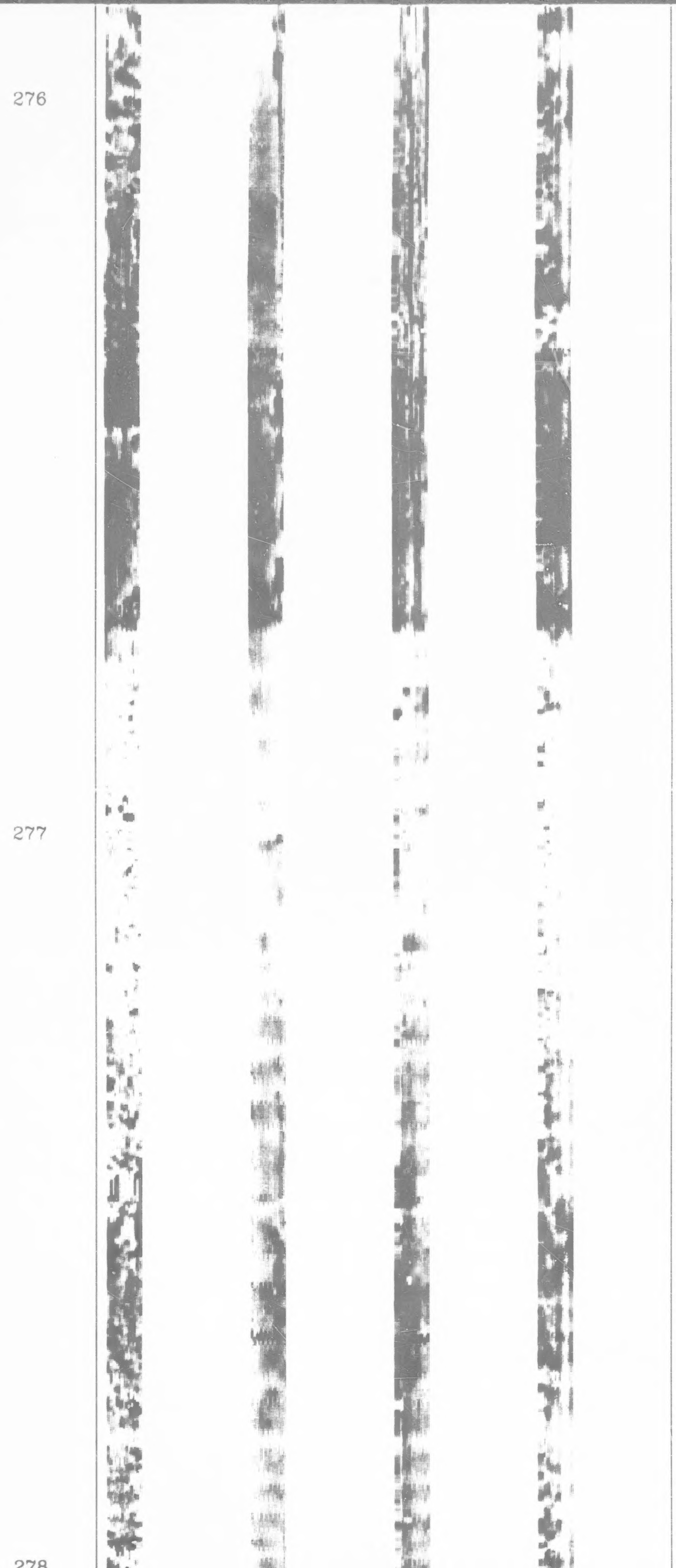
276
277

SCHLUMBERGER

FMS
BOREHOLE
IMAGING

COMPANY	LAMONT DOHERTY
WELL	ODP HOLE 803D
FIELD	ONTONG JAVA PLATEAU
COUNTRY	LEG 130
RUN	2
DATE LOGGED	05 FEB 90
REFERENCE	JAII FS 2 280 306

STATIC NORMALIZATION

PASS 2

FILE : MEST.002

ZONE FROM 306.0 M TO 280.0 M

DEPTH SCALE = 1/ 5

IMAGE SCALE = 1/ 5

BITSIZE = 9.88

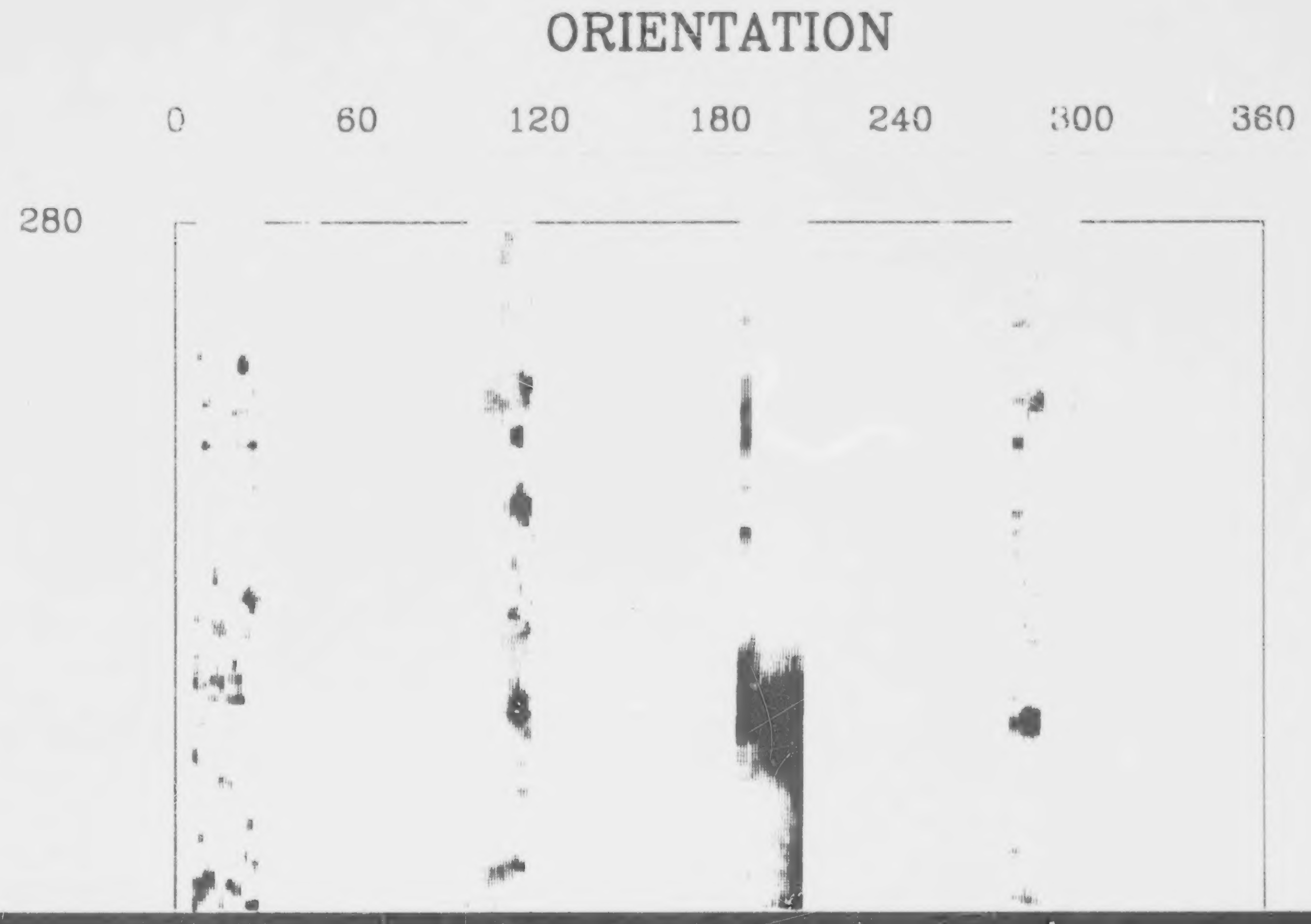

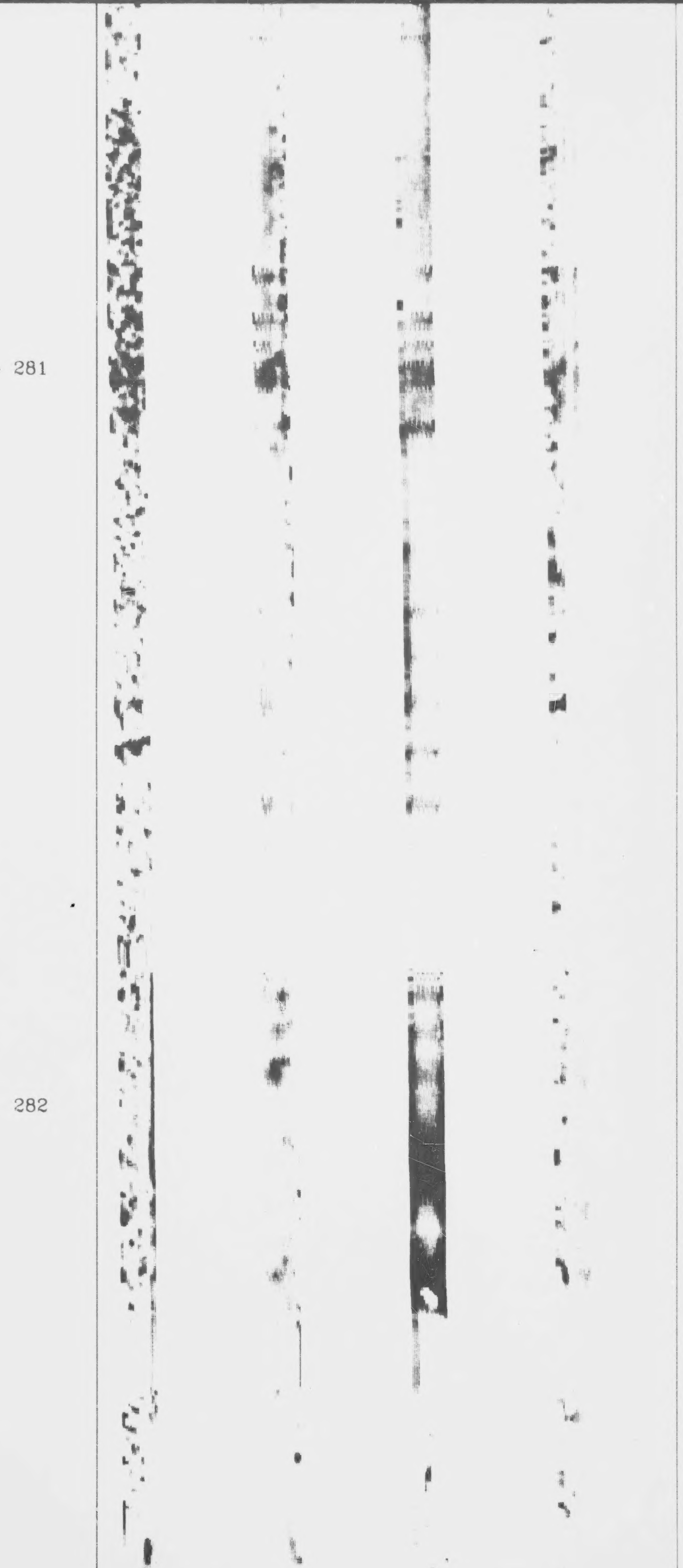
281
282

283 [illegible]

284 [illegible]

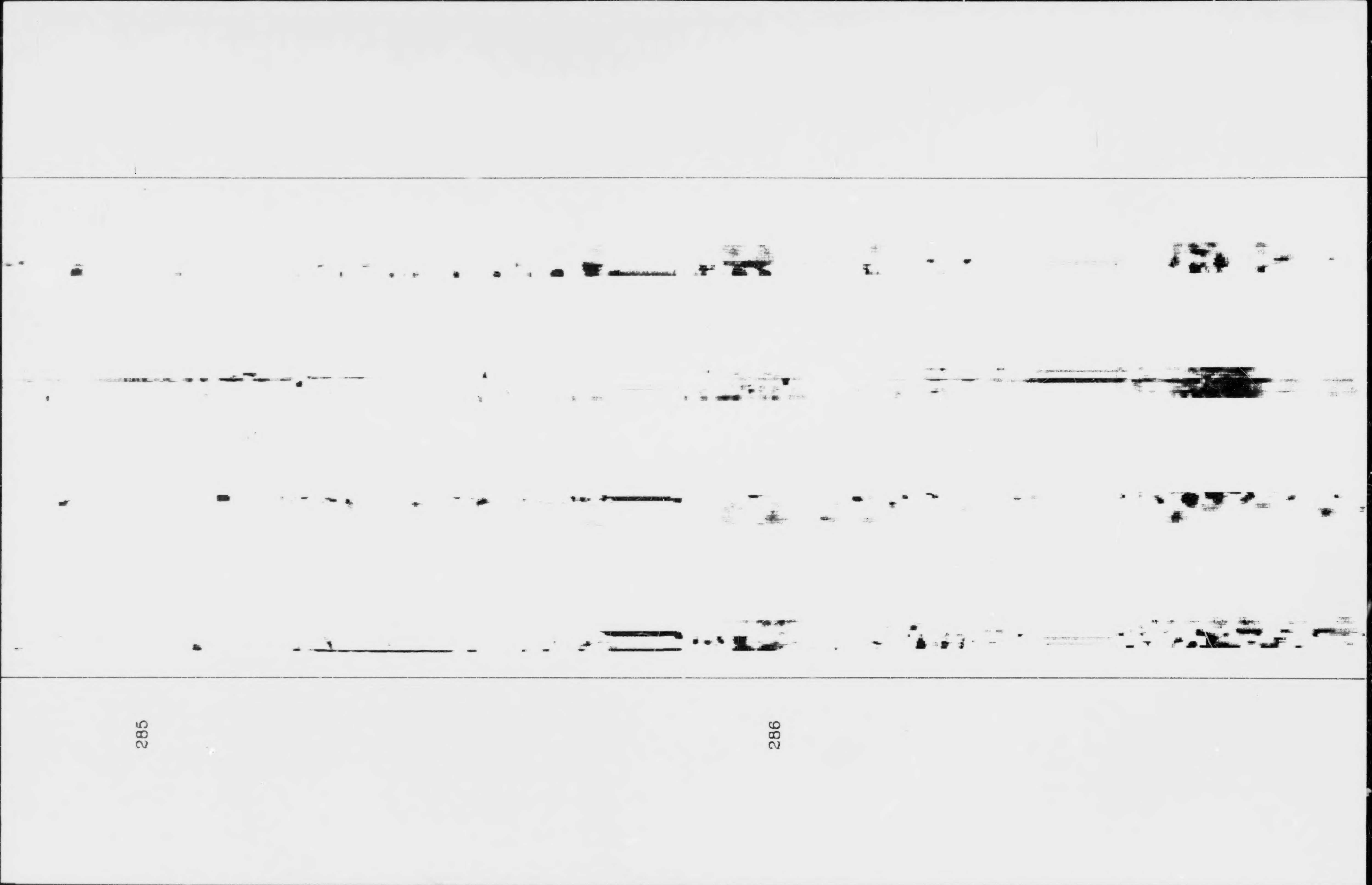
285
286

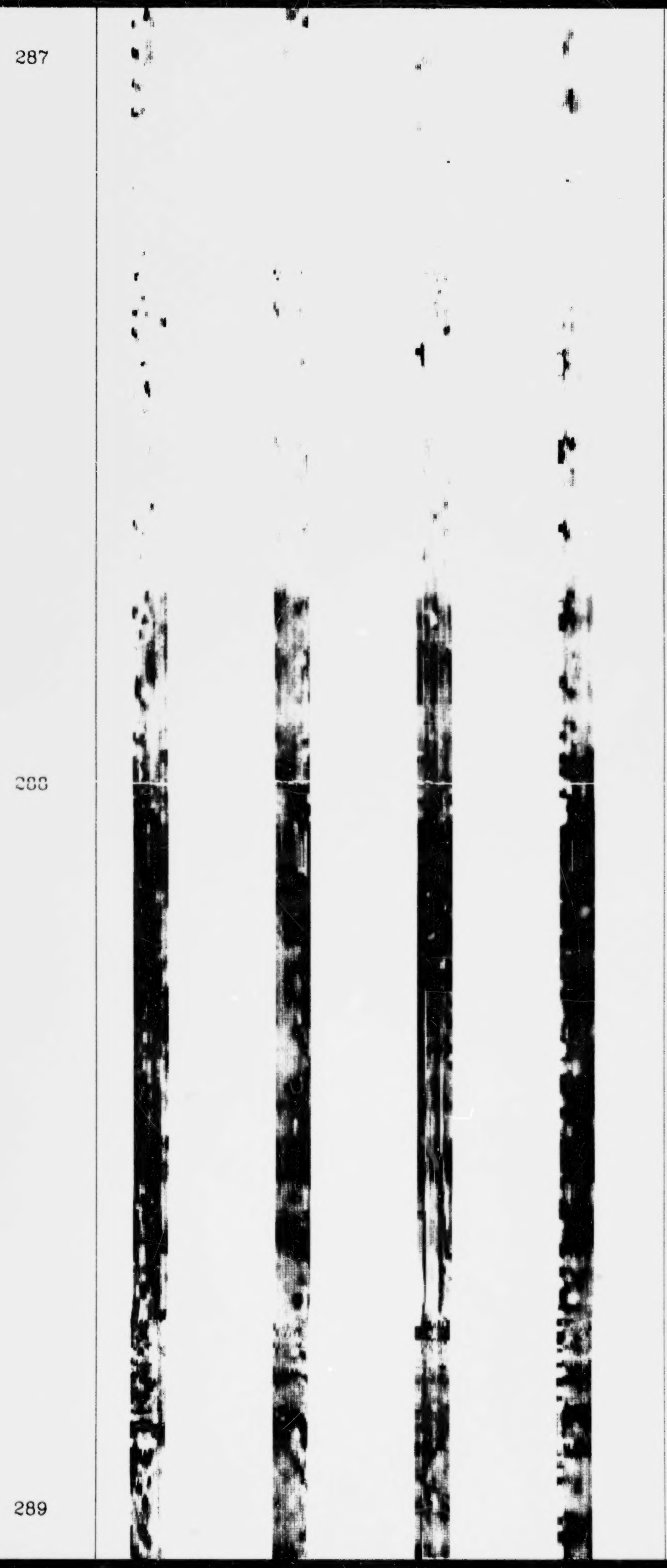
287
288
289

292

293

294

295

302
303
304

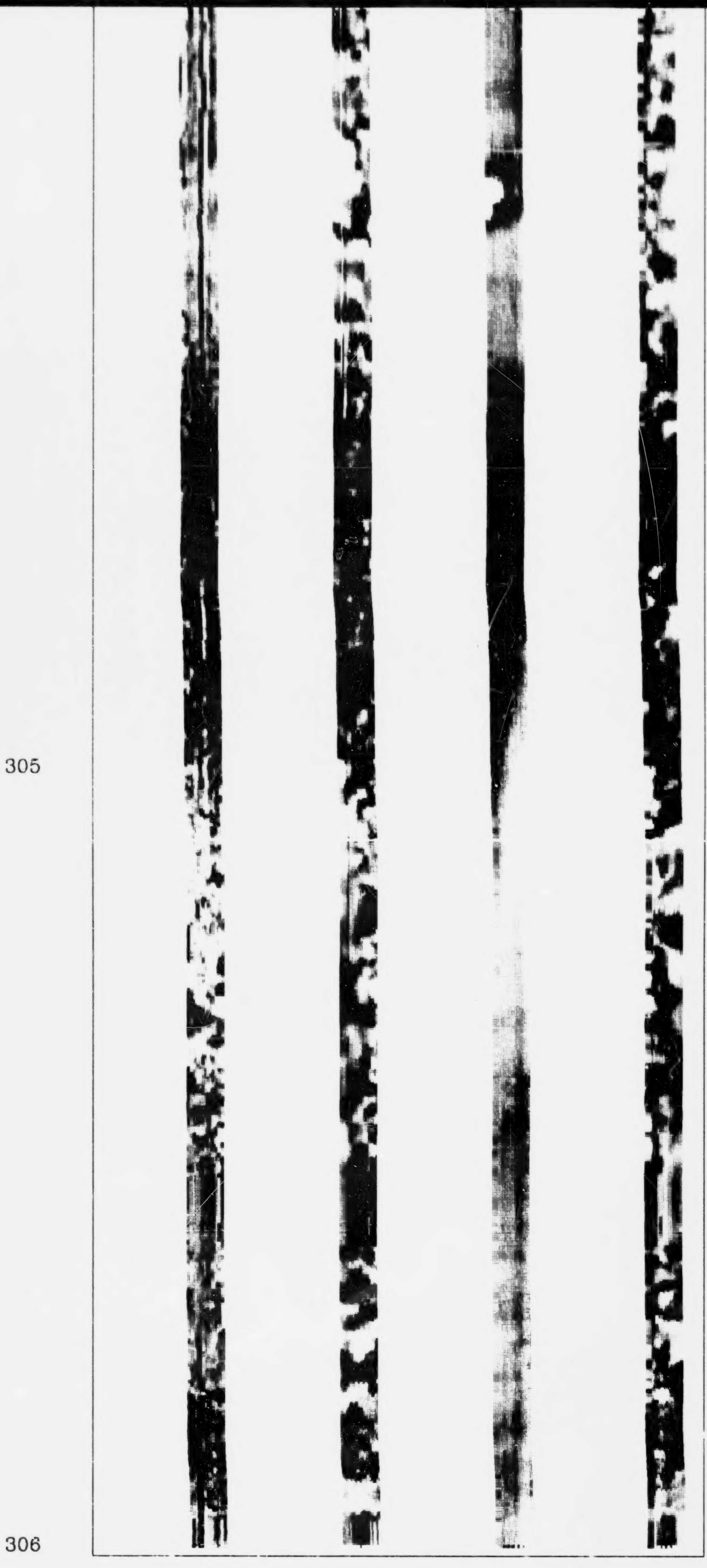
305
306

803-D
MAIN LOG
(PASS 1)

299 - 611
MBSF

Advanced Images, INC.
Rt 22 West Round Valley Plaza
Lebanon, N.J. 08833

SCHLUMBERGER

FMS
BOREHOLE
IMAGING

COMPANY	LAMONT DOHERTY
WELL	ODP HOLE 803D
FIELD	ONTONG JAVA PLATEAU
COUNTRY	LEG 130
RUN	1
DATE LOGGED	05 - FEB - 90
REFERENCE	STATIC PS 1 299 320

STATIC NORMALIZATION

PASS 1 (LAMON)

FILE : MEST.001

ZONE FROM 320.0 M TO 299.8 M

DEPTH SCALE = 1/ 5

IMAGE SCALE = 1/ 5

BITSIZE = 9.88

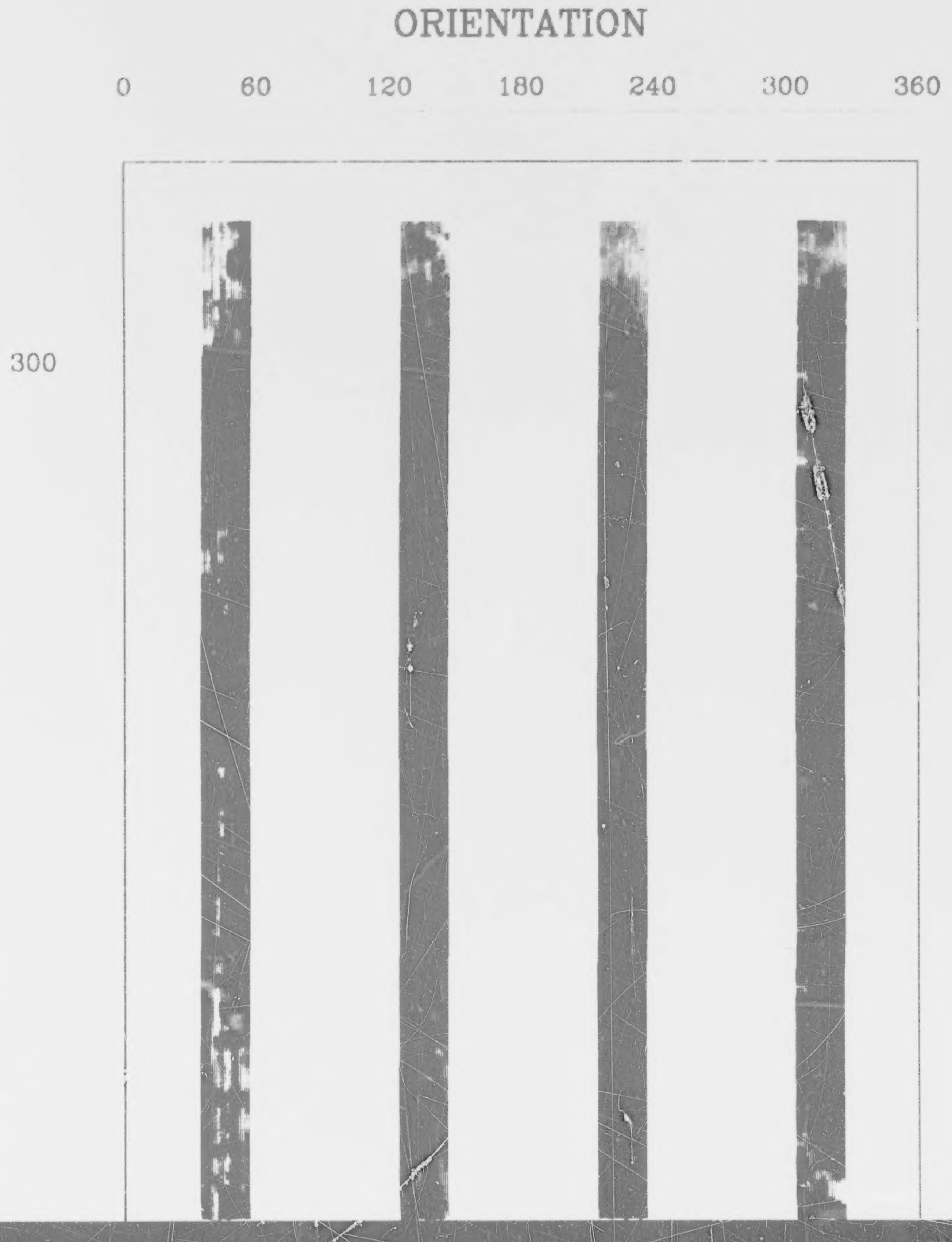

301
302

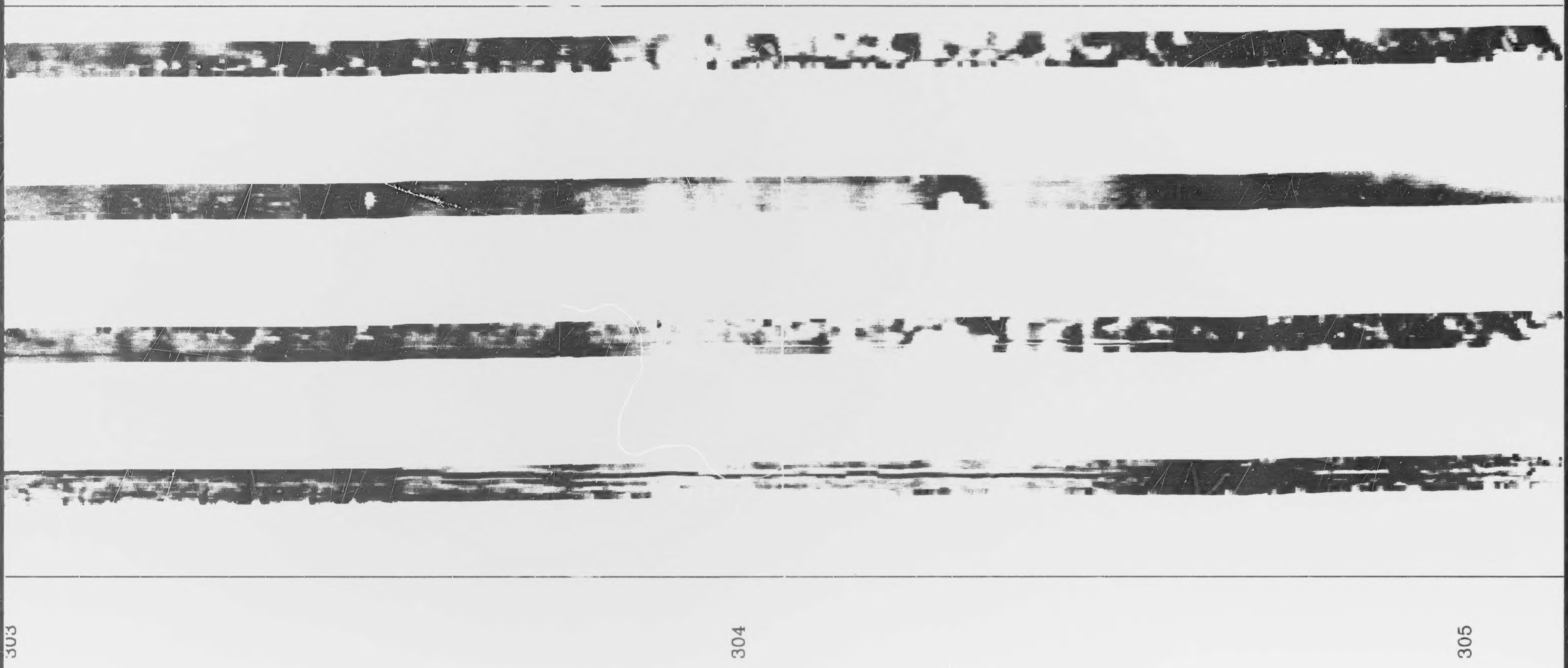
303
304
305

306
307

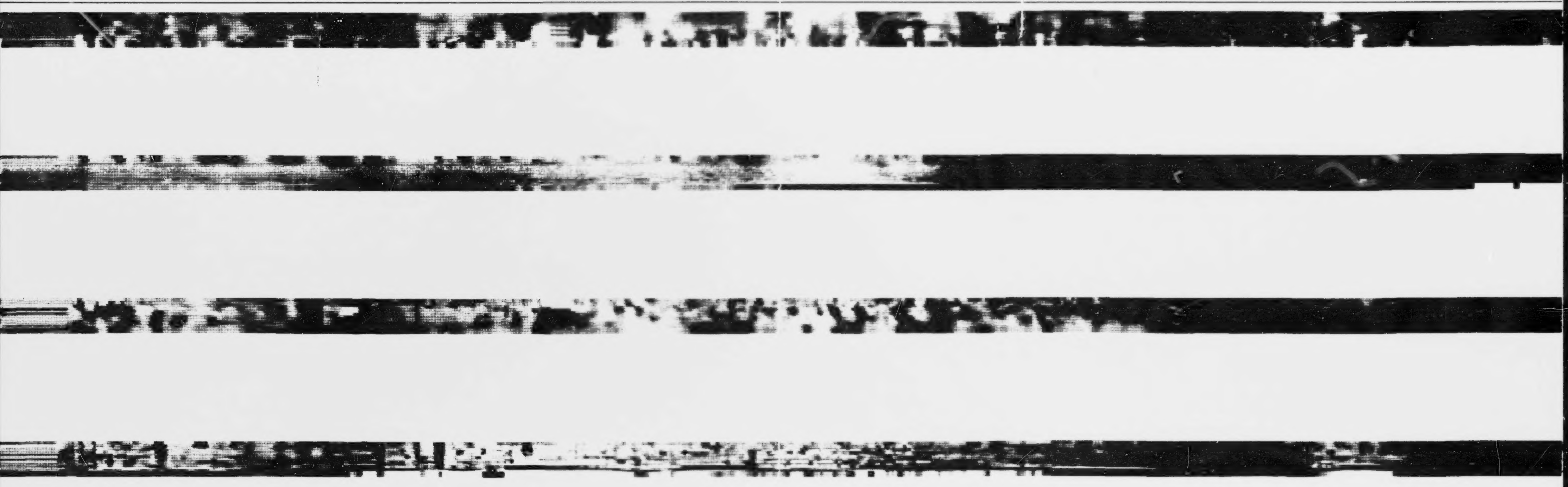

310

311

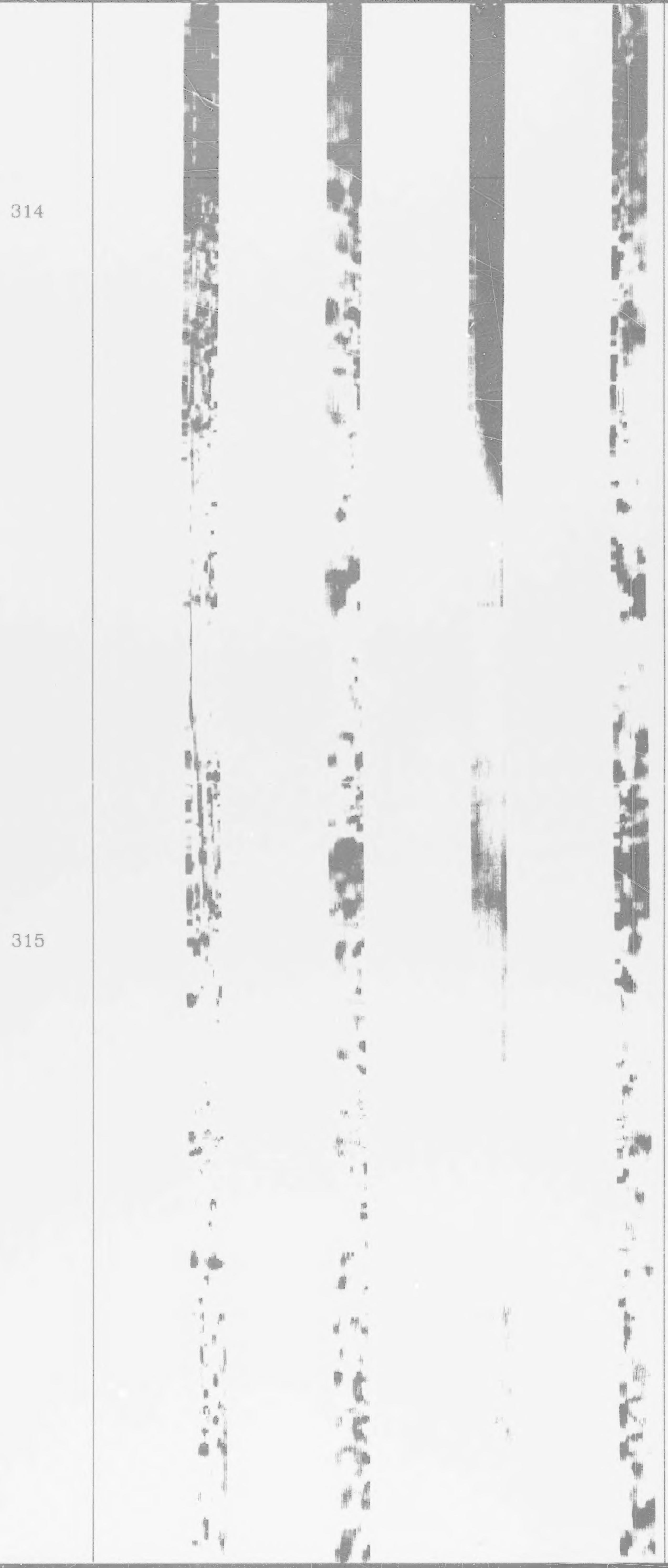
314
315

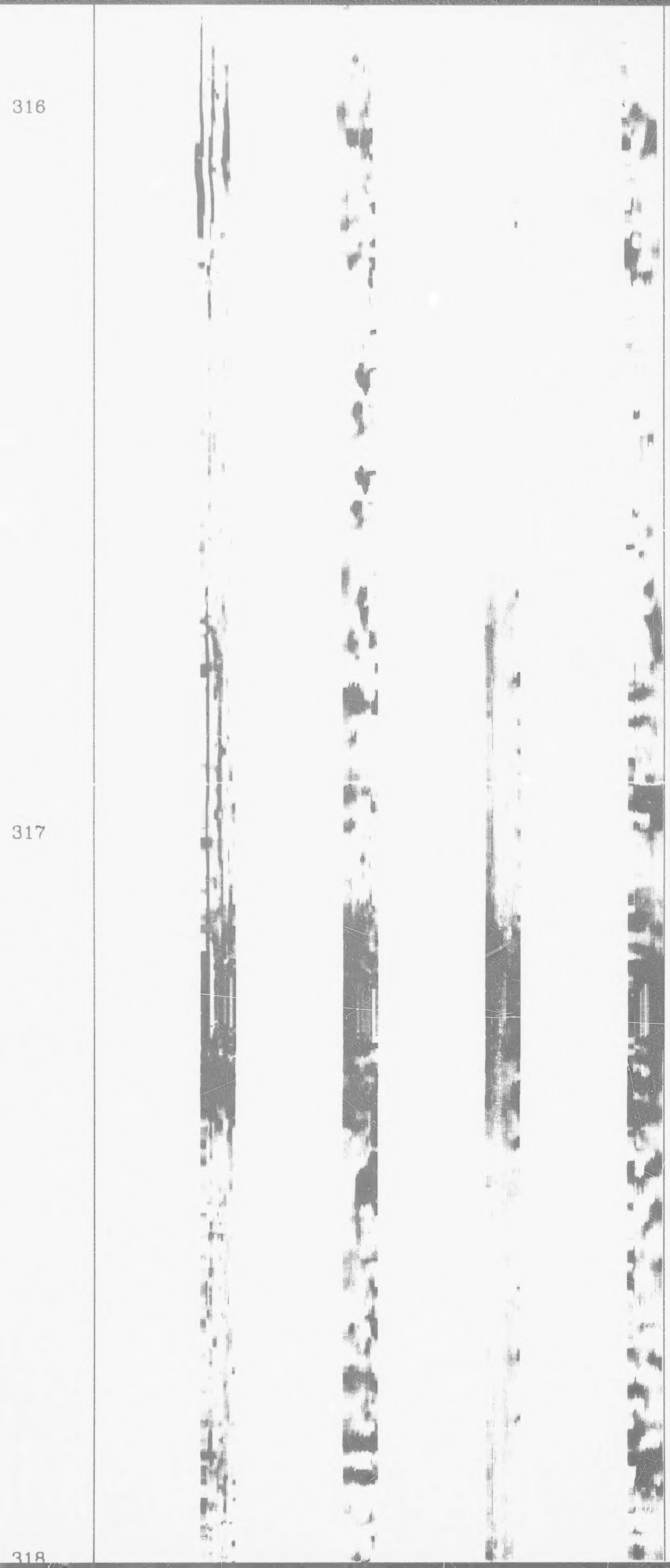
316
317
318

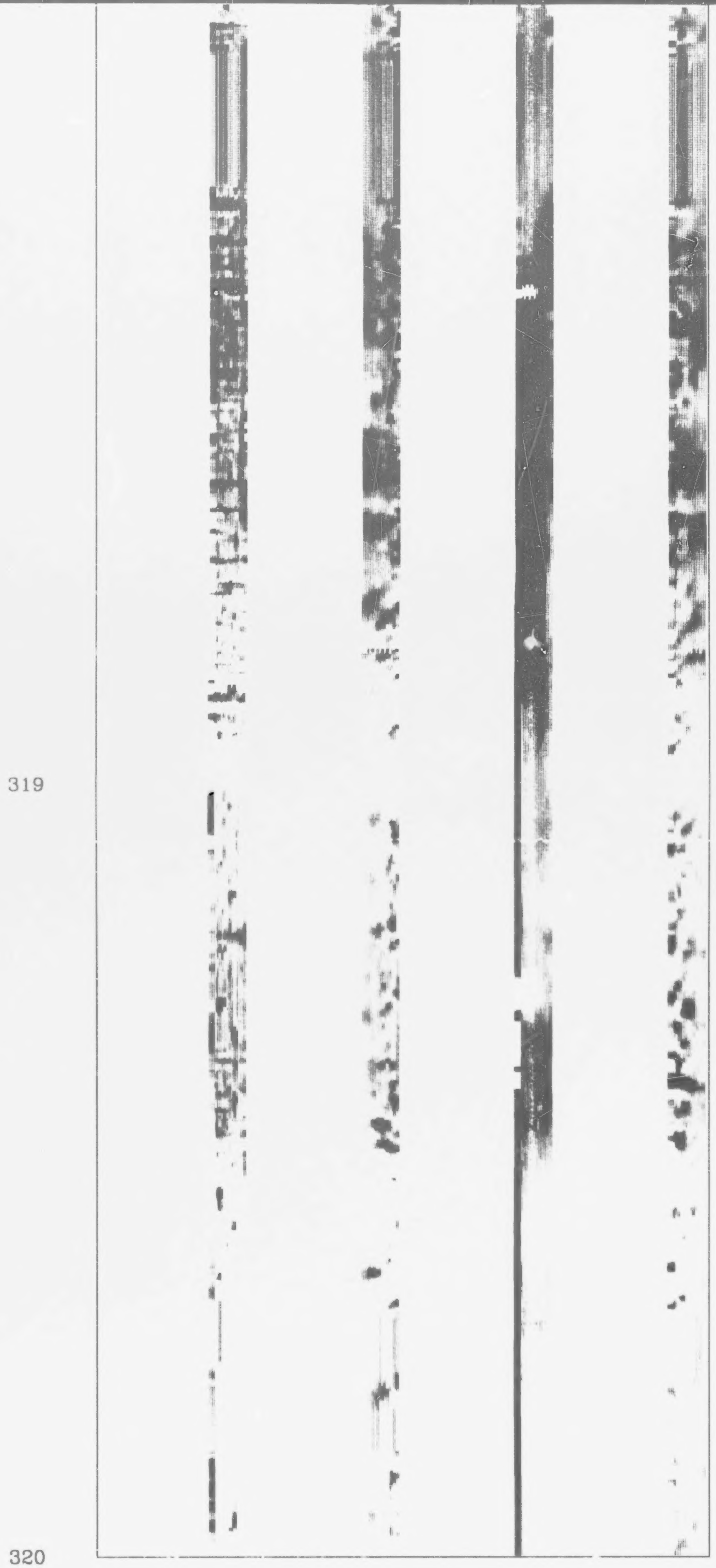
319
320

SCHLUMBERGER

FMS
BOREHOLE
IMAGING

COMPANY	LAMONT DOHERTY
WELL	ODP HOLE 803D
FIELD	ONTONG JAVA PLATEAU
COUNTRY	LEG 130
RUN	1
DATE LOGGED	05 - FEB 90
REFERENCE	STATIC PS 1 320 360

STATIC NORMALIZATION
PASS 1 (LAMON)
FILE : MEST.001

ZONE FROM 360.0 M TO 320.0 M
DEPTH SCALE = 1/ 5
IMAGE SCALE = 1/ 5
BITSIZE = 9.88

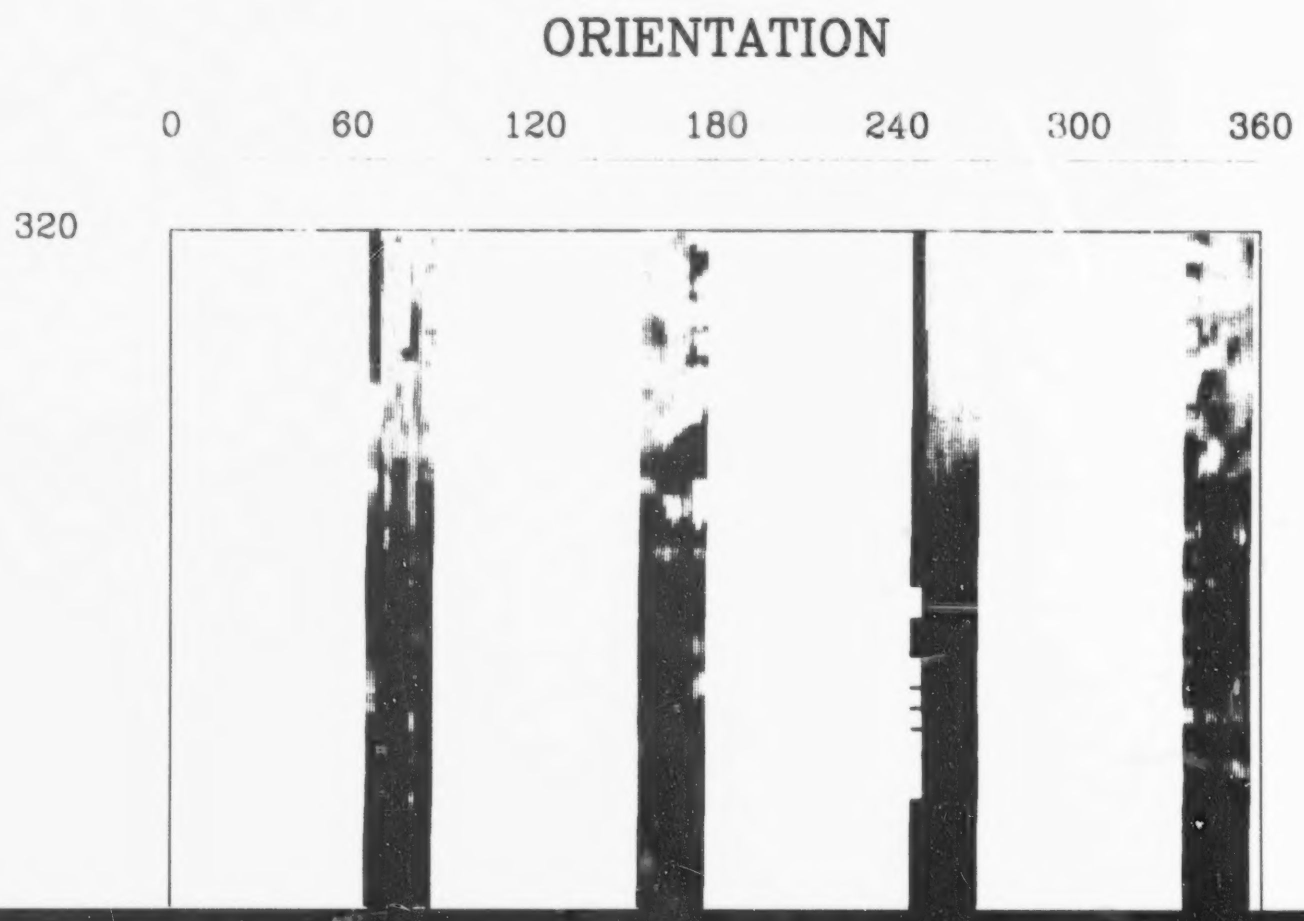

321

322

323

324

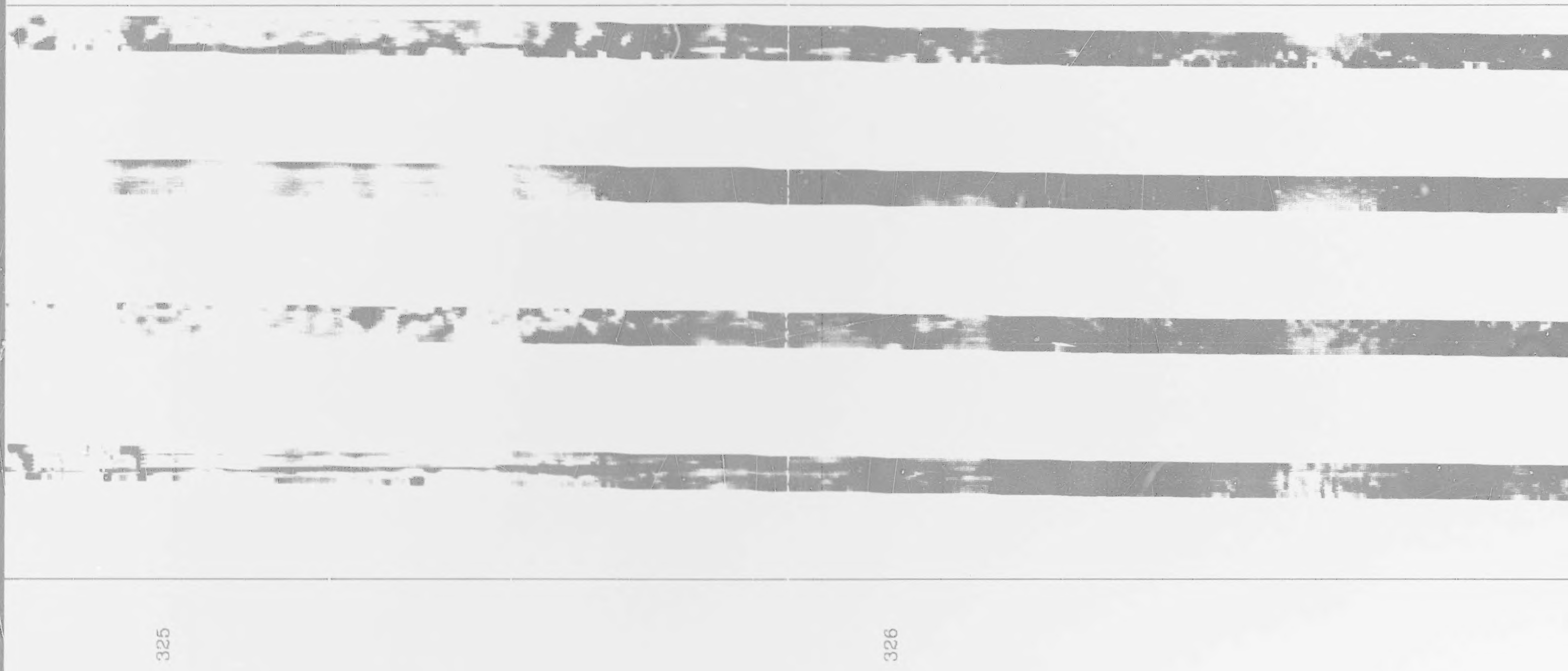
325
326

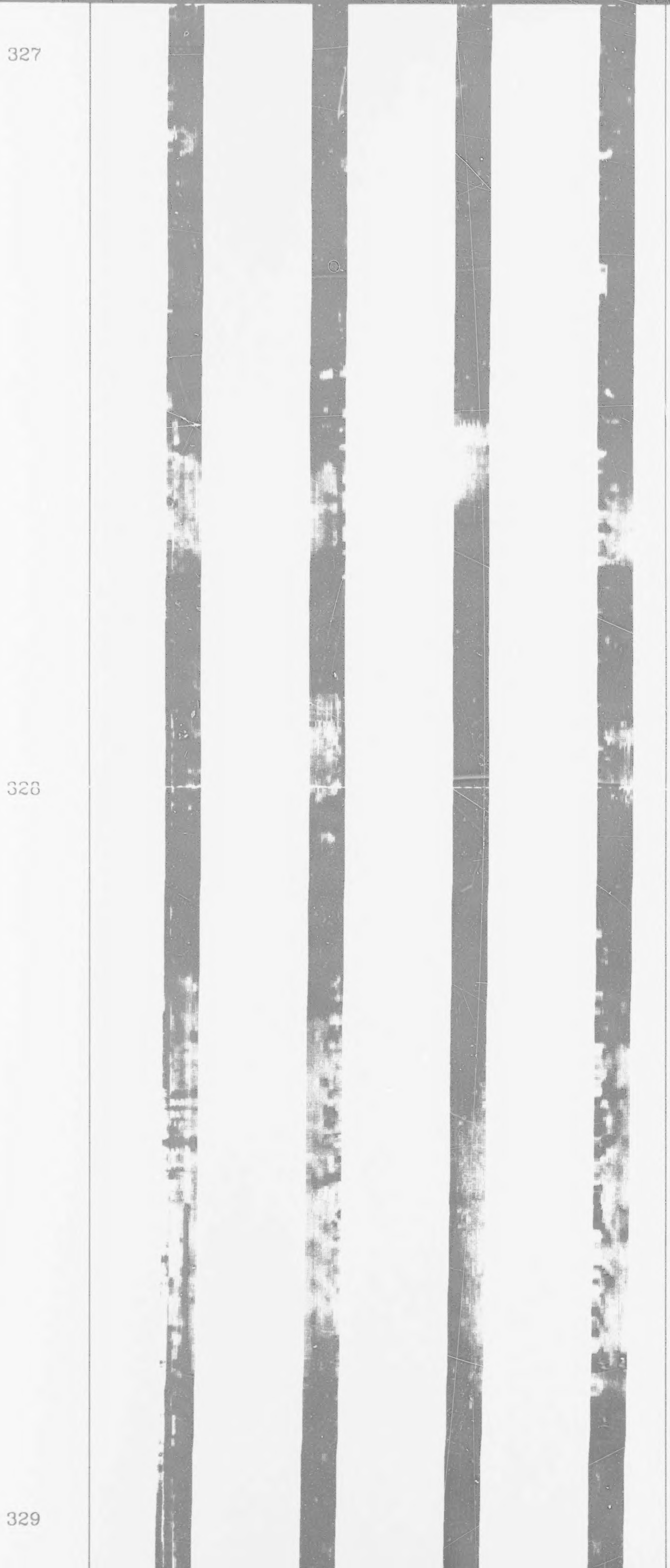
327
328
329

330
331

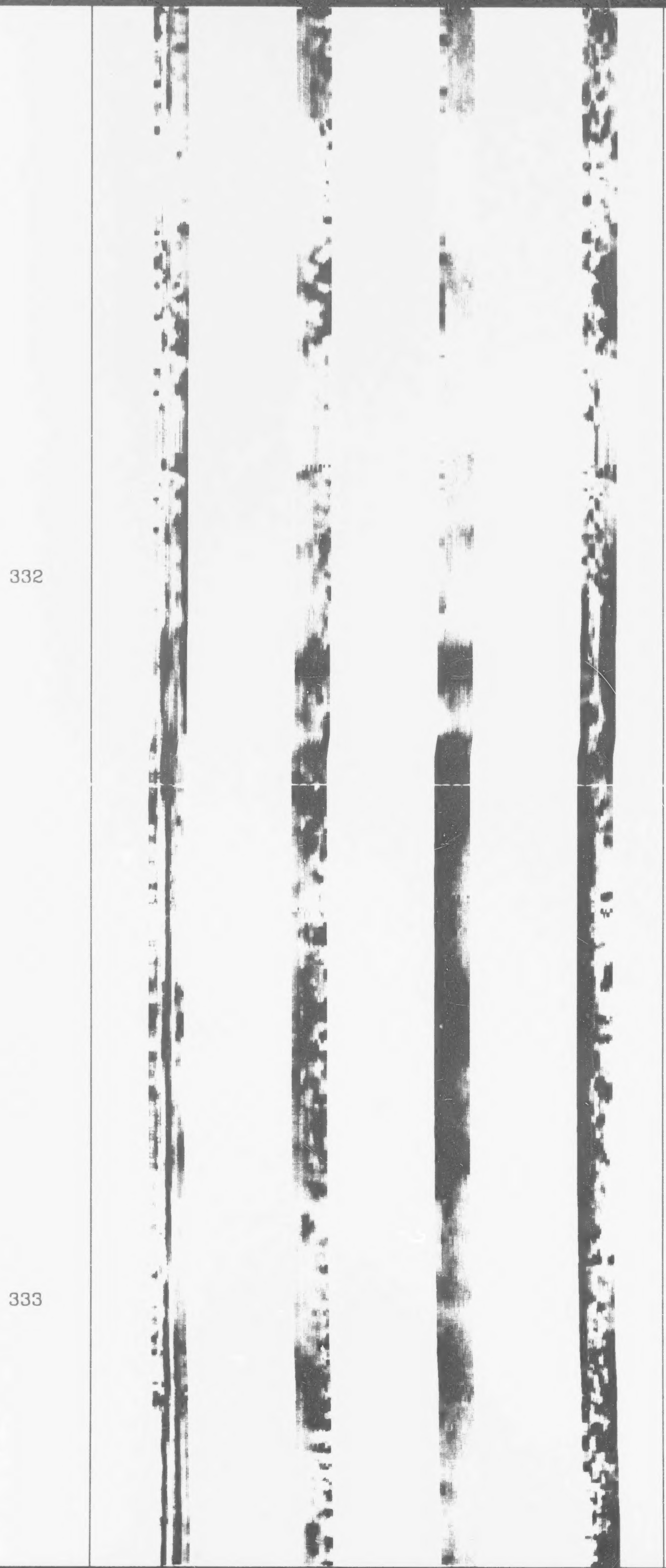
332
333

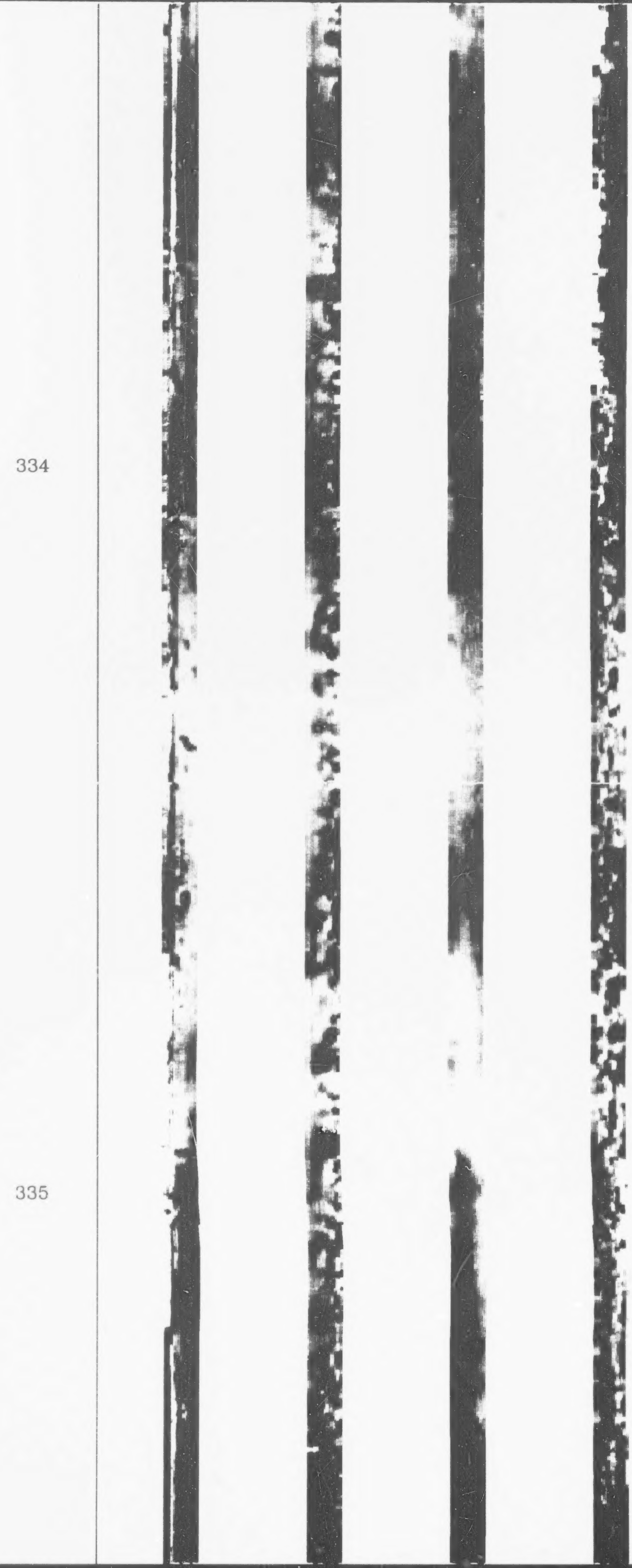
334
335

336
337

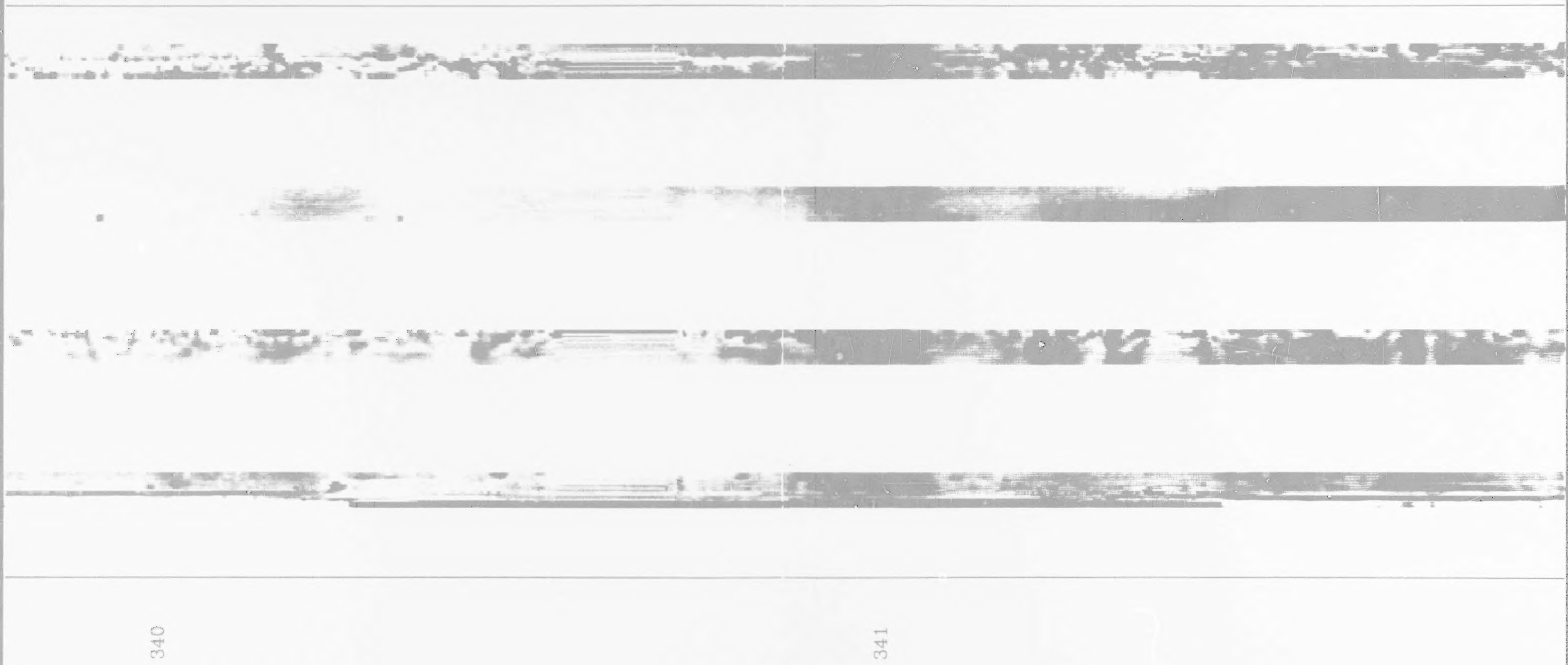
340
341

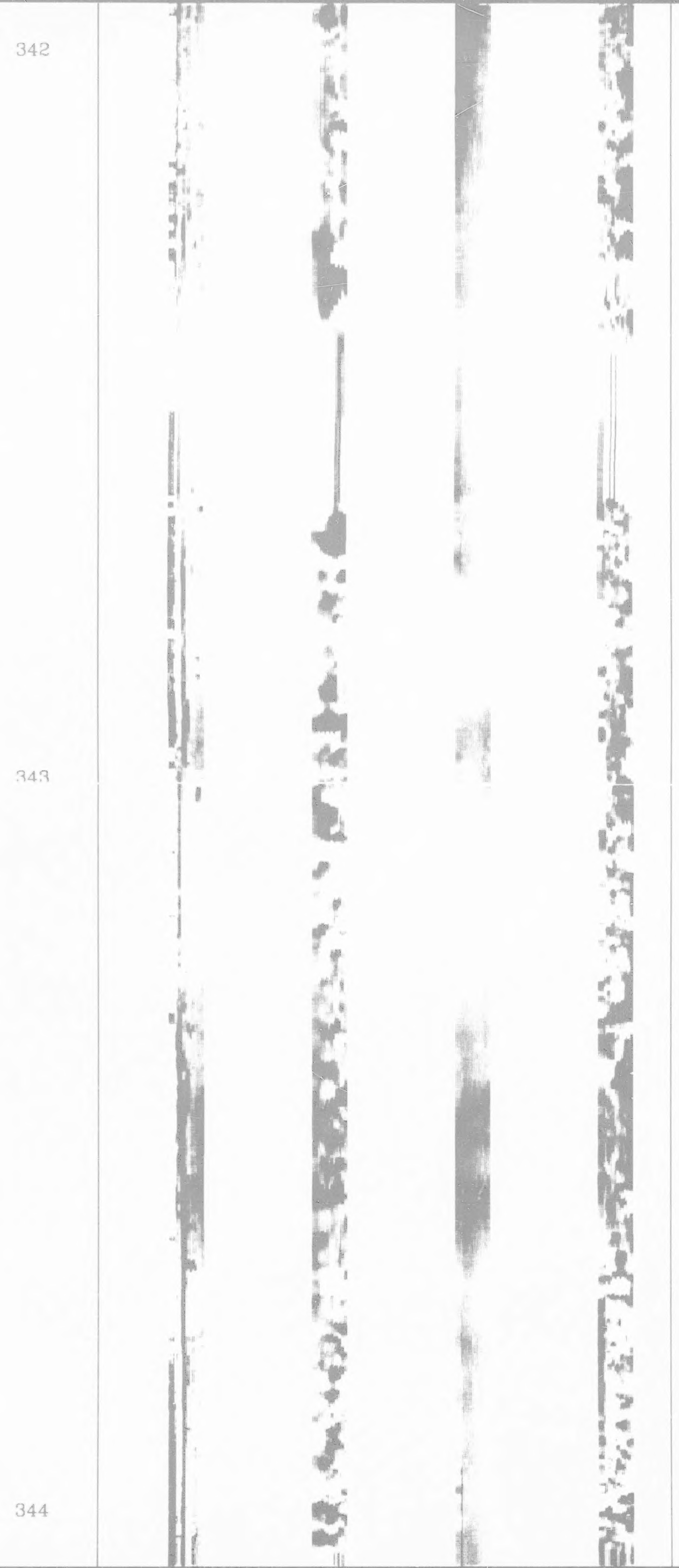
342
343
344

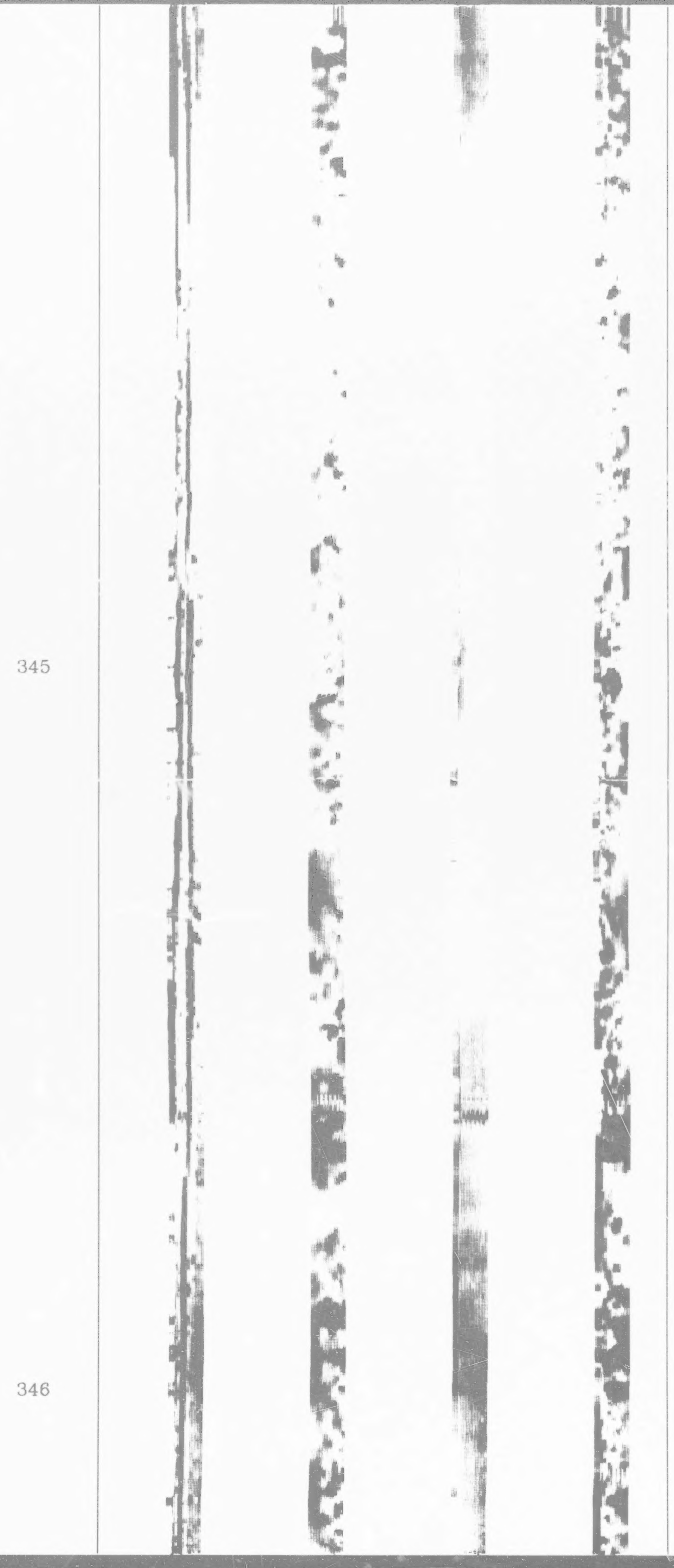

345
346

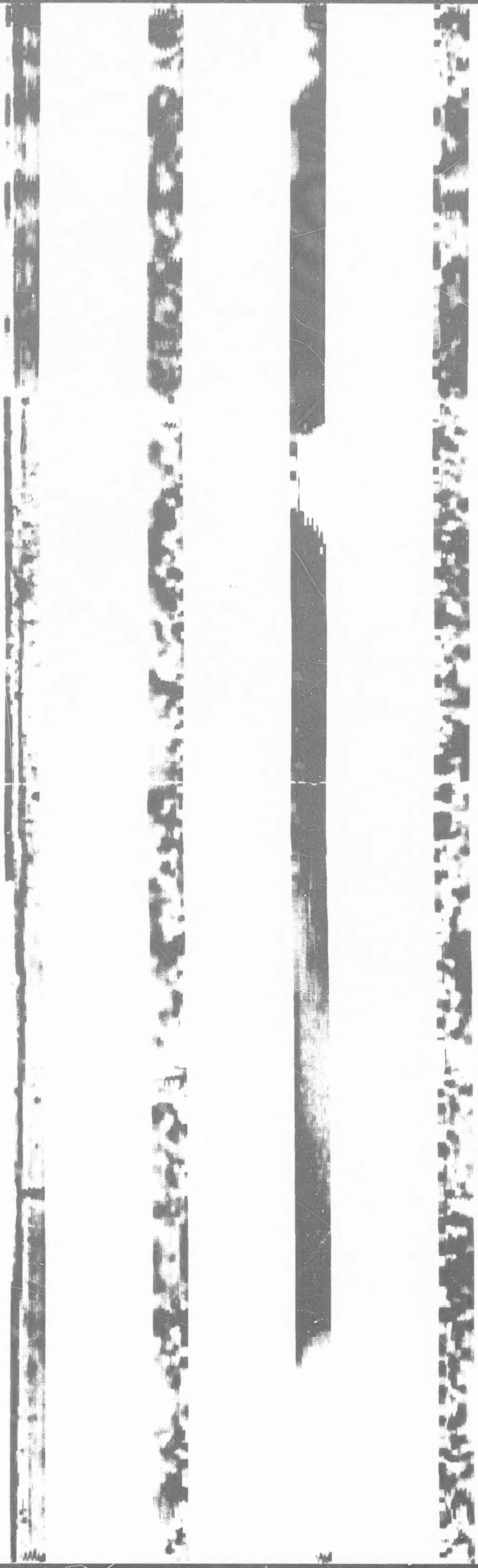
347
348

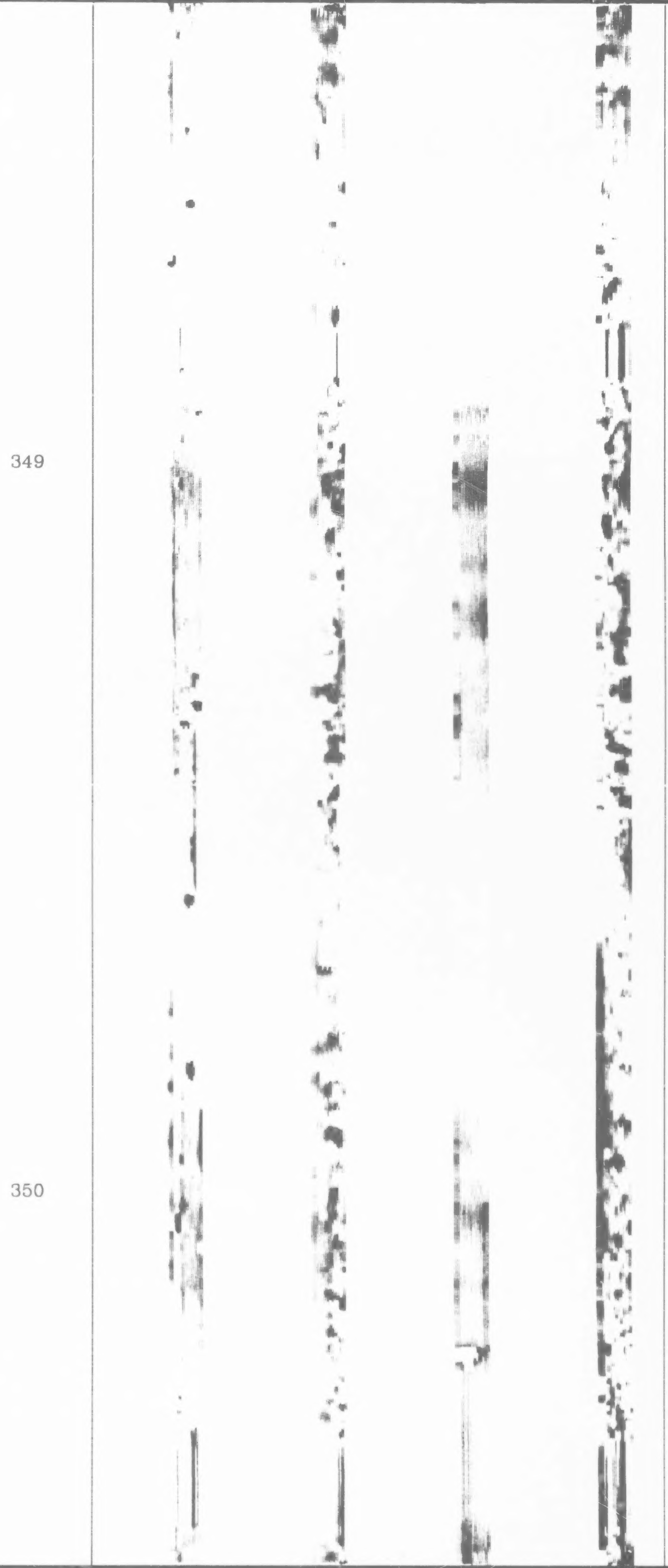
349
350

351
352

353

354

SCHLUMBERGER

FMS
BOREHOLE
IMAGING

COMPANY	LAMONT DOHERTY
WELL	ODP HOLE 803D
FIELD	ONTONG JAVA PLATEAU
COUNTRY	LEG 130
RUN	1
DATE LOGGED	05 – FEB – 90
REFERENCE	STATIC PS 1 360 400

STATIC NORMALIZATION

PASS 1 (LAMON)

FILE : MEST.001

ZONE FROM 400.0 M TO 360.0 M

DEPTH SCALE = 1/ 5

IMAGE SCALE = 1/ 5

BITSIZE = 9.88

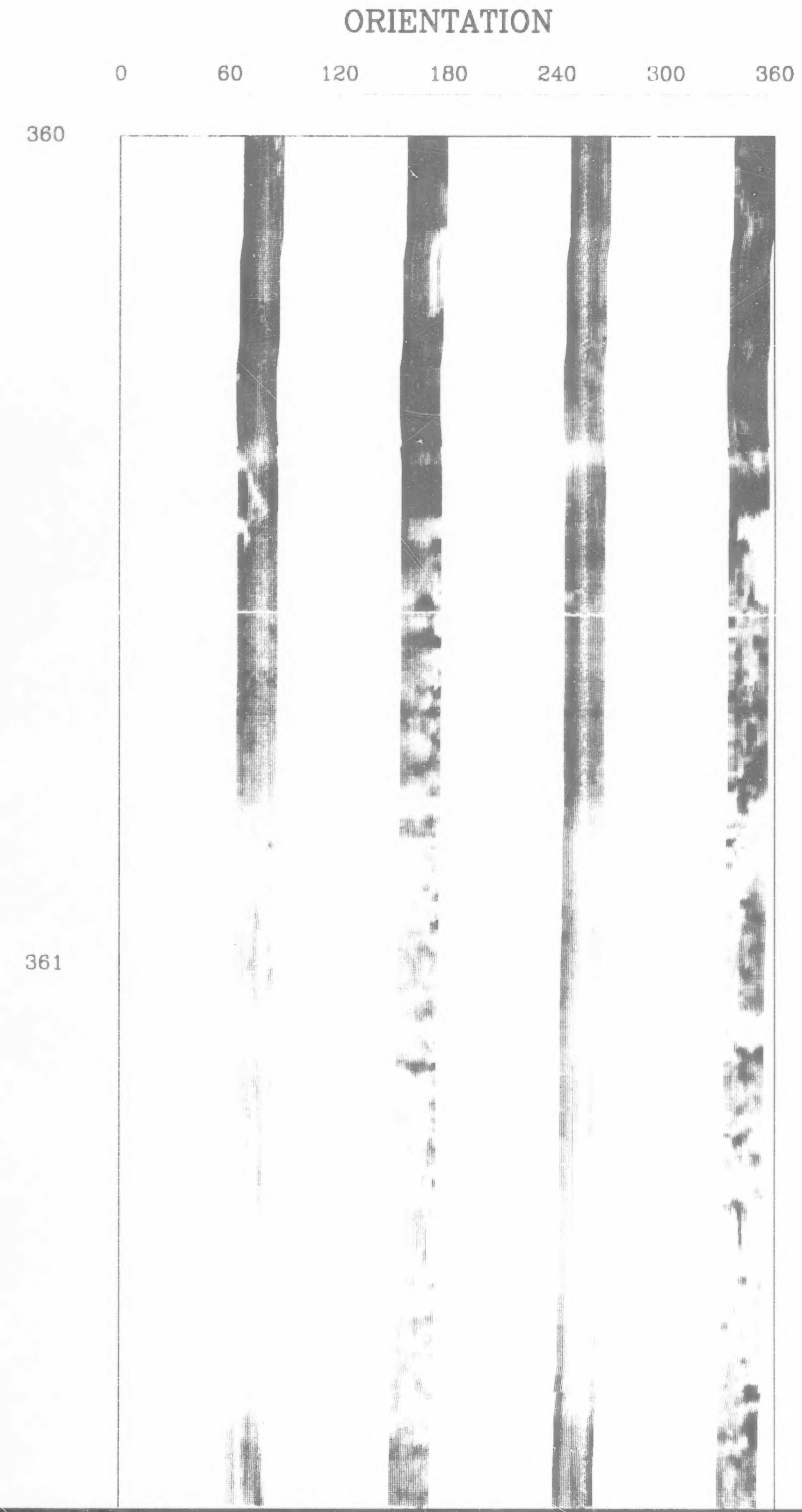

362

363

371

372

373

374

[redacted]

[redacted]

[redacted]

[redacted]

392

393

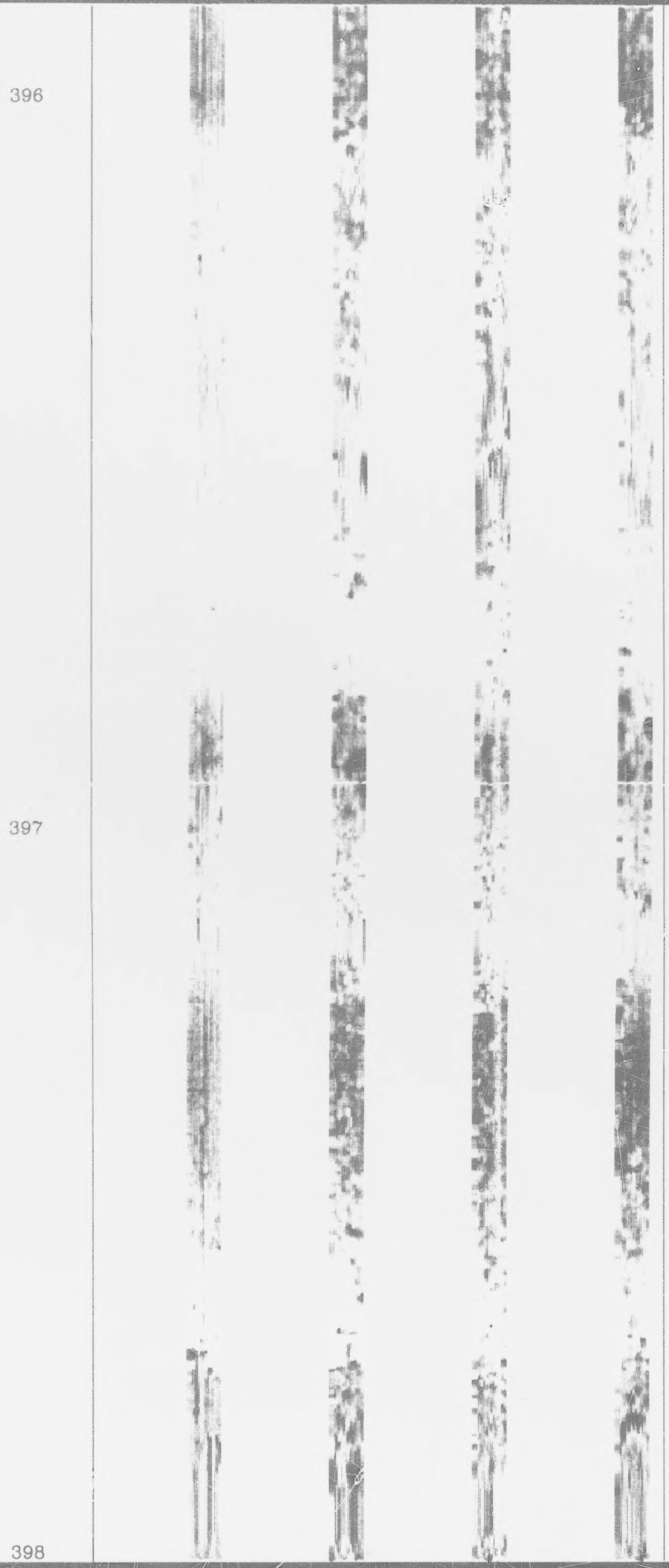
396
397
398

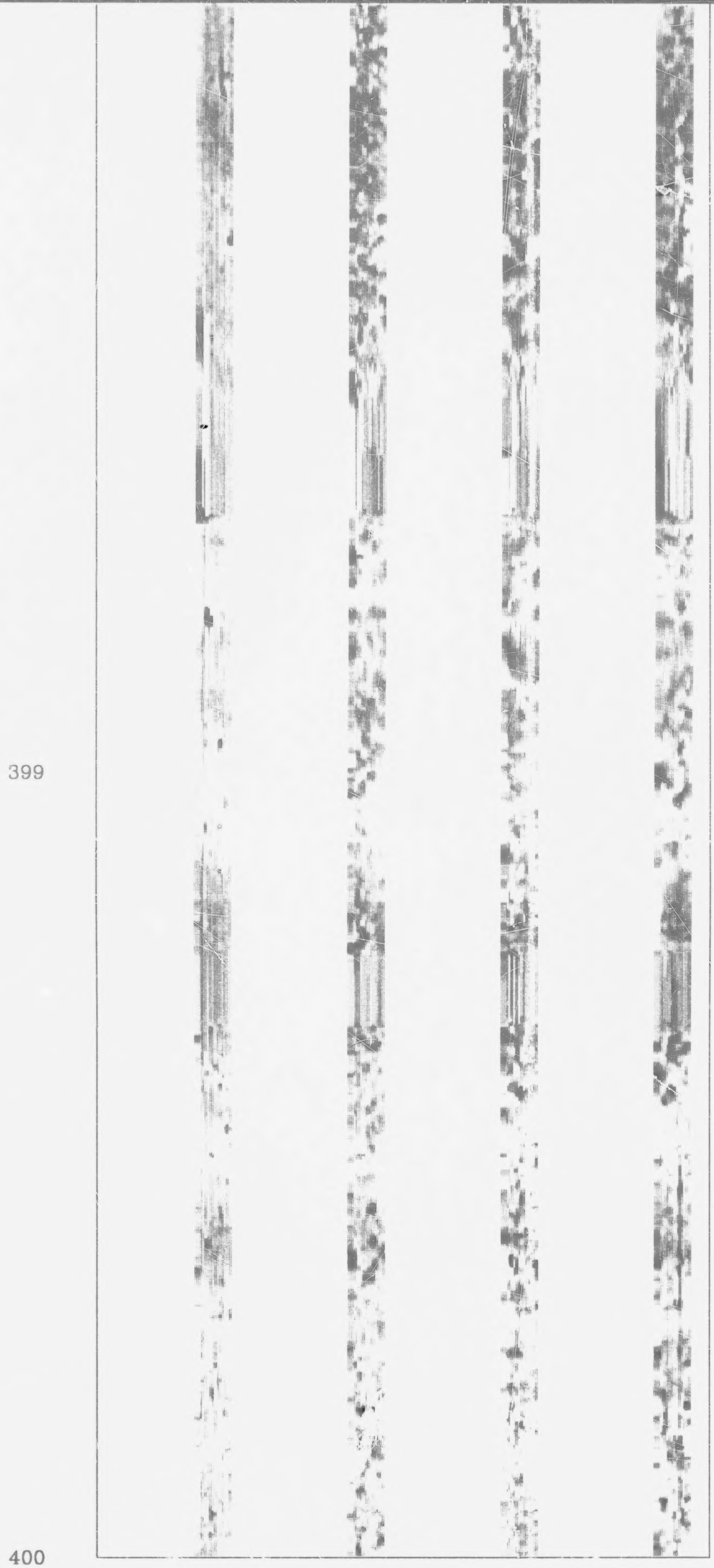
399
400

SCHLUMBERGER

FMS
BOREHOLE
IMAGING

COMPANY	LAMONT DOHERTY
WELL	ODP HOLE 803D
FIELD	ONTONG JAVA PLATEAU
COUNTRY	LEG 130
RUN	1
DATE LOGGED	05 – FEB – 90
REFERENCE	STATIC PS-1 400-440

STATIC NORMALIZATION

FILE : MEST.001

ZONE FROM 440.0 M TO 400.0 M

DEPTH SCALE = 1/ 5

IMAGE SCALE = 1/ 5

BITSIZE = 9.88

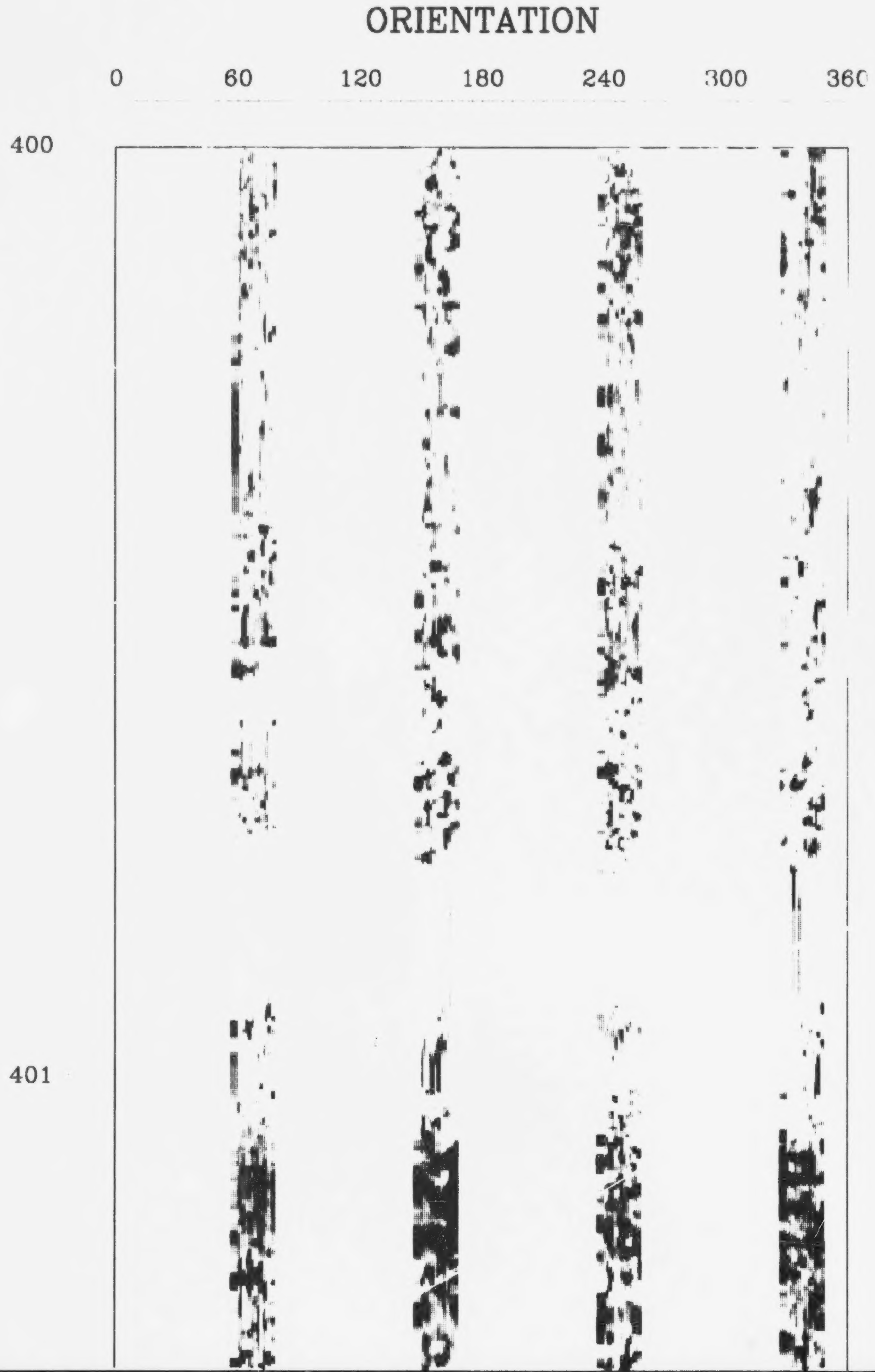

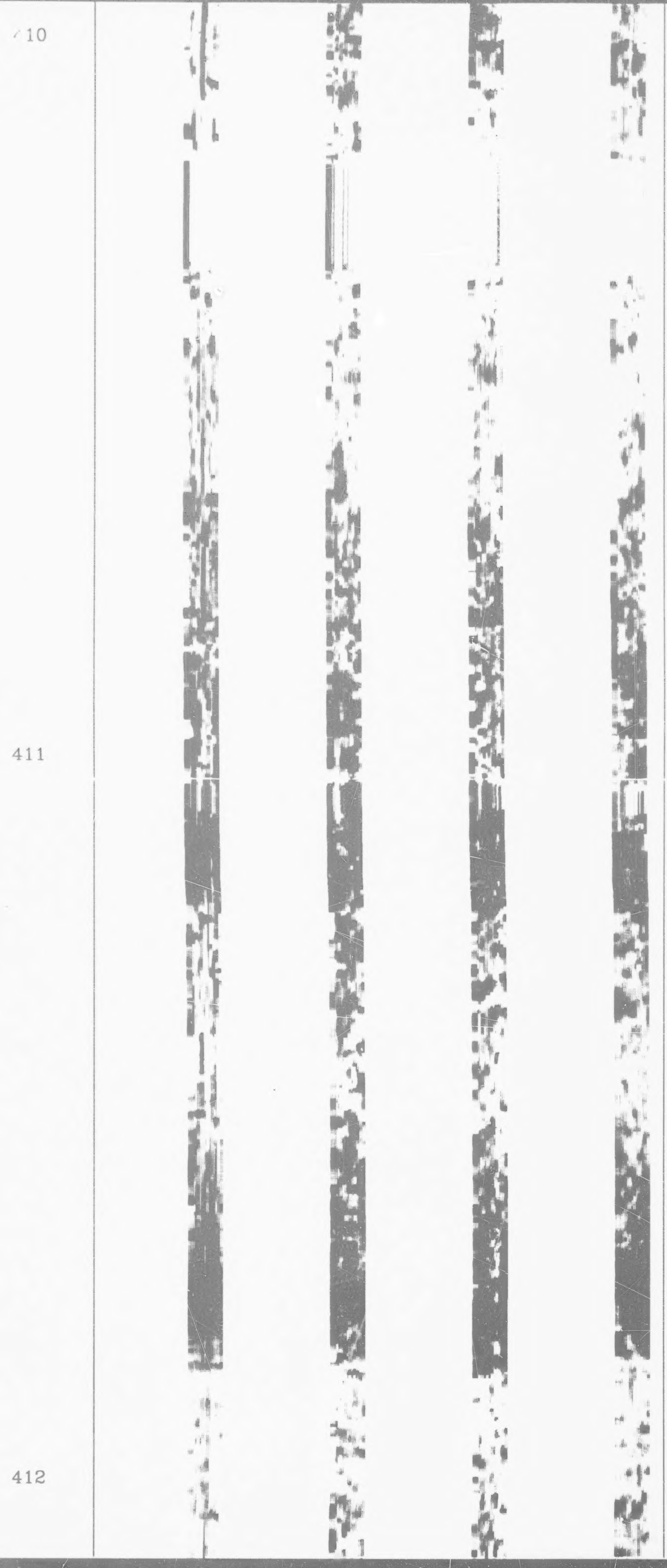
410
411
412

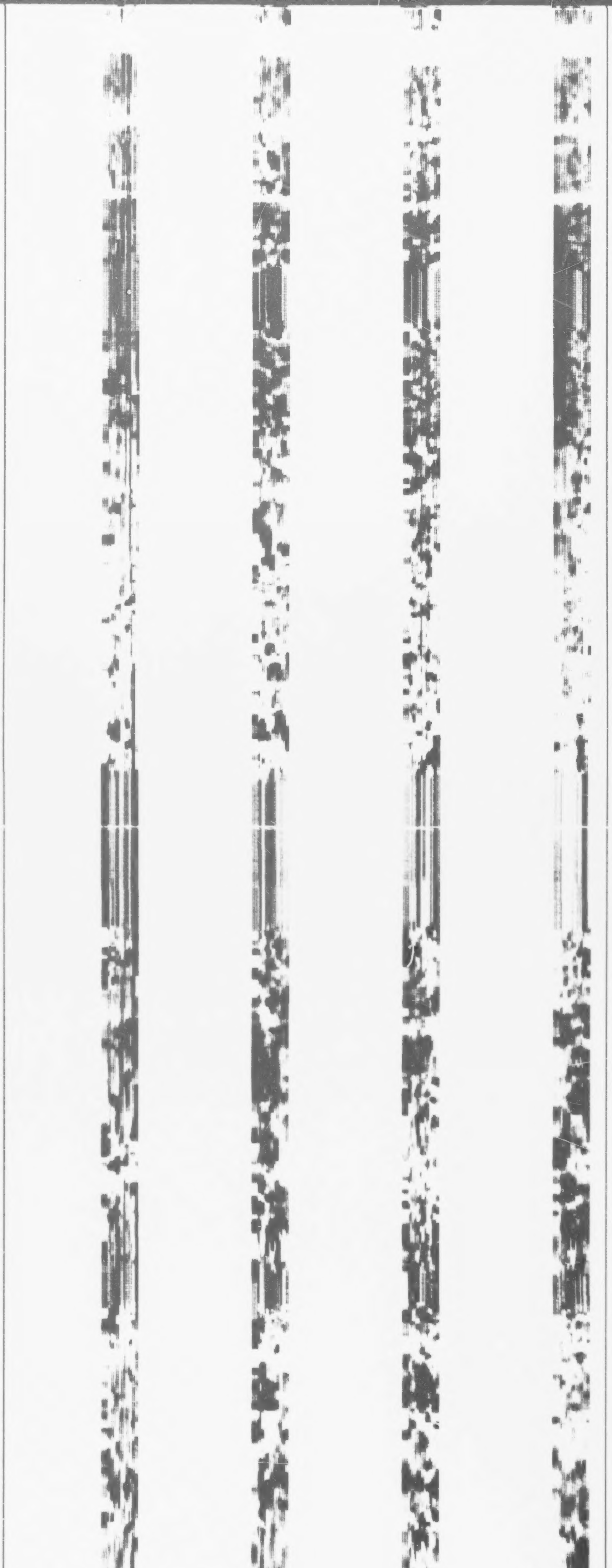

413
414

415

416

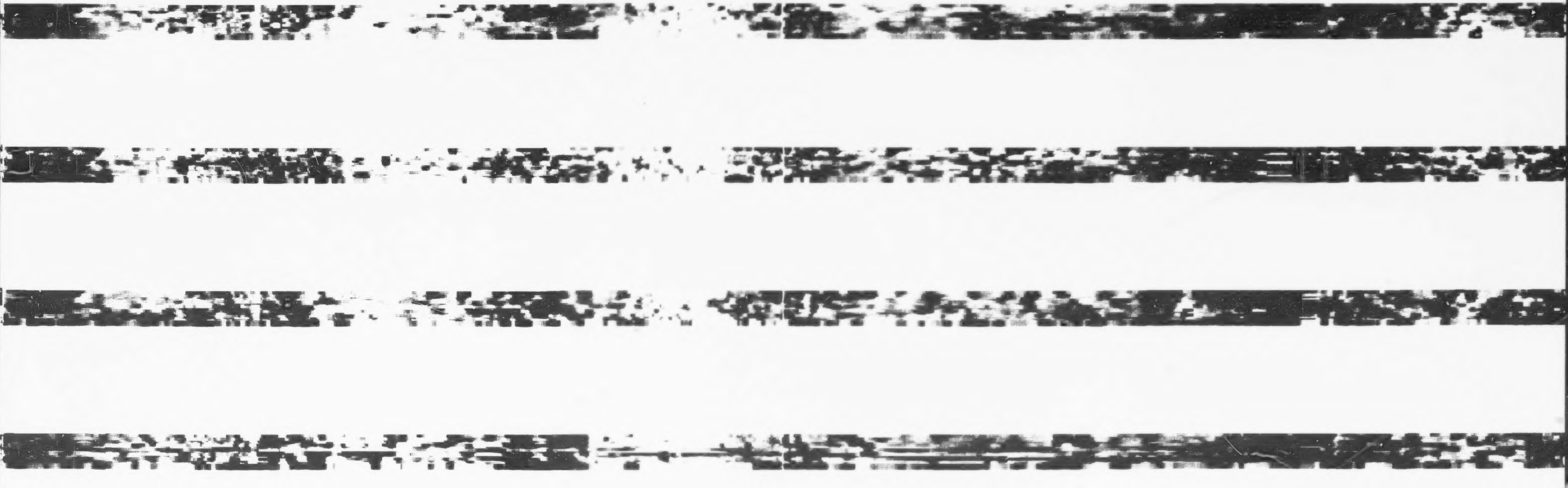

[redacted]

[redacted]

[redacted]

[redacted]

[redacted]

[redacted]

[redacted]

[redacted]

[redacted]

[redacted]

436

437

439
440

SCHLUMBERGER

FMS
BOREHOLE
IMAGING

COMPANY	LAMONT DOHERTY
WELL	ODP HOLE 803D
FIELD	ONTONG JAVA PLATEAU
COUNTRY	LEG 130
RUN	1
DATE LOGGED	05 – FEB – 90
REFERENCE	STATIC PS-1 440-480

STATIC NORMALIZATION

PASS 1 (LAMON)

FILE : MEST.001

ZONE FROM 480.0 M TO 440.0 M

DEPTH SCALE = 1/ 5

IMAGE SCALE = 1/ 5

BITSIZE = 9.88

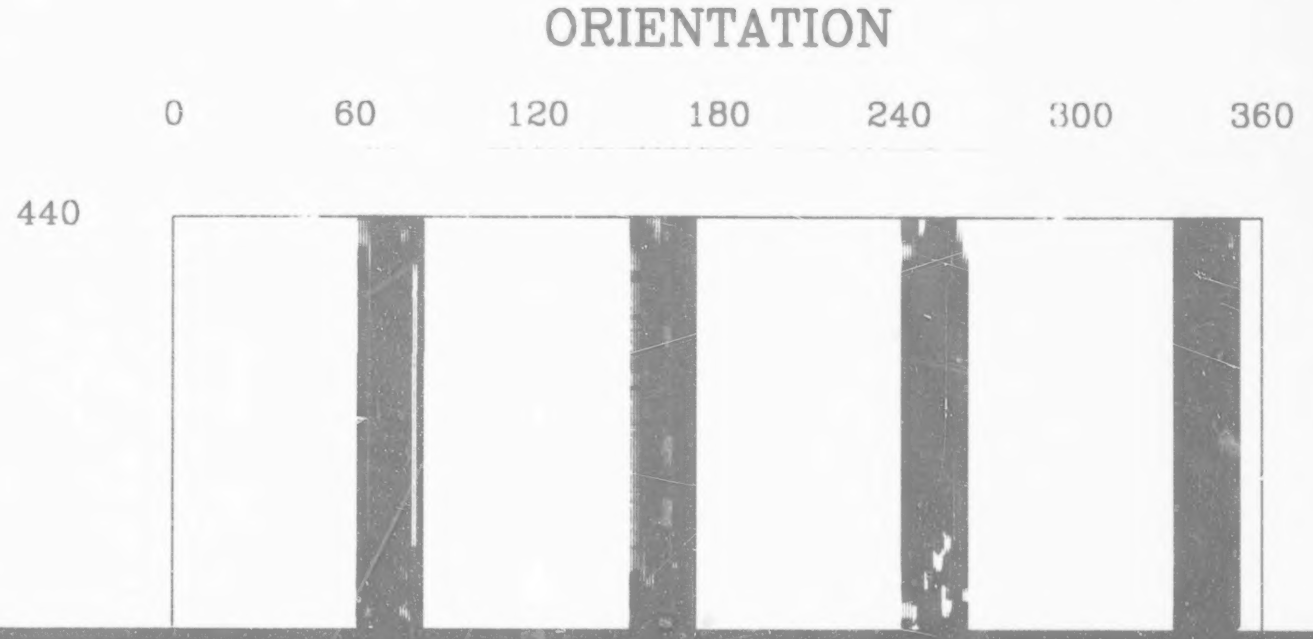

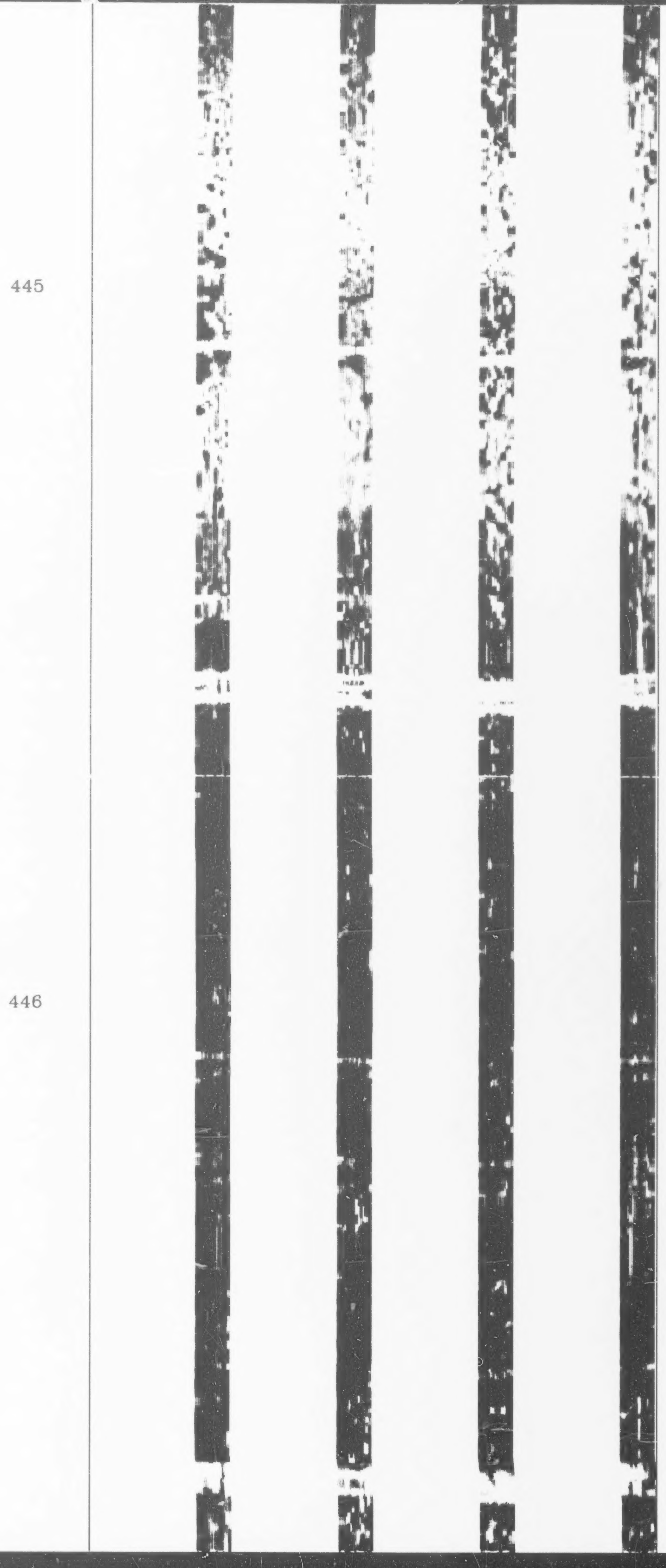
445
446

447

448

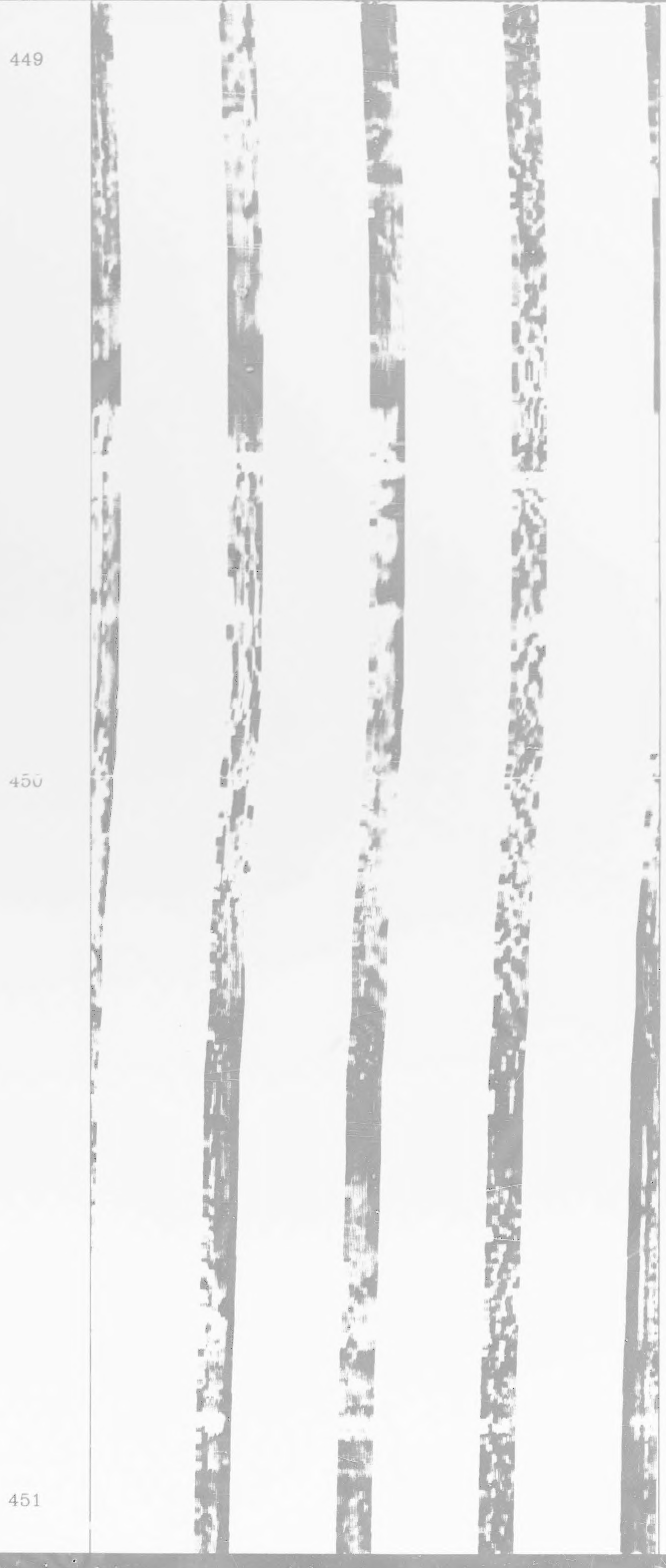
449
450
451

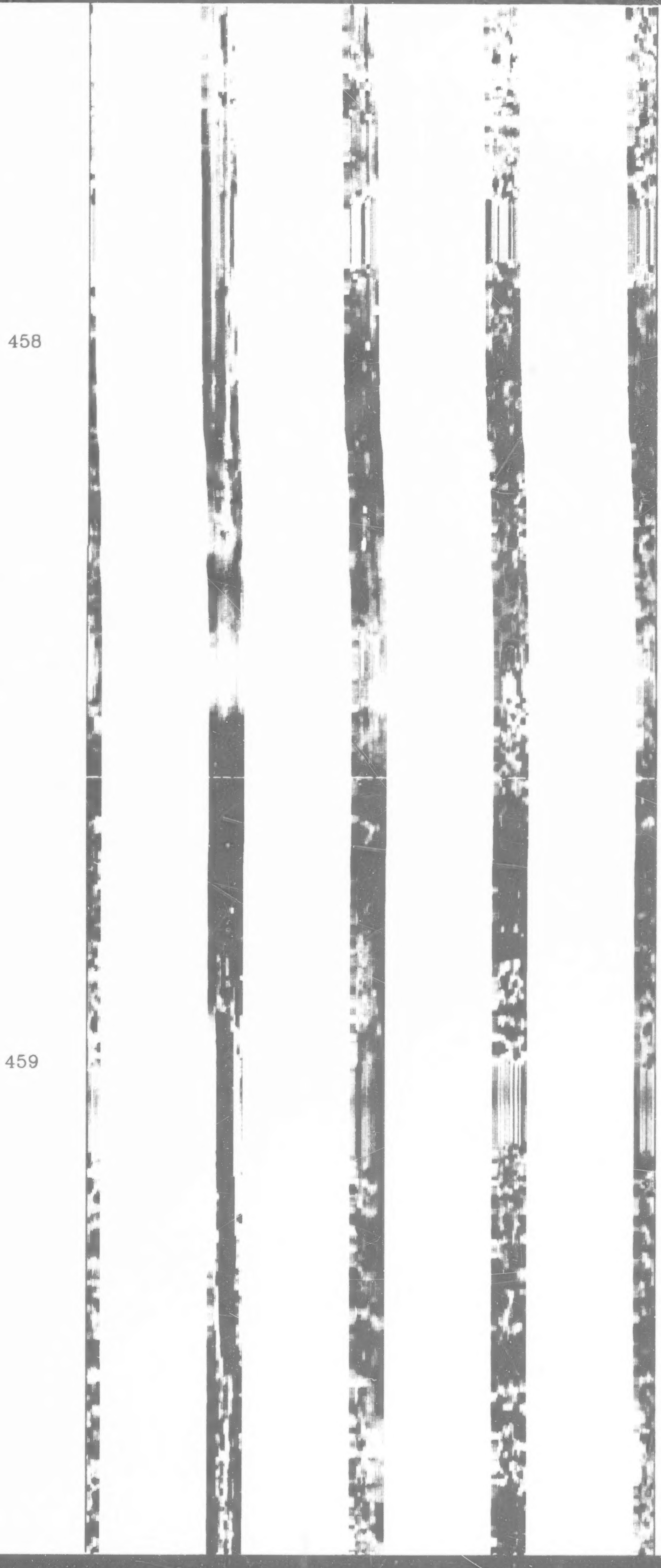
458
459

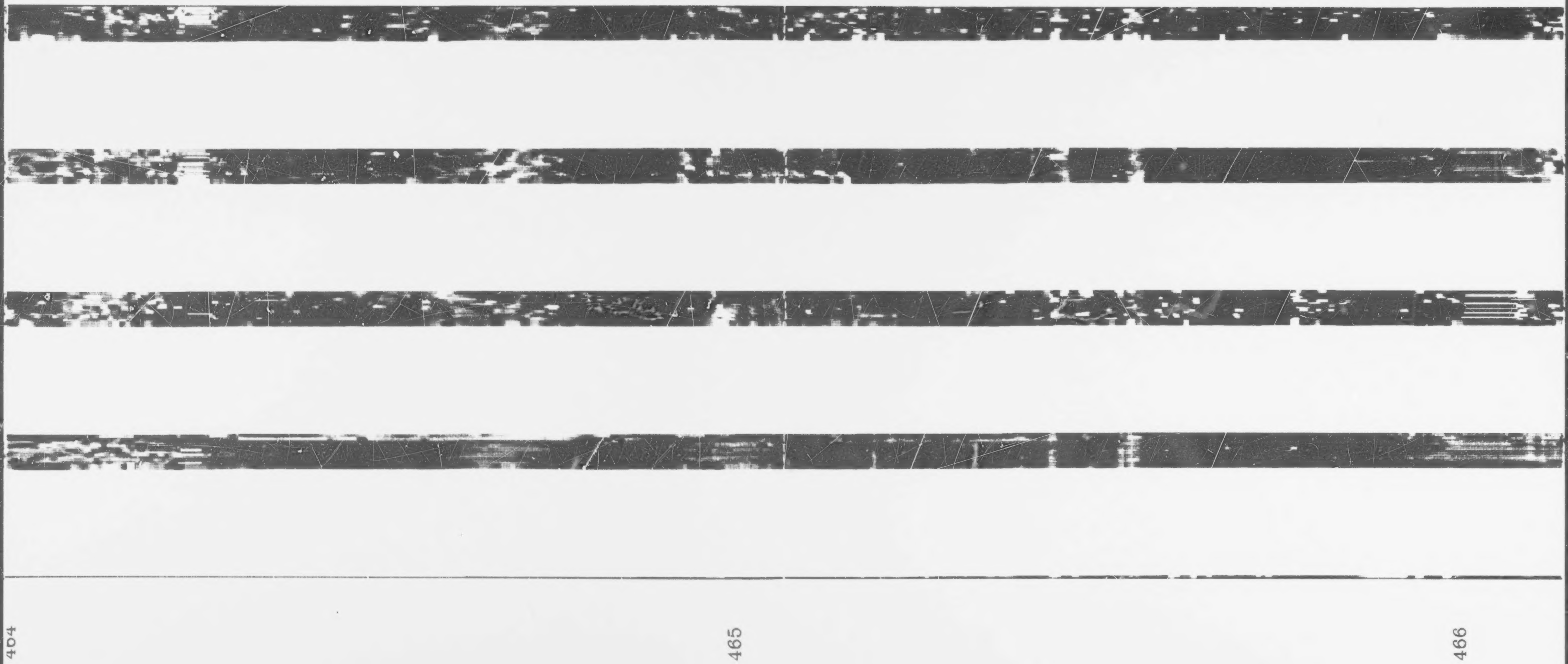
464
465
466

[redacted]

[redacted]

[redacted]

[redacted]

[redacted]

473

474

477

478

479

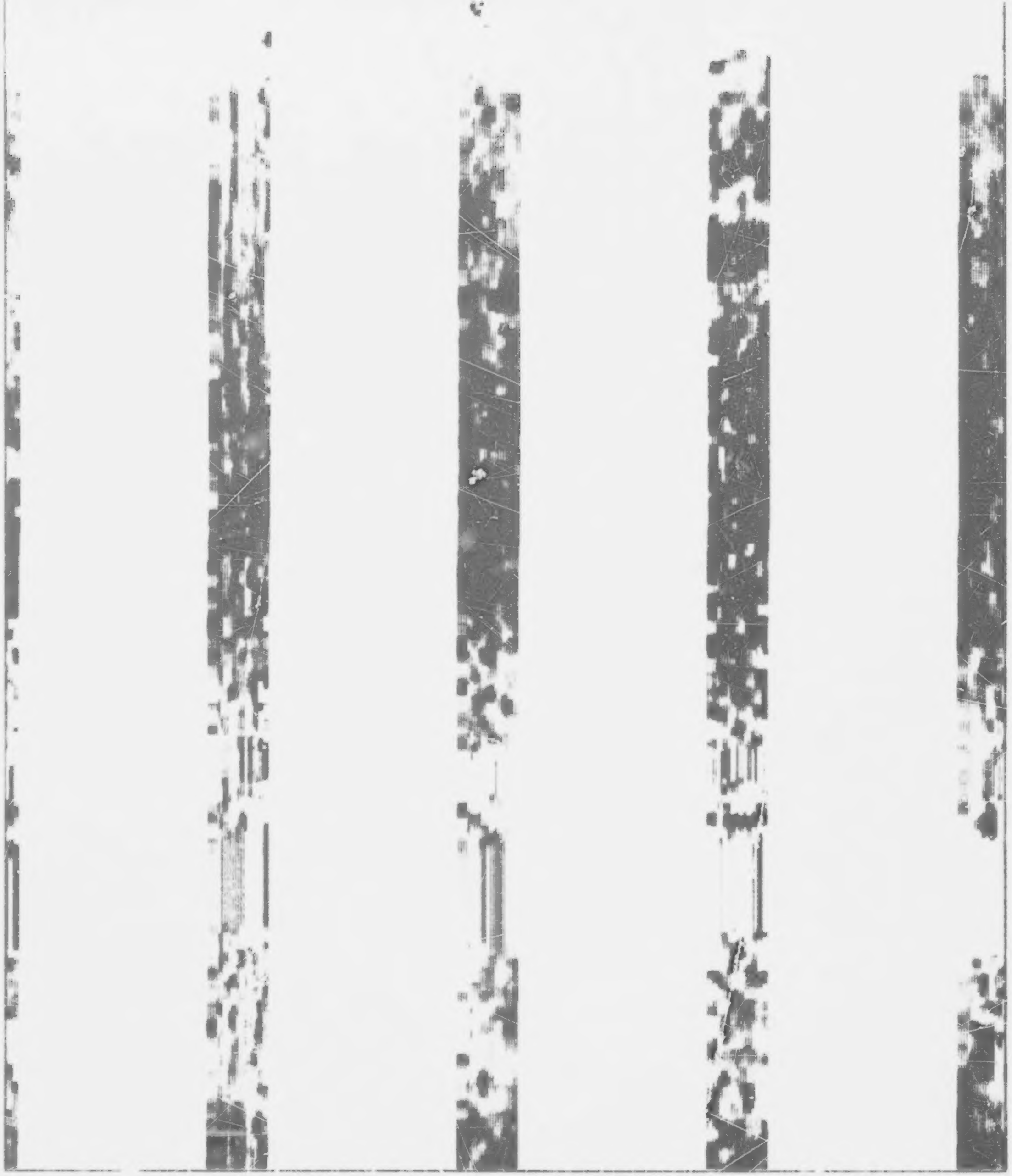

SCHLUMBERGER

FMS
BOREHOLE
IMAGING

COMPANY	LAMONT DOHERTY
WELL	ODP HOLE 803D
FIELD	ONTONG JAVA PLATEAU
COUNTRY	LEG 130
RUN	1
DATE LOGGED	05 - FEB - 90
REFERENCE	STATIC PS-1 480-520

STATIC NORMALIZATION
PASS 1 (LAMON)
FILE : MEST.001

ZONE FROM 520.0 M TO 480.0 M

DEPTH SCALE = 1/ 5

IMAGE SCALE = 1/ 5

BITSIZE = 9.88

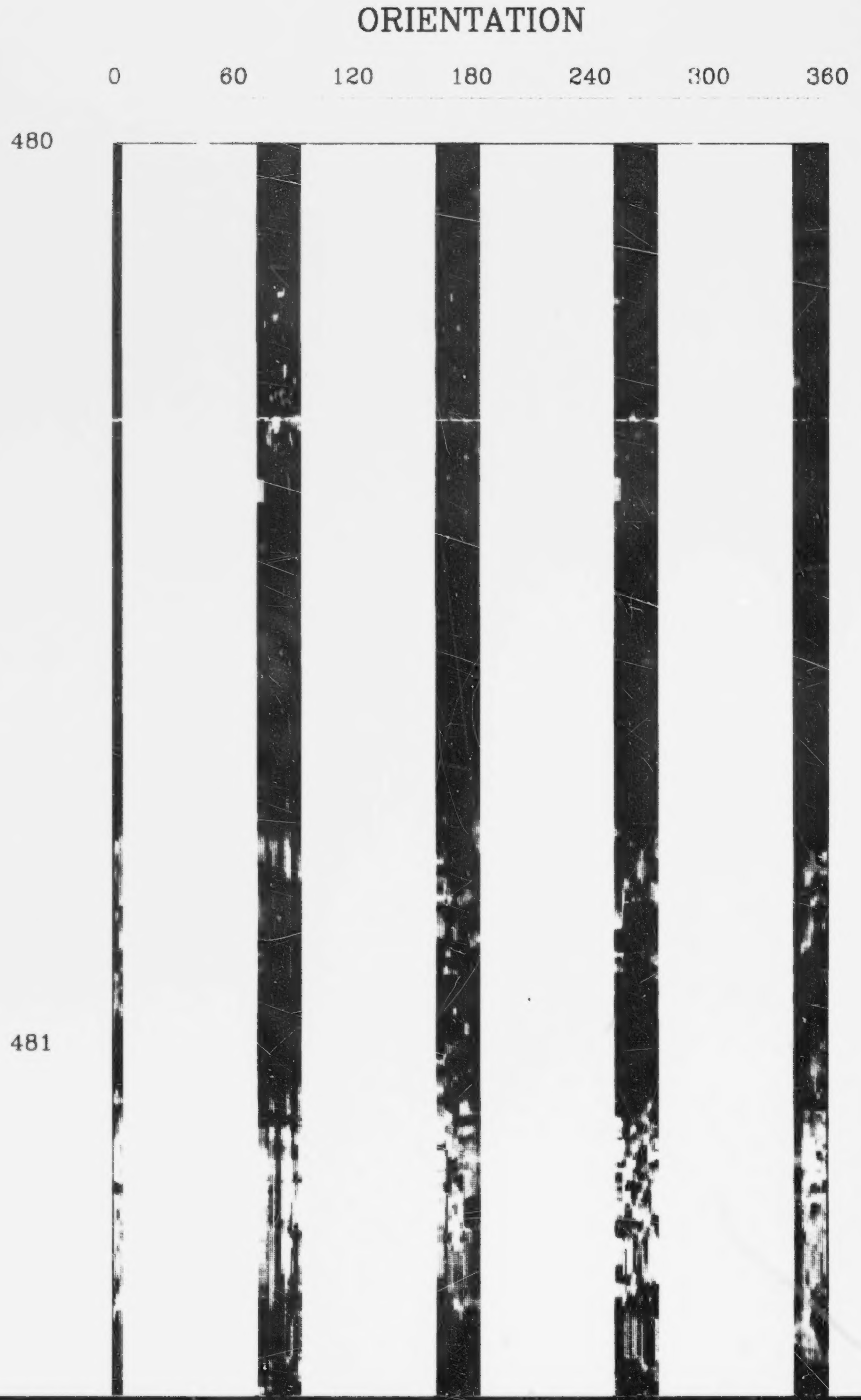

488

489

490

493

494

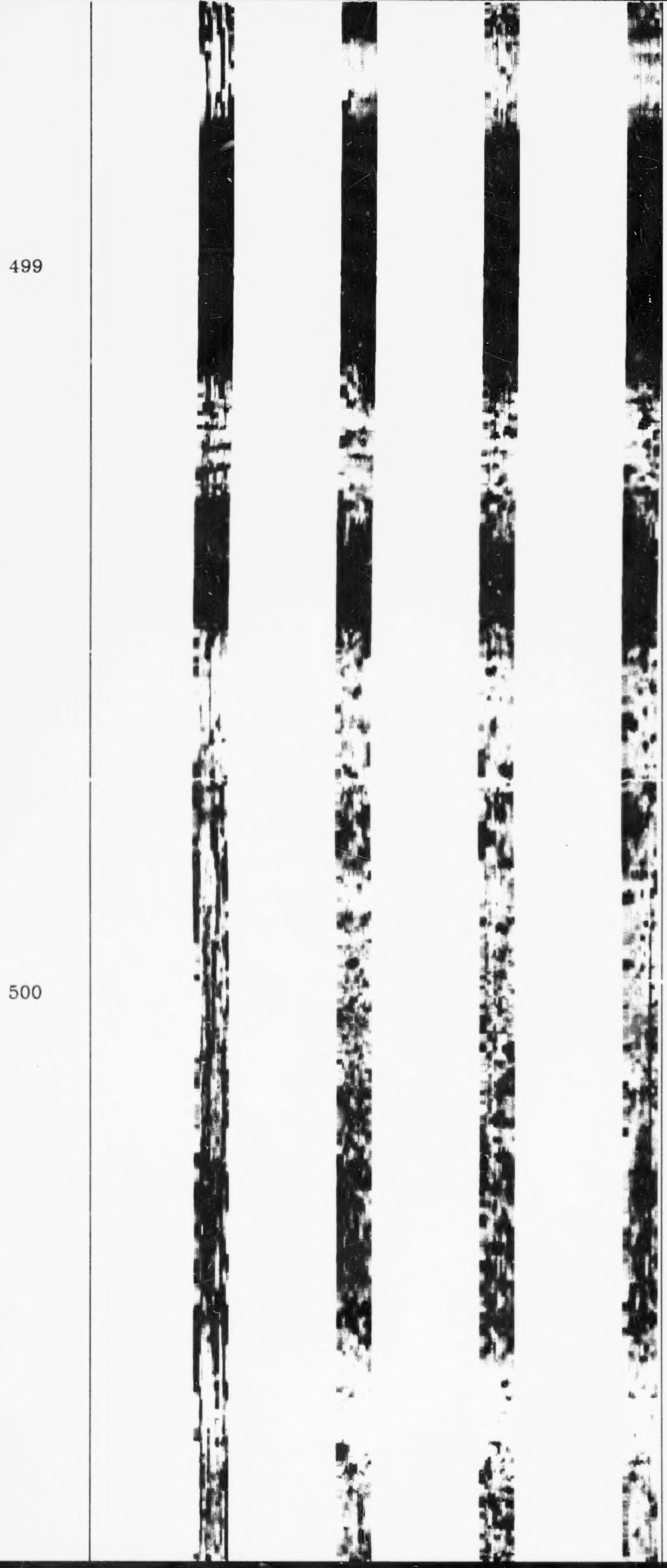
499
500

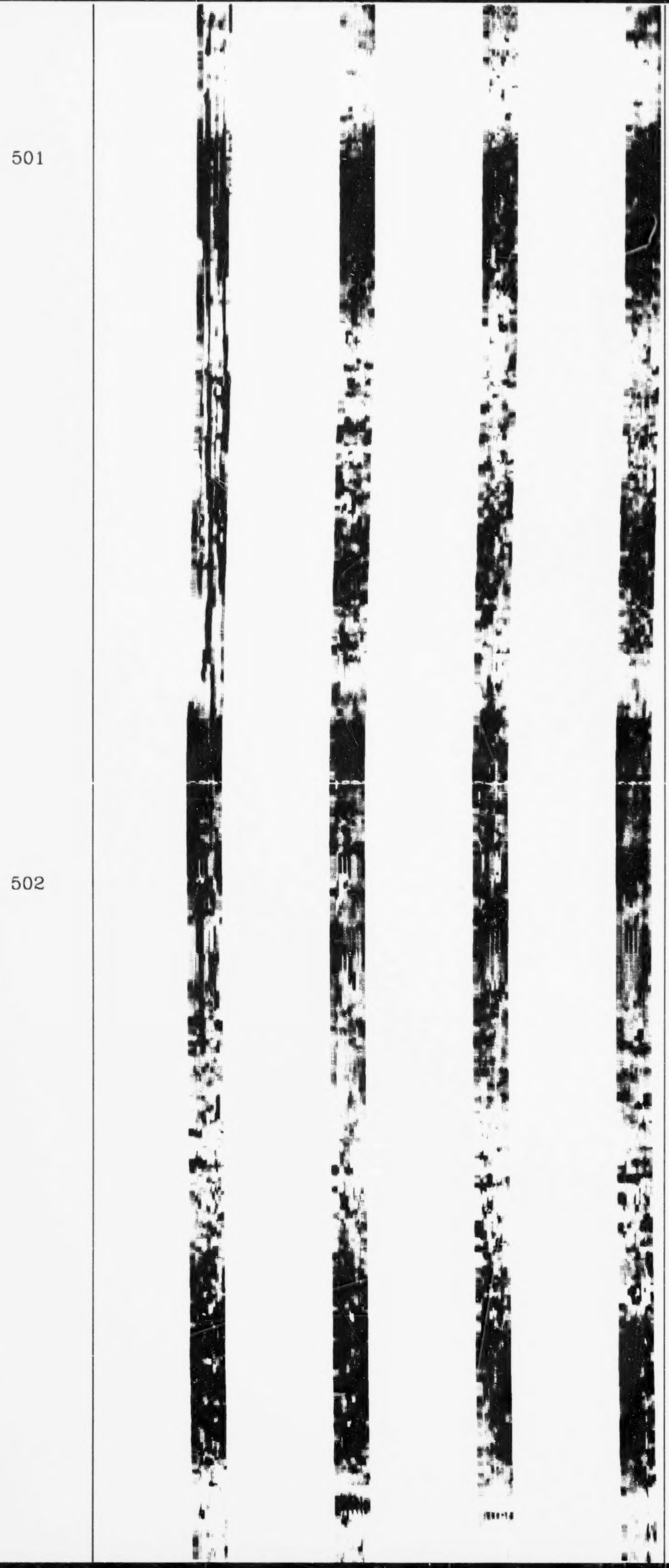
501
502

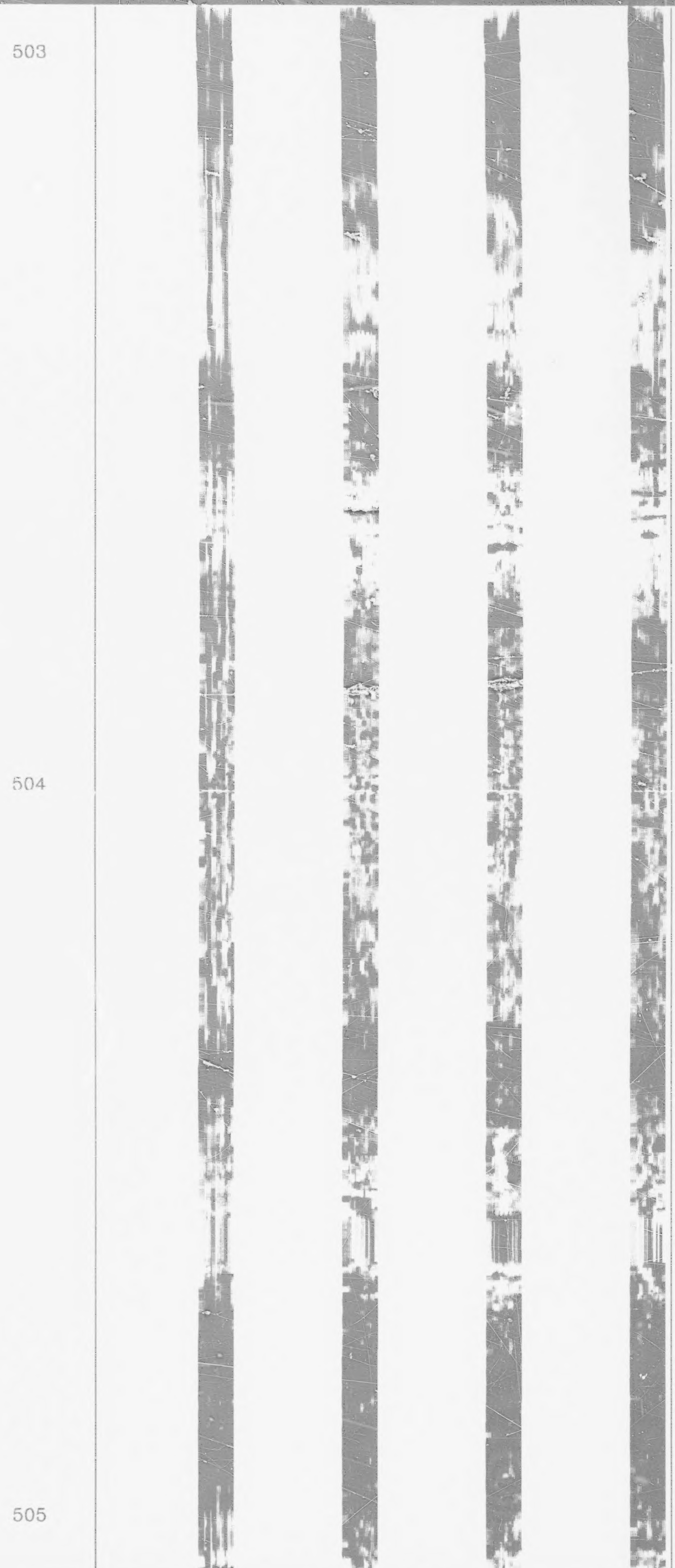
503
504
505

[redacted]

[redacted]

[redacted]

[redacted]

[redacted]

[redacted]

[redacted]

[redacted]

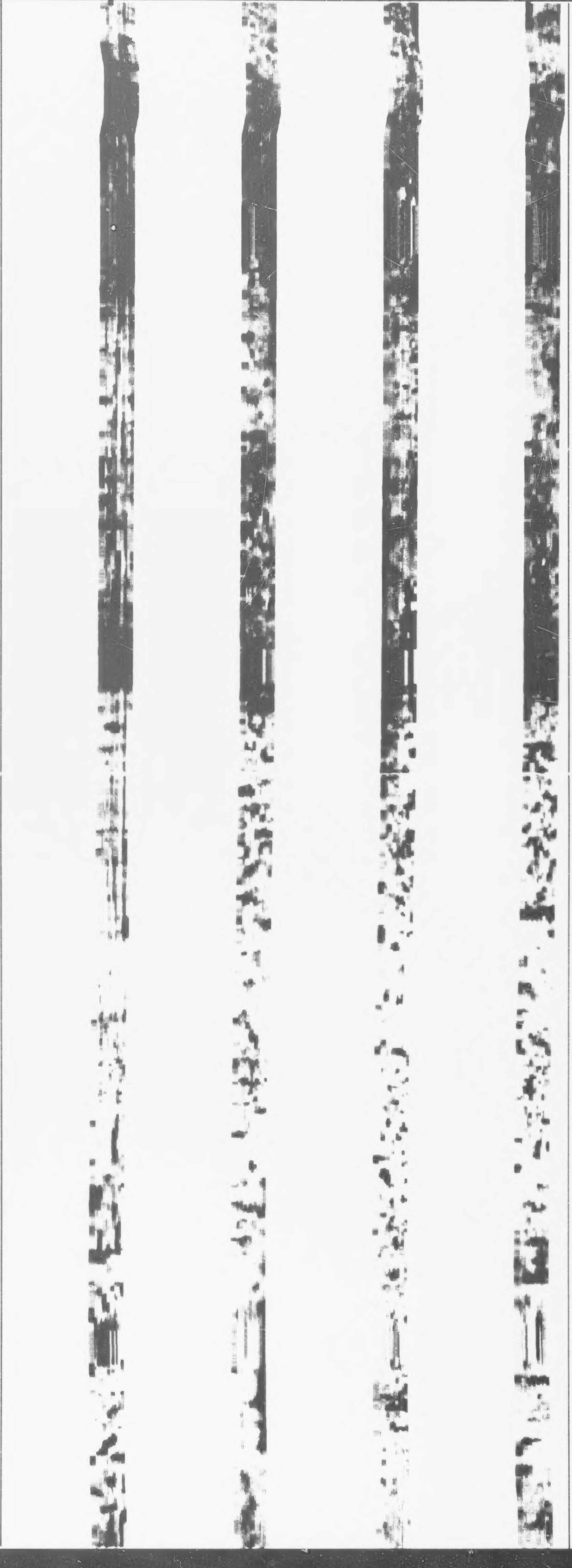
510
511

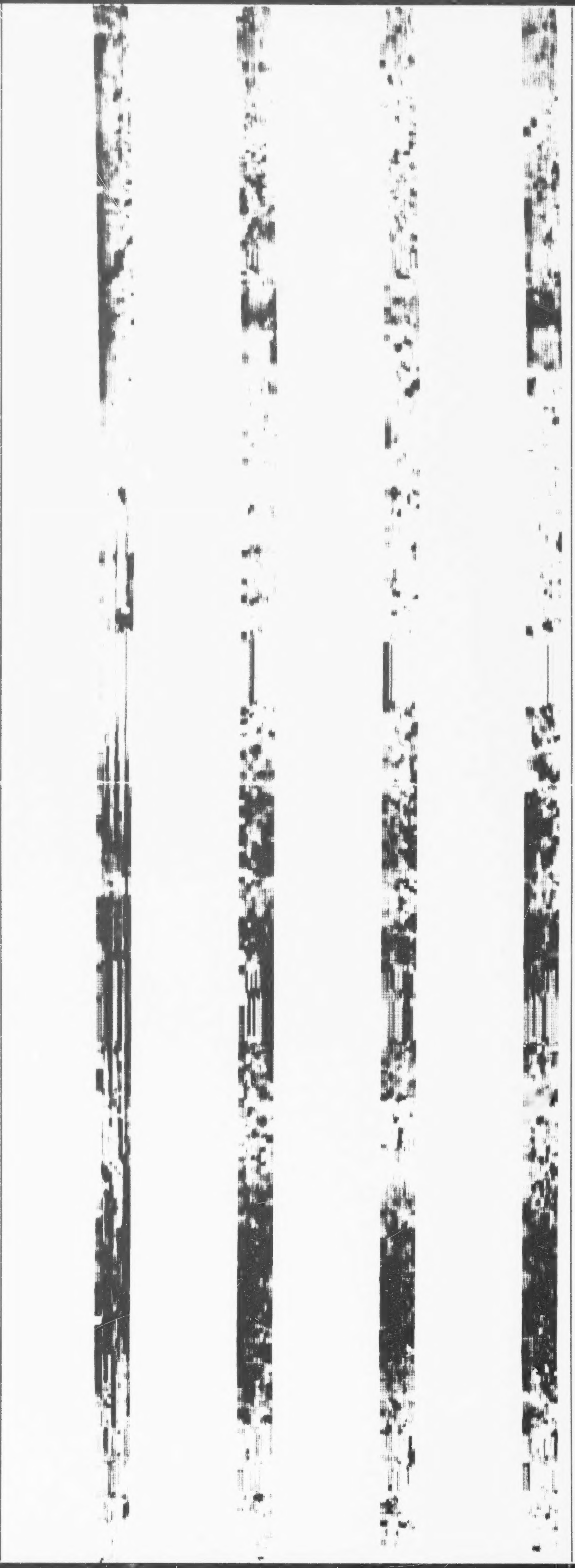
512
513

514

515

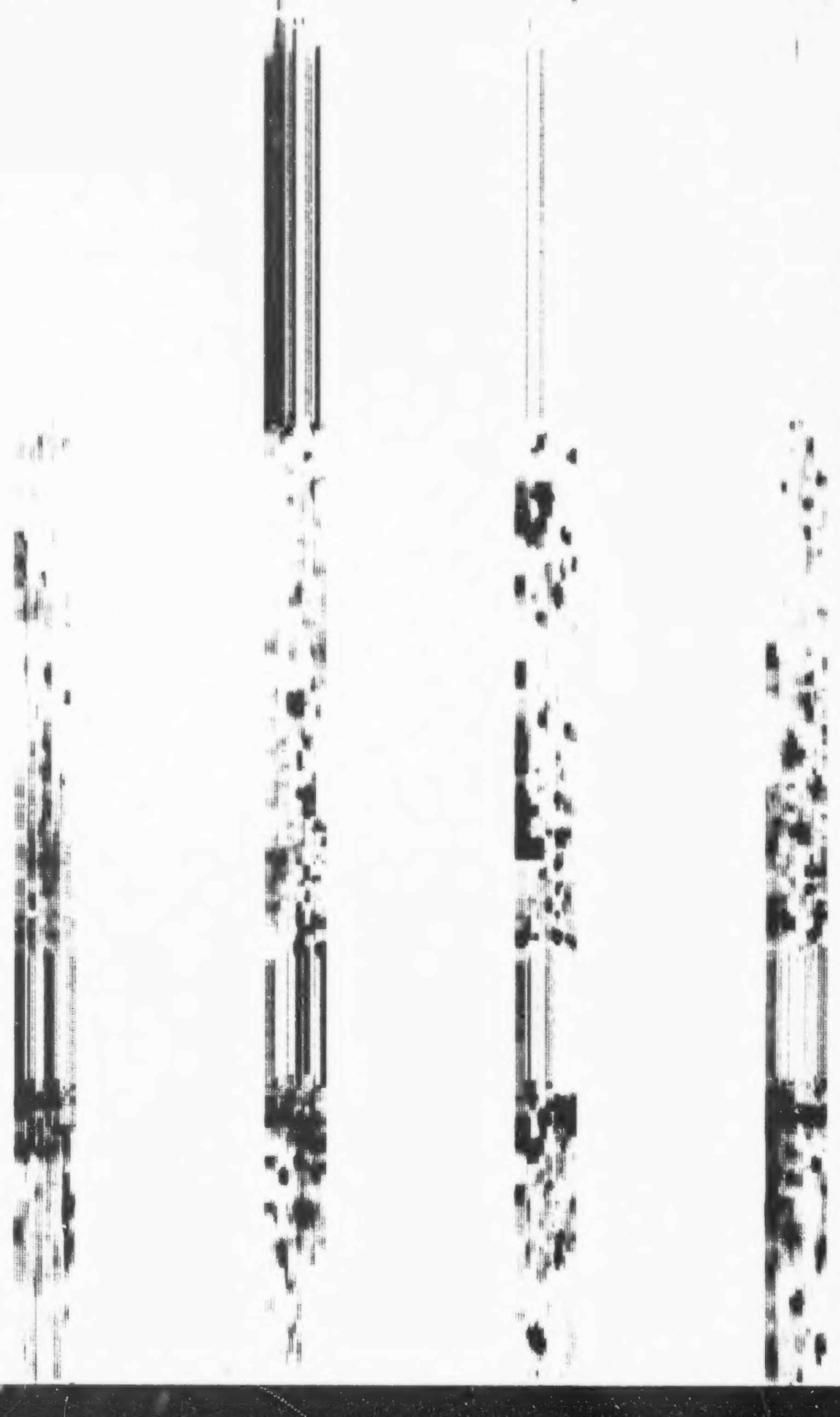

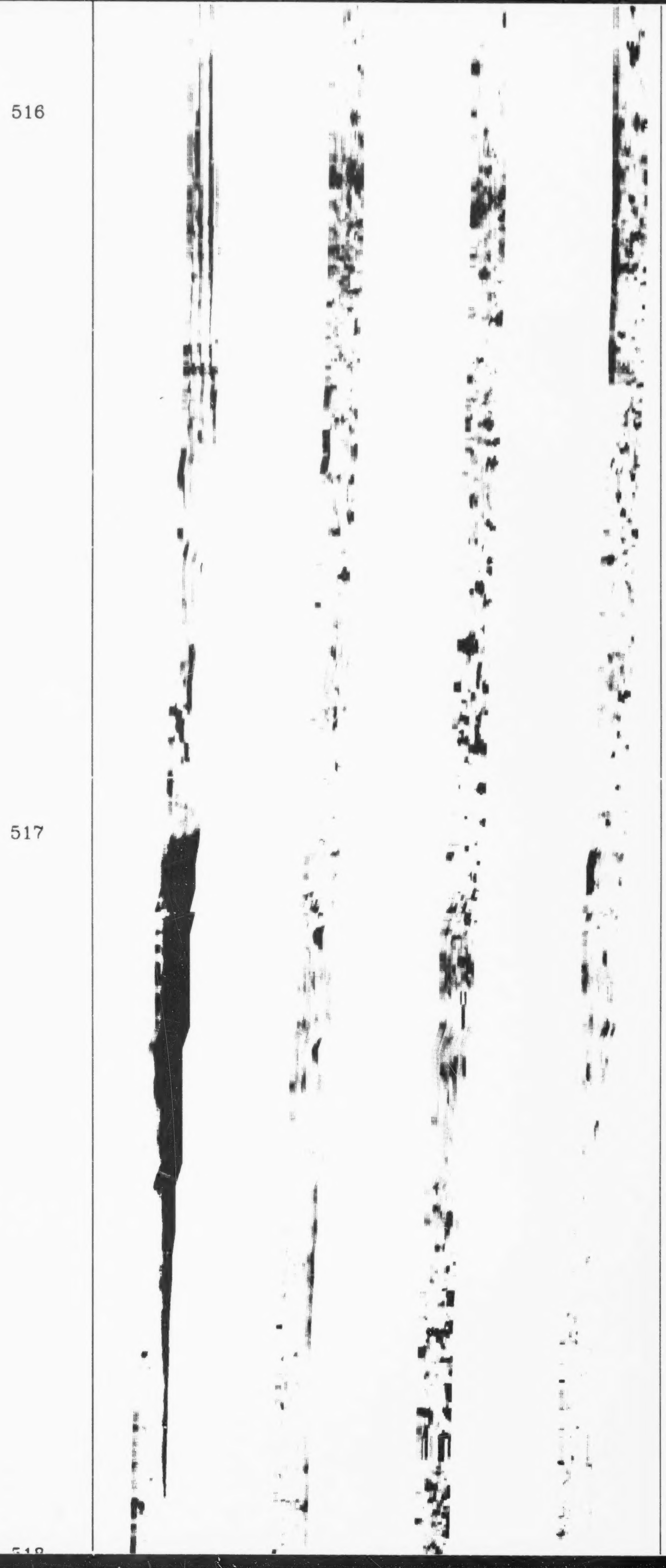
516
517

519
520

SCHLUMBERGER

FMS
BOREHOLE
IMAGING

COMPANY	LAMONT DOHERTY
WELL	ODP HOLE 803D
FIELD	ONTONG JAVA PLATEAU
COUNTRY	LEG 130
RUN	1
DATE LOGGED	05 – FEB – 90
REFERENCE	STATIC PS 1 520 560

STATIC NORMALIZATION
PASS 1 (LAMON)
FILE : MEST.001

ZONE FROM 560.0 M TO 520.0 M
DEPTH SCALE = 1/ 5
IMAGE SCALE = 1/ 5
BITSIZE = 9.88

ORIENTATION

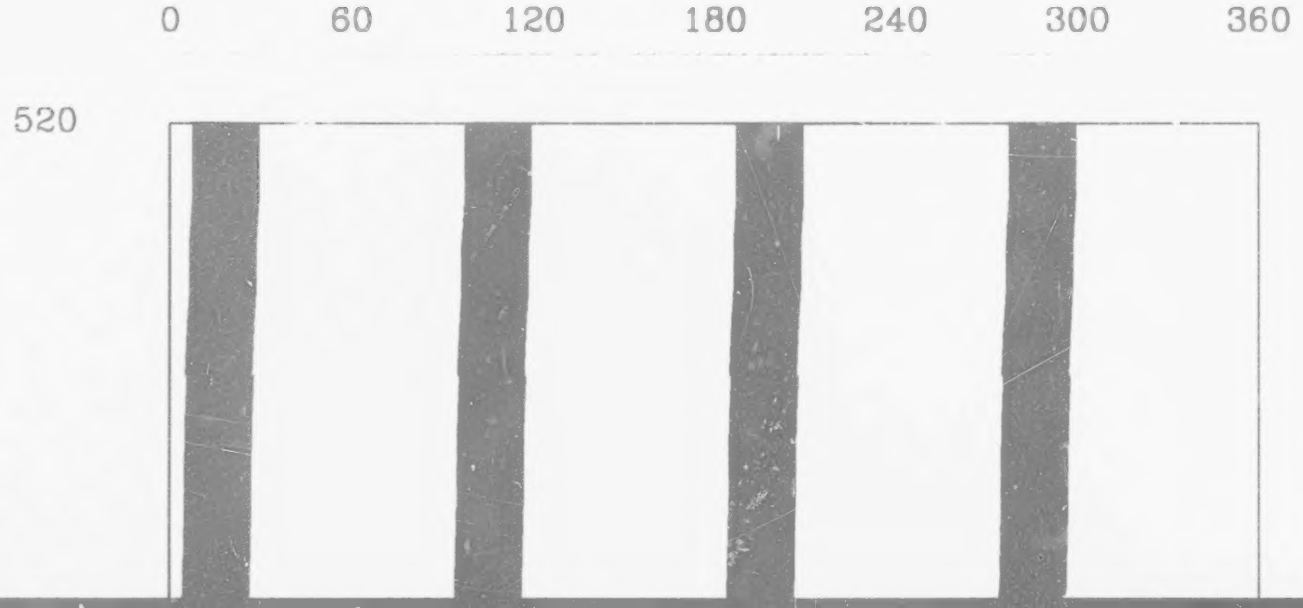

525
526

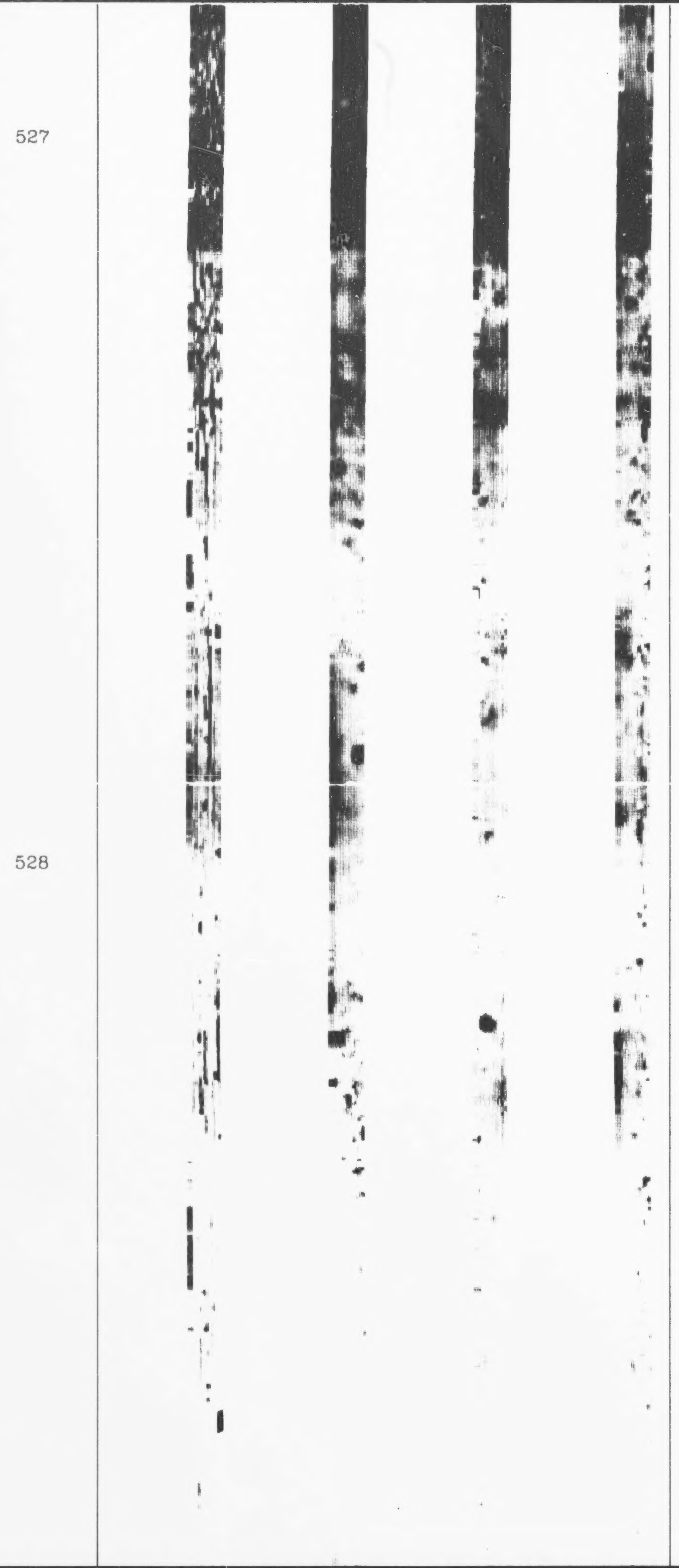
527
528

529
530
531

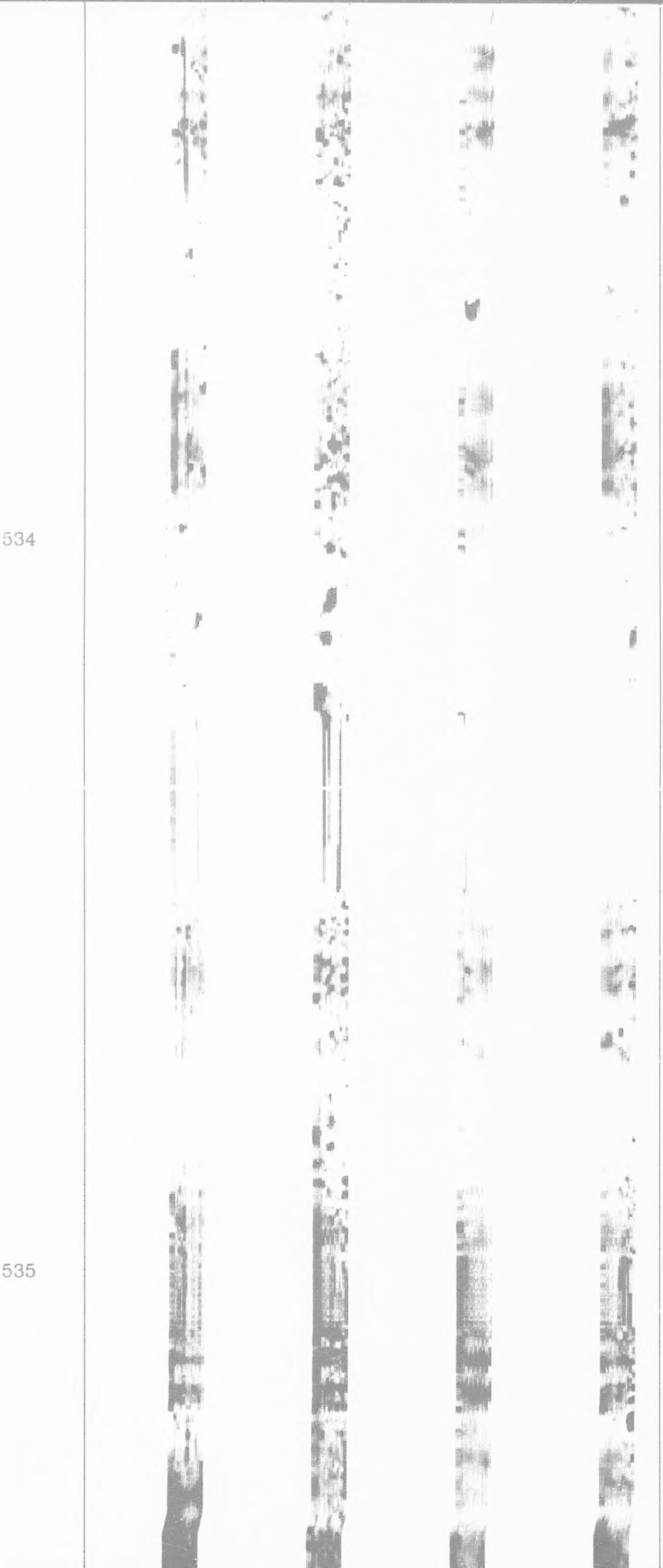
534
535

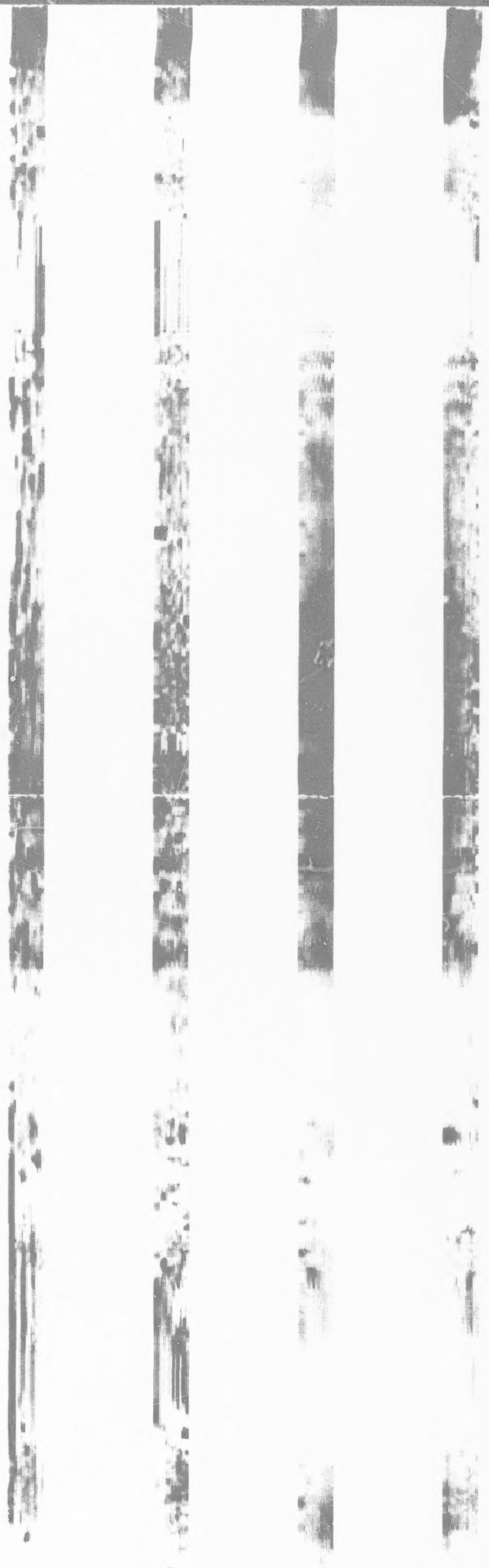
536
537

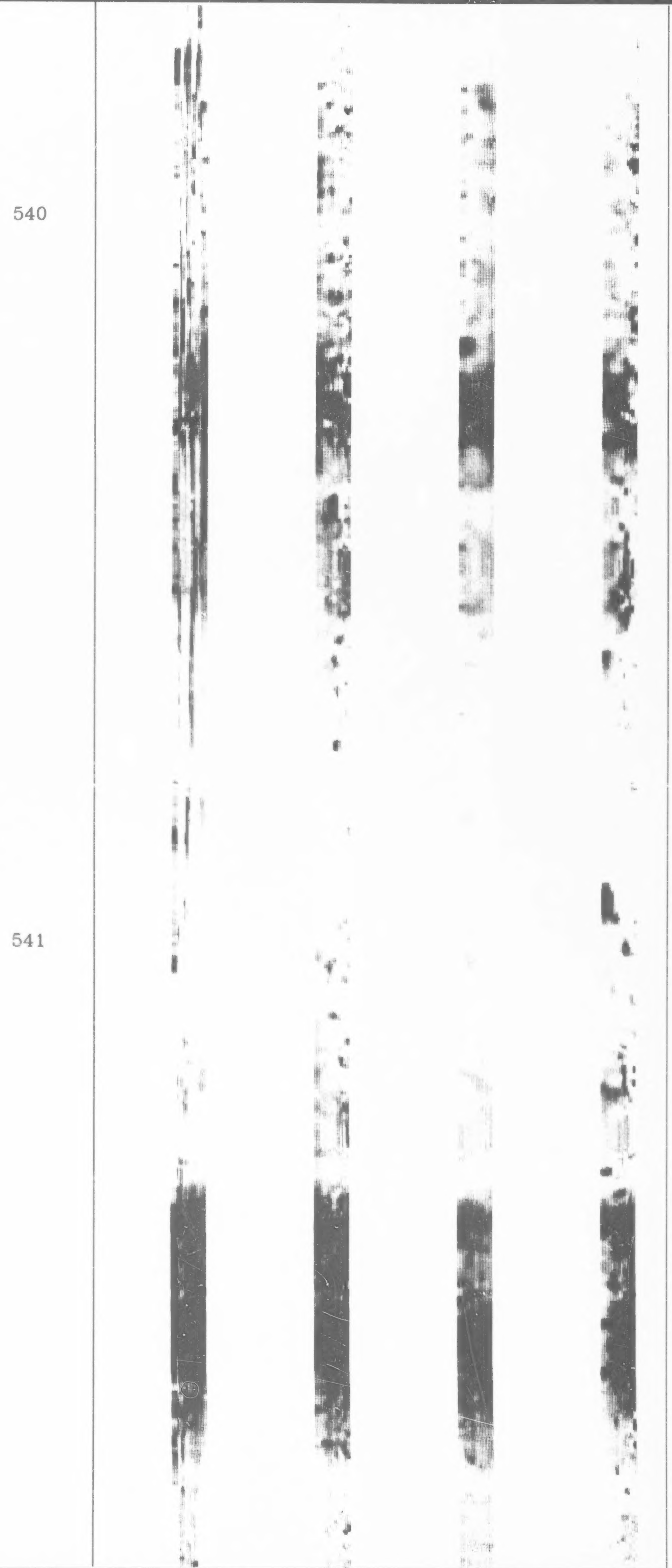
540
541

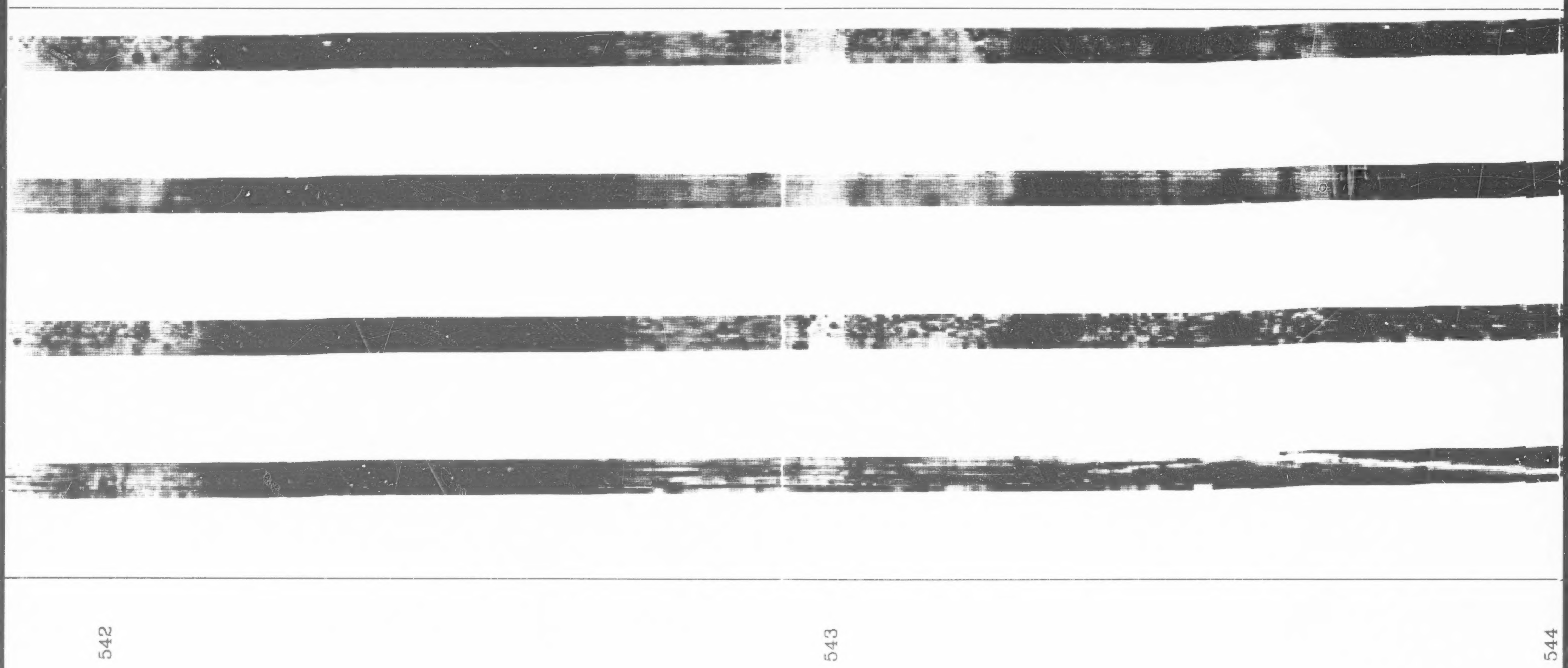
542
543
544

551

552

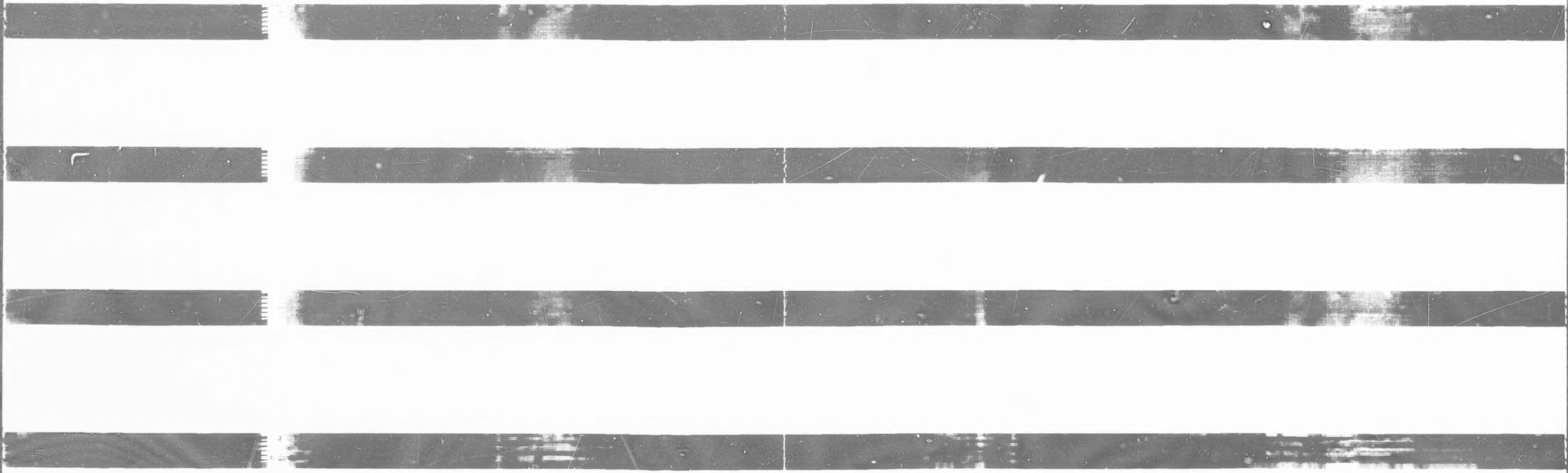

553

554

555

556

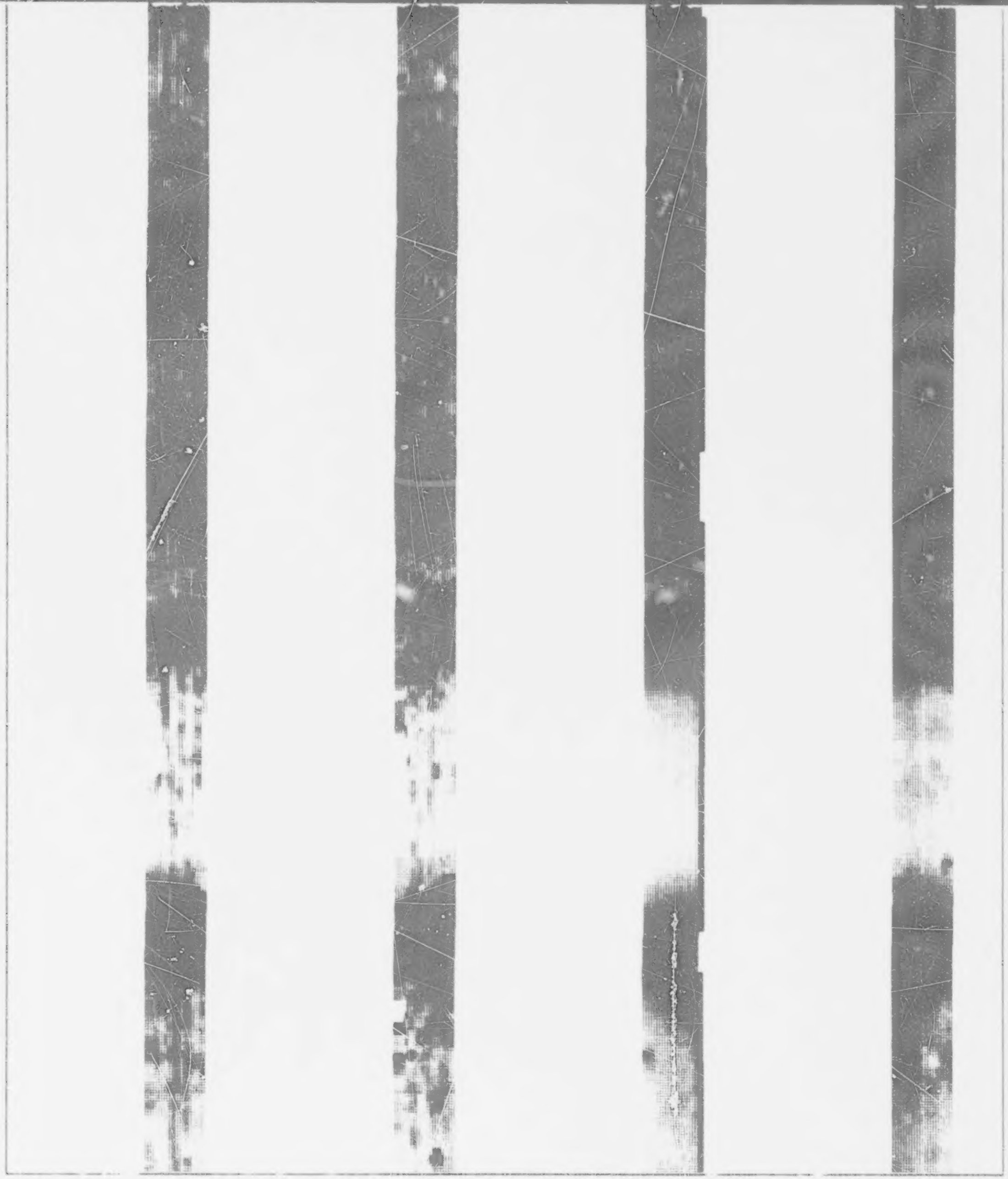

SCHLUMBERGER

FMS
BOREHOLE
IMAGING

COMPANY	LAMONT DOHERTY
WELL	ODP HOLE 803D
FIELD	ONTONG JAVA PLATEAU
COUNTRY	LEG 130
RUN	1
DATE LOGGED	05 – FEB – 90
REFERENCE	STATIC PS 1 560-600

STATIC NORMALIZATION

PASS 1 (LAMON)

FILE : MEST.001

ZONE FROM 600.0 M TO 560.0 M

DEPTH SCALE = 1/ 5

IMAGE SCALE = 1/ 5

BITSIZE = 9.88

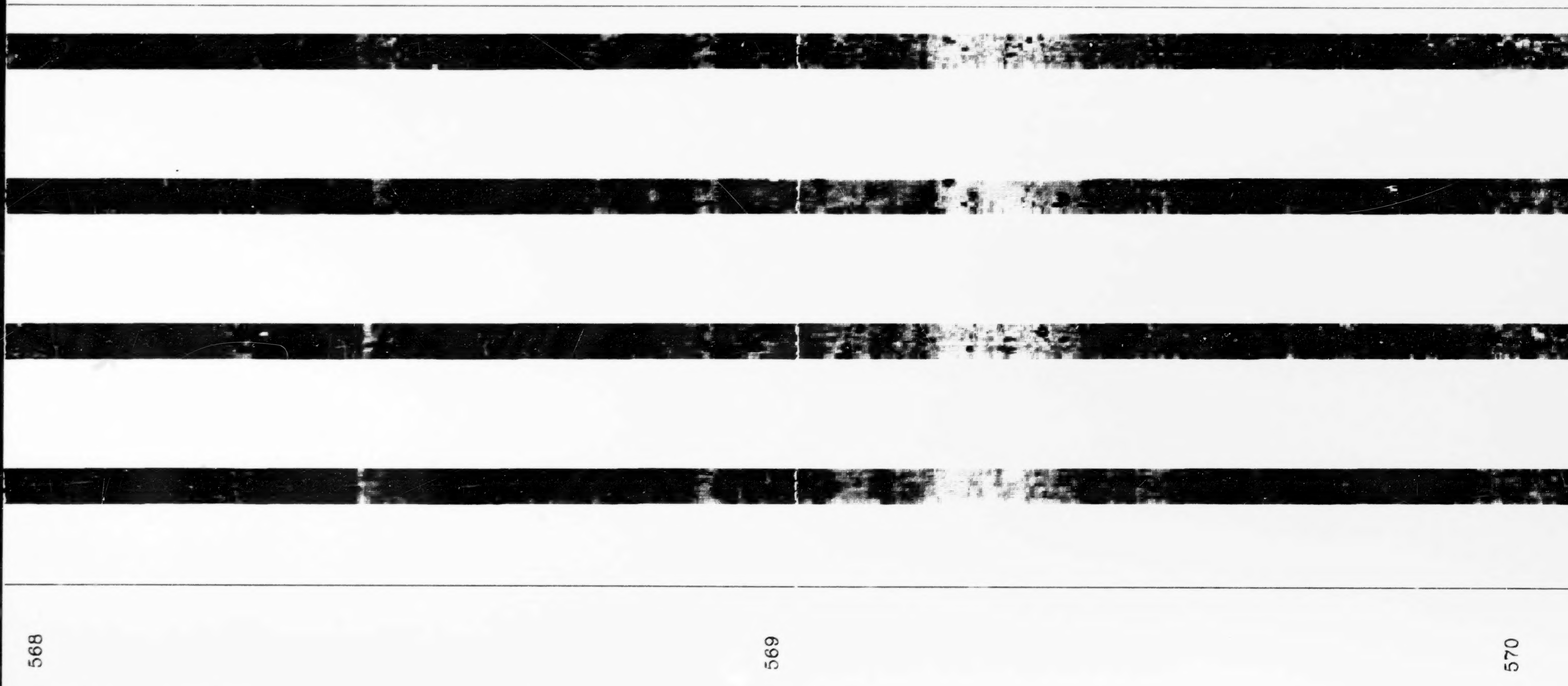

568
569
570

571

572

577

578

579

580

581

582

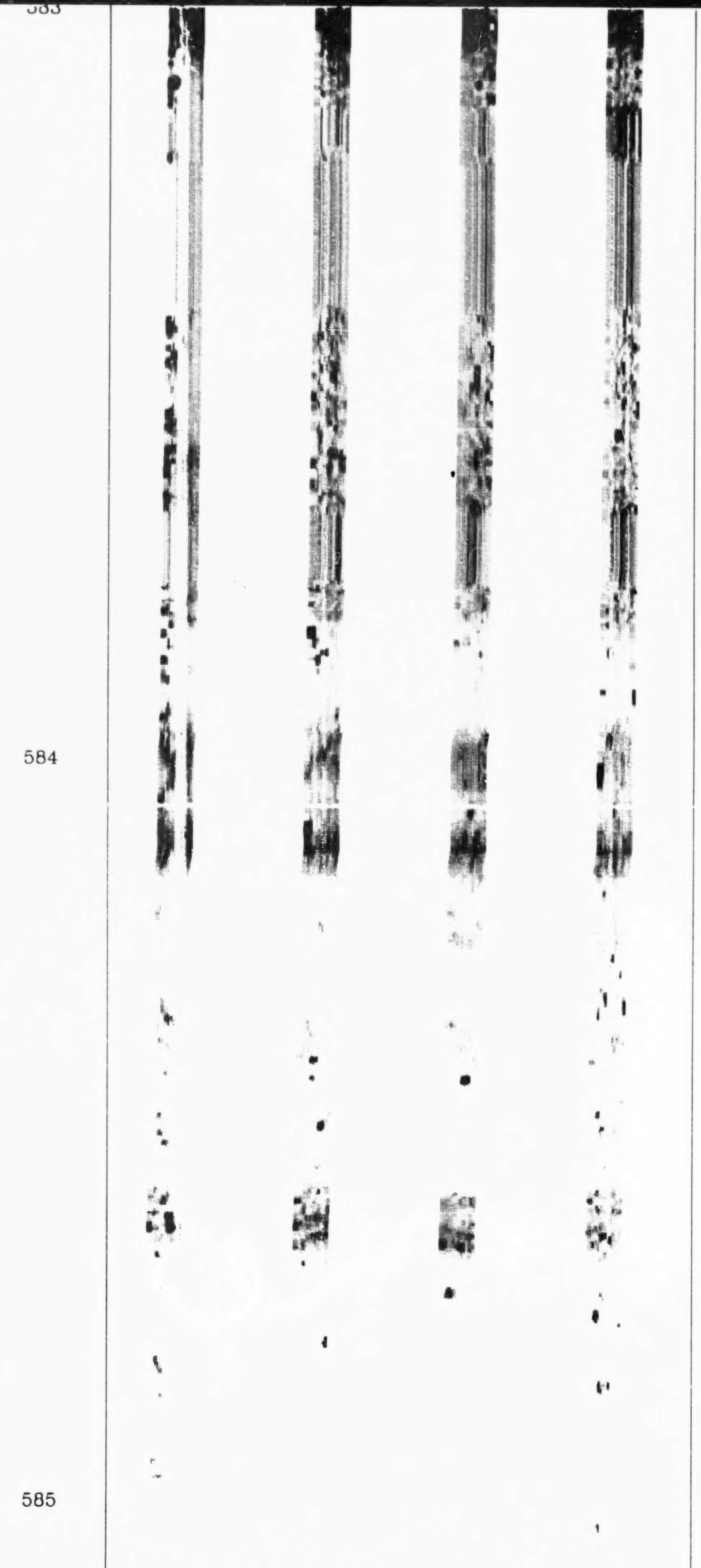
584
585

586

587

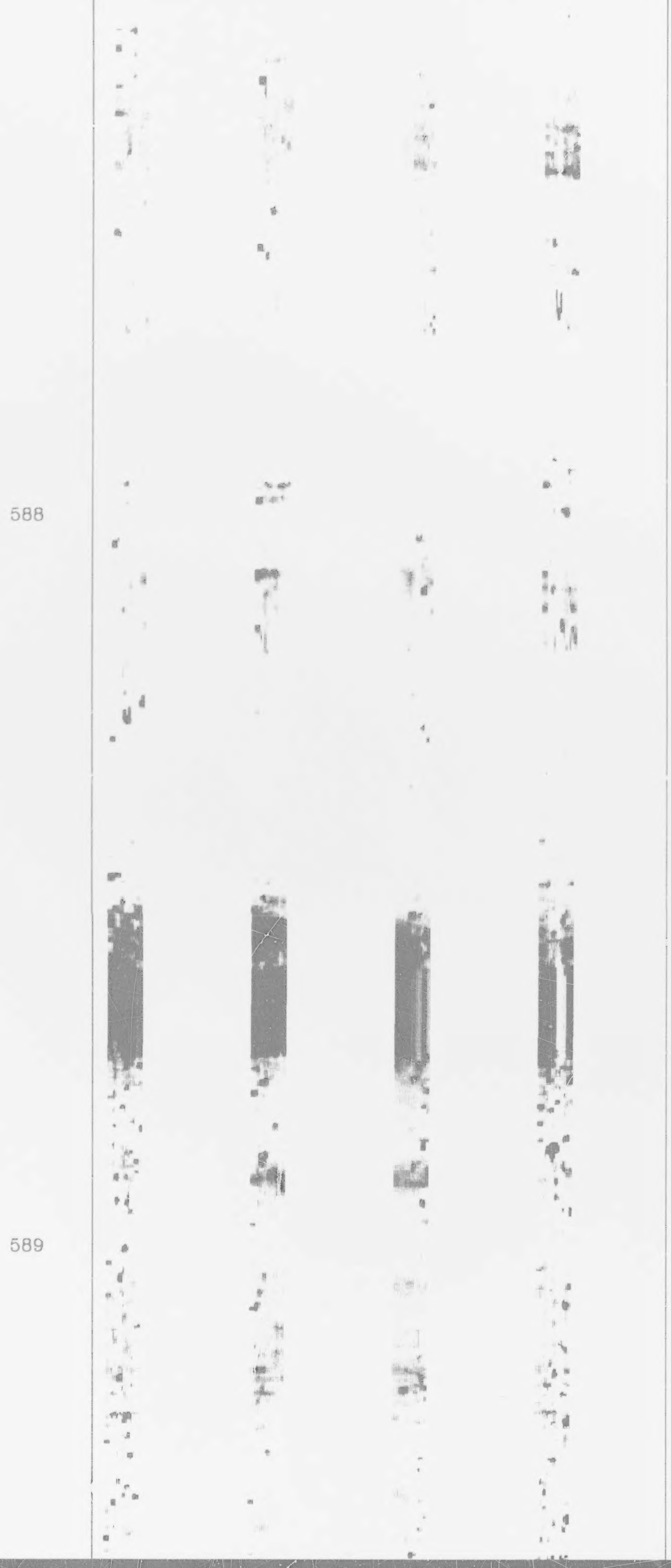
588
589

590 [illegible]

591 [illegible]

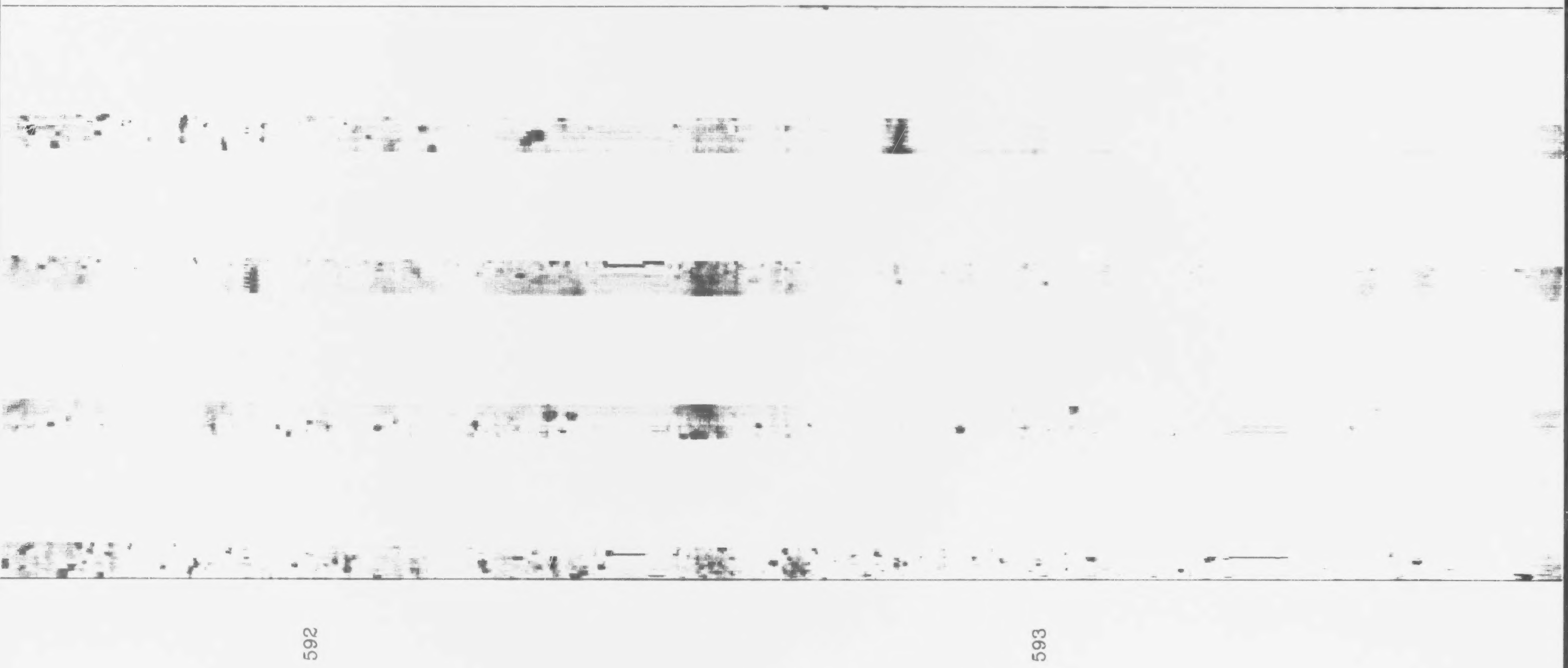
592
593

594
595

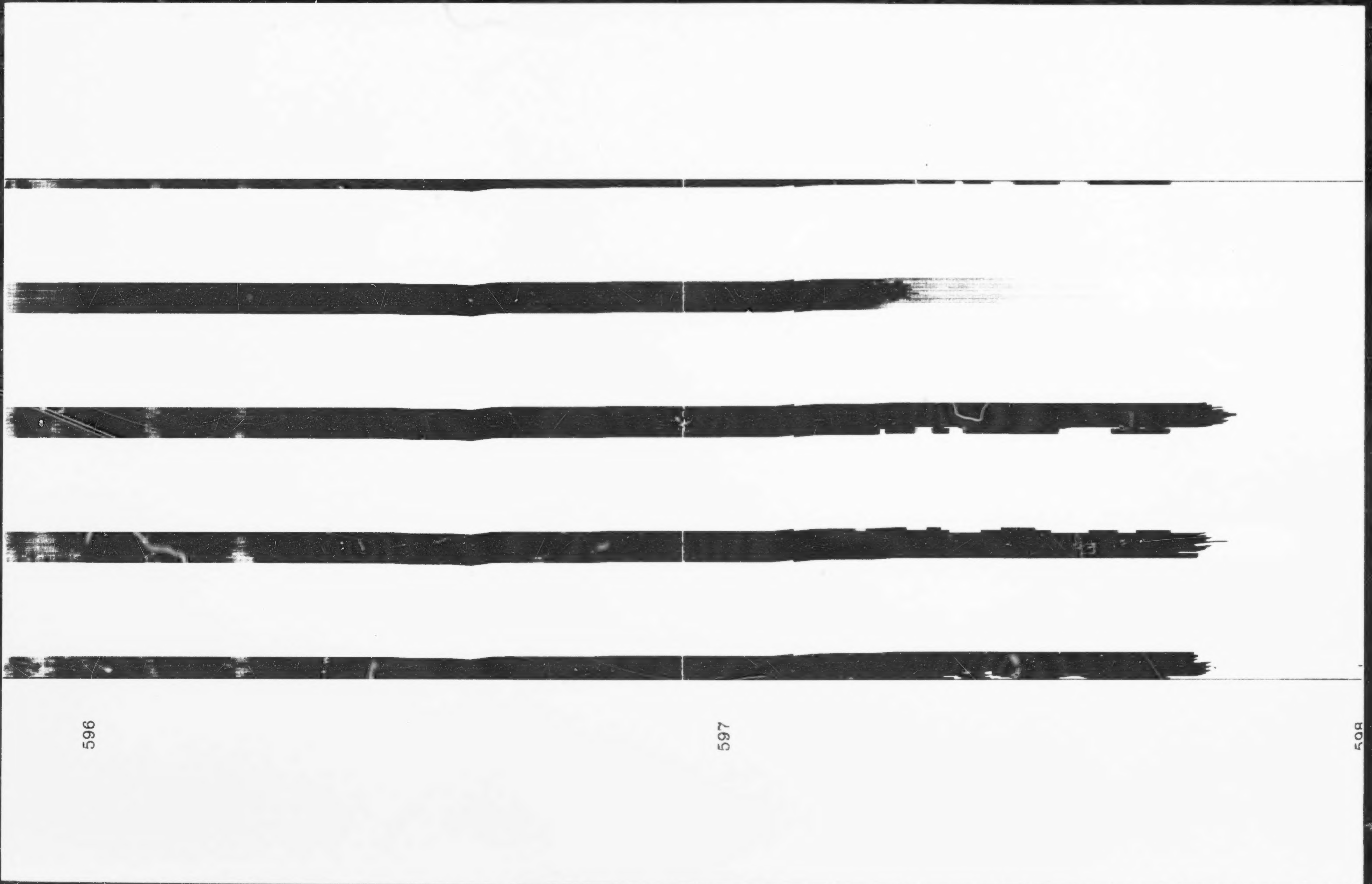
596
597
598

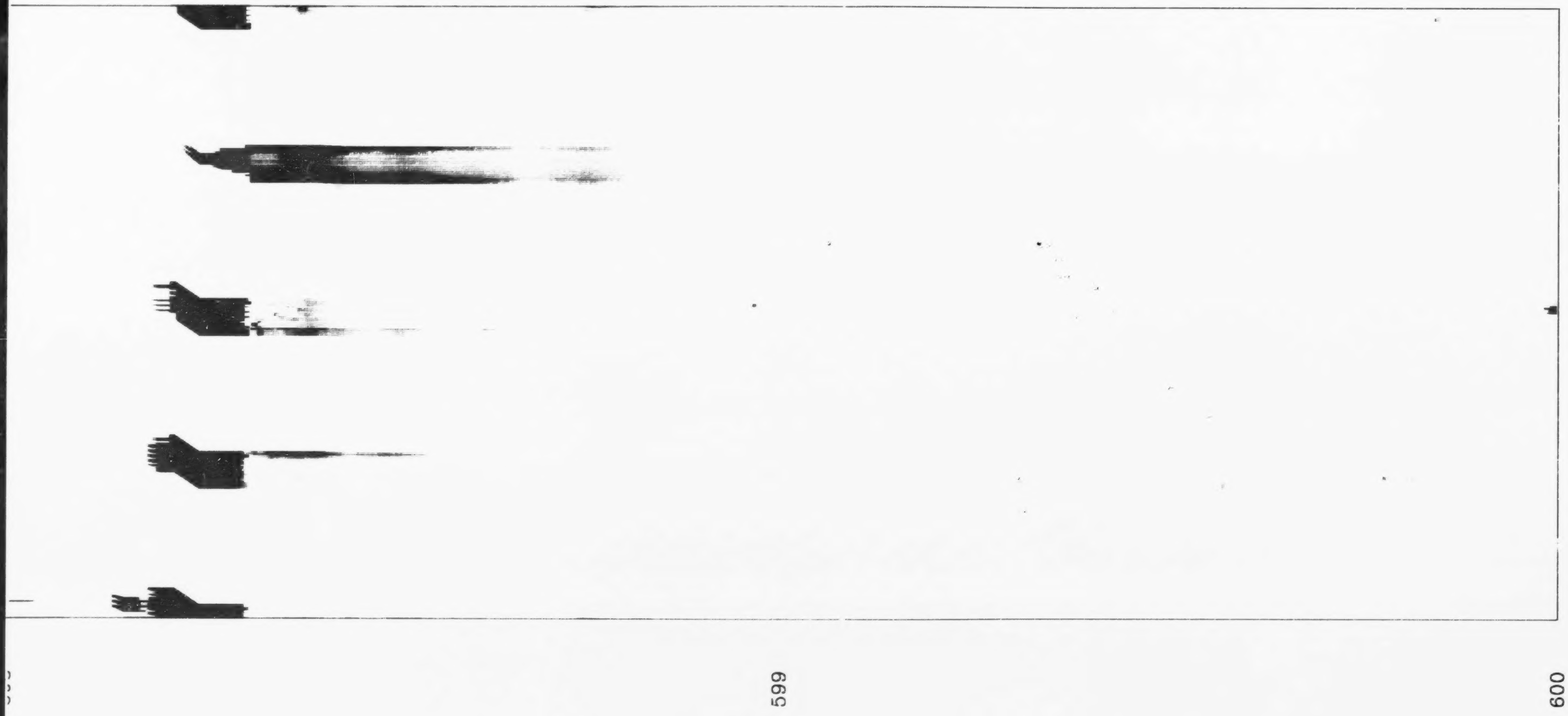
599
600

SCHLUMBERGER

FMS
BOREHOLE
IMAGING

COMPANY	LAMONT DOHERTY
WELL	ODP HOLE 803D
FIELD	ONTONG JAVA PLATEAU
COUNTRY	LEG 130
RUN	1
DATE LOGGED	05 FEB 90
REFERENCE	STATIC PS 1 600 ~~615~~ 611.2

STATIC NORMALIZATION
PASS 1 (LAMON)
FILE : MEST.001

ZONE FROM 611.3 M TO 600.0 M
DEPTH SCALE = 1/ 5
IMAGE SCALE = 1/ 5
BITSIZE = 9.88

ORIENTATION

601

602

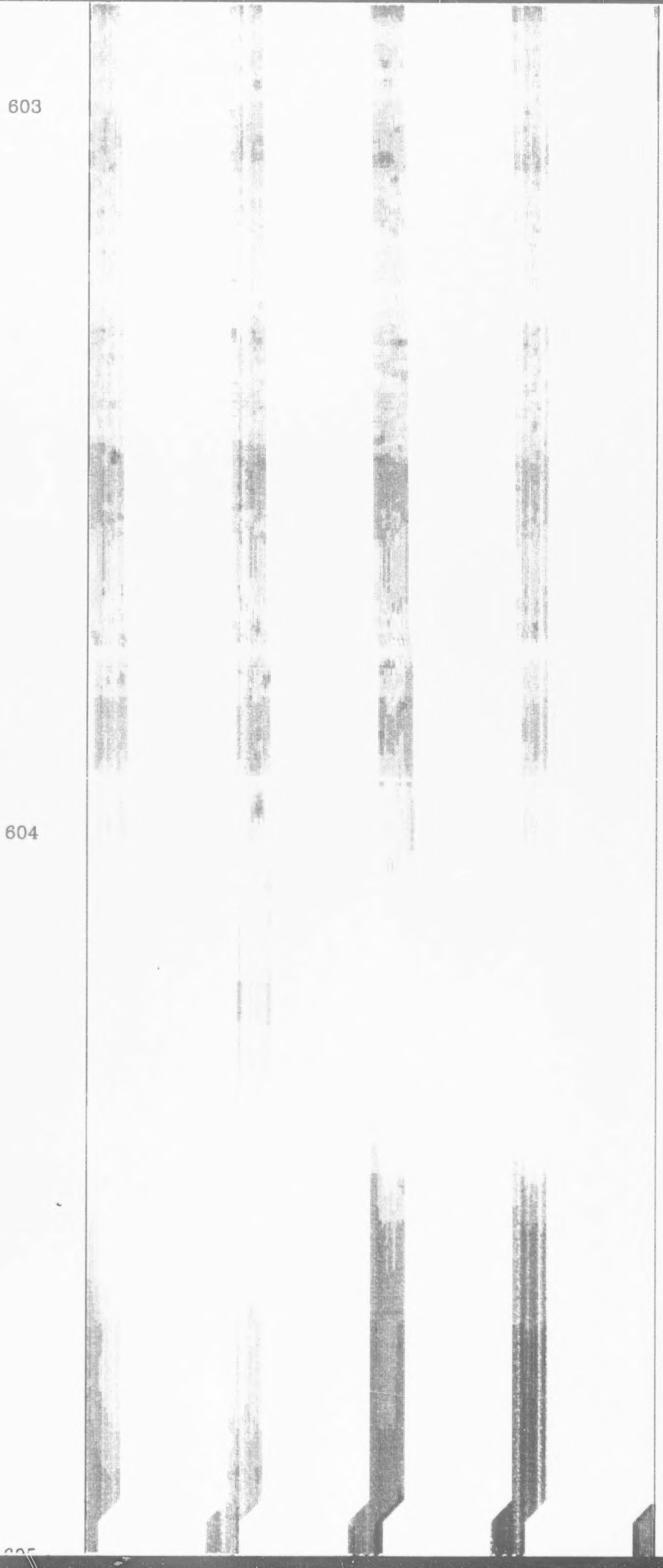
603
604

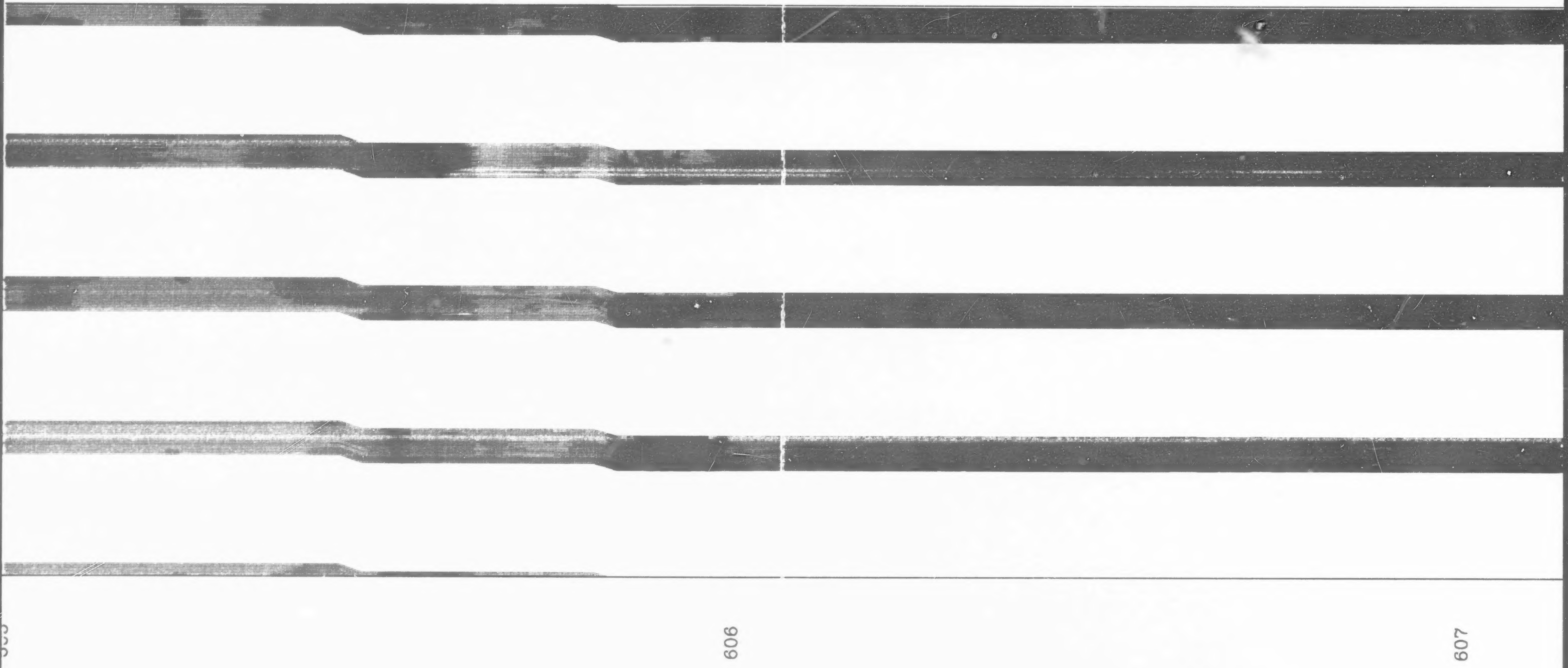
606
607

807-C
MAIN LOG
(PASS 2)

1097-1504
MBSF

Advanced Images, INC.
Rt 22 West Round Valley Plaza
Lebanon, N.J. 08833

SCHLUMBERGER

FMS
BOREHOLE
IMAGING

COMPANY	LAMONT DOHERTY
WELL	ODP HOLE 807-C
FIELD	ONTONG JAVA PLATEAU
COUNTRY	LEG 130
RUN	RUN 2
DATE LOGGED	21 - MAR - 90
REFERENCE	STATIC PASS -2 1138-1097

STATIC NORMALIZATION
PASS– (23761)
FILE : MEST.004

ZONE FROM 1138.0 M TO 1097.2 M
DEPTH SCALE = 1/ 5
IMAGE SCALE = 1/ 5
BITSIZE = 9.88

ORIENTATION

0 60 120 180 240 300 360

1098
1099

[illegible]

[illegible]

[illegible]

[illegible]

[illegible]

1100

1101

[redacted]

[redacted]

1104 [illegible]

1105 [illegible]

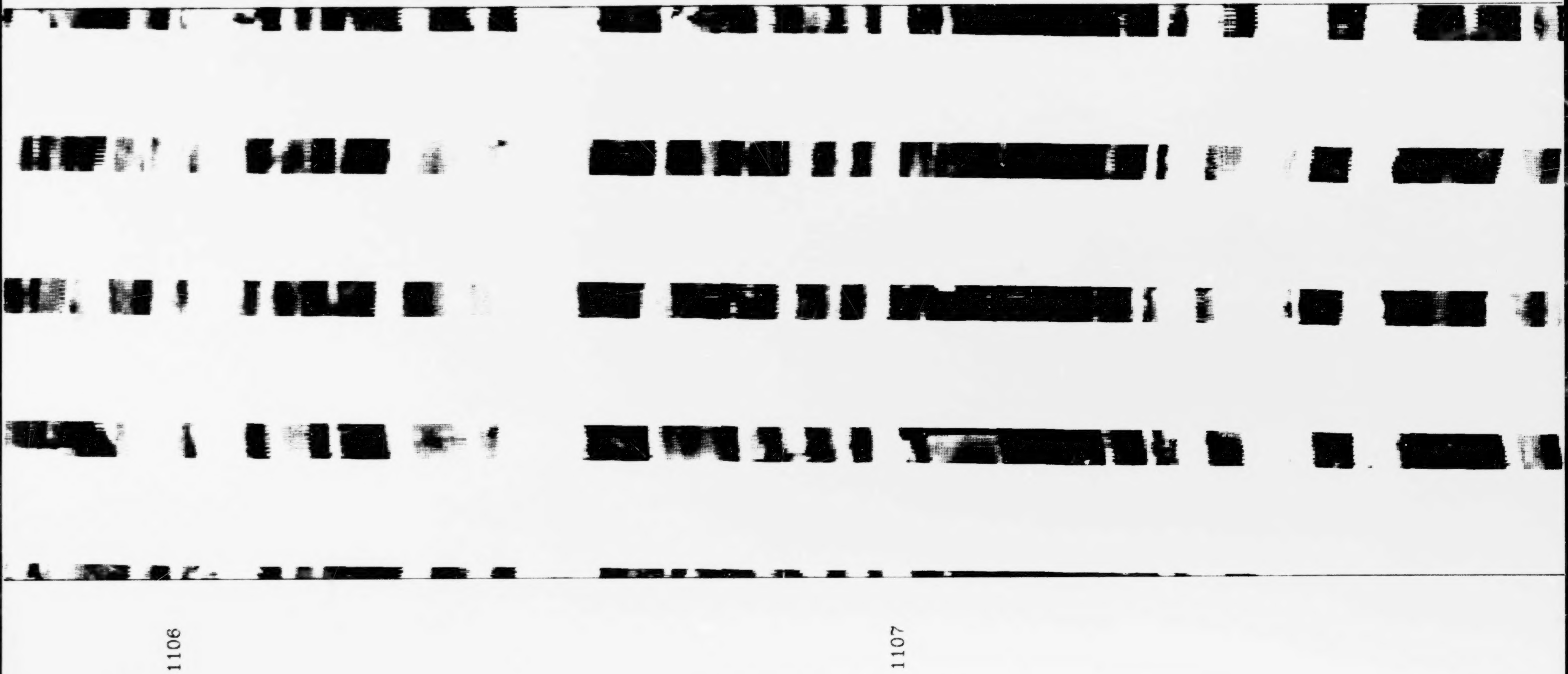
1106
1107

1108

1109

1110

[redacted]

[redacted]

[redacted]

[redacted]

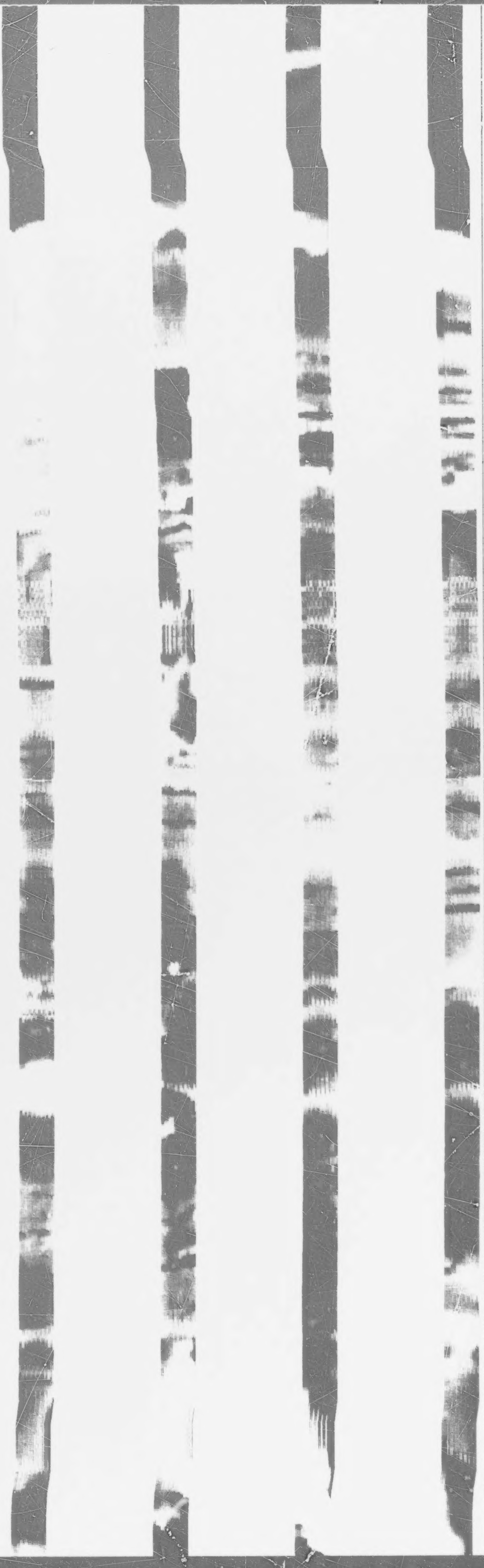
1111
1112

1113

1114

[redacted]

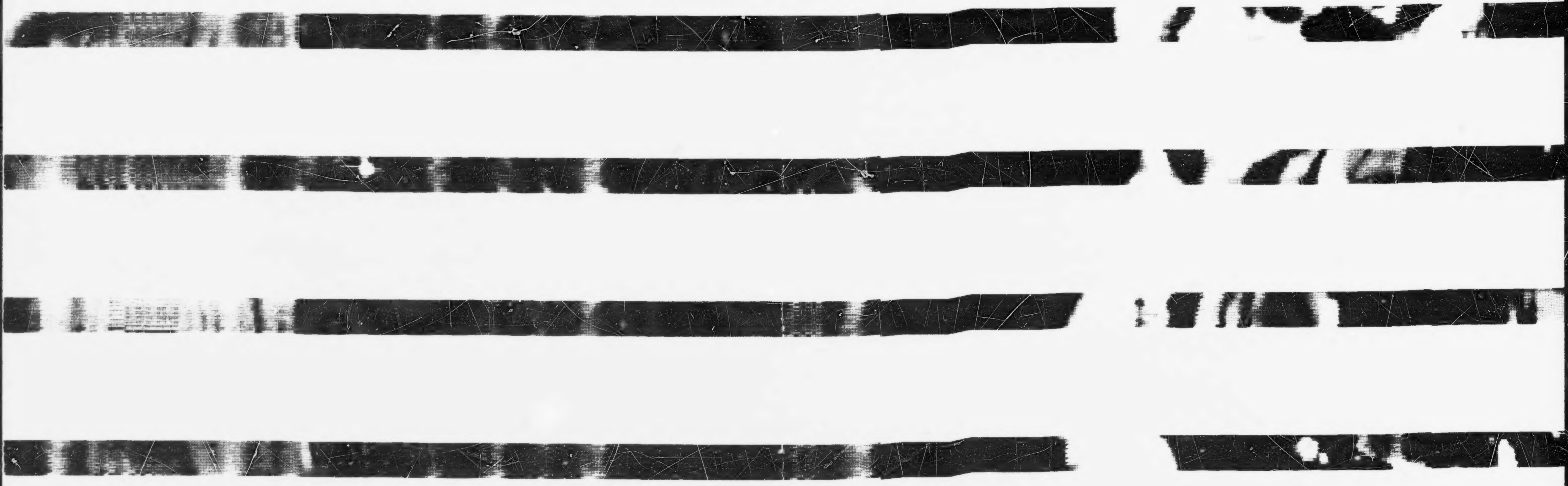

1117

1118

[redacted]

1119

1120

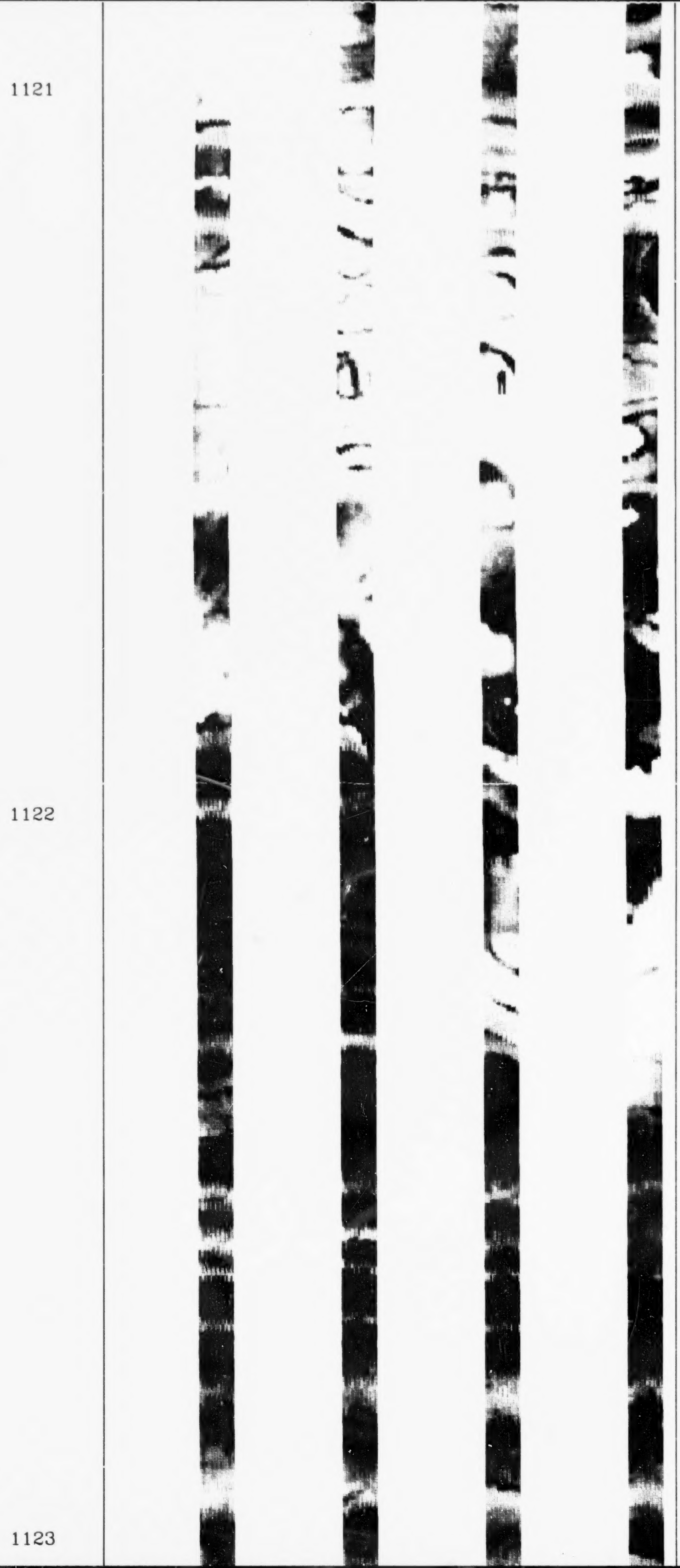
1121
1122
1123

1124
1125

1126 [illegible]

1127 [illegible]

1128
1129

1130

1131

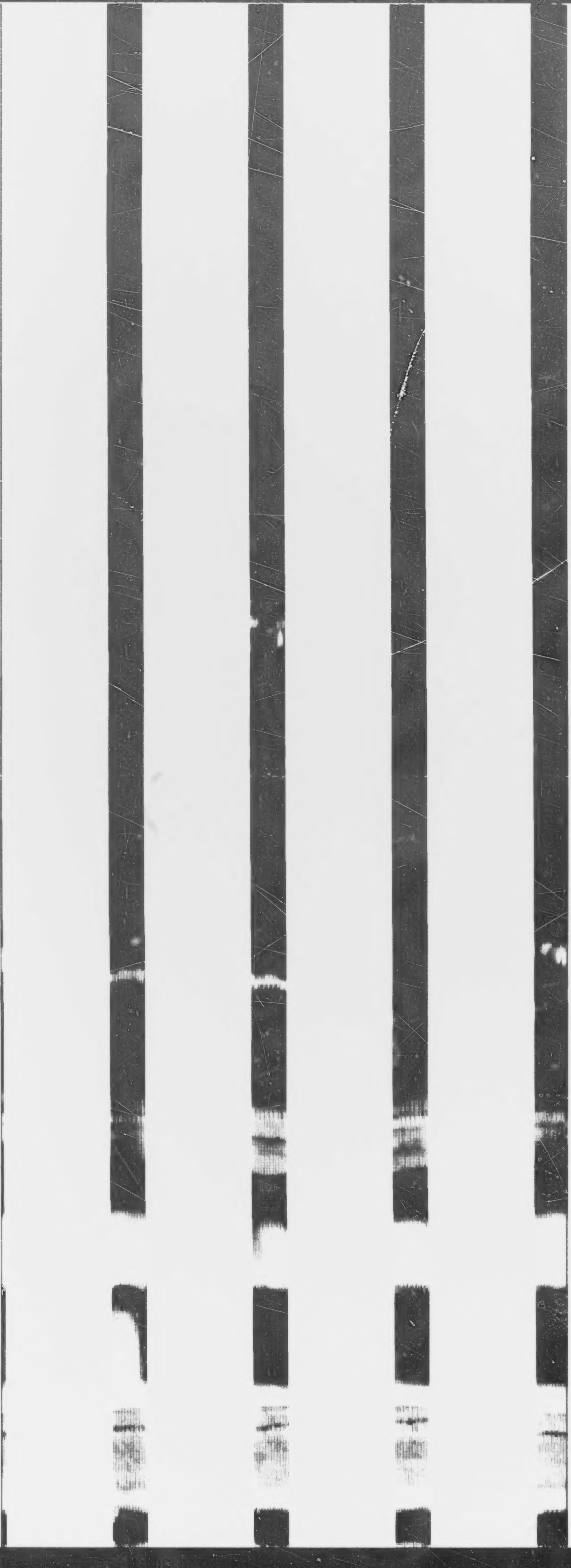

1132

1133

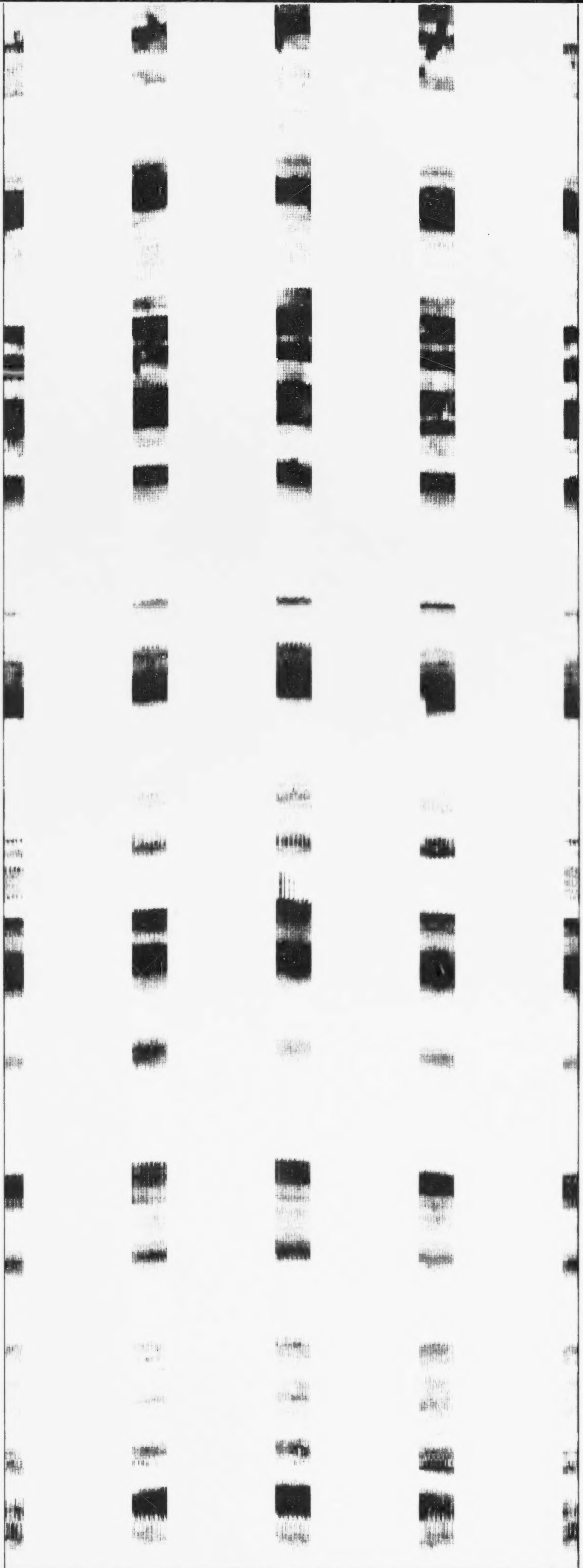
1134
1135

1136
1137
1138

SCHLUMBERGER

FMS
BOREHOLE
IMAGING

COMPANY	LAMONT DOHERTY
WELL	ODP HOLE 807-C
FIELD	ONTONG JAVA PLATEAU
COUNTRY	LEG 130
RUN	RUN 2
DATE LOGGED	21 – MAR – 90
REFERENCE	STATIC PASS-2 1179-1138

STATIC NORMALIZATION
PASS-2 (23761)
FILE : MEST.004

ZONE FROM 1179.0 M TO 1138.2 M
DEPTH SCALE = 1/ 5
IMAGE SCALE = 1/ 5
BITSIZE = 9.88

ORIENTATION

0 60 120 180 240 300 360

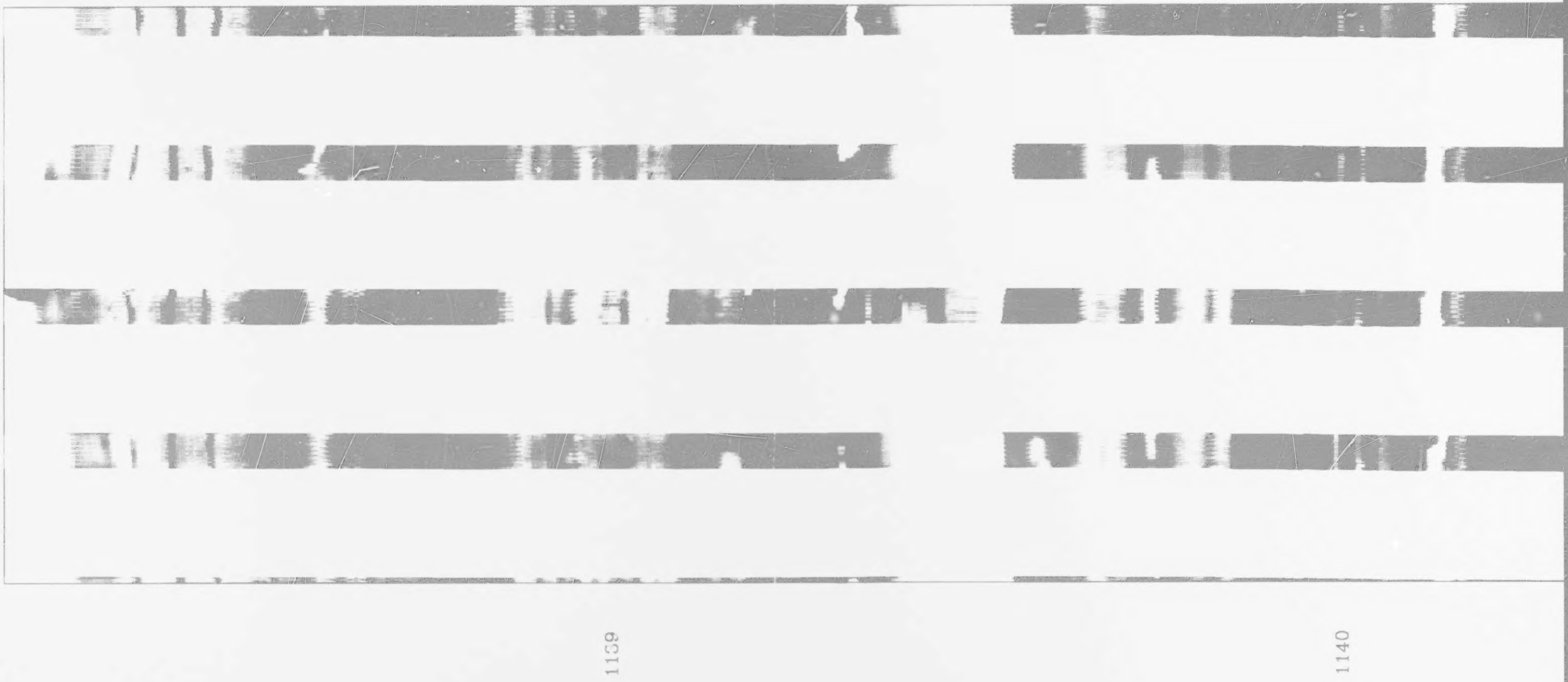
1139
1140

1141

1142

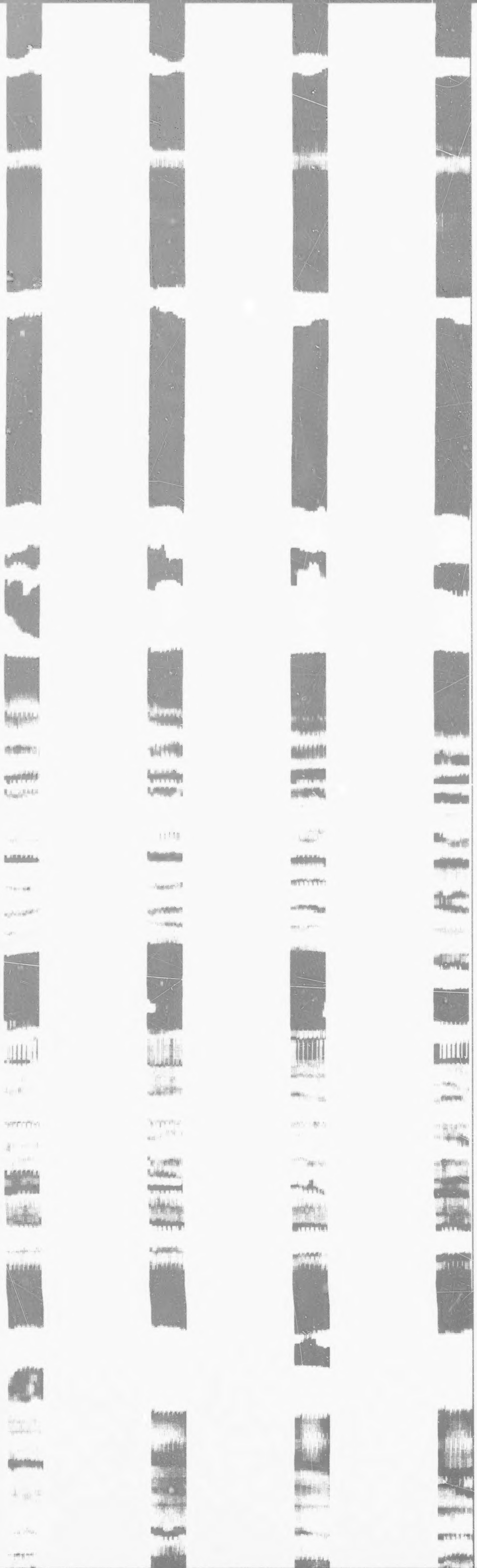

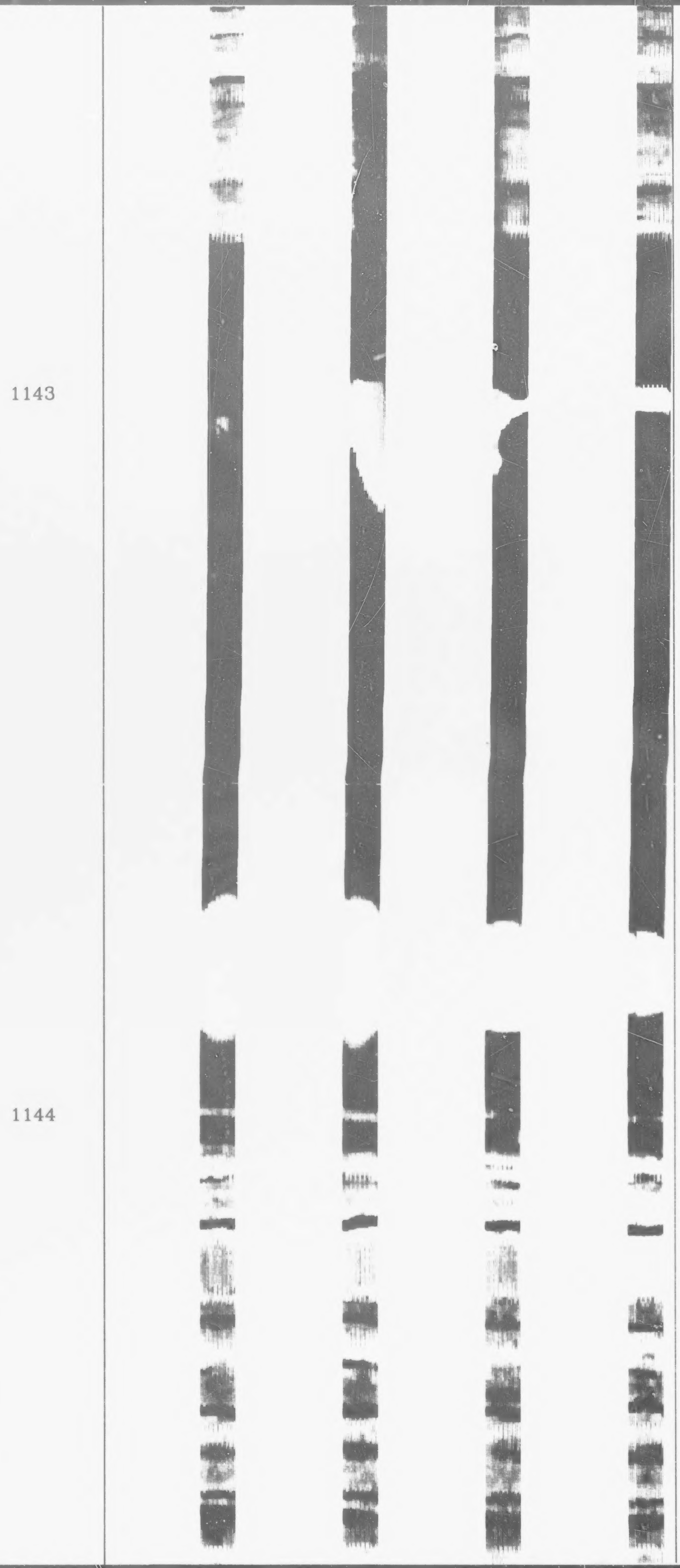
1143
1144

1145

1146

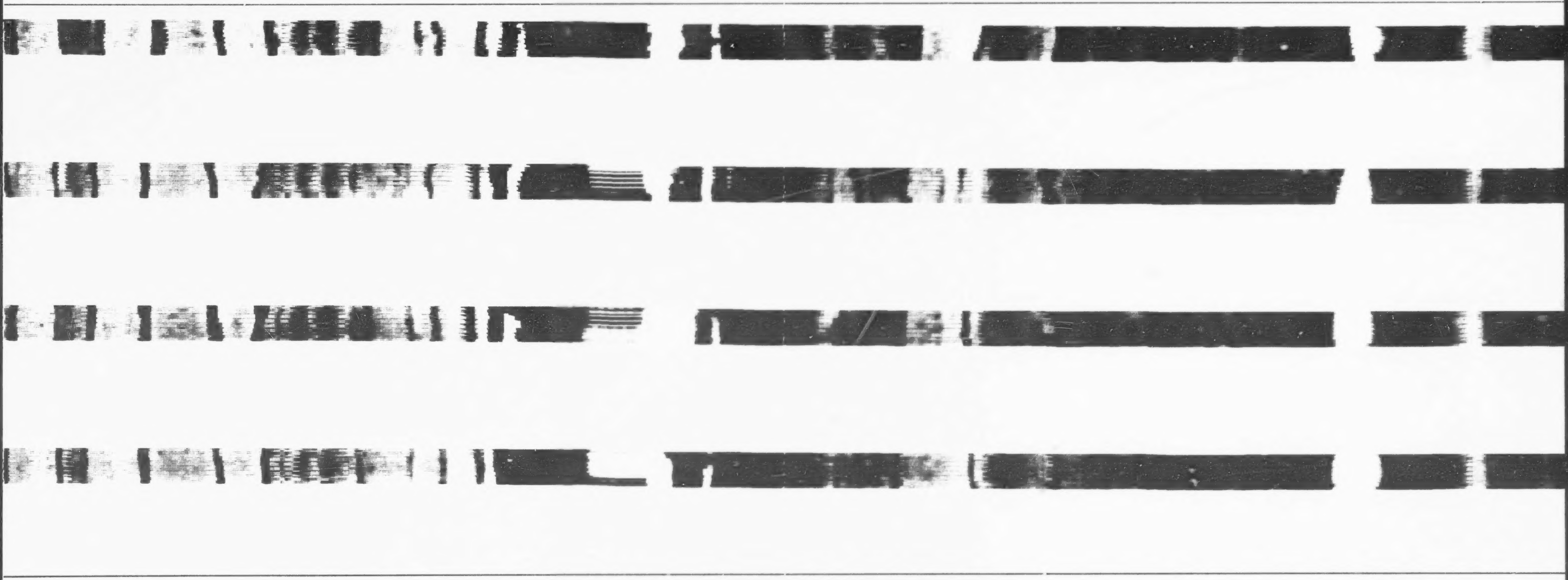
1147
1148

1149
1150
1151

1152

[illegible]

1153

[illegible]

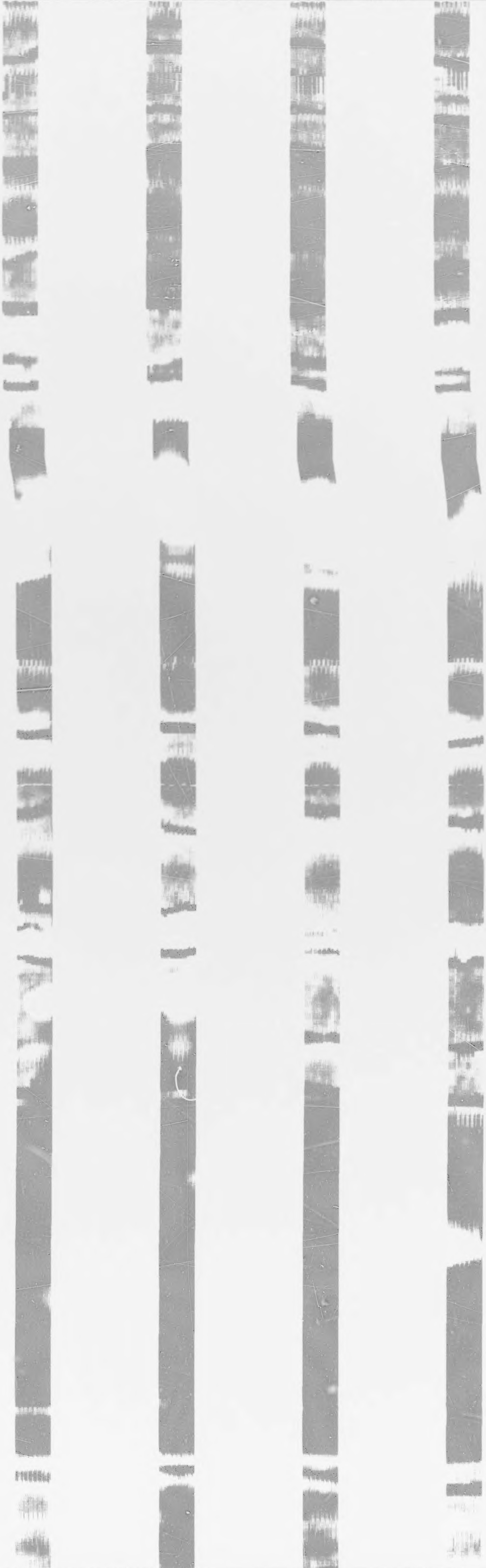
1154
1155

1158

[illegible]

1159

[illegible]

[redacted]

1160

1161

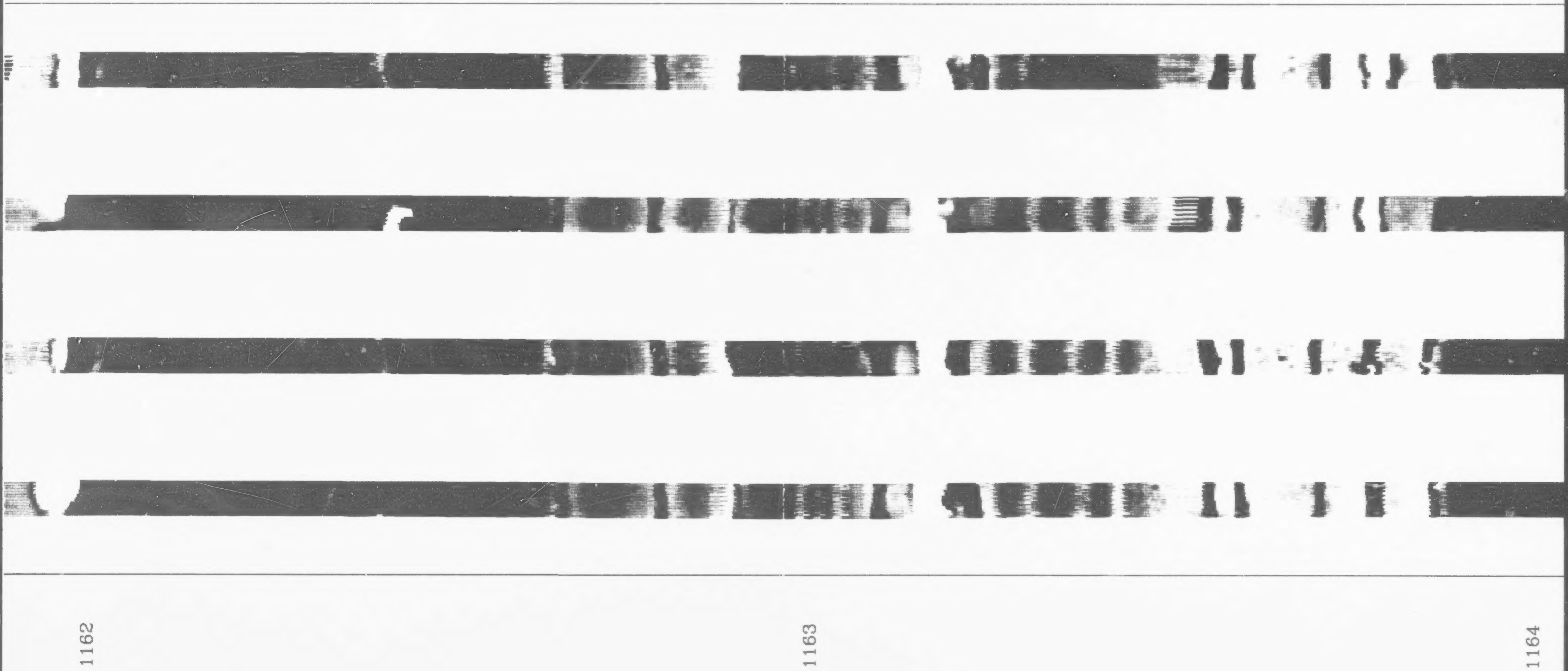
1162
1163
1164

1165
1166

1167

1168

1169

1170

[redacted]

[redacted]

1173

1174

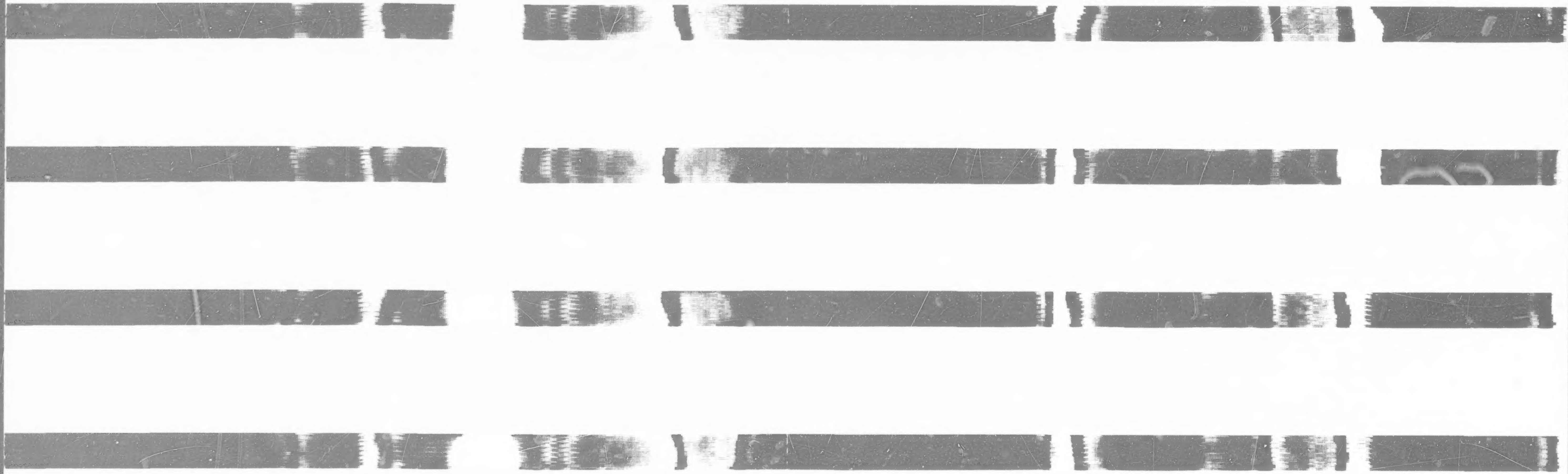

1175

1176

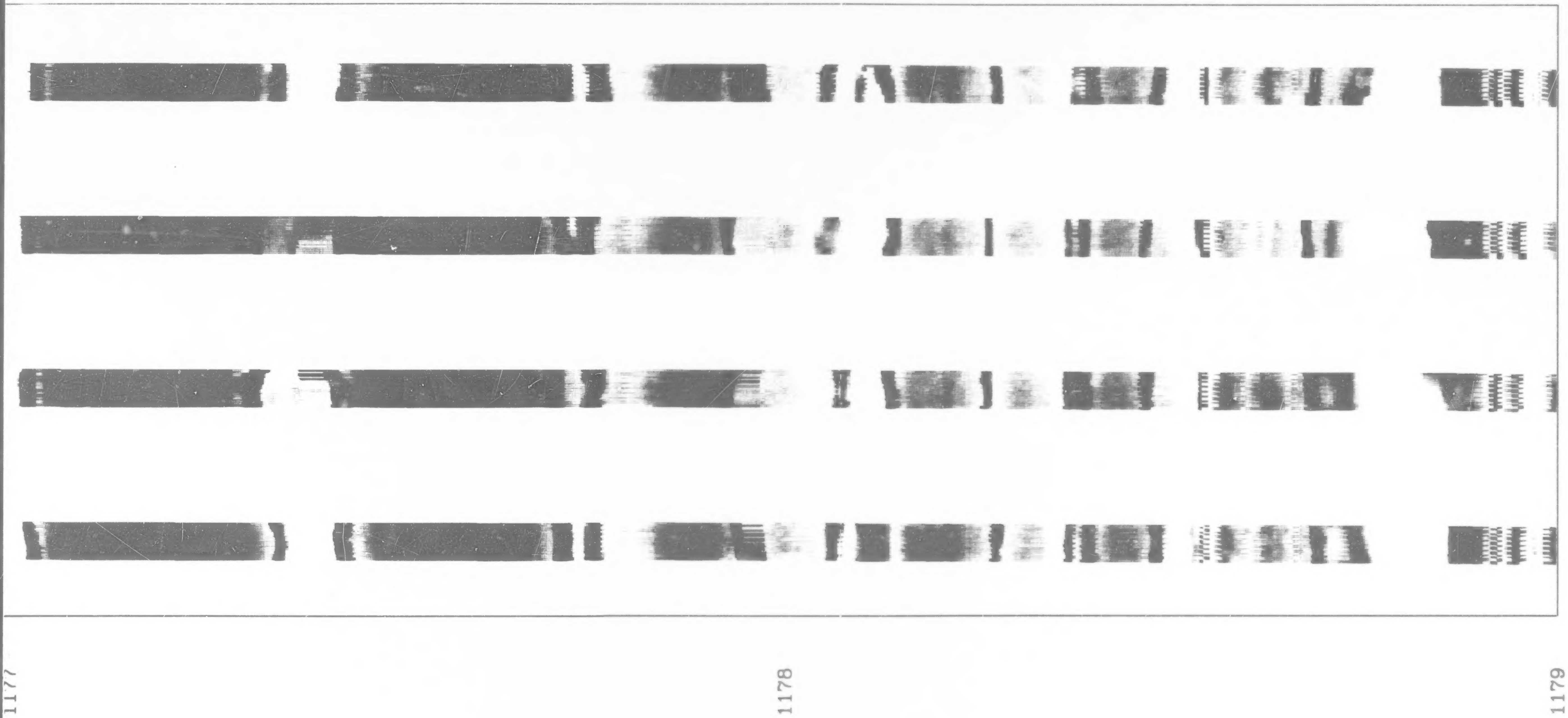
1177
1178
1179

SCHLUMBERGER

FMS
BOREHOLE
IMAGING

COMPANY	LAMONT DOHERTY
WELL	ODP HOLE 807-C
FIELD	ONTONG JAVA PLATEAU
COUNTRY	LEG 130
RUN	RUN 2
DATE LOGGED	21 – MAR – 90
REFERENCE	STATIC PASS-2 1220-1179

STATIC NORMALIZATION

PASS-2 (23761)

FILE : MEST.004

ZONE FROM 1220.0 M TO 1179.2 M

DEPTH SCALE = 1/ 5

IMAGE SCALE = 1/ 5

BITSIZE = 9.88

ORIENTATION

0 60 120 180 240 300 360

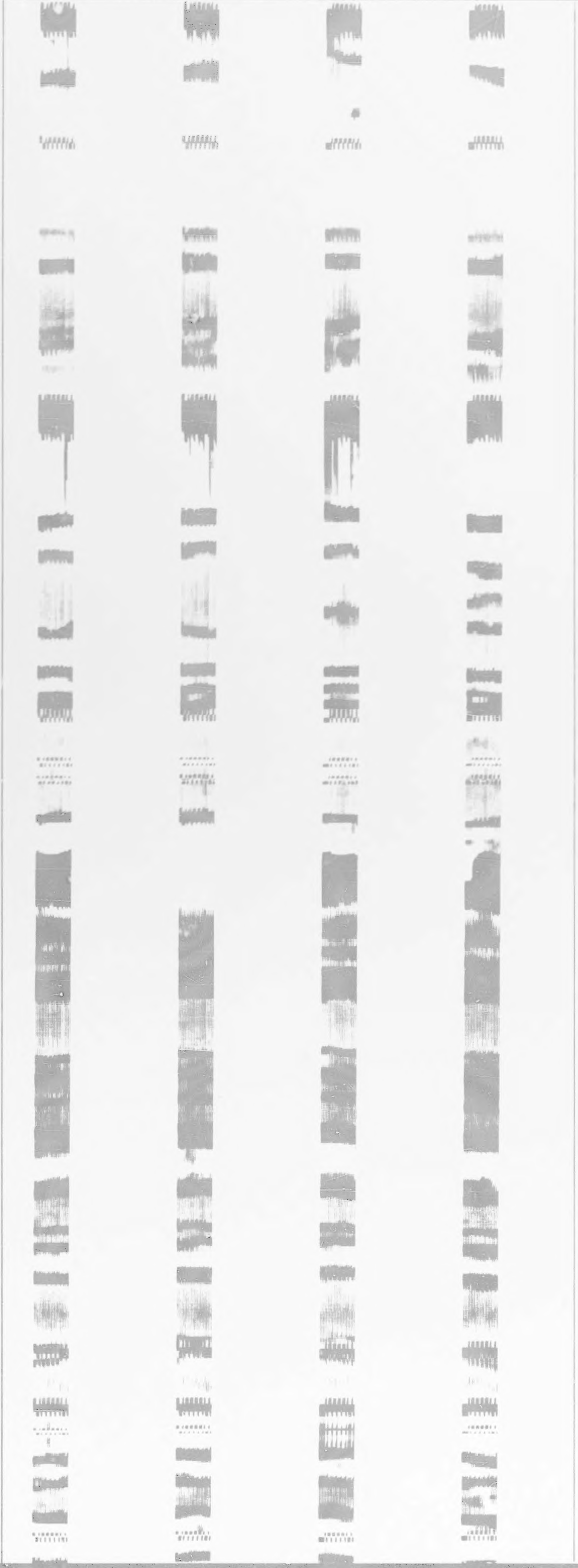
1182
1183

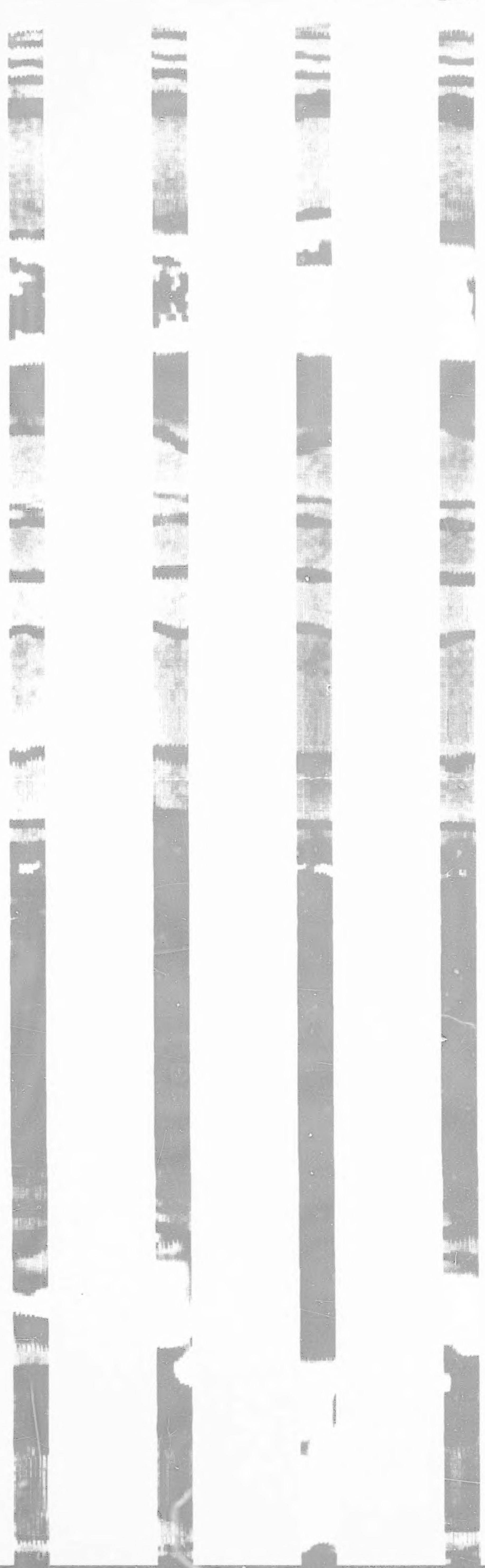
1184
1185

[redacted] [redacted] [redacted]

[redacted] [redacted] [redacted]

[redacted] [redacted] [redacted]

[redacted] [redacted] [redacted]

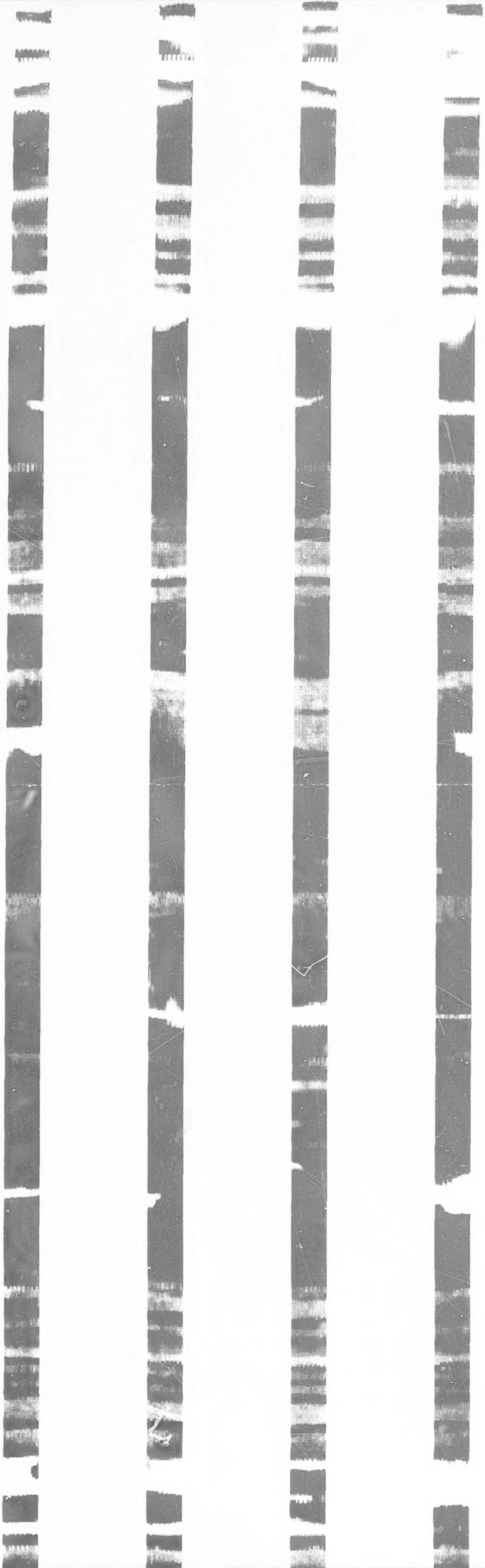
1188
1189

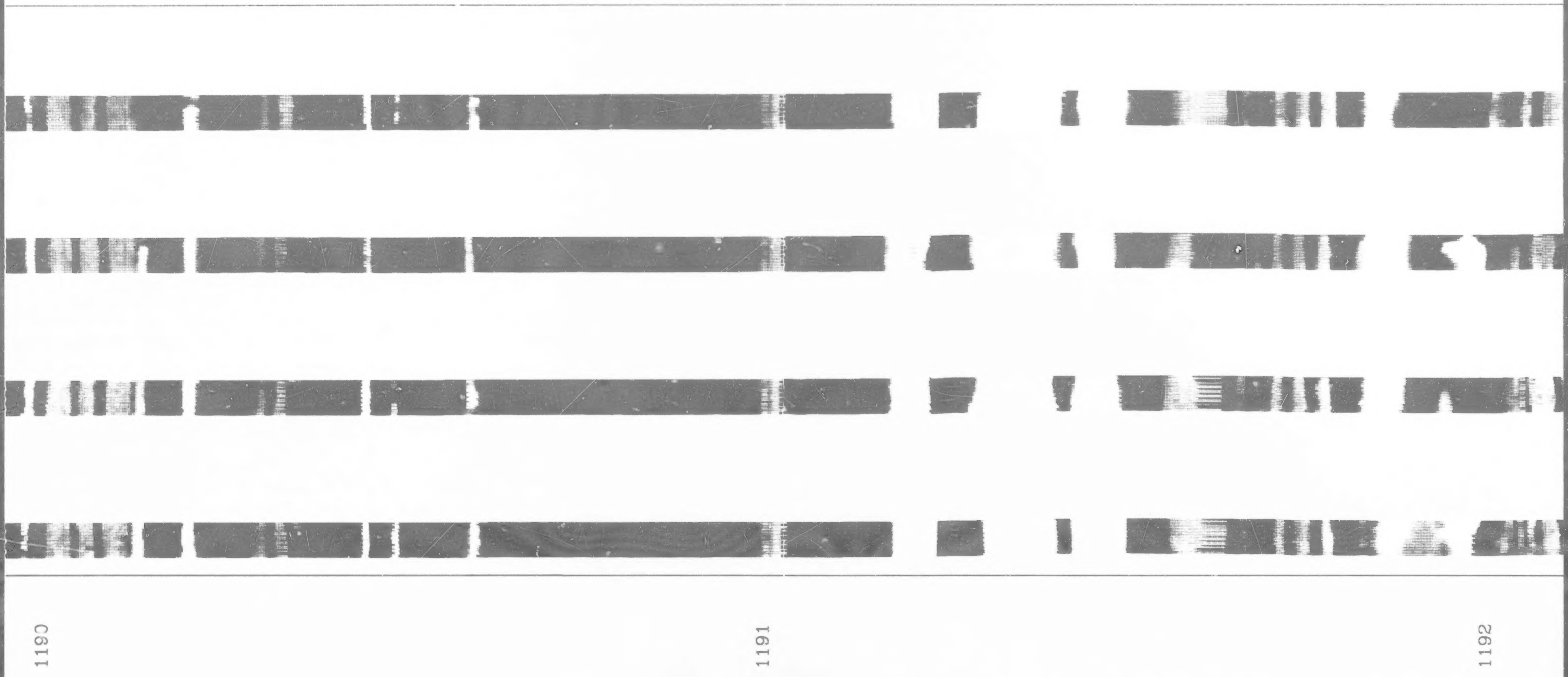
1190
1191
1192

1193

[illegible]

1194

[illegible]

1195

1196

[redacted]

1197

1198

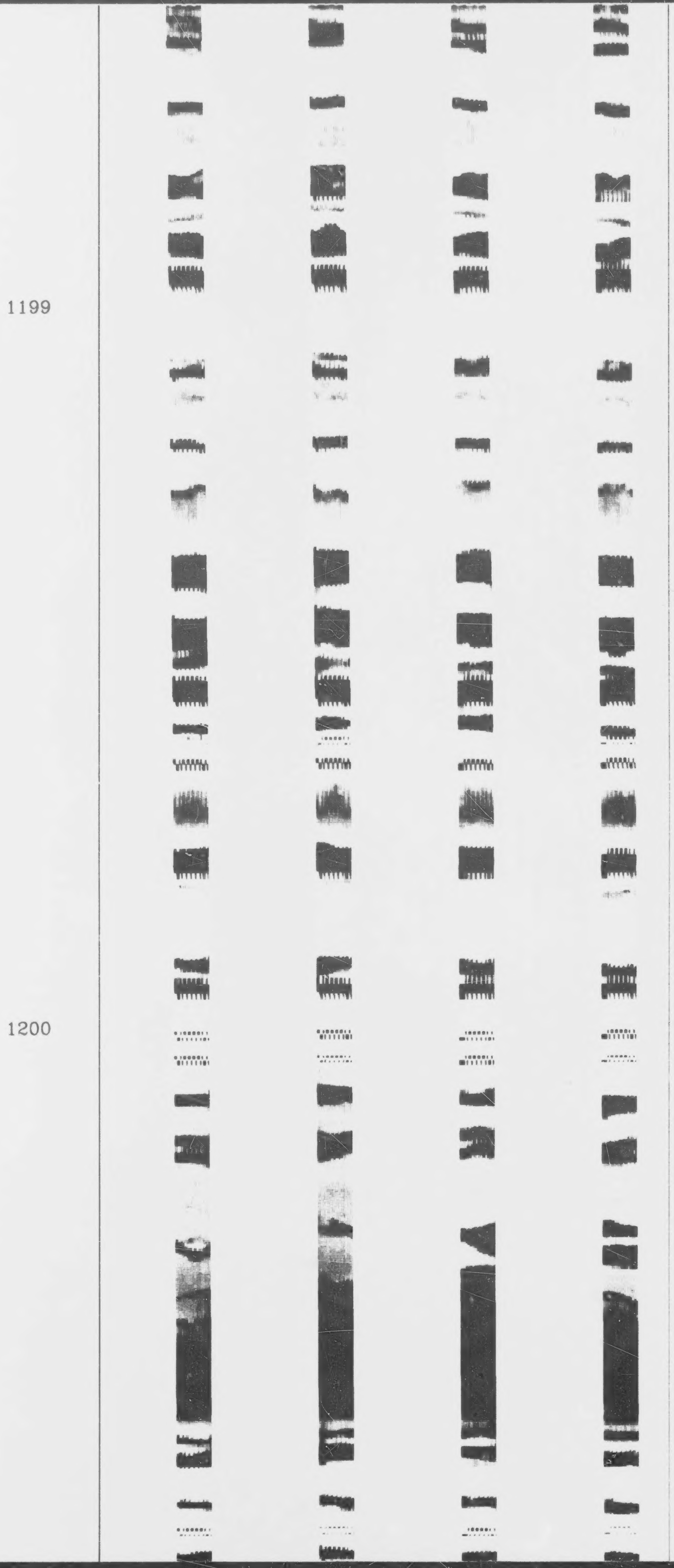
1199
1200

1201

[illegible]

1202

[illegible]

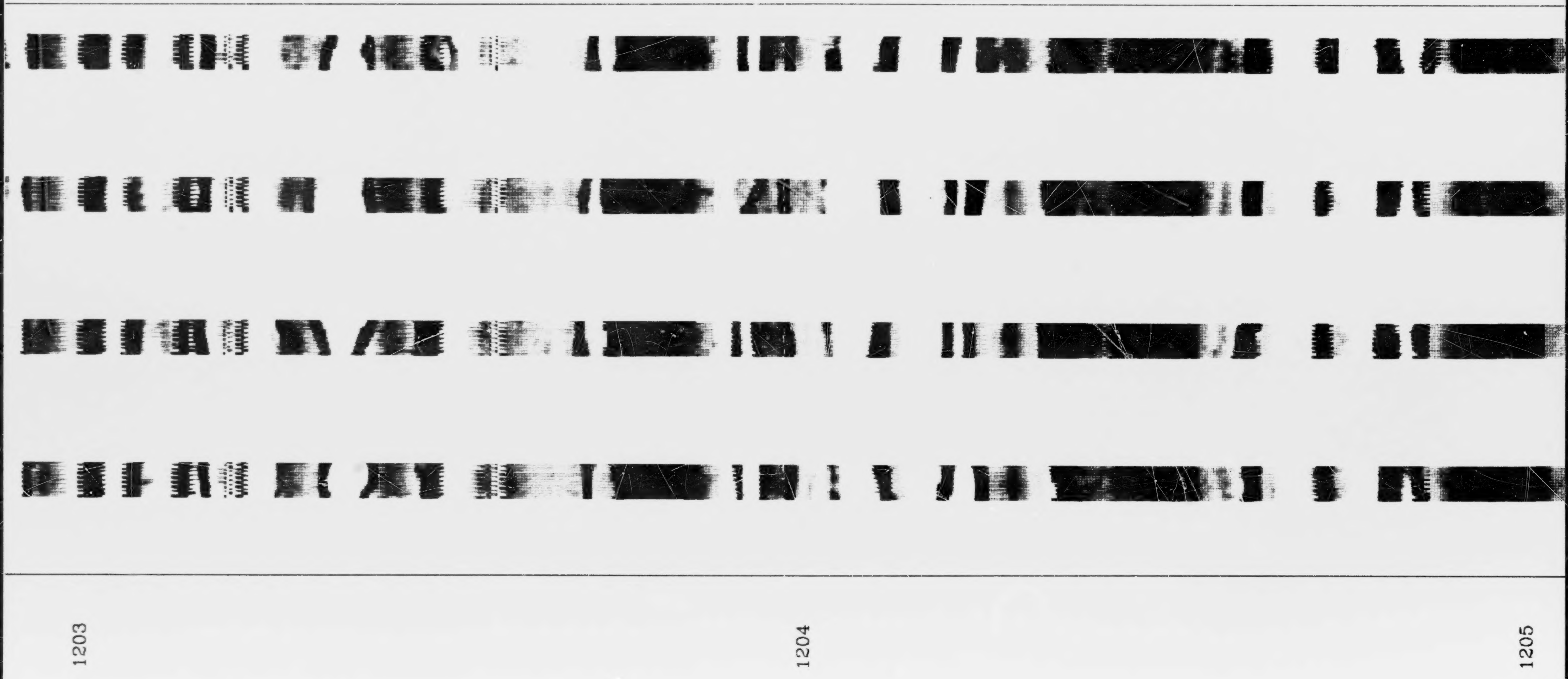
1203
1204
1205

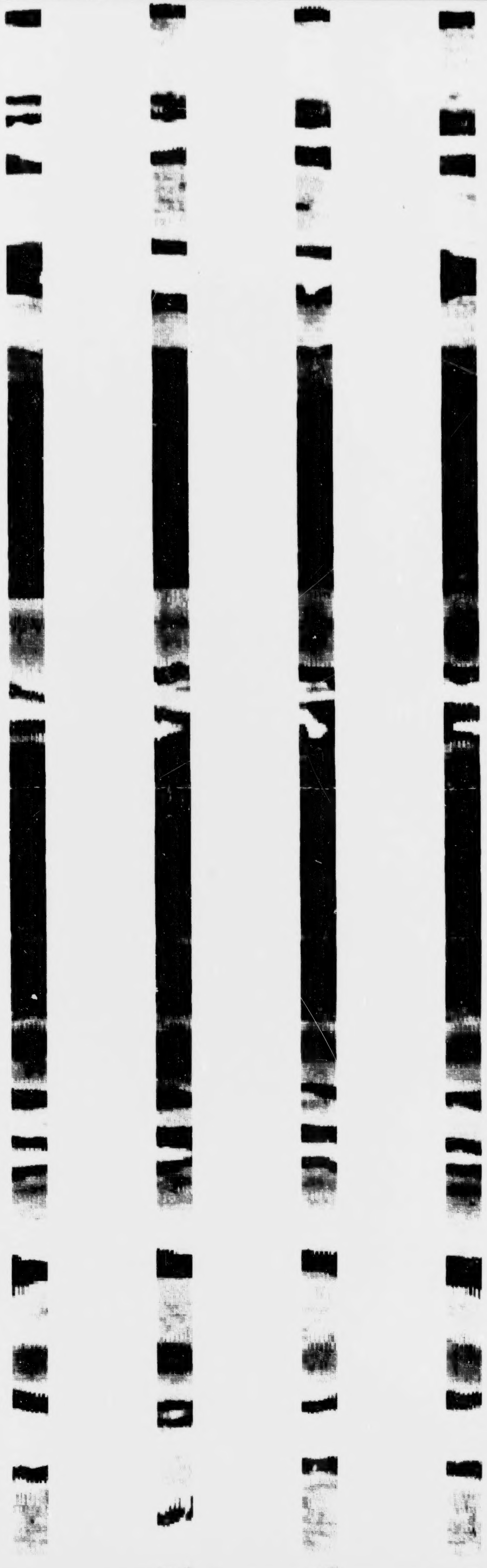

1208

1209

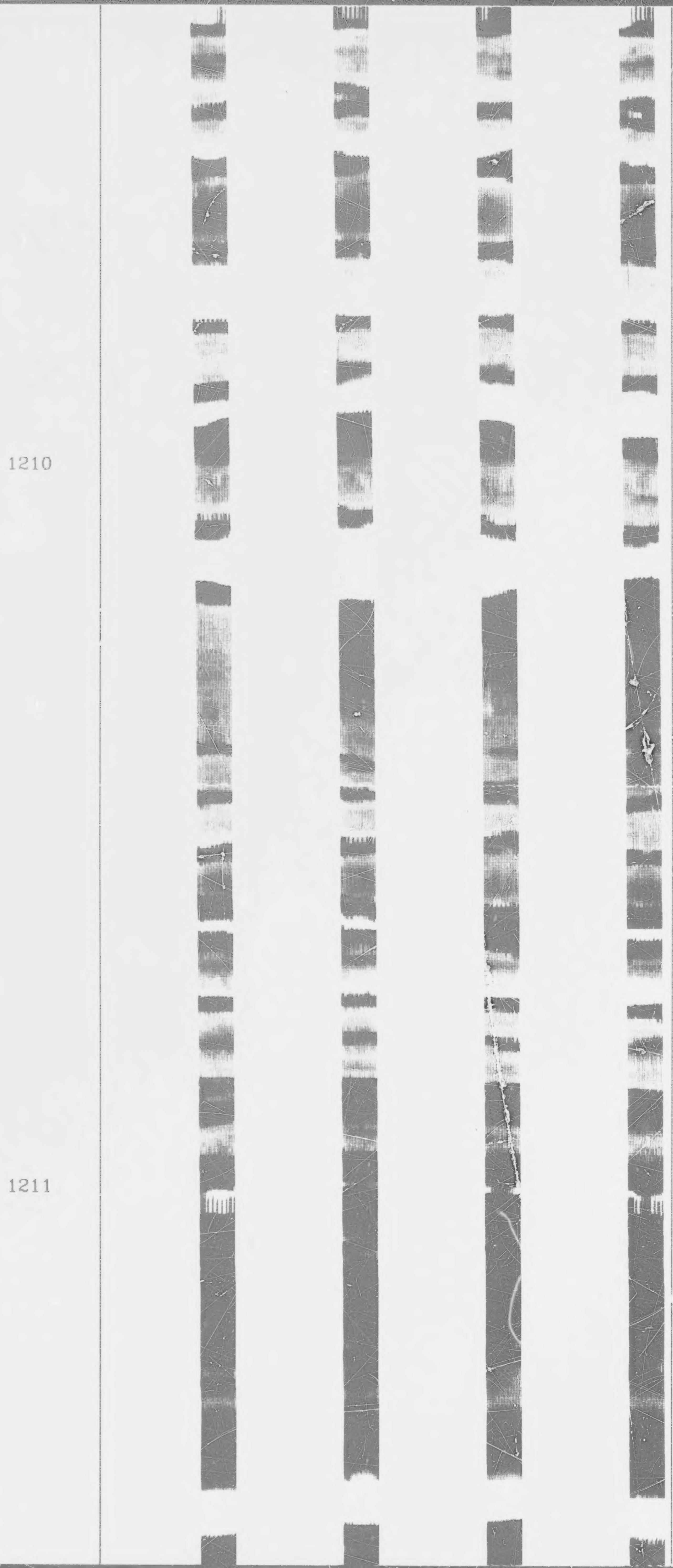
1210
1211

[redacted]

[redacted]

1214

1215

[redacted]

[redacted]

1218
1219
1220

SCHLUMBERGER

FMS
BOREHOLE
IMAGING

COMPANY	LAMONT DOHERTY
WELL	ODP HOLE 807-C
FIELD	ONTONG JAVA PLATEAU
COUNTRY	LEG 130
RUN	RUN 2
DATE LOGGED	21 - MAR - 90
REFERENCE	STATIC PASS 2 1260 1220

STATIC NORMALIZATION

PASS-2 (23761)

FILE : MEST.004

ZONE FROM 1260.0 M TO 1220.0 M

DEPTH SCALE = 1/ 5

IMAGE SCALE = 1/ 5

BITSIZE = 9.88

ORIENTATION

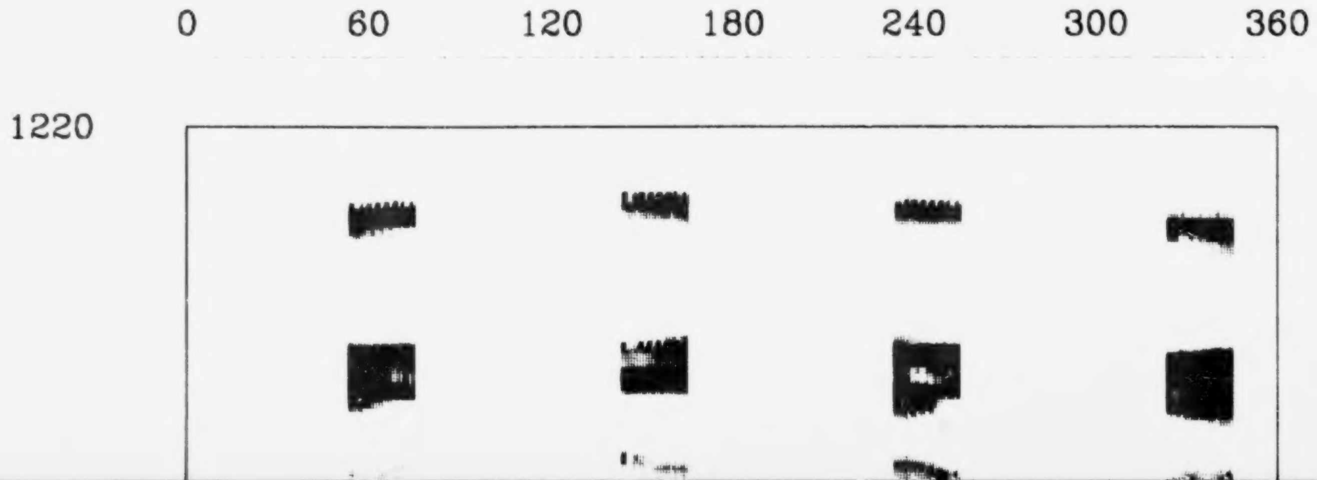

1221

1222

1223

1224

1225

1226

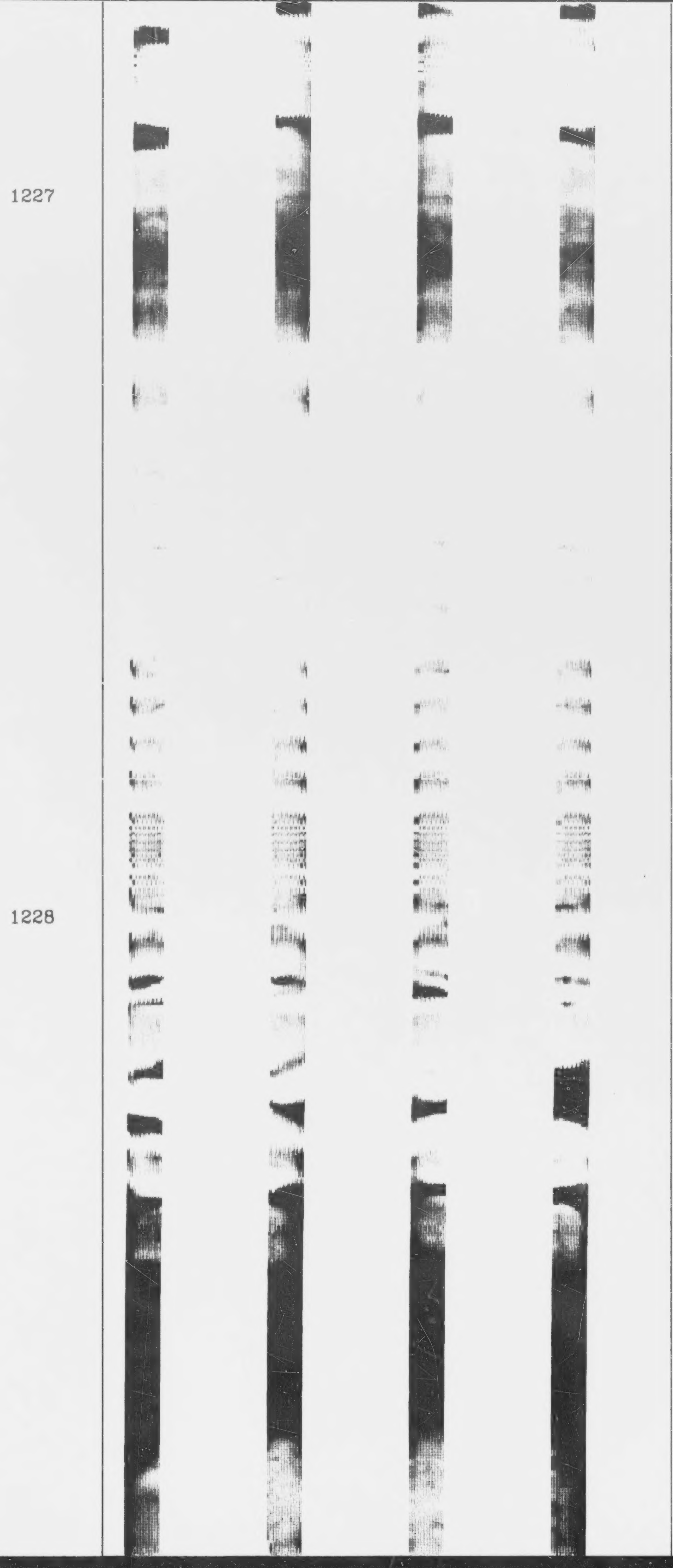
1227
1228

1229

1230

1231

[illegible]

1232

[illegible]

1233

[illegible]

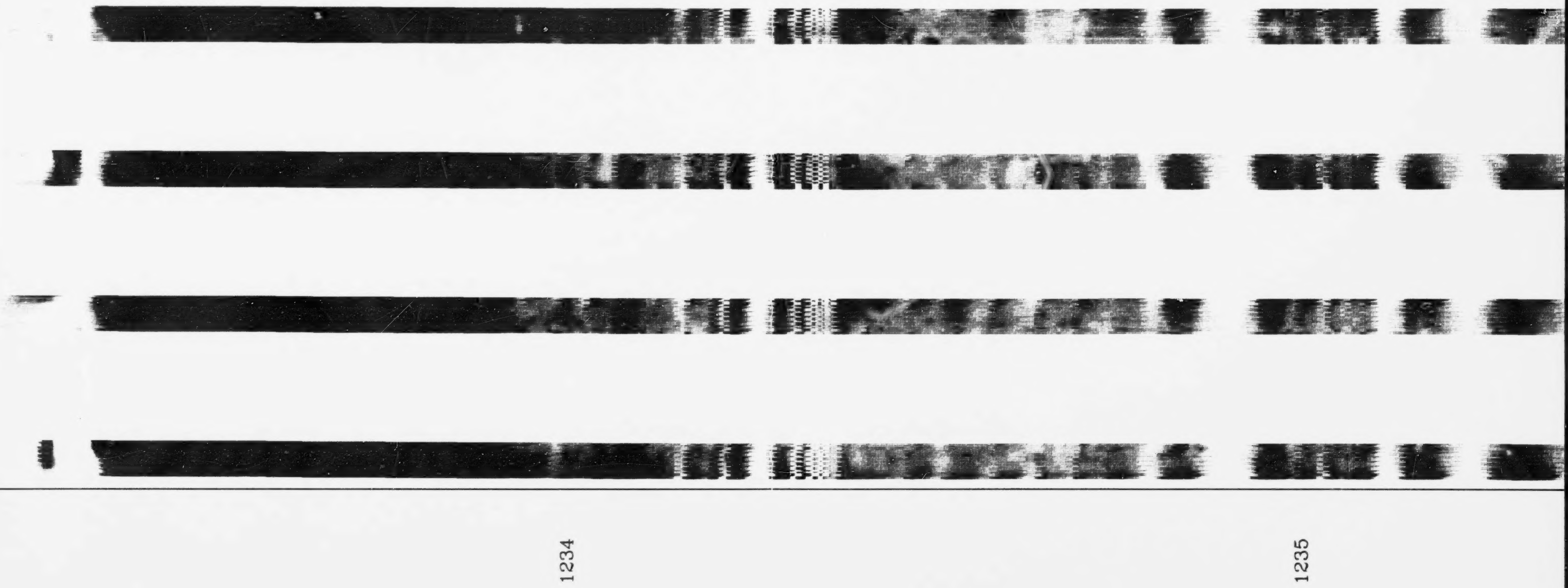
1234
1235

1236

1237

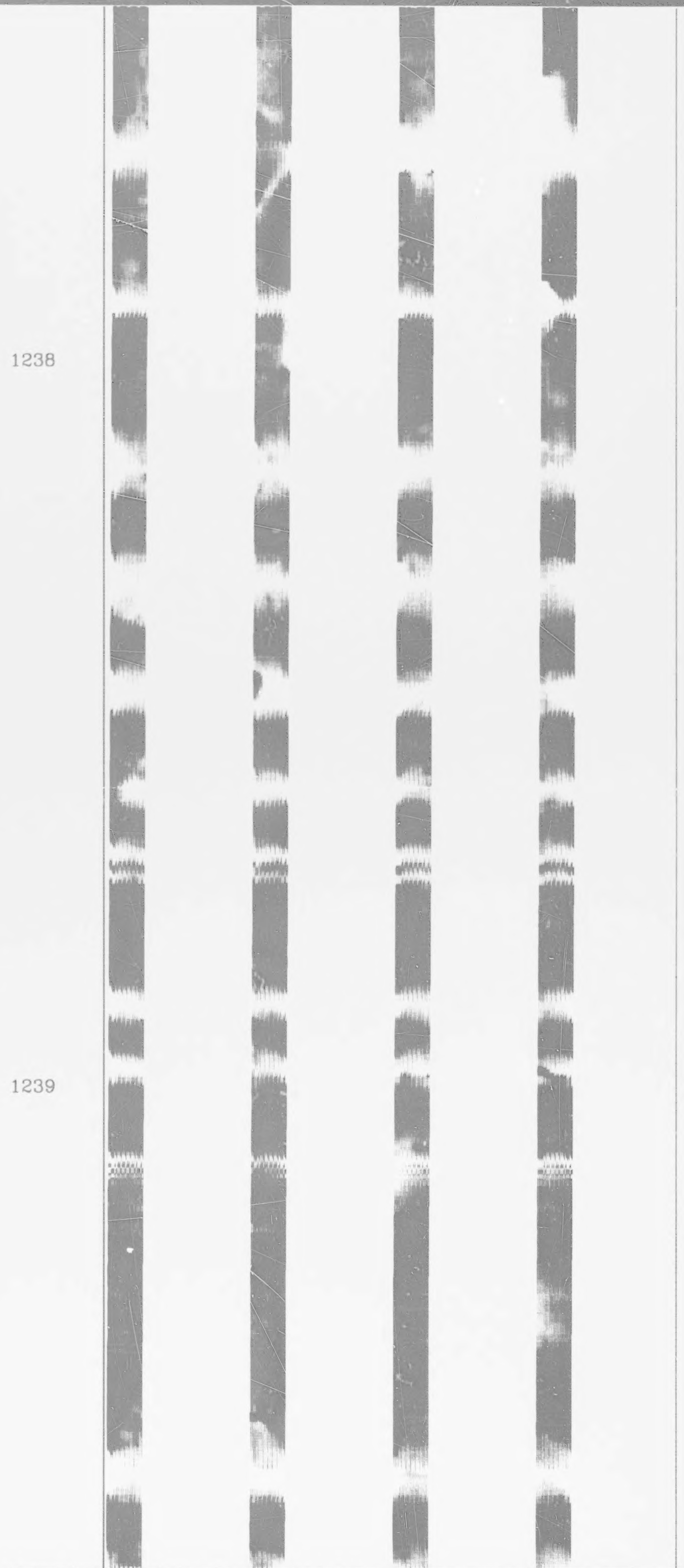
1238
1239

1240

[illegible]

1241

[illegible]

1242

[redacted]

1243

1244
1245
1246

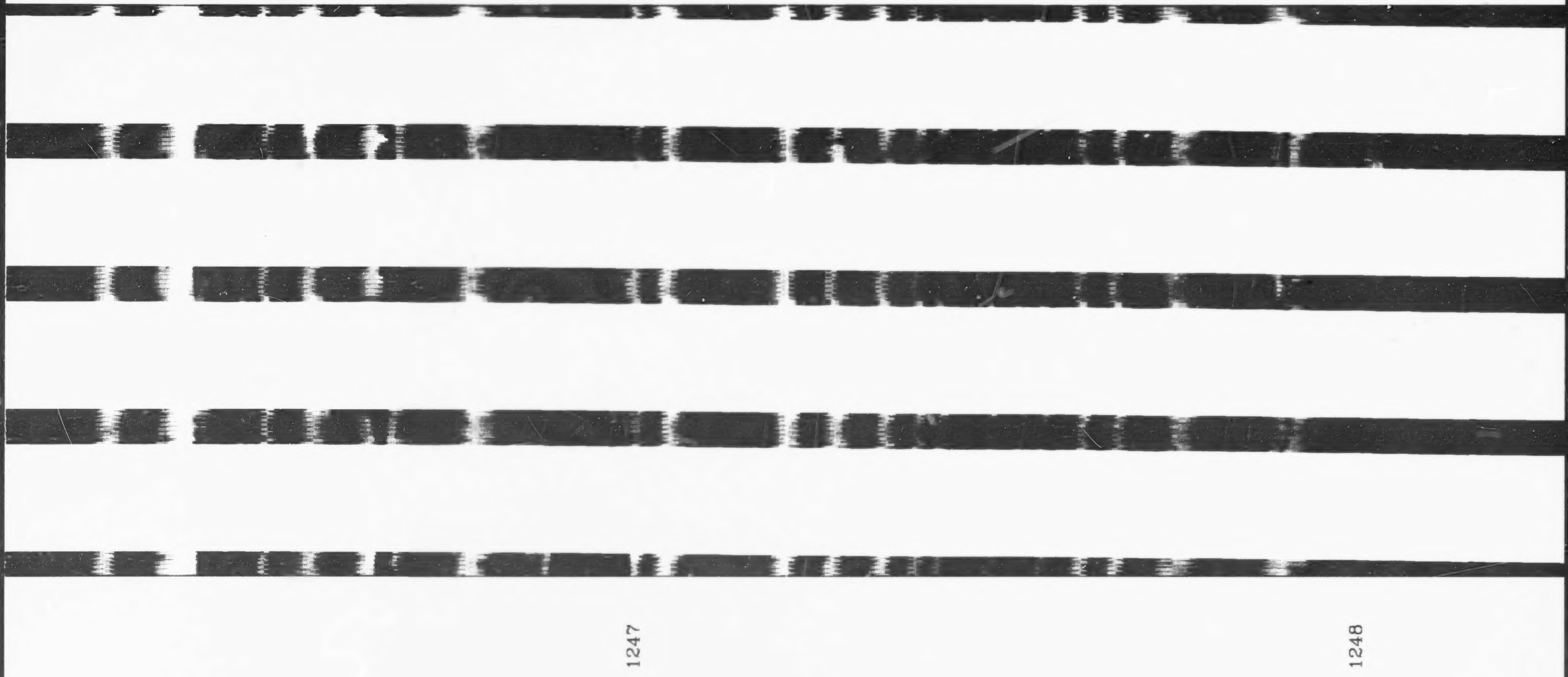
1247
1248

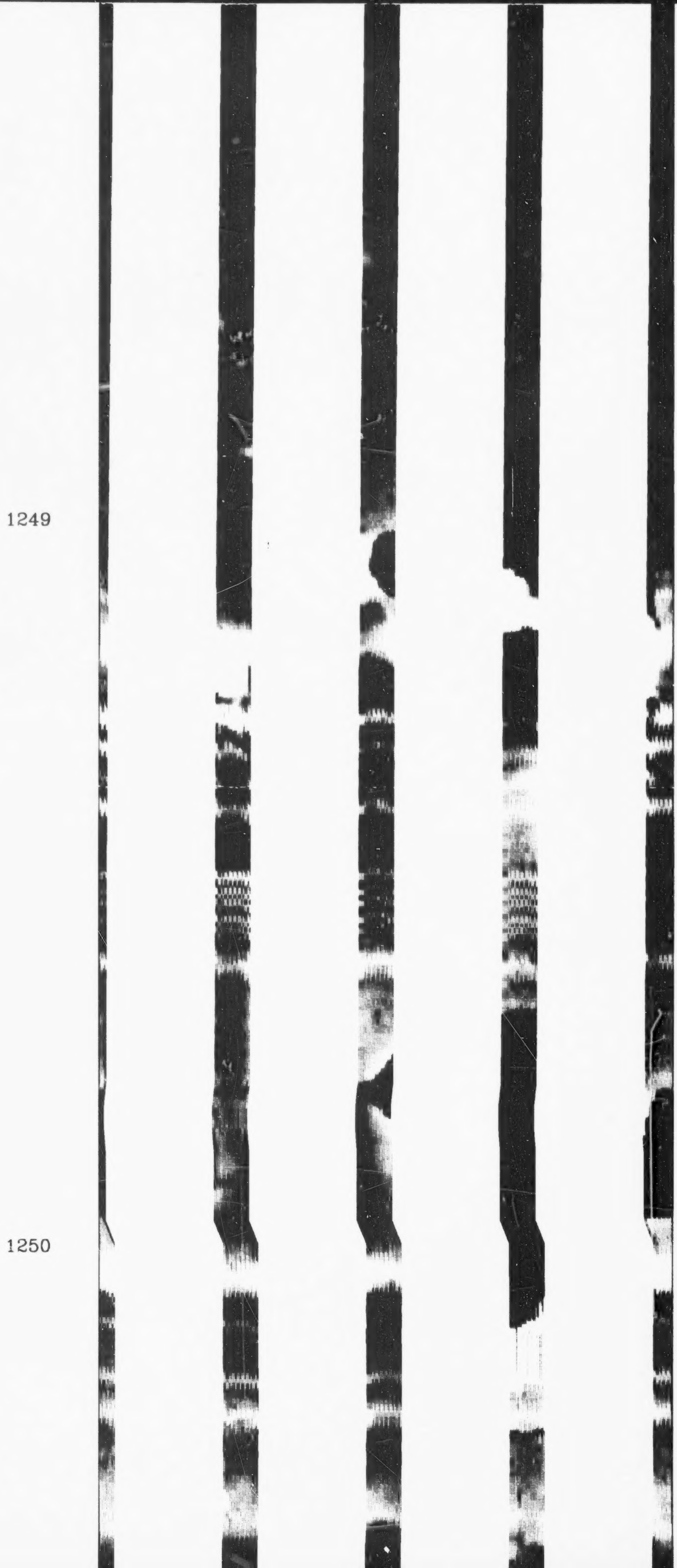
1249
1250

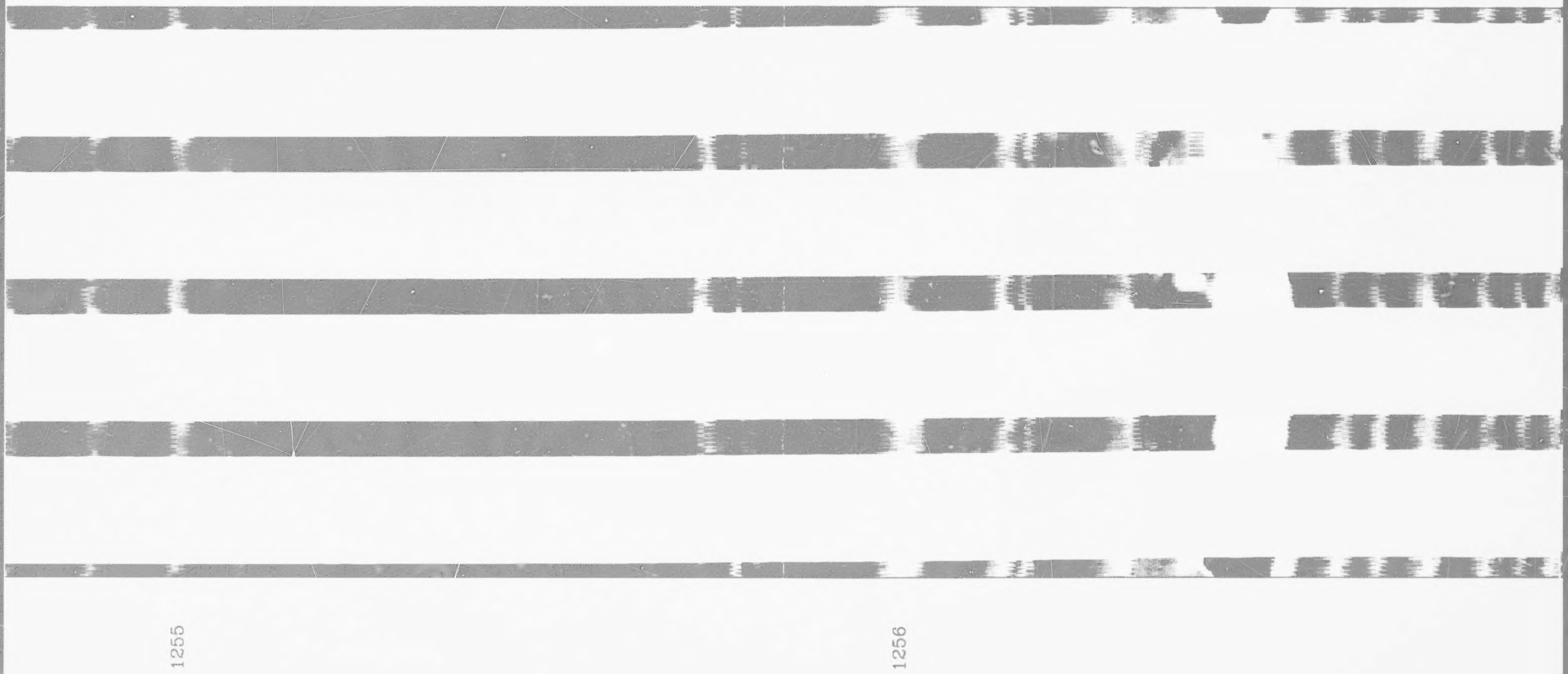
1255
1256

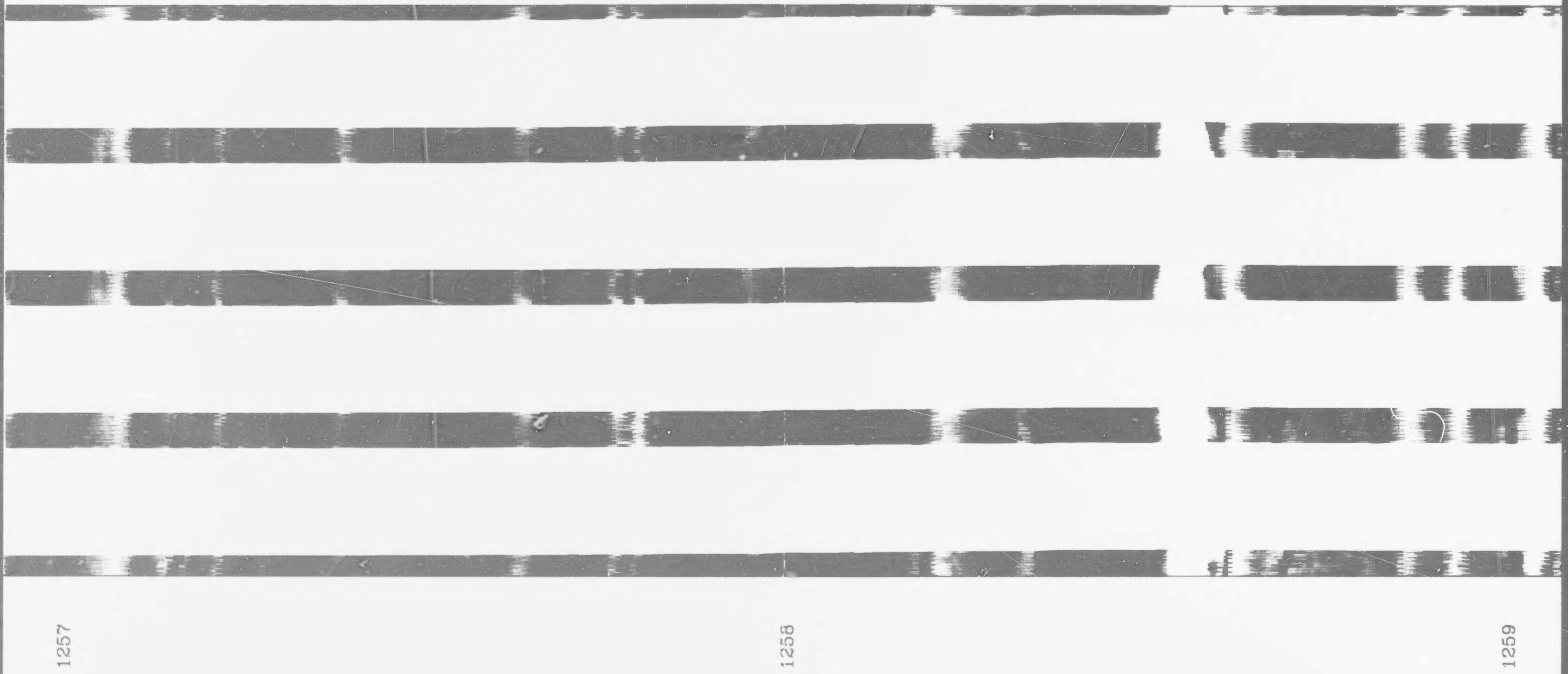
1257
1258
1259

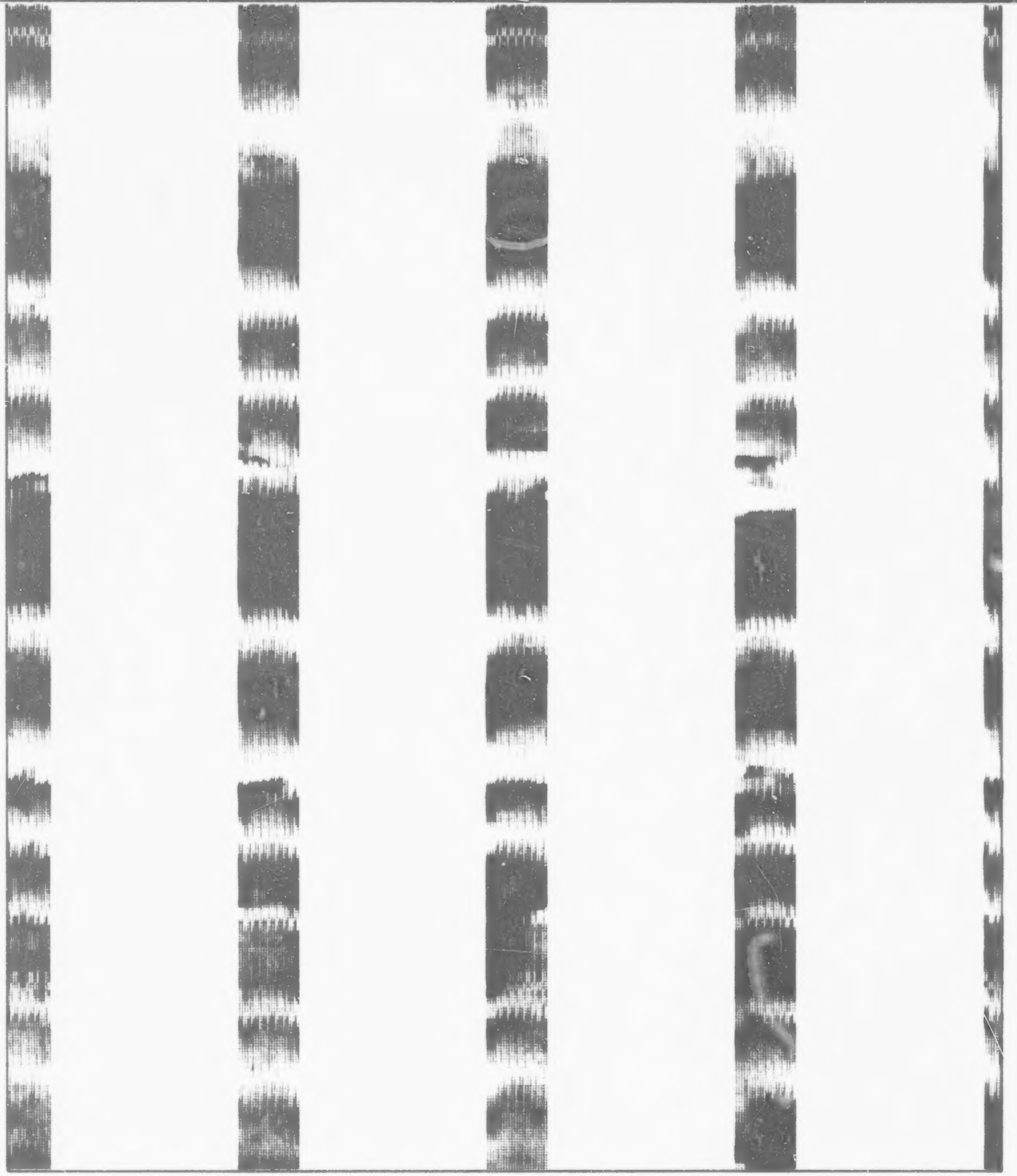

SCHLUMBERGER

FMS
BOREHOLE
IMAGING

COMPANY	LAMONT DOHERTY
WELL	ODP HOLE 807-C
FIELD	ONTONG JAVA PLATEAU
COUNTRY	LEG 130
RUN	RUN 2
DATE LOGGED	21 - MAR - 90
REFERENCE	STATIC PASS-2 1300-1260

STATIC NORMALIZATION
PASS-2 (23761)

FILE : MEST.004

ZONE FROM 1300.0 M TO 1260.0 M

DEPTH SCALE = 1/ 5

IMAGE SCALE = 1/ 5

BITSIZE = 9.88

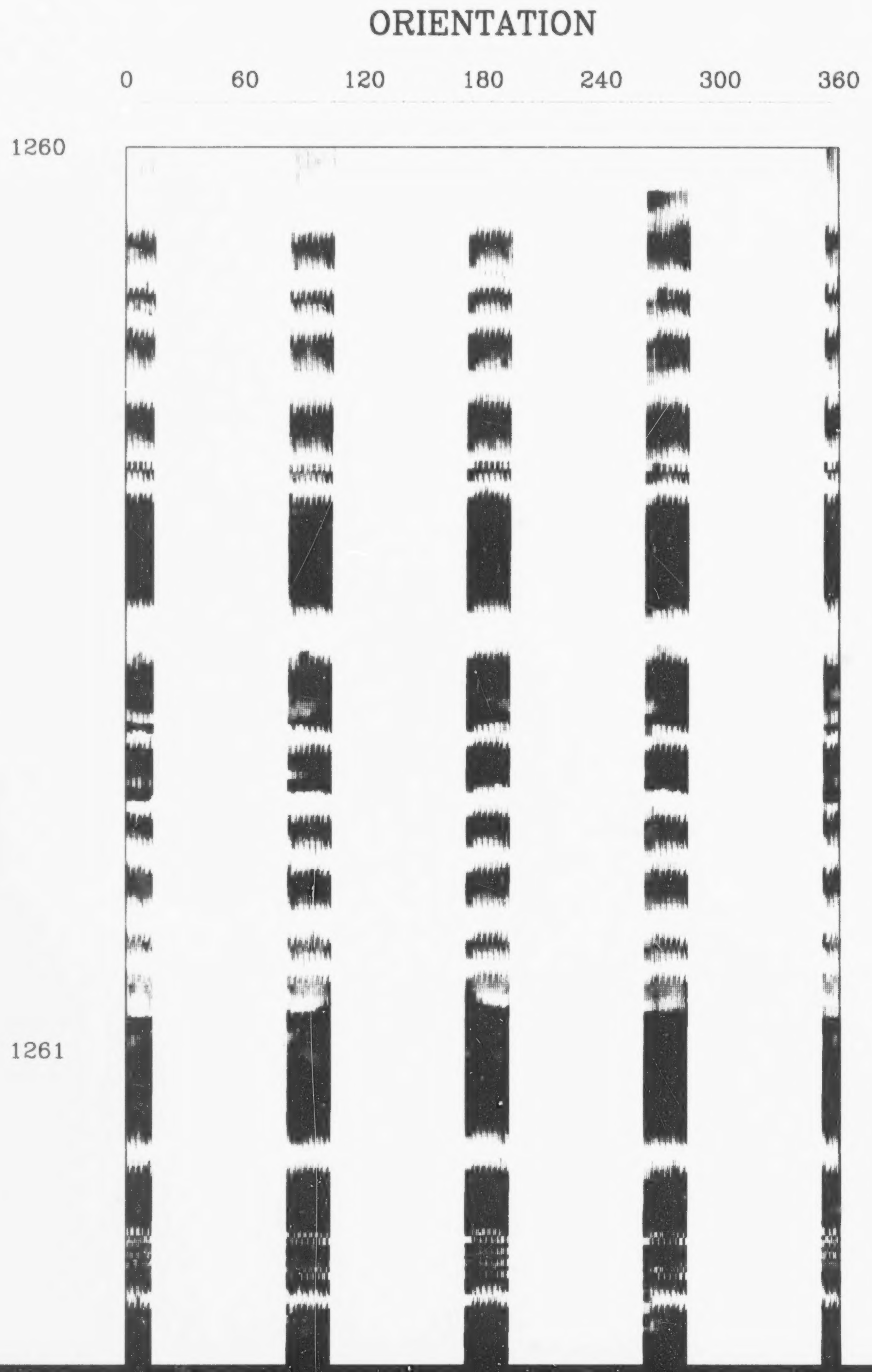

[redacted]

[redacted]

[redacted]

[redacted]

[redacted]

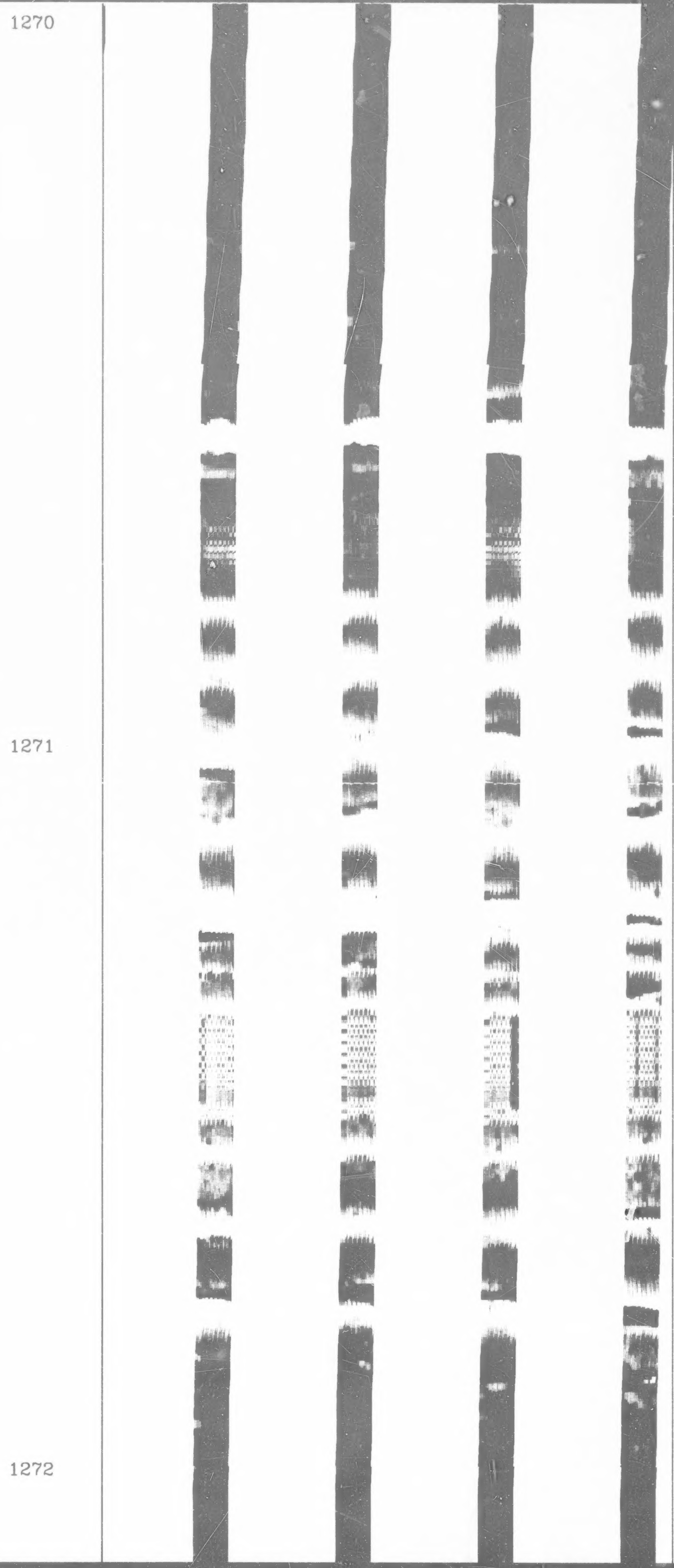
1270
1271
1272

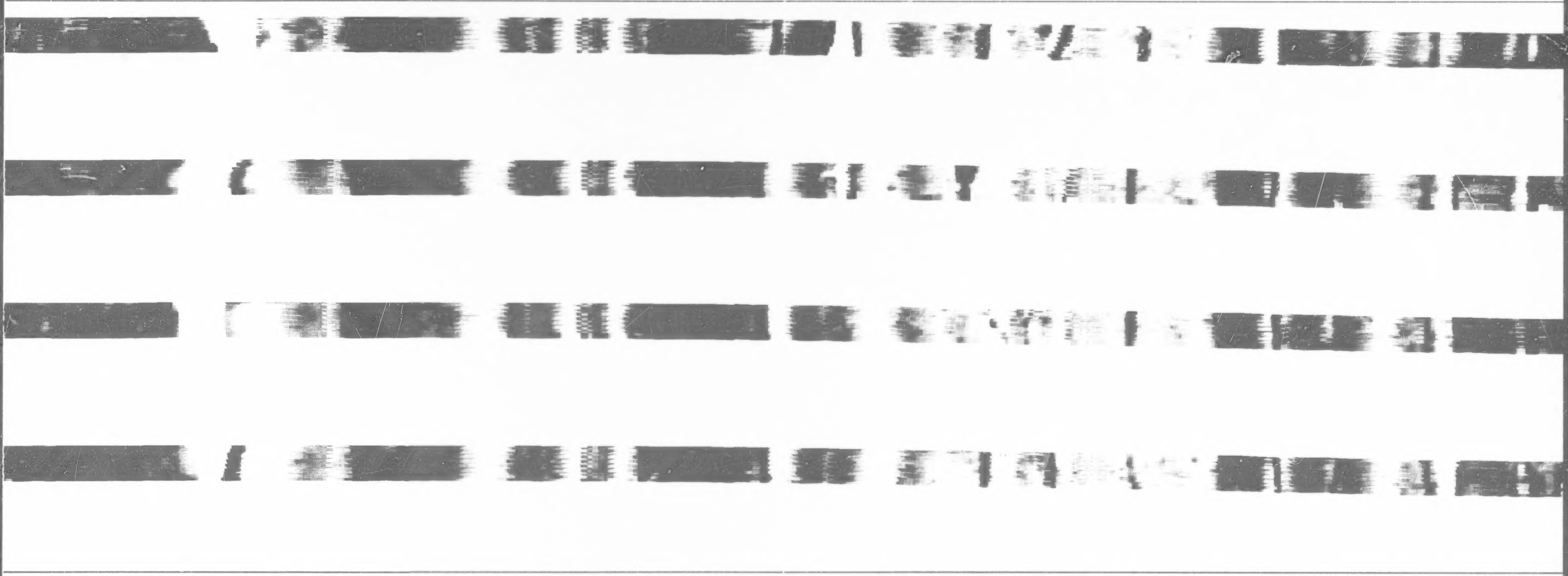
1273
1274

[redacted]

1277

[illegible]

1278

1281 [illegible]

1282 [illegible]

[redacted]

1286

1287

[illegible]

[illegible]

[illegible]

[illegible]

1292

1293

1294

1295

1296

1297

[illegible]

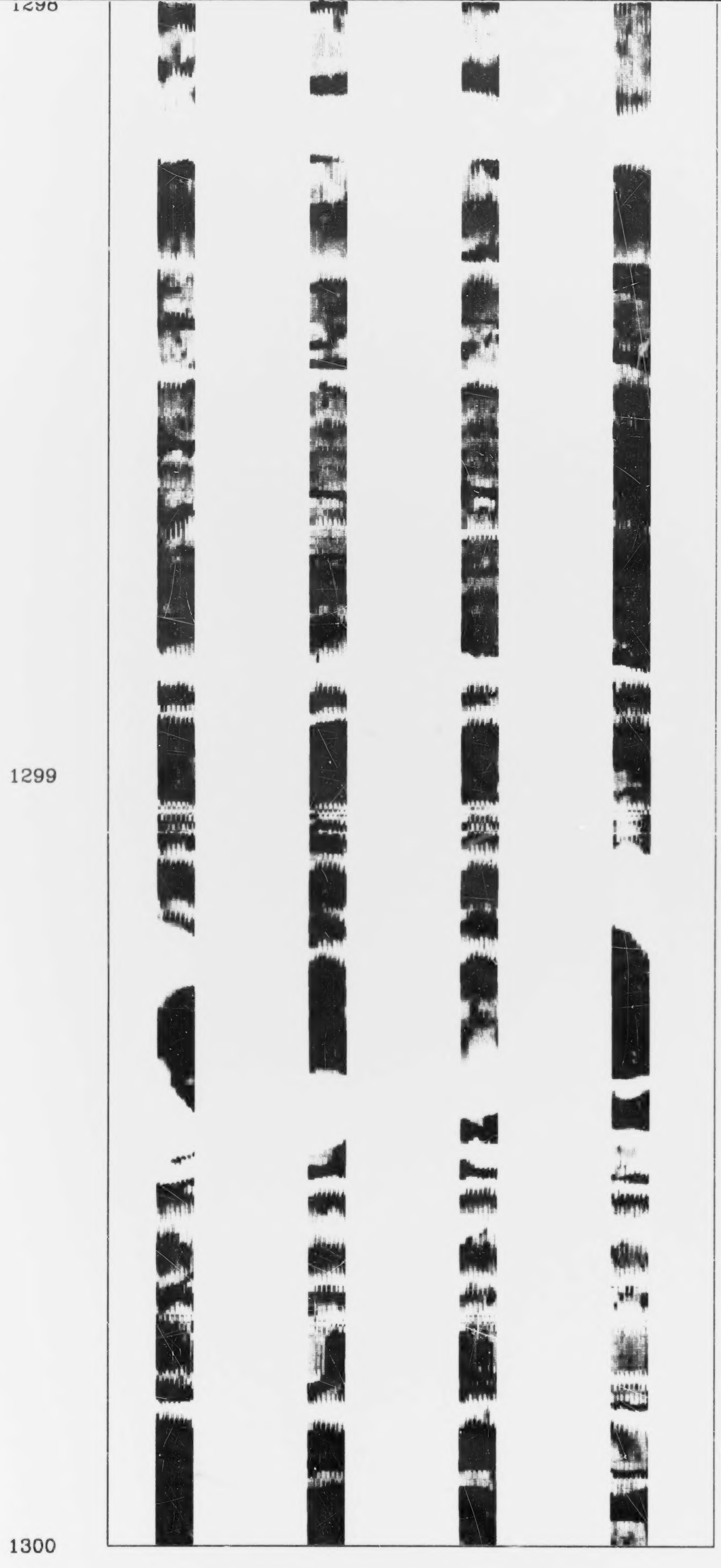
1298
1299
1300

SCHLUMBERGER

FMS
BOREHOLE
IMAGING

COMPANY	LAMONT DOHERTY
WELL	ODP HOLE 807-C
FIELD	ONTONG JAVA PLATEAU
COUNTRY	LEG 130
RUN	RUN 2
DATE LOGGED	21 - MAR - 90
REFERENCE	STATIC PASS 2 1340 1300

STATIC NORMALIZATION

PASS-2 (23761)

FILE : MEST.004

ZONE FROM 1340.0 M TO 1300.0 M

DEPTH SCALE = 1/ 5

IMAGE SCALE = 1/ 5

BITSIZE = 9.88

ORIENTATION

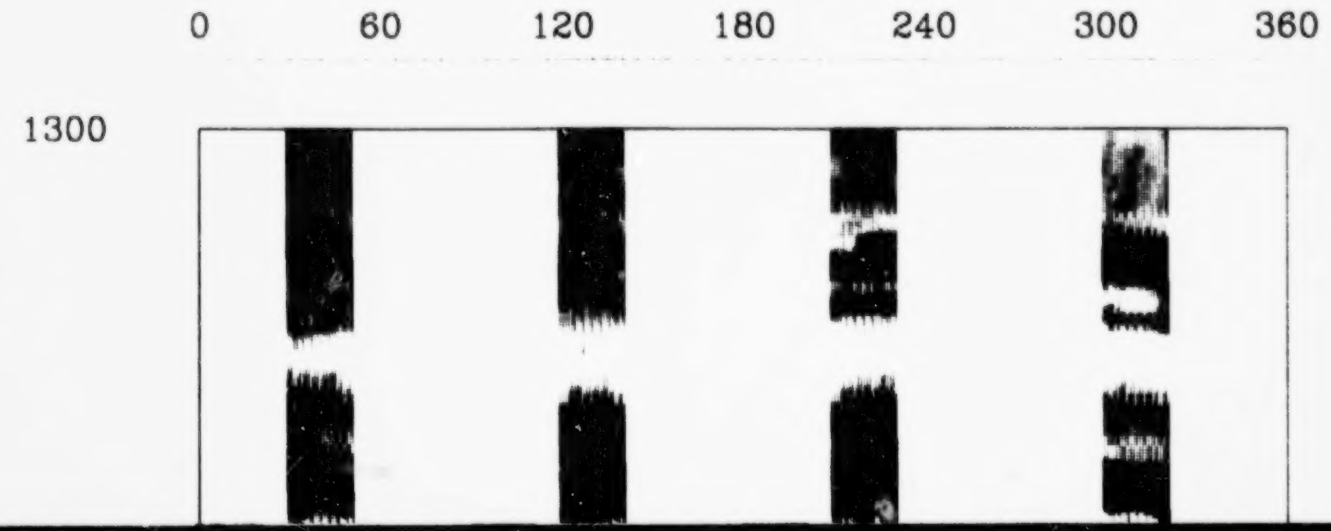

[illegible]

[illegible]

[illegible]

[illegible]

1301

1302

[redacted]

[redacted]

1305

1306

[redacted]

1307

1308

1312

1313

1314

1315

1318 [redacted]

1319

[redacted]

[redacted]

[redacted]

[redacted]

1320

1321

[redacted]

1324 1325 1326

1327

1328

1329 [illegible]

1330 [illegible]

1333

1334

1337

1338

1339

SCHLUMBERGER

FMS
BOREHOLE
IMAGING

COMPANY	LAMONT DOHERTY
WELL	ODP HOLE 807-C
FIELD	ONTONG JAVA PLATEAU
COUNTRY	LEG 130
RUN	RUN 2
DATE LOGGED	21 - MAR - 90
REFERENCE	STATIC PASS-2 1379-1340

STATIC NORMALIZATION

PASS- 2 (23761)

FILE : MEST.004

ZONE FROM 1379.0 M TO 1340.0 M

DEPTH SCALE = 1/ 5

IMAGE SCALE = 1/ 5

BITSIZE = 9.88

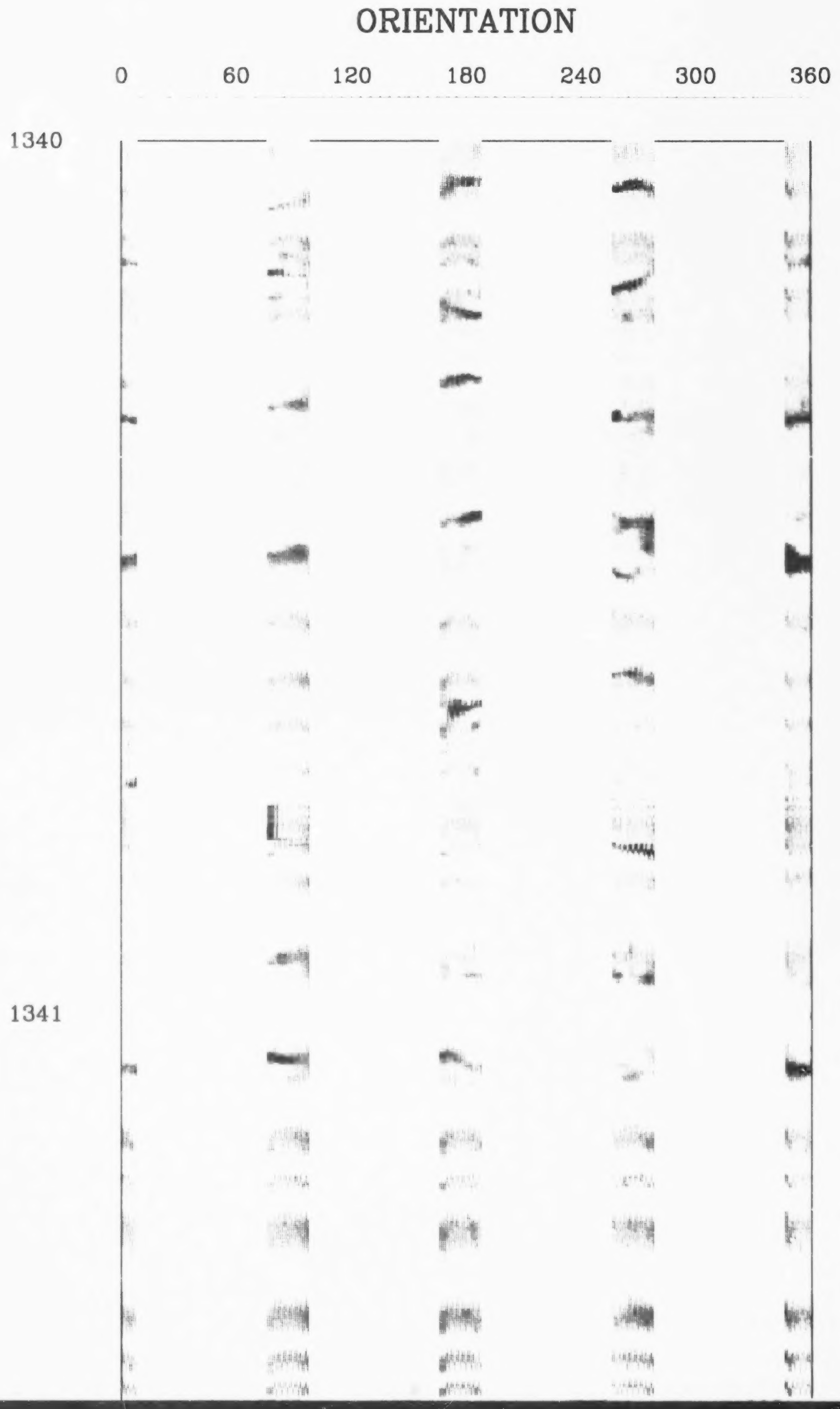

1342

1343

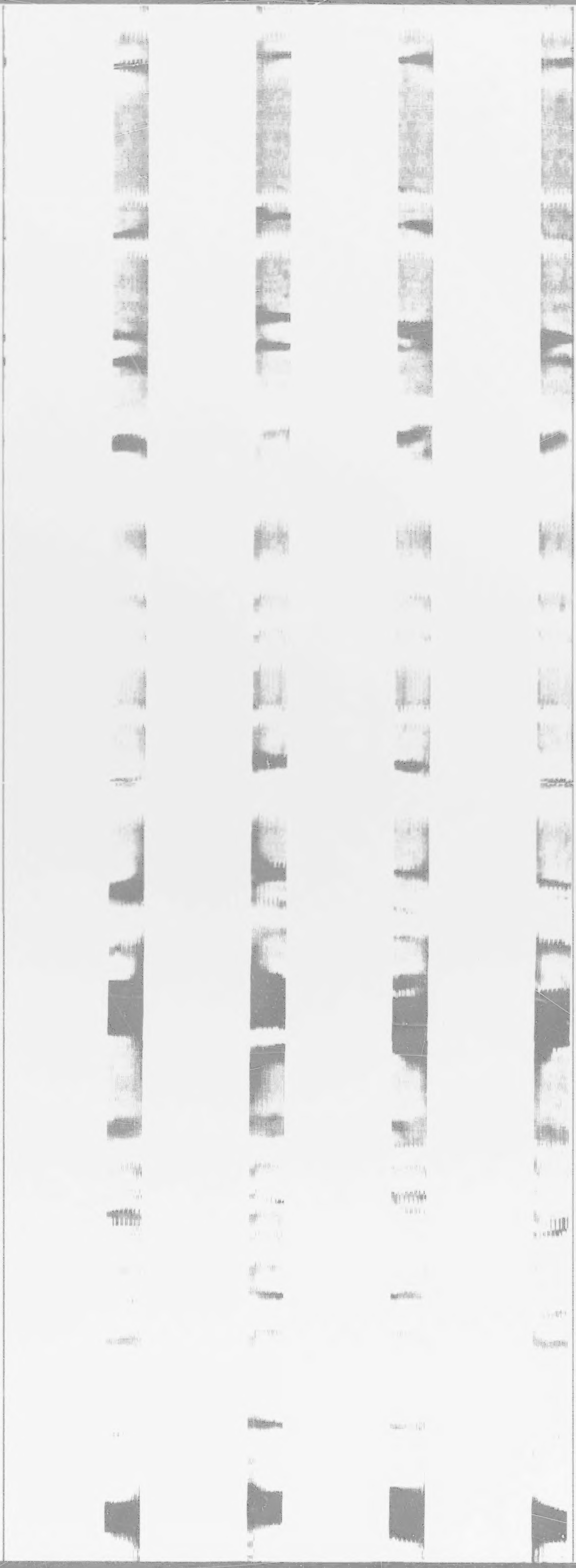

1346
1347

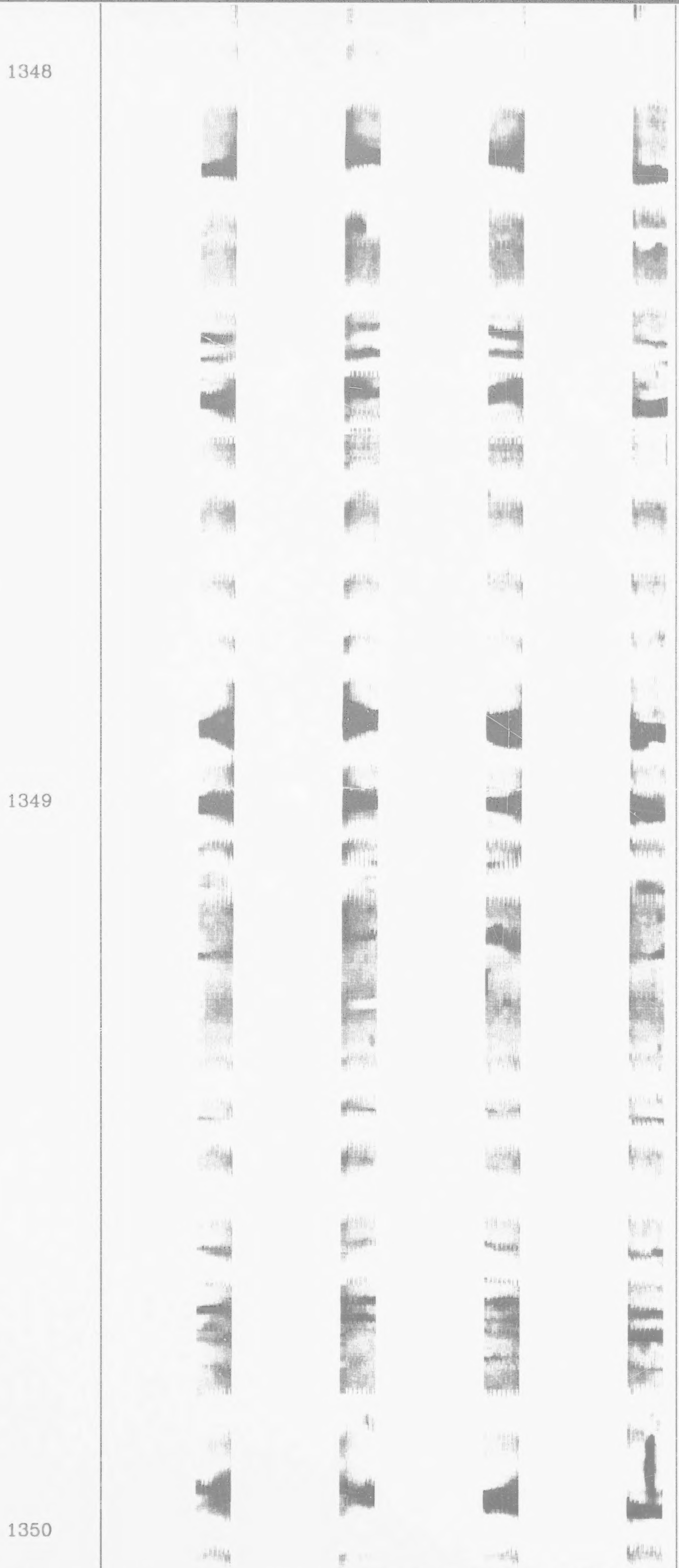
1348
1349
1350

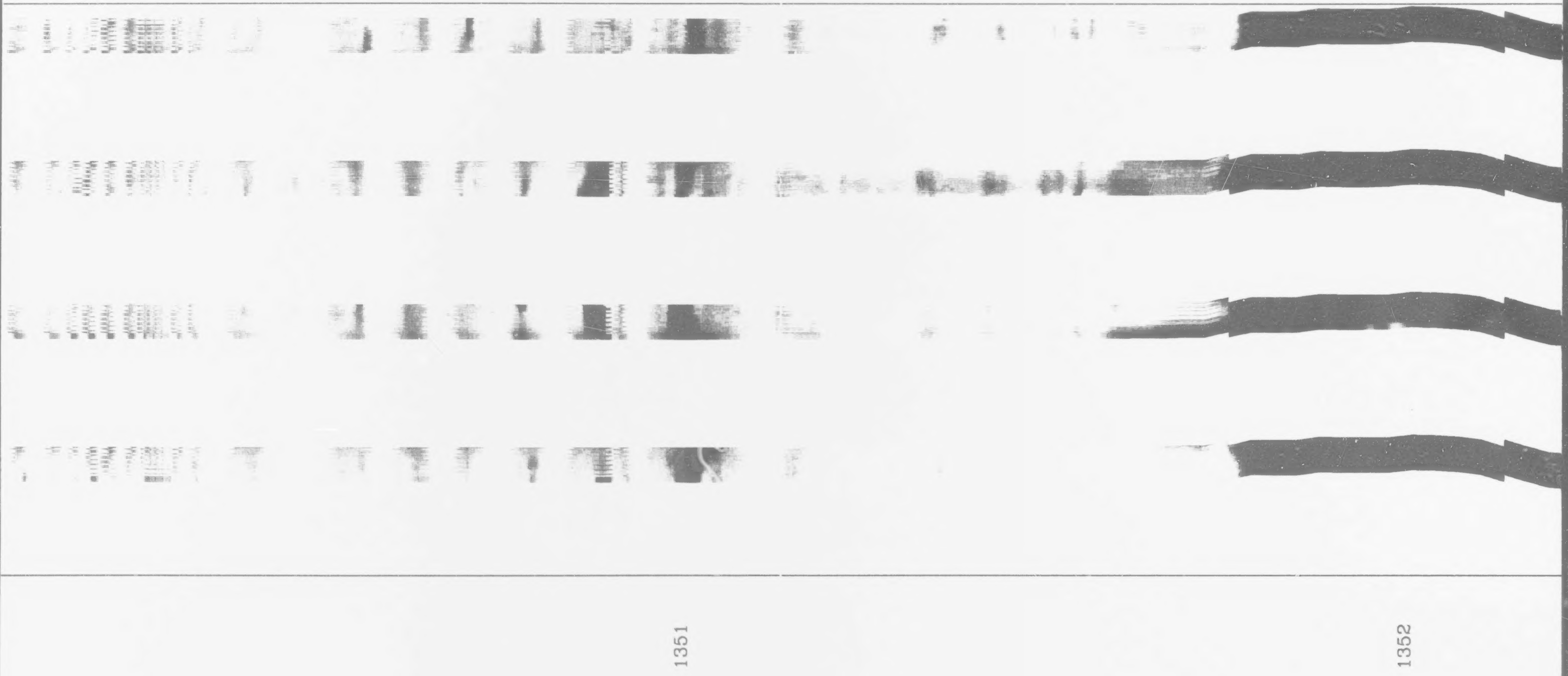
1351
1352

1353
1354

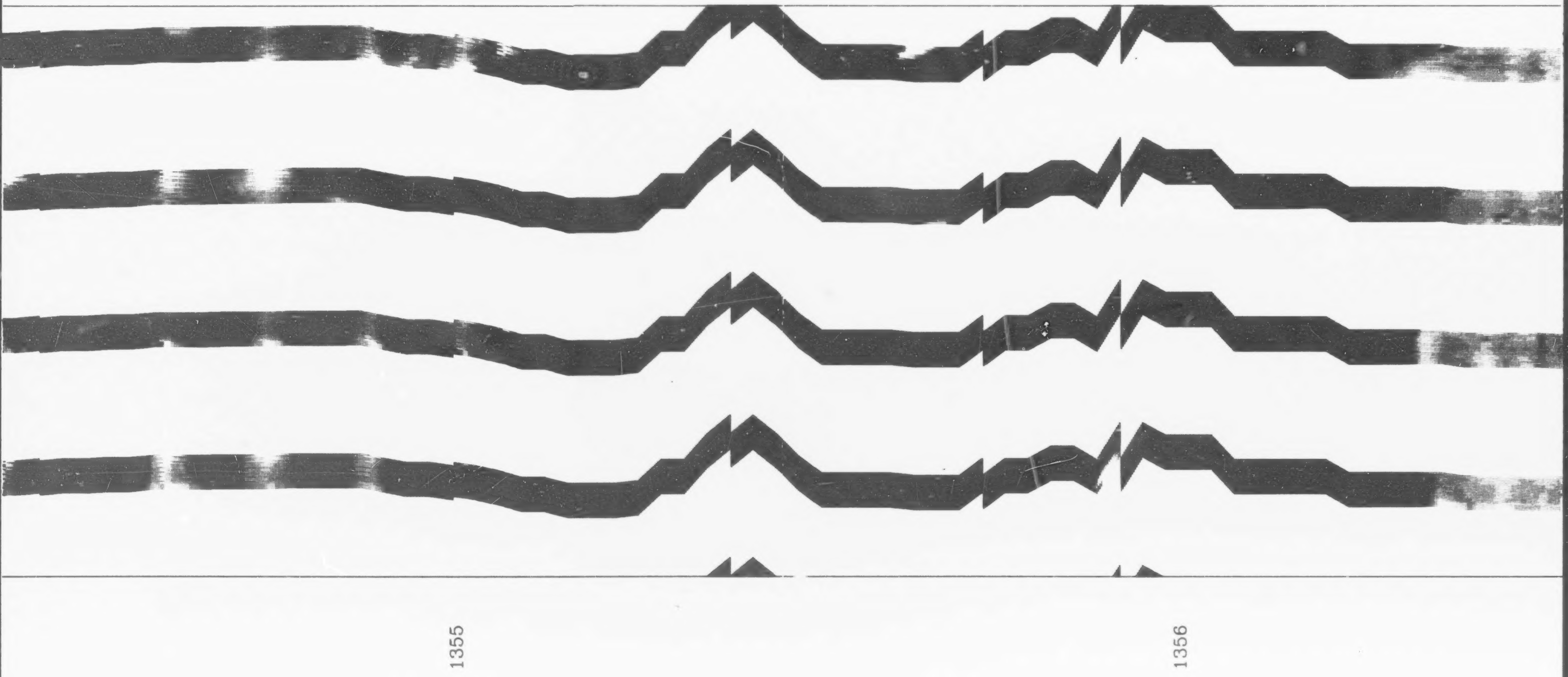
1355
1356

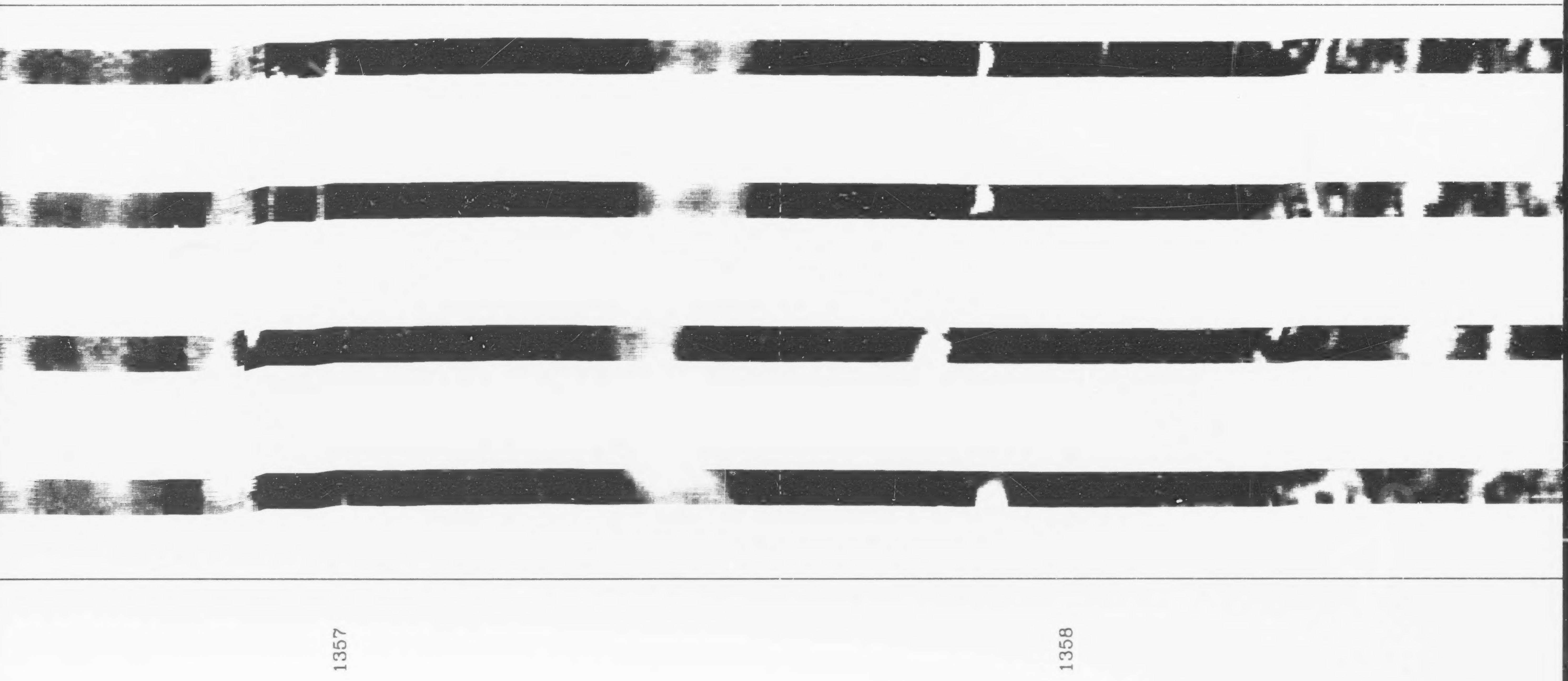
1357
1358

[redacted]

1366

1367

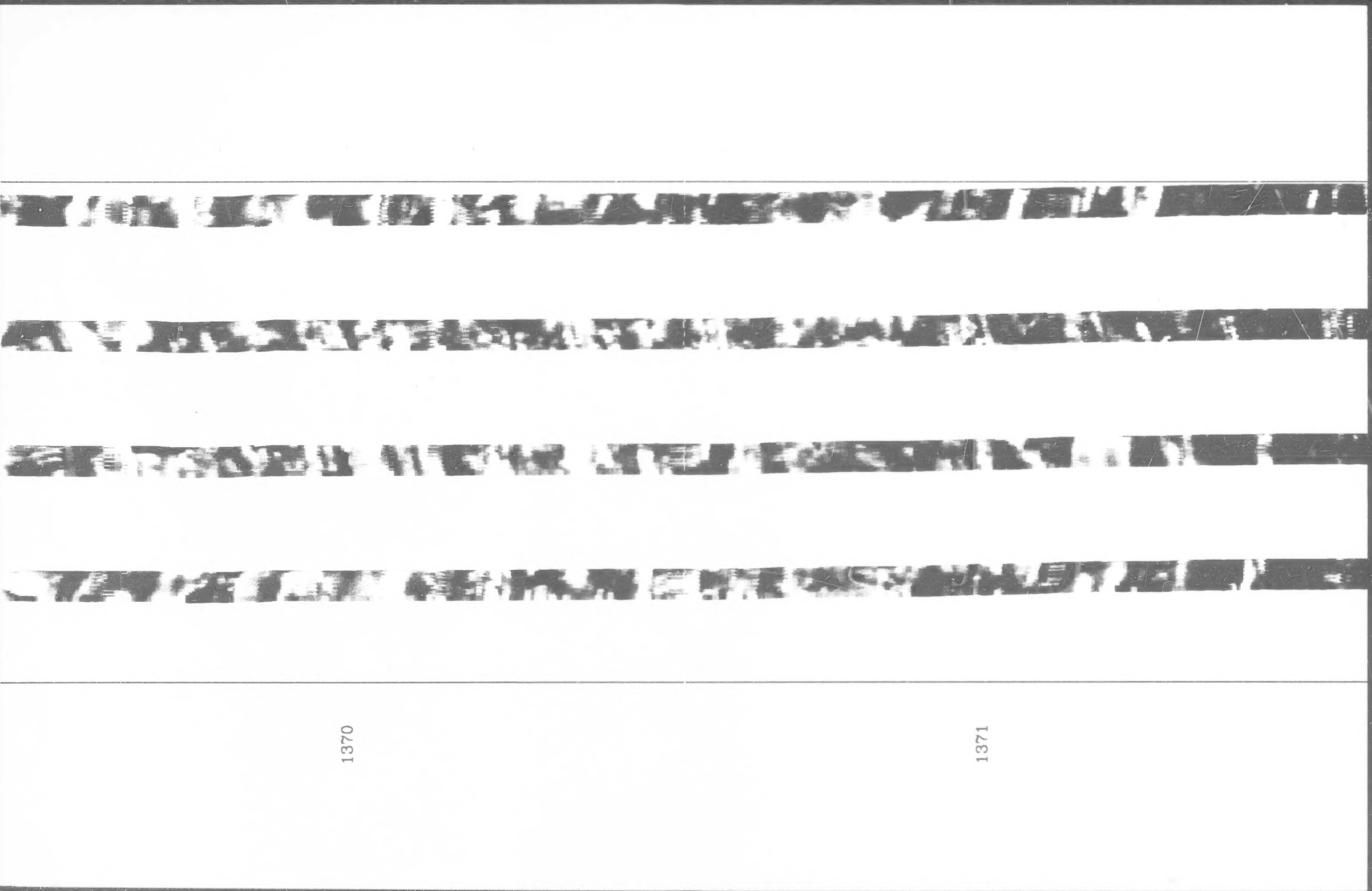
1370
1371

1372

1373

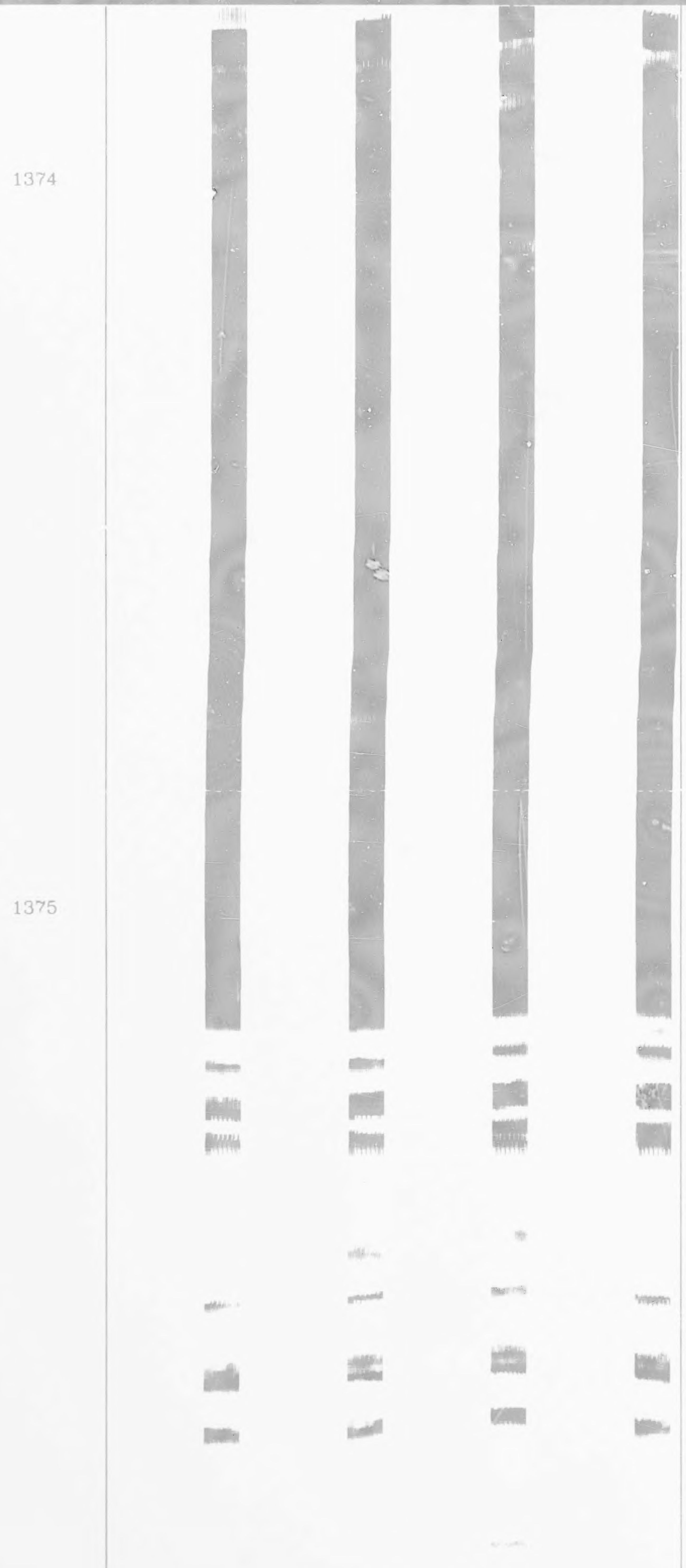
1374
1375

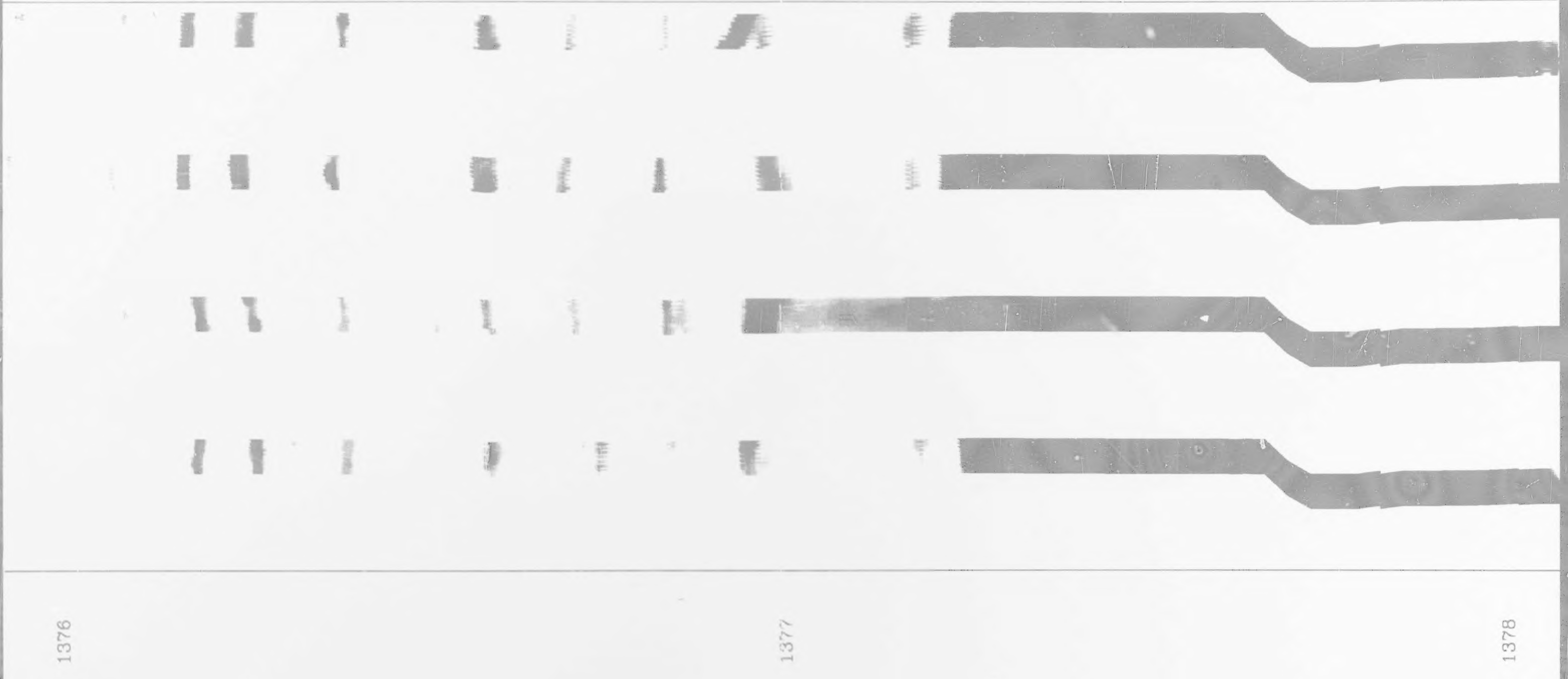
1376
1377
1378

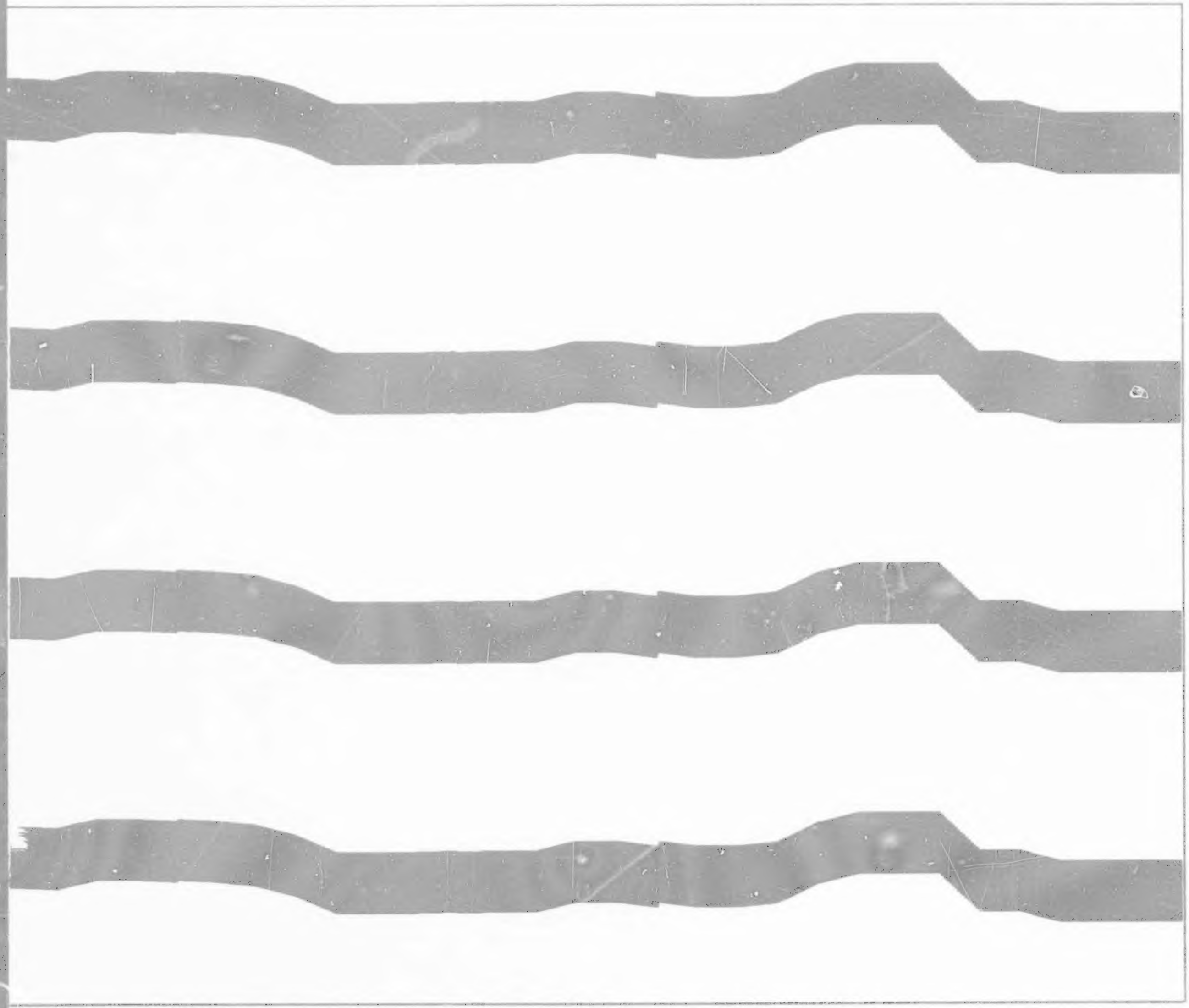

SCHLUMBERGER

FMS
BOREHOLE
IMAGING

COMPANY	LAMONT–DOHERTY BOREHOLE RE
WELL	ODP HOLE 807C
FIELD	ONTONG JAVA PLATEAU
COUNTRY	SOLOMONS
RUN	RUN 2
DATE LOGGED	21 – MAR – 90
REFERENCE	STATIC PASS–2 1379–1410

STATIC NORMALIZATION
PASS 2 (23761)
FILE : MEST.004

ZONE FROM 1410.0 M TO 1379.0 M
DEPTH SCALE = 1/ 5
IMAGE SCALE = 1/ 5
BITSIZE = 9.88

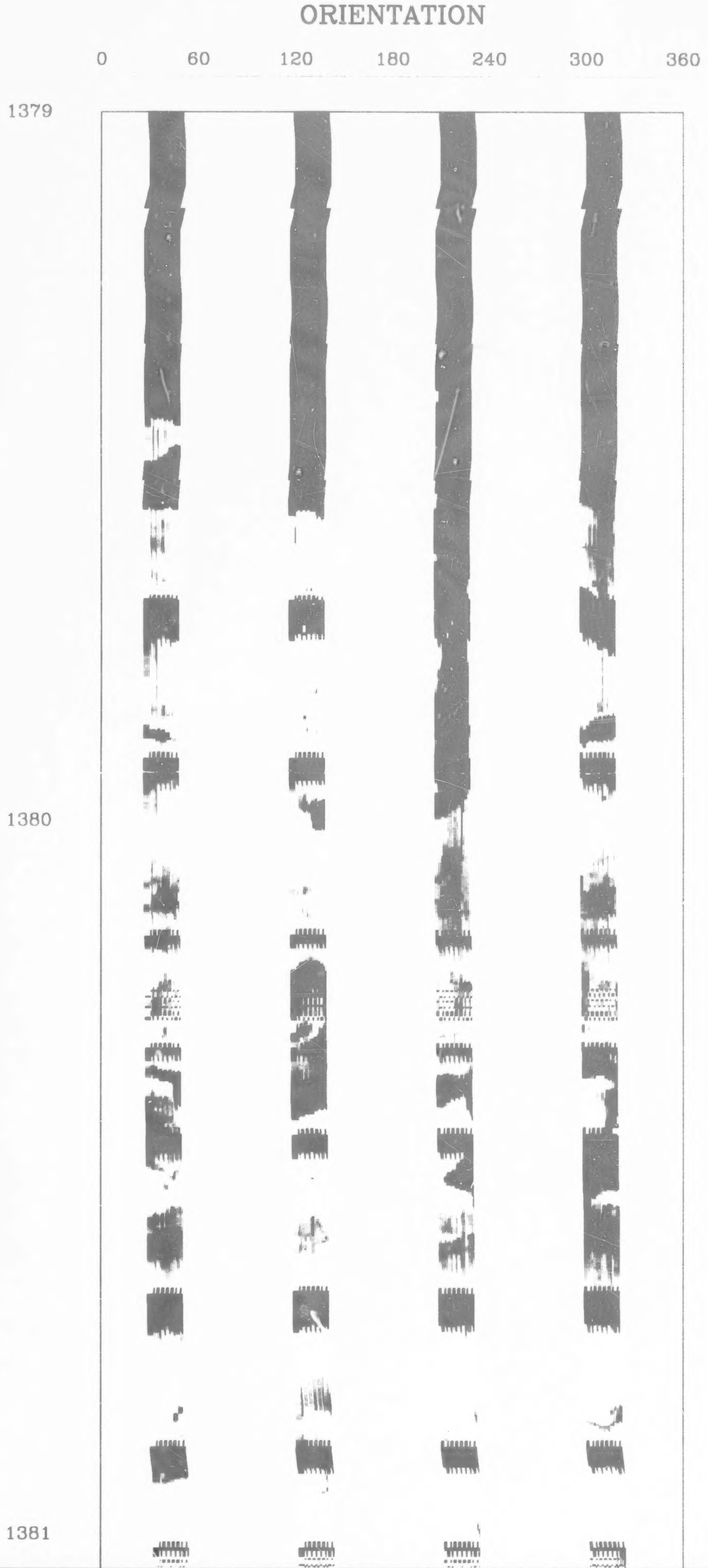
ORIENTATION
0
60
120
180
240
300
360
1379
1380
1381

[redacted]

1382

[redacted]

1383

[redacted]

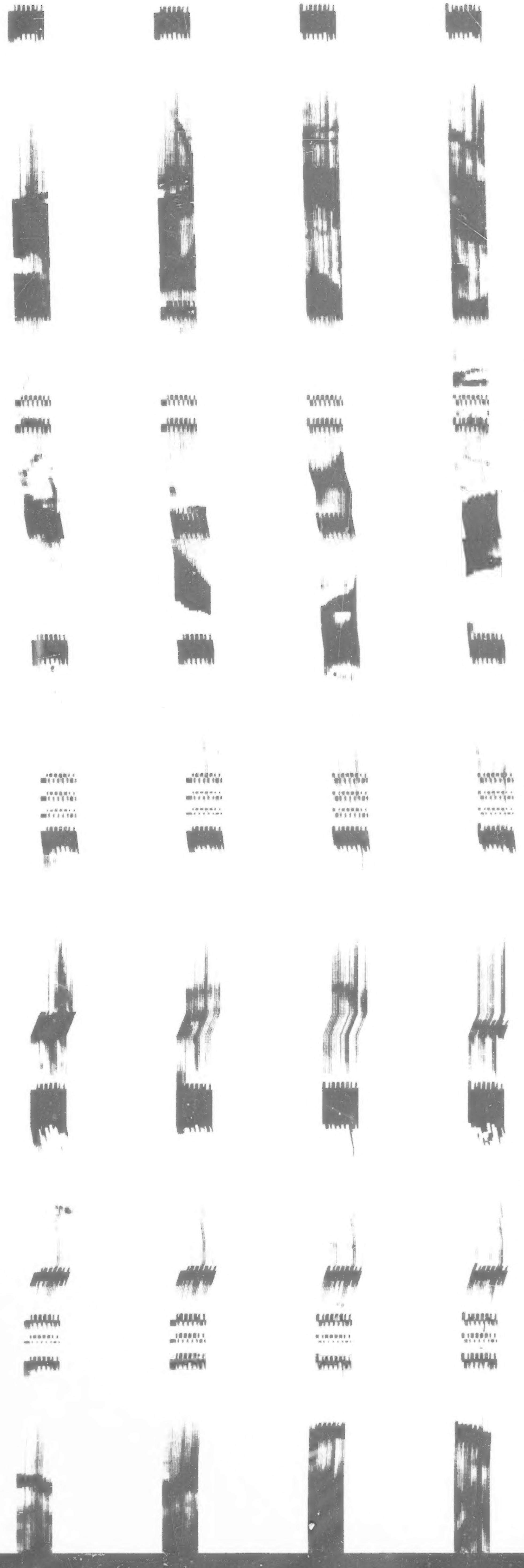

1384

1385

1386

1387

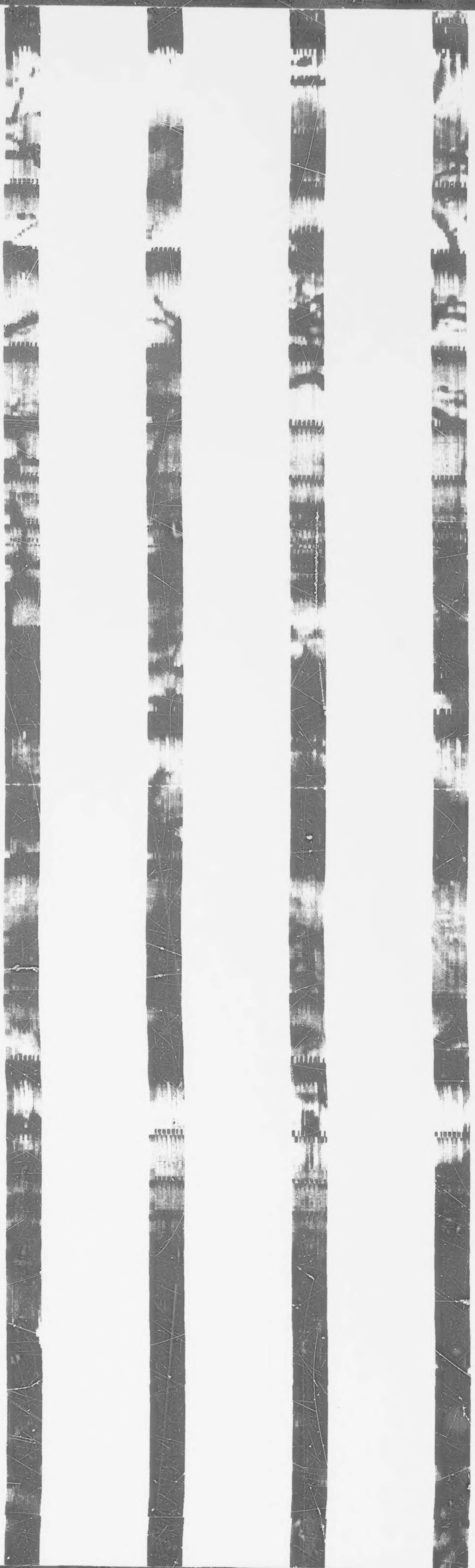

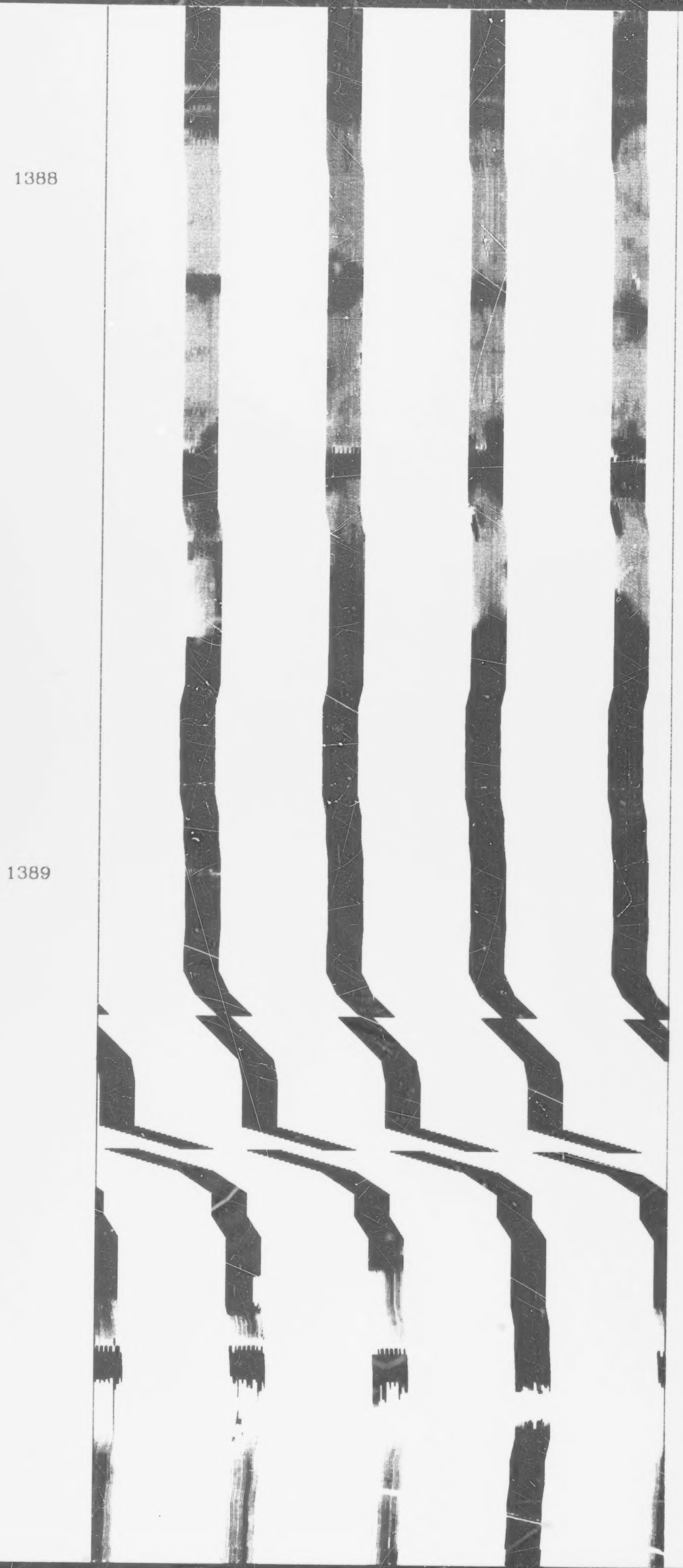
1388
1389

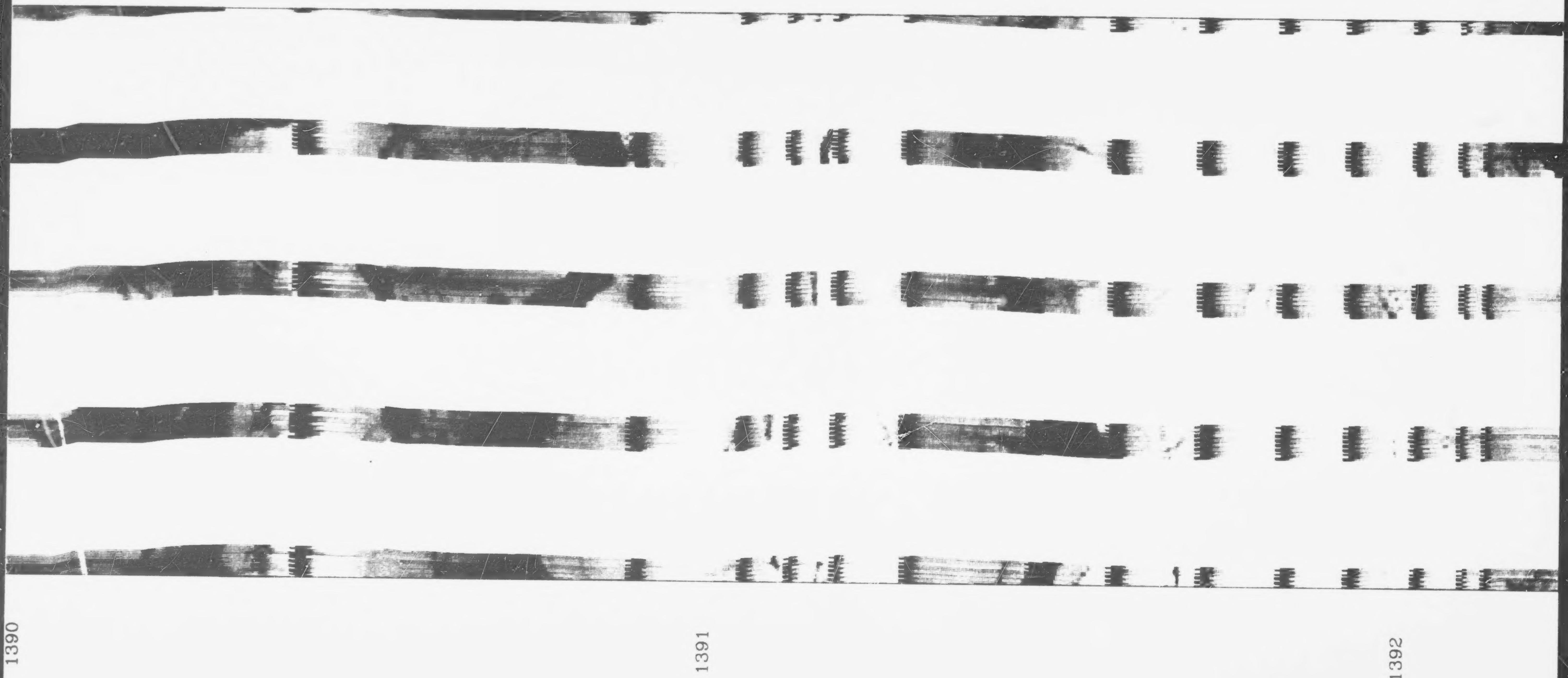
1390
1391
1392

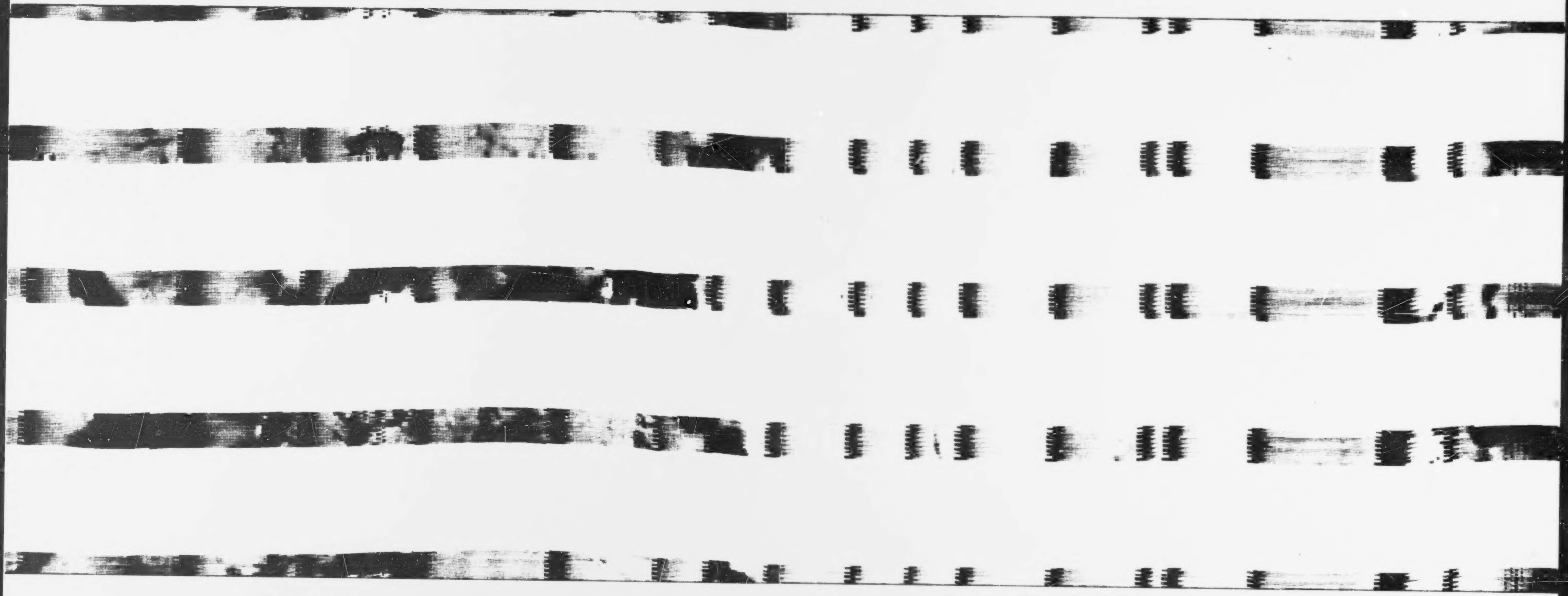

1393
1394

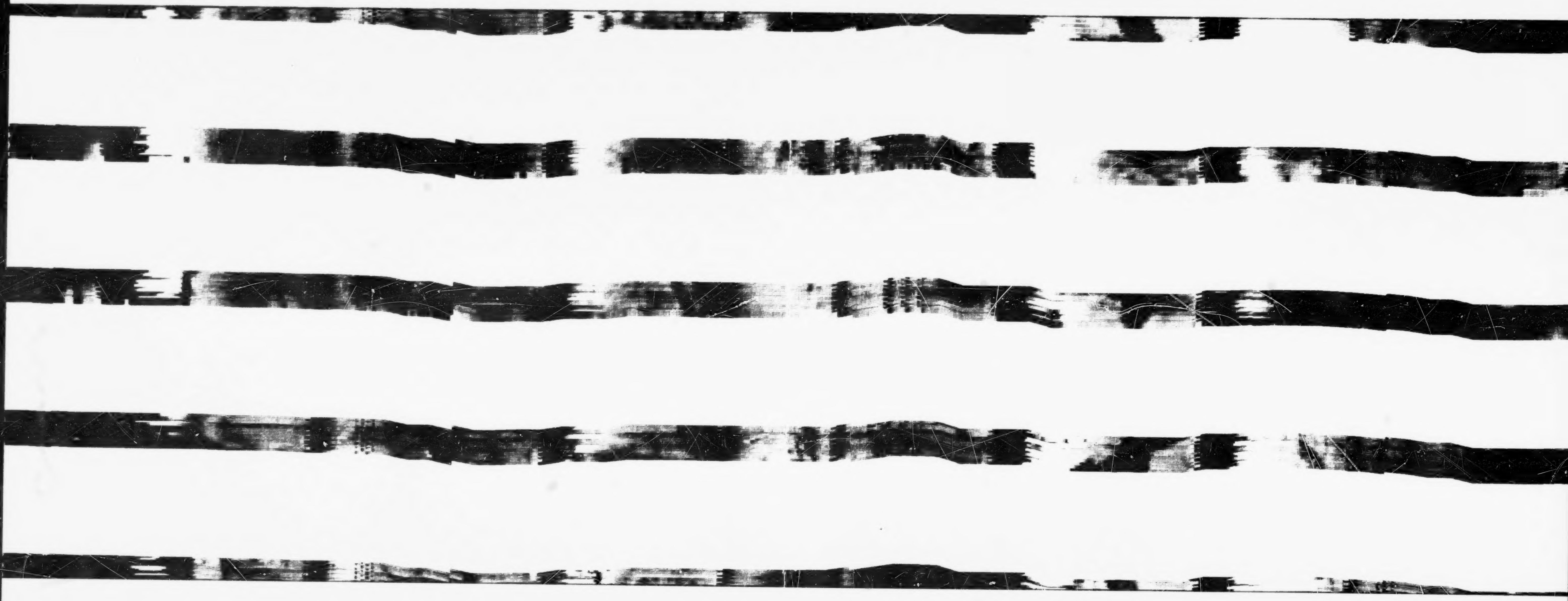

1395
1396

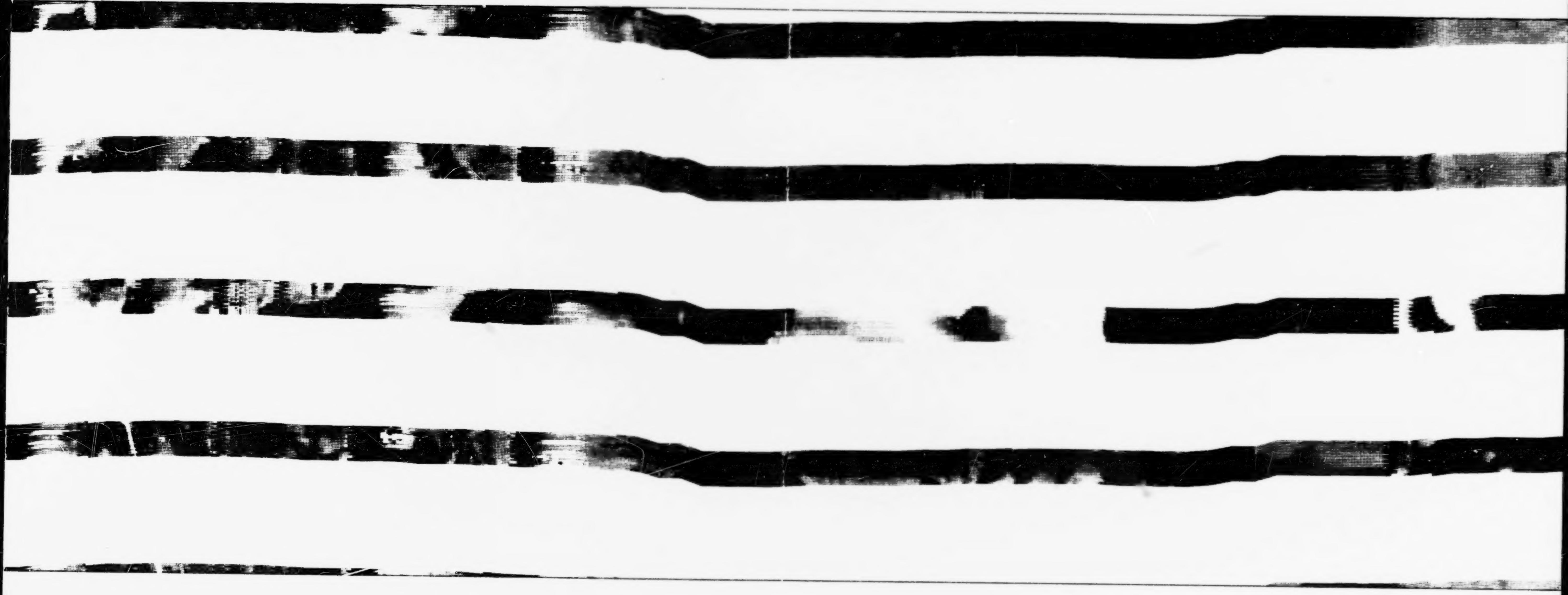

1397

1398

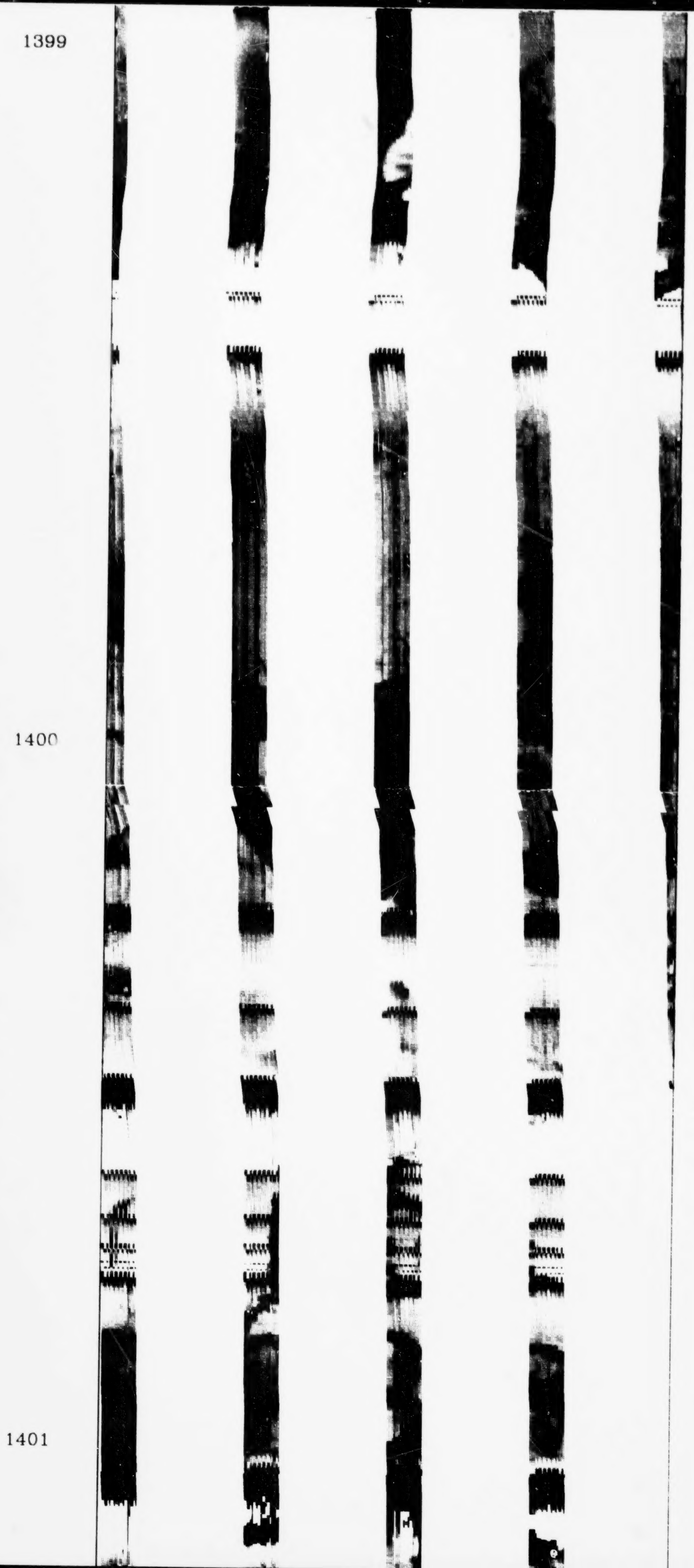
1399
1400
1401

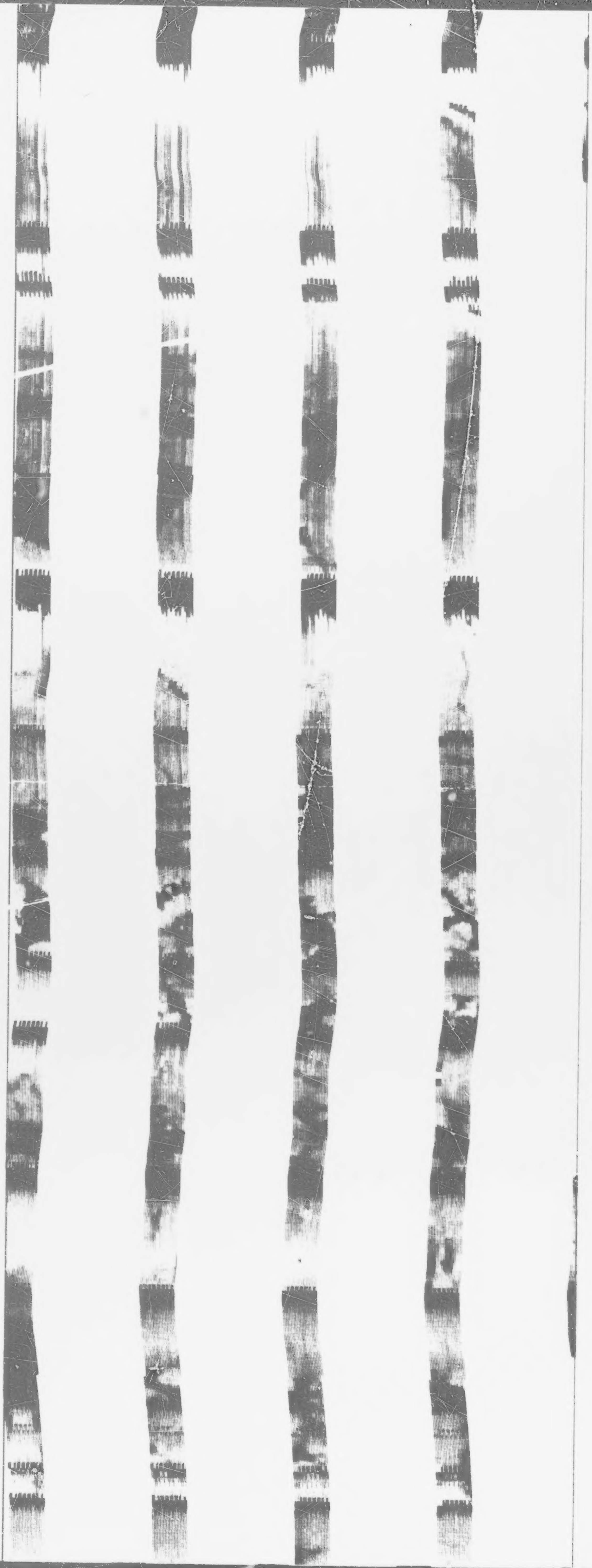
1404
1405

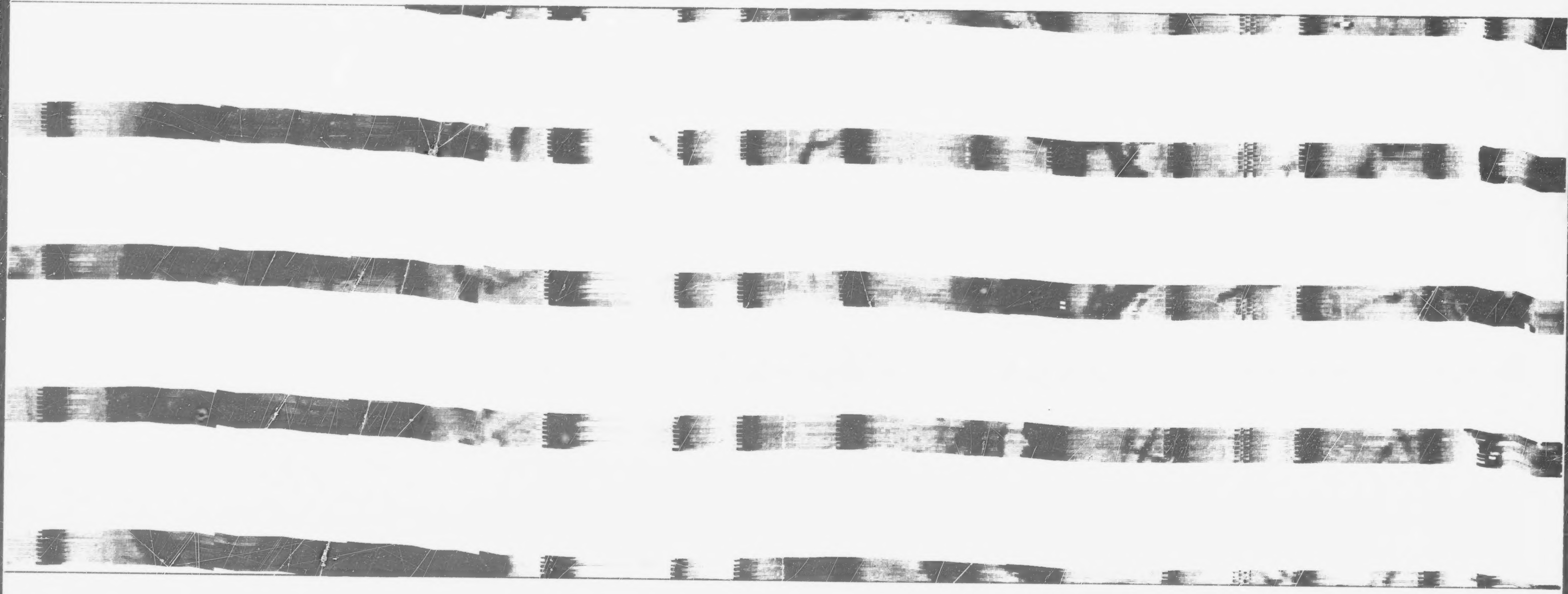
1406
1407

1408
1409
1410

SCHLUMBERGER

FMS
BOREHOLE
IMAGING

COMPANY	LAMONT-DOHERTY BOREHOLE RE
WELL	ODP HOLE 807C
FIELD	ONTONG JAVA PLATEAU
COUNTRY	SOLOMONS
RUN	RUN 2
DATE LOGGED	21 - MAR - 90
REFERENCE	STATIC PASS 2 1410 1440

STATIC NORMALIZATION

PASS 2 (23761)

FILE : MEST.004

ZONE FROM 1440.0 M TO 1410.0 M

DEPTH SCALE = 1/ 5

IMAGE SCALE = 1/ 5

BITSIZE = 9.88

ORIENTATION

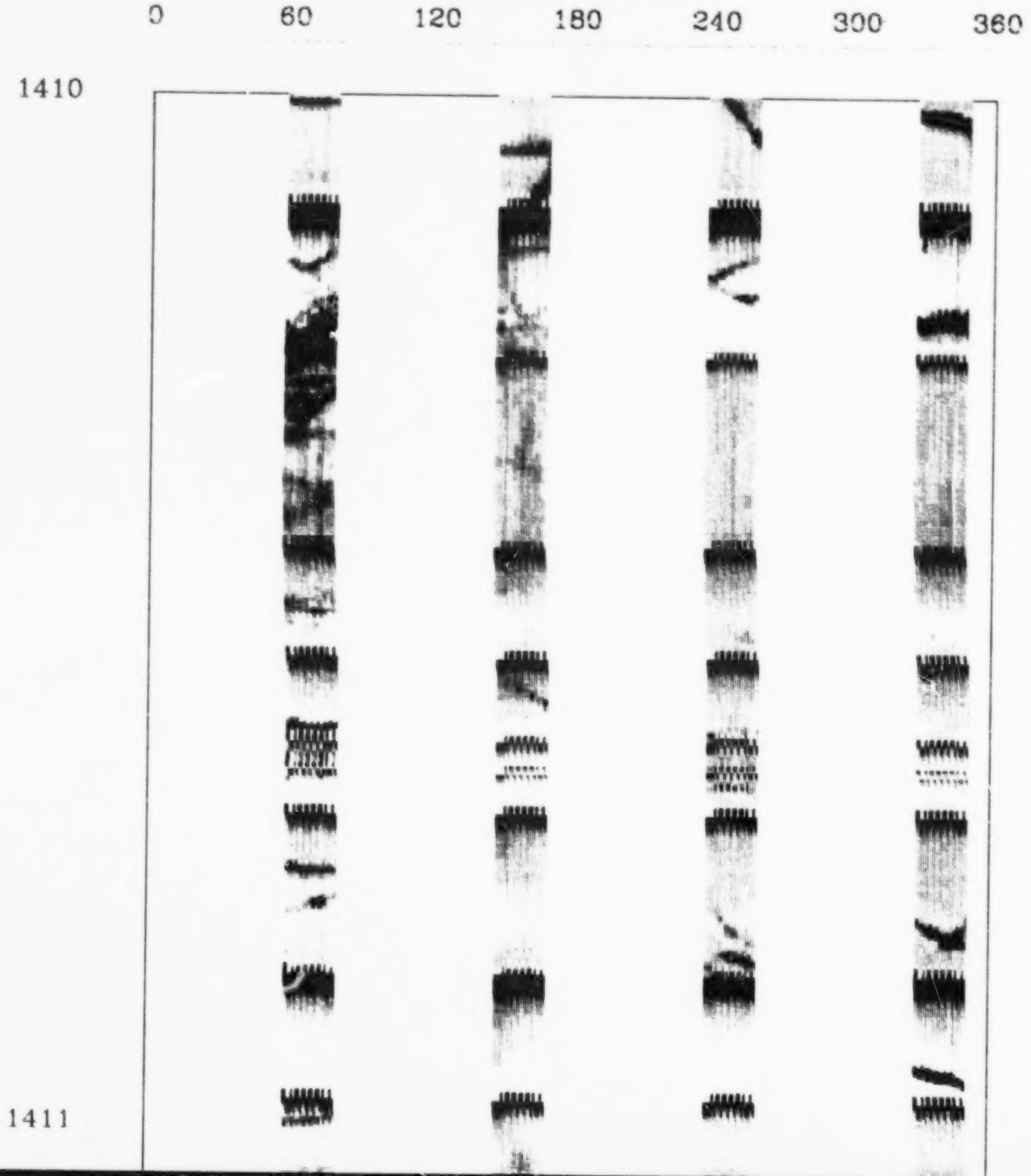

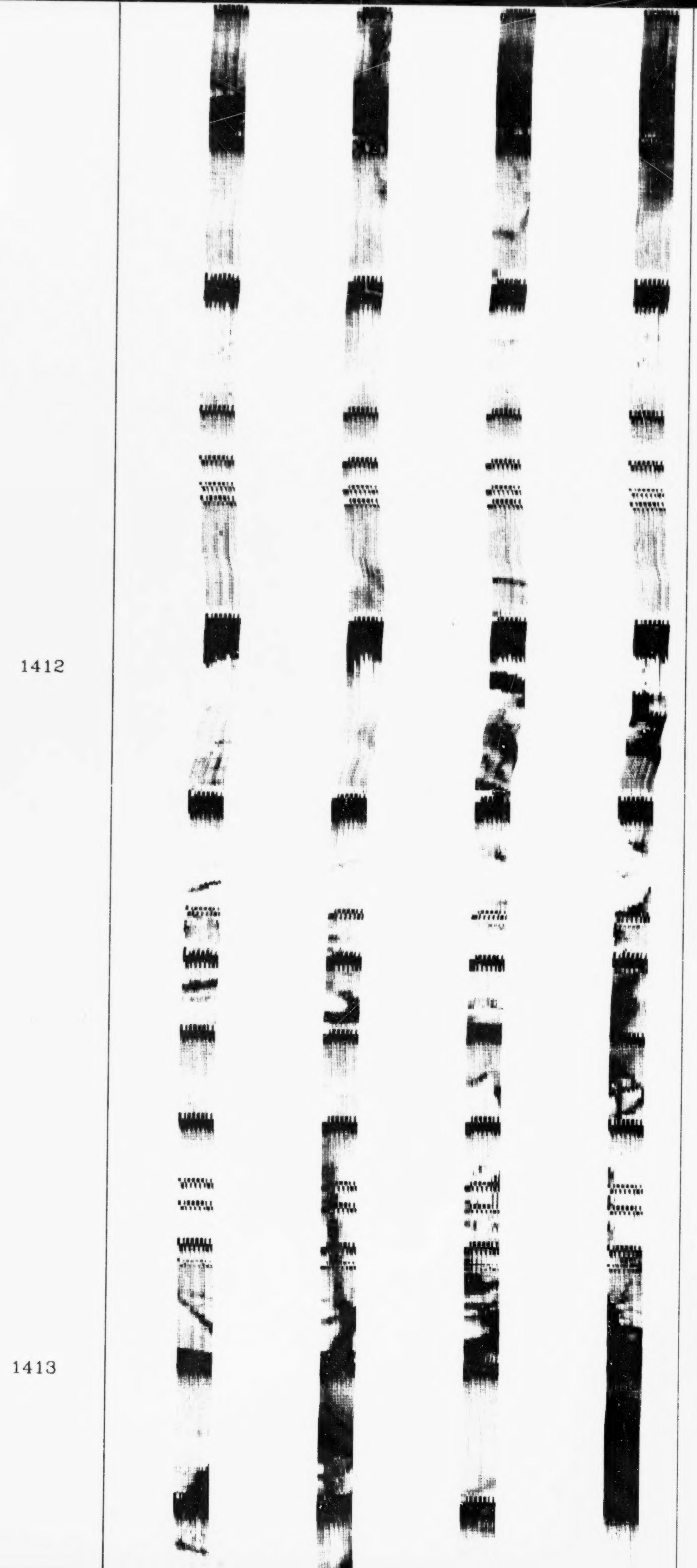
1412
1413

1414

1415

1416

[redacted]

1417

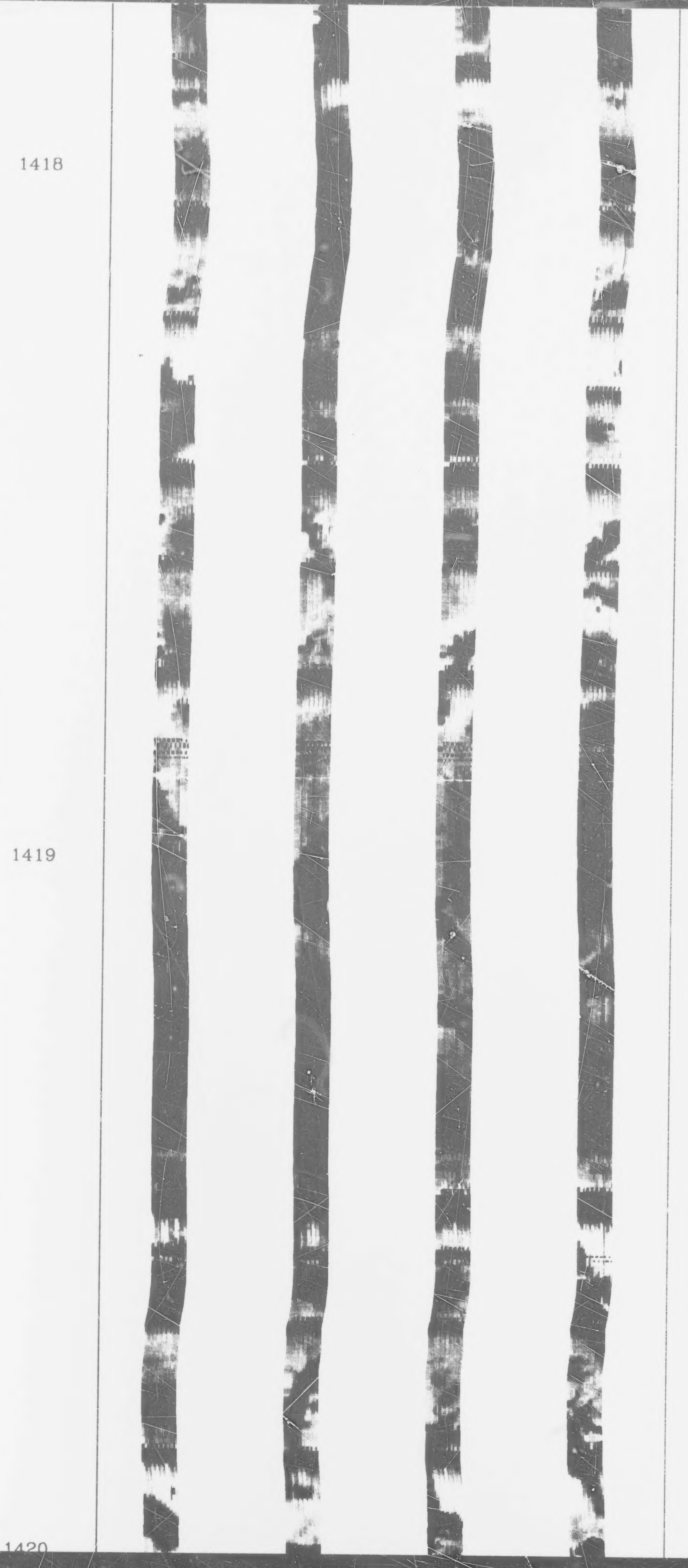
1418
1419
1420

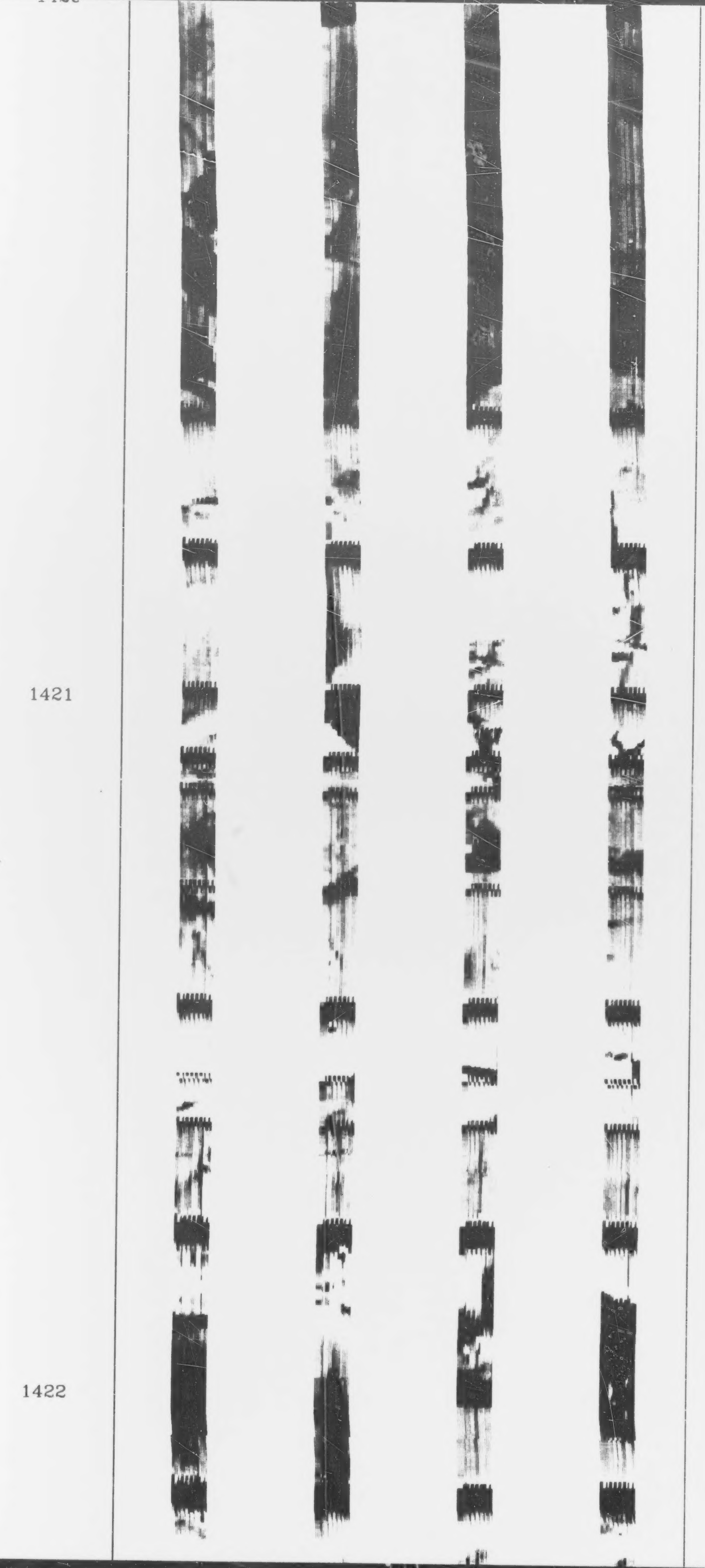
1421
1422

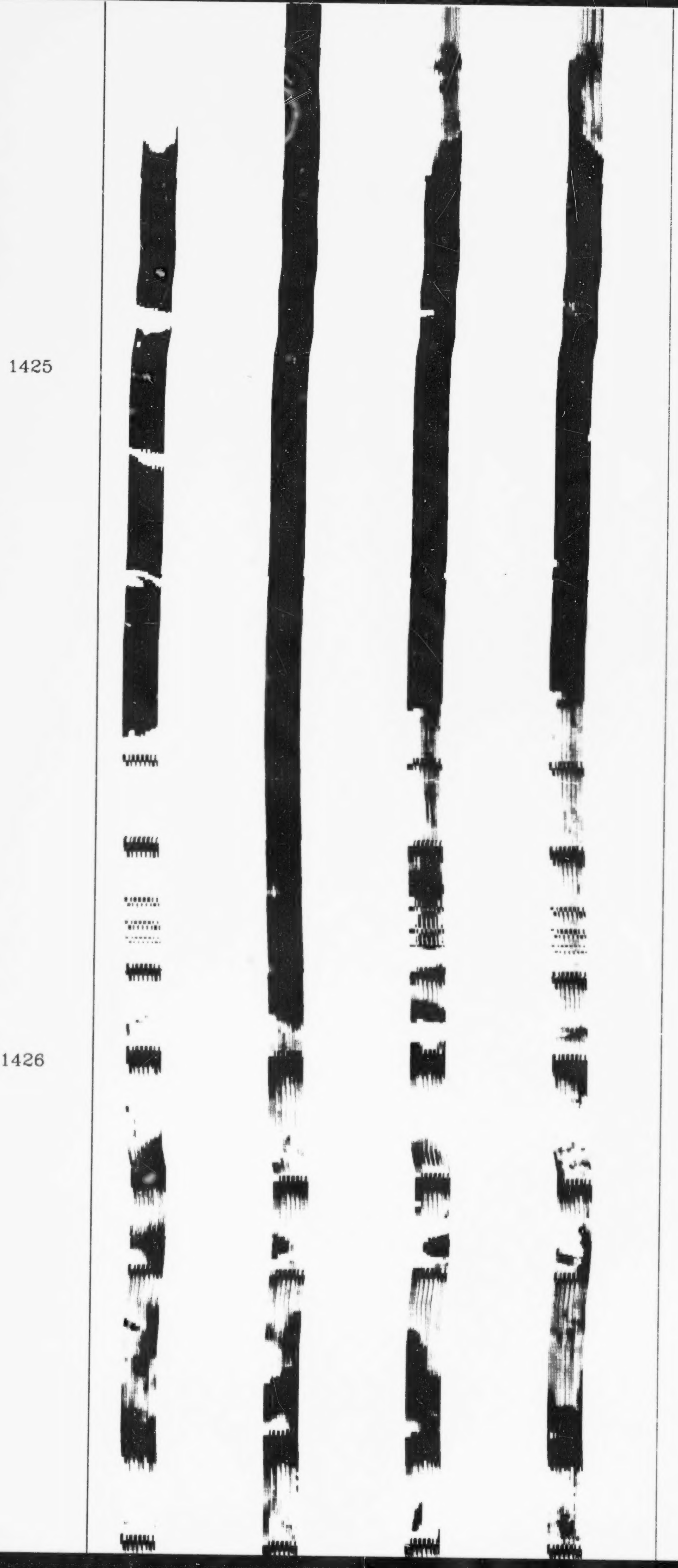
1425
1426

1427

1428

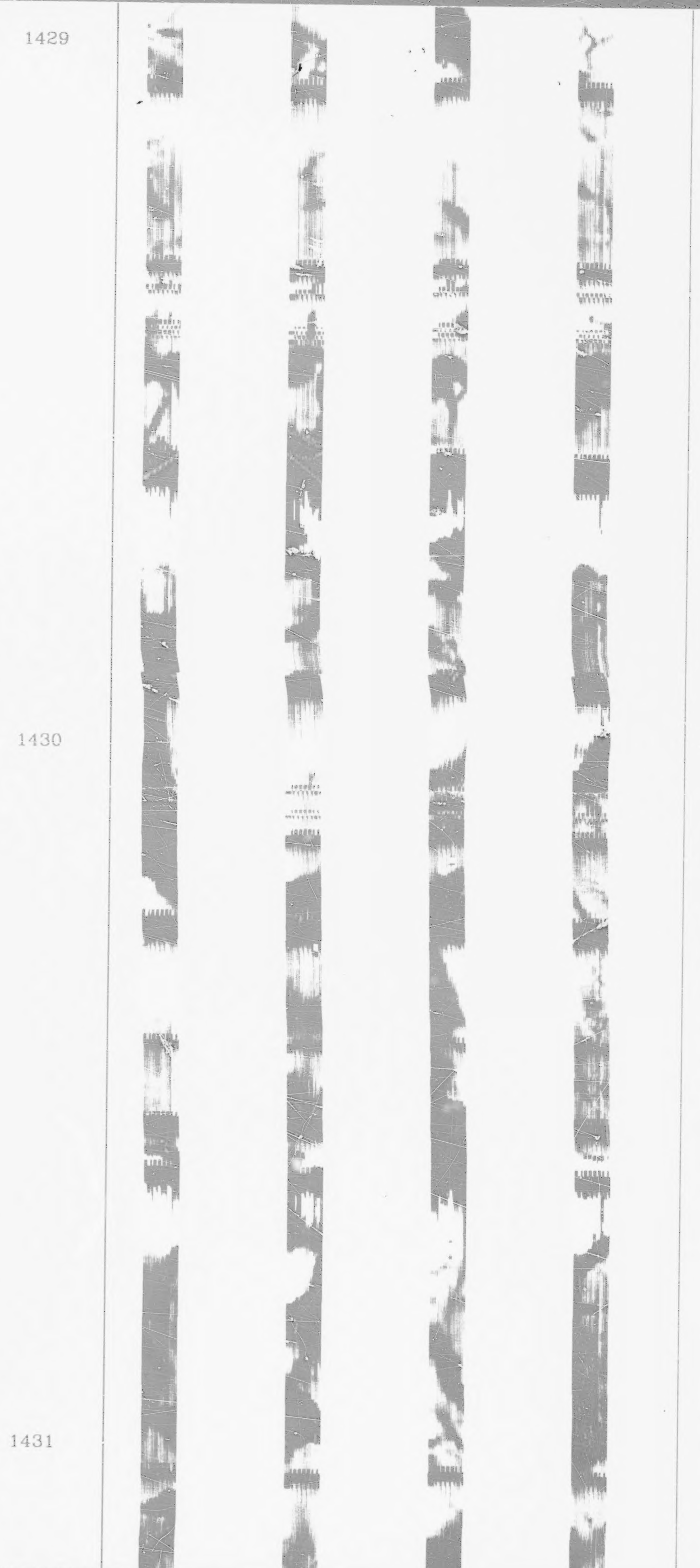
1429
1430
1431

1432

1433

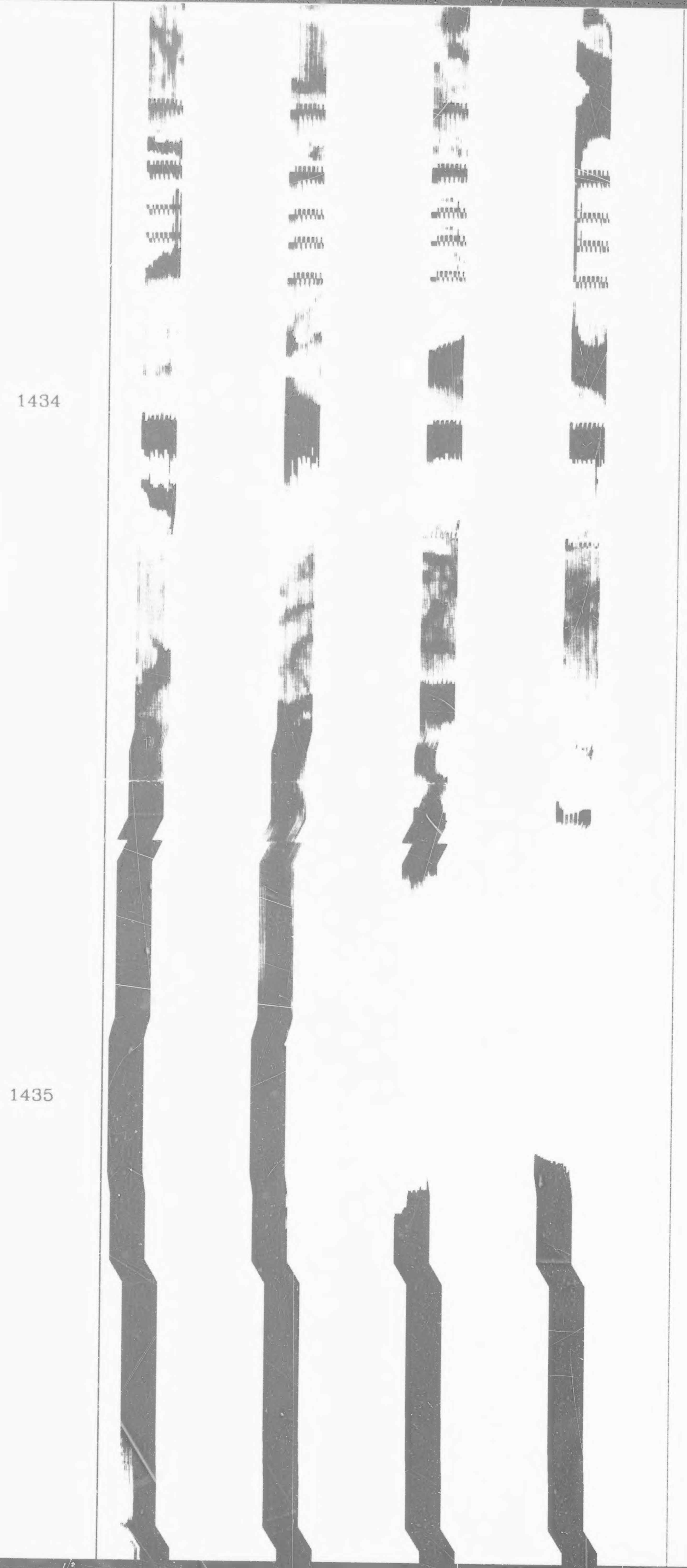
1434
1435

1436
1437

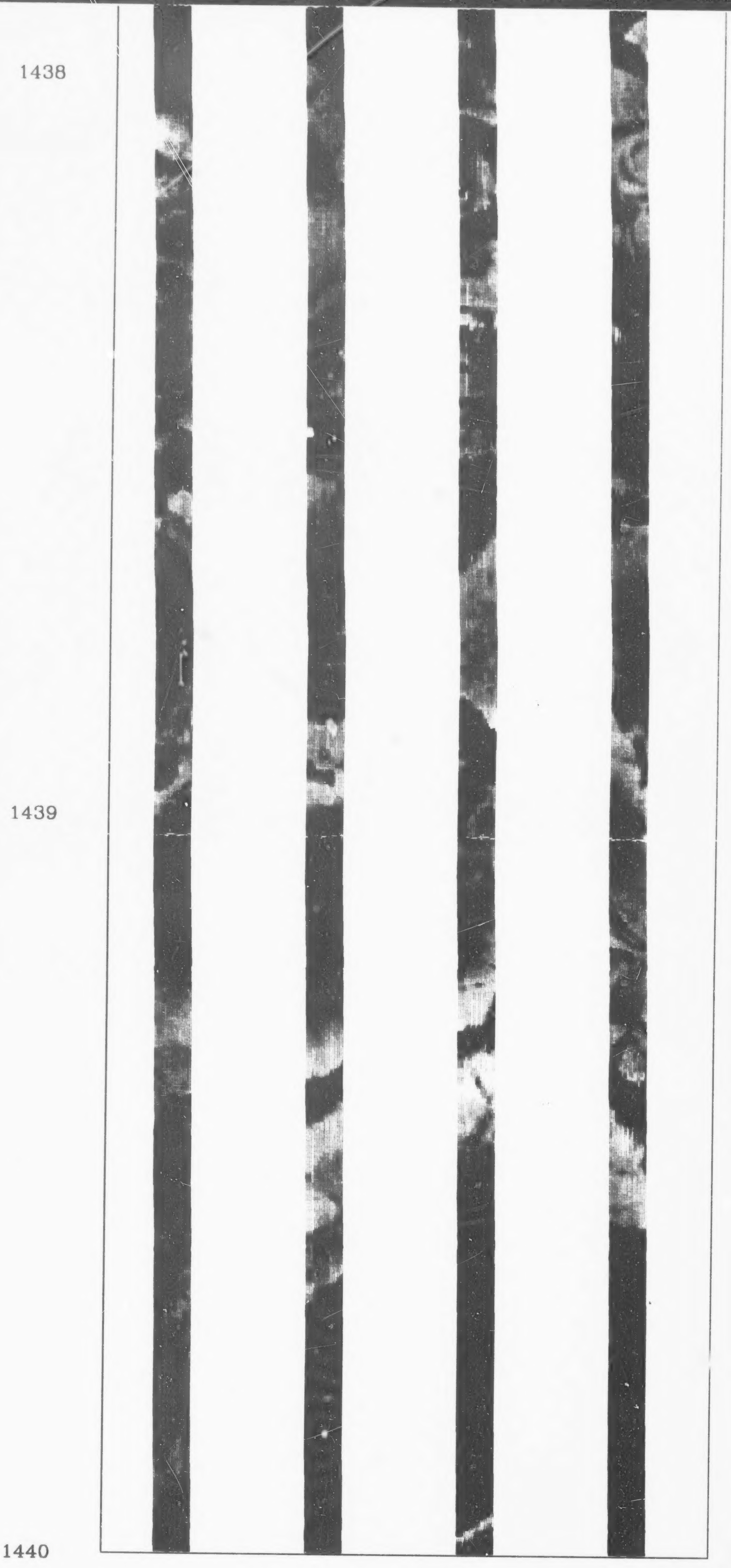
1438
1439
1440

SCHLUMBERGER

FMS
BOREHOLE
IMAGING

COMPANY	LAMONT-DOHERTY BOREHOLE RE
WELL	ODP HOLE 807C
FIELD	ONTONG JAVA PLATEAU
COUNTRY	SOLOMONS
RUN	RUN 2
DATE LOGGED	21 - MAR - 90
REFERENCE	STATIC PASS 2 1440-1470

STATIC NORMALIZATION

PASS 2 (23761)

FILE : MEST.004

ZONE FROM 1470.0 M TO 1440.0 M

DEPTH SCALE = 1/ 5

IMAGE SCALE = 1/ 5

BITSIZE = 9.88

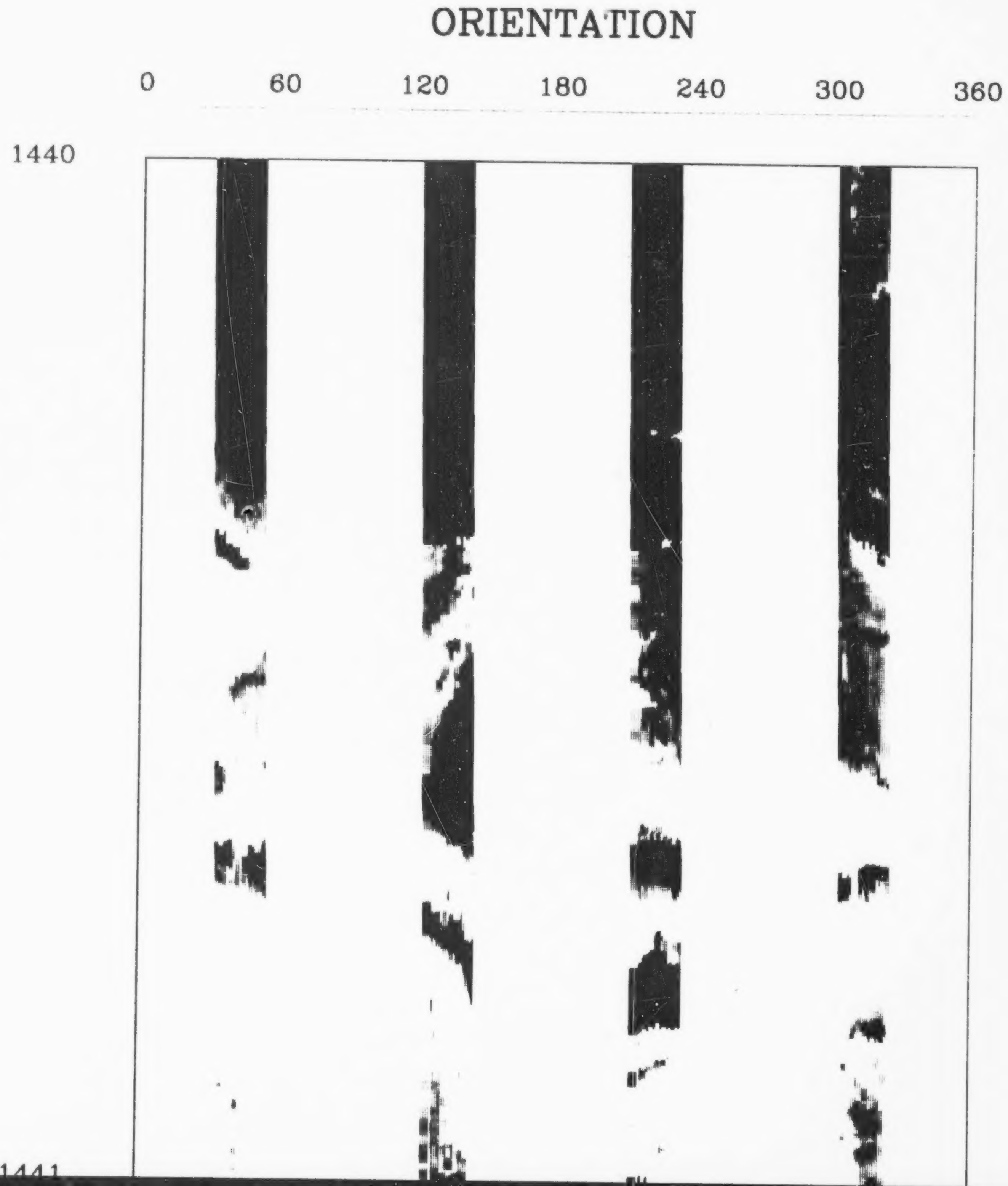

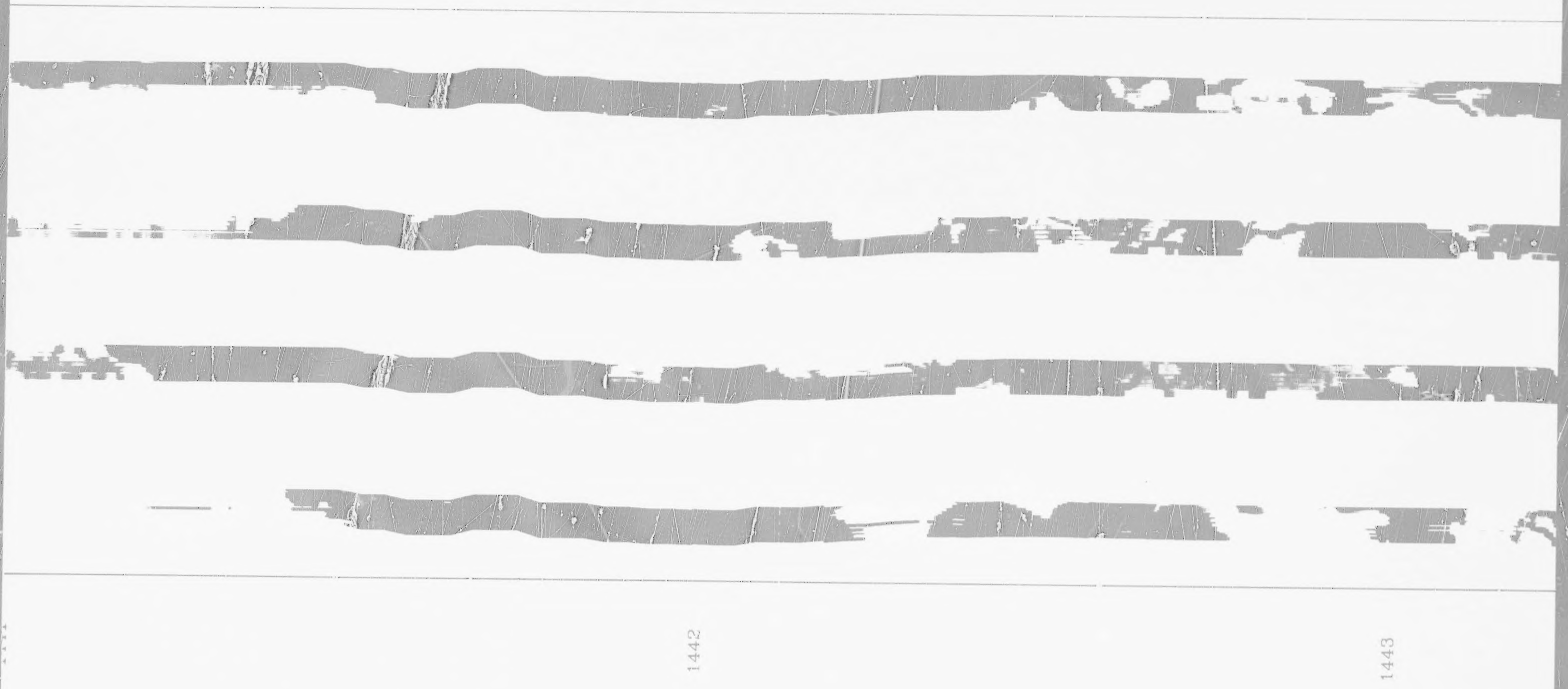
1442
1443

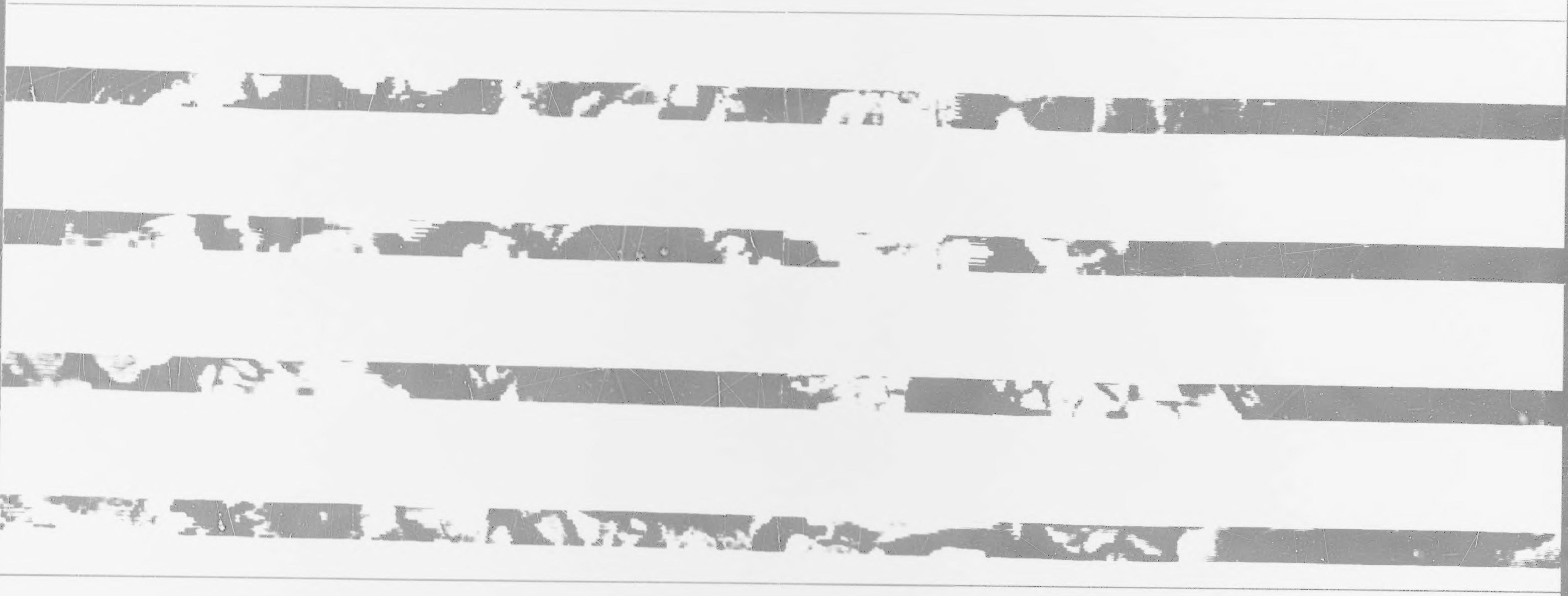

1444
1445

1446

[redacted]

1447

1448
1449

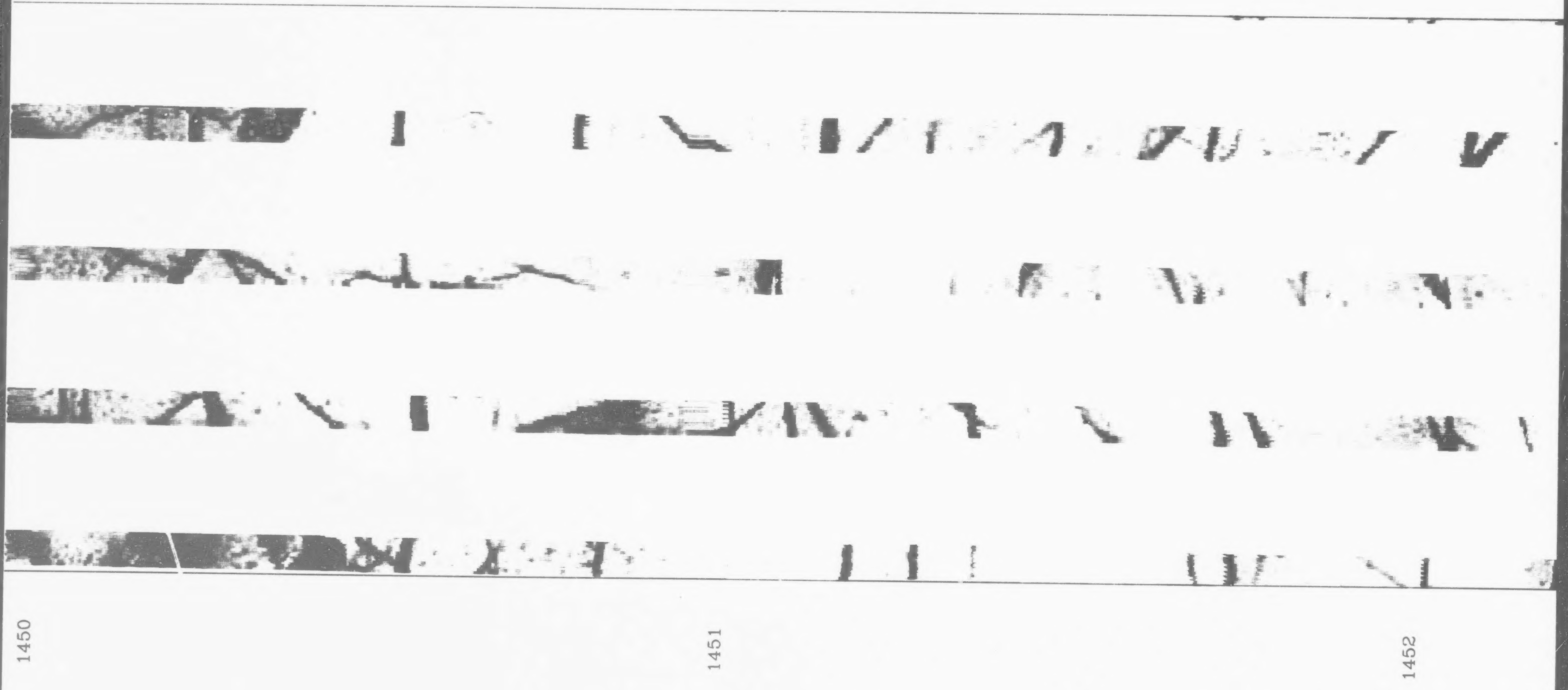
1450
1451
1452

1453
1454

1455
1456

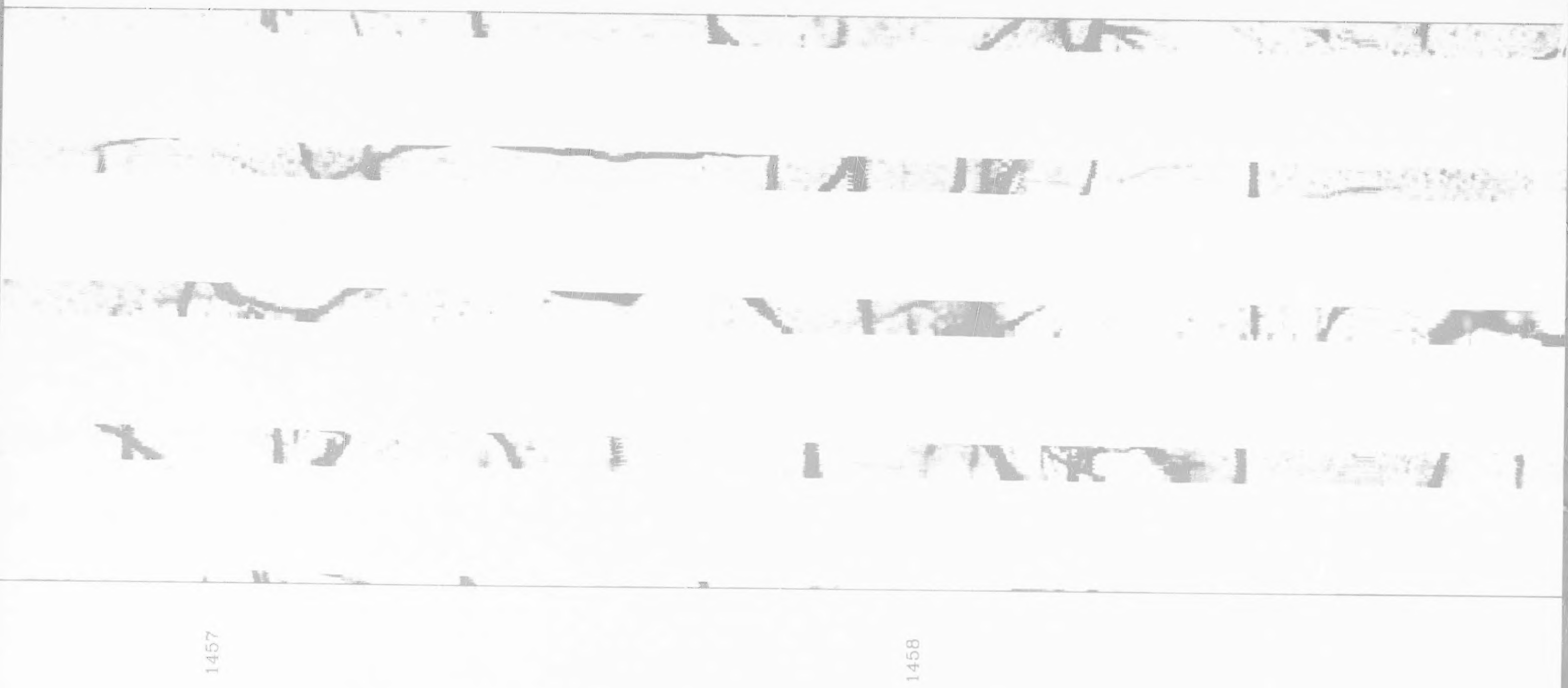
1457
1458

1459
1460
1461

1462
1463

1464

1465

1466
1467

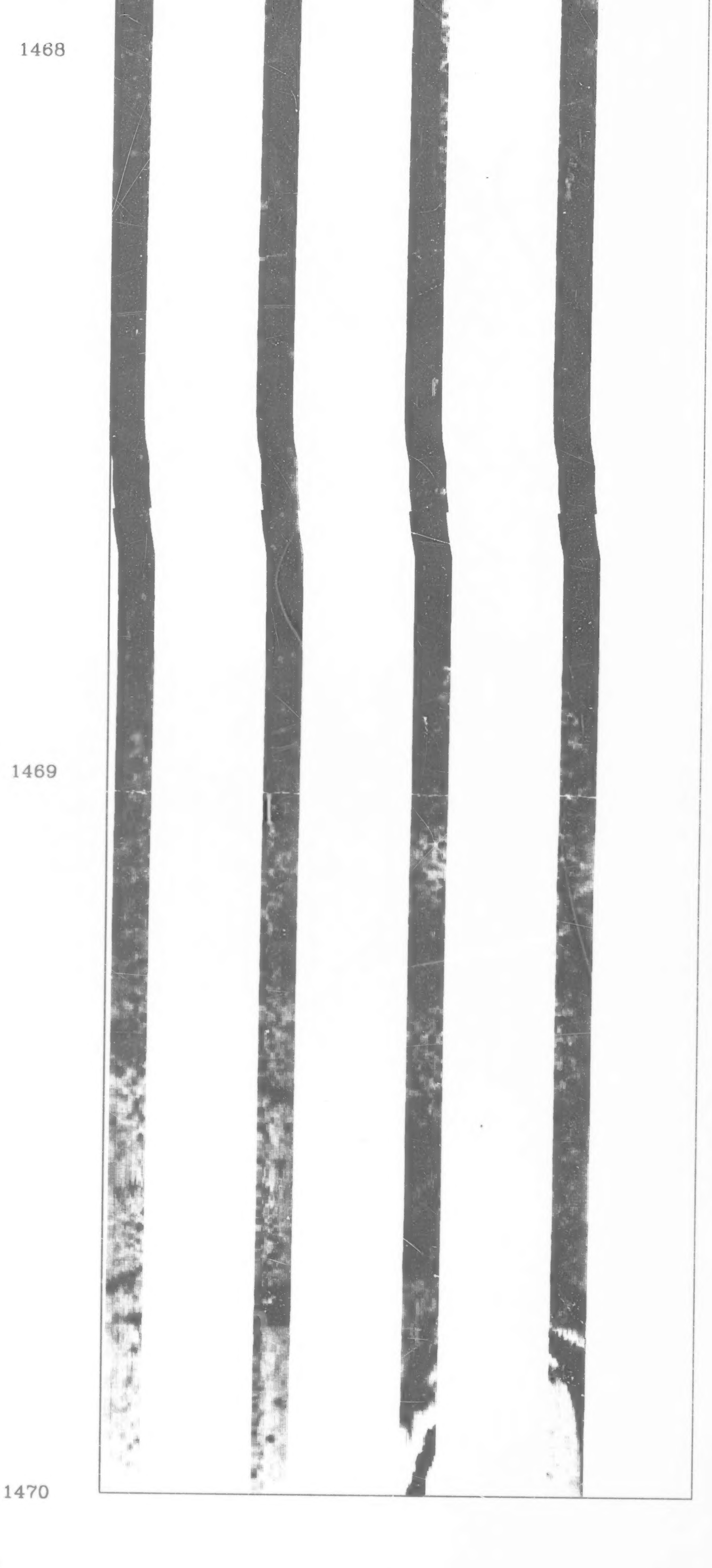
1468
1469
1470

SCHLUMBERGER

FMS
BOREHOLE
IMAGING

COMPANY	LAMONT–DOHERTY BOREHOLE RE
WELL	ODP HOLE 807C
FIELD	ONTONG JAVA PLATEAU
COUNTRY	SOLOMONS
RUN	RUN 2
DATE LOGGED	21 – MAR – 90
REFERENCE	STATIC PASS 2 1470 1504

STATIC NORMALIZATION

PASS 2 (23761)

FILE : MEST.004

ZONE FROM 1503.6 M TO 1470.0 M

DEPTH SCALE = 1/ 5

IMAGE SCALE = 1/ 5

BITSIZE = 9.88

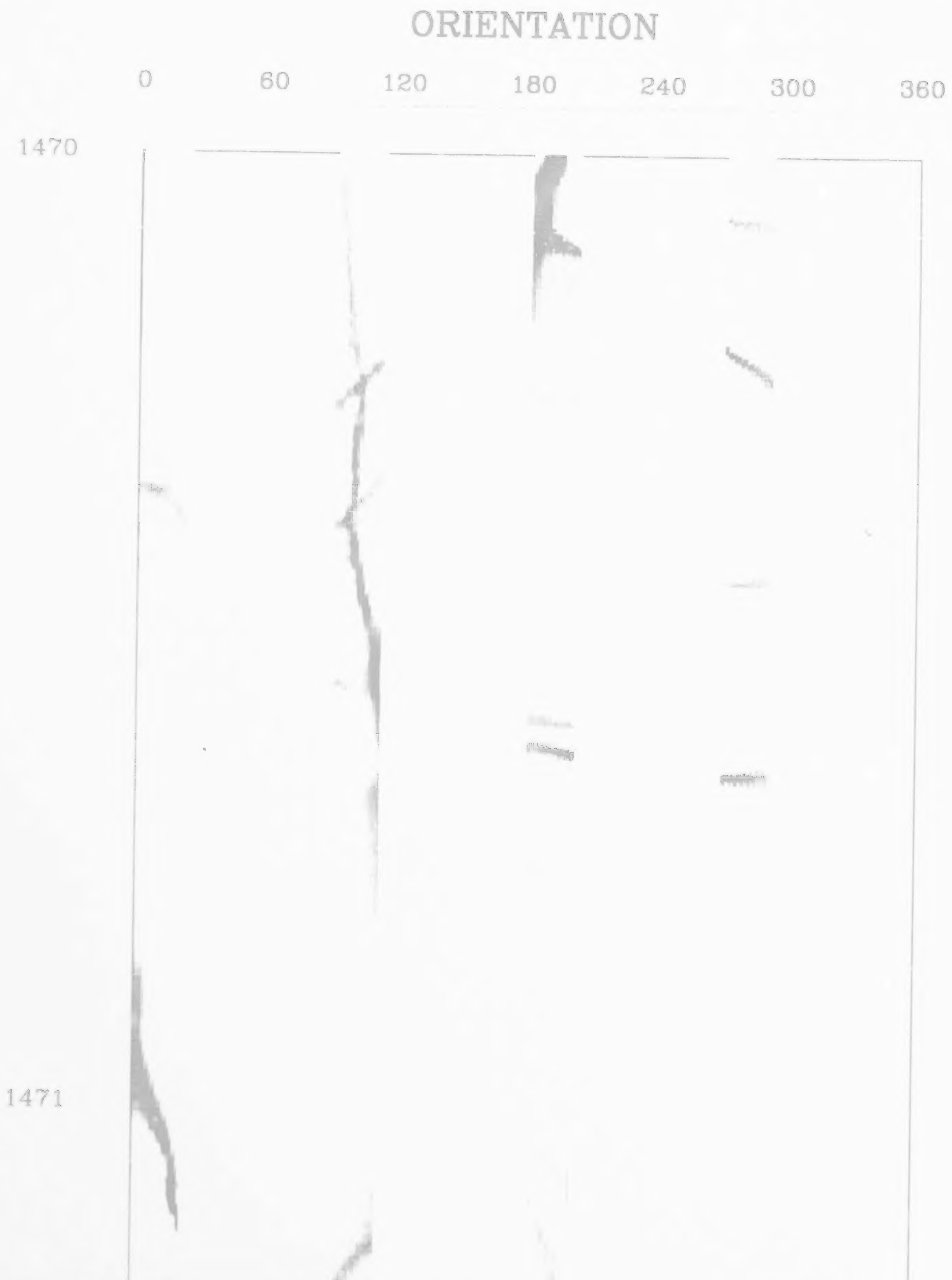

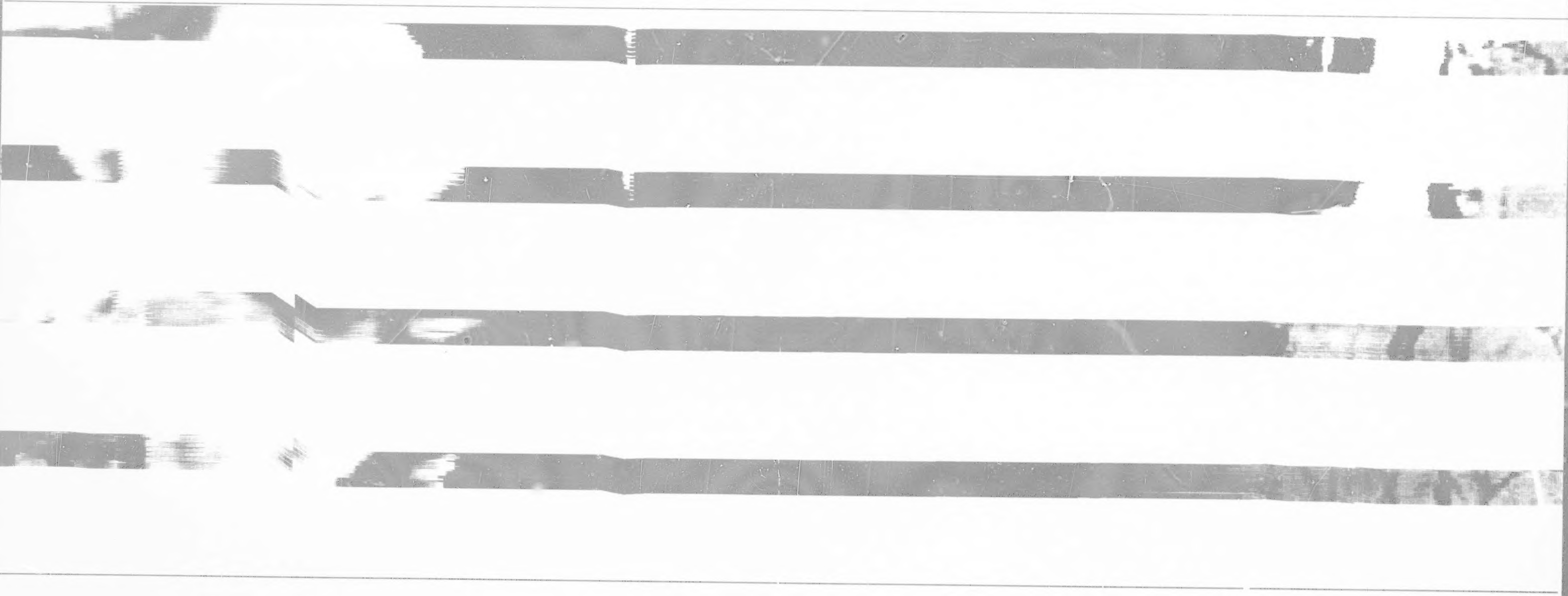

1474

1475

1476
1477

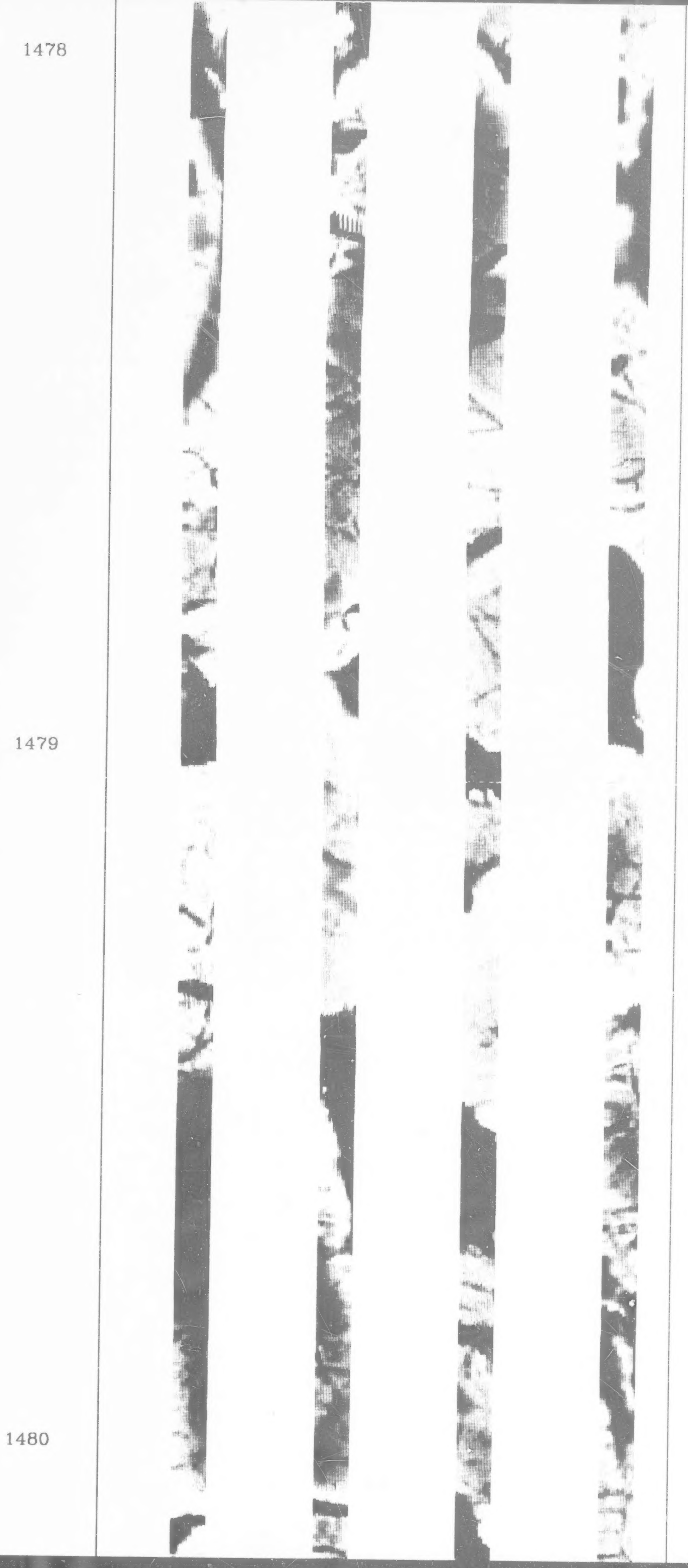
1478
1479
1480

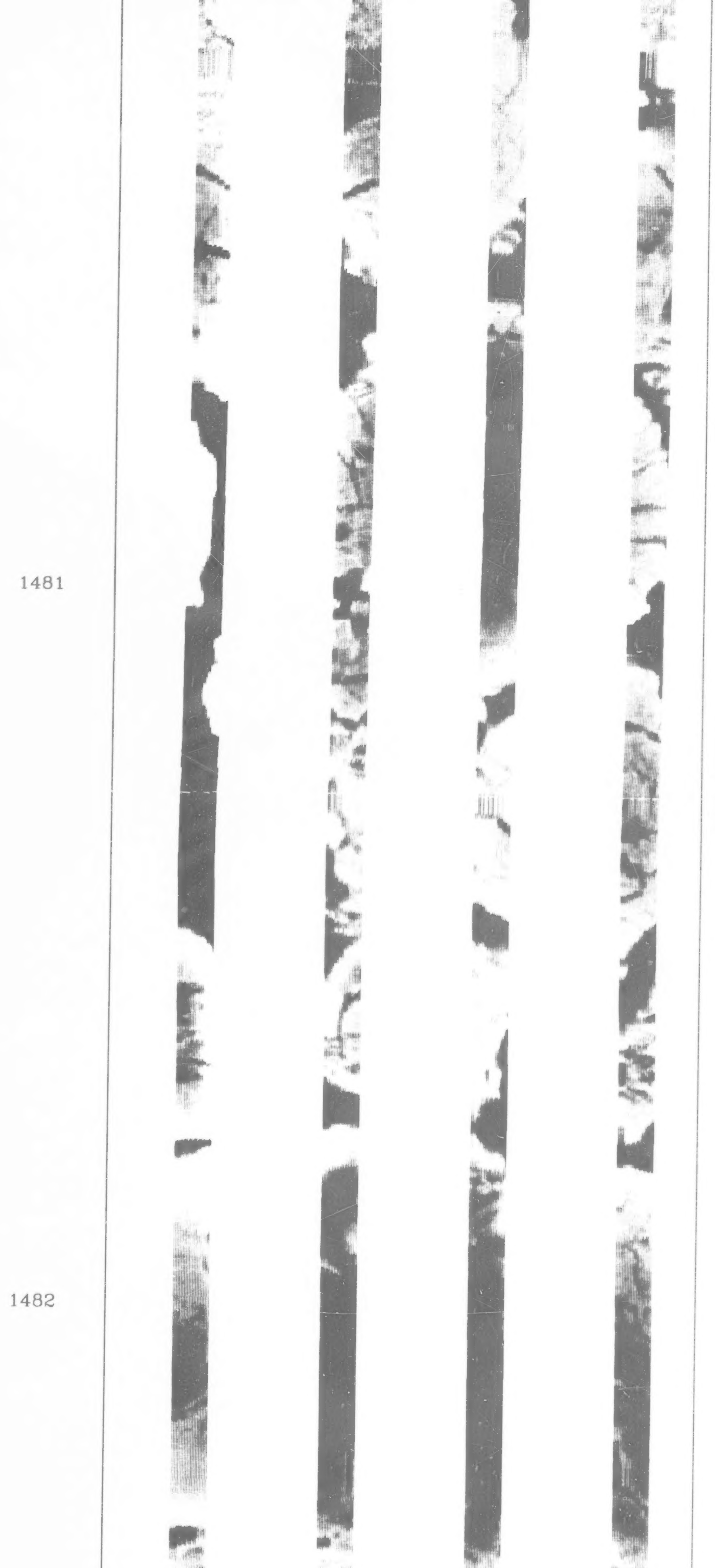
1481
1482

1483

1484

1485

1486

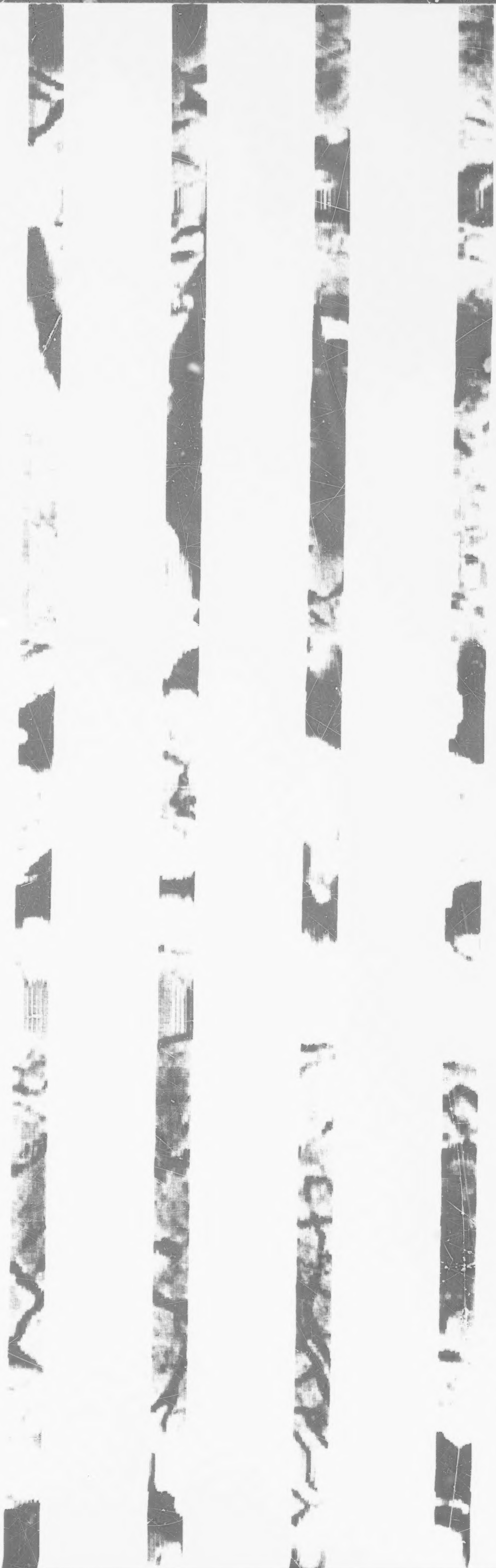

1487
1488
1489

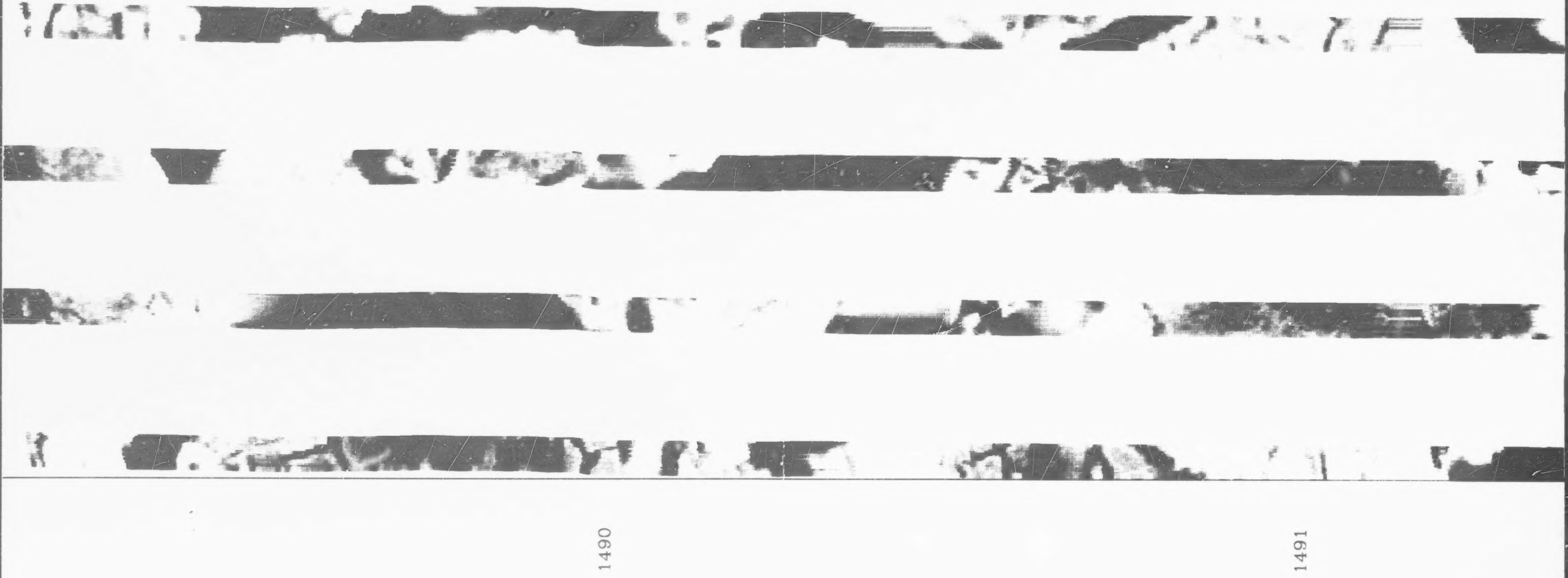
1490
1491

1492
1493

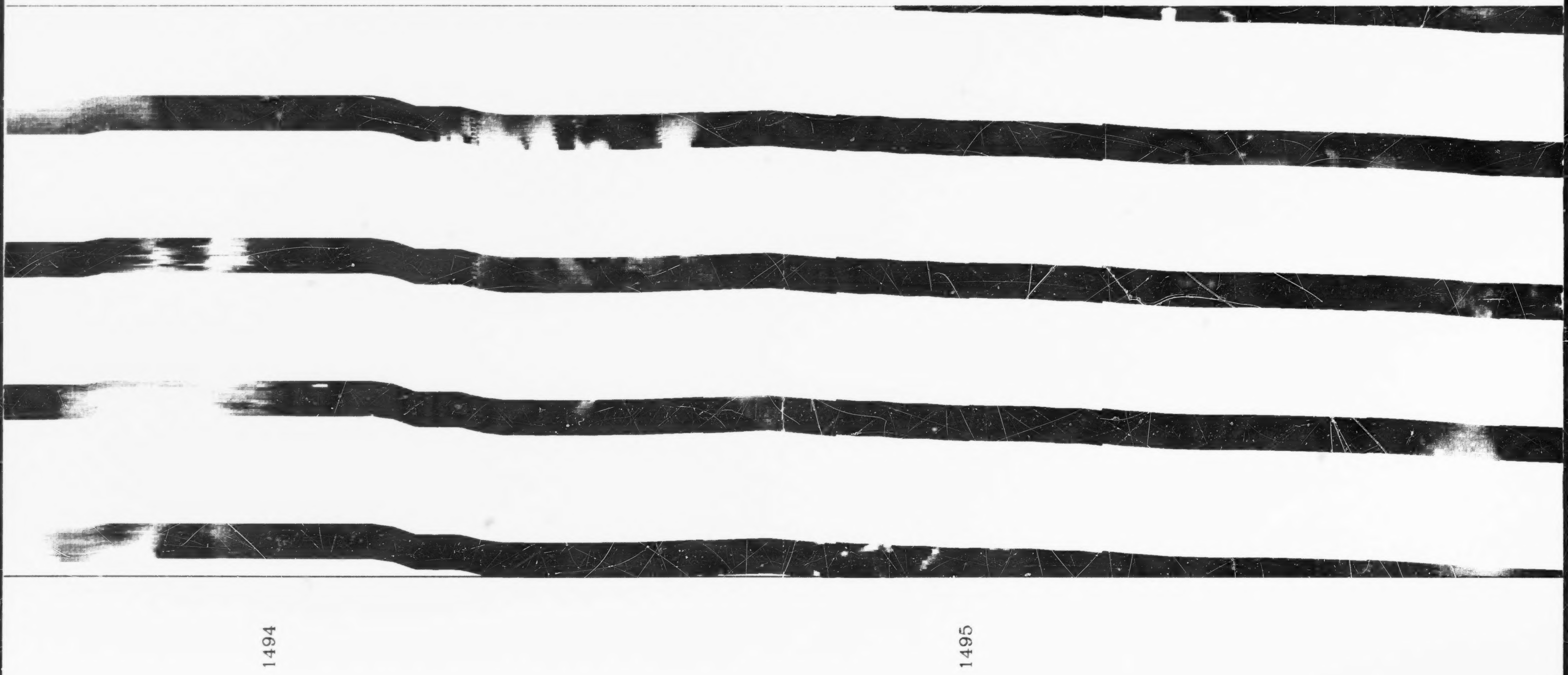
1494
1495

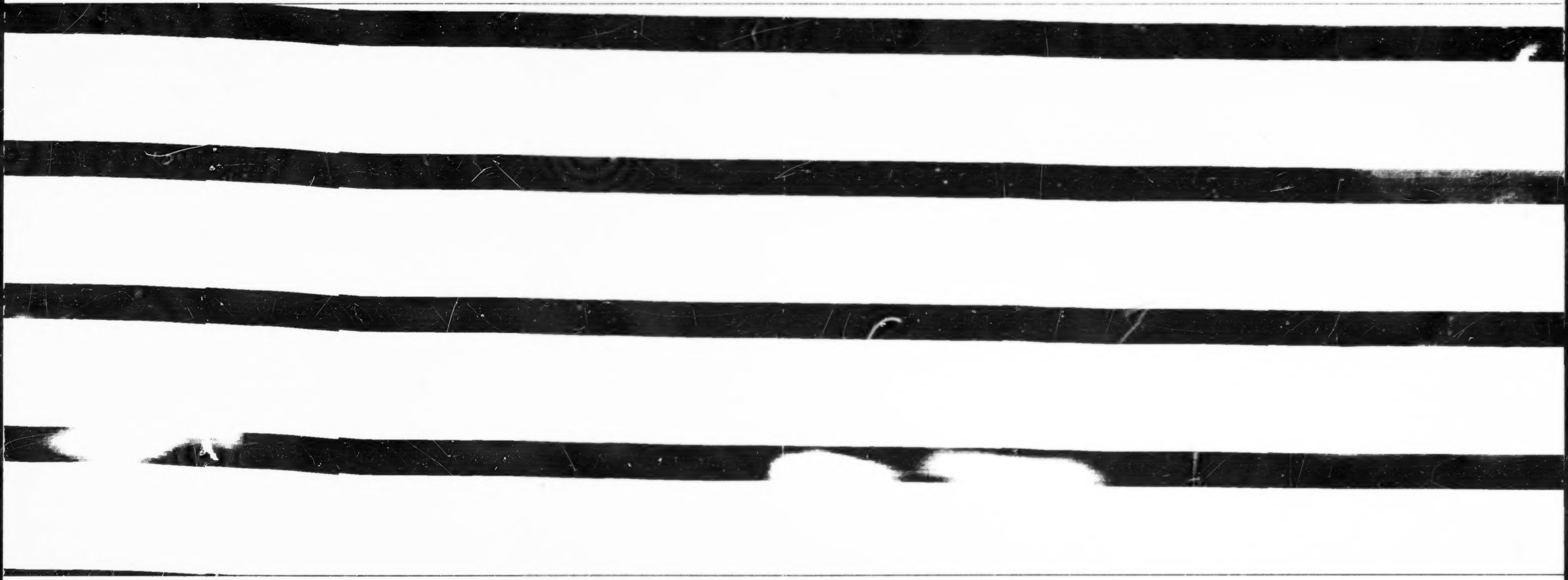

1496
1497
1498

1499

1500

1501

1502

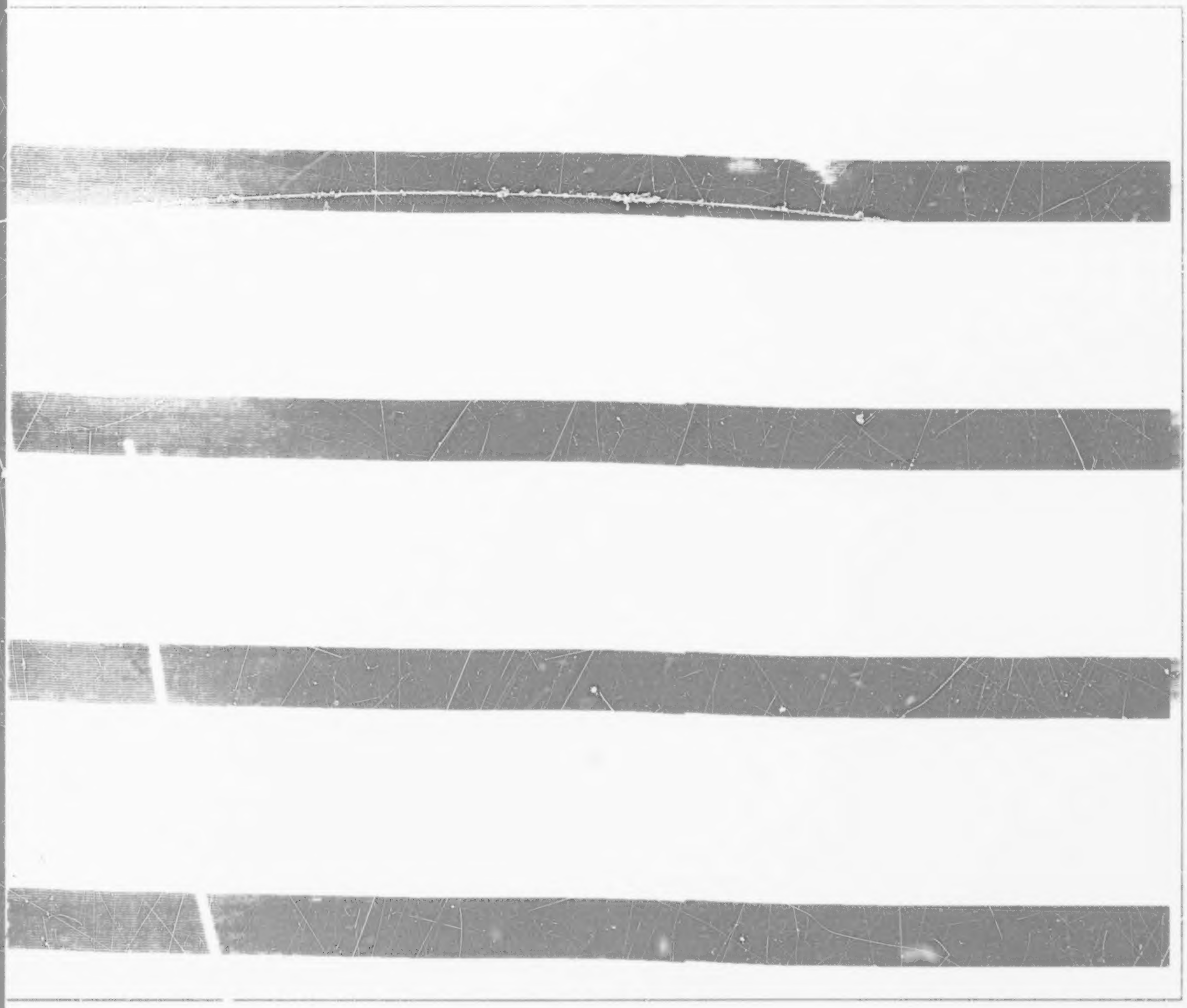

```
#cruise ODP130JR                                              date run: Wed Jul 18 16:38:07 1990          page   1
#
#                          latitude  longitude            actual    drift         dr               prob. error        drift
#da mo  yr    time  deg   min   deg   min       dist speed cse  speed hed  speed cse   cmnt (smajxsmin@az)  dist   time   no.
#- - - - - - - - - - - - - - - - - - - - - - - - - - - - - - - - - - - - - - - - - - - - - - - - - - - - - - - - - - - - - -
 23 01 1990 *0220  13 27.43 144 39.31      0.0   9.7 252    1.5 253   8.2 252   GF    0.00 0.00   0    0.0    0.0      1
 23 01 1990  0222  13 27.3  144 39.0       0.3  11.0 257    1.5 253   9.6 258   c/cs                                   2
 23 01 1990 *0225  13 27.21 144 38.44      0.9  11.1 261    1.6 276   9.6 258   GF    0.00 0.00   0    0.1    0.1      3
 23 01 1990  0226  13 27.2  144 38.3       1.1  11.2 263    1.6 276   9.7 261   c/cs                                   4
 23 01 1990 *0230  13 27.09 144 37.49      1.8  11.7 263    2.0 270   9.7 261   GF    0.00 0.00   0    0.1    0.1      5
 23 01 1990  0231  13 27.1  144 37.3       2.0   9.3 265    2.0 270   7.2 264   c/cs                                   6
 23 01 1990  0233  13 27.0  144 37.0       2.3   9.2 265    2.0 270   7.2 263   c/cs                                   7
 23 01 1990 *0235  13 27.01 144 36.66      2.6   7.6 265    0.4 299   7.2 263   GF    0.00 0.00   0    0.2    0.1      8
 23 01 1990  0236  13 27.0  144 36.5       2.7  10.7 265    0.4 299  10.4 264   c/cs                                   9
 23 01 1990 *0240  13 26.94 144 35.80      3.5  12.6 268    2.4 288  10.4 264   GF    0.00 0.00   0    0.0    0.1     10
 23 01 1990  0240  13 26.9  144 35.8       3.5  13.4 266    2.4 288  11.2 262   c/cs                                  11
 23 01 1990  0242  13 26.9  144 35.3       3.9  11.9 242    2.4 288  10.4 232   c/cs                                  12
 23 01 1990  0243  13 26.8  144 35.2       4.1  11.6 222    2.4 288  10.8 210   c/cs                                  13
 23 01 1990  0244  13 26.7  144 35.0       4.3  10.5 199    2.4 288  10.7 186   c/cs                                  14
 23 01 1990 *0245  13 26.51 144 34.97      4.5  11.2 189    0.7 232  10.7 186   GF    0.00 0.00   0    0.2    0.1     15
 23 01 1990  0246  13 26.3  144 34.9       4.7  11.9 181    0.7 232  11.5 178   c/cs                                  16
 23 01 1990 *0250  13 25.53 144 34.93      5.5  12.5 182    1.3 223  11.5 178   GF    0.00 0.00   0    0.1    0.1     17
 23 01 1990  0254  13 24.7  144 34.9       6.3  12.5 181    1.3 223  11.6 177   c/cs                                  18
 23 01 1990 *0255  13 24.49 144 34.89      6.5  12.1 180    0.8 226  11.6 177   GF    0.00 0.00   0    0.1    0.1     19
 23 01 1990 *0300  13 23.48 144 34.89      7.5  12.2 178    0.7 201  11.6 177   GF    0.00 0.00   0    0.1    0.1     20
 23 01 1990  0301  13 23.3  144 34.9       7.7  12.6 176    0.7 201  12.0 175   c/cs                                  21
 23 01 1990 *0305  13 22.44 144 34.95      8.5  14.3 177    2.4 186  12.0 175   GF    0.00 0.00   0    0.1    0.1     22
 23 01 1990 *0310  13 21.25 144 35.02      9.7  12.8 176    0.8 189  12.0 175   GF    0.00 0.00   0    0.2    0.1     23
 23 01 1990  0312  13 20.8  144 35.1      10.2  12.8 174    0.8 189  12.0 173   c/cs                                  24
 23 01 1990 *0315  13 20.19 144 35.12     10.8  12.8 175    0.9 207  12.0 173   GF    0.00 0.00   0    0.1    0.1     25
 23 01 1990 *0320  13 19.13 144 35.21     11.9  12.2 175    0.5 248  12.0 173   GF    0.00 0.00   0    0.1    0.1     26
 23 01 1990 *0330  13 17.11 144 35.38     13.9  14.5 175    2.5 183  12.0 173   GF    0.00 0.00   0    0.1    0.2     27
 23 01 1990 *0340  13 14.71 144 35.61     16.3  13.9 176    2.0 192  12.0 173   GF    0.00 0.00   0    0.4    0.2     28
 23 01 1990  0342  13 14.2  144 35.6      16.8  13.8 175    2.0 192  11.9 172   c/cs                                  29
 23 01 1990 *0345  13 13.56 144 35.71     17.5  13.4 172    1.5 172  11.9 172   GF    0.00 0.00   0    0.2    0.1     30
 23 01 1990  0347  13 13.1  144 35.8      17.9  13.4 171    1.5 172  11.9 171   c/cs                                  31
 23 01 1990  0349  13 12.7  144 35.8      18.4  12.3 144    1.5 172  11.0 140   c/cs                                  32
 23 01 1990 *0350  13 12.51 144 35.97     18.6  12.2 141    1.2 148  11.0 140   GF    0.00 0.00   0    0.1    0.1     33
 23 01 1990  0351  13 12.4  144 36.1      18.8  12.4 128    1.2 148  11.2 126   c/cs                                  34
 23 01 1990 *0400  13 11.21 144 37.60     20.6  14.7 130    3.6 143  11.2 126   GF    0.00 0.00   0    0.2    0.2     35
 23 01 1990 *0410  13  9.63 144 39.53     23.1  13.9 126    2.6 128  11.2 126   GF    0.00 0.00   0    0.6    0.2     36
 23 01 1990 *0420  13  8.26 144 41.44     25.4  12.5 127    1.3 139  11.2 126   GF    0.00 0.00   0    0.4    0.2     37
 23 01 1990 *0430  13  7.00 144 43.14     27.5  13.6 132    2.6 156  11.2 126   GF    0.00 0.00   0    0.2    0.2     38
 23 01 1990 *0440  13  5.50 144 44.88     29.7  12.7 132    1.9 171  11.2 126   GF    0.00 0.00   0    0.4    0.2     39
 23 01 1990 *0450  13  4.08 144 46.49     31.8  12.2 133    1.7 185  11.2 126   GF    0.00 0.00   0    0.3    0.2     40
 23 01 1990 *0500  13  2.69 144 48.02     33.9  13.7 132    2.8 155  11.2 126   GF    0.00 0.00   0    0.3    0.2     41
 23 01 1990 *0510  13  1.17 144 49.78     36.2  12.5 130    1.5 158  11.2 126   GF    0.00 0.00   0    0.5    0.2     42
 23 01 1990 *0520  12 59.84 144 51.43     38.3  11.9 129    0.9 175  11.2 126   GF    0.00 0.00   0    0.2    0.2     43
 23 01 1990 *0530  12 58.58 144 53.00     40.2  13.6 128    2.4 139  11.2 126   GF    0.00 0.00   0    0.2    0.2     44
 23 01 1990 *0540  12 57.18 144 54.82     42.5  12.7 127    1.4 135  11.2 126   GF    0.00 0.00   0    0.4    0.2     45
 23 01 1990 *0550  12 55.91 144 56.55     44.6  11.8 126    0.6 134  11.2 126   GF    0.00 0.00   0    0.2    0.2     46
 23 01 1990 *0600  12 54.74 144 58.18     46.6  13.5 127    2.2 131  11.2 126   GF    0.00 0.00   0    0.1    0.2     47
 23 01 1990  0605  12 54.1  144 59.1      47.7  13.5 119    2.2 131  11.3 117   c/cs                                  48
 23 01 1990 *0610  12 53.52 145  0.11     48.8  12.7 122    1.7 157  11.3 117   GF    0.00 0.00   0    0.4    0.2     49
 23 01 1990 *0620  12 52.40 145  1.95     50.9  11.3 119    0.5 217  11.3 117   GF    0.00 0.00   0    0.3    0.2     50
 23 01 1990 *0630  12 51.48 145  3.63     52.8  12.2 117    0.9 116  11.3 117   GF    0.00 0.00   0    0.1    0.2     51
 23 01 1990 *0640  12 50.56 145  5.49     54.9  11.5 115    0.5  52  11.3 117   GF    0.00 0.00   0    0.1    0.2     52
 23 01 1990 *0650  12 49.75 145  7.28     56.8  10.9 114    0.8 352  11.3 117   GF    0.00 0.00   0    0.1    0.2     53
```

```
#cruise ODP130JR                                     date run: Wed Jul 18 16:38:07 1990          page   2
#
#                     latitude  longitude               actual    drift         dr                  prob  error          drift
#da mo  yr   time deg   min  deg   min     dist speed cse speed hed speed cse  cmnt (smajxsmin@az)   dist  time   no.
#- - - - - - - - - - - - - - - - - - - - - - - - - - - - - - - - - - - - - - - - - - - - - - - - - - - - - - - - - - -
 23 01 1990 *0700  12 49.02 145  8.99   58.6  12.0 113   1.1  61   11.3 117  GF    0.00 0.00   0    0.1   0.2    54
 23 01 1990  0700  12 49.0  145  9.0    58.6  11.9 119   1.1  61   11.4 123  c/cs                                55
 23 01 1990 *0710  12 48.07 145 10.78   60.6  11.0 120   0.7 357   11.4 123  GF    0.00 0.00   0    0.2   0.2    56
 23 01 1990  0710  12 48.1  145 10.8    60.6  11.0 125   0.7 357   11.5 128  c/cs                                57
 23 01 1990 *0720  12 47.01 145 12.32   62.4  10.2 123   1.6 341   11.5 128  GF    0.00 0.00   0    0.1   0.2    58
 23 01 1990 *0730  12 46.08 145 13.78   64.1  11.4 123   1.0  30   11.5 128  GF    0.00 0.00   0    0.3   0.2    59
 23 01 1990  0739  12 45.2  145 15.2    65.8  11.1 123   1.0  30   11.2 128  c/cs                                60
 23 01 1990 *0740  12 45.05 145 15.41   66.0  10.6 122   1.3   7   11.2 128  GF    0.00 0.00   0    0.2   0.2    61
 23 01 1990 *0750  12 44.11 145 16.95   67.8   9.8 122   1.9 343   11.2 128  GF    0.00 0.00   0    0.2   0.2    62
 23 01 1990  0759  12 43.3  145 18.2    69.3   9.8 123   1.9 343   11.3 129  c/cs                                63
 23 01 1990 *0800  12 43.25 145 18.37   69.4  11.1 124   1.0  28   11.3 129  GF    0.00 0.00   0    0.3   0.2    64
 23 01 1990  0805  12 42.7  145 19.2    70.3  11.1 127   1.0  28   11.3 132  c/cs                                65
 23 01 1990 *0810  12 42.18 145 19.92   71.3  10.6 127   1.2   5   11.3 132  GF    0.00 0.00   0    0.2   0.2    66
 23 01 1990 *0820  12 41.12 145 21.37   73.0  10.1 126   1.6 353   11.3 132  GF    0.00 0.00   0    0.2   0.2    67
 23 01 1990 *0830  12 40.13 145 22.77   74.7  11.4 126   1.1  47   11.3 132  GF    0.00 0.00   0    0.3   0.2    68
 23 01 1990  0835  12 39.6  145 23.6    75.7  11.5 126   1.1  47   11.4 132  c/cs                                69
 23 01 1990  0838  12 39.2  145 24.0    76.3  11.4 125   1.1  47   11.2 131  c/cs                                70
 23 01 1990 *0840  12 39.00 145 24.35   76.6  10.9 123   1.5  24   11.2 131  GF    0.00 0.00   0    0.2   0.2    71
 23 01 1990  0843  12 38.7  145 24.8    77.2  11.0 121   1.5  24   11.3 129  c/cs                                72
 23 01 1990 *0850  12 38.03 145 25.94   78.5  10.2 122   1.8 357   11.3 129  GF    0.00 0.00   0    0.2   0.2    73
 23 01 1990 *0900  12 37.14 145 27.42   80.2  11.9 122   1.5  60   11.3 129  GF    0.00 0.00   0    0.3   0.2    74
 23 01 1990  0902  12 36.9  145 27.8    80.6  11.9 124   1.5  60   11.3 131  c/cs                                75
 23 01 1990  0905  12 36.6  145 28.3    81.2  10.4 122   1.5  60    9.8 130  c/cs                                76
 23 01 1990  0907  12 36.4  145 28.6    81.5  12.0 124   1.5  60   11.4 131  c/cs                                77
 23 01 1990 *0910  12 36.07 145 29.07   82.1  10.9 125   1.2  11   11.4 131  GF    0.00 0.00   0    0.2   0.2    78
 23 01 1990 *0920  12 35.02 145 30.58   83.9  10.2 126   1.5 344   11.4 131  GF    0.00 0.00   0    0.2   0.2    79
 23 01 1990 *0930  12 34.02 145 31.98   85.6  11.5 127   0.9  44   11.4 131  GF    0.00 0.00   0    0.3   0.2    80
 23 01 1990  0933  12 33.7  145 32.5    86.2  11.3 129   0.9  44   11.3 133  c/cs                                81
 23 01 1990 *0940  12 32.85 145 33.51   87.5  11.0 130   0.7  21   11.3 133  GF    0.00 0.00   0    0.1   0.2    82
 23 01 1990  1003  12 30.2  145 36.9    91.7  11.1 130   0.7  21   11.4 133  c/cs                                83
 23 01 1990  1028  12 27.2  145 40.5    96.4  11.0 130   0.7  21   11.3 133  c/cs                                84
 23 01 1990  1055  12 24.1  145 44.4   101.3  11.1 126   0.7  21   11.4 130  c/cs                                85
 23 01 1990 *1100  12 23.50 145 45.20  102.3  11.0 128   0.6 356   11.4 130  GF    0.00 0.00   0    1.0   1.3    86
 23 01 1990  1105  12 22.9  145 45.9   103.2  11.0 126   0.6 356   11.3 128  c/cs                                87
 23 01 1990  1124  12 20.9  145 48.8   106.6   9.8 125   0.6 356   10.2 128  c/cs                                88
 23 01 1990  1126  12 20.7  145 49.1   107.0  10.9 126   0.6 356   11.3 128  c/cs                                89
 23 01 1990 *1130  12 20.30 145 49.70  107.7  11.7 129   0.4 162   11.3 128  GF    0.00 0.00   0    0.3   0.5    90
 23 01 1990  1145  12 18.5  145 52.0   110.6  11.7 129   0.4 162   11.4 128  c/cs                                91
 23 01 1990  1207  12 15.7  145 55.4   114.9  11.5 130   0.4 162   11.1 129  c/cs                                92
 23 01 1990  1235  12 12.3  145 59.6   120.3  11.4 129   0.4 162   11.1 128  c/cs                                93
 23 01 1990  1305  12  8.7  146  4.1   126.0  11.4 127   0.4 162   11.1 126  c/cs                                94
 23 01 1990  1327  12  6.1  146  7.6   130.2  11.5 127   0.4 162   11.1 126  c/cs                                95
 23 01 1990  1355  12  2.9  146 11.9   135.5  11.4 127   0.4 162   11.1 126  c/cs                                96
 23 01 1990  1404  12  1.8  146 13.3   137.3  11.3 127   0.4 162   11.0 126  c/cs                                97
 23 01 1990  1418  12  0.2  146 15.5   139.9  11.5 127   0.4 162   11.1 126  c/cs                                98
 23 01 1990  1448  11 56.8  146 20.1   145.6  11.5 127   0.4 162   11.2 126  c/cs                                99
 23 01 1990  1504  11 54.9  146 22.6   148.7  11.3 126   0.4 162   11.0 125  c/cs                               100
 23 01 1990  1534  11 51.5  146 27.3   154.4  11.4 125   0.4 162   11.1 124  c/cs                               101
 23 01 1990  1602  11 48.5  146 31.7   159.7  11.5 126   0.4 162   11.1 125  c/cs                               102
 23 01 1990  1620  11 46.4  146 34.6   163.2  11.5 127   0.4 162   11.1 126  c/cs                               103
 23 01 1990  1629  11 45.4  146 36.0   164.9  11.6 127   0.4 162   11.3 126  c/cs                               104
 23 01 1990  1645  11 43.5  146 38.5   168.0  11.5 127   0.4 162   11.2 126  c/cs                               105
 23 01 1990  1708  11 40.8  146 42.1   172.4  11.4 127   0.4 162   11.0 126  c/cs                               106
```

```
#cruise ODP130JR                                       date run: Wed Jul 18 16:38:07 1990          page   3
#
#                        latitude   longitude                actual     drift          dr              prob. error          drift
#da mo   yr     time   deg   min    deg   min      dist  speed cse  speed hed   speed cse   cmnt  (smajxsmin@az)    dist   time    no.
#- - - - - - - - - - - - - - - - - - - - - - - - - - - - - - - - - - - - - - - - - - - - - - - - - - - - - - - - - - - - - - - - - -
  23 01 1990   1724    11 39.0   146 44.6     175.4  11.5 127    0.4 162   11.1 126   c/c:                                         107
  23 01 1990   1746    11 36.4   146 48.0     179.7  11.4 126    0.4 162   11.1 125   c/cs                                         108
  23 01 1990   1805    11 34.3   146 51.0     183.3  11.3 124    0.4 162   11.0 123   c/cs                                         109
  23 01 1990   1825    11 32.2   146 54.1     187.0  11.3 124    0.4 162   10.9 123   c/cs                                         110
  23 01 1990   1855    11 29.0   146 58.9     192.7  11.3 125    0.4 162   11.0 124   c/cs                                         111
  23 01 1990  *1900    11 28.43  146 59.68    193.6  13.2 127    2.3 144   11.0 124   GF      0.00 0.00      0     3.3    7.5    112
  23 01 1990   1901    11 28.3   146 59.9     193.8  13.3 127    2.3 144   11.1 123   c/cs                                         113
  23 01 1990  *1905    11 27.77  147  0.58    194.7  11.5 126    0.8 183   11.1 123   GF      0.00 0.00      0     0.2    0.1    114
  23 01 1990  *1910    11 27.20  147  1.37    195.7  11.6 127    0.9 181   11.1 123   GF      0.00 0.00      0     0.1    0.1    115
  23 01 1990  *1915    11 26.62  147  2.16    196.7  11.6 127    0.9 181   11.1 123   GF      0.00 0.00      0     0.1    0.1    116
  23 01 1990  *1920    11 26.04  147  2.95    197.6  11.6 127    0.9 182   11.1 123   GF      0.00 0.00      0     0.1    0.1    117
  23 01 1990  *1925    11 25.46  147  3.74    198.6  10.4 126    1.0 266   11.1 123   GF      0.00 0.00      0     0.1    0.1    118
  23 01 1990  *1930    11 24.95  147  4.45    199.5  13.0 126    2.0 144   11.1 123   GF      0.00 0.00      0     0.1    0.1    119
  23 01 1990   1931    11 24.8   147  4.6     199.7  13.0 125    2.0 144   11.1 122   c/cs                                         120
  23 01 1990  *1935    11 24.32  147  5.35    200.5  11.7 124    0.7 165   11.1 122   GF      0.00 0.00      0     0.2    0.1    121
  23 01 1990  *1940    11 23.77  147  6.17    201.5  11.6 125    0.7 173   11.1 122   GF      0.00 0.00      0     0.1    0.1    122
  23 01 1990  *1945    11 23.22  147  6.98    202.5  11.9 125    0.9 158   11.1 122   GF      0.00 0.00      0     0.1    0.1    123
  23 01 1990  *1950    11 22.66  147  7.81    203.5  11.8 124    0.8 156   11.1 122   GF      0.00 0.00      0     0.1    0.1    124
  23 01 1990  *1955    11 22.11  147  8.64    204.4  10.2 125    1.1 271   11.1 122   GF      0.00 0.00      0     0.1    0.1    125
  23 01 1990  *2000    11 21.62  147  9.35    205.3  13.2 124    2.1 133   11.1 122   GF      0.00 0.00      0     0.1    0.1    126
  23 01 1990   2001    11 21.5   147  9.5     205.5  13.2 124    2.1 133   11.1 122   c/cs                                         127
  23 01 1990  *2005    11 21.01  147 10.28    206.4  11.8 125    0.9 157   11.1 122   GF      0.00 0.00      0     0.2    0.1    128
  23 01 1990  *2010    11 20.45  147 11.11    207.4  11.7 124    0.7 149   11.1 122   GF      0.00 0.00      0     0.1    0.1    129
  23 01 1990  *2015    11 19.91  147 11.94    208.4  11.4 123    0.4 155   11.1 122   GF      0.00 0.00      0     0.1    0.1    130
  23 01 1990   2019    11 19.5   147 12.6     209.1  11.3 124    0.4 155   11.0 123   c/cs                                         131
  23 01 1990  *2020    11 19.39  147 12.75    209.3  10.9 124    0.2 248   11.0 123   GF      0.00 0.00      0     0.0    0.1    132
  23 01 1990  *2030    11 18.38  147 14.29    211.1  12.4 123    1.4 123   11.0 123   GF      0.00 0.00      0     0.0    0.2    133
  23 01 1990  *2040    11 17.25  147 16.06    213.2  11.7 124    0.7 132   11.0 123   GF      0.00 0.00      0     0.2    0.2    134
  23 01 1990   2044    11 16.8   147 16.7     214.0  11.9 124    0.7 132   11.2 123   c/cs                                         135
  23 01 1990   2047    11 16.5   147 17.2     214.6  11.5 124    0.7 132   10.8 123   c/cs                                         136
  23 01 1990  *2050    11 16.17  147 17.72    215.2  10.8 124    0.1 187   10.8 123   GF      0.00 0.00      0     0.1    0.2    137
  23 01 1990   2057    11 15.5   147 18.8     216.4  11.1 123    0.1 187   11.0 122   c/cs                                         138
  23 01 1990  *2100    11 15.17  147 19.27    217.0  12.4 124    1.4 137   11.0 122   GF      0.00 0.00      0     0.0    0.2    139
  23 01 1990  *2110    11 14.03  147 21.02    219.0  11.7 124    0.8 151   11.0 122   GF      0.00 0.00      0     0.2    0.2    140
  23 01 1990   2117    11 13.3   147 22.2     220.4  11.9 126    0.8 151   11.2 124   c/cs                                         141
  23 01 1990  *2120    11 12.92  147 22.67    221.0  11.0 125    0.3 246   11.2 124   GF      0.00 0.00      0     0.1    0.2    142
  23 01 1990  *2130    11 11.86  147 24.20    222.8  12.4 126    1.3 142   11.2 124   GF      0.00 0.00      0     0.0    0.2    143
  23 01 1990   2132    11 11.6   147 24.5     223.2  12.4 126    1.3 142   11.2 124   c/cs                                         144
  23 01 1990   2138    11 10.9   147 25.6     224.5  12.4 126    1.3 142   11.1 124   c/cs                                         145
  23 01 1990  *2140    11 10.65  147 25.91    224.9  11.6 126    0.6 168   11.1 124   GF      0.00 0.00      0     0.2    0.2    146
  23 01 1990  *2150    11  9.52  147 27.50    226.8  10.9 126    0.4 255   11.1 124   GF      0.00 0.00      0     0.1    0.2    147
  23 01 1990   2150    11  9.5   147 27.5     226.8  10.9 126    0.4 255   11.2 124   c/cs                                         148
  23 01 1990   2158    11  8.7   147 28.7     228.3  10.8 126    0.4 255   11.1 124   c/cs                                         149
  23 01 1990  *2200    11  8.46  147 29.00    228.6  11.8 127    0.9 166   11.1 124   GF      0.00 0.00      0     0.1    0.2    150
  23 01 1990   2222    11  5.9   147 32.5     232.9  11.8 127    0.9 166   11.2 124   c/cs                                         151
  23 01 1990  *2230    11  4.93  147 33.80    234.5  11.4 127    0.7 196   11.2 124   GF      0.00 0.00      0     0.4    0.5    152
  23 01 1990  *2240    11  3.78  147 35.34    236.4  11.4 127    0.7 193   11.2 124   GF      0.00 0.00      0     0.1    0.2    153
  23 01 1990   2244    11  3.3   147 36.0     237.2  11.4 126    0.7 193   11.1 123   c/cs                                         154
  23 01 1990   2248    11  2.9   147 36.6     237.9  11.4 126    0.7 193   11.2 123   c/cs                                         155
  23 01 1990  *2250    11  2.64  147 36.89    238.3  10.8 126    0.7 251   11.2 123   GF      0.00 0.00      0     0.1    0.2    156
  23 01 1990  *2300    11  1.59  147 38.37    240.1  12.3 124    1.1 134   11.2 123   GF      0.00 0.00      0     0.1    0.2    157
  23 01 1990   2306    11  0.9   147 39.4     241.3  12.2 123    1.1 134   11.1 122   c/cs                                         158
  23 01 1990  *2310    11  0.46  147 40.10    242.2  11.6 126    0.9 182   11.1 122   GF      0.00 0.00      0     0.2    0.2    159
```

```
#cruise ODP130JR                                         date run: Wed Jul 18 16:38:07 1990        page    4
#
#                                                         actual      drift          dr                prob. error       drift
#                   latitude   longitude                                                                                 
#da mo   yr    time deg   min  deg    min     dist speed cse speed hed speed cse  cmnt (smajxsmin@az)  dist  time  no.
#- - - -  - - - - - - - - - - - - - - - - - - - - - - - - - - - - - - - - - - - - - - - - - - - - - - - - - - - - - -
 23 01 1990 *2320  10 59.33 147 41.69    244.1  10.7 125   0.8 243  11.1 122  GF    0.00 0.00   0   0.2   0.2  160
 23 01 1990  2326  10 58.7  147 42.6     245.2  10.8 126   0.8 243  11.2 123  c/cs                               161
 23 01 1990 *2330  10 58.28 147 43.17    245.9  12.4 126   1.4 152  11.2 123  GF    0.00 0.00   0   0.1   0.2  162
 23 01 1990 *2340  10 57.06 147 44.87    247.9  11.8 126   0.9 168  11.2 123  GF    0.00 0.00   0   0.2   0.2  163
 23 01 1990  2346  10 56.4  147 45.8     249.1  11.7 126   0.9 168  11.0 123  c/cs                               164
 23 01 1990 *2350  10 55.90 147 46.48    249.9  11.0 126   0.6 210  11.0 123  GF    0.00 0.00   0   0.2   0.2  165
 24 01 1990 *0000  10 54.81 147 47.99    251.7  12.3 126   1.4 149  11.0 123  GF    0.00 0.00   0   0.1   0.2  166
 24 01 1990  0000  10 54.8  147 48.0     251.7  12.3 126   1.4 149  11.0 123  c/cs                               167
 24 01 1990  0009  10 53.7  147 49.5     253.6  11.7 125   1.4 149  10.4 122  c/cs                               168
 24 01 1990 *0010  10 53.62 147 49.67    253.8  11.0 126   1.0 179  10.4 122  GF    0.00 0.00   0   0.2   0.2  169
 24 01 1990 *0020  10 52.54 147 51.17    255.6  10.1 127   0.9 232  10.4 122  GF    0.00 0.00   0   0.2   0.2  170
 24 01 1990  0024  10 52.1  147 51.7     256.3  10.1 127   0.9 232  10.4 122  c/cs                               171
 24 01 1990 *0030  10 51.53 147 52.54    257.3  11.4 126   1.3 163  10.4 122  GF    0.00 0.00   0   0.2   0.2  172
 24 01 1990  0034  10 51.1  147 53.2     258.0  11.6 127   1.3 163  10.5 123  c/cs                               173
 24 01 1990 *0040  10 50.38 147 54.10    259.2  11.1 127   1.0 183  10.5 123  GF    0.00 0.00   0   0.2   0.2  174
 24 01 1990 *0050  10 49.26 147 55.59    261.0  10.3 128   0.9 232  10.5 123  GF    0.00 0.00   0   0.2   0.2  175
 24 01 1990  0051  10 49.2  147 55.7     261.2  10.9 127   0.9 232  11.2 122  c/cs                               176
 24 01 1990 *0100  10 48.18 147 57.06    262.9  12.6 127   1.8 160  11.2 122  GF    0.00 0.00   0   0.2   0.2  177
 24 01 1990  0108  10 47.2  147 58.4     264.5  11.7 128   1.8 160  10.2 123  c/cs                               178
 24 01 1990 *0110  10 46.93 147 58.74    264.9  10.8 128   1.0 184  10.2 123  GF    0.00 0.00   0   0.3   0.2  179
 24 01 1990  0110  10 46.9  147 58.7     264.9  11.7 127   1.0 184  11.1 123  c/cs                               180
 24 01 1990 *0120  10 45.75 148  0.31    266.9  10.8 128   1.0 234  11.1 123  GF    0.00 0.00   0   0.2   0.2  181
 24 01 1990  0121  10 45.6  148  0.5     267.0  10.8 128   1.0 234  11.1 123  c/cs                               182
 24 01 1990 *0130  10 44.64 148  1.75    268.7  12.2 129   1.6 171  11.1 123  GF    0.00 0.00   0   0.2   0.2  183
 24 01 1990  0138  10 43.6  148  3.0     270.3  12.2 129   1.6 171  11.1 123  c/cs                               184
 24 01 1990 *0140  10 43.37 148  3.37    270.7  11.5 129   1.3 194  11.1 123  GF    0.00 0.00   0   0.3   0.2  185
 24 01 1990 *0150  10 42.16 148  4.89    272.6  10.9 130   1.3 223  11.1 123  GF    0.00 0.00   0   0.2   0.2  186
 24 01 1990  0152  10 41.9  148  5.2     273.0  10.8 130   1.3 223  10.9 123  c/cs                               187
 24 01 1990 *0200  10 41.01 148  6.30    274.4  12.2 130   1.8 173  10.9 123  GF    0.00 0.00   0   0.2   0.2  188
 24 01 1990  0206  10 40.2  148  7.3     275.6  12.3 130   1.8 173  11.0 123  c/cs                               189
 24 01 1990 *0210  10 39.71 148  7.90    276.5  11.4 129   1.2 197  11.0 123  GF    0.00 0.00   0   0.3   0.2  190
 24 01 1990 *0220  10 38.52 148  9.41    278.4  10.8 129   1.2 229  11.0 123  GF    0.00 0.00   0   0.2   0.2  191
 24 01 1990 *0230  10 37.39 148 10.83    280.2  12.2 129   1.7 172  11.0 123  GF    0.00 0.00   0   0.2   0.2  192
 24 01 1990  0236  10 36.6  148 11.8     281.4  12.2 128   1.7 172  11.1 122  c/cs                               193
 24 01 1990 *0240  10 36.12 148 12.45    282.2  11.6 128   1.4 190  11.1 122  GF    0.00 0.00   0   0.3   0.2  194
 24 01 1990  0247  10 35.3  148 13.5     283.6  11.6 128   1.4 190  11.1 122  c/cs                               195
 24 01 1990 *0250  10 34.92 148 14.00    284.1  10.8 128   1.2 226  11.1 122  GF    0.00 0.00   0   0.2   0.2  196
 24 01 1990 *0300  10 33.80 148 15.44    285.9  12.3 127   1.7 166  11.1 122  GF    0.00 0.00   0   0.2   0.2  197
 24 01 1990  0303  10 33.4  148 15.9     286.6  12.2 125   1.7 166  11.0 119  c/cs                               198
 24 01 1990 *0310  10 32.61 148 17.13    288.0  11.8 125   1.4 182  11.0 119  GF    0.00 0.00   0   0.3   0.2  199
 24 01 1990  0315  10 32.0  148 17.9     289.0  11.5 125   1.4 182  10.8 119  c/cs                               200
 24 01 1990 *0320  10 31.49 148 18.74    289.9  10.5 125   1.1 225  10.8 119  GF    0.00 0.00   0   0.2   0.2  201
 24 01 1990  0327  10 30.8  148 19.8     291.2  10.9 125   1.1 225  11.1 119  c/cs                               202
 24 01 1990 *0330  10 30.48 148 20.22    291.7  13.1 123   2.2 146  11.1 119  GF    0.00 0.00   0   0.2   0.2  203
 24 01 1990 *0335  10 29.88 148 21.15    292.8  11.4 124   1.0 197  11.1 119  GF    0.00 0.00   0   0.2   0.1  204
 24 01 1990 *0340  10 29.35 148 21.95    293.7  11.3 124   1.0 203  11.1 119  GF    0.00 0.00   0   0.1   0.1  205
 24 01 1990  0347  10 28.6  148 23.1     295.1  11.2 124   1.0 203  11.1 119  c/cs                               206
 24 01 1990 *0350  10 28.30 148 23.53    295.6  10.4 124   1.1 246  11.1 119  GF    0.00 0.00   0   0.2   0.2  207
 24 01 1990 *0400  10 27.33 148 25.00    297.4  12.0 123   1.3 167  11.1 119  GF    0.00 0.00   0   0.2   0.2  208
 24 01 1990 *0410  10 26.23 148 26.69    299.3  11.2 124   0.9 202  11.1 119  GF    0.00 0.00   0   0.2   0.2  209
 24 01 1990  0417  10 25.5  148 27.8     300.7  11.2 124   0.9 202  11.0 119  c/cs                               210
 24 01 1990 *0420  10 25.19 148 28.27    301.2  10.4 124   1.0 247  11.0 119  GF    0.00 0.00   0   0.2   0.2  211
 24 01 1990 *0430  10 24.23 148 29.74    303.0  11.7 124   1.2 178  11.0 119  GF    0.00 0.00   0   0.2   0.2  212
```

```
#cruise ODP130JR                               date run: Wed Jul 18 16:38:07 1990        page   5
#
#                     latitude  longitude            actual    drift        dr             prob. error       drift
#da mo   yr   time deg   min deg   min    dist speed cse speed hed speed cse  cmnt (smajxsmin@az)  dist  time  no.
#- - - - - - - - - - - - - - - - - - - - - - - - - - - - - - - - - - - - - - - - - - - - - - - - - - - - - - - - -
 24 01 1990 *0440  10 23.14 148 31.38  304.9  11.1 123   0.9 209  11.0 119  GF    0.00 0.00    0   0.2   0.2  213
 24 01 1990  0442  10 22.9  148 31.7   305.3  11.1 123   0.9 209  11.1 119  c/cs                              214
 24 01 1990 *0450  10 22.12 148 32.95  306.7  10.5 124   1.2 241  11.1 119  GF    0.00 0.00    0   0.1   0.2  215
 24 01 1990 *0500  10 21.13 148 34.42  308.5  12.0 124   1.5 171  11.1 119  GF    0.00 0.00    0   0.2   0.2  216
 24 01 1990  0506  10 20.4  148 35.4   309.7  12.1 126   1.5 171  11.1 121  c/cs                              217
 24 01 1990 *0510  10 19.97 148 36.09  310.5  11.3 126   0.9 202  11.1 121  GF    0.00 0.00    0   0.2   0.2  218
 24 01 1990  0520  10 18.9  148 37.6   312.4  11.2 125   0.9 202  11.0 120  c/cs                              219
 24 01 1990 *0525  10 18.34 148 38.42  313.3  11.3 125   1.1 195  11.0 120  GF    0.00 0.00    0   0.2   0.2  220
 24 01 1990 *0535  10 17.25 148 39.99  315.2  11.4 124   0.9 186  11.0 120  GF    0.00 0.00    0   0.2   0.2  221
 24 01 1990  0538  10 16.9  148 40.5   315.8  11.5 125   0.9 186  11.1 121  c/cs                              222
 24 01 1990 *0545  10 16.16 148 41.59  317.1  11.1 125   0.9 215  11.1 121  GF    0.00 0.00    0   0.1   0.2  223
 24 01 1990  0551  10 15.5  148 42.5   318.2  10.2 127   0.9 215  10.2 122  c/cs                              224
 24 01 1990  0553  10 15.3  148 42.8   318.6  10.9 125   0.9 215  10.9 120  c/cs                              225
 24 01 1990 *0600  10 14.59 148 43.85  319.9  12.0 125   1.4 168  10.9 120  GF    0.00 0.00    0   0.2   0.2  226
 24 01 1990  0608  10 13.7  148 45.2   321.4  11.9 124   1.4 168  10.9 119  c/cs                              227
 24 01 1990 *0610  10 13.45 148 45.51  321.8  11.4 124   1.1 185  10.9 119  GF    0.00 0.00    0   0.2   0.2  228
 24 01 1990 *0620  10 12.38 148 47.11  323.7  10.6 125   1.2 229  10.9 119  GF    0.00 0.00    0   0.2   0.2  229
 24 01 1990 *0630  10 11.37 148 48.58  325.5  11.8 125   1.4 175  10.9 119  GF    0.00 0.00    0   0.2   0.2  230
 24 01 1990  0638  10 10.5  148 49.9   327.1  11.8 125   1.4 175  10.9 119  c/cs                              231
 24 01 1990 *0640  10 10.25 148 50.22  327.5  11.1 125   1.1 202  10.9 119  GF    0.00 0.00    0   0.2   0.2  232
 24 01 1990 *0650  10  9.20 148 51.77  329.3  10.3 124   1.1 243  10.9 119  GF    0.00 0.00    0   0.2   0.2  233
 24 01 1990 *0700  10  8.23 148 53.22  331.1  11.9 124   1.4 168  10.9 119  GF    0.00 0.00    0   0.2   0.2  234
 24 01 1990  0703  10  7.9  148 53.7   331.7  11.8 124   1.4 168  10.9 119  c/cs                              235
 24 01 1990 *0710  10  7.12 148 54.88  333.0  11.2 124   0.9 192  10.9 119  GF    0.00 0.00    0   0.2   0.2  236
 24 01 1990 *0720  10  6.09 148 56.46  334.9  10.3 123   1.0 245  10.9 119  GF    0.00 0.00    0   0.2   0.2  237
 24 01 1990 *0730  10  5.14 148 57.92  336.6  11.9 123   1.2 158  10.9 119  GF    0.00 0.00    0   0.2   0.2  238
 24 01 1990  0731  10  5.0  148 58.1   336.8  11.8 124   1.2 158  10.8 120  c/cs                              239
 24 01 1990 *0740  10  4.05 148 59.59  338.6  11.3 123   0.7 171  10.8 120  GF    0.00 0.00    0   0.2   0.2  240
 24 01 1990  0749  10  3.1  149  1.0   340.3  11.4 122   0.7 171  10.9 119  c/cs                              241
 24 01 1990 *0750  10  3.04 149  1.20  340.5  10.4 123   0.9 244  10.9 119  GF    0.00 0.00    0   0.1   0.2  242
 24 01 1990 *0800  10  2.09 149  2.68  342.2  12.1 122   1.4 151  10.9 119  GF    0.00 0.00    0   0.2   0.2  243
 24 01 1990  0807  10  1.3  149  3.9   343.6  12.3 122   1.4 151  11.1 119  c/cs                              244
 24 01 1990 *0810  10  1.00 149  4.42  344.2  11.4 122   0.7 184  11.1 119  GF    0.00 0.00    0   0.2   0.2  245
 24 01 1990 *0820   9 59.99 149  6.06  346.1  10.7 121   0.6 257  11.1 119  GF    0.00 0.00    0   0.1   0.2  246
 24 01 1990  0821   9 59.9  149  6.2   346.3  10.5 122   0.6 257  11.0 120  c/cs                              247
 24 01 1990 *0830   9 59.05 149  7.57  347.9  12.0 123   1.2 151  11.0 120  GF    0.00 0.00    0   0.1   0.2  248
 24 01 1990  0836   9 58.4  149  8.6   349.1  11.9 125   1.2 151  10.9 122  c/cs                              249
 24 01 1990 *0840   9 57.94 149  9.26  349.9  11.3 125   0.6 175  10.9 122  GF    0.00 0.00    0   0.2   0.2  250
 24 01 1990  0841   9 57.8  149  9.4   350.1  11.3 125   0.6 175  11.0 122  c/cs                              251
 24 01 1990 *0850   9 56.87 149 10.84  351.8  10.7 125   0.6 241  11.0 122  GF    0.00 0.00    0   0.1   0.2  252
 24 01 1990  0855   9 56.4  149 11.6   352.7  10.8 125   0.6 241  11.0 122  c/cs                              253
 24 01 1990 *0900   9 55.85 149 12.33  353.6  12.3 125   1.4 151  11.0 122  GF    0.00 0.00    0   0.1   0.2  254
 24 01 1990  0909   9 54.8  149 13.9   355.4  12.2 125   1.4 151  11.0 122  c/cs                              255
 24 01 1990 *0910   9 54.67 149 14.03  355.6  11.6 126   0.9 175  11.0 122  GF    0.00 0.00    0   0.2   0.2  256
 24 01 1990 *0920   9 53.55 149 15.62  357.6  10.8 125   0.6 235  11.0 122  GF    0.00 0.00    0   0.2   0.2  257
 24 01 1990 *0930   9 52.52 149 17.11  359.4  12.3 125   1.4 145  11.0 122  GF    0.00 0.00    0   0.1   0.2  258
 24 01 1990  0936   9 51.8  149 18.1   360.6  12.2 125   1.4 145  10.9 122  c/cs                              259
 24 01 1990 *0940   9 51.36 149 18.82  361.4  11.4 125   0.8 170  10.9 122  GF    0.00 0.00    0   0.2   0.2  260
 24 01 1990 *0950   9 50.27 149 20.40  363.3  10.4 125   0.7 253  10.9 122  GF    0.00 0.00    0   0.1   0.2  261
 24 01 1990  0952   9 50.1  149 20.7   363.6  10.2 126   0.7 253  10.6 123  c/cs                              262
 24 01 1990 *1000   9 49.27 149 21.80  365.0  11.8 127   1.4 158  10.6 123  GF    0.00 0.00    0   0.1   0.2  263
 24 01 1990  1006   9 48.6  149 22.8   366.2  12.0 128   1.4 158  10.8 124  c/cs                              264
 24 01 1990 *1010   9 48.07 149 23.40  367.0  11.4 128   1.0 180  10.8 124  GF    0.00 0.00    0   0.2   0.2  265
```

```
                                                    date run: Wed Jul 18 16:38:07 1990          page   6
#cruise ODP130JR
#                                                    actual    drift        dr                prob. error          drift
#                     latitude  longitude      dist  speed cse speed hed speed cse  cmnt (smajxsmin@az)      dist  time   no.
#da mo   yr    time deg   min  deg   min - - - - - - - - - - - - - - - - - - - - - - - - - - - - - - - - - - - - - - - - - - - -
#- - - - - - - - - - - - - - - - - - - - - -
 24 01 1990 *1020    9 46.90  149 24.91   368.9  11.4 127   0.9 169  10.8 124  GF    0.00 0.00   0   0.2   0.2   266
 24 01 1990  1021    9 46.8   149 25.1    369.1  11.3 127   0.9 169  10.6 124  c/cs                               267
 24 01 1990  1038    9 44.8   149 27.6    372.3  11.5 125   0.9 169  10.8 122  c/cs                               268
 24 01 1990  1055    9 43.0   149 30.3    375.5  11.4 126   0.9 169  10.7 123  c/cs                               269
 24 01 1990  1102    9 42.2   149 31.4    376.9  10.8 126   0.9 169  10.1 122  c/cs                               270
 24 01 1990  1106    9 41.7   149 32.0    377.6  11.5 126   0.9 169  10.8 123  c/cs                               271
 24 01 1990  1136    9 38.3   149 36.7    383.3  11.5 126   0.9 169  10.8 123  c/cs                               272
 24 01 1990  1154    9 36.3   149 39.5    386.8  11.4 125   0.9 169  10.7 122  c/cs                               273
 24 01 1990  1204    9 35.2   149 41.1    388.7  11.3 125   0.9 169  10.6 122  c/cs                               274
 24 01 1990 *1213    9 34.20  149 42.50   390.4  11.1 126   0.9 184  10.6 122  SF    0.00 0.00   0   1.8   1.9   275
 24 01 1990  1227    9 32.7   149 44.6    393.0  11.3 126   0.9 184  10.8 122  c/cs                               276
 24 01 1990  1247    9 30.4   149 47.7    396.7  11.1 126   0.9 184  10.6 122  c/cs                               277
 24 01 1990  1317    9 27.2   149 52.2    402.3  10.9 127   0.9 184  10.4 123  c/cs                               278
 24 01 1990  1319    9 27.0   149 52.5    402.6  11.1 126   0.9 184  10.7 122  c/cs                               279
 24 01 1990  1336    9 25.1   149 55.1    405.8  11.1 127   0.9 184  10.6 123  c/cs                               280
 24 01 1990  1359    9 22.5   149 58.5    410.0  11.2 126   0.9 184  10.7 122  c/cs                               281
 24 01 1990 *1402    9 22.20  149 59.00   410.6  11.4 126   1.0 175  10.7 122  SF    0.00 0.00   0   1.7   1.8   282
 24 01 1990  1429    9 19.2   150  3.2    415.7  11.1 125   1.0 175  10.5 121  c/cs                               283
 24 01 1990  1437    9 18.3   150  4.4    417.2  11.2 126   1.0 175  10.6 122  c/cs                               284
 24 01 1990  1502    9 15.6   150  8.2    421.9  11.0 126   1.0 175  10.4 122  c/cs                               285
 24 01 1990  1508    9 14.9   150  9.1    423.0  11.2 126   1.0 175  10.5 122  c/cs                               286
 24 01 1990  1530    9 12.5   150 12.5    427.1  11.2 126   1.0 175  10.6 122  c/cs                               287
 24 01 1990  1544    9 11.0   150 14.6    429.7  11.0 126   1.0 175  10.3 122  c/cs                               288
 24 01 1990  1553    9 10.0   150 16.0    431.3  11.1 126   1.0 175  10.4 122  c/cs                               289
 24 01 1990  1607    9  8.5   150 18.1    433.9  11.2 126   1.0 175  10.5 122  c/cs                               290
 24 01 1990  1624    9  6.6   150 20.7    437.1  11.1 125   1.0 175  10.5 121  c/cs                               291
 24 01 1990  1638    9  5.1   150 22.8    439.7  11.3 125   1.0 175  10.7 121  c/cs                               292
 24 01 1990  1650    9  3.8   150 24.7    441.9  11.4 125   1.0 175  10.8 121  c/cs                               293
 24 01 1990  1657    9  3.0   150 25.8    443.3  11.3 126   1.0 175  10.7 122  c/cs                               294
 24 01 1990  1727    8 59.7   150 30.4    448.9  11.4 126   1.0 175  10.8 122  c/cs                               295
 24 01 1990  1732    8 59.1   150 31.2    449.9  11.3 125   1.0 175  10.7 121  c/cs                               296
 24 01 1990  1755    8 56.6   150 34.8    454.2  11.2 126   1.0 175  10.5 122  c/cs                               297
 24 01 1990  1800    8 56.1   150 35.6    455.2  11.2 126   1.0 175  10.5 122  c/cs                               298
 24 01 1990  1830    8 52.8   150 40.1    460.8  11.3 126   1.0 175  10.6 122  c/cs                               299
 24 01 1990  1842    8 51.4   150 42.0    463.0  11.5 128   1.0 175  10.8 124  c/cs                               300
 24 01 1990 *1900    8 49.31  150 44.74   466.5  11.4 129   1.1 181  10.8 124  GF    0.00 0.00   0   5.1   5.0   301
 24 01 1990  1902    8 49.1   150 45.0    466.8  11.6 131   1.1 181  10.9 127  c/cs                               302
 24 01 1990 *1905    8 48.69  150 45.48   467.4  11.5 131   1.0 181  10.9 127  GF    0.00 0.00   0   0.1   0.1   303
 24 01 1990 *1910    8 48.06  150 46.21   468.4  11.6 132   1.1 181  10.9 127  GF    0.00 0.00   0   0.1   0.1   304
 24 01 1990 *1915    8 47.42  150 46.94   469.3  11.8 131   1.2 173  10.9 127  GF    0.00 0.00   0   0.1   0.1   305
 24 01 1990  1916    8 47.3   150 47.1    469.5  11.6 132   1.2 173  10.7 128  c/cs                               306
 24 01 1990 *1920    8 46.77  150 47.67   470.3  10.6 133   0.9 227  10.7 128  GF    0.00 0.00   0   0.1   0.1   307
 24 01 1990  1928    8 45.8   150 48.7    471.7  10.7 133   0.9 227  10.8 128  c/cs                               308
 24 01 1990 *1930    8 45.57  150 48.99   472.1  12.1 133   1.6 165  10.8 128  GF    0.00 0.00   0   0.1   0.2   309
 24 01 1990 *1940    8 44.21  150 50.49   474.1  11.4 133   1.1 186  10.8 128  GF    0.00 0.00   0   0.3   0.2   310
 24 01 1990 *1950    8 42.93  150 51.90   476.0  11.6 132   1.2 172  10.8 128  GF    0.00 0.00   0   0.2   0.2   311
 24 01 1990 *1955    8 42.28  150 52.63   477.0  11.5 133   1.2 184  10.8 128  GF    0.00 0.00   0   0.1   0.1   312
 24 01 1990  1956    8 42.2   150 52.8    477.2  11.6 132   1.2 184  10.9 127  c/cs                               313
 24 01 1990 *2005    8 40.99  150 54.08   478.9  11.5 131   1.0 183  10.9 127  GF    0.00 0.00   0   0.2   0.2   314
 24 01 1990 *2010    8 40.36  150 54.81   479.9  11.3 131   0.8 192  10.9 127  GF    0.00 0.00   0   0.1   0.1   315
 24 01 1990 *2015    8 39.75  150 55.53   480.8  11.4 130   0.8 182  10.9 127  GF    0.00 0.00   0   0.1   0.1   316
 24 01 1990  2019    8 39.3   150 56.1    491.5  11.2 130   0.8 182  10.8 127  c/cs                               317
 24 01 1990 *2020    8 39.14  150 56.26   481.7  10.4 130   0.7 245  10.8 127  GF    0.00 0.00   0   0.1   0.1   318
```

```
#cruise ODP130JR                              date run: Wed Jul 18 16:38:07 1990          page    7
#
#                    latitude  longitude              actual   drift        dr                prob. error        drift
#da mo  yr     time deg   min deg   min      dist  speed cse speed hed  speed cse  cmnt (smajxsmin@az)    dist   time   no.
#- - - - - - - - - - - - - - - - - - - - - - - - - - - - - - - - - - - - - - - - - - - - - - - - - - - - - - - - - - -
  24 01 1990  2029   8 38.1   150 57.5    483.3  10.4 131   0.7 245  10.7 128  c/cs                                319
  24 01 1990 *2030   8 38.01  150 57.60   483.5  11.6 131   1.0 166  10.7 128  GF    0.00 0.00    0    0.1   0.2   320
  24 01 1990 *2045   8 36.11  150 59.80   486.4  11.0 131   0.6 196  10.7 128  GF    0.00 0.00    0    0.3   0.2   321
  24 01 1990  2048   8 35.8   151  0.2    486.9  10.8 130   0.6 196  10.6 127  c/cs                                322
  24 01 1990 *2050   8 35.52  151  0.50   487.3  10.9 130   0.7 191  10.6 127  GF    0.00 0.00    0    0.0   0.1   323
  24 01 1990  2054   8 35.0   151  1.1    488.0  10.8 130   0.7 191  10.5 127  c/cs                                324
  24 01 1990 *2055   8 34.93  151  1.20   488.2  10.9 131   0.9 187  10.5 127  GF    0.00 0.00    0    0.1   0.1   325
  24 01 1990 *2105   8 33.73  151  2.59   490.0  11.3 131   1.2 173  10.5 127  GF    0.00 0.00    0    0.2   0.2   326
  24 01 1990  2108   8 33.4   151  3.0    490.6  12.0 132   1.2 173  11.1 128  c/cs                                327
  24 01 1990 *2110   8 33.09  151  3.32   491.0  11.8 131   1.0 171  11.1 128  GF    0.00 0.00    0    0.1   0.1   328
  24 01 1990 *2115   8 32.44  151  4.07   492.0  11.8 131   0.9 170  11.1 128  GF    0.00 0.00    0    0.1   0.1   329
  24 01 1990 *2120   8 31.80  151  4.82   492.9  11.7 130   0.7 169  11.1 128  GF    0.00 0.00    0    0.1   0.1   330
  24 01 1990 *2125   8 31.17  151  5.57   493.9   9.8 131   1.4 289  11.1 128  GF    0.00 0.00    0    0.1   0.1   331
  24 01 1990  2127   8 31.0   151  5.8    494.2   9.4 131   1.4 289  10.7 128  c/cs                                332
  24 01 1990 *2130   8 30.65  151  6.18   494.7  12.3 131   1.8 152  10.7 128  GF    0.00 0.00    0    0.1   0.1   333
  24 01 1990 *2135   8 29.97  151  6.96   495.7  11.4 131   1.0 172  10.7 128  GF    0.00 0.00    0    0.1   0.1   334
  24 01 1990 *2140   8 29.34  151  7.68   496.7  11.4 131   0.9 171  10.7 128  GF    0.00 0.00    0    0.1   0.1   335
  24 01 1990  2141   8 29.2   151  7.8    496.9  11.5 130   0.9 171  10.9 127  c/cs                                336
  24 01 1990 *2145   8 28.72  151  8.42   497.6  11.4 131   0.9 182  10.9 127  GF    0.00 0.00    0    0.1   0.1   337
  24 01 1990 *2150   8 28.10  151  9.15   498.6  11.4 130   0.8 173  10.9 127  GF    0.00 0.00    0    0.1   0.1   338
  24 01 1990 *2155   8 27.49  151  9.89   499.6  10.1 131   1.0 267  10.9 127  GF    0.00 0.00    0    0.1   0.1   339
  24 01 1990 *2200   8 26.94  151 10.54   500.4  12.0 130   1.2 154  10.9 127  GF    0.00 0.00    0    0.1   0.1   340
  24 01 1990  2203   8 26.6   151 11.0    501.0  12.2 131   1.2 154  11.1 128  c/cs                                341
  24 01 1990 *2210   8 25.63  151 12.10   502.4  11.7 130   0.8 167  11.1 128  GF    0.00 0.00    0    0.2   0.2   342
  24 01 1990 *2215   8 25.00  151 12.85   503.4  11.8 131   1.0 170  11.1 128  GF    0.00 0.00    0    0.1   0.1   343
  24 01 1990 *2220   8 24.35  151 13.60   504.4  11.8 132   1.1 178  11.1 128  GF    0.00 0.00    0    0.1   0.1   344
  24 01 1990  2220   8 24.3   151 13.6    504.4  11.7 132   1.1 178  11.0 128  c/cs                                345
  24 01 1990 *2235   8 22.38  151 15.80   507.3  11.5 133   1.1 193  11.0 128  GF    0.00 0.00    0    0.3   0.2   346
  24 01 1990 *2240   8 21.73  151 16.51   508.3  11.7 132   1.2 179  11.0 128  GF    0.00 0.00    0    0.1   0.1   347
  24 01 1990 *2245   8 21.07  151 17.24   509.3  11.3 133   1.0 201  11.0 128  GF    0.00 0.00    0    0.1   0.1   348
  24 01 1990 *2250   8 20.43  151 17.94   510.2  11.5 132   1.0 190  11.0 128  GF    0.00 0.00    0    0.1   0.1   349
  24 01 1990  2250   8 20.4   151 17.9    510.2  11.4 132   1.0 190  10.9 128  c/cs                                350
  24 01 1990 *2255   8 19.79  151 18.65   511.1  10.1 131   1.0 276  10.9 128  GF    0.00 0.00    0    0.1   0.1   351
  24 01 1990 *2300   8 19.24  151 19.29   512.0  12.3 131   1.5 150  10.9 128  GF    0.00 0.00    0    0.1   0.1   352
  24 01 1990  2300   8 19.2   151 19.3    512.0  12.2 131   1.5 150  10.8 128  c/cs                                353
  24 01 1990 *2310   8 17.91  151 20.85   514.0  11.3 132   0.9 185  10.8 128  GF    0.00 0.00    0    0.3   0.2   354
  24 01 1990 *2315   8 17.28  151 21.56   515.0  11.5 132   1.0 178  10.8 128  GF    0.00 0.00    0    0.1   0.1   355
  24 01 1990  2317   8 17.0   151 21.8    515.3  11.5 132   1.0 178  10.8 128  c/cs                                356
  24 01 1990 *2320   8 16.64  151 22.28   515.9  10.6 133   0.9 231  10.8 128  GF    0.00 0.00    0    0.1   0.1   357
  24 01 1990 *2330   8 15.44  151 23.60   517.7  12.9 132   2.2 149  10.8 128  GF    0.00 0.00    0    0.1   0.2   358
  24 01 1990  2334   8 14.9   151 24.2    518.6  12.9 132   2.2 149  10.8 128  c/cs                                359
  24 01 1990 *2335   8 14.73  151 24.41   518.8  11.5 133   1.1 184  10.8 128  GF    0.00 0.00    0    0.2   0.1   360
  24 01 1990 *2340   8 14.08  151 25.12   519.7  11.6 132   1.1 179  10.8 128  GF    0.00 0.00    0    0.1   0.1   361
  24 01 1990 *2345   8 13.43  151 25.84   520.7  11.6 133   1.3 184  10.8 128  GF    0.00 0.00    0    0.1   0.1   362
  24 01 1990 *2350   8 12.77  151 26.55   521.7  10.8 134   1.0 221  10.8 128  GF    0.00 0.00    0    0.1   0.1   363
  25 01 1990 *0000   8 11.53  151 27.87   523.5  12.1 134   1.7 173  10.8 128  GF    0.00 0.00    0    0.2   0.2   364
  25 01 1990  0000   8 11.5   151 27.9    523.5  12.1 134   1.7 173  10.8 128  c/cs                                365
  25 01 1990  0004   8 11.0   151 28.5    524.3  12.3 134   1.7 173  11.0 128  c/cs                                366
  25 01 1990  0006   8 10.7   151 28.8    524.7  12.0 134   1.7 173  10.7 128  c/cs                                367
  25 01 1990 *0010   8 10.13  151 29.34   525.5  11.5 135   1.6 194  10.7 128  GF    0.00 0.00    0    0.3   0.2   368
  25 01 1990 *0015   8  9.45  151 30.02   526.4  11.7 133   1.4 177  10.7 128  GF    0.00 0.00    0    0.1   0.1   369
  25 01 1990 *0020   8  8.78  151 30.74   527.4  11.5 135   1.6 194  10.7 128  GF    0.00 0.00    0    0.1   0.1   370
  25 01 1990 *0025   8  8.10  151 31.42   528.4  11.7 134   1.5 180  10.7 128  GF    0.00 0.00    0    0.1   0.1   371
```

```
#cruise ODP130JR                            date run: Wed Jul 18 16:38:07 1990         page   8
#
#                      latitude  longitude          actual   drift        dr                  prob. error        drift
#da mo  yr   time deg   min  deg   min     dist speed cse speed hed speed cse  cmnt (smajxsmin@az)  dist  time   no.
#- - - - - - - - - - - - - - - - - - - - - - - - - - - - - - - - - - - - - - - - - - - - - - - - - - - - - - - - - - -
 25 01 1990  0026   8  8.0   151 31.6    528.6  11.7 134   1.5 180  10.8 128  c/cs                                 372
 25 01 1990  0030   8  7.4   151 32.1    529.3  11.9 134   1.5 180  10.9 128  c/cs                                 373
 25 01 1990 *0035   8  6.74  151 32.86   530.3  11.9 134   1.5 183  10.9 128  GF    0.00 0.00   0    0.2    0.2  374
 25 01 1990 *0040   8  6.05  151 33.58   531.3  11.8 134   1.6 186  10.9 128  GF    0.00 0.00   0    0.1    0.1  375
 25 01 1990 *0045   8  5.36  151 34.29   532.3  11.8 135   1.7 190  10.9 128  GF    0.00 0.00   0    0.1    0.1  376
 25 01 1990 *0050   8  4.66  151 34.99   533.3  11.1 135   1.4 214  10.9 128  GF    0.00 0.00   0    0.1    0.1  377
 25 01 1990  0053   8  4.3   151 35.4    533.9  10.9 134   1.4 214  10.8 127  c/cs                                 378
 25 01 1990 *0100   8  3.38  151 36.31   535.1  12.5 133   2.2 165  10.8 127  GF    0.00 0.00   0    0.2    0.2  379
 25 01 1990 *0110   8  1.95  151 37.85   537.2  11.4 134   1.5 195  10.8 127  GF    0.00 0.00   0    0.4    0.2  380
 25 01 1990 *0115   8  1.29  151 38.54   538.2  11.8 135   1.9 189  10.8 127  GF    0.00 0.00   0    0.1    0.1  381
 25 01 1990  0115   8  1.3   151 38.5    538.2  11.7 134   1.9 189  10.7 126  c/cs                                 382
 25 01 1990 *0120   8  0.61  151 39.24   539.1  11.7 131   1.5 175  10.7 126  GF    0.00 0.00   0    0.2    0.1  383
 25 01 1990 *0135   7 58.68  151 41.45   542.1  11.7 131   1.4 173  10.7 126  GF    0.00 0.00   0    0.4    0.2  384
 25 01 1990 *0140   7 58.04  151 42.19   543.0  11.9 131   1.6 165  10.7 126  GF    0.00 0.00   0    0.1    0.1  385
 25 01 1990  0143   7 57.7   151 42.6    543.6  11.9 131   1.6 165  10.7 126  c/cs                                 386
 25 01 1990 *0145   7 57.39  151 42.95   544.0  11.5 131   1.3 178  10.7 126  GF    0.00 0.00   0    0.1    0.1  387
 25 01 1990 *0150   7 56.76  151 43.68   545.0  11.6 131   1.3 173  10.7 126  GF    0.00 0.00   0    0.1    0.1  388
 25 01 1990 *0155   7 56.13  151 44.42   545.9  11.5 130   1.2 173  10.7 126  GF    0.00 0.00   0    0.1    0.1  389
 25 01 1990  0200   7 55.5   151 45.2    546.9  11.4 130   1.2 173  10.6 125  c/cs                                 390
 25 01 1990 *0205   7 54.90  151 45.90   547.9  11.5 131   1.5 181  10.6 125  GF    0.00 0.00   0    0.2    0.2  391
 25 01 1990  0206   7 54.8   151 46.0    548.1  11.5 131   1.5 181  10.6 125  c/cs                                 392
 25 01 1990 *0210   7 54.27  151 46.63   548.8  11.4 131   1.4 181  10.6 125  GF    0.00 0.00   0    0.1    0.1  393
 25 01 1990 *0215   7 53.65  151 47.36   549.8  11.4 130   1.2 176  10.6 125  GF    0.00 0.00   0    0.1    0.1  394
 25 01 1990 *0220   7 53.04  151 48.10   550.7  10.6 130   1.0 216  10.6 125  GF    0.00 0.00   0    0.1    0.1  395
 25 01 1990  0221   7 52.9   151 48.2    550.9  10.6 130   1.0 216  10.6 125  c/cs                                 396
 25 01 1990 *0230   7 51.89  151 49.46   552.5  12.6 129   2.1 150  10.6 125  GF    0.00 0.00   0    0.2    0.2  397
 25 01 1990 *0235   7 51.23  151 50.28   553.5  11.0 128   0.7 182  10.6 125  GF    0.00 0.00   0    0.2    0.1  398
 25 01 1990  0236   7 51.1   151 50.4    553.7  11.1 127   0.7 182  10.7 124  c/cs                                 399
 25 01 1990 *0240   7 50.67  151 51.02   554.5  11.2 128   0.9 182  10.7 124  GF    0.00 0.00   0    0.1    0.1  400
 25 01 1990 *0245   7 50.10  151 51.76   555.4  11.6 127   1.1 156  10.7 124  GF    0.00 0.00   0    0.1    0.1  401
 25 01 1990 *0250   7 49.52  151 52.54   556.4  10.6 127   0.6 225  10.7 124  GF    0.00 0.00   0    0.1    0.1  402
 25 01 1990 *0300   7 48.45  151 53.95   558.1  12.7 127   2.1 144  10.7 124  GF    0.00 0.00   0    0.1    0.2  403
 25 01 1990 *0305   7 47.81  151 54.80   559.2  11.4 128   1.1 172  10.7 124  GF    0.00 0.00   0    0.2    0.1  404
 25 01 1990  0306   7 47.7   151 55.0    559.4  11.5 127   1.1 172  10.8 123  c/cs                                 405
 25 01 1990 *0310   7 47.23  151 55.57   560.1  11.4 128   1.1 180  10.8 123  GF    0.00 0.00   0    0.1    0.1  406
 25 01 1990 *0315   7 46.65  151 56.33   561.1  11.3 127   1.0 180  10.8 123  GF    0.00 0.00   0    0.1    0.1  407
 25 01 1990 *0320   7 46.08  151 57.09   562.0  10.9 128   0.9 207  10.8 123  GF    0.00 0.00   0    0.1    0.1  408
 25 01 1990  0322   7 45.9   151 57.4    562.4  10.7 128   0.9 207  10.6 123  c/cs                                 409
 25 01 1990 *0325   7 45.53  151 57.81   562.9   9.5 128   1.4 270  10.6 123  GF    0.00 0.00   0    0.1    0.1  410
 25 01 1990 *0330   7 45.05  151 58.44   563.7  12.0 128   1.6 160  10.6 123  GF    0.00 0.00   0    0.1    0.1  411
 25 01 1990  0337   7 44.2   151 59.6    565.1  11.9 128   1.6 160  10.6 123  c/cs                                 412
 25 01 1990 *0340   7 43.83  152  0.03   565.7  11.0 128   0.9 191  10.6 123  GF    0.00 0.00   0    0.3    0.2  413
 25 01 1990  0344   7 43.4   152  0.6    566.4  11.0 129   0.9 191  10.6 124  c/cs                                 414
 25 01 1990 *0345   7 43.27  152  0.76   566.6  11.1 127   0.8 181  10.6 124  GF    0.00 0.00   0    0.1    0.1  415
 25 01 1990 *0350   7 42.71  152  1.50   567.6  10.2 127   0.7 255  10.6 124  GF    0.00 0.00   0    0.1    0.1  416
 25 01 1990 *0400   7 41.69  152  2.87   569.3  12.8 127   2.2 141  10.6 124  GF    0.00 0.00   0    0.1    0.2  417
 25 01 1990 *0405   7 41.05  152  3.73   570.3  11.1 127   0.7 171  10.6 124  GF    0.00 0.00   0    0.2    0.1  418
 25 01 1990 *0410   7 40.50  152  4.48   571.2  11.1 126   0.6 164  10.6 124  GF    0.00 0.00   0    0.1    0.1  419
 25 01 1990  0411   7 40.4   152  4.6    571.4  11.0 126   0.6 164  10.6 124  c/cs                                 420
 25 01 1990 *0415   7 39.96  152  5.23   572.2  11.2 125   0.6 138  10.6 124  GF    0.00 0.00   0    0.0    0.1  421
 25 01 1990 *0420   7 39.43  152  6.00   573.1  10.5 126   0.4 225  10.6 124  GF    0.00 0.00   0    0.1    0.1  422
 25 01 1990  0425   7 38.9   152  6.7    574.0  10.5 125   0.4 225  10.6 123  c/cs                                 423
 25 01 1990 *0430   7 38.41  152  7.44   574.8  12.0 125   1.4 137  10.6 123  GF    0.00 0.00   0    0.1    0.2  424
```

```
#cruise ODP130JR                              date run: Wed Jul 18 16:38:07 1990         page   9
#
#                    latitude  longitude              actual    drift        dr                prob. error        drift
#da mo  yr    time deg   min  deg   min      dist speed  cse speed  hed speed  cse   cmnt (smajxsmin@az)   dist  time   no.
#- - - - - - - - - - - - - - - - - - - - - - - - - - - - - - - - - - - - - - - - - - - - - - - - - - - - - - - - - - - - - -
 25 01 1990 *0435    7 37.84 152   8.27   575.8  10.9 125   0.5 179  10.6 123   GF    0.00 0.00    0    0.1   0.1  425
 25 01 1990 *0445    7 36.80 152   9.77   577.7  10.6 125   0.4 212  10.6 123   GF    0.00 0.00    0    0.1   0.2  426
 25 01 1990 *0450    7 36.29 152  10.50   578.5  11.1 125   0.6 157  10.6 123   GF    0.00 0.00    0    0.0   0.1  427
 25 01 1990 *0455    7 35.76 152  11.27   579.5   9.5 125   1.2 290  10.6 123   GF    0.00 0.00    0    0.1   0.1  428
 25 01 1990  0455    7 35.8  152  11.3    579.5   9.7 126   1.2 290  10.8 124   c/cs                                429
 25 01 1990 *0500    7 35.29 152  11.93   580.3  12.7 127   2.0 143  10.8 124   GF    0.00 0.00    0    0.1   0.1  430
 25 01 1990  0504    7 34.8  152  12.6    581.1  12.7 129   2.0 143  10.8 126   c/cs                                431
 25 01 1990 *0505    7 34.65 152  12.78   581.3  11.6 129   0.9 161  10.8 126   GF    0.00 0.00    0    0.2   0.1  432
 25 01 1990 *0510    7 34.05 152  13.54   582.3  11.7 127   0.9 133  10.8 126   GF    0.00 0.00    0    0.1   0.1  433
 25 01 1990 *0515    7 33.47 152  14.33   583.3   9.8 132   1.5 261  10.8 126   GF    0.00 0.00    0    0.1   0.1  434
 25 01 1990 *0520    7 32.92 152  14.94   584.1  11.4 129   0.8 169  10.8 126   GF    0.00 0.00    0    0.1   0.1  435
 25 01 1990  0526    7 32.2  152  15.8    585.2  11.3 130   0.8 169  10.7 127   c/cs                                436
 25 01 1990 *0535    7 31.12 152  17.15   586.9  11.0 130   0.7 186  10.7 127   GF    0.00 0.00    0    0.2   0.2  437
 25 01 1990 *0540    7 30.53 152  17.86   587.8  11.1 130   0.7 183  10.7 127   GF    0.00 0.00    0    0.1   0.1  438
 25 01 1990  0541    7 30.4  152  18.0    588.0  11.2 131   0.7 183  10.8 128   c/cs                                439
 25 01 1990 *0545    7 29.92 152  18.57   588.8  11.5 130   0.9 158  10.8 128   GF    0.00 0.00    0    0.1   0.1  440
 25 01 1990 *0550    7 29.30 152  19.31   589.7  10.2 130   0.7 273  10.8 128   GF    0.00 0.00    0    0.1   0.1  441
 25 01 1990 *0600    7 28.20 152  20.62   591.4  12.8 131   2.1 146  10.8 128   GF    0.00 0.00    0    0.1   0.2  442
 25 01 1990  0602    7 27.9  152  20.9    591.9  13.1 133   2.1 146  11.0 130   c/cs                                443
 25 01 1990 *0605    7 27.48 152  21.43   592.5  11.2 133   0.6 202  11.0 130   GF    0.00 0.00    0    0.2   0.1  444
 25 01 1990 *0610    7 26.84 152  22.12   593.5  11.6 133   0.8 180  11.0 130   GF    0.00 0.00    0    0.1   0.1  445
 25 01 1990 *0615    7 26.18 152  22.83   594.4  11.4 134   0.9 196  11.0 130   GF    0.00 0.00    0    0.1   0.1  446
 25 01 1990 *0620    7 25.52 152  23.52   595.4  11.6 134   0.9 184  11.0 130   GF    0.00 0.00    0    0.1   0.1  447
 25 01 1990  0623    7 25.1  152  23.9    596.0  11.4 134   0.9 184  10.8 130   c/cs                                448
 25 01 1990 *0625    7 24.86 152  24.22   596.3  11.3 134   1.0 190  10.8 130   GF    0.00 0.00    0    0.1   0.1  449
 25 01 1990  0628    7 24.5  152  24.6    596.9  11.5 134   1.0 190  11.0 130   c/cs                                450
 25 01 1990 *0635    7 23.53 152  25.60   598.2  11.4 136   1.2 203  11.0 130   GF    0.00 0.00    0    0.2   0.2  451
 25 01 1990  0638    7 23.1  152  26.0    598.8  11.2 135   1.2 203  10.9 129   c/cs                                452
 25 01 1990 *0640    7 22.86 152  26.27   599.2  11.5 134   1.1 187  10.9 129   GF    0.00 0.00    0    0.1   0.1  453
 25 01 1990 *0645    7 22.20 152  26.97   600.1  11.2 133   0.9 203  10.9 129   GF    0.00 0.00    0    0.1   0.1  454
 25 01 1990 *0650    7 21.56 152  27.65   601.1  10.5 133   0.8 248  10.9 129   GF    0.00 0.00    0    0.1   0.1  455
 25 01 1990  0650    7 21.6  152  27.6    601.1  10.4 133   0.8 248  10.8 129   c/cs                                456
 25 01 1990 *0700    7 20.38 152  28.94   602.8  12.7 134   2.1 159  10.8 129   GF    0.00 0.00    0    0.1   0.2  457
 25 01 1990  0702    7 20.1  152  29.2    603.2  12.8 133   2.1 159  11.0 128   c/cs                                458
 25 01 1990 *0705    7 19.65 152  29.72   603.9  11.3 133   1.0 198  11.0 128   GF    0.00 0.00    0    0.2   0.1  459
 25 01 1990 *0710    7 19.01 152  30.42   604.8  11.2 132   0.9 201  11.0 128   GF    0.00 0.00    0    0.1   0.1  460
 25 01 1990 *0715    7 18.38 152  31.12   605.8  11.4 133   1.1 196  11.0 128   GF    0.00 0.00    0    0.1   0.1  461
 25 01 1990 *0720    7 17.73 152  31.82   606.7  11.2 133   1.0 205  11.0 128   GF    0.00 0.00    0    0.1   0.1  462
 25 01 1990 *0725    7 17.09 152  32.51   607.6   9.8 132   1.3 280  11.0 128   GF    0.00 0.00    0    0.1   0.1  463
 25 01 1990  0727    7 16.9  152  32.8    608.0   9.7 132   1.3 280  10.9 128   c/cs                                464
 25 01 1990 *0730    7 16.55 152  33.12   608.5  12.0 132   1.4 165  10.9 128   GF    0.00 0.00    0    0.1   0.1  465
 25 01 1990 *0740    7 15.21 152  34.62   610.5  11.5 132   1.0 182  10.9 128   GF    0.00 0.00    0    0.2   0.2  466
 25 01 1990  0742    7 15.0  152  34.9    610.8  11.5 133   1.0 182  10.9 129   c/cs                                467
 25 01 1990 *0745    7 14.56 152  35.33   611.4  11.5 132   0.8 173  10.9 129   GF    0.00 0.00    0    0.1   0.1  468
 25 01 1990 *0750    7 13.92 152  36.05   612.4  10.5 132   0.7 262  10.9 129   GF    0.00 0.00    0    0.1   0.1  469
 25 01 1990 *0800    7 12.76 152  37.36   614.1  12.1 133   1.4 162  10.9 129   GF    0.00 0.00    0    0.1   0.2  470
 25 01 1990  0805    7 12.1  152  38.1    615.1  12.2 133   1.4 162  11.0 130   c/cs                                471
 25 01 1990 *0810    7 11.38 152  38.85   616.1  11.3 134   0.8 196  11.0 130   GF    0.00 0.00    0    0.2   0.2  472
 25 01 1990 *0815    7 10.73 152  39.54   617.1  11.2 133   0.7 207  11.0 130   GF    0.00 0.00    0    0.1   0.1  473
 25 01 1990 *0820    7 10.09 152  40.22   618.0  10.5 134   0.9 257  11.0 130   GF    0.00 0.00    0    0.1   0.1  474
 25 01 1990  0828    7  9.1  152  41.2    619.4  10.4 134   0.9 257  10.9 130   c/cs                                475
 25 01 1990 *0830    7  8.88 152  41.49   619.8  12.7 134   1.9 156  10.9 130   GF    0.00 0.00    0    0.1   0.2  476
 25 01 1990 *0835    7  8.15 152  42.26   620.8  11.2 133   0.7 195  10.9 130   GF    0.00 0.00    0    0.2   0.1  477
```

```
                                                                  date run: Wed Jul 18 16:38:07 1990          page  10
#cruise ODP130JR
#
#                         latitude  longitude               actual    drift          dr                 prob. error        drift
#da mo  yr    time deg   min  deg   min        dist speed cse speed hed speed cse   cmnt (smajxsmin@az)   dist  time   no.
#- - - - - - - - - - - - - - - - - - - - - - - - - - - - - - - - - - - - - - - - - - - - - - - - - - - - - - - - - - - - - -
 25 01 1990 *0840    7  7.51 152 42.95    621.8  11.1 134    0.8 212   10.9 130   GF    0.00 0.00    0    0.1    0.1   478
 25 01 1990 *0845    7  6.87 152 43.62    622.7  11.4 134    0.9 191   10.9 130   GF    0.00 0.00    0    0.1    0.1   479
 25 01 1990 *0850    7  6.21 152 44.31    623.6  11.2 134    0.9 203   10.9 130   GF    0.00 0.00    0    0.1    0.1   480
 25 01 1990  0853    7  5.8  152 44.7     624.2  11.3 133    0.9 203   11.0 129   c/cs                                   481
 25 01 1990 *0855    7  5.56 152 44.99    624.6  11.6 134    1.1 187   11.0 129   GF    0.00 0.00    0    0.1    0.1   482
 25 01 1990 *0905    7  4.23 152 46.40    626.5  11.6 134    1.1 190   11.0 129   GF    0.00 0.00    0    0.2    0.2   483
 25 01 1990  0905    7  4.2  152 46.4     626.5  11.6 134    1.1 190   11.0 129   c/cs                                   484
 25 01 1990 *0910    7  3.56 152 47.10    627.5  11.4 134    1.1 198   11.0 129   GF    0.00 0.00    0    0.1    0.1   485
 25 01 1990 *0915    7  2.90 152 47.79    628.4  11.7 133    1.0 177   11.0 129   GF    0.00 0.00    0    0.1    0.1   486
 25 01 1990 *0920    7  2.24 152 48.51    629.4  11.5 133    0.9 186   11.0 129   GF    0.00 0.00    0    0.1    0.1   487
 25 01 1990 *0925    7  1.59 152 49.22    630.3  10.1 134    1.3 268   11.0 129   GF    0.00 0.00    0    0.1    0.1   488
 25 01 1990 *0930    7  1.01 152 49.83    631.2  12.9 133    2.1 152   11.0 129   GF    0.00 0.00    0    0.1    0.1   489
 25 01 1990  0933    7  0.6  152 50.3     631.8  12.8 132    2.1 152   10.9 128   c/cs                                   490
 25 01 1990 *0935    7  0.29 152 50.63    632.3  11.6 131    1.0 172   10.9 128   GF    0.00 0.00    0    0.2    0.1   491
 25 01 1990 *0940    6 59.65 152 51.36    633.2  11.5 132    1.0 179   10.9 128   GF    0.00 0.00    0    0.1    0.1   492
 25 01 1990 *0945    6 59.01 152 52.08    634.2  11.1 130    0.5 190   10.9 128   GF    0.00 0.00    0    0.1    0.1   493
 25 01 1990 *0950    6 58.41 152 52.79    635.1  11.2 132    0.9 195   10.9 128   GF    0.00 0.00    0    0.0    0.1   494
 25 01 1990 *0955    6 57.78 152 53.49    636.0   9.8 132    1.3 274   10.9 128   GF    0.00 0.00    0    0.1    0.1   495
 25 01 1990 *1000    6 57.23 152 54.10    636.9  12.6 131    1.8 148   10.9 128   GF    0.00 0.00    0    0.1    0.1   496
 25 01 1990  1002    6 57.0  152 54.4     637.3  12.7 131    1.8 148   10.9 128   c/cs                                   497
 25 01 1990 *1010    6 55.85 152 55.71    639.0  12.0 131    1.2 158   10.9 128   GF    0.00 0.00    0    0.3    0.2   498
 25 01 1990 *1015    6 55.20 152 56.47    640.0  11.8 131    1.0 161   10.9 128   GF    0.00 0.00    0    0.1    0.1   499
 25 01 1990 *1020    6 54.56 152 57.22    640.9  10.7 131    0.5 240   10.9 128   GF    0.00 0.00    0    0.1    0.1   500
 25 01 1990  1026    6 53.9  152 58.0     642.0  10.6 131    0.5 240   10.8 128   c/cs                                   501
 25 01 1990 *1030    6 53.40 152 58.58    642.7  12.1 130    1.4 145   10.8 128   GF    0.00 0.00    0    0.1    0.2   502
 25 01 1990  1030    6 53.4  152 58.6     642.7  12.2 131    1.4 145   10.9 129   c/cs                                   503
 25 01 1990 *1040    6 52.07 153  0.13    644.8  11.6 131    0.9 161   10.9 129   GF    0.00 0.00    0    0.2    0.2   504
 25 01 1990  1040    6 52.1  153  0.1     644.8  11.6 131    0.9 161   10.8 129   c/cs                                   505
 25 01 1990 *1045    6 51.43 153  0.86    645.7  11.4 131    0.8 166   10.8 129   GF    0.00 0.00    0    0.1    0.1   506
 25 01 1990 *1050    6 50.80 153  1.58    646.7  11.8 130    1.0 139   10.8 129   GF    0.00 0.00    0    0.1    0.1   507
 25 01 1990 *1055    6 50.17 153  2.34    647.7   9.9 132    1.0 281   10.8 129   GF    0.00 0.00    0    0.1    0.1   508
 25 01 1990 *1100    6 49.62 153  2.96    648.5  12.5 131    1.7 141   10.8 129   GF    0.00 0.00    0    0.1    0.1   509
 25 01 1990  1106    6 48.8  153  3.9     649.7  12.3 129    1.7 141   10.7 127   c/cs                                   510
 25 01 1990 *1110    6 48.29 153  4.56    650.6  11.6 128    0.9 135   10.7 127   GF    0.00 0.00    0    0.3    0.2   511
 25 01 1990 *1115    6 47.70 153  5.33    651.5  11.8 129    1.2 145   10.7 127   GF    0.00 0.00    0    0.1    0.1   512
 25 01 1990  1136    6 45.1  153  8.6     655.7  11.9 129    1.2 145   10.7 127   c/cs                                   513
 25 01 1990  1145    6 44.0  153 10.0     657.4  11.9 129    1.2 145   10.8 127   c/cs                                   514
 25 01 1990 *1149    6 43.50 153 10.60    658.2  11.7 129    1.0 151   10.8 127   SF    0.00 0.00    0    0.7    0.6   515
 25 01 1990  1158    6 42.4  153 12.0     660.0  11.2 129    1.0 151   10.3 127   c/cs                                   516
 25 01 1990  1205    6 41.6  153 13.0     661.3  11.7 129    1.0 151   10.8 127   c/cs                                   517
 25 01 1990  1235    6 37.9  153 17.6     667.2  11.7 129    1.0 151   10.8 127   c/cs                                   518
 25 01 1990  1305    6 34.2  153 22.2     673.0  11.8 131    1.0 151   10.9 129   c/cs                                   519
 25 01 1990  1323    6 31.9  153 24.9     676.6  11.8 131    1.0 151   10.8 129   c/cs                                   520
 25 01 1990 *1338    6 29.97 153 27.10    679.5  12.0 128    1.2 118   10.8 129   SF    0.00 0.00    0    1.8    1.8   521
 25 01 1990  1352    6 28.2  153 29.3     682.3  12.3 127    1.2 118   11.1 128   c/cs                                   522
 25 01 1990  1355    6 27.9  153 29.8     682.9  12.2 127    1.2 118   10.9 128   c/cs                                   523
 25 01 1990  1410    6 26.0  153 32.3     686.0  11.6 128    1.2 118   10.3 129   c/cs                                   524
 25 01 1990  1414    6 25.6  153 32.9     686.7  12.1 128    1.2 118   10.9 129   c/cs                                   525
 25 01 1990  1440    6 22.3  153 37.1     692.0  12.1 128    1.2 118   10.9 129   c/cs                                   526
 25 01 1990  1510    6 18.6  153 41.9     698.1  12.1 127    1.2 118   10.8 128   c/cs                                   527
 25 01 1990  1517    6 17.8  153 43.0     699.5  12.0 129    1.2 118   10.8 130   c/cs                                   528
 25 01 1990  1539    6 15.0  153 46.5     703.9  11.9 130    1.2 118   10.7 131   c/cs                                   529
 25 01 1990  1553    6 13.2  153 48.6     706.7  11.7 128    1.2 118   10.5 129   c/cs                                   530
```

```
                                                  date run: Wed Jul 18 16:38:07 1990        page  11
#cruise ODP130JR
#                                                                                          prob. error        drift
#                     latitude  longitude                actual   drift        dr                                              
#da mo  yr    time deg   min  deg   min      dist speed cse speed hed speed cse   cmnt (smajxsmin@az)  dist  time   no.
#- - - - - - - - - - - - - - - - - - - - - - - - - - - - - - - - - - - - - - - - - - - - - - - - - - - - - - - - - - - -
 25 01 1990  1605    6 11.8  153 50.5    709.0  11.7 128   1.2 118  10.5 129  c/cs                                      531
 25 01 1990  1615    6 10.6  153 52.0    711.0  11.9 128   1.2 118  10.6 129  c/cs                                      532
 25 01 1990  1624    6  9.5  153 53.4    712.7  12.0 128   1.2 118  10.8 129  c/cs                                      533
 25 01 1990  1647    6  6.7  153 57.1    717.3  11.9 128   1.2 118  10.7 129  c/cs                                      534
 25 01 1990  1717    6  3.0  154  1.8    723.3  11.8 128   1.2 118  10.6 129  c/cs                                      535
 25 01 1990  1732    6  1.2  154  4.2    726.2  11.9 128   1.2 118  10.7 129  c/cs                                      536
 25 01 1990 *1745    5 59.62 154  6.20   728.8  12.0 131   1.3 144  10.7 129  SF    0.00 0.00    0    5.1   4.1   537
 25 01 1990  1749    5 59.1  154  6.8    729.6  12.0 131   1.3 144  10.8 129  c/cs                                      538
 25 01 1990  1819    5 55.2  154 11.4    735.6  12.0 131   1.3 144  10.8 129  c/cs                                      539
 25 01 1990  1838    5 52.7  154 14.3    739.4  11.9 131   1.3 144  10.6 129  c/cs                                      540
 25 01 1990  1852    5 50.9  154 16.4    742.2  12.1 131   1.3 144  10.8 129  c/cs                                      541
 25 01 1990  1901    5 49.7  154 17.8    744.0  12.0 131   1.3 144  10.7 129  c/cs                                      542
 25 01 1990 *1914    5 48.01 154 19.80   746.6  11.8 132   1.3 162  10.7 129  SF    0.00 0.00    0    2.0   1.5   543
 25 01 1990  1915    5 47.9  154 19.9    746.8  12.0 132   1.3 162  10.9 129  c/cs                                      544
 25 01 1990  1925    5 46.5  154 21.4    748.8  12.2 132   1.3 162  11.1 129  c/cs                                      545
 25 01 1990  1934    5 45.3  154 22.8    750.7  12.1 133   1.3 162  10.9 130  c/cs                                      546
 25 01 1990  2004    5 41.2  154 27.2    756.7  12.0 134   1.3 162  10.9 131  c/cs                                      547
 25 01 1990  2034    5 37.0  154 31.5    762.7  12.1 134   1.3 162  11.0 131  c/cs                                      548
 25 01 1990  2103    5 32.9  154 35.8    768.6  12.2 133   1.3 162  11.0 130  c/cs                                      549
 25 01 1990 *2110    5 31.90 154 36.80   770.0  12.8 128   1.8 117  11.0 130  GF    0.00 0.00    0    2.5   1.7   550
 25 01 1990  2133    5 28.9  154 40.7    774.9  12.6 128   1.8 117  10.9 130  c/cs                                      551
 25 01 1990  2142    5 27.7  154 42.2    776.8  12.7 127   1.8 117  11.0 129  c/cs                                      552
 25 01 1990  2203    5 25.0  154 45.7    781.2  12.8 127   1.8 117  11.1 129  c/cs                                      553
 25 01 1990  2226    5 22.0  154 49.6    786.1  12.9 128   1.8 117  11.2 130  c/cs                                      554
 25 01 1990 *2230    5 21.50 154 50.30   787.0  11.7 131   0.6 144  11.2 130  GF    0.00 0.00    0    2.3   1.3   555
 25 01 1990  2234    5 21.0  154 50.9    787.8  11.6 133   0.6 144  11.0 132  c/cs                                      556
 25 01 1990  2255    5 18.3  154 53.9    791.8  11.6 133   0.6 144  11.0 132  c/cs                                      557
 25 01 1990 *2300    5 17.60 154 54.60   792.8  11.8 133   0.9 143  11.0 132  GF    0.00 0.00    0    0.3   0.5   558
 25 01 1990  2308    5 16.5  154 55.8    794.4  11.8 132   0.9 143  11.0 131  c/cs                                      559
 25 01 1990  2315    5 15.6  154 56.8    795.7  11.8 133   0.9 143  10.9 132  c/cs                                      560
 25 01 1990  2337    5 12.7  154 60.0    800.1  11.8 133   0.9 143  10.9 132  c/cs                                      561
 26 01 1990 *0000    5  9.60 155  3.30   804.6  12.3 131   1.3 121  10.9 132  GF    0.00 0.00    0    0.9   1.0   562
 26 01 1990  0000    5  9.6  155  3.3    804.6  12.3 131   1.3 121  10.9 132  c/cs                                      563
 26 01 1990  0007    5  8.7  155  4.4    806.0  12.4 131   1.3 121  11.1 132  c/cs                                      564
 26 01 1990  0036    5  4.7  155  8.9    812.0  12.4 131   1.3 121  11.0 132  c/cs                                      565
 26 01 1990 *0100    5  1.50 155 12.70   817.0  11.0 131   0.3  42  11.0 132  GF    0.00 0.00    0    1.3   1.0   566
 26 01 1990  0106    5  0.8  155 13.5    818.1  11.2 131   0.3  42  11.2 132  c/cs                                      567
 26 01 1990  0128    4 58.1  155 16.7    822.2  11.2 132   0.3  42  11.2 133  c/cs                                      568
 26 01 1990 *0130    4 57.87 155 16.95   822.5  12.0 132   0.9 115  11.2 133  GF    0.00 0.00    0    0.1   0.5   569
 26 01 1990  0158    4 54.1  155 21.2    828.1  12.0 131   0.9 115  11.2 132  c/cs                                      570
 26 01 1990 *0200    4 53.88 155 21.46   828.5  11 9 130   0.9  98  11.2 132  GF    0.00 0.00    0    0.4   0.5   571
 26 01 1990  0214    4 52.1  155 23.6    831.3  10.3 130   0.9  98   9.6 133  c/cs                                      572
 26 01 1990  0216    4 51.9  155 23.9    831.7  11.9 130   0.9  98  11.1 132  c/cs                                      573
 26 01 1990  0234    4 49.6  155 26.6    835.2  11.9 132   0.9  98  11.2 135  c/cs                                      574
 26 01 1990  0249    4 47.6  155 28.8    838.2  11.6 132   0.9  98  10.8 135  c/cs                                      575
 26 01 1990  0257    4 46.6  155 30.0    839.8  11.6 133   0.9  98  10.9 136  c/cs                                      576
 26 01 1990 *0300    4 46.16 155 30.40   840.3  11.1 134   0.4  73  10.9 136  GF    0.00 0.00    0    0.9   1.0   577
 26 01 1990  0304    4 45.6  155 30.9    841.1  11.3 136   0.4  73  11.1 138  c/cs                                      578
 26 01 1990  0318    4 43.7  155 32.8    843.7  11.4 136   0.4  73  11.2 138  c/cs                                      579
 26 01 1990  0348    4 39.6  155 36.8    849.4  11.6 136   0.4  73  11.4 138  c/cs                                      580
 26 01 1990  0413    4 36.2  155 40.1    854.3  11.5 135   0.4  73  11.3 137  c/cs                                      581
 26 01 1990  0434    4 33.3  155 43.0    858.3  11.4 134   0.4  73  11.2 136  c/cs                                      582
 26 01 1990  0447    4 31.6  155 44.7    860.8  11.6 134   0.4  73  11.4 136  c/cs                                      583
```

```
#cruise ODP130JR                                             date run: Wed Jul 18 16:38:07 1990        page  12
#
#                  latitude longitude          actual    drift       dr            prob. error      drift
#da mo   yr   time deg  min deg   min    dist speed cse speed hed speed cse  cmnt (smajxsmin@az)  dist  time   no.
#- - - - - - - - - - - - - - - - - - - - - - - - - - - - - - - - - - - - - - - - - - - - - - - - - - - - - - - - -
  26 01 1990  0502  4 29.6  155 46.8    863.6  11.5 131   0.4  73  11.3 133  c/cs                              584
  26 01 1990  0525  4 26.7  155 50.2    868.1  11.3 131   0.4  73  11.1 133  c/cs                              585
  26 01 1990  0529  4 26.2  155 50.7    868.8  11.5 131   0.4  73  11.2 133  c/cs                              586
  26 01 1990 *0530  4 26.04 155 50.88   869.0  11.4 134   0.2 179  11.2 133  GF    0.00 0.00   0   1.1   2.5   587
  26 01 1990  0535  4 25.4  155 51.6    870.0  11.1 134   0.2 179  11.0 133  c/cs                              588
  26 01 1990  0539  4 24.9  155 52.1    870.7  11.8 134   0.2 179  11.6 133  c/cs                              589
  26 01 1990  0545  4 24.1  155 53.0    871.9  11.5 134   0.2 179  11.4 133  c/cs                              590
  26 01 1990  0607  4 21.2  155 56.0    876.1  11.3 133   0.2 179  11.2 132  c/cs                              591
  26 01 1990  0634  4 17.7  155 59.8    881.2  11.3 132   0.2 179  11.1 131  c/cs                              592
  26 01 1990 *0700  4 14.46 156  3.41   886.0  11.8 133   0.8 169  11.1 131  GF    0.00 0.00   0   0.3   1.5   593
  26 01 1990  0704  4 13.9  156  4.0    886.8  11.9 133   0.8 169  11.3 131  c/cs                              594
  26 01 1990 *0708  4 13.38 156  4.56   887.6  11.3 134   0.6 214  11.3 131  GF    0.00 0.00   0   0.1   0.1   595
  26 01 1990  0713  4 12.7  156  5.2    888.6  11.4 135   0.6 214  11.3 132  c/cs                              596
  26 01 1990  0734  4  9.9  156  8.1    892.6  11.1 135   0.6 214  11.1 132  c/cs                              597
  26 01 1990  0743  4  8.7  156  9.3    894.2  11.3 135   0.6 214  11.2 132  c/cs                              598
  26 01 1990  0756  4  7.0  156 11.0    896.7  11.4 134   0.6 214  11.3 131  c/cs                              599
  26 01 1990  0823  4  3.4  156 14.7    901.8  11.3 134   0.6 214  11.2 131  c/cs                              600
  26 01 1990  0837  4  1.6  156 16.6    904.5  11.3 133   0.6 214  11.2 130  c/cs                              601
  26 01 1990 *0900  3 58.67 156 19.78   908.8  11.3 133   0.6 211  11.2 130  GF    0.00 0.00   0   1.1   1.9   602
  26 01 1990  0902  3 58.4  156 20.1    909.1  11.3 131   0.6 211  11.2 128  c/cs                              603
  26 01 1990 *0905  3 58.04 156 20.48   909.7  11.0 133   1.1 231  11.2 128  GF    0.00 0.00   0   0.1   0.1   604
  26 01 1990 *0910  3 57.41 156 21.15   910.6  11.5 132   0.8 202  11.2 128  GF    0.00 0.00   0   0.1   0.1   605
  26 01 1990 *0915  3 56.77 156 21.86   911.6  11.7 132   0.9 186  11.2 128  GF    0.00 0.00   0   0.1   0.1   606
  26 01 1990 *0920  3 56.12 156 22.59   912.6  10.8 132   0.8 248  11.2 128  GF    0.00 0.00   0   0.1   0.1   607
  26 01 1990 *0930  3 54.92 156 23.94   914.4  13.0 130   1.8 143  11.2 128  GF    0.00 0.00   0   0.1   0.2   608
  26 01 1990  0932  3 54.6  156 24.3    914.8  13.0 128   1.8 143  11.2 126  c/cs                              609
  26 01 1990 *0935  3 54.24 156 24.78   915.4  11.1 130   0.8 223  11.2 126  GF    0.00 0.00   0   0.2   0.1   610
  26 01 1990 *0940  3 53.64 156 25.49   916.4  11.2 129   0.6 217  11.2 126  GF    0.00 0.00   0   0.1   0.1   611
  26 01 1990  0943  3 53.3  156 25.9    916.9  10.9 129   0.6 217  10.9 126  c/cs                              612
  26 01 1990 *0945  3 53.06 156 26.21   917.3  10.8 129   0.7 223  10.9 126  GF    0.00 0.00   0   0.0   0.1   613
  26 01 1990  0946  3 52.9  156 26.3    917.5  11.2 129   0.7 223  11.3 126  c/cs                              614
  26 01 1990 *0950  3 52.47 156 26.93   918.2  10.5 130   1.1 266  11.3 126  GF    0.00 0.00   0   0.1   0.1   615
  26 01 1990 *1000  3 51.35 156 28.28   920.0  12.4 129   1.3 161  11.3 126  GF    0.00 0.00   0   0.2   0.2   616
  26 01 1990  1000  3 51.3  156 28.3    920.0  12.3 129   1.3 161  11.2 126  c/cs                              617
  26 01 1990 *1005  3 50.70 156 29.07   921.0  11.2 131   1.0 218  11.2 126  GF    0.00 0.00   0   0.1   0.1   618
  26 01 1990  1009  3 50.2  156 29.6    921.7  11.4 133   1.0 218  11.3 128  c/cs                              619
  26 01 1990 *1010  3 50.08 156 29.77   921.9  11.4 133   0.9 217  11.3 128  GF    0.00 0.00   0   0.1   0.1   620
  26 01 1990 *1015  3 49.44 156 30.47   922.9  11.4 132   0.9 217  11.3 128  GF    0.00 0.00   0   0.1   0.1   621
  26 01 1990 *1020  3 48.80 156 31.17   923.8  11.3 132   0.8 218  11.3 128  GF    0.00 0.00   0   0.1   0.1   622
  26 01 1990 *1040  3 46.26 156 33.98   927.6  11.5 132   0.8 208  11.3 128  GF    0.00 0.00   0   0.3   0.3   623
  26 01 1990  1041  3 46.1  156 34.1    927.8  11.5 132   0.8 208  11.3 128  c/cs                              624
  26 01 1990 *1045  3 45.62 156 34.69   928.6  11.4 133   1.1 216  11.3 128  GF    0.00 0.00   0   0.1   0.1   625
  26 01 1990 *1050  3 44.97 156 35.38   929.5   9.4 132   2.0 290  11.3 128  GF    0.00 0.00   0   0.1   0.1   626
  26 01 1990  1051  3 44.9  156 35.5    929.7   7.6 132   2.0 290   9.5 127  c/cs                              627
  26 01 1990 *1100  3 44.11 156 36.35   930.8   6.9 134   2.7 289   9.5 127  GF    0.00 0.00   0   0.3   0.2   628
  26 01 1990  1117  3 42.7  156 37.8    932.8   3.9 138   2.7 289   6.4 126  c/cs                              629
  26 01 1990 *1120  3 42.60 156 37.90   933.0   6.0 134   0.9 244   6.4 126  GF    0.00 0.00   0   0.9   0.3   630
  26 01 1990  1138  3 41.4  156 39.2    934.8   4.9 158   0.9 244   4.9 147  c/cs                              631
  26 01 1990  1139  3 41.3  156 39.2    934.9   6.1 177   0.9 244   5.8 169  c/cs                              632
  26 01 1990  1140  3 41.2  156 39.2    935.0   7.5 203   0.9 244   6.9 198  c/cs                              633
  26 01 1990 *1145  3 40.60 156 39.00   935.6   7.3 207   1.2 271   6.9 198  GF    0.00 0.00   0   0.4   0.4   634
  26 01 1990  1145  3 40.6  156 39.0    935.6   8.1 207   1.2 271   7.6 199  c/cs                              635
  26 01 1990  1156  3 39.3  156 38.3    937.1   7.9 205   1.2 271   7.5 197  c/cs                              636
```

```
#cruise ODP130JR                                   date run: Wed Jul 18 16:38:07 1990        page  13
#
#                  latitude  longitude               actual    drift       dr                prob. error        drift
#da mo  yr   time  deg  min   deg  min      dist  speed cse  speed hed  speed cse  cmnt (smajxsmin@az)   dist  time  no.
#- - - - - - - - - - - - - - - - - - - - - - - - - - - - - - - - - - - - - - - - - - - - - - - - - - - - - - - - - - -
 26 01 1990 *1200   3 38.80 156 38.10  937.6   7.2 216   2.5 303   7.5 197  GF    0.00 0.00   0    0.3   0.2  637
 26 01 1990  1207   3 38.1  156 37.6   938.4   7.5 224   2.5 303   7.4 205  c/cs                              638
 26 01 1990  1232   3 35.9  156 35.4   941.6   7.6 223   2.5 303   7.6 204  c/cs                              639
 26 01 1990  1252   3 34.0  156 33.7   944.1   7.5 223   2.5 303   7.4 204  c/cs                              640
 26 01 1990  1318   3 31.6  156 31.5   947.3   7.3 225   2.5 303   7.2 205  c/cs                              641
 26 01 1990  1321   3 31.4  156 31.2   947.7   7.7 249   2.5 303   6.6 231  c/cs                              642
 26 01 1990  1322   3 31.3  156 31.1   947.8   8.8 273   2.5 303   6.8 262  c/cs                              643
 26 01 1990  1323   3 31.3  156 31.0   948.0   9.0 295   2.5 303   6.6 292  c/cs                              644
 26 01 1990 *1325   3 31.45 156 30.70  948.3   6.5 288   0.5 184   6.6 292  SF    0.00 0.00   0    3.5   1.4  645
 26 01 1990  1327   3 31.5  156 30.5   948.5   6.7 292   0.5 184   6.9 296  c/cs                              646
 26 01 1990  1334   3 31.8  156 29.8   949.3   6.7 285   0.5 184   6.8 289  c/cs                              647
 26 01 1990  1335   3 31.8  156 29.7   949.4   5.8 314   0.5 184   6.1 317  c/cs                              648
 26 01 1990  1336   3 31.9  156 29.6   949.5   5.0 357   0.5 184   5.5 358  c/cs                              649
 26 01 1990  1341   3 32.3  156 29.6   949.9   6.4 359   0.5 184   6.8 359  c/cs                              650
 26 01 1990  1346   3 32.9  156 29.6   950.4   7.4 360   0.5 184   7.9   0  c/cs                              651
 26 01 1990  1352   3 33.6  156 29.6   951.2   7.1   9   0.5 184   7.6   9  c/cs                              652
 26 01 1990  1411   3 35.8  156 29.9   953.4   7.1   7   0.5 184   7.5   7  c/cs                              653
 26 01 1990  1441   3 39.3  156 30.4   957.0   7.0   7   0.5 184   7.5   7  c/cs                              654
 26 01 1990  1452   3 40.6  156 30.5   958.3   6.8  23   0.5 184   7.2  22  c/cs                              655
 26 01 1990  1454   3 40.8  156 30.6   958.5   5.9  62   0.5 184   6.2  58  c/cs                              656
 26 01 1990  1455   3 40.9  156 30.7   958.6   5.5  95   0.5 184   5.6  90  c/cs                              657
 26 01 1990  1457   3 40.8  156 30.9   958.8   7.3 113   0.5 184   7.2 110  c/cs                              658
 26 01 1990  1501   3 40.7  156 31.3   959.3   7.8 117   0.5 184   7.6 114  c/cs                              659
 26 01 1990  1509   3 40.2  156 32.3   960.3   7.2 118   0.5 184   7.1 115  c/cs                              660
 26 01 1990  1514   3 39.9  156 32.8   960.9   6.0 119   0.5 184   5.8 115  c/cs                              661
 26 01 1990  1528   3 39.2  156 34.0   962.3   6.2 119   0.5 184   6.1 115  c/cs                              662
 26 01 1990 *1529   3 39.16 156 34.10  962.4   5.8 121   0.7 234   6.1 115  SF    0.00 0.00   0    1.0   2.1  663
 26 01 1990  1535   3 38.9  156 34.6   963.0   6.2 121   0.7 234   6.5 116  c/cs                              664
 26 01 1990  1543   3 38.4  156 35.3   963.8   7.3 125   0.7 234   7.5 120  c/cs                              665
 26 01 1990  1555   3 37.6  156 36.5   965.3   7.0 125   0.7 234   7.2 120  c/cs                              666
 26 01 1990  1615   3 36.3  156 38.4   967.6   6.8 123   0.7 234   7.1 118  c/cs                              667
 26 01 1990  1633   3 35.2  156 40.1   969.6   6.7 124   0.7 234   6.9 119  c/cs                              668
 26 01 1990  1647   3 34.3  156 41.4   971.2   6.7 123   0.7 234   7.0 118  c/cs                              669
 26 01 1990 *1707   3 33.06 156 43.30  973.4   7.3 124   0.8 186   7.0 118  SF    0.00 0.00   0    1.1   1.6  670
 26 01 1990  1717   3 32.4  156 44.3   974.6   7.3 120   0.8 186   7.1 114  c/cs                              671
 26 01 1990  1722   3 32.1  156 44.8   975.2   7.2 109   0.8 186   7.1 103  c/cs                              672
 26 01 1990  1728   3 31.8  156 45.5   976.0   8.0 108   0.8 186   7.9 103  c/cs                              673
 26 01 1990  1741   3 31.3  156 47.2   977.7   7.7 108   0.8 186   7.6 102  c/cs                              674
 26 01 1990  1756   3 30.7  156 49.0   979.6   7.8 108   0.8 186   7.7 102  c/cs                              675
 26 01 1990  1823   3 29.6  156 52.4   983.2   7.3 108   0.8 186   7.1 102  c/cs                              676
 26 01 1990  1826   3 29.5  156 52.7   983.5   7.9 108   0.8 186   7.7 102  c/cs                              677
 26 01 1990 *1837   3 29.10 156 54.10  985.0   7.7 105   0.4 202   7.7 102  SF    0.00 0.00   0    1.2   1.5  678
 26 01 1990  1856   3 28.5  156 56.5   987.4   7.7 103   0.4 202   7.8 100  c/cs                              679
 26 01 1990  1911   3 28.0  156 58.3   989.3   7.6 103   0.4 202   7.6 100  c/cs                              680
 26 01 1990  1930   3 27.5  157  0.7   991.7   7.6 104   0.4 202   7.7 101  c/cs                              681
 26 01 1990  1956   3 26.7  157  3.9   995.0   6.7 104   0.4 202   6.7 100  c/cs                              682
 26 01 1990 *1959   3 26.60 157  4.20  995.3   6.8 111   1.3 191   6.7 100  SF    0.00 0.00   0    0.6   1.4  683
 26 01 1990  1959   3 26.6  157  4.2   995.3   7.8 111   1.3 191   7.7 101  c/cs                              684
 26 01 1990  2024   3 25.4  157  7.2   998.6   7.5 111   1.3 191   7.4 101  c/cs                              685
 26 01 1990 *2027   3 25.30 157  7.60  999.0   7.4 104   0.4 185   7.4 101  SF    0.00 0.00   0    0.6   0.5  686
 26 01 1990  2033   3 25.1  157  8.3   999.7   7.8 104   0.4 185   7.8 101  c/cs                              687
 26 01 1990  2059   3 24.3  157 11.6  1003.1   7.8 104   0.4 185   7.7 101  c/cs                              688
 26 01 1990 *2100   3 24.27 157 11.75 1003.2   7.4 106   0.8 222   7.7 101  GF    0.00 0.00   0    0.2   0.5  689
```

```
                                                        date run: Wed Jul 18 16:38:07 1990        page  14
#cruise ODP130JR
#                                                       actual    drift      dr              prob. error           drift
#                    latitude  longitude                                          
#da mo  yr   time   deg  min   deg  min     dist  speed cse  speed hed  speed cse  cmnt (smajxsmin@az)   dist   time  no.
#------------------------------------------------------------------------------------------------------------------------
 26 01 1990 *2105    3 24.10  157 12.34  1003.9   7.5 107   0.8 210    7.7 101   GF   0.00 0.00   0    0.1    0.1  690
 26 01 1990 *2110    3 23.92  157 12.94  1004.5   7.6 107   0.8 205    7.7 101   GF   0.00 0.00   0    0.1    0.1  691
 26 01 1990  2112    3 23.8   157 13.2   1004.7   8.1 105   0.8 205    8.2 100   c/cs                                692
 26 01 1990 *2115    3 23.74  157 13.57  1005.1   8.3 105   0.7 186    8.2 100   GF   0.00 0.00   0    0.1    0.1  693
 26 01 1990 *2120    3 23.56  157 14.24  1005.8   8.1 106   0.8 204    8.2 100   GF   0.00 0.00   0    0.1    0.1  694
 26 01 1990 *2125    3 23.38  157 14.89  1006.5   8.2 105   0.6 192    8.2 100   GF   0.00 0.00   0    0.1    0.1  695
 26 01 1990  2131    3 23.2   157 15.7   1007.3   7.9 105   0.6 192    7.9 100   c/cs                                696
 26 01 1990 *2135    3 23.04  157 16.20  1007.9   7.8 106   0.8 198    7.9 100   GF   0.00 0.00   0    0.1    0.2  697
 26 01 1990 *2140    3 22.86  157 16.83  1008.5   8.1 105   0.7 181    7.9 100   GF   0.00 0.00   0    0.1    0.1  698
 26 01 1990 *2145    3 22.69  157 17.48  1009.2   7.8 109   1.2 200    7.9 100   GF   0.00 0.00   0    0.1    0.1  699
 26 01 1990  2146    3 22.6   157 17.6   1009.3   7.2 109   1.2 200    7.3 100   c/cs                                700
 26 01 1990 *2150    3 22.49  157 18.06  1009.8   7.8 103   0.6 139    7.3 100   GF   0.00 0.00   0    0.1    0.1  701
 26 01 1990  2150    3 22.5   157 18.1   1009.8   8.2 103   0.6 139    7.8 101   c/cs                                702
 26 01 1990 *2155    3 22.33  157 18.73  1010.5   7.3 108   1.1 221    7.8 101   GF   0.00 0.00   0    0.0    0.1  703
 26 01 1990 *2200    3 22.14  157 19.31  1011.1   8.4 104   0.7 138    7.8 101   GF   0.00 0.00   0    0.1    0.1  704
 26 01 1990 *2205    3 21.97  157 19.99  1011.8   7.5 109   1.1 212    7.8 101   GF   0.00 0.00   0    0.1    0.1  705
 26 01 1990 *2210    3 21.77  157 20.58  1012.4   8.4 104   0.8 135    7.8 101   GF   0.00 0.00   0    0.1    0.1  706
 26 01 1990  2211    3 21.7   157 20.7   1012.6   8.6 104   0.8 135    7.9 101   c/cs                                707
 26 01 1990 *2215    3 21.60  157 21.27  1013.1   8.1 108   1.0 185    7.9 101   GF   0.00 0.00   0    0.1    0.1  708
 26 01 1990 *2220    3 21.39  157 21.91  1013.8   7.8 108   1.0 201    7.9 101   GF   0.00 0.00   0    0.1    0.1  709
 26 01 1990 *2225    3 21.19  157 22.53  1014.4   7.8 110   1.2 202    7.9 101   GF   0.00 0.00   0    0.1    0.1  710
 26 01 1990 *2230    3 20.97  157 23.14  1015.1   8.3 104   0.6 153    7.9 101   GF   0.00 0.00   0    0.1    0.1  711
 26 01 1990 *2235    3 20.80  157 23.81  1015.8   7.7 108   1.0 208    7.9 101   GF   0.00 0.00   0    0.0    0.1  712
 26 01 1990  2235    3 20.8   157 23.8   1015.8   7.0 108   1.0 208    7.3 100   c/cs                                713
 26 01 1990 *2240    3 20.62  157 24.37  1016.4   7.0 108   1.0 208    7.3 100   GF   0.00 0.00   0    0.1    0.1  714
 26 01 1990 *2245    3 20.44  157 24.93  1017.0   8.0 100   0.7 105    7.3 100   GF   0.00 0.00   0    0.1    0.1  715
 26 01 1990  2253    3 20.2   157 26.0   1018.0   8.0 100   0.7 105    7.3 100   c/cs                                716
 26 01 1990 *2255    3 20.20  157 26.24  1018.3   8.0 103   0.8 133    7.3 100   GF   0.00 0.00   0    0.1    0.2  717
 26 01 1990 *2300    3 20.05  157 26.89  1019.0   7.1 110   1.3 207    7.3 100   GF   0.00 0.00   0    0.1    0.1  718
 26 01 1990  2301    3 20.0   157 27.0   1019.1   7.5 110   1.3 207    7.8 100   c/cs                                719
 26 01 1990 *2305    3 19.84  157 27.47  1019.6   8.1 104   0.6 156    7.8 100   GF   0.00 0.00   0    0.1    0.1  720
 26 01 1990 *2310    3 19.68  157 28.13  1020.2   7.4 107   1.0 215    7.8 100   GF   0.00 0.00   0    0.1    0.1  721
 26 01 1990 *2315    3 19.50  157 28.72  1020.9   7.9 106   0.8 185    7.8 100   GF   0.00 0.00   0    0.1    0.1  722
 26 01 1990  2317    3 19.4   157 29.0   1021.1   7.2 106   0.8 185    7.1 100   c/cs                                723
 26 01 1990 *2320    3 19.33  157 29.32  1021.5   6.9 108   0.9 206    7.1 100   GF   0.00 0.00   0    0.1    0.1  724
 26 01 1990  2320    3 19.3   157 29.3   1021.5   7.4 107   0.9 206    7.6 100   c/cs                                725
 26 01 1990 *2325    3 19.15  157 29.91  1022.1   7.7 107   1.0 191    7.6 100   GF   0.00 0.00   0    0.1    0.1  726
 26 01 1990 *2330    3 18.96  157 30.52  1022.7   7.1 108   1.1 223    7.6 100   GF   0.00 0.00   0    0.1    0.1  727
 26 01 1990 *2335    3 18.78  157 31.08  1023.3   7.6 106   0.9 192    7.6 100   GF   0.00 0.00   0    0.1    0.1  728
 26 01 1990 *2340    3 18.60  157 31.69  1024.0   7.5 108   1.0 197    7.6 100   GF   0.00 0.00   0    0.1    0.1  729
 26 01 1990 *2345    3 18.41  157 32.29  1024.6   7.5 107   0.9 197    7.6 100   GF   0.00 0.00   0    0.1    0.1  730
 26 01 1990  2348    3 18.3   157 32.7   1025.0   7.5 107   0.9 197    7.5 100   c/cs                                731
 26 01 1990 *2350    3 18.23  157 32.89  1025.2   7.2 108   1.1 212    7.5 100   GF   0.00 0.00   0    0.1    0.1  732
 26 01 1990 *2355    3 18.04  157 33.46  1025.8   7.6 106   0.7 188    7.5 100   GF   0.00 0.00   0    0.1    0.1  733
 27 01 1990 *0000    3 17.87  157 34.07  1026.4   7.5 106   0.8 197    7.5 100   GF   0.00 0.00   0    0.1    0.1  734
 27 01 1990  0000    3 17.9   157 34.1   1026.4   7.5 106   0.8 197    7.5 100   c/cs                                735
 27 01 1990 *0005    3 17.70  157 34.67  1027.1   7.4 107   0.9 203    7.5 100   GF   0.00 0.00   0    0.1    0.1  736
 27 01 1990 *0010    3 17.52  157 35.26  1027.7   7.2 106   0.9 212    7.5 100   GF   0.00 0.00   0    0.1    0.1  737
 27 01 1990 *0015    3 17.35  157 35.84  1028.3   7.3 108   1.1 204    7.5 100   GF   0.00 0.00   0    0.1    0.1  738
 27 01 1990  0018    3 17.2   157 36.2   1028.7   7.5 108   1.1 204    7.7 100   c/cs                                739
 27 01 1990 *0020    3 17.16  157 36.43  1028.9   7.5 107   0.9 207    7.7 100   GF   0.00 0.00   0    0.1    0.1  740
 27 01 1990 *0025    3 16.98  157 37.03  1029.5   7.6 106   0.9 200    7.7 100   GF   0.00 0.00   0    0.1    0.1  741
 27 01 1990 *0030    3 16.80  157 37.64  1030.2   7.7 105   0.7 194    7.7 100   GF   0.00 0.00   0    0.1    0.1  742
```

```
#cruise ODP130JR                               date run: Wed Jul 18 16:38:07 1990          page  15
#
#                       latitude  longitude              actual    drift        dr              prob. error      drift
#da mo  yr    time deg   min  deg   min     dist speed cse speed hed speed cse  cmnt (smajxsmin@az)  dist  time   no.
#-- - - - - - - - - - - - - - - - - - - - - - - - - - - - - - - - - - - - - - - - - - - - - - - - - - - - - - - - - -
 27 01 1990 *0035    3 16.63 157 38.26 1030.8   7.6 106   0.8 203   7.7 100  GF     0.00 0.00    0    0.1    0.1  743
 27 01 1990 *0040    3 16.46 157 38.87 1031.4   7.6 106   0.8 202   7.7 100  GF     0.00 0.00    0    0.1    0.1  744
 27 01 1990 *0045    3 16.29 157 39.48 1032.1   7.4 106   0.8 213   7.7 100  GF     0.00 0.00    0    0.1    0.1  745
 27 01 1990  0048    3 16.2  157 39.8  1032.4   7.5 106   0.8 213   7.8 100  c/cs                                  746
 27 01 1990 *0050    3 16.12 157 40.08 1032.7   7.7 104   0.6 205   7.8 100  GF     0.00 0.00    0    0.1    0.1  747
 27 01 1990 *0055    3 15.96 157 40.70 1033.3   7.4 106   0.9 221   7.8 100  GF     0.00 0.00    0    0.1    0.1  748
 27 01 1990 *0100    3 15.79 157 41.29 1033.9   7.7 105   0.7 200   7.8 100  GF     0.00 0.00    0    0.1    0.1  749
 27 01 1990 *0105    3 15.62 157 41.91 1034.6   7.8 105   0.7 191   7.8 100  GF     0.00 0.00    0    0.1    0.1  750
 27 01 1990 *0110    3 15.45 157 42.54 1035.2   8.5 105   1.0 149   7.8 100  GF     0.00 0.00    0    0.1    0.1  751
 27 01 1990 *0113    3 15.34 157 42.95 1035.7   7.6 104   0.6 213   7.8 100  GF     0.00 0.00    0    0.0    0.0  752
 27 01 1990  0113    3 15.3  157 43.0  1035.7   6.8 105   0.6 213   7.0 101  c/cs                                  753
 27 01 1990 *0115    3 15.28 157 43.17 1035.9   6.8 107   0.7 212   7.0 101  GF     0.00 0.00    0    0.0    0.0  754
 27 01 1990  0117    3 15.2  157 43.4  1036.1   7.6 106   0.7 212   7.8 101  c/cs                                  755
 27 01 1990 *0120    3 15.11 157 43.75 1036.5   7.9 105   0.6 178   7.8 101  GF     0.00 0.00    0    0.1    0.1  756
 27 01 1990 *0125    3 14.94 157 44.39 1037.2   7.8 103   0.3 197   7.8 101  GF     0.00 0.00    0    0.0    0.1  757
 27 01 1990 *0130    3 14.79 157 45.02 1037.8   7.7 105   0.6 200   7.8 101  GF     0.00 0.00    0    0.0    0.1  758
 27 01 1990  0147    3 14.2  157 47.1  1040.0   7.7 106   0.6 200   7.8 101  c/cs                                  759
 27 01 1990 *0200    3 13.76 157 48.74 1041.7   7.7 107   0.8 196   7.8 101  GF     0.00 0.00    0    0.3    0.5  760
 27 01 1990  0201    3 13.7  157 48.9  1041.3   8.0 107   0.8 196   8.0 101  c/cs                                  761
 27 01 1990 *0230    3 12.61 157 52.55 1045.6   7.8 108   1.0 205   8.0 101  GF     0.00 0.00    0    0.4    0.5  762
 27 01 1990  0231    3 12.6  157 52.7  1045.8   7.8 107   1.0 205   8.0 100  c/cs                                  763
 27 01 1990  0238    3 12.3  157 53.5  1046.7   7.5 107   1.0 205   7.7 100  c/cs                                  764
 27 01 1990  0245    3 12.0  157 54.4  1047.6   7.7 107   1.0 205   7.9 100  c/cs                                  765
 27 01 1990 *0300    3 11.47 157 56.24 1049.5   9.1 105   1.4 137   7.9 100  GF     0.00 0.00    0    0.5    0.5  766
 27 01 1990  0304    3 11.3  157 56.8  1050.1   8.9 104   1.4 137   7.8  98  c/cs                                  767
 27 01 1990 *0330    3 10.40 158  0.58 1054.0   6.4 103   1.6 256   7.8  98  GF     0.00 0.00    0    0.7    0.5  768
 27 01 1990  0334    3 10.3  158  1.0  1054.4   6.4 104   1.6 256   7.8  99  c/cs                                  769
 27 01 1990 *0400    3  9.61 158  3.69 1057.2   7.7 106   0.9 201   7.8  99  GF     0.00 0.00    0    0.8    0.5  770
 27 01 1990  0402    3  9.5  158  3.9  1057.4   7.5 105   0.9 201   7.6  98  c/cs                                  771
 27 01 1990  0412    3  9.2  158  5.1  1058.7   7.6 105   0.9 201   7.8  98  c/cs                                  772
 27 01 1990  0427    3  8.7  158  7.0  1060.6   7.6 105   0.9 201   7.8  98  c/cs                                  773
 27 01 1990 *0430    3  8.63 158  7.35 1060.9   7.6 105   0.9 203   7.8  98  GF     0.00 0.00    0    0.5    0.5  774
 27 01 1990  0449    3  8.0  158  9.7  1063.4   7.5 106   0.9 203   7.7  99  c/cs                                  775
 27 01 1990 *0500    3  7.64 158 11.01 1064.7   7.5 105   0.8 206   7.7  99  GF     0.00 0.00    0    0.5    0.5  776
 27 01 1990  0506    3  7.4  158 11.7  1065.5   8.1 104   0.8 206   8.3  99  c/cs                                  777
 27 01 1990  0520    3  7.0  158 13.6  1067.4   8.2 104   0.8 206   8.4  99  c/cs                                  778
 27 01 1990 *0530    3  6.64 158 14.90 1068.7   8.6 105   0.8 179   8.4  99  GF     0.00 0.00    0    0.4    0.5  779
 27 01 1990  0550    3  5.9  158 17.7  1071.6   8.6 105   0.8 179   8.4  99  c/cs                                  780
 27 01 1990 *0600    3  5.56 158 19.06 1073.0   8.3 105   0.9 200   8.4  99  GF     0.00 0.00    0    0.4    0.5  781
 27 01 1990  0610    3  5.2  158 20.4  1074.4   8.0 106   0.9 200   8.2  99  c/cs                                  782
 27 01 1990  0617    3  4.9  158 21.3  1075.4   7.7 105   0.9 200   7.8  98  c/cs                                  783
 27 01 1990  0625    3  4.7  158 22.3  1076.4   8.0 105   0.9 200   8.1  98  c/cs                                  784
 27 01 1990 *0630    3  4.51 158 22.94 1077.0   8.0 104   0.9 197   8.1  98  GF     0.00 0.00    0    0.5    0.5  785
 27 01 1990  0649    3  3.9  158 25.4  1079.6   7.6 105   0.9 197   7.7  99  c/cs                                  786
 27 01 1990  0652    3  3.8  158 25.8  1080.0   8.0 105   0.9 197   8.1  99  c/cs                                  787
 27 01 1990 *0700    3  3.51 158 26.81 1081.0   8.0 104   0.8 199   8.1  99  GF     0.00 0.00    0    0.4    0.5  788
 27 01 1990  0722    3  2.8  158 29.6  1084.0   7.7 105   0.8 199   7.8  99  c/cs                                  789
 27 01 1990 *0730    3  2.52 158 30.64 1085.0   8.1 105   0.8 172   7.8  99  GF     0.00 0.00    0    0.4    0.5  790
 27 01 1990  0734    3  2.4  158 31.2  1085.5   8.1 105   0.8 172   7.8  99  c/cs                                  791
 27 01 1990  0754    3  1.7  158 33.8  1088.2   7.8 104   0.8 172   7.5  98  c/cs                                  792
 27 01 1990  0758    3  1.6  158 34.3  1088.7   8.1 104   0.8 172   7.9  98  c/cs                                  793
 27 01 1990 *0800    3  1.52 158 34.55 1089.0   8.2 104   0.9 172   7.9  98  GF     0.00 0.00    0    0.4    0.5  794
 27 01 1990  0809    3  1.2  158 35.7  1090.2   8.0 105   0.9 172   7.7  99  c/cs                                  795
```

```
#cruise ODP130JR                                date run: Wed Jul 18 16:38:07 1990        page  16
#
#                   latitude  longitude              actual    drift          dr                   prob. error       drift
#da mo  yr    time deg   min  deg   min      dist speed cse speed hed speed cse   cmnt (smajxsmin@az)  dist  time    no.
#- - - - - - - - - - - - - - - - - - - - - - - - - - - - - - - - - - - - - - - - - - - - - - - - - - - - - - - - - - - -
 27 01 1990   0813   3  1.1  158 36.3   1090.8    8.3 104   0.9 172   8.0  98   c/cs                                    796
 27 01 1990  *0830   3  0.53 158 38.53  1093.1    8.3 103   0.8 166   8.0  98   GF     0.00 0.00    0    0.4    0.5   797
 27 01 1990   0833   3  0.4  158 38.9   1093.5    7.9 104   0.8 166   7.6  99   c/cs                                    798
 27 01 1990   0836   3  0.3  158 39.3   1093.9    8.3 104   0.8 166   8.0  99   c/cs                                    799
 27 01 1990   0853   2 59.8  158 41.6   1096.3    8.2 104   0.8 166   7.9  99   c/cs                                    800
 27 01 1990  *0900   2 59.55 158 42.55  1097.2    8.0 104   0.7 181   7.9  99   GF     0.00 0.00    0    0.4    0.5   801
 27 01 1990   0917   2 59.0  158 44.8   1099.5    8.2 104   0.7 181   8.1  99   c/cs                                    802
 27 01 1990  *0930   2 58.60 158 46.49  1101.3    8.6 104   0.9 156   8.1  99   GF     0.00 0.00    0    0.3    0.5   803
 27 01 1990   0937   2 58.4  158 47.5   1102.3    8.6 104   0.9 156   8.1  99   c/cs                                    804
 27 01 1990   1004   2 57.4  158 51.2   1106.2    8.3 103   0.9 156   7.8  98   c/cs                                    805
 27 01 1990   1010   2 57.2  158 52.0   1107.0    7.7 103   0.9 156   7.2  98   c/cs                                    806
 27 01 1990   1013   2 57.2  158 52.4   1107.4    8.6 103   0.9 156   8.1  98   c/cs                                    807
 27 01 1990   1035   2 56.5  158 55.5   1110.5    8.4 104   0.9 156   7.9  99   c/cs                                    808
 27 01 1990   1041   2 56.3  158 56.3   1111.4    8.5 104   0.9 156   8.0  99   c/cs                                    809
 27 01 1990   1103   2 55.5  158 59.3   1114.5    8.3 103   0.9 156   7.8  98   c/cs                                    810
 27 01 1990   1111   2 55.3  159  0.4   1115.6    8.4 104   0.9 156   7.9  99   c/cs                                    811
 27 01 1990   1141   2 54.2  159  4.5   1119.8    8.4 104   0.9 156   7.9  99   c/cs                                    812
 27 01 1990   1157   2 53.7  159  6.7   1122.1    8.1 104   0.9 156   7.7  99   c/cs                                    813
 27 01 1990   1206   2 53.4  159  7.9   1123.3    8.1 103   0.9 156   7.6  98   c/cs                                    814
 27 01 1990   1220   2 53.0  159  9.7   1125.2    8.2 104   0.9 156   7.7  99   c/cs                                    815
 27 01 1990   1228   2 52.7  159 10.8   1126.3    8.0 104   0.9 156   7.5  99   c/cs                                    816
 27 01 1990   1234   2 52.5  159 11.6   1127.1    8.4 103   0.9 156   7.9  98   c/cs                                    817
 27 01 1990  *1300   2 51.70 159 15.10  1130.7    8.1 102   0.7 167   7.9  98   SF     0.00 0.00    0    3.0    3.5   818
 27 01 1990   1300   2 51.7  159 15.1   1130.7    8.2 103   0.7 167   7.9  99   c/cs                                    819
 27 01 1990   1330   2 50.7  159 19.1   1134.8    8.1 103   0.7 167   7.8  99   c/cs                                    820
 27 01 1990   1351   2 50.1  159 21.9   1137.6    7.9 104   0.7 167   7.6  99   c/cs                                    821
 27 01 1990   1403   2 49.7  159 23.4   1139.2    8.0 103   0.7 167   7.8  99   c/cs                                    822
 27 01 1990  *1410   2 49.50 159 24.30  1140.1    8.2 105   1.0 165   7.8  99   SF     0.00 0.00    0    0.8    1.2   823
 27 01 1990   1422   2 49.1  159 25.9   1141.8    8.2 105   1.0 165   7.8  99   c/cs                                    824
 27 01 1990   1450   2 48.1  159 29.6   1145.6    8.2 105   1.0 165   7.8  99   c/cs                                    825
 27 01 1990   1511   2 47.3  159 32.4   1148.5    8.0 106   1.0 165   7.5 100   c/cs                                    826
 27 01 1990   1515   2 47.1  159 32.9   1149.0    8.3 105   1.0 165   7.9  99   c/cs                                    827
 27 01 1990   1535   2 46.4  159 35.6   1151.8    8.4 106   1.0 165   8.0 100   c/cs                                    828
 27 01 1990   1547   2 46.0  159 37.2   1153.5    8.0 105   1.0 165   7.6  99   c/cs                                    829
 27 01 1990   1557   2 45.6  159 38.5   1154.8    8.5 105   1.0 165   8.1  99   c/cs                                    830
 27 01 1990   1612   2 45.0  159 40.5   1157.0    8.1 105   1.0 165   7.6  99   c/cs                                    831
 27 01 1990  *1617   2 44.87 159 41.20  1157.6    8.3 104   1.0 150   7.6  99   SF     0.00 0.00    0    2.1    2.1   832
 27 01 1990   1617   2 44.9  159 41.2   1157.6    8.6 104   1.0 150   7.9  99   c/cs                                    833
 27 01 1990   1636   2 44.2  159 43.8   1160.4    8.6 104   1.0 150   7.9  99   c/cs                                    834
 27 01 1990   1652   2 43.6  159 46.1   1162.7    8.5 104   1.0 150   7.9  99   c/cs                                    835
 27 01 1990   1717   2 42.8  159 49.5   1166.2    8.6 104   1.0 150   8.0  99   c/cs                                    836
 27 01 1990   1732   2 42.2  159 51.6   1168.4    8.5 104   1.0 150   7.8  99   c/cs                                    837
 27 01 1990   1738   2 42.0  159 52.4   1169.2    8.8 104   1.0 150   8.1  99   c/cs                                    838
 27 01 1990   1757   2 41.3  159 55.1   1172.0    8.4 104   1.0 150   7.7  99   c/cs                                    839
 27 01 1990  *1804   2 41.10 159 56.10  1173.0    7.8 105   0.9 184   7.7  99   SF     0.00 0.00    0    1.8    1.8   840
 27 01 1990   1804   2 41.1  159 56.1   1173.0    7.9 105   0.9 184   7.8  99   c/cs                                    841
 27 01 1990   1820   2 40.5  159 58.1   1175.1    7.7 105   0.9 184   7.6  99   c/cs                                    842
 27 01 1990   1830   2 40.2  159 59.4   1176.4    7.6 105   0.9 184   7.5  99   c/cs                                    843
 27 01 1990   1848   2 39.6  160  1.6   1178.7    7.8 105   0.9 184   7.7  99   c/cs                                    844
 27 01 1990   1858   2 39.2  160  2.8   1180.0    6.9 105   0.9 184   6.7  98   c/cs                                    845
 27 01 1990   1900   2 39.2  160  3.1   1180.2    7.7 103   0.9 184   7.6  99   c/cs                                    846
 27 01 1990   1917   2 38.6  160  5.2   1182.4    7.3 106   0.9 184   7.2  99   c/cs                                    847
 27 01 1990   1920   2 38.5  160  5.5   1182.8    7.7 105   0.9 184   7.6  99   c/cs                                    848
```

```
#cruise ODP130JR                               date run: Wed Jul 18 16:38:07 1990        page  17
#
#                  latitude   longitude              actual    drift       dr               prob. error        drift
#da mo  yr   time  deg  min   deg  min     dist  speed cse speed hed speed cse  cmnt (smajxsmin@az)  dist  time  no.
#- - - - - - - - - - - - - - - - - - - - - - - - - - - - - - - - - - - - - - - - - - - - - - - - - - - - - - - - - -
 27 01 1990  1950  2 37.5  160  9.2  1186.6   7.6 106   0.9 184   7.5  99  c/cs                              849
 27 01 1990  2019  2 36.5  160 12.8  1190.3   7.5 106   0.9 184   7.3  99  c/cs                              850
 27 01 1990  2025  2 36.3  160 13.5  1191.0   7.6 107   0.9 184   7.5 100  c/cs                              851
 27 01 1990  2036  2 35.9  160 14.9  1192.4   7.2 106   0.9 184   7.1  99  c/cs                              852
 27 01 1990  2042  2 35.7  160 15.6  1193.2   7.7 105   0.9 184   7.6  99  c/cs                              853
 27 01 1990 *2100  2 35.08 160 17.79 1195.5   7.7 104   0.7 185   7.6  99  GF    0.00 0.00   0   2.5   2.9  854
 27 01 1990  2112  2 34.7  160 19.3  1197.0   8.0 104   0.7 185   7.9  99  c/cs                              855
 27 01 1990  2118  2 34.5  160 20.1  1197.8   7.7 105   0.7 185   7.6 100  c/cs                              856
 27 01 1990 *2130  2 34.10 160 21.53 1199.3   7.6 106   0.8 194   7.6 100  GF    0.00 0.00   0   0.4   0.5  857
 27 01 1990  2136  2 33.9  160 22.3  1200.1   7.8 111   0.8 194   7.7 105  c/cs                              858
 27 01 1990  2143  2 33.6  160 23.1  1201.0   7.9 116   0.8 194   7.8 110  c/cs                              859
 27 01 1990  2151  2 33.1  160 24.1  1202.1   7.6 106   0.8 194   7.6 100  c/cs                              860
 27 01 1990 *2200  2 32.77 160 25.15 1203.2   7.9 111   1.6 185   7.6 100  GF    0.00 0.00   0   0.4   0.5  861
 27 01 1990  2221  2 31.8  160 27.7  1206.0   7.9 110   1.6 185   7.7  99  c/cs                              862
 27 01 1990 *2230  2 31.34 160 28.85 1207.2   8.0 102   0.5 150   7.7  99  GF    0.00 0.00   0   0.8   0.5  863
 27 01 1990  2238  2 31.1  160 29.9  1208.2   8.0  98   0.5 150   7.7  95  c/cs                              864
 27 01 1990  2249  2 30.9  160 31.3  1209.7   8.0 114   0.5 150   7.6 112  c/cs                              865
 27 01 1990  2251  2 30.8  160 31.6  1210.0   8.3 142   0.5 150   7.8 142  c/cs                              866
 27 01 1990  2253  2 30.6  160 31.8  1210.2   8.6 142   0.5 150   8.1 141  c/cs                              867
 27 01 1990  2256  2 30.3  160 32.0  1210.7   8.4 124   0.5 150   8.0 123  c/cs                              868
 27 01 1990  2259  2 30.0  160 32.4  1211.1   8.3 122   0.5 150   7.8 120  c/cs                              869
 27 01 1990 *2300  2 29.95 160 32.49 1211.2   7.8 131   1.5 217   7.8 120  GF    0.00 0.00   0   0.2   0.5  870
 27 01 1990  2302  2 29.8  160 32.7  1211.5   8.1 162   1.5 217   7.4 153  c/cs                              871
 27 01 1990  2303  2 29.7  160 32.7  1211.6   9.5 184   1.5 217   8.3 178  c/cs                              872
 27 01 1990  2309  2 28.7  160 32.7  1212.6   8.0 178   1.5 217   6.9 170  c/cs                              873
 27 01 1990  2313  2 28.2  160 32.7  1213.1   6.4 180   1.5 217   5.3 170  c/cs                              874
 27 01 1990  2325  2 26.9  160 32.7  1214.4   6.3 180   1.5 217   5.2 170  c/cs                              875
 27 01 1990 *2330  2 26.36 160 32.70 1214.9   6.4 185   1.9 230   5.2 170  GF    0.00 0.00   0   0.7   0.5  876
 27 01 1990  2335  2 25.8  160 32.7  1215.5   6.5 186   1.9 230   5.3 171  c/cs                              877
 27 01 1990  2355  2 23.7  160 32.4  1217.6   6.8 195   1.9 230   5.3 183  c/cs                              878
 27 01 1990  2358  2 23.4  160 32.3  1217.9   6.7 177   1.9 230   5.8 161  c/cs                              879
 27 01 1990  2359  2 23.2  160 32.3  1218.1   5.9 154   1.9 230   5.8 135  c/cs                              880
 28 01 1990 *0000  2 23.16 160 32.39 1218.2   6.7 137   1.0 150   5.8 135  GF    0.00 0.00   0   1.0   0.5  881
 28 01 1990  0000  2 23.2  160 32.4  1218.2   5.5 101   1.0 150   4.9  93  c/cs                              882
 28 01 1990  0002  2 23.1  160 32.6  1218.3   5.2  74   1.0 150   5.0  63  c/cs                              883
 28 01 1990  0006  2 23.2  160 32.9  1218.7   6.4  67   1.0 150   6.3  58  c/cs                              884
 28 01 1990  0012  2 23.5  160 33.5  1219.3   6.8  92   1.0 150   6.4  85  c/cs                              885
 28 01 1990  0018  2 23.4  160 34.2  1220.0   7.5  98   1.0 150   6.9  92  c/cs                              886
 28 01 1990  0024  2 23.3  160 34.9  1220.7   7.8 109   1.0 150   7.1 104  c/cs                              887
 28 01 1990  0028  2 23.2  160 35.4  1221.3   7.2  88   1.0 150   6.8  81  c/cs                              888
 28 01 1990  0029  2 23.2  160 35.5  1221.4   5.4  51   1.0 150   5.7  41  c/cs                              889
 28 01 1990 *0030  2 23.23 160 35.59 1221.5   5.7  35   0.6 313   5.7  41  GF    0.00 0.00   0   0.5   0.5  890
 28 01 1990  0031  2 23.3  160 35.6  1221.6   6.0  23   0.6 313   5.8  29  c/cs                              891
 28 01 1990  0036  2 23.8  160 35.8  1222.1   6.4  17   0.6 313   6.1  22  c/cs                              892
 28 01 1990  0044  2 24.6  160 36.1  1222.9   6.0   6   0.6 313   5.7  11  c/cs                              893
 28 01 1990  0047  2 24.9  160 36.1  1223.2   6.6 353   0.6 313   6.1 357  c/cs                              894
 28 01 1990  0053  2 25.5  160 36.0  1223.9   6.9 340   0.6 313   6.4 343  c/cs                              895
 28 01 1990  0055  2 25.7  160 36.0  1224.1   7.0 312   0.6 313   6.4 312  c/cs                              896
 28 01 1990  0057  2 25.9  160 35.8  1224.3   7.0 284   0.6 313   6.5 281  c/cs                              897
 28 01 1990  0059  2 26.0  160 35.6  1224.6   6.6 277   0.6 313   6.1 274  c/cs                              898
 28 01 1990 *0100  2 25.97 160 35.46 1224.7   6.8 261   1.6 204   6.1 274  GF    0.00 0.00   0   0.3   0.5  899
 28 01 1990  0109  2 25.8  160 34.4  1225.7   6.6 263   1.6 204   6.0 276  c/cs                              900
 28 01 1990  0126  2 25.6  160 32.6  1227.6   6.3 262   1.6 204   5.6 276  c/cs                              901
```

```
#cruise ODP130JR                                         date run: Wed Jul 18 16:38:07 1990         page  18
#
#                 latitude longitude         actual    drift      dr             prob. error       drift
#da mo   yr  time deg  min deg  min     dist speed cse speed hed speed cse  cmnt (smajxsmin@az)  dist  time   no.
#- - - - - - - - - - - - - - - - - - - - - - - - - - - - - - - - - - - - - - - - - - - - - - - - - - - - - - - -
 28 01 1990  0134  2 25.5  160 31.7  1228.4   6.2 263   1.6 204   5.6 277  c/cs                               902
 28 01 1990  0200  2 25.1  160 29.1  1231.1   3.8  90   1.6 204   4.7  72  c/cs                               903
 28 01 1990  0230  2 25.1  160 31.0  1233.0   1.4  41   1.6 204   2.9  32  c/cs                               904
 28 01 1990  0300  2 25.7  160 31.4  1233.7   1.4  56   1.6 204   2.9  39  c/cs                               905
 28 01 1990  0330  2 26.1  160 32.0  1234.4   1.4  57   1.6 204   2.9  40  c/cs                               906
 28 01 1990  0355  2 26.4  160 32.5  1235.0   1.6 204   1.6 204   0.0  72  c/cs                               907
 28 01 1990 *0400  2 26.26 160 32.48 1235.2   0.0 186   0.0 186   0.0  72  803A  0.00 0.00    0   4.7    3.0  908
 06 02 1990 *1730  2 25.99 160 32.45 1235.4   2.3 157   2.3 157   0.0  72  803D  0.00 0.00    0   0.3  229.5  909
 06 02 1990  1730  2 26.0  160 32.4  1235.4   1.2 150   2.3 157   1.1 343  c/cs                               910
 06 02 1990  1748  2 25.7  160 32.6  1235.8  13.0 144   2.3 157  10.8 141  c/cs                               911
 06 02 1990  1804  2 22.9  160 34.7  1239.2  13.7 144   2.3 157  11.5 141  c/cs                               912
 06 02 1990  1819  2 20.2  160 36.7  1242.6  13.9 144   2.3 157  11.7 142  c/cs                               913
 06 02 1990  1824  2 19.2  160 37.4  1243.8  13.0 145   2.3 157  10.8 142  c/cs                               914
 06 02 1990  1826  2 18.9  160 37.6  1244.2  14.0 144   2.3 157  11.8 142  c/cs                               915
 06 02 1990  1836  2 17.0  160 39.0  1246.6  13.9 144   2.3 157  11.7 142  c/cs                               916
 06 02 1990  1855  2 13.4  160 41.6  1251.0  14.2 145   2.3 157  12.0 143  c/cs                               917
 06 02 1990  1857  2 13.0  160 41.8  1251.4  14.2 144   2.3 157  12.0 142  c/cs                               918
 06 02 1990  1927  2  7.2  160 46.0  1258.5  14.3 143   2.3 157  12.1 141  c/cs                               919
 06 02 1990  1944  2  4.0  160 48.4  1262.6  14.3 143   2.3 157  12.1 141  c/cs                               920
 06 02 1990  2014  1 58.2  160 52.7  1269.8  14.3 143   2.3 157  12.1 141  c/cs                               921
 06 02 1990 *2030  1 55.17 160 54.94 1273.6  15.0 144   3.0 155  12.1 141  GF    0.00 0.00    0   6.8    3.0  922
 06 02 1990 *2035  1 54.16 160 55.68 1274.8  14.1 143   2.0 158  12.1 141  GF    0.00 0.00    0   0.2    0.1  923
 06 02 1990 *2040  1 53.22 160 56.38 1276.0  14.0 143   1.9 156  12.1 141  GF    0.00 0.00    0   0.2    0.1  924
 06 02 1990  2044  1 52.5  160 56.9  1276.9  14.0 143   1.9 156  12.2 141  c/cs                               925
 06 02 1990 *2045  1 52.29 160 57.08 1277.2  14.1 143   1.9 159  12.2 141  GF    0.00 0.00    0   0.2    0.1  926
 06 02 1990 *2050  1 51.35 160 57.78 1278.3  13.4 143   1.3 167  12.2 141  GF    0.00 0.00    0   0.2    0.1  927
 06 02 1990 *2100  1 49.56 160 59.11 1280.6  14.2 143   2.1 157  12.2 141  GF    0.00 0.00    0   0.2    0.2  928
 06 02 1990  2103  1 49.0  160 59.5  1281.3  14.1 143   2.1 157  12.2 140  c/cs                               929
 06 02 1990 *2110  1 47.68 161  0.54 1282.9  13.8 143   1.8 165  12.2 140  GF    0.00 0.00    0   0.3    0.2  930
 06 02 1990  2111  1 47.5  161  0.7  1283.2  13.8 144   1.8 165  12.2 141  c/cs                               931
 06 02 1990 *2115  1 46.75 161  1.22 1284.1  13.8 144   1.7 165  12.2 141  GF    0.00 0.00    0   0.1    0.1  932
 06 02 1990 *2120  1 45.82 161  1.90 1285.2  13.7 145   1.7 172  12.2 141  GF    0.00 0.00    0   0.1    0.1  933
 06 02 1990 *2125  1 44.89 161  2.56 1286.4  12.8 145   1.0 195  12.2 141  GF    0.00 0.00    0   0.1    0.1  934
 06 02 1990 *2130  1 44.02 161  3.18 1287.4  14.4 144   2.3 163  12.2 141  GF    0.00 0.00    0   0.1    0.1  935
 06 02 1990  2133  1 43.4  161  3.6  1288.2  14.5 144   2.3 163  12.3 141  c/cs                               936
 06 02 1990 *2140  1 42.06 161  4.58 1289.8  13.8 144   1.7 165  12.3 141  GF    0.00 0.00    0   0.4    0.2  937
 06 02 1990 *2145  1 41.13 161  5.26 1291.0  14.0 144   1.9 167  12.3 141  GF    0.00 0.00    0   0.1    0.1  938
 06 02 1990 *2150  1 40.18 161  5.94 1292.2  13.3 143   1.2 167  12.3 141  GF    0.00 0.00    0   0.2    0.1  939
 06 02 1990 *2200  1 38.40 161  7.27 1294.4  14.5 143   2.3 156  12.3 141  GF    0.00 0.00    0   0.2    0.2  940
 06 02 1990  2203  1 37.8  161  7.7  1295.1  14.5 143   2.3 156  12.2 141  c/cs                               941
 06 02 1990 *2210  1 36.46 161  8.71 1296.8  13.9 143   1.7 161  12.2 141  GF    0.00 0.00    0   0.4    0.2  942
 06 02 1990 *2215  1 35.53 161  9.40 1298.0  13.9 145   1.8 169  12.2 141  GF    0.00 0.00    0   0.1    0.1  943
 06 02 1990 *2220  1 34.59 161 10.07 1299.1  13.4 144   1.3 174  12.2 141  GF    0.00 0.00    0   0.1    0.1  944
 06 02 1990  2223  1 34.0  161 10.5  1299.8  13.4 144   1.3 174  12.2 141  c/cs                               945
 06 02 1990 *2230  1 32.79 161 11.38 1301.3  14.5 144   2.4 160  12.2 141  GF    0.00 0.00    0   0.2    0.2  946
 06 02 1990 *2240  1 30.83 161 12.80 1303.8  13.8 144   1.7 165  12.2 141  GF    0.00 0.00    0   0.4    0.2  947
 06 02 1990 *2245  1 29.90 161 13.48 1304.9  14.1 144   2.0 163  12.2 141  GF    0.00 0.00    0   0.1    0.1  948
 06 02 1990 *2250  1 28.95 161 14.17 1306.1  14.0 144   1.9 162  12.2 141  GF    0.00 0.00    0   0.2    0.1  949
 06 02 1990  2253  1 28.4  161 14.6  1306.8  13.9 144   1.9 162  12.1 141  c/cs                               950
 06 02 1990 *2255  1 28.01 161 14.86 1307.3  13.8 144   1.8 165  12.1 141  GF    0.00 0.00    0   0.2    0.1  951
 06 02 1990 *2310  1 25.21 161 16.89 1310.7  13.9 144   1.9 164  12.1 141  GF    0.00 0.00    0   0.5    0.2  952
 06 02 1990  2310  1 25.2  161 16.9  1310.7  14.1 144   1.9 164  12.3 141  c/cs                               953
 06 02 1990 *2315  1 24.26 161 17.58 1311.9  14.1 143   1.9 156  12.3 141  GF    0.00 0.00    0   0.2    0.1  954
```

```
#cruise ODP130JR                                    date run: Wed Jul 18 16:38:07 1990        page  19
#                                                    actual   drift        dr                prob. error        drift
#                         latitude  longitude                                                                    
#da mo  yr      time   deg  min   deg  min    dist  speed cse speed hed speed cse  cmnt (smajxsmin@az)   dist  time  no.
#- - - - - - - - - - - - - - - - - - - - - - - - - - - - - - - - - - - - - - - - - - - - - - - - - - - - - - - - - - - -
 06 02 1990 *2320    1 23.32 161 18.29 1313.1  13.9 143   1.7 159  12.3 141  GF    0.00 0.00   0   0.2   0.1   955
 06 02 1990  2322    1 22.9  161 18.6  1313.5  14.0 143   1.7 159  12.4 141  c/cs                              956
 06 02 1990 *2335    1 20.52 161 20.39 1316.6  14.0 143   1.7 155  12.4 141  GF    0.00 0.00   0   0.4   0.2   957
 06 02 1990 *2340    1 19.59 161 21.10 1317.7  13.9 142   1.6 153  12.4 141  GF    0.00 0.00   0   0.1   0.1   958
 06 02 1990 *2345    1 18.67 161 21.81 1318.9  13.8 143   1.5 156  12.4 141  GF    0.00 0.00   0   0.1   0.1   959
 06 02 1990  2349    1 17.9  161 22.4  1319.8  13.7 142   1.5 156  12.3 140  c/cs                              960
 06 02 1990 *2350    1 17.76 161 22.51 1320.0  13.3 143   1.2 176  12.3 140  GF    0.00 0.00   0   0.1   0.1   961
 07 02 1990 *0000    1 15.99 161 23.84 1322.3  14.3 142   2.1 155  12.3 140  GF    0.00 0.00   0   0.2   0.2   962
 07 02 1990  0000    1 16.0  161 23.8  1322.3  14.3 142   2.1 155  12.3 140  c/cs                              963
 07 02 1990  0008    1 14.5  161 25.0  1324.2  14.1 142   2.1 155  12.1 140  c/cs                              964
 07 02 1990 *0010    1 14.11 161 25.30 1324.6  13.4 143   1.4 165  12.1 140  GF    0.00 0.00   0   0.3   0.2   965
 07 02 1990 *0015    1 13.22 161 25.98 1325.8  13.7 142   1.7 158  12.1 140  GF    0.00 0.00   0   0.1   0.1   966
 07 02 1990  0017    1 12.9  161 26.3  1326.2  13.4 142   1.7 158  11.7 140  c/cs                              967
 07 02 1990 *0020    1 12.33 161 26.67 1326.9  12.3 142   0.6 174  11.7 140  GF    0.00 0.00   0   0.1   0.1   968
 07 02 1990  0023    1 11.8  161 27.1  1327.5   9.4 140   0.6 174   8.8 138  c/cs                              969
 07 02 1990  0026    1 11.5  161 27.3  1328.0   7.9 143   0.6 174   7.4 140  c/cs                              970
 07 02 1990 *0030    1 11.07 161 27.67 1328.5   9.2 143   1.8 155   7.4 140  GF    0.00 0.00   0   0.1   0.2   971
 07 02 1990 *0035    1 10.46 161 28.13 1329.3   8.4 141   1.1 152   7.4 140  GF    0.00 0.00   0   0.2   0.1   972
 07 02 1990  0035    1 10.5  161 28.1  1329.3   8.2 143   1.1 152   7.2 142  c/cs                              973
 07 02 1990 *0040    1  9.91 161 28.54 1329.9   8.3 143   1.1 147   7.2 142  GF    0.00 0.00   0   0.1   0.1   974
 07 02 1990 *0045    1  9.36 161 28.96 1330.6   8.4 144   1.2 157   7.2 142  GF    0.00 0.00   0   0.1   0.1   975
 07 02 1990  0047    1  9.1  161 29.1  1330.9   8.4 142   1.2 157   7.2 140  c/cs                              976
 07 02 1990 *0050    1  8.80 161 29.38 1331.3   8.0 143   0.8 170   7.2 140  GF    0.00 0.00   0   0.1   0.1   977
 07 02 1990 *0100    1  7.74 161 30.18 1332.7   9.6 142   2.3 149   7.2 140  GF    0.00 0.00   0   0.1   0.2   978
 07 02 1990 *0105    1  7.11 161 30.67 1333.5   8.6 143   1.4 159   7.2 140  GF    0.00 0.00   0   0.2   0.1   979
 07 02 1990 *0110    1  6.54 161 31.10 1334.2   8.4 143   1.2 162   7.2 140  GF    0.00 0.00   0   0.1   0.1   980
 07 02 1990 *0115    1  5.98 161 31.52 1334.9   8.6 143   1.4 159   7.2 140  GF    0.00 0.00   0   0.1   0.1   981
 07 02 1990 *0120    1  5.41 161 31.95 1335.6   8.6 144   1.4 163   7.2 140  GF    0.00 0.00   0   0.1   0.1   982
 07 02 1990  0120    1  5.4  161 32.0  1335.6   8.5 140   1.4 163   7.2 135  c/cs                              983
 07 02 1990 *0125    1  4.87 161 32.41 1336.3   8.4 139   1.3 163   7.2 135  GF    0.00 0.00   0   0.1   0.1   984
 07 02 1990  0130    1  4.3  161 32.9  1337.0   8.4 138   1.3 163   7.2 134  c/cs                              985
 07 02 1990 *0135    1  3.82 161 33.33 1337.7   8.5 138   1.5 161   7.2 134  GF    0.00 0.00   0   0.2   0.2   986
 07 02 1990 *0140    1  3.29 161 33.80 1338.4   8.7 138   1.6 158   7.2 134  GF    0.00 0.00   0   0.1   0.1   987
 07 02 1990 *0145    1  2.75 161 34.28 1339.1   8.6 139   1.6 162   7.2 134  GF    0.00 0.00   0   0.1   0.1   988
 07 02 1990 *0150    1  2.21 161 34.75 1339.8   9.0 128   2.0 106   7.2 134  GF    0.00 0.00   0   0.1   0.1   989
 07 02 1990  0155    1  1.7  161 35.3  1340.6   7.9 166   2.0 106   7.1 180  c/cs                              990
 07 02 1990 *0205    1  0.47 161 35.65 1341.9   8.9 174   2.0 151   7.1 180  GF    0.00 0.00   0   0.5   0.2   991
 07 02 1990 *0210    0 59.73 161 35.73 1342.6   8.8 175   1.8 156   7.1 180  GF    0.00 0.00   0   0.2   0.1   992
 07 02 1990 *0215    0 59.00 161 35.79 1343.4   8.8 178   1.7 172   7.1 180  GF    0.00 0.00   0   0.1   0.1   993
 07 02 1990 *0220    0 58.27 161 35.81 1344.1   8.9 182   1.8 188   7.1 180  GF    0.00 0.00   0   0.1   0.1   994
 07 02 1990 *0225    0 57.53 161 35.79 1344.8   7.2 180   0.1 203   7.1 180  GF    0.00 0.00   0   0.1   0.1   995
 07 02 1990  0228    0 57.2  161 35.8  1345.2   7.2 179   0.1 203   7.1 179  c/cs                              996
 07 02 1990 *0230    0 56.93 161 35.79 1345.4   8.9 179   1.8 178   7.1 179  GF    0.00 0.00   0   0.0   0.1   997
 07 02 1990 *0236    0 56.04 161 35.81 1346.3   8.8 177   1.7 171   7.1 179  GF    0.00 0.00   0   0.2   0.1   998
 07 02 1990  0238    0 55.7  161 35.8  1346.6   8.9 179   1.7 171   7.2 181  c/cs                              999
 07 02 1990 *0241    0 55.30 161 35.83 1347.1   9.0 182   1.8 188   7.2 181  GF    0.00 0.00   0   0.1   0.1  1000
 07 02 1990 *0246    0 54.55 161 35.80 1347.8   8.5 181   1.3 182   7.2 181  GF    0.00 0.00   0   0.2   0.1  1001
 07 02 1990  0250    0 54.0  161 35.8  1348.4   8.0 179   1.3 182   6.7 179  c/cs                             1002
 07 02 1990 *0251    0 53.85 161 35.79 1348.5   8.0 180   1.4 185   6.7 179  GF    0.00 0.00   0   0.1   0.1  1003
 07 02 1990 *0256    0 53.18 161 35.79 1349.2   8.1 181   1.4 191   6.7 179  GF    0.00 0.00   0   0.1   0.1  1004
 07 02 1990 *0300    0 52.64 161 35.78 1349.7   8.4 176   1.8 164   6.7 179  GF    0.00 0.00   0   0.1   0.1  1005
 07 02 1990 *0301    0 52.50 161 35.79 1349.9   8.4 178   1.7 176   6.7 179  GF    0.00 0.00   0   0.0   0.0  1006
 07 02 1990 *0306    0 51.80 161 35.81 1350.6   8.5 180   1.8 183   6.7 179  GF    0.00 0.00   0   0.1   0.1  1007
```

```
                                                     date run: Wed Jul 18 16:38:07 1990          page  20
#cruise ODP13OJR
#                                                  actual    drift          dr                prob. error        drift
#                    latitude  longitude                                                                               
#da mo  yr    time deg   min  deg   min     dist speed cse speed hed speed cse  cmnt (smajxsmin@az)  dist  time   no.
#- - - - - - - - - - - - - - - - - - - - - - - - - - - - - - - - - - - - - - - - - - - - - - - - - - - - - - - - - -
 07 02 1990  0307   0 51.7  161 35.8  1350.7  8.8 179  1.8 183  7.1 178  c/cs                                    1008
 07 02 1990 *0311   0 51.07 161 35.82 1351.3  8.7 179  1.6 182  7.1 178  GF    0.00 0.00   0    0.1   0.1 1009
 07 02 1990  0313   0 50.8  161 35.8  1351.6  8.8 163  1.6 182  7.3 159  c/cs                                    1010
 07 02 1990  0314   0 50.6  161 35.9  1351.7  7.7 141  1.6 182  6.6 132  c/cs                                    1011
 07 02 1990 *0316   0 50.44 161 36.03 1352.0  7.4 137  1.0 170  6.6 132  GF    0.00 0.00   0    0.1   0.1 1012
 07 02 1990  0316   0 50.4  161 36.0  1352.0  6.7 111  1.0 170  6.3 103  c/cs                                    1013
 07 02 1990  0318   0 50.4  161 36.2  1352.2  6.7  97  1.0 170  6.5  89  c/cs                                    1014
 07 02 1990 *0321   0 50.32 161 36.57 1352.6  7.3  97  1.3 144  6.5  89  GF    0.00 0.00   0    0.1   0.1 1015
 07 02 1990  0325   0 50.3  161 37.1  1353.0  7.6  94  1.3 144  7.0  86  c/cs                                    1016
 07 02 1990 *0330   0 50.21 161 37.70 1353.7  8.5  93  1.7 124  7.0  86  GF    0.00 0.00   0    0.2   0.2 1017
 07 02 1990  0330   0 50.2  161 37.7  1353.7  8.4  90  1.7 124  7.1  82  c/cs                                    1018
 07 02 1990 *0331   0 50.21 161 37.84 1353.8  7.7  89  1.1 141  7.1  82  GF    0.00 0.00   0    0.0   0.0 1019
 07 02 1990 *0336   0 50.22 161 38.48 1354.5  7.8  91  1.4 144  7.1  82  GF    0.00 0.00   0    0.1   0.1 1020
 07 02 1990 *0341   0 50.21 161 39.13 1355.1  7.5  89  1.0 149  7.1  82  GF    0.00 0.00   0    0.1   0.1 1021
 07 02 1990  0345   0 50.2  161 39.6  1355.6  6.6  69  1.0 149  6.5  61  c/cs                                    1022
 07 02 1990 *0346   0 50.26 161 39.73 1355.7  7.1  68  1.0 123  6.5  61  GF    0.00 0.00   0    0.1   0.1 1023
 07 02 1990  0346   0 50.3  161 39.7  1355.7  6.2  43  1.0 123  6.1  33  c/cs                                    1024
 07 02 1990  0348   0 50.4  161 39.9  1355.9  5.2   8  1.0 123  5.7 359  c/cs                                    1025
 07 02 1990 *0351   0 50.67 161 39.91 1356.2  5.8   1  0.2  78  5.7 359  GF    0.00 0.00   0    0.1   0.1 1026
 07 02 1990  0351   0 50.7  161 39.9  1356.2  6.4 359  0.2  78  6.3 357  c/cs                                    1027
 07 02.1990 *0356   0 51.20 161 39.90 1356.7  6.2   6  0.9 100  6.3 357  GF    0.00 0.00   0    0.0   0.1 1028
 07 02 1990 *0400   0 51.61 161 39.94 1357.1  6.9   5  1.0  59  6.3 357  GF    0.00 0.00   0    0.1   0.1 1029
 07 02 1990  0402   0 51.8  161 40.0  1357.4  7.7   5  1.0  59  7.2 358  c/cs                                    1030
 07 02 1990 *0406   0 52.35 161 40.00 1357.9  7.5   2  0.6  54  7.2 358  GF    0.00 0.00   0    0.1   0.1 1031
 07 02 1990  0409   0 52.7  161 40.0  1358.3  7.9 360  0.6  54  7.6 356  c/cs                                    1032
 07 02 1990 *0411   0 52.99 161 40.01 1358.5  7.8   2  0.8  73  7.6 356  GF    0.00 0.00   0    0.0   0.1 1033
 07 02 1990 *0416   0 53.64 161 40.03 1359.2  7.9   1  0.7  62  7.6 356  GF    0.00 0.00   0    0.1   0.1 1034
 07 02 1990 *0421   0 54.30 161 40.04 1359.8  7.5   0  0.5  94  7.6 356  GF    0.00 0.00   0    0.1   0.1 1035
 07 02 1990 *0430   0 55.43 161 40.04 1361.0  8.3   0  0.9  36  7.6 356  GF    0.00 0.00   0    0.1   0.2 1036
 07 02 1990 *0436   0 56.26 161 40.04 1361.8  7.7 358  0.3  59  7.6 356  GF    0.00 0.00   0    0.1   0.1 1037
 07 02 1990  0439   0 56.6  161 40.0  1362.2  7.9 359  0.3  59  7.8 357  c/cs                                    1038
 07 02 1990 *0441   0 56.91 161 40.02 1362.4  7.8   1  0.5  85  7.8 357  GF    0.00 0.00   0    0.0   0.1 1039
 07 02 1990 *0446   0 57.56 161 40.03 1363.1  7.8   0  0.4  84  7.8 357  GF    0.00 0.00   0    0.0   0.1 1040
 07 02 1990 *0451   0 58.21 161 40.03 1363.7  7.7   1  0.6  94  7.8 357  GF    0.00 0.00   0    0.0   0.1 1041
 07 02 1990  0451   0 58.2  161 40.0  1363.7  7.9   0  0.6  94  8.0 356  c/cs                                    1042
 07 02 1990  0458   0 59.1  161 40.0  1364.7  7.7 359  0.6  94  7.8 355  c/cs                                    1043
 07 02 1990 *0500   0 59.39 161 40.03 1364.9  8.4 359  0.8  38  7.8 355  GF    0.00 0.00   0    0.1   0.2 1044
 07 02 1990  0505   1  0.1  161 40.0  1365.6  8.0 336  0.8  38  7.7 331  c/cs                                    1045
 07 02 1990 *0506   1  0.21 161 39.96 1365.8  7.3 324  1.0 217  7.7 331  GF    0.00 0.00   0    0.1   0.1 1046
 07 02 1990  0506   1  0.2  161 40.0  1365.8  7.0 277  1.0 217  6.5 285  c/cs                                    1047
 07 02 1990  0508   1  0.2  161 39.7  1366.0  8.4 270  1.0 217  7.8 276  c/cs                                    1048
 07 02 1990 *0511   1  0.24 161 39.31 1366.4  8.4 275  0.6 261  7.8 276  GF    0.00 0.00   0    0.1   0.1 1049
 07 02 1990 *0516   1  0.30 161 38.61 1367.1  8.8 268  1.5 222  7.8 276  GF    0.00 0.00   0    0.1   0.1 1050
 07 02 1990  0517   1  0.3  161 38.5  1367.3  9.1 267  1.5 222  8.1 274  c/cs                                    1051
 07 02 1990 *0521   1  0.26 161 37.86 1367.9  8.3 271  0.5 212  8.1 274  GF    0.00 0.00   0    0.1   0.1 1052
 07 02 1990  0523   1  0.3  161 37.6  1368.1  8.0 272  0.5 212  7.8 275  c/cs                                    1053
 07 02 1990 *0530   1  0.30 161 36.65 1369.1  9.2 269  1.6 242  7.8 275  GF    0.00 0.00   0    0.1   0.2 1054
 07 02 1990 *0536   1  0.29 161 35.73 1370.0  8.3 270  0.9 218  7.8 275  GF    0.00 0.00   0    0.2   0.1 1055
 07 02 1990 *0541   1  0.29 161 35.04 1370.7  8.6 270  1.1 228  7.8 275  GF    0.00 0.00   0    0.1   0.1 1056
 07 02 1990 *0551   1  0.28 161 33.61 1372.1  8.5 269  1.0 223  7.8 275  GF    0.00 0.00   0    0.2   0.2 1057
 07 02 1990  0553   1  0.3  161 33.3  1372.4  8.3 270  1.0 223  7.7 276  c/cs                                    1058
 07 02 1990 *0556   1  0.28 161 32.91 1372.8  7.2 271  0.8 147  7.7 276  GF    0.00 0.00   0    0.1   0.1 1059
 07 02 1990 *0600   1  0.29 161 32.43 1373.3  9.3 273  1.7 257  7.7 276  GF    0.00 0.00   0    0.1   0.1 1060
```

```
#cruise ODP130JR                                   date run: Wed Jul 18 16:38:07 1990        page  21
#                                                                                          prob. error          drift
#                      latitude  longitude                   actual   drift        dr
#da mo  yr   time deg  min  deg   min      dist speed cse speed hed speed cse  cmnt (smajxsmin@az)  dist  time   no.
#- - - - - - - - - - - - - - - - - - - - - - - - - - - - - - - - - - - - - - - - - - - - - - - - - - - - - - - - - -
 07 02 1990  0604   1  0.3   161 31.8   1373.9   9.4 274   1.7 257   7.8 278  c/cs                                  1061
 07 02 1990  0605   1  0.3   161 31.7   1374.1   9.5 274   1.7 257   7.9 277  c/cs                                  1062
 07 02 1990 *0606   1  0.34  161 31.50  1374.2   7.9 272   0.7 188   7.9 277  GF    0.00 0.00   0   0.2    0.1  1063
 07 02 1990 *0611   1  0.36  161 30.84  1374.9   6.9 282   1.2  66   7.9 277  GF    0.00 0.00   0   0.1    0.1  1064
 07 02 1990 *0616   1  0.48  161 30.28  1375.5   2.6 152   9.6 110   7.9 277  GF    0.00 0.00   0   0.1    0.1  1065
 07 02 1990 *0621   1  0.29  161 30.38  1375.7  10.2  91  18.0  93   7.9 277  GF    0.00 0.00   0   0.8    0.1  1066
 07 02 1990 *0634   1  0.26  161 32.58  1377.9   7.0  89  14.8  93   7.9 277  GF    0.00 0.00   0   3.9    0.2  1067
 07 02 1990 *0700   1  0.29  161 35.62  1380.9   7.9 277   0.0   0   7.9 277   804  0.00 0.00   0   6.4    0.4  1068
 07 02 1990  0700   1  0.3   161 35.6   1380.9   0.0   0   0.0   0   0.0 276  c/cs                                  1069
 10 02 1990 *1011   1  0.29  161 35.62  1380.9   0.1 152   0.1 152   0.0 276   804  0.00 0.00   0   0.0   75.2  1070
 10 02 1990  1112   1  0.2   161 35.7   1381.0   0.0 339   0.1 152   0.1 333  c/cs                                  1071
 10 02 1990  1134   1  0.2   161 35.7   1381.0   0.1 332   0.1 152   0.3 332  c/cs                                  1072
 10 02 1990  1159   1  0.2   161 35.6   1381.1   1.7 288   0.1 152   1.8 291  c/cs                                  1073
 10 02 1990 *1200   1  0.25  161 35.62  1381.1   2.7 256   1.6 216   1.8 291   804  0.00 0.00   0   0.2    1.8  1074
 10 02 1990  1202   1  0.2   161 35.5   1381.2   4.7 224   1.6 216   3.1 228  c/cs                                  1075
 10 02 1990  1206   1  0.0   161 35.3   1381.5   6.1 223   1.6 216   4.5 225  c/cs                                  1076
 10 02 1990  1211   0 59.6   161 35.0   1382.0   7.7 222   1.6 216   6.1 224  c/cs                                  1077
 10 02 1990  1220   0 58.8   161 34.2   1383.2   8.7 223   1.6 216   7.1 224  c/cs                                  1078
 10 02 1990  1231   0 57.6   161 33.1   1384.8   8.5 218   1.6 216   6.9 219  c/cs                                  1079
 10 02 1990  1233   0 57.4   161 32.9   1385.1   8.7 224   1.6 216   7.1 226  c/cs                                  1080
 10 02 1990  1245   0 56.1   161 31.7   1386.8   8.9 213   1.6 216   7.3 212  c/cs                                  1081
 10 02 1990  1247   0 55.9   161 31.5   1387.1   8.2 183   1.6 216   6.9 176  c/cs                                  1082
 10 02 1990  1248   0 55.7   161 31.5   1387.3   5.7 162   1.6 216   4.9 147  c/cs                                  1083
 10 02 1990  1249   0 55.6   161 31.6   1387.4   6.3 133   1.6 216   6.3 118  c/cs                                  1084
 10 02 1990  1250   0 55.6   161 31.6   1387.5   5.3 101   1.6 216   6.2  87  c/cs                                  1085
 10 02 1990 *1254   0 55.50  161 32.00  1387.8   6.3  90   0.4 159   6.2  87  SF    0.00 0.00   0   1.5    0.9  1086
 10 02 1990  1255   0 55.5   161 32.1   1387.9   7.3  91   0.4 159   7 2  88  c/cs                                  1087
 10 02 1990  1325   0 55.5   161 35.8   1391.6   7.5  91   0.4 159   7.3  88  c/cs                                  1088
 10 02 1990  1343   0 55.4   161 38.0   1393.8   7.4  87   0.4 159   7.3  84  c/cs                                  1089
 10 02 1990  1348   0 55.5   161 38.6   1394.4   6.2  53   0.4 159   6.4  50  c/cs                                  1090
 10 02 1990  1349   0 55.5   161 38.7   1394.6   5.9  27   0.4 159   6.2  24  c/cs                                  1091
 10 02 1990  1350   0 55.6   161 38.7   1394.6   5.4   0   0.4 159   5.7 359  c/cs                                  1092
 10 02 1990  1351   0 55.7   161 38.7   1394.7   5.2 319   0.4 159   5.6 320  c/cs                                  1093
 10 02 1990  1356   0 56.0   161 38.5   1395.2   6.1 315   0.4 159   6.5 316  c/cs                                  1094
 10 02 1990  1405   0 56.7   161 37.8   1396.1   6.1 312   0.4 159   6.4 314  c/cs                                  1095
 10 02 1990  1424   0 58.0   161 36.4   1398.0   6.2 311   0.4 159   6.6 313  c/cs                                  1096
 10 02 1990  1444   0 59.3   161 34.8   1400.1   6.0 310   0.4 159   6.4 312  c/cs                                  1097
 10 02 1990  1451   0 59.8   161 34.3   1400.8   6.4 299   0.4 159   6.7 301  c/cs                                  1098
 10 02 1990  1453   0 59.9   161 34.1   1401.0   6.1 259   0.4 159   6.1 262  c/cs                                  1099
 10 02 1990  1456   0 59.8   161 33.8   1401.3   6.2 278   0.4 159   6.4 281  c/cs                                  1100
 10 02 1990 *1500   0 59.90  161 33.40  1401.7   7.7 278   1.3 265   6.4 281  SF    0.00 0.00   0   0.8    2.1  1101
 10 02 1990  1500   0 59.9   161 33.4   1401.7   8.4 275   1.3 265   7.2 277  c/cs                                  1102
 10 02 1990  1507   0 60.0   161 32.4   1402.7   9.0 276   1.3 265   7.8 278  c/cs                                  1103
 10 02 1990  1523   1  0.2   161 30.0   1405.1   8.6 277   1.3 265   7.3 279  c/cs                                  1104
 10 02 1990  1529   1  0.3   161 29.2   1406.0   8.8 277   1.3 265   7.5 279  c/cs                                  1105
 10 02 1990  1559   1  0.9   161 24.8   1410.4   8.9 276   1.3 265   7.7 278  c/cs                                  1106
 10 02 1990  1622   1  1.2   161 21.4   1413.8   8.7 277   1.3 265   7.5 279  c/cs                                  1107
 10 02 1990 *1631   1  1.40  161 20.10  1415.1   8.4 277   1.0 260   7.5 279  SF    0.00 0.00   0   2.0    1.5  1108
 10 02 1990  1633   1  1.4   161 19.8   1415.4   8.6 277   1.0 260   7.6 279  c/cs                                  1109
 10 02 1990  1649   1  1.7   161 17.6   1417.7   7.8 279   1.0 260   6.9 282  c/cs                                  1110
 10 02 1990  1711   1  2.2   161 14.7   1420.5   7.3 279   1.0 260   6.4 282  c/cs                                  1111
 10 02 1990  1741   1  2.7   161 11.1   1424.2   7.3 280   1.0 260   6.4 283  c/cs                                  1112
 10 02 1990  1811   1  3.4   161  7.5   1427.9   7.4 280   1.0 260   6.4 283  c/cs                                  1113
```

```
#cruise ODP130JR                                   date run: Wed Jul 18 16:38:07 1990         page  22
#
#                     latitude  longitude            actual   drift      dr                prob. error       drift
#da mo  yr     time deg   min  deg   min     dist speed cse speed hed speed cse  cmnt (smajxsmin@az)  dist  time   no.
#- - - - - - - - - - - - - - - - - - - - - - - - - - - - - - - - - - - - - - - - - - - - - - - - - - - - - - - - - - -
 10 02 1990  1835   1   3.9  161   4.6  1430.8   7.7 281   1.0 260   6.8 284  c/cs                                 1114
 10 02 1990  1904   1   4.6  161   0.9  1434.6   7.8 279   1.0 260   6.9 282  c/cs                                 1115
 10 02 1990  1911   1   4.8  160  60.0  1435.5   7.6 280   1.0 260   6.7 283  c/cs                                 1116
 10 02 1990  1918   1   4.9  160  59.1  1436.4   7.8 279   1.0 260   6.8 282  c/cs                                 1117
 10 02 1990  1943   1   5.4  160  55.9  1439.6   7.4 278   1.0 260   6.4 281  c/cs                                 1118
 10 02 1990  1946   1   5.5  160  55.6  1440.0   7.8 278   1.0 260   6.9 281  c/cs                                 1119
 10 02 1990 *2008   1   5.90 160  52.71 1442.9   7.7 280   0.8 270   6.9 281  GF    0.00 0.00    0    3.6   3.6 1120
 10 02 1990 *2013   1   6.01 160  52.08 1443.5   7.5 280   0.7 270   6.9 281  GF    0.00 0.00    0    0.1   0.1 1121
 10 02 1990  2016   1   6.1  160  51.7  1443.9   7.6 280   0.7 270   6.9 281  c/cs                                 1122
 10 02 1990 *2018   1   6.12 160  51.46 1444.1   7.8 279   0.9 262   6.9 281  GF    0.00 0.00    0    0.1   0.1 1123
 10 02 1990 *2023   1   6.22 160  50.82 1444.8   6.7 280   0.2 129   6.9 281  GF    0.00 0.00    0    0.1   0.1 1124
 10 02 1990  2029   1   6.3  160  50.2  1445.5   7.7 280   0.2 129   7.9 281  c/cs                                 1125
 10 02 1990 *2030   1   6.36 160  50.03 1445.6   8.8 279   0.9 266   7.9 281  GF    0.00 0.00    0    0.0   0.1 1126
 10 02 1990  2038   1   6.6  160  48.9  1446.8   9.4 280   0.9 266   8.5 281  c/cs                                 1127
 10 02 1990 *2044   1   6.71 160  47.94 1447.7   9.4 280   0.9 266   8.5 281  GF    0.00 0.00    0    0.2   0.2 1128
 10 02 1990 *2049   1   6.84 160  47.17 1448.5   9.5 280   1.0 273   8.5 281  GF    0.00 0.00    0    0.1   0.1 1129
 10 02 1990 *2054   1   6.98 160  46.39 1449.3   9.6 280   1.1 273   8.5 281  GF    0.00 0.00    0    0.1   0.1 1130
 10 02 1990  2057   1   7.1  160  45.9  1449.8  10.2 282   1.1 273   9.1 283  c/cs                                 1131
 10 02 1990 *2100   1   7.17 160  45.42 1450.3  10.3 283   1.2 287   9.1 283  GF    0.00 0.00    0    0.1   0.1 1132
 10 02 1990 *2104   1   7.33 160  44.75 1451.0  10.2 283   1.1 282   9.1 283  GF    0.00 0.00    0    0.1   0.1 1133
 10 02 1990 *2109   1   7.52 160  43.92 1451.8  10.4 283   1.3 280   9.1 283  GF    0.00 0.00    0    0.1   0.1 1134
 10 02 1990 *2114   1   7.71 160  43.07 1452.7  10.4 281   1.3 271   9.1 283  GF    0.00 0.00    0    0.1   0.1 1135
 10 02 1990  2116   1   7.8  160  42.7  1453.0  10.4 282   1.3 271   9.1 284  c/cs                                 1136
 10 02 1990 *2119   1   7.89 160  42.22 1453.5  10.2 282   1.1 267   9.1 284  GF    0.00 0.00    0    0.1   0.1 1137
 10 02 1990 *2124   1   8.07 160  41.39 1454.4  10.0 283   0.9 274   9.1 284  GF    0.00 0.00    0    0.1   0.1 1138
 10 02 1990  2128   1   8.2  160  40.7  1455.1   9.8 282   0.9 274   8.9 283  c/cs                                 1139
 10 02 1990 *2130   1   8.29 160  40.42 1455.4  10.6 283   1.7 283   8.9 283  GF    0.00 0.00    0    0.1   0.1 1140
 10 02 1990 *2134   1   8.45 160  39.73 1456.1   9.9 282   1.0 277   8.9 283  GF    0.00 0.00    0    0.1   0.1 1141
 10 02 1990  2135   1   8.5  160  39.6  1456.3  10.1 282   1.0 277   9.1 283  c/cs                                 1142
 10 02 1990 *2139   1   8.63 160  38.91 1456.9  10.4 282   1.3 275   9.1 283  GF    0.00 0.00    0    0.1   0.1 1143
 10 02 1990 *2144   1   8.81 160  38.06 1457.8  10.2 282   1.1 276   9.1 283  GF    0.00 0.00    0    0.1   0.1 1144
 10 02 1990 *2149   1   8.99 160  37.23 1458.7  10.2 282   1.1 276   9.1 283  GF    0.00 0.00    0    0.1   0.1 1145
 10 02 1990 *2154   1   9.17 160  36.40 1459.5  10.1 282   1.0 277   9.1 283  GF    0.00 0.00    0    0.1   0.1 1146
 10 02 1990 *2159   1   9.35 160  35.58 1460.3   8.6 282   0.5 118   9.1 283  GF    0.00 0.00    0    0.1   0.1 1147
 10 02 1990 *2200   1   9.38 160  35.44 1460.5  10.9 282   1.8 276   9.1 283  GF    0.00 0.00    0    0.0   0.0 1148
 10 02 1990 *2204   1   9.53 160  34.73 1461.2  10.3 281   1.2 265   9.1 283  GF    0.00 0.00    0    0.1   0.1 1149
 10 02 1990  2205   1   9.6  160  34.6  1461.4  10.1 283   1.2 265   9.0 285  c/cs                                 1150
 10 02 1990 *2209   1   9.71 160  33.90 1462.1   9.6 284   0.6 269   9.0 285  GF    0.00 0.00    0    0.1   0.1 1151
 10 02 1990  2210   1   9.7  160  33.7  1462.2   7.6 315   0.6 269   7.2 319  c/cs                                 1152
 10 02 1990  2211   1   9.8  160  33.7  1462.3   6.2 345   0.6 269   6.1 351  c/cs                                 1153
 10 02 1990  2212   1   9.9  160  33.6  1462.5   5.7  18   0.6 269   5.9  24  c/cs                                 1154
 10 02 1990 *2214   1  10.12 160  33.69 1462.6   6.3  25   0.4  38   5.9  24  GF    0.00 0.00    0    0.1   0.1 1155
 10 02 1990  2215   1  10.2  160  33.7  1462.7   6.1 358   0.4  38   5.8 356  c/cs                                 1156
 10 02 1990  2216   1  10.3  160  33.7  1462.8   6.4 325   0.4  38   6.3 322  c/cs                                 1157
 10 02 1990 *2219   1  10.58 160  33.55 1463.2   7.3 319   1.1 300   6.3 322  GF    0.00 0.00    0    0.0   0.1 1158
 10 02 1990  2222   1  10.9  160  33.3  1463.5   7.7 322   1.1 300   6.7 326  c/cs                                 1159
 10 02 1990 *2224   1  11.06 160  33.15 1463.8   7.2 325   0.6 310   6.7 326  GF    0.00 0.00    0    0.1   0.1 1160
 10 02 1990  2228   1  11.5  160  32.9  1464.3   7.3 328   0.6 310   6.8 329  c/cs                                 1161
 10 02 1990 *2230   1  11.66 160  32.74 1464.5   8.2 325   1.5 309   6.8 329  GF    0.00 0.00    0    0.1   0.1 1162
 10 02 1990 *2234   1  12.11 160  32.43 1465.1   7.4 329   0.7 328   6.8 329  GF    0.00 0.00    0    0.1   0.1 1163
 10 02 1990 *2239   1  12.64 160  32.11 1465.7   7.6 329   0.9 325   6.8 329  GF    0.00 0.00    0    0.1   0.1 1164
 10 02 1990 *2244   1  13.18 160  31.78 1466.3   7.5 330   0.7 341   6.8 329  GF    0.00 0.00    0    0.1   0.1 1165
 10 02 1990 *2249   1  13.72 160  31.47 1466.9   7.6 328   0.9 324   6.8 329  GF    0.00 0.00    0    0.1   0.1 1166
```

```
#cruise ODP130JR                                   date run: Wed Jul 18 16:38:07 1990         page  23
#
#                                                          actual    drift          dr              prob. error           drift
#                       latitude  longitude                                                                   
#da mo  yr     time deg   min  deg   min      dist speed cse speed hed speed cse  cmnt (smajxsmin@az)  dist  time   no.
#- - - - - - - - - - - - - - - - - - - - - - - - - - - - - - - - - - - - - - - - - - - - - - - - - - - - - - - - - - - -
                                                                                                                   1167
 10 02 1990  2250    1 13.8  160 31.4  1467.1   7.6 330   0.9 324   6.8 331  c/cs                                   1168
 10 02 1990 *2254    1 14.27 160 31.15 1467.6   7.2 329   0.5 306   6.8 331  GF    0.00 0.00   0   0.1    0.1 1169
 10 02 1990  2257    1 14.6  160 31.0  1467.9   7.3 331   0.5 306   6.9 333  c/cs                                   1170
 10 02 1990 *2300    1 14.90 160 30.79 1468.3   8.3 330   1.5 315   6.9 333  GF    0.00 0.00   0   0.0    0.1 1171
 10 02 1990 *2304    1 15.38 160 30.51 1468.9   6.2 331   0.7 173   6.9 333  GF    0.00 0.00   0   0.1    0.1 1172
 10 02 1990  2313    1 16.2  160 30.1  1469.8   5.9 360   0.7 173   6.6 359  c/cs                                   1173
 10 02 1990  2315    1 16.4  160 30.1  1470.0   5.8  46   0.7 173   6.2  41  c/cs                                   1174
 10 02 1990  2317    1 16.5  160 30.2  1470.2   6.4  87   0.7 173   6.4  81  c/cs                                   1175
 10 02 1990  2319    1 16.5  160 30.4  1470.4   6.5 133   0.7 173   6.0 129  c/cs                                   1176
 10 02 1990  2320    1 16.5  160 30.5  1470.5   5.8 177   0.7 173   5.1 177  c/cs                                   1177
 10 02 1990  2321    1 16.4  160 30.5  1470.6   6.3 193   0.7 173   5.7 195  c/cs                                   1178
 10 02 1990  2324    1 16.1  160 30.4  1470.9   7.4 182   0.7 173   6.7 183  c/cs                                   1179
 10 02 1990  2326    1 15.8  160 30.4  1471.2   7.4 149   0.7 173   6.8 147  c/cs                                   1180
 10 02 1990  2328    1 15.6  160 30.5  1471.4   7.7 142   0.7 173   7.1 139  c/cs                                   1181
 10 02 1990  2331    1 15.3  160 30.8  1471.8   8.2 151   0.7 173   7.6 149  c/cs                                   1182
 10 02 1990  2335    1 14.8  160 31.0  1472.3   8.1 146   0.7 173   7.5 144  c/cs                                   1183
 10 02 1990  2341    1 14.2  160 31.5  1473.1   8.3 150   0.7 173   7.7 148  c/cs                                   1184
 10 02 1990 *2345    1 13.68 160 31.76 1473.7   7.6 148   0.0 328   7.7 148   805  0.00 0.00   0   0.5    0.7 1185
 10 02 1990  2358    1 12.3  160 32.6  1475.3   6.9 148   0.0 328   6.9 148  c/cs                                   1186
 11 02 1990  0000    1 12.1  160 32.8  1475.6   7.8 148   0.0 328   7.8 148  c/cs                                   1187
 11 02 1990  0030    1  8.8  160 34.8  1479.5   0.0 328   0.0 328   0.0   0  c/cs                                   1188
 17 02 1990 *0345    1 13.68 160 31.76 1485.2   0.7 307   0.7 307   0.0   0   805  0.00 0.00   0   5.8  148.0 1189
 17 02 1990  0351    1 13.7  160 31.7  1485.3   3.8 261   0.7 307   3.3 252  c/cs                                   1190
 17 02 1990  0353    1 13.7  160 31.6  1485.4   5.6 236   0.7 307   5.4 228  c/cs                                   1191
 17 02 1990 *0355    1 13.60 160 31.42 1485.6   6.8 229   1.4 231   5.4 228  GF    0.00 0.00   0   0.1    0.2 1192
 17 02 1990  0355    1 13.6  160 31.4  1485.6  10.4 229   1.4 231   9.0 229  c/cs                                   1193
 17 02 1990  0358    1 13.3  160 31.0  1486.1  12.5 229   1.4 231  11.1 229  c/cs                                   1194
 17 02 1990 *0400    1 12.99 160 30.71 1486.6  13.4 230   2.2 233  11.1 229  GF    0.00 0.00   0   0.1    0.1 1195
 17 02 1990 *0405    1 12.27 160 29.86 1487.7  13.2 230   2.1 237  11.1 229  GF    0.00 0.00   0   0.2    0.1 1196
 17 02 1990  0406    1 12.1  160 29.7  1487.9  13.8 229   2.1 237  11.7 228  c/cs                                   1197
 17 02 1990 *0410    1 11.53 160 28.99 1488.8  13.9 230   2.2 238  11.7 228  GF    0.00 0.00   0   0.2    0.1 1198
 17 02 1990 *0415    1 10.78 160 28.11 1490.0  13.7 230   2.0 239  11.7 228  GF    0.00 0.00   0   0.2    0.1 1199
 17 02 1990 *0420    1 10.04 160 27.24 1491.1  13.3 229   1.6 237  11.7 228  GF    0.00 0.00   0   0.2    0.1 1200
 17 02 1990  0426    1  9.2  160 26.2  1492.4  13.3 230   1.6 237  11.7 229  c/cs                                   1201
 17 02 1990 *0430    1  8.60 160 25.56 1493.3  13.7 229   2.0 229  11.7 229  GF    0.00 0.00   0   0.3    0.2 1202
 17 02 1990 *0440    1  7.10 160 23.83 1495.6  13.9 229   2.2 230  11.7 229  GF    0.00 0.00   0   0.3    0.2 1203
 17 02 1990 *0445    1  6.34 160 22.95 1496.8  13.8 229   2.1 228  11.7 229  GF    0.00 0.00   0   0.2    0.1 1204
 17 02 1990  0445    1  6.3  160 23.0  1496.8  14.0 229   2.1 228  12.0 229  c/cs                                   1205
 17 02 1990 *0450    1  5.57 160 22.07 1497.9  13.6 229   1.6 227  12.0 229  GF    0.00 0.00   0   0.2    0.1 1206
 17 02 1990 *0500    1  4.08 160 20.37 1500.2  14.2 226   2.2 225  12.0 229  GF    0.00 0.00   0   0.3    0.2 1207
 17 02 1990 *0510    1  2.51 160 18.60 1502.6  13.9 229   1.9 227  12.0 229  GF    0.00 0.00   0   0.4    0.2 1208
 17 02 1990  0515    1  1.7  160 17.7  1503.7  13.9 229   1.9 227  11.9 229  c/cs                                   1209
 17 02 1990 *0520    1  0.98 160 16.86 1504.9  14.1 228   2.2 226  11.9 229  GF    0.00 0.00   0   0.3    0.2 1210
 17 02 1990 *0525    1  0.20 160 15.98 1506.1  14.0 228   2.1 225  11.9 229  GF    0.00 0.00   0   0.2    0.1 1211
 17 02 1990 *0535    0 58.65 160 14.23 1508.4  14.1 228   2.2 225  11.9 229  GF    0.00 0.00   0   0.3    0.2 1212
 17 02 1990 *0540    0 57.87 160 13.35 1509.6  14.0 229   2.1 228  11.9 229  GF    0.00 0.00   0   0.2    0.1 1213
 17 02 1990 *0545    0 57.10 160 12.47 1510.7  14.1 229   2.1 228  11.9 229  GF    0.00 0.00   0   0.2    0.1 1214
 17 02 1990  0545    0 57.1  160 12.5  1510.7  14.0 229   2.1 228  11.9 229  c/cs                                   1215
 17 02 1990 *0550    0 56.33 160 11.59 1511.9  14.1 228   2.2 225  11.9 229  GF    0.00 0.00   0   0.2    0.1 1216
 17 02 1990 *0555    0 55.55 160 10.71 1513.1  13.3 229   1.4 229  11.9 229  GF    0.00 0.00   0   0.2    0.1 1217
 17 02 1990 *0600    0 54.82 160  9.87 1514.2  14.3 229   2.4 227  11.9 229  GF    0.00 0.00   0   0.1    0.1 1218
 17 02 1990 *0610    0 53.25 160  8.08 1516.6  13.8 229   1.9 231  11.9 229  GF    0.00 0.00   0   0.4    0.2 1219
 17 02 1990 *0615    0 52.50 160  7.21 1517.7  13.7 230   1.7 234  11.9 229  GF    0.00 0.00   0   0.2    0.1
```

```
#cruise ODP130JR                               date run: Wed Jul 18 16:38:07 1990          page  24
#
#                     latitude  longitude              actual    drift        dr                prob. error       drift
#da mo  yr    time  deg   min  deg   min      dist  speed cse  speed hed  speed cse   cmnt  (smajxsmin@az)   dist   time   no.
#- - - - - - - - - - - - - - - - - - - - - - - - - - - - - - - - - - - - - - - - - - - - - - - - - - - - - - - - - - - - - -
 17 02 1990   0615    0 52.5   160  7.2   1517.7   13.7 230    1.7 234   12.0 229   c/cs                                  1220
 17 02 1990  *0620    0 51.76  160  6.34  1518.9   13.2 229    1.2 234   12.0 229   GF     0.00 0.00     0    0.1     0.1 1221
 17 02 1990  *0630    0 50.33  160  4.67  1521.1   13.8 229    1.9 232   12.0 229   GF     0.00 0.00     0    0.2     0.2 1222
 17 02 1990  *0640    0 48.83  160  2.92  1523.4   13.6 229    1.6 231   12.0 229   GF     0.00 0.00     0    0.3     0.2 1223
 17 02 1990  *0645    0 48.09  160  2.06  1524.5   13.8 230    1.8 236   12.0 229   GF     0.00 0.00     0    0.1     0.1 1224
 17 02 1990   0645    0 48.1   160  2.1   1524.5   13.6 229    1.8 236   11.7 228   c/cs                                  1225
 17 02 1990   0649    0 47.5   160  1.4   1525.4   13.8 230    1.8 236   12.0 229   c/cs                                  1226
 17 02 1990  *0650    0 47.35  160  1.20  1525.7   13.6 229    1.6 232   12.0 229   GF     0.00 0.00     0    0.2     0.1 1227
 17 02 1990  *0655    0 46.61  160  0.34  1526.8   12.6 230    0.6 242   12.0 229   GF     0.00 0.00     0    0.1     0.1 1228
 17 02 1990  *0700    0 45.93  159 59.54  1527.8   13.9 230    2.0 236   12.0 229   GF     0.00 0.00     0    0.1     0.1 1229
 17 02 1990   0709    0 44.6   159 57.9   1529.9   13.8 231    2.0 236   11.9 230   c/cs                                  1230
 17 02 1990  *0710    0 44.44  159 57.76  1530.2   13.6 230    1.7 230   11.9 230   GF     0.00 0.00     0    0.3     0.2 1231
 17 02 1990  *0715    0 43.71  159 56.89  1531.3   13.5 231    1.6 242   11.9 230   GF     0.00 0.00     0    0.1     0.1 1232
 17 02 1990  *0720    0 43.01  159 56.01  1532.4   13.5 232    1.7 248   11.9 230   GF     0.00 0.00     0    0.1     0.1 1233
 17 02 1990  *0725    0 42.32  159 55.12  1533.5   13.4 231    1.5 242   11.9 230   GF     0.00 0.00     0    0.1     0.1 1234
 17 02 1990   0727    0 42.0   159 54.8   1534.0   13.5 232    1.5 242   12.0 231   c/cs                                  1235
 17 02 1990  *0735    0 40.94  159 53.35  1535.8   13.6 232    1.6 238   12.0 231   GF     0.00 0.00     0    0.3     0.2 1236
 17 02 1990  *0740    0 40.24  159 52.46  1536.9   13.7 231    1.7 234   12.0 231   GF     0.00 0.00     0    0.1     0.1 1237
 17 02 1990  *0745    0 39.53  159 51.57  1538.1   13.7 232    1.8 237   12.0 231   GF     0.00 0.00     0    0.1     0.1 1238
 17 02 1990  *0750    0 38.82  159 50.67  1539.2   13.2 232    1.2 238   12.0 231   GF     0.00 0.00     0    0.1     0.1 1239
 17 02 1990   0755    0 38.1   159 49.8   1540.3   13.2 232    1.2 238   12.0 231   c/cs                                  1240
 17 02 1990  *0800    0 37.45  159 48.94  1541.4   14.3 232    2.3 236   12.0 231   GF     0.00 0.00     0    0.2     0.2 1241
 17 02 1990  *0810    0 35.98  159 47.07  1543.8   13.8 232    1.8 239   12.0 231   GF     0.00 0.00     0    0.4     0.2 1242
 17 02 1990  *0815    0 35.27  159 46.16  1544.9   14.0 232    2.0 236   12.0 231   GF     0.00 0.00     0    0.2     0.1 1243
 17 02 1990   0815    0 35.3   159 46.2   1544.9   13.9 232    2.0 236   11.9 231   c/cs                                  1244
 17 02 1990  *0820    0 34.55  159 45.25  1546.1   13.4 232    1.4 238   11.9 231   GF     0.00 0.00     0    0.2     0.1 1245
 17 02 1990  *0830    0 33.17  159 43.50  1548.3   14.4 231    2.5 230   11.9 231   GF     0.00 0.00     0    0.2     0.2 1246
 17 02 1990   0833    0 32.7   159 42.9   1549.1   14.4 230    2.5 230   12.0 230   c/cs                                  1247
 17 02 1990  *0840    0 31.63  159 41.65  1550.7   13.8 230    1.8 229   12.0 230   GF     0.00 0.00     0    0.4     0.2 1248
 17 02 1990  *0845    0 30.89  159 40.77  1551.9   13.8 230    1.8 229   12.0 230   GF     0.00 0.00     0    0.2     0.1 1249
 17 02 1990  *0850    0 30.15  159 39.89  1553.0   13.1 229    1.2 224   12.0 230   GF     0.00 0.00     0    0.2     0.1 1250
 17 02 1990  *0900    0 28.73  159 38.23  1555.2   14.5 230    2.6 231   12.0 230   GF     0.00 0.00     0    0.2     0.2 1251
 17 02 1990   0903    0 28.3   159 37.7   1555.9   14.3 229    2.6 231   11.7 229   c/cs                                  1252
 17 02 1990  *0910    0 27.18  159 36.41  1557.6   14.2 229    2.4 229   11.7 229   GF     0.00 0.00     0    0.4     0.2 1253
 17 02 1990   0912    0 26.9   159 36.1   1558.1   13.7 230    2.4 229   11.2 230   c/cs                                  1254
 17 02 1990  *0920    0 25.69  159 34.66  1559.9   12.9 230    1.7 227   11.2 230   GF     0.00 0.00     0    0.4     0.2 1255
 17 02 1990   0921    0 25.6   159 34.5   1560.1   13.0 231    1.7 227   11.3 231   c/cs                                  1256
 17 02 1990   0928    0 24.6   159 33.3   1561.6   13.1 231    1.7 227   11.5 231   c/cs                                  1257
 17 02 1990  *0930    0 24.31  159 32.99  1562.1   14.2 231    2.7 228   11.5 231   GF     0.00 0.00     0    0.3     0.2 1258
 17 02 1990  *0940    0 22.81  159 31.17  1564.4   12.8 230    1.3 225   11.5 231   GF     0.00 0.00     0    0.4     0.2 1259
 17 02 1990   0940    0 22.8   159 31.2   1564.4   10.6 233    1.3 225    9.3 234   c/cs                                  1260
 17 02 1990   0943    0 22.5   159 30.7   1565.0    9.6 234    1.3 225    8.3 235   c/cs                                  1261
 17 02 1990   0946    0 22.2   159 30.4   1565.4    8.6 232    1.3 225    7.3 233   c/cs                                  1262
 17 02 1990  *0950    0 21.85  159 29.91  1566.0    8.1 232    0.8 222    7.3 233   GF     0.00 0.00     0    0.2     0.2 1263
 17 02 1990  *1000    0 21.02  159 28.85  1567.4    9.1 234    1.8 239    7.3 233   GF     0.00 0.00     0    0.1     0.2 1264
 17 02 1990   1001    0 20.9   159 28.7   1567.5    8.7 238    1.8 239    6.9 238   c/cs                                  1265
 17 02 1990   1006    0 20.6   159 28.1   1568.2    8.6 255    1.8 239    6.9 259   c/cs                                  1266
 17 02 1990  *1010    0 20.40  159 27.56  1568.8    8.3 257    1.4 248    6.9 259   GF     0.00 0.00     0    0.3     0.2 1267
 17 02 1990   1013    0 20.3   159 27.2   1569.2    8.9 257    1.4 248    7.5 259   c/cs                                  1268
 17 02 1990  *1020    0 20.08  159 26.14  1570.3    8.3 257    0.8 234    7.5 259   GF     0.00 0.00     0    0.2     0.2 1269
 17 02 1990   1022    0 20.0   159 25.9   1570.5    8.0 257    0.8 234    7.2 259   c/cs                                  1270
 17 02 1990  *1030    0 19.77  159 24.84  1571.6    9.3 257    2.1 250    7.2 259   GF     0.00 0.00     0    0.1     0.2 1271
 17 02 1990   1036    0 19.6   159 23.9   1572.5    9.5 259    2.1 250    7.4 262   c/cs                                  1272
```

```
#cruise ODP130JR                             date run: Wed Jul 18 16:38:07 1990        page  25
#
#                   latitude  longitude          actual    drift      dr              prob. error       drift
#da mo  yr    time deg   min deg   min     dist speed cse speed hed speed cse  cmnt (smajxsmin@az)  dist   time   no.
#- - - - - - - - - - - - - - - - - - - - - - - - - - - - - - - - - - - - - - - - - - - - - - - - - - - - - - - - -
 17 02 1990 *1040   0 19.44 159 23.31 1573.2   7.8 262   0.4 257   7.4 262  GF    0.00 0.00   0   0.4    0.2 1273
 17 02 1990  1052   0 19.2  159 21.8  1574.7   7.8 263   0.4 257   7.4 263  c/cs                                1274
 17 02 1990  1112   0 18.9  159 19.2  1577.3   7.8 263   0.4 257   7.4 263  c/cs                                1275
 17 02 1990  1120   0 18.8  159 18.2  1578.4   8.6  80   0.4 257   9.0  80  c/cs                                1276
 17 02 1990  1200   0 19.7  159 23.8  1584.1   1.7  84   0.4 257   2.1  83  c/cs                                1277
 17 02 1990  1230   0 19.8  159 24.7  1585.0   0.4 257   0.4 257   0.0 263  c/cs                                1278
 17 02 1990  1250   0 19.8  159 24.6  1585.1   0.4 257   0.4 257   0.0   0  c/cs                                1279
 17 02 1990 *2052   0 19.11 159 21.68 1588.1   0.0   0   0.0   0   0.0   0   806  0.00 0.00   0   3.8   10.2 1280
 25 02 1990 *0825   0 19.11 159 21.68 1588.1   1.1 323   1.1 323   0.0   0   806  0.00 0.00   0   0.0  179.5 1281
 25 02 1990  0825   0 19.1  159 21.7  1588.1   1.0 322   1.1 323   0.1 151  c/cs                                1282
 25 02 1990  0900   0 19.6  159 21.3  1588.7   5.3 308   1.1 323   4.2 304  c/cs                                1283
 25 02 1990  0915   0 20.4  159 20.3  1590.0   6.6 319   1.1 323   5.5 318  c/cs                                1284
 25 02 1990 *0917   0 20.57 159 20.12 1590.2   7.0 316   1.6 308   5.5 318  GF    0.00 0.00   0   1.0    0.9 1285
 25 02 1990 *0922   0 20.99 159 19.71 1590.8   7.2 316   1.8 308   5.5 318  GF    0.00 0.00   0   0.1    0.1 1286
 25 02 1990 *0927   0 21.42 159 19.29 1591.4   6.1 316   0.6 301   5.5 318  GF    0.00 0.00   0   0.1    0.1 1287
 25 02 1990 *0930   0 21.64 159 19.08 1591.7   7.0 317   1.5 314   5.5 318  GF    0.00 0.00   0   0.0    0.1 1288
 25 02 1990  0930   0 21.6  159 19.1  1591.7   8.7 316   1.5 314   7.2 317  c/cs                                1289
 25 02 1990 *0932   0 21.85 159 18.88 1592.0   7.1 316   0.1 185   7.2 317  GF    0.00 0.00   0   0.0    0.0 1290
 25 02 1990 *0937   0 22.28 159 18.47 1592.6   7.3 316   0.1 278   7.2 317  GF    0.00 0.00   0   0.0    0.1 1291
 25 02 1990 *0942   0 22.72 159 18.05 1593.2   8.7 316   1.5 309   7.2 317  GF    0.00 0.00   0   0.0    0.1 1292
 25 02 1990  0942   0 22.7  159 18.0  1593.2   7.8 316   1.5 309   6.3 318  c/cs                                1293
 25 02 1990 *0947   0 23.19 159 17.60 1593.9   8.1 316   1.8 310   6.3 318  GF    0 00 0.00   0   0.1    0.1 1294
 25 02 1990 *0952   0 23.68 159 17.13 1594.5   7.8 316   1.5 308   6.3 318  GF    0.00 0.00   0   0.2    0.1 1295
 25 02 1990  0954   0 23.9  159 16.9  1594.8   8.5 317   1.5 308   7.0 319  c/cs                                1296
 25 02 1990 *1000   0 24.49 159 16.37 1595.7   9.6 316   2.6 309   7.0 319  GF    0.00 0.00   0   0.2    0.1 1297
 25 02 1990  1001   0 24.6  159 16.3  1595.8   9.4 316   2.6 309   6.8 319  c/cs                                1298
 25 02 1990  1004   0 24.9  159 15.9  1596.3  10.1 318   2.6 309   7.6 321  c/cs                                1299
 25 02 1990 *1012   0 25.95 159 15.03 1597.6   9.3 320   1.7 314   7.6 321  GF    0.00 0.00   0   0.5    0.2 1300
 25 02 1990 *1017   0 26.54 159 14.53 1598.4   9.3 319   1.8 311   7.6 321  GF    0.00 0.00   0   0.1    0.1 1301
 25 02 1990  1019   0 26.8  159 14.3  1598.7   9.5 320   1.8 311   7.8 322  c/cs                                1302
 25 02 1990 *1022   0 27.14 159 14.02 1599.2   8.7 319   1.0 294   7.8 322  GF    0.00 0.00   0   0.1    0.1 1303
 25 02 1990 *1030   0 28.01 159 13.26 1600.4  10.2 319   2.5 312   7.8 322  GF    0.00 0.00   0   0.1    0.1 1304
 25 02 1990  1033   0 28.4  159 12.9  1600.9  10.1 319   2.5 312   7.6 322  c/cs                                1305
 25 02 1990 *1037   0 28.91 159 12.49 1601.5   9.3 319   1.7 308   7.6 322  GF    0.00 0.00   0   0.3    0.1 1306
 25 02 1990  1040   0 29.3  159 12.2  1602.0   9.3 320   1.7 308   7.7 323  c/cs                                1307
 25 02 1990 *1042   0 29.50 159 11.99 1602.3   9.4 320   1.8 308   7.7 323  GF    0.00 0.00   0   0.1    0.1 1308
 25 02 1990 *1047   0 30.10 159 11.49 1603.1   9.4 320   1.9 306   7.7 323  GF    0.00 0.00   0   0.1    0.1 1309
 25 02 1990 *1052   0 30.70 159 10.98 1603.9   8.6 321   1.0 303   7.7 323  GF    0.00 0.00   0   0.2    0.1 1310
 25 02 1990  1055   0 31.0  159 10.7  1604.3   8.6 321   1.0 303   7.6 323  c/cs                                1311
 25 02 1990 *1100   0 31.59 159 10.25 1605.0   9.8 320   2.2 310   7.6 323  GF    0.00 0.00   0   0.1    0.1 1312
 25 02 1990 *1112   0 33.09 159  9.00 1607.0   9.3 320   1.7 309   7.6 323  GF    0.00 0.00   0   0.4    0.2 1313
 25 02 1990  1113   0 33.2  159  8.9  1607.1   9.0 320   1.7 309   7.3 323  c/cs                                1314
 25 02 1990 *1117   0 33.67 159  8.52 1607.7   8.9 320   1.7 306   7.3 323  GF    0.00 0.00   0   0.1    0.1 1315
 25 02 1990 *1122   0 34.24 159  8.04 1608.5   8.0 321   0.7 305   7.3 323  GF    0.00 0.00   0   0.1    0.1 1316
 25 02 1990  1128   0 34.9  159  7.5  1609.3   8.2 321   0.7 305   7.5 323  c/cs                                1317
 25 02 1990 *1130   0 35.08 159  7.37 1609.6   9.7 320   2.2 311   7.5 323  GF    0.00 0.00   0   0.1    0.1 1318
 25 02 1990  1140   0 36.3  159  6.3  1611.2   9.3 320   2.2 311   7.1 323  c/cs                                1319
 25 02 1990 *1142   0 36.56 159  6.14 1611.5   8.9 321   1.8 313   7.1 323  GF    0.00 0.00   0   0.4    0.2 1320
 25 02 1990  1144   0 36.8  159  6.0  1611.8   9.0 321   1.8 313   7.2 323  c/cs                                1321
 25 02 1990 *1147   0 37.14 159  5.67 1612.2   8.8 319   1.7 304   7.2 323  GF    0.00 0.00   0   0.2    0.1 1322
 25 02 1990 *1152   0 37.70 159  5.19 1613.0   8.6 320   1.4 305   7.2 323  GF    0.00 0.00   0   0.1    0.1 1323
 25 02 1990  1156   0 38.1  159  4.8  1613.5   8.0 320   1.4 305   6.7 323  c/cs                                1324
 25 02 1990 *1157   0 38.24 159  4.74 1613.7   5.8 319   1.0 165   6.7 323  GF    0.00 0.00   0   0.1    0.1 1325
```

```
#cruise ODP130JR                              date run: Wed Jul 18 16:38:07 1990          page  26
#
#                  latitude  longitude            actual    drift        dr                prob. error        drift
#da mo  yr    time deg   min deg   min      dist speed cse speed hed speed cse  cmnt (smajxsmin@az)  dist  time   no.
#- - - - - - - - - - - - - - - - - - - - - - - - - - - - - - - - - - - - - - - - - - - - - - - - - - - - - - - - - -
 25 02 1990 *1200    0 38.46 159   4.55 1614.0   9.4 319   2.7 310   6.7 323  GF    0.00 0.00    0    0.1    0.1 1326
 25 02 1990 *1207    0 39.29 159   3.84 1615.1   8.0 319   1.4 297   6.7 323  GF    0.00 0.00    0    0.3    0.1 1327
 25 02 1990 *1212    0 39.79 159   3.40 1615.7   6.6 319   0.5 215   6.7 323  GF    0.00 0.00    0    0.1    0.1 1328
 25 02 1990  1212    0 39.8  159   3.4  1615.7   6.6 319   0.5 215   6.7 323  c/cs                                1329
 25 02 1990 *1218    0 40.29 159   2.97 1616.4   8.3 319   1.6 303   6.7 323  GF    0.00 0.00    0    0.0    0.1 1330
 25 02 1990 *1223    0 40.81 159   2.52 1617.1   8.1 317   1.6 293   6.7 323  GF    0.00 0.00    0    0.1    0.1 1331
 25 02 1990  1224    0 40.9  159   2.4  1617.2   8.6 318   1.6 293   7.2 323  c/cs                                1332
 25 02 1990  1248    0 43.5  159   0.1  1620.6   8.5 318   1.6 293   7.1 323  c/cs                                1333
 25 02 1990  1305    0 45.2  158  58.5  1623.0   8.6 318   1.6 293   7.2 323  c/cs                                1334
 25 02 1990 *1333    0 48.20 158  55.80 1627.1   8.9 320   1.8 308   7.2 323  SF    0.00 0.00    0    1.9    1.2 1335
 25 02 1990  1335    0 48.4  158  55.6  1627.3   8.9 320   1.8 308   7.1 323  c/cs                                1336
 25 02 1990  1400    0 51.3  158  53.2  1631.0   8.6 321   1.8 308   6.9 324  c/cs                                1337
 25 02 1990  1411    0 52.5  158  52.2  1632.6   8.8 319   1.8 308   7.1 322  c/cs                                1338
 25 02 1990  1417    0 53.2  158  51.7  1633.5   8.9 320   1.8 308   7.2 323  c/cs                                1339
 25 02 1990 *1423    0 53.84 158  51.10 1634.4   8.7 321   1.5 311   7.2 323  GF    0.00 0.00    0    1.5    0.8 1340
 25 02 1990 *1430    0 54.63 158  50.46 1635.4   9.2 321   2.0 315   7.2 323  GF    0.00 0.00    0    0.2    0.1 1341
 25 02 1990 *1438    0 55.59 158  49.69 1636.6   8.8 320   1.6 306   7.2 323  GF    0.00 0.00    0    0.3    0.1 1342
 25 02 1990 *1443    0 56.15 158  49.22 1637.4   8.6 319   1.5 298   7.2 323  GF    0.00 0.00    0    0.1    0.1 1343
 25 02 1990  1447    0 56.6  158  48.8  1637.9   8.6 320   1.5 298   7.2 324  c/cs                                1344
 25 02 1990 *1448    0 56.69 158  48.75 1638.1   8.5 320   1.4 297   7.2 324  GF    0.00 0.00    0    0.1    0.1 1345
 25 02 1990 *1453    0 57.23 158  48.29 1638.8   8.3 320   1.2 295   7.2 324  GF    0.00 0.00    0    0.1    0.1 1346
 25 02 1990 *1500    0 57.97 158  47.67 1639.8   9.2 321   2.0 310   7.2 324  GF    0.00 0.00    0    0.1    0.1 1347
 25 02 1990 *1508    0 58.92 158  46.90 1641.0   8.9 320   1.7 304   7.2 324  GF    0.00 0.00    0    0.3    0.1 1348
 25 02 1990  1512    0 59.4  158  46.5  1641.6   8.9 321   1.7 304   7.3 325  c/cs                                1349
 25 02 1990 *1513    0 59.49 158  46.43 1641.7   8.7 321   1.5 299   7.3 325  GF    0.00 0.00    0    0.1    0.1 1350
 25 02 1990 *1518    1  0.05 158  45.97 1642.4   9.0 321   1.8 304   7.3 325  GF    0.00 0.00    0    0.1    0.1 1351
 25 02 1990 *1523    1  0.63 158  45.50 1643.2   8.3 320   1.2 292   7.3 325  GF    0.00 0.00    0    0.1    0.1 1352
 25 02 1990 *1530    1  1.38 158  44.88 1644.2   9.1 322   1.8 309   7.3 325  GF    0.00 0.00    0    0.1    0.1 1353
 25 02 1990  1537    1  2.2  158  44.2  1645.2   8.9 323   1.8 309   7.1 327  c/cs                                1354
 25 02 1990 *1538    1  2.33 158  44.14 1645.4   8.6 323   1.5 304   7.1 327  GF    0.00 0.00    0    0.2    0.1 1355
 25 02 1990 *1543    1  2.90 158  43.71 1646.1   8.5 325   1.4 313   7.1 327  GF    0.00 0.00    0    0.1    0.1 1356
 25 02 1990 *1548    1  3.48 158  43.30 1646.8   8.6 323   1.5 304   7.1 327  GF    0.00 0.00    0    0.1    0.1 1357
 25 02 1990 *1553    1  4.05 158  42.87 1647.5   8.2 324   1.1 304   7.1 327  GF    0.00 0.00    0    0.1    0.1 1358
 25 02 1990 *1600    1  4.82 158  42.31 1648.5   9.0 323   2.0 308   7.1 327  GF    0.00 0.00    0    0.1    0.1 1359
 25 02 1990  1607    1  5.7  158  41.7  1649.5   9.1 321   2.0 308   7.2 325  c/cs                                1360
 25 02 1990 *1608    1  5.78 158  41.58 1649.7   8.6 322   1.5 310   7.2 325  GF    0.00 0.00    0    0.3    0.1 1361
 25 02 1990 *1613    1  6.35 158  41.14 1650.4   8.5 322   1.5 306   7.2 325  GF    0.00 0.00    0    0.1    0.1 1362
 25 02 1990 *1618    1  6.91 158  40.70 1651.1   8.6 322   1.5 310   7.2 325  GF    0.00 0.00    0    0.1    0.1 1363
 25 02 1990 *1623    1  7.48 158  40.26 1651.8   8.7 323   1.6 313   7.2 325  GF    0.00 0.00    0    0.1    0.1 1364
 25 02 1990 *1628    1  8.06 158  39.82 1652.5   8.8 322   1.7 308   7.2 325  GF    0.00 0.00    0    0.1    0.1 1365
 25 02 1990  1630    1  8.3  158  39.6  1652.8   8.9 321   1.7 308   7.2 324  c/cs                                1366
 25 02 1990 *1638    1  9.21 158  38.89 1654.0   9.0 321   1.8 309   7.2 324  GF    0.00 0.00    0    0.3    0.2 1367
 25 02 1990 *1643    1  9.79 158  38.42 1654.8   8.8 321   1.6 308   7.2 324  GF    0.00 0.00    0    0.1    0.1 1368
 25 02 1990 *1648    1 10.36 158  37.96 1655.5   8.8 321   1.6 308   7.2 324  GF    0.00 0.00    0    0.1    0.1 1369
 25 02 1990 *1653    1 10.93 158  37.50 1656.2   8.0 321   0.9 297   7.2 324  GF    0.00 0.00    0    0.1    0.1 1370
 25 02 1990 *1700    1 11.66 158  36.91 1657.2   9.5 321   2.3 312   7.2 324  GF    0.00 0.00    0    0.1    0.1 1371
 25 02 1990  1700    1 11.7  158  36.9  1657.2   9.4 321   2.3 312   7.2 324  c/cs                                1372
 25 02 1990 *1708    1 12.64 158  36.12 1658.4   9.0 320   1.9 307   7.2 324  GF    0.00 0.00    0    0.3    0.1 1373
 25 02 1990 *1713    1 13.22 158  35.64 1659.2   8.8 321   1.7 309   7.2 324  GF    0.00 0.00    0    0.2    0.1 1374
 25 02 1990 *1718    1 13.79 158  35.18 1659.9   8.8 321   1.7 309   7.2 324  GF    0.00 0.00    0    0.1    0.1 1375
 25 02 1990 *1723    1 14.36 158  34.72 1660.7   9.1 321   1.9 312   7.2 324  GF    0.00 0.00    0    0.1    0.1 1376
 25 02 1990 *1728    1 14.95 158  34.25 1661.4   5.8 321   1.4 155   7.2 324  GF    0.00 0.00    0    0.2    0.1 1377
 25 02 1990 *1730    1 15.10 158  34.13 1661.6   9.4 322   2.2 314   7.2 324  GF    0.00 0.00    0    0.0    0.0 1378
```

```
#cruise ODP130JR                              date run: Wed Jul 18 16:38:07 1990         page  27
#
#                      latitude   longitude               actual     drift        dr                 prob. error       drift
#da mo   yr   time  deg   min   deg   min     dist  speed cse  speed hed  speed cse  cmnt (smajxsmin@az)  dist  time   no.
#- - - - - - - - - - - - - - - - - - - - - - - - - - - - - - - - - - - - - - - - - - - - - - - - - - - - - - - - - - - - -
 25 02 1990  1730    1 15.1   158 34.1   1661.6    9.4 321    2.2 314    7.2 323  c/cs                             1379
 25 02 1990 *1738    1 16.07  158 33.34  1662.9    8.6 319    1.5 300    7.2 323  GF    0.00 0.00    0   0.3   0.1 1380
 25 02 1990 *1743    1 16.61  158 32.87  1663.6    9.2 319    2.2 304    7.2 323  GF    0.00 0.00    0   0.1   0.1 1381
 25 02 1990  1746    1 17.0   158 32.6   1664.0    9.3 319    2.2 304    7.2 323  c/cs                             1382
 25 02 1990 *1748    1 17.19  158 32.36  1664.3    9.0 320    1.8 307    7.2 323  GF    0.00 0.00    0   0.2   0.1 1383
 25 02 1990 *1753    1 17.76  158 31.88  1665.1    8.1 321    0.9 301    7.2 323  GF    0.00 0.00    0   0.1   0.1 1384
 25 02 1990 *1800    1 18.49  158 31.28  1666.0    9.7 321    2.5 314    7.2 323  GF    0.00 0.00    0   0.1   0.1 1385
 25 02 1990 *1813    1 20.12  158 29.94  1668.1    8.8 321    1.6 310    7.2 323  GF    0.00 0.00    0   0.5   0.2 1386
 25 02 1990  1816    1 20.5   158 29.7   1668.6    8.9 321    1.6 310    7.3 323  c/cs                             1387
 25 02 1990 *1818    1 20.69  158 29.47  1668.9    9.1 320    1.9 308    7.3 323  GF    0.00 0.00    0   0.1   0.1 1388
 25 02 1990 *1823    1 21.27  158 28.98  1669.6    8.9 320    1.7 307    7.3 323  GF    0.00 0.00    0   0.2   0.1 1389
 25 02 1990 *1828    1 21.84  158 28.50  1670.4    9.1 319    1.9 305    7.3 323  GF    0.00 0.00    0   0.1   0.1 1390
 25 02 1990 *1838    1 22.99  158 27.51  1671.9    7.5 320    0.5 265    7.3 323  GF    0.00 0.00    0   0.3   0.2 1391
 25 02 1990  1841    1 23.3   158 27.3   1672.3    7.5 319    0.5 265    7.2 322  c/cs                             1392
 25 02 1990 *1844    1 23.56  158 27.02  1672.7    9.2 318    2.0 305    7.2 322  GF    0.00 0.00    0   0.0   0.1 1393
 25 02 1990 *1849    1 24.13  158 26.51  1673.4    9.2 319    2.0 309    7.2 322  GF    0.00 0.00    0   0.2   0.1 1394
 25 02 1990 *1854    1 24.71  158 26.01  1674.2    9.2 318    2.1 303    7.2 322  GF    0.00 0.00    0   0.2   0.1 1395
 25 02 1990  1857    1 25.1   158 25.7   1674.6    9.3 318    2.1 303    7.3 322  c/cs                             1396
 25 02 1990 *1859    1 25.28  158 25.49  1675.0    8.9 318    1.7 300    7.3 322  GF    0.00 0.00    0   0.2   0.1 1397
 25 02 1990 *1900    1 25.39  158 25.39  1675.1    9.1 319    1.9 308    7.3 322  GF    0.00 0.00    0   0.0   0.0 1398
 25 02 1990 *1904    1 25.85  158 24.99  1675.7    9.1 320    1.9 311    7.3 322  GF    0.00 0.00    0   0.1   0.1 1399
 25 02 1990 *1909    1 26.43  158 24.50  1676.5    9.1 320    1.9 311    7.3 322  GF    0.00 0.00    0   0.2   0.1 1400
 25 02 1990 *1914    1 27.01  158 24.01  1677.2    9.0 319    1.8 308    7.3 322  GF    0.00 0.00    0   0.2   0.1 1401
 25 02 1990 *1919    1 27.58  158 23.52  1678.0    9.1 320    1.9 311    7.3 322  GF    0.00 0.00    0   0.1   0.1 1402
 25 02 1990 *1924    1 28.16  158 23.03  1678.7    9.0 320    1.8 311    7.3 322  GF    0.00 0.00    0   0.2   0.1 1403
 25 02 1990  1927    1 28.5   158 22.7   1679.2    9.0 320    1.8 311    7.3 322  c/cs                             1404
 25 02 1990 *1930    1 28.85  158 22.45  1679.6    9.5 320    2.2 311    7.3 322  GF    0.00 0.00    0   0.2   0.1 1405
 25 02 1990 *1934    1 29.33  158 22.04  1680.3    9.1 321    1.8 316    7.3 322  GF    0.00 0.00    0   0.1   0.1 1406
 25 02 1990 *1939    1 29.92  158 21.56  1681.0    9.1 320    1.8 311    7.3 322  GF    0.00 0.00    0   0.2   0.1 1407
 25 02 1990 *1944    1 30.50  158 21.07  1681.8    9.0 320    1.7 314    7.3 322  GF    0.00 0.00    0   0.2   0.1 1408
 25 02 1990 *1949    1 31.08  158 20.59  1682.5    9.1 319    1.8 305    7.3 322  GF    0.00 0.00    0   0.1   0.1 1409
 25 02 1990  1950    1 31.2   158 20.5   1682.7    9.0 319    1.8 305    7.2 323  c/cs                             1410
 25 02 1990 *1954    1 31.65  158 20.10  1683.3    9.0 319    1.9 305    7.2 323  GF    0.00 0.00    0   0.2   0.1 1411
 25 02 1990 *1959    1 32.22  158 19.61  1684.0    7.6 321    0.4 296    7.2 323  GF    0.00 0.00    0   0.2   0.1 1412
 25 02 1990 *2000    1 32.32  158 19.53  1684.2    9.3 320    2.1 309    7.2 323  GF    0.00 0.00    0   0.0   0.0 1413
 25 02 1990 *2009    1 33.39  158 18.63  1685.6    9.1 319    2.0 303    7.2 323  GF    0.00 0.00    0   0.3   0.2 1414
 25 02 1990 *2014    1 33.96  158 18.13  1686.3    9.1 320    1.9 308    7.2 323  GF    0.00 0.00    0   0.2   0.1 1415
 25 02 1990 *2019    1 34.54  158 17.64  1687.1    9.3 319    2.1 307    7.2 323  GF    0.00 0.00    0   0.2   0.1 1416
 25 02 1990  2020    1 34.7   158 17.5   1687.2    9.2 319    2.1 307    7.1 323  c/cs                             1417
 25 02 1990 *2024    1 35.12  158 17.14  1687.9    8.9 320    1.8 307    7.1 323  GF    0.00 0.00    0   0.2   0.1 1418
 25 02 1990  2026    1 35.3   158 16.9   1688.2    8.6 320    1.8 307    6.8 323  c/cs                             1419
 25 02 1990 *2030    1 35.78  158 16.58  1688.7    8.8 320    2.1 308    6.8 323  GF    0.00 0.00    0   0.2   0.1 1420
 25 02 1990  2032    1 36.0   158 16.4   1689.0    9.4 319    2.1 308    7.3 322  c/cs                             1421
 25 02 1990 *2039    1 36.83  158 15.67  1690.1    9.0 319    1.7 308    7.3 322  GF    0.00 0.00    0   0.3   0.2 1422
 25 02 1990 *2044    1 37.40  158 15.18  1690.9    8.9 320    1.6 313    7.3 322  GF    0.00 0.00    0   0.1   0.1 1423
 25 02 1990 *2049    1 37.97  158 14.71  1691.6    9.1 320    1.8 310    7.3 322  GF    0.00 0.00    0   0.1   0.1 1424
 25 02 1990  2049    1 38.0   158 14.7   1691.6    9.0 320    1.8 310    7.2 323  c/cs                             1425
 25 02 1990  2050    1 38.1   158 14.6   1691.8    9.0 320    1.8 310    7.2 323  **** missing data ****           1426
 25 02 1990 *2054    1 38.55  158 14.23  1692.4    8.6 319    1.5 299    7.2 323  GF    0.00 0.00    0   0.2   0.1 1427
 25 02 1990  2058    1 39.0   158 13.9   1692.9    8.8 318    1.5 299    7.4 322  c/cs                             1428
 25 02 1990 *2100    1 39.20  158 13.66  1693.2    9.3 319    1.9 308    7.4 322  GF    0.00 0.00    0   0.1   0.1 1429
 25 02 1990  2108    1 40.1   158 12.8   1694.5    9.0 319    1.9 308    7.1 322  c/cs                             1430
 25 02 1990 *2109    1 40.25  158 12.75  1694.6    8.9 320    1.9 312    7.1 322  GF    0.00 0.00    0   0.3   0.2 1431
```

```
#cruise ODP130JR                                             date run: Wed Jul 18 16:38:07 1990          page  28
#
#                        latitude  longitude              actual   drift      dr             prob. error       drift
#da mo  yr    time  deg   min  deg   min     dist speed cse speed hed speed cse  cmnt (smajxsmin@az)  dist  time  no.
#- - - - - - - - - - - - - - - - - - - - - - - - - - - - - - - - - - - - - - - - - - - - - - - - - - - - - - - - - -
 25 02 1990 *2114   1 40.82 158 12.27 1695.4   9.1 318   2.0 305   7.1 322  GF   0.00 0.00   0   0.2   0.1 1432
 25 02 1990  2116   1 41.0  158 12.1  1695.7   9.2 318   2.0 305   7.2 322  c/cs                               1433
 25 02 1990 *2119   1 41.39 158 11.76 1696.1   8.9 319   1.7 305   7.2 322  GF   0.00 0.00   0   0.2   0.1 1434
 25 02 1990 *2124   1 41.95 158 11.27 1696.9   8.1 318   1.0 293   7.2 322  GF   0.00 0.00   0   0.1   0.1 1435
 25 02 1990 *2130   1 42.56 158 10.73 1697.7   9.3 319   2.1 309   7.2 322  GF   0.00 0.00   0   0.1   0.1 1436
 25 02 1990 *2139   1 43.61 158  9.82 1699.1   8.8 319   1.6 303   7.2 322  GF   0.00 0.00   0   0.3   0.2 1437
 25 02 1990  2142   1 43.9  158  9.5  1699.5   8.8 319   1.6 303   7.3 323  c/cs                               1438
 25 02 1990 *2144   1 44.16 158  9.34 1699.8   8.9 320   1.7 307   7.3 323  GF   0.00 0.00   0   0.1   0.1 1439
 25 02 1990 *2149   1 44.73 158  8.86 1700.5   8.9 320   1.7 307   7.3 323  GF   0.00 0.00   0   0.1   0.1 1440
 25 02 1990 *2154   1 45.30 158  8.38 1701.3   8.2 320   1.0 301   7.3 323  GF   0.00 0.00   0   0.1   0.1 1441
 25 02 1990 *2200   1 45.93 158  7.86 1702.1   9.4 320   2.2 309   7.3 323  GF   0.00 0.00   0   0.1   0.1 1442
 25 02 1990  2202   1 46.2  158  7.7  1702.4   9.5 320   2.2 309   7.4 323  c/cs                               1443
 25 02 1990 *2209   1 47.02 158  6.94 1703.5   8.9 319   1.6 302   7.4 323  GF   0.00 0.00   0   0.3   0.2 1444
 25 02 1990 *2214   1 47.58 158  6.46 1704.3   9.0 319   1.7 304   7.4 323  GF   0.00 0.00   0   0.1   0.1 1445
 25 02 1990  2218   1 48.0  158  6.1  1704.9   8.9 319   1.7 304   7.2 323  c/cs                               1446
 25 02 1990 *2219   1 48.15 158  5.97 1705.0   9.1 319   2.0 303   7.2 323  GF   0.00 0.00   0   0.1   0.1 1447
 25 02 1990 *2224   1 48.72 158  5.47 1705.8   8.0 319   1.0 289   7.2 323  GF   0.00 0.00   0   0.2   0.1 1448
 25 02 1990  2226   1 48.9  158  5.3  1706.0   8.2 318   1.0 289   7.4 322  c/cs                               1449
 25 02 1990 *2230   1 49.33 158  4.93 1706.6   9.5 320   2.2 311   7.4 322  GF   0.00 0.00   0   0.1   0.1 1450
 25 02 1990 *2239   1 50.42 158  4.00 1708.0   8.9 319   1.6 304   7.4 322  GF   0.00 0.00   0   0.3   0.2 1451
 25 02 1990 *2244   1 50.98 158  3.51 1708.8   9.2 320   1.8 314   7.4 322  GF   0.00 0.00   0   0.1   0.1 1452
 25 02 1990 *2249   1 51.57 158  3.02 1709.5   8.9 320   1.6 310   7.4 322  GF   0.00 0.00   0   0.2   0.1 1453
 25 02 1990 *2254   1 52.14 158  2.54 1710.3   8.9 319   1.6 304   7.4 322  GF   0.00 0.00   0   0.1   0.1 1454
 25 02 1990  2256   1 52.4  158  2.3  1710.6   9.0 319   1.6 304   7.4 322  c/cs                               1455
 25 02 1990 *2259   1 52.70 158  2.05 1711.0   9.1 319   1.7 308   7.4 322  GF   0.00 0.00   0   0.1   0.1 1456
 25 02 1990  2304   1 53.3  158  1.6  1711.8   8.7 319   1.7 308   7.0 322  c/cs                               1457
 25 02 1990  2308   1 53.7  158  1.2  1712.4   9.0 320   1.7 308   7.3 323  c/cs                               1458
 25 02 1990 *2309   1 53.83 158  1.08 1712.5   8.8 320   1.6 306   7.3 323  GF   0.00 0.00   0   0.3   0.2 1459
 25 02 1990 *2314   1 54.39 158  0.61 1713.2   8.8 320   1.5 306   7.3 323  GF   0.00 0.00   0   0.1   0.1 1460
 25 02 1990 *2319   1 54.95 158  0.14 1714.0   8.8 319   1.6 303   7.3 323  GF   0.00 0.00   0   0.1   0.1 1461
 25 02 1990 *2324   1 55.51 157 59.66 1714.7   7.7 320   0.6 277   7.3 323  GF   0.00 0.00   0   0.1   0.1 1462
 25 02 1990 *2330   1 56.10 157 59.16 1715.5   9.8 320   2.5 310   7.3 323  GF   0.00 0.00   0   0.1   0.1 1463
 25 02 1990  2336   1 56.8  157 58.5  1716.5   9.7 319   2.5 310   7.2 322  c/cs                               1464
 25 02 1990 *2339   1 57.21 157 58.21 1716.9   9.1 319   1.9 307   7.2 322  GF   0.00 0.00   0   0.4   0.2 1465
 25 02 1990 *2344   1 57.78 157 57.71 1717.7   9.0 319   1.9 306   7.2 322  GF   0.00 0.00   0   0.2   0.1 1466
 25 02 1990  2344   1 57.8  157 57.7  1717.7   9.1 319   1.9 306   7.3 322  c/cs                               1467
 25 02 1990 *2349   1 58.35 157 57.21 1718.5   8.9 319   1.7 305   7.3 322  GF   0.00 0.00   0   0.2   0.1 1468
 25 02 1990 *2354   1 58.91 157 56.72 1719.2   7.7 319   0.6 275   7.3 322  GF   0.00 0.00   0   0.1   0.1 1469
 26 02 1990 *0000   1 59.49 157 56.21 1720.0   9.1 319   1.9 306   7.3 322  GF   0.00 0.00   0   0.1   0.1 1470
 26 02 1990  0000   1 59.5  157 56.2  1720.0   9.1 319   1.9 306   7.3 322  c/cs                               1471
 26 02 1990 *0010   2  0.63 157 55.21 1721.5   9.2 318   2.0 302   7.3 322  GF   0.00 0.00   0   0.3   0.2 1472
 26 02 1990  0014   2  1.1  157 54.8  1722.1   9.3 318   2.0 302   7.4 322  c/cs                               1473
 26 02 1990 *0015   2  1.20 157 54.69 1722.3   9.2 318   1.9 303   7.4 322  GF   0.00 0.00   0   0.2   0.1 1474
 26 02 1990 *0020   2  1.77 157 54.18 1723.0   9.1 319   1.8 305   7.4 322  GF   0.00 0.00   0   0.2   0.1 1475
 26 02 1990 *0025   2  2.34 157 53.68 1723.8   9.1 319   1.8 305   7.4 322  GF   0.00 0.00   0   0.1   0.1 1476
 26 02 1990 *0030   2  2.91 157 53.18 1724.5   9.3 318   2.0 304   7.4 322  GF   0.00 0.00   0   0.1   0.1 1477
 26 02 1990 *0035   2  3.49 157 52.66 1725.3   9.1 319   1.8 305   7.4 322  GF   0.00 0.00   0   0.2   0.1 1478
 26 02 1990 *0040   2  4.06 157 52.16 1726.1   9.1 319   1.8 305   7.4 322  GF   0.00 0.00   0   0.1   0.1 1479
 26 02 1990  0044   2  4.5  157 51.8  1726.7   9.0 319   1.8 305   7.3 322  c/cs                               1480
 26 02 1990 *0045   2  4.60 157 51.66 1726.8   8.9 319   1.7 305   7.3 322  GF   0.00 0.00   0   0.2   0.1 1481
 26 02 1990 *0050   2  5.19 157 51.17 1727.6   9.0 319   1.7 304   7.3 322  GF   0.00 0.00   0   0.1   0.1 1482
 26 02 1990 *0100   2  6.31 157 50.18 1729.1   9.2 318   1.9 304   7.3 322  GF   0.00 0.00   0   0.3   0.2 1483
 26 02 1990 *0105   2  6.83 157 49.67 1729.8   9.0 318   1.8 303   7.3 322  GF   0.00 0.00   0   0.2   0.1 1484
```

```
#cruise ODP130JR
#
#                   latitude  longitude             actual    drift       dr               prob. error        drift
#da mo  yr   time deg   min  deg   min     dist  speed cse speed hed  speed cse   cmnt (smajxsmin@az)   dist   time   no.
#- - - - - - - - - - - - - - - - - - - - - - - - - - - - - - - - - - - - - - - - - - - - - - - - - - - - - - - - - - -
 26 02 1990 *0110   2  7.44 157 49.17 1730.6   9.0 318   1.8 302    7.3 322   GF    0.00 0.00    0    0.1    0.1 1485
 26 02 1990  0114   2  7.9  157 48.8  1731.2   9.0 319   1.8 302    7.3 323   c/cs                               1486
 26 02 1990 *0115   2  8.00 157 48.67 1731.3   8.8 319   1.6 303    7.3 323   GF    0.00 0.00    0    0.1    0.1 1487
 26 02 1990 *0120   2  8.56 157 48.19 1732.1   8.8 319   1.6 300    7.3 323   GF    0.00 0.00    0    0.1    0.1 1488
 26 02 1990 *0130   2  9.67 157 47.22 1733.6   9.2 318   2.0 300    7.3 323   GF    0.00 0.00    0    0.3    0.2 1489
 26 02 1990 *0135   2 10.24 157 46.71 1734.3   9.1 319   1.9 302    7.3 323   GF    0.00 0.00    0    0.2    0.1 1490
 26 02 1990 *0140   2 10.81 157 46.21 1735.1   8.8 319   1.6 300    7.3 323   GF    0.00 0.00    0    0.2    0.1 1491
 26 02 1990  0144   2 11.3  157 45.8  1735.7   8.6 319   1.6 300    7.2 323   c/cs                               1492
 26 02 1990 *0145   2 11.36 157 45.73 1735.8   8.8 319   1.8 305    7.2 323   GF    0.00 0.00    0    0.1    0.1 1493
 26 02 1990 *0150   2 11.92 157 45.25 1736.5   8.8 319   1.7 302    7.2 323   GF    0.00 0.00    0    0.1    0.1 1494
 26 02 1990 *0155   2 12.47 157 44.77 1737.3   8.3 318   1.3 293    7.2 323   GF    0.00 0.00    0    0.1    0.1 1495
 26 02 1990 *0200   2 12.99 157 44.31 1738.0   9.1 318   2.1 299    7.2 323   GF    0.00 0.00    0    0.1    0.1 1496
 26 02 1990  0202   2 13.2  157 44.1  1738.3   9.3 318   2.1 299    7.3 323   c/cs                               1497
 26 02 1990 *0210   2 14.13 157 43.27 1739.5   8.8 318   1.6 297    7.3 323   GF    0.00 0.00    0    0.4    0.2 1498
 26 02 1990 *0215   2 14.68 157 42.78 1740.2   8.9 319   1.7 301    7.3 323   GF    0.00 0.00    0    0.1    0.1 1499
 26 02 1990 *0220   2 15.24 157 42.29 1741.0   8.7 319   1.5 297    7.3 323   GF    0.00 0.00    0    0.1    0.1 1500
 26 02 1990 *0230   2 16.33 157 41.33 1742.4   9.4 318   2.3 300    7.3 323   GF    0.00 0.00    0    0.3    0.2 1501
 26 02 1990  0232   2 16.6  157 41.1  1742.8   9.4 318   2.3 300    7.3 323   c/cs                               1502
 26 02 1990 *0235   2 16.91 157 40.80 1743.2   8.9 319   1 7 301    7.3 323   GF    0.00 0.00    0    0.2    0.1 1503
 26 02 1990 *0240   2 17.47 157 40.31 1744.0   8.9 317   1.8 291    7.3 323   GF    0.00 0.00    0    0.1    0.1 1504
 26 02 1990 *0245   2 18.01 157 39.80 1744.7   8.9 318   1.8 296    7.3 323   GF    0.00 0.00    0    0.2    0.1 1505
 26 02 1990 *0250   2 18.56 157 39.30 1745.5   8.8 317   1.7 291    7.3 323   GF    0.00 0.00    0    0.1    0.1 1506
 26 02 1990  0253   2 18.9  157 39.0  1745.9   8.7 317   1.7 291    7.2 323   c/cs                               1507
 26 02 1990 *0300   2 19.62 157 38.31 1746.9   9.5 318   2.4 303    7.2 323   GF    0.00 0.00    0    0.3    0.2 1508
 26 02 1990 *0305   2 20.21 157 37.78 1747.7   9.0 318   1.9 298    7.2 323   GF    0.00 0.00    0    0.2    0.1 1509
 26 02 1990  0307   2 20.4  157 37.6  1748.0   8.9 319   1.9 298    7.2 325   c/cs                               1510
 26 02 1990 *0310   2 20.77 157 37.29 1748.4   8.9 319   2.0 295    7.2 325   GF    0.00 0.00    0    0.2    0.1 1511
 26 02 1990 *0315   2 21.33 157 36.80 1749.2   8.8 319   1.8 297    7.2 325   GF    0.00 0.00    0    0.2    0.1 1512
 26 02 1990 *0320   2 21.89 157 36.32 1749.9   8.6 319   1.7 291    7.2 325   GF    0.00 0.00    0    0.2    0.1 1513
 26 02 1990 *0330   2 22.97 157 35.37 1751.4   9.5 319   2.5 301    7.2 325   GF    0.00 0.00    0    0.3    0.2 1514
 26 02 1990  0332   2 23.2  157 35.2  1751.7   9.5 320   2.5 301    7.2 326   c/cs                               1515
 26 02 1990 *0340   2 24.18 157 34.34 1753.0   9.0 318   2.1 290    7.2 326   GF    0.00 0.00    0    0.4    0.2 1516
 26 02 1990 *0345   2 24.74 157 33.84 1753.7   9.0 318   2.1 290    7.2 326   GF    0.00 0.00    0    0.2    0.1 1517
 26 02 1990 *0350   2 25.30 157 33.34 1754.5   9.0 319   2.0 295    7.2 326   GF    0.00 0.00    0    0.2    0.1 1518
 26 02 1990 *0355   2 25.87 157 32.85 1755.2   8.0 319   1.2 270    7.2 326   GF    0.00 0.00    0    0.2    0.1 1519
 26 02 1990 *0400   2 26.37 157 32.41 1755.9   9.7 319   2.7 300    7.2 326   GF    0.00 0.00    0    0.1    0.1 1520
 26 02 1990  0402   2 26.6  157 32.2  1756.2   9.7 319   2.7 300    7.2 326   c/cs                               1521
 26 02 1990 *0405   2 26.98 157 31.88 1756.7   8.8 319   1.9 291    7.2 326   GF    0.00 0.00    0    0.2    0.1 1522
 26 02 1990 *0410   2 27.53 157 31.40 1757.4   8.7 318   1.8 287    7.2 326   GF    0.00 0.00    0    0.2    0.1 1523
 26 02 1990 *0415   2 28.07 157 30.92 1758.1   8.5 320   1.6 290    7.2 326   GF    0.00 0.00    0    0.2    0.1 1524
 26 02 1990 *0420   2 28.61 157 30.46 1758.8   8.6 319   1.7 289    7.2 326   GF    0.00 0.00    0    0.1    0.1 1525
 26 02 1990 *0425   2 29.15 157 29.99 1759.6   7.5 320   0.8 257    7.2 326   GF    0.00 0.00    0    0.1    0.1 1526
 26 02 1990  0428   2 29.4  157 29.8  1759.9   7.5 320   0.8 257    7.2 326   c/cs                               1527
 26 02 1990 *0430   2 29.63 157 29.59 1760.2   9.3 321   2.3 303    7.2 326   GF    0.00 0.00    0    0.1    0.1 1528
 26 02 1990 *0440   2 30.83 157 28.60 1761.7   8.5 322   1.5 301    7.2 326   GF    0.00 0.00    0    0.4    0.2 1529
 26 02 1990 *0445   2 31.39 157 28.16 1762.4   8.6 320   1.6 292    7.2 326   GF    0.00 0.00    0    0.1    0.1 1530
 26 02 1990  0445   2 31.4  157 28.2  1762.4   8.5 321   1.6 292    7.1 327   c/cs                               1531
 26 02 1990 *0450   2 31.94 157 27.71 1763.2   8.7 321   1.8 294    7.1 327   GF    0.00 0.00    0    0.1    0.1 1532
 26 02 1990 *0455   2 32.50 157 27.25 1763.9   7.2 322   0.6 237    7.1 327   GF    0.00 0.00    0    0.1    0.1 1533
 26 02 1990 *0500   2 32.97 157 26.88 1764.5   9.3 321   2.3 303    7.1 327   GF    0.00 0.00    0    0.1    0.1 1534
 26 02 1990  0501   2 33.1  157 26.8  1764.6   9.4 321   2.3 303    7.3 327   c/cs                               1535
 26 02 1990 *0505   2 33.58 157 26.39 1765.3   8.4 322   1.3 292    7.3 327   GF    0.00 0.00    0    0.2    0.1 1536
 26 02 1990 *0510   2 34.13 157 25.96 1766.0   8.3 321   1.3 285    7.3 327   GF    0.00 0.00    0    0.1    0.1 1537
```

```
                                                  date run: Wed Jul 18 16:38:07 1990          page  30
#cruise ODP130JR
#
#                       latitude  longitude             actual    drift         dr                prob. error        drift
#dy mo   yr    time deg   min  deg   min      dist speed cse speed hed speed cse   cmnt (smajxsmin@az)  dist  time   no.
#- - - - - - - - - - - - - - - - - - - - - - - - - - - - - - - - - - - - - - - - - - - - - - - - - - - - - - - - - - - -
 26 02 1990 *0515    2 34.67 157 25.52 1766.7   8.4 322   1.3 292   7.3 327  GF   0.00 0.00   0   0.1    0.1 1538
 26 02 1990 *0520    2 35.22 157 25.09 1767.4   7.8 322   0.9 270   7.3 327  GF   0.00 0.00   0   0.1    0.1 1539
 26 02 1990 *0530    2 36.24 157 24.28 1768.7   9.2 322   2.0 302   7.3 327  GF   0.00 0.00   0   0.1    0.2 1540
 26 02 1990  0531    2 36.4  157 24.2  1768.8   9.1 322   2.0 302   7.2 328  c/cs                            1541
 26 02 1990 *0540    2 37.44 157 23.35 1770.2   8.5 323   1.4 294   7.2 328  GF   0.00 0.00   0   0.3    0.2 1542
 26 02 1990 *0545    2 38.00 157 22.92 1770.9   7.0 322   0.8 216   7.2 328  GF   0.00 0.00   0   0.1    0.1 1543
 26 02 1990 *0551    2 38.55 157 22.49 1771.6   8.4 323   1.4 296   7.2 328  GF   0.00 0.00   0   0.1    0.1 1544
 26 02 1990 *0600    2 39.56 157 21.73 1772.8   8.1 324   1.0 295   7.2 328  GF   0.00 0.00   0   0.2    0.2 1545
 26 02 1990 *0601    2 39.67 157 21.65 1773.0   8.9 323   1.8 304   7.2 328  GF   0.00 0.00   0   0.0    0.0 1546
 26 02 1990  0601    2 39.7  157 21.7  1773.0   8.3 324   1.8 304   6.7 329  c/cs                            1547
 26 02 1990 *0606    2 40.23 157 21.24 1773.7   7.9 325   1.3 303   6.7 329  GF   0.00 0.00   0   0.1    0.1 1548
 26 02 1990  0607    2 40.3  157 21.2  1773.8   8.5 325   1.3 303   7.3 329  c/cs                            1549
 26 02 1990 *0611    2 40.80 157 20.84 1774.4   8.3 325   1.2 300   7.3 329  GF   0.00 0.00   0   0.1    0.1 1550
 26 02 1990 *0616    2 41.37 157 20.44 1775.1   8.3 324   1.2 295   7.3 329  GF   0.00 0.00   0   0.1    0.1 1551
 26 02 1990 *0621    2 41.93 157 20.04 1775.7   8.4 324   1.3 298   7.3 329  GF   0.00 0.00   0   0.1    0.1 1552
 26 02 1990 *0626    2 42.50 157 19.63 1776.5   8.1 326   0.9 305   7.3 329  GF   0.00 0.00   0   0.1    0.1 1553
 26 02 1990 *0630    2 42.95 157 19.33 1777.0   9.0 323   1.9 300   7.3 329  GF   0.00 0.00   0   0.1    0.1 1554
 26 02 1990 *0631    2 43.07 157 19.24 1777.1   8.3 324   1.3 293   7.3 329  GF   0.00 0.00   0   0.0    0.0 1555
 26 02 1990 *0636    2 43.63 157 18.83 1777.8   8.4 324   1.3 294   7.3 329  GF   0.00 0.00   0   0.1    0.1 1556
 26 02 1990  0637    2 43.7  157 18.7  1778.0   8.4 323   1.3 294   7.3 328  c/cs                            1557
 26 02 1990 *0641    2 44.19 157 18.41 1778.5   8.6 324   1.4 304   7.3 328  GF   0.00 0.00   0   0.1    0.1 1558
 26 02 1990 *0646    2 44.77 157 17.99 1779.3   8.7 323   1.5 301   7.3 328  GF   0.00 0.00   0   0.1    0.1 1559
 26 02 1990 *0651    2 45.35 157 17.56 1780.0   8.6 322   1.6 295   7.3 328  GF   0.00 0.00   0   0.1    0.1 1560
 26 02 1990 *0656    2 45.92 157 17.12 1780.7   8.5 324   1.3 304   7.3 328  GF   0.00 0.00   0   0.1    0.1 1561
 26 02 1990 *0700    2 46.38 157 16.79 1781.3   8.8 322   1.7 295   7.3 328  GF   0.00 0.00   0   0.1    0.1 1562
 26 02 1990 *0706    2 47.07 157 16.25 1782.1   8.6 324   1.4 303   7.3 328  GF   0.00 0.00   0   0.2    0.1 1563
 26 02 1990  0706    2 47.1  157 16.2  1782.1   8.7 322   1.4 303   7.4 326  c/cs                            1564
 26 02 1990 *0716    2 48.22 157 15.36 1783.6   8.8 322   1.5 304   7.4 326  GF   0.00 0.00   0   0.2    0.2 1565
 26 02 1990 *0721    2 48.80 157 14.91 1784.3   8.9 322   1.6 301   7.4 326  GF   0.00 0.00   0   0.1    0.1 1566
 26 02 1990 *0726    2 49.38 157 14.45 1785.1   8.2 322   1.0 289   7.4 326  GF   0.00 0.00   0   0.1    0.1 1567
 26 02 1990 *0730    2 49.81 157 14.11 1785.6   8.9 320   1.7 296   7.4 326  GF   0.00 0.00   0   0.1    0.1 1568
 26 02 1990 *0736    2 50.50 157 13.54 1786.5   9.0 321   1.7 299   7.4 326  GF   0.00 0.00   0   0.2    0.1 1569
 26 02 1990  0736    2 50.5  157 13.5  1786.5   8.9 321   1.7 299   7.4 326  c/cs                            1570
 26 02 1990 *0741    2 51.08 157 13.07 1737.2   8.7 321   1.5 294   7.4 326  GF   0.00 0.00   0   0.1    0.1 1571
 26 02 1990 *0746    2 51.64 157 12.61 1788.0   8.7 321   1.5 294   7.4 326  GF   0.00 0.00   0   0.1    0.1 1572
 26 02 1990 *0751    2 52.20 157 12.15 1788.7   8.5 321   1.4 291   7.4 326  GF   0.00 0.00   0   0.1    0.1 1573
 26 02 1990 *0800    2 53.19 157 11.34 1790.0   9.4 320   2.2 300   7.4 326  GF   0.00 0.00   0   0.2    0.2 1574
 26 02 1990 *0806    2 53.91 157 10.74 1790.9   8.8 321   1.5 297   7.4 326  GF   0.00 0.00   0   0.2    0.1 1575
 26 02 1990  0806    2 53.9  157 10.7  1790.9   8.8 321   1.5 297   7.4 326  c/cs                            1576
 26 02 1990 *0816    2 55.05 157  9.82 1792.4   8.7 322   1.5 300   7.4 326  GF   0.00 0.00   0   0.3    0.2 1577
 26 02 1990 *0821    2 55.62 157  9.37 1793.1   8.5 322   1.2 296   7.4 326  GF   0.00 0.00   0   0.1    0.1 1578
 26 02 1990 *0830    2 56.62 157  8.58 1794.4   9.4 322   2.1 309   7.4 326  GF   0.00 0.00   0   0.2    0.2 1579
 26 02 1990  0832    2 56.9  157  8.4  1794.7   9.4 321   2.1 309   7.3 324  c/cs                            1580
 26 02 1990 *0836    2 57.35 157  7.99 1795.3   8.9 321   1.6 305   7.3 324  GF   0.00 0.00   0   0.2    0.1 1581
 26 02 1990 *0841    2 57.92 157  7.52 1796.1   8.8 320   1.6 300   7.3 324  GF   0.00 0.00   0   0.1    0.1 1582
 26 02 1990  0843    2 58.1  157  7.3  1796.3   8.4 320   1.6 300   6.9 325  c/cs                            1583
 26 02 1990 *0846    2 58.47 157  7.06 1796.8   8.5 321   1.7 304   6.9 325  GF   0.00 0.00   0   0.1    0.1 1584
 26 02 1990  0847    2 58.6  157  7.0  1796.9   9.0 320   1.7 304   7.4 324  c/cs                            1585
 26 02 1990 *0851    2 59.04 157  6.59 1797.5   8.4 321   1.1 297   7.4 324  GF   0.00 0.00   0   0.1    0.1 1586
 26 02 1990 *0900    3  0.01 157  5.79 1798.8   9.7 321   2.3 311   7.4 324  GF   0.00 0.00   0   0.2    0.2 1587
 26 02 1990 *0906    3  0.76 157  5.18 1799.7   9.1 321   1.8 308   7.4 324  GF   0.00 0.00   0   0.2    0.1 1588
 26 02 1990 *0911    3  1.35 157  4.70 1800.5   8.9 320   1.7 301   7.4 324  GF   0.00 0.00   0   0.1    0.1 1589
 26 02 1990 *0916    3  1.92 157  4.22 1801.2   8.8 321   1.5 303   7.4 324  GF   0.00 0.00   0   0.1    0.1 1590
```

```
                                               date run: Wed Jul 18 16:38:07 1990        page  31
#cruise ODP130JR
#                                                  actual    drift        dr               prob. error      drift
#                   latitude  longitude                                                                         
#da mo  yr   time deg  min  deg  min      dist speed cse speed hed speed cse  cmnt (smajxsmin@az)  dist  time   no.
#- - - - - - - - - - - - - - - - - - - - - - - - - - - - - - - - - - - - - - - - - - - - - - - - - - - - - - - -
 26 02 1990  0917   3  2.0  157  4.1   1801.4   8.9 321   1.5 303   7.5 324  c/cs                                1591
 26 02 1990 *0921   3  2.49 157  3.75  1802.0   8.8 320   1.4 299   7.5 324  GF    0.00 0.00    0    0.1    0.1 1592
 26 02 1990 *0926   3  3.05 157  3.28  1802.7   7.7 320   0.6 252   7.5 324  GF    0.00 0.00    0    0.1    0.1 1593
 26 02 1990 *0930   3  3.44 157  2.95  1803.2   9.6 320   2.2 305   7.5 324  GF    0.00 0.00    0    0.0    0.1 1594
 26 02 1990 *0936   3  4.17 157  2.33  1804.2   8.9 321   1.5 307   7.5 324  GF    0.00 0.00    0    0.2    0.1 1595
 26 02 1990 *0941   3  4.75 157  1.86  1804.9   8.8 319   1.5 296   7.5 324  GF    0.00 0.00    0    0.1    0.1 1596
 26 02 1990 *0946   3  5.31 157  1.38  1805.7   8.8 319   1.5 296   7.5 324  GF    0.00 0.00    0    0.1    0.1 1597
 26 02 1990  0947   3  5.4  157  1.3   1805.8   8.8 320   1.5 296   7.4 325  c/cs                                1598
 26 02 1990 *0951   3  5.87 157  0.91  1806.4   8.2 319   1.1 278   7.4 325  GF    0.00 0.00    0    0.1    0.1 1599
 26 02 1990 *1000   3  6.80 157  0.11  1807.6   9.4 319   2.2 300   7.4 325  GF    0.00 0.00    0    0.2    0.2 1600
 26 02 1990 *1011   3  8.11 156 58.98  1809.3   8.8 320   1.5 296   7.4 325  GF    0.00 0.00    0    0.4    0.2 1601
 26 02 1990 *1016   3  8.67 156 58.51  1810.1   9.1 319   1.9 297   7.4 325  GF    0.00 0.00    0    0.1    0.1 1602
 26 02 1990  1016   3  8.7  156 58.5   1810.1   9.0 319   1.9 297   7.3 325  c/cs                                1603
 26 02 1990 *1021   3  9.24 156 58.02  1810.8   8.2 320   1.2 284   7.3 325  GF    0.00 0.00    0    0.2    0.1 1604
 26 02 1990 *1030   3 10.18 156 57.22  1812.1   9.7 319   2.5 300   7.3 325  GF    0.00 0.00    0    0.2    0.2 1605
 26 02 1990 *1041   3 11.51 156 56.05  1813.8   8.8 320   1.6 297   7.3 325  GF    0.00 0.00    0    0.5    0.2 1606
 26 02 1990  1041   3 11.5  156 56.1   1813.8   8.8 318   1.6 297   7.3 323  c/cs                                1607
 26 02 1990 *1046   3 12.06 156 55.56  1814.6   9.0 318   1.8 299   7.3 323  GF    0.00 0.00    0    0.1    0.1 1608
 26 02 1990 *1051   3 12.62 156 55.06  1815.3   8.9 318   1.7 295   7.3 323  GF    0.00 0.00    0    0.2    0.1 1609
 26 02 1990 *1056   3 13.17 156 54.56  1816.1   7.1 318   0.7 212   7.3 323  GF    0.00 0.00    0    0.1    0.1 1610
 26 02 1990 *1100   3 13.52 156 54.24  1816.5   9.7 319   2.5 306   7.3 323  GF    0.00 0.00    0    0.0    0.1 1611
 26 02 1990 *1111   3 14.86 156 53.06  1818.3   7.6 318   0.7 258   7.3 323  GF    0.00 0.00    0    0.5    0.2 1612
 26 02 1990  1111   3 14.9  156 53.1   1818.3   7.7 319   0.7 258   7.3 324  c/cs                                1613
 26 02 1990 *1117   3 15.44 156 52.56  1819.1   9.0 319   1.8 300   7.3 324  GF    0.00 0.00    0    0.1    0.1 1614
 26 02 1990 *1122   3 16.01 156 52.07  1819.8   8.9 319   1.7 298   7.3 324  GF    0.00 0.00    0    0.1    0.1 1615
 26 02 1990 *1130   3 16.91 156 51.29  1821.0   8.8 319   1.6 294   7.3 324  GF    0.00 0.00    0    0.2    0.1 1616
 26 02 1990 *1137   3 17.68 156 50.61  1822.0   8.9 319   1.7 297   7.3 324  GF    0.00 0.00    0    0.2    0.1 1617
 26 02 1990  1141   3 18.1  156 50.2   1822.6   8.9 318   1.7 297   7.3 323  c/cs                                1618
 26 02 1990 *1142   3 18.24 156 50.12  1822.8   9.0 319   1.7 304   7.3 323  GF    0.00 0.00    0    0.1    0.1 1619
 26 02 1990 *1147   3 18.81 156 49.63  1823.5   8.7 319   1.5 297   7.3 323  GF    0.00 0.00    0    0.1    0.1 1620
 26 02 1990  1159   3 20.1  156 48.5   1825.3   8.7 319   1.5 297   7.3 323  c/cs                                1621
 26 02 1990 *1200   3 20.23 156 48.38  1825.4   8.7 318   1.6 296   7.3 323  GF    0.00 0.00    0    0.3    0.2 1622
 26 02 1990 *1207   3 20.99 156 47.70  1826.5   8.9 319   1.8 305   7.3 323  GF    0.00 0.00    0    0.2    0.1 1623
 26 02 1990  1214   3 21.8  156 47.0   1827.5   8.5 319   1.8 305   6.8 322  c/cs                                1624
 26 02 1990  1218   3 22.2  156 46.6   1828.1   8.8 319   1.8 305   7.2 323  c/cs                                1625
 26 02 1990  1225   3 23.0  156 46.0   1829.1   8.8 320   1.8 305   7.2 324  c/cs                                1626
 26 02 1990 *1248   3 25.60 156 43.80  1832.5   8.7 319   1.6 299   7.2 324  SF    0.00 0.00    0    1.2    0.7 1627
 26 02 1990  1255   3 26.4  156 43.1   1833.5   8.5 319   1.6 299   7.0 324  c/cs                                1628
 26 02 1990  1314   3 28.4  156 41.4   1836.2   8.5 319   1.6 299   7.0 324  c/cs                                1629
 26 02 1990  1326   3 29.7  156 40.3   1837.9   8.0 336   1.6 299   6.7 344  c/cs                                1630
 26 02 1990  1344   3 31.9  156 39.3   1840.3   8.1 336   1.6 299   6.8 344  c/cs                                1631
 26 02 1990 *1407   3 34.72 156 37.98  1843.4   8.6 346   1.7 355   6.8 344  GF    0.00 0.00    0    2.2    1.3 1632
 26 02 1990  1412   3 35.4  156 37.8   1844.1   8.5 345   1.7 355   6.8 343  c/cs                                1633
 26 02 1990 *1417   3 36.10 156 37.63  1844.8   8.1 339   1.4 320   6.8 343  GF    0.00 0.00    0    0.3    0.2 1634
 26 02 1990 *1422   3 36.73 156 37.39  1845.5   7.6 338   1.0 303   6.8 343  GF    0.00 0.00    0    0.1    0.1 1635
 26 02 1990  1428   3 37.4  156 37.1   1846.3   7.5 339   1.0 303   6.8 344  c/cs                                1636
 26 02 1990 *1430   3 37.67 156 37.02  1846.5   8.5 339   1.9 320   6.8 344  GF    0.00 0.00    0    0.1    0.1 1637
 26 02 1990 *1437   3 38.60 156 36.66  1847.5   8.1 339   1.5 316   6.8 344  GF    0.00 0.00    0    0.2    0.1 1638
 26 02 1990 *1442   3 39.23 156 36.42  1848.2   7.7 340   1.1 314   6.8 344  GF    0.00 0.00    0    0.1    0.1 1639
 26 02 1990  1446   3 39.7  156 36.2   1848.7   6.9 359   1.1 314   6.2   6  c/cs                                1640
 26 02 1990 *1447   3 39.83 156 36.24  1848.8   6.5   9   0.5  55   6.2   6  GF    0.00 0.00    0    0.1    0.1 1641
 26 02 1990  1447   3 39.8  156 36.2   1848.8   5.7  49   0.5  55   5.3  48  c/cs                                1642
 26 02 1990  1449   3 40.0  156 36.4   1849.0   6.2  62   0.5  55   5.7  63  c/cs                                1643
```

```
                                                     date run: Wed Jul 18 16:38:07 1990          page  32
#cruise ODP130JR
#
#                    latitude  longitude                actual     drift       dr             prob. error          drift
#da mo  yr    time  deg   min  deg   min    dist  speed cse  speed hed  speed cse  cmnt (smajxsmin@az)   dist   time   no.
#- - - - - - - - - - - - - - - - - - - - - - - - - - - - - - - - - - - - - - - - - - - - - - - - - - - - - - - - - - - -
 26 02 1990 *1452    3 40.10 156 36.66 1849.3   6.1  61   0.4  33   5.7  63  GF   0.00 0.00    0   0.0     0.1 1644
 26 02 1990  1454    3 40.2  156 36.8  1849.5   7.6  62   0.4  33   7.2  64  c/cs                                1645
 26 02 1990 *1500    3 40.55 156 37.51 1850.3   8.3  66   1.1  77   7.2  64  GF   0.00 0.00    0   0.1     0.1 1646
 26 02 1990  1502    3 40.7  156 37.8  1850.6   8.3  74   1.1  77   7.1  74  c/cs                                1647
 26 02 1990 *1507    3 40.85 156 38.43 1851.3   7.7  74   0.6  71   7.1  74  GF   0.00 0.00    0   0.1     0.1 1648
 26 02 1990 *1512    3 41.03 156 39.05 1851.9   7.6  74   0.4  81   7.1  74  GF   0.00 0.00    0   0.0     0.1 1649
 26 02 1990 *1517    3 41.20 156 39.66 1852.5   7.7  74   0.6  71   7.1  74  GF   0.00 0.00    0   0.0     0.1 1650
 26 02 1990 *1522    3 41.38 156 40.28 1853.2   6.7  79   0.8 201   7.1  74  GF   0.00 0.00    0   0.0     0.1 1651
 26 02 1990  1523    3 41.4  156 40.4  1853.3   6.6 112   0.8 201   6.6 105  c/cs                                1652
 26 02 1990  1524    3 41.4  156 40.5  1853.4   6.3 150   0.8 201   5.9 144  c/cs                                1653
 26 02 1990  1525    3 41.3  156 40.5  1853.5   8.5 212   0.8 201   7.7 213  c/cs                                1654
 26 02 1990 *1530    3 40.67 156 40.17 1854.2   9.4 217   1.8 234   7.7 213  GF   0.00 0.00    0   0.1     0.1 1655
 26 02 1990  1534    3 40.2  156 39.8  1854.8   9.0 217   1.8 234   7.3 213  c/cs                                1656
 26 02 1990 *1537    3 39.81 156 39.52 1855.3   7.8 215   0.5 244   7.3 213  GF   0.00 0.00    0   0.2     0.1 1657
 26 02 1990 *1542    3 39.28 156 39.15 1855.9   7.8 214   0.5 224   7.3 213  GF   0.00 0.00    0   0.0     0.1 1658
 26 02 1990 *1547    3 38.74 156 38.79 1856.6   7.7 210   0.6 164   7.3 213  GF   0.00 0.00    0   0.0     0.1 1659
 26 02 1990 *1552    3 38.18 156 38.47 1857.2   7.9 212   0.6 200   7.3 213  GF   0.00 0.00    0   0.0     0.1 1660
 26 02 1990 *1557    3 37.62 156 38.12 1857.9   6.0 217   1.4  17   7.3 213  GF   0.00 0.00    0   0.1     0.1 1661
 26 02 1990 *1600    3 37.38 156 37.94 1858.2   8.4 210   1.2 188   7.3 213  GF   0.00 0.00    0   0.1     0.1 1662
 26 02 1990  1605    3 36.8  156 37.6  1858.9   7.3 196   1.2 188   6.2 198  c/cs                                1663
 26 02 1990 *1608    3 36.42 156 37.49 1859.2   6.2 198   0.0  23   6.2 198   807 0.00 0.00    0   0.2     0.1 1664
 26 02 1990  1611    3 36.1  156 37.4  1859.6   6.4 203   0.0  23   6.4 203  c/cs                                1665
 26 02 1990  1630    3 34.3  156 36.6  1861.6   0.0  23   0.0  23   0.0 205  c/cs                                1666
 23 03 1990 *0000    3 36.39 156 37.49 1863.9   4.0  16   4.0  16   0.0 205   807 0.00 0.00    0   2.3   583.9 1667
 23 03 1990 *0005    3 36.71 156 37.58 1864.2   2.2 300   2.2 300   0.0 205  GF   0.00 0.00    0   0.3     0.1 1668
 23 03 1990 *0010    3 36.80 156 37.42 1864.4   2.9 303   2.9 303   0.0 205  GF   0.00 0.00    0   0.2     0.1 1669
 23 03 1990 *0015    3 36.93 156 37.22 1864.6   3.1 298   3.1 298   0.0 205  GF   0.00 0.00    0   0.2     0.1 1670
 23 03 1990 *0020    3 37.05 156 36.99 1864.9   0.9  33   0.9  33   0.0 205  GF   0.00 0.00    0   0.3     0.1 1671
 23 03 1990  0020    3 37.1  156 37.0  1864.9   3.4 299   0.9  33   3.6 285  c/cs                                1672
 23 03 1990 *0025    3 37.19 156 36.74 1865.2   4.9 293   1.5 313   3.6 285  GF   0.00 0.00    0   0.1     0.1 1673
 23 03 1990 *0030    3 37.35 156 36.36 1865.6   3.3 291   0.5  56   3.6 285  GF   0.00 0.00    0   0.1     0.1 1674
 23 03 1990  0030    3 37.3  156 36.4  1865.6   6.6 292   0.5  56   6.9 289  c/cs                                1675
 23 03 1990 *0035    3 37.56 156 35.85 1866.1   8.2 291   1.3 299   6.9 289  GF   0.00 0.00    0   0.0     0.1 1676
 23 03 1990 *0040    3 37.80 156 35.21 1866.8   8.3 293   1.5 311   6.9 289  GF   0.00 0.00    0   0.1     0.1 1677
 23 03 1990 *0045    3 38.07 156 34.57 1867.5   8.3 291   1.5 301   6.9 289  GF   0.00 0.00    0   0.1     0.1 1678
 23 03 1990 *0050    3 38.32 156 33.92 1868.2   8.3 292   1.5 307   6.9 289  GF   0.00 0.00    0   0.1     0.1 1679
 23 03 1990 *0055    3 38.58 156 33.28 1868.9   8.3 293   1.5 311   6.9 289  GF   0.00 0.00    0   0.1     0.1 1680
 23 03 1990 *0100    3 38.85 156 32.64 1869.6   7.4 291   0.6 321   6.9 289  GF   0.00 0.00    0   0.1     0.1 1681
 23 03 1990  0100    3 38.9  156 32.6  1869.6   8.6 292   0.6 321   8.1 290  c/cs                                1682
 23 03 1990 *0105    3 39.12 156 31.97 1870.3   9.0 291   0.9 302   8.1 290  GF   0.00 0.00    0   0.0     0.1 1683
 23 03 1990 *0110    3 39.39 156 31.27 1871.0   8.9 290   0.8 295   8.1 290  GF   0.00 0.00    0   0.1     0.1 1684
 23 03 1990 *0115    3 39.65 156 30.57 1871.8   8.8 291   0.7 299   8.1 290  GF   0.00 0.00    0   0.1     0.1 1685
 23 03 1990 *0120    3 39.91 156 29.88 1872.5   9.0 290   0.8 294   8.1 290  GF   0.00 0.00    0   0.1     0.1 1686
 23 03 1990 *0125    3 40.17 156 29.18 1873.3   8.9 289   0.7 277   8.1 290  GF   0.00 0.00    0   0.1     0.1 1687
 23 03 1990 *0130    3 40.41 156 28.48 1874.0   8.9 290   0.8 295   8.1 290  GF   0.00 0.00    0   0.1     0.1 1688
 23 03 1990 *0135    3 40.67 156 27.78 1874.8   8.9 290   0.8 287   8.1 290  GF   0.00 0.00    0   0.1     0.1 1689
 23 03 1990 *0140    3 40.92 156 27.08 1875.5   7.7 286   0.7 161   8.1 290  GF   0.00 0.00    0   0.1     0.1 1690
 23 03 1990  0140    3 40.9  156 27.1  1875.5   9.3 299   0.7 161   9.9 302  c/cs                                1691
 23 03 1990 *0145    3 41.30 156 26.40 1876.3   9.8 303   0.1  74   9.9 302  GF   0.00 0.00    0   0.1     0.1 1692
 23 03 1990 *0150    3 41.74 156 25.71 1877.1   9.9 313   1.8  36   9.9 302  GF   0.00 0.00    0   0.0     0.1 1693
 23 03 1990 *0155    3 42.30 156 25.10 1877.9   9.8 304   0.3  57   9.9 302  GF   0.00 0.00    0   0.2     0.1 1694
 23 03 1990 *0200    3 42.75 156 24.42 1878.7  10.2 303   0.4 344   9.9 302  GF   0.00 0.00    0   0.0     0.1 1695
 23 03 1990  0229    3 45.5  156 20.3  1883.6   8.6 296   0.4 344   8.3 294  c/cs                                1696
```

```
#cruise ODP130JR                                 date run: Wed Jul 18 16:38:07 1990          page  33
#
#                     latitude  longitude              actual   drift        dr                 prob. error       drift
#da mo  yr    time deg   min  deg   min      dist speed cse speed hed speed cse   cmnt (smajxsmin@az)  dist  time   no.
#- - - - - - - - - - - - - - - - - - - - - - - - - - - - - - - - - - - - - - - - - - - - - - - - - - - - - - - - - - - -
 23 03 1990   0232    3 45.6   156 19.9   1884.1   8.4 292   0.4 344   8.1 290   c/cs                                   1697
 23 03 1990   0249    3 46.5   156 17.7   1886.4   8.6 291   0.4 344   8.4 289   c/cs                                   1698
 23 03 1990   0304    3 47.3   156 15.7   1888.6   8.4 288   0.4 344   8.2 286   c/cs                                   1699
 23 03 1990  *0310    3 47.56  156 14.91  1889.4   9.2 287   1.0 291   8.2 286   GF     0.00 0.00    0    0.4    1.2  1700
 23 03 1990  *0315    3 47.78  156 14.17  1890.2   9.4 288   1.2 300   8.2 286   GF     0.00 0.00    0    0.1    0.1  1701
 23 03 1990   0317    3 47.9   156 13.9   1890.5   9.5 288   1.2 300   8.3 286   c/cs                                   1702
 23 03 1990  *0320    3 48.02  156 13.42  1891.0   7.9 288   0.5  76   8.3 286   GF     0.00 0.00    0    0.1    0.1  1703
 23 03 1990  *0325    3 48.22  156 12.79  1891.7   9.3 288   1.0 304   8.3 286   GF     0.00 0.00    0    0.0    0.1  1704
 23 03 1990  *0330    3 48.46  156 12.05  1892.4   9.5 288   1.2 306   6.3 286   GF     0.00 0.00    0    0.1    0.1  1705
 23 03 1990  *0335    3 48.71  156 11.30  1893.2   8.8 290   0.8 337   8.3 286   GF     0.00 0.00    0    0.1    0.1  1706
 23 03 1990  *0341    3 49.01  156 10.47  1894.1   9.8 289   1.6 304   8.3 286   GF     0.00 0.00    0    0.1    0.1  1707
 23 03 1990  *0345    3 49.22  156  9.85  1894.8   9.4 289   1.2 314   8.3 286   GF     0.00 0.00    0    0.1    0.1  1708
 23 03 1990   0347    3 49.3   156  9.6   1895.1   9.4 289   1.2 314   8.3 286   c/cs                                   1709
 23 03 1990  *0350    3 49.48  156  9.11  1895.5   9.4 289   1.1 309   8.3 286   GF     0.00 0.00    0    0.1    0.1  1710
 23 03 1990  *0355    3 49.73  156  8.37  1896.3   9.1 288   0.9 313   8.3 286   GF     0.00 0.00    0    0.1    0.1  1711
 23 03 1990  *0400    3 49.97  156  7.65  1897.1   9.3 288   1.0 304   8.3 286   GF     0.00 0.00    0    0.1    0.1  1712
 23 03 1990  *0405    3 50.21  156  6.91  1897.8   9.1 289   1.0 318   8.3 286   GF     0.00 0.00    0    0.1    0.1  1713
 23 03 1990  *0410    3 50.46  156  6.19  1898.6   9.1 289   0.9 319   8.3 286   GF     0.00 0.00    0    0.1    0.1  1714
 23 03 1990  *0415    3 50.71  156  5.47  1899.4   9.0 289   0.8 317   8.3 286   GF     0.00 0.00    0    0.1    0.1  1715
 23 03 1990   0417    3 50.8   156  5.2   1899.7   9.0 289   0.8 317   8.3 286   c/cs                                   1716
 23 03 1990  *0420    3 50.95  156  4.76  1900.1   9.1 288   0.9 312   8.3 286   GF     0.00 0.00    0    0.1    0.1  1717
 23 03 1990  *0425    3 51.19  156  4.04  1900.9   9.1 290   1.0 326   8.3 286   GF     0.00 0.00    0    0.1    0.1  1718
 23 03 1990  *0430    3 51.45  156  3.33  1901.6   9.1 289   1.0 317   8.3 286   GF     0.00 0.00    0    0.1    0.1  1719
 23 03 1990  *0435    3 51.70  156  2.61  1902.4   9.1 289   1.0 316   8.3 286   GF     0.00 0.00    0    0.1    0.1  1720
 23 03 1990  *0440    3 51.95  156  1.89  1903.2   9.3 290   1.2 317   8.3 286   GF     0.00 0.00    0    0.1    0.1  1721
 23 03 1990  *0445    3 52.21  156  1.16  1903.9   9.1 288   0.9 311   8.3 286   GF     0.00 0.00    0    0.1    0.1  1722
 23 03 1990   0447    3 52.3   156  0.9   1904.2   9.0 289   0.9 311   8.2 286   c/cs                                   1723
 23 03 1990  *0450    3 52.45  156  0.44  1904.7   9.3 290   1.2 315   8.2 286   GF     0.00 0.00    0    0.1    0.1  1724
 23 03 1990   0458    3 52.9   155 59.3   1905.9   7.2 291   1.2 315   6.1 286   c/cs                                   1725
 23 03 1990   0459    3 52.9   155 59.2   1906.0   9.4 289   1.2 315   8.3 285   c/cs                                   1726
 23 03 1990  *0500    3 52.96  155 59.01  1906.2   9.0 289   1.0 330   8.3 285   GF     0.00 0.00    0    0.2    0.2  1727
 23 03 1990  *0505    3 53.21  155 58.30  1906.9   9.1 289   1.0 325   8.3 285   GF     0.00 0.00    0    0.1    0.1  1728
 23 03 1990  *0510    3 53.46  155 57.58  1907.7   9.2 290   1.1 328   8.3 285   GF     0.00 0.00    0    0.1    0.1  1729
 23 03 1990  *0515    3 53.72  155 56.86  1908.5   9.4 290   1.4 322   8.3 285   GF     0.00 0.00    0    0.1    0.1  1730
 23 03 1990   0517    3 53.8   155 56.6   1908.8   7.6 292   1.4 322   6.4 286   c/cs                                   1731
 23 03 1990  *0520    3 53.97  155 56.21  1909.2   7.2 292   1.0 329   6.4 286   GF     0.00 0.00    0    0.1    0.1  1732
 23 03 1990  *0525    3 54.19  155 55.65  1909.8   6.7 291   0.6 357   6.4 286   GF     0.00 0.00    0    0.1    0.1  1733
 23 03 1990   0529    3 54.4   155 55.2   1910.2   6.7 290   0.6 357   6.5 285   c/cs                                   1734
 23 03 1990  *0530    3 54.39  155 55.13  1910.3   8.0 291   1.7 315   6.5 285   GF     0.00 0.00    0    0.1    0.1  1735
 23 03 1990  *0535    3 54.63  155 54.51  1911.0   7.3 293   1.3 339   6.5 285   GF     0.00 0.00    0    0.1    0.1  1736
 23 03 1990  *0540    3 54.87  155 53.95  1911.6   7.6 291   1.4 322   6.5 285   GF     0.00 0.00    0    0.1    0.1  1737
 23 03 1990   0540    3 54.9   155 54.0   1911.6   8.9 290   1.4 322   7.8 285   c/cs                                   1738
 23 03 1990  *0545    3 55.13  155 53.25  1912.3   8.9 292   1.4 330   7.8 285   GF     0.00 0.00    0    0.1    0.1  1739
 23 03 1990   0545    3 55.1   155 53.2   1912.3   9.3 290   1.4 330   8.3 284   c/cs                                   1740
 23 03 1990  *0550    3 55.40  155 52.52  1913.1   9.2 289   1.3 328   8.3 284   GF     0.00 0.00    0    0.1    0.1  1741
 23 03 1990  *0600    3 55.91  155 51.07  1914.7   9.3 288   1.2 316   8.3 284   GF     0.00 0.00    0    0.2    0.2  1742
 23 03 1990  *0605    3 56.15  155 50.33  1915.4   9.2 288   1.2 322   8.3 284   GF     0.00 0.00    0    0.1    0.1  1743
 23 03 1990   0609    3 56.3   155 49.7   1916.0   9.2 287   1.2 322   8.3 283   c/cs                                   1744
 23 03 1990  *0610    3 56.39  155 49.60  1916.2   9.2 288   1.2 328   8.3 283   GF     0.00 0.00    0    0.1    0.1  1745
 23 03 1990  *0615    3 56.63  155 48.87  1917.0   9.1 288   1.1 329   8.3 283   GF     0.00 0.00    0    0.1    0.1  1746
 23 03 1990   0624    3 57.1   155 47.6   1918.3   8.7 289   1.1 329   7.9 284   c/cs                                   1747
 23 03 1990  *0625    3 57.10  155 47.43  1918.5   9.1 288   1.4 315   7.9 284   GF     0.00 0.00    0    0.2    0.2  1748
 23 03 1990  *0630    3 57.34  155 46.71  1919.2   8.9 288   1.2 317   7.9 284   GF     0.00 0.00    0    0.1    0.1  1749
```

```
#cruise ODP130JR                                        date run: Wed Jul 18 16:38:07 1990          page  34
#
#                        latitude  longitude              actual    drift        dr              prob. error       drift
#da mo  yr     time deg   min  deg   min      dist    speed cse speed hed  speed cse  cmnt (smajxsmin@az)   dist  time   no.
#- - - - - - - - - - - - - - - - - - - - - - - - - - - - - - - - - - - - - - - - - - - - - - - - - - - - - - - - - - - - - -
23 03 1990  0634   3 57.5  155 46.1   1919.8   9.0 287   1.2 317   8.1 283  c/cs                              1750
23 03 1990 *0635   3 57.57 155 46.00  1920.0   9.1 288   1.3 323   8.1 283  GF    0.00 0.00   0    0.1    0.1 1751
23 03 1990  0639   3 57.8  155 45.4   1920.6   9.1 289   1.3 323   8.0 284  c/cs                              1752
23 03 1990 *0640   3 57.81 155 45.28  1920.7   8.8 288   1.0 324   8.0 284  GF    0.00 0.00   0    0.1    0.1 1753
23 03 1990 *0645   3 58.04 155 44.56  1921.5   8.8 291   1.3 338   8.0 284  GF    0.00 0.00   0    0.1    0.1 1754
23 03 1990 *0650   3 58.30 155 43.89  1922.2   8.6 289   0.9 334   8.0 284  GF    0.00 0.00   0    0.1    0.1 1755
23 03 1990  0650   3 58.3  155 43.9   1922.2   8.9 289   0.9 334   8.3 285  c/cs                              1756
23 03 1990  0654   3 58.5  155 43.3   1922.8   8.9 290   0.9 334   8.2 286  c/cs                              1757
23 03 1990 *0655   3 58.55 155 43.19  1922.9   8.9 289   0.8 322   8.2 286  GF    0.00 0.00   0    0.1    0.1 1758
23 03 1990 *0700   3 58.79 155 42.49  1923.7   8.9 290   0.9 327   8.2 286  GF    0.00 0.00   0    0.1    0.1 1759
23 03 1990 *0705   3 59.04 155 41.79  1924.4   8.9 289   0.8 321   8.2 286  GF    0.00 0.00   0    0.1    0.1 1760
23 03 1990 *0710   3 59.28 155 41.09  1925.2   8.9 289   0.8 323   8.2 286  GF    0.00 0.00   0    0.1    0.1 1761
23 03 1990 *0715   3 59.52 155 40.39  1925.9   9.1 288   0.9 304   8.2 286  GF    0.00 0.00   0    0.1    0.1 1762
23 03 1990 *0720   3 59.75 155 39.67  1926.7   9.0 288   0.8 313   8.2 286  GF    0.00 0.00   0    0.1    0.1 1763
23 03 1990 *0730   4  0.22 155 38.25  1928.1   8.8 287   0.6 309   8.2 286  GF    0.00 0.00   0    0.1    0.2 1764
23 03 1990 *0735   4  0.44 155 37.55  1928.9   9.2 288   1.0 306   8.2 286  GF    0.00 0.00   0    0.0    0.1 1765
23 03 1990  0736   4  0.5  155 37.4   1929.0   8.7 287   1.0 306   7.8 285  c/cs                              1766
23 03 1990 *0740   4  0.66 155 36.85  1929.6   8.7 286   0.9 298   7.8 285  GF    0.00 0.00   0    0.1    0.1 1767
23 03 1990  0740   4  0.7  155 36.8   1929.6   9.0 286   0.9 298   8.1 285  c/cs                              1768
23 03 1990 *0745   4  0.87 155 36.13  1930.4   9.0 287   1.0 304   8.1 285  GF    0.00 0.00   0    0.1    0.1 1769
23 03 1990 *0750   4  1.09 155 35.41  1931.1   9.1 288   1.1 311   8.1 285  GF    0.00 0.00   0    0.1    0.1 1770
23 03 1990  0753   4  1.2  155 35.0   1931.6   8.6 288   1.1 311   7.6 285  c/cs                              1771
23 03 1990  0757   4  1.4  155 34.4   1932.1   9.3 289   1.1 311   8.3 286  c/cs                              1772
23 03 1990 *0800   4  1.56 155 33.99  1932.6   9.1 289   1.0 318   8.3 286  GF    0.00 0.00   0    0.2    0.2 1773
23 03 1990 *0805   4  1.81 155 33.27  1933.4   8.9 289   0.7 324   8.3 286  GF    0.00 0.00   0    0.1    0.1 1774
23 03 1990 *0810   4  2.05 155 32.57  1934.1   8.9 290   0.9 334   8.3 286  GF    0.00 0.00   0    0.1    0.1 1775
23 03 1990 *0815   4  2.31 155 31.87  1934.8   9.0 289   0.9 323   8.3 286  GF    0.00 0.00   0    0.1    0.1 1776
23 03 1990 *0820   4  2.56 155 31.16  1935.6   8.0 289   0.5  49   8.3 286  GF    0.00 0.00   0    0.1    0.1 1777
23 03 1990 *0825   4  2.78 155 30.53  1936.3   9.8 289   1.6 306   8.3 286  GF    0.00 0.00   0    0.0    0.1 1778
23 03 1990  0827   4  2.9  155 30.2   1936.6   9.9 289   1.6 306   8.4 286  c/cs                              1779
23 03 1990 *0830   4  3.05 155 29.75  1937.1   9.0 289   0.8 328   8.4 286  GF    0.00 0.00   0    0.1    0.1 1780
23 03 1990 *0835   4  3.30 155 29.04  1937.8   9.1 290   0.9 332   8.4 286  GF    0.00 0.00   0    0.1    0.1 1781
23 03 1990 *0840   4  3.56 155 28.33  1938.6   9.0 289   0.8 328   8.4 286  GF    0.00 0.00   0    0.1    0.1 1782
23 03 1990 *0845   4  3.81 155 27.62  1939.3   9.2 290   1.0 326   8.4 286  GF    0.00 0.00   0    0.1    0.1 1783
23 03 1990 *0850   4  4.07 155 26.90  1940.1   9.2 289   1.0 319   8.4 286  GF    0.00 0.00   0    0.1    0.1 1784
23 03 1990  0857   4  4.4  155 25.9   1941.2   9.0 291   1.0 319   8.1 288  c/cs                              1785
23 03 1990 *0900   4  4.59 155 25.46  1941.6   9.0 291   1.0 318   8.1 288  GF    0.00 0.00   0    0.2    0.2 1786
23 03 1990 *0905   4  4.86 155 24.76  1942.4   9.0 292   1.1 324   8.1 288  GF    0.00 0.00   0    0.1    0.1 1787
23 03 1990  0905   4  4.9  155 24.8   1942.4   9.2 293   1.1 324   8.3 289  c/cs                              1788
23 03 1990 *0910   4  5.16 155 24.05  1943.2   9.2 294   1.1 333   8.3 289  GF    0.00 0.00   0    0.1    0.1 1789
23 03 1990 *0915   4  5.47 155 23.35  1943.9   9.2 293   1.1 325   8.3 289  GF    0.00 0.00   0    0.1    0.1 1790
23 03 1990 *0920   4  5.77 155 22.64  1944.7   9.3 294   1.2 328   8.3 289  GF    0.00 0.00   0    0.1    0.1 1791
23 03 1990 *0930   4  6.39 155 21.22  1946.2   9.4 294   1.3 324   8.3 289  GF    0.00 0.00   0    0.2    0.2 1792
23 03 1990  0934   4  6.6  155 20.6   1946.9   8.1 295   1.3 324   7.0 290  c/cs                              1793
23 03 1990 *0935   4  6.70 155 20.52  1947.0   8.5 295   1.7 318   7.0 290  GF    0.00 0.00   0    0.1    0.1 1794
23 03 1990  0937   4  6.8  155 20.3   1947.3   9.9 294   1.7 313   8.4 289  c/cs                              1795
23 03 1990 *0940   4  7.02 155 19.81  1947.8   9.1 294   1.1 341   8.4 289  GF    0.00 0.00   0    0.1    0.1 1796
23 03 1990 *0945   4  7.33 155 19.12  1948.5   9.0 294   0.9 338   8.4 289  GF    0.00 0.00   0    0.1    0.1 1797
23 03 1990 *0950   4  7.63 155 18.43  1949.3   9.0 293   1.0 336   8.4 289  GF    0.00 0.00   0    0.1    0.1 1798
23 03 1990  0955   4  7.9  155 17.7   1950.0   8.7 294   1.0 336   8.0 289  c/cs                              1799
23 03 1990 *1000   4  8.22 155 17.07  1950.8   8.6 293   0.8 337   8.0 289  GF    0.00 0.00   0    0.2    0.2 1800
23 03 1990 *1005   4  8.50 155 16.41  1951.5   8.7 292   0.8 320   8.0 289  GF    0.00 0.00   0    0.1    0.1 1801
23 03 1990  1007   4  8.6  155 16.1   1951.8   8.5 291   0.8 320   7.8 288  c/cs                              1802
```

```
#
#                    latitude  longitude              actual    drift       dr               prob. error       drift
#da mo  yr    time deg   min  deg   min     dist speed cse speed hed speed cse  cmnt (smajxsmin@az)  dist  time   no.
#- - - - - - - - - - - - - - - - - - - - - - - - - - - - - - - - - - - - - - - - - - - - - - - - - - - - - - - - - -
 23 03 1990 *1010    4  8.76 155 15.74 1952.2   8.6 291   0.9 321   7.8 288  GF    0.00 0.00    0   0.1   0.1 1803
 23 03 1990 *1015    4  9.02 155 15.07 1952.9   8.2 293   0.8 354   7.8 288  GF    0.00 0.00    0   0.1   0.1 1804
 23 03 1990  1015    4  9.0  155 15.1  1952.9   8.7 293   0.8 354   8.3 288  c/cs                             1805
 23 03 1990 *1020    4  9.30 155 14.40 1953.6   9.2 292   1.0 325   8.3 288  GF    0.00 0.00    0   0.1   0.1 1806
 23 03 1990  1041    4 10.5  155 11.4  1956.8   9.1 292   1.0 325   8.2 288  c/cs                             1807
 23 03 1990  1047    4 10.8  155 10.6  1957.7   9.3 292   1.0 325   8.5 288  c/cs                             1808
 23 03 1990  1052    4 11.1  155  9.9  1958.5   8.7 292   1.0 325   7.9 288  c/cs                             1809
 23 03 1990  1055    4 11.3  155  9.4  1959.0   9.3 292   1.0 325   8.5 288  c/cs                             1810
 23 03 1990 *1105    4 11.87 155  8.00 1960.5   9.2 291   0.8 318   8.5 288  GF    0.00 0.00    0   0.8   0.8 1811
 23 03 1990 *1110    4 12.14 155  7.28 1961.3   9.0 292   0.8 337   8.5 288  GF    0.00 0.00    0   0.1   0.1 1812
 23 03 1990 *1115    4 12.42 155  6.58 1962.0   9.0 291   0.7 333   8.5 288  GF    0.00 0.00    0   0.1   0.1 1813
 23 03 1990  1119    4 12.6  155  6.0  1962.6   8.9 291   0.7 333   8.4 288  c/cs                             1814
 23 03 1990 *1120    4 12.69 155  5.88 1962.8   9.0 291   0.7 329   8.4 288  GF    0.00 0.00    0   0.1   0.1 1815
 23 03 1990 *1130    4 13.23 155  4.48 1964.3   9.0 291   0.7 330   8.4 288  GF    0.00 0.00    0   0.1   0.2 1816
 23 03 1990 *1135    4 13.50 155  3.78 1965.0   8.8 291   0.6 333   8.4 288  GF    0.00 0.00    0   0.1   0.1 1817
 23 03 1990  1137    4 13.6  155  3.5  1965.3   8.8 291   0.6 333   8.4 288  c/cs                             1818
 23 03 1990 *1140    4 13.76 155  3.09 1965.8   8.9 290   0.5 318   8.4 289  GF    0.00 0.00    0   0.0   0.1 1819
 23 03 1990 *1145    4 14.01 155  2.39 1966.5   8.7 291   0.5 346   8.4 288  GF    0.00 0.00    0   0.0   0.1 1820
 23 03 1990 *1150    4 14.27 155  1.71 1967.2   8.1 290   0.4  65   8.4 288  GF    0.00 0.00    0   0.0   0.1 1821
 23 03 1990  1155    4 14.5  155  1.1  1967.9   7.6 290   0.4  65   7.9 288  c/cs                             1822
 23 03 1990  1159    4 14.7  155  0.6  1968.4   7.9 299   0.4  65   8.2 297  c/cs                             1823
 23 03 1990 *1200    4 14.74 155  0.48 1968.5   8.7 303   1.1   2   8.2 297  GF    0.00 0.00    0   0.1   0.2 1824
 23 03 1990  1200    4 14.7  155  0.5  1968.5   8.9 331   1.1   2   8.0 327  c/cs                             1825
 23 03 1990  1204    4 15.3  155  0.2  1969.1   9.1 335   1.1   2   8.2 332  c/cs                             1826
 23 03 1990  1234    4 19.4  154 58.3  1973.7   9.0 335   1.1   2   8.1 332  c/cs                             1827
 23 03 1990 *1235    4 19.53 154 58.22 1973.8   9.2 339   1.5  17   8.1 332  GF    0.00 0.00    0   0.6   0.6 1828
 23 03 1990 *1240    4 20.24 154 57.94 1974.6   9.0 340   1.5  27   8.1 332  GF    0.00 0.00    0   0.1   0.1 1829
 23 03 1990 *1245    4 20.94 154 57.68 1975.4   9.0 335   1.1   2   8.1 332  GF    0.00 0.00    0   0.1   0.1 1830
 23 03 1990  1248    4 21.3  154 57.5  1975.8   8.6 335   1.1   2   7.7 331  c/cs                             1831
 23 03 1990 *1250    4 21.61 154 57.37 1976.1   8.6 337   1.2  14   7.7 331  GF    0.00 0.00    0   0.1   0.1 1832
 23 03 1990  1253    4 22.0  154 57.2  1976.5   9.0 335   1.2  14   8.1 330  c/cs                             1833
 23 03 1990 *1305    4 23.64 154 56.45 1978.3   9.2 332   1.2 342   8.1 330  GF    0.00 0.00    0   0.3   0.2 1834
 23 03 1990  1306    4 23.8  154 56.4  1978.5   9.9 331   1.2 342   8.7 329  c/cs                             1835
 23 03 1990 *1310    4 24.35 154 56.05 1979.1   9.8 331   1.1 344   8.7 329  GF    0.00 0.00    0   0.1   0.1 1836
 23 03 1990 *1315    4 25.06 154 55.65 1979.9   9.7 331   1.1 351   8.7 329  GF    0.00 0.00    0   0.1   0.1 1837
 23 03 1990 *1320    4 25.77 154 55.26 1980.8   9.8 331   1.1 344   8.7 329  GF    0.00 0.00    0   0.1   0.1 1838
 23 03 1990 *1330    4 27.19 154 54.46 1982.4   9.7 330   1.0 342   8.7 329  GF    0.00 0.00    0   0.2   0.2 1839
 23 03 1990  1334    4 27.8  154 54.1  1983.0   9.6 330   1.0 342   8.6 329  c/cs                             1840
 23 03 1990 *1335    4 27.89 154 54.06 1983.2   9.3 331   0.8 353   8.6 329  GF    0.00 0.00    0   0.1   0.1 1841
 23 03 1990 *1340    4 28.57 154 53.68 1984.0   9.6 331   1.0 348   8.6 329  GF    0.00 0.00    0   0.1   0.1 1842
 23 03 1990 *1345    4 29.27 154 53.29 1984.8   9.9 331   1.3 342   8.6 329  GF    0.00 0.00    0   0.1   0.1 1843
 23 03 1990  1348    4 29.7  154 53.0  1985.3   9.5 331   1.3 342   8.2 329  c/cs                             1844
 23 03 1990 *1350    4 29.98 154 52.89 1985.6   9.3 332   1.1 351   8.2 329  GF    0.00 0.00    0   0.1   0.1 1845
 23 03 1990  1351    4 30.1  154 52.8  1985.7   9.8 331   1.1 351   8.8 328  c/cs                             1846
 23 03 1990 *1400    4 31.40 154 52.09 1987.2   9.6 331   1.0 359   8.8 328  GF    0.00 0.00    0   0.2   0.2 1847
 23 03 1990 *1405    4 32.10 154 51.70 1988.0   9.5 330   0.8 349   8.8 328  GF    0.00 0.00    0   0.1   0.1 1848
 23 03 1990 *1410    4 32.78 154 51.30 1988.8   9.5 330   0.9 356   8.8 328  GF    0.00 0.00    0   0.1   0.1 1849
 23 03 1990  1414    4 33.3  154 51.0  1989.4   9.3 331   0.9 356   8.6 329  c/cs                             1850
 23 03 1990 *1415    4 33.47 154 50.91 1989.6   9.5 330   0.9 335   8.6 329  GF    0.00 0.00    0   0.1   0.1 1851
 23 03 1990 *1420    4 34.15 154 50.51 1990.4   9.6 330   1.0 340   8.6 329  GF    0.00 0.00    0   0.1   0.1 1852
 23 03 1990  1424    4 34.7  154 50.2  1991.0   9.6 330   1.0 340   8.6 329  c/cs                             1853
 23 03 1990 *1430    4 35.54 154 49.71 1992.0   9.4 329   0.7 332   8.6 329  GF    0.00 0.00    0   0.2   0.2 1854
 23 03 1990 *1435    4 36.21 154 49.31 1992.8   9.4 330   0.8 344   8.6 329  GF    0.00 0.00    0   0.1   0.1 1855
```

```
#cruise ODP130JR                          date run: Wed Jul 18 16:38:07 1990         page  36
#
#                   latitude  longitude             actual   drift        dr                 prob. error        drift
#da mo   yr    time deg   min deg   min     dist speed cse speed hed speed cse  cmnt (smajxsmin@az)   dist   time   no.
#- - - - - - - - - - - - - - - - - - - - - - - - - - - - - - - - - - - - - - - - - - - - - - - - - - - - - - - - - -
 23 03 1990 *1440    4 36.89 154 48.92 1993.5    9.5 331   0.9 346   8.6 329  GF    0.00 0.00    0    0.1     0.1 1856
 23 03 1990 *1445    4 37.58 154 48.53 1994.3    9.6 329   1.0 327   8.6 329  GF    0.00 0.00    0    0.1     0.1 1857
 23 03 1990  1445    4 37.6  154 48.5  1994.3    9.7 330   1.0 327   8.7 330  c/cs                                 1858
 23 03 1990 *1450    4 38.28 154 48.12 1995.2    9.6 331   0.9 340   8.7 330  GF    0.00 0.00    0    0.1     0.1 1859
 23 03 1990 *1455    4 38.98 154 47.73 1996.0    8.3 331   0.5 134   8.7 330  GF    0.00 0.00    0    0.1     0.1 1860
 23 03 1990  1457    4 39.2  154 47.6  1996.2    7.9 331   0.5 134   8.4 330  c/cs                                 1861
 23 03 1990 *1501    4 39.68 154 47.34 1996.8    9.5 331   1.1 337   8.4 330  GF    0.00 0.00    0    0.0     0.1 1862
 23 03 1990  1505    4 40.2  154 47.0  1997.4    9.8 330   1.1 337   8.7 329  c/cs                                 1863
 23 03 1990 *1506    4 40.37 154 46.95 1997.5    9.6 331   0.9 348   8.7 329  GF    0.00 0.00    0    0.1     0.1 1864
 23 03 1990 *1516    4 41.76 154 46.17 1999.1    9.6 331   1.0 348   8.7 329  GF    0.00 0.00    0    0.2     0.2 1865
 23 03 1990 *1521    4 42.46 154 45.78 1999.9    9.6 331   1.0 348   8.7 329  GF    0.00 0.00    0    0.1     0.1 1866
 23 03 1990 *1526    4 43.16 154 45.39 2000.7    9.7 332   1.1 351   8.7 329  GF    0.00 0.00    0    0.1     0.1 1867
 23 03 1990 *1530    4 43.73 154 45.08 2001.4   10.7 328   2.0 324   8.7 329  GF    0.00 0.00    0    0.1     0.1 1868
 23 03 1990  1531    4 43.9  154 45.0  2001.6   10.5 329   2.0 324   8.5 330  c/cs                                 1869
 23 03 1990 *1536    4 44.63 154 44.53 2002.4    8.7 333   0.5  36   8.5 330  GF    0.00 0.00    0    0.2     0.1 1870
 23 03 1990  1541    4 45.3  154 44.2  2003.2    8.9 333   0.5  36   8.7 330  c/cs                                 1871
 23 03 1990 *1546    4 45.94 154 43.86 2003.9    9.3 333   0.8   2   8.7 330  GF    0.00 0.00    0    0.1     0.2 1872
 23 03 1990 *1551    4 46.63 154 43.50 2004.7   10.0 331   1.4 335   8.7 330  GF    0.00 0.00    0    0.1     0.1 1873
 23 03 1990  1559    4 47.8  154 42.8  2006.0    7.7 331   1.4 335   6.4 330  c/cs                                 1874
 23 03 1990 *1600    4 47.91 154 42.78 2006.2    7.5 332   1.1 340   6.4 330  GF    0.00 0.00    0    0.2     0.2 1875
 23 03 1990  1600    4 47.9  154 42.8  2006.2    9.9 331   1.1 340   8.8 330  c/cs                                 1876
 23 03 1990 *1606    4 48.78 154 42.30 2007.1    9.8 332   1.0 346   8.8 330  GF    0.00 0.00    0    0.1     0.1 1877
 23 03 1990 *1611    4 49.50 154 41.91 2008.0    9.9 331   1.1 339   8.8 330  GF    0.00 0.00    0    0.1     0.1 1878
 23 03 1990 *1616    4 50.22 154 41.51 2008.8   10.0 331   1.2 341   8.8 330  GF    0.00 0.00    0    0.1     0.1 1879
 23 03 1990 *1621    4 50.95 154 41.11 2009.6    9.7 332   0.9 351   8.8 330  GF    0.00 0.00    0    0.1     0.1 1880
 23 03 1990 *1626    4 51.66 154 40.73 2010.4    9.7 330   0.9 333   8.8 330  GF    0.00 0.00    0    0.1     0.1 1881
 23 03 1990 *1630    4 52.22 154 40.41 2011.1   10.0 332   1.2 345   8.8 330  GF    0.00 0.00    0    0.1     0.1 1882
 23 03 1990  1630    4 52.2  154 40.4  2011.1    9.8 331   1.2 345   8.7 329  c/cs                                 1883
 23 03 1990 *1636    4 53.08 154 39.93 2012.1    9.6 331   1.0 349   8.7 329  GF    0.00 0.00    0    0.1     0.1 1884
 23 03 1990 *1641    4 53.78 154 39.54 2012.9    9.7 331   1.1 349   8.7 329  GF    0.00 0.00    0    0.1     0.1 1885
 23 03 1990  1642    4 53.9  154 39.5  2013.0    9.7 331   1.1 349   8.6 329  c/cs                                 1886
 23 03 1990 *1646    4 54.49 154 39.15 2013.7    9.6 331   1.0 352   8.6 329  GF    0.00 0.00    0    0.1     0.1 1887
 23 03 1990  1649    4 54.9  154 38.9  2014.1    9.6 332   1.0 352   8.6 330  c/cs                                 1888
 23 03 1990 *1651    4 55.19 154 38.77 2014.5    9.6 331   1.0 339   8.6 330  GF    0.00 0.00    0    0.1     0.1 1889
 23 03 1990 *1656    4 55.89 154 38.38 2015.3    9.3 331   0.6 346   8.6 330  GF    0.00 0.00    0    0.1     0.1 1890
 23 03 1990 *1700    4 56.43 154 38.08 2015.9    9.7 331   1.1 340   8.6 330  GF    0.00 0.00    0    0.0     0.1 1891
 23 03 1990 *1706    4 57.28 154 37.61 2016.8    9.5 332   0.9 346   8.6 330  GF    0.00 0.00    0    0.1     0.1 1892
 23 03 1990 *1711    4 57.98 154 37.23 2017.6    9.5 332   1.0 353   8.6 330  GF    0.00 0.00    0    0.1     0.1 1893
 23 03 1990  1711    4 58.0  154 37.2  2017.6    9.5 332   1.0 353   8.6 330  c/cs                                 1894
 23 03 1990 *1716    4 58.68 154 36.86 2018.4    9.5 331   0.9 344   8.6 330  GF    0.00 0.00    0    0.1     0.1 1895
 23 03 1990 *1721    4 59.37 154 36.48 2019.2    9.4 332   0.8 350   8.6 330  GF    0.00 0.00    0    0.1     0.1 1896
 23 03 1990 *1730    5  0.61 154 35.81 2020.6   10.1 332   1.5 343   8.6 330  GF    0.00 0.00    0    0.1     0.2 1897
 23 03 1990  1734    5  1.2  154 35.5  2021.3    9.8 332   1.5 343   8.3 330  c/cs                                 1898
 23 03 1990 *1736    5  1.49 154 35.34 2021.6    9.5 331   1.2 340   8.3 330  GF    0.00 0.00    0    0.2     0.1 1899
 23 03 1990  1738    5  1.8  154 35.2  2021.9    9.9 331   1.2 340   8.6 330  c/cs                                 1900
 23 03 1990 *1741    5  2.20 154 34.95 2022.4    9.7 332   1.0 348   8.6 330  GF    0.00 0.00    0    0.1     0.1 1901
 23 03 1990 *1746    5  2.91 154 34.57 2023.2    9.8 332   1.2 349   8.6 330  GF    0.00 0.00    0    0.1     0.1 1902
 23 03 1990 *1751    5  3.63 154 34.19 2024.1   10.0 333   1.4 351   8.6 330  GF    0.00 0.00    0    0.1     0.1 1903
 23 03 1990 *1756    5  4.37 154 33.81 2024.9    9.2 331   0.6 350   8.6 330  GF    0.00 0.00    0    0.1     0.1 1904
 23 03 1990  1758    5  4.6  154 33.7  2025.2    9.1 332   0.6 350   8.5 331  c/cs                                 1905
 23 03 1990 *1800    5  4.91 154 33.52 2025.5   10.0 334   1.6 351   8.5 331  GF    0.00 0.00    0    0.0     0.1 1906
 23 03 1990 *1806    5  5.81 154 33.08 2026.5    9.6 334   1.2   1   8.5 331  GF    0.00 0.00    0    0.2     0.1 1907
 23 03 1990  1809    5  6.2  154 32.9  2027.0    9.8 336   1.2   1   8.7 333  c/cs                                 1908
```

```
#cruise ODP130JR                                    date run: Wed Jul 18 16:38:07 1990         page  37
#
#                  latitude  longitude              actual   drift         dr             prob. error      drift
#da mo  yr    time deg  min  deg  min      dist speed cse speed hed speed cse  cmnt (smajxsmin@az)   dist  time   no.
#- - - - - - - - - - - - - - - - - - - - - - - - - - - - - - - - - - - - - - - - - - - - - - - - - - - - - - - - - -
 23 03 1990 *1811   5  6.54 154 32.74 2027.3   9.7 336  1.1   1  8.7 333  GF   0.00 0.00   0   0.1   0.1 1909
 23 03 1990 *1816   5  7.28 154 32.41 2028.1   9.8 334  1.1 341  8.7 333  GF   0.00 0.00   0   0.1   0.1 1910
 23 03 1990 *1821   5  8.01 154 32.05 2028.9   9.4 335  0.8   1  8.7 333  GF   0.00 0.00   0   0.1   0.1 1911
 23 03 1990  1826   5  8.7  154 31.7  2029.7   9.6 335  0.8   1  8.9 333  c/cs                            1912
 23 03 1990 *1830   5  9.31 154 31.45 2030.4  10.5 334  1.6 342  8.9 333  GF   0.00 0.00   0   0.1   0.2 1913
 23 03 1990  1833   5  9.8  154 31.2  2030.9  10.3 335  1.6 342  8.7 333  c/cs                            1914
 23 03 1990 *1836   5 10.25 154 31.00 2031.4   9.6 334  0.9 345  8.7 333  GF   0.00 0.00   0   0.2   0.1 1915
 23 03 1990 *1841   5 10.97 154 30.65 2032.2   9.8 334  1.1 341  8.7 333  GF   0.00 0.00   0   0.1   0.1 1916
 23 03 1990 *1846   5 11.70 154 30.29 2033.0   9.7 337  1.2   6  8.7 333  GF   0.00 0.00   0   0.1   0.1 1917
 23 03 1990  1850   5 12.3  154 30.0  2033.7   9.6 336  1.2   6  8.6 332  c/cs                            1918
 23 03 1990 *1851   5 12.44 154 29.97 2033.8   9.8 336  1.4   5  8.6 332  GF   0.00 0.00   0   0.1   0.1 1919
 23 03 1990 *1856   5 13.19 154 29.64 2034.6   8.5 338  1.0  72  8.6 332  GF   0.00 0.00   0   0.1   0.1 1920
 23 03 1990  1859   5 13.6  154 29.5  2035.1   8.7 338  1.0  72  8.8 332  c/cs                            1921
 23 03 1990 *1900   5 13.72 154 29.43 2035.2  10.3 334  1.5 347  8.8 332  GF   0.00 0.00   0   0.1   0.1 1922
 23 03 1990  1909   5 15.1  154 28.8  2036.7  10.4 335  1.5 347  9.0 333  c/cs                            1923
 23 03 1990 *1911   5 15.42 154 28.61 2037.1   9.9 336  1.0   0  9.0 333  GF   0.00 0.00   0   0.3   0.2 1924
 23 03 1990 *1916   5 16.17 154 28.27 2037.9   9.9 335  1.0 354  9.0 333  GF   0.00 0.00   0   0.1   0.1 1925
 23 03 1990 *1921   5 16.92 154 27.92 2038.7   9.3 335  0.4  21  9.0 333  GF   0.00 0.00   0   0.1   0.1 1926
 23 03 1990 *1930   5 18.18 154 27.33 2040.1  10.7 336  1.8 350  9.0 333  GF   0.00 0.00   0   0.1   0.2 1927
 23 03 1990 *1936   5 19.16 154 26.89 2041.2   9.9 338  1.2  14  9.0 333  GF   0.00 0.00   0   0.2   0.1 1928
 23 03 1990  1939   5 19.6  154 26.7  2041.7   9.8 337  1.2  14  8.9 332  c/cs                            1929
 23 03 1990 *1941   5 19.92 154 26.57 2042.0   9.8 335  1.1   5  8.9 332  GF   0.00 0.00   0   0.1   0.1 1930
 23 03 1990 *1946   5 20.66 154 26.23 2042.8   9.9 336  1.3   8  8.9 332  GF   0.00 0.00   0   0.1   0.1 1931
 23 03 1990  1948   5 21.0  154 26.1  2043.2   9.8 336  1.3   8  8.7 332  c/cs                            1932
 23 03 1990 *1951   5 21.41 154 25.90 2043.7   9.6 337  0.8  33  8.7 332  GF   0.00 0.00   0   0.1   0.1 1933
 23 03 1990 *2000   5 22.67 154 25.35 2045.0  10.2 336  1.6 358  8.7 332  GF   0.00 0.00   0   0.1   0.2 1934
 23 03 1990  2002   5 23.0  154 25.2  2045.4  10.2 336  1.6 358  8.8 332  c/cs                            1935
 23 03 1990 *2011   5 24.39 154 24.58 2046.9   9.7 336  1.2   4  8.8 332  GF   0.00 0.00   0   0.3   0.2 1936
 23 03 1990 *2016   5 25.14 154 24.24 2047.7   9.7 335  1.0   4  8.8 332  GF   0.00 0.00   0   0.1   0.1 1937
 23 03 1990 *2021   5 25.87 154 23.90 2048.5   9.4 336  1.0  12  8.8 332  GF   0.00 0.00   0   0.1   0.1 1938
 23 03 1990 *2026   5 26.60 154 23.57 2049.3   8.7 335  0.5  80  8.8 332  GF   0.00 0.00   0   0.1   0.1 1939
 23 03 1990  2028   5 26.9  154 23.4  2049.6   6.0 338  0.5  80  6.2 334  c/cs                            1940
 23 03 1990  2029   5 27.0  154 23.4  2049.7   8.8 335  0.5  80  8.9 333  c/cs                            1941
 23 03 1990 *2030   5 27.09 154 23.35 2049.9  10.8 334  1.9 340  8.9 333  GF   0.00 0.00   0   0.0   0.1 1942
 23 03 1990 *2036   5 28.06 154 22.88 2051.0   9.5 333  0.6 337  8.9 333  GF   0.00 0.00   0   0.2   0.1 1943
 23 03 1990 *2041   5 28.77 154 22.52 2051.8   9.7 333  0.6 332  8.9 333  GF   0.00 0.00   0   0.1   0.1 1944
 23 03 1990 *2046   5 29.49 154 22.15 2052.6   9.5 331  0.7 299  8.9 333  GF   0.00 0.00   0   0.1   0.1 1945
 23 03 1990 *2051   5 30.18 154 21.76 2053.4   9.0 334  0.1  31  8.9 333  GF   0.00 0.00   0   0.1   0.1 1946
 23 03 1990  2054   5 30.6  154 21.6  2053.8   8.8 334  0.1  31  8.7 333  c/cs                            1947
 23 03 1990 *2100   5 31.37 154 21.17 2054.7  10.4 334  1.7 336  8.7 333  GF   0.00 0.00   0   0.0   0.2 1948
 23 03 1990  2100   5 31.4  154 21.2  2054.7  10.5 334  1.7 336  8.8 333  c/cs                            1949
 23 03 1990 *2106   5 32.31 154 20.70 2055.7   9.7 334  0.9 346  8.8 333  GF   0.00 0.00   0   0.2   0.1 1950
 23 03 1990  2107   5 32.5  154 20.6  2055.9   9.2 334  0.9 346  8.4 333  c/cs                            1951
 23 03 1990 *2111   5 33.01 154 20.36 2056.5   8.9 334  0.5 342  8.4 333  GF   0.00 0.00   0   0.1   0.1 1952
 23 03 1990  2111   5 33.0  154 20.4  2056.5   9.4 333  0.5 342  8.9 333  c/cs                            1953
 23 03 1990 *2116   5 33.71 154 20.01 2057.3   9.3 333  0.4 338  8.9 333  GF   0.00 0.00   0   0.0   0.1 1954
 23 03 1990 *2121   5 34.40 154 19.66 2058.1   8.7 333  0.2 141  8.9 333  GF   0.00 0.00   0   0.0   0.1 1955
 23 03 1990  2129   5 35.4  154 19.1  2059.2   7.9 333  0.2 141  8.1 333  c/cs                            1956
 23 03 1990 *2130   5 35.55 154 19.08 2059.4   9.4 333  1.4 335  8.1 333  GF   0.00 0.00   0   0.0   0.2 1957
 23 03 1990  2133   5 36.0  154 18.9  2059.8  10.2 333  1.4 335  8.9 333  c/cs                            1958
 23 03 1990 *2141   5 37.19 154 18.25 2061.2   9.4 334  0.5 343  8.9 333  GF   0.00 0.00   0   0.3   0.2 1959
 23 03 1990  2144   5 37.6  154 18.0  2061.7   9.2 333  0.5 343  8.7 332  c/cs                            1960
 23 03 1990 *2146   5 37.88 154 17.90 2062.0   9.2 332  0.6 335  8.7 332  GF   0.00 0.00   0   0.0   0.1 1961
```

```
#cruise ODP130JR                                              date run: Wed Jul 18 16:38:07 1990          page  38
#
#                    latitude  longitude                 actual   drift        dr                prob. error        drift
#da mo  yr    time deg   min  deg   min      dist speed cse speed hed speed cse  cmnt (smajxsmin@az)  dist  time   no.
#- - - - - - - - - - - - - - - - - - - - - - - - - - - - - - - - - - - - - - - - - - - - - - - - - - - - - - - - - - -
 23 03 1990 *2151    5 38.56 154 17.54 2062.7   9.3 334   0.7 353   8.7 332  GF    0.00 0.00   0   0.0   0.1 1962
 23 03 1990  2155    5 39.1  154 17.3  2063.4   8.8 335   0.7 353   8.1 334  c/cs                              1963
 23 03 1990 *2156    5 39.25 154 17.20 2063.5   6.3 333   1.9 156   8.1 334  GF    0.00 0.00   0   0.1   0.1 1964
 23 03 1990  2158    5 39.4  154 17.1  2063.7   4.9 332   1.9 156   6.7 333  c/cs                              1965
 23 03 1990 *2200    5 39.58 154 17.03 2063.9   7.5 333   0.7 328   6.7 333  GF    0.00 0.00   0   0.1   0.1 1966
 23 03 1990  2201    5 39.7  154 17.0  2064.0   7.0 332   0.7 328   6.3 333  c/cs                              1967
 23 03 1990  2202    5 39.8  154 16.9  2064.1   7.7 333   0.7 328   7.0 333  c/cs                              1968
 23 03 1990 *2206    5 40.25 154 16.68 2064.6   6.8 332   0.2 192   7.0 333  GF    0.00 0.00   0   0.1   0.1 1969
 23 03 1990 *2211    5 40.75 154 16.41 2065.2   5.9 333   1.0 152   7.0 333  GF    0.00 0.00   0   0.0   0.1 1970
 23 03 1990 *2217    5 41.28 154 16.14 2065.8   8.0 332   1.0 325   7.0 333  GF    0.00 0.00   0   0.1   0.1 1971
 23 03 1990  2221    5 41.8  154 15.9  2066.3  10.1 332   1.0 325   9.1 333  c/cs                              1972
 23 03 1990 *2222    5 41.90 154 15.81 2066.5   9.6 333   0.5 328   9.1 333  GF    0.00 0.00   0   0.1   0.1 1973
 23 03 1990 *2230    5 43.04 154 15.22 2067.8   9.8 338   1.1  30   9.1 333  GF    0.00 0.00   0   0.1   0.1 1974
 23 03 1990  2230    5 43.0  154 15.2  2067.8   9.5 328   1.1  30   9.1 322  c/cs                              1975
 23 03 1990 *2232    5 43.31 154 15.05 2068.1   9.7 323   0.6 335   9.1 322  GF    0.00 0.00   0   0.0   0.0 1976
 23 03 1990  2232    5 43.3  154 15.1  2068.1   9.7 312   0.6 335   9.1 310  c/cs                              1977
 23 03 1990  2236    5 43.7  154 14.6  2068.7  10.4 314   0.6 335   9.8 313  c/cs                              1978
 23 03 1990 *2237    5 43.86 154 14.44 2068.9  10.2 312   0.4 294   9.8 313  GF    0.00 0.00   0   0.1   0.1 1979
 23 03 1990 *2242    5 44.43 154 13.81 2069.8  10.7 313   0.9 317   9.8 313  GF    0.00 0.00   0   0.0   0.1 1980
 23 03 1990 *2247    5 45.04 154 13.16 2070.6  11.7 313   1.9 313   9.8 313  GF    0.00 0.00   0   0.1   0.1 1981
 23 03 1990  2248    5 45.2  154 13.0  2070.8   3.2 314   1.9 313   1.3 315  c/cs                              1982
 23 03 1990  2249    5 45.2  154 13.0  2070.9  11.8 314   1.9 313   9.8 314  c/cs                              1983
 23 03 1990 *2252    5 45.62 154 12.55 2071.5  10.3 313   0.4 299   9.8 314  GF    0.00 0.00   0   0.2   0.1 1984
 23 03 1990 *2300    5 46.56 154 11.55 2072.9  10.4 314   0.6 306   9.8 314  GF    0.00 0.00   0   0.1   0.1 1985
 23 03 1990  2301    5 46.7  154 11.4  2073.0  10.6 314   0.6 306  10.0 314  c/cs                              1986
 23 03 1990 *2307    5 47.41 154 10.65 2074.1  10.9 313   1.0 301  10.0 314  GF    0.00 0.00   0   0.1   0.1 1987
 23 03 1990  2313    5 48.2  154  9.8  2075.2   7.7 312   1.0 301   6.7 314  c/cs                              1988
 23 03 1990  2314    5 48.2  154  9.7  2075.3  11.5 314   1.0 301  10.6 315  c/cs                              1989
 23 03 1990 *2317    5 48.64 154  9.33 2075.9  11.0 314   0.4 296  10.6 315  GF    0.00 0.00   0   0.2   0.2 1990
 23 03 1990 *2322    5 49.28 154  8.67 2076.8  11.0 314   0.4 296  10.6 315  GF    0.00 0.00   0   0.0   0.1 1991
 23 03 1990 *2327    5 49.92 154  8.01 2077.7  10.7 314   0.3 250  10.6 315  GF    0.00 0.00   0   0.0   0.1 1992
 23 03 1990 *2330    5 50.29 154  7.62 2078.3  11.7 314   1.1 309  10.6 315  GF    0.00 0.00   0   0.0   0.1 1993
 23 03 1990  2336    5 51.1  154  6.8  2079.4  12.2 314   1.1 309  11.1 314  c/cs                              1994
 23 03 1990 *2337    5 51.25 154  6.63 2079.6  11.7 315   0.6 335  11.1 314  GF    0.00 0.00   0   0.1   0.1 1995
 23 03 1990 *2342    5 51.94 154  5.94 2080.6  11.8 315   0.8 331  11.1 314  GF    0.00 0.00   0   0.1   0.1 1996
 23 03 1990 *2347    5 52.64 154  5.24 2081.6  11.9 315   0.8 325  11.1 314  GF    0.00 0.00   0   0.1   0.1 1997
 23 03 1990 *2352    5 53.34 154  4.53 2082.6  11.6 314   0.5 314  11.1 314  GF    0.00 0.00   0   0.1   0.1 1998
 23 03 1990  2357    5 54.0  154  3.8  2083.6  11.6 315   0.5 314  11.1 315  c/cs                              1999
 24 03 1990 *0000    5 54.42 154  3.42 2084.1  12.3 315   1.3 316  11.1 315  GF    0.00 0.00   0   0.1   0.1 2000
 24 03 1990  0000    5 54.4  154  3.4  2084.1  12.3 315   1.3 316  11.1 315  c/cs                              2001
 24 03 1990 *0007    5 55.44 154  2.40 2085.6  11.7 316   0.6 329  11.1 315  GF    0.00 0.00   0   0.1   0.1 2002
 24 03 1990  0007    5 55.4  154  2.4  2085.6  11.9 315   0.6 329  11.4 314  c/cs                              2003
 24 03 1990 *0012    5 56.14 154  1.69 2086.6  12.1 315   0.8 326  11.4 314  GF    0.00 0.00   0   0.1   0.1 2004
 24 03 1990 *0017    5 56.85 154  0.97 2087.6  12.3 316   1.0 334  11.4 314  GF    0.00 0.00   0   0.1   0.1 2005
 24 03 1990 *0022    5 57.58 154  0.25 2088.6  11.7 316   0.5 356  11.4 314  GF    0.00 0.00   0   0.1   0.1 2006
 24 03 1990 *0030    5 58.70 153 59.15 2090.2  12.5 315   1.1 321  11.4 314  GF    0.00 0.00   0   0.1   0.1 2007
 24 03 1990  0033    5 59.1  153 58.7  2090.8  12.6 315   1.1 321  11.5 314  c/cs                              2008
 24 03 1990 *0037    5 59.73 153 58.10 2091.6  12.4 315   0.9 325  11.5 314  GF    0.00 0.00   0   0.1   0.1 2009
 24 03 1990  0040    6  0.2  153 57.7  2092.2  12.1 315   0.9 325  11.3 314  c/cs                              2010
 24 03 1990 *0042    6  0.45 153 57.37 2092.7  11.8 314   0.6 321  11.3 314  GF    0.00 0.00   0   0.1   0.1 2011
 24 03 1990 *0047    6  1.14 153 56.66 2093.6  12.0 315   0.8 326  11.3 314  GF    0.00 0.00   0   0.0   0.1 2012
 24 03 1990  0048    6  1.3  153 56.5  2093.8  12.1 315   0.8 326  11.4 314  c/cs                              2013
 24 03 1990 *0052    6  1.85 153 55.94 2094.6  11.6 314   0.2 306  11.4 314  GF    0.00 0.00   0   0.1   0.1 2014
```

```
#cruise ODP130JR                                      date run: Wed Jul 18 16:38:07 1990          page  39
#
#                        latitude  longitude            actual   drift        dr                prob. error       drift
#da mo  yr    time deg   min  deg   min      dist speed cse speed hed speed cse  cmnt (smajxsmin@az)  dist  time  no.
#- - - - - - - - - - - - - - - - - - - - - - - - - - - - - - - - - - - - - - - - - - - - - - - - - - - - - - - - - -
 24 03 1990 *0100    6  2.92 153 54.82 2096.2  12.8 314   1.4 317  11.4 314  GF   0.00 0.00   0   0.0   0.1 2015
 24 03 1990  0102    6  3.2  153 54.5  2096.6  12.4 314   1.4 317  11.0 314  c/cs                             2016
 24 03 1990 *0107    6  3.94 153 53.77 2097.7  11.7 315   0.8 333  11.0 314  GF   0.00 0.00   0   0.2   0.1 2017
 24 03 1990 *0112    6  4.63 153 53.08 2098.6  11.7 314   0.7 319  11.0 314  GF   0.00 0.00   0   0.1   0.1 2018
 24 03 1990 *0117    6  5.31 153 52.38 2099.6  11.5 316   0.7 343  11.0 314  GF   0.00 0.00   0   0.1   0.1 2019
 24 03 1990  0119    6  5.6  153 52.1  2100.0  11.6 316   0.7 343  11.1 314  c/cs                             2020
 24 03 1990 *0122    6  6.00 153 51.70 2100.6  11.9 316   0.9 335  11.1 314  GF   0.00 0.00   0   0.1   0.1 2021
 24 03 1990 *0127    6  6.71 153 51.00 2101.6  11.1 314   0.1   0  11.1 314  GF   0.00 0.00   0   0.1   0.1 2022
 24 03 1990 *0130    6  7.10 153 50.60 2102.1  12.6 316   1.6 330  11.1 314  GF   0.00 0.00   0   0.0   0.1 2023
 24 03 1990  0135    6  7.9  153 49.9  2103.2  12.8 316   1.6 330  11.3 314  c/cs                             2024
 24 03 1990 *0137    6  8.16 153 49.57 2103.6  12.2 316   1.0 339  11.3 314  GF   0.00 0.00   0   0.2   0.1 2025
 24 03 1990 *C142    6  8.89 153 48.86 2104.6  12.0 316   0.8 345  11.3 314  GF   0.00 0.00   0   0.1   0.1 2026
 24 03 1990 *0147    6  9.61 153 48.16 2105.6  12.4 315   1.1 327  11.3 314  GF   0.00 0.00   0   0.1   0.1 2027
 24 03 1990 *0152    6 10.34 153 47.43 2106.6  11.7 315   0.5 331  11.3 314  GF   0.00 0.00   0   0.1   0.1 2028
 24 03 1990 *0200    6 11.44 153 46.31 2108.2  12.8 315   1.5 321  11.3 314  GF   0.00 0.00   0   0.1   0.1 2029
 24 03 1990  0205    6 12.2  153 45.6  2109.3  12.7 313   1.5 321  11.3 312  c/cs                             2030
 24 03 1990 *0207    6 12.48 153 45.24 2109.7  12.4 314   1.2 332  11.3 312  GF   0.00 0.00   0   0.2   0.1 2031
 24 03 1990 *0212    6 13.20 153 44.49 2110.7  12.2 314   1.0 332  11.3 312  GF   0.00 0.00   0   0.1   0.1 2032
 24 03 1990 *0217    6 13.90 153 43.75 2111.7  11.8 314   0.7 353  11.3 312  GF   0.00 0.00   0   0.1   0.1 2033
 24 03 1990 *0222    6 14.59 153 43.04 2112.7  12.2 313   0.9 322  11.3 312  GF   0.00 0.00   0   0.1   0.1 2034
 24 03 1990 *0227    6 15.28 153 42.29 2113.7  10.1 314   1.2 115  11.3 312  GF   0.00 0.00   0   0.1   0.1 2035
 24 03 1990  0229    6 15.5  153 42.0  2114.1  10.2 313   1.2 115  11.4 311  c/cs                             2036
 24 03 1990 *0230    6 15.63 153 41.92 2114.3  12.9 311   1.5 308  11.4 311  GF   0.00 0.00   0   0.1   0.1 2037
 24 03 1990 *0237    6 16.61 153 40.77 2115.8  12.4 311   1.0 314  11.4 311  GF   0.00 0.00   0   0.2   0.1 2038
 24 03 1990 *0242    6 17.29 153 39.99 2116.8  11.8 312   0.5 329  11.4 311  GF   0.00 0.00   0   0.1   0.1 2039
 24 03 1990  0244    6 17.6  153 39.7  2117.2  12.2 311   0.5 329  11.7 310  c/cs                             2040
 24 03 1990 *0247    6 17.95 153 39.23 2117.8  11.7 310   0.1   1  11.7 310  GF   0.00 0.00   0   0.0   0.1 2041
 24 03 1990 *0300    6 19.60 153 37.28 2120.3  13.3 310   1.6 314  11.7 310  GF   0.00 0.00   0   0.0   0.2 2042
 24 03 1990  0305    6 20.3  153 36.4  2121.4  13.3 311   1.6 314  11.7 311  c/cs                             2043
 24 03 1990 *0307    6 20.61 153 36.10 2121.9  12.4 311   0.7 315  11.7 311  GF   0.00 0.00   0   0.2   0.1 2044
 24 03 1990 *0312    6 21.29 153 35.32 2122.9  12.0 312   0.4 341  11.7 311  GF   0.00 0.00   0   0.1   0.1 2045
 24 03 1990 *0317    6 21.96 153 34.57 2123.9  12.2 311   0.5 316  11.7 311  GF   0.00 0.00   0   0.0   0.1 2046
 24 03 1990 *0322    6 22.63 153 33.80 2124.9  12.1 312   0.5 324  11.7 311  GF   0.00 0.00   0   0.0   0.1 2047
 24 03 1990  0326    6 23.2  153 33.2  2125.7  12.1 312   0.5 324  11.6 311  c/cs                             2048
 24 03 1990 *0327    6 23.30 153 33.04 2125.9  10.2 312   1.5 124  11.6 311  GF   0.00 0.00   0   0.0   0.1 2049
 24 03 1990 *0330    6 23.64 153 32.66 2126.5  13.2 312   1.6 315  11.6 311  GF   0.00 0.00   0   0.1   0.1 2050
 24 03 1990 *0337    6 24.66 153 31.50 2128.0  12.9 312   1.3 323  11.6 311  GF   0.00 0.00   0   0.2   0.1 2051
 24 03 1990  0341    6 25.2  153 30.9  2128.9  10.4 312   1.3 323   9.2 310  c/cs                             2052
 24 03 1990 *0342    6 25.35 153 30.73 2129.0   9.9 311   0.7 323   9.2 310  GF   0.00 0.00   0   0.1   0.1 2053
 24 03 1990  0342    6 25.4  153 30.7  2129.0  12.6 312   0.7 323  11.9 311  c/cs                             2054
 24 03 1990  0345    6 25.8  153 30.3  2129.7  12.2 312   0.7 323  11.5 311  c/cs                             2055
 24 03 1990 *0347    6 26.04 153 29.95 2130.1  12.4 311   0.9 315  11.5 311  GF   0.00 0.00   0   0.1   0.1 2056
 24 03 1990  0348    6 26.2  153 29.8  2130.3  12.4 311   0.9 315  11.5 311  c/cs                             2057
 24 03 1990 *0352    6 26.72 153 29.17 2131.1  11.3 312   0.2  96  11.5 311  GF   0.00 0.00   0   0.1   0.1 2058
 24 03 1990 *0400    6 27.72 153 28.04 2132.6  13.2 312   1.8 317  11.5 311  GF   0.00 0.00   0   0.0   0.1 2059
 24 03 1990 *0407    6 28.75 153 26.88 2134.1  12.5 312   1.0 329  11.5 311  GF   0.00 0.00   0   0.2   0.1 2060
 24 03 1990 *0412    6 29.45 153 26.11 2135.2  12.3 312   0.8 321  11.5 311  GF   0.00 0.00   0   0.1   0.1 2061
 24 03 1990 *0417    6 30.13 153 25.34 2136.2  12.3 312   0.9 325  11.5 311  GF   0.00 0.00   0   0.1   0.1 2062
 24 03 1990  0418    6 30.3  153 25.2  2136.4  12.2 312   0.9 325  11.3 311  c/cs                             2063
 24 03 1990 *0422    6 30.81 153 24.58 2137.2  11.0 312   0.3 100  11.3 311  GF   0.00 0.00   0   0.1   0.1 2064
 24 03 1990 *0430    6 31.79 153 23.48 2138.7  13.4 312   2.1 318  11.3 311  GF   0.00 0.00   0   0.0   0.1 2065
 24 03 1990 *0437    6 32.84 153 22.31 2140.3  12.0 313   0.8 335  11.3 311  GF   0.00 0.00   0   0.3   0.1 2066
 24 03 1990  0441    6 33.4  153 21.7  2141.1  12.4 312   0.8 335  11.6 310  c/cs                             2067
```

```
#cruise ODP130JR                                           date run: Wed Jul 18 16:38:07 1990         page  40
#
#                       latitude  longitude             actual    drift        dr              prob. error       drift
#da mo  yr     time deg   min  deg   min      dist speed cse speed hed speed cse  cmnt (smajxsmin@az)  dist  time  no.
#- - - - - - - - - - - - - - - - - - - - - - - - - - - - - - - - - - - - - - - - - - - - - - - - - - - - - - - - - -
 24 03 1990 *0442    6 33.52 153 21.56 2141.3  12.3 312   0.8 345  11.6 310  GF    0.00 0.00   0    0.1   0.1 2068
 24 03 1990  0444    6 33.8  153 21.3  2141.7  12.1 313   0.8 345  11.4 311  c/cs                                2069
 24 03 1990 *0447    6 34.21 153 20.81 2142.3  12.4 313   1.1 336  11.4 311  GF    0.00 0.00   0    0.1   0.1 2070
 24 03 1990 *0452    6 34.92 153 20.05 2143.3  11.1 312   0.4  87  11.4 311  GF    0.00 0.00   0    0.1   0.1 2071
 24 03 1990  0458    6 35.7  153 19.2  2144.4  11.2 312   0.4  87  11.5 311  c/cs                                2072
 24 03 1990 *0500    6 35.92 153 18.95 2144.8  13.3 313   1.8 324  11.5 311  GF    0.00 0.00   0    0.1   0.1 2073
 24 03 1990 *0512    6 37.72 153 16.99 2147.4  12.3 313   0.9 341  11.5 311  GF    0.00 0.00   0    0.4   0.2 2074
 24 03 1990 *0517    6 38.42 153 16.24 2148.5  12.3 313   0.9 342  11.5 311  GF    0.00 0.00   0    0.1   0.1 2075
 24 03 1990  0521    6 39.0  153 15.6  2149.3  12.2 313   0.9 342  11.4 311  c/cs                                2076
 24 03 1990 *0522    6 39.12 153 15.49 2149.5  10.8 313   0.7  95  11.4 311  GF    0.00 0.00   0    0.1   0.1 2077
 24 03 1990 *0530    6 40.11 153 14.43 2150.9  12.3 312   1.0 329  11.4 311  GF    0.00 0.00   0    0.1   0.1 2078
 24 03 1990  0531    6 40.2  153 14.3  2151.1  12.4 312   1.0 329  11.5 311  c/cs                                2079
 24 03 1990  0535    6 40.8  153 13.7  2152.0  12.3 313   1.0 329  11.4 312  c/cs                                2080
 24 03 1990 *0543    6 41.93 153 12.46 2153.6  12.3 313   1.0 323  11.4 312  GF    0.00 0.00   0    0.2   0.2 2081
 24 03 1990 *0548    6 42.63 153 11.70 2154.6  12.4 313   1.1 329  11.4 312  GF    0.00 0.00   0    0.1   0.1 2082
 24 03 1990  0548    6 42.6  153 11.7  2154.6  12.6 313   1.1 329  11.6 311  c/cs                                2083
 24 03 1990 *0553    6 43.34 153 10.92 2155.7  12.2 313   0.7 345  11.6 311  GF    0.00 0.00   0    0.1   0.1 2084
 24 03 1990 *0558    6 44.03 153 10.17 2156.7  12.1 312   0.5 342  11.6 311  GF    0.00 0.00   0    0.1   0.1 2085
 24 03 1990 *0600    6 44.30 153  9.87 2157.1  12.4 314   1.0 350  11.6 311  GF    0.00 0.00   0    0.0   0.0 2086
 24 03 1990 *0603    6 44.73 153  9.42 2157.7  12.3 313   0.8 342  11.6 311  GF    0.00 0.00   0    0.0   0.1 2087
 24 03 1990  0605    6 45.0  153  9.1  2158.1  12.1 313   0.8 342  11.5 311  c/cs                                2088
 24 03 1990 *0608    6 45.42 153  8.67 2158.7  12.3 313   0.9 343  11.5 311  GF    0.00 0.00   0    0.1   0.1 2089
 24 03 1990 *0613    6 46.12 153  7.92 2159.8  12.5 316   1.4 357  11.5 311  GF    0.00 0.00   0    0.1   0.1 2090
 24 03 1990  0616    6 46.6  153  7.5  2160.4  10.7 301   1.4 357  10.0 294  c/cs                                2091
 24 03 1990  0617    6 46.7  153  7.3  2160.6   9.7 288   1.4 357   9.3 280  c/cs                                2092
 24 03 1990 *0618    6 46.71 153  7.17 2160.7   9.8 283   0.8 330   9.3 280  GF    0.00 0.00   0    0.1   0.1 2093
 24 03 1990  0618    6 46.7  153  7.2  2160.7   7.1 268   0.8 330   6.8 262  c/cs                                2094
 24 03 1990  0622    6 46.7  153  6.7  2161.2   6.1 269   0.8 330   5.8 262  c/cs                                2095
 24 03 1990 *0623    6 46.69 153  6.59 2161.3   5.7 265   0.3   8   5.8 262  GF    0.00 0.00   0    0.1   0.1 2096
 24 03 1990 *0630    6 46.63 153  5.92 2162.0   6.0 262   0.2 272   5.8 262  GF    0.00 0.00   0    0.0   0.1 2097
 24 03 1990 *0633    6 46.59 153  5.62 2162.3   5.5 264   0.3  50   5.8 262  GF    0.00 0.00   0    0.0   0.1 2098
 24 03 1990 *0638    6 46.54 153  5.16 2162.7   5.7 264   0.2  14   5.8 262  GF    0.00 0.00   0    0.0   0.1 2099
 24 03 1990  0638    6 46.5  153  5.2  2162.7   5.6 263   0.2  14   5.7 261  c/cs                                2100
 24 03 1990 *0643    6 46.48 153  4.69 2163.2   5.7 261   0.1  33   5.7 261  GF    0.00 0.00   0    0.0   0.1 2101
 24 03 1990 *0648    6 46.41 153  4.22 2163.7   5.7 260   0.1 151   5.7 261  GF    0.00 0.00   0    0.0   0.1 2102
 24 03 1990 *0653    6 46.33 153  3.75 2164.1   5.6 260   0.2 112   5.7 261  GF    0.00 0.00   0    0.0   0.1 2103
 24 03 1990 *0658    6 46.25 153  3.29 2164.6   5.6 246   1.5 158   5.7 261  GF    0.00 0.00   0    0.0   0.1 2104
 24 03 1990  0658    6 46.3  153  3.3  2164.6   5.1 270   1.5 158   5.8 284  c/cs                                2105
 24 03 1990 *0700    6 46.25 153  3.12 2164.8   7.3 289   1.6 307   5.8 284  GF    0.00 0.00   0    0.1   0.0 2106
 24 03 1990 *0703    6 46.37 153  2.77 2165.1   7.2 286   1.4 295   5.8 284  GF    0.00 0.00   0    0.1   0.1 2107
 24 03 1990  0705    6 46.4  153  2.5  2165.4  11.2 286   1.4 295   9.8 285  c/cs                                2108
 24 03 1990  0707    6 46.5  153  2.2  2165.8  12.5 281   1.4 295  11.1 279  c/cs                                2109
 24 03 1990 *0708    6 46.58 153  1.97 2166.0  11.9 281   0.9 312  11.1 279  GF    0.00 0.00   0    0.1   0.1 2110
 24 03 1990  0712    6 46.7  153  1.2  2166.8  12.6 282   0.9 312  11.8 280  c/cs                                2111
 24 03 1990 *0713    6 46.78 153  0.98 2167.0  12.9 279   1.1 266  11.8 280  GF    0.00 0.00   0    0.1   0.1 2112
 24 03 1990  0716    6 46.9  153  0.3  2167.6  12.1 308   1.1 266  11.3 312  c/cs                                2113
 24 03 1990 *0718    6 47.13 153  0.02 2168.0  12.5 313   1.2 327  11.3 312  GF    0.00 0.00   0    0.1   0.1 2114
 24 03 1990  0719    6 47.3  152 59.9  2168.2  12.7 317   1.2 327  11.5 316  c/cs                                2115
 24 03 1990 *0723    6 47.89 152 59.29 2169.1  11.9 318   0.5   3  11.5 316  GF    0.00 0.00   0    0.1   0.1 2116
 24 03 1990  0728    6 48.6  152 58.6  2170.1  11.9 318   0.5   3  11.6 316  c/cs                                2117
 24 03 1990 *0730    6 48.92 152 58.35 2170.5  12.4 319   1.0 352  11.6 316  GF    0.00 0.00   0    0.1   0.1 2118
 24 03 1990  0758    6 53.3  152 54.5  2176.3  12.3 321   1.0 352  11.5 318  c/cs                                2119
 24 03 1990  0813    6 55.7  152 52.5  2179.3  12.3 321   1.0 352  11.5 319  c/cs                                2120
```

```
                                                    date run: Wed Jul 18 16:38:07 1990          page  41
#cruise ODP130JR
#
#                      latitude   longitude                 actual    drift         dr                 prob. error        drift
#da mo  yr      time deg   min  deg   min       dist speed cse speed hed speed cse   cmnt (smajxsmin@az)  dist  time   no.
#- - - - - - - - - - - - - - - - - - - - - - - - - - - - - - - - - - - - - - - - - - - - - - - - - - - - - - - - - - - -
 24 03 1990   0825   6 57.6   152 51.0   2181.8  12.4 321   1.0 352  11.6 319  c/cs                                    2121
 24 03 1990   0828   6 58.1   152 50.6   2182.4  12.6 321   1.0 352  11.8 319  c/cs                                    2122
 24 03 1990   0844   7  0.7   152 48.5   2185.8  12.4 321   1.0 352  11.6 319  c/cs                                    2123
 24 03 1990   0902   7  3.6   152 46.1   2189.5  12.3 321   1.0 352  11.4 318  c/cs                                    2124
 24 03 1990   0916   7  5.8   152 44.3   2192.4  12.4 321   1.0 352  11.5 319  c/cs                                    2125
 24 03 1990   0923   7  7.0   152 43.4   2193.8  12.4 321   1.0 352  11.6 318  c/cs                                    2126
 24 03 1990  *0932   7  8.40  152 42.20  2195.7  13.3 320   1.8 334  11.6 318  SF    0.00 0.00   0    2.0    2.0 2127
 24 03 1990   0934   7  8.7   152 41.9   2196.1  13.4 318   1.8 334  11.7 315  c/cs                                    2128
 24 03 1990   0949   7 11.2   152 39.6   2199.5  13.4 318   1.8 334  11.7 315  c/cs                                    2129
 24 03 1990   0959   7 12.9   152 38.1   2201.7  10.3 317   1.8 334   8.6 314  c/cs                                    2130
 24 03 1990   1000   7 13.0   152 38.0   2201.9  13.4 316   1.8 334  11.6 313  c/cs                                    2131
 24 03 1990  *1007   7 14.10  152 36.90  2203.5  12.9 317   1.5 347  11.6 313  SF    0.00 0.00   0    1.1    0.6 2132
 24 03 1990   1013   7 15.0   152 36.0   2204.7  12.7 315   1.5 347  11.5 311  c/cs                                    2133
 24 03 1990   1020   7 16.1   152 34.9   2206.2   9.6 316   1.5 347   8.4 311  c/cs                                    2134
 24 03 1990   1021   7 16.2   152 34.8   2206.4  12.8 315   1.5 347  11.6 311  c/cs                                    2135
 24 03 1990   1035   7 18.3   152 32.7   2209.4  12.8 315   1.5 347  11.6 311  c/cs                                    2136
 24 03 1990   1048   7 20.3   152 30.7   2212.2  12.9 315   1.5 347  11.7 311  c/cs                                    2137
 24 03 1990  *1103   7 22.53  152 28.40  2215.4  12.9 314   1.4 345  11.7 311  GF    0.00 0.00   0    1.4    0.9 2138
 24 03 1990  *1108   7 23.28  152 27.63  2216.4  12.8 313   1.2 334  11.7 311  GF    0.00 0.00   0    0.1    0.1 2139
 24 03 1990   1110   7 23.6   152 27.3   2216.9  12.6 310   1.2 334  11.6 308  c/cs                                    2140
 24 03 1990  *1113   7 23.98  152 26.83  2217.5  12.8 311   1.4 337  11.6 308  GF    0.00 0.00   0    0.1    0.1 2141
 24 03 1990  *1118   7 24.68  152 26.02  2218.6  12.8 310   1.4 330  11.6 308  GF    0.00 0.00   0    0.1    0.1 2142
 24 03 1990  *1123   7 25.37  152 25.20  2219.6  12.0 311   0.7   1  11.6 308  GF    0.00 0.00   0    0.1    0.1 2143
 24 03 1990  *1130   7 26.28  152 24.13  2221.0  13.6 309   2.1 314  11.6 308  GF    0.00 0.00   0    0.1    0.1 2144
 24 03 1990   1132   7 26.6   152 23.8   2221.5  13.9 308   2.1 314  11.9 307  c/cs                                    2145
 24 03 1990  *1138   7 27.42  152 22.67  2222.9  13.0 308   1.2 320  11.9 307  GF    0.00 0.00   0    0.3    0.1 2146
 24 03 1990  *1143   7 28.09  152 21.81  2224.0  13.1 308   1.3 316  11.9 307  GF    0.00 0.00   0    0.1    0.1 2147
 24 03 1990  *1148   7 28.76  152 20.94  2225.1  13.0 307   1.2 312  11.9 307  GF    0.00 0.00   0    0.1    0.1 2148
 24 03 1990  *1153   7 29.42  152 20.07  2226.1  12.7 311   1.2 356  11.9 307  GF    0.00 0.00   0    0.1    0.1 2149
 24 03 1990   1159   7 30.3   152 19.1   2227.4  12.8 313   1.2 356  11.9 309  c/cs                                    2150
 24 03 1990  *1203   7 30.84  152 18.48  2228.3  12.7 316   1.7  15  11.9 309  GF    0.00 0.00   0    0.2    0.2 2151
 24 03 1990  *1208   7 31.60  152 17.74  2229.3  13.1 308   1.3 303  11.9 309  GF    0.00 0.00   0    0.1    0.1 2152
 24 03 1990   1214   7 32.4   152 16.7   2230.6   8.5 308   1.3 303   7.3 309  c/cs                                    2153
 24 03 1990   1215   7 32.5   152 16.6   2230.8  13.2 308   1.3 303  12.0 309  c/cs                                    2154
 24 03 1990   1234   7 35.1   152 13.3   2235.0  13.2 308   1.3 303  11.9 309  c/cs                                    2155
 24 03 1990   1257   7 38.2   152  9.3   2240.0  13.2 308   1.3 303  11.9 309  c/cs                                    2156
 24 03 1990   1319   7 41.2   152  5.5   2244.8   9.7 308   1.3 303   8.5 309  c/cs                                    2157
 24 03 1990   1320   7 41.3   152  5.3   2245.0  13.1 308   1.3 303  11.9 309  c/cs                                    2158
 24 03 1990   1350   7 45.4   152  0.1   2251.6  13.1 308   1.3 303  11.9 309  c/cs                                    2159
 24 03 1990  *1358   7 46.52  151 58.76  2253.3  11.3 308   0.7 152  11.9 309  GF    0.00 0.00   0    2.3    1.8 2160
 24 03 1990  *1400   7 46.75  151 58.46  2253.7  13.7 308   1.8 303  11.9 309  GF    0.00 0.00   0    0.0    0.0 2161
 24 03 1990  *1408   7 47.88  151 57.01  2255.5  13.3 308   1.5 303  11.9 309  GF    0.00 0.00   0    0.2    0.1 2162
 24 03 1990  *1413   7 48.57  151 56.13  2256.6  13.3 308   1.5 303  11.9 309  GF    0.00 0.00   0    0.1    0.1 2163
 24 03 1990  *1418   7 49.26  151 55.25  2257.8  13.3 308   1.5 303  11.9 309  GF    0.00 0.00   0    0.1    0.1 2164
 24 03 1990   1420   7 49.5   151 54.9   2258.2  13.3 308   1.5 303  11.9 309  c/cs                                    2165
 24 03 1990  *1423   7 49.95  151 54.37  2258.9  12.9 309   1.0 304  11.9 309  GF    0.00 0.00   0    0.1    0.1 2166
 24 03 1990  *1430   7 50.89  151 53.18  2260.4  13.8 309   1.9 307  11.9 309  GF    0.00 0.00   0    0.1    0.1 2167
 24 03 1990  *1438   7 52.04  151 51.73  2262.2  13.8 310   1.9 315  11.9 309  GF    0.00 0.00   0    0.3    0.1 2168
 24 03 1990   1439   7 52.2   151 51.6   2262.4  12.7 311   1.9 315  10.7 310  c/cs                                    2169
 24 03 1990   1441   7 52.5   151 51.2   2262.9  13.9 310   1.9 315  12.0 309  c/cs                                    2170
 24 03 1990  *1443   7 52.76  151 50.87  2263.3  12.1 302   1.6 221  12.0 309  GF    0.00 0.00   0    0.2    0.1 2171
 24 03 1990  *1448   7 53.29  151 50.00  2264.3  13.2 309   1.2 309  12.0 309  GF    0.00 0.00   0    0.1    0.1 2172
 24 03 1990  *1453   7 53.98  151 49.14  2265.4  12.6 310   0.7 329  12.0 309  GF    0.00 0.00   0    0.1    0.1 2173
```

```
#cruise ODP130JR                                    date run: Wed Jul 18 16:38:07 1990          page  42
#                                                  actual     drift          dr              prob. error        drift
#                   latitude  longitude                                                                                     
#da mo  yr    time deg   min  deg   min      dist speed cse speed hed speed cse   cmnt (smajxsmin@az)  dist  time   no.
#- - - - - - - - - - - - - - - - - - - - - - - - - - - - - - - - - - - - - - - - - - - - - - - - - - - - - - - - - - - -
 24 03 1990 *1500    7 54.93 151 48.00 2266.9  13.3 311   1.4 326  12.0 309  GF    0.00 0.00   0   0.1   0.1 2174
 24 03 1990 *1508    7 56.09 151 46.64 2268.7  13.2 311   1.3 332  12.0 309  GF    0.00 0.00   0   0.2   0.1 2175
 24 03 1990  1511    7 56.5  151 46.1  2269.4  13.1 312   1.3 332  11.9 310  c/cs                            2176
 24 03 1990 *1513    7 56.82 151 45.81 2269.8  13.2 312   1.3 326  11.9 310  GF    0.00 0.00   0   0.1   0.1 2177
 24 03 1990 *1518    7 57.55 151 44.98 2270.9  13.5 312   1.7 324  11.9 310  GF    0.00 0.00   0   0.1   0.1 2178
 24 03 1990 *1523    7 58.30 151 44.13 2272.0  11.8 314   0.8  49  11.9 310  GF    0.00 0.00   0   0.1   0.1 2179
 24 03 1990 *1528    7 58.98 151 43.41 2273.0  12.8 313   1.0 345  11.9 310  GF    0.00 0.00   0   0.1   0.1 2180
 24 03 1990 *1533    7 59.70 151 42.62 2274.1  12.9 312   1.0 332  11.9 310  GF    0.00 0.00   0   0.1   0.1 2181
 24 03 1990  1535    7 60.0  151 42.3  2274.5  12.8 313   1.0 332  11.8 311  c/cs                            2182
 24 03 1990 *1538    8  0.42 151 41.82 2275.1  12.8 312   1.0 327  11.8 311  GF    0.00 0.00   0   0.1   0.1 2183
 24 03 1990 *1543    8  1.14 151 41.02 2276.2  12.9 312   1.1 322  11.8 311  GF    0.00 0.00   0   0.1   0.1 2184
 24 03 1990 *1548    8  1.86 151 40.21 2277.3  13.5 313   1.7 326  11.8 311  GF    0.00 0.00   0   0.1   0.1 2185
 24 03 1990  1549    8  2.0  151 40.0  2277.5  12.1 313   1.7 326  10.4 311  c/cs                            2186
 24 03 1990  1551    8  2.3  151 39.7  2277.9  13.5 312   1.7 326  11.8 310  c/cs                            2187
 24 03 1990 *1553    8  2.59 151 39.41 2278.4  12.9 312   1.2 331  11.8 310  GF    0.00 0.00   0   0.1   0.1 2188
 24 03 1990 *1558    8  3.31 151 38.60 2279.4  10.8 312   1.1 110  11.8 310  GF    0.00 0.00   0   0.1   0.1 2189
 24 03 1990 *1600    8  3.55 151 38.33 2279.8  13.0 312   1.3 336  11.8 310  GF    0.00 0.00   0   0.0   0.0 2190
 24 03 1990 *1608    8  4.72 151 37.04 2281.5  12.8 312   1.1 331  11.8 310  GF    0.00 0.00   0   0.2   0.1 2191
 24 03 1990  1608    8  4.7  151 37.0  2281.5  12.7 313   1.1 331  11.8 311  c/cs                            2192
 24 03 1990 *1613    8  5.44 151 36.25 2282.6  12.8 313   1.2 334  11.8 311  GF    0.00 0.00   0   0.1   0.1 2193
 24 03 1990 *1618    8  6.17 151 35.46 2283.7  12.8 313   1.1 331  11.8 311  GF    0.00 0.00   0   0.1   0.1 2194
 24 03 1990 *1623    8  6.89 151 34.67 2284.7  12.2 313   0.6 348  11.8 311  GF    0.00 0.00   0   0.1   0.1 2195
 24 03 1990 *1630    8  7.86 151 33.61 2286.2  13.1 313   1.5 331  11.8 311  GF    0.00 0.00   0   0.1   0.1 2196
 24 03 1990 *1638    8  9.06 151 32.32 2287.9  12.6 313   0.9 333  11.8 311  GF    0.00 0.00   0   0.2   0.1 2197
 24 03 1990  1638    8  9.1  151 32.3  2287.9  12.6 313   0.9 333  11.7 311  c/cs                            2198
 24 03 1990 *1643    8  9.77 151 31.54 2289.0  13.4 312   1.7 322  11.7 311  GF    0.00 0.00   0   0.1   0.1 2199
 24 03 1990  1645    8 10.1  151 31.2  2289.4   9.3 314   1.7 322   7.7 312  c/cs                            2200
 24 03 1990  1646    8 10.2  151 31.1  2289.6  13.4 312   1.7 322  11.8 311  c/cs                            2201
 24 03 1990 *1648    8 10.48 151 30.76 2290.0  12.5 312   0.8 331  11.8 311  GF    0.00 0.00   0   0.1   0.1 2202
 24 03 1990 *1653    8 11.18 151 29.98 2291.0  12.7 312   1.0 322  11.8 311  GF    0.00 0.00   0   0.1   0.1 2203
 24 03 1990  1653    8 11.2  151 30.0  2291.0  12.6 312   1.0 322  11.6 311  c/cs                            2204
 24 03 1990 *1658    8 11.88 151 29.19 2292.1  11.2 312   0.5 105  11.6 311  GF    0.00 0.00   0   0.1   0.1 2205
 24 03 1990 *1700    8 12.13 151 28.91 2292.5  13.3 312   1.7 320  11.6 311  GF    0.00 0.00   0   0.0   0.0 2206
 24 03 1990  1706    8 13.0  151 27.9  2293.8  13.0 313   1.7 320  11.3 312  c/cs                            2207
 24 03 1990 *1708    8 13.32 151 27.59 2294.2  12.2 312   0.9 318  11.3 312  GF    0.00 0.00   0   0.2   0.1 2208
 24 03 1990  1708    8 13.3  151 27.6  2294.2  12.7 311   0.9 318  11.8 311  c/cs                            2209
 24 03 1990 *1713    8 14.02 151 26.79 2295.3  12.7 312   1.0 328  11.8 311  GF    0.00 0.00   0   0.1   0.1 2210
 24 03 1990  1716    8 14.4  151 26.3  2295.9  12.6 312   1.0 328  11.7 311  c/cs                            2211
 24 03 1990 *1718    8 14.73 151 26.00 2296.4  12.9 312   1.2 317  11.7 311  GF    0.00 0.00   0   0.1   0.1 2212
 24 03 1990 *1723    8 15.44 151 25.19 2297.4  12.8 312   1.1 322  11.7 311  GF    0.00 0.00   0   0.1   0.1 2213
 24 03 1990 *1728    8 16.15 151 24.39 2298.5  11.0 311   0.7 131  11.7 311  GF    0.00 0.00   0   0.1   0.1 2214
 24 03 1990 *1730    8 16.39 151 24.11 2298.9  13.7 311   1.9 312  11.7 311  GF    0.00 0.00   0   0.0   0.0 2215
 24 03 1990 *1733    8 16.84 151 23.59 2299.5  13.0 311   1.3 312  11.7 311  GF    0.00 0.00   0   0.1   0.1 2216
 24 03 1990  1735    8 17.1  151 23.3  2300.0  12.6 311   1.3 312  11.4 311  c/cs                            2217
 24 03 1990 *1738    8 17.54 151 22.78 2300.6  12.5 311   1.1 312  11.4 311  GF    0.00 0.00   0   0.1   0.1 2218
 24 03 1990  1738    8 17.5  151 22.8  2300.6  12.8 311   1.1 312  11.6 311  c/cs                            2219
 24 03 1990 *1743    8 18.24 151 21.97 2301.7  12.8 311   1.1 312  11.6 311  GF    0.00 0.00   0   0.1   0.1 2220
 24 03 1990 *1748    8 18.94 151 21.16 2302.7  13.0 312   1.4 317  11.6 311  GF    0.00 0.00   0   0.1   0.1 2221
 24 03 1990 *1753    8 19.66 151 20.34 2303.8  12.4 311   0.8 309  11.6 311  GF    0.00 0.00   0   0.1   0.1 2222
 24 03 1990 *1800    8 20.61 151 19.23 2305.3  13.4 311   1.7 308  11.6 311  GF    0.00 0.00   0   0.1   0.1 2223
 24 03 1990 *1808    8 21.77 151 17.86 2307.0  12.7 311   1.1 308  11.6 311  GF    0.00 0.00   0   0.2   0.1 2224
 24 03 1990  1808    8 21.8  151 17.9  2307.0  12.9 311   1.1 308  11.8 311  c/cs                            2225
 24 03 1990 *1813    8 22.47 151 17.04 2308.1  13.1 310   1.4 299  11.8 311  GF    0.00 0.00   0   0.1   0.1 2226
```

```
#cruise ODP130JR                                   date run: Wed Jul 18 16:38:07 1990          page  43
#
#                    latitude   longitude              actual    drift        dr           prob. error       drift
#da mo  yr     time deg   min  deg   min    dist  speed cse speed hed speed cse  cmnt (smajxsmin@az)   dist   time   no.
#- - - - - - - - - - - - - - - - - - - - - - - - - - - - - - - - - - - - - - - - - - - - - - - - - - - - - - - - - - - -
24 03 1990 *1818   8 23.17 151 16.19 2309.2  12.9 310   1.1 300  11.8 311  GF    0.00 0.00   0    0.1    0.1 2227
24 03 1990 *1823   8 23.86 151 15.36 2310.3  13.0 310   1.2 297  11.8 311  GF    0.00 0.00   0    0.1    0.1 2228
24 03 1990  1826   8 24.3  151 14.9  2310.9  12.8 309   1.2 297  11.6 310  c/cs                              2229
24 03 1990 *1828   8 24.54 151 14.52 2311.4  10.8 312   0.9 106  11.6 310  GF    0.00 0.00   0    0.1    0.1 2230
24 03 1990 *1830   8 24.78 151 14.25 2311.7  13.4 310   1.8 308  11.6 310  GF    0.00 0.00   0    0.0    0.0 2231
24 03 1990 *1838   8 25.92 151 12.86 2313.5  13.1 309   1.5 304  11.6 310  GF    0.00 0.00   0    0.2    0.1 2232
24 03 1990 *1843   8 26.61 151 12.01 2314.6  13.0 310   1.4 311  11.6 310  GF    0.00 0.00   0    0.1    0.1 2233
24 03 1990 *1848   8 27.31 151 11.17 2315.7  13.2 309   1.6 304  11.6 310  GF    0.00 0.00   0    0.1    0.1 2234
24 03 1990  1852   8 27.9  151 10.5  2316.6  13.3 310   1.6 304  11.7 311  c/cs                              2235
24 03 1990 *1853   8 28.01 151 10.31 2316.8  12.6 312   0.9 322  11.7 311  GF    0.00 0.00   0    0.1    0.1 2236
24 03 1990 *1900   8 28.99 151  9.20 2318.3  14.2 310   2.5 307  11.7 311  GF    0.00 0.00   0    0.1    0.1 2237
24 03 1990 *1903   8 29.45 151  8.65 2319.0  13.1 311   1.4 307  11.7 311  GF    0.00 0.00   0    0.1    0.1 2238
24 03 1990 *1908   8 30.16 151  7.81 2320.1  13.1 311   1.4 306  11.7 311  GF    0.00 0.00   0    0.1    0.1 2239
24 03 1990 *1913   8 30.87 151  6.97 2321.2  13.0 310   1.4 299  11.7 311  GF    0.00 0.00   0    0.1    0.1 2240
24 03 1990  1917   8 31.4  151  6.3  2322.0  12.9 312   1.4 299  11.6 313  c/cs                              2241
24 03 1990 *1918   8 31.57 151  6.13 2322.2  13.4 312   1.8 303  11.6 313  GF    0.00 0.00   0    0.1    0.1 2242
24 03 1990 *1923   8 32.31 151  5.29 2323.4  12.5 312   1.0 300  11.6 313  GF    0.00 0.00   0    0.1    0.1 2243
24 03 1990 *1930   8 33.29 151  4.19 2324.8  13.9 313   2.3 314  11.6 313  GF    0.00 0.00   0    0.1    0.1 2244
24 03 1990  1930   8 33.3  151  4.2  2324.8  12.6 325   2.3 314  10.4 328  c/cs                              2245
24 03 1990  1934   8 34.0  151  3.7  2325.7  13.7 327   2.3 314  11.4 330  c/cs                              2246
24 03 1990 *1938   8 34.75 151  3.21 2326.6  12.5 328   1.2 311  11.4 330  GF    0.00 0.00   0    0.3    0.1 2247
24 03 1990  1938   8 34.7  151  3.2  2326.6  12.4 328   1.2 311  11.3 330  c/cs                              2248
24 03 1990 *1943   8 35.63 151  2.66 2327.6  12.4 329   1.1 320  11.3 330  GF    0.00 0.00   0    0.1    0.1 2249
24 03 1990 *1948   8 36.52 151  2.12 2328.6  12.6 329   1.3 319  11.3 330  GF    0.00 0.00   0    0.1    0.1 2250
24 03 1990 *1953   8 37.42 151  1.57 2329.7  11.9 331   0.6 346  11.3 330  GF    0.00 0.00   0    0.1    0.1 2251
24 03 1990  1957   8 38.1  151  1.2  2330.5  12.3 307   0.6 346  11.9 305  c/cs                              2252
24 03 1990 *2000   8 38.48 151  0.68 2331.1  14.0 305   2.1 304  11.9 305  GF    0.00 0.00   0    0.1    0.1 2253
24 03 1990 *2003   8 38.88 151  0.10 2331.8  13.2 305   1.3 305  11.9 305  GF    0.00 0.00   0    0.1    0.1 2254
24 03 1990 *2008   8 39.51 150 59.19 2332.9  13.0 304   1.2 296  11.9 305  GF    0.00 0.00   0    0.1    0.1 2255
24 03 1990 *2013   8 40.12 150 58.28 2334.0  12.9 304   1.1 298  11.9 305  GF    0.00 0.00   0    0.1    0.1 2256
24 03 1990 *2018   8 40.73 150 57.38 2335.1  12.9 304   1.0 293  11.9 305  GF    0.00 0.00   0    0.1    0.1 2257
24 03 1990  2021   8 41.1  150 56.8  2335.7  13.2 303   1.0 293  12.1 304  c/cs                              2258
24 03 1990 *2023   8 41.33 150 56.47 2336.1  13.3 304   1.2 304  12.1 304  GF    0.00 0.00   0    0.1    0.1 2259
24 03 1990  2025   8 41.6  150 56.1  2336.6  13.0 305   1.2 304  11.8 305  c/cs                              2260
24 03 1990 *2028   8 41.95 150 55.56 2337.2  11.6 305   0.3 131  11.8 305  GF    0.00 0.00   0    0.1    0.1 2261
24 03 1990 *2030   8 42.17 150 55.24 2337.6  13.4 304   1.6 297  11.8 305  GF    0.00 0.00   0    0.0    0.0 2262
24 03 1990 *2038   8 43.17 150 53.74 2339.4  13.3 304   1.5 300  11.8 305  GF    0.00 0.00   0    0.2    0.1 2263
24 03 1990  2039   8 43.3  150 53.6  2339.6  12.2 304   1.5 300  10.7 305  c/cs                              2264
24 03 1990  2041   8 43.5  150 53.2  2340.0  13.4 304   1.5 300  11.9 305  c/cs                              2265
24 03 1990 *2043   8 43.78 150 52.84 2340.5  13.2 305   1.3 305  11.9 305  GF    0.00 0.00   0    0.1    0.1 2266
24 03 1990 *2048   8 44.41 150 51.93 2341.6  13.1 305   1.2 308  11.9 305  GF    0.00 0.00   0    0.1    0.1 2267
24 03 1990 *2053   8 45.04 150 51.03 2342.7  12.6 305   0.7 305  11.9 305  GF    0.00 0.00   0    0.1    0.1 2268
24 03 1990  2059   8 45.8  150 50.0  2343.9  12.6 304   0.7 305  11.9 304  c/cs                              2269
24 03 1990 *2100   8 45.88 150 49.81 2344.1  13.6 305   1.7 312  11.9 304  GF    0.00 0.00   0    0.1    0.1 2270
24 03 1990 *2108   8 46.92 150 48.31 2346.0  13.1 305   1.2 310  11.9 304  GF    0.00 0.00   0    0.2    0.1 2271
24 03 1990 *2113   8 47.54 150 47.40 2347.0  13.3 305   1.4 311  11.9 304  GF    0.00 0.00   0    0.1    0.1 2272
24 03 1990 *2118   8 48.17 150 46.48 2348.2  13.3 305   1.4 317  11.9 304  GF    0.00 0.00   0    0.1    0.1 2273
24 03 1990  2119   8 48.3  150 46.3  2348.4  13.2 305   1.4 317  11.8 304  c/cs                              2274
24 03 1990 *2123   8 48.81 150 45.57 2349.3  13.1 305   1.3 318  11.8 304  GF    0.00 0.00   0    0.1    0.1 2275
24 03 1990 *2128   8 49.44 150 44.67 2350.3  13.3 305   1.5 314  11.8 304  GF    0.00 0.00   0    0.1    0.1 2276
24 03 1990 *2133   8 50.08 150 43.75 2351.5  13.3 305   1.5 317  11.8 304  GF    0.00 0.00   0    0.1    0.1 2277
24 03 1990 *2138   8 50.72 150 42.84 2352.6  13.3 305   1.4 311  11.8 304  GF    0.00 0.00   0    0.1    0.1 2278
24 03 1990 *2143   8 51.35 150 41.92 2353.7  13.3 304   1.5 302  11.8 304  GF    0.00 0.00   0    0.1    0.1 2279
```

```
#cruise ODP130JR                                      date run: Wed Jul 18 16:38:07 1990          page  44
#
#                      latitude  longitude                  actual    drift        dr                prob. error        drift
#da mo   yr    time deg   min  deg   min      dist speed cse speed hed speed cse  cmnt (smajxsmin@az)  dist  time   no.
#- - - - - - - - - - - - - - - - - - - - - - - - - - - - - - - - - - - - - - - - - - - - - - - - - - - - - - - - - - -
 24 03 1990  2143    8 51.3  150 41.9   2353.7  13.3 305   1.5 302  11.8 305  c/cs                                2280
 24 03 1990 *2148    8 51.98 150 41.00  2354.8  13.3 305   1.5 302  11.8 305  GF    0.00 0.00   0   0.1   0.1  2281
 24 03 1990 *2153    8 52.61 150 40.08  2355.9  12.7 305   0.9 305  11.8 305  GF    0.00 0.00   0   0.1   0.1  2282
 24 03 1990 *2200    8 53.46 150 38.85  2357.4  13.7 305   1.9 306  11.8 305  GF    0.00 0.00   0   0.1   0.1  2283
 24 03 1990 *2208    8 54.51 150 37.34  2359.2  13.2 305   1.3 305  11.8 305  GF    0.00 0.00   0   0.2   0.1  2284
 24 03 1990 *2213    8 55.14 150 36.43  2360.3  13.1 305   1.3 309  11.8 305  GF    0.00 0.00   0   0.1   0.1  2285
 24 03 1990  2213    8 55.1  150 36.4   2360.3  13.2 305   1.3 309  11.9 305  c/cs                                2286
 24 03 1990 *2218    8 55.78 150 35.52  2361.4  13.1 305   1.2 301  11.9 305  GF    0.00 0.00   0   0.1   0.1  2287
 24 03 1990 *2223    8 56.40 150 34.61  2362.5  13.1 305   1.2 301  11.9 305  GF    0.00 0.00   0   0.1   0.1  2288
 24 03 1990 *2228    8 57.02 150 33.70  2363.6  11.3 306   0.6 111  11.9 305  GF    0.00 0.00   0   0.1   0.1  2289
 24 03 1990 *2230    8 57.24 150 33.39  2364.0  13.5 305   1.6 303  11.9 305  GF    0.00 0.00   0   0.0   0.0  2290
 24 03 1990  2236    8 58.0  150 32.3   2365.3  13.6 305   1.6 303  12.1 305  c/cs                                2291
 24 03 1990 *2238    8 58.27 150 31.89  2365.8  13.0 304   1.0 294  12.1 305  GF    0.00 0.00   0   0.2   0.1  2292
 24 03 1990 *2243    8 58.88 150 30.98  2366.8  12.8 304   0.7 293  12.1 305  GF    0.00 0.00   0   0.1   0.1  2293
 24 03 1990 *2246    8 59.48 150 30.09  2367.9  12.8 305   0.8 311  12.1 305  GF    0.00 0.00   0   0.1   0.1  2294
 24 03 1990  2252    8 60.0  150 29.4   2368.8  12.8 306   0.8 311  12.0 306  c/cs                                2295
 24 03 1990 *2253    9  0.10 150 29.21  2369.0  12.4 306   0.4 291  12.0 306  GF    0.00 0.00   0   0.1   0.1  2296
 24 03 1990 *2300    9  0.94 150 28.02  2370.4  13.3 305   1.3 298  12.0 306  GF    0.00 0.00   0   0.0   0.1  2297
 24 03 1990  2302    9  1.2  150 27.7   2370.9  13.2 307   1.3 298  11.9 308  c/cs                                2298
 24 03 1990 *2308    9  1.99 150 26.59  2372.2  12.8 307   0.9 300  11.9 308  GF    0.00 0.00   0   0.2   0.1  2299
 24 03 1990 *2313    9  2.64 150 25.73  2373.2  12.7 308   0.8 304  11.9 308  GF    0.00 0.00   0   0.1   0.1  2300
 24 03 1990 *2318    9  3.29 150 24.88  2374.3  12.8 308   0.8 304  11.9 308  GF    0.00 0.00   0   0.1   0.1  2301
 24 03 1990 *2323    9  3.94 150 24.03  2375.4  12.5 308   0.6 299  11.9 308  GF    0.00 0.00   0   0.1   0.1  2302
 24 03 1990 *2330    9  4.83 150 22.86  2376.8  13.4 308   1.5 306  11.9 308  GF    0.00 0.00   0   0.1   0.1  2303
 24 03 1990  2332    9  5.1  150 22.5   2377.3  13.5 308   1.5 306  12.0 308  c/cs                                2304
 24 03 1990 *2338    9  5.93 150 21.42  2378.6  12.7 307   0.7 296  12.0 308  GF    0.00 0.00   0   0.2   0.1  2305
 24 03 1990 *2343    9  6.57 150 20.57  2379.7  12.9 308   0.9 311  12.0 308  GF    0.00 0.00   0   0.1   0.1  2306
 24 03 1990  2346    9  7.0  150 20.1   2380.3  12.9 307   0.9 311  12.0 307  c/cs                                2307
 24 03 1990 *2348    9  7.23 150 19.71  2380.8  12.9 308   0.9 319  12.0 307  GF    0.00 0.00   0   0.1   0.1  2308
 24 03 1990 *2353    9  7.89 150 18.85  2381.8  12.9 308   1.0 317  12.0 307  GF    0.00 0.00   0   0.1   0.1  2309
 25 03 1990  0000    9  8.8  150 17.6   2383.3  12.9 308   1.0 317  12.0 307  c/cs                                2310
 25 03 1990 *0008    9  9.87 150 16.26  2385.1  12.9 309   0.9 330  12.0 307  GF    0.00 0.00   0   0.2   0.2  2311
 25 03 1990 *0013    9 10.54 150 15.41  2386.1  12.5 308   0.6 322  12.0 307  GF    0.00 0.00   0   0.1   0.1  2312
 25 03 1990  0014    9 10.7  150 15.2   2386.4  12.6 307   0.6 322  12.1 306  c/cs                                2313
 25 03 1990 *0018    9 11.17 150 14.56  2387.2  13.1 307   1.1 321  12.1 306  GF    0.00 0.00   0   0.0   0.1  2314
 25 03 1990 *0023    9 11.83 150 13.68  2388.3  13.0 307   0.9 318  12.1 306  GF    0.00 0.00   0   0.1   0.1  2315
 25 03 1990  0024    9 12.0  150 13.5   2388.5  13.0 306   0.9 318  12.1 305  c/cs                                2316
 25 03 1990 *0028    9 12.47 150 12.79  2389.4  11.3 306   0.8 115  12.1 305  GF    0.00 0.00   0   0.1   0.1  2317
 25 03 1990 *0030    9 12.69 150 12.48  2389.7  14.0 306   1.9 313  12.1 305  GF    0.00 0.00   0   0.0   0.0  2318
 25 03 1990 *0038    9 13.79 150 10.95  2391.6  13.1 307   1.0 324  12.1 305  GF    0.00 0.00   0   0.3   0.1  2319
 25 03 1990 *0043    9 14.44 150 10.06  2392.7  13.7 307   1.6 318  12.1 305  GF    0.00 0.00   0   0.1   0.1  2320
 25 03 1990 *0048    9 15.12 150  9.13  2393.9  12.7 308   0.9 350  12.1 305  GF    0.00 0.00   0   0.1   0.1  2321
 25 03 1990 *0053    9 15.77 150  8.28  2394.9  12.5 306   0.5 347  12.1 305  GF    0.00 0.00   0   0.1   0.1  2322
 25 03 1990  0054    9 15.9  150  8.1   2395.1  12.4 307   0.5 347  12.1 306  c/cs                                2323
 25 03 1990 *0100    9 16.65 150  7.11  2396.4  13.9 307   1.9 317  12.1 306  GF    0.00 0.00   0   0.1   0.1  2324
 25 03 1990  0104    9 17.2  150  6.4   2397.3  13.7 307   1.9 317  11.9 305  c/cs                                2325
 25 03 1990 *0108    9 17.76 150  5.62  2398.2  13.2 307   1.4 324  11.9 305  GF    0.00 0.00   0   0.2   0.1  2326
 25 03 1990 *0113    9 18.42 150  4.73  2399.3  13.0 308   1.2 333  11.9 305  GF    0.00 0.00   0   0.1   0.1  2327
 25 03 1990 *0118    9 19.08 150  3.86  2400.4  12.9 306   1.1 322  11.9 305  GF    0.00 0.00   0   0.1   0.1  2328
 25 03 1990  0118    9 19.1  150  3.9   2400.4  12.7 307   1.1 322  11.6 306  c/cs                                2329
 25 03 1990 *0123    9 19.72 150  3.01  2401.4  12.2 308   0.7 348  11.6 306  GF    0.00 0.00   0   0.1   0.1  2330
 25 03 1990 *0130    9 20.60 150  1.88  2402.9  12.9 307   1.3 312  11.6 306  GF    0.00 0.00   0   0.1   0.1  2331
 25 03 1990  0137    9 21.5  150  0.7   2404.4  13.3 306   1.3 312  12.0 305  c/cs                                2332
```

```
#cruise ODP130JR                              date run: Wed Jul 18 16:38:07 1990        page  45
#
#                  latitude  longitude          actual   drift      dr               prob. error     drift
#da mo  yr   time deg   min  deg   min    dist speed cse speed hed speed cse  cmnt (smajxsmin@az) dist  time  no.
#- - - - - - - - - - - - - - - - - - - - - - - - - - - - - - - - - - - - - - - - - - - - - - - - - - - - - - -
 25 03 1990 *0138   9 21.63 150  0.47 2404.6  13.3 307   1.3 321  12.0 305  GF   0.00 0.00   0   0.2   0.1 2333
 25 03 1990 *0143   9 22.29 149 59.57 2405.7  13.2 308   1.4 335  12.0 305  GF   0.00 0.00   0   0.1   0.1 2334
 25 03 1990 *0148   9 22.97 149 58.69 2406.8  13.1 307   1.2 321  12.0 305  GF   0.00 0.00   0   0.1   0.1 2335
 25 03 1990  0148   9 23.0  149 58.7  2406.8  13.1 307   1.2 321  11.9 305  c/cs                           2336
 25 03 1990 *0153   9 23.62 149 57.80 2407.9  12.3 307   0.5 358  11.9 305  GF   0.00 0.00   0   0.1   0.1 2337
 25 03 1990 *0200   9 24.48 149 56.64 2409.3  13.5 308   1.7 332  11.9 305  GF   0.00 0.00   0   0.1   0.1 2338
 25 03 1990  0203   9 24.9  149 56.1  2410.0  13.6 308   1.7 332  12.1 305  c/cs                           2339
 25 03 1990 *0208   9 25.60 149 55.26 2411.1  13.0 307   1.0 330  12.1 305  GF   0.00 0.00   0   0.2   0.1 2340
 25 03 1990 *0213   9 26.25 149 54.32 2412.2  13.2 307   1.3 330  12.1 305  GF   0.00 0.00   0   0.1   0.1 2341
 25 03 1990 *0218   9 26.92 149 53.43 2413.3  12.9 308   1.0 344  12.1 305  GF   0.00 0.00   0   0.1   0.1 2342
 25 03 1990 *0223   9 27.58 149 52.57 2414.4  12.8 307   0.9 345  12.1 305  GF   0.00 0.00   0   0.1   0.1 2343
 25 03 1990  0225   9 27.8  149 52.2  2414.8  12.6 308   0.9 345  12.0 305  c/cs                           2344
 25 03 1990 *0230   9 28.48 149 51.38 2415.9  14.1 308   2.3 325  12.0 305  GF   0.00 0.00   0   0.1   0.1 2345
 25 03 1990 *0238   9 29.64 149 49.88 2417.8  12.9 307   1.1 332  12.0 305  GF   0.00 0.00   0   0.3   0.1 2346
 25 03 1990 *0243   9 30.29 149 49.01 2418.8  13.0 308   1.2 335  12.0 305  GF   0.00 0.00   0   0.1   0.1 2347
 25 03 1990 *0248   9 30.95 149 48.14 2419.9  13.2 306   1.3 318  12.0 305  GF   0.00 0.00   0   0.1   0.1 2348
 25 03 1990 *0253   9 31.60 149 47.24 2421.0  13.0 307   1.1 329  12.0 305  GF   0.00 0.00   0   0.1   0.1 2349
 25 03 1990  0255   9 31.9  149 46.9  2421.5  13.0 308   1.1 329  11.9 306  c/cs                           2350
 25 03 1990 *0258   9 32.26 149 46.37 2422.1  11.5 307   0.5 103  11.9 306  GF   0.00 0.00   0   0.1   0.1 2351
 25 03 1990 *0300   9 32.49 149 46.06 2422.5  13.9 306   2.0 309  11.9 306  GF   0.00 0.00   0   0.0   0.0 2352
 25 03 1990 *0308   9 33.59 149 44.55 2424.3  13.4 306   1.5 307  11.9 306  GF   0.00 0.00   0   0.3   0.1 2353
 25 03 1990 *0313   9 34.25 149 43.63 2425.5  13.6 306   1.7 307  11.9 306  GF   0.00 0.00   0   0.1   0.1 2354
 25 03 1990 *0318   9 34.92 149 42.70 2426.6  13.3 306   1.4 310  11.9 306  GF   0.00 0.00   0   0.1   0.1 2355
 25 03 1990  0320   9 35.2  149 42.3  2427.0  13.3 306   1.4 310  12.0 305  c/cs                           2356
 25 03 1990 *0323   9 35.57 149 41.79 2427.7  12.9 306   0.9 315  12.0 305  GF   0.00 0.00   0   0.1   0.1 2357
 25 03 1990 *0330   9 36.45 149 40.55 2429.2  13.8 306   1.8 309  12.0 305  GF   0.00 0.00   0   0.1   0.1 2358
 25 03 1990 *0338   9 37.52 149 39.03 2431.0  13.2 305   1.2 310  12.0 305  GF   0.00 0.00   0   0.2   0.1 2359
 25 03 1990 *0343   9 38.16 149 38.12 2432.2  13.4 306   1.4 318  12.0 305  GF   0.00 0.00   0   0.1   0.1 2360
 25 03 1990 *0348   9 38.82 149 37.21 2433.3  13.8 305   1.8 306  12.0 305  GF   0.00 0.00   0   0.1   0.1 2361
 25 03 1990  0350   9 39.1  149 36.8  2433.7  13.8 305   1.8 306  12.0 305  c/cs                           2362
 25 03 1990 *0353   9 39.48 149 36.26 2434.4  13.7 305   1.8 306  12.0 305  GF   0.00 0.00   0   0.1   0.1 2363
 25 03 1990 *0358   9 40.14 149 35.31 2435.6  11.6 305   0.4 129  12.0 305  GF   0.00 0.00   0   0.1   0.1 2364
 25 03 1990 *0400   9 40.36 149 34.99 2435.9  13.4 305   1.5 301  12.0 305  GF   0.00 0.00   0   0.0   0.0 2365
 25 03 1990  0402   9 40.6  149 34.6  2436.4  11.9 305   1.5 301  10.4 305  c/cs                           2366
 25 03 1990 *0408   9 41.29 149 33.62 2437.6  12.4 305   1.9 308  10.4 305  GF   0.00 0.00   0   0.2   0.1 2367
 25 03 1990  0412   9 41.8  149 32.9  2438.4  13.7 305   1.9 308  11.8 305  c/cs                           2368
 25 03 1990 *0413   9 41.90 149 32.75 2438.6  13.4 306   1.6 310  11.8 305  GF   0.00 0.00   0   0.2   0.1 2369
 25 03 1990  0417   9 42.4  149 32.0  2439.5  13.4 306   1.6 310  11.8 305  c/cs                           2370
 25 03 1990 *0418   9 42.55 149 31.83 2439.7  13.1 305   1.3 309  11.8 305  GF   0.00 0.00   0   0.1   0.1 2371
 25 03 1990 *0423   9 43.18 149 30.93 2440.8  13.0 305   1.2 305  11.8 305  GF   0.00 0.00   0   0.1   0.1 2372
 25 03 1990 *0430   9 44.05 149 29.67 2442.4  13.8 305   2.0 307  11.8 305  GF   0.00 0.00   0   0.1   0.1 2373
 25 03 1990 *0438   9 45.11 149 28.15 2444.2  13.7 305   1.9 306  11.8 305  GF   0.00 0.00   0   0.3   0.1 2374
 25 03 1990 *0443   9 45.77 149 27.20 2445.3  13.4 306   1.6 311  11.8 305  GF   0.00 0.00   0   0.2   0.1 2375
 25 03 1990  0447   9 46.3  149 26.5  2446.2  13.4 306   1.6 311  11.8 305  c/cs                           2376
 25 03 1990 *0448   9 46.42 149 26.28 2446.4  14.0 311   2.6 342  11.8 305  GF   0.00 0.00   0   0.1   0.1 2377
 25 03 1990  0504   9 48.9  149 23.4  2450.2  14.0 311   2.6 342  11.8 305  c/cs                           2378
 25 03 1990 *0508   9 49.51 149 22.73 2451.1  12.6 301   1.3 254  11.8 305  GF   0.00 0.00   0   0.9   0.3 2379
 25 03 1990  0517   9 50.5  149 21.1  2453.0  12.6 301   1.3 254  11.8 305  c/cs                           2380
 25 03 1990 *0518   9 50.58 149 20.89 2453.2  13.4 308   1.7 331  11.8 305  GF   0.00 0.00   0   0.2   0.2 2381
 25 03 1990 *0523   9 51.27 149 20.00 2454.3  13.3 306   1.5 314  11.8 305  GF   0.00 0.00   0   0.1   0.1 2382
 25 03 1990  0526   9 51.7  149 19.5  2455.0  13.3 306   1.5 314  11.8 305  c/cs                           2383
 25 03 1990 *0528   9 51.92 149 19.09 2455.4  11.5 305   0.3 127  11.8 305  GF   0.00 0.00   0   0.1   0.1 2384
 25 03 1990 *0530   9 52.14 149 18.77 2455.8  13.2 303   1.4 284  11.8 305  GF   0.00 0.00   0   0.0   0.0 2385
```

```
#cruise ODP130JR                                            date run: Wed Jul 18 16:38:07 1990          page  46
#
#                        latitude  longitude               actual    drift         dr                  prob. error        drift
#da mo   yr    time deg   min   deg   min      dist speed cse speed hed speed cse  cmnt (smajxsmin@az)  dist   time   no.
#- - - - - - - - - - - - - - - - - - - - - - - - - - - - - - - - - - - - - - - - - - - - - - - - - - - - - - - - - - - -
 25 03 1990  0535   9 52.7  149 17.8  2456.9  13.2 303   1.4 284  11.8 305  c/cs                                    2386
 25 03 1990 *0538   9 53.09 149 17.27 2457.6  13.4 307   1.6 320  11.8 305  GF     0.00 0.00   0    0.2    0.1 2387
 25 03 1990 *0543   9 53.76 149 16.36 2458.7  13.1 305   1.3 306  11.8 305  GF     0.00 0.00   0    0.1    0.1 2388
 25 03 1990 *0548   9 54.39 149 15.45 2459.8  13.4 304   1.6 295  11.8 305  GF     0.00 0.00   0    0.1    0.1 2389
 25 03 1990 *0553   9 55.01 149 14.51 2460.9  12.7 307   1.0 328  11.8 305  GF     0.00 0.00   0    0.1    0.1 2390
 25 03 1990 *0600   9 55.90 149 13.30 2462.4  12.9 298   1.8 247  11.8 305  GF     0.00 0.00   0    0.1    0.1 2391
 25 03 1990  0604   9 56.3  149 12.5  2463.3  13.1 298   1.8 247  12.0 305  c/cs                                    2392
 25 03 1990 *0608   9 56.72 149 11.75 2464.1  13.3 306   1.3 315  12.0 305  GF     0.00 0.00   0    0.2    0.1 2393
 25 03 1990 *0613   9 57.37 149 10.84 2465.2  13.3 305   1.3 307  12.0 305  GF     0.00 0.00   0    0.1    0.1 2394
 25 03 1990 *0618   9 58.01 149  9.92 2466.4  12.7 306   0.7 322  12.0 305  GF     0.00 0.00   0    0.1    0.1 2395
 25 03 1990 *0623   9 58.63 149  9.05 2467.4  12.8 307   0.9 334  12.0 305  GF     0.00 0.00   0    0.1    0.1 2396
 25 03 1990  0623   9 58.6  149  9.0  2467.4  12.6 307   0.9 334  11.8 305  c/cs                                    2397
 25 03 1990 *0630   9 59.51 149  7.86 2468.9  13.6 305   1.8 306  11.8 305  GF     0.00 0.00   0    0.1    0.1 2398
 25 03 1990 *0638  10  0.55 149  6.36 2470.7  13.4 306   1.6 311  11.8 305  GF     0.00 0.00   0    0.2    0.1 2399
 25 03 1990 *0643  10  1.20 149  5.44 2471.8  12.6 305   0.8 312  11.8 305  GF     0.00 0.00   0    0.1    0.1 2400
 25 03 1990 *0648  10  1.81 149  4.57 2472.8  12.7 306   0.9 316  11.8 305  GF     0.00 0.00   0    0.1    0.1 2401
 25 03 1990  0652  10  2.3  149  3.9  2473.7  12.9 306   0.9 316  11.9 305  c/cs                                    2402
 25 03 1990 *0700  10  3.31 149  2.46 2475.4  13.5 305   1.6 306  11.9 305  GF     0.00 0.00   0    0.2    0.2 2403
 25 03 1990 *0708  10  4.35 149  0.96 2477.2  13.2 306   1.3 311  11.9 305  GF     0.00 0.00   0    0.2    0.1 2404
 25 03 1990 *0713  10  4.99 149  0.05 2478.3  13.4 305   1.5 304  11.9 305  GF     0.00 0.00   0    0.1    0.1 2405
 25 03 1990 *0718  10  5.63 148 59.12 2479.4  13.3 305   1.3 303  11.9 305  GF     0.00 0.00   0    0.1    0.1 2406
 25 03 1990  0722  10  6.1  148 58.4  2480.3  13.1 305   1.3 303  11.7 305  c/cs                                    2407
 25 03 1990 *0723  10  6.26 148 58.20 2480.5  12.3 306   0.6 324  11.7 305  GF     0.00 0.00   0    0.1    0.1 2408
 25 03 1990 *0730  10  7.10 148 57.02 2482.0  13.0 304   1.3 299  11.7 305  GF     0.00 0.00   0    0.1    0.1 2409
 25 03 1990  0733  10  7.5  148 56.5  2482.6  12.7 304   1.3 299  11.5 305  c/cs                                    2410
 25 03 1990  0737  10  7.9  148 55.8  2483.5  13.2 304   1.3 299  11.9 305  c/cs                                    2411
 25 03 1990 *0738  10  8.07 148 55.58 2483.7  13.1 304   1.2 294  11.9 305  GF     0.00 0.00   0    0.2    0.1 2412
 25 03 1990 *0743  10  8.68 148 54.66 2484.8  13.4 304   1.5 299  11.9 305  GF     0.00 0.00   0    0.1    0.1 2413
 25 03 1990 *0748  10  9.31 148 53.72 2485.9  13.6 304   1.8 295  11.9 305  GF     0.00 0.00   0    0.1    0.1 2414
 25 03 1990 *0753  10  9.94 148 52.76 2487.0  13.1 305   1.2 301  11.9 305  GF     0.00 0.00   0    0.1    0.1 2415
 25 03 1990 *0800  10 10.81 148 51.48 2488.6  14.2 306   2.3 308  11.9 305  GF     0.00 0.00   0    0.1    0.1 2416
 25 03 1990  0804  10 11.4  148 50.7  2489.5  14.4 306   2.3 308  12.1 305  c/cs                                    2417
 25 03 1990 *0806  10 11.92 148 49.90 2490.5  14.0 306   1.9 311  12.1 305  GF     0.00 0.00   0    0.3    0.1 2418
 25 03 1990 *0813  10 12.60 148 48.94 2491.6  13.9 305   1.8 302  12.1 305  GF     0.00 0.00   0    0.2    0.1 2419
 25 03 1990 *0818  10 13.26 148 47.97 2492.8  14.5 309   2.7 330  12.1 305  GF     0.00 0.00   0    0.2    0.1 2420
 25 03 1990  0821  10 13.7  148 47.4  2493.5  14.3 310   2.7 330  11.9 306  c/cs                                    2421
 25 03 1990 *0823  10 14.03 148 47.03 2494.0  14.1 309   2.3 324  11.9 306  GF     0.00 0.00   0    0.2    0.1 2422
 25 03 1990 *0828  10 14.77 148 46.10 2495.2  11.6 291   3.1 203  11.9 306  GF     0.00 0.00   0    0.2    0.1 2423
 25 03 1990 *0848  10 16.13 148 42.43 2499.0  14.9 314   3.5 342  11.9 306  GF     0.00 0.00   0    1.0    0.3 2424
 25 03 1990  0851  10 16.6  148 41.9  2499.8  14.9 314   3.5 342  11.9 306  c/cs                                    2425
 25 03 1990 *0900  10 18.20 148 40.25 2502.0  14.5 308   2.6 317  11.9 306  GF     0.00 0.00   0    0.7    0.2 2426
 25 03 1990  0905  10 18.9  148 39.3  2503.2  14.6 308   2.6 317  12.0 306  c/cs                                    2427
 25 03 1990 *0908  10 19.39 148 38.70 2504.0  13.6 308   1.6 320  12.0 306  GF     0.00 0.00   0    0.4    0.1 2428
 25 03 1990 *0913  10 20.08 148 37.79 2505.1  13.4 307   1.5 313  12.0 306  GF     0.00 0.00   0    0.1    0.1 2429
 25 03 1990 *0918  10 20.75 148 36.88 2506.2  13.5 307   1.5 311  12.0 306  GF     0.00 0.00   0    0.1    0.1 2430
 25 03 1990  0920  10 21.0  148 36.5  2506.7  13.6 307   1.5 311  12.1 306  c/cs                                    2431
 25 03 1990 *0923  10 21.42 148 35.96 2507.3  13.1 307   1.1 319  12.1 306  GF     0.00 0.00   0    0.1    0.1 2432
 25 03 1990 *0930  10 22.34 148 34.72 2508.9  14.2 306   2.1 308  12.1 306  GF     0.00 0.00   0    0.1    0.1 2433
 25 03 1990 *0938  10 23.46 148 33.17 2510.8  13.4 306   1.3 303  12.1 306  GF     0.00 0.00   0    0.3    0.1 2434
 25 03 1990 *0943  10 24.11 148 32.25 2511.9  13.4 308   1.4 321  12.1 306  GF     0.00 0.00   0    0.1    0.1 2435
 25 03 1990 *0948  10 24.79 148 31.35 2513.0  12.9 307   0.8 318  12.1 306  GF     0.00 0.00   0    0.1    0.1 2436
 25 03 1990  0950  10 25.0  148 31.0  2513.4  12.8 307   0.8 318  12.0 306  c/cs                                    2437
 25 03 1990 *0953  10 25.43 148 30.48 2514.1  13.1 306   1.1 304  12.0 306  GF     0.00 0.00   0    0.1    0.1 2438
```

```
#cruise ODP130JR                                   date run: Wed Jul 18 16:38:07 1990           page  47
#
#                     latitude  longitude               actual   drift          dr               prob. error          drift
#da mo   yr    time deg   min  deg   min     dist speed cse speed hed speed cse  cmnt (smajxsmin@az)   dist  time   no.
#- - - - - - - - - - - - - - - - - - - - - - - - - - - - - - - - - - - - - - - - - - - - - - - - - - - - - - - - - -
 25 03 1990 *0958  10 26.07 148 29.58 2515.1  10.4 307   1.7 118  12.0 306  GF   0.00 0.00   0    0.1    0.1 2439
 25 03 1990 *1000  10 26.28 148 29.30 2515.5  13.1 306   1.1 300  12.0 306  GF   0.00 0.00   0    0.1    0.0 2440
 25 03 1990  1020  10 28.8  148 25.7  2519.9  13.1 306   1.1 300  12.1 307  c/cs                           2441
 25 03 1990  1039  10 31.3  148 22.3  2524.0  12.8 306   1.1 300  11.8 307  c/cs                           2442
 25 03 1990  1045  10 32.0  148 21.2  2525.3  13.2 306   1.1 300  12.2 307  c/cs                           2443
 25 03 1990 *1048  10 32.44 148 20.70 2526.0  13.3 307   1.1 310  12.2 307  GF   0.00 0.00   0    0.8    0.8 2444
 25 03 1990  1048  10 32.4  148 20.7  2526.0  13.2 306   1.1 310  12.0 306  c/cs                           2445
 25 03 1990 *1053  10 33.09 148 19.80 2527.1  12.6 306   0.5 303  12.0 306  GF   0.00 0.00   0    0.1    0.1 2446
 25 03 1990 *1100  10 33.95 148 18.59 2528.5  13.8 307   1.8 315  12.0 306  GF   0.00 0.00   0    0.1    0.1 2447
 25 03 1990 *1108  10 35.06 148 17.10 2530.4  13.1 307   1.1 316  12.0 306  GF   0.00 0.00   0    0.2    0.1 2448
 25 03 1990  1108  10 35.1  148 17.1  2530.4  13.1 308   1.1 316  12.0 307  c/cs                           2449
 25 03 1990 *1113  10 35.73 148 16.22 2531.4  13.3 306   1.3 301  12.0 307  GF   0.00 0.00   0    0.1    0.1 2450
 25 03 1990 *1118  10 36.39 148 15.31 2532.6  13.1 308   1.0 318  12.0 307  GF   0.00 0.00   0    0.1    0.1 2451
 25 03 1990  1122  10 36.9  148 14.6  2533.4  13.0 309   1.0 318  12.0 308  c/cs                           2452
 25 03 1990 *1123  10 37.06 148 14.44 2533.6  13.2 307   1.3 301  12.0 308  GF   0.00 0.00   0    0.1    0.1 2453
 25 03 1990  1131  10 38.1  148 13.0  2535.4  13.3 307   1.3 301  12.0 308  c/cs                           2454
 25 03 1990  1201  10 42.2  148  7.7  2542.0  13.3 307   1.3 301  12.0 308  c/cs                           2455
 25 03 1990  1205  10 42.7  148  6.9  2542.9  13.3 307   1.3 301  12.0 308  c/cs                           2456
 25 03 1990  1234  10 46.6  148  1.7  2549.4  13.3 307   1.3 301  12.0 308  c/cs                           2457
 25 03 1990  1304  10 50.6  147 56.3  2556.0  13.2 307   1.3 301  12.0 308  c/cs                           2458
 25 03 1990  1329  10 54.0  147 51.9  2561.5  13.4 306   1.3 301  12.2 307  c/cs                           2459
 25 03 1990  1334  10 54.6  147 51.0  2562.6  13.2 307   1.3 301  11.9 308  c/cs                           2460
 25 03 1990  1400  10 58.1  147 46.3  2568.3  13.4 307   1.3 301  12.1 308  c/cs                           2461
 25 03 1990  1430  11  2.2  147 40.9  2575.1  13.4 306   1.3 301  12.1 307  c/cs                           2462
 25 03 1990 *1443  11  3.89 147 38.53 2578.0  13.4 306   1.2 299  12.1 307  GF   0.00 0.00   0    4.3    3.3 2463
 25 03 1990  1443  11  3.9  147 38.5  2578.0  13.3 307   1.2 299  12.1 308  c/cs                           2464
 25 03 1990 *1448  11  4.56 147 37.63 2579.1  13.6 307   1.6 303  12.1 308  GF   0.00 0.00   0    0.1    0.1 2465
 25 03 1990 *1453  11  5.25 147 36.71 2580.2  13.1 308   1.0 307  12.1 308  GF   0.00 0.00   0    0.1    0.1 2466
 25 03 1990 *1508  11  7.26 147 34.08 2583.5  13.7 306   1.6 291  12.1 308  GF   0.00 0.00   0    0.3    0.2 2467
 25 03 1990 *1513  11  7.93 147 33.14 2584.6  13.6 306   1.6 292  12.1 308  GF   0.00 0.00   0    0.1    0.1 2468
 25 03 1990  1513  11  7.9  147 33.1  2584.6  13.7 305   1.6 292  12.2 307  c/cs                           2469
 25 03 1990 *1518  11  8.59 147 32.19 2585.8  12.9 307   0.7 299  12.2 307  GF   0.00 0.00   0    0.1    0.1 2470
 25 03 1990 *1523  11  9.23 147 31.31 2586.8  12.6 307   0.4 310  12.2 307  GF   0.00 0.00   0    0.1    0.1 2471
 25 03 1990  1523  11  9.2  147 31.3  2586.8  12.5 306   0.4 310  12.1 306  c/cs                           2472
 25 03 1990 *1530  11 10.09 147 30.11 2588.3  14.3 306   2.3 305  12.1 306  GF   0.00 0.00   0    0.0    0.1 2473
 25 03 1990 *1538  11 11.21 147 28.53 2590.2  13.5 303   1.6 279  12.1 306  GF   0.00 0.00   0    0.3    0.1 2474
 25 03 1990  1538  11 11.2  147 28.5  2590.2  13.5 303   1.6 279  12.0 306  c/cs                           2475
 25 03 1990 *1543  11 11.82 147 27.57 2591.3  13.6 307   1.6 315  12.0 306  GF   0.00 0.00   0    0.1    0.1 2476
 25 03 1990 *1548  11 12.50 147 26.65 2592.5  13.5 305   1.5 301  12.0 306  GF   0.00 0.00   0    0.1    0.1 2477
 25 03 1990 *1553  11 13.15 147 25.72 2593.6  12.6 306   0.6 300  12.0 306  GF   0.00 0.00   0    0.1    0.1 2478
 25 03 1990 *1600  11 14.01 147 24.50 2595.1  14.5 305   2.5 301  12.0 306  GF   0.00 0.00   0    0.1    0.1 2479
 25 03 1990  1606  11 14.8  147 23.3  2596.5  14.5 304   2.5 301  12.0 305  c/cs                           2480
 25 03 1990 *1613  11 15.80 147 21.87 2598.2  13.3 304   1.3 294  12.0 305  GF   0.00 0.00   0    0.5    0.2 2481
 25 03 1990 *1618  11 16.42 147 20.93 2599.3  13.5 304   1.5 297  12.0 305  GF   0.00 0.00   0    0.1    0.1 2482
 25 03 1990 *1623  11 17.05 147 19.98 2600.4  12.9 304   0.9 290  12.0 305  GF   0.00 0.00   0    0.1    0.1 2483
 25 03 1990 *1630  11 17.89 147 18.71 2601.9  14.4 304   2.4 298  12.0 305  GF   0.00 0.00   0    0.1    0.1 2484
 25 03 1990  1636  11 18.7  147 17.5  2603.4  14.4 304   2.4 298  11.9 305  c/cs                           2485
 25 03 1990 *1638  11 18.96 147 17.08 2603.9  13.6 304   1.7 295  11.9 305  GF   0.00 0.00   0    0.3    0.1 2486
 25 03 1990 *1643  11 19.59 147 16.12 2605.0  12.9 303   1.1 274  11.9 305  GF   0.00 0.00   0    0.1    0.1 2487
 25 03 1990  1646  11 19.9  147 15.6  2605.6  10.4 304   1.1 274   9.5 307  c/cs                           2488
 25 03 1990 *1648  11 20.13 147 15.27 2606.0  10.3 303   1.1 265   9.5 307  GF   0.00 0.00   0    0.1    0.1 2489
 25 03 1990  1649  11 20.2  147 15.1  2606.1   7.7 301   1.1 265   6.8 307  c/cs                           2490
 25 03 1990 *1653  11 20.49 147 14.68 2606.7   7.2 301   0.8 242   6.8 307  GF   0.00 0.00   0    0.1    0.1 2491
```

```
                                                           date run: Wed Jul 18 16:38:07 1990          page  48
#cruise ODP130JR
#                                                          actual    drift       dr              prob  error       drift
#                          latitude  longitude                                                                              
#da mo  yr    time  deg   min  deg   min       dist  speed cse  speed hed  speed cse   cmnt  (smajxsmin@az)    dist  time   no.
#- - - - - - - - - - - - - - - - - - - - - - - - - - - - - - - - - - - - - - - - - - - - - - - - - - - - - - - - - - - - - - -
 25 03 1990   1654  11 20.6   147 14.6   2606.8    6.6 300   0.8 242   6.2 306   c/cs                                   2492
 25 03 1990  *1700  11 20.88  147 13.99  2607.4    8.0 302   1.8 287   6.2 306   GF    0.00 0.00   0    0.1    0.1   2493
 25 03 1990   1700  11 20.9   147 14.0   2607.4    7.9 300   1.8 287   6.2 304   c/cs                                   2494
 25 03 1990  *1708  11 21.41  147 13.06  2608.5    7.3 300   1.2 278   6.2 304   GF    0.00 0.00   0    0.2    0.1   2495
 25 03 1990   1708  11 21.4   147 13.1   2608.5    9.6 301   1.2 278   8.5 304   c/cs                                   2496
 25 03 1990  *1713  11 21.82  147 12.36  2609.3    8.9 304   0.4 300   8.5 304   GF    0.00 0.00   0    0.1    0.1   2497
 25 03 1990   1714  11 21.9   147 12.2   2609.4    9.4 305   0.4 300   9.0 305   c/cs                                   2498
 25 03 1990  *1718  11 22.26  147 11.71  2610.1   10.1 301   1.2 271   9.0 305   GF    0.00 0.00   0    0.0    0.1   2499
 25 03 1990   1720  11 22.4   147 11.4   2610.4    8.6 300   1.2 271   7.5 305   c/cs                                   2500
 25 03 1990  *1723  11 22.65  147 11.04  2610.8    8.1 303   0.6 275   7.5 305   GF    0.00 0.00   0    0.1    0.1   2501
 25 03 1990  *1730  11 23.16  147 10.23  2611.8    9.1 300   1.7 278   7.5 305   GF    0.00 0.00   0    0.1    0.1   2502
 25 03 1990  *1735  11 23.54  147  9.56  2612.5    8.3 303   0.8 283   7.5 305   GF    0.00 0.00   0    0.1    0.1   2503
 25 03 1990   1737  11 23.7   147  9.3   2612.8    7.8 303   0.8 283   7.0 305   c/cs                                   2504
 25 03 1990  *1740  11 23.90  147  8.99  2613.2    8.0 303   1.0 288   7.0 305   GF    0.00 0.00   0    0.1    0.1   2505
 25 03 1990  *1745  11 24.26  147  8.42  2613.9    8.3 301   1.4 283   7.0 305   GF    0.00 0.00   0    0.1    0.1   2506
 25 03 1990  *1750  11 24.62  147  7.82  2614.6    8.4 302   1.5 286   7.0 305   GF    0.00 0.00   0    0.1    0.1   2507
 25 03 1990   1750  11 24.6   147  7.8   2614.6    8.0 302   1.5 286   6.6 305   c/cs                                   2508
 25 03 1990  *1755  11 24.97  147  7.24  2615.2    8.1 298   1.8 271   6.6 305   GF    0.00 0.00   0    0.1    0.1   2509
 25 03 1990   1755  11 25.0   147  7.2   2615.2    8.6 298   1.8 271   7.0 305   c/cs                                   2510
 25 03 1990  *1800  11 25.31  147  6.60  2615.9    8.3 300   1.4 277   7.0 305   GF    0.00 0.00   0    0.1    0.1   2511
 25 03 1990  *1805  11 25.66  147  5.99  2616.6    8.2 303   1.2 291   7.0 305   GF    0.00 0.00   0    0.1    0.1   2512
 25 03 1990   1808  11 25.9   147  5.6   2617.0    8.5 304   1.2 291   7.3 306   c/cs                                   2513
 25 03 1990  *1810  11 26.04  147  5.40  2617.3    8.7 301   1.7 276   7.3 306   GF    0.00 0.00   0    0.1    0.1   2514
 25 03 1990  *1815  11 26.41  147  4.76  2618.0    8.1 306   0.9 307   7.3 306   GF    0.00 0.00   0    0.1    0.1   2515
 25 03 1990  *1820  11 26.81  147  4.20  2618.7    8.6 303   1.4 290   7.3 306   GF    0.00 0.00   0    0.1    0.1   2516
 25 03 1990   1823  11 27.0   147  3.8   2619.2    8.7 307   1.4 290   7.4 310   c/cs                                   2517
 25 03 1990  *1825  11 27.22  147  3.60  2619.4    8.4 307   1.1 286   7.4 310   GF    0.00 0.00   0    0.1    0.1   2518
 25 03 1990   1825  11 27.2   147  3.6   2619.4    8.4 307   1.1 286   7.4 310   c/cs                                   2519
 25 03 1990  *1830  11 27.64  147  3.03  2620.1    8.3 308   1.0 289   7.4 310   GF    0.00 0.00   0    0.1    0.1   2520
 25 03 1990   1834  11 28.0   147  2.6   2620.7    8.3 307   1.0 289   7.4 309   c/cs                                   2521
 25 03 1990  *1835  11 28.06  147  2.47  2620.8    8.6 316   1.5 350   7.4 309   GF    0.00 0.00   0    0.1    0.1   2522
 25 03 1990  *1840  11 28.57  147  1.96  2621.5    9.0 298   2.2 259   7.4 309   GF    0.00 0.00   0    0.1    0.1   2523
 25 03 1990  *1900  11 29.98  146 59.27  2624.5    9.0 305   1.8 287   7.4 309   GF    0.00 0.00   0    0.7    0.3   2524
 25 03 1990   1901  11 30.1   146 59.1   2624.7    8.8 305   1.8 287   7.2 309   c/cs                                   2525
 25 03 1990  *1905  11 30.40  146 58.65  2625.3    8.9 302   2.0 276   7.2 309   GF    0.00 0.00   0    0.1    0.1   2526
 25 03 1990   1906  11 30.5   146 58.5   2625.4    9.1 302   2.0 276   7.3 309   c/cs                                   2527
 25 03 1990  *1910  11 30.80  146 58.00  2626.0    8.4 311   1.1 325   7.3 309   GF    0.00 0.00   0    0.2    0.1   2528
 25 03 1990  *1915  11 31.26  146 57.46  2626.7    8.7 309   1.4 312   7.3 309   GF    0.00 0.00   0    0.1    0.1   2529
 25 03 1990  *1920  11 31.72  146 56.89  2627.5    8.6 307   1.3 296   7.3 309   GF    0.00 0.00   0    0.1    0.1   2530
 25 03 1990  *1925  11 32.15  146 56.31  2628.2    8.7 306   1.5 292   7.3 309   GF    0.00 0.00   0    0.1    0.1   2531
 25 03 1990  *1930  11 32.58  146 55.71  2628.9    9.1 303   1.9 280   7.3 309   GF    0.00 0.00   0    0.1    0.1   2532
 25 03 1990   1933  11 32.8   146 55.3   2629.3    9.1 302   1.9 280   7.4 308   c/cs                                   2533
 25 03 1990  *1935  11 32.99  146 55.06  2629.7    8.4 311   1.1 331   7.4 308   GF    0.00 0.00   0    0.2    0.1   2534
 25 03 1990  *1940  11 33.45  146 54.52  2630.4    8.9 305   1.5 289   7.4 308   GF    0.00 0.00   0    0.1    0.1   2535
 25 03 1990  *1945  11 33.87  146 53.90  2631.1    8.7 306   1.4 297   7.4 308   GF    0.00 0.00   0    0.1    0.1   2536
 25 03 1990  *1950  11 34.30  146 53.30  2631.8    8.9 307   1.5 305   7.4 308   GF    0.00 0.00   0    0.1    0.1   2537
 25 03 1990  *1955  11 34.75  146 52.70  2632.6    8.9 307   1.5 301   7.4 308   GF    0.00 0.00   0    0.1    0.1   2538
 25 03 1990   1957  11 34.9   146 52.5   2632.9    8.7 307   1.5 301   7.2 308   c/cs                                   2539
 25 03 1990  *2000  11 35.19  146 52.10  2633.3    8.7 306   1.5 298   7.2 308   GF    0.00 0.00   0    0.1    0.1   2540
 25 03 1990   2002  11 35.4   146 51.9   2633.6    8.9 307   1.5 298   7.3 309   c/cs                                   2541
 25 03 1990  *2005  11 35.63  146 51.50  2634.0    9.0 306   1.7 293   7.3 309   GF    0.00 0.00   0    0.1    0.1   2542
 25 03 1990  *2010  11 36.07  146 50.88  2634.8    8.6 308   1.3 300   7.3 309   GF    0.00 0.00   0    0.1    0.1   2543
 25 03 1990  *2015  11 36.51  146 50.30  2635.5    9.2 305   1.9 292   7.3 309   GF    0.00 0.00   0    0.1    0.1   2544
```

```
#cruise ODP130JR                                            date run: Wed Jul 18 16:38:07 1990          page  49
#
#                          latitude  longitude                    actual   drift          dr                 prob. error       drift
#da mo  yr      time deg   min  deg   min      dist speed cse speed hed speed cse  cmnt (smajxsmin@az)  dist  time   no.
#- - - - - - - - - - - - - - - - - - - - - - - - - - - - - - - - - - - - - - - - - - - - - - - - - - - - - - - - - - - -
 25 03 1990  2017  11 36.7  146 50.0  2635.8   8.7 305   1.9 292   6.8 309  c/cs                                     2545
 25 03 1990 *2020  11 36.94 146 49.68 2636.2   8.4 306   1.6 291   6.8 309  GF    0.00 0.00   0    0.2     0.1 2546
 25 03 1990  2021  11 37.0  146 49.6  2636.4   9.0 306   1.6 291   7.4 309  c/cs                                     2547
 25 03 1990 *2025  11 37.37 146 49.07 2637.0   8.8 308   1.4 302   7.4 309  GF    0.00 0.00   0    0.1     0.1 2548
 25 03 1990 *2030  11 37.82 146 48.48 2637.7   8.5 308   1.1 298   7.4 309  GF    0.00 0.00   0    0.1     0.1 2549
 25 03 1990 *2035  11 38.25 146 47.91 2638.4   8.8 307   1.4 296   7.4 309  GF    0.00 0.00   0    0.1     0.1 2550
 25 03 1990 *2040  11 38.69 146 47.31 2639.1   8.7 307   1.3 298   7.4 309  GF    0.00 0.00   0    0.1     0.1 2551
 25 03 1990 *2045  11 39.13 146 46.72 2639.9   8.9 307   1.5 299   7.4 309  GF    0.00 0.00   0    0.1     0.1 2552
 25 03 1990 *2050  11 39.58 146 46.12 2640.6   9.0 307   1.6 297   7.4 309  GF    0.00 0.00   0    0.1     0.1 2553
 25 03 1990  2051  11 39.7  146 46.0  2640.8   8.8 307   1.6 297   7.2 309  c/cs                                     2554
 25 03 1990 *2055  11 40.02 146 45.52 2641.3   8.8 308   1.6 303   7.2 309  GF    0.00 0.00   0    0.1     0.1 2555
 25 03 1990 *2100  11 40.47 146 44.93 2642.1   8.3 308   1.2 300   7.2 309  GF    0.00 0.00   0    0.1     0.1 2556
 25 03 1990  2103  11 40.7  146 44.6  2642.5   7.6 308   1.2 300   6.4 309  c/cs                                     2557
 25 03 1990 *2105  11 40.88 146 44.39 2642.8   7.5 307   1.1 298   6.4 309  GF    0.00 0.00   0    0.1     0.1 2558
 25 03 1990 *2110  11 41.26 146 43.88 2643.4   7.3 308   0.9 300   6.4 309  GF    0.00 0.00   0    0.1     0.1 2559
 25 03 1990  2112  11 41.4  146 43.7  2643.6   7.5 308   0.9 300   6.6 309  c/cs                                     2560
 25 03 1990 *2115  11 41.64 146 43.38 2644.0   7.3 308   0.7 294   6.6 309  GF    0.00 0.00   0    0.1     0.1 2561
 25 03 1990 *2120  11 42.01 146 42.89 2644.6   7.6 307   1.0 295   6.6 309  GF    0.00 0.00   0    0.1     0.1 2562
 25 03 1990  2121  11 42.1  146 42.8  2644.7   7.3 307   1.0 295   6.4 309  c/cs                                     2563
 25 03 1990 *2125  11 42.38 146 42.39 2645.2   7.3 308   0.9 298   6.4 309  GF    0.00 0.00   0    0.1     0.1 2564
 25 03 1990 *2130  11 42.75 146 41.90 2645.8   7.6 307   1.3 295   6.4 309  GF    0.00 0.00   0    0.1     0.1 2565
 25 03 1990 *2135  11 43.13 146 41.38 2646.5   7.2 308   0.8 302   6.4 309  GF    0.00 0.00   0    0.1     0.1 2566
 25 03 1990 *2140  11 43.50 146 40.90 2647.1   7.2 306   0.9 282   6.4 309  GF    0.00 0.00   0    0.1     0.1 2567
 25 03 1990 *2145  11 43.85 146 40.40 2647.7   7.6 308   1.2 303   6.4 309  GF    0.00 0.00   0    0.1     0.1 2568
 25 03 1990 *2150  11 44.24 146 39.89 2648.3   6.9 309   0.5 304   6.4 309  GF    0.00 0.00   0    0.1     0.1 2569
 25 03 1990  2152  11 44.4  146 39.7  2648.5   7.0 309   0.5 304   6.4 309  c/cs                                     2570
 25 03 1990 *2155  11 44.60 146 39.43 2648.9   7.5 307   1.1 297   6.4 309  GF    0.00 0.00   0    0.0     0.1 2571
 25 03 1990 *2200  11 44.98 146 38.92 2649.5   7.4 307   0.9 294   6.4 309  GF    0.00 0.00   0    0.1     0.1 2572
 25 03 1990 *2205  11 45.35 146 38.42 2650.1   7.1 309   0.6 307   6.4 309  GF    0.00 0.00   0    0.1     0.1 2573
 25 03 1990 *2210  11 45.72 146 37.95 2650.7   7.2 310   0.7 314   6.4 309  GF    0.00 0.00   0    0.1     0.1 2574
 25 03 1990 *2215  11 46.10 146 37.48 2651.3   7.2 307   0.8 290   6.4 309  GF    0.00 0.00   0    0.1     0.1 2575
 25 03 1990 *2220  11 46.46 146 36.99 2651.9   7.0 309   0.6 307   6.4 309  GF    0.00 0.00   0    0.1     0.1 2576
 25 03 1990  2222  11 46.6  146 36.8  2652.1   7.1 309   0.6 307   6.6 309  c/cs                                     2577
 25 03 1990 *2225  11 46.83 146 36.52 2652.5   7.7 307   1.1 298   6.6 309  GF    0.00 0.00   0    0.0     0.1 2578
 25 03 1990 *2230  11 47.22 146 36.00 2653.1   7.5 308   1.0 305   6.6 309  GF    0.00 0.00   0    0.1     0.1 2579
 25 03 1990  2230  11 47.2  146 36.0  2653.1   8.1 308   1.0 305   7.1 309  c/cs                                     2580
 25 03 1990 *2235  11 47.64 146 35.46 2653.8   8.0 308   1.0 299   7.1 309  GF    0.00 0.00   0    0.1     0.1 2581
 25 03 1990 *2240  11 48.05 146 34.92 2654.5   8.1 308   1.0 305   7.1 309  GF    0.00 0.00   0    0.1     0.1 2582
 25 03 1990 *2245  11 48.47 146 34.38 2655.1   8.0 308   0.9 301   7.1 309  GF    0.00 0.00   0    0.1     0.1 2583
 25 03 1990 *2249  11 48.80 146 33.95 2655.7   7.5 309   0.5 314   7.1 309  GF    0.00 0.00   0    0.1     0.1 2584
 25 03 1990 *2250  11 48.88 146 33.85 2655.8   7.9 309   0.8 307   7.1 309  GF    0.00 0.00   0    0.0     0.0 2585
 25 03 1990 *2255  11 49.29 146 33.33 2656.5   7.9 308   0.8 302   7.1 309  GF    0.00 0.00   0    0.1     0.1 2586
 25 03 1990 *2300  11 49.70 146 32.80 2657.1   8.2 309   1.1 308   7.1 309  GF    0.00 0.00   0    0.1     0.1 2587
 25 03 1990  2300  11 49.7  146 32.8  2657.1   7.8 309   1.1 308   6.8 309  c/cs                                     2588
 25 03 1990 *2305  11 50.11 146 32.28 2657.8   7.6 309   0.9 308   6.8 309  GF    0.00 0.00   0    0.1     0.1 2589
 25 03 1990  2306  11 50.2  146 32.2  2657.9   7.9 309   0.9 308   7.0 309  c/cs                                     2590
 25 03 1990 *2310  11 50.52 146 31.76 2658.4   8.1 307   1.1 295   7.0 309  GF    0.00 0.00   0    0.1     0.1 2591
 25 03 1990  2312  11 50.7  146 31.5  2658.7   7.8 307   1.1 295   6.8 309  c/cs                                     2592
 25 03 1990 *2315  11 50.92 146 31.22 2659.1   7.9 308   1.1 304   6.8 309  GF    0.00 0.00   0    0.1     0.1 2593
 25 03 1990  2317  11 51.1  146 31.0  2659.4   8.0 308   1.1 304   6.9 309  c/cs                                     2594
 25 03 1990 *2320  11 51.33 146 30.69 2659.8   8.2 308   1.3 302   6.9 309  GF    0.00 0.00   0    0.1     0.1 2595
 25 03 1990 *2325  11 51.75 146 30.14 2660.4   8.0 307   1.1 295   6.9 309  GF    0.00 0.00   0    0.1     0.1 2596
 25 03 1990 *2330  11 52.15 146 29.60 2661.1   8.0 308   1.1 300   6.9 309  GF    0.00 0.00   0    0.1     0.1 2597
```

```
#cruise ODP130JR                                date run: Wed Jul 18 16:38:07 1990        page  50
#
#                      latitude  longitude              actual   drift        dr              prob. error         drift
#da mo   yr    time deg    min deg    min     dist speed cse speed hed speed cse  cmnt (smajxsmin@az)  dist  time   no.
#- - - - - - - - - - - - - - - - - - - - - - - - - - - - - - - - - - - - - - - - - - - - - - - - - - - - - - - - - - -
 25 03 1990 *2335  11  52.56 146  29.06 2661.8   8.5 307   1.6 299   6.9 309  GF    0.00 0.00   0   0.1   0.1 2598
 25 03 1990 *2339  11  52.90 146  28.60 2662.3   6.8 309   0.2 149   6.9 309  GF    0.00 0.00   0   0.1   0.1 2599
 25 03 1990 *2340  11  52.97 146  28.51 2662.4   8.1 307   1.2 298   6.9 309  GF    0.00 0.00   0   0.0   0.0 2600
 25 03 1990 *2345  11  53.38 146  27.96 2663.1   8.0 308   1.1 305   6.9 309  GF    0.00 0.00   0   0.1   0.1 2601
 25 03 1990  2347  11  53.5  146  27.7  2663.4   8.1 308   1.1 305   7.0 309  c/cs                                2602
 25 03 1990 *2350  11  53.80 146  27.42 2663.8   7.8 309   0.8 308   7.0 309  GF    0.00 0.00   0   0.1   0.1 2603
 25 03 1990 *2355  11  54.21 146  26.90 2664.5   8.0 307   1.0 293   7.0 309  GF    0.00 0.00   0   0.1   0.1 2604
 26 03 1990 *0000  11  54.61 146  26.36 2665.1   7.9 308   0.9 303   7.0 309  GF    0.00 0.00   0   0.1   0.1 2605
 26 03 1990  0000  11  54.6  146  26.4  2665.1   7.9 308   0.9 303   7.0 309  c/cs                                2606
 26 03 1990 *0005  11  55.02 146  25.83 2665.8   8.0 307   1.0 293   7.0 309  GF    0.00 0.00   0   0.1   0.1 2607
 26 03 1990 *0010  11  55.42 146  25.29 2666.4   7.7 309   0.7 306   7.0 309  GF    0.00 0.00   0   0.1   0.1 2608
 26 03 1990 *0015  11  55.82 146  24.78 2667.1   8.6 307   1.6 301   7.0 309  GF    0.00 0.00   0   0.1   0.1 2609
 26 03 1990  0017  11  56.0  146  24.5  2667.4   8.6 307   1.6 301   7.0 309  c/cs                                2610
 26 03 1990 *0030  11  57.13 146  23.03 2669.2   7.9 308   0.8 296   7.0 309  GF    0.00 0.00   0   0.4   0.2 2611
 26 03 1990 *0035  11  57.53 146  22.50 2669.9   9.0 306   2.0 297   7.0 309  GF    0.00 0.00   0   0.1   0.1 2612
 26 03 1990  0035  11  57.5  146  22.5  2669.9   8.5 306   2.0 297   6.5 309  c/cs                                2613
 26 03 1990  0038  11  57.8  146  22.1  2670.3   9.0 306   2.0 297   7.0 309  c/cs                                2614
 26 03 1990 *0040  11  57.96 146  21.90 2670.6   8.1 305   1.1 283   7.0 309  GF    0.00 0.00   0   0.2   0.1 2615
 26 03 1990 *0045  11  58.35 146  21.34 2671.3   8.5 306   1.5 295   7.0 309  GF    0.00 0.00   0   0.1   0.1 2616
 26 03 1990 *0050  11  58.77 146  20.76 2672.0   8.1 305   1.1 283   7.0 309  GF    0.00 0.00   0   0.1   0.1 2617
 26 03 1990 *0055  11  59.16 146  20.20 2672.7   8.0 308   1.0 300   7.0 309  GF    0.00 0.00   0   0.1   0.1 2618
 26 03 1990 *0100  11  59.57 146  19.66 2673.3   8.1 306   1.2 289   7.0 309  GF    0.00 0.00   0   0.1   0.1 2619
 26 03 1990 *0105  11  59.97 146  19.10 2674.0   8.5 308   1.5 301   7.0 309  GF    0.00 0.00   0   0.1   0.1 2620
 26 03 1990  0108  12   0.2  146  18.8  2674.4   8.4 308   1.5 301   7.0 309  c/cs                                2621
 26 03 1990 *0110  12   0.40 146  18.53 2674.7   7.6 306   0.8 274   7.0 309  GF    0.00 0.00   0   0.1   0.1 2622
 26 03 1990 *0115  12   0.77 146  18.00 2675.4   8.2 307   1.3 295   7.0 309  GF    0.00 0.00   0   0.1   0.1 2623
 26 03 1990 *0120  12   1.18 146  17.44 2676.0   7.9 306   1.0 288   7.0 309  GF    0.00 0.00   0   0.1   0.1 2624
 26 03 1990 *0125  12   1.57 146  16.90 2676.7   8.3 308   1.3 300   7.0 309  GF    0.00 0.00   0   0.1   0.1 2625
 26 03 1990 *0130  12   1.99 146  16.34 2677.4   7.9 307   1.0 294   7.0 309  GF    0.00 0.00   0   0.1   0.1 2626
 26 03 1990 *0135  12   2.39 146  15.80 2678.0   8.2 308   1.2 302   7.0 309  GF    0.00 0.00   0   0.1   0.1 2627
 26 03 1990  0138  12   2.6  146  15.5  2678.5   8.2 308   1.2 302   7.0 309  c/cs                                2628
 26 03 1990 *0140  12   2.81 146  15.25 2678.7   7.4 307   0.4 274   7.0 309  GF    0.00 0.00   0   0.1   0.1 2629
 26 03 1990 *0145  12   3.18 146  14.75 2679.3   7.9 307   1.0 289   7.0 309  GF    0.00 0.00   0   0.0   0.1 2630
 26 03 1990  0148  12   3.4  146  14.4  2679.7   7.6 307   1.0 289   6.6 310  c/cs                                2631
 26 03 1990 *0150  12   3.57 146  14.22 2680.0   7.8 308   1.2 294   6.6 310  GF    0.00 0.00   0   0.1   0.1 2632
 26 03 1990  0152  12   3.7  146  14.0  2680.3   8.1 307   1.2 294   6.9 309  c/cs                                2633
 26 03 1990 *0155  12   3.97 146  13.68 2680.7   7.8 308   0.8 301   6.9 309  GF    0.00 0.00   0   0.1   0.1 2634
 26 03 1990 *0200  12   4.37 146  13.16 2681.3   7.6 309   0.6 313   6.9 309  GF    0.00 0.00   0   0.1   0.1 2635
 26 03 1990 *0205  12   4.77 146  12.66 2681.9   7.7 307   0.8 294   6.9 309  GF    0.00 0.00   0   0.1   0.1 2636
 26 03 1990 *0210  12   5.16 146  12.14 2682.6   8.1 307   1.2 293   6.9 309  GF    0.00 0.00   0   0.1   0.1 2637
 26 03 1990  0213  12   5.4  146  11.8  2683.0   8.0 307   1.2 293   6.9 309  c/cs                                2638
 26 03 1990 *0215  12   5.56 146  11.59 2683.2   7.4 309   0.5 311   6.9 309  GF    0.00 0.00   0   0.1   0.1 2639
 26 03 1990 *0220  12   5.95 146  11.10 2683.9   7.1 306   0.4 254   6.9 309  GF    0.00 0.00   0   0.0   0.1 2640
 26 03 1990 *0225  12   6.30 146  10.61 2684.5   8.0 308   1.2 301   6.9 309  GF    0.00 0.00   0   0.0   0.1 2641
 26 03 1990 *0230  12   6.71 146  10.07 2685.1   6.3 303   0.9 176   6.9 309  GF    0.00 0.00   0   0.1   0.1 2642
 26 03 1990 *0234  12   6.94 146   9.71 2685.5   5.1 306   1.8 138   6.9 309  GF    0.00 0.00   0   0.1   0.1 2643
 26 03 1990 *0235  12   6.99 146   9.64 2685.6   7.8 308   0.9 302   6.9 309  GF    0.00 0.00   0   0.0   0.0 2644
 26 03 1990 *0240  12   7.39 146   9.12 2686.3   8.9 308   2.0 304   6.9 309  GF    0.00 0.00   0   0.1   0.1 2645
 26 03 1990  0243  12   7.7  146   8.8  2686.7   8.8 308   2.0 304   6.8 309  c/cs                                2646
 26 03 1990 *0300  12   9.20 146   6.74 2689.2   6.7 305   0.5 204   6.8 309  GF    0.00 0.00   0   0.7   0.3 2647
 26 03 1990 *0305  12   9.52 146   6.27 2689.8   8.6 306   1.9 295   6.8 309  GF    0.00 0.00   0   0.0   0.1 2648
 26 03 1990  0309  12   9.9  146   5.8  2690.4   8.7 304   1.9 295   6.8 307  c/cs                                2649
 26 03 1990 *0315  12  10.35 146   5.06 2691.2   7.6 304   0.9 275   6.8 307  GF    0.00 0.00   0   0.3   0.2 2650
```

```
#cruise ODP130JR                                    date run: Wed Jul 18 16:38:07 1990          page  51
#
#                      latitude  longitude             actual   drift        dr              prob. error        drift
#da mo  yr     time deg   min  deg   min       dist speed cse speed hed speed cse  cmnt (smajxsmin@az)   dist  time   no.
#- - - - - - - - - - - - - - - - - - - - - - - - - - - - - - - - - - - - - - - - - - - - - - - - - - - - - - - - - - - -
 26 03 1990 *0320   12 10.70 146   4.52 2691.9    7.8 304   1.0 282    6.8 307  GF    0.00 0.00    0    0.1    0.1 2651
 26 03 1990 *0325   12 11.06 146   3.97 2692.5    8.2 304   1.4 289    6.8 307  GF    0.00 0.00    0    0.1    0.1 2652
 26 03 1990  0326   12 11.1  146   3.9  2692.6    7.7 304   1.4 289    6.4 307  c/cs                                2653
 26 03 1990  0329   12 11.4  146   3.5  2693.0    8.2 305   1.4 289    6.9 308  c/cs                                2654
 26 03 1990 *0330   12 11.43 146   3.41 2693.2    7.9 304   1.2 281    6.8 308  GF    0.00 0.00    0    0.1    0.1 2655
 26 03 1990 *0335   12 11.80 146   2.85 2693.8    7.7 304   1.0 277    6.8 308  GF    0.00 0.00    0    0.1    0.1 2656
 26 03 1990 *0340   12 12.16 146   2.31 2694.5    7.7 304   1.0 277    6.8 308  GF    0.00 0.00    0    0.1    0.1 2657
 26 03 1990 *0345   12 12.52 146   1.77 2695.1    8.2 305   1.4 290    6.8 308  GF    0.00 0.00    0    0.1    0.1 2658
 26 03 1990 *0350   12 12.91 146   1.20 2695.8    7.8 306   1.0 291    6.8 308  GF    0.00 0.00    0    0.1    0.1 2659
 26 03 1990 *0355   12 13.29 146   0.66 2696.4    8.0 305   1.2 286    6.8 308  GF    0.00 0.00    0    0.1    0.1 2660
 26 03 1990  0358   12 13.5  146   0.3  2696.8    8.0 305   1.2 286    6.9 308  c/cs                                2661
 26 03 1990 *0400   12 13.67 146   0.10 2697.1    8.1 306   1.2 291    6.9 308  GF    0.00 0.00    0    0.1    0.1 2662
 26 03 1990 *0405   12 14.06 145  59.54 2697.8    7.9 304   1.2 280    6.9 308  GF    0.00 0.00    0    0.1    0.1 2663
 26 03 1990 *0410   12 14.43 145  58.98 2698.4    8.0 305   1.2 286    6.9 308  GF    0.00 0.00    0    0.1    0.1 2664
 26 03 1990 *0415   12 14.81 145  58.42 2699.1    7.7 304   0.9 275    6.9 308  GF    0.00 0.00    0    0.1    0.1 2665
 26 03 1990 *0420   12 15.17 145  57.88 2699.7    8.8 304   2.0 290    6.9 308  GF    0.00 0.00    0    0.1    0.1 2666
 26 03 1990 *0424   12 15.50 145  57.38 2700.3    8.0 305   1.2 286    6.9 308  GF    0.00 0.00    0    0.1    0.1 2667
 26 03 1990  0428   12 15.8  145  56.9  2700.9    8.0 305   1.2 286    6.9 308  c/cs                                2668
 26 03 1990 *0429   12 15.88 145  56.82 2701.0    5.9 307   1.0 132    6.9 308  GF    0.00 0.00    0    0.1    0.1 2669
 26 03 1990 *0430   12 15.94 145  56.74 2701.1    8.1 304   1.3 284    6.9 308  GF    0.00 0.00    0    0.0    0.0 2670
 26 03 1990 *0435   12 16.32 145  56.17 2701.8    8.0 305   1.2 286    6.9 308  GF    0.00 0.00    0    0.1    0.1 2671
 26 03 1990 *0440   12 16.70 145  55.61 2702.4    8.0 305   1.2 286    6.9 308  GF    0.00 0.00    0    0.1    0.1 2672
 26 03 1990 *0445   12 17.08 145  55.05 2703.1    8.0 305   1.2 286    6.9 308  GF    0.00 0.00    0    0.1    0.1 2673
 26 03 1990 *0450   12 17.46 145  54.49 2703.8    8.4 310   1.5 317    6.9 308  GF    0.00 0.00    0    0.1    0.1 2674
 26 03 1990  0458   12 18.2  145  53.6  2704.9    8.4 310   1.5 317    6.9 308  c/cs                                2675
 26 03 1990 *0510   12 19.25 145  52.28 2706.6    8.4 308   1.5 308    6.9 308  GF    0.00 0.00    0    0.5    0.3 2676
 26 03 1990  0511   12 19.3  145  52.2  2706.7    7.7 308   1.5 308    6.2 308  c/cs                                2677
 26 03 1990  0514   12 19.6  145  51.9  2707.1    8.4 307   1.5 308    6.9 307  c/cs                                2678
 26 03 1990 *0515   12 19.66 145  51.74 2707.2    7.9 303   1.1 279    6.9 307  GF    0.00 0.00    0    0.1    0.1 2679
 26 03 1990 *0520   12 20.02 145  51.18 2707.9    8.0 303   1.2 279    6.9 307  GF    0.00 0.00    0    0.1    0.1 2680
 26 03 1990 *0525   12 20.38 145  50.61 2708.6    8.0 306   1.1 299    6.9 307  GF    0.00 0.00    0    0.1    0.1 2681
 26 03 1990 *0530   12 20.77 145  50.06 2709.2    7.9 307   1.1 308    6.9 307  GF    0.00 0.00    0    0.1    0.1 2682
 26 03 1990 *0535   12 21.17 145  49.52 2709.9    8.6 304   1.8 294    6.9 307  GF    0.00 0.00    0    0.1    0.1 2683
 26 03 1990  0536   12 21.3  145  49.4  2710.0    5.2 303   1.8 294    3.4 307  c/cs                                2684
 26 03 1990  0537   12 21.3  145  49.3  2710.1    8.6 304   1.8 294    6.9 307  c/cs                                2685
 26 03 1990 *0540   12 21.54 145  48.96 2710.5    8.3 304   1.5 291    6.9 307  GF    0.00 0.00    0    0.1    0.1 2686
 26 03 1990 *0545   12 21.93 145  48.37 2711.2    8.2 306   1.4 299    6.9 307  GF    0.00 0.00    0    0.1    0.1 2687
 26 03 1990 *0550   12 22.33 145  47.80 2711.9    8.3 305   1.5 297    6.9 307  GF    0.00 0.00    0    0.1    0.1 2688
 26 03 1990 *0555   12 22.73 145  47.22 2712.6    8.2 305   1.3 295    6.9 307  GF    0.00 0.00    0    0.1    0.1 2689
 26 03 1990 *0600   12 23.12 145  46.65 2713.3    6.9 288   2.2 209    6.9 307  GF    0.00 0.00    0    0.1    0.1 2690
 26 03 1990 *0605   12 23.30 145  46.09 2713.9    8.9 303   2.1 288    6.9 307  GF    0.00 0.00    0    0.2    0.1 2691
 26 03 1990  0607   12 23.5  145  45.8  2714.2    8.8 303   2.1 288    6.8 308  c/cs                                2692
 26 03 1990 *0610   12 23.70 145  45.46 2714.6    8.4 307   1.6 304    6.8 308  GF    0.00 0.00    0    0.2    0.1 2693
 26 03 1990 *0614   12 24.04 145  45.00 2715.2    6.0 300   1.2 174    6.8 308  GF    0.00 0.00    0    0.1    0.1 2694
 26 03 1990 *0615   12 24.09 145  44.91 2715.3    7.9 306   1.1 297    6.8 308  GF    0.00 0.00    0    0.0    0.0 2695
 26 03 1990 *0620   12 24.48 145  44.37 2715.9    8.2 304   1.5 288    6.8 308  GF    0.00 0.00    0    0.1    0.1 2696
 26 03 1990  0623   12 24.7  145  44.0  2716.3    8.0 312   1.5 288    6.7 317  c/cs                                2697
 26 03 1990 *0625   12 24.69 145  43.82 2716.6    7.9 314   1.2 295    6.7 317  GF    0.00 0.00    0    0.1    0.1 2698
 26 03 1990  0625   12 24.9  145  43.8  2716.6    7.7 320   1.2 295    6.6 325  c/cs                                2699
 26 03 1990  0628   12 25.2  145  43.6  2717.0    7.3 303   1.2 295    6.1 305  c/cs                                2700
 26 03 1990 *0630   12 25.32 145  43.36 2717.2    7.4 303   1.3 291    6.1 305  GF    0.00 0.00    0    0.1    0.1 2701
 26 03 1990  0631   12 25.4  145  43.3  2717.4    8.1 304   1.3 291    6.8 307  c/cs                                2702
 26 03 1990 *0635   12 25.69 145  42.80 2717.9    8.1 304   1.3 291    6.8 307  GF    0.00 0.00    0    0.1    0.1 2703
```

```
#cruise ODP130JR                              date run: Wed Jul 18 16:38:07 1990          page  52
#
#                     latitude  longitude             actual   drift      dr              prob. error      drift
#da mo  yr   time   deg  min  deg   min    dist  speed cse speed hed speed cse  cmnt (smajxsmin@az)  dist  time   no.
#- - - - - - - - - - - - - - - - - - - - - - - - - - - - - - - - - - - - - - - - - - - - - - - - - - - - - - - - - - -
  26 03 1990 *0640  12 26.07 145 42.23 2718.6   8.2 307   1.4 306   6.8 307  GF    0.00 0.00   0   0.1   0.1 2704
  26 03 1990 *0645  12 26.48 145 41.67 2719.3   8.3 304   1.6 291   6.8 307  GF    0.00 0.00   0   0.1   0.1 2705
  26 03 1990 *0650  12 26.87 145 41.08 2720.0   8.4 305   1.7 296   6.8 307  GF    0.00 0.00   0   0.1   0.1 2706
  26 03 1990  0653  12 27.1  145 40.7  2720.4   8.4 305   1.7 296   6.8 307  c/cs                            2707
  26 03 1990 *0655  12 27.27 145 40.49 2720.7   8.1 306   1.3 302   6.8 307  GF    0.00 0.00   0   0.1   0.1 2708
  26 03 1990 *0700  12 27.67 145 39.93 2721.3   8.3 304   1.5 290   6.8 307  GF    0.00 0.00   0   0.1   0.1 2709
  26 03 1990  0702  12 27.8  145 39.7  2721.6   8.0 305   1.5 290   6.5 308  c/cs                            2710
  26 03 1990 *0705  12 28.05 145 39.36 2722.0   7.8 307   1.3 301   6.5 308  GF    0.00 0.00   0   0.1   0.1 2711
  26 03 1990  0706  12 28.1  145 39.3  2722.1   8.2 306   1.3 301   6.9 307  c/cs                            2712
  26 03 1990 *0710  12 28.45 145 38.80 2722.7   8.1 306   1.2 301   6.9 307  GF    0.00 0.00   0   0.1   0.1 2713
  26 03 1990 *0715  12 28.85 145 38.24 2723.4   8.1 305   1.2 294   6.9 307  GF    0.00 0.00   0   0.1   0.1 2714
  26 03 1990 *0720  12 29.24 145 37.67 2724.0   8.3 306   1.4 303   6.9 307  GF    0.00 0.00   0   0.1   0.1 2715
  26 03 1990 *0725  12 29.65 145 37.10 2724.7   8.1 305   1.1 296   6.9 307  GF    0.00 0.00   0   0.1   0.1 2716
  26 03 1990 *0730  12 30.04 145 36.54 2725.4   7.9 304   1.1 285   6.9 307  GF    0.00 0.00   0   0.1   0.1 2717
  26 03 1990 *0735  12 30.41 145 35.98 2726.1   8.2 307   1.3 309   6.9 307  GF    0.00 0.00   0   0.1   0.1 2718
  26 03 1990  0736  12 30.5  145 35.9  2726.2   8.1 307   1.3 309   6.8 307  c/cs                            2719
  26 03 1990 *0740  12 30.82 145 35.43 2726.7   8.0 305   1.2 292   6.8 307  GF    0.00 0.00   0   0.1   0.1 2720
  26 03 1990 *0745  12 31.20 145 34.87 2727.4   7.8 306   1.0 298   6.8 307  GF    0.00 0.00   0   0.1   0.1 2721
  26 03 1990 *0750  12 31.58 145 34.33 2728.1   8.1 305   1.3 297   6.8 307  GF    0.00 0.00   0   0.1   0.1 2722
  26 03 1990 *0755  12 31.97 145 33.77 2728.7   8.0 308   1.2 313   6.8 307  GF    0.00 0.00   0   0.1   0.1 2723
  26 03 1990 *0800  12 32.38 145 33.23 2729.4   7.7 303   1.1 273   6.8 307  GF    0.00 0.00   0   0.1   0.1 2724
  26 03 1990  0802  12 32.5  145 33.0  2729.7   7.8 303   1.1 273   6.9 307  c/cs                            2725
  26 03 1990 *0805  12 32.73 145 32.67 2730.0   8.0 308   1.1 314   6.9 307  GF    0.00 0.00   0   0.1   0.1 2726
  26 03 1990 *0810  12 33.14 145 32.13 2730.7   8.0 305   1.1 291   6.9 307  GF    0.00 0.00   0   0.1   0.1 2727
  26 03 1990 *0815  12 33.52 145 31.57 2731.4   7.7 304   0.8 281   6.9 307  GF    0.00 0.00   0   0.1   0.1 2728
  26 03 1990 *0820  12 33.88 145 31.03 2732.0   7.9 306   0.9 297   6.9 307  GF    0.00 0.00   0   0.1   0.1 2729
  26 03 1990  0820  12 33.9  145 31.0  2732.0   7.2 306   0.9 297   6.3 307  c/cs                            2730
  26 03 1990 *0825  12 34.23 145 30.53 2732.6   6.2 289   1.9 207   6.3 307  GF    0.00 0.00   0   0.1   0.1 2731
  26 03 1990 *0830  12 34.40 145 30.03 2733.1  12.4 328   6.9 347   6.3 307  GF    0.00 0.00   0   0.2   0.1 2732
  26 03 1990  0831  12 34.6  145 29.9  2733.3  12.3 329   6.9 347   6.1 308  c/cs                            2733
  26 03 1990  0837  12 35.6  145 29.3  2734.6  12.2 328   6.9 347   6.1 307  c/cs                            2734
  26 03 1990 *0840  12 36.15 145 28.94 2735.2   5.4 271   3.6 189   6.1 307  GF    0.00 0.00   0   1.2   0.2 2735
  26 03 1990  0846  12 36.2  145 28.4  2735.7   5.4 274   3.6 189   6.2 309  c/cs                            2736
  26 03 1990 *0850  12 36.19 145 28.02 2736.1   6.6 299   1.1 232   6.2 309  GF    0.00 0.00   0   0.6   0.2 2737
  26 03 1990  0855  12 36.5  145 27.5  2736.6   6.6 297   1.1 232   6.2 307  c/cs                            2738
  26 03 1990 *0900  12 36.71 145 27.03 2737.2   7.0 305   0.9 294   6.2 307  GF    0.00 0.00   0   0.2   0.2 2739
  26 03 1990 *0910  12 37.39 145 26.05 2738.3   6.8 304   0.7 278   6.2 307  GF    0.00 0.00   0   0.1   0.2 2740
  26 03 1990  0915  12 37.7  145 25.6  2738.9   6.8 302   0.7 278   6.1 305  c/cs                            2741
  26 03 1990 *0920  12 38.01 145 25.08 2739.5   7.1 302   1.0 281   6.1 305  GF    0.00 0.00   0   0.1   0.2 2742
  26 03 1990 *0930  12 38.63 145 24.05 2740.7   7.0 304   0.9 296   6.1 305  GF    0.00 0.00   0   0.2   0.2 2743
  26 03 1990  0937  12 39.1  145 23.3  2741.5   7.1 305   0.9 296   6.2 306  c/cs                            2744
  26 03 1990 *0940  12 39.29 145 23.05 2741.8   7.5 305   1.3 298   6.2 306  GF    0.00 0.00   0   0.2   0.2 2745
  26 03 1990  0948  12 39.9  145 22.2  2742.8   4.6 304   1.3 298   3.3 306  c/cs                            2746
  26 03 1990  0949  12 39.9  145 22.1  2742.9   7.4 305   1.3 298   6.1 306  c/cs                            2747
  26 03 1990 *0950  12 39.97 145 22.04 2743.0   7.1 305   1.0 298   6.1 306  GF    0.00 0.00   0   0.2   0.2 2748
  26 03 1990 *1000  12 40.65 145 21.04 2744.2   6.9 298   1.2 252   6.1 306  GF    0.00 0.00   0   0.2   0.2 2749
  26 03 1990  1005  12 40.9  145 20.5  2744.8   6.6 297   1.2 252   5.8 306  c/cs                            2750
  26 03 1990  1009  12 41.1  145 20.1  2745.2   6.9 299   1.2 252   6.2 307  c/cs                            2751
  26 03 1990 *1014  12 41.40 145 19.60 2745.8   7.5 306   1.3 303   6.2 307   SF   0.00 0.00   0   0.3   0.2 2752
  26 03 1990  1039  12 43.2  145 17.0  2748.9   7.5 306   1.3 303   6.1 307  c/cs                            2753
  26 03 1990  1045  12 43.7  145 16.4  2749.7   7.2 306   1.3 303   5.9 307  c/cs                            2754
  26 03 1990  1051  12 44.1  145 15.8  2750.4   7.4 306   1.3 303   6.1 307  c/cs                            2755
  26 03 1990  1118  12 46.1  145 13.1  2753.7   7.4 306   1.3 303   6.1 307  c/cs                            2756
```

```
                                          date run: Wed Jul 18 16:38:07 1990          page  53
#cruise ODP130JR
#                                                    actual    drift        dr              prob. error       drift
#                      latitude  longitude                                                                 
#da mo  yr    time deg   min  deg  min     dist speed cse speed hed speed cse  cmnt (smajxsmin@az)  dist  time  no.
#-- - - - - - - - - - - - - - - - - - - - - - - - - - - - - - - - - - - - - - - - - - - - - - - - - - - - - - - - -
 26 03 1990   1141  12 47.8   145 10.7  2756.6   7.5 306   1.3 303   6.2 307  c/cs                                2757
 26 03 1990  *1208  12 49.80  145  7.90 2760.0   8.0 303   1.9 290   6.2 307   SF   0.00 0.00   0   2.5     1.9 2758
 26 03 1990   1211  12 50.0   145  7.6  2760.4   8.1 303   1.9 290   6.2 307  c/cs                                2759
 26 03 1990   1241  12 52.2   145  4.1  2764.4   8.0 303   1.9 290   6.2 307  c/cs                                2760
 26 03 1990  *1300  12 53.60  145  1.90 2767.0   8.0 303   0.C   0   6.2 307   SF   0.00 0.00   0   1.6     0.9 2762
#previous accum miles      0.000 present accum dist  2766.964 cruise ODP130JR record no  2762
```

VOLUME
130

CHAPTER
5

TABLES
9, 11, 12, AND 13

Table 9. Carbonate and inorganic carbon data, Site 803.

Core, section, interval (cm)	Depth (mbsf)	Inorganic carbon (%)	$CaCO_3$ (%)
130-803A-			
4H-4, 35-36	31.95	10.77	89.7
4H-5, 35-36	33.35	10.59	88.2
4H-6, 35-36	34.85	10.48	87.3
4H-7, 35-36	36.35	10.22	85.1
5H-2, 39-40	38.39	10.54	87.8
5H-3, 39-40	39.89	10.68	89.0
5H-4, 35-36	41.35	10.66	88.8
5H-5, 35-36	42.85	10.24	85.3
5H-6, 39-40	44.39	9.79	81.6
5H-7, 36-37	45.86	10.54	87.8
6H-1, 97-98	46.97	10.20	85.0
6H-2, 45-46	47.95	9.72	81.0
6H-3, 35-36	49.35	10.23	85.2
6H-4, 34-35	50.84	10.34	86.1
6H-5, 40-41	52.40	10.13	84.4
6H-6, 37-38	53.87	10.47	87.2
6H-7, 40-41	55.40	10.46	87.1
130-803B-			
1H-1, 41-42	0.41	10.40	86.6
1H-2, 31-32	1.81	10.32	86.0
1H-3, 36-37	3.36	10.34	86.1
2H-1, 62-64	4.92	10.37	86.4
2H-2, 32-34	6.12	10.64	88.6
2H-3, 35-37	7.65	9.93	82.7
2H-4, 35-37	9.15	10.30	85.8
2H-5, 34-36	10.64	10.67	88.9
2H-6, 34-36	12.14	10.14	84.5
2H-7, 34-36	13.64	10.64	88.6
3H-1, 35-37	14.15	10.31	85.9
3H-2, 35-37	15.65	10.51	87.5
3H-3, 35-37	17.15	10.51	87.5
3H-4, 35-37	18.65	10.50	87.5
3H-5, 34-36	20.14	10.73	89.4
3H-6, 34-36	21.64	10.79	89.9
3H-7, 35-37	23.15	10.49	87.4
4H-1, 35-37	23.65	10.50	87.5
4H-2, 33-35	25.13	10.97	91.4
4H-3, 34-36	26.64	10.93	91.0
4H-4, 34-36	28.14	10.66	88.8
4H-5, 35-37	29.65	10.66	88.8
4H-6, 36-38	31.16	10.69	89.0
4H-7, 35-37	32.65	10.74	89.5
5H-2, 40-42	34.70	10.86	90.5
5H-4, 35-37	37.65	10.49	87.4
5H-5, 34-36	39.14	10.66	88.8
5H-6, 35-37	40.65	10.34	86.1
5H-7, 15-17	41.95	10.38	86.5
6H-2, 46-48	44.26	10.64	88.6
6H-3, 45-47	45.75	9.80	81.6
6H-4, 44-46	47.24	10.38	86.5
6H-5, 31-33	48.61	9.99	83.2
7H-2, 27-29	53.57	10.82	90.1
7H-4, 35-37	56.65	10.94	91.1
7H-5, 35-37	58.15	11.15	92.9
130-803C-			
1H-1, 34-36	19.34	10.39	86.5
1H-3, 40-42	22.40	10.47	87.2
1H-4, 33-35	23.83	10.67	88.5
1H-5, 34-36	25.34	11.03	91.9
1H-6, 35-37	26.85	10.79	89.9
1H-7, 35-37	28.35	10.75	89.5
2H-3, 62-64	32.12	10.51	87.5
2H-4, 24-26	33.24	10.68	89.0
2H-5, 29-31	34.79	10.51	87.5
2H-6, 19-21	36.19	10.86	90.5
3H-2, 37-39	39.87	10.36	86.3
3H-3, 45-47	41.45	10.13	84.4
3H-4, 36-38	42.86	10.68	89.0
3H-5, 29-31	44.29	10.63	88.5
3H-6, 35-37	45.85	9.69	80.7
4H-2, 64-66	49.64	10.65	88.7
4H-3, 49-51	50.99	10.76	89.6

Table 9 (continued).

Core, section, interval (cm)	Depth (mbsf)	Inorganic carbon (%)	$CaCO_3$ (%)
130-803C- (Cont.)			
4H-5, 34-36	53.84	11.01	91.7
4H-6, 34-36	55.34	11.13	92.7
4H-7, 34-36	56.84	11.06	92.1
5H-2, 32-34	58.82	11.12	92.6
5H-3, 44-46	60.44	11.80	98.3
5H-4, 34-36	61.84	11.07	92.2
5H-5, 34-36	63.34	11.10	92.5
5H-6, 38-40	64.88	11.00	91.6
5H-7, 39-41	66.39	10.92	91.0
6H-1, 39-41	66.89	10.54	87.8
6H-2, 37-39	68.37	10.93	91.0
6H-3, 39-41	69.89	9.03	75.2
6H-4, 38-40	71.38	10.85	90.4
6H-5, 35-37	72.85	10.88	90.6
6H-6, 35-37	74.35	10.37	86.4
7H-3, 35-37	79.35	11.13	92.7
7H-4, 48-50	80.98	11.06	92.1
7H-5, 55-57	82.55	11.01	91.7
7H-6, 46-48	83.96	10.89	90.7
7H-7, 35-37	85.35	11.28	94.0
8H-2, 34-36	87.34	11.24	93.6
8H-3, 17-19	88.67	11.05	92.0
8H-4, 25-26	90.25	10.97	91.4
8H-5, 40-41	91.90	10.92	91.0
8H-6, 35-36	93.35	10.88	90.6
8H-7, 35-36	94.85	11.15	92.9
9H-2, 34-36	96.84	11.15	92.9
9H-3, 54-56	98.54	11.12	92.6
9H-5, 44-46	101.44	11.35	94.5
9H-6, 39-41	102.89	11.12	92.6
10H-1, 34-36	104.84	11.19	93.2
10H-2, 34-36	106.34	11.28	94.0
10H-3, 38-40	107.88	11.08	92.3
10H-5, 40-42	110.90	10.95	91.2
10H-6, 40-42	112.40	10.65	88.7
10H-7, 44-46	113.94	10.85	90.4
11H-2, 37-39	115.87	11.17	93.0
11H-3, 33-35	117.33	11.18	93.1
11H-4, 34-36	118.84	11.11	92.5
11H-6, 34-36	121.84	11.22	93.5
11H-7, 44-46	123.44	11.25	93.7
12H-1, 34-36	123.84	11.09	92.4
12H-2, 34-36	125.34	11.10	92.5
12H-4, 33-34	128.33	11.13	92.7
12H-5, 26-28	129.76	10.77	89.7
12H-6, 25-37	131.25	11.19	93.2
12H-6, 35-37	131.35	11.11	92.5
12H-7, 34-36	132.84	11.12	92.6
13H-2, 34-36	134.84	11.25	93.7
13H-3, 34-36	136.34	10.92	91.0
13H-5, 34-36	139.34	10.80	90.0
13H-6, 34-36	140.84	10.82	90.1
13H-7, 44-46	142.44	10.96	91.3
14H-1, 35-37	142.85	10.72	89.3
14H-2, 35-37	144.35	11.14	92.8
14H-3, 34-36	145.84	10.79	89.9
14H-4, 34-36	147.34	10.98	91.5
14H-5, 33-35	148.83	10.55	87.9
14H-6, 32-34	150.32	10.90	90.8
15H-2, 35-37	153.85	10.56	88.0
15H-3, 30-32	155.30	10.77	89.7
15H-4, 36-38	156.86	10.36	86.3
15H-6, 36-38	159.86	10.71	89.2
15H-7, 34-36	161.34	10.65	88.7
16H-2, 36-38	163.36	11.08	92.3
16H-3, 33-35	164.83	10.82	90.1
16H-4, 33-35	166.33	11.20	93.3
16H-5, 33-35	167.83	11.13	92.7
16H-6, 33-35	169.33	11.16	93.0
17H-2, 34-36	172.84	11.17	93.0
17H-3, 34-36	174.34	10.93	91.0
17H-4, 31-33	175.81	11.25	93.7
17H-5, 32-34	177.32	11.09	92.4
17H-6, 32-34	178.82	11.05	92.0
17H-7, 32-34	180.32	11.13	92.7
18H-2, 77-79	182.77	0.39	3.2
18H-3, 32-34	183.82	10.86	90.5

Table 9 (continued).

Core, section, interval (cm)	Depth (mbsf)	Inorganic carbon (%)	$CaCO_3$ (%)
130-803C- (Cont.)			
18H-4, 34-36	185.34	10.93	91.0
18H-5, 35-37	186.85	10.97	91.4
18H-6, 37-39	188.37	10.75	89.5
18H-7, 31-33	189.81	10.67	88.9
19H-1, 36-38	190.36	11.12	92.6
19H-2, 35-37	191.85	11.00	91.6
19H-3, 35-37	193.35	10.87	90.5
19H-4, 39-41	194.89	11.02	91.8
19H-5, 35-37	196.35	11.26	93.8
19H-6, 35-37	197.85	11.01	91.7
19H-7, 23-25	199.23	11.23	93.5
20H-2, 35-37	201.35	11.00	91.6
20H-4, 39-41	204.39	11.05	92.0
20H-6, 35-37	207.35	10.75	89.5
20H-7, 35-37	208.85	10.69	89.0
21H-1, 35-37	209.35	10.20	85.0
21H-2, 34-36	210.84	11.11	92.5
21H-3, 34-36	212.34	10.83	90.2
21H-4, 35-37	213.85	10.66	88.8
21H-5, 40-42	215.40	10.15	84.5
21H-6, 35-37	216.85	10.02	83.5
21H-7, 40-42	218.40	10.32	86.0
22H-1, 34-36	218.84	10.36	86.3
22H-2, 35-36	220.35	10.26	85.5
22H-3, 30-31	221.80	10.50	87.5
22H-4, 35-37	223.35	11.59	96.5
22H-5, 35-37	224.85	11.15	92.9
22H-6, 35-37	226.35	11.04	92.0
23H-1, 70-71	228.70	10.18	84.8
23H-2, 29-30	229.79	10.86	90.5
23H-4, 31-33	232.81	10.33	86.0
23H-5, 33-35	234.33	10.84	90.3
23H-6, 13-14	235.63	10.94	91.1
23H-7, 28-29	237.28	11.07	92.2
130-803D-			
1H-1, 123-125	1.23	10.40	86.6
1H-2, 38-40	1.88	10.52	87.6
2H-1, 110-112	3.60	10.15	84.5
2H-2, 107-109	5.07	10.29	85.7
2H-3, 99-101	6.49	10.19	84.9
2H-4, 44-46	7.44	10.64	88.6
2H-5, 96-98	9.46	10.13	84.4
2H-6, 99-101	10.99	10.62	88.5
2H-7, 39-41	11.89	10.60	88.3
3H-1, 114-116	13.14	9.74	81.1
3H-2, 99-101	14.49	10.44	87.0
3H-3, 103-105	16.03	10.51	87.5
3H-4, 103-105	17.53	10.61	88.4
3H-5, 109-111	19.09	10.80	90.0
3H-6, 109-111	20.59	10.87	90.5
3H-7, 33-35	21.33	10.12	84.3
4H-1, 100-102	22.50	10.61	88.4
4H-2, 35-37	23.35	10.20	85.0
4H-2, 110-112	24.10	10.94	91.1
4H-3, 101-103	25.51	10.85	90.4
4H-4, 99-101	26.99	10.95	91.2
4H-5, 100-102	28.50	10.80	90.0
4H-6, 103-105	30.03	11.08	92.3
4H-7, 29-31	30.79	10.79	89.9
5H-1, 113-115	32.13	10.53	87.7
5H-2, 61-63	33.11	10.27	85.5
5H-3, 113-115	35.13	10.40	86.6
5H-4, 109-111	36.59	10.37	86.4
5H-5, 110-112	38.10	10.86	90.5
5H-6, 110-112	39.60	11.09	92.4
6H-1, 110-112	41.60	10.34	86.1
6H-2, 110-112	43.10	10.69	89.0
6H-3, 36-38	43.86	10.65	88.7
6H-3, 114-116	44.64	10.83	90.2
6H-4, 39-41	45.39	10.43	86.9
7H-1, 36-38	46.46	10.32	86.0
6H-5, 35-37	46.85	9.64	80.3
6H-6, 35-37	48.35	10.76	89.6
7H-2, 110-112	48.70	10.28	85.6
7H-3, 114-116	50.24	10.86	90.5
6H-7, 36-38	49.86	10.25	85.4

Table 9 (continued).

Core, section, interval (cm)	Depth (mbsf)	Inorganic carbon (%)	$CaCO_3$ (%)
130-803D- (Cont.)			
7H-4, 110-112	51.70	10.63	88.5
7H-5, 110-112	53.20	11.02	91.8
7H-6, 110-112	54.70	11.03	91.9
8H-3, 110-112	59.70	10.99	91.5
8H-4, 110-112	61.20	11.03	91.9
8H-5, 110-112	62.70	10.83	90.2
8H-6, 110-112	64.20	10.94	91.1
9H-1, 110-112	66.20	10.61	88.4
9H-2, 109-111	67.69	11.00	91.6
9H-3, 109-111	69.19	10.61	88.4
9H-4, 105-107	70.65	10.79	89.9
9H-5, 113-115	72.23	10.11	84.2
9H-6, 108-110	73.68	10.30	85.8
10H-1, 100-102	75.60	10.97	91.4
10H-2, 107-110	77.17	11.04	92.0
10H-3, 107-109	78.67	11.20	93.3
10H-4, 99-101	80.09	11.07	92.2
10H-5, 108-110	81.68	11.23	93.5
10H-6, 109-111	83.19	10.91	90.9
10H-7, 35-37	83.95	10.95	91.2
11H-2, 109-111	86.69	10.76	89.6
11H-3, 108-110	88.18	10.95	91.2
11H-4, 109-111	89.69	11.01	91.7
11H-5, 108-111	91.18	11.12	92.6
11H-6, 110-112	92.70	11.21	93.4
11H-7, 36-38	93.46	11.11	92.5
12H-1, 109-111	94.69	11.26	93.8
12H-2, 109-111	96.19	11.28	94.0
12H-3, 109-111	97.69	11.36	94.6
12H-5, 110-112	100.70	11.41	95.0
12H-6, 108-110	102.18	11.27	93.9
13H-2, 107-109	105.67	11.11	92.5
13H-3, 107-109	107.17	11.29	94.0
13H-4, 99-101	108.59	11.12	92.6
13H-5, 108-109	110.18	10.95	91.2
13H-6, 108-109	111.68	11.38	94.8
14H-1, 107-109	113.67	11.16	93.0
14H-2, 104-106	115.14	11.21	93.4
14H-3, 98-100	116.58	11.23	93.5
14H-5, 33-35	118.93	10.90	90.3
14H-5, 98-100	119.58	11.22	93.5
14H-6, 32-34	120.42	10.55	87.9
14H-6, 110-112	121.20	11.29	94.0
15H-1, 110-112	123.20	11.22	93.5
15H-2, 108-110	124.68	11.09	92.4
15H-3, 109-111	126.19	11.53	96.0
15H-4, 109-111	127.69	11.24	93.6
15H-5, 103-105	129.13	11.09	92.4
15H-6, 93-95	130.53	11.29	94.0
16H-1, 103-104	132.63	10.81	90.0
16H-2, 109-110	134.19	11.04	92.0
16H-3, 110-111	135.70	11.13	92.7
16H-4, 29-30	136.39	11.11	92.5
16H-5, 108-110	138.68	11.05	92.0
16H-6, 109-111	140.19	11.03	91.9
17H-1, 109-110	142.19	11.05	92.0
17H-2, 97-99	143.57	11.22	93.5
17H-3, 107-108	145.17	11.12	92.6
17H-4, 103-104	146.63	1.23	10.2
17H-5, 110-111	148.20	11.21	93.4
17H-6, 99-101	149.59	10.88	90.6
17H-7, 36-38	150.46	11.34	94.5
18H-1, 109-110	151.69	10.72	89.3
18H-2, 114-116	153.24	10.53	87.7
18H-3, 109-111	154.69	10.55	87.9
18H-4, 110-112	156.20	10.44	87.0
18H-5, 100-102	157.60	10.92	91.0
18H-6, 109-111	159.19	10.73	89.4
19H-1, 110-112	161.20	11.09	92.4
19H-2, 110-112	162.70	10.85	90.4
19H-3, 114-116	164.24	11.25	93.7
19H-4, 100-102	165.60	11.25	93.7
19H-5, 109-111	167.19	10.88	90.6
19H-6, 109-111	168.69	10.95	91.2
20H-1, 110-112	170.70	11.16	93.0
20H-2, 110-112	172.20	10.72	89.3
20H-3, 108-110	173.68	10.98	91.5

Table 9 (continued).

Core, section, interval (cm)	Depth (mbsf)	Inorganic carbon (%)	$CaCO_3$ (%)
130-803D- (Cont.)			
20H-4, 109-111	175.19	10.98	91.5
20H-5, 109-111	176.69	10.96	91.3
20H-6, 95-97	178.05	10.99	91.5
20H-7, 29-31	178.89	10.88	90.6
21H-2, 64-66	181.24	0.87	7.2
21H-3, 103-105	183.13	10.76	89.6
21H-4, 108-110	184.68	10.69	89.0
21H-5, 110-112	186.20	10.72	89.3
21H-6, 41-43	187.01	10.92	91.0
22H-1, 104-106	189.64	11.21	93.4
22H-2, 103-105	191.13	11.17	93.0
22H-3, 103-105	192.63	11.26	93.8
22H-4, 93-95	194.03	10.94	91.1
22H-5, 104-106	195.64	11.23	93.5
22H-6, 105-107	197.15	11.12	92.6
22H-7, 39-41	197.99	11.19	93.2
23H-1, 99-101	199.09	11.02	91.8
23H-2, 99-101	200.59	10.76	89.6
23H-4, 104-106	203.64	10.50	87.5
23H-6, 99-101	206.59	10.48	87.3
23H-7, 38-40	207.48	10.77	89.7
24H-1, 113-115	208.73	10.24	85.3
24H-2, 100-102	210.10	10.71	89.2
24H-3, 103-105	211.63	10.93	91.0
24H-4, 103-105	213.13	10.72	89.3
24H-5, 103-105	214.63	10.79	89.9
24H-6, 103-105	216.13	10.89	90.7
24H-7, 39-41	216.99	10.60	88.3
25X-1, 105-107	218.15	10.66	88.8
25X-2, 37-39	218.97	10.68	89.0
25X-3, 71-73	220.81	10.65	88.7
25X-4, 40-42	222.00	11.04	92.0
26X-1, 32-34	227.12	10.92	91.0
26X-2, 26-28	228.56	11.18	93.1
26X-3, 34-36	230.14	10.67	88.9
26X-4, 62-64	231.92	10.02	83.5
26X-5, 78-80	233.58	10.30	85.8
26X-6, 117-119	235.47	11.35	94.5
27X-1, 73-75	237.23	11.01	91.7
27X-2, 97-99	238.97	10.94	91.1
27X-3, 64-66	240.14	10.89	90.7
28X-2, 84-86	248.24	10.72	89.3
28X-5, 31-33	252.21	11.10	92.5
29X-1, 64-66	256.14	11.13	92.7
29X-2, 55-57	257.55	11.29	94.0
29X-3, 59-61	259.09	11.15	92.9
29X-4, 72-74	260.72	11.34	94.5
29X-5, 29-31	261.79	11.37	94.7
30X-1, 133-135	266.43	11.19	93.2
30X-2, 81-83	267.41	11.27	93.9
30X-3, 75-77	268.85	11.34	94.5
30X-4, 80-82	270.40	10.78	89.8
31X-1, 50-52	275.20	10.69	89.0
31X-2, 90-92	277.10	10.52	87.6
31X-3, 93-95	278.63	11.45	95.4
31X-4, 28-30	279.48	11.16	93.0
32X-1, 89-91	285.19	11.34	94.5
32X-2, 117-119	286.97	10.61	88.4
32X-3, 102-104	288.32	11.19	93.2
32X-4, 67-69	289.47	11.25	93.7
32X-5, 36-38	290.66	10.81	90.0
33X-1, 137-139	295.47	11.25	93.7
33X-2, 101-103	296.61	11.24	93.6
33X-3, 117-119	298.27	11.18	93.1
33X-4, 59-61	299.19	10.75	89.5
33X-5, 48-50	300.58	10.82	90.1
34X-1, 49-51	303.79	10.79	89.9
34X-2, 73-75	305.53	11.21	93.4
34X-3, 71-73	307.01	11.15	92.9
34X-4, 83-85	308.63	10.91	90.9
34X-5, 69-71	309.99	10.75	89.5
34X-6, 137-139	312.17	11.04	92.0
35X-1, 88-90	313.88	10.52	87.6
35X-2, 128-130	315.78	10.37	86.4
35X-3, 87-89	316.87	10.89	90.7
35X-4, 71-73	318.21	11.13	92.7
35X-5, 52-54	319.52	10.95	91.2
35X-6, 48-50	320.98	11.16	93.0

Table 9 (continued).

Core, section, interval (cm)	Depth (mbsf)	Inorganic carbon (%)	$CaCO_3$ (%)
130-803D- (Cont.)			
36X-1, 115-117	323.85	11.27	93.9
36X-2, 71-73	324.91	10.87	90.5
36X-3, 116-118	326.86	10.74	89.5
36X-4, 127-129	328.47	11.17	93.0
36X-5, 125-127	329.95	11.37	94.7
36X-6, 114-116	331.34	11.05	92.0
37X-1, 90-92	333.20	10.67	88.9
37X-2, 104-106	334.84	10.06	83.8
37X-3, 102-104	336.32	10.18	84.8
37X-4, 103-105	337.83	11.12	92.6
37X-5, 99-101	339.29	10.48	87.3
37X-6, 109-111	340.89	10.84	90.3
38X-1, 58-60	342.58	11.01	91.7
38X-4, 133-135	347.83	10.60	88.3
38X-5, 108-110	349.08	10.93	91.0
38X-6, 23-25	349.73	11.09	92.4
39X-1, 126-128	352.86	10.97	91.4
39X-2, 128-130	354.38	10.75	89.5
39X-3, 53-55	355.13	10.98	91.5
39X-4, 53-55	356.63	10.83	90.2
39X-5, 53-55	358.13	10.78	89.8
39X-6, 65-67	359.75	10.66	88.8
40X-2, 90-91	363.70	10.30	85.8
40X-1, 40-41	361.70	10.69	89.0
40X-3, 87-88	365.17	10.23	85.2
40X-4, 91-92	366.71	10.73	89.4
40X-5, 49-50	367.79	10.59	88.2
41X-1, 14-15	371.14	10.88	90.6
41X-2, 70-71	373.20	10.37	86.4
41X-3, 113-114	375.13	10.78	89.8
42X-1, 97-99	381.67	11.12	92.6
42X-2, 32-34	382.52	11.28	94.0
42X-3, 14-16	383.84	11.12	92.6
43X-1, 10-12	390.50	10.90	90.8
43X-2, 87-89	392.77	11.02	91.8
43X-3, 87-89	394.27	10.84	90.3
43X-4, 41-43	395.31	11.14	92.8
43X-5, 21-23	396.61	10.71	89.2
44X-1, 85-87	400.35	11.26	93.8
44X-2, 108-110	402.58	11.42	95.1
44X-3, 70-72	403.70	11.10	92.5
44X-4, 68-70	405.18	11.28	94.0
44X-5, 29-31	406.29	11.21	93.4
45X-1, 88-90	410.58	11.33	94.4
45X-2, 75-77	411.95	11.08	92.3
45X-3, 121-123	413.91	11.15	92.9
45X-4, 73-75	414.93	10.63	88.5
45X-5, 46-48	416.16	11.12	92.6
45X-6, 69-71	417.89	11.05	92.0
46X-1, 120-122	420.50	10.85	90.4
46X-2, 129-131	422.09	10.82	90.1
46X-3, 130-132	423.60	10.41	86.7
46X-5, 56-61	425.86	10.75	89.5
47X-1, 61-63	429.61	11.09	92.4
47X-2, 132-134	431.82	10.89	90.7
47X-3, 119-121	433.19	10.89	90.7
47X-4, 88-90	434.38	10.75	89.5
47X-5, 29-31	435.29	10.98	91.5
48X-1, 19-21	438.79	10.29	85.7
48X-2, 45-47	440.55	10.92	91.0
48X-3, 49-51	442.09	10.59	88.2
48X-4, 50-52	443.60	11.26	93.8
49X-1, 98-100	448.78	11.25	93.7
49X-4, 74-76	453.04	11.21	93.4
49X-2, 80-81	450.10	11.08	92.3
49X-3, 91-93	451.71	10.95	91.2
50X-1, 115-117	458.65	11.00	91.6
50X-2, 37-39	459.37	11.30	94.1
51X-1, 43-45	467.63	11.29	94.0
52X-1, 77-79	477.67	10.94	91.1
52X-2, 79-81	479.19	10.79	89.9
52X-3, 52-54	480.42	10.84	90.3
53X-1, 128-130	487.88	11.12	92.6
53X-2, 141-143	489.51	11.04	92.0
53X-3, 110-112	490.70	11.31	94.2
53X-4, 82-84	491.92	11.04	92.0
54X-1, 76-78	497.06	10.69	89.0

Table 9 (continued).

Core, section, interval (cm)	Depth (mbsf)	Inorganic carbon (%)	$CaCO_3$ (%)
130-803D- (Cont.)			
54X-2, 88-90	498.68	10.60	88.3
54X-3, 77-79	500.07	7.83	65.2
54X-4, 93-95	501.73	10.25	85.4
55X-1, 48-50	506.48	10.28	85.6
55X-2, 47-49	507.97	10.26	85.5
55X-3, 79-81	509.79	10.28	85.6
55X-4, 50-52	511.00	10.83	90.2
56X-1, 112-114	516.72	10.37	86.4
56X-2, 97-99	518.07	10.46	87.1
56X-3, 99-101	519.59	10.47	87.2
56X-4, 107-109	521.17	10.93	91.0
56X-5, 114-116	522.74	10.97	91.4
56X-6, 82-84	523.92	10.64	88.6
57X-1, 91-93	526.21	11.15	92.9
57X-2, 93-95	527.73	11.16	93.0
57X-3, 89-91	529.19	10.96	91.3
58X-1, 22-24	534.82	11.22	93.5
58X-CC, 12-14	535.48	10.12	84.3
59X-1, 59-61	544.89	9.82	81.8
59X-2, 67-69	546.47	10.08	84.0
60X-1, 8-10	554.08	10.81	90.0
60X-2, 9-11	555.59	9.03	75.2
61X-1, 3-5	563.73	10.17	84.7
64X-CC, 10-12	588.80	11.02	91.8
65X-CC, 7-8	598.47	2.48	20.7
66X-CC, 5-7	601.95	10.15	84.5
67R-1, 119-120	613.19	6.45	53.7
68R-3, 52-56	625.32	0.10	0.8
68R-3, 105-109	625.85	0.06	0.5

Table 11. Laboratory vane shear strength, Site 803.

Core, section, interval (cm)	Depth (mbsf)	Peak shear strength (kPa)	Residual shear strength (kPa)
130-803B-			
1H-3, 104	4.04	6	
2H-1, 120	5.50	7.2	
2H-2, 40	6.20	3.8	
2H-2, 120	7.00	5.8	
2H-3, 45	7.75	5.6	
2H-3, 120	8.50	8.8	
2H-4, 45	9.25	9.0	
2H-4, 120	10.00	4.9	
2H-5, 120	11.50	4.9	
2H-6, 120	13.00	9.0	
2H-7, 45	13.75	6.7	2.5
3H-1, 45	14.25	16.6	7.2
3H-1, 120	15.00	25.8	14.6
3H-2, 120	16.50	24.7	10.8
3H-3, 45	17.25	22.0	11.7
3H-4, 120	19.50	21.7	9
3H-5, 120	21.00	16.0	6.7
3H-6, 45	21.75	15.7	
3H-6, 120	22.50	22.5	
4H-1, 45	23.75	11.5	4.9
4H-1, 120	24.50	13.7	6.3
4H-2, 45	25.25	8.5	
4H-2, 120	26.00	9.7	
4H-3, 121	27.51	22.2	
4H-4, 98	28.78	13.0	
4H-5, 114	30.44	12.1	
4H-6, 100	31.80	13.5	6.7
4H-7, 45	32.75	17.6	7.6
5H-1, 131	34.11	4.0	
5H-2, 62	34.92	3.1	
5H-3, 51	36.31	8.8	
5H-3, 119	36.99	14.2	
5H-4, 41	37.71	13.9	
5H-4, 123	38.53	20.6	
5H-5, 43	39.23	20.0	
5H-5, 119	39.99	19.8	
5H-6, 51	40.81	16.4	
5H-6, 119	41.49	23.6	14.2
5H-7, 58	42.38	25.3	
6H-1, 130	43.60	15.3	
6H-2, 31	44.11	21.8	
6H-2, 120	45.00	20.9	
6H-3, 58	45.88	36.4	
6H-4, 54	47.34	29.7	
6H-5, 22	48.52	22.9	
7H-1, 120	53.00	22.2	
7H-2, 44	53.74	18.6	
7H-3, 133	56.13	13.7	
7H-4, 44	56.74	15.7	
7H-5, 28	58.08	13.7	
130-803C-			
1H-1, 118	20.18	12.4	
1H-2, 49	20.99	14.8	7.0
1H-3, 44	22.44	26.5	
1H-4, 45	23.95	18.0	
1H-5, 45	25.45	9.9	
1H-6, 120	27.70	2.1	
1H-7, 45	28.45	12.4	4.0
2H-1, 120	29.70	10.6	2.7
2H-2, 47	30.47	14.8	
2H-3, 69	32.19	18.9	
2H-4, 35	33.35	22.0	8.1
2H-4, 120	34.20	19.1	
2H-6, 41	36.41	24.3	7.9
3H-2, 62	40.12	11.5	
3H-3, 55	41.55	13.9	
3H-4, 47	42.97	16.2	
3H-5, 38	44.38	30.1	
3H-6, 28	45.78	27.4	
3H-7, 28	47.28	30.8	
4H-2, 68	49.68	9.4	4.5
4H-3, 66	51.16	9.0	4.5
130-803C- (Cont.)			
4H-4, 45	52.45	22.5	
4H-5, 26	53.76	18.0	6.9
4H-6, 45	55.45	8.5	4.0
4H-7, 46	56.96	8.3	3.8
5H-2, 25	58.75	7.4	
5H-3, 55	60.55	4.3	
5H-4, 47	61.97	8.5	3.1
5H-5, 45	63.45	11.7	
5H-6, 48	64.98	8.5	3.6
5H-7, 50	66.50	9.9	
6H-1, 50	67.00	10.3	2.6
6H-2, 47	68.47	7.2	
6H-3, 45	69.95	6.7	3.1
6H-4, 120	72.20	13.7	5.5
6H-5, 45	72.95	11.2	5.2
6H-6, 45	74.45	10.8	4.5
7H-2, 113	78.63	8.3	2.5
7H-3, 62	79.62	6.5	
7H-4, 127	81.77	7.9	
7H-5, 45	82.45	7.9	2.7
7H-6, 20	83.70	6.5	
7H-7, 15	85.15	7.0	
8H-1, 110	86.60	2.7	0.9
8H-2, 80	87.80	7.6	1.3
8H-3, 128	89.78	2.7	
8H-5, 120	92.70	6.1	
8H-5, 130	92.80	8.8	2.2
8H-6, 120	94.20	7.6	2.0
8H-7, 45	94.95	6.7	2.2
9H-1, 113	96.13	12.1	3.4
9H-2, 120	97.70	7.9	
9H-3, 120	99.20	9.4	3.8
9H-4, 126	100.76	10.3	4.0
9H-5, 113	102.13	10.3	
9H-6, 119	103.69	8.3	
10H-1, 51	105.01	11.5	3.6
10H-2, 134	107.34	6.5	
10H-3, 118	108.68	5.2	
10H-4, 120	110.20	6.1	
10H-5, 116	111.66	10.3	
10H-6, 125	113.25	7.4	2.9
10H-7, 55	114.05	7.6	2.0
11H-2, 120	116.70	5.6	1.8
11H-3, 45	117.45	6.5	3.6
11H-3, 110	118.10	7.0	2.7
11H-4, 115	119.65	9.4	
11H-5, 110	121.10	7.0	
11H-6, 95	122.45	14.8	
12H-2, 120	126.20	4.5	
12H-3, 120	127.70	4.9	
12H-4, 120	129.20	13.0	4.9
12H-5, 120	130.70	13.7	
12H-6, 123	132.23	13.5	
13H-1, 120	134.20	2.7	
13H-2, 120	135.70	4.5	
13H-3, 120	137.20	9	4.5
13H-4, 120	138.70	10.6	3.4
13H-5, 120	140.20	14.6	4.7
13H-6, 120	141.70	12.1	4.0
13H-7, 55	142.55	13.5	
14H-1, 120	143.70	11.7	
14H-2, 120	145.20	11.9	
14H-3, 115	146.65	11.0	
14H-4, 120	148.20	13.5	
14H-5, 120	149.70	7.2	
14H-6, 120	151.20	11.0	
15H-1, 120	153.20	11.9	
15H-2, 120	154.70	9.0	
15H-3, 120	156.20	7.6	
15H-4, 120	157.70	15.3	
15H-5, 120	159.20	15.7	
15H-6, 120	160.70	24.7	
16H-1, 120	162.70	8.3	
16H-2, 120	164.20	4.0	
16H-3, 120	165.70	12.6	

Table 11 (continued).

Core, section, interval (cm)	Depth (mbsf)	Peak shear strength (kPa)	Residual shear strength (kPa)
130-803C- (Cont.)			
16H-4, 120	167.20	19.8	
16H-5, 120	168.70	13.9	
16H-6, 120	170.20	15.5	
17H-2, 125	173.75	33.7	
17H-3, 120	175.20	30.3	
17H-4, 120	176.70	32.1	
17H-5, 120	178.20	39.3	
17H-6, 120	179.70	27.0	
17H-7, 45	180.45	33.7	
18H-2, 119	183.19	22.9	
18H-3, 118	184.68	23.6	
18H-4, 118	186.18	55.0	
18H-5, 120	187.70	69.6	
18H-6, 102	189.02	47.2	
18H-7, 22	189.72	49.4	
19H-1, 115	191.15	15.7	
19H-2, 18	191.68	24.7	
19H-4, 120	195.70	28.1	
19H-5, 119	197.19	48.3	
19H-6, 118	198.68	32.6	
19H-7, 32	199.32	53.9	
20H-3, 119	203.69	18.0	
20H-4, 117	205.17	29.2	
20H-5, 118	206.68	35.9	
20H-6, 118	208.18	71.9	
21H-1, 120	210.20	51.7	
21H-2, 119	211.69	56.2	
21H-3, 118	213.18	32.1	
21H-4, 118	214.68	58.4	
21H-5, 133	216.33	37.1	
21H-6, 119	217.69	37.7	
21H-7, 25	218.25	33.7	
22H-1, 120	219.70	51.7	
22H-2, 120	221.20	43.8	
22H-3, 120	222.70	56.2	
22H-4, 119	224.19	89.9	
22H-5, 119	225.69	96.6	
22H-6, 98	226.98	46.1	
23H-1, 119	229.19	51.7	
23H-5, 119	235.19	31.5	
23H-6, 120	236.70	69.6	
23H-7, 40	237.40	38.2	
130-803D-			
1H-2, 135	2.85	2.9	0.6
2H-1, 40	2.90	4.3	
2H-1, 130	3.80	3.8	
2H-2, 120	5.20	6.3	2.2
2H-3, 120	6.70	4.9	2.0
2H-4, 80	7.80	6.4	2.7
2H-5, 120	9.70	6.3	1.8
2H-6, 120	11.20	7.0	2.9
2H-7, 55	12.05	7.4	
3H-1, 120	13.20	15.6	
3H-3, 120	16.20	15.3	5.6
3H-4, 120	17.70	15.3	5.4
3H-5, 120	19.20	16.4	5.6
3H-6, 120	20.70	15.3	6.1
3H-7, 40	21.40	22.2	7.6
4H-1, 120	22.70	14.6	
4H-3, 120	25.70	6.7	
4H-5, 127	28.77	14.6	
4H-6, 125	30.25	14.2	5.2
5H-2, 119	33.69	15.1	
5H-3, 115	35.15	15.3	
5H-4, 120	36.70	15.3	7.4
5H-5, 120	38.20	20.4	10.6
5H-6, 120	39.70	23.0	11.2
5H-7, 40	40.40	31.9	16.4
6H-1, 120	41.70	22.2	12.1
6H-2, 120	43.20	13.3	
6H-3, 120	44.70	11.7	
6H-4, 95	45.95	18.6	10.3
6H-5, 125	47.75	22.2	11.2
6H-6, 120	49.20	25.2	13.5

Table 11 (continued).

Core, section, interval (cm)	Depth (mbsf)	Peak shear strength (kPa)	Residual shear strength (kPa)
130-803D- (Cont.)			
6H-7, 45	49.95	19.3	10.1
7H-1, 120	47.30	22.0	
7H-2, 125	48.85	14.8	
7H-3, 120	50.30	6.5	
7H-4, 119	51.79	19.9	7.9
7H-5, 120	53.30	18.4	5.4
7H-6, 120	54.80	8.3	
7H-7, 45	55.55	13.7	5.4
8H-1, 120	56.80	10.8	3.4
8H-2, 120	58.30	7.0	2.0
8H-3, 123	59.83	5.8	
8H-4, 120	61.30	4.0	2.5
8H-5, 120	62.80	12.4	
8H-6, 110	64.20	10.3	5.6
8H-7, 45	65.05	8.5	3.4
9H-1, 120	66.30	16.0	4.5
9H-2, 120	67.80	11.0	4.5
9H-3, 120	69.30	7.0	
9H-4, 120	70.80	9.7	
9H-5, 120	72.30	13.9	
9H-6, 128	73.88	11.7	3.8
10H-1, 120	75.80	11.5	3.8
10H-2, 120	77.30	7.6	3.6
10H-3, 120	78.80	7.6	2.7
10H-4, 110	80.20	7.0	2.5
10H-5, 120	81.80	7.8	3.4
11H-1, 120	85.30	16.6	
11H-2, 120	86.80	5.8	
11H-3, 120	88.30	10.0	3.1
11H-4, 120	89.80	9.9	4.0
11H-5, 120	91.30	9.5	
11H-6, 120	92.80	8.3	2.9
12H-1, 120	94.80	9.4	2.5
12H-2, 120	96.30	9.0	4.0
12H-3, 120	97.80	6.7	3.1
12H-4, 120	99.30	8.1	
12H-5, 120	100.80	6.7	2.7
12H-6, 120	102.30	6.0	2.7
13H-2, 120	105.80	6.3	1.5
13H-3, 120	107.30	6.5	2.0
13H-4, 110	108.70	9.9	
13H-5, 120	110.30	6.3	2.9
13H-6, 120	111.80	9.1	
14H-1, 120	113.80	11.6	
14H-2, 120	115.30	11.6	
14H-3, 120	116.80	7.2	
14H-4, 120	118.30	7.0	
14H-5, 120	119.80	10.3	
14H-6, 120	121.30	8.8	
15H-1, 120	123.30	11.9	
15H-2, 124	124.84	6.9	
15H-3, 120	126.30	10.3	
15H-4, 120	127.80	13.3	
15H-5, 120	129.30	8.3	
15H-6, 120	130.80	7.6	
16H-1, 120	132.80	12.4	
16H-2, 120	134.30	7.6	
16H-3, 119	135.79	12.4	
16H-4, 90	137.00	10.8	
16H-5, 120	138.80	13.6	
16H-6, 120	140.30	14.2	
17H-1, 121	142.31	12.1	
17H-3, 114	145.24	2.6	
17H-4, 120	146.80	13.5	
17H-5, 120	148.30	9.7	
17H-6, 120	149.80	11.5	
17H-7, 55	150.65	12.2	
18H-1, 120	151.80	11.0	
18H-2, 125	153.35	12.4	
18H-3, 120	154.80	13.5	
18H-5, 125	157.85	15.7	
18H-6, 125	159.35	13.5	
19H-1, 117	161.27	17.1	
19H-2, 120	162.80	13.4	
19H-3, 125	164.35	13.3	

Table 11 (continued).

Core, section, interval (cm)	Depth (mbsf)	Peak shear strength (kPa)	Residual shear strength (kPa)
130-803D- (Cont.)			
19H-4, 90	165.50	16.8	
19H-6, 12	167.72	43.8	
20H-1, 121	170.81	42.7	
20H-2, 118	172.28	38.2	
20H-3, 120	173.80	29.2	
20H-4, 123	175.33	34.1	
20H-5, 124	176.84	30.1	
20H-6, 125	178.35	33.7	
21H-2, 120	181.80	18.0	
21H-3, 122	183.32	20.2	
21H-4, 120	184.80	47.2	
21H-5, 121	186.31	66.9	
21H-7, 122	189.32	38.2	
22H-2, 120	191.30	27.0	
22H-3, 122	192.82	34.8	
22H-4, 110	194.20	33.7	
22H-5, 120	195.80	33.7	
22H-6, 120	197.30	38.2	
23H-1, 120	199.30	27.0	
23H-4, 120	203.80	62.5	
23H-5, 120	205.30	64.0	
23H-6, 120	206.80	43.8	
24H-1, 120	208.80	16.8	
24H-2, 122	210.32	18.0	
24H-3, 120	211.80	33.0	
24H-4, 115	213.25	38.2	
24H-5, 120	214.80	83.1	
24H-6, 120	216.30	44.9	

Table 12. Laboratory compressional wave velocity, Site 803.

Core, section, interval (cm)	Depth (mbsf)	Longitudinal *P*-wave velocity (m/s)	Transverse *P*-wave velocity (m/s)
130-803A-			
4H-4, 35	31.85	1515.5	1525.8
4H-4, 110	32.60	1539.1	1535.7
4H-5, 35	33.35	1546.0	1537.3
4H-5, 110	34.10	1559.9	1540.6
4H-6, 35	34.85	1542.5	1529.1
4H-6, 110	35.60		1535.7
4H-7, 35	36.35	1528.9	1532.4
5H-2, 35	38.35	1559.9	1524.2
5H-2, 110	39.10	1556.4	1517.7
5H-3, 35	39.85		1524.2
5H-3, 110	40.60	1567.0	1535.7
5H-4, 35	41.35	1552.9	1532.4
5H-4, 110	42.10		1527.5
5H-5, 35	42.85		1525.8
5H-5, 110	43.60	1535.7	1525.8
5H-6, 35	44.35	1539.1	1522.6
5H-6, 110	45.10	1546.0	1525.8
5H-7, 35	45.85	1535.7	1527.5
6H-1, 98	46.98	1549.4	
6H-2, 45	47.95	1535.7	1512.9
6H-2, 110	48.60	1556.4	1525.8
6H-3, 35	49.35	1542.5	1519.3
6H-3, 108	50.08	1535.7	1516.1
6H-4, 35	50.85	1539.1	1514.5
6H-4, 105	51.55	1535.7	1522.6
6H-5, 39	52.39	1549.4	1524.2
6H-5, 110	53.10	1549.4	1525.8
6H-6, 37	53.87	1532.3	1521.0
6H-6, 105	54.55	1515.5	1517.7
6H-7, 39	55.39	1546.0	1524.2
130-803B-			
1H-1, 41	0.41	1539.0	1556.4
1H-1, 102	1.02	1529.1	1528.9
1H-2, 35	1.85	1539.0	1552.9
1H-2, 110	2.60	1534.0	1539.1
1H-3, 35	3.35	1524.2	1539.1
1H-3, 110	4.10	1522.6	1535.7
2H-1, 65	4.95	1529.1	1532.3
2H-1, 110	5.40	1521.0	1532.3
2H-2, 35	6.15	1562.5	
2H-2, 110	6.90	1534.0	1577.7
2H-3, 35	7.65	1532.4	1539.1
2H-3, 110	8.40	1527.5	1546.0
2H-4, 35	9.15	1542.5	1559.9
2H-4, 110	9.90	1527.5	1535.7
2H-5, 35	10.65	1549.0	1570.6
2H-5, 110	11.40	1559.1	1585.0
2H-6, 35	12.15	1549.0	1570.6
2H-6, 110	12.90	1554.0	1585.0
2H-7, 35	13.65	1550.7	1567.0
3H-1, 35	14.15	1533.7	1556.6
3H-1, 110	14.90	1543.6	1539.1
3H-2, 35	15.65	1560.4	
3H-2, 110	16.40	1553.6	1560.1
3H-3, 34	17.14	1527.1	1556.6
3H-3, 110	17.90	1541.9	1546.0
3H-4, 35	18.65	1555.3	1567.2
3H-4, 110	19.40	1551.9	1553.0
3H-5, 35	20.15	1558.7	1553.0
3H-5, 110	20.90	1551.9	1574.4
3H-6, 35	21.65	1563.8	1560.1
3H-6, 110	22.40	1530.4	1546.0
3H-7, 35	23.15	1533.7	1535.7
4H-1, 35	23.65	1530.4	1535.7
4H-1, 110	24.40	1528.8	1535.7
4H-2, 35	25.15	1541.9	1553.0
4H-2, 110	25.90	1551.9	1581.7
4H-3, 34	26.64	1541.9	
4H-3, 110	27.40	1543.6	1546.0
4H-4, 35	28.15	1528.8	1542.6
4H-4, 110	28.90	1537.0	1553.0
4H-5, 35	29.65	1538.6	1553.0

Table 12 (continued).

Core, section, interval (cm)	Depth (mbsf)	Longitudinal *P*-wave velocity (m/s)	Transverse *P*-wave velocity (m/s)
130-803B- (Cont.)			
4H-5, 108	30.38	1537.0	1549.5
4H-6, 35	31.15	1533.7	1532.2
4H-6, 104	31.84	1538.6	1567.2
4H-7, 35	32.65	1545.3	1535.7
5H-1, 120	34.00	1522.3	1542.6
5H-2, 39	34.69	1512.6	1518.7
5H-2, 110	35.40		1535.7
5H-3, 35	36.15		1542.6
5H-3, 110	36.90		1535.7
5H-4, 35	37.65		1535.7
5H-4, 110	38.40	1527.1	1532.2
5H-5, 35	39.15	1533.7	1522.0
5H-5, 110	39.90	1538.6	1539.1
5H-6, 35	40.65	1525.5	1525.4
5H-6, 110	41.40	1527.1	1508.7
5H-7, 15	41.95	1519.0	1508.7
5H-7, 45	42.25	1528.8	1535.7
6H-1, 120	43.50	1546.9	1570.8
6H-2, 110	44.25	1527.1	1539.1
6H-3, 45	45.75	1528.8	1522.0
6H-3, 110	46.40	1527.1	1539.1
6H-4, 45	47.25	1520.6	1539.1
6H-4, 115	47.95	1525.5	1539.1
6H-5, 30	48.60	1519.0	1525.4
130-803C-			
1H-1, 110	20.10	1545.3	1560.1
1H-2, 35	20.85	1548.6	1549.5
1H-2, 110	21.85	1546.9	1563.7
1H-3, 35	22.35	1551.9	1574.4
1H-3, 110	23.10	1533.7	1546.0
1H-4, 35	23.85	1533.7	1542.6
1H-4, 110	24.60	1535.3	1556.6
1H-5, 35	25.35	1540.3	1570.8
1H-5, 110	26.10	1565.5	1560.1
1H-6, 35	26.85	1538.6	1570.8
1H-6, 110	27.60	1538.6	1563.7
1H-7, 35	28.35	1533.7	1567.2
2H-1, 110	29.60	1535.3	1563.7
2H-2, 35	30.35	1530.4	1542.6
2H-2, 110	31.10	1527.1	1528.8
2H-3, 56	32.08	1527.1	1549.5
2H-3, 110	32.60	1530.4	1549.5
2H-4, 35	33.35	1530.4	1567.2
2H-4, 110	34.10	1548.6	1589.0
2H-5, 30	34.80	1535.3	1567.2
2H-5, 110	35.60	1530.4	1532.2
2H-6, 20	36.20	1541.9	1542.6
2H-6, 110	37.10	1532.0	1553.0
3H-1, 35	38.35	1525.5	1542.6
3H-1, 110	39.10		1532.2
3H-1, 111	39.11		1532.2
3H-2, 45	39.95		1532.2
3H-3, 45	41.45		1556.6
3H-3, 115	42.15		1532.2
3H-4, 36	42.86	1541.9	1542.6
3H-4, 110	43.60	1562.1	1592.7
3H-5, 30	44.30	1553.6	1585.3
3H-5, 110	45.10	1548.6	1563.7
3H-6, 35	45.85	1525.5	1546.0
3H-6, 110	46.60	1533.7	1542.6
3H-7, 30	47.30	1535.3	1570.8
4H-1, 110	48.60	1533.7	1535.7
4H-2, 57	49.57	1520.6	1532.2
4H-2, 128	50.28	1520.6	1525.4
4H-3, 59	51.09	1520.6	1532.2
4H-3, 120	51.70	1512.6	1532.2
4H-4, 35	52.35	1525.5	1539.1
4H-4, 120	53.10	1532.0	1542.6
4H-5, 35	53.85	1528.8	1546.0
4H-5, 110	54.60	1537.0	1539.1
4H-6, 35	55.35	1540.3	1539.1
4H-6, 110	56.10	1533.7	1542.6
4H-7, 35	56.85	1533.7	1549.5

Table 12 (continued).

Core, section, interval (cm)	Depth (mbsf)	Longitudinal *P*-wave velocity (m/s)	Transverse *P*-wave velocity (m/s)
130-803C- (Cont.)			
5H-2, 35	58.85	1528.8	1549.5
5H-2, 110	59.60	1528.8	1539.1
5H-3, 45	60.45	1522.3	1532.2
5H-3, 110	61.10	1543.6	1563.7
5H-4, 35	61.85	1537.0	1546.0
5H-4, 110	62.60	1535.3	1539.1
5H-5, 35	63.35	1532.0	1549.5
5H-5, 110	64.10	1537.0	1560.1
5H-6, 40	64.90	1535.3	1549.5
5H-6, 110	65.60	1532.0	1560.1
5H-7, 40	66.40	1537.0	1560.1
6H-1, 40	66.90	1525.5	1532.2
6H-1, 110	67.60	1512.6	1525.4
6H-2, 35	68.35	1532.0	1542.6
6H-2, 110	69.10	1527.1	1535.7
6H-3, 35	69.85	1535.3	1542.6
6H-3, 110	70.60	1528.8	1539.1
6H-4, 35	71.35	1522.3	1546.0
6H-4, 10	72.10	1528.8	1539.1
6H-5, 35	72.85	1528.8	1549.5
6H-5, 110	73.60	1533.7	1553.0
6H-6, 35	74.35	1522.3	1535.7
6H-6, 110	75.10	1519.0	1549.5
7H-1, 110	77.10	1511.0	1525.4
7H-2, 42	77.92	1514.2	1522.0
7H-2, 100	78.50	1512.6	1518.7
7H-3, 35	79.35	1530.4	1542.6
7H-3, 110	80.10	1522.3	1535.7
7H-4, 48	80.98	1520.6	1532.2
7H-4, 114	81.64	1522.3	1525.4
7H-5, 55	82.55	1530.4	1539.1
7H-5, 100	83.00	1514.2	1528.8
7H-6, 45	83.95	1523.9	1528.8
7H-6, 100	84.50	1520.6	1528.8
7H-7, 35	85.35	1541.9	1553.0
8H-1, 100	86.50		1522.0
8H-2, 35	87.35	1533.7	1542.6
8H-2, 90	87.90	1540.3	1546.0
8H-3, 15	88.65	1520.6	1518.7
8H-3, 113	89.63	1515.8	1522.0
8H-4, 25	90.25	1525.5	1532.2
8H-4, 110	91.10	1528.8	1539.1
8H-5, 39	91.89	1528.8	1528.8
8H-5, 120	92.70	1537.0	1549.5
8H-6, 35	93.35	1525.5	1539.1
8H-6, 115	94.15	1525.5	1546.0
8H-7, 35	94.85	1541.9	1556.6
9H-1, 90	95.90	1522.1	1519.9
9H-2, 35	96.85	1530.3	1526.7
9H-2, 110	97.60	1533.5	1523.3
9H-3, 55	98.55	1541.8	1543.9
9H-3, 110	99.10	1528.6	1537.0
9H-4, 55	100.05	1536.8	1540.4
9H-4, 116	100.66	1530.3	1533.5
9H-5, 45	101.45	1540.1	1547.4
9H-5, 125	102.25	1530.3	1540.4
9H-6, 39.5	102.88	1533.5	1530.1
9H-6, 110	103.60	1531.9	1533.5
10H-1, 35	104.85	1535.2	1540.4
10H-1, 115	105.65	1535.2	1550.9
10H-2, 35	106.35	1531.9	1543.9
10H-2, 105	107.05	1530.3	1540.4
10H-3, 40	107.90	1522.1	1519.9
10H-3, 110	108.60	1520.5	1526.7
10H-4, 23	109.23	1517.3	1519.9
10H-4, 110	110.10	1525.4	1530.1
10H-5, 40	110.90	1530.3	1526.7
10H-5, 110	111.60	1530.3	1533.5
10H-6, 40	112.40	1528.6	1526.7
10H-6, 110	113.10	1531.9	1530.1
10H-7, 45	113.95	1528.6	1530.1
11H-1, 38	114.38	1525.4	1516.6
11H-1, 100	115.00	1527.0	1526.7
11H-6, 35	117.35	1514.1	
11H-3, 100	118.00	1525.4	1523.3

Table 12 (continued).

Core, section, interval (cm)	Depth (mbsf)	Longitudinal *P*-wave velocity (m/s)	Transverse *P*-wave velocity (m/s)
130-803C- (Cont.)			
11H-4, 35	118.85	1523.7	1519.9
11H-4, 100	119.50	1528.6	1519.9
11H-5, 35	120.35	1522.1	1519.9
11H-5, 100	121.00	1528.6	1519.9
11H-6, 35	121.85	1525.4	1526.7
11H-6, 105	122.55	1527.0	1516.6
11H-7, 45	123.45	1538.5	1543.9
12H-1, 35	123.85	1522.1	1516.6
12H-1, 110	124.60	1528.6	1523.3
12H-2, 35	125.35	1528.6	1523.3
12H-3, 35	126.85	1523.7	1513.2
12H-3, 110	127.60	1520.5	1519.9
12H-4, 35	128.35	1527.0	1533.5
12H-4, 110	129.10	1535.2	1533.5
12H-5, 26	129.76	1522.1	
12H-5, 110	130.60	1522.1	1530.1
12H-6, 35	131.35	1545.1	1550.9
12H-6, 110	132.10	1543.5	1550.9
12H-7, 47	132.97	1538.5	1543.9
13H-1, 110	134.10	1527.0	1537.0
13H-2, 35	134.85	1527.0	1526.7
13H-2, 110	135.60	1531.9	1533.5
13H-3, 35	136.35	1533.5	1533.5
13H-3, 110	137.10	1528.6	1526.7
13H-4, 35	137.85	1543.5	1547.4
13H-4, 110	138.60	1533.5	1537.0
13H-5, 35	139.35	1567.1	1575.9
13H-5, 110	140.10		1565.1
13H-6, 35	140.85	1558.6	1594.2
13H-6, 110	141.60	1560.3	1586.8
13H-7, 45	142.45	1558.6	1568.7
14H-1, 35	142.85	1550.1	1605.4
14H-1, 110	143.60	1563.7	1572.3
14H-2, 35	144.35	1596.8	1601.7
14H-2, 110	145.10	1582.7	1526.7
14H-3, 35	145.85	1563.7	1583.2
14H-3, 102	146.52	1586.2	1620.6
14H-4, 35	147.35	1574.0	1597.9
14H-4, 110	148.10	1555.2	1557.9
14H-5, 35	148.85	1553.5	1568.7
14H-5, 110	149.60	1550.1	1557.9
14H-6, 35	150.35	1556.9	1572.3
14H-6, 110	151.10	1546.8	1561.5
15H-1, 110	153.10	1543.5	1543.9
15H-2, 35	153.85		1572.3
15H-2, 110	154.60	1541.8	1554.4
15H-3, 35	155.35	1533.5	1572.3
15H-3, 110	156.10	1541.8	1561.5
15H-4, 35	156.85	1545.1	1575.9
15H-4, 110	157.60	1550.1	1583.2
15H-5, 35	158.35	1550.1	1561.5
15H-5, 110	159.10	1558.6	1575.9
15H-6, 35	159.85	1546.8	1568.7
15H-6, 110	160.60	1545.1	1579.5
15H-7, 35	161.35	1556.9	1583.2
16H-2, 35	163.35		1561.5
16H-2, 110	164.10	1541.8	1550.9
16H-3, 35	164.85		1561.5
16H-3, 110	165.60	1555.2	1561.5
16H-4, 35	166.35	1553.5	1568.7
16H-4, 110	167.10	1556.9	1583.2
16H-5, 35	167.85	1546.8	1572.3
16H-5, 110	168.60	1548.5	1579.5
16H-6, 35	169.35	1553.5	1590.5
16H-6, 110	170.10	1550.1	1597.9
17H-2, 110	173.60	1540.1	1579.5
17H-3, 35	174.35		1540.4
17H-3, 110	175.10		1561.5
17H-4, 35	175.85		1586.8
17H-4, 110	176.60		1572.3
17H-5, 35	177.35		1601.7
17H-5, 110	178.10		1586.8
17H-6, 35	178.85		1609.2
17H-6, 110	179.60		1605.4
17H-7, 35	180.35		1609.2

Table 12 (continued).

Core, section, interval (cm)	Depth (mbsf)	Longitudinal *P*-wave velocity (m/s)	Transverse *P*-wave velocity (m/s)
130-803C- (Cont.)			
18H-2, 80	182.80		1604.3
18H-2, 110	183.10		1571.2
18H-3, 110	184.60		1560.5
18H-4, 35	185.35		1582.1
18H-4, 110	186.10		1600.6
18H-5, 35	186.85		1585.8
18H-5, 110	187.60		1600.6
18H-6, 36	188.36		1600.6
18H-6, 110	189.10		1608.1
18H-7, 30	189.80		1611.9
19H-1, 35	190.35		1600.6
19H-1, 110	191.10		1600.6
19H-2, 35	191.85		1593.2
19H-2, 110	192.60		1646.8
19H-3, 35	193.35		1608.1
19H-3, 110	194.10		1582.1
19H-4, 35	194.85		1619.5
19H-4, 100	195.50		1596.9
19H-5, 35	196.35		1670.9
19H-5, 110	197.10		1658.7
19H-6, 110	198.60		1704.1
19H-7, 25	199.25		1658.7
20H-3, 35	202.85		1589.5
20H-3, 109	203.59		1596.9
20H-4, 40	204.40		1593.2
20H-4, 110	205.10		1596.9
20H-5, 36	205.86		1574.8
20H-5, 111	206.61		1593.2
20H-6, 35	207.35		1638.9
20H-6, 110	208.10		1627.2
20H-7, 35	208.85		1556.9
21H-1, 35	209.35		1519.0
21H-1, 111	210.11		1574.8
21H-2, 35	210.85		1589.5
21H-2, 100	211.50		1582.1
21H-3, 35	212.35		1596.9
21H-3, 110	213.10		1574.8
21H-4, 35	213.85		1608.1
21H-4, 110	214.60		1608.1
21H-5, 40	215.40		1619.5
21H-5, 110	216.10		1604.3
21H-5, 110	216.10		1593.2
21H-6, 35	216.85		1615.7
21H-6, 100	217.50		1608.1
21H-7, 40	218.40		1596.9
22H-1, 35	218.85		1589.5
22H-1, 35	218.85		1589.5
22H-1, 100	219.50		1519.0
22H-2, 35	220.35		1593.2
22H-2, 100	221.00		1549.9
22H-2, 100	221.00		1585.8
22H-3, 30	221.80		1582.1
22H-3, 110	222.60		1623.4
22H-4, 35	223.35		1608.1
22H-4, 110	224.10		1638.9
22H-5, 35	224.85		1650.7
22H-5, 110	225.60		1615.7
22H-6, 35	226.35		1627.2
22H-6, 90	226.90		1638.9
23H-1, 70	228.70		1596.9
23H-4, 35	232.85		1549.9
23H-4, 100	233.50		1604.3
23H-5, 30	234.30		1585.8
23H-5, 99	234.99		1608.1
23H-6, 20	235.70		1635.0
23H-6, 100	236.50		1608.1
23H-7, 25	237.25		1623.4
23H-7, 25	237.25		1615.7
130-803D-			
1H-1, 125	1.25	1554.8	1572.9
1H-2, 40	1.90	1548.1	1580.8
2H-1, 35	2.85	1543.1	1545.7
2H-1, 110	3.60	1526.7	1541.8

Table 12 (continued).

Core, section, interval (cm)	Depth (mbsf)	Longitudinal *P*-wave velocity (m/s)	Transverse *P*-wave velocity (m/s)
130-803D- (Cont.)			
2H-2, 45	4.45	1554.8	1580.8
2H-2, 108	5.08	1529.9	1541.8
2H-3, 45	5.95	1538.1	1553.3
2H-3, 100	6.50	1529.9	1538.0
2H-4, 45	7.45	1548.1	1565.0
2H-5, 45	8.95	1544.8	1565.0
2H-5, 96	9.46	1538.1	1553.3
2H-6, 35	10.35	1553.1	1565.0
2H-6, 100	11.00	1551.5	1588.9
2H-7, 40	11.90	1554.8	1572.9
3H-1, 35	12.35	1541.4	1557.2
3H-1, 110	13.10	1551.5	1580.8
3H-2, 35	13.85	1539.8	1545.7
3H-2, 100	14.50	1553.1	1565.0
3H-3, 30	15.30	1553.1	1561.1
3H-3, 110	16.10		1545.7
3H-4, 24	16.74	1517.0	1545.7
3H-4, 105	17.55	1554.8	1565.0
3H-5, 35	18.35	1554.8	1557.2
3H-5, 110	19.10	1561.6	1576.9
3H-6, 40	19.90	1549.8	1553.3
3H-6, 110	20.60	1553.1	1580.8
3H-7, 34	21.34	1546.4	1553.3
4H-1, 110	22.60		1533.5
4H-2, 35	23.35	1525.4	1523.3
4H-2, 110	24.10	1535.2	1543.9
4H-3, 35	24.85	1554.8	1584.8
4H-4, 35	26.35		1553.3
4H-4, 100	27.00	1548.1	1576.9
4H-5, 39	27.89	1539.8	1549.5
4H-5, 100	28.50	1538.1	1565.0
4H-6, 45	29.45	1539.8	1565.0
4H-6, 104	30.04	1539.8	1561.1
4H-7, 30	30.80	1541.4	1565.0
5H-1, 105	32.15	1528.3	1541.8
5H-2, 60	33.10	1515.4	1519.4
5H-2, 130	33.80	1536.5	1541.8
5H-3, 35	34.35	1523.4	
5H-3, 105	35.05	1529.9	1534.3
5H-4, 35	35.85	1528.3	1538.0
5H-4, 110	36.60	1531.6	1541.8
5H-5, 35	37.35	1533.2	1545.7
5H-5, 110	38.10	1531.6	
5H-6, 35	38.85	1525.1	1530.5
5H-6, 110	39.60	1529.9	1538.0
5H-7, 35	40.35	1531.6	1534.3
6H-1, 110	41.60	1528.3	1526.8
6H-2, 35	42.35	1528.3	1541.8
6H-2, 110	43.10	1551.5	1545.7
6H-3, 35	43.85	1536.5	1557.2
6H-3, 105	44.55	1543.1	1565.0
6H-4, 35	45.35	1546.4	1572.9
6H-4, 110	46.10	1525.1	1545.7
7H-1, 35	46.45	1529.9	1545.7
6H-5, 35	46.85	1529.9	1538.0
7H-1, 110	47.20	1539.8	1557.2
6H-5, 110	47.60	1523.4	1549.5
7H-2, 35	47.95	1533.2	1549.5
6H-6, 35	48.35	1536.5	1549.5
7H-2, 110	48.70	1505.8	1561.1
6H-6, 110	49.10	1539.8	1545.7
7H-3, 35	49.45	1531.6	1557.2
6H-7, 35	49.85	1526.7	1549.5
7H-3, 115	50.25	1538.1	1572.9
7H-4, 33	50.93	1549.8	1561.1
7H-4, 110	51.70	1544.8	1568.9
7H-5, 35	52.45	1533.2	1568.9
7H-5, 110	53.20	1551.5	1568.9
7H-6, 35	53.95	1538.1	1576.9
7H-6, 110	54.70	1529.9	1549.5
7H-7, 35	55.45	1543.1	1565.0
8H-1, 110	56.70	1533.2	1545.7
8H-2, 35	57.45	1566.7	1584.8
8H-2, 110	58.20	1544.8	1545.7
8H-3, 35	58.95	1549.8	1557.2

Table 12 (continued).

Core, section, interval (cm)	Depth (mbsf)	Longitudinal *P*-wave velocity (m/s)	Transverse *P*-wave velocity (m/s)
130-803D- (Cont.)			
8H-3, 110	59.70	1544.8	1549.5
8H-4, 35	60.45	1531.6	1549.5
8H-4, 110	61.20	1544.8	1565.0
8H-5, 35	61.95	1541.4	1549.5
8H-5, 110	62.70	1539.8	1553.3
8H-6, 35	63.45	1541.4	1549.5
8H-6, 110	64.20	1551.5	1588.9
8H-7, 35	64.95	1546.4	1545.7
9H-1, 35	65.45	1531.6	1534.3
9H-1, 110	66.20	1536.5	1538.0
9H-2, 35	66.95	1543.1	1549.5
9H-2, 110	67.70	1536.5	1545.7
9H-3, 35	68.45	1534.8	1545.7
9H-3, 110	69.20	1534.8	1545.7
9H-4, 35	69.95	1538.1	1557.2
9H-4, 105	70.65	1538.1	1557.2
9H-5, 37	71.47	1544.8	1557.2
9H-5, 113	72.23	1528.3	1553.3
9H-6, 35	72.95	1539.8	1557.2
9H-6, 109	73.69	1534.8	1565.0
9H-7, 35	74.45	1525.1	
10H-1, 35	74.95	1528.3	1545.7
10H-1, 110	75.70	1541.4	1561.1
10H-2, 35	76.45	1529.9	1549.5
10H-2, 110	77.20	1538.1	1549.5
10H-3, 35	77.95	1536.5	1549.5
10H-3, 100	78.60	1546.4	1557.2
10H-4, 35	79.45	1543.1	1561.1
10H-4, 100	80.10	1543.1	1580.8
10H-5, 35	80.95	1543.1	1557.2
10H-5, 110	81.70	1553.1	1565.0
10H-6, 35	82.45	1543.1	1576.9
10H-6, 110	83.20	1538.1	1549.5
10H-7, 35	83.95	1539.8	1545.7
11H-1, 35	84.45	1538.1	1553.3
11H-1, 110	85.20	1539.8	1576.9
11H-2, 35	85.95	1536.5	1568.9
11H-2, 110	86.70	1546.4	1572.9
11H-3, 35	87.45	1536.5	1572.9
11H-3, 110	88.20	1543.1	1584.8
11H-4, 35	88.95	1531.6	1557.2
11H-4, 110	89.70	1531.6	1572.9
11H-5, 35	90.45	1539.8	1576.9
11H-5, 110	91.20	1546.4	1580.8
11H-6, 35	91.95	1543.1	1561.1
11H-6, 110	92.70	1536.5	1572.9
11H-7, 35	93.45	1543.1	1572.9
12H-1, 110	94.70	1549.8	1565.0
12H-2, 35	95.45	1549.8	1568.9
12H-2, 110	96.20	1558.2	1576.9
12H-3, 35	96.95	1541.4	1572.9
12H-3, 110	97.70	1551.5	1561.1
12H-4, 35	98.45	1549.8	1565.0
12H-4, 110	99.20	1548.1	1565.0
12H-5, 35	99.95	1543.1	1553.3
12H-5, 110	100.70	1536.5	1561.1
12H-6, 35	101.45	1548.1	1568.9
12H-6, 110	102.20	1543.1	1565.0
13H-2, 35	104.95	1525.1	1553.3
13H-2, 110	105.70	1543.1	1553.3
13H-3, 45	106.55	1573.6	1597.0
13H-3, 45	106.55	1573.6	1597.0
13H-3, 110	107.20	1577.0	1584.8
13H-3, 110	107.20	1577.0	1584.8
13H-4, 35	107.95	1543.1	1561.1
13H-4, 100	108.60	1541.4	1549.5
13H-5, 35	109.45	1538.1	1549.5
13H-5, 110	110.20	1538.1	1549.5
13H-6, 35	110.95	1541.4	1549.5
13H-6, 110	111.70	1539.8	1561.1
13H-7, 35	112.45	1536.5	1557.2
14H-1, 35	112.95	1538.1	1557.2
14H-1, 110	113.70	1539.8	1568.9
14H-2, 35	114.45	1544.8	1545.7
14H-2, 110	115.20	1544.8	1545.7

Table 12 (continued).

Core, section, interval (cm)	Depth (mbsf)	Longitudinal *P*-wave velocity (m/s)	Transverse *P*-wave velocity (m/s)
130-803D- (Cont.)			
14H-3, 35	115.95	1544.8	1553.3
14H-3, 100	116.60	1538.1	1549.5
14H-4, 30	117.40	1541.4	1557.2
14H-4, 105	118.15	1538.1	1553.3
14H-5, 35	118.95	1528.3	1538.0
14H-5, 100	119.60	1536.5	1549.5
14H-6, 40	120.50	1533.2	1541.8
14H-6, 110	121.20	1541.4	1557.2
15H-1, 110	123.20	1533.2	1538.0
15H-2, 35	123.95	1534.8	1538.0
15H-2, 110	124.70	1534.8	1538.0
15H-3, 35	125.45	1534.8	1534.3
15H-3, 110	126.20	1541.4	1553.3
15H-4, 39	126.99	1539.8	1549.5
15H-4, 110	127.70	1544.8	1545.7
15H-5, 44	128.54	1533.2	1541.8
15H-5, 105	129.15	1541.4	1549.5
15H-6, 30	129.90	1531.6	1545.7
15H-6, 105	130.65	1534.8	1553.3
16H-1, 60	132.20	1526.7	1530.5
16H-1, 105	132.65	1533.2	1545.7
16H-2, 40	133.50	1543.1	1557.2
16H-2, 110	134.20	1538.1	1541.8
16H-3, 35	134.95	1538.1	1545.7
16H-3, 110	135.70	1541.4	1545.7
16H-4, 30	136.40	1546.4	1549.5
16H-4, 80	136.90	1538.1	1538.0
16H-5 35	137.95	1577	1576.9
16H-5, 110	138.70	1570.1	1601.1
16H-6, 11	139.21	1573.6	1572.9
16H-6, 35	139.45	1556.5	1609.3
17H-1, 35	141.45	1571.9	1613.5
17H-1, 110	142.20	1578.8	1588.9
17H-2, 35	142.95	1573.6	1597.0
17H-2, 99	143.59	1559.9	1580.8
17H-4, 37	145.97	1573.6	1592.9
17H-4, 104	146.64	1585.8	1617.7
17H-5, 29	147.39	1598.1	1638.9
17H-5, 110	148.20	1549.8	1561.1
17H-6, 35	148.95	1543.1	1557.2
17H-6, 100	149.60	1536.5	1553.3
17H-7, 35	150.45	1548.1	1572.9
18H-1, 110	151.70	1526.7	1538.0
18H-2, 115	153.25	1529.9	1530.5
18H-3, 30	153.90	1541.4	1530.5
18H-3, 110	154.70	1529.9	1526.8
18H-4, 35	155.13	1541.4	
18H-4, 110	156.20	1539.8	1561.1
18H-5, 35	156.95	1543.1	1561.1
18H-5, 110	157.70	1551.5	1565.0
18H-6, 35	158.45	1541.4	1557.2
18H-6, 110	159.20	1536.5	1534.3
19H-1, 35	160.45	1549.8	1565.0
19H-1, 110	161.20	1533.2	1557.2
19H-2, 35	161.95	1531.6	1549.5
19H-2, 110	162.70	1543.1	1553.3
19H-3, 40	163.50	1536.5	1549.5
19H-3, 115	164.25	1546.4	1557.2
19H-4, 35	164.95	1538.1	1576.9
19H-4, 100	165.60	1544.8	1568.9
19H-5, 35	166.45	1543.1	1588.9
19H-5, 110	167.20	1539.8	1572.9
19H-6, 35	167.95	1543.1	1568.9
19H-6, 110	168.70	1544.8	1592.9
20H-1, 35	169.95	1549.8	1576.9
20H-1, 110	170.70	1539.8	1545.7
20H-2, 35	171.45	1544.8	1557.2
20H-2, 110	172.20	1543.1	1545.7
20H-3, 35	172.95	1544.8	1572.9
20H-3, 110	173.70	1548.1	1568.9
20H-4, 35	174.45	1546.4	1561.1
20H-4, 110	175.20	1534.8	1568.9
20H-5, 35	175.95		1580.8
20H-5, 110	176.70	1538.1	1584.8
20H-6, 35	177.45		1580.8

Table 12 (continued).

Core, section, interval (cm)	Depth (mbsf)	Longitudinal *P*-wave velocity (m/s)	Transverse *P*-wave velocity (m/s)
130-803D- (Cont.)			
20H-6, 95	178.05	1529.9	1588.9
20H-7, 30	178.96	1549.8	1597.0
21H-2, 67	181.27	1539.8	1597.0
21H-3, 35	182.45		1561.1
21H-3, 95	183.05		1565.0
21H-4, 35	183.95	1533.2	1572.9
21H-4, 100	184.60		1613.5
21H-5, 40	185.50		1580.8
21H-5, 110	186.20		1609.3
21H-6, 35	186.95		1605.2
22H-1, 100	189.60		1630.3
22H-2, 35	190.46		1621.9
22H-2, 100	191.10		1626.1
22H-3, 35	191.95		1621.9
22H-3, 100	192.60		1630.3
22H-4, 45	193.55		1656.2
22H-4, 90	194.00		1630.3
22H-5, 33	194.93		1617.7
22H-5, 100	195.60		1597.0
22H-6, 105	197.15		1621.9
22H-7, 35	197.95		1651.9
23H-1, 35	198.45		1565.0
23H-1, 100	199.10		1568.9
23H-2, 35	199.95		1553.3
23H-2, 100	200.60		1561.1
23H-4, 35	202.95		1609.3
23H-4, 105	203.65		1584.8
23H-5, 35	204.45		1609.3
23H-5, 100	205.10		1597.0
23H-6, 35	205.95		1580.8
23H-6, 100	206.60		1605.2
23H-7, 35	207.45		1605.2
24H-1, 35	207.95		1549.5
24H-1, 110	208.70		1561.1
24H-2, 100	210.10		1572.9
24H-3, 35	210.95		1576.9
24H-3, 100	211.60		1588.9
24H-4, 35	212.45		1588.9
24H-4, 100	213.10		1605.2
24H-5, 35	213.95		1647.5
24H-5, 100	214.60		1609.3
24H-6, 35	215.45		1609.3
24H-6, 100	216.10		1609.3
24H-7, 40	217.00		1613.5
25X-2, 38	218.98		1562.9
25X-3, 73	220.83		1578.7
26X-1, 32	227.12	1598.5	1592.1
26X-2, 30	228.60	1603.3	1610.4
26X-3, 35	230.15	1609.5	1596.3
26X-4, 64	231.94	1612.7	1588.4
26X-5, 79	233.59	1598.7	1645.5
27X-1, 74	237.24	1681.1	1580.2
27X-2, 98	238.98	1639.1	1627.4
28X-1, 85	246.75	1550.9	1567.2
29X-1, 65	256.15		1661.8
29X-2, 56	257.56	1643.1	1635.6
29X-3, 60	259.10		1637.4
29X-4, 73	260.73		1599.5
29X-5, 30	261.80		1582.2
30X-1, 134	266.44	1586.6	1608.4
30X-2, 81	267.41		1582.4
30X-3, 76	268.86		1597.3
31X-3, 94	278.64		1596.2
32X-1, 90	285.20		1543.0
32X-2, 118	286.98		1611.3
32X-3, 102	288.32	1576.0	1596.0
32X-5, 37	290.67		1571.9
33X-1, 138	295.48		1581.1
33X-2, 102	296.62	1590.1	1582.1
33X-3, 118	298.28	1556.7	1627.0
33X-4, 60	299.20	1585.0	1603.0
34X- , 50	303.80		1611.5
34X-3, 72	307.02	1614.0	1605.4
34X-4, 83	308.63	1653.0	1640.6
34X-5, 70	310.00	1625.9	1665.0

Table 12 (continued).

Core, section, interval (cm)	Depth (mbsf)	Longitudinal *P*-wave velocity (m/s)	Transverse *P*-wave velocity (m/s)
130-803D- (Cont.)			
34X-6, 138	312.18	1617.5	1636.3
35X-1, 91	313.91	1635.8	1704.0
35X-2, 130	315.80	1642.4	1726.3
35X-3, 87	316.87	1724.2	1676.3
35X-4, 72	318.22	1638.8	1731.4
35X-5, 53	319.53	1700.2	1700.2
35X-6, 49	320.99	1583.4	1704.7
36X-1, 114	323.84	1644.0	1678.4
36X-2, 72	324.92		1691.0
36X-3, 117	326.87	1687.8	1744.7
36X-4, 128	328.48	1678.7	1675.6
36X-5, 126	329.96	1686.2	1710.8
36X-6, 115	331.35		1663.3
37X-1, 91	333.21	1716.1	1781.0
37X-2, 105	334.85	1666.9	1720.3
37X-3, 103	336.33	1616.3	1669.9
37X-4, 104	337.84	1624.9	1701.9
37X-5, 100	339.30	1721.3	1732.0
37X-6, 110	340.90	1750.5	1754.8
38X-1, 60	342.60		1684.2
38X-4, 134	347.84	1677.2	1690.8
38X-5, 108	349.08	1660.0	1684.9
38X-6, 23	349.73	1622.7	1680.1
39X-1, 126	352.86	1639.1	1726.8
39X-2, 130	354.40	1692.3	1757.9
39X-3, 54	355.14		1699.0
39X-4, 53	356.63	1641.1	1705.7
39X-5, 54	358.14	1708.8	1739.8
39X-6, 66	359.76	1699.7	1677.9
40X-1, 40	361.70	1681.4	1755.6
40X-2, 90	363.70	1685.2	1711.9
40X-3, 87	365.17		1800.6
40X-4, 90	366.70	1736.4	1790.2
40X-5, 50	367.80	1691.0	1730.2
41X-1, 14	371.14		1615.2
41X-2, 74	373.24	1529.2	1546.2
41X-3, 115	375.15	1543.2	
42X-1, 34	381.04	1550.3	1578.4
42X-1, 99	381.69	1565.2	1551.2
42X-3, 15	383.85		1519.3
42X-3, 115	384.85	1547.0	
43X-1, 12	390.52	1738.3	1763.9
43X-2, 90	392.80	1817.1	1767.8
43X-3, 41	393.81		1741.2
43X-3, 87	394.27	1765.8	
43X-4, 41	395.31		1782.4
43X-5, 22	396.62	1775.8	1886.7
44X-1, 90	400.90	1826.6	1859.6
44X-2, 114	402.64	1779.0	1735.5
44X-3, 73	403.73	1697.0	1690.1
44X-4, 72	405.22	1825.4	1791.9
44X-5, 30	406.30	1822.0	1849.6
45X-1, 82	410.52	1860.6	1832.0
45X-2, 71	411.91	1787.8	1854.4
45X-3, 118	413.88	1737.8	1742.1
45X-4, 70	414.90	1792.8	1850.3
45X-5, 50	416.20	1782.3	1790.2
45X-6, 68	417.88	1747.0	1737.9
46X-1, 118	420.48	1863.9	1855.8
46X-2, 128	422.08	1748.7	1731.3
46X-3, 128	423.58	1717.0	1775.6
46X-5, 62	425.92	1767.9	1739.7
47X-1, 65	429.65	1699.3	1658.1
47X-2, 133	431.83	1843.2	1796.3
47X-3, 118	433.18	1745.5	1782.6
47X-4, 88	434.38	1688.9	1781.4
47X-5, 27	435.27	1793.2	1869.8
48X-1, 22	438.82	1700.5	1749.1
48X-2, 48	440.58	1800.8	1780.1
48X-3, 49	442.09	1782.4	1812.5
48X-4, 48	443.58	1767.1	1767.1
49X-1, 95	448.75	1575.7	1738.1
49X-2, 83	450.13	1897.5	1783.7
49X-4, 77	453.07	1748.6	1770.0

Table 12 (continued).

Core, section, interval (cm)	Depth (mbsf)	Longitudinal *P*-wave velocity (m/s)	Transverse *P*-wave velocity (m/s)
130-803D- (Cont.)			
50X-1, 120	458.70		1750.8
50X-2, 29	459.29		1766.7
50X-3, 148	461.98	1862.6	1684.9
50X-4, 109	463.09		1744.3
52X-2, 78	479.18	1817.1	1916.0
52X-3, 53	480.43	1923.3	1811.4
53X-1, 129	487.89	1840.1	1872.7
53X-2, 142	489.52	1959.5	1847.5
53X-3, 112	490.72	1741.4	1843.0
53X-4, 83	491.93	2035.5	
54X-1, 76	497.06	1907.0	1916.0
54X-2, 87	498.67	1824.9	1906.4
54X-3, 76	500.06	2006.3	1997.0
54X-4, 93	501.73	1959.9	1922.9
55X-1, 48	506.48	2139.1	1966.7
55X-2, 47	507.97	1817.1	1988.9
55X-3, 80	509.80	1889.0	1923.8
55X-4, 55	511.05	1907.0	2004.6
56X-1, 115	516.75	1873.3	1974.5
56X-2, 100	518.10	1969.0	1971.5
56X-3, 100	519.60	1872.7	2057.1
56X-4, 108	521.18	2076.1	1997.4
56X-5, 115	522.75	2015.9	2065.7
56X-6, 83	523.93	2015.8	2097.3
57X-1, 92	526.22	1987.4	2128.0
57X-2, 95	527.75	1996.8	2099.2
57X-3, 91	529.21	2227.6	2222.8
58X-1, 21	534.81	2341.9	2287.7
58X-CC, 10	535.46	2264.7	2251.2
59X-1, 60	544.90	1831.3	1873.3
59X-2, 67	546.47	1987.4	2035.1
60X-1, 10	554.10	2055.4	2045.2
60X-2, 22	555.72	1812.8	2049.7
61X-1, 5	563.75	2016.1	1951.1
64X-CC, 10	588.80	2064.6	2312.6
65X-CC, 10	598.50		1807.9
66X-CC, 5	601.95	2170.6	2366.3
67X-1, 117	613.17	1694.2	1649.2
67X-CC, 15	614.39		2520.5
68X-1, 18	621.98		1865.4
68X-3, 128	626.08	1640.1	
69X-1, 88	632.28	4313.3	4178.4

Table 13. Discrete index properties, Site 803.

Core, section, interval (cm)	Depth (mbsf)	Bulk density (g/cm^3)	Grain density (g/cm^3)	Water content (% dry wt)	Porosity (%)	Dry density (g/cm^3)
130-803A-						
4H-4, 35	31.85	1.56	2.69	80.4	67.7	0.86
4H-4, 110	32.60	1.58	2.69	75.1	66.1	0.90
4H-5, 35	33.35	1.59	2.68	73.1	65.5	0.92
4H-5, 110	34.10	1.57	2.66	76.8	66.4	0.89
4H-6, 35	34.85	1.56	2.69	78.5	67.1	0.88
4H-6, 110	35.60	1.59	2.70	73.8	65.8	0.91
4H-7, 35	36.35	1.58	2.68	74.1	65.7	0.91
5H-2, 39	38.39	1.60	2.73	73.2	65.9	0.92
5H-2, 115	39.15	1.75	2.68	48.9	56.0	1.17
5H-3, 39	39.89	1.58	2.67	74.6	65.8	0.90
5H-3, 115	40.65	1.57	2.69	77.8	67.0	0.88
5H-4, 35	41.35	1.58	2.68	75.6	66.2	0.90
5H-4, 110	42.10	1.59	2.74	75.3	66.6	0.91
5H-5, 35	42.85	1.58	2.65	73.4	65.3	0.91
5H-5, 110	43.50	1.57	2.69	78.1	67.0	0.88
5H-6, 39	44.39	1.58	2.68	74.5	65.8	0.91
5H-6, 110	45.10	1.61	2.69	69.7	64.5	0.95
5H-7, 36	45.86	1.60	2.71	72.2	65.4	0.93
6H-1, 97	46.97	1.52	2.68	87.2	69.3	0.81
6H-2, 45	47.95	1.50	2.66	93.7	70.6	0.77
6H-2, 109	48.59	1.59	2.69	72.5	65.3	0.92
6H-3, 35	49.35	1.59	2.67	71.7	64.9	0.93
6H-4, 34	50.84	1.58	2.68	74.3	65.8	0.91
6H-4, 104	51.54	1.59	2.69	74.1	65.9	0.91
6H-5, 40	52.40	1.60	2.70	72.4	65.4	0.93
6H-5, 110	53.10	1.59	2.67	72.0	65.0	0.92
6H-6, 37	53.87	1.60	2.71	72.8	65.6	0.92
6H-7, 40	55.40	1.60	2.69	71.1	64.9	0.94
130-803B-						
1H-1, 41	0.41	1.46	2.66	102.7	72.5	0.72
1H-1, 112	1.12	1.53	2.70	86.2	69.2	0.82
1H-2, 31	1.81	1.47	2.70	102.1	72.7	0.73
1H-2, 107	2.57	1.55	2.76	84.7	69.3	0.84
1H-3, 36	3.36			77.0		
1H-3, 110	4.10			87.2		
2H-1, 62	4.92	1.56	2.70	79.8	67.5	0.87
2H-1, 109	5.39	1.56	2.69	79.4	67.4	0.87
2H-2, 32	6.12	1.54	2.70	84.6	68.8	0.83
2H-2, 108	6.88	1.53	2.69	85.7	69.0	0.83
2H-3, 35	7.75	1.54	2.69	83.2	68.4	0.84
2H-3, 99	8.29	1.58	2.72	76.0	66.7	0.90
2H-4, 35	9.15	1.56	2.66	77.1	66.4	0.88
2H-4, 109	9.89	1.61	2.71	70.7	64.9	0.94
2H-5, 34	10.64	1.57	2.64	75.7	65.9	0.89
2H-5, 109	11.39	1.53	2.67	86.0	68.9	0.82
2H-6, 34	11.84	1.53	2.69	85.8	69.1	0.82
2H-6, 109	12.89	1.53	2.71	87.5	69.6	0.82
2H-7, 34	13.64	1.55	2.68	81.8	67.9	0.85
3H-1, 35	14.15	1.58	2.66	73.8	65.5	0.91
3H-1, 109	14.89	1.59	2.71	74.0	66.0	0.91
3H-2, 35	15.65			86.2		
3H-2, 110	16.40			86.2		
3H-3, 35	17.15	1.60	2.70	72.2	65.3	0.93
3H-3, 110	17.90	1.53	2.73	88.9	70.1	0.81
3H-4, 35	18.65	1.56	2.67	79.7	67.3	0.87
3H-4, 110	19.40	1.58	2.78	79.2	68.0	0.88
3H-5, 34	20.14	1.53	2.72	86.4	69.4	0.82
3H-5, 110	20.90	1.58	2.74	77.5	67.3	0.89
3H-6, 34	21.64	1.56	2.68	79.5	67.3	0.87
3H-6, 110	22.40			70.3		
3H-7, 35	23.15	1.61	2.66	67.3	63.4	0.97
4H-1, 35	23.65	1.51	2.67	68.8	64.0	0.95
4H-1, 110	24.40			65.5		
4H-2, 33	25.13	1.59	2.75	75.0	66.6	0.91
4H-2, 109	25.89	1.47	2.68	102.0	72.5	0.73
4H-3, 34	26.64	1.54	2.68	83.3	68.3	0.84
4H-3, 110	27.40	1.57	2.69	78.0	67.0	0.88
4H-4, 34	28.14	1.56	2.66	77.7	66.6	0.88
4H-4, 109	28.89	1.55	2.68	81.1	67.7	0.86
4H-5, 35	29.65	1.56	2.66	78.2	66.8	0.88
4H-5, 108	30.38	1.55	2.69	80.8	67.8	0.86
4H-6, 36	31.16	1.56	2.69	79.9	67.5	0.87
4H-7, 35	32.65	1.58	2.70	74.5	66.0	0.91
5H-1, 120	34.00	1.55	2.67	80.1	67.4	0.86

Table 13 (continued).

Core, section, interval (cm)	Depth (mbsf)	Bulk density (g/cm^3)	Grain density (g/cm^3)	Water content (% dry wt)	Porosity (%)	Dry density (g/cm^3)
130-803B- (Cont.)						
5H-2, 40	34.70	1.58	2.69	74.5	66.0	0.91
5H-2, 111	35.41	1.57	2.71	77.8	67.1	0.88
5H-3, 36	36.16			74.4		
5H-3, 111	36.91	1.59	2.75	74.8	66.5	0.91
5H-4, 35	37.65	1.60	2.72	72.9	65.8	0.92
5H-4, 110	38.40	1.60	2.69	72.1	65.2	0.93
5H-5, 34	39.14	1.60	2.76	74.4	66.5	0.92
5H-5, 110	39.90	1.58	2.71	75.1	66.3	0.90
5H-6, 35	40.65	1.59	2.68	73.7	65.6	0.91
5H-6, 110	41.40	1.60	2.67	69.5	64.2	0.95
5H-7, 15	41.95	1.62	2.77	71.3	65.6	0.94
5H-7, 45	42.25	1.58	2.67	73.7	65.5	0.92
6H-1, 127	43.57	1.57	2.67	76.6	66.4	0.89
6H-2, 46	44.26	1.59	2.73	73.7	66.1	0.92
6H-2, 109	44.89			81.3		
6H-3, 45	45.75	1.56	2.69	80.4	67.7	0.86
6H-3, 109	46.39	1.58	2.70	74.9	66.1	0.90
6H-4, 44	47.24	1.60	2.74	73.6	66.1	0.92
6H-4, 114	47.94			70.3		
6H-5, 31	48.61	1.60	2.75	73.5	66.2	0.92
7H-1, 110	52.90	1.59	2.71	73.1	65.7	0.92
7H-2, 27	53.57	1.62	2.71	68.8	64.3	0.96
7H-2, 111	54.41	1.63	2.73	67.0	63.9	0.98
7H-3, 124	56.04	1.60	2.71	72.6	65.6	0.93
7H-4, 35	56.65	1.27	2.70	219.0	84.9	0.40
7H-4, 110	57.40	1.64	2.76	66.0	63.8	0.99
7H-5, 35	58.15	1.61	2.71	70.2	64.8	0.95
130-803C-						
1H-1, 34	19.34	1.56	2.76	82.0	68.6	0.86
1H-1, 109	20.09	1.54	2.71	85.2	69.1	0.83
1H-2, 34	20.84	1.58	2.78	77.9	67.7	0.89
1H-2, 104	21.54	1.58	2.71	76.0	66.6	0.90
1H-3, 40	22.40	1.63	2.78	69.4	65.1	0.96
1H-5, 34	25.34	1.56	2.71	79.4	67.5	0.87
1H-5, 110	26.10	1.52	2.73	90.3	70.4	0.80
1H-6, 35	26.85	1.56	2.73	81.2	68.2	0.86
1H-7, 35	28.35	1.52	2.68	88.3	69.6	0.81
2H-1, 110	29.60	1.52	2.75	90.8	70.7	0.80
2H-2, 34	30.34	1.58	2.76	77.0	67.3	0.89
2H-2, 104	31.04	1.58	2.66	74.6	65.7	0.90
2H-3, 62	32.12	1.55	2.61	78.4	66.5	0.87
2H-3, 110	32.60	1.56	2.70	79.4	67.5	0.87
2H-4, 24	33.24	1.60	2.72	72.6	65.7	0.93
2H-4, 108	34.08	1.58	2.68	75.5	66.2	0.90
2H-5, 29	34.79	1.61	2.72	71.4	65.3	0.94
2H-5, 109	35.59	1.60	2.70	71.0	[illegible]	0.94
2H-6, 19	36.19	1.55	2.69	82.0	68.0	0.85
2H-6, 109	37.09	1.58	2.72	75.9	66.6	0.90
3H-1, 35	38.35	1.59	2.68	72.0	65.1	0.93
3H-1, 113	39.13	1.56	2.72	80.4	67.9	0.87
3H-2, 37	39.87	1.57	2.65	75.0	65.8	0.90
3H-2, 109	40.59	1.54	2.66	82.7	68.0	0.84
3H-3, 45	41.45	1.58	2.73	77.5	67.2	0.89
3H-3, 114	42.14	1.57	2.70	77.3	66.9	0.89
3H-4, 36	42.86	1.58	2.68	75.3	66.1	0.90
3H-4, 111	43.61	1.57	2.78	80.9	68.5	0.87
3H-5, 29	44.29	1.60	2.74	73.9	66.2	0.92
3H-5, 109	45.09	1.58	2.69	76.1	66.5	0.90
3H-6, 35	45.85	1.54	2.66	82.1	67.9	0.85
3H-6, 110	46.60	1.58	2.68	74.1	65.8	0.91
3H-7, 29	47.29	1.61	2.69	70.1	64.6	0.94
4H-1, 116	48.66	1.57	2.74	79.3	67.8	0.88
4H-2, 64	49.64	1.58	2.69	74.4	65.9	0.91
4H-2, 126	50.26	1.55	2.67	80.3	67.5	0.86
4H-3, 49	50.99	1.58	2.66	73.8	65.6	0.91
4H-3, 123	51.73	1.58	2.69	74.7	66.1	0.91
4H-4, 36	52.36	1.57	2.69	76.5	66.5	0.89
4H-4, 109	53.09	1.59	2.70	73.1	65.6	0.92
4H-5, 34	53.84	1.61	2.70	69.7	64.5	0.95
4H-5, 109	54.59	1.62	2.68	66.8	63.4	0.97
4H-6, 109	56.09	1.62	2.68	66.7	63.4	0.97
4H-6, 34	55.34	1.52	2.69	89.1	69.8	0.80
4H-7, 34	56.84	1.58	2.71	76.8	66.8	0.89
5H-2, 32	58.82	1.61	2.69	68.9	64.2	0.95
5H-2, 109	59.59	1.59	2.64	70.8	64.4	0.93

Table 13 (continued).

Core, section, interval (cm)	Depth (mbsf)	Bulk density (g/cm^3)	Grain density (g/cm^3)	Water content (% dry wt)	Porosity (%)	Dry density (g/cm^3)
130-803C- (Cont.)						
5H-3, 44	60.44	1.58	2.65	74.4	65.6	0.90
5H-3, 109	61.09	1.62	2.76	70.9	65.4	0.95
5H-4, 34	61.84	1.61	2.70	69.8	64.6	0.95
5H-4, 109	62.59	1.58	2.66	74.0	65.6	0.91
5H-5, 34	63.34	1.60	2.72	71.9	65.4	0.93
5H-5, 109	64.09	1.57	2.67	77.4	66.7	0.88
5H-6, 38	64.88	1.60	2.65	69.2	64.0	0.95
5H-6, 109	65.59	1.59	2.66	71.9	64.9	0.92
5H-7, 39	66.39			71.2		
6H-1, 39	66.89	1.56	2.66	73.9	65.5	0.91
6H-1, 110	67.60	1.54	2.65	83.4	68.1	0.84
6H-2, 110	69.10	1.57	2.66	76.0	66.1	0.89
6H-3, 39	69.89	1.58	2.74	76.3	66.9	0.90
6H-3, 110	70.60	1.61	2.73	70.1	64.9	0.95
6H-4, 38	71.38	1.56	2.57	74.3	64.9	0.89
6H-4, 110	72.10	1.62	2.73	69.5	64.8	0.95
6H-5, 35	72.85	1.61	2.68	69.5	64.3	0.95
6H-5, 110	73.60	1.58	2.67	73.7	65.6	0.91
6H-6, 35	74.35	1.61	2.77	71.4	65.6	0.94
6H-6, 110	75.10	1.59	2.68	73.0	65.4	0.92
7H-1, 110	77.10	1.59	2.64	71.7	64.7	0.92
7H-2, 40	77.90	1.73	2.72	52.7	58.1	1.13
7H-2, 99	78.49	1.57	2.63	75.5	65.8	0.89
7H-3, 35	79.35			68.3		
7H-3, 110	80.10	1.63	2.74	68.2	64.4	0.97
7H-4, 48	80.98			62.1		
7H-4, 113	81.63	1.64	2.70	63.7	62.5	1.00
7H-5, 55	82.55	1.66	2.72	62.5	62.2	1.02
7H-5, 100	83.00	1.56	2.72	81.6	68.2	0.86
7H-6, 46	83.96	1.64	2.83	68.4	65.2	0.98
7H-6, 100	84.50	1.58	2.67	73.5	65.5	0.91
7H-7, 35	85.35	1.62	2.68	67.9	63.8	0.96
8H-1, 99	86.49	1.59	2.67	72.2	65.1	0.92
8H-2, 34	87.34	1.62	2.67	66.4	63.2	0.98
8H-2, 90	87.90	1.62	2.69	66.9	63.6	0.97
8H-3, 17	88.67	1.62	2.69	67.6	63.8	0.97
8H-3, 114	89.64	1.60	2.70	72.1	65.3	0.93
8H-4, 25	90.25	1.60	2.67	70.4	64.5	0.94
8H-4, 109	91.09	1.64	2.67	64.0	62.4	1.00
8H-5, 40	91.90	1.62	2.68	67.4	63.6	0.97
8H-5, 120	92.70	1.62	2.67	67.2	63.5	0.97
8H-6, 35	93.35	1.62	2.68	67.6	63.7	0.97
8H-6, 114	94.14	1.61	2.68	68.8	64.1	0.95
9H-1, 90	95.90	1.63	2.72	67.0	63.8	0.98
9H-2, 34	96.84	1.65	2.70	62.6	62.1	1.02
9H-2, 107	97.57	1.61	2.67	68.1	63.8	0.96
9H-3, 54	98.54	1.68	2.69	58.2	60.3	1.06
9H-3, 108	99.08	1.66	2.72	61.3	61.7	1.03
9H-4, 55	100.05	1.66	[illegible]	[illegible]	61.8	1.03
9H-4, 115	100.65	1.65	2.71	63.6	62.5	1.01
9H-5, 44	101.44	1.67	2.73	61.0	61.7	1.04
9H-5, 124	102.24	1.68	2.69	58.9	60.6	1.05
9H-6, 39	102.89	1.64	2.66	62.8	61.9	1.01
9H-6, 109	103.59	1.64	2.69	64.0	62.5	1.00
10H-1, 34	104.84	1.65	2.70	62.5	62.0	1.02
10H-1, 115	105.65	1.64	2.64	61.8	61.3	1.02
10H-2, 34	106.34	1.65	2.65	60.6	60.9	1.03
10H-3, 38	107.88	1.62	2.71	67.7	64.0	0.97
10H-3, 108	108.58	1.63	2.66	63.9	62.2	1.00
10H-4, 22	109.22	1.62	2.71	67.9	64.0	0.97
10H-4, 108	110.08	1.64	2.69	64.6	62.7	1.00
10H-6, 40	112.40	1.64	2.66	63.9	62.2	1.00
10H-6, 110	113.10	1.64	2.67	64.0	62.4	1.00
10H-7, 44	113.94	1.67	2.70	60.2	61.1	1.04
11H-2, 37	115.87	1.63	2.63	63.1	61.7	1.00
11H-2, 99	116.49	1.67	2.70	59.5	60.9	1.05
11H-3, 33	117.33	1.59	2.68	71.8	65.1	0.93
11H-3, 99	117.99	1.66	2.72	62.8	62.3	1.02
11H-5, 100	121.00	1.66	2.65	59.8	60.6	1.04
11H-6, 34	121.84	1.67	2.70	59.5	60.9	1.05
11H-6, 104	122.54	1.65	2.67	62.1	61.6	1.02
11H-7, 44	123.44	1.65	2.70	63.2	62.3	1.01
12H-1, 34	123.84			63.3		
12H-1, 109	124.59	1.66	2.69	60.6	61.3	1.03
12H-3, 108	127.58	1.62	2.70	68.3	64.1	0.96
12H-4, 33	128.33	1.66	2.68	61.1	61.3	1.03
12H-4, 109	129.09			65.0		

Table 13 (continued).

Core, section, interval (cm)	Depth (mbsf)	Bulk density (g/cm^3)	Grain density (g/cm^3)	Water content (% dry wt)	Porosity (%)	Dry density (g/cm^3)
130-803C- (Cont.)						
12H-5, 26	129.76	1.61	2.69	68.5	64.1	0.96
12H-5, 109	130.59	1.61	2.62	65.7	62.5	0.97
12H-6, 35	131.35	1.61	2.61	67.1	62.9	0.96
12H-6, 110	132.10			72.6		
12H-7, 46	132.96	1.63	2.69	65.7	63.1	0.98
13H-1, 111	134.11	1.59	2.73	73.7	66.0	0.92
13H-2, 34	134.84	1.63	2.67	64.9	62.7	0.99
13H-2, 110	135.60	1.60	2.65	70.4	64.3	0.94
13H-3, 34	136.34	1.64	2.73	65.8	63.5	0.99
13H-3, 110	137.10	1.63	2.69	65.9	63.2	0.98
13H-4, 34	137.84	1.68	2.69	58.1	60.2	1.06
13H-4, 110	138.60	1.65	2.68	62.5	61.9	1.01
13H-5, 34	139.34	1.63	2.63	63.7	61.9	0.99
13H-5, 111	140.11	1.58	2.67	73.5	65.5	0.91
13H-6, 34	140.84	1.62	2.69	67.0	63.6	0.97
13H-6, 112	141.62	1.62	2.67	66.6	63.3	0.97
13H-7, 34	142.34	1.64	2.70	65.2	63.1	0.99
14H-1, 35	142.85	1.59	2.78	76.4	67.2	0.90
14H-1, 110	143.60	1.61	2.68	69.5	64.3	0.95
14H-2, 35	144.35			64.9		
14H-2, 110	145.10	1.63	2.70	66.3	63.5	0.98
14H-3, 34	145.84	1.58	2.67	74.8	65.9	0.90
14H-3, 109	146.59	1.62	2.64	65.7	62.7	0.98
14H-4, 34	147.34	1.61	2.65	67.2	63.3	0.96
14H-4, 108	148.08	1.66	2.67	59.8	60.8	1.04
14H-5, 33	148.83	1.63	2.68	65.7	63.0	0.98
14H-5, 111	149.61	1.65	2.70	63.0	62.3	1.01
14H-6, 32	150.32	1.63	2.71	66.4	63.5	0.98
14H-6, 113	151.13	1.66	2.69	61.1	61.4	1.03
15H-1, 102	153.02	1.54	2.65	82.3	67.8	0.84
15H-2, 35	153.85	1.59	2.68	73.7	65.6	0.91
15H-2, 110	154.60	1.61	2.68	68.4	64.0	0.96
15H-3, 30	155.30	1.62	2.66	66.3	63.1	0.90
15H-3, 109	156.09	1.62	2.65	66.2	62.9	0.97
15H-4, 36	156.86	1.59	2.63	70.8	64.3	0.93
15H-4, 110	157.60	1.62	2.71	68.6	64.3	0.96
15H-5, 35	158.35	1.63	2.67	65.4	62.9	0.98
15H-5, 111	159.11	1.64	2.67	63.8	62.3	1.00
15H-6, 36	159.86	1.62	2.70	67.1	63.6	0.97
15H-6, 110	160.60	1.61	2.68	69.1	64.2	0.95
15H-7, 34	161.34	1.78	2.70	46.2	54.8	1.21
16H-1, 109	162.59	1.62	2.68	67.7	63.7	0.96
16H-2, 36	163.36	1.67	2.82	63.8	63.6	1.02
16H-2, 109	164.09	1.61	2.72	69.5	64.6	0.95
16H-3, 33	164.83	1.63	2.64	63.2	61.8	1.00
16H-3, 109	165.59	1.62	2.67	67.3	63.5	0.97
16H-4, 33	166.33	1.66	2.69	60.2	61.1	1.04
16H-4, 110	167.10	1.69	2.72	58.0	60.5	1.07
16H-5, 33	167.83	1.67	2.73	61.5	61.9	1.03
16H-5, 110	168.60	1.64	2.66	63.9	62.2	1.00
16H-6, 33	169.33	1.69	2.68	56.6	59.6	1.08
16H-6, 110	170.10	1.70	2.71	56.5	59.8	1.08
16H-7, 33	170.83	1.71	2.69	54.4	58.7	1.11
17H-2, 34	172.84	1.68	2.71	58.1	60.4	1.07
17H-2, 109	173.59	1.67	2.63	57.9	59.6	1.06
17H-3, 34	174.34	1.65	2.68	61.9	61.6	1.02
17H-3, 107	175.07	1.67	2.74	60.6	61.7	1.04
17H-4, 31	175.81	1.67	2.65	58.4	60.0	1.05
17H-4, 107	176.57	1.66	2.70	60.8	61.4	1.03
17H-5, 32	177.32	1.68	2.69	57.9	60.1	1.06
17H-5, 107	178.07	1.67	2.69	59.8	60.9	1.04
17H-6, 32	178.82	1.66	2.67	60.9	61.2	1.03
17H-6, 107	179.57	1.72	2.70	53.3	58.3	1.12
17H-7, 32	180.32	1.66	2.69	61.7	61.7	1.02
18H-2, 77	182.77	1.52	2.85	94.3	72.2	0.78
18H-2, 110	183.10	1.66	2.73	62.7	62.4	1.02
18H-3, 32	183.82	1.68	2.70	58.8	60.6	1.06
18H-3, 109	184.59	1.66	2.70	61.5	61.7	1.03
18H-4, 34	185.34	1.70	2.73	56.6	60.0	1.09
18H-4, 109	186.09	1.72	2.71	53.6	58.5	1.12
18H-5, 35	186.85	1.74	2.77	52.8	58.7	1.14
18H-6, 37	188.37	1.67	2.67	58.9	60.4	1.05
18H-6, 109	189.09	1.70	2.76	57.5	60.6	1.00
18H-7, 31	189.81	1.66	2.66	60.1	60.8	1.04
19H-1, 36	190.36	1.68	2.78	60.8	62.1	1.05
19H-1, 111	191.11			53.6		
19H-2, 35	191.85	1.72	2.71	52.8	58.1	1.13

Table 13 (continued).

Core, section, interval (cm)	Depth (mbsf)	Bulk density (g/cm^3)	Grain density (g/cm^3)	Water content (% dry wt)	Porosity (%)	Dry density (g/cm^3)
130-803C- (Cont.)						
19H-2, 110	192.60	1.73	2.69	51.7	57.5	1.14
19H-3, 35	193.35	1.72	2.71	53.2	58.3	1.12
19H-4, 39	194.89	1.71	2.71	55.1	59.2	1.10
19H-4, 99	195.49	1.64	2.66	63.9	62.2	1.00
19H-5, 35	196.35	1.78	2.78	48.5	56.7	1.20
19H-5, 110	197.10	1.75	2.77	51.0	57.8	1.16
19H-6, 35	197.85	1.73	2.69	51.8	57.5	1.14
19H-6, 108	198.58	1.72	2.72	53.7	58.6	1.12
19H-7, 23	199.23	1.74	2.73	50.9	57.4	1.16
20H-3, 35	202.85			54.1		
20H-3, 108	203.58	1.67	2.68	59.8	60.9	1.04
20H-4, 39	204.39	1.71	2.66	52.8	57.7	1.12
20H-4, 110	205.10	1.68	2.68	57.0	59.7	1.07
20H-5, 35	205.85	1.66	2.70	61.2	61.6	1.03
20H-5, 110	206.60	1.66	2.75	63.1	62.7	1.02
20H-6, 35	207.35	1.68	2.70	57.9	60.3	1.07
20H-6, 110	208.10	1.66	2.68	60.5	61.1	1.04
20H-7, 35	208.85	1.67	2.70	59.2	60.7	1.05
21H-1, 35	209.35	1.63	2.70	66.3	63.4	0.98
21H-1, 110	209.11	1.67	2.76	62.0	62.4	1.03
21H-2, 34	210.84	1.65	2.69	62.6	62.0	1.02
21H-2, 64	211.14	1.64	2.70	63.7	62.4	1.00
21H-3, 34	212.34	1.70	2.70	55.3	59.2	1.10
21H-3, 109	213.09			59.7		
21H-4, 35	213.85	1.70	2.68	55.4	59.0	1.09
21H-4, 110	214.60	1.65	2.68	61.8	61.6	1.02
21H-5, 40	215.40	1.72	2.77	55.1	59.7	1.11
21H-5, 110	216.10	1.67	2.70	59.6	61.0	1.05
21H-6, 35	216.85	1.62	2.66	65.8	62.9	0.98
21H-6, 100	217.50	1.67	2.68	58.5	60.3	1.06
21H-7, 40	218.40	1.67	2.70	59.6	60.9	1.05
22H-1, 34	218.84	1.69	2.67	56.5	59.5	1.08
22H-1, 99	219.49	1.65	2.66	60.6	61.0	1.03
22H-2, 35	220.35	1.66	2.68	60.8	51.2	1.03
22H-3, 30	221.80	1.67	2.69	60.1	61.1	1.04
22H-3, 99	222.49	1.65	2.72	63.9	62.8	1.01
22H-3, 113	222.63	1.65	2.68	62.5	61.9	1.02
22H-4, 35	223.35	1.73	2.70	52.0	57.7	1.14
22H-4, 112	224.12	1.73	2.72	52.0	57.9	1.14
22H-5, 35	224.85	1.73	2.73	52.5	58.2	1.13
22H-5, 110	225.60	1.73	2.75	53.4	58.8	1.13
22H-6, 35	226.35	1.76	2.70	47.4	55.4	1.20
23H-1, 70	228.70			53.7		
23H-1, 110	229.10	1.71	2.72	54.9	59.1	1.10
23H-2, 29	229.79	1.77	2.84	50.7	58.3	1.18
23H-4, 31	232.81	1.70	2.67	54.4	58.5	1.10
23H-4, 103	233.53	1.76	2.69	47.4	55.3	1.19
23H-5, 33	234.33	1.77	2.75	48.3	56.3	1.19
23H-5, 98	234.98	1.75	2.75	51.2	57.7	1.16
23H-6, 13	235.63	1.77	2.73	48.0	56.0	1.20
23H-6, 104	236.54	1.67	2.65	58.4	60.0	1.05
23H-7, 28	237.28	1.70	2.68	54.8	58.8	1.10
130-803D-						
1H-1, 123	1.23	1.45	2.68	108.0	73.6	0.70
1H-2, 38	1.88	1.47	2.67	103.2	72.7	0.72
2H-2, 107	5.07	1.55	2.68	81.8	67.9	0.85
2H-3, 99	6.49	1.52	2.69	89.5	70.0	0.80
2H-6, 99	10.99	1.56	2.79	84.3	69.5	0.84
2H-7, 39	11.89	1.57	2.64	75.6	65.9	0.89
3H-1, 114	13.14	1.52	2.65	87.4	69.1	0.81
3H-2, 99	14.49	1.53	2.61	82.0	67.4	0.84
3H-3, 103	16.03	1.58	2.67	75.3	66.1	0.90
3H-4, 103	17.53	1.56	2.69	80.1	67.6	0.86
3H-5, 109	19.09	1.54	2.68	83.5	68.4	0.84
3H-6, 109	20.59	1.56	2.65	77.2	66.4	0.88
3H-7, 33	21.33	1.61	2.62	66.8	62.9	0.97
4H-1, 100	22.50	1.58	2.70	74.5	66.0	0.91
4H-2, 110	24.10	1.57	2.77	80.7	68.3	0.87
4H-2, 35	23.35	1.59	2.76	76.4	67.1	0.90
4H-3, 101	25.51	1.52	2.77	91.6	71.1	0.79
4H-4, 99	26.99	1.56	2.74	80.2	68.0	0.87
4H-5, 100	28.50	1.61	2.70	69.1	64.4	0.95
4H-6, 103	30.03	1.58	2.73	76.5	66.9	0.90
4H-7, 29	30.79	1.56	2.70	79.3	67.4	0.87
5H-1, 113	32.13	1.58	2.73	77.5	67.2	0.89
5H-2, 61	33.11	1.58	2.71	75.1	66.3	0.90

Table 13 (continued).

Core, section, interval (cm)	Depth (mbsf)	Bulk density (g/cm³)	Grain density (g/cm³)	Water content (% dry wt)	Porosity (%)	Dry density (g/cm³)
130-803D- (Cont.)						
5H-3, 113	35.13	1.60	2.73	72.4	65.7	0.93
5H-4, 109	36.59	1.60	2.73	73.6	66.0	0.92
5H-5, 110	38.10	1.57	2.78	79.9	68.2	0.87
5H-6, 110	39.60	1.60	2.77	73.9	66.4	0.92
6H-1, 110	41.10	1.56	2.69	79.5	67.4	0.87
6H-2, 110	42.60	1.57	2.75	80.5	68.2	0.87
6H-3, 36	43.36	1.55	2.69	81.5	67.9	0.85
6H-3, 114	44.14	1.58	2.72	76.8	66.9	0.89
6H-4, 39	44.89	1.58	2.74	76.8	67.1	0.89
6H-5, 35	46.35	1.57	2.72	78.0	67.2	0.88
6H-6, 35	47.85	1.59	2.69	72.1	65.2	0.93
6H-7, 36	49.36	1.58	2.74	78.1	67.4	0.88
7H-1, 36	46.46	1.58	2.67	75.2	66.1	0.90
7H-2, 110	48.70	1.58	2.70	76.0	66.5	0.90
7H-3, 114	50.24	1.56	2.70	80.8	67.9	0.86
7H-4, 110	51.70	1.62	2.72	69.1	64.5	0.96
7H-5, 110	53.20	1.62	2.72	68.1	64.2	0.97
7H-6, 110	54.70	1.60	2.70	71.0	64.9	0.94
8H-1, 110	56.70	1.60	2.69	70.4	64.7	0.94
8H-2, 110	58.20	1.60	2.70	70.9	64.9	0.94
8H-3, 110	59.70	1.59	2.76	75.3	66.8	0.91
8H-4, 110	61.20	1.55	2.63	79.6	66.9	0.86
8H-5, 110	62.70	1.60	2.67	71.1	64.7	0.93
8H-6, 110	64.20	1.60	2.70	72.6	65.5	0.92
9H-2, 110	67.70	1.60	2.68	71.1	64.9	0.94
9H-3, 110	69.20	1.54	2.60	81.0	67.1	0.85
9H-4, 105	70.65	1.60	2.67	70.7	64.6	0.94
9H-5, 113	72.23	1.58	2.69	75.1	66.1	0.90
9H-6, 108	73.68	1.59	2.66	72.0	65.0	0.92
10H-1, 100	75.60	1.63	2.70	66.7	63.5	0.98
10H-2, 107	77.17	1.63	2.68	64.9	62.7	0.99
10H-3, 107	78.67	1.62	2.72	68.0	64.2	0.97
10H-4, 99	80.09	1.59	2.69	72.9	65.5	0.92
10H-5, 108	81.68	1.63	2.67	65.1	62.7	0.99
10H-6, 109	83.19	1.62	2.71	68.9	64.4	0.96
10H-7, 3[illegible]	83.95	1.64	2.71	64.6	62.9	1.00
11H-1, 110	85.20	1.64	2.75	66.5	63.9	0.98
11H-2, 109	86.69	1.65	2.73	64.0	62.9	1.01
11H-3, 108	88.18	1.62	2.69	68.3	64.0	0.96
11H-4, 109	89.69	1.62	2.72	67.7	64.0	0.97
11H-5, 108	91.18	1.65	2.72	63.4	62.5	1.01
11H-6, 110	92.70	1.64	2.69	63.4	62.3	1.01
12H-1, 110	94.70	1.67	2.72	60.6	61.5	1.04
12H-2, 110	96.20	1.65	2.70	62.2	61.9	1.02
12H-3, 110	97.70	1.64	2.71	64.1	62.7	1.00
12H-4, 110	99.20	1.65	2.72	63.5	62.6	1.01
12H-5, 110	100.70	1.66	2.71	60.9	61.5	1.03
12H-6, 110	102.20	1.66	2.67	59.7	60.8	1.04
13H-2, 108	105.68			70.2		
13H-3, 108	107.18	1.68	2.68	57.7	60.0	1.07
13H-4, 99	108.59	1.65	2.69	62.6	62.0	1.01
13H-5, 108	110.18	1.63	2.71	66.7	63.7	0.98
13H-6, 108	111.68	1.63	2.66	65.2	62.7	0.98
14H-1, 107	113.67	1.65	2.73	64.7	63.1	1.00
14H-2, 104	115.14	1.66	2.69	61.2	61.5	1.03
14H-3, 98	116.58	1.67	2.73	61.1	61.8	1.04
14H-4, 104	118.14	1.67	2.71	60.0	61.2	1.04
14H-5, 98	119.58	1.67	2.70	59.7	61.0	1.05
14H-6, 109	121.19	1.68	2.70	58.7	60.6	1.06
15H-1, 110	123.20	1.65	2.70	62.8	62.2	1.01
15H-2, 108	124.68	1.64	2.70	65.2	63.0	0.99
15H-3, 109	126.19	1.63	2.69	66.3	63.3	0.98
15H-4, 109	127.69	1.67	2.66	58.6	60.2	1.05
15H-5, 103	129.13	1.67	2.73	60.3	61.5	1.04
15H-6, 93	130.53	1.63	2.71	67.5	63.9	0.97
16H-1, 103	132.63	1.55	2.61	78.7	66.6	0.87
16H-2, 109	134.19	1.62	2.70	68.4	64.2	0.96
16H-3, 110	135.70	1.66	2.69	61.4	61.6	1.03
16H-4, 29	136.39	1.67	2.69	59.6	60.8	1.05
16H-5, 108	138.68	1.62	2.68	67.2	63.6	0.97
16H-6, 109	140.19	1.61	2.70	69.7	64.5	0.95
17H-1, 109	142.19	1.61	2.68	68.6	64.0	0.96
17H-2, 97	143.57	1.62	2.68	67.6	63.7	0.97
17H-3, 107	145.17	1.63	2.71	66.6	63.6	0.98
17H-4, 103	146.63	1.62	2.69	67.4	63.7	0.97
17H-5, 110	148.20	1.67	2.68	59.3	60.6	1.05
17H-6, 99	149.59	1.62	2.68	67.8	63.8	0.96

Table 13 (continued).

Core, section, interval (cm)	Depth (mbsf)	Bulk density (g/cm^3)	Grain density (g/cm^3)	Water content (% dry wt)	Porosity (%)	Dry density (g/cm^3)
130-803D- (Cont.)						
17H-7, 36	150.46	1.64	2.68	63.7	62.3	1.00
18H-1, 109	151.69	1.58	2.66	74.2	65.6	0.91
18H-2, 114	153.24	1.59	2.68	73.5	65.6	0.91
18H-3, 109	154.69	1.61	2.67	68.6	64.0	0.96
18H-4, 110	156.20	1.61	2.68	69.6	64.3	0.95
18H-5, 100	157.60	1.62	2.68	67.8	63.8	0.96
18H-6, 109	159.19	1.57	2.63	75.5	65.7	0.89
19H-1, 110	161.20	1.67	2.69	58.9	60.6	1.05
19H-3, 114	164.24	1.69	2.70	57.8	60.2	1.07
19H-4, 100	165.60	1.70	2.70	55.4	59.2	1.09
19H-5, 109	167.19	1.67	2.67	59.0	60.4	1.05
19H-6, 110	168.70	1.68	2.69	57.7	60.1	1.07
20H-1, 110	170.70	1.66	2.68	60.3	61.0	1.04
20H-2, 110	172.20	1.68	2.66	57.3	59.6	1.07
20H-3, 109	173.69	1.67	2.68	59.1	60.6	1.05
20H-4, 110	175.20	1.66	2.69	61.4	61.5	1.03
20H-5, 110	176.70	1.69	2.69	57.3	59.9	1.07
20H-6, 96	178.06	1.69	2.70	57.0	59.9	1.08
20H-7, 30	178.90	1.68	2.68	57.2	59.8	1.07
21H-2, 64	181.24	1.45	2.74	111.7	74.7	0.68
21H-3, 103	183.13	1.65	2.72	64.3	62.9	1.00
21H-4, 108	184.68	1.70	2.69	55.2	59.0	1.09
21H-5, 110	186.20	1.71	2.70	54.3	58.7	1.11
21H-6, 41	187.01	1.65	2.70	63.6	62.4	1.01
22H-1, 104	189.64	1.73	2.70	51.8	57.6	1.14
22H-2, 103	191.13	1.68	2.68	58.2	60.2	1.06
22H-3, 103	192.63	1.75	2.71	49.9	56.7	1.17
22H-4, 93	194.03	1.69	2.67	56.1	59.3	1.08
22H-5, 104	195.64	1.70	2.68	54.3	58.5	1.10
22H-6, 105	197.15	1.72	2.70	53.3	58.3	1.12
22H-7, 39	197.99	1.74	2.70	50.8	57.1	1.15
23H-1, 99	199.09	1.68	2.68	57.6	59.9	1.07
23H-2, 99	200.59	1.65	2.64	61.5	61.2	1.02
23H-4, 104	203.64	1.68	2.72	59.5	61.0	1.05
23H-5, 99	205.09	1.61	2.66	67.8	63.6	0.96
23H-6, 99	206.59	1.65	2.64	61.1	61.0	1.02
23H-7, 38	207.48	1.63	2.66	64.4	62.4	0.99
24H-1, 113	208.73	1.62	2.66	66.1	63.0	0.98
24H-3, 103	211.63	1.67	2.69	60.1	61.0	1.04
24H-4, 103	213.13	1.67	2.70	59.2	60.8	1.05
24H-5, 103	214.63	1.69	2.68	56.2	59.3	1.08
24H-6, 103	216.13	1.69	2.70	57.6	60.1	1.07
24H-7, 39	216.99	1.67	2.66	58.6	60.2	1.05
25X-1, 105	218.15	1.67	2.68	59.2	60.6	1.05
25X-2, 37	218.97	1.65	2.67	61.7	61.5	1.02
25X-3, 72	220.82	1.67	2.68	59.2	60.6	1.05
25X-4, 40	222.00	1.69	2.68	55.8	59.2	1.09
26X-1, 31	227.11	1.73	2.69	50.9	57.1	1.15
26X-2, 29	228.59	1.72	2.62	49.9	55.9	1.15
26X-3, 34	230.14	1.73	2.68	51.0	57.0	1.15
26X-4, 63	231.93	1.69	2.66	56.1	59.2	1.08
26X-5, 78	233.58	1.73	2.68	50.4	56.7	1.15
26X-6, 118	235.48	1.75	2.70	48.9	56.2	1.16
27X-1, 73	237.23	1.72	2.73	54.1	58.9	1.11
27X-2, 97	238.97	1.71	2.70	53.5	58.3	1.12
27X-3, 64	240.14	1.78	2.79	48.3	56.7	1.20
28X-2, 84	248.24	1.74	2.67	49.4	56.1	1.16
28X-5, 31	252.21	1.78	2.67	44.3	53.5	1.24
29X-1, 64	256.14	1.85	2.69	38.8	50.4	1.33
29X-2, 55	257.55	1.87	2.70	37.0	49.3	1.36
29X-3, 59	259.09	1.86	2.73	38.2	50.3	1.35
29X-4, 72	260.72	1.83	2.72	41.1	52.0	1.30
29X-5, 29	261.79	1.80	2.73	44.7	54.2	1.24
30X-1, 133	266.43	1.86	2.79	40.2	52.1	1.33
30X-2, 80	267.40	1.83	2.74	41.8	52.6	1.29
30X-3, 75	268.85	1.83	2.75	41.8	52.7	1.29
30X-4, 80	270.40	1.79	2.70	44.5	53.8	1.24
31X-1, 50	275.20	1.80	2.74	44.6	54.3	1.25
31X-2, 90	277.10	1.84	2.80	42.5	53.5	1.29
31X-3, 93	278.63	1.83	2.75	41.6	52.6	1.30
31X-4, 28	279.48	1.80	2.75	45.0	54.6	1.24
32X-1, 89	285.19	1.86	2.76	39.7	51.6	1.33
32X-2, 117	286.97	1.83	2.75	42.0	52.9	1.29
32X-3, 102	288.32	1.81	2.77	44.7	54.6	1.25
32X-2, 67	286.47	1.82	2.72	42.4	52.8	1.28
32X-5, 36	290.66	1.82	2.77	43.3	53.8	1.27
33X-1, 137	295.47	1.84	2.76	41.0	52.4	1.31

Table 13 (continued).

Core, section, interval (cm)	Depth (mbsf)	Bulk density (g/cm^3)	Grain density (g/cm^3)	Water content (% dry wt)	Porosity (%)	Dry density (g/cm^3)
130-803D- (Cont.)						
33X-2, 101	296.61	1.85	2.81	42.2	53.5	1.30
33X-3, 117	298.27	1.81	2.69	42.2	52.4	1.27
33X-4, 59	299.19	1.81	2.73	43.1	53.3	1.27
33X-5, 48	300.58	1.79	2.74	46.0	55.0	1.23
34X-1, 50	303.80	1.79	2.66	42.8	52.5	1.26
34X-2, 73	305.53	1.83	2.68	40.3	51.2	1.30
34X-3, 71	307.01	1.82	2.70	41.1	51.9	1.29
34X-4, 89	308.69	1.80	2.68	43.2	52.9	1.26
34X-5, 67	309.97	1.75	2.64	47.3	54.8	1.19
34X-6, 133	312.13	1.79	2.69	43.9	53.4	1.25
35X-1, 91	313.91	1.80	2.71	43.5	53.3	1.26
35X-2, 130	315.80	1.79	2.66	43.6	53.0	1.24
35X-3, 86	316.86	1.84	2.72	40.3	51.6	1.31
35X-4, 70	318.20	1.81	2.66	41.1	51.6	1.28
35X-5, 60	319.60	1.82	2.66	40.6	51.2	1.29
35X-6, 48	320.98	1.80	2.67	42.4	52.4	1.27
36X-1, 115	323.85	1.83	2.73	41.7	52.5	1.29
36X-2, 71	324.91	1.82	2.67	40.5	51.3	1.30
36X-3, 116	326.86	1.81	2.67	41.5	51.8	1.28
36X-4, 127	328.47	1.83	2.68	40.3	51.2	1.30
36X-5, 125	329.95	1.83	2.71	40.9	51.9	1.30
36X-6, 114	331.34	1.80	2.66	42.9	52.6	1.26
37X-1, 90	333.20	1.81	2.69	42.5	52.6	1.27
37X-2, 104	334.84	1.78	2.63	43.2	52.5	1.24
37X-3, 102	336.32	1.77	2.64	44.7	53.4	1.22
37X-4, 103	337.83	1.80	2.65	41.6	51.7	1.28
37X-5, 99	339.29	1.81	2.67	41.2	51.6	1.28
37X-6, 109	340.89	1.85	2.69	37.9	49.8	1.34
38X-1, 59	342.59	1.86	2.71	37.8	49.9	1.35
38X-4, 134	347.84	1.83	2.69	39.8	51.0	1.31
38X-6, 23	349.73			40.7		
39X-1, 25	351.85	1.80	2.69	43.8	53.4	1.25
39X-2, 129	354.39	1.86	2.70	38.0	49.9	1.35
39X-3, 53	355.13	1.87	2.72	37.5	49.7	1.36
39X-4, 57	356.67	1.84	2.68	39.1	50.5	1.32
39X-6, 66	359.76	1.83	2.69	40.2	51.2	1.30
40X-1, 40	361.70	1.83	2.67	40.0	50.9	1.30
40X-2, 90	363.70	1.83	2.67	39.6	50.7	1.31
40X-3, 87	365.17	1.85	2.67	38.1	49.7	1.34
40X-4, 91	366.71	1.90	2.71	34.3	47.4	1.42
41X-1, 14	371.14	1.88	2.72	36.8	49.3	1.37
41X-2, 70	373.20	1.77	2.67	45.3	54.0	1.22
41X-3, 113	375.13	1.81	2.69	42.2	52.4	1.27
42X-1, 97	381.67	1.82	2.67	40.9	51.5	1.29
42X-2, 32	382.52	1.80	2.70	43.3	53.2	1.26
42X-3, 14	383.84	1.81	2.71	42.7	52.9	1.27
43X-1, 110	390.50	1.85	2.65	37.3	49.0	1.35
43X-2, 87	392.77	1.82	2.68	40.9	51.6	1.29
43X-3, 87	394.27	1.84	2.69	39.0	50.5	1.33
43X-4, 41	395.31	1.87	2.68	36.4	48.7	1.37
43X-5, 21	396.61	1.89	2.70	35.0	47.9	1.40
44X-1, 85	400.85	1.87	2.72	37.5	49.8	1.36
44X-2, 108	402.58	1.84	2.65	38.4	49.7	1.33
44X-3, 70	403.70	1.86	2.69	37.2	49.3	1.36
44X-4, 68	405.18			34.0		
44X-5, 29	406.29	1.88	2.71	36.2	48.8	1.38
45X-1, 88	410.58	1.87	2.71	37.4	49.6	1.36
45X-2, 75	411.95	1.89	2.69	34.7	47.6	1.40
45X-3, 121	413.91	1.86	2.70	37.6	49.7	1.35
45X-4, 73	414.93	1.85	2.67	37.9	49.6	1.34
45X-5, 46	416.16	1.85	2.71	38.8	50.5	1.33
45X-6, 69	417.89	1.84	2.68	39.3	50.7	1.32
46X-1, 110	420.40	1.87	2.67	36.4	48.5	1.37
46X-2, 129	422.09	1.84	2.65	38.5	49.8	1.33
46X-3, 130	423.60	1.81	2.60	39.3	49.8	1.30
46X-5, 59	425.89	1.85	2.70	38.8	50.5	1.33
47X-1, 61	429.61	1.84	2.67	38.7	50.1	1.32
47X-3, 119	433.19	1.86	2.70	38.1	50.0	1.35
47X-4, 88	434.38	1.83	2.69	40.5	51.4	1.30
47X-5, 29	435.29	1.83	2.67	39.2	50.5	1.32
48X-1, 19	438.79	1.84	2.68	39.3	50.6	1.32
48X-2, 45	440.55	1.85	2.66	37.3	49.0	1.35
48X-3, 49	442.09	1.84	2.67	38.4	49.9	1.33
48X-4, 50	443.60	1.87	2.77	38.9	51.1	1.35
49X-1, 98	448.78	1.84	2.71	39.9	51.3	1.32
49X-2, 80	450.10	1.88	2.67	34.8	47.4	1.40
49X-3, 91	451.71	1.84	2.65	37.6	49.2	1.34

Table 13 (continued).

Core, section, interval (cm)	Depth (mbsf)	Bulk density (g/cm^3)	Grain density (g/cm^3)	Water content (% dry wt)	Porosity (%)	Dry density (g/cm^3)
130-803D- (Cont.)						
49X-4, 75	453.05	1.87	2.68	36.0	48.3	1.38
50X-1, 115	458.65	1.87	2.69	36.6	48.9	1.37
50X-2, 37	459.37	1.86	2.72	38.5	50.4	1.34
50X-4, 11	462.11	1.84	2.69	39.2	50.6	1.32
51X-1, 44	467.64	1.82	2.69	40.9	51.7	1.30
52X-1, 78	477.68	1.86	2.71	38.0	50.0	1.35
52X-2, 77	479.17	1.89	2.66	33.9	46.8	1.41
52X-3, 52	480.42	1.86	2.62	35.4	47.4	1.37
53X-1, 129	487.89	1.83	2.66	39.4	50.5	1.31
53X-2, 139	489.49	1.86	2.67	36.7	48.8	1.36
53X-3, 109	490.69	1.82	2.66	40.2	51.0	1.30
53X-4, 81	491.91	1.87	2.67	35.8	48.2	1.38
54X-1, 76	497.06	1.85	2.67	37.4	49.2	1.35
54X-2, 89	498.69	1.89	2.65	33.6	46.4	1.41
54X-3, 75	500.05	1.90	2.68	33.5	46.6	1.43
54X-4, 91	501.71	1.89	2.64	32.8	45.7	1.43
55X-1, 47	506.47	1.80	2.63	41.3	51.3	1.27
55X-2, 47	507.97	1.78	2.63	43.4	52.6	1.24
55X-3, 79	509.79	1.83	2.62	37.5	48.8	1.33
55X-4, 50	511.00	1.86	2.62	35.1	47.2	1.38
56X-1, 111	516.71	1.81	2.61	39.9	50.3	1.29
56X-2, 97	518.07	1.81	2.66	40.9	51.4	1.29
56X-3, 101	519.61	1.80	2.66	42.0	52.0	1.27
56X-4, 105	521.15	1.82	2.69	41.3	51.9	1.29
56X-5, 113	522.73	1.82	2.68	40.7	51.5	1.30
56X-6, 87	523.97	1.88	2.68	35.6	48.1	1.38
57X-1, 93	526.23	1.82	2.69	41.2	51.9	1.29
57X-2, 93	527.73	1.87	2.70	36.7	49.1	1.37
57X-3, 89	529.19	1.92	2.71	32.9	46.5	1.45
58X-1, 22	534.82	1.87	2.72	37.5	49.8	1.36
58X-CC, 12	535.48	1.87	2.71	37.1	49.5	1.36
59X-1, 61	544.91	1.85	2.64	36.7	48.5	1.35
59X-2, 67	546.47	1.91	2.66	32.4	45.5	1.44
60X-1, 8	554.08	1.94	2.66	30.4	44.0	1.48
60X-2, 9	555.59	1.85	2.61	35.5	47.3	1.37
61X-1, 4	563.74	1.94	2.63	28.8	42.4	1.51
64X-CC, 10	588.80	2.04	2.63	22.2	36.2	1.67
65X-CC, 7	598.47	1.46	2.24	80.8	63.7	0.81
66X-CC, 5	601.95	2.05	2.65	22.3	36.6	1.68
67X-1, 119	613.19	1.77	2.43	36.6	46.4	1.30
67X-CC, 5	614.19	1.95	2.12	8.7	15.2	1.80
68X-1, 15	621.95	1.94	2.67	30.5	44.3	1.48
68X-1, 17	624.97	1.83	2.72	41.7	52.4	1.29
69X-1, 88	632.28	2.70	2.88	3.8	9.70	2.60

VOLUME
130

CHAPTER
6

TABLES
5, 7, 9, AND 10

Table 5. Carbonate and inorganic carbon data, Hole 804A.

Core, section, interval (cm)	Depth (mbsf)	Inorganic carbon (%)	$CaCO_3$ (%)
130-804A-			
1H-1, 34-36	0.34	9.68	80.60
2H-1, 109-111	2.29	8.87	73.90
2H-2, 34-36	3.04	9.26	77.10
2H-3, 35-37	4.55	9.97	83.10
2H-4, 35-37	6.05	10.34	86.10
2H-5, 45-47	7.65	9.74	81.10
2H-6, 34-36	9.04	9.58	79.80
2H-7, 35-37	10.55	10.55	87.90
3H-1, 35-37	11.05	10.08	84.00
3H-2, 35-37	12.55	9.23	76.90
3H-3, 35-37	14.05	7.02	58.50
3H-4, 35-37	15.55	9.92	82.60
3H-5, 35-37	17.05	10.40	86.60
3H-6, 34-36	18.54	10.12	84.30
3H-7, 35-37	20.05	10.61	88.40
4H-1, 50-52	20.70	10.04	83.60
4H-2, 35-37	22.05	9.38	78.10
4H-3, 35-37	23.55	9.89	82.40
4H-4, 29-31	24.99	6.55	54.60
4H-5, 34-36	26.54	10.68	89.00
4H-6, 34-36	28.04	10.34	86.10
4H-7, 35-37	29.55	10.17	84.70
5H-1, 68-70	30.38	9.96	83.00
5H-2, 40-42	31.60	10.13	84.40
5H-3, 40-42	33.10	10.50	87.50
5H-4, 37-39	34.57	9.36	78.00
5H-5, 45-47	36.15	9.69	80.70
5H-6, 33-35	37.53	9.53	79.40
5H-7, 32-34	39.02	9.99	83.20
6H-1, 124-125	40.44	10.21	85.00
6H-2, 40-41	41.10	10.40	86.60
6H-3, 57-58	42.77	10.23	85.20
6H-4, 29-30	43.99	10.77	89.70
6H-5, 39-40	45.59	11.19	93.20
6H-6, 13-14	46.83	10.91	90.90
130-804B-			
5H-1, 119-121	34.39	10.80	90.00
5H-2, 34-36	35.04	10.03	83.50
5H-3, 36-38	36.56	8.59	71.60
5H-4, 40-42	38.10	9.31	77.60
5H-5, 29-31	39.49	8.08	67.30
5H-6, 29-31	40.99	9.73	81.10
5H-7, 45-47	42.65	9.33	77.70
6H-1, 35-37	43.05	9.78	81.50
6H-2, 38-40	44.58	9.48	79.00
6H-3, 34-36	46.04	10.86	90.50
6H-4, 34-36	47.54	10.87	90.50
6H-5, 34-36	49.04	10.86	90.50
6H-6, 35-37	50.55	10.92	91.00
6H-7, 34-36	52.04	10.77	89.70
7H-1, 35-37	52.55	10.78	89.80
7H-2, 33-35	54.03	8.23	68.60
7H-3, 34-36	55.54	11.26	93.80
7H-4, 35-37	57.05	11.40	95.00
7H-5, 36-38	58.56	11.27	93.90
7H-6, 34-36	60.04	10.85	90.40
7H-7, 34-36	61.54	10.92	91.00
8H-1, 109-111	62.79	10.90	90.80
8H-2, 34-36	63.54	11.19	93.20
8H-3, 35-37	65.05	10.94	91.10
8H-4, 34-36	66.54	10.86	90.50
8H-5, 35-37	68.05	11.07	92.20
8H-6, 34-36	69.54	10.69	89.00
8H-7, 35-37	71.05	10.44	87.00
9H-1, 34-36	71.54	10.22	85.10
9H-2, 33-35	73.03	10.41	86.70
9H-3, 34-36	74.54	10.98	91.50
9H-4, 34-36	76.04	10.80	90.00
9H-5, 34-36	77.54	10.49	87.40
9H-6, 34-36	79.04	10.74	89.50
9H-7, 35-37	80.55	10.89	90.70
10H-1, 109-111	81.79	10.99	91.50
10H-2, 33-35	82.53	10.55	87.90
130-804B- (Cont.)			
10H-3, 34-36	84.04	10.79	89.90
10H-4, 35-37	85.55	9.23	76.90
10H-5, 34-36	87.04	10.98	91.50
10H-6, 33-35	88.53	11.03	91.90
10H-7, 38-40	90.08	10.74	89.50
11H-1, 34-36	90.54	10.05	83.70
11H-2, 48-50	92.18	10.00	83.30
11H-3, 36-38	93.56	10.82	90.10
11H-4, 34-36	95.04	10.71	89.20
11H-5, 34-36	96.54	10.78	89.80
11H-6, 36-38	98.06	10.68	89.00
11H-7, 36-38	99.56	10.98	91.50
12H-1, 109-111	100.79	11.10	92.50
12H-2, 34-36	101.54	11.08	92.30
12H-3, 34-36	103.04	11.08	92.30
12H-4, 34-36	104.54	11.24	93.60
12H-5, 34-36	106.04	11.05	92.00
12H-6, 34-36	107.54	10.99	91.50
12H-7, 34-36	109.04	11.04	92.00
13H-1, 109-111	110.29	10.79	89.90
13H-2, 98-100	111.68	11.11	92.50
13H-3, 34-36	112.54	10.46	87.10
13H-4, 34-36	114.04	10.94	91.10
14H-1, 100-102	119.70	11.13	92.70
14H-2, 34-36	120.54	10.95	91.20
14H-3, 34-36	122.04	11.12	92.60
14H-4, 34-36	123.54	11.20	93.30
14H-5, 34-36	125.04	11.10	92.50
14H-6, 37-39	126.57	11.14	92.80
14H-7, 36-38	128.06	11.03	91.90
15H-1, 34-36	128.54	11.43	95.20
15H-2, 34-35	130.04	10.58	88.10
15H-3, 34-35	131.54	10.95	91.20
15H-4, 27-28	132.97	11.15	92.90
15H-5, 35-36	134.55	11.70	97.50
15H-6, 35-36	136.05	10.85	90.40
15H-7, 40-41	137.60	11.05	92.00
130-804C-			
15X-1, 108-110	130.88	11.34	94.50
15X-2, 109-111	132.39	10.59	88.20
15X-3, 99-101	133.79	10.78	89.80
16X-1, 95-97	140.25	10.49	87.40
16X-2, 54-56	141.34	10.43	86.90
17X-1, 109-111	149.89	11.12	92.60
17X-2, 109-111	151.39	10.55	87.90
17X-3, 101-103	152.81	11.08	92.30
17X-4, 109-111	154.39	11.08	92.30
17X-5, 109-111	155.89	11.08	92.30
17X-6, 109-111	157.39	10.82	90.10
18X-1, 98-100	159.28	9.70	80.80
18X-2, 99-101	160.79	10.17	84.70
18X-3, 99-101	162.29	10.40	86.60
18X-3, 129-131	162.59	10.86	90.50
18X-5, 100-102	165.30	10.75	89.50
18X-6, 22-24	166.02	10.36	86.30
19X-1, 99-101	168.99	10.83	90.20
19X-2, 98-100	170.48	10.74	89.50
19X-3, 104-106	172.04	10.82	90.10
19X-4, 104-106	173.54	10.54	87.80
19X-5, 110-112	175.10	10.02	83.50
19X-6, 40-42	175.90	10.02	83.50
20X-1, 108-110	178.78	9.78	81.50
20X-2, 121-123	180.41	10.29	85.70
20X-3, 106-108	181.76	11.11	92.50
20X-4, 106-108	183.26	10.90	90.80
20X-5, 106-108	184.76	10.43	86.90
21X-1, 100-102	188.40	9.46	78.80
21X-2, 100-102	189.90	10.14	84.50
21X-3, 100-102	191.40	10.04	83.60
21X-4, 100-102	192.90	10.80	90.00
22X-1, 102-104	198.12	8.52	71.00
22X-2, 80-82	199.40	10.01	83.40
22X-4, 38-40	201.98	9.19	76.60
22X-5, 4-6	203.14	7.80	65.00

Table 5 (continued).

Core, section, interval (cm)	Depth (mbsf)	Inorganic carbon (%)	$CaCO_3$ (%)
130-804C- (Cont.)			
23X-1, 71–73	207.51	9.08	75.60
23X-3, 42–44	210.22	8.97	74.70
23X-4, 32–34	211.62	10.13	84.40
23X-5, 39–41	213.19	11.16	93.00
24X-1, 87–89	217.37	11.23	93.50
24X-2, 95–97	218.95	11.04	92.00
25X-2, 102–104	228.72	9.94	82.80
25X-3, 51–53	229.71	9.84	82.00
25X-4, 100–102	231.70	10.81	90.00
25X-5, 71–73	232.91	9.80	81.60
25X-6, 26–28	233.96	10.55	87.90
26X-1, 103–105	236.83	9.37	78.10
26X-2, 85–87	238.15	9.98	83.10
26X-3, 121–123	240.01	10.76	89.60
26X-4, 52–54	240.82	10.58	88.10
26X-5, 65–67	242.45	9.94	82.80
27X-1, 66–68	246.06	10.83	90.20
27X-3, 93–94	249.33	10.78	89.80
27X-6, 58–60	253.48	9.72	81.00
28X-1, 116–118	256.26	7.87	65.60
28X-2, 94–96	257.54	10.36	86.30
28X-5, 110–112	262.20	9.77	81.40
28X-6, 65–67	263.25	10.74	89.50
29X-4, 120–122	270.40	8.03	66.90
29X-5, 61–63	271.31	9.56	79.60
30X-1, 110–112	275.50	7.91	65.90
30X-2, 95–97	276.85	10.74	89.50
30X-3, 17–19	277.57	11.28	94.00
30X-4, 44–46	279.34	11.07	92.20
31X-1, 146–148	285.46	10.95	91.20
31X-2, 122–124	286.72	11.08	92.30
31X-4, 35–37	288.85	11.10	92.50
32X-1, 115–117	294.85	11.20	93.30
32X-2, 119–121	296.39	11.19	93.20
32X-3, 106–108	297.76	11.24	93.60
32X-4, 34–36	298.54	11.31	94.20
33X-1, 100–102	304.30	9.95	82.90
33X-2, 82–84	305.41	10.35	86.20
33X-3, 82–84	306.91	10.13	84.40
33X-4, 63–65	308.22	10.46	87.10
33X-5, 21–23	309.30	9.58	79.80

Table 7. Shear strength data, Site 804.

Core, section, interval (cm)	Depth (mbsf)	Peak shear (kPa)	Residual strength (kPa)
130-804A-			
1H-1, 45	0.45	4.7	2.2
2H-1, 120	2.40	7.3	3.1
2H-2, 120	3.90	9.0	4.5
2H-3, 120	5.40	7.0	3.6
2H-4, 120	6.90	9.3	5.2
2H-5, 120	8.40	7.9	5.2
3H-1, 120	11.90	17.4	9.2
3H-2, 120	13.40	11.8	6.3
3H-3, 80	14.50	8.0	4.3
3H-4, 120	16.40	17.6	8.1
3H-5, 120	17.90	18.3	9.9
3H-6, 130	19.50	31.8	15.5
4H-1, 120	21.40	12.7	5.6
4H-2, 120	22.90	11.6	5.4
4H-3, 120	24.40	9.5	3.4
4H-4, 110	25.80	13.6	6.3
4H-4, 120	25.90	23.5	9.9
4H-5, 120	27.40	22.2	9.9
5H-1, 132	31.02	18.8	
5H-2, 132	32.52	22.0	9.1
5H-3, 133	34.03	24.7	
5H-4, 133	35.53	17.3	12.5
5H-5, 140	37.10	29.4	9.7
5H-6, 130	38.50	38.2	20.2
5H-7, 18	38.88	50.5	22.5
6H-1, 138	40.58	16.8	13.5
6H-2, 140	42.10	16.8	10.1
6H-3, 138	43.58	16.8	10.1
6H-4, 128	44.98	14.6	5.6
6H-5, 128	46.48	23.5	14.2
6H-6, 35	47.05	17.1	7.4
6H-6, 128	47.98	12.0	5.6
130-804B-			
1H-3, 103	4.03	8.2	4.2
2H-1, 138	6.08	10.7	4.9
2H-2, 140	7.60	11.8	6.3
2H-3, 136	9.06	9.2	4.7
2H-4, 80	10.00	10.2	4.9
2H-5, 110	11.80	11.0	6.7
2H-6, 139	13.59	13.2	9.2
2H-7, 66	14.36	14.5	7.0
3H-1, 140	15.60	10.2	4.5
3H-2, 136	17.06	13.7	6.3
3H-3, 140	18.60	8.2	3.6
3H-4, 131	20.01	17.9	10.3
3H-5, 97	21.17	21.8	10.1
3H-7, 58	23.78	35.3	16.8
4H-1, 130	25.00	25.2	12.4
4H-2, 132	26.52	21.5	7.9
4H-3, 132	28.02	13.0	4.5
4H-4, 128	29.48	18.0	9.0
4H-5, 116	30.86	24.7	11.2
4H-6, 120	32.40	25.2	11.2
4H-7, 50	33.20	32.6	15.7
5H-1, 134	34.54	22.5	12.4
5H-2, 135	36.05	18.0	
5H-3, 135	37.55	16.8	
5H-4, 80	38.50	28.1	13.5
5H-5, 140	40.60	33.7	19.1
5H-6, 118	41.88	30.3	13.5
6H-1, 120	43.90	29.2	15.7
6H-2, 122	45.42	19.1	5.6
6H-3, 122	46.92	12.4	6.7
6H-4, 120	48.40	15.7	6.7
6H-5, 120	49.90	7.9	2.2
6H-6, 120	51.40	6.3	4.5
7H-1, 120	53.40	8.8	4.0
7H-3, 120	56.40	8.9	3.4
7H-4, 120	57.90	9.0	4.3
7H-5, 120	59.40	7.2	2.9
7H-6, 120	60.90	8.8	4.3
8H-1, 120	62.90	12.6	4.5
8H-2, 120	64.40	13.5	
130-804B- (Cont.)			
8H-3, 120	65.90	11.3	5.2
8H-4, 120	67.40	16.4	4.5
8H-5, 120	68.90	12.4	4.7
8H-6, 120	70.40	12.5	6.1
9H-1, 120	72.40	9.3	2.2
9H-2, 120	73.90	9.4	2.5
9H-3, 120	75.40	10.1	2.9
9H-4, 120	76.90	10.1	3.6
9H-5, 120	78.40	10.6	3.4
9H-6, 120	79.90	7.8	3.3
10H-1, 120	81.90	10.2	3.8
10H-2, 120	83.40	16.0	6.3
10H-3, 120	84.90	16.4	6.7
10H-4, 120	86.40	12.5	5.2
10H-5, 120	87.90	11.2	4.5
10H-6, 125	89.45	12.8	5.6
11H-1, 128	93.08	25.2	
11H-2, 140	94.70	14.6	5.3
11H-3, 125	96.05	12.8	4.5
11H-4, 140	97.70	16.2	5.6
11H-5, 125	99.05	27.0	9.9
11H-6, 125	100.55	20.2	6.1
12H-1, 125	102.55	19.8	6.1
12H-2, 119	103.99	14.2	4.5
12H-3, 120	105.50	14.5	6.5
12H-4, 115	106.95	28.5	8.8
12H-5, 115	108.45	24.7	9.4
12H-6, 135	110.15	35.9	16.8
13H-1, 128	110.48	20.2	11.2
13H-2, 39	111.09	27.4	15.7
13H-3, 125	113.45	39.8	20.2
14H-2, 132	121.52	20.2	11.2
14H-3, 134	123.04	18.0	9.0
14H-4, 134	124.54	16.8	7.9
14H-5, 133	126.03	21.8	11.2
14H-6, 133	127.53	27.0	10.1
15H-1, 134	129.54	33.2	11.2
15H-2, 130	131.00	47.2	18.0
15H-3, 136	132.56	41.6	10.1
15H-4, 82	133.52	34.8	15.7
15H-5, 133	135.53	52.3	24.7
15H-6, 135	137.05	52.3	20.2
130A-804C-			
1H-1, 138	1.38	6.1	2.2
1H-2, 136	2.86	5.6	2.5
1H-3, 131	4.31	6.8	4.0
1H-4, 136	5.86	10.0	5.6
2H-1, 139	7.69	7.1	2.9
2H-2, 140	9.20	6.7	3.6
2H-3, 140	10.70	7.0	3.1
2H-4, 140	12.20	11.0	5.8
2H-5, 135	13.65	8.3	4.0
2H-6, 141	15.21	14.2	7.2
3H-1, 140	17.20	13.9	6.1
3H-2, 140	18.70	10.8	5.4
3H-3, 132	20.12	14.2	7.0
3H-3, 139	20.19	18.2	9.2
3H-4, 140	21.70	14.2	6.1
3H-5, 140	23.20	16.6	9.8
3H-6, 131	24.61	25.8	12.2
4H-4, 119	30.99	19.1	10.8
4H-5, 134	32.64	23.6	
4H-6, 146	34.26	30.3	9.7
4H-7, 32	34.62	20.9	7.3
6H-2, 137	47.17	15.3	6.3
6H-2, 141	47.21	11.2	5.6
6H-3, 141	48.71	11.9	4.7
6H-4, 141	50.21	11.2	5.1
6H-5, 140	51.70	7.8	4.3
6H-6, 142	53.22	9.1	3.9
6H-7, 78	54.08	9.7	4.5
7H-2, 140	56.70	15.5	5.3
7H-3, 127	58.07	9.4	3.6
130-804C- (Cont.)			
7H-4, 140	59.70	11.7	3.1
7H-5, 139	61.19	12.0	3.6
7H-6, 139	62.69	17.5	5.6
8H-1, 140	64.70	23.1	5.8
8H-2, 134	66.14	18.8	5.2
8H-3, 140	67.70	16.2	4.7
8H-4, 136	69.16	19.5	5.4
8H-5, 140	70.70	14.3	5.2
8H-6, 140	72.20	11.6	3.8
9H-1, 144	74.24	10.6	
9H-2, 140	75.70	9.4	2.7
9H-3, 140	77.20	14.2	3.7
9H-4, 120	78.50	13.5	4.2
9H-5, 122	80.02	11.8	1.9
10H-1, 119	83.49	13.7	2.2
10H-2, 120	85.00	16.2	1.7
10H-2, 128	85.08	22.5	
10H-3, 120	86.50	18.5	4.3
10H-5, 130	89.60	19.8	6.7
11H-1, 130	93.60	30.1	11.2
11H-2, 120	94.50	22.5	14.6
11H-3, 120	96.00	16.8	9.0
11H-4, 120	97.50	18.0	11.2
11H-5, 120	99.00	18.6	7.9
11H-6, 100	100.30	16.4	6.7
12H-2, 120	104.00	15.3	5.8
12H-4, 120	107.00	24.0	8.1
12H-5, 120	108.50	28.3	9.0
12H-6, 120	110.00	12.8	4.7
13H-1, 110	111.90	19.8	6.7
13H-1, 120	112.00	21.5	7.9
13H-2, 120	113.50	16.6	6.4
13H-4, 120	116.50	23.1	9.0
13H-5, 120	118.00	20.9	6.7
13H-6, 120	119.50	21.8	4.5
14H-1, 120	121.50	13.5	2.2
14H-2, 120	123.00	8.5	
14H-3, 120	124.50	7.9	3.4
14H-4, 120	126.00	14.8	3.4
15H-1, 120	131.00	16.0	
15H-2, 120	132.50	13.5	4.9
15H-3, 120	134.00	18.0	5.8
16H-1, 114	140.44	13.5	7.9
17X-1, 122	150.02	22.5	8.1
17X-2, 120	151.50	23.1	14.6
17X-3, 123	153.03	25.8	11.2
17X-4, 123	154.53	25.8	14.6
17X-5, 120	156.00	31.5	16.8
17X-6, 120	157.50	27.0	12.4
18X-1, 120	160.00	23.6	13.0

Table 9. Index properties data, Site 804.

Core, section, interval (cm)	Depth (mbsf)	Wet-bulk density (g/cm^3)	Grain density (g/cm^3)	Water content (% dry wt)	Porosity (%)	Dry-bulk density (g/cm^3)
130-804A-						
1H-1, 35	0.35	1.51	2.66	89.5	69.7	0.80
2H-1, 33	1.53	1.49	2.68	96.0	71.3	0.76
2H-1, 109	2.29	1.49	2.72	96.8	71.7	0.76
2H-2, 34	3.04	1.52	2.69	88.1	69.6	0.81
2H-2, 109	3.79	1.48	2.70	101.6	72.6	0.73
2H-3, 35	4.55	1.53	2.73	88.0	69.9	0.81
2H-3, 106	5.26	1.51	2.72	93.6	71.1	0.78
2H-4, 35	6.05	1.52	2.67	88.8	69.6	0.80
2H-4, 110	6.80	1.54	2.71	84.3	68.8	0.84
2H-5, 45	7.65	1.53	2.69	85.7	69.0	0.83
2H-5, 110	8.30	1.52	2.69	89.0	69.8	0.80
2H-6, 34	9.04	1.51	2.68	89.9	69.9	0.80
2H-6, 109	9.79	1.54	2.72	84.0	68.9	0.84
2H-7, 35	10.55	1.56	2.68	79.3	67.2	0.87
3H-1, 35	11.05	1.52	2.63	86.0	68.6	0.82
3H-1, 109	11.79	1.51	2.68	89.6	69.8	0.80
3H-2, 35	12.55	1.51	2.68	90.8	70.1	0.79
3H-2, 109	13.29	1.57	2.63	75.4	65.7	0.89
3H-3, 35	14.05	1.45	2.65	107.2	73.2	0.70
3H-4, 35	15.55	1.50	2.68	93.7	70.8	0.77
3H-4, 109	16.29	1.56	2.65	77.7	66.6	0.88
3H-5, 35	17.05	1.54	2.70	83.5	68.5	0.84
3H-5, 109	17.79	1.53	2.69	85.8	69.0	0.82
3H-6, 34	18.54	1.57	2.73	78.1	67.3	0.88
3H-6, 109	19.29	1.53	2.67	85.2	68.7	0.83
3H-7, 35	20.05	1.59	2.68	71.7	65.0	0.93
4H-1, 50	20.70	1.54	2.70	85.1	68.9	0.83
4H-1, 109	21.29	1.52	2.72	90.4	70.3	0.80
4H-2, 35	22.05	1.50	2.69	94.4	71.0	0.77
4H-2, 109	22.79	1.62	2.72	68.0	64.2	0.97
4H-3, 35	23.55	1.53	2.66	85.4	68.7	0.82
4H-3, 109	24.29	1.52	2.70	88.0	69.7	0.81
4H-4, 29	24.99	1.51	2.66	89.5	69.7	0.80
4H-4, 109	25.79	1.52	2.65	87.0	69.0	0.81
4H-5, 34	26.54	1.57	2.68	76.6	66.5	0.89
4H-5, 105	27.25	1.57	2.56	76.7	66.3	0.89
4H-6, 34	28.04	1.57	2.67	77.4	66.7	0.88
4H-6, 109	28.79	1.52	2.68	88.4	69.6	0.81
4H-7, 35	29.55	1.53	2.67	85.4	68.8	0.82
5H-1, 68	30.38	1.52	2.68	88.8	69.7	0.80
5H-1, 119	30.89	1.46	2.65	105.3	72.9	0.71
5H-2, 40	31.60	1.55	2.67	80.9	67.6	0.86
5H-2, 105	32.25	1.51	2.68	92.3	70.5	0.78
5H-3, 40	33.10	1.55	2.67	80.1	67.4	0.86
5H-3, 112	33.82	1.46	2.69	106.3	73.4	0.71
5H-4, 37	34.57	1.47	2.65	100.7	72.0	0.73
5H-4, 124	35.44	1.49	2.65	94.0	70.7	0.77
5H-5, 45	36.15	1.52	2.64	85.4	68.5	0.82
5H-5, 115	36.85	1.58	2.72	76.6	66.8	0.89
5H-6, 33	37.53	1.49	2.65	94.8	70.8	0.77
5H-6, 119	38.39	1.42	2.64	119.4	75.2	0.65
5H-7, 32	39.02	1.54	2.70	85.3	69.0	0.83
6H-1, 124	40.44	1.54	2.69	83.9	68.6	0.84
6H-2, 40	41.10	1.55	2.69	81.7	68.0	0.85
6H-2, 110	41.80	1.47	2.68	101.0	72.3	0.73
6H-3, 57	42.77	1.53	2.70	86.2	69.2	0.82
6H-3, 127	43.47	1.55	2.71	81.9	68.2	0.85
6H-4, 29	43.99	1.54	2.68	83.2	68.3	0.84
6H-4, 108	44.78	1.58	2.68	73.8	65.7	0.91
6H-5, 39	45.59	1.58	2.68	74.2	65.8	0.91
6H-5, 108	46.28	1.57	2.65	75.0	65.8	0.90
6H-6, 13	46.83	1.58	2.70	75.6	66.4	0.90
6H-6, 115	47.85	1.62	2.69	68.2	64.0	0.96
130-804B-						
1H-1, 32	0.32	1.49	2.67	94.6	70.9	0.77
1H-1, 103	1.03	1.50	2.65	93.1	70.5	0.78
1H-2, 24	1.74	1.51	2.69	92.6	70.7	0.78
1H-2, 104	2.54	1.53	2.72	87.8	69.7	0.81
1H-3, 34	3.34	1.50	2.66	91.6	70.2	0.79
1H-3, 119	4.19	1.51	2.67	90.1	69.9	0.79
2H-1, 48	5.18	1.49	2.64	95.5	70.9	0.76
2H-1, 110	5.80	1.54	2.67	82.8	68.1	0.84
2H-2, 34	6.54	1.54	2.69	83.5	68.4	0.84

Table 9 (continued).

Core, section, interval (cm)	Depth (mbsf)	Wet-bulk density (g/cm^3)	Grain density (g/cm^3)	Water content (% dry wt)	Porosity (%)	Dry-bulk density (g/cm^3)
130-804B- (Cont.)						
2H-2, 114	7.34	1.55	2.67	80.9	67.6	0.86
2H-3, 24	7.94	1.52	2.67	88.3	69.5	0.81
2H-3, 118	8.88	1.53	2.66	84.2	68.4	0.83
2H-4, 24	9.44	1.55	2.66	80.2	67.5	0.86
2H-4, 103	10.23	1.55	2.70	82.5	[illegible]	[illegible]
2H-5, 29	10.99	1.49	2.65	93.9	70.6	0.77
2H-5, 128	11.98	1.54	2.7	84.7	68.9	0.83
2H-6, 24	12.44	1.53	2.69	87.1	69.3	0.82
2H-6, 115	13.35	1.53	2.67	85.1	68.7	0.83
2H-7, 50	14.20	1.55	2.68	81.0	67.7	0.86
3H-1, 115	15.35	1.55	2.66	81.3	[illegible]	0.85
3H-2, 34	16.04	1.51	2.71	91.0	70.4	0.79
3H-3, 40	17.60	1.55	2.69	81.9	68.0	0.85
3H-3, 116	18.36	1.52	2.63	86.7	68.8	0.81
3H-4, 29	19.09	1.53	2.68	86.0	69.0	0.82
3H-4, 104	19.74	1.53	2.69	86.1	69.1	0.82
3H-5, 34	20.54	1.53	2.66	85.1	68.6	0.83
3H-5, 107	21.27	1.54	2.54	80.9	67.4	0.85
3H-6, 39	22.09	1.56	2.67	77.4	66.6	0.88
3H-6, 108	22.78	1.58	2.70	76.3	66.6	0.89
3H-7, 44	23.64	1.57	2.64	74.8	65.7	0.90
4H-1, 44	24.14	1.50	2.65	92.8	70.4	0.78
4H-1, 107	24.77	1.56	2.68	79.7	67.3	0.87
4H-2, 34	25.54	1.52	2.63	85.2	63.4	0.82
4H-2, 107	26.27	1.57	2.68	77.7	66.8	0.88
4H-3, 40	27.10	1.58	2.71	76.0	66.6	0.90
4H-3, 103	27.73	1.55	2.68	81.9	68.0	0.85
4H-4, 29	28.49	1.56	2.67	78.5	67.0	0.87
4H-4, 108	29.28	1.55	2.67	80.7	67.5	0.86
4H-5, 29	29.99	1.51	2.66	89.3	69.6	0.80
4H-5, 108	30.78	1.50	2.66	93.4	70.6	0.77
4H-6, 34	31.54	1.52	2.65	87.5	69.1	0.81
4H-6, 109	32.29	1.45	2.63	106.3	73.0	0.70
4H-7, 35	33.05	1.49	2.63	95.0	70.7	0.76
5H-1, 119	34.39	1.56	2.71	81.3	68.1	0.86
5H-2, 34	35.04	1.51	2.66	89.6	69.7	0.80
5H-2, 107	35.77	1.47	2.67	102.7	72.6	0.72
5H-3, 36	36.56	1.46	2.64	105.2	72.8	0.71
5H-3, 126	37.46	1.55	2.67	81.4	67.8	0.85
5H-4, 40	38.10	1.49	2.66	94.3	70.8	0.77
5H-4, 109	38.79	1.58	2.74	76.2	66.9	0.90
5H-5, 29	39.49	1.42	2.65	119.1	75.2	0.65
5H-5, 115	40.35	1.45	2.67	108.0	73.5	0.70
5H-6, 29	40.99	1.47	2.69	104.0	72.9	0.72
5H-6, 108	41.78	1.51	2.69	90.3	70.1	0.79
5H-7, 45	42.65	1.48	2.69	99.6	72.1	0.74
6H-1, 112	43.82			83.6		
6H-1, 35	43.05	1.51	2.71	91.4	70.5	[illegible]
6H-2, 38	44.58	1.50	2.71	95.3	71.4	[illegible]
6H-2, 110	45.30	1.55	2.69	82.2	68.1	0.85
6H-3, 34	46.04	1.54	2.69	84.7	68.8	0.83
6H-3, 106	46.76	1.60	2.64	68.9	63.8	0.95
6H-4, 34	47.54	1.58	2.68	74.5	65.9	0.91
6H-4, 109	48.29	1.63	2.70	66.6	63.5	0.98
6H-5, 34	49.04	1.61	2.70	69.3	64.5	0.95
6H-5, 110	49.80	1.63	2.70	67.0	63.7	0.97
6H-6, 35	50.55	1.64	2.71	64.6	62.9	1.00
6H-6, 109	51.29	1.60	2.70	71.2	65.0	0.94
6H-7, 34	52.04	1.58	2.67	73.9	65.6	0.91
7H-1, 35	52.55	1.60	2.69	70.7	[illegible]	0.94
7H-1, 110	53.30	1.63	2.69	65.6	[illegible]	0.99
7H-2, 33	54.03	1.62	2.70	68.5	[illegible]	0.96
7H-2, 108	54.78	1.66	2.70	61.5	[illegible]	1.03
7H-3, 34	55.54	1.65	2.67	62.2	[illegible]	1.02
7H-3, 109	56.29	1.66	2.71	61.5	[illegible]	1.03
7H-4, 35	57.05	1.66	2.69	60.7	[illegible]	1.03
7H-4, 109	57.79	1.65	2.68	61.9	[illegible]	1.02
7H-5, 36	58.56	1.66	2.68	61.0	[illegible]	1.03
7H-5, 108	59.28	1.64	2.72	65.3	63.2	0.99
7H-6, 34	60.04	1.60	2.68	[illegible]	64.6	0.94
7H-6, 109	60.79	1.67	2.69	59.5	60.8	1.05
7H-7, 34	[illegible]	1.62	2.67	[illegible]	63.4	0.97
8H-1, 109	62.79	1.65	2.68	[illegible]	61.6	1.02
8H-2, 34	63.54	1.66	2.68	[illegible]	61.4	1.03

Table 9 (continued).

Core, section, interval (cm)	Depth (mbsf)	Wet-bulk density (g/cm^3)	Grain density (g/cm^3)	Water content (% dry wt)	Porosity (%)	Dry-bulk density (g/cm^3)
130-804B- (Cont.)						
8H-2, 109	64.29	1.66	2.68	60.9	61.3	1.03
8H-3, 35	65.05	1.70	2.67	54.9	58.7	1.10
8H-3, 108	65.78	1.63	2.66	64.7	62.5	0.99
8H-4, 34	66.54			56.0		
8H-4, 109	67.29	1.68	2.65	56.6	59.3	1.07
8H-5, 35	68.05	1.69	2.70	56.8	59.7	1.08
8H-5, 109	68.79	1.70	2.68	55.4	59.0	1.09
8H-6, 34	69.54	1.64	2.69	65.0	62.9	0.99
8H-6, 109	70.29	1.63	2.69	65.9	63.2	0.98
8H-7, 35	71.05			70.4		
9H-1, 34	71.54	1.55	2.63	79.5	66.9	0.86
9H-1, 109	72.29	1.61	2.68	69.2	64.2	0.95
9H-2, 33	73.03	1.59	2.67	72.9	65.4	0.92
9H-2, 107	73.77			68.3		
9H-3, 34	74.54	1.62	2.68	66.8	63.4	0.97
9H-3, 109	75.29	1.59	2.64	71.3	64.6	0.93
9H-4, 34	76.04	1.63	2.68	65.7	63.0	0.98
9H-4, 108	76.78	1.63	2.68	65.3	62.9	0.99
9H-5, 34	77.54	1.58	2.66	74.1	65.6	0.91
9H-5, 108	78.28	1.61	2.68	68.2	63.9	0.96
9H-6, 34	79.04			68.7		
9H-6, 109	79.79	1.64	2.70	63.7	62.5	1.00
9H-7, 35	80.55			65.8		
10H-1, 109	81.79	1.63	2.66	64.3	62.4	0.99
10H-2, 33	82.53	1.61	2.66	68.4	63.8	0.96
10H-2, 109	83.29	1.59	2.64	71.5	64.7	0.93
10H-3, 34	84.04			61.9		
10H-3, 109	84.79	1.62	2.70	67.3	63.8	0.97
10H-4, 35	85.55	1.60	2.67	70.0	64.4	0.94
10H-4, 110	86.30	1.64	2.69	64.0	62.6	1.00
10H-5, 34	87.04	1.67	2.70	60.0	61.1	1.04
10H-5, 109	87.79	1.66	2.69	61.6	61.6	1.02
10H-6, 33	88.53	1.64	2.68	64.5	62.6	0.99
10H-6, 102	89.22	1.65	2.71	63.1	62.3	1.01
10H-7, 38	90.08	1.65	2.67	61.8	61.6	1.02
11H-1, 34	90.54	1.56	2.62	76.7	66.1	0.88
11H-1, 105	91.25	1.52	2.58	83.3	67.5	0.83
11H-2, 48	92.18	1.58	2.63	73.0	65.1	0.91
11H-2, 131	93.01	1.58	2.64	73.9	65.4	0.91
11H-3, 36	93.56	1.60	2.63	69.3	63.9	0.94
11H-3, 115	94.35			69.5		
11H-4, 34	95.04	1.64	2.65	63.2	61.9	1.00
11H-4, 113	95.83	1.64	2.65	63.4	62.0	1.00
11H-5, 34	96.54	1.62	2.64	65.8	62.7	0.98
11H-5, 113	97.33	1.65	2.67	61.2	61.3	1.03
11H-6, 36	98.06	1.67	2.69	58.8	60.5	1.05
11H-6, 113	98.83	1.68	2.68	57.5	59.9	1.07
11H-7, 38	99.58	1.65	2.70	63.1	62.2	1.01
11H-2, 111	92.81	1.55	2.64	80.6	67.3	0.86
12H-1, 109	100.79	1.64	2.69	63.3	62.2	1.01
12H-2, 34	101.54	1.63	2.68	65.4	62.9	0.99
12H-2, 109	102.29	1.66	2.68	60.4	61.1	1.04
12H-3, 34	103.04	1.67	2.67	59.1	60.5	1.05
12H-3, 109	103.79	1.66	2.68	60.5	61.2	1.03
12H-4, 34	104.54	1.68	2.70	58.4	60.4	1.06
12H-4, 105	105.25	1.70	2.68	55.4	59.0	1.09
12H-5, 34	106.04	1.70	2.68	54.5	58.6	1.10
12H-5, 109	106.79			56.9		
12H-6, 34	107.54	1.69	2.68	56.2	59.3	1.08
12H-6, 109	108.29	1.66	2.61	58.1	59.6	1.05
12H-7, 34	109.04	1.68	2.66	56.2	59.1	1.08
13H-1, 109	110.29	1.67	2.69	59.9	61.0	1.04
13H-2, 136	112.08	1.62	2.67	67.2	63.4	0.97
13H-2, 98	111.68	1.69	2.67	55.4	58.9	1.09
13H-3, 34	112.54	1.62	2.66	67.1	63.4	0.97
13H-3, 109	113.29	1.62	2.66	66.3	63.1	0.97
13H-4, 34	114.04	1.66	2.69	60.8	61.3	1.03
13H-4, 135	115.05	1.63	2.70	65.8	63.3	0.98
14X-1, 100	119.70	1.51	2.71	91.9	70.6	0.79
14X-2, 34	120.54	1.58	2.68	74.1	65.8	0.91
14X-2, 107	121.27	1.67	2.70	60.6	61.3	1.04
14X-3, 34	122.04	1.67	2.70	59.5	60.9	1.05
14X-3, 108	122.78	1.66	2.68	60.5	61.1	1.03
14X-4, 34	123.54	1.67	2.66	58.4	60.1	1.05
14X-4, 107	124.27	1.67	2.69	60.1	61.0	1.04

Table 9 (continued).

Core, section, interval (cm)	Depth (mbsf)	Wet-bulk density (g/cm^3)	Grain density (g/cm^3)	Water content (% dry wt)	Porosity (%)	Dry-bulk density (g/cm^3)
130-804B- (Cont.)						
14X-5, 34	125.04	1.67	2.70	59.2	60.8	1.05
14X-5, 107	125.77	2.01	2.68	25.7	40.1	1.60
14X-6, 37	126.57	1.69	2.69	56.6	59.6	1.08
14X-6, 107	127.27	1.70	2.71	56.4	59.7	1.08
14X-7, 36	128.06	1.69	2.68	56.7	59.6	1.08
15X-1, 34	128.54	1.72	2.68	52.5	57.8	1.13
15X-1, 105	129.25	1.63	2.67	64.5	62.5	0.99
15X-2, 34	130.04	1.61	2.65	67.7	63.5	0.96
15X-2, 105	130.75	1.64	2.71	65.2	63.2	0.99
15X-3, 34	131.54	1.62	2.68	66.4	63.2	0.98
15X-3, 108	132.28	1.58	2.68	74.1	65.7	0.91
15X-4, 27	132.97	1.61	2.66	69.2	64.1	0.95
15X-4, 99	133.69	1.58	2.63	73.5	65.1	0.91
15X-5, 35	134.55	1.63	2.71	67.2	63.8	0.97
15X-5, 106	135.26	1.59	2.66	72.3	65.1	0.92
15X-6, 35	136.05	1.60	2.68	71.3	64.9	0.93
15X-6, 107	136.77	1.61	2.67	69.5	64.2	0.95
15X-7, 40	137.60	1.58	2.66	73.2	65.4	0.91
130-804C-						
1H-1, 90	0.90	1.48	2.67	99.7	71.9	0.74
1H-2, 106	2.56	1.50	2.68	94.4	71.0	0.77
1H-3, 120	4.20	1.53	2.69	85.7	69.0	0.82
1H-4, 100	5.50	1.53	2.67	84.7	68.6	0.83
2H-1, 99	7.29	1.46	2.70	105.5	73.3	0.71
2H-2, 101	8.81	1.53	2.68	85.1	68.8	0.83
2H-3, 96	10.26	1.57	2.71	78.8	67.4	0.88
2H-4, 100	11.80	1.55	2.71	82.0	68.2	0.85
2H-5, 100	13.30	1.53	2.68	86.0	69.0	0.82
2H-6, 101	14.81	1.52	2.68	88.4	69.6	0.81
3H-1, 99	16.79	1.53	2.70	86.0	69.1	0.82
3H-2, 104	18.34	1.58	2.68	75.1	66.1	0.90
3H-3, 99	19.79	1.51	2.70	91.3	70.4	0.79
3H-4, 98	21.28	1.54	2.69	85.0	68.9	0.83
3H-5, 100	22.80	1.53	2.70	86.4	69.2	0.82
3H-6, 40	23.70	1.50	2.68	92.5	70.6	0.78
4H-3, 127	29.57	1.53	2.67	85.2	68.8	0.83
4H-4, 107	30.87	1.48	2.69	99.8	72.1	0.74
4H-5, 98	32.28	1.53	2.70	86.7	69.3	0.82
4H-6, 100	33.80	1.54	2.68	83.8	68.4	0.84
6H-2, 100	46.80			66.3		
6H-3, 100	48.30			61.5		
6H-4, 99	49.79	1.65	2.72	63.2	62.5	1.01
6H-5, 98	51.28			64.0		
6H-6, 100	52.80			63.8		
7H-2, 99	56.29	1.66	2.72	62.3	62.2	1.02
7H-3, 99	57.79	1.65	2.69	61.8	61.7	1.02
7H-4, 122	59.52	1.63	2.68	65.4	62.9	0.99
7H-5, 100	60.80	1.70	2.70	56.0	59.4	1.09
7H-6, 100	62.30	1.70	2.73	56.6	60.0	1.09
7H-7, 27	63.07	1.62	2.67	67.1	63.4	0.97
8H-1, 99	64.29	1.71	2.68	52.8	57.8	1.12
8H-2, 99	65.79	1.68	2.65	56.8	59.4	1.07
8H-3, 103	67.33	1.64	2.71	64.7	62.9	1.00
8H-4, 99	68.79	1.63	2.67	65.9	63.0	0.98
8H-5, 99	70.29	1.61	2.64	67.5	63.3	0.96
8H-6, 98	71.78	1.62	2.68	67.9	63.8	0.96
8H-7, 39	72.69	1.60	2.67	70.8	64.7	0.94
9H-1, 125	74.05	1.61	2.70	69.8	64.6	0.95
9H-2, 106	75.36	1.64	2.72	64.7	63.0	1.00
9H-3, 113	76.93	1.66	2.70	61.8	61.8	1.02
9H-4, 109	78.39	1.66	2.70	60.8	61.5	1.03
9H-5, 114	79.94	1.63	2.68	65.7	63.0	0.98
10H-1, 110	83.40	1.63	2.70	65.9	63.3	0.98
10H-2, 109	84.89	1.62	2.69	67.1	63.6	0.97

Table 9 (continued).

Core, section, interval (cm)	Depth (mbsf)	Wet-bulk density (g/cm^3)	Grain density (g/cm^3)	Water content (% dry wt)	Porosity (%)	Dry-bulk density (g/cm^3)
130-804C- (Cont.)						
10H-3, 109	86.39	1.66	2.72	62.1	62.1	1.02
10H-4, 115	87.95	1.63	2.68	65.0	62.8	0.99
10H-5, 110	89.40	1.58	2.66	74.4	65.7	0.90
11H-1, 109	92.89	1.51	2.61	88.0	68.9	0.80
11H-2, 108	94.38	1.66	2.69	61.1	61.4	1.03
11H-3, 109	95.89	1.63	2.69	65.8	63.2	0.98
11H-4, 109	97.39	1.67	2.70	60.7	61.4	1.04
11H-5, 109	98.89	1.68	2.69	58.6	60.4	1.06
11H-6, 90	100.20	1.72	2.70	52.9	58.1	1.12
12H-1, 108	102.38	1.68	2.71	59.4	60.9	1.05
12H-2, 110	103.90	1.68	2.69	57.8	60.2	1.07
12H-3, 109	105.39	1.72	2.69	52.2	57.7	1.13
12H-4, 110	106.90	1.70	2.68	55.0	58.8	1.10
12H-5, 109	108.39	1.66	2.68	61.1	61.4	1.03
12H-6, 109	109.89	1.65	2.69	62.1	61.8	1.02
13H-1, 99	111.79	1.62	2.67	66.7	63.3	0.97
13H-2, 109	113.39	1.62	2.64	65.4	62.6	0.98
13H-3, 110	114.90	1.58	2.67	75.1	66.0	0.90
13H-4, 109	116.39	1.62	2.68	66.5	63.3	0.98
13H-5, 109	117.89	1.63	2.67	64.7	62.6	0.99
13H-6, 109	119.39	1.63	2.69	65.6	63.1	0.99
14X-1, 109	121.39	1.64	2.69	63.9	62.5	1.00
14X-2, 109	122.89	1.63	2.69	66.2	63.3	0.98
14X-3, 109	124.39	1.65	2.67	62.0	61.6	1.02
14X-4, 109	125.89	1.63	2.68	64.8	62.7	0.99
15X-1, 108	130.88	1.69	2.73	58.2	60.6	1.07
15X-2, 109	132.39	1.58	2.65	74.3	65.6	0.90
15X-3, 99	133.79	1.58	2.68	74.1	65.8	0.91
16X-1, 95	140.25	1.58	2.69	75.0	66.1	0.90
16X-2, 54	141.34	1.57	2.71	77.7	67.1	0.88
17X-1, 109	149.89	1.66	2.70	60.6	61.3	1.04
17X-2, 109	151.39	1.67	2.65	57.8	59.7	1.06
17X-3, 101	152.81	1.68	2.68	58.0	60.1	1.06
17X-4, 109	154.39	1.70	2.68	54.6	58.6	1.10
17X-5, 109	155.89	1.68	2.70	58.6	60.5	1.06
17X-6, 110	157.40	1.71	2.69	53.6	58.3	1.11
18X-1, 98	159.78	1.59	2.68	73.4	65.6	0.92
18X-2, 99	161.29	1.60	2.67	70.6	64.6	0.94
18X-3, 99	162.79	1.58	2.68	74.9	66.0	0.90
18X-4, 129	164.59	1.68	2.68	58.2	60.2	1.06
18X-5, 100	165.80	1.61	2.69	70.0	64.5	0.95
18X-6, 20	166.50	1.63	2.63	63.6	61.9	1.00
19X-1, 99	168.99	1.64	2.68	64.4	62.6	0.99
19X-2, 98	170.48	1.67	2.67	59.3	60.6	1.05
19X-3, 104	172.04	1.59	2.64	70.4	64.3	0.94
19X-4, 104	173.54	1.63	2.66	64.9	62.6	0.99
19X-5, 110	175.10			71.6		
19X-6, 40	175.90	1.59	2.68	72.3	65.2	0.92
20X-1, 108	178.78	1.62	2.66	65.7	62.8	0.98
20X-2, 121	180.41	1.65	2.65	61.2	61.1	1.02
20X-3, 106	181.76	1.69	2.69	56.2	59.5	1.08
20X-4, 106	183.26	1.67	2.68	59.4	60.7	1.05
20X-5, 100	184.70	1.60	2.67	69.9	64.4	0.94
21X-1, 100	188.40	1.56	2.65	77.8	66.6	0.88
21X-2, 100	189.90	1.64	2.67	63.2	62.0	1.01
21X-3, 100	191.40	1.59	2.65	71.2	64.7	0.93
21X-4, 100	192.90	1.71	2.67	52.7	57.7	1.12
22X-1, 102	198.12	1.62	2.64	64.9	62.4	0.98
22X-2, 80	199.40	1.68	2.75	60.5	61.7	1.05
22X-4, 38	201.98					
22X-5, 4	203.14	1.52	2.59	83.5	67.6	0.83
23X-1, 71	207.51	1.58	2.62	71.4	64.4	0.92
23X-3, 42	210.22	1.57	2.65	75.3	65.9	0.90
23X-4, 32	211.62	1.68	2.72	59.8	61.2	1.05
23X-5, 39	213.19	1.70	2.78	58.6	61.2	1.07
24X-1, 87	217.37	1.76	2.75	49.3	56.8	1.18
24X-2, 95	218.95	1.68	2.71	58.0	60.3	1.07
25X-2, 102	228.72	1.67	2.54	54.1	57.2	1.08
25X-3, 51	229.71	1.67	2.65	58.2	59.9	1.06
25X-4, 100	231.70	1.81	2.72	42.9	53.2	1.27
25X-5, 71	232.91	1.71	2.71	54.9	59.1	1.10
25X-6, 26	233.96	1.77	2.77	49.0	56.8	1.19
26X-1, 103	236.83	1.68	2.78	61.2	62.3	1.04
26X-2, 85	238.15	1.68	2.66	56.2	59.2	1.08
26X-3, 121	240.01	1.77	2.70	47.0	55.2	1.20

Table 9 (continued).

Core, section, interval (cm)	Depth (mbsf)	Wet-bulk density (g/cm^3)	Grain density (g/cm^3)	Water content (% dry wt)	Porosity (%)	Dry-bulk density (g/cm^3)
130-804C- (Cont.)						
26X-4, 52	240.82	1.72	2.70	52.2	57.8	1.13
26X-5, 65	242.45	1.67	2.66	58.4	60.1	1.05
27X-1, 66	246.06	1.74	2.65	48.7	55.6	1.17
27X-3, 93	249.33	1.80	2.66	42.0	52.1	1.27
27X-6, 58	253.48	1.72	2.65	50.4	56.4	1.15
28X-1, 116	256.26	1.64	2.65	62.8	61.8	1.01
28X-2, 94	257.54	1.71	2.51	46.7	53.2	1.17
28X-5, 110	262.20	1.82	2.65	40.1	50.8	1.30
29X-4, 120	270.40	1.63	2.58	62.0	60.8	1.00
29X-5, 61	271.31	1.71	2.66	53.3	57.9	1.11
30X-2, 95	276.85	1.81	2.68	42.1	52.3	1.27
30X-3, 17	277.57	1.79	2.78	47.7	56.3	1.21
30X-4, 44	279.34	1.85	2.69	38.4	50.1	1.34
31X-1, 146	285.46	1.79	2.70	44.6	53.9	1.24
31X-2, 122	286.72	1.97	2.68	28.5	42.6	1.53
31X-4, 35	288.85	1.81	2.65	40.9	51.3	1.29
32X-1, 115	294.85	1.80	2.69	43.5	53.2	1.25
32X-2, 119	296.39	1.78	2.72	46.8	55.3	1.21
32X-3, 106	297.76	1.76	2.69	47.6	55.4	1.19
32X-4, 34	298.54	1.83	2.71	40.6	51.7	1.30
33X-1, 100	304.30	1.68	2.64	55.6	58.7	1.08
33X-2, 82	305.62	1.69	2.65	55.0	58.6	1.09
33X-3, 82	307.12	1.71	2.65	52.6	57.4	1.12
33X-4, 63	308.43	1.70	2.68	55.6	59.1	1.09
33X-5, 21	309.51	1.66	2.61	58.7	59.8	1.04

Table 10. *P*-wave velocity data, Site 804.

Core, section, interval (cm)	Depth (mbsf)	Vertical *P*-wave velocity (m/s)	Horizontal *P*-wave velocity (m/s)
130-804A-			
1H-1, 35	0.35	1531.8	1528.0
2H-1, 35	1.55	1536.8	1534.8
2H-1, 110	2.30	1517.2	1534.8
2H-2, 35	3.05	1514.0	1528.0
2H-2, 110	3.80	1517.2	1521.2
2H-3, 35	4.55	1526.9	1534.8
2H-3, 110	5.30	1523.7	1517.8
2H-4, 110	6.80	1514.0	1528.0
2H-4, 110	6.80	1551.8	1573.6
2H-5, 35	7.55	1520.4	1528.0
2H-5, 110	8.30	1515.6	1528.0
2H-6, 10	8.80		1528.0
2H-6, 35	9.05	1526.9	1534.8
2H-6, 110	9.80	1522.1	
2H-7, 5	10.25		1534.8
2H-7, 35	10.55	1540.1	
3H-1, 35	11.05	1531.8	1559.3
3H-1, 110	11.80	1523.7	1531.4
3H-2, 35	12.55	1528.6	1528.0
3H-2, 110	13.30	1531.8	1541.7
3H-3, 5	13.75		1534.8
3H-3, 35	14.05	1528.6	
3H-4, 35	15.55	1526.9	1534.8
3H-4, 110	16.30	1528.6	1534.8
3H-5, 35	17.05	1540.1	1534.8
3H-5, 110	17.80		1538.2
3H-6, 35	18.55	1535.1	1541.7
3H-6, 110	19.30	1538.4	1552.2
3H-7, 35	20.05	1526.9	1548.7
4H-1, 35	20.55	1518.8	
4H-1, 110	21.30		1524.6
4H-2, 35	22.05		1545.2
4H-2, 110	22.80		1548.7
4H-3, 35	23.55		1538.2
4H-3, 110	24.30		1534.8
4H-4, 30	25.00		1534.8
4H-4, 110	25.80		1541.7
4H-5, 35	26.55		1545.2
4H-5, 110	27.30	1523.7	1555.7
4H-6, 35	28.05	1526.9	1534.8
4H-6, 110	28.80	1515.8	1548.7
4H-7, 35	29.55	1523.7	1534.8
5H-1, 60	30.30		1545.2
5H-1, 112	30.82		1538.2
5H-2, 41	31.61		1528.0
5H-2, 110	32.30		1524.6
5H-3, 41	33.11	1522.1	1531.4
5H-4, 37	34.57		1517.8
5H-4, 125	35.45	1520.4	1538.2
5H-5, 45	36.15	1523.7	1531.4
5H-5, 115	36.85	1515.6	1521.2
5H-6, 34	37.54	1520.4	1528.0
5H-6, 125	38.45	1510.8	1528.0
5H-7, 40	39.10		1528.0
6H-1, 125	40.45	1517.2	
6H-2, 40	41.10	1520.4	
6H-2, 110	41.80		1521.2
6H-3, 58	42.78		1514.4
6H-3, 125	43.45	1512.4	1528.0
6H-4, 30	44.00	1515.6	1524.6
6H-4, 109	44.79	1515.6	1514.4
6H-5, 40	45.60	1538.4	1559.3
6H-5, 109	46.29	1525.3	1534.8
6H-6, 115	47.85	1526.9	1531.4
130-804B-			
1H-1, 35	0.35	1522.1	1534.8
1H-1, 105	1.05		1514.4
1H-2, 25	1.75	1531.8	1531.4
1H-2, 105	2.55	1541.7	1566.4
1H-3, 35	3.35		1517.8
2H-1, 50	5.20	1531.8	1524.6
2H-1, 110	5.80	1514.0	
2H-2, 35	6.55	1535.1	1548.7
2H-2, 115	7.35	1510.8	1528.0
2H-3, 25	7.95	1525.3	1541.7
2H-3, 120	8.90	1514.0	1517.8
2H-4, 25	9.45	1518.8	1517.8
2H-4, 105	10.25	1523.7	1517.8
2H-5, 30	11.00	1522.1	1528.0
2H-5, 130	12.00	1540.1	1541.7
2H-6, 25	12.45	1541.7	1545.2
2H-6, 115	13.35	1526.9	1545.2
2H-7, 50	14.20	1530.2	1534.8
3H-1, 115	15.35	1525.3	1531.4
3H-2, 35	16.05	1523.7	1524.6
3H-2, 115	16.85		1531.4
3H-3, 40	17.60		1534.8
3H-3, 117	18.37		1528.0
3H-4, 40	19.10		1541.7
3H-4, 105	19.75	1531.8	1552.2
3H-5, 35	20.55		1534.8
3H-5, 109	21.29	1518.8	1521.2
3H-6, 40	22.10	1520.4	1528.0
3H-6, 109	22.79	1518.8	1524.6
3H-7, 45	23.65	1518.8	1538.2
4H-1, 45	24.15	1538.4	1538.2
4H-1, 109	24.79	1530.2	1528.0
4H-2, 35	25.55		1521.2
4H-2, 109	26.29	1525.3	1524.6
4H-3, 40	27.10		1531.4
4H-3, 104	27.74		1517.8
4H-4, 30	28.50	1522.1	1521.2
4H-4, 109	29.29		1566.4
4H-5, 30	30.00	1515.6	1521.2
4H-5, 109	30.79	1517.2	1514.4
4H-6, 35	31.55	1518.8	1528.0
4H-6, 110	32.30		1517.8
4H-7, 35	33.05	1517.2	1514.4
5H-1, 120	34.40	1514.0	1521.2
5H-2, 109	35.79		1517.8
5H-3, 29	36.49		1517.8
5H-3, 125	37.45		1521.2
5H-4, 40	38.10		1521.2
5H-4, 110	38.90	1533.5	
5H-5, 30	39.50	1515.6	1524.6
5H-5, 115	40.35	1512.4	1534.8
5H-6, 35	41.05	1517.2	1534.8
5H 6, 109	41.79		1538.2
5H-7, 45	42.65	1517.2	1521.2
6H-1, 35	43.05	1531.0	1570.0
6H-1, 110	43.80		1555.7
6H-2, 35	44.55	1531.8	1555.7
6H-2, 35	44.55		1552.2
6H-2, 110	45.30		1552.2
6H-2, 110	45.30		1552.2
6H-4, 35	47.55	1536.8	1541.7
6H-4, 110	48.30	1543.4	1566.4
6H-5, 35	49.05	1531.8	1552.2
6H-5, 110	49.80	1533.5	1570.0
6H-6, 35	50.55	1543.4	1559.3
6H-6, 110	51.30	1525.3	1541.7
6H-7, 35	52.05	1525.3	1545.2
7H-1, 35	52.55	1540.1	1552.2
7H-1, 110	53.30	1531.8	1559.3
7H-2, 35	54.05	1543.4	1534.8
7H-2, 110	54.80	1536.8	1566.4
7H-3, 35	55.55	1553.5	1570.0
7H-3, 110	56.30	1536.8	1566.4
7H-4, 35	57.05	1541.7	1566.4
7H-4, 110	57.80	1548.4	1566.4
7H-5, 35	58.55	1533.5	1552.2
7H-5, 110	59.30	1528.6	1555.7
7H-6, 35	60.05	1553.5	
7H-6, 110	60.80	1541.7	1570.0
7H-7, 35	61.55	1555.1	1599.3
8H-1, 110	62.80	1545.1	1562.8
8H-2, 35	63.55	1560.2	1573.6
8H-2, 110	64.30	1577.4	1603.0
8H-3, 35	65.05	1570.5	1603.0
8H-3, 110	65.80	1556.8	1577.2
8H-4, 35	66.55	1574.0	1588.2
8H-4, 110	67.30	1560.2	1618.2
8H-5, 35	68.05	1548.4	1588.2
8H-5, 110	68.80	1570.5	1595.6
8H-6, 35	69.55	1541.7	1570.0
8H-6, 110	70.30	1541.7	1573.6
8H-7, 35	71.05	1546.7	1562.8
9H-1, 35	71.55	1538.4	1548.7
9H-1, 110	72.30	1541.7	1562.8
9H-2, 35	73.05	1530.2	1552.2
9H-2, 110	73.80	1541.7	1552.2
9H-3, 35	74.55	1531.8	1552.2
9H-3, 110	75.30	1535.1	1545.2
9H-4, 35	76.05	1533.5	1555.7
9H-4, 110	76.80	1541.7	1555.7
9H-5, 35	77.55	1535.1	1559.3
9H-5, 110	78.30	1535.1	1548.7
9H-6, 35	79.05	1538.4	1552.2
9H-6, 110	79.80	1545.1	1552.2
9H-7, 35	80.55	1543.4	1555.7
10H-1, 110	81.80	1545.1	1555.7
10H-2, 35	82.55	1555.1	1566.4
10H-2, 110	83.30	1545.1	1580.8
10H-3, 35	84.05	1545.1	1566.4
10H-3, 110	84.80	1540.1	1566.4
10H-4, 35	85.55	1538.4	1552.2
10H-4, 110	86.30	1541.7	1562.8
10H-5, 35	87.05	1546.7	1566.4
10H-5, 110	87.80	1536.8	1559.3
10H-6, 35	88.55	1533.5	1562.8
10H-6, 104	89.24	1531.8	1562.8
10H-7, 39	90.09	1538.4	1552.2
11H-1, 36	90.56	1536.8	1588.2
11H-1, 105	91.25	1535.1	1588.2
11H-2, 36	92.06	1536.8	1570.0
11H-2, 111	92.81	1579.2	1641.5
11H-2, 132	93.02	1545.1	1577.2
11H-3, 36	93.56	1546.7	1591.9
11H-3, 115	94.35	1548.4	1584.5
11H-4, 35	95.05	1545.1	1603.0
11H-4, 115	95.85	1515.6	1591.9
11H-5, 35	96.55	1530.2	1577.2
11H-5, 115	97.35	1545.1	1591.9
11H-6, 35	98.05	1531.8	1584.5
11H-6, 115	98.85	1550.1	1599.3
11H-7, 35	99.55	1570.5	1614.4
12H-1, 110	100.80	1551.8	1606.8
12H-2, 35	101.55	1548.4	1603.0
12H-2, 110	102.30	1561.9	1622.0
12H-3, 35	103.05	1567.1	1606.8
12H-3, 110	103.80	1558.5	1606.8
12H-4, 35	104.55	1584.4	1622.0
12H-4, 105	105.25	1555.1	1595.6
12H-5, 35	106.05	1570.5	1649.4
12H-5, 110	106.80	1555.1	1614.4
12H-6, 35	107.55	1546.4	1633.6
12H-6, 110	108.30	1551.8	1603.0
12H-7, 35	109.05	1561.9	1645.4
13H-1, 110	110.30	1543.4	1599.3
13H-2, 97	111.67		1633.6
13H-3, 35	112.55	1545.1	1610.6
13H-3, 110	113.30	1550.1	1584.5
13H-4, 35	114.05	1548.4	1610.6
13H-4, 136	115.06	1546.7	1595.6
14H-1, 100	119.70		1552.2
14H-2, 35	120.55		1577.2
14H-2, 108	121.28	1548.4	1591.9
14H-3, 35	122.05	1560.2	1588.2
14H-3, 108	122.78	1558.5	1570.0
14H-4, 35	123.55	1565.4	1599.3
14H-4, 108	124.28		1584.5
14H-5, 35	125.05		1591.9
14H-5, 108	125.78	1561.9	1591.9

Table 10 (continued).

Core, section, interval (cm)	Depth (mbsf)	Vertical *P*-wave velocity (m/s)	Horizontal *P*-wave velocity (m/s)
130-804B- (Cont.)			
14H-6, 38	126.58		1625.9
14H-6, 38	126.58		1618.2
14H-6, 108	127.28	1579.2	1618.2
14H-7, 51	128.21		1618.2
15H-1, 35	128.55		1649.4
15H-1, 105	129.25		1573.6
15H-2, 35	130.05	1523.7	1584.5
15H-2, 105	130.75	1528.6	1570.0
15H-3, 35	131.55		1588.2
15H-3, 108	132.28		1573.6
15H-4, 28	132.98	1520.4	1591.9
15H-4, 100	133.70	1540.1	1577.2
15H-5, 35	134.55		1595.6
15H-5, 105	135.25	1541.7	1584.5
15H-6, 108	136.78	1538.4	1588.2
15H-7, 40	137.60	1538.4	1595.6
130-804C-			
1H-3, 30	3.30	1518.00	1521.40
1H-3, 120	4.20	1526.10	1538.50
1H-4, 40	4.90	1521.20	1524.80
1H-4, 100	5.50	1529.40	1531.60
2H-1, 50	6.80	1531.00	1531.60
2H-1, 100	7.30	1534.30	1545.40
2H-2, 40	8.20	1526.10	1538.50
2H-2, 100	8.80	1527.70	1531.60
2H-3, 40	9.70	1518.00	1518.00
2H-3, 97	10.27	1521.20	1535.10
2H-4, 38	11.18	1527.70	1531.60
2H-4, 100	11.80	1545.90	1559.50
2H-5, 40	12.70	1521.20	1528.20
2H-5, 100	13.30	1540.90	1552.40
2H-6, 40	14.20	1527.70	1531.60
2H-6, 100	14.80	1544.20	1538.50
3H-1, 100	16.80	1531.00	1535.10
3H-2, 40	17.70	1519.60	1535.10
3H-2, 105	18.35	1537.60	1538.50
3H-3, 40	19.20	1529.40	1545.40
3H-3, 100	19.80	1526.10	1531.60
3H-4, 35	20.65	1537.60	1542.00
3H-4, 100	21.30		1524.80
3H-5, 35	22.15		1511.30
3H-5, 100	22.80		1518.00
3H-6, 40	23.70	1516.40	1524.80
3H-6, 100	24.30	1537.60	1531.60
4H-3, 120	29.50	1511.60	
4H-4, 40	30.20	1518.00	1518.00
4H-4, 100	30.80	1518.00	1524.80
4H-5, 100	32.30	1519.60	1528.20
4H-6, 35	33.15		1528.20
4H-6, 100	33.80	1518.00	1528.20
4H-7, 40	34.70	1514.80	1535.10
6H-2, 40	46.20	1532.60	1531.60
6H-2, 100	46.80	1524.50	1535.10
6H-3, 35	47.65	1526.10	1535.10
6H-3, 100	48.30	1532.60	1531.60
6H-4, 40	49.20	1532.60	1538.50
6H-4, 100	49.80	1532.60	1531.60
6H-5, 40	50.70	1534.30	1531.60
6H-5, 100	51.30	1535.90	1531.60
6H-6, 40	52.20	1529.40	1524.80
6H-6, 100	52.80	1531.00	1531.60
6H-7, 48	53.78	1540.90	1552.40
7H-2, 40	55.70	1526.10	1531.60
7H-2, 100	56.30	1531.00	1521.40
7H-3, 40	57.20	1524.50	1521.40
7H-3, 100	57.80	1529.40	1535.10
7H-4, 40	58.70	1537.60	1548.90
7H-4, 125	59.55	1545.90	1552.40
7H-5, 40	60.20	1544.20	1556.00
7H-5, 100	60.80	1549.30	1552.40
7H-6, 40	61.70	1540.90	1545.40
7H-6, 100	62.30	1549.30	1556.00
7H-7, 27	63.07	1542.60	1542.00

Table 10 (continued).

Core, section, interval (cm)	Depth (mbsf)	Vertical *P*-wave velocity (m/s)	Horizontal *P*-wave velocity (m/s)
130-804C- (Cont.)			
8H-1, 40	63.70	1545.90	1542.00
8H-1, 100	64.30	1561.10	1573.90
8H-2, 40	65.20	1549.30	1573.90
8H-2, 100	65.80	1554.30	1566.70
8H-3, 20	66.50	1551.00	
8H-3, 100	67.30	1524.50	1552.40
8H-3, 105	67.35		1524.80
8H-4, 40	68.20	1529.40	1535.10
8H-4, 100	68.80	1531.00	1535.10
8H-5, 37	69.67	1519.60	1521.40
8H-5, 100	70.30	1532.60	1531.60
8H-6, 40	71.20	1531.00	1524.80
8H-6, 100	71.80	1535.90	1542.00
8H-7, 40	72.70	1524.50	1535.10
9H-1, 125	74.05	1521.20	1521.40
9H-2, 35	74.65	1534.30	1545.40
9H-2, 110	75.40	1534.30	1545.40
9H-3, 35	76.15	1531.00	1538.50
9H-3, 115	76.95	1539.30	1542.00
9H-4, 35	77.65	1547.60	1581.10
9H-4, 110	78.40	1540.90	1545.40
9H-5, 35	79.15	1544.20	1566.70
9H-5, 115	79.95	1534.30	1545.40
10H-1, 110	83.40	1537.60	1545.40
10H-2, 35	84.15	1531.00	1542.00
10H-2, 110	84.90	1532.60	1548.90
10H-3, 35	85.65	1539.30	1556.00
10H-3, 110	86.40	1544.20	1552.40
10H-4, 35	87.15	1537.60	1559.50
10H-4, 117	87.97	1540.90	1559.50
10H-5, 35	88.65	1547.60	1552.40
10H-5, 110	89.40	1540.90	1556.00
11H-1, 35	92.15	1527.70	1535.10
11H-1, 110	92.90	1531.00	1552.40
11H-2, 35	93.65	1551.00	
11H-2, 108	94.38	1545.90	1556.00
11H-3, 35	95.15	1551.00	1595.90
11H-3, 110	95.90	1537.60	1570.20
11H-4, 35	96.65	1544.20	1545.40
11H-4, 100	97.30	1544.20	
11H-4, 110	97.40	1544.20	1607.10
11H-5, 35	98.15	1535.90	1538.50
11H-5, 110	98.90	1549.30	1588.40
11H-5, 110	98.90	1551.00	
11H-6, 35	99.65	1545.90	1577.50
11H-6, 110	100.40	1557.70	1581.10
12H-1, 110	102.40	1557.70	1610.90
12H-2, 35	103.15	1562.80	1607.10
12H-2, 110	103.90	1569.70	1607.10
12H-3, 35	104.65	1576.60	1622.30
12H-3, 110	105.40	1559.40	1599.60
12H-4, 35	106.15	1544.20	1610.90
12H-4, 110	106.90	1554.30	1603.30
12H-5, 35	107.65	1547.60	1588.40
12H-5, 110	108.40	1552.60	1599.60
12H-6, 35	109.15	1559.40	1595.90
12H-6, 110	109.90	1545.90	1614.70
12H-7, 35	110.65	1549.30	1603.30
13H-1, 35	111.15		1566.70
13H-1, 110	111.90	1535.90	
13H-2, 35	112.65	1537.60	1548.90
13H-2, 110	113.40		1581.10
13H-3, 35	114.15		1559.50
13H-3, 110	114.90		1563.10
13H-4, 35	115.65	1542.60	1563.10
13H-4, 110	116.40		1573.90
13H-5, 35	117.15		1566.70
13H-5, 110	117.90	1544.20	1573.90
13H-6, 35	118.65	1545.90	1595.90
13H-6, 110	119.40	1556.00	1581.10
14X-1, 35	120.65	1556.00	1563.10
14X-1, 110	121.40		1581.10
14X-2, 35	122.15	1549.30	1559.50
14X-2, 110	122.90	1549.30	1552.40
14X-3, 35	123.65	1564.50	1577.50

Table 10 (continued).

Core, section, interval (cm)	Depth (mbsf)	Vertical *P*-wave velocity (m/s)	Horizontal *P*-wave velocity (m/s)
130-804C- (Cont.)			
14X-3, 110	124.40	1566.30	1603.30
14X-4, 35	125.15	1557.70	1577.50
14X-4, 110	125.90	1556.00	1588.40
14X-5, 35	126.65	1551.00	1584.80
15X-1, 110	130.90	1564.50	1607.10
15X-2, 35	131.65	1527.70	1548.90
15X-2, 110	132.40	1524.50	1538.50
15X-3, 35	133.15		1521.40
15X-3, 110	133.90	1519.60	
16X-1, 37	139.67	1532.60	1535.10
16X-1, 105	140.35	1521.20	1542.00
16X-2, 54	141.34	1519.60	1542.00
17X-1, 35	149.15	1580.10	
17X-1, 110	149.90	1587.20	1599.60
17X-2, 110	151.40	1580.10	1573.90
17X-3, 35	152.15	1569.70	1595.90
17X-3, 113	152.93	1603.20	1599.60
17X-4, 37	153.67	1571.40	
17X-4, 110	154.40	1581.90	1622.30
17X-5, 35	155.15	1578.40	1599.60
17X-5, 110	155.90	1578.40	1614.70
17X-6, 35	156.65	1576.60	1581.10
17X-6, 110	157.40	1581.90	1610.90
18X-1, 110	159.40	1532.60	1528.20
18X-2, 35	160.15	1524.50	
18X-4, 130	164.10		1577.50
19X-1, 100	169.00		1657.60
19X-3, 35	171.35	1580.10	1626.20
19X-3, 105	172.05	1603.20	1649.70
19X-4, 35	172.85		1559.50
19X-4, 105	173.55	1585.40	1610.90
19X-5, 110	175.10		1573.90
20X-1, 35	178.05		1588.40
20X-1, 110	178.80		1618.50
20X-2, 29	179.49		1614.70
20X-3, 30	181.00		1521.40
20X-5, 90	184.60		1557.90
21X-1, 82	188.22	1562.70	1581.20
21X-2, 79	189.69		1546.40
21X-3, 81	191.21		1559.00
21X-4, 89	192.79		1566.50
22X-1, 104	198.14		1530.00
22X-2, 81	199.41		1525.90
22X-4, 40	202.00	1550.30	1558.10
22X-5, 2	203.12	1546.10	1523.20
23X-1, 75	207.55	1522.80	
23X-2, 70	209.00	1512.50	
23X-3, 48	210.28	1540.90	
23X-4, 28	211.58	1563.50	
23X-5, 35	213.15	1528.60	
24X-1, 94	217.44	1518.00	
24X-2, 94	218.94	1567.90	
25X-2, 98	228.68	1614.30	1620.90
25X-3, 56	229.76	1607.20	1597.80
25X-4, 96	231.66	1601.90	1607.50
25X-5, 76	232.96		1596.00
25X-6, 27	233.97		1555.60
26X-1, 102	236.82		1607.70
26X-2, 87	238.17		1591.90
26X-3, 122	240.02		1549.80
26X-4, 50	240.80	1559.40	1549.20
26X-5, 60	242.40		1568.70
27X-1, 60	246.00		1567.70
27X-3, 94	249.34		1741.80
27X-6, 60	253.50		1571.00
28X-1, 148	256.58		1531.90
28X-2, 119	257.79		1575.70
28X-4, 100	260.60		1552.80
28X-5, 111	262.21		1661.70
28X-6, 64	263.24		1604.10
29X-4, 120	270.40	1512.70	1523.50
29X-5, 58	271.28	1533.80	1555.80
30X-1, 109	275.49	1527.20	1555.80
30X-2, 96	276.86	1586.20	1559.10
30X-3, 18	277.58	1710.60	1607.30

Table 10 (continued).

Core, section, interval (cm)	Depth (mbsf)	Vertical *P*-wave velocity (m/s)	Horizontal *P*-wave velocity (m/s)
130-804C- (Cont.)			
30X-4, 45	279.35	1622.90	1597.90
31X-2, 123	286.73	1723.70	1744.50
32X-1, 116	294.86		1620.70
32X-2, 120	296.40	1700.20	1697.80
32X-3, 107	297.77	1617.70	1657.70
32X-4, 35	298.55		1632.00
32X-4, 36	298.56		1585.10
32X-CC, 13	301.09	1753.60	1832.80
33X-1, 101	304.31	1572.20	1583.20
33X-2, 83	305.42	1606.30	1542.20
33X-3, 83	306.92	1596.70	1584.20
33X-4, 64	308.23		1518.70
33X-5, 22	309.31	1566.40	1579.90

VOLUME
130

CHAPTER
7

TABLES
8, 9, 10, AND 11

Table 8. Carbonate and inorganic carbon data, Holes 805B and 805C.

Core, section, interval (cm)	Depth (mbsf)	Inorganic carbon (%)	$CaCO_3$ (%)
130-805B-			
1H-1, 109-111	1.09	10.29	85.70
1H-2, 109-111	2.59	10.58	88.10
1H-3, 109-111	4.09	10.74	89.50
1H-4, 109-111	5.59	9.86	82.10
1H-5, 25-27	6.25	10.18	84.80
2H-1, 106-108	7.76	10.34	86.10
2H-2, 111-113	9.31	10.73	89.40
2H-3, 117-119	10.87	10.14	84.50
2H-4, 109-111	12.29	10.35	86.20
2H-5, 110-112	13.80	10.25	85.40
2H-6, 110-112	15.30	10.52	87.60
3H-1, 109-111	17.29	10.33	86.00
3H-2, 110-112	18.80	10.98	91.50
3H-3, 110-112	20.30	10.86	90.50
3H-4, 110-112	21.80	10.60	88.30
3H-5, 110-112	23.30	10.55	87.90
3H-6, 109-111	24.79	10.34	86.10
4H-2, 109-111	28.29	10.19	84.90
4H-3, 109-111	29.79	10.51	87.50
4H-4, 109-111	31.29	10.43	86.90
4H-5, 110-112	32.80	10.56	88.00
4H-6, 109-111	34.29	10.82	90.10
5H-1, 109-111	36.29	11.03	91.90
5H-2, 109-111	37.79	10.63	88.50
5H-3, 109-111	39.29	10.54	87.80
5H-4, 109-111	40.79	11.02	91.80
5H-5, 109-111	42.29	10.86	90.50
5H-6, 109-111	43.79	10.87	90.50
6H-2, 109-111	47.29	10.45	87.00
6H-3, 109-111	48.79	10.96	91.30
6H-4, 109-111	50.29	10.59	88.20
6H-5, 109-111	51.79	10.91	90.90
6H-6, 109-111	53.29	11.03	91.90
7H-3, 132-134	58.52	10.55	87.90
7H-4, 45-46	59.15	10.96	91.30
7H-4, 105-106	59.75	11.10	92.50
7H-5, 104-105	61.24	11.07	92.20
8H-2, 105-107	66.25	11.05	92.00
8H-3, 104-106	67.74	10.84	90.30
8H-4, 105-107	69.25	10.83	90.20
8H-5, 100-102	70.70	10.87	90.50
8H-6, 90-92	72.10	10.88	90.60
9H-1, 104-106	74.24	10.40	86.60
9H-2, 104-106	75.74	10.87	90.50
9H-3, 106-108	77.26	10.77	89.70
9H-4, 104-106	78.74	10.80	90.00
9H-5, 104-106	80.24	10.69	89.00
9H-6, 104-106	81.74	10.78	89.80
10H-1, 104-106	83.74	10.60	88.30
10H-2, 104-106	85.24	10.56	88.00
10H-3, 104-106	86.74	11.12	92.60
10H-4, 104-106	88.24	10.67	88.90
10H-5, 104-106	89.74	10.70	89.10
10H-6, 104-106	91.24	10.83	90.20
10H-7, 59-61	92.29	11.03	91.90
11H-1, 104-106	93.24	11.00	91.60
11H-2, 104-106	94.74	10.97	91.40
11H-3, 104-106	96.24	10.84	90.30
11H-4, 104-106	97.74	10.72	89.30
11H-5, 104-106	99.24	10.73	89.40
11H-6, 104-106	100.74	11.27	93.90
12H-2, 104-106	104.24	10.93	91.00
12H-3, 104-106	105.74	11.18	93.10
12H-4, 104-106	107.24	10.86	90.50
12H-5, 110-112	108.80	10.81	90.00
12H-6, 110-112	110.30	11.07	92.20
13H-1, 110-112	112.30	10.86	90.50
13H-2, 109-111	113.79	10.97	91.40
13H-3, 110-112	115.30	11.10	92.50
13H-4, 109-111	116.79	10.78	89.80
13H-5, 109-111	118.29	10.97	91.40
13H-6, 108-110	119.78	10.78	89.80
14H-1, 110-112	121.80	10.85	90.40
14H-2, 110-112	123.30	11.02	91.80
130-805B- (Cont)			
14H-3, 110-112	124.80	10.74	89.50
14H-4, 116-118	126.36	10.96	91.30
14H-5, 108-110	127.78	10.40	86.60
14H-6, 109-111	129.29	10.79	89.90
14H-7, 44-46	130.14	11.20	93.30
15H-1, 110-112	131.30	11.25	93.70
15H-2, 35-37	132.05	11.08	92.30
15H-3, 35-37	133.55	10.93	91.00
15H-4, 37-39	135.07	11.07	92.20
15H-5, 35-37	136.55	11.09	92.40
15H-6, 35-37	138.05	11.26	93.80
16H-1, 35-37	140.05	11.23	93.50
16H-2, 33-35	141.53	11.21	93.40
16H-3, 33-35	143.03	11.13	92.70
16H-4, 33-35	144.53	11.15	92.90
16H-5, 34-35	146.04	11.15	92.90
16H-6, 35-37	147.55	11.21	93.40
16H-7, 33-35	149.03	11.14	92.80
17H-1, 33-35	149.53	10.87	90.50
17H-2, 34-36	151.04	11.09	92.40
17H-3, 35-37	152.55	11.10	92.50
17H-4, 35-37	154.05	11.16	93.00
17H-5, 35-37	155.55	11.10	92.50
17H-6, 34-36	157.04	11.44	95.30
17H-7, 33-35	158.53	11.33	94.40
18H-1, 108-110	159.78	11.32	94.30
18H-2, 35-37	160.55	11.16	93.00
18H-3, 35-37	162.05	11.33	94.40
18H-4, 33-35	163.53	11.40	95.00
18H-5, 35-37	165.05	11.31	94.20
18H-6, 34-36	166.54	11.34	94.50
19H-1, 110-112	169.30	11.27	93.90
19H-2, 35-37	170.05	11.18	93.10
19H-3, 34-36	171.54	11.45	95.40
19H-4, 59-61	173.29	11.30	94.10
19H-5, 57-59	174.77	11.23	93.50
19H-6, 29-31	175.99	11.26	93.80
20H-1, 51-53	178.21	11.31	94.20
20H-2, 31-33	179.51	11.20	93.30
20H-3, 33-35	181.03	11.15	92.90
20H-4, 34-36	182.54	11.06	92.10
20H-5, 32-34	184.02	11.14	92.80
20H-6, 34-36	185.54	11.20	93.30
21H-2, 34-36	189.04	11.34	94.50
21H-3, 34-36	190.54	11.27	93.90
21H-4, 34-36	192.04	11.21	93.40
21H-5, 35-37	193.55	11.11	92.50
21H-6, 35-37	195.05	11.11	92.50
22H-1, 109-111	197.79	11.20	93.30
22H-2, 35-37	198.55	11.31	94.20
22H-3, 33-35	200.03	11.19	93.20
22H-4, 33-35	201.53	11.03	91.90
22H-5, 35-37	203.05	11.06	92.10
22H-6, 34-36	204.54	11.20	93.30
22H-7, 34-36	206.04	10.93	91.00
23H-1, 34-36	206.54	11.06	92.10
23H-3, 34-36	209.54	10.99	91.50
23H-3, 35-37	209.55	11.15	92.90
23H-4, 34-36	211.04	10.85	90.40
23H-5, 34-36	212.54	11.17	93.00
23H-6, 44-46	214.14	10.95	91.20
23H-7, 26-28	215.46	11.14	92.80
24H-2, 67-69	217.87	11.15	92.90
24H-3, 34-36	219.04	10.79	89.90
24H-4, 40-42	220.60	10.69	89.00
24H-5, 39-41	222.09	10.77	89.70
24H-6, 34-36	223.54	10.94	91.10
24H-7, 34-36	225.04	10.79	89.90
25H-1, 110-111	226.30	10.91	90.90
25H-2, 105-107	227.75	10.35	86.20
25H-3, 107-108	229.27	10.97	91.40
25H-4, 104-107	230.74	11.10	92.50
25H-5, 108-109	232.28	11.65	97.00
25H-6, 103-104	233.73	11.39	94.90
26H-2, 107-108	237.27	10.99	91.50
26H-3, 113-114	238.83	10.96	91.30

Table 8 (continued).

Core, section, interval (cm)	Depth (mbsf)	Inorganic carbon (%)	$CaCO_3$ (%)
130-805B- (Cont)			
26H-4, 86–87	240.06	10.61	88.40
26H-5, 101–102	241.71	10.83	90.20
26H-6, 106–107	243.26	10.03	83.50
27H-3, 118–119	246.97	10.85	90.40
27H-4, 98–99	248.27	10.73	89.40
27H-5, 109–110	249.88	10.75	89.50
27H-7, 106–107	252.85	10.95	91.20
27H-8, 35–36	253.64	11.02	91.80
28H-1, 99–101	254.69	10.99	91.50
28H-2, 99–101	256.19	11.23	93.50
28H-3, 99–101	257.69	11.38	94.80
28H-4, 60–62	258.80	11.04	92.00
28H-6, 99–101	262.19	11.04	92.00
28H-7, 41–43	263.11	11.19	93.20
29X-1, 32–34	263.52	11.09	92.40
29X-2, 45–47	265.15	11.20	93.30
29X-3, 45–47	266.65	11.64	97.00
29X-4, 44–46	268.14	10.97	91.40
29X-5, 45–47	269.65	10.61	88.40
29X-6, 19–21	270.89	11.16	93.00
30X-1, 119–121	274.09	11.09	92.40
30X-4, 60–62	278.00	11.09	92.40
30X-5, 60–62	279.50	11.20	93.30
30X-6, 65–67	281.05	11.15	92.90
31X-2, 97–99	284.97	10.69	89.00
31X-5, 83–85	289.33	11.04	92.00
32X-2, 88–89	294.58	11.03	91.90
32X-3, 68–70	295.88	11.05	92.00
32X-4, 96–97	297.66	11.04	92.00
33X-2, 129–131	304.19	10.78	89.80
33X-4, 129–131	307.19	11.02	91.80
33X-6, 44–45	309.34	10.78	89.80
34X-1, 47–49	311.47	10.54	87.80
34X-2, 14–16	312.64	11.11	92.50
34X-3, 31–33	314.31	11.02	91.80
34X-4, 26–28	315.76	10.76	89.60
34X-5, 95–97	317.95	11.45	95.40
35X-1, 12–14	320.62	10.39	86.50
35X-2, 14–16	322.14	11.01	91.70
35X-3, 48–50	323.98	10.96	91.30
36X-1, 11–13	330.11	10.86	90.50
36X-2, 46–48	331.96	10.35	86.20
36X-3, 73–75	333.73	10.89	90.70
36X-4, 16–18	334.66	10.92	91.00
36X-5, 105–107	337.05	11.11	92.50
40X-1, 138–140	370.08	11.01	91.70
40X-2, 135–137	371.55	10.21	85.00
40X-3, 135–137	373.05	10.33	86.00
40X-4, 120–122	374.40	11.17	93.00
40X-5, 140–142	376.10	11.15	92.90
41X-1, 80–82	379.10	11.17	93.00
41X-2, 80–82	380.60	10.52	87.60
41X-3, 77–79	382.07	10.93	91.00
41X-4, 77–79	383.57	11.04	92.00
42X-1, 90–92	388.90	10.68	89.00
42X-2, 91–93	390.41	10.17	84.70
42X-3, 84–86	391.84	10.91	90.90
42X-4, 76–78	393.26	11.07	92.20
42X-5, 79–81	394.79	10.87	90.50
43X-1, 99–101	398.69	11.14	92.80
43X-2, 102–104	400.22	10.69	89.00
43X-3, 116–118	401.86	10.78	89.80
43X-4, 99–101	403.19	10.82	90.10
43X-5, 117–118	404.87	10.87	90.50
43X-6, 113–115	406.33	11.08	92.30
44X-1, 44–46	407.74	10.98	91.50
44X-2, 42–44	409.22	11.24	93.60
44X-3, 45–47	410.75	11.22	93.50
44X-4, 42–44	412.22	11.08	92.30
44X-5, 47–49	413.77	11.28	94.00
44X-6, 27–29	415.07	11.38	94.80
45X-1, 120–122	418.20	11.09	92.40
45X-3, 121–123	421.21	11.20	93.30
45X-4, 126–128	422.76	10.77	89.70
45X-5, 112–114	424.12	11.36	94.60

Table 8 (continued).

Core, section, interval (cm)	Depth (mbsf)	Inorganic carbon (%)	$CaCO_3$ (%)
130-805B- (Cont)			
45X-6, 64–66	425.14	11.40	95.00
46X-1, 126–128	427.76	11.29	94.00
46X-4, 80–82	431.80	11.08	92.30
47X-1, 23–25	436.23	11.05	92.00
48X-1, 85–87	446.35	10.76	89.60
48X-2, 109–111	448.09	11.13	92.70
48X-3, 102–104	449.52	11.28	94.00
48X-4, 80–82	450.80	11.07	92.20
48X-5, 53–55	452.03	10.91	90.90
49X-2, 93–94	457.53	11.36	94.60
49X-3, 88–90	458.98	11.40	95.00
49X-4, 42–44	460.02	10.96	91.30
49X-5, 139–141	462.49	11.36	94.60
49X-6, 59–61	463.19	11.13	92.70
50X-2, 128–130	467.58	10.76	89.60
50X-3, 98–100	468.78	11.32	94.30
50X-4, 62–64	469.92	11.47	95.50
130-805C-			
1H-1, 74–76	0.74	10.49	87.40
1H-2, 74–76	2.24	10.07	83.90
1H-3, 74–76	3.74	10.29	85.70
1H-4, 74–76	5.24	10.02	83.50
1H-5, 74–76	6.74	10.52	87.60
2H-3, 71–73	11.51	10.36	86.30
2H-4, 71–73	13.01	10.41	86.70
2H-5, 71–73	14.51	10.51	87.50
2H-6, 71–73	16.01	10.71	89.20
3H-2, 73–75	19.53	10.34	86.10
3H-3, 73–75	21.03	10.42	86.80
3H-5, 73–75	24.03	10.62	88.50
3H-6, 73–75	25.53	10.66	88.80
4H-1, 72–74	27.52	10.81	90.00
4H-2, 72–74	29.02	10.71	89.20
4H-5, 72–74	33.52	10.66	88.80
4H-6, 72–74	35.02	10.65	88.70
5H-2, 60–62	38.40	10.94	91.10
5H-3, 72–74	40.02	10.84	90.30
5H-4, 35–37	41.15	11.06	92.10
5H-5, 99–101	43.29	10.98	91.50
5H-6, 97–99	44.77	10.74	89.50
6H-1, 99–101	46.79	10.79	89.90
6H-2, 111–113	48.41	10.80	90.00
6H-3, 110–112	49.90	10.94	91.10
6H-4, 104–106	51.34	10.86	90.50
6H-5, 109–111	52.89	10.64	88.60
6H-6, 96–98	54.26	10.74	89.50
7H-6, 109–111	63.89	10.98	91.50
7H-7, 33–35	64.63	11.27	93.90
9H-1, 114–116	75.44	10.99	91.50
9H-2, 114–116	76.94	10.56	88.00
9H-3, 114–116	78.44	10.87	90.50
9H-4, 114–116	79.94	10.46	87.10
9H-5, 104–106	81.34	10.46	87.10
9H-6, 115–117	82.95	10.73	89.40
9H-7, 33–35	83.63	10.79	89.90
10H-5, 114–116	90.94	10.56	88.00
10H-6, 114–116	92.44	11.02	91.80
12H-1, 114–116	103.94	11.07	92.20
12H-2, 114–116	105.44	11.16	93.00
12H-3, 114–116	106.94	11.12	92.60
12H-4, 113–115	108.43	11.20	93.30
12H-5, 114–116	109.94	11.10	92.50
12H-6, 97–99	111.27	11.30	94.10
12H-7, 35–37	112.15	10.96	91.30
13H-3, 108–111	116.38	10.89	90.70
13H-4, 108–110	117.88	10.94	91.10
13H-5, 104–106	119.34	10.94	91.10
13H-6, 108–110	120.88	10.97	91.40
13H-7, 22–24	121.52	10.60	88.30
14H-3, 116–118	125.96	10.93	91.00
14H-4, 108–110	127.38	10.55	87.90
14H-5, 110–112	128.90	10.40	86.60
14H-6, 108–110	130.38	11.14	92.80

Table 8 (continued).

Core, section, interval (cm)	Depth (mbsf)	Inorganic carbon (%)	$CaCO_3$ (%)
130-805C- (Cont)			
14H-7, 35-37	131.15	10.97	91.40
15H-1, 108-110	132.38	10.97	91.40
15H-2, 108-110	133.88	10.88	90.60
15H-3, 109-111	135.39	11.20	93.30
15H-4, 97-99	136.77	11.28	94.00
15H-5, 109-111	138.39	11.22	93.50
15H-6, 114-116	139.94	11.44	95.30
16H-1, 114-116	141.94	11.16	93.00
16H-2, 113-115	143.43	11.31	94.20
16H-3, 112-114	144.92	11.25	93.70
16H-4, 115-117	146.45	11.29	94.00
16H-5, 115-117	147.95	11.17	93.00
16H-6, 115-117	149.45	11.11	92.50
17H-1, 115-117	151.45	11.13	92.70
17H-2, 115-117	152.95	11.22	93.50
17H-3, 115-117	154.45	11.17	93.00
17H-4, 115-117	155.95	11.24	93.60
17H-5, 115-117	157.45	11.23	93.50
17H-6, 115-117	158.95	11.23	93.50
18H-1, 115-117	160.95	11.25	93.70
18H-2, 115-117	162.45	11.28	94.00
18H-3, 115-117	163.95	11.34	94.50
18H-4, 94-96	165.24	11.13	92.70
18H-5, 115-117	166.95	11.27	93.90
18H-6, 115-117	168.45	11.32	94.30
19H-1, 115-117	170.45	11.29	94.00
19H-2, 115-117	171.95	11.36	94.60
19H-3, 115-117	173.45	11.22	93.50
19H-4, 115-117	174.95	11.29	94.00
19H-5, 115-117	176.45	11.14	92.80
19H-6, 110-112	177.90	11.10	92.50
19H-7, 26-28	178.56	11.10	92.50
20H-2, 104-106	181.34	11.32	94.30
20H-3, 104-106	182.84	11.22	93.50
20H-4, 90-92	184.20	11.24	93.60
20H-5, 74-76	185.54	11.28	94.00
20H-6, 105-107	187.35	11.10	92.50
21H-1, 105-107	189.35	11.35	94.50
21H-2, 105-107	190.85	11.43	95.20
21H-3, 105-107	192.35	11.37	94.70
21H-4, 105-107	193.85	11.51	95.90
21H-5, 105-107	195.35	11.49	95.70
21H-6, 105-107	196.85	11.37	94.70
22H-1, 105-106	198.85	11.09	92.40
22H-2, 105-106	200.35	11.16	93.00
22H-3, 105-106	201.85	11.08	92.30
22H-4, 90-91	203.20	11.04	92.00
22H-5, 104-105	204.84	10.87	90.50
22H-7, 34-35	207.14	11.04	92.00
23H-1, 105-106	208.35	11.23	93.50
23H-2, 30-31	209.10	10.47	87.20
24H-1, 35-36	217.15	10.81	90.00
24H-2, 105-106	219.35	10.97	91.40
24H-3, 38-39	220.18	10.66	88.80
24H-4, 35-36	221.65	10.62	88.50
24H-5, 104-105	223.84	10.65	88.70
24H-6, 105-106	225.35	10.78	89.80
25H-4, 105-107	231.85	10.99	91.50
25H-5, 95-97	233.25	11.17	93.00
25H-6, 99-101	234.79	11.22	93.50
25H-7, 44-46	235.74	11.16	93.00
26X-1, 99-101	236.79	10.87	90.50
26X-3, 131-133	240.11	10.66	88.80
26X-4, 107-109	241.37	10.56	88.00
26X-5, 119-121	242.99	10.77	89.70
26X-6, 106-108	244.36	10.83	90.20
27X-1, 102-104	246.42	10.84	90.30
28X-2, 104-106	257.64	11.21	93.40
28X-3, 45-47	258.55	11.34	94.50
28X-4, 42-44	260.02	11.21	93.40
28X-6, 19-21	262.79	11.00	91.60
29X-2, 94-96	267.14	11.06	92.10
29X-3, 96-98	268.66	11.05	92.00
29X-4, 113-115	270.33	10.55	87.90
29X-5, 91-93	271.61	11.02	91.80

Table 8 (continued).

Core, section, interval (cm)	Depth (mbsf)	Inorganic carbon (%)	$CaCO_3$ (%)
130-805C- (Cont)			
29X-6, 82-84	273.02	11.36	94.60
30X-1, 87-89	275.27	11.18	93.10
30X-2, 71-73	276.61	11.10	92.50
30X-3 69-71	278.09	11.20	93.30
30X-4, 49-51	279.39	10.96	91.30
30X-5, 92-94	281.32	10.86	90.50
31X-1, 107-108	285.07	11.09	92.40
31X-2, 73-75	286.23	10.94	91.10
31X-3, 122-124	288.22	10.93	91.00
32X-1, 120-122	294.90	11.02	91.80
32X-2, 141-143	296.61	11.19	93.20
32X-3, 121-123	297.91	11.15	92.90
32X-4, 93-95	299.13	11.28	94.00
32X-6, 13-15	301.33	11.09	92.40
33X-1, 35-37	303.25	10.67	88.90
33X-2, 4-6	304.44	11.05	92.00
33X-3, 50-52	306.40	11.15	92.90
33X-4, 131-133	308.71	11.10	92.50
33X-5, 139-141	310.29	11.05	92.00
34X-2, 46-48	314.56	11.00	91.60
34X-3, 139-141	316.99	10.59	88.20
34X-4, 28-30	317.38	10.48	87.30
34X-5, 43-45	319.03	10.54	87.80
35X-2, 80-82	324.60	11.23	93.50
35X-3, 112-114	326.42	10.94	91.10
35X-4, 114-116	327.94	11.02	91.80
35X-5, 49-51	328.79	11.60	96.60
36X-1, 66-68	332.46	10.86	90.50
36X-2, 63-65	333.93	11.26	93.80
36X-3, 62-64	335.42	11.28	94.00
36X-4, 79-81	337.09	11.07	92.20
36X-5, 99-101	338.79	10.86	90.50
36X-6, 69-71	339.99	11.16	93.00
37X-1, 61-63	342.11	10.77	89.70
37X-2, 56-58	343.56	11.24	93.60
37X-3, 14-16	344.64	11.21	93.40
37X-5, 94-96	348.44	11.21	93.40
38X-1, 72-74	351.92	11.10	92.50
38X-2, 57-59	353.27	11.14	92.80
38X-3, 52-54	354.72	10.83	90.20
38X-4, 99-101	356.69	11.27	93.90
38X-5, 46-47	357.66	11.24	93.60
38X-6, 98-100	359.68	11.27	93.90
39X-1, 59-61	361.49	10.83	90.20
39X-3, 79-81	364.69	10.41	86.70
39X-4, 94-96	366.34	10.70	89.10
39X-5, 115-117	368.05	10.56	88.00
39X-6, 109-111	369.49	11.14	92.80
40X-1, 98-100	371.58	11.05	92.00
40X-2, 125-127	373.35	11.31	94.20
40X-3, 25-27	373.85	10.23	85.20
40X-4, 123-125	376.33	11.18	93.10
40X-5, 133-135	377.93	11.26	93.80
41X-1, 110-112	381.40	11.04	92.00
41X-2, 61-63	382.41	10.83	90.20
41X-3, 43-45	383.73	10.94	91.10
41X-4, 71-73	385.51	10.62	88.50
42X-1, 67-69	390.57	10.42	86.80
42X-3, 40-42	393.30	11.35	94.50
43X-1, 34-36	399.84	11.18	93.10
43X-2, 33-35	401.33	11.06	92.10
43X-3, 77-79	403.27	11.24	93.60
43X-4, 50-52	404.50	10.88	90.60
43X-5, 25-27	405.75	11.08	92.30
43X-6, 13-15	407.13	11.09	92.40
44X-1, 26-28	409.36	11.06	92.10
44X-2, 38-40	410.98	11.33	94.40
44X-4, 54-56	414.14	11.23	93.50
44X-5, 10-12	415.20	11.46	95.50
44X-6, 8-10	416.68	11.17	93.00
45X-1, 103-105	419.73	11.35	94.50
45X-2, 24-26	420.44	11.09	92.40
45X-3, 123-125	422.93	10.86	90.50
45X-4, 137-139	424.57	11.20	93.30
45X-5, 146-148	426.16	11.06	92.10

Table 8 (continued).

Core, section, interval (cm)	Depth (mbsf)	Inorganic carbon (%)	$CaCO_3$ (%)
130-805C- (Cont)			
46X-1, 84-86	429.24	11.17	93.00
46X-2, 96-98	430.86	10.72	89.30
46X-3, 83-85	432.23	11.15	92.90
46X-4, 54-56	433.44	11.13	92.70
46X-5, 35-37	434.75	11.27	93.90
46X-6, 32-34	436.22	11.13	92.70
47X-1, 95-97	439.05	11.02	91.80
47X-2, 81-83	440.41	11.11	92.50
47X-3, 79-81	441.89	10.98	91.50
47X-4, 81-83	443.41	10.35	86.20
47X-5, 52-54	444.62	10.54	87.80
47X-6, 90-92	446.50	11.22	93.50
48X-1, 96-98	448.66	11.16	93.00
48X-2, 98-100	450.18	11.15	92.90
48X-3, 90-92	451.60	11.03	91.90
48X-4, 94-96	453.14	11.09	92.40
48X-5, 86-88	454.56	11.20	93.30
49X-2, 83-85	459.73	10.77	89.70
49X-3, 103-105	461.43	11.00	91.60
50X-1, 128-130	468.28	11.35	94.50
50X-2, 94-96	469.44	11.46	95.50
50X-3, 90-92	470.90	11.28	94.00
50X-4, 75-77	472.25	11.26	93.80
51X-1, 137-139	476.87	10.79	89.90
51X-2, 115-117	478.15	11.11	92.50
51X-3, 106-108	479.56	11.07	92.20
51X-4, 78-80	480.78	11.02	91.80
51X-5, 74-76	482.24	11.15	92.90
52X-1, 105-107	486.25	11.14	92.80
52X-2, 60-62	487.30	11.08	92.30
52X-3, 88-90	489.08	11.13	92.70
52X-4, 48-50	490.18	10.90	90.80
53X-1, 88-90	495.78	11.24	93.60
53X-2, 72-74	497.12	11.14	92.80
53X-3, 9-11	497.99	11.11	92.50
53X-4, 84-86	500.24	10.91	90.90
53X-5, 55-57	501.45	10.93	91.00
54X-1, 55-57	505.15	11.24	93.60
54X-2, 72-74	506.82	11.32	94.30
54X-3, 109-111	508.69	11.04	92.00
54X-4, 59-61	509.69	10.28	85.60
55X-1, 66-68	514.86	11.14	92.80
55X-2, 46-48	516.16	11.35	94.50
55X-3, 43-45	517.63	10.74	89.50
55X-CC, 33-35	518.29	10.96	91.30
57X-1, 55-57	534.05	10.98	91.50
57X-2, 83-85	535.83	11.02	91.80
58X-1, 45-47	543.65	11.43	95.20
59X-1, 13-15	553.03	10.56	88.00
59X-2, 19-21	554.59	10.72	89.30
60X-1, 44-46	563.04	11.26	93.80
61X-1, 29-31	572.59	11.20	93.30
61X-2, 63-65	574.43	10.53	87.70
61X-3, 108-110	576.38	11.30	94.10
61X-5, 133-135	579.63	11.31	94.20
62X-1, 121-123	583.21	11.08	92.30
62X-2, 122-124	584.72	11.40	95.00
62X-3, 114-116	586.14	11.02	91.80
63X-1, 105-107	592.75	11.44	95.30
63X-2, 49-51	593.69	11.34	94.50
64X-1, 12-14	601.42	11.25	93.70

Table 9. Laboratory vane shear strength, Holes 805B and 805C.

Core, section, interval (cm)	Depth (mbsf)	Peak shear strength (kPa)	Residual shear strength (kPa)
130-805B-			
22H-6, 120	205.40	9	5
23H-2, 120	208.90	15	2
23H-3, 120	210.40	16	2
23H-4, 110	211.80	11	
23H-5, 120	213.40	13	
23H-6, 120	214.90	8	
23H-7, 50	215.70	12	3
24H-1, 140	217.10	16	4
24H-3, 139	220.09	13	4
25H-5, 122	232.42	13	4
25H-6, 122	233.92	16	
25H-7, 60	234.80	11	3
130-805C-			
1H-1, 44	0.44	4	2
1H-1, 104	1.04	5	2
1H-2, 44	1.94	5	2
1H-2, 104	2.54	5	
1H-3, 104	4.04	3	
1H-4, 104	5.54	17	
1H-5, 45	6.45	14	7
2H-3, 44	11.24	7	
2H-3, 104	11.84	9	3
2H-4, 45	12.75	9	
2H-4, 108	13.38	9	4
2H-5, 45	14.25	14	7
2H-5, 105	14.85	9	3
2H-6, 43	15.73	12	6
2H-6, 104	16.34	11	
2H-7, 45	17.25	9	4
3H-2, 45	19.25	12	2
3H-2, 105	19.85	7	2
3H-3, 105	21.35	12	
3H-5, 45	23.75	9	
3H-4, 45	22.25	13	
3H-4, 105	22.85	14	
3H-5, 43	23.73	22	
3H-5, 103	24.33	16	
3H-6, 45	25.25	16	
3H-6, 105	25.85	16	5
4H-1, 45	27.25	14	5
4H-1, 105	27.85	16	7
4H-2, 45	28.75	11	4
4H-2, 105	29.35	6	3
4H-5, 105	33.85	14	6
4H-7, 35	36.15	17	6
5H-2, 105	38.85	10	5
5H-3, 105	40.35	13	
5H-4, 105	41.85	12	3
5H-5, 105	43.35	13	2
5H-6, 45	44.25	20	
5H-6, 105	44.85	9	
6H-1, 110	46.90	10	2
6H-2, 128	48.58	10	
6H-3, 120	50.00	9	3
6H-4, 115	51.45	8	
6H-5, 120	53.00	9	3
6H-6, 120	54.50	5	2
7H-6, 122	64.02	8	2
9H-1, 105	75.35	13	3
9H-2, 105	76.85	15	
9H-3, 105	78.35	12	
9H-4, 105	79.85	17	
9H-5, 105	81.35	10	
9H-6, 105	82.85	14	
10H-5, 105	90.85	2	
10H-6, 105	92.35	10	3
11H-1, 105	94.35	10	2
11H-2, 105	95.85	11	
11H-3, 105	97.35	8	
11H-4, 105	98.85	8	
11H-5, 105	100.35	8	
130-805C- (Cont)			
11H-6, 105	101.85	10	3
13H-3, 18	115.48	11	1
13H-4, 123	118.03	11	
13H-5, 121	119.51	19	3
13H-6, 121	121.01	19	
14H-3, 123	126.03	15	3
14H-4, 121	127.51	20	
14H-5, 123	129.03	17	
14H-6, 117	130.47	11	
15H-1, 122	132.52	16	
15H-2, 121	134.01	15	
15H-3, 121	135.51	13	
15H-4, 105	136.85	10	
15H-5, 121	138.51	12	4
15H-6, 119	139.99	8	
16H-1, 105	141.85	10	
16H-2, 105	143.35	8	
16H-3, 105	144.85	9	2
16H-4, 105	146.35	14	
16H-5, 105	147.85	17	
16H-6, 105	149.35	15	
17H-2, 105	152.85	7	
17H-3, 105	154.35	11	
17H-4, 105	155.85	14	2
17H-5, 105	157.35	10	
17H-6, 105	158.85	8	3
18H-1, 105	160.85	15	
18H-2, 105	162.35	13	
18H-3, 105	163.85	10	
18H-4, 105	165.35	11	
18H-5, 105	166.85	8	
18H-6, 105	168.35	11	
19H-1, 105	170.35	15	
19H-2, 105	171.85	10	
19H-3, 105	173.35	6	
19H-4, 105	174.85	10	
19H-5, 105	176.35	10	
19H-6, 105	177.85	15	
19H-7, 45	178.75	19	
20H-2, 130	181.60	8	
20H-3, 130	183.10	9	
20H-4, 130	184.60	6	
20H-5, 125	186.05	11	
20H-6, 130	187.60	13	
21H-1, 135	189.65	8	
21H-2, 131	191.11	13	
21H-3, 131	192.61	11	
21H-4, 131	194.11	12	
21H-5, 130	195.60	16	
21H-6, 135	197.15	10	3
22H-1, 140	199.20	13	
22H-2, 140	200.70	13	
22H-3, 140	202.20	16	
22H-4, 140	203.70	9	2
22H-5, 130	205.10	7	
22H-6, 140	206.70	16	
22H-7, 60	207.40	14	
23H-1, 140	208.70	19	
23H-2, 40	209.20	14	
24H-1, 140	218.20	17	
24H-2, 141	219.71	21	
24H-3, 140	221.20	22	
24H-4, 140	222.70	24	
24H-5, 130	224.10	19	
24H-6, 139	225.69	10	
24H-7, 40	226.20	9	
25H-3, 140	230.70	17	
25H-4, 135	232.15	11	

Table 10. Discrete index properties, Holes 805B and 805C.

Core, section, interval (cm)	Depth (mbsf)	Wet-bulk density (g/cm³)	Grain density (g/cm³)	Water content (% dry wt)	Porosity (%)	Dry-bulk density (g/cm³)
130-805B-						
1H-1, 109	1.09	1.45	2.66	107.	73.3	0.70
1H-2, 109	2.59	1.51	2.70	90.	70.2	0.79
1H-3, 109	4.09	1.52	2.67	87.6	69.3	0.81
1H-4, 109	5.59	1.49	2.71	96.5	71.6	0.76
1H-5, 25	6.25	1.54	2.70	83.1	68.4	0.84
2H-1, 106	7.76	1.53	2.70	86.6	69.3	0.82
2H-2, 111	9.31	1.55	2.69	81.1	68.0	0.85
2H-3, 117	10.87	1.55	2.73	84.0	68.9	0.84
2H-4, 109	12.29	1.54	2.67	82.2	68.0	0.85
2H-5, 110	13.80	1.55	2.68	81.1	67.8	0.86
2H-6, 110	15.30	1.59	2.71	74.6	66.2	0.91
3H-1, 109	17.29	1.51	2.70	96.8	70.3	0.79
3H-2, 110	18.80	1.55	2.76	85.7	69.0	0.84
3H-3, 110	20.30	1.53	2.68	86.0	69.0	0.82
3H-4, 110	21.80	1.51	2.74	92.4	71.0	0.79
3H-5, 110	23.30	1.55	2.74	84.6	69.1	0.84
3H-6, 109	24.79	1.56	2.71	79.2	67.5	0.87
4H-2, 109	28.29	1.53	2.68	86.3	69.1	0.82
4H-3, 109	29.79	1.56	2.70	78.9	67.3	0.87
4H-4, 109	31.29	1.58	2.70	76.2	66.6	0.89
4H-5, 110	32.80	1.55	2.70	82.1	68.2	0.85
4H-6, 109	34.29	1.51	2.69	92.4	70.6	0.78
5H-1, 109	36.29	1.60	2.69	70.7	64.8	0.94
5H-2, 109	37.79	1.57	2.68	76.7	66.6	0.89
5H-3, 109	39.29	1.62	2.65	67.1	63.	0.97
5H-4, 109	40.79	1.62	2.72	68.8	64.4	0.96
5H-6, 109	43.79	1.53	2.74	89.2	70.2	0.81
6H-2, 109	47.29	1.57	2.70	78.0	67.0	0.88
6H-3, 109	48.79	1.56	2.66	77.3	66.6	0.88
6H-4, 109	50.29	1.62	2.71	68.3	64.2	0.96
6H-5, 109	51.79	1.58	2.70	75.3	66.3	0.90
6H-6, 109	53.29	1.59	2.72	74.6	66.3	0.91
7H-3, 132	58.52	1.55	2.67	80.5	67.5	0.86
7H-4, 45	59.15	1.59	2.72	74.1	66.1	0.91
7H-5, 105	61.25	1.52	2.69	88.1	69.6	0.81
7H-6, 104	62.74	1.57	2.70	77.4	66.9	0.89
8H-2, 105	66.25	1.58	2.68	74.6	65.9	0.91
8H-3, 104	67.74	1.59	2.73	75.2	66.5	0.91
8H-4, 105	69.25	1.59	2.68	72.7	65.4	0.92
8H-5, 100	70.70	1.59	2.73	75.2	66.5	0.91
8H-6, 90	72.10	1.58	2.68	75.0	66.3	0.96
9H-1, 104	74.24	1.57	2.66	75.6	66.0	0.89
9H-2, 104	75.74	1.57	2.68	76.1	66.4	0.89
9H-3, 104	77.24	1.57	2.77	80.7	68.4	0.87
9H-4, 104	78.74	1.59	2.67	72.7	65.3	0.92
9H-5, 104	80.24	1.60	2.69	70.8	64.9	0.94
9H-6, 104	81.74	1.59	2.68	72.1	65.1	0.93
10H-1, 104	83.74	1.58	2.69	74.3	65.9	0.91
10H-2, 104	85.24	1.60	2.70	71.4	65.1	0.93
10H-3, 104	86.74	1.59	2.72	73.8	66.0	0.92
10H-4, 104	88.24	1.59	2.67	72.7	65.2	0.92
10H-5, 104	89.74	1.60	2.69	72.1	65.3	0.93
10H-6, 104	91.24	1.62	2.69	67.1	63.6	0.97
10H-7, 59	92.29	1.61	2.70	70.1	64.7	0.95
11H-1, 104	93.24	1.59	2.70	73.0	65.6	0.92
11H-2, 104	94.74	1.60	2.73	72.1	65.6	0.93
11H-3, 104	96.24	1.64	2.68	64.0	62.4	1.00
11H-4, 104	97.74	1.61	2.69	69.9	64.5	0.95
11H-5, 104	99.24	1.64	2.74	66.7	63.9	0.98
11H-6, 104	100.74	1.61	2.71	69.6	64.6	0.95
12H-2, 104	104.24	1.65	2.70	63.5	62.4	1.01
12H-3, 104	105.74	1.64	2.69	64.1	62.6	1.00
12H-4, 104	107.24	1.59	2.71	74.4	66.1	0.91
12H-5, 110	108.80	1.61	2.71	69.7	64.7	0.95
12H-6, 110	110.30	1.62	2.69	68.4	64.1	0.96
13H-1, 110	112.30	1.64	2.72	65.9	63.4	0.99
13H-2, 109	113.79	1.61	2.69	69.6	64.4	0.95
13H-3, 110	115.30	1.63	2.69	66.2	63.3	0.98
13H-4, 109	116.79	1.64	2.68	64.3	62.5	1.00
13H-5, 109	118.29	1.65	2.69	63.0	62.2	1.01
13H-6, 108	119.78	1.63	2.70	67.4	63.8	0.97
14H-1, 110	121.80	1.67	2.72	58.5	60.6	1.06
14H-2, 110	123.30	1.68	2.71	58.9	60.7	1.06
14H-3, 110	124.80	1.66	2.72	61.3	61.7	1.03

Table 10 (continued).

Core, section, interval (cm)	Depth (mbsf)	Wet-bulk density (g/cm³)	Grain density (g/cm³)	Water content (% dry wt)	Porosity (%)	Dry-bulk density (g/cm³)
130-805B- (Cont)						
14H-4, 116	126.36	1.64	2.70	64.6	62.8	1.00
14H-5, 108	127.78	1.61	2.73	70.3	65.0	0.95
14H-6, 109	129.29	1.67	2.73	61.0	61.7	1.04
14H-7, 44	130.14	1.66	2.70	61.2	61.5	1.03
15H-1, 110	131.30	1.63	2.67	64.3	62.4	1.00
15H-2, 35	132.05	1.67	2.68	59.4	60.7	1.05
15H-2, 108	132.78	1.66	2.69	61.5	61.5	1.03
15H-3, 35	133.55	1.64	2.70	64.7	62.9	1.00
15H-3, 109	134.29	1.57	2.72	78.4	67.4	0.88
15H-4, 37	135.07	1.67	2.72	59.8	61.2	1.05
15H-4, 109	135.79	1.66	2.72	62.3	62.1	1.02
15H-5, 35	136.55	1.65	2.67	61.4	61.4	1.02
15H-5, 110	137.30	1.68	2.72	59.1	60.9	1.06
15H-6, 35	138.05	1.68	2.70	58.4	60.5	1.06
15H-6, 105	138.75	1.67	2.69	60.1	61.1	1.04
16H-1, 35	140.05	1.64	2.72	65.4	63.2	0.99
16H-1, 110	140.80	1.65	2.70	62.1	61.9	1.02
16H-2, 33	141.53	1.64	2.69	64.5	62.7	1.00
16H-2, 110	142.30	1.64	2.72	65.3	63.2	0.99
16H-3, 33	143.03	1.61	2.69	68.3	64.2	0.96
16H-3, 110	143.80	1.63	2.69	65.9	63.2	0.98
16H-4, 33	144.53	1.68	2.68	57.0	59.6	1.07
16H-4, 110	145.30	1.67	2.70	60.2	61.1	1.04
16H-5, 34	146.04	1.68	2.68	58.4	60.3	1.06
16H-5, 110	146.80	1.66	2.71	62.5	62.1	1.02
16H-6, 35	147.55	1.70	2.68	55.0	58.9	1.10
16H-6, 110	148.30	1.68	2.70	58.7	60.6	1.06
16H-7, 33	149.03	1.65	2.69	62.4	62.0	1.02
17H-1, 33	149.53	1.62	2.68	67.8	63.8	0.96
17H-1, 109	150.29	1.65	2.69	61.8	61.7	1.02
17H-2, 34	151.04	1.71	2.70	54.6	58.8	1.10
17H-2, 109	151.79	1.68	2.71	59.2	60.9	1.05
17H-3, 35	152.55	1.71	2.70	53.8	58.5	1.11
17H-3, 109	153.29	1.66	2.69	60.5	61.2	1.04
17H-4, 35	154.05	1.68	2.70	59.0	60.7	1.05
17H-4, 109	154.79	1.68	2.70	58.4	60.4	1.06
17H-5, 35	155.55	1.66	2.69	60.9	61.4	1.03
17H-5, 109	156.29	1.70	2.68	54.5	58.6	1.10
17H-6, 34	157.04	1.69	2.70	57.4	60.0	1.07
17H-6, 109	157.79	1.68	2.67	57.3	59.8	1.07
17H-7, 33	158.53	1.71	2.71	54.8	59.0	1.10
18H-1, 108	159.78	1.67	2.69	59.4	60.8	1.05
18H-2, 35	160.55	1.68	2.70	58.5	60.4	1.06
18H-2, 108	161.28	1.70	2.69	55.6	59.2	1.09
18H-3, 109	162.79	1.67	2.70	59.6	61.0	1.05
18H-4, 33	163.53	1.68	2.71	58.9	60.8	1.06
18H-4, 106	164.26	1.67	2.69	60.3	61.1	1.04
18H-5, 35	165.05	1.70	2.71	56.0	59.5	1.09
18H-5, 108	165.78	1.67	2.71	59.4	60.9	1.05
18H-6, 34	166.54	1.70	2.69	55.3	59.1	1.09
18H-6, 109	167.29	1.69	2.71	58.0	60.4	1.07
19H-1, 110	169.30	1.70	2.67	53.9	58.3	1.11
19H-2, 35	170.05	1.65	2.67	61.3	61.4	1.03
19H-2, 108	170.78	1.68	2.71	57.9	60.3	1.07
19H-3, 34	171.54	1.69	2.70	56.4	59.6	1.08
19H-3, 108	172.28	1.68	2.72	59.4	61.1	1.05
19H-4, 59	173.29	1.69	2.69	57.0	59.8	1.08
19H-4, 119	173.89	1.68	2.70	58.1	60.4	1.06
19H-5, 57	174.77	1.69	2.68	55.8	59.2	1.09
19H-5, 111	175.31	1.67	2.68	59.5	60.7	1.05
19H-6, 29	175.99	1.67	2.68	58.8	60.4	1.05
20H-1, 51	178.21	1.65	2.66	60.9	61.1	1.03
20H-1, 105	178.75	1.66	2.70	61.0	61.5	1.03
20H-2, 34	179.54	1.65	2.67	61.6	61.4	1.02
20H-2, 104	180.24	1.70	2.71	55.2	59.2	1.10
20H-3, 33	181.03	1.69	2.7[illegible]	58.1	60.6	1.07
20H-3, 104	181.74	1.67	2.69	60.5	61.1	1.04
20H-4, 34	182.54	1.68	2.79	60.[illegible]	62.1	1.05
20H-4, 104	183.24	1.66	2.73	61.5	62.0	1.03
20H-5, 32	184.02	1.70	2.74	56.3	60.1	1.09
20H-5, 104	184.74	1.69	2.72	57.6	60.3	1.07
20H-6, 34	185.54	1.71	2.72	54.1	58.9	1.11
20H-6, 112	186.32	1.74	2.73	51.[illegible]	57.8	1.14
21H-1, 34	187.54	1.70	2.71	55.[illegible]	59.4	1.09

Table 10 (continued).

Core, section, interval (cm)	Depth (mbsf)	Wet-bulk density (g/cm^3)	Grain density (g/cm^3)	Water content (% dry wt)	Porosity (%)	Dry-bulk density (g/cm^3)
130-805B- (Cont)						
21H-1, 103	188.23	1.72	2.70	53.4	58.3	1.12
21H-2, 34	189.04	1.68	2.71	58.9	60.7	1.06
21H-2, 111	189.81	1.67	2.73	60.9	61.7	1.04
21H-3, 34	190.54	1.72	2.69	52.7	57.9	1.13
21H-3, 109	191.29	1.69	2.65	55.0	58.6	1.09
21H-4, 34	192.04	1.72	2.70	52.6	58.0	1.13
21H-4, 112	192.82	1.71	2.74	55.8	59.8	1.10
21H-5, 35	193.55	1.70	2.70	56.1	59.5	1.09
21H-5, 109	194.29	1.73	2.71	52.2	57.8	1.14
21H-6, 35	195.05	1.70	2.69	55.3	59.0	1.09
21H-6, 110	195.80	1.69	2.69	56.5	59.6	1.08
22H-1, 109	197.79	1.67	2.66	58.9	60.4	1.05
22H-2, 35	198.55	1.69	2.70	56.7	59.7	1.08
22H-2, 113	199.33	1.64	2.67	64.1	62.4	1.00
22H-3, 33	200.03	1.67	2.69	60.0	61.0	1.04
22H-3, 108	200.78	1.69	2.70	56.4	59.6	1.08
22H-4, 33	201.53	1.68	2.71	58.0	60.3	1.07
22H-4, 109	202.29	1.66	2.67	59.8	60.7	1.04
22H-5, 35	203.05	1.69	2.63	54.6	58.2	1.09
22H-6, 34	204.54	1.62	2.70	67.9	64.0	0.97
22H-6, 109	205.29	1.67	2.70	59.5	60.8	1.05
22H-7, 34	206.04	1.69	2.72	57.7	60.4	1.07
23H-1, 34	206.54	1.65	2.69	62.5	61.9	1.01
23H-1, 109	207.29	1.65	2.69	62.2	61.8	1.02
23H-2, 34	208.04	1.61	2.70	69.0	64.4	0.96
23H-2, 108	208.78	1.68	2.67	57.9	60.0	1.06
23H-3, 35	209.55	1.65	2.70	63.1	62.2	1.01
23H-3, 110	210.30	1.65	2.67	61.4	61.4	1.02
23H-4, 34	211.04	1.66	2.72	61.8	61.9	1.03
23H-4, 98	211.68	1.65	2.69	62.7	62.1	1.01
23H-5, 34	212.54	1.69	2.71	57.0	59.9	1.08
23H-5, 108	213.28	1.64	2.65	63.3	61.9	1.00
23H-6, 44	214.14	1.67	2.69	58.9	60.6	1.05
23H-6, 104	214.74	1.67	2.70	59.7	61.0	1.05
23H-7, 26	215.46	1.68	2.66	56.3	59.2	1.08
24H-2, 67	217.87	1.71	2.71	54.4	58.8	1.11
24H-2, 109	218.29	1.71	2.68	54.3	58.6	1.11
24H-3, 34	219.04	1.64	2.67	64.1	62.4	1.00
24H-3, 108	219.78	1.67	2.72	61.0	61.7	1.04
24H-4, 40	220.60	1.64	2.65	62.8	61.7	1.01
24H-4, 109	221.29	1.66	2.67	59.7	60.7	1.04
24H-5, 39	222.09	1.66	2.67	60.2	61.0	1.04
24H-5, 104	222.74	1.68	2.69	57.3	59.9	1.07
24H-6, 34	223.54	1.66	2.67	59.8	60.7	1.04
24H-6, 100	224.20	1.70	2.64	53.5	57.8	1.11
24H-7, 34	225.04	1.66	2.66	59.5	60.5	1.04
25H-1, 130	226.50	1.69	2.70	57.5	60.1	1.07
25H-2, 105	227.75	1.63	2.68	65.4	62.9	0.99
25H-3, 107	229.27	1.64	2.67	64.1	62.4	1.00
25H-4, 104	230.74	1.64	2.68	63.3	62.2	1.01
25H-5, 108	232.28	1.68	2.69	58.1	60.2	1.06
25H-6, 103	233.73	1.69	2.70	56.2	59.5	1.08
26H-2, 107	237.27	1.66	2.65	59.5	60.4	1.04
26H-3, 113	236.83	1.63	2.71	65.8	63.3	0.99
26H-4, 86	240.06	1.61	2.63	67.3	63.1	0.96
26H-5, 100	241.70	1.68	2.67	56.7	59.5	1.07
26H-6, 106	243.26	1.65	2.66	62.1	61.5	1.02
27H-3, 118	248.38	1.65	2.66	61.2	61.3	1.02
27H-4, 98	249.68	1.64	2.67	63.8	62.3	1.00
27H-5, 109	251.29	1.63	2.66	65.1	62.6	0.99
27H-6, 109	252.79	1.66	2.66	60.1	60.8	1.04
27H-7, 106	254.26	1.72	2.68	51.8	57.5	1.14
27H-CC, 35		1.71	2.69	54.4	58.7	1.11
28H-1, 99	254.69	1.64	2.70	63.8	62.5	1.00
28H-2, 99	256.19	1.72	2.69	52.2	57.7	1.13
28H-3, 99	257.69	1.72	2.70	52.7	57.9	1.13
28H-4, 60	258.80	1.69	2.72	57.1	60.1	1.08
28H-6, 99	262.19	1.73	2.70	51.2	57.3	1.15
28H-7, 92	263.62	1.70	2.73	55.9	59.7	1.09
29X-1, 32	263.52	1.73	2.69	51.7	57.4	1.14
29X-2, 45	265.15			58.6		
29X-3, 45	266.65	1.70	2.70	55.4	59.2	1.09
29X-4, 44	268.14	1.73	2.70	52.0	57.7	1.14
29X-5, 45	269.65	1.69	2.72	57.4	60.3	1.07

Table 10 (continued).

Core, section, interval (cm)	Depth (mbsf)	Wet-bulk density (g/cm^3)	Grain density (g/cm^3)	Water content (% dry wt)	Porosity (%)	Dry-bulk density (g/cm^3)
130-805B- (Cont)						
29X-6, 19	270.89	1.70	2.67	54.1	58.3	1.10
30X-1, 119	274.09	1.68	2.69	57.4	59.9	1.07
30X-4, 60	278.00	1.74	2.72	51.1	57.4	1.15
30X-5, 60	279.50	1.70	2.69	54.5	58.7	1.10
30X-6, 65	281.05	1.73	2.79	54.0	59.4	1.13
31X-2, 97	284.97	1.74	2.69	49.8	56.5	1.16
31X-5, 83	289.33	1.76	2.75	49.8	57.1	1.17
32X-2, 88	294.58	1.77	2.70	46.6	55.0	1.21
32X-3, 69	295.89	1.77	2.70	47.4	55.4	1.20
33X-1, 127	302.67	1.68	2.65	56.1	59.0	1.08
33X-2, 129	304.19	1.68	2.62	54.9	58.3	1.09
33X-4, 129	307.19	1.74	2.63	48.0	55.1	1.18
33X-6, 44	309.34			43.9		
34X-1, 47	311.47	1.69	2.67	55.7	59.1	1.09
34X-2, 14	312.64	1.71	2.64	51.9	57.1	1.13
34X-3, 31	314.31	1.72	2.75	54.6	59.3	1.11
34X-4, 26	315.76	1.72	2.66	52.1	57.4	1.13
34X-5, 95	317.95	1.69	2.69	56.2	59.5	1.08
35X-1, 12	320.62	1.69	2.67	56.3	59.3	1.08
35X-2, 42	322.42	1.71	2.72	54.5	59.0	1.11
35X-3, 48	323.98	1.71	2.69	53.5	58.2	1.12
35X-4, 41	325.41	1.77	2.72	47.2	55.5	1.20
35X-5, 14	326.64	1.74	2.67	48.9	55.9	1.17
36X-1, 11	330.11			52.2		
36X-2, 46	331.96	1.77	2.69	46.8	55.0	1.20
36X-3, 73	333.73	1.78	2.69	45.8	54.4	1.22
36X-4, 15	334.65	1.78	2.65	44.1	53.1	1.24
36X-5, 105	337.05	1.80	2.70	43.2	53.1	1.26
37X-1, 52	340.22	1.75	2.70	48.7	56.1	1.18
37X-2, 81	342.01	1.74	2.67	49.5	56.1	1.16
37X-3, 67	343.37	1.76	2.73	48.6	56.3	1.19
37X-4, 75	344.95	1.83	2.69	40.2	51.3	1.31
37X-5, 89	346.59	1.76	2.71	48.4	56.0	1.19
38X-1, 141	350.81	1.71	2.67	53.4	58.0	1.11
38X-2, 116	352.06	1.75	2.70	48.8	56.1	1.18
38X-3, 86	353.26	1.81	2.69	42.6	52.6	1.27
38X-4, 98	354.88	1.78	2.70	45.8	54.6	1.22
39X-1, 100	360.00	1.74	2.69	50.6	56.9	1.15
39X-2, 121	361.71	1.79	2.67	43.7	53.1	1.24
39X-3, 50	362.50	1.76	2.68	47.7	55.3	1.19
39X-4, 89	364.39	1.74	2.64	48.4	55.3	1.17
39X-5, 64	365.64	1.78	2.72	46.5	55.1	1.21
39X-6, 40	366.90	1.75	2.72	50.3	57.0	1.16
40X-1, 138	370.08	1.74	2.71	50.6	57.1	1.16
40X-3, 135	373.05	1.74	2.70	50.8	57.1	1.15
40X-4, 120	374.40	1.73	2.66	49.7	56.2	1.16
40X-5, 140	376.10	1.78	2.68	45.0	53.9	1.23
41X-1, 80	379.10	1.82	2.73	42.5	53.0	1.28
41X-2, 80	380.60	1.87	2.68	36.4	48.6	1.37
41X-3, 77	382.07	1.92	2.72	33.5	47.0	1.44
41X-4, 77	383.57	1.88	2.69	36.2	48.6	1.38
42X-1, 90	388.90	1.93	2.77	33.8	47.7	1.44
42X-2, 91	390.41	1.83	2.73	41.2	52.2	1.30
42X-3, 84	391.84	1.93	2.67	31.0	44.6	1.47
42X-4, 76	393.26	1.78	2.74	46.7	55.4	1.21
42X-5, 79	394.79	1.88	2.68	35.9	48.3	1.38
43X-1, 99	398.69	1.81	2.69	42.6	52.7	1.27
43X-2, 102	400.22	1.88	2.67	35.4	47.9	1.39
43X-3, 116	401.86	1.84	2.69	39.6	50.9	1.31
43X-4, 99	403.19	1.82	2.66	40.6	51.2	1.29
43X-5, 117	404.87	1.88	2.72	36.8	49.3	1.37
43X-6, 113	406.33	1.92	2.65	31.6	44.8	1.46
44X-1, 43	407.73	1.94	2.69	30.9	44.7	1.48
44X-2, 42	409.22	1.85	2.72	39.1	50.8	1.33
44X-3, 45	410.75	1.86	2.72	38.3	50.3	1.35
44X-4, 42	412.22	1.84	2.68	39.1	50.5	1.32
44X-5, 47	413.77	1.83	2.70	40.7	51.6	1.30
44X-6, 27	415.07	1.89	2.74	36.2	49.1	1.39
45X-1, 120	418.20	1.83	2.68	39.5	50.7	1.31
45X-2, 122	419.72	1.82	2.72	42.1	52.7	1.28
45X-3, 121	421.21	1.77	2.71	47.6	55.6	1.20
45X-4, 126	422.76	1.89	2.71	35.4	48.3	1.40
45X-5, 112	424.12	1.76	2.69	47.3	55.3	1.20
45X-6, 64	425.14	1.79	2.70	45.1	54.2	1.23

Table 10 (continued).

Core, section, interval (cm)	Depth (mbsf)	Wet-bulk density (g/cm^3)	Grain density (g/cm^3)	Water content (% dry wt)	Porosity (%)	Dry-bulk density (g/cm^3)
130-805B- (Cont)						
46X-1, 126	427.76	1.80	2.70	43.9	53.5	1.25
46X-2, 122	429.22	1.78	2.69	45.5	54.3	1.22
46X-3, 106	430.56	1.81	2.70	43.0	53.0	1.26
46X-4, 80	431.80	1.90	2.76	36.0	49.1	1.40
46X-5, 53	433.03	1.82	2.70	41.8	52.3	1.28
46X-6, 32	434.32	1.89	2.68	34.6	47.4	1.40
47X-1, 35	436.35	1.92	2.69	32.4	45.9	1.45
48X-1, 87	446.37	1.90	2.71	34.5	47.6	1.41
48X-2, 110	448.10	1.84	2.68	39.1	50.5	1.32
48X-3, 102	449.52	1.85	2.69	38.8	50.4	1.33
48X-4, 80	450.80	1.84	2.69	39.4	50.7	1.32
48X-5, 53	452.03	1.88	2.69	35.5	48.2	1.39
49X-2, 93	457.53	1.88	2.72	36.5	49.1	1.38
49X-3, 88	458.98	1.91	2.71	33.9	47.1	1.42
49X-4, 42	460.02	1.91	2.70	33.6	46.9	1.43
49X-5, 139	462.49	1.87	2.69	36.9	49.1	1.36
49X-6, 59	463.19	1.89	2.68	35.0	47.8	1.40
50X-2, 128	467.58	1.86	2.70	38.3	50.1	1.34
50X-3, 98	468.78	1.84	2.70	39.8	51.1	1.31
50X-4, 62	469.92	1.89	2.72	35.7	48.5	1.39
130-805C-						
1H-1, 74	0.74	1.47	2.71	104.0	73.1	0.72
1H-2, 74	2.24	1.47	2.72	103.1	73.0	0.73
1H-3, 74	3.74	1.51	2.72	91.5	70.6	0.79
1H-4, 74	5.24	1.52	2.70	90.0	70.1	0.80
1H-5, 74	6.74	1.50	2.59	90.3	69.3	0.79
2H-3, 71	11.51	1.54	2.76	86.5	69.7	0.83
2H-[illegible] 71	13.01	1.53	2.65	84.4	68.4	0.83
2H-5, 61	14.41	1.53	2.66	85.8	68.8	0.82
2H-6, 71	16.01	1.55	2.79	85.4	69.7	0.84
3H-2, 7[illegible]	19.53	1.54	2.69	84.1	68.7	0.84
3H-3, 73	21.03	1.55	2.71	83.4	68.6	0.84
3H-5, 73	24.03			96.2		
3H-6, 73	25.53	1.55	2.71	82.6	68.3	0.85
4H-1, 72	27.52	1.59	2.70	72.6	65.5	0.92
4H-2, 72	29.02	1.51	2.66	89.8	69.8	0.80
4[illegible], 72	33.52	1.53	2.66	84.5	68.5	0.83
4H-6, 72	35.02	1.54	2.68	83.1	68.3	0.84
5H-2, 60	38.40	1.56	2.71	79.8	67.7	0.87
5H-3, 72	40.02	1.58	2.60	71.4	64.3	0.92
5H-4, 35	41.15	1.55	2.63	79.5	66.9	0.86
5H-5, 99	43.29	1.52	2.70	89.3	69.9	0.80
5H-6, 97	44.77	1.44	2.47	101.7	70.8	0.71
6H-1, 99	46.79	1.60	2.68	70.3	64.6	0.94
6H-2, 111	48.41	1.53	2.65	85.7	68.7	0.82
6H-3, 110	49.90	1.61	2.72	70.0	64.8	0.95
6H-4, 104	51.34	1.58	2.67	75.1	66.0	0.90
6H-5, 109	52.89	1.55	2.68	80.1	67.4	0.86
6H-6, 96	54.26	1.59	2.71	73.8	66.0	0.92
7H-6, 109	63.89	1.57	2.73	79.0	67.6	0.88
7H-7, 33	64.63	1.59	2.73	75.2	66.5	0.91
9H-1, 114	75.44	1.57	2.69	76.2	66.4	0.89
9H-2, 114	76.94	1.56	2.68	79.6	67.4	0.87
9H-3, 114	78.44	1.62	2.70	68.7	64.2	0.96
9H-4, 114	79.94	1.62	2.70	67.5	63.8	0.97
9H-5, 104	81.34	1.49	2.73	97.9	72.0	0.75
9H-6, 115	82.95	1.60	2.71	72.4	65.5	0.93
9H-7, 33	83.63	1.60	2.67	70.3	64.5	0.94
10H-5, 114	90.94	1.61	2.72	71.1	65.1	0.94
10H-6, 114	92.44	1.65	2.70	63.3	62.3	1.01
12H-1, 114	103.94	1.65	2.72	63.6	62.6	1.01
12H-2, 114	105.44	1.63	2.72	66.8	63.7	0.98
12H-3, 114	106.94	1.61	2.67	69.6	64.3	0.95
12H-4, 113	108.43	1.64	2.71	65.4	63.2	0.99
12H-5, 114	109.94	1.64	2.69	64.7	62.7	0.99
12H-6, 97	111.27	1.62	2.70	67.1	63.7	0.97
12H-7, 35	112.15	1.63	2.68	66.3	63.3	0.98
13H-3, 108	116.38	1.61	2.70	69.8	64.6	0.95
13H-4, 108	117.88	1.67	2.71	59.7	61.0	1.05
13H-5, 104	119.34	1.69	2.74	58.6	60.9	1.06
13H-6, 108	120.88	1.66	2.74	63.7	62.9	1.01
13H-7, 22	121.52	1.63	2.73	66.9	63.9	0.98
14H-3, 116	125.96	1.65	2.70	63.2	62.3	1.01

Table 10 (continued).

Core, section, interval (cm)	Depth (mbsf)	Wet-bulk density (g/cm^3)	Grain density (g/cm^3)	Water content (% dry wt)	Porosity (%)	Dry-bulk density (g/cm^3)
130-805C- (Cont)						
14H-4, 108	127.38	1.63	2.70	65.5	63.1	0.99
14H-5, 110	128.90	1.64	2.73	66.1	63.6	0.99
14H-6, 108	130.38	1.67	2.73	61.5	61.9	1.03
14H-7, 35	131.15	1.64	2.71	64.9	63.0	0.99
15H-1, 108	132.38	1.68	2.71	58.5	60.6	1.06
15H-2, 108	133.88	1.67	2.73	61.0	61.7	1.04
15H-3, 109	135.39	1.68	2.71	58.4	60.6	1.06
15H-4, 97	136.77	1.67	2.71	60.5	61.4	1.04
15H-5, 109	138.39	1.69	2.69	56.6	59.6	1.08
15H-6, 114	139.94	1.64	2.70	64.5	62.8	1.00
16H-1, 114	141.94	1.67	2.70	59.7	61.0	1.05
16H-2, 113	143.43	1.67	2.70	60.5	61.3	1.04
16H-3, 112	144.92			60.7		
16H-4, 115	146.45	1.69	2.69	56.5	59.6	1.08
16H-5, 114	147.94	1.67	2.71	59.4	60.9	1.05
16H-6, 115	149.45	1.67	2.70	59.4	60.9	1.05
17H-1, 115	151.45	1.67	2.71	60.9	61.6	1.04
17H-2, 115	152.95	1.71	2.69	53.8	58.4	1.11
17H-3, 115	154.45	1.66	2.71	61.1	61.6	1.03
17H-4, 115	155.95	1.69	2.72	58.0	60.5	1.07
17H-5, 115	157.45	1.67	2.70	60.5	61.3	1.04
17H-6, 115	158.95	1.68	2.71	58.0	60.4	1.07
18H-1, 115	160.95	1.69	2.70	57.1	60.0	1.08
18H-2, 115	162.45	1.69	2.74	57.8	60.5	1.07
18H-3, 115	163.95	1.72	2.72	53.9	58.7	1.12
18H-4, 94	165.24	1.78	2.70	46.1	54.8	1.22
18H-5, 115	166.95	1.68	2.69	58.0	60.2	1.06
18H-6, 115	168.45	1.70	2.73	55.9	59.6	1.09
19H-1, 115	170.45	1.73	2.72	52.3	58.0	1.14
19H-2, 115	171.95	1.70	2.73	56.7	60.0	1.08
19H-3, 115	173.45	1.66	2.71	62.4	62.1	1.02
19H-4, 115	174.95	1.67	2.71	59.6	61.0	1.05
19H-5, 115	176.45	1.67	2.71	59.7	61.1	1.05
19H-6, 110	177.90	1.67	2.71	59.4	60.9	1.05
19H-7, 26	178.56	1.69	2.70	57.6	60.1	1.07
20H-2, 104	181.34	1.71	2.72	55.2	59.3	1.10
20H-3, 104	182.84	1.69	2.70	57.4	60.1	1.07
20H-4, 90	184.20	1.70	2.72	56.6	59.9	1.08
20H-5, 74	185.54	1.70	2.70	56.1	59.5	1.09
20H-6, 105	187.35	1.71	2.74	55.7	59.7	1.10
21H-1, 105	189.35	1.70	2.68	55.0	58.9	1.10
21H-2, 105	190.85	1.72	2.70	52.2	57.7	1.13
21H-3, 105	192.35	1.70	2.70	55.8	59.4	1.09
21H-4, 105	193.85	1.73	2.72	51.6	57.6	1.14
21H-5, 105	195.35	1.69	2.70	57.1	59.9	1.07
21H-6, 105	196.85	1.68	2.71	59.4	61.0	1.05
22H-1, 105	198.85	1.67	2.67	58.6	60.3	1.05
22H-2, 105	200.35	1.70	2.70	55.6	59.3	1.09
22H-3, 105	201.85	1.67	2.68	59.7	60.8	1.04
22H-4, 90	203.20	1.69	2.71	57.4	60.1	1.07
22H-5, 104	204.84	1.65	2.72	63.6	62.6	1.01
22H-6, 121	206.51	1.64	2.71	65.1	63.1	0.99
22H-7, 34	207.14	1.64	2.69	63.4	62.3	1.01
23H-1, 105	208.35	1.65	2.71	63.0	62.3	1.01
23H-2, 30	209.10	1.59	2.64	71.0	64.5	0.93
24H-1, 35	217.15	1.73	2.72	52.0	57.8	1.14
24H-2, 105	219.35	1.69	2.68	56.7	59.6	1.08
24H-3, 38	220.18	1.66	2.68	60.8	61.3	1.03
24H-4, 35	221.65	1.68	2.70	57.9	60.3	1.07
24H-5, 104	223.84	1.69	2.69	57.0	59.8	1.07
24H-6, 105	225.35	1.66	2.69	61.0	61.4	1.03
25H-3, 129	230.59	1.68	2.68	58.4	60.3	1.06
25H-4, 105	231.85	1.68	2.68	57.8	60.1	1.06
25H-5, 95	233.25	1.71	2.67	52.8	57.7	1.12
25H-6, 90	234.70	1.69	2.69	56.5	59.6	1.08
25H-7, 44	235.74	1.68	2.70	59.0	60.7	1.05
26X-1, 99	236.79	1.65	2.67	61.2	61.3	1.03
26X-3, 131	240.11	1.64	2.66	62.2	61.5	1.01
26X-4, 107	241.37	1.62	2.67	66.5	63.3	0.97
26X-5, 119	242.99	1.66	2.69	61.6	61.6	1.03
26X-6, 106	244.36	1.67	2.65	58.2	60.0	1.06
27X-1, 102	246.42	1.68	2.67	56.9	59.6	1.07
28X-1, 119	256.29	1.66	2.72	62.6	62.3	1.02
28X-2, 104	257.64	1.67	2.69	58.7	60.4	1.06

Table 10 (continued).

Core, section, interval (cm)	Depth (mbsf)	Wet-bulk density (g/cm^3)	Grain density (g/cm^3)	Water content (% dry wt)	Porosity (%)	Dry-bulk density (g/cm^3)
130-805C- (Cont)						
28X-3, 45	258.55	1.66	2.68	60.2	61.0	1.04
28X-4, 22	259.82	1.69	2.70	56.6	59.7	1.08
28X-6, 19	262.79	1.72	2.70	53.0	58.1	1.12
29X-2, 94	267.14	1.68	2.65	56.8	59.3	1.07
29X-3, 96	268.66	1.68	2.68	57.6	59.9	1.07
29X-4, 113	270.33	1.77	2.71	47.6	55.6	1.20
29X-5, 91	271.61	1.69	2.69	56.1	59.4	1.08
29X-6, 82	273.02	1.71	2.70	54.7	58.9	1.10
30X-1, 87	275.27	1.65	2.71	63.3	62.5	1.01
30X-2, 71	276.61	1.72	2.70	53.4	58.3	1.12
30X-3, 69	278.09	1.73	2.71	51.6	57.6	1.14
30X-4, 49	279.39	1.66	2.70	61.6	61.7	1.03
30X-5, 92	281.32	1.65	2.68	61.5	61.5	1.02
31X-1, 107	285.07	1.70	2.67	53.9	58.3	1.11
31X-2, 73	286.23	1.75	2.68	48.3	55.7	1.18
31X-3, 122	288.22	1.77	2.70	46.9	55.1	1.20
32X-1, 120	294.90	1.77	2.70	46.8	55.0	1.21
32X-2, 141	296.61	1.69	2.65	55.6	58.8	1.08
32X-3, 121	297.91	1.77	2.69	46.8	55.0	1.20
32X-4, 93	299.13	1.72	2.68	51.9	57.4	1.13
32X-6, 13	301.33	1.70	2.67	55.3	58.9	1.09
33X-1, 35	303.25	1.69	2.70	57.4	60.0	1.07
33X-2, 4	304.44	1.67	2.63	56.8	59.1	1.07
33X-3, 50	306.40	1.72	2.71	52.5	57.9	1.13
33X-4, 131	308.71	1.66	2.66	59.5	60.6	1.04
33X-5, 139	310.29	1.70	2.68	55.5	59.1	1.09
33X-7, 9	311.99	1.70	2.71	55.7	59.4	1.09
34X-2, 46	314.56	1.73	2.70	51.2	57.3	1.15
34X-3, 439	319.99	1.70	2.67	54.3	58.4	1.10
34X-4, 28	317.38	1.63	2.58	62.0	60.8	1.01
34X-5, 43	319.03	1.70	2.65	53.2	57.7	1.11
35X-2, 82	324.62	1.75	2.76	51.6	58.0	1.15
35X-3, 112	326.42	1.73	2.66	50.7	56.7	1.15
35X-4, 114	327.94	1.71	2.71	54.5	58.9	1.11
35X-5, 49	328.79	1.71	2.70	53.9	58.5	1.11
36X-1, 66	332.46	1.79	2.71	45.5	54.5	1.23
36X-2, 63	333.93	1.72	2.69	52.6	57.9	1.13
36X-3, 62	335.42	1.75	2.67	47.9	55.4	1.19
36X-4, 79	337.09	1.78	2.72	46.1	54.9	1.22
36X-5, 99	338.79	1.79	2.69	43.9	53.5	1.25
36X-6, 69	339.99	1.74	2.69	49.6	56.4	1.17
37X-1, 61	342.11	1.76	2.70	47.7	55.6	1.19
37X-2, 56	343.56	1.74	2.69	49.7	56.5	1.16
37X-3, 14	344.64	1.74	2.70	50.7	57.1	1.15
37X-5, 94	348.44	1.74	2.71	50.4	57.0	1.16
38X-1, 72	351.92	1.80	2.71	44.3	53.8	1.24
38X-2, 57	353.27	1.78	2.73	46.3	55.1	1.22
38X-3, 52	354.72	1.79	2.68	44.2	53.5	1.24
38X-4, 99	356.69	1.77	2.70	47.4	55.4	1.20
38X-5, 45	357.65	1.71	2.70	53.8	58.5	1.11
38X-6, 98	359.68	1.74	2.70	50.0	56.7	1.16
39X-1, 59	361.49	1.81	2.69	42.5	52.6	1.27
39X-3, 79	364.69	1.74	2.65	48.3	55.4	1.17
39X-4, 94	366.34	1.72	2.70	52.8	58.1	1.13
39X-5, 115	368.05	1.79	2.66	43.1	52.7	1.25
39X-6, 109	369.49	1.73	2.68	51.1	57.0	1.14
40X-1, 98	371.58	1.78	2.68	45.5	54.2	1.22
40X-2, 125	373.35	1.76	2.71	48.0	55.9	1.19
40X-3, 25	373.85	1.75	2.64	47.4	54.9	1.19
40X-4, 123	376.33	1.82	2.70	41.8	52.3	1.28
40X-5, 133	377.93	1.77	2.69	47.0	55.1	1.20
41X-1, 110	381.40	1.78	2.67	45.0	53.8	1.23
41X-2, 61	382.41	1.92	2.67	31.4	44.9	1.46
41X-3, 43	383.73	1.81	2.69	42.4	52.5	1.27
41X-4, 71	385.51	1.89	2.68	34.8	47.6	1.40
42X-1, 67	390.57	1.86	2.69	37.2	49.2	1.36
43X-3, 40	402.90	1.82	2.72	42.1	52.6	1.28
43X-1, 34	399.84	1.81	2.70	42.2	52.5	1.28
43X-2, 33	401.33	1.83	2.68	40.1	51.0	1.30
43X-3, 77	403.27	1.90	2.71	34.2	47.4	1.42
43X-4, 50	404.50	1.89	2.66	34.0	46.8	1.41
43X-5, 25	405.75	1.91	2.69	33.0	46.3	1.44
43X-6, 13	407.13	1.92	2.72	33.6	47.0	1.43
44X-1, 26	409.36	1.89	2.69	35.2	47.9	1.40

Table 10 (continued).

Core, section, interval (cm)	Depth (mbsf)	Wet-bulk density (g/cm^3)	Grain density (g/cm^3)	Water content (% dry wt)	Porosity (%)	Dry-bulk density (g/cm^3)
130-805C- (Cont)						
44X-2, 38	410.98	1.85	2.67	37.4	49.3	1.35
44X-4, 54	414.14	1.91	2.70	33.2	46.6	1.44
44X-5, 10	415.20	1.85	2.68	37.8	49.6	1.34
44X-6, 8	416.68	1.91	2.69	33.4	46.6	1.43
45X-1, 103	419.73	1.79	2.69	44.1	53.6	1.24
45X-2, 24	420.44	1.87	2.71	37.6	49.8	1.36
45X-3, 123	422.93	1.87	2.66	35.4	47.8	1.38
45X-4, 137	424.57	1.83	2.71	41.0	51.9	1.30
45X-5, 146	426.16	1.90	2.72	35.1	48.1	1.40
46X-1, 84	429.24	1.85	2.72	39.1	50.8	1.33
46X-2, 96	430.86	1.89	2.69	34.6	47.5	1.41
46X-3, 83	432.23	1.86	2.71	37.7	49.8	1.35
46X-4, 34	433.24	1.85	2.73	39.9	51.4	1.32
46X-5, 35	434.75	1.83	2.70	40.0	51.2	1.31
46X-6, 31	436.21	1.93	2.70	31.7	45.4	1.47
47X-1, 95	439.05	1.89	2.71	35.2	48.1	1.40
47X-2, 81	440.41	1.82	2.69	41.1	51.8	1.29
47X-3, 79	441.89	1.79	2.70	44.3	53.8	1.24
47X-4, 84	443.44	1.88	2.67	35.3	47.8	1.39
47X-5, 52	444.62			36.1		
47X-6, 91	446.51			40.1		
48X-1, 99	448.69			38.8		
48X-2, 98	450.18	1.82	2.69	41.3	51.9	1.29
48X-3, 91	451.61	1.85	2.66	37.2	49.0	1.35
48X-4, 94	453.14			35.6		
48X-5, 85	454.55			37.7		
49X-2, 83	459.73			32.1		
49X-3, 103	461.43			32.3		
50X-1, 128	468.28	1.88	2.71	36.4	48.9	1.38
50X-2, 94	469.44	1.85	2.71	38.6	50.4	1.34
50X-3, 90	470.90			36.8		
50X-4, 75	472.25			41.6		
51X-1, 137	476.87	1.89	2.71	35.7	48.4	1.39
51X-2, 115	478.15	1.90	2.70	34.7	47.7	1.41
51X-3, 106	479.56	1.86	2.69	37.4	49.4	1.36
51X-4, 78	480.78	1.82	2.67	40.4	51.2	1.30
51X-5, 74	482.24	1.83	2.71	40.7	51.7	1.30
52X-1, 105	486.25	1.88	2.69	35.8	48.3	1.38
52X-2, 60	487.30	1.87	2.71	37.5	49.7	1.36
52X-3, 88	489.08	1.88	2.72	36.5	49.1	1.38
52X-4, 48	490.18	1.83	2.69	40.4	51.3	1.30
53X-1, 88	495.78	1.85	2.70	38.4	50.2	1.34
53X-2, 72	497.12	1.74	2.56	45.6	53.1	1.19
53X-3, 9	497.99	1.79	2.70	44.3	53.8	1.24
53X-4, 84	500.24	1.86	2.68	36.8	49.0	1.36
53X-5, 55	501.45	1.92	2.71	32.8	46.4	1.45
54X-1, 131	505.91	1.85	2.75	40.4	51.9	1.31
54X-2, 72	506.82	1.82	2.69	41.1	51.8	1.29
54X-3, 109	508.69	1.93	2.71	32.6	46.3	1.45
54X-4, 59	509.69	1.92	2.75	34.5	48.0	1.43
55X-1, 66	514.86	1.89	2.71	35.3	48.2	1.40
55X-2, 46	516.16	1.91	2.67	32.9	46.1	1.44
55X-3, 43	517.63	1.93	2.66	30.5	44.1	1.48
56X-7, 33	533.23	1.93	2.67	31.0	44.6	1.47
57X-1, 55	534.05	1.85	2.74	39.6	51.4	1.33
57X-2, 83	535.83	1.89	2.67	34.6	47.3	1.40
58X-1, 45	543.65	1.94	2.70	31.5	45.3	1.47
59X-1, 13	553.03	1.94	2.66	30.0	43.7	1.49
59X-2, 19	554.59	2.00	2.70	27.2	41.7	1.57
60X-1, 44	563.04	1.90	2.71	34.4	47.5	1.41
61X-1, 29	572.59	1.95	2.70	30.3	44.3	1.50
61X-2, 63	574.43	1.97	2.70	29.1	43.3	1.52
61X-3, 108	576.38	1.90	2.72	35.3	48.3	1.40
61X-5, 133	579.63	1.93	2.71	32.7	46.3	1.45
62X-1, 121	583.21	1.94	2.71	31.5	45.4	1.48
62X-2, 122	584.72	1.95	2.70	30.4	44.4	1.50
62X-3, 114	586.14	1.98	2.71	28.3	42.7	1.54
63X-1, 105	592.75	1.96	2.73	30.9	45.0	1.49
63X-2, 49	593.69	1.93	2.69	31.6	45.3	1.47
64X-1, 12	601.42	1.97	2.69	28.9	43.0	1.53

Table 11. ***P*-wave velocity data, Holes 805B and 805C.**

Core, section, interval (cm)	Depth (mbsf)	Vertical *P*-wave velocity (m/s)	Horizontal *P*-wave velocity (m/s)
130-805B-			
1H-1, 35	0.35	1553 2	1578.0
1H-1, 110	1.10	1541.4	1535.5
1H-4, 35	4.85		1511.7
1H-4, 130	5.80	1521.7	1532.1
1H-5, 25	6.25		1508.4
2H-1, 35	7.05		1498.5
2H-1, 107	7.77	1523.4	1528.6
2H-2, 35	8.55	1515.3	1525.2
2H-2, 110	9.30	1515.3	1518.4
2H-3, 35	10.05	1549.8	1538.9
2H-3, 117	10.87	1510.5	1515.1
2H-4, 37	11.57	1523.4	1515.1
2H-4, 110	12.30	1516.9	1508.4
2H-5, 35	13.05	1523.4	1511.7
2H-5, 110	13.80	1515.3	1515.1
2H-6, 35	14.55	1534.8	1532.1
2H-6, 110	15.30	1518.5	1511.7
2H-7, 21	15.91	1516.9	1528.6
3H-1, 110	17.30		1505.1
3H-2, 35	18.05	1546.4	1505.1
3H-2, 110	18.80	1563.4	1567.2
3H-3, 110	20.30	1543.1	1549.4
3H-4, 110	21.80	1534.8	1538.9
3H-5, 110	23.30	1553.2	1528.6
3H-5, 110	23.30	1543.1	1521.8
3H-6, 35	24.05	1543.1	1525.2
3H-6, 110	24.80	1520.1	1511.7
4H-2, 35	27.55	1526.6	1505.1
4H-2, 110	28.30	1521.7	1508.4
4H-3, 110	29.80	1516.9	1515.1
4H-4, 35	30.55	1534.8	1545.9
4H-4, 106	31.26	1525.0	1535.5
4H-5, 35	32.05	1538.7	1567.9
4H-5, 110	32.80	1550.5	1550.1
4H-6, 35	33.55	1552.1	1578.8
4H-6, 110	34.30	1560.6	1593.6
5H-1, 110	36.30	1543.7	1553.7
5H-2, 35	37.05	1548.8	1557.2
5H-2, 110	37.80	1542.1	1546.6
5H-3, 35	38.55	1540.4	1557.2
5H-3, 110	39.30	1538.7	1567.9
5H-4, 35	40.05	1532.1	1536.2
5H-4, 110	40.80	1538.7	1539.6
5H-5, 35	41.55	1564.1	1578.8
5H-5, 110	42.30	1540.4	1553.7
5H-6, 35	43.05	1574.5	1582.5
5H-7, 35	44.55	1532.1	1543.1
6H-2, 35	46.55	1533.8	1536.2
6H-2, 110	47.30	1542.1	1539.6
6H-4, 35	49.55	1525.5	1543.1
6H-4, 110	50.30	1542.1	1553.7
6H-5, 35	51.05	1540.4	1571.6
6H-5, 110	51.80	1532.1	1546.6
6H-6, 35	52.55	1537.1	1543.1
6H-6, 110	53.30	1543.7	1564.3
6H-7, 35	54.05	1548.8	1564.3
7H-3, 133	58.53	1539.5	1539.5
7H-4, 45	59.15	1542.8	1564.2
7H-4, 105	59.75	1537.8	1546.5
7H-5, 35	60.55	1549.5	1550.0
7H-5, 105	61.25	1551.1	1567.7
7H-6, 35	62.05	1536.1	1536.1
7H-6, 105	62.75	1542.8	1546.5
8H-2, 35	65.55	1539.5	1546.5
8H-2, 105	66.25	1532.8	1539.5
8H-3, 35	67.05	1547.8	1550.0
8H-3, 105	67.75	1536.1	1539.5
8H-4, 35	68.55	1529.6	1532.7
8H-4, 105	69.25	1537.8	
8H-5, 27	69.97	1532.8	1539.5
Table 11 (continued).			
130-805B- (Cont)			
8H-5, 100	70.70	1541.1	1543.0
8H-6, 29	71.49	1539.5	1546.5
8H-6, 0	72.10	1539.5	1536.1
9H-1, 105	74.25	1529.6	1529.2
9H-2, 35	75.05	1532.8	1543.0
9H-2, 105	75.75	1536.1	1536.1
9H-3, 35	76.55	1527.9	1532.7
9H-3, 108	77.28	1536.1	1536.1
9H-4, 35	78.05	1541.1	1546.5
9H-4, 105	78.75	1541.1	1550.0
9H-5, 35	79.55	1532.8	1532.7
9H-5, 105	80.25	1537.8	1539.5
9H-6, 35	81.05	1531.2	1532.7
9H-6, 105	81.75	1524.7	1536.1
10H-1, 105	83.75	1524.7	1522.4
10H-2, 30	84.50	1531.2	1532.7
10H-2, 105	85.25	1527.9	1529.2
10H-3, 35	86.05	1526.3	1529.2
10H-3, 106	86.76	1542.8	1536.1
10H-4, 35	87.55	1529.6	1529.2
10H-4, 105	88.25	1546.1	1550.0
10H-5, 35	89.05	1534.5	1532.7
10H-5, 105	89.75	1539.5	1532.7
10H-6, 35	90.55	1526.3	1536.1
10H-6, 105	91.25	1541.1	1546.5
10H-7, 60	92.30	1544.4	1553.5
11H-1, 105	93.25	1532.8	1525.8
11H-2, 50	94.20	1546.1	1546.5
11H-2, 105	94.75	1524.7	1515.7
11H-3, 35	95.55	1551.1	1543.0
11H-3, 105	96.25	1542.8	1543.0
11H-4, 35	97.05	1547.8	1543.0
11H-4, 105	97.75	1536.1	1532.7
11H-5, 35	98.55	1541.1	1553.5
11H-5, 105	99.25	1532.8	1532.7
11H-6, 35	100.05	1541.1	1539.5
11H-6, 105	100.75	1537.8	1546.5
11H-7, 35	101.55	1532.8	1543.0
12H-1, 35	102.05	1557.9	1557.0
12H-1, 105	102.75	1537.8	1532.7
12H-3, 35	105.05	1549.5	1550.0
12H-3, 105	105.75	1563.0	1567.7
12H-4, 35	106.55	1549.5	1550.0
12H-4, 105	107.25	1547.8	1560.6
12H-5, 35	108.05	1539.5	1564.2
12H-5, 110	108.80	1547.8	1553.5
12H-6, 35	109.55	1539.5	1564.2
12H-6, 110	110.30	1544.4	1560.6
12H-7, 20	110.90	1534.5	1539.5
13H-1, 49	111.69	1542.8	1539.5
13H-1, 110	112.30	1546.1	1546.5
13H-2, 35	113.05	1539.5	1543.0
13H-2, 110	113.80	1554.5	1567.7
13H-3, 45	114.65	1542.8	1557.0
13H-3, 110	115.30	1557.9	1567.7
13H-4, 28	115.98	1557.9	1567.7
13H-4, 110	116.80	1547.8	1532.7
13H-5, 35	117.55	1537.8	1550.0
13H-5, 110	118.30	1552.8	1567.7
13H-6, 35	119.05	1534.5	1557.0
13H-6, 110	119.80	1532.8	1546.5
13H-7, 35	120.55	1544.4	1550.0
14H-1, 110	121.80	1532.8	1550.0
14H-2, 35	122.55	1529.6	1543.0
14H-2, 109	123.29	1537.8	1546.5
14H-3, 50	124.20	1534.5	1546.5
14H-3, 110	124.80	1542.8	1550.0
14H-4, 35	125.55	1536.1	1557.0
14H-4, 105	126.25	1537.8	1560.6
14H-5, 35	127.05	1544.4	1553.5
14H-5, 110	127.80	1531.2	1543.0
14H-6, 35	128.55	1561.3	1582.2

Table 11 (continued).

Core, section, interval (cm)	Depth (mbsf)	Vertical *P*-wave velocity (m/s)	Horizontal *P*-wave velocity (m/s)
130-805B- (Cont)			
14H-6, 110	129.30	1544.4	1553.5
14H-7, 45	130.15	1539.5	1550.0
15H-2, 35	132.05	1544.4	1543.0
15H-2, 110	132.80	1544.4	1557.0
15H-3, 35	133.55	1534.5	1543.0
15H-3, 110	134.30	1544.4	1546.5
15H-4, 35	135.05	1544.4	1550.0
15H-4, 110	135.80	1546.1	1564.2
15H-5, 35	136.55	1537.8	1532.7
15H-5, 110	137.30	1554.5	1567.7
15H-6, 35	138.05	1547.8	1560.6
15H-6, 110	138.80	1552.8	1553.5
16H-1, 35	140.05	1556.2	1585.9
16H-1, 110	140.80	1542.8	1550.0
16H-2, 35	141.55	1531.2	1532.7
16H-2, 110	142.30	1544.4	1550.0
16H-3, 35	143.05	1552.8	1571.3
16H-3, 110	143.80	1564.7	1574.9
16H-4, 35	144.55	1541.1	1553.5
16H-4, 110	145.30	1557.9	1578.6
16H-5, 35	146.05	1568.2	1578.6
16H-6, 35	147.55		1578.6
16H-6, 110	148.30	1578.6	1650.9
16H-7, 35	149.05	1552.8	1567.7
17H-1, 35	149.55	1554.5	1564.2
17H-1, 110	150.30	1546.1	1557.0
17H-2, 35	151.05	1556.2	1567.7
17H-2, 110	151.80	1564.7	1564.2
17H-3, 35	152.55	1563.0	1574.9
17H-3, 110	153.30	1544.4	1546.5
17H-4, 35	154.05	1539.5	1546.5
17H-4, 110	154.80	1544.4	1557.0
17H-5, 35	155.55	1539.5	1550.0
17H-5, 110	156.30	1544.4	1557.0
17H-6, 35	157.05	1551.1	1557.0
17H-7, 35	158.55	1549.5	1553.5
18H-1, 110	159.80	1561.3	1578.6
18H-2, 35	160.55	1539.5	1550.0
18H-2, 110	161.30	1566.5	1574.9
18H-3, 35	162.05	1552.8	1564.2
18H-3, 110	162.80	1556.2	1560.6
18H-4, 35	163.55	1561.3	1564.2
18H-4, 110	164.30	1551.1	1550.0
18H-5, 35	165.05	1549.5	1550.0
18H-5, 110	165.80	1563.0	1578.6
18H-6, 35	166.55	1556.2	1564.2
18H-6, 110	167.30	1544.4	1550.0
19H-1, 110	169.30	1552.8	1571.3
19H-2, 35	170.05	1549.5	1543.0
19H-2, 107	170.77	1544.4	1557.0
19H-3, 35	171.55	1551.1	1567.7
19H-3, 110	172.30	1549.5	1567.7
19H-4, 60	173.30	1546.1	1560.6
19H-4, 120	173.90	1556.2	1571.3
19H-5, 30	174.50	1551.1	1564.2
19H-5, 110	175.30	1554.5	1567.7
20H-1, 50	178.20	1549.5	1557.0
20H-1, 105	178.75	1544.4	1553.5
20H-2, 10	179.30	1549.5	1553.5
20H-2, 105	180.25	1557.9	
20H-3, 35	181.05	1552.8	1564.2
20H-3, 105	181.75	1541.1	1546.5
20H-4, 35	182.55	1556.2	1550.0
20H-4, 105	183.25	1542.8	1543.0
20H-5, 35	184.05	1561.3	1571.3
20H-5, 105	184.75	1561.3	1612.0
20H-6, 35	185.55	1556.2	1550.0
20H-6, 110	186.30	1569.9	1585.9
21H-1, 105	188.25	1542.8	1560.6
21H-2, 35	189.05	1546.1	1550.0
21H-2, 110	189.80	1549.5	1557.0
21H-3, 35	190.55	1564.7	1578.6
21H-3, 110	191.30	1561.3	1567.7

Table 11 (continued).

Core, section, interval (cm)	Depth (mbsf)	Vertical *P*-wave velocity (m/s)	Horizontal *P*-wave velocity (m/s)
130-805B- (Cont)			
21H-4, 35	192.05	1551.1	1557.0
21H-4, 115	192.85	1552.8	1553.5
21H-5, 35	193.55	1564.7	1560.6
21H-5, 110	194.30	1561.3	1560.6
21H-6, 35	195.05	1557.9	1564.2
21H-6, 110	195.80	1563.0	1557.0
22H-1, 110	197.80	1556.2	1557.0
22H-2, 35	198.55	1563.0	1557.0
22H-2, 110	199.30	1534.5	1546.5
22H-3, 35	200.05	1559.6	1553.5
22H-3, 110	200.80	1559.6	1557.0
22H-4, 35	201.55	1554.5	1560.6
22H-4, 110	202.30	1575.1	1571.3
22H-5, 35	203.05	1559.6	1571.3
22H-5, 110	203.80	1551.1	1557.0
22H-6, 35	204.55	1554.5	1560.6
22H-6, 110	205.30	1573.4	1567.7
22H-7, 35	206.05	1554.5	1564.2
23H-1, 35	206.55	1556.2	1567.7
23H-1, 110	207.30	1561.3	1567.7
23H-2, 35	208.05	1587.3	1593.3
23H-2, 110	208.80	1561.3	1578.6
23H-3, 35	209.55	1566.5	1585.9
23H-3, 110	210.30	1546.1	1553.5
23H-4, 35	211.05	1552.8	
23H-5, 35	212.55	1561.3	1564.2
23H-5, 110	213.30	1557.9	1519.1
23H-6, 45	214.15		1536.1
23H-6, 105	214.75	1556.2	1550.0
23H-7, 25	215.45	1564.7	1567.7
24H-1, 60	216.30	1552.8	1553.5
24H-1, 110	216.80	1556.2	1560.6
24H-3, 35	219.05	1544.4	1546.5
24H-3, 108	219.78	1554.5	1546.5
24H-4, 35	220.55	1546.1	1546.5
24H-4, 110	221.30	1568.2	1567.7
24H-5, 40	222.10	1556.2	1560.6
24H-5, 105	222.75	1561.3	1567.7
24H-6, 35	223.55	1563.0	1564.2
24H-6, 101	224.21	1561.3	1557.0
24H-7, 35	225.05	1549.5	1560.6
25H-1, 124	226.44	1541.1	1560.6
25H-2, 35	227.05		1557.0
25H-2, 105	227.75	1559.6	1557.0
25H-3, 35	228.55	1551.1	1550.0
25H-3, 108	229.28	1563.0	1578.6
25H-4, 35	230.05		1585.9
25H-4, 105	230.75	1578.6	1582.2
25H-5, 35	231.55		1564.2
25H-5, 105	232.25	1556.2	1560.6
25H-5, 108	232.28	1564.7	1560.6
26H-2, 35	236.55	1551.1	1560.6
26H-2, 107	237.27	1552.8	1564.2
26H-3, 110	237.80		1597.0
26H-3, 115	238.85		1560.6
26H-4, 25	239.45		1567.7
26H-4, 86	240.06	1571.6	1593.3
26H-5, 35	241.05	1563.0	1578.6
26H-5, 100	241.70	1554.5	1589.6
26H-6, 35	242.55	1568.2	1571.3
26H-6, 105	243.25	1568.2	1600.7
27H-3, 47	246.26		1560.6
27H-3, 112	246.91		1543.0
27H-4, 53	247.82		1593.3
27H-4, 105	248.34		1567.7
27H-5, 35	249.14	1563.0	1567.7
27H-5, 105	249.84	1539.5	1600.7
27H-6, 55	250.84		1571.3
27H-6, 108	251.37	1563.0	1553.5
27H-7, 35	252.14	1559.6	1567.7
27H-7, 105	252.84	1563.0	1585.9
27H-8, 35	253.64	1561.3	1589.6
28H-1, 100	254.70	1557.9	1574.9

Table 11 (continued).

Core, section, interval (cm)	Depth (mbsf)	Vertical P-wave velocity (m/s)	Horizontal P-wave velocity (m/s)
130-805B- (Cont)			
28H-2, 100	256.20	1557.9	1574.9
28H-3, 100	257.70	1559.6	1574.9
28H-4, 60	258.80	1552.8	1582.2
28H-6, 100	262.20	1576.8	1612.0
28H-7, 40	263.10	1580.3	1604.5
29X-1, 39	263.59	1592.6	1597.0
29X-2, 45	265.15	1583.8	1582.2
29X-3, 45	266.65	1571.6	1574.9
29X-4, 45	268.15	1561.3	1574.9
29X-5, 45	269.65		1571.3
29X-6, 20	270.90		1582.2
30X-1, 110	274.00	1547.8	
30X-2, 130	275.70		1557.0
30X-4, 60	278.00	1566.5	1585.9
30X-5, 60	279.50	1557.9	1582.2
30X-5, 65	281.05		1582.2
32X-2, 91	294.61		1623.6
32X-3, 72	295.92	1540.8	1576.3
32X-4, 93	297.63	1630.2	1636.5
33X-1, 131	302.71	1580.8	1579.5
33X-2, 128	304.18		1573.8
33X-4, 130	307.20		1596.2
33X-6, 45	309.35	1672.9	
34X-1, 48	311.48	1586.0	1582.3
34X-2, 15	312.65	1565.2	1610.0
34X-3, 32	314.32	1630.5	1578.5
34X-4, 27	315.77	1653.9	1653.7
34X-5, 96	317.96	1653.4	1625.1
35X-1, 12	320.62	1566.4	1569.8
35X-2, 42	322.42	1626.1	1605.5
35X-3, 49	323.99	1569.1	1521.8
35X-4, 42	325.42	1584.1	1591.5
35X-5, 13	326.63	1635.2	
36X-1, 12	330.12	1695.4	1710.5
36X-2, 47	331.97	1634.2	1686.7
36X-3, 74	333.74	1706.6	
36X-4, 16	334.66	1717.1	1655.9
36X-5, 106	337.06	1673.9	1653.7
37X-1, 53	340.23	1940.8	1809.4
37X-2, 82	342.02	1684.9	
37X-3, 68	343.38	1812.3	1778.0
37X-4, 82	345.02	1773.3	1641.5
37X-5, 90	346.60	1764.7	1661.7
38X-1, 142	350.82	1672.8	1618.7
38X-2, 117	352.07	1784.0	
38X-3, 87	353.27	1761.2	1716.6
38X-4, 99	354.89	1634.9	1644.5
39X-1, 101	360.01	1693.8	1601.1
39X-2, 122	361.72	1774.2	1664.4
39X-3, 51	362.51	1705.9	1691.5
39X-4, 90	364.40	1765.7	1706.1
39X-5, 65	365.65	1793.8	1584.9
39X-6, 41	366.91	1870.4	1714.2
40X-1, 139	370.09	1914.4	1737.0
40X-2, 136	371.56	1744.3	1651.0
40X-3, 136	373.06	1804.3	1681.0
40X-4, 121	374.41	1871.0	1854.3
40X-5, 141	376.11	1862.6	1781.9
41X-1, 81	379.11		1754.3
41X-2, 81	380.61	1746.5	1714.2
41X-3, 78	382.08		1906.1
41X-4, 78	383.58	1996.7	1789.1
42X-1, 91	388.91	1646.4	1751.6
42X-2, 92	390.42	1660.0	1730.6
42X-3, 85	391.85	1756.3	1828.6
42X-4, 77	393.27	1620.4	1647.2
42X-5, 81	394.81	1618.0	1697.7
43X-1, 100	398.70	1631.7	1680.8
43X-2, 103	400.23	1774.2	1788.8
43X-2, 103	400.23	1702.9	
43X-3, 115	401.85	1622.8	
43X-4, 100	403.20	1671.1	1682.0
43X-5, 118	404.88	1737.6	1708.7

Table 11 (continued).

Core, section, interval (cm)	Depth (mbsf)	Vertical P-wave velocity (m/s)	Horizontal P-wave velocity (m/s)
130-805B- (Cont)			
43X-6, 114	406.34	1710.3	1813.3
44X-1, 44	407.74	1746.9	1730.4
44X-2, 43	409.23	1797.3	1677.9
44X-3, 46	410.76	1715.4	1616.1
44X-4, 43	412.23	1821.8	1640.9
44X-6, 28	415.08		1706.2
45X-1, 121	418.21	1821.1	1721.6
45X-2, 123	419.73	1597.9	1652.6
45X-3, 122	421.22	1853.7	1675.4
45X-4, 127	422.77	1752.8	1777.1
45X-5, 113	424.13	1741.1	1611.6
45X-6, 65	425.15	1813.1	1641.7
46X-1, 127	427.77	1748.5	1527.9
46X-2, 123	429.23	1820.3	1644.9
46X-3, 107	430.57	1905.7	1763.5
46X-4, 81	431.81	1823.4	1822.2
46X-5, 54	433.04	1837.2	1630.9
46X-6, 33	434.33		2020.9
47X-1, 36	436.36	1950.2	1824.5
48X-1, 88	446.38	1950.2	1851.2
48X-2, 111	448.11	1889.0	1795.1
48X-3, 101	449.51	1820.3	
48X-4, 81	450.81	1862.6	1676.7
48X-5, 54	452.04	1896.6	1856.9
49X-2, 95	457.55		1674.6
49X-3, 90	459.00	1789.8	1721.0
49X-4, 44	460.04	1714.6	1705.8
49X-5, 141	462.51	1767.8	1691.2
49X-6, 60	463.20	1778.7	1697.5
50X-3, 99	468.79		1743.8
50X-4, 60	469.90	1809.5	1698.7
50X-5, 99	472.40	1770.9	
130-805C-			
1H-1, 30	0.30	1547.8	
1H-1, 73	0.73		1571.3
1H-2, 74	2.24	1547.8	1543.0
1H-3, 74	3.74	1551.1	1557.0
1H-4, 73	5.23	1546.1	1543.0
1H-5, 73	6.73	1552.8	1574.9
2H-3, 73	11.53	1552.8	1560.6
2H-4, 73	13.03	1537.8	1539.5
2H-6, 73	16.03	1546.1	1550.0
3H-2, 73	19.53	1542.8	1550.0
3H-3, 73	21.03	1532.8	1529.2
3H-5, 73	24.03	1566.5	1571.3
3H-6, 73	25.53	1552.8	1539.5
4H-1, 73	27.53	1551.1	1567.7
4H-5, 73	33.53	1563.0	1574.9
4H-6, 73	35.03	1546.1	1539.5
5H-2, 61	38.41	1536.1	1543.0
5H-3, 73	40.03	1539.5	1543.0
5H-4, 35	41.15	1564.7	1585.9
5H-4, 100	41.80	1539.5	1546.5
5H-5, 35	42.65	1541.1	1550.0
5H-5, 100	43.30	1551.1	1574.9
5H-6, 35	44.15	1539.5	1539.5
5H-6, 98	44.78	1549.5	1560.6
6H-1, 100	46.80	1536.1	1539.5
6H-2, 62	47.92	1527.9	1536.1
6H-2, 110	48.40	1546.1	1560.6
6H-3, 35	49.15	1531.2	1522.4
6H-3, 110	49.90	1539.5	1529.2
6H-4, 35	50.65	1541.1	1536.1
6H-4, 105	51.35	1542.8	1546.5
6H-5, 35	52.15	1527.9	1529.2
6H-5, 110	52.90	1532.8	1529.2
6H-6, 35	53.65	1523.0	1539.5
6H-6, 97	54.27	1531.2	1539.5
6H-7, 45	55.25	1523.0	1522.4
7H-6, 110	63.90	1539.5	1550.0
7H-7, 35	64.65	1526.3	1536.1

Table 11 (continued).

Core, section, interval (cm)	Depth (mbsf)	Vertical *P*-wave velocity (m/s)	Horizontal *P*-wave velocity (m/s)
130-805C- (Cont)			
9H-1, 35	74.65	1536.1	1539.5
9H-1, 115	75.45	1521.4	1536.1
9H-2, 35	76.15	1524.7	1536.1
9H-2, 115	76.95	1519.8	1519.1
9H-3, 35	77.65	1531.2	1532.7
9H-3, 115	78.45	1541.1	1539.5
9H-4, 35	79.15	1531.2	1546.5
9H-4, 115	79.95	1531.2	1550.0
9H-5, 35	80.65	1527.9	1536.1
9H-5, 105	81.35	1523.0	1519.1
9H-6, 35	82.15	1541.1	1539.5
9H-6, 115	82.95	1531.2	1539.5
9H-7, 35	83.65	1541.1	1543.0
10H-5, 35	90.15	1541.1	1553.5
10H-5, 115	90.95	1534.5	1539.5
10H-6, 35	91.65	1556.2	1557.0
10H-6, 115	92.45	1547.8	1550.0
10H-7, 35	93.15	1536.1	1550.0
12H-1, 115	103.95	1552.8	1564.2
12H-2, 35	104.65	1564.7	
12H-2, 115	105.45	1566.5	1578.6
12H-3, 35	106.15	1557.9	1567.7
12H-3, 115	106.95	1554.5	1567.7
12H-4, 35	107.65	1532.8	1539.5
12H-4, 115	108.45	1569.9	1582.2
12H-5, 35	109.15	1547.8	1543.0
12H-5, 115	109.95	1564.7	1578.6
12H-6, 35	110.65	1527.9	1546.5
12H-6, 97	111.27	1534.5	1553.5
12H-7, 35	112.15	1544.4	1557.0
13H-3, 110	116.40	1534.5	1553.5
13H-4, 35	117.15	1536.1	1553.5
13H-4, 110	117.90	1539.5	1553.5
13H-5, 35	118.65	1542.8	1560.6
13H-5, 105	119.35	1554.5	1585.9
13H-6, 22	120.02	1544.4	1564.2
13H-6, 110	120.90	1544.4	1578.6
13H-7, 23	121.53	1521.4	
14H-3, 117	125.97	1546.1	1557.0
14H-4, 35	126.65	1542.8	1557.0
14H-4, 110	127.40	1527.9	1553.5
14H-5, 45	128.25	1529.6	1546.5
14H-5, 110	128.90	1531.2	1557.0
14H-6, 35	129.65	1539.5	1553.5
14H-6, 108	130.38	1541.1	1553.5
14H-7, 35	131.15	1529.6	1529.2
15H-1, 110	132.40	1546.1	1571.3
15H-2, 35	133.15	1531.2	1557.0
15H-2, 105	133.85	1541.1	1553.5
15H-3, 35	134.65	1539.5	1557.0
15H-3, 110	135.40	1552.8	1567.7
15H-4, 35	136.15	1534.5	1557.0
15H-4, 98	136.78	1544.4	1557.0
15H-5, 35	137.65	1536.1	1550.0
15H-5, 110	138.40	1557.9	1567.7
15H-6, 35	139.15	1539.5	1550.0
15H-6, 115	139.95	1571.6	1571.3
15H-7, 35	140.65	1544.4	1557.0
16H-1, 35	141.15	1551.1	1546.5
16H-1, 115	141.95	1547.8	1553.5
16H-2, 35	142.65	1546.1	1546.5
16H-2, 115	143.45	1561.3	1557.0
16H-3, 35	144.15	1559.6	1564.2
16H-3, 115	144.95	1587.3	1589.6
16H-4, 35	145.65		1585.9
16H-4, 115	146.45	1561.3	
16H-5, 35	147.15	1566.5	1564.2
16H-5, 115	147.95	1568.2	1578.6
16H-6, 5	148.35	1569.9	1546.5
16H-6, 115	149.45	1569.9	1567.7
16H-7, 35	150.15	1546.1	1560.6
17H-1, 35	150.65	1556.2	1557.0
17H-1, 115	151.45	1551.1	1550.0

Table 11 (continued).

Core, section, interval (cm)	Depth (mbsf)	Vertical *P*-wave velocity (m/s)	Horizontal *P*-wave velocity (m/s)
130-805C- (Cont)			
17H-2, 35	152.15	1556.2	1550.0
17H-2, 115	152.95	1561.3	1553.5
17H-3, 35	153.65	1552.8	1553.5
17H-3, 115	154.45	1563.0	1578.6
17H-4, 35	155.15	1544.4	1553.5
17H-4, 115	155.95	1554.5	1557.0
17H-5, 35	156.65	1546.1	1546.5
17H-5, 115	157.45	1534.5	1543.0
17H-6, 35	158.15	1561.3	1567.7
17H-6, 115	158.95	1554.5	1543.0
17H-7, 35	159.65	1542.8	1550.0
18H-1, 115	160.95	1552.8	1550.0
18H-2, 35	161.65	1561.3	1578.6
18H-2, 115	162.45	1568.2	1564.2
18H-3, 35	163.15	1556.2	1553.5
18H-3, 115	163.95	1556.2	1557.0
18H-4, 115	165.45	1542.8	1557.0
18H-5, 35	166.15	1544.4	1539.5
18H-5, 115	166.95	1568.2	1574.9
18H-6, 35	167.65	1534.5	1539.5
18H-6, 115	168.45	1563.0	1553.5
18H-7, 35	169.15	1552.8	1553.5
19H-1, 35	169.65	1549.5	
19H-1, 115	170.45	1563.0	1571.3
19H-2, 35	171.15	1541.1	1553.5
19H-2, 115	171.95	1566.5	1560.6
19H-3, 35	172.65	1547.8	1553.5
19H-3, 115	173.45		1546.5
19H-4, 35	174.15	1539.5	1550.0
19H-4, 115	174.95	1552.8	1553.5
19H-5, 35	175.65	1547.8	1543.0
19H-5, 115	176.45	1546.1	1543.0
19H-6, 35	177.15	1556.2	1543.0
19H-6, 110	177.90	1546.1	1550.0
19H-7, 25	178.55	1551.1	1557.0
20H-2, 35	180.65	1546.1	1546.5
20H-2, 105	181.35	1544.4	1546.5
20H-3, 35	182.15	1544.4	1543.0
20H-3, 105	182.85	1539.5	1546.5
20H-4, 90	184.20	1544.4	1539.5
20H-5, 75	185.55	1542.8	1543.0
20H-6, 35	186.65	1552.8	1553.5
20H-6, 105	187.35	1539.5	1536.1
21H-1, 35	188.65	1556.2	1564.2
21H-1, 105	189.35	1544.4	1543.0
21H-2, 40	190.20	1549.5	1553.5
21H-2, 105	190.85	1546.1	1550.0
21H-3, 35	191.65	1556.2	1560.6
21H-3, 105	192.35	1554.5	1553.5
21H-4, 35	193.15	1537.8	1553.5
21H-4, 105	193.85	1564.7	1564.2
21H-5, 25	194.55	1554.5	1550.0
21H-5, 105	195.35	1559.6	1553.5
21H-6, 35	196.15	1559.6	1553.5
21H-6, 105	196.85	1564.7	1543.0
22H-1, 35	198.15	1561.3	1567.7
22H-1, 105	198.85	1547.8	1560.6
22H-2, 35	199.65	1559.6	1567.7
22H-2, 105	200.35	1549.5	1560.6
22H-3, 40	201.20	1539.5	1539.5
23H-1, 35	207.65	1550.7	1561.8
23H-1, 105	208.35	1564.3	1579.8
23H-2, 30	209.10	1549.1	1568.9
24H-1, 35	217.15	1562.6	1587.1
24H-1, 105	217.85	1557.5	1565.3
24H-2, 35	218.65	1550.7	1572.5
24H-2, 105	219.35	1557.5	1583.4
24H-3, 35	220.15	1549.1	1568.9
24H-3, 132	221.12	1555.8	1561.8
24H-4, 35	221.65	1559.2	1579.8
24H-4, 105	222.35	1554.1	1576.2
24H-5, 35	223.15	1557.5	1579.8
24H-5, 104	223.84	1566.1	1598.2

Table 11 (continued).

Core, section, interval (cm)	Depth (mbsf)	Vertical *P*-wave velocity (m/s)	Horizontal *P*-wave velocity (m/s)
130-805C- (Cont)			
24H-6, 35	224.65	1566.1	1587.1
24H-6, 105	225.35	1549.1	1565.3
25H-3, 130	230.60	1569.5	1551.2
25H-4, 45	231.25	1562.6	1576.2
25H-4, 105	231.85	1564.3	1579.8
25H-5, 40	232.70	1569.5	1576.2
25H-5, 95	233.25	1562.6	1576.2
25H-6, 40	234.20	1560.9	1590.8
25H-6, 100	234.80	1569.5	1583.4
25H-7, 45	235.75	1566.1	1594.5
26X-1, 35	236.15	1571.2	1594.5
26X-1, 100	236.80		1598.2
26X-3, 52	239.32		1565.3
26X-3, 131	240.11	1569.5	1598.2
26X-4, 52	240.82		1594.5
26X-4, 107	241.37	1552.4	1576.2
26X-5, 40	242.20	1564.3	1558.2
26X-5, 120	243.00	1555.8	1587.1
26X-6, 40	243.70		1572.5
26X-6, 107	244.37	1521.0	1561.8
27X-1, 104	246.44		1576.2
28X-1, 45	255.55	1557.5	1568.9
28X-1, 120	256.30	1557.5	1565.3
28X-2, 45	257.05		1561.8
28X-2, 105	257.65	1559.2	1572.5
28X-3, 45	258.55		1576.2
28X-3, 105	259.15	1549.1	1561.8
28X-4, 23	259.83		1583.4
28X-4, 90	260.50	1559.2	1576.2
28X-6, 20	262.80	1562.6	1554.7
28X-6, 90	263.50	1573.0	1602.0
29X-2, 95	267.15	1585.2	
29X-3, 90	268.60	1578.2	1605.7
29X-4, 120	270.40		1587.1
29X-5, 92	271.62	1554.1	1583.4
29X-6, 82	273.02		1598.2
30X-1, 80	275.20		1579.8
30X-2, 66	276.56		1617.1
30X-3, 76	278.16		1579.8
30X-4, 56	279.46		1605.7
30X-5, 93	281.33		1587.1
31X-1, 111	285.11		1550.6
31X-2, 78	286.28		1548.3
31X-3, 125	288.25		1560.0
32X-1, 122	294.92		1590.8
32X-2, 143	296.63		1595.2
32X-3, 119	297.89	1694.7	1629.5
32X-4, 94	299.14	1668.8	
32X-6, 14	301.34	1635.7	1589.9
33X-1, 36	303.26	1626.1	
33X-2, 5	304.45	1635.7	1584.0
33X-2, 50	304.90	1664.7	1635.5
33X-4, 132	308.72	1593.2	1587.8
33X-5, 140	310.30	1648.0	1622.3
33X-CC, 10	311.91	1666.0	1619.0
34X-1, 105	313.65	1767.7	1666.8
34X-2, 47	314.57	1538.3	1582.3
34X-3, 140	317.00	1608.8	1544.4
34X-4, 30	317.40	1673.1	1610.2
34X-5, 45	319.05	1603.3	
35X-2, 78	324.58	1540.2	1560.0
35X-3, 112	326.42	1551.2	1558.0
35X-4, 114	327.94	1582.4	1603.8
35X-5, 50	328.80	1524.9	
36X-1, 67	332.47	1601.6	1593.1
36X-2, 64	333.94	1652.9	1709.8
36X-3, 63	335.43	1614.3	1624.9
36X-4, 80	337.10	1648.0	1643.3
36X-5, 102	338.82	1706.2	1700.8
36X-6, 70	340.00	1690.7	1652.8
37X-1, 62	342.12	1649.2	1676.1
37X-2, 57	343.57	1674.1	1662.4
37X-3, 15	344.65	1727.3	1683.5

Table 11 (continued).

Core, section, interval (cm)	Depth (mbsf)	Vertical *P*-wave velocity (m/s)	Horizontal *P*-wave velocity (m/s)
130-805C- (Cont)			
37X-5, 95	348.45	1716.2	1619.3
38X-1, 73	351.93	1668.1	1655.2
38X-2, 58	353.28	1647.4	1657.1
38X-3, 53	354.73	1583.6	1611.1
38X-4, 100	356.70	1698.9	1710.1
38X-5, 46	357.66	1762.6	1679.4
38X-6, 99	359.69	1797.3	1661.4
39X-1, 60	361.50	1822.6	1814.7
39X-3, 80	364.70	1691.8	1622.2
39X-4, 95	366.35	1743.3	1640.1
39X-5, 116	368.06	1691.2	1680.2
39X-6, 110	369.50	1871.6	1748.2
40X-1, 99	371.59	1871.6	1706.2
40X-2, 126	373.36	1806.0	1701.6
40X-3, 126	374.86	1799.1	1772.5
40X-4, 124	376.34	1862.0	1777.7
40X-5, 134	377.94	1837.9	1810.7
41X-1, 111	381.41	1932.1	1791.3
41X-2, 62	382.42	1987.4	1989.9
41X-3, 44	383.74	1896.1	1785.2
41X-4, 72	385.52	1862.6	1803.8
42X-1, 68	390.58	1791.4	1713.3
42X-3, 41	393.31	1711.9	
43X-1, 35	399.85	1640.9	1673.6
43X-2, 36	401.36	1636.9	1677.7
43X-3, 78	403.28	1707.0	1743.8
43X-4, 51	404.51	1687.3	1737.9
43X-5, 26	405.76	1698.1	1709.9
43X-6, 14	407.14	1746.1	1788.5
44X-1, 27	409.37	1734.8	1757.8
44X-2, 39	410.99	1705.4	1743.8
44X-4, 55	414.15	1726.5	1723.0
44X-5, 11	415.21	1675.1	1715.8
44X-6, 9	416.69	1662.8	1694.2
45X-1, 104	419.74	1686.4	1657.4
45X-2, 25	420.45	1908.5	1671.2
45X-3, 124	422.94	1692.0	
45X-3, 138	423.08	1692.0	1719.3
45X-5, 147	426.17	1731.5	1724.7
46X-1, 85	429.25	1661.2	
46X-2, 97	430.87	1778.7	1779.0
46X-3, 84	432.24	1798.2	1767.1
46X-4, 35	433.25	1665.7	1633.7
46X-5, 36	434.76	2035.5	1874.2
47X-1, 96	439.06	1914.8	1791.6
47X-2, 82	440.42	1759.2	1581.9
47X-3, 78	441.88	1905.3	1776.4
47X-4, 85	443.45	1862.6	1827.3
47X-5, 53	444.63	1822.6	1799.0
47X-6, 32	445.92	1888.5	1876.6
47X-6, 92	446.52	1837.9	1683.0
48X-1, 98	448.68	1795.6	
48X-2, 99	450.19		1704.6
48X-3, 92	451.62	1871.0	
48X-4, 95	453.15	1777.1	1749.6
48X-5, 86	454.56	1905.7	1691.1
49X-2, 86	459.76	1932.1	1788.0
50X-1, 129	468.29		1685.3
50X-2, 95	469.45	1896.6	1691.4
50X-3, 91	470.91	1854.3	1598.0
50X-4, 76	472.26		1634.2
51X-1, 138	476.88	1968.7	1938.1
51X-2, 116	478.16	1813.1	1664.7
51X-3, 107	479.57	1923.6	1662.6
51X-4, 79	480.79		1734.7
51X-5, 75	482.25	1871.0	1772.7
52X-1, 106	486.26	1862.1	1663.1
52X-2, 60	487.30	1845.5	1804.1
52X-3, 90	489.10	1724.8	
52X-4, 49	490.19	1691.2	1664.0
53X-1, 90	495.80	1670.0	1678.5
53X-2, 74	497.14	1679.3	1715.5

Table 11 (continued).

Core, section, interval (cm)	Depth (mbsf)	Vertical *P*-wave velocity (m/s)	Horizontal *P*-wave velocity (m/s)
130-805C- (Cont)			
53X-3, 8	497.98	1794.8	1704.5
53X-4, 84	500.24	1857.4	1933.4
53X-5, 56	501.46	1966.0	1961.8
54X-1, 133	505.93	1925.8	1948.9
54X-2, 74	506.84	1826.1	1747.5
54X-3, 112	508.72	1857.1	1825.2
54X-4, 57	509.67	1853.8	1732.7
55X-1, 66	514.86	1756.5	1855.4
55X-2, 47	516.17	1958.6	1807.4
55X-3, 41	517.61	1803.4	1890.2
56X-CC, 35	524.56	1830.5	1871.7
57X-1, 56	534.06	1883.6	1799.2
57X-2, 84	535.84	1900.2	1842.5
58X-1, 45	543.65	1926.4	1868.0
59X-1, 14	553.04	1877.5	1919.1
59X-2, 19	554.59	1880.5	1834.6
60X-1, 45	563.05	1837.6	1861.5
61X-1, 32	572.62	1985.4	1908.2
61X-2, 53	574.33	1843.7	1922.9
61X-3, 110	576.40	1917.7	
61X-5, 134	579.64	1959.1	1840.8
62X-1, 122	583.22	1865.3	1923.1
62X-2, 120	584.70	1983.6	1912.6
63X-1, 105	592.75	1874.3	1918.0
63X-2, 50	593.70	1833.1	1870.3
64X-1, 13	601.43	1865.6	1898.3

VOLUME
130

CHAPTER
8

TABLES
6, 7, 8, AND 9

Table 6. Concentrations of total carbon and inorganic carbon, Hole 806B.

Core, section, interval (cm)	Depth (mbsf)	Inorganic carbon (%)	CaCO$_3$ (%)	Total carbon (%)	Total organic carbon (%)
130-806B-					
1H-1, 111-113	1.11	10.41	86.70	10.58	0.17
1H-2, 34-36	1.84	10.02	83.50		
1H-3, 34-36	3.34	10.12	84.30	10.52	0.40
1H-4, 35-37	4.85	10.21	85.00		
2H-1, 108-110	7.58	10.58	88.10	10.71	0.13
2H-2, 35-37	8.35	10.61	88.40		
2H-3, 34-36	9.84	10.25	85.40	10.54	0.29
2H-4, 34-36	11.34	10.50	87.50		
2H-5, 35-37	12.85	10.75	89.50		
2H-6, 31-33	14.31	10.65	88.70		
3H-1, 34-36	16.34	10.49	87.40	10.70	0.21
3H-2, 34-36	17.84	10.26	85.50		
3H-3, 34-36	19.34	10.69	89.00		
3H-4, 34-36	20.84	10.96	91.30		
3H-5, 34-36	22.34	10.81	90.00	10.81	0.00
3H-6, 34-36	23.84	10.59	88.20		
3H-7, 34-36	25.34	10.50	87.50		
4H-1, 109-111	26.59	10.58	88.10		
4H-2, 32-34	27.32	10.58	88.10	10.63	0.05
4H-3, 34-36	28.84	10.80	90.00		
4H-4, 34-36	30.34	10.73	89.40		
4H-5, 34-36	31.84	10.71	89.20		
4H-6, 34-36	33.34	10.87	90.50		
4H-7, 34-36	34.84	10.67	88.90		
5H-1, 33-35	35.33	10.78	89.80	11.00	0.22
5H-2, 34-36	36.84	10.84	90.30		
5H-3, 35-37	38.35	10.68	89.00		
5H-4, 34-36	39.84	10.82	90.10		
5H-5, 34-36	41.34	10.80	90.00		
5H-6, 34-36	42.84	10.86	90.50		
5H-7, 33-35	44.33	10.07	83.90		
6H-1, 110-112	45.60	10.93	91.00		
6H-2, 110-112	47.10	10.69	89.00		
6H-3, 34-36	47.84	10.82	90.10		
6H-4, 40-42	49.40	10.88	90.60		
6H-5, 40-42	50.90	10.85	90.40		
6H-6, 40-42	52.40	11.04	92.00		
6H-7, 40-42	53.90	11.04	92.00		
7H-1, 109-110	55.09	10.70	89.10	10.84	0.14
7H-2, 39-40	55.89	10.77	89.70		
7H-3, 40-41	57.40	10.78	89.80		
7H-4, 39-40	58.89	10.91	90.90		
7H-5, 40-41	60.40	10.91	90.90		
7H-6, 39-40	61.89	11.07	92.20		
7H-7, 39-40	63.39	10.86	90.50		
8H-1, 38-40	63.88	10.80	90.00		
8H-2, 38-40	65.38	10.32	86.00	10.96	0.64
8H-3, 38-40	66.88	10.89	90.70		
8H-4, 38-40	68.38	10.87	90.50		
8H-5, 38-40	69.88	10.76	89.60		
8H-6, 38-40	71.38	10.99	91.50		
8H-7, 38-40	72.88	10.98	91.50		
9H-1, 110-112	74.10	10.85	90.40		
9H-2, 38-40	74.88	10.90	90.80		
9H-3, 38-40	76.38	10.98	91.50		
9H-4, 38-40	77.88	11.04	92.00		
9H-5, 39-41	79.39	10.94	91.10		
9H-6, 39-41	80.89	11.06	92.10		
9H-7, 49-51	82.49	11.14	92.80		
10H-1, 69-71	83.19	11.18	93.10		
10H-2, 38-40	84.38	11.12	92.60		
10H-3, 38-40	85.88	10.93	91.00		
10H-4, 39-41	87.39	10.97	91.40		
10H-5, 39-41	88.89	11.20	93.30		
10H-6, 39-41	90.39	11.06	92.10		
10H-7, 30-34	91.80	11.05	92.00		
11H-1, 110-112	93.10	11.09	92.40	11.13	0.04
11H-2, 39-41	93.89	11.20	93.30		
11H-3, 38-40	95.38	11.10	92.50		
11H-4, 40-42	96.90	10.94	91.10		
11H-5, 40-42	98.40	10.80	90.00		
11H-6, 40-42	99.90	10.90	90.80		
11H-7, 73-75	101.73	10.73	89.40		

Table 6 (continued).

Core, section, interval (cm)	Depth (mbsf)	Inorganic carbon (%)	CaCO$_3$ (%)	Total carbon (%)	Total organic carbon (%)
130-806B- (Cont.)					
12H-1, 39-41	101.89	11.23	93.50		
12H-2, 38-40	103.38	10.88	90.60	10.93	0.05
12H-3, 37-39	104.87	10.94	91.10		
12H-4, 33-35	106.33	10.80	90.00		
12H-5, 40-42	107.90	10.91	90.90		
12H-6, 39-42	109.39	10.73	89.40		
12H-7, 59-61	111.09	10.66	88.80		
13H-1, 37-39	111.37	10.32	86.00		
13H-2, 36-38	112.86	10.93	91.00		
13H-3, 34-36	114.34	11.04	92.00		
13H-4, 34-36	115.84	10.92	91.00		
13H-5, 34-36	117.34	10.98	91.50		
13H-6, 34-36	118.84	10.93	91.00		
13H-7, 64-67	120.64	11.09	92.40		
14H-1, 111-113	121.61	11.22	93.50		
14H-2, 41-43	122.41	11.22	93.50		
14H-3, 36-38	123.86	11.05	92.00	11.10	0.05
14H-4, 33-35	125.33	11.26	93.80		
14H-5, 32-34	126.82	11.20	93.30		
14H-6, 34-36	128.34	11.00	91.60		
14H-7, 23-25	129.73	10.87	90.50		
15H-1, 34-36	130.34	11.01	91.70		
15H-2, 33-35	131.83	11.03	91.90		
15H-3, 34-36	133.34	11.05	92.00	11.25	0.20
15H-4, 39-41	134.89	11.22	93.50		
15H-5, 40-42	136.40	11.09	92.40		
15H-6, 39-41	137.89	11.36	94.60		
15H-7, 40-42	139.40	11.29	94.00		
16H-1, 108-110	140.58	11.39	94.90	11.61	0.22
16H-2, 108-110	142.08	11.17	93.00		
16H-3, 108-110	143.58	11.33	94.40		
16H-4, 107-109	145.07	11.16	93.00		
16H-5, 108-110	146.58	11.19	93.20		
16H-6, 109-111	148.09	10.99	91.50		
17H-1, 109-111	150.09	11.37	94.70		
17H-2, 108-110	151.58	11.11	92.50		
17H-3, 107-109	153.07	11.12	92.60		
17H-4, 108-110	154.58	11.13	92.70		
17H-5, 109-111	156.09	10.86	90.50		
17H-6, 109-111	157.59	11.00	91.60		
17H-7, 39-41	158.39	10.90	90.80		
18H-1, 108-110	159.58	10.88	90.60	11.35	0.47
18H-2, 107-109	161.07	10.98	91.50		
18H-3, 110-112	162.60	10.98	91.50		
18H-4, 89-91	163.89	10.99	91.50		
18H-5, 110-112	165.60	11.25	93.70		
18H-6, 110-112	167.10	11.06	92.10		
18H-7, 44-46	167.94	10.82	90.10		
19H-1, 110-112	169.10	11.02	91.80	11.34	0.32
19H-2, 109-111	170.59	11.21	93.40		
19H-3, 111-113	172.11	11.10	92.50		
19H-4, 111-113	173.61	11.28	94.00		
19H-5, 110-112	175.10	11.05	92.00		
19H-6, 109-111	176.59	11.07	92.20		
19H-7, 40-42	177.40	11.00	91.60		
20H-1, 111-113	178.61	11.32	94.30	11.47	0.15
20H-2, 109-111	180.09	11.09	92.40		
20H-3, 109-111	181.59	11.34	94.50		
20H-4, 109-111	183.09	11.18	93.10		
20H-5, 110-112	184.60	11.16	93.00		
20H-6, 109-111	186.09	11.41	95.00		
21H-1, 108-110	188.08	11.11	92.50	11.23	0.12
21H-2, 108-110	189.58	11.44	95.30		
21H-3, 109-111	191.09	11.21	93.40		
21H-4, 109-111	192.59	11.05	92.00		
21H-5, 108-110	194.08	11.17	93.00		
21H-6, 108-110	195.58	11.33	94.40		
22H-1, 108-110	197.58	11.29	94.00	11.33	0.04
22H-2, 109-111	199.09	11.12	92.60		
22H-3, 109-111	200.59	11.29	94.00		
22H-4, 110-112	202.10	11.14	92.80		
22H-5, 109-111	203.59	11.29	94.00		
22H-6, 110-112	205.10	11.16	93.00		
23H-1, 105-107	207.05	11.09	92.40	11.55	0.46
23H-3, 38-40	209.38	11.26	93.80		

Table 6 (continued).

Core, section, interval (cm)	Depth (mbsf)	Inorganic carbon (%)	$CaCO_3$ (%)	Total carbon (%)	Total organic carbon (%)
130-806B- (Cont.)					
23H-4, 109-111	211.59	11.30	94.10		
23H-5, 105-107	213.05	11.47	95.50		
23H-6, 109-111	214.59	11.23	93.50		
24H-1, 110-112	216.60	11.41	95.00	11.45	0.04
24H-2, 110-112	218.10	11.23	93.50		
24H-3, 109-111	219.59	11.41	95.00		
24H-4, 106-108	221.06	11.15	92.90		
24H-5, 110-111	222.60	11.51	95.90		
24H-6, 110-112	224.10	11.12	92.60		
24H-7, 40-42	224.90	11.38	94.80		
25H-2, 108-111	227.58	11.09	92.40	11.49	0.40
25H-3, 108-111	229.08	11.39	94.90		
25H-4, 109-112	230.59	11.36	94.60		
25H-5, 119-122	232.19	11.42	95.10		
25H-6, 111-114	233.61	11.30	94.10		
25H-7, 48-52	234.48	11.12	92.60		
26H-1, 108-110	235.58	11.18	93.10	11.19	0.01
26H-2, 104-106	237.04	11.20	93.30		
26H-3, 109-111	238.59	11.31	94.20		
26H-4, 109-111	240.09	11.33	94.40		
26H-5, 110-112	241.60	11.23	93.50		
26H-6, 109-111	243.09	11.24	93.60		
26H-7, 39-41	243.89	11.08	92.30		
27H-1, 29-31	244.29	11.37	94.70	11.52	0.15
27H-3, 109-111	248.09	11.40	95.00		
27H-4, 104-106	249.54	11.41	95.00		
27H-5, 104-106	251.04	11.27	93.90		
27H-6, 107-109	252.57	11.38	94.80		
27H-7, 38-40	253.38	11.42	95.10		
28H-1, 109-111	254.59	11.39	94.90	11.42	0.03
28H-2, 109-111	256.09	11.38	94.80		
28H-3, 115-117	257.65	11.47	95.50		
28H-4, 109-111	259.09	11.43	95.20		
28H-5, 115-117	260.65	11.38	94.80		
28H-6, 109-111	262.09	11.34	94.50		
29H-1, 109-111	264.09	11.23	93.50	11.34	0.11
29H-2, 109-111	265.59	11.26	93.80		
29H-3, 113-115	267.13	11.17	93.00		
29H-4, 99-101	268.49	11.28	94.00		
29H-5, 104-106	270.04	11.25	93.70		
29H-6, 115-117	271.65	11.26	93.80		
30H-1, 110-112	273.60	11.24	93.60		
30H-2, 23-25	274.23	11.25	93.70		
30H-3, 129-131	276.79	10.71	89.20		
30H-4, 109-111	278.09	11.18	93.10		
30H-5, 28-30	278.78	11.26	93.80		
30H-6, 105-107	281.05	11.27	93.90		
30H-7, 38-40	281.88	11.14	92.80		
31H-1, 108-110	283.08	10.71	89.20	10.90	0.19
31H-2, 29-31	283.79	11.19	93.20		
31H-3, 109-111	286.09	11.22	93.50		
31H-4, 105-107	287.55	11.08	92.30		
31H-5, 108-110	289.08	11.26	93.80		
31H-6, 116-118	290.66	11.19	93.20		
31H-7, 39-41	291.39	11.04	92.00		
32H-1, 35-37	291.85	11.14	92.80		
32H-1, 116-118	292.66	11.11	92.50		
32H-2, 107-109	294.07	11.22	93.50		
32H-3, 107-109	295.57	11.07	92.20		
32H-4, 114-116	297.14	11.22	93.50		
32H-5, 114-116	298.64	11.25	93.70		
32H-6, 110-112	300.10	11.48	95.60		
33H-1, 112-114	302.12	11.27	93.90		
33H-2, 106-108	303.56	11.19	93.20		
33H-3, 126-128	305.26	11.15	92.90		
33H-4, 102-104	306.52	10.80	90.00		
33H-5, 127-129	308.27	11.10	92.50		
33H-6, 115-117	309.65	10.95	91.20		
34H-1, 101-103	311.51	10.88	90.60		
34H-2, 108-110	313.08	10.68	89.00	10.71	0.03
34H-3, 109-111	314.59	11.06	92.10		
34H-4, 108-110	316.08	10.99	91.50		
34H-5, 109-111	317.59	11.14	92.80		
34H-6, 109-111	319.09	10.98	91.50		
35X-1, 105-107	321.05	11.08	92.30		
35X-2, 105-107	322.55	11.40	95.00		
35X-3, 107-109	324.07	11.20	93.30		
35X-4, 107-109	325.57	11.18	93.10		
35X-5, 109-111	327.09	11.37	94.70		
35X-6, 107-109	328.57	11.30	94.10		
36X-2, 104-106	332.24	11.36	94.60		
36X-3, 105-109	333.75	11.31	94.20		
36X-4, 104-106	335.24	11.21	93.40		
36X-5, 104-106	336.74	11.28	94.00		
36X-6, 104-106	338.24	11.33	94.40		
37X-1, 118-120	340.58	11.30	94.10		
37X-3, 118-120	343.58	11.32	94.30	11.41	0.09
37X-5, 109-111	346.49	11.24	93.60		
38X-2, 86-88	351.46	11.20	93.30	11.21	0.01
38X-4, 63-65	354.23	11.37	94.70		
39X-1, 98-99	359.78	11.32	94.30		
39X-2, 98-100	361.28	11.31	94.20		
39X-3, 79-81	362.59	11.18	93.10		
39X-5, 94-96	365.74	11.30	94.10		
40X-1, 33-35	368.83	11.34	94.50		
40X-2, 32-34	370.32	11.13	92.70	11.19	0.06
40X-CC, 11-13	375.81	11.10	92.50		
41X-1, 79-81	378.99	11.08	92.30		
41X-2, 74-76	380.44	11.13	92.70		
41X-3, 63-65	381.83	10.94	91.10		
42X-1, 63-65	388.53	11.07	92.20		
42X-4, 51-53	392.91	11.29	94.00		
42X-6, 129-131	396.69	11.31	94.20		
43X-1, 80-82	398.30	11.18	93.10		
43X-2, 26-28	399.26	11.17	93.00		
43X-3, 93-95	401.43	11.07	92.20		
43X-6, 123-125	406.23	11.14	92.80		
44X-1, 82-84	408.02	10.96	91.30		
44X-2, 94-96	409.64	10.95	91.20		
44X-3, 79-81	410.99	10.99	91.50		
44X-5, 88-90	414.08	11.12	92.60		
44X-6, 128-130	415.98	11.05	92.00		
45X-1, 47-49	417.37	11.08	92.30		
45X-2, 84-86	419.24	11.09	92.40	11.12	0.03
45X-3, 42-45	420.32	11.13	92.70		
45X-4, 107-109	422.47	11.10	92.50		
46X-1, 65-67	427.15	11.34	94.50		
46X-2, 55-57	428.55	11.32	94.30	11.46	0.14
46X-3, 107-109	430.57	11.22	93.50		
46X-4, 104-106	432.04	11.43	95.20		
46X-5, 57-59	433.07	11.35	94.50		
46X-6, 66-68	434.66	11.06	92.10		
47X-1, 34-36	436.44	10.87	90.50		
47X-3, 110-112	440.20	11.02	91.80		
47X-4, 92-94	441.52	10.99	91.50		
48X-1, 16-18	445.96	10.68	89.00		
49X-1, 9-11	455.59	10.91	90.90		
49X-2, 20-22	457.20	11.14	92.80		
49X-6, 64-66	463.64	11.31	94.20		
50X-1, 44-46	464.04	11.20	93.30		
50X-3, 92-94	467.52	10.84	90.30		
50X-6, 67-69	471.77	10.95	91.20		
51X-1, 9-11	473.39	11.44	95.30		
51X-2, 115-117	475.95	11.00	91.60	11.22	0.22
52X-1, 21-23	482.81	11.15	92.90		
52X-2, 71-73	484.81	11.29	94.00		
52X-3, 56-58	486.16	11.22	93.50		
52X-5, 5-7	488.65	11.13	92.70		
53X-1, 4-6	492.34	11.22	93.50		
53X-2, 4-6	493.84	11.11	92.50	11.20	0.09
53X-4, 147-149	498.27	11.43	95.20		
54X-1, 2-4	501.92	11.16	93.00		
54X-3, 124-126	506.14	11.16	93.00	11.27	0.11
55X-1, 2-4	511.62	10.61	88.40		
55X-3, 5-7	514.65	11.48	95.60		
55X-4, 31-33	516.41	11.35	94.50		
55X-6, 49-51	519.59	11.43	95.20		
56X-1, 108-111	522.38	10.96	91.30		
56X-2, 108-110	523.88	11.26	93.80	11.34	0.08
56X-4, 43-45	526.23	10.56	88.00		

Table 6 (continued).

Core, section, interval (cm)	Depth (mbsf)	Inorganic carbon (%)	$CaCO_3$ (%)	Total carbon (%)	Total organic carbon (%)
130-806B- (Cont.)					
57X-1, 13-16	531.03	10.70	89.10		
57X-3, 31-33	534.21	11.22	93.50		
58X-1, 4-6	540.54	10.88	90.60		
58X-3, 42-44	543.92	10.81	90.00	10.90	0.09
59X-1, 14-16	550.34	10.84	90.30		
59X-2, 146-148	553.16	11.16	93.00	11.20	0.04
59X-3, 63-65	553.83	10.94	91.10		
60X-1, 140-141	561.30	10.92	91.00		
60X-2, 118-120	562.58	11.12	92.60	11.22	0.10
60X-4, 89-91	565.29	10.99	91.50		
61X-2, 65-67	571.75	11.14	92.80	11.29	0.15
61X-4, 53-55	574.63	11.00	91.60		
63X-3, 11-13	592.11	11.22	93.50		
63X-6, 25-27	596.75	11.20	93.30		
64X-2, 48-50	600.58	11.06	92.10	11.35	0.29
66X-1, 11-13	618.01	11.34	94.50		
66X-5, 11-13	624.01	11.32	94.30	11.42	0.10
66X-7, 13-15	627.03	11.51	95.90		
67X-1, 22-24	627.72	11.34	94.50		
67X-2, 29-31	629.29	11.37	94.70		
68X-1, 23-25	637.43	11.36	94.60	11.42	0.06
69X-1, 23-25	646.73	11.08	92.30		
69X-4, 17-19	651.17	11.36	94.60		
70X-1, 13-15	656.33	11.02	91.80		
70X-2, 16-18	657.86	11.28	94.00		
70X-3, 13-15	659.33	11.39	94.90		
70X-4, 16-18	660.86	11.37	94.70		
71X-1, 68-70	666.48	11.04	92.00	11.17	0.13
72X-1, 5-7	675.55	11.23	93.50		
72X-2, 33-35	677.33	11.19	93.20	11.27	0.08
72X-3, 30-32	678.80	11.30	94.10		
72X-4, 40-42	680.40	10.71	89.20		
73X-1, 97-99	686.17	11.42	95.10		
73X-2, 62-64	687.32	11.59	96.50	11.65	0.06
73X-3, 31-33	688.51	11.56	96.30		
74X-1, 95-97	695.75	11.47	95.50		
74X-2, 105-107	697.35	11.24	93.60	11.40	0.16
74X-3, 105-107	698.85	11.35	94.50		
75X-1, 20-22	704.70	11.25	93.70		
75X-4, 119-121	710.19	10.69	89.00		
76X-1, 46-48	714.56	10.69	89.00		
76X-2, 48-50	716.08	11.30	94.10	11.39	0.09
76X-3, 31-33	717.41	11.42	95.10		
78X-1, 7-9	733.47	11.41	95.00		

Note: Calcium carbonate and organic carbon contents are calculated as noted in the "Explanatory Notes" chapter (this volume).

Table 7. Shear strength data, Holes 806B and 806C.

Core, section, interval (cm)	Depth (mbsf)	Peak shear strength (kPa)	Residual shear strength (kPa)
130-806B-			
1H-1, 120	1.20	5.17	1.91
1H-2, 120	2.70	5.39	1.12
1H-3, 120	4.20	8.76	3.37
1H-4, 120	5.70	10.56	4.94
2H-1, 120	7.70	6.07	2.02
2H-2, 120	9.20	4.49	1.57
2H-3, 120	10.70	10.33	4.04
2H-4, 120	12.20	8.09	3.26
2H-5, 120	13.70	7.53	3.37
2H-6, 120	15.20	14.15	5.62
3H-1, 121	17.21	7.53	2.92
3H-2, 122	18.72	8.20	2.92
3H-3, 120	20.20	6.63	2.47
3H-4, 14	20.64	11.01	3.15
3H-5, 118	23.18	18.65	7.86
3H-6, 121	24.71	13.93	6.29
4H-1, 117	26.67	8.76	3.82
4H-1, 120	26.70	10.00	4.72
4H-2, 120	28.20	11.68	2.92
4H-3, 118	29.68	12.02	4.94
4H-5, 120	32.70	15.28	6.74
4H-6, 120	34.20	11.68	3.82
5H-1, 120	36.20	15.50	4.94
5H-2, 120	37.70	8.31	2.92
5H-3, 120	39.20	6.51	1.68
5H-4, 120	40.70	6.29	1.57
5H-5, 120	42.20	7.86	2.92
5H-6, 120	43.70	7.86	2.47
6H-1, 120	45.70	6.40	1.80
6H-2, 120	47.20	7.86	3.15
6H-3, 120	48.70	8.99	3.71
6H-4, 100	50.00	7.86	3.15
6H-5, 110	51.60	5.73	2.25
6H-6, 120	53.20	9.32	3.59
7H-2, 140	56.90	10.22	2.36
7H-3, 140	58.40	8.20	1.68
7H-4, 140	59.90	9.66	2.25
7H-5, 140	61.40	11.68	2.92
7H-6, 140	62.90	9.77	2.58
7H-7, 65	63.65	10.56	3.48
8H-1, 140	64.90	7.64	2.47
8H-2, 140	66.40	14.15	4.49
8H-3, 140	67.90	11.01	3.37
8H-4, 140	69.40	11.46	3.82
8H-5, 140	70.90	8.31	1.80
8H-6, 140	72.40	12.13	3.15
8H-7, 50	73.00	9.77	
9H-1, 140	74.40	8.99	3.15
9H-2, 140	75.90	6.96	2.81
9H-3, 141	77.41	10.67	3.15
9H-4, 114	78.64	8.31	2.47
9H-5, 140	80.40	6.07	1.57
9H-7, 80	82.80	9.55	1.68
10H-2, 140	85.40	4.72	1.12
10H-3, 140	86.90	7.30	2.36
10H-4, 140	88.40	9.66	2.25
10H-5, 136	89.86	10.22	1.57
10H-6, 140	91.40	12.36	3.15
11H-1, 140	93.40	8.42	3.59
11H-2, 140	94.90	5.62	2.02
11H-3, 134	96.34	9.77	3.82
11H-4, 140	97.90	9.88	1.12
11H-5, 140	99.40	11.46	2.25
11H-6, 140	100.90	17.97	4.94
11H-7, 64	101.64	13.82	3.37
11H-7, 79	101.79	19.10	4.94
12H-2, 140	104.40	10.00	3.03
12H-3, 140	105.90	13.03	4.72
12H-4, 115	107.15	9.10	4.04
12H-5, 140	108.90	10.90	4.38
12H-6, 135	110.35	20.44	7.19
12H-7, 70	111.20	14.38	5.84
13H-1, 120	112.20	11.01	3.15
13H-2, 120	113.70	17.52	3.37
13H-3, 118	115.18	7.53	2.47
13H-4, 120	116.70	14.27	3.82
13H-5, 118	118.18	16.40	
13H-6, 119	119.69	15.05	
13H-7, 118	121.18	15.05	5.39
14H-2, 119	123.19	13.03	
14H-3, 121	124.71	14.60	3.59
14H-4, 126	126.26	10.78	1.80
14H-5, 122	127.72	15.28	1.80
14H-6, 122	129.22	10.78	3.26
14H-7, 29	129.79	8.65	1.80
15H-1, 121	131.21	10.56	
15H-2, 120	132.70	9.66	2.92
15H-3, 120	134.20	10.33	1.57
15H-4, 108	135.58	7.53	2.02
15H-5, 110	137.10	5.17	1.68
15H-6, 120	138.70	11.01	
16H-2, 120	142.20	5.05	1.57
16H-3, 120	143.70	4.38	1.46
16H-4, 120	145.20	6.29	1.46
16H-5, 120	146.70	7.19	2.70
16H-6, 120	148.20	9.88	3.59
17H-1, 118	150.18	6.85	2.13
17H-3, 120	153.20	4.38	0.90
17H-4, 120	154.70	11.12	2.47
17H-5, 120	156.20	13.82	3.26
17H-6, 120	157.70	13.37	
18H-1, 120	159.70	9.10	1.68
18H-3, 121	162.71	9.66	4.49
18H-4, 120	164.20	6.85	1.68
18H-5, 114	165.64	11.91	2.47
18H-6, 130	167.30	17.30	5.17
18H-7, 74	168.24	13.93	
19H-1, 121	169.21	15.28	3.59
19H-2, 121	170.71	15.16	
19H-3, 124	172.24	10.45	2.13
19H-4, 122	173.72	13.03	2.36
19H-5, 121	175.21	14.04	3.59
19H-6, 123	176.73	17.41	4.04
19H-7, 52	177.52	17.75	4.72
20H-1, 123	178.73	12.58	
20H-2, 119	180.19	8.87	2.81
20H-3, 119	181.69	11.91	
20H-4, 121	183.21	11.23	2.13
20H-5, 120	184.70	16.74	3.59
20H-6, 121	186.21	11.46	2.92
21H-1, 120	188.20	8.87	2.25
21H-2, 120	189.70	8.20	1.91
21H-3, 120	191.20	9.66	3.37
21H-4, 120	192.70	5.62	2.25
21H-5, 120	194.20	10.56	
21H-6, 125	195.75	11.34	4.83
22H-1, 120	197.70	10.78	2.70
22H-2, 120	199.20	9.55	2.70
22H-3, 120	200.70	13.82	4.94
22H-4, 120	202.20	10.22	2.81
22H-5, 120	203.70	16.51	
22H-6, 120	205.20	15.73	
23H-1, 120	207.20	15.28	1.80
23H-2, 120	208.70	12.47	2.70
23H-3, 120	210.20	6.07	3.48
23H-4, 120	211.70	4.38	2.81
23H-5, 120	213.20	8.42	2.81
23H-6, 120	214.70	14.94	5.39
23H-7, 70	215.70	11.79	5.95
24H-1, 140	216.90	8.09	3.37
24H-2, 125	218.25	14.38	4.04
24H-3, 121	219.71	14.94	
24H-4, 111	221.11	12.47	2.47
24H-5, 140	222.90	12.24	5.39
24H-6, 140	224.40	9.88	3.15
24H-7, 65	225.15	15.39	3.03
25H-1, 140	226.40	9.10	3.15
25H-2, 140	227.90	10.78	2.70
25H-3, 138	229.38	14.60	5.39
25H-4, 140	230.90	12.13	4.49
25H-6, 140	233.90	17.07	4.72
25H-7, 80	234.80	17.41	3.48
26H-1, 140	235.90	11.57	2.92
26H-3, 140	238.90	20.89	
26H-4, 140	240.40	11.23	3.59
26H-5, 140	241.90	12.36	4.49
26H-6, 140	243.40	11.91	4.49
26H-7, 60	244.10	14.38	3.48
27H-3, 140	248.40	15.05	3.15
27H-4, 115	249.65	8.99	2.25
27H-5, 140	251.40	15.73	4.49
27H-7, 70	253.70	11.68	1.24
28H-1, 140	254.90	15.50	
28H-2, 140	256.40	10.67	3.82
28H-3, 140	257.90	10.11	2.47
28H-4, 140	259.40	12.58	2.92
28H-5, 140	260.90	12.13	2.70
28H-6, 140	262.40	13.37	2.58
29H-1, 140	264.40	18.08	
29H-2, 140	265.90	18.42	
29H-3, 140	267.40	15.39	
29H-4, 140	268.90	13.25	
29H-5, 140	270.40	14.49	3.37
30H-1, 140	273.90	18.76	
30H-2, 140	275.40	16.74	5.39
30H-3, 140	276.90	13.25	2.81
30H-6, 130	281.30	23.14	
30H-7, 80	282.30	39.31	5.62
31H-1, 140	283.40	20.22	
31H-2, 130	284.80	5.62	
31H-3, 140	286.40	20.22	1.12
31H-4, 140	287.90	13.48	
31H-5, 140	289.40	20.22	3.37
31H-6, 140	290.90	14.60	
31H-7, 70	291.70	16.85	
32H-1, 140	292.90	17.97	4.49
32H-3, 143	295.93	20.22	3.37
32H-4, 135	297.35	15.73	
32H-5, 130	298.80	16.85	1.12
32H-6, 123	300.23	24.71	2.25
33H-1, 126	302.26	22.46	
33H-2, 129	303.79	12.36	2.25
33H-3, 129	305.29	15.73	
33H-4, 108	306.58	17.97	
33H-5, 132	308.32	25.83	4.49
33H-6, 131	309.81	26.96	8.99
34H-1, 128	311.78	10.11	2.25
34H-2, 125	313.25	19.10	6.74
34H-3, 128	314.78	14.60	5.62
34H-4, 134	316.34	23.59	6.74
130-806C-			
1H-2, 120	1.20	1.62	0.79
1H-3, 120	4.20	7.08	0.22
2H-2, 137	8.47	8.87	1.91
2H-3, 140	10.00	10.67	3.37
2H-4, 144	11.54	11.01	3.71
2H-5, 140	13.00	6.74	1.80
2H-6, 140	14.50	9.88	3.59
2H-7, 70	15.30	8.65	3.15
3H-2, 141	18.01	9.44	3.37
3H-3, 140	19.50	10.78	3.59
3H-4, 140	21.00	10.67	3.59
3H-5, 140	22.50	11.57	4.27
3H-6, 144	24.04	9.10	3.26
3H-7, 75	24.85	17.75	5.39
4H-1, 140	26.00	13.93	6.40
4H-3, 127	28.87	10.45	4.27
4H-4, 140	30.50	6.74	2.02
4H-5, 131	31.91	11.23	4.72

Table 7 (continued).

Core, section, interval (cm)	Depth (mbsf)	Peak shear strength (kPa)	Residual shear strength (kPa)
130-806C- (Cont.)			
4H-6, 140	33.50	12.80	3.03
4H-7, 62	34.22	9.44	
5H-1, 142	35.52	8.76	3.82
5H-2, 141	37.01	7.86	2.36
5H-3, 140	38.50	8.20	3.26
5H-5, 142	41.52	10.78	3.59
6H-1, 144	45.04	9.44	3.37
6H-4, 140	49.50	7.41	2.13
6H-5, 140	51.00	11.12	3.82
6H-6, 140	52.50	10.78	2.47
7H-2, 140	56.00	7.86	1.80
7H-3, 140	57.50	10.11	4.27
7H-4, 140	59.00	13.37	3.93
7H-5, 140	60.50	10.33	3.71
7H-6, 140	62.00	10.56	3.15
8H-2, 140	65.50	10.11	2.25
8H-3, 118	66.78	8.99	2.02
8H-4, 126	68.36	11.34	2.58
8H-5, 123	69.83	15.16	4.49
8H-6, 120	71.30	4.72	1.46
9H-2, 120	74.80	6.63	2.13
9H-3, 120	76.30	5.73	1.57
9H-4, 120	77.80	9.44	1.80
9H-5, 121	79.31	11.68	2.92
9H-6, 120	80.80	12.80	2.47
10H-1, 121	82.81	8.31	2.47
10H-2, 120	84.30	10.22	3.71
10H-3, 120	85.80	11.46	3.15
10H-4, 120	87.30	8.31	2.02
10H-5, 120	88.80	7.08	1.57
10H-6, 120	90.30	8.99	3.15
11H-1, 120	92.30	11.34	2.92
11H-2, 118	93.78	12.58	3.82
11H-3, 119	95.29	7.86	1.91
11H-4, 120	96.80	12.58	2.81
11H-5, 118	98.28	19.99	
11H-6, 115	99.75	19.54	
12H-1, 121	101.81	12.36	5.62
12H-2, 120	103.30	11.91	4.94
12H-3, 121	104.81	9.77	3.48
12H-4, 120	106.30	16.17	6.29
12H-5, 122	107.82	11.68	4.04
12H-6, 137	109.47	14.49	
12H-7, 14	109.74	17.52	
13H-1, 119	111.29	11.68	5.39
13H-2, 120	112.80	10.11	3.59
13H-3, 121	114.31	10.78	3.71
13H-4, 120	115.80	15.73	5.84
13H-5, 121	117.31	15.95	
13H-6, 122	118.82	13.25	4.38
14H-1, 121	120.81	12.69	5.17
14H-2, 121	122.31	8.65	2.70
14H-3, 121	123.81	12.02	4.27
14H-4, 120	125.30	11.46	4.49
14H-5, 121	126.81	5.62	1.57
14H-6, 121	128.31	10.11	3.48
15H-2, 120	131.80	9.44	1.80
15H-3, 121	133.31	7.41	1.80
15H-4, 121	134.81	6.40	0.79
15H-5, 120	136.30	11.01	1.80
15H-6, 121	137.81	9.88	2.92
16H-1, 122	139.82	11.01	3.71
16H-2, 115	141.25	6.74	
16H-3, 120	142.80	10.56	
16H-4, 120	144.30	8.54	
16H-6, 122	147.32	10.90	1.57
17H-1, 122	149.32	8.54	1.46
17H-2, 120	150.80	5.95	1.57
17H-3, 121	152.31	10.11	
17H-4, 120	153.80	10.56	
18H-2, 120	160.30	13.93	
18H-3, 120	161.80	12.80	
18H-5, 120	164.80	9.21	1.68
18H-6, 120	166.30	7.19	
19H-1, 120	168.30	14.38	
19H-2, 120	169.80	11.91	
19H-3, 120	171.30	10.45	
19H-4, 120	172.80	13.59	
19H-5, 120	174.30	12.47	
19H-6, 120	175.80	16.62	
20H-1, 120	177.80	8.31	2.92
20H-2, 120	179.30	7.41	2.70
20H-3, 120	180.80	6.74	3.82
20H-4, 120	182.30	9.77	
20H-5, 120	183.80	11.46	3.37
20H-6, 120	185.30	8.42	2.70
21H-1, 120	187.30	8.09	3.37
21H-2, 120	188.80	7.86	2.13
21H-3, 120	190.30	8.54	2.47
21H-4, 120	191.80	9.44	4.04
21H-5, 120	193.30	13.70	4.49
21H-6, 120	194.80	13.93	5.62
22H-1, 120	196.80	15.05	
22H-2, 121	198.31	11.12	2.36
22H-3, 121	199.81	11.01	
22H-4, 121	201.31	8.76	3.93
22H-5, 122	202.82	14.38	0.25
23H-1, 122	206.32	10.45	2.02
23H-3, 122	209.32	4.94	1.24
23H-4, 130	210.90	13.03	4.38
23H-5, 122	212.32	11.12	2.81
23H-6, 122	213.82	12.92	4.38
24H-1, 122	215.82	9.44	2.70
24H-2, 120	217.30	12.02	
24H-3, 121	218.81	14.94	3.26
24H-4, 120	220.30	16.40	3.15
24H-5, 122	221.82	11.57	2.70
24H-6, 118	223.28	12.36	3.15
25H-1, 120	225.30	6.63	3.59
25H-2, 120	226.80	11.01	2.70
25H-3, 120	228.30	18.65	
25H-4, 120	229.80	11.91	2.92
25H-5, 120	231.30	9.66	
25H-6, 120	232.80	6.96	1.80
26H-2, 120	236.30	9.66	0.90
26H-3, 120	237.80	11.01	1.80
26H-4, 120	239.30	13.48	
26H-6, 120	242.30	12.47	3.93
27H-1, 120	244.30	15.05	5.62
27H-2, 120	245.80	9.66	3.59
27H-3, 120	247.30	12.80	
27H-4, 120	248.80	12.13	3.59
27H-5, 120	250.30	14.94	
27H-6, 120	251.80	10.78	3.59
28H-2, 120	255.30	4.04	1.57
28H-3, 120	256.80	12.13	1.12
28H-4, 120	258.30	14.15	0.90
28H-5, 120	259.80	10.33	
28H-6, 120	261.30	11.01	3.82
28H-7, 120	262.80	10.90	2.70
29H-1, 140	263.50	17.63	8.31
29H-2, 134	264.94	10.00	2.92
29H-3, 140	266.50	16.17	
29H-4, 140	268.00	13.70	4.49
29H-5, 140	269.50	13.70	
30H-3, 140	276.00	16.85	
30H-4, 140	277.50	13.70	2.92
30H-5, 140	279.00	18.20	4.04
30H-6, 140	280.50	24.04	
31H-1, 138	282.48	9.3[illegible]	
31H-3, 140	285.50	23.59	
31H-4, 140	287.00	12.58	
31H-5, 137	288.47	18.42	
32H-2, 140	293.50	11.46	2.70
32H-3, 140	295.00	8.99	4.49
32H-4, 140	296.50	20.22	5.62
32H-5, 140	298.00	26.96	
32H-6, 140	299.50	33.70	
33H-1, 137	301.47	8.99	2.25
33H-1, 145	301.55	8.99	2.25
33H-2, 140	303.00	11.23	2.25
33H-4, 140	306.00	19.10	
33H-5, 145	307.55	22.46	

Table 8. Index properties data, Holes 806B and 806C.

Core, section, interval (cm)	Depth (mbsf)	Wet-bulk density (g/cm^3)	Grain density (g/cm^3)	Water content (% dry wt)	Porosity (%)	Dry-bulk density (g/cm^3)
130-806B-						
1H-1, 111	1.11	1.50	2.74	96.3	71.8	0.76
1H-2, 34	1.84	1.50	2.72	96.3	71.7	0.76
1H-2, 109	2.59	1.47	2.61	99.7	71.5	0.73
1H-3, 34	3.34	1.50	2.71	94.4	71.2	0.77
1H-3, 95	3.95	1.54	2.73	86.0	69.4	0.83
1H-4, 35	4.85	1.52	2.71	88.5	69.9	0.81
1H-4, 109	5.59	1.52	2.72	90.1	70.3	0.80
2H-1, 108	7.58	1.53	2.70	85.5	69.0	0.83
2H-2, 35	8.35	1.52	2.71	88.7	69.9	0.81
2H-2, 108	9.08	1.53	2.73	87.8	69.8	0.81
2H-3, 34	9.84	1.57	2.90	85.4	70.5	0.85
2H-3, 109	10.59	1.54	2.76	86.2	69.7	0.83
2H-4, 34	11.34	1.53	2.72	86.3	69.4	0.82
2H-4, 109	12.09	1.56	2.76	80.9	68.3	0.86
2H-5, 35	12.85	1.56	2.72	81.5	68.2	0.86
2H-5, 110	13.60	1.51	2.71	91.1	70.4	0.79
2H-6, 31	14.31	1.54	2.70	84.9	68.9	0.83
2H-6, 109	15.09	1.55	2.70	82.4	68.3	0.85
3H-1, 34	16.34	1.55	2.69	81.8	68.0	0.85
3H-1, 110	17.10	1.58	2.72	76.0	66.7	0.90
3H-2, 34	17.84	1.54	2.76	85.8	69.6	0.83
3H-2, 91	18.41	1.56	2.69	79.1	67.3	0.87
3H-3, 34	19.34	1.59	2.71	74.0	66.0	0.91
3H-3, 109	20.09	1.58	2.70	75.4	66.3	0.90
3H-4, 34	20.84	1.56	2.73	80.7	68.1	0.86
3H-4, 107	21.57	1.54	2.71	84.1	68.8	0.84
3H-5, 34	22.34	1.58	2.71	76.5	66.7	0.89
3H-5, 109	23.09	1.58	2.72	77.2	67.0	0.89
3H-6, 34	23.84	1.56	2.76	81.5	68.5	0.86
3H-6, 103	24.53	1.57	2.72	78.0	67.2	0.88
3H-7, 34	25.34	1.56	2.74	80.5	68.1	0.87
4H-1, 109	26.59	1.56	2.74	80.5	68.0	0.87
4H-2, 32	27.32	1.54	2.76	86.5	69.7	0.83
4H-2, 112	28.12	1.59	2.73	75.1	66.5	0.91
4H-3, 34	28.84	1.52	2.73	91.4	70.6	0.79
4H-3, 110	29.60	1.58	2.79	78.4	67.9	0.89
4H-4, 34	30.34	1.57	2.69	78.1	67.0	0.88
4H-4, 108	31.08	1.56	2.72	79.6	67.6	0.87
4H-5, 34	31.84	1.56	2.75	81.6	68.5	0.86
4H-5, 110	32.60	1.54	2.74	85.6	69.4	0.83
4H-6, 34	33.34	1.56	2.72	80.6	67.9	0.86
4H-6, 110	34.10	1.59	2.73	75.3	66.6	0.90
4H-7, 34	34.84	1.57	2.77	80.0	68.1	0.87
5H-1, 33	35.33	1.58	2.73	77.6	67.2	0.89
5H-1, 110	36.10	1.60	2.74	72.4	65.8	0.93
5H-2, 34	36.84	1.59	2.71	73.9	66.0	0.91
5H-2, 109	37.59	1.55	2.73	82.2	68.4	0.85
5H-3, 35	38.35	1.55	2.69	81.5	68.0	0.85
5H-3, 110	39.10	1.53	2.74	88.3	70.0	0.81
5H-4, 34	39.84	1.57	2.74	79.2	67.7	0.88
5H-4, 108	40.58	1.57	2.74	79.4	67.7	0.87
5H-5, 34	41.34	1.56	2.71	79.5	67.6	0.87
5H-5, 110	42.10	1.56	2.71	79.8	67.7	0.87
5H-6, 34	42.84	1.54	2.72	85.6	69.2	0.83
5H-6, 110	43.60	1.54	2.73	86.7	69.6	0.82
5H-7, 33	44.33	1.53	2.69	85.2	68.9	0.83
6H-1, 110	45.60	1.64	2.71	65.5	63.2	0.99
6H-2, 110	47.10	1.57	2.73	78.4	67.4	0.88
6H-3, 34	47.84	1.55	2.71	82.7	68.4	0.85
6H-3, 110	48.60	1.56	2.74	80.3	68.0	0.87
6H-4, 40	49.40	1.58	2.75	77.7	67.4	0.89
6H-4, 110	50.10	1.58	2.73	77.4	67.1	0.89
6H-5, 40	50.90	1.56	2.71	80.3	67.8	0.86
6H-5, 120	51.70	1.60	2.72	73.1	65.8	0.92
6H-6, 40	52.40	1.63	2.73	67.9	64.2	0.97
6H-6, 120	53.20	1.62	2.75	70.5	65.2	0.95
6H-7, 40	53.90	1.58	2.69	74.6	66.0	0.91
7H-1, 109	55.09	1.52	2.71	90.7	70.3	0.79
7H-2, 39	55.89	1.55	2.70	81.3	68.0	0.86
7H-2, 110	56.60	1.57	2.65	75.8	66.0	0.89
7H-3, 40	57.40	1.62	2.72	69.2	64.6	0.96
7H-3, 110	58.10	1.57	2.74	78.2	67.4	0.88
7H-4, 39	58.89	1.58	2.72	75.4	66.5	0.90
7H-4, 109	59.59	1.58	2.72	76.9	66.9	0.89
7H-5, 40	60.40	1.58	2.70	75.9	66.5	0.90

Table 8 (continued).

Core, section, interval (cm)	Depth (mbsf)	Wet-bulk density (g/cm^3)	Grain density (g/cm^3)	Water content (% dry wt)	Porosity (%)	Dry-bulk density (g/cm^3)
130-806B- (Cont.)						
7H-5, 111	61.11	1.62	2.69	68.2	64.0	0.96
7H-6, 39	61.89	1.59	2.69	74.0	65.8	0.91
7H-6, 109	62.59	1.60	2.73	73.6	66.0	0.92
7H-7, 39	63.39	1.60	2.74	73.8	66.2	0.92
8H-2, 38	65.38	1.56	2.69	78.5	67.1	0.88
8H-1, 110	64.60	1.58	2.77	78.4	67.7	0.89
8H-2, 110	66.10	1.56	2.72	80.5	67.9	0.86
8H-3, 110	67.60	1.59	2.73	75.2	66.6	0.91
8H-3, 38	66.88	1.58	2.74	76.5	67.0	0.90
8H-4, 38	68.38	1.56	2.72	81.5	68.1	0.86
8H-4, 110	69.10	1.57	2.72	78.2	67.3	0.88
8H-5, 110	70.60	1.57	2.72	77.8	67.2	0.88
8H-5, 38	69.88	1.57	2.72	78.7	67.4	0.88
8H-6, 38	71.38	1.54	2.72	84.8	69.0	0.83
8H-6, 110	72.10	1.56	2.72	80.7	67.9	0.86
8H-7, 38	72.88	1.57	2.73	78.3	67.4	0.88
9H-1, 110	74.10	1.56	2.74	80.7	68.2	0.87
9H-2, 38	74.88	1.56	2.73	81.4	68.2	0.86
9H-2, 109	75.59	1.55	2.69	80.9	67.8	0.86
9H-3, 38	76.38	1.54	2.70	85.3	69.0	0.83
9H-3, 109	77.09	1.56	2.72	81.4	68.2	0.86
9H-4, 38	77.88	1.57	2.69	76.8	66.6	0.89
9H-4, 109	78.59	1.56	2.68	79.0	67.2	0.87
9H-5, 39	79.39	1.56	2.74	81.8	68.4	0.86
9H-5, 109	80.09	1.60	2.69	71.0	64.9	0.94
9H-6, 39	80.89	1.56	2.70	79.2	67.4	0.87
9H-6, 109	81.59	1.58	2.71	76.4	66.7	0.89
9H-7, 49	82.49	1.59	2.72	75.5	66.5	0.90
10H-1, 69	83.19	1.55	2.73	83.9	68.9	0.84
10H-2, 38	84.38	1.57	2.75	80.1	68.0	0.87
10H-2, 110	85.10	1.56	2.74	81.1	68.2	0.86
10H-3, 38	85.88	1.57	2.71	78.7	67.4	0.88
10H-3, 109	86.59	1.56	2.71	79.6	67.6	0.87
10H-4, 39	87.39	1.57	2.71	77.2	66.9	0.89
10H-4, 109	88.09	1.57	2.74	79.1	67.7	0.88
10H-5, 39	88.89	1.59	2.72	74.3	66.1	0.91
10H-5, 110	89.60	1.56	2.71	80.5	67.8	0.86
10H-6, 109	91.09	1.58	2.73	76.5	66.9	0.90
10H-6, 39	90.39	1.60	2.73	73.4	66.0	0.92
10H-7, 32	91.82	1.57	2.70	76.8	66.7	0.89
11H-1, 110	93.10	1.60	2.73	72.4	65.7	0.93
11H-2, 39	93.89	1.61	2.72	71.1	65.2	0.94
11H-2, 110	94.60	1.60	2.73	72.0	65.5	0.93
11H-3, 38	95.38	1.56	2.74	82.1	68.5	0.86
11H-3, 109	96.09	1.58	2.71	76.7	66.7	0.89
11H-4, 40	96.90	1.58	2.70	74.4	66.0	0.91
11H-4, 125	97.75	1.58	2.70	75.5	66.4	0.90
11H-5, 40	98.40	1.61	2.76	71.1	65.5	0.94
11H-5, 111	99.11	1.62	2.75	69.3	64.9	0.96
11H-6, 40	99.90	1.60	2.76	73.4	66.2	0.92
11H-6, 110	100.60	1.64	2.74	66.4	63.8	0.98
11H-7, 73	101.73	1.60	2.73	73.3	65.9	0.92
12H-1, 39	101.89	1.64	2.72	65.3	63.3	0.99
12H-1, 111	102.61	1.60	2.75	72.9	66.0	0.93
12H-2, 110	104.10	1.58	2.70	76.5	66.6	0.89
12H-3, 37	104.87	1.58	2.73	75.9	66.7	0.90
12H-3, 109	105.59	1.60	2.70	72.0	65.3	0.93
12H-4, 33	106.33	1.58	2.70	75.9	66.5	0.90
12H-4, 109	107.09	1.59	2.70	73.4	65.7	0.92
12H-5, 40	107.90	1.59	2.71	72.9	65.6	0.92
12H-5, 112	108.62	1.63	2.73	67.8	64.1	0.97
12H-6, 39	109.39	1.60	2.70	71.8	65.3	0.93
12H-6, 109	110.09	1.60	2.71	71.7	65.3	0.93
12H-7, 59	111.09	1.60	2.74	72.8	65.9	0.93
13H-1, 37	111.37	1.60	2.72	71.9	65.4	0.93
13H-1, 113	112.13	1.61	2.71	71.0	65.1	0.94
13H-2, 36	112.86	1.58	2.73	77.9	67.3	0.89
13H-2, 112	113.62	1.61	2.73	71.0	65.2	0.94
13H-3, 34	114.34	1.61	2.73	71.1	65.3	0.94
13H-3, 109	115.09	1.58	2.71	75.2	66.3	0.90
13H-4, 34	115.84	1.61	2.74	70.8	65.2	0.94
13H-4, 109	116.59	1.60	2.72	71.6	65.3	0.93
13H-5, 34	117.34	1.61	2.70	70.3	64.7	0.94
13H-5, 111	118.11	1.60	2.69	72.2	65.3	0.93
13H-6, 34	118.84	1.63	2.70	66.6	63.5	0.98

Table 8 (continued).

Core, section, interval (cm)	Depth (mbsf)	Wet-bulk density (g/cm^3)	Grain density (g/cm^3)	Water content (% dry wt)	Porosity (%)	Dry-bulk density (g/cm^3)
130-806B- (Cont.)						
13H-6, 110	119.60	1.61	2.69	69.8	64.5	0.95
13H-7, 64	120.64	1.60	2.73	72.8	65.8	0.93
14H-1, 111	121.61	1.63	2.71	66.6	63.6	0.98
14H-2, 41	122.41	1.65	2.74	65.2	63.3	1.00
14H-2, 110	123.10	1.62	2.74	69.0	64.7	0.96
14H-3, 36	123.86	1.59	2.71	74.0	66.0	0.91
14H-3, 109	124.59	1.61	2.73	71.3	65.3	0.94
14H-4, 33	125.33	1.62	2.72	68.6	64.4	0.96
14H-4, 109	126.09	1.62	2.72	69.1	64.5	0.96
14H-5, 32	126.82	1.61	2.71	70.3	64.8	0.94
14H-5, 109	127.59	1.64	2.75	67.2	64.1	0.98
14H-6, 34	128.34	1.60	2.71	71.6	65.3	0.93
14H-6, 110	129.10	1.61	2.71	70.1	64.8	0.95
14H-7, 23	129.73	1.58	2.72	76.8	66.9	0.89
15H-1, 34	130.34	1.63	2.70	66.9	63.7	0.97
15H-1, 108	131.08	1.61	2.72	71.1	65.2	0.94
15H-2, 33	131.83	1.60	2.69	71.1	64.9	0.94
15H-2, 108	132.58	1.63	2.72	67.8	64.1	0.97
15H-3, 34	133.34	1.62	2.70	68.2	64.1	0.96
15H-3, 108	134.08	1.58	2.72	76.1	66.7	0.90
15H-4, 39	134.89	1.63	2.70	66.3	63.4	0.98
15H-4, 98	135.48	1.63	2.70	66.7	63.6	0.98
15H-5, 40	136.40	1.61	2.72	69.8	64.7	0.95
15H-5, 108	137. 8	1.67	2.72	61.0	61.7	1.04
15H-6, 39	137.89	1.63	2.71	66.2	63.5	0.98
15H-6, 108	138.58	1.63	2.70	66.6	63.5	0.98
15H-7, 40	139.40	1.66	2.71	62.3	62.9	1.02
16H-1, 108	140.58	1.63	2.70	66.4	63.5	0.98
16H-2, 108	142.08	1.60	2.69	70.6	64.7	0.94
16H-3, 108	143.58	1.60	2.69	71.6	65.1	0.93
16H-4, 107	145.07	1.60	2.69	70.6	64.8	0.94
16H-5, 108	146.58	1.59	2.69	72.7	65.4	0.92
16H-6, 109	148.09	1.64	2.72	65.4	63.2	0.99
17H-1, 109	150.09	1.60	2.69	71.8	65.2	0.93
17H-2, 108	151.58	1.61	2.70	69.8	64.6	0.95
17H-3, 107	153.07	1.60	2.71	71.4	65.2	0.93
17H-4, 108	154.58	1.63	2.71	67.4	63.9	0.97
17H-5, 109	156.09	1.60	2.70	71.1	65.9	0.94
17H-6, 109	157.59	1.63	2.72	66.6	63.7	0.98
17H-7, 39	158.39	1.63	2.68	65.0	62.8	0.99
18H-2, 107	161.07	1.61	2.71	70.5	64.9	0.94
18H-3, 110	162.60	1.63	2.72	67.4	63.9	0.97
18H-4, 89	163.89	1.61	2.72	71.2	65.2	0.94
18H-5, 110	165.60	1.67	2.75	61.8	62.2	1.03
18H-6, 110	167.10	1.65	2.72	62.9	62.4	1.02
18H-7, 44	167.94	1.61	2.69	68.9	64.2	0.96
19H-1, 110	169.10	1.64	2.72	66.1	63.5	0.99
19H-2, 109	170.59	1.64	2.71	65.0	63.9	0.99
19H-3, 111	172.11	1.67	2.73	60.8	61.6	1.04
19H-4, 111	173.61	1.64	2.70	65.4	63.1	0.99
19H-5, 110	175.10	1.64	2.72	66.0	63.5	0.99
19H-6, 109	176.59	1.64	2.70	64.0	62.6	1.00
19H-7, 40	177.40	1.68	2.72	59.3	61.9	1.05
20H-1, 111	178.61	1.65	2.74	64.8	63.3	1.00
20H-2, 109	180.09	1.65	2.71	64.2	62.8	1.00
20H-3, 109	181.59	1.65	2.72	63.2	62.5	1.01
20H-4, 109	183.09	1.66	2.72	61.9	62.9	1.03
20H-6, 109	186.09	1.67	2.74	61.7	62.1	1.03
21H-1, 108	188.08	1.63	2.72	66.8	63.7	0.98
21H-2, 108	189.58	1.70	2.73	57.0	60.2	1.08
21H-3, 109	191.09	1.65	2.70	63.6	62.4	1.01
21H-4, 109	192.59	1.66	2.74	62.2	62.3	1.03
21H-5, 108	194.08	1.64	2.68	64.3	62.6	1.00
21H-6, 108	195.58	1.64	2.72	64.9	63.1	1.00
22H-1, 108	197.58	1.66	2.73	62.4	62.3	1.02
22H-2, 109	199.09	1.62	2.72	68.1	64.2	0.97
22H-3, 109	200.59	1.65	2.73	63.4	62.6	1.01
22H-4, 110	202.10	1.66	2.70	61.9	61.8	1.02
22H-5, 109	203.59	1.65	2.69	62.1	61.8	1.02
22H-6, 110	205.10	1.65	2.72	63.2	62.5	1.01
23H-1, 105	207.05	1.64	2.72	65.4	63.3	0.99
23H-2, 109	208.59	1.66	2.71	62.1	62.9	1.02
23H-3, 38	209.38	1.67	2.75	62.3	62.4	1.03
23H-4, 109	211.59	1.66	2.73	62.6	62.4	1.02
23H-5, 105	213.05	1.67	2.71	60.9	61.5	1.04

Table 8 (continued).

Core, section, interval (cm)	Depth (mbsf)	Wet-bulk density (g/cm^3)	Grain density (g/cm^3)	Water content (% dry wt)	Porosity (%)	Dry-bulk density (g/cm^3)
130-806B- (Cont.)						
23H-6, 109	214.59	1.66	2.73	62.8	62.4	1.02
24H-1, 110	216.60	1.67	2.68	59.2	60.6	1.05
24H-2, 110	218.10	1.73	2.70	51.2	57.2	1.15
24H-3, 109	219.59	1.66	2.71	62.0	62.9	1.02
24H-4, 106	221.06	1.67	2.74	60.9	61.8	1.04
24H-5, 110	222.60	1.68	2.75	59.8	61.5	1.05
24H-6, 110	224.10	1.68	2.70	58.2	60.4	1.06
24H-7, 40	224.90	1.69	2.72	58.4	60.6	1.06
25H-2, 108	227.58	1.67	2.69	58.9	60.5	1.05
25H-3, 108	229.08	1.65	2.69	62.1	61.8	1.02
25H-4, 109	230.59	1.66	2.70	60.7	61.4	1.04
25H-5, 119	232.19	1.68	2.72	58.7	60.8	1.06
25H-6, 111	233.61	1.68	2.69	58.7	60.5	1.06
25H-7, 48	234.48	1.69	2.73	58.4	60.7	1.06
26H-1, 108	235.58	1.67	2.69	59.2	60.7	1.05
26H-2, 104	237.04	1.65	2.69	62.8	62.0	1.01
26H-3, 109	238.59	1.66	2.70	60.9	61.4	1.03
26H-4, 109	240.09	1.66	2.70	61.0	61.4	1.03
26H-5, 110	241.60	1.66	2.70	60.7	61.4	1.04
26H-6, 109	243.09	1.66	2.73	63.1	62.5	1.01
26H-7, 39	243.89	1.65	2.69	62.2	61.9	1.02
27H-1, 29	244.29	1.70	2.67	55.3	58.9	1.09
27H-3, 109	248.09	1.70	2.70	55.9	59.4	1.09
27H-4, 104	249.54	1.67	2.71	59.7	61.1	1.05
27H-5, 104	251.04	1.66	2.66	60.4	60.9	1.03
27H-6, 107	252.57	1.67	2.67	59.2	60.5	1.05
27H-7, 38	253.38	1.68	2.72	58.7	60.7	1.06
28H-1, 109	254.59	1.68	2.70	58.2	60.3	1.06
28H-2, 109	256.09	1.67	2.67	58.3	60.2	1.06
28H-3, 115	257.65	1.70	2.69	55.8	59.3	1.09
28H-4, 109	259.09	1.69	2.68	55.8	59.2	1.09
28H-5, 115	260.65	1.67	2.69	59.2	60.7	1.05
28H-6, 109	262.09	1.66	2.68	60.2	61.0	1.04
29H-1, 109	264.09	1.66	2.70	61.5	61.7	1.03
29H-2, 109	265.59	1.68	2.70	58.5	60.4	1.06
29H-3, 113	267.13	1.62	2.69	67.4	63.7	0.97
29H-4, 99	268.49	1.65	2.71	62.6	62.1	1.02
29H-5, 104	270.04	1.63	2.68	65.5	62.9	0.98
29H-6, 115	271.65	1.61	2.67	67.9	63.7	0.96
30H-1, 110	273.60	1.66	2.71	62.0	61.9	1.02
30H-2, 23	274.23	1.66	2.69	60.9	61.4	1.03
30H-3, 129	276.79	1.66	2.68	60.1	61.0	1.04
30H-4, 109	278.09	1.66	2.69	60.6	61.3	1.03
30H-5, 28	278.78	1.70	2.71	56.4	59.7	1.08
30H-6, 105	281.05	1.68	2.67	56.7	59.5	1.07
30H-7, 38	281.88	1.65	2.69	62.4	61.9	1.02
31H-1, 108	283.08	1.66	2.67	60.6	61.1	1.03
31H-2, 29	283.79	1.67	2.70	59.8	61.0	1.05
31H-3, 109	286.09	1.67	2.70	59.8	61.1	1.05
31H-4, 105	287.55	1.64	2.66	63.2	62.0	1.01
31H-5, 108	289.08	1.70	2.70	55.8	59.4	1.09
31H-6, 116	290.66	1.65	2.68	62.6	61.9	1.01
31H-7, 39	291.39	1.65	2.68	62.4	61.8	1.01
32H-1, 35	291.85	1.65	2.69	63.4	62.3	1.01
32H-1, 116	292.66	1.66	2.70	61.1	61.5	1.03
32H-2, 107	294.07	1.63	2.68	64.8	62.7	0.99
32H-3, 107	295.57	1.63	2.71	67.2	63.8	0.97
32H-4, 114	297.14	1.66	2.70	61.6	61.7	1.03
32H-5, 114	298.64	1.68	2.69	58.2	60.2	1.06
32H-6, 110	300.10	1.72	2.70	52.7	58.0	1.13
33H-1, 112	302.12	1.69	2.71	58.0	60.4	1.07
33H-2, 106	303.56	1.66	2.68	60.5	61.1	1.03
33H-3, 126	305.26	1.65	2.67	62.5	61.8	1.01
33H-4, 102	306.52	1.63	2.70	66.0	63.3	0.98
33H-5, 127	308.27	1.67	2.68	59.1	60.6	1.05
33H-6, 115	309.65	1.64	2.68	63.5	62.3	1.00
34X-1, 101	311.51	1.66	2.69	61.1	61.4	1.03
34X-2, 108	313.08	1.65	2.68	62.2	61.8	1.02
34X-3, 109	314.59	1.63	2.67	65.4	62.8	0.98
34X-4, 108	316.08	1.64	2.69	64.0	62.5	1.00
34X-5, 109	317.59	1.66	2.72	61.5	61.8	1.03
34X-6, 109	319.09	1.63	2.67	65.6	62.9	0.98
35X-1, 105	321.05	1.68	2.71	58.9	60.7	1.06
35X-2, 105	322.55	1.70	2.66	53.8	58.2	1.11
35X-3, 107	324.07	1.70	2.70	56.1	59.5	1.09

Table 8 (continued).

Core, section, interval (cm)	Depth (mbsf)	Wet-bulk density (g/cm^3)	Grain density (g/cm^3)	Water content (% dry wt)	Porosity (%)	Dry-bulk density (g/cm^3)
130-806B- (Cont.)						
35X-4, 107	325.57	1.68	2.70	58.9	60.6	1.05
35X-5, 109	327.09	1.65	2.68	62.1	61.7	1.02
35X-6, 107	328.57	1.70	2.70	55.8	59.4	1.09
36X-1, 103	330.73	1.72	2.71	52.6	58.0	1.13
36X-2, 104	332.24	1.69	2.71	57.7	60.3	1.07
36X-3, 105	333.75	1.66	2.68	60.0	60.9	1.04
36X-4, 104	335.24	1.66	2.71	62.5	62.1	1.02
36X-5, 104	336.74	1.72	2.70	53.4	58.3	1.12
36X-6, 104	338.24	1.68	2.69	58.2	60.3	1.06
37X-1, 118	340.58	1.71	2.70	54.8	58.9	1.10
37X-3, 118	343.58	1.66	2.69	60.2	61.0	1.04
37X-5, 109	346.49	1.61	2.66	67.3	63.4	0.97
38X-2, 86	351.46	1.69	2.71	56.9	59.9	1.08
38X-4, 63	354.23	1.68	2.70	57.5	60.1	1.07
39X-1, 96	359.76	1.68	2.69	57.9	60.2	1.06
39X-2, 98	361.28	1.75	2.67	48.0	55.4	1.18
39X-3, 79	362.59	1.71	2.69	54.0	58.5	1.11
39X-5, 94	365.74	1.72	2.69	52.8	57.9	1.12
40X-1, 33	368.83	1.68	2.65	56.6	59.2	1.07
40X-2, 32	370.32	1.68	2.70	57.8	60.2	1.07
41X-1, 79	378.99	1.72	2.71	53.4	58.4	1.12
41X-2, 74	380.44	1.71	2.68	53.6	58.2	1.11
41X-3, 63	381.83	1.73	2.72	52.7	58.2	1.13
42X-1, 63	388.53	1.73	2.72	52.2	58.0	1.14
42X-4, 51	392.91	1.71	2.69	54.3	58.6	1.11
42X-6, 129	396.69	1.70	2.70	55.0	59.0	1.10
43X-1, 80	398.30	1.69	2.70	56.8	59.8	1.08
43X-2, 26	399.26	1.74	2.69	50.6	56.9	1.15
43X-3, 93	401.43	1.68	2.68	56.8	59.6	1.07
43X-6, 123	406.23	1.67	2.67	58.4	60.2	1.06
44X-1, 82	408.02	1.68	2.68	57.4	59.8	1.07
44X-2, 94	409.64	1.71	2.68	53.4	58.2	1.12
44X-3, 79	410.99	1.80	2.68	43.0	52.8	1.26
44X-5, 88	414.08	1.71	2.69	53.0	58.0	1.12
44X-6, 128	415.98	1.73	2.68	51.4	57.3	1.14
45X-1, 47	417.37	1.66	2.66	59.9	60.7	1.04
45X-2, 84	419.24	1.70	2.69	55.6	59.1	1.09
45X-3, 42	420.32	1.70	2.69	54.9	58.9	1.10
45X-4, 107	422.47	1.71	2.68	53.3	58.1	1.12
46X-1, 65	427.15	1.70	2.68	55.1	58.9	1.10
46X-2, 55	428.55	1.73	2.68	50.9	56.9	1.15
46X-3, 107	430.57	1.72	2.68	52.7	57.8	1.12
46X-4, 104	432.04	1.74	2.69	50.4	56.9	1.16
46X-5, 57	433.07	1.71	2.69	54.6	58.8	1.10
46X-6, 66	434.66	1.71	2.68	54.1	58.5	1.11
47X-1, 34	436.44	1.70	2.69	55.4	59.1	1.09
47X-3, 110	440.20	1.69	2.66	55.5	58.8	1.09
47X-4, 92	441.52	1.73	2.66	50.8	56.8	1.14
48X-1, 16	445.96	1.67	2.63	57.9	59.7	1.06
49X-1, 9	455.59	1.69	2.68	56.7	59.6	1.08
49X-2, 20	457.20	1.74	2.70	50.4	56.9	1.16
49X-6, 64	463.64	1.70	2.66	53.5	58.0	1.11
50X-1, 44	464.04	1.72	2.66	51.0	56.8	1.14
50X-3, 92	467.52	1.74	2.63	47.9	55.0	1.18
50X-6, 67	471.77	1.72	2.70	52.9	58.1	1.13
51X-1, 9	473.39	1.75	2.72	49.1	56.4	1.18
51X-2, 115	475.95	1.78	2.70	46.3	54.8	1.21
52X-1, 21	482.81	1.75	2.69	49.2	56.2	1.17
52X-2, 71	484.81	1.75	2.70	49.4	56.4	1.17
52X-3, 56	486.16	1.76	2.69	47.8	55.5	1.19
52X-5, 5	488.65	1.71	2.68	52.9	57.9	1.12
53X-1, 4	492.34	1.75	2.67	48.3	55.7	1.18
53X-2, 4	493.84	1.76	2.70	48.4	55.9	1.18
53X-4, 147	498.27	1.75	2.70	49.2	56.3	1.17
54X-1, 2	501.92	1.76	2.73	49.0	56.5	1.18
54X-3, 124	506.14	1.77	2.70	46.7	55.0	1.21
55X-1, 2	511.62	1.83	2.67	39.7	50.7	1.31
55X-3, 5	514.65	1.76	2.67	47.0	54.9	1.20
55X-4, 31	516.41	1.78	2.72	46.3	55.0	1.22
55X-6, 49	519.59	1.75	2.69	49.3	56.2	1.17
56X-1, 108	522.38	1.81	2.69	41.8	52.2	1.28
56X-2, 108	523.88	1.77	2.67	45.4	54.1	1.22
56X-4, 43	526.23	1.76	2.66	47.0	54.8	1.20
57X-1, 13	531.03	1.78	2.64	44.3	53.2	1.23
57X-3, 31	534.21	1.71	2.70	54.8	58.9	1.10

Table 8 (continued).

Core, section, interval (cm)	Depth (mbsf)	Wet-bulk density (g/cm^3)	Grain density (g/cm^3)	Water content (% dry wt)	Porosity (%)	Dry-bulk density (g/cm^3)
130-806B- (Cont.)						
58X-1, 4	540.54	1.82	2.65	40.5	51.1	1.29
58X-3, 42	543.92	1.77	2.69	46.1	54.6	1.21
59X-1, 14	550.34	1.84	2.69	39.9	51.1	1.31
59X-2, 146	553.16	1.77	2.69	46.9	55.0	1.20
59X-3, 63	553.83	1.78	2.73	46.8	55.4	1.21
60X-1, 140	561.30	1.79	2.59	44.6	53.8	1.24
60X-2, 118	562.[illegible]8	1.65	2.67	61.7	61.4	1.02
60X-4, 89	565.29	1.77	2.67	45.4	54.1	1.22
60X-5, 17	566.07	1.79	2.68	44.0	53.4	1.24
61X-2, 65	571.75	1.80	2.70	43.4	53.2	1.26
61X-4, 53	574.63	1.81	2.68	42.3	52.4	1.27
63X-3, 11	592.11	1.81	2.71	42.9	53.1	1.27
63X-6, 25	596.75	1.83	2.73	41.7	52.5	1.29
64X-2, 48	600.58	1.87	2.74	38.0	50.3	1.36
66X-1, 11	618.01	1.86	2.72	38.1	50.2	1.35
66X-5, 11	624.01	1.83	2.70	40.4	51.5	1.31
66X-7, 13	627.03	1.83	2.68	40.4	51.3	1.30
67X-1, 22	627.72	1.83	2.69	39.8	51.0	1.31
67X-2, 29	629.29	1.84	2.69	39.4	50.7	1.32
68X-1, 23	637.43	1.89	2.69	34.5	47.5	1.41
69X-1, 23	646.73	1.85	2.71	38.8	50.5	1.33
69X-4, 17	651.17	1.85	2.71	39.0	50.7	1.33
70X-1, 13	656.33	1.86	2.70	38.1	50.0	1.35
70X-2, 16	657.86	1.89	2.68	34.8	47.5	1.40
70X-3, 13	659.33	1.88	2.69	35.8	48.3	1.38
70X-4, 16	660.86	1.88	2.70	35.8	48.5	1.39
71X-1, 68	666.48	1.89	2.67	34.4	47.2	1.40
72X-1, 5	675.55	1.91	2.72	34.3	47.6	1.42
72X-2, 33	677.33	1.88	2.68	35.4	47.9	1.39
72X-3, 30	678.80	1.87	2.70	36.4	48.8	1.37
72X-4, 40	680.40	1.98	2.71	29.0	43.3	1.53
73X-1, 97	686.17	1.92	2.72	33.5	47.0	1.44
73X-2, 62	687.32	1.90	2.73	34.9	48.1	1.41
73X-3, 31	688.51	1.92	2.77	35.0	48.5	1.42
74X-1, 95	695.75	1.87	2.68	36.3	48.6	1.37
74X-2, 105	697.35	1.90	2.70	34.1	47.2	1.42
74X-3, 105	698.85	1.91	2.72	34.0	47.3	1.43
75X-1, 20	704.70	1.88	2.69	35.5	48.1	1.39
75X-4, 119	710.19	1.88	2.66	34.8	47.3	1.39
76X-1, 46	714.56	1.86	2.66	36.6	48.6	1.36
76X-2, 48	716.08	1.90	2.66	32.9	46.0	1.43
76X-3, 31	717.41	1.92	2.70	32.7	46.3	1.45
78X-1, 7	733.47	1.94	2.72	32.1	46.0	1.46
130-806C-						
1H-1, 109	1.09	1.50	2.69	94.7	71.1	0.77
1H-2, 109	2.59	1.48	2.68	100.7	72.2	0.74
1H-3, 109	4.09	1.50	2.71	95.2	71.3	0.77
2H-2, 109	8.19	1.48	2.68	99.1	71.9	0.74
2H-3, 109	9.69	1.52	2.69	88.1	69.6	0.81
2H-4, 109	11.19	1.54	2.72	85.1	69.1	0.83
2H-5, 109	12.69	1.53	2.69	86.8	69.3	0.82
2H-6, 109	14.19	1.54	2.69	83.6	68.5	0.84
2H-7, 39	14.99	1.55	2.72	83.5	68.7	0.84
3H-3, 108	19.18	1.58	2.72	75.2	66.4	0.90
3H-4, 106	20.66	1.56	2.67	78.2	66.9	0.88
3H-5, 108	22.18	1.53	2.64	84.3	68.3	0.83
3H-6, 115	23.75	1.54	2.69	83.1	68.4	0.84
3H-7, 32	24.42	1.58	2.73	77.8	67.3	0.89
4H-1, 109	25.69	1.55	2.71	83.0	68.4	0.85
4H-2, 109	27.19	1.57	2.71	78.8	67.4	0.88
4H-3, 109	28.69	1.53	2.73	87.7	69.8	0.82
4H-4, 108	30.18	1.52	2.71	89.6	70.1	0.80
4H-5, 108	31.68	1.56	2.71	80.4	67.8	0.86
4H-6, 108	33.18	1.56	2.72	80.0	67.8	0.87
4H-7, 35	33.95	1.55	2.70	82.4	68.3	0.85
5H-1, 107	35.17	1.55	2.70	82.4	68.3	0.85
5H-2, 107	36.67	1.57	2.75	79.8	68.0	0.87
5H-3, 103	38.13	1.54	2.71	84.3	68.8	0.84
5H-4, 100	39.60	1.56	2.70	79.5	67.5	0.87
5H-5, 108	41.18	1.54	2.69	83.3	68.4	0.84
5H-6, 120	42.80	1.56	2.70	78.7	67.2	0.88
6H-1, 110	44.70	1.61	2.70	69.8	64.6	0.95
6H-2, 39	45.49	1.58	2.70	76.4	66.6	0.89
6H-2, 103	46.13	1.56	2.70	79.0	67.3	0.87

Table 8 (continued).

Core, section, interval (cm)	Depth (mbsf)	Wet-bulk density (g/cm^3)	Grain density (g/cm^3)	Water content (% dry wt)	Porosity (%)	Dry-bulk density (g/cm^3)
130-806C- (Cont.)						
6H-3, 99	47.59	1.58	2.72	76.6	66.9	0.89
6H-4, 107	49.17	1.56	2.72	79.4	67.6	0.87
6H-5, 107	50.67	1.59	2.71	73.1	65.7	0.92
6H-6, 107	52.17	1.59	2.73	74.9	66.4	0.91
7H-1, 110	54.20	1.56	2.74	81.7	68.4	0.86
7H-2, 108	55.68	1.57	2.71	78.9	67.4	0.87
7H-3, 108	57.18	1.59	2.71	74.7	66.2	0.91
7H-4, 128	58.88	1.55	2.70	82.2	68.2	0.85
7H-5, 97	60.07	1.60	2.71	71.3	65.1	0.94
7H-6, 108	61.68	1.56	2.72	80.9	68.0	0.86
7H-7, 40	62.50	1.59	2.68	72.2	65.2	0.92
8H-2, 110	65.20	1.56	2.70	78.7	67.2	0.88
8H-3, 110	66.70	1.55	2.73	82.8	68.6	0.85
8H-4, 109	68.19	1.59	2.70	73.2	65.6	0.92
8H-5, 110	69.70	1.57	2.70	77.1	66.8	0.89
8H-6, 109	71.19	1.55	2.69	80.8	67.7	0.86
9H-2, 109	74.69	1.53	2.70	87.8	69.6	0.81
9H-4, 110	77.70	1.55	2.68	81.7	67.9	0.85
9H-5, 110	79.20	1.54	2.71	83.9	68.7	0.84
9H-6, 109	80.69	1.56	2.71	79.1	67.5	0.87
10H-1, 109	82.69	1.57	2.71	78.9	67.4	0.88
10H-2, 107	84.17	1.57	2.70	77.0	66.8	0.89
10H-3, 108	85.68	1.57	2.71	78.3	67.3	0.88
10H-4, 104	87.14	1.58	2.67	73.8	65.6	0.91
10H-5, 109	88.69	1.57	2.70	78.6	67.2	0.88
10H-6, 109	90.19	1.57	2.69	76.2	66.5	0.89
11H-1, 109	92.19	1.60	2.67	70.1	64.4	0.94
11H-2, 109	93.69	1.59	2.70	73.2	65.7	0.92
11H-3, 95	95.05	1.59	2.70	72.8	65.6	0.92
11H-4, 109	96.69	1.56	2.69	78.7	67.2	0.87
11H-5, 109	98.19	1.60	2.69	71.5	65.1	0.93
11H-6, 105	99.65	1.62	2.69	67.1	63.6	0.97
12H-1, 105	101.65	1.63	2.71	66.7	63.6	0.98
12H-2, 108	103.18	1.59	2.72	73.4	65.9	0.92
12H-3, 107	104.67	1.61	2.74	71.1	65.3	0.94
12H-4, 108	106.18	1.58	2.66	73.9	65.5	0.91
12H-5, 107	107.67	1.57	2.70	77.3	66.9	0.89
12H-6, 107	109.17	1.59	2.69	72.7	65.4	0.92
13H-1, 105	111.15	1.60	2.70	72.2	65.4	0.93
13H-2, 107	112.67	1.60	2.71	72.3	65.5	0.93
13H-3, 108	114.18	1.59	2.71	73.9	66.0	0.91
13H-4, 109	115.69	1.62	2.73	68.7	64.5	0.96
13H-5, 110	117.20	1.59	2.72	74.8	66.3	0.91
13H-6, 109	118.69	1.59	2.70	73.3	65.7	0.92
14H-1, 109	120.69	1.59	2.70	72.7	65.5	0.92
14H-2, 109	122.19	1.65	2.71	63.1	62.4	1.01
14H-3, 108	123.68	1.59	2.69	72.9	65.5	0.92
14H-4, 107	125.17	1.62	2.71	68.6	64.3	0.96
14H-5, 108	126.68	1.60	2.71	71.8	65.3	0.93
14H-6, 105	128.15	1.60	2.68	70.2	64.5	0.94
15H-1, 109	130.19	1.61	2.70	69.1	64.3	0.95
15H-2, 109	131.69	1.59	2.70	73.8	65.8	0.91
15H-3, 108	133.18	1.61	2.69	68.8	64.2	0.96
15H-4, 108	134.68	1.61	2.69	68.7	64.2	0.96
15H-5, 108	136.18	1.61	2.71	70.8	65.0	0.94
15H-6, 108	137.68	1.61	2.69	69.3	64.3	0.95
16H-1, 108	139.68	1.62	2.71	69.3	64.5	0.95
16H-2, 107	141.17	1.62	2.69	68.4	64.1	0.96
16H-3, 108	142.68	1.62	2.71	68.6	64.3	0.96
16H-4, 108	144.18	1.62	2.70	68.4	64.2	0.96
16H-6, 114	147.24	1.60	2.69	72.0	65.2	0.93
17H-1, 107	149.17	1.61	2.70	70.3	64.8	0.94
17H-2, 109	150.69	1.62	2.70	67.3	63.8	0.97
17H-3, 112	152.22	1.61	2.67	68.0	63.8	0.96
17H-4, 104	153.64	1.62	2.71	68.0	64.1	0.96
17H-5, 108	155.18	1.63	2.72	66.1	63.5	0.98
17H-6, 108	156.68	1.63	2.69	65.5	63.1	0.99
18H-1, 109	158.69	1.64	2.71	64.1	62.7	1.00
18H-2, 109	160.19	1.65	2.66	61.9	61.5	1.02
18H-3, 109	161.69	1.65	2.70	63.5	62.4	1.01
18H-4, 109	163.19	1.63	2.68	65.8	63.1	0.98
18H-5, 109	164.69	1.62	2.70	68.2	64.0	0.96
18H-6, 109	166.19	1.63	2.70	65.4	63.1	0.99
19H-1, 109	168.19	1.62	2.69	66.9	63.6	0.97
19H-2, 109	169.69	1.71	2.68	53.1	58.0	1.12

Table 8 (continued).

Core, section, interval (cm)	Depth (mbsf)	Wet-bulk density (g/cm^3)	Grain density (g/cm^3)	Water content (% dry wt)	Porosity (%)	Dry-bulk density (g/cm^3)
130-806C- (Cont.)						
19H-3, 109	171.19	1.65	2.73	64.6	63.1	1.00
19H-4, 108	172.68	1.63	2.68	65.2	62.9	0.99
19H-5, 108	174.18	1.65	2.70	62.8	62.1	1.01
19H-6, 108	175.68	1.62	2.70	67.3	63.7	0.97
20H-1, 108	177.68	1.63	2.69	66.4	63.4	0.98
20H-2, 108	179.18	1.63	2.69	65.8	63.2	0.98
20H-3, 108	180.68	1.62	2.68	68.0	63.8	0.96
20H-4, 108	182.18	1.63	2.70	65.5	63.2	0.99
20H-5, 108	183.68	1.67	2.68	59.5	60.7	1.05
20H-6, 108	185.18	1.65	2.68	63.1	62.1	1.01
21H-1, 108	187.18	1.65	2.69	63.0	62.1	1.01
21H-2, 108	188.68	1.67	2.71	60.7	61.4	1.04
21H-3, 108	190.18	1.63	2.67	65.8	63.0	0.98
21H-4, 108	191.68	1.64	2.67	64.0	62.3	1.00
21H-5, 108	193.18	1.63	2.73	66.8	63.8	0.98
21H-6, 108	194.68	1.65	2.70	63.7	62.5	1.01
22H-1, 109	196.69	1.67	2.71	60.8	61.5	1.04
22H-2, 108	198.18	1.61	2.67	68.7	64.0	0.95
22H-3, 100	199.60	1.64	2.71	65.0	63.0	0.99
22H-4, 109	201.19	1.63	2.70	65.6	63.2	0.99
22H-5, 111	202.71	1.63	2.69	65.5	63.1	0.99
22H-6, 123	204.33	1.65	2.71	63.4	62.4	1.01
23H-1, 103	206.13	1.64	2.70	65.3	63.1	0.99
23H-2, 107	207.67	1.63	2.69	65.4	63.0	0.99
23H-3, 110	209.20	1.62	2.70	68.4	64.1	0.96
23H-4, 134	210.94	1.68	2.68	58.0	60.1	1.06
23H-5, 110	212.20	1.68	2.71	58.4	60.5	1.06
23H-6, 112	213.72	1.66	2.70	62.0	61.9	1.02
24H-1, 112	215.72	1.67	2.71	61.1	61.7	1.03
24H-2, 112	217.22	1.67	2.69	59.4	60.7	1.05
24H-3, 109	218.69	1.66	2.71	61.0	61.6	1.03
24H-4, 110	220.20	1.68	2.70	58.4	60.4	1.06
24H-5, 110	221.70	1.67	2.71	60.3	61.2	1.04
24H-6, 110	223.20	1.68	2.71	58.1	60.4	1.07
25H-1, 110	225.20	1.65	2.71	63.1	62.3	1.01
25H-2, 108	226.68	1.65	2.70	62.5	62.0	1.02
25H-3, 109	228.19	1.70	2.70	54.9	59.0	1.10
25H-4, 108	229.68	1.69	2.70	56.9	59.8	1.08
25H-5, 109	231.19	1.68	2.70	58.1	60.3	1.06
25H-6, 110	232.70	1.66	2.69	60.9	61.4	1.03
26H-2, 109	236.19	1.64	2.68	63.8	62.3	1.00
26H-3, 109	237.69	1.66	2.70	61.3	61.6	1.03
26H-4, 109	239.19	1.66	2.68	61.0	61.3	1.03
26H-5, 109	240.69	1.65	2.67	62.4	61.8	1.01
26H-6, 109	242.19	1.65	2.71	62.9	62.3	1.01
27H-1, 109	244.19	1.69	2.70	56.6	59.7	1.08
27H-2, 109	245.69	1.70	2.70	55.1	59.1	1.10
27H-3, 109	247.19	1.70	2.71	56.1	59.6	1.09
27H-4, 109	248.69	1.68	2.72	59.1	60.9	1.06
27H-5, 109	250.19	1.73	2.70	52.1	57.7	1.14
27H-6, 109	251.69	1.67	2.70	60.5	61.3	1.04
28H-2, 109	255.19	1.65	2.71	63.6	62.5	1.01
28H-3, 109	256.69	1.70	2.68	55.6	59.1	1.09
28H-4, 109	258.19	1.69	2.73	58.7	60.8	1.06
28H-5, 109	259.69	1.69	2.70	57.6	60.2	1.07
28H-6, 109	261.19	1.68	2.69	58.1	60.2	1.06
28H-7, 109	262.69	1.68	2.72	58.5	60.7	1.06
29H-1, 96	263.06	1.67	2.71	60.7	61.5	1.04
29H-2, 98	264.58	1.67	2.69	59.6	60.8	1.04
29H-3, 108	266.18	1.67	2.72	60.8	61.6	1.04
29H-4, 107	267.67	1.65	2.72	64.5	63.0	1.00
29H-5, 100	269.10	1.66	2.71	62.1	62.0	1.02
29H-6, 108	270.68	1.64	2.68	64.1	62.5	1.00
30H-1, 107	272.67	1.65	2.70	63.1	62.2	1.01
30H-2, 107	274.17	1.67	2.71	59.9	61.2	1.05
30H-3, 107	275.67	1.66	2.70	61.6	61.7	1.03
30H-4, 107	277.17	1.69	2.68	56.3	59.4	1.08
30H-5, 107	278.67	1.69	2.70	57.2	59.9	1.07
30H-6, 107	280.17	1.71	2.67	52.6	57.7	1.12
31H-1, 103	282.13	1.61	2.69	69.0	64.3	0.95
31H-2, 107	283.67	1.73	2.68	51.2	57.1	1.14
31H-3, 107	285.17	1.66	2.68	60.5	61.1	1.03
31H-4, 107	286.67	1.62	2.65	66.4	63.1	0.97
31H-5, 106	288.16	1.71	2.71	54.7	59.0	1.10
31H-6, 106	289.66	1.66	2.67	60.3	60.9	1.04
32H-1, 103	291.63	1.61	2.68	69.5	64.3	0.95

Table 8 (continued).

Core, section, interval (cm)	Depth (mbsf)	Wet-bulk density (g/cm^3)	Grain density (g/cm^3)	Water content (% dry wt)	Porosity (%)	Dry-bulk density (g/cm^3)
130-806C- (Cont.)						
32H-2, 107	293.17	.69	2.70	57.3	60.0	1.07
32H-3, 107	294.67	1.66	2.68	60.4	61.1	1.04
32H-4, 107	296.17	1.64	2.71	65.4	63.1	0.99
32H-5, 113	297.73	1.69	2.69	56.8	59.7	1.08
32H-6, 107	299.17	1.74	2.72	50.6	57.2	1.16
33H-1, 107	301.17	1.65	2.68	61.8	61.6	1.02
33H-2, 104	302.64	1.68	2.69	58.2	60.3	1.06
33H-3, 107	304.17	1.64	2.67	63.0	62.0	1.01
33H-4, 110	305.70	1.65	2.72	64.1	62.8	1.00
33H-5, 73	306.83	1.65	2.71	63.0	62.3	1.01
33H-6, 59	308.19	1.64	2.69	63.3	62.3	1.01
35X-2, 50	321.30	1.72	2.68	52.8	57.9	1.12
35X-3, 111	323.41	1.64	2.68	63.5	62.3	1.00
35X-4, 116	324.96	1.67	2.67	59.4	60.6	1.05
36X-1, 73	329.63	1.72	2.79	55.2	59.9	1.11
36X-2, 73	331.13	1.64	2.70	64.4	62.8	1.00
36X-3, 74	332.64	1.66	2.66	59.7	60.6	1.04
36X-4, 75	334.15	1.63	2.67	64.8	62.6	0.99
36X-6, 74	337.14	1.67	2.68	58.7	60.4	1.05
37X-1, 74	339.24	1.69	2.71	56.4	59.7	1.08
37X-2, 74	340.74	1.66	2.68	60.9	61.3	1.03
37X-3, 74	342.24	1.66	2.69	60.1	61.0	1.04
37X-5, 59	345.09	1.70	2.68	54.4	58.6	1.10
38X-1, 74	348.94	1.73	2.76	54.0	59.1	1.12
38X-2, 74	350.44	1.62	2.70	67.7	63.9	0.97
38X-3, 74	351.94	1.62	2.68	66.6	63.4	0.97
38X-4, 74	353.44	1.70	2.68	54.5	58.6	1.10
38X-5, 74	354.94	1.63	2.68	64.9	62.8	0.99
39X-1, 72	358.62	1.69	2.70	57.0	59.9	1.08
39X-2, 72	360.12	1.69	2.69	55.9	59.3	1.09
39X-3, 72	361.62	1.70	2.68	55.3	58.9	1.09
39X-4, 72	363.12	1.69	2.70	57.1	59.9	1.07
39X-5, 74	364.64	1.69	2.71	58.0	60.4	1.07
40X-1, 74	368.34	1.56	2.66	78.0	66.8	0.88
40X-2, 74	369.84	1.69	2.66	55.1	58.7	1.09
40X-3, 74	371.34	1.73	2.70	51.3	57.4	1.15
40X-4, 74	372.84	1.67	2.71	60.1	61.2	1.04
41X-1, 68	377.98	1.68	2.68	58.2	60.2	1.06
41X-2, 74	379.54	1.73	2.68	51.4	57.2	1.14
41X-3, 74	381.04	1.68	2.70	58.7	60.6	1.06
41X-4, 74	382.54	1.65	2.67	61.5	61.5	1.02
41X-5, 35	383.65	1.68	2.63	56.1	58.9	1.08
42X-1, 22	387.22	1.73	2.69	51.5	57.3	1.14
42X-2, 103	389.53	1.72	2.70	53.3	58.3	1.12
42X-3, 60	390.60	1.69	2.68	56.8	59.6	1.08
42X-4, 19	391.69	1.68	2.66	57.7	59.8	1.06
42X-6, 37	394.87	1.72	2.69	52.7	57.9	1.13
43X-1, 134	398.04	1.69	2.66	56.0	59.1	1.08
43X-2, 100	399.20	1.73	2.68	50.5	56.7	1.15
43X-3, 31	400.01	1.73	2.70	52.2	57.8	1.13
43X-4, 116	402.36	1.68	2.67	57.3	59.8	1.07
43X-5, 116	403.86	1.72	2.77	55.5	59.8	1.11
43X-6, 34	404.54	1.71	2.69	54.5	58.8	1.10
44X-1, 76	407.06	1.70	2.67	55.1	58.8	1.09
44X-2, 69	408.49	1.68	2.68	58.0	60.1	1.06
44X-3, 35	409.65	1.69	2.63	54.8	58.3	1.09
44X-4, 106	411.86	1.67	2.66	57.7	59.8	1.06
44X-5, 68	412.98	1.71	2.67	53.5	58.0	1.11
44X-6, 13	413.93	1.71	2.69	53.7	58.4	1.11
45X-2, 135	418.75	1.68	2.67	57.3	59.7	1.07
45X-3, 126	420.16	1.72	2.65	51.3	56.9	1.14
45X-4, 139	421.79	1.71	2.68	52.8	57.8	1.12
45X-5, 55	422.45	1.70	2.68	54.6	58.7	1.10
46X-1, 123	426.83	1.70	2.68	54.7	58.7	1.10
46X-2, 92	428.02	1.70	2.67	54.0	58.3	1.11
46X-3, 25	428.85	1.71	2.69	54.4	58.6	1.10
46X-4, 95	431.05	1.73	2.72	52.8	58.2	1.13
46X-5, 121	432.81	1.72	2.67	51.8	57.3	1.13
46X-6, 81	433.91	1.71	2.65	52.3	57.4	1.12
47X-1, 107	436.27	1.68	2.66	56.4	59.2	1.08
47X-2, 125	437.95	1.66	2.67	60.3	61.0	1.04
47X-3, 82	439.02	1.71	2.71	54.0	58.7	1.11
47X-5, 10	441.30	1.73	2.72	52.3	58.0	1.14
47X-6, 57	443.27	1.67	2.67	58.7	60.3	1.05
48X-2, 94	447.34	1.72	2.70	53.2	58.2	1.12

Table 8 (continued).

Core, section, interval (cm)	Depth (mbsf)	Wet-bulk density (g/cm³)	Grain density (g/cm³)	Water content (% dry wt)	Porosity (%)	Dry-bulk density (g/cm³)
130-806C- (Cont.)						
48X-3, 29	448.19	1.69	2.68	55.9	59.2	1.09
49X-2, 128	457.38	1.71	2.68	53.0	57.9	1.12
49X-3, 96	458.56	1.74	2.72	51.0	57.4	1.15
49X-4, 80	459.90	1.73	2.65	50.2	56.3	1.15
50X-1, 68	465.18	1.69	2.70	56.9	59.8	1.08
50X-2, 104	467.04	1.70	2.66	53.6	58.1	1.11
50X-3, 117	468.67	1.72	2.68	52.3	57.6	1.13
50X-4, 122	470.22	1.75	2.69	48.4	55.8	1.18
50X-5, 97	471.47	1.73	2.66	50.6	56.6	1.15
50X-6, 126	473.26	1.76	2.71	48.5	56.0	1.18
51X-1, 136	475.66	1.76	2.69	48.0	55.6	1.19
51X-2, 88	476.68	1.73	2.68	50.4	56.7	1.15
51X-3, 127	478.57	1.69	2.70	57.0	59.9	1.08
51X-4, 109	479.89	1.72	2.70	52.2	57.7	1.13
52X-1, 65	484.35	1.81	2.72	42.9	53.2	1.27
52X-2, 35	485.55	1.75	2.70	49.9	56.7	1.16
52X-3, 55	487.25	1.74	2.68	50.0	56.6	1.16
53X-1, 60	493.90	1.78	2.69	45.0	54.0	1.23
53X-2, 50	495.30	1.78	2.70	46.0	54.7	1.22
53X-3, 82	497.12	1.77	2.70	46.6	55.0	1.21
53X-4, 132	499.12	1.80	2.68	43.6	53.2	1.25
53X-5, 145	500.75	1.80	2.68	43.1	52.9	1.26
54X-2, 118	505.98	1.79	2.68	44.5	53.7	1.24
54X-3, 137	507.67	1.81	2.69	42.6	52.7	1.27
55X-2, 144	515.64	1.79	2.70	44.4	53.8	1.24
55X-3, 145	517.15	1.76	2.64	46.3	54.3	1.20
55X-4, 125	518.45	1.78	2.70	45.4	54.3	1.23
56X-1, 117	523.57	1.75	2.67	47.9	55.4	1.18
56X-2, 107	524.97	1.78	2.70	45.4	54.3	1.23
56X-3, 125	526.65	1.79	2.71	44.4	53.8	1.24
56X-4, 111	528.01	1.77	2.69	47.1	55.2	1.20
56X-5, 127	529.67	1.79	2.68	44.4	53.6	1.24
56X-6, 122	531.12	1.77	2.69	46.4	54.8	1.21
57X-2, 54	534.04	1.77	2.69	45.9	54.5	1.22
57X-3, 144	536.44	1.77	2.71	46.7	55.1	1.21
57X-4, 81	537.31	1.76	2.69	47.9	55.6	1.19
57X-5, 50	538.50	1.79	2.66	43.5	52.9	1.25
57X-6, 94	540.44	1.84	2.71	39.6	51.1	1.32
58X-3, 132	603.32	1.88	2.72	37.1	49.5	1.37
39X-5, 13	746.13	1.91	2.68	33.1	46.3	1.43
61X-1, 38	759.58	1.94	2.71	31.5	45.3	1.47
61X-2, 105	761.75	1.94	2.72	31.8	45.7	1.47
61X-4, 93	764.63	1.94	2.69	31.1	44.9	1.48
61X-6, 57	767.27	1.93	2.70	31.9	45.6	1.46
62X-1, 30	767.00	1.96	2.69	29.4	43.4	1.51

Table 9. *P*-wave velocity data, Holes 806B and 806C.

Core, section interval (cm)	Depth (mbsf)	Vertical *P*-wave velocity (m/s)	Horizontal *P*-wave velocity (m/s)
130-806B-			
1H-1, 120	1.20		1580.3
1H-2, 35	1.85	1570.0	1587.6
1H-2, 110	2.60	1587.4	
1H-2, 120	2.70		1527.4
1H-4, 35	4.85	1561.4	1555.1
1H-4, 110	5.60	1566.5	1583.9
2H-1, 120	7.70	1542.8	1555.1
2H-2, 35	8.35	1566.5	1580.3
2H-2, 110	9.10	1564.8	1591.3
2H-3, 35	9.85	1528.0	1548.1
2H-3, 110	10.60	1566.5	1558.7
2H-4, 35	11.35	1564.8	1576.6
2H-4, 110	12.10	1547.9	1555.1
2H-5, 35	12.85	1559.7	1573.0
2H-5, 110	13.60	1587.4	1587.6
2H-6, 35	14.35	1551.2	1573.0
2H-6, 110	15.10	1559.7	1591.3
3H-1, 35	16.35	1576.9	1573.0
3H-1, 110	17.10	1559.7	1562.2
3H-2, 35	17.85	1561.4	1591.3
3H-2, 110	18.60	1563.1	1583.9
3H-3, 35	19.35	1536.2	1551.6
3H-3, 110	20.10	1529.6	1544.6
3H-4, 35	20.85	1547.9	1569.4
3H-4, 109	21.59	1559.7	1598.8
3H-4, 109	21.59	1561.4	
3H-5, 35	22.35	1539.5	1551.6
3H-5, 110	23.10	1566.5	1610.0
3H-6, 35	23.85	1566.5	1580.3
3H-6, 104	24.54	1573.4	1558.7
3H-7, 35	25.35	1564.8	1580.3
4H-1, 110	26.60	1539.5	1565.8
4H-2, 32	27.32	1542.8	1551.6
4H-2, 112	28.12	1547.9	1569.4
4H-3, 35	28.85	1556.3	1569.4
4H-3, 110	29.60	1570.0	
4H-4, 35	30.35	1556.3	1587.6
4H-4, 110	31.10	1547.9	1569.4
4H-5, 35	31.85	1564.8	1591.3
4H-5, 110	32.60	1564.8	1591.3
4H-6, 35	33.35	1575.2	1587.6
4H-6, 110	34.10	1556.3	1583.9
4H-7, 35	34.85	1556.3	1569.4
5H-1, 35	35.35	1549.5	1558.7
5H-1, 110	36.10	1556.3	1548.1
5H-2, 35	36.85	1558.0	1569.4
5H-2, 110	37.60	1558.0	1569.4
5H-3, 35	38.35	1576.9	1580.3
5H-3, 110	39.10	1589.2	1595.0
5H-4, 35	39.85	1561.4	1583.9
5H-4, 110	40.60	1571.7	1565.8
5H-5, 35	41.35	1573.4	1595.0
5H-5, 110	42.10	1564.8	1587.6
5H-6, 35	42.85	1576.9	1580.3
5H-6, 110	43.60	1571.7	1527.4
5H-7, 35	44.35	1547.9	1548.1
6H-1, 110	45.60	1531.3	1537.7
6H-2, 110	47.10	1544.5	1576.6
6H-3, 35	47.85	1531.3	1541.1
6H-3, 110	48.60	1563.1	1573.0
6H-4, 40	49.40	1559.7	1569.4
6H-4, 110	50.10	1559.7	1569.4
6H-5, 35	50.85	1559.7	1562.2
6H-5, 120	51.70	1542.8	1562.2
6H-6, 40	52.40	1556.3	1555.1
6H-6, 110	53.10	1575.2	1573.0
6H-7, 40	53.90	1566.5	1576.6
7H-1, 110	55.10	1552.9	1591.3
7H-2, 40	55.90	1552.9	1562.2
7H-2, 110	56.60	1536.2	1551.6
7H-3, 40	57.40	1528.0	1534.2
7H-3, 110	58.10	1558.0	1583.9
7H-4, 40	58.90	1554.6	1558.7
7H-4, 110	59.60	1568.3	1587.6
7H-5, 40	60.40	1552.9	1565.8
7H-5, 110	61.10	1531.3	1537.7
7H-6, 40	61.90	1563.1	1580.3
7H-6, 110	62.60	1549.5	1562.2
7H-7, 40	63.40	1541.2	1558.7
8H-1, 40	63.90	1546.2	1558.7
8H-1, 110	64.60	1559.7	1551.6
8H-2, 40	65.40	1542.8	1555.1
8H-2, 110	66.10	1552.9	1569.4
8H-3, 40	66.90	1544.5	1562.2
8H-3, 110	67.60	1542.8	1555.1
8H-4, 40	68.40	1544.5	1558.7
8H-4, 110	69.10	1536.2	1555.1
8H-5, 40	69.90	1534.6	1555.1
8H-5, 110	70.60	1544.5	1551.6
8H-6, 40	71.40	1547.9	1562.2
8H-6, 110	72.10	1556.3	1565.8
8H-7, 40	72.90	1563.1	1562.2
9H-1, 110	74.10	1551.2	1558.7
9H-2, 40	74.90	1529.6	1555.1
9H-2, 110	75.60	1552.9	1576.6
9H-3, 40	76.40	1556.3	1580.3
9H-3, 110	77.10	1549.5	1562.2
9H-4, 40	77.90	1552.9	1569.4
9H-4, 110	78.60	1551.2	1573.0
9H-5, 40	79.40	1563.1	1565.8
9H-5, 110	80.10	1532.9	1537.7
9H-6, 40	80.90	1544.5	1562.2
9H-6, 40	80.90	1547.9	
9H-6, 110	81.60	1558.0	1569.4
9H-7, 50	82.50	1546.2	1565.8
10H-1, 70	83.20	1547.9	1548.1
10H-2, 40	84.40	1542.8	1558.7
10H-2, 110	85.10	1556.3	1569.4
10H-3, 40	85.90	1526.4	1541.1
10H-3, 110	86.60	1541.2	1551.6
10H-4, 40	87.40	1539.5	1551.6
10H-4, 110	88.10	1558.0	1576.6
10H-5, 40	88.90	1544.5	1562.2
10H-5, 110	89.60	1546.2	1565.8
10H-6, 40	90.40	1534.6	1548.1
10H-6, 110	91.10	1547.9	1569.4
10H-7, 30	91.80	1563.1	1580.3
11H-1, 40	92.40	1551.2	1555.1
11H-1, 110	93.10	1554.6	1551.6
11H-2, 40	93.90	1556.3	1587.6
11H-2, 110	94.60	1561.4	1595.0
11H-3, 110	96.10	1554.6	1573.0
11H-4, 40	96.90	1532.9	1548.1
11H-4, 125	97.75	1544.5	1555.1
11H-5, 40	98.40	1532.9	1544.6
11H-5, 110	99.10	1541.2	1548.1
11H-6, 40	99.90	1542.8	1555.1
11H-6, 110	100.60	1536.2	1544.6
11H-7, 73	101.73	1529.6	1537.7
12H-1, 40	101.90	1546.2	1558.7
12H-1, 110	102.60	1556.3	1569.4
12H-2, 40	103.40	1547.9	1565.8
12H-2, 110	104.10	1539.5	1537.7
12H-3, 40	104.90	1544.5	1558.7
12H-3, 110	105.60	1549.5	1555.1
12H-4, 35	106.35	1561.4	1591.3
12H-4, 110	107.10	1563.1	1583.9
12H-5, 40	107.90	1546.2	1558.7
12H-5, 110	108.60	1531.3	1537.7
12H-6, 40	109.40	1546.2	1580.3
12H-6, 110	110.10	1559.7	1583.9
12H-7, 60	111.10	1564.8	1591.3
13H-1, 35	111.35	1566.5	1602.5
13H-1, 110	112.10	1554.6	1580.3
13H-2, 35	112.85	1554.6	1598.8
13H-2, 110	113.60	1551.2	1573.0
13H-3, 35	114.35	1558.0	1595.0
13H-3, 110	115.10	1549.5	1591.3
13H-4, 35	115.85	1554.6	1591.3
13H-4, 110	116.60	1551.2	1580.3
13H-5, 35	117.35	1544.5	1565.8
13H-5, 110	118.10	1552.9	1587.6
13H-6, 35	118.85	1541.2	1551.6
13H-6, 110	119.60	1561.4	1606.3
13H-7, 64	120.64	1559.7	1583.9
14H-1, 110	121.60	1552.9	1569.4
14H-2, 39	122.39	1568.3	1580.3
14H-2, 109	123.09	1559.7	1576.6
14H-3, 35	123.85	1544.5	1565.8
14H-3, 110	124.60	1544.5	1541.1
14H-4, 35	125.35	1576.9	1606.3
14H-4, 110	126.10	1541.2	1548.1
14H-5, 35	126.85	1556.3	1569.4
14H-5, 110	127.60	1566.5	1534.2
14H-6, 35	128.35	1551.2	
14H-6, 110	129.10	1554.6	1580.3
14H-7, 23	129.73	1551.2	1591.3
15H-1, 35	130.35	1537.9	1569.4
15H-1, 110	131.10	1552.9	1591.3
15H-2, 35	131.85	1558.0	1591.3
15H-2, 110	132.60	1537.9	1555.1
15H-3, 35	133.35	1551.2	1576.6
15H-3, 110	134.10	1549.5	1569.4
15H-4, 35	134.85	1564.8	1580.3
15H-4, 110	135.60	1570.0	1580.3
15H-5, 40	136.40	1556.3	1569.4
15H-5, 100	137.00	1576.9	1602.5
15H-6, 40	137.90	1596.3	1541.1
15H-6, 110	138.60	1561.4	1576.6
15H-7, 40	139.40	1564.8	1591.3
16H-1, 40	139.90	1566.5	1580.3
16H-1, 110	140.60	1578.7	1606.3
16H-2, 40	141.40	1591.0	1583.9
16H-2, 110	142.10	1563.1	1580.3
16H-3, 40	142.90	1580.4	1621.5
16H-3, 110	143.60	1559.7	1580.3
16H-4, 40	144.40	1566.5	1587.6
16H-4, 110	145.10	1587.4	1595.0
16H-5, 40	145.90	1546.2	1569.4
16H-5, 110	146.60	1575.2	1595.0
16H-6, 40	147.40	1585.7	1595.0
16H-6, 110	148.10	1573.4	1573.0
16H-7, 40	148.90	1576.9	1606.3
17H-1, 110	150.10	1575.2	1587.6
17H-2, 40	150.90	1568.3	1625.3
17H-2, 110	151.60	1585.7	1591.3
17H-3, 40	152.40	1582.2	1602.5
17H-3, 110	153.10	1578.7	1591.3
17H-4, 40	153.90	1573.4	1602.5
17H-4, 110	154.60	1582.2	1613.8
17H-5, 40	155.40	1575.2	1606.3
17H-5, 110	156.10	1547.9	1576.6
17H-6, 40	156.90	1559.7	1580.3
17H-6, 110	157.60	1547.9	1576.6
17H-7, 40	158.40	1568.3	1583.9
18H-1, 110	159.60	1580.4	1610.0
18H-2, 40	160.40	1573.4	1587.6
18H-2, 110	161.10	1529.6	1573.0
18H-3, 40	161.90	1561.4	1565.8
18H-3, 110	162.60	1551.2	1558.7
18H-4, 35	163.35	1570.0	1598.8
18H-4, 89	163.89	1575.2	1598.8
18H-5, 35	164.85	1551.2	1573.0
18H-5, 110	165.60	1585.7	1633.1
18H-6, 40	166.40	1571.7	1598.8
18H-6, 110	167.10	1575.2	1617.7
18H-7, 45	167.95	1558.0	1583.9
19H-1, 40	168.40	1546.2	1576.6
19H-1, 110	169.10	1578.7	1617.7
19H-2, 40	169.90	1552.9	1573.0

Table 9. (continued).

Core, section interval (cm)	Depth (mbsf)	Vertical *P*-wave velocity (m/s)	Horizontal *P*-wave velocity (m/s)
130-806B- (Cont.)			
19H-2, 110	170.60	1549.5	1576.6
19H-3, 40	171.40	1537.9	1565.8
19H-3, 110	172.10	1566.5	1583.9
19H-4, 40	172.90	1566.5	1602.5
19H-4, 110	173.60	1554.6	1558.7
19H-5, 40	174.40	1591.0	1602.5
19H-5, 110	175.10	1558.0	1576.6
19H-6, 40	175.90	1570.0	1598.8
19H-6, 110	176.60	1547.9	1562.2
19H-7, 40	177.40	1571.7	1606.3
20H-1, 45	177.95	1585.7	1629.2
20H-1, 110	178.60	1571.7	1606.3
20H-2, 40	179.40	1546.2	1551.6
20H-2, 110	180.10	1563.1	1598.8
20H-3, 40	180.90	1561.4	1583.9
20H-3, 40	180.90		1583.9
20H-3, 110	181.60	1551.2	1555.1
20H-4, 45	182.45	1578.7	1617.7
20H-4, 110	183.10	1587.4	1633.1
20H-5, 40	183.90	1573.4	1573.0
20H-5, 110	184.60	1591.0	1640.9
20H-6, 40	185.40	1568.3	1562.2
20H-6, 110	186.10	1570.0	1602.5
21H-1, 110	188.10	1551.2	1558.7
21H-2, 40	188.90	1564.8	1565.8
21H-2, 110	189.60	1589.2	1617.7
21H-3, 40	190.40	1580.4	1602.5
21H-3, 110	191.10	1554.6	1558.7
21H-4, 40	191.90	1589.2	1610.0
21H-4, 110	192.60	1564.8	1565.8
21H-5, 40	193.40	1596.3	1613.8
21H-5, 110	194.10	1589.2	1602.5
21H-6, 40	194.90	1589.2	1606.3
21H-6, 110	195.60	1589.2	1613.8
21H-7, 40	196.40	1591.0	1613.8
22H-1, 110	197.60	1575.2	1617.7
22H-2, 40	198.40	1563.1	1602.5
22H-2, 110	199.10	1583.9	
22H-3, 40	199.90	1591.0	
22H-3, 110	200.60	1556.3	1573.0
22H-4, 40	201.40	1556.3	1580.3
22H-4, 110	202.10	1583.9	1587.6
22H-5, 40	202.90	1583.9	
22H-5, 110	203.60	1591.0	1617.7
22H-6, 40	204.40	1578.7	1610.0
22H-6, 110	205.10	1564.8	1580.3
22H-7, 40	205.90	1561.4	1576.6
23H-1, 40	206.40	1564.8	
23H-1, 110	207.10	1589.2	1602.5
23H-2, 40	207.90	1587.4	1610.0
23H-2, 110	208.60	1576.9	1602.5
23H-3, 40	209.40	1571.7	1602.5
23H-3, 40	209.40		1580.3
23H-4, 40	210.90	1563.1	1591.3
23H-4, 110	211.60	1566.5	1587.6
23H-5, 40	212.40	1591.0	1555.1
23H-5, 110	213.10	1583.9	1587.6
23H-6, 40	213.90	1566.5	1587.6
23H-6, 110	214.60	1575.2	1595.0
24H-1, 40	215.90	1546.2	1555.1
24H-1, 110	216.60	1583.9	1591.3
24H-2, 30	217.30	1587.4	1598.8
24H-2, 110	218.10	1578.7	1591.3
24H-3, 40	218.90	1578.7	1595.0
24H-3, 110	219.60	1585.7	1613.8
24H-4, 40	220.40	1566.5	1598.8
24H-4, 110	221.10	1594.5	1598.8
24H-5, 30	221.80	1594.5	1633.1
24H-5, 110	222.60	1587.4	1613.8
24H-6, 30	223.30	1576.9	1595.0
24H-6, 110	224.10	1585.7	1629.2
24H-7, 40	224.90	1559.7	1565.8
25H-2, 40	226.90	1549.5	1580.3
25H-2, 110	227.60	1585.7	1598.8
25H-3, 40	228.40	1568.3	1580.3
25H-3, 110	229.10	1575.2	1595.0
25H-4, 33	229.83	1554.6	1573.0
25H-4, 110	230.60	1578.7	1591.3
25H-5, 30	231.30	1571.7	1587.6
25H-5, 110	232.10	1580.4	1569.4
25H-6, 40	232.90	1582.2	1598.8
25H-6, 110	233.60	1589.2	1606.3
25H-7, 50	234.50	1559.7	1576.6
26H-1, 110	235.60	1559.7	1573.0
26H-2, 40	236.40	1571.7	
26H-2, 110	237.10	1573.4	1598.8
26H-3, 40	237.90	1570.0	1544.6
26H-3, 110	238.60	1589.2	1610.0
26H-4, 40	239.40	1585.7	1595.0
26H-4, 110	240.10	1589.2	1587.6
26H-5, 40	240.90	1575.2	1606.3
26H-5, 105	241.55	1578.7	1602.5
26H-6, 30	242.30	1570.0	1598.8
26H-6, 110	243.10	1587.4	
26H-7, 40	243.90		1595.0
27H-1, 30	244.30	1587.4	1613.8
27H-3, 110	248.10	1573.4	1591.3
27H-4, 20	248.70	1591.0	1583.9
27H-4, 105	249.55	1571.7	1591.3
27H-5, 40	250.40	1587.4	1606.3
27H-5, 105	251.05	1575.2	1558.7
27H-6, 40	251.90	1573.4	1602.5
27H-6, 108	252.58	1566.5	1569.4
27H-7, 40	253.40	1573.4	1565.8
28H-1, 110	254.60	1571.7	1591.3
28H-2, 40	255.40		1591.3
28H-2, 110	256.10	1582.2	1595.0
28H-3, 10	256.60	1578.7	1595.0
28H-3, 115	257.65	1564.8	1587.6
28H-4, 35	258.35	1566.5	1591.3
28H-4, 110	259.10	1594.5	1617.7
28H-5, 20	259.70	1583.9	1613.8
28H-5, 115	260.65	1568.3	1602.5
28H-6, 40	261.40	1573.4	1591.3
28H-6, 110	262.10	1573.4	1587.6
29H-1, 40	263.40	1582.2	
29H-1, 110	264.10	1576.9	1602.5
29H-2, 40	264.90	1605.3	1637.0
29H-2, 110	265.60	1585.7	1598.8
29H-3, 40	266.40	1594.5	1621.5
29H-3, 110	267.10	1571.7	1621.5
29H-4, 110	268.60	1576.9	1580.3
29H-5, 50	269.50	1563.1	1583.9
29H-5, 110	270.10	1566.5	1602.5
29H-6, 25	270.75	1582.2	1606.3
29H-6, 108	271.58	1576.9	1602.5
30H-1, 40	272.90	1566.5	1598.8
30H-1, 110	273.60	1591.0	1610.0
30H-2, 25	274.25	1566.5	1595.0
30H-3, 25	275.75	1589.2	
30H-3, 130	276.80	1580.4	1625.3
30H-4, 40	277.40	1583.9	1602.5
30H-4, 110	278.10	1582.2	
30H-5, 40	278.90	1585.7	1606.3
30H-5, 104	279.54	1601.7	1613.8
30H-6, 30	280.30	1599.9	1610.0
30H-6, 105	281.05	1583.9	1621.5
30H-7, 40	281.90	1589.2	1606.3
31H-1, 40	282.40		1591.3
31H-1, 108	283.08	1576.9	1591.3
31H-2, 30	283.80	1570.0	1551.6
31H-3, 46	285.46	1556.3	1580.3
31H-3, 46	285.46	1570.0	1562.2
31H-4, 32	286.82		1591.3
31H-4, 105	287.55	1566.5	1565.8
31H-5, 30	288.30	1580.4	1606.3
31H-5, 108	289.08	1576.9	1610.0
31H-6, 30	289.80	1589.2	1598.8
31H-6, 115	290.65	1575.2	1583.9
32H-1, 35	291.85	1575.2	
32H-1, 115	292.65	1583.9	
32H-2, 108	294.08		1602.5
32H-4, 110	297.10		1595.0
32H-5, 41	297.91		1633.1
32H-5, 110	298.60		1637.0
32H-6, 42	299.42		1625.3
32H-6, 110	300.10		1617.7
32H-7, 40	300.90		1633.1
33H-1, 40	301.40		1629.2
33H-1, 40	301.40		1610.0
33H-1, 110	302.10		1613.8
33H-2, 40	302.90		1598.8
33H-2, 110	303.60		1625.3
33H-3, 40	304.40		1602.5
33H-3, 123	305.23		1598.8
33H-4, 22	305.72		1644.9
33H-4, 97	306.47		1602.5
33H-5, 41	307.41		1633.1
33H-5, 123	308.23		1610.0
33H-6, 49	308.99		1562.2
33H-6, 49	308.99		1625.3
33H-6, 110	309.60		1617.7
33H-7, 33	310.33		1606.3
34H-1, 40	310.90		1648.9
34H-1, 110	311.60		1591.3
34H-2, 109	313.09		1681.3
34H-3, 37	313.87		1637.0
34H-3, 110	314.60		1602.5
34H-4, 40	315.40		1633.1
34H-5, 40	316.90		1710.7
35X-3, 109	324.09		1695.0
35X-4, 109	325.59		1541.4
36X-2, 105	332.25		1546.5
37X-1, 119	340.59		1559.3
38X-4, 64	354.24		1522.8
39X-1, 97	359.77	1652.3	1645.2
39X-2, 99	361.29	1666.0	1683.5
39X-3, 80	362.60	1631.1	1636.6
39X-5, 95	365.75	1724.1	1718.9
40X-1, 34	368.84	1620.3	1618.2
40X-2, 33	370.33	1588.7	1550.9
41X-1, 80	379.00	1581.0	1587.7
41X-2, 75	380.45	1660.9	
41X-3, 64	381.84	1650.2	1600.9
42X-1, 64	388.54	1688.8	1598.0
42X-4, 52	392.92	1580.7	
43X-1, 81	398.31		1628.1
43X-2, 27	399.27		1625.6
43X-3, 94	401.44		1615.4
43X-6, 124	406.24		1623.2
44X-1, 83	408.03	1753.8	1654.9
44X-2, 95	409.65		1863.2
44X-2, 95	409.65		1779.3
44X-3, 80	411.00	1949.9	1612.8
44X-5, 90	414.10	1689.3	
44X-6, 129	415.99	1846.8	1711.1
45X-1, 48	417.38	1780.9	1611.5
45X-2, 85	419.25	1688.0	
45X-3, 43	420.33	1737.3	
45X-4, 108	422.48	1750.7	
46X-1, 66	427.16	1686.2	
46X-2, 56	428.56	1761.6	
46X-3, 108	430.58	1701.3	
46X-4, 105	432.05	1708.2	
46X-5, 58	433.08	1748.5	
46X-6, 67	434.67	1743.3	
47X-1, 35	436.45	1715.4	
47X-3, 111	440.21	1813.9	
47X-4, 93	441.53	1696.3	
48X-1, 17	445.97	1888.5	1718.6
49X-1, 18	455.68	1831.1	1734.6
49X-1, 18	455.68		1747.0

Table 9. (continued).

Core, section interval (cm)	Depth (mbsf)	Vertical *P*-wave velocity (m/s)	Horizontal *P*-wave velocity (m/s)
130-806B- (Cont.)			
49X-2, 18	457.18	1789.7	1759.8
49X-6, 65	463.65		1768.5
50X-1, 44	464.04	1769.5	
50X-3, 95	467.55	1741.5	
50X-6, 68	471.78	1710.3	1676.9
51X-1, 10	473.40	1727.6	1691.2
51X-2, 116	475.96	1767.7	
52X-1, 22	482.82	1897.1	1856.3
52X-2, 71	484.81	1842.4	1792.7
52X-3, 58	486.18	1759.2	1727.9
52X-5, 4	488.64	1693.3	1825.3
53X-1, 4	492.34	1716.3	1777.4
53X-2, 4	493.84	1777.9	1722.1
53X-4, 148	498.28	1716.9	
54X-1, 4	501.94	1824.2	1763.7
54X-3, 124	506.14	1740.6	1644.6
54X-6, 15	509.55	1760.3	1698.4
55X-1, 4	511.64	1716.8	1739.8
55X-3, 8	514.68	1748.3	1719.4
55X-4, 33	516.43	1791.4	
55X-6, 150	520.60	1778.8	
56X-1, 108	522.38	1881.4	1885.0
56X-2, 111	523.91	1816.3	
56X-4, 44	526.24	1695.7	1765.4
57X-1, 10	531.00	1840.2	1791.7
57X-3, 32	534.22	1729.8	
58X-1, 4	540.54	1874.3	
58X-3, 43	543.93	1742.0	
59X-1, 15	550.35	1843.6	1895.7
59X-2, 149	553.19	1664.9	
59X-3, 66	553.86	1658.4	
60X-1, 143	561.33	1844.6	1736.2
60X-2, 118	562.58	1808.5	1711.2
60X-4, 90	565.30	1751.9	1743.7
60X-CC, 17	566.70	2001.5	1809.0
63X-1, 42	589.42	1880.7	1777.9
63X-3, 11	592.11		1814.0
63X-6, 26	596.76	1910.4	1930.1
64X-1, 54	599.14	2026.4	1937.2
64X-2, 49	600.59	2081.6	
64X-CC, 11	601.46	2062.6	1996.0
65X-1, 7	508.37	2002.5	1887.4
65X-4, 94	613.74	1888.3	
65X-6, 20	616.00	1880.0	
66X-1, 13	618.03	1816.0	1819.6
66X-5, 12	624.02	1769.3	1813.9
66X-7, 14	627.04	1787.2	1833.8
67X-1, 25	627.75	1901.1	1939.7
67X-2, 30	629.30	1864.2	1882.2
68X-1, 23	637.43	1915.1	
69X-1, 24	646.74		1959.9
69X-4, 18	651.18	1808.4	1919.9
70X-1, 12	656.32	1994.1	2106.7
70X-2, 17	657.87	2176.1	2200.2
70X-3, 14	659.34	2105.8	2090.5
70X-4, 17	660.87	1997.8	2024.3
71X-1, 69	666.49	2012.8	2085.9
71X-2, 24	667.54		2087.5
71X-2, 34	667.64	1967.3	
72X-1, 6	675.56	1827.1	1875.8
72X-3, 31	678.81	2035.8	2087.2
72X-4, 41	680.41	2251.2	
73X-1, 98	686.18	2232.2	
73X-2, 63	687.33		1996.8
74X-1, 96	695.76	2027.8	2027.5
74X-2, 106	697.36	2418.2	2344.0
74X-3, 106	698.86	2300.1	2208.1
75X-1, 21	704.71	2338.3	
75X-4, 120	710.20		2070.7
76X-1, 47	714.57	2137.7	2166.3
76X-2, 49	716.09	2194.0	
76X-2, 49	716.09	2110.9	
130-806B- (Cont.)			
76X-3, 32	717.42	2240.6	
78X-1, 8	733.48	2287.7	2234.5
130-806C-			
1H-1, 110	1.10		1596.0
1H-2, 35	1.85	1555.4	1563.2
1H-2, 110	2.60	1607.9	
1H-3, 35	3.35	1581.2	1603.5
1H-3, 110	4.10	1557.1	1570.3
1H-4, 35	4.85	1569.0	
2H-2, 40	7.50	1541.9	1549.0
2H-2, 108	8.18	1538.6	1563.2
2H-3, 41	9.01	1530.4	1552.5
2H-3, 108	9.68	1528.7	1542.0
2H-4, 40	10.50	1558.8	1577.6
2H-4, 108	11.18	1535.3	1556.1
2H-5, 40	12.00	1543.6	1574.0
2H-5, 108	12.68	1530.4	1556.1
2H-6, 40	13.50	1558.8	1577.6
2H-6, 108	14.18	1537.0	1552.5
2H-7, 40	15.00	1548.6	1577.6
3H-3, 46	18.56	1548.6	1592.3
3H-3, 108	19.18	1530.4	1538.6
3H-4, 40	20.00	1532.0	1545.5
3H-4, 108	20.68	1520.6	1521.4
3H-5, 40	21.50	1540.3	1552.5
3H-5, 108	22.18	1546.9	1566.8
3H-6, 40	23.00	1546.9	1559.6
3H-6, 108	23.68	1553.7	1574.0
3H-7, 32	24.42	1528.7	1552.5
4H-1, 108	25.68	1552.0	1588.6
4H-2, 35	26.45	1548.6	1581.2
4H-2, 108	27.18	1550.3	1574.0
4H-3, 40	28.00	1540.3	1549.0
4H-3, 108	28.68	1545.3	1581.2
4H-4, 40	29.50	1562.2	1577.6
4H-4, 108	30.18	1540.3	1556.1
4H-5, 40	31.00	1540.3	1559.6
4H-5, 108	31.68	1528.7	1542.0
4H-6, 38	32.48	1540.3	1556.1
4H-6, 108	33.18	1546.9	1566.8
4H-7, 30	33.90	1537.0	1563.2
5H-1, 108	35.18	1541.8	1556.5
5H-2, 46	36.06	1550.1	1567.2
5H-2, 108	36.68	1536.8	1546.0
5H-3, 40	37.50	1543.5	1589.0
5H-3, 105	38.15	1563.7	1556.5
5H-4, 40	39.00	1550.1	1556.5
5H-4, 101	39.61	1546.8	1553.0
5H-5, 35	40.45	1546.8	1560.1
5H-5, 108	41.18	1548.5	1556.5
5H-6, 40	42.00	1565.4	1600.1
5H-6, 120	42.80	1562.0	1556.5
6H-1, 108	44.68	1545.1	1556.5
6H-2, 40	45.50	1548.5	1567.2
6H-2, 103	46.13	1522.1	1518.6
6H-3, 40	47.00	1543.5	1539.1
6H-3, 101	47.61	1550.1	1560.1
6H-4, 40	48.50	1535.2	1532.2
6H-4, 108	49.18	1533.5	1539.1
6H-5, 40	50.00	1543.5	1553.0
6H-5, 108	50.68	1541.8	1556.5
6H-6, 35	51.43	1551.8	1570.8
6H-6, 108	52.18	1548.5	1549.5
7H-1, 110	54.20	1543.5	1539.1
7H-2, 40	55.00	1543.5	1560.1
7H-2, 108	55.68	1538.5	1553.0
7H-3, 40	56.50	1528.6	1532.2
7H-3, 108	57.18	1558.6	1581.7
7H-4, 35	57.95	1550.1	1567.2
7H-4, 130	58.90	1540.1	1553.0
7H-5, 40	59.50	1550.1	1574.4
7H-5, 100	60.10	1535.2	1535.6
130-806C- (Cont.)			
7H-6, 30	60.90	1548.5	1563.6
7H-6, 108	61.68	1548.5	1556.5
7H-7, 40	62.50	1530.3	1532.2
8H-2, 38	64.48	1540.1	1539.1
8H-2, 110	65.20	1543.5	1556.5
8H-3, 40	66.00	1546.8	1560.1
8H-3, 110	66.70	1540.1	1563.6
8H-4, 42	67.52	1546.8	1574.4
8H-4, 110	68.20	1545.1	1574.4
8H-5, 40	69.00	1536.8	1560.1
8H-5, 110	69.70	1528.6	1546.0
8H-6, 40	70.50	1550.1	1574.4
8H-6, 110	71.20	1553.5	1578.0
8H-7, 40	72.00	1541.8	1578.0
9H-2, 35	73.95		1549.5
9H-2, 110	74.70	1548.5	1553.0
9H-3, 35	75.45	1548.5	1563.6
9H-3, 110	76.20	1556.9	1570.8
9H-4, 40	77.00	1546.8	1556.5
9H-4, 110	77.70	1546.8	1570.8
9H-5, 40	78.50	1540.1	1570.8
9H-5, 110	79.20	1555.2	
9H-6, 40	80.00	1551.8	1574.4
9H-6, 110	80.70	1546.8	1578.0
9H-7, 40	81.50	1546.8	1574.4
10H-1, 35	81.95	1550.1	1560.1
10H-1, 110	82.70	1536.8	1553.0
10H-2, 35	83.45	1551.8	1553.0
10H-2, 110	84.20	1556.9	1567.2
10H-3, 35	84.95		1549.5
10H-3, 110	85.70	1536.8	1556.5
10H-4, 35	86.45	1555.2	1560.1
10H-4, 110	87.20	1550.1	1556.5
10H-5, 35	87.95	1536.8	1546.0
10H-5, 110	88.70	1550.1	1560.1
10H-6, 35	89.45	1565.4	1574.4
10H-6, 110	90.20	1584.4	1611.4
10H-7, 35	90.95	1541.8	1574.4
11H-1, 110	92.20	1538.5	1553.0
11H-2, 110	93.70	1553.5	1585.3
11H-3, 96	95.06	1548.5	1574.4
11H-4, 110	96.70	1541.8	
11H-5, 110	98.20	1540.1	1556.5
11H-6, 105	99.65	1533.5	1556.5
12H-1, 105	101.65	1548.0	1546.8
12H-2, 40	102.50	1536.4	
12H-2, 108	103.18	1533.1	1543.3
12H-3, 40	104.00	1538.0	1564.5
12H-3, 108	104.68	1546.3	
12H-4, 40	105.50	1546.3	1560.9
12H-4, 108	106.18	1533.1	1539.8
12H-5, 40	107.00	1548.0	1571.7
12H-5, 108	107.68	1549.6	1550.3
12H-6, 40	108.50	1549.6	1557.4
12H-6, 108	109.18	1548.0	1550.3
12H-7, 49	110.09	1549.6	1564.5
13H-1, 105	111.15	1548.0	1575.3
13H-2, 110	112.70	1553.0	1575.3
13H-3, 110	114.20	1558.1	1582.6
13H-4, 110	115.70	1559.7	1586.3
13H-5, 110	117.20	1553.0	1578.9
13H-6, 110	118.70	1563.1	1589.9
14H-1, 110	120.70	1556.4	1586.3
14H-2, 110	122.20	1548.0	1557.4
14H-3, 110	123.70	1558.1	1589.9
14H-4, 110	125.20	1558.1	1582.6
14H-5, 110	126.70	1549.6	1575.3
14H-6, 110	128.20	1539.7	1543.3
15H-1, 110	130.20	1543.0	1560.9
15H-2, 110	131.70	1559.7	1582.6
15H-3, 110	133.20	1554.7	1586.3
15H-4, 110	134.70	1556.4	1586.3
15H-5, 110	136.20	1554.7	1586.3
15H-6, 110	137.70	1580.3	1623.9

Table 9. (continued).

Core, section interval (cm)	Depth (mbsf)	Vertical *P*-wave velocity (m/s)	Horizontal *P*-wave velocity (m/s)
130-806C- (Cont.)			
16H-1, 110	139.70	1559.7	1589.9
16H-2, 110	141.20	1571.7	1601.1
16H-3, 110	142.70	1570.0	1589.9
16H-4, 110	144.20	1571.7	1604.9
16H-6, 113	147.23	1570.0	1604.9
17H-1, 110	149.20	1578.6	1620.1
17H-2, 110	150.70	1578.6	1623.9
17H-3, 113	152.23	1580.3	1593.6
17H-4, 105	153.65	1571.7	1578.9
17H-5, 110	155.20	1563.1	1589.9
17H-6, 110	156.70	1548.0	1578.9
18H-1, 110	158.70	1578.6	1586.3
18H-2, 110	160.20	1570.0	1582.6
18H-3, 110	161.70	1546.3	1571.7
18H-4, 110	163.20	1571.7	1597.4
18H-5, 110	164.70	1575.1	1589.9
18H-6, 110	166.20	1578.6	1601.1
19H-1, 110	168.20	1573.4	1597.4
19H-2, 110	169.70	1566.6	1586.3
19H-3, 110	171.20	1585.6	1589.9
19H-4, 110	172.70	1548.0	1571.7
19H-5, 110	174.20	1580.3	1601.1
19H-6, 110	175.70	1563.1	1586.3
20H-1, 110	177.70	1570.0	1586.3
20H-2, 110	179.20	1570.0	1586.3
20H-3, 110	180.70	1576.9	1601.1
20H-4, 110	182.20	1580.3	1612.4
20H-5, 110	183.70	1594.4	1612.4
20H-6, 110	185.20	1575.1	1593.6
21H-1, 110	187.20	1605.1	1612.4
21H-2, 110	188.70	1597.9	1608.6
21H-3, 110	190.20	1596.2	1612.4
21H-4, 110	191.70	1580.3	1601.1
21H-5, 110	193.20	1568.3	1593.6
21H-6, 110	194.70	1592.6	1620.1
22H-1, 110	196.70	1612.3	1631.7
22H-2, 108	198.18	1590.8	
22H-3, 107	199.67	1580.3	1604.9
22H-4, 110	201.20	1578.6	1604.9
22H-5, 112	202.72	1575.1	1601.1
22H-6, 112	204.22	1589.1	1612.4
23H-1, 106	206.16	1573.4	1620.1
23H-2, 108	207.68	1589.1	1612.4
23H-3, 97	209.07	1606.9	1623.9
23H-4, 135	210.95	1596.2	1616.2
23H-5, 111	212.21	1585.6	1601.1
23H-6, 113	213.73	1597.9	
24H-1, 113	215.73	1596.2	1582.6
24H-2, 112	217.22	1582.1	1623.9
24H-3, 110	218.70	1597.9	1655.4
24H-4, 110	220.20	1605.1	1651.4
24H-5, 110	221.70	1583.8	1601.1
24H-6, 110	223.20	1612.3	1651.4
25H-1, 110	225.20	1568.3	1597.4
25H-2, 110	226.70	1597.9	1604.9
25H-3, 110	228.20	1568.3	1597.4
25H-4, 110	229.70	1587.3	1597.4
25H-5, 110	231.20	1599.7	1616.2
25H-6, 110	232.70	1596.2	1586.3
26H-2, 110	236.20	1583.8	1623.9
26H-3, 110	237.70	1585.6	1601.1
26H-4, 110	239.20	1592.6	1659.4
26H-5, 110	240.70	1606.9	1623.9
26H-6, 110	242.20	1570.0	1589.9
27H-1, 110	244.20	1582.1	1620.1
27H-2, 110	245.70	1597.9	1631.7
27H-3, 110	247.20	1566.6	1589.9
27H-4, 110	248.70	1617.7	
27H-5, 110	250.20	1605.1	1627.8
27H-6, 110	251.70	1597.9	1616.2
28H-1, 110	253.70	1594.4	1620.1
28H-3, 110	255.35	1619.6	1635.6
28H-4, 110	256.85	1608.7	1631.7
28H-5, 110	258.35	1601.5	1616.2
28H-6, 110	259.85	1592.6	1616.2
28H-7, 110	261.35	1592.6	1620.1
29H-1, 108	263.18	1573.4	1597.4
29H-2, 50	264.10	1596.2	1623.9
29H-2, 108	264.68	1603.3	1612.4
29H-3, 40	265.50	1576.9	1601.1
29H-3, 108	266.18	1590.8	1616.2
29H-4, 40	267.00	1583.8	1620.1
29H-4, 108	267.68	1573.4	1604.9
29H-5, 40	268.50	1585.6	1582.6
29H-5, 108	269.18		1601.1
29H-6, 40	270.00	1576.9	1597.4
29H-6, 108	270.68	1580.3	
30H-1, 40	272.00	1582.1	1612.4
30H-1, 108	272.68	1585.6	1604.9
30H-2, 40	273.50	1587.3	1620.1
30H-2, 108	274.18	1578.6	1604.9
30H-3, 40	275.00		1616.2
30H-3, 108	275.68		1578.9
30H-4, 40	276.50	1583.8	1627.8
30H-4, 108	277.18	1594.4	1620.1
30H-5, 40	278.00	1582.1	1616.2
30H-5, 108	278.68	1589.1	1623.9
30H-6, 40	279.50	1590.8	1623.9
30H-6, 108	280.18	1603.3	1659.4
31H-1, 40	281.50	1582.1	1612.4
31H-1, 105	282.15	1573.4	1608.6
31H-2, 40	283.00	1575.1	1601.1
31H-2, 108	283.68	1589.1	
31H-3, 40	284.50	1526.6	1586.3
31H-3, 108	285.18		1597.4
31H-4, 40	286.00	1566.6	1608.6
31H-4, 108	286.68	1573.4	
31H-4, 108	286.68	1585.6	
31H-5, 34	287.44	1587.3	1608.6
31H-5, 108	288.18	1594.4	1608.6
31H-6, 50	289.10	1573.4	1608.6
31H-6, 108	289.68	1580.3	1589.9
32H-1, 40	291.00	1548.0	1631.7
32H-1, 104	291.64		1597.4
32H-2, 40	292.50	1544.6	
32H-2, 108	293.18	1592.6	1612.4
32H-3, 40	294.00		1593.6
32H-3, 108	294.68	1548.0	1631.7
32H-4, 40	295.50	1587.3	1608.6
32H-4, 107	296.17	1599.7	1639.5
32H-5, 33	296.93	1556.4	1623.9
32H-5, 105	297.65	1594.4	1631.7
33H-1, 28	300.38	1597.9	1597.4
33H-2, 38	301.98		1597.4
33H-2, 105	302.65	1596.2	1597.4
33H-4, 40	305.00	1583.8	1643.4
33H-4, 110	305.70		1593.6
33H-5, 68	306.78		1601.1
33H-6, 51	308.11		1593.6
35X-2, 60	321.40	1580.9	1666.2
35X-3, 103	323.33	1629.5	1666.2
35X-4, 104	324.84	1605.7	1646.2
36X-1, 75	329.65		1662.1
36X-2, 75	331.15		1626.7
36X-3, 75	332.65		1560.1
36X-4, 75	334.15		1650.1
36X-5, 75	335.65		1518.6
36X-6, 75	337.15		1695.0
37X-1, 75	339.25		1634.4
37X-2, 75	340.75		1592.7
37X-3, 10	341.60		1622.8
37X-5, 60	345.10		1638.3
38X-1, 75	348.95		1592.7
38X-2, 75	350.45		1622.8
38X-3, 75	351.95		1670.2
38X-4, 75	353.45		1666.2
38X-5, 75	354.95		1703.4
39X-1, 75	358.65		1622.8
39X-2, 75	360.15		1695.0
39X-3, 75	361.65		1695.0
39X-4, 75	363.15		1603.9
39X-5, 75	364.65		1670.2
40X-1, 75	368.35		1662.1
40X-2, 75	369.85		1622.8
40X-4, 75	372.85		1662.1
42X-1, 22	387.22	1695.2	1661.3
42X-2, 104	389.54	1661.7	1582.0
42X-3, 61	390.61	1644.8	1588.2
42X-4, 20	391.70	1608.8	1597.3
42X-6, 39	394.89	1664.9	1589.0
43X-1, 136	398.06	1597.9	1584.4
43X-2, 101	399.21	1676.1	
43X-3, 32	400.02	1642.1	1628.3
43X-4, 117	402.37	1643.0	
43X-5, 117	403.87	1667.4	1556.7
43X-6, 35	404.55	1634.3	1570.6
44X-1, 77	407.07	1675.1	1640.9
44X-2, 70	408.50	1730.3	1667.5
44X-3, 36	409.66	1713.2	1729.1
44X-5, 70	413.00	1744.8	1669.3
44X-6, 17	413.97	1734.2	1659.1
45X-2, 139	418.79	1633.7	
45X-3, 127	420.17	1730.0	1648.4
45X-4, 140	421.80	1683.9	1666.2
45X-5, 56	422.46	1777.9	1643.6
46X-1, 124	426.84	1651.4	
46X-2, 94	428.04	1695.2	
46X-3, 26	428.86	1691.9	1621.2
46X-4, 96	431.06	1760.0	
46X-5, 122	432.82	1745.4	1653.7
46X-6, 82	433.92	1712.8	1653.7
47X-1, 108	436.28	1720.1	1581.7
47X-2, 126	437.96	1763.9	1669.3
47X-3, 83	439.03	1833.2	1756.7
47X-5, 11	441.31	1729.5	1672.5
47X-6, 57	443.27	1734.5	1644.4
48X-2, 94	447.34	1783.0	1712.9
48X-3, 30	448.20	1824.3	1721.0
49X-2, 130	457.40	1715.4	1646.5
49X-3, 97	458.57	1777.9	1747.3
49X-4, 84	459.94	1951.6	1781.3
50X-1, 68	465.18	1742.6	1631.1
50X-2, 105	467.05	1868.9	1873.5
50X-3, 118	468.68	1674.8	
50X-4, 122	470.22	1842.2	1679.6
50X-5, 98	471.48	1786.2	1715.0
50X-6, 126	473.26	1712.8	1621.6
51X-1, 138	475.68	1771.7	
51X-2, 89	476.69	1939.3	1810.6
51X-3, 129	478.59	1778.5	
52X-1, 66	484.36	1957.6	1846.0
52X-2, 36	485.56	1948.5	1866.5
52X-3, 56	487.26	19[illegible]7.8	1949.1
53X-1, 61	493.91	1907.1	1751.5
53X-2, 51	495.31		1711.9
53X-3, 82	497.12	1861.5	1693.3
53X-4, 133	499.13	1908.0	1821.9
53X-5, 145	500.75	1857.6	1750.4
54X-2, 122	505.72	1673.1	
54X-3, 139	507.39	1753.0	1706.1
55X-2, 143	515.63	1804.2	1799.1
55X-3, 125	516.95	1891.7	17[illegible]5.7
55X-4, 126	518.46	1946.3	1785.0
56X-1, 120	523.60	1971.4	1845.2
56X-2, 110	525.00	1727.0	1668.2
56X-3, 126	526.66	1895.7	1738.9
56X-4, 114	528.04	1786.2	1677.9
56X-5, 130	529.70	1890.4	1834.0
56X-6, 126	531.16	1919.8	1885.2
57X-2, 55	534.05	1947.2	1773.3
57X-3, 145	536.45	1877.2	
57X-4, 82	537.32	1752.9	1694.9

Table 9. (continued).

Core, section interval (cm)	Depth (mbsf)	Vertical *P*-wave velocity (m/s)	Horizontal *P*-wave velocity (m/s)
130-806C- (Cont.)			
57X-5, 50	538.50	1848.1	1744.0
57X-6, 95	540.45	1829.6	1762.5
58X-3, 133	603.33	1980.8	1965.2
58X-4, 132	604.82	1951.8	1994.7
59X-CC, 15	740.65	1989.4	1968.4
60X-1, 16	749.66	2091.6	2111.7
61X-1, 38	759.58	2122.0	2275.3
61X-2, 106	761.76	2079.9	2022.6
61X-3, 82	763.02	2044.7	2233.5
61X-4, [illegible]	764.64	2132.0	
62X-1, 31	767.01	1921.7	2178.0
61X-6, 56	767.26	1964.5	1945.3

VOLUME
130

CHAPTER
9

TABLE
14

Table 14. *P*-wave velocity data, Site 807.

Core, section, interval (cm)	Depth (mbsf)	Vertical *P*-wave velocity (m/s)	Horizontal *P*-wave velocity (m/s)
130-807A-			
1H-1, 95	0.95	1561.4	1563.9
1H-2, 12	1.62	1554.6	1567.5
1H-2, 95	2.45	1564.8	1582.0
1H-3, 15	3.15	1544.6	1546.2
1H-3, 95	3.95	1568.2	1582.0
1H-4, 15	4.65	1541.3	1539.3
1H-4, 95	5.45	1539.6	1556.8
1H-5, 15	6.15	1549.6	1563.9
1H-5, 95	6.95	1549.6	1563.9
2H-1, 95	8.35	1575.1	1596.8
2H-2, 15	9.05	1559.7	1567.5
2H-2, 95	9.85	1580.3	1615.6
2H-3, 15	10.55	1549.6	1563.9
2H-3, 95	11.35	1575.1	1585.7
2H-4, 15	12.05	1552.9	1556.8
2H-4, 95	12.85	1569.9	1589.3
2H-5, 15	13.55	1566.5	1623.3
2H-5, 95	14.35	1573.3	1593.0
2H-6, 15	15.05	1563.1	
2H-6, 95	15.85	1575.1	1593.0
2H-7, 15	16.55	1561.4	1585.7
3H-1, 110	18.00	1540.0	1533.0
3H-2, 15	18.55	1575.1	1604.3
3H-2, 95	19.35	1578.5	1608.0
3H-3, 15	20.05	1582.0	1560.3
3H-3, 95	20.85	1561.4	1585.7
3H-4, 15	21.55	1568.2	1563.9
3H-4, 95	22.35	1526.5	1556.8
3H-5, 15	23.05	1552.9	1574.7
3H-5, 95	23.85	1563.1	1593.0
3H-6, 15	24.55	1549.6	1556.8
3H-6, 95	25.35	1559.7	1582.0
3H-7, 15	26.05	1590.8	1631.0
4H-1, 95	27.35		1574.7
4H-2, 15	28.05	1546.2	1553.3
4H-2, 95	28.85	1542.9	1578.3
4H-3, 15	29.55	1576.8	1600.5
4H-3, 95	30.35	1559.7	1600.5
4H-4, 5	30.95	1573.3	1600.5
4H-4, 95	31.85	1571.6	1504.3
4H-5, 15	32.55	1569.9	1508.0
4H-5, 95	33.35	1575.1	1604.3
4H-6, 15	34.05	1561.4	1542.7
4H-6, 95	34.85	1556.3	1574.7
4H-7, 30	35.70	1568.2	1596.8
5H-1, 110	37.00	1554.6	1593.0
5H-2, 35	37.75	1566.5	1589.3
5H-2, 110	38.50	1563.1	1571.1
5H-3, 40	39.30	1549.6	1571.1
5H-3, 111	40.01	1552.9	1571.1
5H-4, 40	40.80	1580.3	1608.0
5H-4, 110	41.50	1564.8	1589.3
5H-5, 40	42.30	1571.6	1608.0
5H-5, 110	43.00	1564.8	1582.0
5H-6, 40	43.80	1556.3	1574.7
5H-6, 110	44.50	1559.7	1600.5
5H-7, 30	45.20	1566.5	1608.0
6H-1, 35	45.75	1582.0	1596.8
6H-1, 110	46.50	1571.6	1518.8
6H-3, 35	48.75	1571.6	1582.0
6H-3, 110	49.50		1553.3
6H-4, 110	51.00	1540.0	1568.2
6H-4, 110	51.00	1576.8	1593.0
6H-5, 35	51.75	1571.6	1593.0
6H-5, 110	52.50	1569.9	1589.3
6H-6, 35	53.25	1566.5	1593.0
6H-6, 110	54.00	1561.4	1589.3
7H-1, 110	56.00	1521.7	1567.5
7H-2, 35	56.75	1575.1	1578.3
7H-2, 110	57.50	1549.6	1553.3
7H-3, 10	58.00	1580.3	1593.0
7H-3, 35	58.25	1571.6	1604.3
7H-4, 35	59.75	1569.9	1593.0
7H-4, 110	60.50	1546.2	1563.9
7H-5, 35	61.25	1559.7	1589.3
7H-5, 110	62.00	1569.9	1611.8
7H-6, 35	62.75	1541.3	1585.7
7H-6, 110	63.50	1546.2	1578.3
8H-1, 110	65.50	1566.5	1571.1
8H-2, 35	66.25	1569.9	1604.3
8H-2, 110	67.00	1556.3	1578.3
8H-3, 34	67.74	1546.2	1553.3
8H-3, 110	68.50	1552.9	1589.3
8H-4, 42	69.32	1546.2	1567.5
8H-4, 110	70.00	1549.6	1571.1
8H-5, 39	70.79	1547.9	1567.5
8H-5, 110	71.50	1549.6	1578.3
8H-6, 40	72.30	1549.6	1571.1
8H-6, 100	72.90	1566.5	1604.3
8H-7, 35	73.75	1563.1	1600.5
9H-1, 35	74.25	1556.3	1567.5
9H-1, 110	75.00	1556.3	1560.3
9H-2, 35	75.75	1546.2	1556.8
9H-2, 110	76.50	1554.6	1556.8
9H-3, 35	77.25		1553.3
9H-3, 110	78.00		1556.8
9H-4, 35	78.75	1558.0	1549.7
9H-4, 110	79.50	1576.8	1604.3
9H-5, 35	80.25	1556.3	1585.7
9H-5, 110	81.00	1529.8	1549.7
9H-6, 35	81.75	1551.3	1560.3
9H-6, 110	82.50	1533.0	1563.9
10H-1, 110	84.50	1575.1	1585.7
10H-2, 110	86.00	1542.9	1589.3
10H-3, 110	87.50	1551.3	1589.3
10H-4, 110	89.00	1563.1	1589.3
10H-5, 110	90.50	1554.6	1589.3
10H-6, 110	92.00	1571.6	1593.0
11H-1, 108	93.98	1520.1	1542.7
11H-2, 15	94.55		1549.7
11H-2, 108	95.48	1552.9	1553.3
11H-3, 15	96.05	1538.0	1567.5
11H-3, 108	96.98	1554.6	1556.8
11H-4, 15	97.55	1549.6	1574.7
11H-4, 108	98.48	1558.0	1567.5
11H-5, 15	99.05	1568.2	
11H-5, 108	99.98	1552.9	1578.3
11H-6, 15	100.55	1546.2	1563.9
11H-6, 108	101.48	1552.9	
12H-1, 108	103.48	1527.2	1535.7
12H-2, 25	104.15	1532.1	1546.1
12H-2, 108	104.98	1520.7	1532.2
12H-3, 25	105.65	1533.0	1541.6
12H-3, 108	106.48	1520.1	
12H-4, 25	107.15	1528.2	1545.1
12H-5, 25	108.65	1538.0	1559.1
12H-5, 107	109.47	1533.0	1548.6
12H-6, 36	110.26	1546.3	1566.3
12H-6, 107	110.97	1523.3	1534.7
13H-2, 107	114.47	1538.7	1558.5
13H-3, 25	115.15	1535.4	1544.5
13H-3, 108	115.98	1535.4	1551.5
13H-4, 20	116.60	1520.7	1527.2
13H-4, 107	117.47	1532.1	
13H-5, 25	118.15	1563.5	1586.4
13H-5, 106	118.96	1561.8	1597.5
13H-6, 25	119.65	1556.7	1582.7
13H-6, 108	120.48	1566.9	1593.7
14H-3, 25	124.65	1568.6	1605.0
14H-3, 108	125.48	1553.3	1579.0
14H-4, 25	126.15	1575.5	1605.0
14H-4, 108	126.98	1551.6	1557.5
14H-5, 25	127.65	1553.3	1582.7
14H-5, 108	128.48	1566.9	1590.0
14H-6, 25	129.15	1558.4	1575.4
14H-6, 108	129.98	1550.0	1579.0
15H-3, 108	133.73	1546.6	1561.0
15H-4, 35	134.50	1572.1	1608.7

Table 14 (continued).

Core, section, interval (cm)	Depth (mbsf)	Vertical *P*-wave velocity (m/s)	Horizontal *P*-wave velocity (m/s)
15H-4, 108	135.23	1563.5	1579.0
15H-5, 30	135.95	1575.5	1597.5
15H-5, 108	136.73	1546.6	1553.9
15H-6, 25	137.40	1565.2	1582.7
15H-6, 108	138.23	1548.3	1550.4
15H-7, 30	138.95	1565.2	1582.7
15H-7, 108	139.73	1558.4	1564.6
16H-1, 108	141.48	1556.7	1553.9
16H-2, 25	142.15	1548.3	1561.0
16H-2, 108	142.98	1560.1	1593.7
16H-3, 20	143.60	1548.3	1557.5
16H-3, 108	144.48	1555.0	1557.5
16H-4, 25	145.15	1553.3	1561.0
16H-4, 107	145.97	1594.8	1605.0
16H-5, 24	146.64	1553.3	1568.2
16H-5, 108	147.48	1579.0	1590.0
16H-6, 25	148.15	1593.0	1601.2
16H-6, 123	149.13	1589.5	1605.0
17H-1, 75	150.65	1570.3	1597.5
17H-2, 90	152.30	1561.8	1597.5
17H-3, 75	153.65	1563.5	1568.2
17H-5, 75	156.65	1575.5	1593.7
17H-6, 75	158.15	1584.2	1624.0
18H-1, 75	160.15	1579.0	1605.0
18H-2, 75	161.65	1568.6	1590.0
18H-3, 75	163.15	1565.2	1601.2
18H-4, 75	164.65	1548.3	1553.9
18H-5, 75	166.15	1566.9	1575.4
18H-6, 75	167.65	1573.8	1597.5
19H-1, 75	169.65	1566.9	1579.0
19H-2, 75	171.15	1565.2	1579.0
19H-3, 75	172.65	1572.1	1586.4
19H-4, 86	174.26	1551.6	1568.2
19H-5, 75	175.65	1580.7	1605.0
19H-6, 75	177.15	1591.3	1608.7
20H-1, 75	179.15	1580.7	1608.7
20H-2, 75	180.65	1572.1	1593.7
20H-3, 75	182.15	1560.1	1575.4
20H-4, 75	183.65	1573.8	1590.0
20H-5, 75	185.15	1573.8	1582.7
20H-6, 75	186.65	1591.3	1616.3
21H-1, 112	189.02	1566.9	1586.4
21H-2, 108	190.48	1565.2	1593.7
21H-3, 110	192.00	1565.2	1590.0
21H-4, 90	193.30	1560.1	
21H-5, 108	194.98	1556.7	1561.0
21H-6, 110	196.50	1551.6	1546.9
22H-1, 108	198.48	1568.6	1590.0
22H-2, 100	199.90	1565.2	1579.0
22H-3, 110	201.50	1577.2	1608.7
22H-4, 110	203.00	1565.2	1586.4
22H-5, 110	204.50	1565.2	1575.4
22H-6, 112	206.02	1591.3	1620.2
23H-1, 106	207.96	1573.5	1612.5
23H-2, 110	209.50	1572.1	1590.0
23H-3, 110	211.00	1586.0	1631.8
23H-4, 110	212.50	1582.5	1631.8
23H-5, 110	214.00	1614.5	1675.7
23H-6, 110	215.50	1591.3	1608.7
24H-1, 110	217.50	1612.7	1643.5
24H-2, 110	219.00	1600.1	1612.5
24H-3, 110	220.50	1589.5	
24H-4, 110	222.00	1577.2	1593.7
24H-5, 110	223.50	1603.7	1639.6
25H-2, 110	228.50	1587.7	1601.2
25H-3, 110	230.00	1587.7	1612.5
25H-4, 110	231.50	1593.0	1539.9
25H-5, 110	233.00	1575.5	1597.5
25H-6, 110	234.50	1580.7	1616.3
26H-1, 110	236.50	1589.5	1624.0
26H-3, 110	239.50	1572.1	1627.9
26H-5, 110	242.50	1593.0	1627.9
26H-6, 110	244.00	1584.2	1616.3
27H-1, 110	246.00	1584.2	
27H-3, 110	249.00	1593.0	

Table 14 (continued).

Core, section, interval (cm)	Depth (mbsf)	Vertical *P*-wave velocity (m/s)	Horizontal *P*-wave velocity (m/s)
27H-4, 110	250.50	1605.5	1663.5
27H-5, 110	252.00	1587.7	1651.5
27H-6, 110	253.50		1643.5
28X-1, 106	255.46	1582.0	1662.8
28X-2, 32	256.22		1560.3
28X-2, 103	256.93		1604.3
28X-3, 63	258.03		1600.5
28X-4, 32	259.22	1569.9	1611.8
28X-4, 103	259.93		1679.1
28X-5, 33	260.73		1627.2
28X-5, 107	261.47		1662.8
28X-6, 28	262.18		1650.7
28X-6, 80	262.70		1634.9
29X-1, 49	264.59		1646.7
29X-1, 103	265.13	1587.3	1585.7
29X-2, 32	265.92	1571.6	1574.7
29X-2, 100	266.60		1638.9
29X-3, 70	267.80	1583.8	1611.8
29X-4, 79	269.39	1592.5	1608.0
29X-5, 85	270.95	1569.9	1593.0
29X-6, 75	272.35	1569.9	1589.3
30X-5, 56	280.36	1527.2	
31X-1, 89	284.39	1539.3	1539.4
31X-2, 127	286.27	1537.6	
31X-3, 72	287.22	1558.0	1567.5
31X-4, 60	288.60	1596.1	1631.0
31X-5, 63	290.13	1564.8	1571.1
32X-1, 147	294.17	1665.5	1579.3
32X-2, 111	295.31	1629.9	1564.9
32X-3, 127	296.97	1596.3	1534.6
32X-4, 98	298.18	1652.3	1613.6
33X-1, 37	302.67	1655.1	1631.9
33X-2, 135	305.15	1699.7	1584.3
33X-3, 57	305.87	1679.1	1606.7
33X-4, 128	308.08	1689.6	1648.5
33X-5, 148	309.78	1600.2	1543.3
33X-6, 76	310.56	1682.4	
34X-1, 70	312.70	1606.3	1616.2
34X-2, 72	314.22	1724.0	1624.4
34X-3, 99	315.99	1655.1	1539.5
34X-4, 99	317.49	1689.2	
34X-4, 108	317.58		1600.9
34X-5, 43	318.43	1571.6	
34X-6, 132	320.82	1615.9	
35X-1, 135	322.55	1659.1	1546.7
35X-2, 142	324.12	1669.2	1578.9
35X-3, 114	325.34	1655.7	1576.1
35X-4, 146	327.16	1655.7	1544.3
35X-5, 106	328.26	1665.7	1568.6
36X-1, 135	332.25	1668.9	
36X-2, 141	333.81	1717.9	1649.4
36X-3, 109	334.99	1689.2	1646.9
36X-4, 133	336.73	1787.1	1666.2
36X-5, 114	338.04	1727.6	1664.9
36X-6, 84	339.24	1674.9	1604.0
37X-2, 93	343.03	1716.6	
37X-3, 97	344.57	1638.9	1620.0
37X-4, 52	345.62	1699.3	1611.5
37X-5, 11	346.71	1584.0	
38X-1, 142	351.62	1671.4	1591.0
38X-2, 112	352.82	1738.9	1640.0
38X-3, 143	354.63	1685.0	1620.0
38X-4, 97	355.67	1668.1	1633.6
38X-5, 80	357.00	1671.7	1595.0
39X-1, 136	361.26	1757.0	1696.5
39X-2, 92	362.32	1706.3	1641.0
39X-4, 50	364.90	1757.0	1649.3
39X-5, 141	367.31	1707.0	1616.5
39X-6, 40	367.80	1798.2	1697.4
40X-1, 78	370.48	1873.9	1785.5
40X-2, 58	371.78	1902.1	1773.5
40X-3, 62	373.32	1802.5	1690.9
40X-4, 148	375.68	1811.3	1638.5
40X-5, 123	376.93	1678.5	
40X-6, 107	378.27	1845.9	1609.7

Table 14 (continued).

Core, section, interval (cm)	Depth (mbsf)	Vertical *P*-wave velocity (m/s)	Horizontal *P*-wave velocity (m/s)
41X-1, 97	380.47	1798.2	1688.0
41X-2, 81	381.81	1714.5	1714.9
41X-3, 77	383.27	1783.0	1775.3
41X-4, 80	384.80	1745.9	1732.4
41X-5, 92	386.42	1751.9	1766.1
41X-6, 85	387.85	1699.7	1729.4
42X-1, 107	390.27	1837.4	1848.2
42X-2, 105	391.75	1829.5	1887.7
42X-3, 107	393.27	1767.9	
42X-4, 80	394.50	1705.8	1661.1
42X-5, 61	395.81	1794.0	1764.8
42X-6, 41	397.11	1745.9	1722.2
43X-1, 82	399.72	1862.0	
43X-2, 70	401.10	1950.2	
43X-3, 70	402.60	1977.8	1887.4
43X-4, 70	404.10	1959.1	1863.2
43X-5, 77	405.67	1897.5	1824.0
44X-1, 76	409.36	1782.8	1680.0
44X-2, 142	411.52	1822.6	
44X-2, 142	411.52	1808.4	
44X-3, 111	412.71	1829.1	
44X-5, 125	415.85	2086.0	
45X-1, 99	419.29	1941.1	1840.6
45X-2, 98	420.78	1864.5	1828.2
45X-3, 91	422.21	1932.5	2005.5
45X-4, 96	423.76	1949.7	
45X-5, 58	424.88	1923.3	
45X-6, 66	426.46	1950.2	
46X-1, 117	428.97	1887.0	
46X-2, 113	430.43	1905.7	
46X-3, 108	431.88	1855.6	1844.9
46X-4, 109	433.39	1896.1	
46X-5, 82	434.62	1888.5	
46X-6, 79	436.09	1922.9	
47X-1, 112	438.62	1846.1	1661.2
47X-2, 123	440.23	1786.8	
47X-3, 111	441.61	1940.8	
47X-4, 114	443.14	1897.5	
47X-5, 104	444.54	1931.8	
47X-6, 52	445.52	1978.0	1864.3
48X-1, 101	448.11	1761.0	1776.9
48X-2, 102	449.62	1693.3	1741.2
48X-3, 102	451.12	1775.8	1821.2
48X-4, 94	452.54	1790.7	1845.1
48X-5, 85	453.95	1797.4	1766.9
48X-6, 101	455.62	1794.0	1783.9
49X-1, 54	457.34	1771.4	1701.6
49X-2, 93	459.23	1849.0	1829.1
49X-3, 66	460.46	1863.6	1900.6
49X-4, 73	462.03	1817.0	1817.0
49X-5, 73	463.53	1718.0	1782.5
50X-1, 90	467.30	1686.1	1674.2
50X-2, 94	468.84	1778.9	1776.0
50X-3, 91	470.31	1753.3	1693.2
50X-4, 101	471.91	1673.4	1722.4
50X-5, 98	473.38	1790.6	1751.4
50X-6, 99	474.89	1732.0	1697.6
51X-1, 34	476.44	1949.9	
51X-2, 42	478.02	1888.0	
51X-3, 42	479.53	1941.1	1777.2
51X-4, 39	480.99	1987.2	
51X-5, 34	482.44	1931.5	
51X-6, 19	483.79	1862.0	
52X-1, 109	486.89	1751.7	
52X-3, 15	488.95	1848.9	
52X-5, 62	492.42	2110.2	
53X-1, 106	496.46	1889.5	
53X-2, 94	497.84	1820.3	
53X-3, 98	499.38	1968.5	
53X-4, 91	500.81	1811.4	
54X-1, 97	506.07	1855.6	
54X-2, 98	507.58	1923.3	
54X-3, 115	509.25	1837.2	
54X-4, 114	510.74	1838.7	
54X-5, 81	511.91	1733.1	

Table 14 (continued).

Core, section, interval (cm)	Depth (mbsf)	Vertical *P*-wave velocity (m/s)	Horizontal *P*-wave velocity (m/s)
54X-6, 29	512.89	1849.0	1692.9
55X-2, 116	517.46	1862.1	1685.8
55X-3, 62	518.42	1660.9	1563.0
55X-4, 66	519.96	1933.7	1727.5
55X-5, 104	521.84	1895.3	1805.9
55X-6, 43	522.73	1908.0	1809.4
56X-1, 147	525.47	1737.2	
56X-2, 110	526.60	1772.1	1617.7
56X-3, 53	527.53	1810.3	1676.6
56X-4, 132	529.82	1809.4	1710.6
56X-6, 50	532.00	1801.7	1703.7
57X-1, 86	534.56	1790.6	
57X-2, 86	536.06	1834.0	1713.1
57X-3, 96	537.66	1738.9	1721.2
57X-4, 66	538.86	1857.4	1653.5
57X-5, 57	540.27	1750.0	1725.0
58X-1, 106	544.46	1690.4	1713.5
58X-2, 105	545.95	1682.8	1714.4
58X-3, 144	547.84	1696.5	1690.1
58X-4, 137	549.27	1775.3	1684.1
59X-2, 126	555.76	1762.3	1700.5
59X-3, 108	557.08	1739.7	1711.5
59X-4, 133	558.83	1697.7	1639.4
60X-1, 10	562.70	1806.0	
60X-3, 141	567.01	1721.4	1718.3
60X-4, 75	567.85	1690.9	1720.9
60X-4, 75	567.85	1754.0	1707.4
61X-1, 98	573.28	1671.6	1710.6
61X-1, 98	573.28	1674.2	
61X-3, 125	576.55		1679.8
61X-4, 147	578.27	1698.1	1779.8
61X-4, 147	578.27	1749.4	1798.2
61X-5, 146	579.76	1907.0	1937.6
61X-5, 146	579.76	2036.3	1988.3
61X-6, 93	580.73	1972.6	1937.6
61X-6, 93	580.73	1809.4	
62X-2, 114	584.54	1728.2	1787.5
62X-3, 101	585.91	1750.2	1747.4
62X-4, 95	587.35	1788.2	1837.2
62X-5, 89	588.79	1775.6	1820.5
63X-1, 111	592.71	1754.2	1756.0
63X-2, 53	593.63	1725.8	1773.3
63X-3, 33	594.93	1813.6	1724.6
63X-4, 60	596.70	1791.5	
63X-5, 47	598.07	1854.3	1764.3
64X-1, 11	601.41	1728.2	1766.7
64X-2, 112	603.92	1823.9	1935.3
64X-3, 125	605.55	1816.9	1897.8
64X-4, 82	606.62	1790.7	1815.8
64X-5, 60	607.90	1865.0	1831.6
65X-1, 68	611.68	1862.4	1814.3
65X-2, 63	613.13	1810.2	1826.8
65X-4, 66	616.16	1996.8	
65X-4, 66	616.16	1803.1	
65X-5, 53	617.53	1941.4	1868.0
66X-1, 86	621.46	1959.3	
66X-3, 80	624.40	2025.5	
66X-4, 86	625.96	1941.4	
67X-3, 93	634.23	1996.8	
68X-1, 106	640.96	2035.6	
68X-2, 112	642.52	2086.5	
68X-3, 106	643.96	2025.7	
68X-4, 90	645.30	2096.0	
70X-3, 61	662.81	2006.3	
70X-4, 18	663.88	2096.0	
70X-5, 71	665.91	2085.6	
71X-1, 127	670.17	1831.8	1822.8
71X-2, 126	671.66	1753.7	1828.8
71X-3, 110	673.00	1756.9	1805.5
71X-4, 113	674.53	1768.3	1848.1
71X-5, 109	675.99	1807.6	1820.6
72X-1, 75	678.95	1895.3	1957.3
72X-2, 67	680.37	1810.2	1795.2
72X-3, 79	681.99	1832.7	1999.7
72X-4, 66	683.36	1843.4	1829.5

Table 14 (continued).

Core, section, interval (cm)	Depth (mbsf)	Vertical *P*-wave velocity (m/s)	Horizontal *P*-wave velocity (m/s)
73X-2, 41	689.71	1779.0	
73X-2, 91	690.21		1842.3
73X-3, 86	691.66	1839.7	1919.1
73X-4, 79	693.09	1790.7	1778.2
73X-5, 76	694.56	1894.4	1977.8
73X-6, 36	695.66	1946.5	2073.5
74X-1, 63	698.13	2263.3	
74X-2, 60	699.60	2138.4	2024.4
74X-3, 64	701.14	1968.8	
75X-1, 74	707.94	1950.4	2015.1
75X-2, 87	709.57	2025.9	1770.7
75X-3, 73	710.93	2066.5	
75X-4, 84	712.54	1814.7	2023.1
76X-1, 95	717.85	2172.3	2155.5
76X-2, 121	719.61	2278.4	
76X-3, 115	721.05	2230.0	2063.7
76X-4, 96	722.36	2193.0	2085.6
76X-5, 83	723.73	2148.6	
77X-1, 84	727.34	2252.6	2055.4
77X-2, 106	729.06	2171.5	
77X-3, 79	730.29	2195.0	2029.6
77X-4, 76	731.76	2194.0	1980.7
77X-5, 74	733.24	2239.4	1981.5
78X-1, 108	737.28	2099.4	
78X-2, 89	738.59	1879.6	1978.1
78X-3, 28	739.48	1912.5	1803.4
78X-4, 112	741.82	1979.0	2000.6
78X-5, 66	742.86	1960.6	2003.4
79X-1, 36	745.86	2013.9	1994.9
79X-CC, 31	747.71	2227.6	2141.8
80X-1, 44	755.64	1881.8	1707.3
80X-1, 44	755.64		1794.0
80X-2, 94	757.64		1917.4
80X-2, 94	757.64		2022.7
80X-3, 90	759.10	1960.6	1915.6
82X-2, 72	776.72	1956.9	2006.2
82X-4, 72	779.72	1931.5	1728.0
83X-2, 7	785.77	1934.0	1855.5
83X-3, 4	787.24	1840.8	1869.4
83X-4, 23	788.93	1916.1	1835.7
130-807B-			
1H-1, 35	0.35	1548.3	1575.4
1H-1, 110	1.10	1573.8	
1H-2, 105	2.55	1572.1	1597.5
2H-1, 110	4.20	1556.7	1579.0
2H-2, 96	5.56	1553.3	1575.4
2H-3, 112	7.22	1565.2	1597.5
2H-4, 107	8.67	1563.5	1590.0
2H-5, 110	10.20	1550.0	1579.0
2H-6, 110	11.70	1556.7	1586.4
3H-2, 110	15.20	1546.6	1586.4
3H-3, 110	16.70	1556.7	1582.7
3H-4, 110	18.20	1560.1	1601.2
3H-5, 113	19.73	1558.4	1593.7
3H-6, 110	21.20	1568.6	1586.4
4H-1, 128	23.38	1548.3	1597.5
4H-2, 110	24.70	1561.8	1579.0
4H-3, 137	26.47	1546.6	1575.4
4H-4, 106	27.66	1565.2	1593.7
4H-5, 110	29.20	1555.0	1586.4
4H-6, 110	30.70	1568.6	1601.2
5H-1, 110	32.70	1551.6	1579.0
5H-2, 107	34.17	1551.6	1579.0
5H-3, 110	35.70	1540.0	1564.6
5H-5, 127	38.87	1536.7	1536.5
5H-6, 110	40.20	1551.6	1571.8
6H-2, 110	43.70	1553.3	1590.0
6H-3, 113	45.23	1540.0	1550.4
6H-4, 110	46.70	1563.5	1579.0
6H-5, 110	48.20	1558.4	1582.7
6H-6, 110	49.70	1541.6	1564.6
7H-1, 110	51.70	1573.8	1590.0
7H-2, 110	53.20	1563.5	1568.2
7H-3, 110	54.70	1555.0	1582.7

Table 14 (continued).

Core, section, interval (cm)	Depth (mbsf)	Vertical *P*-wave velocity (m/s)	Horizontal *P*-wave velocity (m/s)
7H-4, 110	56.20	1555.0	1579.0
7H-5, 110	57.70	1575.5	1586.4
7H-6, 110	59.20	1558.4	1582.7
8H-1, 110	61.20	1545.0	1553.9
8H-2, 110	62.70	1543.3	1550.4
8H-3, 110	64.20	1558.4	1571.8
8H-4, 110	65.70	1541.6	1550.4
8H-5, 110	67.20	1543.3	1553.9
8H-6, 110	68.70	1568.6	1582.7
9H-1, 110	70.70	1550.0	1568.2
9H-2, 110	72.20	1587.7	1627.9
9H-3, 110	73.70	1561.8	1597.5
9H-4, 110	75.20	1533.4	1557.5
9H-5, 110	76.70	1566.9	1593.7
9H-6, 110	78.20	1531.8	1550.4
10H-1, 110	80.20	1553.3	1561.0
10H-2, 110	81.70	1556.7	1557.5
10H-3, 110	83.20	1545.0	1553.9
10H-4, 110	84.70	1548.3	1564.6
10H-6, 110	87.70	1555.0	1590.0
11H-1, 110	89.70	1570.3	1571.8
11H-2, 10	90.20		1601.2
11H-2, 110	91.20	1558.4	
11H-3, 110	92.70	1566.9	1590.0
11H-4, 110	94.20	1573.8	
11H-5, 110	95.70	1568.6	1590.0
11H-6, 11	96.21		1586.4
11H-6, 110	97.20	1561.8	
12H-1, 110	99.20	1548.3	1571.8
12H-2, 110	100.70	1535.0	1553.9
12H-3, 110	102.20	1550.0	1553.9
12H-4, 110	103.70	1535.0	1561.0
12H-5, 110	105.20	1556.7	1568.2
12H-6, 110	106.70	1570.3	1605.0
12H-6, 110	106.70		1522.8
12H-6, 110	106.70		1601.2
13H-1, 110	108.70	1570.3	1590.0
13H-2, 110	110.20	1582.5	1601.2
13H-3, 112	111.72	1556.7	1590.0
13H-4, 110	113.20	1560.1	1612.5
13H-5, 110	114.70	1551.6	1586.4
13H-6, 110	116.20	1551.6	1543.4
14H-1, 110	118.20	1573.8	1608.7
14H-2, 110	119.70	1550.0	1561.0
14H-3, 105	121.15	1550.0	1557.5
14H-4, 110	122.70	1558.4	1593.7
14H-5, 106	124.16	1553.3	
14H-6, 106	125.66	1565.2	1582.7
15H-1, 110	127.70	1553.3	1561.0
15H-2, 110	129.20	1551.6	1550.4
15H-3, 110	130.70	1546.6	1571.8
15H-4, 110	132.20	1545.0	1579.0
15H-5, 110	133.70	1540.0	1557.5
15H-6, 110	135.20	1558.4	1553.9
16H-1, 110	137.20	1575.5	1568.2
16H-2, 110	138.70	1572.1	1575.4
16H-3, 110	140.20	1550.0	1553.9
16H-4, 110	141.70	1563.5	1597.5
16H-4, 110	141.70	1575.5	
16H-5, 110	143.20	1535.0	1550.4
16H-6, 110	144.70	1560.1	1564.6
17H-1, 110	146.70	1560.1	1593.7
17H-2, 110	148.20	1568.6	1605.0
17H-3, 110	149.70	1598.3	1627.9
17H-4, 110	151.20	1570.3	1601.2
17H-5, 110	152.70	1580.7	1620.2
17H-6, 110	154.20	1556.7	1564.6
18H-1, 104	156.14	1594.8	1624.0
18H-2, 108	157.68	1565.2	1631.8
18H-3, 108	159.18	1560.1	1593.7
18H-3, 108	159.18	1568.6	
18H-4, 108	160.68	1566.9	1564.6
18H-5, 108	162.18	1568.6	1575.4
18H-6, 108	163.68	1546.6	1543.4
19H-1, 108	165.68	1575.5	1593.7

Table 14 (continued).

Core, section, interval (cm)	Depth (mbsf)	Vertical *P*-wave velocity (m/s)	Horizontal *P*-wave velocity (m/s)
19H-2, 108	167.18	1560.1	1575.4
19H-3, 108	168.68	1563.5	1586.4
19H-4, 108	170.18	1558.4	1575.4
19H-5, 85	171.45	1558.4	1582.7
20H-1, 108	175.18	1575.5	1601.2
20H-2, 108	176.68	1572.1	1590.0
20H-3, 108	178.18	1572.1	1593.7
20H-4, 52	179.12	1566.9	1586.4
21H-1, 108	184.68	1573.8	
21H-2, 108	186.18	1565.2	1582.7
21H-3, 108	187.68	1550.0	1571.8
21H-4, 108	189.18	1556.7	1590.0
21H-5, 108	190.68	1573.8	1582.7
21H-6, 108	192.18	1572.1	1575.4
22H-1, 108	194.18	1568.6	1590.0
22H-2, 108	195.68	1566.9	1579.0
22H-3, 108	197.18	1556.7	1571.8
22H-4, 108	198.68	1572.1	1605.0
22H-5, 108	200.18	1560.1	1568.2
22H-6, 108	201.68	1558.4	1568.2
23H-1, 108	203.68	1568.6	1597.5
23H-2, 108	205.18	1580.7	1586.4
23H-3, 108	206.68	1573.8	1597.5
23H-4, 108	208.18	1570.3	1575.4
23H-5, 108	209.68	1591.3	1620.2
23H-6, 108	211.18	1575.5	1579.0
24H-1, 108	213.18	1575.2	1579.0
24H-2, 108	214.68	1587.5	1593.8
24H-3, 108	216.18		1557.4
24H-4, 108	217.68	1566.6	1582.7
24H-5, 108	219.18	1573.5	1616.4
24H-6, 108	220.68	1566.6	1579.0
25H-1, 108	222.68	1575.2	1608.8
25H-3, 108	225.68	1573.5	1597.5
25H-4, 108	227.18	1561.5	1586.4
25H-5, 108	228.68		1616.4
25H-6, 108	230.18	1568.4	1597.5
26H-1, 108	232.18	1580.5	1601.3
26H-2, 108	233.68	1568.4	1582.7
26H-3, 108	235.18	1558.1	1575.4
26H-4, 108	236.68	1571.8	1582.7
26H-6, 108	239.68	1566.6	1564.6
27H-1, 108	241.68	1575.2	1579.0
27H-2, 108	243.18	1566.6	1557.4
27H-3, 108	244.68	1583.9	1590.1
27H-4, 108	246.18	1583.9	1593.8
27H-5, 102	247.62	1594.5	1568.2
27H-6, 108	249.18	1573.5	1586.4
28H-1, 103	251.13	1568.4	1608.8
28H-2, 108	252.68		1635.8
28H-3, 108	254.18	1587.5	1582.7
28H-4, 108	255.68		1582.7
28H-5, 108	257.18		1616.4
28H-6, 76	258.36		1571.8
29H-1, 110	260.70	1585.7	1612.6
29H-2, 110	262.20	1587.5	1593.8
29H-3, 110	263.70	1583.9	1631.9
29H-4, 110	265.20	1580.5	1605.0
29H-5, 110	266.70		1612.6
29H-6, 110	268.20		1659.6
30H-1, 110	270.20	1587.5	1593.8
30H-2, 110	271.70	1515.3	1586.4
30H-3, 110	273.20	1558.1	1620.3
30H-4, 110	274.70	1564.9	1608.8
30H-5, 110	276.20	1566.6	1620.3
30H-6, 110	277.70	1561.5	1612.6
130-807C-			
2R-1, 36	790.06	1789.8	1813.8
2R-2, 27	791.47	1676.8	1790.6
4R-1, 56	809.56	1840.2	1856.6
4R-2, 67	811.17	1794.1	1809.2
6R-1, 92	829.22	1752.9	1798.5
6R-2, 93	830.73	1839.7	1914.6
6R-3, 92	832.22	1925.9	1863.5

Table 14 (continued).

Core, section, interval (cm)	Depth (mbsf)	Vertical *P*-wave velocity (m/s)	Horizontal *P*-wave velocity (m/s)
6R-4, 92	833.72	1782.3	1872.4
6R-5, 81	835.11	1837.8	1886.4
9R-1, 24	857.64	1851.8	1852.7
12R-1, 28	876.88	1927.9	1771.3
15R-1, 18	894.08	1995.9	1925.3
16R-1, 59	899.49	1856.6	2005.2
17R-1, 32	904.22	1742.4	1752.3
17R-2, 48	905.88	1868.6	1835.2
19R-1, 32	914.22	1789.8	1824.3
21R-1, 5	923.95	1759.3	1838.3
23R-1, 50	939.20	1856.1	1897.8
23R-2, 43	940.63	1915.5	2015.1
23R-3, 44	942.14	1813.5	1918.5
23R-4, 38	943.58	1904.2	1934.8
24R-1, 71	944.41	1914.1	1838.4
24R-2, 71	945.91	1856.0	1804.4
25R-1, 36	948.76	1851.4	1902.0
26R-1, 57	958.67	1930.3	2002.9
30R-1, 35	997.15	1860.4	1981.9
30R-2, 50	998.06	1932.8	1970.8
31R-1, 24	1006.74	2372.5	
31R-1, 27	1006.77		2715.5
35R-1, 21	1044.51	1817.1	1772.2
37R-1, 5	1063.75	2329.1	
38R-1, 39	1073.59	2194.0	
40R-1, 90	1092.90	2489.1	
41R-1, 33	1098.03	2833.6	
42R-1, 42	1102.82	3234.1	
43R-1, 19	1106.59	3100.3	
44R-1, 45	1116.45	2329.8	2520.1
45R-1, 63	1126.23	2698.0	2576.2
45R-2, 50	1127.60	2991.6	3280.0
46R-1, 45	1135.65		4262.5
46R-1, 49	1135.69	3572.5	
46R-2, 55	1137.25	3552.4	
46R-2, 55	1137.25	3713.3	
46R-3, 3	1138.23	3466.8	3520.0
47R-1, 88	1141.08	4186.2	4771.5
47R-1, 88	1141.08		4305.3
47R-2, 66	1142.36	3490.4	3799.3
48R-1, 118	1146.38	3951.0	4158.0
48R-2, 99	1147.69	3793.9	3725.7
49R-1, 78	1150.98	3718.6	
50R-1, 72	1155.92	4302.3	
51R-1, 71	1160.91	4101.0	3971.6
51R-2, 68	1162.38	4161.0	4349.3
51R-3, 72	1163.92	4804.1	4589.1
52R-1, 83	1170.63	3868.6	3928.1
52R-2, 121	1172.51	3980.2	4460.3
53R-1, 69	1180.09	4265.5	4270.3
53R-2, 75	1181.65	4867.6	5328.6
53R-3, 63	1183.03	4692.5	4329.1
53R-4, 123	1185.10	3862.0	4053.4
56R-1, 134	1207.94	3885.4	4124.1
56R-2, 140	1209.50	4170.7	3688.1
56R-3, 50	1210.10	3372.3	3759.5
57R-1, 116	1217.46	4285.4	4292.7
57R-2, 99	1218.79	3830.7	4261.1
58R-1, 11	1222.61	4305.4	4598.2
59R-1, 56	1232.76	3020.9	3325.9
59R-2, 67	1234.37	2935.1	3137.6
61R-1, 57	1252.07	3293.7	3673.3
61R-2, 89	1253.89	3900.7	3895.3
62R-1, 83	1262.03	3089.6	3434.2
62R-2, 64	1263.34	3364.5	3418.8
62R-3, 95	1265.15	3358.3	
63R-1, 29	1271.09	3183.1	3774.9
63R-2, 58	1272.88	3359.8	3565.2
63R-3, 86	1274.66	3256.8	3581.7
64R-1, 96	1281.46	3537.7	3804.5
64R-2, 73	1282.73	3145.5	3392.6
65R-1, 54	1290.64	3784.4	3514.8
65R-2, 42	1292.02	3222.3	3664.8
66R-1, 128	1301.08	3314.4	3426.1
66R-2, 75	1302.05	3224.8	3546.0

Table 14 (continued).

Core, section, interval (cm)	Depth (mbsf)	Vertical *P*-wave velocity (m/s)	Horizontal *P*-wave velocity (m/s)
66R-3, 85	1303.65	3130.9	3464.0
67R-1, 76	1310.26	3049.0	3366.1
67R-2, 110	1312.04	3636.7	3442.2
67R-3, 74	1313.18	3793.9	
67R-4, 38	1314.32		3810.8
67R-4, 67	1314.61	3381.6	
67R-5, 38	1315.82	3403.5	3569.8
68R-1, 68	1319.78	3186.0	3360.6
68R-2, 28	1320.88	3177.2	3481.9
68R-3, 58	1322.68	3272.4	3830.1
69R-2, 107	1331.37	3383.1	3599.8
69R-3, 4	1331.84	3631.9	3934.8
69R-4, 87	1334.17	3503.4	3797.5
69R-5, 17	1334.97	3370.7	3938.0
70R-1, 70	1339.10	3581.5	3887.3
70R-2, 108	1340.98	3519.7	3784.3
70R-3, 98	1342.38	3320.5	3481.0
70R-4, 52	1343.42	3704.7	3662.7
71R-1, 46	1348.46	3330.8	3565.8
71R-2, 131	1350.81	2603.1	3143.7
71R-3, 107	1352.07	1938.5	
71R-4, 60	1353.10	1829.3	2519.0
71R-5, 48	1354.48	1897.6	2308.0
71R-6, 28	1355.78	2033.0	2628.5
72R-2, 43	1359.63	1978.6	2268.6
73R-1, 68	1368.08	2029.8	2021.2
73R-2, 58	1369.48	2264.4	2773.3
76R-1, 109	1395.89	5234.4	4795.0
77R-1, 112	1405.62	4927.9	5057.7
78R-1, 69	1410.19	5359.7	5384.8
79R-2, 135	1417.25	4826.5	3480.4
80R-1, 53	1424.43	5603.4	4985.5
81R-2, 75	1435.85	4947.1	4846.4
83R-2, 29	1448.40	5572.8	5343.6